Amperometric Determination of Cobalt as Tungstate

By V. D. ANAND*, G. S. DESHMUKH and A. JOSEPH

(Received November 29, 1960)

The use of sodium tungstate as a precipitant for the quantitative determination of cobalt was recently reported by Anand[1]. The method was based on the reaction studied by Smith and Bradbury[2]. A conductometric titration procedure for cobalt[3] based on the precipitation of cobalt as tungstate was also developed. Consequent upon the development of an amperometric titration method for the determination of cobalt as tellurite[4] it was considered worthwhile to examine the validity of the results of gravimetric and conductometric studies on the determination of cobalt as tungstate by the application of the amperometric technique to this precipitation reaction. A further confirmation of the composition of cobalt tungstate was also sought.

Experimental and Results

Solutions.—Sodium tungstate: An approximately 0.1 M solution was prepared from B. D. H. reagent grade sample. It was standardized by precipitating tungsten as the benzidine complex[5] and final weighing as WO_3 after incineration above 1000°C.

Cobalt(II) chloride solution was about 0.1 M and was standardized by the anthranillate procedure[6] and checked by the α-nitroso β-naphtol method[7].

Gelatin solution was prepared according to the details given by Meites[8] and was 0.1%. Fresh solutions of gelatin were prepared every day. B. D. H. Analar salt was used for preparing a stock 1.0 M solution of potassium chloride.

Apparatus. — A Fisher elecdropode (catalog No. 9-317) was used for recording the current potential characteristics during the amperometric determination of cobalt as tungstate. The instrument has a built in galvanometer and works on 115 V. A. C. supply. It is used in conjunction with the dropping mercury electrode. The working of the instrument involves the increment method which makes it necessary merely to obtain current values at a limited number of points both before and after equivalence point in order to carry out an analysis.

Determinations of Cobalt as Tungstate. — In a supporting electrolyte consisting of 0.1 M potassium chloride, having 0.01% gelatin and enough alcohol to give an overall concentration

TABLE I. AMPEROMETRIC DETERMINATION OF COBALT AS TUNGSTATE

No.	Strength of cobalt solution mM	Strength of tungstate solution mM	Amount of cobalt Taken mg.	Amount of cobalt Found mg.	Error %
1	9.938	98.31	14.64	14.62	−0.14
2	8.944	88.48	13.18	13.18	—
3	7.950	78.65	11.71	11.70	−0.08
4	6.957	68.72	10.25	10.24	−0.09
5	5.963	58.97	8.78	8.79	+0.11
6	4.969	49.16	7.32	7.28	−0.51
7	3.975	39.32	5.86	5.88	+0.34
8	2.981	29.49	4.39	4.39	—
9	1.988	19.66	2.93	2.93	—
10	0.994	9.83	1.46	1.47	+0.69
11	0.497	4.92	0.733	0.74	+0.95
12	0.248	2.46	0.366	0.37	+1.10

* Present address: Indian Institute of Technology, Kanpur, India.

1) V. D. Anand, *Ann. Chim. (Rome)*, **50**, 432 (1960).
2) E. F. Smith and R. H. Bradbury, *Ber.*, **24**, 2930 (1891).
3) G. S. Deshmukh, V. D. Anand and A. K. Vishwanath, *Ann. Chim. (Rome)*, **50**, 439 (1960).
4) G. S. Deshmukh, V. D. Anand and A. Joseph, *Z. anal. Chem.*, in press.
5) G. von Knore, ibid., **47**, 37 (1908); *Ber.*, **38**, 783 (1905).
6) P. E. Wenger, C. Cimmerman and A. Corbaz, *Mikrochim. Acta*, **2**, 314 (1938).
7) A. I. Vogal, "A Text Book of Quantitative Inorganic Analysis", Longman Green, New York (1953), p. 461.
8) L. Meites, "Polarographic Techniques", Interscience, New York (1955), p. 135.

of 50% was taken an aliquot of the cobalt-(II) solution. The mixture was thoroughly deaerated by a slow stream of purified nitrogen. Necessary connections were made and the drop time adjusted to a drop of mercury every three seconds. A potential of −1.5 V. vs. S. C. E. was applied to the dropping mercury cathode and the mean galvanometer deflection noted.

The process was repeated after every addition of the tungstate solution from a microburette. The mixture was thoroughly mixed and deaerated by a rapid stream of nitrogen and the precipitate allowed to settle for one minute before observing the current reading. The strength of the tungstate solution was maintained at approximately 10 times stronger than that of cobalt to eliminate the dilution effects. Correction factor for volume error $i_{obs}\{(V+v)/V\}$ was however, applied for greater accuracy. Point of intersection of the graph obtained by plotting the current against the volume of the titrant was read at the volume axis to get the equivalence point. Results of the titrations of cobalt solutions varying in concentration from 0.2∼10 mM are given in Table I.

The effect of addition of alcohol on the equivalence point of the precipitation of cobalt as tungstate was also studied. Alcohol concentrations were varied from 30∼90%. The results are presented in Table II and shown in Fig. 1, which also represents the mode of the titration curves obtained in the amperometric determination of cobalt as tungstate.

TABLE II. EFFECT OF ALCOHOL CONCENTRATION ON AMPEROMETRIC TITRATION OF COBALT AS TUNGSTATE

No.	Concn. of alcohol %	Amount of cobalt		Error %
		Taken mg.	Found mg.	
I	90	14.64	14.66	+0.14
II	80	14.64	14.65	+0.07
III	70	14.64	14.64	—
IV	60	14.64	14.65	+0.07
V	50	14.64	14.64	—
VI	40	14.64	14.55	−0.38
VII	30	14.64	14.51	−0.89

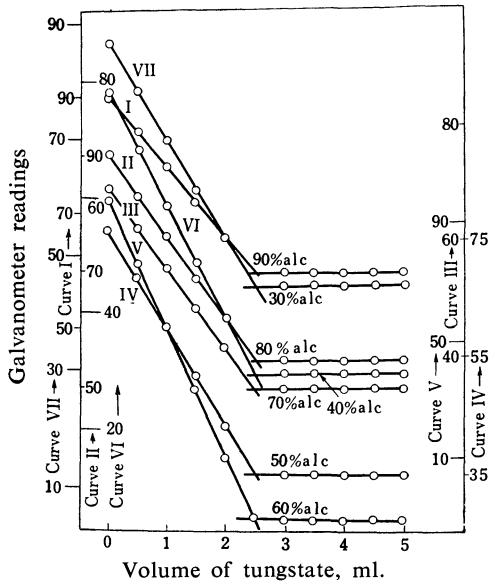


Fig. 1

Discussion

Von Stackelberg et al.[9] studied the polarography of tungsten(VI) in conentrated hydrochloric acid and reported only a single reduction wave. In neutral or alkaline media tungsten does not produce any reduction wave[10]. Cobalt, however, is not reducible in hydrochloric acid[11]. There were accordingly two possibilities for the choice of a suitable supporting electrolyte in the amperometric titration of cobalt as tungstate. Either concentrated hydrochloric acid could be employed as the supporting medium, in which case the reducible ion would be tungsten(VI) ; or a supporting electrolyte in which cobalt ion is reduced at the dropping mercury electrode. The WO_4^{2-} ion was, however, reported to exist only alkaline media[12]. As such hydrochloric acid could not be used as the supporting electrolyte, because the precipitation of cobalt tungstate would be inhibited. Potassium chloride was, therefore, chosen as the medium, in view of its earlier use in the amperometric titrations of cobalt as tellurite[4], and also because earlier work on cobalt tungstate had been done in normal aqueous solutions[1,3].

In potassium chloride the $E_{1/2}$ vs. S. C. E. for cobalt was −1.2 V. and though the wave was reportedly irreversible, the magnitude of the current was found to be proportional to cobalt concentration over a considerable range[13] (up to 15 mM). For actual titrations a potential of −1.5 V. was applied during the amperometric titrations of cobalt as tungstate.

The diffusion current due to cobalt fell as more and more of the precipitant was added

9) V. Stackelberg, M. P. Klinger, W. Koch and E. Krath, *Forschungberichte Tech. Mitt. Krupp., Essen*, 2, 59 (1939).
10) I. M. Kolthoff and J. J. Lingane, "Polarography", Vol. II, Interscience, New York (1952), p. 461.
11) L. Meites and T. Meites, unpublished experiments in "Polarographic Techniques", Interscience, New York (1955), Appendix B., p. 303,
12) H. J. Emelius and J. S. Anderson, "Modern Aspects in Inorganic Chemistry", Routledge and Kegan Paul, London (1952), p. 212.
13) J. J. Lingane and H. Kerlinger, *Ind. Eng. Chem., Anal. Ed.*, 13, 77 (1941).

and this continued till the whole of the cobalt in the test solution had been precipitated. Beyond the equivalence point, the current approached the residual current value due to the titration medium.

At low concentrations of cobalt encountered in these studies, the solubility of cobalt tungstate was significant. To overcome this effect, the addition of some non-aqueous medium was necessary. Alcohol up to 50% overall concentration was used in the conductometric studies reported earlier[3]. The effect of varying alcohol concentrations ranging from 30~90% was studied (cf. Table II, Fig. 1) to determine alcohol concentration required in these studies for getting reproducible results. Best results were obtained with alcohol concentrations above 50%. This concentration of alcohol was, therefore, used in the amperometric titration of cobalt.

The titrations for cobalt as tungstate were performed for different cobalt concentrations. In a series of 12 determination involving 0.2~10 mM Co, precision was better than 1%; with very dilute samples, however, it was poorer. The concentration limits for cobalt determination by the present technique were found to lie between 0.1~50 mM. Stronger solutions could be handled after proper dilutions. The method was not applicable in the presence of other cations giving insoluble tungstates.

Amounts of tungstate required during the amperometric titrations agreed with the molar ratio Co : W of unity and agreed with the observations of Smith and Bradbury[2] and Anthon[14], and also of the present author's[1,3] earlier reports. This confirms the composition of the precipitate formed to be $CoWO_4$ i. e. the normal tungstate.

Grateful thanks of the authors are due to Professor S. S. Joshi for keen interest and to Professor G. B. Singh, Head of the Chemistry Department for necessary facilities. The award of a Senior Scholarship to one of us (V. D. A.) from the Ministry of Scientific Research and Cultural Affairs is also acknowledged.

Department of Chemistry
Banaras Hindu University
Banaras-5, India

14) E. F. Anthon, *J. prakt. Chem.*, (1) **9**, 314 (1836).

Infrared and Raman Spectra of Ethylidene Dialkyl Ethers

By Kenkichi NUKADA

(Received April 21, 1961)

The author has investigated the infrared and Raman spectra of dialkoxymethanes such as $CH_3OCH_2OCH_3$, $CH_3OCH_2OC_2H_5$, $C_2H_5OCH_2 \cdot OC_2H_5$ and $(CH_3)_2CHOCH_2OCH(CH_3)_2$ in various phases. He has concluded that dimethoxy methane ($CH_3OCH_2OCH_3$) takes one forms in both its vapor and liquid phases, at least near room temperature, and that the different figures of the vapor and liquid spectra are not due to the existence of rotational isomerism but to different intermolecular forces in the two phases. It was not clear whether or not in the other dialkoxy methanes such a conclusion is also reasonable, but from the similarity of behavior of spectra in various conditions he assumed that in the other dialkoxy methanes the molecule exists as one form in both the vapor and liquid phases[1]. With this assumption, the assignment of spectra of these compounds has been undertaken[1-3].

It is now interesting to study the rotational isomerism in ethylidene dialkyl ethers ($R_1OCH(CH_3)OR_2$), in which one hydrogen atom of the central OCH_2O group of dialkoxy methanes is replaced by a methyl group. In this paper, he presents the infrared spectra of ethylidene dimethyl ether ($CH_3OCH(CH_3)OCH_3$), ethlidene methyl ethyl ether ($CH_3OCH(CH_3)OC_2H_5$), and ethylidene diethyl ether ($C_2H_5OCH(CH_3)OC_2H_5$) in vapor at various temperatures, and in carbon tetrachloride and acetonitrile solutions. They are abbreviated as EDM, EME and EDE, respectively.

From a comparison of the spectra obtained, he has found that ethylidene dialkyl ethers

1) K. Nukada, This Bulletin, **34**, 1615 (1961).

2) K. Nukada, *Spectrochim. Acta*, to be published.

3) K. Nukada, This Bulletin, **34**, 1624 (1961).

have a possibility of having two or more rotational isomers in their vapor and liquid phases.

Raman spectra of these compounds were also obtained, and the assignment of spectra is presented with the observation that rotational isomerism could exist in these molecules.

Experimental

EDM and EDE were prepared from methanol and acetoaldehyde, and from ethanol and acetoaldehyde, respectively. EME was prepared from a mixture of methanol and ethanol and acetoaldehyde[4]. A detailed description of the preparation of EME will be given elsewhere. The purity of samples was checked by a gas-chromatograph.

Infrared spectra of vapor and liquid phases were taken by using a Perkin Elmer 21 spectrophotometer equipped with a sodium chloride prism. Vapor spectra at elevated temperatures were obtained by means of a high temperature gas cell designed and constructed by Tomita of the author's laboratory[5]. It must be noticed that ethylidene dialkyl ethers are decomposed very quickly at the vapor phase in the presence of oxygen at elevated temperatures, so the high temperature cell should be completely deoxygenized before using.

Raman spectra of pure liquid were taken by using a Cary 81 spectrophotometer. The degree of depolarization was obtained by wrapping two types of silver chloride polarizers around a Raman tube alternately.

Results and Discussion

Infrared Spectra of Ethylidene Dialkyl Ethers. — *Ethylidene Dimethyl Ether.* — The relative

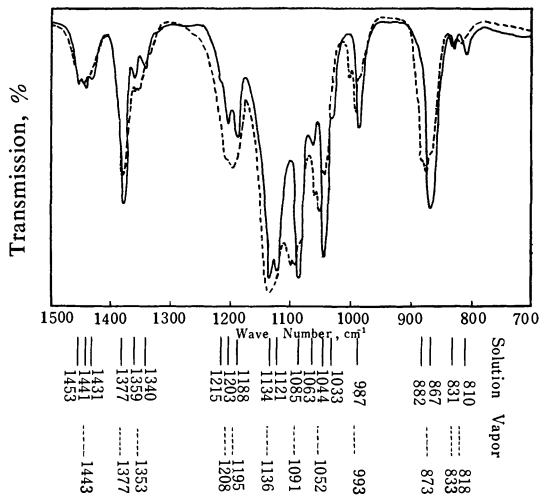


Fig. 1. Infrared spectra of ethylidene dimethyl ether ($CH_3OCH(CH_3)OCH_3$). Solid line, CCl_4 and CS_2 solutions, cell thickness: 0.15 mm., 2%. Dashed line, vapor.

4) K. Nukada, *Reports Gov. Chem. Ind. Research Inst. Tokyo*, 55, 99 (1960).
5) H. Tomita, unpublished.

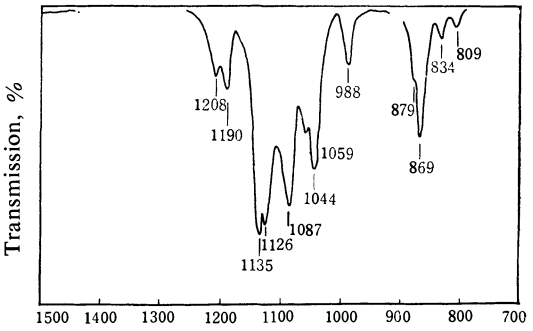


Fig. 2. Infrared spectrum of ethylidene dimethyl ether ($CH_3OCH(CH_3)OCH_3$). Acetonitrile solution, cell thickness: 0.015 mm., 20%.

intensity of the bands at 1121 and 1052 cm^{-1} decreases in the vapor phase, and that of the band at 1087 cm^{-1} in acetonitrile solution decreases slightly, as compared with that of the corresponding band in carbon tetrachloride solution (Figs. 1 and 2). The vapor spectra at elevated temperatures, however, show no appreciable change. Therefore, in EDE, there is no definite evidence that this molecule has two or more rotational isomers in its vapor and liquid phases.

Ethylidene Methyl Ethyl Ether.—The relative intensity of the bands at 1083, 1050 and 942 cm^{-1} decreases in the vapor phase, and that of the corresponding bands in acetonitrile solution definitely increases, as compared with that of the carbon tetrachloride solution bands (Figs. 4 and 5). In vapor spectra at elevated temperatures, the positions of maximum absorption are shifted from 1111 to 1098 cm^{-1} and from 935 cm^{-1} to a higher frequcncy, respectively (Fig. 6).

To interpret these results, the following theory is reasonable.

In this molecule, there are two rotational isomers, one with a less and the other with a more polar configuration both in the vapor and liquid phases. The bands at 1083, 1050 and at 942 cm^{-1} are due to the more polar form, while the band at 1105 cm^{-1} is due to the less polar form. From Figs. 4 and 5, it is clear that the abundance ratio of the more polar form to the less in acetonitrile solution is greater than that in carbon tetrachloride solution. In the vapor phase at low temperatures, the less polar form is predominant, but at higher temperature the number of molecules having the more polar form increases. In carbon tetrachloride solution, both forms exist almost equally.

Ethylidene Diethyl Ether.—The relative intensity of the band at 1095 cm^{-1} decreases in the

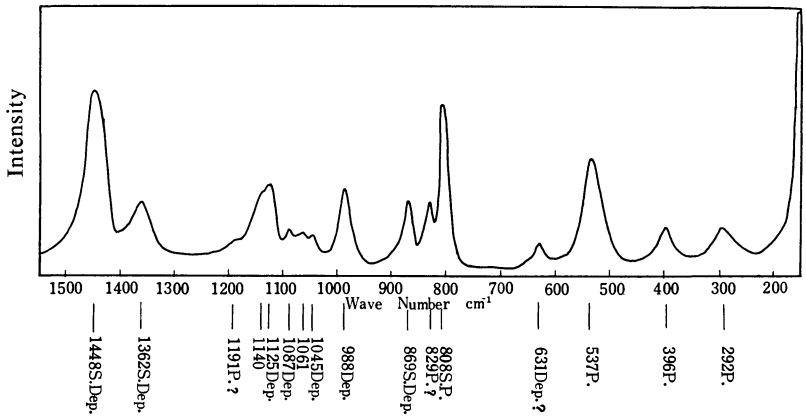


Fig. 3. Raman spectrum of ethylidene dimethyl ether ($CH_3OCH(CH_3)OCH_3$).

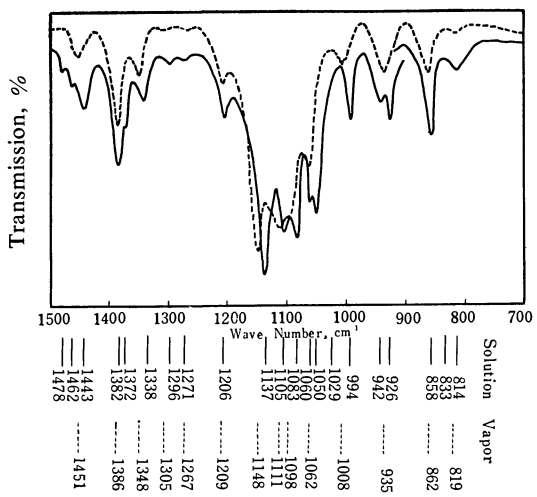


Fig. 4. Infrared spectra of ethylidene methyl ethyl ether ($CH_3OCH(CH_3)OC_2H_5$). Solid line: CCl_4 and CS_2 solutions, cell thickness: 0.15 mm., 2%. Dashed line: vapor.

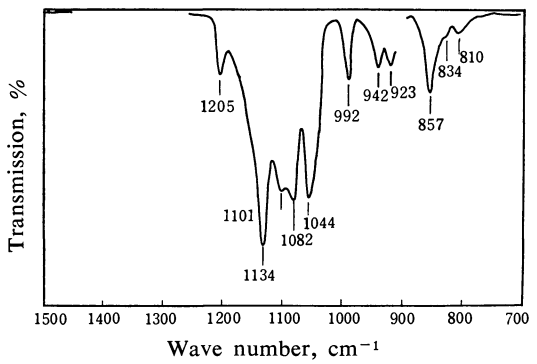


Fig. 5. Infrared spectrum of ethylidene methyl ethyl ether ($CH_3OCH(CH_3)OC_2H_5$). Acetonitrile solution, cell thickness: 0.015 mm., 20%.

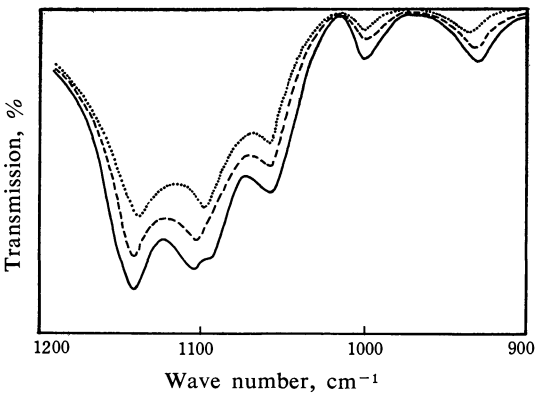


Fig. 6. Infrared spectra of ethylidene methyl ethyl ether ($CH_3OCH(CH_3)OC_2H_5$). Vapor.
—— 24°C ---- 85°C ····· 145°C

vapor phase, and that of the corresponding band in acetonitrile solution increases (Figs. 8 and 9) as compared with that of the carbon tetrachloride solution band. In vapor spectra at elevated temperatures, the position of maximum absorption is shifted from 1109 to 1095 cm^{-1} (Fig. 10).

Hence, as in the case of EME, it is reasonable to assume that in EDE there also exists rotational isomerism. The bands at 1080 and 1060 cm^{-1} are due to a more polar form, and the band at 1099 cm^{-1} is due to a less polar form. The more polar form is predominant in acetonitrile solution and in vapor at higher temperatures. In carbon tetrachloride solution, both forms are mixed almost equally.

Next the author will consider the molecular configuration of these compounds by assuming the existence of rotational isomerism. As one can easily understand from the actual molecular model, a planar zigzag form and a gauche-gauche form, in which terminal alkoxy groups rotate counterclockwise about 120° from the

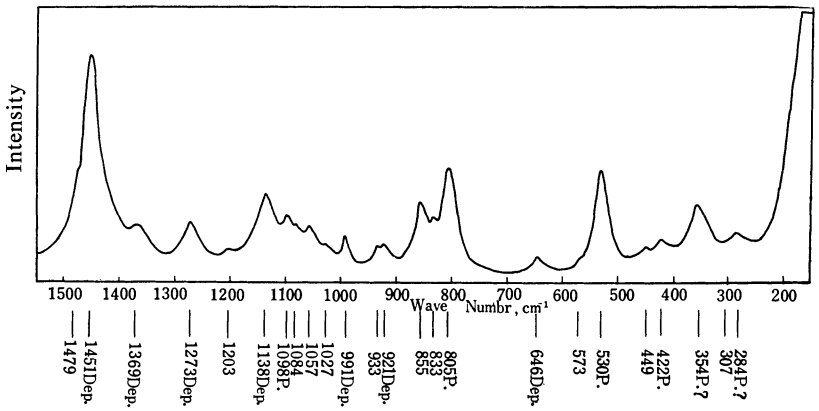


Fig. 7. Raman spectrum of ethylidene methyl ethyl ether ($CH_3OCH(CH_3)OC_2H_5$).

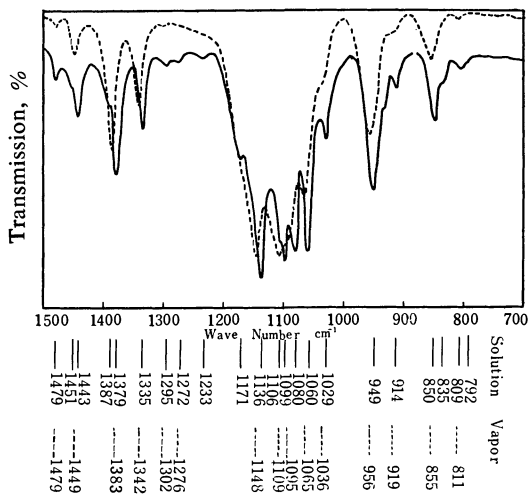


Fig. 8. Infrared spectra of ethylidene diethyl ether ($C_2H_5OCH(CH_3)OC_2H_5$). Solid line: CCl_4 and CS_2 solutions, cell thickness: 0.15 mm., 2%. Dashed line: vapor.

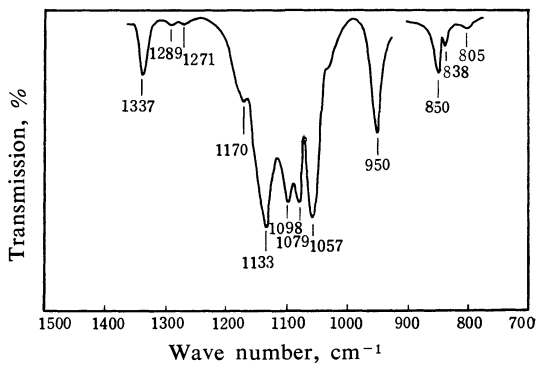


Fig. 9. Infrared spectrum of ethylidene diethyl ether ($C_2H_5OCH(CH_3)OC_2H_5$). Acetonitrile solution, cell thickness: 0.015 mm., 20%.

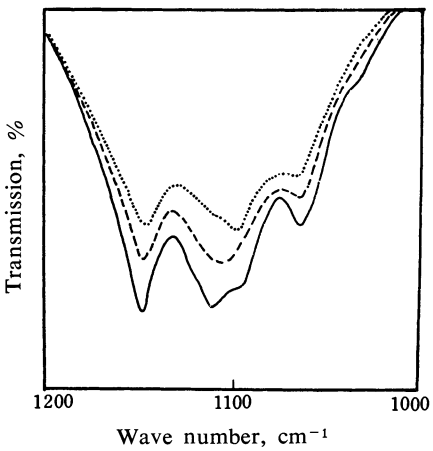


Fig. 10. Infrared spectra of ethylidene diethyl ether ($C_2H_5OCH(CH_3)OC_2H_5$). Vapor.
—— 24°C ---- 78°C ····· 155°C

central OCO plane, could not exist, since the repulsion between central methyl ($OCH(CH_3)O$) and terminal alkyl groups is fairly large. Kubo has produced a diagram showing the relation between the dipole moment of a R_1–O–C–O–R_2 type molecule and the azimuthal angles φ and ϕ of terminal alkoxy groups from the central OCO plane. From the observed value of the dipole moment of EDE in the vapor phase, Kubo has suggested that the molecule has a configuration in which $\varphi=120°$ and $\phi=240°$ (A form), or one in which $\varphi=180°$ and $\phi=240°$ (B form)[6]. From the diagram given by Kubo, it is concluded that the more polar form is the A form and the less polar one is the B form, if rotational isomerism exists in EME and EDE.

6) M. Kubo, *Sci. Papers Inst. Phys. Chem. Research*, **30**, 169 (1936).

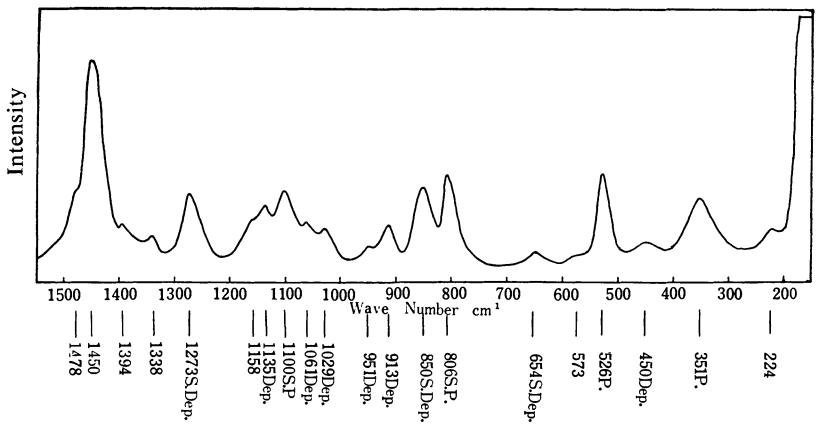


Fig. 11. Raman spectrum of ethylidene diethyl ether ($C_2H_5OCH(CH_3)OC_2H_5$).

As in the case of dialkoxy methanes, however, the difference in intermolecular interaction could produce some changes in the appearance of spectra in various phases[1]. Hence, a rigorous conclusion regarding the existence of rotational isomerism in EME and EDE in not obtained only from the present observation. To examine the reliability of the present interpretation of infrared spectra, the accurate measurement of the dipole moment in both the vapor and liquid phases at various temperatures is necessary, as in the case of dimethoxy methanes[1].

Assignment of Spectra of Ethylidene Dialkyl Ethers.—In this section, the assignment of the spectra of EDM, EME and EDE will be described by referring to that of dialkoxy methanes and related compounds. As discussed in detail in the preceding section, there is a possibility of the existence of rotational isomerism in EME and EDE. But in the assignment of these two compounds it is very difficult to decide one by one which band is due to which configuration, except for the few bands mentioned in the preceding section. So in the following description, an assignment to a definite molecular configuration is not presented except for a few cases. Raman spectra are shown in Figs. 3, 7 and 11.

A very weak infrared and medium Raman band appears at 1478~11479 cm^{-1} in EME and EDE, but no band appears at this frequency in EDM. As was discussed in detail in another paper[3], this band is assigned to the methylene scissoring of the ethoxy group.

From the study of the spectra of diethoxy methane[3] and dimethoxy methane[2], an asymmetrical methyl deformation of the ethoxy and methoxy groups is expected to appear at 1460 and 1455 cm^{-1} respectively. A symmetrical methyl deformation of methoxy group should exist at 1460 cm^{-1}, according to Nakagawa[7], Sheppard[8] and Nukada[3]. The position of the asymmetrical methyl deformation of central $OCH(CH_3)O$ group is not clear, but presumably it exists near 1460 cm^{-1}. Therefore, at least four kinds of vibrations could exist around 1460 cm^{-1}, and it is not possible to assign the spectra of EDM, EME and EDE in this region definitely. If spectra of deuterated compounds were obtained, one could assign the bands in this region clearly.

The strong infrared band at 1377 cm^{-1} (having no corresponding Raman band) in EDM completely disappears in dimethoxy methane[3]. Therefore, this band is due to the $OCH(CH_3)O$ group. Since the CH deformation is expected to appear at a much lower frequency, this band is assigned to the symmetrical methyl deformation of $OCH(CH_3)O$ group. In EME and EDE, strong infrared bands are observed also at 1382 and 1379 cm^{-1} respectively which have no corresponding Raman bands. The medium Raman bands appear at 1362, 1369 and 1394 cm^{-1} in EDM, EME and EDE respectively; they have corresponding very weak infrared bands. As there is no other appropriate mode at this frequency, these bands are also assigned to the symmetrical methyl deformation of $OCH(CH_3)O$ group. To interpret these results reasonably, it is better to conclude that these two types of bands correspond to two different types of rotational isomers. Since the more polar form (A form as defined in the preceding section) and the less polar form (B form) belong to the Cs and C_1 point groups (ignoring the species of terminal alkyl groups), the former band (strong in infrared and no Raman) is assigned to the

7) I. Nakagawa, *J. Chem. Soc. Japan, Pure Chem. Sec.* (*Nippon Kagaku Zasshi*), **77**, 68 (1956).
8) N. Sheppard, *Trans. Faraday Soc.*, **51**, 1465 (1955).

TABLE I. VIBRATIONAL FREQUENCIES

EDM			EME		
IR		Raman	IR		Raman
Vapor	Liq.		Vapor	Liq.	
				1478(w)	1479(m)
	1453(m)	1448(s) Dep.		1462(w)	
1443(m)	1441(m)		1451(m)	1443(m)	1451(m) Dep.
	1431(m)				
1377(s)	1377(s)		1386(s)	1382(s)	
1353(w)	1359(w)	1362(m) Dep.		1372(w)	1369(mb) Dep.
	1340(w)		1348(m)	1338(m)	
			1305(w)	1296(w)	
			1267(w)	1271(w)	1273(s) Dep.
1208(m)	1215(sh)				
1195(s)	1203(m)	1191(w) P. ?	1209(w)	1206(m)	1203(w)
	1188(m)				
1136(s)	1134(s)	1140(m, sh)	1148(s)	1137(s)	1138(s) Dep.
	1121(s)	1125(s) Dep.	1111(s)	1105(s)	1098(m) P.
			1098(w)	1083(s)	1084(w)
1091(s)	1085(s)	1087(s)	1062(m)	1060(s)	1057(m)
	1063(w)	Dep.		1050(s)	
1052(s)	1044(s)	1061(w)			
	1033(sh)	1045(w) Dep.		1029(sh)	1027(w)
993(m)	987(m)	988(s) Dep.	1008(m)	994(m)	991(m) Dep.
				942(m)	933(m)
			935(m)	926(m)	921(m) Dep.
873(s)	882(sh)	869(s) S. Dep.	862(m)	858(s)	855(s) S. Dep.
	867(s)				
833(w)	831(w)	829(m) P. ?		833(vw)	833(w)
818(w)	810(w)	808(s) S. P.	819(w)	814(m)	805(s) S. P.
		631(m) Dep. ?			646(m) Dep.
		537(s) P.			530(s) P.
		396(s) P.			354(m) P.?
		292(s) P.			284(w) P.?
					573(vw)
					449(w)
					422(w) P.
					307(vw)

* s, m, mb, w and vw mean the qualitative intensities, strong, medium, medium and broad, weak and very weak. P., S. P., Dep. and S. Dep. mean the qualitative degree of depolarization,

more polar form and the latter one (strong in Raman and very weak in infrared) to the less polar form.

The medium infrared band at 1338~1335 cm^{-1} in EME and EDE is assigned to the methylene wagging of ethoxy group by analogy with diethoxy methane[4]. The origin of the very weak band at 1340 cm^{-1} in EDM is not clear at present.

The very weak infrared bands at 1295~1296 (with no corresponding Raman band) and 1271~1272 cm^{-1} (the corresponding Raman band being strong and depolarized) both in EME and EDE are assigned to the methylene rocking and twisting of the ethoxy group respectively, because no band appears in this region in EDM and the appearance of the spectra is similar to that of diethoxy methane and diethoxy methane-d_2[4].

The bands at 1215 and 1203 cm^{-1} and one at 1206 cm^{-1} in EDM and EME are assigned to the methyl rocking of the methoxy group, as will be explained in detail in another paper[2].

OF ETHYLIDENE DIALKYL ETHERS*

EDE			
IR		Raman	Assignment
Vapor	Liq.		
1479(w)	1479(w)	1478(m)	CH_2 scissoring (EtO)
	1451(w)		Asym. CH_3 deformation ($OCH(CH_3)O$, MeO, EtO)
1449(s)	1443(m)	1450(s)	Sym. CH_3 deformation (MeO)
1383(s)	1379(s)		Sym. CH_3 deformation ($OCH(CH_3)O$, EtO) L-form
	1387(w)	1394(mb)	Sym. CH_3 deformation ($OCH(CH_3)O$, EtO) M-form
1342(m)	1335(m)	1338(w)	CH_2 wagging (EtO)
1302(w)	1295(w)		CH_2 rocking (EtO)
1276(w)	1272(w)	1273(s) S. Dep.	CH_2 twisting (EtO)
	1233(w)		
			CH_3 rocking (MeO)
	1171(w)		
		1158(sh)	
1148(s)	1136(s)	1135(m) Dep.	Asym. COCOC stretching
1109(s)	1106(sh)	1100(s) S. P.	L-form
	1099(s)		sym. COCOC stretching
1095(w)	1080(s)		M-form
1065(m)	1060(s)	1061(m) Dep.	Asym. COCOC stretching M-form
1036(w)	1029(m)	1029(m) Dep.	CC stretching ($OCH(CH_3)O$)
			CH_3 rocking (MeO)
956(m)	949(s)	951(w) Dep. ?	CC stretching,
	935(sh)		CH_3 rocking (EtO)
919(w)	914(m)	913(m) Dep.	
855(m)	850(m)	850(s) S. Dep.	Asym. COCOC stretching
	835(sh)		
	792(w)		
811(w)	809(m)	806(s) S. P.	Sym. COCOC stretching
		654(m) S. Dep.	Asym. COCOC deformation
		526(s) P.	Sym. COCOC deformation
		351(s) P.	Sym. COCOC deformation
		573(vw)	Combination or overtone of torsional vibrations,
		450(w)	skeletal deformations
		224(sh)	Torsional vibration

polarized, strongly polarized, depolarized and strongly depolarized.

Skeletal stretchings are expected to appear between 1150 and 700 cm^{-1} as in the case of dialkoxy methanes[1,2].

The strong infrared band (with a corresponding medium or strong and depolarized Raman band) around 1135 cm^{-1} in EDM, EME and EDE is assigned to an asymmetrical COCOC skeletal stretching. Since the intensity of this band does not change in vapor, and in carbon tetrachloride and acetonitrile solutions, it is not clear to which molecular configuration this band belongs.

The bands at 1105 cm^{-1} in EDM and one at 1099 cm^{-1} in EDE (strong in infrared and medium or strong and polarized in Raman) are due to the less polar configuration, as described in the last section. Since the Raman band is strongly polarized, these bands are assigned to a symmetrical COCOC skeletal stretching.

The band at 1083 cm^{-1} in EME and that at 1080 cm^{-1} in EDE (strong in infrared and very weak in Raman) are due to the more polar configuration, as described in the last

section. Since the Raman band is depolarized (in EDE), these bands are assigned to an asymmetrical COCOC skeletal stretching.

Within the above-mentioned frequency region, the observed infrared and Raman bands of EDM do not correlate with those of EME and EDE. The band at 1121 cm^{-1} (strong both in liquid infrared and Raman and depolarized in Raman) in EDM is assigned to a symmetrical COCOC skeletal stretching, since the intensity of the vapor infrared band is very weak and that of the Raman band is strong. Although the definite assignment of the bands at 1085 and 1052 cm^{-1} in EDM is difficult, they have been assigned to asymmetrical stretchings since the intensity of the vapor and liquid infrared bands is very strong and that of the Raman bands is weak. It is not clear either that these bands are branches of doublet being caused by Fermi resonance, or that they are due to different molecular forms.

The weak or medium infrared bands around 1030 cm^{-1} (with depolarized Raman bands) in EDM, EME and EDE are assigned to a CC stretching of the $OCH(CH_3)O$ group.

The medium infrared bands around 990 cm^{-1} (with corresponding medium or strong and depolarized Raman bands) in EDM and EME are assigned to the methyl rocking of the methoxyl group.

There are three infrared bands between 960 and 910 cm^{-1} in EME and EDE. As no band appears in EDM and a few bands appear in diethoxy methane and diethoxy methane-d_2 in this region[3], they are assigned to vibrations due to the ethoxy group. More detailed assignment is quite hard, but they are presumably CC stretching or methyl rocking.

Between 870 and 850 cm^{-1}, strong and strongly depolarized Raman bands appear in EDM, EME and EDE. These bands have corresponding strong or medium infrared bands. As Raman bands are strongly depolarized. they are assigned to an asymmetrical COCOC skeletal stretching.

The Raman bands around 815 cm^{-1} are the strongest ones below 1300 cm^{-1} in EDM, EME and EDE. They are strongly polarized and have cerresponding medium or weak infrared bands. These bands are therefore definitely assigned to a symmetrical COCOC skeletal stretching.

In EDM, the number of bands assigned to the asymmetrical skeletal stretching exceeds two, so 1) at least two of them are the branches of doublet being caused by Fermi resonance, or 2) they are due to two rotational isomers.

The appearance of Raman spectra below 700 cm^{-1} is quite similar among EDM, EME and EDE; that is, the strongest and polarized bands appear around 530 cm^{-1}, while two medium or strong bands appear around 640 cm^{-1} (depolarized) and at 400~290 cm^{-1} (polarized). The position and the degree of depolarization of the bands are similar to those of dimethoxy methane, diethoxy methane and the deuterated compounds[2,3]. In accordance with the assignment of the spectra of dialkoxy methanes and the degree of depolarization observed, the following assignment has been obtained.

The bands around 640 cm^{-1} are assigned to the asymmetrical COCOC skeletal deformation because they are strongly depolarized. The strongest bands around 530 cm^{-1} and the next strongest bands between 400 and 280 cm^{-1} are assigned to the symmetrical COCOC deformations. In EDM, two bands having almost equal intensities appear, and it is not possible to give a more definite assignment for them at present.

Many weak bands appear below 600 cm^{-1} in EME and EDE; they should be 1) CH_3–C skeletal deformation, 2) overtone and/or combination of torsional vibrations, and 3) the skeletal deformations of the rotational isomers which are less predominant in the liquid phase.

Torsional vibrations are expected to exist below 250 cm^{-1}, but only one band was observed at this region in EDE.

The assignments thus obtained are tabulated in Table I.

Summary

Infrared spectra of three kinds of ethylidene dialkyl ethers ($CH_3OCH(CH_3)OCH_3$; EDM, $CH_3OCH(CH_3)OC_2H_5$; EME and $C_2H_5OCH\cdot(CH_3)OC_2H_5$; EDE), of vapor at various temperatures, and of carbon tetrachloride and acetonitrile solutions are presented.

From a comparison of the spectra obtained, it has been concluded that rotational isomerism could at least exist in EME and EDE.

Raman spectra of pure liquid have been obtained, together with the degree of depolarization.

The assignment of these spectra is given by referring to those of the homologues, such as dialkoxy methanes.

The author wishes to express his sincere thanks to Dr. Y. Mashiko for his valuable discussion, and to Mr. T. Suzuki for his help in the laboratory work.

Government Chemical Industrial Research Institute
Shibuya-ku, Tokyo

Effect of Hyperconjugation on the Decomposition of N-Alkyl-N-nitrosoacetamide

By Masuo MURAKAMI, Katsuhiko AKAGI and Yonosuke MORI

(Received April 4, 1961)

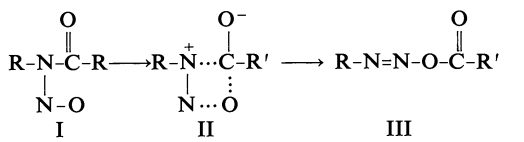
In the decomposition of *N*-alkyl-*N*-nitrosoacetamide, the β-phenyl group has been found, in an earlier paper, to decrease the heat of activation. This decrease in the heat of activation was explained by the stabilization of the transition state, involving second order hyperconjugation.

The effect of the β-phenyl group on the decomposition of *N-sec*-alkyl-*N*-nitrosoacetamide was found to be more pronounced when the alkyl group was cyclohexyl than when it was isopropyl, and the heat of activation of *N*-cyclohexyl-*N*-nitrosoacetamide was smaller than that of *N*-isopropyl-*N*-nitrosoacetamide. Hence the second order hyperconjugation was suggested as more probable for the cycloalkyl group. This hypothesis was supported by a hydrogen deuterium isotope effect experiment in which the rates of decomposition of *N*-cyclohexyl-*N*-nitrosoamides were found to be 1.1 ~2.8 times higher than those of corresponding deuterated homologues.

The thermal decomposition of *N*-alkyl-*N*-nitrosoamide has been known to result either in the formation of nitrogen and ester or in that of nitrogen, carboxylic acid and olefin as in the following equation (1).

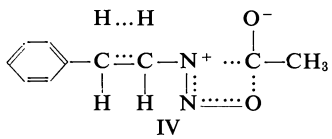
$$\mathrm{RN(NO)COR'} \begin{cases} \rightarrow \mathrm{N_2 + ROCOR'} \\ \rightarrow \mathrm{N_2 + R'CO_2H + olefins\ (corresponding\ to\ R)} \end{cases} \quad (1)$$

This decomposition has been considered to proceed through an intermediate, III, diazoester, while the rate-determining step was suggested to involve a four-membered ring, II[1].



(2)

In an earlier work[2] we have shown that the rate and the heat of activation of decomposition of *N*-ω-phenyl-*n*-alkyl-*N*-nitrosoacetamide varied with the increase of methylene linkages, and that the heat of activation of *N*-2-phenylethyl-*N*-nitrosoacetamide was smaller than those of *N*-benzyl- and *N*-3-phenyl-*n*-propyl-*N*-nitrosoacetamides. The heat of activation of *N*-2-phenylethyl-*N*-nitrosoacetamide was found to be 3 kcal. smaller than that of *N-n*-propyl-*N*-nitrosoacetamide. We suggested that the transition state IV of the decomposition of *N*-2-phenylethyl-*N*-nitrosoacetamide is



IV

more stable than those of the others because the double bonds in the phenyl group can conjugate with the π-electrons in the four-membered ring by means of the second-order hyperconjugation[3].

In this paper, the decompositions of several *N*-alkyl-*N*-nitrosoacetamides are examined in order to confirm our hypothesis and to find the nature of the hyperconjugation which occurs in the alkyl group, especially in the cyclic alkyl group.

Results and Discussion

The rates of decomposition of the *N-n*-alkyl-*N*-nitrosoacetamides were measured in xylene, while those of the *N-sec*-alkyl-*N*-nitrosoacetamides were done in benzene. All the nitrosoamides examined decomposed following first order kinetics. At the same temperature duplicate rate measurements were carried out. The maximum deviation of rate constants obtained in each experiment fell within $\pm 1\%$. Thus, the error of the heat of activation was calculated to be ± 0.2 kcal. per mol.[4]

1) R. Huisgen, *Ann.*, **574**, 184 (1951), and four earlier papers; D. H. Hey, J. Stuart-webb and G. H. Williams, *J. Chem. Soc.*, **1952**, 4657; E. H. White, *J. Am. Chem. Soc.*, 77, 6014 (1955).

2) M. Murakami and K. Akagi, *J. Chem. Soc. Japan, Pure Chem. Sec.* (*Nippon Kagaku Zasshi*), **75**, 532 (1954).

3) E. Berliner and F. Berliner, *J. Am. Chem. Soc.*, **71**, 1195 (1949); M. J. S. Dewer, "The Electronic Theory of Organic Chemistry", Oxford Univ. Press, (1950), p. 158; (Later, however, Dewar himself seems to have changed his original thought. See M. J. S. Dewar and H. N. Schmeising, *Tetrahedron*, **5**, 166 (1959)).

4) T. I. Crowell and L. P. Hammett, *J. Am. Chem. Soc.*, **70**, 3444 (1948); P. M. Dumber and L. P. Hammett, ibid., **72**, 109 (1950); R. K. Brinton, ibid., 77, 842 (1955).

The Effect of β-Phenyl Group of *N*-2-Phenyl-*sec*-alkyl-*N*-nitrosoacetamide.—A similar effect by the β-phenyl group was observed in the decompositions of both *N*-2-phenyl-isopropyl- and *trans*-*N*-2-phenylcyclohexyl-*N*-nitrosoacetamides in benzene. The results obtained are shown in Table I.

TABLE I. DECOMPOSITION RATE, HEAT AND ENTROPY OF ACTIVATION OF *N*-2-PHENYL-*sec*-ALKYL-*N*-NITROSOACETAMIDE IN BENZENE

RN(NO)COCH$_3$ R	Temp. °C	$10^4 \times k$ sec^{-1}	$\Delta H^{\neq}$ kcal. mol^{-1}	$\Delta S^{\neq}$ e.u.
sec-Butyl	34.8	0.677	23.9	− 4.5
	44.7	2.35		
	54.9	7.91		
2-Phenyl-isopropyl[2]	50.0	2.53	20.6	−13.5
	60.0	7.08		
	70.0	17.5		
2-Cyclohexyl-isopropyl	34.8	0.408	23.5	− 5.0
	44.7	1.39		
	55.1	4.55		
trans-2-Cyclohexyl-cyclohexyl	34.8	1.30	21.8	− 8.1
	44.7	3.95		
	54.9	12.2		
trans-2-Phenyl-cyclohexyl	34.8	0.642	17.6	−22.5
	44.7	1.34		
	54.9	3.24		

As will be shown in the latter part of this paper, the rate of reaction was found to increase, decreasing the heat of activation by the steric effect of a α-substituent of *N*-alkyl group in the decomposition of nitrosoamide[5].

However, a β-alkyl substituent does not seem to have a steric effect; the heats of activation of *N*-2-cyclohexyl-isopropyl-*N*-nitrosoacetamide and *N*-*sec*-butyl-*N*-nitrosoacetamide were the same as that of *N*-isopropyl-*N*-nitrosoacetamide (23.7 kcal./mol.).

The phenyl group at the β-position apparently decreased the heat of activation of the decomposition. The decrease by the β-phenyl group, which can not be explained by steric effect, is probably caused by the greater stability at the transition state, which involves second order hyperconjugation between the phenyl group and four membered ring.

It is very interesting to note that the effect of β-phenyl on the heat of activation is greater in a cyclohexyl system than in an open chain system. The difference in the heat of activation between *N*-2-cyclohexyl-isopropyl- and *N*-2-phenyl-isopropyl-*N*-nitrosoacetamide was 3 kcal. per mol., while the difference in the heat of activation between *trans*-*N*-2-cyclohexylcyclohexyl- and *trans*-*N*-2-phenylcyclohexyl-*N*-nitrosoacetamides was 4 kcal. per mol.

5) R. Huisgen, *Ann.*, **595**, 55 (1955).

Although all these compounds have one hydrogen atom at the α-carbon atom of the *N*-alkyl group, the β-carbon atom of *N*-2-phenyl-isopropyl-*N*-nitrosoacetamide has two hydrogen atoms which are available for hyperconjugation with the benzene ring in the transition state, while *N*-2-phenylcyclohexyl-*N*-nitrosoacetamide has only one. Therefore, if the magnitude of second order hyperconjugation is dependent on the number of available hydrogen atoms, the effect of β-phenyl could be expected to be larger in the *N*-isopropyl compound than in the *N*-cyclohexyl compound. However, the observed result was contrary to our expection.

We would like to suggest that the magnitude of second order hyperconjugation is not determined by the number of available hydrogen atoms but rather by the structure of the ethylene linkage which is involved. In other words, hyperconjugation would be larger in cyclic alkane than in open chain alkane.

Decomposition of *N*-*n*-Alkyl-, *N*-*sec*-Alkyl- and *N*-Cycloalkyl-*N*-nitrosoacetamides.—There were large differences in the rate and the heat of activation in decompositions of *N*-*n*-propyl-, *N*-*sec*-butyl- and *N*-cyclohexyl-*N*-nitrosoacetamides. The decompositions of some *N*-*n*-alkyl-, *sec*-alkyl- and cycloalkyl-*N*-nitrosoacetamides were also examined in order to find if the reactivity of the nitrosoamide is affected by hyperconjugation which is caused by π-electrons in the four-membered ring at the transition state. The results obtained are shown in Tables II, III and IV.

The heats of activation on *N*-*n*-alkyl-*N*-nitrosoacetamides, as shown in Table II, had no correlation with the number of hydrogen atoms available for hyperconjugation, all

TABLE II. DECOMPOSITION RATE, HEAT AND ENTROPY OF ACTIVATION OF *N*-*n*-ALKYL-*N*-NITROSOACETAMIDE IN XYLENE

RN(NO)COCH$_3$ R	Temp. °C	$10^4 \times k$ sec^{-1}	$\Delta H^{\neq}$ kcal. mol^{-1}	$\Delta S^{\neq}$ e.u.
Methyl	80.0	0.165	27.5	−5.3
	90.2	0.525		
	100.2	1.46		
Ethyl	70.2	0.313	27.0	−3.4
	80.0	0.975		
	90.2	2.925		
n-Propyl[a]	70.0	0.365	28.5	−1.2
	90.0	3.85		
n-Butyl	70.1	0.349	27.7	−0.9
	80.1	1.10		
	90.0	3.45		
Isobutyl	59.9	0.229	27.1	−1.0
	70.0	0.793		
	80.0	2.43		
	90.2	7.75		

a) Ref. 2

Table III. Decomposition rate, heat and entropy of activation of *N*-*sec*-alkyl-*N*-nitrosoacetamide in benzene

$RN(NO)COCH_3$ R	Temp. °C	$10^4 \times k$ sec^{-1}	$\Delta H^{\neq}$ kcal. mol^{-1}	$\Delta S^{\neq}$ e.u.
Isopropyl	24.9	0.235	23.7	−2.6
	34.8	0.848		
	44.7	3.04		
sec-Butyl	34.8	0.677	23.9	−4.2
	44.6	2.35		
	54.9	7.91		
1-Ethyl-propyl	25.0	0.212	24.3	−0.2
	35.0	0.809		
	45.0	2.95		

Table IV. Decomposition rate, heat and entropy of activation of *N*-cycloalkyl-*N*-nitrosoacetamide in xylene

$RN(NO)COCH_3$ R	Temp. °C	$10^4 \times k$ sec^{-1}	$\Delta H^{\neq}$ kcal. mol^{-1}	$\Delta S^{\neq}$ e.u.
Cyclobutyl	30.0	0.245	21.5	−11.2
	45.0	1.38		
	55.0	4.01		
Cyclopentyl	24.9	0.406	21.7	− 8.3
	34.8	1.27		
	44.7	4.26		
Cyclohexyl	24.9	0.712	20.8	−10.3
	34.8	2.16		
	44.7	6.76		
Cycloheptyl	24.9	0.283	22.6	− 5.9
	34.8	1.04		
	44.7	3.32		
	54.9	10.32		
Cyclooctyl	29.3	0.406	23.8	− 6.2
	34.8	0.860		
	44.7	3.01		
	54.9	9.78		

substances giving almost the same value (within the bounds of experimental error) except for the *N*-*n*-propyl compound. In the decomposition of *N*-*sec*-alkyl-*N*-nitrosoacetamides (Table III), the differences in heats of activation were very small, although there seems to be a trend for the heat of activation to increase with the decrease in the number of the available hydrogen atoms for the second order hyperconjugation. (All these compounds have one hydrogen atom for the first order hyperconjugation.) Therefore, in the decomposition of *N*-normal and *sec*-alkyl-*N*-nitrosoacetamides, the effect of hypercojugation is not large enough to effect the heat of activation. However, the situation was different when the *N*-alkyl group was cyclic. The heat of activation of *N*-cycloalkyl-*N*-nitrosoacetamides changed with the change in the ring size, the *N*-cyclohexyl compound being the most reactive.

Now let us look at the differences in the heat of activation (Table V) which appeared clearly in three alkyl series, *n*-alkyls, *sec*-alkyls, and cycloalkyls that are smaller than the seven-membered ring.

Table V. Heat of activation of *n*-alkyl-, *sec*-alkyl- and cycloalkyl-nitrosoacetamide

$RN(NO)COCH_3$ R	$\Delta H^{\neq}$ kcal. mol^{-1}
n-Alkyl	27.0～28.5
sec-Alkyl	23.7～24.3
Cycloalkyl	20.8～22.6

Huisgen[5] explained the difference between *N*-*n*-alkyl- and *N*-*sec*-alkyl-*N*-nitrosoamides as follows: the energy level of the ground state of *N*-*sec*-alkyl-*N*-nitrosoamide is higher than that of *N*-*n*-alkyl-*N*-nitrosoamide because the former has some steric strain as a result of the interaction of the branched alkyl group and the nitroso group, but the latter has not, while the energy levels of the transition states of the two compounds are the same.

While the difference in heat of activation between *N*-*n*-alkyl- and *N*-*sec*-alkylnitrosoamides can be accounted for by such a steric strain of the ground state, the difference between the heat of activation of *N*-*sec*-alkylnitrosoamide and that of *N*-cyclic alkyl nitrosoamide is hard to explain by a similar steric strain, because the acetamide group of the cyclic compound is at the equatrial position, thus causing no change in the steric strain.

Here again the second order hyperconjugation seems to offer a better explanation, because quasi-π-bond formation would be more favored in puckered cycloalkyl groups than in open chain compounds.

Decomposition of *N*-1- or 2-Deuterated Cyclohexyl-*N*-nitrosoacetamides.—If the assumption dercribed above is correct, it can be expected that the decomposition rate of *N*-cyclohexyl-*N*-nitrosoacetamide will decrease when 1- or 2-hydrogen atoms of cyclohexyl are replaced by deuterium atoms. The results obtained are exactly as expected and are presented in Table VI:

Table VI. Decomposition rates of *N*-cyclohexyl- and *N*-1- or 2-deuterated cyclohexyl-*N*-nitrosoacetamide in benzene

$RN(NO)COCH_3$ R	$10^4 \times k$ sec^{-1}	D atoms per molecule
Cyclohexyl	6.76	
1-Deuterated cyclohexyl	6.08	0.297
2-Deuterated cyclohexyl	2.43	2.54

The rate of acetolysis of cyclopentyl tosylate is known to be retarded[6] by the sustitution

6) A. Streitwieser, Jr., R. H. Jagow and S. Suzuki, *J. Am. Chem. Soc.*, 77, 6713 (1955).

of deuterium at the 2-position. The difference in free energy of activation per a deuterium atom was found to be ca. 100 cal. From this value it would be adequate to assume that the second order hyperconjugation can explain the decreased reactivities of *N*-deuterated cyclohexyl-*N*-nitrosoacetamides, because the second order hyperconjugation might be of the same order of magnitude as the first order hyperconjugation[7].

Experimental

Preparation of Amines.—Methyl-, ethyl-, *n*-propyl-, *n*-butyl-, isobutyl-, and cyclohexyl-amines were all commercially available products. *trans*-2-Phenylcyclohexylamine[8] (b. p. 116~118°C/6 mmHg., hydrochloride m. p. 247°C), *trans*-2-cyclohexyl-cyclohexylamine[8] (b. p. 110~110.5°C/4 mmHg), *sec*-butylamine[9] (b. p. 63°C), cyclopentylamine (b. p. 104~106°C) and cycloheptylamine (b. p. 85°C/75 mmHg, hydrochloride m. p. 245~246°C) were prepared from the corresponding oximes by reduction, using sodium and absolute ethanol[8]. Cyclooctylamine[9] (b. p. 72°C/12 mmHg, picrate m. p. 191~192°C), and 2-cyclohexyl-isopropylamine[10] (b. p. 85~87°C/21 mmHg, n_D^{20} 1.4615) were prepared by catalytic reduction from cyclooctanoneoxime and 2-phenylisopropylamine respectively. 1-Ethyl-*n*-propylamine (b. p. 90°C, picrate m. p. 167~168°C) and cyclobutylamine (b. p. 80~81°C) were prepared by the Schmidt reaction from α-ethylbutyric acid and cyclobutanecarboxylic acid respectively.

1-Deuterated Cyclohexylamine.—It has been reported that only 1-hydrogen atoms were exchanged by deuterium in the treatment of carboxylic acid with D_2SO_4. A mixture of 12 g. of cyclohexanecarboxylic acid (b. p. 113°C/6 mmHg, m. p. 29~30°C) and 18 g. of ice-cooled D_2SO_4 in a sealed tube was kept at 50°C for 300 hr. The resultant dark-brown mixture was poured into ice-water. The acid was extracted with ether and then was dissolved in a diluted aqueous sodium hydroxide solution. This solution was acidified with sulfuric acid and extracted with ether again. After drying the extract and removing the ether, the residue was distilled under reduced pressure, and 10.6 g. of 1-deuterated cyclohexanecarboxylic acid (b.p. 135°C/25 mmHg) was obtained. This substance has an absorption at 2195 cm^{-1} for carbon-deuterium bond. From 7.5 g. of this acid, 5 g. of 1-deuterated cyclohexylamine (b. p. 134°C) was obtained by the Schmidt reaction, using sulfuric acid. This amine has an absorption at 2170 cm^{-1} for carbon-deuterium bond.

2-Deuterated Cyclohexylamine.—2-Deuterated cyclohexanone was prepared by the method described in a previous work[12]. Twenty grams of cyclohexanone was added to ice-cooled D_2SO_4 (40 g.), and the mixture was kept at 20°C for 90 min. The resultant mixture was poured into ice-water and then extracted with ether. From the extract 5.2 g. of 2-deuterated cyclohexanone was obtained. This substance has an absorption at 2190 cm^{-1} for carbon-deuterium bond. From this ketone 2.2 g. of 2-deuterated cyclohexylamine (b. p. 133~134°C) was obtained by the usual oximation method, using

TABLE VII. *N*-ALKYLACETAMIDES, $RNHCOCH_3$

R	Formula	B.p./mmHg or m.p., °C	C, %		H, %		N, %	
			Calcd.	Found	Calcd.	Found	Calcd.	Found
Methyl	C_3H_7NO	65/8						
Ethyl	C_4N_9NO	80~82/5						
n-Propyl	$C_5H_{11}NO$	122/25						
Isopropyl	$C_5H_{11}NO$	82/9						
n-Butyl	$C_6H_{13}NO$	110/3					12.16	12.00
Isobutyl	$C_6H_{13}NO$	93/2	62.57	62.81	11.38	10.84	12.16	12.15
sec-Butyl	$C_6H_{13}NO$	87/3	62.57	62.32	11.38	11.07	12.16	11.93
1-Ethyl propyl	$C_7H_{15}NO$	66	65.07	65.15	11.70	11.54	10.84	10.34
Cyclobutyl	$C_6H_{11}NO$	44	63.68	64.01	9.80	9.78	12.39	11.98
Cyclopentyl	$C_7H_{13}NO$	143/16	66.10	65.79	10.30	10.15	11.09	10.93
Cyclohexyl	$C_8H_{15}NO$	107	68.04	68.12	10.71	10.46	9.92	9.99
Cycloheptyl	$C_9H_{17}NO$	147~148/3	69.63	69.55	11.04	10.80	9.02	8.68
Cyclooctyl	$C_{10}H_{19}NO$	162/4					8.28	8.05
2-Cyclohexylisopropyl	$C_{11}H_{21}NO$	97					7.64	7.95
trans-2-Phenyl-cyclohexyl	$C_{14}H_{19}NO$	135	77.38	77.34	8.81	8.69	6.45	6.32
trans-2-Cyclo-hexylcyclohexyl	$C_{14}H_{25}NO$	147	75.28	75.63	11.28	11.33	6.27	6.12

7) M. M. Kreevoy and H. Eyring, ibid., **79**, 5121 (1957).
8) D. V. Nightingale, J. D. Kerr, J. A. Gallagher and M. Maienthal, *J. Org. Chem.*, **17**, 1017 (1952).
9) E. Rohrmann and H. A. Shonle, *J. Am. Chem. Soc.*, **66**, 1516 (1944).
10) B. L. Zenitz, E. B. Macks and M. L. Moore, ibid., **69**, 1117 (1947).
11) V. N. Setkina and E. V. Byova, *Doklady Acad. Nauk. S.S.S.R.*, **92**, 341 (1953); *Chem. Abstr.*, **49**, 164 (1955).
12) D. N. Kursanov and V. N. Setkina, *Doklady Akad. Nauk. S.S.S.R.*, **94**, 69 (1954); *Chem. Abstr.*, **49**, 844 (1955).

hydroxylamine hydrochloride, and reduction of the resultant oxime, using sodium and absolute ethanol. This amine has a strong absorption at 2175 cm^{-1} for carbon-deuterium bond.

Preparation of Acetamides.—Acetamides were prepared by acetylating the amines with acetic anhydride in ether. After washing with water, aqueous potassium carbonate solution, and water successively the mixture was dried over magnesium sulfate. Removal of the ether and distillation under reduced pressure gave the expected products. Recrystallization from a mixture of ligroin and chloroform gave the products in a pure form. Table VII lists the boiling points or the melting points and analytical data of the acetamides.

Water obtained from the combustion of 1- or 2-deuterated cyclohexyl acetamides contained 1.96 atom % and 16.5 atom % of deuterium respectively.

Nitrosation[13] of Amides.—Into an ice-cooled mixture of 0.01 mol. of acetamide and 0.03 mol. of anhydrous sodium acetate in carbon tetrachloride, a solution of 0.015 mol. of nitrogen tetraoxide in carbon tetrachloride, cooled to $-10\sim-15$°C, was stirred. After 30~60 min. at 0°C, the mixture was poured into ice-water. The carbon tetrachloride layer was washed with water, 5% aqueous solution of potassium carbonate, and water successively and dried over anhydrous sodium sulfate. The solvent was removed under reduced pressure at 0°C to give nitrosoacetamide, as yellow or reddish-yellow oil. Since nitrosoamide decomposes very easily, it was used immediately, without further purification, for the measurement of the rate.

Table VIII. Rate constant for the decomposition of *N*-methyl-*N*-nitrosoacetamide in xylene at 100.2°C

Time sec.	$V_\infty - V_t$ cc.	$10^4 \times k$ sec^{-1}
0	87.73	
300	83.91	1.49
600	80.43	1.45
900	77.01	1.44
1200	73.78	1.45
1500	70.55	1.45
1800	67.56	1.43
2100	64.92	1.47
2400	61.70	1.45
2700	59.29	1.45
3000	56.73	1.46
3300	54.27	1.46
3600	51.85	1.46
3900	49.65	1.46
4200	47.47	1.46
4500	45.47	1.47
4800	43.44	1.47
5100	41.52	1.45
Average value		1.46 ± 0.01

Table IX. Rate constant for the decomposition of *N*-cycloheptyl-*N*-nitrosoacetamide in benzene at 24.9°C

Time sec.	$V_\infty - V_t$ cc.	$10^4 \times k$ sec^{-1}
0	103.21	
1800	98.10	0.282
3000	94.45	0.281
4200	91.68	0.283
5400	88.59	0.283
6180	86.68	0.283
6600	85.65	0.283
8400	81.34	0.283
10200	77.33	0.283
11400	74.73	0.283
12600	72.22	0.283
13920	69.53	0.284
15000	67.34	0.285
20280	58.02	0.284
25200	50.45	0.284
32100	41.22	0.285
Average value		0.283 ± 0.001

Kinetic Studies.—The decomposition rates were measured volumetrically. A 50 cc. azotometer and 50% aqueous solution of potassium hydroxide were used for the measurement of the volume of nitrogen evolved from a solution of 0.004~0.007 mol. of nitrosoacetamide in 100 cc. of benzene or xylene. The thermostat was adjusted so as to maintain the temperature within ±0.01°C. The first order rate constant was calculated according to the following equation;

$$k = 2.303/t \cdot \log\{V_\infty/(V_\infty - V_t)\}$$

in which V_t and V_∞ are the volumes having evolved at time t and at the time when the decomposition ceased, usually ten-fold half the life of the reaction. The energy and entropy of activation were calculated by the least square method. Rate data for typical determination are shown in Tables VIII and IX.

The authors wish to thank Mr. Sotoo Yamamoto for his analysis of heavy water and Miss Kayo Kabazawa for her infrared spectral measurements. They are also grateful to the Ministry of Education for the grant-in-aid for the scientific research.

The Institute of Scientific and Industrial Research
Osaka University
Sakai-shi, Osaka

13) E. H. White, *J. Am. Chem. Soc.*, 77, 6008 (1955).

Photosensitized Oxidation of Leuco-uranine and the Identification of the Photobleached Product of Uranine in Ethanol Solution

By Kengo UCHIDA, Shunji KATO and Masao KOIZUMI

(Received April 24, 1961)

According to Imamura and Koizumi[1,2], the reductive photobleaching of xanthene dyes such as eosine and uranine takes place when the degassed solutions of such dyes in ethanol are irradiated by visible light. They studied the primary processes of this reaction to some extent, but did not undertake the identification of the final product, suspecting that the dye structure might be completely destroyed since the dye is not restored by the introduction of air after the reaction. There remains, however, a possibility that the leuco dye itself is stable and exists as such in the presence of air, and even in case the above speculation be true, it seems at least possible that the decomposition would take place after the formation of leuco dye; the transient existence of a rather stable semiquinone has been established by the flash technique[3], and this makes more plausible the ultimate formation of leuco dye through disproportionation reaction.

With regard to leuco-uranine, Kul'berg and Matveev[4] had reported that this compound, being rather stable in the presence of air, can be conveniently utilized for the quantitative analysis of a minute quantity of oxidant. The present authors have now found that this leuco compound is easily converted photochemically to uranine by the use of some dyes and acridine as photosensitizers. Moreover, this reaction, contrary to our expectation, has proved to take place more rapidly under the deaerated condition. A similar reaction was found to occur with the photobleached product in question; this and some other facts have now unambiguously confirmed that most of the photobleached product exists as leuco dye.

Preparation of Leuco-uranine and Some of its Physico-chemical Properties

Preparation.—*Reagents.* — 1) Sodium amalgam: Prepared from Merck's sodium and distilled mercury.

2) Sodium hydroxide solution: Saturated solution was prepared by dissolving Wako Pure Chemical Industries' G. R. grade sodium hydroxide. To minimize the contamination of sodium carbonate, the supernatant liquid was used.

3) Fluorescein: For the preparation of leuco-uranine, Hikotaro Shudzui & Co. G. R. grade fluorescein was used without further purification. For chromatography, polarography and sensitized reaction, the above sample was neutralized and then twice recrystallized from ethanol by evaporating the solvent without heating. The uranine crystal thus obtained was desiccated in a high vacuum. This sample has an extinction coefficient of 8.2×10^4 at 490 mμ, the highest value ever obtained[5]; this assures its high purity.

Procedure. — Fluorescein was dissolved in water, neutralizing it with a small excess of sodium hydroxide, and then reduced by sodium amalgam. When the dye color became quite faint, the amalgam was removed from the solution and the precipitate of leuco-fluorescein was obtained by adding dilute hydrochloric acid. The precipitate had a tint of yellow at first but gradually turned brown. It is a sticky resin-like material but solidifies by slight cooling.

This substance, after being dissolved in 99% ethanol, was neutralized with an equimolar sodium hydroxide pellet; evaporation of the solvent under reduced pressure gave a crystalline substance.

Further purification was performed to remove the sodum carbonate and the small amount remaining of the oxidized form of uranine. The latter substance, being more soluble in ethanol than leuco dye, can be washed out by a small quantity of ethanol. Then the substance is dissolved in a large quantity of ethanol; sodium carbonate which is insoluble in ethanol can be eliminated by this procedure. The solvent was distilled off in a high vacuum, and the crystal deposited was treated further in the above way several times. The final evacuation was continued for more than ten hours to remove any trace of ethanol; this was continued until the ethanol vapor could not be detected by Geissler's tube.

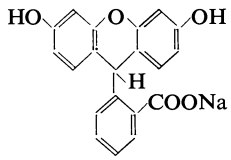
It is, of course, necessary to perform all the above procedures under a safety lamp. Heating in the course of dissolution and precipitation is undesirable since it tends to promote the decomposition of the sample. Only at the last stage of desiccation was the sample heated up to 40°C.

The final substance obtained with a slight tint of brown is very deliquescent; hence, it was preserved in a sealed ampoule and was kept in the dark.

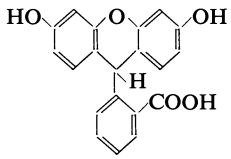
1) M. Imamura and M. Koizumi, This Bulletin, **28**, 117 (1955); ibid., **29**, 899 (1956); ibid., **29**, 913 (1956).
2) M. Imamura, ibid., **30**, 249 (1957).
3) S. Kato and M. Koizumi, *Nature*, **184**, 1620 (1959); S. Kato, T. Watanabe, S. Nagaki and M. Koizumi, This Bulletin, **33**, 262 (1960).
4) L. Kul'berg and L. Matveev, *J. Gen. Chem.* (*U.S.S.R.*), **17**, 457 (1947); *Chem. Abstr.*, **42**, 478 (1948).
5) M. Imamura, This Bulletin. **31**, 962 (1958).

The crystal does not melt up to 210°C.

Analysis of Leuco-uranine. — The sample is considered to be practically pure (I) from the results of acid and base titration.



I



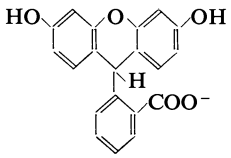
II

The sample was transformed into II by adding hydrochloric acid and, after washing with water and after desiccation through pumping in a high vacuum, was submitted to elementary analysis. The result is as follows:

Found: C, 68.06; H, 4.89. (a) Calcd. for II: C, 71.85; H, 4.22. (b) Calcd. for II with one mole of water (as crystalline water): C, 68.18; H, 4.58%.

The experimental value closely approximates the one for b.

Some Physico-chemical Properties of Leuco-uranine.—*Polarographic Studies.*—According to Delahay[6], who studied the polarogram of fluorescein in the pH range 2.00~10.83, two-stage waves appear only in the alkaline region; this indicates a two-steps reduction involving the formation of stable semiquinone. He considered the ultimate form of leuco dye to be III.



III

To ascertain that the same III is obtained by treating our sample of fluorescein with sodium amalgam, our starting substance, fluorescein was re-examined polarographically in the alkaline region. The result gave two-stage waves, the half-wave potentials being −1.12 and −1.36 V. at pH 10.5, and −1.16 and −1.60 V. in a 1.2 N sodium hydroxide solution (referred to as S. C. E.). Delahay's value at pH 10.5 (interpolated value) is −1.18 V.

It is most plausible from the above results that the treatment of fluorescein with sodium amalgam in the alkaline solution gives I as a final product.

Absorption Spectra.—As shown in Fig. 1, the absorption spectra of leuco-uranine have two peaks, at 280 mμ ($\varepsilon \sim 5\times10^3$) and at 210 mμ. The extinction in the visible region is different

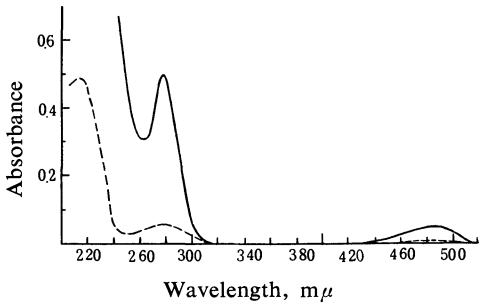


Fig. 1. Absorption spectra of leuco-uranine.
—— 1.0×10^{-4} M; ---- 1.0×10^{-5} M

from sample to sample, probably because of being contaminated with a different quantity of uranine, which has a large absorption maximum at 490 mμ. The second peak of leuco-uranine at 210 mμ is not so clear-cut, since it is superposed by the absorption of coexisting uranine.

Measurement of pK of Leuco-uranine. — For the measurement of pH, a Hitachi pH-meter E. H. P-1 was used. Acid and alkaline titration of leuco-uranine gave the two-step curves as shown in Fig. 2.

The two pK values obtained were $pK_1=3.8$ and $pK_2=9.6$ at 30°C. The first of these surely corresponds to the dissociation of the carboxyl group, II $\rightleftarrows$ III, in view of the fact that the pK values of benzoic acid, 2-ethylbenzoic acid

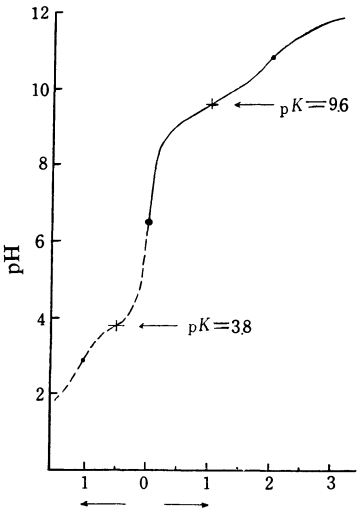
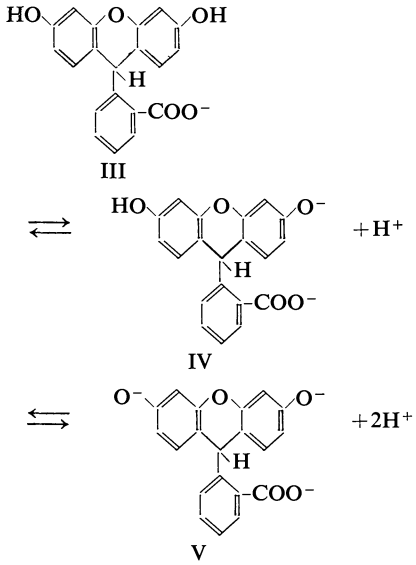


Fig. 2. An example of the titration curve of leuco-uranine.
Concn. of leuco-uranine: 2.76×10^{-2} M (25 ml.)
—— Alkali titration, NaOH 0.335 N
---- Acid titration, HCl 1.09 N

6) P. Delahay, *Bull. soc. chim. France*, **15**, 348 (1948).

and 2-*tert*-butylbenzoic aid are respectively 4.2, 3.8[7] and 3.5[8].

The second value is most certainly an average of the two p*K* values corresponding to the following two dissociation processes:



Strong evidence for this is the fact that about two equivalents of sodium hydroxide are needed for neutralization. The value is reasonable in view of the p*K* value of phenol, 10.0. Table I gives a comparison of the above values with those of fluorescein. It seems worth while to note that leuco dye has somewhat different values.

TABLE I. p*K*-VALUES OF FLUORESCEIN AND ITS LEUCO COMPOUND

	Fluorescein		Leuco compound
	Zanker[9]	Lindqvist[10]	
Cation~Neutral	1.95	2.2	
Neutral~Univalent anion	5.05	4.4	3.8
Univalent~Divalent	7.00	6.7	9.6
Divalent~Tervalent			

Photosensitized Oxidation of Leuco-uranine

It was found that leuco-uranine in the aqueous solution is photochemically oxidized to uranine by adding some substances as sensitizers. Quite unexpectedly, the reaction was further found to take place more promptly in the deaerated condition. Acridine, xanthene dyes such as uranine, eosine, erythrosine and thiazine dyes such as methylene blue and thionine are more or less effective sensitizers. Some azo dyes and rhodamine were found to be not effective.

Detailed studies were made using acridine, uranine and methylene blue.

Materials.—*Acridine.*—Tokyo Kasei G. R. grade acridine was submitted to repeated crystallization using a water-ethanol mixture. The concentration of acridine employed as a sensitizer was usually 1.5×10^{-4} M.

Methylene Blue.—Grübler's sample was twice recrystallized from *n*-butanol.

Other Dyes. — Commercial reagents were used without further purification.

Water.—Twice distilled.

Ethanol.—Wako Pure Chemical Industries' G. R. grade ethanol was used without further purification.

The concentration of leuco-uranine was usually 1×10^{-5} M.

The solution for each experiment was prepared by diluting the stock solution of 1.0×10^{-4} M. The stock solution when kept in the dark scarcely showed any change.

Apparatus.—In the case of acridine being employed as a sensitizer, the irradiating light was 365 mμ from a high pressure mercury lamp, passed through a ultraviolet filter (D-2). When the sensitizer was uranine or methylene blue, a 75 V.-500 W tungsten lamp was used at 45.0 V., the light $<$360 mμ being cut off in the former case with a ultraviolet-cut off-filter, and the light $<$600 mμ in the latter case with a Walz R-2 filter. The degree of coloration was measured by a Hitachi spectrophotometer EPU-2A, using a $1\times1\times4$ cm. Terex cell which was designed for evacuation. Degassing of the sample was done by use of a mercury diffusion pump, melting and freezing (in a dry-ice bath) being repeated five or six times.

The aqueous solution of acridine has an absorption maximum at 355 mμ, at which there exists no absorption of leuco-uranine or uranine; hence, 365 mμ of mercury lamp is very convenient for studying this system. This is the reason that acridine was chiefly used as a sensitizer.

Results

When the aerated solution containing leuco-uranine and acridine was irradiated with 365 mμ light, the coloration due to the restoration of uranine took place, but it did not go over 40%; further irradiation after evacuation never induced any more coloration. Examination of this material by paper chromatography proved the absence of leuco-uranine. Thus, it seems plausible that the decomposition of the dye took place, perhaps photochemically, following the formation of uranine.

The absorption spectra of the irradiated solution completely coincide with those of uranine in the visible region, with a maximum at 490 mμ and a shoulder near 460 mμ.

7) "International Critical Table", VI, McGraw-Hill, New York (1929), p. 291.
8) J. B. Shoesmith and A. Mackie, *J. Chem. Soc.*, **1936**, 300.
9) V. Zanker and W. Peter, *Chem, Ber.*, **91**, 572 (1958).
10) L. Lindqvist, *Arkiv. Kemi.*, **16**, 79 (1960).

Scarcely any change was perceived in the spectra of acridine (in the ultraviolet region).

The unexpected coloration which takes place in the highly degassed system proceeds with a much greater speed, and, moreover, it is almost quantitative.

In Fig. 3 the absorption spectra before and

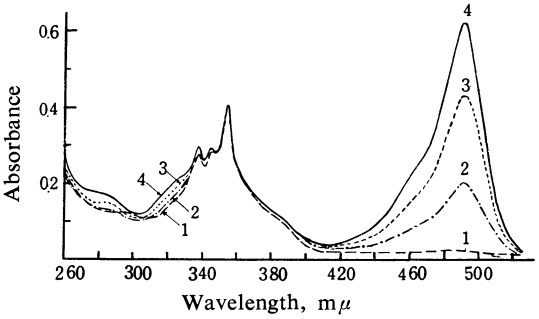


Fig. 3. Absorption spectra of leuco-uranine +acridine (sensitizer) at various irradiation times.

1 ——— Before irradiation
2 —·—· 1 min. irradiation
3 ------ 4 min. irradiation
4 ——— 30 min. irradiation

after the irradiation are shown. It is remarkable that there is no change in the absorption spectra of acridine, which precludes the hydrogenation of acridine taking place. There is no evolution of hydrogen*, but the exact nature of this reaction is quite unknown at the present time.

In the case of uranine as a sensitizer (with light $>360\,m\mu$), the reaction was also accele-

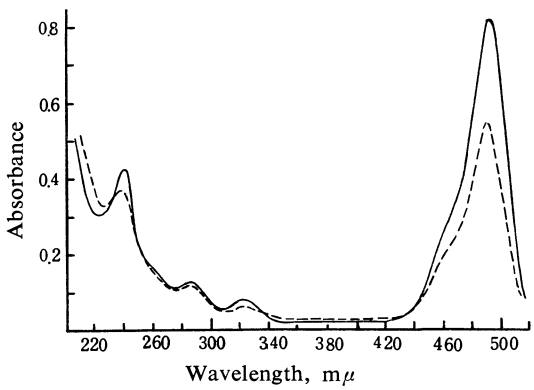


Fig. 4. Comparison between the absorption spectra of uranine and those of the irradiated product of leuco-uranine (a small quantity of uranine having been added previously as a sensitizer).

—— Uranine
---- The irradiated product of leucc-uranine

rated, so to speak in this case, autocatalytically. In this case also, degassing promotes the coloration and makes it more complete. The absorption spectra of the irradiated solution, as shown in Fig. 4, are quite similar to those of uranine. In the aerated solution, the coloration did not exceed 50%, whence the optical density at $490\,m\mu$ gradually declined, perhaps due to the irreversible photoöxidation.

When methylene blue was used as a sensitizer under the irradiation with light $>600\,m\mu$, the absorption spectra of uranine with a maximum at $490\,m\mu$ also grew with a moderate speed. In the presence of air, no appreciable change was observed in the absorption spectra of methylene blue, with only a slight decrease of optical dentity, probable due to photoöxidation[11].

In case of the evacuated solution, methylene blue is photoreduced to leuco, dye accompanied by the change of leuco-uranine to uranine. Its rate is very large, as is seen from Fig. 5A, which shows the absorption spectra of the solution at various irradiation times. The maximum of methylene blue at $665\,m\mu$ gradually declines even when the solution is kept in the dark, but the decline is very rapid when the solution is irradiated, and it is restored up to about 96% when air is introduced after the reaction. The maximum at $490\,m\mu$, which is due to uranine, grows gradually when the solution is kept in the dark. For example, the decrease of methylene blue and the increase of uranine when the solution is kept in the dark for four hours after evacuation, are respectively 0.33×10^{-8} mol. and 0.17×10^{-8} mol. The excess of the former over the latter is perhaps due to the adsorption of methylene blue to the cell wall. Irradiation accelerates the rate very much. The introduction of air causes a slight increase of absorbance at $490\,m\mu$, which is probably due to the absorption of methylene blue restored having a small extinction in this region.

In the ultraviolet region, the absorption spectra of methylene blue, leuco methylene blue, uranine and leuco-uranine overlap each other, complicating the change of the entire absorption spectra. Subtracting the absorption spectra due to uranine and leuco-uranine from the entire spectra, one gets the resultant spectra shown in Fig. 5B.

Although some degree of error is unavoidable in this treatment, it is clear that the absorption maxima at 293 and $248\,m\mu$ of methylene blue existent prior to irradiation disappear and that in their place a new maximum appears at $256\,m\mu$ in the irradiated solution.

* The experiment concerning this will be published shortly.

11) H. Obata, K. Kogasaka and M. Koizumi, This Bulletin, 32, 125 (1959).

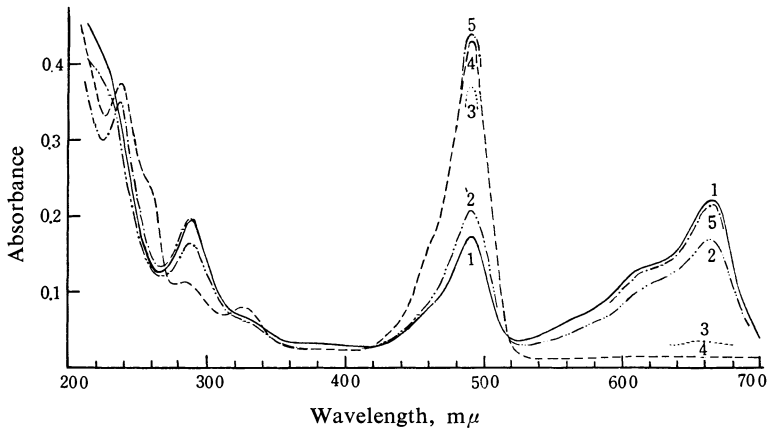


Fig. 5A. Absorption spectra of the solution containing leuco-uranine and methylene blue (sensitizer).

1 ——— Directly after deaeration
2 —··— After 4 hr. in the dark
3 ------ 10 sec. irradiation
4 ——— 90 sec. irradiation
5 —·—· After introduction of air

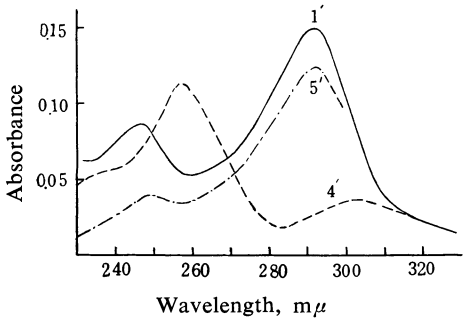


Fig. 5B. The resultant absorption spectra (240 ~320 mμ) when the contributions of leuco-uranine or uranine are subtracted from the observed spectra (Fig. 5A.).

1′ ——— Before irradiation
4′ ------ After irradiation
5′ —·—· After introduction of air

This is exactly equal to that of leuco methylene blue[12]. When the air is introduced after the reaction, the latter disappears and the two maxima due to methylene blue again come to exist.

The oxidation of leuco-uranine proceeds quite rapidly as long as methylene blue exists, but it becomes very slow when almost all the methylene blue turns into leuco form.

The quantity of methylene blue and leuco-uranine having reacted can be evaluated separately by the use of the extinction coefficients of methylene blue (6.0×10^4 at 665 mμ) and of uranine (8.2×10^4 at 490 mμ). Calculation showed that during the irradiation for 1.5 min., 1.4×10^{-8} mol. of methylene blue has disappeared and 1.2×10^{-8} mol. of uranine has been produced. The two values coincide well within the range of experimental error.

The reactions with the use of methylene blue are quite reasonable, since the oxidation-reduction potential of methylene blue and uranine are respectively ca. 0 and <-1 V.

Identification of the Photobleached Product of Imamura and Koizumi with Leuco-uranine

As to the photobleached product when the ethanol solution of uranine or eosine is irradiated by a visible light, Imamura and Koizumi suggested that the structure of the dye might be decomposed[1,2]. Now it is evident, however, from the results described above that the leuco dye is not so reactive, and hence there is ample possibility for the final product to be nothing but leuco dye. Therefore, the comparison between the chemically prepared leuco dye and the photobleached compound was undertaken spectroscopically and especially in respect to the photosensitized oxidation, which is highly specific.

Besides, paper-chromatographic comparison between them was tried.

Photosensitized Oxidation of the Photobleached Product.—The absorption spectra of the photobleached product, as shown in Fig. 6, resemble those of leuco-uranine, with maxima at 285 mμ and <220 mμ.

The photobleached product was prepared by irradiating the ethanol solution of uranine in the usual way. It was then separated from ethanol by distilling the latter in vacuo; to its alkaline solution was added acridine, and then the solution was irradiated by a 365 mμ

12) Y. Usui, H. Obata and M. Koizumi, ibid., 34, 1049 (1961).

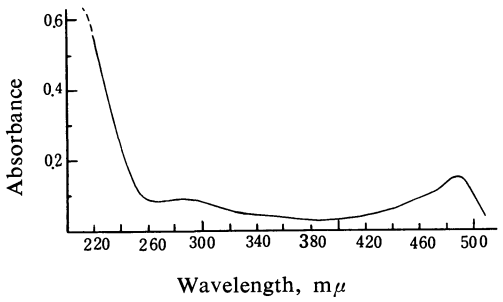


Fig. 6. Absorption spectra of the photobleached product of uranine as dissolved in a weak alkaline aqueous solution.

light. The formation of uranine was observed up to about 25% of the original quantity. In contrast to this result obtained for the aerated solution, degassing of the system accelerated the reaction, and the recovery attained about 60%. This indicates that at least more than 60% of the photobleached product exists as leuco dye.

It is to be added, however, that the restoration of color is slower than that of the chemically prepared leuco dye, the rate in the aerated and deaerated solution being respectively about half and one-fifth of that of the latter. This might be due to the inhibiting action of a certain substance produced during the photobleaching.

An analogous comparison was made with eosine.

The photosensitized coloration of the chemically prepared leuco-eosine in the deaerated alkaline solution was only about 70% of the total quantity. For the photobleached product it was about 35%. From these results it can be said that about half of the photobleached product exists as leuco dye.

In the aerated solution the result is not so clear-cut, the coloration in both the photobleached and chemically prepared samples being only 15~20%.

It is to be added that, in these cases, the shift of the maximum is accompanied by the oxidation of the leuco dye. Thus, the absorption peak of the recovered dye is 506~505 mμ compared with 514 mμ of eosine in the alkaline solution. This is due to the debromination reaction occurring in the alkaline solution[13]; this reaction would take place during the photosensitized oxidation and, moreover, might occur in the course of the preparation of leuco dye, which was done in a 1.3 N alkaline solution to make easy its reduction by sodium amalgam. According to Oster[14], dibromofluorescein has a peak at 506 mμ, which is exactly the same as the above value.

Analysis by Means of Paper Chromatography. —Taylor's method[15] was employed except that the composition of the developer was somewhat modified. Our composition was 28% ammonia water 10 vol.%, ethanol 15 vol.%, water 75 vol.%. Since the concentration of both uranine and leuco-uranine was low, the position after the development was decided by the fluorescence emitted by ultraviolet irradiation.

The ascending method was employed, and the filter papers used were Toyo Roshi (filter paper) No. 50. All the procedures were done in the dark room.

The results obtained for uranine are shown in Table II. It is clear that the result for the photobleached product is quite the same as that of leuco-uranine except for the existence of a certain substance with $R_f=0.935$. This unknown substance emits fluorescence with a white tint. 0.79 of leuco-uranine and the photobleached product, without doubt, is due to contaminated uranine. The R_f of leuco compound (0.86) is easily ascertained, since it is oxidized to uranine when irradiated (after development) and emits the fluorescence characteristic to uranine. Samples c and d usually give only $R_f=0.78$, but in addition they sometimes give $R_f=0.86$ of leuco-uranine, though its quantity is always very small.

Table II. The results of paper chromatography for uranine and related compounds

	R_f	
a) Uranine	0.78	
b) Leuco-uranine	0.79	0.86
c) The material obtained from leuco dye by oxidation in air	0.78	
d) The material obtained from leuco dye by oxidation in vacuo	0.79	0.86 (very little)
e) The photobleached product from uranine	0.79	0.85 0.935(?)

In case of eosine the results are more complicated and the reproducibility of the R_f-values is not so good. It can be said, however, from the results of more than ten tests, that the photobleached product contains an appreciable quantity of leuco-eosine. The material obtained by the photosensitized oxidation of leuco-eosine gives spots other than those of eosine, which may perhaps be attributed to dibromofluorescein.

13) M. Imamura and M. Koizumi, ibid., **29**, 913 (1956). Eosine, when, irradiated in the alkaline water-ethanol mixture, undergoes a rapid debromination.

14) A. H. Adelman and G. Oster, *J. Am. Chem. Soc.*, **78**, 3977 (1956).

15) K. B. Taylor, *Nature*, **185**, 243 (1960).

Summary

Leuco-uranine was prepared by reducing uranine with sodium amalgam, and some of its properties were investigated. The aqueous solution of leuco-uranine is stable in the presence of air irrespective of its low oxidation-reduction potential.

It was found that leuco-uranine is photo-oxidized to uranine by the use of acridine and some dyes as sensitizers. The reaction may be attributed to the dissolved oxygen and is very reasonable. A quite unexpected result was, however, that a similar reaction takes place more rapidly and more quantitatively in the degassed solution than in the aerated solution. The uranine and acridine employed as sensitizers in this case were ascertained not to sustain any change. The nature of the reaction is not known at the present time.

It was further established that the photo-bleached product obtained by irradiating the deaerated ethanol solution of xanthene dyes, consists mainly of leuco dye. This was ascertained by comparing their absorption spectra, by the photosensitized coloration, acridine being used as a sensitizer, and, in addition, by means of paper chromatography.

The authors wish to thank Miss Chieko Iwanaga for her assistance.

Department of Chemistry
Faculty of Science
Tohoku University
Katahira-cho, Sendai

Electrometric Study on Thorium-Arsenite System as a Function of the pH

By Ram Sahai SAXENA and G. P. SAXENA

(Received February 22, 1961)

The reaction between thorium nitrate and sodium(meta)arsenite solutions at different pH values has been studied by E.M.F. measurements reactants, using bright platinum as indicator involving potentiometric titrations between the electrode. The electrometric experiments give definite evidence of the formation of three arsenite compounds having the molecular formulae, $ThO_2 \cdot 2As_2O_3$; $ThO_2 \cdot As_2O_3$ and $3ThO_2 \cdot 2As_2O_3$ at pH 9.85, 11.25 and 12.28 respectively. The proportion of ThO_2 increases with the concentration of alkali used in the preparation of alkali arsenites and the formation of thorium arsenites is thus a function of the hydrogen ion concentration. The potentiometric titration curves are regular in form ; a pronounced maxima in dE/dV occurs at the end point, with either of the reagents used as the titrant and the results are accurate and reproducible. The effect of alcohol and electrolytes on the end point has been studied. The behavior of the indicator electrode and the mechanism of the electrode reaction have been discussed.

The precipitation of sodium arsenite solutions with heavy metal salts causes the formation of complex arsenites whose composition is mainly governed by the pH. The investigations of these compoundis made difficult by the adsoption of arsenic oxide by the metallic hydroxide; the conversion of ortho arsenite to pyro and meta arsenite takes place with great ease and these dissolve in excess of alkali or acid[1]. consequently analytical methods have failed to give a correct view of their composition. A survey of literature reveals that there are very few references to rare-metals arsenites and the earlier workers[2-4] mainly confined themselves to the analytical investigations of the precipitates formed by mixing metal salts and alkali arsenites under different conditions. Besides, it appears that the formation of arsenites has not been studied at different hydrogen ion concentration of the medium which plays an important role in their precipitation. Moreover, there is hardly any reference in literature to the study of this system by electrometric techniques which have provided more conclusive evidences on the composition of such metal complexes (Saxena et al.)[5] and hence the present investigation has been initiated.

1) Fritz Ephraim, "Text book of Inorganic Chemistry" (translated by P. C. L.Thorne and E. R. Robarts), Gurney and Jackson, London (1949), p. 745.
2) A. Stavenhagen. *J. prakt. Chem.*, **2**, 51 (1895).
3) C. Reichard, *Ber.*, **27**, 1024 (1894); **31**, 2166 (1898).
4) H. Wilke, *Kolloid. Z.*, **34**, 83 (1924).
5) R.S. Saxena et al., *J. Inorg. Nucl. Chem.*, **12**, 38 (1959); *Naturwiss*, **46**, 575 (1959); *Z. anorg. u. allgem. Chem.*, **303**, 12 (1960); **297**, 146 (1958); *Z. physik. Chem.*, [*N. F.*], **19**, 94 (1959); *Anal. Chim. Acta*, **20**, 494 (1959); *Z. Naturforsch.*, **130**, 557 (1958).

TABLE I. SUMMARY OF RESULTS OF POTENTIOMETRIC TITRATIONS

Molarity of solution		Equivalence point (ml.) Calc.	Obs. from dE/dV in presence of			Formula supported
			Alcohol		KNO_3 2 g.	
$NaAsO_2$	$Th(NO_3)_4$		0%	20%		
Direct titrations						
$NaAsO_2$ soln. at pH 9.85 added to 20 ml. of $Th(NO_3)_4$ soln. pH 5.6 (Fig. 1)						
M/5	M/120	3.33	3.38	3.35	3.36	$Th(AsO_2)_4$
M/10	M/200	4.0	4.08	4.08	4.05	or
M/15	M/400	3.0	3.04	3.02	3.03	$ThO_2 \cdot 2As_2O_3$
$Na_4As_2O_5(2NaAsO_2+2NaOH)$ soln. at pH 11.25 added to 20 ml. of $Th(NO_3)_4$ (Fig. 2)						
M/10	M/45	4.44	4.48	4.46	4.46	$ThAs_2O_5$
M/20	M/120	3.33	3.37	3.35	3.34	or
M/40	M/300	2.66	2.70	2.67	2.68	$ThO_2 \cdot As_2O_3$
$Na_3AsO_3(2NaAsO_2+4NaOH)$ soln. at pH 12.28 added to 20 ml. of $Th(NO_3)_4$ soln. (Fig. 3)						
M/10	M/100	2.66	2.68	2.66	2.68	$Th_3(AsO_3)_4$
M/20	M/180	2.96	3.0	2.98	2.98	or
M/50	M/300	4.44	4.52	4.47	4.48	$3ThO_2 \cdot 2As_2O_3$
Reverse titrations						
$Th(NO_3)_4$ soln. at pH 4.6 added to 20 ml. of $NaAsO_2$ soln. at pH 9.85 (Fig. 4)						
M/40	M/20	2.50	2.47	2.50	2.48	$Th(AsO_2)_4$
M/75	M/40	2.66	2.62	2.65	2.64	or
M/100	M/60	3.0	2.96	2.99	2.98	$ThO \cdot 2As_2O_3$
$Th(NO_3)_4$ soln. added to 20 ml. of $Na_4As_2O_5(2NaAsO_2+2NaOH)$ soln. at pH 11.25 (Fig. 5)						
M/80	M/10	2.50	2.46	2.48	2.48	$ThAs_2O_5$
M/100	M/20	4.0	3.95	3.98	3.96	or
M/200	M/30	3.0	2.97	2.98	3.0	$ThO_2 \cdot As_2O_3$
$Th(NO_3)_4$ soln. added to 20 ml. of $Na_3AsO_3(4NaOH+2NaAsO_2)$ soln. pH 12.28 (Fig. 6)						
M/60	M/14	3.50	3.44	3.48	3.46	$Th_3(AsO_3)_4$
M/100	M/20	3.0	2.98	3.0	2.98	or
M/400	M/60	2.25	2.21	2.24	2.22	$3ThO_2 \cdot 2As_2O_3$

Experimental

Merck's guarateed extra-pure reagents thorium nitrate and $NaAsO_2$ were used. Thorium was estimated as thorium oxalate and its subsequent ignition to thorium oxide[6]. The strength of sodium arsenite solutions was checked by titrating against standardized iodine solution. The pH of $NaAsO_2$ solutions was measured using a glass electrode of the range (1~13 pH) with the help of buffer solution. Calculated amounts of sodium hydroxide were added to sodium arsenite solutions in definite molecular proportions to vary the pH.

Using differnt concentrations of thorium nitrate and alkali arsenite solution at pH levels 9.85, 11.25 and 12.28, potentiometric titrations were carried out both by the direct and the inverse methods, i. e. when the alkalized arsenite solutions from the micro-burette were add to thorium salt in the electrode vessel and vice versa. A bright platinum foil was dipped in the solution to be titrated and used as an indicator electrode in conjunction with saturated calomel electrode through potassium nitrate salt-bridge. The titration cell was kept in an electrically maintained thermostat. The E. M. F. was measured on a Cambridge (null deflection type) pH-meter. The titer solution was continuously stirred by a magnetic stirrer. Curves were plotted between the E(obs.) and the volume of the titrant added in ml. and from the sharp break in potential indicated by the titration curves, the equivalence point was obtained. This was further checked by calculating the maximum value of dE/dV in each case. The titrations were also performed in presence of varying concentrations of ethanol and electrolytes as potassium nitrate. Twenty milliliters of the reagent was taken in the cell each time (see Table I).

Discussion

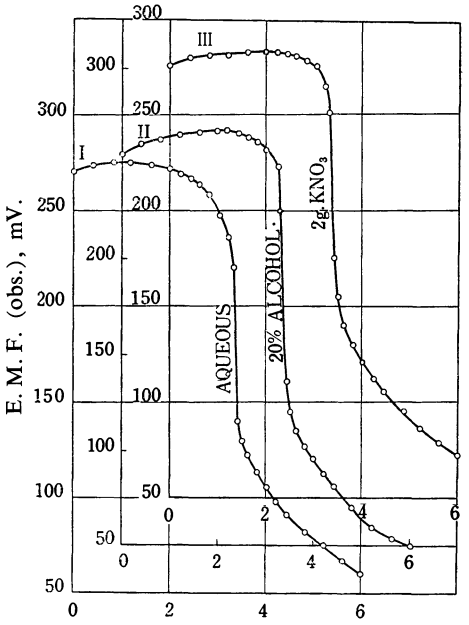
The pH of stock solution of sodium arsenite was measured by glass electrode and found to be 9.85. The variations of the latter were obtained by the progressive additions of calculated

6) A. I. Vogel, "Quantitative Inorganic Analysis", p. 472.

quantities of sodium hydroxide solution to sodium arsenite. When sodium hydroxide is mixed with sodium arsenite in the molecular ratio 1 : 1 and 2 : 1, the corresponding compounds formed are $Na_4As_2O_5$ (sodium pyroarsenite) and Na_3AsO_3 (sodium orthoarsenite) and the pH of their solutions were found to be 11.25 and 12.28 respectively.

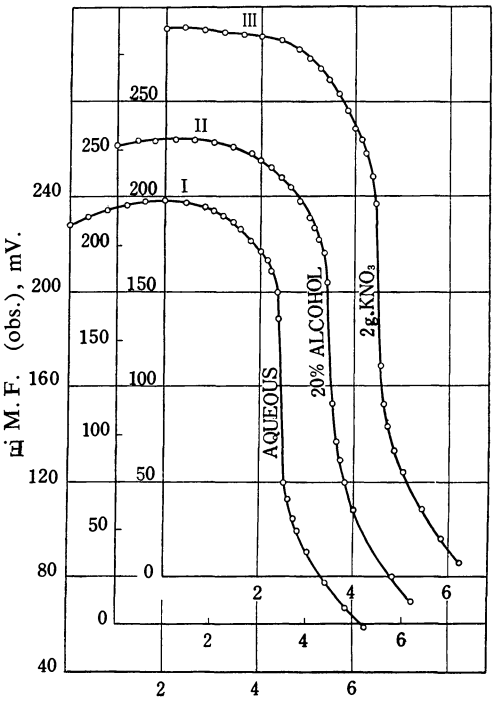
It is clear from Figs. 1 and 4 and from the summary of observations in Table I that when sodium arsenite solution at pH 9.85 is added to thorium nitrate solution and vice versa and the potential between a platinum indicator electrode and the calomel half-cell, measured and plotted against the volume of the titrant added in ml., a sharp deflection in curve occurs at a point where the molecular ratio of sodium arsenite and thorium nitrate is 4 : 1, corresponding to the formation of thick gelatinous precipitate of thorium metaarsenite $Th(AsO_2)_4$ or $ThO_2 \cdot 2As_2O_3$. At pH 11.25, the potentiometric titrations between $Th(NO_3)_4$ and $Na_4As_2O_5$ suggest the formation of thorium orthoarsenite having the molecular formula $ThAs_2O_5$ or $ThO_2 \cdot As_2O_3$ (Figs. 2 and 5). The titrations of thorium salt and Na_3AsO_3 ($2NaOH + NaAsO_2$) pH 12.28 show a sharp break in potential at the point of equivalence and the compound formed corresponds very closely to the normal compound $Th_3(AsO_3)_4$ or $3ThO_2 \cdot 2As_2O_3$ (vide Figs. 3 and 6).

In these titrations, the behavior of indicator electrode with bright platinum as electrodic metal in contact with thorium ions and



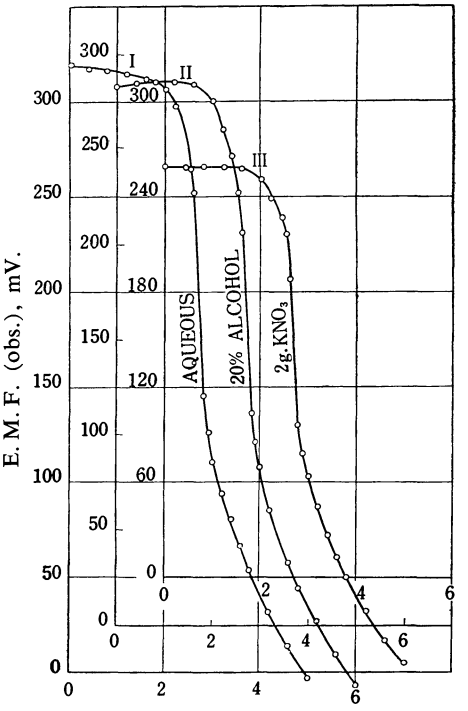
M/5 $NaAsO_2$ added to 20 cc. of M/120 $Th(NO_3)_4$ soln. in cc. (pH 9.85)

Fig. 1. Direct titration.



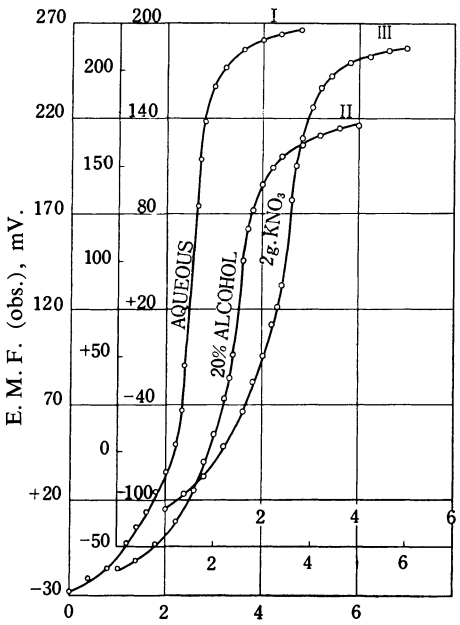
M/10 $Na_4As_2O_5$ added to 20 cc. of M/45 $Th(NO_3)_4$ soln. in cc. (pH 11.25)

Fig. 2. Direct titration.



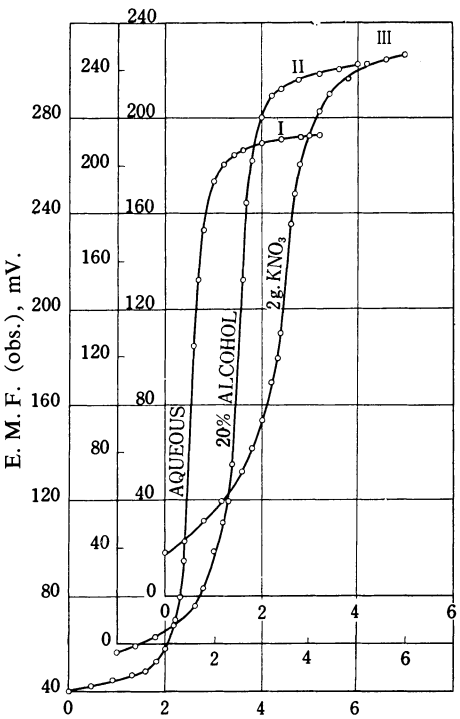
M/10 Na_3AsO_3 added to 20 cc. of M/100 $Th(NO_3)_4$ soln. in cc. (pH 12.28)

Fig. 3. Direct titration.



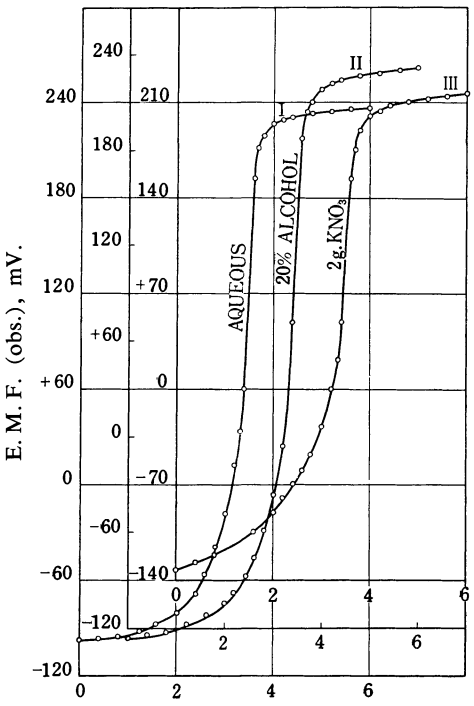
M/20 $Th(NO_3)_4$ added to 20 cc. of M/40 $NaAsO_2$ soln. in cc. (pH 9.85)

Fig. 4. Reverse titration.



M/10 $Th(NO_3)_4$ added to 20 cc. of M/80 $Na_4As_2O_5$ soln. in cc. (pH 11.25)

Fig. 5. Reverse titration.



M/14 $Th(NO_3)_4$ added to 20 cc. of M/60 Na_3AsO_3 soln. in cc. (pH 12.28)

Fig. 6. Reverse titration.

slightly soluble thorium oxide, could be interpreted as that of metal-metal oxide electrode (in this case Th-ThO_2), whose potential depends to a great extent upon the concentration of thorium ions which is groverned by its hydrogen ion concentration. The mechanism of the electrode reaction may be visualized as follows:

$$Th + 4AsO_2^- = ThO_2 \cdot 2As_2O_3 + 4e$$

$$ThO_2 + 4H + 4e \rightleftarrows Th^{4+} + 2H_2O$$

from which

$$\frac{[Th^{4+}]}{[ThO_2][H^+]^4} = K$$

and as $[ThO_2]$ (being slightly soluble) is a constant,

$$[Th^{4+}] = K'[H^+]^4$$

The potential of the electrode can therefore be represented by the Nernst equation

$$E = E_0 + 0.059/2 \log [Th^{4+}]$$

In the direct titrations, the electrode dipped in acidic thorium nitrate solution (pH 5.6), is positive. When alkalized arsenite solutions at different pH values are added from the microburette to thorium nitrate solutions, the concentration of thorium ions gradually decreases owing to their removal from solution by precipitation as thorium arsenites and consequently the E. M. F. slightly decreases after each addition of

the reagent. At the point of equivalence when all the thorium ions are removed, a sharp downward jump in potential is observed which is indicated by the steep portion of the titration curves (Figs. 1—3). In the case of inverse titrations, an equilibrium is established after the additon of a few drops of thorium nitrate solution to the titration cell containing arsenite solutions. The E. M. F. shows a gradual rise from the beginning of the reaction, till in the vicinity of the end point when the last traces of arsenite have been removed by precipitation, the first excess of thorium ions added causes a sudden leap in potential indicating the end point, after which the E. M. F. assumes more or less a constant value (Figs. 4—6).

It is noted that after each addition of the reagent, the E. M. F. readily becomes steady. A thorough stirring in the neighborhood of the end point has a favorable effect. Each titration takes about half an hour for completion. The addition of alcohol in varying concentrations improves the end point as the presence of alcohol reduces the adsorption of AsO_2^- ions and also the solubility of thorium arsenite precipitates and hence a closer approach to the theoretical values is envisaged in the experimental results in aqueous-alcoholic solutions (see Table I). The presence of electrolytes such as potassium nitrate has also a favorable effect on the end point as it curtails the time for titration by coagulating the arsenite sol formed in the reaction mixture and thus increasing the sensitiveness of the titration.

Potentiometric titration curves are symmetrical on both sides of the point of equivalence; a pronounced maxima in dE/dV is obtained at the end point and the results are accurate and reproducible. The reaction between alkali arsenites and thorium salts can be successfully studied potentiometrically. There is, however, no appreciable affect of alcohol or electrolytes on the nature of the curves or the magnitude of the break in potential.

It is observed that on mixing thorium nitrate and alkalized arsenite solutions different arsenites of thorium are formed, the composition of which depends on the conditions of precipitation, particularly the concentration of sodium hydroxide in sodium arsenite. Further, the arsenite precipitates dissolve in excess of alkali and also in acids and hence the precipitation of one or the other compound is a function of the hydrogen ion concentration of the medium. The disagreement between the views of previous workers on the molecular composition of thiorum arsenite compounds as reported earlier in literature (loc. cit.) seems to be due to the fact that the experiments were not performed at definite pH values of arsenite solutions.

The reactions between thorium nitrate and thorium arsenite at different pH levels can be represented as follows:

$$4NaAsO_2(2Na_2O+2As_2O_3)+Th(NO_3)_4 = Th(AsO_2)_4[ThO_2\cdot 2As_2O_3]+4NaNO_3$$

pH 9.85

$$2Na_4As_2O_5(4Na_2O+2As_2O_3)+2Th(NO_3)_4 = 2ThAs_2O_5[ThO_2\cdot 2As_2O_3]+NaNO_3$$

pH 11.25

$$4Na_3AsO_3(6Na_2O+2As_2O_3+3Th(NO_3)_4 = Th_3(AsO_3)_4[3ThO_2\cdot 2As_2O_3]+12NaNO_3$$

pH 12.28

The composition of thorium arsenites can thus be represented by the general formula $xThO_2\cdot As_2O_3$ and the amount of thorium oxide is proportional to the quantity of sodium oxide in sodium arsenite and its proportion increases with the concentration of alkali used in the preparation of arsenite solutions or, in other words, with the pH of the medium.

Chemical Laboratories
Government College
Kota (Rajasthan), India

Spectroscopic Studies on Molecular Configurations of Some Aliphatic Dinitriles. III. Infrared Spectra of Adiponitrile and Bis-(adiponitrilo)copper(I) Nitrate

By Ikuo MATSUBARA

(Received April 24, 1961)

Recently the author has studied the infrared spectra of some copper(I) complexes of aliphatic dinitriles and showed that they are quite useful in understanding the spectra and molecular configurations of free dinitriles[1,2]. In the course of the spectroscopic studies on the molecular configurations of the series of aliphatic dinitriles, the infrared spectra of adiponitrile and bis(adiponitrilo)copper(I) nitrate, $[Cu\{NC-(CH_2)_4-CN\}_2]NO_3$, have been investigated. Because adiponitrile has three internal axes of rotation, the number of possible staggered rotational isomers becomes large[3], and the complexity of the liquid-state spectrum of this compound may be explained as due to the coexistence of these rotational isomers. X-Ray analysis of bis(adiponitrilo)-copper(I) nitrate[4] has revealed that the ligand adiponitrile takes the planar all-trans(TTT*) configuration in the crystals of this complex. The infrared spectrum of bis(adiponitrilo)-copper(I) nitrate has been explained satisfactorily on the basis of this result, and interpretation of the spectra of adiponitrile both in the liquid and in the crystalline solid states has been made possible by comparing them with that of the complex. The results of the previous spectroscopic studies on other molecules of the type $X-(CH_2)_4-X$ such as *n*-hexane[5-7], tetramethylene halides[8] and adipic acid[9] were also useful in the assignment of the vibrational frequencies of adiponitrile.

Experimental

Bis(adiponitrilo)copper(I) nitrate was prepared in the same way as described in the previous paper[4].

The infrared spectra in the 4000~400 cm^{-1} region of adiponitrile and the complex were obtained by using a Perkin-Elmer Model 21 and a Perkin-Elmer Model 13 spectrophotometer (with sodium chloride and potassium bromide optics respectively). The spectrum of adiponitrile in the liquid state is shown in Fig. 1a. The spectral simplification

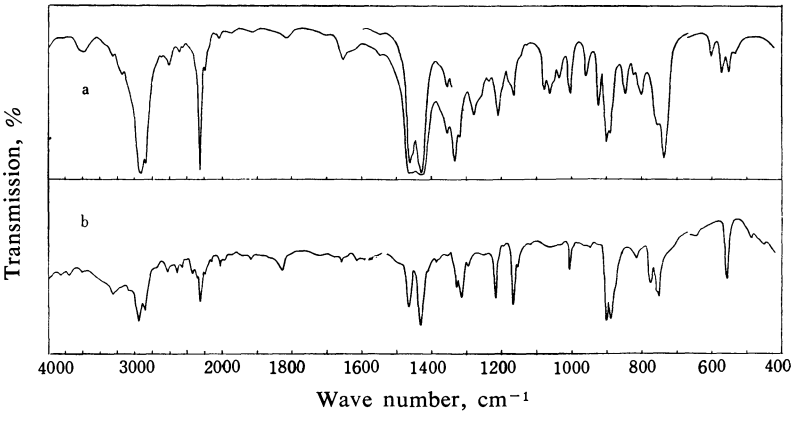


Fig. 1. Infrared spectra of adiponitrile.
(a) at room temperature (liquid); (b) at −20°C (solid).

1) I. Matsubara, This Bulletin, **34**, 1710 (1961).
2) I. Matsubara, ibid., **34**, 1719 (1961).
3) See for example S. Mizushima, "Structure of Molecules and Internal Rotation", Academic Press Inc., New York (1954), Part I, Chap. V.
4) Y. Kinoshita, I. Matsubara, T. Higuchi and Y. Saito, This Bulletin, **32**, 1221 (1959).
* For the nomenclature of rotational isomers see Ref. 3.
5) D. W. E. Axford and D. H. Rank, *J. Chem. Phys.*, **18**, 51 (1950).
6) J. K. Brown, N. Sheppard and D. M. Simpson, *Discussions Faraday Soc.*, No. **9**, 261 (1950).
7) H. Tschamler, *J. Chem. Phys.*, **22**, 1845 (1954).
8) J. K. Brown and N. Sheppard, *Proc. Roy. Soc.*, **A231**, 555 (1955).
9) H. Susi, *Spectrochim. Acta*, **15**, 1063 (1959).

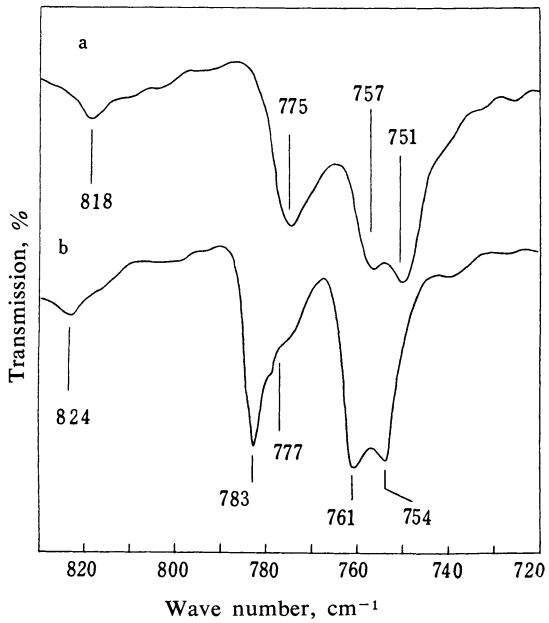


Fig. 2. Infrared spectra in the 830~720 cm^{-1} region of the solid adiponitrile.
(a) at −20°C; (b) at −150°C.

which occurred when the liquid was cooled down to −20°C is shown in Fig. 1b. The solid-state spectrum of adiponitrile undergoes a reversible change depending on the temperature, although the main features of the spectrum remain the same and no discrete change of the spectrum as observed in the case of glutaronitrile[2] takes place. In Fig. 2 is shown the spectral change in the 830~720 cm^{-1} region which occurred when the temperature was lowered from −20°C to −150°C. The behavior of adiponitrile is anomalous in that the liquid, if it contains a trace of water, forms a transparent solid phase when rapidly cooled. This has the spectrum shown in Fig. 3. When the solid was warmed up to ca. −20°C, a transition occurred, giving the normal crystalline solid phase which has the spectrum shown in Fig. 1b. The spectrum of bis(adiponitrilo)copper(I) nitrate was obtained using both Nujol mull and potassium bromide disk techniques. Nujol mulls of the complex gave different spectra depending on the type of alkali halide cell windows used as supporting plates. The use of KRS-5 plates and sodium chloride plates resulted in spectra which were at first identical with each other, but the one obtained by using sodium chloride plates soon began to change gradually. When potassium bromide plates were used, the change took place more quickly than in the case of sodium chloride plates. These changes must be attributed to the reaction of the complex with sodium chloride and potassium bromide plates. In Fig. 4a is shown the spectrum obtained by using KRS-5 plates. The spectra in Figs. 4b and 4c are those obtained respectively by the use of sodium chloride and potassium bromide plates. (These two spectra were recorded after the specimens had been placed in the laboratory for one day.) The spectrum obtained from a potassium bromide disk of the complex is shown in Fig. 5. This spectrum agrees quite well with that obtained from Nujol mull by the use of potassium bromide supporting plates (Fig. 4c), showing that the type of reaction which occurs between the complex and potassium bromide is the same in both cases. The absorption frequencies of adiponitrile and bis-(adiponitrilo)copper(I) nitrate are listed in Table I, together with the assignment.

Results and Discussion

The symmetry types and the selection rules for the fundamental vibrations of adiponitrile in the 1400~400 cm^{-1} region are given in Table II[10,11]. Only the rotational isomers with the planar $C\diagdown C\diagup C\diagdown C$ skeleton are included here, because these are considered the most important among all the isomers of adiponitrile. For the TTT(C_{2h}) and the GTG′(C_1) isomers the existence of a center of symmetry makes the Raman and infrared active fundamentals mutually exclusive, and only nine infrared active modes are expected in this region. For the other isomers, all the fundamentals are expected to be active in both the Raman and infrared spectra. The spectrum of bis(adiponitrilo)-copper(I) nitrate can be explained on the basis of the result of X-ray analysis; the ligand

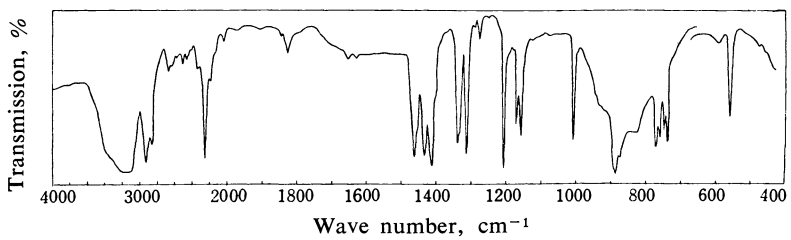


Fig. 3. Infrared spectrum obtained by rapid cooling of adiponitrile containing a trace of water down to −120°C.

10) J. K. Brown, N. Sheppard and D. M. Simpson, *Phil. Trans. Roy. Soc. London*, A 247, 35 (1954).

11) E. Funck, *Z. Elektrochem.*, 62, 901 (1958).

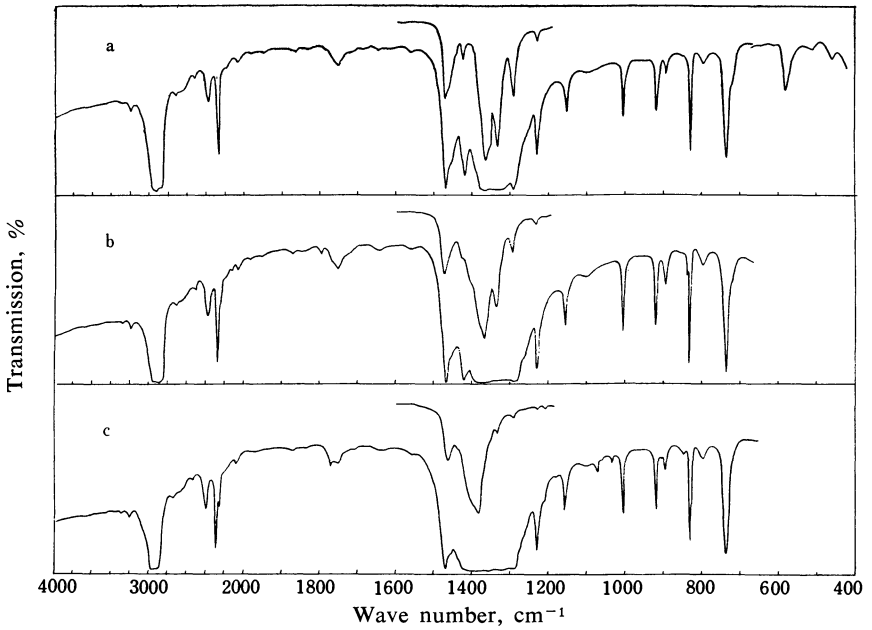


Fig. 4. Infrared spectra obtained from Nujol mulls of bis(adiponitrilo)copper(I) nitrate by using (a) KRS-5, (b) NaCl and (c) KBr supporting plates.

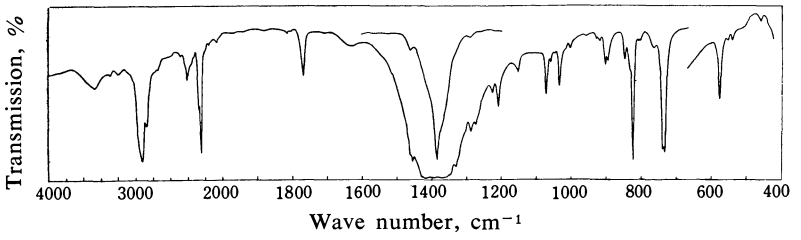


Fig. 5. Infrared spectrum obtained from a KBr disk of bis(adiponitrilo)copper(I) nitrate.

adiponitrile molecule takes the TTT configuration[4]. The Nujol mull spectrum of bis(adiponitrilo)copper(I) nitrate (Fig. 4a) shows quite simple features in good agreement with the selection rules for the centrosymmetric structure. The appearance of an intense band at 737 cm^{-1} is strong evidence for the TTT configuration of adiponitrile, because this band must correspond to the CH_2 rocking vibration of the methylene chain of the planar all-trans configuration[7,10]. Vibrational assignment of the individual bands is made with reference to the spectra of like molecules such as *n*-hexane[5-7]. Thus the strong bands at 1333 and 1290 cm^{-1} are assigned to the CH_2 wagging modes, and those at 1229 and 1155 cm^{-1} to the CH_2 twisting modes. The bands of medium intensity at 1006 and 921 cm^{-1} may correspond to the C–C stretching modes. As mentioned above, the strong band at 737 cm^{-1} is assigned with confidence to one of the CH_2 rocking modes, and the weak band at 895 cm^{-1} may be assigned to another CH_2 rocking mode. The relatively strong band at 581 cm^{-1} should be ascribed to the C–C–C bending mode. A broad weak band at 797 cm^{-1} may be an overtone or combination of some skeletal deformation modes, as has been suggested by Fujiyama and Shimanouchi[12], but no conclusive evidence in support of this view can be found at this stage of investigation.

The strong bands at 1364/57 and 830 cm^{-1} are assigned to the infrared active fundamentals of the nitrate ion, and the weak band at 1751 cm^{-1} must also be correlated with some nitrate vibration. When sodium chloride plates were used to support the mull, new bands appeared at 1795, 1362 and 836 cm^{-1}, as is shown in Fig. 4b. These frequencies correspond well to those of sodium nitrate[13]. In the Nujol mull spectrum obtained by the use

12) T. Fujiyama and T. Shimanouchi, paper presented at the 14th Annual Meeting of the Chemical Society of Japan, Tokyo, April, 1961.
13) F. A. Miller and C. H. Wilkins, *Anal. Chem.*, **24**, 1253 (1952).

TABLE I. INFRARED ABSORPTION BANDS OF ADIPONITRILE AND BIS(ADIPONITRILO)COPPER(I) NITRATE

Adiponitrile		Bis(adiponitrilo)-copper(I) nitrate			
Liquid (room temp.)	Solid (−20°C)	Nujol mull[a)]	KBr disk	Assignment	
	3861 vw				
	3759 vw				
	3591 vw				
3268 vw	3247 mw	3268 vw	3279 vw		
		3195 w	3205 vw		
3155 vw					
2941 vs	2950 ms		2933 s	TTT, GTG′	C–H stretch.
2874 ms	2882 m		2874 m	TTT, GTG′	C–H stretch.
		2725 vw			
2611 vw	2618 w				
		2513 vw			
2494 vw	2506 w		2488 vw		
2451 vw	2463 w		2433 w sh		
			2404 mw		
		2381 mw			
2315 vw sh	2331 w				
	2278 w				
		2273 ms	2273 m sh	TTT	C≡N stretch. (bound)
2247 vs	2247 ms		2252 ms	TTT, GTG′	C≡N stretch. (free)
2198 w	2193 w	2208 w			
2165 vw sh			2169 vw		
2119 vw	2128 vw				
		2062 vw	2070 vw		
2033 vw	2024 mw				
1972 vw					
1916 vw	1916 vw				
		1866 vw			
1815 vw	1828 mw		1815 vw		
1701 vw					
1653 vw	1658 w	1645 vw			
1548 vw		1560 vw			
1464 vs	1468 ms		1456 s	TTT, GTG′	CH_2 bend.
1456 s sh					
1429 vs	1431 s	1422 ms		TTT, GTG′	CH_2 bend.
	1408 vw				
1377 vw sh	1387 vw				
1357 m					
1335 s	1328 m	1333 vs	1335 s	TTT, GTG′	CH_2 wag.
1319 m	1314 ms			GTG′	CH_2 wag.
1307 vw sh	1295 vw				
1280 mw		1290 s	1289 ms	TTT	CH_2 wag.
			1277 m sh		
1266 vw sh			1267 mw sh		
1258 vw					
1235 vw		1229 ms	1229 mw	TTT	CH_2 twist.
1209 m	1217 ms		1209 m	GTG′	CH_2 twist.
1198 vw sh	1193 vw				
1179 w					
1167 w	1167 s		1163 vw sh	GTG′	CH_2 twist.
1152 vw	1153 w	1155 mw	1156 mw	TTT	CH_2 twist.
1129 vw					
		1101 vw			

TABLE I. (Continued)

Adiponitrile		Bis(adiponitrilo)-copper(I) nitrate		Assignment	
Liquid (room temp.)	Solid (−20°C)	Nujol mull[a]	KBr disk		
1080 mw			1073 m		
1064 mw			1063 w		
1054 w sh			1049 vw		
1038 w		1044 vw	1035 m		
1032 vw sh			1021 vw		
1005 m	1007 m	1006 m	1005 w	TTT, GTG′	C–C stretch.
		971 vw			
960 mw			962 vw		
954 vw sh	948 vw				
			930 w		
923 m		921 m	920 w	TTT	C–C stretch.
900 ms	900 s		905 mw	GTG′	CH_2 rock.
891 m	888 s	895 w	897 mw	TTT GTG′	CH_2 rock. C–C stretch.
883 vw sh	876 m sh				
848 mw			849 mw		
			833 w sh		
821 vw	818 w		810 vw		
803 mw		797 w	807 vw		
	775 m				
	757 ms			GTG′	CH_2 rock.
752 m sh	751 ms		763 w		
734 s		737 s	736 s	TTT	CH_2 rock.
			732 s		
602 w					
573 mw		581 mw	576 mw	TTT	C–C–C bend.
553 mw	556 ms		553 vw	GTG′	C–C–C bend.
535 vw			539 vw		
	486 vw				
	457 vw	459 vw	459 vw		

a) KRS-5 supporting plates were used to obtain the spectrum.

of potassium bromide plates and in the potassium bromide disk spectrum, new bands appear at 1770, 1383 and 824 cm^{-1}, as is shown in Figs. 4c and 5 respectively. These frequencies agree well with those of potassium nitrate[13]. It can be concluded from the above results that the mechanism of reaction of the complex and alkali halides should be ascribed largely to an ion interchange between the two phases. The spectra in Figs. 4c and 5 show absorptions which correspond to those of the liquid adiponitrile (Fig. 1a). This suggests that interaction between the complex and alkali halides results in the isolation of free adiponitrile.

The sharp band observed at 2273 cm^{-1} in the Nujol mull spectrum (Fig. 4a) corresponds to the C≡N stretching mode of the complex. The C≡N vibrational shift of 26 cm^{-1} towards higher frequencies by complex formation may be explained in the same way as in the cases of the lower homologues of this complex series[1,2]. Namely, X-ray analysis of this complex has revealed that the C–N bond distance is 1.13 Å and that the Cu–N–C–CH_2 group is close to linear, from which it is to be expected that the C–N bond is essentially of a triple-bond character, the contributions of polar resonance structures such as $-C^+=N^-$ being decreased and the C≡N stretching frequency being thereby increased. The effect of the interaction with the Cu-N stretching vibration, though small, may also contribute to the increase in the C≡N stretching frequency. As is evident from Figs. 4b, 4c and 5, reaction with alkali halides results in the appearance of the band at 2252 cm^{-1} which is attributed to the C≡N stretching frequency of free adiponitrile. The band observed at 2381 cm^{-1} may correspond to a vibration characteristic of the tetrahedral configuration of the complex[1,2].

Adiponitrile shows a marked spectral simplification on passing from the liquid to the crystalline solid state, as is shown in Fig. 1b.

TABLE II. THE SYMMETRY TYPES AND SELECTION RULES FOR THE FUNDAMENTAL VIBRATIONS OF ADIPONITRILE IN THE 1400～400 cm^{-1} region[a]

Types of symmetry coordinates	TTT(C_{2h})				GTG′ (C_i)		GTG(C_2)		TTG(C_1)
	A_g	B_g	A_u	B_u	A_g	A_u	A	B	
CH_2 wagging	2	0	0	2	2	2	2	2	4
CH_2 twisting	0	2	2	0	2	2	2	2	4
C–C stretching	3	0	0	2	3	2	3	2	5
CH_2 rocking	0	2	2	0	2	2	2	2	4
C–C–C bending	1	0	0	1	1	1	1	1	2
Selection rules IR	−	−	+	+	−	+	+	+	+
Selection rules Raman	+	+	−	−	+	−	+	+	+

a) Only the isomers with the planar C\C/C\C skeleton are included.

The isomer of adiponitrile stable in the crystalline solid state is considered to have a center of symmetry, as the number of prominent absorption peaks is close to that expected for such a configuration and much smaller than that required for a less symmetrical form (see Table II). Consideration of the selection rules for the skeletal deformation vibrations is particularly useful for the confirmation of this view. The fact that no strong band other than that at 556cm^{-1} is observed in the 600～450cm^{-1} region gives strong support to this conclusion, because only one vibration corresponding to the C–C–C bending mode is to be expected to appear in this region in a centrosymmetric structure. Determination of the isomeric form of adiponitrile in the crystalline solid state can then be made by comparing its spectrum (Fig. 1b) with that of bis(adiponitrilo)copper-(I) nitrate (Fig. 4a). The two spectra are evidently very different from each other. For example, the C–C–C bending frequency of 556 cm^{-1} in the crystalline adiponitrile is much lower than the corresponding value of 581 cm^{-1} in the complex. The band observed at 757/51 cm^{-1} in the spectrum of the crystalline adiponitrile must be assigned to the CH_2 rocking mode, while the absorption corresponding to this mode appears at 737 cm^{-1} in the case of the complex. As the frequencies of these two types of vibration are known to change conspicuously with the azimuthal angle of internal rotation[1,2], such differences in the observed values will serve to exclude the possibility that adiponitrile takes the TTT form in the crystalline solid state. Therefore, it can be concluded that the isomer of adiponitrile stable in the crystalline solid state is another centrosymmetric one, the GTG′ form. The vibrational assignment of the crystalline adiponitrile may be carried out with reference to the work of Brown and Sheppard[8] on tetramethylene halides, which are known to take the GTG′ configuration in the crystalline solid state. The fact that the spectral features of the crystalline adiponitrile are quite similar to those of tetramethylene halides may give additional support for the GTG′ configuration of the former. Thus, the bands observed at 1468 and 1431 cm^{-1} in the solid-state spectrum (Fig. 1b) are assigned to the CH_2 bending modes. The bands at 1328 and 1314 cm^{-1} may be ascribed to the CH_2 wagging modes, and those at 1217 and 1167 cm^{-1} to the CH_2 twisting modes. The bands at 1007 and 888 cm^{-1} may correspond to the C–C stretching modes. The band at 757/51 cm^{-1} must be assigned to one of the CH_2 rocking modes, and that at 900 cm^{-1} may correspond to another CH_2 rocking mode. As mentioned above, the band at 556 cm^{-1} should be ascribed to the C–C–C bending mode. By analogy with the cases of the lower homologues of the dinitrile series[1,2], the energetical contributions of both the C–C–C bending and C–C≡N bending motions are considered to be important in this vibration. The bands observed at 818 and 775 cm^{-1} may be explained as overtones or combinations of some skeletal deformation vibrations. Although the 775 cm^{-1} band seems too intense to be interpreted as such vibrations, this assignment is nevertheless not unreasonable, because the overtone or combination bands of this type are expected to become remarkably intense at low temperatures, as has been observed in the case of succinonitrile[1].

As shown in Fig. 2, the solid-state spectrum of adiponitrile undergoes a reversible change depending on the temperature, which suggests the occurrence of a change in the crystal structure. However, as the change is not discrete and the overall spectral features are essentially the same at all temperatures, it may not be attributed to a transition to different isomeric forms, as in the case of glutaronitrile[2].

The anomalous spectrum in Fig. 3 which is obtained when adiponitrile containing a trace of water is rapidly cooled may correspond to some metastable crystalline solid phase. Although this spectrum seems at first sight to

be very different from that of the normal crystalline solid phase (Fig. 1b), the one to one correspondence of the individual bands in the two spectra is quite good, showing that adiponitrile also takes the GTG′ form in this metastable solid state.

Many of the bands in the liquid-state spectrum of adiponitrile can be explained as due to the vibrations of the TTT and the GTG′ isomers, as is shown in Table I. Considering the number of the unassigned bands, at least one more isomer can be expected to exist in the liquid state. Determination of the configuration of this isomer will not be attempted here, however, as it would require much more detailed analysis of the spectrum based on a normal coordinate treatment.

Summary

The infrared spectra of adiponitrile and bis-(adiponitrilo)copper(I) nitrate, $[Cu\{NC-(CH_2)_4-CN\}_2]NO_3$, have been studied. The spectrum of the complex has been analyzed on the basis of the result of X-ray analysis which disclosed that the ligand adiponitrile takes the TTT(C_{2h}) configuration in the crystals of this compound. This complex reacts with alkali halides such as sodium chloride and potassium bromide, resulting in the isolation of free adiponitrile. Considering the frequency shifts of the nitrate vibrations, the reaction of the complex with alkali halides should be ascribed largely to an ion interchange between the two phases. The increase of 26 cm^{-1} in the C≡N stretching frequency by complex formation may be understood by considering the linear structure of the Cu–N–C–CH_2 group, which suggests that the carbon-nitrogen bond is essentially of a triple-bond character, the contributions of polar resonance structures such as $-C^+=N^-$ being decreased. Adiponitrile shows a marked spectral simplification on passing from the liquid to the crystalline solid state. From a comparison of the solid-state spectrum with that of the complex, and from a consideration of the vibrational selection rules, it has been concluded that adiponitrile takes the GTG′(C_i) configuration in the crystalline solid state. The fact that the solid-state spectrum of adiponitrile is subject to a reversible change depending on the temperature may be explained as due to a slight change in the crystal structure. Many of the bands in the liquid-state spectrum of adiponitrile have been assigned to the vibrations of the TTT and the GTG′ isomers, and the number of the remaining bands suggests the existence of at least one more isomer in the liquid state.

The author wishes to express his sincere thanks to Professor S. Imanishi of Kyushu University for his kind encouragement throughout the course of this study. He also wishes to thank Dr. T. Yoshino of Toyo Rayon Co., Ltd. for many valuable suggestions, and to Messrs. T. Ito, H. Kataoka and K. Shirasaki of Toyo Rayon Co., Ltd. for their assistance in the experiments.

Central Research Laboratories
Toyo Rayon Co., Ltd.
Otsu, Shiga-ken

A Theoretical Treatment of Molecular Complexes. II. Iodine-Aromatic Hydrocarbon Complexes

By Kenichi FUKUI, Akira IMAMURA, Teijiro YONEZAWA and Chikayoshi NAGATA

(Received April 28, 1961)

Theoretical and experimental research into the benzene-iodine complex has derived many welcome conclusions. With regard to the configuration of benzene-iodine complex for instance, Mulliken[1] had considered the symmetries of the molecular orbitals of electron donor and acceptor and predicted the resting model in which the iodine molecule is situated above the benzene molecule, with its axis parallel to the benzene plane and its center on the sixfold axis of the benzene molecule. This model, however, was contradictory to the

1) R. S. Mulliken, *J. Am. Chem. Soc.*, **74**, 811 (1952).

results of the study of X-ray diffraction[2] and of infrared spectra[3]. Both of these results supported the axial model in which the axis of iodine molecule was coincident with the sixfold axis of benzene. The reason for this discrepancy was pointed out by Aono[4], who calculated the magnitude of the overlap integral between a benzene molecule and an iodine molecule and made it clear that the error in the estimation of the overlap integral in Mulliken's treatment might be the reason for this discrepancy. Further, a numerical calculation for the benzene-iodine complex was made with respect to the axial model by using experimental data such as the ionization potential, so that a considerable agreement was found between the theoretical values and the experimental data of dipole moment, charge transfer spectra, and so on.

Another discrepancy between the theoretical and experimental data was found concering the intensity of the charge transfer spectra for the complex of iodine-benzene derivatives. From a theoretical point of view, the intensity of the charge transfer spectra would be expected to increase in proportion to the basicity of the aromatic molecule. On the other hand, experimental data showed the opposite[5]. In order to elucidate this experimental result the concept of the contact charge transfer spectra was introduced by Mulliken[6]. On the other hand, a statistical consideration of the configuration of aromatic compound-iodine complexs was made by Murakami, and numerical calculations of the intensity of the charge transfer spectra which were carried out on the basis of the statistical consideration showed a clear correlation with the experimental result[7].

It has recently been pointed out by many authors that the ease of complex formation depends not only on the charge transfer spectra, but also on the magnitude of other intermolecular interactions, such as dispersion force, exchange repulsion energy, and electrostatic force[6,7]. In many cases, the discussions of molecular complex formation in which these factors were taken into account seemed to be rather qualitative than quantitative. A more detailed discussion is in order.

In this paper we intend to apply aromatic hydrocarbon-iodine complex to the delocalization method that has already been used for aromatic compound-silver complexes[8], and to compare the results of numerical calculation with the experimental results, bearing the effects of the dispersion force in mind.

Model and Formulation

The procedure used in this paper is the same as has been described in a previous paper[8], that is, the delocalization method. In order to execute the theoretical treatment for aromatic compound-iodine complexes, the model adopted is the axial one in which the axis of the iodine molecule is coincident with the sixfold axis of one of the benzene rings in an aromatic compound; this model was supported by X-ray diffraction[3] as well as by infrared spectra[4] for benzene-iodine or benzene-bromine complexes.

In this model the stabilization energy due to the delocalization of π electrons from the aromatic compound to the iodine molecule is obtained by the perturbation method, in the same way as has been described in the previous paper.

Prior to the formulation, the electronic configuration of the iodine molecule should be discussed. The six outer-shell molecular orbitals of iodine molecule may approximately be written as a linear combination of two $5p_x$, $5p_y$ and $5p_z$ orbitals, as is shown in Eq. 1 (normalized factors are omitted).

$$\left.\begin{array}{ll} \phi_1 \approx 5p_x + 5p_x' & \phi_4 \approx 5p_y - 5p_y' \\ \phi_2 \approx 5p_y + 5p'_y & \phi_5 \approx 5p_z - 5p_z' \\ \phi_3 \approx 5p_z + 5p_z' & \phi_6 \approx 5p_x - 5p_x' \end{array}\right\} \quad (1)$$

In which $5p_x$, $5p_y$ and $5p_z$ are the atomic orbitals of iodine atoms and the x axis is taken to be the molecular axis of the iodine molecule. Therefore, the orbital ϕ_1 is nothing but the σ-bonding orbital, and ϕ_6, the σ-antibonding orbital.

At the stage of the first approximation, only ϕ_1 and ϕ_6 are involved in the linear combination of the atomic orbital for the total system of the complex, and the conjugations between the aromatic compound and one of ϕ_2, ϕ_3, ϕ_4 and ϕ_5 are neglected since the magnitude of overlap integrals between the $5p_y$ as well as the $5p_z$ and $2p\pi$ atomic orbital in aromatic compounds may reasonably be expected to be much smaller than that between $5p_x$ and $2p\pi$ in the axial model.

The secular equation for this model is written in a simple LCAO MO treatment (overlap neglected) in the following form:

2) E. E. Ferguson, *J. Chem. Phys.*, 25, 577 (1956).
3) O. Hassel, *Molecular Phys.* **1**, 241 (1958).
4) S. Aono, *Progr. Theoret. Phys. Japan*, **22**, 313 (1959).
5) L. J. Andrews and R. M. Keefer, *J. Am. Chem. Soc.*, **74**, 4500 (1952).
6) R. S. Mulliken, *Rec. trav. chim.*, **75**, 845 (1956); L. E. Orgel and R. S. Mulliken, *J. Am. Chem. Soc.*, **79**, 4839 (1957).
7) H. Murakami, This Bulletin, **28**, 577 (1955), ibid., **28**, 581 (1955), *J. Chem. Phys.*, **23**, 1957 (1955).
8) K. Fukui, A. Imamura, T. Yonezawa and C. Nagata, This Bulletin, **34**, 1076 (1961).

$$D(\lambda)=\begin{vmatrix} h-\lambda & l & 0\cdots\cdots & 0 \\ l & h-\lambda & \gamma\cdots\cdots\ \gamma & 0\cdots\cdots\ 0 \\ 0 & \gamma & a_{11}-\lambda\ \ a_{12}\cdots\cdots\ a_{16}\cdots\cdots & a_{1n} \\ \vdots & \vdots & a_{21}\ \ a_{22}-\lambda\cdots a_{26}\cdots\cdots & a_{2n} \\ \vdots & \vdots & \vdots\ \ \vdots\ \ \vdots & \vdots \\ \vdots & \gamma & a_{61}\ \ a_{62}\cdots\cdots\ a_{66}-\lambda\cdots & a_{6n} \\ \vdots & 0 & \vdots\ \ \vdots\ \ \vdots & \vdots \\ 0 & 0 & a_{n1}\ \ a_{n2}\cdots\cdots a_{n6}\cdots\cdots & a_{nn}-\gamma \end{vmatrix}$$

$$=\{(h-\lambda)^2-l^2\}\Delta(\lambda)+(h-\lambda)\gamma^2\sum_{r,s=1}^{6}(-1)^{r+s+1}\Delta_{rs}(\lambda) \qquad (2)$$

in which

$$\Delta(\lambda)=\begin{vmatrix} a_{11}-\lambda & a_{12}\cdots\cdots a_{1n} \\ a_{21} & a_{22}-\lambda\cdots\cdots a_{2n} \\ \cdots\cdots & \cdots\cdots \\ a_{n1} & a_{n2}\cdots\cdots a_{nn}-\lambda \end{vmatrix} \qquad (3)$$

is the secular determinant for the isolated aromatic molecule and $\Delta_{rs}(\lambda)$ denotes the secular determinant with row r and column s struck out, and a_{ii} and $a_{ij}(i\neq j)$ are the Coulomb and the resonance integrals respectively; h and l are the Coulomb and the resonance integrals of 5p orbital in iodine molecule respectively, and γ is the resonance integral between the $2p\pi$ orbital of carbon atom in the aromatic compound and the $5p_x$ orbital of the iodine atom, which is the one of two iodine atoms nearer to the aromatic molecule. The suffixes $1, 2, 3\cdots\cdots, 6$ of the Coulomb and the resonance integrals in Eq. 2 correspond to the numbers of the constituent atoms of the benzene ring above which the iodine molecule is located.

Since the magnitude of γ is small, the perturbation method can be applied in this treatment, as has been shown in the previous paper.

Case 1: When neither $h+l$ nor $h-l$ is equal to any λ_j, the roots of Eq. 2, $\lambda^{(1)}, \lambda^{(2)}\cdots\cdots, \lambda^{(n)}$; $\lambda'^{(1)}$ and $\lambda'^{(2)}$ are represented by:

$$\lambda^{(j)}=\lambda_j+\frac{(\lambda_j-h)}{(\lambda_j-h)^2-l^2}\times(c_1{}^j+c_2{}^j+\cdots+c_6{}^j)^2\gamma^2+[\gamma^4]\quad(j=1, 2, \cdots, n) \qquad (4)$$

$$\lambda'^{(k)}=\lambda'_k+\frac{1}{2}\sum_{j=1}^{n}\frac{(c_1{}^j+c_2{}^j+\cdots\cdots+c_6{}^j)^2}{\lambda'_k-\lambda_j}\times\gamma^2+[\gamma^4]\quad(k=1, 2)$$

in which λ_j is the root of $\Delta(\lambda)=0$, and λ_1' λ_2' are equal to $h+l$ and $h-l$ respectively; $c_r{}^j$ is the coefficient of the rth atomic orbital in the jth molecular orbital; and $[\gamma^4]$ denotes the higher term. The delocalization energy for complex formation that was defined for silver-aromatic hydrocarbon complexes in the previous paper[8] may be described for the iodine-aromatic molecular complex as follows:

$$\Delta E=\left\{\sum_{j=1}^{m}\frac{2(\lambda_j-h)}{(\lambda_j-h)^2-l^2}(c_1{}^j+c_2{}^j+\cdots\cdots+c_6{}^j)^2+\sum_{j=1}^{n}\frac{(c_1{}^j+c_2{}^j+\cdots\cdots+c_6{}^j)^2}{h+l-\lambda_j}\right\}\gamma^2+[\gamma^4] \qquad (5)$$

in which $\lambda_1, \lambda_2, \cdots\cdots, \lambda_m$ correspond to the occupied orbitals.

Case 2: When $h-l$ is equal to the highest occupied orbital, λ_m, of the isolated aromatic molecule, the roots of Eq. 2 are represented by:

$$\left.\begin{matrix}\lambda^{(m)} \\ \lambda'^{(2)}\end{matrix}\right\}=\lambda_m\pm\frac{1}{\sqrt{2}}|c_1{}^j+c_2{}^j+\cdots\cdots+c_6{}^j|\gamma+[\gamma^2]$$

$$\lambda^{(j)}=\lambda_j+\frac{(\lambda_j-h)}{(\lambda_j-h)^2-l^2}(c_1{}^j+c_2{}^j+\cdots\cdots+c_6{}^j)^2\gamma^2+[\gamma_4]\quad(j=1, 2, \cdots\cdots, n;\ j\neq m) \qquad (6)$$

$$\lambda'^{(1)}=\lambda_1'+\frac{1}{2}\sum_{j=1}^{n}\frac{(c_1{}^j+c_2{}^j+\cdots\cdots+c_6{}^j)^2}{\lambda_1'-\lambda_j}\gamma^2+[\gamma^4]$$

In presenting the value of energies, we make the zero point equal to the Coulomb integral of the benzene carbon atom and express them in units of $(-\beta)$, which is the resonance integral of the benzene C–C bond.

In both cases, 1 and 2, the formulas for the delocalization energy indicate that the magnitude of delocalization energy depends upon the symmetry of the benzene ring combined with the iodine molecule; this conclusion is quite coincident with that of Mulliken's theory. This circumstance is similar to the case of silver-aromatic hydrocarbon complexes, as has been pointed out in the previous paper[8].

Result and Discussion

Benzene-Iodine Complex.—With regard to the benzene-iodine complex, many theoretical and experimental studies had been carried out as has been described in the introduction. In this paper we carry out the numerical calculation for the comparison with the experimental data of benzene-iodine complex, making use of the delocalization method. For the charge transfer spectrum, the transition of the π electron may occur from the lowest occupied π orbital of benzene to the lowest vacant orbital of the iodine molecule, and the transition from the highest occupied π orbital of benzene to the lowest vacant orbital of iodine is forbidden for the sake of the symmetry of complex of the axial model. Accordingly, the frequency of the charge transfer spectrum is given by:

$$h\nu = \left\{2 + \frac{6(2-h)}{(2-h+l)(2-h-l)}\gamma^2\right\} - \left\{(h-l) + \frac{3}{h-l-2}\gamma^2\right\} + [\gamma^4] \qquad (7)$$

in which h is Planck's constant and ν is the charge transfer frequency, and the first term and the second term correspond to the energy of the lowest occupied π orbital of benzene and that of the lowest vacant orbital of iodine molecule respectively. The energy is represented in units of $(-\beta)$ in Eq. 7.

In order to determine the value of h, l and γ, we adopt the semi-empirical treatment, that is, the value of l and γ are obtained on the assumption that the resonance integral is proportional to the corresponding overlap integral, and h is determined bearing in mind the fact that the value of $h-l$ is nothing but the electron affinity of the iodine molecule. The values used in the calculation have been taken as follows after a consideration of many experimental data:

The resonance integral of the benzene C–C bond: 2.39 eV.[9]
The electron affinity of the iodine molecule: 7.0 eV.[10]
The distance of the iodine-iodine bond in iodine molecule: 2.67 Å
The distance between the nearer iodine atom and a carbon atom of the benzene ring in the axial model; 3.7 Å*

Adopting these parameters in calculation, we can get the values of h, l and γ as follows:

$$h=1.45 \qquad l=1.39 \qquad \gamma^2=0.021 \qquad (8)$$

The frequency of the charge transfer spectrum and the magnitude of dipole moment of this complex are calculated and listed in Table I in comparison with the experimental results.

TABLE I. FREQUENCY OF THE CHARGE TRANSFER SPECTRUM AND THE DIPOLE MOMENT OF BENZENE-IODINE COMPLEX

	Calcd.	Obs.
Dipole moment (Debye unit)	1.31	0.72
Charge transfer spectrum, cm^{-1}	37.1×10^3	36.5×10^3

The solvent effect is taken into account to compare the observed value of charge transfer spectrum with that calculated in Table I, that is, $36.5\times10^3\,cm^{-1}$ in Table I is obtained by adding $2\times10^3\,cm^{-1}$ to the experimental value**.

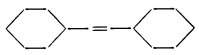
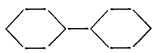
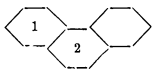
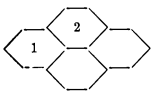
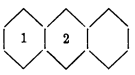
The good agreement between experimental and calculated values is rather striking, since in this approximation the electron-electron repulsion is entirely neglected and the calculation is carried out by a method which is not more accurate than simple LCAO MO. Such a result may probably be attributed to the fact that the estimation of the Coulomb and resonance integrals is semi-empirically made so as to involve the effect of electron-electron repulsion implicitly.

As to the dipole moment, on the other hand, the agreement between experimental and calculated values is not good. This discrepancy is probably caused by two main factors. The first is the fact that the electron transfer from the occupied orbital of the iodine molecule to the vacant orbitals of the benzene is neglected in the calculation. The second is the ambiguity engendered in the process of determining the magnitude of many integrals in such a semi-empirical treatment. As is well known, the parameters used for the discussion of chemical reactivity in the simple LCAO MO treatment are often found not suitable for estimating the value of dipole moment, and in this case the reason of this discrepancy may perhaps be that parameters determined semi-empirically are not appropriate for the calculation of dipole moment.

Polycondensed Aromatic Hydrocarbon-Iodine Complexes.—Many experimental studies for polycondensed aromatic hydrocarbon-iodine complexes have been performed. The electric conductivity of these complexes was measured especially, and it was found that a remarkable increase in conductivity was caused by the molecular complex formation. In this paper we calculate the delocalization energy, making use of Eq. 5, in order to get a clue to elucidate the physical properties of these complexes. The delocalization energies obtained are listed in Table II, together with the equilibrium constant[11] of the complex formation and the energy of the highest occupied orbital of aromatic hydrocarbons. The parallelism between the magnitude of the theoretical index and the equilibrium constant is not complete. This discrepancy is owing to many factors pointed out in the previous paper. The most important factor among these seems to be the dispersion force. To estimate roughly the magnitude of the dispersion force, we calculate the potential due to the dispersion force for the benzene-iodine complex by making use of London's formula. London's formula is represented as:

9) R. Pariser and R. G. Parr, *J. Chem. Phys.*, **21**, 767 (1953).
10) S. Nagakura and J. Tanaka, ibid., **22**, 563 (1954).
* The value of the carbon-iodine distance is estimated by considering the results of X-ray analysis of the bromine-benzene complex[3].
** N. S. Bayliss, *J. Chem. Phys.*, **18**, 292 (1950).
11) R. Bhattacharya and S. Basu, *Trans. Faraday Soc.*, **54**, 1286 (1958).

TABLE II. THE VALUES OF THE THEORETICAL INDEX AND THE EQUILIBRIUM CONSTANT FOR THE COMPLEX FORMATION BETWEEN AROMATIC HYDROCARBON AND IODINE

Aromatic compound	Ring number*	K[11]	Delocalization energy**	Energy of the highest occupied orbital
		0.34	1.615	0.504
		0.37	1.579	0.705
		0.62	1.511	0.618
	1	1.06	1.547	0.605
	2	1.06	1.479	0.605
	1	36.49	1.517	0.445
	2	36.49	1.547	0.445
	1	52.35	1.505	0.414
	2	52.35	1.457	0.414

* Ring number indicates the ring that is assumed to associate with the iodine molecule in axial model.

** The value of localization energy listed in Table II is the coefficient of the second order perturbation term in Eq. 5.

$$E_{\text{disp}} = -\frac{3}{2R^6}\frac{I_1 \cdot I_2}{I_1 + I_2}\alpha_1^0\alpha_2^0 \qquad (9)$$

in which I and α^0 are the ionization potential and the static polarizability respectively, and the suffixes 1 and 2 denote the molecules 1 and 2 respectively, and R is the distance between the two molecules. For the benzene-iodine complex, the values of the ionization potential, static polarizability and distance used in calculation are listed in Table III. The dispersion energy is discovered to be 1.48 kcal.

TABLE III. THE IONIZATION POTENTIAL AND STATIC POLARIZABILITY AND ATOMIC DISTANCE FOR BENZENE AND IODINE MOLECULE AND THEIR COMPLEX

	Benzene	Iodine molecule
Ionization potential, eV.	9.24	9.41
Static polarizability*, cm^3	107×10^{-25}	105×10^{-25}
Distance between benzene and iodine molecule, Å	4.8	

* The static polarizability of iodine molecule is estimated from the value of atomic refraction of iodine atom.

Taking the magnitude of the dispersion force of the benzene-iodine complex into account, we may attain to the following conclusion. It is probably not only the delocalization energy but also the dispersion force and other factors that decides the case of complex formation for the iodine-aromatic hydrocarbon complexes. A detailed discussion of this point will be made in the future.

The Relation between the Delocalization Method and Mulliken's Theory

In both the previous and the present papers, we have proposed the delocalization method and applied this method to the problem of aromatic compound-silver and aromatic hydrocarbon-iodine complexes. The formulas of delocalization energy obtained for both complexes were coincident with Mulliken's theory in its symmetry character, as was earlier pointed out.

In Mulliken's theory the magnitude of charge transfer force was not given in an explicit form, and the symmetry consideration characteristic of his theory is substantially limited to the compound which has some symmetry.

Mulliken's theory was developed by Brown in order to apply to electrophilic aromatic substitutions[12]. The mathematical interrelation between the chemical reactivity indexes of the frontier theory and Brown's theory was pointed out by some of the present authors[13]. An analogous relation may be expected between the delocalization method and Mulliken's

12) R. D. Brown, *J. Chem. Soc.*, **1959**, 2224, 2232.
13) K. Fukui, K. Morokuma, T. Yonezawa and C. Nagata, *J. Chem. Phys.*, **32**, 1743 (1960).

theory in the case of molecular complex formation if Mulliken's theory is developed in a manner similar to Brown's. This point will be discussed later.

Faculty of Engineering
Kyoto University
Sakyo-ku, Kyoto

σ-Electronic Structure in Conjugated Systems

By Kenichi FUKUI, Hiroshi KATO, Teijiro YONEZAWA, Keiji MOROKUMA, Akira IMAMURA and Chikayoshi NAGATA

(Received May 18, 1961)

In the last quarter of a century, the electronic structures of numerous unsaturated compounds have been calculated quantum-mechanically by either a non-empirical or a semi-empirical method; electronic spectra, chemical reactivities and other physical properties of these compounds have also been interpreted with sufficient accuracy in terms of their electronic behavior.

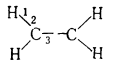
In those calculations, however, except for some simpler compounds such as carbon dioxide, formaldehyde, ethylene and benzene, σ electrons have not been treated explicitly but, rather, have been looked upon as constructing a framework of potential in which π electrons move.

Some physico-chemical properties of unsaturated compounds, however, for example, the proton shift in the high resolution nuclear magnetic resonance spectroscopy, the frequency shift in the pure quadrupole resonance, the dipole moment, the polarographic reduction potential, the reactivity in the halogen substitution reaction, and inductive and hyperconjugative effects of substituents, can not be interpreted without an explicit consideration of the σ electrons in the system. Consequently, the appearance of a simple method of calculating the σ electronic structures of large unsaturated molecules has been loked for.

Recently Sandorfy[1] and the present authors[2] have computed the electronic states of saturated hydrocarbons and halides by a simple LCAO MO method where the molecular orbitals (MO's) are written as a linear combination of the atomic orbitals (LCAO) of the carbon, halogen and hydrogen atoms.

At this time, by extending the simple method stated above, the present authors have calculated the σ electronic structures in large

TABLE I. CALCULATED σ ORBITAL ENERGIES AND ELECTRON DISTRIBUTIONS

(a) Ethylene 

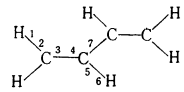
Sym.	λ_j*	H_1	C_2	C_3
A	−1.31812	0.03874	0.05482	0.31288
AA**	−1.21430	0.22617	0.27383	0
S	−0.94858	0.14860	0.09424	0.01433
A	−0.66410	0.13385	0.03263	0.16703
S	+0.63769	0.07059	0.05606	0.24669
AA**	+0.65430	0.27383	0.22617	0
A	+1.16221	0.07741	0.16256	0.02007
S	+1.49089	0.03081	0.09970	0.23898

* λ_j is the coefficient in $\varepsilon_j=\alpha+\lambda_j\beta$, where ε_j is the jth molecular orbital energy.
** AA denotes the antisymmetric orbital with respect to C-C bonding axis. In this orbital, bonding electrons localize only C-H bond.

1) C. Sandorfy, *Can. J. Chem.*, 33, 1337 (1955).

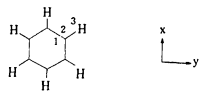
2) K. Fukui, H. Kato and T. Yonezawa, This Bulletin, 34, 442, 1111 (1961).

TABLE I (Continued)

(b) Butadiene 

j	Sym.	λ_j	H_1	C_2	C_3	C_4	C_5	H_6	C_7
18	A	−1.35539	0.0117	0.0177	0.1153	0.1290	0.0026	0.0017	0.1926
17	S	−1.30690	0.0192	0.0266	0.1455	0.1403	0.0710	0.0512	0.0003
16	A	−1.27763	0.0061	0.0080	0.0390	0.0339	0.1707	0.1299	0.0983
14,15	AA*	−1.21430	0.2262	0.2738	0	0	0	0	0
13	S	−1.05520	0.0347	0.0287	0.0321	0.0036	0.1497	0.1808	0.0068
12	A	−0.92480	0.0968	0.0576	0.0029	0.0175	0.0350	0.0589	0.0769
11	S	−0.74484	0.1058	0.0356	0.0608	0.1069	0.0103	0.0305	0.0087
10	A	−0.57576	0.0472	0.0075	0.1017	0.0623	0.0157	0.0982	0.1127
9	S	+0.62850	0.0314	0.0244	0.1132	0.1091	0.0035	0.0044	0.1582
8	A	+0.64104	0.0285	0.0228	0.0986	0.0999	0.0884	0.1104	0
7	S	+0.64650	0.0070	0.0057	0.0237	0.0246	0.1602	0.1976	0.0685
5,6	AA*	+0.65430	0.2738	0.2262	0	0	0	0	0
4	A	+1.03757	0.0342	0.0593	0.0013	0.0496	0.1577	0.0910	0.0134
3	S	+1.23235	0.0449	0.1043	0.0401	0	0.0396	0.0171	0.1048
2	A	+1.43497	0.0255	0.0771	0.1413	0.1078	0.0298	0.0099	0.0061
1	S	+1.57953	0.0069	0.0247	0.0845	0.1154	0.0657	0.0183	0.1528

* See Table I (a).

(c) Benzene 

j	Sym. xy	λ_j	C_1	C_2	H_3
24	AA	−1.38000	0.0833	0	0
22,23	SA, AS	−1.32743	0.1236	0.0509	0.0354
20,21	SS, AA	−1.28027	0.0613	0.1199	0.0908
19	SA	−1.27004	0.0232	0.0679	0.0524
18	SS	−1.09917	0.0018	0.0779	0.0851
16,17	SA, AS	−1.01199	0.0457	0.1033	0.1385
14,15	SS, AA	−0.71938	0.1029	0.0298	0.0978
13	SA	−0.50125	0.0547	0.0053	0.0520
12	AS	+0.62000	0.0833	0	0
10,11	SS, AA	+0.63752	0.0840	0.0732	0.0922
8,9	SA, AS	+0.64612	0.0409	0.1126	0.1390
7	SS	+0.64780	0.0162	0.0602	0.0740
6	SA	+0.95129	0.0055	0.0934	0.0623
4,5	SS, AA	+1.16119	0.0852	0.1104	0.0526
2,3	SA, AS	+1.49330	0.1232	0.0665	0.0205
1	SS	+1.63137	0.0653	0.0286	0.0075

substituted as well as non-substituted unsaturated compounds. In the present paper, as in the first of the series, the σ electronic structures of ethylene, butadiene, propylene, benzene, naphthalene and toluene will be discussed and some characteristics of the σ MO's in these compounds will be given.

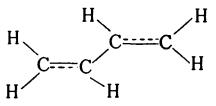
Method of Calculation

The method of calculation is similar to the one that has been employed in previous papers where the electronic structures of saturated compounds have been discussed[2].

The σ molecular orbitals in a conjugated hydrocarbon are represented by the linear combinations of atomic orbitals, the sp^2 hybridized orbitals of the carbon atoms and the 1s atomic orbitals of the hydrogen atoms. Thus, the jth σ MO is written as follows:

$$\psi_j=\sum_r^n C_{rj}\phi_{C,r}+\sum_l^m C_{lj}\phi_{H,l} \qquad (1)$$

in which C_{rj} denotes the coefficient of the



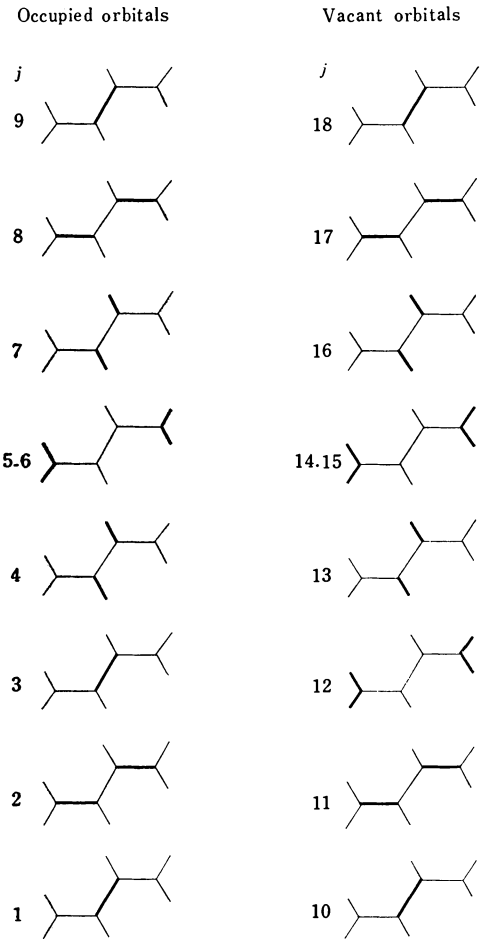
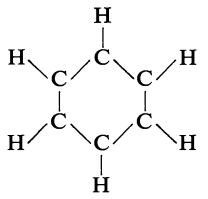


Fig. 1a. The σ electron distributions in butadiene. (Thick lines denote the most densely populated bonds.)



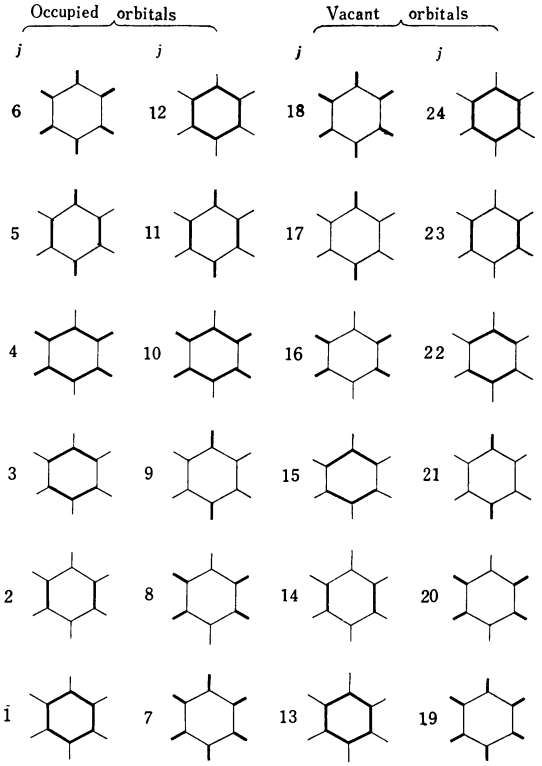


Fig. 1b. The σ electron distributions in benzene. (Thick lines denote the most densely populated bonds.)

rth sp^2 hybridized orbital of carbon in the jth MO, and C_{lj} denoted that of the 1s orbital of the lth hydrogen atom.

Referring to the simple LCAO MO approximation (the Hückel approximation) in the treatment of π electrons, the electronic interaction is not also explicitly considered in this σ problem. The overlap integrals between σ atomic orbitals are also neglected.

Furthermore, the σ electrons are assumed to be independent of the electronic distribution of π electrons. This neglect of so-called σ-π interaction is permissible in the present "simple" LCAO MO treatment.

The Coulomb and the resonance integrals are taken as follows:

The Coulomb integrals:

$$\int \phi_{C,r} H \phi_{C,r}\, d\tau = \alpha$$

$$\int \phi_{H,l} H \phi_{H,l}\, d\tau = \alpha - 0.2\beta$$

The resonance integrals:

$$\int \phi_{C,r} H \phi_{C,r+1}\, d\tau = \beta$$

(r and $r+1$ belonging to neighboring carbons)

$$\int \phi_{C,r} H \phi_{C,r+1}\, d\tau = m\beta = 0.38\beta$$

(r and $r+1$ belonging to the same carbon)

$$\int \phi_{C,r} H \phi_{H,r+1}\, d\tau = \beta_{sp^2-H} = 0.94\beta \qquad (2)$$

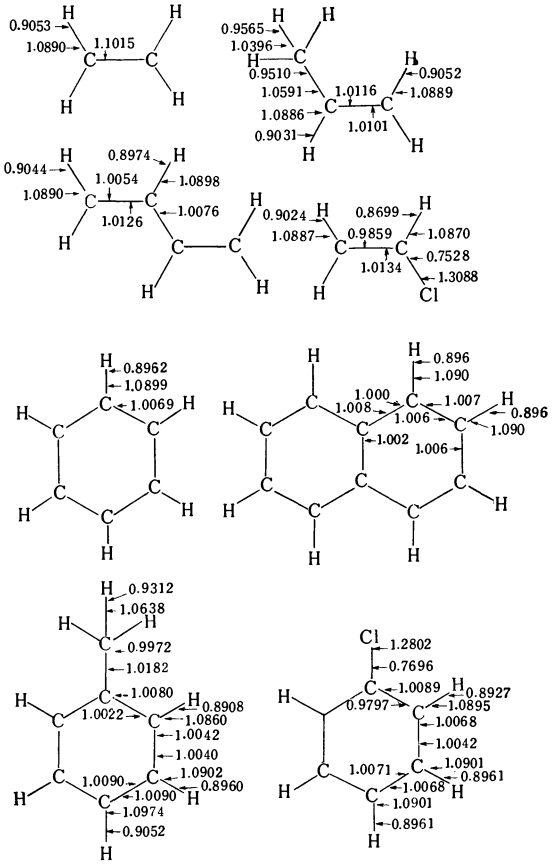


Fig. 2. The values of total σ electron densities of bonding orbitals (q_r^O) in some conjugated compounds.

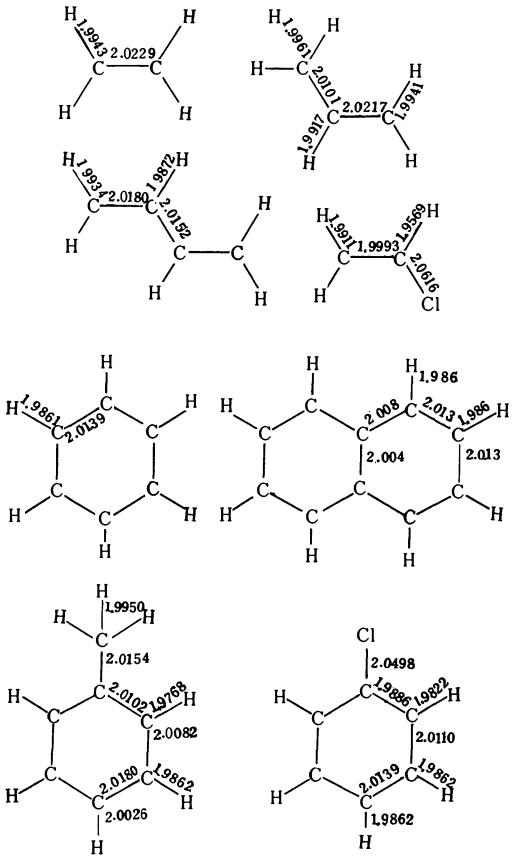


Fig. 3. The values of total σ electron densities of bonds (q_r^B) in some conjugated compounds.

in which H is the one electron hamiltonian of a σ electron. The value of m is determined by considering the degree of hybridization from the similar value of saturated hydrocarbons in previous papers[2,3]. The value of β_{sp^2-H} is estimated from the overlap integrals of a C–C and a C–H bond as calculated by Mulliken[4]. Further, α_H is determined so as to explain the C–H bond moment.

In treating propylene and toluene, the integrals containing the sp^3 hybridized orbital of carbon are needed. They are estimated from the electron affinity and the ionization potential of valence states and also from overlap integrals, resulting in

$$\left.\begin{aligned}
&\int \phi_{sp^3,r} H \phi_{sp^3,r}\, d\tau = \alpha - 0.1\beta \\
&\int \phi_{sp^3,r} H \phi_{sp^2,r+1}\, d\tau = 0.92\beta \\
&\int \phi_{sp^3,r} H \phi_{sp^3,r+1}\, d\tau = m(sp^3)\beta = 0.29\beta \\
&\int \phi_{sp^3,r} H \phi_{H,r+1}\, d\tau = \beta_{sp^3-H} = 0.93\beta
\end{aligned}\right\} \quad (3)$$

in which α and β are the integrals of the sp^2 orbitals defined in Eq. 2.

Electronic Structure of the σ-Skeleton in a Conjugated System

The calculated values of the energy level and the charge distribution of each orbital are listed in Table I for ethylene, butadiene and benzene. The characteristics of the σ-electronic structure of the polyene are found to be similar to those of the normal aliphatic hydrocarbons discussed in a previous paper[2].

On investigating Table I and Figs. 1—4, the following conclusions may be derived.

a) The bonding electrons belonging to each orbital tend to localize in certain particular bonds. For instance, the charge distribution of each orbital for butadiene, benzene, and so on, shows the above-mentioned characteristics, as is

3) H. Yoshizumi, *Trans. Faraday Soc.*, 53, 125 (1957).
4) R. S. Mulliken, C. A. Rieke, D. Orloff and H. Orloff, *J. Chem. Phys.*, 17, 1248 (1949); R. S. Mulliken, *J. Am. Chem. Soc.*, 72, 4493 (1950).

clearly seen in Fig. 1. Namely, the electron densities in the highest occupied orbital as well as in the lowest vacant orbital are largest in the carbon-carbon σ bond. Such general trend is also seen in benzene, naphthalene and chlorobenzene, where electrons belonging to the highest occupied orbital localize completely in carbon-carbon σ bonds.

b) The energy gap between the highest occupied orbital and the lowest vacant one is much greater than that of the π-orbitals. This point is discussed in detail in the following section.

c) Generally speaking, the charge distribution is not uniform. The values of the total electron density of the carbon hybridized orbital or hydrogen 1s orbital (q_r^{O}), the electron density of each bond (q_r^{B}), and the net charge of each atom (Q_r) for some compounds are indicated in Figs. 2, 3 and 4. The quantities of q_r^{O}, q_r^{B} and Q_r are given in the following formulas:

$$\left.\begin{aligned} q_r^{O} &= 2\sum_{i}^{occ} C_{ir}^{2} \\ q_r^{B} &= q_s^{O} + q_{s+1}^{O} \\ Q_r &= (\text{valence number of the } r\text{th atom}) \\ &\quad - \sum{}' q_s^{O} \end{aligned}\right\} \quad (4)$$

in which $\sum'$ denotes the summation carried out over all valence orbitals belonging to the rth atom.

It is worthy of notice that the magnitudes of the total electron densities of hydrogen atoms of benzene and naphthalene are smaller than those of ethylene and butadiene. The following interesting conclusion may accordingly be derived. In σ electron systems the benzene ring exerts an electron-attracting effect. Further, the hydrogen atoms belonging to the methyl group of propylene and toluene have larger electron densities than those of the hydrogen atoms attached to the sp^2 hybridized carbon orbital.

d) The order of magnitude of I-effect for many substituents can be indicated by referring to the values of Q_r listed in Fig. 4 for toluene, chlorobenzene* and so on. The more electronegative the substituent is, the larger the electron density of the substituent. The effect of the substituent, however, becomes smaller in the distant atom from the substituent, and the magnitude of the change in electron density effected by a substituent is approximately proportional to m^{2n}, where n is the number of atoms along the carbon chain from the substituent to the atom in question**. In this case the remarkable effect of the bond alteration is not revealed.

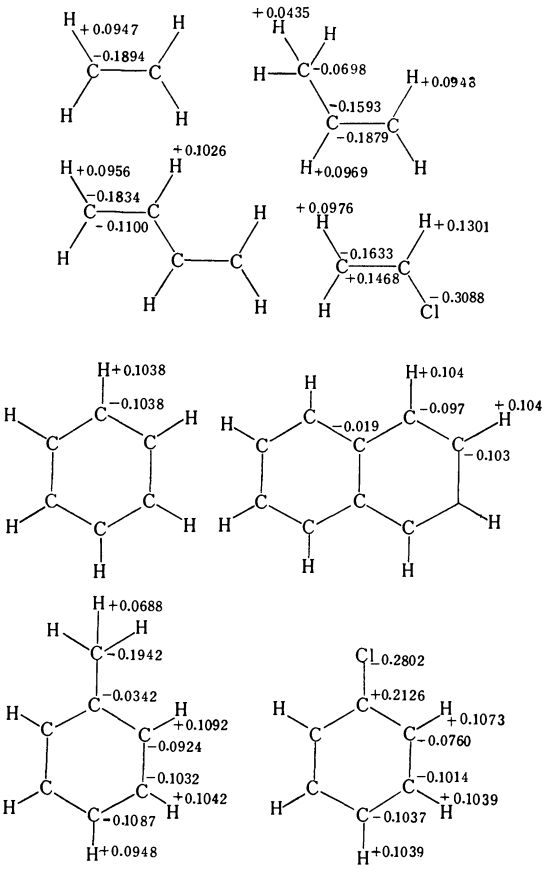


Fig. 4. The values of net charges of atoms (Q_r) in some conjugated compounds.

Comparative Discussion on σ- and π-Electronic Structures

Energy of σ-MO's

It has been believed that the energies of σ- and π-molecular orbitals increase in the following order:

$$\sigma\text{-occupied} < \pi\text{-occupied} < \pi\text{-unoccupied} < \sigma\text{-unoccupied orbitals}$$

Hence, it is required that the energy gap between the lowest vacant and the highest occupied σ-orbitals be large enough to include all the π-orbitals within it. The calculated energies of these σ-orbitals in some compounds

* The values of the Coulomb and the resonance integrals of a chlorine atom are put tentatively at $\alpha_{Cl}=\alpha+0.3\beta$ and $\beta_{C\text{-}Cl}=0.6\beta$ respectively.

** In the case of a simple LCAO MO treatment of the π electron systems, the I-effect upon the Coulomb integral is taken as $(1/3)^n$ by Dewar[5]. This approximation seems to be reasonable on the basis of the result obtained in the present paper.

5) M. J. S. Dewar, *J. Chem. Soc.*, **1949**, 463.

TABLE II. THE CALCULATED VALUES OF ENERGIES OF HIGHEST OCCUPIED (ho) AND LOWEST VACANT (lv) ORBITALS OF σ, AND OF ENERGIES OF LOWEST OCCUPIED (lo) AND HIGHEST VACANT (hv) ORBITALS OF π ELECTRONS OF SOME CONJUGATED COMPOUNDS

	σ (in unit of β_{sp^2})		π (in unit of β_p)	
	λ_{ho}	λ_{lv}	λ_{lo}	λ_{hv}
Ethylene	0.6377	−0.6641	1.000	−1.000
Butadiene	0.6258	−0.5758	1.618	−1.618
Propylene	0.5853	−0.6031	1.414	−1.414*
Benzene	0.6200	−0.5013	2.000	−2.000
Naphthalene	0.6200	−0.4428	2.300	−2.300
Toluene	0.6057	−0.4805	2.000	−2.000*

* These values were obtained by neglecting hyperconjugation of methyl group.

which are summarized in Table II show that the energy gap amounts to 1.1∼1.4 in units of $-\beta_{sp^2}$ or 11∼14 eV., which is sufficiently large to include all the π-MO's of ordinary conjugated compounds since in these the energies of the π-MO's lie in the range of $\alpha_p+2.5\beta_p$ to $\alpha_p-2.5\beta_p$*.

In some exceptional cases, however, the lowest vacant σ-orbital, whose energy is $\alpha_{sp^2}-0.2\beta_{sp^2}$ lies in proximity to the nonbonding π-MO of zero energy. Thus the lowest vacant σ-MO may be situated below the lowest vacant π-orbital in these compounds. This fact may have an important bearing on the chemical reaction and the polarographic reduction. The details of these facts will be published in the future.

σ-Electron Density

In the alternant hydrocarbon, the total π-electron density at the carbon atom is always equal to unity, whereas the σ-electron density at the carbon atom (Eq. 4), in the σ-skeleton of conjugated molecules is not necessarily uniform, as has been pointed out by the present authors[2].

It may be reasonable, therefore, to consider that this σ-electron distribution modifies the Coulomb integral of the π-electron system and causes an alteration of the π-electron density. In this connection a comprehensive SCF treatment, including both σ-electrons and π electrons, should be carried out.

One should bear in mind that the position of attack in the reaction is never determined by the magnitude of the σ-electron density, even when the π-electron distribution is uniform. Thus, in butadiene, the σ-electron densities, at positions 1 and 4, are larger than those at positions 2 and 3, as is shown in Fig. 4. This distribution appears to indicate that positions 1 and 4 are more susceptible to electro philic attack than positions 2 and 3, in agreement with experience. However, this distribution is incompatible with the fact that nucleophilic attack also takes place at positions 1 and 4. According to the self-consistency consideration, this σ-electron distribution may bring about a decrease in π-electron densities at positions 1 and 4 and an increase of those at 2 and 3. This result leads us again to a contradiction to the experimental facts in electrophilic substitutions. Also, in naphthalene, the σ-electron density increases in the order

$$9\text{-} < 1\text{-} < 2\text{-position}$$

which is reverse to the order of reactivity in electrophilic substitutions. In toluene, the calculated σ-electron density increases in the order

$$\text{ortho} < \text{meta} < \text{para}$$

which is not consistent with the *o*, *p*-directing property of this compound. All of these facts show that the σ-electron density has no direct concern with the chemical reaction and that the electron which plays an important role is not the σ-electron but the π-electron.

The σ-electron distribution stated above may be provide us with an indirect support of the validity of the π approximation in discussing the reactivity of conjugated molecules.

With respect to propylene and toluene, the σ-electron distribution of some σ occupied orbitals is shown in Table III. The molecular orbitals localized in the methyl group are closely similar to a normal π-type orbital and are orthogonal to each other. The mode of this distribution suggests that hyperconjugation may take place in these compounds, as has been pointed out by Mulliken[6] and Coulson[7].

Other Problems

Many other facts are successfully explained by the present results. Some of these will be described here. Full details of each topic will be published in the future.

Proton Shift

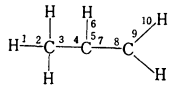
The calculated density of σ-electrons at the hydrogen atom will provide us with information about the local diamagnetic shielding of the proton in nuclear magnetic resonance spectra.

* See, for example, B. Pullman and A. Pullman, "Les Théories Electroniques de la Chimie Organique", Masson & Cie, Paris (1952).

6) R. S. Mulliken, C. A. Rieke and W. G. Brown, *J. Am. Chem. Soc.*, **63**, 41 (1941).

7) C. A. Coulson and V. A. Crawford, *J. Chem. Soc.*, **1953**, 2052; C. A. Coulson, *Quart. Rev.*, **1**, 144 (1947).

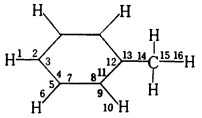
TABLE III (a). SOME σ OCCUPIED ORBITALS OF PROPYLENE



λ_j	H_1	C_2	C_3	C_4	C_5	H_6	C_7	C_8	C_9	H_{10}
+0.58534*	0.03218	0.02295	0.27069	0.28179	0.04471	0.06406	0.05312	0.06568	0.01121	0.01606
+0.63984**	0.36721	0.29946	0	0	0	0	0	0	0	0
+0.64174	0.00042	0.00034	0.00307	0.00388	0.20291	0.25305	0.17756	0.17467	0.04062	0.05066
+0.65430	0	0	0	0	0	0	0	0	0.22617	0.27383
+1.09543	0.02628	0.05100	0.00165	0.07096	0.20094	0.10580	0.04894	0.00086	0.11104	0.05846

* Highest occupied orbital ** Localized orbital in CH_3 group

TABLE III (b-1). SOME σ OCCUPIED ORBITALS OF TOLUENE

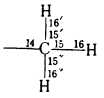


λ_j	H_1	C_2	C_3	C_4	C_5	H_6	C_7	C_8
+0.60570*	0.0047	0.0034	0.0014	0.0010	0.0046	0.0062	0.0140	0.0119
+0.61264**	0	0	0	0	0	0	0	0
+0.62000	0	0	0.0833	0.0833	0	0	0.0833	0.0833
+0.63752	0	0	0.0619	0.0641	0.0549	0.0692	0	0
+0.64070	0.1278	0.1022	0.0298	0.0277	0.0078	0.0097	0.0685	0.0700

λ_j	C_9	H_{10}	C_{11}	C_{12}	C_{13}	C_{14}	C_{15}	H_{16}
+0.60570*	0.0094	0.0128	0.0548	0.0484	0.2355	0.2512	0.0270	0.0319
+0.61264**	0	0	0	0	0	0	0.3083	0.3584
+0.62000	0	0	0.0833	0.0833	0	0	0	0
+0.63752	0.0549	0.0692	0.0641	0.0619	0	0	0	0
+0.64070	0.0735	0.0919	0.0008	0.0004	0.0036	0.0035	0.0004	0.0005

* Highest occupied orbital ** Localized orbital in CH_3 group

TABLE III (b-2). ORBITALS LOCALIZED IN CH_3 GROUP



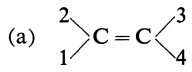
λ_j	C_{15}	H_{16}	$C_{15'}$	$H_{16'}$	$C_{15''}$	$H_{16''}$
0.61264	0.3083	0.3584	0.0771	0.0896	0.0771	0.0896
0.61264	0	0	0.2312	0.2688	0.2312	0.2688

In the case of benzene and naphthalene (Fig. 2), the σ-electron densities at each hydrogen atom do not vary much according to the position attached. Therefore, it is considered that the difference in the chemical shift between α- and β-hydrogen atoms in naphthalene is ascribable to the unequal contribution of the induced π-ring current.

The σ-electron densities and values of chemical shifts in propylene and toluene are indicated in Table IV. In both cases, σ-electron densities at methyl hydrogen atoms are greater than those at other hydrogen atoms. These results coincide with the experimental fact that the resonance fields for methyl protons is higher than those for other protons.

In conclusion, a more quantitative explanation of the proton chemical shift is possible by the present procedure. The results will be published in the future.

TABLE IV. CHEMICAL SHIFTS AND σ ELECTRON DENSITIES OF HYDROGEN ATOMS IN SOME COMPOUNDS

(a) 

		Shift[1]*	Density
Ethylene	H_2	−0.9	0.905
	H_3	−0.9	0.905
	H_4	−0.9	0.905
Propylene	H_2	−0.8	0.903
	H_3	−0.2	0.905
	H_4	−0.1	0.905
	CH_3	+3.3	0.957

(b)

Benzene	Ring proton	−2.52	0.896
Toluene	Ring proton	−2.35	0.905∼0.891
	CH_3 Proton	+2.45	0.931

1) J. A. Pople, W. G. Schneider and H. J. Bernstein, "High-resolution Nuclear Magnetic Resonance", McGraw-Hill, London (1959).

* In p.p.m. referred to water.

Dipole Moment

The dipole moment of conjugated molecules has hitherto been calculated as the sum of π moment obtained theoretically and the σ moment estimated empirically. The present treatment enables us to calculate the σ moment theoretically. According to our results, the σ dipole moments of toluene and propylene become 0.57 D and 0.05 D respectively*. Though it needs further investigation to decide whether these values are reasonable or not, the calculated result clearly indicates that conjugated compounds containing both sp^2 and sp^3 hybridized carbon atoms may have a σ moment of an appreciable magnitude. At least the usual procedure for explaining the dipole moment of these compounds only by hyperconjugation must be re-examined.

Summary

The σ-electronic structures and σ-electron densities of σ skeletons in some conjugated compounds are calculated by a simple LCAO MO method developed by the present authors. The inductive and hyperconjugative effects, dipole moment, proton shift, and so on, are briefly discussed. Agreements of the results with experiments seem to be almost entirely satisfactory.

A part of the calculation has been carried out with the KDC-I digital computer of Kyoto University.

Faculty of Engineering
Kyoto University
Sakyo-ku, Kyoto

* The values of the Coulomb integral of the H atom in the CH_3 group in toluene and propylene are tentatively put $\alpha_H=\alpha-0.25\beta$ and $\alpha-0.2\beta$ respectively. Thus, the difference of σ-electron densities at these atoms is partially dependent on the difference of the values of parameters. In calculating the values of σ dipole moments in these compounds, the center of gravity of sp^3 and sp^2 hybridzed orbital is located at the positions of 0.44 Å and 0.41 Å apart from the carbon nucleus respectively.

Syntheses of γ-Ionone Analogues. III. Diels-Alder Reaction Involving a Mixture of 3, 4-Dimethyl-1, 3-pentadiene and 2, 3-Dimethyl-1, 3-pentadiene, and Some Derivatives from 2-Benzyloxymethyl-4, 5, 6-trimethylcyclohexa-1, 4-dienylmethanal

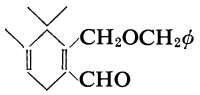
By Atsuaki ARAI and Iwao ICHIKIZAKI

(Received April 13, 1961)

As described in a previous paper[1], 2-methylene-4, 5-dimethylcyclohexylmethanol, an analogue of γ-cyclogeraniol, can be conveniently synthesized, in five steps, from a Diels-Alder adduct prepared by the condensation of 2, 3-dimethyl-1, 3-butadiene with 4-benzyloxy-2-butyn-1-al (I), $C_6H_5CH_2OCH_2C{\equiv}CCHO$. It is to be expected, therefore, that a similar condensation of 3, 4-dimethyl-1, 3-pentadiene (III) with I will yield 2-benzyloxymethyl - 3, 3, 4 - trimethylcyclohexa - 1, 4 - dienyl methanal (VI) and contribute an easy approach

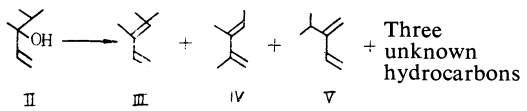
1) A. Arai and I. Ichikizaki, This Bulletin, **34**, 1571 (1961).

to either 6-methyl-γ-cyclogeraniol or, further, to γ-irone itself.



VI

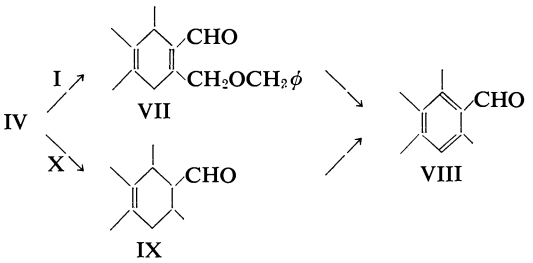
The studies under various conditions to prepare III revealed that the dehydration of 3, 4-dimethyl-1-penten-3-ol (II)[2,3] with potassium hydrogen sulfate afforded totally, in a 75% yield, a diene mixture containing III, 2, 3-dimethyl-1, 3-pentadiene (IV) and 2-isopropyl-1, 3-butadiene (V) in a ratio of approximately 18 : 21 : 53, with unkown three hydrocarbons of minor quantities.



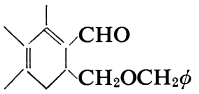
II III IV V

The composition of these hydrocarbons scarcely changed during many dehydrations at 140~180°C. Since the effective separation of III from IV was particularly difficult even by careful fractionations through an efficient column, a mixture consisting of 37.5% III and 62.5% IV, b. p. 107.5~108°C/753 mmHg, n_D^{20} 1.4664, was employed for the Diels-Alder reaction in the early stage of this research.

When a benzene solution of the mixed diene in the presence of a little amount of hydroquinone was heated for 10 hr. at 155°C with I, a doubly unsaturated aldehyde, $C_{18}H_{22}O_2$, ν_{max}^{film} 2750 and 1670 cm^{-1}, was obtained in a 64% yield. The light absorption band (in ethanol) at 236 mμ (ε 5900) revealed that the unsaturated aldehyde contains an α, β- and an isolated unsaturated linkage. The quantitatively yielded phenylsemicarbazone was readily hydrolyzed by super heated steam in the presence of both phthalic and sulfric acids to be converted with the elimination of benzyl alcohol into 2, 3, 4, 6-tetramethylbenzaldehyde (VIII). The aldehyde VIII was also prepared from the sulfur dehydrogenation of 2, 3, 4, 6-tetramethyl-3-cyclohexenylmethanal (IX), which had been obtained in a 52% yield by a similar treatment of the same mixed diene with crotonaldehyde (X). Consequently, the structure of the adduct was reasonably concluded to be 2-benzyloxymethyl-4, 5, 6-trimethylcyclohexa-1, 4-dienylmethanal (VII). The aldehyde VII was readily converted by the action of diluted sulfuric acid into an isomer which



was presumed to be 6-benzyloxymethyl-2, 3, 4-trimethylcyclohexa-1, 3-dienylmethanal (XI).



XI

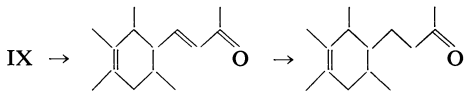
All the results obtained above clearly indicated that only IV could participate in this reaction, that III could not practically react with the dienophiles, and, moreover, that a high degree of specificity was exhibited in the direction of the addition of IV to either I or X. And from the higher yield of VII than that expected, it was considered that III was partly isomerized to IV under the given conditions. In order to fully test the ability of III as a Diels-Alder diene, the authors employed for the reaction with X a specially enriched sample, b. p. 109.2~110°C/758 mmHg, n_D^{20} 1.4722, which had been confirmed to consist of 94.7% III, 5.3% IV and no other dienes; they then found that III was partly polymerized and mostly recovered after isomerizing to IV, whereas the addition product obtained in a slight yield was proved to consist largely of IX. On the other hand, a similar reaction at 125°C with a mixture, b. p. 106.3~106.6°C/760 mmHg, n_D^{20} 1.4634, containing 91.4% IV and 8.6% III, afforded IX in a 42% yield.

Naves[2], Nazarov[3] and their associates claimed that the Diels-Alder reaction between so-called 3, 4-dimethyl-1, 3-pentadiene and X gave an adduct which resulted directly from III itself as a main product, although as to the direction of the addition their conclusions were contradictory. It is still obscure, for the present, why the opinions about the Diels-Alder reaction involving III do not agree with one another; however, it should be emphasized that both the diene samples used by the European investigators, showing n_D^{20} 1.4560 and 1.4691 respectively, might be more heterogeneous and clearly more deficient in III than the one employed by the authors for the above test. Several problems concerning the diene III will be discussed in detail in a following paper.

2) Y. R. Naves and P. Ardizio, *Helv. Chim. Acta*, **31**, 2256 (1948).
3) I. N. Nazarov and M. V. Mavrov, *Zhur. Obshchei Khim.*, **29**, 1158 (1959).

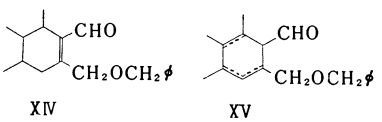
The Diels-Alder adducts, VII and IX, gave several derivatives, some of which were proved to have an odor.

The aldehyde IX freshly regenerated from its phenylsemicarbazone afforded, on condensation with acetone, 4-(2′, 3′, 4′, 6′-tetramethyl-3′-cyclohexenyl)-but-3-en-2-one (XII) in an 82.2% yield. The catalytic hydrogenation of XII over platinum oxide catalyst gave, in an 81% yield, 4-(2′, 3′, 4′, 6′-tetramethyl-3′-cyclohexenyl)-butan-2-one (XIII). Both XII and XIII have a pleasant odor.

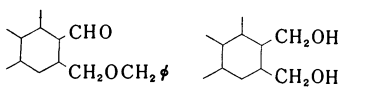


XII XIII

On the partial hydrogenation of VII in the presence of a palladium-calcium carbonate catalyst, when one mole of hydrogen was consumed, an α, β-unsaturated aldehyde XIV and appreciable amounts of an unconjugated unsaturated aldehyde XV were obtained, although the location of the double bond in the latter has not been confirmed. With a palladium-barium carbonate catalyst, after absorbing two moles of hydrogen, VII afforded 6-benzyl-oxymethyl-2, 3, 4-trimethylcyclohexylmethanal (XVI). In the meanwhile, when hydrogenation was carried out under pressure in the presence of a Raney nickel catalyst, it afforded the saturated diol XVII in a yield of 73%.

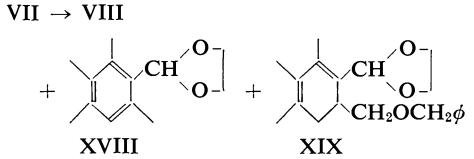


XIV XV



XVI XVII

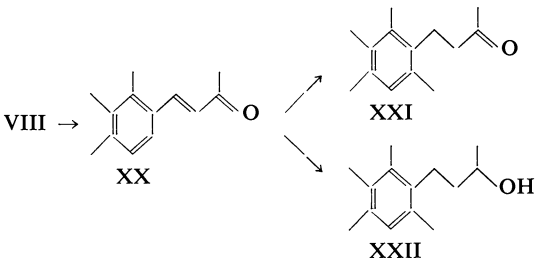
Treatment of VII with ethylene glycol[4] in the presence of *p*-toluenesulfonic acid gave VIII, the ethylene acetal XVIII and, in only a 3% yield, an acetal which was presumed to be XIX, an isomer of the desired acetal.



XVIII XIX

4) E. I. Salmi, *Ber.*, **71**, 1803 (1938).

Finally, when VIII was condensed with acetone in the usual way 4-(2′, 3′, 4′, 6′-tetramethylphenyl)-but-3-en-2-one (XX), with a weak violet-like odor, was obtained in a 92% yield. On partial hydrogenation over platinum oxide catalyst XX afforded, in an excellent yield, 4-(2′, 3′, 4′, 6′-tetramethylphenyl)-butan-2-one (XXI), and, on further hydrogenation with a Raney nickel catalyst under pressure, it gave 4-(2′, 3′, 4′, 6′-tetramethylphenyl)-butan-2-ol (XXII).



XX XXI XXII

Experimental[5]

3, 4-Dimethyl-1-penten-3-ol (II).—3, 4-Dimethyl-1-penten-3-ol (II) was prepared in an 85~89% yield by hydrogenation of 3, 4-dimethyl-1-pentyn-3-ol, b. p. 134.5°C/760 mmHg, n_D^{20} 1.4362 (lit.[3] b. p. 134~134.5°C/752 mmHg, n_D^{20} 1.4370), with a palladium-on-calcium carbonate catalyst. The carbinol II had b. p. 134.7~135°C/760 mmHg and n_D^{20} 1.4335 (lit.[3] b. p. 130.7~131°C/748 mmHg, n_D^{20} 1.4361).

Dehydration of 3, 4-Dimethyl-1-penten-3-ol (II) with Potassium Hydrogen Sulfate.—The carbinol II (77 g.) was stirred, drop by drop, into potassium hydrogen sulfate (fused, 20 g.) over a period of 7 hr. at 175~180°C under a nitrogen atmosphere and simultaneous distillation of the dehydration products through a 25 cm. Vigreux column. After separating the aqueous layer, the distillate was dried over calcium chloride, then simply redistilled through a 30 cm. column, and a fraction boiled at 82 to 108°C was collected. The yield was 43.7 g. (75%). There remained a brown tarry oil (ca. 10 g.) containing unchanged II in a distilling flask. Vapor phase chromatography at 90°C showed that the above fraction consists of six components containing 3, 4-dimethyl-1, 3-pentadiene (III), 2, 3-dimethyl-1, 3-pentadiene (IV) and 2-isopropyl-1, 3-butadiene (V) in a ratio of approximately 18 : 21 : 53, with three unknown hydrocarbons of minor quantities (Fig. 1).

The above fraction was carefully fractionated through a 100 cm. modified Todd fractionating column to give the following representatitive fractions :

5) All m. p.'s were determined on the Kofleir hot-stage and are uncorrected. The ultraviolet absorption spectra were determined with a Hitachi spectrophotometer model EPU-2A, while the infrared absorption spectra were obtained with a Perkin-Elmer model 112, a Kōken model DS-301 and a Nippon Bunkō model IR-S recording spectrophotometer using sodium chloride optics. Vapor phase chromatographic analyses were carried out with a Kotaki Super Fractioner model GU-21 using a 200 mm. × 8 mm. φ copper tube packed with Celite DM-13 A which was coated with Carbowax-4000.

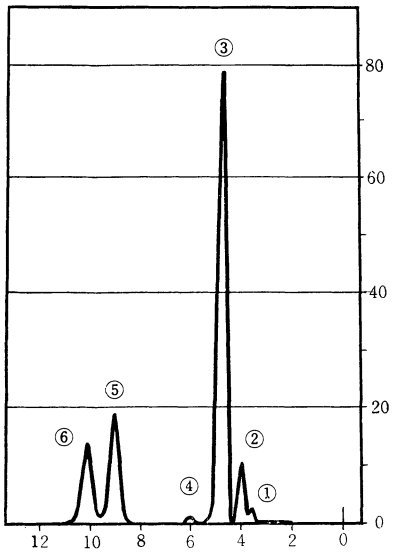


Fig. 1. Vapor phase chromatogram of the dehydration products of 3,4-dimethyl-1-penten-3-ol (II) with potassium hydrogen sulfate at 175~180°C.
①, ② and ④: Unknown hydrocarbons
③: 2-Isopropyl-1,3-butadiene (V)
⑤: 2,3-Dimethyl-1,3-pentadiene (IV)
⑥: 3,4-Dimethyl-1,3-pentadiene (III)

F. No.	B. p. °C/760 mmHg	n_D^{20}	Yield g.	Composition, % III : IV : V		
3	86~87	1.4326	16.0			98
7	104~106	1.4552~1.4617	1.8	6	72	15
8	106~106.5	1.4635	2.9	7.5	85	4.5
9	106.5~107.5	1.4635~1.4660	2.5	17	82	
10	107.5~108.5	1.4664~1.4671	5.3	42	58	
11	108.5	1.4680	1.4	52	48	

The diene V was easily isolated from the other components after two redistillations through the same column, whereas III and IV could not be separated from each other even by the repeated redistillations. The enriched sample of III which was thus obtained had b. p. 109.2~110°C/758 mmHg and n_D^{20} 1.4722 and consisted of 94.7% III and 5.3% IV; that of IV had b. p. 106.3~106.6°C/760mmHg and n_D^{20} 1.4634 and was composed of 91.4% IV and 8.6% III.

Many dehydrations of II with potassium hydrogen sulfate carried out in the range at 140 to 180°C showed that the composition of the hydrocarbons was practically constant and did not change with the temperature.

A mixed diene consisting of 37.5% III and 62.5% IV, b. p. 107.5~108°C/753 mmHg, n_D^{20} 1.4664, which was easily obtained, was employed for the next Diels-Alder reactions.

2-Benzyloxymethyl-4,5,6-trimethylcyclohexa-1,4-dienylmethanal (VII).—A mixture of 4-benzyloxy-2-butyn-1-al (I) (34.8 g.), the mixed diene (20.2 g.) and benzene (30 ml.) was heated with a little hydroquinone for 10 hr. at 155°C under nitrogen in a glass bomb. Concentration of the reaction mixture under reduced pressure, followed by distillation, gave a small amount of unchanged I and a pale yellow oil (36.0 g.), b. p. 133~135°C/2.2×10^{-3} mmHg, n_D^{20} 1.5496. There remained a considerable amount of a dark-red resinous matter. In order to investigate the homogeneity of the above fraction, the 2,4-dinitrophenylhydrazone was directly prepared from the above fraction (0.34 g.), and the excess of water was added to the reaction mixture to precipitate any methanol-soluble materials. When the precipitate (0.36 g.) was dissolved in chloroform (1.5 ml.) and chromatographed on alumina (200 mm.×18 mm. ϕ) from benzene, a weak red-orange band at the top of the column and then a strong yellow-orange band were obtained. The lower zone afforded orange silk-like needles (270 mg.), m. p. 155~156°C, after being crystallized from ethanol-ethyl acetate.

Found: N, 12.42. Calcd. for $C_{24}H_{27}O_5N_4$: N, 12.44%.

The upper band gave red-orange needles (10 mg.), m. p. 128~129.8°C, after crystallization from methanol.

Found: N, 12.60%.

The phenylsemicarbazone was prepared from the above fraction (1.0 g.) in the usual manner, and an excess of water was added and allowed to stand overnight. The crystalline solid was collected and crystallized from ethanol to give colorless needles (1.27 g.) melting at 163~164°C, λ_{max}^{EtOH} 235 mμ (ε, 17700), 285 (32100), which could be converted into the 2,4-dinitrophenylhydrazone, m. p. 155~156°C, described above.

Found: N, 10.46. Calcd. for $C_{25}H_{29}O_2N_3$: N, 10.41%.

From the mother liquor, colorless needles (60 mg.) melting at 139 to 141°C were isolated.

Found: N, 10.38%.

The crude pale yellow oil mentioned above was twice redistilled carefully under nitrogen to afford VII as a pale yellow viscous liquid, b. p. 133~134°C/2×10^{-3} mmHg, n_D^{20} 1.5494. ν_{max}^{film} 2750, 1670 (CHO, conju.), 1640 (C=C, conju.), 1070 (C-O-C), 3025, 1502, 742 and 705 cm^{-1} (phenyl group). λ_{max}^{EtOH} 236 mμ (ε 5900).

Found: C, 79.80; H, 8.27. Calcd. for $C_{18}H_{22}O_2$: C, 79.96; H, 8.20%.

From the above fraction, only the 2,4-dinitrophenylhydrazone, m. p. 155~156°C, was obtained.

Treatment of the Aldehyde VII with Diluted Sulfuric Acid.—The aldehyde VII (0.3 g.), dissolved in a solution of concentrated sulfuric acid (0.2 ml.) in 80% aqueous methanol (2 ml.), was warmed at 60°C for 5 min. A saturated solution of potassium acetate in methanol was added dropwise to the cooled reaction mixture until the precipitation of potassium sulfate was completed. The mixture was filtered, and the filtrate was then concentrated and treated with a solution of phenylsemicarbazide (0.4 g.) in methanol (5 ml.). After

this was kept overnight at room temperature, a solid derivative was collected and crystallized from 50% aqueous ethanol to yield what is believed to be the phenylsemicarbazone of 6-benzyloxymethyl-2, 3, 4 - trimethylcyclohexa - 1, 3 - dienylmethanal (XI) (0.26 g.) as long needles, m. p. 167~169°C; this showed a marked depression in melting point on admixture with that of VII, m. p. 163~164°C.

Found: N, 10.37. Calcd. for $C_{25}H_{29}O_2N_3$: N, 10.41%.

2, 3, 4, 6 - Tetramethyl - 3 - cyclohexenylmethanal (IX).—*a) From the Mixed Diene (b. p. 107.5~108°C/753 mmHg) and Crotonaldehyde (X).*—A mixture of mixed diene (16.2 g.), X (10.5 g.) and benzene (10 ml.) were heated with a small amount of hydroquinone for 7 hr. at 155°C in a 50 ml. glass bomb. After removal of the solvent, the residue was distilled to afford a colorless liquid (13.0 g.), b. p. 72~74.5°C/3.5 mmHg, n_D^{20} 1.4778.

Found: C, 79.16; H, 11.15. Calcd. for $C_{11}H_{18}O$: C, 79.46; H, 10.92%.

Treatment of the above fraction with the Brady reagent gave a yellow 2, 4-dinitrophenylhydrazone, m. p. 181~182°C, after crystallization from methanol.

Found: N, 16.16. Calcd. for $C_{17}H_{22}O_4N_4$: N, 16.18%.

From the mother liquor a small number of orange-yellow needles, m. p. 128.5~136°C, which have not been further investigated, were separated.

The phenylsemicarbazone obtained from the above fraction was crystallized from aqueous ethanol to give needles, m. p. 133~135°C, in a 62% yield.

Found: N, 14.23. Calcd. for $C_{18}H_{25}ON_3$: N, 14.04%.

From the mother liquor an appreciable amount of a crystalline solid melted at 115 to 121°C was separated.

The phenylsemicarbazone (6.7 g.) obtained above as the main product was mixed with *o*-phthalic acid (14 g.), ethylene glycol (6 ml.) and water (100 ml.), and distilled in steam. The distillate was extracted with ether, and the ether extract was then washed with a 10% aqueous sodium carbonate solution and with water, dried and evaporated. Distillation of the residue afforded the aldehyde IX (2.6 g., 68%), b. p. 61~63.5°C/1.5 mmHg, n_D^{20} 1.4795, which gave only 2, 4-dinitrophenylhydrazone melting at 181~182°C.

Found: C, 79.34; H, 11.08. Calcd. for $C_{11}H_{18}O$: C, 79.46; H, 10.92%.

b) From the Mixed Diene (b. p. 109.2~110°C/758 mmHg) and X.—A mixture of the mixed diene (2.5 g.), X (1.9 g.) and benzene (10 ml.) was heated with a small amount of hydroquinone for 30 hr. at 125°C in a 50 ml. glass bomb. After removal of the solvent, the residual oil was distilled through a 10 cm. Vigreux column to afford a considerable amount of fore-run consisting of the unchanged starting materials and an oil (0.3 g.), b. p. 71~73°C/3 mmHg, n_D^{20} 1.4796, whose vapor phase chromatogram showed that this fraction consisted mainly of IX and of an appreciable amount of some unknown components.

Found: C, 79.78; H, 11.12. Calcd. for $C_{11}H_{18}O$: C, 79.46; H, 10.92%.

From the vapor phase chromatography, it was shown that the fore-run obtained above contains the diene III and IV in the proportion of 1 : 5, besides unchanged crotonaldehyde (X).

When the same reaction mixture as above was heated for 6 hr. at 200°C, the compositions of product became more complicated. In all cases, a gummy matter, which on cooling solidified gradually to give a white amorphous polymer, softened at ca. 130°C.

c) From the Mixed Diene (b.p. 106.3~106.6°C/760 mmHg) and X.—A mixture of the mixed diene (2.5 g.), X (1.9 g.) and benzene (10 ml.) was heated with a small amount of hydroquinone for 12 hr. at 125°C in a 50 ml. glass bomb. After removal of the solvent, the residue was distilled through an 8 cm. Vigreux column under nitrogen to afford a fore-run consisting largely of the unchanged starting materials and a colorless oil (1.8 g.), b. p. 76~78°C/4 mmHg, n_D^{20} 1.4791. Redistillation gave pure IX (1.52 g.), b. p. 75.5°C/4 mmHg, n_D^{21} 1.4791. ν_{max}^{film} 2740, 1721 (CHO), 1468 (CH_2) and 1387 cm^{-1} (CH_3).

Found: C, 79.42; H, 11.12. Calcd. for $C_{11}H_{18}O$: C, 79.46; H, 10.92%.

Upon treatment with the Brady reagent, IX gave a yellow 2, 4 - dinitrophenylhydrazone, m. p. 181~182°C, which showed no melting point depression on admixture with that prepared in a).

2, 3, 4, 6-Tetramethylbenzaldehyde (VIII).—*a) Acid Hydrolysis of the Phenylsemicarbazone of VII Melted at 163~164°C.*—A mixture of this derivative (7.0 g.), *o*-phthalic acid (7.0 g.), ethylene glycol (50 g.), concentrated sulfuric acid (15 g.) and water (50 ml.) was distilled in steam until no more organic materials passed over (7 hr. were required for this). The distillate (1300 ml.) was extracted with ether, and the ether extract was washed with water, dried over sodium sulfate and concentrated. Fractional distillation of the residual oil afforded a fore-run (0.6 g.), b. p. 49~55°C/1.2 mmHg, and 2, 3, 4, 6-tetramethylbenzaldehyde (VIII) (2.0 g., 69%) as a colorless oil, b. p. 92~94°C/1.2 mmHg, n_D^{20} 1.5482. ν_{max}^{film} 1709 (C=O), 867 cm^{-1} (penta-substituted phenyl group). λ_{max}^{EtOH} 268.5 and 306 mμ (lit.[6] λ_{max}^{EtOH} 267 mμ (log ε, 4.00), 306 (3.32)).

Found: C, 80.75; H, 8.89. Calcd. for $C_{11}H_{14}O$: C, 81.44; H, 8.70%.

The semicarbazone crystallized from 50% aqueous methanol in the form of needles, melted at 189°C to a liquid which quickly solidified and then remelted at 259~260°C with partial decomposition. λ_{max}^{EtOH} 219 mμ (ε, 19200), 275 (12000).

Found: C, 65.72; H, 7.64; N, 19.12. Calcd. for $C_{12}H_{17}ON_3$: C, 65.72; H, 7.81; N, 19.16%.

The 2, 4-dinitrophenylhydrazone crystallized from ethanol-ethyl acetate in the form of orange-yellow needles, m. p. 222~223°C.

Found: C, 59.57; H, 5.15; N, 16.35. Calcd. for $C_{17}H_{18}O_4N_4$: C, 59.64; H, 5.30; N, 16.37%.

b) Sulfur Dehydrogenation of 2, 3, 4, 6-Tetramethyl-3-cyclohexenylmethanal (IX).—The aldehyde IX (3.3

6) N. J. Leonard and E. R. Blout, *J. Am. Chem. Soc.*, 72, 486 (1950).

g.) prepared in the method of c) was heated under reflux with sulfur (1.6 g.) at 220~230°C under a nitrogen atmosphere until the evolution of hydrogen sulfide ceased (40 min. were required). The volatile materials were distilled under reduced pressure. The yellow distillate, b. p. 120~130°C/8.2 mmHg, thus obtained, on further distillation under nitrogen through a 7 cm. Vigreux column, yielded 2,3,4,6-tetramethylbenzaldehyde (VIII) (1.0 g., 31%) which had b. p. 127°C/8.2 mmHg and n_D^{20} 1.5740. There remained black tarry materials (ca. 1.3 g.) in the distilling flask.

The semicarbazone crystallized from aqueous methanol in prisms melted at 187~188°C to a liquid which rapidly solidified and then remelted at 259°C with partial decomposition; it gave no melting point depression on admixture with that prepared in a).

The 2, 4-dinitrophenylhydrazone prepared in the usual manner was chromatographed on alumina from benzene and crystallized twice from methanol-ethyl acetate to yield orange-yellow needles, m. p. 221~222°C, which showed no melting point depression on admixture with that obtained in a).

4-(2′,3′,4′,6′-Tetramethyl-3′-cyclohexenyl)-but-3-en-2-one (XII).—The aldehyde IX (2.3 g.) regenerated from the phenylsemicarbazone described above in acetone (7.0 ml.) was added dropwise to a boiled solution of barium hydroxide (0.4 g.) in 80% aqueous acetone (20 ml.) and refluxed for 19 hr. After the bulk of the solvent had been removed, the residue was dissolved in ether. The ethereal solution was washed successively with 10% hydrochloric acid and water, dried over magnesium sulfate and evaporated. Distillation afforded the unsaturated ketone XII (2.35 g., 82.2%) as a colorless liquid with a pleasant odor, b. p. 98~100°C/1.2 mmHg, n_D^{20} 1.4979. ν_{max}^{film} 1680 (C=O), 1622 (C=C), 1257 (CH_3CO) and 984 cm^{-1} (-CH=CH-, *trans*).

Found: C, 81.63; H, 10.86. Calcd. for $C_{14}H_{22}O$: C, 81.50; H, 10.75%.

The phenylsemicarbazone crystallized from ethanol in the form of feather-like needles, m. p. 149~151°C.

Found: N, 12.33. Calcd. for $C_{21}H_{29}ON_3$: N, 12.38%.

The 2, 4-dinitrophenylhydrazone crystallized from ethanol-ethyl acetate in the form of ruby-red needles, m. p. 141~142°C.

Found: N, 14.51. Calcd. for $C_{20}H_{26}O_4N_4$: N, 14.50%.

4-(2′,3′,4′,6′-Tetramethyl-3′-cyclohexenyl)-butan-2-one (XIII).—The ketone XII (1.45 g.) in ethyl acetate (40 ml.) was hydrogenated at ordinary pressure in the presence of a platinum oxide catalyst (50 mg.) until one molar equivalent (170 ml. at 20°C) of hydrogen had been absorbed. Removal of the catalyst and solvent, followed by distillation of the residue, afforded XIII (1.18 g., 80.5%) as a colorless liquid with a pleasant odor, b. p. 97~99°C/1.5 mmHg, n_D^{20} 1.4769.

Found: C, 80.50; H, 11.77. Calcd. for $C_{14}H_{24}O$: C, 80.71; H, 11.61%.

The semicarbazone crystallized from 40% aqueous methanol in the form of needles, m. p. 152.5~153.5°C.

Found: C, 68.00; H, 10.09; N, 15.76. Calcd. for $C_{15}H_{27}ON_3$: C, 67.88; H, 10.26; N, 15.83%.

The 2,4-dinitrophenylhydrazone crystallized from ethanol-ethyl acetate in the form of bright yellow prisms, m. p. 150~150.5°C.

Found: C, 61.57; H, 7.11; N, 14.60. Calcd. for $C_{20}H_{28}O_4N_4$: C, 61.84; H, 7.27; N, 14.42%.

2-Benzyloxymethyl-4, 5, 6-trimethyl-1-cyclohexenylmethanal (XIV).—The aldehyde VII (5.4 g.) in ethanol (10 ml.) was hydrogenated in the presence of a palladium-on-calcium carbonate catalyst (2.5% Pd, 2.0 g.) until 1.1 mol. equivalents (508 ml. at 8°C and 754 mmHg) of hydrogen had been absorbed. Removal of the catalyst and solvent, followed by distillation of the residue, afforded a pale yellow liquid (3.6 g.), b. p. 124~126°C/9×10^{-3} mmHg, n_D^{20} 1.5388.

Found: C, 78.71; H, 8.72. Calcd. for $C_{18}H_{24}O_2$: C, 79.37; H, 8.88%.

The phenylsemicarbazone crystallized from ethanol in the form of needles, m. p. 173.5~174.5°C. λ_{max}^{EtOH} 232 mμ (ε 29400), 292 (22200).

Found: N, 10.46. Calcd. for $C_{25}H_{31}O_2N_3$: N, 10.36%.

The crude 2,4-dinitrophenylhydrazone prepared directly from the above hydrogenation product (0.4 g.) in the usual manner was chromatographed on alumina from benzene. The lower, main red-orange zone gave the 2,4-dinitrophenylhydrazone of XIV as orange-red needles, m. p. 164~165°C (0.33 g.), after recrystallization from ethanol-ethyl acetate.

Found: N, 12.52. Calcd. for $C_{24}H_{28}O_5N_4$: N, 12.38%.

The upper, slight yellow band yielded, after being crystallized from ethanol-ethyl acetate, a 2,4-dinitrophenylhydrazone (10 mg.), m. p. 193~194°C, which is believed to be that of 6-benzyloxymethyl-2,3,4-trimethylcyclohexenylmethanal (XV), although the location of the double bond has not been determined.

Found: N, 12.38%.

6-Benzyloxymethyl-2, 3, 4-trimethylcyclohexylmethanal (XVI).—The aldehyde VII (2.70 g.) in ethanol (20 ml.) was hydrogenated at one atmosphere in the presence of a palladium-on-barium carbonate catalyst (2.5% Pd, 1.0 g.) until 2.05 mol. equivalents (470 ml. at 9.5°C) of hydrogen had been absorbed. Removal of the catalyst and solvent, followed by distillation of the residue, afforded the saturated aldehyde XVI (2.10 g., 76.6%) as a colorless liquid, b. p. 115~117°C/5×10^{-3} mmHg, n_D^{20} 1.5290. ν_{max}^{film} 2710, 1724 (CHO), 1099 (C-O-C), 741 and 703 cm^{-1} (mono-substituted phenyl group).

Found: C, 78.74; H, 9.29. Calcd. for $C_{18}H_{26}O_2$: C, 78.79; H, 9.55%.

The phenylsemicarbazone crystallized from ethanol in the form of fine needles, m. p. 134~135°C. λ_{max}^{EtOH} 248 mμ (ε 28400).

Found: N, 10.47. Calcd. for $C_{25}H_{33}O_2N_3$: N, 10.31%.

The 2,4-dinitrophenylhydrazone crystallized from ethyl acetate in the form of orange-yellow needles, m. p. 105°C.

Found: N, 12.54. Calcd. for $C_{24}H_{30}O_5N_4$: N, 12.33%.

1, 2 - Bishydroxymethyl - 3, 4, 5 - trimethylcyclohexane (XVII).—The aldehyde VII (2.7 g.) in ethanol (30 ml.) was hydrogenated in the presence of a Raney nickel catalyst (1.0 g.) for 4 hr. at 150°C and 195 kg./cm². After the catalyst had been removed, the filtrate was again hydrogenated with a palladium-on-charcoal catalyst (5% Pd, 1.0 g.) for 2 hr. at 130°C and 150 kg./cm². Removal of the catalyst and solvent, followed by distillation of the residue, gave the diol XVII (1.36 g., 73%), b. p. 113~115°C/4×10^{-3} mmHg, n_D^{25} 1.4860. ν_{max}^{film} 3333 and 1054 cm^{-1} (OH).

Found: C, 71.32; H, 11.75. Calcd. for $C_{11}H_{22}O_2$: C, 70.29; H, 11.90%.

The bisphenylurethane crystallized from benzene-ethyl acetate in the form of needles, m. p. 173°C.

Found: C, 67.88; H, 7.59; N, 6.42. Calcd. for $C_{25}H_{32}O_4N_2\cdot H_2O$: C, 67.85; H, 7.75; N, 6.33%.

Attempted Acetalation of 2-Benzyloxymethyl-4, 5, 6-trimethylcyclohexa-1, 4-dienylmethanal (VII) with Ethylene Glycol.—A mixture of the aldehyde VII (13.5 g.), ethylene glycol (15 g.), *p*-toluenesulfonic acid (0.25 g.) and benzene (60 ml.) was heated under reflux in an oil bath at a temperature of 120°C for 4 hr. with an azeotroper. The reaction mixture was cooled and the benzene layer separated. The ethylene glycol layer was extracted with benzene. The combined benzene solution was washed with a 10% aqueous sodium carbonate solution and with water, dried over sodium sulfate and evaporated. The residue was fractionated through a 7 cm. Vigreux column to give three representative fractions: i) 2, 3, 4, 6-Tetramethylbenzaldehyde (VIII) (3.3 g., 40.0%), b. p. 106~107°C/2.2 mmHg, n_D^{20} 1.5482, whose infrared spectrum was identical with that of the authentic VIII described above.

Found: C, 81.34; H, 8.77%.

ii) 2, 3, 4, 6 - Tetramethylbenzaldehyde ethylene acetal (XVIII) (1.0 g., 17%), a colorless oil, b. p. 123~125°C/2.2 mmHg, which solidified quickly to give prisms melting at 58°C after being crystallized from petroleum ether.

Found: C, 75.32; H, 8.69. Calcd. for $C_{13}H_{18}O_2$: C, 75.69; H, 8.80%.

Treated with the Brady reagent, XVIII gave 2, 4-dinitrophenylhydrazone, m. p. 221°C, which showed no melting point depression on admixture with that of VIII.

iii) 6-Benzyloxymethyl-2, 3, 4-trimethylcyclohexa-1, 3-dienylmethanal ethylene acetal (XIX) (0.5 g., 3%), a pale yellow viscous oil, b. p. 147~150°C/2 $\times10^{-2}$ mmHg, n_D^{20} 1.5630.

Found: C, 76.20; H, 8.30. Calcd. for $C_{20}H_{26}O_3$: C, 76.40; H, 8.34%.

4-(2', 3', 4', 6' - Tetramethylphenyl)-but-3-en-2-one (XX).—The aldehyde VIII (1.0 g.) in acetone (5 ml.) was added dropwise to a boiled 80% aqueous acetone (10 ml.) containing barium hydroxide (0.2 g.), and the resultant mixture was refluxed for 21 hr. The cooled reaction mixture was neutrallized with 1 N hydrochloric acid and concentrated under reduced pressure. The pale yellow crystalline residue (1.25 g.) was crystallized from 80% aqueous methanol to give the unsaturated ketone XX (1.15 g., 92.2%) as colorless fine long needles with a weak violet-like odor, m. p. 80°C. ν_{max}^{KBr} 1658 (C=O, conju.), 1611 (C=C, conju.), 1255 (CH_3CO), 1004 (-CH=CH-, *trans*) and 878 cm^{-1} (penta-substituted phenyl group). λ_{max}^{EtOH} 218 mμ (ε 20500), 295 (11700).

Found: C, 82.88; H, 9.08. Calcd. for $C_{14}H_{18}O$: C, 83.12; H, 8.97%.

The semicarbazone crystallized from ethanol-ethyl acetate in leaflets, m. p. 225~226°C (partly decomp.). λ_{max}^{EtOH} 286 mμ (ε 31000).

Found: C, 69.27; H, 8.25; N, 16.05. Calcd. for $C_{15}H_{21}ON_3$: C, 69.46; H, 8.16; N, 16.21%.

The 2, 4-dinitrophenylhydrazone crystallized from ethanol-ethyl acetate in the form of dark-red prisms, m. p. 174~175°C.

Found: N, 14.58. Calcd. for $C_{20}H_{22}O_4N_4$: N, 14.65%.

4-(2', 3', 4', 6' - Tetramethylphenyl) - butan - 2 - one (XXI).—The ketone XX (50.6 mg.) in ethanol (20 ml.) was hydrogenated in the presence of a platinum oxide catalyst (30 mg.) until 1.05 mol. equivalents (5.9 ml. at 10°C and 754 mmHg) of hydrogen had been absorbed. Removal of the catalyst and solvent, followed by recrystallization of the residual solid from petroleum ether, gave the ketone XXI (47.0 mg., 93%) as colorless needles, m. p. 62.5~63.5°C.

Found: C, 82.54; H, 9.90. Calcd. for $C_{14}H_{20}O$: C, 82.30; H, 9.87%.

The 2, 4-dinitrophenylhydrazone crystallized from ethanol-ethyl acetate in the form of yellow needles, m. p. 166~167°C.

Found: C, 62.12; H, 6.26. Calcd. for $C_{20}H_{24}O_4N_4$: C, 62.48; H, 6.29%.

4 - (2', 3', 4', 6' - Tetramethylphenyl) - butan - 2 - ol (XXII).—The ketone XX (0.7 g.) in ethanol (50 ml.) was hydrogenated in the presence of a Raney nickel catalyst (1.2 g.) for 1.5 hr. at 120~130°C and 110 kg./cm² in a 100 ml. autoclave. Removal of the catalyst and solvent, followed by crystallization of the residue from methanol, yielded the carbinol XXII (0.66 g., 92.6%) as colorless needles, m. p. 79°C. ν_{max}^{KBr} 3356, 1089 (OH), 867 and 857 cm^{-1} (penta-substituted phenyl group).

Found: C, 80.75; H, 10.74. Calcd. for $C_{14}H_{22}O$; C, 81.50; H, 10.75%.

We wish to thank Dr. Asaji Kondo of the Tokyo Institute of Technology for his elementary analyses, and Dr. Tadashi Sato of Waseda University and Dr. Kenji Kuratani of the Aeronautical Research Institute, the University of Tokyo, for their infrared spectral measurements.

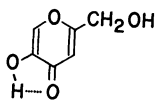
Laboratory of Organic Chemistry
Kobayasi Institute of Physical Research
Kokubunji, Tokyo

Complexing Behavior of Kojic Acid with Metal Ions. I. Mg(II) and Mn(II) Chelates[*1,*2]

By Yukito MURAKAMI

(Received May 4, 1961)

In recent years, the investigation of the metal complexes of tropolone and its derivatives has been in much progress and has brought about the information that these organic compounds form metal complexes of much greater stability than those of β-diketones of comparable acidity. Since kojic acid (I) forms a



I

five-membered chelate ring with hydrogen or metal ion, which is the same as tropolone, it was expected that kojic acid would react with metal ions to produce metal chelates or relatively high stability. Thus, Fernelius and his coworker[1] have carried out an investigation on this subject and found out that kojic acid forms metal chelates whose stabilities were greater than, or at least equal to, those of β-diketones of the same acidity.

To avoid such an ambiguity brought about by their use of non-aqueous solvent[1] (50% dioxane) for the determination of the stability constants, it was intended in this work to employ an aqueous system to clarify the interaction between kojic acid and metal ions.

Experimental

Reagents.—Kojic acid was purchased from the Tokyo Kasei Kogyo Co., Ltd., and was purified by sublimation in vacuo: m. p. 156~156.6°C; reported 154~156°C[1], 154°C[2].

This purified substance was used to prepare an aqueous stock solution which was standardized by potentiometric titration with standard base. Analytical grade $Mg(NO_3)_2 \cdot 6H_2O$ and $MnSO_4 \cdot nH_2O$, purchased from the Wako Pure Chemical Industries, Ltd., were used to make up stock solutions and standardized by the usual technique of chelatometric titration[3].

Potentiometric Measurements.—An HRL Model P pH meter (made by the Horiba Instruments Inc., Kyoto) with extension glass and calomel electrodes was used to measure hydrogen ion concentration after being calibrated with acetic acid buffer as well as standard hydrochloric acid and sodium hydroxide. Measurements were carried out at 25.0 $\pm$0.1°C, and the ionic strength was maintained at approximately 0.10 M with potassium nitrate. Solutions under investigation were kept in a nitrogen atmosphere by circulation of purified nitrogen through the jacketed titration cell.

Mathematical Treatment

In this investigation, metal species were found to exist in three forms: $M(H_2O)_4^{2+}$, $MA(H_2O)_2^{+}$, and MA_2. Therefore, the solution equilibria may be expressed in terms of the following equations:

$$HA \rightleftarrows H^+ + A^- \qquad K_D = \frac{[H^+]\,[A^-]}{[HA]} \tag{1}$$

$$M(H_2O)_4^{2+} + A^- \rightleftarrows MA(H_2O)_2^{+} + 2H_2O$$

$$K_1 = \frac{[MA^+]}{[M^{2+}]\,[A^-]} \tag{2}$$

$$MA(H_2O)_4^{+} + A^- \rightleftarrows MA_2 + 2H_2O$$

$$K_2 = \frac{[MA_2]}{[MA^+]\,[A^-]} \tag{3}$$

in which M represents a metal ion and HA indicates an undissociated form of a ligand.

The amount and distributing ratio of these chelate species may be calculated from the equilibrium relationships and the stoichiometric relations shown in the following paragraph.

If T_A and T_M represent the total concentration of the ligand species and of the metal species respectively, then

$$T_A = [HA] + [A^-] + [MA^+] + 2[MA_2] \tag{4}$$

$$T_M = [M^{2+}] + [MA^+] + [MA_2] \tag{5}$$

T_{OH}, the hydroxide added to a solution during the titration, introduces the relationship:

$$[H^+] - [OH^-] + T_{OH} = [A^-] + [MA^+] + 2[MA_2] \tag{6}$$

From Eq. 5 in combination with equilibrium relations 2 and 3, it results in

$$\frac{T_M}{[M^{2+}]} = 1 + K_1[A^-] + K_1K_2[A^-]^2 \tag{7}$$

---

*1 Contribution No. 19 from Department of Organic Synthesis, Faculty of Engineering, Kyushu University.

*2 Presented at the 14th Annual Meeting of the Chemical Society of Japan, Tokyo, April, 1961.

1) B. E. Bryant and W. C. Fernelius, *J. Am. Chem. Soc.*, **76**, 5351 (1954).

2) F. Challenger, T. Klein and T. K. Walker, *J. Chem. Soc.*, **1929**, 1498.

3) K. Ueno, "Chelatometric Titration" (in Japanese), Nankodo, Ltd., Tokyo (1960), pp. 274, 278.

The combination of Eqs. 1, 4 and 6 gives

$$[A^-] = \frac{K_D}{[H^+]}\left\{T_A - [H^+] + [OH^-] - T_{OH}\right\} \quad (8)$$

The quantity of free metal ion M^{2+} may be shown in terms of T_A, [HA], $[A^-]$, K_1 and K_2 from Eqs. 2, 3 and 4:

$$[M^{2+}] = \frac{T_A - [HA] - [A^-]}{K_1[A^-] + 2K_1K_2[A^-]^2} \quad (9)$$

Thus, substitution of the relationship 9 into Eq. 7 results in the final equation:

$$(F-1)[A^-]K_1 + (2F-1)[A^-]^2K_1K_2 = 1 \quad (10)$$

where

$$F = \frac{T_M}{T_A - [HA] - [A^-]}$$

Equation 10 means that K_1 may be plotted as a function of K_1K_2 corresponding to each experimental point on the titration curve. The intercept on the vertical axis is $1/(F-1)[A^-]$ and that on the horizontal axis is $1/(2F-1)[A^-]^2$. Straight lines obtained from a number of experimental points are to intersect at one point, which represents the solution of the simultaneous equations. The ordinate at this point is equal to K_1 and the abscissa is equal to K_1K_2. This method was employed for the determination of stability constants of the magnesium chelates. There is another graphical method for the evaluation of K_1 and K_2 employing Eq. 10. Equation 10 may be rewritten as

$$\alpha = K_1 + K_1K_2\beta \quad (11)$$

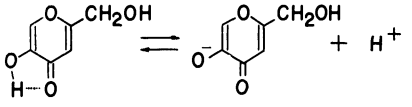
where

$$\alpha = 1/(F-1)[A^-];\ \beta = (2F-1)[A^-]/(F-1)$$

Thus if chelate formation reactions shown by Eqs. 2 and 3 occur, when α is plotted against β, a straight line is obtained the slope of which is equal to K_1K_2 and in which the intercept at $\beta = 0$ is equal to K_1. This alternate method was used for the evaluation of the stability constants of the manganese chelates.

Results and Discussion

Kojic Acid.—Potentiometric titration of kojic acid provides only one sharp inflection which corresponds to the following dissocciation:



The pK value of 7.68 is much smaller than the value of 9.40 obtained by Bryant and Fernelius[1] in 50% aqueous dioxane. This difference in pK value is to be expected because an acidic proton of an organic compound is more labile in aqueous system than in mixed aqueous systems.

Interaction of Mg(II) Ion with Kojic Acid.—Titration curves are illustrated in Fig. 1 for the kojate chelates of Mg(II) at 1 : 1 and 2 : 1 ratios of ligand to metal ion. In both titrations the total concentration of kojic acid was maintained constant.

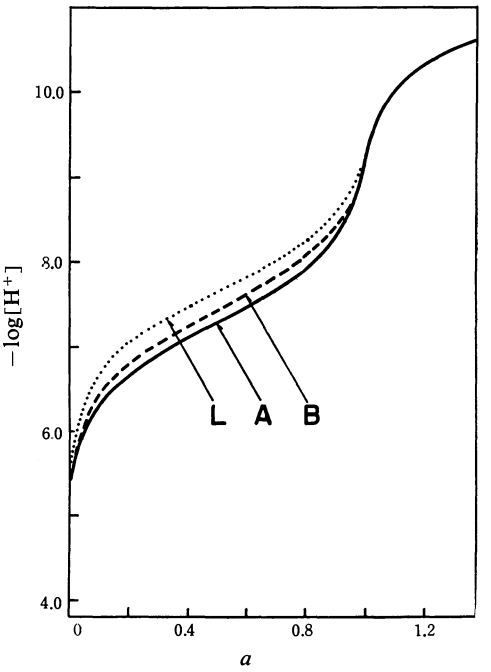


Fig. 1. Potentiometric titration of Mg(II)-kojate chelates at the total ligand concentration of 2.20×10^{-3} M, with these molar ratios of ligand to metal ion: A, 1 : 1; B, 2 : 1; L, ligand (kojic acid) alone; a = moles of base added per mole of ligand; t=25°C; μ=0.1 (KNO_3).

The apparent depression of the titration curves in the buffer region indicates the formation of the metal chelate species. The titration curve for the 2 : 1 ratio behaves similarly to that for the 1 : 1 ratio, thus suggesting the simultaneous formation of MgA and MgA_2. No precipitates were found throughout the titrations. Mg(II) ion undergoes hydrolysis in accordance with the equation:

$$Mg^{2+} + H_2O \rightleftarrows Mg(OH)^+ + H^+$$

However, the contribution of such a reaction is expected to be negligible in the buffer region where the two chelate formation reactions take place, for the K value is as much as $10^{-12.8}$ at 30°C and μ=0.1[4].

4) S. Chaberek, Jr., R. C. Courtney and A. E. Martell, *J. Am. Chem. Soc.*, 74, 5057 (1952).

TABLE I. STABILITY CONSTANTS OF THE METAL CHELATES

Metal ion	Ligand	Temp., °C	μ	pK_D	log K_1	log K_2
Mg(II)	Kojic acid (HA)	25	0.10	7.68	2.92	2.19
	Acetylacetone[a] (HA)	30	→0	8.95	3.63	2.54
	Tiron[b] (H_2A)	20	0.1	7.66	1.98	
Mn(II)	Kojic acid (HA)	25	0.10	7.68	3.95	2.83
	Acetylacetone[a] (HA)	30	→0	8.95	4.18	3.07

K_D=first dissociation constant; $K_1=\frac{[MA]}{[M][A]}$; $K_2=\frac{[MA_2]}{[MA][A]}$

K_1 value for the Tiron chelate is shown for equilibrium: $\frac{[MHA]}{[M][HA]}$

a) See Ref. 5; b) See Ref. 6

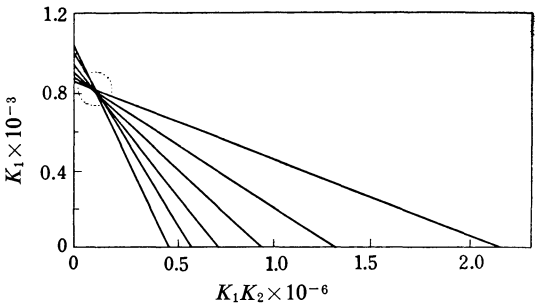


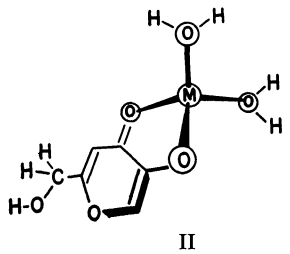
Fig. 2. Graphical determination of the formation constants for Mg(II)-kojate system.

In order to evaluate the formation constants of the chelates, Eq. 10 was employed and K_1 and K_2 values were obtained graphically in Fig. 2. All the straight lines intersect satisfactorily at one point which verifies the formation of the two chelate species, MgA^+ and MgA_2.

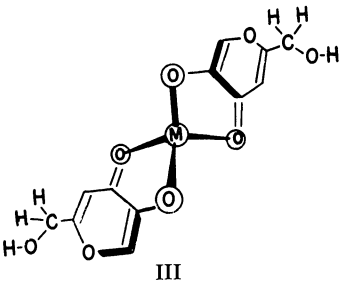
Although such differences were not critical, very slight deviations in K_1 and K_2 values, which depended upon the ligand to metal ratio, were noticed. Nevertheless, K_1 and K_2 values with reasonable accuracy may be obtained from 1 : 1 and 2 : 1 titration curves respectively. The values thus estimated are shown in Table I.

Formation of a tetracoördinated Mg(II) complex with tetrahedral configuration utilizing its $3s3p^3$ orbitals has been widely accepted. The 1 : 1 and 2 : 1 chelates probably have the structures indicated by II and III respectively.

The stability of the kojate chelate of Mg(II) may be compared with those of other Mg(II)



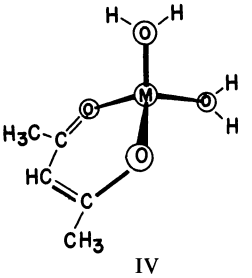
II



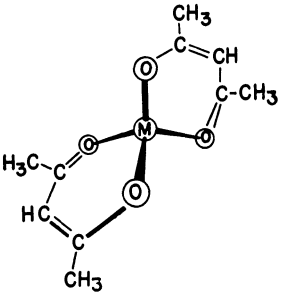
III

chelates having a similar configuration of the chelate ring.

Acetylacetone forms chelates with Mg(II)[5] the structure of which are shown by IV and V. These formation constants for IV and V are slightly greater than those for the corresponding kojate chelates. These formation constants of slightly greater values for the acetylacetonate complexes may be considered



IV

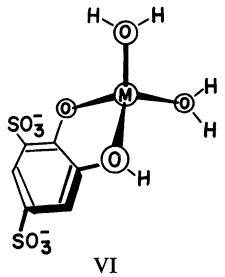


V

5) R. M. Izatt, W. C. Fernelius and B. P. Block, *J. Phys. Chem.*, **59**, 80 (1955).

due to the higher basicity of the enol group and the resonance stabilization of the heterocyclic chelate ring, while such resonance stabilization is prohibited for the kojate complexes.

Meanwhile, the Tiron chelate[6] indicated by VI is obtained with smaller stability in com-



VI

parison with the kojate chelate in spite of the fact that both kojic acid and the first phenol group of Tiron have almost the same magnitude of dissociation constants. Thus, this difference in stability is solely due to the difference in donor property of alcoholic oxygen and carbonyl oxygen toward Mg(II) ion.

Interaction of Mn(II) Ion with Kojic Acid.— A family of titration curves for solutions containing various amounts of kojic acid per mole of Mn(II) ion are shown in Fig. 3. Distinctive inflections were observed at m values corresponding to the complete neutralization of protons liberated from kojic acid.

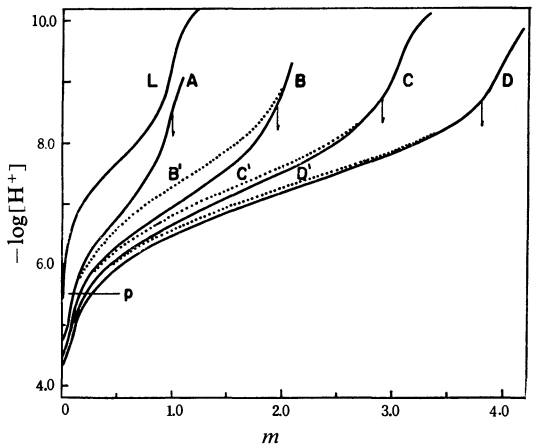


Fig. 3. Potentiometric titration of Mn(II)-kojate chelate system at the total metal concentration of 1.14×10^{-3} M, with these molar ratios of ligand to metal ion: A, 1 : 1; B, 2 : 1; C, 3 : 1; D, 4 : 1; L, ligand (kojic acid) alone; m=moles of base added per mole of metal ion; t=25°C; μ=0.1(KNO_3). Dotted curves represent superimposition of two titration curves: B', A+L; C', B+L; D', C+L. Arrows indicate points where pH drifting became noticeable, while titration curves below p represent non-equilibrated data.

The color of the titrating solutions was pale yellow and slightly deepened as pH went up. Precipitation was observed at very high pH beyond inflection regions. In all cases, the solutions did not come to equilibrium immediately in the pH($-\log[H^+]$) region below 5.5 and above 8.5. Thus, experimental titration curves lying between these pH values were actually used in pursuing the chelating behavior of kojic acid with the metal ion.

Curves obtained by superimposition of the titration curve of free kojic acid on adequate experimental titration curves are shown, together with experimental titration curves for solutions containing the same total concentrations of metal ion and ligand. The depression of pH is significant for the 2 : 1 ratio, and such depression decreases as the molar ratio of the ligand increases. However, such phenomena are not adequate enough to verify the chelate species formed at different molar ratios of kojic acid to Mn(II) ion.

As a first step in determining the Mn(II)-kojate chelate species, 1 : 1 titration curves were obtained over a four-fold concentration range as shown in Fig. 4.

The hydrolytic tendency of manganese(II) ion indicated by the equation:

$$Mn^{2+}+H_2O \rightleftarrows Mn(OH)^+ + H^+$$

does not seem to influence the complexing behavior of this metal ion with the ligand under

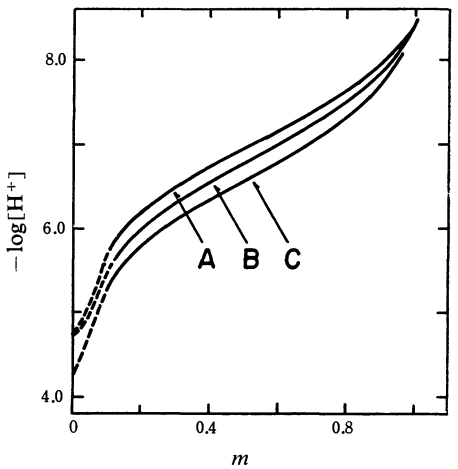


Fig. 4. Potentiometric titration of 1 : 1 Mn(II)-kojate chelate system: A, 5.68×10^{-4} M; B, 1.14×10^{-3} M; C, 2.28×10^{-3} M; m=moles of base added per mole of metal ion; t=25°C; μ=0.1(KNO_3). Dotted lines indicate non-equilibrated data.

6) G. Schwarzenbach and A. Willi, unpublished results; J. Bjerrum, G. Schwarzenbach and L. G. Sillén, "Stability Constants, Part I Organic Ligands", the Chemical Society, London (1956), p. 45.

experimental conditions of the present investigation since the K value is as small as $10^{-10.6}$ at 30°C and $\mu=0.1$[4]).

Mathematical treatment of the data employing Eq. 11 yielded the plots shown in Fig. 5. Good conformity with a straight line was obtained, and the slight fluctuation from the straight line for the data of lower concentration does not seem to disturb the evaluation of the formation constants. The same mathematical treatment performed for the titration curves of solutions containing 2 : 1 and 3 : 1 molar ratios of ligand to metal ion results in a satisfactory linear relationship as indicated

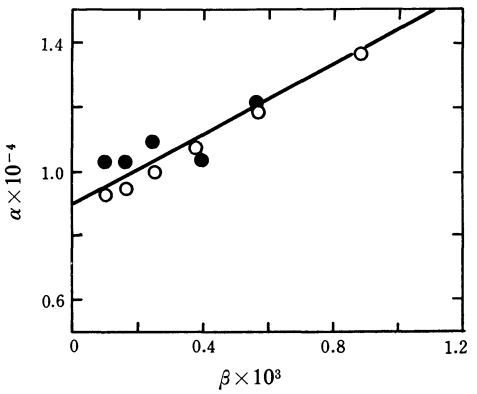


Fig. 5. Graphical determination of the formation constants for Mn(II)-kojate chelate system from titration data obtained for Mn(II)/kojic acid=1 in connection with Eq. 11. Concentrations of metal ion : ○, 2.28×10^{-3} M ; ●, 1.14×10^{-3} M.

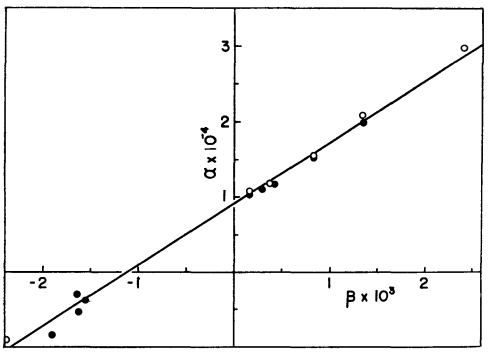


Fig. 6. Graphical determination of the formation constants for Mn(II)-kojate chelate system from titration data obtained for ligand to metal ratios : ○, 2 : 1 ; ●, 3 : 1.

in Fig. 6. With the same reason as mentioned above for the interaction of Mg(II) ion with the ligand, K_1 value was evaluated from the calculated data shown in Fig. 5 while K_2 value was determined from the data in Fig. 6. The results are summarized in Table I.

Satisfactory linear relationship in Fig. 6 provides the conclusive support for the formation of a chelate species containing two moles of ligand per mole of metal ion and not more than two moles of ligand. Manganese(II) ion could be expected to form a hexacoördinated chelate compound having octahedral configuration. In the case of hexacoördinated manganese(II) ion, the metal ion should utilize its $3d^24s4p^3$ atomic orbitals for the coördinate bond formation. Such a five-membered chelate ring formation that takes up two oxygens as donor atoms toward manganese(II) ion does not seem to supply enough energy to transfer the five 3d electrons into three degenerate t_{2g} orbitals. Instead, $4s4p^3$ atomic orbitals of manganese(II) ion could be utilized for the formation of four chelate bonds in the atmosphere of weak ligand field produced by kojate ion. The structures of Mn(II)-kojate chelates may be represented by II and III having tetrahedral configuration.

Mn(II)-kojate chelates possess slighly greater values of formation constant than Mg(II)-kojate chelates as observed in other Mn(II) chelates involving oxygen atoms as donor atoms[7]).

In conclusion, manganese(II) ion frequently behaves like magnesium(II) ion with a similar magnitude of chelate formation constants in aqueous system in spite of the fact that manganese(II) ion is a member of the first transition series.

Summary

Chelating tendencies of kojic acid toward divalent magnesium and manganese ions have been investigated in aqueous media at 25.0 ±0.1°C and 0.10 M of ionic strength. In spite of the difference in their electronic configurations, both metal ions formed similar chelate compounds and indicated an optimum coördination number of four. Both metal ions formed kojate chelates whose stabilities are nearly equal to the corresponding metal chelates of β-diketones of the same acidity.

This work was supported in part by the scientific research grant of the Ministry of Education, which grant is gratefully acknowledged.

Department of Organic Synthesis
Faculty of Engineering
Kyushu University
Hakozaki, Fukuoka

7) J. Bjerrum, G. Schwarzenbach and L. G. Sillén, Loc. cit.

Vinyl Copolymerization. I. Copolymerization of Acrylonitrile with Methyl Methacrylate

By Momotaro SUZUKI, Hajime MIYAMA and Shiro FUJIMOTO

(Received April 28, 1961)

In previous papers[1,2], investigations on the rate of copolymerization of VA (vinyl acetate)-MM (methyl methacrylate), St (styrene)-VA and MM-St by the thermistor method[3] were reported. Usually the rate of copolymerization is measured by weighing the copolymer's weight in the copolymerization system after a difinite time of reaction, but this method is not accurate because the concentration of each monomer changes during this definite period. On the other hand, the thermistor method can measure accurately the initial rate of copolymerization within ten seconds. In the VA-MM and St-VA systems, the large difference between the reactivity ratios of the two monomers caused a large error limit of ϕ, the ratio of the rate constant for "crossed" termination to the geometric mean of the rate constants of the chain termination of each monomer alone, so that we could not find any essential regularities in the variation of ϕ with successive mixing ratios. In the MM-St system, however, where the difference of the two reactivity ratios is not so large, we could determine the value of ϕ more precisely and obtain a concrete confirmation of Arlman's theory[4].

In this experiment, an AN (acrylonitrile)-MM pair was chosen for the rate measurement.

Experimental

The procedure and the treatment of the experimental results are almost the same as those described in detail in previous papers[1-3]. The temperature was 30.5°C and the fluctuation of the thermostat temperature was controlled within ±0.001°C. The sensitizer for photopolymerization was 1,1'-azobiscyclohexanecarbonitrile at a concentration of 7.56×10^{-3} mol./l.

The rate of polymerization was found by multiplication of the rate of temperature increase by the factor $1/\Delta t$ as follows[1,2]:

$$1/\Delta t=(S\times H)/(\Delta H_c\times M) \qquad (1)$$

Here, M, H, S and ΔH_c are molecular weight, specific heat, specific gravity and heat of polymerization, respectively, of the copolymerization system. The quantities M, H and S are related by:

$$M=(M_1f_1+M_2f_2)/(f_1+f_2) \qquad (2)$$

$$H=(H_1f_1+H_2f_2)/(f_1+f_2) \qquad (3)$$

$$S=(M_1f_1+M_2f_2)S_1S_2/(S_2M_1f_1+S_1M_2f_2) \qquad (4)$$

in which f's are the mole fractions of each monomer. According to Alfrey[4], ΔH_c is given by the following equation:

$$\Delta H_c=\frac{1-[1-F_2(1-F_2)(1-r_1r_2)]^{1/2}}{2(1-r_1r_2)}\times(\Delta H_{12}+\Delta H_{21}-\Delta H_{11}-\Delta H_{22})+F_1\Delta H_{11}+F_2\Delta H_{22} \qquad (5)$$

in which F's are the mole frations of each monomer in copolymer, r's are the reactivity ratios of each monomer, and the suffixes 1 and 2 denote the values of each monomer. ΔH_{11}, ΔH_{12}, ΔH_{21} and ΔH_{22} are heats of copolymerization corresponding to the following four different chain-propagation processes between monomers (M_1 or M_2) and radicals (M_1* or M_2*).

$$-M_1^* + M_1 \rightarrow -M_1-M_1^* \qquad \Delta H_{11}$$

$$-M_1^* + M_2 \rightarrow -M_1-M_2^* \qquad \Delta H_{12}$$

$$-M_2^* + M_1 \rightarrow -M_2-M_1^* \qquad \Delta H_{21}$$

$$-M_2^* + M_2 \rightarrow -M_2-M_2^* \qquad \Delta H_{22}$$

Although the values of ΔH_{11} and ΔH_{22} can be measured for the polymerization of each monomer alone, nothing is known about the values of ΔH_{12} and ΔH_{21}. As described in previous papers[5,6], the values of $\Delta H_{12}+\Delta H_{21}$, and also ΔH_c, can be obtained by comparing the rate of temperature rise with the rate of copolymerization. The rate of the temperature rise was measured every minute for 15 min. by the thermistor method, and the rate of copolymerization was obtained from the results of

TABLE I. VALUES OF CONSTANTS OF EACH MONOMER IN AN-MM SYSTEM AT 30.5°C

$M_1=53.06$	$M_2=100$	g./mol.
$H_1=26.53$[7]	$H_2=49.00$[8]	cal./mol. °C
$S_1=0.7944$[7]	$S_2=0.9305$[9]	g./cc.
$r_1=0.18$[10]	$r_2=1.35$[10]	

1) M. Suzuki, H. Miyama and S. Fujimoto, *J. Polymer Sci.*, **32**, 445 (1958).
1) Ibid., **37**, 533 (1959).
3) H. Miyama, This Bulletin, **29**, 711 (1956).
4) T. Alfrey, *J. Polymer Sci.*, **4**, 222 (1949).
5) M. Suzuki, H. Miyama and S. Fujimoto, ibid., **31**, 212 (1958).
6) M. Suzuki, H. Miyama and S. Fujimoto, *J. Chem. Soc. Japan, Pure Chem. Sec.* (*Nippon Kagaku Zasshi*), **79**, 609 (1958).
7) H. S. Davis and O. F. Wiedman, *Ind. Eng. Chem.*, **37**, 482 (1945).
8) W. I. Bengough and H. W. Melville, *Proc. Roy. Soc.*, **A 225**, 330 (1954).
9) M. S. Matheson, E. E. Auer, E. B. Bevilacqua and E. J. Hart, *J. Am. Chem. Soc.*, **71**, 497 (1949).
10) F. M. Lewis and W. F. Hulse, ibid., **67**, 170 (1945).

Table II. Values of rate of temperature rise, rate of copolymerization, ΔH_c and $\Delta H_{12}+\Delta H_{21}$ at 30.4°C

Mole fraction of AN f_1	Rate of temp. rise 10^{-3} °C/sec.	Rate of copolymerization 10^{-4} mol./l. sec.	ΔH_c kcal./mol.	$\Delta H_{12}+\Delta H_{21}$ kcal./mol.
0	5.60	1.87	13.65 ($=\Delta H_{22}$)	
0.15	5.00	1.70	13.22	23.17
0.29	5.15	1.65	13.86	28.31
0.41	5.27	1.65	14.00	29.11
0.52	5.31	1.60	14.35	29.18
0.62	5.53	1.58	14.92	29.96
0.79	7.05	2.01	14.53	27.75
0.94	13.10	3.26	16.25	31.38
1.00	23.94	5.68	16.75 ($=\Delta H_{11}$)	
				Av. 28.40

analysis in which the copolymerization system was dissolved in a mixture of acetone and dimethylformamide after the photocopolymerization had proceeded 15 min.

In Table I, the necessary data for the calculation of $1/\Delta t$ are shown.

Results and Discussion

Heat of Copolymerization. — The values of the rate of temperature rise, the rate of copolymerization, ΔH_c and $\Delta H_{12}+\Delta H_{21}$ are shown in Table II. Details of the calculation of ΔH_c and $\Delta H_{12}+\Delta H_{21}$ have been described in previous papers[5,6].

From the fact that the values of $\Delta H_{12}+\Delta H_{21}$ are almost constant in Table II, the application of Eq. 5 in this system seems reasonable. By substituting the average value 28.40 kcal./mol. of $\Delta H_{12}+\Delta H_{21}$, the values of ΔH_{11} and ΔH_{22} of Table II and the values of r_1 and r_2 of Table I in Eq. 5, ΔH_c can be expressed as follows:

$$\Delta H_c = -1.32\,[1-(1-3.03F_1F_2)^{1/2}] + 16.75F_1 + 13.65F_2 \qquad (6)$$

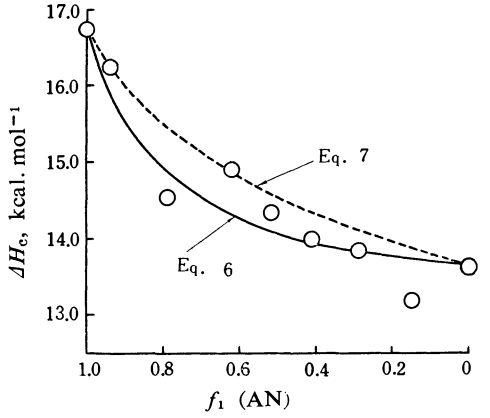


Fig. 1. Variation of ΔH_c with f_1.

○ Experimental values

Note: f_1 is a mole fraction of AN in the feed.

As shown in Fig. 1, the values of ΔH_c in Table II agree with the full line expressing Eq. 6. The dashed line in this figure is drawn by using the following equation:

$$\Delta H_c = F_1\Delta H_{11} + F_2\Delta H_{22} \qquad (7)$$

The results of calculation by using 6 and 7 give almost the same curve as shown in Fig. 1. Therefore, the application of 7 instead of 6 in this systems seem approximately correct.

Rate of Copolymerization. — In Fig. 2, the values of $1/\Delta t$ calculated from Eq. 1 are plotted against f_1, where Eq. 6 is used to obtain the value of ΔH_c. The values of the rate of polymerization as shown in Table III were calculated by a multiplication of the rate of temperature increase by this factor, $1/\Delta t$, where the rate of temperature increase was measured within 10 sec. of the instant polymerization starts by the thermistor method.

As shown in Fig. 3, the rate is minimum at the molar fraction of about 0.7 of AN. The

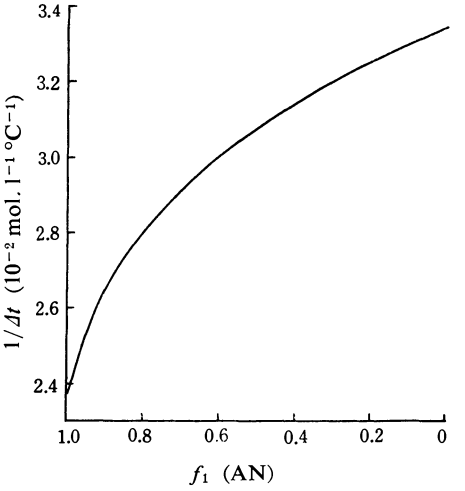


Fig. 2. Variation of $1/\Delta t$ with f_1.

TABLE III. VALUES OF THE RATE OF COPOLYMERIZATION AND ϕ VALUES

Mole fraction of AN f_1	Rate of copolymerization 10^{-4} mol./sec. l.	ϕ_{exp}
0	1.96	
0.15	1.72	24
0.29	1.69	18
0.41	1.69	16
0.52	1.68	15
0.62	1.66	14
0.79	1.83	10
0.94	2.51	6
1.00	4.94	
		Av. 15

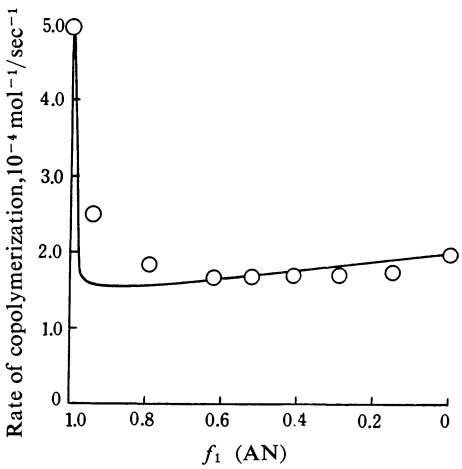


Fig. 3. Variation of rate of copolymerization with f_1.
○ Experimental values
— Walling's equation with $\phi=15$

rate of copolymerization is given by the following equation of Walling[11]:

$$V=\frac{(r_1[M_1]^2+2[M_1][M_2]+r_2[M_2]^2)I^{1/2}}{\left\{\begin{array}{c}((\delta_1^2r_1^2[M_1]^2+2\phi\delta_1\delta_2r_1r_2[M_1][M_2]\\+\delta_2^2r_2^2[M_2]^2)^{1/2}\end{array}\right\}} \quad (8)$$

The nomenclature of which is described in detail in Walling's paper[11] or in our previous papers[1,2]. Although ϕ in this equation should be constant, the values of ϕ calculated from Walling's equation (expressed as ϕ_{exp} in Table III) vary with the mole fraction of AN. The theoretical curve obtained by substituting $\phi=15$ (the average value of ϕ_{exp} in Table III) into Eq. 8 agrees with the experimental values as shown in Fig. 3. However, in order to explain the nonconstancy of ϕ, the application of Arlman's equation[12] to these data must be considered[2]. Arlman considered in his theory the following two cross-termination reactions:

(I) ~~~ BB· + ·A ~~~ k_{tbba}

(II) ~~~ AB· + ·A ~~~ k_{taba}

Reaction I is a usual cross-termination reaction, but in reaction II the existence of the penultimate unit A in the first free radical somewhat retards the termination reaction. Postulating these reactions, Arlman derived the equation:

$$(f_1\chi+r_2f_2)/(f_1+r_2f_2)=\phi_{exp}/\phi_n \quad (9)$$

χ and ϕ_n are related by:

$$\chi=k_{taba}/k_{tbba}<1 \quad (10)$$

$$1/\phi_n=(k_{taa}k_{tbb})^{1/2}/k_{tbba} \quad (11)$$

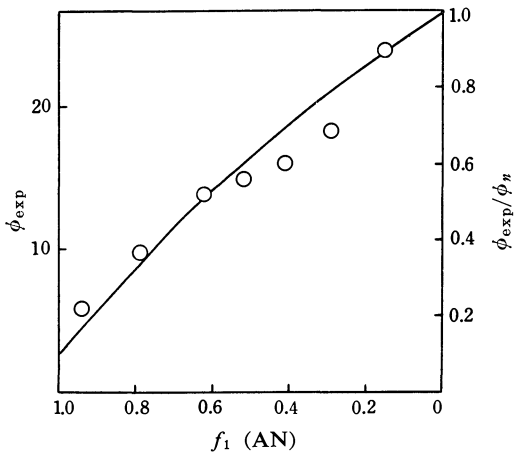


Fig. 4. Variation of ϕ_{exp} and ϕ_{exp}/ϕ_n with f_1.
○ Experimental values
— Arlman's equation with $\chi=0.1$ and $r_2=1.35$.

Here, k_{taa} and k_{tbb} are the termination constants of each monomer, and ϕ_{exp} is obtained from experimental data by a calculation according to Wallings' equation. Using Eq. 9, the curve shown in Fig. 4 was constructed; a χ with which the experimental and theoretical value in this figure agreed most satisfactorily was chosen. This value of χ is 0.1, and the corresponding value of ϕ_n is 27. Since k_{taa} and k_{tbb}, the termination constants of AN and MM, are known, k_{tbba} can be calculated by the substitution of these values and $\phi_n=27$ in Eq. 11. We took k_{taa} as 1.22×10^7 [13] and k_{tbb} as 2.32×10^7 [9] respectively at 25°C because no activation energy is available for the termination constant of AN, and, therefore, correction to the values for our polymerization temperature 30.5°C is impossible. The resulting value was $k_{tbba}=4.55\times10^8$. From

11) F. M. Lewis and C. Walling, ibid., **71**, 747 (1949).
12) J. Arlman and H. W. Melville, *Proc. Roy. Soc.*, **A203**, 301 (1950).
13) W. I. Bengough, *J. Polymer Sci.*, **28**, 476 (1958).

Eq. 10, using $\chi=0.1$, $k_{taba}=4.55\times10^7$ was obtained. Therefore, the termination constants for mixed radicals are larger than those for homogeneous radicals, and furthermore, the rate constant of reaction I is about ten times as large as that of reaction II.

Summary

Rates of copolymerization, of AN-MM for various mixing ratios of the two monomers were measured by the thermistor method. The heat of copolymerization, which was obtained by comparing the results of the thermistor method with those of the usual analytical method, agrees very well with Alfrey's equation. Also, the non-constancy of ϕ can be explained by Arlman's theory. It is concluded that the termination constants for mixed radicals are larger than those homogenous radicals and, furthermore, that the rate constant for a normal cross-termination reaction is about ten times as large as that of the cross-termination reaction having a penultimate unit.

The authors wish to thanks Mr. Shinichi Taira of Tokyo Metropolitan University for the preparation of 1,1′-azobiscyclohexanecarbonitrile.

Department of Chemistry
Defense Academy
Yokosuka

Vinyl Copolymerization. II. Copolymerization of Acrylonitrile with Styrene and Vinyl Acetate

By Momotaro SUZUKI, Hajime MIYAMA and Shiro FUJIMOTO

(Received April 28, 1961)

In the previous paper[1], an investigation of the rate of copolymerization of AN(acrylonitrile)-MM(methyl methacrylate) by the thermistor method[2] was reported. In this experiment, two pairs, i. e., AN-St (styrene) and VA (vinyl acetate)-AN have been chosen for rate measurement.

The procedure and the treatment of the experimental results are the same as those in previous paper[1]. For both of the copolymerization systems, the temperature was 20.0°C and the sensitizer for photopolymerization was 1, 1'-azobiscyclohexanecarbonitrile at a concentration of 7.56×10^{-3} mol./l. The necessary data for the calculation of the factor $1/\Delta t$, which is used for converting the rate of temperature increase into the rate of copolymerization, are shown in Table I.

TABLE I. VALUES OF CONSTANTS OF EACH MONOMER IN THE AN-St AND VA-AN SYSTEMS AT 20.0°C

	Copolymerization system	
	AN-St	VA-AN
Molecular weight, g./mol.		
M_1	53.06	86.05
M_2	104.14	53.06
Specific heat, cal./mol. °C		
H_1	26.53[3]	40.50[7]
H_2	43.31[4]	26.53[3]
Specific gravity, g./cc.		
S_1	0.8060[3]	0.9319[8]
S_2	0.9050[5]	0.8060[3]
Reactivity ratio		
r_1	0.04[6]	0.06[9]
r_2	0.41[6]	4.05[9]

Results and Discussion

Heat of Copolymerization.—The values of the rate of temperature rise, the rate of copolymerization, ΔH_c and $\Delta H_{12}+\Delta H_{21}$ are shown in Table II and III. Details of the meaning and calculation of these quantities were described in the previous paper[1].

1) M. Suzuki, H. Miyama and S. Fujimoto, This Bulletin, **35**, 57 (1962).
2) H. Miyama, ibid., **29**, 711 (1956).
3) H. S. Davis and O. F. Wiedman, *Ind. Eng. Chem.*, **37**, 482 (1945).
4) R. H. Boundy and R. F. Boyer, "Styrene", Reinhold. New York (1952), p. 67.
5) M. S. Matheson, E. E. Auer, E. B. Bevilacqua and E. J. Hart, *J. Am. Chem. Soc.*, **67**, 1701 (1945).
6) F. M. Lewis, F. R. Mayo and W. F. Hulse, ibid., **67**, 1701 (1945).
7) W. I. Bengough and H. W. Melville, *Proc. Roy. Soc.*, **A225**, 330 (1954).
8) M. S. Matheson, E. E. Auer, E. B. Bevilacqua and E. J. Hart, *J. Am. Chem. Soc.*, **71**, 2610 (1949).
9) F. R. Mayo, F. M. Lewis, C. Walling and W. F. Hulse, ibid., **70**, 1523 (1948).

TABLE II. VALUES OF RATE OF TEMPERATURE RISE, RATE OF COPOLYMERIZATION, ΔH_c AND $\Delta H_{12}+\Delta H_{21}$ IN THE AN-St SYSTEM AT 20.0°C

Mole fraction of AN f_1	Rate of temp. rise 10^{-2} °C/sec.	Rate of copolymerization 10^{-4} mol./l. sec.	ΔH_c kcal./mol.	$\Delta H_{12}+\Delta H_{21}$ kcal./mol.
1.0	1.83	4.61	16.03 ($=\Delta H_{11}$)	
0.94	0.65	1.57	16.48	33.75
0.88	0.59	1.40	16.67	33.60
0.72	0.51	1.19	16.81	33.67
0.64	0.50	1.13	17.29	34.63
0.54	0.50	1.10	17.62	35.66
0.30	0.40	0.85	17.92	37.10
0.16	0.29	0.65	16.99	34.30
0	0.20	0.45	16.73 ($=\Delta H_{22}$)	
				Av. 34.67

TABLE III. VALUES OF RATE OF TEMPERATURE RISE, RATE OF COPOLYMERIZATION, ΔH_c AND $\Delta H_{12}+\Delta H_{21}$ IN THE VA-AN SYSTEM AT 20.0°C

Mole fraction of VA f_1	Rate of temp. rise 10^{-2} °C/sec.	Rate of copolymerization 10^{-4} mol./l. sec.	ΔH_c kcal./mol.	$\Delta H_{12}+\Delta H_{21}$ kcal./mol.
1.0	2.03	3.96	22.49 ($=\Delta H_{11}$)	
0.87	0.56	1.22	19.81	40.45
0.63	0.78	1.84	18.08	38.98
0.42	0.88	2.18	17.00	35.51
0.32	0.97	2.37	17.00	35.45
0.23	0.98	2.38	17.28	40.40
0.07	1.30	3.04	17.29	58.80*
0	1.90	4.56	16.80 ($=\Delta H_{22}$)	
				Av. 38.15

* Note: This value is omitted in calculating the average value of $\Delta H_{12}+\Delta H_{21}$ because of its large deviation.

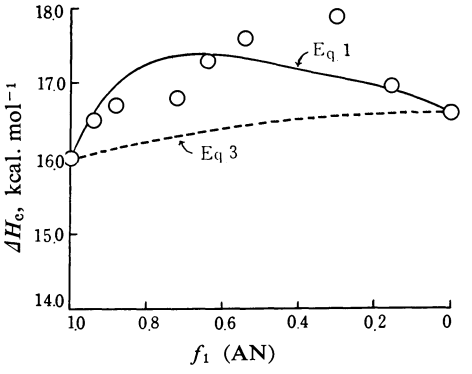


Fig. 1. Variation of ΔH_c with f_1 in the AN-St system.
○ experimental values
Note: f_1 is a mole fraction of AN in the feed.

By using these results and Alfrey's equation[10], the heat of copolymerization ΔH_c can be expressed as follows:

$$\Delta H_c = 1.02\,[1-(1-3.93F_1F_2)^{1/2}] + 16.03F_1 + 16.73F_2 \quad \text{for AN-St} \quad (1)$$

10) T. Alfrey, *J. Polymer Sci.*, 4, 222 (1949).

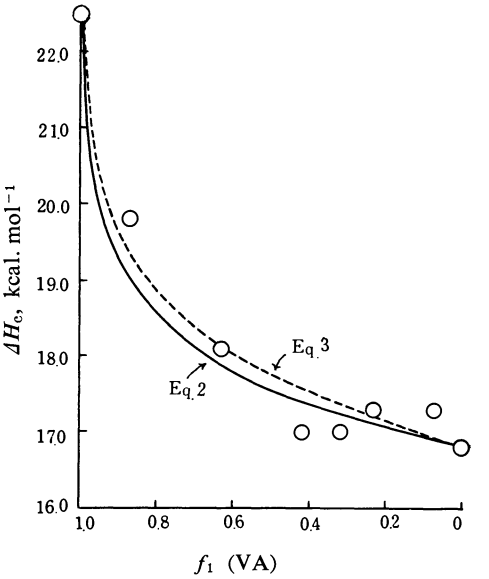


Fig. 2. Variation of ΔH_c with f_1 in the VA-AN system.
○ experimental values
Note: f_1 is a mole fraction of VA in the feed.

$$\Delta H_c = -0.76\,[1-(1-3.03F_1F_2)^{1/2}] + 22.49F_1 + 16.80F_2 \quad \text{for VA-AN} \quad (2)$$

As shown in Figs. 1 and 2, the values of ΔH_c in Tables II and III agree with the full lines expressing Eqs. 1 and 2. The dashed lines in these figures are drawn according to the following equation:

$$\Delta H_c = F_1\Delta H_{11} + F_2\Delta H_{22} \quad (3)$$

Rate of Copolymerization.—In Tables IV and V, the values of $1/\Delta t$, the rate of copolymerization and ϕ are shown, the details of calculation of which were shown in the previous paper[1].

As shown in Figs. 3 and 4, the theoretical curves obtained by substituting $\phi=80$ and $\phi=53$ (average values of ϕ_{exp}) into Walling's equation[11] agree with the experimental values. However, in order to explain the non-constancy of ϕ, the application of Arlman's[12] equation to these data must be considered. In the AN-St system, the curve shown in Fig. 5 was constructed by using Arlman's equation. The value of χ[1,12] is 0.05, and the corresponding value of ϕ_n[1,12] is 266. By using termination constants k_{taa} and k_{tbb} of each monomer alone, normal cross-termination constant k_{tbba} and constant k_{taba} of the cross-termination reaction having a penultimate unit are calculated[1]. These values are shown in Table VI.

Here, we took the values of k_{taa} and k_{tbb} at 25°C because the termination constant of AN is known only at 25°C and no activation energy

TABLE IV. VALUES OF $1/\Delta t$, THE RATE OF COPOLYMERIZATION AND ϕ IN THE AN-St SYSTEM AT 20.0°C

Mole fraction of AN f_1	$1/\Delta t$ 10^{-2} mol./l. °C	Rate of copolymerization 10^{-4} mol./l. sec.	ϕ_{exp}
1.00	2.53	4.48	
0.94	2.37	1.54	19
0.88	2.30	1.38	28
0.72	2.27	1.18	53
0.64	2.26	1.06	77
0.54	2.24	1.05	76
0.30	2.23	0.78	120
0.16	2.22	0.62	186
0	2.26	0.50	
			Av. 80

TABLE V. VALUES OF $1/\Delta t$, THE RATE OF COPOLYMERIZATION AND ϕ IN THE VA-AN SYSTEM AT 20.0°C

Mole fraction of VA f_1	$1/\Delta t$ 10^{-2} mol./l. °C	Rate of copolymerization 10^{-4} mol./l. sec.	ϕ_{exp}
1.00	1.95	4.97	
0.87	2.27	1.41	11
0.63	2.38	1.83	19
0.42	2.41	2.19	49
0.32	2.41	2.34	83
0.23	2.39	2.70	103
0.07	2.39	3.01	488*
0	2.40	4.08	
			Av. 53

* Note: This value is omitted in calculating the avevage value of ϕ because of it's large deviation.

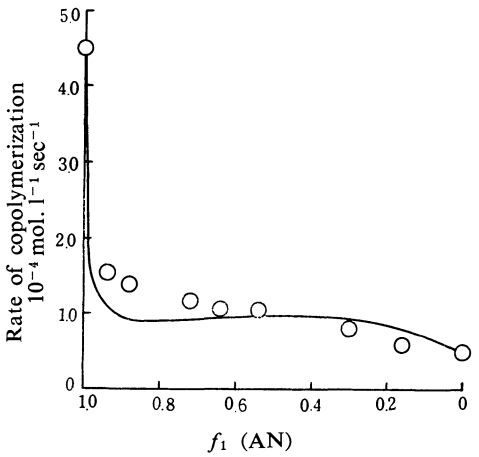


Fig. 3. Variation of rate of copolymerization with f_1 in the AN-St system.
○ experimental values
— Walling's equation with $\phi=80$

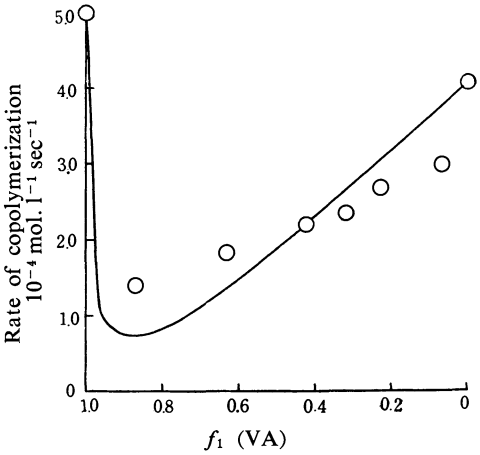


Fig. 4. Variation of rate of copolymerization with f_1 in the VA-AN system.
○, experimental values
—, Walling's equation with $\phi=15$

11) F. M. Lewis and C. Walling, *J. Am. Chem Soc.*, **71**, 747 (1949).

12) J. Arlman and H. W. Melville, *Proc. Roy. Soc.*, **A203**, 301 (1950).

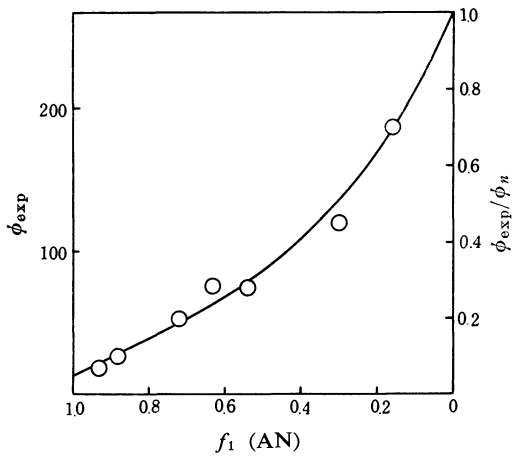


Fig. 5. Variation of ϕ_{exp} and ϕ_{exp}/ϕ_n with f_1 in the AN-St system.

○ experimental values
— Arlman's equation with $\chi=0.05$ and $r_2=0.41$

TABLE VI. VALUES OF k_{taa}, k_{tbb}, k_{tbba} AND k_{taba} FOR AN-St SYSTEM AT 25°C

$k_{taa}=1.22\times10^{7}$ [13] $k_{tbb}=2.79\times10^{6}$ [14]
$k_{tbba}=1.55\times10^{9}$ $k_{taba}=7.75\times10^{7}$

is available. From the results of Table VI, it is obvious that in the AN-St system, termination constants for mixed radicals are larger than those for homogeneous radicals and that the ratio of the normal cross-termination constant to the constant of the cross-termination having a penultimate unit is 20.

On the other hand, in the VA-AN system, the application of Arlman's equation was impossible. As explained in the case of the St-VA system[15], this seems to be due to the large difference between the reactivity ratios of the two monomers, which difference causes a large error limit in the calculated values of ϕ.

Summary

Rates of copolymerization of AN-St and VA-AN for various mixing ratios of the two monomers were measured by the thermistor method. The heat of copolymerization, which was obtained by comparing the results of the thermistor method with those of the usual analytical method, agrees very well with Alfrey's equation. Also, the non-constancy of ϕ in the AN-St system can be explained by Arlman's theory; it is concluded that the termination constants for mixed radicals are larger than those for homogeneous radicals and, furthermore, that the ratio of a normal cross-termintion constant to a constant of the cross-termination having a penultimate unit is 20.

However, in the VA-NA system, the application of Arlman's equation was impossible because the large difference between the reactivity ratios of the two monomers causes a large error limit in the calculated values of ϕ.

Department of Chemistry
Defense Academy
Yokosuka

13) W. I. Bengough, *J. Polymer Sci.*, **28**, 476 (1958).
14) C. H. Bamford and M. J. S. Dewar, *Proc. Roy. Soc.* **A193**, 309 (1948).
15) M. Suzuki, H. Miyama and S. Fujimoto, *J. Polymer Sci.*, **37**, 533 (1959).

Hot-Atom Chemistry of Halogens in Cobaltammine Complex Salts. II. Hot-Atom Chemistry of Radiobromine in Pentammine Cobalt(III) Bromides and Bisethylenediamine Cobalt(III) Bromides

By Nobufusa SAITO, Takeshi TOMINAGA and Hirotoshi SANO

(Received May 2, 1961)

Among a number of studies of the hot-atom chemistry of complex compounds, only a few have contributed to elucidate the recoil reactions of ligand atoms or outer anions[1-6].

In the first paper of this series[2], the present authors reported on the behavior of radiobromine recoils in some neutron-irradiated bromopentammine cobalt(III) complex salts. They

1) A. W. Adamson and J. M. Grunland, *J. Am. Chem. Soc.*, **73**, 5508 (1951).
2) N. Saito, H. Sano and T. Tominaga, This Bulletin, **33**, 20 (1960).
3) N. Saito, T. Tominaga and H. Sano, ibid., **33**, 120 (1960).
4) H. Rauscher, N. Sutin and J. M. Miller, *J. Inorg. & Nuclear Chem.*, **12**, 378 (1960).
5) N. Ikeda, K. Yoshihara and S. Yamagishi, This Bulletin, **34**, 139 (1961).
6) G. Harbottle, Paper presented at the IAEA Symposium on the Chemical Effects of Nuclear Transformations, Prague, October, 1960.

found that radiobromine recoil atoms arising from thermal-neutron capture in outer anions of cobaltammine bromides could substitute in the cobalt co-ordination sphere to produce radiobromine-labeled complex cations[3].

In order to investigate the mechanism of such substitution of ligands by radiobromine recoil atoms, the present authors irradiated, with slow neutrons, solid complex salts of the formulas $[Co(NH_3)_5X]Br_{2,3}$ and $[Co(en)_2X_2]\cdot Br_{1,3}$, all of which contained different kinds of ligand (X), and bromine atoms outside the co-ordination sphere. It was found that the fraction of total radiobromine produced finally retained in ligands varied with the kind of ligand group, X, in each complex. A model has been proposed by the present authors to explain the experimental results.

Experimental

Sample.—Seventeen cobaltammine complex salts were prepared by well-known methods described in the literature:

1) $[Co(NH_3)_6]Br_3$[7]
2) $[Co(NH_3)_5NCS]Br_2$[8]
3) $[Co(NH_3)_5NO_2]Br_2$[9]
4) $[Co(NH_3)_5OH_2]Br_3$[10]
5) $[Co(NH_3)_5ONO]Br_2$[11]
6) $[Co(NH_3)_5ONO_2]Br_2$[12]
7) $[Co(NH_3)_5F]Br_2$[13]
8) $[Co(NH_3)_5Cl]Br_2$[14]
9) $[Co(NH_3)_5I]Br_2$[15]
10) $[Co(NH_3)_5Br]Br_2$[16]
11) $[Co(en)_3]Br_3\cdot 3H_2O$[17]
12) *trans*-$[Co(en)_2(NH_3)_2]Br_3\cdot H_2O$[18]
13) *trans*-$[Co(en)_2(NCS)_2]Br\cdot 1^1/_2\ H_2O$[19]
14) *cis*-$[Co(en)_2(NCS)_2]Br\cdot H_2O$[20]
15) *trans*-$[Co(en)_2Cl_2]Br$[21]
16) *cis*-$[Co(en)_2Cl_2]Br\cdot H_2O$[22]
17) *trans*-$[Co(en)_2Br_2]Br$[23]

Their composition and purity were checked by the spectrophotometric method and by the determination of halogen contents.

Irradiation.—Bombardments were made under conditions previously described[2].

Procedures of Separation.—The procedures of separation were similar to those employed for solid samples in the previous paper[2]. Two fractions were separated by means of a procedure involving a cation-exchange resin after dissolution of the activated salt. The first fraction contained bromide ions in the sample solution and anionic radiobromine. The second fraction contained ligand bromine, including its radioisotopes, which had been aquotized through digestion on a warm-bath and then extracted with water.

Measurements were made on each fraction with respect to the gross activity of ^{80m}Br (actually, of its daughter, ^{80}Br, in equilibrium) and ^{82}Br, and to the bromine content. The methods of determination have all been described previouly[2]. Although the hot-atom effects of ^{80m}Br and ^{82}Br, both arising from (n, γ) reactions, were observed at the same time, the contribution of ^{82}Br to the gross activity was, practically, small.

For convenience of discussion, the authors have defined the quantity "ligand yield", which indicates the fraction of the total activity produced retained in ligands of complex ions. "Ligand yield" was calculated as follows:

$$\text{Ligand yield} = \frac{\left(\begin{array}{c}\text{the activity of the}\\ \text{2nd fraction}\end{array}\right)}{\left(\begin{array}{c}\text{sum of the activtiy of the}\\ \text{1st and the 2nd fraction}\end{array}\right)} \times 100$$

Results and Discussion

Ligand Yield.—It was found by the present authors that energetic radiobromine atoms arising from the outside of the co-ordination sphere could substitute for ligands in these cobaltammine complex salts. The fraction of the radiobromine atoms retained in the ligands, or the ligand yield, is shown in Tables I and II.

As various complexes labeled with radiobromine (Br*) might be produced through reactions of hot radiobromine atoms with the target complex, the observed ligand yield was expected to be the sum of the fractions of radiobromine retained in ligands of such labeled complexes. Thus, on the irradiation of the complex salts of the formula $[Co(NH_3)_5\cdot X]Br_{2,3}$, some unstable radiobromine-labeled complexes ($[Co(NH_3)_4XBr^*]^{1,2+}$, etc.) of which the present authors have not yet confirmed the existence, might possibly be formed at first as

7) W. C. Fernelius, "Inorganic Syntheses", Vol. 2, McGraw-Hill Book Co., Inc., New York (1946), p. 216.
8) A. Werner and H. Müller, *Z. anorg. Chem.*, **22**, 108 (1900).
9) A. Werner and A. Miolati, *Z. physik. Chem.*, **12**, 43 (1893).
10) S. M. Jörgensen, *J. prakt. Chem.*, [2], **31**, 62 (1885).
11) The salt was precipitated by ammonium bromide from an aqueous solution of chloride prepared by the method of Jörgensen (*Z. anorg. Chem.*, **5**, 168 (1894).).
12) S. M. Jörgensen, *J. prakt. Chem.*, [2], **23**, 227 (1881).
13) M. Linhard and M. Weigel, *Z. anorg. Chem.*, **266**, 49 (1951).
14) S. M. Jörgensen, *J. prakt. Chem.*, [2], **18**, 221 (1878).
15) R. G. Yalman, *J. Am. Chem. Soc.*, **77**, 3219 (1955).
16) H. S. Booth, "Inorganic Syntheses", Vol. 1, McGraw-Hill Book Co., Inc., New York (1939), p.186.
17) A. Werner, *Ber.*, **45**, 121 (1912).
18) A. Werner, *Ann.*, **386**, 194 (1912).
19) A. Werner and Braünlich, *Z. anorg. Chem.*, **22**, 139 (1900).
20) A. Werner and Braünlich, ibid., **22**, 147 (1900).
21) S. M. Jörgensen, *J. prakt. Chem.*, [2], **41**, 441 (1890); W. C. Fernelius, "Inorganic Syntheses", Vol. 2, McGraw-Hill Book Co., Inc., New York (1946), p. 222.
22) W. C. Fernelius, ibid., Vol. 2, p. 223; P. Larisch, Dissertation, Zürich (1904), p. 87.
23) A. Werner, L. Gerb, S. Lorie and J. Rapiport, *Ann.*, **386**, 111 (1912).

Table I. Ligand yield of irradiated complex salts, $[Co(NH_3)_5X]Br_{2,3}$

No.	Irradiated salt	Ligand yield[a], %	Enrichment factor
1	$[Co(NH_3)_6]Br_3$	4.8±0.2	4×10^2
2	$[Co(NH_3)_5NCS]Br_2$	5.7±0.3	1.2×10^2
3	$[Co(NH_3)_5NO_2]Br_2$	8.0±0.3	4×10^2
4	$[Co(NH_3)_5OH_2]Br_3$	7.1±0.7	0.2×10^2
5	$[Co(NH_3)_5ONO]Br_2$	8.8±0.1	9×10^2
6	$[Co(NH_3)_5ONO_2]Br_2$	9.0±0.3	0.3×10^2
7	$[Co(NH_3)_5F]Br_2$	7.3±0.6	6×10^2
8	$[Co(NH_3)_5Cl]Br_2$	15.2±0.4	3×10^2
9	$[Co(NH_3)_5I]Br_2$	15.8±0.4	5×10^2
10	$[Co(NH_3)_5Br]Br_2$	17.3±0.6	—

a) The ligand yield is nearly identical with the fraction (%) of radiobromine in the form of $[Co(NH_3)_5Br^*]^{2+}$.

Table II. Ligand yield of irradiated complex salts, $[Co(en)_2X_2]Br_{1,3}$

No.	Irradiated salt	Ligand yield[b], %	Enrichment factor
11	$[Co(en)_3]Br_3 \cdot 3H_2O$	0.0±0.1	—
12	*trans*-$[Co(en)_2(NH_3)_2] \cdot Br_3 \cdot H_2O$	0.8±0.1	0.8×10^2
13	*trans*-$[Co(en)_2(NCS)_2] \cdot Br \cdot 1^1/_2H_2O$	4.5±0.2	6×10^2
14	*cis*-$[Co(en)_2(NCS)_2]Br \cdot H_2O$	5.0±0.1	4×10^2
15	*trans*-$[Co(en)_2Cl_2]Br$	16.6±0.3	5×10^3
16	*cis*-$[Co(en)_2Cl_2]Br \cdot H_2O$	17.9±0.3	4×10^3
17	*trans*-$[Co(en)_2Br_2]Br$	37 ±2	—

b) The ligand yield denotes the fraction (%) of radiobromine in the form of $[Co(en)_2XBr^*]^{1,2+}$

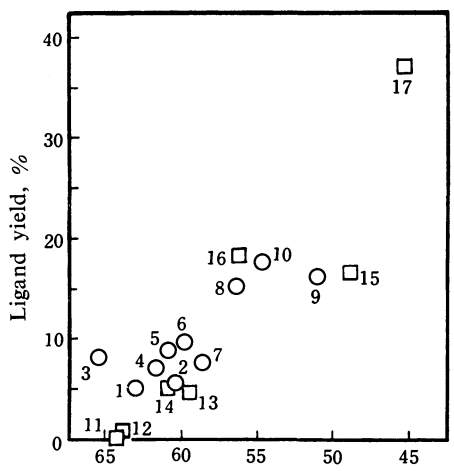
well as the complex $[Co(NH_3)_5Br^*]^{2+}$. However, almost all radiobromine-labeled complexes other than $[Co(NH_3)_5Br^*]^{2+}$ were extremely unstable in aquotization, and adequate procedures of separation made it possible to determine the ligand yield as nearly entirely due to the stable complex $[Co(NH_3)_5Br^*]^{2+}$, without any appreciable contribution from unstable complexes.

In this investigation, the irradiated complex salts had been kept standing in aqueous solutions at room temperature for a sufficiently long time before the completion of the separation of the first fraction. By this treatment, most of the unstable radiobromine-labeled complexes, if they did exist at all, were aquotized and the labile radiobromine atoms extracted as anions into the first fraction, whereas the complex $[Co(NH_3)_5Br^*]^{2+}$ was not aquotized practically, keeping the radiobromine in ligands (i. e., in the second fraction). Therefore, the ligand yield shown in Table I may be considered to be nearly identical with the fraction of radiobromine in the form of $[Co(NH_3)_5Br^*]^{2+}$, which might be synthesized through replacement of X in $[Co(NH_3)_5X]^{2,3+}$ by Br*.

On the irradiation of the salts of the formula $[Co(en)_2X_2]Br_{1,3}$, the probability of the replacement of ethylenediamine molecules with radiobromine seemed to be very small (Table II). Thus, the ligand yield shown in Table II may be taken as indicating the fraction of radiobromine in the form of $[Co(en)_2XBr^*]^{1,2+}$.

Mechanism of Substitution of Ligands by Hot Radiobromine Atoms.—For both groups of complex salts shown in Tables I and II, the ligand yield was found to vary with the kind of ligand, X. Attempts to find the relationship between the ligand yield and the chemical or physical properties of the ligand X, might contribute to clarifying the mechanism by which radiobromine atoms substitute for ligands of the complex salts.

If radioactive complexes, $[Co(NH_3)_5Br^*]^{2+}$ and $[Co(en)_2XBr^*]^{1,2+}$, were produced through substitution of X in the target complex by a hot radiobromine atom (Br*), the ligand yields in the forms of such labeled complexes might be related to the stability of the ligand, X. With the cobalt complex salts studied in the present work, the relationship between their stability and the wavelength of the maximum in their optical absorption bands has been known as the spectrochemical series. In Fig. 1, the ligand yield was plotted against the frequency



Frequency of the maximum in the first absorption band, 10^{13}/sec.

Fig. 1. The relationship between the ligand yield and the frequency of the maximum in the first absorption band.
○ $[Co(NH_3)_5X]Br_{2,3}$
□ $[Co(en)_2X_2]Br_{1,3}$
Numbers in Figs. 1 and 2 correspond to those in Tables I and II.

of the maximum in the first absorption band of the target complex. Fig. 1 shows that the ligand yield roughly tends to increase with the decrease in the frequency of the maximum in the first absorption band or with the decrease in the stability of the ligand, X: the less stable the ligand X is, the more easily it is substituted for by hot radiobromine. However, the ligand yield in some complex salts was incompatible with the general tendency. For example, the ligand yield in $[Co(NH_3)_5 \cdot NO_2]Br_2$, which contained a very stable ligand NO_2, was considerably high, and the ligand yield in $[Co(NH_3)_5F]Br_2$, $[Co(NH_3)_5Cl]Br_2$, $[Co(NH_3)_5Br]Br_2$ and $[Co(NH_3)_5I]Br_2$, all of which contained halogen atoms (F, Cl, Br, I), did not increase in the order of the spectrochemical series.

As the maximum recoil energy of radiobromine resulting from slow neutron capture was calculated to be 174 eV.[24], most radiobromine atoms would recoil with energies larger than those which were involved in ordinary thermal reactions. Therefore, the present authors assumed a model in which collisions of a hot bromine atom with the donor atom in ligand X played an important role. When the masses of the donor atom in ligand X and of a bromine atom are M and M′ respectively, the fraction of the maximum possible loss in the recoiling energy of a hot bromine atom in an elastic collision with the donor atom is given as:

$$\gamma = 4MM'/(M+M')^2. \quad (1)$$

The calculated values of γ for donor atoms in different ligands, X, are shown in Table III. Fig. 2 shows the relationship between the ligand yield and the γ value for the complex salts listed in Tables I and II. As each complex molecule of the salts of the formula $[Co(en)_2X_2]Br_{1,3}$ contains more X's in ligands than that of $[Co(NH_3)_5X]Br_{2,3}$, the probability of the collision of a hot radiobromine atom with X may be somewhat larger for the salts

TABLE III. CALCULATED VALUES OF γ FOR THE DONOR ATOM IN LIGAND X IN A COLLISION WITH A HOT BROMINE ATOM

X	Donor atom	$\gamma=4MM'/(M+M')^2$
NH_3, NCS, NO_2	N	0.50
OH_2, ONO, ONO_2	O	0.56
F	F	0.64
Cl	Cl	0.85
I	I	0.95
Br	Br	1.00

24) A. C. Wahl and N. A. Bonner, "Radioactivity Applied to Chemistry", John Wiley & Sons, Inc., New York (1951), p. 247.

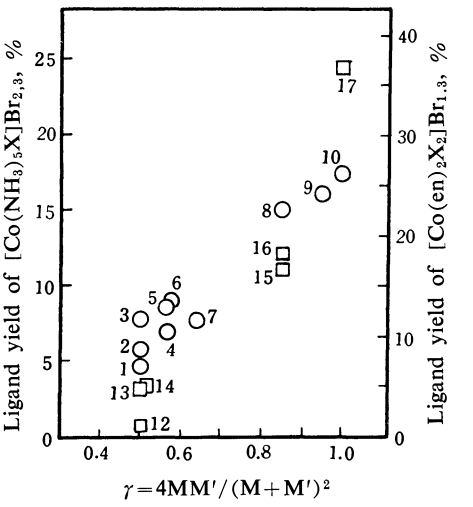


Fig. 2. The relationship between the ligand yield and the value of γ.
○ $[Co(NH_3)_5X]Br_{2,3}$
□ $[Co(en)_2X_2]Br_{1,3}$

of the former series*. Based on the available crystallochemical data, the ratio of relative collision cross sections of a bromine atom with X in ligands was estimated as about 1.5 : 1 for $[Co(en)_2X_2]Br$ and $[Co(NH_3)_5X]Br_2$. For convenience of comparison, these two series of complex salts, which did not seem much alike in crystal structure, are both shown in Fig. 2. Different ligand yield scales were used in Fig. 2 for the two series, considering the ratio of collision cross sections shown above. It is seen in Fig. 2 that the ligand yield tends to increase as the value of γ of the donor atom in ligands increases: the efficiency of replacement of X by a hot radiobromine atom depends mainly on γ.

It can be predicted on the collision model that a ligand group with the donor atom of a larger γ-value is more readily replaced by a hot radiobromine atom. As the experimental results are well explained by this model, the present authors presume that the kinetic processes might play an important role in determining the fate of hot radiobromine atoms, at least in the above solid complex salts. In addition to the kinetic processes, some chemical processes might contribute to determine the ligand yield at some stages in recoil reactions. However, it has not been unequivocally shown in the present work how much contribution such chemical processes make to the recoil reaction.

* Though the presence of crystalline water in some of the salts of the $[Co(en)_2X_2]Br_{1,2}$ series might possibly have more or less influence upon recoil reactions, the effect is not fully investigated in the present work.

Summary

The fate of energetic radiobromine atoms arising from the (n, γ) reaction on bromine in solid complex salts of the formulas $[Co(NH_3)_5X]Br_{2,3}$ and $[Co(en)_2X_2]Br_{1,3}$, was investigated. The fraction of the total radiobromine produced finally retained in ligands (ligand yield) was found to increase with a function of the mass of the donor atom in ligand X. Therefore, it was suggested that the kinetic processes might play an important role in recoil reaction in the solid complex salts.

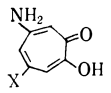
Department of Chemistry
Faculty of Science
The University of Tokyo
Hongo, Tokyo

*Diazo Reactions of 4-Aminotropolones**

By Kozo Doi

(Received May 9, 1961)

Recently the author[1] has synthesized 4-aminotropolone (I), 4-amino-6-methyltropolone (II) and 4-amino-6-isopropyltropolone (III) by an application of the elimination-addition mechanism[2] involving benzyne-type intermediate to the corresponding 3-iodotropolone. The author has also reported further synthetic methods of the aminotropolones, which include applications of the Curtius reaction to 4-carboxytropolones[1] and of the Schmidt reaction to acetyl, formyl and isopropenyl derivatives of tropolones[3], and the reaction of 4-bromotropolone and ammonia[4].



I: X=H II: X=Me
III: X=*iso*-Pr

On the other hand, there have been rare observations of the reactivities of 4-aminotropolones, except in the case of the diazotization of a methyl analogue II, in which instance the corresponding hydroxytropolone (V) was obtained without detecting the intermediate diazonium salt[5]. In the previous papers the author stated in brief some synthetic applications of the aminotropolone (I), involving preparations of some pyridotropolones[6] and of 4-aminotropone[7]. Furthermore, the author has very recently reported that the aminotropolone (I), differing from the isomeric 3- and 5-aminotropolones, undergoes some electrophilic substitutions to give normal nuclear substitution products[8].

It is well-known that diazotization of 5-aminotropolones results in formation of diazonium salts, which undergo the Sandmeyer reaction in the presence of cuprous salt to replace the amino group by halogen, nitrile and alkoxyl groups[9]. On the other hand, the diazotization of 3-aminotropolones is also known to undergo the Sandmeyer reaction[10], although accompanied by aromatization into the corresponding salicylic acid[11], forming 3-halogenotropolones and 3-hydroxytropolones under a certain reaction condition[12].

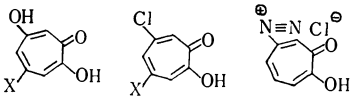
In this communication the author wishes to describe the diazotizations of the above three 4-aminotropolones in comparison with those of the 3- and 5-isomers.

On diazotization in a sulfuric acid solution the aminotropolones afford the corresponding hydroxytropolones, in neither case of which the addition of alkaline β-naphthol to the diazotized solution causes red coloration, as observed by Haworth and his co-workers[5]. The melting points and ultraviolet absorptions

* This work was presented at the 12th Annual Meeting of the Chemical Society of Japan, Kyoto, April, 1959.

1) K. Doi, This Bulletin, **34**, 497 (1961).
2) J. D. Roberts et al., *J. Am. Chem. Soc.*, **75**, 3290 (1953); ibid., **78**, 601 (1956).
3) K. Doi, This Bulletin, **34**, 501 (1961).
4) K. Doi, ibid., **34**, 504 (1961).
5) W. D. Crow, R. D. Haworth and P. R. Jefferies, *J. Chem. Soc.*, **1952**, 3705.
6) K. Doi, *Bull. Chem. Res. Inst. Non-Aqueous Solutions, Tohoku Univ.*, **9**, 19 (1959).
7) K. Doi, This Bulletin, **33**, 887 (1960).
8) K. Doi, ibid., **34**, 1410 (1961).
9) P. L. Pauson, *Chem. Revs.*, **55**, 9 (1955); T. Nozoe, S. Seto, S. Ebine and S. Ito, *J. Am. Chem. Soc.*, **73**, 1895 (1951).
10) T. Nozoe, Y. Kitahara and K. Doi, *Proc. Japan Acad.*, **27**, 282 (1951).
11) R. D. Haworth and P. R. Jefferies, *J. Chem. Soc.*, **1951**, 2067; T. Nozoe, Y. Kitahara and K. Doi, *J. Am. Chem. Soc.*, **73**, 1895 (1951).
12) T. Nozoe, Y. Kitahara and K. Doi, *Science Repts. Tohoku Univ., Ser. I*, **40**, 121 (1957).

of 4-hydroxytropolone[13] (IV) and 4-hydroxy-6-methyltropolone[5] (V) respectively are in essentially good agreement with those reported. 4-Hydroxy-6-isopropyltropolone (VI) was also ascertained to agree with reaction product[14], obtained by high temperature alkaline hydrolysis of 3-bromo-6-isopropyltropolone.

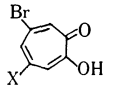


IV: X=H VII: X=H
V: X=Me VIII: X=Me X
VI: X=*iso*-Pr IX: X=*iso*-Pr

On diazotization in a dilute hydrochloric acid solution in place of sulfuric acid, the aminotropolones form corresponding 4-chlorotropolones in a good yield, even without any catalyst such as cuprous chloride or copper. 4-Chlorotropolone (VII) is in good agreement with an authentic sample[15] in both its melting point and ultraviolet absorption spectrum. The structures of 4-chloro-6-methyl-VIII and 4-chloro-6-isopropyltropolones (IX) are reasonably understood from the comparison of their ultraviolet absorptions with that of VII.

An isolation of a stable diazonium salt was possible in some cases. For instance, in a concentrated hydrochloric acid solution, 4-aminotropolone (I) results in facile diazotization, even in a state of suspension, and converts into yellow tropolone-4-diazonium chloride (X), which undergoes red coloration with alkaline β-naphthol. This diazonium salt gives the chloro derivative VII on being heated with copper powder under the vigorous evolution of nitrogen, 4-methoxytropolone on being heated with methanol, and 4-cyanotropolone on reaction with cuprous cyanide. From alkyl derivatives II and III, the corresponding diazonium salt has not been isolated in a solid state, but it seems to be formed as an intermediate in the above reactions.

In a similar manner, the use of hydrobromic acid in place of hydrochloric acid in the diazotization results also in the formation of corresponding bromotropolones without any catalyst. 4-Bromotropolone (XI) was identified with an authentic specimen[4] by the determination of the mixed melting point and by a comparison of the ultraviolet absorption. The structures of the other reaction products XII and XIII are assumed from the similarity of their ultraviolet absorptions to that of XI.



XI: X=H XII: X=Me
XIII: X=*iso*-Pr

Fig. 1 indicates the ultraviolet absorption spectra of hydroxyl (IV), chloro (VII), and bromo (XI) derivatives obtained from 4-aminotropolone (I). The ultraviolet spectra of the alkyl derivatives of the above three products resemble essentially that of the respective product from I.

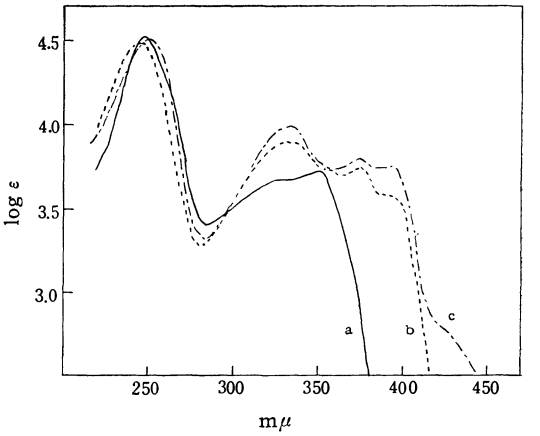
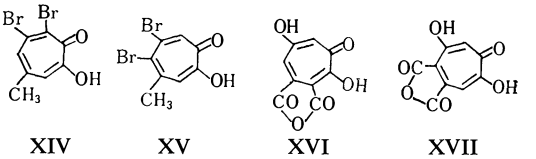


Fig. 1. The ultraviolet absorption spectra.
a: 4-Hydroxytropolone (IV)
b: 4-Chlorotropolone (VII)
c: 4-Bromotropolone (XI)

When diazotized in an concentrated hydrobromic acid solution, 4-amino-6-methyltropolone (II) has been found to yield not only 4-bromo-6-methyltropolone (XI) but also an unexpected



XIV XV XVI XVII

product, dibromo-methyltropolone. The ultraviolet absorption spectrum of this anomalously produced dibromotropolone resembles not so much that of 3,6-dibromotropolone as that of the 4-bromo derivative XI, although indicating a bathochromic shift by the introduction of one bromine atom (Fig. 2). For the above reason, the dibromo-methyltropolone is probably a nuclear substitution product, namely XIV or XV.

Whether the dibromotropolone is XIV or XV is reasonably suggested by its infrared absorption spectra. Table I indicates the absorption bands in the CH out-of-plane vibration regions

13) Y. Kitahara, ibid., **39**, 258 (1956).
14) T. Toda, private communication.
15) T. Sato, *J. Chem. Soc. Japan, Pure Chem. Sec.* (*Nippon Kagaku Zasshi*), **80**, 1171 (1959).

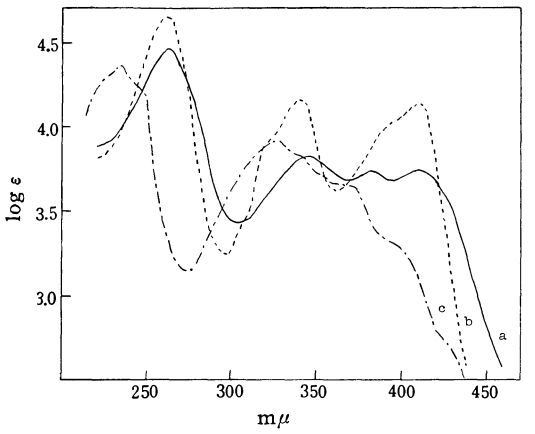


Fig. 2. The ultraviolet absorption spectra.
a: 3, 4-Dibromo-6-methyltropolone (XIV)
b: 3, 6-Dibromotropolone
c: 5-(β-Chloro-β-cyanoethyl)tropolone (XVIII)

TABLE I. FREQUENCIES IN THE CH OUT-OF-PLANE VIBRATION REGION OF THE INFRARED SPECTRA OF SOME TRISUBSTITUTED TROPOLONES (cm^{-1})

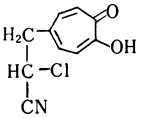
XIV	896	867	823	795	735
XVI	896	865	806	774	730
XVII	—	—	814	763, 782	740

of the infrared spectra of the dibromotropolone, 6-hydroxytropolone-3, 4-dicarboxylic anhydride[16] (XVI) (3, 4, 6-trisubstituted tropolone), and stipitatonic acid[16] (XVII) (4, 5, 6-trisubstituted tropolone). Undoubtedly these absorptions of the dibromo-methyltropolone resemble not so much those of XVII as of XVI, and therefore, the dibromotropolone seems to be 3, 4-dibromo-6-methyltropolone (XIV) rather than 4, 5-dibromo-6-methyltropolone (XV).

The formation of this dibromotropolone (XIV) is probably interpreted to be due to further bromination of XI, which has been produced normally in the diazotization, with free bromine formed by an oxidation of hydrobromic acid with nitrous acid. A similar example was reported in the formation of 3, 5-dibromotropolone from 3- and 5-nitrotropolone when heated with hydrobromic acid[17].

The above description has demonstrated that the diazotizations of 4-aminotropolones result in the formation of diazonium salt, which reacts immediately with anions of the acid used to give the halogeno- or hydroxytropolones without any catalyst such as cuprous salt or copper. Such a fact has not been found in the other isomeric aminotropolones. This is probably to be understood as a competitive action of an electron-withdrawing effect of the diazonium group and a conjugate acid-forming effect of the tropolone ring with the acid used, resulting in promotion of the formation of a carbonium ion, which combines immediately with anions from the acid used to form substitution product.

In relation to the diazotization of the 4-aminotropolones, the author has investigated the reaction of 5-diazotized aminotropolone and acrylonitrile under the Meerwein condition to obtain 5-(β-chloro-β-cyanoethyl)tropolone (XVIII), although in a poor yield. The structure of this product XVIII is probably supported by the resemblance of the ultraviolet absorption (Fig. 2) to those of 5-alkyltropolones and by the result obtained in the reaction of diazotized aniline and acrylonitrile[18].



XVIII

Experimental

All of the ultraviolet absorption spectra were measured in methanol solution with a Beckman model DU quartz spectrophotometer. The infrared spectra were measured on potassium bromide disks with a Perkin-Elmer model 21 infrared spectrometer, using a rock salt prism.

4-Hydroxytropolone (IV).—A solution of sodium nitrite (70 mg.) and water (1 ml.) was added, drop by drop, for 5 min. into a cold suspension of 4-aminotropolone (I, 140 mg.), concentrated sulfuric acid (0.5 ml.) and water (5 ml.). After 30 min., the reaction mixture was gradually warmed up to 50°C, by which means a complete solution was effected. Then the mixture was diluted with water (20 ml.) and extracted continuously with ether for 8 hr. The residue obtained by the evaporation of the ether extract, after sublimation in vacuo and subsequent crystallization from acetic acid, afforded IV (60 mg.) as colorless needles, m. p. 230~231°C, undepressed on admixture with an authentic sample[13].

4-Hydroxy-6-methyltropolone (V).—A solution of sodium nitrite (70 mg.) and water (1 ml.) was added dropwise into a cold, stirred solution of 4-amino-6-methyltropolone (II, 150 mg.), concentrated sulfuric acid (0.5 ml.) and water (10 ml.). The reaction mixture was then treated as in the above case, and V (60 mg.) was obtained as colorless prisms, m. p. 241~242°C, undepressed on admixture with an authentic specimen[5].

4-Hydroxy-6-isopropyltropolone (VI).—A solution of sodium nitrite (70 mg.) and water (1 ml.) was added dropwise into a cold, stirred solution of 4-amino-6-isopropyltropolone (III, 180 mg.), concentrated sulfuric acid (0.5 ml.), and water (10 ml.) for 5 min. After 30 min., the reaction mixture was

16) K. Doi and Y. Kitahara, This Bulletin, 31, 788 (1958).
17) T. Nozoe, Y. Kitahara, K. Doi and T. Arai, *Bull. Chem. Res. Inst. Non-Aqueous Solutions, Tohoku Univ.*, 7, 13 (1957).
18) C. F. Koelsch, *J. Am. Chem. Soc.*, 65, 57 (1943).

extracted with three 20-ml. portions of chloroform, and the residue obtained by evaporation of the chloroform extract was sublimed in vacuo. Recrystallization of the sublimate from dilute methanol gave VI (100 mg.) as colorless prisms, m.p. 178~179°C, undepressed on admixture with an authentic sample[14].

4-Chlorotropolone (VIII).—To a cold, stirred mixture of 4-aminotropolone (I, 70 mg.), concentrated hydrochloric acid (1 ml.) and water (2 ml.) was added dropwise for 5 min. a solution of sodium nitrite (40 mg.) and water (0.5 ml). Then the mixture was warmed gradually to 40°C, by which the suspended solid dissolved with evolution of gas to form a clear solution. This solution was extracted with three 3-ml. portions of chloroform, and the residue therefrom was recrystallized from cyclohexane. VII (50 mg.) was obtained as pale yellow needles, m. p. 78~79°C, undepressed on admixture with an authentic sample[15].

4-Chloro-6-methyltropolone (VIII).—A solution of sodium nitrite (70 mg.) and water (1 ml.) was added dropwise into a cold, stirred solution of 4-amino-6-methyltropolone (II, 150 mg.), concentrated hydrochloric acid (5 ml.), and water (2 ml.). With the progress of the diazotization, the colorless solid separated out from the reaction mixture. After stirring for 2 hr., the reaction mixture was diluted with water (10 ml.) and extracted with three 20-ml. portions of chloroform. The residue obtained by evaporation of the extract, after sublimation in vacuo and subsequent crystallization from cyclohexane, yielded VIII (120 mg.) as colorless needles, m. p. 117°C.

Found: C, 56.19; H, 4.62. Calcd. for $C_8H_7O_2Cl$: C, 56.30; H, 4.16%. λ_{max} mμ (log ε): 246 (4.49), 334 (3.90), 373 (3.78).

4-Chloro-6-isopropyltropolone (IX).—To a cold, stirred solution of 4-amino-6-isopropyltropolone (III, 180 mg.), concentrated hydrochloric acid (2 ml.) and water (2 ml.), was added dropwise a solution of sodium nitrite (70 mg.) and water (1 ml.). With the progress of the diazotization, the colorless solid precipitated out. The reaction mixture was treated as above and recrystallization of the final sublimate from petroleum ether (b. p. 40~60°C) afforded IX (110 mg.) as pale yellow needles, m. p. 42~43°C.

Found: C, 60.23; H, 5.86. Calcd. for $C_{10}H_{11}O_2Cl$: C, 60.46; H, 5.59%. λ_{max} mμ (log ε): 248 (4.51), 334 (3.94), 373 (3.78).

Tropolone-4-diazonium Chloride (X).—A solution of sodium nitrite (280 mg.) and water (1 ml.) was added dropwise into a cold, stirred mixture of 4-aminotropolone (I, 550 mg.), concentrated hydrochloric acid (20 ml.) and water (6 ml.), and then the reaction mixture was stirred for an hour at 0°C. The colorless solid turned gradually into a yellow solid with the progress of the diazotization. The residual yellow solid was collected by filtration to give X (0.31 g.), m. p. 100~103°C (decomp.). From the filtrate 4-chlorotropolone (120 mg.) was obtained.

The diazonium salt X showed red coloration on being added into an alkaline solution of β-naphthol, and yielded 4-chlorotropolone on being heated with copper bronze in benzene.

4-Methoxytropolone from X.—To a cold, stirred mixture of the diazonium salt (X, 100 mg.) and methanol (5 ml.) was added copper bronze (10 mg.). The reaction mixture turned into a deep red solution with the evolution of nitrogen, and then it was stirred for an hour at room temperature. The filtrate, after removal of copper, evaporation of the solvent, sublimation in vacuo and subsequent crystallization from methamol, gave 4-methoxytropolone (20 mg.) as colorless leaflets, m. p. 95°C, undepressed on admixture with an authentic sample[13].

4-Cyanotropolone from X.—To a stirred mixture of potassium cyanide (700 mg.), cuprous cyanide (450 mg.) and water (2 ml.), was added the diazonium salt (X, 400 mg.) at room temperature. The mixture was stirred for another hour and then warmed gradually to 50°C. Hydrogen sulfide was passed through the mixture, chloroform (10 ml.) was added, and some insoluble matter was removed by filtration. The chlorform solution, after evaporation of the solvent in vacuo, gave 4-cyanotropolone (40 mg.) as yellow needles, m. p. 194°C, undepressed on admixture with an authentic sample[4].

4-Bromotropolone (XI).—A solution of sodium nitrite (70 mg.) and water (1 ml.) was added dropwise under cooling into a stirred mixture of the aminotropolone (I, 140 mg.), concentrated hydrobromic acid (4 ml.) and water (2 ml.). With the progress of the diazotization, the reaction mixture became a clear solution under evolution of nitrogen. After 2 hr., the reaction mixture was diluted with water (40 ml.) and extracted with three 30-ml. portions of chloroform. The residue obtained by evaporation of the solvent of the extract, after sublimation in vacuo and subsquent crystallization from cyclohexane, afforded XI (100 mg.) as pale yellow needles, m. p. 85~86°C, undepressed on admixture with an authentic specimen[4].

4-Bromo-6-methyltropolone (XII).—A mixture of the aminotropolone (II, 150 mg.), concentrated hydrobromic acid (2 ml.) and water (4 ml.) was diazotized with a solution of sodium nitrite (70 mg.) and water (1 ml.). As treated similarly to the above case, the reaction mixture afforded XII (120 mg.) as pale yellow needles (cyclohexane), m. p. 116~117°C.

Found: C, 44.50; H, 3.34. Calcd. for $C_8H_7O_2Br$: C, 44.68; H, 3.28%. λ_{max} mμ (log ε): 253 (4.50), 336 (3.87), 370 (3.76), 395 (3.49).

4-Bromo-6-isopropyltropolone (XIII).—A solution of the aminotropolone (III, 90 mg.), concentrated hydrobromic acid (1 ml.) and water (2 ml.) was diazotized with a solution of sodium nitrite (40 mg.) and water (1 ml.). The procedure followed for isolating the product was essentially the same as above, and the reaction product XIII (20 mg.) was obtained. Analytical sample was crystallized from petroleum ether (b. p. 40~60°C) as pale yellow needles, m. p. 52~53°C.

Found: C, 49.19; H, 4.32. Calcd. for $C_{10}H_{11}O_2Br$: C, 49.38; H, 4.52%. λ_{max} mμ (log ε): 255 (4.49), 335 (3.38), 370 (3.74), 393 (3.48).

3, 4-Dibromo-6-methyltropolone (XIV).—A solution of sodium nitrite (70 mg.) and water (1 ml.) was added dropwise into a cold, stirred mixture of the aminotropolone (II, 150 mg.), concentrated hydrobromic acid (8 ml.) and water (2 ml.). After

being stirred for 3 hr. further, the reaction mixture was diluted with water (20 ml.), extracted with three 20-ml. portions of chloroform, and the solvent of the extract was evaporated in vacuo. The residual solid, m. p. 104~110°C, was dissolved in cyclohexane (50 ml.) and chromatographed on a column of silica gel (1.5×20 cm.). From the more soluble eluate, the monobromotropolone (XII, 40 mg., m. p. and mixed m. p. 116~117°C), was obtained, and from the less soluble eluate the dibromotropolone (XIV, 60 mg.) was obtained as pale yellow prisms (from ligroin), m. p. 127°C.

Found: C, 32.41; H, 2.31. Calcd. for $C_8H_6O_2Br_2$: C, 32.69; H, 2.06%. λ_{max} mμ (log ε): 264 (4.47), 345 (3.83), 383 (3.74), 410 (3.74).

5-(β-Chloro-β-cyanoethyl)tropolone (XVIII).—A cold solution of 5-aminotropolone (4.1 g.), concentrated hydrochloric acid (6 ml.), water (12 ml.), and dioxane (10 ml.) was diazotized with a solution of sodium nitrite (2.2 g.) and water (4 ml.). This diazonium salt solution was added dropwise under cooling to a stirred mixture of acrylonitrile (1.6 g.), sodium acetate trihydrate (4.1 g), cupric chloride (4 g.), water (6 ml.), and acetone (50 ml.), and the reaction mixture was stirred overnight at room temperature. Then the mixture was separated by filtration into the solid and the filtrate. The former afforded, after treatment with hydrogen sulfide, 5-chlorotropolone, m. p. and mixed[9] m. p. 180~181°C.

The filtrate was diluted with water (50 ml.), extracted with three 50-ml. portions of chloroform, and hydrogen sulfide was introduced into this extract. The chloroform solution, from which copper sulfide was removed, was evaporated in vacuo and the residual resinous matter was re-extracted with hot cyclohexane (100 ml.). The residue obtained on evaporation of the cyclohexane extract was separated by fractional sublimation into the two parts, A, which sublimed up to 120°C/2 mmHg (bath temp.), and B, which sublimed up to 170°C. The fraction. A was crystallized from cyclohexane to afford XVIII (20 mg.) as colorless leaflets, m. p. 119~120°C.

Found: C, 57.40; H, 3.72; N, 6.73. Calcd. for $C_{10}H_8O_2NCl$: C, 57.29; H, 3.80; N, 6.67%. λ_{max} mμ (log ε): 235 (4.36), 325 (2.92).

From the fraction B, 5-chlorotropolone (0.7 g.) was obtained.

The author wishes to express his deep gratitude to Professor Yoshio Kitahara for his kind guidance, to Professor Sekio Mitsui for supplying acrylonitrile, to Mr. Hideji Aono for infrared spectral measurements, and to Messrs. Shin-ichi Ohyama, Kuni Kato and Ayako Iwanaga for microanalyses.

The Chemical Research Institute of Non-Aqueous Solutions
Tohoku University
Katahira-cho, Sendai

Dehydration Reaction of Hydroxamic Acids with Unsaturated Ethers

By Teruaki MUKAIYAMA, Hiroyuki NOHIRA and Siro ASANO

(Received May 18, 1961)

In a preceding paper[1] a successful method for the conversion of hydroxamic acids into isocyanates by means of a ketene dimer has been described. It is one of the improved methods of Lossen rearrangement. In the present study, the dehydration of hydroxamic acids with organic reagents is extended to some unsaturated ethers. The dehydration by means of acetylenic ether was tried first, since acetylenic ether is hydrated to give carboxylic ester, which is unreactive with isocyanate and is known to be an effective reagent for the dehydrations of carboxylic acids, phosphoric acids[2], primary nitroparaffins[3,4] and aldoximes[4,5] into carboxylic acid anhydrides, pyrophosphoric acids, nitrile oxides and nitriles, respectively. It has also been confirmed that initially-formed addition compounds of acetylenic ether with the above-mentioned compounds are the necessary intermediate for these reactions.

It has been now established that without a catalyst benzhydroxamic acid does not react with ethoxyacetylene, but the reaction is carried out easily at about 40~50°C in the presence of a catalytic amount of boron trifluoride in tetrahydrofuran to give an addition compound. After removal of the solvent, the

1) T. Mukaiyama and H. Nohira, *J. Org. Chem.*, **26**, 782 (1961).
2) J. F. Arens and T. Doornbos, *Rec. trav. chim.*, **74**, 79 (1955).
3) T. Mukaiyama and T. Hoshino, *J. Am. Chem. Soc.*, **82**, 5339 (1960).
4) T. Mukaiyama and T. Hata, This Bulletin, **33**, 1382 (1960).
5) T. Mukaiyama and T. Hata, ibid., **33**, 1712 (1960).

TABLE I. REACTION OF HYDROXAMIC ACIDS WITH ETHOXYACETYLENE

Hydroxamic acid $R-C(=O)NHOH$, R =	g.	EA* g.	Pyrolysis condition: Temp. °C	Pyrolysis condition: Pressure mmHg	Isocyanate: Distilling range °C	Isocyanate: Yield %
$C_6H_5CH_2-$	2.0	1.4	100~120	12~15	75~90	55
p-$CH_3OC_6H_4-$	2.0	1.2	85~100	0.5~1	54~57	65
p-$CH_3C_6H_4-$	2.0	1.4	80~ 90	11~12	69~72	70
p-ClC_6H_4-	1.3	0.9	100~120	1.5	43~45	60
m-$NO_2C_6H_4-$	2.0	1.1	100~120	0.5~1	71~80	50
p-$NO_2C_6H_4-$	2.0	0.95	90~110	0.5~1	80~85	45

* EA = Ethoxyacetylene

adduct is obtained as a viscous liquid which decomposes at about 90°C. When it was decomposed in a Claisen flask at a temperature between 90~110°C under reduced pressure, phenyl isocyanate was obtained in a 65% yield along with ethyl acetate.

$$CH{\equiv}COC_2H_5 + R{-}\overset{\overset{O}{\|}}{C}NHOH \longrightarrow$$

$$\left(CH_2{=}C\begin{matrix}OC_2H_5\\ ONHC{-}R\\ \quad\|\\ \quad O\end{matrix}\right) \longrightarrow CH_3{-}\overset{\overset{O}{\|}}{C}{-}OC_2H_5 + R{-}NCO$$

I

In order to obtain a variety of isocyanates by this process, the reactions of hydroxamic acids with acetylenic ether were examined, and successful results were obtained. The results of the experiments are summarized in Table I.

In the next place, dehydration with methylketone diethylacetal, a compound which possesses a similar dehydrating ability, was tried. In this connection, the dehydration of aldoximes with methylketone diethylacetal has been already examined, and an interesting reaction, to give isonitriles, rearranged products, has been reported[4,6]. It was found that a variety of hydroxamic acids react with methylketene diethylacetal at 30~50°C without a catalyst to give addition compounds. These adducts II are unstable, viscous liquids and could not be isolated as pure liquids or crystaline substances. However, by their decomposition at 80~100°C under reduced pressure, the corresponding isocyanates are obtained in good yields along with ethyl propionate and ethanol.

In the course of attempts to isolate the adducts II, a crystalline substance (m. p. 86~86.5°C decomp.) was obtained from the reaction mixture of p-nitrobenzhydroxamic acid and methylketene diethylacetal. From the results of the elementary analyses, the infrared spectra and some other examinations, the structure of this substance was concluded to be III, 1-ethoxypropenyl-1-p-nitrobenzhydroxamate. It decomposes into p-nitrophenyl isocyanate and ethyl propionate almost quantitatively. In addition, the same substance is obtained by the reaction of p-nitrobenzhydroxamic acid and ethyl orthopropionate; this reaction is also considered to proceed through the same intermediate II, as is shown in the following equations:

$$CH_3CH{=}C\begin{matrix}OC_2H_5\\ OC_2H_5\end{matrix} + R{-}\overset{\overset{O}{\|}}{C}NHOH \longrightarrow \left(CH_3CH_2C\begin{matrix}OC_2H_2\\ OC_2H_5\\ ONHC{-}R\\ \quad\|\\ \quad O\end{matrix}\right)$$

or

$$CH_3CH_2{-}C\begin{matrix}OC_2H_5\\ OC_2H_5\\ OC_2H_5\end{matrix}$$

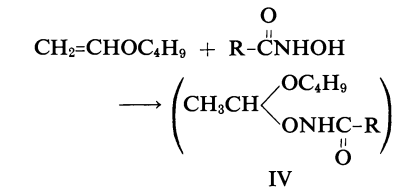
II

$$CH_3CH{=}C\begin{matrix}OC_2H_5\\ ONHC{-}R\\ \quad\|\\ \quad O\end{matrix} \longrightarrow CH_3CH_2\overset{\overset{O}{\|}}{C}OC_2H_5 + R{-}NCO + C_2H_5OH$$

III

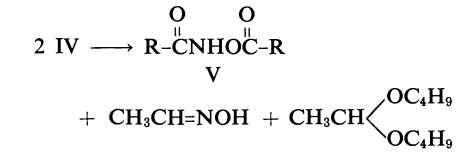
Finally, the dehydration of hydroxamic acids with vinyl ether, which has been confirmed to be an effective reagent for the dehydration of benzaldoxime into benzonitrile[5], was examined. Analogous to the reaction described above, benzhydroxamic acid reacts with n-butylvinyl ether in the presence of a catalytic amount of phosphoric acid to give an adduct as a viscous liquid.

6) T. Mukaiyama, K. Tonooka and K. Inoue, *J. Org. Chem.*, **26**, 2202 (1961).



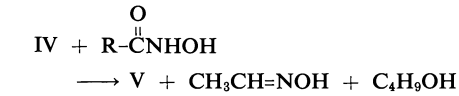
IV

This adduct could not be isolated pure, but it was confirmed to possess the structure of IV from its infrared spectrum. It decomposes, against expectation, however, at a relatively low temperature (50~70°C) into dibenzhydroxamic acid (or benzoyl benzhydroxamate) (V), acetaldoxime, acetaldehyde dibutylacetal and butanol. The formation of these products may be explained by the following two equations:



V

and

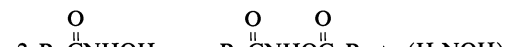


Dibenzhydroxamic acid (m. p. 163~164°C) is identified with an authentic sample, showing no depression in mixed melting points. The presence of acetaldoxime, acetaldehyde dibutylacetal and butanol is confirmed by fractional distillation and gas-chromatographic analysis.

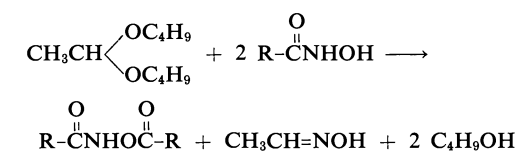
This type of reaction, to produce dihydroxamic acids from hydroxamic acids by the action of ethyl acetoacetate or potassium cyanide, has been reported by Moissan[7], wherein it was suggested that this reaction is equivalent to 1 mol. dehydroxylamination from 2 mol. of hydroxamic acids. But some points concerning the mechanism of the reaction have remained unclarified.

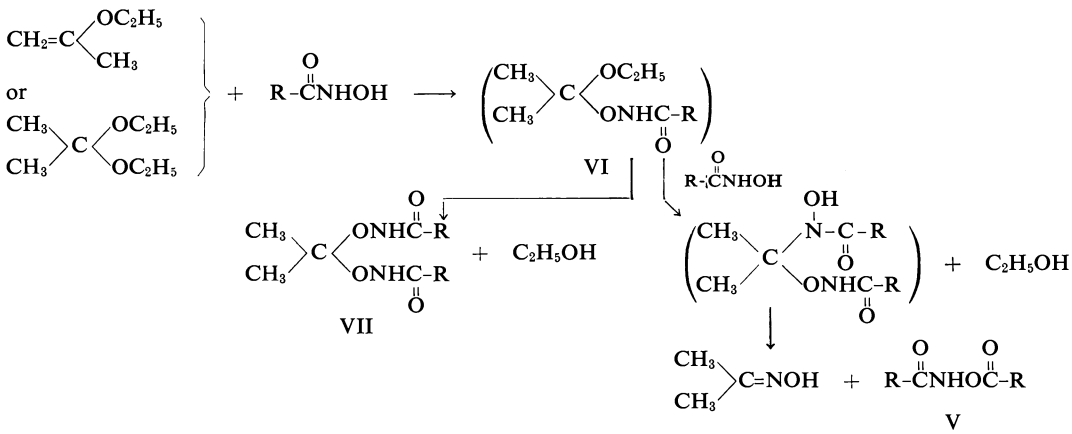
Table II. Reactions to give dihydroxamic acids

Hydroxamic acid R-CNHOH (R=)	Dehydroxylaminating reagent	Dihydroxamic acid R-CNHOC-R Yield %	M. p. °C
$C_6H_5CH_2$-	*n*-Butyl vinyl ether	37	150~151
p-$CH_3OC_6H_4$-	*n*-Butyl vinyl ether	47	143~143.5
p-$CH_3C_6H_4$-	*n*-Butyl vinyl ether	52	156~157
p-$NO_2C_6H_4$-	*n*-Butyl vinyl ether	27	174.5
C_6H_5-	*o*-Nitrobenzaldehyde	38	163~164
C_6H_5-	Acetaldehyde di-*n*-butylacetal	77	163~164



It is now established that a variety of hydroxamic acids react with *n*-butyl vinyl ether under the same condition as has been mentioned in the case of benzhydroxamic acid to give corresponding dihydroxamic acids (Table II). Further experiments were tried in order to ascertain whether or not carbonyl compounds or their derivatives, which are able to react with hydroxylamine to give oximes, are effective in this type of reaction. Analogous to the reaction of vinyl ether, dibenzhydroxamic acid has been obtained by the reaction of benzhydroxamic acid with acetaldehyde dibutylacetal, *o*-nitrobenzaldehyde, ethylpropenyl ether or acetone diethylketal. When acetaldehyde dibutylacetal is used, for example, the reaction is shown by the following equation.





7) M. U. Moissan, *Compt. rend.*, **140**, 1398 (1905).

In this case, the reaction is thought to proceed through the intermediate IV, and this result, together with the formation of III from ethyl orthopropionate, suggests that the ethoxyl group in orthoester or acetal is easily replaced by the -ONHCO-R group. This has been further confirmed by the following evidence.

When ethyl propenyl ether or acetone diethylketal was used, a crystalline product which melts at 160~161°C was isolated along with dibenzhydroxamic acid and identified as isopropylidene bis-benzhydroxamic acid, VII. Therefore these reactions are thought to proceed via the intermediate VI, which in turn changes into V or VII.

Experimental

Reaction of Benzhydroxamic Acid with Ethoxyacetylene.—A solution of ethoxyacetylene (1.1 g., 0.016 mol.) in 7 ml. of dry tetrahydrofuran was added dropwise with stirring over a period of 10 min. into a suspension of benzhydroxamic acid (2.0 g., 0.015 mol.) and 3 drops of boron trifluoride etherate in 8 ml. of tetrahydrofuran at 40°C. After the addition was completed, the mixture was stirred for an additional hour. The solvent was subsequently removed under reduced pressure, and an adduct I ($R = C_6H_5-$) was obtained as a viscous liquid which decomposed at about 100°C. By the decomposition of this adduct in a Claisen flask at 90~100°C under reduced pressure (12~15 mmHg), 1.1 g. (65%) of phenyl isocyanate was obtained, along with 0.8 g. (60%) of ethyl acetate.

Similarly, benzyl-, *p*-anisyl-, *p*-tolyl-, *p*-chlorophenyl-, *p*-nitrophenyl and *m*-nitrophenyl isocyanate were obtained from corresponding hydroxamic acids. Their experimental conditions and yields are listed in Table I.

Reaction of Benzhydroxamic Acid with Methylketene Diethylacetal.—A mixture of benzhydroxamic acid (4.11 g., 0.03 mol.) and methylketene diethylacetal (7.8 g., 0.06 mol.) in 30 ml. of dry ether was stirred for 3 hr. at 30°C. After the mixture became homogeneous, the solvent was removed under reduced pressure, and an adduct II ($R = C_6H_5-$) was obtained as a colorless, viscous liquid. By a similar pyrolytic process, it decomposed into ethyl propionate, phenyl isocyanate and ethanol in a high yield. Phenyl isocyanate was converted into diphenylurea by the addition of aniline (2.81 g., 0.03 mol.) to the pyrolyzate, which was collected in a cooled trap; 5.28 g. (83%, m. p. 238~239°C) of sym-diphenylurea was obtained.

Similarly, benzyl- and *p*-anisyl isocyanate were obtained from corresponding hydroxamic acids in yields ranging from 50 to 85%.

Formation of 1-Ethoxyprophenyl-1-*p*-nitrobenzhydroxamate (III).—A mixture of *p*-nitrobenzhydroxamic acid (6.6 g., 0.036 mol.) and methylketene diethylacetal (8.0 g., 0.062 mol.) in 70 ml. of dry ether was stirred for 4 hr. at 30°C. After the mixture became homogeneous, the solvent was removed under reduced pressure, and 8.9 g. (92%) of III ($R = NO_2-C_6H_4-$), was obtained as pale yellow crystalline. It was recrystallized from ether, m. p. 86~86.5°C, decomp.

Found: C, 54.41; H, 5.39; N, 10.62. Calcd. for $C_{12}H_{14}N_2O_5$; C, 54.13; H, 5.30; N, 10.52%.

It was readily soluble in ether, ethanol and sparingly in benzene and carbon tetrachloride. Its hydrolysis in dilute hydrochloric acid and ethanol gave *p*-nitrobenzhydroxamic acid, which was confirmed by its characteristic color reaction with ferric chloride. The infrared absorption bands are 3060~3125 cm^{-1} m (broad), 2986m, 2930m, 1635w (shoulder), 1600s, 1520w (shoulder), 1435m, 1310m, 1235s, 1155s, 1109w, 1075s, 1030w, 972s, 943m, 870m, 857m, 810m, (Nujol or carbon tetrachloride solution, s=strong, m=medium, w=weak).

Similarly, the same substance III was obtained from the reaction of *p*-nitrobenzhydroxamic acid with ethyl orthopropionate in an 82% yield.

Decomposition of III.—The above-mentioned III (5.32 g., 0.02 mol.) was decomposed under reduced pressure (17~18 mmHg) in a 50 ml. Claisen flask heated in an oil bath (150°C). The low boiling part of the pyrolyzate was collected in a cooled trap, from which 1.54 g. (75%, b. p. 98~99°C) of ethyl propionate was obtained by distillation. Separately, 2.73 g. (91%, m. p. 53~55°C) of *p*-nitrophenyl isocyanate was obtained from the pyrolysate which remained in the flask (recrystallization from chloroform).

Reaction of Benzhydroxamic Acid with *n*-Butyl Vinyl Ether.—A mixture of benzhydroxamic acid (2.75 g., 0.02 mol.), *n*-butyl vinyl ether (2.0 g., 0.02 mol.) and 2 drops of phosphoric acid (85%) in 11 ml. of ethyl acetate was refluxed for 3 hr., cooled and filtered. The precipitate of dibenzhydroxamic acid was washed with warm water and recrystallized from ethyl acetate (yield, 1.35 g. 56%, m. p. 163~164°C). By fractional distillation of the filtrate, two fractions of A (37~42°C/12.5 mmHg, 0.62 g.) and B (65~75°C/12.5 mmHg, 0.45 g.) were obtained. The fraction A was identified as a mixture of acetaldoxime and *n*-butanol by gas-chromatographic analysis, while the B was acetaldehyde di-*n*-butylacetal.

Similarly, a variety of dibenzhydroxamic acids were obtained from the reaction of corresponding hydroxamic acids with *n*-butyl vinyl ether or some other reagents. The results of all the experiments are summarized in Table II.

Formation of the Intermediate IV.—A mixture of benzhydroxamic acid (2.75 g. 0.02 mol.), *n*-butyl vinyl ether (2.0 g., 0.02 mol.) and 2 drops of phosphoric acid was warmed without a solvent at 50°C for an hour, and an adduct IV ($R = C_6H_5-$) was obtained as a viscous liquid. The infrared absorption bands of a carbon tetrachloride solution are at 3404 cm^{-1}(w) attributed to the free N-H group and at 3225 cm^{-1}(m) (broad) to the associated N-H group. Bands due either to the O-H group of hydroxamic acid or to the $C{=}CH_2$ group of vinyl ether were not observed. This intermediate IV decomposed to give dihydroxamic acid on heating, and even at room temperature it changed slowly to give dihydroxamic acid.

Formation of Isopropylidene-bis-benzhydroxamic Acid VII.—A mixture of benzhydroxamic acid

(2.75 g., 0.02 mol.) and isopropenyl ether (1.72 g., 0.02 mol.) in 10 ml. of ethyl acetate was refluxed for an hour in the presence of *p*-toluenesulfonic acid (0.03 g.). The solvent was removed under reduced pressure, and the residue was washed with ether and subsequently with warm water. It was then dried and weighed (1.1 g., m. p. 140~146°C). By fractional crystallization from ethyl acetate, 0.5 g. of VII (R = C_6H_5-, m. p. 160~161°C) and 0.1 g. of dibenzhydroxamic acid (m. p. 163~164°C) were obtained.

Found (for VII): C, 65.02; H, 5.89; N, 9.17. Calcd. for $C_{17}H_{18}N_2O_4$: C, 64.95; H, 5.77; N, 8.91%.

The infrared absorption bands are 3175 cm^{-1} m (broad), 2955s, 2890m, 1658s, 1592m, 1326m, 1205w, 1159m (Nujol or carbon tetrachloride solution).

Similarly, the same substance VII was obtained from the reaction of benzhydroxamic acid with acetone diethylketal in a good yield (75%), along with a trace of dibenzhydroxamic acid.

Summary

Dehydration reactions of hydroxamic acids with unsaturated ethers have been studied. The reaction of hydroxamic acids with ethoxyacetylene or methylketene diethylacetal led to the formation of corresponding isocyanates, along with ethyl acetate or ethyl propionate and ethanol, through the intermediate of addition compounds of hydroxamic acids and the dehydrating reagents.

The reaction of hydroxamic acids with *n*-butyl vinyl ether, on the other hand, led to the formation of dihydroxamic acids, along with acetaldoxime and acetaldehyde dibutylacetal. This type of reaction was further extended to the reactions of hydroxamic acids with propenyl ether, acetals and aldehydes, and the formation of dihydroxamic acids was confirmed.

Department of Chemistry
Tokyo Institute of Technology
Meguro-ku, Tokyo

The Cobalt(III) Complexes of Ethylenediaminediacetic and Ammoniadiacetic Acids[1]

By Motoshichi MORI, Muraji SHIBATA, Eishin KYUNO and Fukun MARUYAMA

(Received March 3, 1961)

In previous papers[2] of this series, some methods of preparation of the cobalt(III) complexes of ethylenediaminetetracetic acid and ammoniatriacetic acid were reported. The present paper is to report preparation of the cobalt(III) complexes of ethylenediaminediacetic and ammoniadiacetic acids. Since ethylenediaminediacetate ion commonly acts as a quadridentate ligand, the participation of its one molecule in the bonding to a cobalt(III) ion would be expected to be most regular. On the other hand, ammoniadiacetate ion usually acts as a tridentate ligand, and consequently the participation of the two molecules would seem most possible. Both of these possibilities are realized in this research.

1) Part VI : On the Syntheses of Metal Complexes. Previous paper on this series : V.: M. Mori, M. Shibata, E. Kyuno and M. Kanaya, This Bulletin, **34**, 1837 (1961). Presented at the 12th Annual Meeting of the Chemical Society of Japan, Tokyo, April, 1959.

2) M. Mori, M. Shibata, E. Kyuno and H. Nakajima, This Bulletin, **29**, 887 (1956); M. Mori, M. Shibata, E. Kyuno and Y. Okubo, ibid., **31**, 940 (1958).

Experimental

Chelating Agent. — Ethylenediaminediacetic acid (EDDA) was prepared by the action of monochloracetic acid on ethylenediamine. A solution of 10 g. monochloracetic acid in 10 ml. water was carefully neutralized with 17 g. of sodium bicarbonate, and then 7.5 g. of ethylenediamine (85%) was added to the solution. This was allowed to warm at about 50°C and a solution of 8 g. sodium hydroxide in 10 ml. water was added to it. After standing for few minutes, the solution was acidified with 6 N hydrochloric acid and then evaporated in vacuo, whereby some sodium chloride separated out. After the removal of the salt by filtration, two or three volumes of ethanol were added to the filtrate and the mixture kept in a refrigerator until white precipitates appeared. These were recrystallized from water. The nitrogen analysis and the potentiometric titration of this material gave satisfactory results for the desired ethylenediaminediacetic acid. Ammoniadiacetic acid (ADA) was provided by the Dojin Institute of Pharmaceutical Chemistry through the courtesy of Dr. K. Ueno.

Preparation. — *1) Potassium Bisammoniadiacetatocobaltate(III), $K[Co(ada)_2]\cdot 4H_2O$*.* — About 2 g. of ADA was suspended in 5 ml. of water, and the solution was neutralized with 2 g. of potassium bicarbonate. To this solution were added a solution of 2 g. $CoCl_2\cdot 6H_2O$ in a little water and 2 ml. of hydrogen peroxide (10%), and the mixture was warmed on a water bath to nearly 40°C, whereupon the color of the solution became red-violet. By cooling this solution in a refrigerator, red-violet crystals of the desired complex were obtained. Yield, about 0.5 g.

Found: Co, 14.7; N, 6.5. Calcd. for $K[Co(ada)_2]\cdot 4H_2O$: Co, 14.6; N, 6.49%.

*2) Potassium Carbonatoethylenediaminediacetatocobaltate(III), $K[Co(edda)(CO_3)]\cdot H_2O$***. — To a solution of the potassium tricarbonatocobaltate prepared by the method of a previous paper[3] were added equimoles of EDDA, and the mixture was warmed on a waterbath of 50°C for a few minutes. The resulting solution was evaporated in vacuo, whereby some salts were deposited. After the removal of these salts by filtration, about three volumes of ethanol were added to the filtrate, and it was kept in a refrigerator until red-violet crystals separated out.

Found: Co, 17.4. Calcd. for $K[Co(edda)(CO_3)]\cdot H_2O$: Co, 17.7%.

3) Ethylenediamminediacetatodiaquocobalt(III) perchlorate, $[Co(edda)(OH_2)_2]ClO_4$.—A solution of the carbonato-complex obtained in 2) was acidified with dilute hydrochloric acid, and then a certain amount of perchloric acid was added to it. After the removal of insoluble materials by filtration, the filtrate was treated in the same manner as mentioned in 2). In this case, some violet precipitates which may be regarded as the diaquo-complex were obtained, but the purity of the complex was not satisfactory.

Found: Co, 15.0. Calcd. for $[Co(edda)(OH_2)_2]\cdot ClO_4$: Co, 16.0%.

4) Potassium Dinitroethylenediaminediacetatocobaltate(III) $K[Co(edda)(NO_2)_2]\cdot H_2O$. — This was prepared by using the above-mentioned diaquo-complex. To a solution of the diaquo-complex was added the necessary amount of potassium nitrite, and the mixture was warmed to 50°C for some time until the color of the solution changed to yellow-brown. The solution was filtered once and the filtrate treated with ethanol in the same manner as mentioned in 2). The product was recrystallized from water in the form of red-brown prisms.

Found: Co, 15.2; N, 7.81. Calcd. for $K[Co(edda)(NO_2)_2]\cdot H_2O$: Co, 15.4; N, 7.36%.

For the determination of the chemical formulae of these complexes, chemical and thermal analyses, coagulation of ferric oxide sol and spectroscopic measurements were used in the same manner as described in previous papers[3,4].

Results and Discussion

Coagulation Value.—The values obtained in the present experiment were 4.1 mF for the $[Co(ada)_2]^-$, 3.4 mF for the $[Co(edda)(CO_3)]^-$, and 4.2 mF for the $[Co(edda)(NO_2)_2]^-$. These values were somewhat lower than the average value, 6.6 mF, for univalent complex anions, but far too high for that of bivalent anions (0.48 mF)[5]. Therefore, these complex anions may be regarded as univalent.

Absorption Spectra. — The visible and ultraviolet absorption spectra of these complexes are shown in Fig. 1 and the numerical data are given in Table I. Based upon these data, some discussion is possible about the geometrical structures of the complexes. In the case of the $[Co(ada)_2]^-$, two geometrically different structures, cis and trans in respect to the coordinated nitrogen atoms, are possible,

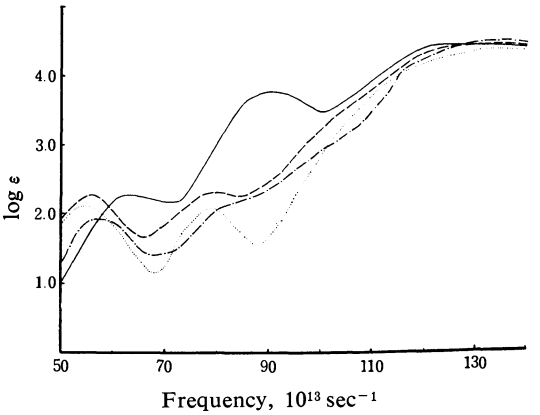
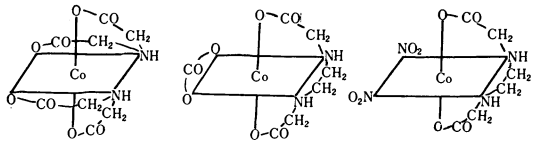


Fig. 1. Absorption spectra of:
·····: $K[Co(ada)_2]\cdot 4H_2O$
—·—·: $K[Co(edda)CO_3]\cdot H_2O$
– – –: $[Co(edda)(OH_2)_2]ClO_4$
———: $K[Co(edda)(NO_2)_2]\cdot H_2O$

TABLE I. ABSORPTION MAXIMA AND log ε (10^{13}/sec.)

	ν_1	log ε_1	ν_2 or ν_{sp}	log(ε_2 or ε_{sp})	ν_3	log ε_3
$K[Co(ada)_2]\cdot 4H_2O$	53.8	2.13	79.4	2.08	134.5	4.40
$K[Co(edda)(CO_3)]\cdot H_2O$	57.0	1.94	79.0	2.08	136.4	4.38
$[Co(edda)(OH_2)_2]ClO_4$	55.4	2.27	79.8	2.30	132.1	4.49
$K[Co(edda)(NO_2)_2]\cdot H_2O$	62.8	2.29	90.4	3.74	122.5	4.47

* "ada" stands for ammoniadiacetate ion.
** "edda" stands for ethylenediaminediacetate ion.
3) M. Mori, M. Shibata, E. Kyuno and T. Adachi, This Bulletin, **29**, 883 (1956).
4) M. Mori, M. Shibata, E. Kyuno and K. Hoshiyama, This Bulletin, **31**, 291 (1958).
5) S. Nakahara, K. Nakamoto and R. Tsuchida, *J. Chem. Soc. Japan, Pure Chem. Sec.* (*Nippon Kagaku Zasshi*), **74**, 488 (1953).



a b c

Fig. 2. Probable structures.

but the cis structure illustrated by a in Fig. 2 must be adopted for the present complex ion because the absorption maxima of this complex ion are similar to those of the α-$[Co(NH_3)_2 \cdot (C_2O_4)_2]^-$ regarded as cis isomer in the previous paper[4]. As the most probable structure, formula b in the figure may be assigned to the $[Co(edda)(CO_3)]^-$, because ethylenediaminediacetate ion usually acts as a quadridentate ligand and carbonate ion as a bidentate ligand. The dinitro-complex ion $[Co(edda)(NO_2)_2]^-$ which can be derived from the corresponding carbonatocomplex, probably has a structure illustrated by c. Evidence for the validity of this assignment lies in the fact that the absorption maxima of this complex ion are more similar to those of the cis isomer of the [Co en ox$(NO_2)_2]^-$ [6]. For *cis*-[Co en ox$(NO_2)_2]^-$: ν_1, 63.3; ν_{sp}, 90.9; ν_3, 121.0. For *trans*-[Co en ox$(NO_2)_2]^-$: ν_1, 63.3; ν_{sp}, 85.7; ν_3, 116.3.

In order to check the coordination of the carboxylate ions, the infrared spectra of the $K[Co(ada)_2] \cdot 4H_2O$ and the $K[Co(edda)(NO_2)_2] \cdot H_2O$ as well as the free acids of the chelating agents were measured. For the ammoniadiacetic acid, strong split bands were observed at 1718 and 1585 cm^{-1}, and for the ethylenediaminediacetic acid, at 1721 and 1605 cm^{-1}. On the other hand, the ammoniadiacetato- and the ethylenediaminediacetato-complex showed strong absorption arising from the coordinated carboxylate ions at 1623 and 1619 cm^{-1} respectively.

Table II is a summary of the absorption maxima of the first bands for several complexes which belong to the $[CoN_2 \cdot O_4]$-type and which are also regarded as cis form with respect to the coordinated nitrogen atoms. Among these complexes, the tetraaquo-complexes $[Co(NH_3)_2(OH_2)_4](ClO_4)_3$ and [Co en $(OH_2)_4](ClO_4)_3$ were prepared from the corresponding dichlorodiaquo-complexes[7] by treating with glacial acetic acid. Both of these were quite hygroscopic and difficult to be isolated as crystals, but the complex ions were completely held on a cation exchanger from the solutions. If the maximum value ν_1^0 for the $[Co(NH_3)_2(OH_2)_4]^{3+}$ is chosen as a standard absorption for the $[CoN_2 \cdot O_4]$-type complexes, the deviations of the maximum values for the other complexes from this standard value, $\alpha = \nu_1^0 - \nu_1$, may be regarded as a measure for the chelation effect.

Table II. Absorption maxima of $[CoN_2 \cdot O_4]$-type complexes

		ν_1	α
1	$[Co(NH_3)_2(CO_3)_2]^-$	52.2	1.3
2	$[Co\ en(CO_3)_2]^-$	53.2	0.3
3	$[Co(NH_3)_2\ ox\ CO_3]^-$	53.4	0.1
4	$[Co(NH_3)_2(OH_2)_4]^{3+}$	53.5	0
5	$[Co(ada)_2]^-$	53.8	−0.3
6	$[Co(NH_3)_2\ ox_2]^-$	54.4	−0.9
7	$[Co\ en(OH_2)_4]^{3+}$	54.8	−1.2
8	$[Co\ en\ ox_2]^-$	55.6	−2.1
9	$[Co(edta)]^-$	55.9	−2.4
10	$[Co(edda)(CO_3)]^-$	57.0	−3.5

Summary

The cobalt(III) complexes containing ammoniadiacetate group (ada) and ethylene diaminediacetate group (edda) have been prepared:

1) $K[Co(ada)_2] \cdot 4H_2O$ Red-violet
2) $K[Co(edda)(CO_3)] \cdot H_2O$ Red-violet
3) $[Co(edda)(OH_2)_2]ClO_4$ Violet
4) $K[Co(edda)(NO_2)_2] \cdot H_2O$ Yellow-brown

The visible and the ultraviolet absorption spectra as well as the infrared spectra of these complexes have been measured and discussed in relation to the structures of these complex ions.

Department of Chemistry
Faculty of Science
Kanazawa University, Kanazawa

6) E. Kyuno, ibid., **80**, 981 (1959).

7) E. Kyuno, ibid., **80**, 724 (1959).

Physicochemical Studies on Cobalt Salts of Higher Fatty Acids. V. Appearances, Densities, and X-Ray Analysis of Crystal Structures of Cobalt Soaps

By Hirotaro KAMBE*

(Received March 15, 1961)

In the previous papers of this study[1], three species of cobalt soap with different colors were investigated. They differ so much from each other to the eye and also, more especially, to the touch, that their crystallinities must be distinguishable. In the present parer, microphotographs of their appearances are shown, and apparent densities in air and in acetone, and true densities are measured. Moreover, X-ray analysis of these soaps is carried out.

X-Ray analysis of cobalt stearate and palmitate was executed by Vold and Hattiangdi[2]. However, as they had dried their soaps in an oven, their samples perhaps took a melted form which showed only an amorphous halo in the X-ray pattern. Our soaps, prepared in cold, are truly crystalline. But unfortunately, no adequate solvent was found for them, so single crystals of cobalt soaps have not yet been obtained. Complete X-ray analysis of their crystal structures must be reserved for the future.

Experimental

Materials. — The same cobalt stearates in three typical colors were used, as in the previous papers[1].

Microphotography.—Soap powder, passed through a sieve of 100 meshes per inch, was scattered on a glass plate in the field of a microscope. Microphotographs of 300 magnifications were taken with transmitted light.

Density Measurement. — The apparent packing densities of cobalt soap powders in air were measured in a graduated glass tube. Apparent volume was measured directly after the settling of the powder and after a gentle tapping of about 300 times. Finally the tube was inverted and the packing of the powder was observed. The sedimentation volume of soap powder in acetone was measured with the lapse of time in the same tube. Apparent densities in acetone were calculated. True densities of powder were measured with a substitution method in acetone. Acetone was chosen because the color of soaps did not change at all in it.

Powder X-Ray Analysis. — Debye-Scherrer's method was applied to soap powders*2. Powder was pushed into a glass capillary and extruded by a wire. A cylinder formed by soap with a length of 1~2 mm. and a diameter of about 0.5 mm. was barely attached to a sample holder at the center of a cylindrical camera. The camera radius, R, was 57.44 mm. The radiation used was CuKα with a nickel filter.

X-Ray diffraction patterns were analyzed with a microphotometer, and the diffraction angle θ was calculated by the formula:

$$L=2\theta\cdot R \qquad (1)$$

in which L is the distance of a diffraction line from the center of the film. Lattice spacing d was calculated by Bragg's formula:

$$2d\sin\theta=n\lambda \qquad (2)$$

in which n is an order of diffraction, λ is a wavelength of incident X-rays; in this case $\lambda(\mathrm{CuK}\alpha)=1.539$ Å.

Results and Discussion

Appearances.—Blue cobalt stearate was clearly crystalline and easily removable from filter paper in a dry state, but it was hard to pulverize it. Pink soap was rather plastic to the touch, like fatty acid, and adhered to filter paper after drying. Often it was charged electrically when it was removed from filter paper. When pulverized, it became a fluffy powder. Red soap was most easily pulverized, did not stick together, and freely flowed.

Crystal forms of powdered red and blue cobalt stearates are shown in microphotographs in Fig. 1. In blue soap powder some prismatic crystals are found, but in red soap only plate-like crystals exist in the field. Crystal forms of red soap are very similar to that of stearic acid.

Densities.—The apparent densities of cobalt stearates with different colors were distinguishable from each other. Packing densities in air are shown in Table I. In this state blue soap is much denser than red soap, and pink soap is between them. This is because of the difference in their crystalline forms.

*1 Present address: Aeronautical Research Institute, the University of Tokyo, Meguro-ku, Tokyo.

1) H. Kambe, This Bulletin, **34**, 1786, 1790, 1794 (1961); H. Kambe and I. Mita, ibid., **34**, 1797 (1961).

2) R. D. Vold and G. S. Hattiangdi, *Ind. Eng. Chem.*, **41**, 2311 (1949).

*2 X-Ray measurements were carried out at Physics Department, Inst. Sci. Techn., following the advice of Mr. T. Sakurai.

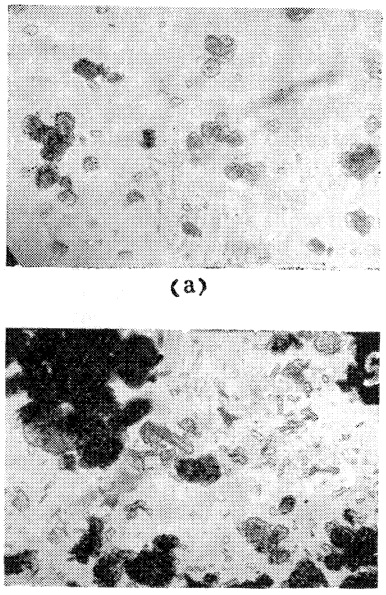


Fig. 1. Appearances of cobalt stearate crystals.
(a) Red dihydrate; (b) Blue anhydrate

TABLE I. APPARENT DENSITIES OF COBALT STEARATE POWDERS IN AIR (g./ml.)

Color of cobalt soap	After settling	After tapping 300 times	After inversion
Blue	0.195	0.333	0.221
Red	0.150	0.246	0.149
Pink	0.173	0.278	0.179

The apparent densities in acetone are shown in Table II. Sedimentation volumes of cobalt soaps in acetone gradually become smaller. In this case, the density of the blue form is also the highest, as in air. But red and pink soaps reverse their densities in acetone and air. Red form was apparently much denser in acetone.

True densities, measured with a substitution method in acetone at 25°C, are tabulated in Table III. It is found that the density of red soap is slightly larger than that of blue soap, in contrast with the apparent densities. This may be due to the difference in their crystalline structure.

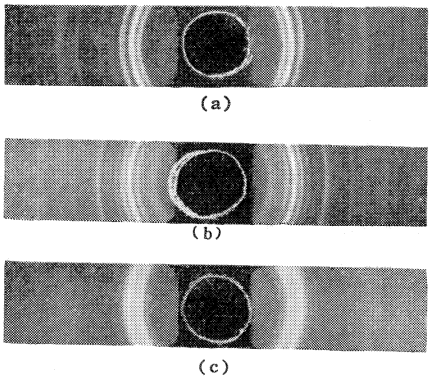


Fig. 2. X-Ray diffraction patterns of cobalt soaps.
(a) Stearic acid; (b) Red cobalt stearate dihydrate; (c) Blue cobalt stearate anhydrate

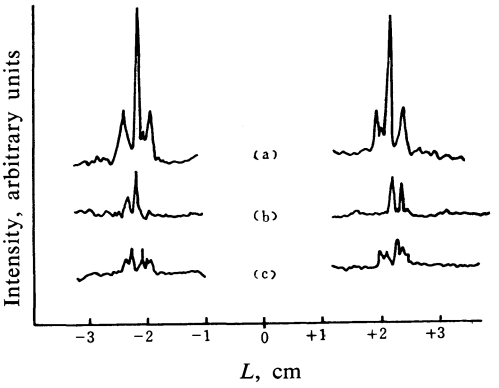


Fig. 3. Microphotometric curves of X-ray patterns.
(a) Stearic acid; (b) Red cobalt stearate dihydrate; (c) Blue cobalt stearate anhydrate

X-Ray Analysis. — The X-ray diffraction patterns of blue and red cobalt soaps and stearic acid are shown in Fig. 2, and their microphotometric curves are shown in Fig. 3. The main diffraction lines are tabulated in Table IV.

Red soap shows a pattern which is very

TABLE II. APPARENT DENSITIES OF COBALT STEARATE POWDERS IN ACETONE (g./ml.)

Color of cobalt soap	Weight, g.		Directly	After				
	Soap	Acetone		20 min.	2 hr.	4.5 hr.	2 days	6 days
Blue	1.015	6.871	0.139	0.156	0.171	0.181	0.209	0.228
Red	0.468	7.253	0.096	0.170	0.184	0.195	0.204	0.213
Pink	0.934	7.080	0.139	0.144	0.144	0.148	0.158	0.164

TABLE III. TRUE DENSITIES OF COBALT STEARATES (25°C)

Red soap:	1.251, 1.321, 1.229, 1.232, 1.281	Av. 1.263
Blue soap:	1.185, 1.222, 1.207, 1.304, 1.195, 1.199, 1.187, 1.205	Av. 1.213

TABLE IV. X-RAY DIFFRACTION LINES OF TYPICAL COBALT STEARATES AND STEARIC ACID*1

Stearic acid*2			Red soap			Blue soap	
	$\sin\theta$	d/n		$\sin\theta$	d/n	$\sin\theta$	d/n
w	0.092	8.37*3					
m	0.169	4.56	(4.12)*4	w 0.129	5.97*3		
w	0.178	4.32		w 0.172	4.47	(4.04)*4	
vs	0.187	4.12		s 0.190	4.05	s 0.171	4.50
s	0.208	3.70		m 0.205	3.75	s 0.178	4.32
w	0.236	3.26		w 0.217	3.54	s 0.182	4.23
w	0.273	2.82		w 0.241	3.19	vs 0.198	3.89
w	0.311	2.47		w 0.260	2.96	s 0.205	3.75
				w 0.274	2.81	s 0.208	3.70

*1 s: strong; vs: very strong; m: medium; w: weak.
*2 Without nickel filter.
*3 Higher order of long spacing.
*4 The values in parentheses were calculated as CuKβ (λ=1.389 Å) diffraction. These lines were weakened by a nickel filter.

similar to that of stearic acid. It is characteristic of this pattern that a strong line exists between two medium lines, the inner one of which was weakened by the attachment of a nickel filter. Blue soap shows a quite different pattern, in which two groups of strong lines are characteristic.

Fatty acid and its derivatives usually exhibit crystals of a monoclinic system. Their crystal structure is composed alternately of ionic layers and hydrocarbon layers, stacked on one another. The resemblance of the X-ray pattern of red soap to that of fatty acid means that this species also has such a layer structure. Pink soap also shows such a layer structure pattern, and so it is evident that there is a similarity of structure between these soaps. The water molecules contained in red dihydrate must be attached directly to cobalt ion. The coordination number of six, which has been found by magnetic measurement on red soap[1], must be fulfilled by joining two cobalt ions together by carboxylate ions. Such a structure has been proposed by Stanley[3] for calcium stearate monohydrate.

It is certain, because of the difference in coordination numbers and X-ray patterns, that blue soap has a different structure from pink and red soaps, but X-ray analysis of crystals has not yet been executed on single crystals. The confirmation of the exact crystal structure must therefore be postponed.

Purple soaps, which were obtained from red or pink soaps immersed in absolute ethanol, showed a diffraction pattern from the blue type, but violet soap, which was half turning red from blue, showed a red-type pattern. Melted soap always showed a diffuse halo, as shown by Vold and Hattiangdi[2].

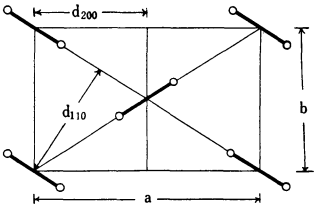


Fig. 4. Schematic diagram of a besal plane of unit cell in red cobalt stearate dihydrate. Dumbbells show orientations of paraffinic chains in crystal lattice.

The diffraction pattern of red soap was analyzed in the same way as Müller[4] had done on normal paraffins. A basal plane of paraffinic lattice may be described as Fig. 4. A lattice spacing obtained from the most intense diffraction line in an X-ray pattern of this type was identified as d_{110}; the outer medium line was d_{200}, and the inner medium CuKβ-diffraction of d_{110}, which was weakened line was by a nickel filter.

From the observed values of diffraction angles in red soap, d_{110}=4.05 Å and d_{200}=3.75 Å. From these, the lattice constants of red cobalt stearate were calculated as $a=2d_{200}$=7.50 Å, and b=4.81 Å. In the same way, stearic acid shows d_{110}=4.12 and d_{200}=3.70 Å. Therefore, in stearic acid, a=7.40 and b=4.96 Å. The lattice of red soap is broadened a little along the b axis and shortened along the a axis compared with acid.

Summary

Crystallinities of cobalt stearates with different colors have been compared. Blue soap

3) E. Stanley, *Nature*, **175**, 165 (1955).

4) A. Müller, *Proc. Roy. Soc.*, **A138**, 514 (1932).

shows a prismatic crystal form, but red soap a plate-like form. The apparent density of blue soap in air is much denser than other soaps. Red soap shows a larger density in acetone than in air. True densities measured in acetone show that the density of red soap is higher than that of blue soap.

X-Ray diffraction patterns show the difference between red or pink soap and blue soap. Red soap has a lamellar structure like that of fatty acid, while blue soap shows a quite different structure. Exact X-ray analysis was not executed, however, because single crystals of cobalt soaps have not yet been obtained.

The author wishes to express his thanks to Professor Bunnosuke Yamaguchi for his kind advice throughout this work, and to Mr. Toshio Sakurai for his cooperation in X-ray measurements. He is also indebted to Mr. Masami Ozaki for microphotography.

Institute for Science and Technology
The University of Tokyo
Meguro-ku, Tokyo

Physicochemical Studies on Cobalt Salts of Higher Fatty Acids. VI. Some Observations on Thermal Transitions of Cobalt Soaps, by Differential Thermal Analysis, Thermogravimetry, and Magnetic Measurement

By Hirotaro KAMBE*1, Takeo OZAWA*2, Masao ONOUE*3 and Shoichi IGARASHI*1

(Received March 29, 1961)

Cobalt soaps with different colors, obtained and examined in previous papers[1], are crystalline at room temperatures, but they melt at higher temperatures. In the present paper, their melting behaviors are investigated by differential thermal analysis, thermogravimetry, and the measurement of magnetic susceptibility at various temperatures.

Cobalt soap decomposes at extremely high temperatures. Thermogravimetric analysis is applied also to this process.

Soap which has been cooled from a molten state takes the form of a glassy mass. The characteristics of once-melted soap are examined by reflection spectroscopy, X-ray analysis, and the measurement of magnetic moment.

Experimental

Materials.—Cobalt stearate with different colors were used as in the previous papers[1].

Differential Thermal Analysis.—Soap sample and liquid paraffin, as a reference, were heated simultaneously in coaxial cylinder cells of stainless steel, as Vold has described[2]. Cells were put into holes of a copper block placed at the center of a vertical electric furnace, within an atmosphere of nitrogen. The difference of temperature between sample and reference was measured by a thermocouple of chromel-constantan with two pairs in series. Differential thermo-electric motive force was recorded on the chart of an electric recorder through a D. C. amplifier.

The temperature of the electric furnace was elevated continuously by a program controller at a constant heating rate of 2/3°C/min. The furnace temperature was measured by another thermocouple of chromel-alumel and directly recorded on the same chart as the record of differential temperature. Cooling curves were taken on free cooling.

Thermogravimetry. — An automatic recording thermobalance, with a differential transformer as a detector of the elongation of a spring balance, which will be described elsewhere, was used to record the weight changes during the elevation of the sample temperature at a constant rate of heating of 1°C/min. within an atmosphere of nitrogen. The weight changes by dehydration and by decomposition of cobalt soaps were observed. The sample weight was about 90 mg.

Magnetic Measurement.—Magnetic susceptibilities at various temperatures were measured with Gouy's method*4. Magnetic moments were calculated as in Part IV[1].

*1 Present address : Aeronautical Research Institute, The University of Tokyo.
*2 Present address : Electrotechnical Laboratory, Tanashi, Tokyo.
*3 Present address : Daido Kogyo Co., Nishi-ku, Osaka.
1) H. Kambe, This Bulletin, 34, 1786, 1790, 1794 (1961); 35, 78 (1962); H. Kambe and I. Mita, ibid., 34, 1797 (1961).
2) M. J. Vold, *Anal. Chem.*, 21, 683 (1949).

*4 Magnetic measurements were executed by Mr. H. Honda, at the Resources Research Institute, and by Dr. Y. Matsunaga, at the Department of Chemistry, Faculty of Science, The University of Tokyo.

Reflection Spectroscopy and X-Ray Analysis.—These measurements were carried out as in Parts III and V[1].

Results and Discussion

Differential Thermal Analysis.—Differential thermograms of cobalt stearates are shown in Figs. 1—3. Heating curves at a constant rate of heating and cooling curves at free cooling are shown on opposite sides of the base lines.

Blue anhydrous cobalt stearate (Fig. 1) showed two peaks at 99 and 108°C in the first heating curve, while on cooling two peaks appeared at 89 and 47°C. When cooled soap was heated again, it showed a low-temperature peak at 54C° and two high-temperature peaks at 90 and 100°C. The former of the high-temperature peaks was smaller than in the first heating curve, and the low-temperature peak appeared as a substitute for it.

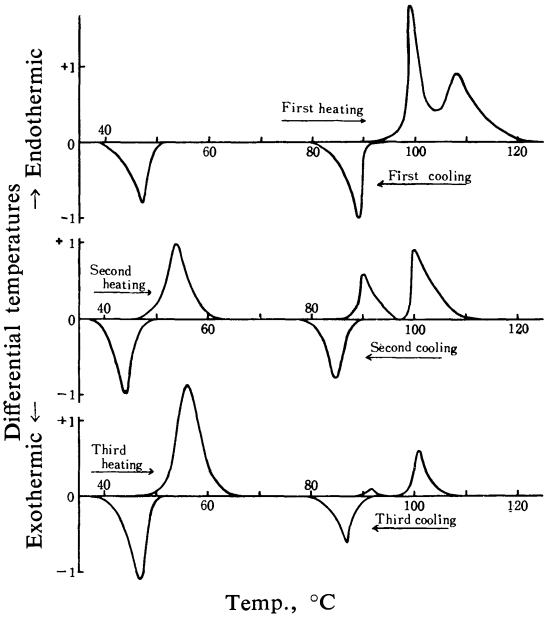


Fig. 1 Differential thermograms of blue cobalt stearate anhydrate. Heating rate: 2/3°C/min.

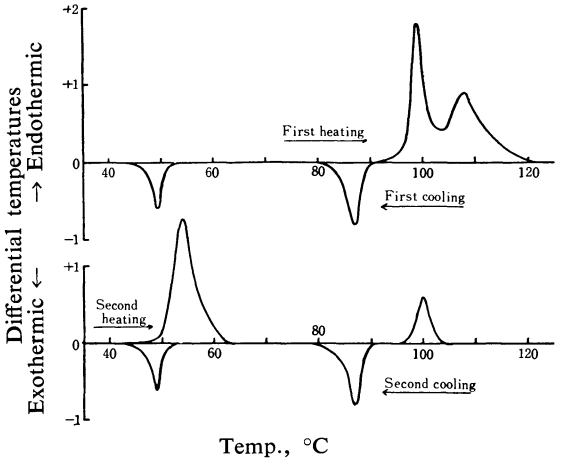


Fig. 2. Differential thermograms of blue cobalt stearate anhydrate. First cooling was done after heating at 120°C for one hour.

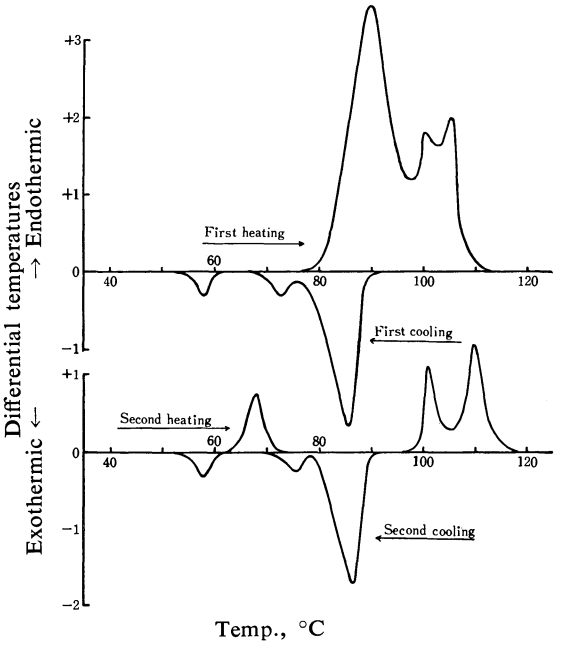


Fig. 3. Differential thermograms of red cobalt stearate dihydrate.

When the twice melted soap was cooled again, two peaks appeared at 85 and 44°C in the cooling curve. The soap generally showed a tendency to be supercooled in cooling curves, and peaks appeared at considerably lower temperatures than in heating curves. The high-temperature peak was not divided into two peaks, as in heating curves.

At the third heating, the low-temperature peak at 46°C was magnified, while the first high-temperature peak almost disappeared. On cooling two peaks appeared at 87 and 47°C.

From these facts, it is concluded that heating has the effect of reducing the high-temperature peaks, especially the lower of them, and extending the low-temperature peak. During heating, the mechanism of the first high-temperature transition might be replaced by that of a low-temperature transition.

When blue cobalt soap was held at 120°C for one hour, this process was advanced considerably, as shown in Fig. 2. In Fig. 2, the first heating and subsequent cooling curves were similar to that in Fig. 1, but in the second heating the low-temperature peak was much

intensified, while the first high-temperature peak disappeared completely, as had been expected.

In the first heating curve, red cobalt stearate dihydrate (Fig. 3) showed a very large peak at 90°C and two high-temperature peaks at 100 and 110°C, as did blue soap. On cooling, a low-temperature peak appeared at 58°C and the high-temperature peaks were displaced to 86°C and 76°C. In the cooling curve of red soap, the high-temperature peak was also divided into two peaks as in heating, in contrast with blue soap. In the second heating curve, a low-temperature peak clearly appeared, while high temperature peaks became smaller although they remained as they were.

In red soap the large peak at 90°C in the first heating curve must correspond to dehydration. This was confirmed by thermogravimetry, as will be discussed below.

Koenig[3] measured visually the melting point of cobalt stearate as 73~75°C. Hattiangdi, Vold and Vold[4] carried out a differential thermal analysis of cobalt soaps by heating at rate of 1.5°C/min. until 150°C, above which decomposition of the soap was feared. They found transition points at 59°C(ΔH=13440 cal./mol.) and at 92°C(probably second-order transition) in cobalt stearate. They also described the visual melting point of cobalt stearate as 80°C. In a free cooling curve, they found only a transition at 57°C. Their sample was perhaps a melted amorphous form, as Vold and Hattiangdi[5] observed only an amorphous halo in a powder X-ray pattern of this soap, as stated in Part V[1]. The peaks obtained by them might correspond to our low-temperatue peak and second high-temperature peak.

Hattiangdi, Vold and Vold[4] have concluded that cobalt soaps are in a mesomorphic state at room temperatures. A revised mechanism of the phase transitions of cobalt soap is proposed as follows:

Crystalline blue anhydrous soap melts at first heating in two stages. The first transition, which may be called premelting, is a phase transition from a crystalline to a plastic mesomorphic state, while the second transition corresponds to true melting. When blue soap is cooled from a melted state, it transforms to an (upper) mesomorphic state with some supercooling, but at a lower temperature a second transition occurs and the soap phase changes to a lower mesomorphic state.

At the second heating, soap transforms from a lower mesomorphic state to an upper mesomorphic state at low temperature transition, as described before. At a higher temperature region, the same two peaks appear as in the first heating. The first of them becomes smaller, however.

It is concluded, therefore, that although the upper transition peak was not apparently divided into two peaks in the first cooling curve, some of soap was transformed from an upper mesomorphic state to a true crystalline form, and it appeared in the second heating curve as a smaller first high-temperature peak. Repeated or prolonged melting suppressed this transition so much that the first high-temperature peak was faded markedly, while the low-temperature peak became eminent.

Crystalline red cobalt stearate shows a large dehydration peak, but thereafter it behaves as an anhydrous soap. The following processes are completely similar to those in the anhydrous blue soap. However, it shows high-temperature peak in the cooling curve, in contrast to blue soap.

Thermogravimetry.—Thermogravimetric curves of blue cobalt stearate anhydrate and red dihydrate are shown in Figs. 4 and 5. In these curves the weight loss (%) observed is plotted

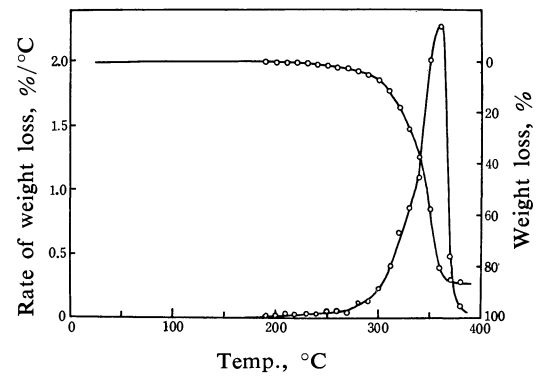


Fig. 4. Thermogravimetric curve of blue cobalt stearate anhydrate.

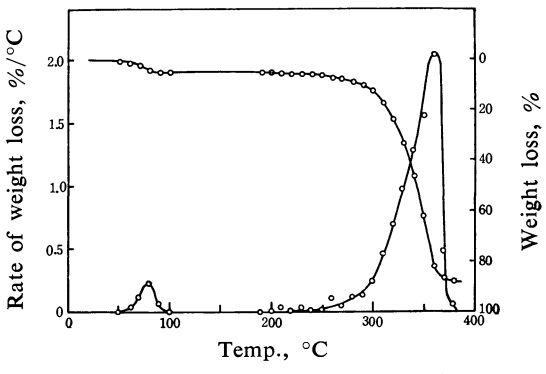


Fig. 5. Thermogravimetric curve of red cobalt stearate dihydrate.

3) A. E. Koenig, *J. Am. Chem. Soc.*, **36**, 931 (1914).
4) G. S. Hattiangdi, M. J. Vold and R. D. Vold, *Ind. Eng. Chem.*, **41**, 2320 (1949).
5) R. D. Vold and G. S. Hattiangdi, ibid., **41**, 2311 (1949).

against temperature. The rate of weight loss (%/°C) was obtained by a graphical differentiation of weight loss curve and is also plotted in the same figure.

Blue soap (Fig. 4) did not show any weight loss at the melting point, but red soap (Fig. 5) showed a weight loss of about 4.4% at about 80°C. Even if somewhat smaller, this is correspondent with the loss of hydrate water from cobalt stearate dihydrate (calcd. 5.46%). This process is also correspondent with the first large peak of differential thermogram of red soap.

Differential thermogravimetric curves of both soaps showed a significant weight loss, which commenced at about 200°C and reached a maximum rate of weight loss at about 360°C. This weight loss is evidently caused by the decomposition of soap. In this process some white crystalline powder was condensed at the cold part of a glass tube, which enveloped an inert atmosphere around the sample. This powder melts at 87.5~88.5°C. This was identified with stearone $(C_{17}H_{35})_2CO$, the melting point of which is 88.5°C. In the sample cell remained a black mass, which was identified as cobalt oxide.

Magnetic Measurement. — The reciprocal molar susceptibility of red cobalt soap was plotted against temperature, as shown in Fig. 6. It was found that the magnetic susceptibility of cobalt soap changed abruptly at the melting point. Below this temperature, Curie's law

$$\chi_M = \frac{C}{T} \qquad (1)$$

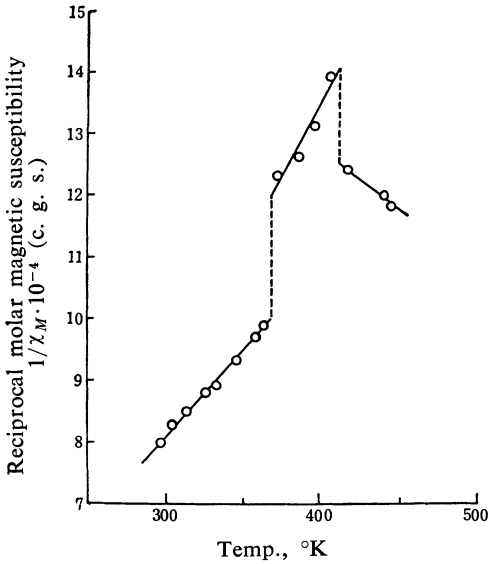


Fig. 6. Temperature dependence of magnetic susceptibility of red cobalt stearate dihydrate.

where C is a constant, held.

Herron and Pink[6] measured the thermal change of the magnetic susceptibility of cobalt soaps and found that Curie-Weiss' law

$$\chi_M = \frac{C}{T-\theta} \qquad (2)$$

where C and θ are constants, held below 320°K. They obtained Weiss' temperature $-\theta$ as 18.5°K in cobalt stearate. It is difficult to estimate Weiss' temperature from our experiments, which were conducted only above room temperatures.

Properties of Melted Soap.—When cobalt soap was cooled from its melted state, it took a mesomorphic state, as stated above. An X-ray diffraction pattern of melted soap is shown in Fig. 7. It is evident that there is only an amorphous halo, as Vold and Hattiangdi[5] pointed out. The color of melted soap is dark red. Its reflection curve is shown in Fig. 8, where its dominant wavelength is 546c mμ, its purity is 18%, and its brightness is 34.95% (cf. Part III[1]). The color is like that of red soap rather than blue soap. This is because the ground state of the spectral terms is seriously affected by the change of the crystal field on melting. The magnetic moment of melted cobalt stearate, calculated as in Part IV[1], was



Fig. 7. X-Ray diffraction pattern of melted cobalt stearate.

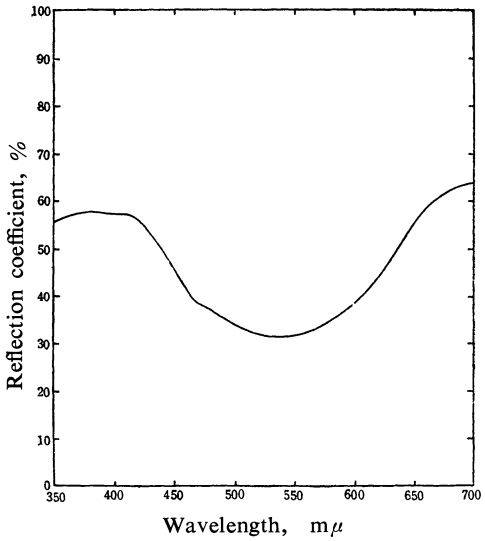


Fig. 8. Reflection curve of cobalt stearate, cooled from melt.

6) R. C. Herron and R. C. Pink, *J. Chem. Soc.*, **1956**, 3948.

4.86 B. M., in which there is a considerable orbital contribution.

Summary

The thermal transitions of red dihydrate and blue anhydrate of cobalt stearate have been measured by differential thermal analysis, thermogravimetry, and magnetic measurement.

Differential thermograms of anhydrous blue soap showed two peaks at high temperatures (about 100°C). When it was heated repeatedly, a new peak appeared at a lower temperature (about 50°C). A low temperature transition is considered to be a transition between mesomorphic phases. The first high-temperature transition corresponds to a transition from a crystalline to an upper mesomorphic state, which disappeared on repeated heating. Red dihydrate soap showed a large peak at 90°C owing to the removal of hydration water. Thereafter it appeared in an anhydrous state.

Thermogravimetric analysis showed the dehydration process in red soap, but not in blue anhydrate. The decomposition of cobalt stearates to stearone and cobalt oxide was found in thermogravimetric curves.

The magnetic susceptibility of cobalt soap obeys Curie-Weiss' law below the melting temperature, but above it the susceptibility decreases abruptly and anomalous behavior is observed.

Melted soap is in an amorphous state, which was certified by X-ray measurement. Its color and magnetic moment show that melted soap is different in nature from red and blue soaps.

The authors wish to express their gratitude to Professor Bunnosuke Yamaguchi for his advice throughout this work, and to Dr. Hidemasa Honda and Dr. Yoshio Matsunaga for their accomplishments in magnetic measurement.

Institute for Science and Technology
and Aeronautical Research Institute
The University of Tokyo
Meguro-ku, Tokyo

Molecular Association and the Dielectric Constant of a Solution

By Ko KIMURA and Ryoichi FUJISHIRO

(Received May 12, 1961)

It may be expected that much useful information about the intermolecular force is obtained by an examination of the dielectric behavior of solutions. Only a few studies based on this point of view have been carried out because of the difficulty of taking into account the contributions of both the long- and short-range intermolecular forces to the dielectric constant of a solution. Buckingham and Raas[1] tried to examine the short-range intermolecular force between solutes by the help of the dielectric virial coefficients of solutions. They showed that, to some extent, the dielectric virial coefficients gave valuable information about the intermolecular configuration as well as the intermolecular force. The results obtained by them agree fairly well with spectroscopic data, but some questions still remain about the application of the virial expansion method[2] of the total dielectric polarization of a gas to solutions.

In this report, the dimerization of a nitrocompound in carbon tetrachloride will be discussed in detail, because De Maine et al.[3] suggested from spectroscopic measurements the dimerization of nitromethane due to the charge transfer force in solutions. Unfortunately, the dielectric constants of the concentrated solutions, as well as the pure liquid of nitromethane, varied with time during the measurements. This was probably due to the isomerization of nitromethane to methylnitrite[4]. Hence, this article describes the dimerization of nitrobenzene (instead of nitromethane) in carbon tetrachloride, which dimerization is estimated on the basis of some assumptions from the observed dielectric constant of the solution.

1) A. D. Buckingham and R. E. Raas, *Trans. Faraday Soc.*, **55**, 377 (1959).
2) A. D. Buckingham and J. A. Pople, ibid., **51**, 1029 (1955).
3) P. A. D. De Maine, M. M. De Maine and A. G. Golbe, ibid., **53**, 427 (1957).
4) G. Geiseler und M. Rätzsch, *Z. physik. Chem.* [*N. F.*], **26**, 131 (1960).

Experimental

The apparatus for the dielectric measurement has already been described elsewhere[5]. The dielectric cell used in this work was of a Sayce-Briscoe type, the electric capacity of which was about 5 pF. All material were purified according to standard methods[6].

Experimental Results

The dielectric constant of the mixture of nitrobenzene and carbon tetrachloride has already been measured by some authors[7], but we repeated the measurement in order to examine the temperature dependence of the dielectric constant of the solution. The observed results are shown in Table I.

TABLE I. THE DIELECTRIC CONSTANTS ε OF SOLUTIONS

Mol. fraction of nitrobenzene x	ε(25°C)	ε(40°C)	x	ε(60°C)
0	2.23	2.20	0	2.17
0.0610	3.52	3.39	0.0160	3.26
0.1277	5.06	4.83	0.1277	4.57
0.2712	8.82	8.32	0.2712	7.74
0.3613	11.39	10.68	0.3613	9.88
0.4712	14.76	13.79	0.4890	13.23
0.6995	22.45	20.85	0.5997	16.30
0.7966	26.04	24.15	0.7323	20.18
0.8467	27.95	25.87	0.8382	23.46
1	34.16	31.47	1	28.76

Discussion

Determination of the Formation Constant of the Nitrobenzene Dimer in the Solution from the Observed Dielectric Data.—We can roughly estimate the formation constant K of the nitrobenzene dimer in the solution from the observed dielectric constant on the assumption that the difference between the observed dielectric constant and the calculated one obtained by the use of Scholte's model[8] is due to molecular association. We regard the monomer and the dimer of nitrobenzene as spheroidal in form and consider the spheroidal cavity of the molecular dimension in the dielectric. The surroundings of the spheroidal cavity are replaced as usual by the continuum of the macroscopic dielectric constant. The point dipole is located along the long axis. The dipole moment of the dimer is zero or twice the monomer moment according to the antiparallel or the parallel orientation of two dipoles. The long and short axes of the spheroids for the monomer and for the dimer are determined by the atomic distances and van der Waals radii of constituent atoms of a nitrobenzene molecule. Those for the monomer are easily obtained, whereas those for the dimer can not be obtained without assuming a tentative configuration for the dimer. In order to make the observed dielectric constant agree with the calculated one, only the parallel orientation of two dipoles is allowed for the configuration of the dimer. Therefore, we calculated the formation constant in each concentration by assuming some plausible configuration for the dimer with the parallel orientation of two dipoles. The most probable configuration of the dimer would indicate a small dependence of K on concentrations. Formulas required for this calculation are derived in quite the same way as in a paper already published[9].

When we use 0, 1 and 2 as suffixes expressing the nonpolar solvent, the monomer and the dimer, respectively, we obtain the following formula:

$$\varepsilon-1=4\pi\left[\sum_{i=1}^{2}N_i\frac{\varepsilon}{\varepsilon+(1-\varepsilon)A_i}\left\{\frac{\mu_i^2}{(1-\alpha_i g_i)^2 3\boldsymbol{k}T}+\frac{\alpha_i}{1-\alpha_i g_i}\right\}+N_0\frac{\varepsilon(n_0^2-1)}{2\varepsilon+n_0^2}a_0^3\right] \quad (1)$$

in which the notations are the same as those used in the previous paper[9]. In calculating N_1 and N_2 from Eq. 1, polarizability α_2 was assumed to be twice α_1, both α_1 and α_2 being isotropic, and volume change on mixing was ignored. When N_1 and N_2 are calculated from Eq. 1 by means of the observed dielectric constant, the formation constant is easily obtained,

$$K=\frac{N_2}{N_1^2}\cdot\frac{\boldsymbol{N}}{10^3}\ (\text{l./mol.}) \quad (2)$$

in which $\boldsymbol{N}$ is the Avogadro number. Table II shows some of the calculated results of K for the two plausible configurations of the dimer at different temperatures. When the ratio a_2/b_2 for the dimer is equal to 1, the variation of K with concentrations is comparatively small. This ratio a_2/b_2 for the dimer corresponds to a configuration such as that in which constituent dipoles of the dimer take a parallel orientation and in which one of them lies upon another one. The value of K is very small compared with that for hydrogen bonding and is kept almost constant at

5) K. Kimura and R. Fujishiro, This Bulletin, **32**, 433 (1959).
6) A. Weissberger et al., "Organic Solvents", Interscience Publishers, Inc., New York (1955).
7) T. Hanai et al., *J. Chem. Soc. Japan, Pure Chem. Sec.* (*Nippon Kagaku Zasshi*), **80**, 17 (1959); N. N. Pal, *Phil. Mag.*, (7) **10**, 265 (1930).
8) T. G. Scholte, *Physica*, **15**, 437 (1949).
9) K. Kimura and R. Fujishiro, This Bulletin, **32**, 1237 (1959).

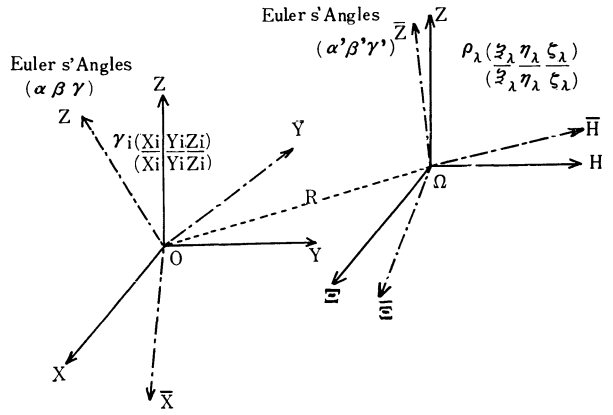


Fig. 1. The coordinate systems.

TABLE II. THE FORMATION CONSTANT K OF THE DIMER

Monomer a/b=1.72 Dimer a/b=1.74		Monomer a/b=1.72 Dimer a/b=1			
x	K (25°C)	K (40°C)	K (25°C)	x	K (60°C)
0.1277	0.016	0.0077	—		
0.2712	0.019	0.0078	0.0087	0.2712	0.0074
0.3613	—	0.0082	—		
0.4712	0.027	0.009	0.0093	0.4890	0.0094
0.6995	—	0.010	—		
0.7966	—	0.011	—	0.7323	0.011
0.8467	0.050	0.011	0.011		
1	0.068	0.012	0.012	1	0.012

any temperature between 25°C and 60°C. The latter result means that the heat of the formation of the dimer is of the same order of magnitude as kT. These results may probably be attributable to the electrostatic force by considering the large dipole moment of the solute molecule. In the next two sections, discussion will be given over mainly to electrostatic force.

Intermolecular Electrostatic Energy and the Sign of $\langle\cos\varphi_{12}\rangle$.—Let it be supposed that two dipoles form an angle φ_{12} in vacuo. The average value of $\langle\cos\varphi_{12}\rangle$ is given by

$$\langle\cos\varphi_{12}\rangle=\frac{\int\cos\varphi_{12}\,e^{-U/kT}\,d\omega}{\int e^{-U/kT}\,d\omega} \qquad (3)$$

where ω is a solid angle and U is the electrostatic potential energy. If the coordinate systems depicted in Fig. 1 are used, and coordinates of a charge e_i and those of a charge e_λ are r_i (x_i, y_i, z_i) in the O-coordinate system and ρ_λ $(\xi_\lambda, \eta_\lambda, \zeta_\lambda)$ in the Ω-coordinate system, respectively, U is given by the following formula[10],

$$U=-\frac{1}{R^3}\sum_{i,\lambda}e_ie_\lambda(2z_i\zeta_\lambda-x_i\xi_\lambda-y_i\eta_\lambda)+\frac{1}{2R^4}\sum_{i,\lambda}e_ie_\lambda\{r_i^2\zeta_\lambda-\rho_\lambda^2z_i+(2x_i\xi_\lambda+2y_i\eta_\lambda-3z_i\zeta_\lambda)(z_i-\zeta_\lambda)\}+\cdots \qquad (4)$$

The first term of the above formula corresponds to the dipole-dipole interaction energy, the second term to the dipole-quadrupole interaction, and so on. Generally speaking, non-electrostatic forces such as dispersion and repulsive forces must be included in the function U. However, if these non-electrostatic forces are assumed to have spherical symmetry, they have no effect on the averaging process over ω. In calculating the right hand side of Eq. 3, it is convenient to introduce rotating coordinate systems $\overline{X}$, $\overline{Y}$, $\overline{Z}$ of the origin O and $\overline{\Xi}$, $\overline{H}$, $\overline{Z}$ of the origin Ω. The direction of a dipole located at the origin O and that of another dipole located at the origin Ω are taken along the axes $\overline{Z}$ and $\overline{Z}$, respectively. Angles (α, β, γ) or $(\alpha', \beta', \gamma')$ express Eulerian angles of the axes $\overline{X}$, $\overline{Y}$, $\overline{Z}$ to X, Y, Z or those of the axes $\overline{\Xi}$, $\overline{H}$, $\overline{Z}$ to Ξ, H, Z. When we express the coordinates of e_i and e_λ by the rotating coordinate systems, coordinates of e_i $(\bar{x}_i, \bar{y}_i, \bar{z}_i)$ and e_λ $(\bar{\xi}_\lambda, \bar{\eta}_\lambda, \bar{\zeta}_\lambda)$ do not vary with the averaging process. Hence, the average value is obtained by carrying out integration over Eulerian angles only. If we introduce the following transformation matrix,

$$T=\begin{pmatrix}\cos\alpha\cos\gamma-\sin\alpha\sin\gamma\cos\beta, & -\cos\alpha\sin\gamma-\sin\alpha\cos\gamma\cos\beta, & \sin\alpha\sin\beta\\ \sin\alpha\cos\gamma+\cos\alpha\sin\gamma\cos\beta, & -\sin\alpha\sin\gamma+\cos\alpha\cos\gamma\cos\beta, & -\cos\alpha\sin\beta\\ \sin\gamma\sin\beta & \cos\gamma\sin\beta & \cos\beta\end{pmatrix} \qquad (5)$$

10) H. Margenau and V. W. Myers, *Phys. Rev.*, **66**, 307 (1944).

TABLE III. THE STABILIZATION ENERGY DUE TO THE SURROUNDING DIELECTRIC

[A] → →, [B] ⇄, [C] ⇉, [D] → ←

	$x=1$, $\varepsilon=34.16$, $\Delta G_1=-2.44$ kcal./mol.		$x=0.6995$, $\varepsilon=22.45$, $\Delta G_1=-2.38$		$x=0.2712$, $\varepsilon=8.82$, $\Delta G_1=-2.12$	
	ΔG_2	$1/2(\Delta W+\Delta G_2)-\Delta G_1$	ΔG_2	$1/2(\Delta W+\Delta G_2)-\Delta G_1$	ΔG_2	$1/2(\Delta W+\Delta G_2)-\Delta G_1$
[A]	−3.01	+0.65	−2.95	+0.62	−2.07	+0.80
[B]	0	+1.69	0	+1.62	0	+1.37
[C]	−9.46	−1.65	−9.16	−1.56	−7.81	−1.14
[D]	0	+2.70	0	+2.65	0	+2.39

we can transform the coordinate systems X, Y, Z and Ξ, H, Z to the new coordinate systems $\overline{X}$, $\overline{Y}$, $\overline{Z}$ and $\overline{\Xi}$, $\overline{H}$, $\overline{Z}$, respectively. The function $\cos\varphi_{12}$ is expressed by the use of Eulerian angles as follows:

$$\cos\varphi_{12}=\sin\alpha\sin\beta\sin\alpha'\sin\beta'+\cos\alpha\sin\beta\cos\alpha'\sin\beta'+\cos\beta\cos\beta' \quad (6)$$

Substituting Eqs. 4 and 6 into Eq. 3, integration is carried out over ω. Because the denominator of Eq. 3 is always positive, the numerator decides the sign of $\langle\cos\varphi_{12}\rangle$. If we expand the numerator of Eq. 3 in power series and retain only the dipole-dipole term of U, we have

$$\int\cos\varphi_{12}\,e^{-U/kT}\,d\omega=\frac{\pi^4}{3!}\cdot\frac{1024}{25}\cdot\left(\frac{\mu^2}{R^3kT}\right)^3+\frac{\pi^4}{5!}\cdot\frac{196608}{49}\cdot\left(\frac{\mu^2}{R^3kT}\right)^5+\cdots=452+204+\cdots>0 \quad (7)$$

where R is determined by the density of nitrobenzene at 25°C and μ is taken to be 4.27 D. The positive sign of $\langle\cos\varphi_{12}\rangle$ agrees with the experimental results. In order to confirm the minor effect of higher multipoles, the dipole-quadrupole term was included in Eq. 7. The result is as follows:

$$\int\cos\varphi_{12}\,e^{-U/kT}\,d\omega=-\frac{\pi^4}{2!}\cdot\frac{512}{75}\left(\frac{3\mu\Theta_{zz}}{2R^4kT}\right)^2+\frac{\pi^4}{3!}\cdot\frac{1024}{25}\left(\frac{\mu^2}{R^3kT}\right)^3+\frac{\pi^4}{5!}\cdot\frac{196608}{49}\left(\frac{\mu^2}{R^3kT}\right)^5+\cdots=-80+452+204+\cdots>0 \quad (8)$$

The above equation is derived on the assumption that the charge distribution of a molecule and that of another one are symmetrical about the axes $\overline{Z}$ and $\overline{Z}$, respectively and Θ_{zz} is presumed to be of the order of 10^{-25}. The series in Eq. 8 will converge gradually and be positive, even if the polarizability of molecules and the interaction energy between higher multipoles are taken into account. The result obtained experimentally in the previous section was confirmed theoretically.

The Dipole-Dipole Interaction Energy and the Stabilization Energy due to the Surrounding Dielectric—When two dipoles with polarizability α_1 are at distance R from each other in vacuo, the dipole-dipole interaction energy with respect to each of the four simple cases depicted in the upper part of Table III, is given by,

$$[A]\quad \Delta W_A=-\frac{2\mu_1^2}{R^3_A(1-2\alpha_1/R^3_A)}=-0.56 \text{ kcal./mol.}$$

$$[B]\quad \Delta W_B=-\frac{\mu_1^2}{R^3_B(1-\alpha_1/R^3_B)}=-1.51$$

$$[C]\quad \Delta W_C=\frac{\mu_1^2}{R^3_C(1+\alpha_1/R^3_C)}=1.29$$

$$[D]\quad \Delta W_D=\frac{2\mu_1^2}{R^3_D(1+2\alpha_1/R^3_D)}=0.53$$

If these dimers are introduced into the continuum of dielectric, there is the free energy of stabilization due to the reaction field. This energy ΔG_i (ΔG_1 for the monomer and ΔG_2 for the dimer), is

$$\Delta G_i=-\frac{1}{2}\cdot\frac{g_i\mu_i^2}{1-\alpha_i g_i} \quad (9)$$

The values of ΔG_2 for the four simple cases and those of ΔG_1 are shown in Table III in respective concentrations at 25°C. Apart from including dispersion energy, the values of $1/2(\Delta W+\Delta G_2)-\Delta G_1$ are considered as a measure of the stability of the dimer in solutions about the four configurations, although the stabilization energy ΔG_i is overestimated owing to the rough model. The most probable configuration of the dimer in solutions corresponds to the case [C]. This result of the semi-quantitative calculation thus agrees with the experimentally determined configuration of the dimer. Strictly speaking, the association of n-molecules ($n\geqq3$) will occur especially in concentrated solutions, but the dielectric behavior of solutions is, as a first approximation, interpreted in terms of dimerization.

Summary

The formation constant of the nitrobenzene dimer in carbon tetrachloride was estimated as of the order of 0.01 from the dielectric constant of the solution by the use of Scholte's model. The configuration of the dimer is probably such that one of the constituent molecules lies upon the other. The small formation constant and the configuration of the dimer suggest that there is no need to consider some special forces between molecules such as the charge transfer force. The results deduced experimentally are interpreted satisfactorily in terms of the electrostatic force.

The expenses for this work have been partly defrayed by a grant from the Ministry of Education.

Department of Chemistry
Faculty of Science
Osaka City University
Kita-ku, Osaka

Analysis of the Variation in Coil Character by Carbonized Coal with Q-Meter

By Sadaharu TOYODA

(Received April 27, 1961)

It is well known that the variation of character of a circuit, containing a coil or a condenser-type electrode, can be utilized to find a neutralization point on high frequency titration, though many other applications of the coil have been reported in several papers[1-11]. Many significant results[12,13] have been obtained by considering the variation of coil character, which is caused by inserting an aqueous solution into the coil. Recently, the calculation[14] of the relation between the variable resistance of platinum wire and the resistance of an aqueous solution has been extended on the basis of Ref. 12. However, some of the calculated values have not agreed with the experimental values in the case of a coil-type instrument. As a result of calculation, it has also been shown that the consideration of the dielectric constant of a sample solution would help to solve this problem.

The Q-change of the coil with aqueous solution has been explained in another paper[15]. The variation of coil character when a substance is inserted into the coil is visualized in Fig. 1. According to the experimental result, the value of Q/Q_1 for an aqueous solution ($\varepsilon'=80$) changes with the resistance of the solution, as is shown by the full-line in Fig. 2. This variation seems to be explained by the equivalent circuit (Fig. 4 in Ref. 15) and the following relation (Eq. 15 in Ref. 15), which are based on Refs. 13, 16 and 14:

$$\frac{Q}{Q_1} \fallingdotseq \frac{1}{1+\alpha\left(\frac{px}{1+x^2}+\frac{1}{pMx}\right)\frac{\omega L}{R_1}} \tag{1}$$

where

$$x \equiv \omega(\varepsilon' C_1 + C_0)R, \quad R \equiv kr, \quad p \equiv \frac{C_0}{\varepsilon' C_1 + C_0}$$

$$\alpha \equiv \omega^2 L C_0$$

After some calculation using the above relation, the dotted line in Fig. 2 is obtained in the case of a low dielectric constant (for example, $\varepsilon'=1$). Comparing these two curves, the minimum value of Q/Q_1 in the dotted line is smaller than the value in the full-line, while the maximum value of Q/Q_1 does not depend

1) F. Bloch, *Phys. Rev.*, **70**, 460 (1946); F. Bloch, W. W. Hausen and M. Packard, ibid., **70**, 474 (1946).
2) N. Bloembergen, E. M. Purcell and R. V. Pound, ibid., **73**, 679 (1948).
3) R. V. Pound and W. D. Knight, *Rev. Sci. Instr.*, **21**, 219 (1950).
4) P. W. West, T. Robichaux and T. S. Burkhalter, *Anal. Chem.*, **23**, 1625 (1951).
5) P. W. West, P. Senise and T. S. Burkhalter, ibid., **24**, 1250 (1952).
6) M. Honda, *J. Chem. Soc. Japan, Pure Chem. Sec.* (*Nippon Kagaku Zasshi*), **73**, 529 (1952); **74**, 371 (1953).
7) H. Honda, S. Toyoda and Y. Hirose, *J. Fuel Soc., Japan* (*Nenryō Kyokaishi*), **35**, 526 (1956).
8) H. Honda, 2nd Int. Coal Preparation Congress, Essen (1957), C 9,
9) F. J. Schmidt, *Anal. Chem.*, **29**, 1060 (1957).
10) Isidore Bady, *J. App. Phys.*, **29**, 393 (1958).
11) R. D. Ray, *B. C. U. R. A. Mon. Bull.*, **24**, 117 (1960).
12) K. Nakano, *J. Chem. Soc. Japan, Pure Chem. Sec.* (*Nippon Kagaku Zasshi*), **75**, 776 (1954).
13) M. Honda, K. Nakano and A. Satsuka, ibid., **75**, 1299 (1954).
14) S. Toyoda, This Bulletin, **33**, 504 (1960).
15) S. Toyoda, ibid., **34**, 944 (1961).
16) W. J. Blaedel et al., *Anal. Chem.*, **24**, 198 (1952).

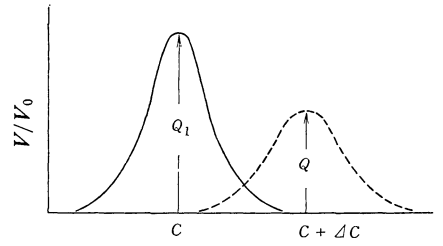


Fig. 1. Two curves showing variation of coil character.

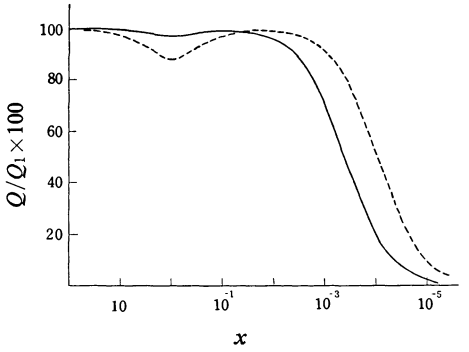


Fig. 2. Curves of Q/Q_1-change ($x \equiv \omega(\varepsilon' C_1 + C_0)R$, $R \equiv kr$), full-line ($\varepsilon' = 80$), dotted line ($\varepsilon' = 1$) at 3×10^6-cycle.

on the dielectric constant. The present paper is concerned with the variation in coil character caused by carbonized coal. The experimental results seem to be understandable by taking account of the above-described difference between the full-line and the dotted line.

Experimental Equipment and Method

Fig. 3 shows an experimental apparatus. The explanation of the parts except a furnace (a) and its accessories are omitted, since they have been reported in Ref. 15. Although a long quartz pipe (b) shown in Fig. 3 has not been illustrated in Ref. 15, it had been attached to a quartz vessel of a sample solution. The length of the quartz pipe is about 45 cm., and the outside diameter, 2.5 cm. A three-way cock (c), suspended by a

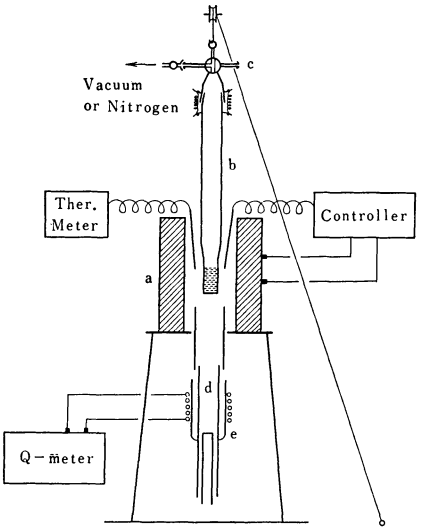


Fig. 3. Apparatus for experiment.
a Furnace b Quartz pipe
c Three-way cock
d Quartz pipe serving as a guide
e Quartz pipe for coil

string and a pulley as shown in Fig. 3, is connected to another end of the quartz pipe with a spring, and so the coal sample in the quartz vessel is located in the center of the furnace, which is regulated at the heating rate of 2°C per minute. When the temperature of the coal sample is raised to an appointed temperature, the connection to a vacuum or a nitrogen system is set off, and the heated quartz vessel containing the coal is inserted into a coil by using the string and the pulley. After measuring the Q-value of the coil as fast as possible, the quartz vessel is pulled up to the original position, the three-way cock is connected again to the vacuum or the nitrogen system, and the quartz vessel with the coal is heated to the next desired temperature.

When the heated quartz vessel is inserted into the coil, the Q of the coil is apt to decrease due to the heat conduction and the radiation from the vessel, in addition to the Q-change caused by the character of carbonized coal. The following method

TABLE I. ANALYSIS OF VARIOUS COALS

Coal	Proximate analysis, %				Ultimate analysis (d.a.f.), %		
	Moisture	Ash	VM	Fixed carbon	C	H	O+N+S
Tempoku	—	2.07*	—	—	68.12	5.63	26.25
Nakagō	13.32	3.96	38.03	44.69	74.33	5.26	20.41
Takamatsu	4.45	2.63	41.42	51.50	79.52	5.53	14.95
Yūbari	1.13	2.67	44.85	51.35	84.85	6.16	8.99
Shikamachi	1.16	2.52	21.16	75.16	88.76	4.70	6.54
Yatake	1.67	11.82	19.06	67.45	88.95	4.93	6.12
Uonuki	1.68	1.80	10.80	85.72	91.16	3.97	4.87
Hongei (Indo-China)	1.92	1.08	6.25	90.75	92.65	3.48	3.87

* Dry basis

was employed in order to suppress this tendency caused by the heat conduction and the radiation. Taking account of the heat conduction, the quartz tube (d) serving as a guide for the vessel containing the sample as shown in Fig. 3, is attached inside the quartz tube (e) on which the coil is wound; moreover, because of the radiation, the outside surface of the transparent quartz tube (d) is frosted. In spite of these attentions, the Q-change of the coil still remains somewhat, so that the coil must be cooled by a fan after the heated quartz vessel with coal is drawn up.

The coal specimens were pulverized to pass through a 30- and stand on a 60-Tyler mesh sieve. The vitrain of coals of specific gravity less than 1.30, except for Yatake coal, was isolated by the float-or-sink method using mixtures of benzene and carbon tetrachloride. Shikamachi and Yatake coals were pulverized to pass through a 200-Tyler mesh sieve. All samples were dried in air for several days. The characteristics[17] of the various coals are listed in Table I. Taking account of the loss in weight of coal by carbonization as shown in Fig. 4, the initial coal sample length in the quartz vessel was made longer than 6.5 cm. (refer to Table III and Ref. 15).

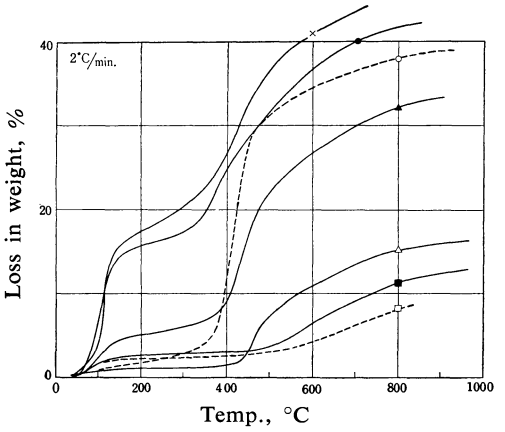


Fig. 4.

● Tempoku △ Shikamachi
× Nakagō ■ Uonuki
▲ Takamatsu □ Hongei
○ Yūbari

In the previous experiment (Ref. 15), the Q-value did not change when the quartz vessel without a sample solution was inserted into the coil. This seems to be attributable to the high resistance or low loss of the quartz vessel at 3×10^6 cycle. On the contrary, it can be imagined that the properties of the quartz vessel will change in the present case because the vessel is heated to about 1000°C. Therefore, it is necessary to investigate the variation in coil character due to the property change of the heated quartz vessel without a sample. The Q of the coil is measured when the heated quartz vessel without a sample is put into the coil; the results obtained are shown in Table II.

17) H. Honda and Y. Hirose, *Fuel*, **37**, 323 (1958).

TABLE II

Temp °C	Quartz vessel Q/Q_1 ×100	Shikamachi Q/Q_1 ×100	Shikamachi $\Delta C'$ (pF)	Yatake Q/Q_1 ×100	Yatake $\Delta C'$ (pF)
20	100	99.5	−0.10	99.2	−0.17
100	〃	—	—	—	—
200	〃	99.9	−0.11	99.5	−0.24
300	〃	—	—	—	—
400	〃	99.9	−0.10	99.2	−0.20
500	〃	〃	−0.12	99.5	−0.22
550	〃	99.7	−0.11	98.9	−0.20
600	〃	〃	−0.18	95.1	−0.38
625	〃	96.7	−0.22	93.5	−0.42
640	—	—	—	94.8	−0.53
650	100	98.2	−0.19	99.0	−0.54
675	〃	91.7	−0.44	89.4	−0.56
690	—	96.8	−0.53	—	—
700	100	98.7	−0.47	82.6	−0.63
725	—	98.4	−0.54	—	—
750	100	98.7	−0.54	45.7	−0.62
775	—	55.6	−0.64	—	—
800	99.7	40.5	(−0.44)	≈5	—
825	—	15.6	—	—	—
850	99.5	≈5	—	—	—
900	99.2	≈8	—	≈2.5	—

The notation Q_1 means the Q-value of the coil without a quartz vessel, just before measuring the Q-value of the heated quartz vessel with or without coal. In order to measure the Q-value correctly, the capacity of the condenser in the Q-meter most be adjusted at the tuning point, but it is not changed when measuring the heated quartz vessel without coal, after adjusting it without the vessel. It may be considered that the Q/Q_1-value of the heated quartz vessel, at least, would not be smaller than the one in Table II, because the V/V_0-value of coil has a tendency to decrease when the capacity of condenser is not tuned. According to the experimental result, the decrease of the Q-value is so small that it can not be detected up to 750°C, while the value of Q/Q_1 decreases slightly with the increase of temperature in the range from 800 to 900°C. Therefore, it may be concluded that the variation in Q-value caused by carbonized coal is hardly affected by the heated quartz vessel, because the variation due to the carbonized coal is much larger than that due to the heated quartz vessel at a high temperature.

When the Q-value is measured, as mentioned above, the capacity of the condenser must be adjusted again after the heated quartz vessel with coal sample is inserted into the coil. It is not unreasonable to assume that the tuning capacity of the condenser has a tendency to decrease when carbonized coal is inserted into the coil, because an aqueous solution has the same tendency. Thus, the capacity of the condenser decreases at a suitable rate from the tuning capacity without the heated vessel, and the maximum value of V/V_0, that is to say, the Q of the coil, is measured after the heated vessel with coal is put into the coil.

The time required for each measurement of Q-value is usually less than five seconds. The temperature at which the Q-value is measured is selected according to the quantity of variation of Q. As the temperature of the heated coal decreases when the coal is inserted into the coil, the next measurement of Q-value must be carried out after enough time to recover the decline in temperature and keep the heating rate of 2°C per minute on an average. Therefore, the narrowest interval of temperature for measurement has been decided as 20°C. The reading of the thermometer goes down about 5°C to 20°C over the range from 500°C to 900°C after the quartz vessel containing the coal is withdrawn into the furnace, but this decrease is recovered and the reading of the thermometer becomes the desired value after 2 to 5 min. In the measurement at higher temperatures, there is still a small decrease of Q_1, in spite of cooling the coil with the fan after the Q-value is measured and withdrawing the heated quartz vessel as fast as possible. It must be remembered, however, that this decay of Q_1 does not interfere with the following experiment, since the ratio, Q/Q_1, is discussed instead of the Q-value, and the variation in the Q-value due to the coal sample is rather large in the higher temperature range.

Experimental Results

The measurements were made of the samples under vacuum, and the results are shown by the dotted lines in Figs. 5a—5d. There is a slight danger under a vacuum condition that some of the coal samples may suddenly expand and lose packing uniformity by the gas given off on thermal decomposition. In order to avoid these errors, the variation of the Q-value was also measured for the sample in a nitrogen atmosphere (1 atm.) substituted for the air around the coal before the start of heating. In this case, the initial coal sample in the quartz vessel has a length of 10 cm., as is shown in Table III. The experimental results in the nitrogen atmosphere are shown by the full-lines in Figs. 5a—5d. Minimum and maximum values of the full-line and the dotted line in Figs. 5a—5d are listed in Table III, together with the temperature at which they were measured. These values are classified into first and second values by depth of minimum value. The shape of the curves which have one minimum is similar to that of aqueous solution, as shown in Ref. 13 and Fig. 2. As the length of coal in the quartz vessel changes with heating, the variation of Q/Q_1 and tuning capacity ($\Delta C'$) must be measured for an aqueous solution with the corresponding length in order to compare the results of coal with those of aqueous solution. They are listed in Table IV. It can be concluded from Table IV that the concentration of an aqueous solution which shows a minimum or a maximum has nothing to do with the change of length. However, the minimum value of Q/Q_1 slightly changes with the length, while the maximum value is

TABLE III

Coal	Initial sample length, cm.		Minimum and maximum values of Q/Q_1, % Temperature at each value, °C							
			Nitrogen				Vacuum			
			1st		2nd		1st		2nd	
	Nitrogen	Vacuum	min.	max.	min.	max.	min.	max.	min.	max.
Tempoku	10	10	97.4 475	98.7 540	90.5 640	93.2 680	96.8 500	97.9 550	89.8 620	96.8 680
Nakagō	〃	〃	97.6 510	98.7 560	—	—	97.3 500	98.1 550	91.4 620	98.1 690
Takamatsu	〃	8	—	—	92.4 600	96.7 670	96.3 520	97.7 580	92.6 640	95.0 680
Yūbari	〃	〃	—	—	92.3 570	96.5 660	95.7 570	96.5 600	92.9 640	93.5 660
Shikamachi	〃	7.5	—	—	88.5 600	96.2 660	—	—	90.1 615	94.2 675
Shikamachi (1000 kg./cm²)	6.5	—	96.7 625	98.2 650	91.7 675	98.7 700	—	—	—	—
S-550°C	—	6.5	—	—	—	—	—	—	91.0 590	97.8 660
Yatake (10% Graphite, 1000 kg./cm²)	6.5	—	—	—	93.5 625	99.0 650	—	—	—	—
Y-550°C	—	6.5	—	—	—	—	—	—	91.0 570	98.7 650
Uonuki	10	10	—	—	90.8 640	95.4 710	96.3 580	98.4 620	88.0 680	93.1 740
Hongei	〃	7.5	—	—	89.7 580	96.5 740	96.1 375	97.2 500	90.6 640	96.7 760

TABLE IV

Aq. Soln. KCl (N)	Aq. Soln. HCl (N)	$l_0=5.5$ cm. $Q/Q_1\times100$	$l_0=5.5$ cm. $\Delta C'$ (pF)	$l_0=6.5$ cm. $Q/Q_1\times100$	$l_0=6.5$ cm. $\Delta C'$ (pF)	$l_0=7.5$ cm. $Q/Q_1\times100$	$l_0=7.5$ cm. $\Delta C'$ (pF)	$l_0=8.5$ cm. $Q/Q_1\times100$	$l_0=8.5$ cm. $\Delta C'$ (pF)	$l_0=10$ cm. $Q/Q_1\times100$	$l_0=10$ cm. $\Delta C'$ (pF)
(Dist. water)		99.7	−0.42	99.7	−0.44	99.5	−0.43	99.5	−0.44	99.2	−0.46
10^{-5}		〃	〃	〃	−0.43	99.3	−0.44	99.6	−0.45	99.0	−0.47
	10^{-5}	99.2	−0.43	99.0	〃	98.7	〃	98.8	〃	98.3	〃
10^{-4}		98.7	−0.42	98.5	−0.44	98.5	−0.45	98.3	−0.47	97.9	−0.50
	10^{-4}	98.3	−0.44	98.3	〃	97.9	−0.46	97.8	−0.46	97.4	−0.55
3×10^{-4}		97.9	〃	97.8	−0.46	97.1	(−0.44)	96.9	−0.48	96.7	−0.56
10^{-3}		96.9	−0.47	96.5	−0.49	96.0	−0.50	94·8	−0.50	93.8	〃
	10^{-3}	97.4	−0.52	97.0	−0.52	96.4	−0.52	95.8	−0.54	94.8	(−0.66)
3×10^{-3}		98.1	−0.50	97.3	−0.54	96.3	−0.50	95.7	−0.52	94.7	−0.59
0.01		97.9	(−0.47)	97.7	〃	97.2	−0.56	97.4	−0.56	96.2	−0.66
0.03		99.0	−0.53	98.1	−0.56	97.9	−0.60	98.7	−0.62	98.9	−0.64
	0.01	97.3	−0.54	97.5	−0.55	97.3	〃	97.0	−0.70	95.6	−0.69
0.1		95.2	−0.50	95.2	〃	95.1	−0.66	94.7	〃	93.2	−0.74
0.3		91.9	−0.54	91.2	−0.61	90.0	−0.74	89.5	−0.74	87.4	−0.80
	0.1	90.8	−0.52	89.7	〃	89.6	−0.73	87.9	−0.79	85.9	−0.90
1		83.3	−0.66	82.6	−0.76	82.1	−0.80	81.7	−0.84	82.2	−0.86
3		69.7	−0.69	69.5	−0.94	69.2	−0.86	69.2	−0.88	69.4	−1.05
	1	67.0	−0.80	66.9	−0.97	67.4	−1.00	68.5	−0.99	68.3	−1.07

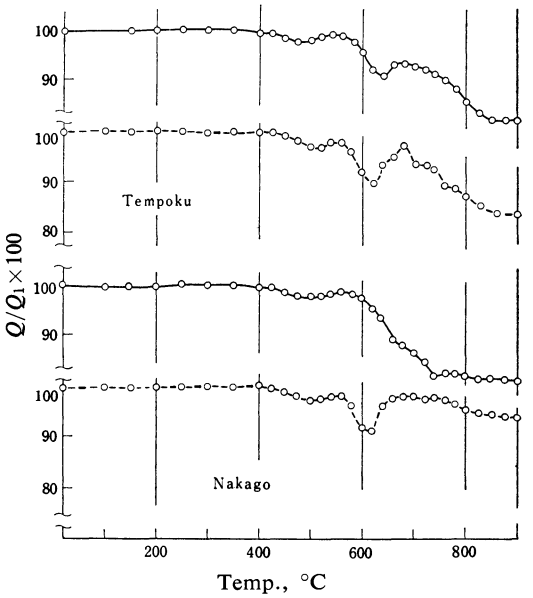


Fig. 5a. Tempoku and Nakagō coals.

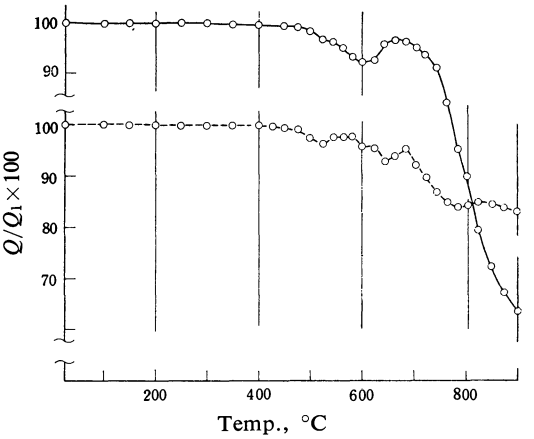


Fig. 5b. Takamatsu coal.

approximately constant. The value of the tuning capacity decreases with the increase of the concentration of the aqueous solution, although it becomes slightly smaller with the increase in the length of solution.

It seems impossible to neglect the change of length in a discussion of the experimental results of coal obtained under heating. Therefore, the following experiments were made. The powder of Shikamachi or Yatake coals was moulded like brick[18] under a pressure of 1000 kg./cm^2, and it was cut into the proper size for blocks. They were buried in other coal powder, and their temperatures were raised at a suitable rate so as to prevent oxidation and expansion by the gas evolved. In order to keep the heating uniform, they are kept in the last-desired temperature for one hour. After cooling, a cylindrical bar of carbonized coal was made by lathe. The length and the diameter are 6.5 cm. and 1.70 cm. respectively. The results made by measuring these samples at room temperature, are shown by the full-lines in Fig. 6 (refer to Table II, except 640

18) H. Honda, N. Mochida and Y. Sanada, *Rep. Resources Res. Inst.*, No. 44 (1958).

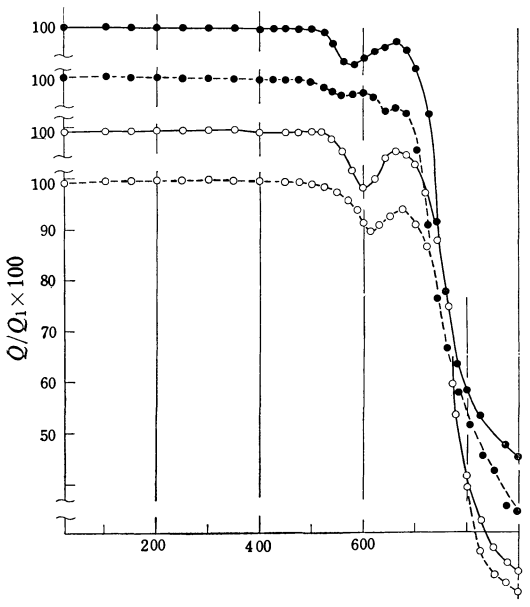


Fig. 5c. Yūbari and Shikamachi coals.
● Yūbari ○ Shikamachi

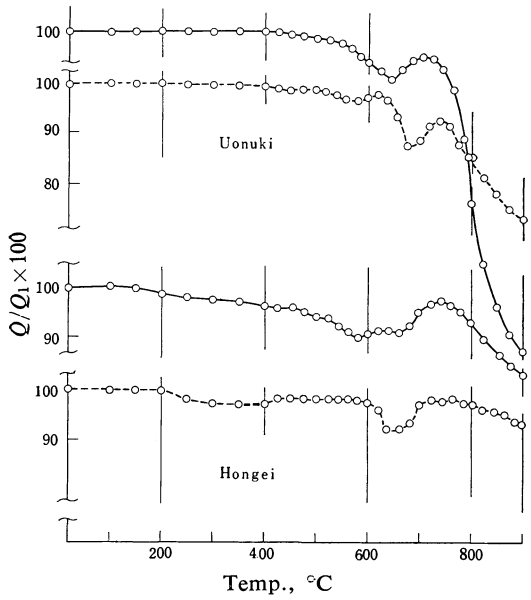


Fig. 5d. Uonuki and Hongei coals.

and 690°C). There exists at least one minimum value near 675°C (Shikamachi) or 625°C (Yatake). To make sure of the depth of the minimum, the bar of Shikamachi or Yatake coal, which had already been heated up to 550°C, was put into the quartz vessel and heated again from room temperature at the rate of 1°C per minute in vacuo. The results obtained are also shown by the dotted lines in Fig. 6.

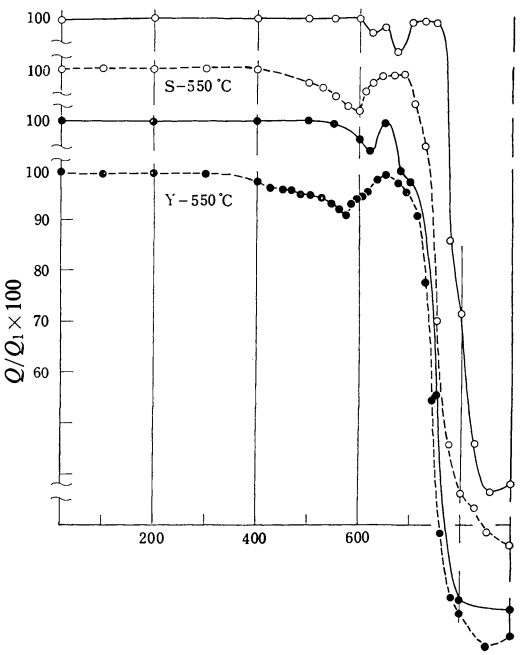


Fig. 6. Shikamachi and Yatake coal bars
○ Shikamachi ● Yatake

Discussion

There exist several papers[19-25] on the subject of the dielectric sonstant of coal. According to Ref. 19, the dielectric constant and loss factor of various coals were measured at room temperature. Each of the test pieces was cut from the vitreous portion of a large block of coal and then carefully made into the form of a circular plate about 4 cm. in diameter. The test pieces thus prepared were kept in the desiccator over phosphoric anhydride for three or four months. The present writer measured the dielectric constant and the dielectric loss factor of various coals by using the above-mentioned method, as shown in Fig. 7. There have been few papers[26-28] concerning the

19) I. Miyasita, *Bull. Res. Inst. Appl. Elec., Hokkaido Univ.*, **5**, 123 (1953); **6**, 117 (1954); **7**, 17 (1955).
20) M. P. Groenewege, J. Schuyer and D. W. Van Krevelen, *Fuel*, **34**, 339 (1955).
21) I. Miyasita, R. Miura and K. Higasi, This Bulletin, **28**, 148 (1955).
22) I. Miyasita and K. Higasi, ibid., **30**, 513 (1957).
23) K. Higasi, I. Miyasita and Y. Ozawa, ibid., **30**, 546 (1957); I. Miyasita, K. Higasi and M. Kugo, ibid., **30**, 550 (1957).
24) K. Higasi, Y. Higasi and I. Miyasita, ibid., **30**, 556 (1957).
25) K. Chitoku and K. Higasi., ibid., **34**, 320 (1961).
26) Y. Zyomoto and K. Higasi, *Kagaku*, **26**, 638 (1956).
27) Y. Zyomoto, *J. Fuel Soc., Japan*, (*Nenryō Kyokaishi*), **37**, 248 (1958).
28) D. K. Sen, S. K. Sengupta, K. A. Kini and A. Lahiri, *J. Sci. Ind. Research*, **19 B**, 184 (1960).

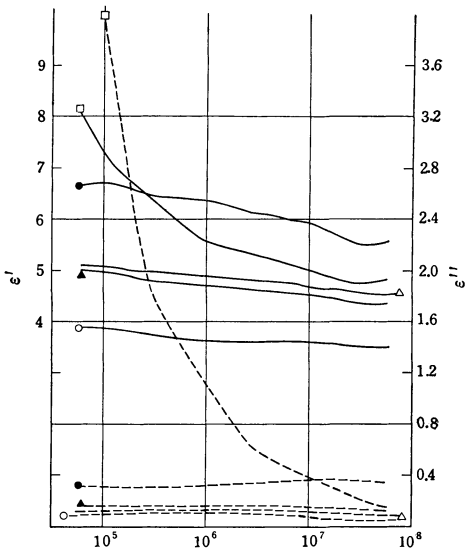


Fig. 7. Frequency dependence of dielectric constant (full-line) and loss factor (dotted line) of various coals.

● Tempoku △ Shikamachi
▲ Takamatsu □ Hongei
○ Yūbari

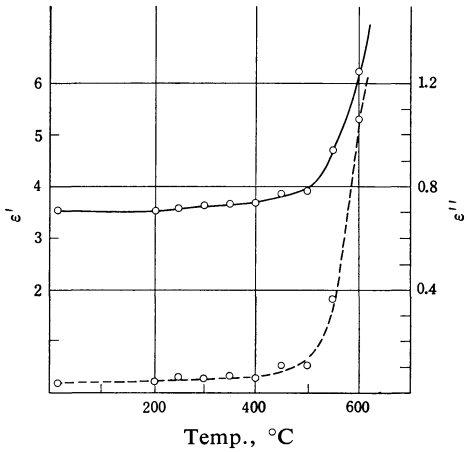


Fig. 8. Relation between dielectric constant (full-line), loss factor (dotted line) and carbonization temperature of Shikamachi coal (circular plate) at 3×10^6 cycle.

dielectric constant of carbonized coal. According to Ref. 26, a method using the powder of carbonized coal and paraffin was adopted for measuring the dielectric constant of carbonized bituminous coal. It has been described how the dielectric constant of the mixture increases beyond 600°C, while the dielectric loss factor increases with the temperature to a maximum at about 650°C, above which it decreases with the temperature, reaching a minimum at about 700°C; there is then a sudden increase above about 700°C. According to Ref. 28, a sudden increase in the dielectric constant of the original coals was observed at 600°C. Therefore, the present writer prepared many test pieces of circular plates (5.1 cm. in diameter, about 0.6 cm. in thickness) by pressing the powder of Shikamachi coal under 1400 kg./cm^2. These samples were carbonized up to the desired temperature at the heating rate of 1°C per minute. The dielectric constant and the loss factor of the sample were measured at room temperature by the method in Ref. 19, but the measurement was rather difficult for the sample beyond 550°C. The results are illustrated in Fig. 8.

It has been implied in Ref. 19 that Japanese coals are constituted mainly of non-polar substances. Furthermore, in Ref. 23, brown coals are found to have a moment near to that of one O–H group and that the polarity of bituminous coal is in general too small to be distinguishable from zero. According to Ref. 20, the ε' values of coals were found to rise very rapidly above 88% carbon content, and the rise was ascribed to a progressive increase in electrical conductance. The dielectric constant of coals used in the present experiment is less than ten, as is shown in Fig. 7. In Ref. 28, the sudden increase in the dielectric constant at 600°C has been attributed to an increase in the electrical conductivity of coals in the region of this temperature. Taking the above-mentioned results into account, it is unlikely that the ε' value of carbonized coal or coal being heated increases to a large value due to the mechanism shown by such polar molecules as water or methyl alcohol.

The specific resistance, r, at 3×10^6 cycle of carbonized Shikamachi and Yatake coal bars was obtained by the following method. The coal bar, of which a tin-foil with a short wire is attached to each side, was connected parallel to the variable condenser of Q-meter to measure the Q-value, so that the next relation (Eq. 18 in Ref. 15) can be used:

$$r=\frac{1}{\omega C}\cdot\frac{QQ_1}{Q_1-Q}\cdot\frac{\sigma}{h} \qquad (2)$$

in which σ is the section area of the coal bar and h its length. There is no sample having the value of $10^2\sim10^4\ \Omega\cdot$cm., so that the coal bars, S-675°C and Y-625 shown in Table II, are heated again up to 690 and 640°C respectively in vacuo. These results are listed in Table V, and the relation between the value of Q/Q_1 and the specific resistance is shown in Fig. 9 together with that of aqueous solution. The value of specific resistance at direct current

TABLE V

Temp. °C	Shikamachi r, Ω·cm. D. C.	Shikamachi r, Ω·cm. 3×10^6 cycle	Shikamachi $\varepsilon'C_1+C_0$ pF	Shikamachi ε' 3×10^6-cycle	Yatake (10% Graphite) r, Ω·cm. D. C.	Yatake (10% Graphite) r, Ω·cm. 3×10^6 cycle	Yatake (10% Graphite) $\varepsilon'C_1+C_0$ pF	Yatake (10% Graphite) ε' 3×10^6 cycle
500					1.4×10^6	6.6×10^5	0.643	4.8
550						3.6×10^5	0.625	4.1
600	5×10^6	9.7×10^5	0.687	6.5	1.7×10^5	5.6×10^4	0.672	5.9
625	7×10^5	9.5×10^4	0.644	4.8	5.9×10^4	3.0×10^4	0.752	9.0
640	—	—	—	—	7.3×10^3	4.7×10^3	1.30	31
650	1.75×10^6	$1.9_6\times10^6$	0.607	3.3	275	300		
675	3.2×10^4	$2.0_3\times10^4$	0.738	8.5	11.9	*13.3		
690	6.5×10^3	$3.5_8\times10^3$	2.33	71	—	—	—	—
700	270				6.6	*7.5		
725	130				—	—		
750	240				0.43	*1.3		
775	3.1	*2.07			—	—		
800	0.366	*1.07			0.034			
825	0.10				—	—		
850					—	—		
900	0.040				0.016			

* Calculated value obtained by Eq. 1.

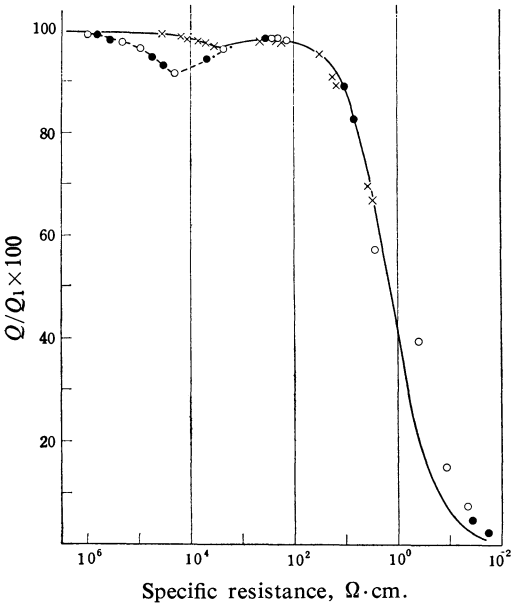


Fig. 9. Relation between $Q/Q_1\times100$ and specific resistance of carbonized coal or aqueous solution at 3×10^6 cycle.

○ Shikamachi ● Yatake
× Aqueous solution

for some coals carbonized at a higher temperature is used instead of that at 3×10^6 cycle since the latter can not be obtained by using the Q-meter. This manipulation results in several points in Fig. 9 not being located on the curve obtained by Eq. 1 over the range of lower specific resistance. The minimum value of carbonized coals in Fig. 9 is smaller than that of the aqueous solution. The description as shown in Ref. 15, "the minimum value of Q/Q_1 depends on the dielectric constant", is very helpful in understanding this difference in minimum value, because the original coal sample used in the present experiment has a dielectric constant value of less than ten. Therefore, this fact may support the view that there must be the dotted line as shown in Fig. 2 obtained by calculation. The dielectric constant of some of the carbonized coals is calculated by using the value of r at 3×10^6 cycle in Table V and Eq. 1. Above about 2×10^4 Ω·cm., in Table V, the values of ε' of the carbonized Shikamachi and Yatake coals are less than ten, but at the specific resistance lower than this value, they increase rapidly.

The calculation of the dielectric loss factor was done for the carbonized Shikamachi coal bar using the following relation from Ref. 15 and the value of $r(=\rho)$ as shown in Table V:

$$\frac{1}{\rho}=\frac{f(\varepsilon'/\varepsilon_0)\tan\delta}{1.8\times10^{12}}$$

or

$$(\varepsilon'/\varepsilon_0)\tan\delta=\frac{1.8\times10^{12}}{\rho f} \qquad (3)$$

From these values, ε' in Table V and Fig. 8, the variation in the dielectric property of the circular plate and the cylindrical bar of Shikamachi coal for carbonization temperature are visualized in Fig. 10, although the value of ε'' of the circular plate and the cylindrical bar at 600°C is slightly different since the value of

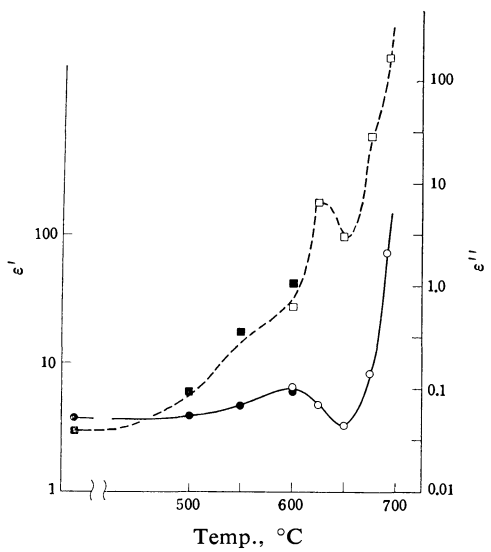


Fig. 10. Relation between dielectric constant (full-line), loss factor (dotted line) and carbonization temperature of Shikamachi coal at 3×10^6-cycle.

● ■ Circular plate
○ □ Cylindrical bar

ε'' of Shikamachi coal increases greatly in the vicinity of this temperature. The dielectric constant not only slightly increases from room temperature to 400°C, but also increases substantially beyond 400°C (refer to Fig. 8), shows a maximum and minimum at 600 and 650°C respectively, and then increases again rapidly. There is a similar tendency in the variation of the dielectric loss factor. However, the dielectric constant decreases in the neighboring range of 625°C, at which the dielectric loss factor shows a maximum value. It seems that this relation has something to do with the anomalous dispersion of carbonized coal shown at about 700°C in Refs. 26 and 27.

Returning to Fig. 6, the Q/Q_1 value of the full-line of the Shikamachi coal bar hardly changes over the range from room temperature to 500°C, since it may be considered that the values of ε' and r do not change greatly over this temperature range. Moreover, the Q/Q_1 value of the full-line has only a little change at the interval of 500~600°C, although the values of ε' and r changes substantially in this range. The variation of Q/Q_1 due to the effect of r appears beyond 600°C. In this case, the value of r, at which the dotted line in Fig. 9 begins to show the decrease of Q/Q_1, is larger than that of the aqueous solution, owing to the difference of dielectric constant between the carbonized coal and the aqueous solution. The Q/Q_1 value of the full-line of the Shikamachi coal bar in Fig. 6 increases in the range of 625~650°C, because the value of r increases greatly in spite of the decrease of ε', and then decreases to the minimum value. Under the conditions of the increase of ε' and the decrease of r, the value of Q/Q_1 increases from this minimum value to the maximum value determined by the effect of the eddy current in the coal sample. Furthermore, the eddy current causes a sudden decrease in the value of Q/Q_1 at a higher temperature, as deduced from the descriptions in Refs. 12—15, because the powders in the coal sample connect with each other owing to the strong caking property of coal. The first minimum of the full-line of the Yatake coal bar is not found in Fig. 6, although it might exist near 600°C. The dotted lines in Fig. 6 have not the first minimum. This result may be considered as due to the fact that the specific resistance in the sample is not uniform because of the low heat conductivity of this sample. It is reasonable that the temperature at the minimum value of Q/Q_1 shifts to the lower temperature side, comparing the dotted line with the full-line since the measurement was done at a high temperature with lower heating rate. The second minimum of the dotted lines in Fig. 6 seems to correspond to the minimum of the dotted line in Fig. 9. According to Table IV in Ref. 15, it is likely that the ε' values of S-550°C at 590°C and Y-550°C at 570°C are the order of 9~10.

The results of the coals in Figs. 5a—5d under the carbonization process show many different curves depending on the grade of coal. They may be caused by the different chemical structures of coal, as deduced from the result of analysis in Table I and the above-mentioned dielectric character. All the curves in Fig. 5a have the first and the second minima except Nakagō's full-line which has no second minimum, the reason for which is difficult to ascertain. These first minimums may be understood by considering the increase of r-value near 500°C, although the length of the samples changes during the carbonization process. Takamatsu coal does not show the first minimum on the full-line in Fig. 5b. It may be considered that the value of ε' would be less than about twenty over the range from room temperature to the second minimum temperature. The sudden decrease of Q/Q_1 in the full-line appears in the range of higher temperatures, whereas the one in the dotted line can not be located. The Yūbari coal lines in Fig. 5c are similar to those of Takamatsu coal as far as the first minimum is concerned. The value of Q/Q_1 of both the lines at higher temperatures sharply decreases to near zero, as do those of Shikamachi and Yatake coals

in Figs. 5c and 6. It may be considered that these decreases have shown the effect of eddy current due to the strong caking property of the coals. The ε' value of the carbonized Yūbari coal may be less than twenty till near 560°C. In Fig. 5c, the ε' value of the carbonized Shikamachi coal may be as small as the one of the original coal till the second minimum temperature. The value of Q/Q_1 of Uonuki coal in Fig. 5d decreases quite a bit at higher temperatures, although Uonuki coal is not a strong caking coal. The second minimum value is small, as is that on the full-line of Shikamachi coal in Fig. 5c. It seems that the value of ε' is less than ten at the second minimum temperature. The temperature, at which the first minimum value is shown, is below 600°C except that of Shikamachi coal. Above all, the first minimum value of Hongei (anthracite) under vacuum is located at rather a lower temperature. Both lines for Hongei coal in Fig. 5d begin to change the value of Q/Q_1 from a lower temperature than do those of other coals. These phenomena seem to be attributable to the special chemical structure Hongei coal, as imagined from the frequency dependence of the dielectric constant and the loss factor shown in Fig. 7. Although the coal samples change their length by thermal decomposition, the second minimum values are less than 93.8 per cent, which corresponds to the minimum value of aqueous solution having the length of 10 cm. This fact seems to support the deduction about the dotted line in Fig. 9, by taking it into account that the dielectric constant of the coals under carbonization would be quite a bit less than eighty over the range from room temperature to the respective temperature of the minimum.

Finally, the value of the variation in tuning capacity of carbonized Shikamachi and Yatake coals in Table II decreases with the increase of carbonization temperature over 600°C. It can be considered that these value seems to decrease monotonously with the increase of the dielectric loss factor, because the aqueous solution shows the same relation in Table IV. Comparing the carbonized coal and the distilled water, the variation in the tuning capacity of carbonized Shikamachi and Yatake coals, having a specific resistance of the same order or larger than that of distilled water, is less than that of distilled water, owing to the difference in the dielectric constant between the coal and the distilled water, as expected by Eq. 14 in Ref. 15.

Summary

The relation between the value of Q/Q_1 and the carbonization temperature of coal has been studied for various coals. The shape of the curve depends on the grade of coal. It is significant that the Q/Q_1 value of both the full-line and the dotted line in strongly caking coal suddenly decreases at higher temperatures. Most of the curves have a second minimum value which is smaller than that of the curve for the aqueous solution. This can be understood by taking account of the difference in dielectric constant between the coal and the aqueous solution. This result seems to support the existence of the dotted line in Fig. 2, as well as the opinion in Ref. 14 that the factor, p, would be very important.

The author desires to thank Dr. Hidemasa Honda and Mr. Naoyuki Mochida for their kind discussion and support.

Shigengijutsu Shikenjo
Resources Research Institute
Kawaguchi-shi, Saitama

The Crystal Structure of Nickel Dialpha-amino Isobutyrate Tetrahydrate

By Teruo NOGUCHI*

(Received May 16, 1961)

Recently the present author succeeded in constructing an electronic device[1] to compute the minimum-functions[1] proposed by Buerger[2]. The present paper will give a structure analysis of nickel(II) α-amino isobutyrate tetrahydrate, which seemed to present a suitable problem for applying this device.

A good deal of the structures of amino acids has been elucidated in the past several years, but not so much has been done for the amino acid salts. The differences in the configuration of acid groups between the free acid and salt might be one of the most interesting problems from the chemical point of view. This paper will present its findings by reviewing the X-ray analysis of nickel α-amino isobutyrate tetrahydrate.

Experimental

The crystals used in this investigation were prepared by adding an excess of freshly prepared nickel(II) hydroxide to a warm aqueous solution of α-amino isobutyric acid. The solution was then filtered and allowed to evaporate slowly. This procedure made it possible to obtain blue needle-like crystals, the direction of elongation being along the a-axis.

Crystallographic Data

Laue, oscillation and Weissenberg photographs taken with copper K_α radiation (λ= 1.542 Å) confirmed the unit cell dimensions of the crystal reported by Hirokawa et al.[3,4]:

$a=9.92\pm0.02$ Å $\quad c=11.42\pm0.02$ Å

$b=14.24\pm0.05$ Å $\quad \beta=107.5\pm0.5°$

The space group of the crystal was concluded to be $P2_1/a$ from the systematic absences of the following spectra: $(h\,k\,l)$ for all, $(0\,k\,0)$ for $k=2n+1$, and $(h\,0\,l)$ for $h=2n+1$.

The density of the crystal, measured by the floatation method, was found to be 1.48 g./cc., corresponding to four formula units, $4Ni(NH_2\cdot(CH_3)_2C\cdot COO)_2\cdot 4H_2O$, in the unit cell. There are two kinds of amino acid groups and four kinds of water molecules which are crystallographically non-equivalent.

Determination of the Structure

The intensities of the $(0\,k\,l)$, $(h\,0\,l)$ and $(h\,k\,0)$ reflections were estimated visually from Weissenberg photographs. The intensities of the reflections on different films were put on the same scale by comparing the intensities of the same reflections appearing on successive photographs.

No correction were made for absorption, because the crystals used were cut into suitable sizes and shapes, having dimensions less than 0.2 mm.×0.4 mm. in cross section.

After a correction for the Lorentz and polarization factors, the measured intensities were converted to an absolute scale by using Wilson's statistical method (Wilson, 1949)[5].

Using the F^2 values thus obtained, three sets of Patterson syntheses were computed along the a-, b- and c-axis. The minimum-function method (Buerger, 1951) was applied first to $P(v, w)$, using the image seeker described in a preceding paper[1]. The obtained minimum function (M_2) is given in Fig. 1. It gives a clue to the structure, giving approximate

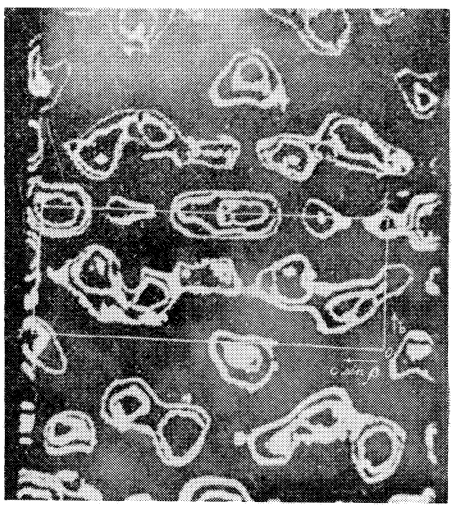


Fig. 1. M_2-Map from $P(v, w)$ obtained by the application of the newly designed image-seeker.

* Present address : Koa Oil Company, Marunouchi, Tokyo.

1) T. Noguchi, to be published in Ōyōbutsuri, 1961.

2) M. J. Buerger, *Acta Cryst.*, **4**, 531 (1951).

3) S. Hirokawa, and S. Kuribayashi, *Annual Report of the Institute for Fibre Research, Osaka University*, **5**, 4 (1950).

4) S. Hirokawa, S. Kuribayashi and I. Nitta, This Bulletin, **25**, 192 (1952).

5) A. J. C. Wilson, *Nature*, **150**, 151 (1949).

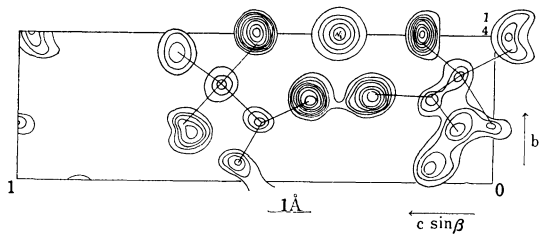


Fig. 2. Fourier projection $\rho(y,z)$. Contours for lighter atoms are drawn at equal intervals on an arbitrary scale.

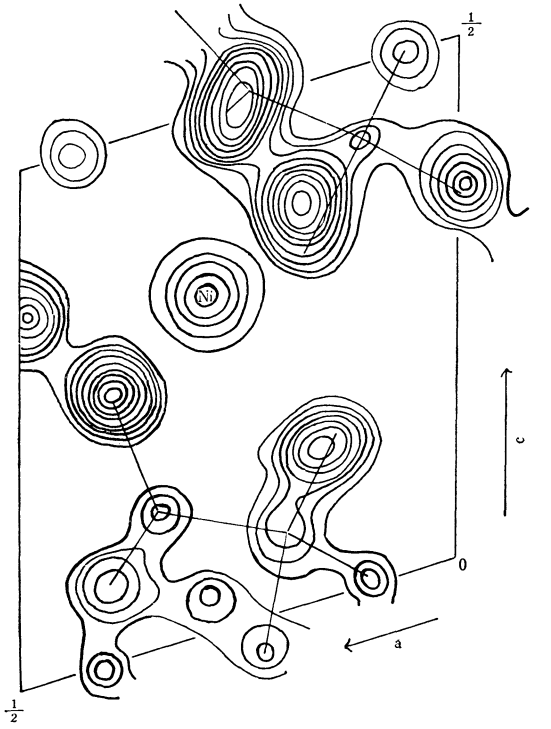


Fig. 3. Fourier projection $\rho(x,z)$. Contours for lighter atoms are drawn at equal intervals on an arbitrary scale.

values of the y- and z-coordinates not only for the nickel atom but also for several light atoms. The same procedures were applied to $P(u,v)$ and $P(u,w)$. Though the obtained maps were rather poor to resolve the location of each atom, a rough lay-out of the structure was obtained from the interpretation of these three minimum function maps.

Structure factors for $(0\,k\,l)$, $(h0l)$ and $(hk0)$ were calculated using the parameters found from the three sets of M_2-maps. These parameter-values were first refined by the Fourier syntheses. The locations of some atoms on the projected electron-density maps were obscured on account of overlappings. The coordinates of these atoms were obtained by successive refinement, using the trial-and-error method.

TABLE I. ATOMIC COORDINATES

		x	y	z
	Ni	0.285	0.250	0.326
A	O_2	0.395	0.152	0.252
	O_3 (H_2O)	0.387	0.363	0.263
B	O_4	0·175	0.140	0.392
	O_5 (H_2O)	0.177	0.350	0.383
A	O_6	0.397	0.092	0.075
B	O_7	0.233	0.032	0.532
	O_8 (H_2O)	0.017	0.077	0.630
	O_9 (H_2O)	0.170	0.475	0.135
A	N_{10}	0.133	0.238	0.152
B	N_{11}	0.439	0.237	0.498
A	C_{12}	0.338	0.149	0.132
A	C_{13}	0.192	0.182	0.071
A	C_{14}	0.218	0.229	0.963
A	C_{15}	0.095	0.100	0.005
B	C_{16}	0.263	0.105	0.490
B	C_{17}	0.392	0.165	0.572
B	C_{18}	0.496	0.091	0.652
B	C_{19}	0.328	0.218	0.667

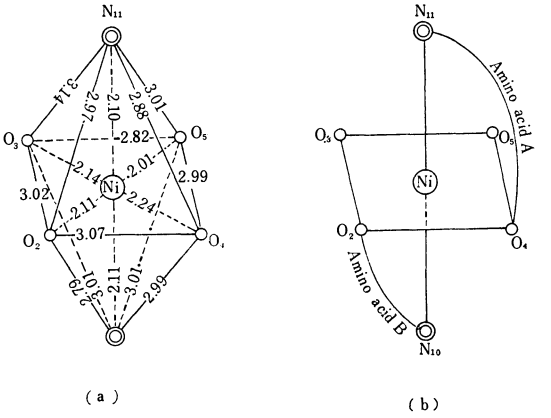


Fig. 4. (a) Interatomic distances around the nickel ion.
(b) The chelation of the amino acid molecules around the nickeous ion.

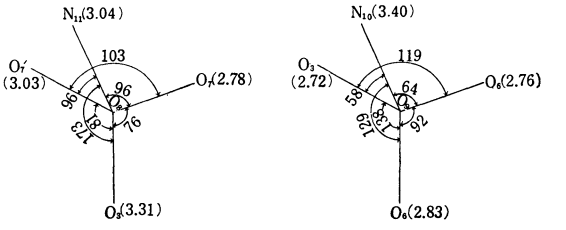


Fig. 5. The interatomic distances and angles around two water molecules, which bind the structure.

Fourier projections $\rho(y,z)$ and $\rho(x,z)$ are shown in Figs. 2 and 3. The atomic coordinates are tabulated in Table I, where A and B denote two different amino-radicals in the crystal respectively.

TABLE II. COMPARISON OF OBSERVED AND CALCULATED STRUCTURE FACTORS

$h\,k\,l$	F_o	F_c	$h\,k\,l$	F_o	F_c	$h\,k\,l$	F_o	F_c	$h\,k\,l$	F_o	F_c
0 0 1	78.5	−94.8	0 4 0	8.7	0.4	0 8 0	80.3	83.0	0 12 4	11.5	−16.3
0 0 2	22.0	23.4	0 4 1	2.9	− 7.1	0 8 1	24.1	−25.0	0 12 5	7.6	− 8.4
0 0 3	83.1	82.0	0 4 2	6.5	−11.0	0 8 2	21.5	−27.8	0 12 6	10.9	13.3
0 0 4	54.1	−51.8	0 4 3	7.6	− 6.8	0 8 3	22.1	19.8	0 12 7	4.1	− 8.5
0 0 5	57.9	−52.0	0 4 4	5.9	−11.8	0 8 4	5.0	1.9	0 12 8	7.6	− 8.6
0 0 6	47.6	45.2	0 4 5	53.9	−62.4	0 8 5	22.1	−24.9	0 12 9	8.8	7.1
0 0 7	21.2	−21.4	0 4 6	81.2	88.2	0 8 6	42.9	35.2	0 12 10	< 2.4	− 2.1
0 0 8	11.7	22.9	0 4 7	< 2.9	0.5	0 8 7	< 4.1	6.3			
0 0 9	< 2.9	0.7	0 4 8	34.4	−41.0	0 8 8	< 4.1	3.7	0 13 1	14.1	−14.9
0 0 10	8.8	−14.8	0 4 9	28.2	29.1	0 8 9	< 4.1	5·5	0 13 2	< 4.1	− 6.4
0 0 11	20.2	−16.7	0 4 10	5.0	− 8.3	0 8 10	< 2.9	0.3	0 13 3	< 4.1	− 3.3
0 0 12	20.5	17.4	0 4 11	19.4	−25.1	0 8 11	16.2	−16.0	0 13 4	20.9	−26.0
0 0 13	< 2.9	3.1	0 4 12	13.2	5.0	0 8 12	10.6	9.5	0 13 5	10.3	15.8
			0 4 13	< 2.9	− 1.7				0 13 6	4.1	5.2
0 1 1	127.1	−162.2				0 9 1	74.1	−86.9	0 13 7	20.6	−19.7
0 1 2	2.9	− 0.8	0 5 1	9.7	19.2	0 9 2	47.9	53.2	0 13 8	10.6	9.3
0 1 3	7.6	5.3	0 5 2	18.5	−22.3	0 9 3	4.1	9.3	0 13 9	5.0	5.7
0 1 4	47.0	−48.6	0 5 3	9.7	15.0	0 9 4	23.5	−19.7			
0 1 5	38.8	26.4	0 5 4	31.7	−26.6	0 9 5	48.8	55.8	0 14 0	12.3	−13.3
0 1 6	16.8	17.9	0 5 5	44.7	54.6	0 9 6	< 4.1	2.4	0 14 1	4.1	0.9
0 1 7	5.0	5.7	0 5 6	30.3	35.6	0 9 7	< 4.1	6.7	0 14 2	< 4.1	− 9.9
0 1 8	6.5	− 0.3	0 5 7	49.4	−51.7	0 9 8	< 4.1	− 4.4	0 14 3	5.9	0.7
0 1 9	< 2.9	1.4	0 5 8	17.1	14.4	0 9 9	< 4.1	− 8.7	0 14 4	5.0	− 4.8
0 1 10	5.9	− 0.2	0 5 9	21.7	29.0	0 9 10	10.6	−14.4	0 14 5	15.3	18.1
0 1 11	10.3	8.3	0 5 10	30.6	−31.9	0 9 11	5.9	5.6	0 14 6	20.3	−20.2
0 1 12	22.3	19.3	0 5 11	14.1	13.5	0 9 12	5.9	3.2	0 14 7	5.0	2.0
0 1 13	12.9	−12.0	0 5 12	< 2.9	4.8				0 14 8	12.9	12.9
			0 5 13	7.1	− 3.8	0 10 0	64.7	−63.5			
0 2 0	109.4	−132.7				0 10 1	30.9	31.7	0 15 1	8.2	7.7
0 2 1	27.1	28.6	0 6 0	67.3	−64.8	0 10 2	28.8	34.3	0 15 2	10.9	−16.8
0 2 2	47.9	54.5	0 6 1	14.1	12.8	0 10 3	25.9	−13.9	0 15 3	< 2.9	− 0.6
0 2 3	76.5	−80.4	0 6 2	< 4.1	− 6.1	0 10 4	13.5	13.5	0 15 4	15.0	16.6
0 2 4	< 4.1	− 6.0	0 6 3	53.8	−64.7	0 10 5	6.5	7.3	0 15 5	9.7	−10.6
0 2 5	29.1	−29.7	0 6 4	13.5	7.5	0 10 6	7.6	− 7.4	0 15 6	2.9	0.7
0 2 6	48.8	−42.8	0 6 5	38.5	42.4	0 10 7	6.5	− 9.9	0 15 7	20.3	19.3
0 2 7	6.5	7.4	0 6 6	63.2	−76.5	0 10 8	< 2.9	− 2.1			
0 2 8	27.0	28.7	0 6 7	24.7	32.3	0 10 9	8.2	− 1.9	0 16 0	< 3.2	− 8.7
0 2 9	15.9	−10.8	0 6 8	18.2	19.9	0 10 10	< 2.9	5.0	0 16 1	< 2.9	− 3.0
0 2 10	< 4.1	2.0	0 6 9	18.5	−17.2	0 10 11	10.6	12.3	0 16 2	11.5	−10.7
0 2 11	23.2	23.1	0 6 10	< 2.9	− 1.8				0 16 3	13.5	8.5
0 2 12	21.5	−19.4	0 6 11	9.4	8.2	0 11 1	37.7	33.5	0 16 4	2.9	− 1.0
0 2 13	< 2.9	− 4.6	0 6 12	12.3	−14.4	0 11 2	25.3	−24.9	0 16 5	8.2	− 5.8
			0 6 13	< 2.4	1.3	0 11 3	7.1	−10.0	0 16 6	13.5	5.5
0 3 1	43.5	46.6				0 11 4	19.7	20.8			
0 3 2	77.6	−92.0	0 7 1	37.9	34.1	0 11 5	15.3	−13.2	0 17 1	16.2	−12.6
0 3 3	12.0	−13.9	0 7 2	41.5	−42.8	0 11 6	4.1	− 6.3	0 17 2	9.7	8.4
0 3 4	19.4	19.8	0 7 3	< 4.1	1.9	0 11 7	10.3	14.2	0 17 3	< 2.4	0.4
0 3 5	66.1	−73.9	0 7 4	18.2	13.6	0 11 8	10.6	−10.1	0 17 4	7.6	− 8.1
0 3 6	10.3	−13.3	0 7 5	17.3	− 3.6	0 11 9	< 2.9	− 0.7			
0 3 7	46.7	44.1	0 7 6	21.5	−24.2	0 11 10	7.6	6.5	0 18 0	16.4	−15.8
0 3 8	23.8	−29.3	0 7 7	38.5	37.2	0 11 11	4.1	− 4.7	0 18 1	4.1	4.4
0 3 9	4.1	− 2.9	0 7 8	13.5	−16.1						
0 3 10	16.8	12.9	0 7 9	7.6	−10.9	0 1 20	40.6	41.0	2 0 $\bar{1}$	3.8	2.7
0 3 11	10.9	−10.3	0 7 10	11.5	8.1	0 1 21	10.3	− 7.7	2 0 $\bar{2}$	16.7	−26.1
0 3 12	2.9	− 3.7	0 7 11	6.5	− 4.4	0 1 22	13.8	− 6.9	2 0 $\bar{3}$	57.9	64.1
0 3 13	5.9	3.8	0 7 12	9.7	− 6.8	0 1 23	20.6	25.3	2 0 $\bar{4}$	44.5	−45.6

TABLE II. (Continued)

hkl	F_o	F_c	hkl	F_o	F_c	hkl	F_o	F_c	hkl	F_o	F_c
2 0 $\bar{5}$	11.1	−11.7	6 0 $\bar{3}$	2.7	1.8	10 0 $\bar{8}$	< 1.9	− 1.8	2 14 0	18.0	19.8
2 0 $\bar{6}$	27.4	−22.5	6 0 $\bar{4}$	93.9	−100.7	10 0 $\bar{9}$	5.5	2.6	2 15 0	< 5.0	0.6
2 0 $\bar{7}$	7.9	−10.9	6 0 $\bar{5}$	80.7	69.5	10 0 $\bar{10}$	9.0	− 5.9	2 16 0	9.1	− 6.1
2 0 $\bar{8}$	50.1	51.8	6 0 $\bar{6}$	14.3	13.8	10 0 $\bar{11}$	< 1.1	2.3	2 17 0	< 5.0	− 1.1
2 0 $\bar{9}$	22.0	−20.3	6 0 $\bar{7}$	51.4	−56.8	10 0 $\bar{12}$	10.8	16.5			
2 0 $\bar{10}$	4.8	2.6	6 0 $\bar{8}$	25.0	30.3				3 1 0	33.3	32.9
2 0 $\bar{11}$	28.1	35.1	6 0 $\bar{9}$	< 1.9	− 6.2	10 0 0	20.0	21.2	3 2 0	17.8	−26.4
2 0 $\bar{12}$	11.2	− 7.1	6 0 $\bar{10}$	36.4	−34.4	10 0 1	16.1	24.6	3 3 0	< 5.0	9.3
2 0 $\bar{13}$	14.2	−13.8	6 0 $\bar{11}$	4.8	− 5.2	10 0 2	25.9	−23.8	3 4 0	9.4	4.2
2 0 $\bar{14}$	16.9	19.8	6 0 $\bar{12}$	5.7	−11.5	10 0 3	21.5	25.9	3 5 0	< 5.0	4.4
			6 0 $\bar{13}$	2.3	− 4.0	10 0 4	9.7	9.7	3 6 0	12.0	11.3
2 0 0	123.6	−129.6	6 0 $\bar{14}$	2.3	1.7	10 0 5	2.3	− 0.9	3 7 0	11.0	9.8
2 0 1	33.7	46.5							3 8 0	24.0	14.7
2 0 2	4.3	7.0	6 0 0	1.9	4.9	12 0 $\bar{1}$	1.9	1.2	3 9 0	12.0	−15.1
2 0 3	86.6	−101.8	6 0 1	21.8	17.6	12 0 $\bar{2}$	< 1.7	− 1.3	3 10 0	14.6	20.0
2 0 4	72.5	74.7	6 0 2	41.6	−47.6	12 0 $\bar{3}$	< 1.7	3.7	3 11 0	< 5.0	3.9
2 0 5	61.0	76.2	6 0 3	10.8	19.2	12 0 $\bar{4}$	< 1.7	− 6.1	3 12 0	11.3	6.6
2 0 6	51.6	−45.2	6 0 4	38.4	−47.6	12 0 $\bar{5}$	2.3	4.0	3 13 0	5.0	8.1
2 0 7	8.9	3.9	6 0 5	5.3	− 8.0	12 0 $\bar{6}$	3.6	− 3.9	3 14 0	14.7	−14.4
2 0 8	< 1.9	2.8	6 0 6	9.7	− 6.3	12 0 $\bar{7}$	5.0	10.3	3 15 0	< 5.0	0.6
2 0 9	7.0	− 7.4	6 0 7	27.9	29.1	12 0 $\bar{8}$	7.9	9.4	3 16 0	< 5.0	1.8
2 0 10	3.4	− 1.2	6 0 8	4.1	1.5	12 0 $\bar{9}$	8.1	− 4.7			
2 0 11	13.4	13.5	6 0 9	5.6	− 2.2				4 1 0	10.0	17.8
2 0 12	2.7	1.3	6 0 10	8.3	8.4	12 0 0	1.2	0.7	4 2 0	5.0	5.8
2 0 13	1.1	1.3							4 3 0	36.0	42.1
			8 0 $\bar{1}$	36.8	41.0	1 1 0	14.7	−23.3	4 4 0	64.0	64.0
4 0 $\bar{1}$	87.9	−104.7	8 0 $\bar{2}$	31.0	−25.2	1 2 0	77.5	−110.6	4 5 0	45.3	−47.7
4 0 $\bar{2}$	7.8	13.7	8 0 $\bar{3}$	8.9	− 9.4	1 3 0	20.0	21.1	4 6 0	64.0	−56.8
4 0 $\bar{3}$	16.2	7.7	8 0 $\bar{4}$	39.2	49.6	1 4 0	14.4	24.6	4 7 0	49.3	45.0
4 0 $\bar{4}$	15.0	14.6	8 0 $\bar{5}$	9.7	− 4.9	1 5 0	21.3	−20.6	4 8 0	< 5.0	− 0.3
4 0 $\bar{5}$	31.7	−29.5	8 0 $\bar{6}$	13.8	−14.0	1 6 0	4.5	−13.2	4 9 0	< 5.0	8.8
4 0 $\bar{6}$	39.2	36.0	8 0 $\bar{7}$	24.7	27.0	1 7 0	8.7	−10.5	4 10 0	< 5.0	2.6
4 0 $\bar{7}$	16.4	16.2	8 0 $\bar{8}$	9.4	−10.6	1 8 0	14.3	25.4	4 11 0	11.3	10.9
4 0 $\bar{8}$	43.1	−40.7	8 0 $\bar{9}$	< 1.9	5.1	1 9 0	< 5.0	2.9	4 12 0	9.3	8.3
4 0 $\bar{9}$	13.2	10.1	8 0 $\bar{10}$	< 1.7	− 7.6	1 10 0	< 5.0	− 6.4	4 13 0	10.4	− 6.5
4 0 $\bar{10}$	40.1	37.6	8 0 $\bar{11}$	< 1.4	4.8	1 11 0	< 5.0	− 4.0	4 14 0	18.0	−15.4
4 0 $\bar{11}$	9.7	− 8.9	8 0 $\bar{12}$	6.3	− 9.8	1 12 0	6.4	4.1	4 15 0	17.0	11.7
4 0 $\bar{12}$	< 1.2	− 1.7	8 0 $\bar{13}$	14.9	12.6	1 13 0	5.0	− 8.8	4 16 0	8.7	9.0
4 0 $\bar{13}$	6.6	4.5				1 14 0	< 5.0	−13.2			
4 0 $\bar{14}$	11.2	−12.0	8 0 0	< 1.9	1.8	1 15 0	7.0	11.6	5 1 0	8.0	11.2
			8 0 1	34.8	−37.7	1 16 0	< 5.0	9.8	5 2 0	< 5.0	−13.6
4 0 0	10.0	−10.8	8 0 2	11.7	10.0	1 17 0	< 5.0	5.6	5 3 0	13.0	−11.2
4 0 1	52.2	−46.9	8 0 3	< 1.9	− 5.0				5 4 0	23.9	−30.5
4 0 2	39.2	32.9	8 0 4	9.1	− 9.0	2 1 0	40.6	62.9	5 5 0	5.3	7.5
4 0 3	52.5	57.9	8 0 5	4.8	3.5	2 2 0	74.3	82.7	5 6 0	< 5.3	−11.1
4 0 4	21.2	−21.2	8 0 6	< 1.7	0.4	2 3 0	24.7	−23.6	5 7 0	< 5.3	− 8.2
4 0 5	3.4	−11.4	8 0 7	6.1	− 7.1	2 4 0	80.7	−82.3	5 8 0	< 5.0	− 3.0
4 0 6	58.9	59.9	8 0 8	< 1.1	6.1	2 5 0	8.6	−13.1	5 9 0	< 5.0	−16.8
4 0 7	55.7	−65.9				2 6 0	6.2	− 5.1	5 10 0	< 5.0	− 8.6
4 0 8	2.7	− 2.1	10 0 $\bar{1}$	21.0	−22.3	2 7 0	24.7	−31.3	5 11 0	< 5.0	4.6
4 0 9	12.2	11.9	10 0 $\bar{2}$	9.6	14.6	2 8 0	62.6	−54.3	5 12 0	< 5.0	− 8.8
4 0 10	13.5	−15.6	10 0 $\bar{3}$	21.3	21.7	2 9 0	10.6	7.1	5 13 0	< 5.0	6.0
4 0 11	< 1.1	− 3.0	10 0 $\bar{4}$	19.7	−19.5	2 10 0	36.0	39.6	5 14 0	< 5.0	− 4.5
			10 0 $\bar{5}$	3.0	6.5	2 11 0	22.0	−22.5	5 15 0	< 5.0	− 1.3
6 0 $\bar{1}$	11.3	−17.3	10 0 $\bar{6}$	7.0	−13.8	2 12 0	10.3	− 2.0			
6 0 $\bar{2}$	22.3	15.3	10 0 $\bar{7}$	13.0	−11.7	2 13 0	< 5.0	1.6	6 1 0	11.0	12.1

TABLE II. (Continued)

hkl	F_o	F_c	hkl	F_o	F_c	hkl	F_o	F_c	hkl	F_o	F_c
6 2 0	< 5.0	6.3	7 4 0	8.0	13.6	8 7 0	24.0	17.0	9 11 0	12.0	−12.5
6 3 0	64.0	−61.6	7 5 0	< 5.0	− 8.5	8 8 0	< 5.0	− 4.3			
6 4 0	< 6.0	− 8.1	7 6 0	< 5.0	1.4	8 9 0	19.3	−17.0	10 1 0	20.0	12.1
6 5 0	55.4	54.4	7 7 0	11.3	− 3.2	8 10 0	< 5.3	6.8	10 2 0	< 5.0	− 7.5
6 6 0	15.3	19.2	7 8 0	< 5.0	7.3	8 11 0	23.3	17.9	10 3 0	< 5.0	1.8
6 7 0	45.3	−45.7	7 9 0	< 5.0	1.3	8 12 0	< 5.0	2.4	10 4 0	< 5.0	− 6.7
6 8 0	11.3	− 9.8	7 10 0	< 5.0	0.2	8 13 0	15.5	− 9.7	10 5 0	< 5.0	− 8.8
6 9 0	8.0	15.9	7 11 0	< 5.0	− 1.9				10 6 0	< 5.0	− 6.9
6 10 0	< 5.0	− 5.3	7 12 0	12.7	11.6	9 1 0	< 5.0	6.3	10 7 0	< 5.0	− 4.4
6 11 0	11.3	−10.5	7 13 0	< 5.0	3.8	9 2 0	< 5.0	1.7	10 8 0	< 5.0	1.4
6 12 0	8.8	− 3.5	7 14 0	8.7	10.3	9 3 0	< 5.0	5.5	10 9 0	11.3	9.9
6 13 0	16.0	15.4				9 4 0	< 5.0	− 8.7			
6 14 0	14.7	13.9	8 1 0	39.3	−33.1	9 5 0	< 5.0	13.0	11 1 0	< 5.0	− 5.2
6 15 0	16.7	−15.9	8 2 0	11.0	17.3	9 6 0	< 5.0	− 2.6	11 2 0	< 5.0	− 3.8
			8 3 0	14.0	6.8	9 7 0	< 5.0	− 1.9	11 3 0	< 5.0	− 0.9
7 1 0	12.0	− 7.8	8 4 0	11.3	−15.0	9 8 0	< 5.0	− 0.6	11 4 0	< 5.0	− 2.7
7 2 0	12.3	10.1	8 5 0	< 5.0	− 8.3	9 9 0	< 5.0	5.3	11 5 0	< 5.0	− 5.7
7 3 0	< 5.0	− 3.2	8 6 0	9.3	− 9.5	9 10 0	< 5.0	− 1.6			

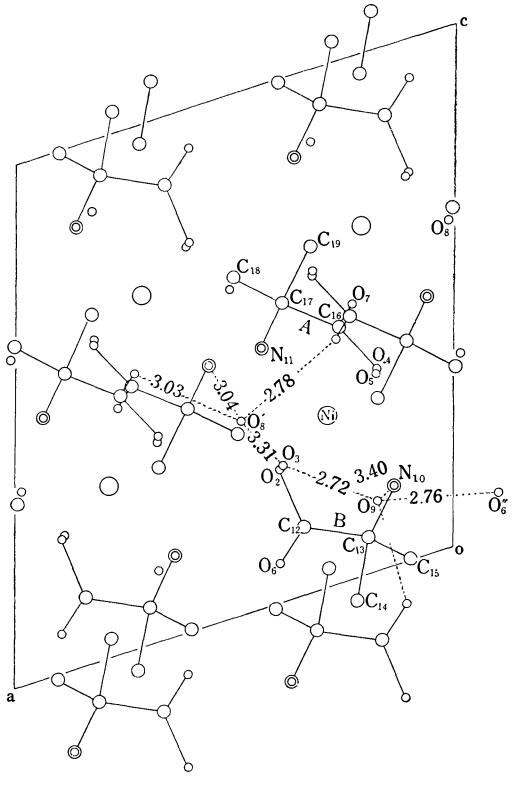


Fig. 6. The structure of nickel dialpha-amino isobutyrate tetrahydrate viewed along the b-axis.

○ Ni ∘ O ◎ N ○ C

Comparison of F_o are tabulated in Table II, where the F_c-values include the overall temperature factor ($-3.15 \sin^2\theta/\lambda^2$).

The reliability index, neglecting unobserved reflections, is 16.8, 15.7 and 18.1% respectively for the ($0kl$), ($h0l$) and ($hk0$) reflections.

Discussion of the Structure

The Amino Acid Radicals.—The interatomic distances and the bond angles for the two kinds of acid groups are given in Table III. Standard deviations were estimated to be ±0.05 Å for distances and ±5° for angles. For comparison, the reported values for the free acid (Hirokawa, 1952) are given in the last column of Table III.

In the structure of α-amino isobutyric acid (Hirokawa et al., 1952), the carboxyl group, C_α and N, is almost coplanar. The most characteristic feature of the structure of the nickel salt is that the nitrogen atoms are definitely out of the plane, the angles of twist around the C_α–C_o bonds being 17.8° and 24.1° respectively for groups A and B. It is interesting to note that the configurations and the dimensions of the two kinds of the amino acid groups are almost the same. The twist around the C_α–C_o bond may be caused by the coordination of amino groups around the nickel ion.

The nearest neighbors surrounding the nickel ion are two carboxylic oxygen atoms, two nitrogen atoms and two water molecules. They form a distorted octahedron, having the structural dimensions which are given in Table IV and Fig. 4 (a).

The two kinds of the amino acid groups form chelate rings with the nickel ion by the nitrogen atoms in the amino groups and by the carboxylic oxygen atoms, assuming a cis-configuration (Fig. 4 (b)).

TABLE III. MOLECULAR DIMENSIONS OF THE α-AMINO ACIDS

	Group A	Group B	Free molecule
(a) Interatomic distances, Å			
O_c-C_c	1.32	1.30	1.26
	1.29	1.22	1.20
C_c-C_α	1.48	1.58	1.52
C_α-N	1.47	1.48	1.49
C_α-C_β	1.50	1.57	1.53
	1.55	1.60	1.54
(b) Bond angles, °			
O_c-C_c-O_c	115	119	125
O_c-C_c-C_α	122	121	118
	119	119	118
C_c-C_α-N	113	112	109
C_c-C_α-C_β	114	105	114
	98	104	109
N-C_α-C_β	114	122	108
	118	109	105
C_β-C_α-C_β	100	104	112

TABLE IV. INTERATOMIC DISTANCES AROUND THE NICKEL ION, Å

Ni-O_2	2.11	N_{10}-O_5	3.01
Ni-O_3	2.14	N_{11}-O_2	2.97
Ni-O_4	2.24	N_{11}-O_3	3.14
Ni-O_5	2.01	N_{11}-O_4	2.88
Ni-N_{10}	2.11	N_{11}-O_5	3.01
Ni-N_{11}	2.10	O_2-O_3	3.02
N_{10}-O_2	2.79	O_2-O_4	3.07
N_{10}-O_3	3.03	O_3-O_5	2.82
N_{10}-O_4	2.99	O_4-O_5	2.99

Thus, two of the four water molecules are coordinated to the nickel ion, and the remaining two are found between these octahedra, playing the role of binding them. Each of the latter two water molecules has three carboxylic oxygen atoms and one nitrogen atom as its nearest neighbors. The interatomic distances and angles around these water molecules are shown in Fig. 5. It is rather difficult to say which of these contacts are hydrogen bonds, though the interatomic distances suggest they are O_7—$H_2O(O_8)$, O_3—$H_2O(O_9)$ and O'_6—$H_2O(O_9)$. These features may be compared to the hydrogen bonds in the structure of ice.

The structures viewed along the b-axis are shown in Fig. 6, where one can easily see the following structural features: the two amino acids and the two H_2O molecules are coordinated to the nickel ion, forming a complex. These groups are held together along the [101] and [100] directions by the other H_2O molecules, making short contacts between them.

Summary

The unit cell of nickel(II) dialpha-amino isobutyrate tetrahydrate has the follwing dimensions; a=9.92, b=14.24, c=11.42 Å, β=107.5°, and contains four chemical units. The space group is determined to be $P2_1/a$.

Buerger's minimum-function method was applied to the structure analysis, and the newly designed image-seeker was used. Two of the four water molecules are coordinated to the nickel ion, forming a distorted octahedron with the carboxylic oxygen and the amino nitrogen atoms. The other two water molecules play the role of binders for these octahedrons. The chelation of the amino acid molecules is of the cis-form. The structure of the skeleton of α-amino propionic acid in this complex is not planar, in contrast to that of its free acid.

The author is indebted to Professor Isamu Nitta, Professor Tokunosuke Watanabe and Professor Sakutaro Hirokawa, who encouraged him throughout this investigation. He also wishes to express his heartfelt thanks to Professor Masao Sawada, who showed a deep interest in this structure analysis.

Department of Physics
Faculty of Science
Osaka University, Osaka

*Biochemical Studies on Oils and Fats. X. Toxicity of Thermally Denatured Ethyl Linolenate**

By Noboru MATSUO

(Received May 19, 1961)

In previous papers the author has reported that thermally denatured fish oil (cuttle fish oil)[1,2], rape-seed oil[3], and the ethyl esters of highly unsaturated fatty acids[4] show toxicity due to monomeric cyclization products formed as a result of heating.

For the purpose of elucidating the properties and structure of the cyclic products, experiments were conducted to investigate whether or not ethyl linolenate shows a similar toxicity when thermally denatured. The present paper describes the results of the experiments.

Experimental and Results

Separation of Linolenic Acid from Linseed Oil.—Refined linseed oil, whose properties are shown in Table I, was saponified by the ordinary method, and the separated fatty acids were dissolved in ether. Bromine was dropped into the ether solution with cooling. The precipitated bromide was collected by filtration, washed with cold ether, and then dried. For purification, the bromide was dissolved in a large quantity of benzene, and the solution was boiled on a hot water bath. The hexabromide of linolenic acid was then obtained as white precipitate on cooling. The precipitate was collected, washed with cold ether and dried. The hexabromide thus obtained was treated with zinc, ethanol and hydrochloric acid to effect debromination and esterification simultaneously. The ester mixture was distilled in vacuo (1.5 mmHg), and the fraction boiling at 167~170°C was used in the experiment. The properties of this fraction are shown in Table I.

Thermal Denaturation of Ethyl Linolenate and Separation of Cyclic Monomer.—Thermal denaturation of ethyl linolenate was carried out by heating it for 40 hr. at 250°C in a carbon dioxide stream. During this process the iodine value decreased from 242.5 to 157.5, as is shown in Fig. 1. Straight chain ester and cyclic ester were separated from the denatured ethyl linolenate by the urea adduct method[1]. The yields of the straight chain ester and the cyclic ester were 21.2 and 63.3% respectively. By vacuum distillation, the latter was separated into distillate (153~175°C/1.8~2.0 mmHg) and residue. The distillate is a transparent light yellow, and its yield was 24.7% of the total cyclic ester. The residue is somewhat viscous, transparent, and reddish brown, and its yield was 70.8%.

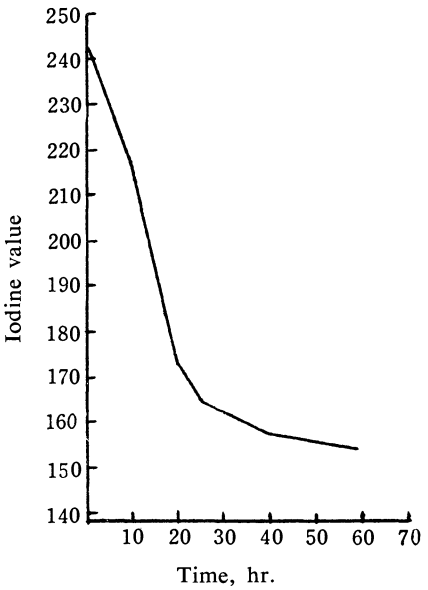


Fig. 1. Change in iodine value of ethyl linolenate due to thermal denaturation.

TABLE I. PROPERTIES OF LINSEED OIL AND ETHYL LINOLENATE

	n_D^{20}	Iodine value (Wijs)	Sap. value	Acid value	Molecular weight (Rast)
Linseed oil	1.4833	191.8	186.9	0	—
Ethyl linolenate	1.4688	242.5	183.1	1.0	302

* IX: N. Matsuo, *J. Biochemistry*, **49**, 635 (1961).

1) N. Matsuo, *J. Biochemistry (Japan)*, **29**, 885 (1958).
2) N. Matsuo, *Food and Nutrition (Japan)*, **10**, 255 (1958).
3) N. Matsuo, ibid., **12**, 118 (1958).
4) N. Matsuo, *J. Japan Oil Chemists' Soc.*, **9**, 37 (1960).

Animal Experiments with Various Esters.— An animal experiment was conducted in which rats, each weighing about 60 g., were fed on the basal diet containing 20% of a sample ester, as shown in Table II.

TABLE II. COMPOSITION OF DIET (%)

Starch (rice powder):	65
Casein (ether extracted):	9
McCollum salt mixture:	3
Yeast	3
Liver oil:	One drop a day
Ester	20

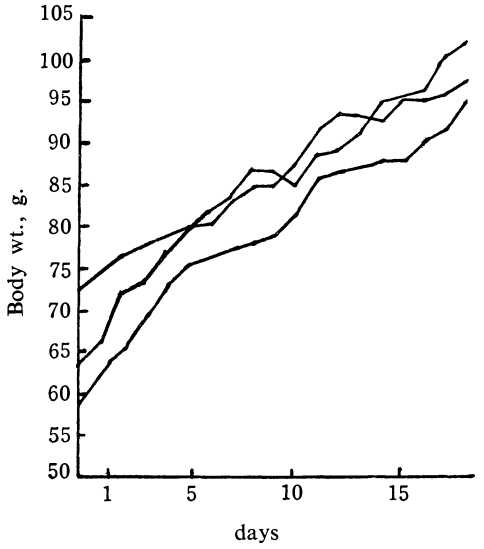


Fig. 2. Growth of rats fed on basal diet containing 20% ethyl linolenate.

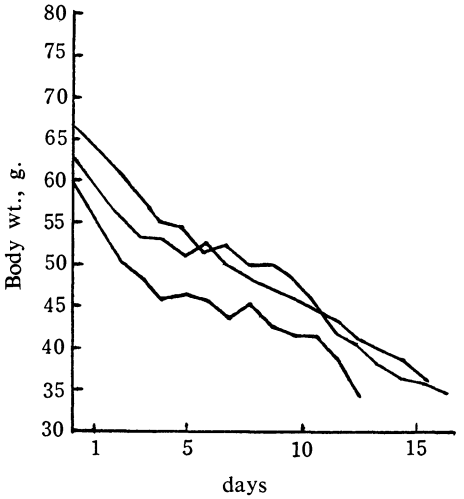


Fig. 3. Growth of rats fed on basal diet containing 20% denatured ethyl linolenate. (All rats died at the ends of the curves.)

Ethyl Linolenate. — The rats fed on a diet containing ethyl linolenate showed a healthy growth, as is seen in Fig. 2.

Denatured Ethyl Linolenate. — As shown in Fig. 3, these rats gradually became thinner and died in 15 days or so.

Distilled Cyclic Ester and Residual Cyclic Ester. — When rats were fed on a basal diet containing 20% distilled cyclic ester, extremely acute toxicity was shown, and all rats died in three or four days. However, no particular change was noticed in the appearance of the rats. In the case of feeding on a basal diet containing 20% residual cyclic ester, toxicity was considerably weaker, and there were some increases in the weight of the rats, although they excreted soft feces (Fig. 4).

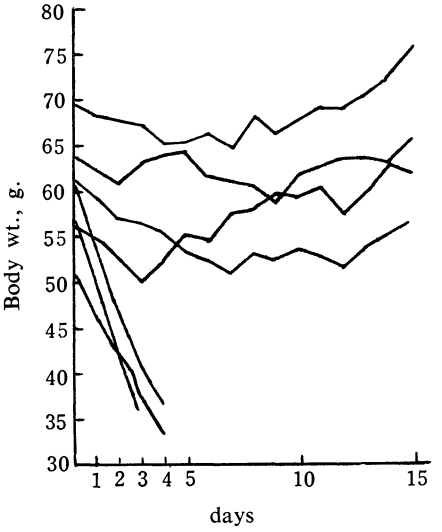


Fig. 4. Growth of rats fed on basal diet containing 20% of distilled cyclic ester (A) and residual cyclic ester (B). (A: all rats died at the ends of the curves.)

From these observations, it was apparent that distilled cyclic ester was severely toxic.

Properties of Various Esters.—The properties of these esters are shown in Table III.

From the iodine value 242.5 of ethyl linolenate (theoretical value: 247.4), it is assumed that the linolenate contained about 6% ethyl linoleate if the contaminant was only ethyl linoleate. The saponification value of this ethyl linolenate was 183.1 (theoretical value: 183.0) and its molecular weight 302 (theoretical value: 306).

The molecular weight of the distilled cyclic ester was 293. From its boiling point, the main component of this cyclic ester is considered a cyclic monomer. Since its iodine value was 159.4, it seems that the original

TABLE III. PROPERTIES OF ESTERS

	n_D^{20}	Iodine value (Wijs)	Sap. value	Acid value	Molecular weight (rast)
Ethyl linolenate	1.4688	242.5	183.1	1.0	302
Denatured ethyl linolenate	1.4838	157.5	170.1	6.5	
Straight chain ester	1.4692	201.5	177.4	0.4	
Cyclic ester	1.4891	142.5	168.6	7.3	
Distilled ester	1.4751	159.4	171.0	7.4	293
Residual ester	1.4948	135.8	168.5	8.2	

linolenate with three double bonds lost one on cyclization. The iodine value of ethyl linoleate, with two double bonds, is 166.0.

Infrared Absorption Spectra of Ethyl Linolenate and Distilled Cyclic Ester.—The infrared absorption spectra of ethyl linolenate and distilled cyclic ester are shown in Fig. 5, I and II, respectively, measured with the Baird B type. The absorption band at about 14 μ for ethyl linolenate is considerably intense and is attributable to cis double bonds.

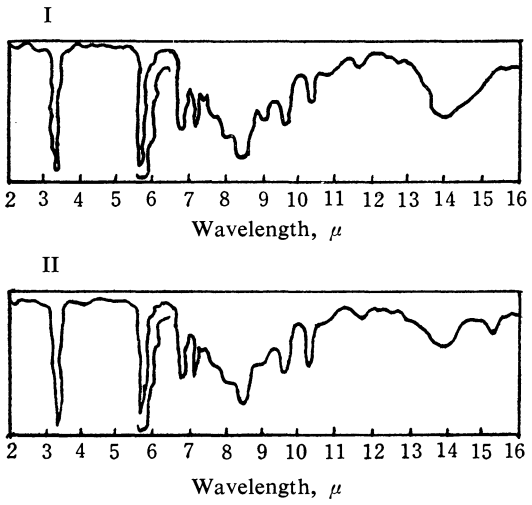


Fig. 5. Infrared absorption spectrum of ethyl linolenate (I) and distilled cyclic ester (II).

Linolenic acid has cis double bonds naturally. When it is separated by the bromination method, however, isomerization takes place to some extent, and an absorption band of 10.3 μ (970 cm^{-1}) attributable to trans double bonds appears. When the absorption band near 6 μ was examined with an increased concentration of the sample, a small absorption was noticed. This absorption is also considered to be attributable to cis double bonds.

When the infrared absorption spectrum (Fig. 5-II) of the distilled cyclic ester is compared with that (Fig. 5-I) of ethyl linolenate, it is found that the absorption attributed to cis double bonds is considerably weaker. This seems to be due to the disappearance of some double bonds. A new absorption band at 15.2 μ (660 cm^{-1}) was observed. Cyclohexene shows a band at 670 cm^{-1} (14.97 μ)[5]. Bands at 663 and 671 cm^{-1} (15.1 and 14.9 μ) are characteristic of Δ^2- and Δ^3-steroids respectively[6], *cis*-α-Ionone[7] also absorbs in this region. So this absorption band is considered to be attributable to the formation of a cyclohexene ring as a result of cyclization. This absorption band was also ascertained by MacDonald[5] in the monomeric, non-urea-adduct-forming material resulting from the ethanolysis of heated linseed oil.

Absorption due to trans double bonds became somewhat greater, but no significant change was observed. Examination of the absorption near 6 μ observed with the higher concentration of the sample showed the existence of two small bands. It seems that the new absorption band at about 6.1 μ (1650 cm^{-1}) originates from the cyclic compound.

Discussion

Acute toxicity is shown by the distilled cyclic ester separated from the denatured product obtained by heating ethyl linolenate for 40 hr. at 250°C. From its molecular weight and infrared absorption spectrum, this distilled ester is considered to be a cyclic monomer with a cyclohexene ring.

Paschke, Wheeler[8] and Rivett[9] have reported the possibility of the formation of intermolecular cyclic compounds. Apparent toxicity was shown also in an experiment feeding animals on a certain synthesized compound containing a cyclohexene ring and one double bond outside the ring[10,11].

Cyclic compounds showed toxicity also in an experiment[4] on highly unsaturated fatty acid

5) J. A. MacDonald, *J. Am. Oil Chemists' Soc.* 33, 394 (1956).
6) R. N. Jones and F. Herling, *J. Org. Chem.*, 19, 1252 (1954).
7) G. Buchi and N. C. Yang, *Helv. Chim. Acta*, 38, 1338 (1955).
8) R. F. Paschke and D. H. Wheeler, *J. Am. Oil Chemists' Soc.*, 32, 473 (1955).
9) D. E. A. Rivett, ibid., 33, 635 (1956).
10) N. Matsuo, *J. Chem. Soc. Japan, Pure Chem. Sec.* (*Nippon Kagaku Zasshi*), 81, 469 (1960).
11) N. Matsuo, *Food and Nutrition* (*Japan*), 12, 86 (1959).

from fish oil; a monomeric cyclization product, separated by vacuum distillation, was the main origin of the toxicity.

From the result of the experiment on ethyl linolenate, it can be concluded that the origin of toxicity is a monomeric cyclization product, and that the main component of this product is a compound having a cyclohexene ring.

Summary

When ethyl linolenate is thermally denatured at 250°C for 40 hr. in a carbon dioxide stream, the product is toxic to rats. The origin of the toxicity of thermally denatured ethyl linolenate is a monomeric cyclization product, which is mainly a compound having a cyclohexene ring.

The author expresses his deep appreciation to Dr. Keizo Kodama, President of Tokushima University, for his guidance during this work.

Thanks are also due to Dr. Seishi Tanaka, instructor at the Engineering Research Institute, Faculty of Engineering, The University of Tokyo, to whom the author is greatly indebted for the infrared absorption spectra.

Department of Chemistry
Seikei University
Musashino, Tokyo

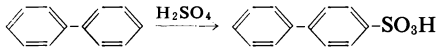
Synthesis of n-Alkyl p-Diphenyl Ethers and Aryl p-Diphenyl Ethers

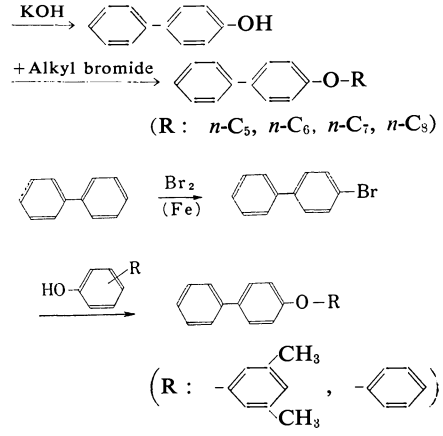
By Hajime SUZUMURA

(Received May 4, 1961)

n-Alkyl *p*-diphenyl ethers[1] whose alkyl group consists of either C_1, C_2, C_3, C_4 and C_5, and aryl *p*-diphenyl ethers whose aryl group includes phenyl[2], *p*-tolyl[3] and benzyl[1] have hitherto been reported on in the literature. Their melting points are shown in Tables I and II.

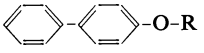
The melting points, except for those of allyl, benzyl and *p*-tolyl ether, are within a relatively narrow range. In order to examine the physical properties of the ethers which have a longer alkyl chain or a methylated benzene ring, the author newly synthesized *n*-alkyl ethers (*n*-C_6, *n*-C_7 and *n*-C_8) and an aryl ether (3, 5-dimethylphenyl) along with the known *n*-amyl and *p*-phenyl ethers by the scheme shown below.





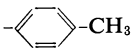
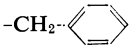
Diphenyl was first sulfonated in nitrobenzene[4], and the resulting sulfonic acid was

TABLE I. ALKYL DIPHENYL ETHERS



R	CH_3	C_2H_5	*n*-C_3H_7	*iso*-C_3H_7	-CH=CH-CH_3	*n*-C_4H_9	*n*-C_5H_{11}
M. p. of the ether, °C	90	76, 78	76~77	73	86	74~75	64~65

TABLE II. ARYL DIPHENYL ETHERS

R			
M. p. of the ether, °C	68	94~96	136

1) C. M. Brewster et al., *J. Am. Chem. Soc.*, **61**, 3083 (1939).
2) A. Luttringkhaus, *Chem. Ber.*, **89**, 463 (1956).
3) R. L. Huang, *J. Chem. Soc.*, **1954**, 3084.
4) E. Gebauer-Fülnegg et al., *Monatsh.*, **49**, 41 (1928).

TABLE III

	n-Amyl	*n*-Hexyl	*n*-Heptyl	*n*-Octyl	Phenyl	3, 5-Dimethylphenyl
Appearance	Colorless flakes	Colorless flakes	Colorless flakes	Colorless flakes	Colorless flakes	Colorless needles
B. p., °C/2 mmHg	178.5～179.5	187～188	201～201.3	208		210～213
M. p., °C	64～65	63.5～64.3	70.7～71.7	68～69	67～68	65.5～66.5
Elementary analysis						
C, %	84.88	84.74	85.17	85.26	—	87.74
H, %	8.25	8.46	8.99	9.42	—	6.49
Calculated for	$C_{17}H_{20}O$	$C_{18}H_{22}O$	$C_{19}H_{24}O$	$C_{20}H_{26}O$	—	$C_{20}H_{18}O$
C, %	84.95	84.99	85.02	85.05	—	87.56
H, %	8.39	8.72	9.01	9.28	—	6.61

fused with potassium hydroxide to give *p*-phenylphenol, which was condensed with *n*-alkyl bromide in ethanol in the presence of sodium hydroxide.

In the case of aryl ethers, diphenyl dissolved in carbon tetrachloride was treated with bromine in the presence of iron powder, and the resulting *p*-bromodiphenyl was condensed with phenols in the presence of copper powder.

The properties of the purified specimens are shown in Table III.

Experimental

Materials.—*Diphenyl*[5].—A sample supplied by Yawata Chemical Industry Co. was recrystallized from ethanol in the form of white leaflets, m. p. 68～69.2°C.

n-Octanol[6].—A commercial reagent was redistilled, b. p. 194～196°C, n_D^{25} 1.4266.

n-Amyl Bromide[7].—A commercial reagent was redistilled, b. p. 126.5～128°C (757 mmHg) (uncorr.).

n-Hexyl Bromide[8].—A commercial reagent was redistilled, b. p. 155～157°C (757 mmHg), n_D^{20} 1.4469.

n-Heptyl Bromide[9].—A mixture of *n*-heptyl alcohol (20 g.), 72 g. of hydrobromic acid and 18.2 g. of concentrated sulfuric acid was refluxed for 6 hr., then washed with water and dilute sodium carbonate solution and finally dried over calcium chloride; yield 22.87 g., 75%, n_D^{25} 1.4482.

n-Octyl Bromide[10].—It was prepared in the same manner as above. From a mixture of *n*-octanol (18.6 g.), 65 g. of hydrobromic acid, 17.0 g. of concentrated sulfuric acid, and 9.6 g. of a fraction boiling at 195～203°C were obtained; $n_D^{19.5}$ 1.454.

1, 3, 5-Xylenol[11].—Commercial reagent; m. p. 61°C.

Bromine, Potassium Hydroxide, Sulfuric Acid.—Commercial reagent.

Synthesis of *n*-Alkyl *p*-Diphenyl Ether.—*Sulfonation of Biphenyl.*—Biphenyl (30 g.), 40 cc. of nitrobenzene and 19 g. of concentrated sulfuric acid were kept at 80～90°C while being stirred for 6.5 hr. Unreacted diphenyl and nitrobenzene were steam distilled, and sodium salt of diphenyl-*p*-sulfonic acid (20.7 g.) was obtained by the addition of a sodium hydroxide solution to the residue. 8.1 g. of diphenyl was recovered. The yield of the sulfonic acid based on the consumed diphenyl was about 57%.

Alkali Fusion of the Sulfonate.—Into potassium hydroxide melted in an nickel crucible at 290～300°C the sodium sulfonate was gradually stirred, and the heating was continued for a while. The mixture was then allowed to cool and dissolved in water. Upon the addition of hydrochloric acid to this solution, a precipitate of crude *p*-phenylphenol was obtained. The results of the potassium hydroxide fusion are shown in Table IV.

TABLE IV

Na-sulfonate g.	KOH g.	Time of fusion min. at 290～300°C	Time of fusion min. at 320～330°C	*p*-Phenylphenol Amount g.	*p*-Phenylphenol Yield %
7.7	25.0	10	15	4.15	81
12.0	46.5	15	5	6.80	85
9.6	32.0	10	5	5.60	88

The crude phenylphenol was distilled in vacuo to give a distillate which boiled at 184～190°C (18 mmHg) and melted at 159～162°C (uncorr.).

Condensation.—It was carried out by the Williamson reaction. A mixture of *p*-phenylphenol, ethanol, sodium hydroxide and *n*-alkyl bromide was refluxed, and the mixture was poured into water. On the addition of an aqueous solution of sodium hydroxide, the crude ether was separated from the phenylphenol which had been recovered by the acidification of the filtrate. The crude ether was purified by recrystallization from ethanol. The results are shown in Table V.

Synthesis of Aryl *p*-Diphenyl Ether.—*Synthesis of p-Bromodiphenyl*[12].—Bromine (90 g.) was gradually stirred into a mixture of diphenyl (86 g.), 260 cc. of carbon tetrachloride and 2 g. of iron powder, and heating was continued at 45～55°C for 11 hr. The solvent was then distilled off and the

5) I. Heilbron, "Dictionary of Organic Compounds", Vol. 2, Oxford University Press, New York (1953), p. 401.
6) Ibid., Vol. 4, p. 13.
7) Ibid., Vol. 1, p. 152.
8) Ibid., Vol. 1, p. 329.
9) Ibid., Vol. 1, p. 329.
10) Ibid., Vol. 4, p. 14.
11) Ibid., Vol. 4, p. 680.
12) L. Gattermann and H. Wieland, "Laboratory Methods of Organic Chemistry" (English Ed.), Walter de Gruyter, Berlin (1952), p. 102.

TABLE V

Alkyl	Alkyl-bromide g.	*p*-Phenyl-phenol g.	NaOH g.	EtOH cc.	Time hr.	Crude ether g.	Recrystallized ether: Amount g.	Yield %	M. p. °C	Mol. wt.: Found	Calcd.
n-Amyl	3.4	3.4	1	33	2	3.9	2.19	46	64~65	236	240
n-Hexyl	3.4	3.4	0.75	30	3	2.4	1.16	23	63~63.5	247	254
//	4.2	3.4	1	33	2	2.4	0.93	18	63.5~64.3		
n-Heptyl	4.0	3.4	1	40	2	4.1	3.5	66	70.7~71.7	265	268
n-Octyl	5.0	5.0	1.3	52	1	5.1	8.85	53	68~69	283	282
//	5.0	5.0	1.3	52	2.5	6.0					

residue distilled in vacuo, the distillate was recrystallized to give 66.7 g. of *p*-bromodiphenyl; yield 51%, m. p. 86~88.5°C.

p-Diphenylphenyl Ether.—A mixture of *p*-bromodiphenyl (47 g.), 27 g. of phenol, 12 g. of potassium hydroxide and 2 g. of copper powder was heated at 184~240°C for 6 hr. The mixture was extracted with benzene, and the benzene extract was concentrated and distilled in vacuo. Recrystallization of the distillate yielded 37.5 g. (76%) of the crude ether, m. p. 60~68°C which was further recrystallized from ethanol to give a purified specimen, m. p. 67~68°C.

Synthesis of 3, 5-Dimethylphenyl p-Diphenyl Ether.—A mixture of *p*-bromodiphenyl (8.7 g.), 2.2 g. of potassium hydroxide, 4.78 g. of 1, 3, 5-xylenol and 0.05 g. of copper powder was heated at 160~200°C for 2.5 hr. The mixture, when treated in the usual manner, gave 3.33 g. of colorless flakes; yield 33%, m. p. 65.5~66.5°C.

Found: C, 87.74; H, 6.49. Mol. wt., 273. Calcd. for $C_{20}H_{18}O$: C, 87.56; H, 6.61%. Mol. wt., 274.

Infrared Spectra of the p-Diphenyl Ethers.—The spectra of *n*-alkyl (C_5, C_6, C_7, C_8) and aryl (C_8) ethers are shown in Figs. 1, 2, 3, 4 and 5. The absorption bands common to these ethers are as follows: a band at 8 μ (1250 cm^{-1}) is assigned to the C-O stretching of the ether linkage, and an appearance of a band in the vicinity of 12.05 μ which corresponds to two adjacent hydrogen atoms in the benzene ring shows that the ethers are all substituted at the para position of diphenyl. Also,

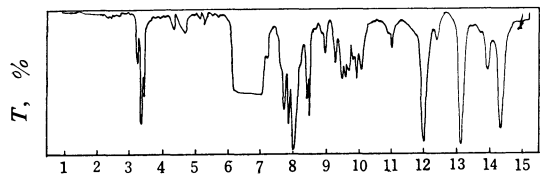


Fig. 1. *n*-Amyl *p*-diphenyl ether.

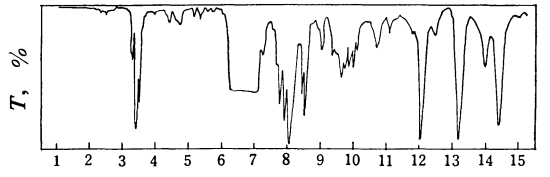


Fig. 2. *n*-Hexyl *p*-diphenyl ether.

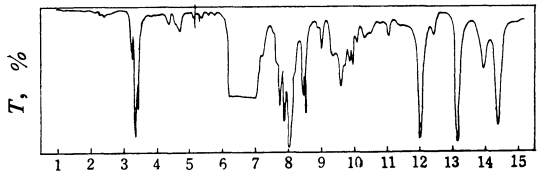


Fig. 3. *n*-Heptyl *p*-diphenyl ether.

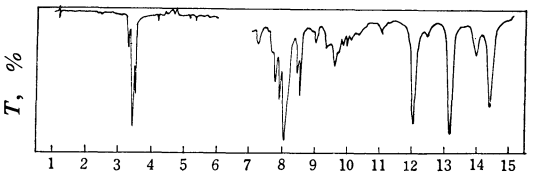


Fig. 4. *n*-Octyl *p*-diphenyl ether.

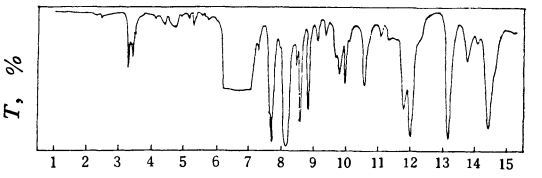


Fig. 5. 3,5-Dimethylphenyl *p*-diphenyl ether.

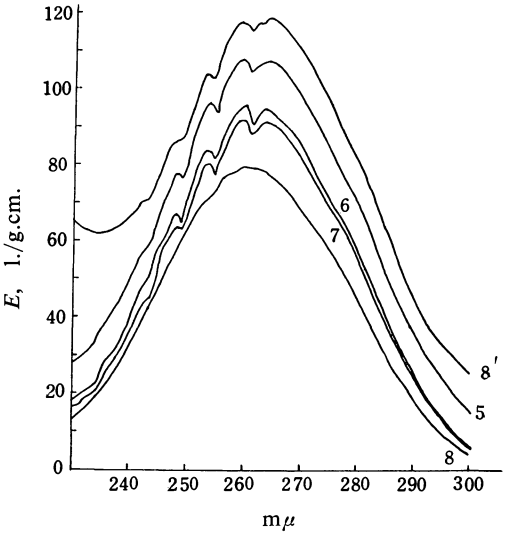


Fig. 6. *p*-Diphenyl ethers.

5; *n*-Amyl (E+10) 6; *n*-Hexyl 7; *n*-Heptyl 8; *n*-Octyl 8'; 3,5-Dimethylphenyl (E+20)

an absorption band due to the rocking motion of a methylene group in the *n*-alkyl chain appears at the same wavelength in all the *n*-alkyl ethers, as is shown below.

No. of C atoms of *n*-alkyl ether	5	6	7	8
Absorption, μ	13.94	13.95	13.93	13.95

A strong band near 1250 cm^{-1} of the *n*-alkyl ethers is shifted to a slightly shorter wavelength compared with that of the aryl ethers.

	n-Alkyl ether			
The ethers	*n*-C_5	*n*-C_6	*n*-C_7	*n*-C_8
Absorption, μ	8.05	8.07	8.06	8.07

	Aryl ether		
The ethers	Phenyl	3,5-Dimethyl-phenyl	*p*,*p*'-Diphenyl
Absorption, μ	8.15	8.20	8.15

Ultraviolet Spectra.—The spectra in cyclohexane are shown in Fig. 6. Showing almost the same pattern, bands appearing at 248, 254, 260 and 264 mμ are common to these ethers, except for *n*-octyl ether, and the maximum absorption is at a longer wavelength than that of *p*-diphenyl methyl ether, which has been reported to be 259 mμ in cyclohexane. The absorption maximum of *p*-terphenyl, which may be regarded as a phenyl derivative of diphenyl, is at 276 mμ in hexane. Thus the introduction of a phenoxyl group, i. e. an ether linkage, to diphenyl is less bathochromic than a phenyl.

Solubility.—The new alkyl ethers (C_6, C_7, C_8) are only with difficulty soluble in cold ethanol but are readily soluble in benzene. 3,5-Dimethylphenyl ether is with more difficulty soluble in ethanol than *n*-alkyl ethers but is readily soluble in benzene.

The author is indebted to Professor Ryozo Goto of Kyoto University for his helpful discussion and criticisms of this work, and to Professor Sakujiro Kimura for his advice and encouragement.

Tokyo Laboratory of Research Center
Yawata Chemical Industry Co.
Chuo-ku, Tokyo

Syntheses and Ultraviolet Spectra of Aromatic Azo Compounds. II. Azobenzenecarboxylic Acids, Methylazobenzenecarboxylic Acids and their Ethyl Esters

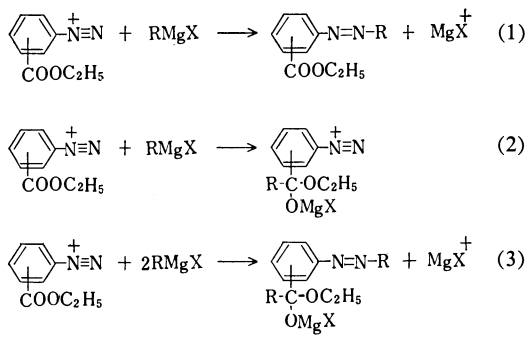
By Yujiro NOMURA and Hiroyuki ANZAI

(Received May 30, 1961)

In the preceding paper of this series[1] the syntheses of twelve bromomethylazobenzenes involving ten new substances by reactions of Grignard reagents with the zinc chloride double salts of diazonium chlorides were reported. We would now like to report our extension of this investigations with the aim of preparing a number of new azobenzene derivatives carrying an ethoxycarbonyl or carboxyl group.

In the reaction of Grignard reagent with ethoxycarbonylbenzenediazonium ion, it was considered that not only the reaction 1 but also the reaction 2 or/and 3 might occur simultaneously in whichever ethoxycarbonyl group was attacked by a Grignard reagent.

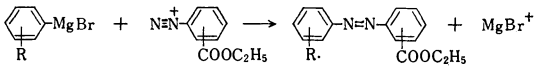
Fortunately, however, the azo compound formed by 1 could be readily isolated from the ether solution of the reaction mixture, since the reaction products by 2 and 3 are insoluble in the ether employed as a solvent in this reaction.



General Procedure.—The suspension of 1.25 mol. of the zinc chloride double salt of ethoxycarbonylbenzenediazonium chloride in ether was vigorously stirred and the ethereal solution of phenyl- or tolylmagnesium bromide prepared from 1 mol. of bromobenzene or bromotoluene and the excess of magnesium was added slowly to it at a rate necessary to maintain reflux. The mixture was stirred for an additional 60 min. at room temperature,

1) Y. Nomura, This Bulletin, **34**, 1648 (1960).

TABLE I. ETHYL AZOBENZENECARBOXYLATES PREPARED BY THE REACTION:



	R	$COOC_2H_5$	[M. p.], (B. p.)[a]	Color	Found: N, %[b]	Yield, %[c]
I	H	2-	(ca. 200°C/18 mmHg)	Red	—[d]	—[d]
II	H	3-	(210°C/25 mmHg)[e]	Red	11.29	42.8
III	H	4-	[83.5~84°C][f]	Red	11.02	42.4
IV	2'-CH_3	2-	(200°C/9 mmHg)	Deep red	10.85	36.3
V	2'-CH_3	3-	[36~37°C]	Red	10.32	56.5
VI	2'-CH_3	4-	[59~60°C]	Orange red	10.70	63.0
VII	3'-CH_3	2-	(195°C/9 mmHg)	Deep red	9.72	45.0
VIII	3'-CH_3	3-	(220°C/15 mmHg)	Deep red	10.01	53.0
IX	3'-CH_3	4-	[76~77°C]	Orange red	10.86	42.5
X	4'-CH_3	2-	(205°C/15 mmHg)	Deep red	9.72	49.5
XI	4'-CH_3	3-	[72~73°C]	Orange yellow	10.22	47.7
XII	4'-CH_3	4-	[102.5~103.5°C]	Orange	10.60	45.3

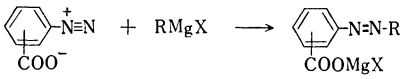
a M. p. and b. p. are uncorrected.
b Calcd. N % for ethyl azobenzenecarboxylate $C_{15}H_{14}N_2O_2$ (I—III): 11.02.
Calcd. N % for ethyl methylazobenzenecarboxylate $C_{16}H_{16}N_2O_2$ (IV—XII): 10.44.
c Based on bromobenzene or bromotoluene used to prepare Grignard reagent.
d The yield was poor, and an analytically pure sample could not be obtained even after repeated distillation in vacuo. Its structure was confirmed, however, by converting it to the known free acid (XIII).
e The reported[2] b. p. of II is 248°C/38 mmHg; it was prepared by the esterification of azobenzene-3-carboxylic acid.
f The reported[3] m. p. of III is 85~86°C; it was prepared from silver azobenzene-4-carboxylate and ethyl iodide.

and the dark red ether solution was then separated by filtration with suction from the unreacted diazonium salt and solid products, which were washed several times with ether. The ether filtrate and washings were combined and washed with dilute hydrochloric acid and then with water, dried and evaporated to get azo compounds as red crystals or oil, which were purified either by recrystallization from alcohol and then from ligroin or by distillation under reduced pressure, depending on their nature.

The ethyl azobenzenecarboxylates prepared by this method are shown in Table I. They are all new compounds except ethyl azobenzene-3-carboxylate (II) and 4-carboxylate (III).

Azobenzenecarboxylic acids and methylazobenzenecarboxylic acids, which were prepared by the hydrolysis of the corresponding ethyl esters in almost quantitative yields, are listed in Table II.

An attempt to prepare azobenzenecarboxylic acid from diazotized aminobenzoic acid and Grignard reagent in ether was fruitless. The ether layer remained almost colorless when the Grignard reagent was added to the suspension of diazonium salt in ether, while diazonium salt turned red brown and from it only a trace amount of azobenzenecarboxylic acid was isolated. The formation of ether-insoluble magnesium salt of azobenzenecarboxylic acid according to reaction 4 and the covering of the surface of solid diazonium salt by it was considered to be responsible for such a poor yield of azo compound.



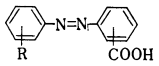
(4)

The wavelength and the molecular extinction coefficients, ε, of the absorption maxima of ethyl azobenzenecarboxylates and their free acids are listed in Table III.

Experimental

Zinc Chloride Double Salt of Ethoxycarbonylbenzenediazonium Chloride. — Following the procedure described in the previous paper[1], the mixture of ethyl aminobenzoate (1 mol.) and 6 N hydrochloric acid (3 mol.) was diazotized at 0°C with aqueous sodium nitrite, and zinc chloride double salt was precipitated by adding solid zinc chloride (0.65 mol.) to the diazotized solution. Thus, from 16.5 g. of ethyl *p*-aminobenzoate, 67 ml. of 6 N hydrochloric acid and 7 g. of zinc chloride 21.8 g. of the double salt in the form of colorless crystals was obtained. In the same way, from 13.2 g. of ethyl *m*-aminobenzoate and 18.2 g. of ethyl *o*-aminobenzoate 22.0 and 24.0 g. of the respective double salt were obtained.

2) M. H. Duval, *Bull. soc. chim. France* [4]. **11**, 19 (1912).
3) P. Jacobson and A. Steinbrenk, *Ann.*, **303**, 387 (1899).

TABLE II. AZOBENZENECARBOXYLIC ACIDS 

	R	COOH	M. p., °C[a]	Color	Found : N, %[b]
XIII	H	2-	95[c]	Yellow	12.41
XIV	H	3-	168.5~169[d]	Orange yellow	12.47
XV	H	4-	237.5~238.5[e]	Orange	12.09
XVI	2'-CH_3	2-	138	Orange	11.74
XVII	2'-CH_3	3-	162.5~163	Orange	11.46
XVIII	2'-CH_3	4-	231~232	Orange	11.66
XIX	3'-CH_3	2-	97~ 98	Yellow	11.69
XX	3'-CH_3	3-	164~165	Orange yellow	11.48
XXI	3'-CH_3	4-	211~213	Orange	11.67
XXII	4'-CH_3	2-	116~117[f]	Yellow	11.38
XXIII	4'-CH_3	3-	200~201[g]	Yellow	11.61
XXIV	4'-CH_3	4-	330	Orange	11.86

a Melting points are uncorrected.
b Calcd. N % for azobenzenecarboxylic acid $C_{13}H_{10}N_2O_2$ (XIII—XV): 12.38.
Calcd. N % for methylazobenzenecarboxylic acid $C_{14}H_{12}N_2O_2$ (XVI—XXIV): 11.66.
c The reported[4] m. p. of XIII is 95°C; it was synthesized by the hydrolysis of methyl azobenzene-2-carboxylate prepared from methyl anthranilate and nitrosobenzene.
d The reported[5] m. p. of XIV is 170~171°C; it was synthesized by the hydrolysis of methyl azobenzene-3-carboxylate, m. p. 58°C, prepared from methyl *m*-aminobenzoate and nitrosobenzene.
e The reported[6] m. p. of XV is 238°C; it was prepared from *p*-aminobenzoic acid and nitrosobenzene.
f The reported[7] m. p. of XXII is 115°C; it was synthesized by the oxidation of 2-*p*-tolylindazole.
g The reported[8] m. p. of XXIII is 192°C; it was prepared from *p*-toluidine and *m*-nitrosobenzoic acid.

TABLE III. WAVELENGTHS AND INTENSITIES OF ELECTRONIC ABSORPTION MAXIMA

	λ, mμ	ε	λ, mμ	ε	λ, mμ	ε		λ, mμ	ε	λ, mμ	ε	λ, mμ	ε
II	228	6960	316.5	10400	437	438	XIV	224	9720	317.5	15200	438	633
III	228	11200	323.5	22100	445	536	XV	230	12900	325	23700	443	848
IV	226.5*	9550	319	8480	430	436	XVI	230*	8990	323.5	12750	421	589
V	227*	11050	323.5	14900	440	559	XVII	229*	7690	325	8140	441	813
VI	228	9720	330	20000	449	623	XVIII	229.5	5210	322	10900	452	964
VII	242*	7560	303	10200	428	355	XIX	232*	11100	320	13600	429	471
VIII	232*	16300	319	13800	435	690	XX	230*	14500	320	15500	437	675
IX	259	7240	326	24300	444	857	XXI	230.7	7790	326	15150	443	692
X	235.5	10000	320	10800	428	484	XXII	229.5	16200	329	19200	432.5	995
XI	231.5	15800	327.5	13500	440	858	XXIII	226	14500	326	20900	436	439
XII	229	9100	335	20000	443	718	XXIV	231.5	8230	333	12200	440	590
XIII	223.5	13400	319	17700	427	504							

* Wavelength of shoulder. Methylazobenzenecarboxylic acids and their ethyl esters, in which methyl and carboxyl or ethoxycarbonyl groups are not situated in the para position with respect to the azo group, have no maximum but do have a shoulder at the 220~250 mμ region.

Ethyl Azobenzenecarboxylates. — Twelve ethyl azobenzenecarboxylates were prepared following the general procedure described above. They have been summarized in Table I.

Azobenzenecarboxylic Acids. — A solution of ethyl azobenzenecarboxylate (1 mol.) in alcohol containing sodium hydroxide (1.5 mol.) was warmed on the water bath for an hour, diluted with four times its volume of water and acidified with dilute hydrochloric acid to precipitate azobenzenecarboxylic acid. The products obtained in this manner were almost pure in most cases, and analytically pure samples could be obtained by recrystallization from alcohol. They have been summarized in

4) M. P. Freundler, *Bull. soc. chim. France*, [4], **1**, 219 (1907).
5) M. P. Freundler, *Compt. rend.*, **143**, 910 (1906).
6) H. D. Anspon, "Org. Syntheses", **25**, 86 (1946).
7) C. Paal and E. Fritzweiler, *Ber.*, **25**, 3170 (1892).
8) F. J. Alway, ibid., **37**, 335 (1904).

Table II. Yields were almost theoretical in all cases.

Measurement of Spectra.—The absorption spectra were measured in an alcoholic solution with a Hitachi EPU 2 type spectrophotometer using a 1 cm. quartz cell.

Summary

1) The zinc chloride double salts of ethoxycarbonylbenzenediazonium chlorides reacted with aryl Grignard reagents to give ethyl azobenzenecarboxylates. This provides a new method for the preparation of these compounds, as has been demonstrated by the preparation of twelve azo compounds, including ten substances not hitherto known.

2) A group of azobenzenecarboxylic acids was prepared by the hydrolysis of the corresponding ethyl esters obtained above; seven of them are new compounds.

3) The ultraviolet absorption spectra of these esters and free acids were measured.

Department of Chemistry
College of General Education
The University of Tokyo
Meguro-ku, Tokyo

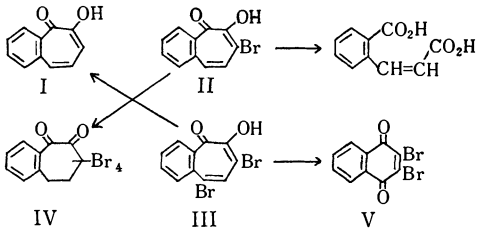
*3, 4-Benzotropolone and Related Compounds. I. Bromo Derivatives of 3, 4-Benzotropolone**

By Seiji EBINE

(Received April 24, 1961)

3, 4-Benzotropolone (I) was synthesized first by Cook et al.[1], later by Moroe et al.[2], and some of its substitution products were reported on by Nozoe et al.[3] Some other benzologs of tropolone and hydroxytropones, such as 4, 5-benzotropolone[4], 4-hydroxy-2, 3-benzotropone[5], and hydroxydibenzotropone[6,7], have recently been reported on. Of these compounds, I is most closely related to the parent tropolone. It seems, therefore, of interest to compare the chemical behavior of I with that of monocyclic tropolone and thereby to examine how the condensed benzene ring influences the character of the tropolone nucleus of I. From this point of view, the present author has undertaken a more detailed study of I and its derivatives. As a part of this work, this paper deals with bromo-3, 4-benzotropolones and their brominated products.

I and its monobromo- and dibromo-derivatives, II and III, the materials for this study, were prepared according to Cook's method[1] starting with 3, 4-benzocycloheptene-1, 2-dione. I, II and III gave ultraviolet spectra characteristic of troponoid compounds (Fig. 1)[8] and exhibited infrared absorption bands of their carbonyl groups within the same region as other troponoid carbonyl groups (as given in the experimental section).



Concerning the position of the bromine atoms in bromo-3, 4-benzotropolones, Cook et al.[1] have reasonably suggested, though without any experimental evidence, that II is 7-substituted and that III is 5, 7-disubstituted. Their prediction is now proved to be true by studies of the oxidation of II and III with alkaline

* Presented at the 12th Annual Meeting of the Chemical Society of Japan, Kyoto, April, 1959.

1) J. W. Cook and A. R. Sommerville, *Nature*, **163**, 410 (1949); J. W. Cook, A. R. Gibb, R. A. Raphael and A. R. Sommerville, *J. Chem. Soc.*, **1952**, 603.

2) T. Moroe, T. Matsushima and O. Miyamoto, *J. Pharm. Soc. Japan* (*Yakugaku Zasshi*), **72**, 1238 (1952).

3) T. Nozoe, Y. Kitahara and T. Ando, *Proc. Japan Acad.*, **27**, 107 (1951).

4) D. S. Tarbell, G. P. Scott and A. D. Kemp, *J. Am. Chem. Soc.*, **72**, 379 (1950); D. S. Tarbell and J. C. Bill, ibid., **74**, 1234 (1952); G. A. Nicholls and D. S. Tarbell, ibid., **74**, 4935 (1952); H. Fernholz, E. Hartwig and J. -C. Salfeld, *Ann.*, **576**, 131 (1952).

5) a) G. L. Buchanan, *J. Chem. Soc.*, **1954**, 1060; b) G. L. Buchanan and J. K. Sutherland, ibid., **1956**, 2620.

6) T. Sakan and M. Nakazaki, *J. Inst. Polytech. Osaka City Univ.*, I, No. 2, 23 (1950): *Chem. Abstr.*, **46**, 5036 (1952).

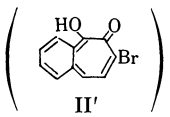
7) J. Rigaudy and L. Nédélec, a) *Compt. rend.*, **236**, 1287 (1953); b) *Bull. soc. chim. France*, **1959**, 638, 659.

8) The ultraviolet spectrum of I was given previously. J. W. Cook et al., loc. cit.

hydrogen peroxide to *o*-carboxycinnamic acid and phthalic acid respectively. An attempt was made to obtain 5-bromo-3,4-benzotropolone by catalytic hydrogenolysis of III with one mole of hydrogen. However, this resulted only in the formation of one-half an equivalent of I, the remainder being recovered unchanged and no monobromo derivative being obtained.

I, II and III are less acidic than monocyclic tropolone and bromotropolones. I formed an unstable amine salt which was decomposed readily to its components on recrystallization from solvents. II and III formed stable salts with aliphatic amines but did not with aromatic amines, whereas monocyclic bromotropolones were known to combine firmly with both aliphatic and aromatic amines[9]. The lesser acidity of benzotropolones may be ascribed to the fact that the condensed benzene ring restricts the resonance of the tropolone nucleus. On the other hand, I, II and III behaved as weak bases and dissolved in concentrated sulfuric acid, from which they were recovered unchanged on dilution with water. Such an amphoteric property is characteristic of troponoid compounds.

As reported by Nozoe et al.[10], 3-bromotropolone exists as a tautomeric mixture with 7-bromotropolone, and is methylated to produce the two corresponding isomeric methyl ethers. However, II, a benzolog of 3-bromotropolone, was methylated to give only one methyl ether, 6-bromo-7-methoxy-2,3-benzotropone, indicating that II exists in only one form, unlike the monocyclic bromotropolones. A tautomeric form (II′) of II could not exist because its benzene ring is not aromatic but quinonoid.



II′

III was similarly methylated, affording 4,6-dibromo-7-methoxy-2,3-benzotropone as the sole product. These methyl ethers, like II and III, exhibited ultraviolet spectra characteristic of troponoid compounds (Fig. 1). As compared with monocyclic bromotropolone methyl ethers, bromobenzotropolone methyl ethers were more stable towards hydrolysis and were not affected when heated with hydrobromic acid in a methanolic solution for an hour, but hydrolyzed when heated with 47% hydrobromic acid without methanol for two hours. The methyl ether of II was debrominated by catalytic hydrogenolysis to give an oily methyl ether of I, which failed to crystallize[11]. The methyl ether of I afforded a picrate and a 2,4-dinitrophenylhydrazone. II and III gave acetates which were readily hydrolyzed when their methanolic solutions containing a little hydrochloric acid, were refluxed for 5 min.

II was brominated in acetic acid solution to yield III as previously described[1]. In contrast, II was brominated in chloroform solution to yield an addition product assumed to be tetrabromo-3,4-benzocycloheptene-1,2-dione (IV) based upon its spectrum (Fig. 1), which was crystallized unchanged from petroleum ether but was decomposed to yield III on crystallization from acetic acid. III and bromine in chloroform gave an unstable addition product, from which III was regenerated on crystallization from solvents.

III was subjected to exhaustive bromination by heating its acetic acid solution with excess bromine on a water bath for fifteen hours, 2,3-dibromo-1,4-naphthoquinone (V) being unexpectedly produced. V was identified by mixed melting point determination and by agreement in ultraviolet and infrared spectra with an authentic sample. An anilino derivative of V also showed no melting point depression on admixture with an authentic 2-bromo-3-anilino-1,4-naphthoquinone. The structure of V was further elucidated by converting it to 2-bromo-3-*p*-toluidino-1,4-naphthoquinone, 2-bromo-3-hydroxy-1,4-naphthoquinone, 2-bromo- and 2,

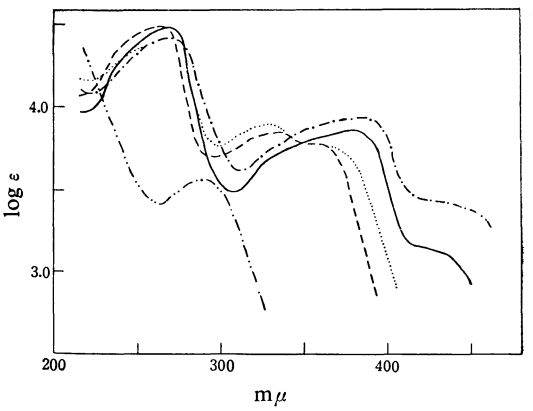


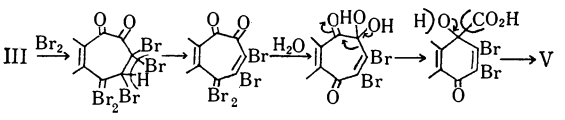
Fig. 1. Ultraviolet spectra of 7-bromo-3,4-benzotropolone (II) (——), 5,7-dibromo-3,4-benzotropolone (III) (-·-·), the methyl ether of II (----), the methyl ether of III (·····) in methanol and tetrabromo-3,4-benzocycloheptene-1,2-dione (IV) (-···) in cyclohexane.

9) T. Nozoe, T. Mukai and K. Takase, *Proc. Japan Acad.*, **26** No. 8, 22 (1950); T. Nozoe, E. Sebe, S. Mayama and S. Iwamoto, *Sci. Repts. Tohoku Univ., Ser. I*, **36**, 194 (1952).

10) T. Nozoe, Y. Kitahara and S. Masamune, *Proc. Japan Acad.*, **27**, 649 (1951); T. Sato, *J. Chem. Soc. Japan, Pure Chem. Sec.* (*Nippon Kagaku Zasshi*), **80**, 1340 (1959).

11) Nozoe et al. (Ref. 3) have obtained the methyl ether of I, m.p. 82.5~83.5°C, by the action of ethereal diazomethane on I, while Cook et al. (Ref. 1) have reported that I reacts very sluggishly with diazomethane and smoothly with methyl *p*-toluenesulfonate to yield an oily methyl ether of I.

3-dibromo-1, 4-diacetoxynaphthalenes. The tentative mechanism of this transformation may be represented by the following scheme:



Closely related ring contractions of hydroxytropones into quinones have been reported: 5, 7-dibromo-4-hydroxy-2, 3-benzotropone is transformed on heating with alkali to 2-hydroxy-1, 4-naphthoquinone[5b], and 4-hydroxy-2, 3:6, 7-dibenzotropone in alkaline solution is oxidized by air to anthraquinone[7b].

Experimental

7-Bromo- and 5, 7-Dibromo-3, 4-benzotropolones (II and III). — Prepared according to Cook and others' method[1]. 7-Bromo-3, 4-benzotropolone (II), yellow prisms from ethanol, m. p. 149°C (reported m. p.'s 143~144[1] and 148~149°C[3]), (Found: C, 52.72; H, 3.02. Calcd. for $C_{11}H_7O_2Br$: C, 52.61; H, 2.81%), infrared ν(KBr): 1612, 1600, 1547 cm^{-1}.

5, 7-Dibromo-3, 4-benzotropolone (III), yellow needles, m. p. 127°C (reported m. p. 119~121°C[1]), (Found: C, 40.31; H, 2.08. Calcd. for $C_{11}H_6O_2Br_2$: C, 40.03; H, 1.83%), infrared ν(KBr): 1612, 1585, 1550 cm^{-1}.

The Amine Salts.—A solution of a 50-mg. sample and 0.2 g. of an amine in 1 ml. of ethanol was warmed on a water bath for 5 min. The solution was concentrated, and the product which separated on cooling was collected and recrystallized from ethanol. The amine salts thus obtained were decomposed to regenerate bromobenzotropolones when dissolved in ethanol containing a little hydrochloric acid.

Amine Salts of II. — Diethylamine salt, yellow scales, m. p. 130.5~131.5°C.

Found: C, 55.30; H, 5.57; N, 4.53. Calcd. for $C_{11}H_7O_2Br \cdot C_4H_{11}N$: C, 55.57; H, 5.60; N, 4.32%.

Ethylenediamine salt, yellow scales decomposing at 157°C.

Found: C, 50.86; H, 3.95; N, 5.03. Calcd. for $(C_{11}H_7O_2Br)_2 \cdot C_2H_8N_2$: C, 51.26; H, 3.94; N, 4.98%.

Benzylamine salt, yellow, silky needles, m. p. 143°C.

Found: C, 60.36; H, 4.32; N, 4.29. Calcd. for $C_{11}H_7O_2Br \cdot C_7H_9N$: C, 60.36; H, 4.50; N, 3.91%.

Amine Salts of III. — Diethylamine salt, yellow needles, m. p. 146~147°C.

Found: C, 44.58; H, 4.25; N, 3.71. Calcd. for $C_{11}H_6O_2Br_2 \cdot C_4H_{11}N$: C, 44.69; H, 4.25; N, 3.48%.

Ethylenediamine salt, a yellow crystalline powder, m. p. above 300°C.

Benzylamine salt, yellow, silky needles, m. p. 142°C (decomp.).

Found: C, 49.65; H, 3.40; N, 3.41. Calcd. for $C_{11}H_6O_2Br_2 \cdot C_7H_9N$: C, 49.46; H, 3.46; N, 3.21%.

The Methyl Ethers.—Prepared by methylation of II and III with ethereal diazomethane in the usual manner. Methyl ether of II, colorless needles from dilute methanol, m. p. 86~87°C (reported m. p. 84~85°C[1]), infrared $\nu(CCl_4)$: 1635, 1598, 1565 cm^{-1}.

Found: C, 54.54; H, 3.56. Calcd. for $C_{12}H_9O_2Br$: C, 54.36; H, 3.42%.

Methyl ether of III, pale yellow needles, m. p. 120°C, infrared $\nu(CCl_4)$: 1650, 1589, 1565 cm^{-1}.

Found: C, 42.19; H, 2.56. Calcd. for $C_{12}H_8O_2Br_2$: C, 41.89; H, 2.34%.

The Acetates.—A solution of a 50-mg. sample in 1 ml. of acetic anhydride containing a trace of concentrated sulfuric acid was heated on a water bath for 5 min., the excess acetic anhydride was decomposed with ice, and the product was crystallized from methanol. Acetate of II, colorless crystals, m. p. 91°C.

Found: C, 52.96; H, 3.13. Calcd. for $C_{13}H_8O_3Br$: C, 53.27; H, 3.10%.

Acetate of III, colorless crystals, m. p. 92°C.

Found: C, 41.90; H, 2.33. Calcd. for $C_{13}H_8O_3Br_2$: C, 41.97; H, 2.17%.

3, 4-Benzotropolone Methyl Ether. — A solution of 500 mg. of the methyl ether of II in 10 ml. of ethanol was shaken with hydrogen in the presence of 0.5 ml. of diethylamine and 50 mg. of 10% palladium-on-charcoal at ordinary temperature and pressure. After uptake of 1 mol. equivalent of hydrogen, the catalyst was removed and the solvent was evaporated. The crude product thus obtained was converted to its picrate, orange prismatic needles from carbon tetrachloride, m. p. 84~85°C.

Found: C, 52.24; H, 3.23; N, 9.97. Calcd. for $C_{12}H_{10}O_2 \cdot C_6H_3O_7N_3$: C, 52.05; H, 3.16; N, 10.12%.

The picrate was decomposed by passing its chloroform solution through an alumina column to yield 130 mg. (37%) of 3, 4-benzotropolone methyl ether, a pale yellow oil, which gave a 2, 4-dinitrophenylhydrazone[1], m. p. 238~240°C. In this experiment, there was produced a solid by-product, presumably a more hydrogenated product, which was not studied.

Attempted Monodebromination of III.—A solution of 500 mg. of III in 10 ml. of ethanol containing 0.3 ml. of 33% aqueous dimethylamine was shaken with hydrogen over 50 mg. of 10% palladium-on-charcoal until 1 mol. equivalent of hydrogen had been absorbed. The catalyst was removed, the solution was diluted with water, and the crystalline precipitate which separated was recrystallized from ethanol to yield 220 mg. (44%) of unchanged II, m. p. and mixed m. p. 125~126°C. The mother liquor from the above recrystallization was evaporated, and the residue was crystallized from petroleum ether to afford 80 mg. (30%) of I, pale yellow crystals, m. p. and mixed m. p. 84~85°C. No monobromo derivative could be obtained.

Oxidation of II and III.—To a stirred suspension of 200 mg. of II in 40 ml. of 0.2 N sodium hydroxide was added dropwise 2 ml. of 35% hydrogen peroxide, and the resulting mixture was set aside under continued stirring at room temperature. The suspension went into solution in 10 min. and the yellow color of the solution disappeared in an hour. Acidification with 6 N sulfuric acid produced a precipitate

which was collected and crystallized from dilute acetic acid to yield 70 mg. (46%) of colorless needles of *o*-carboxycinnamic acid. Found: C, 62.48; H, 4.33. Calcd. for $C_{10}H_8O_4$: C, 62.50; H, 4.20%), m. p. 187~189°C.

The melting point was undepressed on admixture with an authentic sample[12].

Oxidation under the same conditions was applied to 200 mg. of III, affording 74 mg. (74%) of phthalic acid, m. p. and mixed m. p. 199~201°C (decomp.).

Addition of Bromine to II and III.—A solution of 100 mg. of II and 0.1 ml. of bromine in 3 ml. of chloroform was left to stand for 10 min., the chloroform and excess bromine were evaporated, and the solid residue was crystallized from petroleum ether to give 140 mg. (72%) of tetrabromo-3,4-benzocycloheptene-1,2-dione (IV), a pale yellow, crystalline powder, decomposing at 115~118°C.

Found: C, 27.36; H, 1.45. Calcd. for $C_{11}H_6O_2 \cdot Br_4$: C, 26.98; H, 1.24%.

The product was insoluble in alkali, showed no ferric chloride coloration, and was decomposed to III, m. p. and mixed m. p. 126°C, on recrystallization from acetic acid.

A similar bromination of III gave an addition product, decomposing at 111°C, which could not be purified owing to its facile decomposition to regenerate III on crystallization from solvents.

Exhaustive Bromination of III.—A solution of 1 g. of III and 0.5 ml. of bromine in 15 ml. of acetic acid was heated on a water bath for 5 hr., and to this were added two additional 0.5-ml. portions of bromine at intervals of 5 hr. under continued heating. Dilution with water caused precipitation of the product, which was collected and crystallized from acetic acid, affording 775 mg. (81%) of yellow needles of 2,3-dibromo-1,4-naphthoquinone (V), melting at 218.5°C. (Found: C, 38.27; H, 1.38. Calcd. for $C_{10}H_4O_2Br_2$: C, 38.01; H, 1.28%). The melting point was not depressed on admixture with an authentic sample[13].

Derivatives of V. — 2-Bromo-3-anilino-1,4-naphthoquinone[13], 2-bromo-3-hydroxy-1,4-naphthoquinone[13] and 2,3-dibromo-1,4-diacetoxynaphthalene[14] derived from V showed no melting point depression on admixture with authentic samples. 2-Bromo-3-*p*-toluidino-1,4-naphthoquinone was prepared by warming 50 mg. of V and 170 mg. of *p*-toluidine in 2 ml. of ethanol for 5 min. Dark red plates from ethanol, m. p. 190.5°C.

Found: C, 59.83; H, 3.46; N, 4.35. Calcd. for $C_{17}H_{12}O_2NBr$: C, 59.66; H, 3.53; N, 4.09%.

2-Bromo-1,4-diacetoxynaphthalene was prepared by heating a mixture of 200 mg. of V, 600 mg. of zinc powder, 400 mg. of fused sodium acetate and 3 ml. of acetic anhydride on a water bath for 10 min. Colorless, granular crystals from ethanol, m. p. 146°C.

Found: C, 52.11; H, 3.62. Calcd. for $C_{14}H_{11} \cdot O_4Br$: C, 52.03; H, 3.43%.

The author wishes to express his sincere thanks to Professor Tetsuo Nozoe of Tohoku University for his guidance and encouragement throughout this work. The author is also indebted to Dr. Eishiro Tamate of the Nitto Institute of Chemical Research for infrared measurements, and to Mrs. Kuniko Kodaira and Miss Ayako Iwanaga of Tohoku University for microanalyses.

Department of Chemistry
Saitama University
Urawa, Saitama

12) J. Boesekin et al., *Rec. trav. chim.*, **30**, 145 (1911).

13) C. Liebermann and S. Schlossberg, *Ber.*, **32**, 2097 (1899).

14) R. Melodola and F. Huges, *J. Chem. Soc.*, **57**, 810 (1890).

3,4-Benzotropolone and Related Compounds. II[1]. *Chloro and Iodo Derivatives of 3,4-Benzotropolone**

By Seiji EBINE

(Received April 24, 1961)

Nozoe and collaborators[2] have presented a short communication on the substitution of 3,4-benzotropolone (I) describing how I can be chlorinated to yield monochloro-3,4-benzotropolone. The chlorination and the iodination of I have now been studied in more detail and are described herein.

When treated with one molar equivalent of chlorine, I afforded 5,7-dichloro-3,4-benzotropolone (V) in a low yield besides the recovery of unchanged material, no monochloro derivative being isolated. Treatment of I with two molar equivalents of chlorine afforded V in a

* Presented at the 14th Annual Meeting of the Chemical Society of Japan, Tokyo, April, 1961.

1) Part I: This Bulletin, 35, 114 (1962).

2) T. Nozoe. Y. Kitahara and T. Ando, *Proc. Japan Acad.*, 27, 107 (1951).

TABLE I. M. P. AND MIXED M. P. OF CHLORO- AND BROMO-3,4-BENZOTROPOLONES

Chloro deriv.	M. p., °C	Bromo deriv.	M. p., °C	Mixed m. p., °C
7-Chloro-	151	7-Bromo-	148	148~149
methyl ether	97	methyl ether	87	87~ 89
acetate	101.5	acetate	91	90~ 91
5,7-Dichloro-	136	5,7-Dibromo-	126	122~126
methyl ether	106	methyl ether	120	104~109
5-Chloro-7-bromo-	111~114	5-Bromo-7-chloro-	122.5	116~119

fair yield. The monochlorination of 7-bromo-3,4-benzotropolone (II) gave 5-chloro-7-bromo-3,4-benzotropolone (VI). The passage of the excess chlorine into an acetic acid solution of II furnished 5,6,7-trichloro-7-bromo-3,4-benzocycloheptene-1,2-dione (VIII), which exhibited two infrared carbonyl absorption bands at 1753 and 1700 cm^{-1} and an ultraviolet spectrum closely similar to that of the parent 3,4-benzocycloheptene-1,2-dione (Fig. 2). When treated with a large excess of chlorine, 5,7-dibromo-3,4-benzotropolone (III) was transformed into 2,3-dichloro-1,4-naphthoquinone, identified by comparison with an authentic sample[3]. This ring contraction is analogous to that observed in the exhaustive bromination of III described in the preceding paper[1].

Heating II with concentrated hydrochloric acid gave 7-chloro-3,4-benzotropolone (IV) in a good yield which could not be obtained by the direct chlorination of I. A similar treatment of III gave V. The bromination of IV furnished 5-bromo-7-chloro-3,4-benzotropolone (VII). On slight warming with hydrochloric acid in methanol, 5-bromo- and 5,7-dibromo-3,4-benzotropolone methyl ethers, II′ and III′, easily underwent a halogen-exchange reaction to afford 5-chloro and 5,7-dichloro-3,4-benzotropolone methyl ethers, IV′ and V′, respectively. Under the same conditions, II and III remained unchanged and their acetates suffered hydrolysis their bromine atoms remaining intact. The ultraviolet spectra of IV, V, IV′ and V′ are analogous to those of general troponoid compounds as given in Fig. 1. II was allowed to react with thionyl chloride, producing an adduct which decomposed to give V on recrystallization from ethanol. The adduct, to which the structure IX was tentatively assigned, gave no coloration with ferric chloride and exhibited an ultraviolet spectrum entirly different from that of a troponoid compound (Fig. 2). III and thionyl chloride afforded the same V. It should be noted that, although monocyclic tropolones and their bromo derivatives react with thionyl chloride to form chlorotropones[4], II and III react with the same reagent to afford chlorobenzotropolones their hydroxyl groups remaining unreplaced[5]. The susceptibility of the bromine atoms at 5- and 7-positions and the inertness of hydroxyl and methoxyl groups at 1-position of bromobenzotropolones and their methyl ethers towards anionoid substitution may be ascribed to the resonance structures of these compounds to which formula A contributes mainly and formula B contributes only to a less extent because the benzene ring of formula A is aromatic, whereas that of formula B is quinonoid.

Bromo- and chloro-3,4-benzotropolones, like monocyclic halotropolones[6], possess melting points close to each other and show obscure mixed melting point depression, as is shown in Table I.

I was treated with sodium iodide and sodium iodate in an acetic acid solution to yield 7-iodo-3,4-benzotropolone (X). X was produced even when an excess of iodinating reagent was employed. Under the same conditions, II was not iodinated. II and III were heated with hydriodic acid to produce I and 5-bromo-3,4-benzotropolone (XII) respectively, instead of the expected iodobenzotropolones. The bromination of XII gave III. Analogously with the reaction of bromobenzotropolone methyl ethers with hydrochloric acid, II′ and III′ reacted with hydroiodic acid in methanol to give 7-iodo-3,4-benzotropolone methyl ether (X′) and 5-bromo-7-iodo-3,4-benzotropolone methyl ether (XI) respectively. XI was identified by converting it into methyl 1-hydroxy-4-bromo-2-naphthoate[7]. In these reactions, the 5-position of I and II was not iodinated, and 5-bromine atom of III and III′ remained unaffected, presumably because the action of an iodide ion on the 5-position was sterically hindered by the *peri* position of the condensed benzene ring.

It has been found that, as in the benzenoid compounds, the out-of-plane CH deformation

3) A. Bertheim, *Ber.*, **34**, 1554 (1901).

4) W. von E. Doering and L. H. Knox, *J. Am. Chem. Soc.*, **74**, 5683 (1952); B. J. Abadir, J. W. Cook, J. D. Loudon and D. K. V. Steel, *J. Chem. Soc.*, **1952**, 2350.

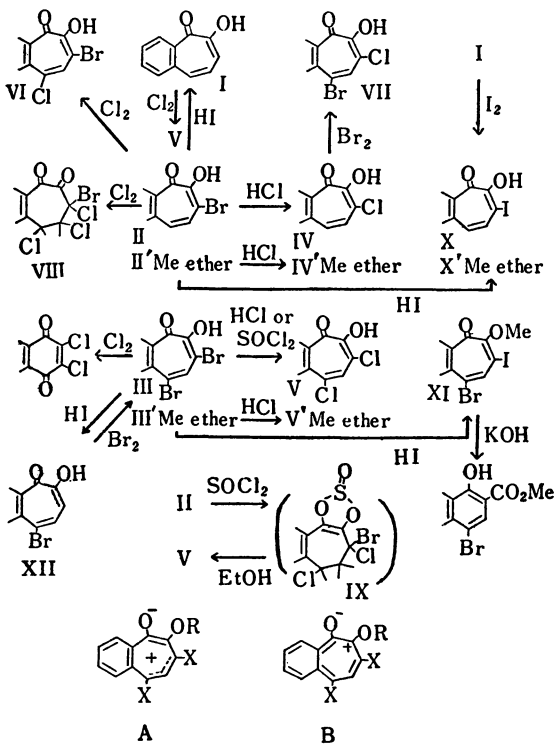
5) It has recently been reported that 3,4- and 4,5-benzotropolones fail to react with thionyl chloride. W. E. Parham, D. A. Bolon and E. E. Sweizer, *J. Am. Chem. Soc.*, **83**, 603 (1961).

6) E. Sebe, T. Nozoe, P. -Y. Yeh and S. Iwamoto, *Sci. Repts. Tohoku* Univ., *I*, **36**, 307 (1952).

7) Part IV: This Bulletin, to be published.

TABLE II. OUT-OF-PLANE CH DEFORMATION VIBRATIONS OF HALO-3,4-BENZOTROPOLONES

Compound	One isolated troponoid H 910~850 cm^{-1}	Two adjacent troponoid H 845~790 cm^{-1}	Four adjacent benzenoid H 770~735 cm^{-1}
7-Chloro-		802	747
methyl ether		795	742
acetate		806	740
7-Bromo-		807	753
methyl ether		794	742
acetate		808	739
5-Bromo-		832	754
methyl ether		840	750
7-Iodo-		795	737
methyl ether		795	742
5,7-Dichloro-	854		745
5,7-Dibromo-	907		760
methyl ether	858		756
5-Bromo-7-iodo-, methyl ether	866		756



vibrations of troponoid compounds are correlated to the positions of their substituents[8]. A similar correlation is also found in halobenzotropolones, as is shown in Table II.

Experimental

7-Chloro-3, 4-benzotropolone (IV).—A mixture of 300 mg. of 7-bromo-3,4-benzotropolone (II), 3 ml. of concentrated hydrochloric acid and 9 ml. of acetic acid was heated in a sealed tube at 120~130°C for 5 hr. The product deposited on cooling. Concentration of the filtrate gave a further crop of the product. The combined products were recrystallized from ethanol to give yellow prisms of m. p. 151°C. Yield, 215 mg. (88%). IV gave a brown coloration with ferric chloride in amyl alcohol solution. ν(KBr): 1617, 1605, 1583 cm^{-1}. λ(MeOH), mμ (log ε): 245(4.40), 262(4.44), 345(3.80), 370(3.85).

Found: C, 63.84; H, 3.29. Calcd. for $C_{11}H_7O_2Cl$: C, 63.94; H, 3.42%.

IV was also obtained in an 84% yield by refluxing a mixture of 100 mg. of 7-bromo-3,4-benzotropolone methyl ether (II'), 3 ml. of acetic acid and 15 ml. of concentrated hydrochloric acid for 5 hr.

The Acetate of IV. — Colorless prisms from methanol, m. p. 101.5°C.

Found: C, 62.62; H, 3.54. Calcd. for $C_{13}H_9O_3Cl$: C, 62.79; H, 3.65%.

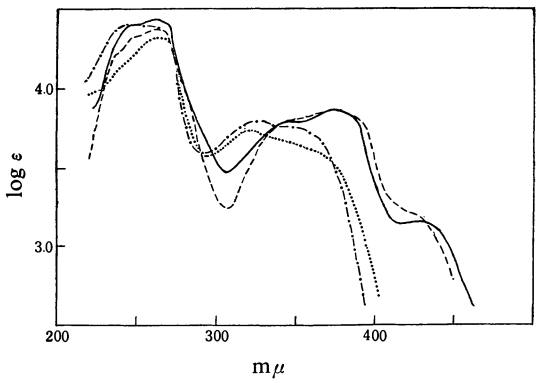


Fig. 1. Ultraviolet spectra of 7-chloro-3,4-benzotropolone (IV) (——), its methyl ether (IV') (-·-·), 5,7-dichloro-3,4-benzotropolone (V) (----) and its methyl ether (V') (·····) in methanol.

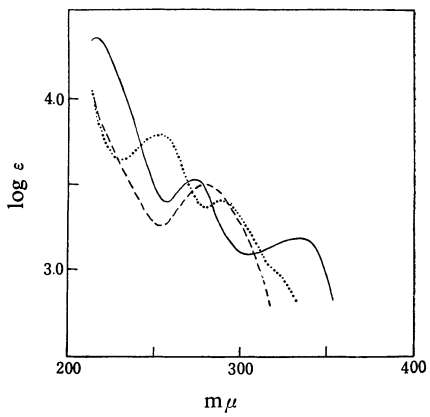


Fig. 2. Ultraviolet spectra of 3,4-benzocycloheptene-1,2-dione (·····), its 5,6,7-trichloro-7-bromo derivative (VIII) (——) in methanol and 7-bromo-3,4-benzotropolone-thionyl chloride adduct (IX) (----) in cyclohexane.

8) Y. Kitahara, *Sci. Repts. Tohoku Univ., I*, **39**, 275 (1956).

5, 7-Dichloro-3, 4-benzotropolone (V).—*From 3,4-Benzotropolone (I).* — To 100 mg. of I dissolved in 1.5 ml. of acetic acid was added an acetic acid solution of 82 mg. (2 mol. equiv.) of chlorine*. After standing for an hour at room temperature, the acetic acid was removed under reduced pressure below 30°C, leaving a crystalline residue which was washed with water and recrystallized from methanol to give 85 mg. (61%) of V, yellow needles, m. p. 135~136°C. V gave a brown coloration with ferric chloride in amyl alcohol solution. ν(Nujol): 1630, 1580 cm^{-1}. λ(MeOH), mμ(log ε): 266(4.40), 352 (3.85), 376(3.87).

Found: C, 54.85; H, 2.40. Calcd. for $C_{11}H_6O_2Cl_2$: C, 54.80; H, 2.51%.

Treatment of 100 mg. of I with 41 mg. (1 mol. equiv.) of chlorine in an acetic acid solution at room temperature gave 45 mg. (32%) of V and 30 mg. of an unidentified product with a m. p. 120~126°C, besides the recovery of 15 mg. of unchanged material.

From 7-Bromo-3, 4-benzotropolone (II).—A 300-mg. sample of II was dissolved in 3 ml. of thionyl chloride, and the solution was allowed to stand overnight at room temperature. Removal of the thionyl chloride under reduced pressure left an oily residue which solidified on trituration with ligroin. Recrystallization of the product from ligroin gave 320 mg. (73%) of yellow prisms of the addition product, m. p. 148°C (mixed m. p. with II, 107~111°C).

Found: C, 35.77; H, 1.80. Calcd. for $C_{11}H_7O_2Br \cdot SOCl_2$: C, 35.69; H, 1.91%.

On recrystallization from ethanol the adduct changed into V, m. p. 137°C. Yield, 190 mg. (66% based on II).

From 5,7-Dibromo-3,4-benzotropolone (III) and Hydrochloric Acid. — A mixture of 150 mg. of III, 1.5 ml. of concentrated hydrochloric acid and 6 ml. of acetic acid was heated in a sealed tube at 110~120°C for 5 hr. and worked up as described above for the preparation of IV, affording 100 mg. (90%) of V, m. p. 136°C.

V was also obtained by refluxing a mixture of 100 mg. of 5,7-dibromo-3,4-benzotropolone methyl ether (III'), 3 ml. of acetic acid and 15 ml. of concentrated hydrochloric acid for 5 hr., followed by recrystallization of the product from methanol.

From III and Thionyl Chloride. — A treatment of 300 mg. of III with 3 ml. of thionyl chloride similar to that described above afforded 140 mg. (64%) of V, m. p. 137°C.

7-Chloro-3, 4-benzotropolone Methyl Ether (IV') and 5, 7-Dichloro-3, 4-benzotropolone Methyl Ether (V').—*From IV and V.*—IV', colorless needles, m. p. 96~97°C. ν(Nujol): 1625, 1597, 1560 cm^{-1}. λ(MeOH), mμ(log ε): 243(4.40), 330(3.81).

Found: C, 65.30; H, 4.06. Calcd. for $C_{12}H_9O_2Cl$: C, 65.31; H, 4.11%.

V', pale yellow needles, m. p. 106°C. λ(MeOH), mμ(log ε): 262(4.34), 318(3.75).

Found: C, 56.46; H, 3.11. Calcd. for $C_{12}H_8O_2Cl_2$: C, 56.49; H, 3.16%.

* The content of chlorine in acetic acid solution was determined by iodometric titration.

From 7-Bromo- and 5,7-Dibromo-3,4-benzotropolone Methyl Ethers (II' and III').—A mixture of 50 mg. of II', 5 ml. of methanol and 2 ml. of concentrated hydrochloric acid was refluxed for 15 min. The product separated on dilution with water. This was then recrystallized from dilute methanol to yield 35 mg. (83%) of IV', m. p. 96°C. A similar treatment of III' with hydrochloric acid in methanol gave V', m. p. 106°C, in an 80% yield.

5-Chloro-7-bromo-3, 4-benzotropolone (VI). — II (200 mg.) dissolved in 15 ml. of acetic acid was treated with an acetic acid solution of 56 mg. (1 mol. equiv.) of chlorine at room temperature for an hour. The solution was then concentrated to 5 ml. in vacuo and diluted with an equal volume of water, forming a precipitate (190 mg.) of a crude product, which on recrystallization from methanol yielded 110 mg. (48%) of VI as yellow needles, m. p. 111~115°C, besides 25 mg. of unchanged material. VI gave a brown coloration with ferric chloride in amyl alcohol solution.

Found: C, 46.37; H, 2.27. Calcd. for $C_{11}H_6O_2 \cdot BrCl$: C, 46.27; H, 2.12%.

5-Bromo-7-chloro-3, 4-benzotropolone (VII). — A solution of 100 mg. of IV and 80 mg. (1 mol. equiv.) of bromine in 1 ml. of acetic acid was heated on a water bath for 2 hr. The crystalline product which separated on cooling was collected and recrystallized from methanol to give V as yellow needles, m. p. 122.5°C. Yield, 115 mg. (83%). VII gave a brown coloration with ferric chloride in amyl alcohol solution.

Found: C, 46.07; H, 2.08. Calcd. for $C_{11}H_6O_2 \cdot BrCl$: C, 46.27; H, 2.12%.

5, 6, 7-Trichloro-7-bromo-3, 4-benzocycloheptene-1, 2-dione (VIII).—Chlorine gas was bubbled into a solution of 400 mg. of II in 25 ml. of acetic acid at room temperature for an hour, the excess chlorine removed under reduced pressure, and 50 ml. of water added. A crude product (420 mg., m. p. 113~117°C) separated after standing overnight. This was collected and recrystallized from methanol to yield yellow prisms of VIII, m. p. 124~125°C. VIII gave no coloration with ferric chloride. ν ($CHCl_3$): 1753, 1700 cm^{-1}. λ(MeOH), mμ(log ε): 215(4.14), 275(3.32), 340(3.02).

Found: C, 37.12; H, 1.72. Calcd. for $C_{11}H_6O_2 \cdot BrCl_3$: C, 37.06; H, 1.70%.

2, 3-Dichloro-1, 4-naphthoquinone from III.—Into a solution of 250 mg. of III in 15 ml. of acetic acid was passed chlorine gas for 1.5 hr. at room temperature. After the removal of excess chlorine under diminished pressure, the solution was concentrated to 5 ml. and diluted with water to produce a precipitate. Sublimation at 110~120°C/7mmHg, followed by recrystallization from ethanol, gave yellow needles of 2,3-dichloro-1,4-naphthoquinone, m. p. 196~197°C, the melting point of which was undepressed on admixture with an authentic sample[3] prepared by chlorination of α-naphthoquinone. Yield, 60 mg. (35%).

3, 4-Benzotropolone (I) from 7-Bromo-3, 4-benzotropolone (II) and Hydriodic Acid. — A solution of 400 mg. of potassium iodide in 0.5 ml. of water was added to a suspension of 200 mg. of II in 5 ml. of acetic acid, and the mixture was heated in a

sealed tube at 120~130°C for 2 hr. Dilution of the reaction mixture with water gave a brown precipitate, which was collected and dissolved in ether. The ethereal solution was shaken with sodium thiosulfate solution, the ether removed, and the residue recrystallized from petroleum ether to give 100 mg. (73%) of I, m. p. and mixed m. p. 83.5~84°C.

5-Bromo-3, 4-benzotropolone (XII). — A solution of 300 mg. of potassium iodide in 0.5 ml. of water was added to a suspension of 200 mg. of 5,7-dibromo-3,4-benzotropolone (III) in 5 ml. of acetic acid, and the mixture was heated on a water bath for 5 hr. The product which separated on cooling was collected and recrystallized from methanol to yield 130 mg. (85%) of yellow needles, m. p. 140°C. ν(Nujol): 1635, 1588, 1558 cm^{-1}. λ(MeOH), mμ (log ε): 238(4.41), 263(4.33), 350(3.97), 375(3.99), 430(2.90).

Found: C, 52.86; H, 2.67. Calcd. for $C_{11}H_7O_2Br$: C, 52.61; H, 2.81%.

5-Bromo-3,4-benzotropolone Methyl Ether. — Colorless needles, m. p. 69~70°C. ν(Nujol): 1623, 1600, 1572 cm^{-1}. λ(MeOH), mμ(log ε): 240(4.18), 325 (3.82), 360~370(3.65).

Found: C, 54.02; H, 3.23. Calcd. for $C_{12}H_9O_2Br$: C, 54.36; H, 3.42%.

7-Iodo-3, 4-benzotropolone (X). — A mixture of 220 mg. of sodium iodide and 60 mg. of sodium iodate was added to a solution of 100 mg. of I in 5 ml. of acetic acid and 1.6 ml. of 2 N sulfuric acid. After standing for 10 min., the solution was diluted with water to produce a precipitate. An ethereal solution of the precipitate was shaken with sodium thiosulfate solution and the ether evaporated. The residue was recrystallized from methanol to give orange yellow crystals, m. p. 124~127°C. Yield, 70 mg. (40%). ν(Nujol): 1612, 1590, 1550 cm^{-1}. λ(MeOH), mμ(log ε): 268(4.32), 345(3.69), 360 (3.90), 380(3.75).

Found: C, 44.57; H, 2.50. Calcd. for $C_{11}H_7O_2I$: C, 44.31; H, 2.37%.

7-Iodo-3,4-benzotropolone Methyl Ether (X'). — A mixture of 100 mg. of 7-bromo-3,4-benzotropolone methyl ether (II'), 2 ml. of hydriodic acid and 2 ml. of methanol was heated for 10 min. on a water bath. Dilution with water gave a solid product. An ethereal solution of the product was shaken with sodium thiosulfate solution. The ether was evaporated and the residue recrystallized from dilute methanol. Yellow scales, m. p. 99~100°C. Yield, 100 mg. (85%). ν(Nujol): 1622, 1598, 1562 cm^{-1}. λ(MeOH), mμ(log ε): 268(4.32), 350~355 (3.66).

Found: C, 46.14; H, 3.18. Calcd. for $C_{12}H_9O_2I$: C, 46.17; H, 2.91%.

5-Bromo-7-iodo-3, 4-benzotropolone Methyl Ether (XI). — A mixture of 100 mg. of 5,7-dibromo-3,4-benzotropolone methyl ether (III'), 2 ml. of hydriodic acid and 10 ml. of methanol was refluxed for 5 hr., and then the resulting solution was worked up in the same way as above. Yellow scales, m. p. 130~131°C. Yield, 80 mg. (68%). ν(Nujol): 1631, 1602, 1582, 1560 cm^{-1}. λ(MeOH), mμ(log ε): 267(4.40), 320(3.88).

Found: C, 36.69; H, 2.07. Calcd. for $C_{12}H_8O_2BrI$: C, 36.86; H, 2.06%.

Methyl 1-Hydroxy-4-bromo-2-naphthoate from XI. —To a solution of 200 mg. of XI in 18 ml. of methanol was added a solution of 280 mg. of potassium hydroxide in 0.8 ml. of water; the resulting solution was heated for 5 hr. on a water bath. The solution was acidified with 6 N hydrochloric acid, the methanol evaporated and the residue recrystallized from methanol to yield 100 mg. (70%) of colorless needles, m. p. 119.5~120.5°C, the melting point of which was undepressed on admixture with an authentic sample[7].

The author gratefully acknowledges his indebtedness to Professor Tetsuo Nozoe of Tohoku University for his kind guidance throughout the course of this work. Thanks are also due to Dr. Eishiro Tamate of the Nitto Institute of Chemical Research for infrared spectra and to Mrs. Kuniko Kodaira and Miss Ayako Iwanaga of Tohoku University for microanalyses.

Department of Chemistry
Saitama University
Urawa, Saitama

3, 4-Benzotropolone and Related Compounds. III[1]. *Nitration of 3, 4-Benzotropolone**

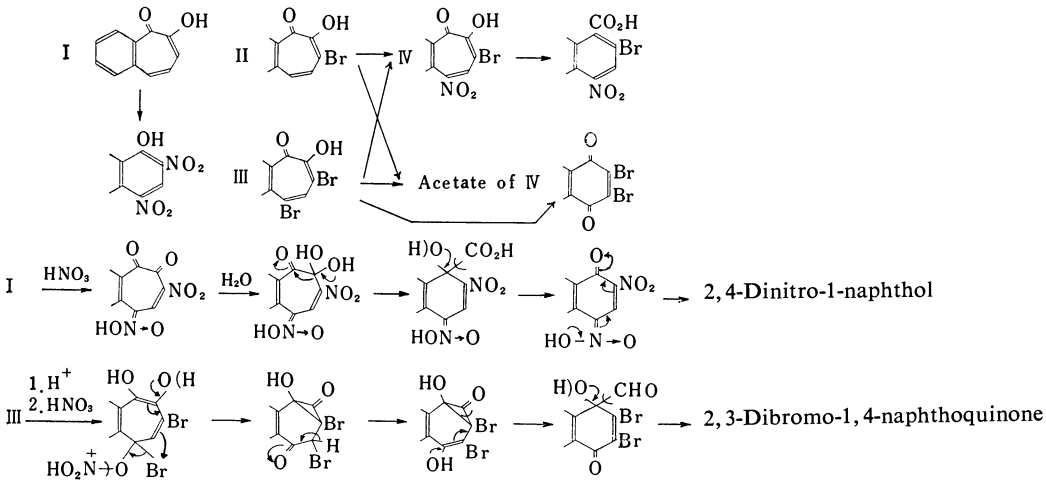
By Seiji EBINE

(Received April 24, 1961)

It has been reported that 3, 4-benzotropolone (I) can be nitrated to produce dinitro-3, 4-benzotropolone[2]. This nitration will now be re-examined.

Nitration of I with nitric acid in an acetic acid solution unexpectedly produced 2, 4-dinitro-1-naphthol, which was identified by mixed melting point determination and further by infrared-spectral agreement with an authentic sample[3]. No nitro derivative of I was isolated from the nitration product. I gave the same product in a lower yield even when one molar equivalent of nitric acid was employed. This transformation may be represented by the scheme described below. A similar type of ring contraction has been observed in the iodination of tropolone with sodium hypoiodite to produce 2, 4, 6-triiodophenol[4].

7-Bromo-3, 4-benzotropolone (II) was nitrated in an acetic acid solution to yield 5-nitro-7-bromo-3, 4-benzotropolone (IV). Since IV was highly susceptible to resinification during nitration, it was collected by filtration as soon as the reaction was completed. The yield of IV was somewhat improved when the reaction mixture was poured into a sodium bicarbonate solution before the filtration of the product. IV showed a brown coloration with ferric chloride, gave methyl ether and underwent rearrangement with alkali into 2-bromo-4-nitro-1-naphthoic acid. This behavior is characteristic of nitrotropolones. Nitration of II in acetic anhydride afforded the acetate of IV, which was hydrolyzed and then methylated to give the same methyl ether of IV as was obtained above. It has been known that monocyclic tropolones resist nitration in a concentrated sulfuric acid solution owing to the formation of a tropolonium (dihydroxytropylium) cation[5]. Nevertheless, II was successfully nitrated in concentrated sulfuric acid to afford IV. This fact indicates that II is less basic than monocyclic tropolones presumably because the condensed benzene ring restricts the resonance of the tropolone ring. III, although its tropolone ring is blocked by



* Presented at the 13th Annual Meeting of the Chemical Society of Japan, Tokyo, April, 1960.

1) Part II: This Bulletin, **35**, 117 (1962).

2) T. Nozoe, Y. Kitahara and T. Ando, *Proc. Japan Acad.*, **27**, 107 (1951).

3) F. Bender, *Ber.*, **22**, 996 (1889).

4) W. von E. Doering and L. H. Knox, *J. Am. Chem. Soc.*, **73**, 828 (1951); J. W. Cook, A. R. Gibb and R. A. Raphael, *J. Chem. Soc.*, **1951**, 2244. Formation of 6-quinolinol derivative by bromination of 8-isopropylpyrido(3,2-d)-tropolone has been reportrd by K. Yamane, 13th Annual Meeting of Chem. Soc. Japan, 1960.

5) T. Nozoe, *Proc. Japan Acad.*, **26** (9), 32 (1950); J. W. Cook. J. D. Loudon and D. K. V. Steel, *J. Chem. Soc.*, **1954**, 530.

bromo substituents, reacted with nitric acid in an acetic acid solution in such a manner that one of its two bromine atoms was replaced by a nitro group to yield IV. Similarly, nitration of III in acetic anhydride gave the acetate of IV. The nitration of III in concentrated sulfuric acid did not take place at room temperature, but was effected at 100°C, resulting in the unexpected formation of 2,3-dibromo-1,4-naphthoquinone, which showed no melting point depression on admixture with an authentic sample[6]. Under the same conditions, 5,7-dichloro-3,4-benzotropolone was also transformed into 2,3-dichloro-1,4-naphthoquinone which was identical with an authentic sample[7]. This reaction may include oxidation with nitric acid followed by migration of bromine atom, as described above. Treatment of II and III with nitric acid under more drastic conditions gave phthalic acid. In all nitrations mentioned above, the condensed benzene ring remained not nitrated.

Experimental

2,4-Dinitro-1-naphthol from 3,4-Benzotropolone (I).—To an ice-cooled solution of 200 mg. of I in 0.5 ml. of acetic acid was added 0.18 ml. (2 mol. equiv.) of concentrated nitric acid diluted with an equal volume of acetic acid. After standing for 10 min. with ice-cooling, the solution was diluted with 1 ml. of water to produce a precipitate. This was collected, washed with a small amount of cold methanol in order to remove a resinous material and then recrystallized from methanol to give 70 mg. (26%) of greenish yellow prisms of the dinitronaphthol, m. p. 137.5~138°C (decomposed at 140°C with effervescence), the melting point of which was undepressed on admixture with an authentic sample[8] prepared by the nitration of α-naphthol. (Found: C, 51.34; H, 2.60; N, 11.83. Calcd. for $C_{10}H_6O_5N_2$: C, 51.29; H, 2.58; N, 11.96%.)

5-Nitro-7-bromo-3,4-benzotropolone (IV).—*a) Nitration of 7-Bromo-3,4-benzotropolone (II).—In Acetic Acid:* To a mixture of 0.085 ml. (0.95 mol. equiv.) of concentrated nitric acid and 0.9 ml. of acetic acid was added 300 mg. of II. On stirring at room temperature, the suspension went into solution in a few minutes and then in an additional several minutes there separated out a crystalline powder (140 mg.), which was collected by filtration. On dilution with water, the filtrate gave a further crop of the product (10 mg.) which was also collected. The combined products were washed with a small amount of methanol to remove a resinous material and recrystallized from methanol to afford 110 mg. (30%) of IV as yellow scales decomposing at 161°C with effervescence. On rapid heating, the decomposition point was raised to 167°C. The mother liquor gave 30 mg. of unchanged material.

In another experiment, soon after the nitration had been completed, the reaction mixture was poured into a saturated sodium bicarbonate solution; the product was then collected and recrystallized from methanol to give 140 mg. (40%) of IV. λ(MeOH), mμ(log ε): 215(4.19), 268(3.92), 485 (4.20).

Found: C, 44.63; H, 2.33; N, 4.88. Calcd. for $C_{11}H_6O_4NBr$: C, 44.62; H, 2.04; N, 4.73%.

In Concentrated Sulfuric Acid: A mixture of 0.085 ml. (0.95 mol. equiv.) of concentrated nitric acid and an equal volume of concentrated sulfuric acid was added to 300 mg. of II dissolved in 1.5 ml. of concentrated sulfuric acid, and the solution was left aside for 10 min. at room temperature. On pouring it on crushed ice, a resinous product separated, which was collected and washed with 2 ml. of methanol, leaving a crystalline mass. Recrystallization from methanol afforded 105 mg. (29%) of IV decomposing at 160°C, as well as 65 mg. of unchanged material.

The nitration in concentrated sulfuric acid at 100°C resulted in resinification of a greater part of II besides the recovery of a minute amount of unchanged material.

b) Nitration of 5,7-Dibromo-3,4-benzotropolone (III).—A 300-mg. sample of III was treated with a mixture of 0.068 ml. (1 mol. equiv.) of concentrated nitric acid and 0.6 ml. of acetic acid in the same manner as above, affording IV in a lower yield (45 mg., 16%).

Attempted nitration of III in concentrated sulfuric acid at room temperature resulted in the recovery of unchanged material.

The nitration products of II and III obtained above proved to be the same from mixed melting point determination of their methyl ethers.

The Methyl Ether of IV.—Yellow prisms from dilute methanol, m. p. 146.5°C.

Found: C, 46.47; H, 2.81; N, 4.85. Calcd. for $C_{12}H_8O_4NBr$: C, 46.48; H, 2.60; N, 4.52%.

The p-Toluidine Salt of IV.—A red crystalline powder which darkened at 124°C and decomposed at 161°C with effervescence.

Found: C, 53.98; H, 3.98; N, 7.27. Calcd. for $C_{11}H_6O_4NBr \cdot C_7H_9N$: C, 53.62; H, 3.75; N, 6.95%.

The Acetate of IV.—*Nitration of II in Acetic Anhydride.*—A mixture of 0.085 ml. (0.95 mol. equiv.) of concentrated nitric acid and 0.34 ml. of acetic anhydride was added to 300 mg. of II suspended in 1.5 ml. of acetic anhydride. The suspension was warmed for a while until it went into solution. The acetic anhydride was decomposed with ice, and the product was then collected, washed with a small amount of methanol and recrystallized from methanol to afford 110 mg. (27%) of the acetate of IV as yellow prisms decomposing at 164°C with effervescence.

Found: C, 46.40; H, 2.22; N, 3.92. Calcd. for $C_{13}H_8O_5NBr$: C, 46.18; H, 2.39; N, 4.14%.

Nitration of III in Acetic Anhydride.—A suspension of 200 mg. of III in acetic anhydride was treated with a mixture of 0.046 ml. of concentrated nitric acid and 0.18 ml. of acetic anhydride in the same manner as above, affording 35 mg. (18%) of the acetate of IV.

6) C. Liebermann and S. Schlossberg, *Ber.*, **32**, 2097 (1899).
7) J. B. Conant and L. F. Fieser, *J. Am. Chem. Soc.*, **46**, 1873 (1924).

The acetate of IV obtained above was hydrolyzed by refluxing its methanolic solution in the presence of a few drops of concentrated hydrochloric acid, the product was treated with ethereal diazomethane to yield the methyl ether of IV.

2-Bromo-4-nitro-1-naphthoic Acid from IV.—A 100-mg. sample of IV was dissolved in 5 ml. of 2 N potassium hydroxide, and the solution was allowed to stand for 10 min. at room temperature. Acidification of the solution with hydrochloric acid and recrystallization of the product from methanol gave 80 mg. (80%) of yellow, granular crystals, m. p. 190°C. λ(MeOH), mμ(log ε): 220(4.76), 255(4.24), 285(3.67), 320(3.68), 340(3.80).

Found: C, 44.77; H, 2.01; N, 4.79. Calcd. for $C_{11}H_6O_4NBr$: C, 44.62; H, 2.04; N, 4.73%.

Formation of 2, 3-Dibromo-1, 4-naphthoquinone from 5, 7-Dibromo-3, 4-benzotropolone (III).—To a solution of 200 mg. of III in 1 ml. of concentrated sulfuric acid was added a mixture of 0.046 ml. (1 mol. equiv.) of concentrated nitric acid and 0.4 ml. of concentrated sulfuric acid. The solution was heated at 100°C for 10 min. and then poured on ice, producing a resinous product. Recrystallization of the product from methanol afforded 55 mg. (29%) of deep yellow needles of the dibromonaphthoquinone, m. p. 218°C, the melting point of which was undepressed on admixture with an authentic sample[6]. (Found: C, 37.77; H, 1.56%. Calcd. for $C_{10}H_4O_2Br_2$: C, 38.01; H, 1.28%.) Unchanged material (65 mg.) was also recovered.

2, 3-Dichloro-1, 4-naphthoquinone from 5, 7-Dichloro-3, 4-benzotropolone.—A similar treatment of 100 mg. of 5, 7-dichloro-3, 4-benzotropolone with 0.032 ml. (1 mol. equiv.) of concentrated nitric acid in concentrated sulfuric acid gave 15 mg. (16%) of yellow needles of the dichloronaphthoquinone, m. p. 195~196°C, identified by mixed melting point determination with an authentic sample[7], besides 25 mg. of unchanged material.

Oxidation of III with Nitric Acid.—A 200-mg. sample of III was heated with 0.5 ml. of concentrated nitric acid at 100°C for 10 hr. The product which separated on cooling was collected and recrystallized from water to yield 40 mg. of phthalic acid, m. p. and mixed m. p. 200~201°C (decomp.).

The author wishes to express his sincere gratitude to Professor Tetsuo Nozoe of Tohoku University for his kind guidance in carrying out this work. The author is also grateful to Mrs. Kuniko Kodaira and Miss Ayako Iwanaga of Tohoku University for microanalyses.

Department of Chemistry
Saitama University
Urawa, Saitama

Potentiometric Determination of the Formation Constants of Thiocyanato Complexes of Mercury(II)

By Nobuyuki TANAKA, Kazuko EBATA and Teisuke MURAYAMA

(Received May 15, 1961)

Although a number of investigations have been carried out on the formation constant of the tetrathiocyanatomercurate(II) complex, the values reported are not in satisfactory agreement with each other[1]. As for the formation constants of the dithiocyanatomercury(II) and trithiocyanatomercurate(II) complexes, only a few papers have been published[1].

In the present communication, the potentiometric determination of the formation constants of the dithiocyanatomercury(II) and tri- and tetrathiocyanatomercurate(II) complexes and some thermodynamic data for the formation reactions of these complexes are presented. Although Nyman and Alberts[2] reported the formation constants of these complexes during the course of this study, the scope of their study was limited to the determination of the formation constants at 25°C.

Experimental

A stock solution of 0.05 M mercury(II) was prepared by dissolving mercury(II) nitrate of a guaranteed reagent grade in 0.3 N nitric acid. Its concentration was determined by titrating with the standard solution of sodium chloride, using sodium nitroprusside as indicator[3]. A solution of potassium thiocyanate was obtained by dissolving

1) J. Bjerrum, G. Schwarzenbach and L. G. Sillén, "Stability Constants of Metal Ion Complexes, Part II, Inorganic Ligands", Chemical Society, London (1958), p. 42.

2) C. J. Nyman and G. S. Alberts, *Anal. Chem.*, 32, 207 (1960).

3) I. M. Kolthoff and V. A. Stenger, "Volumetric Analysis", Vol. II. Interscience Publishers, New York (1947), p. 332.

an appropriate amount of potassium thiocyanate of a guaranteed reagent grade. The concentration of thiocyanate was determined by the Volhard method[4]. All other chemicals used were also of a guaranteed reagent grade.

A conventional manual apparatus similar to that of Kolthoff and Lingane[5] was used for the measurement of the current-potential curve. The dropping mercury electrode used had an m value of 2.109 mg./sec. and a drop time t_d of 4.22 sec., being measured in a de-aerated 0.2 M potassium nitrate solution at -0.5 V. vs. SCE at 59 cm. of the mercury height. A saturated calomel electrode (SCE) with a large surface area was used for the reference electrode; to this the electrolytic solution was connected with a Hume and Harris type salt bridge[6]. The measurements were carried out in the thermostat at 15, 25 and 35°C. The solutions prepared for the potentiometric determination contained 0.532 mM of mercury(II) and 0.016 to 0.03 M of thiocyanate, unless otherwise stated. The ionic strength of the solutions was adjusted to 0.2 with potassium nitrate. The residual current was obtained with a 0.2 M potassium nitrate solution. After the correction for the residual current and for the internal resistance (iR drop) across the electrolysis cell, the zero-current potential, i. e. the potential at which the current equals zero, was determined within the limits of ± 0.5 mV.

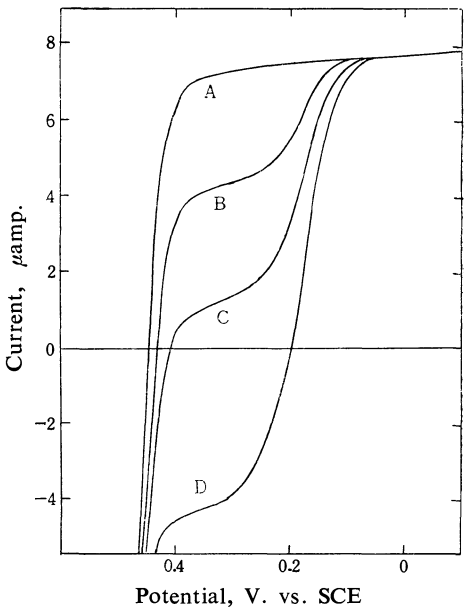


Fig. 1. Current-potential curves of 1.06_3 mM mercury(II) obtained at 25°C and $\mu=0.2$ without (curve A) and with 0.841 mM (B), 1.68 mM (C) and 2.94 mM (D) of thiocyanate. The residual current is not corrected.

Results

The current-potential curves of 1 mM mercury(II) obtained in the absence and in the presence of thiocyanate of various concentrations are reproduced in Fig. 1. The solution containing 1 mM of mercury(II) and less than 2 mM of thiocyanate gave a double wave. With the increasing concentration of thiocyanate at a constant concentration of mercury(II), the waves shifted to more negative potentials and the height of the first wave decreased, while the total height of both waves remained almost the same. The first wave was considered as due to the reduction of the free (hydrated) mercury(II) ion, and the second, to that of the thiocyanatomercury(II) complexes.

Since the limiting current of each wave was nearly completely dependent on the square root of the effective height of the mercury head, it was considered that the limiting currents are controlled by diffusion and are proportional to the concentrations of the hydrated and the complex mercury(II) ions in the bulk of solution respectively. The relation between the added concentration of the thiocyanate and the height of the wave showed that the complex which is formed under such conditions has two thiocyanate ions coordinating to the central metal ion. When the thiocyanate concentration exceeded 2 mM in the solution containing 1mM of mercury(II), the first wave became anodic, which is due to the dissolution of electrode mercury with the formation of thiocyanato complexes. These observations clearly showed that, in the concentration range employed in the present experiments, the presence of the mono-coordinated species $Hg(SCN)^+$ was negligible.

The relation between the zero-current potential ε and the thiocyanate concentration is given by the following equation:

$$\varepsilon = E^\circ + \frac{RT}{2F} \ln f_{Hg^{2+}} + \frac{RT}{2F} \ln \sum_j [Hg(SCN)_j^{2-j}] - \frac{RT}{2F} \ln \sum_j K_j^c [SCN^-]^j, \quad (0 \leqq j \leqq 4) \quad (1)$$

in which E° is the standard potential of the reaction,

$$Hg^{2+} + 2e = Hg$$

$f_{Hg^{2+}}$ the activity coefficient of the species Hg^{2+}, and K_j^c the formation constant of the complex $Hg(SCN)_j^{2-j}$ in terms of concentration. (When j equals zero, K_j^c is unity.) At the potential ε, the concentrations of the ions at the electrode surface are the same as those in the bulk of the solution.

4) I. M. Kolthoff and V. A. Stenger, ibid., Vol. II, p. 278.
5) I. M. Kolthoff and J. J. Lingane, "Polarography", Interscience Publishers, New York (1952), p. 297.
6) D. N. Hume and W. E. Harris, *Ind. Eng. Chem., Anal. Ed.*, 15, 465 (1943).

In the absence of thiocyanate, the potential ε° is expressed as

$$\varepsilon^\circ = E^\circ + \frac{RT}{2F} \ln f_{Hg^{2+}} + \frac{RT}{2F} \ln [Hg^{2+}]. \quad (2)$$

Since the value of ε° could not be obtained experimentally, it was calculated by means of Eq. 2. The standard oxidation-reduction potential of the system Hg(0)-Hg(II) at 25°C was taken as 0.850 V. vs. NHE, which had been obtained by Hietanen and Sillén[7] taking into account the complex formation between mercury(II) and nitrate ions. The standard potentials at 15° and 35° were calculated using the value at 25°C and the enthalpy change of the system at 25°C[8]. The ε° values calculated are given in Table I.

At the constant concentration of total mercury(II), Leden's F_0 function[9] was obtained from Eqs. 1 and 2 as:

$$F_0 \equiv \sum_j K_j^c [SCN^-]^j = \text{antilog}\left[0.435 \cdot \frac{2F}{RT} (\varepsilon^\circ - \varepsilon) \right] \quad (3)$$

Since the presence of hydrated mercury(II) and mono-coordinated thiocyanatocomplex ions was negligible compared to other species in the concentration range employed, the following F_2 function was obtained:

$$F_2 = \frac{F_0}{[SCN^-]^2} = K_2^c + K_3^c [SCN^-] + K_4^c [SCN^-]^2 \quad (4)$$

If the values of F_2 obtained experimentally are plotted against $[SCN^-]$, the value of K_2^c can be determined by extrapolation of the plot to a zero thiocyanate concentration. Using the K_2^c value thus obtained, the values of K_3^c and K_4^c can be determined by a similar graphical method with the aid of the following equation:

$$F_3 = \frac{F_2 - K_2^c}{[SCN^-]} = K_3^c + K_4^c [SCN^-] \quad (5)$$

In the above procedure the concentration of free (uncoordinated) thiocyanate $[SCN^-]$ must

TABLE I. VALUES OF ε° OF 0.532 mM MERCURY(II) NITRATE SOLUTION AT IONIC STRENGTH 0.2

Temperature °C	ε°, V. vs. SCE
15	0.493_3
25	0.492_9
35	0.492_6

TABLE II. VARIATIONS OF ε, F_2 AND F_3 AS A FUNCTION OF THIOCYANATE CONCENTRATION

$[SCN^-]_t$* mol./l.	ε V. vs. SCE	$[SCN^-]$ mol./l.	F_2	F_3
0.0315	0.0451	0.0296	1.63×10^{18}	5.42×10^{19}
0.0263	0.0548	0.0243	1.13×10^{18}	4.53×10^{19}
0.0210**	0.0795	0.0173	6.55×10^{17}	3.64×10^{19}
0.0189**	0.0854	0.0152	5.34×10^{17}	3.33×10^{19}
0.0168**	0.0919	0.0131	4.31×10^{17}	3.07×10^{19}
0.0147**	0.0993	0.0111	3.38×10^{17}	2.80×10^{19}
0.0126**	0.1076	0.00910	2.65×10^{17}	2.61×10^{19}
0.00946	0.1052	0.00774	2.21×10^{17}	2.50×10^{19}
0.0105**	0.1182	0.00712	1.90×10^{17}	2.28×10^{19}
0.00841	0.1116	0.00673	1.77×10^{17}	2.24×10^{19}
0.00946**	0.1242	0.00614	1.60×10^{17}	2.16×10^{19}
0.00631	0.1261	0.00471	1.17×10^{17}	1.92×10^{19}
0.00525	0.1337	0.00371	1.04×10^{17}	2.08×10^{19}
0.00420	0.1456	0.00273	7.62×10^{16}	1.80×10^{19}
0.00273	0.1684	0.00140	4.90×10^{16}	1.57×10^{19}

* $[SCN^-]_t$ is the added concentration of potassium thiocyanate.

** In these experiments the added concentration of mercury nitrate is 1.06_3 mM.

TABLE III. CONCENTRATION FORMATION CONSTANTS OF $Hg(SCN)_n^{2-n}$ AT IONIC STRENGTH 0.2

Temperature °C	K_2^c	K_3^c	K_4^c
15	$(1.8\pm0.2)\times10^{17}$	$(7.1\pm0.3)\times10^{19}$	$(1.11\pm0.02)\times10^{22}$
25	$(2.7\pm0.2)\times10^{16}$	$(1.39\pm0.03)\times10^{19}$	$(1.32\pm0.02)\times10^{21}$
35	$(5.5\pm0.2)\times10^{15}$	$(2.43\pm0.05)\times10^{18}$	$(1.68\pm0.04)\times10^{20}$

7) S. Hietanen and L. G. Sillén, *Arkiv Kemi*, **10**, 103 (1956).

8) W. M. Latimer, "Oxidation Potentials", Prentice-Hall, New York (1952), p. 176.

9) I. Z. Leden, *Z. phisik. Chem.*, **188A**, 160 (1941).

be known. Since the concentration of the thiocyanate that is consumed by complexing cannot be ignored, the free thiocyanate concentration must be calculated from the added concentrations of the thiocyanate and mercury-(II) nitrate. At first, [SCN^-] was calculated with appropriate coordination numbers (2 or 3) assumed tentatively. When a set of approximate values of the formation constants were available, the concentration of free thiocyanate was computed again with those constants. Such a procedure of stepwise approximation was repeated until self-consistent values of the formation constants were obtained. As an example, the data at 25°C are presented in Table II. Similar sets of data are also obtained at 15 and 35°C, and the final values of K_2^c, K_3^c and K_4^c at 15, 25 and 35°C are given in Table III.

The plots of F_2 and F_3 versus [SCN^-] obtained at 25°C are given in Fig. 2. The

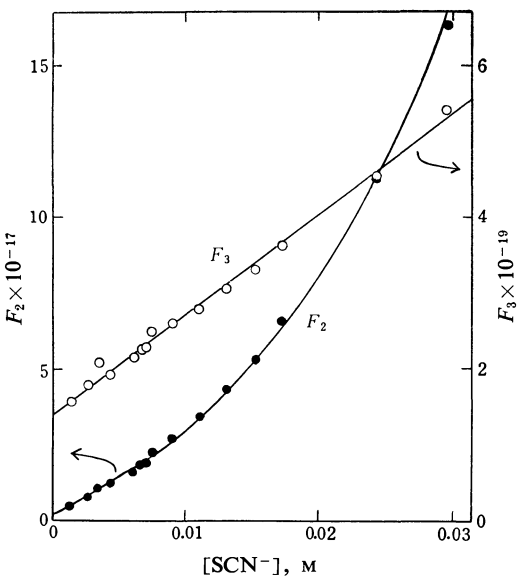


Fig. 2. F_2(Eq. 4) and F_3(Eq. 5) as functions of the thiocyanate ion concentration. (at 25°C). The solid line was calculated with the formation constants given in Table III.

solid line represents the theoretical curve which was calculated with the formation constants given in Table III. It is clearly seen that both F_2 and F_3 curves fit satisfactorily with the observed points plotted. This indicates that the formation constants obtained are proper ones.

Discussion

It is estimated from the experiments that, in a solution containing 0.532 mM of mercury-(II) and 0.03 M thiocyanate, the mean coordination number with respect to thiocyanate ion is approximately 3.7 and that some 70 per cent of the mercury(II) in the solution exists in the form of $Hg(SCN)_4^{2-}$. Hence, the range of the thiocyanate concentration chosen in the present investigation is considered sufficient for the determination of the formation constants of the three complex species, $Hg(SCN)_2$, $Hg(SCN)_3^-$ and $Hg(SCN)_4^{2-}$. The measurements at higher thiocyanate concentrations were not taken into account, because it seemed better, for the following reasons, to avoid varying the composition of the medium widely:

1. The residual current was measured with a solution containing 0.2 M potassium nitrate. With a solution containing thiocyanate, the oxidation of the electrode mercury occurs at almost the same potential as when mercury(II) nitrate is added to the solution.

2. The liquid junction potential will not stay constant with the increase of thiocyanate concentrations.

3. The activity coefficient will not be the same with the change in the composition of medium, even though the ionic strength of the medium is held constant at 0.2.

Using the activity coefficients of the ions, the formation constants given in Table III were reduced to thermodynamic formation constants, which are given in Table IV. The

Table IV. Thermodynamic formation constants of $Hg(SCN)_n^{2-n}$

Temperature °C	K_2	K_3	K_4
15	1.2×10^{18}	4.6×10^{20}	4.1×10^{22}
25	1.8×10^{17}	9.3×10^{19}	4.9×10^{21}
35	3.8×10^{16}	1.7×10^{19}	6.8×10^{20}

activity coefficients were evaluated with the equation[10],

$$\log f_i=\frac{-Az_i^2\sqrt{\Gamma}}{1+Ba_i\sqrt{\Gamma}}$$

in which A and B are constants at a given temperature[11], a_i is the mean distance of the nearest approach of the ions measured in Å, and Γ, the ionic concentration of the solution[11]. As for the mean distance of the nearest approach, the values given in Kielland's table[10] are used for the Hg^{2+} and SCN^- ions. For the $Hg(SCN)_3^-$ and $Hg(SCN)_4^{2-}$ ions, the a_i values were estimated from the data given in the same table[10].

From the thermodynamic formation constants, the free energy change ΔF, the enthalpy

10) I. Kielland, *J. Am. Chem. Soc.* **59**, 1675 (1937).
11) G. Kortüm and J. O'M. Bockris, "Textbook of Electrochemistry", Vol. II, Elsvier Publishing Co., New York (1951), p. 645.

change ΔH and the entropy change ΔS for the reaction,

$$Hg^{2+}(aq.) + n\,SCN^{-}(aq.) \rightleftarrows Hg(SCN)_n^{2-n}(aq.) \quad (6)$$

were evaluated, as given in Table V.

TABLE V. THERMODYNAMIC DATA FOR REACTION 6 AT 25°C

	ΔH, kcal./mol.	ΔF, kcal./mol.	ΔS, cal./deg. mol.
$n=2$	−30	−23.6	−20
$n=3$	−29	−27.2	− 6
$n=4$	−36	−29.6	−20

In Table VI are presented the formation constants of thiocyanatomercury(II) complexes which are reported in the literature. Among them there are the formation constants K_2, K_3 and K_4 which were reported by Nyman and Alberts. They obtained those constants from the study of the polarographic anodic wave of mercury(II) which appeared in the presence of thiocyanate ions. Although the ionic strength of the solution in their study is not the same as that in our experiments, it is nevertheless reasonable to conclude that their values of the formation constants are in good agreement with ours. The values given by Korshunov and Shchennikova[13] and those by Yatsimirski and Tukhlov[16] are discussed by Nyman and Alberts in their paper[2]. Most of the formation constants given in Table VI were determined without taking into consideration the ionic strength of the medium. Therefore, those are not compared with the values obtained in this study. The constants k_3 and k_4 given by Gallais and Mounier[17] are the third and the fourth successive formation constants corresponding to the reactions

$$Hg(SCN)_2 + SCN^{-} \rightleftarrows Hg(SCN)_3^{-}$$
$$Hg(SCN)_3^{-} + SCN^{-} \rightleftarrows Hg(SCN)_4^{2-}$$

respectively. However, they are undoubtedly too small compared with the others.

Besides the values in Table VI, Toropova[12] reported the thermodynamic formation constant of $Hg(SCN)_4^{2-}$ at 25°C to be 7.8×10^{21}, which is greater than our value for K_4 by about 1.6 times. She also estimated the enthalpy change and the entropy change for reaction 6 to be −35 kcal./mol. and −20 cal./deg. mol. respectively for $n=4$ at 25°C; these figures are in good agreement with the values in Table V.

In the case of halo and pseudohalo complexes of mercury(II), it is known that the species with two anions coordinated, in general, are relatively more stable[19]. This tendency is clearly recognized in the formation constants of thiocyanato complexes of mercury(II) obtained in the present study.

Summary

The formation constants of dithiocyanatomercury(II) and tri- and tetrathiocyanatomercurate(II) complexes have been determined by the potentiometric method with a dropping

TABLE VI. FORMATION CONSTANTS OF THIOCYANATOCOMPLEXES OF MERCURY(II) OBTAINED BY VARIOUS INVESTIGATORS

Medium	Temp., °C	Method	K_2^c	K_3^c	K_4^c	Investigators
1 M $KClO_4$	25	polarography	1.18×10^{16}	8.9×10^{18}	8.7×10^{20}	Nyman and Alberts[2]
0.3 M $NaNO_3$	20	e. m. f.	—	—	4.68×10^{21}	Toropova[12]
	25	〃	—	—	1.70×10^{21}	
	30	〃	—	—	6.30×10^{20}	
var.	18	polarography	—	—	2.0×10^{19}	Korshunov and Shchennikova[13]
var.	18	e. m. f.	—	—	2.5×10^{22}	Grossmann[14]
var.	25	〃	—	—	9.7×10^{21}	Sherrill and Skowronski[15]
Br^-	25	Spectrophotometry	2.95×10^{17}	—	—	Yatsimirski and Tukhlov[16]
Cl^-	25	〃	1.32×10^{17}	—	—	
var.	16	Faraday effect	$k_3=4.78\times10$, $k_4=5.25$			Gallais and Mounier[17]
var.	20	e. m. f.	—	—	4.43×10^{21}	Golub and Tsitsurina[18]

12) V. F. Toropova, *Zhur. Neorg. Khim.*, **1**, 243 (1956); *Chem. Abstr.*, **51**, 4192 (1957).
13) I. A. Korshunov and M. K. Shchennikova, *Zhur. Obshcheĭ Khim.*, **19**, 1820 (1949); *Chem. Abstr.*, **44**, 909 (1950).
14) H. Grossmann, *Z. anorg. Chem.*, **43**, 356 (1905).
15) M. S. Sherrill and S. Skowronski, *J. Am. Chem. Soc.*, **27**, 30 (1905).
16) K. B. Yatsimirski and B. D. Tukhlov, *Zhur. Obshcheĭ Khim.*, **26**, 356 (1956); *Chem. Abstr.*, **50**, 13643 (1956).
17) F. Gallais and J. Mounier, *Compt. rend.*, **223**, 790 (1946).
18) A. M. Golub and T. I. Tsitsurina, *Nauk. Zapiski, Kiïv. Derzhav. Univ. im. T. G. Shevchenka*, **16**, No. 15, *Zbirnik Khim. Fak.*, No. 8, 101 (1957); *Chem. Abstr.*, **53**, 9881 (1959).
19) F. Basolo and R. G. Pearson, "Mechanisms of Inorganic Reactions", John Willey & Sons, New York (1958), p. 4.

mercury electrode at ionic strength 0.2 and at 15, 25 and 35°C. The values obtained are:

at 15°C, $K^c_{Hg(SCN)_2}=1.8\times10^{17}$,
$K^c_{Hg(SCN)_3}=7.1\times10^{19}$,
$K^c_{Hg(SCN)_4}=1.11\times10^{22}$;

at 25°C, $K^c_{Hg(SCN)_2}=2.7\times10^{16}$,
$K^c_{Hg(SCN)_3}=1.39\times10^{19}$,
$K^c_{Hg(SCN)_4}=1.32\times10^{21}$;

at 35°C, $K^c_{Hg(SCN)_2}=5.5\times10^{15}$,
$K^c_{Hg(SCN)_3}=2.43\times10^{18}$,
$K^c_{Hg(SCN)_4}=1.68\times10^{20}$.

The thermodynamic formation constants of these complexes and the free energy change, the enthalpy change and the entropy change of the formation reactions of these complexes have been calculated.

The authors thank the Ministry of Education for the financial support granted for this research.

Department of Chemistry
Faculty of Science
Tohoku University
Katahira-cho, Sendai

The Decomposition of Methyl N-Nitroso-p-acetamidobenz[^{14}C]oate in Benzene. The Determination of the Products by the Isotopic Dilution Method

By Takashi INUKAI, Kenjiro KIMURA, Osamu SIMAMURA and Tadashi SUEHIRO

(Received May 23, 1961)

Nitrosoacylarylamines decompose in a liquid aromatic compound (Ar'H) to yield biaryls (Ar-Ar') as follows[1]:

$$ArN(NO)COR + Ar'H \longrightarrow Ar\text{-}Ar' + N_2 + RCOOH$$

The homolytic nature of this reaction is now widely accepted[2]; the biaryl is thought to be formed by substitution of Ar'H by aryl radicals (Ar·) homolytically produced from the nitroso compound. However, the yield of the biaryl is far from quantitative, and an appreciable quantity of tar is usually formed. In some cases a compound (ArH) resulting from abstraction of a hydrogen atom by the aryl radical was isolated[3]. Further, it was observed that about 3% of azobenzene was formed in the decomposition of *N*-nitrosoacetanilide in benzene[4]. In view of the complex nature of this reaction, it seemed of interest to determine the yields of various by-products from the decomposition of *N*-nitrosoacylarylamines. We report the results of isotopic dilution analysis of the products from decomposition of labelled methyl *N*-nitroso-*p*-acetamidobenzoate in benzene.

Methyl *N*-nitroso-*p*-acetamidobenz[^{14}C]oate (4.48 mmol.) was dissolved in benzene (405 mmol.) and left to stand for four days at 17~18°C; by the end of this period 76 cc. (0°, 1 atm., 76% of the theoretical amount) of nitrogen had been evolved. The reaction mixture was then worked up, and the yields of methyl benzoate, methyl *p*-acetoxybenzoate, methyl 4-biphenylcarboxylate etc. were determined by isotopic dilution analysis as will be described in the experimental part. The results are summarized in Table I.

Methyl 4-biphenylcarboxylate is obviously the product of the homolytic substitution of benzene by 4-methoxycarbonylphenyl radicals, although the detailed mechanism of this reaction is still obscure. Its yield, viz., 53.3%, definitely precludes the possibility, which has already come to be regarded as unlikely, that methyl 4-biphenylcarboxylate is formed exclusively by combination of 4-methoxycarbonylphenyl with phenyl radicals produced from benzene by hydrogen abstraction by the former radical. The low yield of methyl benzoate, which is formed by this abstraction, also supports this conclusion.

1) W. S. M. Grieve and D. H. Hey, *J. Chem. Soc.*, **1934**, 1798; H. France, I. M. Heilbron and D. H. Hey, ibid., **1940**, 369.
2) G. H. Williams, "Homolytic Aromatic Substitution", Pergamon Press, Oxford (1960), p. 29.
3) I. M. Heilbron, D. H. Hey and A. Lambert, *J. Chem. Soc.*, **1940**, 1279; J. W. Haworth and D. H. Hey, ibid., **1940**, 361; H. France, I. M. Heilbron and D. H. Hey, ibid., **1939**, 1284; J. Elks and D. H. Hey, ibid., **1943**, 441.
4) D. F. DeTar and H. J. Scheifele, *J. Am. Chem. Soc.*, **73**, 1442 (1951).

Dimethyl 4, 4′-biphenyldicarboxylate may have been produced by homolytic substitution of the methyl benzoate formed during the reaction by *p*-methoxycarbonylphenyl radicals. The extent of this substitution can be estimated as follows: The concentration of methyl benzoate may be assumed to be $0.013\times4.48\times0.5/405=7.2\times10^{-5}$ mol. per mole of benzene throughout the reaction, and as the partial rate factor of the para position of the methyl benzoate for the homolytic phenylation should be about 5[5] and the yield of methyl 4-biphenylcarboxylate was 53%, the yield of dimethyl 4, 4′-biphenyldicarboxylate by the substitution mechanism is expected to be of the order of $53\times7.2\times10^{-5}\times5/6=0.0032\%$. The experimentally found value of 0.024% therefore suggests that dimethyl 4, 4′-biphenyldicarboxylate must have been afforded largely by dimerization of *p*-methoxycarbonylphenyl radicals. But the possibility of induced decomposition by these radicals of the original *N*-nitroso-compound or of the rearranged diazoacetate could not be ruled out.

TABLE I. YIELDS OF VARIOUS PRODUCTS FROM THE DECOMPOSITION OF METHYL *N*-NITROSO-*p*-ACETAMIDOBENZ[^{14}C]OATE IN BENZENE

Product	yield, %
Methyl 4-biphenylcarboxylate	53.3
Methyl 4-acetoxybenzoate	0.046
Methyl benzoate	1.30
Dimethyl 4, 4′-biphenyldicarboxylate	0.024
Dimethyl 4, 4′-azobenzenedicarboxylate	0.46
Methyl 2-biphenylcarboxylate	<0.0074

The yields of dimethyl 4, 2′- and 4, 3′-biphenylcarboxylate, although no attempt was made at their determination, must have been small, since the homolytic arylation usually gives three isomerides in comparable amounts.

Methyl benzoate is thought to have been formed by hydrogen abstraction by *p*-methoxycarbonylphenyl radicals. Some of it must have reacted with *p*-methoxycarbonylphenyl radicals, giving three isomeric dimethyl biphenyldicarboxylates, but the extent of this reaction seems to have been exceedingly small, as is indicated by the low yield of dimethyl 4, 4′-biphenyldicarboxylate. The same is true of the substitution of methyl benzoate by any phenyl radicals to be generated from benzene by hydrogen abstraction by radicals, methyl 2-biphenylcarboxylate, one of the anticipated products of the phenylation, being formed in a negligible quantity, if at all. The yield of the meta isomeride would have been shown to be virtually nil, too. The conclusion is therefore drawn that the observed yield of methyl benzoate gives a practical estimate of the extent of the hydrogen abstraction by *p*-methoxycarbonylphenyl radicals.

5) A value estimated from the partial rate factors of ethyl benzoate for phenylation (unpublished work).

Experimental

Methyl *p*-Acetamidobenz[^{14}C]oate. — *p*-Aminobenz[^{14}C]oic acid was prepared according to the procedure described by Murry et al.[6] The labelled acid (0.357 g.) was dissolved in 37 cc. of anhydrous methanol and 1 cc. of acetyl chloride, the solution left to stand overnight, and the solvent removed on a water bath. The remaining methyl *p*-aminobenz-[^{14}C]oate hydrochloride was dissolved in water; the solution was treated with a little active charcoal, filtered, made slightly alkaline with sodium carbonate and stirred with acetic anhydride. The resulting precipitate was collected on a filter paper to give 0.352 g. of methyl *p*-acetamidobenz[^{14}C]oate, m. p. 129.7~130.5°C. A specimen of the non-labelled acid (Found: N, 7.25. Calcd. for $C_{10}H_{11}\cdot NO_3$: N, 7.25%) which was similarly prepared had the same melting point[7]. The labelled methyl ester was diluted with the inactive specimen and recrystallized from hot water containing 10% of methanol to give 990 mg. of methyl *p*-acetamidobenz-[^{14}C]oate (activity, 27.25 ± 0.545 mc./mol.), which was used for the preparation of the *N*-nitroso compound.

Methyl *N*-Nitroso-*p*-acetamidobenz[^{14}C]oate.— The above methyl *p*-acetamidobenz[^{14}C]oate (943.5 mg.) was dissolved in 6 cc. of a mixture (1 to 1 by volume) of acetic anhydride and acetic acid, containing 1.8 g. of potassium acetate and a little phosphorus pentoxide; this mixture was cooled with ice and water and nitrosated by adding dropwise 3 cc. of a solution of nitrosyl chloride (1 cc.) in acetic anhydride (4.3 cc.). The reaction mixture was stirred into 30 cc. of water, and the yellow precipitate was filtered off, washed with water and dried on a porous plate for 2 hr. and a half in an evacuated desiccator (3 mmHg) containing concentrated sulphuric acid, to give 1.004 g. of methyl *N*-nitroso-*p*-acetamidobenz[^{14}C]oate, m. p. 73~74°C with decomposition. This was immediately assayed for purity and subjected to decomposition in benzene. The purity of this specimen was estimated at $94.8\pm2.5\%$, as is described below. On the addition of 8.59 mg. of the labelled nitroso compound to a solution of 14 mg. of β-naphthol in 5 cc. of methanol, labelled 1-(*p*-methoxycarbonylphenylazo)-2-naphthol began to precipitate. The reaction mixture was allowed to stand for two days, 102.15 mg. of inactive 1-(*p*-methoxycarbonylphenylazo)-2-naphthol and 150 cc. of methanol were added, and the mixture was heated on a water bath to effect dissolution and then cooled. The precipitated azo compound was filtered off and repeatedly crystallized from methanol to a constant

6) A. Murray, W. W. Foreman and W. Langham, *J. Am. Chem. Soc.*, **70**, 1037 (1948).

7) N. W. Hirwe and P. Y. Kulkarni (*Proc. Indian Acad. Sci.*, **16A**, 294 (1942); *Chem. Abstr.*, **37**, 4061 (1943)) reported a m. p. of 114°C, but G. W. K. Cavill and J. M. Vincent (*J. Soc. Chem. Ind.* (London), **67**, 25 (1948); *Chem. Abstr.*, **42**, 4701b (1948)) reported a m.p. of 128°C.

activity of 2.70±0.043 mc./mol. The non-radioactive azo compound used as a carrier for the dilution analysis was prepared by coupling methyl *N*-nitroso-*p*-acetamidobenzoate with β-naphthol in methanol, m. p. 185.3~186.8°C (from methanol) (Found: N, 9.37. Calcd. for $C_{18}H_{14}N_2O_3$: N, 9.15%).

Decomposition of Methyl *N*-Nitroso-*p*-acetamidobenz[^{14}C]oate in Benzene.—The labelled nitroso compound (994.5 mg., 4.48 mmol.) was dissolved in 36 cc. of benzene (405 mmol.) containing a little anhydrous sodium sulphate and allowed to decompose at 17~18°C; at the end of four days the nitrogen evolved had amounted to 76 cc. (0°C, 1 atmosphere).

The solution was decanted from the sodium sulphate, which was then washed with benzene. To the combined benzene solutions, 753.35 mg. of methyl benzoate was added, and the benzene was removed on a water bath. The residue, after addition of 496.20 mg. of methyl *p*-acetoxybenzoate, m. p. 82.9~83.9°C, (lit.[8] m. p. 85°C), and 941.73 mg. of methyl 4-biphenylcarboxylate, m. p. 117~118°C, (lit.[9] m. p. 116~117°C), was subjected to distillation under diminished pressure. The following fractions were obtained: Methyl benzoate, b. p. 90.6~90.9°C at 21 mmHg, methyl *p*-acetoxybenzoate, b. p. 144~160°C at 9 mmHg, and methyl 4-biphenylcarboxylate, b. p. 179~180°C at 9 mmHg.

The methyl benzoate was hydrolyzed with alkali, and the resulting benzoic acid was repeatedly crystallized from hot water to a constant activity of 0.283±0.0099 mc./mol. The yield of methyl benzoate from the decomposition of the nitroso compound in benzene was therefore 7.91 mg., or 1.30% based on the nitroso compound.

The methyl 4-biphenylcarboxylate was purified by repeated crystallizations from methanol; the activity was found to be 9.55±0.191 mc./mol., corresponding to a yield of 53.3%.

It was found difficult to purify the methyl *p*-acetoxybenzoate by recrystallization from methanol on account of the contamination with methyl 4-biphenylcarboxylate. Accordingly, the fraction containing methyl *p*-acetoxybenzoate was dissolved in benzene, and the solution was washed with dilute aqueous alkali to remove any phenolic substance which might have been formed owing to unknown causes, washed with water, dried with anhydrous sodium sulphate and filtered through a column of alumina. Methyl 4-biphenylcarboxylate passed through, and on elution with ether 0.2 g. of methyl *p*-hydroxybenzoate was recovered. It was ascertained by a separate experiment that methyl *p*-acetoxybenzoate is deacetylated on alumina under those experimental conditions. The eluted methyl *p*-hydroxybenzoate was dissolved in benzene and extracted with dilute aqueous alkali, and the extract was washed with benzene and acidified with dilute sulfuric acid to precipitate methyl *p*-hydroxybenzoate, m. p. 131°C, (lit.[8] m. p. 131°C). Two crystallizations from water afforded a specimen with an activity of 0.0223 mc./mol. We were unable to pursue the purification to a constant activity on account of the dearth of the material. The activity of 0.0223 mc./mol. corresponds to a yield of 0.046%.

The mother liquors from the purification of methyl 4-biphenylcarboxylate were combined, and methanol was removed. The residue was combined with that from evaporation of the fraction containing 4-biphenylcarboxylate from the above chromatographic separation, and 750.15 mg. of methyl 2-biphenylcarboxylate, b. p. 173.5°C (18 mmHg), was added. The whole was dissolved in benzene and the solution washed with 0.05 N sodium hydroxide solution and then with water, dried with calcium chloride and filtered through a column of alumina to remove most of the methyl 4-biphenylcarboxylate. Benzene was removed from the filtrate, the remaining ester hydrolyzed by boiling for about five hours with sodium hydroxide in dilute alcohol, and hydrochloric acid added. The precipitated 2-biphenylcarboxylic acid was filtered off, dried (706 mg.), and heated for ten minutes with 4 cc. of concentrated sulphuric acid on a water bath. The reaction mixture was added to water, the precipitate filtered off and dissolved in ether, the solution washed thoroughly with dilute sodium carbonate and dried with anhydrous calcium chloride, and the ether removed on a water bath to give 0.50 g. of fluorenone. Repeated crystallizations from petroleum ether gave a specimen, m. p. 84°C (lit.[10] m. p. 84~86°C), with an activity of 1.1 μc./mol. with a reliable error of ±1.6 μc./mol. Therefore, the yield of methyl 2-biphenylcarboxylate is estimated to be less than 0.0074%.

The upper part of the chromatographic column for the separation of methyl 4-biphenylcarboxylate and methyl *p*-acetoxybenzoate showed an orange color. This part was extracted three times with hot 94% alcohol, and the combined extracts were evaporated. The residue was added, together with 175.5 mg. of dimethyl 4, 4'-azobenzenedicarboxylate, m.p. 242~242°C (lit.[11] m.p. 242°C), 365.1 mg. of methyl 4-azobenzencarboxylate, m.p. 123~124°C (lit.[12] m.p. 123~124°C), and 115.1 mg. of dimethyl 4,4'-biphenyldicarboxylate, m.p. 213~214°C (lit.[13] m.p. 212~213°C), to a benzene solution of the residue from the fractional distillation. The benzene solution was heated, and, on concentration to about 40 cc., dimethyl 4, 4'-azobenzenedicarboxylate crystallized out in small scales. This was filtered off and recrystallized from benzene to a constant activity of 0.947±0.018 mc./mol., corresponding to a yield of 0.46%. The mother liquor was chromatographed on alumina in order to effect a further separation. But, as no substances were eluted owing to strong adsorption, the alumina was boiled with methanol and 17.0 mg. of dimethyl 4, 4'-biphenyldicarboxylate recovered. This was diluted with 176 mg. of inactive ester and recrystallized from benzene to a constant activity of 0.0060±0.0006 mc./mol., corresponding to a yield of 0.024%. Purification of methyl 4-azobenzenecarboxylate failed owing to its greater

8) C. H. V. Hoessle, *J. prakt. Chem.*, (2), **49**, 502 (1894).
9) R. L. Dannley and B. Zaremsky, *J. Am. Chem. Soc.*, **77**, 1588 (1955).
10) J. Schmidt and H. Wagner, *Ber.*, **43**, 1797 (1910).
11) F. Meyer and K. Dahlem, *Ann.*, **326**, 338 (1903).
12) P. Jacobson and A. Steinbrenk, ibid., **303**, 387 (1898).
13) M. Weiler, *Ber.*, **32**, 1061 (1899).

solubility than those of the other compounds added as carriers.

Radioactivity Determination.—Radiocarbon assays were carried out by oxidizing samples according to the method of Van Slyke and Folch[14] and by converting the resulting carbon dioxide into barium carbonate, the activity of which was counted with an end-window Geiger-Müller counter on an "infinitely thick" layer with a surface area of 4.9 cm^2, the counts being all corrected for background and compared with the count of a standard barium carbonate with a known activity.

14) D. D. Van Slyke and J. Folch, *J. Biol. Chem.*, **136**, 509 (1940).

Summary

Methyl *N*-nitroso-*p*-acetamidobenz [^{14}C] oate was decomposed in benzene, and the product was analyzed by the isotopic dilution method. The results are shown in Table I, and the mechanistic implication is discussed.

Department of Chemistry
Faculty of Science
The University of Tokyo
Hongo, Tokyo

Dimer-Monomer Equilibrium Constants for Acetic Acid and the Three Chloroacetic Acids in Benzene

By Yoichiro NAGAI and Osamu SIMAMURA

(Received May 23, 1961)

An accurate value of the equilibrium constant for the association of monomeric dichloroacetic acid to the dimeric form in benzene was required for a kinetic study being carried out in this laboratory. A search of the literature showed that a number of workers[1-5] had already been concerned with the problem of determining the association constants of acetic acid and the three chloroacetic acids in various non-polar solvents. In view of the lack of a reliable value for our present purpose, however, we have now determined, by infrared absorption measurement, the dimer-monomer equilibrium constant for dichloroacetic acid in benzene at 20°C, together with those for acetic, monochloroacetic, and trichloroacetic acid.

Experimental

Materials.—Benzene was shaken with concentrated sulphuric acid and with water, dried with calcium chloride and fractionated over sodium. Acetic acid was refluxed with potassium permanganate, distilled, and subjected to fractional crystallizations until a product with a constant freezing point, 16.5°C, was obtained; this material was distilled before use, b. p. 117°C. Monochloroacetic acid was recrystallized three times from benzene, dried over phosphorus pentoxide in an Abderhalden apparatus, m. p. 63.0°C, and distilled, b. p. 186°C. Dichloroacetic acid was prepared by Cope, Clark, and Connor's procedure[6] and fractionated three times under reduced pressure, b. p. 86.6~87.0°C/13mmHg. Trichloroacetic acid was distilled four times, b. p. 195.5~195.8°C.

Absorption Measurement.—The measurements were carried out at 20°C on benzene solutions of the acids in concentrations ranging from 0.01 to 1 mol./l., a Perkin-Elmer grating spectrophotometer Model 112G being used. A 1 mm. measuring cell was used for solutions of acetic, monochloroacetic, and dichloroacetic acid and an 0.1 mm. cell for solutions of trichloroacetic acid. The absorption spectra were measured in the region between 3250 and 3550 cm^{-1}, in which the peak of a band due to a free OH stretching vibration usually appears, with a spectral slit width of 1.0 cm^{-1} being used.

Results and Discussion

The absorption frequencies observed in benzene corresponding to the stretching mode of the free OH group of acetic acid and the three chloroacetic acids are listed in Table I, together with the values in carbon tetrachloride reported in the literature.

1) J. T. Harris, Jr. and M. E. Hobbs, *J. Am. Chem. Soc.*, **76**, 1419 (1954).
2) J. Wenograd and R. A. Spurr, ibid., **79**, 5844 (1957).
3) C. P. Brown and A. R. Mathieson, *J. Chem. Soc.*, **1957**, 3625; C. P. Brown and A. R. Mathieson, *J. Phys. Chem.*, **58**, 1057 (1954).
4) H. A. Pohl, M. E. Hobbs and P. M. Gross, ibid., **9**, 408 (1941); R. J. W. Le Fèvre and H. Vine, *J. Chem. Soc.*, **1938**, 1795.
5) M. M. Davies and G. B. B. M. Sutherland, *J. Chem. Phys.*, **6**, 755 (1938).
6) A. C. Cope, J. R. Clark and R. Connor, "Organic Syntheses", Coll. Vol. II (1948), p. 181.

TABLE I. ABSORPTION FREQUENCIES (cm^{-1})

Acid	Present work in C_6H_6	Ref. 1 in CCl_4	Ref. 7 in CCl_4	pK_a[8] in H_2O
CH_3COOH	3472	3548	3533	4.76
$CH_2ClCOOH$	3438	3539	3522	2.86
$CHCl_2COOH$	3410	3529	3511	1.29
CCl_3COOH	3389	3526	3505	0.3

Table I shows that the free OH vibration frequency of the stronger acid is lower than that of the weaker one both in benzene and in carbon tetrachloride. There is a linear relation between the OH vibration frequencies in benzene and the pK_a values[8], as is shown in Fig. 1. A similar relation has also been observed in carbon tetrachloride solution[7].

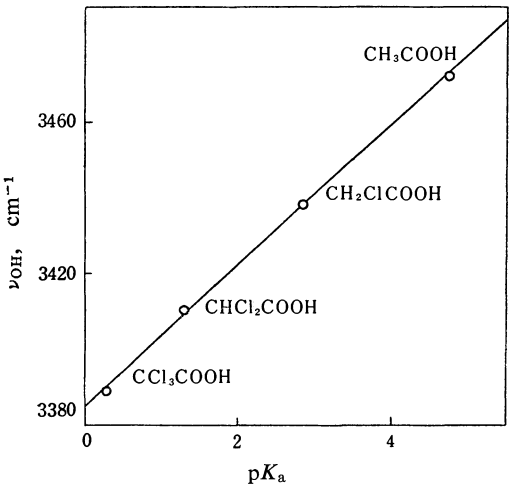


Fig. 1. Relation between the OH vibration frequency of the monomeric acid in benzene and the pK_a value.

Further, the observed frequencies are considerably lower in benzene than in carbon tetrachloride. This shift in the OH frequency is obviously attributable to an interaction, similar to hydrogen bond formation, between the hydroxyl of a carboxyl group and the π-electron system of a benzene nucleus. Since the relative affinity of the acid for benzene is considered to be parallel to the acid strength, it is expected that the more highly chlorinated acids interact more strongly with benzene, resulting in a larger shift in frequency; this has been borne out, as is shown in Fig. 1. Such a shift has also been observed for methanol-d[9] and phenols[10], and a similar one has been observed in the NH frequency for *N*-methylacetamide[11].

The dimer-monomer equilibrium constants were calculated from the change in the apparent molar extinction coefficient of the OH absorption band with the acid concentration by using the equations,

$$d = l\varepsilon C = lEM$$

$$K = 2M^2/(C-M)$$

In these equations d is the optical density, l the absorption path length, ε the apparent molar extinction coefficient, E the molar extinction coefficient of the monomeric acid, C the concentration of the acid taken, M the concentration of the acid monomer, and K the equilibrium constant. Combination of the above equations and rearrangement gives

$$\varepsilon C = (KE^2/2)(1/\varepsilon) - KE/2$$

It follows from this equation that a graph of εC at the particular OH absorption frequency against $1/\varepsilon$ should give a straight line of slope $KE^2/2$ and intercept $KE/2$. The experimental data are shown numerically in Table II and graphically in Fig. 2. The apparent molar extinction coefficient ε increases with a decreasing concentration of the acid, showing that the frequencies which have been measured are due to the OH vibration of the monomeric acids. Since there are satisfactory linear relations between εC and $1/\varepsilon$, as is shown in Fig. 2, it is evident that the assumption of a dimer-monomer equilibrium is well-founded.

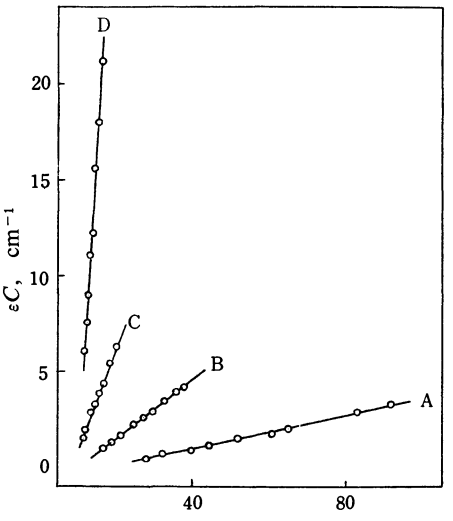


Fig. 2. Relation between εC and $1/\varepsilon$.
A : CH_3COOH B : $CH_2ClCOOH$
C : $CHCl_2COOH$ D : CCl_3COOH

7) J. P. S. Goulden, *Spectrochim. Acta*, **6**, 129 (1954).
8) E. J. P. Dippy, *Chem. Revs.*, **25**, 151 (1939).
9) M. Tamres, *J. Am. Chem. Soc.*, **74**, 3375 (1952).
10) M. Ōki, H. Iwamura and Y. Urushibara, this Bulletin, **31**, 769 (1958); R. West, ibid., **81**, 1641 (1959).
11) I. Suzuki, M. Tsuboi, T. Shimanouchi and S. Mizushima, *J. Chem. Phys.*, **31**, 1437 (1959); I. Suzuki, M. Tsuboi and T. Shimanouchi, ibid., **32**, 1263 (1960).

TABLE II. THE APPARENT MOLAR EXTINCTION COEFFICIENTS (ε IN l. mol^{-1} cm^{-1}) AT VARIOUS ACID CONCENTRATIONS (C IN mol./l.)

CH_3COOH		$CH_2ClCOOH$		$CHCl_2COOH$		CCl_3COOH	
C	ε	C	ε	C	ε	C	ε
0.309	10.9	0.159	26.3	0.124	50.4	1.174	42.8
0.247	12.0	0.143	27.7	0.0993	54.2	0.587	52.3
0.129	15.5	0.123	29.3	0.0931	54.5	0.528	55.5
0.124	15.9	0.114	30.1	0.0827	57.4	0.440	56.4
0.103	16.4	0.0858	33.2	0.0744	58.6	0.411	57.7
0.0772	19.2	0.0715	36.2	0.0620	62.5	0.352	60.2
0.0515	22.5	0.0572	39.5	0.0558	65.4	0.261	65.2
0.0483	23.2	0.0476	40.9	0.0496	66.9	0.235	66.5
0.0322	24.9	0.0357	46.2	0.0414	72.3	0.176	69.3
0.0215	30.8	0.0286	47.9	0.0372	73.4	0.147	75.7
0.0129	35.7	0.0238	52.6	0.0248	79.4	0.117	76.7
		0.0159	59.2	0.0186	82.8	0.0978	77.7
				0.0165	86.5	0.0733	83.2

The values of E and K calculated from the slopes and intercepts of the lines in Fig. 2 determined by the method of least squares are given in Table III. Harris and Hobbs[1] have estimated, by means of infrared absorption measurement, the equilibrium constants in carbon tetrachloride at 25°C at 2.5×10^{-4}, 6.2×10^{-4}, 9.3×10^{-4}, and 19×10^{-4} mol./l. for acetic, monochloroacetic, dichloroacetic, and trichloroacetic acid, respectively. Comparison with the present values indicates that these acids are very much more associated in carbon tetrachloride than in benzene. The larger dissociation in the latter solvent is evidently attributable to the same cause that has been adduced above to account for the shift in the hydroxyl frequency in benzene from that in carbon tetrachloride; the stabilizing interaction of a hydroxyl group with a molecule of benzene tends to bring about the dissociation of the dimeric form.

TABLE III. MOLAR EXTINCTION COEFFICIENTS AND DIMER-MONOMER EQUILIBRIUM CONSTANTS IN BENZENE AT 20°C

Acid	E l.mol^{-1} cm^{-1}	K mol./l.
CH_3COOH	50.8	0.036
$CH_2ClCOOH$	87.7	0.041
$CHCl_2COOH$	110.9	0.092
CCl_3COOH	92.2	0.91

Summary

Acetic, monochloroacetic, dichloroacetic, and trichloroacetic acid in benzene show an infrared absorption band due to the OH stretching vibration of the monomeric form at 3472, 3438, 3410, and 3389 cm^{-1}, respectively. The dimer-monomer equilibrium constants for these acids in benzene at 20°C have been evaluated, from the change in intensity of these bands with the acid concentration, to be 0.036, 0.041, 0.092, and 0.91 mol./l., respectively.

The observed shift in frequency indicates that there is an interaction, similar to hydrogen bond formation, between the hydroxyl of a carboxyl group and the π-electron system of a benzene nucleus and that the stronger acid interacts more strongly with benzene, resulting in a larger shift in frequency.

The authors are indebted to Professor Takehiko Shimanouchi for valuable suggestions.

Department of Chemistry
Faculty of Science
The University of Tokyo
Hongo, Tokyo

Alternant Conjugate Systems. III. Syntheses of Stereoisomeric p, p'-Distyrylstilbenes and Related Compounds

By Sōichi MISUMI, Motoyuki KUWANA and Masazumi NAKAGAWA

(Received March 7, 1961)

In Part II[1] of this series, the present authors reported the syntheses of alternatively conjugated compounds containing three benzene rings in the conjugate system. The appearance of absorption maxima at ca. 270 mμ in the ultraviolet spectra of these compounds could be attributed either to the so-called "cis-peak"[2] or to the partial chromophore[3] which became operative at the presence of steric hindrance. As it seems to be possible to distinguish the two possibilities stated above by an examination of the ultraviolet spectra of the longer alternant conjugate system, the authors have carried out the syntheses of stereoisomeric *p, p'*-distyrylstilbenes and the related compounds containing four benzene nuclei in the system.

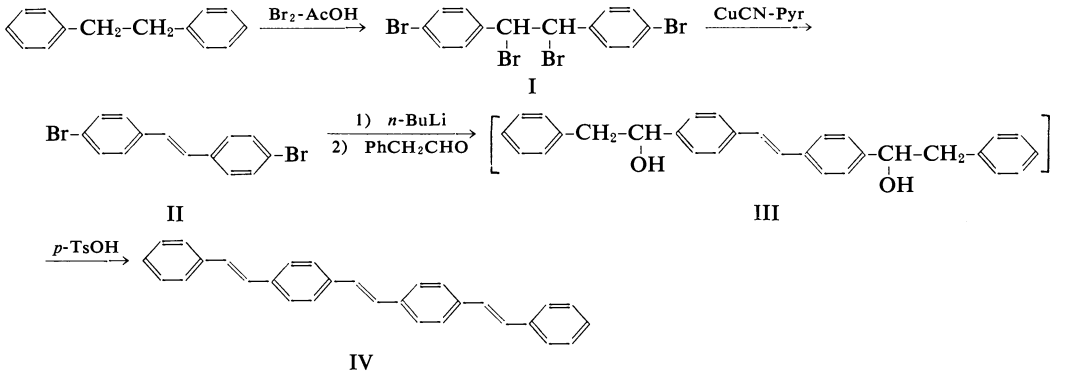
Theoretically, eighteen stereoisomers are possible in the alternant conjugate system containing four benzene nuclei which are linked with each other by double or triple bonds in their para-positions. The present paper deals with the syntheses of ten of the eighteen stereoisomers of this series.

The all-trans isomers has been synthesized by Dale[4] through the Meerwein reaction of *p, p'*-diaminostilbene and by Drefahl and his co-worker[5] through the Grignard reaction of *p, p'*-stilbenedialdehyde. The present authors have synthesized the all-trans isomer according to the following scheme[6].

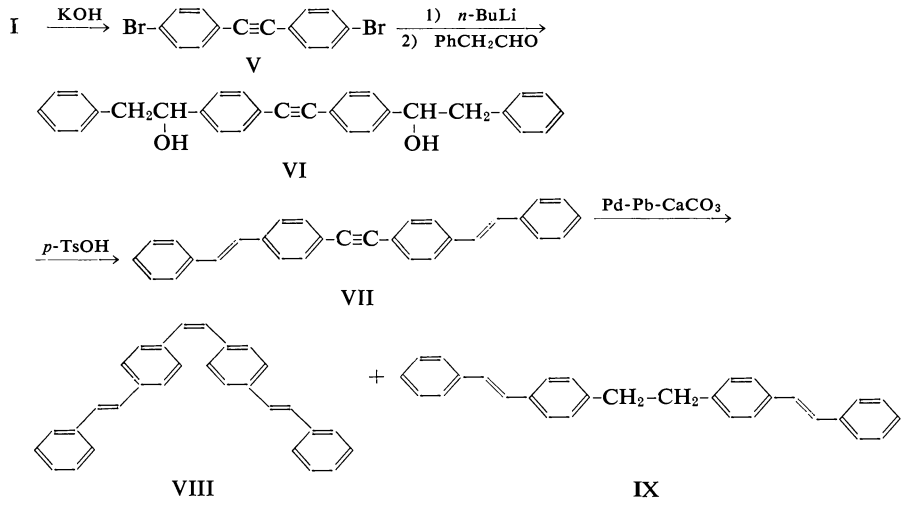
p, p'-Dibromostilbene (II) was derived from the tetrabromide (I) by treatment with cuprous cyanide[7]. The crude glycol (III) which was obtained by the metalation of the stilbene (II) and the subsequent reaction with phenylacetaldehyde was dehydrated without further purification, yielding trans, trans, trans-*p, p'*-distyrylstilbene (IV) as yellow crystals with green fluorescence.

Two different methods, a half-reduction of the corresponding acetylenic analogues and the Wittig reaction of the appropriate aldehyde with a phosphonium halide, were employed for the syntheses of trans, cis, trans- and trans, trans, cis-isomers of *p, p'*-distyrylstilbene (abbreviated as t-c-t and t-t-c).

The t-c-t isomer was synthesized according to the following scheme: *p, p'*-Dibromotolan (V) was obtained in an almost quantitative yield by the dehydrobromination[8] of the tetrabromide (I). Successive reactions of *n*-butyllithium with dibromotolan (V) and then with phenylacetaldehyde yielded the glycol (VI). The glycol (V) was dehydrated in boiling toluene in the presence of *p*-toluenesulfonic acid to yield *trans, trans-p, p'*-distyryltolan



1) Part II: S. Misumi, M. Kuwana, K. Murashima and M. Nakagawa, This Bulletin, **34**, 1833 (1961).
2) L. Zechmeister, L. Pauling et al., *J. Am. Chem. Soc.*, **65**, 1940 (1943); L. Zechmeister, *Chem. Revs.*, **34**, 267 (1944); *Experientia*, **10**, 1 (1954).
3) W. Oroshnik and A. D. Mebane, *J. Am. Chem. Soc.*, **76**, 5719 (1954). cf. P. Karrer et al., *Helv. Chim. Acta*, **35**, 1850 (1952); **36**, 562 (1953).
4) J. Dale, *Acta Chem. Scand.*, **11**, 971 (1957).
5) G. Drefahl and G. Plötner, *Chem. Ber.*, **91**, 1274 (1958).
6) S. Misumi and M. Kuwana, presented at the 12th Annual Meeting of the Chemical Society of Japan, Kyoto, April, 1959.
7) S. Bance, H. J. Barker and A. M. Woolman, *J. Chem. Soc.*, **1943**, 1.
8) H. J. Barker and R. Slack, ibid., **1944**, 612.



(VII)[6] (abbreviated as t-A-t).

t-A-t (VII) was found to be sparingly soluble in common solvents for catalytic hydrogenation. Therefore, VII was dissolved in a large amount of tetrahydrofuran (solubility: 3 mg. in 43 ml.) and hydrogenated in a dark place over a large amount of Lindlar's catalyst[9] (about the same weight as VII). The progress of hydrogenation was followed, measuring the change of the ultraviolet absorption at a certain time interval. The hydrogenation product from several runs was combined (300 mg.) and recrystallized from benzene. This substance yielded almost pure t-c-t isomer by chromatographic purification over alumina. The configuration of this material was inferred from the following evidence: (1) Analytical data, (2) definite and sharp melting point, (3) thermal isomerization to all-trans isomer, and (4) photoisomerization to all-trans isomer.

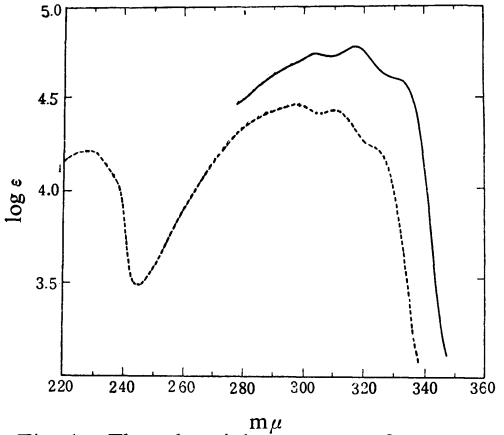
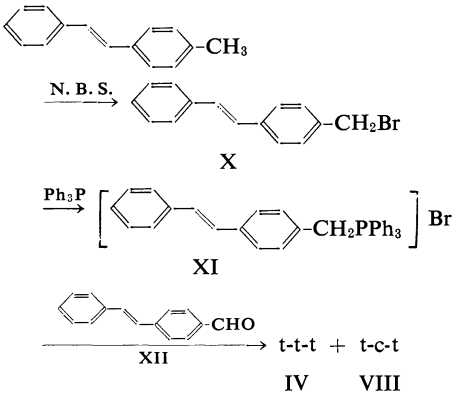


Fig. 1. The ultraviolet spectra of IX (——) (in benzene) and *p*-methylstilbene (·····) (in *n*-hexane).

9) H. Lindlar, *Helv. Chim. Acta*, 35, 446 (1952).

Pale yellow needles with green fluorescence (m. p. 262°C.) were obtained from the first mother liquor of the recrystallization of t-c-t isomer. The solubility in organic solvents and the closely related ultraviolet spectrum of this compound with that of *p*-methylstilbene (maxima at almost the same positions with two-fold intensities) suggest that the substance with the melting point of 262°C is *p*,*p*'-distyryldibenzyl (IX) (Fig. 1 and Table I).

The t-t-t and t-c-t isomers were also prepared by the Wittig reaction. The reaction of the phosphonium salt XI, derived quantitatively from *p*-bromomethylstilbene (X), with *p*-stilbenealdehyde (XII)[10] resulted in a mixture of



t-t-t (IV) and t-c-t isomer VIII. Recrystallization and chromatography over alumina of the mixture afforded pure t-t-t and t-c-t isomer.

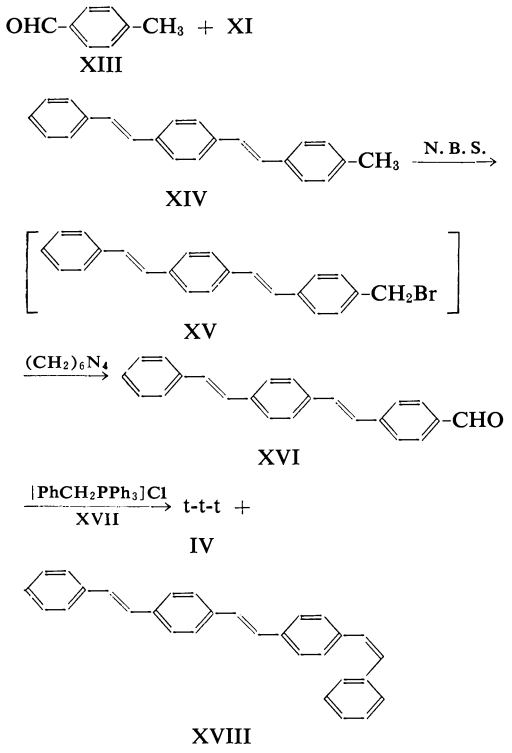
The synthesis of the third isomer, t-t-c (XVIII), was performed starting from *p*-tolualdehyde (XIII)[11]. *p*-Methyldistyrylbenzene (XIV)[5] was prepared by the Wittig reaction

10) Part I: S. Misumi, This Bulletin, 34, 1827 (1961).
11) G. H. Coleman and D. Craig, "Organic Syntheses", Col. Vol. II, 583 (1943).

Table I. The ultraviolet spectra of IX and *p*-methylstilbene

	λ_{max}, mμ (ε_{max})				
IX		303 (55100)	317 (60900)	(benzene)	
p-Methylstilbene	229 (16100)	298 (29400)	310 (28000)	(*n*-hexane)	

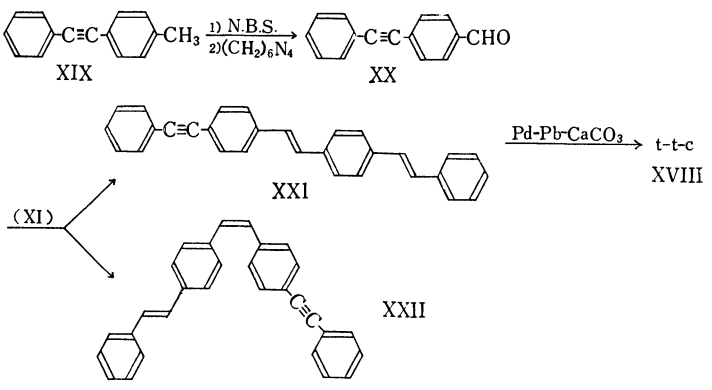
of *p*-tolualdehyde (XIII) with the phosphonium bromide (XI) and converted to *p*-bromomethyl derivative XV by the reaction with *N*-bromosuccinimide. Distyrylbenzenealdehyde (XVI) was prepared according to Drefahl's procedure[5] with the slight modification of employing the crude bromide XV. The Wittig reaction of the aldehyde XVI with benzyltriphenylphosphonium chloride (XVII) was carried out in a dark place. Recrystallization and chromatography of the reaction product resulted in the separation of t-t-t (IV) and t-t-c isomer XVIII.



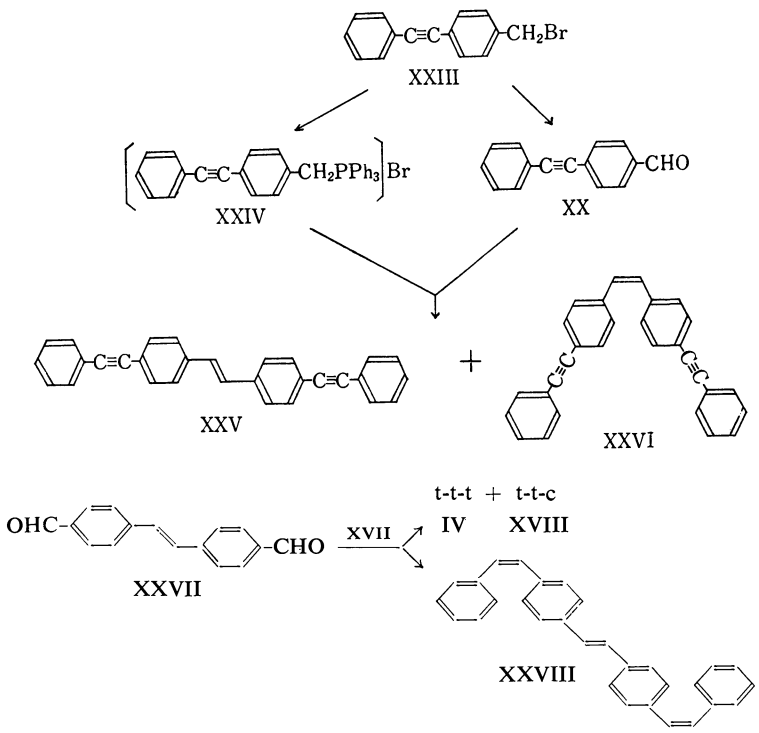
The t-t-c isomer XVIII showed a characteristic behavior which could not be observed in the other cis-isomer. When the temperature of a heating bath was gradually raised, a gradual sintering of the crystals was observed at ca. 227°C and the crystals melted at the melting point of the t-t-t isomer. On the other hand, when the bath temperature was rapidly elevated, the crystals melted at 227~230°C and the molten substance immediately resolidified. This solid showed an identical melting point with the all-trans isomer. Therefore, the definite melting point of the t-t-c isomer could not be determined owing to the above-mentioned thermal instability.

The t-t-c isomer XVIII was also prepared by the half-reduction of the corresponding acetylenic compound. *p*-Tolanaldehyde (XX)[1,12] obtained from *p*-methyltolan (XIX) was treated with *p*-styrylbenzyltriphenylphosphonium bromide (XI). A chromatographic purification of the reaction product afforded *p*-phenylethynyl-*p'*-styryl-*trans*-stilbene (XXI) (t-t-A) and *p*-phenylethynyl-*p'*-styryl-*cis*-stilbene (XXII) (t-c-A) in a yield of 40% and 30% respectively.

The structure of the t-c-A isomer was inferred from the analytical data and from the thermal- and photo-isomerizations to the t-t-A isomer. Owing to the poor solubility in common organic solvents, the catalytic half-hydrogenation of the t-t-A compound to the t-t-c isomer was performed in tetrahydrofuran as for the reduction of the t-A-t isomer. The t-t-c compound (XVIII) obtained by this method was proved to be identical with the specimen,



12) G. Drefahl and G. Plötner, *Chem. Ber.*, 93, 990 (1960).



which was prepared by the above-mentioned Wittig reaction, by the mixed melting point determination and by a comparison of the ultraviolet spectra.

With the purpose of comparing the ultraviolet spectroscopic properties with those of analogous alternant triene or alternant dienyne compounds, *cis*- and *trans*-*p*,*p*'-bisphenylethynylstilbenes (XXVI, A-c-A and XXV, A-t-A[12]) were synthesized by the reaction of phosphonium salt XXIV with tolanaldehyde (XX), both of which are derived from *p*-bromomethyltolan (XXIII). The structure of the cis-isomer was determined by the analytical data and the thermal- and photo-isomerizations to the A-t-A isomer.

The fourth isomer of *p*,*p*'-distyrylstilbene, c-t-c (XXVIII), was obtained by a double Wittig reaction of *p*,*p*'-stilbenedialdehyde (XXVII) together with t-t-t (IV) and t-t-c (XVIII). The structure of this isomer was confirmed by elementary analysis and the thermal- and photo-isomerizations to the t-t-t isomer. It is interesting to note that this isomer is thermally more stable than t-c-t (VIII) and t-t-c (XVIII).

Generally, a slightly larger or almost the same amount of cis-isomer as compared with that of trans-isomer could be isolated from the products of the Wittig reactions of these types of compound. This fact seems to be attributable to the difficult isolation and purification of the sparingly soluble trans-isomer from the unreacted phosphonium salt in contrast with the case of the more soluble cis-isomer.

The ultraviolet spectra of the above-mentioned ten compounds, t-t-t, t-t-c, t-c-t, c-t-c, t-t-A, t-A-t, A-t-A, A-c-A, t-c-A and A-A-A, are illustrated in Figs. 2, 3 and 4. The physical properties of these compounds are presented in Table II. A detailed discussion on the ultraviolet spectra and the photoisomerizations of these compounds will be presented in a following paper.

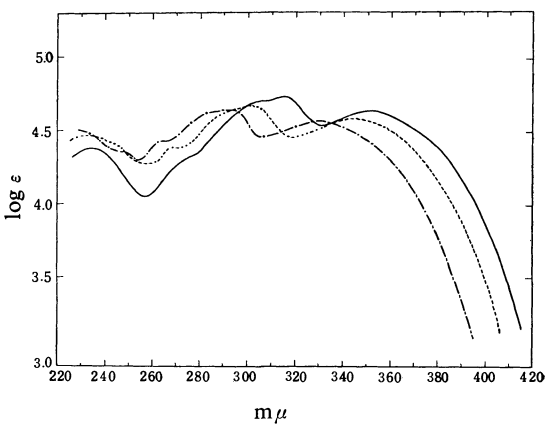


Fig. 2. The ultraviolet spectra of t-c-t (VIII, ——), t-c-A (XXII, ·····) and A-c-A (XXVI, —·—·) in tetrahydrofuran.

TABLE II. PROPERTIES OF STEREOISOMERIC *p,p'*-DISTYRYLSTILBENES AND RELATED COMPOUNDS

	M. p., °C	Color	Fluorescence in solution	Ultraviolet spectrum λ_{max} in mμ ($\varepsilon_{max} \times 10^{-3}$) in tetrahydrofuran			
t-t-t	334~336	Green yellow	Intense blueviolet	238 (35.9)	270 (18.6)		384 (89.3)
t-t-A	308~309	Light green yellow	Intense blueviolet	237 (32.1)	266 (20.8)		374 (78.7)
t-A-t	305~308	Light green yellow	Intense blueviolet	243 (43.2)			361 (84.3)
A-t-A	278~279	Light green yellow	Blueviolet	235 (29.7)	262 (14.4)		362 (80.1)
t-t-c	227~230	Light green yellow	Blueviolet	237 (28.5)			372 (68.1)
t-c-t	227~228	Light yellow	Light greenblue	236 (22.9)	316 (52.1)		353 (41.0)
c-t-c	111~112	Pale yellow	Colorless	238 (36.8)			359 (48.8)
t-c-A	198~199	Light yellow	Colorless	235 (29.0)	270 (24.1)	302 (45.7)	346 (37.6)
A-c-A	151~152	Colorless	Colorless		295 (45.3)		330 (36.5)

c, t and A denote cis-ethylenic, trans-ethylenic and acetylenic linkage respectively.

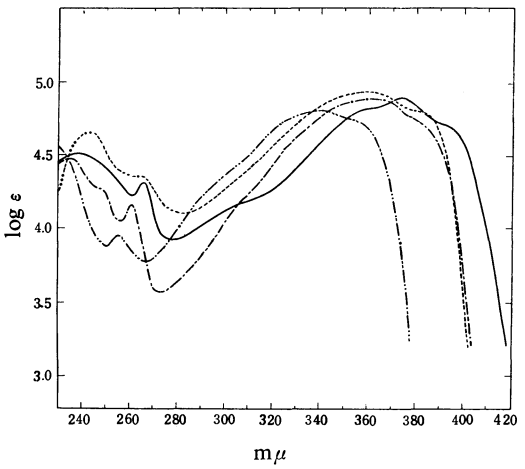


Fig. 3. The ultraviolet spectra of t-t-A (XXI, ——), t-A-t (VII, ·····), A-t-A (XXV —·—·) (in tetrahydrofuran) and A-A-A (—··—··) (in chloroform).

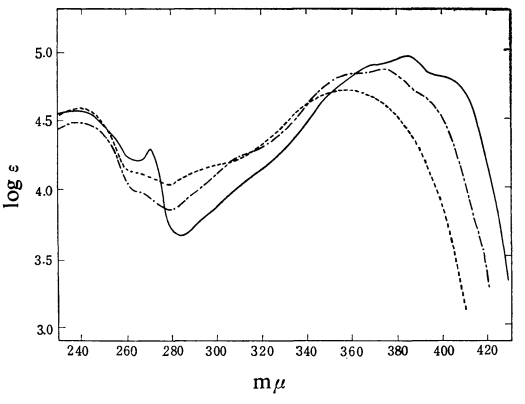


Fig. 4. The ultraviolet spectra of *p,p'*-distyrylstilbenes (t-t-t, IV, ——; t-t-c, XVIII, —·—·; c-t-c, XXVIII, ·····) in tetrahydrofuran.

Experimental*

***trans, trans, trans-p, p'*-Distyrylstilbene (t-t-t) (IV).** — *a) From p,p'-Dibromostilbene (II).* — The debromination of *p,p',α,α'*-tetrabromodibenzyl (I) according to the method of Bance et al. yielded *p,p'*-dibromostilbene (II), in the form of lustrous colorless plates, m. p. 207.5~209°C (81.7%) (lit., m. p. 206~210°C, 72%)[7]. A small excess of *n*-butyllithium in dry ether was slowly stirred into a suspension of dibromostilbene (II, 16.6 g., 0.049 mol.) in dry ether (170 ml.) in an atmosphere of pure nitrogen. The reaction mixture was kept overnight at room temperature, and then freshly distilled phenylacetaldehyde (15.0 g., 0.125 mol.) in dry ether (170 ml.) was slowly stirred into the mixture over a period of 1 hr. The stirring was continued for a further 10 hr., and then the mixture was refluxed for 4 hr. A slow stream of pure nitrogen was introduced continuously into the reaction flask throughout these operations. A saturated aqueous solution of ammonium chloride (10.7 g.) was added to the cooled reaction mixture. The crystals accumulated on the intersurface of organic and aqueous layers were collected by filtration (16.4 g.). The aqueous layer was extracted with ether. The extract was combined with the ethereal layer and washed with water. The solvent was removed from the dried ethereal solution, yielding crude glycol III (19.4 g.). The crude material was combined (35.8 g.) and dissolved in toluene (450 ml.). The toluene solution was refluxed for 7 hr. in the presence of a small amount of *p*-toluenesulfonic acid, and the water formed was removed continuously by means of a water-separator. Deposition of yellow crystals was observed during the course of dehydration. The mixture was cooled, and the crystals deposited were filtered. The crude crystals were recrystallized from chlorobenzene to give IV, on greenish yellow plates, m. p. 295~305°C,

* All melting points were measured on a Kofler block and were not corrected.

6.7 g. (35.6%). This material was recrystallized twice from the same solvent to yield pure IV, m. p. 334~336°C.

Found: C, 93.38; H, 5.99. Calcd. for $C_{30}H_{24}$: C, 93.71; H, 6.29%.

b) By the Wittig Reaction.—IV was also obtained as a by-product of the syntheses of *trans, cis, trans-*, *trans, trans, cis-*, *cis, trans, cis-p, p'*-distyrylstilbenes according to the Wittig reaction. The experimental details will be described in section b) on the syntheses of VIII and XVIII and the synthesis of XXVIII.

***trans, trans-p, p'*-Distyryltolan (t-A-t) (VII.)**—*p, p'-Dibromotolan (V).*—Finely powdered tetrabromide (I, 40 g., 0.08 mol.) was added to a solution of sodium ethoxide in absolute ethanol (sodium, 38 g., 1.65 mol. in absolute ethanol, 600 ml.), and the mixture was refluxed for 1 hr. The reaction mixture was poured into water (1.5 l.) and the precipitate formed filtered. The dried precipitate was recrystallized from chloroform to yield dibromotolan (V), on lustrous plates, m. p. 182~183°C, 25.6 g. (95.2%) (lit., m. p. 182~184°C, 74%[8]). Further recrystallization gave the analytically pure sample, m. p. 184.5~185°C.

Found: Br, 47.84. Calcd. for $C_{14}H_8Br_2$: Br, 47.57%.

p, p'-Bis(α-hydroxy-β-phenylethyl)tolan (VI).—The glycol (VI) was obtained through the metalation of the dibromotolan (V, 13.5 g., 0.04 mol.) and the subsequent reaction with phenylacetaldehyde (11.5 g., 0.096 mol.) as for the synthesis of t-t-t (IV). The crude glycol (20.7 g.) was twice recrystallized from benzene-light petroleum (1 : 3) to give pure VI, in the form of colorless fine crystals, m. p. 155.5~157.5°C, 4.6 g. (27.2%).

Found: C, 85.90; H, 6.32. Calcd. for $C_{30}H_{26}O_2$: C, 86.09; H, 6.26%.

$IR_{max}(cm^{-1})$ 3350 (νOH), 1052 (δOH).

t-A-t (VII).—A solution of the acetylenic glycol (VI, 2.5 g.) and *p*-toluenesulfonic acid (1.0 g.) in dry toluene (150 ml.) was refluxed for 2 hr., with a continuous removal of water. The crystals separated on cooling were filtered and recrystallized twice from chlorobenzene, yielding VII, in the form of pale greenish yellow leaflets, m. p. 305~308°C, 1.6 g. (70%).

Found: C, 94.19; H, 5.72. Calcd. for $C_{30}H_{22}$: C, 94.20; H, 5.80%.

***trans, cis, trans-p, p'*-Distyrylstilbene (t-c-t) (VIII).**—*a) From t-A-t (VII) by Partial Reduction.*—t-A-t (VII) in a large amount of tetrahydrofuran was hydrogenated over Lindlar's catalyst (about the same amount as VII) by shaking a dark brown flask in a dark place. The progress of hydrogenation was followed by measuring the change of the ultraviolet spectrum at 30 min. intervals instead of by observing the change of the absorption curve of hydrogen. It required about 2.5 hr. to complete the half-reduction. The reduction products from several runs were combined (ca. 300 mg.) and digested with hot benzene. The hot solution was filtered to remove the insoluble material (a mixture of t-A-t and t-t-t). Pale yellow crystals, m. p. 210~220°C, were obtained on cooling the filtrate. The crystals were dissolved in benzene and chromatographed on alumina in a dark place. The column was eluted first with benzene, then with benzene-alcohol and finally with alcohol. Fractions 1 and 2, eluted with benzene gave crystals of m. p. 225~227°C, whereas fractions 3—6, eluted with benzene, gave crystals of m. p. 261~262°C. Fraction 8, eluted with benzene-alcohol, furnished crystals of m. p. ca. 300°C. (sublime). The crystals obtained from the fractions 1 and 2 were recrystallized from benzene, resulting in t-c-t (VIII), in the form of pale yellow plates with a pale green fluorescence, m. p. 227~228°C.

Found: C, 93.50; H, 6.30. Calcd. for $C_{30}H_{24}$: C, 93.71; H, 6.29%.

Resolidification was observed when VIII was kept in a molten state for several minutes. The resolidified material began to sublime near 300°C and melted ca. 320°C, indicating the thermal isomerization to all-trans isomer (m. p. 334~336°C). Also an identical ultraviolet absorption curve with that of t-t-t isomer was obtained after the insolation of a solution of VIII in *n*-hexane.

The crystals obtained from fractions 3—6 were recrystallized from chlorobenzene, yielding IX, in the form of pale yellow needles, m. p. 262°C. An analysis could not be performed, however, because of the small amount.

b) From p-Stilbenealdehyde by the Wittig Reaction.—*p-Styrylbenzyltriphenylphosphonium Bromide (XI).*—A mixture of *p*-methylstilbene (15 g., 0.077 mol.), *N*-bromosuccinimide (15 g., 0.084 mol.)[13] and benzoyl peroxide (200 mg.) in carbon tetrachloride (150 ml.) was stirred for 8 hr. under reflux. The cooled reaction mixture was filtered to remove the succinimide. The imide was washed repeatedly with carbon tetrachloride. The combined filtrate and washing were concentrated under reduced pressure. The crystals thus obtained were washed with ethanol, resulting in colorless crystals, m. p. 119~121°C, 12.5 g. (57%). Finely powdered triphenylphosphine (20 g., 0.076 mol.) was added to a solution of the crude bromide (8 g., 0.029 mol.) in xylene (150 ml.), and the mixture was stirred for 4 hr. with gentle refluxing. The crystals deposited on cooling the reaction mixture were filtered and washed with ethanol, resulting in phosphonium bromide, XI, in the form of colorless fine needless, m. p. 286~288°C, 14.5 g. (92%).

trans, cis, trans-p, p'-Distyrylstilbene (t-c-t) (VIII) and trans, trans, trans-p, p'-Distyrylstilbene (t-t-t) (IV).—To a stirred suspension of *p*-stilbenealdehyde (XII, 2.0 g., 9.6 mmol.) and the phosphonium bromide (XI, 6.0 g., 11.2 mmol.) in absolute ethanol (120 ml.) was added a solution of lithium ethoxide in absolute ethanol (from 0.15 g. of lithium and 70 ml. of absolute ethanol). Fine yellow crystals were gradually deposited as the phosphonium salt disappeared. The crystals were filtered without suction and digested with hot benzene. The insoluble portion was recrystallized from chlorobenzene, yielding t-t-t isomer, IV, in the form of greenish yellow plates, m. p. 328~330°C, 0.08 g. A melting point depression was not observed on admixture with the authentic t-t-t isomer.

The benzene soluble portion was chromatographed

13) Y. Yukawa and U. Suzuki, *Mem. Inst. of Sci. Ind. Research, Osaka*, **10**, 190 (1952).

over alumina in a dark place, and the column was eluted with benzene. The column was exposed occasionally to ultraviolet light for a short time, and the shift of the absorption band was located by observing the fluorescence which is characteristic of the t-c-t isomer. Fractions 1 and 2, eluted with benzene, afforded VIII, in the form of light yellow plates, m. p. 227~228°C. The mixed melting point showed no depression on admixture with an authentic specimen obtained by the partial reduction of the t-A-t isomer VII. Also, the ultraviolet spectra of these two samples were found to be identical.

***trans, trans*-p-Phenylethynyl-*p'*-styrylstilbene (t-t-A) (XXI) and *trans, cis*-*p*-Phenylethynyl-*p'*-styrylstilbene (t-c-A) (XXII).**—To a mixture of *p*-tolanaldehyde (XX, 1.0 g., 4.9 mmol.) and finely powdered phosphonium salt (XI, 3.0 g., 5.6 mmol.) was added an excess of lithium ethoxide in absolute ethanol. After 30 min., the mixture was heated to 50~60°C for 2 hr. The solid deposited on cooling the reaction mixture was filtered and washed with ethanol. This was crystallized from chlorobenzene, yielding t-t-A (XXI), in the form of light greenish yellow plates, m. p. 308~309°C, 0.76 g. (40.6%).

Found: C, 94.25; H, 5.95. Calcd. for $C_{30}H_{22}$: C, 94.20; H, 5.80%.

The filtrate was concentrated to dryness under reduced pressure. The residual solid was dissolved in benzene and chromatographed over alumina in a dark place. The first fraction, eluted with benzene, gave t-c-A (XXII), in the form of light yellow plates, m. p. 198~199°C, 0.56 g. (29.9%). An analytical sample, melted at the same temperature, was obtained on recrystallization from benzene.

Found: C, 94.38; H, 5.91. Calcd. for $C_{30}H_{20}$: C, 94.20; H, 5.80%.

This substance isomerized to the t-t-A isomer XXI at its melting point. Also, the photoisomerization of XXII to XXI was confirmed by the observation of the ultraviolet spectrum of XXII on an insolation of the solution.

***trans, trans, cis-p, p'*-Distyrylstilbene (t-t-c) (XVIII).**—*a) From t-t-A (XXI) by Partial Reduction.*—The solubility of XXI in tetrahydrofuran was found to be 1 mg./9 ml. The hydrogenation was carried out in the same manner as described in the case of t-A-t isomer VII. The benzene solution of the reduction product was chromatographed over alumina and eluted with the same solvent. The crystals of m. p. ca. 227°C obtained from the eluate was recrystallized from benzene, resulting in XVIII, in the form of light yellow prisms, m. p. 226~229°C. The mixed melting point determination proved the identity of this substance with the specimen obtained by method b).

b) From p-Styryl-[p'-formylstyryl]benzene (XVI) by the Wittig Reaction.—p-Styryl-[p'-methylstyryl]-benzene (XIV).—An excess of lithium ethoxide in ethanol (0.2 g. of lithium and 130 ml. of absolute ethanol) was stirred into a mixture of *p*-tolualdehyde[11] (XIII, 2.8 g., 0.022 mol.), powdered phosphonium salt (XI, 11 g., 0.021 mol.) and absolute ethanol (130 ml.), and the mixture was refluxed gently for 5 hr. The crystals deposited from the cooled reaction mixture were filtered, yielding crude XIV. The second crop of XIV was obtained from the filtrate on exposure to sunlight to convert the cis-isomer to the trans compound. The combined crude XIV was washed with ethanol and recrystallized from chlorobenzene, yielding light yellow plates with a green fluorescence, m. p. 264~265°C, 1.8 g. (29.6%).

p-Styryl-[p'-formylstyryl]benzene (XVI).—A mixture of XIV (2 g., 6.7 mmol.) and *N*-bromosuccinimide (1.4 g., 7.8 mmol.) in chloroform (200 ml.) was refluxed for 8 hr. in the presence of benzoyl peroxide (200 mg.). After cooling the reaction mixture (a deposition of crystalline mass was observed), hexamethylenetetramine (3.5 g., 0.025 mol.) in chloroform (35 ml.) was added and the mixture was refluxed for 4 hr. The amine complex deposited on cooling the reaction mixture was filtered and mixed with aqueous acetic acid (160 ml.). The mixture was refluxed for 2 hr. to hydrolyze the complex. The crystals deposited from the cooled reaction mixture were washed with a small amount of ethanol and recrystallized from chlorobenzene, resulting in XVI, in the form of yellow thin plates, m. p. 250~253°C.

Found: C, 88.63; H, 5.84. Calcd. for $C_{23}H_{18}O$: C, 88.99; H, 5.84%.

UV_{max} ($m\mu$) 242 (ε=20000), 273 (61400) (in dioxane).

IR_{max} (cm^{-1}) 1702, 1166 (-CHO).

t-t-c (XVIII) and t-t-t (IV).—A solution of the above-mentioned aldehyde (XVI, 370 mg.) in dry tetrahydrofuran (250 ml.) was mixed with benzyltriphenylphosphonium chloride (XVII, 650 mg.) in ethanol (40 ml.). A small excess of lithium ethoxide in ethanol (15 ml.) was stirred drop by drop into the mixture at room temperature. Then, the mixture was heated at 40~50°C for 8 hr. while continually being stirred. The crystals deposited from the cooled reaction mixture were filtered and identified as all-trans isomer IV by means of a mixed melting point determination. The residue obtained on concentrating the filtrate under reduced pressure was dissolved in benzene and chromatographed over alumina. The fractions 3—5, eluted with benzene, gave crystals of m. p. 224~226°C*. The fractions 3—7, eluted with benzene, resulted in crystals of m. p. 224~228°C*. This was recrystallized carefully from benzene to give XVIII, in the form of light yellow prisms, m. p. 227~230°C*.

Found: C, 93.57; H, 6.46. Calcd. for $C_{30}H_{24}$: C, 93.71; H, 6.29%.

***trans*- and *cis*-Bis(*p*-phenylethynyl)stilbenes (A-t-A, XXV and A-c-A, XXVI).**—*p-Phenylethynylbenzyl-triphenylphosphonium Bromide (XXIV).*—A mixture of *p*-methyltolan[14] (7 g., 0.031 mol.), *N*-bromosuccinimide (7 g., 0.039 mol.) and benzoyl peroxide (200 mg.) in carbon tetrachloride (80 ml.) was stirred under reflux for 6~7 hr. The succinimide deposited on cooling was removed. The oily material admixed with crystals was obtained by

* The t-t-c isomer was found to be thermally unstable. The melting point was determined by a rapid elevation of the temperature of the heating bath to avoid a rearrangement to all-trans isomer; otherwise the t-t-c isomer showed the melting point of the t-t-t isomer.

14) G. Drefahl and G. Plötner, *Chem. Ber.*, **93**, 990 (1960).

concentration of the filtrate and dissolved in benzene. The solution was passed through a short column of alumina and the solvent removed in vacuo. To a toluene solution of the residue was added triphenylphosphine (8 g., 0.031 mol.). The mixture was refluxed for 7 hr. under stirring. The solid deposited from the cooled reaction mixture was washed three times with ethanol, yielding XXIV, a colorless amorphous solid, m. p. 286~288°C, 7.0 g. (36%).

A-t-A (XXV) and A-c-A (XXVI).—A small excess of lithium ethoxide in absolute ethanol (80 ml.) was added dropwise to a suspension of the phosphonium salt (XXIV, 3.0 g., 5.6 mmol.) and tolanaldehyde[1,12] (XX, 1.0 g., 4.8 mmol.) in absolute ethanol (150 ml.) at room temperature, and the mixture was stirred for 20 hr. The crude crystals deposited from the reaction mixture were digested with hot benzene and filtered (Filtrate A). The insoluble crystalline mass was recrystallized twice from chlorobenzene, yielding XXV, in the form of light yellow needles with a green fluorescence, m. p. 278~279°C, 0.30 g. (16.5%).

Found: C, 94.25; H, 5.32. Calcd. for $C_{30}H_{20}$: C, 94.70; H, 5.30%.

The filtrate A was chromatographed oved alumina. The fractions 1 and 2, eluted with benzene, gave crystals of m. p. 149~151°C. This was recrystallized from ethanol-benzene (9 : 1) to give XXVI, in the form of colorless plates, m. p. 151~152°C, 0.34 g. (18.7%).

Found: C, 94.61; H, 5.31. Calcd. for $C_{30}H_{20}$: C, 94.70; H, 5.30%.

The ultraviolet spectrum of XXVI changed to that of XXV on the insolation of the solution.

The total yield of the Wittig reaction was found to be 0.46 g. (35%).

***cis, trans, cis-*, *trans, trans, trans-* and *trans, trans, cis-p, p'*-Distyrylstilbenes (XXVIII, IV and XVIII).** — *p, p'-Stilbenedialdehyde (XXVII).* — The dialdehyde (XXVII) was prepared according to the usual method. The crude dibromide obtained by the reaction of *p,p'*-dimethylstilbene with *N*-bromosuccinimide was converted without purification to XXIX by the Sommelet reaction. The product was recrystallized from acetic acid to give pure XXVII, in the form of long yellow needles, m. p. 170~171°C, 3.5 g. (19.3%) (lit. value[14], 169~170°C, 8% yield).

Found: C, 80.95; H, 5.16. Calcd. for $C_{16}H_{12}O_2$: C, 81.34; H, 5.12%.

c-t-c (XXVIII), t-t-t (IV) and t-t-c (XVIII).—To the stirred suspension of benzyltriphenylphosphonium chloride (XVII, 3.6 g., 9.3 mmol.) in absolute alcohol (30 ml.) was added excess of lithium ethoxide (from 0.2 g. of lithium) in absolute alcohol (40 ml.). After stirring for 1 hr., tetrahydrofuran (30 ml.) was added and stirred for 30 min. To the stirred mixture was added dropwise stilbenedialdehyde (XXVII, 1.0 g., 4.2 mmol.) in tetrahydrofuran (80 ml.) and absolute alcohol (10 ml.). The mixture was stirred for 2 hr. at room temperature and 8 hr. at 40~50°C. After cooling, the crystals deposited were filtered, and the filtrate was diluted with water (ca. 1 l.), precipitating the crystals. The combined crystals were dried, extracted with hot benzene and filtered. The cooled filtrate was filtered to remove the crystals A deposited and chromatographed over alumina in a dark place. Fractions 2 and 3, eluted with benzene, afforded XXVIII, m. p. 109~111°C, which was recrystallized from alcohol to give greenish yellow plates with a green fluorescence, m. p. 111~112°C, 0.18 g. (11%).

Found: C, 93.71; H, 6.27. Calcd. for $C_{30}H_{24}$: C, 93.71; H, 6.29%.

This substance, thermally more stable than t-c-t and t-t-c, isomerized to t-t-t isomer at 170°C and photoisomerized to t-t-t on the insolation of the solution.

Fractions 4—6, m. p. 224~228°C, were recrystallized from benzene, yielding light yellow prisms with a green fluorescence 2.0 g. (12%), and were found to be identical with t-t-c (XVIII) by the determination of the ultraviolet spectrum and the mixed melting point.

The insoluble crystals, m. p. 310~320°C, 0.15 g. (9%), in hot benzene, showed an identical ultraviolet spectrum with t-t-t (IV) and the crystals A were found to be a mixture of t-t-c and the recovered aldehyde (XXVII).

The cost of this research was partly defrayed by the Scientific Research Expenditure Fund of the Ministry of Education, to which authors' thanks are due.

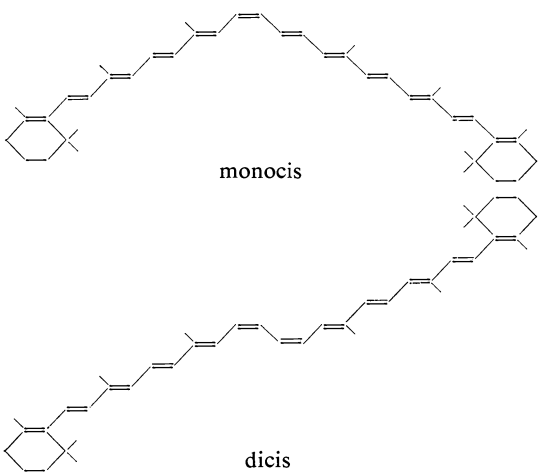
Department of Chemistry
Faculty of Science
Osaka University
Kita-ku, Osaka

Alternant Conjugate Systems. IV. Ultraviolet Spectroscopic Properties and Photoisomerization of Geometrical Isomers of p-Distyrylbenzenes, p, p'-Distyrylstilbenes and Related Compounds

By Sōichi MISUMI, Motoyuki KUWANA and Masazumi NAKAGAWA

(Received March 23, 1961)

Zechmeister and his co-workers have observed the appearance of a new absorption maximum in the near ultraviolet region when various kinds of all trans isoprenic conjugated polyolefins were irradiated[1]. They have attributed the new absorption band to the presence of unhindered cis ethylenic linkage formed by a photochemical stereomutation of trans linkage. The so-called " cis-peak rule " was proposed by them to correlate the wavelength and the intensity of the new absorption maximum with the geometry of the cis-isomer. It has been proved that this rule is valid for a wide variety of carotenoids, such as central cis-β-carotene, central cis-bixin methyl ester, monocis- and dicis-homo-β-carotenes (I)[2] and the straight conjugated system, i. e., diphenylpolyenes[1].



Homo-β-carotene (I)

Recently Dale has shown that the wavelength of minor bands, (λ_s), including the so-called cis-peak in the spectrum of a polyene with n conjugated double bonds, lies very close to the wavelength of the main band of a corresponding polyene with n/s conjugated double bonds (where n/s does not need to be an integral)[3]. He has also shown that this simple relationship holds also in the conjugated system containing benzene nuclei such as diphenylbutadiene, stilbene, etc. From these results, he has concluded that the appearance of minor bands in a conjugated polyene can not be attributed to the operation of independent partial chromophores, but is ascribable to the higher order transition of the total chromophore system. According to this argument, Zechmeister's cis-peak can be regarded as the first overtone band of the full chromophore system.

On the other hand, it has been found that isoprenic diphenylpolyenes containing sterically hindered cis ethylenic linkage exhibit no distinct cis-peak[4]. Oroshnik and his coworkers[5] have attributed the absorption band at a shorter wavelength in the spectra of hindered retrovitamin A methyl ether and related compounds to an overlap of the cis-peak with an absorption arising from the partial chromophore systems. He has pointed out that the contribution of the cis-peak and the partial chromophore can not be distinguished in these cases and that Zechmeister's cis-peak rule seems to be inapplicable in its original form to a conjugated system with sterically hindered cis olefinic linkage.

As reported in the preceding papers of this series[6], the present authors have synthesized several geometrical isomers of stilbene homologues and the acetylenic analogues, including sterically hindered cis-isomers (Fig. 1). The

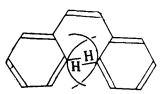


Fig. 1

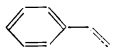
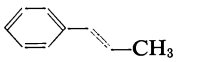
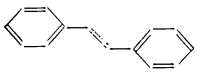
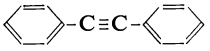
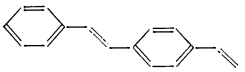
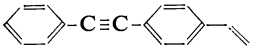
1) L. Zechmeister, L. Pauling et al., *J. Am. Chem. Soc.*, **65**, 1940 (1943); L. Zechmeister, *Chem. Revs.*, **34**, 267 (1944); *Experientia*, **10**, 1 (1954).
2) H. H. Inhoffen et al., *Ann.*, **570**, 54 (1940); **573**, 1 (1951); **592**, 214 (1955); L. Zechmeister, *Fortschr. Chem. org. Naturstoffe*, **18**, 223 (1960).
3) J. Dale, *Acta Chem. Scand.*, **8**, 1235 (1954); **11**, 971 (1957).
4) P. Karrer et al., *Helv. Chim. Acta*, **35**, 1850 (1952); **36**, 562 (1953).
5) W. Oroshnik et al., *J. Am. Chem. Soc.*, **76**, 5719 (1954).
6) Part II and III, This Bulletin, **34**, 1833 (1961); **35**, 135 (1962).

present paper deals with the ultraviolet spectroscopic properties and the photoisomerization of these geometrical isomers.

Spectroscopic Properties. — In the series of *p*-distyrylbenzene, the t-t isomer* showed a main maximum at the longest wavelength as compared with other geometrical isomers and the acetylenic analogues, as illustrated in Figs. 1 and 2 in Part II of this series. (The numerical data are summarized in Table I of Part II.) Substitution of the trans-linkage with cis- or acetylenic bonds caused a shift of the absorption maximum to shorter wavelength and a decrease of the absorption intensity. The decrease of absorption intensity was found to be much larger in the case of the insertion of cis-linkage than that of acetylenic bond, in spite of the same degree of hypsochromic shift in both cases. This fact is quite understandable from the fact that the coplanarity of the cis-molecule is broken as the result of the steric hindrance of hydrogen atoms in the *o*- and *o'*-positions of the benzene rings adjacent to the cis-linkage (Fig. 1). On the contrary, the absorption intensity of the band near 230 mμ is larger in the case of the cis-isomer than in that of the trans-isomer. The sequence of intensity of this absorption peak was found to be c-c>t-c>t-t and A-c>A-t. The ultraviolet spectra of the three compounds containing no cis-linkage, i. e., t-t, t-A and A-A, each exhibit a distinct absorption minimum in the region of 250~290 mμ. But an absorption maximum at about 270 mμ was observed in the spectra of the corresponding cis-isomers, i. e., t-c, c-c and A-c. An examination of the spectra of reference substances which can be regarded as the possible partial chromophores of the above-mentioned *p*-distyrylbenzenes and *p*-styryltolan indicates that the absorption maximum at ca. 270 mμ can not be attributed to a contribution of any partial chromophores (Table I). For instance, styrene, stilbene and vinylstilbene may be the possible partial chromophores for the t-c isomer, but it seems to be quite difficult to find out the contribution of the ultraviolet absorption of these compounds from the spectrum of the t-c isomer. Tolan, styrene and vinyltolan may be the possible partial chromophores of A-c isomer. Also, the shape of the absorption curve of the A-c isomer indicates that the participation of the partial chromophores is negligible.

The same situation was found in the spectra of the higher homologues; the isomeric *p,p'*-distyrylstilbenes and the related compounds (t-c-t, t-c-A and A-c-A) exhibit broad and most intense absorption maxima at the wavelength region of 280~320 mμ (cf. Fig. 2 in Part III of this series). An examination of the spectra of the reference substances corresponding to the partial chromophores also

TABLE I. ULTRAVIOLET ABSORPTION OF POSSIBLE PARTIAL CHROMOPHORES

	λ_{max} mμ	ε_{max}	Solv.*	Ref.
	198 255	8000 230	b	
	244 282	12600 500	a	7
	250 284 293	17300 1100 780	a	8
	226 295 310	15000 27000 25000	a	9
	265 281 289 298	21000 29000 20000 25000	c	10
	323	34000	b	11
	301	43000	b	11

* a=alcohol, b=hexane, c=cyclohexane.

* t, c and A denote trans-, cis- and acetylenic bonds respectively. Therefore, for example, t-t isomer and t-c-A isomer represent *trans*, *trans-p*-distyrylbenzene and *p-trans*-styryl-*p'*-phenylethynyl-*cis*-stilbene respectively.

7) H. P. Koch, *J. Chem. Soc.*, **1949**, 387; W. W. Robertson and F. A. Matsen, *J. Am. Chem. Soc.*, **72**, 5250 (1950).

8) R. Y. Mixer, R. F. Hech, S. Winstein and W. G. Young, *J. Am. Chem. Soc.*, **75**, 4094 (1953).

9) A. Eucken and K. H. Hellwege, "Landolt-Börnstein Zahlenwerte und Funktionen aus Physik, Chemie, Astronomie, Geophysik und Technik", 6 Aufl., Band I, Teil. 3, Springer-Verlag (1951).

10) R. A. Friedel and M. Orchin, "Ultraviolet Spectra of Aromatic Compounds", John Wiley & Sons, Inc. (1951).

11) G. Drefahl, G. Plötner and F. Rudolph, *Chem. Ber.*, **93**, 998 (1960).

TABLE II. ULTRAVIOLET ABSORPTION OF STEREOISOMERIC *p,p'*-DISTYRYLSTILBENES AND RELATED COMPOUNDS

	λ_{max}, mμ ($\varepsilon_{max}\times10^{-2}$)				Solv.*
t-t-t	238(359)	270(186)		384(893)	a
t-t-A	237(321)	266(208)		374(787)	a
t-A-t	243(432)			361(843)	a
A-t-A	235(297)	262(144)		362(801)	a
A-A-A	236(370)	256(89)		340(709)	c
t-t-c	237(285)			372(681)	a
t-c-t	236(229)		316(521)	353(410)	a
	232(224)		312(492)	348(409)	b
c-t-c	238(368)			359(488)	a
t-c-A	235(290)	270(241)	302(457)	346(376)	a
	232(271)	268(230)	298(457)	341(387)	b
A-c-A			295(453)	330(365)	a

* a=tetrahydrofuran, b=*n*-hexane, c=chloroform

reveals that the operation of partial chromophores is not reflected in the spectra of the distyrylstilbenes and their analogues. The absorption maximum at 312 mμ and the inflection at ca. 300 mμ in the spectrum of the t-c-t isomer seem to be attributable to the participation of the absorption of stilbene, an possible partial chromophore, which has a strong maxima at 297 and 310 mμ, while the presence of an absorption minimum at 326 mμ in the spectrum of t-c-t isomer excludes the possible operation of another partial chromophore, vinylstilbene, which has a strong maximum at the same wavelength (323 mμ). Also, the attribution of the λ_{max} at 293 mμ and the $\lambda_{infl.}$ at ca. 283 mμ in the spectrum of the A-c-A isomer to the contribution of a partial chromophore, tolan (λ_{max} 281 and 298 mμ), is inconsistent with the fact that the spectrum of this isomer shows a distinct λ_{min} at 307 mμ, while the spectrum of vinyltolan, another possible partial chromophore, exhibits a strong λ_{max} at about the same wavelength (301 mμ). Similarly, the absorption of the t-c-A isomer (λ_{max} 298 mμ, $\lambda_{infl.}$ ca. 290 mμ) could not be explained by the participation of either pair of the partial chromophores, stilbene-vinyltolan or tolan-vinylstilbene. Furthermore, the close resemblance of the shape of the absorption curve of the unsymmetrical t-c-A isomer to those of the symmetrical isomers (t-c-t and A-c-A) in this wavelength region seems to indicate the negligible participation of the partial chromophores. It may be reasonable to conclude from these observed results that the absorption maxima at ca. 270 mμ and at 280~320 mμ in the spectra of the three benzene and the four benzene systems do not arise from the participation of partial chromophores, but arise from the second order electronic transitions of the total chromophore.

The absorption curves of the t-c and A-c each form a distinct peak at 270 mμ, while the spectrum of the c-c isomer forms a plateau at the same wavelength (Fig. 1 in Part II). Also, the t-c-t, t-c-A and A-c-A isomers each showed a very strong absorption at 280~320 mμ (Fig. 2 in Part III). On the other hand, the t-t-c and c-t-c isomers did not exhibit a marked absorption peak at this region (Fig. 4 in Part III). These facts indicate that the probability of the second order transition is strongly affected by the geometry of the molecule. As illustrated in Fig. 2, the A-c and t-c isomers may have a dipolemoment perpendicular to the long axis of the conjugated system, whereas the most probable configuration of c-c isomer (a) has no dipolemoment perpendicular to the long axis, and the contribution of a configuration such as (b) which has the

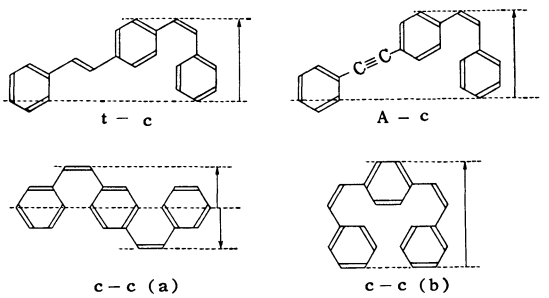


Fig. 2

above-mentioned dipolemoment seems to be highly improbable owing to its great steric hindrance. Similarly, the t-c-t, t-c-A and A-c-A isomers which may have large dipolemoment perpendicular to the long axis exhibit a distinct second order absorption maximum, and the t-t-c and c-t-c isomers having minor dipolemoment show only a weak shoulder at the corresponding wavelength position. The same trend has been pointed out by Zechmeister[1] in carotenoid series containing unhindered cis-linkage or cis-linkages.

If the appearance of the second absorption maximum in the spectra of cis-compounds could be attributed to the second order transition of the total chromophore, the all-trans isomer and the acetylene-trans compounds would also have an absorption in the same wavelength, even if it is extremely weak in its intensity. In fact, the spectra of t-t, t-A and A-A compounds exhibit a weak inflection at ca. 270 mμ (Figs. 1 and 2 in Part II). In the same way, a weak inflection at 290~310 mμ was observed in the spectra of t-t-t, t-A-t, t-t-A, A-t-A and A-A-A compounds (Figs. 3 and 4 in Part III). The existence of these inflections at the wavelength corresponding to the second absorption maximum of the cis-compound clearly indicates that the second order transition contributes to the spectra of the alternant conjugate systems lacking cis-linkage.

All compounds belonging to the four benzene system showed an absorption maximum at the wavelength of 260~280 mμ. This maximum was observed as a weak inflection in the cis-series. On the other hand, a fairly distinct peak was observed in the spectra of the trans- and acetylene-series. This absorption and the absorption at a shorter wavelength (235~245 mμ) can also be satisfactorily explained in terms of a third and of still higher order transitions of the total chromophore. It is to be noted that the probability of the xth order transition is larger in trans and/or acetylenic series than the corresponding cis-compounds when x is an even number. Conversely, when

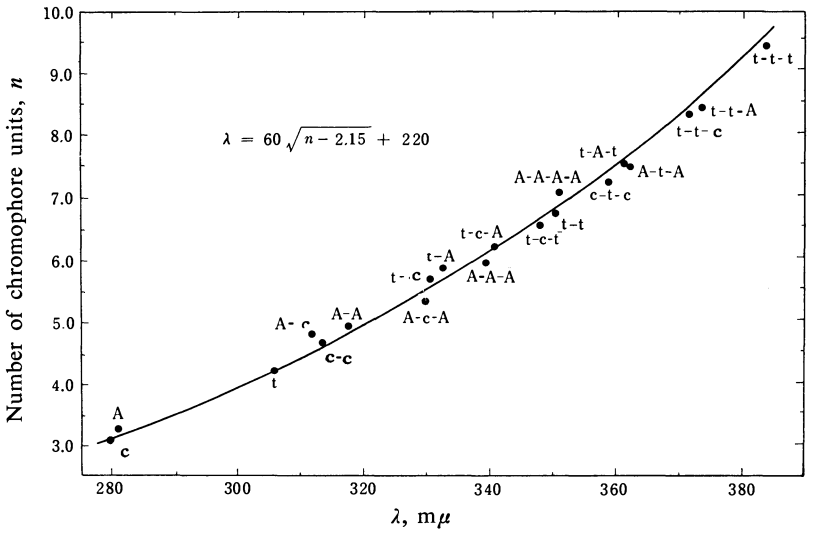


Fig. 3. The wavelength positions of the longest wavelength bands of the stereoisomers plotted against number of chromophore units.

TABLE III. CALCULATED AND OBSERVED VALUES OF LONGEST WAVELENGTH BANDS

	Number of chromophore units, n	Calcd. mμ	Obs. mμ	Solv.*
t	4.20	306	306	d
c	3.13	279	280	a
A	3.26	283	281	a
t-t	6.80	349	350	d
t-c	5.73	334	331	d
c-c	4.66	315	314	d
t-A	5.86	336	333	d
c-A	4.79	316	312	d
A-A	4.91	320	318	a
t-t-t	9.40	382	384	e
t-t-c	8.33	369	372	e
t-c-t	6.59	346	348	d
c-t-c	7.26	356	359	e
t-t-A	8.46	371	374	e
t-A-t	7.57	360	361	e
A-t-A	7.51	359	362	e
t-c-A	6.28	342	341	d
A-c-A	5.33	327	330	e
A-A-A	6.01	338	340	c
A-A-A-A	7.10	353	351	b

t, c and A denote trans-, cis- and acetylenic bond, respectively.
* a=alcohol, b=benzene, c=chloroform, d=*n*-hexane, e=tetrahydrofuran

x is an odd number, cis-compounds have larger xth order absorption maxima than the corresponding trans and/or acetylenic compounds (Figs. 3 and 4 in Part III).

As illustrated in Fig. 3, a smooth curve was obtained by plotting the position of the absorption maxima of the longest wavelength (λ_{max}) against the number of chromophore units (n), where an ethylenic bond is taken as an unit, and each benzene ring and acetylenic bond is set equal to the 1.6 and 0.6 ethylenic bond respectively, and the effect of the blue shift caused by the presence of cis- and acetylenic bonds is corrected by introducing cis- ($f_C=0.33$) and acetylenic ($f_A=0.66$) factors. The calculated chromophore units of this series of compounds are summarized in Table III. The relationship between λ_{max} and n is well represented by the following empirical Eq. 1.

$$\lambda=60\sqrt{n-2.15}+220 \qquad (1)$$

A fairly good agreement of the calculated values with the observed values was obtained for almost all compounds of this series, as shown in Table III. The minor deviation of the calculated values in the four benzene series seems to be attributable to a solvent effect, since the spectra were measured using tetrahydrofuran or benzene as the solvent. *n*-Hexane and ethanol could not be used owing to the poor solubility of the compounds to these solvents. A red shift of about 2~5 mμ was generally observed in the case of a solution in tetrahydrofuran or benzene as compared with those in aliphatic hydrocarbons. A slightly larger deviation between the predicted and observed values was observed in the cases of polytolans.

Photoisomerization. — In order to determine the relative rates of photoisomerization and to know the isomer ratios in the equilibrated mixtures, dilute solutions of each pair of the above-mentioned alternant conjugate systems

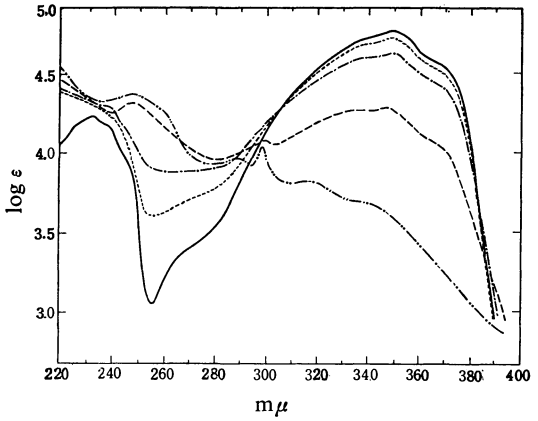


Fig. 4. The change of ultraviolet spectra on irradiation of *trans*, *trans*-*p*-distyrylbenzene (0 hr., ——; 1 hr., ------; 27 hr., —·—·; 100 hr., ----; 240 hr., —··—··) in *n*-hexane.

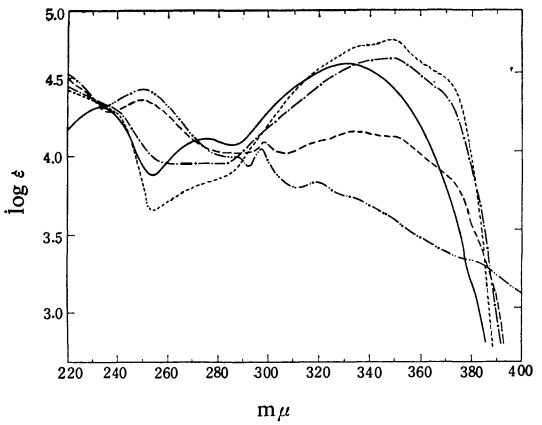


Fig. 5. The change of ultraviolet spectra on irradiation of *trans*, *cis*-*p*-distyrylbenzene (0 hr., ——; 1 hr., ------; 27 hr., —·—; 100 hr., ----; 240 hr., —··—··) in *n*-hexane.

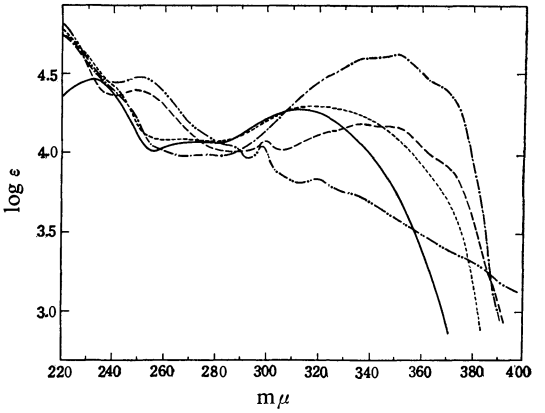


Fig. 6. The change of ultraviolet spectra on irradiation of *cis*, *cis*-*p*-distyrylbenzene in *n*-hexane (0 hr., ——; 1 hr., ------; 27 hr., —·—·; 100 hr., ----; 240 hr., —··—··).

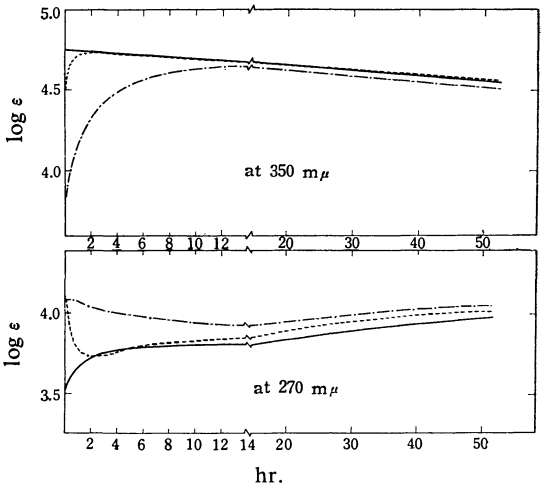


Fig. 7. The change of the extinction values of the ultraviolet spectra of three isomeric *p*-distyrylbenzenes in *n*-hexane by exposure to light at 10 cm. (t-t, ——; t-c, ------; c-c, —·—·).

were exposed to the light of a fluorescent tube under controlled conditions and the course of photoisomerization was followed, measuring the change of the spectra. It was observed that some kind of photocyclization presumably accompanied with photodegradation occurs on a prolonged irradiation. As a result of these side-reactions, it was found to be impossible to determine the composition of the equilibrium mixture.

The changes of ultraviolet spectra on irradiation of the three geometrical isomers of *p*-distyrylbenzene (t-t, t-c and c-c) are illustrated in Figs. 4, 5 and 6, and those of absorption intensities at 350 and 270 mμ of each isomer are shown in Fig. 7. The bands at the longest wavelength in the t-c and c-c isomer shifted to the red side, increasing their intensities in accord with the period of irradiation. It was observed that the t-c isomer is converted to an approximate equilibrium with the t-t isomer after 1 hr. of irradiation. On the other hand, in the case of the c-c isomer, an approximate equilibrium with the t-t isomer was attained only after 13 hr. irradiation. It is to be noted that the rate of photoisomerization is much slower in the case of the more hindered c-c isomer than the case of the less hindered t-c isomer.

Further change of the spectra were observed on prolonged irradiation. A slow decrease of the intensity at 350 mμ was accompanied with a gradual increase of the intensity at 232 mμ, and the latter maximum was buried in the

strong absorption which appeared in the shorter wavelength region. The appearance of new inflections at 250 and 297 mμ was observed after exposure for ca. 54 hr. These inflections grew to the intense absorption maxima after exposure for 100 hr.

Also, the A-c and A-t isomers showed a distinct fine structure in their spectra after irradiation for a long time, suggesting the formation of phenanthrene nucleus by photochemical cyclization[12] (Figs. 8 and 9).

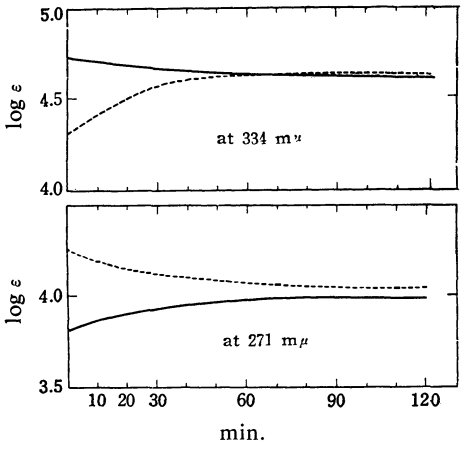


Fig. 8. The change of the extinction values of the ultraviolet spectra of stereoisomeric *p*-styryltolans in *n*-hexane by exposure to light at 10 cm. (A-t, ——; A-c, ------).

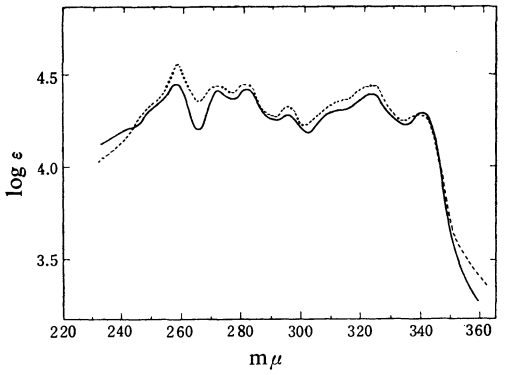


Fig. 9. The ultraviolet spectra of stereoisomeric *p*-styryltolans after irradiation for 213 hr. at 10 cm. (A-t, ——; A-c, ------).

The change of absorption intensities at three points of wavelength according to the progress of photoisomerization of the four geometrical isomers of *p,p'*-distyrylstilbene is illustrated in Fig. 10. The sequence of the rate of photochemical stereomutation was found to be

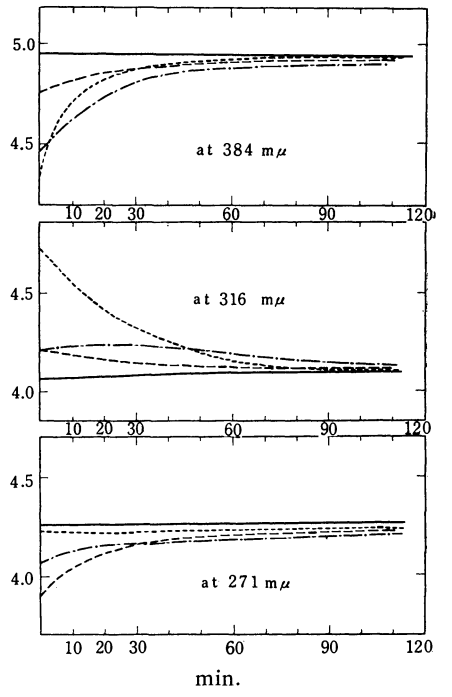


Fig. 10. The change of the extinction values of the ultraviolet spectra of four isomeric *p,p'*-distyrylstilbenes in tetrahydrofuran by exposure to light at 20 cm. (t-t-t, ——; t-c-t, ----; t-t-c, ------; c-t-c, —·—·).

t-c-t>t-t-c>c-t-c. The fact that the most hindered c-t-c isomer is most stable is consistent with the case of the c-c isomer. Also, it is an interesting fact that the isomer having a more intense cis-peak (in another word, absorption due to the second order transition of total chromophore) shows a larger rate of photoisomerization.

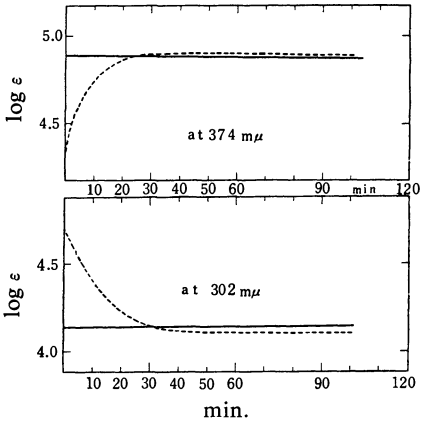


Fig. 11. The change of the extinction values of the ultraviolet spectra of isomeric *p*-styryl-*p'*-phenylethynyl-stilbenes in tetrahydrofuran by exposure to light at 10 cm. (t-t-A, ——; t-c-A, ------).

12) A. Smakula, *Z. physik. Chem.*, **B25**, 90 (1934); R. E. Buckles, *J. Am. Chem. Soc.*, **77**, 1041 (1955); P. Hugelshofer, J. Kalvoda and K. Schaffner, *Helv. Chim. Acta*, **43**, 1322 (1960).

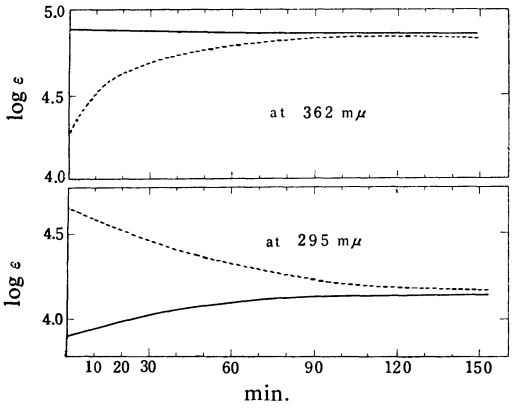


Fig. 12. The change of the extinction values of the ultraviolet spectra of isomeric *p*-bis-(phenylethynyl)stilbenes in tetrahydrofuran by exposure to light at 20 cm. (A-t-A, ——; A-c-A, ------).

The changes of the spectra by irradiation of other pairs of isomers of the four benzene series, t-t-A : t-c-A and A-c-A : A-t-A, are presented in Figs. 11 and 12. After prolonged irradiation, the spectra of these compounds showed distinct fine structures, indicating the formation of a condensed aromatic system.

The present authors are continuing the photochemical cyclization of these series of compounds.

Experimental

General Method of Photoisomerization. — The spectrum was measured in a sealed fused silica cell of 1.0 cm. thickness using a dilute solution (ca. 1 mg. of substance in 1000 ml. of solvent). Spectral grade *n*-hexane was used in the case of the compounds of the three benzene series. The compound of the four benzene series were dissolved in purified tetrahydrofuran. Two cells containing the solutions of the pair of isomers were irradiated with a fluorescent tube (10 W. daylight type). The change of spectrum and the change of intensities at particular wavelength were measured at an appropriate interval.

The authors are grateful to the Ministry of Education for the financial support for this wark.

Department of Chemistry
Faculty of Science
Osaka University
Nakanoshima, Osaka

Synthetic Studies on the Benzofuran Derivatives. VII. A New Synthesis of Angelicin and 4-Methylangelicin

By Yoshiyuki KAWASE, Mitsuru NAKAYAMA* and Hiroko TAMATSUKURI

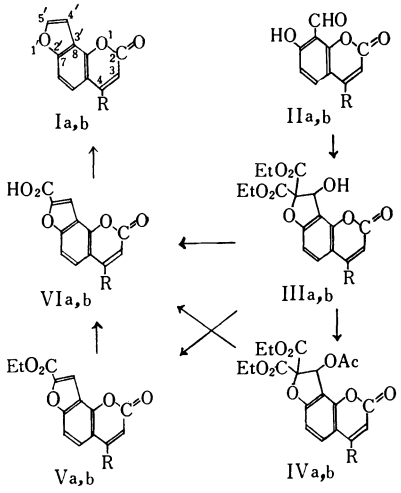
(Received June 1, 1961)

Angelicin, a furocoumarin isolated from *Angelica archangelica*[1-4] and *Psoralea corylifolia*[5], is an interesting compound because of its fluorescence and biological activity. Its chemical structure was established by Späth and Pesta[4] to be represented by the formula Ia. For the synthesis of Ia, several methods were reported by Späth and Pailer[6], Limaye[7], Naik and Thakor[8] and Seshadri et al.[9], and recently the synthesis of 4-methylangelicin (Ib) also has been reported by Antonello[10].

The present paper describes a new synthesis of Ia and Ib accomplished with more ease and furnishing higher yields following Tanaka's method[11] for benzofuran synthesis, as shown in the chart.

* Present address : Faculty of Science, Hiroshima University, Higashisenda-machi, Hiroshima.

1) L. A. Buchner, *Ann.*, **42**, 226 (1842).
2) C. Brimer, ibid., **180**, 269 (1876).
3) E. Bocker and A. Hahn, *J. prakt. Chem.*, (2) **83**, 243 (1911).
4) E. Späth and O. Pesta, *Ber.*, **67**, 853 (1934).
5) H. S. Jois and B. L. Manjunath, *Proc. Indian Sci. Congress*, **21**, 243 (1934); ibid., **22**, 147 (1935); *Ber.*, **69B**, 964 (1936).
6) E. Späth and M. Pailer, ibid., **67**, 1212 (1934); ibid., **68**, 940 (1935).
7) D. B. Limaye, *Rasayanam*, **1**, 1 (1936); *Chem. Abstr.*, **31**, 2206 (1937).
8) R. M. Naik and V. M. Thakor, *J. Org. Chem.*, **22**, 1696 (1957).
9) T. R. Seshadri et al., *Tetrahedron*, **4**, 256 (1958).
10) C. Antonello, *Gazz. chim. ital.*, **88**, 430 (1958); *Chem. Abstr.*, **53**, 20046 (1959).
11) S. Tanaka, *J. Am. Chem. Soc.*, **73**, 872 (1951).



For I—VI; a) R=H, b) R=Me

The starting material is 8-formyl-7-hydroxycoumarin[6] (IIa) and 8-formyl-7-hydroxy-4-methylcoumarin[7] (IIb) as in the syntheses of Späth and Pailer, Naik and Thakor and Antonello. As the aldehydes were obtained only in poor yields by the formylation of coumarins following the hexamine method[6,12] attempts were made to improve the formylation by the glyceroboric acid-hexamine method[13] and by the dimethylformamide method[14], but they resulted only in failure.

The aldehyde, IIa or IIb, was made to react with ethyl bromomalonate and potassium carbonate in ethyl methyl ketone. Procedures of very little difference, namely, refluxing either with or without stirring, gave two different products: a higher melting ester (Va, m. p. 212~213°C or Vb, m. p. 194~195°C) with stirring and a lower melting ester (IIIa, m. p. 178~180°C or IIIb, m. p. 175~176°C) without stirring. Analysis and infrared spectroscopy proved that the latter is a hydroxy-diester IIIa or IIIb because it showed a sharp OH band (IIIa, 3226 cm^{-1}; IIIb, 3185 cm^{-1}) and ester CO bands (IIIa, 1767, 1727 cm^{-1}; IIIb, 1773, 1730 cm^{-1}), and that the former is an ester Va or Vb without a hydroxy-group because it showed the ester CO band (Va, 1718 cm^{-1}; Vb, 1724 cm^{-1}) and no OH band. As hydroxy-ester IIIa (or IIIb) was converted into ester Va (or Vb) by further action of potassium carbonate in ethyl methyl ketone under reflux with stirring, IIIa (or IIIb) seems to be the intermediate compound to Va (or Vb); the compound of this type has been reported in some cases[15]. Ester IIIa (or IIIb) was converted into Va (or Vb) also by the action of phosphoric acid, but was not affected by 10% hydrochloric acid and by *p*-toluenesulfonyl chloride, and was converted only into its acetate IVa or IVb by acetic anhydride with or without sodium acetate.

Alkaline hydrolysis of the esters IIIa, IVa, and Va or IIIb, IVb, and Vb furnished the same corresponding acid VIa or VIb, which was decarboxylated in quinoline into compound Ia, m. p. 137~138°C, or Ib, m. p. 190~192°C, in a good yield.

Experimental[16]

5', 5'-Diethoxycarbonyl-4'-hydroxy-4', 5'-dihydroangelicin (IIIa). — To a solution of 8-formyl-7-hydroxycoumarin[6] (IIa, m. p. 184~185°C, 0.5 g.) and ethyl bromomalonate (1 g.) in anhydrous ethyl methyl ketone (60 ml.) was added anhydrous potassium carbonate (1.5 g.); the mixture was refluxed for 8 hr. in a steam bath. The resulting mixture was freed from precipitates, and the solvent was distilled off. The residual product was recrystallized from ethanol to give IIIa in the form of colorless microcrystals, m. p. 178~180°C, giving a negative ferric reaction; yield 0.5 g. (54.9%).

Found: C, 58.83; H, 4.67. Calcd. for $C_{17}H_{16}O_8$: C, 58.62; H, 4.63%.

Acetate IVa was prepared quantitatively by refluxing IIIa (0.1 g.) and acetic anhydride (10 ml.) with or without anhydrous sodium acetate (0.1 g.), m. p. 140~141°C (from ethanol).

Found: C, 58.62; H, 4.65. Calcd. for $C_{19}H_{18}O_9$: C, 58.46; H, 4.69%.

5', 5'-Diethoxycarbonyl-4'-hydroxy-4', 5'-dihydro-4-methylangelicin (IIIb).—By a method similar to that described for IIIa, IIIb was obtained from 8-formyl-7-hydroxy-4-methylcoumarin[7] (IIb, m. p. 176~177°C, 2 g.), ethyl bromomalonate (2.3 g.), anhydrous potassium carbonate (4.8 g.) and anhydrous ethyl methyl ketone (150 ml.); colorless microcrystals, m. p. 175~176°C (from ethanol), giving a negative ferric reaction; yield 2 g. (56.5%).

Found: C, 59.84; H, 5.14. Calcd. for $C_{18}H_{18}O_8$: C, 59.66; H, 5.01%.

Acetate IVb: M. p. 189~190°C (from ethanol).

Found: C, 59.57; H, 4.97. Calcd. for $C_{20}H_{20}O_9$: C, 59.40; H, 4.99%.

5'-Ethoxycarbonyl-angelicin (Va).—*From Aldehyde IIa.*—A mixture of IIa (0.3 g.), ethyl bromomalonate (0.6 g.), potassium carbonate (0.8 g.) and ethyl methyl ketone (60 ml.) was refluxed with stirring for 8 hr. in a steam bath. The resulting mixture was treated similarly to IIIa; colorless needles, m. p. 212~213°C (from ethanol); yield 0.2 g. (50%).

12) T. R. Seshadri et al., *Proc. Indian Acad. Sci.*, **6A**, 112 (1937); *Chem. Abstr.*, **32**, 559 (1938); A. N. Nesmeyanov et al., *J. Gen. Chem. (U. S. S. R.)*, **7**, 2767 (1937); *Chem. Abstr.*, **32**, 2915 (1938).

13) J. C. Duff, *J. Chem. Soc.*, **1941**, 547.

14) E. Campaigne and W. L. Archer, *J. Am. Chem. Soc.*, **75**, 989 (1953).

15) T. Matsumoto and K. Fukui, This Bulletin., **30**, 3 (1957).

16) Melting points are uncorrected, and IR spectra were taken by the Nujol method.

Found: C, 65.06; H, 4.07. Calcd. for $C_{14}H_{10}O_5$: C, 65.12; H, 3.90%.

From Hydroxy-ester IIIa.—1) By the Action of Potassium Carbonate.—A solution of IIIa (0.1 g.) in ethyl methyl ketone (20 ml.) was refluxed for 8 hr. while anhydrous potassium carbonate (0.5 g.) was stirred in and then treated as before to give Va, m. p. 210~211°C. *2) By the Action of Phosphoric Acid.*—A mixture of IIIa (0.1 g.) and phosphoric acid (40 ml.) was heated for 30 min. in a steam bath. The cooled mixture was poured into water, and the solid product was recrystallized from ethanol to give Va, m. p. 210~212°C.

5'-Ethoxycarbonyl-4-methylangelicin (Vb).—*From Aldehyde IIb.*—By a method similar to that described for Va, Vb was obtained from IIb (1 g.), ethyl bromomalonate (1.2 g.), potassium carbonate (2.4 g.) and ethyl methyl ketone (70 ml.); colorless needles, m. p. 194~195°C (from ethanol); yield 0.65 g. (48.9%). Reported m. p. is 192°C[10].

Found: C, 65.86; H, 4.48. Calcd. for $C_{15}H_{12}O_5$: C, 66.15; H, 4.45%.

From Hydroxy-ester IIIb.—1) By the Action of Potassium Carbonate.—Vb was obtained similarly to Va; m. p. 193~194°C. *2) By the Action of Phosphoric Acid.*—Vb was obtained similarly to Va; m. p. 193~194°C.

5'-Carboxy-angelicin (VIa).—*a) From Ester Va.*—A mixture of Va (0.4 g.) and a 5% potassium hydroxide solution in 50% aqueous methanol (20 ml.) was refluxed for 30 min. in a steam bath. The resulting mixture was filtered and acidified with dilute hydrochloric acid, and the precipitates were collected and recrystallized from ethanol to give VIa in the form of colorless needles, m. p. 320~325°C (decomp.); yield 0.35 g. (98.3%). Reported m. p. is 315°C[8].

Found: C, 62.30; H, 2.73. Calcd. for $C_{12}H_6O_5$: C, 62.66; H, 2.63%.

b) From Hydroxy-ester IIIa.—By a treatment similar to a), VIa was obtained from IIIa (0.1 g.); m. p. 315~320°C (decomp.).

c) From Acetoxy-ester IVa.—By a similar treatment, VIa was obtained from IVa (0.1 g.); m. p. 320°C (decomp.).

5'-Carboxy-4-methylangelicin (VIb).—*From Ester Vb.*—By a method similar to that described for VIa, VIb was obtained from Vb (0.6 g.) and a 5% potassium hydroxide solution in 50% aqueous methanol (25 ml.); colorless needles, m. p. 295~299°C (decomp.) (from ethanol); yield 0.5 g. (92.6%).

Found: C, 63.85; H, 3.45. Calcd. for $C_{13}H_8O_5$: C, 63.94; H, 3.30%.

From Hydroxy-ester IIIb.—VIb was obtained similarly; m. p. 290~295°C (decomp.).

From Acetoxy-ester IVb.—VIb was obtained similarly; m. p. 290~295°C (decomp.).

Angelicin (Ia).—A mixture of acid Va (0.3 g.), copper powder (0.5 g.) and quinoline (40 ml.) was heated while being stirred in an atmosphere of nitrogen at 200~220° until evolution of carbon dioxide ceased. The quinoline was distilled off by steam-distillation from the resulting mixture, the copper was filtered off while hot, and the precipitates obtained on cooling were collected and recrystallized from dilute ethanol to give Ia in the form of colorless needles, m. p. 137~138°C; this was not depressed on admixture with a natural specimen; yield 0.1 g. (41.7%).

Found: C, 70.84; H, 3.33. Calcd. for $C_{11}H_6O_3$: C, 70.95; H, 3.25%.

4-Methylangelicin (Ib).—By a method similar to that described for Ia, Ib was obtained from Vb (0.5 g.), copper powder (0.8 g.) and quinoline (40 ml.); colorless needles, m. p. 190~192°C (from petroleum benzine or methanol); yield 0.2 g. (50%). Reported m. p. is 194°C[10].

Found: C, 71.88; H, 4.08. Calcd. for $C_{12}H_8O_3$: C, 71.99; H, 4.03%.

The authors are grateful to Professor Minoru Nakajima of Kyoto University for infrared spectroscopy, and to the members of Faculty of Pharmacology of this University for microanalyses.

Faculty of Literature and Science
Toyama University
Hasumachi, Toyama

On the Structures of p-tert-Butylphenol Resin and α-Naphthol Resin. III. Infrared Absorption Spectra of Resins of p-tert-Butylphenol and α-Naphthol

By Reisuke SODA

(Received March 8, 1961)

Polymer synthesized from *p-tert*-butylphenol and formaldehyde with ammonia was used as a suitable material for coating the fiber of a dust respirator to raise its efficiency; it showed an anomalous behavior in benzene solution[1]. Infrared spectra of the polymer in solid and in various solutions have been observed and its structure discussed[1], but there

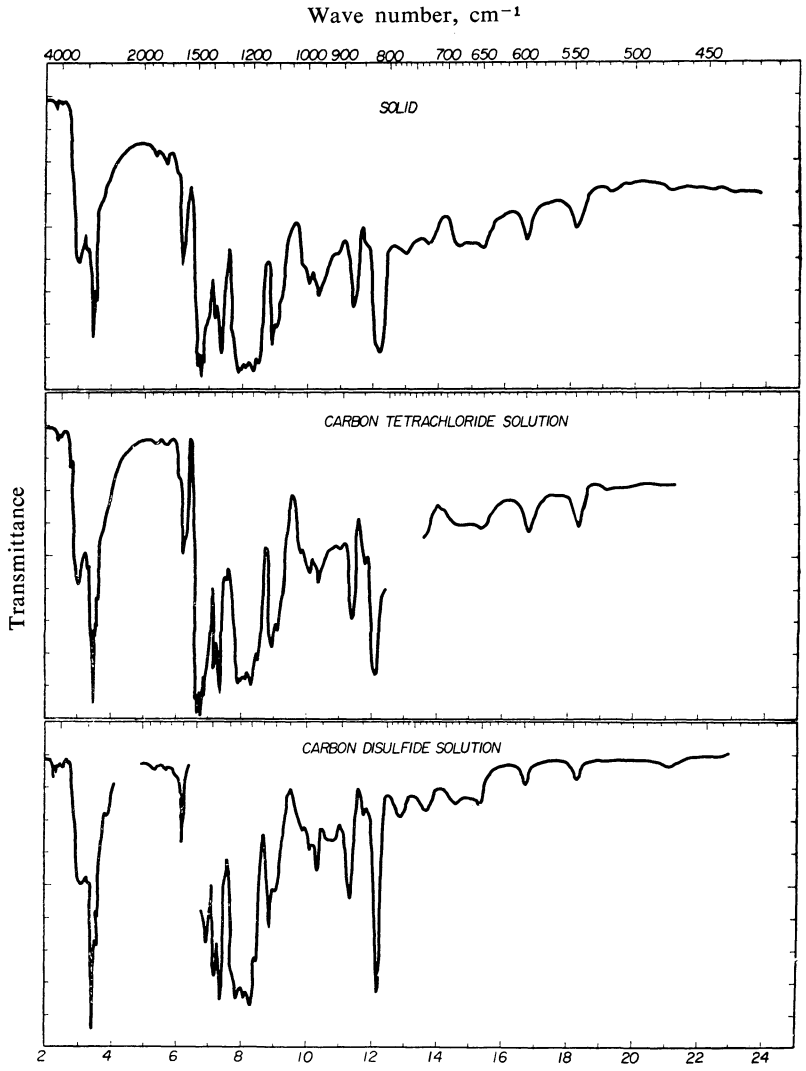


Fig. 1. Spectra of *p-tert*-butylphenol resin in solid and solutions. Spectrum is cut off in the region of interference due to solvents. Concentration of solution is about 15% in carbon tetrachloride and 10% in carbon disulfide.

1) R. Soda, *Bull. Nat. Inst. Ind. Health*, No. 3, 40 (1960).

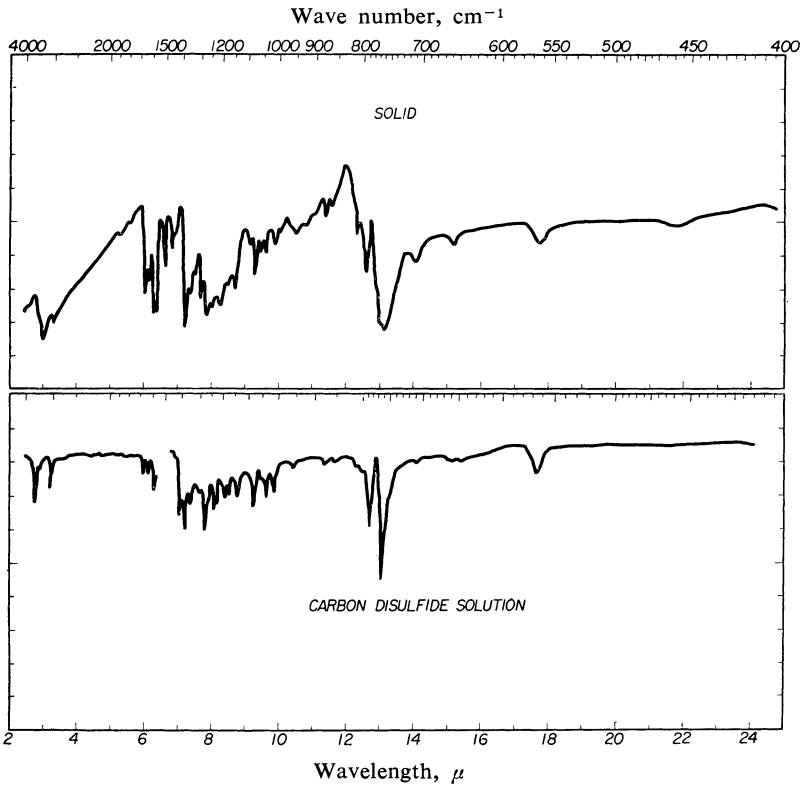


Fig. 2. Spectra of α-naphthol resin in solid and solution. Spectrum is cut off in the region of interference due to solvent. Concentration of solution is about 2%.

still remain some ambiguities in the assignment of those spectral bands. In order to eliminate the doubtfulness in the previous paper, infrared spectra of phenol, *p-tert*-butylphenol and α-naphthol were observed in more detail, and the band assignment and their structures were discussed more precisely[2]. The present paper deals with the band assignment of the spectra of the polymers of *p-tert*-butylphenol and α-naphthol, comparing them with information obtained already[2], particularly about the O–H deformation vibrations of those polymers.

Experimental

p-tert-Butylphenol formaldehyde resin and α-naphthol formaldehyde resin were supplied from S. Koshi. The former was synthesized from *p-tert*-butylphenol and formaline with ammonia as catalyst, and the latter, from α-naphthol and formaline. These polymers were purified from their benzene solutions. The color of *p-tert*-butylphenol polymer was yellowish brown, while that of α-naphthol polymer was dark brown or black.

The solvents used were benzene, acetone, carbon tetrachloride and carbon disulfide, each being distilled once. Only benzene and acetone were used as solvents for *p-tert*-butylphenol polymer. Spectra of the solvents were the same as those reported in the literature.

Solid spectrum of *p-tert*-butylphenol polymer was observed by sandwiched film which was resolidified between two window plates. α-Naphthol polymer did not fuse without decomposition; therefore, its solid spectrum was observed by potassium bromide disk alone. Some spectra of *p-tert*-butylphenol polymer were also obtained with this potassium bromide disk.

A Perkin-Elmer Model 137 infracord spectrophotometer, a Perkin-Elmer Model 21 spectrophotometer (cesium bromide region), and a Perkin-Elmer Model 221 spectrophotometer were used in the present experiment.

Results

***p-tert*-Butylphenol Polymer.**—Spectra of *p-tert*-butylphenol polymer in solid and in solutions of carbon tetrachloride and carbon disulfide are shown in Fig. 1. Solid spectrum of the polymer in cesium bromide region is shown in Fig. 3. The solution spectrum of *p-tert*-butylphenol polymer is almost the same as its solid spectrum, and no significant change in the bands is found when the concentration is altered, except a little change in the 3 and 8 μ regions, as is shown in Figs. 5 and 6. In solid the polymer gives rise to a broad

2) R. Soda, This Bulletin, **34**, 1842 (1961).

band near 3300 cm^{-1} which shows no appreciable change even if the polymer is dissolved in several solvents and the concentration of the solution varies. Only in the cases of carbon tetrachloride and benzene solutions is a weak but sharp band observed near 3600 cm^{-1} as a shoulder of the broad 3300 cm^{-1} band. In other solvents, such as acetone and carbon disulfide, it does not give rise to any band at 3600 cm^{-1}. The intensity of the band at 3600 cm^{-1} increases slightly as the concentration decreases, but the increment is so small that the quantitative relation with the concentration cannot be confirmed.

In the 8 μ region, this polymer gives rise to the bands at 1425, near 1232 and 1205 cm^{-1} in solid and in solution. Those bands in the 3 and 8 μ regions may be concerned in O–H vibration modes, but as far as the present experiment shows, a solvent cannot be found in which all O–H bonds are set free by dilution.

In the region of 600 to 400 cm^{-1}, and some

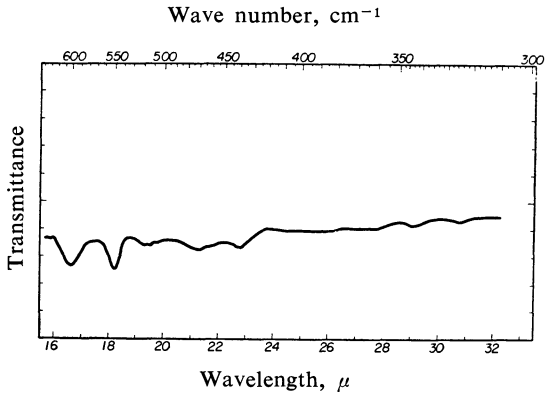


Fig. 3. Spectrum of *p-tert*-butylphenol resin in CsBr region (fused film).

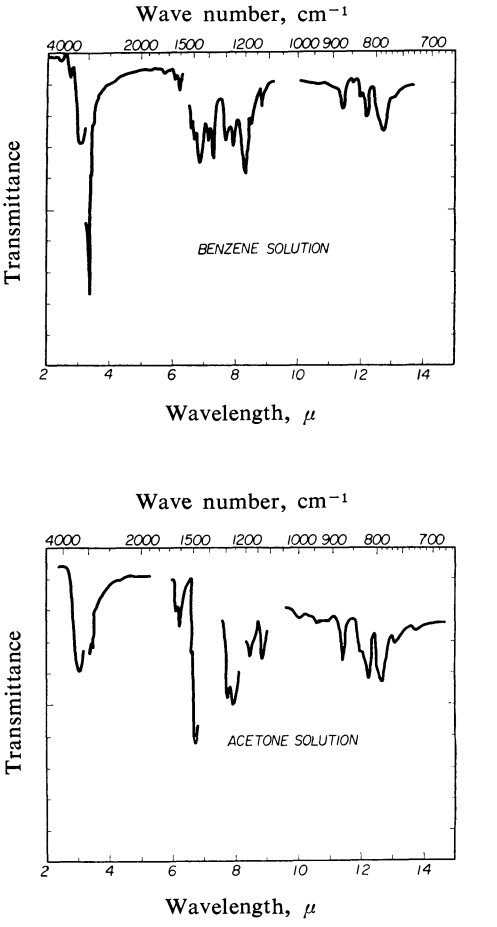


Fig. 4. Spectra of *p-tert*-butylphenol resin in benzene and acetone. Spectrum is cut off in the region of interference due to solvents. Concentration of solution is about 5% in benzene and 5% in acetone.

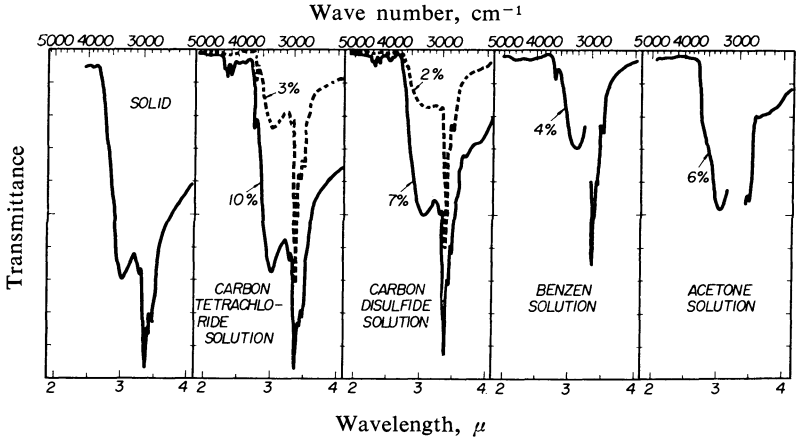


Fig. 5. Spectra of *p-tert*-butylphenol resin in 3 μ region. Spectrum is cut off in the region of interference due to solvents.

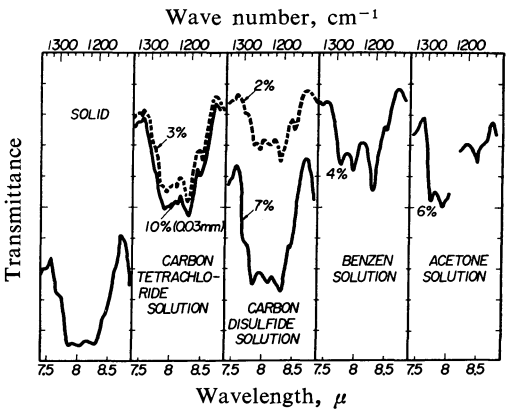


Fig. 6. Spectra of *p-tert*-butylphenol resin in the region near 1200 cm^{-1}. Spectrum is cut off in the region of interference due to solvents.

other regions, such a change of spectra with phase cannot be observed. The observed bands and their assignments are summarized in Table I.

α-Naphthol Polymer. — α-Naphthol polymer is insoluble or scarcely soluble in a non-polar solvent such as carbon tetrachloride; therefore, only a spectrum of a dilute solution of carbon disulfide was observed, as is shown in Fig. 2. The solution spectrum is considerably different from that of solid. This difference is so large that it cannot be explained as an impurity effect due to insufficient purification. In the region of the bands concerned with the C–H out-of-plane vibration mode, the strong bands occur at 765 and 755 cm^{-1}. In 3 μ, the solid gives rise to a very broad band near 3380 cm^{-1}, but the solution gives rise to a sharp (strong) band at 3600 cm^{-1} and a broader (weak) band at 3450 cm^{-1}. In the 8 μ region, several bands are observed, and the bands at 1441 and 1240 cm^{-1} in solid are considered to shift to 1385 or 1370 and 1176 cm^{-1} in solution respectively. In the lower wave number regions, no significant shift or chang is observed between solid and solution.

Discussion

***p-tert*-Butylphenol Polymer.** — *p-tert*-Butylphenol polymer is composed of *p-tert*-butylphenol and a methylene bridge at the ortho positions of phenol ring, and both sides of the linear polymer chain are probably *p-tert*-butylphenol residues[1,3-5]. The polymer has in it a methylene group, 1, 2, 3, 5-tetra- and 1, 2, 4-tri-substituted benzene rings, aromatic O–H and a *tert*-butyl group. *p-tert*-Butylphenol has in it a 1, 4-di-substituted benzene ring, aromatic O–H and a *tert*-butyl group. The polymer gives rise to the bands concerned with those group vibration modes, and the spectral difference between the polymer and *p-tert*-butylphenol may be attributed to the difference between groups or ring structures in these compounds.

The change of the bands concerned in the

Table I. Band positions and assignment of spectrum of *p-tert*-butylphenol resin

Bands, cm^{-1}		Assignment
Solid	Solution	
	(3610)	ν(O–H), free?
3300	3311 to 3200	ν(O–H), bonded
3030	3030	ν(C–H), aromatic
2950	2960	ν(C–H), $-CH_3$
2910	2910	ν(C–H), $-CH_2-$
2870	2870	ν(C–H), $-CH_3$
2830	2830	ν(C–H), $-CH_2-$
1613	1613	Ring vibration
1598	1597	Ring vibration
1534	1536	Ring vibration
1511	1513	Ring vibration
1484	1484	δ(C–H), $-CH_3$
1462	1462	δ(C–H), $-CH_3$ or $-CH_2-$
1450	1453	δ(C–H), $-CH_3$ or $-CH_2-$
1425	1427	δ(O–H), bonded and ν(C–O)
1394	1395	δ(O–H), $-CH_3$ or $-CH_2-$
1362	1363	Skeletal vibration
1328	1327	$-CH_2-$ Twisting
1294	1294	$-CH_2-$ Twisting?
1270	1273	Skeletal vibration
1257	1258	$C-CH_3$ Rocking
1238	1233	δ(O–H), bonded and ν(C–O)
1206	1204	δ(C–H), aromatic?
1181	1179	δ(C–H), aromatic
1125	1125	δ(C–H), aromatic
1106	1107	δ(C–H), aromatic
1010	1015	δ(C–H), aromatic
990	992	Skeletal vibration
968	970	Skeletal vibration
920	918	ν(C–C), $C-CH_3$
880	882	δ(C–H), out of plane
848	850	ν(C–C), $C-CH_3$
822	825	δ(C–H), out of plane
818	820	δ(C–H), aromatic or ν(C–C), $C-CH_3$
778	777	
730	730	$-CH_2-$ Rocking
685	685	Substituent characteristic
654	653	Substituent characteristic
600	600	
550	548	δ(O–H), out of plane
521	522	δ(O–H), out of plane
474	475	

3) R. J. Grisemthwaite and R. F. Hunter, *J. Applied Chem.*, **6**, 324 (1956).
4) W. J. Wurke and S. J. Ruetman, *J. Polymer Sci.*, **32**, 22 (1958).
5) A. Rosenthal, F. Lederer and K. Gilson, *Can. J. Chem.*, **34**, 679 (1956).

O–H vibration modes in the polymer with the phase or the concentration of solution is different from that of *p-tert*-butylphenol. The spectrum of the polymer shows no obvious difference between solution and solid. Solid and acetone solutions give rise to a broad band at 3300 cm^{-1} but carbon tetrachloride and benzene solutions give rise to a weak band at 3600 cm^{-1} near the 3300 cm^{-1} band. *p-tert*-Butylphenol gives rise to the broad band at 3300 cm^{-1} in solid and a sharp band at 3600 cm^{-1} besides the broader band at 3400 cm^{-1}. These bands are assigned to the O–H stretching vibration mode, the band at 3600 cm^{-1} is assigned to the vibration of free O–H, and the band at 3400 to 3300 cm^{-1}, to that of bonded O–H. Therefore, the O–H bond in the polymer is considered to be bound by very strong intramolecular H-bonding; this H-bonding cannot be easily broken into a free O–H bond in the solution. Only in a non-polar solvent, with interaction between the non-polar group of the polymer and the solvent, can the polymer chain extend to some extent and some O–H bond perhaps exist in a free state. The hydrogen bonded O–H bond of the polymer cannot be loosened by a hydrogen acceptor solvent such as acetone. Accordingly, in the case of the *p-tert*-butylphenol polymer, an appreciable change by the phase change cannot be expected in the bands concerned with O–H vibration modes.

The bands are assigned by comparing them with spectral data of various aromatic O–H compounds[4-6], particularly that of *p-tert*-butylphenol[2]. The assignment in Table I is carried out in such a way.

p-tert-Butylphenol in solid gives rise to the bands at 1389 and 1222 cm^{-1}, and those are assigned to the O–H in-plane deformation vibration, coupled with a C–O stretching vibration. Therefore, the bands at 1425 and 1232 cm^{-1} in the polymer are assumed to be assigned to those vibration modes. In a similar way, the bands at 548 and 520 cm^{-1} are assumed to be concerned with O–H out-of-plane deformation vibration.

The other bands at 600 to 400 cm^{-1} may be attributed to characteristics of 1, 2, 4, 6-tetra- and 1, 2, 4-tri-substitutions.

α-Naphthol Polymer.—Polymerization of α-naphthol and formaldehyde may take place at various positions of the α-naphthol nucleus. Position 1 of naphthalene ring is occupied by the O–H group, and there are two types of adjacent free hydrogen atom groups in α-naphthol. The methylene bridge can occupy several positions of the α-naphthol ring, for example, 2, 4, 6 and 8. The type of adjacent free hydrogen atom group is assumed to be as shown in Fig. 7.

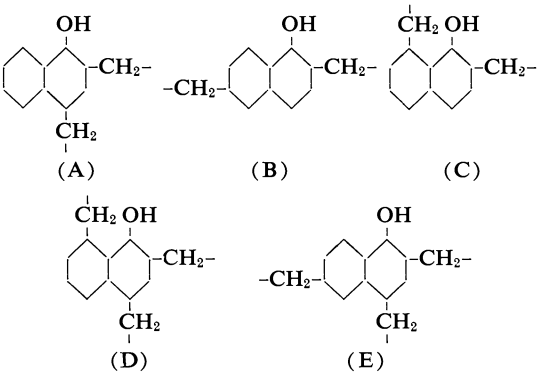


Fig. 7. Diagram regards to several types of methylene bridge in α-naphthol resin.

Out-of-plane bending vibration and some in-plane bending of aromatic C–H bond give rise to bands in the region of 950 to 650 cm^{-1}, and the band positions obey an empirical rule of the spectrum of substituted aromatic derivatives[7-11]. With several substituted naphthalene derivatives in which two sorts of adjacent free hydrogen atom groups exist, the intense band arise in the region of 860 to 800 cm^{-1} and 750 to 700 cm^{-1}. In the case of four adjacent free hydrogen atoms, the compound also gives rise to the bands in the region of 770 to 735 cm^{-1} and 730 to 710 cm^{-1}. With three adjacent aromatic hydrogen atoms, the characteristic bands appear at 810 to 750 cm^{-1} and 730 to 680 cm^{-1}. One isolated hydrogen atom attached to aromatic ring gives rise to the band at 900 to 850 cm^{-1}. From those rules of spectral bands concerned with out-of-plane C–H bending, the polymer may be considered to have a linear but a partly cross-linked chain structure in which the methylene bridge group mainly occupies the 2 and 4 or 6 positions of the naphthalene ring. The main structures may be drawn as shown by I and II in Fig. 8. Bands 850 and 870 cm^{-1} are assigned to out-of-plane bending of the isolated C–H group, bands 810 and 760 or 710 cm^{-1} to that of two adjacent free hydrogen atoms, and bands 770 and 760 or 710 cm^{-1} to that of four adjacent free hydrogen atoms. The band at 790 cm^{-1} is weak, and if the polymer has

6) H. Kammerer, *Angew. Chem.*, **70**, 390 (1958).

7) L. J. Bellamy, "The Infrared Spectra of Complex Molecules", Metheu & Co., Ltd., London, J. Wiley & Sons Inc., New York (1954), pp. 64-69 and p. 96.

8) "Chemical Application of Spectroscopy", Ed. by W. West, Interscience Pub. Ltd., London (1956), pp. 388-434.

9) H. Kamata and S. Tanaka, *Japan Analyst*, **5**, 98 (1956).

10) R. W. Bayer and E. J. O'Reily, *J. Phys. Chem.*, **62**, 504 (1958).

11) H. Luther and H. Gunzler, *Z. Naturforsch.*, **10b**, 445 (1955).

structure I in Fig. 8, this band can be assigned to the vibration of three adjacent free hydrogen atoms in the end of the polymer chain.

In the region of 3 μ, the band at 3380 cm^{-1} is assigned to H-bonded O-H stretching vibration, that at 3450 cm^{-1} to that of weakly H-bonded O-H bond, and that at 3600 cm^{-1} to free O-H stretching vibration. The O-H bonds in the solid polymer may all be bound with each other by intermolecular hydrogen bonding, and in carbon disulfide solution, the polymer has a large number of free O-H bonds and a very small number of H-bonded O-H bonds. It may be assumed that the O-H bonds in the molecule of the α-naphthol polymer find it difficult to approach near enough to each other to build up a strong intramolecular hydrogen bonding.

Table II. Band positions and assignment of spectrum of α-naphthol resin

Bands, cm^{-1} Solid	Bands, cm^{-1} Solution	Assignment
	3600	ν(O-H), free
	3510	ν(O-H), bonded
3380		ν(O-H), bonded
3030	3060	ν(C-H), aromatic
1650	1664	Ring vibration
1626	1629	Ring vibration
1587	1597	Ring vibration
1575	—	Ring vibration
1508	—	Ring vibration
1460	—	δ(C-H), $-CH_2-$
1441	1403 ?	δ(O-H), bonded and ν(C-O)
1385	1385	δ(C-H), $-CH_2-$ or skeletal vibration
	1357	δ(O-H), free and ν(C-O)
1353		
1335		$-CH_2-$ Twisting or skeletal vibration
1302	1297	$-CH_2-$ Twisting or skeletal vibration
1269	1276	Skeletal vibration
1241	1242 and 1233	δ(O-H), bonded and ν(C-O)
1203	1199	δ(C-H), aromatic
1179		
	1176	δ(O-H), free and ν(C-O)
1142	1143	ν(C-C), aromatic
1081	1080	ν(C-C), aromatic
1051	1051	δ(C-H), aromatic
1014	1014	δ(C-H), aromatic
953	955	Skeletal vibration
930		Skeletal vibration
876	876	Skeletal vibration or δ(C-H), out of plane
859	853	δ(C-H), out of plane
809	812	δ(C-H), out of plane
792	788	δ(C-H), out of plane
765	767	δ(C-H), out of plane
755	757	δ(C-H), out of plane
711	710	δ(C-H), out of plane
661	659	Substituent characteristic skeletal vibration
567	568	δ(O-H), out of plane ?

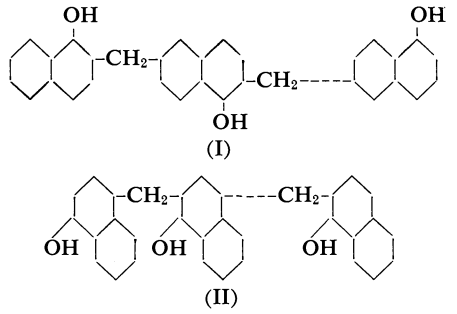


Fig. 8. Possible structures of α-naphthol resin prepared in this work.

From the comparison of the spectra of *p-tert*-butylphenol and its polymer, the bands at 1460, 1385 or 1353, 1335, 1300 and 750 cm^{-1} are assigned to the methylene group vibration[6,7]. O-H deformation vibration may be coupled with C-O stretching vibration. The bands 1385 or 1353 and 1176 cm^{-1} are assigned to the vibration of the free O-H bond, and the bands at 1441 and 1240 cm^{-1}, to those of H-bonded O-H. The bands at 568 cm^{-1} may be concerned with O-H out-of-plane bending. The other bands are attributed to the vibration of the condensed aromatic ring. The band positions and assignments are summarized in Table II.

Summary

Polymers of *p-tert*-butylphenol with formaldehyde and α-naphthol with formaldehyde have been synthesized, and infrared spectra have been observed in solid and in solutions. The following conclusions have been obtained concerning band assignments and the polymer structures.

(1) *p-tert*-Butylphenol polymer is a linear chain polymer connected with the methylene bridge, and O-H bonds restrict each other by a strong intramolecular hydrogen bonding. This hydrogen bonding is partly loosened in a benzene and carbon tetrachloride solution, but not in an acetone solution.

(2) With *p-tert*-butylphenol polymer the bands at 1425 and 1205 cm^{-1} are assigned to the deformation vibration of the O-H bond coupled with the C-O stretching vibration. Out-of-plane O-H bending is considered to give rise to the bands in the 550 to 500 cm^{-1} region, and the bands at 548 and 520 cm^{-1} are

assumed to be concerned with those vibrations.

(3) The O–H bond in α-naphthol polymer is bound by an intramolecular hydrogen bonding in solid, but in solution almost all the O–H bonds are liberated from the H-bonding. The polymer is considered to be a linear chain molecule whose O–H bonds can only with difficulty interact with each other to make an intramolecular hydrogen bonding.

(4) In-plane O–H deformation vibration coupled with C–O stretching vibration of α-naphthol polymer gives rise to the bands at 1385 or 1357 and 1176 cm^{-1}. The bands at 560 cm^{-1} may be concerned in out-of-plane O–H bending vibration.

The author wishes to express his hearty thanks to Assistant Professor Tatsuo Miyazawa and his collaborators at the Institute for Protein Research, Osaka University, for their kind permission to use their Perkin-Elmer Model 221 spectrophotometer. He also wishes to thank Mr. Michio Kawano, at the Railway Technical Research Institute, for the measurement of the spectrum in the cesium bromide region.

National Institute of Industrial Health
Kizuki-Sumiyoshi-cho, Kawasaki-shi

Dehydration of Bile Acids and their Derivatives. IX. Oxidation of Methyl 3α-Acetoxy-Δ⁷-cholenate with Selenium Dioxide

By Ryuzaburo OSAWA

(Received February 27, 1961)

Previously Fieser et al.[1] reported that the selenium dioxide oxidation of Δ^7-cholestene-3β-ol acetate in benzene-ether or ether-acetic acid affords, along with allylic rearrangement and acetylation, $\Delta^{8(14)}$-cholestene-3β, 7α-diol diacetate. Saucy et al.[2] found later that the same oxidation of $\Delta^{7,22}$-ergostadiene-3β-ol acetate in boiling ether containing a little acetic acid gives, as expected, not only $\Delta^{8(14),22}$-ergostadiene-3β, 7α-diol diacetate, but also $\Delta^{7,22}$-ergostadiene-3β, 9ξ-diol monoacetate. In his preceding paper, Fieser[3] had concluded that among the various steroids tested, 5α- or Δ^5-steroids having a double bond adjacent to the C-14 hydrogen atom give positive results in his selenium dioxide test, while none of the 5β-isomers does. Accidentally Professor Yamasaki has noticed that, contrary to Fieser's conclusion, some of the unsaturated bile acids (5β) give apparently positive results in the selenium dioxide test reported by Fieser[3]. These results are summarized in Table I.

It is interesting to note that not only the bile acids with a double bond adjacent to the C-14 hydrogen atom, but also those having a $\Delta^{8(14)}$ double bond afforded positive results in the selenium dioxide test.

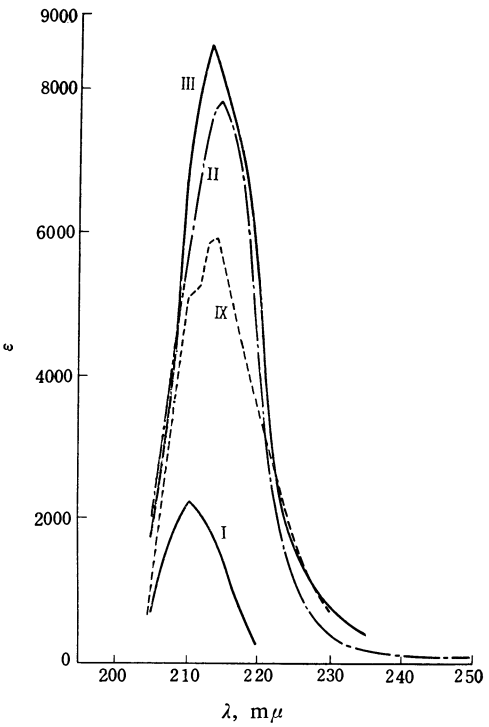


Fig. 1. Absorption spectra of: Methyl 3α-acetoxy-Δ^7-cholenate (I); substance B (II) and its acetate (III); methyl 3α-acetoxy-$\Delta^{8(14)}$-cholenate (IX, for reference).

1) L. F. Fieser and G. Ourisson, *J. Am. Chem. Soc.*, **75**, 4404 (1953).
2) G. Saucy, P. Geistlich, R. Helbling and H. Heusser, *Helv. Chem. Acta*, **37**, 250 (1954).
3) L. F. Fieser, *J. Am. Chem. Soc.*, **75**, 4395 (1953).

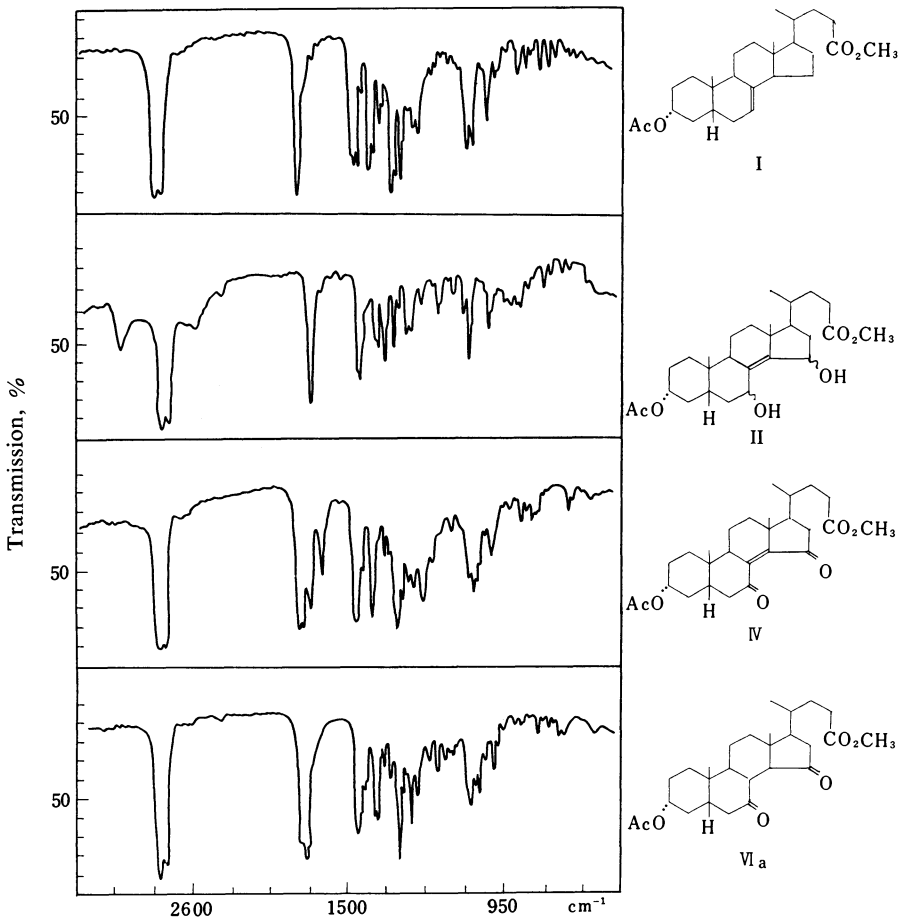


Fig. 2. IR-spectra of: Methyl 3α-acetoxy-Δ^7-cholenate (I); substance B (II); the oxidation product of II (IV); the zinc dust-reduction product of IV (VIa).

TABLE I. SELENIUM DIOXIDE TEST OF SOME BILE ACIDS

Bile acid	SeO_2 test	Ref.
3α-Hydroxy-Δ^7-cholenic acid	++	5
Methyl 3α-acetoxy-Δ^7-cholenate	++	5
Methyl 3α-hydroxy-$\Delta^{8(14)}$-cholenate	++	6
Methyl 3α-acetoxy-$\Delta^{8(14)}$-cholenate	++	6
Apocholic acid	++	a
Methyl 3α-acetoxy-Δ^8-cholenate	+	b
Methyl 3α-acetoxy-$\Delta^{9(11)}$-cholenate	—	c
Methyl 3α-acetoxy-Δ^{14}-cholenate	—	5
Methyl 3α-acetoxy-Δ^6-cholenate	—	d
Methyl 3α-acetoxy-$\Delta^{7,9(11)}$-choladienate	++	c

+: Turns yellow within 20 min.
++: Turns yellow within 10~15 min.
The reaction is more intense in acetic acid than in benzene.

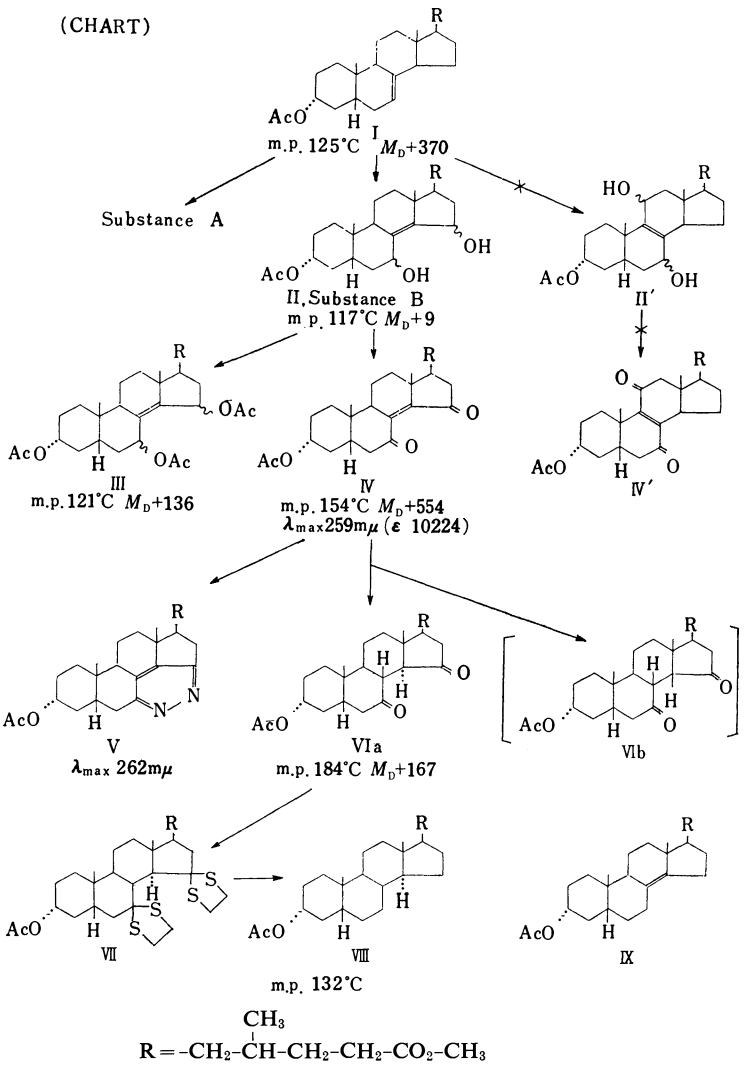
a) Fr. Bödecker, *Ber.*, **53**, 1852 (1920).
b) L. F. Fieser, W. P. Schneider and W. Y. Huang, *J. Am. Chem. Soc.*, **75**, 124 (1953).
c) L. F. Fieser and S. Rajagopalan, ibid., **73**, 118 (1951).
d) S. L. Hsia, J. T. Matschiner, T. A. Mahowald, W. H. Elliot and E. A. Doisy, *J. Biol. Chem.*, **226**, 667 (1957).

The present author has sought to isolate the selenium dioxide oxidation products of methyl 3α-acetoxy-Δ^7-cholenate. The crude crystalline oxidation product was dissolved in benzene and chromatographed to give three crystalline substances. The substance eluted first proved to be the recovered starting material (melting point; mixed melting point; the infrared spectrum).

Substance A, eluted immediately after the starting material, was in the form of colorless needles (m. p. 174°C), the infrared spectrum of which indicated that the acetyl group and the double bond of the starting material were eliminated. No further evidence on the structure of this product has yet been obtained, since the amount of the product is too small for further study.

Substance B (II), in the form of colorless prisms (m. p. 114°C), eluted with a mixture of ether-methanol (4 : 1) showed a high absorption maximum at 214 mμ (ε_{max}^{EtOH} 7804). This characteristic absorption seems to indicate the presence of a tetra-substituted, exocyclic

(CHART)



ethylenic linkage in the molecule, as has been shown by Bladon et al.[4] and Osawa et al.[5,6]; indeed, the ultraviolet absorption spectrum of this substance was found to be quite similar to that of methyl 3α-acetoxy-$\Delta^{8(14)}$-cholenate[6] (IX) derived from apocholic acid (Fig. 1). From these observations and the structure of the starting material, it is highly probable that substance B has a double bond shifted to the position between C-8 and C-14, just like apocholic acid.

The infrared spectrum of substance B showed a distinct band at 3400 cm^{-1}, indicative of the presence of a hydroxyl group or groups (Fig. 2, II). This band disappeared when substance B was acetylated in the usual way, which indicates that the hydroxyl group or groups are not of tertiary, but probably of secondary nature. Analytical data of this acetylated substance correspond well to a tri-acetate, $C_{25}H_{37}O_5 \cdot (CH_3CO)_3$ (III). From these results it has been concluded that substance B contains no tertiary hydroxyl group unlike the oxidation product of $\Delta^{7,22}$-ergostadiene-3β-ol acetate[2], and that it probably has two acylable hydroxyl groups newly introduced at the positions adjacent to the double bond ($\Delta^{8(14)}$) as formulated as II.

The secondary nature of these hydroxyl groups was confirmed by the fact that chromic acid oxidation gave a diketone IV, which afforded a dioxime.

This unsaturated diketone IV showed an absorption maximum at 259 mμ with a characteristic extinction coefficient (ε_{max}^{EtOH} 10224)

4) P. Bladon, H. B. Henbest anb G. W. Wood, *J. Chem. Soc.*, **1952**, 2737.
5) R. Osawa and K. Yamasaki, This Bulletin, **32**, 1302 (1959).
6) F. Nakada, R. Osawa and K. Yamasaki, ibid., **34**, 538 (1961).

TABLE II

Substance	M. p., °C	α_D	Absorption maximum, λ	Ref.
Methyl 3α-acetoxy-7,11-diketo-Δ^8-cholenate (IV′)	147~149	+ 32° (chf.)	272 mμ* ε_{max}^{EtOH} 5012	10
The oxidation product of substance B (IV)	154~155	+120.4°(chf.)	259 mμ ε_{max}^{EtOH} 10224	—
7,15-Dioxoergosta-$\Delta^{8(14),22}$-diene-3β-ol acetate	180~181	+ 36° (chf.)	259 mμ ε_{max}^{EtOH} 11300	7

* A sample of m. p. 136~143°C showed an absorption maximum ε_{max}^{EtOH} 8139 at 272 mμ[10].

quite similar to that shown by 7,15-dioxo-ergosta-$\Delta^{8(14),22}$-diene-3β-ol acetate[7].

On the basis of these results, it appears highly probable that the resulting diketone IV is methyl 3β-acetoxy-7,15-diketo-$\Delta^{8(14)}$-cholenate. Furthermore, the presence of an ene-1,4-dione system in the diketone was substantiated by the fact that the diketone not only gave a pyridazine derivative, characterized by the absorption maximum at 262 mμ (ε_{max}^{EtOH} 2440)[7,8], but also was reduced at room temperature by zinc and acetic acid like the dioxo-ergostadiene derivative[7]. This reduction product no longer showed such a characteristic absorption at 259 mμ (Fig. 3), and two kinds of crystalls

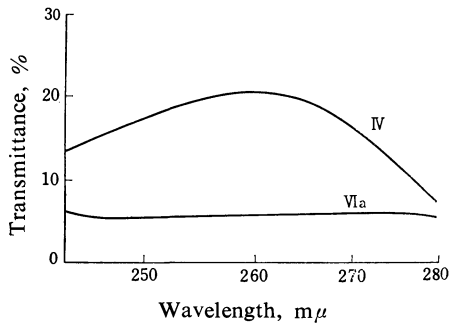


Fig. 3. Absorption spectra of: The oxidation product of substance B (IV) (1/1000% w/v MeOH) and its zinc dust-reduction product (VIa) (1/100% w/v MeOH).

were obtained, the one melting at 184°C and the other at 111°C. The former saturated diketone VIa, the major product, remained unchanged by treatment with alkali followed by esterification and acetylation, and it gave a bisthioketal (VII)[9] which in turn, by desulfuration with Raney nickel, was converted into methyl 3α-acetoxycholanate (VIII) (Identification: melting point; mixed melting point; infrared spectrum). These findings strongly indicate that the C/D ring fusion in this diketone is trans (14α-hydrogen), just like the usual bile acid. The other product of m. p. 111°C had been expected to have the structure of cis C/D fusion, as formulated as VIb, but the amount of the product was too small to elucidate the structure.

Furthermore, not only the unsaturated diketone IV but also the saturated diketone VIa showed characteristic infrared spectra, indicative of α,β-unsaturated (1692 cm^{-1}, 1634 cm^{-1}) and saturated (1732 cm^{-1}, 1717 cm^{-1}) ketonic groups in a five- and a six-membered ring respectively (Fig. 2).

From these experimental results the major product (substance B) of the selenium dioxide oxidation of methyl 3α-acetoxy-Δ^7-cholenate has been proved to be methyl 3α-acetoxy-7,15-dihydroxy-$\Delta^{8(14)}$-cholenate (II).

The fact that substance B (II) and its oxidation product IV showed great absorptions in the ultraviolet region, as indicated above, is consistent with Formulae II and IV, and not with Formulae II′[4] and IV′[10] respectively. The other physical constants of the oxidation product of substance B are also quite different from those of methyl 3α-acetoxy-7,11-diketo-Δ^8-cholenate[10] (IV′) (Table II).

The configurations of the newly introduced hydroxyl groups at C-7 and C-15 of substance B have not yet been established. Since the rear attack of selenium dioxide will be a very probable mode of action, as was the case in the oxidation of Δ^7-cholestene-3β-ol acetate[1], the C-7 hydroxyl group of substance B might be α-oriented (M_D contribution −79). If this were so, the M_D contributions of the hydroxyl and acetyl groups at C-15 could be calculated to be −162 and +30 respectively, indicating that the C-15 OH is α-oriented. Methyl 3α-acetoxy-$\Delta^{8(14)}$-cholenate (M_D +250)[6] has here been taken as a point of reference.

7) D. H. R. Barton and G. F. Laws, *J. Chem. Soc.*, **1954**, 52.
8) H. E. Stavely and C. N. Bollenback, *J. Am. Chem. Soc.*, **65**, 1285 (1943).
9) H. Hauptmann, ibid., **69**, 562 (1947); L. F. Fieser, ibid., **75**, 4386 (1953).
10) H. Heusser, K. Eichenberger, P. Kurath, H. R. Dällenbach and O. Jeger, *Helv. Chim. Acta*, **34**, 2106 (1951); C. S. Barnes and D. H. R. Barton, *J. Chem. Soc.*, **1953**, 1419.

Experimental

Oxidation of Methyl 3α-Acetoxy-Δ^7-cholenate.—To a solution of methyl 3α-acetoxy-Δ^7-cholenate (I) (m. p. 126°C; 2 g.) in 50 ml. of absolute ether was added 92 ml. of a solution of 0.1 M selenium dioxide in acetic acid[1], and the mixture was kept at room temperature (18~25°C) overnight. Then the reaction mixture was poured carefully into 1 l. of water and extracted thoroughly with ether. The ethereal extract was washed with water, with sodium carbonate solution and again with water successively, and dried over sodium sulfate. Removal of the solvent gave a crystalline residue, which, dissolved in 4~5 ml. of benzene, was allowed to pass through a Brockmann-alumina column and eluted with petroleum ether, benzene, ether and methanol successively. The first portions (Fraction 1—4) of the eluate contained the starting material (yield: 55% as an average) and substance A of a higher melting point, while substance B of a lower melting point (yield: 15% as an average) was obtained from the fractions eluted with ether-methanol (4:1, v/v). Substance A and B were separately treated and refluxed in acetone with precipitated silver for about 3 hr. to remove colloidal selenium. Removal of the solvent of these solutions gave crystalline residues.

Methyl 3α-Acetoxy-7ξ, 15ξ-dihyroxy-$\Delta^{8(14)}$-cholenate (II).—Substance B was recrystallized repeatedly from methanol. Yield, 230 mg., m. p. 114~117°C, $\alpha_D^{29}=+2.0°$ (chf.); λ_{max} 214 mμ (ε_{max}^{EtOH} 7804). The infrared spectrum of this substance had a distinct hydroxyl absorption band at 3400 cm^{-1}. Substance B showed a melting point depression on admixture with the starting material and no more positive result in the selenium dioxide test.

Found: C, 69.78; H, 9.02. Calcd. for $C_{27}H_{42}O_6$ (462.61): C, 70.10; H, 9.15%.

Methyl 3α, 7ξ, 15ξ-Triacetoxy-$\Delta^{8(14)}$-cholenate (III).—Substance B (200 mg.) dissolved in 2 ml. of pyridine with 1 ml. of acetic anhydride was allowed to stand at room temperature. After 24 hr. the reaction mixture was warmed for 20 min. on a water bath and some concentrated hydrochloric acid was added. The separated solid was then collected. Recrystallized once from methanol, the product was obtained as colorless needles of m. p. 120~121°C, $\alpha_D^{28}=+25.0°$ (chf.); λ_{max} 214 mμ (ε_{max}^{EtOH} 8610). Yield, 188 mg. The hydroxyl absorption at 3400 cm^{-1} was not observed in the infrared spectrum of III.

Found: C, 68.16; H, 8.58. Calcd. for $C_{31}H_{46}O_8$ (546.68): C, 68.10; H, 8.48%.

Methyl 3α-Acetoxy-7, 15-diketo-$\Delta^{8(14)}$-cholenate (IV).—Substance B (400 mg.) in 40 ml. of acetone was oxidized with the chromium trioxide-sulfuric acid mixture (3.2 ml.) according to the method of Bladon et al.[4] After completion of the oxidation (3~4 min.), the excess of the oxidant was reduced with a small amount of methanol. The reaction mixture was diluted with water and extracted thoroughly with ether. The ethereal extract was washed with water, with sodium carbonate solution and again with water successively, dried over sodium sulfate and evaporated. Recrystallization from methanol and then aqueous methanol afforded yellowish crystals of m. p. 154~155°C; $\alpha_D^{28}=+120.4°$ (chf.); λ_{max} 259 mμ (ε_{max}^{EtOH} 10224). The infrared spectrum showed four carbonyl absorption bands, two of which indicated α, β-unsaturated 5- and 6-membered rings (1692, 1634 cm^{-1}).

Found: C, 70.77; H, 8.31. Calcd. for $C_{27}H_{38}O_6$ (458.57): C, 70.71; H, 8.35%.

Oxime of IV.—The diketone (100 mg.) in 20 ml. of methanol was treated with an aqueous solution of hydroxylamine (a mixture of 5 M sodium acetate, 4 ml. and 5 M hydroxylamine hydrochloride, 4 ml.). The mixture was refluxed for 2 hr. and then poured into 100 ml. of water, and the product was collected. The product failed to be crystallized, but repeated precipitations from aqueous methanol afforded a satisfactorily pure sample (87 mg.).

Found: N, 5.46. Calcd. for $C_{27}H_{40}O_6N_2$ (488.33): N, 5.73%.

Pyridazine Derivative of IV.—The diketone IV (200 mg.) in 33 ml. of methanol was refluxed for 6 hr. with 0.6 ml. of hydrazine hydrate (42%). Removal of the solvent left a residue which became crystalline when treated with a small amount of ether. The crystalline material dissolved in benzene was chromatographed (Florisil). M. p. 158°C; yield, 76 mg. λ_{max} 262 mμ (ε_{max}^{EtOH} 2440).

The infrared spectrum of the resulting product indicated that the acetyl group of the diketone IV was removed by the above treatment.

Found: C, 72.20; H, 8.88; N, 6.46. Calcd. for $C_{25}H_{38}O_3N_2$ (414.30): C, 72.42; H, 9.24; N, 6.76%.

Zinc Dust Reduction of IV.—*Methyl 3α-Acetoxy-7, 15-diketo-cholanate (VIa).*—A solution of the $\Delta^{8(14)}$-diketone (IV) (200 mg.) in 20 ml. of acetic acid was stirred with 1 g. of zinc dust for 5 hr. at room temperature. After removal of zinc dust the solution was diluted with water and extracted with ether. The ethereal extract was washed with water, with sodium carbonate and again with water successively and then evaporated to dryness. Recrystallized from methanol, the product was obtained as platelets of m. p. 184°C, $\alpha_D^{16}=+36.4°$ (chf.). Yield, 122 mg.

Found: C, 70.26, 70.40; H, 8.84, 8.73. Calcd. for $C_{27}H_{40}O_6$ (460.59): C, 70.40; H, 8.75%.

The infrared spectrum of the product showed characteristic bands of a saturated ketone: ν_{max}^{Nujol} 1750 cm^{-1} (ester), 1732 cm^{-1} (5-membered ring ketone), 1717 cm^{-1} (6-membered ring ketone); 1254, 1225 cm^{-1} (acetate).

Chromatography of the filtrate gave a further crop (35 mg.) of m. p. 182°C. Total yield, 157 mg. A small amount of another kind of crystals (m. p. 110°C) was also obtained; this yield, however, was not enough for its identification.

A solution of the ketone (50 mg., m. p. 184°C) in 2 ml. of 5% methanolic potassium hydroxide was refluxed for 1 hr. in an atmosphere of nitrogen, and then the solution was neutralized with dilute acetic acid. The precipitate was collected and esterified with diazomethane, followed by the usual acetylation (acetic anhydride and pyridine). Recrystallized from methanol, the product melted at 182°C, showing no melting point depression on admixture with the starting material.

Bisthioketal (VII) of VIa. — The saturated diketone (m. p. 184°C) (200 mg.) was allowed to react with 1 ml. each of ethanedithiol and borofluoride etherate at room temperature. After 72 hr. the reaction mixture was poured into 20 ml. of ice-cold water and extracted with ether. The ethereal extract was washed, dried and evaporated to dryness. After removal of residual ethanedithiol by steam distillation, the product was extracted with ethyl acetate and the solvent removed. Recrystallization from methanol gave needles of m. p. 178°C. Yield, 110 mg.

Found: S, 20.92. Calcd. for $C_{51}H_{48}O_4S_4$ (612.95): S, 21.32%.

Desulfuration of the Bisthioketal (VII).—*Methyl 3α-Acetoxycholanate (VIII).* — A solution of the thioketal VII (100 mg.) in 4 ml. of methanol was refluxed with Raney nickel (1 g.) for 8 hr. on a water bath. Chromatography of the product gave needles of m. p. 132°C (32 mg.). No melting point depression was observed on admixture with an authentic sample of methyl 3α-acetoxycholanate (m. p. 133°C).

Found: C, 75.02; H, 10.03. Calcd. for $C_{27}H_{44}O_4$ (432.626): C, 74.95; H, 10.25%.

Substance A. — Substance A was recrystallized from methanol or acetone-water and melted at 174°C; $\alpha_D^{29.5} = +136°$ (EtOH); λ_{max} 273 mμ; 240 mμ (ε_{max}^{EtOH} 11492, 7681). The substance in acetic acid absorbed bromine to turn dark brown in color. It was found to be resistant to catalytical hydrogenation as well as to chromic acid oxidation at room temperature. (Found: C, 65.04; H, 7.13%).

Summary

Carefully repeated experiments have shown that, contrary to Fieser's report[3], methyl 3α-acetoxy-Δ^7-cholenate and some other unsaturated bile acids (5β) listed in Table I give positive results in the selenium dioxide test. This finding was substantiated by the fact that two oxidation products of methyl 3α-acetoxy-Δ^7-cholenate were isolated, one of which was proved to be methyl 3α-acetoxy-7ξ, 15ξ-dihydroxy-$\Delta^{8(14)}$-cholenate.

It is very interesting to note that, unlike the Δ^7-steroids of the 5α-series, not only C_7-H, but C_{15}-H of the unsaturated bile acid mentioned above was oxidized with selenium dioxide to give hydroxyl groups, both of which remained without being acetylated under the experimental conditions described.

Department of Biochemistry
Tottori University School of Medicine
Yonago & Laboratory of
the Nippon Eiyô Kagaku Co.
Katsushika-ku, Tokyo

Dielectric Properties of Monohalogenobenzenes in the Microwave Region

By Hideo OKABAYASHI

(Received June 6, 1961)

The assumption of the local field plays an important rôle in the theory of the anomalous dispersion of a dielectric constant and the absorption of electric waves by a polar liquid.

Debye was the first to succeed in explaining theoretically the phenomena concerning the dielectric relaxation of polar liquids[1]. Debye's assumption for the local field explains inadequately the experimental results of dielectric constants, however. Nevertheless, the assumption of a single relaxation time seems to be at least approximately valid in the cases of many polar liquids from the experimental point of view[2].

Recently Yasumi and Komooka have derived a formula of the local field in liquids[3]. Applying the formula, they have shown that the validity of the assumption of a single relaxation time is justified in the case of polar liquids, which consist of molecules with a spherical shape and isotropic polarizability, and that the critical frequency ν_c is related to the relaxation time τ as follows:

$$2\pi\nu_c\tau=1$$

Thereafter, the formula for the local field has been extended to the case of liquids which consist of molecules with a ellipsoidal shape and anisotropic polarizability, and the formula for the static dielectric constant[4] and that for the Kerr constant of pure liquid[5] have been

1) P. Debye, "Polare Molekeln", Hirzel, Leipzig (1929).
2) F. H. Müller, *Ergeb. exakt. Naturw.*, **17**, 164 (1938); A. Schallachmach, *Trans. Faraday Soc.*, **42A**, 180 (1946); C. H. Collie, J. B. Hasted and D. M. Ritson, *Proc. Phys. Soc.*, **60**, 145 (1948); J. B. Hasted, G. H. Haggis and P. Hutton, *Trans. Faraday Soc.*, **47**, 577 (1951); G. H. Haggis, J. B. Hasted and T. J. Buchanan, *J. Chem. Phys.*, **20**, 1452 (1952); J. A. Saxton, *Proc. Roy. Soc.*, **A213**, 473 (1952).
3) M. Yasumi and H. Komooka, This Bulletin, **29**, 407 (1956).
4) M. Yasumi, H. Okabayashi and H. Komooka, ibid., **31**, 402 (1958).
5) H. Okabayashi, ibid., **34**, 1010 (1961).

derived. In the cases of liquid chloro-, bromo- and iodo-benzene, these formulae explain the experimental facts fairly well.

In the present work, the complex dielectric constants of liquid monohalogenobenzenes are measured in the microwave region; the paper's results are discussed on the basis of the formula of the local field derived by Yasumi and Komooka. The free wave method developed by Yasumi[6] and the waveguide method of Surber[7] are used.

Materials

Chloro- and bromo-benzene were fractionally distilled.

Iodobenzene was three times vacuum distilled.

	B. p., °C
Chlorobenzene	130.9
Bromobenzene	155.3
Iodobenzene	42.8 under the pressure of 3 mmHg.

Experimental

Free Wave Method. — This method has been theoretically developed in detail by Yasumi[6], and in his laboratory the dielectric properties of various liquids have been investigated in the microwave region[8-11].

In this work, the dielectric constant and the loss factor of halogenobenzenes were measured by the free wave method at the wavelength of 1.38 cm. The apparatus has been reported on in detail in a previous paper[11].

If R^2 is denoted as the reflection coefficient of a system consisting of a liquid layer of the thickness d on mercury, and λ is the wavelength of an electric wave in vacuo, the reflection coefficient is represented as follows:

$$R_2=\frac{\sinh^2\left(2\pi k\frac{d}{\lambda}+\frac{1}{2}\ln R_{12}\right)+\cos^2\left(2\pi n\frac{d}{\lambda}-\frac{\gamma}{2}\right)}{\sinh^2\left(2\pi k\frac{d}{\lambda}-\frac{1}{2}\ln R_{12}\right)+\cos^2\left(2\pi n\frac{d}{\lambda}+\frac{\gamma}{2}\right)} \tag{1}$$

in which n and k are the refractive index and the absorption coefficient of the liquid respectively, and, further, R_{12} and γ are expressed as

$$R_{12}^2=\frac{(n-1)^2+k^2}{(n+1)^2+k^2},\qquad \tan\gamma=\frac{2k}{n^2-1+k^2} \tag{2}$$

The real part ε' and the imaginary part ε'' of the complex dielectric constant are related to n and k in the following manner:

$$\varepsilon'=n^2-k^2,\qquad \varepsilon''=2nk \tag{3}$$

The values of ε' and ε'' can be determined from the observed curve of R versus d/λ by the same way as described in the previous paper[11].

The observed values of R at different thicknesses of the liquid layer of chlorobenzene (at $t=13$°C and $\lambda=1.38$ cm.) are shown in Fig. 1, together with the calculated curve for the determined values of n and k.

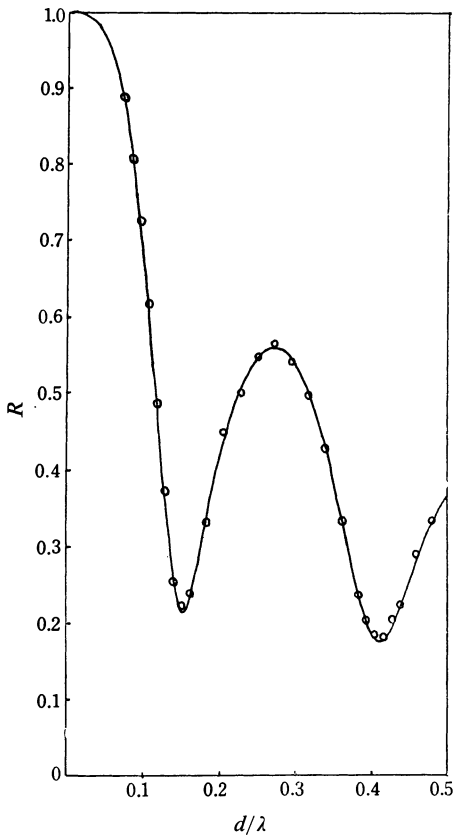


Fig. 1. The square root of the reflection coefficient of the chlorobenzene layer of the thickness d/λ measured at 13°C and the wavelength of 1.38 cm. and the calculated curve corresponding to $n=1.86$ and $k=0.36$.

The errors of ε' and ε'' are probably within ±1.5 and ±2.5% respectively.

Waveguide Method.—The dielectric constant and the loss factor at the wavelengths of 3.30 and 4.35 cm. were measured by means of the waveguide method. Each apparatus was similar to the one used by Crouch[12], by Smyth[13], or by Koizumi[14]. A block diagram of the apparatus is shown in Fig. 2.

The directional coupler picks up the reflected wave from the liquid-filled waveguide cell. The reflected power P corresponding to a liquid layer of the thickness d can be known by the detector

6) M. Yasumi, ibid., **24**, 53 (1951).
7) W. H. Surber, *J. Appl. Phys.*, **19**, 541 (1948).
8) M. Yasumi, K. Nukazawa and S. Mizushima, This Bulletin, **24**, 60 (1951).
9) M. Yasumi, H. Okabayashi, M. Shirai and S. Mizushima, *J. Chem. Phys.*, **19**, 978 (1951).
10) M. Yasumi, M. Shirai and S. Mizushima, This Bulletin, **25**, 133 (1952).
11) H. Okabayashi, ibid., **28**, 312 (1955).
12) G. E. Crouch, *J. Chem. Phys.*, **16**, 364 (1948).
13) H. L. Lacquer and C. P. Smyth, *J. Am. Chem. Soc.*, 70, 4097 (1948).
14) N. Koizumi, *J. Chem. Phys.*, **27**, 625 (1957).

TABLE I. THE OBSERVED VALUE OF P/P_∞ FOR LIQUID BROMOBENZENE LAYER OF THE THICKNESS d/λ ($t=25°C$ AND $\lambda=3.29$ cm.) AND THE CALCULATED VALUE CORRESPONDING TO $n_w=1.898$ AND $k_w=0.363$

d/λ	$(P/P_\infty)_{obs}$	$(P/P_\infty)_{calcd}$	d/λ	$(P/P_\infty)_{obs}$	$(P/P_\infty)_{calcd}$
0.0169	2.094	2.215	0.4172	1.504	1.501
0.0206	1.967	2.064	0.4233	1.475	1.471
0.0254	1.882	1.961	0.4263	1.457	1.453
0.0290	1.863	1.932	0.4293	1.437	1.434
0.0339	1.878	1.936			
0.0393	1.927	1.978	0.5019	0.800	0.805
0.0454	2.012	2.052	0.5049	0.785	0.788
			0.5079	0.770	0.774
0.0877	2.626	2.624	0.5110	0.756	0.760
0.0937	2.689	2.683	0.5140	0.745	0.749
0.0998	2.744	2.735	0.5176	0.734	0.739
0.1058	2.789	2.778	0.5212	0.726	0.731
0.1119	2.822	2.814	0.5249	0.722	0.726
0.1191	2.852	2.846	0.5285	0.721	0.724
0.1246	2.864	2.861	0.5321	0.722	0.724
0.1300	2.870	2.869	0.5358	0.724	0.727
0.1355	2.870	2.869	0.5412	0.731	0.736
0.1409	2.864	2.859	0.5472	0.747	0.751
0.1482	2.834	2.831	0.5533	0.770	0.772
0.1542	2.798	2.794	0.5593	0.793	0.796
0.1602	2.744	2.743			
0.1633	2.714	2.710	0.6259	1.108	1.106
0.1663	2.671	2.671	0.6349	1.132	1.130
			0.6398	1.143	1.140
0.2540	0.297	0.295	0.6446	1.150	1.148
0.2558	0.272	0.272	0.6513	1.157	1.156
0.2576	0.251	0.252	0.6567	1.161	1.159
0.2594	0.236	0.235	0.6603	1.161	1.160
0.2618	0.219	0.218	0.6658	1.161	1.159
0.2643	0.207	0.207	0.6718	1.157	1.155
0.2673	0.203	0.202	0.6773	1.149	1.149
0.2691	0.204	0.203	0.6833	1.139	1.140
0.2721	0.212	0.211	0.6894	1.128	1.128
0.2739	0.220	0.219	0.6954	1.114	1.115
0.2757	0.231	0.230			
0.2782	0.248	0.249	0.7649	0.935	0.937
0.2812	0.278	0.277	0.7698	0.928	0.930
0.2842	0.312	0.310	0.7746	0.922	0.924
			0.7819	0.914	0.918
0.3628	1.418	1.413	0.7891	0.913	0.915
0.3689	1.462	1.456	0.7940	0.913	0.915
0.3779	1.513	1.505	0.7988	0.915	0.916
0.3828	1.529	1.523	0.8042	0.917	0.918
0.3882	1.543	1.537	0.8103	0.920	0.922
0.3955	1.548	1.545	0.8163	0.927	0.928
0.4009	1.545	1.544	0.8194	0.929	0.931
0.4088	1.533	1.530	0.8224	0.932	0.935
0.4112	1.526	1.523			

system. When the thickness of the layer is changed, P is also changed, and the curve, P versus d/λ, is obtained. By an analysis of the curve thus obtained, the values of ε' and ε'' of the liquid can be determined.

Reflex klystrons of the types Raytheon RK5976 and Raytheon 2K25 were used as the oscillator tubes at the wavelengths of 4.35 and 3.30 cm. respectively.

The plunger in the liquid-filled waveguide is of the open circuit-terminated type and is constructed of a teflon block whose length is a quarter of the

TABLE II. THE OBSERVED VALUE OF P/P_∞ FOR LIQUID IODOBENZENE LAYER OF THE THICKNESS d/λ (t=25°C AND λ=4.347 cm.) AND THE CALCULATED VALUE CORRESPONDING TO n_w=1.794 AND k_w=0.259

d/λ	$(P/P_\infty)_{obs}$	$(P/P_\infty)_{calcd}$	d/λ	$(P/P_\infty)_{obs}$	$(P/P_\infty)_{calcd}$
0.0242	3.554	3.566	0.4264	2.183	2.185
0.0260	3.489	3.500	0.4307	2.172	2.172
0.0292	3.396	3.413	0.4344	2.153	2.156
0.0320	3.352	3.358	0.4455	2.069	2.078
0.0348	3.320	3.325	0.4574	1.948	1.949
0.0366	3.309	3.312	0.4666	1.814	1.818
0.0421	3.302	3.303			
0.0439	3.309	3.309	0.5471	0.464	0.460
0.0458	3.316	3.318	0.5526	0.431	0.430
0.0508	3.356	3.358	0.5567	0.418	0.417
0.0550	3.403	3.403	0.5604	0.413	0.412
0.0596	3.453	3.458	0.5641	0.412	0.414
0.0642	3.514	3.520	0.5673	0.417	0.419
			0.5705	0.426	0.429
0.1037	4.020	4.009	0.5769	0.458	0.461
0.1079	4.061	4.047	0.5815	0.490	0.492
0.1125	4.093	4.084	0.5861	0.526	0.529
0.1171	4.124	4.116	0.5907	0.566	0.571
0.1207	4.142	4.137			
0.1244	4.161	4.156	0.6620	1.321	1.322
0.1276	4.179	4.170	0.6730	1.392	1.388
0.1304	4.188	4.179	0.6795	1.420	1.411
0.1373	4.197	4.192	0.6850	1.433	1.434
0.1428	4.192	4.192	0.6892	1.446	1.444
0.1493	4.174	4.179	0.6947	1.452	1.451
0.1539	4.156	4.159	0.6961	1.454	1.451
0.1585	4.133	4.131	0.7002	1.454	1.453
0.1631	4.097	4.094	0.7057	1.452	1.449
0.1677	4.043	4.041	0.7099	1.443	1.444
			0.7149	1.433	1.431
0.2757	0.072	0.070	0.7241	1.402	1.398
0.2776	0.044	0.045	0.7310	1.368	1.365
0.2803	0.015	0.019	0.7402	1.311	1.311
0.2831	0.001	0.004			
0.2854	0.000	0.0006	0.8115	0.809	0.804
0.2886	0.008	0.008	0.8207	0.774	0.770
0.2927	0.035	0.037	0.8276	0.753	0.752
0.2964	0.078	0.079	0.8313	0.750	0.746
0.3010	0.154	0.151	0.8345	0.744	0.742
			0.8372	0.743	0.741
0.3838	1.960	1.968	0.8428	0.741	0.742
0.3953	2.083	2.088	0.8487	0.748	0.747
0.4031	2.142	2.144	0.8552	0.759	0.758
0.4082	2.167	2.169	0.8621	0.776	0.777
0.4123	2.183	2.183	0.8713	0.808	0.809
0.4183	2.192	2.192			

wavelength in the teflon-filled waveguide. The mica sheet of the thickness of about 3/100 mm. is inserted between the liquid cell and the waveguide connected to it in order to separate them. Two attenuators decrease the power level of the wave, which propagates towards the sample, about 30 db in order to loose the coupling between the klystron oscillator and the waveguide cell, because the reflection coefficient of the liquid-filled cell varies from unity to zoro.

The temperature of the liquid sample was controlled by water which circulated in the jacket surrounding the waveguide system and the thermostat, the fluctuation of the temperature was within ±0.1°C.

Before the liquid sample was poured into the

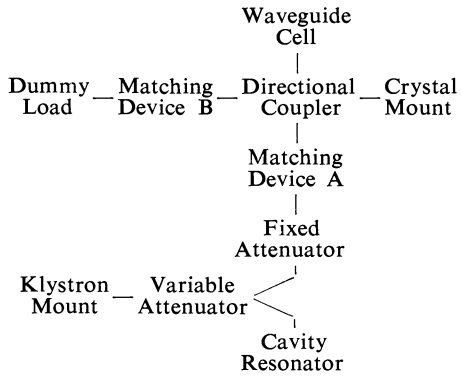


Fig. 2. The block diagram of the apparatus by the waveguide method.

waveguide cell, the following adjustments were made: After the movable dummy load of about 1.01 V. S. W. R. was inserted instead of the plunger in the waveguide cell, the matching device B (see Fig. 2) was adjusted so as to minimize the variation in the reading of the detector when the position of the dummy load was changed. After the plunger was set up in the waveguide cell, the matching device A (see Fig. 2) was adjusted so as to minimize the variation in the reading of the detector when the position of the plunger was changed.

If the effect of the mica sheet can be ignored, the reflection coefficient R_w^2 of the liquid layer in the waveguide cell has the following expression*1:

$$R_w^2=\frac{\sinh^2\left(2\pi k_w\frac{d}{\lambda}+\frac{1}{2}\ln R_{w12}\right)+\sin^2\left(2\pi n_w\frac{d}{\lambda}-\frac{\gamma_w}{2}\right)}{\sinh^2\left(2\pi k_w\frac{d}{\lambda}-\frac{1}{2}\ln R_{w12}\right)+\sin^2\left(2\pi n_w\frac{d}{\lambda}+\frac{\gamma_w}{2}\right)} \quad (4)$$

In this case R_{w12} and γ_w are related to n_w and k_w as follows:

$$R_{w12}^2=\frac{(n_w-n_{w1})^2+k_w^2}{(n_w+n_{w1})^2+k_w^2}$$

$$\tan\gamma_w=\frac{2n_{w1}k_w}{n_w^2-n_{w1}^2+k_w^2}$$

$$n_{w1}=\left\{1-\left(\frac{\lambda}{\lambda_c}\right)^2\right\}^{1/2} \quad (5)$$

in which λ_c is the cut-off wavelength characteristic of the waveguide. ε' and ε'' have the following relationship to n_w and k_w:

$$\varepsilon'=n_w^2-k_w^2+(\lambda/\lambda_c)^2,\quad \varepsilon''=2n_wk_w \quad (6)$$

If the reading of the detector system of the apparatus is proportional to the square of the field strength, it is also proportional to the reflection coefficient of the liquid layer in the waveguide. As the standard of the power, the power P_∞ for the liquid layer of infinite thickness is taken.

In this work, the values of n_w and k_w, and therefore ε' and ε'', were determined in the following way: Near the maximum and minimum points of the curve, P/P_∞ versus d/λ, the values of the power P were measured at short intervals. In Tables I and II some examples of the observed values of P/P_∞ are shown. The value of n_w was determined roughly from the separations of the maximum points. Next, the value of k_w was roughly determined from the values of P/P_∞ at the maximum points. Finally, the values of n_w and k_w were chosen in order to fit the observed values of P/P_∞ at different thicknesses of the liquid layer in the waveguide.

Various factors may contribute to the experimental error. One of the sources of error may be the disturbance of the wave by the mica sheet. This sheet forms a multiple layer with the liquid layer and the teflon-block in the waveguide*2. The effect can be checked by the theoretical calculation of the reflection coefficient of a multiple layer placed on a metal. The theoretical calculation shows that the effect of the mica sheet is negligible at the present stage of the accuracy.

When the values of n_w and k_w were determined, the value of P/P_∞ at the first minimum point was not taken into account*3.

Table III. Dielectric properties of some halogenobenzenes observed by the free wave method

Substance	Temp. °C	λ cm.	n	k	ε'	ε''
Chlorobenzene	26	3.24[1)]	2.18	0.33	4.64	1.44
	14	3.24[1)]	2.16	0.365	4.54	1.58
	13	1.38	1.86	0.36	3.33	1.34
Bromobenzene	23	1.39	1.75_5	0.28_5	3.00	1.00

1) M. Yasumi and M. Shirai, to be published.

Table IV. Dielectric properties of some halogenobenzenes observed by the waveguide method*

Substance	Temp. °C	λ cm.	n_w	k_w	ε'	ε''
Chlorobenzene	25	3.295	2.06_5	0.345	4.66	1.43
		4.347	2.16_4	0.287	4.99	1.24
	40	3.295	2.06_4	0.297	4.69	1.22
		4.347	2.14_2	0.242	4.92	1.04
Bromobenzene	25	3.295	1.89_8	0.363	3.99	1.38
		4.347	2.01_6	0.328	4.35	1.32
	40	3.295	1.92_0	0.332	4.09	1.27
		4.347	2.02_5	0.288	4.41	1.17
Iodobenzene	25	3.295	1.68_5	0.253	3.29	0.85
		4.347	1.79_4	0.259	3.54	0.93

* The values of λ_c for the apparatus at the wavelengths of 3.295 and 4.347 cm. are 4.58_0 and 6.97_0 cm. respectively.

*1 Yasumi's theoretical treatment concerning the free wave method can be conveniently applied to the waveguide method with a few modifications. For example, n_w and k_w in this case correspond to n and k, and the refractive index of vacuum (which is unity) should be replaced by $n_{w1}(\neq 1)$. ε'' is related to n_w and k_w by Eq. 6.

*2 The length of the teflon block is a quarter of the wavelength in the teflon-filled waveguide. In this work the samples with high absorption coefficients were tested. Therefore, the error due to the teflon block seems to be negligible.

*3 The details will be reported on elsewhere.

The errors of ε' and ε'' were within $\pm 1\%$.

The obtained values of ε' and ε'' of liquid monohalogenobenzenes are tabulated in Tables III and IV. On the other hand, Yasumi and Shirai have measured the complex dielectric constant of liquid chlorobenzene by the free wave method at the wavelength of 3.24 cm. These values are shown in Table III for comparison. The results by the waveguide method shows an fair agreement with those obtained by the free wave method.

Theoretical Discussion

A molecule of monohalogenobenzene is rigid, and each principal axis of its polarizability ellipsoid coincides with each of the principal axes of the molecular ellipsoid. In such a case, the component of the local field $\vec{F}$ has the following expression[4]:

$$\left.\begin{aligned} F_i &= \left(1-\frac{\varphi_i\alpha_i}{v}\right)^{-1}\left(E_i e^{i\omega t}+\frac{\varphi_i\mu_{0i}}{v}\right) \\ &= \gamma_i\left(E_i e^{i\omega t}+\frac{\varphi_i\mu_{0i}}{v}\right) \\ \varphi_i &= 2\pi a_1 a_2 a_3 \\ &\quad \times\int_0^\infty \frac{du}{(a_i^2+u)\sqrt{(a_1^2+u)(a_2^2+u)(a_3^2+u)}} \end{aligned}\right\} \quad (7)$$

in which $\vec{E}e^{i\omega t}$ is the field strength in the medium, ω is the angular frequency of an applied field, $\vec{\mu}_0$ is the permanent dipole moment. α_i is the principal component of the polarizability tensor along the principal axis of the molecular ellipsoid, v is molecular volume, and $2a_i$ is the length of the principal axis of the molecular ellipsoid.

Perrin[15] treated the dielectric relaxation of a polar liquid consisting of ellipsoidal molecules from the point of view of hydrodynamics, and derived a partial differential equation which determines the distribution function of dipole orientation. The equation of Perrin will be applied to Eq. 7.

If the potential energy of a dipole under the influence of the electric field is denoted by U, we have

$$U=-\left(\frac{1}{2}\sum \alpha_i F_i^2+\sum \mu_{0i}F_i\right) \quad (8)$$

If only the term proportional to E is retained, the torques L_i about each principal axis of the molecular ellipsoid have the following expressions:

$$\left.\begin{aligned} L_1 &= Ee^{i\omega t}(\mu_{02}\gamma_2^2\zeta_3-\mu_{03}\gamma_3^2\zeta_2) \\ L_2 &= Ee^{i\omega t}(\mu_{03}\gamma_3^2\zeta_1-\mu_{01}\gamma_1^2\zeta_3) \\ L_3 &= Ee^{i\omega t}(\mu_{01}\gamma_1^2\zeta_2-\mu_{02}\gamma_2^2\zeta_1) \end{aligned}\right\} \quad (9)$$

15) F. Perrin, *J. phys.*, 5, 497 (1934).

in which ζ_1, ζ_2 and ζ_3 are the direction cosines of the electric field $\vec{E}$ with respect to the principal axes of molecular ellipsoid respectively.

Inserting Eqs. 9 into Perrin's equation, we have the following expression of the probability function f as the approximate solution of the differential equation:

$$f=f_0+f_0\frac{Ee^{i\omega t}}{kT}\sum\frac{\mu_{0i}\gamma_i^2}{1+i\omega\tau_i}\zeta_i \quad (10)$$

f_0 denotes the distribution function when no electric field is applied. τ_i is the relaxation time and is related to the viscosity coefficient of liquid η as follows:

$$\left.\begin{aligned} \tau_i &= \frac{C_{jk}}{2kT} \\ \frac{2}{C_{jk}} &= \frac{1}{C_j}+\frac{1}{C_k} \\ C_i &= \frac{32\pi^2}{3}a_1a_2a_3\frac{\left(\frac{a_j}{a_1}\right)^2+\left(\frac{a_k}{a_1}\right)^2}{\left(\frac{a_j}{a_1}\right)^2\varphi_j+\left(\frac{a_k}{a_1}\right)^2\varphi_k}\eta \end{aligned}\right\} \quad (11)$$

The total electric moment of the molecule $\vec{\mu}$ is the sum of the permanent dipole moment and the induced dipole moment.

$$\mu_i=\mu_{0i}+\alpha_i F_i \quad (12)$$

If the component of $\vec{\mu}$ along the direction $\vec{E}$ is denoted by μ_E, and the statistical mean value of μ_E is denoted by $\langle\mu_E\rangle$, we have

$$\mu_E=\sum\mu_i\frac{E_i}{E}=\sum\gamma_i(\alpha_i Ee^{i\omega t}+\mu_{0i})\frac{E_i}{E} \quad (13)$$

and

$$\langle\mu_E\rangle=\frac{\int f\mu_E\,d\Omega}{\int f\,d\Omega} \quad (14)$$

in which $d\Omega$ is an elementary solid angle.

Inserting Eqs. 10 and 13 into Eq. 14, we have

$$\langle\mu_E\rangle=\left(\frac{\sum\alpha_i\gamma_i}{3}+\frac{1}{3kT}\sum\frac{\mu_{0i}\gamma_i^3}{1+i\omega\tau_i}\right)Ee^{i\omega t} \quad (15)$$

The complex dielectric constant ε is related to $\langle\mu_E\rangle$ by the following equation:

$$(\varepsilon-1)Ee^{i\omega t}=4\pi N_c\langle\mu_E\rangle \quad (16)$$

in which N_c is the number of molecules in a unit volume.

Accordingly, the dielectric constant ε' and the loss factor ε'' have the following expressions:

$$\left.\begin{aligned}\varepsilon' &= \varepsilon_\infty + \frac{4\pi N_c}{3kT}\sum \frac{\mu_{0i}^2\gamma_i^3}{1+\omega^2\tau_i^2}\\ \varepsilon'' &= \frac{4\pi N_c}{3kT}\sum \frac{\mu_{0i}^2\gamma_i^3}{1+\omega^2\tau_i^2}\omega\tau_i\\ \varepsilon_\infty &= 1+4\pi N_c\sum\frac{\alpha_i\gamma_i}{3}\end{aligned}\right\} \quad (17)$$

Equations 17 show that generally there are three relaxation times.

If the direction of the permanent dipole moment coincides with one of the principal axes of the molecular ellipsoid, the Eqs. 17 are simplified as follows:

$$\left.\begin{aligned}\varepsilon' &= \varepsilon_\infty + \frac{\varepsilon_0-\varepsilon_\infty}{1+\omega^2\tau^2}\\ \varepsilon'' &= \frac{\varepsilon_0-\varepsilon_\infty}{1+\omega^2\tau^2}\omega\tau\end{aligned}\right\} \quad (18)$$

in which ε_0 is the static dielectric constant of a polar liquid. It is assumed that the polarizability is independent of frequency.

In Tables V and VI the values of ε_∞ and τ obtained from the experimental values of the complex dielectric constant are tabulated, together with the value of the static dielectric constant ε_0 and that of the square of the refractive index n_D^2.

In Table VII the values of ε_∞ evaluated from the sum of the electronic polarization P_E and the atomic polarization P_A are tabulated. It is assumed that the Lorentz-Lorenz law is valid.

The values of ε_∞ evaluated from the experimental values of ε' and ε'' at different wavelengths coincide with each other within the limits of experimental error.

Yasumi, Shirai and Mizushima[10] hava measured the dielectric constant and the loss factor of liquid aliphatic alcohols at the wavelength of 3.24 cm. and have shown that the value of ε_∞ evaluated according to Eqs. 18 is considerably larger than the square of the refractive index for the sodium D line (n_D^2). This interesting result has been confirmed by the measurements at the wavelength of 1.38 cm.[11]

Table V. The values of ε_∞ and τ of halogenobenzenes evaluated from the experimental values of ε' and ε'' by the free wave method

Substance	Temp. °C	λ cm.	ε_0	n_D^2	ε_∞	$\tau\times10^{11}$ sec.
Chlorobenzene	26[1]	3.24	5.61[2]	2.32	2.50±0.15	1.16
	14[1]	3.24	5.86[2]	2.33	2.65±0.10	1.44
	13	1.38	5.89[2]	2.33	2.63±0.08	1.40
Bromobenzene	23	1.39	5.42[2]	2.43	2.59±0.07	1.80

1) M. Yasumi and M. Shirai, to be published.
2) W. A. Hestone, E. T. Hennelly and C. P. Smyth, *J. Am. Chem. Soc.*, **72**, 207(1950).

Table VI. The values of ε_∞ and τ of halogenobenzene evaluated from the experimental values of ε' and ε'' by the waveguide method

Substance	Temp. °C	λ cm.	ε_0	n_D^2	ε_∞	$\tau\times10^{11}$ sec.
Chlorobenzene	5[1]	3.25	6.06[2]	2.35	2.59±0.05	1.62
	25	3.30	5.63[2]	2.32	2.55±0.10	1.19
		4.35			2.6 ±0.2	1.19
	40	3.30	5.31[2]	2.29	2.3 ±0.2	0.89
		4.35			2.2 ±0.3	0.84
Bromobenzene	5[1]	3.25	5.68[2]	2.46	2.69±0.04	2.37
	25	3.30	5.39[2]	2.43	2.63±0.03	1.77
		4.35			2.67±0.06	1.81
	40	3.30	5.18[2]	2.40	2.61±0.05	1.51
		4.35			2.63±0.09	1.52
Iodobenzene	25	3.30	4.62[3]	2.62	2.75±0.03	2.75
		4.35			2.74±0.03	2.68

1) T. Kato and H. Okabayashi, to be published.
2) W. A. Hestone, E. T. Hennelly and C. P. Smyth, *J. Am. Chem. Soc.*, **72**, 207(1950).
3) A. Audsley and F. R. Goss, *J. Chem. Soc.*, **1942**, 497; C. R. K. Murty, *J. Sci. Ind. Research (India)*, **18B**, 268 (1959).

Table VII. The values of ε_∞ at 25°C evaluated from the value of (P_E+P_A)

Substance	(P_E+P_A)[1] cc.	ε_∞
Chlorobenzene	34.9	2.56
Bromobenzene	35.6	2.53
Iodobenzene	41.4	2.76

1) C. G. Le Fèvre and R. J. W. Le Fèvre, *J. Chem. Soc.*, **1954**, 1577.

However, in the case of liquid monohalogenobenzene the value of ε_∞ is much closer to the value of n_D^2 and, moreover, is almost equal to the value ε_∞ evaluated from the value of (P_E+P_A).

From Tables V and VI the validity of Eqs. 18 seems to be justified in the cases of liquid monohalogenobenzenes; i. e. the dielectric relaxation is explained by the single relaxation time, and ε_∞ in Eqs. 18 has a value almost the same as the value of n_D^2.

According to Fqs. 11, the effective volume of a molecule v_e for the molecular rotation can be evaluated from the observed relaxation time if the ratios of the lengths of the principal axes of the molecular ellipsoid are known. In Table VIII the values of the effective volume v_e of the molecules at 25°C are shown, together with those of the volume $v_{(van\ der\ Waals)}$ of the molecular ellipsoid (the model which is assumed in order to determine the axial ratios). Also, the values of the molecular volume v

TABLE VIII. THE EFFECTIVE VOLUME v_e OF A MOLECULE, THE VOLUME $v_{(van\ der\ Waals)}$ OF THE ASSUMED MOLECULAR ELLIPSOID AND THE MOLECULAR VOLUME v EVALUATED FROM THE MOLAR VOLUME AT 25°C

Substance	Chlorobenzene	Bromobenzene	Iodobenzene
$\tau \times 10^{11}$, sec.	1.19	1.79	2.72
Assumed axial ratio	1 : 0.77 : 0.43	1 : 0.75 : 0.45	1 : 0.69 : 0.45
$\eta \times 10^3$ (poise)[1]	7.53	10.8	15.3
v_e, Å^3	15.1	15.7	17.4
$v_{(van\ der\ Waals)}$, Å^3	107	117	135
v, Å^3	170	175	186
$v_e/v_{(van\ der\ Waals)}$	0.141	0.133	0.131
v_e/v	0.089	0.090	0.094

1) K. Shiba, "Butsuri Jōsūhyō", Iwanami-shoten (1947).

evaluated from the molar volume are shown for reference.

The value of v_e is only about 13% of the value of $v_{(van\ der\ Waals)}$. The reason why the value of v_e is so small is obscure as yet.

Summary

The dielectric constants and the loss factors of liquid monohalogenobenzenes were measured in the microwave region by the free wave method and the waveguide method. The experimental results were discussed on the basis of the formula of the local field previously proposed. In the cases of liquid monohalogenobenzenes, the experimental facts can be explained by a single relaxation time.

The author is grateful to Professor Masasi Yasumi for his kind guidance and encouragement throughout this work, and to Dr. Naokazu Koizumi, Dr. Michiro Shirai and Mr. Hitoshi Komooka for their advice. The author also wishes to thank Mr. Taketoshi Kato, who assisted the author in the experiment at the wavelength of 3.30 cm., and Mr. Yasuhiro Kawanishi, who prepared the samples used in these experiments.

The present work has been supported partly by the Scientific Research Grant from the Ministry of Education.

Aeronautical Research Institute
The University of Tokyo
Meguro-ku, Tokyo

SHORT COMMUNICATIONS

Polycondensation of Tripeptide with Bis-o-phenylene Pyrophosphite

By Toshiyuki FURUYAMA[1], Shumpei SAKAKIBARA and Shiro AKABORI

(Received November 20, 1961)

Many attempts to prepare high molecular polypeptides, in which amino acid residues were arranged in a regular order, have been made thus far[2-10]. These methods will be divided into two types. The one is the use of peptide derivative, e. g. peptide ester, *N*-carbothiophenylpeptide, as a monomer[2-7,9], and the other is the use of free peptide in the presence of the reagents which form peptide linkage, such as dicyclohexyl carbodiimide[8], tetraethyl pyrophosphite[9], or phosphorus pentoxide[10]. Among them, the carbothiophenyl method[7] and the tetraethyl pyrophosphite method[9] gave rather favorable results.

The present authors found a very handy procedure for the polycondensation of oligopeptides by the aid of bis-*o*-phenylene pyrophosphite. The present reagent was used previously for the peptide bond formation between acylamino acids and amino acid esters by Crofts et al.[11] In the present communication, polycondensation of L-leucylglycylglycine is described. Bis-*o*-phenylene pyrophosphite[12] resembles tetraethyl pyrophosphite[13] in the chemical nature, but the synthesis of the former reagent was much easier than that of the latter.

L-Leucylglycylglycine (m. p. 215~216°C with decomp. Found: C, 49.08; H, 7.96; N, 17.06. Calcd. for $C_{10}H_{19}O_4N_3$: C, 48.96; H, 7.81; N, 17.13%.) was synthesized from carbobenzoxy-L-leucine and glycylglycine ethyl ester by the use of isobutyl chloroformate, subsequent saponification and catalytic hydrogenation. Bis-*o*-phenylene pyrophosphite was synthesized according to the method of Crofts et al.[12]

A mixture of 1 g. of L-leucylglycylglycine, 1.2 g. of bis-*o*-phenylene pyrophosphite (an equimolar ratio) and 6 ml. of dry pyridine was heated at 100°C for 6 hr. in a sealed tube. During the reaction, the solution gradually gelled and became pale yellow. After the reaction completed, the product was poured into a flask containing 30 ml. of water. Then pyridine and water were removed in vacuo. The residues were dissolved in a small amount of ethanol, and an equal volume of water was added to the solution to decompose the terminal activated groups and the solvents were removed in vacuo. These procedures were repeated. An oily material remained was suspended in ethanol. Dry ether was added to the suspension and the syrupy material resulted was centrifuged off, washed several times with ethanol and ether*1, and finally dried. The weight of the dried material was 770 mg. The crude polypeptide was partly dissolved in hot dimethylformamide and precipitated by the addition of ether. In order to decompose the activated end groups completely, the precipitate was dissolved in 80% aqueous phenol*2 (5 ml.) and 1% aqueous ammonia (15 ml.) was added to the solution. The above solution was dialyzed against deionized water for 50 hr. in a cellophane tube. The precipitate obtained during dialysis was centrifuged off (fraction 1, which amounted to approximately 9% for L-leucylglycylglycine in weight) and the supernatant was lyophilized (fraction 2, which amounted to about 8%).

The polypeptide (fraction 1) was soluble in 80% aqueous phenol and 85% aqueous formic acid, and insoluble in glacial acetic acid,

1) Asahi Chemical Industry Company Fellow.
2) E. Pacsu and E. J. Wilson, Jr., *J. Org. Chem.*, **7**, 117, 126 (1942).
3) M. Z. Magee and K. Hofmann, *J. Am. Chem. Soc.*, **71**, 1515 (1949).
4) M. Winitz and J. S. Fruton, ibid., **75**, 3041 (1953).
5) T. Wieland and H. Bernhard, *Ann.*, **582**, 218 (1953).
6) R. A. Boissonas and I. Schumann, *Helv. Chim. Acta*, **35**, 2229 (1952).
7) J. Noguchi and T. Hayakawa, *J. Am. Chem. Soc.*, **76**, 2846 (1954).
8) V. Bruchner, M. Szekerke and J. Kovács, *Naturwiss.*, **43**, 107 (1956).
9) H. Kitaoka, S. Sakakibara and H. Tani, This Bulletin, **31**, 802 (1958).
10) G. Schramm and H. Wisomann, *Chem. Ber.*, **91**, 1075 (1958).
11) P. C. Crofts, J. H. H. Markes and H. N. Rydon, *J. Chem. Soc.*, **1959**, 3610.
12) P. C. Crofts, J. H. H. Markes and H. N. Rydon, ibid., **1958**, 4250.
13) G. W. Anderson, J. Blodinger and A. D. Welcher, *J. Am. Chem. Soc.*, **74**, 5309 (1952).

*1 By these procedures the syrupy material changed gradually into powder.
*2 Sometimes the precipitate can dissolve in hot dimethylformamide.

pyridine, dimethylformamide, hot ethanol, water, benzene, chloroform and ethyl acetate. Found: C, 49.30; H, 7.41; N, 16.56. Calcd. for $(C_{13}H_{17}O_3N_3 \cdot H_2O)_n$: C, 48.96; H, 7.81; N, 17.13%*3. The phosphorus content of this material was determined by the method of Allen[14], and the value of 0.99% was obtained*4.

The average molecular weight of the polypeptides, fraction 1 and fraction 2 of poly-(L-leucylglycylglycine), was determined by titrating the end carboxyl groups with sodium methoxide in dimethylformamide[15], and the values of 3220 and 1730 were obtained for the fractions 1 and 2 respectively.

The infrared absoption bands which were characteristic for polypeptides could be observed at 3290, 1660, 1540 and 1250 cm^{-1}, especially in the fraction 1.

Further investigations on this condensation reaction are now in progress and details will be presented elsewhere.

Institute for Protein Research
Osaka University
Kita-ku, Osaka

*3 On the elementary analysis, the polypeptide gave 3.78% of the incombustible material.

*4 In turn, the phosphorus content of the fraction 2 was determined in a fashion analogous to the fraction 1, and the value of 18.0% was obtained. It appeared to be probable that the phosphorus might affect the elementary analysis of C, H and N considerably. Found: C, 39.38; H, 6.88; N, 12.81%. On the analysis, the incombustible material amounted to 7.67% in weight.

14) R. J. L. Allen, *Biochem. J.*, **34**, 858 (1940).

15) M. Sela and A. Berger, *J. Am. Chem. Soc.*, **77**, 1895 (1955).

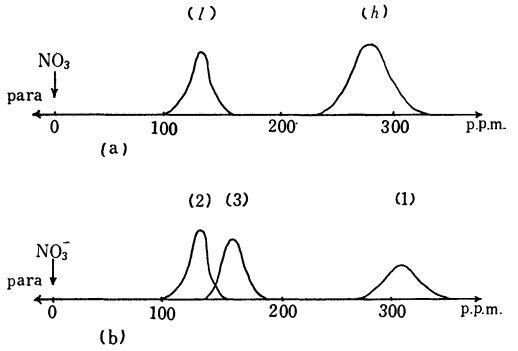


Fig. 1. NMR spectra of NaN_3 in aq. sol. (a) and $C_2H_5N_3$ (b).

Nuclear Magnetic Resonance of Azides

By Teinosuke KANDA, Yushiro SAITO and Kazutami KAWAMURA

(Received December 9, 1961)

We have measured, in a field of 16250 gauss, the chemical shift σ and the spin-lattice relaxation time T_1 of the N^{14} nuclear magnetic resonance (NMR) of the sodium azide in aqueous solution and of the ethyl azide.

As shown in Fig. 1 (a), NaN_3 gives two resonance lines. σ of the line of lower field side (*l*) is 130 p. p. m. and that of higher field side (*h*) is 280 p. p. m. where the origin of σ is resonance point of NO_3^-. The line width of *l* is narrower than that of *h* and the ratio of the absorption areas of *l* and *h* is equal to 1 : 2. As the atomic groups containing nitrogens which present in aqueous solution of NaN_3 we can cite three kinds, N_3^-, HN_3 and NaN_3, but the first is overwhelming in its quantity. The structure of the N_3^- is known to be linear[1] and so *l* must be the line of central nitrogen and *h* that of the both ends of the N_3^-. The origin of the line widths is mainly the spin-lattice relaxation and the T_1 values measured by the saturation method are 5.8 and 3.6 m. sec. for *l* and *h*, respectively.

Ethyl azide gives three lines, as shown in Fig. 1 (b), of equal intensity of which the σ's are 130, 160 and 310 p. p. m. respectively. The line widths increase in order from lower field one to higher one and their T_1 values are measured to be 4.5, 2.2 and 1.1 m. sec., respectively.

In methyl azide three nitrogen atoms are colinear and the angle CNN is 120° [1]. We expect that the ethyl azide might have the same structure as the methyl azide and we number the three nitrogen atoms 1, 2 and 3 from the carbon atom side.

The spectral position of the lowest line is just the same as the line *l* of the N_3^- and so this line is considered to arise from the central nitrogen (2). For the assignment of the other two lines, consider the electronic structures A and C given by Pauling[1],

A: $R-\ddot{N}=N^+=\ddot{N}^-:$

C: $R-\ddot{N}-N^+\equiv N:$

and calculate the number of unbalanced p-electron U_p by the method analogous to Townes and Dailey's[2]. As the atomic wave function of σ bonds we use the sp^2 hybridized orbital for nitrogen atom 1 and sp hybridized orbitals for 2 and 3.

1) L. Pauling, "The Nature of the Chemical Bond", 3rd Ed., Cornell University Press, p. 271.

In the Table I, the first and the second row show the U_p's of three N-atoms for the structure A and C respectively, and the last for the structure in which A and C are equally mixed.

TABLE I. NUMBER OF UNBALANCED p-ELECTRON OF NITROGEN ATOMS 1, 2 AND 3 OF AZIDE FOR THE STRUCTURES A AND C AND ALSO FOR THEIR EQUALLY MIXED STRUCTURE

	1	2	3
A	−2/3	0	0
C	−1/6	0	−1/2
	−5/12	0	−1/4

Since the spin-lattice relaxation is originated from the intramolecular quadrupole coupling, the inverse T_1 should be proportional to (e^2qQ^2) and hence to U_p^2. Therefore, we conclude that the line having the shortest T_1 is caused by the nitrogen atom 1 and the line having the medium T_1 by the atom 3. The assignment of three lines is indicated in Fig. 1 (b).

Several authors[3] have discussed on the NMR spectra of nitrogen. The spectra are separated into two groups; the first is the ammonia group distributing around the position $\sigma=300$ p. p. m. and the second is the nitro and CN-group around the position $\sigma=0$. It is remarkable that the azides have the lines belonging to each group. The diamagnetic shift due to *one* 1s electron or *one* 2s electron is calculated to be +120 and +17 p. p. m. respectively, and the paramagnetic shift due to *one* 2p electron to be −460 p. p. m. assuming the mean excitation energy of 5 eV. The chemical shift beyond 200 p. p. m. as displayed by the azides should be attributed to the paramagnetic shift of the 2p electron and so be proportional to U_p. But the experimental results are just in opposite direction; the line of the N-atom (1) having the largest U_p is the most diamagnetic. Such a contradiction was already found by Masuda[4] in the case of molecular chlorine compounds and the azides give the second example.

Part of this research was supported by the Scientific Research Fund granted by the Ministry of Education.

Department of Physics
Faculty of Science
Kobe University
Mikage, Kobe

2) C. H. Townes and B. P. Dailey, *J. Chem. Phys.*, **17**, 782 (1949).

3) For example, B. M. Schmidt, L. C. Brown and D. Williams, *J. Mol. Spectroscopy*, **2**, 551 (1958).

4) Y. Masuda, *J. Phys. Soc. Japan*, **11**, 670 (1956).

On the Mechanism of Pulp Bleaching. II[1]. *On the Residual Lignosulfonic Acid Existing Undissolved in Unbleached Sulfite Pulp*

By Koichiro SATO and Hiroshi MIKAWA

(Received December 19, 1960)

In order to make clear the mechanism of pulp bleaching, it is most important to know the chemical and physical nature of the residual lignin in unbleached pulp, in so far as it is the main material to be bleached. Knowledge about this residual lignin can be expected also to contribute to better understanding of the cooking mechanism of wood inasmuch as it will give information why some amount of lignin always remain undissolved in the pulp after the cooking.

Although there exist a few investigations into this lignin, not much is known as yet. Kawamura[2] prepared acetylated thiolignin from acetylated beech kraft pulp and showed that the thiolignin is chemically combined with xylose. Kratzl[3] compared the acid lignin obtained from unbleached pulp with that obtained from wood, concluding that they are at least partly identical. By nitrobenzene oxidation Bland[4] showed that there exists not much difference between the nuclear structures of the lignins in wood, in waste liquor and in unbleached pulp. Kullgren[5] extracted lignosulfonic acid from unbleached sulfite pulp by prolonged washing of the pulp and showed that the lignin thus obtained contained one carboxyl group per sulfonic acid group.

As for the reasons for the difficulty of dissolution of the total amount of lignin in the case of the sulfite process, one or several of the following reasons is conceivable.

1) Residual lignin is not sulfonated sufficiently, 2) it is firmly combined to carbohydrate, 3) it goes into solution with difficulty because of the morphological structure of its fiber, and 4) it is condensed to other lignin units during the digestion. As has been reported preliminarily before[6], we have succeeded in dissolving residual lignosulfonic acid from unbleached sulfite pulp by a drastic beating in water, which causes the fibrillation of the fiber. By this treatment any morphological hindrance to the dissolution of the lignin can be expected to be diminished. As is well known, the primary wall and the other layer of the secondary wall are said to be distructed successively by beating, while the fibrillation proceeds gradually into the middle layer of the secondary wall[7], thus enabling the dissolution of the low sulfonated residual lignosulfonic acid.

Residual lignosulfonic acid was isolated from the unbleached sulfite pulp prepared from a mixture of *Picea jezoensis* (spruce) and *Abies mariana* (fir), and the chemical nature of the isolated residual lignosulfonic acid was investigated. The isolable yield of the residual lignosulfonic acid thus obtained from the unbleached pulp is about one fifth of the total amount of lignin present in the pulp.

Experimental

Extraction of the Residual Lignosulfonic Acid.—540 g. of unbleached sulfite pulp from the mixture of *Picea jezoensis* and *Abies mariana* (Sieber Zahl 52, cuproammonium disperse viscosity (Japan Industrial Standard) 18.0 were suspended in water (21 l.) and beaten with a Niagara type 1 to 1/2 pound beater (TAPPI-Standard T200 m-45) for up to 20 hr. During the course of the beating, the SR-value, chlorine absorption[8], permanganate number (TAPPI-Standard T214m-50), specific surface area and degree of polymerization of the beaten pulp were measured and are shown by curves I, II, III, IV and V respectively in Fig. 1. The relative viscosity of the pulp was measured according to the Japan Industrial Standard, the specific outer surface area, by immersing the pulp in a solution of benzo fast scarlet 4BS and measuring the decrease of the absorption at 506 mμ[9], and the degree of polymerization, according to Okada's method[10].

Curve I shows that the SR-value approaches 100 after 10~12 hr., while the chlorine absorption (curve II) and the permanganate number (curve III) decrease monotonously. Although the SR-value reaches its maximum after 10~12 hr., the specific surface area of the fiber (curve IV) continues to increase, showing the progress of fibrillation. The degree of polymerization of the beaten pulp decreases along curve V.

1) Presented briefly in this Bulletin, **31**, 660 (1958).
2) I. Kawamura and T. Higuchi, *J. Soc. Textile Cellulose Ind. (Japan)*, **9**, 454 (1953).
3) K. Kratzl and A. Graf, *Holzforsch. u. Holzverwert*, **9**, No. 4, 60 (1957); *Chem. Abstr.*, **52**, 1604i (1958).
4) D. E. Bland and C. Stamp, *The World's Paper Trade Review*, **21**, April, 1293 (1955).
5) C. Kullgren, *Svensk Papperstidn.*, **55**, 1 (1952).
6) K. Sato, K. Ebisawa and H. Mikawa, This Bulletin, **31**, 660 (1958).
7) H. W. Emerton, *Tappi*, **40**, No. 7, 542 (1957).
8) H. Okada and E. Hayakawa, *Cellulose Chem.*, **13**, 33 (1933).
9) E. F. Thode, J. W. Bedmesderfer and A. J. Chase, *Tappi*, **35**, No. 8, 379 (1952).
10) H. Okada, *Rayon World (Japan)*, **3**, 194 (1935).

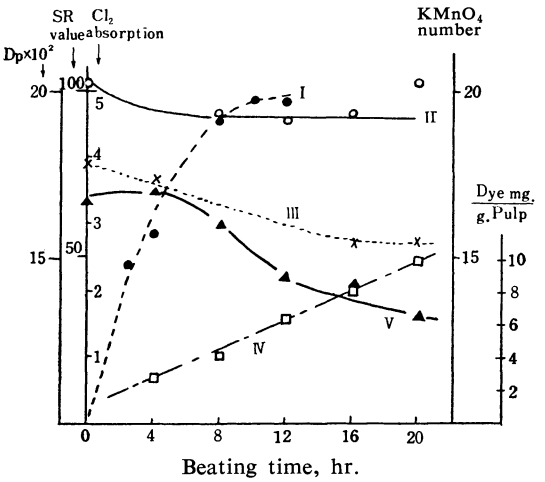


Fig. 1. Properties of the beaten unbleached sulfite pulp versus beating time. I, SR-value; II, Chlorine absorption; III, Permanganate number, IV, Specific surface; V, Degree of polymerization

The dissolution of the residual lignosulfonic acid was measured by the ultraviolet absorption spectra of the filtrate of the beaten pulp, which was diluted three times with water. Curve II in Fig. 2 shows the optical density at 280 mμ thus obtained, and curve III, the total amount of the dissolved lignosulfonic acid calculated from the optical density, assuming the molar extinction and methoxyl content of the lignosulfonic acid as 3000 and 11% respectively. As shown by curve II, the dissolved amount of lignosulfonic acid reaches its maximum at about 10~12 hr., although as stated previously the fibrillation continues to proceed even after this period of time. Curve I here is the same curve as curve I in Fig. 1.

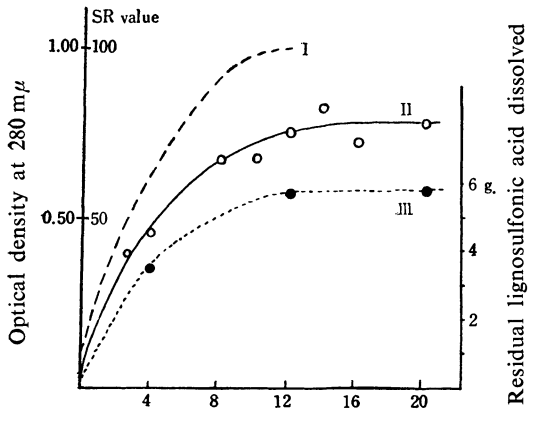


Fig. 2. Properties of beating water versus beating time. I, SR-value; II, Optical density of the beating water after being diluted three times with water; III, Calculated amount of the dissolved residual lignosulfonic acid.

After having been beaten for 20 hr., the pulp was separated by a centrifuge and washed with water, and the combined mother liquor and the washings (ca. 40 l.) were concentrated to 2 l. under 40°C in vacuo, centrifuged again in order to remove fine flocculating pulp fibers, and passed through ion exchange resin IR-120 in hydrogen form, after which the lignosulfonic acid was precipitated by adding 1-(*N*-piperidinoacetylamino)-naphthalene sulphate[11]. The precipitate was washed well with water, to which was added dilute sodium hydroxide solution until pH 8~9. After about one hour the separated free base was filtered and the filtrate passed through ion exchange resin IR-120 in hydrogen form, neutralized with barium carbonate until pH 6, centrifuged and poured into alcohol. The precipitated barium lignosulfonate was separated by centrifuge and then washed twice with alcohol, ether and petroleum ether successively. The yield was 5.5 g., which is not much less than the dissolved amount estimated from the optical density of the beating water (curve II, Fig. 2). As the total amount of the residual lignosulfonic acid contained in the pulp used is estimated as about 27.5 g., the isolated amount corresponds to about 20% of the total. The existence of no carbohydrate components in the sample was confirmed by paper chromatography after hydrolyzing the sample with 2% sulfuric acid at 100°C for 5 hr.[12] Anal. C, 45.36; H, 5.09; S, 3.73; Ba, 12.80; CH_3O, 11.12%.

Functional Groups of the Residual Lignosulfonic Acid.—As is well known, the conductometric titration curve of the lignosulfonic acid has two "breaks", the first being the completion of the neutralization of the sulfonic acid group. Richtzenhain proved[13] that lignin contains at least two types of phenolic hydroxyl groups; one is the phenolic hydroxyl group of the simple guaiacyl type (type I), and the other is that having a C–C side chain at the ortho position to the phenolic hydroxyl group of the guaiacyl type (type II). As was found by some of the present authors[14], the type I phenolic hydroxyl group was conductometrically titratable, while type II was untitratable; the second break represents the complete neutralization of the carboxyl group plus the type I phenolic hydroxyl group. It is possible to estimate the amount of both the types I and II phenolic hydroxyl groups separately by measuring the change in the $\Delta\varepsilon$-value[15] of the solution during the conductometric titration.

Barium salt of the residual lignosulfonic acid (500 mg.) was passed through ion exchange resin IR-120 in hydrogen form. The eluate was made up to 50 ml. and was titrated conductometrically with sodium hydroxide as usual (curve I, Fig. 3). The amount of sodium hydroxide consumed until the first break gives the amount of the sulfonic acid group, and that consumed between the first and the second break the amount of the carboxyl group

11) B. Leopold, *Acta Chem. Scand.*, **6**, 64 (1952).
12) H. Toda and C. Hamada, *J. Jap. TAPPI*, **12**, No. 5, 324 (1958).
13) H. Richtzenhain, *Ber.*, **83**, 488 (1950).
14) H. Mikawa, K. Sato, C. Takasaki and K. Ebisawa, This Bulletin, **29**, 245 (1956).
15) G. A. Erdtman, *Svensk Papperstidn*, **55**, 745 (1952).

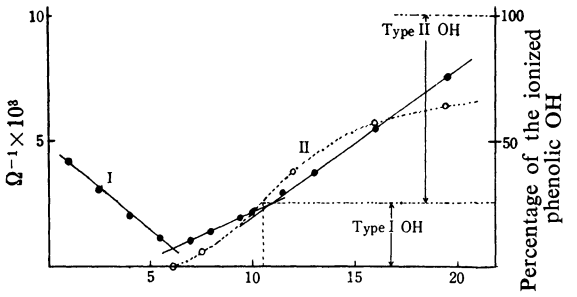


Fig. 3. Conductometric titration of the residual lignosulfonic acid. I, Conductivity; II, Ionization of phenolic hydroxyl group

plus the type I phenolic hydroxyl group. During the course of the titration the ultraviolet absorption spectra of the solution were measured by using a quartz cell 0.07 mm. thick. Curve II of Fig. 3 represents the percentage of the ionized phenolic hydroxyl group thus obtained. About 25% of the total phenolic hydroxyl group is ionized at the second break.

The amount of the type I phenolic hydroxyl group and the amount of the type II phenolic hydroxyl group were calculated separately, as was stated in a previous report[14]. Because, according to the $\Delta\varepsilon$-method of Erdtman[15], the amount of the total phenolic hydroxyl group is estimated as 0.23~0.19/CH_3O, the amount of the type I phenolic hydroxyl group is 0.06~0.05/CH_3O, that of type II, 0.17~0.14/CH_3O, and that of carboxyl group, 0.21/CH_3O. The amount of the sulfonic acid group is 0.32/CH_3O. The molecular formula of the residual lignosulfonic acid is thus expressed as follows:

$$C_9H_{10.55}O_{3.57}(CH_3O)_{0.95}(SO_3Ba/2)_{0.30}S^{neut}_{0.00}Ba^{excess}_{0.09}$$

in which $S^{neut}_{0.00}$ means non-acidic sulfur and $Ba^{excess}_{0.09}$, the amount of barium which is not combined with the sulfonic acid group.

Further Sulfonation of the Residual Lignosulfonic Acid.—As has been stated above, the degree of sulfonation of the residual lignosulfonic acid was only 0.32/CH_3O, much lower than the 0.6 of the ordinary lignosulfonic acid separated from the waste liquor. In order to know whether the residual lignosulfonic acid no longer has any sulfonatable group or if it has but remained unsulfonated during the sulfite cooking by, say, morphological reasons, further sulfonation of the residual lignosulfonic acid was attempted in a homogeneous solution.

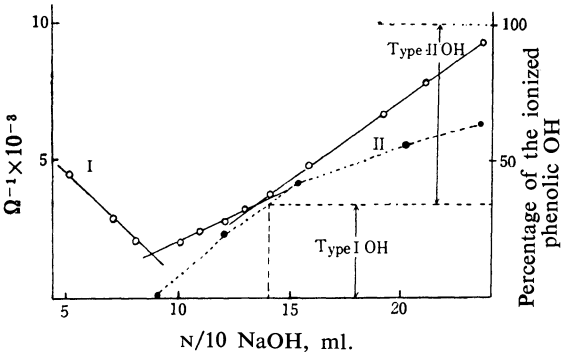


Fig. 4. Conductometric titration of the further sulfonated residual lignosulfonic acid. I, Conductivity; II, Ionization of phenolic OH

Residual lignosulfonic acid (2 g.) was dissolved in a cooking liquor of pH 1.8 (60 ml.) prepared from 5% sodium hydroxide solution and sulfur dioxide and heated at 135°C for 9 hr. The sulfonic acid was separated with 1-(*N*-piperidinoacetylamino)-naphthalene as usual and was obtained as barium salt. Anal. C, 39.92; H, 4.80; S, 5.28; Ba, 15.14; CH_3O, 10.30%. Total phenolic hydroxyl group, 0.24~0.19/CH_3O; type I phenolic hydroxyl group, 0.08~0.07/CH_3O; type II phenolic hydroxyl group, 0.16~0.12/CH_3O; carboxyl group, 0.26~0.25/CH_3O; SO_3H, 0.49/CH_3O. The molecular formula is as follows:

$$C_9H_{11.4}O_{4.08}(CH_3O)_{1.00}(SO_3Ba/2)_{0.49}S^{neut}_{0.01}Ba^{excess}_{0.08}$$

Discussion

The fact that the residual lignosulfonic acid in the unbleached sulfite pulp was at least partly dissolved out by drastic beating of the fiber in water seems to support strongly the thesis that this part of residual lignosulfonic acid remained undissolved in the fiber during the cooking because of morphological reasons. It is said that the residual lignin in the unbleached sulfite pulp is distributed across the whole section of the fiber, but the amount is larger near the outer surface[16] and near the inner surface around the lumen. As has been made evident in the present report, the dissolution of the residual lignosulfonic acid reaches its maximum when the SR-value of the beaten pulp reaches its maximum value of 100. Even though the outer specific surface of the fiber estimated by dye absorption continues to increase by prolonged beating, dissolution of any significant amount of the residual lignosulfonic acid was not observed any more. This fact will be well understood from the fact that during the beating process fibrillation proceeds from the surface of the fiber and that the amount of the residual lignin is comparatively larger near the outer surface of the fiber. As is shown in Table I, the residual lignosulfonic acid prepared carefully in the present paper contained no carbohydrates, although that prepared previously contained some. It seems, therefore, to be certain that there exists no chemical linkage between carbohydrates and the residual lignosulfonic acid obtained by beating.

16) G. Jayme and A. V. Köppen, *Das Papier*, **4**, 455 (1950).

TABLE I. FUNCTIONAL GROUPS OF THE RESIDUAL LIGNOSULFONIC ACID AND THE FURTHER SULFONATED PRODUCTS OBTAINED THEREFROM

C_9 basis	Sample			
	Residual lignosulfonic acid		Further sulfonated residual lignosulfonic acid	
	A	B	Prepared from A	Prepared from B
Total S	0.31	0.31	0.68	0.50
$SO_3Ba/2$	0.28	0.30	0.66	0.49
Neutral S	0.03	0.00	0.02	0.01
CH_3O	0.91	0.95	0.96	1.00
Ba excess	0.02	0.09	0.04	0.08
Total OH*	0.20～0.16	0.22～0.18	0.23～0.19	0.24～0.19
Type I OH*	0.05～0.04	0.06～0.05	0.09～0.07	0.08～0.07
Type II OH*	0.16～0.12	0.17～0.14	0.15～0.12	0.16～0.12
COOH	0.12～0.11	0.16～0.15	0.23～0.21	0.26～0.25
Type I/Type II	1/3	1/3	1/2	1/2
Molecular formula	**	***	****	*****

* Means phenolic hydroxyl group.

A Residual lignosulfonic acid prepared previously[6]. Values are corrected for the contamination of carbohydrate, which was estimated chromatographically. The amount of xylan, mannan and glucan was 1.23, 0.79 and 0.59% respectively.

B The same prepared in the present communication. Carbohydrate was not detected.

** $C_9H_{9.15}O_{3.74}(CH_3O)_{0.91}(SO_3Ba/2)_{0.28}S^{neut}_{0.03}Ba^{excess}_{0.02}$

*** $C_9H_{10.55}O_{3.57}(CH_3O)_{0.95}(SO_3Ba/2)_{0.30}S^{neut}_{0.00}Ba^{excess}_{0.09}$

**** $C_9H_{10.5}O_{3.31}(CH_3O)_{0.96}(SO_3Ba/2)_{0.66}S^{neut}_{0.02}Ba^{excess}_{0.04}$

***** $C_9H_{11.4}O_{4.08}(CH_3O)_{1.00}(SO_3Ba/2)_{0.49}S^{neut}_{0.01}Ba^{excess}_{0.08}$

Functional groups of the residual lignosulfonic acid and of the further sulfonated products obtained therefrom are summarized in Table I. The amount of the sulfonic acid group of the residual lignosulfonic acid, ca. 0.3 per C_9-unit, is low, of the same order of magnitude with that of the so-called low sulfonated lignosulfonic acid prepared from sulfonated wood by the Kullgren procedure, and also approximately half the amount of the sulfonic acid group of the ordinary lignosulfonic acid separated from waste liquor. 0.3 sulfonic acid groups per C_9-unit will be the lower limit of the degree of sulfonation which renders the lignin soluble. The degree of sulfonation could doubled by sulfonating further in the homogenous phase. Nearly half of the sulfonatable groups in lignin seems, therefore, to remain intact in the residual lignosulfonic acid.

The amount of the carboxyl group, 0.11～0.16, of the residual lignosulfonic acid is higher than that of low sulfonated lignosulfonic acid (0.08～0.1) and somewhat lower than that of ordinary lignosulfonic acid (0.16～0.17). The comparatively low degree of sulfonation and the low content of the carboxyl group in residual lignosulfonic acid seem to suggest that the action of the cooking acid is somewhat milder on the lignin in the fiber. The fact that the rather drastic condition of 135°C, for 9 hr., which nearly doubles the content of the carbonyl group in lignin, was required to elevate the degree of sulfonation to 0.5～0.6 seems to suggest that the sulfonatable group remaining in residual lignosulfonic acid is rather difficult to sulfonate in nature.

The ratio of the type I phenolic hydroxyl group to type II is about 1/3, being approximately the same as gymnosperm[17] α-lignosulfonic acid. The value is distinctly lower than that of low sulfonated lignosulfonic acid and of birch α-lignosulfonic acid. The total amount of the phenolic hydroxyl group is about the same as that of the ordinary α-lignosulfonic acid. Although the ratio of the type I phenolic hydroxyl group to type II, I/II, decreases somewhat with the further sulfonation of the low sulfonated lignosulfonic acid, the ratio increases from 1/3 to 1/2 with the further sulfonation of the residual lignosulfonic acid.

The authors wish to express their sincere thanks to Professor Yoshikazu Hachihama of Osaka University, for his unfailing kindness

17) H. Mikawa, K. Sato, C. Takasaki and K. Ebisawa, This Bulletin, **28**, 653 (1955).

in encouraging this work, and to Mr. Toshio Yuki, vice director of this laboratory, for his permission to publish this paper.

Research Laboratory
Kokusaku Pulp Ind. Co., Ltd.
Shinjuku-ku, Tokyo

Fundamentals of Statistical Thermodynamics

By Noboru NAGASAKO

(Received June 15, 1961)

Physico-chemical phenomena in stationary states obey not only thermodynamics, but also the theoretical probability distributions of mathematical statistics. These two branches of science can be connected more closely by a new definition of entropy.

1. Probability of Microscopic States. — We confine our attention to a homogeneous system in a stationary state which has been placed for a long period of time in a thermostat of temperature T. Let $\varepsilon_i (i=0, 1, \cdots\cdots, r)$ denote the energy level of a single particle, and n_i the number of particles in state ε_i. If the particles are independent, the probability of the microscopic states assigned by $n_0, n_1, \cdots\cdots, n_r$ will be given by

$$p(n_0, n_1, \cdots\cdots, n_r) = W \cdot {p_0}^{n_0} {p_1}^{n_1} \cdots\cdots {p_r}^{n_r} / \Xi \quad (1.1)$$

in which p_i denotes the relative probability of finding a particle in state ε_i, W a statistical weight or the number of complexions, and Ξ a normalizing factor.

For example, if we set $p_0+p_1+\cdots\cdots+p_r=1$, we have

$$1=(\sum_i p_i)^N=\sum \frac{N!}{n_0!\, n_1! \cdots n_r!} {p_0}^{n_0} {p_1}^{n_1} \cdots {p_r}^{n_r}$$

We have, therefore, as the multinomial distribution for N independent events, $(0<p_i<1)$,

$$p(n_0, n_1, \cdots\cdots, n_r) = \frac{N!}{n_0!\, n_1! \cdots\cdots n_r!} {p_0}^{n_0} {p_1}^{n_1} \cdots\cdots {p_r}^{n_r} \quad (1.2)$$

in which $N=\sum_i n_i=\sum_i \bar{n}_i$ and $\Xi=1$.

If every state ε_i is g_i-fold degenerate, and if we set $\sum_i g_i p_i=1$, in place of $\sum_i p_i=1$, we have

$$p(n_0, n_1, \cdots\cdots, n_r) = N! \frac{{g_0}^{n_0} {g_1}^{n_1} \cdots\cdots {g_r}^{n_r}}{n_0!\, n_1! \cdots\cdots n_r!} {p_0}^{n_0} {p_1}^{n_1} \cdots\cdots {p_r}^{n_r} \quad (1.3)$$

On the other hand, we have by binomial expansions

$$1=(1+p)^g/(1+p)^g=\sum \binom{g}{n} p^n/(1+p)^g$$

and $$1=(1-p)^{-g}/(1-p)^{-g} = \sum \binom{g+n-1}{n} p^n/(1-p)^{-g}$$

We have, therefore, as the product of binomial distributions

$$p(n_0, n_1, \cdots\cdots, n_r) = \prod_i \binom{g_i}{n_i} {p_i}^{n_i}/(1+p_i)^{g_i} \quad (0<p_i) \quad (1.4)$$

and $$p(n_0, n_1, \cdots\cdots, n_r) = \prod_i \binom{g_i+n_i-1}{n_i} {p_i}^{n_i}/(1-p_i)^{-g_i} \quad (0<p_i<1) \quad (1.5)$$

For (1.4) and (1.5) we have $\bar{N}=\sum_i \bar{n}_i$

and $$\Xi=\prod_i (1 \pm p_i)^{\pm g_i} \quad (1.6)$$

When $p_i \ll 1$, both (1.4) and (1.5) lead to the multiple Poisson distribution given by

$$p(n_0, n_1 \cdots\cdots n_r) = \exp[-\bar{N}] \times \frac{{g_0}^{n_0} {g_1}^{n_1} \cdots\cdots {g_r}^{n_r}}{n_0!\, n_1! \cdots\cdots n_r!} {p_0}^{n_0} {p_1}^{n_1} \cdots\cdots {p_r}^{n_r} \quad (1.7)$$

It is evident that these theoretical probability distributions may be reduced to (1.1). In place of the ergodic hypothesis by Boltzmann, the equal a priori probability of finding a particle in each energy level of a single particle has been postulated by ${p_i}^{n_i}$ of (1.1).

When a probability distribution is given, we can obtain the mean value and the other moments by a moment-generating function[1] defined by $\Phi=\sum p(x)\exp[xt]$, where $p(x)$ denotes the probability of a random variable x. Hence, we have

1) P. G. Hoel, "Introduction to Mathematical Statistics", John Wiley and Sons, Inc., New York (1951).

$$\Phi=\sum_x p(x)(1+xt+\cdots\cdots+x^m t^m/m!+\cdots\cdots)$$

$$=1+\bar{x}t+\cdots\cdots+\overline{x^m}t^m/m!+\cdots\cdots$$

Differentiating Φ with respect to t, and putting $t=0$,

$$\overline{x^m}=\left.\frac{\partial^m\Phi}{\partial t^m}\right|_{t=0} \tag{1.8}$$

The moment-generating function for the multinomial distribution will be given by

$$\Phi=(p_0+p_1+\cdots\cdots+e^t p_i+\cdots\cdots+p_r)^N \tag{1.9}$$

Hence, $$\bar{n}_i=\left.\frac{\partial\Phi}{\partial t}\right|_{t=0}=Np_i \tag{1.10}$$

The moment-generating function for the binomial distributions will be given by

$$\Phi=(1\pm e^t p_i)^{\pm g_i}(1\pm p_i)^{\mp g_i} \tag{1.11}$$

Hence, $$\bar{n}_i=\left.\frac{\partial\Phi}{\partial t}\right|_{t=0}=g_i p_i/(1\pm p_i) \tag{1.12}$$

2. Probability and Entropy. — The probability (1.1) is given in a form $W\times P$, where

$$P=p_0^{n_0}p_1^{n_1}\cdots\cdots p_r^{n_r}/\Xi$$

denotes the probability of a set of microscopic states. Taking the logarithm of P, we have

$$\ln P=\sum_i n_i\ln p_i-\ln\Xi$$

The mean value of $\ln P$ is given by

$$\overline{\ln P}=\sum_i \bar{n}_i\ln p_i-\ln\Xi$$

We define the entropy not by $S=k\ln W$, but by

$$S=-k\overline{\ln P}$$

i. e., $$S=-k\sum_i \bar{n}_i\ln p_i+k\ln\Xi \tag{2.1}$$

in which k denotes Boltzmann's constant.

We have, therefore, by (1.2)

$$S=-k\sum_i \bar{n}_i\ln p_i \tag{2.2}$$

and then we have by (1.10)

$$S=-kN\sum_i p_i\ln p_i$$

or $$S=-k\sum_i \bar{n}_i\ln\bar{n}_i+k\sum_i \bar{n}_i\ln N \tag{2.3}$$

We have by (1.6) and (2.1)

$$S=-k\sum_i \bar{n}_i\ln p_i\pm k\sum_i g_i\ln(1\pm p_i) \tag{2.4}$$

and then we have by (1.12)

$$S=-k\sum_i \bar{n}_i\ln\bar{n}_i\pm k\sum_i g_i\ln g_i$$

$$\mp k\sum_i(g_i\mp\bar{n}_i)\ln(g_i\mp\bar{n}_i) \tag{2.5}$$

Thus we obtain the entropies, nearly identical with the familiar expressions, without the aid of Stirling's approximation formula.

By differentiation of (2.2) we have

$$dS=-k\sum_i \ln p_i d\bar{n}_i$$

Since every g_i is maintained constant at constant volume, we have by differentiation of (2.4) at constant volume V

$$(dS)_V=-k\sum_i \ln p_i(d\bar{n}_i)_V$$

We may generalize the above results by differentiation of (2.1), which gives

$$dS=-k\sum_i \ln p_i d\bar{n}_i-k\sum_i \bar{n}_i d\ln p_i+k d\ln\Xi$$

We have, therefore,

$$dS=-k\sum_i \ln p_i d\bar{n}_i \tag{2.6}$$

if we may write

$$\sum_i \bar{n}_i d\ln p_i=0 \quad\text{and}\quad d\ln\Xi=0 \tag{2.7}$$

which is fulfilled to obtain (2.6) form (2.2). We have also

$$(dS)_V=-k\sum_i \ln p_i(d\bar{n}_i)_V \tag{2.8}$$

if we may write

$$\sum_i \bar{n}_i(d\ln p_i)_V=(d\ln\Xi)_V$$

i. e., $$\bar{n}_i=(\partial\ln\Xi/\partial\ln p_i)_V \tag{2.9}$$

which is fulfilled to obtain (2.8) from (2.4).

Now let us assume that a system obeys the thermodynamic equation

$$dU=TdS-pdV+\mu dN_t \tag{2.10}$$

in which U denotes the energy, p the pressure, μ the chemical potential, and N_t the total number of particles of the system. We have, therefore, at constant volume

$$(dU)_V=T(dS)_V+\mu(dN_t)_V \tag{2.11}$$

When the particles are independent, we may write

$$E=\varepsilon_0 n_0+\varepsilon_1 n_1+\cdots\cdots+\varepsilon_r n_r \tag{2.12}$$

and $$\bar{E}=\varepsilon_0\bar{n}_0+\varepsilon_1\bar{n}_1+\cdots\cdots+\varepsilon_r\bar{n}_r \tag{2.13}$$

in which E denotes the total energy of the system and $\bar{E}$ its mean value. Writing $U=\bar{E}$, we have

$$dU=\sum_i \varepsilon_i d\bar{n}_i+\sum_i \bar{n}_i d\varepsilon_i$$

Since we may write, in general, $d\varepsilon_i=0$ for $dV=0$, it follows that

$$(dU)_V=\sum_i \varepsilon_i(d\bar{n}_i)_V \tag{2.14}$$

Moreover, we may write

$$dN_t=\sum_i d\bar{n}_i \tag{2.15}$$

Substituting (2.8), (2.14) and (2.15) into (2.11), we have

$$\sum_i(\varepsilon_i+kT\ln p_i-\mu)(d\bar{n}_i)_V=0$$

Since we may write, in general, $(d\bar{n}_i) \neq 0$, it follows that

$$\varepsilon_i + \boldsymbol{kT} \ln p_i - \mu = 0$$

or
$$p_i = \exp[(\mu - \varepsilon_i)/\boldsymbol{kT}] \qquad (2.16)$$

which enormously simplifies the discussions.

Substituting (2.16) into (2.1), we obtain as the general equation of statistical-thermodynamic entropy

$$\boldsymbol{S} = \bar{E}/T - \mu \sum_i \bar{n}_i/T + \boldsymbol{k} \ln \Xi \qquad (2.17)$$

Since the Gibbs free energy of a homogeneous system will be given by $G = \mu \sum_i \bar{n}_i$, it follows that

$$pV = \boldsymbol{kT} \ln \Xi \qquad (2.18)$$

3. Fermi-Dirac and Bose-Einstein Statistics. —Dividing the $2f$-dimensional μ-space into many cells with the volume $\boldsymbol{h}^f$, where $\boldsymbol{h}$ denotes Planck's constant and f the degrees of freedom for a single particle, we shall find g_i cells for the same energy ε_i, when a state ε_i is g_i-fold degenerate. We now try to discover the law of probability by which these cells will be occupied by the particles.

If there are n_i particles in a g_i-fold degenerate energy level ε_i, and if the particles obey the Fermi-Dirac statistics, it is known that the number of complexions will be given by[2]

$$W(\text{Fermi-Dirac}) = \prod_i \binom{g_i}{n_i} \qquad (3.1)$$

and for the Bose-Einstein statistics

$$W(\text{Bose-Einstein}) = \prod_i \binom{g_i + n_i - 1}{n_i} \qquad (3.2)$$

We may consider by (1.1) and (3.1) that the probability distribution for the Fermi-Dirac statistics will be given by (1.4), the product of positive binomial distributions. Similarly, by (3.2) we obtain (1.5), the product of negative binomial distributions, for the Bose-Einstein statistics. Moreover, it is assumed by (1.4) and by (1.5) that the particles occupy each energy level independently.

The translational energy of an independent material particle of mass m in a state described by the three quantum numbers, k_x, k_y, k_z, is given by $\varepsilon_i = \boldsymbol{h}^2(k^2_x + k^2_y + k^2_z)/8mV^{2/3}$, which gives $d\varepsilon_i = 0$ for $dV = 0$. The energy of a photon in given by $\varepsilon_i = \boldsymbol{h}\nu$, i. e., $d\varepsilon_i = 0$. We may use (2.14), therefore, to obtain (2.16).

We may write for material particles $g_i = 4\pi V q^2 dq/\boldsymbol{h}^3$, in which q denotes the momentum of a single particle, and for photons, $g_i = (8\pi V/c^3)\nu^2 d\nu$. At constant volume, therefore, every g_i remains constant. Taking the logarithm of (1.6) for the probability distributions (1.4) and (1.5), we have

$$\ln \Xi = \pm \sum_i g_i \ln(1 \pm p_i)$$

Hence, $$(d \ln \Xi)_V = \sum_i g_i dp_i/(1 \pm p_i)$$

Since we have by (1.12)

$$\bar{n}_i = g_i p_i/(1 \pm p_i)$$

it follows that

$$\bar{n}_i = (\partial \ln \Xi/\partial \ln p_i)_V$$

which is the condition (2.9) to obtain (2.8).

Having examined the derivation of (2.16), and substituting (2.16) into (1.6), we have

$$\Xi = \prod_i (1 \pm \exp[(\mu - \varepsilon_i)/\boldsymbol{kT}])^{\pm g_i} \qquad (3.3)$$

Substituting (3.3) into (2.17), we obtain as the statistical-thermodynamic entropy of the Fermi-Dirac and the Bose-Einstein system

$$\boldsymbol{S} = \bar{E}/T - \mu \bar{N}/T \pm \boldsymbol{k} \sum_i g_i \ln(1 \pm \exp[(\mu - \varepsilon_i)/\boldsymbol{kT}]) \qquad (3.4)$$

Substituting (3.3) into (2.18), we obtain

$$pV = \pm \boldsymbol{kT} \sum_i g_i \ln(1 \pm \exp[(\mu - \varepsilon_i)/\boldsymbol{kT}]) \qquad (3.5)$$

Substituting (2.16) into (1.12), we obtain as the distribution law

$$\bar{n}_i = g_i \exp[(\mu - \varepsilon_i)/\boldsymbol{kT}] / (1 \pm \exp[(\mu - \varepsilon_i)/\boldsymbol{kT}]) \qquad (3.6)$$

Although a different method has been used to obtain (3.4), (3.5) and (3.6), these equations are identical with those proposed by Fowler and Guggenheim[3].

When $p_i \ll 1$, we have by (1.6)

$$\Xi = \exp[\sum_i g_i p_i]$$

and by (1.12)

$$\bar{n}_i = g_i p_i \qquad (3.7)$$

Hence, $$\Xi = \exp[\sum \bar{n}_i]_i = \exp[\bar{N}] \qquad (3.8)$$

The probability distribution for this case is given, therefore, by the multiple Poisson distribution (1.7), in which

$$W = \prod_i g_i^{n_i}/n_i ! \qquad (3.9)$$

Substituting (3.8) into (2.17), we have

$$\boldsymbol{S} = \bar{E}/T - \mu \bar{N}/T + \boldsymbol{k}\bar{N} \qquad (3.10)$$

Substituting (3.8) into (2.18), we obtain the equation of the state of an ideal gas given by $pV = \boldsymbol{kT}\bar{N}$.

Substituting (2.16) into (3.7), we obtain the Boltzmann distribution law for an ideal gas given by

2) J. E. Mayer and M. G. Mayer, "Statistical Mechanics", John Wiley & Sons, Inc., New York (1940), p. 111.

3) R. H. Fowler and E. A. Guggenheim, "Statistical Thermodynamics", Cambridge University Press (1939). pp. 50-67, 234.

$$\bar{n}_i = g_i \exp[(\mu - \varepsilon_i)/\boldsymbol{k}T] \quad (3.11)$$

Hence, $$\bar{N} = \sum_i \bar{n}_i = (p.f.)\exp[\mu/\boldsymbol{k}T] \quad (3.12)$$

where $(p.f.)$ denotes the partition function. We can eliminate, therefore, μ from (3.10) by (3.12) to obtain

$$S = \bar{E}/T + \boldsymbol{k}\bar{N}\ln[(p.f.)/\bar{N}] + \boldsymbol{k}\bar{N} \quad (3.13)$$

which is identical with the Sackur-Tetrode equation for the entropy of an ideal gas.

4. Multinomial Distributions.—In statistical mechanics the number of complexions was given first by

$$W = N!/n_0!\ n_1!\cdots\cdots n_r! \quad (4.1)$$

which may be interpreted as the number of ways that $n_0, n_1, \cdots\cdots, n_r$ identical particles with energies $\varepsilon_0, \varepsilon_1, \cdots\cdots, \varepsilon_r$ will be placed in N numbered, i. e., physically distinguishable, cells, one particle to each cell. The particles may or may not be localized, although the application of (4.1) has been restricted to the localized particles by Fowler and Guggenheim[4].

When W is given by (4.1), we obtain the multinomial distribution (1.2), with $\Xi = 1$. It may be noticed that we have $\Xi = (\sum_i p_i)^N$ for (4.1), if we set $\sum_i p_i \neq 1$. However, we can reduce this probability distribution to (1.2), if W is given by (4.1). When every state ε_i is g_i-fold degenerate, we have the probability distribution (1.3)

and $$W = N! \prod_i g_i^{n_i}/n_i! \quad (4.2)$$

Substituting $\Xi = 1$ into (3.18), we obtain $pV = 0$. We may apply the probability distributions (1.2) and (1.3), therefore, to the vibrational and rotational motions of gas molecules, since these motions have nothing to do with pV. In these cases we may omit the term $p\mathrm{d}V$ in (2.10) and may write $\mathrm{d}\varepsilon_i = 0$, i. e.,

$$\mathrm{d}U = \sum_i \varepsilon_i \mathrm{d}\bar{n}_i \quad (4.3)$$

We have, therefore, by (2.10), (4.3), (2.6) and (2.15)

$$\sum_i (\varepsilon_i + \boldsymbol{k}T \ln p_i - \mu_0)\mathrm{d}\bar{n}_i = 0$$

or $$p_i = \exp[(\mu_0 - \varepsilon_i)/\boldsymbol{k}T] \quad (4.4)$$

Substituting $\Xi = 1$ and (4.4) into (2.1), we have

$$S = \bar{E}/T - \mu_0 N/T \quad (4.5)$$

which is also obtained by substituting $\Xi = 1$ into (2.17). Denoting by A the Helmholtz free energy, we have, therefore, $\mu_0 = A/N$ which holds for the systems with $pV = 0$ and which has been distinguished from $\mu = G/N$.

Substituting (4.4) into $\sum_i p_i = 1$ of (1.2) and into $\sum_i g_i p_i = 1$ of (1.3), we have

$$1 = (p.f.)\exp[\mu_0/\boldsymbol{k}T] \quad (4.6)$$

We can eliminate, therefore, μ_0 from (4.5) by (4.6) to obtain

$$S = \bar{E}/T + \boldsymbol{k}\ln[(p.f.)^N] \quad (4.7)$$

For the non-localized gas molecules, the entropy due to vibrations of atoms and that due to rotations can be calculated by (4.7); these results have been verified by experiments.

Substituting (4.4) into (1.10), we have again the Boltzmann distribution law given by

$$\bar{n}_i = N \exp[(\mu_0 - \varepsilon_i)/\boldsymbol{k}T] \quad (4.8)$$

For the probability distribution (1.3), we have

$$\bar{n}_i = N g_i \exp[(\mu_0 - \varepsilon_i)/\boldsymbol{k}T] \quad (4.9)$$

We could also apply the probability distribution (1.2) and (1.3) to the localized oscillators in a crystal at low pressures.

If the number of complexions is given by (3.9), we can construct another probability distribution, i. e., the multinomial distribution for the translational motions of an ideal gas. If we set $N = \sum_i g_i p_i$, we have

$$1 = (\sum_i g_i p_i/N)^N = (N!/N^N)\sum \prod_i g_i^{n_i} p_i^{n_i}/n_i! \quad (4.10)$$

Hence,

$$p(n_0, n_1, \cdots\cdots, n_r) = (N!/N^N)\prod_i g_i^{n_i} p_i^{n_i}/n_i! \quad (4.11)$$

and $\bar{n}_i = g_i p_i$ which is identical with (3.7).

Substituting $\Xi = N^N/N!$ and (3.7) into (2.1), we have

$$S = -\boldsymbol{k}\sum_i g_i p_i \ln p_i + \boldsymbol{k}\ln(N^N/N!) \quad (4.12)$$

Differentiating (4.12) at constant V and N, we have

$$(\mathrm{d}S)_{N,V} = -\boldsymbol{k}\sum_i \ln p_i (\mathrm{d}\bar{n}_i)_{N,V} \quad (4.13)$$

Substituting (2.14) and (4.13) into the thermodynamic equation $(\mathrm{d}U)_{N,V} = T(\mathrm{d}S)_{N,V}$, we have

$$\sum_i (\varepsilon_i + \boldsymbol{k}T \ln p_i)(\mathrm{d}\bar{n}_i)_{N,V} = 0$$

Since $\sum_i (\mathrm{d}\bar{n}_i)_{N,V} = 0$, we may write

$$\varepsilon_i + \boldsymbol{k}T \ln p_i = \mu' \text{ (constant)}$$

or $$p_i = \exp[(\mu' - \varepsilon_i)/\boldsymbol{k}T] \quad (4.14)$$

Substituting (4.14) into (4.12), we have

$$S = \bar{E}/T - \mu' N/T + \boldsymbol{k}\ln(N^N/N!) \quad (4.15)$$

Since $N = \sum_i g_i p_i$, it follows that

$$N = (p.f.)\exp[\mu'/\boldsymbol{k}T] \quad (4.16)$$

Now we can eliminate μ' from (4.15) by (4.16) to obtain

4) R. H. Fowler and E. A. Guggenheim, loc. cit., pp. 20-29.

$$S=\bar{E}/T+\boldsymbol{k}\ln[(p.f.)^N/N!] \qquad (4.17)$$

which is identical with (3.13), when $\bar{N}=N\gg 1$.

Comparing (4.7) with (4.17), we find the well known difference, $N!$, in the divisor, which is often introduced ambiguously to obtain (4.17) from (4.7). It is evident that the number of complexions ((4.1) or (4.2)) and the entropy (4.7) can be applied solely to the system with $pV=0$. It is not legitimate, therefore, to try to obtain (4.17) for $pV=\boldsymbol{k}TN$ from (4.7) for $pV=0$, although the difference between these equations is apparently simple.

5. Grand-canonical and Canonical Distributions. — Substituting (2.16) into (1.1) and considering (2.12) and (2.18), we have

$$p(n_0, n_1, \cdots\cdots, n_r) = W\exp[(\mu N-E-pV)/\boldsymbol{k}T] \qquad (5.1)$$

Denoting by Ω the total number of complexions for the given N, E, and by $\sum_c$ the conditioned sum of W of which $n_0, n_1, \cdots\cdots, n_r$ satisfy the given N, E, we may write

$$\Omega(N, E)=\sum_c W(n_0, n_1, \cdots\cdots, n_r) \qquad (5.2)$$

The probability that the system contains N particles and is in state E is given, therefore, by

$$p(N, E)=\Omega(N, E)\exp[(\mu N-E-pV)/\boldsymbol{k}T] \qquad (5.3)$$

which corresponds to the Gibbs grand ensemble canonically distributed[5], i. e., the grand-canonical distribution. The probability distributions ((1.4), (1.5) for the Fermi-Dirac and Bose-Einstein statistics and (1.7) for an ideal gas) lead, therefore, to the grand-canonical distributions.

Substituting $\Xi=1$ and (4.4) into (1.1), we have

$$p(n_0, n_1, \cdots\cdots, n_r)=W\exp[(\mu_0 N-E)/\boldsymbol{k}T] \qquad (5.4)$$

The probability that the system is in state E is given, therefore, by

$$p(E)=\Omega(N, E)\exp[(A-E)/\boldsymbol{k}T] \qquad (5.5)$$

which corresponds to the Gibbs canonical distribution. The multinomial distributions ((1.2) and (1.3)) lead, therefore, to the canonical distributions.

Substituting (4.14) into (1.1), we have

$$p(n_0, n_1, \cdots\cdots, n_r) = W\exp[(\mu' N-E-\boldsymbol{k}T\ln\Xi)/\boldsymbol{k}T] \qquad (5.6)$$

Since we may write by (4.15) $A=\mu' N-\boldsymbol{k}T\ln\Xi$, we have again (5.5) for $p(E)$. The probability distribution (4.11) for an ideal gas leads, therefore, to the canonical distribution. It may be mentioned that it is difficult to treat the Fermi-Dirac and the Bose-Einstein statistics canonically, since, for these statistics, there is no simple probability distribution in which the total number of particles is maintained constant, while the total energy is variable.

For the linear harmonic oscillators with frequency ν, i. e., $\varepsilon_i=\boldsymbol{h}\nu/2+i\boldsymbol{h}\nu (i=0, 1, \cdots\cdots, \infty)$, we have by (4.4)

$$\begin{aligned} 1&=(\sum_i p_i)^N \\ &=(1-\exp[-\boldsymbol{h}\nu/\boldsymbol{k}T])^{-N}\cdot \\ &\quad \exp[\mu_0 N/\boldsymbol{k}T-N\boldsymbol{h}\nu/2\boldsymbol{k}T] \\ &=\sum_{J=0}^{\infty}\binom{N+J-1}{J}\exp[(A-E)/\boldsymbol{k}T] \end{aligned}$$

in which $E=N\boldsymbol{h}\nu/2+J\boldsymbol{h}\nu (J=0, 1, \cdots\cdots, \infty)$. We have, therefore the canonical distribution in a compact form

$$p(E)=\binom{N+J-1}{J}\exp[(A-E)/\boldsymbol{k}T] \qquad (5.7)$$

for which we may write by (5.2) and (5.5)

$$\Omega(N, E)=\binom{N+J-1}{J}=\sum_c N!/n_0!\ n_1!\cdots\cdots n_r!$$

Thus we obtain, in general, either the canonical or the grand-canonical distribution by the probability distribution (1.1).

6. Fluctuations. — By means of a moment-generating function we can calculate fluctuations. We have by (1.8) as the variance

$$\sigma^2=(\overline{x^2})-(\bar{x})^2=\frac{\partial^2\Phi}{\partial t^2}\bigg|_{t=0}-\left(\frac{\partial\Phi}{\partial t}\right)^2\bigg|_{t=0}$$

Calculations will be performed more simply by the following relations:

$$\frac{\partial\ln\Phi}{\partial t}=\frac{1}{\Phi}\frac{\partial\Phi}{\partial t}$$

and

$$\frac{\partial^2\ln\Phi}{\partial t^2}=\frac{1}{\Phi}\frac{\partial^2\Phi}{\partial t^2}-\frac{1}{\Phi^2}\left(\frac{\partial\Phi}{\partial t}\right)^2$$

Since $\Phi(t=0)=1$, it follows that

$$\bar{x}=\frac{\partial\ln\Phi}{\partial t}\bigg|_{t=0}$$

and

$$\sigma^2=\frac{\partial^2\ln\Phi}{\partial t^2}\bigg|_{t=0} \qquad (6.1)$$

For the binomial distributions (1.4) and (1.5), we have by (6.1) and the moment-generating function (1.11)

$$\sigma^2=(\overline{n_i^2})-(\bar{n}_i)^2=g_i p_i/(1\pm p_i)^2 \qquad (6.2)$$

Since the particles occupy each energy level independently, we have for $N=\sum_i n_i$

5) J. W. Gibbs, "Elementary Rrinciples in Statistical Mechanics", Yale University Press (1902).

$$\sigma^2{}_N=\overline{(N^2)}-(\overline{N})^2=\sum_i g_i p_i/(1\pm p_i)^2 \quad (6.3)$$

and for $E=\sum_i \varepsilon_i n_i$

$$\sigma^2{}_E=\overline{(E^2)}-(\overline{E})^2=\sum_i \varepsilon^2{}_i g_i p_i/(1\pm p_i)^2 \quad (6.4)$$

For the multiple Poisson distribution (1.7), in which $p_i \ll 1$, we have

$$\sigma^2{}_N=\sum_i g_i p_i=\overline{N}$$

and

$$\sigma^2{}_E=\sum_i \varepsilon^2{}_i g_i p_i=\sum_i \varepsilon^2{}_i \bar{n}_i \quad (6.5)$$

Applying (1.7) to an ideal gas, and setting $g_i=4\pi V\, q^2 \mathrm{d}q/\boldsymbol{h}^3$, we have by (2.13) and (3.11)

$$\overline{E}=\exp[\mu/\boldsymbol{kT}]\cdot(2\pi V/m\boldsymbol{h}^3)$$
$$\times\int_0^\infty q^2\exp[-q^2/2m\boldsymbol{kT}]\cdot \mathrm{d}q$$
$$=\exp[\mu/\boldsymbol{kT}]\cdot(3/2)\boldsymbol{kT}\cdot V(2\pi m\boldsymbol{kT})^{3/2}/\boldsymbol{h}^3$$

Since $(p.f.)=V(2\pi m\boldsymbol{kT})^{3/2}/\boldsymbol{h}^3$, we have by (3.12)

$$\overline{E}=\overline{N}(3/2)\boldsymbol{kT} \quad (6.6)$$

We have by (3.11) and (6.5)

$$\sigma^2{}_E=\overline{N}(15/4)(\boldsymbol{kT})^2$$

i. e.,

$$\sigma_E=\sqrt{\overline{N}}(\sqrt{15}/2)\boldsymbol{kT} \quad (6.7)$$

On the other hand, we have, in general, with respect to the variance

$$\sigma^2=\int_{-\infty}^{\infty}(x-\bar{x})^2 p(x)\mathrm{d}x=\int_{|x-\bar{x}|\geqq\xi\sigma}+\int_{|x-\bar{x}|<\xi\sigma}$$

Since

$$\int_{|x-\bar{x}|\geqq\xi\sigma}\geqq\xi^2\sigma^2 p(|x-\bar{x}|\geqq\xi\sigma)$$

we obtain Tchebychev's theorem given by

$$p(|x-\bar{x}|\geqq\xi\sigma)\leqq 1/\xi^2$$

where $p(|x-\bar{x}|\geqq\xi\sigma)$ denotes the probability that the deviation from the mean value $x-\bar{x}$ is greater than $\xi\sigma$.

We have, therefore, as the estimations for the grand ensemble

$$p(|N-\overline{N}|\geqq 100\sigma_N)\leqq 0.0001$$

and

$$p(|E-\overline{E}|\geqq 100\sigma_E)\leqq 0.0001 \quad (6.8)$$

For an ideal gas obeying (1.7), we may write $\overline{N}=2.7\times10^{19}$/cc. at N. T. P and by (6.5) $\sigma_N=\sqrt{\overline{N}}=5.2\times10^9$. $\overline{E}$ is given by (6.6) proportional to $\overline{N}$. σ_E is given by (6.7) proportional to $\sqrt{\overline{N}}$. It is evident, therefore, that we may neglect the probability of finding a system with N, E deviated from the physically observable mean values $\overline{N}, \overline{E}$. In other words, there is no significant difference between the grand ensemble from (1.7) for an ideal gas and the micro-canonical ensemble in which the total number of particles is fixed and the total energy falls within the narrow limits between E and $E+\Delta E$.

This is also the case with the Fermi-Dirac statistics. Comparing (6.3) and (6.4) with (6.5), it is seen that the probability distribution (1.4) for the Fermi-Dirac statistics is more sharply concentrated near the mean values than the distribution (1.7).

The probability distribution (1.5) for the Bose-Einstein statistics is more broadly distributed than the distribution (1.7). Applying the distribution (1.5) to the temperature radiation, and setting $g_i=(8\pi V/c^3)\,\nu^2\mathrm{d}\nu$, $\mu=0$ and $x=\boldsymbol{h}\nu/\boldsymbol{kT}$, we have by (3.6)

$$\overline{N}=(8\pi V/c^3)\int_0^\infty \nu^2 \mathrm{e}^{-x}(1-\mathrm{e}^{-x})^{-1}\mathrm{d}\nu$$
$$=16\pi^4(\boldsymbol{kT})^3 V/(25.8)c^3\boldsymbol{h}^3 \quad (6.9)$$

Hence, we obtain $\overline{N}=2.03\times10^{13}$/cc. at $T=1000°$K. We have also by (6.3)

$$\sigma^2{}_N=8\pi^3(\boldsymbol{kT})^3 V/3c^3\boldsymbol{h}^3=1.37\overline{N}$$

i. e.,

$$\sigma_N=1.17\sqrt{\overline{N}}$$

by (2.13) and (6.9)

$$\overline{E}=8\pi^5(\boldsymbol{kT})^4 V/15c^3\boldsymbol{h}^3=2.70\overline{N}\boldsymbol{kT}$$

and by (6.4)

$$\sigma^2{}_E=32\pi^5(\boldsymbol{kT})^5 V/15c^3\boldsymbol{h}^3=10.8\overline{N}(\boldsymbol{kT})^2$$

i. e.,

$$\sigma_E=3.29\sqrt{\overline{N}}\boldsymbol{kT}$$

Combining the above results with the estimations (6.8), we may consider that there is, in general, no significant difference between the grand ensemble from (1.5) for the temperature radiation and the micro-canonical.

Analytically the canonical and the grand-canonical distributions are much more manageable than the micro-canonical. It is especially simple and exact when we employ the theoretical probability distribution of mathematical statistics reducible to Eq. 1.1 to describe the probability of microscopic states and we define the entropy by Eq. 2.1.

It is possible to extend the present method to more complicated physico-chemical phenomena, such as chemical equilibria, adsorption and cooperative phenomena.

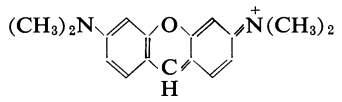
Tokyo Institute of Technology
Meguro-ku, Tokyo

Some Spectral Studies of the Aqueous Solution of Pyronine G

By Kōnosuke FUJIKI, Chieko IWANAGA and Masao KOIZUMI

(Received April 13, 1961)

Pyronine G is a xanthene dye with a positive charge, as againt anionic eosine and uranine, and it has a simpler structure than the latter dye ions, as is shown below:



We have studied some of its optical properties in an aqueous solution as a preparatory step for studying its photochemical behavior; this paper concerns the following three phenomena: I) dimerization, II) formation of carbinol as studied from the absorption spectra (pH dependence of the absorption spectra), and III) pH dependence of the fluorescent behavior.

I. Dimerization

Not long ago, one of the present authors studied the dimerization of this dye in relation to metachromasy[1] and observed a typical spectral change due to the dimerization. In this paper, special attention has been paid to the interaction between the dye cation and inorganic anion.

Dimer bands, when observed, usually lie on the shorter wavelength side of monomer bands; this phenomenon has been interpreted on the basis of Förster's model[2]. Thus, when the dimer is formed from two monomeric ions lying close together, with their molecular planes opposite each other, the excited level is split into two, of which two only the higher level has an appreciable transition moment, causing the blue shift of the dimer-band. But it is not quite certain how, if at all, the anion takes part in the dimerization. Simpson et al.[3] observed that in the case of 1, 1'-diethyl-2, 2'-pyriodocyanine, iodide and perchlorate have different association constants and that, moreover, the position of the dimer band is different in the two cases; from these facts they concluded that anions are involved in the dimerization. They further inferred that the ionic pair is formed in both monomer- and dimer- forms, but in the former case, it can only occur at the expense of the resonance energy of dye ion (due to the electrical charge), while in the latter, the univalent anion is sandwiched between two dye ions, each with half a unit charge; this partly contributes to the stability of the dimer. Ramette[4] studied the association of rhodamine B, and from the finding that the dimerization constant is different for chloride, bromide and perchlorate (they studied in particular the variation of an orange-band which is due to a two-protonated species), they also surmised the participation of the ionic pair in the dimerization.

It may now be possible in principle to decide whether the molecular species involved in the dimerization are an ionic pair or free ions and what their ionic values are, if the effect of the ionic strength on the association constant is carefully investigated. Denoting monomer and dimer as M (or M' if in a different state) and MM', the thermodynamic dimerization constant for

$$M + M' \rightleftharpoons MM'$$

would be given as follows:

$$K_a = K\frac{f_{MM'}}{f_M f_{M'}}$$

$$\log K = \log K_a + \log f_M + \log f_{M'} - \log f_{MM'} \qquad (1)$$

in which K is the apparent association constant and f's, the activity coefficients.

If Debye-Hückel's theory in its simple form is applied to f's as an approximation, then

$$\log f_i = -aZ_i^2\sqrt{J} \qquad (2)$$

The combination of 1 and 2 would enable us to predict how the apparent dimerization constant is affected by the ionic strength. Some of the conceivable cases will be cited below:

a) Participation of no anion

$$\log K = \log K_a + 2a\sqrt{J}$$

or approximately

$$\log K = \log K_a + \sqrt{J}$$

b) Participation of a univalent anion (X^-)

i) if M=DX M'=DX

$$\log K = \log K_a$$

1) M. Koizumi and N. Mataga, This Bulletin, **27**, 194 (1954).
2) Th. Förster and E. Konig, *Z. Elektrochem.*, **61**, 344 (1957).
3) G. S. Levinson, W. T. Simpson and W. Curtis, *J. Am. Chem. Soc.*, **79**, 4314 (1957).
4) R.W. Ramette and E. B. Sandell, ibid., **78**, 4872 (1956).

ii) if $M=DX$ $M'=D^+$

$$\log K=\log K_a$$

c) Participation of a bivalent anion (Y^{2-})

i) if $M=M'=DY^-$

$$\log K=\log K_a+\sqrt{J}$$

ii) if $M=DY^-$, $M'=D^+$

$$\log K=\log K_a-\sqrt{J}$$

In the above classification, case b ii) and case c ii) will perhaps correspond to the sandwich-model of Simpson, while b i) and c i) will be cases in which a 1 : 1 ion pair is formed between the dye and the anion, those perhaps occupying lateral position in both monomer and dimer.

From such a view, the effects of the addition of some salts such as potassium chloride, potassium nitrate, magnesium sulfate, potassium iodide, potassium perchlorate and sodim perchlorate were investigated. As a supplement, the effect of pH on the dimerization was also examined.

Experimental.—*Sample.*—Merck's reagent was used without further purification. $\varepsilon\approx1.2\times10^4$. Later, for the sample in parts II and III, purification was made by repeated crystallization, giving an appreicable increase of ε; this indicated the crudeness of above sample. Hence, the absolute value of the dimerization constant is not very reliable, but discussion on the salt effect will nevertheless be permissible since it is essentially based on the relative rather than the absolute quantity.

The Method of Determining the Association Constant.—The absorption spectra are measured by a Hitachi spectrophotometer EPU-2, using cells 1, 0.3 or 0.1 cm. in thickness according to the concentration of dye (from ca. 10^{-5} to 10^{-3} M). Putting the analytical concentration of dye as C_0 and the molar fraction of dimer as x in a monomer unit, the apparent association constant is given by;

$$K=\frac{x}{2C_0(1-x)^2}$$

If one measures the apparent molar absorbance ε and determines in a suitable way the molar absorbance of monomer and dimer, ε_m and ε_d, then K can be evaluated from the following equation[5]:

$$\log C_0(\varepsilon_m-\varepsilon)=\log\frac{2K}{(\varepsilon_m-\varepsilon_d/2)}+2\log C_0(\varepsilon-\varepsilon_d/2) \quad (3)$$

In the case where further polymerization as well as dimerization occurs among three monomers and four monomers and so on, the following formula may hold if the absorbance of all the polymers can be disregarded:

$$C_0(\varepsilon_m-\varepsilon)=\frac{2K_1}{\varepsilon_m}(C_0\varepsilon)^2+\frac{3K_1K_2}{\varepsilon_m^2}(C_0\varepsilon)^3+\frac{4K_1K_2K_3}{\varepsilon_m^3}(C_0\varepsilon)^4+\cdots\cdots \quad (4)$$

5) N. Mataga, This Bulletin, **30**, 375 (1957).

in which K_1, K_2, K_3,…… are respectively the equilibrium constants for each successive polymerization.

For most of the experimental results a linear relation holds between $C_0(\varepsilon_0-\varepsilon)$ and $(C_0\varepsilon)^2$, whence it can be concluded that $K_2=K_2=\cdots\cdots=0$, and, further, that $\varepsilon_d\approx0$.

This method, which is satisfactory for the majority of cases, gives $2K_1/\varepsilon_m$ as a solpe of the plot.

Results and Discussion.—The dependence of the absorption spectra of pyronine G on pH is shown in Fig. 1. It is evident that in the

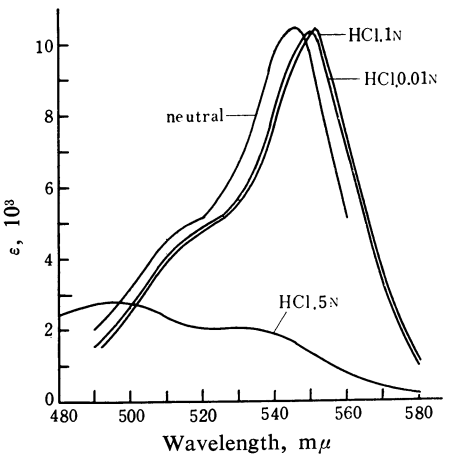


Fig. 1. pH dependence of the absorption spectra of pyronine G (2.12×10^{-5} M).

region $0<pH<3$, the maximum shifts several mμ towards red without any appreciable change in the entire feature. This would perhaps be due to the attachment of one proton to the $N(CH_3)_2$ group. A remarkable change was found to occur in the 5 N hydrochloric acid solution, the absorption spectra turning into a broad band with a maximum at 495 mμ. The exact assignment of this band was not undertaken, but in view of a large blue shift this would probably be due to the attachment of another proton to the C- or O- atom of the central ring. The case for $pH>7$ will be described in Part II. No particular attention was paid to the pH of the solution in studying the salt effect on the dimerization.

i) Potassium Chloride, Potassium Nitrate, Magnesium Sulfate.—In order to determine the salt effect on the dimerization constant, the absorption spectra of pyronine G in the aqueous solution were measured, adding various amounts of these salts and changing the dye concentration from ca. 2×10^{-5} to 9×10^{-4} M. Fig. 2 shows the case of 0.3 M potassium nitrate as an example. The position of the dimer band is practically the same for magnesium nitrate, potassium chloride or without any salt. The K-values evaluated from 3 or 4 (disregarding ε_d) are shown in Table I. In Fig. 3 the cases

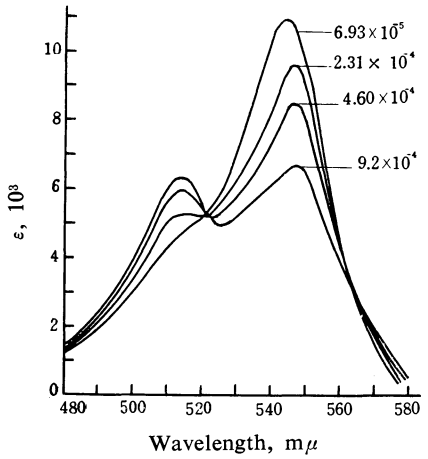


Fig. 2. The absorption spectra of pyronine G in the aqueous solution containing 0.3M KNO_3.

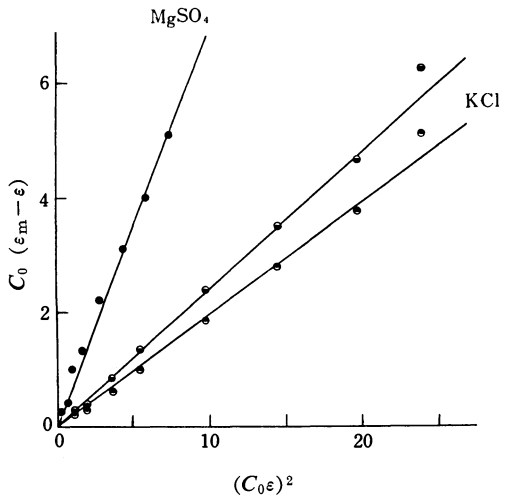


Fig. 3. Plot of $C_0(\varepsilon_m-\varepsilon)$ against $(C_0\varepsilon)^2$.
◒ $\varepsilon_m=12.0\times10^3$, ◓ $\varepsilon_m=10.9\times10^3$

of potassium chloride and magnesium sulfate are shown. These results are not satisfactorily accurate, the main cause of error perhaps lying in the fluctuation of ε_m. The K-value for the simple aqueous solution is quite smaller than that reported before[1] (1.6×10^3 at 27°C). This is probably due to the circumstance that in the previous case, the ε_d-value evaluated from the extrapolation of the ε-value in the higher concentration region was used for calculating the K-value. The present results are considered more reliable in view of the fact that a disregard of ε_d can give a satisfactory analysis in most cases.

Figs. 4a and 4b give plots of the log K-value at 20°C against the ionic strength and the molarity of the solution respectively. These

TABLE I

Temp.	Salt	Concn., M	K	log K
20°C		0	720～900	2.86～2.95
			～510	～2.71
	KCl	0.5	620～710	2.80～2.85
			580～650	2.76～2.81
		1	1100～1300	3.04～3.11
		2.2	1900～1950	3.28～3.29
	KNO_3	0.3	450～510	2.65～2.71
		0.5	560～620	2.75～2.79
		1	680～730	2.83～2.86
			730～780	2.86～2.89
	$MgSO_4$	0.25	700～820	2.85～2.91
		0.5	690～750	2.84～2.87
		1.0	1200～1900	3.08～3.28
		2.0	～2980	～3.47
30°C		0	600～650	2.78～2.81
	KCl	1	1200～1320	3.08～3.12
	$MgSO_3$	1	1560～1700	3.19～3.23

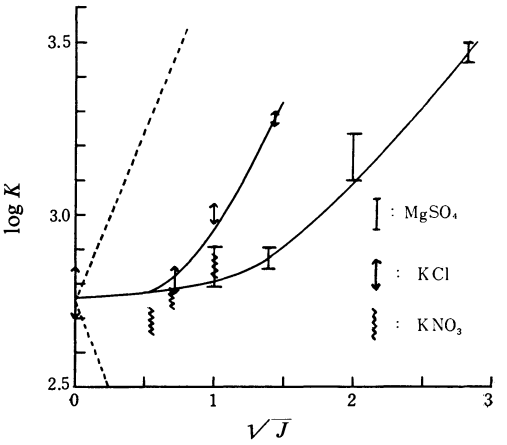


Fig. 4a. The dependence of log K on $\sqrt{J}$.

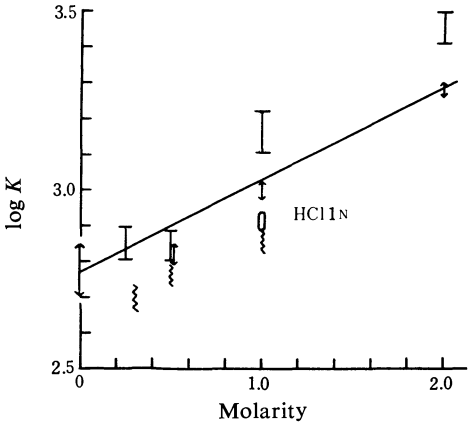


Fig. 4b. The dependence of log K on molarity.

figures show clearly the specificity in the effect of anions. Apart from the region of great ionic strength where Debye-Hückel's formula does

not hold, $\log K$ is almost independent of J (in the region $\sqrt{J} \ll 1$). The dotted lines in Fig. 4a are written with an inclination of ± 1.

Thus, the results obtained obviate the possibility of a reaction between free ions (case a) in the case of a univalent anion, while in the case of bivalent anions both case c i) and case c ii) do not match the experimental results, not to speak of the case of free ions. If the sandwich-model is generally to be adopted, case c ii) should hold for the bivalent anion, but this proved not to be the case. Hence, by analogy this model may also be rejected for the univalent anion (case b ii). This conclusion is also supported by the constancy of the position of the dimer band irrespective of the various anions.

Taking all this into consideration, it is most plausible that the dimerization in this case takes place as shown in Fig. 5.

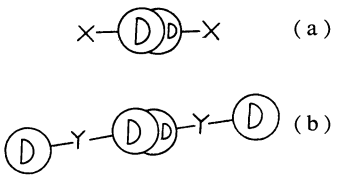


Fig. 5. Plausible models of a dimer.

Fig. 5a corresponds to the aforementioned case b i) of a univalent anion, but Fig. 5b for a bivalent anion Y^{2-} corresponds to neither c i) nor c ii).

ii) Potassium Iodide, Potassium Perchlorate, Sodium Perchlorate.—The specificity of the anion mentioned above is particularly prominent in the case of I^- and of ClO_4^-.

The measurements were made for 0.05, 0.1, 0.3, 0.5 and 1 M solutions of potassium iodide.

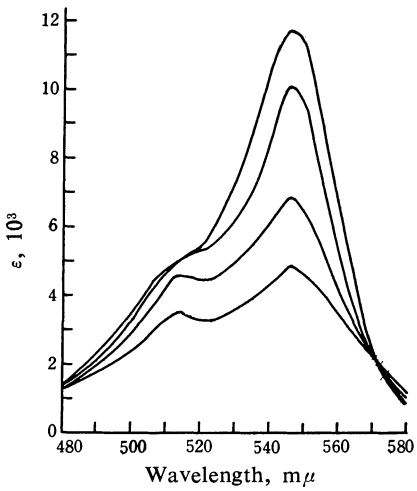


Fig. 6. The absorption spectra of pyronine G in the aqueous solution containing 0.1 M KI.

In all cases the dimer band somewhat increases up to $(2.3 \sim 3.0) \times 10^{-4}$ M in the dye concentration, but beyond this the entire absorption curve declines noticeably, accompaied by a slight red-shift of the maximum. No new band appears, at least in the region 400~780 mμ. The increase of the salt concentration does not essentially affect the above behavior. Fig. 6 shows the result for 0.1 M potassium iodide.

As for ClO_4^-, the measurements were made in 0.5 and 1 M. In both cases, the absorption band declines monotonously with the increase of the dye concentration from 2.11×10^{-5} to 9.2×10^{-4} M. Even a slight growth of the dimer band is not observable (Fig. 7). A similar change is observed when the dye concentration is kept constant and the quantity of sodium perchlorate is varied.

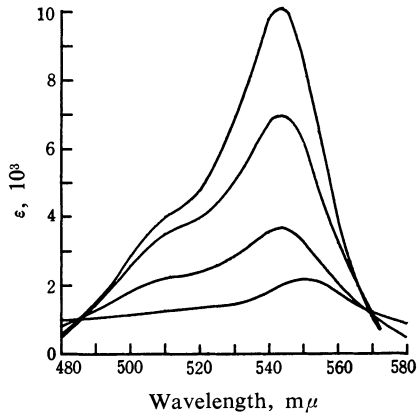


Fig. 7. The absorption spectra of pyronine G in the aqueous solution containing 0.5 M $NaClO_4$.

For the above two cases, perhaps polymers of higher association would be produced in view of the weak and broad absorption band.

The reason that only dimerization occurs in the case of Cl^- and of SO_4^{2-} may lie in the bulky size of such ions due to the high degree of hydration, these ions laterally attached to the dimer cation probably prohibiting the further approach of other dye ions. In the case of I^- and of ClO_4^-, for which the hydration is small at most, the lateral attachment of these ions close to the dye cation might not inhibit the alignment of many dye ions face to face and thus allow the high polymer to be formed.

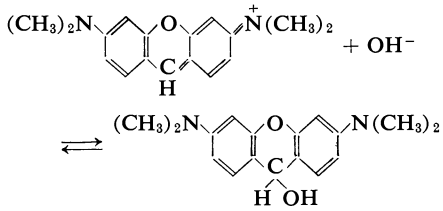
iii) Hydrochloric Acid.—Similar experiments were made using 5 N hydrochloric acid, 1 N hydrochloric acid (potassium chloride 1 M) and 0.001 N hydrochloric acid (potassium chloride 0.1 M) solutions. Qualitatively the dimer formation is quite the same in the case of 0.001 N and of 0.1 N hydrochloric acid as for the neutral solution. One notable fact is that in spite of a shift of the monomer band (toward red),

the position of the dimer band completely coincides with that in the neutral solution. The K-values were found to be 785 and 1300 for 1 N (20°C) and 0.001 N respectively. Taking into account the somewhat larger error of these experiments, it may be said that the above values do not differ much from those in the neutral solution.

The result is quite different in the case of 5 N hydrochloric acid. The absorption spectra, which are shown in Fig. 1, never change through the variation of dye concentration from 2.8×10^{-5} to 9.2×10^{-4} M. The cause for this different behavior is not known at present.

II. The Equilibrium Constant of Carbinol Formation Evaluated from the pH Effect on the Absorption Spectra

The color of the acidic or neutral solution of pyronine G is red, while the alkaline solution is colorless; this change is reversible. As described below, the maximum absorption at 546 mμ in the neutral solution turns into a broader one with a new maximum at 390 mμ. A shift as large as 156 mμ clearly suggests the disappearance of the conjugation in the pyronine cation and may be inferred to be due to the formation of carbinol.



In xanthene dyes there seems to exist no detailed study about the formation of carbinol, but it is well known that triphenylmethane dyes easily form carbinols such as, the carbinol of phenolphthalein[6] crystal violet[7].

The reason for the easy formation of carbinol in the case of pyronine G and the rapid establishment of its equilibrium may perhaps be that it is a positive ion and has no steric hindrance, as judged from its rather simple structure.

In this paper, the equilibrium constant of the carbinol formation is determined at several temperatures from the variation of the absorption spectra due to pH change. From the results, some thermodynamic constants are estimated.

Experimental.—Pyronine G of Merck was dissolved in ethanol and recrystallised by evaporating the solution spontaneously. The crystal obtained was dried in a descicator. $\varepsilon_{max}\approx70000$. Sodium hydroxide, G. R. was used without further purification. Borate and Na_2HPO_4, both G. R., were recrystallized. The buffer solutions employed were the $NaOH\text{-}Na_2B_4O_7$ system and the $NaOH\text{-}Na_2HPO_4$ system. The former was used for the preliminary experiment in the range pH 9.24~12.25 and the latter, for more accurate measurements between pH 11.0 and 12.0. The pH of the solution was measured by a Hitachi pH meter prior to the measurement of the absorption spectra. The glass electrode used was GL-13 for the alkaline solution. Quartz cells were used for spectral measusement in order to minimize the adsorption of dye on the cell wall. The spectrophotometer used was a Hitachi EPU-2. The wavelength width was always maintained at 0.5 mμ. The temperature was controlled by circulating the water from the constant temperature bath.

Results and Discussion.—The pH change of absorption spectra is shown in Fig. 8. As seen from the figure, the peak at 546 mμ in the neutral solution declines with the increase of pH, and a broad band with a peak at 390 mμ gradually rises ($\varepsilon\approx10000$) with an isosbestic point at 445 mμ, which supports the existence of the equilibrium.

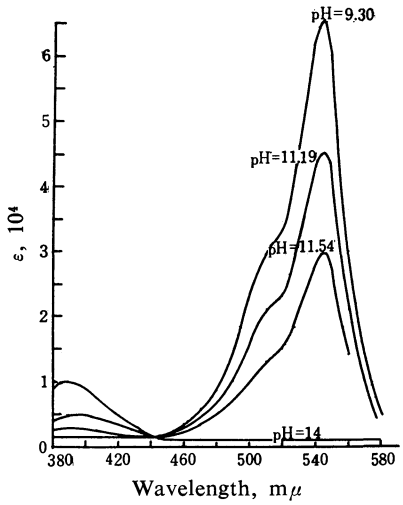


Fig. 8. pH change of absorption spectra of pyronine G.

From the data the equilibrium constant was determined by the following procedure[8]. Writing pyronine G cation as A^+ and carbinol as B, the reaction is represented by

$$A^+ + OH^- \rightleftharpoons B \qquad (5)$$

From a mass action law

$$K=\frac{[B]}{[A^+][OH^-]}=\frac{[B][H^+]}{[A^+]K_w} \qquad (6)$$

where K_w is the ionic product of water.

6) Cf., e. g., M. D. Barnes and V. K. LaMer, *J. Am. Chem. Soc.*, **64**, 2312 (1942).
7) S. Hochberg and V. K. LaMer, ibid., **63**, 3110 (1941).
8) This is a slight modification of the method usually employed for the case of Base+$H^+\rightleftarrows$Acid. Cf., e. g., H. H. Perkampus and Th. Rössel, *Z. Elektrochem.*, **60**, 1102 (1956).

TABLE II. THE VARIATION OF THE OPTICAL DENSITY AT 546 mμ THROUGH pH-CHANGE
(dye concentration: 2×10^{-5} M)

20°C	pH	(9.25)	11.38	11.65	11.83	12.00	(14.0)	
	O. D.	1.35	0.80	0.655	0.513	0.379	0.052	
22.5°C	pH	(9.25)	11.17	11.34	11.53	11.66	11.88	(14.0)
	O. D.	1.30	0.96	0.81	0.66	0.518	0.389	0.055
25°C	pH	(9.30)	10.94	11.19	11.34	11.54	(14.0)	
	O. D.	1.30	1.06	0.90	0.79	0.590	0.020	
27.5°C	pH	(9.30)	10.97	11.21	11.42	11.57	11.78	(14.0)
	O. D.	1.35	1.06	0.925	0.72	0.529	0.360	0.024
30°C	pH	(9.30)	10.93	11.15	11.43	11.60	11.81	(14.0)
(a)	O. D.	1.36	1.14	1.04	0.91	0.76	0.495	0.024
30°C	pH	(9.30)	11.07	11.19	11.39	11.58	11.75	(14.0)
(b)	O. D.	1.30	0.85	0.78	0.570	0.416	0.304	0.056

TABLE III. pK VALUES AT VARIOUS TEMPERATURES

Temp., °C.,	20	22.5	25	27.5	30
pK	-2.52 ± 0.02	-2.47 ± 0.02	-2.45 ± 0.02	-2.37 ± 0.02	-2.06 ± 0.04 -2.48 ± 0.02

Of course, K in 6 is not a rigorous equilibrium constant in the thermodynamical sense but only an apparent one in the phosphate buffer solution in the pH range 11~12.

Taking logarithm of Eq. 6

$$\log K=\log[H^+]-\log K_w+\log([B]/[A^+])$$

or

$$pK=pH+\log K_w-\log([B]/[A^+]) \qquad (7)$$

the application of Beer's law for each molecular species leads to Eq. 8 in which ε_{A^+}, ε_B and ε are respectively, the molar absorbancy of A^+ and of B and the apparent molar absorbancy at the corresponding pH.

$$pK=pH+\log K_w-\log\frac{\varepsilon_{A^+}-\varepsilon}{\varepsilon-\varepsilon_B} \qquad (8)$$

For ε_{A^+} and ε_B, one can use respectively the molar absorbancy in the neutral solution and in the strong alkaline solution. Plotting $\log(\varepsilon_{A^+}-\varepsilon)/(\varepsilon-\varepsilon_B)$ against pH, one obtains a straight line with a slope of 45°, and the pH-value at intercept, combined with $\log K_w$[9], gives the pK-value.

The experimental results in the phosphate buffer solution are given in Table II.

Using the above data and putting ε_B as 0.02, pK was calculated from 8. An example of the plot is shown in Fig. 9, and the results are given in Table III.

From these (the values at 30°C were omitted because they are less reliable), ΔG^0, ΔS^0 and ΔH^0 were calculated using the relations,

$$\Delta G=2.303\,RT\,pK,\quad \Delta S=-(\partial\Delta G/\partial T)$$
$$\Delta H=4.56\{\partial pK/\partial(1/T)\}$$

The results are

ΔG(kcal.): -3.38(20°C) -3.35(22.5°C)
-3.34(25°C) -3.30(27.5°C)

ΔS=ca. -12 cal./deg.mol.

$\Delta H=-8\pm3$ kcal./mol.

These values are not very accurate, but it is certain that the formation of carbinol in the phosphate buffer is an exothermic reaction with a small decrease of entropy.

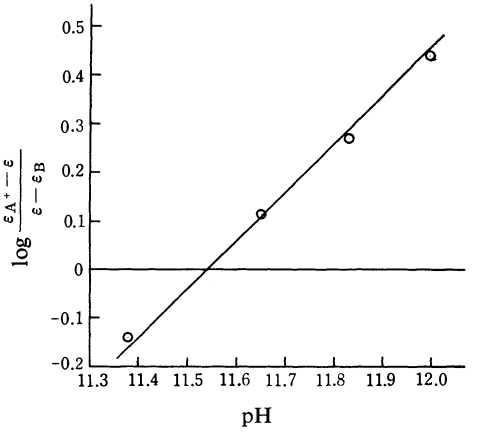


Fig. 9. Plot of $\log\frac{\varepsilon_{A^+}-\varepsilon}{\varepsilon-\varepsilon_B}$ against pH (20°C).

9) Beilstein, International Critial Table, Vol. VI, (1929), p. 152.

III. The Fluorescent Behaviors of the Aqueous Solution of Pyronine G

The formation of cabinol, which was established by the pH variation of the absorption spectra would not occur so promptly as does the proton addition or its detachment. Hence, the same equilibrium constant is to be expected from the pH variation of fluorescence if it can be measured. This was confirmed by the present investigation; in addition, the excitation spectra were measured.

Experimental.—*Sample.*—Same as the absorption experiment. The concentration is 2×10^{-5} M unless otherwise described.

Procedure.—The fluorescence spectra were measured with the fluorescence accessory of a Hitachi spectrophotometer EPU-2; hence, they are not genuine fluorescence spectra. The measurements were made at room temperature. The exciting light is 365 mμ from a high pressure mercury lamp (100 W). In order to obtain the pK-value of the carbinol formation from the pH variation of the fluorescence intensity, a newly constructed fluorometer was used which had been designed on the principle of the optical zero-method and which enables one to measure the action spectra of the fluorescence[10]. As the light source, a 200W tungsten filament lamp (projection lamp) was used. Its intensity distribution was calculated by the use of Planck's formula for black body radiation[11], in

$$N_\lambda = \frac{2\pi c}{\lambda^4}\left\{\exp\left(\frac{hc}{k\lambda T}\right)-1\right\}^{-1}$$

which c, λ and T are light velocity, wavelength (μ), and absolute temperature respectivery; the dimension of N_λ is photons/cm^2 sec. μ. The color temperature of the tungsten lamp (100 V.) was determined in such a way as to make the action spectra of eosine and uranine, of which the quantum yield is known to be independent of wavelength, as similar to the absorption spectra as possible. It was found that $T=2800$°K gives a satisfactory result, as is shown in Fig. 10.

The wavelength width was taken into account.

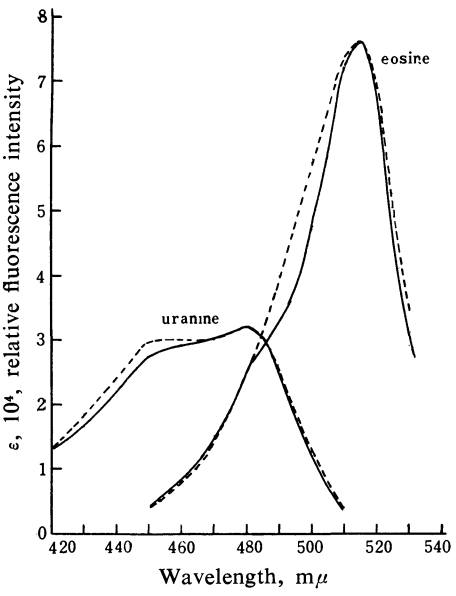


Fig. 10. Action spectra (------) and absorption spectra (——) of eosine and uranine.

Results.—*pH Variation of the Fluorescence Spectra.*—An example is shown in Fig. 11. The

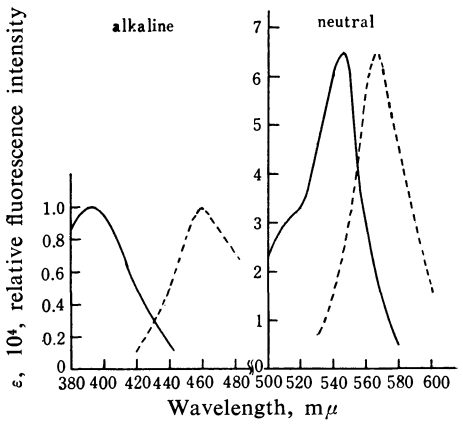


Fig. 11. Fluorescence spectra of pyronine G.

maximum of the fluorescence spectra in the neutral solution lies at 566 mμ, which is displaced about 20 mμ from the absorption maximum. The result that there exists no shoulder corresponding to a dimer is naturally to be expected, since the dimer in most dyes has no power of emission. The alkaline solution, on the other hand, gives a fluorescence spectra with a maximum at 460 mμ corresponding to 390 mμ of the absorption spectra. Stokes' shift of 70 mμ is much larger than the 20 mμ of the

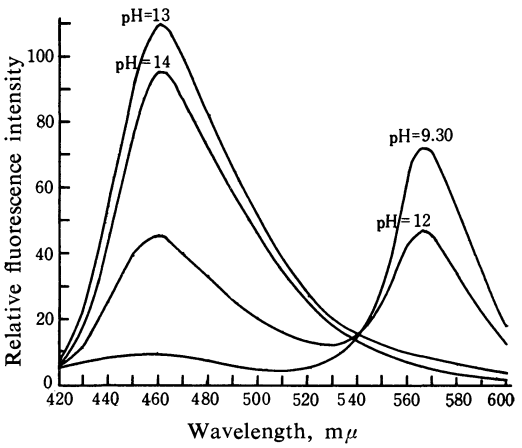


Fig. 12. The pH dependence of the flourescence spectra of pyronine G.

10) To be published elsewhere.
11) A. N. Lowan and G. Blauch, *J. Opt. Soc. Am.*, **30**, 70 (1940).

TABLE IV. pH CHANGE OF THE FRUORESCENCE INTENSITY

20°C	pH	9.30	10.95	11.37	11.51	11.87	12.00	14
	I	563	380	355	251	174	112	1.00
25°C	pH	9.30	11.12	11.35	11.45	11.60	12.06	14
	I	38	25.12	17.8	16.6	7.58	6.45	1.00
30°C	pH	9.30	11.0	11.19	11.37	11.54	11.76	14
	I	44.7	30.2	24.0	17.4	10.5	7.08	1.00

neutral solution. The spectra at various pH cross at a point near 540 mμ, which indicates, analogous to the isosbestic point in the case of absorption spectra, that two molecular species existent in equilibrium give rise to an independent fluorescence. This is shown in Fig. 12. The fluorescence of carbinol declines somewhat at pH 13 ; this may perhaps be due to the quenching by the OH^- ion.

The Determination of pK from the pH Change of Fluorescence Intensity.—Since pyronine G cation and carbinol each emit a separate fluorescence, the quantitative investigation of the pH change of the fluorescence intensity of one component will make it possible to determine the equilibrium constant of the carbinol formation. To make the calculation feasible, λ of the exciting light was chosen at 445 mμ, which is an isosbestic point. A photographic filter (0-2) which cuts $\lambda<560$ mμ was used to remove the exciting light.

The calculation was made as follows, taking into account the fact that the fluorescence of the two molecular species slightly overlap. Putting the molar fraction of the cation and carbinol as X_{A^+} and X_B respectively, and denoting the relative intensity as I_{A^+} and I_B, the measured intensity can be expressed by

$$I=I_{A^+}X_{A^+}+I_BX_B$$
$$=I_{A^+}\frac{[A^+]}{[A^+]+[B]}+I_B\frac{[B]}{[A^+]+[B]}$$

Combining this with

$$K=\frac{[B]}{[A^+][OH^-]}$$

one gets

$$pK=-\log\frac{I_{A^+}-I}{I-I_B}+pH+\log K_w$$

This is quite analogous to the formula for the absorption spectra. The results are given in Table IV. An example is shown in Fig. 13. From the above data, pK and the related thermodynamic quantities were calculated as follows:

pK: -2.66 ± 0.03(20°C), -2.59 ± 0.05(25°C), -2.50 ± 0.02(30°C)

ΔG: -3.60(20°C), -3.52(25°C), -3.45(30°C)

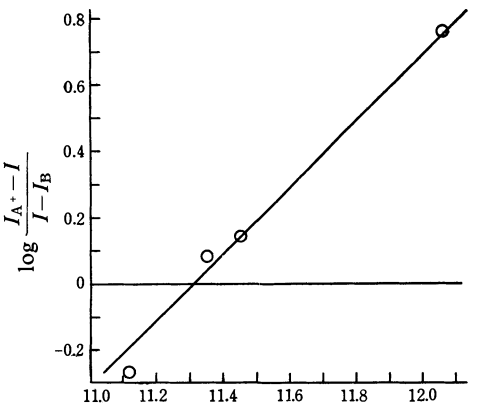


Fig. 13. Plot of $\log\frac{I_{A^+}-I}{I-I_B}$ against pH (25°C).

$\Delta H=-6.5\pm1.5$ kcal./mol.
$\Delta S=-14\pm3$ kcal./mol.

All the above data are nearly equal to those obtained from the absorption spectra. Above pH=13 the fluorescence intensity shows a decrease with the increase of $[OH^-]$, but in the above pH region this effect may perhaps be so small that it can be disregarded.

Action Spectra.—Excitation spectra of fluorsecence in the aqueous solution of pyronine G were measured by a newly constructed fluorometer. The result, as shown in Fig. 14, largely

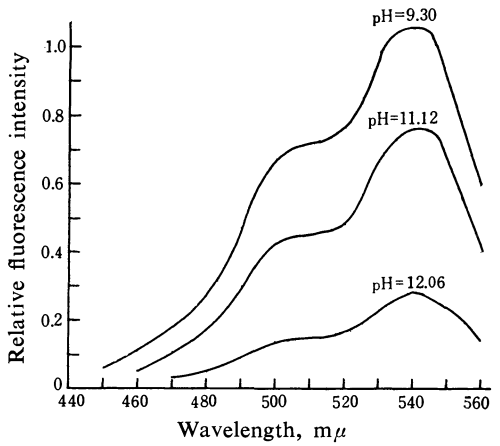


Fig. 14. Excitation spectra of fluorescence in the aqueous solution of pyronine G.

coincides with the absorption spectra, indicating that the quantum yield of fluorescence is independent of the wavelength. It is, however, worth while to note that a shoulder similar to that of the absorption is existent in the action spectra. This is somewhat curious in view of the fact that a dimer, which is the source of this shoulder, is commonly considered to be non-fluorescent, and there is indeed no shoulder in the fluorescence spectra. The reason for this is not yet certain ; it might be that the exciting energy is transferred to a neighboring monomer or that the excited dimer rapidly dissociates into monomers (in an excited and ground state) and then the emission takes place. Further studies are required.

Summary

Th effect of inorganic anions on the dimerization constant of pyronine G in an aqueous solution was examined. It was found that the effect is very specific and can not be explained simply by the effect of the ionic strength. The analysis led to the conclusion that a dimer exists as an ion-pair with the anions attached laterally to dye ions instead of being sandwiched between two dye ions.

The change of absorption spectra in the alkaline solution was interpreted to be due to the formation of carbinol, and from its analysis the formation constant of carbinol was determined.

Carbinol was found to have also its proper fluorescence, and from the pH change of fluorescence spectra the formation constant of carbinol was again decided, the value of which coincided well with that obtained from the absorption spectra.

Department of Chemistry
Faculty of Science
Tohoku University
Katahira-cho, Sendai

Anionic Polymerization of Vinylidene Chloride. I. Susceptibilities of Vinyl Monomers to Initiation by Ionic Catalysis

By Akio KONISHI

(Received May 10, 1961)

The reactivity of the vinyl monomers in the radical polymerization have been theoretically discussed in a number of publications which have dealt with the problem using the molecular orbital method[1,2], the frontier electron theory[3-5], a Q-e or q-ε scheme[6-8], or a polarity parameter[9]. It is considered in ionic polymerization that monomers form an intermediate ionic complex with the catalyst; the mutual relationship between the monomer and the catalyst seems to be more important in ionic polymerization than in free radical polymerization. This paper is intended to make a survey of the susceptibility of vinyl monomers to ionic catalysis.

Theoretical

Susceptibility and Q-e or q-ε Map. — Alfrey and Price have presented polarity (e) and resonance (Q) factors for vinyl monomers derived from copolymerization data to explain the monomer reactivity ratios; they have reported Q and e values on thirty one monomers[6,7]. This concept has been theoretically extended and generalized, and a new set of parameter q for resonance and ε for polarity has been proposed for one hundred and ten monomers[8]. Walling[10] and Furukawa[11] pointed out that there is a linear relationship between relative reactivities or polarity factor

1) M. G. Evans, J. Gergely and E. C. Seaman, *J. Polymer Sci.*, **3**, 886 (1948).
2) T. Fueno, T. Tsuruta and J. Furukawa, *J. Chem. Soc. Japan, Pure Chem. Sec.* (*Nippon Kagaku Zasshi*), **78**, 1075 (1957).
3) T. Yonezawa, T. Higashimura, K. Katagiri, S. Okamura and K. Fukui, *Chem. High Polymers* (*Kobunshi Kagaku*), **14**, 533 (1957).
4) K. Hayashi, T. Yonezawa, C. Nagata, S. Okamura and K. Fukui, *J. Polymer Sci.*, **20**, 537 (1956).
5) T. Yonezawa, K. Hayashi, C. Nagata, S. Okamura and K. Fukui, ibid., **14**, 312 (1954).
6) T. Alfrey and C. C. Price, ibid., **2**, 101 (1947).
7) C. C. Price, ibid., **3**, 772 (1948).
8) T. C. Schwan and C. C. Price, ibid., **40**, 457 (1959).
9) C. H. Bamford, A. D. Jenkins and R. Johnston, *Trans. Faraday Soc.*, **55**, 418 (1959).
10) C. Walling, E. R. Briggs, K. B. Wolfstirn and F. R. Mayo, *J. Am. Chem. Soc.*, **70**, 1537 (1948).
11) J. Furukawa and T. Tsuruta, *J. Polymer Sci.*, **36**, 275 (1959).

e and Hammett sigma constants of ionic reaction, and Price[8] has also shown a good linear relation between ε values of styrene derivatives and Hammett sigma constants. Although such a good linearity as this has not been obtained in the case of ethylene derivatives, the effect caused by a substituent of the phenyl group on the double bond of styrene is assumed to correspond to the effect caused by the substituent of ethylene derivatives on their double bond, and the polarity parameter *e* or ε should reasonably be applied for indicating the ionic reactivity of vinyl monomers in ionic polymerization as well as in radical polymerization.

Although numerous experimental data have been reported on the susceptibilities of various monomers to homopolymerization under anionic, free radical, and cationic conditions, Schildknecht's table[12] is taken here as a reliable reference; here he has classified the susceptibilities of fifty four monomers.

The relationship between the susceptibility and the *Q-e* values of fourteen monomers obtained from the original *Q-e* table[7] is illustrated in Fig. 1. Furukawa[11] has presumed that monomers having a large plus *e* value ($e>1.5$) are likely to be polymerized in an anionic condition; on the contrary, monomers having large negative *e* values ($e>-1.0$) are likely to be polymerized in a cationic condition. However, it seems rather difficult to explain the behavior of monomers (such as styrene, butadiene and methyl vinyl ketone) which can be polymerized in both radical and ionic conditions. The susceptibility arranged according to Price's new parameter *q*-ε for twenty two monomers is illustrated in Fig. 2.

In general, cationic polymerization takes place with monomers whose double bond is negatively polarized and has an affinity to electrophillic reagents, whereas the double bond of anionic polymerizable monomers is positively polarized and reacts with nucleophillic reagents. As a first approximation, the magnitude of polarization in an ionic condition seems to correspond to the polarity expressed by the polarity factor *e* or ε. With the resonance factor *Q* or *q*, such a good relationship as ε vs. sigma has not yet been obtained, but the *Q* or *q* factor is closely connected with the reactive pi electrons of the vinyl bond, namely, with the electron donating or accepting characters of the vinyl bond, and if the electronic field is so large as to induce the polarization of pi electrons, the magnitude of such electrodynamic polarity here induced may serve to form an ionic complex with an ionic catalyst. Accordingly, the *Q* or *q* factor may also be regarded as a reactivity determining factor in ionic reactions, and both the *e*(ε) and *Q*(*q*) factors may be helpful in explaining

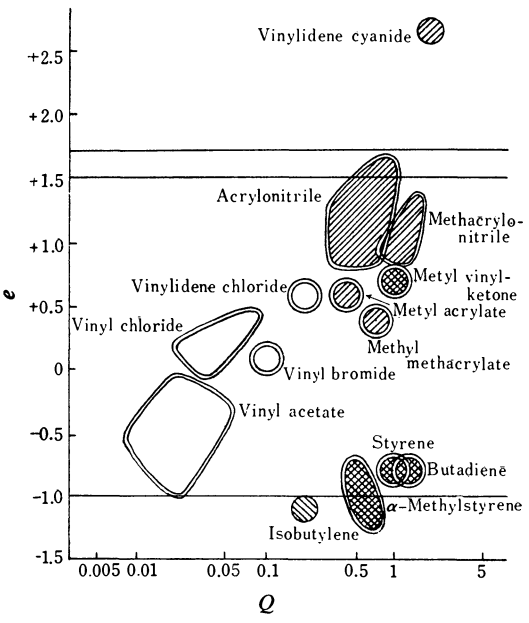


Fig. 1. Relationship between susceptibility and *Q-e* map. Susceptible to radical ◎, anion ▨ and cation ▩.

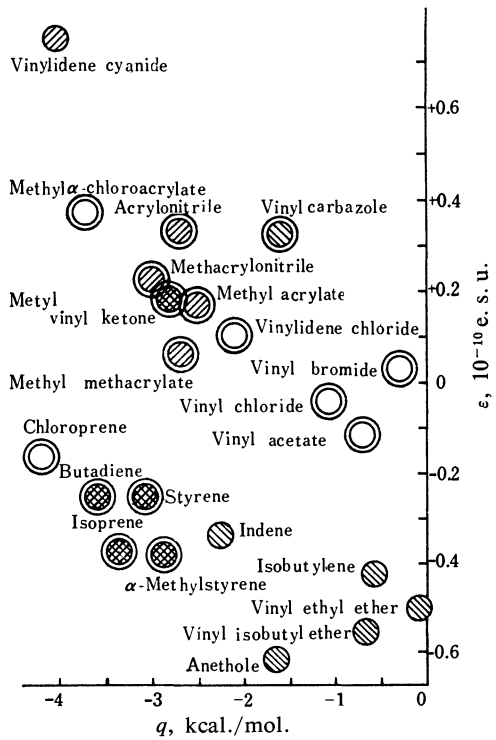


Fig. 2. Relationship between susceptibility and *q*-ε map. Susceptible to radical ◎, anion ▨ and cation ▩.

12) C. E. Schildknecht, *Ind. Eng. Chem.*, **50**, 107 (1958).

the susceptibility of a monomer in an ionic polymerization reaction. Hence, Q-e or q-ε maps can be related to the susceptibilities of vinyl monomers to initiation by an ionic catalyst. Monomers like styrene or butadiene, which has a conjugated double bond, are polymerized by either a cationic or anionic catalyst.

Another factor affecting polymerizability may be steric effect, but the order of its magnitude is difficult to estimate quantitatively. As the matter of fact, the steric factor should be involved implicity in the Q-e or q-ε factors, because the latter factors are experimentally determined.

The propagating macro anions seem to be relatively stable because the living polymer has been obtained in the anionic polymerization of styrene[13]. It is deduced that the larger the value of e (or ε) and Q (or q) of the monomers, the greater the susceptibilities of the monomers toward the ionic catalyst.

The relative susceptibilities can be shown as in Fig. 3 (q-ε map) and Fig. 4 (Q-e map), in which the Q-e values of vinyl ethyl ether[14], vinyl chloride[15], vinylidene chloride[15], acrylonitrile[15], chlorotrifluoroethylene[16] and vinylidene cyanide[17] are added, besides the values listed in Refs. 7 and 8. The values were converted by the following equations,

$$q = -2\times10^{-3}\,T\ln Q - 3.1$$

$$\varepsilon = 1.66\times10^{-12}\,T^{1/2}\,e$$

in which T=323°K. The area of the map is determined from the following monomers: vinylidene cyanide, anethole, 2, 3-dichloro-1, 3-butadiene and diphenylacetylene (Ref. 8).

In the map, the diagonal line along which the monomers are distributed shows the relative susceptibilities of monomers to catalysts: at first vinylidene cyanide is located at the upper left corner, followed by acrylonitrile, methacrylonitrile, methyl acrylate, methyl methacrylate (in the order of decreasing susceptibility to anion); styrene, butadiene, isoprene (susceptible to anion, radical and cation and located near the center parallel to the diagonal line); vinylidene chloride, vinyl chloride, vinyl acetate (susceptible to radical); isobutylene, indene, and finally vinyl ether (in the order of decreasing susceptibility to cation). The susceptibility of methyl vinyl ketone (to either cation, radical or anion) and vinylcarbazole (to both radical and cation) are understandable considering that they are located in the central part of the map.

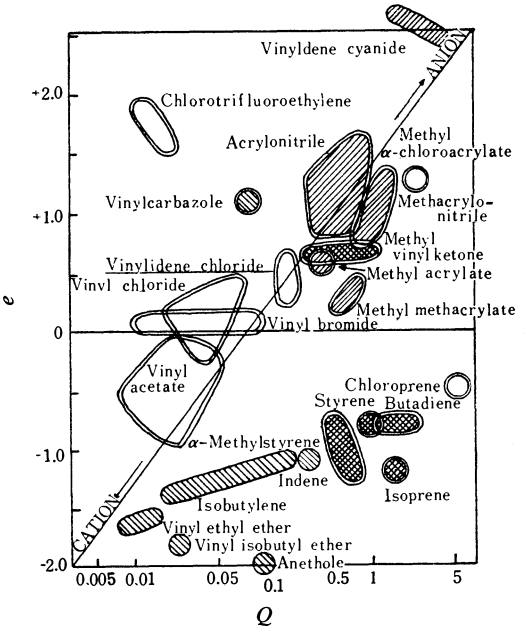


Fig. 4. Relationship between susceptibility and Q-e map. Susceptible to radical ◎, anion ▨ and cation ▧.

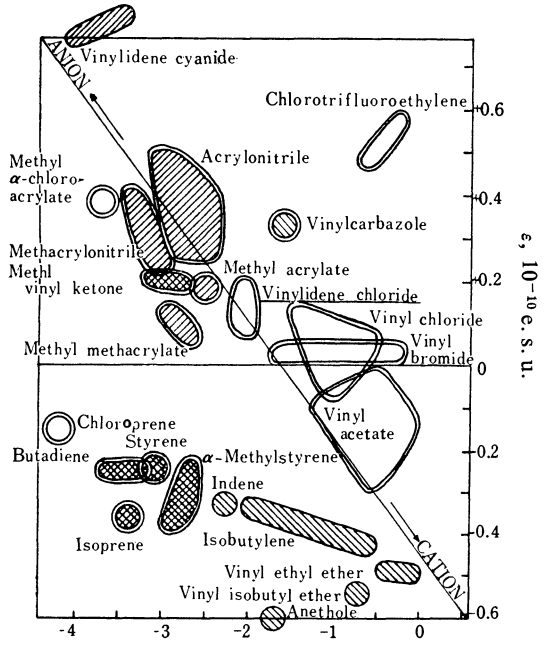


Fig. 3. Relationship between susceptibility and q-ε map. Susceptible to radical ◎, anion ▨ and cation ▧.

13) M. Szwarc, M. Levy and R. Milkovich, *J. Am. Chem. Soc.*, **78**, 2656 (1956).
14) C. C. Price and T. C. Schwan, *J. Polymer Sci.*, **16**, 577 (1955).
15) B. R. Thompson and R. H. Raines, idid., **41**, 265 (1959).
16) N. Kliman and M. Lozàr, *Chem. prûmysl.*, **9**, 668 (1959).
17) H. Gilbert, *J. Am. Chem. Soc.*, **78**, 1669 (1956).

Application of *Q-e* or *q-ε* Map. — It is considered that all monomers can be polymerized by either a anionic, radical or cationic catalyst under proper ionic conditions where undesired side reactions between the initiating ion (or its counter ion) and the polar substituents of the monomer can be eliminated as much as possible.

New Polymerization Reaction.—There are a considerable number of monomers which have not been polymerized by ionic reagents. Some of these which are not classified in Ref. 12 are shown in the map, Fig. 5. It can be predicted from the map that cationic polymerization should be possible for such monomers as hexene-1, hexyne-1, *N*-vinylpyrrolidone and stilbene, and for isostilbene, vinyl formate and vinyl acetate with some difficulty. Anionic polymerization will be possible for acrylamide, acrolein, vinylcarbazole, and vinylidene chloride, and either anionic or cationic polymerization of 1,1-diphenylethylene, methyl isopropenyl ketone, methacrolein, acrolein, and 2- and 4-vinylpyridines will be possible. The author has succeeded in the polymerization of vinylidene chloride in anionic mechanism; the details will be reported on in Parts II and III of this report.

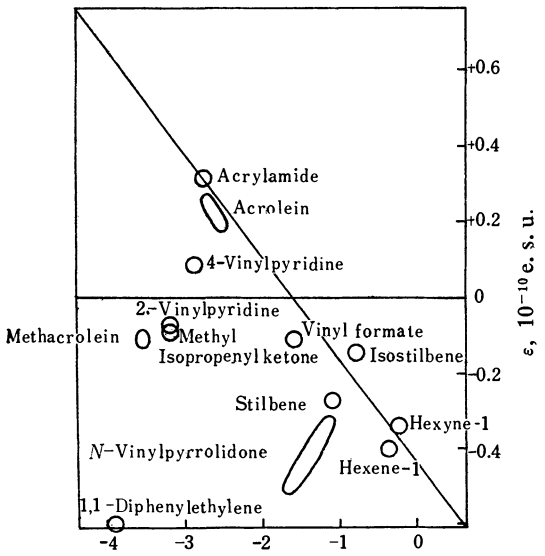


Fig. 5. Locations of several monomers in *q-ε* map.

Ionic Copolymerization.—Data of the monomer reactivity ratios in ionic polymerization[18,19] are very interesting since the relative reactivity of monomers in the ionic reaction can be estimated from them. Although data are less available and are more uncertain than in the case of radical copolymerization, it can be seen qualitatively that in cationic copolymerization the monomer reactivity ratios of the monomer seated near the lower right corner are larger than the comonomer, and in anionic copolymerization the monomer reactivity ratios of the monomer located near the upper left corner are larger than the comonomer; the arrow in Figs. 6 and 7 shows the monomers whose monomer reactivity ratios are larger in the pair. The case of styrene-vinyl acetate is

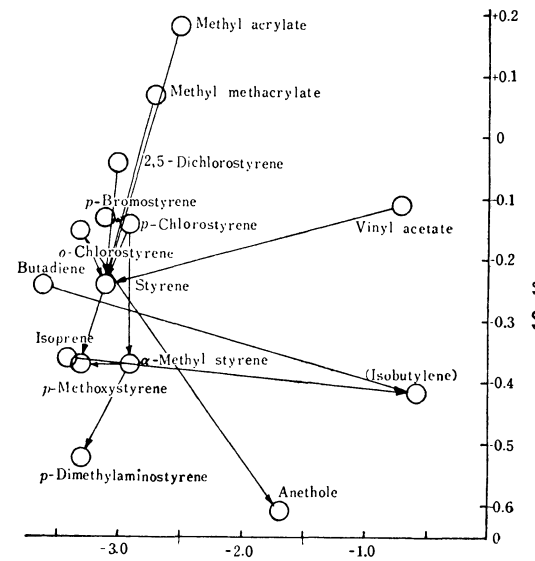


Fig. 6. Relative reactivities of monomers in cationic copolymerization.

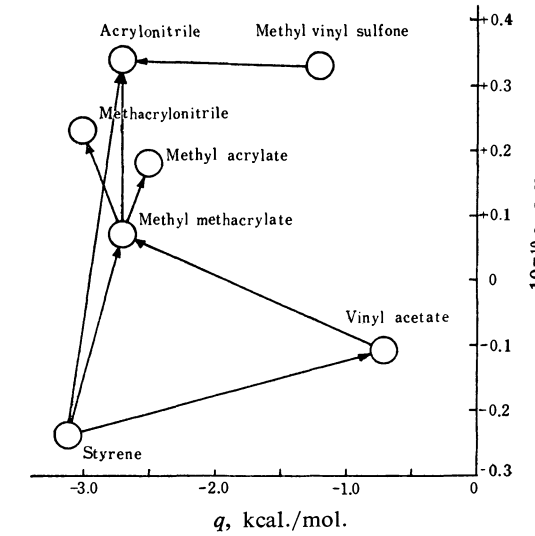


Fig. 7. Relative reactivities of monomers in anionic copolymerization.

18) D. C. Pepper, *Quart. Rev.*, 8, 88 (1954).
19) N. L. Zutty and F. J. Welch, *J. Polymer Sci.*, 43, 445 (1960).

somewhat abnormal, for in this case both r_1 and r_2 are far smaller than unity. It is possible to predict the relative tendency between two monomers which enter into copolymerization under an ionic condition, and the results on the anionic copolymerization of vinylidene chloride, which will be reported on in Part III, will present an experimental evidence of this scheme.

Summary

The relative reactivities of vinyl monomers under ionic conditions have been discussed using a Q-e or q-ε map. It has been deduced that the larger the value of the polarity factor e (or ε) and the resonance factor Q (or q) of the monomer, the greater the susceptibility of the monomers to ionic catalysis. The possibility of new ionic polymerization reaction and the relative reactivity of monomers in ionic copolymerization have been discussed. As the result of this scheme, it seems that the anionic polymerization of vinylidene chloride is possible.

Tokyo Laboratory
Kureha Kasei Co., Ltd.
Shinjuku-ku, Tokyo

Anionic Polymerization of Vinylidene Chloride. II. Homopolymerization Initiated by n-Butyllithium

By Akio KONISHI

(Received May 10, 1961)

A number of attempts to polymerize various vinyl monomers by *n*-butyllithium have recently been reported on such monomers as butadiene[2-4], isoprene[5-9], styrene[10-16], methyl methacrylate[12,13], acrylonitrile[12,13], vinyl chloride[13,17], methyl and butyl acrylates[12], dimethyl maleate[12], vinyl acetate[12,13], allyl acetate[12] and vinyl *n*-butyl ether[13], though successful results have not yet been obtained in the last five monomers. From the copolymerization data it has been proposed that the polymerization initiated by this catalyst is of anionic mechanism[18,19].

An attempt to polymerize vinylidene chloride under anionic conditions by *n*-butyllithium has been made because the monomer is considered to be susceptible to anionic catalysis, as has been discussed in a previous paper[1].

Experimental

A vinylidene chloride monomer produced by the Kureha Kasei Co. was repurified by drying it over calcium hydride and then distilling it under an argon atmosphere in the presence of copper stearate immediately before use. *n*-Hexane and *n*-butyl bromide were dried over calcium hydride and distilled immediately before use. Argon was freed from the oxygen by passing it through an alkaline solution of pyrogallol and drying it with concentrated sulfuric acid.

n-Butyllithium, prepared in *n*-hexane by the reaction of *n*-butyl bromide with lithium metal by a method similar to that of Gilman[20], was kept standing in the Schlenk apparatus and its concentration checked by titration[21] before use.

From half to one mole of monomer was used in every run. The addition of the reagents and the polymerizations were carried out under argon. Into

1) A. Konishi, This Bulletin, 35, 193 (1962).
2) A. A. Korotkov, *Angew. Chem.*, 70, 85 (1958).
3) V. A. Kropachev, B. A. Kolgolosk and N. I. Nikolaev, *Doklady Akad. Nauk, S. S. S. R.*, 115, 516 (1957).
4) I. Kuntz and A. Gerber, *J. Polymer Sci.*, 42, 299 (1960).
5) H. Hsieh and A. V. Tobolsky, ibid., 25, 245 (1957).
6) H. Hsieh, D. J. Kelley and A. V. Tobolsky, ibid., 26, 240 (1957).
7) H. Morita and A. V. Tobolsky, *J. Am. Chem. Soc.*, 79, 5853 (1957).
8) R. S. Stearns and L. E. Forman, *J. Polymer Sci.*, 41, 381 (1959).
9) A. A. Korotkov, N. N. Chesnokova and L. B. Trukhanova, *Visokomolekulyarnye Soedineniya*, 1, 46 (1959).
10) A. Zilkha, M. Albeck and M. Frankel, *J. Chem. Educ.*, 35, 345 (1958).
11) H. Sinn, C. Lundborg and K. Kirchner, *Angew. Chem.*, 70, 744 (1958).
12) M. Frankel, A. Ottolenghi, M. Albeck and A. Zikka. *J. Chem. Soc.*, 1959, 3858.
13) J. Furukawa, T. Tsuruta, K. Ito, I. Kashiuchi and A. Kawasaki, *J. Chem. Soc. Japan, Ind. Chem. Sec.* (*Kogyo Kagaku Zasshi*), 63, 96 (1960).
14) K. F. O'Driscoll and A. V. Tobolsky, *J. Polymer Sci.*, 35, 259 (1959).
15) F. J. Welch, *J. Am. Chem. Soc.*, 81, 1345 (1959).
16) R. J. Kern, *Nature*, 187, 410 (1960).
17) S. A. Solvic, Belg. Pat. 566529 (Oct. 15, 1958).
18) K. F. O'Driscoll and A. V. Tobolsky, *J. Polymer Sci.*, 37, 363 (1959).
19) N. L. Zutty and F. J. Welch, ibid., 43, 445 (1960).
20) H. Gilman, J. A. Beel, C. G. Branner, M. W. Bullock, G. E. Dunn and L. S. Miller, *J. Am. Chem. Soc.*, 71, 1499 (1949).
21) M. Frankel, J. Rabani and A. Zilkha, *J. Polymer Sci.*, 28, 387 (1958).

a four-necked flask fitted with a stirrer, thermometer, and a gas inlet as well as an outlet for the argon, the required amounts of monomer and solvent were added. At above 30°C the polymerizations were carried out in a 150 cc. glass ampoule as a polymerization apparatus, and the reagents used were all added at −70°C under argon. The polymerization was stopped after the required time interval by adding methanol, followed by the pouring in of excess methanol. The polymer precipitated was filtered off with a glass filter, washed with methanol and water successively, and then dried to a constant weight in a vacuum-desiccator at 40°C. The rate of polymerization was determined gravimetrically.

Intrinsic viscosities were measured in cyclohexanone at 30°C, using an Ubbelohde dilution viscometer. The chlorine content of the polymer was measured by the combustion method with a Shimadzu universal micro determination apparatus type UM-2. The infrared spectra of the pressed potassium bromide disk containing the above samples were measured by a Perkin-Elmer model 13 infrared spectrophotometer.

Results

Polymerizations were carried out with *n*-hexane as a solvent, and the influences of monomer concentration (M), catalyst concentration (BuLi) and polymerization temperature on the rate of polymerization (R_p), intrinsic viscosity [η] and chlorine content were investigated. The initial slope of conversion vs. time curve was taken as the rate of polymerization. The rate was markedly influenced by the method of the addition of the catalyst, as is illustrated in Fig. 1. In this paper, however, the author will report on the rate of polymerization induced by adding all the catalyst at the beginning of the reaction.

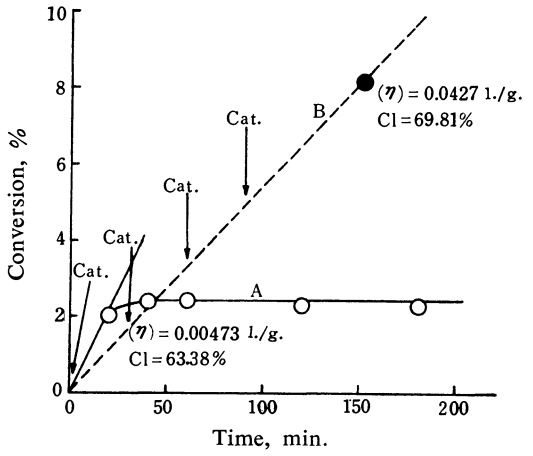


Fig. 1. Conversion vs. time curve.
Temp., 25°C ; A : (M) = 11.13 mol./l., (BuLi) = 0.111 mol./l., whole amount of the catalyst was added initially; B : (M) = 11.44 mol./l., (BuLi) (final) = 0.0917 mol./l., each quarter of the whole amount of the catalyst was successfully added in every 30 min.

As listed in Table I, hydroquinone, a typical radical scavenger, showed little effect on the rate of polymerization, whereas dibenzoyl peroxide, a typical peroxide, reacted immediately with the catalyst and showed an inhibiting effect. This is thought to be an experimental evidence of the ionic character of the polymerization.

In Fig. 2 it is shown that, for a given monomer concentration, the rate is independent of the catalyst concentration above the critical

TABLE I. EFFECT OF INGREDIENTS
Temp., 25°C ; time, 30 min.; (M) = 5.00 mol./l., (BuLi) = 0.100 mol./l.

Ingredient	Concn. mol./l.	Conv. %	[η] l./g.
None	—	1.81	0.0064
Hydroquinone	0.050	2.06	0.0036
Dibenzoyl peroxide	0.050	0.017	0.0048

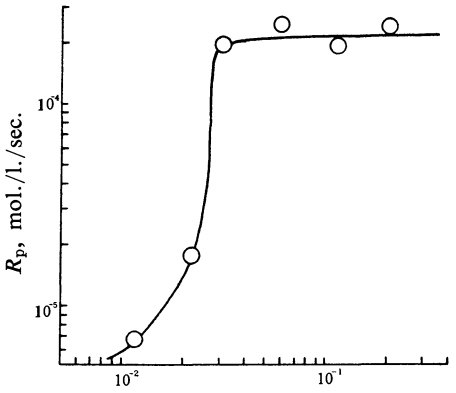


Fig. 2. The rate vs. catalyst concentration.
Temp., 25°C ; (M) = 10.0∼12.1 mol./l.

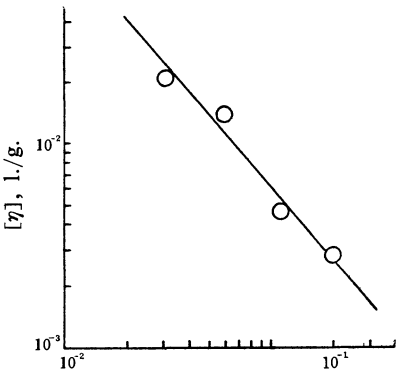
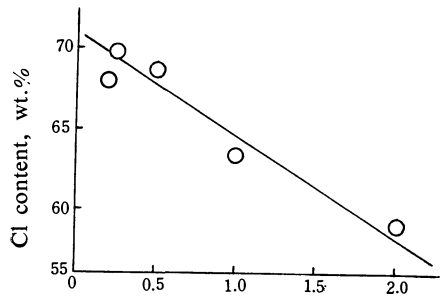


Fig. 3. Intrinsic viscosity vs. catalyst concentration. Condition, the same as in Fig. 2.

value (0.03 mol./l. in the case). The decrease in viscosity and chlorine content are inversely proportional to the increment of the concentration of the catalyst, as is shown in Figs. 3 and 4 respectively. Figure 4 also suggests that the polar chlorine atom reacted with the catalyst.

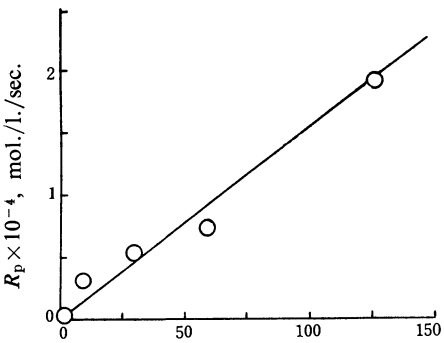
The rate of polymerization is proportional to the square of the monomer concentration, as in Fig. 5. Intrinsic viscosity decreases with the increasing monomer concentration, as in Fig. 6.

The effect of temperature on the rate was investigated in a range between −30 and +50°C, and the activation energy of the overall rate of polymerization was calculated to be 10.7 kcal./mol. from the Arrhenius plot, as is shown in Fig. 7. This relatively small value agrees with the activation energy found in methyl methacrylate (7.6 kcal./mol.)[13] and vinyl chloride (8.8 kcal./mol.)[13]. Intrinsic viscosity passed through a maximum at +10°C, as in Fig. 8. Chlorine content is almost independent of the temperature.



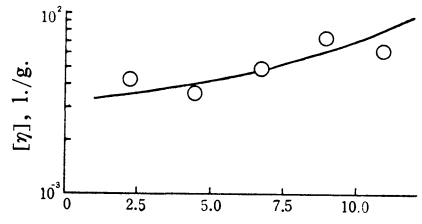
(BuLi), mol. % to monomer

Fig. 4. Cl content vs. catalyst concentration. Condition, the same as in Fig. 2.



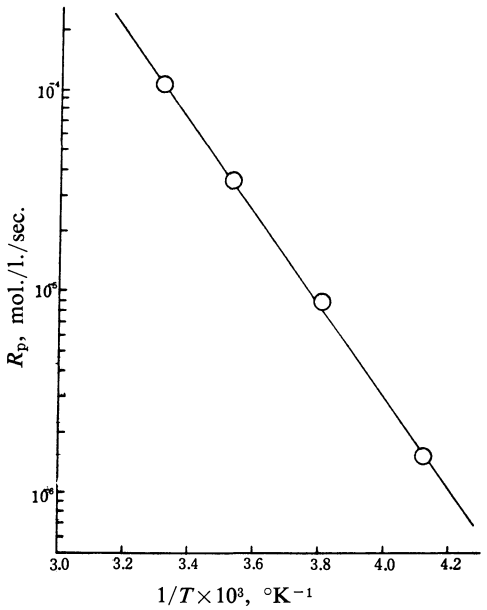
$(M)^2$, mol^2/l^2

Fig. 5. The rate vs. monomer concentration. Temp., 25°C ; (BuLi) = 1.00 mol.% to monomer.



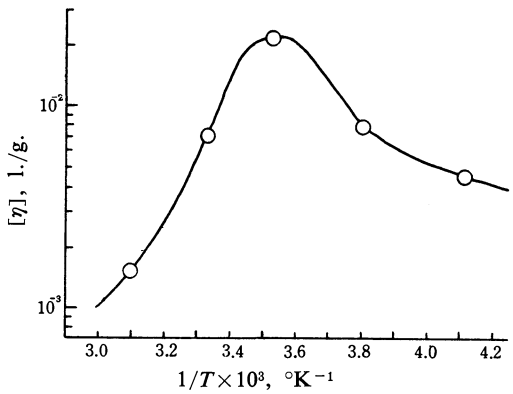
(M), mol./l.

Fig. 6. Intrinsic viscosity vs. monomer concentration.
Temp., 25°C ; (BuLi) = 0.1086 mol./l.



$1/T \times 10^3$, °K^{-1}

Fig. 7. The rate vs. temperature.
(M) = 8.91 mol./l.; (BuLi) = 0.0893 mol./l.



$1/T \times 10^3$, °K^{-1}

Fig. 8. Intrinsic viscosity vs. temperature. Condition, the same as in Fig. 7.

Discussion

The kinetics of anionic polymerization of some other monomers initiated by *n*-butyllithium have been presented by O'Driscoll[14], Welch[15], Furukawa[13] and Korotkov[9], though they have not coincided with one another at

several points. The following mechanism is suggested:

$$(BuLi)_n \rightleftarrows BuLi + (BuLi)_{n-1} \quad (1)$$

$$BuLi + M \xrightarrow{k_I} BuM^- + Li^+ \quad (2)$$

$$BuM^- + M + Li^+ \xrightarrow{k_p} \cdots \xrightarrow{k_p} Bu(M)_n^- + Li^+ \quad (3)$$

In a propagating step, the structure of the growing polymer chain seems to be not so simple as that expressed in an ion-pair form like 4, but it is assumed to be a complex one like cyclic structure 5 or like ionic quadrapole 6, as suggested by Cram[22] or Mark[23] in the stereospecific polymerization of methyl methacrylate or diene:

$$Bu\text{-}(\text{-}CH_2\text{-}CCl_2\text{-})_m\text{-}CH_2\text{-}\underset{\displaystyle Cl}{\overset{\displaystyle Cl}{\overset{|}{\underset{|}{C}}}}{}^{-} : Li^+ \quad (4)$$

$$Bu\text{-}(\text{-}CH_2\text{-}CCl_2\text{-})_m\text{-}CH_2\text{-}\underset{\displaystyle Cl}{\overset{\displaystyle Cl}{\overset{|}{\underset{|}{C}}}}{}^{-} \cdots Li^+ \quad (5)$$

$$Bu\text{-}(\text{-}CH_2\text{-}CCl_2\text{-})_m\text{-}CH_2\text{-}\underset{\displaystyle Li^+}{\overset{\displaystyle Li^+}{\overset{|}{\underset{|}{C}}}}{}^{-} : Bu^- \quad (6)$$

Since poly(vinylidene chloride) has no assymmetric centers, the problem of the tacticity of the polymer will not arise, the crystallinity of the polymer here obtained being similar to the polymer obtained by radical polymerization from X-ray study. It seems that structure 5 or 6 serves to stabilize the growing polymer anion. The termination probably occur by association reaction as follows:

$$Bu(M)_n^- + Li^+ + (BuLi) \xrightarrow{k_{t_1}} Bu(M)_nLi(BuLi) \quad (7)$$

or, less probably,

$$Bu(M)_n^-Li^+ \xrightarrow{k_{t_2}} Bu(M)_nLi \quad (8)$$

Since the elimination of chlorine is very remarkable, the following termination reactions are also suggested:

$$Bu\text{-}(\text{-}CH_2\text{-}CCl_2\text{-})_m\text{-}CH_2\text{-}\underset{\displaystyle Cl}{\overset{\displaystyle Cl^{\delta-}}{\overset{|}{\underset{|}{C}}}}{}^{-} : Li^+ \xrightarrow{k_{t_3}} Bu\text{-}(\text{-}CH_2\text{-}CCl_2\text{-})_m\text{-}CH_2\text{-}\underset{\displaystyle Cl}{\overset{\displaystyle Cl}{\overset{|}{\underset{|}{C}}}}{}^{-} + LiCl \quad (9)$$

then

$$\xrightarrow{H\text{-}R} Bu\text{-}(\text{-}CH_2\text{-}CCl_2\text{-})_m\text{-}CH_2\text{-}CHCl \quad (10)$$

or

$$\longrightarrow Bu\text{-}(\text{-}CH_2\text{-}CCl_2\text{-})_m\text{-}CH\text{=}CHCl \quad (11)$$

Other side reactions which induce the abstraction of chlorine from the polymer chain may be:

$$\text{-}CH_2\text{-}\underset{\displaystyle Cl}{\overset{\displaystyle Cl^{-\delta}}{\overset{|}{\underset{|}{C}}}}\text{-} + Li^+ \longrightarrow \text{-}CH_2\text{-}\underset{\displaystyle Cl}{\overset{\displaystyle Cl}{\overset{|}{\underset{|}{C}}}}{}^{+}\text{-} + LiCl \quad (12)$$

$$\xrightarrow{Bu} \text{-}CH_2\text{-}\underset{\displaystyle Cl}{\overset{\displaystyle Bu}{\overset{|}{\underset{|}{C}}}}\text{-} \quad (13)$$

$$\xrightarrow{H\text{-}R} \text{-}CH_2\text{-}CHCl\text{-} \quad (14)$$

The decrease in the chlorine content of the polymer can probably be attributed to reactions 9 and 12, in which the chlorine atom is eliminated as lithium chloride from the polymer chain.

Making the steady state assumption for the chain reaction:

$$k_i(M)(BuLi) = k_{t_1}(BuLi)(Bu(M)_n^-Li^+) + k_{t_2}(Bu(M)_n^-Li^+) + k_{t_3}(Bu(M)_n^-Li^+)$$
$$= (Bu(M)_n^-Li^+)\{k_{t_1}(BuLi) + k_{t_2} + k_{t_3}\} \quad (15)$$

$$(Bu(M)_n^-Li^+) = k_i(M)(BuLi)/\{k_{t_1}(BuLi) + k_{t_2} + k_{t_3}\} \quad (16)$$

$$R_p = k_p(Bu(M)_n^-Li^+)(M) = k_ik_p(M)^2(BuLi)/\{k_{t_1}(BuLi) + k_{t_2} + k_{t_3}\} \quad (17)$$

Supposing $k_{t_2}, k_{t_2} \ll k_{t_1}(BuLi)$ (18)

$$R_p \propto (M)^2 \quad (19)$$

Kinetic chain length $\overline{X}_n$ is written as

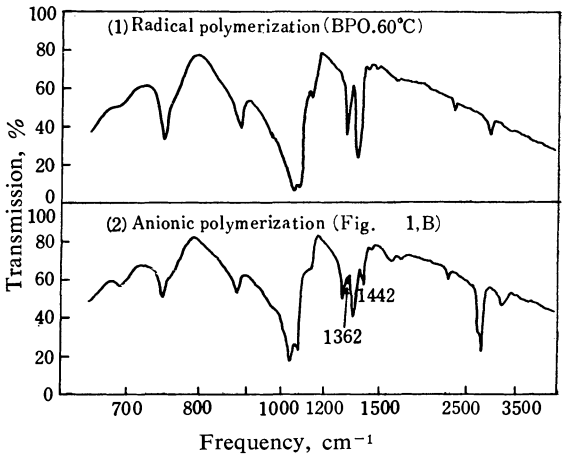


Fig. 9. Infrared spectrum of poly(vinylidene chloride).

23) S. Krim, *Fortschr. Hochpolym.-Forsch.*, **2**, 51 (1960).
22) D. J. Cram and K. R. Kopecky, *J. Am. Chem. Soc.*, **81**, 2748 (1959).

$$\overline{X}_n = R_p/R_t = k_p(\mathrm{Bu}(M)_n{}^-\mathrm{Li}^+)(M)/$$
$$(\mathrm{Bu}(M)_n{}^-\mathrm{Li}^+)\{k_{t_1}(\mathrm{BuLi}) + k_{t_2} + k_{t_3}\}$$
$$= k_p(M)/\{k_{t_1}(\mathrm{BuLi}) + k_{t_2} + k_{t_3}\} \quad (20)$$
$$\log[\eta] \propto \overline{X}_n \propto (M)/(\mathrm{BuLi}) \quad (21)$$

Namely, 19 and 21 accord with the experimental results qualitatively.

Infrared spectra of the polymer are compared with that of the polymer polymerized by dibenzoyl peroxide at 60°C, as is shown in Fig. 9. Characteristic differences observed at 1362 and 1442 cm^{-1}, are attributed to the methyl group in the terminal and pendant butyl groups of the polymer. These absorptions are thought to have been shifted by chlorine from the 1375 and 1457 cm^{-1} which were observed in polyethylene[23].

Summary

The polymerization of vinylidene chloride initiated by *n*-butyllithium in *n*-hexane has been investigated. It has been found that the initial rate of polymerization is independent of the catalyst concentration above a critical value and is proportional to the square of the monomer concentration. The activation energy of the over-all rate was 10.7 kcal./mol. The chlorine content of the polymer decreased inversely with the increase of catalyst concentration. An anionic mechanism is suggested for the polymerization kinetics.

Tokyo Laboratory
Kureha Kasei Co., Ltd.
Shinjuku-ku, Tokyo

Some Addition Compounds of Salicylaldehyde-ethylenediimine-copper. VI[1]. *The Absorption Spectra of 5,5'-Disubstituted Salicylaldehyde-ethylenediimine-coppers*

By Tsuguo TANAKA

(Received April 15, 1961)

It had been reported previously that the positions of the absorption maxima of the spectra of salicylaldehyde-ethylenediimine-copper were shifted in regular ways according to the nature of the solvents in which the absorption spectra were measured[2]. Now the absorption spectra of 5,5'-dichloro-[2], 5,5'-dibromo-, 5,5'-diiodo-salicylaldehyde-ethylenediimine-coppers[3] have been measured in various solvents, and some close relations have been observed between the position of the absorption maxima of band I and band II[4] of these chelates and their tendencies to form addition compounds with the solvents.

Measurement and Results

The absorption spectra were measured with a Hitachi EPU 2A spectrophotometer (cell depth 1.0 cm.). All solvents were purified according to the method of Weissberger[5]. The results are listed in Table I.

Discussion

Band I.—Although many discussions[6] have been presented by different authors about the origin of the visible band of the metal chelates, satisfactory experimental evidence for them have not yet been obtained. It is now frequently assumed, however, that the greatest factor leading to this absorption is the vibration of the non-bonding electron of the metal ion.

Martell and Ueno[7] measured the absorption spectra of the metal chelates of bisacetylacetone-ethylenediimine and its derivatives and found that the band I of copper chelates which appeared between 540~575 mμ is the characteristic absorption of the copper ion. Analogous observations had previously been reported by Sone[8] about the absorption spectra of the bidentate chelates.

1) Bissalicylaldehyde-ethylenediimine-copper. Part V. *J. Chem. Soc. Japan, Pure. Chem. Sec.* (*Nippon Kagaku Zasshi*), **81**, 1013 (1960).
2) T. Tanaka, *J. Am. Chem. Soc.*, **80**, 4108 (1958).
3) T. Tanaka, This Bulletin, **33**, 259 (1960).
4) T. Tsumaki. ibid., **13**, 252 (1938); A. v. Kiss, P. Csokan and G. Nyiri., *Z. physik. Chem., Abt. A.*, **190**, 65 (1942).
5) A. Weissberger and E. S. Proskauer, "Organic Solvents", Interscience Publishers, Inc., New York, N. Y. (1955).
6) Cf., for example, L. Pauling, *J. Am. Chem. Soc.*, **53**, 1367 (1931); A. Mead, *Trans. Faraday. Soc.*, **30**, 1052 (1934).
7) K. Ueno and A. E. Martell, *J. Phys. Chem.*, **61**, 257 (1957).
8) K. Sone, *J. Am. Chem.* Soc., **75**, 5207 (1953).

TABLE I. THE ABSORPTION SPECTRA OF SALICYLALDEHYDE-ETHYLENEDIIMINE-COPPER DERIVATIVES

Solvent	Substituent	Absorption maximum in mμ (log ε), shift in mμ					
		Band I	Shift	Band II	Shift	Band III	Shift
Benzene	5,5'-H	572(2.34)[d]		372(3.68)[d]		276(4.66)	
	5,5'-Cl	575(1.88)		379(3.49)		276(3.74)	
	5,5'-Br	566(2.01)		379(3.51)		275(3.87)	
	5,5'-I	549(2.30)		379~381(3.96)[b]		276(4.42)	
Pyridine	5,5'-H	603(2.67)[d]	+31[c]	372(4.27)[d]	0	299.5(3.60)	+23.5
	5,5'-Cl	593(2.46)	+18[c]	379(4.15)	0	299(3.72)	+23
	5,5'-Br	589(2.51)	+23	379(4.54)	0	301(3.29)	+26
	5,5'-I	594(2.44)	+45	379(3.71)	0	300(3.54)	+24
Chloroform	5,5'-H	564(2.55)[d]	−8	365~370(4.01)[d]	−(2~7)	276(4.47) 245(4.59)	0 −31
	5,5'-Cl	552(2.41)	−23	375~377(2.72)	−(2~4)	245(4.32)	−31
	5,5'-Br	553(2.58)	−13	374~379(4.35)	−(0~5)	242~246(5.03)	−(29~33)
	5,5'-I	544(2.42)	−5	377(3.75)	−2	244.5(4.48)	−31.5
Propionic acid	5,5'-H	560(2.17)[d]	−12	350(3.89)[d]	−22	271(4.83)	−5
	5,5'-Cl	554(2.34)	−21	359(3.40)	−20	247(4.37)	−29
	5,5'-Br	549(2.34)	−17	357~361(3.71)	−(18~22)	255~258(4.30)	−(17~20)
	5,5'-I	548(2.34)	−1	361(3.27)	−18	249(3.96)	−27
Propionic acid-Benzene[a]	5,5'-H	559(2.30)[d]	−13	356(4.30)[d]	−16	276(4.38)	0
	5,5'-Cl	557(2.32)	−18	368(3.94)	−11	276(4.27)	0
	5,5'-Br	559(2.44)	−7	365~370(4.21)	−(9~14)	275(4.61)	0
	5,5'-I	555(2.36)	+6	370(4.11)	−9	276(4.63)	0
Phenol-Benzene[a]	5,5'-H	550(2.38)[d]	−22	358~359(4.19)[d]	−(13~14)	293(3.80)	+17
	5,5'-Cl	552(2.38)	−23	368(3.89)	−11	293(3.80)	+17
	5,5'-Br	553(2.48)	−13	369(3.82)	−10	293(3.77)	+18
	5,5'-I	542(2.46)	−7	369(3.60)	−10	293(3.66)	+17

a 3 M (acid or phenol) solution in benzene.
b 379 mμ was taken as the standard.
c + indicates the red shift and − the blue shift.
d These values were previously reported (cf. Ref. 2).

TABLE II. ADDITION COMPOUNDS OF SALICYLALDEHYDE-ETHYLENEDIIMINE-COPPER DERIVATIVES[2,3]

Substituent	Addition compound			
	Pyridine	Propionic acid	Chloroform	Phenol
5,5'-H	—	Stable	—	Stable
5,5'-Cl	—	—	Least stable	Less stable
5,5'-Br	—	—	Less stable	Stable
5,5'-I	—	Stable	Stable	Stable

Calvin et al.[9] reported that band I of the copper chelates of bisacetylacetone and its 3-ethyl variant is composed of a set of three Gaussian components whose positions and intensities were shown to depend primarily upon solvent basicity; these component bands were identified with the transitions of the 3d electrons of the copper ion predicted from the crystal field and molecular orbital theories.

In this report, it is examined whether there are any relations between the tendencies of 5, 5'-dichloro-, 5, 5'-dibromo- and 5, 5'-diiodo-salicylaldehyde-ethylenediimine-coppers to form addition compounds with propionic acid, phenol and chloroform and the positions of band I of these chelates observed in these solvents.

The wavelengths of the absorption maxima of band I of these chelates in benzene solutions, as listed in Table I, increase in the order

$$5,5'\text{-I} < 5,5'\text{-Br} < 5,5'\text{-Cl}$$

which is the order of decreasing basicity[10];

9) R. L. Belford, M. Calvin and G. Belford, *J. Chem. Phys.*, **26**, 1165 (1957).

10) R. L. Belford, A. E. Martell and M. Calvin, *J. Inorg. & Nuclear Chem.*, **2**, 11 (1956).

that of the unsubstituted one lies between those of 5, 5'-dichloro- and 5, 5'-dibromo-derivatives, the order is

$$5,5'\text{-I} < 5,5'\text{-Br} < 5,5'\text{-H} < 5,5'\text{-Cl}$$

The extinction coefficients of band I as well as those of band II and band III of these chelates observed in the same solvent decrease in the order

$$5,5'\text{-I} > 5,5'\text{-Br} > 5,5'\text{-Cl}$$

The shifts listed in Table I were calculated as the deviations of the wavelengths of the absorption maxima measured in various solvents from those measured in benzene solutions.

In the pyridine solutions, red shifts of the absorption maxima of the band I were observed of these chelates. The magnitudes of the red shifts decrease in the order

$$5,5'\text{-I} > 5,5'\text{-H} > 5,5'\text{-Br} > 5,5'\text{-Cl}$$

On the other hand, in chloroform and propionic acid solutions, blue shifts were observed. The magnitudes of the blue shifts increase in the order

$$5,5'\text{-I} < 5,5'\text{-H} < 5,5'\text{-Br} < 5,5'\text{-Cl}$$

that is, the chelates which are characterized by the larger red shifts in pyridine solutions are those characterized by the smaller blue shifts in chloroform and propionic acid solutions.

It can be seen that these orders are the same as that of the tendency of the formation of the addition compounds which was reported previously[3].

In the cases of the propionic acid-benzene and of the phenol-benzene solutions, the order of the shifts is somewhat different from those discussed above; it is the same as that of the wavelengths of these chelates in benzene solutions. The blue shifts increase in the order

$$5,5'\text{-I} < 5,5'\text{-Br} < 5,5'\text{-H} < 5,5'\text{-Cl}$$

It is remarkable that a red shift is observed in the case of 5, 5'-diiodo-chelate in the propionic acid-benzene solution in contrast with the blue shifts of 5, 5'-dichloro- and 5, 5'-dibromo-chelates.

These results indicate that the energy changes of the 3d electrons which may be induced both by the ligands and the solvents are closely related to the tendency of the formation of the addition compounds. The circumstances are, however, somewhat more complicated in the case of the mixed solvents containing benzene and require further examination. It is also important to inquire whether there are any relations between the stabilities of the addition compounds of these chelates with solvents and the wavelengths of the absorption maxima of band I of the chelates in the respective solvents.

In the chloroform solutions, the absorption maxima are 544 mμ for 5, 5'-diiodo-chelate and 553 and 552 mμ for 5, 5'-dibromo, 5, 5'-dichloro-chelates, corresponding to the formation of stable and less stable addition compounds respectively, and 564 mμ for the unsubstituted chelate of which the addition compound cannot be isolated.

On the other hand, band III of the unsubstituted chelate in a chloroform solution consists of two maxima, i. e., a band at 245 mμ which seems to originate from the unstable addition compound of the chelate with chloroform and a band at 276 mμ which seems to originate from the original chelate; the former is analogous to band III of the substituted chelates in chloroform, while the latter is analogous to the absorption maxima of the unsubstituted chelate in a benzene solution. Therefore, the chelate is considered to exist in the chloroform solution as an equilibrium mixture of the original chelate with the unstable addition compound with chloroform.

In the phenol-benzene solutions, the maxima are 542 mμ for 5, 5'-diiodo-chelate corresponding to the formation of a stable addition compound with phenol, 550 mμ for an unsubstituted one, and 553 and 552 mμ for 5, 5'-dibromo- and 5, 5'-dichloro-chelates corresponding to less stable addition compounds.

These results seem to indicate that the shorter the wavelength of the absorption maximum of a chelate observed in a solvent, the greater the stability of the addition compound of the chelate with the solvent.

Band II.—In contrast with those of band I and band III, the wavelengths of the absorption maxima of band II in the spectra of 5, 5'-dichloro-, 5,5'-dibromo- and 5,5'-diiodo-chelates were found at 379 mμ in both benzene and pyridine solutions.

The flat maximum of 5, 5'-diiodo-chelate in benzene from 379 to 381 mμ was an abnormal case of which no appropriate explanation can be made at present.

The blue shifts of 2 mμ for 5, 5'-diiodo-chelate, 0$\sim$5 mμ for 5, 5'-dibromo-chelate and 2$\sim$4 mμ for 5, 5'-dichloro-chelate in the chloroform solutions, corresponding to stable, less stable and least stable addition compounds of these chelates with chloroform respectively, represent a series. Analogous series of the blue shifts of the wavelength of the absorption maxima of band II were observed in the propionic acid solutions as well as in the propionic acid-benzene solutions. The shifts in propionic acid solutions are, respectively, 18 mμ for 5, 5'-diiodo-chelate which can form

an addition compound with propionic acid, and 18~22 and 20 mμ for 5, 5'-dibromo- and 5, 5'-dichloro-chelates which can not form addition compounds with propionic acid; those in propionic acid-benzene solutions are 9 mμ for 5, 5'-diiodo-, 9~14 mμ for 5, 5'-dibromo- and 11 mμ for 5, 5'-dichloro-chelates. In the phenol-benzene solutions, the blue shifts are 10 mμ for 5, 5'-diiodo- and 5, 5'-dibromo-chelates and 11 mμ for 5, 5'-dichloro-chelates, all of which can form addition compounds with phenol.

From these results, it is assumed that the smallest shifts for 5, 5'-diiodo-chelate observed in chloroform as well as in propionic acid and in propionic acid-benzene solutions are related to the formation of the stable addition compounds of this chelate with these solvents, and the larger shifts for 5, 5'-dichloro-chelate correspond to the formation of unstable associated structures. The flat maxima of band II of 5, 5'-dibromo-chelate in these solvents, which are characterized by blue shifts ranging from the largest to the smallest values may be due to the properties of this chelate which are intermediate between those of 5, 5'-diiodo- and 5, 5'-dichloro-chelates.

It is also important to notice that 5, 5'-halogen substituents in comparison with that of the unsubstituted chelate, produce a marked influence on the wavelengths of band II.

Band III.—Some different orders are observed of the absorption maxima of band III of these chelates. Larger shifts of the wavelengths of the absorption maxima of 5, 5'-dibromo-chelate than those of the others were observed in the pyridine as well as in the phenol-benzene solutions. A smaller blue shift of 5, 5'-dibromo-chelate than those of the others was also observed in the propionic acid solution, while a flat maximum of 5, 5'-dibromo-chelate, with a blue shift ranging from 29 to 33 mμ in chloroform solution, was contrasted with those of the blue shifts of 31 mμ of 5, 5'-dichloro-chelate and 31.5 mμ of 5, 5'-diiodo-chelate in the same solvent. No shifts of the band III of these three chelates were observed in the propionic acid-benzene solutions.

It is important to notice that band III of the unsubstituted chelate in the chloroform solution consists of two maxima (cf. the discussions for band I).

From these results, it is supposed that 5, 5'-halogen substituents do not exert a marked influence on the origin of band III[7,11].

Department of Chemistry
Faculty of Liberal Arts
Saga University
Honjo, Saga-shi

11) T. Tsumaki and R. Tsuchida, This Bulletin, **13**, 527 (1938).

The Chemical Reaction in Silent Electric Discharge. II. The Frequency Effect on Ozone Formation

By Kihei MORINAGA and Momotaro SUZUKI

(Received May 16, 1961)

Numerous accounts have been published on silent discharge[1-11], the majority dealing with the electric characteristics of the ozonizer[1-6]. In the oscillographic study of the discharge[1-4] that was originated by Klemenc et al.[1], the rapid impulse with a "fringe"[2] structure was noticed, and the relation between the pulse and the discharge spot that appeared on the photographic plate in the gap space was investigated[3]. Fillipov et al. derived a equation[5,6] for the effective current in an ozonizer from a knowledge of the static and dynamic characteristics of discharge, and recently[7] they have combined this equation

1) A. Klemenc et al., *Z. Elektrochem.*, **43**, 708 (1937).
2) V. Spreter and E. Briner, *Helv. Chim. Acta*, **32**, 2524 (1949).
3) M. Suzuki and Y. Naito, *Proc. Japan Acad.*, **28**, 469 (1959).
4) K. Honda and Y. Naito, *J. Phys. Soc. Japan*, **10**, 1007 (1955).
5) Yu. V. Fillipov and Yu. M. Emel'yanov, *Zhur. Fiz. Khim.*, **31**, 896 (1956); **32**, 2817 (1958); **33**, 1780 (1959).
6) Yu. M. Emel'yanov and Yu. V. Fillipov, ibid., **31**, 1628 (1957); **33**, 1042 (1959).
7) Yu. V. Fillipov, *Vestnik. Moskov. Univ. Ser. Mat., Mekh., Astron., Fiz. i. Khim.*, **14**, 153 (1959).
8) J. C. Devins, *J. Electrochem. Soc.*, **103**, 460 (1956).
9) M. Suzuki, S. Okazaki and T. Yamamoto, *Advance Chem. Ser.*, **21**, 331 (1959).
10) R. W. Lunt, ibid., **21**, 286 (1959).
11) K. Morinaga and M. Suzuki, This Bulletin, **34**, 157 (1961).

with the intensity of the formation and decomposition of ozone in an ozonizer. Lunt has pointed out[10] the gaps in knowledge which hinder the identification of the reaction mechanism.

In the previous paper the ozone formation through silent discharge (50 c/sec.) was studied with its relation to the pulse current, the gap length and the discharge electrode area. The results showed that the ozone yield is proportional to the pulse current and that the ozone formation rate per unit pulse current has a linear relationship with A/d, where A is the effective discharge area and d, the discharge gap distance.

In the case of the 50 c/sec. electric source of the previous work[11], the pulse current was restricted up to 200 μamp. on account of possible damage to the discharge tube due to electrical breakdown. Furthermore, upon increasing the pulse current beyond the above value, the wave form of the secondary current became more irregular, making rather ambiguous the measurement of the pulse current by means of pulse heights.

In the present work, a relatively high and variable frequency electric source is applied. Accordingly, the pulse current range, upon applying a relatively high frequency current, could be extended up to 0~1300 μamp. The frequency dependence of the ozone formation that clarifies the effect of the pulse current on ozone formation was also pursued.

Experimental

All experiments were performed in an atmospheric flow system. The equipment and procedure were similar in principle to those described in the previous work. The glass discharge tubes had a discharge area of 50~200 cm^2 and a gap of 1~3 mm. respectively. The variable frequency electric source was supplied by a high frequency generator of 32 poles. The number of cycles could be adjusted from 500 to 2000 c/sec. by changing the number of revolutions of the armature. The output voltage could be regulated between 50 and 100 V. The applied high tension to the discharge tube was obtained from a core type transformer which had been designed in order to diminish the core loss of the current. The wave form of the output current remained steady, even with frequencies up to 2000 c/sec.

The frequency measurement of the source current was performed by both the tachometer and oscillographic methods. The frequency deviation in each run was controlled within a limit of ±3% by regulating the field current of the driving D. C. motor. The procedure for taking measurements of the pulse current was the same as in the previous work. The time constant of the leakage resistance and the integral condenser of the oscillogram circuit was 2.7×10^{-6} sec.

The ozone, after leaving the discharge tube, was led into a neutral potassium iodide solution and then analyzed in the usual method.

Results

The Effect of the Frequency.—In the course of the research for the frequency effect on ozone formation, the experiments were carried out with the value of variables as follows: the pulse current covering 0~1300 μamp., resident time 0.3~10 sec., and the total discharge current 0~16 mamp. using a discharge tube with an effective discharge area of 100 cm^2 (in one electrode side) and a gap length of 1 mm. This resulted in almost identical curves of ozone concentration vs. resident time τ in the various frequencies. The asymptotes on the curves of ozone concentration vs. resident time at $\tau=0$ give the value of the initial ozone formation rate. In Fig. 1, the ozone formation rates at

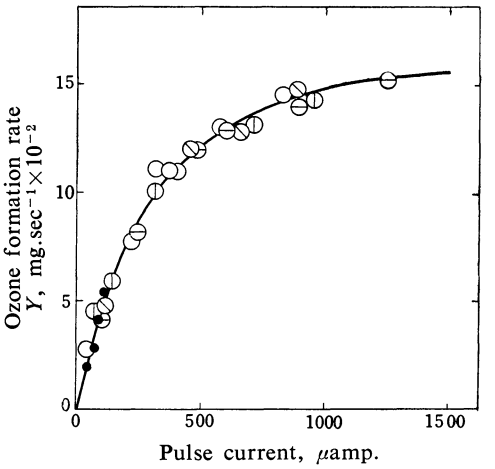


Fig. 1. Ozone formation rates at various frequencies electric source against pulse current. Discharge are a 100 cm^2, Discharge gap length 1 mm.

⊖ 2000, ○ 1000, ● 50, ① 1500, ⊘ 500 sec.

various frequencies against pulse current are given. The ozone formation rate is expressed in one diagram independent of the frequencies of the current. If the above rates are plotted against other parameters, such as total discharge current, secondary voltage etc., then the diagram does not show any unified form but rather appears as separate curves according to the frequency used.

In the previous report[11] the same ozone formation rate at 50 c/sec. current, under otherwise identical conditions, varied linearly with the pulse current, whereas in the present case the diagram starts at first linearly, then with the increase of the pulse current, bends

gradually downwards until it approaches a certain definite value. It should be noted that in the former case a high value of pulse current was precluded because of the reasons described elsewhere above, while in the present case the high frequency current enables a more intense flow of the pulse current.

In a discharge of a low pulse current the linear relationship will validly hold no matter how the frequency alters, but in the region of a high discharge current the rate value will be smaller than is anticipated from a linear relationship unaffected by a change of the frequency.

The Effect of Discharge Area and Gap Length.—Figures. 2, 3 and 4 show a relationship similar to that given in Fig. 1 for a certain current frequency (1000 c/sec.) and for various electrode areas, in which each diagram corresponds to values of a certain gap length. The operational specifications are the same as for the foregoing series, but the areas are changed 50, 100 and 200 cm^2 and the gap lengths are changed 1, 2, 3 mm. respectively. The whole aspect of the diagrams somewhat resembles that of Fig. 1.

The region where the curves leave the linear property depends upon the discharge area, and the values of the corresponding pulse current are around or less than 200 μamp.

To compare these results with those in the previous work, the authors denoted as before the ozone formation rates per unit pulse

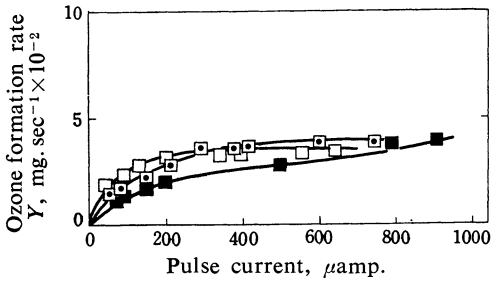


Fig. 2. Ozone formation rates against pulse current. Frequency 1000 c/sec., Discharge area 50 cm^2, Discharge gap lengths 1, 2, 3 mm.

■ Gap 1 mm., area 50 cm^2
◉ Gap 2 mm., area 50 cm^2
□ Gap 3 mm., area 50 cm^2

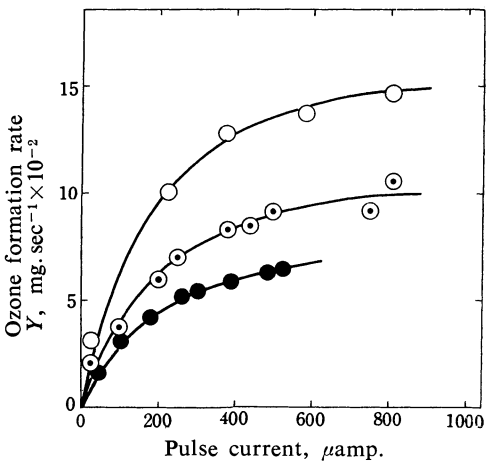


Fig. 3. Ozon formation rates against pulse current. Frequency 1000 c/sec., Discharge gap length 1, 2, 3 mm.

● Gap 1 mm., area 100 cm^2
⊙ Gap 2 mm., area 100 cm^2
○ Gap 3 mm., area 100 cm^2

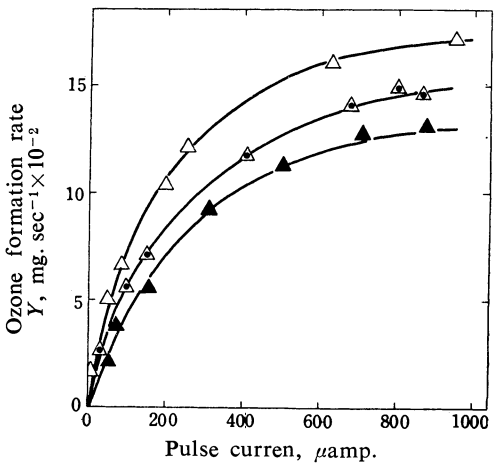


Fig. 4. Ozone formation rate against pulse current. Frequency 1000 c/sec., Discharge area 200 cm^2, Discharge gap length 1, 2, 3 mm.

▲ Gap 1 mm., area 200 cm^2
△ Gap 2 mm., area 200 cm^2
△ Gap 3 mm., area 200 cm^2

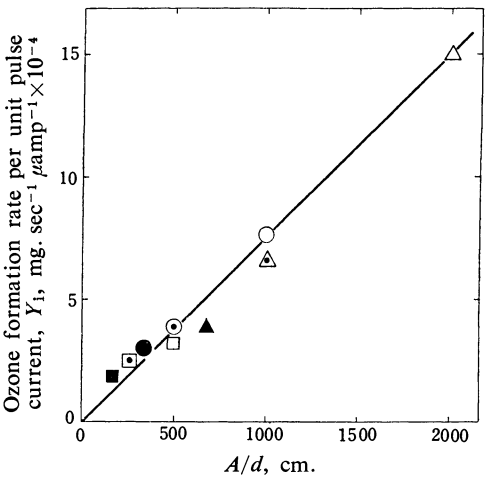


Fig. 5. Ozone formation rate per unit pulse current Y_I against A/d. The plots represents as in Figs, 2, 3 and 4.

current at a low pulse current region as Y_i. The relation between Y_i and A/d is shown in Fig. 5. The linear feature, independent of the value of frequency, appears here again as in the previous case of a 50 c/sec. current discharge. This linear relationship seemed to be valid for the frequency up to 200 c/sec. The slope was found to be 7.5×10^{-7} mg. sec^{-1} μamp^{-1} cm^{-1} whereas the corresponding value in the previous paper is 7.0×10^{-7} mg. sec^{-1} μamp^{-1} cm^{-1}; they therefore seem essentially equal.

Discussion

In the high frequency silent discharge, pulses were not noticeable up to a certain value of the total discharge current, and as long as the pulses were not observed, there was no gain of ozone. The above discharge region of missing pulses had hardly been noticed in the previous work of 50 c/sec. electric source frequency.

It seems that the electric source frequencies of the present studies would not be concerned with the ozone formation or with appropriate representation of the extent of silent discharge by the pulse current. Thus, as shown in Fig. 1, the ozone formation rates are solely dependent on the value of the pulse current and independent of the electric source frequencies used here.

The relationship between pulse current and initial ozone formation rate, which was reported in the previous paper[11], was revealed to be essentially consistent even in the high frequency discharge area studied here, i. e. 500~2000 c/sec., and with the pulse current up to 200 μamp. The ozone formation rate per unit pulse current Y_i at a low pulse current region changes along with the value of A/d linearly.

There have been observed, nevertheless, some discrepancies from the previous work. As is shown in Fig. 1, the linear relationship between the initial ozone formation rate Y and pulse current I_p holds up to a certain value of I_p independent of the frequency value. As is shown in Figs. 2, 3 and 4, however, the linear relationship is not valid from a certain current value upwards. The values where this linearity does not hold remain appreciably unaffected by the change of value of the discharge area. With an increasing discharge area, the pulse current region at which the curve departs from the linear relationship between Y and I_p, comes to assume a higher value.

Concerning the spot number, it was seemingly conceivable, as was discussed in the previous work[11], that the increase of discharge area led to the increase in spot number, because the increase of the discharge area implies that the spots are distributed more sporadically, thus offering more chance for the generation of new spot sites. As long as the number of the electrons ejected from a spot does not exceed the number of molecules just in front of the spot and as for as the more the generation of spots with an increasing pulse current is permitted, the formation of ozone may possibly be proportional to the number of electrons or, further, to the pulse current. The larger the area of the discharge electrodes is, the larger the region of the pulse current where are fulfilled the above conditions. Consequently, with an increase in the discharge area, the deviation from the linear relations tends to appear in a higher pulse current region than is the case in a smaller discharge area.

Concerning a lower pulse current region than the above discussion, the ozone formation rates per unit pulse current in high frequency discharge showed the same behavior as in the previous work, and the dependence on A/d was explainable in the same manner as in the previous paper.

The results which have been obtained in the present work are explainable by the above discussion, and the discussion also evidently supports the discussion of the previous paper.

Summary

1. The ozone formation in the silent electric discharge was investigated with a current of higher frequency. The rate is independent of the electric source frequency but dependent solely upon the value of the pulse current, and the rate per pulse current is linear in relation to the electrode area divided by the gap length. The above findings are similar to those in the case of 50 c/sec.

2. At a higher value of pulse current, the ozone formation rate is no longer linear to the pulse current and shows a type of saturation curve.

3. Some relations at a high frequency discharge among pulse current, electrode area and gap length have been discussed.

Department of Chemistry
Defense Academy
Yokosuka

The Synthesis of Alkyltin Halides by Direct Reaction between Tin and Alkyl Halides[1)]

By Sumio MATSUDA and Haruo MATSUDA

(Received April 24, 1961)

Organotin compounds are widely used as stabilizers for polyvinylchloride or as antifungicides, and many patents or reports have been published about the synthesis of alkyltin halides, R_nSnX_{4-n}, which are the most important intermediates of these organotin compounds.

To obtain dialkyltin or trialkyltin halides, the redistribution reaction between tetraalkyltin and stannic chloride or the halogenation of tetraalkyltin has conveniently been employed. There have been, however, a few studies attempting to prepare these compounds from tin and alkyl halides by direct methods; with these, however, a considerable yield could be obtained only in the limited case where an alloy of tin was used.

In this report a modified direct synthesis of alkyltin halides will be described in which the reaction is carried out by adding a trace of magnesium or zinc and a small amount of alcohol, ester or an ether such as tetrahydrofuran. For its ease and the high yield of alkyltin halides, this method can be considered the most excellent one among the direct methods reported thus far.

For example, tin foil and butyl iodide were reacted at ordinary pressure in the presence of magnesium (0.2~0.3% to tin) and *n*-butanol (3% to butyl iodide); then almost all the tin foil was converted to dibutyltin diiodide.

By a similar reaction, alkyl bromide could convert tin almost completely to R_nSnBr_{4-n} (n=1—3) in an autoclave, but in this case it was found neccessary to add alkyl iodide (ca. 5% to alkyl bromide) besides magnesium and *n*-butanol.

The reaction of an alkyl chloride, for example, methyl chloride, with tin foil in the presence of magnesium, *n*-butanol or tetrahydrofuran and butyl iodide gave dimethyltin dichloride in a high yield of ca. 92%.

When aryl halides were used instead of alkyl halides, no reaction product was obtained.

1) This paper is a summarized report of four articles published in Japanese: S. Matsuda and H. Matsuda, *J. Chem. Soc. Japan, Ind. Chem. Sec.* (*Kogyo Kagaku Zasshi*), **63**, 114 (1960); H. Matsuda and S. Matsuda, ibid., **63**, 1958, 1965 (1960); H. Matsuda, H. Taniguchi and S. Matsuda, idid., **64**, 541 (1961).

Experimental

Materials.—The tin foil and the metals used as additives were 99.99 and 99.9% pure respectively. The alkyl halides and solvents used were purified by distillation.

Typical examples of the precedures are as follows.

Reaction of Tin and Butyl Iodide.—In a three-necked flask of 1 l. were placed 100 g. (0.843 mol.) of tin foil, 372 g. (0.843×2.4 mol.) of butyl iodide, 0.3 g. (0.3% to tin) of magnesium, and 11.2 g. (3% to butyl iodide) of *n*-butanol; then the mixture was heated to 130~135°C for three hours with being stirred. After the reaction, a small amount of solid was filtered off (98% of the tin was consumed). The fractionation of the remaining liquid gave unreacted butyl iodide and dibutyltin diiodide (b. p. 143~145°C/3 mmHg; yield 381 g., 95% to the reacted tin).

Reaction of Tin and Butyl Bromide.—A mixture of tin foil (30 g.: 0.253 mol.), butyl bromide (83~104 g.: 0.253×(2.4~3.0)mol.) and a catalytic amount of magnesium, butyl iodide and *n*-butanol was heated at 135~170°C in a stainless autoclave of 500 ml. After the reaction, the solid, which mainly consisted of unreacted tin, was filtered off. Fractionations through a helices-packed column of about thirty theoretical plates gave three fractions: unreacted butyl bromide, fraction I (95~100°C/2 mmHg) and fraction II (120~125°C/2 mmHg). Fraction I consisted of butyltin tribromide, while fraction II was a mixture of dibutyltin dibromide and tributyltin bromide.

The added butyl iodide was considered to have been converted to higher boiling substances.

Under optimum conditions (tin 30 g., butyl bromide 104 g., butyl iodide 5 g., *n*-butanol 2.5 g., and magnesium 0.12 g. were allowed to react at 160°C for 8 hr.), the tin was consumed completely and 27 g. of butyltin tribromide, 60 g. of dibutyltin dibromide and 6 g. of tributyltin bromide were obtained (yields: 26, 60 and 7% respectively).

Reaction of Tin and Methyl Chloride.—Methyl chloride 50~60 g. (ca. 1.0~1.2 mol.) was introduced into a stainless autoclave of 100 ml. in which 20 g. (0.169 mol.) of tin foil, magnesium, butyl iodide and *n*-butanol or tetrahydrofuran were charged. The temperature was kept at 190°C for six hours; then the reaction product was separated from the unreacted tin by filtration or sublimation under reduced pressure. The white crystal thus obtained was found to be dimethyltin dichloride. M. p. 105~106.5°C.

Found: Sn, 54.35; Cl, 32.32. Calcd. for $C_2H_6SnCl_2$: Sn, 54.03; Cl, 32.28%.

Analyses.—Halogen was determined by high frequency titration[2] with an aqueous silver nitrate solution. Gas chromatography was also applied[3] for identification of some of the products.

Results

Alkyltin Iodides.—In the reaction of tin and butyl iodide, the effect of the amount of magnesium and *n*-butanol vs. the tin conversion (see A and B), as well as the amount of the tin conversions by using various kinds of metal additives and solvents, are shown in Fig. 1. Usually 90~95% of dibutyltin diiodide was found in the reaction product.

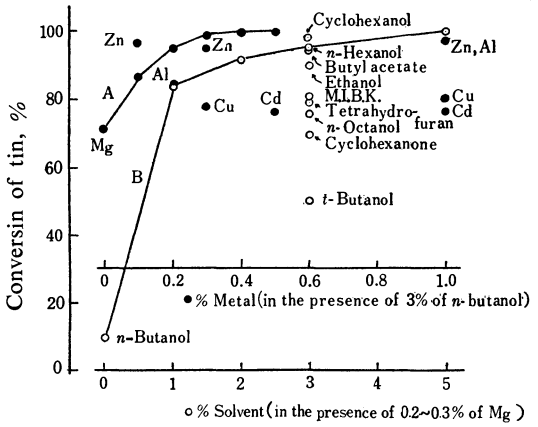


Fig. 1. The effect of the additives for the conversion of tin.

Figure 1 also shows that magnesium and zinc are two of the most effective additives in cooperation with alcohols such as *n*-butanol or cyclohexanol. The preferable amount of the metal seemed to be 0.1~0.3% to tin; an excessive addition caused an unfavourable discoloring of the product.

Methyl iodide and tin could be reacted completely in an autoclave within two hours in the presence of magnesium and methanol or *n*-butanol. Vacuum distillation gave a mixture of trimethyltin iodide, dimethyltin diiodide and methyltin triiodide in yields of 25~30, 40~46 and 20~27% respectively, and no appreciable change in composition was observed after changing the ratios of the reaction components, the amount of the additives, the reaction temperature or the reaction time.

Similarly, from tin and ethyl iodide, triethyltin iodide, diethyltin diiodide and ethyltin triiodide were obtained in yields of 14~18, 63~67 and 3~6% respectively.

Other alkyl iodides could be used as well as butyl iodide. In these reactions almost the same conversions were obtained as in the case

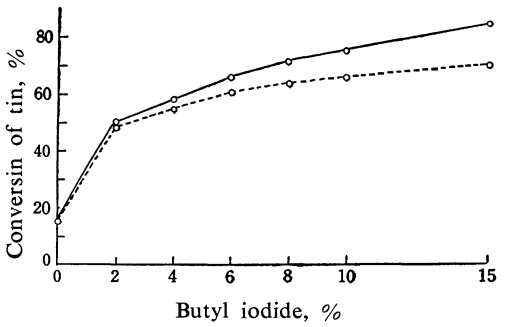


Fig. 2. The effect of butyl iodide for the reaction of tin and butyl bromide.
Butyl bromide (mol.)/tin (mol.) = 2.4, magnesium 0.06 g. (0.2% to tin), *n*-butanol 2.5 g. (6% to butyl bromide), reaction temperature 170°C, reaction time 4 hr.
—— The observed conversion of tin by butyl bromide and added butyl iodide.
---- The calculated conversion of tin by butyl bromide.

Table I. The effect of additives in the reaction between tin and methyl chloride

Tin, 20 g.; Methyl chloride, 50~60 g.; Reaction temp., 190°C; Reaction time, 6 hr.

Amount of additives				Tin conversion	$(CH_3)_2SnCl_2$	Yield
Magnesium	*n*-Butanol	Tetrahydro-furan	Butyl iodide			
g.	g.	g.	g.	%	g.	%
0.06	1.7	14	3.4	100	34.3	92.7
0.06	1.7	0	3.4	100	33.5	90.6
0.06	0	14	3.4	100	34.4	92.8
0.06	0	14	0	45.0	—	—
0.06	0	0	3.4	21.0	—	—
0.06	1.7	0	0	4.0	—	—
0	1.7	0	3.4	26.0	—	—
0.06	0	7	3.4	100	33.8	91.3
0.06	0	3.5	3.4	74.0	—	—

2) H. Matsuda and S. Matsuda, ibid., **64**, 539 (1961).

3) H. Matsuda and S. Matsuda, ibid., **63**, 1960 (1960).

TABLE II. PHYSICAL PROPERTIES[a] OF ALKYLTIN HALIDES

Compound	B. p., °C/mmHg	M. p., °C	n_D^{20}	d_4^{20}	Anal. Sn% (Calcd.)
$(CH_3)_3SnI$	61~62/14 (67~68/15)		1.5726 (1.5724)	2.1205	40.52[c] (40.83)
$(C_2H_5)_3SnCl$	147~149/130 (94/13)		1.5072 (1.5055)	1.4396	49.60 (49.18)
$(C_2H_5)_3SnI$	78~80/3 (117.5/13)		1.5615[b]	1.8232	35.98[d] (35.67)
$(n\text{-}C_4H_9)_3SnCl$	147~149/130 (145~147/5)		1.4909[b]	1.2072	36.23 (36.47)
$(n\text{-}C_4H_9)_3SnBr$	139~140/4.5 (163/12)		1.5028[b]	1.3421[b]	31.48 (32.08)
$(n\text{-}C_4H_9)_3SnI$	138~140/2.5 (168/8)		1.5302 (1.5345)	1.4810	28.03 (28.47)
$(n\text{-}C_3H_7)_2SnI_2$	103~104/2.5 (166~167/10)		1.6309	2.2099	—
$(i\text{-}C_3H_7)_2SnI_2$	95.5~96/2 (153~156/5)		1.6350	2.2088	—
$(n\text{-}C_4H_9)_2SnI_2$	143~145/3		1.6054	2.0198	24.93[e] (24.39)
$(i\text{-}C_4H_9)_2SnCl_2$	107/3.9 (135.5/15)		1.5090	1.4213	39.77 (39.07)
$(i\text{-}C_4H_9)_2SnBr_2$	118/4 (144/15)		1.5424	1.7578	29.85 (30.22)
$(i\text{-}C_4H_9)_2SnI_2$	124~126/3 (290~295/760)		1.6127	2.0738	—
$(s\text{-}C_4H_9)_2SnCl_2$	113/4		1.5218	1.4357	38.39 (39.07)
$(s\text{-}C_4H_9)_2SnBr_2$	122~124/4.5		1.5575	1.7836	29.93 (30.22)
$(s\text{-}C_4H_9)_2SnI_2$	113.5/3		1.6294	2.0999	25.42 (24.39)
$(i\text{-}C_5H_{11})_2SnCl_2$	129~135/4		1.5072	1.3402	35.18 (35.76)
$(i\text{-}C_5H_{11})_2SnBr_2$	137~139/4		1.5357	1.6688	28.72 (28.21)
$(i\text{-}C_5H_{11})_2SnI_2$	120.5~121/2 (202~205/8)		1.5964	1.9237	23.50 (23.06)
$(n\text{-}C_6H_{13})_2SnBr_2$	149~151/2				26.50 (26.45)
$(n\text{-}C_8H_{17})_2SnBr_2$	183~185/1.5	22~24			24.14 (23.41)
$(n\text{-}C_{10}H_{21})_2SnCl_2$	220~223/3.5	45~48			24.85 (25.16)
$(n\text{-}C_{10}H_{21})SnBr_2$	215~218/2	35~36			20.41 (21.17)
$(n\text{-}C_{12}H_{25})_2SnI_2$		46.5~48			
CH_3SnI_3	122~125/5.5	86.5~88.0 (86.5)			23.09 (23.07)
$n\text{-}C_4H_9SnBr_3$	120/8		1.5933	2.3652	28.79[f] (28.56)

a) Data in parenthesis are cited from Ref. 4.
b) Data at other temperatures were reported in Ref. 4.
c) Anal. Found: C, 12.94; H, 3.22. Calcd.: C, 12.39; H, 3.12
d) Anal. Found: C, 21.08; H, 4.80. Calcd.: C, 21.65; H, 4.54
e) Anal. Found: C, 20.22; H, 4.07. Calcd.: C, 19.74; H, 3.74
f) Anal. Found: C, 11.85; H, 2.29. Calcd.: C, 11.56; H, 2.18

of adding *n*-butanol by adding the alcohol with the same alkyl group as the iodide.

However, the rate of conversion of tin and the yield of dialkyltin diiodides decreased with the increasing size of the alkyl group. For example, *n*-dodecyl iodide converted 49% of tin and yielded di(*n*-dodecyl)tin diiodide corresponding to 59% of the tin consumed.

Alkyltin Bromides.—The reaction of tin with butyl bromide in the presence of magnesium and

n-butanol can be carried out by adding alkyl iodide. The effect of butyl iodide is shown in Fig. 2.

The reactions shown in Fig. 2 were carried out at 170°C for four hours, but the highest conversion of tin was observed in the experiment at 160°C for eight hours. It was also found that in this reaction the metal additives were not as effective as in the reaction of tin and butyl iodide; the amount of magnesium neccessary increased slightly, and zinc was found to be practically ineffective.

The reaction product from tin and butyl bromide, in contrast that of butyl iodide, was a mixture of three alkyltin bromides.

Ethyl bromide could react with tin under similar conditions; thus, from 30 g. of tin were obtained 34 g. of diethyltin dibromide and 32 g. of a mixture of triethyltin bromide (ca. 30%) and ethyltin tribromide (ca. 70%).

Long chain alkyl bromides such as *n*-octyl bromide could be reacted under ordinary pressure as well as in an autoclave, but the amount of conversion decreased with the increasing size of the alkyl group.

Alkyltin Chlorides.—The effect ot additives in the reaction between tin and methyl chloride is shown in Table I.

It can easily be seen from Table I that the three additives, magnesium, alkyl iodide and *n*-butanol or tetrahydrofuran, are indispensable for this reaction to proceed.

The high yield of dimethyltin dichloride obtained by this method is of special note.

Butyl chloride was treated with tin by a similar procedure, but the reaction was found to be unsuccessful because of side reactions.

The physical properties of the alkyltin halides obtained in these experiments are listed in Table II, together with the data which appeared also in a recent article[4].

Faculty of Engineering
Osaka University
Miyakojima-ku, Osaka

4) R. K. Ingham, S. D. Rosenberg and H. Gilman, *Chem. Revs.*, **60**, 459 (1961).

Spark Ionization of Semi-metallic and Metallic Elements and of Ionic-crystals

By Toshiyoshi YUASA

(Received April 21, 1961)

Inghram et al.[1-3] and Honig[4] have observed polyatomic molecular ions of carbon, silicon, and germanium by means of a mass spectrometer with a high-temperature effusion cell. These molecular ions have also been observed by Dörnenburg and Hintenberger[5] and by Sasaki et al.[6] using a double-focusing Mattauch-type mass spectrometer with a high frequency spark ionization source. However, the mechanism of the production of the molecular ion is still not clear. Therefore, primarily to find out qualitatively what kinds of electrode elements are capable of producing such molecular ions, experiments on the electrodes of semi-metallic and metallic elements and on ionic-crystals were performed by the author. In addition, some measurements for thermal ionization were also made in connection with the spark ionization.

Experimental

A double-focusing Mattauch-type mass spectrometer with a high frequency spark ionization source, which had been constructed by Sasaki et al.[6-8], was used. The sample to be examined was prepared in the form of rods. Two such rods for each sample were mounted in the spark ionization source with their tips approximately 1 mm. apart. The source was evacuated and, when the pressure had fallen to about 10^{-6} mmHg, spark voltage of 20 kV. was applied to the sample rods. The mass spectrum

1) W. A. Chupka and M. G. Inghram, *J. Chem. Phys.*, **21**, 1313 (1953).
2) J. Drowart, G. De Maria, A. J. H. Boerboom and M. G. Inghram, ibid., **30**, 308 (1959).
3) I. Drowart, R. P. Burns, G. De Maria and M. G. Inghram, ibid., **31**, 1131 (1959).
4) R. E. Honig, ibid., **22**, 1610 (1954).
5) E. Dörnenburg and H. Hintenberger, *Z. Naturforsch.*, **14**, 765 (1959).
6) N. Sasaki, M. Onchi and J. Kai, *Mass Spectroscopy (Shitsuryo Bunseki)*, No. **12**, 69 (1959).
7) N. Sasaki, M. Onchi, J. Kai and Y. Abe, ibid., No. **12**, 61 (1959).
8) N. Sasaki and J. Kai, ibid., No. **12**, 64 (1959).

TABLE I

Samples	Ions found
C	C_5^+, C_4^+, C_3^+, C_2^+, C^+, C^{2+}
Si	Si_6^+, Si_5^+, Si_4^+, Si_3^+, Si_2^+, Si^+, Si^{2+}
Ge	Ge_4^+, Ge_3^+, Ge_2^+, Ge^+, Ge^{2+}, Ge^{3+}, Ge^{4+}
Se	Se_3^+, Se_2^+, Se^+, Se^{2+}
Te	Te_2^+, Te^+, Te^{2+}
Sb	Sb_2^+, Sb^+, Sb^{2+}, Sb^{3+}, Sb^{4+}
Bi	Bi^+, Bi^{2+}, Bi^{3+}, Bi^{4+}, Bi^{5+}, Bi^{6+}
Al	Al^+, Al^{2+}
Ti	Ti^+, Ti^{2+}
Fe	Fe^+, Fe^{2+}, Fe^{3+}
Ni	Ni^+, Ni^{2+}, Ni^{3+}
Cu	Cu^+, Cu^{2+}
Zn	Zn^+, Zn^{2+}, Zn^{3+}
Zr	Zr^+, Zr^{2+}, Zr^{3+}
In	In^+, In^{2+}, In^{3+}
Sn	Sn^+, Sn^{2+}, Sn^{3+}
Pt	Pt^+, Pt^{2+}, Pt^{3+}, Pt^{4+}
Pt(Cu), Pt(Cu)	Pt^+, Pt^{2+}, Cu^+, Cu^{2+}
Au	Au^+, Au^{2+}, Au^{3+}
NaCl	Na^+, Na^{2+}, Cl^+
LiF	Li^+, Li^{2+}, Li^{3+}, Li^{4+}, F^+
KBr	K^+, K^{2+}, K^{3+}, Br^+
C, Si	$C_3^+ \sim C^+$, $Si_3^+ \sim Si^+ \sim Si^{2+}$
C, Ge	$C_4^+ \sim C^+$, $Ge_3^+ \sim Ge^+ \sim Ge^{4+}$
C, Pt	$C_3^+ \sim C^+$, $Pt^+ \sim Pt^{2+}$
Ge, Pt	$Ge_3^+ \sim Ge^+ \sim Ge^{4+}$, $Pt^+ \sim Pt^{4+}$
Ni, Pt	$Ni^+ \sim Ni^{3+}$, $Pt^+ \sim Pt^{4+}$
NaCl, KBr	$Na^+ \sim Na^{2+}$, $K^+ \sim K^{3+}$, Cl^+, Br^+
LiF, KBr	$Li^+ \sim Li^{4+}$, $K^+ \sim K^{3+}$, F^+, Br^+

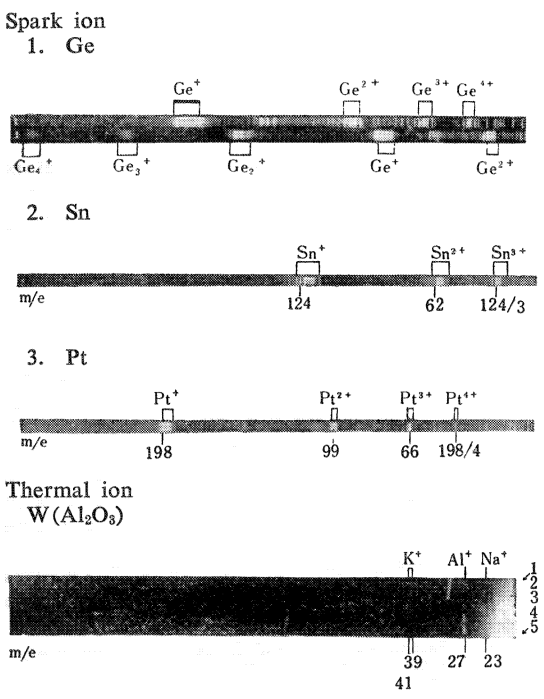


Fig. 1. Mass spectra.

Spark ion

1. Ge

2. Sn

3. Pt

Thermal ion

$W(Al_2O_3)$

was recorded, at the ion-accelerating voltage of 16 kV., on an Ilford Q-2 photographic plate. The time of exposure required for taking mass spectrographs clearly for the samples of elements and of ionic-crystals were 1~5 min. and 10 min. respectively. Typical results obtained for samples of germanium, tin (white tin), and platinum are given in Fig. 1. Gaseous species for each sample were examined on the mass spectrograph; those results are summarized in Table I, in which the sample Pt(Cu) is a platinium rod plated with copper. The results obtained in the spark between the electrodes of the different kinds of sample rods are also given in Table I.

Furthermore, mass spectra of positive ions emitted by electrical heating from a filament which has been mounted at both ends of the sample holder of the electrodes were investigated.

The thermal ionization source $W(Al_2O_3)$ shown in Fig. 1 is an alumina-coated tungsten filament, 0.055 mm. in diameter.

Results and Discussion

Thermal Ionization.—The mass spectrographs (Nos. 1—5) of the thermal ion given in Fig. 1 were taken during the gradual rise of temperature in one filament. The observed color of the filament and the time of exposure at each

temperature were as follows: 1) dark red, 10 min.; 2) red, 10 min.; 3) yellowish red, 10 min.; 4) yellow, 5 min.; 5) yellowish white, 5 min. The experimental results can be summarized as follows.

The positive ions emitted from the filament are Na^+ and K^+ (39) at somewhat low tempertures, and K^+(41) and Al^+ in addition to Na^+ and K^+(39) at still higher temperatures, perhaps above 1000° C. At still higher temperatures these impure ions of alkali disappear and the emission of the only Al^+ ion is rich. Thus, the variation in positive ion emission caused by the gradual rise in temperature of the filament was successfully tracked out by taking a mass spectrograph of the ion emitted.

For the ion source of the platinum filament, 0.06 mm. in diameter, only alkali ions such as Na^+ and K^+ were observed.

Spark between Different Kinds of Electrode Elements.—Species found in the spark between the electrodes of different kind were found in just the same mixture as had been produced in the sparks of each electrode. For instance, in the spark between the electrodes of carbon and silicon elements no molecular ion such as silicon carbide was observed (cf. Table I).

Spark between the Same Kind of Electrode Elements.—Multiply-charged monatomic ions are given for all samples, whereas polyatomic ions are given only for several kinds of samples, and these are only singly charged ones (cf. Table I). This seems to show that monatomic molecules in the gas phase can be readily ionized to multiply-charged ions, whereas polyatomic molecules are too unstable to form doubly-charged ions without decomposition of the molecules.

Polyatomic ions are produced only for the semi-metallic elements (cf. Table I). (This result was obtained in a significant concentration of mass spectra under experimental conditions concerning spark voltage, the time of exposure, etc., such as has been described in the experimental section. No experiments under other conditions were carried out.)

Spark between the Electrodes of Ionic-crystal.—When the spark voltage was applied to the electrodes of an alkali halide single crystal, the crystals were brightly colored in the run, violet for sodium chloride, yellow for lithium fluoride, and cobalt blue for potassium bromide.

As shown in Table I, the gaseous species for each crystal are positive ions of alkali and halogen, including their isotopes, and the concentration of the spectral line of halogen ions is, in general, less then that of the corresponding alkali ions. For alkalis, their multiply-charged monatomic ions are given, whereas for halogens, only singly-charged monatomic ions are given. Molecular ions such as $NaCl^+$ and Na_2^+, for instance, were not observed.

When the crystals were taken out from the spark source after sparking, it was observed that the crystals still held their original shape and, moreover, that color centers had been formed finely, yellow for sodium chloride, yellowish brown for lithium fluoride, and cobalt blue for potassium bromide. These color centers seem to have been formed by electron impact on the crystals.

The species found in the spark between electrodes of different kinds (e. g., sodium chloride and potassium bromide) were in just the same mixture as what had been produced in the sparks of each electrode (cf. Table I). Similar results to the case of the same kind of electrodes were also obtained in the matters of the brightness of crystals during sparking and of the color centers after sparking.

Concentration of Mass Spectral Line of Spark Ion.—The results obtained from an examination of the mass spectral line in the significant concentration are as follows:

For all elements, as shown in Fig. 1, for instance, their isotopes are simultaneously given in the spark, and the relative intensity in the lines of an isotope corresponds approximately to their abundance ratio.

For each sample element (X), the relative intensity of multiply-charged monatomic ions is $X^+ > X^{2+} > X^{3+} \cdots\cdots$. In the case of polyatomic molecular ions, the relative intensity is $X^+ > X_2^+ > X_3^+ \cdots\cdots$ for silicon, germanium, and selenium, $X^+ > X_2^+$ for tellurium and antimony, and $X^+ > X_3^+ > X_2^+ > X_5^+ > X_4^+$ for carbon. Furthermore, the intensity of polyatomic ions is, in general, less than that of multiply-charged monatomic ions of the same element.

Discussion.—Gaseous species observed in the thermal ionization were usually singly-charged monatomic ions for the ion sources of alumina-coated tungsten filament, bare platinum filament, etc.[9-11], whereas, in the spark, multiply-charged monatomic ions were always observed. In addition, an estimation of quite a high temperature can be given for the tips of element rods during sparking, for, the tips have been observed in a melting state after sparking. These results seem to show a difference between the mechanism of ion formation by sparking and that by thermal ionization[9-11]. In the case of a spark, as is well known, electrons are produced through a kind of chain reaction, and most of the experimental results obtained here can well be understood as an effect of the

9) T. Yuasa, *J. Chem. Soc. Japan, Pure Chem. Sec.* (*Nippon Kagaku Zasshi*), **79**, 996 (1958).
10) T. Yuasa, ibid., **79**, 999 (1958).
11) T. Yuasa, ibid., **80**, 1117 (1959).

electron impact on the electrodes or gaseous particles.

In the condition of such an electron impact on gaseous particles, the ionization (or decomposition) process for the atom, ion, or molecule seems to overcome other processes such as the recombination of atom and ion.

Therefore, one of the two alternative mechanisms considered—the formation of polyatomic ions by recombining the atom with the ion in the gas phase—seems to be unlikely, and another formation process appears probable. That is, first, large gaseous molecules are emitted from the rods, then the substances are decomposed in the gas phase; thus a series of molecular ions as given in Table I are produced, or such a series of ions may be sublimated simultaneously from the first. (These two processes may take place simultaneously.) If this process, in which no polyatomic ions can be formed as long as polymerized substances are not sublimated from the solid, is applied to the experimental results, the conclusion can be drawn that the sublimation products from the metallic crystal are only a group of free monoatomic molecules, whereas for the semi-metallic crystal with a covalent bond some gaseous polymer must exist in the sublimation products.

Summary

Using a mass spectrometer, the nature of the mass spectrum produced by the spark ionization source of semi-metallic and metallic elements and of ionic-crystals was studied, and it was found that only semi-metallic elements are capable of producing their polyatomic ions in a significant concentration.

When the samples of alkali halide single crystals were taken out from the spark source after sparking, it was observed that the crystals held their shape and, moreover, that color centers had been formed finely.

In the light of the experimental results, the mechanism of the ion formation in the spark was discussed, and it was pointed out that some relation might exist between the crystal structure of the solid sample and the formation of the gaseous molecular ion.

The author wishes to express his thanks to Mr. S. Nas for his cooperation in the experiments.

Department of Chemistry
School of General Studies
Kyoto University, Kyoto

Separation of Uranium from Fission Products using Cellulose

By Noboru Oi

(Received May 20, 1961)

Cellulose column chromatography has been extensively used for the separation of uranium from other metals[1], thorium from rare earths[2], uranium from thorium[3], uranium from plutonium[4] and so on.

This method has the advantage that minor components or impurities are adsorbed and collected onto cellulose. This is the opposite of the ion exchange or solvent extraction method, which extracts the main component, such as uranium or thorium.

The applicability of this method to the separation of uranium from fission products has been briefly mentioned by the author[5]. Because the amounts of fission products in irradiated uranium are very small, this method seems especially suitable for this separation. In this paper a detailed treatment of this program is presented.

Experimental

Reagents.—*Cellulose.*—Cellulose powder, 100~200 meshes for chromatography, was obtained from Toyo Roshi Co., Ltd., and was used after treatment with dilute nitric acid according to the method of Burstall[1].

The irradiation of the uranium was performed in a JRR-1 reactor. A uranium(IV) oxide pellet was irradiated for one week, and after a coling period of 30 to 100 days it was dissolved in nitric acid; then the excess nitric acid and water were evaporated off, leaving the uranyl nitrate hexahydrate.

Separation by Column Method.—One gram of cellulose was packed in a glass tube 18 mm. in

1) F. H. Burstall and R. A. Wells, *Analyst*, **76**, 396 (1951).
2) N. F. Kember, ibid., **77**, 78 (1952).
3) C. A. Barnett, E. Furby and A. M. Thomas, AERE C/R 1183.
4) J. A. F. Delsiel, AERE C/R 704.
5) N. Oi, This Bulletin, **33**, 1617 (1960).

diameter. Uranyl nitrate containing fission products was dissolved in an organic solvent keeping the concentration of uraniun about 0.2 M, and this solution was passed through the column. Then the column was washed with ten milliliters of the organic solvent, and then 30 ml. of one molar nitric acid was passed to elute the adsorbed fission products. The fractions of the organic solution, nitric acid and remaining cellulose were analyzed by a single-channel γ-scintillation spectrometer.

Separation by Batch Methed.—To obtain the distribution ratios of individual fission products at various uranium concentrations in an organic solvent, the following method was employed. About one microcurie of nuclides in nitric acid was evaporated to dryness in a beaker under an infrared lamp. Then, various concentrations of uranyl nitrate in organic solution were added, and the nuclide was dissolved by stirring. This solution was then transferred to a graduated glass cylinder with a stopper, and 100~200 mg. of cellulose was added. The activities of the solution before and after the equilibration (one hour was enough) were measured by a scintillation counter, and the K_d value was calculated by the following equation:

$$K_d = \frac{\text{Activity adsorbed per g. of cellulose (c.p.m./g.)}}{\left(\begin{array}{c}\text{Activity per ml. in solution at equilibrium} \\ \text{(c.p.m./ml.)}\end{array}\right)}$$

Results

Selection of the Solvent. — Almost all the works ever published on cellulose column separation have used as an organic solvent, either ethyl ether, isopropyl ether, or, in some cases, ethyl methyl ketone. In order to establish a rule for the selection of the organic solvent, about forty solvents which can dissolve uranyl nitrate were tested (Table I). In this experiment, one gram of uranyl nitrate hexahydrate was dissolved in 30 ml. of organic solvent together with cerium-144 and was passed through the column. The eluted organic fraction was counted to calculate the percentage of the eluted cerium. The K_d values obtained for cesium-137 proved more clearly the rule for the selection of the organic solvent, as shown in Fig. 1. These two results agreed well in that the solubility of water in the solvent here plays a main role in the separation. A water-insoluble ether or an acetate, such as ethylether, *n*-butylacetate or isoamylacetate, showed good results. On the other hand, alcohols, acetone and tri-*n*-butylphosphate did not give good results.

Influence of Nitric Acid and Water.—All of the published works have used a mixture of inorganic acid and an organic solvent, such as nitric acid and ether, hydrofluoric acid and ethyl methyl ketone. As to the influence of nitric acid, Burstall and Wells[1] pointed out that nitric acid was necessary for the quantitative recovery of uranium or thorium, while large amounts of nitric acid caused an increase in the solubility of other metals.

In this work we used only organic solvent. For the separation of uranium from fission products, free nitric acid must be eliminated. In this case, however, the complete recovery

TABLE I. SEPARATION OF URANIUM FROM CERIUM-144. SELECTION OF THE SOLVENT

Organic solvent	Cerium-144 eluted %	Solubility of water in the solvent*
Alcohol		
Methanol	98	∞
Ethanol	96	∞
Isopropanol	13	∞
n-Butyl alcohol	18	20.1
Isobutyl alcohol	12	15
Isoamyl alcohol	29	2.6
n-Hexyl alcohol	29	7.2
2-Ethylhexyl alcohol	0	2.6
Cyclohexanol	65	—
Ketone		
Acetone	67	∞
Ethyl methyl ketone	28	11.8
Methyl propyl ketone	0	3.3
Isobutyl methyl ketone	0	1.8
Amyl methyl ketone	0	1.5
Diacetonealcohol	90	∞
Cyclohexanol	50	8.7
Mesityloxide	9	3.4
Isophorone	11	4.3
Acethylacetone	35	—
Ester		
Ethyl formate	10	4.5
Ethyl acetate	4	3.3
n-Butyl acetate	0	1.2
Isopropyl acetate	0	1.8
Isoamyl acetate	0	1.0
2-Ethoxyethyl acetate	20	—
Ethyl acetoacetate	70	4.9
Tri-*n*-butyl phosphate	42	7.0
Cellusolve		
Methylcellusolve	99	∞
Ethylcellusolve	96	∞
Butylcellusolve	76	∞
Ether		
Ethyl ether	0	1.3
Isopropyl ether	0	0.57
Butyl ether	0	0.17
Dioxane	21	
Nitromethane	5	—

* These data were taken from "Physical Properties: Synthetic Organic Chemicals", the Union Carbide Chemicals Co. (1961).

Table II. Influence of nitric acid

Solvent	Content of nitric acid vol, %*	γ-Activity eluted %	Ratios of eluted nuclides**			
			$^{144-1}$Ce	$^{103-6}$Ru	^{131}I	^{95}Zr-Nb
Ethyl ether	0	1.2	1	1	1	1
	3	4.5	1	18	1.5	1
	5	6.6	1	27	1.5	1
n-Butyl acetate	0	1.7	1	1	1	1
	3	4.4	1	6.5	1.5	1

* d=1.38 nitric acid
** No nitric acid was taken as unity.
*** One week irradiated, four weeks cooled uranium was used. Uranyl nitrate hexahydrate, one gram.

Table III. Influence of water

Crystal water of uranyl nitrate	Water present in this system mg.	Eluted γ-activity, %	Decontamination factor		Uranium loss mg.
			$^{103-6}$Ru	^{95}Zr-Nb	
$2H_2O$	72	2.1	18	50	1.0
$3H_2O$	108	0.88	37	110	1.8
$6H_2O$	248	0.31	59	380	16
$6H_2O$*	700	0.23	43	400	23

Uranium: One gram as uranyl nitrate hexahydrate
Solvent: *n*-Butyl acetate
Fission products: Mixed fission products (ORNL)~10^8 γ c.p.m.
* Solvent was saturated with water.

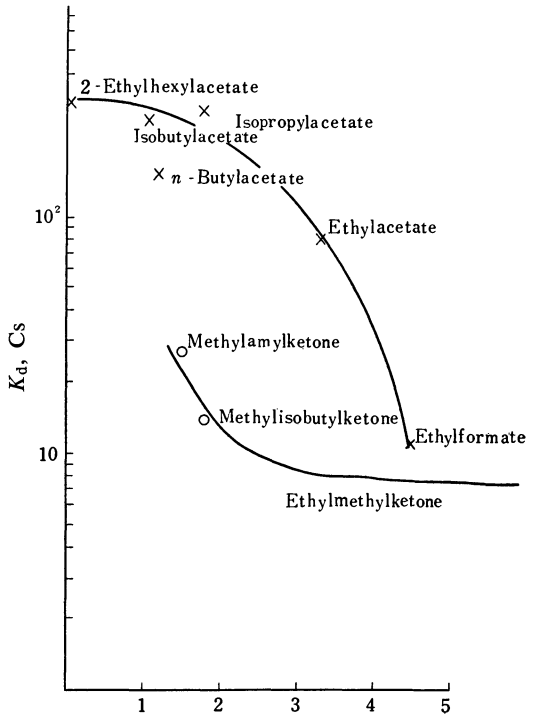


Fig. 1. Distribution ratios of cesium-137 as a function of water-in solubility of the solvent.

of uranium becomes difficult. From Table II, it is clear that the adsorption of fission products, especially ruthenium, decreased rapidly with the addition of nitric acid. The adsorption of uranium and its daughter nuclides also decreased, while adsorptions of cerium[6] and zirconium were little influenced. The increase in the elution of ruthenium is perhaps due to the formation of a trinitrato nitrosyl complex.

On the contrary, the presence of water is necessary for this separation, as is shown in Table III. This indicates also that water, namely partition, is a key factor for the adsorption. But the addition of water in excess must be avoided because the loss of uranium will increase.

Distribution Ratios for Individual Nuclides. — Irradiated uranyl nitrate cooled for four weeks was dissolved in *n*-butyl acetate and was passed through the cellulose column. Eluted fractions were collected and analyzed for uranium and fission products. The results are shown in Fig. 2. This pattern indicates that the adsorption of fission products onto cellulose is influenced by the concentration of uranium in the organic solvent. This phenomenon becomes clear with the determination of the K_d values of the fission products. Figure

6) Ce-144 was completely retained on the cellulose when 20% of HNO_3 in ethylether was used.

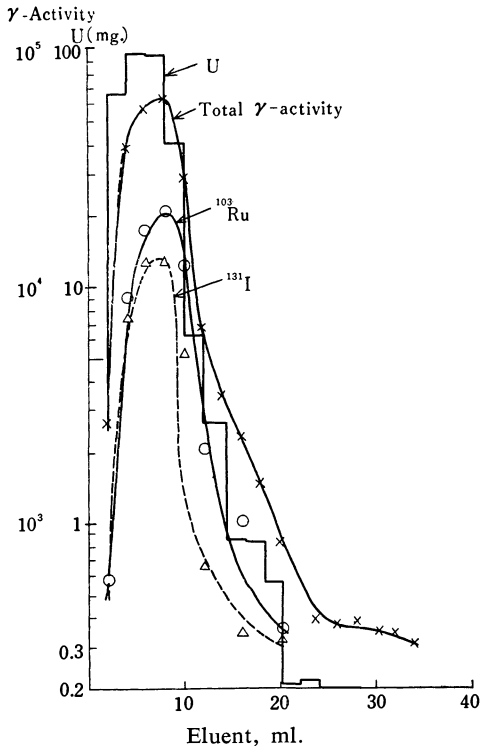


Fig. 2. Elution of uranium and fission products using *n*-butyl acetate.

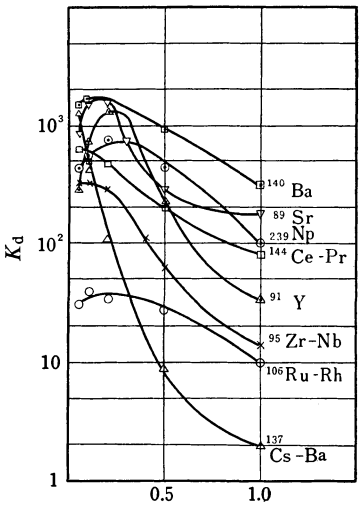


Fig. 3. Distribution ratios of fission products and neptunium as a function of uranium concentration in *n*-butyl acetate.

3 shows the K_d values for comparatively long-lived fission products and neptunium at various concentrations of uranium in *n*-butyl acetate. Here, the adsorption of fission products decreased rapidly with an increase in the uranium concentration. These values correspond well to the behavior of the nuclides in the column. Ruthenium is the most troublesome nuclide, and its degree of adsorption always determines the decontamination factor for total gamma activity. Cesium was found to elute when the uranium concentration was high. Consequently, uranium concentrations which passed through the column were limited to below 0.2 M.

Treatment of Irradiated Uranium. — As an example, the treatment of one-week-irradiated and 100 day-cooled uranium was conducted. The results are shown in Table IV. It must be noted that these results are valid only for this amount of uranium. Figure 4 shows the γ-spectrographs for the sample of uranium, the eluted organic solution and the activity remaining on the cellulose after the passage of one molar nitric acid. About 20~40% of zirconium was found to remain on cellulose without its being eluted by nitric acid.

Table IV. Treatment of 100 day-cooled uranium

Solvent	Eluted γ-activity, %	Decontamination factor $^{103-6}$Ru	Decontamination factor ^{95}Zr-Nb
Ethyl ether	0.42	47	1360
n-Butyl acetate	0.68	37	1700
Isoamyl acetate	0.89	12	5000
Isopropyl acetate	1.1	11	1800
Isobutyl methyl ketone	3.1	6	320

Uranyl nitrate hexahydrate : 1 g.
(10^8 γ-c.p.m.)

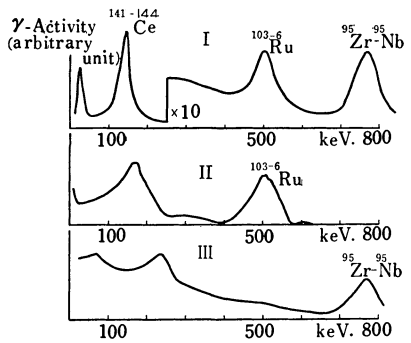


Fig. 4. Treatment of 100 day-cooled, irradiated uranium using *n*-butyl acetate.
I Total activity (sample of uranium)
II Eluted organic solution
III Activity remained on cellulose after the passage of one molar nitric acid

Discussion

As has been mentioned, for the separation of uranium from fission products by cellulose,

we can not use nitric acid to keep off the elution of ruthenium. For this reason, large amounts of organic solvent are necessary for the complete recovery of uranium. But when one to two grams of uranium are to be treated, 99% or more of uranium recovery and 99% or more of fission products removal can be accomplished easily by using less than 40 ml. of organic solvent and one gram of cellulose.

As to the treatment of large amounts of irradiated uranium, it requires much further investigation. Because the K_d values for fission products nuclides are of the order of 10^2 to 10^3, even at a uranium concentration of 0.2 M the amount of uranium to be treated by one gram of cellulose seems to be limited.

This method has the advantage that the fission products are collected onto cellulose. This makes easier further treatment such as waste disposal or the recovery of potential radioisotopes. The selective elution of fission products nuclides from cellulose will be made possible by the use of a combination of complexing agents. This remains for further investigation.

The mechanism of this separation is not yet known. As has been mentioned, partition will be a large factor, while adsorption by ion exchange seems to be a factor, too.

Summary

The separation of uranium from fission products by using cellulose has been demonstrated. Uranyl nitrate hexahydrate containing fission products was dissolved in an organic solvent that had low solubility of water, and this solution was passed through the column of cellulose. Almost all the fission products were retained on the cellulose, while uranium passed almost unadsorbed. The most labile nuclides were found to be ruthenium and cesium. Free nitric acid must be eliminated to prevent the elution of ruthenium.

The distribution ratios of individual fission products and neptunium between cellulose and an uranyl nitrate solution in *n*-butyl acetate were determined, and it was found that the adsorption of fission products decreased with the increase in the uranium concentration of the organic solvent. Therefore, the concentration of uranium that passed through the column was limited to below 0.2 M.

It was also found that water was necessary. This indicated partition as one of the mechanisms of this separation.

In this method the mass transfer of uranium between two different phases is not performed, so the contamination of fission products is rather small. Moreover, uranium can be easily recovered and fission products are condensed on a small amount of cellulose.

The author wishes to express his sincere thanks to Dr. Kakuzo Tada of the Central Research Laboratory, Tokyo Shibaura Electric Co., Ltd., for his fruitful discussions and encouragement.

Central Research Laboratory
Tokyo Shibaura Electric Co., Ltd.
Kawasaki

Energy Distribution of Secondary Electrons from Copper-Beryllium Alloy by Bombardment of Positive Ions of Inert Gases. II. Activated Copper-Beryllium

By Toshio SUGIURA

(Received April 1, 1961)

In a previous communication[1], study of the electron ejection from the electro-polished copper-beryllium by the bombardment of the positive ions of inert gases has been reported on. In that work, the energy distribution of secondary electrons was measured, and the mechanism of the secondary electron ejection from the electro-polished copper-beryllium surface was discussed. It was found that the general features of the distribution curves show the kinetic ejection, and that the energy distribution of secondary electrons has a correlation with the ionization potential of the impacted ions. These results indicate that the mechanism of the secondary ejection in that study is not satisfactorily explained by the

1) T. Sugiura, This Bulletin, **34**, 1475 (1961).

simple kinetic ejections; the contribution of the potential ejection must also be taken into consideration. In an earlier communication[2], it has been reported that the secondary electron yield from the copper-beryllium surface impacted by positive ions is markedly increased by the activation treatment of the copper-beryllium surface, and that quite a thick layer of beryllium oxide is newly formed by the activation in the neighborhood of the surface.

It is, therefore, of interest to the present author to investigate the energy distribution of the secondary electrons emitted from the activated copper-beryllium surface, since such an investigation would make possible a comparison with the results reported in the previous communication[1] and with the information on the mechanism of the secondary electron ejection from the activated copper-beryllium surface.

Experimental

Apparatus and Procedure. — The apparatus and the procedure have already been described in the previous communication[1].

Preparation of Ion Target. — The activation treatment of the ion target was carried out in a quartz tube (45 mm. in inner diameter and 500 mm. in length) connected by a water-cooled taper joint to the vacuum system, the reservoir of purified oxygen, and a McLeod gauge. The quartz tube was heated in an electrical furnace, and the temperature was measured with an alumel-chromel thermocouple enclosed in this quartz tube. The shaped and electro-polished ion target was put into the quartz tube and evacuated to lower than 5×10^{-6} mmHg at about 800°C for about three hours. After the evacuation, the temperature in the quartz tube was lowered to the required temperature (400°C in this study), then a known quantity of oxygen was introduced into the quartz tube. The initial pressure of oxygen was about 5×10^{-2} mmHg.

Materials. — The inert gases were the same as those described in the previous communication[1]. Oxygen used for the activation of the ion target was prepared by the thermal decomposition of potassium permanganate and was purified by passing it through a trap cooled by liquid nitrogen.

Results

Contact Potential between Gold and Activated Copper-Beryllium. — The contact potential between gold and activated copper-beryllium was determined for the purpose of the correction of the energy scale for the secondary electrons. Typical results on the retarding potential measured in a manner similar to that described in the previous communication[1] are shown in Fig. 1, in which the circular points indicate the retarding potential curve between the tungsten filament and the gold surface, while the square points show the retarding potential curve between the tungsten filament and the activated copper-beryllium surface. As seen in Fig. 1, the retarding potential portion had been observed to be linear from 0.75 to 1.25 V. for the tungsten~copper-beryllium system, and the value of the retarding potential for the tungsten~gold system well coincides with that obtained in the previous communication. As shown by arrows in each curve in Fig. 1, the point of zero field has beeen determined by the intersection of each extrapolated straight lines with the saturated current and the retarding portion. The observed value of the contact potential difference between gold and activated copper-beryllium is 0.25 eV; namely, the surface potential of activated copper-beryllium is 0.25 eV. more positive than that of gold.

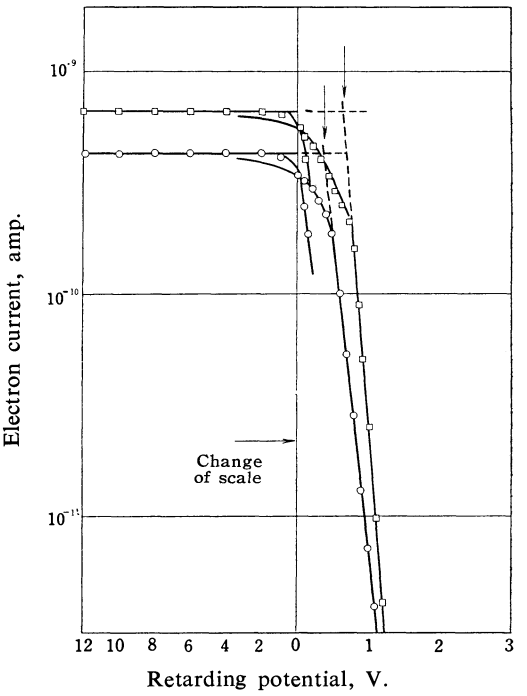


Fig. 1. Retarding potential curves of thermoionic electron from the heated tungsten used to determine the contact potential difference between gold and activated Cu-Be. The circular devices show the Au~W system, the square devices show the activated Cu-Be~W system. The vertical arrows on each curve indicate the values for the zero field in each systems.

Energy Distribution of Secondary Electrons. — The distribution curves of the kinetic energy of secondary electrons by singly-charged argon ions are shown in Fig. 2. In this figure, the results obtained for the incident ion energy of 1240, 840 and 540 V. are indicated by circular,

2) T. Sugiura and T. Hayakawa, ibid., 34, 58 (1961).

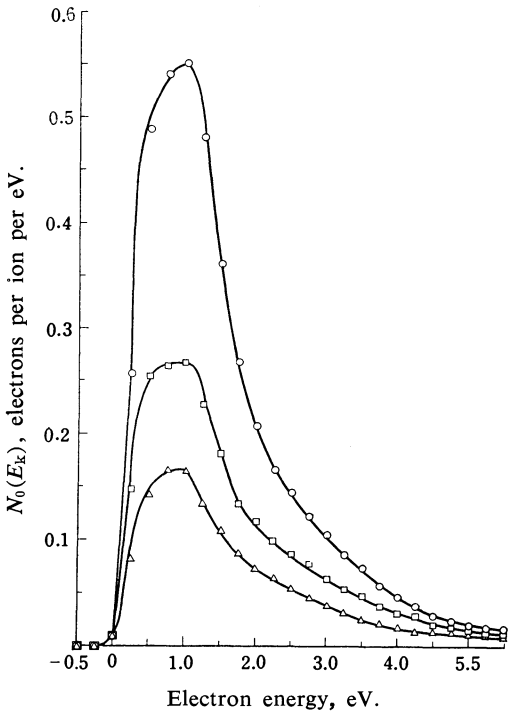


Fig. 2. Energy distributions of electron ejected from activated Cu-Be by singly charged argon ions of 1240, 840 and 540 V. incident kinetic energies, indicate by circular, square and triangular devices, respectively.

square and triangular devices respectively. The electron energy scale (V_r) in this figure was corrected to the contact potential difference between the ion target and the electron collector, as described above. The distribution curves of the kinetic energy of secondary electrons by doubly-charged argon ions, singly- and doubly-charged neon ions and singly charged helium ions have been also obtained; these distribution curves, which have been abbreviated in this paper, have a shape similar to and have the same tendency as the curves in Fig. 2. The distribution of the kinetic energy of the secondary electrons obtained in this study represented by half the width of each distribution curve and the yield of secondary electrons are summarized in Table I. As seen in Fig. 2, these distribution curves show no low energy tail, the fringing field of the analyzing magnet of the mass spectrometer having no observable influence on low energy electrons.

Discussion

General Features of Energy Distribution Curves. — As seen Fig. 2, the general features of the distribution curves of the secondary

TABLE I. VARIATION OF THE HALF WIDTH OF THE ENERGY DISTRIBUTION CURVES AND YIELDS OF SECONDARY ELECTRONS FROM ACTIVATED Cu-Be SURFACE WITH ION ENERGIES OF INERT GAS IONS

	Half width of distribution curves of secondary electron energy in eV.			Yields of secondary electrons γ_1 in electrons per ion		
Ion energy / ion	1240	840	540	1240	840	540
A^+	1.50	1.55	1.60	1.08	0.56	0.32
A^{2+}	1.55	1.60	1.65	1.02	0.67	0.42
Ne^+	1.70	1.80	1.90	1.18	0.83	0.49
Ne^{2+}	2.00	2.20	2.40	1.86	1.45	1.00
He^+	2.40	2.50	2.70	2.40	1.74	1.07

electrons from the activated copper-beryllium surface are similar to those obtained for those of non-activated copper-beryllium surface already reported on in the previous paper[1]. But, as seen in Table I, the half-widths of the distribution curves increased about 10 to 50% by the activation of the copper-beryllium in each case, together with the increase in the secondary electron yield

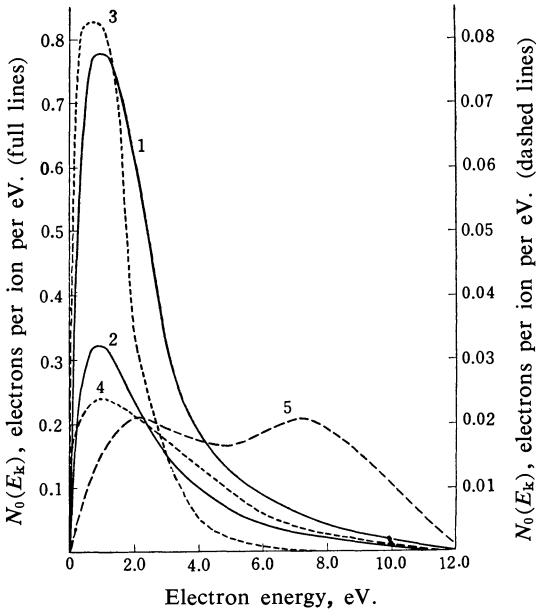


Fig. 3. Energy distributions of electrons ejected from activated Cu-Be by singly-charged helium ions of 1240 (curve 1) and 540 eV. (curve 2), and energy distributions of electrons ejected by 10 eV. helium ions from germanium (111) surface in various cleaning conditions obtained by Hagstrum[3] (curves 3, 4 and 5), the cleaning conditions of germanium surface described in the text.

3) H. D. Hagstrum, *J. Phys. Chem. Solid*, **14**, 33 (1960).

Recently, Hagstrum et al. have reported investigations into the interaction between the slowly moving helium ion and the germanium[3] and the silicon[4]; he was interested to find the procedures necessary for the preparation of clean semiconductor surfaces. In Fig. 3, the energy distribution curves 1 and 2 of secondary electrons ejected from activated copper-beryllium by 1240 and 540 eV. helium ions obtained in the present study are compared with the results of Hagstrum (curves 3, 4 and 5) with 10 eV. helium ions from the (111) face of germanium. Curve 3 in Fig. 3 was obtained for the face of etched germanium, and curve 4 was obtained for the germanium surface treated in the following manner: after being heated to 1125°K for 4 hr., the target was exposed with dry nitrogen at atmospheric pressure and successively repumped for about 100 hr. without any target heating. As seen in Fig. 3, the energy distribution curves of the secondary electrons are gradually broadened from curve 3 to curve 4 by target heating, but the area of the distribution curve is markedly decreased by the heat treatment i. e., the electron yield decreases as a result of target heating. Curve 5 in Fig. 3 was obtained for the germanium surface after heating at 940~1170°K for about 180 hr. and subsequent sputtering of about 100 layers of germanium at a 4 mA/cm^2 current intensity for 90 min.; Hagstrum has considered that curve 5 is the distribution curve of a secondary electron emitted from the atomically clean germanium surface. Hagstrum has obtained similar results for a silicon surface[4].

Figure 3 indicates that distribution curves 1 and 2 show a great similarity to distribution curves 3 and 4 rather than to the distribution curve of the kinetic ejection obtained by Waters[5]. These results imply that the emission of secondary electrons from activated copper-beryllium is followed by the Auger ejection in spite of the fact that the surface is not atomically clean. Further comparison reveals that the yields of secondary electrons in the present experiments are about one order greater than the results of Hagstrum, and distribution curves 1 and 2 are both broader than curve 3, though narrower than curve 4. These results suggest that the cleanliness of the target in the present study may correspond to that about the middle of curve 3 and of curve 4 in Fig. 3. In the present study, the ion target was heated to about 800°C by electron bombardment of the background pressure of 1×10^{-6} mmHg for about 10 min. It is clear that this treatment did not result in an atomically clean surface, but some adsorped layers of residual or foreign gases were removed. Allen[4] has studied the nature of the silicon surface by means of the field emission microscope connected with the investigations of Hagstrum; he has observed that the high intensity random spots from the unheated surface and the secondary electrons emitted by ions from this surface have an energy similar to that shown on curve 3 in Fig. 3. These high intensity spots were eliminated by heating of the silicon, and this surface then emitted secondary electrons having an energy similar to that shown on curve 4 in Fig. 3. Allen has described how these high intensity spots are emitted from the cluster of adsorption layers. From this study, the difference between curves 3 and 4 in Fig. 3 is considered to arise from the fact that the respective surface have and do not have the cluster of adsorption layers. In a comparison of the curves shown in Fig. 3, the energy of each secondary electron shown by curves 3 and 4 is considered to shift to a low energy compared with the energy of the secondary electrons shown by curve 5, and it is supposed that secondary electrons emitted from the ion target lose their kinetic energy in collisions with the adsorbed molecules or atoms. In these surfaces, it is supposed that the influence of the surface characteristics on the energy of the secondary electrons emitted by ions is obscured by the action of the adsorption layers. From the consideration described above, it may be considered that the cluster on the ion target in the present study is removed by the heating of the electron bombardment.

The influence of the ion kinetic energy, the ion species and the ionic charge on the distribution curves of the electron energy has a tendency similar to the results on the electro-polished surface reported on in the previous paper[1].

Influence of Target Activation of the Energy Distribution Curves. — By the activation of copper-beryllium, the yield of secondary electrons was greatly increased. For the purpose of obtaining information about the emission characteristics of the secondary electrons emitted from activated copper-beryllium, the energy distribution curves of the secondary electrons increased by target activation were plotted from the results both of the present study and of the previous communication[1].

Figures 4, 5 and 6 show the plot of the difference in the energy distribution $\Delta N_0(E_k)$ of secondary electrons at each electron energy E_k obtained for the activated and electro-polished

4) F. G. Allen, J. Eisinger, H. D. Hagstrum and J. T. Law, *J. Appl. Phys.*, **10**, 1563 (1959).
5) P. M. Waters, *Phys. Rev.*, **109**, 1053 (1958); **111**, 1466 (1958).

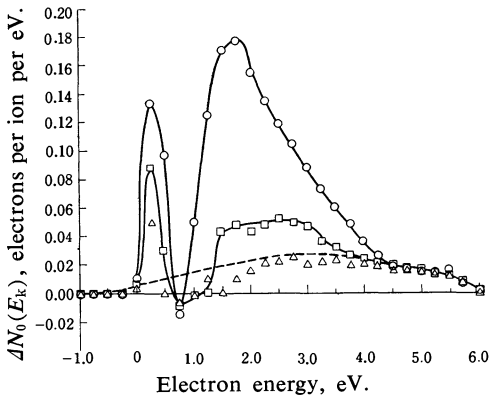


Fig. 4. Plots of the differences between energy distribution ejected from activated and electro-polished Cu-Be impacted by singly-charged argon ions. Circular, square and triangular devices indicate the kinetic energy of incident ions of 1240, 840 and 540 eV., respectively. The dashed curve shows the distribution curve of Auger electron ejected by singly charged argon ions of 10 eV. from atomically clean W surface obtained by Hagstrum[6].

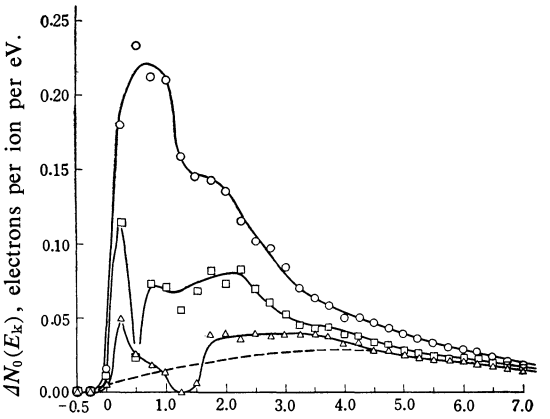


Fig. 5. Plots of the differences between energy distribution ejected from activated and electro-polished Cu-Be impacted by singly-charged neon ions. Circular, square and triangular devices indicate the kinetic energy of incident ions of 1240, 840 and 540 eV., respectively. The dashed curve shows the distribution of Auger electron ejected by singly neon ions of 10 eV. from atomically clean W surface obtained by Hagstrum[6].

copper-beryllium target impacted by the singly-charged argon, neon and helium ions respectively. In these figures, circular, square and triangular devices indicate the energy distributions by the incident ions of 1240, 840 and 540 eV. kinetic energy respectively. For comparison, the energy distribution curves of secondary electrons from an atomically clean tungsten surface impacted by 10 eV. inert gas ions obtained by Hagstrum[6] are shown by dashed lines in Figs. 4, 5 and 6.

The distribution curves of $\Delta N_0(E_k)$ were very different from that obtained from activated copper-beryllium. The distribution curves of the singly-charged ions, especially in the case of the slow ions shown in the figures, have two maxima, and the peak of the lower energy side is very narrow, while the distribution of the higher energy side is relatively broad and has a high energy tail. The emission processes of secondary electrons shown in these distributions must thus be considered separately in three parts.

The distribution curves higher than about 4 eV. in electron energy show a great similarity to the distribution curves of Hagstrum indicated by dashed line in each figure, and this distribution is independent of the kinetic energy of the incident ions. From this similarity, the distribution curve under the dashed line may be considered that of the secondary electrons emitted by the Auger

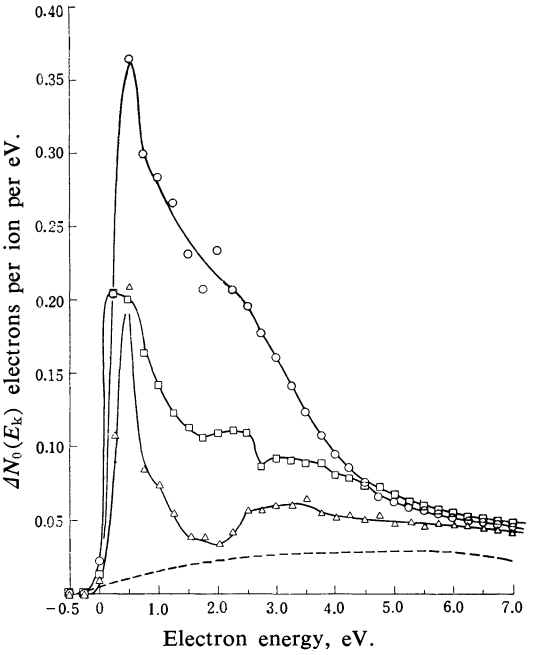


Fig. 6. Plots of the differences between energy distribution ejected from activated and electro-polished Cu-Be impacted by singly-charged helium ions. Circular, square and triangular devices indicate the kinetic energy of incident ions of 1240, 840 and 540 eV., respectively. The dashed curve shows the distribution of Auger electron ejected by 10 eV. singly-charged helium ions from atomically clean W surface obtained by Hagstrum[6].

6) H. D. Hagstrum, ibid., **104**, 317 (1956).

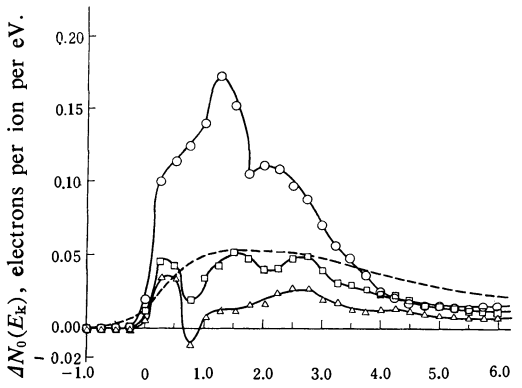


Fig. 7. Plots of the differences between energy distribution ejected from activated and electro-polished Cu-Be impacted by doubly-charged argon ions. Circular, square and triangular devices indicate the kinetic energy of incident ions of 1240, 840 and 540 eV., respectively. The dashed curve shows the distribution of Auger electron ejected by 200 eV. doubly-charged argon ions from atomically clean W surface obtained by Hagstrum[7].

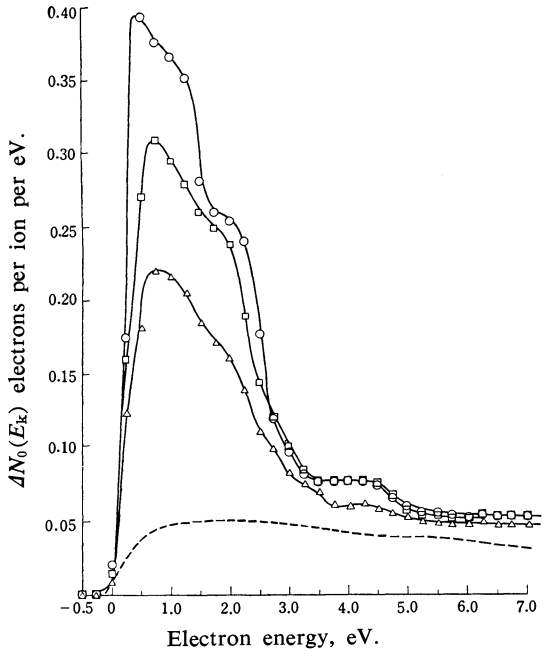


Fig. 8. Plots of the differences between energy distribution ejected from activated and electro-polished Cu-Be impacted by doubly-charged neon ions. Circular, square and triangular devices indicate the kinetic energy of incident ions of 1240, 840 and 540 eV., respectively. The dashed curve shows the distribution of Auger electron ejected by 200 eV. doubly-charged argon ions from atomically clean W surface obtained by Hagstrum[7].

process described by Hagstrum[7]. According to the earlier study by electron diffraction analysis of the activated and electro-polished copper-beryllium surface[2], the quite thick layers of the beryllium oxide were formed on the surface, replacing the copper oxide, by the activation treatment, and the results of the surface configuration suggested that the Auger ejection from activated copper-berillium might be contributed by the beryllium oxide layers mentioned above.

As seen in Figs. 4, 5 and 6, electron distributions exist above the dashed curve in each figure, and these distributions have relatively high energy as compared with distributions obtained from activated surface; the quantity of $\Delta N_0(E_k)$ depends on the kinetic energy of the incident ions. These phenomena show that secondary electrons emitted from activated copper-beryllium have a relatively a higher energy than those emitted from an electro-polished surface. Consequently, higher energy electrons markedly increased by the target activation may be formed relatively near the surface of the ion target. It is also supposed that the stopping cross-section of beryllium oxide for low speed ions in the present study may be greater than that of cupric oxide, although it is difficult to evaluate the values of the stopping cross-section of low energy ions.

The lower energy side of the distribution curves of $\Delta N_0(E_k)$ greatly depends on the kinetic energy of the incident ions, as seen in Figs. 4, 5 and 6; the low energy part of these distribution curves may imply the following interpretation. Part of the secondary electrons are produced in the deeper layer of the ion target by penetrated ions, and these secondary electrons thus produced pass through the considerable length of beryllium oxide produced near the surface of the ion target by target activation, and that part of these secondary electrons with sufficient energy may be ejected from the ion target. Assuming that the stopping power for the electrons of the beryllium oxide is greater than that of the copper oxide, the ejected electrons from the activated copper-beryllium may lose their energy more than those from the electro-polished copper-beryllium surface, as has been suggested by Sternglass[8]. A part of the ejected electrons from activated copper-beryllium may be shifted to the low energy side, in contrast to those from the electro-polished surface.

The distribution curves of $\Delta N_0(E_k)$ for doubly-charged argon and neon ions are shown in Figs. 7 and 8 respectively. As seen in Fig.

7) H. D. Hagstrum, ibid., **96**, 336 (1954).

8) E. J. Sternglass, ibid., **108**, 1 (1957).

7, for the doubly-charged argon ions the high energy tail in the present distribution curve is smaller than that of Hagstrum indicated by the dashed line in Fig. 7, and the separation of the distribution curve is not clear. In the case of the doubly-charged neon ions as seen in Fig. 8, the separation of the distribution curve is not clear for any incident ion energy. As seen from the results of Hagstrum[9] on the 200 eV. doubly-charged argon and neon ions shown by the dashed line in Figs. 7 and 8 respectively, the distribution curve by the Auger ejection processes of the doubly-charged inert gas ions has shifted to the lower energy side as compared with the distribution curves of singly-charged ions. Hagstrum has considered that the faster electrons may be ejected by highly charged ions in the Auger process and that the mean energy of the ejected electrons is practically independent of the ionic charges; he has explained his results by saying that the Auger neutralization of the highly charged ions by the metal surface occurs in steps. From the fact that this explanation may also be fitted to apply to the present result of the doubly-charged ions, it is considered that the distribution of $\Delta N_0(E_k)$ results from the shift of electron energy to the low energy side.

The phenomena in this study can not be attributed to the surface of the ion target not being atomically clean, but it is not unreasonable to consider that the secondary electron emission from activated copper-beryllium includes the contribution of the Auger ejection together with the kinetic ejection.

Summary

The distribution curves of the kinetic energis of secondary electrons from the activated copper-beryllium surface impacted by inert gas ions were together with the yield of the secondary electrons, measured by the retarding potential method. The contact potential difference between the ion target (activated copper-beryllium) and the electron collector (gold) was also measured by the retarding potential method for the thermal electrons from tungsten, and the correction to the kinetic energies of secondary electrons by this contact potential difference was made. For the purpose of obtaining information about the emission characteristics of the increase in the yield of secondary electrons by target activation, the distribution of $\Delta N_0(E_k)$, which is the difference in the secondary electrons emitted from activated and from electro-polished copper-beryllium, was plotted by electron energies. The main results obtained are as follows:

(1) The contact potential difference between activated copper-beryllium and gold is 0.25 eV. (gold, negative).

(2) The general features of the distribution curves of the secondary electrons emitted from activated copper-beryllium show a tendency similar to that of the secondary electrons emitted from electro-polished copper-beryllium, and they also show a great similarity to the distribution curves obtained from the not atomically clean semiconductor surface (germanium or silicon) by Hagstrum.

(3) The distribution of $\Delta N_0(E_k)$ show a remarkable difference from the distribution curves for activated copper-beryllium. Distribution curves of $\Delta N_0(E_k)$ higher than about 4 eV. in electron energies showed a great similarity to the distribution curves of the Auger electron obtained by Hagstrum. Moreover, the distribution of $\Delta N_0(E_k)$ for singly-charged ions shows clearly a separation in the electron energy scale; this result was explained by the fact that the stopping cross-section of the beryllium oxide is greater than that of the cupric oxide.

(4) From the explanation of the distribution of $\Delta N_0(E_k)$, it is considered that the increase in the yield of secondary electrons by target activation depends on the stopping cross-section of beryllium oxide and on the Auger process of electron emission.

The author wishes to acknowledge his indebtedness to Professor Shoji Shida of Tokyo Institute of Technology, and to Professor Teruo Hayakawa and Professor Osamu Toyama of University of Osaka Prefecture; under their direction and guidance this work was carried out. The expense has been defrayed in part from a grant given by the Ministry of Education, to which the author's thanks are also due.

Department of Applied Chemistry
College of Engineering
University of Osaka Prefecture
Sakai, Osaka

9) H. D. Hagstrum, ibid., **96**, 325 (1954).

*A New Method of Decomposition for Refractory Minerals and its Application to the Determination of Ferrous Iron and Alkalies**

By Jun Ito

(Received May 18, 1961)

The common ferrous minerals noted for their resistance to attack by a boiling mixture of hydrofluoric and sulfuric acids[1] are staurolite, tourmaline, axinite, kornerupine, sapphirine, ilmenite, chromite, spinels, columbite-tantalite and chrysoberyl. The determination of the ferrous oxide content in these minerals has long been a difficult problem in mineralogy as well as in analytical chemistry.

Among many attempts by analysts and mineralogists to solve this problem, the Mitscherlich method[2], involving decomposition with sulfuric acid in a heated sealed glass tube, and the Rowledge method[3], employing fusion with sodium metafluoborate in a sealed pyrex glass tube or a Vycor tube (Juulinen's modification)[4] or in a stream of carbon dioxide in a platinum boat[5] (Groves's modification), have been considered to be the best. None of these methods however, is simple. The sealing of the glass tubing, fusion under special conditions, continuous boiling of the titrant, etc. are all very time-consuming and are very likely sources of error unless done by well qualified analysts.

The writer noticed the strong resistivity of Teflon against hydrofluoric acid and sulfuric acid as well as its durability at a high temperature (260°C) and pressure and used it as a liner in a high temperature-pressure steel bomb. In this way, a new method of the decomposition of minerals in hydrofluoric acid and sulfuric acid at elevated temperatures and under fairly high pressures was established. This is very simple, less subject to error, and suprisingly efficient method for refractory minerals.

On the other hand, the recent developement of flame photometry has changed entirely the method of determination of alkalies, and the classical Laurence Smith decomposition has been largely replaced by simple acid decomposition, because the complete separation of the other elements has become unnecessary. For refractory minerals such as mentioned above, however, the Laurence Smith method has still been believed to be superior and indispensable. The writer's method offers a much simpler and more suitable way of decomposition with minimum contamination; also the results of an analysis of the alkalies in refractory materials should be more accurate than before. Using many pure minerals and standards available at Harvard Mineralogical Musem, the writer obtained the results given in the following section.

Experimental

Apparatus.—The electric furnace employed was of a vertical type, with chromel-alumel winding. It was operated at 110 V. AC, with Variac control.

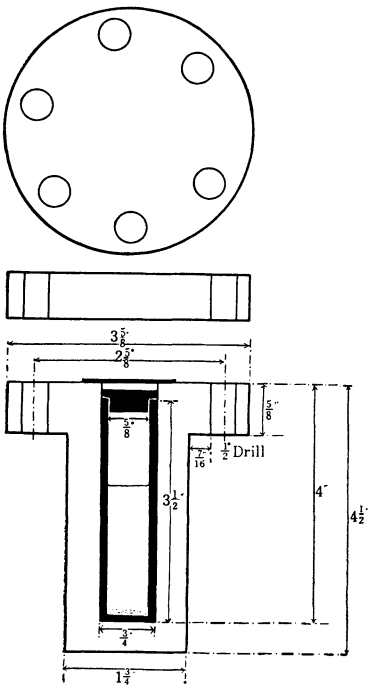


Fig. 1. Steel bomb and teflon liner.

* This work was done while the writer was at the Department of Mineralogy, Harvard University, U. S. A.

1) J. H. Pratt, *Am. J. Sci.*, (3), 48, 149 (1894).

2) W. F. Hillebrand and G. E. F. Lundell, "Applied Inorganic Chemical Analysis", John Wiley, New York (1953), p. 911; Mitscherlich, *J. prakt. Chem.*, **81**, 116 (1860).

3) H. P. Rowledge, *S. Roy. Soc. W. Australia.* **20**. 169 (1934).

4) A. Juulinen, *Ann. Acad. Scient. Fennicaes*, A III **47**, 19 (1956).

5) A. W. Groves, "Silicates Analysis", 2nd ed., London (1956), pp. 184-186.

Table I. Results of ferrous iron determination by both new and conventional methods in silicates

Sample	mg.	Heating time	FeO	Fe_2O_3	FeO, conventional
Tourmaline Newry, Maine	200	2	11.70	nil	Insoluble
	300	3	11.73		
Axinite, H. M. 86113 Roseberry, Tasmania	200	2	9.65	nil	Insoluble
	300	3	9.72		
W-1 Diabase	300	3	8.92 (mean of 3 determinations)	—	8.97 (Recommended value 8.72)
Staurolite Fanning Co., Georgia, U. S. A.	300	3	12.56	1.20	Incomplete decomposition
Staurolite, Kootenay Lake, British Columbia	300	3	10.81	1.73	9.92
Kornerupine, H. M. 46934 Itrongahy, Madagascar	200	4	2.39	nil	1.47
Chrysoberyl, H. M. 96545 Tokowaja Lake, Urals	100	3	2.1	—	—
Garnet (Almandite), Davis, New Hampshire, U. S. A.	300	3	31.70	nil	31.37
Garnet (Almandite), North County, N. H., U. S. A.	300	3	21.42	nil	20.65

The temperature was measured with a thermometer.

The steel bomb (Fig. 1) was machined by Arthur and Harold Ames (Dunbar Lab., Harvard) from 316 stainless steel. The bomb was roasted in air for 24 hr. at 450°C to provide a protective oxide coating.

The Teflon liner (tetrafluoethylene) (Fig. 1) was machined by Dr. I. Barnes from 3/4 inch round Teflon stock. The rod was turned to 5/8 inch O. D. and bored with a 19/32 inch drill. The Teflon cap was turned to 5/8 inch O. D. on the upper end and 9/15 inch on the lower end. The Teflon gasket was cut from a 1/32 inch sheet of teflon. The length of the Teflon cup with cap in place was 3 1/2 inches. The bolts were Allen caps the screws 1/2 inch and 3 inch.

Reagents.

H_2SO_4	1 : 1
HF	48%
H_3BO_3	Saturated aqueous solution
$KMnO_4$	0.1 N Standard solution

Procedure.—1) Transfer 0.300 g. of the fine powdered sample to a Teflon liner. 2) Add 5 ml. sulfuric acid (1 : 1), 5 ml. hydrofuoric acid. 3) Stir well with a thin platinum spatula and then wash it with a few drops of pure water. 4) Cover the liner and place in the bomb. 5) Place the gasket and cover on the bomb. 6) Tighten the cover with bolts, using a vise and a rachet wrench. 7) Place the bomb in a preheated furnace at 240°C and leave for 3~4 hr. 8) Take out, cool and open the bomb. 9) Pull out the teflon liner from the bomb using a thin needle. 10) a) For ferrous oxide determination, transfer the acid solution into a 500 ml. beaker filled with 300 ml. of distilled water and 10 ml. of saturated boric acid, then titarte with potassium permanganate standard solution. b) For alkali determination, transfer the acid solution into a platinum basin and heat until all the hydrofluoric acid is driven off, then follow the regular procedure for flame photometric determination.

Results

Diabase standard W-1[6] was analyzed for ferrous oxide (Table I) to check on the accuracy of the method. The results seem to be a little higher (0.1%) than the average analysis. The average value is not necessarily the true value, especially in terms of ferrous oxide determination with conventional methods, but a slight reduction of ferric iron to ferrous iron by pyrite ferrous sulfide could be suspected. Pyrite partly decomposed with this procedure.

Tourmaline from Newry, Maine, U. S. A., Axinite from Tasmania and Kornerupine from Madagascar were analyzed totally using the new method. The calculated formulae from the chemical analysis indicates that the iron present in these minerals is divalent, replacing magnesium manganese in the structure. Axinite definitely does not contain alkalies.

The iron in kornerupine and chrysoberyl is divalent; this explains their bluish color.

Fig. 2. shows that contamination of the iron by the steel of the bomb is remarkably low. Aparently the hydro fluoric acid and sulfuric acid were kept inside of Teflon liner well.

The blank consumption of potassium permanganate solution increases with the time of heating. For ferrous oxide determination, therefore, the heating should be limited to 4 hr. (Fig. 3) if possible.

Among the refractory minerals mentioned above, only tourmaline and kornerupine contain appreciable amounts of alkalies. The

6) H. W. Fairbairn and others, "A Cooperative Investigation of Precision and Accuracy in Chemical, Spectrochemical and Modal Analysis of Silicate Rock", U. S. Geological Survey Bulletin 980 (Analysis of Diabase W-1), (1953).

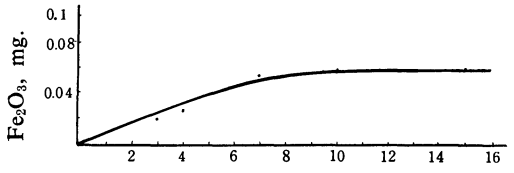


Fig. 2. Iron contamination during the decomposition with new method.

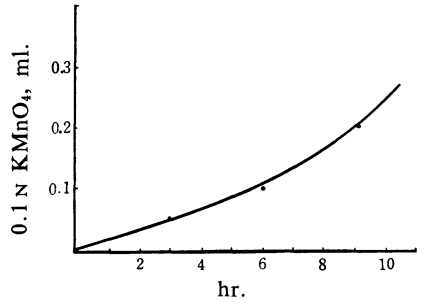


Fig. 3. Blank consumption of 0.1 N $KMnO_4$ after the heating of solution of H_2SO_4+HF with 1 ml of 5 N $Fe_2(SO_4)_3$ solution.

results of the alkali determination are shown in Table II. Blank values of contamination from the new procedure did not exceed the values obtained by the conventional procedure. Actually, the new method decomposed minerals more completely than the other method, and subsequent flame photometric determination was very easily carried out. Although none of the refractory oxide minerals which will be mentioned in the following section contain appreciable amount of alkalies, this method should be very suitable when their alkali content is in question.

Discussion

The principle of the method is somewhat similar to that of the Mitscherlich method, but the use of hydrofluoric acid inside a sealed vessel at an elevated temperature and pressure has never been attempted before for lack of a suitable liner such as Teflon.

As the results show, the reaction between minerals and acids under the stated conditions were carried out completely, and the difficulty of the ferrous ion and alkali determination of the refractory minerals was reduced.

The acid solution in a Teflon-lined bomb can be heated safely as long as the sample requires. Iron and alkali contamination are not detected, although consumption of the potassium permanganate standard solution gradually increases due to the very slight decomposition of the Teflon container. Also, there is no chance for any other contamination of the cation from outside.

Neither appreciable oxidation nor reduction occurred during the heating within a limited time, and the oxygen (air) contained in the partly-filled bomb does not significantly affect the results. The air can be replaced by nitrogen gas if desired.

The apparatus can be designed on a large industrial scale as well as on a microchemical scale, and there is no danger of breakage during the entire procedure because no glassware is involved.

In addition, the writer has extended these

Table II. Results of alkali determination

Mineral	Element	Number of analyses	%
Tourmaline Newry, Maine	Na_2O	3	1.78
	K_2O	3	0.09
Axinite, Roseberry, Tasmania	Na_2O	2	nil
	K_2O	2	nil
Kornerupine, Madagascar	Na_2O	3	0.30
	K_2O	3	0.12
Blank alkalies	Na_2O	3	0.5 ppm in final 100 ml test solution
	K_2O	3	0.5 ppm in final 100 ml test solution

Table III. Decomposition of non-silicates

Mineral	Heating time, hr.	FeO	Grade of decomposition
Magnetite, $FeOFe_2O_3$	4	29.9	Complete, Fe^3 hydrolyzed
Pyrite, FeS_2	5	—	Very incomplete
Ilmenite, $FeOTiO_2$	6	45.1	Complete, Ti^4 hydrolyzed
Chromite, $FeOCr_2O_3$	6	32.9	Complete, clean solution
Tantalite, $(FeMn)(TaCb)_2O_6$	8	7.9	Complete, Fe^3 hydrolyzed
Columbite	8	12.2	Complete, Fe^3 hydrolyzed
Baddeleyite, ZrO_2	12	—	Complete, clean solution
Rutile, TiO_2	16	—	Complete, clean solution
Corundum, Al_2O_3	4	—	Complete, small amount of Al salt precipitated
Zircon, $ZrSiO_4$	10	—	Only HF was used. Complete

experiments toward non-silicate minerals that are mostly oxides and the most difficult materials to dissolve in acids.

Chromite, ilmenite, baddeleyite, columbite-tantalite, rutile and corundum were readily decomposed by the same treatment, although pyrite and zircon were only partly decomposed.

Recently the writer has tried to decompose zircon ($ZrSiO_4$) in various ways and has finally found that it decomposes in the same vessel after 10 hr. of heating at 240°C, using hydrofluoric acid alone instead of a mixture of sulfuric acid and hydrofluoric acid.

The method is good not only for chemical analysis, but also various industrial uses may be found for it.

Finally, the use of strong alkalies instead of acids (Teflon is stable in alkalies too) should be studied.

The writer is indebted to Professor Clifford Frondel, Department of Mineralogy, Harvard University, for his kind advice and encouragement, to Dr. Ivan Barnes, now of the U. S. Geological Survey, for his help in supplying the bomb and furnace, and to Mr. A. Carpenter for his assistance in preparing many specimens used for this experiment.

Also, thanks are due to Dr. J. Frondel and Dr. K. Fuwa for their critical reading of the manuscript.

Department of Chemistry
College of General Education
The University of Tokyo
Meguro-ku, Tokyo

Differences in the Catalytic Activity of Nickel, Platinum and Palladium as Observed in the Isotopic Exchange Reaction of Paraxylene with Deuterium Oxide

By Kozo HIROTA and Tomiko UEDA

(Received May 23, 1961)

In our former reports on the isotopic exchange reaction of paraxylene with deuterium oxide, it was established that nickel powder exchanges the hydrogen of the methyl groups of paraxylene at 55~100°C with a much higher velocity than it does the hydrogen attached to the benzene ring[1], while platinum black can exchange both hydrogens under similar experimental conditions, as was reported preliminarily[2]. These results are interesting, because such a reaction would serve as an example wherein the difference in catalytic nature between nickel and platinum is shown definitely. Therefore, research has been extended to other metals and to nickel supported on several oxide carriers, using the NMR method for the analysis of products in addition to the infrared and mass-spectrometric methods hitherto adopted. The aims of the present paper are to confirm the above-mentioned difference in the catalytic activity of platinum and nickel and and further to investigate that of the palladium catalyst and the effects of carriers on the activity.

1) K. Hirota, K. Kuwata and T. Ueda, *J. Chem. Soc. Japan, Pure Chem. Soc.* (*Nippon Kagaku Zasshi*), **81**, 362 (1960); K. Hirota, H. Kusumoto and T. Ueda, This Bulletin, **33**, 423 (1960); H. Kusumoto, J. Itoh, K. Hirota and T. Ueda, *J. Phys. Soc. Japan*, **15**, 728 (1960).

2) K. Hirota and T. Ueda, Abstr. of the 7th Symposium on IR and Raman Spectroscopy (Japan), **60** (1960); K. Hirota, T. Ueda, K. Kuwata and M. Hatada, *Catalyst* (*Tokyo*), **2**, 181 (1960).

Experimental

Materials.—Deuterium oxide obtained from the Norsk Hydro Co. (99.7% D_2O) was used without any further purification.

Paraxylene (technical grade) was shaken with mercury to make it free from sulfur compounds and was separated from *o*- and *m*-xylene by recrystallization which was repeated five times. The paraxylene thus purified was dried over metallic sodium and distilled into a store vessel.

Raney nickel was developed from Ni-Al alloy consisting of 50% nickel by the method of W-2.

Ni-kieselguhr catalyst, K. S. Y.-6-FC, which had been prepared by the Nikko Co. (Tokyo) was used without any further treatment.

Nickel-alumina and nickel-silica were prepared by decomposing nickel formate supported on alumina and on silica at 270°C, according to the method already reported[1]. The preparation of the nickel-formate-alumina was as follows: 80% formic acid was added to a nickel carbonate solution in which alumina was suspended. In order to complete the

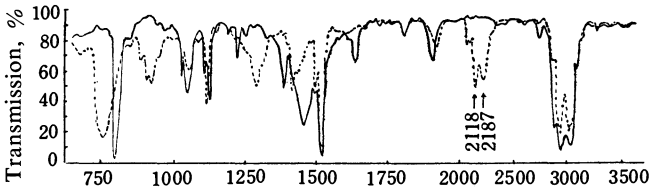


Fig. 1. IR spectra for the liquid samples.
—— Normal *p*-xylene, ---- Partially deuterated *p*-xylene on Raney Ni catalyst (No. 1) (NaCl prism)

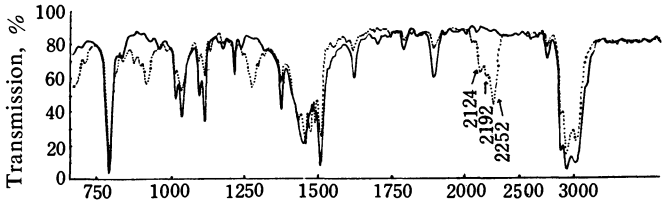


Fig. 2. IR spectra for the liquid samples.
—— Normal *p*-xylene, ---- Partially deuterated *p*-xylene on Pt catalyst (No. 11) (NaCl prism)

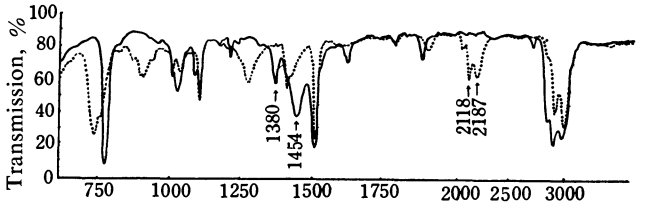


Fig. 3. IR spectra for the liquid samples.
—— Normal *p*-xylene, ---- Partially deuterated *p*-xylene on Ni catalyst (No. 0) prepared from nickel formate (NaCl prism)

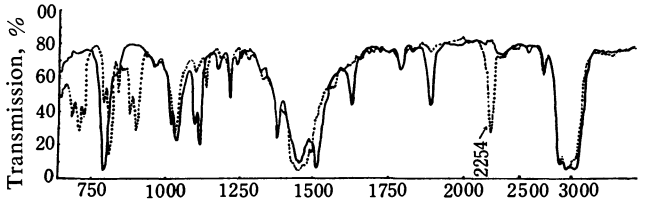


Fig. 4. IR spectra for the liquid samples.
—— Normal *p*-xylene, ---- Partially deuterated *p*-xylene on D_2SO_4 catalyst (NaCl prism)

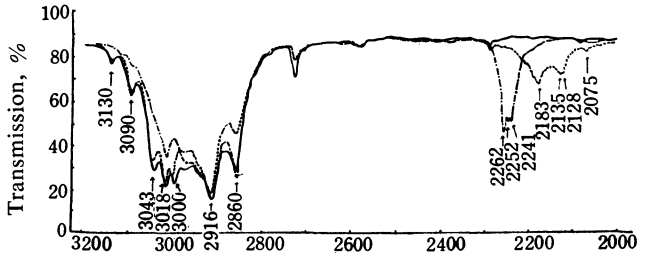


Fig. 5. IR spectra for the liquid samples.
—— Normal *p*-xylene, ---- Partially deuterated *p*-xylene on Ni catalyst, —·—· Partially deuterated *p*-xylene on D_2SO_4 catalyst (LiF prism)

Table I. Experimental conditions

Exp. No.	Catalyst	Weight of samples			Conditions of the reaction	
		Catalyst	*p*-Xylene	D_2O	Temp., °C	Time, hr.
1	Raney Ni	2.06	0.544	0.611	100	150
2	Ni-kieselguhr (1 : 1)	10.1	0.587	0.576	〃	〃
3	Ni-SiO_2 (1 : 10)	22*	0.616	0.666	〃	〃
4	Ni-Al_2O_3[a] (1 : 1)	10*	0.458	0.446	〃	〃
5	〃 (1 : 3)	20*	0.527	0.547	〃	〃
6	〃 (3 : 1)	6.7*	0.525	0.582	〃	〃
7	Ni-Al_2O_3[b] (1 : 1)	10*	0.525	0.523	〃	〃
8	Al_2O_3[a]	5.1	0.660	0.475	〃	〃
9	Al_2O_3[b]	5.0	0.449	0.477	〃	〃
10	Pt black	0.64	0.534	0.520	〃	285
11	〃 〃	〃	0.757	0.725	80	300
12	Pd black	0.99_4	0.568	0.741	100	150

* These numerals denote the estimated values of the produced catalyst after the decomposition of $Ni(HCO_2)_2$-Al_2O_3.

precipitation of nickel formate on alumina, acetone was added to the solution. Two kinds of alumina were used as the carrier: (a) Al_2O_3[a]: commercial activated γ-alumina (Wako Co. (Osaka)); (b) Al_2O_3[b]: pure alumina obtained by dehydration of alumina gel, which was made by adding ammonia solution to aluminium nitrate and letting dry air flow over it for 10 hr. at 500°C. Nickelformate-silica was prepared by the same method as in the case of nickelformate-alumina, by the use of commercial silica gel (Mallinckrodt Chemical Works) in this case instead of alumina.

Platinum black was prepared by reducing chloroplatinic acid made from platinum with formaldehyde and potassium hydroxide.

Commercial palladium black was used (Mitsuwa Kagaku Yakuhin Co.).

Procedure. — Since the procedure has been described in detail in previous reports[1], only the essential points will be mentioned. The catalyst was always prepared in a reaction tube, in which *p*-xylene and deuterium oxide were charged by distillation from their store vessels. The tube was kept at the reaction temperature in a thermostat. After the reaction both *p*-xylene and deuterium oxide were separated from the catalyst by distillation. Paraxylene was pipetted out from the upper part of the distillate, which formed two liquid layers; the paraxylene was then dehydrated with calcium chloride and distillated into another vessel. By infrared spectrometry the deuterated positions of the *p*-xylene molecules were determined, but quantitative analysis of the degree of deuteration was made by resorting to the NMR method. The mass-spectrometric method was also adopted for the same purpose.

The experimental conditions of all the runs are summarized in Table I, where the ratios in parentheses denote those in weight. Infrared spectra were obtained by using Hilger H 800 and Hitachi EPI-2 spectrophotometers equipped with sodium chloride or lithium fluoride prism. The NMR analysis was made by resorting to a high resolution spectrometer (Varian 4300 B; 40 Mc/sec.). The mass-spectrometric analysis was conducted with a Hitachi RMU-5 mass-spectrometer.

Results and Discussion

Difference of Activity among Nickel Catalysts, Platinum Black and Palladium Black.— Before the particular discussion on all the runs, it will be convenient to explain the general tendency of the differences in catalytic activity, taking the runs of Raney nickel (No. 1) and platinum black (Nos. 10 and 11) as examples.

The infrared spectra of the reaction products of Nos. 1 and 11 are shown in Figs. 1 and 2 respectively. The former is quite similar to the one shown in Fig. 3, which was the spectrum of the product when a nickel catalyst prepared from nickel formate was used[1]. It will be evident from a comparison of Figs. 1 and 3 that only hydrogen molecules of the methyl group were catalytically exchanged by nickel, while a new band appeared at 2252 cm^{-1} in the spectrum (Fig. 2) of the sample after the exchange reaction in the presence of platinum at 80°C (No. 11*). The same band was observed in the spectrum of No. 10 when the reaction was carried out at 100°C. It perfectly coincides with that of the deuterated product[3] of *p*-xylene with deuterosulfuric acid D_2SO_4, as is shown in Fig. 4. Since it is a well-known fact that only ring hydrogen can be exchanged with deuterium oxide by an acid catalyst[4], this new band must be due to the stretching vibration of the C–D bond in the

* A similar conclusion has been obtained recently by A. Ozaki et al., (Abstr. Papers of the 14th Annual Meeting of Chem. Soc. Japan, p. 185 (1961)) in the system of toluene and deuterium oxide.

3) T. Ueda, *Catalyst (Tokyo)*, **1**, 1 (1959).

4) C. K. Ingold et al., *J. Chem. Soc.*, **1946**, 222.

ring. Two other bands, which appear at 2192 and 2124 cm^{-1} by deuteration, seem to coincide with those appearing at 2187 and 2118 cm^{-1} in Figs. 1 and 3, i. e., in the samples catalyzed by nickel. (When a lithium fluoride prism was used, the 2187 and 2118 cm^{-1} bands were found to be at 2183 and 2128 cm^{-1} respectively (Fig. 5).) These bands therefore can be ascribed to those of the stretching vibrations of the methyl C–D bond.

The characteristics of the activities of all the catalysts investigated in this research are summarized in Table II, with No. 0 indicating the previous data on nickel prepared by the decomposition of nickel-formate. It will be noted that the activity of palladium black (No. 12) is similar qualitatively to that of platinum, but lies between those of nickel and platinum. The above conclusion can be derived quantitatively from the data of the mass-spectrometric method shown in Table III, where deuterium distribution in the reacted samples was tabulated as d_i (=% of *p*-xylene molecules containing *i* deuterium atoms). The existence of highly deuterated xylene in the cases of platinum and palladium catalysts indicates that all the hydrogen molecules in *p*-xylene are exchangeable, and especially so in the case of platinum.

Table II. Characteristics of catalysts on hydrogen exchange of paraxylene with deuterium oxide

Exp. No.	Catalyst	Benzene ring	Methyl group
0	Ni powder	−	+
1	Raney Ni	−	+
2	Ni-kieselguhr	−	+
3	$Ni-SiO_2$	−	+
4	$Ni-Al_2O_3$[a] (1 : 1)	+	+
5	〃 (1 : 3)	+	+
6	〃 (3 : 1)	+	+
7	$Ni-Al_2O_3$[b] (1 : 1)	+	+
8	Al_2O_3[a]	−	−
9	Al_2O_3[b]	−	−
10	Pt black	+	+
11	〃 〃	+	+
12	Pd black	+	+

N. B. + Exchangeable, − Not exchangeable

Table III. Mass-spectrometric analysis of the reacted samples, when Ni, Pt and Pd catalysts were used

Catalyst	Exp. No.	d_0	d_1	d_2	d_3	d_4	d_5	d_6	d_7	d_8	d_9	d_{10}	ϕ
Ni powder	0	0.2	2.0	9.0	23.5	32.6	24.7	7.9	0.1	—	—	—	39.0
Pt black	11	29.1	2.2	2.7	5.8	10.2	14.1	15.7	11.5	6.1	2.2	0.4	38.4
Pd black	12	7.2	3.9	12.0	21.6	25.7	20.1	10.8	3.9	0.8	0.3	—	39.5

$\phi = (1/10)\sum_{i=1}^{10} i d_i$ (average deuterium content %)

Table IV. Deuterium distribution in the reacted samples

A. Mass-spectrometric analysis

Exp. No.	d_0	d_1	d_2	d_3	d_4	d_5	d_6	d_7	d_8	d_9	ϕ
6	1.4	4.1	14.2	27.7	29.9	17.7	4.8	0.2			35.4
4	3.1	9.7	21.1	28.7	21.5	11.1	3.8	0.9	0.1		30.9
5	0.1	7.2	15.4	25.7	25.4	16.3	7.1	2.2	0.5	0.1	36.1
7	1.3	4.9	14.7	23.7	25.3	17.8	8.8	2.8	0.7		37.4

$\phi = (1/10)\sum_{i=1}^{10} i d_i$ (Average deuterium content %)

B. NMR method analysis*

Exp. No.	Catalyst	Deuterium fraction in benzene ring, %	Deuterium fraction in methyl groups, %
6	$Ni-Al_2O_3$[a] (3 : 1)	1	34
4	〃 (1 : 1)	7	24
5	〃 (1 : 3)	11	25
7	$Ni-Al_2O_3$[b] (1 : 1)	13	25
11	Pt black	15	23
12	Pd black	9	30

* Both fractions were determined by allotting ϕ proportionally to the height of NMR signals of methyl and ring hydrogens.

Another point to be mentioned here is the fact that nickel has no activity with the hydrogen atoms of benzene ring. This is apparently in contradiction to the finding of Horiuti and Polanyi[5] that benzene can exchange hydrogen with heavy water in the presence of nickel powder. According to our experiment[2], where nickel powder was prepared by the procedure adopted in the case of xylene, a similar degree of exchange could be found in the case of benzene under the same experimental conditions. Therefore, it must be considered that the activity of ring hydrogen is decreased by the introduction of methyl groups. Such a decrease may be explained by the "geometric" factor rather than by the "electronic" factor, because if it is assumed that the exchange of methyl hydrogen can be realized by dissociative chemisorption of the methyl group ($-CH_3 \rightarrow -CH_2 + H$) on a nickel surface, it will be difficult from the structural reason that a part of the benzene ring is chemisorbed simultaneously. However, the reason why platinum and palladium have the catalytic activity with both hydrogen atoms cannot be answered at the present state of investigation.

Effect of Carriers on Nickel.—As shown in Table II, in the presence of Ni-kieselgulr (No. 2) or Ni–SiO_2 (No. 3) the catalytic exchange of methyl hydrogen occurred in a way similar to the case when no carrier was used (Nos. 0 and 1); i.e., no qualitative effect of these carriers could be found in the infrared spectrum. On the other hand, the results obtained on the Ni-Al_2O_3catalysts (Nos. 4~7) were the same in nature as those obtained on the platinum and palladium catalysts (Nos. 10~12); i.e., both kinds of hydrogen atoms were exchanged, though no exchange could be observed in two runs of the alumina catalyst (Nos. 8 and 9). It is interesting that the catalytic activities of Ni-$Al_2O_3{}^a$ (No. 4) and Ni–$Al_2O_3{}^b$ (No. 7) were nearly the same, irrespective of the differences in their methods of preparation. In order to confirm quantitatively the above results obtained by the IR method, both mass-spectrometric and NMR methods were utilized, the results being shown in Tables IV A and B.

It must also be mentioned regarding Table IV B that the activity of the nickel-alumina catalysts obviously changes according to the ratio of the two components. From a comparison of Nos. 4, 5 and 6, it can be noted that No. 5, the catalyst of the least nickel content, shows the largest activity with ring hydrogen and that the degree of activity is similar to that of platinum black.

Such peculiar effects of alumina as a carrier make it difficult to classify this oxide in the same category as silica and kieselguhr, because it cannot be explained by the difference in surface area between these catalysts. According to Rubinishtein et al. and Morikawa et al.[6], when alumina coexists with nickel, it interacts with nickel more strongly than silica gel[6] does. If so, it is not surprising that nickel catalyst can change its activity when supported on alumina. Another explanation is the change in the valency state of nickel, as proposed by Selwood et al.[7] in the case of nickel oxide-alumina. From their magnetic susceptibility measurement, they concluded that the valency of some nickel atoms changes into +3 in the presence of alumina. Considering the infrared measurement of Eischens[8] that the chemisorbed state of carbon monoxide on platinum-alumina differs from that on platinum-silica, a valency change due to carriers may be possible. Such being the situation, it will be required hereafter to investigate the change in activity from the standpoint of the electronic factor.

Summary

It has been confirmed that nickel can exchange catalytically only hydrogen atoms of methyl groups of paraxylene with deuterium oxide, irrespective of the method of preparation, while platinum and palladium can exchange hydrogen atoms of both methyl groups and benzene ring under similar experimental conditions.

It has been found that the catalytic activity of nickel becomes similar to that of platinum and palladium if nickel is supported on alumina, but remains unchanged if it is supported on silica or kieselguhr.

It has been shown to be difficult to explain these two findings perfectly.

The authors wish to express their sincere thanks to Mr. Motoyoshi Hatada and Mr. Shiro Sato for the mass-spectrometric and NMR measurements of this research project.

Department of Chemistry
Faculty of Science
Osaka University
Nakanoshima, Osaka

5) J. Horiuti and M. Polanyi, *Trans. Faraday Soc.*, **30**. 1163 (1934).

6) A. M. Rubinshtein, L. Kh. Freidlin and V. N. Borunova, *Izvest. Akad. Nauk. S.S.S.R., Otdel. Khim. Nauk*, **1955**, 766; cf. *Chem. Abstr.*, **50**, 2262 (1956). K. Morikawa and F. Nozaki, Abstr. of the 9th Symposium on Catalysis (Japan), 19 (1960).

7) F. N. Hill and. F. W. Selwood, *J. Am. Chem. Soc.*, **71**, 2522 (1949).

8) R. P. Eischens and W. A. Pliskin, *Advances in Catalysis*, **10**, 18 (1958).

Studies on Solvent Extraction using Radioactive Isotopes. VIII[1]. *Solvent Extraction of Cerium with Acetylacetone*

By Nobuo SUZUKI and Shohachiro OKI

(Received March 23, 1961)

The separation of cerium by solvent extraction with ethyl ether or methyl isobutyl ketone from a nitric acid medium has been studied by Imre[1] and by others[3-5], but their methods are tedious in order to avoid the hazard of an explosion of the solvent by concentrated nitric acid. Recently, however, an extraction with di(2-ethylhexyl) orthophosphoric acid and thenoyltrifluoroacetone has been reported[6,7].

It has been known that acetylacetone forms with cerium a chelate compound such as $Ce(C_5H_7O_2)_4$ which dissolves in organic solvents[8,9]. There is no report, however, on the extraction behavior of cerium with acetylacetone. The authors have therefore investigated the various conditions such as acetylacetonate, having an effect on the extraction of cerium.

Experimental

Reagents.—Acetylacetone on the market usually contains considerable amounts of acetic acid; therefore, it was purified as follows: One liter of acetylacetone was washed with 100 ml. of ammonia water (1 : 10), then washed twice with 100 ml. portions of water, and distilled. The distillation fraction of 138°C was collected and used. Carrier-free cerium-144 ($^{144}CeCl_3$) used as a tracer was imported from England; a part of this was diluted to 1 M nitric acid with an activity of about 10^6 c. p. m./ml.

Cerium stock solutions (10^{-2} M) of cerium(III) and cerium(IV) were prepared by dissolving the guaranteed-grade reagents of cerous nitrate and ceric sulfate in 1 M nitric acid respectively; the concentrations of the stock solutions were determined by titration with ferrous sulfate potentiometrically. More dilute solutions were prepared fresh before use from the stock solutions.

Sodium bromate, sodium acetate and other reagents were all guaranteed-grade reagents.

Redistilled water was used.

Apparatus.—For measurements of radioactivity, a well-type scintillation counter, Model RSP-1, made by Kobe Kogyo Co., Japan, was employed. For measurements of the pH of the aqueous phase, a glass electrode pH meter, Model GU-1, made by Shimadzu Co., Japan, was used.

General Procedure.—The general procedure is, unless otherwise stated, as follows: To a stoppered Erlynmeyer flask containing cerium (5×10^{-6} M) and ^{144}Ce, add sodium bromate, acetylacetone, and acetate buffer (20 ml.), and make up the volume to a constant (40 ml.) with water. Mix well for two minutes and let it stand. Every suitable period take out an aliquot (5 ml.) into a separatory funnel and extract the cerium acetylacetonate with 2 ml. of benzene by shaking for one minute. After the phases have separated, transfer the organic and the aqueous phases into two test tubes and let them stand for more than four hours till the radioactive equilibrium of ^{144}Ce and ^{144}Pr has been established; then measure the radioactivity of both phases and the pH of the aqueous phase.

Results and Discussion

Concentration of Acetylacetone.—As will be shown in the later part of this paper, cerous cerium is not extracted with acetylacetone by shaking for 40 min. Accordingly, it is necessary to oxidize cerium to the ceric state. The

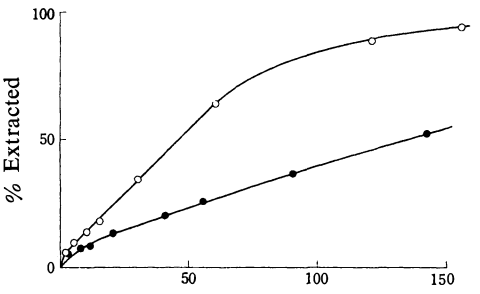


Fig. 1. Effect of concentration of HA.
(HA : Acetylacetone)
○ : [HA] 1.2 M
● : [HA] 0.61 M
[$NaBrO_3$] 0.15 M

1) Paper VII of this series : N. Suzuki, *J. Chem. Soc. Japan, Pure Chem. Sec.* (*Nippon Kagaku Zasshi*), **81**, 437 (1960).
2) L. Imre, *Z. anorg. u. allgem. Chem.*, **151**, 214 (1927).
3) A. W. Wylie, *J. Chem. Soc.*, **1951**, 1417.
4) E. C. Pitzer, U. S. Pat. 2615798 (Oct. 28, 1952).
5) L. E. Glendenin, K. F. Flynn, R. F. Buchanan and E. P. Steinberg, *Anal. Chem.*, **27**, 59 (1955).
6) D. F. Peppard, G. W. Mason and S. W. Moline, *J. Inorg. Nucl. Chem.*, **5**, 141 (1957).
7) G. W. Smith and F. L. Moore, *Anal. Chem.*, **29**, 448 (1957).
8) Beilsteins Handbuch der Organischen Chemie, 4. Aufl., Bd. 1, p. 402, Julius Springer, Berlin.
9) W. C. Fernelius, "Inorganic Synthesis", Vol. II, McGraw-Hill Book Co., Inc., New York (1946), p. 13.

authors used sodium bromate as an oxidizing agent.

The relation between the amounts of the chelate extracted and the reaction time is shown in Fig. 1. The reaction rate of cerium with acetylacetone is quite slow at room temperature. Even though the large excess of acetylacetone, such as 0.6 M acetylacetone, is used, complete extraction is not obtained.

Concentration of Bromate.—The concentration of bromate has a great influence on the oxidation of cerium, viz., on the extraction from cerous state, as is shown in Fig. 2. It is conceivable from the results in Figs. 1 and 2 that the rate of increase in the extraction

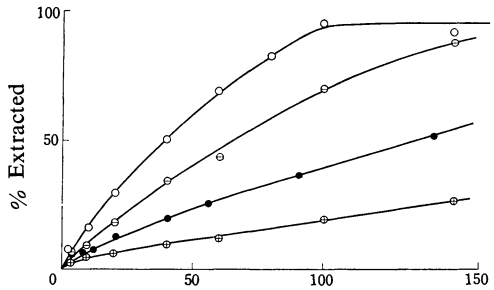


Fig. 2. Effect of concentration of $NaBrO_3$.

[$NaBrO_3$] ○: 0.65 M, ⊖: 0.33 M, ●: 0.16 M, ⊕: 0.065 M

[HA] : 0.61 M

percentage against the time elapsed is approximately proportional to the concentration of acetylacetone and bromate, but the discrepancy from the linear proportionality in the case of bromate of a higher concentration can be presumed to be due to the formation of complexes of ceric ion with bromate ion or bromide ion.

Direct Extraction with Acetylacetone in Benzene.—A comparison was made between the following two cases:

(1) Acetylacetone was added to the aqueous solution and left to standing for 2.5 hr. Every suitable period, the chelate was extracted with benzene as described in the general procedure.

(2) Acetylacetone was added as benzene solution, and direct extraction of the chelate was carried out by shaking for a suitable period.

The amounts of acetylacetone used in the two cases were equal. As is shown in Fig. 3, the results of the two cases are, however, considerably different; the results in the latter case are lower. This may be expected from Fig. 1; i. e., the concentration of the acetylacetone distributed in the aqueous phase is decreased by the presence of benzene.

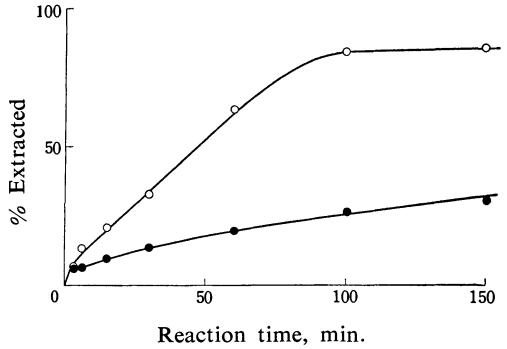


Fig. 3. Comparison of two types of extraction.

○: Extraction by benzene after acetylacetone was added to aqueous solution

●: Direct extraction with acetylacetone in benzene

Oxidation State.—In order to confirm the effects of the oxidation state and the oxidation process, the authors carried out some experiments on various combinations of carrier cerium and ^{144}Ce.

(1) Cerium(III) and ^{144}Ce with 0.61 M acetylacetone.

(2) Cerium(IV) and ^{144}Ce with 0.61 M acetylacetone.

(3) Cerium(IV) and ^{144}Ce with 0.61 M acetylacetone, but in this case ^{144}Ce was pretreated by being left standing overnight in a solution of 0.17 M bromate at pH 2.2.

(4) Cerium(IV) and ^{144}Ce with 0.61 M acetylacetone, but in this case ^{144}Ce was pretreated by being left standing overnight in a solution of 0.17 M bromate and 1 M nitric acid.

(5) Cerium(IV) and ^{144}Ce the same as Exp. 3, except that the concentration of acetylacetone was 1.2 M.

In all cases the concentration of cerium(III) and cerium(IV) was 1.0×10^{-6} M. The results are presented in Fig. 4. It can be observed that cerium in a cerous state can not be extracted with acetylacetone without an oxidizing agent. When cerium(IV) and pretreated ^{144}Ce are used, 50% extraction is obtained as a maximum. This is probably owing to the hydrolysis of cerium(IV). Therefore, though ceric cerium is extracted with acetylacetone, it is not desirable to oxidize cerium before the addition of acetylacetone.

The result of Exp. 2 shows that the exchange reaction is fairly slow. Consequently, in spite of the long reaction time, the apparent extraction remains low.

When an aqueous solution containing carrier-free ^{144}Ce is shaken with acetylacetone in

benzene, ^{144}Ce is rapidly extracted[10]. On the basis of the results in Exp. 1, cerous cerium in ordinary concentration can not be extracted.

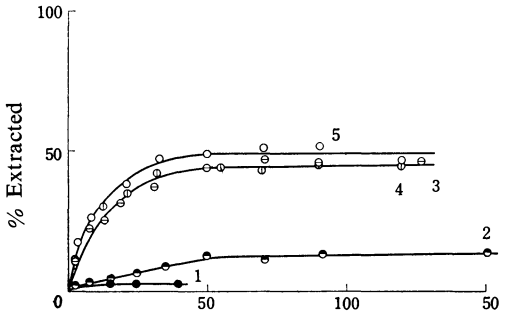


Fig. 4. Effect of oxidation states of carrier and tracer cerium. [HA] ; 0.61 M

	Oxidation state	
	Carrier	Tracer
(1)	III	III
(2)	IV	III
(3), (4), (5)*	IV	IV

* [HA] ; 1.2 M

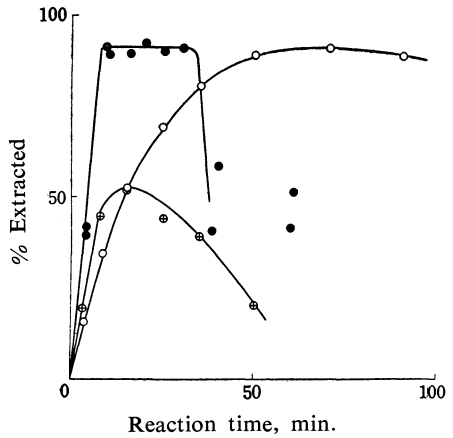


Fig. 5. Effect of concentration of reagents at 40°C.

	[HA], M	[$NaBrO_3$], M
●	0.61	0.33
⊕	0.61	0.065
○	0.15	0.33

This is one of the most characteristic features of the carrier-free ^{144}Ce. The details of this problem are now being examined.

Effect of Heating. — As described in the previous part, a fairly long time is necessary for complete extraction, but the reaction is accelerated by heating. After cooling to room temperature, the extraction with benzene was carried out. The effect of the concentration of reagents at 40°C is shown in Fig. 5.

The results with various concentrations of cerium at 40°C are shown in Fig. 6. Though heating is effective, the yield is low at about 5×10^{-5} M cerium. In every case in Figs. 5 and 6, the effect of heating is accompanied by the

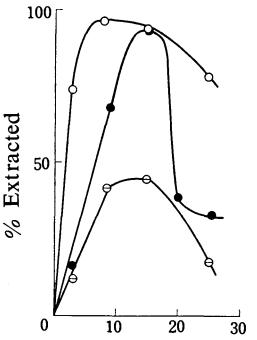


Fig. 6. Extraction of various concentration of cerium carrier (at 40°C).
[HA] ; 0.98 M, [$NaBrO_3$] ; 0.40 M
[Ce^{3+}] { ○ : 5×10^{-6} M ● : 2.5×10^{-5} M ⊖ : 5×10^{-5} M

simultaneous disadvantage of the destruction of the chelate compound by hydrolysis. Care should be taken not to heat too long. Ten minutes heating is the best. At room temperature, however, the chelate is found to be fairly stable in the organic phase.

The authors arranged the standard procedure for extraction as follows: A mixture containing 1 ml. of cerium(III)[11], 1 ml. of 2 M sodium bromate, 0.5 ml. of acetylacetone, and 2.5 ml. of the acetate buffer solution is heated at 40°C for the minutes. After cooling to room temperature, the chelate is extracted with 2 ml. of benzene by shaking for one minute.

Extraction and Back-extraction. — The extraction curve of cerium by the standard procedure is shown in Fig. 7. In comparison with the extraction curve of carrier-free ^{144}Ce[10], the optimum pH range is quite narrow, but it is not difficult to adjust the pH of the aqueous phase to about 5~6 with an acetate buffer solution.

In order to investigate the distribution of cerium between benzene and the aqueous phase, and in order to find the suitable conditions for the back-extraction of cerium, an aliquot (2 ml.) of the benzene solution containing chelate prepared by the standard procedure was shaken for 1 min.[12] with each 5 ml.

10) This is shown in Part IX of this series, This Bulletin, 35, 237 (1961).

11) In the final aqueous solution the concentration of Ce(III) is 5×10^{-6} M.

12) One minute was found to be enough for the extraction.

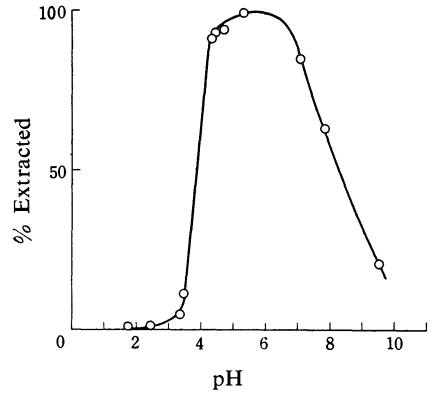


Fig. 7. Extraction curve of cerium. [HA] ; 0.81 M, [$NaBrO_3$] ; 0.33 M

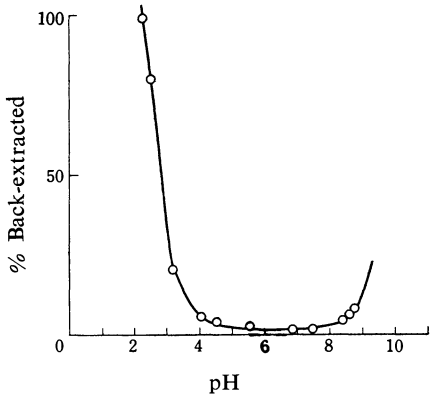


Fig. 8. Back-extraction of cerium from organic phase.

of the buffer solution or with dilute nitric acid.

As shown in Fig. 8, cerium extracted in benzene is easily stripped with a dilute acid, e. g., 0.1 M nitric acid. The chelate in the organic phase is not appreciably influenced by washing with the buffer solution of pH 4~8. The pH range is considerably wider than that of the extraction (cf. Fig. 7), but it is almost the same as the extraction curve of carrier-free ^{144}Ce[10]. Consequently, it is proper to consider that cerium was hydrolyzed in the region of pH 7~8.

Coexisting Substances. — Table I shows the effects of inorganic salts and organic acids. Of the substances tried phosphate, oxalic acid, citric acid, tartaric acid, and EDTA (disodium salt) cause severe interference, even with such a low concentration as ca. 10^{-2} M. A little

Table I. Effects of coexisting substances

Salt or acid	Concn., M	Acetylacetonate % extracted
$NaNO_3$	0.03	97.4
	0.08	94.4
	0.2	91.6
Na_2SO_4	0.03	92.1
	0.07	90.7
NaCl	0.03	71.0
	0.08	48.5
KH_2PO_4	0.03	9.2
	0.08	4.2
Oxalic acid	0.007	3.6
	0.02	0.6
Citric acid	0.007	4.9
	0.02	1.2
Tartaric acid	0.03	7.6
EDTA	4×10^{-4}	1.0

interference is observed with nitrate and sulfate. Chloride shows a more complicated interference. This is perhaps owing to the reduction effect of chloride ion in the case of cerium.

Summary

The extraction of cerium with acetylacetone was studied, using ^{144}Ce as a tracer. Cerous cerium can not be extracted without an oxidizing agent. After the mixture of 0.61 M acetylacetone, 0.65 M sodium bromate and 5×10^{-6} M cerium had been left standing for 100 min. at pH 5~6, 95% of the cerium was extracted in benzene. The reaction was accelerated by heating, e. g., at 40°C, or by increasing the concentration of acetylacetone and bromate. Care should be taken not to heat too long, thus avoiding the decomposition of the chelate by hydrolysis. The presence of phosphate, oxalic acid, citric acid, tartaric acid and EDTA caused severe interference.

The authors wish to express their hearty thanks to Professor Shin'ichiro Hakomori and Professor Kunio Seto for their kind suggestions in the course of this work.

Department of Chemistry
Faculty of Science
Tohoku University
Katahira-cho, Sendai

Studies on Solvent Extraction using Radioactive Isotopes. IX[1]. *Solvent Extraction of Carrier-free Cerium-144 with Acetylacetone*

By Nobuo SUZUKI and Shohachiro OKI

(Received March 23, 1961)

Several methods for the extraction of cerium have been developed[2,3]. A few applications have also been made to the separation of carrier-free ^{144}Ce from fission products[4]. The separation of a daughter nuclide of a short half-life such as ^{144}Pr from her parent is a very difficult problem on account of the requirement of rapidity. For this purpose, solvent extraction is one of the most proper methods.

In a previous paper[1] the solvent extraction of cerium with acetylacetone was studied. In the course of the work, the carrier-free ^{144}Ce was found to show peculiar features. The authors intend not only to investigate the solvent extraction of ^{144}Ce from fission products, but also to visualize the outlines of the peculiar behaviors of the carrier-free ^{144}Ce compared with cerium of the ordinary concentration reported on in the previous paper.

In addition, because of the rapidity and the simplicity of the method, the separation of ^{144}Pr was found to be possible with acetylacetone.

Experimental

Reagents and Apparatus.—Reagents and apparatus were the same as those of the previous paper. The hydrogen ion concentration of the aqueous phase was adjusted with an acetate buffer solution (ca. 0.1 M for sodium acetate), sodium hydroxide (1 M), and/or nitric acid (1 M). The washing solution for the organic phase consisted of an 0.1 M acetate buffer solution with or without sodium bromate (ca. 0.3 M); this solution was pre-saturated with 20% acetylacetone in carbon tetrachloride or in benzene.

General Procedure.—Unless otherwise stated, the general procedure was as follows: To 5 ml. of an acetate solution containing ^{144}Ce in a separatory funnel, 1 ml. of a 1 M sodium bromate solution was added, and the pH of the aqueous phase was adjusted to 5~6, after which 3 ml. of 20% acetylacetone in carbon tetrachloride or in benzene solution was added. Equilibration was achieved by shaking. After the phases had disengaged the phases were transferred into two test tubes. If necessary, the organic phase was washed with the washing solution.

Results and Discussion

Shaking Time.—^{144}Ce is completely extracted by shaking for about 3 min., especially in the presence of bromate (Table I). It is strange that carrier-free ^{144}Ce is extracted without an oxidizing agent such as bromate. Smith and Pitzer have noticed that tracer amounts of cerium were oxidized by dichromate, but this phenomenon is not expected from the oxidation potential data of a cerous-ceric couple. Cerous cerium can not be extracted with acetylacetone[1], so it may be considered that ^{144}Ce is oxidized to a ceric state without an oxidizing agent and is extracted as acetylacetonate. This is very characteristic behavior of tracer amounts of cerium. This problem is now being examined. It may be noticed in Table I that it takes a longer shaking time for complete extraction without bromate.

TABLE I. THE EFFECT OF SHAKING TIME

Shaking time min.	% Extracted With $NaBrO_3$	% Extracted Without $NaBrO_3$
1	97.5	92.4
2	98.6	93.4
4	99.3	91.9
8	99.3	96.8
15	99.0	95.3

Concentration of Reagents.—The effect of the concentration of the reagents was examined. The results are summarized in Table II, but the relation between the amounts of bromate and the yield is not clear.

TABLE II. EFFECTS OF CONCENTRATIONS OF ACETYLACETONE AND BROMATE

Concn. of acetylacetone %	% Extracted Amounts of 1 M $NaBrO_3$ added, ml. 0	0.5	1.0	2.0
5	83.0	97.0	90.6	97.0
10	88.9	98.0	98.9	98.6
20	94.5	98.9	99.3	98.2

Extraction Solvents.—It is expected that extractability would vary with different solvents.

1) Part VIII of this series, This Bulletin, 35, 233 (1962).
2) E. C. Pitzer, U. S. Pat. 2615798 (Oct. 28, 1952).
3) D. F. Peppard, G. W. Mason and S. W. Moline, *J. Inorg. Nucl. Chem.*, 5, 141 (1957).
4) G. W. Smith and F. L. Moore, *Anal. Chem.*, 29, 448 (1957).

Table III. Extraction by various solvents

Solvent	% Extracted
Carbon tetrachloride	98.5
Benzene	98.9
Chloroform	97.8
Xylene	96.9
Isoamyl acetate	94.6
Methyl isobutyl ketone	93.0
Isopropyl ether	78.6

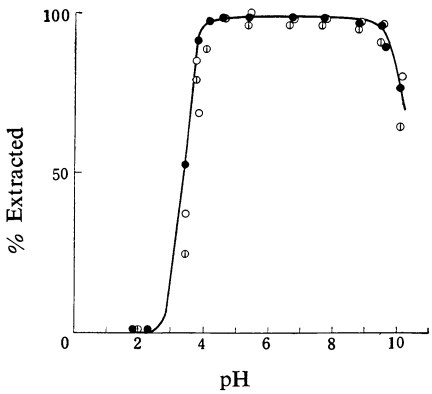


Fig. 1. Extraction curve of ^{144}Ce.
○ Benzene
● Carbon tetrachloride
◑ Xylene

The results of the extraction with 20% acetylacetone in various solvents are summarized in Table III. Carbon tetrachloride and benzene are found to be more effective for extraction.

Extraction and Back-extraction.—The extraction curves of ^{144}Ce by the general procedure with carbon tetrachloride, benzene and xylene are shown in Fig. 1. ^{144}Ce is completely extracted in the range of pH 4~9, and the range is wider than the case of the extraction of carrier cerium[1], but the pH range in the back extraction curve in the latter case is similar to that of the extraction curve of carrier-free ^{144}Ce.

In order to investigate the suitable conditions for the stripping of ^{144}Ce, an aliquot of the organic solution containing the chelate prepared by the general procedure was shaken with mineral acid or a hydrogen peroxide solution for one minute. After the aqueous phase had been removed, the remaining organic phase was shaken again with fresh mineral acid (second stripping). The results are summarized in Tables IV and V. ^{144}Ce in organic phase is readily stripped by dilute acid or hydrogen peroxide solution of about 10%.

Table IV. Back-extraction with mineral acids

Stripping soln.	CCl_4 as solvent		Benzene as solvent	
	1st stripping	2nd*	1st	2nd*
	%	%	%	%
0.1 N H_2SO_4	99.0	100.0	95.1	99.1
1 N H_2SO_4	99.4	100.0	92.8	98.2
0.1 N HCl	99.3	100.0	96.5	99.7
1 N HCl	99.8	100.0	93.7	99.5
0.1 N HNO_3	99.9	100.0	97.2	100.0
1 N HNO_3	98.8	100.0	96.7	99.8

* The total of 1st and 2nd stripping.

Table V. Back-extraction with hydrogen peroxide

Concn. of H_2O_2, %	Back-extracted, %
2	20.1
4	36.9
6	76.9
8	96.6
10	95.0

Decontamination from Fission Products.—The elements found in fission products were tested for their degree of separation from ^{144}Ce. Each pure nuclide was examined individually by the general procedure, and after the completion of this procedure the organic phase was washed with an equal volume of acetate buffer solution (pH 5.6) containing bromate, then the organic phase was shaken with 2 ml. of 0.1 M nitric acid. The results are summarized in Table VI. Decontamination from ^{90}Sr (^{90}Y), ^{106}Ru, ^{137}Cs and rare earth nuclides (e. g., $^{152,154}Eu$), except ^{95}Zr (^{95}Nb), is complete. ^{95}Zr (^{95}Nb) is extracted in the range of pH 2~7[5]; therefore, it is unavoidable that some ^{95}Zr (^{95}Nb) is joined with ^{144}Ce.

For the separation of ^{144}Ce from ^{95}Zr (^{95}Nb), the authors devised two tentative schemes;

Table VI. Behavior of other nuclides (expressed as percentage found in 0.1 M HNO_3 phase)

Nuclide	CCl_4 as solvent	Benzene as solvent
Sr-Y-90	0.07	0.01
Zr-Nb-95	22.5	—
Ru-106	0.1	0.1
Cs-137	0.2	0.1
Eu-152, 154	0.01	0.07
Ce-144	99.1	99.6

Table VII. The effect of $NaNO_3$ on stripping

Nuclide	Concn. of $NaNO_3$ M	Remained in org. phase
Ce-144	1	1.0
	2	1.2
Zr-Nb-95	1	70.5
	2	82.1

5) N. Suzuki and T. Omori, This Bulletin, unpublished.

(a) and (b). Scheme (a) was designed on the basis of the following experimental results: ^{95}Zr (^{95}Nb) extracted in the organic phase is not practically stripped with the mixed solution of 0.01 M nitric acid and 2 M sodium nitrate; on the other hand, ^{144}Ce is stripped quantitatively with the same solution (cf. Table VII). ^{95}Zr (^{95}Nb) stripped in the aqueous phase is extracted again less than 60%, while ^{144}Ce is re-extracted more than 90%. By repeating the extraction-washing cycle twice, the radiochemically pure ^{144}Ce can be prepared from fission products.

In scheme (b), thiocyanate ion serves as a complete masking agent for cerium in the case of acetylacetone extraction[6], while ^{95}Zr (^{95}Nb) is not affected by the presence of thiocyanate[5]. Thiocyanate ions are easily destroyed with nitric acid. Then ^{144}Ce is extracted from the aqueous phase by adjusting the pH with an acetate buffer solution.

By either of the methods nearly 90% of the ^{144}Ce was recovered, while ^{95}Zr (^{95}Nb) was present less than 1% of the initial amount. Fortunately, fission products aged for two years or so have a smaller content of ^{95}Zr (^{95}Nb) than ^{144}Ce; therefore, the contamination by ^{95}Zr (^{95}Nb) is practically negligible. The purity of the ^{144}Ce obtained from such fission products by these methods is expected to be higher than that of ^{144}Ce separated from the mixture (ca. 1 : 1) of ^{144}Ce and ^{95}Zr (^{95}Nb). ^{144}Ce of a radiochemical purity of over 99% was obtained from the fission products with a high yield.

Separation of ^{144}Pr from ^{144}Ce. — As praseodymium is not extractable, the effective separation of a short-life daughter ^{144}Pr from its parent ^{144}Ce is possible. After the radioactive equilibrium of ^{144}Ce (^{144}Pr) in the organic phase has been established, an aliquot of the organic phase is shaken with 3 ml. of the washing solution with or without bromate, and then ^{144}Pr is brought into the aqueous phase. The aqueous phase is washed with carbon tetrachloride; then the radioactivity is measured by a well-type scintillation counter. The radiochemical purity of ^{144}Pr is measured at more than 99.5%. The separation takes only 3 min. or so. The results are summarized in Table VIII, together with the elapsed time after the preparation of the organic phase containing ^{144}Ce. As is shown in Table VIII, bromate is not always necessary to avoid the contamination of ^{144}Ce, and, for practical purposes, it is better not to add bromate to the washing solution. Milking of ^{144}Pr is possible succesively, and the results of the half life of ^{144}Pr show a good agreement with the literature's value (17.5 min), as shown in Fig. 2.

TABLE VIII. RADIOCHEMICAL PURITY OF Pr-144 OBTAINED BY WASHING

Solvent	Standing time after preparation, hr.	Purity %
Benzene	8	99.4
	15	99.2
	22	98.6
	50	97.6*
CCl_4	25	99.1
	33	99.8*
	50	99.6*

* The washing solution contains $NaBrO_3$.

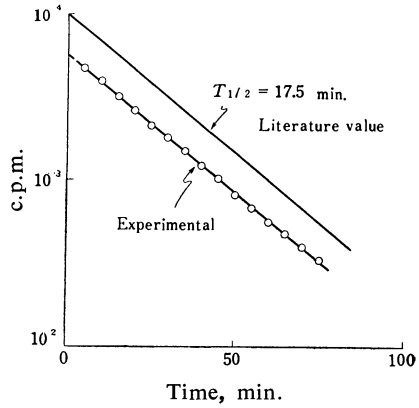


Fig. 2. Decay of ^{144}Pr.

Summary

^{144}Ce was extracted with acetylacetone in a benzene or in a carbon tetrachloride solution by shaking for 3 min. at a pH range of 4~9. Though an oxidizing agent such as bromate was not always necessary, the presence of bromate makes the time for extraction shorter. Decontamination from other fission products, ^{90}Sr (^{90}Y), ^{106}Ru, ^{137}Cs, and rare earths (e.g., $^{152,154}Eu$), except ^{95}Zr (^{95}Nb), was found to be negligible. The contamination of ^{95}Zr (^{95}Nb) was reduced to a negligible amount by repeating the cycle of extraction and stripping or by masking ^{144}Ce with thiocyanate. The separation of ^{144}Ce from fission products with acetylacetone was attempted. ^{144}Pr with a radiochemical purity of more than 99% was easily obtained by washing the organic phase with an acetate buffer solution of pH 5~8.

The authors wish to express their hearty thanks to Professor Shin'ichiro Hakomori and Professor Kunio Seto for their kind suggestions in the course of this work.

Department of Chemistry
Faculty of Science
Tohoku University
Katahira-cho, Sendai

6) At the concentrations of 1 and 2 M KSCN, ^{144}Ce is extracted at only 3 and 2% respectively.

On the Mode of Interaction of Surface Active Agents with Gelatin

By Toshizo ISEMURA, Fumikatsu TOKIWA* and Shoichi IKEDA

(Received May 23, 1961)

There are a number of studies on the interaction of surface active agents with high polymers and proteins. It is well known that proteins exhibit a markedly strong affinity for both cationic and anionic detergents. Among various proteins, gelatin is suitable for investigating the nature of the affinity of polypeptide chains with detergents and the mechanism of their mutual interaction. It is readily available. It has no organized conformation as globular proteins have, and it behaves as a random coil, at least, at elevated temperatures (higher than about 30°C).

Pankhurst and his coworkers[1-4] have extensively investigated the interaction of gelatin with various detergents, particularly with sodium dodecyl sulfate, by examining the precipitation of a complex as a function of mixing ratio. They have pointed out that gelatin binds with detergents to form a complex and that the binding ratio of detergent to gelatin is of importance in elucidating the mode of interaction. Tamaki and Tamamushi[5] have also obtained the same conclusion from the determination of two detergents, sodium dodecyl sulfate and dodecylamine hydrochloride, bound to precipitated gelatin on the acidic and alkaline sides of the isoionic point of gelatin respectively.

However, the mode of binding of detergents by gelatin before precipitate formation can not be known by means of such a solubility determination. Detergents should interact and combine with gelatin even without precipitation, since the formation of precipitates would arise from the enhanced hydrophobicity of the gelatin-detergent complex with an increasing amount of detergent bound to gelatin. Evidence for the combination of detergents with other proteins in a region wherein precipitation does not occur has been obtained from studies by electrophoresis[6-8], equilibrium dialysis[6,9], ultracentrifugation[10], viscosity[5,9], solubilization[11], etc.

For solutions of low detergent-gelatin ratios in which no precipitation occurred, studies by electrophoresis and equilibrium dialysis were attempted in order to find quantitatively the amount of detergent bound to gelatin. With the experiment by electophoresis, however, two peaks appeared in the electrophoretic pattern for gelatin alone. It is supposed that the pattern would be more complicated in a gelatin solution mixed with detergent and that its interpretation will be more difficult. Thus electrophoretic investigation was abandoned. In this work, therefore, the mode of binding of detergent by gelatin has been studied by means of equilibrium dialysis in the range of low detergent concentrations at various values of pH. This paper concerns the interaction of gelatin with an anionic detergent, sodium dodecylbenzene sulfonate, and two cationic detergents, dodecyl pyridinium bromide and cetyl pyridinium chloride.

Experimental

Materials.—Commercial photographic gelatin was purified according to the method of James et al.[12] A gelatin solution (2%) was passed through a column of mixed resins (5 parts of Amberlite IRA-400 to 2 parts of Amberlite IR-120) at 30~35°C. The pH of the gelatin solution thus purified was 4.9. The concentration of the stock solution was determined by dry weight.

Sodium dodecylbenzene sulfonate (SDBS), which was prepared by the sulfonation of dodecylbenzene (Oronite Chemical Co., U. S. A.), was obtained from the Japan Surfactant Association. To remove the lower homologues and inorganic salts, it was extracted with distilled water and then with ethyl alcohol. The pH of a 1% solution of the purified SDBS was 7.0. Dodecyl pyridinium bromide (DPB)

* Present address : Research Laboratory, Kao Soap Co., Ltd., Wakayama.

1) K. G. A. Pankhurst and R. C. M. Smith, *Trans. Faraday Soc.*, **41**. 630 (1945).
2) K. G. A. Pankhurst, *Discussions Faraday Soc.*, **No. 6**, 52 (1949).
3) K. G. A. Pankhurst and R. C. M. Smith, *Trans. Faraday Soc.*, **43**, 511 (1947).
4) K. G. A. Pankhurst and R. C. M. Smith, ibid., **40**, 565 (1944); K. G. A. Pankhurst, *Research*, "Surface Chemistry" (1949), p. 109.
5) K. Tamaki and B. Tamamushi, This Bulletin, **28**, 555 (1955).
6) J. T. Yang and J. F. Foster, *J. Am. Chem. Soc.*, **75**, 5560 (1953); **75**, 5743 (1953).
7) K. Aoki and J. Hori, This Bulletin, **29**, 104 (1956); **29**, 369 (1956).
8) T. Isemura and T. Takagi, *J. Biochem.*, **46**, 1637 (1959).
9) J. F. Foster and J. T. Yang, *J. Am. Chem. Soc.*, **76**, 1015 (1954).
10) K. Aoki and J. Hori, ibid., **81**, 1885 (1959).
11) I. Blei, *J. Colloid Sci.*, **15**, 370 (1960); M. Breuer and U. P. Strauss, *J. Phys. Chem.*, **64**, 228 (1960).
12) J. W. James, A. W. Kenlkington and A. G. Ward, *Research*, **4**, 247 (1953).

supplied by the Kao Soap Co. was recrystallized twice from acetone. Cetyl pyridinium chloride (CPC) was prepared from cetyl alcohol of high purity and recrystallized several times from acetone.

Equilibrium Dialysis. — A dialysis cell consists of two compartments of equal volume, separated by a membrane. As a membrane, Vising cellulose casings (diameter of a pore: ca. 24 Å) were used after rinsing them with warm distilled water. A 10 ml. portion of a detergent solution was placed in one compartment of the cell and equilibrated against an equal volume of gelatin solution in the other compartment. Dialysis was carried out at 30 or 43°C for 3 to 4 days, with an occasional shaking of the cell. The concentration of gelatin was kept constant, 0.2%, and the pH of solution was adjusted by hydrochloric acid or sodium hydroxide. It was confirmed by a Horiba model M3 pH-meter that no change in the pH of the solutions was observed before and after dialysis, except for a slight difference of pH in the case of the binding of SDBS at the isoionic point of gelatin. After the attainment of equilibrium, the detergent concentration in the compartment containing no-gelatin was determined spectrophotometrically, because the molar extinction coefficient of detergent was greatly affected by the presence of gelatin. Since 0.1 M sodium chloride was added to all solutions to eliminate the correction for Donnan's effect, the amount of bound detergent was directly calculable from an analytical value. A control experiment with detergent alone was always carried out to minimize analytical errors. This dialysis method is applicable only to dilute solutions of detergent, since the detergent formed micelles at some high concentrations and was difficult to permeat through membrane[13].

Determination of Concentration of Detergents. —A spectrophotometric method has been developed to determine the concentration of detergents having benzene or pyridinium rings as low as 10^{-5} M[14]. Measurements of the ultraviolet absorption were made by means of a Hitachi type EPU-2A spectrophotometer at a wavelength of 230 mμ with SDBS (molar extinction coefficient, $\varepsilon_{SDBS}=8.75\times10^3$) or at a wavelength of 259 mμ with DPB and CPC ($\varepsilon_{DPB}=4.48\times10^3$ and $\varepsilon_{CPC}=4.59\times10^3$).

Results

The Binding of an Anionic Detergent, SDBS, by Gelatin.—The permeability of SDBS through dialysis membrane decreased with increasing concentration on account of the micelle formation and further decreased with the addition of neutral salts such as sodium chloride because of the lowering of the critical micelle concentration[15]. SDBS was permeable to membrane with difficulty at concentrations above 1.3×10^{-3} when 0.1 M sodium chloride was added. In addition, on the acidic side of the isoionic point of gelatin, precipitation occurred when gelatin was added to a relatively concentrated solution of SDBS. Accordingly, all the experiments were carried out at concentrations of SDBS lower than 1.0×10^{-3} M.

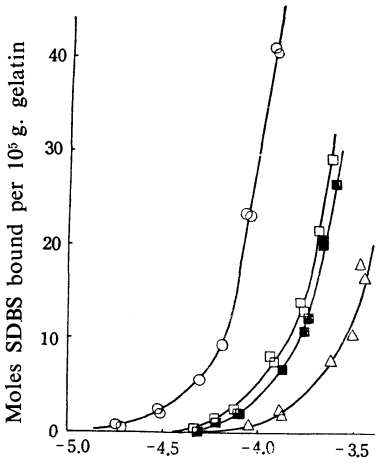


Fig. 1. Binding curves of SDBS by gelatin. ○, pH 2.7, 30°C; □, pH 5.0, 30°C; ■, pH 5.0, 43°C; △, pH 8.0, 30°C

Figure 1 illustrates the binding curves in which the number of moles bound SDBS per 10^5 g. of gelatin, r is plotted against the logarithm of the concentration of free SDBS, $\log c$. The amount of binding of SDBS increases acceleratively with increasing concentration. As the pH of the solution is lowered, the binding of SDBS is enhanced, but even on the alkaline side of the isoionic point of gelatin, SDBS combines with gelatin to a considerable extent. This indicates that gelatin has a strong affinity for SDBS, as other proteins have for long chain alkyl sulfate and alkylaryl sulfonate[4,6,7,11].

The Binding of Cationic Detergents, DPB and CPC, with Gelatin. — Since the critical micelle concentration of DPB lies in such a high concentration as 10.5×10^{-3} M[16], dialysis experiments were possible up to relatively high concentrations. However, experiments with CPC were carried out only at a low concentration region because of its low critical micelle concentration, i. e., 0.9×10^{-3} M[17].

Figure 2 shows the curves for the binding of DPB and CPC by gelatin. CPC combines with gelatin at the isoionic point as well as on the alkaline side of it, but not on the acidic side. DPB is, however, less bound with gelatin

13) B. S. Harrap and I. J. O'Donnell, *J. Phys. Chem.*, **58**, 1097 (1954).
14) J. T. Yang and J. F. Foster, ibid., **57**, 628 (1953).
15) M. L. Corrin and W. D. Harkins, *J. Am. Chem. Soc.*, **69**, 683 (1947).
16) T. Ino, T. Kondo and K. Meguro, *J. Chem. Soc. Japan, Pure Chem. Sec.* (*Nippon Kagaku Zasshi*), **76**, 200 (1955).
17) Cf. N. K. Adam and H. L. Shute, *Trans. Faraday Soc.*, **34**, 758 (1938).

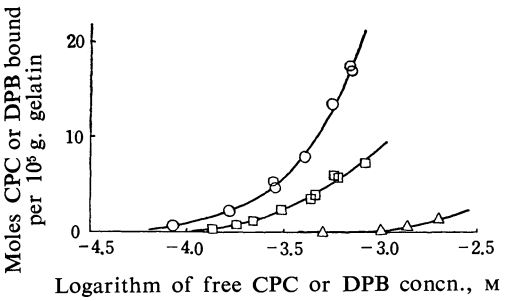


Fig. 2. Binding curves of DPB and CPC by gelatin at 30°C. ○, CPC, pH 7.0; □, CPC, pH 4.9; △, DPB, pH 7.0

even on the alkaline side. Both cationic detergents can bind with gelatin only to a less extent than the anionic detergent, SDBS. It has been observed[9] that proteins other than gelatin also have a weaker affinity for cationic detergents than for anionic detergents.

Discussion

Binding Isotherm. — If detergent ions bound with protein have no interaction with one another, the equation for the binding is written as

$$r=\frac{kmc}{1+kc} \qquad (1)$$

where k is a binding constant and m is the maximum amount of binding[18]. Eq. 1 implies that r approaches to a saturated value, m, when c is increased and that a plot of $1/r$ vs. c or r/c vs. r should be linear. It was found, however, that the binding data of detergents, SDBS and CPC, with gelatin could not fit Eq. 1. Since detergent ions can combine acceleratively with increasing concentration, detergent ions already bound seem to promote the succeeding binding; that is, the bound detergent ions interact with one another.

When the binding takes place cooperatively, Eq. 1 should be modified to[19-21]

$$r=\frac{kmc^n}{1+kc^n} \quad (n>1) \qquad (2)$$

where n is a constant characteristic of the kind of binding, and is greater than unity if the interaction is operative towards stabilization. Eq. 2 can be rewritten as

$$\frac{r}{m-r}=kc^n \qquad (3)$$

18) I. M. Klotz, F. M. Walker and R. B. Pivan, *J. Am. Chem. Soc.*, **68**, 1486 (1946).
19) I. M. Klotz, "The Chemistry of Proteins", Ed. by S. Akabori and S. Mizushima, Vol. 4, Kyoritsu Shuppan Co., Ltd., Tokyo (1956), p. 15.
20) I. M. Klotz, "The Proteins", Ed. by H. Neurath and K. Bailey, Vol. 1, Academic Press, New York (1953), p. 769.
21) M. Kubo, *Proc. Japan Acad.*, **29**, 156 (1953).

The present experiments are concerned with the low detergent-gelatin ratios at which no precipitation occurs. Since the phase separation or precipitation occurs only at relatively high detergent-gelatin ratios, the amount of bound detergent in the present experiment is expected to be far less than the maximum amount of binding. The increasing steepness of the binding curves also suggests that the saturated amount of binding or the number of the binding sites is very large, if it exists at all. Based on these experimental facts, it may be assumed that r is small compared with m. Then Eq. 3 reduces to

$$r=Kc^n \quad (K=km) \qquad (4)$$

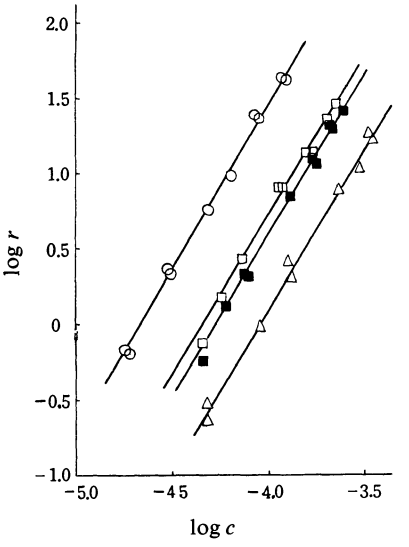


Fig. 3. The log r vs. log c diagram for the binding of SDBS by gelatin. ○, pH 2.7, 30°C; □, pH 5.0, 30°C; ■, pH 5.0, 43°C; △, pH 8.0, 30°C

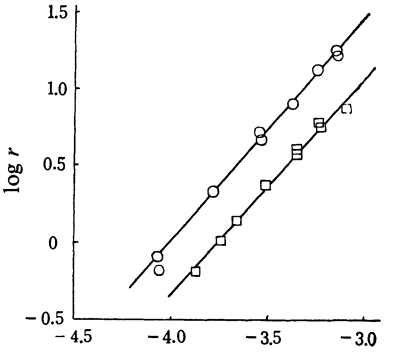


Fig. 4. The log r vs. log c diagram for the binding of CPC by gelatin at 30°C. ○, pH 7.0; □, pH 4.9

which is formally identical with the Freundlich adsorption isotherm, although n is greater than unity. Then a plot of $\log r$ vs. $\log c$ should be linear.

If the data of the binding of detergents, SDBS and CPC, with gelatin are replotted in a logarithmic scale, straight lines are obtained for all cases, as is shown in Figs. 3 and 4. Thus cooperative stabilization is effective for the binding of these detergents by gelatin. The values of the constants, K and n, which can be estimated from the intercept and slope of the straight line, are listed in Table I.

TABLE I. DEPENDENCE OF n AND K ON pH

Detergent	Temp. °C	pH	n	K	$\log K$
SDBS	30	2.7	2.13	8.71×10^{9}	9.94
	30	5.0	2.13	1.74×10^{9}	9.24
	30	8.0	2.10	2.95×10^{8}	8.47
	43	5.0	2.12	1.15×10^{9}	9.06
CPC	30	4.9	1.40	1.82×10^{5}	5.26
	30	7.0	1.44	6.03×10^{5}	5.78

Significance of the Constants, K and n. — Equation 2 can be expressed by an alternate form[21]

$$\frac{r}{m}=\frac{1}{2}\left\{1+\tanh\left(\frac{n}{2}\ln\frac{c}{c_{1/2}}\right)\right\} \qquad (5)$$

in which $c_{1/2}$ represents the concentration of free detergent ions at half saturation ($r=m/2$). Equation 5 can be identified with Eq. 2, if

$$k=c_{1/2}{}^{-n} \qquad (6)$$

Hence, in Eq. 4 for $m\gg r$,

$$K=mc_{1/2}{}^{-n} \qquad (7)$$

In this respect, K is regarded as a measure of the ability of binding or the extent of affinity.

On the other hand, the physical meaning of n is not explicit; the value of n depends on the strength of mutual interaction between bound detergent ions. If n is greater than unity, there occurs a cooperative interaction stabilizing the protein bound with detergent, so that the uptake of one ion makes another ion bind easier[20,21].

Dependence of K and n on pH and the Nature of the Binding. — As is shown in Table I, the value of K increases with the lowering of pH in the case of the binding of SDBS by gelatin. A linear relationship is found between $\log K$ and pH, as is shown in Fig. 5, which is represented by

$$\log K=10.7-0.27\,\mathrm{pH} \qquad \text{at } 30°\mathrm{C}$$

Thus the magnitude of K is related to the interaction of DBS anions with gelatin. This suggests that an electrostatic attraction between

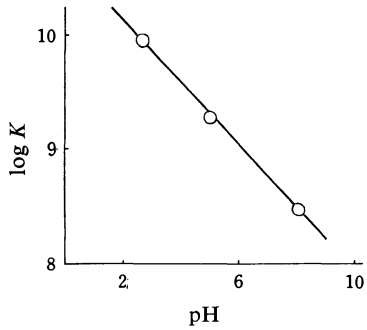


Fig. 5. Relationship between $\log K$ and pH for the binding of SDBS by gelatin.

DBS anions and positively charged groups of gelatin is partly responsible for the binding. Even on the alkaline side gelatin has positively charged sites and binds a finite number of DBS anions.

The value of n is about 2.1 and is independent of pH. This means that the uptake of DBS anions by gelatin favors further binding of other DBS anions in the vicinity of the binding site on gelatin, probably because of the hydrophobic cohesion between DBS anions. Thus, DBS anions form aggregates like micelles on a gelatin molecule. This might have some relation with the increase in the solubilizing power of sodium dodecyl sulfate in the presence of gelatin[22]. Generally, the binding of detergents on synthetic polymers is also interpreted as essentially due to the formation of this kind of micelles on a polymer molecule[23].

It may be concluded that a DBS anion combines with a positively charged group of gelatin and that its binding promotes the further binding of DBS anions around this site due to hydrophobic cohesion. Bound DBS anions form micelle-like aggregates on a gelatin molecule. The former binding will be mostly related to pH's while the latter will be influenced by the length of the alkyl chain of detergent. The effect of the length of alkyl chain has been investigated for anionic detergent-protein systems[4,7], and it is known[4] that the increase in chain length makes the detergent-gelatin ratio lower above which a precipitate separates out. This would also support the concept of the micelle formation on gelatin.

The binding isotherm of SDBS by gelatin can be expressed by

$$\log r=10.7-0.27\,\mathrm{pH}+2.13\log c \qquad \text{at } 30°\mathrm{C}$$

Temperature elevation scarcely influences the

22) S. Saito, *Kolloid-Z.*, **158**, 120 (1958).
23) S. Saito, ibid., **154**, 19 (1957).

value of n, but it does decrease the value of K by a small amount.

On the other hand, the value of K for CPC is considerably smaller than that for SDBS, and it increases with pH. Further, the value of n for CPC, 1.4, is independent of pH and smaller than that for SDBS, 2.1. These are an indication of the lower affinity of CPC for gelatin; that is, CPC and DPB are less bound to gelatin than SDBS. Generally, a cationic detergent exhibits less affinity for proteins and polymers than an anionic detergent[9,22].

The dependence of the value of K upon pH suggests that the binding of CPC by gelatin is of electrostatic nature. According to Pankhurst[2], an ion-ion binding is responsible for the combination between gelatin and CPC, but an ion-dipole binding can not occur at the peptide bonds of gelatin owing to a steric effect. However, the difference in the binding behavior of DPB from that of CPC, i. e., the insignificant binding of DPB as compared with CPC, implies that the length of the alkyl chain, i. e., the hydrophobic cohesion, is of primary importance even with the sufficiently long alkyl chain in the case of cationic detergents.

Summary

The mode of the binding of detergents, SDBS, CPC and DPB, by gelatin in the region of low detergent-gelatin ratios, where solutions are stable without precipitation, was investigated by determining the bound detergents by means of equilibrium dialysis.

Detergents bind with gelatin in accordance with the isotherm $r=Kc^n$, where K and n (>1) are constants which measure an affinity for the binding and an extent of cooperative interaction respectively. The value of K, which is dependent on pH and temperature, decreases with increasing pH for the binding of SDBS and vice versa for CPC. The value of n is characteristic of a given detergent. The value of n for SDBS is significantly greater than that for CPC. Thus the extent of the cooperative stabilization of a bound detergent is higher for SDBS than for CPC.

Both anionic SDBS and cationic CPC combine with gelatin, but cationic DPB scarcely combines with it. Further, it was inferred that a detergent, especially SDBS, binds with gelatin, forming aggregates on it in such a manner as the micelle formation.

The sign of charge of the detergent is of essential importance for the binding of the detergent by gelatin, and the length of the alkyl chain of detergent also has additional effects on the binding. The effect of chain length was examined with cationic detergents.

Institute for Protein Research
(T. I. & F. T.)
and
Faculty of Science
(T. I. & S. I.)
Osaka University, Osaka

The Structural Assignments for the Geometrical Isomers of α, α'-Dimethylstilbene

By Yoichiro NAGAI, Osamu SIMAMURA* and Leo EHARA

(Received May 23, 1961)

Wessely and Welleba[1] assigned to α, α'-dimethylstilbene of m. p. 107°C the trans- and to the isomer of m. p. 67°C the cis-configuration on the basis of their dipole moment measurement, although without giving any experimental details. Some ambiguity, however, yet exists in the application of this method to the present case, because the substances examined are hydrocarbons probably with a small dipole moment value at most, even for the cis-compound. Suzuki[2] reached the same assignments by a theoretical consideration of their ultraviolet absorption spectra in relation to the shift of the absorption maximum due to the change in conjugation caused by the steric requirement of the substituent groups. It seemed desirable to confirm these conclusions by an unambiguous method. We now report the synthesis of *cis*- and *trans*-4, 4'-dinitro-α, α'-

* To whom inquiries regarding this paper should be directed.

1) F. v. Wessely and H. Welleba, *Ber.*, **74**, 777 (1941).

2) H. Suzuki, This Bulletin, **25**, 145 (1952).

dimethylstilbene, whose geometrical configurations have been determined unequivocally by dipole moment measurement, and their conversion into *cis*- and *trans*-α,α'-dimethylstilbene. This constitutes chemical evidence in favor of the already assumed configuration of isomeric α,α'-dimethylstilbenes.

4, 4'-Dinitro-α,α'-dimethylstilbene was prepared from *p*-nitroacetophenone hydrazone with a method similar to that of Vargha and Kovacs's synthesis[3] of some substituted diethylstilbenes. The product was fractionated by recrystallization into the trans-, m. p. 222.4°C, and the cis-isomer, m. p. 151.8°C. The geometrical configurations were derived from dipole moment measurement in benzene[4], the former having a dipole moment of 0.68D and the latter a dipole moment of 6.88D. For the oxidation of the hydrazone to *p*-nitrophenyldiazoethane, one of the intermediates, we found that lead dioxide was much more efficient than mercuric oxide originally[3] used.

Catalytic reduction of *trans*-4, 4'-dinitro-α,α'-dimethylstilbene in the presence of a Raney nickel catalyst yielded 58% of 4, 4'-diamino-α,α'-dimethylstilbene (I), m. p. 157.5°C, and an oily mixture, which gave, on treatment with salicylaldehyde, two isomeric *N*, *N'*-disalicylidene derivatives (III and IV) in 6 and 13% yield, respectively, based on the dinitro compound used. In a separate experiment, pure diamine I gave disalicylidene derivative III in a nearly quantitative yield, but never gave the isomeric derivative IV; therefore, the latter was presumed to be formed only from the geometrically isomeric diamine II, which could not be isolated as such in this study.

$$(p\text{-}O_2NC_6H_4CMe:)_2 \downarrow$$
$$(p\text{-}H_2NC_6H_4CMe:)_2 \rightarrow (o\text{-}HOC_6H_4CH:NC_6H_4CMe:)_2$$
I (trans) | or II (cis) III (trans) or IV (cis)
$$\downarrow$$
$$(C_6H_5CMe:)_2$$

Although the assignment of configuration to the salicylidene derivatives is irrelevant to the main theme of the present report, it is obvious that the geometrical configurations of these compounds (III and IV) correspond with those of diamines I and II, respectively, since it is impossible for the complete inversion to the other configuration to take place in both cis- and trans-isomer.

Similarly reduced, *cis*-4, 4'-dinitro-α,α'-dimethylstilbene gave an oily mixture, which afforded *N*, *N'*-disalicylidene derivatives III and IV in yields of 12 and 61%, respectively, indicating the formation of diamine II in a yield of over 61%.

Although the catalytic reduction of 4, 4'-dinitro-α,α'-dimethylstilbene was thus accompanied by cis-trans isomerization, it follows from the above results that diamine I corresponds to the trans- and diamine II to the cis-configuration. If diamine I which was isolated from the reduction product of the trans-dinitro compound in a yield of at least 58% had had the cis-configuration, the equilibrium mixture of the isomeric diamines after stereomutation under the obtaining experimental conditions would have contained 58% or more of the cis-form, and, consequently, this compound (diamine I) should have been formed from the cis-dinitro compound in a yield of at least 58%, which is impossible because the other isomer (diamine II) was formed in 61% yield.

trans-Diamine I was diazotized and reduced with hypophosphorous acid, giving (67.4% of) α,α'-dimethylstilbene, m. p. 107°C, as the sole isolable product. This result shows that little, if any, stereomutation took place in the course of the deamination; extensive stereomutation would have given a mixture which melted much lower and, finally, an equilibrium mixture containing about 45%[5] of the lower melting isomer. Similarly, the diamine mixture (containing at least 61% of the cis form) from the catalytic reduction of *cis*-dinitrodimethylstilbene gave (58% of) a mixture of isomeric α,α'-dimethylstilbenes consisting of 78% (or 70%) of the form, m. p. 67°C, and 22% (or 30%) of the form, m. p. 107°C. These results establish that dimethylstilbene, m.p. 107°C, has the trans- and the isomer, m. p. 67°C, the cis-configuration.

Experimental

Melting points are corrected.

***cis*- and *trans*-4,4'-Dinitro-α,α'-dimethylstilbene.** —*p*-Nitroacetophenone hydrazone (10 g.) and lead dioxide (100 g.) were stirred in benzene (500 ml.) for 5 hr. at room temperature, the mixture was filtered, and sulphur dioxide was passed into the red filtrate until the solution turned light yellow. Removal of the benzene on a water-bath gave a solid product, which, recrystallized from acetic acid, afforded *trans*-4, 4'-dinitro-α,α'-dimethylstilbene (5.0 g., 60.1%) in colorless crystals, m. p. 221.6~222.4°C (Found: N, 9.71. $C_{16}H_{14}N_2O_4$ requires N, 9.40%). On slow evaporation at room temperature, the mother liquor deposited a mixture of the trans- and the cis-dinitro compound in large crystalline forms; the cis-isomer was picked out and recrystallized from acetone, giving *cis*-4, 4'-dinitro-α,α'-dimethylstilbene in pale yellow prisms (1.9 g., 22.8%), m.p. 150.8~151.8°C (Found: N, 9.56. $C_{16}H_{14}N_2O_4$ requires N, 9.40%). When light

3) L. v. Vargha and E. Kovács, *Ber.*, **75**, 794 (1942).
4) T. Simozawa and Y. Nagai, *J. Chem. Soc. Japan, Pure Chem. Sec.* (*Nippon Kagaku Zasshi*), **81**, 22 (1960).
5) O. Simamura and H. Suzuki, This Bulletin, **28**, 231 (1954).

petroleum was used instead of benzene in the above preparation and the solvent was allowed to evaporate at room temperature from the filtered reaction mixture, 1-*p*-nitrophenyldiazoethane was obtained in red needles, m. p. 84.5~87.5°C (decomp.) (Found: N, 23.69. $C_8H_7O_2N_3$ requires N, 23.73%). Passage of sulphur dioxide into a solution of 1-*p*-nitrophenyldiazoethane in light petroleum gave a white precipitate of 1, 2-bis-(*p*-nitrophenyl)-1, 2-dimethylethylene sulphone which was difficult to purify, decomposition at 130~200°C (Found: N, 8.31. $C_{16}H_{14}N_2O_6S$ requires N, 7.73%).

Reduction of *trans*-4, 4'-Dinitro-α, α'-dimethylstilbene.—*With Stannous Chloride.*—Powdered *trans*-4, 4'-dinitro-α, α'-dimethylstilbene (1.43 g.) was allowed to stand overnight with anhydrous stannous chloride (18 g.) in acetic acid (80 ml.) saturated with hydrogen chloride. The mixture was heated for 1 hr. on a water-bath and cooled. The precipitate was filtered off and dissolved in hot water, and the solution made alkaline with sodium hydroxide. The white precipitate was filtered off and recrystallized from benzene, affording *trans*-4, 4'-diamino-α, α'-dimethylstilbene (I) (1.149 g., 98%) in needles, m. p. 156.6~157.6°C (recrystallized from ethanol) (lit[6]., m. p. 146°C) (Found: N, 12.1. Calcd. for $C_{16}H_{18}N_2$: N, 11.8%).

This diamine and excess of salicylaldehyde in ethanol gave a nearly quantitative yield of *N, N'*-disalicylidene-4, 4'-diamino-α, α'-dimethylstilbene (III) (0.74 g.), m. p. 222.5~226.1°C (from benzene) (Found: N, 6.52. $C_{30}H_{26}N_2O_2$ requires N, 6.28%).

Catalytic Reduction.—The catalyst was a Raney nickel prepared according to the directions for W6 catalyst[7], washed with acetone and stored in it. The nitro compound (1.373 g.) was reduced with hydrogen in the presence of the nickel catalyst (from 4 g. of Raney alloy) in ethanol (20 ml.) under cooling with water. After the catalyst was filtered off, concentration of the filtrate gave *trans*-4, 4'-diamino-α, α'-dimethylstilbene (I) (0.635 g., 57.8%), m. p. 157.6°C. Removal of the ethanol from the mother liquor gave an oil which, on treatment with salicylaldehyde and fractional crystallization of the product from ethanol-benzene, yielded *trans-N, N'*-disalicylidene-4, 4'-diamino-α, α'-dimethylstilbene (III) (0.130 g., 6.3%) and the cis-isomer (IV) (0.282 g., 13.2%), m. p. 150.0~153.5°C (Found: N, 6.53%. $C_{30}H_{26}N_2O_2$ requires N, 6.28%).

Catalytic Reduction of *cis*-4, 4'-Dinitro-α, α'-dimethylstilbene.—Catalytic reduction of the *cis*-dinitro compound (1.12 g.) gave only an oil (0.8 g., 87%), which was converted into a mixture of *N, N'*-disalicylidene derivatives (1.57 g., m. p. 145~171°C). Fractional crystallization from ethanol-benzene gave the *cis*-disalicylidene derivative IV (1.06 g., 61% based on the dinitro compound subjected to the reduction) and the trans-isomer III (0.21 g., 12%).

Deamination of 4, 4'-Diamino-α, α'-dimethylstilbenes.—The *trans*-diamino compound I (0.474 g.) was diazotized with sodium nitrite (0.4 g.) in diluted hydrochloric acid (H_2O 40 ml. and concd. HCl 5 ml.) at 0°C. The solution was added to aqueous sodium hypophosphite (10 g. in H_2O 10 ml. and concd. HCl 10 ml.) and the mixture left overnight in a refrigerator. The solution was extracted with ether, the extract washed and dried ($CaCl_2$), and the ether removed. The residue was chromatographed in light petroleum on alumina, giving α, α'-dimethylstilbene (0.277 g., 67.4%), m. p. and mixed m. p. 104.5~.107°C

The product (0.484 g.) from the catalytic reduction of *cis*-4, 4'-dinitro-α, α'-dimethylstilbene was subjected to deamination as described above, yielding α, α'-dimethylstilbene (0.246 g., 58%), m. p. 52~60°C. This melting behavior indicates that the dimethylstilbene formed contained about 78% (or 70%) of the low melting isomer (see the accompanying figure).

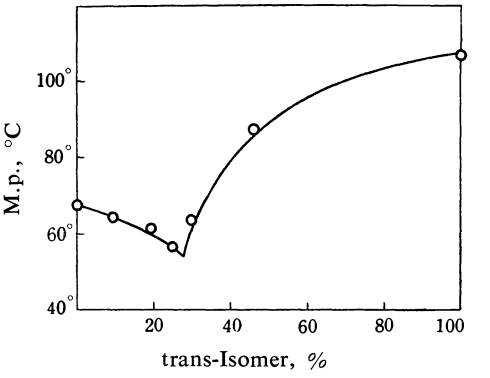


Fig. 1. Melting point—composition curve for a mixture of *cis*- and *trans*-α, α'-dimethylstilbene.

Summary

cis- and *trans*-4, 4'-Dinitro-α, α'-dimethylstilbene were prepared by oxidation of *p*-nitroacetophenone hydrazone with lead dioxide in benzene, followed by treatment with sulphur dioxide. Catalytic reduction of the *trans*-dinitro compound gave at least 64% of *trans*-4, 4'-diamino-α, α'-dimethylstilbene, m. p. 157.6°C, and a similar reduction of the cis-dinitro compound afforded a mixture of the cis- and trans-diamino compound which was shown to contain at least 61% of the cis-isomer. On deamination, the trans-diamino compound yielded α, α'-dimethylstilbene melting at 107°C, and the above mixture of the cis- and trans-isomer, a mixture of the isomeric α, α'-dimethylstilbenes in which the lower melting form predominated (at least 70%). These findings establish that α, α'-dimethylstilbene, m.p. 107°C, has the trans- and the isomer, m. p. 67°C, the cis-configuration.

Department of Chemistry
Faculty of Science
The University of Tokyo
Hongo, Tokyo

6) M. J. Allen and A. H. Corwin, *J. Am. Chem. Soc.*, **72**, 117 (1950).
7) "Organic Syntheses", Coll. Vol. 3, (1955), p. 176.

The Micro and Rapid Determination of Cobalt Carbonyl Anion in Organic Solvents by Titration with Methylene Blue

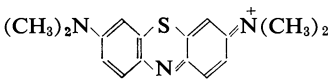
By Ryoji IWANAGA

(Received May 30, 1961)

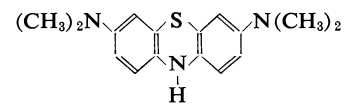
In the course of an investigation of catalysts for oxo reactions, the rate of which seems to be dependent to a large extent on the rate of regeneration of cobalt hydrocarbonyl during the reaction, it was desired to measure rapidly a small amount of cobalt hydrocarbonyl or of cobalt carbonyl anion in various organic solvents. For a quantitative determination of cobalt carbonyl anion, the gasometric method of Sternberg et al.[1] and the gravimetric method of Hieber et al.[2] have been proposed. Neither of these methods, however, is suitable for a determination of the micrograms of the anion in Lewis-base solutions such as methanol and acetone, owing to the difficulty of a quantitative precipitation of the complex salt of the anion in Lewis-base solutions.

Reppe[3] mentioned briefly that "the acidimetric value of cobalt hydrocarbonyl with sodium hydroxide shows practical agreement with the reduction value titrated with methylene blue in the acid pH range", but quantitative results were not presented. The present author has, therefore, investigated on the conditions for titrimetric determination of the micrograms of the cobalt carbonyl anion in various organic solvents, especially in Lewis bases such as alcohols, ketones or aldehydes with methylene blue.

The cobalt carbonyl anion in the aqueous solution was primarily oxidized to dicobalt octacarbonyl by weak oxidizing reagents such as air, methyl orange, methyl red, ferric chloride or cupric sulfate[4]. Methylene blue also may oxidize the anion, and then a leuco-compound may be produced as follows:



$$+ H^+ + 2[Co(CO)_4]^-$$



$$+ Co_2(CO)_8 \qquad (1)$$

In the preliminary test it was observed that the above reaction did not take place quantitatively in a strong acid or in an alkaline medium.

The author has first investigated the effect of the pH of the titration medium on the stoichiometry of the titration of the anion with methylene blue. The end point of this titration was easily detected at the point where the blue color of the methylene blue added to the solution does not disappear for several minutes. By the titration of the anion in aqueous solutions of various pH, it was found that the stoichiometric reaction given by Eq. 1 can be held only at the pH range from 1.9 to 5.2 of titration solutions; at a higher pH range than 5.2 the molar ratio of the added methylene blue to the anion decreases below 1:2 with the increasing pH, and at a lower pH range than 1.9 it increases over 1:2 with the decreasing pH. From these results it was found that the quantitative titration of the anion with methylene blue according to Eq. 1 can be performed only in the pH range from 1.9 to 5.2.

Examining further a titration in a nonaqueous medium by using glacial acetic acid as a solvent for methylene blue titrant and for the titration medium, it was found that the titration could also be performed in good agreement with the reaction given by Eq. 1.

When a titration of the anion in Lewis bases such as methanol and acetone is carried out, methylene blue may be consumed excessively in more than the above ratio, in which case the end point becomes indistinguishable. This may be due to the occurrence of "the base reaction"[5], i.e., the reaction between dicobalt octacarbonyl formed from the anion according to Eq. 1 and a Lewis base, during the titration.

1) H. W. Sternberg, I. Wender and M. Orchin, *Anal. Chem.*, **24**, 174 (1952).
2) W. Hieber and H. Frankel, *Ber.*, **86**, 710 (1953).
3) W. Reppe, "Neue Entwicklung auf dem Gebiet der Chemie des Acetylens und Kohlenoxyds", Springer-Verlag (1949), p. 120; W. Reppe, *Ann.*, **582**, 122 (1953).
4) W. Hieber and W. Hübel, *Z. Elektrochem.*, **57**, 331 (1953).
5) W. Hieber et al., *Ber.*, **86**, 700 (1953); **87**, 25, 789 (1954); **91**, 1146, 1156 (1958). Alcohols, ketones, cyclic ethers, nitriles and isonitriles, as well as amines, react with dicobalt octacarbonyl and produce cobalt carbonyl anion as follows:
$3Co_2(CO)_8 + 2x\,\text{Base} \rightarrow 2[Co(\text{Base})_x][Co(CO)_4]_2 + 8CO$

The author has thus then investigated the conditions needed to decrease "the base reaction" with methanol, because methanol is one of the Lewis bases which reacts rapidly with dicobalt octacarbonyl, and has found that the influence of "the base reaction" on the analysis of the anion could be decreased effectively by diminishing the rate of the base reaction, by diluting the sample solution with a 1 : 1 mixture of glacial acetic acid and toluene, and by lowering the treating temperature as low as possible, about 0°C being satisfactory (see Fig. 4). On the basis of the above results, the author proposes a rapid and simplified method for determining a small amount of the anion in organic solvents, especially in Lewis bases. The author examined the proposed method for the titration of samples of a known concentration of the anion in the presence of water, methanol, acetone, dicobalt octacarbonyl and acetoaldehyde, and could determine the anion in all within a percentage of error of only about one percent.

Experimental and Results

Titration of Cobalt Hydrocarbonyl and Cobalt Carbonyl Anion

Reagents.—A test solution of a known concentration of cobalt hydrocarbonyl was prepared as follows: about 1 g. of dicobalt octacarbonyl was dissolved in 5 ml. of pyridine; after the solution turned clear pink, 1 : 1 aqueous sulfuric acid was dropped into the solution at about −5°C, and the cobalt hydrocarbonyl gas evolved was introduced, together with oxygen-free nitrogen, into an oxygen-free water or methanol through a U-tube filled with phosphorus pentaoxide and a trap cooled at −20°C. The concentration of cobalt hydrocarbonyl in the solution was determined by total cobalt analysis, and this value showed quite a good agreement with a value obtained from the titration with sodium hydroxide[6]. The test solution of cobalt carbonyl anion was also prepared by introducing the cobalt hydrocarbonyl gas evolved as described above into an oxygen-free aqueous or methanol solution of sodium hydroxide, until the solution was neutralized with phenolphthalein as an indicator; the concentration of this was also determined from the total cobalt content.

Standard methylene blue titrant of 1 meq./l. was prepared by dissolving 374 mg. of the special grade crystals of $C_{16}H_{18}N_3SCl \cdot 3\,H_2O$ (Junsei Pure Chemicals Co., Ltd.) into 500 ml. of oxygen-free glacial acetic acid and then filling the container with oxygen-free toluene to 1 l.

All of the above-mentioned oxygen-free solvents were prepared by being refluxed for 1 hr., cooled to room temperature and reserved under a slightly more positive pressure of nitrogen than the atmosphere.

6) This titration was made according to the procedure reported by W. Hieber and W. Hübel, *Z. Elektrochem.*, **57**, 235 (1953).

Apparatus.—Figure 1 illustrates a titration apparatus. Titration is carried out in a 100 ml. Erlenmeyer flask with two holes on each side, one of which holes is for inserting a thermometer and another for introducing the samples and the solvent. To the stopper of the flask, a 25 ml. buret and two glass tubes are attached, one of which is an inlet for nitrogen and another an outlet, the outer end of which is closed by a mercury valve.

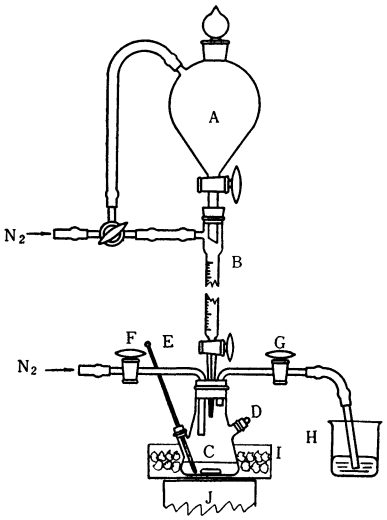


Fig. 1. Apparatus for titration of cobalt carbonyl anion.
A Titrant holder
B Buret
C Titration flask
D Inlet of sample
E Thermometer
F Inlet tube of N_2
G Outlet tube of gas
H Mercury valve
I Ice-water bath
J Magnetic stirrer

Procedures.—Because cobalt carbonyl anion in solutions is very sensitive and easily oxidized with air, a sample to be analyzed, as well as the titration solvents and the methylene blue titrant, must be strictly protected from the air. After all the system has been flushed with nitrogen, the standard methylene blue titrant is introduced into a holder A under a counter-current flow of nitrogen and poured into a buret B. Twenty milliliters of a mixture of glacial acetic acid and toluene are then introduced into the titration flask, which is placed in an ice-water bath, through a side hole D under a counter-current flow of nitrogen; this is cooled to about 0°C by stirring. After the solvent has been cooled, a suitable aliquot of the solution to be analyzed is pipetted into the solvent through D and titrated immediately with the methylene blue titrant while being stirred. While the blue color of methlene blue dropped disappears immediately, the solution titrated becomes light brown due to the formation of dicobalt octacarbonyl, and as soon as its color changes to light green, the titration is

TABLE I. TITRATIONS OF $HCo(CO)_4$ AND $Na[Co(CO)_4]$ IN TOLUENE-ACETIC ACID SOLVENT WITH 1 meq./l. METHYLENE BLUE TITRANT

Sample	ml.	Compound added	$[Co(CO)_4]^-$ obtained from total amount of Co	(μ.eq.) found	Std. dev. %
$HCo(CO)_4$ in water	1	—	7.29	7.26	−0.4
$Na[Co(CO)_4]$ in water	1	—	20.75	20.58	−0.8
$HCo(CO)_4$ in methanol	1	—	21.40	21.40	0
$HCo(CO)_4$ in methanol	2	Methanol 10 ml.	42.80	42.80	0
$Na[Co(CO)_4]$ in methanol	1	—	26.70	26.60	−0.4
$HCo(CO)_4$ in methanol	1	Acetone 10 ml.	21.40	21.40	0
$HCo(CO)_4$ in methanol	1	$Co_2(CO)_8$ 1 mg. Toluene 10 ml.	21.40	21.55	+0.7
$HCo(CO)_4$ in methanol	1	Acetaldehyde 1 ml.	21.40	21.40	0
Oxo product*1	3		34.56*2	36.78	+6.4

*1 This product was obtained as follows: a solution containing 2 eq./l. of methylacrylate and 9.11 meq./l. of $Co_2(CO)_8$ in toluene was treated with 1 : 1 CO and H_2 under 200 kg./cm^2 at 120°C.

*2 The amount of $[Co(CO)_4]^-$ was measured by *o*-phenanthroline method.

stopped. Weights of the anion in the sample are calculated as follows:

mg. of $[Co(CO)_4]^- =$

ml. of methylene blue titrant added $\times 0.342$

Results.—In order to examine the present method, aliquots of a solution of a known concentration of $HCo(CO)_4$ or $Na[Co(CO)_4]$ were pipetted and titrated, alone or in the presence of a large amount of methanol, acetone or dicobalt octacarbonyl. In addition, a titration in the presence of acetoaldehyde was tested. The results of these analyses, listed in Table I, are shown to be in good agreement with the values obtained from the total cobalt contents within a deviation of 1%. The larger deviation on the practical oxo reaction product (in Table I) was presumably due to the inaccuracy of the value obtained from the precipitate of Co-*o*-phenanthroline complex salt with the anion.

Effect of Hydrogen Ion

A pH determination was made by means of a glass electrode which was inserted into a 200 ml. titration flask. After all the system had been flushed with nitrogen, 50 ml. of oxygen-free distilled water were first introduced into the flask, and to this solution was added sulfuric acid, acetic acid or sodium hydroxide under a counter-current flow of nitrogen to give various pH values. Then, 1 ml. aqueous solution of $Na[Co(CO)_4]$ was added and titrated with 1 meq./l. aqueous methylene blue titrant at 20°C. At the end point of titration, the pH of the solution was measured. Figure 2 shows the curve of the molar ratio of methylene blue reacting with the anion at various pH values at the end point.

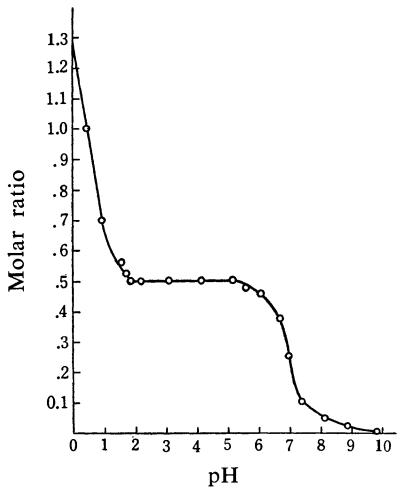


Fig. 2. Variations of molar ratio of methylene blue reacted with $[Co(CO)_4]^-$ at the end point of a titration as a function of pH.

Rates of Base Reaction of Dicobalt Octacarbonyl with Methanol in Various Solvents

Dicobalt octacarbonyl was recrystallized from oxygen-free toluene before use. Reactions of dicobalt octacarbonyl with methanol were carried out in a 100 ml. Erlenmeyer flask, as is shown in Fig. 1, at 20 and 0°C. After the flask had been thoroughly flushed with oxygen-free nitrogen, 25 ml. of oxygen-free methanol and 25 ml. of the oxygen-free solvent to be tested were introduced into the flask and kept at the temperature to be tested. Then a solid of about 0.5 g. of dicobalt octacarbonyl was vigorously stirred in at the controlled temperature. After various periods of reaction

time, 1 ml. of the solution was pipetted out, and the amount of the anion formed in it was determined by the titration described above. Figure 3 shows the rates of formation of the anion in various solvents at 20 and 0°C. In Fig. 3, $[Co]_0$ gives the concentration of the total cobalt in the solution, and $[[Co(CO)_4]^-]_t$ is of the anion formed after the reaction had proceeded for t minutes.

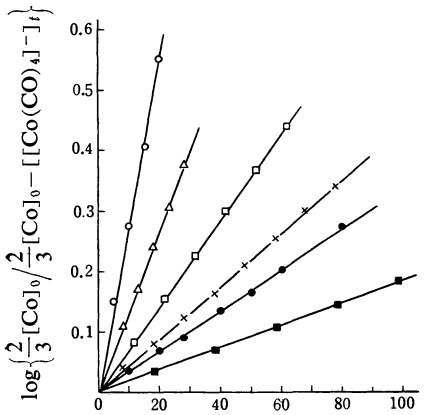


Fig. 3. Effect of solvent and temperature on the rate of base reaction.
- ○ Methanol 50 ml. at 20°C
- ● Methanol 50 ml. at 0°C
- △ Methanol 25 ml. and toluene 25 ml. at 20°C
- × Methanol 25 ml. and glacial acetic acid 25 ml. at 20°C
- □ Methanol 25 ml. and 1 : 1 glacial acetic acid and toluene 25 ml. at 20°C
- ■ Methanol 25 ml. and 1 : 1 glacial acetic acid and toluene 25 ml. at 0°C

Discussion

This titration is based upon the reduction of one-valenced methylene blue cation into a no-valenced leuco-compound with cobalt carbonyl anion in an acid pH range. However, Fig. 2 shows that the stoichiometry of the reaction of titration as given by Eq. 1 does not always exist in the whole pH range. It may be due to other types of reactions of methylene blue in addition to the above reaction, the possibility of the former being postulated from the different redox-potentials of methylene blue at various pH's[7]. Therefore, it is convenient to use a mixture of acetic acid and toluene as the solvent, because the pH of the solution to be titrated does not have to be adjusted to 1.9~5.2. Furthermore, this solvent has the advantages over aqueous acetic acid or glacial acetic acid not only of its miscibility with the anion dissolved in organic solvents, but also of its lower freezing point.

It was found from Fig. 3 that the base reaction of dicobalt octacarbonyl with methanol is of the first order with respect to a concentration of dicobalt octacarbonyl, that the rate of the reaction is most effectively decreased by lowering the reaction temperature, and that in the base reaction at 0°C by using a 1 : 1 mixture of glacial acetic acid and toluene as solvent, the amount of the anion formed by the base reaction in a minute can be decreased by less than 0.1 mol. % of the cobalt of dicobalt octacarbonyl.

If a base reaction thoroughly proceeds during the titration, the amount of methylene blue which may be consumed may be triple that corresponding to the initial amount of cobalt carbonyl anion. The author could really observe such a result when a methanol solution of $Na[Co(CO)_4]$ was titrated for a long time at an atmospheric temperature. Therefore, for determining the anion in Lewis-base solutions, it is important to cool the sample and titrate it as rapidly as possible.

If substances easily oxidized with methylene blue are presented in the sample to be analyzed, it is impossible to determine the anion in the sample by this method. However, from the fact as is shown in Table I that no significant interference of aldehydes was observed under the conditions in this method, it seems to be possible to determine the anion in an oxo reaction product. Furthermore, this method may be especially suitable for the determination of the anion in solutions during oxo, base or other reactions, as it requires only a small amount of the anion (less than 1 mg. as a sample) and takes only about 0.5 to 1 min. for one titration.

Summary

An accurate and rapid method is described for the direct titration of cobalt carbonyl anion in organic solvents. This method is based upon the oxidation reaction of the anion with methylene blue in acid media. The stoichiometry of the reaction of 2 mol. of the anion with 1 mol. of methylene blue is found only at the pH range from 1.9 to 5.2 or in the acetic acid medium. By using a 1 : 1 acetic acid-toluene mixture as solvent, and by carrying out the titration at about 0°C, the anion in Lewis bases such as methanol and acetone is titrated successively without any interference by the base reaction. This method is very suitable for the

7) L. Michaelis and S. Granick, *J. Am. Chem. Soc.*, **63**, 1636 (1941); H. W. Meyer and W. D. Treadwell, *Helv., Chim. Acta*, **35**, 1444 (1952).

determination of the cobalt carbonyl anion in solutions in the course of various reactions.

The author wishes to express his sincere thanks to Professor S. Murahashi, Dr. T. Yoshida and Mr. J. Kato for their kind guidance and encouragement throughout this work. The author is also indebted to Mr. T. Fujii for his assistance in this experiment.

Central Research Laboratory
Ajinomoto Co., Inc.
Suzuki-cho, Kawasaki

Estimation of Micellar Charge from Conductivity Data of Aqueous Detergent Solutions

By Hideo KIMIZUKA and Iwao SATAKE

(Received July 20, 1961)

The micellar molecular weight and the critical micelle concentration (CMC) are essential quantities in the study of the physicochemical properties of detergents. There are a number of methods for determining the CMC, while only a few methods are available for estimating the micellar molecular weight. This is true because of the complex nature of detergent solution, which contains the single detergent ion and the gegen ion in addition to the micellar aggregate in the concentration above the CMC.

The light scattering method is the most profitable one and is widely employed for the measurement of the micellar molecular weight. It is of interest, however, to estimate the micellar molecular weight from a measurement other than that of light scattering. Some authors have attempted the estimation of micellar size from the measurement of the diffusion coefficient[1], and attempts to determine the micellar charge have also been made by using the data of conductivity[2] and cataphoresis[3].

Since the measurement of conductivity has widely been employed for study of the solutions of ionic detergent, it is advantageous to estimate the micellar charge or the micellar aggregation number by using the conductivity data if possible. Therefore, we have started to obtain a method for determining the micellar charge based on assumptions somewhat different from those of the early studies[2,3].

For simplicity we assume, as did, e.g., Hutchinson[2], that above the CMC there is only one kind of micelle, containing a n unit of detergent ion and possessing a charge Z_m, and assume that the concentration of detergent ion in the micellar form is $C-C_m$, where C is the concentration in the gram formula weight per liter and C_m, the critical micelle concentration. It is well known that below the CMC the equivalent conductivity, Λ, of the ionic detergent solution is linear against the ionic strength, I, of the solution:

$$\Lambda=\Lambda_o-\alpha\sqrt{I} \tag{1}$$

$$I=\frac{1}{2}\sum_i C_i Z_i^2 \tag{2}$$

where Λ_o is the equivalent conductivity at infinite dilution, α, a constant for a given detergent, and C_i and Z_i, the concentration and valency of ith ion respectively. Here we assume that in dilute solutions Eq. 1 holds, even in concentrations above the CMC. This involves believing that an abrupt change in conductivity just above the CMC is to be attributed to the presence of the high valent micellar ion, which increases the ionic strength of the detergent solution.

Let us consider an ionic detergent $D_{\nu_d}^{z_d}G_{\nu_g}^{z_g}\rightleftarrows \nu_d D^{z_d\pm}+\nu_g G^{z_g\mp}$, where D and G denote the detergent ion and the gegen ion respectively.

At the CMC,

$$\Lambda_m=\Lambda_o-\alpha\sqrt{I_m} \tag{3}$$

where m refers to the CMC. By comparing Eq. 1 with Eq. 3 we obtain

$$(\Lambda_o-\Lambda/\Lambda_o-\Lambda_m)^2=I/I_m \tag{4}$$

In the concentration above the CMC,

1) D. Stigter, R. J. Williams and K. J. Mysels, *J. Phys. Chem.*, **59**, 330 (1955); G. S. Hartley and D. F. Runnicles, *Proc. Roy. Soc.*, **A168**, 420 (1938); M. E. L. McBain, *J. Phys. Chem.*, **48**, 237 (1944), etc.

2) P. van Rysselberghe, *J. Phys. Chem.*, **48**, 62 (1944); E. Hutchinson, *J. Colloid Sci.*, **9**, 191 (1954).

3) D. Stigter and K. J. Mysels, *J. Phys. Chem.*, **59**, 45 (1955).

the concentration of micelle $=\nu_d(C-C_m)/n$ (5a)

the concentration of the single detergent ion
$=\nu_d C_m$ (5b)

the concentration of the gegen ion
$=\nu_g C-(C-C_m)(Z_d-Z_m/n)\times(\nu_d/Z_g)$ (5c)

The ratio of the fixed gegen ion to micelle was taken into account in Eq. 5c.

The ionic strengths of the solutions above and at the CMC are therefore given as follows:

$$2I=\{C(Z_g+Z_c)+C_m(Z_d-Z_c)\}\nu_d Z_d \quad (6)$$

$$Z_c=\{Z_m^2-Z_g(nZ_d-Z_m)\}/nZ_d \quad (7)$$

$$2I_m=(Z_g+Z_d)\nu_d Z_d C_m \quad (8)$$

Substituting Eqs. 6 and 8 into Eq. 4,

$$(\Lambda_o-\Lambda/\Lambda_o-\Lambda_m)^2=\{(Z_d-Z_c)+(Z_d+Z_c)C/C_m\}/(Z_g+Z_d) \quad (9)$$

The last term on the right hand side of Eq. 7,

$$r=(nZ_d-Z_m)/nZ_d \quad (10)$$

expresses the ratio of the charge of the fixed gegen ion to that of the micelle. If r is zero and, consequently, Z_m is nZ_d, Z_c becomes nZ_d, which is the charge of the micelle having no fixed gegen ions. It may be pointed out here that we shall be able to obtain a similar expression with Eq. 4 for other properties of a detergent solution, e.g.,

$$(\ln f_g/\ln f_{gm})^2=I/I_m \quad (11)$$

where f_g denotes an activity coefficient of the gegen ion. But, unfortunately, we have no exact data on f_g.

Check of the Theory and Discussion

The conductivity data employed in the estimation of the micellar charge were taken from those reports which gave numerical data[4-7], although a number of studies have already been carried out for the conductivities of ionic detergent solutions.

In Figs. 1, 2 and 3, the calculated values of $(\Lambda_o-\Lambda/\Lambda_o-\Lambda_m)^2$ are plotted against C/C_m. The linearity of these lines is satisfactory to some extent above the CMC. The deviation from linearity appearing in higher concentrations probably comes from the assumption of the limiting law as expressed in Eq. 1. This

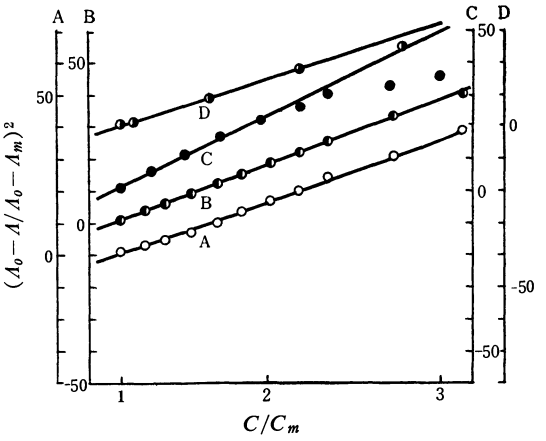


Fig. 1. Test of Eq. 9. A; silver dodecyl sulfate, B; sodium dodecyl sulfate, C; sodium tetradecyl sulfate, D; sodium hexadecyl sulfate.

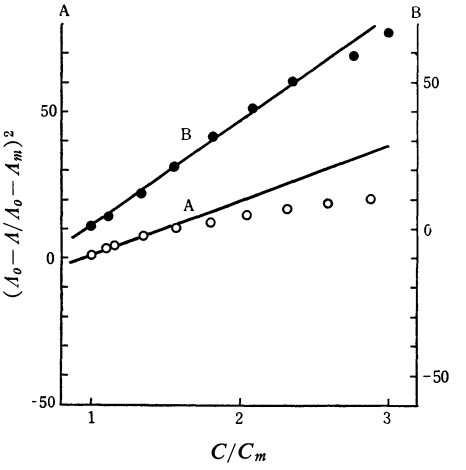


Fig. 2. Test of Eq. 9. A; sodium dodecyl sulfonate, B; sodium tetradecyl sulfonate.

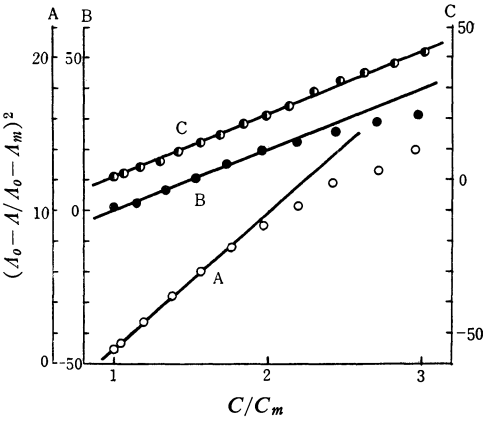


Fig. 3. Test of Eq. 9. A; trimethyl dodecylammonium sulfate, B; dodecylammonium chloride, C; trimethyl octadecylammonium chloride.

4) A. Lottermoser and F. Püschel, *Kolloid-Z.*, **63**, 175 (1933).
5) K. A. Wright, A. D. Abbott, V. Sivertz and H. V. Tartar, *J. Am. Chem. Soc.*, **61**, 549 (1939).
6) G. L. Brown, P. F. Griezer and C. A. Kraus, ibid., **71**, 95 (1949).
7) J. F, Voekes and H. V. Tartar, *J. Phys. Chem.*, **59**, 1190 (1955).

TABLE I. MICELLAR CHARGES OBTAINED FROM CONDUCTIVITY DATA AND MICELLAR AGGREGATE NUMBERS OBTAINED FROM LIGHT SCATTERING DATA

Detergent	CMC, mol./1.	Temp.	Z_c	Ref.	Temp.	n_l	Ref.	r
SDS	6.4×10^{-3}	40	37	4)	23	40	9)	0.04
STS	3×10^{-3}	40	49	4)	23	43	8)	
SHS	5.76×10^{-4}	40	29	4)				
AgDS	6.4×10^{-3}	40	33	4)				
SDS*	1.26×10^{-2}	40	37	5)	40	45	9)	0.09
STS*	2.7×10^{-3}	40	70	5)	60	80	8)	0.06
DAC	1.48×10^{-2}	25	39	6)		55	10)	0.15
TMOAC	3.4×10^{-4}	25	42	6)				
TMDAS	1.64×10^{-2}	25	25	7)	23	65	8)	0.38

SDS: Sodium dodecyl sulfate; STS: Sodium tetradecyl sulfate; SHS: Sodium hexadecyl sulfate; AgDS: Silver dodecyl sulfate; SDS*: Sodium dodecyl sulfonate; STS*: Sodium tetradecyl sulfonate; DAC: Dodecylammonium chloride; TMOAC: Trimethyl octadecylammonium chloride; TMDAS: Trimethyl dodecylammonium sulfate.

agrees well with the result that the reduced concentration, C/C_m at which the deviations are observed to begin becomes lower as the CMC of the detergent solution increases. The value of Z_c may be obtained from the slope of each linear portion according to Eq. 9.

Table I shows the value of Z_c and r, together with the value of n_l, the micellar aggregation number observed by means of the light scattering technique[8-10]. r was calculated from Eqs. 7 and 10 by using the value of n_l in place of n in these equations. As is seen in this table, the values of the Z_c of anionic detergent are almost the same as those of n_l. This would suggest that the micellar aggregate of the anionic detergent ion behaves as if it were *a* polyvalent ion with few fixed gegen ions.

Thus, Z_c gives approximately the micellar aggregation number; we can therefore estimate the micellar aggregation number from the conductivity data as described in the present study. We were unable to obtain a linear portion near the CMC in the plot, $(\Lambda_o-\Lambda/\Lambda_o-\Lambda_m)^2$ vs. C/C_m, for sodium decyl sulfonate. This probably comes from the fact that the CMC of sodium decyl sulfonate is relatively high, 6.25×10^{-2} mol./1., where the limiting law does not hold any more. The values of r for cationic detergents are somewhat higher than those for anionic detergents. This agrees with the conclusion obtained by Hartley[11].

8) H. V. Tartar and A. L. M. Lelong, ibid., **59**, 1185 (1955).
9) H. V. Tartar, *J. Colloid Sci.*, **14**, 115 (1959).
10) P. Debye, *J. Phys. & Colloid Chem.*, **53**, 1 (1949).
11) G. S. Hartley, *Kolloid-Z.*, **88**, 22 (1939).

Summary

An equation relating the micellar charge to the conductivity data was derived for the ionic detergent solutions. It was found that the calculated values of the micellar charge were approximately the same as the micellar aggregation number observed by means of the light scattering technique. The ratio of the fixed gegen ion to the micelle was also estimated.

The authors wish to express their thanks to Professor Ryohei Matuura of this department for his kind advice and discussion in the course of this study.

Department of Chemistry
Faculty of Science
Kyushu University
Hakozaki, Fukuoka

ESR Study of the Radiation Chemical Process in Polyethylene

By Shun-ichi OHNISHI

(Received July 17, 1961)

Several works[1-10] have already been published on the ESR spectrum of irradiated polyethylene (PE). The results of these works have revealed that at least three kinds of radicals are produced in irradiated PE. The short-living component of the radicals (decay: 1 day) gives a sextet spectrum of ΔH_{hfs} (hyperfine separation) = 30 gauss and is assigned to the $-CH_2-\dot{C}H-CH_2-$ radical (FR_{VI})[1,3,4,7,9,10]. The radical of a longer life-time (decay: months) shows a septet spectrum ($\Delta H_{hfs}=18$ gauss) with further complex splittings, probably a doublet structure ($\Delta H_{hfs}=7$ gauss) and is identified with the $-CH_2-\dot{C}H-CH=CH-CH_2-$ radical (FR_{VII})[3,9,10]. The interpretation of the septet spectrum is, admittedly, not as well established as the sextet, about which there is no doubt in its identification. Lawton et al.[4] have expressed their view that the spectrum is a quintet with very "fine" struture and perhaps corresponds to the $-CH_2\cdot : \cdot CH_2-$ radical. Their view, however, does not seem to be well supported. The third component of the radicals has a very long life-time (half-life: 30 min. at 150°C) and gives only a singlet spectrum of ΔH_{msl} (line width at maximum slope) = 25 gauss. This is assigned to the polyenyl radical $-CH_2-\dot{C}H-(-CH=CH-)_n-CH_2-$[5,8]. The spectra of these radicals are summarized in Fig. 1.

In the present investigation PE was irradiated in vacuo at −196°C with a variety of doses, and the change in the obtained ESR spectrum with the rising temperature was followed. The results are discussed from the standpoint of the mechanism of the radiation-chemical changes in the irradiated PE.

Experimental

Material. — Marlex 50 inflation film ~30 μ in thickness was used. The inflation film had some internal strain; therefore, it expanded by about 5% in the extruded direction when put into boiling water.

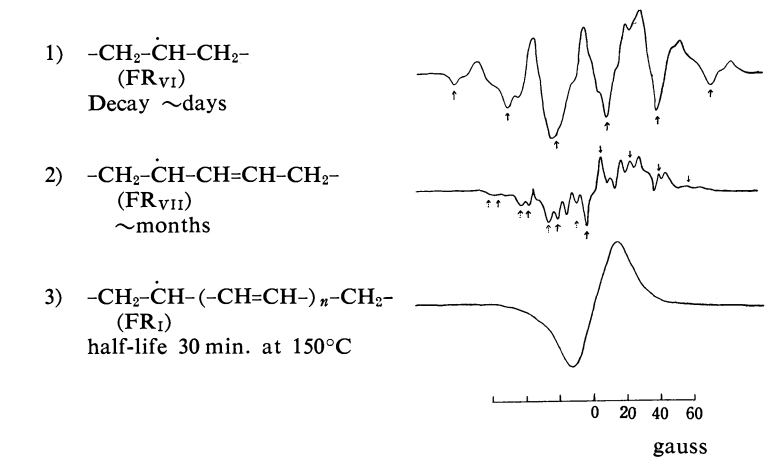


Fig. 1. ESR spectra and free radicals identified from the spectra in irradiated polyethylene.

1) B. Smaller and M. S. Matheson, *J. Chem. Phys.*, **28**, 1169 (1958).
2) R. J. Abraham and D. H. Whiffen, *Trans. Faraday Soc.*, **54**, 1291 (1858).
3) A. T. Koritzky, Yu. N. Molin, V. N. Shamshev, N. Ya. Bouben and V. V. Voevodsky, *Vysokomolec. Soed.*, **1**, 1182 (1959).
4) E. J. Lawton, J. S. Balwit and R. S. Powell, *J. Chem. Phys.*, **33**, 395 (1960).
5) E. J. Lawton, J. S. Balwit and R. S. Powell, ibid., **33**, 405 (1960).
6) H. Kashiwabara and K. Shinohara, *J. Phys. Soc. Japan*, **15**, 1129 (1960).
7) B. R. Loy, *J. Polymer Sci.*, **44**, 341 (1960).
8) S. Ohnishi, Y. Ikeda, S. Sugimoto and I. Nitta, ibid., **47**, 503 (1960).
9) A. G. Kiselev, M. A. Mokul'skii and Yu. S. Lazurkin, *Vysokomolec. Soed.*, **2**, 1678 (1960).
10) S. Ohnishi, Y. Ikeda, M. Kashiwagi and I. Nitta, *Polymer*, **2**, 119 (1961).

Irradiations.—Electron irradiation by a 2 MeV. Van de Graaff accelerator was carried out in vacuo at −196°C as follows: Samples were sealed in a glass ampoule ~4 mm. in diameter under a high vacuum (~10^{-5} mmHg). The glass ampoule was adjusted to float about 1 mm. under the surface of liquid nitrogen so as to be located within the range of the 2 MeV. beam.

In some experiments samples were 'reirradiated'. Samples, preirradiated at a variety of doses, were heated at some high temperature (125°C for FR_{VII} and 250°C for FR_{I}) so that the free radicals produced by the irradiation could decay almost entirely. After the heat-treatment, the samples were irradiated again at −196°C.

The irradiation dose was calculated by referring to the calorimetry experiment. Hydrogen gas evolved by irradiation from PE was removed by evacuation at −196°C.

ESR Measurement.—ESR signal was recorded at −196°C on a Varian V-4500 spectrometer with Liquid Nitrogen Accessory. All spectra were recorded at a small power level (~1 mW) to avoid the power saturation effect[11]. The decay curve at room temperature was determined by storing the sample at room temperature for a certain time and then recording the spectrum at −196°C. The concentration of the free radicals was determined by comparing the ESR signal intensity at room temperature with that from a DPPH benzene solution (~1×10^{-5} mol./g.). Sufficient attention was paid to those fractors[12] which often lead to an erroneous estimation.

Results and Discussion

Spectrum of Irradiated PE at −196°C.—PE, irradiated at various doses at −196°C, has shown a broad sextet spectrum, as is shown in Fig. 2 (1). Comparing this sextet with that obtained from PE irradiated at room temperature (Fig. 1 (1)), the broadness of the former spectrum can be clearly seen. This arises from the spin-spin interaction and might correspond to the circumstance that such radicals are closely spaced[4]. It is to be added that, in the irradiated methane, both a broad and a narrow quartet spectrum were obtained and that the interpretation of such differences might be the same[13] as has been indicated above.

On warming to room temperature, the broad sextet decayed quickly, and the spectrum remaining after 2.5 hr. was a narrow sextet (see Fig. 2 (2)). After 7 days (Fig. 2 (5)), the sextet spectrum had decayed almost entirely and there only remained the septet spectrum, which hardly decays at all at room temperature.

Comparing the spectral change at room temperature of samples irradiated at higher doses with those irradiated at lower doses (cf. Fig. 2A with 2B), it can be concluded that FR_{VI} decays faster in those samples irradiated at larger doses. This result might be due to the existence of more 'defects', such as a cross-linked point or a double bond, caused by irradiation in the polymer, defects somewhat facilitating the motion of free radicals in the crystalline region[14]. It should be remembered in this connection that the ESR spectrum observed on γ-irradiation at room temperature was sextet at small doses <~1 Mrad and septet only in the intermediate dose range (10 ~100 Mrad)[10]. At higher doses (~3000 Mrad), only a singlet spectrum was observed. The phenomenon might be interpreted, at least in part, on the basis of the increased mobility of the free radicals with increasing doses. In the intermediate doses, for example, FR_{VI} as well as FR_{VII} were produced, but, owing to the increased rate of decay in PE irradiated with larger doses, the sextet spectrum was not observed on ESR recording.

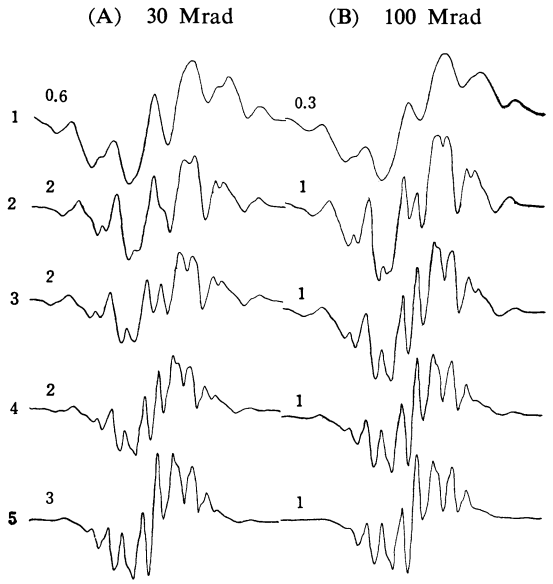


Fig. 2. Change of ESR spectrum of irradiated polyethylene on storage at room temperature. Spectra were recorded at −196°C. Irradiation was carried out in vacuo at −196°C with doses of (A) 30 Mrad and (B) 100 Mrad. The evolved H_2 gas was removed by evacuation. 1) Immediately after irradiation. 2) After 2.5 hr. at room temperature. 3) After 16 hr. 4) After 1 day, 15 hr. 5) After 7 days, 10 hr. Figures show the magnification factor of the amplifier.

11) S. Ohnishi, Y. Ikeda, S. Sugimoto and I. Nitta, *Ann. Repts. Japanese Association for Radiation Research on Polymers (JARRP)*, **2**, 215 (1960).
12) S. Ohnishi, Y. Ikeda, S. Sugimoto and I. Nitta, ibid., **2**, 219 (1960).
13) L. A. Wall, D. W. Brown and R. E. Florin, *J. Phys. Chem.*, **63**, 1762 (1959).
14) For example, R. E. Glick, R. P. Gupta, J. A. Sauer and A. E. Woodward, *Polymer*, **1**, 340 (1960).

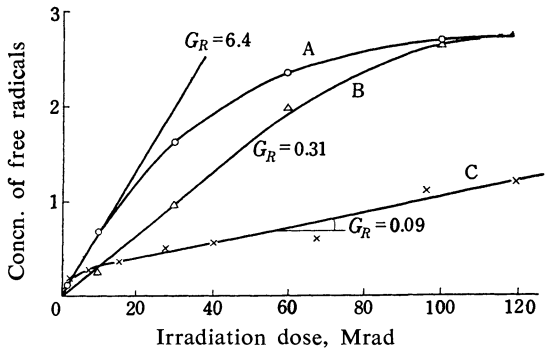


Fig. 3. Free radical formation curve for irradiated polyethylene. Curve A at −196°C by electron irradiation. Curve B for the $-CH_2-\dot{C}H-CH=CH-CH_2-$ radical remaining on storage at room temperature. Curve C at room temperature by γ-irradiation. The ordinate scale for curve A is 10 times larger than that for curves B and C.

$\times 10^{-4}$ mol./g. for ○
$\times 10^{-5}$ mol./g. for △ and ×

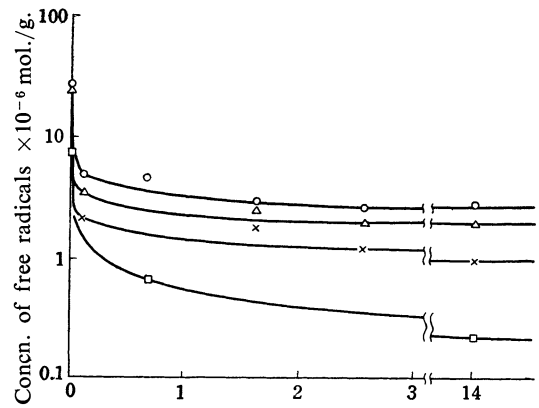


Fig. 4. Free radical decay curve at room temperature for polyethylene irradiated at −196°C with various doses.

—○— 100 Mrad —△— 60 Mrad
—×— 30 Mrad —□— 10 Mrad

Free Radical Formation Curve. — The concentration of free radicals produced by irradiation at −196°C was plotted against the dosage (see Fig. 3 curve A). The curve does not make a straight line, in contrast with the expectation based on a complete trapping of the primary radical at −196°C. This deviation from linearity might suggest that one part of the primary radicals, FR_{VI} showing the broad sextet in our case, reacts during irradiation even at −196°C. This component of FR_{VI} will be referred to as FR^{I}_{VI} (FR_{VI} reacting instantaneously at −196°C) in this paper. The occurrence of the reaction of FR^{I}_{VI} at −196°C might not be unreasonable in view of the fact that most FR_{VI}'s were produced by irradiation in close proximity and also that probably most of them were in 'hot' states.

The decay curve at room temperature is shown in Fig. 4 for samples irradiated with various doses at −196°C (cf. Fig. 2). It shows a quick decay of FR_{VI} and long life-time for the remaining FR_{VII}. This result can be interpreted to show that the free radicals in irradiated PE at −196°C consisted of about 90% FR_{VI} and 10% FR_{VII}. The concentration of the remaining FR_{VII} was plotted against the dosage in Fig. 3 (curve B). It should be noted that the decay curve given in Fig. 4 was for that in vacuo; the evolved hydrogen gas had been removed by reevacuation at −196°C. If the evolved gas was not removed, the decay of FR_{VI} and also of FR_{VII} were accelerated to a small but definite extent, showing a possibility of the backreaction of H_2 with the radicals.

The G_R values were estimated from the initial slope of the formation curve. G_R(total) was found to be 6.4 from curve A, and $G_R(FR_{VII})$ was 0.31 from curve B. It is assumed that $G_R(FR_{VI}) = G_R(\text{total}) - G_R(FR_{VII}) = 6.1$. Lawton et al.[4] obtained $G_R = 3.6$ at −196°C calculated at a dose of 40 Mrad. If we calculate the value at the dose of 40 Mrad, where the formation curve deviates from the straight line of slope $G_R = 6.4$, our result gives a value of 4.6. Voevodsky et al.[3] gave a value of 2.9±0.6 for FR_{VI} at 178°K and 0.16 for FR_{VII} at 323°K. The G_R value, estimated by the scavenger method for the lower aliphatic hydrocarbons[15], ranged from 6 to 8. This range is very close to that for irradiated PE at −196°C and shows that the yield of primary radicals in low and high molecular hydrocarbons is nearly the same.

In Fig. 3 the formation curve in the case of γ-irradiation at room temperatures[12] is shown for comparison (curve C). The G_R value 1.6 estimated from the initial slope corresponds almost exactly to that for FR_{VI}, and the value 0.09 determined from the slope of the curve in the intermediate dose ranges (10∼100 Mrad), to that for FR_{VII}.

The difference between the straight line with the slope $G_R = 6.4$ and the experimentally obtained curve A will correspond to the FR^{I}_{VI} disappearing during irradiation at −196°C. The G_R value for FR^{I}_{VI} was calculated from the amount of deviation to be 2.2 at a dose of 50 Mrad. Therefore, the G_R value for FR_{VI} reacting on being warmed to room temperature should be $G_R(FR_{VI}) - G_R(FR^{I}_{VI}) = 4$. The G_R

15) See, for example, A. J. Swarrow, "Radiation Chemistry of Organic Compounds", Pergamon Press, New York (1960), p. 19.

TABLE I. ESTIMATED G VALUE

$-CH_2-\dot{C}H-CH_2-$	6.1 (LN)	1.6 (RT)
$-CH_2-\dot{C}H-CH=CH-CH_2-$	0.31 (LN)	0.09 (RT)
$(-CH_2-\dot{C}H-CH_2-)_{inst}$	2.2 (LN)*	
Instantaneous crosslinking	1.1 (LN)*	(=2.2/2)
Crosslinking on warming to room temperature	2.0**	(=1/2(6.1−1.1))
Total crosslinking	3 (RT)	(=6.1/2=1.1+2.0)

* The $-CH_2-\dot{C}H-CH_2-$ radical reacting and disappearing instantaneously during irradiation at −196°C. Estimated from the deviation from linearity in the formation curve at a dose of 50 Mard. G (crosslinking) was estimated from G_R $(-CH_2-\dot{C}H-CH_2-)/2$.

** Estimated from the $G_R(-CH_2-\dot{C}H-CH_2-)$ value corresponding to the radical disappearing on warming the sample from −196°C to room temperature.

LN: Liquid nitrogen temperature. RT: Room temperature.

TABLE II. CONCENTRATION OF FREE RADICALS PRODUCED ON 'REIRRADIATION' WITH 30 MRAD AT −196°C

Preirradiation dose (Mrad)	Immediately after irradiation at −196°C*	$-CH_2-\dot{C}H-CH=CH-CH_2-$**
0	1.6×10^{-4} mol./g.	9.6×10^{-6} mol./g.
10	1.2×10^{-4}	8.9×10^{-6}
30	1.3×10^{-4}	9.0×10^{-6}
60	1.3×10^{-4}	1.3×10^{-5}
100	1.1×10^{-4}	1.1×10^{-5}
3000	1.2×10^{-4}	3.5×10^{-5}***

* $-CH_2-\dot{C}H-CH_2-$ + $-CH_2-\dot{C}H-CH=CH-CH_2-$. Corresponds nearly to $-CH_2-\dot{C}H-CH_2-$ except in the case of 3000 Mrad.

** Remaining component on storage of the samples at room temperature for a week or more.

*** Corresponds to polyenyl radical. Concentration of the $-CH_2-\dot{C}H-CH_2-$ radical 8.8×10^{-5} mol./g.

values obtained in the present investigation are summarized in Table I.

Formation of $-CH_2-\dot{C}H-CH=CH-CH_2-$ Radical.—The $G_R(FR_{VII})$ was found to be 0.31 for electron irradiation at −196°C and 0.09 for γ-irradiation at room temperature. The difference in the values might be due to the decay of FR_{VII} in the presence of evolved H_2 during irradiation, since γ-irradiation takes more time than electron irradiation. On the other hand, it is a well-known fact that irradiation produces a transvinylene group in PE. The G value was estimated to be 2.2 by Dole et al.[16] Comparing the values, it may be concluded that FR_{VII} is produced to a lesser extent, about 0.31/2.2=0.14, than the unsaturated group.

As for the mechanism of FR_{VII} formation, we do not yet have any definite picture. Several possible mechanisms will now be discussed, however,

1) Free radical migration such as

$$-CH_2-\dot{C}H-CH_2- \cdots\cdots -CH_2-CH=CH-$$
$$\rightarrow -CH_2-CH_2-CH_2- \cdots\cdots -\dot{C}H-CH=CH-$$

This mechanism might be essentially the same as that suggested by Voevodsky et al.[3], who had some experimental evidence that 'reirradiation' increased the $G_R(FR_{VII})$ to 3.2. Our result does not seem to support this mechanism strongly. First, FR_{VII} is produced in only 14% of the unsaturated group, as is stated above. Secondly, our results of the reirradiation experiment, summarized in Table II, cannot be interpreted to show that free radical migration is a predominant mechanism for FR_{VII} formation. As the preirradiation dose increased, more unsaturated groups existed in the irradiated polymer. Therefore, on reirradiation at the same dose (30 Mrad), samples preirradiated at higher doses should have a higher FR_{VII} concentration if the migration mechanism prevailed. The results given in Table II show a tendency toward a slightly increasing concentration of FR_{VII}, but it is not certain that the data provide strong evidence for mechanism 1. The

16) M. Dole, D. C. Milner and T. F. Williams, *J. Am. Chem. Soc.*, **80**, 1580 (1958).

spectrum obtained from the reirradiated samples was more or less the same as that from the virgin sample except one preirradiated with 3000 Mrad (see Fig. 5). PE irradiated with 3000 Mrad had shown a singlet spectrum. On reirradiation at −196°C with 30 Mrad, the sample (Sample I) gave the spectrum as shown in Fig. 5 (2A), with somewhat different features from those preirradiated with 0 to 100 Mrad. Immediately after being warmed to room temperature, Sample I gave only singlet spectrum (Fig. 5 (2B)). The subtracted curve (A–B) was almost a sextet. That conjugated double bond which exists in Sample I might have something to do with the different features observed.

2) Hydrogen abstraction; $-CH_2-CH=CH- + H \longrightarrow -\dot{C}H-CH=CH- + H_2$. This reaction requires an activation energy of the order of 5 kcal./mol.[17] and hence does not seem to occur easily at −196°C or at room temperature. Hot H atoms could abstract combined H to form FR_{VII} and H_2 even at −196°C, but the probability of H atoms finding double bonds before they cooled or before other reactions, such as the abstraction of H from the neighboring $-CH_2-CH_2-CH_2-$ chain, had occurred, would seem to be very small. Mechanism 3 may also be mentioned as possible:

$$-CH_2-CH_2-CH_2-CH_2- \rightsquigarrow (-CH_2-\dot{C}H-CH_2-CH_2-)_{hot} \longrightarrow -CH_2-\dot{C}H-CH=CH- + H_2$$

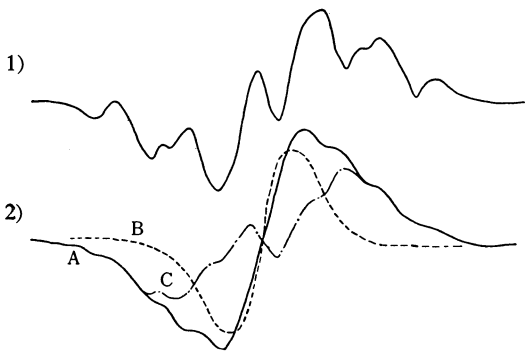


Fig. 5. Spectrum of polyethylene 'reirradiated' with 30 Mrad at −196°C. 1) For sample preirradiated with 100 Mrad. 2) For sample preirradiated with 3000 Mrad. A: Immediately after irradiation. B: After storage at room temperature for 25 min., spectrum being recorded at −196°C. C: Subtracted curve A–B, showing the decayed component to be nearly a sextet spectrum.

17) See, for example, E. W. R. Steacie, "Atomic and Free Radical Reactions", 2nd Ed. Vol. 1, Reinhold Publishing Corporation, New York (1954).

or

$$-CH_2-CH_2-CH_2-CH_2- \rightsquigarrow -CH_2-\overset{+}{C}H-CH_2-CH_2- + H + e$$

$$-CH_2-\overset{+}{C}H-CH_2-CH_2- \longrightarrow -CH_2-\overset{+}{C}H-CH=CH- + H_2$$

$$-CH_2-\overset{+}{C}H-CH=CH- + e \longrightarrow -CH_2-\dot{C}H-CH=CH-$$

The molecular elimination reaction of H_2 from the thermal $-CH_2-\dot{C}H-CH_2-CH_2-$ radical requires an activation energy of about 30 kcal./mol.[18] Some hot radicals could overcome the barrier and could produce FR_{VII} even at −196°C.

Other mechanisms than these three could be thought of, but as yet we have no experimental background available for further discussion.

Radiation Chemical Process in Polyethylene; a Concluding Remark.—The present ESR result could be interpreted to suggest the following features of the radiation chemical process in PE. Primarily irradiation produces the $-CH_2-\dot{C}H-CH-$ radicals (FR_{VI}) clustered in a spur with a G value of 6.4; it also produces the trans-vinylene unsaturated group by the molecular H_2 detatchment process with a G value of 2.2. The $-CH_2-\dot{C}H-CH_2-$ radicals are 'hot', and the excess energy might distribute over a certain range. Most of the $-CH_2-\dot{C}H-CH_2-$ radicals are produced in close proximity, giving the broad sextet spectrum, and the distance distribution among the radicals might be given by a certain function. The excess energy of the hot radicals would cool very rapidly ($\sim 10^{-12}$ sec.). Some hot radicals with sufficient excess energy decompose before cooling to give $-CH_2-\dot{C}H-CH=CH-$ and H_2, with a G value of 0.31. Other hot radicals located very closely within a certain range can react with each other during irradiation even at −196°C and form crosslinks. The rest of the hot radicals will only cool without reacting and so be trapped. They will, however, react to form crosslinks as the temperature is raised. Thus the reaction process can be represented as:

$$-CH_2-CH_2-CH_2-CH_2- \overset{1)}{\underset{G=6.4}{\rightsquigarrow}} (-CH_2-\dot{C}H-CH_2-CH_2-)_{hot} + H$$

$$\overset{2)}{\underset{G=2.2}{\rightsquigarrow}} -CH_2-CH=CH-CH_2- + H_2$$

$$(-CH_2-\dot{C}H-CH_2-CH_2-)_{hot}$$

18) A. S. Gordon and S. R. Smith, *J. Chem. Phys.*, **34**, 331 (1961).

$$\xrightarrow[G=0.31]{\text{3) sufficiently hot}} -CH_2-\dot{C}H-CH=CH- + H_2$$

$$\xrightarrow[\text{at } -196°C]{\text{4) located close together}} 1/2$$

$$-CH_2-CH-CH_2-CH_2-$$
$$|$$
$$-CH_2-\dot{C}H-CH_2-CH_2-$$

$$\xrightarrow[\text{cool at } -196°C]{\text{5) located apart}} -CH_2-\dot{C}H-CH_2-CH_2-$$

$$\downarrow \text{as temp. is raised}$$

$$1/2 \quad \begin{matrix} -CH_2-CH-CH_2-CH_2- \\ | \\ -CH_2-CH-CH_2-CH_2- \end{matrix}$$

The G value for the instantaneous crosslinking at $-196°C$ (Eq. 4) can be calculated from $G_R(FR^{I}_{VI})$ divided by 2 and so becomes 1.1. The G value for crosslinking ($G(X)$) resulted from being warmed to room temperature (Eq. 5) is calculated to $1/2(G_R(FR_{VI})-G_R(FR^{I}_{VI}))=2$. On irradiation at room temperature the $G(X)$ will then become $2+1.1=3.1$.

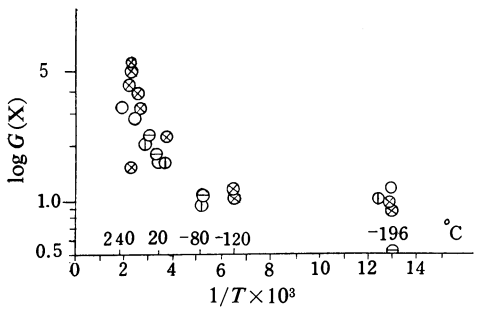


Fig. 6. An Arrhenius plot of the crosslinking yields obtained by various authors, compiled by A. Chapiro[19].

- ⊖ Black 1956
- ⊗ Charlesby Davison 1957
- ⊕ Pravednikov Medvedev 1958
- ○ Lawton et al. 1958

Comparing the crosslinking G value expected from the present ESR result with those obtained experimentally by several other authors, the agreement is found to be satisfactory. Chapiro[19] has summarized the $G(X)$ values by several authors as in Fig. 6. The data show the $G(X)$ at $-196°C$ to be nearly 1 and the value at 40°C to be 3, in agreement with the present suggestion. Such agreement may well show the reasonableness of the present picture of the radiation chemistry of PE. As Fig. 6 suggests, the crosslinking reaction below $-40°C$ proceeds with an activation energy of nearly zero. In order to explain this particular nature of the crosslinking reaction, some authors have suggested an 'ionic' mechanism[19,20]. Pravednikov et al.[21], on the other hand, proposed a 'hot' radical mechanism. Our result is in favor of the latter opinion. Production of the 'hot' $-CH_2-\dot{C}H-CH_2-$ radicals in close proximity is a characteristic of chemical reaction caused by ionizing radiation. They cannot react with oxygen, as has been revealed by us[22], and cannot react with radical scavengers such as DPPH, because, before the arrival of such scavengers, they react with each other almost instantaneously. The $-CH_2-\dot{C}H-CH_2-$ radicals produced apart from each other or diffused out of the spur, thus making 'background' radicals in Magee's sense[23], behave in a way similar to the so-called free radical reaction or photochemical reaction. They may react with oxygen or radical scavengers.

In irradiated poly(vinyl chloride)[24], poly(vinyl alchohol)[12], and nylon[12], the free radical formation curves deviated from straight line in a way quite similar to that of PE. This might suggest, as in the case of PE, the occurrence of the reaction of some hot radicals at $-196°C$. The G_R values were estimated from the initial slope to be 7.1, 8.0 and 10 respectively, Irradiated polypropylene[25] was an exceptional case where the free radical formation curve at $-196°C$ was nearly a straight line ($G_R=6.2$) up to 100 Mrad, showing an almost complete trapping of the primary radicals. This rather exceptional behavior might have something to do with the shrinkage of the spiral main chain on scission.

The author would like to express his sincere thanks to Professor Isamu Nitta for his discussions and also to Professor Shuzo Seki for his encouragement. Thanks are also due to Mr. Yohta Nakai of this Association for his determination of the irradiation dose.

Osaka Laboratories
Japanese Association for
Radiation Research on Polymers
Neyagawa, Osaka

19) A. Chapiro, *Isotopes and Radiation*, 3, 423 (1960).

20) For example, J. Weiss, *J. Polymer Sci.*, 29, 425 (1958).

21) A. N. Pravednikov, Yin-Shen-Kan and S. S. Medvedev, *Proc. 2nd Conf. on Peaceful Uses of Atomic Energy*, P/2294 (1958).

22) S. Ohnishi, S. Sugimoto and I. Nitta, *J. Polymer Sci.*, in press.

23) J. L. Magee, *J. Am. Chem. Soc.*, 73, 3270 (1951).

24) S. Ohnishi, Y. Nakajima and I. Nitta, *J. Appl. Polymer Sci.*, in press.

25) Y. Shioji, S. Ohnishi and I. Nitta, *Ann. Repts. JARRP*, 2, 253 (1960).

*Electron Spin Resonance Hyperfine Spectra of Diphenyl Nitric Oxide**

By Yasuo DEGUCHI**

(Received June 30, 1961)

Many electron spin resonance spectra of organic free radicals have been reported by many investigators[1]. Hoskins[2], for instance, has reported that he could observe the proton hyperfine spectra of diphenyl nitric oxide (DPNO) during the oxidation of diphenylamine. The spectrum showed that it was composed of three groups, each of which consisted of more than thirteen sharp lines. His explanation of this result was that the separation into three groups was caused by the interaction of the nuclear magnetic moment of nitrogen (^{14}N) with that of electron and that each sharp line in any of the three groups occurred from the proton-electron hyperfine interaction. Thus, he obtained 10.3 gauss as the isotropic hyperfine interaction coefficient of ^{14}N and $g=2.0062$. However, he did not explain the proton hyperfine spectra in detail.

We have synthesized DPNO and studied the exchange narrowing effect and the crystal anisotropy effect on the spectra in crystalline states[3]. In this paper we shall report on the results of electron spin resonance measurements in liquid solutions of DPNO.

Experimental

The synthetic method of DPNO has already been described in a previous paper[3],***. The same compounds, in which either the para- or the meta-position in the two benzene rings was deuterized, were also synthesized.

The ESR spectrometer employed here is the new high-resolution apparatus constructed by Professor J. Townsend, of the Department of Physics of Washington University. The microwave length is 3 cm., and the cavity is a reflex cylindrical type. The static magnetic field is generated by a Varian electro-magnet with 12 pole faces. The magnetic field modulation frequency is 100 kc. An aqueous solution of peroxylamine disulfonate[4] was used as a standard of the g-value and the magnetic field. Especially for the precise measurement of the nitrogen and proton isotropic hyperfine splittings, a glass capillary filled with an aqueous solution of peroxylamine disulfonate was attached to a sample tube, a 2.5 mm. (I. D.) $\times$ 200 mm. pyrex glass tube sealed at one end.

Solutions of DPNO were made with various kinds of organic solvents, i. e., cyclohexane, ethyl ether, ethyl alcohol, dimethoxyethane, tetrahydrofurane and mixtures of ethyl alcohol and glycerol[5], either in vacuum-sealed glass tubes[6] or under ordinary pressure atmosphere conditions.

Results and Discussion

The Case of Samples Prepared under the Normal Pressure Atmosphere.—We determined the suitable concentration for obtaining well-resolved hyperfine spectra. Of the different concentrations of cyclohexane solutions, a 0.1 mol./l. solution showed a single absorption line, a 0.01 mol./l. solution began to reveal hyperfine spectra slightly, a 0.001 mol./l. solution had three broad absorption lines due to ^{14}N and a 0.0001 mol./l. solution also had three broad lines but never revealed further splittings due to protons. The measured g-values are 2.0078 for the 0.1 mol./l. solution, 2.0069 for the 0.01 mol./l. solution, 2.0106 for the 0.001 mol./l. solution, and 2.0100 for the 0.0001 mol./l. solution. The isotropic hyperfine splitting coefficient of ^{14}N is 9.55 gauss. In the 0.00001 mol./l. solution, no absorption spectra could be obtained, since at this concentration the noise level of the apparatus was much higher than the signal level. Solutions of ethyl ether, ethyl alcohol, dimethoxyethane and tetrahydrofurane behaved just the same as did the cyclohexane solution. In the case of a mixed solution of ethyl alcohol and glycerol, however, we obtained proton hyperfine spectra similar to those of Hoskins[2]. The remarkable difference between our spectra and Hoskins' is that our spectrum is asymmetric with respect to the center group lines, while Hoskins' is not, as is shown in Fig. 1. In Fig. 1, the absorption lines in the central group

* This work was supported by the U. S. Air Force through the Air Force Office of Scientific Research of the Air Research and Development Command under contract. Reproduction in whole or in part is permitted for any purpose of the U. S. Government.

** Present address : Department of Chemistry, Kyoto University, Sakyo-ku, Kyoto.

1) Cf. J. E. Wertz, *Chem. Revs.*, 55, 828 (1955); D. J. E. Ingram, "Free Radicals", Academic Press (1958).
2) R. Hoskins, *J. Chem. Phys.*, 25, 788 (1956).
3) Y. Deguchi, This Bulletin, 34, 910 (1961).

*** The crystals and solutions of DPNO are rather unstable if they are kept at room temperature, but stable if kept in a refrigerator. We synthesized it about a year ago, but it has stayed stable in a refrigerator since.

4) G. E. Pake, J. Townsend and S. I. Weissman, *Phys. Rev.*, 85, 682 (1952).
5) K. H. Hausser, *Z. Naturforsch.*, 14A, 425 (1959).
6) Y. Deguchi, *J. Chem. Phys.*, 32, 1584 (1960).



Fig. 1. ESR proton hyperfine spectrum of DPNO in a mixed solvent of ethyl alcohol and glycerol with a mixed ratio 3 : 2.

are the sharpest compared with the groups in both sides. Also, each line in the lower field side is sharper than the one in the higher field side. Each group overlaps at the tail of the other.

This phenomenon can be explained according to McConnel[7], as the effect of anisotropic hyperfine interaction on the paramagnetic relaxation in liquid. Further experiments will be made and discussed elsewhere in the near future.

The Case of Samples Prepared in Vacuum.— As reported before[6], diphenylpicrylhydrazyl (DPPH) revealed a well-resolved proton hyperfine structure in the ESR spectrum when its sample was prepared in vaccum. DPNO also shows a more detailed proton hyperfine structure when prepared in vacuo, as is shown in Fig. 2.



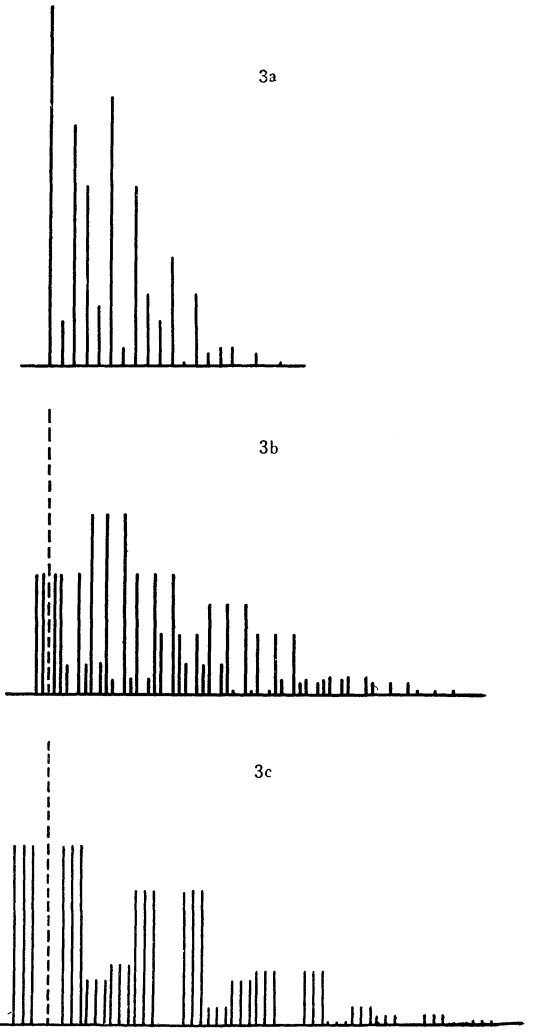
2a 2b

Figs. 2a and 2b. ESR protone hyperfine spectra of DPNO in degassed ethyl alcohol. Fig. 2b. is a half spectrum of the lower magnetic field side group where the concentration of the sample is a little more concentrated than the one in Fig. 2a.

From Fig. 2a, we can not determine exactly the total numbers of lines in each group, because the concentration of the sample is rather small for obtaining the weaker lines in the ends far from the center. Thus, by making a little more concentrated sample, Fig. 2b was obtained. From Figs. 2a and 2b, one could finally find that each group consisted of seventeen lines due to the proton hyperfine interaction.

In other solvents, such as dimethoxyethane, tetrahydrofuran cyclohexane, methylcyclohexane, carbon disulfide, toluene, etc., the same spectra as that of the ethyl alcohol solution have been obtained, except that small variations in the nitrogen and proton isotropic splitting coefficients appear from one solvent to another.

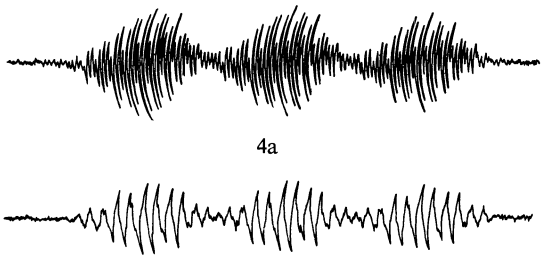
In order to explain these spectra, we assume



Figs. 3a, 3b and 3c. One halves of calculated intensities of the proton hyperfine spectra of DPNO in one of the three groups: (a) Non-deuterized DPNO; (b) Para-deuterized DPNO; (c) Meta-deuterized DPNO.

that the odd electron spin densities at the para- and ortho-position carbon adjacent to the proton in the benzene ring are equal to one another and nearly twice as large as the one at the meta-position. The relative intensities thus calculated are shown in Fig. 3a. The measured isotropic splitting coefficients due to the para- or ortho-position spin density and that of the meta-position are 1.89 gauss ($\Delta H_{p,o}$) and 0.83 gauss (ΔH_m) respectively, i. e., $\Delta H_{p,o} \gtrsim 2\Delta H_m$. To verify further the validity of our assumption, we observed the ESR spectra of deuterized DPNO, in which one of the para- or meta-protons of the benzene rings was substituted for by a deuterium, as is shown in

7) H. M. McConnell, ibid., 25, 709 (1956).



4a

4b

Figs. 4a and 4b. ESR spectra of para- or meta-deuterized DPNO in ethyl alcohol. Fig. 4a is the spectrum of the para-deuterized DPNO and Fig. 4b is the one of the meta-deuterized DPNO.

Figs. 4a and 4b. While each hyperfine line splits further into three lines by the substitution for the proton at the para-position of the deuteron ($I=1$) (cf. Fig. 4a), the appearance of the triple splitting in each line is very weak in the case of meta-deuterized DPNO. These results confirm that the aforementioned assumption about spin density is valid. Figures 3b and 3c are the calculated relative intensity diagrams for para- and meta-deuterized DPNO based upon the aforementioned assumption.

Hereafter we shall apply Kivelson's theory[8] to calculate the line width of each hyperfine line in the spectrum of DPNO. As has been described in the preceding paper[3], we will have

$$\omega=\omega_0-\Delta$$

$$\omega_0=\gamma B_0+\sum_\lambda a_\lambda M_\lambda-\frac{S(S+1)K'}{3}$$

where K' is the same as K as defined in the preceding paper[3] although $A_\lambda=a_\lambda$, a_λ is an isotropic hyperfine splitting factor for the λth nucleus and Δ is a nonsecular shift.

The integrated intensity of each line (I) is

$$I=\frac{NS(S+1)\gamma g_M}{3}$$

where N and g_M are defined as in the preceding paper[3].

Assuming $\tau_c^2 a_\lambda^2 \ll 1$ and $\gamma B_0 \gg a_\lambda$, $T_1'(IS)$ and $T_2'(IS)$ are given by

$$\begin{aligned}T_2'^{-1}(IS)=&\frac{3\tau_c}{20}\sum_\lambda(2S^2+2S+1)\sigma_{\lambda\lambda'}^2\\&\times[\ll J_\lambda(J_\lambda+1)\gg_{M_\lambda}-M_\lambda^2]\\&+\tau_c\sum_\lambda\sum_{\lambda'}\{\sigma_{\lambda\lambda'}^2M_\lambda M_{\lambda'}\}\\&+\frac{4\tau_c}{15}\left\{\frac{(\Delta\gamma B_0)^2}{3}+(\delta\gamma B_0)^2\right\}\\&-\frac{4\tau_c}{15}\sum_\lambda\{\Delta\gamma B_0 b_\lambda M_\lambda+2\delta\gamma B_0(c_\lambda+c_\lambda^*)M_\lambda\}\end{aligned}$$

$$\begin{aligned}T_1'^{-1}(IS)=&\tau_c[1+\omega_0^2\tau_c^2]^{-1}\left\{\frac{1}{15}(\Delta\gamma B_0)^2\right.\\&+\frac{1}{5}(\delta\gamma B_0)^2-\sum_\lambda\left[\frac{1}{5}\Delta\gamma B_0 b_\lambda M_\lambda\right.\\&+\frac{2}{5}\delta\gamma B_0(c_\lambda+c_\lambda^*)M_\lambda\\&+\frac{7}{40}(8S^2+8S-1)\sigma_{\lambda\lambda'}^2[\ll J_\lambda(J_\lambda+1)\gg_{M_\lambda}\\&\left.-M_\lambda^2]\right]+\sum_\lambda\sum_{\lambda'}\frac{3}{4}\sigma_{\lambda\lambda'}^2M_\lambda M_{\lambda'}\left.\right\}\end{aligned}$$

where

$$\sigma_{\lambda\lambda'}=\frac{1}{5}\left[b_\lambda b_{\lambda'}+\frac{8}{3}(c_\lambda^*c_{\lambda'}+c_\lambda c_{\lambda'}^*+d_\lambda^*d_{\lambda'}+d_\lambda d_{\lambda'}^*)\right]$$

If $\delta\gamma=c=d=0$, then

$$\begin{aligned}T_2'^{-1}(IS)=&\frac{3\tau_c}{20}\sum_\lambda(2S^2+2S+1)\\&\times\frac{b_\lambda^2}{5}[\ll J_\lambda(J_\lambda+1)\gg_{M_\lambda}-M_\lambda^2]\\&+\tau_c\sum_\lambda\sum_{\lambda'}\left(\frac{b_\lambda b_{\lambda'}}{5}M_\lambda M_{\lambda'}\right)\\&+\frac{4\tau_c}{45}(\Delta\gamma B_0)^2-\frac{4\tau_c}{15}\sum_\lambda(\Delta\gamma B_0 b_\lambda M_\lambda)\end{aligned}$$

$$\begin{aligned}T_1'^{-1}(IS)=&\tau_c[1+\omega_0^2\tau_c^2]^{-1}\left\{\frac{(\Delta\gamma B_0)^2}{15}\right.\\&-\sum_\lambda\left[\frac{1}{5}\Delta\gamma B_0 b_\lambda M_\lambda\right.\\&+\frac{7}{40}(8S^2+8S-1)\frac{b_\lambda^2}{25}\\&\left.\times[\ll J_\lambda(J_\lambda+1)\gg_{M_\lambda}-M_\lambda^2]\right]\\&\left.+\sum_\lambda\sum_{\lambda'}\frac{3b_\lambda b_{\lambda'}}{100}M_\lambda M_{\lambda'}\right\}\end{aligned}$$

where

$$\ll J_\lambda(J_\lambda+1)\gg_{M_\lambda}=\sum_{I_\lambda=M_\lambda}^{n_\lambda I_\lambda}J_\lambda(J_\lambda+1)\frac{g'_{J_\lambda}-g'_{J_\lambda+1})}{g_M}$$

$$g'_{J_\lambda}=[W(n_\lambda,J_\lambda,I_\lambda)]\prod_\lambda(2I_\lambda+1)^{-n_\lambda}$$

$$g_M=\prod_\lambda W(n_\lambda,J_\lambda,I_\lambda)(2I_\lambda+1)^{-n_\lambda}$$

In the case of diphenyl nitric oxide, we have one nitrogen atom and 6 para- and ortho-protons and 4 meta-protons; i. e.,

$$n_N=1,\quad I_N=1;\quad S=\frac{1}{2}$$

$$n_{p,o}=6,\quad I_{p,o}=\frac{1}{2}$$

$$n_m=4,\quad I_m=\frac{1}{2}$$

8) D. Kivelson, ibid., 33, 1094 (1960).

Also, as assumed in the preceding section, the electron spin density at the para- or ortho-position is about twice as large as that at the meta-position.

In the formula for ω_o, the term $\sum_\lambda a_\lambda M_\lambda$ gives the hyperfine structure in spectra. In our case, we have three different equivalent groups of niclei, i.e., one nitrogen, 6 para- and ortho-protons, and 4 meta-protons. One nitrogen has I_{zN}: $1, 0, -1$; 6 para- and ortho-protons, $I_{zp,o}$: $\pm3, \pm2, \pm1, 0$; 4 meta-protons, I_{zm}: $\pm2, \pm1, 0$. One thus obtains 105 absorption lines, but some of them will be so weak that one can not observe them in the spectra.

It is tedious to calculate the $\ll J_\lambda(J_\lambda+1)\gg_{M_\lambda}$ of all the component lines. Thus we shall calculate only those referred to the three center lines of each group. These lines are given as follows:

1. For $M_N=1$, there exist three different combination of $M_{p,o}$ and M_m, i.e.,

$$\begin{cases} M_{p,o}=0 \\ M_m=2 \end{cases} \quad \begin{cases} M_{p,o}=1 \\ M_m=-2 \end{cases} \quad \begin{cases} M_{p,o}=-1 \\ M_m=2 \end{cases}$$

2. For $M_N=0$ (this corresponds to the center group),

$$\begin{cases} M_{p,o}=0 \\ M_m=0 \end{cases} \quad \begin{cases} M_{p,o}=1 \\ M_m=-2 \end{cases} \quad \begin{cases} M_{p,o}=-1 \\ M_m=2 \end{cases}$$

3. For $M_N=-1$,

$$\begin{cases} M_{p,o}=0 \\ M_m=0 \end{cases} \quad \begin{cases} M_{p,o}=1 \\ M_m=-2 \end{cases} \quad \begin{cases} M_{p,o}=-1 \\ M_m=2 \end{cases}$$

Each combination has its own T_1', T_2' and integrated intensity I, which are given above. In order to evaluate a correlation time (τ_c) for the molecular tumbling, evidently we cannot assume the DPNO molecule as a sphere, but rather must regard it as a prolate ellipsoid. The dimensions thus determined are

$$a=4.84\,\text{Å}$$
$$b=2.10\,\text{Å}$$

where a and b are the longer and the shorter axes. According to Perrin's theory[9],

$$\frac{\tau_a}{\tau_o}=\frac{2(1-q^4)}{\dfrac{3q^2(2-q^2)}{\sqrt{1-q^2}}\ln\left\{\dfrac{1+\sqrt{1-q^2}}{q}\right\}-3q^2}$$

$$\frac{\tau_b}{\tau_o}=\frac{4(1-q^4)}{\dfrac{3q^2(2q^2-1)}{\sqrt{1-q^2}}\ln\left\{\dfrac{1+\sqrt{1-q^2}}{q}\right\}+3}$$

where τ_a: the correlation time for the molecular tumbling around the b-axis. τ_b: the correlation time for the molecular tumbling around the a-axis. τ_o: the correlation time for a hypothetical sphere with a volume equivalent to that of the actual ellipsoid.

$$\tau_o=\frac{4\pi\eta ab^2}{3KT}$$

q: an axial ratio given by

$$b/a$$

η: the viscosity of a solvent in poise, T: absolute temperature (°K).

In the case of ethyl alcohol at $T=293$°K,

$$\eta=1.20\times10^{-2}\ \text{poise}^{10)}$$

Thus we get

$$\tau_a=4.608\times10^{-11}\ \text{sec.}$$
$$\tau_b=4.256\times10^{-11}\ \text{sec.}$$

The numerical values of a_N, $a_{p,o}$, a_m, b_N, $b_{p,o}$, b_m, $\Delta\gamma$ and H_o have been given in the preceding paper[3]. The results thus obtained are tabulated in Table I. As can be seen in Table I, the angular quantum number dependency of the spectra for the center line in each group can be explained by this theory, but the two outside lines next to the center line in each group are one-eighth the intensity of the center lines, while their calculated widths are about five times broader than the center lines. Thus we

Table I

		Half-width at max. slope gauss	
		Calcd.	Obs.
Lower magnetic field side group	$M_N=1$, $M_{p,o}=0$, $M_m=0$	0.152	0.169
	$M_N=1$, $M_{p,o}=1$, $M_m=-2$	0.764	—
	$M_N=1$, $M_{p,o}=-1$, $M_m=2$	0.751	—
Central group	$M_N=0$, $M_{p,o}=0$, $M_m=0$	0.107	0.122
	$M_N=0$, $M_{p,o}=1$, $M_m=-2$	0.408	—
	$M_N=0$, $M_{p,o}=-1$, $M_m=2$	0.553	—
Higher magnetic field side group	$M_N=-1$, $M_{p,o}=0$, $M_m=0$	0.242	0.203
	$M_N=1$, $M_{p,o}=1$, $M_m=-2$	0.823	—
	$M_N=-1$, $M_{p,o}=-1$, $M_m=2$	0.790	—

9) J. Perrin, *J. Phys. Radium.*, (7) 5, 497 (1934).

10) "Handbook of Phys. & Chem.", 39th Ed., Chem. Rubber Publishing Co.

can not expect well-resolved absorption lines. This is the case in the actual spectra.

Effect of a Methyl Group Attached to the Benzene Ring either at the para-, meta- or ortho-Position. — Using bromo-toluene instead of bromo-benzene, these radicals were synthesized by the same procedure as has been described above. Among three methylized radicals, the ESR spectra of the para- or meta-methylized ones show that an attached methyl group adds extra proton hyperfine lines to the original spectra of DPNO, while the ortho-methylized one exhibits a drastic modification in the spectra, as is shown in Fig. 5. Only four broad lines instead of seventeen sharp lines appear in each group. From this spectra, one can conclude that the electron spin densities at the nitrogen and methyl groups are much greater than those at the other ring carbons.

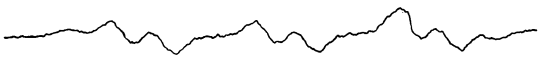


Fig. 5. ESR spectrum of the ortho-methylized DPNO in ethyl alcohol.

In order to clarify this remarkable effect, further investigations, such as optical measurements and ESR measurement of its crystalline state, are now being undertaken.

Effect of Solvents on the Widths of Nitrogen and Proton Hyperfine Splittings. — During the course of the present study, it was found that the widths of nitrogen and proton hyperfine splittings vary from one solvent to other. These results are shown in Fig. 6. In this figure, the magnitudes of the dielectric constants of the solvents were conveniently taken as an abscissa scale. From this diagram, it can be seen that nitrogen and proton isotropic splittings are approximately linearly proportional to the dielectric constants of the solvents. This result can be qualitatively understood if one considers as follows:

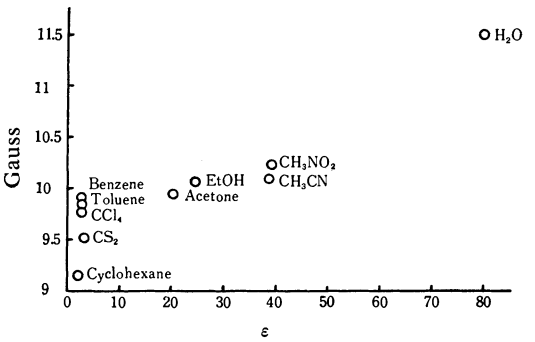


Fig. 6. Dependence of the nitrogen isotropic hyperfine splittings on dielectric constants of various kinds of solvent.

According to the valence bond theory, one will have various kinds of ionic structure besides the covalent bond structure, as is shown in Fig. 7.

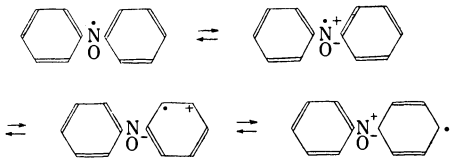


Fig. 7. Various resonance structures of DPNO.

The second structure gives the nitrogen splitting, and the third and fourth structures, the proton splitting. Thus, by the presence of polar solvents, the ionic structures among the above resonant ones will be favored.

In order to put this consideration on a rigorous theoretical basis, a further investigation is now under way.

Summary

Liquid solutions of diphenyl nitric oxide reveal well-resolved proton hyperfine spectra either in mixed solvents of glycerine and ethyl alcohol in a suitable mixed ratio or in vacuum-sealed, degassed solvents.

Assuming odd electron spin densities at the ring carbon atoms and applying Kivelson's theory, one can explain the experimental results. Moreover, the effect on the ESR spectra of the addition of a methyl group to a benzene ring has been reported on.

Finally, the solvent effect on the ESR spectra has been discussed.

The author is much obliged to Professor S. I. Weissman for his helpful discussions and encouragement during the course of this work. He is also indebted to Professor J. Townsend for offering him a chance to use the ESR apparatus. He also appreciates Dr. A. Holtzer's suggestion of the molecular tumbling-correlation time estimation method.

Department of Chemistry
Washington University
St. Louis, Mo., U. S. A.

Physicochemical Studies on Cobalt Salts of Higher Fatty Acids. VII. Effects of Solvents on Cobalt Soaps. Solubilities and Color Changes of Cobalt Soaps in Solvents, and Adsorption of Water Vapor on Cobalt Soaps

By Hirotaro KAMBE*

(Received March 29, 1961)

Cobalt stearates with red and blue colors have been prepared and investigated in the previous papers[1]. Cobalt soaps do not readily dissolve in common solvents when cold, as has been stated in Part V. Boner[2] dissolved cobalt stearate in hot paraffinic oils and observed gelatinization after cooling. He described how cobalt stearate, dissolved in pyridine, made a red complex with the pyridine which decomposed in air on being heated. Lawrence[3] used this complex as a means of the purification of cobalt soaps. Koenig[4] described how cobalt stearate showed solubilities over 1% in chloroform, carbon tetrachloride, liquid paraffin, *n*-heptane, benzene, toluene, amyl alcohol and pyridine, and of about 0.01% in ethyl ether and carbon disulfide. It was stated to be insoluble in methanol, acetone and ethyl acetate.

In preliminary observation, some typical solubility characteristics were observed. Cobalt soaps did not dissolve in water. Because water did not wet them, they floated on its surface. Ethanol did wet them, but they did not show any solubility in it, even if it was hot. If cobalt soaps were immersed in cold ethanol for a long time, they changed purple, as stated in Part III. In benzene, cobalt soaps did not dissolve at room temperatures, but in hot benzene, a blue solution was obtained which appeared silky when it was stirred. A purple jelly was obtained after cooling. In hot toluene, cobalt soaps dissolved considerably, but the colors of the solutions changed to a dirty yellow.

In the present paper, the solubility characteristics and color changes of cobalt soaps in various solvents will be observed. Additionally, the adsorption of water vapor on cobalt soaps will be measured.

Experimental

Materials.—The same cobalt stearates were used as in previous papers[1]. Solvents (cf. Table I) were chemically pure reagents. They were used without special purifications.

Observations on Solubilities and Color Changes.—An amount (usually 10 mg.) of cobalt soap was sealed and shaken with various solvents (usually 5 ml.) in glass tubes. The changes in appearance and color were observed at cold temperatures. Then the solutions were heated in an air bath at 90~100°C for 3~4 hr. and cooled again. They were observed occasionally during these processes.

Adsorption of Water Vapor.—The same quartz spring balance was used as in determining the amount of hydrate water in Part II. The relative humidity (RH) in the atmosphere of the sample was controlled by aqueous solutions of sulfuric acid. Measurements of the amount of adsorbed water, x(g.), were carried out at room temperatures at about 25 and 30°C. The saturated vapor pressure, p_s, was obtained from International Critical Tables. The weight of the sample, m(g.), was 40~100 mg. Specific adsorption, x/m, was calculated and plotted against relative humidity to get an adsorption isotherm.

Results and Discussion

Solubilities.—The solubility characteristics of red dihydrate and blue anhydrate of cobalt stearate were almost identical. Although, in a cold solution, the red soap swelled and suspended more easily in many solvents than blue soap, at higher temperatures the difference of color did not significantly affect the appearance of the soaps. The results of observations on the changes in appearance of red cobalt soaps were tabulated in Table I. Much the same data were obtained for blue soap. The differences in characteristics between these tables were so minor that the latter table was eliminated.

There were several solvents in which cobalt soaps showed considerable solubilities. Among the solvents investigated, pyridine and bromoform were the most effective solvents for cobalt soaps, followed by benzyl alcohol, nitrobenzene, chlorobenzene and aniline.

* Present address: Aeronautical Research Institute, the University of Tokyo, Meguro-ku, Tokyo.

1) H. Kambe, This Bulletin, 34, 1786, 1790, 1794 (1961); 35, 78 (1962); H. Kambe and I. Mita, ibid., 34, 1797 (1961); H. Kambe, T. Ozawa, M. Onoue and S. Igarashi, ibid., 35, 81 (1962).
2) C. J. Boner, *Ind. End. Chem.*, 29, 56 (1937).
3) A. S. C. Lawrence, *Trans. Faraday Soc.*, 34, 669 (1938).
4) A. E. Koenig, *J. Am. Chem. Soc.*, 36, 951 (1914).

TABLE I. SOLUBILITY CHARACTERISTICS OF RED COBALT STEARATE DIHYDRATE IN VARIOUS SOLVENTS*
(10 mg. soap/5 ml. solvent)

Solvent	At room temp.	At 90°C	After cooling
Water	insol. float.	insol. melting	insol. float.
Methanol	insol. cloudy dispers. pink ppt.	sol. yellow soln.	colorless soln. pale pink ppt.
Ethanol	alm. insol. cloudy dispers. purple ppt.	sl. insol. gray susp.	colorless soln. violet ppt.
Butanol	insol. cloudy dispers. purple ppt.	sol. yellow soln.	
Benzyl alcohol	insol. brown ppt.	sol. pink soln.	brown soln. violet ppt.
Phenol	insol. float. dispers.	sol. brown soln.	
Ethylene glycol	alm. insol. float. indispers.	alm. insol. pink soln. ppt.	cloudy dispers.
Diethylene glycol	alm. insol. float. indispers.	insol. pink soln. ppt.	cloudy dispers.
Dioxane	alm. insol. cloudy dispers. red ppt.	sol. yellow soln.	brown soln. black ppt.
Methyl Cellosolve	alm. insol. dispers.	sol. yellow soln.	brown ppt.
Chloroform	insol. float. dispers.	sol. light blue soln.	pink susp.
Bromoform	alm. sol. brown soln.	sol. green soln.	yellow soln.
Carbon tetrachloride	insol. float. dispers.	sol. colorless soln.	colorless jelly
1, 2-Dichloro-ethane	alm. insol. dispers. brown ppt.	alm. sol. brown soln.	brown soln.
Trichloroethylene	alm. insol.	alm. sol.	pink jelly
Acetone	alm. insol. dispers. purple ppt.	insol. white susp.	colorless soln. pink ppt.
Ethyl methyl ketone	insol.	sol. brown soln	yellow soln. ppt.
Isoamyl acetate	alm. insol.	sl. insol. cloudy pink ppt.	red ppt.
n-Butyl acetate	insol.	sol. pink soln.	brown susp.
Ethyl ether	insol.		colorless soln. dark red ppt.
Benzene	insol. dispers. purple ppt.	sol. purple soln.	pink jelly
Toluene	insol. dispers. purple ppt.	sol. dark blue soln.	
p-Xylene	sl. insol. cloudy red ppt.		green soln. black ppt.
Chlorobenzene	sl. insol. dispers.	sol. blue soln.	
Nitrobenzene	sl. insol. dispers.	sl. insol. dark red soln.	
Aniline	sl. insol. float.	sol. yellow susp.	dark red ppt.
Pyridine	alm. sol. pink soln.	sol. violet soln.	yellow soln.
Cyclohexane	insol. purple ppt.		red jelly cloudy
n-Heptane	insol. cloudy purple ppt.		brown jelly cloudy

* sol. : soluble ; insol. : insoluble ; alm. : almost ; sl. : slightly ; ppt. : precipitate ; soln. : solution ; susp. : suspension ; dispers. : dispersible ; indispers. : indispersible ; float. : floating.

Water showed absolutely no influences on cobalt soaps. Acetone was also a relatively indifferent solvent to them. In a hot state, halogen compounds and aromatic hydrocarbons were fairly good solvents for cobalt soaps. Glycols were poor.

When hot solutions in some comparatively good solvents were cooled, jellies were obtained. These solvents were carbon tetrachloride, trichloroethylene, benzene, toluene and chlorobenzene. Sometimes solutions became a dirty yellow or brown in which dark precipitates appeared.

As cobalt soaps did not readily dissolve in common solvents, it was difficult to get a single crystal from these solvents, as has been stated in Part V.

Color Change.—Several types of color change were observed. (i) No change of color was observed in water or in acetone. (ii) The color of red soap turned blue or gained a tinge of blue in ethanol, and violet in benzene. The color of blue soap in these solvents approaches to the color of changed red soap. (iii) The color of blue soap turned pale pink in methanol, and red in pyridine. Red soap also approached these colors in them. (iv) The color changed to a dirty yellow, brown, or green in *n*-butanol, toluene, *p*-xylene, *n*-heptane, dioxane (at first, red), cyclohexane (at first, blue), and in ethyl ether. The absorption spectra of solutions of cobalt stearates in dioxane and in xylene are shown in Fig. 1. Absorption maxima appeared

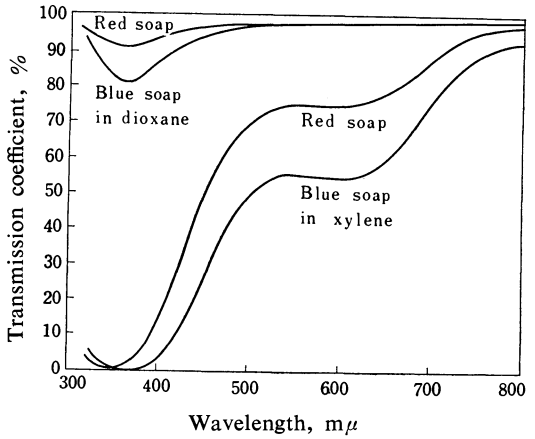


Fig. 1. Absorption spectra of cobalt stearate solutions in xylene and in dioxane.

at 360 mμ. In these systems, the addition of water did not recover soaps of the original color. It is suggested that some change in the electronic configuration of cobalt ion occurred in these solutions. (v) The solution gelatinized after cooling. Purple jelly was obtained in benzene, but dirty yellow or brown jellies grew in toluene, *n*-hexane, *p*-xylene and cyclohexane. These jellies were thixotropic and syneretic and gradually recovered their fluidities for a long time. (vi) In hot pyridine, cobalt stearates dissolved easily, but they soon turned red. Red crystals precipitated on cooling. These were complexes of cobalt soaps with pyridine[2].

In aqueous ethanol the color of blue cobalt soap gradually turned red. The effects of the addition of electrolytes to these systems were examined. Suspensions of red and blue cobalt stearate in mixtures of ethanol with water in 80, 50 and 40 wt.%, with the addition of potassium chloride, potassium nitrate, cobalt chloride and cobalt nitrate, were shaken with a machine at room temperatures. Cobalt stearates in all systems turned completely red after two or three days. Some bluish tint remained in red soaps in systems to which potassium salts had been added without regard to concentrations of ethanol. In other systems red soap did not change its color. In absolute ethanol, red and blue soaps became pale purple in systems with potassium salts, but with cobalt salts the color turned violet.

In benzene, hot solutions of cobalt soaps gelatinized after cooling. Red or blue cobalt soap was sealed in glass tubes with benzene, at various concentrations of 0.05~5.00 wt.%. When they were heated at 100°C for one hour, pale blue solutions were obtained in which some gelatinized mass floated. After subsequent cooling, they gelatinized soon. These processes were repeated three or four times. The appearances of jellies were observed. Below concentration of 0.12 wt.%, the jelly showed a considerable fluidity at 20°C, but above this concentration the system solidified as purple jelly. Red soap in benzene systems with concentrations above 0.28% were heterogeneous and turbid. Blue soap systems were clear and transparent.

When ethanol was added to benzene, the gelatinization was much suppressed. When various amounts of ethanol above 2 vol.% were added, solutions of cobalt stearates in benzene, with a concentration of 0.3%, did not solidify. Purple flocculates grew within the solution. Long after, the color of soap remained a reddish violet in pure benzene, but in other systems soap turned blue completely.

In pyridine red and blue soap dissolved above 10% and reddish violet solutions were obtained. Red crystals of complex precipitated from the solution.

Adsorption of Water Vapor.—The amounts of water adsorbed on red and blue cobalt stearates are shown in Table II and in Fig. 2. Red soap adsorbed much more water than blue soap, but the difference of temperature at

TABLE II. ADSORPTION OF WATER VAPOR ON COBALT STEARATES

Red soap, at 30°C
m=42.3 mg. p_s=31.8 mmHg

RH p/p_s %	Adsorbed amount x mg.	Specific adsorption x/m %
86	1.1	2.6
74	0.5	1.2
63	1.1	2.6
49	0.8	1.9
40	0.5	1.2
29	0.5	1.2
14	0.3	0.7
8	0.1	0.2

Blue soap, at 25°C
m=94.7 mg. p_s=23.8 mmHg

RH p/p_s %	Adsorbed amount x mg.	Specific adsorption x/m %
91	0.9	0.95
77	—	—
59.5	0.4	0.42
37.5	0.1	0.1
16.5	0.1	0.1
2.5	—	—

measurement must also be considered. The forms of the adsorption isotherm are apparently different from each other. The mechanisms of adsorption seem also to be different. Since the accuracy of measurement is insufficient, however, particularly in blue soap, the significance of these results must be minimized.

Summary

The effects of various solvents on cobalt soaps were investigated. The solubility of cobalt soap was low in general. In pyridine and bromoform, it showed a considerable value. In a hot state, several solvents dissolved cobalt soaps fairly well. In some solvents, jellies were obtained on cooling. In other solvents, the color changed to a dirty yellow. Absorption spectra showed that the absorption maxima in these solutions were displaced for a shorter wavelength. This means that a change of the electronic configuration occurred.

Adsorption of water vapor on cobalt soaps was measured. Red dihydrate seemed to adsorb much more water vapor than blue anhydrate.

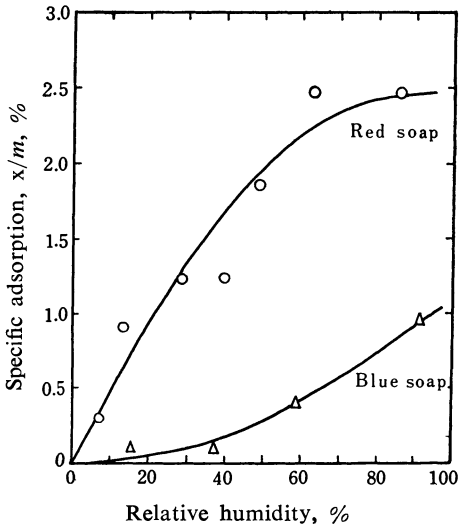


Fig. 2. Adsorption isotherms of water on cobalt stearates.

The author expresses his gratitude to Professor Bunnosuke Yamaguchi for his advice throughout this work, and to Mr. Itaru Mita for his help in the measurement of solubility.

Institute for Science and Technology
the University of Tokyo
Meguro-ku, Tokyo

Physicochemical Studies on Cobalt Salts of Higher Fatty Acids. VIII. Some Rheological Properties of Solutions of Cobalt Soaps. Specific Viscosities and Non-Newtonian Flow

By Hirotaro KAMBE*

(Received March 29, 1961)

It has been shown in the preceding part of this series[1] that cobalt is hard to dissolve in common solvents at room temperatures. It shows relatively higher solubilities in hot aromatic hydrocarbons, but these solutions gelatintize after cooling. The flow properties of these gelatinous solutions are investigated in the present paper. Intrinsic viscosities of red and blue cobalt stearates were obtained from specific viscosities of dilute benzene solutions. Jellies, formed by solutions in benzene, were peptized by adding a small amount of ethanol. It was observed in specific viscosities.

The non-Newtonian flow of concentrated solutions of cobalt soaps in benzene, toluene, xylene and *n*-heptane were measured with capillary viscometers. These solutions, particularly with higher concentrations, were gelatinized, and the capillary was often blocked by a slump of jelly. The jelly was so thixotropic and syneretic that the reproducibility of measurement was poor.

Experimental

Materials.—Cobalt stearates were used as in previous papers. Benzene, toluene, xylene and *n*-heptane, used as solvents, were purified as usual. Soap was mixed with an appropriate amount of solvent and dissolved by shaking while hot. Jellies or viscoelastic solutions were obtained after cooling in the viscometer.

Viscometry. — Specific viscosities of the dilute solution, η_{sp}, at several concentrations, were measured with an Ubbelohde suspended-level viscometer[2]. Intrinsic viscosity, $[\eta]$, was obtained by an extrapolation of the linear plots of reciprocal reduced viscosity, c/η_{sp}, against concentration, c, as applied by Gray and Alexander[3] to solutions of aluminum soap in benzene, using the following formula:

$$\frac{c}{\eta_{sp}}=\frac{1}{[\eta]}-k'c \qquad (1)$$

The non-Newtonian flow of solutions was measured by using a Tsuda[4] or Philippoff[5] viscometer of horizontal capillary with a manostat. Shearing stress $P_R=R\Delta P/2L$ and nominal rate of shear $\dot{e}_R=4Q/\pi R^3 t$ at wall were calculated and plotted as a flow curve; where R and L are radius and length of the capillary respectively, Δp is a pressure difference at both ends of the capillary, and Q is a volume of liquid flowing through the capillary during time t. Kinetic energy corrections are negligible. The dimensions of the capillaries are shown in Table I.

TABLE I. DIMENSIONS OF VISCOMETERS

Type	V cm^3	L cm.	R cm.
Tsuda	1.295	8.0	0.0554
Philippoff A	1.000	11.6	0.025
Philippoff B	1.000	12.1	0.052

Results and Discussion

Specific Viscosity. — Specific viscosities of solutions of red cobalt stearate dihydrate and blue cobalt stearate anhydrate in benzene are

TABLE II. SPECIFIC VISCOSITIES OF COBALT STEARATES IN BENZENE, AT 30°C
$\eta_0=0.563$ cp.

Concn. c g./dl.	Viscosity η cp.	Specific viscosity η_{sp}	Reduced viscosity η_{sp}/c dl./g.	Reciprocal reduced viscosity c/η_{sp} g./dl.
(Red soap)				
0.0431	0.830	0.474	11.0	0.091
0.0294	0.702	0.247	8.40	0.119
0.0220	0.622	0.105	4.77	0.210
0.017	0.606	0.076	4.37	0.229
0.0147	0.599	0.064	4.35	0.230
(Blue soap)				
0.0237	0.629	0.117	4.94	0.202
0.0158	0.612	0.087	5.50	0.182
0.0118	0.606	0.076	6.45	0.155
0.0095	0.577	0.025	2.63	0.380
0.0075	0.575	0.021	2.80	0.357
0.0068	0.569	0.011	1.62	0.617

* Present address: Aeronautical Research Institute, the University of Tokyo, Meguro-ku, Tokyo.

1) H. Kambe, This Bulletin, **34**, 1786, 1790, 1794 (1961); **35**, 78, 265 (1962); H. Kambe and I. Mita, ibid., **34**, 1797 (1661); H. Kambe, T. Ozawa, M. Onoue and S. Igarashi, ibid, **35**, 81 (1962).

2) L. Ubbelohde, *Ind. Eng. Chem., Anal. Ed.*, **9**, 35 (1937).

3) V. R. Gray and A. E. Alexander, *J. Phys. Coll. Chem.*, **53**, 9 (1949).

4) S. Tsuda, *Kolloid-Z.*, **45**, 325 (1928).

5) W. Philippoff, ibid., **75**, 155 (1936).

TABLE III. VISCOSITIES OF COBALT STEARATES IN MIXTURES OF BENZENE AND ETHANOL, AT 20°C

Mixed solvent			Soap solution		
Concn. of ethanol vol. %	Viscosity of solvent η_0 cp.	Concn. of soap c g./dl.	Viscosity of soln. η cp.	Specific viscosity η_{sp}	Reduced viscosity η_{sp}/c dl./g.
(Red soap)					
0	0.620	0.0456	0.969	0.563	11.095
2	0.616	0.0460	0.620	0.0063	0.137
4	0.613	0.0448	0.618	0.0068	0.151
6	0.611	0.0454	0.617	0.0093	0.204
8	0.610	0.0460	0.615	0.0110	0.217
10	0.609	0.0450	0.612	0.0064	0.140
(Blue soap)					
0	0.620	0.0266	0.762	0.229	8.57
2	0.616	0.0290	0.638	0.0369	1.260
4	0.613	0.0264	0.614	0.0024	0.091
6	0.611	0.0266	0.613	0.0016	0.060
8	0.610	0.0272	0.611	0.0027	0.099
10	0.609	0.0264	0.610	0.0023	0.087

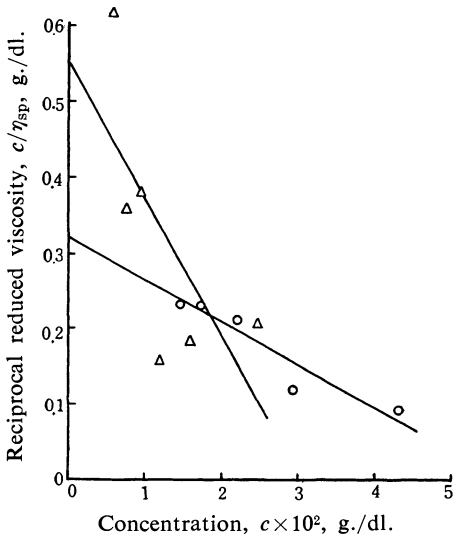


Fig. 1. Concentration dependency of reduced viscosities of solutions of cobalt soap.
○ Red soap △ Blue soap

shown in Table II and are plotted in Fig. 1. Intrinsic viscosity was obtained by applying Eq. 1 to Fig. 1. The coefficients of Eq. 1 were determined by the least-square method. The following formulas were obtained for each soap:

$$c/\eta_{sp}=(0.32\pm0.02)-(0.005\pm0.005)c$$

for red soap.

$$c/\eta_{sp}=(0.55\pm0.10)-(0.18\pm0.07)c$$

for blue soap.

The values of $[\eta]$ are 3.13 for red soap and 1.81 for blue soap. They were larger than the value obtained for aluminum stearate in benzene by Gray and Alexander[3]. This discrepancy is because of the gelatinous character of cobalt soap in benzene.

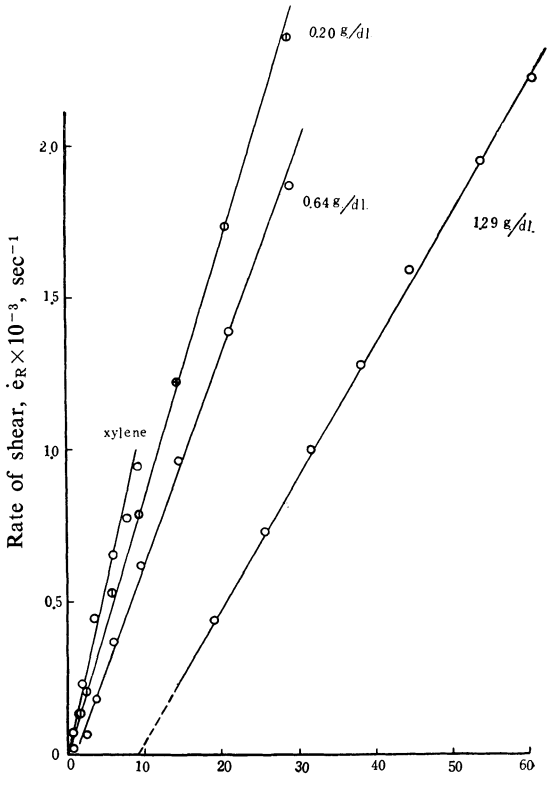


Fig. 2. Flow curves of solutions of red cobalt stearate in xylene, at 20°C.

Specific viscosities of cobalt stearates in mixtures of benzene and ethanol are shown in Table III. At a concentration of 0.045 g./dl. for red soap and 0.036 g./dl. for blue soap, the viscosity of the solution is markedly lowered by the addition of a little ethanol. The viscosity of a solution in a mixed solvent containing ethanol above 2% by volume is essentially the same as that of the mixed solvent itself. Additions of ethanol prevent the gelatinization of the system, and the solubility of soap is so much suppressed that the cobalt soap is almost removed from the solution by being deposited on the wall of the vessel.

Non-Newtonian Flow. — Solutions of cobalt stearate in xylene are dark violet at boiling, but solidify to jellies after cooling. Below concentrations of 2.0 g./dl., the solution is slightly fluid, and below 1.0 g./dl., it is so thixotropic that it increases its fluidity when it was shaken.

The viscosities of these solutions at concentrations of 1.29, 0.62 and 0.20 g./dl. were measured with a Tsuda viscometer at a range of rate of shear, as shown in Fig. 2, and the apparent viscosities, calculated from $\eta_{app}=p_R/\dot{e}_R$, are plotted in Fig. 3 against rate of shear. In Fig. 2, a flow curve of the solution at 1.29

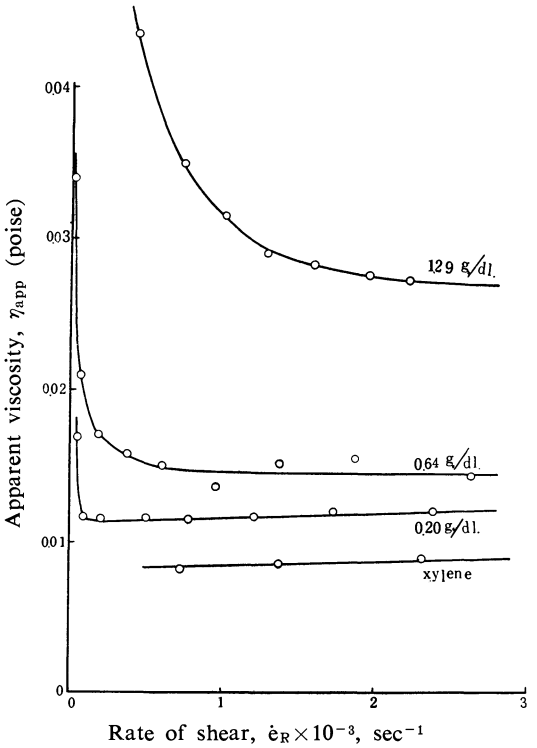


Fig. 3. Shear-rate dependency of apparent viscosity of solutions of red cobalt stearate in xylene, at 20°C.

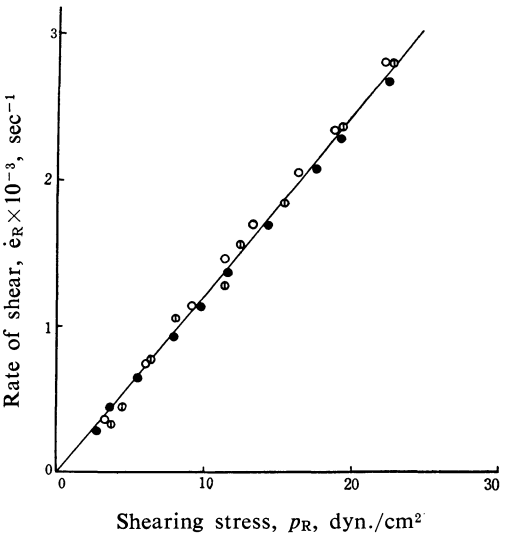


Fig. 4. Flow curve of solutions of cobalt stearate in benzene, at 30°C.
○ 0.020 g./dl. ⦶ 0.043 g./dl.
● 0.097 g./dl.

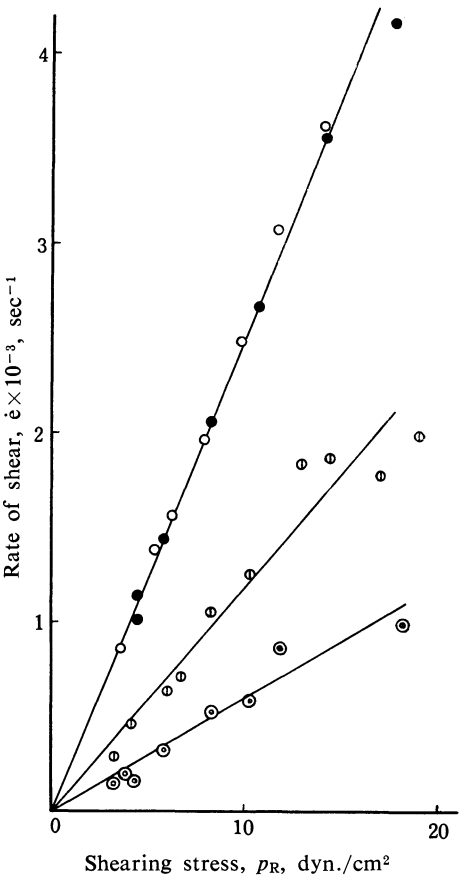


Fig. 5. Flow curves of solutions of cobalt stearate in *n*-heptane and in toluene.
In *n*-heptane ○ 0.057 g./dl. ● 0.17 g./dl.
In toluene ⦶ 0.08 g./dl. ◎ 0.12 g./dl.

g./dl. shows a typical form of the Bingham plastic flow, with a yield value of about 8.5 dyn./cm^2. At other concentrations, there appears no yield value. But in Fig. 3, it is evident that they also show structural viscosity at a low rate of shear range, which does not appear clearly in Fig. 2.

Non-Newtonian behaviors of benzene solutions, with concentrations of 0.097, 0.043 and 0.02 g./dl. at 30°C, were measured with Philippoff viscometers and are shown in Fig. 4. These solutions are blue when hot, but solidify after cooling to pink jellies. These jellies are viscoelastic, thixotropic and highly syneretic. Owing to their insufficient strength, they are easily crushed to pieces and their flow properties are poorly reproducible.

The flow curves of these systems are consistent with each other in this range of concentrations. It is apparently a Newtonian flow. The value of its apparent viscosity is obtained from Fig. 4 as 0.82 cp., which is not markedly different from that of pure benzene. In this case it is the viscosity of a saturated solution of a small concentration that is being measured.

Flow curves in *n*-heptane, shown in Fig. 5 at concentrations of 0.057 and 0.17 g./dl., are almost consistent with each other, as are benzene solutions. However, the flow curves of solutions in toluene, shown in the same figure at 0.08 and 0.12 g./dl., are considerably separated from each other. The apparent viscosity of the toluene solution at 0.12 g./dl. is considerably htgher than the other. Since this solution is most easily gelatinized, the capillary tube of viscometer was often blocked by a piece of gel in the solution. The low fluidity of xylene solution at a high concentration may be caused by such blockage.

The flow curves of benzene solutions at 0.152 g./dl. were measured with different capillaries in which R is 0.25 and 0.52 mm., as shown in Fig. 6. The flow curve must be principally unique to a material. The inconsistency of flow curves obtained with different bores might be caused by the slippage of the solution. In this case, the curve obtained with a large bore would be expected to show a large viscosity[6], and this holds true in Fig. 6.

Thixotropic effects often appeared in these systems. However, sometimes an antithixotropic hysteresis also appeared, as shown in Fig. 7. In this system, the viscosily becomes larger in the down-curve than in the up-curve. The origin of this behavior was not clarified, but blockage by gel is a conceivable cause.

6) M. Reiner, "Deformation and Flow", H. K. Lewis, London (1949), Chap. VIII.

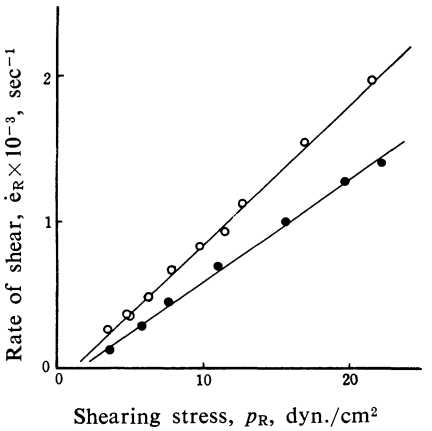


Fig. 6. Slip effect observed in the solution of cobalt stearate in benzene (0.152 g./dl.), at 20°C.

	Capillary	R, mm.
○	A	0.25
●	B	0.52

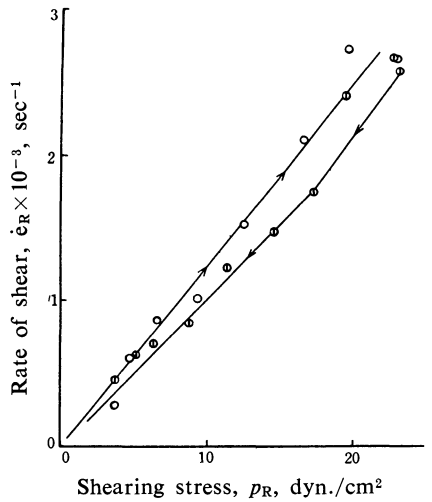


Fig. 7. Antithixotropic hysteresis in flow curve of a solution of cobalt stearate in benzene (0.17 g./dl.), at 20°C.
○ Up-curve ⓘ Down-curve

Summary

The specific viscosity of dilute solution of cobalt stearate in benzene has been measured. Intrinsic viscosities are 3.13 for red soap and 1.81 for blue soap. The specific viscosity of benzene solution is decreased markedly by the addition of a small amount of ethanol, owing to the subsequent decrease of solubility.

The non-Newtonian flow behavior of solutions in xylene, benzene, *n*-heptane and toluene are shown. At higher concentrations, in particular in xylene, these solutions are Bingham plastic. In benzene and *n*-heptane,

flow curves with different concentrations are consistent with a flow curve of Newtonian behavior, which corresponds to that of a saturated solution in benzene. In toluene, flow curves are scattered, possibly due to the blockage of the capillary by a piece of gel.

Different flow curves are sometimes obtained with capillaries of different bores, owing to slippage at the wall. An antithixotropic flow curve was obtained in some solutions.

The author expresses his gratitude to Professor Bunnosuke Yamaguchi for his advice throughout this work, and to Messrs. Minoru Kawano and Masamichi Sato for their help in the experiments.

Institute for Science and Technology
The University of Tokyo
Meguro-ku, Tokyo

The Systematic Analysis of Silicate Rocks using Ion Exchange Resin

By Yasue Ôki*, Shôhachirô Ôki** and Hidekata Shibata

(Received June 5, 1961)

The many varieties of rock-forming-elements have necessitated the repetition of cycles of absorption and elution, which requires much time and effots for the analysis of silicate rocks using ion exchange resin[1,2]. In order to analyze many samples of ordinary silicate rocks, the present authors have developed a rapid and simple method of analysis using an ion exchange column and a solvent extraction technique. A complete analysis of an ordinary rock or silicate mineral can be carried out in only 3 days by this method.

Experimental

Chemicals and Ion Exchange Resin.—Amberlite IR-120 in 100~150 mesh was employed. The column was 18 cm. long and 1 cm. in diameter. The flow rate was 1 ml. per minute. Fractions were collected every 20 ml.

Constant boiling hydrochloric acid was used as 6 N acid.

Guaranteed-grade chemicals and distilled water were used.

Procedure.—*Decomposition.*—The analytical procedure is schematically illustrated in Fig. 1.

Weigh 100 mg. of the fine powder of the rock sample into a platinum dish, then add a few milliliter of water and dilute hydrofluoric acid. Mix and heat the dish on a sand bath, carefully at first, then more strongly, until fumes of sulfuric acid are given off. Cool, wash the side of the dish with a little water, and add 2 ml. of 1 : 1 sulfuric acid and 5 ml. of hydrofluoric acid. Evaporate again to dryness. Add 20 ml. of 6 N hydrochloric acid and warm until all soluble materials have been taken into solution. Remove the solution into a quartz dish. Cover with a watch glass, add 3 ml. of 3% hydrogen peroxide, and boil gently for a minute or two. After washing the watch glass with a little water, evaporate the solution to less than 10 ml.

Extraction Separation of Iron.—Cool the solution and transfer it to a 50 ml. separatory funnel. Make the solution less than 20 ml. and adjust the concentration of hydrochloric acid to 6 N hydrochloric acid. Shake thoroughly for two minutes. Allow the layers to settle and then separate the two layers. Repeat the extraction twice, and collect the ether layer containing iron in another separatory funnel. Strip the ferric iron into 10 ml. of water. Repeat stripping with 5 ml. of water. Transfer the aqueous layer into a 200 ml. Erlenmeyer flask and add 3 ml. of 6 N hydrochloric acid and 50 ml. of water. After gently boiling the aqueous solution to expel the ether, determine the total iron by the Zimmermann-Reinhard method.

Chromatographic Separation of Elements.—Evaporate the sample solution from which iron had been removed by extraction nearly to dryness (1~2 ml.). Care should be taken not to evaporate the contents; otherwise, titanium will be lost as insoluble materials to water. Add 20 ml. of water and pass through the column.

Pass 160 and 150 ml. of 0.4 N hydrochloric acid through the column to elute the sodium and potassium successively. Pass another 10 ml. of 8 N sulfuric acid for the detection of titanium by the hydrogen peroxide-sulfuric acid method. When no titanium is present, add the fraction to the effluent containing potassium and determine the sodium and potassium by flame photometry.

* Present address: Hot Spring Research Institute of Kanagawa Prefecture, Odawara.

** Present address: Department of Chemistry, Faculty of Science, Tohoku University, Sendai.

1) J. Yoshimura and H. Waki, *Japan Analyst*, **6**, 362 (1957).

2) E. Minami, *J. Chem. Soc. Japan, Pure Chem. Sec.* (*Nippon Kagaku Zasshi*), **74**, 740 (1953).

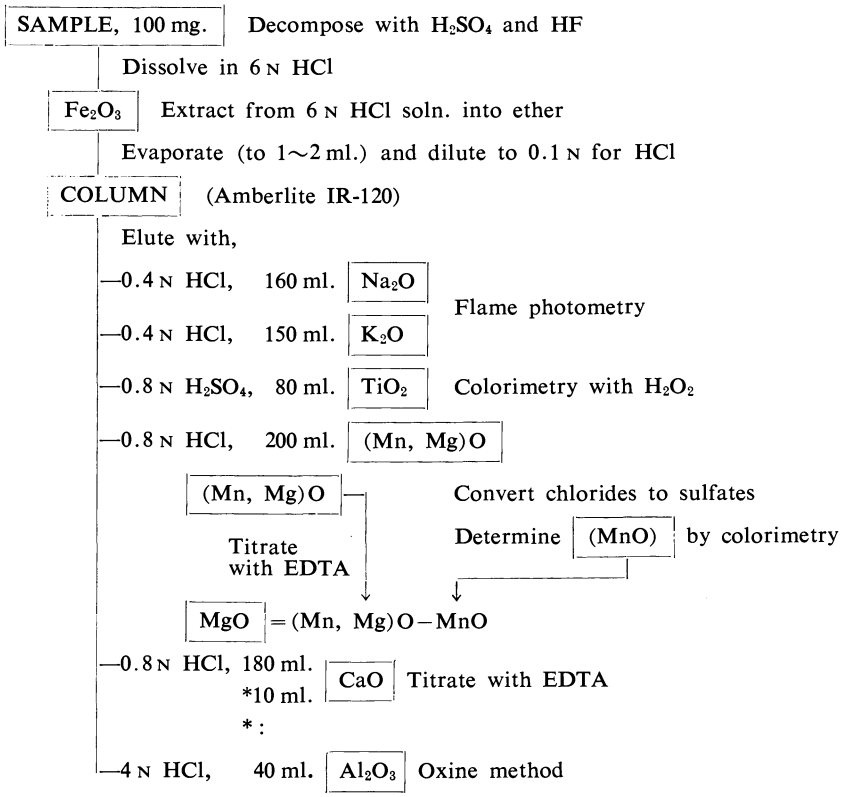


Fig. 1. The scheme of the analytical procedure.

* Detect Al with alizaline-S.

Table I. Ionic radius of rock forming elements

Element	Na	K	Ti(IV)	Mg	Fe(II)	Mn(II)	Ca	Fe(III)	Al
Ionic radius, Å[4].	0.98	1.33	0.68	0.78	0.83	0.91	1.06	0.67	0.57

Liberate the titanium with 70 ml. of 0.8 N sulfuric acid. Add 10 ml. of 1 : 1 sulfuric acid and 5 ml. of 3% hydrogen peroxide to the effluent and dilute the solution to 100 ml. in a volumetric flask. Determine the titanium by measuring the transmittancy of the solution at 420~430 mμ.

Pass 200 ml. of 0.8 N hydrochloric acid to elute the magnesium and manganese. Divide this effluent into two parts, and with the one part titrate the mixture of magnesium and manganese by the EDTA method. To the other part of the effluent, adding a few drops of dilute sulfuric acid to convert the chlorides into sulfates, evaporate it nearly to dryness. Determine the manganese colorimetrically by the permanganate method.

Elute the calcium by the 0.8 N hydrochloric acid. Test the absence of calcium in the first 40 ml. fraction. To make sure, pass fractionally 80, 40 and 20 ml. of 0.8 N hydrochloric acid. Determine the calcium for each fraction by the EDTA (Mg-EDTA) method. Ditect the aluminum with alizaline-S in each following 10 ml. fraction. When no aluminum is present, titrate the calcium.

Elute the aluminum with 40 ml. of 4 N hydrochloric acid. Evaporate the effluent nearly to dryness, and add 30 ml. of water. Warm at 70°C and add an excess of 8-hydroxyquinoline, and determine the aluminum by gravimetry.

Determination of Silica and Phosphorus.—Determine the silica by the ordinary gravimetric method by sodium carbonate fusion.

To determine phosphorus, take out one portion of the filtrate. The solution will conveniently contain less than 10 p. p. m. of phosphorus. Dilute with water, and pass through the column. Pass 50 ml. of 0.1 N hydrochloric acid to liberate the phosphorus completely. Evaporate the effluent nearly to dryness, and determine the phosphorus colorimetrically by the heteropoly-blue-method.

Discussion

Until recently, for the total analysis of a silicate rock, a long column or a set of columns consisting of two or more of them has been required. Aiming at simplicity and rapidity, the present authors adopted a short column (18 cm. long and 1 cm. in diameter) and constant-boiling hydrochloric acid as 6 N acid.

Titanium which is eluted with 0.8 N sulfuric acid as in Fig. 2 could also be eluted with 0.8 N hydrochloric acid. In this case, 0.8 N sulfuric acid is preferable for the colorimetric determination of titanium with hydrogen peroxide.

Following Sweet et al., a long column was used for the separation of the sodium and potassium with 0.7 N hydrochloric acid[3]. The present authors obtained good results with 0.4 N hydrochloric acid as shown in Fig. 2 with

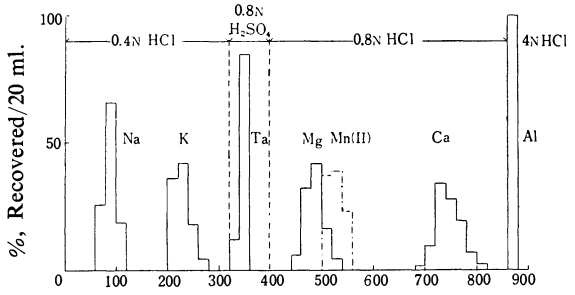


Fig. 2. Chromatographic separation of rock forming elements.

such a short column. Hydrochloric acid over 0.6 N causes the cross contamination of sodium (not shown).

Except for titanium, the order of elution is proved to be the order of increase in valence, and at constant valence, the order of increase in ionic radious (Table I).

Magnesium(II) and iron(II) and manganese-(II) are eluted with 0.8 N hydrochloric acid in almost the same position, as is shown in Fig. 2. The ionic radii of these ions are 0.78 for magnesium(II), 0.83 for manganese(II), and 0.91 Å for iron(II) respectively[4]. The similar size of the ionic radii of these ions inevitably causes the cross contamination of them with

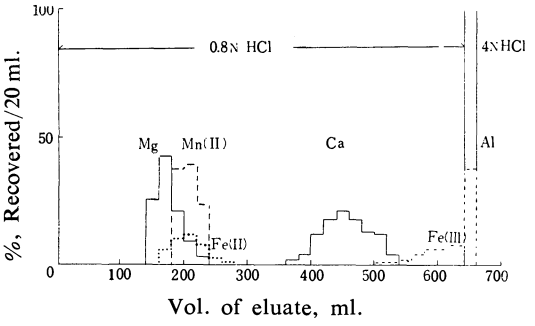


Fig. 3. Contamination of iron.

3) R. C. Sweet, W. Rieman, III, and J. Beukenkamp, *Anal. Chem.*, **24**, 952 (1952).
4) V. M. Goldschmidt, *Geochemische Verteilungsgesetze der Elemente*, **8**, 69 (1926).

Table II. Examples of analyses of standard samples

	Taken, mg.	Found, mg. 1	2	3
TiO_2	0.38	0.35	0.35	0.40
Al_2O_3	20.55	20.12	20.43	20.43
Fe_2O_3	5.93	5.85	5.88	5.87
MgO	2.03	2.00	2.10	2.08
MnO	0.20	0.19	0.22	n.d.
CaO	2.05	2.09	2.06	2.08
Na_2O	5.00	4.90	5.10	5.15
K_2O	5.00	4.80	4.72	4.90

Table III. The practical applications to a silicate rock

	Run 1 mg.	2 mg.	3 mg.	4 mg.
SiO_2	58.52			
TiO_2	0.91	0.90	0.91	0.90
Al_2O_3	16.40	16.35	16.75	16.31
Fe_2O_3	5.75	5.60	5.61	5.60
MnO	0.11	0.11	0.08	0.11
MgO	3.08	3.07	3.06	3.02
CaO	6.03	5.87	5.80	5.79
Na_2O	2.85	2.80	2.94	2.88
K_2O	2.33	2.44	2.41	2.33
H_2O	3.14			
H_2O	0.93			
P_2O_5	0.14			
Total	100.14			

Hypersthene andesite from Dogamori, Mt. Ishizuti, Ehime Prefecture (Collected by K. Horikoshi, Sp. No. 443). Note: FeO is calculated as Fe_2O_3. Analyst: K. Horikoshi, Y. Ôki.

such a short column. This disadvantage was overcome by the extraction of iron with ether before the chromatographic separation and by the respective determination of magnesium and manganese, as is shown in Fig. 1.

Aluminum and iron(III) are also eluted at the same time with 0.8 N hydrochloric acid (Fig. 3). This problem, however can be overcome by the extraction of the iron beforehand.

Titanium(IV) is hydrolyzed in dilute mineral acids to the titanyl ion. Accordingly, titanium should be ranked among the divalent ions.

Applicaton of this procedure was justified with the standard solution containing similar amounts of sodium, potassium, calcium, magnesium, manganese, iron, titanium and aluminum in 100~150 mg. of the ordinary igneous rocks (Table II). The practical applications of this method gave satisfactory results, which are summarized in Table III. A complete analysis of an ordinary rock sample can be carried out in only 3 days.

Summary

An accurate and rapid systematic analysis of ordinary silicate rocks was studied with a column of an ion exchange resin (Amberlite IR-120). A powdered rock sample was decomposed by the usual method of Berzelius. Iron was extracted from 6 N hydrochloric acid solution into ether before chromatographic separation Metal ions absorbed on the column are eluted as follows: With 0.4 N HCl Na and K, with 0.8 N H_2SO_4 Ti(IV), with 0.8 N HCl Mg, Mn(II), and Ca, and with 4 N HCl Al are eluted successively. A complete analysis of an ordinary rock sample can be carried out in only 3 days by this method.

The authors wish to express their gratitude to Dr. Shôhei Tamura of the Institute for Solid State Physics, the University of Tokyo, for his helpful suggestions. Thanks are also due to Mr. Yutaro Sakakibara of Tokyo University of Education and Assistant Professor Kazue Horikoshi of Ehime University, for their great help. A part of the expense of the study was defrayed by a grant-in-aid for science research of the Ministry of Education.

Geological and Mineralogical Institute
Faculty of Science
Tokyo University of Education
Otsuka, Tokyo

Infrared Spectra of Succinimide and Maleimide in the Crystalline State

By Toyozo UNO and Katsunosuke MACHIDA

(Received July 18, 1961)

Although the infrared spectra of succinimide[1-4] and maleimide[5,6] have been discussed in many papers, no investigation concerning the spectral change on deuteration has been made for these compounds. In a series of studies on the infrared spectra of acyclic imides[7-10], we have given assignments to the characteristic frequencies of the trans-trans -CONHCO- group. In contrast with the case of acyclic imides, the -CONHCO- group in cyclic imides is expected to be nearly in the cis-cis configuration. Under these circumstances, the present paper deals with succinimide and maleimide with a view of discussing the characteristic frequencies of the cis-cis -CONH·CO- group. The infrared spectra of both the undeuterated and the *N*-deuterated species of these compounds in the crystalline state have been measured in the region 4000 to 400 cm^{-1}, and several bands have been found to result from the vibrations of the -CONHCO- group. The spectral change on the addition of potassium iodide has also been examined for succinimide and succinimide-*d*.

Results and Discussion

Molecular Structure and Infrared Spectra.— By X-ray diffraction study, the molecular structure of succinimide in the crystalline state has been established to be planar except for the positions of the hydrogen atoms[11]. Furthermore, the sum of the three interbond angles around the nitrogen atom has been calculated to be 358°. Thus, in the following discussions, the cis-cis configuration of the -CONHCO- group will be adopted as a good approximation for succinimide. Although the molecular structure of maleimide has not been determined crystallographically, it may be reasonable to assume that the -CONHCO- group of this molecule in the crystalline state is also nearly in the cis-cis configuration.

Thus, the most symmetric arrangement of atoms in the molecule affords the point group C_{2v}, although the actual molecules may be of a somewhat lower symmetry. In fact, according to Mason[11] and Mirone[5], the crystals of succinimide and of maleimide consist of cyclic dimers, each of which involves two equivalent hydrogen bonds, so a molecule contains botb

1) H. M. Randall, R. G. Fowler, N. Fuson and J. R. Dangle, "Infrared Determination of Organic Structures", D. Van Nostrand, New York (1949).
2) H. Lenormant, *Bull. soc. chim. France*, (5) **15**, 33 (1948).
3) J. Chouteau, ibid., (5) **20**, 1148 (1953).
4) A. W. Baker, *J. Phys. Chem.*, **61**, 453 (1957).
5) P. Chiorboli and P. Mirone, *Ann. chim. (Rome)*, **42**, 681 (1952).
6) P. Mirone, ibid., **46**, 39 (1956).
7) T. Uno and K. Machida, This Bulletin, **34**, 545 (1961).
8) T. Uno and K. Machida, ibid., **34**, 551 (1961).
9) T. Uno and K. Machida, ibid., **34**, 821 (1961).
10) T. Uno, K. Machida and I. Hamanaka, ibid., **34**, 1448 (1961).
11) R. Mason, *Acta Cryst.*, **9**, 405 (1956).

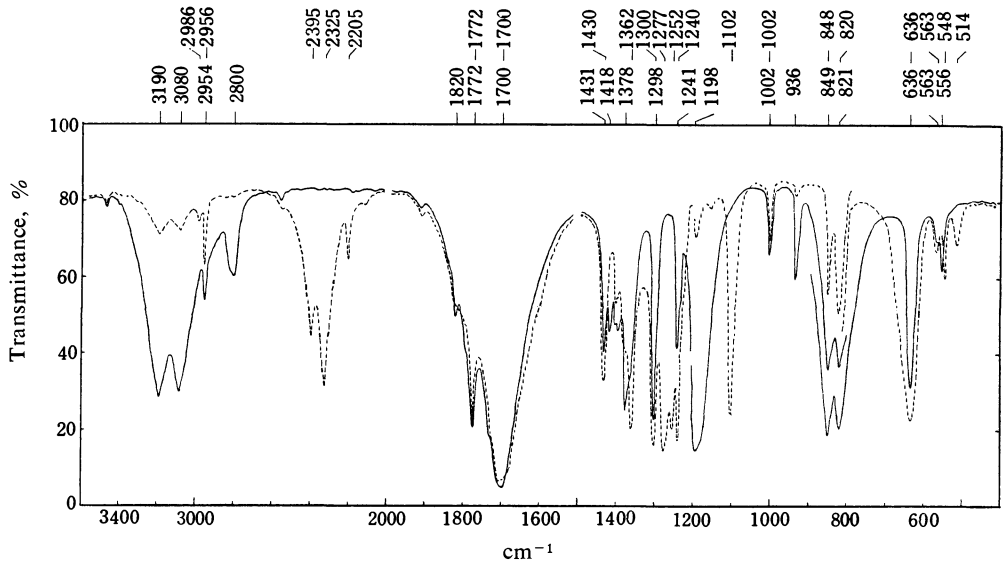


Fig. 1.* Infrared spectra of succinimide (solid line) and succinimide-*d* (broken line).
* (3600～2000 cm^{-1} and 1500～1200 cm^{-1}) hexachlorobutadiene pastes; (2000～1500 cm^{-1} and 1200～400 cm^{-1}) Nujol pastes.

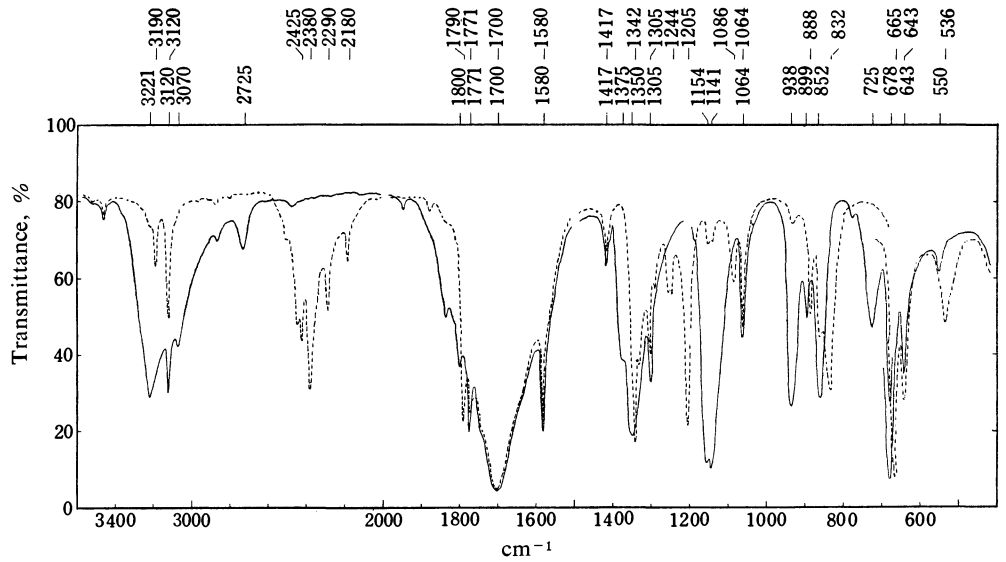


Fig. 2.* Infrared spectra of maleimide (solid line) and maleimide-*d* (broken line).
* (3600～2000 cm^{-1} and 1500～1200 cm^{-1}) hexachlorobutadiene pastes; (2000～1500 cm^{-1} and 1200～400 cm^{-1}) Nujol pastes.

bonded and free C=O bonds. This means both that the two C=O bonds in the –CONHCO– group are not equivalent to each other in the crystalline state and that the molecular symmetry of these compounds deviates appreciably from C_{2v}. This deviation from C_{2v} may or may not affect the feature of an absorption band according to the nature of vibration related to the band under consideration. The infrared spectra of succinimide and succinimide-*d* are shown in Fig. 1, while those of maleimide and maleimide-*d* are shown in Fig. 2. Table I shows the characteristic frequencies of succinimide and succinimide-*d*, together with their assignments. Similarly, Table II is concerned with maleimide and maleimide-*d*. The non-characteristic frequencies of these compounds are listed in Tables IV and V. In the region below 1100 cm^{-1}, the infrared spectrum of maleimide in the crystalline state measured in

TABLE I. THE CHARACTERISTIC FREQUENCIES OF SUCCINIMIDE AND SUCCINIMIDE-*d* (in cm^{-1})*1

Undeut. compd.	*N*-Deut. compd.	Assignments*2	Symmetry*3 species
3190 s, br.*4		ν_{N-H}	
3080 s, br.		1700+1418	
2800 w		1418+1378	
	2395 w	1277+1102	
	2325 s	ν_{N-D}	
	2205 w	1102×2	
1772 m	1772 m	$\nu_{C=O}$ (Imide I) free	
1700 vs, br.	1700 vs, br.	$\nu_{C=O}$ (Imide I) bonded	
1418 m		$\delta_{N-H}+\nu_{C-N-C}$ (antisym)	A′
1378 s		ν_{C-N-C} (sym)	
	1362 s	ν_{C-N-C} (sym)	
	1277 s	ν_{C-N-C} (antisym)	
1198 s		$\delta_{N-H}+\nu_{C-N-C}$ (antisym)	
	1102 s	δ_{N-D}+skeletal	
936 m		Skeletal*5	
	820 m	δ_{N-D}+skeletal	
636 m	636 m, br.	$\delta_{C=O}$ (Imide IV)	
849 s		π_{N-H} (Imide V)	
	(636)*6	π_{N-D} (Imide V′)	A″
556 w		$\pi_{C=O}$ (Imide VI)	
	548 w	$\pi_{C=O}$ (Imide VI′)	

TABLE II. THE CHARACTERISTIC FREQUENCIES OF MALEIMIDE AND MALEIMIDE-*d* (in cm^{-1})*1

Undeut. compd.	*N*-Deut. compd.	Assignments*2	Symmetry*3 species
3221 s, br.*4		ν_{N-H}	
3070 sh		1700+1375	
2725 w		1375+1350	
	2425 w	1342+1086 or 1205×2	
	2380 s	ν_{N-D}	
	2290 w	1205+1086	
	2180 w	1086×2	
1771 m	1771 m	$\nu_{C=O}$ (Imide I) free	
1700 vs, br.	1700 vs, br.	$\nu_{C=O}$ (Imide I) bonded	
1375 sh		$\delta_{N-H}+\nu_{C-N-C}$ (antisym)	A′
1350 s, br.		ν_{C-N-C} (sym)	
	1342 s	ν_{C-N-C} (sym)	
	1205 s	ν_{C-N-C} (antisym)	
1154, 1141 s, db.		$\delta_{N-H}+\nu_{C-N-C}$ (antisym)	
	1086 w	δ_{N-D}+skeletal	
938 s		Skeletal*5	
	832 s	δ_{N-D}+skeletal	
643 m	643 m	$\delta_{C=O}$ (Imide IV)	
725 m, br.		π_{N-H} (Imide V)	
	536 w, br.	π_{N-D} (Imide V′)	A″
550 w		$\pi_{C=O}$ (Imide VI)	

*1 The combination and the overtone frequencies above 2000 cm^{-1} are also listed here.
*2 Greek letters denote the following vibrational modes: ν, stretching; δ, in-plane deformation; π, out-of-plane deformation.
*3 The symmetry species are based on the point group C_s obtained by eliminating the C_2 axis from C_{2v}.
*4 Abbreviations indicating the absorption intensities and the band shapes are as follows: vs, very strong; s, strong; m, medium; w, weak; sh, shoulder; br., broad; db., doublet.
*5 This frequency is listed here so that the behavior on deuteration may be indicated explicitly.
*6 Parentheses show the overlapped frequencies.

the present study is somewhat different from that reported by Chiorboli and Mirone[5]. Thus, their interpretation of the absorption bands below 1100 cm^{-1} is not consistent with the results discussed below.

The In-plane Characteristic Frequencies Below 2000 cm^{-1}. — For both succinimide[1,2] and maleimide[5], the strongest band near 1700 cm^{-1} and the medium band near 1770 cm^{-1} have been assigned to the bonded and the free C=O stretching vibration respectively. Although there remains a question regarding how far the vibrational coupling contributes to the separation (ca. 70 cm^{-1}) between the two C=O stretching frequencies, no attempt will be made to discuss this problem further. The following discussion will be focussed on the absorption frequencies sensitive to the azimutal angles around the C–N bonds of the –CONHCO– group. In this respect, it is interesting to compare the infrared spectra of these cyclic imides with those of the acyclic imides reported in preceding papers[7,8]. A similarity in the characteristic bands between the trans-trans –CONHCO– and the trans –CONH– group has already been pointed out[8]. Thus, the spectral changes on deuteration for the cis-cis –CONH–CO– group may be expected to be analogous with those for the cis –CONH– group. The normal coordinate analysis for the cis *N*-methylacetamide[12] has shown that the coupling between the N–H in-plane deformation and the C–N stretching vibration is less significant for the cis –CONH– group than for the trans –CONH– group. This difference in the coupling results in the characteristic frequencies of the cis –CONH– group being markedly different from those of the trans –CONH– group. The most important difference is that the former does not show the amide II band which has been well established for the latter in the region near 1550 cm^{-1}. That a similar situation holds also for the –CONHCO– group is confirmed by the fact that neither succinimide nor maleimide shows any band in the region 1600 to 1450 cm^{-1}, whereas the trans-trans and the trans-cis –CONHCO– group show the strong imide II band which disappears on deuteration[7,8]. Instead, succinimide and maleimide show a band in the region 1380 to 1340 cm^{-1} which undergoes a low-frequency shift by 8~16 cm^{-1} on deuteration. A similar spectral change on deuteration has been reported for monosubstituted amides containing the cis –CONH– group[12]. As a consequence of these spectral features, the cis-cis –CONHCO– group is expected to show two fundamentals due to the C–N–C stretching vibrations in the region 1500 to 1000 cm^{-1}. Since it is quite probable that a marked coupling occurs among the stretching vibrations of adjacent bonds with similar bond orders, one of these vibrations may be more symmetric or less antisymmetric in nature than the other vibration. Analogy with the cis –CONH– group suggests that the band in the region 1380 to 1340 cm^{-1} observed for both the undeuterated and the *N*-deuterated species of succinimide and maleimide results essentially from the symmetric C–N–C stretching vibration. On the other hand, the antisymmetric C–N–C stretching vibration of the undeuterated species seems to be involved in an appreciable coupling with the N–H in-plane deformation vibration. This is suggested from the fact that two absorptions, which disappear on deuteration, are observed in the region 1450 to 1100 cm^{-1} for both of these cyclic imides. With respect to succinimide, these are the medium but well-resolved band at 1418 cm^{-1} and the strong and broad band near 1200 cm^{-1}. The high- and low-frequency counterparts of maleimide are observed at 1375 cm^{-1} as a shoulder of the broad symmetric C–N–C stretching band and near 1150 cm^{-1} as a strong doublet (1154 and 1141 cm^{-1}), respectively. These bands are considered to result from coupling between the N–H in-plane deformation and the antisymmetric C–N–C stretching vibration. Although the high-frequency bands are not so strong, the assignment to an in-plane vibration within the –CONHCO– group is confirmed, as will be discussed later, by an examination of the combination tone near the N–H stretching frequency. It is expected that the *N*-deuterated species will show a band contributed mainly from the antisymmetric C–N–C stretching vibration which is involved in the coupling for the undeuterated species. The bands at 1277 and 1205 cm^{-1} observed for succinimide-*d* and maleimide-*d* respectively are assigned to this vibration, so the product rule holds well. The other bands appearing on deuteration in this region may be considered not to be fundamentals.

The N–D in-plane deformation vibration has been reported to couple with other vibrations for the cis –CONH– group[12]. This situation seems to hold also for cyclic imides. The strong band at 1102 cm^{-1} for succinimide-*d* and the weak band at 1086 cm^{-1} for maleimide-*d* are undoubtedly contributed from the N–D in-plane deformation vibration. These frequencies, however, in comparison with the N–D in-plane deformation (imide III′) frequencies of the trans-trans –CONDCO– group (ca. 960 cm^{-1}), seem to be so high that they can only with difficulty be assigned to the pure N–D

12) T. Miyazawa, *J. Mol. Spectroscopy*, 4, 155 (1960).

in-plane deformation vibration. Thus, an appreciable coupling with other vibrations is expected to be the case with these frequencies. This is confirmed by the fact that the band near 936 cm^{-1} (medium for succinimide and strong for maleimide) of the undeuterated species disappears on deuteration. The alternative frequencies which satisfy the product rule can be found at 820 and 832 cm^{-1} for succinimide-*d* and maleimide-*d* respectively. These bands may also be contributed from the N–D in-plane deformation vibration. The marked difference in intensity in the corresponding bands between succinimide-*d* and maleimide-*d* may be due to the structural difference in the hydrocarbon residues of these two compounds.

The band near 640 cm^{-1} observed for both succinimide and maleimide remains unchanged on deuteration. Comparison with the other related compounds leads to the assigment of this band to the C=O in-plane deformation (the imide IV) vibration. Thus, nearly complete assignments have been made for the characteristic in-plane vibrations of succinimide, maleimide and their *N*-deuterated compounds. It is seen that succinimide and maleimide show quite analogous frequencies as far as the characteristic vibrations are concerned.

The Out-of-plane Characteristic Frequencies.—The broad bands at 849 and 725 bm^{-1}, observed respectively for succinimide and maleimide, disappear on deuteration, suggesting that they are due mainly to the N–H out-of-plane deformation (imide V) vibration. As alternative N–D out-of-plane deformation (imide V′) frequencies, the band at 636 cm^{-1} of succinimide-*d* and the band at 536 cm^{-1} of maleimide-*d* are quite probable. The sharp medium band at 556 cm^{-1} observed for succinimide shifts to 548 cm^{-1} on deuteration. These bands may be due to the C=O out-of-plane deformation (imide VI and VI′) vibration. The corresponding band for maleimide may be that observed at 550 cm^{-1}. However, this band's shift on deuteration is not obvious owing to the overlapping of the broad imide V′ band at 536 cm^{-1}. The marked differences in the imide V and V′ frequencies between succinimide and maleimide suggest that there is an appreciable difference in the strength of the hydrogen bond between the crystals of these compounds. This is consistent with the information from the N–H and N–D stretching frequencies, which will be discussed later. It is to be noticed here that similar differences in the N–H and N–D out-of-plane deformation frequencies have been pointed out also for monosubstituted amides[13] and acyclic imides[10].

The Product Rule.—The theoretical product rule ratios for species A′ and A″ are calculated from the principal moments of inertia, which, in turn, may be calculated for succinimide from Mason's data on the molecular structure[11]. On the other hand, the theoretical ratio for the frequencies above 2000 cm^{-1} may be given by $(\mu_N+\mu_H)^{1/2}/(\mu_N+\mu_D)^{1/2}$, since in this case only the N–H and the N–D stretching frequencies are involved. This ratio, together with the above-obtained ratio for all A′ frequencies, leads to the evaluation of the theoretical ratio for the A′ frequencies of succinimide below 2000 cm^{-1}. Table III shows these three theoretical ratios, together with the experimental ratios obtained from the frequencies which undergo an appreciable shift on deuteration. The theoretical ratios for maleimide are expected to be not far from the corresponding ratios for succinimide. It is seen that the observed ratios agree well with the theoretical ones. This result gives support to the assignment of the characteristic frequencies proposed in the present paper.

TABLE III. THE PRODUCT RULE RATIOS
(Undeut. compd./*N*-Deut. compd.)

		Succinimide		Maleimide	
		Theor.	Obs.*	Theor.	Obs.*
A′	(ν_{N-H}/ν_{N-D})	1.37	1.38	1.37	1.35
A′	($<2000\ cm^{-1}$)	1.44	1.40	—	1.38
A″		1.38	1.35	—	1.38

* The frequencies used are as follows: succinimide (A′) 3190, 1418, 1378, 1198, 936, (A″) 849, 556; succinimide-*d* (A′) 2325, 1362, 1277, 1102, 820, (A″) 636, 548; maleimide (A′) 3221, 1375, 1350, 1148 (the mean value of 1154 and 1141), 938, 899, (A″) 725, 678; maleimide-*d* (A′) 2380, 1342, 1205, 1086, 888, 832, (A″) 665, 536.

The N–H and N–D Stretching Frequencies.—As seen from Figs. 1 and 2, the N–H and the N–D stretching bands show quite different features from each other for these two cyclic imides. Similar phenomena have been observed for several acyclic imides and interpreted in terms of the Fermi resonance[9]. As shown in Tables I and II, the features of the N–H and the N–D stretching bands of cyclic imides in the present study can also be well elucidated from analogous points of view. The broad doublet (3190 and 3080 cm^{-1}) of succinimide is considered to result from the Fermi resonance between the the N–H stretching vibration and the combination tone of the lower characteristic fundamentals (1700 and 1418 cm^{-1}). The sum of these fundamental frequencies

13) T. Miyazawa, T. Shimanouchi and S. Mizushima. *J. Chem. Phys.*, 24, 408 (1956).

($3118\,cm^{-1}$) exceeds the frequency of the lower peak ($3080\,cm^{-1}$) by about $40\,cm^{-1}$, suggesting that the resonance is considerable. This is consistent with the fact that the peaks at 3190 and $3080\,cm^{-1}$ show almost the same intensity. The difference between the unperturbed and the perturbed frequency is expected to be the same for the N–H stretching frequency as for the combination frequency involved in the Fermi resonance[14]. Thus, the unperturbed N–H stretching frequency of succinimide may be estimated to be near $3150\,cm^{-1}$, that is, $40\,cm^{-1}$ lower than the frequency of the higher peak ($3190\,cm^{-1}$). Nakamoto et al. have pointed out the linear dependence of the N–H stretching frequencies on the N···O distances in the N–H···O hydrogen bond[15]. In this connection, the present result is nearly consistent with the crystallographic data, according to which the N···O distance is 2.85 Å for succinimide[11].

On the other hand, the weakness of the band at $3070\,cm^{-1}$ of maleimide, as well as the small difference between the observed ($3070\,cm^{-1}$) and the combined ($1700+1375=3075\,cm^{-1}$) frequencies, indicates that the Fermi resonance is less significant for this molecule. This means that the unperturbed N–H stretching frequency of maleimide is not far from the observed frequency ($3221\,cm^{-1}$). From these results it is seen that there is an appreciable difference (ca. $70\,cm^{-1}$) in the unperturbed N–H stretching frequencies between succinimide and maleimide. Thus, it may be suggested that the hydrogen bond involved in succinimide is stronger than that involved in maleimide. This results is consistent with the information from the spectral differences between these compounds in the potassium bromide region.

The weak peaks associated with the N–D stretching band can be interpreted as overtone or combination bands related to the characteristic frequencies in the region 1400 to 1000 cm^{-1}. This means that these characteristic frequencies of the –CONHCO– group are distinguished from the non-characteristic frequencies not only by their sensitivity to deuteration but also by their tendency to give rise to overtone or combination bands.

Frequencies Due to the Hydrocarbon Residues. —It is observed that the ring strain raises the C–H strecthing frequencies of these compounds by 60 to $100\,cm^{-1}$ from the ordinary positions for the structures $-CH_2-$ and $=CH-$[16]. However, the effect of the ring strain on the C–H deformation frequencies of these compounds is not so obvious as that on the stretching frequencies. If the symmetry C_{2v} is assumed, succinimide is expected to show six C–H deformation frequencies, since in this case the A_2 CH_2 twisting and the A_2 CH_2 rocking vibration are infrared inactive. Furthermore, the B_1 CH_2 bending and the A_1 CH_2 wagging frequencies may not be observed owing to the small transition moments for the corresponding vibrations. In fact, succinimide shows four bands, at 1431, 1298, 1241 and $1002\,cm^{-1}$, which remain unshifted on deuteration. These bands are assigned to the C–H deformation vibrations, as shown in Table IV. Thus, in contrast with the case of the vibrations related to the –CONHCO– group, the deviation from C_{2v} seems to be negligible with respect to the C–H deformation vibrations. Similarly, the three C–H deformation frequencies of maleimide may be assigned as shown in Table V. It should be noticed here that the C–H out-of-plane deformation frequency undergoes an appreciable shift on deuteration. The bands left unassigned so far in the region 1000 to $800\,cm^{-1}$ may be due to the in-plane ring skeletal vibrations, to which the contribution of the stretching of the C–C bonds is significant.

Table IV. The non-characteristic frequencies of succinimide and succinimide-*d* (in cm^{-1})

Undeut. compd.	*N*-Deut. compd.	Assignments
	2986 w	ν_{CH_2}
2954 w	2956 w	
1431 m	1430 m	CH_2 bend.
1298 s	1300 s	CH_2 wag.
1241 m	1240 m	CH_2 twist.
1002 m	1002 m	CH_2 rock.
	1252 sh	?
(849)	848 m	Skeletal
821 s	(820)	

Table V. The non-characteristic frequencies of maleimide and maleimide-*d* (in cm^{-1})

Undeut. compd.	*N*-Deut. compd.	Assignments
	3190 w	ν_{C-H}
3120 s	3120 s	
1580 m	1580 m	$\nu_{C=C}$
1417 w	1417 w	δ_{C-H}
1305 m	1305 m	δ_{C-H}
	1255, 1244 m, db.	?
1064 m	1064 m	Skeletal
899 m	888 m	
852 s	852 sh	
678 s	665 s	π_{C-H}

14) T. Miyazawa, *J. Mol. Spectroscopy*, **4**, 168 (1960).
15) K. Nakamoto. M. Margoshes and R. E. Rundle, *J. Am. Chem. Soc.*, **77**, 6480 (1955).
16) L. J. Bellamy, "The Infra-red Spectra of Complex Molecules", John Wiley & Sons, Inc., New York (1958), pp. 15, 34.

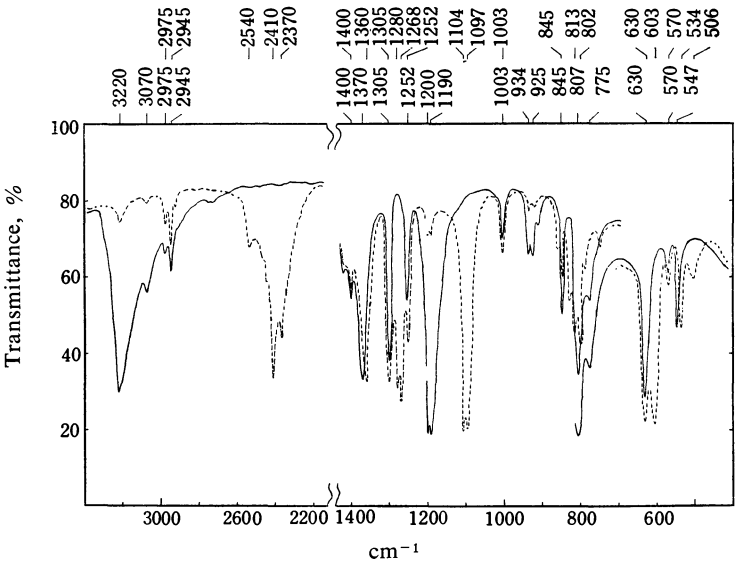


Fig. 3. Infrared spectra of succinimide (solid line) and succinimide-*d* (broken line) mixed with potassium iodide.

Interaction with Potassium Iodide.—Baker has reported that succinimide undergoes a marked spectral change on the change of matrix in the disk technique from potassium bromide to potassium iodide[4]. The anomalous infrared spectrum of succinimide measured with potassium iodide disks has been given for the region 1400 to 750 cm^{-1}. We have obtained an anomalous spectrum identical with that shown in Baker's paper by using a sample obtained by removing water from an aqueous solution of succinimide and potassium iodide. This procedure can be used to obtain the anomalous spectrum of the *N*-deuterated compounds corresponding to that of the undeuterated species. These anomalous spectra are shown in Fig. 3. From this spectral change due to potassium iodide, the several interesting results following concerning the characteristic frequencies have been obtained:

(1) The high-frequency shift of the N–H (N–D) stretching band and the low-frequency shift of the imide V (V′) band are observed on the spectral change due to potassium iodide. This suggests that the N–H hydrogen atom is involved in the interaction with the iodide anion, as in the case of diacetamide[10]. (2) The weak overtone or combination bands near the N–D stretching band also undergo a frequency shift according to the change in the lower characteristic fundamentals. (3) The overlapping of the imide IV and V′ bands at 634 cm^{-1} of the *N*-deuterated species is removed by the low-frequency shift of the latter band. Thus, it is explicitly observed that the former band remains unshifted on deuteration. (4) The band near 830 cm^{-1} observed for the *N*-deuterated species splits according to the splitting of the band at 936 cm^{-1} of the undeuterated species. This may be taken as indicating that the band at 936 cm^{-1} of the undeuterated species actually shifts to 820 cm^{-1} on deuteration. This frequency shift is not obvious in the ordinary spectra owing to the presence of the band at 820 cm^{-1} for both the undeuterated and the *N*-deuterated species. (5) The band at 1198 cm^{-1} of the undeuterated species and the band at 1102 cm^{-1} of the *N*-deuterated species split in a similar way, suggesting that these bands are contributed from vibrations of a similar nature. These results are consistent with the interpretation of the absorption bands given in the present paper, thus giving supports to the assignments made in Tables I, II, IV and V.

Experimental

Materials and Measurement.—G. P. grade succinimide was recrystallized from ethylmethylketone, m. p. 125°C. Maleimide was prepared from dimethyl maleate through maleindiamide, according to Rinkes' method[17], and purified by sublimation under reduced pressure, m. p. 93°C. No spectral change was observed for either of these compounds on crystallization from water. Thus, succinimide-*d* and maleimide-*d* were prepared by the usual exchange reaction with deuterium oxide. A Koken DS-301 infrared spectrophotometer equipped with rock salt or potassium bromide prisms was used. The measurements were carried out on pastes in

17) I. J. Rinkes, *Rec. trav. chim.*, **46**, 272 (1927); **48**, 961 (1929).

Nujol or hexachlorobutadiene under the same conditions as those reported previously[7].

Interaction with Potassium Iodide.—A small amount of an aqueous solution of succinimide and potassium iodide was evaporated to dryness under reduced pressure (ca. 5 mmHg) at 80~90°C. The samples thus obtained were measured immediately as pastes. The anomalous spectrum for the *N*-deuterated species was obtained by the same procedure, using deuterium oxide instead of water.

The authors wish to express their thanks to Dr. Tatsuo Miyazawa of Osaka University and to Dr. Kiyoshi Nakamura of the Research Laboratory, Dainippon & Co., Ltd., for their kind advice throughout this work.

Faculty of Pharmacy
Kyoto University
Sakyo-ku Kyoto

Carboxyl Group as a Proton Donor in the Interaction between Hydroxyl Group and π-Electrons[1]

By Michinori Ōki and Hiizu Iwamura

(Received June 19, 1961)

Since carboxylic acids form stable dimers due to the strong hydrogen bonding and are generally considered to be stronger proton donors than alcohols and phenols, it is natural to expect that the carboxyl group will also be a proton donor in the interaction with the π-electrons. As to the intramolecular interaction, no example seems to be available in this class, but the report by Suzuki et al.[2] which reveals that *N*-methylphenylacetamide possesses this kind of interaction may be taken as an analogous phenomenon.

In this respect, the authors measured the O–H stretching absorptions (ν_{O-H}) of carboxylic acids which might exhibit the intramolecular interaction due to proximity of the carboxyl group to the aromatic nucleus. The carbonyl stretching absorptions ($\nu_{C=O}$) of the carboxylic acids were also measured, since it was found in this laboratory that the $\nu_{C=O}$ of the free carbonyl group in the " trans " carboxyl group[3] appears at as high as 1790 cm^{-1} [4].

Experimental

The materials used in this work were all known compounds and prepared or purified according to the literature. The physical constants were checked prior to the measurement.

The spectral measurements were carried out with a Perkin Elmer 112G grating infrared spectrometer, the samples being dissolved in carbon tetrachloride unless otherwise specified. The concentration of the solution was made up ca. 0.5 mmol./l. as a compromise between the convenient absorption and the minimum effect of the dimer. A quartz cell of 5 cm. optical length and a sodium chloride cell of 2.45 cm. length were used for the ν_{O-H} region, and the latter and another sodium chloride cell of 0.10 cm. length for the $\nu_{C=O}$ region.

Results and Discussion

The results of the measurements with a series of compounds are listed in Table I.

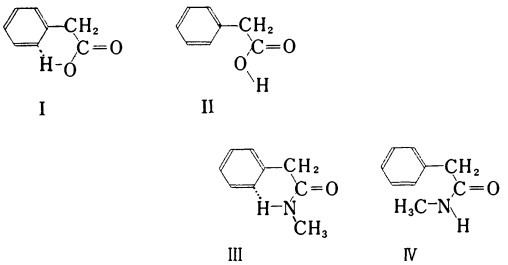


TABLE I. THE ν_{O-H} AND $\nu_{C=O}$ DATA OF SOME CARBOXYLIC ACIDS

Carboxylic acid	ν_{O-H} cm^{-1}	ε^{a}	$\nu_{C=O}$ cm^{-1}
$PhCH_2CO_2H$	3531.5	61.7	1762.7
Ph_2CHCO_2H	3526.7	68.3	1757.5
Ph_3CCO_2H	3520.9	79.4	1752.2
$PhCH_2CH_2CO_2H$	3532.8	63.8	1758.4
o-$PhC_6H_4CO_2H$	3529.9	81.1	1750.4 1736.9

1) This article is the fifteenth paper pertaining to the intramolecular interaction between hydroxyl group and π-electrons. For the preceding paper see: This Bulletin, **34**, 1395 (1961).

2) I. Suzuki, M. Tsuboi and T. Shimanouchi, *Spectrochim. Acta*, **16**, 467 (1960).

3) The nomenclature, " cis " and " trans " of a carboxyl group, is according to C. P. Smyth, " Dielectric Behavior and Structure ", McGraw-Hill Book Co., Inc., New York (1955), p. 306.

4) M. Ōki and M. Hirota, This Bulletin, **34**, 374 (1961).

In the first place, phenylacetic acid has been considered to be a carboxylic acid which should possess the intramolecular interaction from the structural analogy between the acid I and the methylamide III[2]. Contrary to the expectation, no intramolecular interaction between the carboxyl group and π-electrons is observed. Phenylacetic acid shows single ν_{O-H} and single $\nu_{C=O}$ at the ordinary regions assigned to the monomeric carboxylic acids.

It has been shown that the statistical factors obtained by considering the rotational isomerism about the single bonds play an important role in the intramolecular interaction. For example tribenzylcarbinol has no free hydroxyl group[5], whereas benzyldimethylcarbinol includes ca. 57% free form, provided that the absorption intensities per molecule due to O–H stretching are the same in both free and interacting forms. Triphenylacetic acid must favor the intramolecular interaction as far as the statistical factor is concerned. The results indicate, however, even diphenyl- and triphenylacetic acids possess a single peak for the ν_{O-H} and the $\nu_{C=O}$, respectively. The absorption maxima are in good agreement with those assigned to the monomeric "cis" forms.

Hydrocinnamic acid and *o*-carboxybiphenyl show free carboxyl group only, indicating that the absence of the interaction in phenylacetic acid is not due to the unfavorable ring member. Otherwise, sterically advantageous *o*-carboxybiphenyl should possess the interaction. The doublet $\nu_{C=O}$ of *o*-carboxybiphenyl can not be ascribed to the interaction, but is common for the *o*-substituted benzoic acids[6].

The carboxyl group is known to assume "cis" and "trans" structures[3], examples of which are illustrated by I and II, respectively. Establishment of the intramolecular interaction requires the "trans" form of the carboxyl group and this requirement may be the reason why phenylacetic acid does not show the interaction. Namely no matter what configuration is taken, the "cis" structure is disadvantageous.

The "cis" configuration is known to be more stable than the "trans" by several kcal./mol.[7] On the other hand, it is found in this laboratory that a lone pair electrons of a rather highly basic atom is needed to convert the "cis" structure into the "trans"[4], the phenomenon being suggestive of the comparable energies in O–H···O hydrogen bond and in the "cis" structure. π-Electron system, acting as a proton acceptor, is a weak base and can not compensate the required stabilization energy as is suggested by the energy measurement of the O–H···π interactions[8]. The energy of the intramolecular interaction between hydroxyl group and π-electrons has never been higher than 2.5 kcal./mol.[9] and is too low to compete with the stabilization energy of the "cis" structure. In this manner, it is also possible to account for the presence of the intramolecular interaction in *N*-methylphenylacetamide, since the "trans" structure III is more stable than the "cis" IV in the secondary amides[10].

Recently, Nagai and Simamura[11] reported that acetic acid and its halogenated derivatives in carbon tetrachloride show a second ν_{O-H} on addition of benzene and attributed the phenomenon to the intermolecular association between the carboxyl group and the π-electrons of the benzene nucleus. Since the entropy requirement is rather severe in the intermolecular hydrogen bonding[12], it seems unreasonable from this standpoint that the interaction which has not been observed intramolecularly is taking place intermolecularly. The acetic acid-benzene system has therefore been reinvestigated and the results are summarized in Table II together with those of the other aromatic solvents.

TABLE II. ν_{O-H} AND $\nu_{C=O}$ OF THE MONOMERIC ACETIC ACID IN SEVERAL SOLVENTS

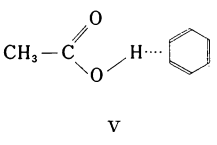
Solvent	ν_{O-H}, cm^{-1}	$\nu_{C=O}$, cm^{-1}
Carbon tetrachloride	3538.2	1769.3
Bromobenzene	3484.8	—
Benzene	3463.1	1763.2
Toluene	3458.8	1762.3
p-Xylene	3447.5	—
Mesitylene	3433.4	—

On dissolution of benzene, monomeric ν_{O-H} of acetic acid in carbon tetrachloride diminishes in its intensity and instead a second ν_{O-H} at ca. 3465 cm^{-1} arises. The intensity of the latter band grows as the concentration of benzene increases and the former disappears when the spectrum was measured in benzene. It can be seen from Table II that ν_{O-H} depends upon the basicity of the benzenoid π-electrons. Thus when the π-electron density in the benzene ring of the solvent molecule is decreased

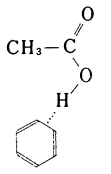
5) M. Ōki and H. Iwamura, ibid., 33, 1600 (1960).
6) C. I. W. Brooks, G. Eglinton and J. F. Morman, *J. Chem. Soc.*, 1961, 106.
7) M. M. Davies, *Trans. Faraday Soc.*, 36, 333 (1940).
8) M. Ōki and H. Iwamura, This Bulletin, 33, 717 (1960).
9) This highest energy has been obtained for 2-hydroxy-4-nitrobiphenyl. See, M. Ōki, H. Iwamura and Y. Urushibara, ibid., 31, 769 (1958).
10) I. Suzuki, M. Tsuboi, T. Shimanouchi and S. Mizushima, *Spectrochim. Acta*, 16, 471 (1960).
11) Y. Nagai and O. Simamura, presented at the 13th Annual Meeting of the Chemical Society of Japan, Tokyo, April, 1961. This Bulletin, 35, 132 (1962).
12) H. H. Jaffe, *J. Am. Chem. Soc.*, 79, 2373 (1957).

by halogen substitution, ν_{O-H} of acetic acid appears at higher frequency than in benzene, indicating the weakening of the interaction. On the other hand, when the π-electron density in the benzene ring is raised by substituting with the alkyl group, ν_{O-H} shifts to the lower frequency corresponding to the stronger interaction. The phenomenon is in parallel with those of ν_{N-H} of *N*-methylacetamide[13] and ν_{O-H} of phenol[14] in aromatic solvents, and adds strong support to the notion of the intermolecular interaction between the carboxyl group and π-electrons.

In spite of a rather large shift in ν_{O-H}, $\nu_{C=O}$ shifts little. The wave number (1763 cm^{-1}) is the place where the ordinary monomeric $\nu_{C=O}$ of "cis" configuration appears and too low to be assigned to the "trans" configuration which has the $\nu_{C=O}$ at around 1790 cm^{-1}[14]. Therefore it is tentatively concluded that in the intermolecular interaction between carboxyl group and π-electrons the "cis" configuration is maintained (V and not VI).



V



VI

The authors are indebted to Professor Yoshiyuki Urushibara and Professor Takehiko Shimanouchi for their encouragement and discussion throughout this work. The authors' thanks are also due to the Ministry of Education for the grant-in-aid for Fundamental Scientific Research.

Department of Chemistry
Faculty of Science
The University of Tokyo
Hongo, Tokyo

13) I. Suzuki, M. Tsuboi and T. Shimanouchi, *J. Chem. Phys.*, **32**, 1263 (1960).
14) R. West, *J. Am. Chem. Soc.*, **81**, 1614 (1959).

Physicochemical Studies of Stearic Acid Monolayer-Aluminum Ion Interaction. I. The Surface Pressure

By Kinsi MOTOMURA and Ryohei MATUURA

(Received May 22, 1961)

There exist a number of reports on the interaction of the monolayers of fatty acid with aluminum ion[1-12], but no work has succeeded in establishing a complete picture of the structure and constitution of the monolayers resulting from the interaction. Schulman et al.[5-7], studying the effect of the presence of aluminum ion in underlying solutions on monolayers, suggested that the solidification of monolayers could be brought about by hydrogen bonding between the monolayer soaps produced through the dissociated monolayers-basic aluminum ion interaction. Spink and Sanders[8] could not arrive at any conclusion as to the interaction of the stearic acid monolayer with aluminum ion, reporting that the interaction was obviously complicated and further work was required. It was shown by Ekwall and Bruun[9-12] that the final product of the interaction was dibasic aluminum soaps. On the other hand, Sasaki and Matuura[2,3] ascribed the rigid expanded monolayer resulting from the interaction to a complicated polymeric structure in which the backbone of -Al-O- would lie flat on the surface. We think it reasonable that the interaction should be considered from the standpoint of the adoption of aluminum ion on the monolayer as well as

1) I. Langmuir and V. J. Schaefer, *J. Am. Chem. Soc.*, **59**, 2400 (1937).
2) T. Sasaki and R. Matuura, This Bulletin, **24**, 274 (1951).
3) R. Matuura, ibid., **24**, 278 (1951).
4) H. Kimizuka, ibid., **29**, 123 (1956).
5) G. A. Wolstenholme and J. H. Schulman, *Trans. Faraday Soc.*, **46**, 475 (1950).
6) G. A. Wolstenholme and J. H. Schulman, ibid., **47**, 788 (1951).
7) J. G. N. Thomas and J. H. Schulman, ibid., **50**, 1131 (1954).
8) J. A. Spink and J. V. Sanders, ibid., **51**, 1154 (1955).
9) P. Ekwall and H. Bruun, *Acta Chem. Scand.*, **9**, 412 (1955).
10) P. Ekwall and H. Bruun, ibid., **9**, 424 (1955).
11) P. Ekwall and H. Bruun, ibid., **9**, 1057 (1955).
12) P. Ekwall and H. Bruun, ibid., **9**, 1069 (1955).

of the formation of aluminum soaps in the monolayers.

In the following series of investigations, our object is to determine, with the aid of surface pressure and viscoelasticity measurements, the structure and constitution of the stearic acid monolayers which have interacted with aluminum ion in the underlying solution. For this purpose the monolayers of aluminum distearate on water and aluminum salt solutions have also been investigated. It is also attempted in this paper to report the results of the surface pressure measurement and to find how they can be accounted for.

Experimental

The monolayers of stearic acid and aluminum distearate were prepared from benzene solutions on substrate solutions, and their surface pressures were measured by the modified Wilhelmy type surface balance described elsewhere[13]. The stearic acid was purified by repeated recrystallization from ethanol. The aluminum distearate was prepared by the addition of an excess of aluminum chloride solution to a solution of potassium soap. This was washed with water until the filtrate was free from chloride, thoroughly extracted free or loosely bound stearic acid with dried acetone and dried over phosphorus pentoxide for a few days. It was found by analyzing the aluminum content that the aluminum distearate thus obtained was almost in accord with the theoretical composition.

Redistilled water was used for preparing the substrate solution. The concentration of aluminum chloride was kept at 10^{-4} mol./l. The pH was adjusted with hydrochloric acid or sodium hydroxide over a wide range. The use of buffer salts was avoided so that they might not lead to an anomalous result due to their interaction with the monolayers. As the pH value of the solution, a mean value before and after the experiment was taken, but the deviation did not exceed 0.1 pH unit.

In order to maintain the experimental temperature constant, a constant temperature box was used. All the experiments were carried out in this box, kept at 25 ± 0.5°C.

The monolayers were left to stand for thirty minutes after spreading, and then their compression was started. The monolayers of stearic acid and aluminum distearate on aluminum chloride solutions were almost stable over the whole range of areas studied. On the contrary, the surface pressure of the aluminum distearate monolayer on distilled water varied distinguishably with time. As the surface pressure of this monolayer, therefore, we, for convenience's sake, read the value which the monolayer exhibited when left to stand for one minute.

Results

Stearic Acid Monolayer on Aluminum Chloride Solution.—The variation of surface pressure of the stearic acid monolayer on aluminum chloride solutions with the area occupied by a stearic acid molecule was measured over a range of pH values of the solution. Typical surface pressure-area curves are shown in Fig. 1, in which the numerals represent the pH

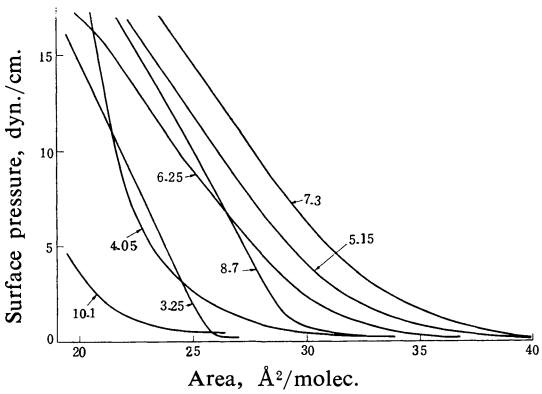


Fig. 1. Effect of pH on the pressure-area curves of stearic acid monolayer spread on 10^{-4} mol./l. aluminum chloride solution at 25°C.

values. It was found that the folds of the film were visibly detected at smaller areas than the inflection point of the pressure-area curves. It is obvious from this figure that the influence of aluminum ion is extremely characteristic for the pH, which suggests that it depends on the state of aluminum ion in the solution. This may be more clearly elucidated by plotting a limiting area, which we define as the area at which an appreciable rise in surface pressure occurs when the monolayer is compressed, against the pH of the solution. This relation is given by the curve 1 in Fig. 4. It is seen that the curve has two maxima and one minimum. In the previous work[2] only one maximum was found; another maximum and a minimum were overlooked since the intervals of pH were so coarse there. The shape of the curve characterizing the interaction between the stearic acid monolayer and aluminum ion is very similar to that already shown by Spink and Sanders[8], although in the magnitude of limiting areas there is a great difference, which might arise from the use of different aluminum salts or from other artificial causes. There is, however, no obtaining of further information on the reaction in the monolayer with only this finding. To gain a deeper insight into the problem, we investigated the monolayer of aluminum distearate which had been known to have a polymeric structure in the hydrocarbon solution as well as in the solid state.

Aluminum Distearate Monolayer on Distilled

13) R. Matuura and I. Hayasi, *Memoirs Fac. Sci., Kyushu Univ., Ser. C*, **1**, 31 (1948).

Water.—The monolayer of aluminum distearate on distilled water at various pH values was unstable, as has been previously stated, but it was revealed by the talc method that the monolayer was solid expanded at pH values between about 4.5 and 9.0. Figure 2 illustrates

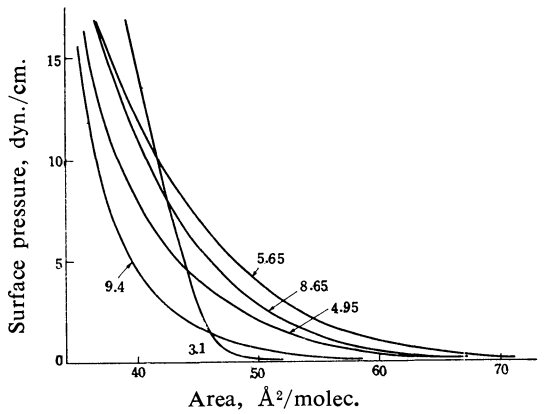


Fig. 2. Effect of pH on the pressure-area curves of aluminum distearate monolayer on distilled water at 25°C.

some pressure-area curves of the monolayer. These curves are less expanded than that of stearic acid on aluminum chloride solution when the area per chain of aluminum distearate is compared with that occupied by a stearic acid. In the same way as in the case of the stearic acid monolayer, the limiting area-pH curve is depicted in the Fig. 4 curve 2. This curve resembles curve 1 in shape; this might be considered to suggest that the reaction of the stearic acid monolayer with aluminum ion in the underlying solution forms aluminum distearate in the monolayer. However, there are considerable differences in the value of the

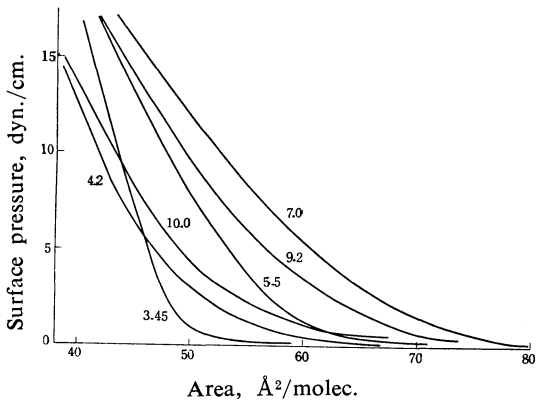


Fig. 3. Effect of pH on the pressure-area curves of aluminum distearate monolayer on 10^{-4} mol./l. aluminum chloride solution at 25°C.

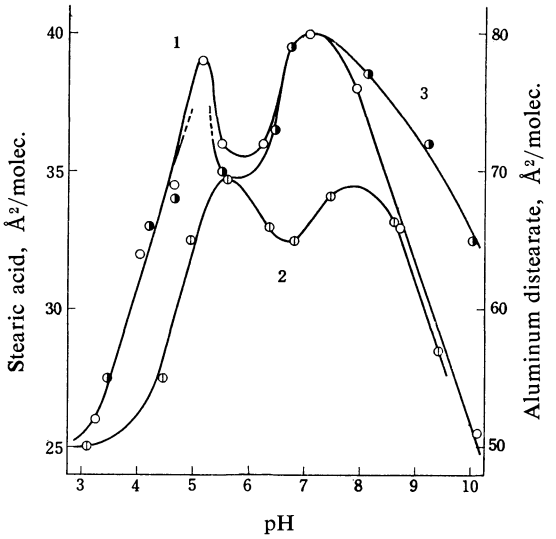


Fig. 4. Comparison among limiting area-pH curves of the monolayers of stearic acid and aluminum distearate on underlying solutions at 25°C: (1) Stearic acid on aluminum ion (○); (2) Aluminum distearate on water (◐); (3) Aluminum distearate on aluminum ion (◑).

areas between the two curves. In order to interpret this difference, it seems necessary to study the interaction of the aluminum distearate monolayer with the aluminum ion in the solution.

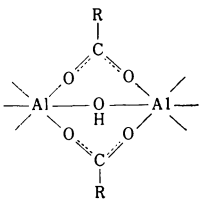
Aluminum Distearate Monolayer on Aluminum Chloride Solution.—The results obtained for the influence of aluminum ion at various pH values on the pressure-area curve of the aluminum distearate monolayer are shown in Fig. 3. The behavior of these pressure-area curves is typically solid-expanded and is extremely similar, not to that of the aluminum distearate monolayer on water, but to that of the stearic acid monolayer on aluminum ion. The limiting area-pH curve produced from Fig. 3 is curve 3 in Fig. 4. This curve is partially a little different from curve 1, but there seems to be essentially no difference between them.

Discussion

The interaction of the monolayers of fatty acids with various metal ions has been discussed from the standpoint of the formation of metallic soaps in the monolayers ever since Langmuir and Schaefer[1], and many investigators have tried to shed light on the compositions of the interacted monolayers from only the results of chemical analysis carried out on

the matter collected after the monolayers were compressed to collapse. Through the investigation of tanning by chromium ion of various monolayers, e. g., the myristic acid monolayer, practicing at the same time the chemical analysis of them, Schulman and Dogan[14] thought it likely that the structure of solid monolayers can be brought about by the interlinking between chromium monosoap molecules by hydrogen bonding between two hydroxyl groups attached to the chromium ion or between hydroxyl and carbonyl in the carboxyl group. A similar investigation was made by Ekwall and Bruun[11,12] of the interaction of the myristic acid monolayer with aluminum ion; they concluded that the final product of the interaction seemed to be a dibasic aluminum monomyristate with regard to the composition of the interacted monolayer. The matter used by these authors for the analysis was, however, that which had been removed with a scoop at the very small area where the monolayers might be collapsed and, moreover, perhaps included physically adsorbed metal ions. Therefore, it seems doubtful whether the monolayer compositions thus estimated will express the true ones even if the physically adsorbed metal ions are taken into account experimentally. It is a well-known fact that the reaction of alkali salts of a fatty acid such as stearic acid with aluminum ion in an aqueous medium always results in aluminum disoap. It is conceivable, therefore, that when the stearic acid monolayer is spread on the solution containing aluminum ion at certain pH values, the former will combine with the latter to form aluminum distearate in the monolayer.

With aluminum disoap investigated by many workers from various viewpoints, it has been made clear that the structure of aluminum disoap is polymeric in its hydrocarbon solutions as well as in the solid state. Bauer et al.[15,16] elucidated by means of the technique of the infrared absorption spectra that the polymeric structure of aluminum disoaps is constituted not through hydrogen bonding between hydroxyl groups but through a coordinate bond between aluminum and oxygen in the hydroxyl group. Taking account of experimental results of various kinds, a reliable polymeric structure of aluminum disoap may be that of Leger et al.[17], similar to that of Bauer et al., i. e.,



in which R represents the hydrocarbon part. When aluminum distearate is spread on the substrate from the benzene solution, it is natural that the aluminum distearate will, in the monolayer state, hold the polymeric structure, the backbone chain of which will attach to or be immersed in the underlying solution. It was found that the pressure-area curve of a aluminum distearate monolayer spread on a sodium fluoride solution became less expanded with an increasing sodium fluoride concentration and finally coincided with that of stearic acid on water (i. e., it contained no aluminum ion) at about 10^{-3} mol./l. sodium fluoride solution. This is considered to show that the coordinate bond was cut by the fluorine ion which preferentially coordinates on aluminum ion[18]. Further discussions from the rheological aspect of the aluminum distearate monolayer will appear in part II of this series.

If the two-dimensional polymeric structure of aluminum distearate monolayer on distilled water is valid, its unstable behavior on compression can be ascribed to the fact that the rearrangement of aluminum distearate into the true equilibrium state takes a long time. Therefore, the pressure-area curves in Fig. 2 and the limiting area-pH curve illustrated by curve 2 in Fig. 4 may not be referable to those of the equilibrium, but some properties characteristic of the aluminum distearate monolayer would be disclosed in these curves. In this stage it is not easy to say what monolayer structures are corresponding to these pressure-area curves at respective pH values. However, the depression of the limiting area of the monolayer at the acidic side may be explained by its decomposition into stearic acid and aluminum ion, and at the alkaline side by its dissolution into water as sodium stearate.

Comparing the findings concerning the stearic acid monolayer on aluminum ion with those concerning the aluminum distearate monolayer on distilled water, we find a not negligible difference, even though they resemble each other in shape, as is clearly shown in Fig. 4. If only aluminum distearate was formed in the monolayer of stearic acid on aluminum ion and no other effects were exerted, the film 1 should agree with the film 2. In fact, the film

14) J. H. Schulman and M. Z. Dogan, *Discussions Faraday Soc.*, **16**, 158 (1954).
15) F. A. Scott, J. Goldenson, S. E. Wiberley and W. H. Bauer, *J. Phys. Chem.*, **58**, 61 (1954).
16) W. O. Ludke, S. E. Wiberley, J. Goldenson and W. H. Bauer, ibid., **59**, 222 (1955).
17) A. E. Leger, R. L. Haines, C. E. Hubley, J. C. Hyde and H. Sheffer, *Can. J. Chem.*, **35**, 799 (1957).
18) K. Motomura and R. Matuura, to be published soon.

1 is very much analogous to film 3 in various properties. This suggests that the interacted stearic acid monolayer may be that in which aluminum ion is adsorbed on the aluminum distearate monolayer. In the limiting area-pH curves, however, there seems to be a little partial disagreement between curves 1 and 3 in Fig. 4. Perhaps this disagreement may be not essential. It is accordingly conceivable that these two curves would fall into agreement with each other if all the measurements of surface pressure were carried out on the monolayers which attained to a state of complete equilibrium after very long times.

In view of the above discussion, it may be concluded that the interaction of the stearic acid monolayer with aluminum ion in the underlying solution occurs only over a characteristic pH range, below which the acid monolayer does not dissociate enough to interact appreciably and above which the monolayer tends to dissolve in the underlying solution; the solid expanded film brought about through the interaction is quite similar to the polymeric aluminum distearate monolayer adsorbing aluminum ion.

In part II of this series we present a further discussion on the interaction by making use of the results of surface rheological measurements.

Summary

In order to throw light on the interaction of the stearic acid monolayer with aluminum ion in underlying solutions, surface pressure measurements were carried out on (1) the stearic acid monolayer spread on 10^{-4} mol./l. aluminum chloride solution, (2) the aluminum distearate monolayer spread on distilled water, and (3) the aluminum distearate monolayer spread on 10^{-4} mol./l. aluminum chloride. It was found that their pressure-area curves were all solid expanded films over characteristic pH ranges, with the curve of 1 especially analogous to that of 3. In the limiting area-pH curves, there seemed to be a little partial disagreement between them which would not be essential. From these results it was concluded that the monolayer of stearic acid interacting with aluminum ion might be analogous to the two-dimensional polymeric aluminum distearate adsorbing aluminum ion.

Department of Chemistry
Faculty of Science
Kyushu University
Fukuoka

Physicochemical Studies of Stearic Acid Monolayer-Aluminum Ion Interaction. II. The Surface Viscoelasticity

By Kinsi MOTOMURA and Ryohei MATUURA

(Received May 22, 1961)

In the preceding paper[1] we investigated the interaction of the stearic acid monolayer with aluminum ion in underlying solutions by means of surface pressure measurement and concluded that the interacted monolayer had an analogous structure to the polymeric aluminum distearate monolayer adsorbed by aluminum ion. In order to confirm and further to develop this conclusion, it is most desirable to measure the surface rheological property of the monolayer, because a two-dimensional polymeric structure is most clearly revealed by surface viscoelasticity. Qualitative investigations have alcready been performed[2,3], but no quantitative study has been done with this system. Many investigators have tried to shed light on the rheological behavior of the monolayers of synthetic high polymers and proteins by making use of the aperiodic torsion pendulum[4-7] or the oscillating torsion pendulum[8,9], and it has been shown that these methods indeed give useful information about the structure of the monolayer. However, since the methods used by

1) K. Motomura and R. Matuura, This Bulletin, **35**, 285 (1962).
2) R. Matuura, ibid., **24**, 278 (1951).
3) H. Kimizuka, ibid., **29**, 123 (1956).
4) K. Inokuchi, ibid., **28**, 453 (1955).
5) K. Inokuchi, ibid., **26**, 500 (1953).
6) T. Tachibana and K. Inokuchi, *J. Colloid Sci.*, **8**, 341 (1953).
7) T. Tachibana. K. Inokuchi and T. Inokuchi, *Kolloid-Z.*, **167**, 141 (1959).
8) C. W. N. Cumper and A. E. Alexander, *Trans. Faraday Soc.*, **46**, 235 (1950).
9) N. W. Tschoegl and A. E. Alexander, *J. Colloid Sci.*, **15**, 168 (1960).

these authors are either instrumentally unsatisfactory or mathematically only approximate in analysis, a new and more exact treatment seems to be required in order to obtain more detailed information about the molecular structure of the monolayer. Here we employed a ring torsion pendulum method similar to that used by Kimizuka[3] and performed an exact mathematical analysis based on Oka and Sato's equation[10]. The object of this paper is to show, from the results of rheological measurements, the structure and constitution of the stearic acid monolayer formed on the substrate solution containing aluminum ion.

Theoretical

The viscoelasticity of a monolayer is usefully expressed by a mechanical model made up of various combinations of springs indicating elasticity and dashpots indicating viscosity. Two examples of models are shown in Fig. 2. In order to evaluate the viscoelasticity, it is necessary to obtain the deformation-time curve of the monolayer under surface shearing stress and to analyze it through a given mechanical model.

Let us now imagine a system in which the monolayer is spread between the ring of radius R_1, suspended with a very fine wire of phosphorus bronze just so its lower edge touches the underlying solution, and that of radius R_2, as shown in Fig. 1. When the head of the suspending wire is twisted at a given angle ϕ,

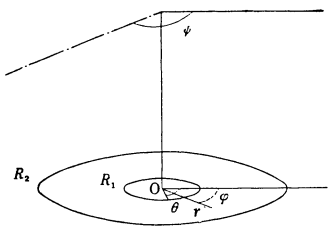


Fig. 1. Schematic diagram of the apparatus.

the ring R_1 will turn round by θ after the time t, and at the same time the monolayer being distant r from the origin O will also be displaced at an angle φ. Suppose, moreover, that the monolayer gets surface shear strain γ under the surface shearing stress S, which is brought about by the restoring torque of the suspending wire. If the monolayer is expressed by a certain mechanical model, we can obtain

$$L\gamma = MS \tag{1}$$

in which L and M are the operators characteristic of the mechanical model. The shear strain γ is subject to the relation

$$\gamma = -r\frac{\partial\varphi}{\partial r} \tag{2}$$

And then the shearing stress is expressed by

$$\sigma\frac{\partial^2\varphi}{\partial t^2} = -\frac{1}{r^3}\frac{\partial}{\partial r}(Sr^2) \tag{3}$$

in which σ is the surface density of the monolayer which is often neglected because of its small value. Using Eqs. 1, 2 and 3, φ can be given in the form of the function of r and t. From this φ and Eqs. 1 and 2, the relation between S and θ becomes

$$2\pi R_1^2 MS = CL\theta \tag{4}$$

by making use of the expression

$$\theta(t) = \varphi(R_1, t) \tag{5}$$

In Eq. 4 C is given by

$$C = 4\pi\Big/\left(\frac{1}{R_1^2} - \frac{1}{R_2^2}\right) \tag{6}$$

On the other hand, if I is the moment of inertia of the ring R_1 and κ the torsion constant of the suspending wire, the equation of motion with regard to the ring R_1 is given by

$$I\frac{d^2\theta}{dt^2} = \kappa(\phi - \theta) - 2\pi R_1^2 S \tag{7}$$

By substituting from 4 into 7, this becomes

$$IM\frac{d^2\theta}{dt^2} = \kappa M(\phi - \theta) - CL\theta^{10)} \tag{8}$$

When the monolayer is very rigid, then $d^2\theta/dt^2$ becomes negligibly small. Hence, Eq. 8 reduces to a simple form

$$\kappa M(\phi - \theta) - CL\theta = 0 \tag{9}$$

with sufficient accuracy. The approximate formula 9 is to be used throughout this paper, since the monolayer studied in the present experiment is so rigid that the condition for Eq. 9 is almost completely fulfilled. The general equation 8 will be used in another paper

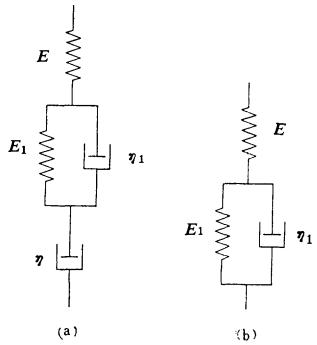


Fig. 2. Mechanical models: (a) four-parameter model; (b) three-parameter model (elasticity+Voigt element).

10) S. Oka and Y. Sato, *Bull. Kobayashi Inst. Phys. Res.*, 5, 96 (1955).

for the study of the rheological behavior of high polymer monolayers (which are not so rigid as in the present case).

In the first place let us consider the general mechanical model, i. e., the four-parameter model illustrated by a in Fig. 2. The relation between γ and S for the model is given by

$$\eta_1\frac{d^2\gamma}{dt^2}+E_1\frac{d\gamma}{dt}=\frac{\eta_1}{E}\frac{d^2S}{dt^2}+\left(1+\frac{E_1}{E}+\frac{\eta_1}{\eta}\right)\frac{dS}{dt}+\frac{E_1}{\eta}S \tag{10}$$

It follows thus that the operators $\boldsymbol{L}$ and $\boldsymbol{M}$ are expressed dy

$$\boldsymbol{L}=\eta_1\frac{d^2}{dt^2}+E_1\frac{d}{dt} \tag{11}$$

and

$$\boldsymbol{M}=\frac{\eta_1}{E}\frac{d^2}{dt^2}+\left(1+\frac{E_1}{E}+\frac{\eta_1}{\eta}\right)\frac{d}{dt}+\frac{E_1}{\eta} \tag{12}$$

when Eq. 10 is compared with Eq. 1. Inserting the operators into Eq. 9 and arranging, we can obtain a differential equation

$$\frac{d^2\theta}{dt^2}+b\frac{d\theta}{dt}+d\theta=d\phi \tag{13}$$

where

$$b=\frac{\kappa}{\kappa+CE}\left(\frac{E}{\eta_1}+\frac{E_1}{\eta_1}+\frac{E}{\eta}+\frac{C}{\kappa}\frac{EE_1}{\eta_1}\right) \tag{14}$$

and

$$d=\frac{\kappa}{\kappa+CE}\frac{EE_1}{\eta\eta_1} \tag{15}$$

It can easily be found that the solution of Eq. 13 is

$$\theta=\phi-Ae^{-\alpha t}-Be^{-\beta t} \tag{16}$$

in which A and B are arbitrary constants, and α and β are expressed by

$$\alpha=\frac{b-\sqrt{b^2-4d}}{2} \tag{17}$$

and

$$\beta=\frac{b+\sqrt{b^2-4d}}{2} \tag{18}$$

When α is much smaller than unity, Eq. 16 can be written in the form of

$$\theta=\phi-A+A\alpha t-Be^{-\beta t} \tag{19}$$

for small values of t. If the θ-t curve obtained experimentally of a certain monolayer coincides with the expression 16 or 19, it is thought natural that the rheological behavior of this monolayer can be analyzed by the four-parameter model. It is possible, therefore, to estimate the values of A, B, α and β, and, further, of b and d by making use of

$$b=\alpha+\beta \quad \text{and} \quad d=\alpha\beta \tag{20}$$

Thus using the values of A, B, b and d, we can evaluate the viscoelasticity by means of equations

$$E=\frac{\kappa}{C}\cdot\frac{A+B}{\phi-A-B} \tag{21}$$

$$E_1=1\Big/\left(\frac{C}{\kappa}\frac{\phi-A}{A}-\frac{1}{E}\right) \tag{22}$$

$$\eta_1=\frac{\kappa}{\kappa+CE}\cdot\frac{E+E_1+(C/\kappa)EE_1}{b} \tag{23}$$

and

$$\eta=\frac{\kappa}{\kappa+CE}\cdot\frac{EE_1}{d\eta_1} \tag{24}$$

Let us next consider the three-parameter model, the elasticity being accompanied by the Voigt model, as shown by b in Fig. 2. In a way similar as to that of the four-parameter model, it is readily found that for the three-parameter model

$$\boldsymbol{L}=\eta_1\frac{d}{dt}+E_1 \tag{25}$$

and

$$\boldsymbol{M}=\frac{\eta_1}{E}\frac{d}{dt}+\left(1+\frac{E_1}{E}\right) \tag{26}$$

By substituting the operators into Eq. 9, the expression for this model corresponding to Eq. 13 for the four-parameter model is given by

$$\frac{d\theta}{dt}+b\theta=d\phi \tag{27}$$

in which

$$b=\frac{\kappa}{\kappa+CE}\left(\frac{E}{\eta_1}+\frac{E_1}{\eta_1}+\frac{C}{\kappa}\frac{EE_1}{\eta_1}\right) \tag{28}$$

and

$$d=\frac{\kappa}{\kappa+CE}\left(\frac{E}{\eta_1}+\frac{E_1}{\eta_1}\right) \tag{29}$$

Then we, by solving Eq. 27, obtain

$$\theta=\frac{d}{b}\phi-Ae^{-bt} \tag{30}$$

A being an arbitrary constant. In the same way as the four-parameter model, from a comparison of the θ-t curve obtained experimentally with the expression 30 the evaluation of A, b and d is made easily. And hence the viscoelasticity can be evaluated by relations

$$E=\frac{\kappa}{C}\cdot\frac{(1-d/b)\phi+A}{(d/b)\phi-A} \tag{31}$$

$$E_1=(b-d)E\Big/\left(\frac{\kappa+CE}{\kappa}d-b\right) \tag{32}$$

and

$$\eta_1=\frac{\kappa}{\kappa+CE}\cdot\frac{E+E_1}{d} \tag{33}$$

This treatment for the three-parameter model leads to the same result as that which has been used to investigate the rheological properties of adsorbed films by Sasaki and Kimizuka[11].

In the third place, let us consider the monolayer having elasticity only. The operators as a matter of course are given by

$$\boldsymbol{L}=1 \tag{34}$$

and

$$\boldsymbol{M}=1/E \tag{35}$$

Therefore, we directly obtain the expression

$$E=\frac{\kappa}{C}\cdot\frac{\psi-\theta}{\theta} \tag{36}$$

from Eq. 9, where θ is independent of t.

Experimental

The measurement of surface viscoelasticity was carried out with the aid of the ring torsion pendulum apparatus used by Kimizuka[2] as shown schematically in Fig. 1. The ring R_1 was a platinum ring 2 cm. in diameter suspended with a phosphorus bronze wire, the torsion constant of which was 1.23 dyn. cm. As for the ring R_2, it was assumed that the radius was replaced by the distance from the origin 0 to the brim of the trough, i. e., 7.5 cm., with sufficient accuracy. The deflection angle θ of the ring R_1 was read by means of the lamp scale method and expressed by the moving distance on the scale.

The experiment was made on the stearic acid monolayer on a 10^{-4} mol./l. aluminum chloride solution and the aluminum distearate monolayer on both water and a 10^{-4} mol./l. aluminum chloride solution as described in the preceding paper[1]. All experimental conditions were entirely the same as in the preceding paper, except that the pH of the underlying solutions was kept constant at 5.5, which is in the region of maximum expansion of the monolayers.

After being spread on the substrate solutions, the monolayers were left to stand for 60 min. before the ring R_1 was deposited and then allowed to stand for another 30 min. because it was found that the values of viscoelasticity depended on the time of film aging.

Results and Discussion

It was found that the monolayer of aluminum distearate shows remarkable viscoelastic behavior even at considerably large areas. Fig. 3 illustrates an example of the θ-t relation obtained at 81.8 Å^2/molec. of the aluminum distearate monolayer on water. This relation

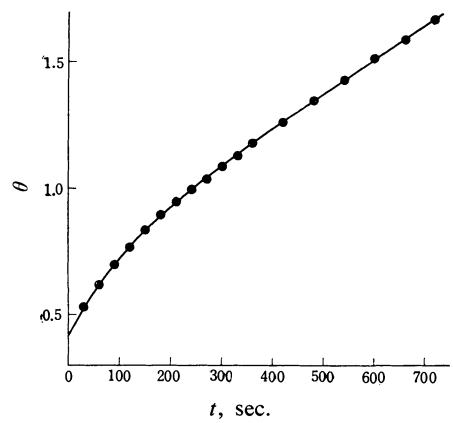


Fig. 3. θ-t curve of the aluminum distearate monolayer on water. Area 81.8 Å^2/molec.; Temperature 25°C.

is well expressed by the equation

$$\theta=0.714+0.00133\,t-0.297\,e^{-0.00882t} \tag{37}$$

which is shown as a full line in Fig. 3. Eq. 37 is in the same form as Eq. 19. We can say, therefore, that the surface rheological behavior of aluminum distearate can be explained in terms of the four-parameter model. From this result the values of viscoelasticity can be easily evaluated by applying Eqs. 21, 22, 23 and 24 in the manner described previously. We thus obtain 18.1 dyn./cm., 25.3 dyn./cm., 2.87×10^3 dyn. sec./cm. and 5.65×10^3 dyn. sec./cm. for E, E_1, η_1 and η respectively. These values are large enough to be compared with those of nylon 6 film at an area smaller than the limiting area as studied by Inokuchi[5]. Therefore, it is evident that the aluminum distearate spread on water holds the polymeric structure in the monolayer as well as in bulk and that its surface rheological behavior is due to a two-dimensional network brought about by its linear polymeric structure. Another proof comes from the studies on the aluminum distearate monolayer spread on sodium fluoride solution[12]. The viscoelasticity decreases with increase in the concentration of sodium fluoride, and at 10^{-3} mol./l. no rheological behavior is found anywhere over the area by means of this method. This may be explained by the destruction of the polymer chain through the bonding of fluorine with the aluminum atom in the chain, as stated in the preceding paper. The measured θ-t curves of the aluminum distearate monolayer on water at other areas than 81.8 Å^2/molec. are in shape quite similar to that illustrated in Fig. 3. By the same procedure as above, the values

11) T. Sasaki and H. Kimizuka, This Bulletin, 25, 318 (1952).

12) K. Motomura and R. Matuura, to be published soon.

of viscoelasticity were calculated for various areas of the monolayer. The results are shown in Fig. 4, where these values are plotted against the area per aluminum distearate molecule. It is seen that the viscoelasticity increases first gradually and then a little steeply as the area decreases.

If we accept the view that aluminum distearate is formed in the monolayer when the stearic acid monolayer was spread on aluminum ion, as discussed in the preceding paper, the interacted monolayer will show a rheological behavior. It was really found that the viscoelasticity of the stearic acid monolayer was so large as to be measured by the apparatus described here. Fig. 5 illustrates a typical θ-t curve for the monolayer of stearic acid on aluminum ion of 10^{-4} mol./l. at the area 38.9 Å^2/molec. The curve is essentially similar to that of the aluminum distearate monolayer on water. Furthermore, the curve is represented by

$$\theta = 0.552 + 0.00302\,t - 0.143\,e^{-0.0103t} \qquad (38)$$

bearing a resemblance to Eq. 37. Hence, this monolayer can also be analyzed in terms of the four-parameter model. We, in a like manner, obtained the similar θ-t curves at various areas. In Fig. 6, the values of E, E_1, η_1 and η evaluated from these curves are plotted against the area. It will be seen from Fig. 6

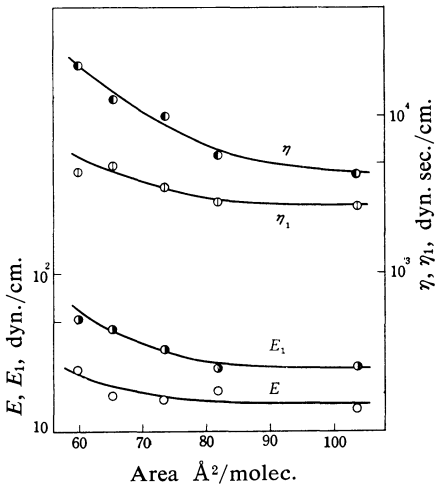


Fig. 4. Viscoelasticity-area curve of the aluminum distearate monolayer on water at 25°C.

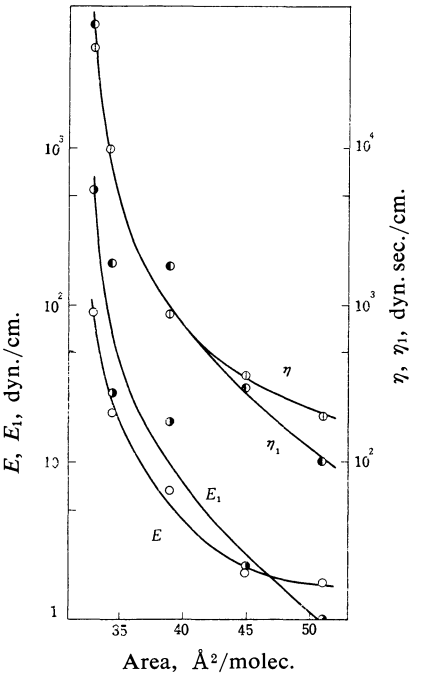


Fig. 6. Viscoelasticity-area curve of the stearic acid monolayer on 10^{-4} mol./l. aluminum chloride solution at 25°C.

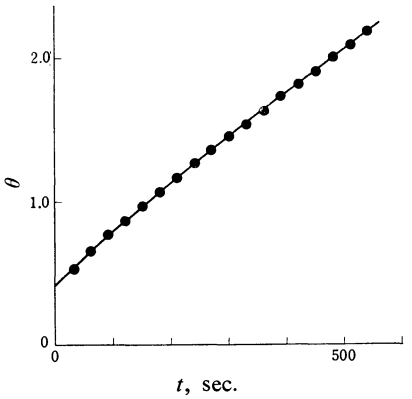


Fig. 5. θ-t curve of the stearic acid monolayer on 10^{-4} mol./l. aluminum chloride solution. Area 38.9 Å^2/molec.; Temperature 25°C.

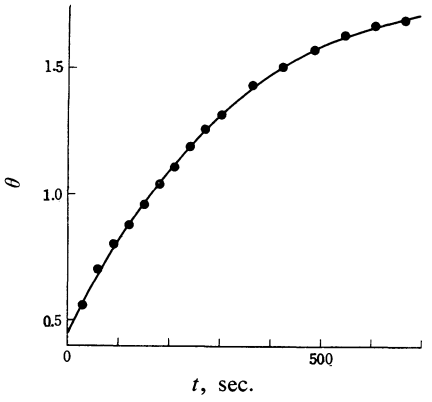


Fig. 7. θ-t curve of the aluminum distearate monolayer on 10^{-4} mol./l. aluminum chloride solution. Area 98.9 Å^2/molec.; Temperature 25°C.

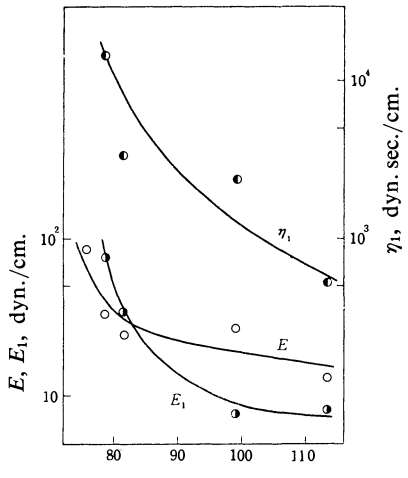


Fig. 8. Viscoelasticity-area curve of the aluminum distearate monolayer on 10^{-4} mol./l. aluminum chloride solution at 25°C.

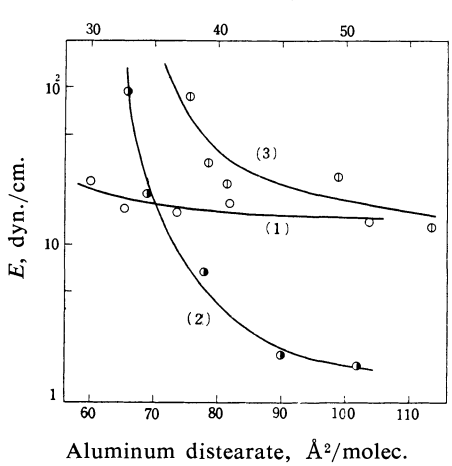


Fig. 9. Comparison among E-area curves of the monolayers of stearic acid and aluminum distearate on underlying solutions at 25°C:
(1) Aluminum distearate on water (○);
(2) Stearic acid on aluminum ion (◑);
(3) Aluminum distearate on aluminum ion (⊕).

that the curves, in contrast with those of aluminum distearate monolayer, rise steeply with a decrease in the area. In addition, it is to be noticed, when Fig. 6 is compared with Fig. 4, that the curves are lower than the latter at larger areas whereas higher at smaller areas. This fact may be more clearly revealed by the comparison between curves 1 and 2 in Fig. 9, which are the E-area curves for the aluminum distearate monolayer on water and the stearic acid monlayer on aluminum ion respectively. This difference leads us to the conclusion that, although the polymeric soaps are probably formed on water between stearic acid and aluminum ion, the structure of the monolayer thus formed is not just the same as that of aluminum distearate.

Now it is necessary to know the action of aluminum ion in the underlying solutions on the aluminum distearate monolayer. As an example of the viscoelastic behavior of the aluminum distearate monolayer on aluminum ion of 10^{-4} mol./l. over larger areas, the θ-t curve at the area 98.9 Å²/molec. is given in Fig. 7. It will be at once recognized that the curve behaves unlike those of Figs. 3 and 5. Since the curve can be represented in the form of the equation

$$\theta = 1.89 - 1.47\, e^{-0.00320t} \qquad (39)$$

which has just the same form as Eq. 30, the behavior of the monolayer must be expressed with the three-parameter model, the values E, E_1 and η_1 of which are calculated according to Eqs. 31, 32 and 33. In a smaller area, e. g., 75.6 Å²/molec., on the other hand, it was found that the value of θ kept constant throughout the measuring time within experimental errors. This means pure elasticity. Hence, the value is evaluated by use of Eq. 36. The values of elasticity at much smaller areas were too large to be measured by making use of this apparatus. In Fig. 8, the values of viscoelasticity in this system are plotted against the area. In comparing the curves in Fig. 8 with the corresponding curves in Fig. 4, it will be found that the former curves are incomparably higher than the latter at small areas, while equal to or rather a little less than the latter at large areas. It may be possible to say, therefore, that the aluminum ion in underlying solutions acts on the aluminum distearate monolayer through changing the four-parameter model into the three-parameter model, or pure elasticity, and making its values extremely large at smaller areas. In other words, we may be able to conclude that the aluminum ion is adsorbed on the monolayer of polymeric aluminum distearate, probably in a form of basic ion, and strengthens its two-dimensional network structure.

In the preceding paper, in which the interaction of stearic acid monolayer with aluminum ion was discussed from the viewpoint of surface pressure, it was suggested that the interacted monolayer might have the structure of the polymeric aluminum distearate adsorbing aluminum ion. According to this theory, the rheological behavior of both the stearic acid and aluminum distearate monolayers on

aluminum ion can be expected to agree. An appreciable difference exists, however, between them, e. g., curves 2 and 3 in Fig. 9, although aluminum distearate seems undoubtedly to be formed in the stearic acid monolayer. In Fig. 9 it is clear that the E of film 2 gets greater than that of film 1 and approaches to that of film 3 as the area decreases, while the former is lower than the latter two at large areas. It is quite possible that at much smaller areas the viscoelastic behavior of stearic acid monolayer on aluminum ion finally turns into the elastic one and that films 2 and 3 perfectly agree with each other. Therefore, this difference may be ascribed to the fact that the polymeric aluminum distearate formed in the interacted stearic acid monolayer is of a chain length shorter than that prepared in bulk. As elucidated by Singer's[13] or our[14] equation of state for high polymer, the effect of the chain length on surface pressure is very little when the high polymer has a fairly long one. The above result is not thought, therefore, to conflict with the well agreed results of surface pressure measurement between them. It thus may be concluded that the interacted monolayer of stearic acid with aluminum ion in underlying solution is constructed from the monolayer of polymeric aluminum distearate of a short chain length adsorbing basic aluminum ion.

13) S. J. Singer, *J. Chem. Phys.*, **16**, 872 (1948).
14) K. Motomura and R. Matuura, to be published.

Summary

By using the ring torsion pendulum method and applying the correct mathematical analysis, surface viscoelasticity measurements were carried out on the monolayers of (1) stearic acid on a 10^{-4} mol./l. aluminum chloride solution, (2) aluminum distearate on distilled water, and (3) aluminum distearate on a 10^{-4} mol./l. aluminum chloride solution. It was found that the rheological behavior of 1 and 2 could be analyzed in terms of the four-parameter model and of 3 by the three-parameter model or elasticity. Also, with regard to the values of viscoelasticity, it was shown that at large areas 1 was smaller than both 2 and 3, and at small areas 1 approaches to 3. From the viewpoint of these results, it was concluded that the interacted monolyer of stearic acid with aluminum ion in an underlying solution might be analogous to the monolayer of aluminum distearate with a short chain length adsorbing basic aluminum ion.

Department of Chemistry
Faculty of Science
Kyushu University
Fukuoka

The Very Weak Visible Absorption Band of p-Benzoquinone

By Akira KUBOYAMA

(Received July 10, 1961)

Recently, in various carbonyl compounds[1-7] and azines[8], very weak absorption bands at the long wavelength sides of the $n\rightarrow\pi^*$ singlet-singlet absorption bands have been found and safely assigned as $n\rightarrow\pi^*$ singlet-triplet absorption bands from the phosphorescence spectra, the temperature-independency, the solvent effect and the substitution effect. Previously, Sidman[9], in his study of the low temperature crystalline spectrum of *p*-benzoquinone, found a very weak absorption band at the long wavelength side of the $n\rightarrow\pi^*$ singlet-singlet absorption band and tentatively assigned it to the $n\rightarrow\pi^*$ singlet-triplet absorption band. Apart from his study, the $n\rightarrow\pi^*$ singlet-triplet absorption bands of quinones have not been studied. Thus, we have studied this very weak visible absorption band of *p*-benzoquinone in solution. Our results are now reported on.

1) J. W. Sidman, *Chem. Revs.*, **58**, 689 (1958).
2) a) J. C. D. Brand, *J. Chem. Soc.*, **1958**, 858; b) A. D. Cohen and C. Reid, *J. Chem. Phys.*, **24**, 85 (1956); c) G. W. Robinson, *Can. J. Phys.*, **34**, 699 (1956).
3) R. A. Ford, *Spectrochim. Acta*, **13**, 394 (1959).
4) D. S. McClure and P. L. Hanst, *J. Chem. Phys.*, **23**, 1772 (1955).
5) J. C. D. Brand, *Trans. Faraday Soc.*, **50**, 431 (1954).
6) a) J. W. Sidman and D. S. McClure, *J. Am. Chem. Soc.*, **77**, 6461 (1955); b) L. S. Forster, *J. Chem. Phys.*, **26**, 1761 (1957).
7) R. A. Ford and F. Parry, *Spectrochim. Acta*, **12**, 78 (1958).
8) C. Reid, *J. Chem. Phys.*, **18**, 1673 (1950); D. F. Evance, *J. Chem. Soc.*, **1957**, 3385; L. Goodman and M. Kasha, *J. Mol. Spec.*, **2**, 58 (1958); R. C. Hirt, *Spectrochim. Acta*, **12**, 114 (1958).
9) J. W. Sidman, *J. Am. Chem. Soc.*, **78**, 2363 (1956).

Experimental

Measurements. — The absorption spectra were measured with a Cary recording spectrophotometer 14 M with 1, 5, 10 cm. path quartz cells. For the measurements of the very weak absorption bands, the slidewire for the scale expansion, the accessory, was used. A thermostated cell jacket was used for measurements at 5 and 42°C.

Materials.—The solvents were purified according to the methods described in our previous work[10]. Ethyl iodide (a commercial product) was washed with a 1N aqueous solution of potassium hyroxide and repeatedly with water, and distilled after being dried over calcium chloride. *p*-Benzoquinone, toluquinone and *p*-xylo-*p*-quinone (commercial products) were purified by cautious sublimation. *o*-[11] and *m*-xylo-*p*-quinones[12] were prepared according to the methods described in the literature and were purified by cautious sublimation. α-Naphthoquinone was prepared according to Fieser's method[13] and purified by charcoal treatment in an ether solution. 2,5- and 2,6-dichlor-*p*-benzoquinones (commercial products) were recrystallized from ethanol and *n*-heptane, successively*1.

Melting Points (corr.) — *p*-ebnzoquinone 115~116°C, toluquinone 69°C, *o*-xylo-*p*-quinone 56.5~57.5°C, *m*-xylo-*p*-quinone 72.5~73°C, *p*-xylo-*p*-quinone 125°C, α-naphthoquinone 124°C, 2,5-dichloro-*p*-benzoquinone 121.5~122.5°C, 2,6-dichloro-*p*-benzoquinone 162~163°C.

Results

The absorption spectra obtained are given in Figs. 1—6. In these figures ε represents the molecular extinction coefficient.

Discussion

As seen in Figs. 1, 2, 3, 4, 5 and 6, *p*-benzoquinone and its derivatives have very weak adsorption bands (ε_{max} ~0.2) at the long wavelength sides of the $n\rightarrow\pi^*$ singlet-singlet absorption bands. In the following remarks, this band is called the α-band. In many carbonyl compounds (formaldehyde[2], acetaldehyde[3], benzophenone[4], glyoxal[5], diacetyl[6] and camphorquinone[7], very weak absorption bands similar to the α-band, at the long wavelength sides of the $n\rightarrow\pi^*$ singlet-singlet absorption bands, have been found and safely assigned to the $n\rightarrow\pi^*$ singlet-triplet absorption bands by many people on the basis of the phosphorescence spectra, the temperature-independency, the solvent effect and the substitution effect. The maximum molecular extinction coefficient of the α-band (ca. 0.2) is of the same order of magnitude as those of comphorquinone (ca. 0.1) and diacetyl (ca. 0.05), but it is far larger

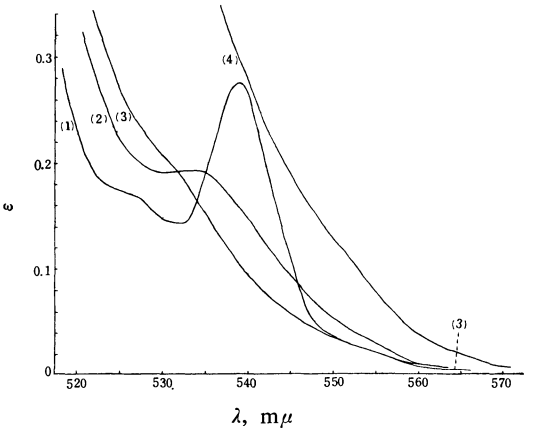


Fig. 1. *p*-Benzoquinone, solvent (1) *n*-heptane; (2) carbon tetrachloride; (3) benzene; (4) ethyl iodide.

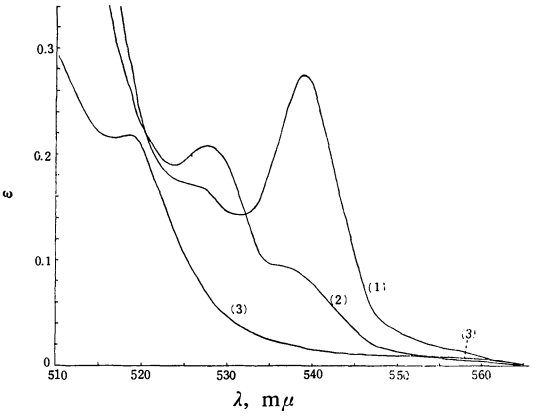


Fig. 2. (1) *p*-Benzoquinone; (2) toluquinone; (3) *p*-xylo-*p*-quinone, solvent *n*-heptane.

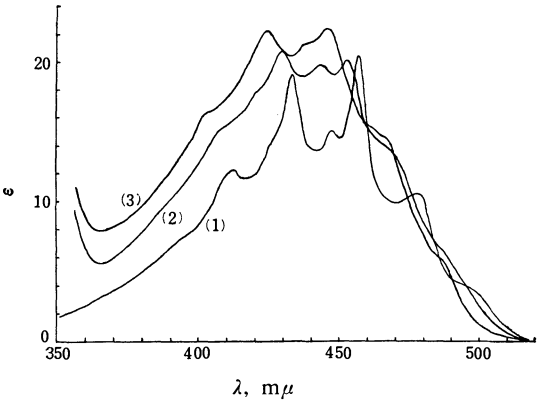


Fig. 3. (1) *p*-Benzoquinone; (2) toluquinone; (3) *p*-xylo-*p*-quinone, solvent *n*-heptane.

10) A. Kuboyama, This Bulletin, **33**, 1027 (1960); *J. Chem. Soc. Japan, Pure Chem. Sec.* (*Nippon Kagaku Zasshi*), **81**, 558 (1960).
11) O. H. Emerson and L. I. Smith, *J. Am. Chem. Soc.*, **62**, 141 (1940).
12) L. I. Smith et al., ibid., **63**, 1038 (1941).
13) L. F. Fieser, "Experiments in Organic Chemistry", D. C. Heath and Co., Boston (1941), p. 23.
*1 In 2,5-dichloro-*p*-benzoquinone, a mixed solvent of *n*-heptane and benzene was used instead of *n*-heptane alone.

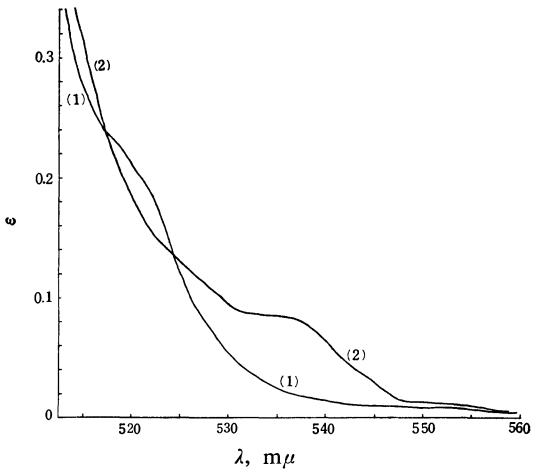


Fig. 4. (1) *o*-Xylo-*p*-quinone; (2) *m*-xylo-*p*-quinone, solvent *n*-heptane.

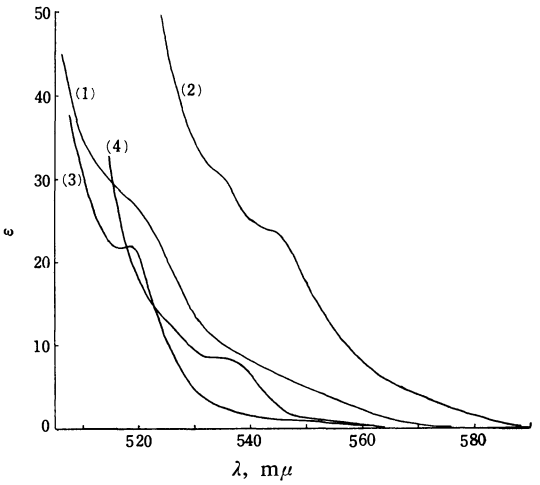


Fig. 5. (1) 2,5-Dichloro-*p*-benzoquinone; (2) 2,6-dichloro-*p*-benzoquinone; (3) *p*-xylo-*p*-quinone; (4) *m*-xylo-*p*-quinone, solvent *n*-heptane.

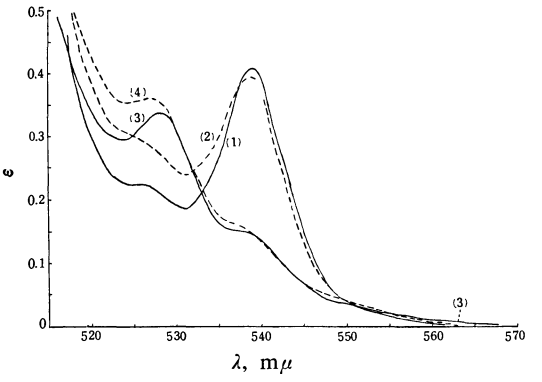


Fig. 6. (1), (2) *p*-Benzoquinone; (3), (4) toluquinone; (1), (3) 4 °C; (2), (4) 42°C, solvent *n*-heptane.

than that of acetaldehyde (ca. 0.0001). For *p*-benzoquinone, the distance*2 (wave number) between the peak (at 539 mμ) of the α-band and the longest wavelength peak (at 479 mμ) of the $n\rightarrow\pi^*$ singlet-singlet band in *n*-heptane is 2330 cm^{-1}. If this value is regarded as the separation between the $n\rightarrow\pi^*$ singlet and triplet excited states, it is of the same order of magnitude as the reported values (2000~3000 cm^{-1}) for the above carbonyl compounds. As seen in Fig. 1, the α-band of *p*-benzoquinone is partly masked by the tail of the $n\rightarrow\pi^*$ singlet-singlet absorption band, and, especially in ethyl iodide, the α-band is so almost entirely masked that the spin-orbit interaction effect of iodine atom on the α-band cannot be examined. In *n*-heptane one peak and one shoulder are observed at 539 mμ and ca. 527.5 mμ respectively. The distance between the peak and the shoulder is ca. 410 cm^{-1}; this vibrational sequence probably corresponds to that in the crystalline spectrum assigned to the totally symmetric ring deformation vibration of the *p*-benzoquinone molecule by Sidman[9]. The α-band shifts toward shorter wavelengths in the order of *n*-heptane, carbon tetrachloride, and benzene, like the $n\rightarrow\pi^*$ singlet-singlet absorption band of *p*-benzoquinone. On the other hand, the $\pi\rightarrow\pi^*$ adsorption bands of the quinones are at shorter wavelengths in *n*-heptane than in carbon tetrachloride and in benzene. As for the methyl group substitution effect, in Fig. 2 the peak of the α-band shifts towards shorter wavelengths as the number of methyl groups increases, in the same manner as in the $n\rightarrow\pi^*$ singlet-singlet bands in Fig. 3. This fact is characteristic of the $n\rightarrow\pi^*$ absorption band[14]. The peaks of the α-band of toluquinone and *p*-xylo-*p*-quinone in *n*-heptane are at 528 and 519 mμ respectively*3. From the solvent effect and the methyl group substitution effect, the α-band is safely assigned to the $n\rightarrow\pi^*$ absorption band. As seen in Fig. 2, toluquinone alone has a shoulder at the long wavelength side of the peak. In the $n\rightarrow\pi^*$ singlet-singlet bands in Fig. 3, such an abnormality of toluquinone as the above cannot be observed. Therefore, this abnormality of toluquinone seems to be intrinsic to the α-band. In Fig. 4, the α-band of *o*-xylo-*p*-quinone is similar to that of *p*-xylo-*p*-quinone, while the band of *m*-xylo-*p*-quinone has a shoulder similar to that of toluquinone. Therefore, it is concluded that

*2 The corresponding one in the crystalline state, studied by Sidman[9], was 2060 cm^{-1}.

14) H. Baba, *J. Chem. Soc. Japan, Pure Chem. Sec.* (*Nippon Kagaku Zasshi*), **72**, 341 (1951); S. Nagakura, This Bulletin, **25**, 164 (1952); A. Kuboyama, *J. Chem. Soc. Japan, Pure Chem. Sec.* (*Nippon Kagaku Zasshi*), **77**, 1062 (1956).

*3 α-Naphthoquinone has a peak at 491 mμ in *n*-heptane, similar to that of *p*-xylo-*p*-quinone.

these shoulders are characteristic of the structure where two carbonyl groups of *p*-benzoquinone are not equivalent. As seen in Fig. 2, *p*-benzoquinone has a tail which extends over the long wavelength side of the peak. This tail may be enhanced to become the shoulders in toluquinone and *m*-xylo-*p*-quinone mentioned above. It is uncertain whether this tail and the α-band are due to the same electronic transition or not. As seen in Fig. 5, in dichloro-*p*-benzoquinones the intensities of the α-band are considerably enhanced in comparison with those of dimethyl-*p*-benzoquinones. This enhancement of the intensity of the α-band is surely to be attributed to the spin-orbit interaction effect of chlorine atoms. Therefore, this fact is indicative of the α-band being the singlet-triplet absorption band. Further, we have examined the temperature-dependency of the α-band of *p*-benzoquinone and toluquinone. Though, as seen in Fig. 6, owing to the tails of the $n\rightarrow\pi^*$ singlet-singlet bands the temperature-dependency cannot be fully examined, it seems that no noticeable temperature-dependency can be observed in the temperature range 4~42°C. In conclusion, from the results obtained in this work, the α-band is reasonably assigned to the $n\rightarrow\pi^*$ singlet-triplet absorption band.

Summary

The very weak absorption bands at the long wavelength sides of the $n\rightarrow\pi^*$ singlet-singlet absorption bands of *p*-benzoquinone and its derivatives were examined with regard to the solvent effect, the substitution effect and the temperature-dependency. From the obtained results, this absorption band is reasonably assigned to the $n\rightarrow\pi^*$ singlet-triplet absorption band. As for its absorption curve, a distinct difference between the structure where the two carbonyl groups of *p*-benzoquinone are equivalent and that where the two carbonyl groups are not equivalent is observed.

The author wishes to express his sincere thanks to Professor Saburo Nagakura and Dr. Hiroshi Tsubomura of The University of Tokyo for their helpful advices and to Dr. Yoichiro Mashiko of this Institute for his kind offices. The author's thanks are also due to Mr. Akio Suzuki and Mr. Hiroshi Wakikawa of this Institute for their kind assistances in this work.

Government Chemical Industrial Research Institute of Tokyo
Shibuya-ku, Tokyo

Absorption Spectra and Catalytic Behavior of the Copper(II) Chelates of Some Alkylated Ethylenediamines

By Heijirô OJIMA and Kôzô SONE

(Received July 12, 1961)

The copper chelates of various alkylated ethylenediamines were studied first by Pfeiffer and Glaser[1], and then by Irving and Griffiths[2], and especially by Basolo and his collaborators[3]. Comparative studies of the absorption spectra of some of these chelates have been carried out recently by the present authors, together with some experiments on their activities to catalyze the chemiluminescent reaction of luminol with hydrogen peroxide in alkaline solution. The results of these experiments will be described and discussed in the present paper.

1) P. Pfeiffer and H. Glaser, *J. prakt. Chem.*, **151**, 134 (1938).
2) H. Irving and J. M. M. Griffiths, *J. Chem. Soc.*, **1954**, 213.
3) F. Basolo and R. K. Murmann, *J. Am. Chem. Soc.*, **74**, 5243 (1952); **76**, 211 (1954); F. Basolo, Y. T. Chen and R. K. Murmann, ibid., **76**, 956 (1954).

Experimental

Materials. — The samples of $[Cu\,en_2](ClO_4)_2$, $[Cu\,pn_2](ClO_4)_2$ and $[Cu(N,N\text{-diethyl-en})_2](ClO_4)_2$ were prepared and purified according to the methods of the literature[1], while those of $[Cu(\text{tetramethyl-en})_2]I_2$, $[Cu(N\text{-propyl-en})_2]Br_2$ and $[Cu(N,N'\text{-dipropyl-en})_2](NO_3)_2$ were kindly presented by Prof. Fred Basolo of Northwestern University (Evanston, Ill., U. S. A.) to one of the authors (K. S.). The spectrum of $[Cu(N\text{-hydroxyethyl-en})_2]^{2+}$ was measured with a solution containing $CuSO_4$ (5×10^{-3} M) and purified ligand amine in the molar ratio of 1 : 2 (ionic strength : 0.5 with KNO_3).

Absorption Spectra.—A Shimadzu QR-50 quartz spectrophotometer with cells 10 mm. in thickness

was used throughout this study. 5×10^{-3} M solutions of the chelates were used in the spectral measurements; their ionic strength was kept at 0.5 by adding potassium nitrate. The measurements were mostly carried out at approx. 27°C.

Paper Electrophoresis.—Filter paper strips (6× 22 cm²) were dipped in electrolyte solutions containing various amounts of NaOH up to 5×10^{-2} M (ionic strength: 5×10^{-2} with potassium nitrate for 10 hr., and small amounts of aqueous solutions of the chelates (approx. 10^{-7} mol.) were spotted at their centers. Electrophoresis experiments with these strips were then carried out by means of the horizontal open strip method, with a potential of 10 V./cm. and at 25°C for 30 min. The migration distances of the spots were measured, and corrections were made of the flow of the liquid phase caused by electroösmosis and evaporation effects, by comparing the data with those of *o*-nitroaniline obtained under the same conditions. The corrected data were plotted against the alkali concentration (cf. Fig. 5).

Catalytic Activity for the Chemiluminescence of Luminol. — Seven milliliters portions of various sodium hydroxide solutions ($0\sim5\times10^{-2}$ M; ionic strength: 0.1 with potassium nitrate) containing luminol (10^{-5} mol.) and each one of the chelates (5×10^{-6} mol.) were kept in a thermostat at 25°C, and 0.5 ml. portion of a hydrogen peroxide solution (containing 1.6×10^{-4} mol.) was poured rapidly into each of them. The intensities of the chemiluminescence emitted by these mixtures were measured by means of a selenium photocell-galvanometer circuit, and the maxima of the galvanometer readings, which were obtained several seconds after the addition of the hydrogen peroxide solution, were plotted against the alkali concentration (cf. Fig. 6).

Results and Discussion

Visible Absorption Spectra.—The visible absorption spectra of the chelates in their aqueous solutions are shown in Fig. 1, and the maximum frequencies and molar extinction coefficients (ν_{max} and ε_{max}) calculated from these curves are shown in Table I, together with the values of their stability constants taken from the literature[2,3]. It can be seen that there is an approximately linear relationship between ν_{max} and log k_1k_2 (or log k_2), so that the more stable a chelate is, the larger is its ν_{max} value, in accord with the general trend observed in many Co(III) and Cr(III) complexes as well as in certain complexes of

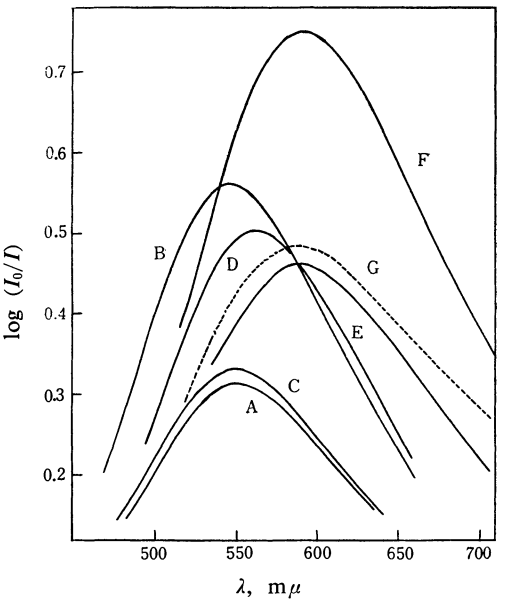


Fig. 1. Absorption spectra of the chelates. A, B,....., G: cf. Table I. Concn.: 5×10^{-3} M.

Table I

	Chelates	ν_{max} (10^{13} sec^{-1}) in H_2O ( ): ε_{max}*	in EtOH	log k_1	log k_2**
(A)	$[Cu\,en_2]^{2+}$	54.5 (64)	54.5	10.76	9.37[3]
(B)	$[Cu(tetramethyl\text{-}en)_2]^{2+}$	55.0 (112)	52.6	11.63	10.24[3]
(C)	$[Cu\,pn_2]^{2+}$	54.5 (66)	—	10.78	9.28[3]
(D)	$[Cu(N\text{-}propyl\text{-}en)_2]^{2+}$	53.2 (101)	50.0	9.98	8.16[3]
(E)	$[Cu(N, N'\text{-}dipropyl\text{-}en\text{-}_2]^{2+}$	50.8 (93)	51.8	8.79	5.55[3]
(F)	$[Cu(N, N\text{-}diethyl\text{-}en)_2]^{2+}$	50.6 (150)	53.0	8.17	5.55[2]
(G)	$[Cu(N\text{-}hydroxyethyl\text{-}en)_2]^{2+}$	50.9 (97)	—	—	—

* The ε_{max} values in this table are those calculated from the curves of Fig. 1; the exact values of the more unstable chelates may be somewhat higher than these. In fact, while the addition of an excess of ethylenediamine (Cu: en=approx. 1:10) to a solution of $[Cu\,en_2]^{2+}$ has almost no effect on its spectra, the addition of *N*, *N*-diethyl-ethylenediamine to a solution of $[Cu(N, N\text{-diethyl-en})_2]^{2+}$ causes a small but noticeable increase in the intensity (up to approx. 15% when Cu: amine=1:8) of its absorption band, indicating the partial dissociation of the latter chelate in its solution.

** The log *k* values are all those at 25°C and at an ionic strength of 0.5, except in (F), where the ionic strength is 0.1. The log *k* values of $[Cu(N, N'\text{-dimethyl-en})_2]^{2+}$ in Fig. 2 are those of Basolo et al.[3], which were obtained under the same conditions.

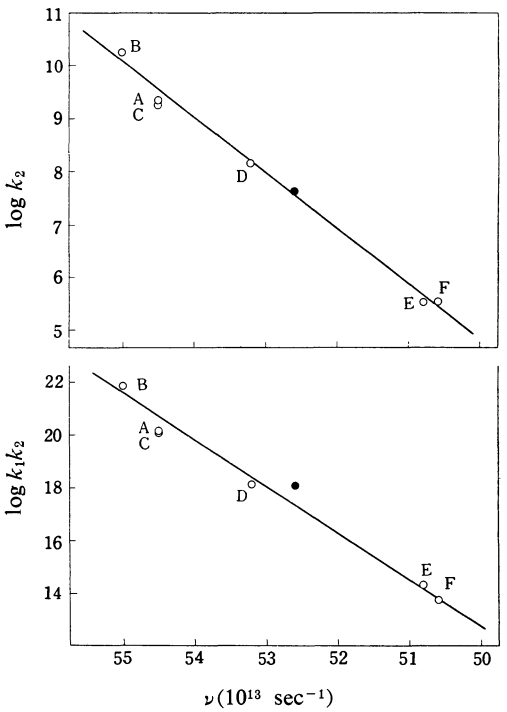


Fig. 2. Relation between ν_{max} and log k values of the chelates. A, B,···, F: cf. Table I. Black circles correspond to $[Cu(N,N'\text{-dimethyl-en})_2]^{2+}$, the value of which were taken from the literature[2,3] (cf. Footnote of Table I).

Ni(II) and Cu(II)[4] (cf. Fig. 2). It can also be seen that the absorption intensities of the alkylated chelates are generally much higher than that of $[Cu\,en_2]^{2+}$.

It was formerly observed by Sone and Kato[5] that a striking color change from blue-violet to yellow took place when the alcoholic solutions (or aqueous solutions containing sodium perchlorate) of $[Ni\,en_2]^{2+}$ and $[Ni\cdot pn_2]^{2+}$ were heated, and this change was ascribed to the existence of the equilibrium

$$[Ni\,en_2A_2]^{2+} \rightleftarrows \underset{\text{blue-violet}}{} [Ni\,en_2]^{2+} + 2A \quad (A: H_2O \text{ or EtOH})$$
yellow

in these media[5]. On the other hand, no such drastic spectral change was observed when the copper chelates studied here were treated in the same manner; only small shifts and intensity changes in their absorption curve occurred. Some data on the absorption bands in alcoholic solutions are given in Table I. It may be of interest that the bands of the two unstable chelates shift to shorter wavelengths in alcohol, while the bands of the other chelates generally shift in the opposite direction. The natures of these shifts were not studied in greater detail, however, partly because some of these chelates were sparingly soluble in such media, and also because of the lack of sufficient quantities for such a study.

It is also of some interest to compare the absorption curve of the chelate $[Cu(N\text{-propyl-en})_2]^{2+}$ with that of $[Cu(N\text{-hydroxyethyl-en})_2]^{2+}$, the ligand of which contains an -OH group instead of $-CH_3$ at the end of the *N*-substituent radical. It has already been shown by Harvey, Hall et al.[6,7] that the latter complex is formed predominantly in a solution containing Cu^{2+} and *N*-hydroxyethyl-ethylenediamine in the ratio of 1:2; the absorption curve of such a mixture measured by the present authors (curve G, Fig. 1) agreed well with the data of these earlier investigators, showing a band at 590 mμ which lies at a much longer wavelength than the band of the *N*-propyl chelate, This difference is very probably due to the 5- (or possibly 6-) coordinated structure of the *N*-hydroxyethyl chelate, in which also the -OH group is taking part in coordination, since a number of instances showing that the formation of a 5- or 6-coordinated structure in a copper complex is generally accompanied by a shift of its absorption band to a longer wavelength is already known in the literature[8-11]. For example, Rosenblatt[8] found that the addition of a large quantity of NH_3 to a solution of $[Cu\cdot en_2]^{2+}$ produced a shift of its band at 550 mμ to ~610 mμ, owing to the formation of the complex $[Cu\,en_2NH_3]^{2+}$, and Jonassen et al.[9] observed a similar shift in solutions containing $[Cu\,en_2]^{2+}$ and NaOH, owing to the formation of $[Cu\,en_2OH]^{+}$ in such media.

Effect of Added Alkali on the Spectra.—In their study of copper complexes of *N*-alkylated ethanolamines, the present authors found that the spectral data indicate the presence of at least two types of complexes, a chelate and a non-chelate, in their solutions containing various amounts of ligand and sodium hydroxide[12].

4) Cf. e. g., R. Tsuchida, "Color and Structure of Metallic Compounds", Zoshindo, Osaka (1947); H. Ito, *J. Chem. Soc. Japan, Pure Chem. Sec.* (*Nippon Kagaku Zasshi*), **77**, 1383 (1956).
5) K. Sone and M. Kato, *Z. anorg. u. allgem. Chem.*, **301**, 277 (1959).
6) J. L. Harvey, C. I. Tewksbury and H. M. Haendler, *J. Am. Chem. Soc.*, **71**, 3641 (1949).
7) J. L. Hall and W. E. Dean, ibid., **80**, 4183 (1958).
8) F. Rosenblatt, *Z. anorg. u. allgem. Chem.*, **204**, 351 (1932).
9) H. B. Jonassen, R. E. Reeves and L. Segal, *J. Am. Chem. Soc.*, **77**, 2748 (1955).
10) S. Yamada and R. Tsuchida, This Bulletin, **29**, 289 (1956).
11) H. Ito, Ref. 4.
12) H. Ojima and K. Sone, *Z. anorg. u. allgem. Chem.*, **309**, 110 (1961).

The effect of added alkali on the spectra of the alkylated ethylenediamine chelates, which were studied in a manner similar to that of Jonassen et al. cited above, is now shown in Figs. 3 and 4; it can be seen that the situation is quite different here from that in ethanolamine complexes, owing to the increased stability of the chelate rings formed by the diamine molecules[13].

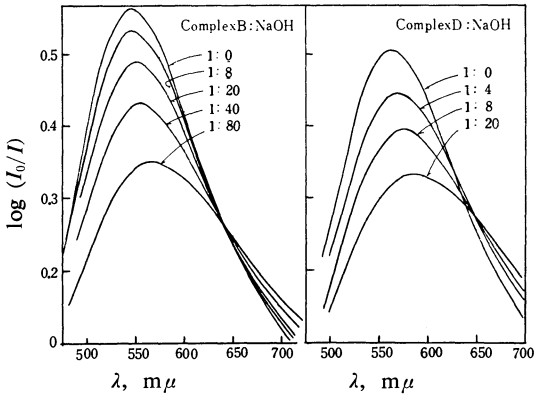


Fig. 3. Effect of added alkali on the spectra of $[Cu(tetramethyl\text{-}en)_2]^{2+}$ (B) and $[Cu\cdot(N\text{-}propyl\text{-}en)_2]^{2+}$ (D).

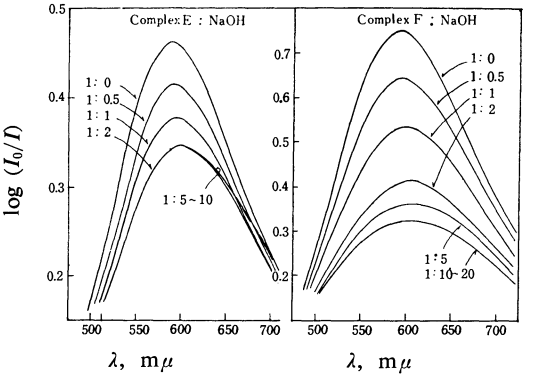


Fig. 4. Effect of added alkali on the spectra of $[Cu(N, N'\text{-}dipropyl\text{-}en)_2]^{2+}$ (E) and $[Cu(N, N\text{-}diethyl\text{-}en)_2]^{2+}$ (F).

In the case of tetramethyl and *N*-propyl chelates (Fig. 3), it can be seen that the appearance of the spectral changes is very similar to that of $[Cu\,en_2]^{2+}$ described by Jonassen et al.; this indicates the gradual formation of the complexes of the type $[Cu\,en_2\cdot OH]^{+}$ with an increasing OH^- concentration. Approximate values of their formation constants can be estimated at ~2 and 15 respectively from analysis of the curves in Fig. 3.

13) The precipitation of $Cu(OH)_2$, which frequently occurs in mixtures containing OH^- ions and *N*-alkylated ethanolamine complexes (cf. Ref. 12), is not observed in the solutions of the compositions shown in Figs. 3 and 4.

On the other hand, the situation is somewhat different in the case of *N, N'*-dipropyl and *N, N*-diethyl chelates. The curves in Fig. 4 show that even relatively small amounts of sodium hydroxide can cause a great decrease in their absorption intensities; as soon as only two moles of OH^- ions are added to one mole of the chelate, the change seems to become more or less complete.

Now the drastic spectral changes of these chelates can be explained in the following manner: because there are so many and such large alkyl groups around the coordination center, it is to be expected that the formation of the $[Cu\,en_2OH]^{+}$-type complexes would be strongly hindered in these chelates; however, the steric interactions of these groups make these chelates themselves unstable (cf. $\log k$ values in Table 1), so that they are easily decomposed by relatively small amounts of OH^- ions, probaly through the following successive steps:

$$[Cu(R_2\text{-}en)_2]^{2+} + OH^- + H_2O \longrightarrow \left[(R_2\text{-}en)Cu\begin{matrix}OH\\ \cdot\cdot OH_2\end{matrix}\right]^{+} + R_2\text{-}en$$

I

$$2\,I \longrightarrow \left[(R_2\text{-}en)Cu\begin{matrix}OH\cdot\cdot\\ \cdot\cdot OH\end{matrix}Cu(R_2\text{-}en)\right]^{2+}$$

II

$$+2H_2O$$

$$\left.\begin{matrix}I & +OH^-\\ II/2 & +OH^-\end{matrix}\right\} \longrightarrow [(R_2\text{-}en)Cu(OH)_2]^0$$

III

In fact, Pfeiffer and Glaser[1] obtained binuclear complexes like II by using *N, N'*-trialkylated ethylenediamines as ligands, and Martell et al.[14] recently studied the equilibria involving chelates of types I, II and III by using ligands which are very similar to those in this study.

Therefore, it seems probable that the spectral changes in Fig. 4 are due to these decomposition reactions, which lead eventually to the complexes of the type $[Cu\,en(OH)_2]$ with no electric charge. Experimental data supporting this point of view are also obtained from the studies of the behaviors of these chelates in paper electrophoresis.

Paper Electrophoresis Studies.—It was found by Maki[15] and also Ojima[16] that there is a marked parallel between the migration velocities

14) A. E. Martell, S. Chaberek, R. Courtney, S. Westerback and H. Hyytiainen, *J. Am. Chem. Soc.*, **79**, 3036 (1957); R. C. Courtney, R. L. Gustafson, S. Chaberek, Jr. and A. E. Martell, ibid., **81**, 519 (1959); R. L. Gustafson and A. E. Martell, ibid., **81**, 525 (1959).

15) M. Maki, *Japan Analyst (Bunseki Kagaku)*, **4**, 217 (1955).

16) H. Ojima, *J. Chem. Soc. Japan, Pure Chem. Sec. (Nippon Kagaku Zasshi)*, **78**, 1331 (1957).

of ionic complexes in paper electrophoresis experiments and the magnitudes of their electric charges, if complexes with similar structures are used for comparison. The results of such experiments on the chelates studied here, carried out in solutions containing various amounts of sodium hydroxide, are shown in Fig. 5. In solutions containing no sodium

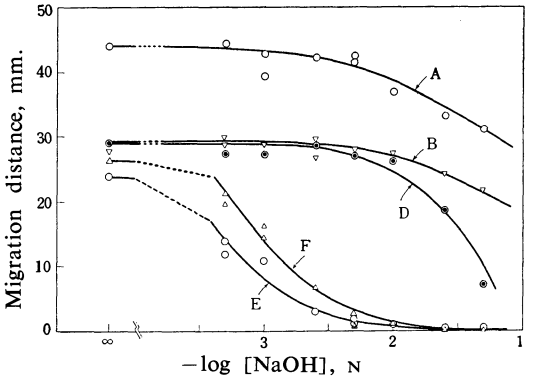


Fig. 5. Relation between migration distance and alkali concentration. A, B, ···, F: cf. Table I.

hydroxide, the mobilities of the alkylated chelates are all smaller than that of $[Cu\cdot en_2]^{2+}$ and are not very different from one another, although it seems that the mobility becomes smaller with the increase in substituted alkyl groups. The mobilities of the more stable chelates of ethylenediamine and tetramethyl- and *N*-propyl-ethylenediamines do not change very much with the addition of OH^- ions, and they gradually decrease when the alkali concentration becomes large, probably owing to the formation of $[Cu\,en_2OH]^+$-type complexes. On the other hand, the mobilities of the two other chelates begin to drop quickly and approach zero with an increasing alkali concentration, indicating the final formation of uncharged complexes. The color of the spots indicates, however, that there is no precipitation of $Cu(OH)_2$, and the tailing of the spots observed when the alkali concentration is $5\sim25\times10^{-4}$ N suggests the coexistence of two or more complex species in solution. All these findings are in accord with the foregoing considerations based on the spectral changes of these chelates.

Catalytic Behavior in the Chemiluminescence of Luminol.—It was shown earlier by Ojima[17,18] that the chemiluminescence emitted in the reaction between luminol (5-aminophthalaz-1, 4-dione) and hydrogen peroxide in alkaline solution is remarkably intensified by various amine complexes of copper. The mode of this catalytic action depends strongly on the nature of the amine used; NH_3, pyridine, and primary aliphatic amines are all effective, but complex solutions containing these ligands in a great excess (Cu: amine=1: several hundreds when the concentration of Cu^{2+} is 5×10^{-6} g. ion/7 ml.) must be used to obtain the maximum effect. On the other hand, only a small quantity of ethylenediamine (Cu: en=approx. 1:2) is sufficient to create an effect of similar magnitude, and the luminescence is markedly hindered when ethylenediamine is added in excess.

On the basis of these and other results, Ojima postulated the formation of an intermediate complex $[Cu\cdot en\cdot(\text{luminolate anion})]^+$ in such media, which reacts more easily with hydrogen peroxide than free luminol, emitting a stronger luminescence than that of the latter.

It was found that all the chelates studied here show the same catalytic effect; the relation between the observed luminescent intensities and alkali concentrations are shown in Fig. 6, and the relation between the maximum intensities in this figure and the chelate stabilities is shown in Fig. 7. It is clear from these data that the catalytic activity increases with the decreasing chelate stability; this fact is also in conformity with the mechanism postulated above, since the formation of the complex $[Cu\cdot en\cdot(\text{luminolate anion})]^+$ will be facilitated by the instability of the original chelate.

It is certain that many further studies are

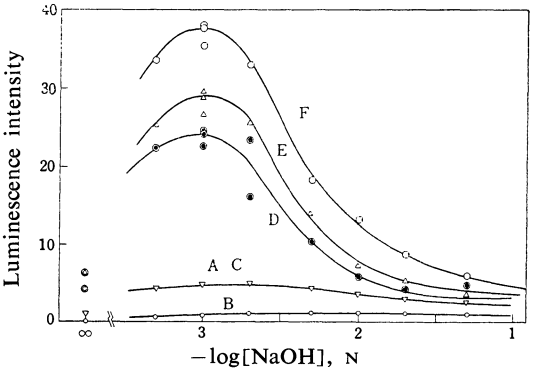


Fig. 6. Relation between chemiluminescence intensity and alkali concentration in the reaction mixture. A, B, ···, F: cf. Table I.

17) H. Ojima, ibid., **79**, 1076 (1958); **80**, 965, 1371 (1959); **81**, 1785 (1960).

18) Recently, the authors found that the data of B. Kirson (*Bull. soc. chim. France*, **1956**, 1793; **1957**, 257) on the catalytic decomposition of H_2O_2 by copper complexes are of special interest in connection with this problem. Some data on the absorption spectra of Cu-ammine complexes are also given in his papers. However, the possible relation of his results to those of the authors will be discussed more fully elsewhere.

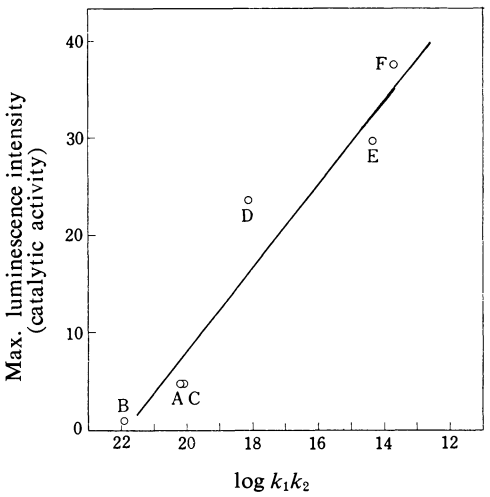


Fig. 7. Relation between catalytic activity and chelate stability. A, B,···, F: cf. Table I.

needed to get a clear understanding of this complicated reaction; however, even apart from the discussions of the reaction mechanism, the data in Figs. 6 and 7 are of practical interest, because they suggest a new method of estimating chelate stabilities with the aid of chemiluminescence measurements, although its application will be limited to certain favorable cases like the present ones.

Summary

The absorption spectra of the copper chelates of ethylenediamine and several alkylated ethylenediamines were studied in their aqueous solutions, and an approximately linear relationship was found between the frequencies of their absorption maxima and the logarithms of their stability constants. The spectral changes caused by the addition of a strong base (sodium hydroxide) to these solutions, and the activities of these chelates to catalyze the chemiluminescent reaction of luminol with sodium peroxide in an alkaline solution, were also studied; it was shown that the chelates with smaller stabilities show, in general, more drastic spectral changes and higher catalytic activities than those with larger stabilities.

The authors are grateful to Professor Fred Basolo of Northwestern University, Evanston, Ill., U. S. A., for his invaluable gift of chelate samples, and also to Professor Hatsusaka Kato of their University for his encouragement throughout this study.

Aichi Gakugei University
Chemical Laboratories
Okazaki and Nagoya

*Polymerization of Olefines by Ziegler Catalyst. II. Polymerization of Ethylene by $AlEt_3$-$TiCl_4$ Catalyst**

By Kenichi FUKUI, Tsutomu KAGIYA, Sueo MACHI, Takeo SHIMIDZU and Sachio YUASA

(Received June 13, 1961)

Since polymerization of ethylene at low pressure and temperature in the presence of the catalyst obtained from the interaction of titanium tetrachloride with aluminum trialkyl has been discovered by Ziegler[1], several studies on this type of polymerization have been reported.

The present paper concerns a study on ethylene polymerization with $AlEt_3$-$TiCl_4$ catalyst as an extension of the investigation previously reported[2] for propylene polymerization with the same catalyst. The reaction conditions are correlated with the polymerization rate as well as with the properties of polymers.

Experimental

Ethylene was produced by dehydrating ethanol over activated alumina at 350°C and then liquefied under pressure and distilled. The purity of the gas is more than 99.9%. Other materials and the apparatus were exactly the same as those described

* Presented at the 11th Annual Meeting of the Chemical Society of Japan, Tokyo, April, 1958.

1) K. Ziegler, Belg. Pat. 533362 (1954).

2) S. Kodama, T. Kagiya, S. Machi, T. Shimidzu, S. Yuasa and K. Fukui, *J. Appl. Polymer Sci.*, 3, 20 (1960).

in the previous paper[2]. Introduction of catalyst into the reaction vessel was made in a nitrogen stream by pipetting a definite amount of titanium tetrachloride solution (0.15 M. solution in *n*-heptane) followed by adding triethyl aluminum solution (0.9 or 3.0 M solution in *n*-heptane) at room temperature (15~20°C). Immediately after the addition of the catalyst, the inner nitrogen was purged under reduced pressure. After the temperature was raised to the desired one, the pressure was then raised to a definite one by introducing compressed ethylene gas. The polymerization then started. It always took 20 min. from the addition of the catalyst to the introduction of ethylene gas. The pressure decreased during the reaction, and was recorded to estimate the reaction rate. In addition, some experiments were carried out under constant pressure.

The number average molecular weight, $\overline{M}_n$, was estimated by the intrinsic viscosity measurement in tetralin at 130°C, using Tung's formula[3],

$$[\eta] = 5.10 \times 10^{-4} \overline{M}_n^{0.725}$$

Results and Discussion

The experimental results obtained are shown in the following several figures. The discussions will be made in regard to two items; namely, the molecular weight and the polymerization rate.

Molecular Weight.—The dependence of the molecular weight on the various factors is shown in Figs. 1, 2 and 3, which make it clear that the important factors affecting the molecular weight are the ratio of triethylaluminum to titanum tetrachloride. The increase in the reaction temperature and the amount of catalyst makes the molecular weight decreased to some extent, as shown in Fig. 1, where the ratio of triethylaluminum to titanium tetrachloride is kept constant. As shown in Fig. 2, the molecular weight also increases sharply with the ratio of triethylaluminum to titanium

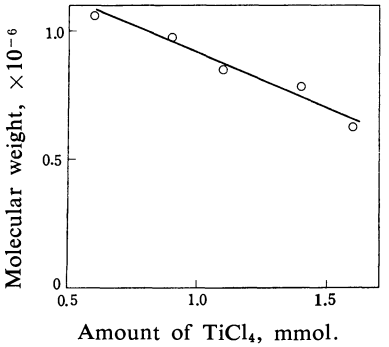


Fig. 1. Molecular weight vs. amount of $TiCl_4$. ($AlEt_3/TiCl_4$, 6.7; Solvent, 16 ml.; Temperature, 50°C; Initial pressure, 43 kg./cm²; Reaction time, 120 min.)

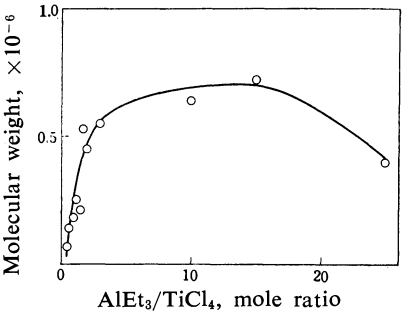


Fig. 2. Molecular weight vs. $AlEt_3/TiCl_4$ ratio. ($TiCl_4$, 1.2 mmol.; Solvent, 16 ml.; Temperature, 50°C; Initial pressure, 43 kg./cm²; Reaction time, 120 min.)

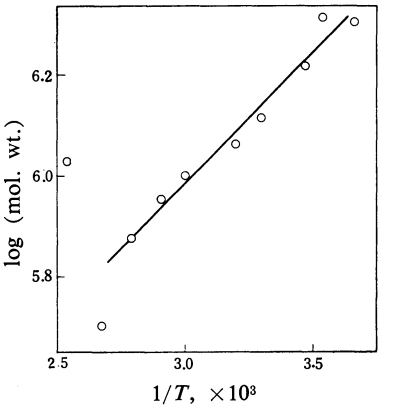


Fig. 3. Molecular weight vs. reaction temperature.
($TiCl_4$, 1.2 mmol.; $AlEt_3$, 8.0 mmol.; Solvent, 16 ml.; Initial pressure, 43 kg./cm².; Reaction time, 120 min.)

tetrachloride in the range from 0 to 3, but it is only slightly affected with more addition of trithylaluminum, where the amount of titanium tetrachloride is kept constant. The molecular weight decreases nearly exponentially with temperature rise. As shown in Fig. 3, the plot of the logarithm of molecular weight versus the reciprocal of absolute temperature gives a straight line. The dependences of the molecular weight on the temperature and the ratio of two components of catalyst are almost the same as the case of polypropylene produced by the same catalyst[2].

Recently, Badin[4] reported that the molecular weight of polyethylene produced by $TiCl_4$-Al·(i-C_4H_9)$_3$ catalyst, was decreased with raising reaction temperature, with increased ratio of $TiCl_4$ to Al(i-C_4H_9)$_3$, and with increasing amount of catalyst. These are coincident with our present results.

Rate of Polymerization. — Several pressure-reaction time curves are shown in Fig. 4. This

3) L. H. Tung, *J. Polymer Sci.*, **24**, 333 (1957).

4) E. J. Badin, *J. Am. Chem. Soc.*, **80**, 6545 (1958).

experiment is carried out in a batch type reaction vessel. These curves, of course, represent the diminishing ethylene pressure which causes the fall of polymerization rate. But, as was previously observed in the polymerization of propylene with the same catalyst, the polymerization rate falls even at a constant ethylene pressure. An experiment is carried out at a constant ethylene pressure, and the result is shown in Fig. 5.

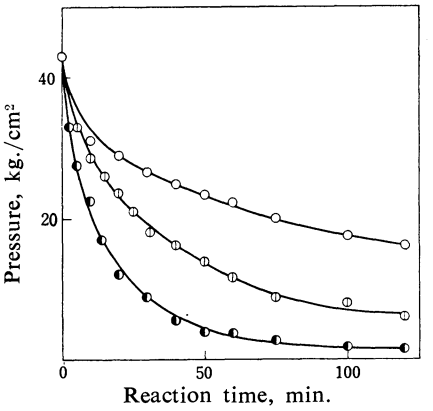


Fig. 4. Pressure vs. reaction time.
○ $TiCl_4$, 1.2 mmol.; $AlEt_3$, 0.96 mmol.;
◐ $TiCl_4$, 1.1 mmol.; $AlEt_3$, 7.4 mmol.;
◑ $TiCl_4$, 1.6 mmol.; $AlEt_3$, 10.7 mmol.;
Solvent, 16 ml; Temperature, 50°C.

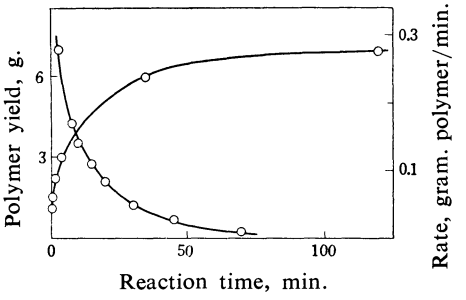


Fig. 5. Polymer yield vs. reaction time.
($TiCl_4$, 0.68 mmol.; $AlEt_3$, 4.65 mmol.; Solvent, 16 ml.; Temperature, 30°C; Pressure, 11 kg./cm².)

In order to decide the dependence of the rate on ethylene pressure, the initial rate is analyzed. Figure 6 shows that the initial rate is almost proportional to the ethylene pressure over the range of 0~30 kg./cm² (Ludlum et al.[5] reported that the rate of ethylene polymerization with $TiCl_4$-$LiAlR_4$ catalyst was also proportional to ethylene pressure). Thus the "specific" rate should be defined by the rate divided by ethylene pressure. The estimation

5) D. B. Ludlum, A. W. Anderson and C. E. Ashby, ibid., **80**, 1380 (1958).

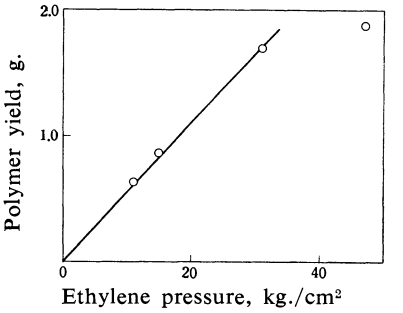


Fig. 6. Polymer yield during initial 90 sec. vs. reaction pressure.
($TiCl_4$, 0.6 mmol.; $AlEt_3$, 3.6 mmol.; Solvent, 16 ml.; Temperature, 30°C; Reaction time, 90 sec.)

of the rate of polymerization from the curves of Fig. 4 is made in the same manner as described in the previous paper. Namely, the pressure drop during the first 30 min. divided by the mean pressure times the duration of reaction (30 min.) is used as a measure of the rate. This value is indicated in Figs. 7, 8 and 9 as the "mean specific rate".

Dependence of Rate on the Amount of Catalyst. —Figure 7 indicates that the mean specific rate is almost proportional to the amount of titanium tetrachloride, where the ratio of triethylaluminum to titanium is kept constant. This result is the same as that obtained in the polymerization of propylene. That this curve does not pass through the origin might be due to the impurities.

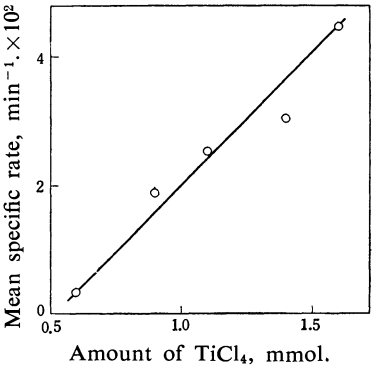


Fig. 7. Mean specific rate vs. amount of $TiCl_4$.
($AlEt_3/TiCl_4$, 6.7; Solvent, 16 ml.; Temperature, 50°C; Initial pressure, 43 kg./cm².)

Dependence of Rate on Catalyst Composition. —With a definite amount of titanium tetrachloride, the rate varies with the amount of triethylaluminum added as shown in Fig. 8. The rate increases rapidly with the increase in the amount of triethylaluminum and then maintains an almost constant value over the range of which the ratio of triethylaluminum

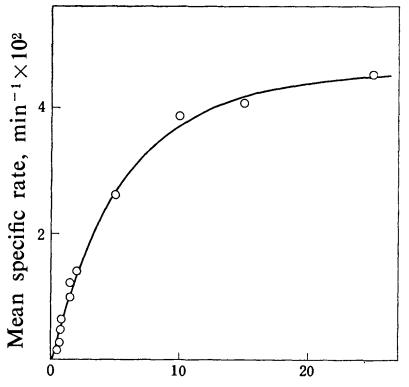


Fig. 8. Mean specific rate vs. $AlEt_3/TiCl_4$ ratio.
($TiCl_4$, 1.2 mmol.; Solvent, 16 ml.; Temperature, 50°C; Initial pressure, 43 kg./cm^2)

to titanium tetrachloride is from 10 to 25.

Temperature Dependence of Rate.—The plot of the logarithm of the rate against the reciprocal of absolute temperature is shown in Fig. 9. The rate first increases with temperature rise and then falls off at higher temperatures. The temperature to give the maximum rate is 85°C. The straight line in the range from 0 to 85°C gives an "apparent" activation energy of 1.0 kcal./mol. To estimate the value of activation energy corresponding to the pure polymerization step in the liquid phase, the heat of solution of ethylene in *n*-heptane is calculated from known data[6], which amounts to −1.7 kcal./mol. Consequently, 2.7 kcal./mol. for the activation energy of polymerization in the liquid phase is obtained.

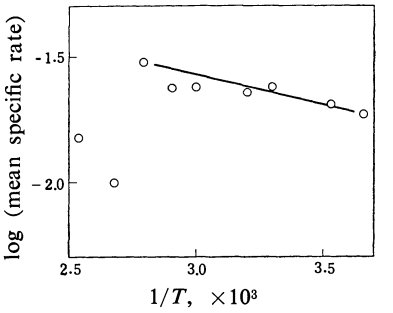


Fig. 9. Mean specific rate vs. reaction temperature.
($TiCl_4$, 1.2 mmol.; $AlEt_3$, 8.0 mmol.; Solvent, 16 ml.; Initial pressure, 43 kg./cm^2)

The decrease of the rate at higher temperatures may be due to the deterioration of the catalyst as has been observed in the propylene polymerization by $AlEt_3$-$TiCl_4$ catalyst[2].

Faculty of Engineering
Kyoto University
Sakyo-ku, Kyoto

6) "International Critical Table," Vol. 3, 269 (1928).

*Polymerization of Olefines by Ziegler Catalyst. III. Polymerization of Ethylene by $AlEt_3$-$TiCl_3$ Catalyst**

By Kenichi FUKUI, Tsutomu KAGIYA, Sueo MACHI, Takeo SHIMIDZU and Sachio YUASA

(Received June 13, 1961)

As an extension of the investigation previously reported for ethylene[1] and propylene[2] polymerization with $AlEt_3$-$TiCl_4$ catalyst, a study on the polymerization of ethylene by means of $AlEt_3$-$TiCl_3$ catalyst is described in the present paper. No report of the study on the ethylene polymerization with $AlEt_3$-$TiCl_3$ catalyst is found, while the polymerization of propylene with the same catalyst has been studied by Natta et al.[3]

Experimental

The apparatus and the procedure adopted was utterly the same as those described in the previous paper[1,2]. Titanium trichloride was due to the Sumitomo Chemical Co., Ltd. Introduction of the catalyst components into the autoclave was made by pipetting an amount of a dispersion of titanium trichloride in *n*-heptane (78 g. titanium trichloride

* Presented at the 7th Annual Meeting of the High Polymer Chemical Society, Tokyo, May, 1958.

1) K. Fukui, T. Kagiya, S. Machi, T. Shimidzu and S. Yuasa, This Bulletin, 35, 303 (1962).

2) S. Kodama, T. Kagiya, S. Machi, T. Shimidzu, S. Yuasa and K. Fukui, *J. Appl. Polymer Sci.*, 3, 20 (1960).

3) G. Natta, I. Pasquon and E. Giachetti, *Angew. Chem.*, 69, 213 (1957).

in 1000 ml. *n*-heptane) followed by addition of triethylaluminum solution (0.9 mol. solution in *n*-heptane), and then a suitable amount of *n*-heptane), was added to make the total volume of solvent 16 ml. The number average molecular weight, $\bar{M}_n$, is estimated by the intrinsic viscosity at 130°C in tetralin solution, using Tung's formula[4],

$$[\eta] = 5.10 \times 10^{-4} \times \bar{M}_n^{0.725}$$

Result and Discussion

Molecular Weight.—Figures 1, 2 and 3 indicate that important factors affecting the molecular weight of polyethylene are the reaction temperature and the amount of catalyst. Figure 1 shows that the melecular weight decreases with the increase in the amount of titanium trichloride where the ratio of triethylaluminum to titanium trichloride is kept constant. The dependence of the molecular weight on the amount of catalyst is almost the same as in the case of ethylene polymerization using $AlEt_3$-$TiCl_4$ catalyst. It may be a characteristic feature of the Ziegler type catalysts that the molecular weight decreases with the amount of the catalyst. As shown in Fig. 2, the molecular weight is but little affected by the quantity of triethylaluminium with a constant amount of titanium trichloride. But, in the range of 6~25 of $AlEt_3/TiCl_3$ ratio a tendency is observed that the molecular weight decreases slightly with the increase in the amount of triethylaluminum. The plot of the logarithm of the molecular weight versus the reciprocal of reaction temperature in an absolute scale is shown in Fig. 3. A decrease in the molecular weight with the increase in temperature has also been observed in the present case, as in the preceding two papers[1,2].

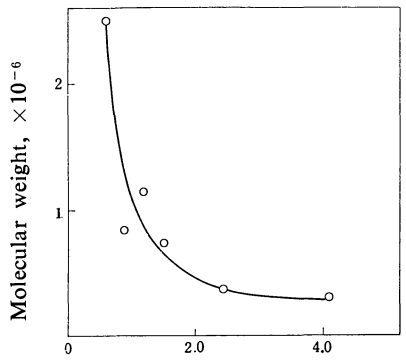


Fig. 1. Molecular weight vs. amount of $TiCl_3$. ($AlEt_3/TiCl_3$, 6.7; Temperature, 50°C; Initial pressure, 42 kg./cm²: Reaction time, 120 min.)

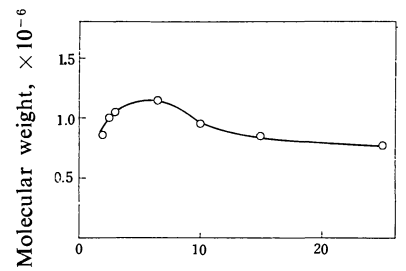


Fig. 2. Molecular weight vs. $AlEt_3/TiCl_3$ ratio. ($TiCl_3$, 1.2 mmol.; Temperature, 50°C; Initial pressure, 42 kg./cm²; Reaction time 120 min.)

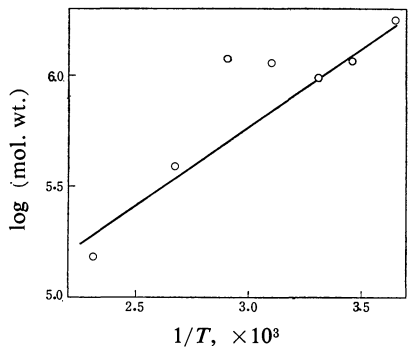


Fig. 3. Molecular weight vs. reaction temperature.
($TiCl_3$, 1.2 mmol.; $AlEt_3$, 8.0 mmol.; Temperature, 50°C; Initial pressure, 42 kg./cm²; Reaction time, 120 min.)

Rate of Polymerization.—The pressure drop was observed at every moment with regard to each run of an experiment. As shown in Fig. 4, the plot of $\log(P_0/P)$ versus reaction time

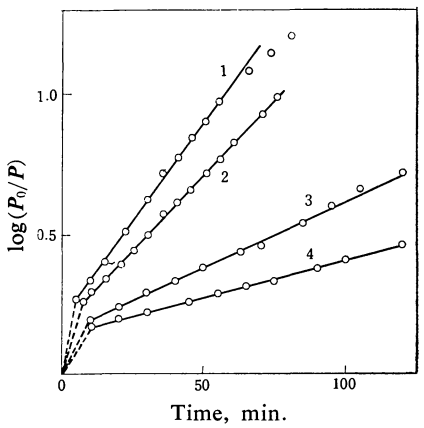


Fig. 4. $\log(P_0/P)$ vs. reaction time.

	$TiCl_3$ mmol.	$AlEt_3$ mmol.	Temperature °C
(1)	1.2	12.0	50
(2)	1.2	8.0	50
(3)	1.2	3.6	50
(4)	1.2	8.0	50

P_0, 42 kg./cm²

4) L. H. Tung, *J. Polymer Sci.*, **24**, 333 (1957).

gives almost a straight line. This means that the rate is approximately proportional to the pressure except an initial short interval of reaction time.

In regard to all runs of an experiment, the specific rate is calculated and is related to the various factors as follows.

Dependence of Rate on the Amount of Catalyst. —Figure 5 indicates that the relation between the specific rate and the amount of catalyst is almost linear, where the ratio of triethylaluminum to titanium trichloride is kept constant.

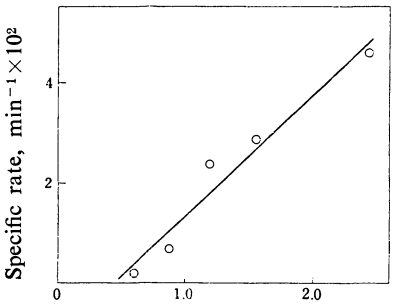


Fig. 5. Specific rate vs. amount of $TiCl_3$. ($AlEt_3/TiCl_3$, 6.7; Temperature, 50°C; Initial pressure, 42 kg./cm^2)

Dependence of Rate on Catalyst Composition. —With a constant amount of titanium trichloride, the rate grows with the increasing amount of triethylaluminum used, as shown in Fig. 6. The curve is very simple in comparison with that of the polymerization by means of $AlEt_3$-$TiCl_4$ catalyst. Natta et al.[3] already reported that the ratio of triethylaluminum to titanium trichloride did not affect the rate in the polymerization of propylene.

Temperature Dependence of Rate.—The logarithm of the rate is plotted against the reciprocal of absolute temperatue in Fig. 7. The straight line, obtained at 0~100°C, gives an apparent activation energy of 1.6 kcal./mol.

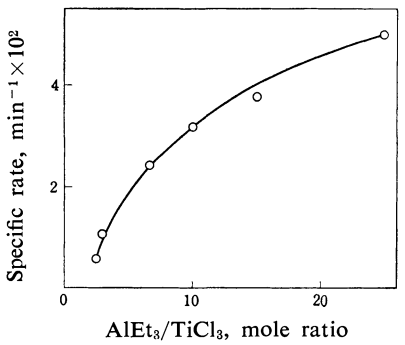


Fig. 6. Specific rate vs. $AlEt_3/TiCl_3$ ratio. ($TiCl_3$, 1.2 mmol.; Temperature, 50°C; Initial pressure, 42 kg./cm^2)

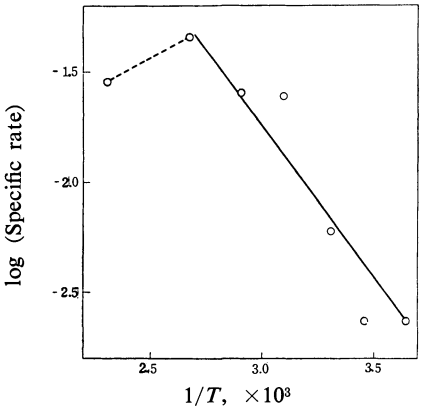


Fig. 7. Specific rate vs. reaction temperature. ($TiCl_3$, 1.2 mmol.; $AlEt_3$, 8.0 mmol.; Initial pressure, 42 kg./cm^2)

If the heat of solution of ethylene in the solvent, *n*-heptane, is added to the above value, 7.8 kcal./mol. is obtained as the activation energy of polymerization. Optimum temperature is 100°C and at higher temperatures a fouling up of the catalyst arises as has been observed in $AlEt_3$-$TiCl_4$ catalyst[2].

Faculty of Engineering
Kyoto University
Sakyo-ku, Kyoto

Rheological Properties of Thermo-reversible Gels

By Kiyoshi ARAKAWA

(Received June, 23, 1961)

In the preceding papers[1-3] the results of stress relaxation studies made on various kinds of thermo-reversible gels (for example, the gels of polyvinyl alcohol-glycerin-water system[1], the gels of polyvinyl alcohol-Congo red-water system[2], and the hydrogels of agar-agar[3]), were reported on.

In the present paper the author reports on the results of a more comprehensive study on the rheological properties of the thermo-reversible gels above described, including the results of a stress relaxation experiment on hydrogels of gelatin.

Experimental

A chainomatic balance relaxometer was used to measure the relaxation Young's modulus of hydrogels of gelatin, which was the same one as was used previously[1-3]. The intrinsic viscosity $[\eta]_{55°C}$ of a powder sample of gelatin in the presence of 0.15 M sodium chloride and at pH 7 was determined to be 0.21 (100 cc./g.) by means of a capillary viscometer of the Ostwald type, and the molecular weight M_n was estimated from the value to be about 2×10^4, according to the relation between M_n and $[\eta]_{55°C}$ which had been reported previously by Scatchard et al.[4] Cylindrical specimens of 17.5 wt.% were prepared and aged at about 0°C in liquid paraffin for more than two weeks. Before the experiment each specimen gel was brought to and kept at the temperature of measurement for five hours[5], and then the observation of the relaxation Young's modulus was started.

Results and Discussion

Stress Relaxation Data of Gelatin Gels.—The data of the relaxation Young's modulus of 17.5% gelatin gel under a constant compressional strain are given in Fig. 1. The amount of strain was 15% for all specimens. The mechanical behavior of the gel may be represented by a six-parameter model as shown in Fig. 2, and the relaxation Young's modulus $E_r(t)$ under constant strain is expressed by the following Eq. 1:

$$E_r(t)=E_1e^{-t/\tau_1}+E_2e^{-t/\tau_2}+E_3e^{-t/\tau_3} \quad (1)$$

in which

$$\tau_1 > \tau_2 > \tau_3$$

The values of the parameters obtained are given in Table I.

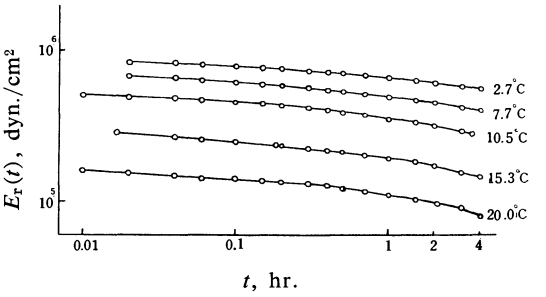


Fig. 1. Relaxation Young's modulus of 17.5% gelatin gel.

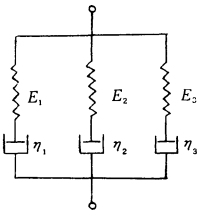


Fig. 2. Mechanical model.
$E_1/\eta_1=\tau_1$, $E_2/\eta_2=\tau_2$, $E_3/\eta_3=\tau_3$

Applcation of the Modified Time-Temperature Superposition Principle. — For the gels of the polyvinyl alcohol-glycerin-water system and those of the polyvinyl alcohol-Congo red-water system, the time temperature superposition principle[6] was applied successfully as has been reported previously[1,2] but the circumstances were found to be different in the hydrogels of agar-agar[3,7]; they were also found to be so in the hydrogels of gelatin, as is seen in Fig. 1.

Recently Nagamatsu, Takemura et al. have proposed the modified time-temperature superposition principle for crystalline polymers which include the vertical shift $\log b_T$ along

1) K. Arakawa, This Bulletin, **31**, 842 (1958).
2) K. Arakawa, ibid., **32**, 1248 (1959); **33**, 1568 (1960).
3) K. Arakawa and K. Atsumi, *J. Chem. Soc. Japan. Pure Chem. Sec.* (*Nippon Kagaku Zasshi*), **80**, 133 (1959),
4) G. Scatchard, J. L. Oncley, J. W. Williams and A. Brown, *J. Am. Chem. Soc.*, **66**, 1980 (1944).
5) J. D. Ferry, ibid., **70**, 2244 (1948).
6) J. D. Ferry, ibid., **72**, 3746 (1950); A. V. Tobolsky, *J. Appl. Phys.*, **27**, 673 (1956); C. A. Dahlquist and M. R. Hatfield, *J. Colloid Sci.*, **7**, 253 (1952).
7) K. Arakawa, This Bulletin, **34**, 1233 (1961).

TABLE I. VALUES OF PARAMETERS OF 17.5% GELATIN GEL

T °C	E_1 10^5 dyn./cm^2	E_2 10^5 dyn./cm^2	E_3 10^5 dyn./cm^2	τ_1 hr.	τ_2 min.	τ_3 min.
2.7	6.6	1.3	1.6	7.8	17	0.6
7.7	5.1	1.4	1.0	6.3	8	0.5
10.5	3.8	1.0_5	0.6_5	5.3	$8._3$	0.6
15.3	2.0_5	0.5_3	0.6_2	4.6	9	0.8
20.0	1.2_3	0.2_5	0.3_2	4.0	$8._4$	0.4

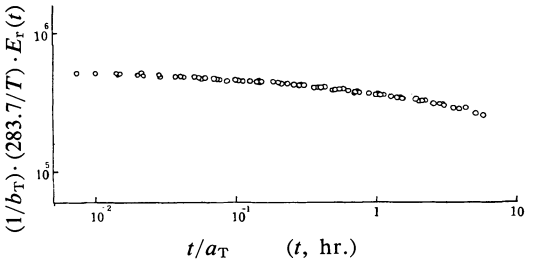


Fig. 3(a). Composite relaxation curve of 17.5% gelatin gel at 10.5°C.

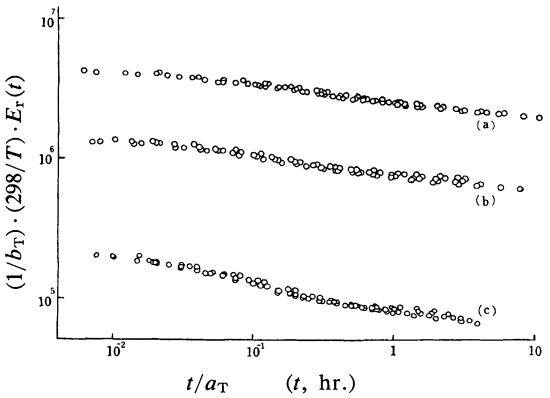


Fig. 3(b). Composite relaxation curves of agar-agar gel at 25°C.

(a) 4.1%, mol. wt. 8×10^3
(b) 2.6%, mol. wt. 4×10^4
(c) 1.0%, mol. wt. 8×10^3

TABLE II. SHIFT FACTORS $\log a_T$ AND $\log b_T$

17.5% Gelatin gel (mol. wt. 2×10^4)			2.6% Agar-agar gel (mol. wt. 4×10^4)		
T	$\log a_T$	$\log b_T$	T	$\log a_T$	$\log b_T$
2.7	0.44	0.22	5.0	0.15_4	0.03_5
7.7	0.16	0.13	14.7	0.04_8	0.01_9
15.3	−0.10	−0.26	35.7	-0.12_7	-0.12_4
20.0	-0.15_2	−0.50	44.6	−0.27	-0.15_4
4.1% Agar-agar gel (mol. wt. 8×10^3)			1.0% Agar-agar gel (mol. wt. 8×10^3)		
1.3	0.22	0.07_5	1.4	0.29	0.08
14.4	0.13_5	0.05	15.4	0.12	0.02_5
38.2	−0.31	−0.04	35.8	−0.10	-0.02_5
46.8	−0.48	−0.16	46.1	-0.18_5	-0.09_2
55.5	−0.73	−0.25	54.8	−0.25	−0.26
			59.0	−0.28	−0.30

the log E_r axis as well as the usual horizontal shift log a_T along the log time axis[8].

The composite relaxation curve of 17.5% gelatin gels which has been obtained from the relaxation curves shown in Fig. 1 by the application of the modified superposition principle described above is shown in Fig. 3(a). Those of hydrogels of agar-agar which have been obtained according to the same procedure from the data previously reported[3,7] are also shown in Fig. 3(b). The values of the two kinds of shift factors log a_T and log b_T, are tabulated in Table II.

Structure of Thermo-reversible Gels.—Concerning those thermo-reversible gels which make the sol-gel transition reversibly, it may be generally said that the junctions supporting the network structure in the gels are of a secondary nature, rather than of a primary nature (covalent bond) as in swollen gels, for example, the swollen gels of vulcanized rubber. Therefore, it may be also said that in the stress relaxation experiment of thermo-reversible gels, scission of network chains occurs at the junctions rather than along the network stands.

In a rubber network with N_0 moles of effective network chains, the relaxation Young's modulus $E_r(t)$ under constant strain is proportional to the moles of effective network chains $N(t)$ at the time t as follows:

$$\frac{E_r(t)}{E_r(0)}=\frac{N(t)}{N_0} \tag{2}$$

and with the assumption that the rate of bond cleavage at network junctions is of a first order:

$$-\frac{dN(t)}{dt}=kN(t) \tag{3}$$

in which k is the rate constant of the bond cleavage reaction. Then we obtain from Eqs. 2 and 3:

$$E_r(t)=E_r(0)e^{-kt} \tag{4}$$

Therefore, the reciprocal of k is found to be

8) K. Nagamatsu, T. Yoshitomi and T. Takemoto, *Memoirs Fac. Eng. Kyushu Univ.*, **30**, 259 (1958); K. Nagamatsu, T. Takemura, T. Yoshitomi and T. Takemoto, *J. Polymer Sci.*, **33**, 515 (1958); T. Takemura, ibid., **38**, 471 (1959).

equal to τ_1, which is obtained graphically[3] from the experimental curve according to Eq. 1, and then the activation energy $\Delta\bar{H}$ as an average, which is obtained from the the $\log \tau_1$ vs. $1/T$ relation, may be regarded as the activation energy of the bond cleavage reaction at the junctions. An example[2] the $\log \tau_1$ vs. $1/T$ relation is shown in Fig. 4.

$$\Delta\bar{H}=R\frac{\partial \ln \tau_1}{\partial(1/T)} \qquad (5)$$

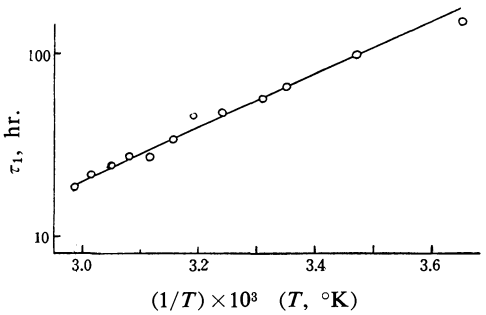


Fig. 4. τ_1, vs. $1/T$ relation of polyvinyl alcohol-Congo red-water gel.
Mol. wt. of PVA, 4.9×10^4
Composition: PVA, 17.5 wt. %
1.75 wt. %

TABLE III. VALUES OF ACTIVATION ENERGY $\Delta\bar{H}$

PVA-glycerin-water gel

Mol. wt. of PVA	Concn. of PVA %	$\Delta\bar{H}$ kcal./mol.
1.1×10^4	8.3	4.6
	9.9	4.0
	12.1	4.6
8.5×10^4	7.95	4.8
	9.07	4.0

PVA-Congo red-water gel

Mol. wt. of PVA	Concn. of PVA, %	Concn. of C. R., %	$\Delta\bar{H}$ kcal./mol.
8.5×10^4	15.0	1.50	7.9
	17.5	1.75	8.5
3.5×10^4	17.5	1.75	7.5
4.9×10^4	17.5	1.75	7.0
9.8×10^4	17.5	1.75	7.0

Agar-agar gel

Mol. wt. of agar-agar	Concn. of agar-agar, %	$\Delta\bar{H}$ kcal./mol.
8×10^3	1.0	4.8
	2.6	5.8
	4.1	4.5
4×10^4	2.6	6.6

Gelatin gel

Mol. wt. of gelatin	Concn. of gelatin, %	$\Delta\bar{H}$ kcal./mol.
2×10^4	17.5	5.8

The values of $\Delta\bar{H}$ thus obtained for various kinds of thermo-reversible gels are tabulated in Table III. Those for the gels of the polyvinyl alcohol-glycerin-water system[1,9] and the gels of the polyvinyl alcohol-Congo red-water system[2] are calculated from the data previously reported[1,2,9] by the six-parameter model analysis and Eq. 5, while those for the agar-agar gels are quoted from a previous paper[7]. The value for the gelation gel is calculated from the values of τ_1 given in Table I.

It is clearly seen in Table III that the values of $\Delta\bar{H}$ for the gels of the polyvinyl alcohol-glycerin-water system, those for the hydrogels of agar-agar, and the value for the gelatin gel are all substantially equal with each other irrespective of the difference in chemical species and, of course, of the differencce in molecular weight. It is also seen that the values of $\Delta\bar{H}$ of the gels above described are substantially equal to the activation energy for the hydrogen bond between water molecules, 4.5 kcal./mol.[10], and to the one for the hydrogen bond between ethyl alcohol molecules, 6.2 kcal./mol.[10] The values $\Delta\bar{H}$ for the gels of the polyvinyl alcohol-Congo red-water system are found in Table III to be a little larger than those values for the hydrogen bonds described above, and to be nearly equal to the value for the hydrogen bond in the micelle of neutral cellulose[11], for example.

Therefore, in the gels of the polyvinyl alcohol-glycerin-water system in which no ions or ionic groups are present, it may be said that the hydrogen bonds play the principal part as the linkages between chain molecules.

In the hydrogels of agar-agar and those of gelatin, considering that the relaxation curves behave like those of other crystalline polymers concerning the application of the modified superposition principle as described above, and that the values of $\Delta\bar{H}$ are substantially equal to those of polyvinyl alcohol-glycerin-water gels, it may be also tentatively said that the hydrogen bonds in the micelles play a more important part as the linkages in the network than ionic groups do.

In the gels of the polyvinyl alcohol-Congo red-water system, Congo red molecules are supposed to play an important role in the formation of the network structure[12]. Probably in this case the hydrogen bond is also important.

9) K. Arakawa, This Bulletin, **34**, 1549 (1961).
10) L. Pauling, "The Nature of Chemical Bond", Cornell University Press, Ithaca, N. Y. (1940), Chap. 9.
11) N. Saito, "High Polymer Physics (Kobunshi Butsurigaku)", Shokabo, Tokyo (1958), p. 8.
12) C. Ditmar and W. J. Priest, *J. Polymer Sci.*, **18**, 275 (1955).

Summary

From the stress relaxation data of various kinds of thermo-reversible gels obtained by means of a chainomatic balance relaxometer, it has been found that:

1) The modified time-temperature superposition principle which includes the vertical shift along the $\log E_r(t)$ axis as well as along the log time axis can be successfully applied to the hydrogels of agar-agar and gelatin, and composite relaxation curves are obtained with good coincidence;

2) The activation energy $\Delta\overline{H}$ which is obtained from the τ_1 vs. $1/T$ relation and which is regarded as the activation energy of the bond cleavage process at the junctions in the network is substantially equal to the value of the hydrogen bond in water and ethyl alcohol for the gels of the polyvinyl alcohol-glycerin-water system and for the hydrogels of agar-agar and gelatin; the value of $\Delta\overline{H}$ is, however, a little larger for the gels of the polyvinyl alcohol-Congo red-water system.

Department of Chemistry
Faculty of Engineering
Shizuoka University
Oiwake, Hamamatsu

Periodic Acid Oxidation on N-Arylamino Alcohols

By Kiyoshi HATTORI, Hirokiti HARADA and Yoshimasa HIRATA

(Received June 28, 1961)

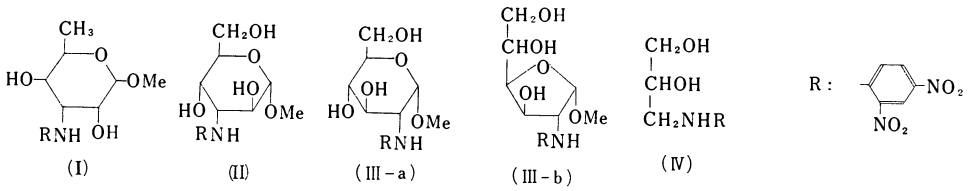
It has been known that the primary and secondary α-amino alcohols[1] are cleft by periodic acid like the vicinal glycols, whereas the tertiary α-amino alcohols are not, excepting a few examples[2]. Upon the periodic acid oxidation, the side reactions take place depending on the quantity of oxidant, temperature, pH, and even light. Some examples of such reactions have also been reported with phenols[3] and aromaitc amines[4] not containing the α-glycol or α-amino alcohol group.

The preparation of the *N*-2, 4-dinitrophenyl derivative of amine is widely used for the purpose of the isolation of amine from its mixture. We have also obtained an amino sugar in the form of *N*-2, 4-dinitrophenyl derivative from the antibiotic trichomycin. Investigations showed that this dinitrophenylamino sugar was not attacked by periodic acid[5] and was identical with the *N*-2, 4-dinitrophenyl derivative of mycosamine methyl glycoside obtained from pimaricin[6].

The cleavage reaction of the *N*-alkylamino alcohol group by periodic acid is well known[7], but that of the *N*-arylamino alcohol group is hardly known. In order to check the unreactivity of the above mentioned *N*-2, 4-dinitrophenyl derivative of mycosamine methyl glycoside (I), other *N*-2, 4-dinitrophenyl derivatives of amino alcohols have been examined.

Since it has been known that the *trans*-glycol group is difficultly attacked by periodic acid, methyl *N*-2, 4-dinitrophenyl-3-amino-3-deoxy-altroside (I) containing both cis and trans amino alcohol groups was studied. This compound was not attacked and the same applies for the *N*-2, 4-dinitrophenyl derivatives of D, L-serine and ethanolamine. These results indicated that the unreactivity of these compounds do not depend on the difference of the configuration of the amino and hydroxyl groups. Therefore, it can be said that the substitution of the *N*-2, 4-dinitrophenyl group on an amino alcohol almost protects the compound from the periodate oxidation. In general, the presence of an hydrogen atom on the amino nitrogen atom is important for the cleavage reaction of an amino alcohol by periodic acid, and in the case of the *N*-acetylated amino alcohol the reactivity is also reduced and no reaction occurs. Therefore, it might be inferred that one reason for the unreactivity of the *N*-2, 4-dinitrophenyl derivative is very similar to that

1) B. E. Nicolet and L. A. Shinn, *J. Am. Chem. Soc.*, **61**, 1615 (1939).
2) E. H. Flynn, M. V. Sigal, Jr, B. F. Wiley and K. Gerzon, ibid., **76**, 3121 (1954).
3) J. P. Feifer, M. A. Smith and B. R. Willeford, *J. Org. Chem.*, **24**, 90 (1959).
4) H. Tanabe, *J. Pharm. Soc. Japan* (*Yakugaku Zasshi*), **76**, 1023 (1956); **78**, 410 (1958).
5) H. Nakano, *J. Antibiotics, Ser. A*, **12**, 72 (1961).
6) J. B. Patrick, R. B. Williams and J. S. Webb, *J. Am. Chem. Soc.*, **80**, 6689 (1958).
7) P. Fleury, J. Courtois and M. Grandchamp, *Bull. soc. chim. France*, **1949** 88.



of the *N*-acyl substituent and lies in the strongly electron attracting property of the nitro group.

Jeanloz and Forchielli[8] reported that about six and two mole equivalents of periodic acid were consumed by one mole each of *N*-acetyl glucosamine and methyl *N*-acetyl glucosamide, respectively at 25°C. Similarly, as shown in Fig. 1, we observed that *N*-2, 4-dinitrophenyl-

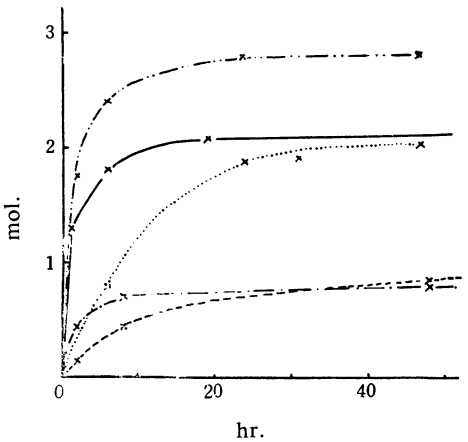


Fig. 1. Periodate consumption curves.
—··— *N*-2,4-Dinitrophenyl glucosamine
------ (III-a) mole ratio, 1 : 2
..... (III-a) mole ratio, 1 : 5
·—·— (III-b) mole ratio, 1 : 5
——— (IV)

D-α-methyl-glucopyranosamide (III-a) consumed one mole equivalent of the oxidant at 4°C, when the mole ratio of the reagent and sample was two. But anomalously when the mole ratio was increased to five, another one mole was consumed.

Another unusual example has been reported by Neuberger[9]; namely, *N*-benzoyl glucosamine was observed to be overoxidized by lead tetra-acetate. Since we had assumed the *N*-2, 4-dinitrophenyl substitution of α-amino alcohols had a masking effect towards periodic acid oxidation, the reactivity of compound III-a consuming two moles of the oxidant was unexpected. Further, the above-mentioned examples appeared to be very analogous, too. Besides, it was shown that 2, 4-dinitroanilino-1-propane-2, 3-diol (IV) consumed two mole equivalents of periodic acid, and that formaldeyde and formic acid were detected as the reaction products. The formation of formaldehyde was due to the normal cleavage of the α-glycol group. In order to avoid the side reaction, all experiments were run under the selected condition[10] in which the oxidation from aldehyde to acid did not occur. Therefore, the additional one mole consumption of periodic acid was caused by the cleavage reaction of the newly produced α-amino aldehyde group. With methyl *N*-2, 4-dinitrophenyl glucofuranosamide (III-b) having no possibility to produce the α-amino aldehyde group, the consumption of periodic acid was only one mole. From these results it might be said that the *N*-2, 4-dinitrophenyl derivative of the α-amino aldehyde group can be attacked by periodic acid, but that of the α-amino alcohol group can not be cleft under this condition even when the quantity of the oxidant is increased.

The unreactivity of the *N*-2, 4-dinitrophenyl-α-amino alcohol group towards periodate oxidation might suggest that the electron density of the amino nitrogen atom which is reduced by the nitro substitution has an important role in this reaction. In order to examine this effect of the nitro group, two mono-substituted aryl-amino alcohols were investigated as shown in Fig. 2. Since *N*-*p*-nitrophenylethanolamine consumed one mole equivalent of the oxidant, while *N*-*o*-nitrophenylethanolamine consumed only a small amount, it was presumed that the ortho substituted phenyl group might have a much greater masking effect against the attack

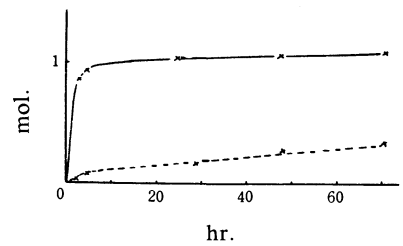


Fig. 2. Periodate consumption curves of *N*-*p*-nitrophenylethanolamine (——) and *N*-*o*-nitrophenylethanolamine (----).

8) R. W. Jeanloz and E. Forchielli, *J. Biol. Chem.*, **188**, 361 (1951).
9) A. Neuberger, *J. Chem. Soc.*, **1941**, 47.
10) C. F. Huebner, S. R. Ames and E. C. Bubl, *J. Am. Chem. Soc.*, **68**, 1621 (1946); L. Hough, T. J. Taylor, C. H. S. Thomas and B. M. Woods, *J. Chem. Soc.*, **1958**, 1212.

of periodic acid than the para substituted isomer. Accordingly, the influence of various ortho substituents were investigated.

As shown in Fig. 3, all substituents excepting the nitro group showed no masking effect and gave the abnormally high consumption value

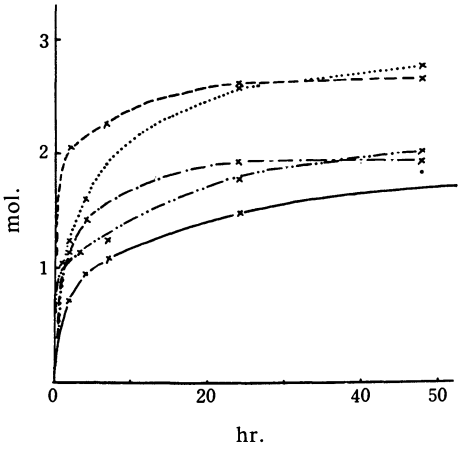
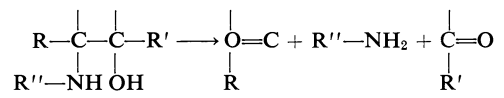


Fig. 3. Periodate cosumption curves.



X; OMe ·····, NH_2 ------,
Cl —·—, CH_3 ·—·—
H ———

of the oxidant. This tendency to afford the high consumption value was more apparent for the introduction of an amino or a methoxy group. As the pH of the reaction medium had some influence on the reaction curve as shown in Fig. 4, these measurements were all carried out in a constant buffer solution of pH 4.5. One of the factors giving such abnormally high consumption values might be considered to be the difference in electron negativity of the amino nitrogen atom, but other factors should be also considered, since the order of consumption and electron negativity was not parallelled, and the order was reversed for *N*-phenylethanolamine and *N*-*o*-chlorophenylethanolamine. The p*K* value of each amines was as follows; *N*-phenylethanolamine (3.8), *N*-*o*-nitrophenylethanolamine and *N*-*p*-nitrophenylethanolamine (below 2.5), *N*-*o*-methoxyphenylethanolamine (4.8), *N*-*o*-aminophenylethanolamine (4.6), *N*-*o*-chlorophenylethanolamine(2.6) in aqueous methanol (33%).



From the reaction scheme of α-amino alcohol[11] the abnormal consumption of periodic acid upon the *N*-arylamino alcohols might be caused by the oxidation of the newly produced aromatic amines. Tanabe has already investigated the periodate oxidation of aromatic amines in detail[4]. Thus we have examined the periodate oxidation of the aromatic amines which were expected to be produced by the oxidation of the *N*-arylamino alcohols, and straightforward results were obtained. An example shown in Fig. 5 indicated that the difference in the oxidation curves of *N*-*o*-chlorophenylethanolamine and *o*-chloroaniline gave the normal consumption value. The normal consumption curve of *N*-*o*-nitrophenylethanolamine was probably due to the property of *o*-nitroaniline which was not oxidized by periodic acid. Thus it was proved that the over-oxidation of *N*-arylaminoalcohols by periodic acid is due to the oxidation of the newly produced aromatic amine.

We are also investigating the masking property of other substituents including steric requirements, and will report on this subsequently.

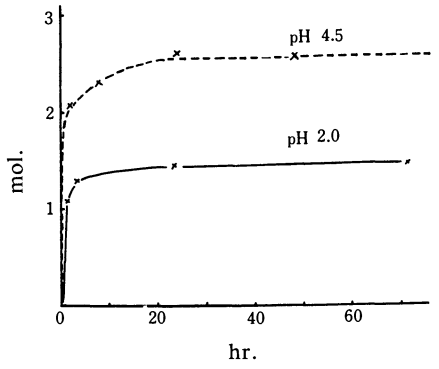


Fig. 4 Periodate consumption curves of *N*-*o*-aminophenylethanolamine at different pH.

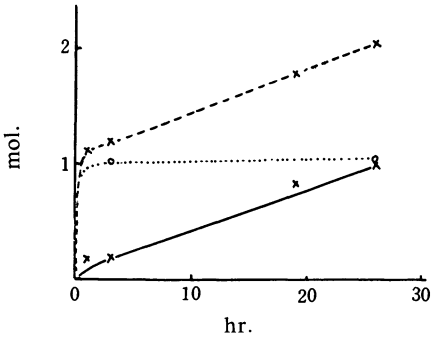


Fig. 5. Periodate consumption curves of *N*-*o*-chlorophenylethanolamine (----) and *o*-chloraniline (——); difference (·····).

11) L. A. Shinn, B. H. Nicolet, *J. Biol. Chem.*, **139**, 687 (1941).

Experimental

Preparation of Amino alcohols. — *N-2, 4-Dinitrophenyl Derivatives.*—Those were prepared by the usual condensation method of a primary amine and 2, 4-dinitrofluorobenzene in an alkaline medium. *N*-2, 4-Dinitrophenyl-D, L-serine[12], pale yellow crystals from aqueous ethanol, m. p. 198~201°C : *N*-2, 4-dinitrophenylethanolamine[13], yellow crystals from ether-methanol, m. p. 89~91°C : *N*-2, 4-dinitrophenyl glucosamine[14], pale yellow needle from benzene-methanol, m. p. 194~197°C : methyl *N*-2, 4-dinitrophenyl glucopyranosamide[14], yellow needle from acetone-ether, m. p. 212~214°C : methyl *N*-2, 4-dinitrophenyl glucofuranosamide[14], pale yellow needle from aqueous ethanol, m. p. 164~166°C : methyl *N*-2, 4-dinitrophenyl-3-amino-3-deoxy-D-altroside, yellow needle from aqueous methanol, m. p. 176~179°C : *N*-2, 4-dinitrophenyl-1-aminopropane-2, 3-diol, yellow crystals from aqueous ethanol, m. p. 82~83°C.

Found : N, 16.21. Calcd. for $C_9H_{11}N_3O_6$: N, 16.34%.

N-Phenylethanolamine.—This was prepared from aniline and ethylene chlorohydrin by the method of Knorr[15]. Pale yellowish viscid liquid of b. p. 151~156°C (16 mmHg). Benzoyl derivative, m. p. 90~92°C.

N-Nitrophenylethanolamine. — This was prepared from nitrochlorobenzene and ethanolamine as described by Kremer[16]. *N-o*-Nitrophenylethanolamine; deep orange needle from ethanol, m. p. 74~76°C.

Found : N, 15.44. Calcd. for $C_8H_{10}N_2O_3$: N, 15.38%.

N-p-Nitrophenylethanolamine ; golden yellow plate from ethyl acetate, m. p. 109~111°C.

Found : N, 15.51. Calcd. for $C_8H_{10}N_2O_3$: N, 15.38%.

N-o-Aminophenylethanolamine : By reduction of *o*-nitrophenylethanolamine with zinc and dilute acetic acid at 40°C, colorless plate crystals were obtained from benzene extraction and were recrystallized from benzene-ethanol, m. p. 105~107°C[17]. By the method of reductive acetylation, this compound was converted into *N, N'*-diacetyl-*o*-aminophenylethanolamine ; colorless needle, m. p. 128~130°C.

Found : C, 60.98 ; H, 6.71 ; N, 11.92. Calcd. for $C_{12}H_{16}N_2O_3$: C, 61.00 ; H, 6.83 ; N, 11.86%.

Further acetylation of this derivative changed to be *N, N', O*-triacetyl derivative ; colorless needle, m. p. 137~138°C.

Found : C, 60.23 ; H, 6.67 ; N, 10.28. Calcd. for $C_{14}H_{18}N_2O_4$: C, 60.42 ; H, 6.52 ; N, 10.02%.

N-o-Methoxyphenylethanolamine. — This was prepared by the method of Knorr[15] as pale yellowish liquid of b. p. 210~225°C (18 mmHg). This hydrochloride ; colorless crystals from ethanol, m. p. 149~153°C.

Found : N, 7.11. Calcd. for $C_9H_{13}O_2N \cdot HCl$: N, 6.91%.

N-o-Chlorophenylethanolamine.—This was prepared by the method of Dashen[18]. A fraction of b. p. 180~190°C (18 mmHg) was collected and converted into its hydrochloride ; colorless crystals from ethanol, m. p. 116~117°C.

Found : C, 45.99 ; H, 5.32 ; N, 6.88. Calcd. for $C_8H_{10}NOCl \cdot HCl$: C, 46.15 ; H, 5.33 ; N, 6.77%.

N-o-Tolylethanolamine.—After heating of a mixture of *o*-toluidine and ethylene chlorohydrin at 120°C for 6 hr., the fraction of b. p. 140~170°C (17 mmHg) was collected and dissolved in ethanol.

The insoluble fraction was *N, N'*-bistolylpiperazine ; sublimate at 166~168°C.

Found : C, 81.43 ; H, 8.49 ; N, 10.20. Calcd. for $C_{18}H_{22}N_2$: C, 81.16 ; H, 8.33 ; N, 10.52%.

The ethanol soluble fraction gave colorless crystals by treating with hydrochloric acid and ether. This was *N-o*-tolylethanolamine hydrochloride, recrystallized from ethanol, m. p. 134~135°C.

Found : C, 57.63 ; H, 7.46 ; N, 7.57. Calcd. for $C_9H_{13}NO \cdot HCl$: C, 57.59 ; H, 7.51 ; N, 7.46%.

Benzoyl derivative, m. p. 141~142°C.

Oxydation by Periodic Acid.—A quantity (about 0.02~0.03 mmol.) sample was dissolved in 2 cc. of methanol and added with about 3 equiv. of periodic acid, then the volume made up to 10 cc. with addition of pH 4.5 acetate buffer. The oxidation was carried out in a dark place at 4°C. A blank test was carried out similarly with the same concentration of periodic acid and no sample, and titration was practiced every times during the course of the oxidation. For the measurement of periodate consumption, 1 cc. of aliquot was pipetted into 3 cc. of saturated aqueous sodium bicarbonate solution, added with 2 cc. of N/100 arsenious acid solution and 1 cc. of potassium iodide (10%), and titrated with N/100 iodine solution.

N-2, 4-Dinitrophenyl derivatives of serine, ethanolamine, methylamine and methyl 3-amino-3-deoxy-altroside did not consume periodic acid after 72 hr., whenever the reaction temperature changed to 9°C or room temperature (about 20°C), and the quantity of oxidant changed to about six mole equivalents.

Production of formaldehyde was identified by making its 2, 4-dinitrophenylhydrazone and dimedone derivatives, and paper chromatographic analysis and mercuric chloride method[19] was applied for the detection of formic acid.

Sample	Mol. equiv. of periodate consumption, hr.
N-DNP-glucosamine	1.77(2), 2.41(6), 2.83(24), 2.83(31), 2.83(47)
N-DNP-glucosamide (III-a) mole ratio (1 : 5),	0.78 (6), 1.79(24), 1.80(31), 2.02(47)
(1 : 2),	0.16 (2), 0.37 (8), 0.79(48), 0.77(72)

12) F. C. Green and L. M. Key, *Anal. Chem.*, **24**, 727 (1952).
13) K. F. Wadkoetter, *Rec. trav. chim.*, **57**, 1294 (1938) ; *Chem. Abstr.*, **33**, 1286 (1939).
14) P. F. Lloyd and M. Stacey, *Tetrahedron*, **9**, 120 (1960).
15) L. Knorr, *Ber.*, **22**. 2092 (1889).
16) C. B. Kremer, *J. Am. Chem. Soc.*, **59**, 1681 (1937).
17) G. R. Ramage and G. Trappe, *J. Chem. Soc.*, **1952**, 4406.
18) L. Dashen and R. Q. Brewster, *Trans. Kansas Acad. Sci.*, **40**, 103 (1937) ; *Chem. Abstr.*, **33**, 5395 (1939).
19) J. R. Dyer, "Methods of Biochemical Analysis", (1954), p. 131.

N-DNP-glucosamide (III-b)
mole ratio (1 : 5), 0.49 (2), 0.73 (8), 0.70(48), 0.93(72)

N-DNP-1-aminopropane-2,3-diol (IV)
1.33 (1), 1.86 (6), 2.13(19), 2.38(73)

N-Arylethanolamine derivatives

p-Nitrophenyl	0.86(2), 0.94(4), 1.07(24), 1.09(48), 1.10(72)
o-Nitrophenyl	0.03(2), 0.10(4), 0.19(24), 0.27(48), 0.34(72)
Phenyl	0.73(1), 0.96(4), 1.10(7), 1.49(24), 1.83(72)
o-Tolyl	1.19(2), 1.41(4), 1.94(24), 1.95(48)
o-Methoxyphenyl	1.32(2), 1.66(4), 2.55(24), 2.75(48)
o-Chlorophenyl	1.09(1), 1.20(3), 1.37(7), 1.79(25), 2.03(48)
o-Aminophenyl	2.09(2), 2.30(7), 2.64(24), 2.59(48), 2.61(96)
(pH 2.0)	1.12(1), 1.31(3), 1.45(24), 1.46(72)

For Fig. 5

o-Chloroaniline	0.19(1), 0.18(3), 0.82(19), 0.99(26)
N-*o*-Chlorophenylethanolamine	1.13(1), 1.19(3), 1.77(19), 2.03(26)

Summary

The authors have examined the cleavage reaction with periodic acid of the *N*-aryl-α-amino alcohols. It has been seen that the α-amino alcohols do not react with the oxidant when substituted by the *N*-2, 4-dinitrophenyl or *o*-nitrophenyl group. When *N*-aryl-α-amino aldehyde groups were produced during the course of oxidation, the normal cleavage reaction took place even if the substituent was a *N*-2, 4-dinitrophenyl group. An over-oxidation was observed in the periodate oxidation of other *N*-aryl-α-amino alcohols, and it was proved that the cause of such high consumption of periodic acid was due to the oxidation of the aromatic amine that was produced by the normal cleavage of the *N*-aryl-α-amino alcohol group.

The authors are indebted to Mr. S. Ohta for microanalyses, and to Dr. G. Huber for a sample of methyl 3-amino-3-deoxy-altroside, and we also wish to thank Dr. M. Ohara for his encouragement.

Research Laboratory of
Fujisawa Pharmaceutical Co. Ltd.
Higashi-yodogawa-ku
Osaka (H. H. & K. H.)

Chemical Department of
Nagoya University
Chikusa-ku, Nagoya
(Y. H.)

The Ignition of Methane-Oxygen Mixture by Reflected Shock Wave

By Momotaro SUZUKI, Hajime MIYAMA, Shiro FUJIMOTO and Tsuneo KASE

(Received June 26, 1961)

In a previous paper[1], measurements about the shock ignition of methane-oxygen mixture with a shock tube of 2.5 cm. internal diameter were reported. This time, measurements of the ignition of CH_4+2O_2 by reflected shock wave have been carried out with a shock tube which has a square cross section with an inside lateral of 5 cm. The tube is divided into three portions, a reservoir chamber 60 cm. in length, a buffer chamber 60 cm. in length and a test chamber 120 cm. in length. The buffer chamber was used to eliminate the effect of puncturing the membrane and was separated from a reservoir chamber by sheets of cellophane films and from a test chamber by a shutter. Details of the experimental procedure have been described elswhere[1-3]. The driver gas was air, the buffer gas a mixture of 88.8%

1) M. Suzuki, H. Miyama and S. Fujimoto, This Bulletin, **31**, 232 (1958).

2) M. Suzuki, H. Miyama and S. Fujimoto, ibid., **31**, 819 (1958).

3) M. Steinberg and W. E. Kaskan, "Fifth Symposium on Combustion", The Williams and Wilkins Co., Baltimore (1953), p. 664.

methane and 11.2% nitrogen, and the test gas a mixture of CH_4+2O_2. It was confirmed, as a result of piezo-electric measurements that almost all of ignitions were caused by the reflected shock waves[2] only the case of ignitions by reflected shock wave will be considered here, however.

The minimum pressures of the reservoir chamber necessary for igniting the detonable gas of the definite initial pressure were measured. By using the results of these measurements, the temperature T_r and pressure P_r behind the reflected shock wave were calculated[4]. In this calculation, a constant value of heat capacity of detonable gas was assumed because the variation of heat capacity caused a temperature decrease of less than 4% under our experimental conditions. In Fig. 1,

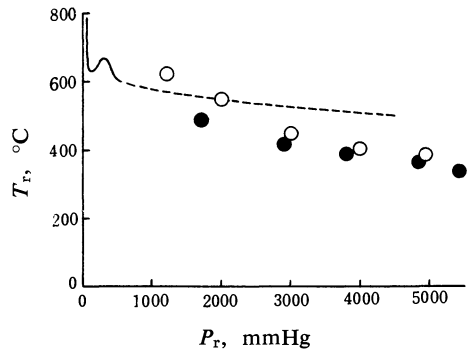


Fig. 1. Shock ignition limit expressed by T_r and P_r, where T_r and P_r are temperature and pressure behind reflected shock wave.
- ○ Shock ignition limit with a shock tube of 5 cm. inside lateral,
- ● Shock ignition limit with a shock tube of 2.5 cm. diameter[1],
- —— Thermal ignition limit by Neumann and Serbinoff[5],
- ------ Thermal ignition limit by Sagulin[6]

the explosion boundary is shown in terms of T_r and P_r. In the previous paper[1], it was shown that the shock ignition temperature is remarkably lower than the thermal ignition temperature. However, there was a mistake because the initial pressure of detonable gas was used instead of P_r. Corrected values from the previous data are shown in Fig. 1 for comparison. From this figure, it is obvious that the difference between the shock ignition and thermal temperatures[5,6] is not remarkable.

Sagulin[6] found that there is the following relationship in the reaction between aliphatic hydrocarbon and oxygen:

$$\log (P/T) = A/T + B$$

in which P is pressure (cmHg), T, ignition temperature (°K), and A and B are constants. Yamazaki and Kato[7] also found that this relationship can be applied to the cases of the ignitions of a propane-oxygen mixture by incident shock waves with a shock tube 2.6 cm. in diameter. In the present case, this relationship can be also observed, as is shown in Fig. 2, where Sagulin and Yamazaki's data are

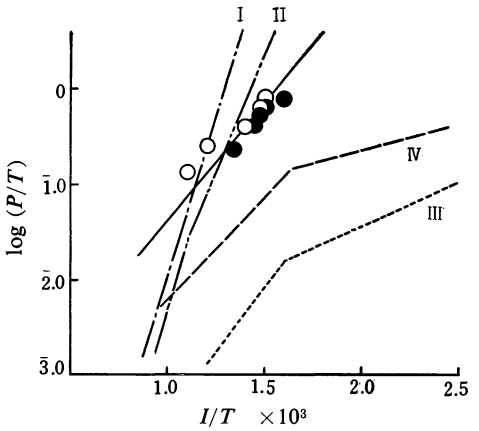


Fig. 2. Variation of log (P/T) with $1/T$ for the reaction of aliphatic hydrocarbon and oxygen.
- ○ Experimental values about CH_4+2O_2 with a shock tube of 5 cm. inside lateral,
- ● Experimental values about CH_4+2O_2 with a shock tube of 2.5 cm. diameter[1],
- I Sagulin's data about CH_4+2O_2[6],
- II Sagulin's data about $C_3H_8+5O_2$[6],
- III Yamazaki's data about propane-oxygen[7],
- IV Corrected Yamazaki's data about propane-oxygen

shown for comparison. The slope of our line is very different from that of Sagulin's but similar to the slope of the initial part of Yamazaki's line III, although the position of our line is very far from that of line III. Although Yamazaki et al. used the initial pressure in their calculation, the pressure behind the incident shock wave should have been used. Therefore, we recalculated those values by using the pressure behind the incident shock wave and obtained line IV of Fig. 2. This corrected line is much closer to

4) I. I. Glass, W. Martin and G. N. Patterson, "A Theoretical and Experimental Study of the Shock Tube", UTIA Report No. 2, Nov., 1953.
5) N. Semenoff, "Chemical Kinetics and Chain Reaction", Oxford at the Clarendon Press., London (1955), p. 308.
6) A. B. Sagulin, *Z. physik. Chem.*, **B1**, 275 (1928).
7) K. Yamazaki and Y. Kato, *J. Chem. Soc. Japan, Ind. Chem. Sec. (Kogyo Kagaku Zasshi)*, **63**, 2124 (1960).

our line, and the slope of the initial part of this line is almost the same as that of our line about methane-oxygen. This result seems to confirm their conclusion that the mechanism of the breaking C–H bond is predominant at the lower pressure of a propane-oxygen mixture*.

Department of Chemistry
Defense Academy
Yokosuka

* Sagulin found that the above-described linear relationship for ethane, propane and pentane consists of two parts, one at the lower pressure (i. e., at the lower value of P/T) and another at the higher pressure (i. e., at the higher value of P/T). Although the slope of the line at the higher pressure is different for the different hydrocarbons, the slope at the lower pressure is the same for ethane, propane and pentane; it is also as same as the slope for methane. From this result, Sagulin (and also Yamazaki et al.) concluded that the mechanism of the breaking C–H bond is predominant at the lower pressure and that of the breaking C–C bond at the higher pressure. Details are described in Refs. 6 and 7.

Electronic Spectra of Polynitrophenols and their Anions

By Takehiro ABE

(Received June 26, 1961)

In previous papers[1] it has been reported that, for *m*-dinitro- and 1, 3, 5-trinitro-benzene, a 260 mμ band of nitrobenzene shifted toward blue in the order of the increasing numbers of the nitro group, although substitution had been considered to shift in general the absorption of a parent molecule to longer wavelengths. High-intensity absorption bands of mono- and di-substituted benzenes, each containing only a strongly electron-attracting substituent, have been interpreted by Nagakura and Tanaka[2-5] in terms of the intramolecular charge transfer spectra. In the present paper, an attempt has been made to expand Nagakura and Tanaka's theory into high-intensity absorption bands of polynitrophenols and their anions, which contain two or three electron-attracting substituents. The absorption spectra of the polynitrophenols and their anions have been indicated in the Landolt-Börnstein table[6]. However, the spectra are not complete. In this work, the absorption spectra of *p*-nitrophenol, 2, 4-dinitrophenol and picric acid, all in water, were measured, if necessary, in the presence of either hydrochloric acid or sodium hydroxide in order to obtain the spectra of these polynitrophenols and their anions.

1) T. Abe, This Bulletin, **31**, 904 (1958); **32**. 339 (1959); **33**, 220 (1960).
2) S. Nagakura and J. Tanaka, *J. Chem. Phys.*, **22**, 236 (1954); *J. Chem. Soc. Japan, Pure Chem. Sec.* (*Nippon Kagaku Zasshi*), **75**, 331 (1954).
3) S. Nagakura, ibid., **75**, 822 (1954); *J. Chem. Phys.*, **23**, 1441 (1955).
4) J. Tanaka and S. Nagakura, ibid., **24**, 1274 (1956); *J. Chem. Soc. Japan, Pure Chem. Sec.* (*Nippon Kagaku Zasshi*), **78**, 1200 (1957).
5) J. Tanaka, S. Nagakura and M. Kobayashi, *J. Chem. Phys.*, **24**, 311 (1956).
6) Landolt-Börnstein, " Physikalisch-chemische Tabellen ", 6th Ed., Part 3 (II), Springer, Berlin (1951), p. 269.

Experimental

Commercial grade polynitrophenols were recrystallized several times from water. Commercial grade hydrochloric acid and sodium hydroxide were used without further purification. The spectra of solutions were measured using a Hitachi EPU-2 spectrophotometer at room temperature. The length of absorption cells was 1 cm.

Results

The results of the measurements of the absorption spectra are shown in Fig. 1 and Table I. The spectrum of an aqueous picric acid solution (2.69×10^{-5} M) containing hydrochloric acid at a concentration 4.8 N is considered to be due almost entirely to the undissociated picric acid, because the spectrum is nearly identical with that of a hydrochloric acid concentration of 7.2 N. Therefore, *p*-nitrophenol and 2, 4-dinitrophenol, whose dissociation constants are smaller than that of picric acid, are not dissociated in water containing 4.8 N hydrochloric acid. Aqueous solutions both of 4.8 N hydrochloric acid and of 4.2×10^{-2} N sodium hydroxide scarcely absorb in wavelength regions above 230 mμ. An absorption at 31300 cm^{-1} for *p*-nitrophenol is only slightly more intense in the aqueous hydrochloric acid solution (4.8 N) than in pure water, so that it is known that *p*-nitrophenol is mostly undissociated in water at room temperature (ca. 25°C). 2, 4-Dinitrophenol absorbs somewhat more strongly at 27600 cm^{-1} and slightly more weakly at

TABLE I. ULTRAVIOLET ABSORPTION BANDS OF THE POLYNITROPHENOLS AND THEIR ANIONS (IN cm^{-1})

p-Nitrophenol	31300*	44300			
p-Nitrophenolate anion	24900*	38000^s	41000^s		
2,4-Dinitrophenol	33000^s	37900*			
2,4-Dinitrophenolate anion	25000^s	27600*	38600 ?	45000	
Picric acid	29100	35000^s	42000*		
Picrate anion		25000^s	28300*	41000^s	45000^s

The marks of * and ^{s} denote the long wavelength absorption maxima (except for the case of picric acid) and the absorption shoulders, respectively.

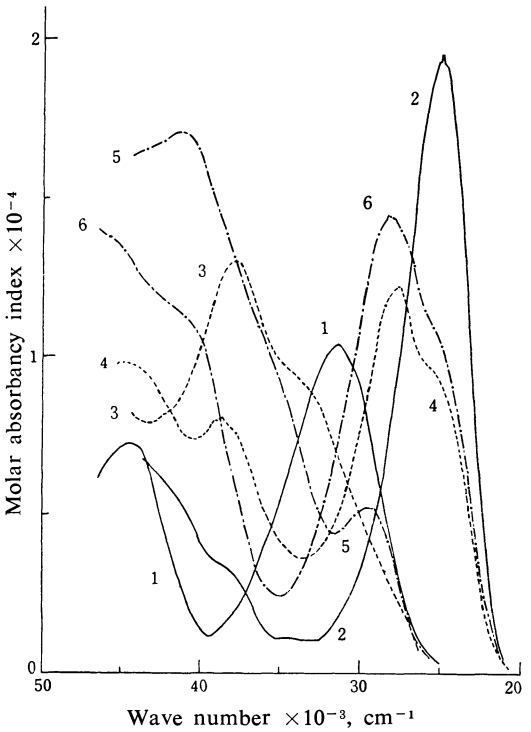


Fig. 1. Absorption spectra of aqueous solutions of the polynitrophenols.

1 An aqueous solution of *p*-nitrophenol (*p*-nitrophenol)
2 An aqueous 4.2×10^{-2} N sodium hydroxide solution of *p*-nitrophenol (*p*-nitrophenolate anion)
3 An aqueous 4.8 N hydrochloric acid solution of 2,4-dinitrophenol (2,4-dinitrophenol)
4 An aqueous solution of 2,4-dinitrophenol (2,4-dinitrophenolate anion)
5 An aqueous 4.8 N hydrochloric acid solution of picric acid (picric acid)
6 An aqueous solution of picric acid (picrate anion)

38600 cm^{-1} in the aqueous sodium hydroxide solution (4.2×10^{-2} N) than in water. From this it follows that 2,4-dinitrophenol (2.77×10^{-5} M) is dissociated to a large extent in water at room temperature, giving the 27600 cm^{-1} band, although it is not so distinct that the 2,4-dinitrophenolate anion also gives a band at 38600 cm^{-1}. A 28300 cm^{-1} band of picric acid has almost the same intensity in water as in an aqueous sodium hydroxide solution (4.2×10^{-2} N). This means that picric acid (2.69×10^{-5} M) is almost dissociated in water at room temperature. From the above results one can conclude that the absorption curves 1—6 in Fig. 1 are due to *p*-nitrophenol, *p*-nitrophenolate anion, 2,4-dinitrophenol, 2,4-dinitrophenolate anion, picric acid and picrate anion respectively, except for the 38600 cm^{-1} band in absorption curve 4.

In the present work, the absorption spectra of both 2,4-dinitrophenol and picric acid may probably be affected both by intramolecular hydrogen bonds and by intermolecular ones, since it is well known that the formation of a hydrogen bond has an effect on the near ultraviolet absorption spectra of many aromatic compounds*.

In addition to the hydrogen bonds, it is to be expected that, in both 2,4-dinitrophenol and picric acid, steric hindrances between the hydroxyl groups and the adjacent nitro groups will occur, affecting their spectra.

According to the Landolt-Börnstein table[6], *p*-nitrophenol and its anion show absorption shoulders near 36000 and 28000 cm^{-1} respectivery. These shoulders, although they seem to appear, can not be perceived distinctly in absorption curves 1 and 2 in Fig. 1.

From Fig. 1 and Table I one can see that the long wavelength absorption maxima of the polynitrophenols shift toward blue in the order of *p*-nitrophenol, 2,4-dinitrophenol and picric acid, all having increasing molar absorbancy indexes in the same order, and that the absorption maxima of these polynitrophenolate anions similarly shift toward blue with the increasing number of the nitro groups. The absorption maximum of each anion lies at a longer wavelength than does that of the corresponding polynitrophenol. This red shift is greater with the increasing number of the nitro group.

* For example: a) S. Nagakura and H. Baba, *J. Chem. Soc. Japan, Pure Chem. Sec.* (*Nippon Kagaku Zasshi*), 71, 527, 560, 610 (1950); 72, 3 (1951); *J. Am. Chem. Soc.*, 74, 5693 (1952). b) N. D. Coggeshall and E. M. Lang, ibid., 70, 3233 (1948).

Discussion

The longer wavelength absorption maximum of *p*-nitrophenol has been interpreted by Nagakura and Tanaka[3,4] in terms of the intramolecular charge transfer involving an excitation of a bonding π-electron of the highest occupied energy-level of phenol to a vacant energy-level of the nitro group, as illustrated in Fig. 2. According to Nagakura and Tanaka's theory[2-5], all high intensity absorption bands of the polynitrophenols and their anions may be similarly interpreted as due to intramolecular charge transfers. From the viewpoint of the theory, these bands will be briefly discussed below.

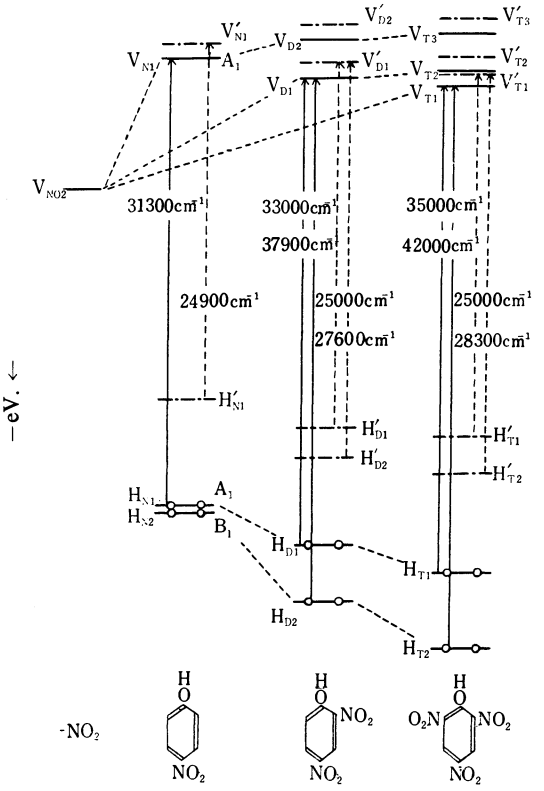


Fig. 2. The highest occupied and lowest vacant energy-levels for the polynitrophenols (——) and their anions (—·—).

When one more nitro group is substituted for hydrogen in a 2-carbon atom of *p*-nitrophenol, the highest occupied π-levels (H_{N1} and H_{N2}) of *p*-nitrophenol can be expected to interact mainly with the vacant energy-level V_{NO2} of the second entering nitro group, because both H_{N1} and H_{N2} are widely separated from the occupied energy-levels of the nitro group or have no interaction with them. H_{N1} lies close to H_{N2}. According to Nagakura and Tanaka, as the result of the interaction with V_{NO2}, the highest occupied energy-level H_N ($=H_{N1}$ or H_{N2}) is shifted by the following amount:

$$\Delta E_N = 1/2 \cdot [(V_{NO2} - H_N) - \{(H_N - V_{NO2})^2 + 4C_N^2 C_{NO2}^2 \beta^2\}^{1/2}] \quad (1)$$

Here C_N is a coefficient of an atomic orbital of the 2-carbon atom in a molecular orbital of H_N, C_{NO2}, a coefficient of an atomic orbital of a nitrogen atom in a molecular orbital of V_{NO2}, and β, a resonance integral between the two atomic orbitals of the carbon atom and the nitrogen. Similarly, V_{NO2} may interact mainly with H_{N1}, H_{N2} and V_{N1}, which are relatively near V_{NO2}. V_{N1} is the lowest vacant energy-level in *p*-nitrophenol. In 2, 4-dinitrophenol, therefore, V_{NO2} of the second nitro group may be sifted as follows:

$$\begin{aligned}\Delta E_{NO2} = {} & 1/2 \cdot [(H_{N1} - V_{NO2}) \\ & + \{(H_{N1} - V_{NO2})^2 + 4C_{N1}^2 C_{NO2}^2 \beta^2\}^{1/2}] \\ & + 1/2 \cdot [(H_{N2} - V_{NO2}) \\ & + \{(H_{N2} - V_{NO2})^2 + 4C_{N2}^2 C_{NO2}^2 \beta^2\}^{1/2}] \\ & + 1/2 \cdot [(V_{N1} - V_{NO2}) \\ & - \{(V_{N1} - V_{NO2})^2 + 4C_{VN1}^2 C_{NO2}^2 \beta^2\}^{1/2}]\end{aligned} \quad (2)$$

in which formula C_{VN1} is a coefficient of an atomic orbital of the 2-carbon atom in a molecular orbital of V_{N1}. By the simple LCAO MO method Nagakura[3] calculated the square values of the coefficients for *p*-nitrophenol as $C_{N1}^2 = 0.100$, $C_{N2}^2 = 0.250$ and $C_{VN1}^2 = 0.009$. By putting these values in Eq. (1), one knows that H_{N2} interacts more strongly with V_{NO2} than does H_{N1}. This suggests that an intramolecular charge transfer band due to an $H_{N2} \rightarrow V_{NO2}$ ($H_{D2} \rightarrow V_{D1}$) transition appears at a shorter wavelength than that for an $H_{N1} \rightarrow V_{NO2}$ ($H_{D1} \rightarrow V_{D1}$) transition. The two bands at 33000 and 379000 cm^{-1} for 2, 4-dinitrophenol may be associated with the transitions, $H_{D1} \rightarrow V_{D1}$ and $H_{D2} \rightarrow V_{D1}$, respectively. According to Eq. 2, the main interactions of V_{NO2} with H_{N1} and H_{N2} can be expected to raise V_{NO2} considerably, since C_{VN1}^2 is negligibly smaller than either C_{N1}^2 or C_{N2}^2. The support for this expectation comes from the fact that the band due to the $H_{D1} \rightarrow V_{D1}$ transition in dinitrophenol is at a shorter wavelength than for the $H_{N1} \rightarrow V_{N1}$ transition in nitrophenol; from this blue shift it follows that $(H_{N1} - H_{D1}) > (V_{N1} - V_{D2})$. From the above discussion, the observed 33000 and 37900 cm^{-1} bands of 2, 4-dinitrophenol may be interpreted as indicated in Fig. 2.

Next, the substitution of the third nitro group in a 6-carbon atom of 2, 4-dinitrophenol can be roughly thought to move H_{D1}, H_{D2} and

V_{D1} of dinitrophenol and V_{NO2} of the third nitro group in the same directions by the same mechanism as for the substitution of the second nitro group in *p*-nitrophenol, since picric acid belongs to the symmetry group C_{2v}. It is, however, to be expected that the square values of the coefficients of the 6-carbon atom in the molecular orbitals of H_{D1} and H_{D2} in 2, 4-dinitrophenol are smaller than C_{N1}^2 and C_{N2}^2 respectively, owing to the strong electron-attracting nature of the second entering nitro group. Moreover, interactions of V_{NO2} of the third nitro group with V_{D1} and V_{D2}, although weak, may lower the V_{NO2}. Accordingly, it may be expected that H_{D1} and H_{D2} of dinitrophenol and V_{NO2} of the third nitro group are shifted to a lesser extent in picric acid than H_{N1} and H_{N2} of *p*-nitrophenol and V_{NO2} of the second nitro group in 2, 4-dinitrophenol respectively. Consequently, one may predict that the intramolecular charge transfer bands due to the $H_{T1}\rightarrow V_{T1}$ and $H_{T2}\rightarrow V_{T1}$ transitions in picric acid will appear at shorter wavelengths than do those for the $H_{D1}\rightarrow V_{D1}$ and $H_{D2}\rightarrow V_{D1}$ transitions respectively, although the respective blue shifts are smaller than the corresponding shifts of *p*-nitrophenol for 2, 4-dinitrophenol. The $H_{T1}\rightarrow V_{T1}$ and $H_{T2}\rightarrow V_{T1}$ transitions are most likely to produce high-intensity bands at 35000 and 42000 cm^{-1} respectively. The above expectation is in agreement with the experimental result.

In addition to the above intramolecular charge transfer bands, absorption bands due to the transitions $H_{D1}\rightarrow V_{D2}$ and $H_{D2}\rightarrow V_{D2}$ in 2, 4-dinitrophenol and those due to the transitions $H_{T1}\rightarrow V_{T2}$, $H_{T2}\rightarrow V_{T2}$, $H_{T1}\rightarrow V_{T3}$ and $H_{T2}\rightarrow V_{T3}$ in picric acid would be expected to appear, although they are not distinguished in Fig. 1.

A predominating difference in π-electron structure between each polynitrophenol and its anion can be ascribed to the fact that the electronegativity of an oxygen atom belonging to the hydroxyl group in the polynitrophenol is greater than that for the polynitrophenolate anion. It may, therefore, be approximately assumed that the dissociation of each polynitrophenol reduces only the coulomb term for the oxygen atom by $\Delta\alpha_0$ through the decrease in electronegatively. Then, according to Coulson and Longuet-Higgins[7], if an inductive effect is disregarded, each orbital of the polynitrophenol is raised by the following amount in the polynitrophenolate anion:

$$\Delta E = C_0^2 \cdot \Delta\alpha_0 \qquad (3)$$

Here C_0 is a coefficient of an atomic orbital of the oxygen atom belonging to the hydroxyl group in the molecular orbital of each level.

The calculation[3] for *p*-nitrophenol gave values of C_0^2 for H_{N1}, H_{N2} and V_{N1} of 0.127, 0 and 0.012 respectively. Putting these values in Eq. 3, it follows that in *p*-nitrophenolate anion H_{N1} is raised more greatly than V_{N1}. It is, therefore, to be expected that an intramolecular charge transfer band of *p*-nitrophenolate anion appears at a longer wavelength than that of *p*-nitrophenol. This agrees with the experimental data.

The great red shifts of the high-intensity absorptions of 2, 4-dinitrophenol on dissociation lead to the suggestion that, in 2, 4-dinitrophenolate anion, H_{D1} and H_{D2} are raised more greatly to H'_{D1} and H'_{D2} respectively than V_{D1} and V_{D2}, as is shown in Fig. 2. The 25000 and 27600 cm^{-1} bands are possibly asssigned to the transitions $H'_{D1}\rightarrow V'_{D1}$ and $H'_{D2}\rightarrow V'_{D1}$ respectively.

When picric acid is dissociated, the energy-levels of picric acid may be raised in the same way as in the case of 2, 4-dinitrophenol. The transitions indicated by the dotted lines in Fig. 2 may produce the observed 25000 and 28300 cm^{-1} bands.

The red shifts of the intramolecular charge transfer bands of each polynitrophenol for its anion are greater with the increasing number of the nitro group. This means that the two highest occupied orbitals of each polynitrophenol are more greatly raised in its anion as the number of the nitro group increases. This, with Eq. 3, suggests that the values of C_0^2 in the molecular orbitals of these occupied levels in each polynitrophenol are greater with the increasing number of the nitro group.

Summary

The absorption spectra of *p*-nitrophenol, 2, 4-dinitrophenol, picric acid and their anions, all in water, were measured in the presence or absence of either hydrochloric acid or sodium hydroxide. The long wavelength absorption maxima of these polynitrophenols shift toward blue in the order of *p*-nitrophenol, 2, 4-dinitrophenol and picric acid, with increasing molar absorbancy indexes in the same order. The absorption maxima of the anions similarly shift toward blue. The absorption maxima of each anion lie at longer wavelengths than do those of the corresponding polynitrophenol. These red shifts are greater with the increasing number of the nitro group. The high-intensity bands of these nitro compounds containing two or three electron-attracting substituents are interpreted from the viewpoint of Nagakura and Tanaka's theory of the intramolecular charge transfer spectra.

7) C. A. Coulson and H. C. Longuet-Higgins, *Proc. Roy. Soc.*, **A191**, 39 (1947).

The author is particularly indebted to Professor Yōkan Nomura for his suggestions and encouragement.

Department of Chemistry
Defense Academy
Yokosuka

The Assignment of the Molecular Vibrations of Hexachlorobenzene

By Shinnosuke SAËKI

(Received June 3, 1961)

The Raman spectrum of hexachlorobenzene has been studied by Dadieu and his colleagues[1] and by Murray and Andrews[2], and the infrared absorption spectrum of the same substance, by Plyler and his collaborators[3]. But, in all of these papers, only the results of observations (vibrational frequencies, intensities, depolarization ratios of Raman lines, etc.) have been presented, and no discussion has been given concerning the assignment of the observed lines or bands. In this paper, the Raman spectra of hexachlorobenzene in various solutions, the qualitative depolarization ratio of each Raman line, and infrared absorption spectra in gaseous state are reported on, and an assignment of these observed lines and bands is proposed.

Experimental and Results

Hexachlorobenzene of extra pure grade on the market was recrystallized from ethanol three times and used for the measurement of the spectra.

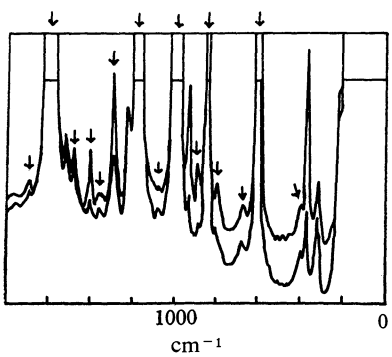


Fig. 1. Raman spectra of hexachlorobenzene (0.25 g. in 5 ml. benzene).
The upper curve: cross
The lower curve: parallel

The Raman spectra were measured using a Cary model 81 Raman spectrophotometer. The qualitative depolarization ratios were observed by the two-exposure method, using polaroid cylinders. As the solubility of this substance is not enough to obtain an adequately clear spectrum, not only benzene and carbon tetrachloride, but also carbon disulfide were used as the solvents in order to make the measurements as accurate as possible. To prepare the

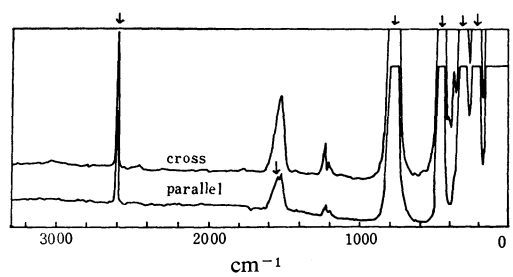


Fig. 2. Raman spectra of hexachlorobenzene (0.2 g. in 5 ml. carbon tetrachloride).

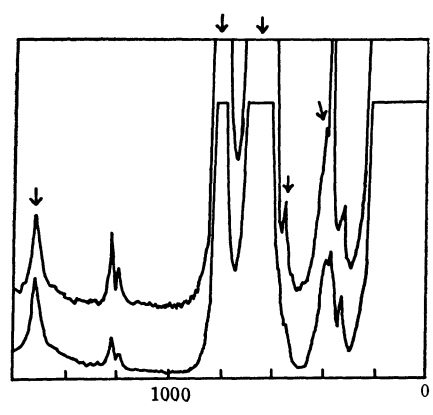


Fig. 3. Raman spectra of hexachlorobenzene (0.2 g. in 5 ml. carbon disulfide).
The upper curve: cross
The lower curve: parallel

1) A. Dadieu, K. W. F. Kohlrausch and A. Pongratz, *Monatsh.*, **61**, 426 (1932).
2) J. W. Murray and D. H. Andrews, *J. Chem. Phys.*, **2**, 119 (1934).
3) E. K. Plyler, H. C. Allen, Jr. and E. D. Tidwell, *J. Res. Nat. Bur. Standards*, **58**, 255 (1958).

TABLE I. RAMAN LINES OF HEXACHLOROBENZENE

Benzene soln.			CCl_4 soln.			CS_2 soln.		
	Intensity			Intensity			Intensity	
ν, cm^{-1}	Cross	Parallel	ν, cm^{-1}	Cross	Parallel	ν, cm^{-1}	Cross	Parallel
213	sh 1	sh 1						
322	31	35				322	25	22
342	1	1						
373	80	30	371	26	sh 10 ?	371	>60	20
			572	2	—			
			1196	8	3	1194	12	5
1224	27	12	1226	22	9	1225	27	11
1248	sh 1	—						
1522	15	17	1521	masked	15	1518	33	32
			2453	2	+			
			3042	1	—			

sample solutions, 0.2~0.25 g. solute was dissolved in 5 ml. solvent in all cases. The obtained Raman spectra are shown in Figs. 1—3, and the frequencies of the observed lines are shown in Table I. The small arrows in the figures point out the Raman lines of the solvent and the mercury lines from the source lamp.

The infrared absorption specta were measured using a Perkin-Elmer model 21 spectrophotometer equipped with sodium chloride or a cesium bromide prism over the region of 4000~300 cm^{-1}. The far infrared spectrum was measured in the region of 300~100 cm^{-1} using the grating spectrophotometer installed at the laboratory of Professor Yoshinaga of Osaka University[4].

As the vapor pressure of hexachlorobenzene is quite low, a high temperature and long path length cell was necessary to measure the spectrum in a gaseous state. The spectra in the sodium chloride region were measured using a long path and high temperature cell of the multiple reflection type. This cell has an optical system quite similar to that of the Perkin-Elmer long path gas cell, but all its mirrors are spattered with gold to prevent corrosion. The path length used in the measurements was 720 cm. The cell can be used at any desired temperature below 120°C by the aid of a transformer and the heaters which are coiled over the outside surface of the cell body. In the measurement, the specimen was put in the cell, and the air in the cell was replaced by nitrogen from the bomb in order to make the absorption by the atmospheric water vapor as weak as possible*. Then, after keeping the cell at a desired temperature for two or three hours in order to saturate the vapor pressure of the sample substance, the spectrum was measured.

The spectrum in the cesium bromide region was measured using the 85 mm. high temperature cell with cesium bromide windows 50 mm. in diameter. The design of this cell is almost the same as that described previously[5].

In the far infrared region, since a high temperature cell could not be used because of the complete difference in the type of spectrometer, the spectrum was taken as the Nujol mull sandwiched between two thick sheets of polyethylene. However, no absorption band was observed in this region. Since this molecule certainly has some vibrations of low frequency which are active to the infrared

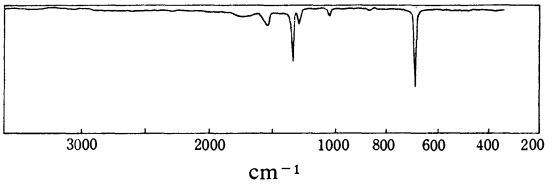


Fig. 4. Infrared absorption spectrum of hexachlorobenzene (in gaseous state).

TABLE II. INFRARED ABSORPTION BANDS OF HEXACHLOROBENZENE

ν, cm^{-1}	Intensity
1396	m
1350	s
1307	m
1053	w
1012	w
874.4	w
696.2	s
687.6	w

4) H. Yoshinaga, S. Fujita, S. Minami, A. Mitzuishi, R. A. Oetjen and Y. Yamada, *J. Opt. Soc. Am.*, **48**, 315 (1958).

* Because of a slight leakage of the cell, the spectra could not be observed in vacuo.

5) S. Saëki, This Bulletin, **33**, 1021 (1960).

TABLE III. NORMAL VIBRATIONS OF HEXACHLOROBENZENE

Species	Activity	No.	Mode	Observed frequency cm^{-1}
A_{1g}	Raman	ν_1	C–Cl stretching	1225
		ν_2	Breathing	372
A_{2u}	Infrared	ν_4	C–Cl out-of-plane bending	—
E_{1g}	Raman	ν_{11}	C–Cl out-of-plane bending	213
E_{1u}	Infrared	ν_{12}	Ring stretching	1350
		ν_{13}	C–Cl stretching	696
		ν_{14}	C–Cl in-plane bending	—
E_{2g}	Raman	ν_{15}	Ring stretching	1522
		ν_{16}	C–Cl stretching	—
		ν_{17}	Ring in-plane deformation	340
		ν_{18}	C–Cl in-plane bending	322

absorption, this fact might be because the intensity of these vibrations is too low to be observed.

The infrared absorption spectra in the sodium chloride and cesium bromide regions are shown in Fig. 4, and the frequencies of the observed bands are listed in Table II.

Assignment

Assuming the symmetry D_{6h} for the molecule of hexachlorobenzene, the normal vibrations are classified as:

$$\text{In-plane vibrations}: 2A_{1g}+A_{2g}+2B_{1u}+2B_{2u}+3E_{1u}+4E_{2g}$$

$$\text{Out-of-plane vibrations}: A_{2u}+2B_{2g}+E_{1g}+2E_{2u}$$

Among these vibrations, those belonging to the species A_{1g}, E_{1g} and E_{2g} are active in the Raman effect, and those belonging to the species A_{2u} and E_{1u} are active in the infrared absorption spectrum. Consequently, seven Raman lines and four infrared absorption bands are expected for this molecule. These are listed in Table III.

Raman Spectrum.—*Species A_{1g}.*—Two vibrations belong to this species. One is the breathing vibration of the molecule as a whole, and the other is the symmetric stretching vibration of the C–Cl bands. Though the former would empirically be expected to have a frequency about 1000 cm^{-1} and the latter about 600 cm^{-1}, this expectation is not realized in this case. As is shown in Table I, two strong and polarized lines were observed at 372 and 1225 cm^{-1}. The third polarized line at 1195 cm^{-1} was much weaker than the first two and should be considered as an overtone or a combination. The observed frequencies of both ν_1 and ν_2 are completely different from the above, expected values. Since the two totally symmetric vibrations can be regarded as linear combinations of the breathing vibrations of two rings, that is, the rings consisting of six carbon atoms and six chlorine atoms respectively, the line at 1225 cm^{-1} can be assigned to the antiphase linear combination of these breathings, namely, the symmetric stretching vibration of the C–Cl bonds (ν_1), while the line at 372 cm^{-1} can be assigned to the same-phase linear combination of these breathings, namely, the breathing vibration of the molecule as a whole.

Species E_{1g}.—Only one vibration, ν_{11}, belongs to this species. As this is the out-of-plane bending vibration of the C–Cl bonds, the line observed at 213 cm^{-1} was assigned to it.

Species E_{2g}.—The line at 1522 cm^{-1} was apparently assigned to the stretching vibration of the benzene ring, ν_{15}. Though this line was not very clearly observed in the carbon tetrachloride and carbon disulfide solutions because of the overlapping with lines of solvents, it was clearly observed in benzene solution and its depolarization ratio could be confirmed to be large.

The C–Cl stretching vibration, ν_{16}, was expected to appear near 700 cm^{-1}, but no line was observed around there. In the carbon tetrachloride solution a weak line was observed at 572 cm^{-1}, but this line was found to be polarized and could not be regarded as a fundamental. Though no fundamental line was found which might give an overtone at 572 cm^{-1}, it might possibly still be an overtone since there are many fundamentals inactive in both Raman and infrared spectra.

The weak line at 340 cm^{-1} was assigned to the deformation vibration of the ring, ν_{17}. This line probably corresponds to a fundamental vibration irrespective of its extremely low intensity, for its frequency is too low to be considered as an overtone or a combination.

The remarkable line at 322 cm^{-1} was assigned to the in-plane bending vibration of the C–Cl bonds, ν_{18}.

Overtones and Combinations.—The five lines at 3042, 2452, 1248, 1195 and 572 cm^{-1} which were not assigned to fundamentals are all polarized and were considered to be overtones. The first two are apparently the overtones of ν_{15} (1522 cm^{-1}) and ν_1 (1225 cm^{-1}). The other three are not overtones of observed fundamentals, but they might be the overtones of inactive fundamentals of the frequencies about 624, 598 and 286 cm^{-1}. However, of course, the above-mentioned observed bands can by no means be adequate evidence for the existence of these fundamental frequencies.

Infrared Absorption Specta.—*Species* A_{2u}.—Only the out-of-plane bending vibration of C–Cl bonds, ν_4, belongs to this species. Though this vibration was expected to appear near 200 cm^{-1}, no absorption band was observed in the far infrared region, as has already been mentioned. This might be due to the difficulty in the measuring technics* and to the low intensity of this band.

Species E_{1u}.—Three vibrations, ν_{12}, ν_{13} and ν_{14}, belong to this species. The modes of these vibrations might be rather complicated in this case, and it is difficult to visualize these modes because of extreme mixing of the stretching and deformation vibrations of the ring and the C–Cl bonds. Though the simple modes are given for these vibrations in Table III, this is simply for the sake of convenience; actually such simple notations might by no means describe the true modes faithfully. On account of such complexity in the vibrational mode, the empirical estimation of the normal frequencies might be very difficult for this species. However, one can find an analogy in the case of the species E_{1u} of benzene. The mode of ν_{12} of benzene is nearly the stretching vibration of C–H bonds, that of ν_{13} is nearly the stretching vibration of the carbon ring, and that of ν_{14} is the vibration between the carbon ring and the ring consisting of six hydrogen atoms[6]. The observed frequencies for these vibrations are 3099, 1485 and 1037 cm^{-1} respectively. The first two are just the frequencies to be expected from the modes, but it is interesting that the third is the frequency empirically expected for a C–H in-plane bending vibration. Provided that the analogy can be applied to the case of hexachlorobenzene, irrespective of the large difference between the masses of hydrogen and chlorine atom, the vibration ν_{12}, ν_{13} and ν_{14} might have the frequencies of the ring stretching vibration, of C–Cl stretching vibration and of C–Cl in-plane bending vibration respectively. In the infrared absorption spectrum, two strong absorption bands were really observed at 1350 and 696.2 cm^{-1}. Consequently, the former can be assigned to ν_{12} and the latter to ν_{13}. However, though ν_{14} could be expected to appear at 200~300 cm^{-1} according to the above-mentioned analogy, no band was observed in the far infrared region, as has already been mentioned. This is probably because ν_{14} has a very low intensity.

Combination Bands.—A considerable number of combination bands were observed in the infrared absorption spectra, as is shown in Table II. As this molecule has a center of symmetry, only the vibrations belonging to the ungerade species are active to the infrared absorption. Since the first overtone of a fundamental of any species belongs to a gerade species, and since second overtones and higher might not have observable intensities, the observed absorption bands not corresponding to fundamentals should be regarded as combination bands between a gerade fundamental and an ungerade fundamental. However, the clear explanation of these combination bands is not easy in this case. The molecule of hexachlorobenzene has ten fundamental frequencies belonging to the ungerade species, but only two of them were observed; the others were inactive or unobserved. Also, of the vibrations belonging to the gerade species, only a few were observed. Under such conditions, it is not possible to explain all of the combination bands, and it seems to be rather insignificant to present the explanations for only a few combination bands. Thus, discussion of the combination bands has been entirely omitted.

The above-mentioned assignment for the normal vibrations is shown in the last column of Table III.

Summary

The infrared absorption spectra of hexachlorobenzene were measured in a gaseous state from 4000 to 300 cm^{-1}, and in solid state from 300 to 100 cm^{-1}. The Raman spectra of the same substance were measured in solutions in benzene, carbon tetrachloride and carbon disulfide. The depolarization ratio of each Raman line was also observed qualitatively. The assignment of the observed absorption bands and Raman lines was determined, partly by referring to that of benzene.

The author wishes to express his appreciation to Professor H. Yoshinaga and Dr.

* The measurement had to be carried out in vacuo in order to avoid the extreme masking effect of the strong absorption of water vapor in the atmosphere. However, as the window material of the sample holder was polyethylene, it was not certain that the proper thickness and homogeneity of the Nujol paste layer was preserved even in vacuo.

6) G. Herzberg, "Molecular Spectra and Molecular Structure II", D. Van Nostrand Co. (1954), p. 118.

Mitzuishi for the use of the far infrared spectrometer, and to Dr. Y. Mashiko for his helpful suggestions.

The Government Chemical Industrial Research Institute, Tokyo
Shibuya-ku, Tokyo

The Infrared Absorption Spectra of p-Dichlorobenzene and p-Dichlorobenzene-d_4

By Shinnosuke SAËKI

(Received June 26, 1961)

A report has previously been published by the author[1] concerning the infrared absorption spectra of *p*-dichlorobenzene and *p*-dichlorobenzene-d_4 in the regions of the lithium fluoride, sodium chloride and potassium bromide prisms. Recently the author carried out the measurement of the infrared spectra in the farther region, that is, from 400 to 300 cm^{-1} which a cesium bromide prism and from 300 to 100 cm^{-1} with gratings. In addition, the shape of each absorption band observed between 1700 and 700 cm^{-1} was also measured by the aid of a high-temperature long-path cell. The results of these measurements and the new assignment determined on the basis of these experimental results are reported in this paper. The assignment proposed in the previous paper was revised in several points in the new assignment proposed here.

Experimental

Far Infrared Absorption Spectra.—The measurement in the cesium bromide prism region was carried out from 670 to 300 cm^{-1} using a Perkin-Elmer model 21 spectrophotometer and a 85 mm. high temperature gas cell almost identical with that described in the previous paper[1], except that the window material was cesium bromide. The method of measurement need not be mentioned, since it was quite similar to the previous case[1]. The measurement was done at about 210°C. As a number of intense bands of atmospheric water vapor made the 100% line uneven, especially beyond 330 cm^{-1}, and as the infrared radiation from the cell and the hot sample vapor itself made the base line also uneven, it was necessary to measure the 100% and base lines, as well as the absorption curve for each measurement, in order to obtain a correct spectrum.

The spectra between 300 and 100 cm^{-1} were measured using the grating spectrophotometer installed in the laboratory of Professor Yoshinaga of Osaka University[2]. As the construction of the spectrometer did not allow the measurement in a gaseous state, the spectra were taken in the state of Nujol mull sandwiched between two polyethylene sheets (1 mm. thick)*. As the specimen, on measurement, was placed in a vaccum in order to avoid disturbance by the strong absorption of atmospheric water, some extent of inhomogenity of thickness might occur in the layer of Nujol mull due to the insufficient rigidity of the polyethylene sheet. However, this inhomogenity, if any, gave rise to no obstacle to simple, accurate observation of the frequencies of absorption bands.

Observation of Band Shapes.—It is very desirable for the determination of the assignment to observe the correct shapes of the band envelopes. However, using the 85 mm. high temperature cell, it proved to be impossible to observe the clear band envelopes. This failure might be attributed to the high temperature at which the measurements were carried out more than to the poor resolution of the spectrometer. If the 85 mm. high temperature cell was used, it was necessary to raise the temperature over the boiling points of these sample substances, that is, at 200 or 300°C, to obtain an enough strong absorption curve. But at high temperatures the width of an absorption band becomes large**, and a clear envelope can not be observed, even if a small slit width is used. Also, because of the extremely low vapor pressures of the sample substances, the use of an ordinary long path cell of the multiple reflection type (for example, a ten-meter gas cell) at room temperature was not sufficient to obtain a strong enough absorption curve. Thus it proved necessary, in order to obtain a sufficiently clear spectrum, to carry out a measurement at a temperature not extremely high, using a high temperature long path cell.

The high temperature long path cell constructed in our laboratory has the same optical alignment as that of the Perkin-Elmer ten-meter cell, but all its mirrors were spattered with gold to secure them from corrosion by the heat and by the sample

1) S. Saëki, This Bulletin, 33, 1021 (1960).

2) H. Yoshinaga, S. Fujita, S. Minami, A. Mitsuishi, R. A. Oetjen and Y. Yamada, *J. Opt. Soc. Am.*, **48**, 315 (1958).

* To prepare the specimen, the method of compounding the substance with hot polyethylene was not available in this case because of the high volatility of the sample substance. The method of making the solid solution in paraffin was also found to be impossible.

** This might be due to the increasing collision between molecules and to the increasing population at the levels of higher *J* values.

gases. The cell was coiled with heaters on the whole outside surface and then covered with several layers of asbestors for the sake of heat insulation. The entrance and exit openings were doubly closed by potassium bromide plates in order to prevent the condensing of the sample gas on the inner surfaces of the windows. The temperature of the cell could be raised up to about 110°C without any risk of decomposing the binding and sealing materials. A slight leakage at the stopcock, however, did not allow the maintenance of the vacuum over the whole period of scanning the spectrum. The 720 cm. path length was used for the measurements, and the sufficiently clear spectra were obtained at 60~80°C for *p*-dichlorobenzene. Although the large amount of energy loss due to multiple reflections in the cell obliged the use of considerably wide slits, the obtained spectra were much clearer than those obtained using the 85 mm. high temperature cell, and many absorption bands which could not be resolved previously were newly observed by the aid of this 720 cm. cell. The absorption curves for the bands at 1417 and 1393 cm^{-1} of *p*-dichlorobenzene obtained using these two cells of different types are shown in Fig. 1 for comparison.

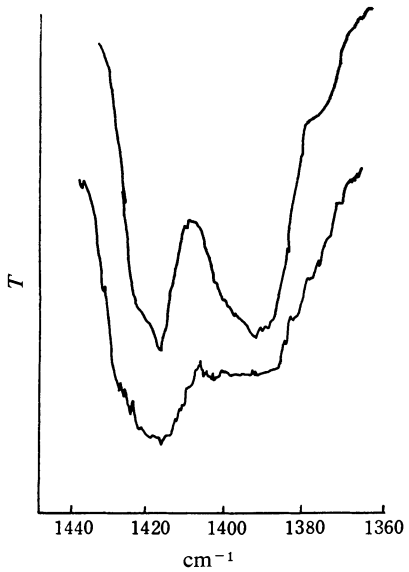


Fig. 1. The infrared absorption spectra of *p*-dichlorobenzene near 1400 cm^{-1} measured using the long path and short path gas cells.
The upper curve: spectrum measured using the 720 cm. cell (slit width: 70 μ)
The lower curve: spectrum measured using the 85 mm. cell (slit width: 40 μ)

Although every effort was made to reduce the absorption due to atmospheric water vapor, a remarkable amount of absorption, which necessarily remained because of the design of the long-path cell, made difficult the observation of band envelopes in the 6 μ region. The adsorption of the sample gas on the inner surface of the cell required the paying of a good deal of attention to the washing of the cell after measurements. It proved to be necessary in the case of *p*-dichlorobenzene, when measurement was over, to drive the sample gas out by nitrogen as completely as possible; then the cell was demounted and kept open for forty hours at a high temperature. Even after such a drastic washing, on the next use, the absorption bands of desorbed gas were often observed with considerable intensities when the measurement was carried out over a long period of time. Accordingly, on the analysis of the spectra taken under such conditions, much attention was required to rule out the undesired band.

Results

The observed spectra of *p*-dichlorobenzene and *p*-dichlorobenzene-d_4 are shown in Fig. 2. The curves beyond 300 cm^{-1} are fragmental because of the necessity of frequent exchanges of the gratings and filters with the decreasing frequency during the measurement.

The observation of band envelopes was successful for some of the bands observed in the region of cesium bromide prism, while it is impossible in principle in the region of the gratings, where the spectra were observed in the solid state.

The spectra of *p*-dichlorobenzene-d_4 observed using the 720 cm. high temperature cell are shown in Fig. 3 for the region where the principal bands appeared.

The frequencies, intensities and types of the observed bands are shown in Table I. However, it should be mentioned here that the strong band at 1170 cm^{-1} of *p*-dichlorobenzene-d_4 proved to originate in a substance other than *p*-dichlorobenzenes. A comparison with the spectrum of the solutions and an examination of the time dependent change of the spectrum revealed this. Accordingly, no further consideration should be given to this band.

Discussion and Assignment

Band Envelopes.—In the case of *p*-dichlorobenzene, the three principal axes of the moment of inertia coincide with the three symmetry axes of the molecule because of the high symmetry. Taking the x-axis perpendicular to the molecular plane, the z-axis along the line combining two chlorine atoms, and the y-axis perpendicular to these two, the moments of inertia are calculated to be:

	$C_6H_4Cl_2$	$C_6D_4Cl_2$	
I_x	823	848	
I_y	735	741	
I_z	88	106	(in physical atomic weight·Å^2)

Therefore, vibrations belonging to species B_{1u}, B_{2u} an B_{3u} give absorption bands of type A, B and C respectively. In the actual spectrum,

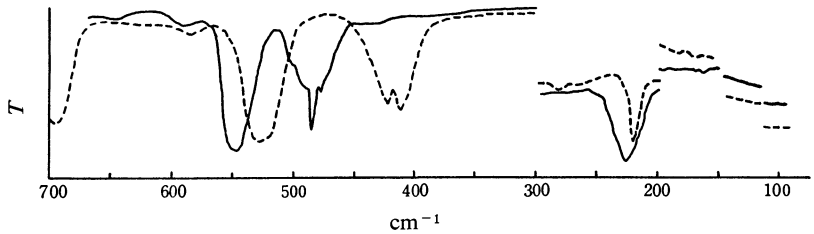


Fig. 2. Far infrared absorption spectra of ordinary and deuterated *p*-dichlorobenzenes.
$C_6H_4Cl_2$ —— $C_6D_4Cl_2$ ----

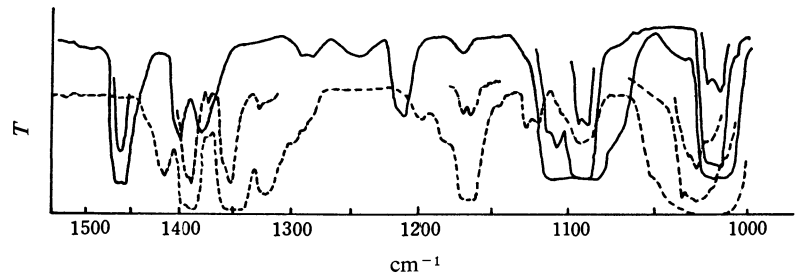


Fig. 3. Infrared absorption spectra of ordinary and deuterated *p*-dichlorobenzenes.
$C_6H_4Cl_2$ —— $C_6D_4Cl_2$ ----

TABLE I. INFRARED ABSORPTION BANDS OF *p*-DICHLOROBENZENE AND *p*-DICHLOROBENZENE-d_4

$C_6D_4Cl_2$			$C_6H_4Cl_2$		
Wave number	Type	Intensity	Wave number	Type	Intensity
3098	B	2	2301		3
3037	A	sh 1	2289		0
1888	B	4	1622	A	2
1758	A	3	1568	B	4
1656	B	sh 2			
1625	A	5	1434	A	4
1509	A or B	3	1405		12
1478	B or A	10	1366	B or A	14
1417	A	8	1373		
1393	A	5	1334 {1337, 1331}	B	5
1297	B	1	1315 {1319, 1310}	B	sh 1
1253	A	1	1205		sh 2
1217		4	1187		sh 1
1173	B?	1	1170 ?	B	12
1112 {1115, 1109}	B	3	1127 {1131, 1123}	B	3
1094 {1096, 1091}	B	15	1096	A	4
1017 {1021, 1014}	B	12	834.7, 821.8, 811.7		7
819.2	C	20	694.8	C	10
774.2	B	sh 1			
588	A	m	581.7	A	w
545.2	A or B	s	527.4	A	s
480.7	C	s	418.4	B ?	s
225.2		s	221.2		s

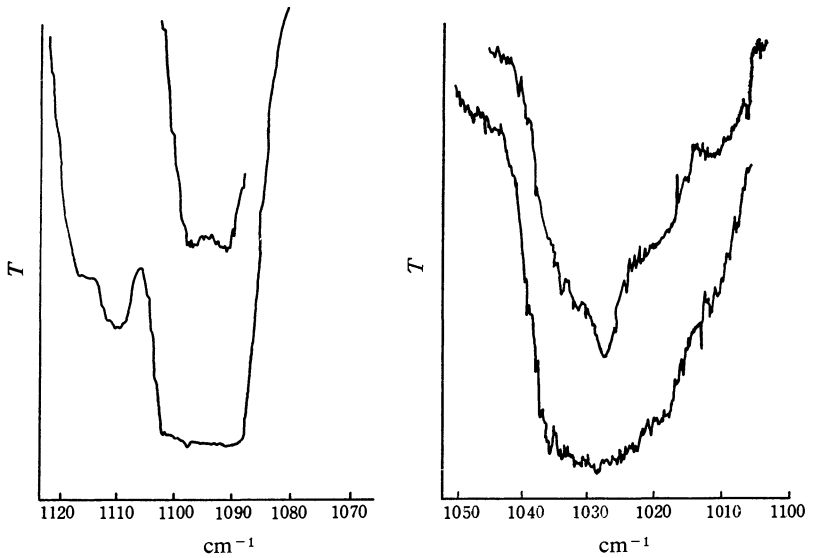


Fig. 4. The shapes of the bands at 1094 cm^{-1} of ordinary *p*-dichlorobenzene and at 1028 cm^{-1} of deuterated *p*-dichlorobenzene.

relatively clear band envelopes were observed for type C bands, for, as was expected from their vibrational modes, all of them appeared in a lower frequency region, where the resolution of the spectrometer is relatively high. However, for the bands of the other species, when they appeared in the higher frequency region, the observed envelopes were not adequately clear to distinguish them as type A or B. In Table I, bands having somewhat pointed peaks are descibed as type A bands, and bands having somewhat round peaks, as type B bands. On the contrary, envelopes were clearly observed for the bands which appeared in the region below 1100 cm^{-1}, except for a few bands. Examples will be shown below.

The band of $C_6H_4Cl_2$ at 1094 cm^{-1}, which certainly corresponds to 1028 cm^{-1} of $C_6D_4Cl_2$*, is shown in Fig. 4. This appeared to be a type B band showing a clear absorption minimum at the center, while the band of $C_6D_4Cl_2$ at 1028 cm^{-1} could be explained only as a type A band because of its clear Q branch, as is seen in the figure. This fact suggests that too much significance should not be attached to the observed band envelopes on determining the assignment, at least when their apparent shapes are considered.

In the observed spectra, there were many asymmetrical absorption bands consisting of two branches of unequal intensity. The band of *p*-dichlorobenzene observed at 1217 cm^{-1} is shown in Fig. 5 as a typical example. Considering the existence of two branches, they might be regarded as type B bands, but if the stronger branch is regarded as an overlap of the Q and R branches, such a band should be considered as a type A or C band. As will be mentioned later, the band of $C_6D_4Cl_2$ at 414 cm^{-1} also showed such an envelope and appeared to be a type B band, but it was revealed to be a type C band by a consideration of the product rule and of the correspondence with a band of $C_6H_4Cl_2$. There were many other bands like this, of which the type could not be determined clearly.

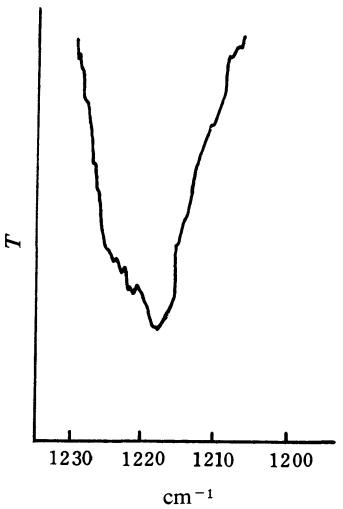


Fig. 5. The shape of the band at 1217 cm^{-1} of *p*-dichlorobenzene.

* This correspondence between bands satisfied the product rule, as will be shown later.

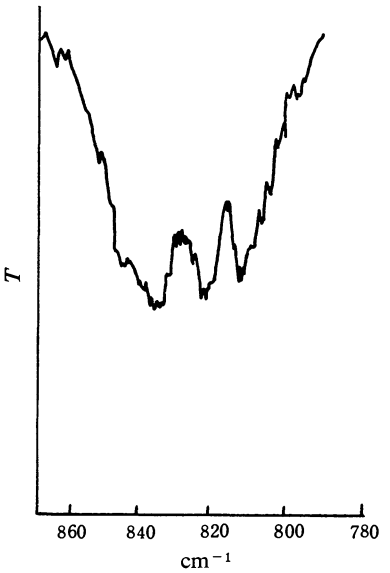


Fig. 6. The shape of the band at 820 cm^{-1} of *p*-dichlorobenzene-d_4.

Another difficult band was observed in the spectrum of deuterated *p*-dichlorobenzene. In Fig. 6 is shown a band observed around 820 cm^{-1}. The large spacing between the three absorption maxima (see the figure) could be explained neither as three branches of a single band, nor as three separate absorption bands, because of the resultant absence of the branches of each band. However, in the spectra of solutions, three closely positioned weak bands were observed in this frequency region; these may be separate bands, the branches of which overlap, one with the others.

Assignment.—Taking account of the product rule, and on the basis of the above-mentioned results concerning the envelopes of principal bands, the assignment of the observed bands was determined as is shown in Table II.

Some revisions of the previous assignment were required to be consistent with the above-mentioned new experimental results. In our previous paper[1], the band at 483 cm^{-1} of $C_6H_4Cl_2$ (414 cm^{-1} for $C_6D_4Cl_2$) was assigned

TABLE II. ASSIGNMENT OF THE INFRARED ABSORPTION BANDS OF *p*-DICHLOROBENZENE AND *p*-DICHLOROBENZENE-d_4

Wave number		Assignment	Mode
$C_6H_4Cl_2$	$C_6D_4Cl_2$		
3098	2301	$\nu_{10}(b_{1u})$	C-H or C-D stretching
3098	2289	$\nu_{18}(b_{2u})$	C-H or C-D stretching
1888	1622	$\nu_7(a_u)+\nu_{15}(b_{2g})$	
1758		$\nu_2(a_g)+\nu_{30}(b_{3u})$	
1656		$\nu_4(a_g)+\nu_{14}(b_{1u})$	
1625		$\nu_9(b_{1g})+\nu_{28}(b_{3u})$	
	1568	$\nu_3(a_g)+\nu_{28}(b_{3u})$	
1509		$\nu_{12}(b_{1u})+\nu_{16}(b_{2g})$	
	1434	$\nu_{13}(b_{1u})+\nu_{26}(b_{3g})$	
1478	1370	$\nu_{11}(b_{1u})$	Ring stretching
1417	1405	$\nu_{19}(b_{2u})$	Ring stretching
1393	1334	$\nu_{20}(b_{2u})$	Ring stretching
	1315	$\nu_{13}(b_{1u})+\nu_{17}(b_{2g})$	
1297		$\nu_9(b_{1g})+\nu_{29}(b_{3u})$	
1253		$\nu_7(a_u)+\nu_{17}(b_{2g})$	
1217		$\nu_4(a_g)+\nu_{29}(b_{3u})$	
	1205	$\nu_{13}(b_{1u})+\nu_{16}(b_{2g})$	
1173		$\nu_{14}(b_{1u})+\nu_{26}(b_{3g})$	
	1127	$\nu_4(a_g)+\nu_{29}(b_{3u})$	
1112	811.7	$\nu_{21}(b_{2u})$	C-H or C-D in-plane bending
	1096	$\nu_3(a_g)+\nu_{30}(b_{3u})$	
1094	1028	$\nu_{12}(b_{1u})$	Ring in-plane deformation
1017	821.8	$\nu_{13}(b_{1u})$	C-H or C-D in-plane bending
819.2	694.8	$\nu_{28}(b_{3u})$	C-H or C-D out-of-plane bending
774.2		$\nu_{17}(b_{2g})+\nu_{29}(b_{3u})$	
588	581.7	$\nu_6(a_g)+\nu_{22}(b_{2u})$ or $\nu_{22}(b_{2u})+\nu_{27}(b_{3g})$	
545.2	527.4	$\nu_{14}(b_{1u})$	C-Cl stretching
480.7	418.4	$\nu_{29}(b_{3u})$	Ring out-of-plane deformation
225.2	221.2	$\nu_{30}(b_{3u})$	C-Cl out-of-plane bending

to ν_{14} of the species B_{1u}, and the band at 544 cm^{-1} of $C_6H_4Cl_2$ (526 cm^{-1} for $C_6D_4Cl_2$) was assigned to ν_{29} of species B_{3u}. However, as the bands at 481 cm^{-1} of $C_6H_4Cl_2$ and at 418 cm^{-1} of $C_6D_4Cl_2$ proved to be type C bands in this study, it became clear that the 481 cm^{-1} and the 418 cm^{-1} should be assigned to ν_{29} and the 545 cm^{-1} and 527 cm^{-1} should be assigned to ν_{14}, inverting the previous assignment.

Furthermore, in our previous assignment, the pair of bands at 1014 and 800 cm^{-1} was assigned to the ring deformation vibration ν_{20} of species B_{2u}. However, as is clear from a consideration of the vibrational mode, this vibration is necessarily accompanied with the ring stretching one, and, consequently, the frequency of this vibration must be relatively high. From this viewpoint, the bands at 1393 cm^{-1} of $C_6H_4Cl_2$ and at 1334 cm^{-1} of $C_6D_4Cl_2$ were assigned to this vibration, ν_{20}.

As the large frequency shifts observed for the bands at 1017 and 1112 cm^{-1} of $C_6H_4Cl_2$ on the deuteration (to 821.8 and 811.7 cm^{-1} of $C_6D_4Cl_2$ respectively) suggest that these vibrations mainly concern the motions of the C–H bonds, they are assigned to the C–H in-plane bending vibrations.

The assignment of the combination bands is also shown in Table II. Of these combination bands, a brief discussion should be given about the assignment of the band at 588 cm^{-1} of $C_6H_4Cl_2$ which appearently corresponds to the band at 581.7 cm^{-1} of $C_6D_4Cl_2$. This pair of bands is difficult to explain as any combination of the observed fundamentals. The unobserved low frequency fundamental of the gerade species is ν_{27} of $C_6D_4Cl_2$* (b_{3g}, Raman active), and those of ungerade species are $\nu_8(a_u)$ and $\nu_{22}(b_{2u})$ of each substance. Therefore, the possible assignments for 588 and 581.7 cm^{-1} are as follows:

$$\nu_6(a_g)+\nu_{22}(b_{2u})$$
$$\nu_{22}(b_{2u})+\nu_{27}(b_{3g})$$
$$\nu_8(a_u)+\nu_{17}(b_{2g})$$
$$\nu_8(a_u)+\nu_{27}(b_{3g})$$

However, as $\nu_8(a_u)$, being the out-of-plane deformation vibration of the ring, may have a frequency higher than 300 cm^{-1} at the lowest, the last two assignments appear to be impossible. The remaining two assignments seem to have similar possibilities. If the first assignment is taken up, the frequencies of ν_{22}'s are calculated from the frequencies of ν_6's to be 259 and 258 cm^{-1} for $C_6H_4Cl_2$ and $C_6D_4Cl_2$ respectively. If the second assignment is taken up, 239 cm^{-1} is obtained as the frequencies of ν_{22} for $C_6H_4Cl_2$, while the frequency of ν_{22} for $C_6D_4Cl_2$, can not be calculated, for the frequency of ν_{27} was not observed for $C_6D_4Cl_2$. However, if the above-mentioned frequency of 340 cm^{-1} for the ν_{27} of $C_6D_4Cl_2$ (see the last footnote) is used, ν_{22} can be calculated to be 242 cm^{-1} for $C_6D_4Cl_2$. Since, from a theoretical viewpoint, the frequency must be lower for $C_6D_4Cl_2$ than for $C_6H_4Cl_2$, the frequencies of ν_{22} and ν_{27} for $C_6D_4Cl_2$ should be determined to be 239 and 343 cm^{-1}. After all, two possible pairs of ν_{22} for each substance are obtained, that is, 259 and 258 cm^{-1}, and 239 and 239 cm^{-1}. As both of these two pairs are plausible for the C–Cl in-plane bending vibrations, it is very difficult to distinguish which pair is the true one, while one of these two pairs is certainly true. Since the influence of these two assignments on the ratio of the products of the frequencies is very small, even the product rule sheds little light on the determination of this question.

Product Rule.—The ratios of products of the frequency required by the theorem of Teller and Redlich are as follows:

1.972 for species B_{1u}

1.972 for species B_{2u}

1.395 for species B_{3u}

The ratios calculated from the observed frequencies are 1.977 for species B_{1u} and 1.379 for species B_{3u}, showing good accordances with the above theoretical values. As for species B_{2u}, since ν_{22} was observed for neither $C_6H_4Cl_2$ nor $C_6D_4Cl_2$, the perfect application of the product rule was impossible. However, taking account of the fact that a low frequency vibration such as ν_{22} is little influenced by deuteration, the ratio of ν_{22}'s for both substance could be estimated to be little larger than 1. This estimation seems to be justified by the calculated pairs of frequencies for ν_{22}'s in the previous paragraphs. With this assumption, the ratio of the products of the frequencies can be calculated to be 1.953 for species B_{2u}; the accordance with the theoretical value is also very good in this case. From such considerations, the assignment proposed here proves to have much reliability.

Summary

The infrared absorption spectra of *p*-dichlorobenzene and *p*-dichlorobenzene-d_4 were measured from 300 to 700 cm^{-1} in a gaseous state with cesium bromide prism, from 300 to 100 cm^{-1} in a solid state with gratings, and, using a newly constructed long path (720 cm.) high

* ν_{27} of $C_6H_4Cl_2$ was observed at 349 cm^{-1}. Applying the product rule using this frequency, the frequency of ν_{27} of $C_6D_4Cl_2$ is calculated to be about 340 cm^{-1}.

temperature cell, from 1700 to 700 cm^{-1} in a gaseous state with a sodium chloride prism. The frequencies and band envelopes of observed absorption bands were reported.

On the basis of these results, the assignment of the infrared active normal vibrations of these molecules was determined. The assignment was checked by means of the application of the product rule, and the correctness was verified by the good agreement between the theoretical and experimental values.

The assignment was also determined for the observed combination bands, using the Raman fundamental frequencies presented in the previous paper as well as infrared frequencies.

The author wishes to express his indebtedness to Professor H. Yoshinaga and Dr. A. Mitzuishi for the use of the far infrared grating spectrometer, and to Dr. Y. Mashiko for his advice and encouragement.

Government Chemical Industrial Research Institute, Tokyo
Shibuya-ku, Tokyo

Infrared Absorption Spectra of Hydrazides. I. Hydrazides of Aromatic Acids

By Mitsuo MASHIMA

(Received June 8, 1961)

The infrared absorption spectra of a number of mono-substituted amides and their related compounds have been studied[1], and the characteristic bands of mono-substituted amides have been reported on in detail[2]. Bands amide I, amide II and amide III in the rock salt region have been associated with CONH group of non-cyclic secondary amides. Amide frequencies of difomylhydrozine[2,3] and diacetylhydrazine[2,4] have recently been studied, and amide I and amide II bands have been observed to shift abnormally to the lower frequencies in the spectra of these hydrazides. However, the number of the hydrazides examined has been rather limited. The aim ot the present study is to examine in detail the amide bands of various aromatic hydrazides containing a CONHNHCO group.

Experimental

Acetylbenzoylhydrazine was synthesized with acetic anhydride and benzoylhydrazine[5] and purified by recrystallization from ethanol, m. p. 171°C. Benzoylhydrazine was prepared with ethylbenzoate and hydrazine hydrate[6] and purified by recrystallization from benzene, m. p. 111°C. Trichloroacetylbenzoylhydrazine was synthesized with trichloroacetylchloride and benzoylhydrazine[7] and purified by recrystallization from benzene, m. p. 164°C. Dibenzoylhydrazine was synthesized with benzoylchloride and hydrazine hydrate[8] and purified by recrystallization from ethanol, m. p. 238°C. Benzamide was prepared by recrystallization of the material of G. R. grade from ethanol, m. p. 130°C. *N*-Deuterated derivatives examined were prepared in sealed tubes in the presence of heavy water (99.8%). The excess of heavy water was evaporated in vacuo.

The spectra of hydrazides which were insoluble in non-polar solvents, such as carbon disulfide and carbon tetrachloride, were obtained with acetonitrile as a solvent and cells of 0.1 mm. in the optical path. The solid spectra of all compounds were studied with potassium bromide disk. A double-beam Hitachi infrared spectrophotometer Type EPI-2 was used in the rock salt region.

Results and Discussion

Acetylbenzoylhydrazine (ABH).—The infrared absorption spectra of ABH are given in Fig. 1, in which a solid curve shows the solid spectrum, a dotted curve, the solution spectrum and a dashed curve, the spectrum of *N*-deuterated ABH (ABH-d_2) in the solid state. The solution spectrum of ABH was obtained with a saturated solution (ca. 0.1 mol./l.) in acetonitrile.

The 3000 cm^{-1} Region. — Two strong bands were found at 3180 and 3000 cm^{-1} in the spectrum of solid ABH. Probably an ABH molecule is planar in the solid state, and the two

1) See, for instance, L. J. Bellamy, "The Infrared Spectra of Complex Molecules", Methuen and Company, Ltd., London (1954).
2) T. Miyazawa, T. Shimanouchi and S. Mizushima, *J. Chem. Phys.*, **24**, 408 (1956).
3) T. Miyazawa, *J. Chem. Soc. Japan, Pure Chem. Sec.* (*Nippon Kagaku Zasshi*), **76**, 341 (1955).
4) A. Yamaguchi, ibid., **79**, 880 (1958).
5) T. Curtius, *J. prakt. Chem.*, [2] **50**, 280 (1894).
6) T. Curtius, ibid., [2] **50**, 278 (1894).
7) L. Spiegel and P. Spiegel, *Ber.*, **40**, 1739 (1907).
8) R. Stolle and A. Benrath, *J. prakt. Chem.*, [2] **70**, 268 (1904).

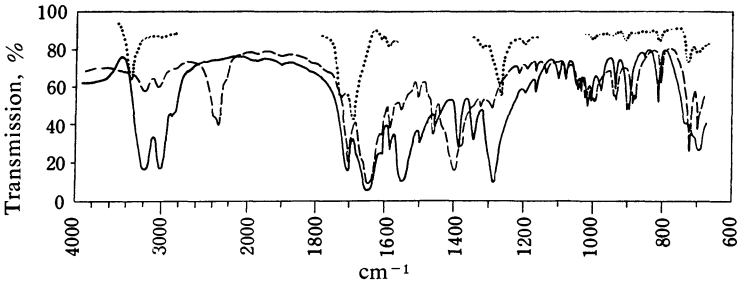


Fig. 1. Infrared absorption spectra of ABH in the rock salt region. The solid curve indicates the solid spectrum, the dotted curve partly represented is the solution spectrum of ABH (0.1 mol./l., 0.1 mm. cell), and the dashed curve shows the spectrum of ABH-d_2 in the solid state.

frequencies can be ascribed to the N–H stretching vibration. The abnormally low frequencies for the N–H vibration may be attributed to the coupling between two N–H vibrations in the CONHNHCO group of point group C_{2h}. On the other hand, only one band at 3320 cm^{-1} was found in this region for the solution spectrum. Probably the molecule is nonplanar in the solution, and the increase in frequency in the solution spectrum may be due to a decrease in the interaction between the two N–H vibrations. A band corresponding to them in the spectrum of *N*-deuterated ABH was found at 2310 cm^{-1}, which band was accompanied by two shoulder bands near 2340 and 2380 cm^{-1}. They are assigned to ν(N–D). ABH also has two weak bands at 2860 and 2830 cm^{-1} which are assigned to ν(C–H). Bands corresponding to them are found at 2830 and 2800 cm^{-1} for ABH-d_2.

The 1700~1450 cm^{-1} Region.—ABH has two bands which must be ascribed to the C=O stretching vibration. They are 1707 and 1644 cm^{-1} in the solid spectrum and 1720 and 1683 cm^{-1} in the solution spectrum. ABH-d_2 has bands at 1697 and 1645 cm^{-1} corresponding to them. The splitting of ν(C=O) may be due to the interaction of two vibrations which are two related C=O groups. However, the frequencies are rather higher than those of the hydrazides studied already, i. e., at 1610 cm^{-1} for diformylhydrazine[3] and 1597 cm^{-1} for diacetylhydrazine[4] in the solid state. The bands of those frequencies are called amide I.

There was also a strong band at 1527 cm^{-1} in the solid spectrum of ABH ascribed to the amide II band. A band corresponding to it is found at 1393 cm^{-1} in the spectrum of ABH-d_2 and called amide II′ according to Miyazawa et al.[2], the ratio ν_H/ν_D being 1.096. It was impossible to check this band in the solution spectrum because of interference by solvent absorption.

In this region two comparatively strong bands are also found at 1607 and 1582 cm^{-1} in the solid spectrum and at 1603 and 1583 cm^{-1} in the solution spectrum. Bands corresponding to them are found at 1607 and 1581 cm^{-1} in the solid ABH-d_2 spectrum. These bands can be assigned to aromatic ring vibrations. Two other bands are found at 1493 and 1450 cm^{-1} in the spectrum of ABH and are also ascribed to aromatic ring vibrations. In the spectrum of ABH-d_2 bands corresponding to them are found at 1497 and 1453 cm^{-1} respectively.

The 1450~1200 cm^{-1} Region. — Deformation frequencies of a CH_3 group are expected to concern two bands in this region. In the spectrum of ABH a band at 1381 cm^{-1} may be taken as the symmetric vibration $\delta_s(CH_3)$ and a shoulder at 1442 cm^{-1} of the band at 1450 cm^{-1}, ν(aromatic C–C), is probably due to the asymmetric $\delta_{as}(CH_3)$. In the spectrum of ABH-d_2 the corresponding bands are found at 1372 and near 1430 cm^{-1}, which are both observed as shoulders on the low- and high-frequency sides of the 1393 cm^{-1} band, amide II′.

The most intense band at 1281 cm^{-1} in this region of the solid spectrum is assigned to the amide III band. A relatively weak band at 1337 cm^{-1} is also probably an amide III. Two bands corresponding to them are found at 1256 and 1313 cm^{-1} in the solution spectrum. The splitting of amide III may be due to coupling between two N–H vibrations; this finding is in accordance with that discussed already in connection with the N–H stretching frequencies.

The 1200~690 cm^{-1} Region. — Owing to the complexity of the spectral pattern in this region, the observed bands will be assigned through a comparison of the spectrum with those of related compounds. Strong and relatively weak bands have been found in this region in the spectra of aromatic compounds; the strong bands may generally be ascribed to the out-of-plane C–H deformation vibrations. In the solid ABH spectrum the most intense

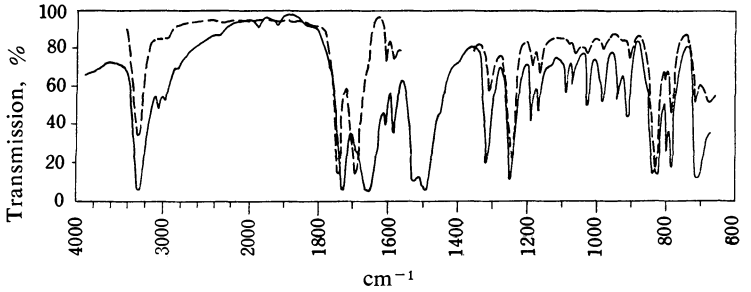


Fig. 2. Infrared absorption spectra of TCABH in the solid state (solid curve) and in a 0.2 mol./l. solution (dashed curve).

band in this region is found at 687 cm^{-1}, which band is accompanied by two well-defined shoulders at 702 and 724 cm^{-1}. ABH in solution has two bands at 691 and 717 cm^{-1}, while ABH-d_2 has them at 691 and 715 cm^{-1}. Since these frequencies are, in general, within or near the range of 700±10 cm^{-1} [1], the two bands can be attributed to the out-of-plane C–H deformation vibrations.

The out-of-plane C–H deformation vibrations of the mono-substituted benzene ring give rise to another band generally within the range 770~730 cm^{-1} [1]. Kross et al.[9] studied the influence of substituents of mono-substituted benzene on the positions of the C–H deformation bands and pointed out that the introduction of electrophilic substituents tends to increase the C–H band in frequency. A band at 803 cm^{-1} of the ABH spectrum can, therefore, be attributed to the C–H out-of-plane vibration. A band corresponding to it is found at 794 cm^{-1} in the ABH-d_2 spectrum.

Other relatively weak bands in this region can not be interpreted with confidence because of the complexity of the spectrum.

Trichloroacetylbenzoylhydrazine (TCABH). —The infrared absorption spectrum of TCABH was studied in the rock salt region in the solid state and in a solution in acetonitrile (0.2 mol./l.). The spectra obtained are illustrated in Fig. 2.

In the solid spectrum TCABH has a band 3280 cm^{-1} which lies in the range 3320~3270 cm^{-1} characteristic to ν(N–H) of many secondary amides[1], and the band can surely be ascribed to ν(N–H). Its appearence as a single band might depend on a decrease in the interaction between two N–H stretching vibrations. However, it must be pointed out that the ν(N–H) frequency does not change in value in the solution spectrum. That is one of the characteristics of the TCABH spectrum different from the ABH spectrum shown in Fig. 1.

TCABH has its amide I bands at 1731 and 1658 cm^{-1} in the solid spectrum and at 1742 and 1694 cm^{-1} in the solution spectrum. This suggests that there is a coupling between two C=O stretching vibrations. It is very interesting to compare the amide I frequencies with those of ABH. The amide I frequencies are collected in Table II. An increase of ν(C=O) due to α-halogen substitution of organic acids has been found to be of the order of 20 cm^{-1} [1]. Such an increase in ν(C=O) is also observed here, e.g., for the higher frequency band of amide I an increase by 24 cm^{-1} is seen between the solid spectra of TCABH and ABH and an increase by 22 cm^{-1} between their solution spectra.

Let us consider next the effect of solvent on the splitting of the amide I band. In the case of ABH the spacing of the splitting is 63 cm^{-1} in the solid and 37 cm^{-1} in solution, and that for TCABH is found to be 73 cm^{-1} in the solid and 48 cm^{-1} in solution. The differences between the values of the splitting in the solid state and solution are, accordingly, relatively very close, i.e., about 25 cm^{-1}. Although obtaining nearly the same values in the splitting of the amide I bands of ABH and TCABH may be accidental because of the different environments of the molecules in the crystalline state and in solution, the phenomenon seems to be worth describing here.

Two bands corresponding to the amide II bands are observed at 1524 and 1492 cm^{-1} in the solid spectrum, and, accordingly, the coupling between two C–N stretching frequencies must be taken into account, although the doublet splitting of amide II was not seen in the ABH spectrum. In solution no amide II band was observed because of interference by the absorption of solvent.

Furthermore, the splitting of the amide III band is also observed; i.e., two bands appear at 1317 and 1248 cm^{-1} in the solid spectrum and at 1305 and 1241 cm^{-1} in the solution spectrum. Thus, it can easily be concluded

9) R. D. Kross, V. A. Fassel and M. Margoshes, *J. Am. Chem. Soc.*, **78**, 1332 (1956).

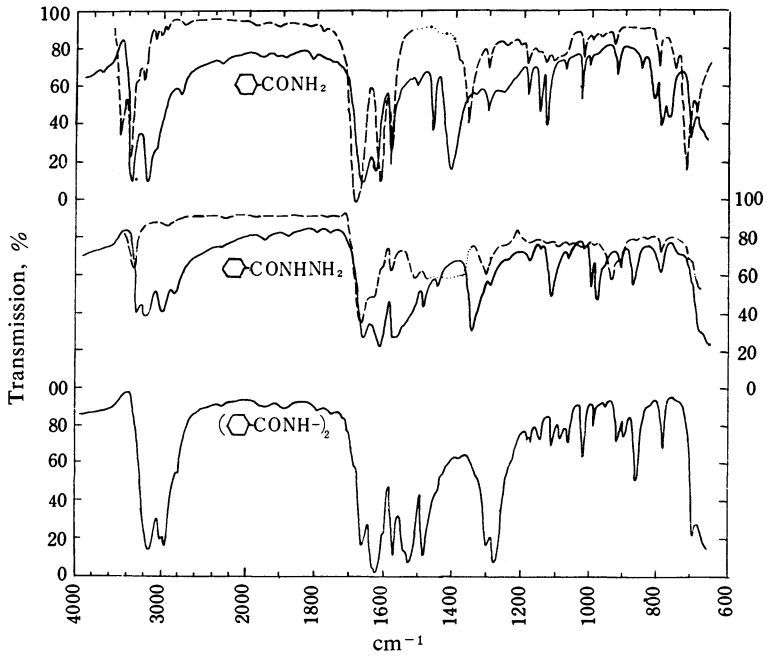


Fig. 3. Infrared absorption spectra of hydrazides and benzamide. The solid curves indicate the solid spectra in KBr disk, and the dashed curves show the solution spectra in acetonitrile.

that there is also a coupling between the two amide III frequencies of the CONHNHCO group.

In the solid spectrum TCABH has a very intense band with two peaks at 835 and 824 cm^{-1}, and a band corresponding to it is found at 827 cm^{-1} in the solution spectrum. This band may be due to the C–Cl stretching frequencies since no corresponding band is observed in the ABH spectrum, as is indicated in Fig. 1.

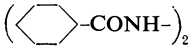
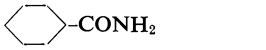
Other bands, especially due to vibrations of the aromatic ring, will be considered in the next section.

Dibenzoylhydrazine (DBH) and Relating Compounds. — The infrared absorption spectra of DBH and its related compounds are shown in Fig. 3, in which solid curves show the solid spectra and dashed curves indicate the solution spectra. The solution spectrum of DBH could not be observed because no appropriate solvent was found.

The 3000 cm^{-1} Region.—DBH has two intense bands at 3170 and 2980 cm^{-1} which may be assigned to N–H vibrations analogous to the bands at 3180 and 3000 cm^{-1} of ABH mentioned already. In the solid state benzamide also has two absorption bands of an NH_2 group at 3330 and 3140 cm^{-1}, to which correspond two bands at 3460 and 3350 cm^{-1} in the solution spectrum. These bands are naturally due to the asymmetric and symmetric N–H stretching frequencies. On the other hand, benzoylhydrazine (BH) has three bands at 3280, 3180 and 3010 cm^{-1}, of which the latter two bands have nearly the same frequencies as those of DBH and ABH. Moreover, it is interesting to see that only one band, at 3350 cm^{-1}, in the solution spectrum of BH corresponds to those three NH bands. The primary amides having an NH_2 group indicate generally two bands in the solid state and in solution[1]. They are also found in the benzamide absorption, while BH containing an NH_2 group adjacent to the CONH group has the three bands as mentioned above. It is impossible to give a reasonable interpretation for such a feature of ν(N–H) of BH without further observations, but the following explanation may tentatively be presented. In the solid state at least two of the three NH vibrations of BH may interact with each other, and hence bands similar to those of DBH and ABH may appear. The coupling between the two N–H vibrations decreases in solution, and hence BH has only one N–H band. The N–H stretching frequencies of the hydrazides and their related compounds are collhcted in Table I.

Other relatively weak bands in this region probably are due to C–H stretching frequencies, but their full assignment can not yet be completely given.

TABLE I. ν(N-H) VALUES IN cm^{-1}

Molecule	Solid	In CH_3CN
	3280, 3050	3280
	3180, 3000	3320
	3170, 2980	—
	3280, 3180, 3010	3350
	3340, 3140	3460, 3350

The Amide Frequencies. — DBH has bands at 1669 and 1636 cm^{-1}. Although DBH is examined only in the solid state, these two bands may be ascribed to C=O stretching frequencies (amide I) by comparison of the solid spectrum with those of TCABH and ABH.

Benzamide also has two bands at 1656 and 1623 cm^{-1} in the solid spectrum, while in the solution spectrum, bands corresponding to them are seen at 1682 and 1608 cm^{-1}. The 1656 cm^{-1} band is assigned to an amide I, and the 1623 cm^{-1} band to NH_2 deformation vibration.

In this region BH also has two bands at 1664 and 1618 cm^{-1} in the solid state, of which the latter is more intense, while in the solution spectrum a band at 1672 cm^{-1} is stronger than that at 1634 cm^{-1}. BH has an NH_2 group, and an NH_2 deformation vibration will give rise to a band near 1590 cm^{-1} as sustituted hydrazines[10]. In addition to it, an amide I band should also be found in this region. The 1664 cm^{-1} band of solid BH may correspond to the 1672 cm^{-1} band in solution, and, accordingly, it is probably due to the C=O vibration. On the other hand, the 1618 cm^{-1} band of solid BH probably corresponds to the 1634 cm^{-1} band in solution, but it is difficult to discuss its assignment from the present observation only. For instance, three absorption bands characteristic to mono-acid hydrazides in this region were reported by Jensen[11], and one of them was seen to appear at 1620 cm^{-1}. Moreover, a band of the same frequency was seen in solution.

DBH has a band at 1535 cm^{-1} which can undoubtedly be assigned to an amide II band since the frequency is very close to that of the corresponding band of ABH. This region of the spectrum of BH is complicated by bands due to the vibrations of the aromatic ring. Nevertheless, it is not difficult to find bands due to the ring vibrations by comparison of the spectrum with those of relating compounds. The ring absorption bands will soon be discussed. BH has an intense band at 1568 cm^{-1} which is accompanied by a band at 1527 cm^{-1}. In the solution spectrum a corresponding band may appear in the lower frequencies, but it would be impossible to observe it because of interference by solvent absorption.

DBH has bands at 1305 and 1285 cm^{-1} of which the latter is stronger, and they are both ascribed to amide III bands by comparison of frequencies and their relative intensities with those of the corresponding bands of ABH. This suggests that there also is the coupling of two identical vibrations of the CONHNHCO group. In the solid state BH has an intense band isolated at 1349 cm^{-1} which is higher than the amide III frequencies of secondary amides. The frequency value decreases to 1311 cm^{-1} in the solution spectrum. Benzamide has an intense absorption at 1403 cm^{-1}, while a band at 1356 cm^{-1} is considered to correspond to it in the solution spectrum. This frequency is within the range of 1420~1400 cm^{-1} in which many primary amides have bands of frequencies characteristic to them[1]. The amide frequencies shown by the hydrazides examined are collected in Table II. Frequencies of BH and benzamide similar in value to them are also indicated in the lower part on the table.

In order to ascertain the assignment of characteristic bands of these hydrazides, absorption bands due to the ring vibrations will be discussed. The identification of these bands was made by a comparison of the spectra of all materials examined.

Four bands produced by skeletal stretching vibrations are easily found in spite of the superposition of other strong absorption bands. They lie near 1600, 1580, 1500 and 1450 cm^{-1}, as usually found in ordinary aromatic compounds[1]. The intensity of the 1580 cm^{-1} band is seen to be enhanced in the spectra of the compounds examined. This fact is regarded as a positive indication[1] of the conjugation of the C=O bond with the aromatic ring.

Strong bands assigned to the out-of-plane C–H deformation vibrations are little difficult to detect if shifts of the bands to higher frequencies are taken into account. A band near

10) D. W. E. Axford, G. J. Janz and K. E. Russell, *J. Chem. Phys.*, **19**, 704 (1951); E. E. Shull, J. L. Wood, J. G. Aston and D. H. Rank, ibid., **22**, 1191 (1954).
11) J. B. Jensen, *Acta Chem. Scand.*, **10**, 667 (1956).

TABLE II. AMIDE FREQUENCIES (in cm^{-1})

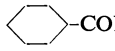
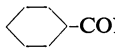
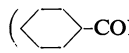
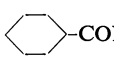
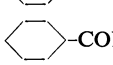
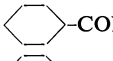
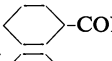
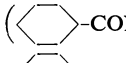
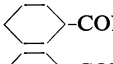
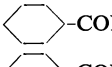
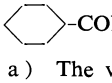
Molecule and state		Amide I	Amide II	Amide III
 -CONHNHCOCl$_3$	Solid	1731, 1658	1524, 1492	1317, 1248
	In CH_3CN	1742, 1694	——	1305, 1241
 -CONHNHCOCH$_3$	Solid	1707, 1644	1527	1337, 1281
	In CH_3CN	1720, 1683	——	1313, 1256
 -CONH-)$_2$	Solid	1669, 1636	1535	1305, 1285
 -CONHNH$_2$	Solid	1664, 1618	1568, 1527	1349
	In CH_3CN	1672, 1634	——	1311
 -CONH$_2$	Solid	1656, 1623		1403
	In CH_3CN	1682, 1608		1356

TABLE III. FREQUENCIES DUE TO THE AROMATIC RING IN THE RANGE 1600~690 cm^{-1} a) (in cm^{-1})

Molecule	ν(Aromatic C-C) b)	π(C-H) b)
 -CONH$_2$	— 1578, 1497, 1451	811, 793, 770, 705
 -CONHNH$_2$	1608, 1582, 1492, 1450	801, 747, 190
 -CONH-)$_2$	1607, 1579, 1490, 1450	796, 707
 -CONHNHCOCH$_3$	1607, 1582, 1493, 1450	803, 724, 702, 687
 -CONDNDCOCH$_3$	1607, 1581, 1497, 1453	794, 715, 691
 -CONHNHCOCCl$_3$	1607, 1585, 1500, 1453	798, 783, 708

a) The values in the solid state. b) ν; stretching, π; out-of-plane deformation.

800 cm^{-1} is commonly found for all materials with a C=O group directly attached to the ring, as has been pointed out by Kross et al.[9]

The C-H in-plane deformation vibrations will concern bands in the range 1225~950 cm^{-1}, but they are not always found because of the superposion of many relatively weak bands in this region.

Characteristic Bands. — The features of the amide frequencies of the hydrazides of aromatic acids are summarized as follows: (1) The splitting of the C=O stretching vibration (amide I) is observed in both solid and solution spectra. The spacing of the splitting of these two frequencies depends on radicals attached to the CONHNHCO group. (2) The amide II absorption band is found on the lower frequency side of the normal range of the corresponding band of secondary amides. The splitting of the amide II frequency was observed for TCABH, but not for ABH and DBH. It is noteworthy that TCABH has a single N-H stretching absorption band, while ABH and DBH have two N-H bands each. (3) The splitting of the amide III absorption band is seen for all of the hydrazides examined in both solid and solution, as it is for amide I. The frequencies of these two bands are in the normal range 1305~1200 cm^{-1}, in which many secondary amides have their characteristic frequencies of vibrations[1].

Summary

The infrared absorption spectra of acetylbenzoylhydrazine, trichloroacetylbenzoylhydrazine and dibenzoylhydrazine have been studied in the rock salt region. The assignment of the amide frequencies characteristic to the hydrazides RCONHNHCOR′ and the coupling between vibrations due to two CONH groups have been discussed.

The author is grateful to Professor Sunao Imanishi of Kyushu University for his generous permission to use the spectrophotometer, and to Dr. Yoshiya Kanda of Kyushu University for his encouragement throughout the work. He is also indebted to the Ministry of Education for financial support.

Department of Literature and Science
Saga University
Saga

Infrared Absorption Spectra of Hydrazides. II. Sodium Hydrazides

By Mitsuo MASHIMA

(Received June 17, 1961)

In a previous paper[1] amide frequencies of aromatic hydrazides have been studied. In the present study, the influence on the amide frequencies of the ionized group of $CONHNCO^-$ of the substitution for a hydrogen atom of a sodium ion will be discussed.

Experimental

Diformylhydrazine was synthesized with sodium formate and hydrazine sulfate[2] and purified by recrystallization from ethanol, m. p. 155°C. Diacetylhydrazine was prepared with acetic anhydride and hydrazine hydrate[3] and purified by recrystallization from ethanol, m. p. 137°C. The syntheses of acetylbenzoylhydrazine and dibenzoylhydrazine have been described previously[1]. Sodium salts of these hydrazides were obtained by heating their ethanol solutions with sodium ethoxide and repeatedly washing them with a large quantity of ethanol. The salts obtained were examined analytically*1. Calcd. for $HCONHNCOH \cdot Na$: C, 21.8; H, 2.75; N, 25.5; Na, 20.9%. Found: C, 22.4; H, 3.16; N, 22.6; Na, 22.0%. Calcd. for $CH_3 \cdot CONHNCOCH_3 \cdot Na$: C, 34.8; H, 5.1; N, 20.3; Na, 16.7%. Found: C, 34.6; H, 5.4; N, 20.0; Na, 17.3%. Calcd. for $CH_3CONHNCOC_6H_5 \cdot Na$: C, 54.0; H, 4.53; N, 14.0; Na, 11.5%. Found: C, 54.0; H, 4.68; N, 13.8; Na, 12.1%. Calcd. for $C_6H_5CONHNCOC_6H_5 \cdot Na$: C, 64.1; H, 4.23; N, 10.7; Na, 8.77%. Found: C, 61.8; H, 4.23; N, 10.3; Na, 8.44%. Deuterium-containing salts were prepared in sealed tubes in the presence of heavy water (99.8%), of which the excess was evaporated in vacuo after the exchange reaction. A Hitachi infrared spectrophotometer type EPI-2 with a rock salt prism was used throughout the work.

Results and Discussion

Sodium Diformylhydrazine (SDFH).—The infrared absorption spectrum of diformylhydrazine[4] was reasonably explaned with a model of a transplanar configuration. It may be assumed that an ion $(HCONHNCOH)^-$ also has a planar configuration. It has only one plane of symmetry of point group C_s, and all twenty-one $(3N-6)$ fundamental modes will be active in the infrared. Of these, fifteen modes are of species A′ and six of species A″. Five of those will give rise to bands outside of the rock salt region. They may be torsional, τ(N–N), $\tau(C_1\text{–}N)$*2 and $\tau(C_2\text{–}N)$ (species A″), and deformation vibrations, $\delta(C_1\text{–}N\text{–}N)$ and $\delta(C_2\text{–}N\text{–}N)$ (species A′), because the τ(N–N) frequency of NH_2NH_2 is 377 cm^{-1} [5], and the δ(C–N–N) frequency of CH_3NHNH_2 is 433 $^{-1}$ [6]. In consequence, sixteen bands are expected to appear in the rock salt region.

The infrared absorption spectra of SDFH and SDFH-d are illustrated in Fig. 1. Let us first consider the frequencies related to the C–H bond, such as bond stretching ν(C–H), in-plane bending δ(C–H) and out-of-plane bending π(C–H). For diformylhydrazine Miyazawa[4] obtained a ν(C–H) frequency of 2900 cm^{-1} and a δ(C–H) frequency of 1368 cm^{-1}, while no π(C–H) frequency was found. SDFH has bands at 2870 and 1357 cm^{-1} and, accordingly, they are ascribed to ν(C–H) and δ(C–H) respectively. Bands corresponding to them are found at 2870 and 1354 cm^{-1} in the SDFH-d spectrum, respectively. For the ion $(HCONHNCOH)^-$ twe bands may be expected to appear as ν(C–H) or δ(C–H). However, only a single band due to ν(C–H) was observed on the background of absorption. On the other hand, a band appears at 1380 cm^{-1} in the SDFH spectrum which may be assigned to δ(C–H), while a band corresponding to it is seen at 1378 cm^{-1} for SDFH-d. SDFH has two bands at 1026 and 974 cm^{-1} which are easily ascribed to π(C–H), because bands corresponding to them were obtained at 1050 cm^{-1} for formamide[7], 1037 cm^{-1} for formamidoxime[8] and 1015 cm^{-1} for *N*-methyl formamide[9].

Other vibrational modes involving a hydrogen atom will be ν(N–H), δ(N–H) and π(N–H).

1) M. Mashima, This Bulletin, **35**, 332 (1962).
2) G. Peillizzari, *Gazz. chim. ital.*, **39**, I, 529 (1909).
3) R. Stolle, *J. prakt. chem.*, [2] **69**, 145 (1904).
*1 The analyses of C, H and N were made by the Elementary Analysis Centre of Kyushu University, the analysis of Na, by Mr. H. Waki, Faculty of Science, Kyushu University.
4) T. Miyazawa, *J. Chem. Soc. Japan, Pure Chem. Sec.* (*Nippon Kagaku Zasshi*), **76**, 341 (1955), and see also T. Miyazawa, T. Shimanouchi and S. Mizushima, *J. Chem. Phys.*, **24**, 408 (1956).
*2 For C_1 and C_2 see Fig. 2.
5) A. Yamaguchi, I. Ichishima, T. Shimanouchi and S. Mizushima, *J. Chem. Phys.*, **31**, 843 (1959).
6) D. W. E. Axford, G. J. Janz and K. E. Russell, ibid., **19**, 704 (1951).
7) J. C. Evans, ibid., **22**, 1228 (1954).
8) W. J. Oriville-Thomas and A. E. Parsons, *Trans. Faraday Soc.*, **54**, 460 (1958).
9) T. Miyazawa, *J. Chem. Soc. Japan, Pure Chem. Sec.* (*Nippon Kagaku Zasshi*), **77**, 171 (1957).

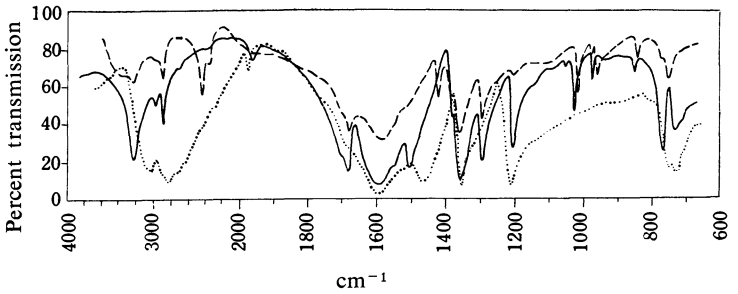


Fig. 1. Infrared absorption spectra of sodium diformylhydrazine (the solid curve), its *N*-deuterated derivative (the dashed curve) and diformylhydrazine (the dotted curve) in the solid state (KBr disk).

SDFH has a band at 3210 cm^{-1}, while a band at 2410 cm^{-1} corresponds to it in the spectrum of SDFH-d, the ratio ν_H/ν_D being 1.33. The band of 3210 cm^{-1} can, therefore, be easily assigned to ν(N-H). The identification of δ(N-H) will be considered later. The 785 cm^{-1} band of SDFH is not very different in frequency from the 770 cm^{-1} band of π(N-H) of diformylhydrazine[4], and, further no band corresponding to it is seen in the SDFH-d spectrum. It may, therefore, be taken as π(N-H).

Next the amide bands will be considered. In the range 1700~1200 cm^{-1} SDFH has bands at 1683, 1592, 1507, 1295, and 1202 cm^{-1} (except for the bands at 1380 and 1357 cm^{-1} which have already been ascribed to δ(C-H)). Three of the five bands scarcely change in frequency on *N*-deuteration; i. e., bands at 1676, 1588, and 1288 cm^{-1} in the spectrum of SDFH-d correspond to the bands at 1683, 1592, and 1295 cm^{-1} of SDFH respectively. On the other hand, two bands at 1417 and 955 cm^{-1} of SDFH-d correspond to the two remaining bands at 1507 and 1202 cm^{-1} respectively. Therefore, these two bands can be assigned without difficulty. The 1507 cm^{-1} band can be taken as an amide II band, because it is close in frequency to the corresponding bands of secondary amides, which generally show frequencies within 1570~1515 cm^{-1} [10]. Moreover, the wave number ratio is 1.063. This is close in value to 1.106 for diformylhydrazine[4]. The 1202 cm^{-1} band can be ascribed to an amide III band, the ratio ν_H/ν_D being 1.258, which is close to 1.248 for diformylhydrazine[4]. In addition to the amide II and amide III bands due to the CONH group of the ionized group $CONHNCO^-$, an amide I band will be expected to appear. It can be identified with the 1683 cm^{-1} band because the value of frequency is very close to the upper limit of the range 1680~1630 cm^{-1} in which many secondary amides have amide I frequencies. In consequence, the amide bands I, II, and III due to the CONH group are located in their own characteristic regions. It may, therefore, be concluded that the vibrations relating to the CONH group are not much influenced by an electronic charge stored in another part of the $CONHNCO^-$ group, and hence the NCO^- group probably has its own absorption frequencies. It is reasonable to expect that in the ion $(RCONHNCOR')^-$ there is a resonance between the two structures as indicated in Fig. 2. Therefore, absorptions due to the NCO^- group will be somewhat similar to those of the ionized group COO^-. The antisymmetrical and symmetrical vibrations of the COO^- structure concern two bands within the ranges 1610~1550 cm^{-1} and 1420~1300 cm^{-1} respectively[10]. In the range 1700~1200 cm^{-1} of SDFH two bands at 1592 and 1295 cm^{-1} remain to be assigned. We may ascribe the bands at 1592 and 1295 cm^{-1} to $\nu'(NCO^-)$ and $\nu''(NCO^-)$ respectively. The modes of vibrations of $\nu'(NCO^-)$ and $\nu''(NCO^-)$ may be assumed to be similar to those of ν_{as} and ν_s of a COO^- group respectively.

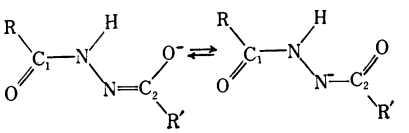


Fig. 2.

There remain three fundamentals unaccounted for, i. e., δ(O-C_1-N), δ(O-C_2-N), and ν(N-N). SDFH has a band at 731 cm^{-1} which can possibly be assigned to δ(O-C_1-N), because a band corresponding to it is observed at 753 cm^{-1} in the diformylhydrazine spectrum[4] and 746 cm^{-1} for SDFH-d. A ν(N-N) band was observed at 1100 cm^{-1} for HCONDNHCOH[4] and at 1165 cm^{-1} for $(CH_3CONH-)_2 \cdot H_2O$[11].

10) L. J. Bellamy, "The Infrared Spectra of Complex Molecules", Methuen and Company, Ltd., London (1954).

11) A. Yamaguchi, *J. Chem. Soc. Japan, Pure Chem. Sec.* (*Nippon Kagaku Zasshi*), **79**, 880 (1958).

TABLE I. INFRARED FREQUENCIES OF Na·HCONHNCOH AND Na·HCONDNCOH IN THE ROCK SALT REGION (in cm^{-1})

Species	Mode	Na·HCONHNCOH	Na·HCONDNCOH	Wave number ratio ν_H/ν_D
	ν(N-H), ν(N-D)	3200	2410	1.336
	ν(C-H)	2870	2870	1.000
	Amide I	1683	1676	1.004
	ν'(NCO^-)	1592	1588	1.003
	Amide II	1507	1417	1.092
	ν''(NCO^-)	1295	1288	1.005
A'	Amide III	1202	955	1.259
	δ(C-H)	1380	1378	1.001
		1357	1354	1.002
	ν(N-N)	(1000)	(1000)	
	δ(N-C_2-O)	843	837	1.007
	δ(N-C_1-O)	732	746	0.981
	δ(N-N-C_2)			
	δ(N-N-C_1)			
	π(C-H)	1026	1012	1.014
		974	973	1.001
	π(N-H)	767	—	
A''	τ(C_1-N)			
	τ(C_2-N)			
	τ(N-N)			

ν: stretching, δ: in-plane bending, π: out-of-plane bending, τ: torsional.
Values in parentheses are no exact ones.

SDFH and SDFH-d also have a band near 1100 cm^{-1}, but the definite frequency can not be determined because of its broad absorption pattern. Now, only one fundamental, δ(O-C_2-N), remains to be located. The 843 cm^{-1} band not yet interpreted may be ascribed to δ(O-C_2-N), a corresponding band being at 837 cm^{-1} for SDFH-d. The observed frequencies and their assignments are summarized in Table I.

In order to check the validity of these assignments, the Teller-Redlich product rule[12] is applied to the frequencies of species A'. The structure of $(HCONHNCOH)^-$ is not definitely determined, but the dimensions used in calculating moments of inertia are assumed as follows; for the HCONH-N part[4] N-H 1.00 Å, C-N 1.32 Å, C-O 1.21 Å, C-H 1.07 Å, N-N 1.38 Å, ∠C-N-N- 116°, ∠H-N-C 122°, ∠N-N-H 122°, ∠O-C-N 124°, ∠H-C-O 118°, ∠N-C-H 118°, for the HCON-N part C-N 1.21 Å, C-O 1.27 Å, C-H 1.07 Å, ∠N-N-C 118°, ∠H-C-O 118°, ∠N-C-O 124°. For the HCON the C-O distance and N-C-O angle are assumed to be equal to the C-O distance and O-C-O angle of sodium formate[13], and the C-N distance and N-N-C angle are chosen as equal to the C-N distance and H-N-C angle of HNCO[14]. In applying the product rule, it is assumed that the ratio ν_H/ν_D is 1.024*3 for δ(C-N-N) due to the HCONH-N part and that the values of δ(C-N-N) related to the HCONH-N part and ν(N-N) of SDFH-d are the same as those of SDFH. The observed product ratio is 0.530, while the calculated ratio is 0.509. Although the agreement is not very good, a much better value could be calculated if more reasonable estimates of the ratios of δ(C-N-N) and ν(N-N) could be made.

Sodium Diacetylhydrazine (SDAH). — The infrared absorption spectra of SDAH and SDAH-d in the solid state are shown in Fig. 3, in which the spectrum of diacetylhydrazine is also given for comparison. Let us chiefly consider the location of bands due to vibrations relating to the ionized group $CONHNCO^-$. SDAH has a band at 3290 cm^{-1} which is easily assigned to ν(N-H), while a band corresponding to it is at 2390 cm^{-1} for SDAH-d, the ratio ν_H/ν_D being 1.34.

A complicated spectral pattern is seen in the region of 1650~1250 cm^{-1}, and bands in that region will reflect vibrations relating to the $CONHNCO^-$ and CH_3 groups. There are bands at 1656, 1552*4, 1513, 1428, 1392, 1339,

12) G. Herzberg, "Infrared and Raman Spectra", D. Van Nostrand Company, Inc., New York (1947), p. 232.
13) W. H. Zachariasen, *Phys. Rev.*, 53, 917 (1938).
14) L. H. Jones, J. N. Shooler, R. G. Shulman and D. M. Yost, *J. Chem. Phys.*, 18, 990 (1950).
*3 It was postulated by Miyazawa (Ref. 3).
*4 This is a mean value of the two peak frequencies at 1563 and 1541 cm^{-1}.

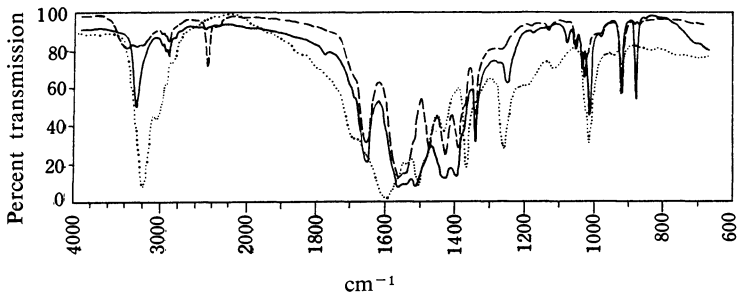


Fig. 3. Infrared absorption spectra of sodium diacetylhydrazine (the solid curve), its *N*-deuterated derivative (the dashed curve), and diacetylhydrazine (the dotted curve) in KBr disk.

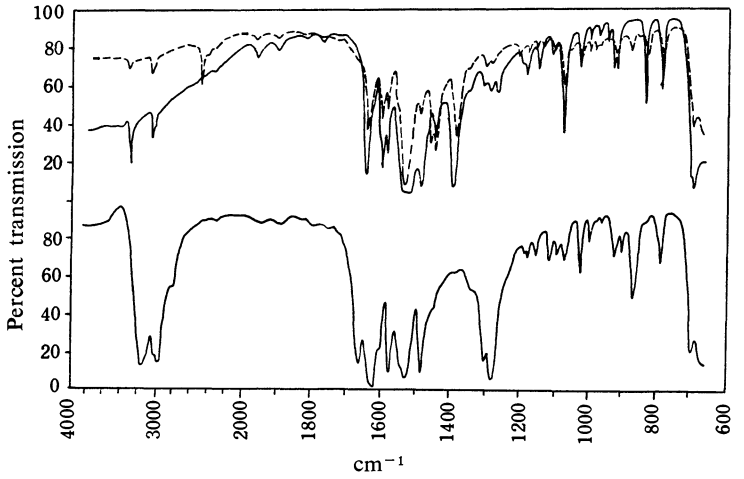


Fig. 4. Infrared absorption spectra of sodium dibenzoylhydrazine (the upper solid curve), its *N*-deuterated derivative (the dashed curve) and dibenzoylhydrazine (the lower solid curve) in KBr disk.

and 1249 cm^{-1} for SDAH. Of these seven bands the 1513 cm^{-1} band seems to correspond to a band at 1473 cm^{-1} of the SDAH-d spectrum, while the 1249 cm^{-1} band has no counterpart in the SDAH-d spectrum. The former is very close in frequency to the amide II band at 1506 cm^{-1} for diacetylhydrazine[11], and hence it may be taken as the amide II band relating to the CONH group of the ion $(CH_3CONHNCOCH_3)^-$. The latter may be taken as the amide III band of the CONH group because a band corresponding to it was found at 1260 cm^{-1} for diacetylhydrazine[11].

On the other hand, the five remaining bands of SDAH have respective counterparts of nearly the same frequencies in the SDAH-d spectrum. Their assignments can be made by comparison of the SDAH spectrum with that of SDFH. The rather weak band at 1656 cm^{-1} corresponds to the 1683 cm^{-1} band of SDFH and, accordingly, may be ascribed to the C=O vibration relating to the CONH group. Although the occurrence of two peaks as indicated in the footnote is not reasonably explained the 1552 cm^{-1} band corresponds in frequency and especially in intensity to the 1592 cm^{-1} band of SDFH. In consequence, it is probably ascribed to ν' as mentioned in the previous section. Further, two bands at 1428 and 1392 cm^{-1} can be assigned to the asymmetrical and symmetrical CH_3 deformation vibrations respectively; a detailed assignment will be given in a later section. Only the 1339 cm^{-1} band is not yet accounted for in the region 1650~1250 cm^{-1}. It can probably be ascribed to ν'' of the NCO^- group like the 1295 cm^{-1} band of SDFH. This assignment is corroborated by the fact that no corresponding band has been observed for diacetylhydrazine[11].

Sodium Dibenzoylhydrazine (SDBH).—The infrared absorption spectra of SDBH and SDBH-d are shown in Fig. 4, the solid spectrum of dibenzoylhydrazine (DBH) is also given for comparison.

In the 3000 cm^{-1} region, SDBH has a band at 3290 cm^{-1} and a relatively weak band at

3030 cm^{-1}. The former is within the normal range 3320~3270 cm^{-1} of secondary amides[10], and a band corresponding to it is found at 2480 cm^{-1} in the SDBH-d spectrum. Therefore, the 3290 cm^{-1} and 2480 cm^{-1} bands are ascribed to ν(N-H) and ν(N-D) respectively, the ratio ν_H/ν_D being 1.326. The 3030 cm^{-1} band can be attributed to the aromatic C-H stretching vibrations, because its corresponding band is seen at 3040 cm^{-1} in the SDBH-d spectrum. Since the ionized group $CONHNCO^-$ has one N-H group, only a single N-H band is expected to appear. In fact, it is observed at 3290 cm^{-1}, as indicated above.

Next we will consider amide bands. As pointed out previously[1], DBH has amide I bands at 1669 and 1636 cm^{-1}, while SDBH has a band at 1637 cm^{-1} and a band of the same frequency is found in the SDBH-d spectrum. All the bands lie within the normal range (1680~1630 cm^{-1}) of the amide I band of the secondary amides. In consequence, the 1637 cm^{-1} band should be taken as the amide I band due to the CONH group of $CONHNCO^-$.

The amide III absorption has also been found as two bands at 1302 cm^{-1} and 1285 cm^{-1} in the DBH spectrum[1], while SDBH has a band at 1264 cm^{-1} (very weak) and no corresponding band is seen in the SDBH-d spectrum. Therefore, the 1264 cm^{-1} band is taken as the amide III band of the CONH part of the $CONHNCO^-$ group.

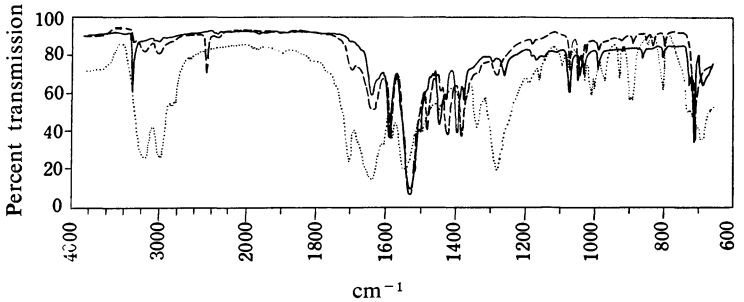


Fig. 5. Infrared absorption spectra of sodium acetylbenzoylhydrazine, its (solid curve), its *N*-deuterated derivative (dashed curve), and acetylbenzoylhydrazine (dotted curve) in KBr disk.

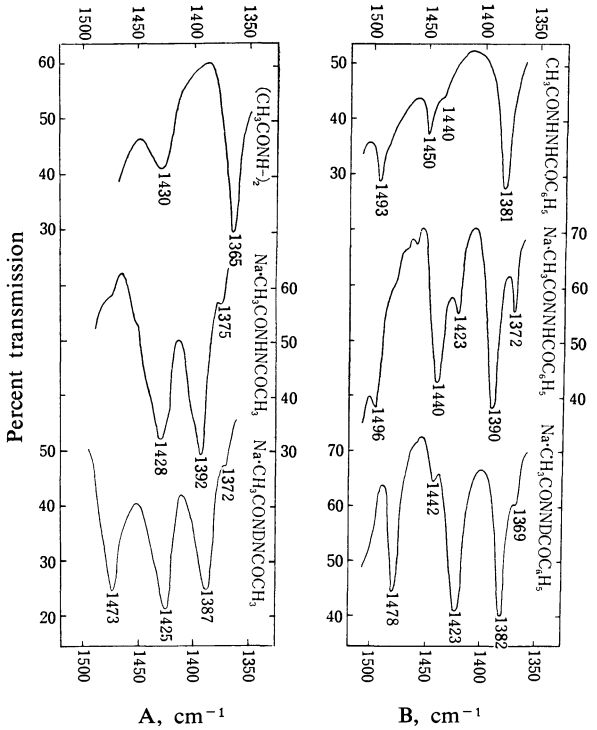


Fig. 6. Infrared spectra in the region of methyl bending vibrations.

The presence of the aromatic ring absorption in the 1600～1450 cm^{-1} region makes the spectrum much more complicated, but the amide bands in that region can be located without difficulty by comparison of the spectral patterns in Fig. 4 with each other. The 1535 cm^{-1} band of DBH[1] has been assigned to the amide II band. SDBH has a very strong absorption band at 1528 cm^{-1} and, further, a band at 1390 cm^{-1}, while SDBH-d has corresponding bands at 1527 and 1383 cm^{-1}. Moreover, a band at 1485 cm^{-1} of SDBH is too intense to be ascribed to an aromatic ring vibration of about 1500 cm^{-1} [10]. In the SDBH-d spectrum a relatively weak band at 1487 cm^{-1} may correspond to it, and in addition a band of 1442 cm^{-1} appears. Therefore, the 1485 cm^{-1} band of SDBH is ascribed to the amide II band of the CONH group. In consequence, both bands, at 1528 and 1390 cm^{-1} of SDBH, are ascribed to vibrations of the NCO^- group. They can probably be attributed to ν' and ν'', as indicated in the previous sections.

Sodium Acetylbenzoylhydrazine (SABH).— The infrared absorption spectra of SABH and SABH-d are illustrated in Fig. 5. The spectrum of acetylbenzoylhydrazine is also shown for comparison.

SABH has an isolated absorption band at 3300 cm^{-1} which can easily be assigned to ν(N–H). A corresponding band is located at 2460 cm^{-1} for *N*-deuterated SABH, the ratio ν_H/ν_D being 1.34.

The 1637 cm^{-1} band of SABH is in good accordance in frequency and in relative intensity with the 1637 cm^{-1} of SDBH assigned to the amide I. A corresponding band is found at 1638 cm^{-1} for SABH-d. Therefore, both bands are ascribed to the amide I band.

Acetylbenzoylhydrazine[1] has an amide III band at 1281 cm^{-1}. A corresponding band is seen at 1256 cm^{-1} in the spectrum of SABH, but it is very weak in intensity. In the SABH-d spectrum a band at 1046 cm^{-1} may correspond to it. Therefore, the 1256 cm^{-1} band of SABH is taken as the amide III absorption.

SABH shows the most intense band at 1527 cm^{-1} among its spectral bands. It is in good accordance with the 1528 cm^{-1} band of SDBH in frequency, and a band of the same frequency is seen for SABH-d similar to that of SDBH-d. Hence, it is ascribed to $\nu'(NCO^-)$ like the 1528 cm^{-1} band of SDBH. On the other hand, it is difficult to fix a band due to $\nu''(NCO^-)$. Since SABH has a methyl group, deformation vibrations of the methyl group give rise to bands generally in the region of 1500～1350 cm^{-1}, and, moreover, SABH may also have bands of $\nu''(NCO^-)$ and aromatic ring frequencies in that region. The infrared spectra in the region of methyl bending vibrations of diacetylhydrazine, SDAH, and SDAH-d are illustrated in Fig. 6A, while those of acetylbenzoylhydrazine, SABH, and SABH-d are given in Fig. 6B. Acetylbenzoylhydrazine[1] has a band at 1381 cm^{-1} which is undoubtedly due to $\delta_s(CH_3)$. However, SABH has bands corresponding to it at 1390 and 1372 cm^{-1}, and SABH-d has them at 1382 and 1369 cm^{-1}. Similar bands are also observed in the spectra of diacetylhydrazine and its sodium salt, as is shown in Fig. 6A. Diacetylhydrazine shows a band due to $\delta_s(CH_3)$ at 1365 cm^{-1}. Bands corresponding to it are observed at 1392 and 1375 cm^{-1} in the spectrum of SDAH and at 1387 and 1372 cm^{-1} of SDAH-d. In general, the bands due to $\delta_s(CH_3)$ appear at nearly the same position. In the spectrum of SABH appearances of two bands due to $\delta_s(CH_3)$ can not be interpreted with confidence. However, these two bands can probably be ascribed to $\delta_s(CH_3)$, since they are in good agreement in frequency and relative intensity with those of the spectra SABH, SABH-d, SDAH, and SDAH-d. The compounds containing a methyl group generally show another absorption band near 1460 cm^{-1} arising from the asymmetrical deformation $\delta_{as}(CH_3)$. Diacetylhydrazine shows a corresponding band at 1430 cm^{-1}. SDAH also has an absorption band at 1428 cm^{-1}, and SDAH-d, at 1425 cm^{-1}. On the other hand, it is difficult to locate a band of $\delta_{as}(CH_3)$ in the spectra of SABH and of SABH-d, because aromatic ring vibrations also give rise to bands near 1450 cm^{-1}. In the spectrum of acetylbenzoylhydrazine, a band which appeared as a shoulder of the 1450 cm^{-1} band was ascribed to $\delta_{as}(CH_3)$ in the previous paper[1]. However, SABH shows two bands at 1423 and 1440 cm^{-1} (relatively strong), and, also, SABH-d has bands at 1423 (more intense) and 1442 cm^{-1}. These two bands of SABH are in good agreement with the corresponding bands of SABH-d in frequency but in an inverse intensity ratio. As mentioned above, diacetylhydrazine and its salt show a single band each assigned to $\delta_{as}(CH_3)$, i. e., 1430 and 1428 cm^{-1} respectively, while acetylbenzoylhydrazine has a single band at 1440 cm^{-1}. On the other hand, it can be expected that in SABH and SABH-d the absorption due to $\delta_{as}(CH_3)$ is overlapped by the absorption due to the aromatic ring vibrations and further $\nu''(NCO^-)$ vibrations. In consequence, it is impossible to locate these three vibrations definitely. The 1478 cm^{-1} band of SABH-d is not yet accounted for. No corresponding band is observed in the spectrum of SABH and also of acetylbenzoylhydrazine.

TABLE II. OBSERVED FREQUENCIES AND THEIR ASSIGNMENTS (in cm^{-1})

Group	Assignment	DFH	SDF	DAFH	SDAH	DBH	SDBH	ABH	SABH
	Amide I	1610	1683	1598	1656	1669 1636	1637	1707 1646	1637
CONH	Amide II	1480	1507	1506	1513	1535	1485	1527	1510
	Amide III	1229	1202	1260	1249	1285 1305	1264	1281 1337	1256
NCO^-	ν'		1592		1552		1528		1528
	ν''		1295		1339		1390		—

Furthermore, its frequency value is too low to be ascribed to aromatic ring vibrations whose bands generally appear near 1500 cm^{-1}. The ring vibrations were observed at 1493 cm^{-1} and 1497 cm^{-1} for acetylbenzoylhydrazine and its *N*-deuterated derivative respectively. SABH also shows a band at 1496 cm^{-1}. Thus, the 1478 cm^{-1} band of SABH-d can be ascribed to the amide II′ absorption relating to the COND part of the ionized group $CONDNCO^-$. A corresponding band for SABH can be taken as a poorly defined shoulder (near 1510 cm^{-1}) which is accompanied by the 1528 cm^{-1} band.

Characteristic Frequencies.—In the solid state the sodium hydrazides can be expected to exist in a form $Na^+RCONHNCOR'^-$. The amide bands will, therefore, be shown by the group CONH in their infrared spectra. In addition to them, absorption bands due to the ionized group NCO^- will also be observed.

The observed frequencies and their assignments are summarized in Table II. For comparison the amide frequencies of the hydrazides are also represented in that table.

Secondary amides[10] in the solid state have the amide I and amide II bands in the ranges 1680～1630 cm^{-1} and 1570～1515 cm^{-1} respectively, and the amide III band near 1290 cm^{-1}. The hydrazides of aliphatic acids[15] have bands shifted towards lower frequencies. However, SDFH and SDAH show amide frequencies somewhat different from those of the corresponding hydrazides, i. e., the amide I band increased distinctly in frequency but decreased a little in intensity, the amide II band increased a little in frequency, and the amide III band decreased in frequency.

On the other hand, the hydrazides of aromatic acids[1] in the solid state showed the amide I band within the range of secondary amides but split into two bands, which bands are attributable to coupling between two C=O vibrations. Further, the amide II and amide III bands are seen within the normal ranges of secondary amides, but the latter splits into two bands. As for SDBH and SABH, their amide I bands are in good agreement in frequency each other, and they can be ascribed to the C=O group adjacent to the benzene ring. Further, these salts show that the amide II band has decreased in frequency, while the amide III bands of SDBH and SABH are nearly equal in frequency. Therefore, it may be understood that the amide bands due to the CONH group of the ions $(RCONHNCOR')^-$ appear generally in the normal range of secondary amides, so that the vibrations relating to CONH group are little affected by an electronic charge stored in the NCO^- group. In the NCO^- group resonance will be possible between the C–N and C–O bonds. In consequence, the NCO^- structure gives rise to two bands similar to those of the COO^- group as represented in Table II.

Furthermore, it is noteworthy that an N–H stretching vibration concerns a band near 3300 cm^{-1} in the spectra of the sodium hydrazides. The value of frequency lies in the normal range 3320～3270 cm^{-1} of the secondary amides[10].

Summary

The infrared absorption spectra of $HCONH \cdot NCOH \cdot Na$, $CH_3CONHNCOCH_3 \cdot Na$, $CH_3CONHNCOC_6H_5 \cdot Na$, and $C_6H_5CONHNCOC_6H_5 \cdot Na$ and their *N*-deuterated derivatives have been examined in the rock salt region. The characteristic frequencies of the ions $(RCONHNCOR')^-$ have been obtained, and the influence of an electronic charge on the amide frequencies has been discussed.

The author is grateful to Professor Sunao Imanishi of Kyushu University for his generous permission to use the spectrophotometer, and to Dr. Yoshiya Kanda of Kyushu University for his encouragement throughout the work. Thanks are also due to Mr. Hirohiko Waki of Kyushu University for his analyses of Na contents, and to Mr. Michio Sido, Miss Yukiko Indo and Miss Takeko Tahara of the Centre of Elementary Analyses, Kyushu University, for their analyses of C, H, and N contents. The author is indebted to the Ministry of Education for financial support.

Department of Literature and Science
Saga University, Saga

15) To be published elsewhere.

The Reaction of Hydrogen and Oxygen through a Silent Electric Discharge. I. The Formation of Hydrogen Peroxide

By Kihei MORINAGA

(Received June 26, 1961)

The formation of hydrogen peroxide from a hydrogen-oxygen gas mixture through a high frequency silent discharge has been investigated with the intention of obtaining a reaction pattern in connection with an accompanying pulse current. The features of the peroxide formation more resembles that of ozone formation in a silent discharge[1,2] than that of both gases in a low pressure glow discharge.

Experimental

All the measurements were carried out under atmospheric pressure using the flow method.

The reaction mixture of hydrogen and oxygen gas (4.5% vol. O_2) was held in a gas holder of ca. 1 m^3. The gas mixture was dried by passing it through a 4 m. glass tube filled with calcium chloride and silica gel and then was served for use. The humidity of the gas on the final issue was about $-20°C$.

The electric circuit was similar to that which had been used in the previous work[2]. The high frequency electric current was provided by a 32 pole generator with the R. P. M. selected so as to obtain an output frequency of from 500 c./sec. to 2000 c./sec.

The discharge tubes were of the Siemens type, made of Telex glass, with a length and diameter of 40 and 4 cm. respectively. The gap length was varied between 1, 2 and 3 mm., and the discharge area could be varied by applying an adequate expansion of a tin foil patch on the outside of the glass tube.

After being exposed to the electric discharge, the reactant gas was cooled in a condensation trap where the hydrogen peroxide and water were caught by freezing. The cooling agents of the condensation trap were a salt-ice mixture or liquid air. The former was used mainly for the constant flow system, and the latter for the variable rapid flow system. The condensate was weighed and analyzed by iodometry, using ammonium molybdate as a decomposition catalyst for the hydrogen peroxide.

Results

1) The effect of the change of frequencies of the discharge current on the formation of peroxide is shown in Fig. 1, where the pulse current is scaled on the abscissa and the rate of conversion of reactant oxygen gas to hydrogen peroxide, on the ordinate. The flow rate, or the time (τ) of the residence in the discharge tube, is the same throughout the runs — 5.0 sec. for each run. The measurements were conducted up to the high frequency pulse current value of 600 μamp., this being the safety limit to prevent damage to the discharge tube. The area of the electrode and the gap length have values of 233 cm^2 and 3 mm. respectively.

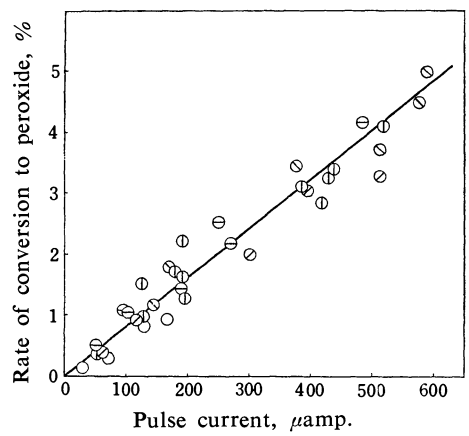


Fig. 1. The rate of conversion to the peroxide under the discharge of various frequencies against pulse current.
$A=233$ cm^2; $d=3$ mm.
○ 50 c./sec. ⊖ 500 c./sec. ◐ 1000 c./sec.
⊘ 1500 c./sec. ⊗ 2000 c./sec.

As shown in Fig. 1, the above rate, plotted against the pulse current, shows as a straight line and is independent of the frequency of the discharge current. The exclusive products of the reaction were water and hydrogen peroxide. The concentration of the hydrogen peroxide in the product solution was about 60% by wt., which percentage does not vary extensively in accordance with the different values of frequencies.

2) The rate of peroxide formation in various shaped discharge tubes was measured with respect to the pulse current. The values of the time of residence ($\tau=5.0$ sec.) and the frequency of discharge current (1000 c./sec.) were kept constant.

1) K. Morinaga and M. Suzuki, This Bulletin, 34, 157 (1961).
2) K. Morinaga and M. Suzuki, ibid., 35, 204 (1962).

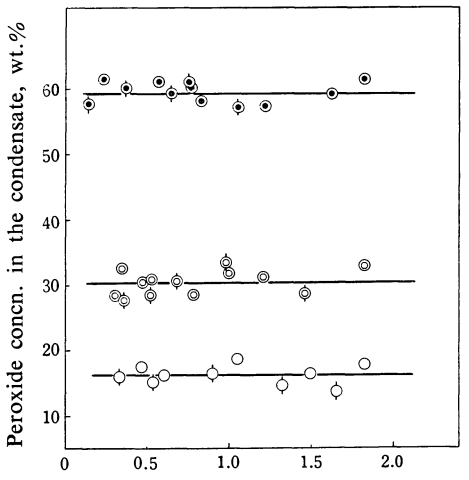


Fig. 2. The peroxide concentration in the condensate against the pulse current per unit discharge area. A and d varies.
○ d=1 mm., A=120 cm²
◎ d=2 mm., A=120 cm²
⊙ d=3 mm., A=120 cm²
○ d=1 mm., A=250 cm²
◎ d=2 mm., A=250 cm²
⊙ d=3 mm., A=250 cm²

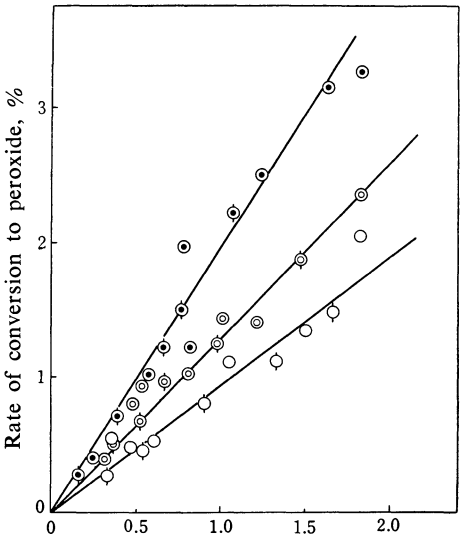


Fig. 3. The rate of conversion to the peroxide against the pulse current per unit discharge area. A and d are varied. Each of the plots represents such the discharge tube as is noted in Fig. 2.

In Fig. 2, the concentration of the hydrogen peroxide in the condensate is plotted against the pulse current per unit electrode area. The concentration does not depend on the pulse current, or on the electrode area, but rather depends on the gap length of the discharge tube. In Figs. 3, 4 and 5, the pulse current per unit electrode area is plotted on the abscissa. The conversion rate of the peroxide and water are increased linearly with respect to the pulse current per unit electrode area but does not depend on the electrode area. In these figures, one gap length corresponds to

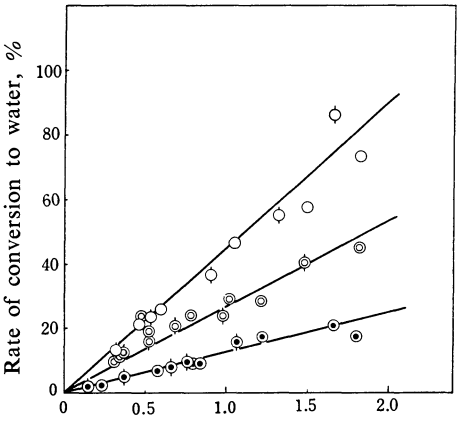


Fig. 4. The rate of conversion to water against pulse current per unit discharge area. A and d are varied. Each of the plots represents such the discharge tube as is noted in Fig. 2.

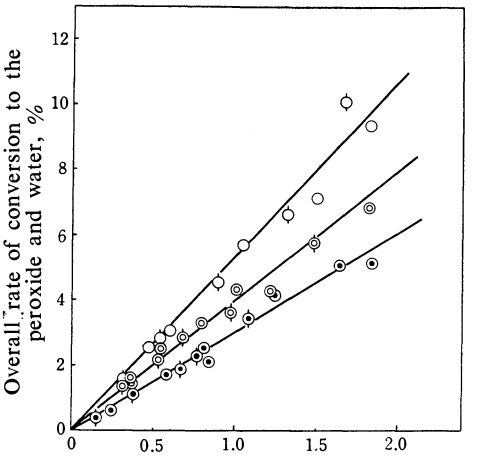


Fig. 5. The overall conversion rate to the peroxide and water, against pulse current per unit discharge area. A and d are varied. Each of the plots represents such the discharge tube as is noted in Fig. 2.

one straight line. The rate of conversion of the peroxide is larger with the larger gap length, while, on the other hand, that of water is larger in the shorter gap length. In Fig. 5, the overall conversion rate is summarized. So far as the constant resident time (ca. 5 sec.) is concerned, the results obtained using both liquid air or salt-ice coolants were entirely identical.

3) In the following experiments, the results of which are shown in Figs. 6, 7 and 8, the gap length of the discharge tubes were 1, 2 and 3 mm. and the discharge area was 250 cm^2. In these figures, the peroxide concentration

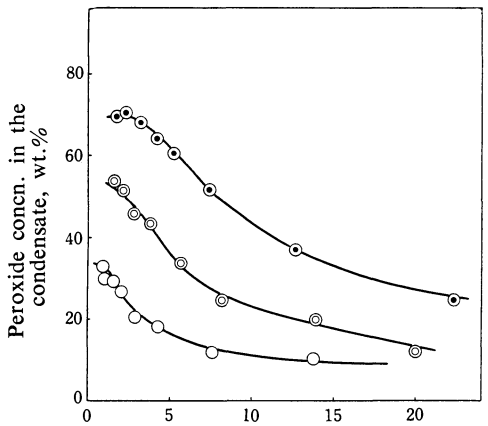


Fig. 6. Peroxide concentration in the condensate against time of residence. d is varied.
○ d=1 mm., A=250 cm^2
◎ d=2 mm., A=250 cm^2
⊙ d=3 mm., A=250 cm^2

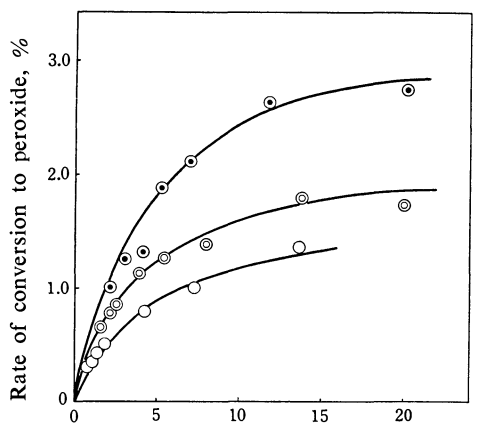


Fig. 7. Rate of conversion to peroxide against time of residence. d is varied. Each of the plots represents such the discharge tube as is noted in Fig. 6.

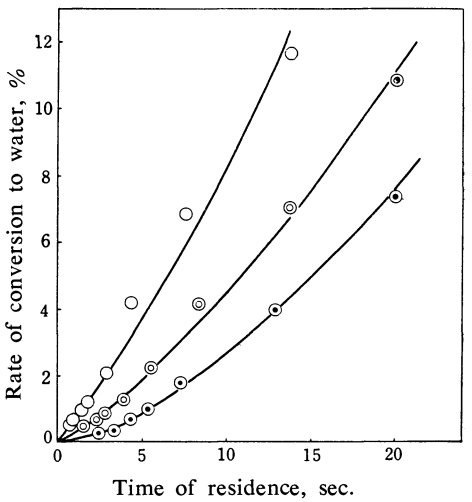


Fig. 8. Rate of conversion to water against time of residence. d is varied. Each of the plots represents such the discharge tube as is noted in Fig. 6.

and the rate of conversion of peroxide and water are plotted against the time of residence, the pulse current per area being ca. 0.85 μamp./cm^2. For each case, a run corresponding to a certain gap length is represented by a curve. In the runs where the flow velocities vary, that is, when the time of residence is occasionally very short, the condensate product was trapped by liquid air freezing. The peroxide concentration in the condensate decreases with increasing resident time, as is shown in Fig. 6, and the conversion rate to the peroxide plotted in Fig. 7, showed a kind of saturation-like behavior against the resident time. On the other hand, the conversion rate to water shows a different behavior than Fig. 7.

Discussion

From Fig. 1, one may conclude that the mechanism of the rate of formation of hydrogen peroxide is the same for all reactions, regardless of the output frequency (between 50 c./sec. and 2000 c./sec.). The same applies to the formation of water under identical conditions, for the rate of water formation versus pulse current has about the same characteristics as those of peroxide formation.

The whole pattern which is apparent in the above-mentioned figures is very much like those of ozone formation. In the reaction between hydrogen and oxygen, the elementary processes which govern the rate of formation of the entire series would be, then, the one wherein an electron participates.

According to the generally accepted mechanism[3-8], the simplest reaction scheme to explain these essential features may be written as follows:

$$H_2+e=2H+e \quad (1)$$

$$O_2+e=2O+e \quad (2)$$

$$H+O_2=OH+O \quad (3)$$

$$O+H_2=OH+H \quad (4)$$

$$OH+H_2=H_2O+H \quad (5)$$

$$OH+OH=H_2O_2 \quad (6)$$

$$H_2O_2+H=H_2O+OH \quad (7)$$

The reaction involving H atoms and the OH radical may be of importance here. If the pressure under which the reaction proceeds is rather high, then the concentration of the H atom is not likely to be high; on the other hand, if the amount of oxygen in the starting mixture is small, then the number of oxygen atoms will also be small. Because reactions 3 and 4 are fast, an equilibrium concentration for the OH radical may be established which will govern the overall reaction rate and, simultaneously, be governed by the molecular entities of the collision product with electrons.

It seems to be irrelevant to go into more detail in each of these elementary processes; it will suffice to explore the obtained results from the postulate concerning the behavior of issued electrons and their first-step elementary act. Therefore, in this pattern of reaction mechanism, the overall rate of formation should keep a linear relationship with the quantity of electrons carried through the discharge zone or the pulse current which is in accord with Figs. 3, 4 and 5.

The fact that, in Fig. 2, the concentration of the produced hydrogen peroxide remains constant, independent of the value of the pulse current, agrees with the features of the diagrams in Figs. 3, 4 and 5. The reaction rate at a certain flow velocity ($\tau=5.0$ sec.), and under a certain frequency of discharge current, is again proportional to the pulse current. In conclusion, the ratio of produced hydrogen peroxide to the whole reaction product should remain constant regardless of the pulse current per unit area.

Each straight line in Figs. 3, 4 and 5 is assigned to a certain value of gap length because the rate of reaction should receive considerable influence from the gap length between the electrodes.

The curves for the relationship between concentration and flow velocities (Figs. 6, 7 and 8) are those usually known for such cases. As the flow rate becomes smaller, the composition of the product tends to approach a limiting value which is expected to be an equilibrium value between formation and destruction at an approximately static state.

As has been pointed out in the ozone formation process[1], the initiation of the reaction is started in a small column by an individual discharge lasting half the period of every discharge frequency. The remaining space in the whole discharge zone serves partly as a destruction area for the hydrogen peroxide which is the result of the sequence of processes in the discharge column. The larger the gap length is, then, the more the small discharge column will be expanded; in other words, the field of formation is relatively larger than that of destruction. The postulate is then concordant with the results.

The elucidation of the detailed behavior of the reacting molecular species in connection with the accepted elementary processes is not yet fully feasible because of the lack of detailed knowledge of the discharge phenomena which accompany chemical reactions.

Summary

1) The reaction between hydrogen and oxygen in a silent electric discharge of high frequency was investigated. The product, in the course of reaction, is solely hydrogen peroxide and water.

2) The linear relationship, independent of the frequency of the current, between the rate of formation of hydrogen peroxide or of water and the pulse current was established.

3) The composition of the hydrogen peroxide-water solution is constant so long as the gap length is constant.

4) The flow rate and the said composition relation were measured.

5) The reaction pattern in the discharge zone was briefly discussed.

The author would like to express his deep appreciation to Professor Momotaro Suzuki of the Defense Academy for his encouragement, helpful advice and guidance throughout this investigation.

Department of Chemistry
Defense Academy
Yokosuka

3) C. N. Hinshelwood and A. T. Williamson, "The Reaction between Hydrogen and Oxygen", Oxford Univ. Press, London (1934).
4) G. von Elbe and B. Lewis, *J. Chem. Phys.*, **10**, 366 (1942).
5) C. F. Cullis and C. N. Hinshelwood, *Proc. Roy. Soc.*, **186A**, 462 (1946).
6) C. N. Hinshelwood, ibid., **188A**, 1 (1946).
7) A. H. Willbourn and C. N. Hinshelwood, ibid., **188A** 353, 369, 376 (1946).
8) W. Forst and P. A. Giguère, *J. Phys. Chem.*, **62**, 340 (1958).

The Reaction of Tropoids and Quinone Derivatives. II. Reaction of Several Tropolones and p-Benzoquinone

By Shuichi SETO and Humio SATO

(Received June 13, 1961)

Preceding paper of this series[1] reported the reaction of several kinds of tropolones and *p*-benzoquinone dibenzenesulfonimide. The use of *p*-benzoquinone in place of *p*-benzoquinone dibenzenesulfonimide results in rather complicated reactions but under certain reaction conditions, products having a tropolone ring were found to be formed. The present paper reports on the structure of products obtained by the reaction of tropolone and its bromo derivatives with *p*-benzoquinone.

A solution of tropolone and *p*-benzoquinone dissolved in methanol containing a small amount of acetic acid afforded at room temperature, orange crystals (A) and colorless crystals (B). Analytical values of B corresponded to the molecular formula of $C_{13}H_{10}O_4$ and, from its coloration to ferric chloride and ultraviolet absorption spectrum, it was found to retain the tropolone ring. Methylation of B with diazomethane afforded a monomethyl ether (C) and dimethyl ether (D). Hydrolysis of C reverted it to B, but that of D afforded a monomethyl ether (E) different from C. C and D do not show the characteristic coloration to ferric chloride but E does so. Methylation of B with dimethyl sulfate, in the presence of potassium hydroxide afforded monomethyl ether (E), whose further methylation with diazomethane gave D. These facts show that B possesses two hydroxyl groups, one of which is phenolic and the other is the hydroxyl in the tropolone ring. In order to determine the structure of B, the tropolone ring was made to undergo rearrangement to form a benzoic acid derivative. D was led to the 2-bromotropone derivative through the hydrazino derivative[2] and treated with alkali to form a benzoic acid derivative which showed no depression of the melting point on admixture with 4-(4′-methoxyphenoxy)benzoic acid (VII)[3] and ultraviolet absorption spectra of these two substances were in good agreement. Consequently, the foregoing 2-bromotropone and hydrazino derivatives would respectively be 2-bromo-5-(4′-methoxyphenoxy) tropone (VI) and 2-hydrazino-5-(4′-methoxyphenoxy)tropone (V). The methyl ethers, C, D and E would then be 2-methoxy-5-(4′-hydroxyphenoxy)tropone (II), and 2-methoxy-5-(4′-methoxyphenoxy)-tropone (III), and 5-(4′-methoxyphenoxy)-tropolone (IV). It has therefore been proved that B is 5-(4′-hydroxyphenoxy)tropolone (I).

The analytical values of the orange crystals (A) agreed with the formula of $C_{13}H_8O_4$ and this substance was also found to retain the tropolone ring from its coloration to ferric chloride and ultraviolet absorption spectrum. Its infrared spectrum exhibited absorption of $\nu_{C=O}$ of *p*-benzoquinone at 1657 and 1651 cm^{-1}. These facts suggest that A is a compound formed by carbon-carbon bonding of tropolone and *p*-benzoquinone. As for the position of its bonding, there is only one possible position in *p*-benzoquinone but three positions, 3, 4 and 5, are possible in the tropolone ring. It was proved, by the experiments to be iterated below, that the bonding position in the tropolone ring is at 3 and that A is 3-(*p*-benzoquinonyl)tropolone (VIII).

Catalytic reduction of A over palladium-carbon or treatment with sodium dithionite affords a dihydroxyphenyltropolone (IX), whose methylation with dimethyl sulfate gives dimethoxyphenyltropolone (X). X forms two kinds of 2-methoxytropone derivative (XI and XII) by treatment with diazomethane which indicates that the aryl group is bonded to a position other than 5 in the tropolone ring. Similar to the foregoing case, 2-methoxytropone (XI) was led to 2-chlorotropone (XIV) via 2-hydrazinotropone (XIII) and alkali treatment of XIV gave a benzoic acid derivative (F). F was identified with 2-(2′, 5′-dimethoxyphenyl)-benzoic acid (XV), synthesized by the following route, by mixed fusion and comparison of infrared and ultraviolet absorption spectra.

In accordance with the preparation of 4-(2′,-5′-dihydroxyphenyl)acetophenone from 4-aminoacetophenone and *p*-benzoquinone[4], the diazonium salt obtained from methyl anthranilate was reacted with *p*-benzoquinone, in the

1) S. Seto, H. Yamazaki and Y. Nishiyama, This Bulletin, 33, 1081 (1960).
2) S. Seto, *Sci Repts. Tohoku Univ., First Ser.*, 37, 292 (1953).
3) C. R. Harrington, *Biochem. J.*, 20, 300 (1926).
4) G. A. Reynolds and J. A. VanAllen, "Organic Syntheses", 34, 1 (1954).

presence of sodium hydrogencarbonate and reduction of its product with sodium dithionite afforded colorless crystals (G), whose analytical values corresponded to the formula of $C_{13}H_8O_3$ and which formed phthalic acid by oxidation with potassium permanganate. Methylation of G with dimethyl sulfate in the presence of potassium carbonate gave a monomethyl ether. Therefore G would be 2-hydroxybenzo[c]coumarin (XVI) and its monomethyl ether, 2-methoxybenzo[c]coumarin (XVII). Methylation of XVI with dimethyl sulfate with heating in the presence of potassium hydroxide, resulted in opening of the lactone ring to form 2-(2′, 5′-dimethoxyphenyl)benzoic acid (XV).

Since the structure of F is 2-(2′, 5′-dimethoxyphenyl)benzoic acid, the structure of A would be 3-(*p*-benzoquinonyl)tropolone (VIII).

The reduction product of A, 3-(2′, 5′-dihydroxyphenyl)tropolone (IX), easily undergoes dehydration when warmed with *p*-toluenesulfonic acid and changes into 2-hydroxybenzofuro[2, 3-b]tropone (XVIII). This reaction also supports the above structure. Methylation of XVIII with dimethyl sulfate in the presence of potassium carbonate, affords 2-methoxybenzofuro[2, 3-b]tropone (XIX).

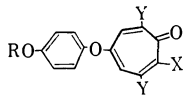
3-Bromotropolone also undergoes reaction with *p*-benzoquinone to form *p*-benzoquinonyl-3-bromotropolone (XX) whose catalytic reduction over palladium-carbon or treatment with sodium dithionite affords a dihydroxyphenyl derivative (XXI). Hydrogenolysis of XXI in ethanol containing diethanolamine, with palladium-carbon catalyst, gives 3-(2′, 5′-dihydroxyphenyl)tropolone (IX). Consequently, XX is proved to be 3-bromo-7-(*p*-benzoquinonyl)tropolone.

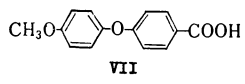
Methylation of XXI with dimethyl sulfate in acetone, in the presence of potassium carbonate, results in rearrangement of the tropolone ring to benzoic acid and 2-methoxy-7-bromobenzo[c]coumarin (XXIV) is obtained. Treatment of XXI with *p*-toluensulfonic acid affords 2-hydroxy-7-bromobenzofuro[2, 3-b]tropone (XXII) and its methylation as above produces 2-mehoxy-7-bromobenzofuro[2, 3-b]tropone (XXIII) and dimethyl ether (XXV) of 3-bromo-7-(2′, 5′-dihydroxyphenyl)tropolone (XXI) without such a rearrangement.

The ultraviolet absorption spectra of benzocoumarin derivatives and benzofuro-tropone derivatives are similar in the wavelength of absorption maxima but there is a distinct difference in the infrared spectra of these two series. The infrared spectra of benzocoumarin derivatives show strong absorptions in the range of 1690~1720 cm^{-1} (at 1696 cm^{-1} in XVI, at 1709 cm^{-1} in XVII, and at 1721 cm^{-1} in XXIV) while that of benzofuro-tropone derivatives does not show any absorption in this region.

Reaction of 3, 7-dibromotropolone with *p*-benzoquinone first precipitated crystals of 3, 7-dibromotropolone and methylation of its mother liquor, without purification, with dimethyl sulfate in the presence of potassium hydroxide and fractional crystallization of the potassium salt of its product afforded 3, 7-dibromo-5,(4′-methoxyphenoxy)tropolone (XXVII). The structure of XXVII is clear from its analytical values and formation of 5-(4′-methoxyphenoxy)-tropolone (IV) by its hydrogenolysis. Consequently, the product obtained by the reaction of 3, 7-dibromotropolone and *p*-benzoquinone would be 3, 7-dibromo-5-(4′-hydroxyphenoxy)-tropolone (XXVI).

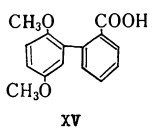
Reaction of *p*-benzoquinone and tropolones in the presence of a weak base affords a product corresponding to 1 : 1 molar compound of *p*-benzoquinone and tropolone. This compound does not show the properties of a tropolone



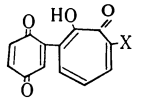


VII

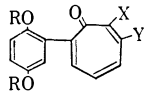
I :	R=H,	X=OH,	Y=H
II :	R=H,	X=OCH_3,	Y=H
III :	R=CH_3,	X=OCH_3,	Y=H
IV :	R=CH_3,	X=OH,	Y=H
V :	R=CH_3,	X=$NHNH_2$,	Y=H
VI :	R=CH_3,	X=Br,	Y=H
XXVI :	R=H,	X=OH,	Y=Br
XXVII :	R=CH_3,	X=OH,	Y=Br



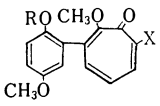
XV



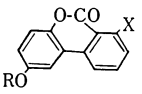
VIII : X=H
XX : X=Br



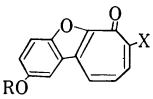
IX :	R=H,	X=OH,	Y=H
X :	R=CH_3,	X=OH,	Y=H
XI :	R=CH_3,	X=OCH_3,	Y=H
XIII :	R=CH_3,	X=$NHNH_2$,	Y=H
XIV :	R=CH_3,	X=Cl,	Y=H
XXI :	R=H,	X=OH,	Y=Br



XII : R=CH_3, X=H
XXV : R=H, X=Br



XVI: R=X=H
XVII: R=CH_3, X=H
XXIV: R=CH_3, X=Br



XVIII: R=X=H
XIX: R=CH_3, X=H
XXII: R=H, X=Br
XXIII: R=CH_3, X=Br

derivative. Examinations are now under way on its structure.

Experimental[5]

3-(*p*-Benzoquinonyl)tropolone (VIII) and 5-(4'-Hydroxyphenoxy)tropolone (I).—A solution of 5 g. of tropolone, 2.1 g. of *p*-benzoquinone, and 2 ml. of acetic acid dissolved in 10 ml. of methanol was allowed to stand in a room temperature. After several hours, orange crystals precipitated out. After standing for 4 days, the orange crystals (A) (1.58 g.), m. p. 160~165°C, were collected, washed with methanol, and recrystallized from ethyl acetate to 1.3 g. of 3-(*p*-benzoquinonyl)tropolone (VIII), m. p. 169~170°C.

Found: C, 68.24; H, 3.52. Calcd. for $C_{13}H_8O_4$: C, 68.42; H, 3.57%. λ_{max}^{MeOH} mμ (log ε): 242 (4.45), 328(3.87), 335(3.88), 361(3.66), 376(3.71).

The filtrate left after separation of A was allowed to stand and 0.52 g. of colorless crystals (B), m. p. 195~197°C, precipitated out. Recrystallization of B from methanol afforded 5-(4'-hydroxyphenoxy)-tropolone (I) as colorless crystals, m. p. 196~197°C.

Found: C, 67.82; H, 4.38. Calcd. for $C_{13}H_{10}O_4$: C, 67.91; H, 4.49%. λ_{max}^{MeOH} mμ (log ε): 238 (4.54), 340 (4.24), 390 (3.91), 410 (3.83).

The filtrate left after separation of B was evaporated and sublimation of its residue at 80°C (bath temperature) at 2 mmHg, afforded 2.5 g. of recovered tropolone.

Reaction of I and Diazomethane.—Ether solution of diazomethane was added to 0.1 g. of I suspended in methanol and the mixture was allowed to stand over night. The crystals that precipitated out were collected and recrystallized from a mixture of benzene and acetone to give 2-methoxy-5-(4'-hydroxyphenoxy)tropone (II) as pale yellow prisms, m. p. 164~166°C. Yield, 60 mg.

Found: C, 68.82; H, 5.30. Calcd. for $C_{14}H_{12}O_4$: C, 68.84; H, 4.95%. λ_{max}^{MeOH} mμ (log ε): 231 (4.48), 330 (4.10).

II did not show any coloration with ferric chloride.

The filtrate left after separation of II was evaporated to dryness, the residue was dissolved in benzene, and the solution was purified by passing through an alumina column. From its effluent, 2-methoxy-5-(4'-methoxyphenoxy)tropone (III) was obtained as pale yellow crystals, m. p. 89~91°C. Yield, 30 mg.

Found: C, 70.20; H, 5.21. Calcd. for $C_{15}H_{14}O_4$: C, 69.75; H, 5.46%. λ_{max}^{MeOH} mμ (log ε): 234 (4.53), 330 (4.16).

III also did not undergo coloration with ferric chloride.

Hydrolysis of II.—A mixture of 10 mg. of II in 0.1 ml. of 2 N sodium hydroxide and 0.1 ml. of methanol was heated on a water bath for 1 hr., methanol was evaporated, and residual solution was acidified with dilute hydrochloric acid. The precipitate that formed was collected and sublimed at 200°C (bath temperature) at 1.5 mmHg, from which 5 mg. of colorless crystals, m. p. 192~193°C, was obtained. This showed no melting point depression on admixture with I.

Hydrolysis of III.—The same treatment as above of 20 mg. of III afforded 15 mg. of 5-(4'-methoxyphenoxy)tropolone (IV), m. p. 129~130°C.

Found: C, 68.62; H, 4.83. Calcd. for $C_{14}H_{12}O_4$: C, 68.84; H, 4.95%. λ_{max}^{MeOH} mμ (log ε): 235 (4.50), 345(4.23), 390 (3.82).

Methylation of I with Dimethyl Sulfate.—A mixture of 0.2 g. of I, 0.6 g. of potassium hydroxide, and 5 ml. of water was heated on a water bath and 0.2 g. of dimethyl sulfate was added while stirring. After 30 min., the reaction mixture was cooled, acidified with dilute hydrochloric acid, and the precipitate thereby formed was collected. The proddct was sublimed at 200°C (bath temperature) and 1.5 mmHg, and the sublimate was recrystallized from benzene-petroleum ether mixture to give 150 mg. of colorless crystals, m. p. 128~129°C, undepressed on admixture with IV obtained by hydrolysis of III.

Reaction of IV and Diazomethane.—Ether solution of diazomethane was added to a solution of 0.1 g. of IV dissolved in 15 ml. of ether and the solution was allowed to stand over night. The solvent was evaporated and the residue was sublimed at 200°C (bath temperature) and 1.5 mmHg. The sublimate was recrystallized from ether to give 75 mg. of pale yellow crystals, m. p. 89~90°C, undepressed on admixture with III.

2-Hydrazino-5-(4'-methoxyphenoxy)tropone (V).—A mixture of 80 mg. of III and 30 mg. of hydrazine hydrate (80%) in 0.4 ml. of methanol was warmed on a water bath for 30 min., methanol was evaporated, and the residue was diluted with a small amount of water. The precipitate that formed was collected and recrystallized from methanol to 55 mg. of yellow crystals, m. p. 123~124°C.

Found: C, 64.92; H, 5.48; N, 11.19. Calcd. for $C_{14}H_{14}O_3N_2$: C, 65.10; H, 5.46; N, 10.85%. λ_{max}^{MeOH} mμ (log ε): 231 (4.22), 250 (4.30), 348 (4.12), 424 (3.89).

2-Bromo-5-(4'-methoxyphenoxy)tropone (VI).—A solution of 0.5 g. of copper sulfate dissolved in 0.8 ml. of water with heating was maintained at 120°C and a mixture of 50 mg. of V and 0.5 ml. of concentrated hydrobromic acid was added to it while

5) All melting points are not corrected. Microanalyses were carried out by Misses Yôko Endô and Yukiko Endô of this Institute. Measurements of ultraviolet and infrared spectra were made respectively by a Hitachi EPU-2A type spectrophotometer and by a Perkin-Elmer Model 21 infrared spectrophotometer in potassium bromide disk.

stirring. A vigorous evolution of nitrogen occurred and the liquid turned black. After maintaining the mixture at 120°C for 5 min., it was cooled, 5 ml. of water and 30 ml. of chloroform were added, and the whole was shaken thoroughly. The mixture was filtered, chloroform layer was separated from the filtrate, and dried over anhydrous sodium sulfate. The dried chloroform solution was purified by passage through an alumina column and the product obtained from its effluent was recrystallized from petroleum ether, affording 30 mg. of pale yellow crystals, m. p. 95~97°C.

Found: C, 55.15; H, 3.99. Calcd. for $C_{14}H_{11}O_3Br$: C, 54.72; H, 3.61%. λ_{max}^{MeOH} mμ (log ε): 225 (4.48), 247 (4.30), 341 (4.19).

Rearrangement Reaction of VI with Alkali.—A mixture of 10 mg. of VI in 0.5 ml. of dioxane and 0.5 ml. of 0.2 N sodium hydroxide was heated on a water bath for 1 hr., the solvent was evaporated in reduced pressure, and the residue was treated with activated carbon after dilution with 0.2 ml. of water. The pale yellow aqueous solution so obtained was acidified with dilute sulfuric acid and this was allowed to stand over night in an ice chamber. The crystals that separated out were collected and sublimed at 160°C (bath temperature) and 2 mmHg, affording 5 mg. of colorless crystals, m. p. 173~174°C, underpressed on admixture with 4-(4'-methoxyphenoxy)benzoic acid (VII), m. p. 176~176.5°C, prepared through a known process[3]. The ultraviolet absorption spectra of these two compounds were also in good agreement.

λ_{max}^{MeOH} mμ (log ε): 252 (4.22).

3-(2', 5'-Dihydroxyphenyl)tropolone (IX).—a) A solution of 0.4 g. of sodium dithionite dissolved in 2 ml. of water was added while stirring into 0.2 g. of VIII, reduced to a powder in a mortar, suspended in 5 ml. of water and the mixture was warmed to 40°C. The color of the suspension changed from orange to yellow. After stirring for 10 min., the mixture was cooled, the precipitation was collected by filtration, and washed with water to 0.2 g. of a yellow substance, m. p. 285°C. Recrystallization from methanol afforded 0.18 g. of pale yellow microcrystals, m. p. 289~290°C.

Found: C, 67.29; H, 4.14. Calcd. for $C_{13}H_{10}O_4$: C, 67.82; H, 4.38%. λ_{max}^{MeOH} mμ (log ε): 227 (4.34), 330 (4.00), 375 (3.88)

b) A solution of 0.1 g. of VIII dissolved in 50 ml. of ethanol in the presence of 40 mg. of palladium-carbon was shaken in hydrogen atmosphere at room temperature. When the absorption of hydrogen ceased, the catalyst was filtered off and the filtrate was concentrated, affording 95 mg. of pale yellow crystals, m. p. 288~290°C, undepressed on admixture with the product obtained in a).

3-(2', 5'-Dimethoxyphenyl)tropolone (X).—A solution of 0.6 g. of sodium hydroxide in 5 ml. of water was added to a mixture of 0.1 g. of IX and 0.5 g. of dimethyl sulfate while stirring. After stirring the mixture for 30 min. at room temperature and for 1 hr. on a water bath, the reaction mixture was cooled and shaken with 5 ml. of ether. The yellow crystals that separated out were collected, dissolved in 2 ml. of water, and the solution was acidified with dilute hydrochloric acid. The oil that separated solidified into crystals, when allowed to stand in an ice box. The crystals were collected, sublimed at 200°C (bath temperature) and 2 mmHg, and the sublimate was recrystallized from ether-petroleum ether mixture to 60 mg. of pale yellow needles, m. p. 82~84°C.

Found: C, 69.56; H, 5.16. Calcd. for $C_{15}H_{14}O_4$: C, 69.75; H, 5.46%. λ_{max}^{MeOH} mμ (log ε): 225 (4.41), 325 (3.96), 350 (3.86), 372 (3.84).

Reaction of X and Diazomethane.—Ether solution of diazomethane was added to 0.26 g. of X dissolved in 10 ml. of ether and the mixture was allowed to stand over night. The crystals that separated out were collected and recrystallized from acetone to 140 mg. of pale yellow needles, m. p. 145~146°C.

Found: C, 70.39; H, 5.73. Calcd. for $C_{16}H_{16}O_4$: C, 70.57; H, 5.92%. λ_{max}^{MeOH} mμ (log ε): 223 (4.26), 320 (3.83), 350(3.79).

The ether solution left after separation of foregoing crystals was evaporated to remove excess of diazomethane, passed through a column of alumina, and the column was eluted with ether. From the initial effluent, 70 mg. of colorless crystals, m. p. 116~117°C, was obtained and later fraction afforded 20 mg. of crystals, m. p. 145°C.

Crystals of m. p. 116~117°C.

Found: C, 70.24; H, 5.90. Calcd. for $C_{16}H_{16}O_4$: C, 70.57; H, 5.92%. λ_{max}^{MeOH} mμ (log ε): 223 (4.44), 325 (4.05).

Neither of these two kinds of crystals colored with ferric chloride. Assuming from their solubility, shape of their ultraviolet absorption spectra, and ease or difficulty of elution in chromatography, the structure of these products was assumed to be 2-methoxy-7-(2', 5'-dimethoxyphenyl)tropone (XI) for the product of m. p. 145~146°C and 2-methoxy-3-(2', 5'-dimethoxyphenyl)tropone (XII) for that of m. p. 116~117°C.

2-Hydrazino-7-(2', 5'-dimethoxyphenyl)tropone (XIII).—A mixture of 70 mg. of methoxytropone (XI) of m. p. 145~146°C, 1 ml. of methanol, and 80 mg. of hydrazine hydrate (80%) was warmed on a water bath for 30 min., cooled, and crystals that separated out were collected. Recrystallization from methanol gave 55 mg. of yellow prisms, m. p. 194~195°C.

Found: C, 65.74; H, 5.50; N, 10.66. Calcd. for $C_{14}H_{16}O_3N_2$: C, 66.16; H, 5.92; N, 10.29%. λ_{max}^{MeOH} mμ (log ε): 223 (4.24), 252 (4.19), 345 (3.93), 412 (4.01).

2-Chloro-7-(2', 5'-dimethoxyphenyl)tropone (XIV).—To a solution of 0.4 g. of crystalline copper sulfate in 1 ml. of water and maintained at 120°C, a mixture of 50 mg. of XIII in 0.5 ml. of concentrated hydrochloric acid was added while stirring, the mixture was cooled after 5 min., and 10 ml. of water and 20 ml. of chloroform were added. This mixture was shaken thoroughly, filtered, and the chloroform layer was separated from the filtrate. After drying over anhydrous sodium sulfate, the chloroform layer was passed through an alumina column and the solvent was evaporated from effluents. The crystalline residue was recrystallized from petroleum ether to 45 mg. of pale yellow prisms, m. p. 114~115°C.

Found : C, 65.25 ; H, 4.72. Calcd. for $C_{15}H_{13}O_3Cl$: C, 65.08 ; H, 4.74%. λ_{max}^{MeOH} mμ (log ε) : 265 (3.92), 320 (3.95).

Rearrangement Reaction of XIV with Alkali.—A mixture of 40 mg. of XIV, 2 ml. of water, 0.2 g. of sodium hydroxide, and 1 ml. of ethanol was heated on a water bath for 2 hr., ethanol was evaporated, and the residual solution was extracted with ether to remove neutral substance. The aqueous layer was acidified with dilute hydrochloric acid, extracted with ether to collect an acid substance, and the ether extract was esterified by addithon of ether solution of diazomethane. The product therefrom was purified through an alumina column, the column was eluted with ether, and the initial eluate afforded 30 mg. of colorless oil.

A mixture of this oily product with 0.1 g. of sodium hydroxide, 5 ml. of water, and 2 ml. of methanol was refluxed on a water bath for 3 hr., methanol was evaporated, and the residue was treated with activated carbon. The solution so obtained was acidified with dilute hydrochloric acid and the crystals that separated out were recrystallized from 50% methanol to 15 mg. of colorless needles, m. p. 152~153°C, undepressed on admixture with 2-(2′, 5′-dimethoxyphenyl)benzoic acid (XV) prepared in a different way. Infrared spectra of these two were in good agreement.

2-Hydroxybenzo[c]coumarin (XVI).—A solution of 1.38 g. of sodium nitrite in 6.6 ml. of water was added to a mixture of 3.8 g. of methyl anthranilate hydrochloride, 4 ml. of concentrated hydrochloric acid, and 2 g. of ice, while stirring under cooling, to effect diazotization and the pale yellow solution so obtained was added dropwise into a suspension of 2 g. of *p*-benzoquinone in a mixture of 3.4 g. of sodium hydrogencarbonate, 5 ml. of water, and 5 g. of ice, while stirring under ice-cooling. Vigorous evolution of carbon dioxide and nitrogen was noticed. The dropwise addition was made during about 1 hr., the mixture was stirred at room temperature for a further 1 hr., and the yellow solid that separated was collected by filtration. This yellow solid was difficult to purify, so that it was dissolved in 20 ml. of chloroform, a solution of 5 g. of sodium dithionite in 50 ml. of water was added to it while stirring, the mixture was stirred for 1 hr., and allowed to stand over night. The colorless crystals that separated out were collected and washed with a small amount of chloroform and water to give 2.5 g. of colorless crystals, m. p. 195~198°C. Recrystallization from methanol-benzene mixture raised the melting point to 218~220°C.

Found : C, 72.45 ; H, 3.79. Calcd. for $C_{13}H_8O_3$: C, 73.58 ; H, 3.80%. λ_{max}^{MeOH} mμ (log ε) : 230 (4.54), 263 (4.11), 317 (3.81), 325 (3.82).

Oxidation of XVI with Potassium Permanganate.—A solution of 1 g. of XVI dissolved in 4 ml. of pyridine with 12 ml. of 5% aqueous solution of potassium permanganate added was warmed on a water bath for 2 hr., and evaporated to dryness in a reduced pressure. The residue was diluted with 5 ml. of water, filtered, and the filtrate was acidified with dilute hydrochloric acid. This was extracted with ethyl acetate, the solvent was evaporated from this extract, and 0.1 ml. of acetic anhydride was added to its residue. After warming this mixture on a water bath the product was sublimed at 60°C (bath temperature) and 20 mmHg, and 60 mg. of colorless prisms, m. p. 129~131°C, was obtained, showing no depression of the melting point on admixture with phthalic anhydride.

2-Methoxybenzo[c]coumarin (XVII).—A mixture of 0.8 g. of XVI, 25 ml. of acetone, 1.7 g. of dimethyl sulfate, and 4.5 g. of potassium carbonate was refluxed for 2 hr. while stirring, acetone was evaporated in a reduced pressure, and 10 ml. of water was added to the residue. The crystals were collected by filtration, dissolved in methanol, and treated with activated carbon. Evaporation of methanol afforded 0.7 g. of colorless needles, m. p. 118~119°C.

Found : C, 74.20 ; H, 4.41. Calcd. for $C_{14}H_{10}O_3$: C, 74.33 ; H, 4.46%. λ_{max}^{MeOH} mμ (log ε) : 231 (4.62), 260 (4.14), 270 (4.06), 316 (3.88), 326 (3.88).

2-(2′, 5′-Dimethoxyphenyl)benzoic Acid (XV).—To 1.2 g. of XVI being stirred on a water bath, a solution of 2.24 g. of potassium hydroxide in 10 ml. of water and 1.26 g. of dimethyl sulfate were added in four portions at an interval of 30 min. The mixture was heated for 1 hr. after the final addition, cooled, and extracted with ether to remove neutral substane. The aqueous layer was acidified with dilute hydrochloric acid, the solid (0.73 g.) that separated was collected, and dissolved in ether. Ether solution of diazomethane was added to it to effect esterification and the product was purified by passage through an alumina column.

The oily product (0.5 g.) so obtained was hydrolyzed with 0.75 g. of sodium hydroxide in 5 ml. each of methanol and water by heating on a water bath for 1 hr., methanol was evaporated from the reaction mixture, and the aqueous solution was extracted with benzene to remove neutral substance. This aqueous solution was treated with activated carbon, acidified with dilute hydrochloric acid, and 0.32 g. of colorless crystals that separated out was recrystallized from 50% methanol to colorless needles, m. p. 152~154°C.

Found : C, 69.92 ; H, 4.85. Calcd. for $C_{15}H_{14}O_4$: C, 69.75 ; H, 5.46%. λ_{max}^{MeOH} mμ (log ε) : 305 (3.65).

2-Hydroxybenzofuro[2, 3-b]tropone (XVIII).—A mixture of 70 mg. of IX and 0.2 g. of *p*-toluenesulfonic acid was heated in an oil bath at 110~120°C, by which the solution turned red, heated for 20 min., and cooled. The reaction mixture solidified into a pale yellow mass, 2 ml. of water was added to it, and the solid was collected by filtration. Recrystallization from acetone-methanol mixture afforded 60 mg. of pale yellow prisms, m. p. 287~290°C.

Found : C, 72.76 ; H, 3.63. Calcd. for $C_{13}H_8O_3$: C, 73.58 ; H, 3.80. λ_{max}^{MeOH} mμ (log ε) : 275 (4.61), 325 (4.40).

2-Methoxybenzofuro[2, 3-b]tropone (XIX).—A mixture of 0.17 g. of XVIII in 10 ml. of acetone, 0.4 g. of dimethyl sulfate, and 2 g. of potassium carbonate was refluxed for 1 hr. with stirring. Acetone was evaporated from this mixture, 10 ml. of water was added to the residue, and 0.12 g. of insoluble substance so obtained was recrystallized

from methanol to 80 mg. of colorless needles, m. p. 179~180°C.

Found: C, 73.80; H, 4.46. Calcd. for $C_{14}H_{10}O_3$: C, 74.33; H, 4.46%. λ_{max}^{MeOH} mμ (log ε): 267 (4.38), 325 (4.22).

3-Bromo-7-(*p*-benzoquinonyl)tropolone (XX).—A mixture of 3 g. of 3-bromotropolone, 1 g. of *p*-benzoquinone, 10 ml. of methanol, and 1 ml. of acetic acid was warmed slightly to effect solution and allowed to stand over night, by which orange plate crystals separated out. After standing the mixture for 2 days, 0.82 g. of crystals were collected and recrystallized from a mixture of methanol and ethyl acetate to give orange scales (XX), m. p. 175~181°C.

Found: C, 50.82; H, 2.63. Calcd. for $C_{13}H_7O_4Br$: C, 50.82; H, 2.30%. λ_{max}^{MeOH} mμ (log ε): 255 (4.51), 338 (3.99), 408 (3.91).

The mother liquor left after removal of the orange plate was evaporated and the residue was sublimed at 120°C (bath temperature) and 1 mmHg, from which 2 g. of 3-bromotropolone was recovered.

3-Bromo-7-(2', 5'-dihydroxyphenyl)tropolone (XXI).—a) To a suspension of 0.2 g. of XX, reduced to a powder in a mortar, in 5 ml. of water, a solution of sodium dithionite in 2 ml. of water was added while stirring at 40°C, by which color of the suspension changed from orange to yellow. After stirring for 20 min., the mixture was cooled, and filtered to collect a pale yellow powder, which was washed with water. Recrystallization from methanol afforded 0.18 g. of pale yellow crystals, m. p. 237~240°C.

Found: C, 50.21; H, 2.95. Calcd. for $C_{13}H_9O_4Br$: C, 50.48; H, 2.93%. λ_{max}^{MeOH} mμ (log ε): 260 (4.34), 330 (3.98), 385 (3.80), 408 (3.77).

b) A suspension of 0.1 g. of XX in 100 ml. of ethanol and added with 50 mg. of palladium-carbon was shaken in hydrogen atmosphere. Absorption of hydrogen ceased after 2 hr. The catalyst was filtered off and evaporation of the filtrate afforded 90 mg. of pale yellow crystals, m. p. 240~242°C, undepressed on admixture with the product obtained by the method a).

Hydrogenolysis of XX.—A mixture of 0.1 g. of XX, 0.1 ml. of diethanolamine, and 50 mg. of palladium-carbon in 100 ml. of ethanol was shaken in hydrogen atmosphere. The catalyst was filtered off, when absorption of hydrogen ceased, 0.2 ml. of acetic acid was added to the filtrate, and the solution was evaporated to dryness. To its residue, 5 ml. of water was added, insoluble matter was collected, and recrystallized from a mixture of methanol and ethyl acetate to give 60 mg. of pale yellow crystals, m. p. 288~289°C, undepressed on admixture with IX.

2-Hydroxy-7-bromobenzofuro [2, 3-b] tropone (XXII).—A mixture of 0.27 g. of XX and 0.81 g. of *p*-toluenesulfonic acid was heated at 125°C while stirring for 20 min., by which the solution turned red. This was cooled, 5 ml. of water was added, and insoluble matter was collected by filtration. This was washed with water and 0.26 g. of crude crystals melting at 288~290°C so obtained was recrystallized from methanol to give crystals of m. p. 300~303°C.

Found: C, 53.44; H, 2.50. Calcd. for $C_{13}H_7O_3Br$: C, 53.61; H, 2.42%. λ_{max}^{MeOH} mμ (log ε): 280 (4.54), 334 (4.23).

2-Methoxy-7-bromobenzofuro [2, 3-b] tropone (XXIII).—a) Ether solution of diazomethane was added to 0.12 g. of XXII suspended in 10 ml. of methanol and the mixture was allowed to stand for 2 days. The mixture was evaporated and the residue was fractionally crystallized from methanol. From the sparingly soluble portion, 65 mg. of XXII was recovered. An easily soluble portion afforded 40 mg. of pale yellow needles (XXIII), m. p. 222~224°C.

Found: C, 55.06; H, 2.95. Calcd. for $C_{14}H_9O_3Br$: C, 55.09; H, 2.97%. λ_{max}^{MeOH} mμ (log ε): 278 (4.52), 330 (4.18).

b) A mixture of 0.37 g. of XXII in 20 ml. of acetone, 0.8 g. of dimethyl sulfate, and 4 g. of potassium carbonate was refluxed for 1 hr. while stirring, acetone was evaporated from the reaction mixture, and the residue was diluted with 10 ml. of water, separating 0.34 g. of insoluble matter, m. p. 150~190°C. This was dissolved in methanol, treated with activated carbon, and fractional recrystallization afforded 80 mg. of pale yellow needles, m. p. 223~225°C, undepressed on admixture with XXIII prepared by the method a).

Easily soluble portion afforded 50 mg. of pale yellow crystals, m. p. 118~120°C, which was assumed to be XXV from the shape of its ultraviolet absorption spectrum, its analytical values and no coloration with ferric chloride.

Found: C, 53.32; H, 3.87. Calcd. for $C_{15}H_{13}O_4Br$: C, 53.41; H, 3.88%. λ_{max}^{MeOH} mμ (log ε): 220 (4.26), 256 (4.37), 334 (4.08), 380 (3.84).

2-Methoxy-7-bromobenzo[c]coumarin (XXIV).—A mixture of 170 mg. of XXI, 12 ml. of acetone, 0.6 g. of dimethyl sulfate, and 1.1 g. of potassium carbonate was refluxed for 2 hr. while stirring, acetone was evaporated from the reaction mixture, and 5 ml. of water was added to the residue. The insoluble matter was collected, dissolved in methanol, and treated with activated carbon. Evaporation of the filtrate afforded 80 mg. of colorless crystals, m. p. 176~177°C.

Found: C, 54.91; H, 3.08. Calcd. for $C_{14}H_9O_3Br$: C, 55.09; H, 2.97%. λ_{max}^{MeOH} mμ (log ε): 238 (4.51), 268 (4.06), 330 (3.93).

Hydrogenolysis of XXIII.—A solution of 30 mg. of XXIII dissolved in 100 ml. of ethanol, added with 30 mg. of sodium acetate and 20 mg. of palladium-carbon, was shaken in hydrogen atmosphere, the catalyst was filtered off when absorption of hydrogen ceased, and the filtrate was evaporated in a reduced pressure. To its residue, 2 ml. of water was added, insoluble matter was collected, and recrystallized from methanol to 10 mg. of crystals melting at 175~178°C, alone and in admixture with XIX.

Hydrogenolysis of XXIV.—XXIV (20 mg.) was treated in the same manner as in hydrogenolysis of XXIII and 10 mg. of crystals, m. p. 113~117°C, was obtained. It showed no depression of the melting point on admixture with XVII.

Reaction of 3, 7-Dibromotropolone and *p*-Benzoquinone.—A mixture of 3 g. of 3, 7-dibromotropolone, 1 g. of *p*-benzoquinone. 30 ml. of methanol, and

2 ml. of acetic acid was heated at 60°C for 5 hr., cooled to the room temperature, and 1.14 g. of crystals, m. p. 146~152°C, was obtained. This was found by admixture to be the starting tropolone. Concentration of the filtrate left after separation of these crystals afforded 1.27 g. of recovered 3, 7-dibromotropolone.

This filtrate was evaporated to dryness, 13 ml. of 5 N potassium hydroxide and 7 g. of dimethyl sulfate were added to its residue, and the mixture was heated on a water bath for 8 hr. while stirring. When cooled, 1.25 g. of yellow potassium salt separated which was dissolved in 100 ml. of water, dark insoluble matter was filtered off, and the filtrate was concentrated to 50 ml. On cooling this solution, 0.4 g. of the salt was obtained. This salt was suspended in water, acidified with dilute hydrochloric acid, and the separated crystals were collected. Recrystallization from methanol gave 0.15 g. of pale yellow crystals, m. p. 130~135°C. This is 3, 7-dibromo-5-(4'-methoxyphenoxy)tropolone (XXVII).

Found : C, 41.47 ; H, 2.79. Calcd. for $C_{14}H_{10}O_4Br_2$: C, 41.80 ; H, 2.51%. λ_{max}^{MeOH} mμ (log ε) : 268 (4.49), 348 (4.10), 446 (3.90).

Hydrogenolysis of XXVII.—A mixture of 30 mg. of XXVII, 30 mg. of potassium hydroxide, and 40 ml. of water, with 30 mg. of palladium-carbon added, was shaken in hydrogen atmosphere until absorption of hydrogen had ceased. The catalyst was filtered off, the filtrate was acidified, and the crystals that separated out were collected to 10 mg. of crystals melting at 125~127°C, alone and on admixture with 5-(4'-methoxyphenoxy)tropolone (IV).

Summary

Reaction of tropolone and *p*-benzoquinone was carried out in methanol containing acetic acid and the structure of products so obtained was determined. Tropolone gave 5-(4'-hydroxyphenoxy)tropolone and 3-(*p*-benzoquinonyl)-tropolone, 3-bromotropolone gave 3-bromo-7-(*p*-benzoquinonyl)tropolone, and 3, 7-dibromotropolone gave 3, 7-dibromo-5-(4'-hydroxyphenoxy)tropolone by this reaction. Benzofurotropones were derived from benzoquinonyltropolones.

In order to prove the structure of the product by admixture, benzocoumarin derivative was prepared by the reaction of the diazonium salt of anthranilate and *p*-benzoquinone.

The present work was aided by financial assistance from the Sankyo Co., Ltd. The authors are indebted to Mr. Yusaku Ikegami for infrared spectral analyses.

The Chemical Research Institute of Non-Aqueous Solutions
Tohoku University
Katahira-cho, Sendai

De-localization of Bond Eigenfunctions in π-Electronic Systems. I. Proposal of an Approximate Method for the Calculation of the π-Electronic States of Molecules

By Shozaburo TAKEKIYO

(Received October 21, 1960)

If in complex π-electronic systems all kinds of linearly independent resonance structures were taken as a set of canonical structures, the calculation of the various physical quantities (for example, energy levels, π-electron densities, or bond orders) would be extremely laborious. For the sake of diminishing such difficulties, various approximate treatments have been proposed. In most of them, however, only a small number of resonance structures, which are expected to be comparatively important, have almost intuitively been taken as a set of canonical structures[1-3].

One of these treatments is the Heitler-London method, where only the covalent structures are considered. One of the greatest defects of this method is that by this method it is impossible to explain the migration effects of the π-electrons from the substituents of mono-substituted benzenes (phenol, aniline, chlorobenzene, etc.) to the benzene nuclei[4].

Importance of the ionic structures has been emphasized by Daudel and Daudel[5], and a few calculations including them have been carried out[6]. But these attempts are very qualitative,

1) L. Pauling and G. W. Wheland, *J. Chem. Phys.*, **1**, 362 (1933).
2) A. L. Sklar, ibid., **5**, 669 (1937).
3) D. P. Craig, *Proc. Roy. Soc.*, **A200**, 401 (1950).
4) L. Pauling and G. W. Wheland, *J. Am. Chem. Soc.*, **57**, 2086 (1935).
5) P. Daudel and R. Daudel, *J. Chem. Phys.*, **16**, 639 (1948).
6) J. A. A. Ketelaar, *Rec. trav. chim.*, **58**, 266 (1939); See also Refs. 2 and 3.

and the number of ionic structures considered is also extremely small.

Now, it is well known that the molecular orbital method and the Heitler-London method are the two extreme approximations, in which the contributions of the ionic structures are too much emphasized and too much neglected respectively. Therefore, a new approximate method is desirable one, which corresponds to the middle point of view of the two methods.

The approximate method which is proposed by us stands on this middle ground and is as follows: all the resonance structures under consideration are sorted out into a few classes, suitable functions which are the linear combinations of the bond eigenfunctions for the structures in each class are found, and the wave functions for the molecule are represented by linear combinations of them.

By this method the degree of the energy determinants is more diminished than in the straightforward method. Hence, the problem can be simplified in cases when a great number of resonance structures are included.

Since there are various manners for the classification of the resonance structures, one particular manner must be selected. The appraisal of multiple exchange integrals is however, made prior to this, since it directly relates to our manner of classification.

Appraisal of Multiple Exchange Integrals

Multiple exchange integrals, which appear by way of the computation of the π-electronic energy levels of polyatomic molecules based on the valence bond method, have hitherto been neglected[2,3]. It does not seem, moreover, that satisfactory appraisals of them have been made, in spite of the emphasis on their importance[7].

Accordingly, in this paragraph the influence of the multiple exchange integrals upon the energy matrix with respect to the bond eigenfunctions is discussed by means of illustrations

TABLE I. COMPARISON OF RESONANCE INTEGRALS*

Kind of interacting structures**	Resonance integrals	Multiple exchange integrals not included (I)	Multiple exchange integrals included (II)	Difference (II-I)
		trans-Butadiene		
N-N	(*ad* : *bc*-*ad* : *bc*)	−46.83703	−46.92960	−0.09257
	(*ab* : *cd*-*ac* : *bd*)	+25.23109	+25.26019	+0.02909
N-M	(*ab* : *cd*-*aa* : *cd*)	−18.97761	−20.85919	−1.88158
	(*ab* : *cd*-*ac* : *bb*)	+ 4.15071	+ 4.12262	−0.02809
N-D	(*ab* : *cd*-*bb* : *cc*)	− 9.40144	− 8.78519	+0.61624
	(*ac* : *bd*-*aa* : *dd*)	+ 4.71797	+ 4.71817	+0.00019
M-M	(*ab* : *cc*-*aa* : *bd*)	+ 0.63185	− 1.85967	−2.49153
	(*aa* : *bd*-*aa* : *bd*)	−33.94508	−33.94215	+0.00293
M-D	(*aa* : *cd*-*bb* : *dd*)	0	− 2.03915	−2.03915
	(*aa* : *bd*-*aa* : *dd*)	− 2.55372	− 2.55374	−0.00002
D-D	(*aa* : *cc*-*bb* : *dd*)	0	− 0.46832	−0.46832
	(*aa* : *dd*-*aa* : *dd*)	−29.17000	−29.17000	−0.00000
		Cyclobutadiene		
N-N	(*ab* : *cd*-*ab* : *cd*)	−61.90093	−57.08229	+4.81863
	(*ab* : *cd*-*ac* : *bd*)	+28.76985	+25.24667	−3.52318
N-M	(*ab* : *cd*-*ab* : *cc*)	−20.51222	−19.89659	+0.61563
	(*ab* : *cd*-*aa* : *bd*)	+ 1.59245	+ 1.33355	−0.25890
N-D	(*ab* : *cd*-*aa* : *bb*)	+ 5.65218	+ 3.77742	−1.87477
	(*ac* : *bd*-*aa* : *bb*)	+ 3.27535	+ 3.91720	+0.64186
M-M	(*ab* : *cc*-*bd* : *cc*)	−15.84698	−13.36064	+2.48634
	(*ab* : *cc*-*ac* : *bb*)	+12.30104	+12.62430	+0.32326
M-D	(*ab* : *cc*-*cc* : *dd*)	− 2.67620	− 0.68669	+1.98951
	(*ab* : *cc*-*bb* : *dd*)	0	+ 0.00740	+0.00740
D-D	(*aa* : *cc*-*aa* : *bb*)	− 4.59603	− 3.53324	+1.06278
	(*aa* : *cc*-*bb* : *dd*)	0	+ 0.00492	+0.00492

* Values are in electron volts.

** N, M and D mean non-polar, mono-polar, and di-polar structures respectively.

7) C. A. Coulson, "Valence", Oxford University Press, Oxford (1952), p. 237.

of *trans*-butadiene and cyclobutadiene molecules.

When the numerical values of the molecular integrals are taken from Parr and Mulliken[8] for *trans*-butadiene and from Craig[9] for cyclobutadiene, the results of Table I for the resonance integrals are obtained. In the table *a*, *b*, *c* and *d* are carbon atoms and are marked in order from one end of the molecule to the other for *trans*-butadiene and clockwise beginning with the left upper atom for cyclobutadiene. $ij : kl$ $(i \neq j, k \neq l)$ is the resonance structure in which there are π-electronic covalent bonds between atoms i and j, k and l. $ii : kl$ is that in which an atom i possesses a lone pair of π-electrons. $(ij : kl - pq : rs)$ means the interaction between structures $ij : kl$ and $pq : rs$.

$$(ij : kl - pq : rs) = \int \Psi_{ij:kl} H \Psi_{pq:rs} \mathrm{d}v_1 \mathrm{d}v_2 \mathrm{d}v_3 \mathrm{d}v_4$$

were $\Psi ij : kl$ is the normalized bond eigenfunction corresponding to the structure $ij : kl$, $\mathrm{d}v_i$ is the volume element for electron i, and H is the Hamiltonian operator commonly employed in considerations of π-electronic system

$$H = \sum_i H_{\mathrm{core}}(i) + (1/2) \sum_{\substack{i,j \\ i \neq j}} (e^2/r_{ij})$$

where

$$H_{\mathrm{core}}(i) = T(i) + U_{\mathrm{core}}(i)$$

$T(i)$ is the kinetic energy operator for electron i, and $U_{\mathrm{core}}(i)$ is the potential energy operator for this electron in the field of the core.

Numerical values in column 3 in Table I are results obtained by neglecting the multiple exchange integrals*. The integrals taken into account are of the following type:

$$Q_0 = \int \cdots\cdots a(1)b(2)c(3)d(4)e(5)f(6) \cdots\cdots H \cdots\cdots a(1)b(2)c(3)d(4)e(5)f(6) \cdots\cdots \mathrm{d}\tau$$

$$Q_1 = \int \cdots\cdots a(1)b(2)c(3)c(4)e(5)f(6) \cdots\cdots H \cdots\cdots a(1)b(2)c(3)c(4)e(5)f(6) \cdots\cdots \mathrm{d}\tau$$

$$Q_2 = \int \cdots\cdots a(1)b(2)b(3)d(4)d(5)f(6) \cdots\cdots H \cdots\cdots a(1)b(2)b(3)d(4)d(5)f(6) \cdots\cdots \mathrm{d}\tau$$

and the coulomb integrals Q_i's for the other higher polar structures:

$$K = \int \cdots\cdots a(1)b(2)c(3)d(4)e(5)f(6) \cdots\cdots H \cdots\cdots a(1)b(2)c(3)c(4)e(5)f(6) \cdots\cdots \mathrm{d}\tau$$

$$J_0 = \int \cdots\cdots a(1)b(2)c(3)d(4)e(5)f(6) \cdots\cdots H \cdots\cdots a(1)b(2)d(3)c(4)e(5)f(6) \cdots\cdots \mathrm{d}\tau$$

$$J_1 = \int \cdots\cdots a(1)b(2)c(3)d(4)e(5)f(6) \cdots\cdots H \cdots\cdots a(1)b(2)b(3)d(4)d(5)f(6) \cdots\cdots \mathrm{d}\tau$$

$$J_2 = \int \cdots\cdots a(1)b(2)b(3)d(4)e(5)f(6) \cdots\cdots H \cdots\cdots a(1)b(2)c(3)d(4)d(5)f(6) \cdots\cdots \mathrm{d}\tau$$

where $k(i)$ is the atomic orbital of the i-th electron on atom k and $\mathrm{d}\tau$ is the product of the volume elements for all the π-electrons.

Values in column 4 in the same table are results in which all types of integrals have been taken into account in the calculations.

In this table, only the results for the interactions of the resonance structures are shown in which the differences in the results for the approximate treatment from those for the exact one are the largest or the smallest for each kind.

Numerical values of the last column in Table I are of the same order as the penetration and coulomb-exchange integrals over atomic orbitals[8,9]. Particularly, in interactions between ionic structures and covalent structures or ionic structures, the lowest order of multiple exchange integrals L_i's appear, namely:

$$L_1 = \int \cdots a(1)b(2)c(3)d(4)e(5)f(6)g(7)h(8) \cdots H \cdots a(1)b(2)d(3)c(4)e(5)e(6)g(7)h(8) \cdots \mathrm{d}\tau$$

$$L_2 = \int \cdots a(1)b(2)c(3)d(4)e(5)f(6)g(7)h(8) \cdots H \cdots a(1)b(2)b(3)d(4)d(5)f(6)f(7)h(8) \cdots \mathrm{d}\tau$$

$$L_3 = \int \cdots a(1)b(2)c(3)c(4)e(5)f(6)g(7)h(8) \cdots H \cdots a(1)b(2)d(3)d(4)e(5)e(6)g(7)h(8) \cdots \mathrm{d}\tau$$

In the computations in which this kind of integral appears frequently, the influence of the multiple exchange integrals will be larger than that in the Heitler-London method because in the Heitler-London method the J_i' type of integrals,

$$J_0' = \int \cdots a(1)b(2)c(3)d(4)e(5)f(6)g(7)h(8) \cdots H \cdots a(1)b(2)d(3)c(4)f(5)e(6)g(7)h(8) \cdots \mathrm{d}\tau$$

$$J_1' = \int \cdots a(1)b(2)d(3)c(4)e(5)f(6)g(7)h(8) \cdots H \cdots a(1)b(2)c(3)d(4)f(5)e(6)g(7)h(8) \cdots \mathrm{d}\tau$$

appear as the lowest order multiple exchange integrals and are approximately equal to L_iS, where S is the overlap integral**.

8) R. G. Parr and R. S. Mulliken, *J. Chem. Phys.*, **18**, 1338 (1950).

9) D. P. Craig, *Proc. Roy. Soc.*, **A202**, 498 (1950).

* The use here of the term "multiple exchange integral" is not strictly correct. It is used conveniently for the higher orders of integrals, whose corresponding integrals, When the Hamiltonian operator is substituted for the unit operator, are more than the three order of overlap integrals.

** It will go without saying that the multiple exchange integrals which appear among atoms with nearer distances are more important than the non-multiple exchange integrals in the farther ones.

Use of the Orthogonalized Atomic Orbitals and Classification of Resonance Structures

From these considerations it seems that for quantitative or at least semi-quantitative computations of the π-electronic states of molecules, including the ionic structures besides the covalent ones, multiple exchange integrals must be taken into consideration.

One of the manners of classification of resonance structures which may easily be thought of is that in which covalent structures, monopolar structures, and di-polar structures, etc., are assigned to respective classes. It is, however, entirely inadequate to apply this manner to the quantitative calculations of polyatomic molecules, because in complex molecules the explicit evaluations of the multiple exchange integrals are extremely troublesome. Orthogonalized atomic orbitals[10] are, therefore, generally used to avoid this difficulty.

Actually, when only the covalent structures are assigned to a class, the integral types appearing in calculations are Q_0, J_0 and the other higher order ones. In cases when orthogonalized atomic orbitals are used, Q_0 is a mere additive term in each energy level and J_0 is generally repulsive, as can be inferred from the following expanded expression:

$$\overline{J_0}=\sum_{\substack{k\\ k\neq c,d}}\overline{\alpha}_k\overline{S}^2_{cd}+2\overline{\beta}_{cd}\overline{S}_{cd}+(1/2)\sum_{\substack{k,l\\ k\neq c,d\\ l\neq c,d,k}}(\overline{k}\overline{k}\mid\overline{l}\overline{l})\overline{S}^2_{cd}$$
$$+2\sum_{\substack{l\\ l\neq c,d}}(\overline{c}\overline{d}\mid\overline{l}\overline{l})\overline{S}_{cd}+(\overline{c}\overline{d}\mid\overline{c}\overline{d}),$$

where

$$\overline{\alpha}_k=\int\overline{k}(i)H_{\mathrm{core}}(i)\overline{k}(i)\mathrm{d}v_i$$

$$\overline{\beta}_{kl}=\int\overline{k}(i)H_{\mathrm{core}}(i)\overline{l}(i)\mathrm{d}v_i$$

$$\overline{S}_{kl}=\int\overline{k}(i)\overline{l}(i)\mathrm{d}v_i$$

$$(\overline{k}\overline{l}\mid\overline{p}\overline{q})=e^2\int(1/r_{ij})\overline{k}(i)\overline{l}(i)\overline{p}(j)\overline{q}(j)\mathrm{d}v_i\mathrm{d}v_j$$

where $\overline{k}(i)$ is the orthogonalized atomic orbital for the atomic orbital $k(i)$.

It will be understood by a procedure similar to that for $\overline{J_0}$ that the other higher order multiple exchange integrals lead to zeros.

It is ultimately deduced that, when the orthogonalized atomic orbitals are employed, the integral type, playing the most important role for the resonance effect of a molecule, is type $\overline{K}$, whose expanded expression is

$$\overline{K}=\sum_{\substack{k\\ k\neq d}}\overline{\alpha}_k\overline{S}_{cd}+\overline{\beta}_{cd}+(1/2)\sum_{\substack{k,l\\ k\neq d\\ l\neq d,k}}(\overline{k}\overline{k}\mid\overline{l}\overline{l})S_{cd}$$
$$+\sum_{\substack{l\\ l\neq d}}(\overline{c}\overline{d}\mid\overline{l}\overline{l})$$

It can be understood from the integral form of type K that, when including this type of integral in calculations, the ionic structures must always be included in each class of the classification.

From these considerations, the following manner of classification of resonance structures is proposed.

A covalent structure K and all the ionic structures, in which the two π-electrons on a certain bond in the structure K occupy the same atomic orbital on either side of the atom for the bond, are assigned to class K. Then the normalized bond eigenfunctions Ψ_L's corresponding to all the resonance structures I's belonging to this class are combined linearly, viz.,

$$\phi_i^K=\sum_L C_L^K\Psi_L$$

C_L^K is the coefficient of the bond eigenfunction Ψ_L and is determined by the variational method together with the normalization condition. ϕ_i^K is the function associated with class K, and the corresponding energy is E_i^K.

The function ϕ_i^K may be derived from the other covalent structures. Wave functions Φ_j's for the electronic states of the molecule are assumed to be linear combinations of the linearly independent ϕ_i^K's,

$$\Phi_j=\sum_K C_i^K\Phi_i^K$$

The values of the coefficients C_i^K's are, again, determined by the use of the variational method and the normalization condition. The resulting energies are denoted by E_j's.

Probabilities of Resonance Structures, π-Electron Densities and Bond Orders

Electron density and bond order have been discussed and have also been defined variously from the points of view of the molecular orbital method and the valence bond method[11]. Since, however, analyses of these definitions are not our principal purpose, in this paper the contributive probabilities of resonance structures, π-electron densities, and bond orders are first defined for the straightforward HLSP valence bond method by the most conventional

10) P. O. Löwdin, *J. Chem. Phys.*, **18**, 365 (1950); **21**, 496 (1953).

11) L. Pauling, L. O. Brockway and J. Y. Beach, *J. Am. Chem. Soc.*, **57**, 2705 (1935); C. A. Coulson and H. C. Longuet-Higgins, *Proc. Roy. Soc.*, **A191**, 39 (1947); W. G. Penny, ibid., **A158**, 306 (1937); R. McWeeny, ibid., **A223**, 63 (1954).

expressions, and then a definition of them on the basis of our approximate method is made on that basis.

The Straightforward HLSP Method.—When the wave function Φ_G for the ground state of a molecule is represented by

$$\Phi_G=\sum_L C_L\Psi_L$$

where Ψ_L is the normalized bond eigenfunction for structure L and C_L is the coefficient, the probability P_L for structure L is

$$P_L=C_L\sum_J C_J\int\Psi_L\Psi_J\mathrm{d}\tau$$

and the π-electron density D_i in atom i is

$$D_i=\sum_L P_L m(i)_L$$

where $m(i)_L$ is the number of π-electrons in atom i in structure L. The bond order B_{ij} between atoms i and j is

$$B_{ij}=\sum_L P_L\,[n(ij)_L+1]$$

where $n(ij)_L$ is the number of π-electronic covalent bonds between atoms i and j in structure L.

The approximate method.—1) The probability P_L^K of structure L in class K is

$$P_L^K=C_L^K\sum_J C_J^K\int\Psi_L\Psi_J\mathrm{d}\tau$$

where C_L^K is the coefficient of the bond eigenfunction Ψ_L in the wave function ϕ_1^K for the ground state of this class.

The π-electron density D_i^K in atom i in the ground state of class K is

$$\mathrm{D}_i^K=\sum_J P_J^K m(i)_J^K$$

where $m(i)_J^K$ is the number of π-electrons in atom i in structure J in class K. The bond order B_{ij}^K between atoms i and j in this state of class K is

$$B_{ij}^K=\sum_J P_J^K\,[n(ij)_J^K+1]$$

where $n(ij)_J^K$ is the number of π-electronic covalent bonds between atoms i and j in structure J in class K.

2) The probability P^K of the class K in the ground state of the molecule under consideration is represented by

$$P^K=C_1^K\sum_J C_1^J\int\phi_1^K\phi_1^J\mathrm{d}\tau$$

Therefore, the probability P_L of structure L is

$$P_L=\sum_J P^J P_L^J$$

the π-electron density D_i of atom i is

$$D_i=\sum_J P^J D_i^J$$

and the bond order B_{ij} between atoms i and j is

$$B_{ij}=\sum_J P^J B_{ij}^J$$

Survey of the Approximate Method and the Excited States

It must now be explained to what kind approach our method belongs. When a conjugated molecule is interpreted to be due to the σ-bond between parts, each of which contains a double bond, the wave functions representing the π-electronic states of this hypothetical molecule K are ϕ_i^K's in our approximation, and the energy values E_i^K's are obtained by solving the following equation:

$$H\phi_i^K=E_i^K\phi_i^K$$

Since, from the point of view of the valence bond method, the parts due to the π-bond between two non-neighboring atoms may be supposed, such hypothetical molecules K's can be found by the same number as all the π-type covalent structures conceivable for the molecule under consideration. The corresponding wave functions are ϕ_i^K's for all the class K's in our approximation. Wave functions Φ_i's for the electronic states of the entire molecule may, therefore, be represented by linear combinations of these linearly independent functions ϕ_i^K's.

Our approximate method is based on a hypothetical interpretation of the structures of molecules rather than on a mathematical approximation. In the Heitler-London method the basic functions Ψ_K's correspond to covalent structures. On the other hand, the functions ϕ_i^K's in our method mean that the π-bond between the two atoms is not the so-called "covalent bond", but is partly ionic.

For obtaining wave functions corresponding to the excited states of a molecule, number of wave functions in each class should be considered as a step in calculating the interaction of classes. It is not easy to find such wave functions however. In the practical calculations given in a later paper, therefore, an assumption will be made that the wave functions ϕ_i^K's for the lowest energies belonging to the respective symmetries in class K are employed as the wave functions associated with this class.

Our method may now also be applied successfully to computations using non-orthogonal atomic orbitals and Slater functions, as well as the orthogonalized atomic orbitals. An example based on the non-orthogonal atomic orbitals will be shown in Part II, where the energy levels evaluated by our approximaxe method are lower than the corresponding ones obtained by the Heitler-London method.

In the examples of Parts II–IV, the orthogonalization of the atomic orbitals is not made,

except in cases where it is especially required. This is because, since the approximate procedure is generally made for the orthogonalization, the accuracy of the results is lower than that for calculations based on the non-orthogonal atomic orbitals, considering all the overlap and exchange integrals. Particularly for a molecule with a lower symmetry, matrix S does not commute with matrix H[10], and the procedure for the orthogonalization is more troublesome than expected.

Summary

The influence of the multiple exchange integrals in the HLSP method for the π-electronic systems has been investigated by means of the illustrations of *trans*-butadiene and cyclobutadiene molecules. Their importance for the theory, including ionic structures, has been emphasized. For avoiding difficulties in calculations due to the presence of many resonance structures in complex compounds, an approximate method has been proposed. In that method, the degree of energy determinants is diminished.

The author wishes to express his sincere thanks to Professor Kyosuke Omori, Kyushu University, for his continual encouragement and helpful, discussions on the subjects. Thanks are also due to Professor Saburo Nagakura, The University of Tokyo, suggestions and criticisms, and to Professor Eiichi Ishiguro, Ochanomizu University, for his extremely helpful discussions and readings of the manuscripts.

Faculty of Liberal Arts
Nagasaki University
Ohashi, Nagasaki

De-localization of Bond Eigenfunctions in π-Electronic Systems. II. Non-Empirical Calculation of the π-Electronic States of the trans-Butadiene Molecule

By Shozaburo TAKEKIYO

(Received October 21, 1960)

trans-Butadiene is a simple molecule, suitable for considering the π-electronic states of conjugated chain compounds consisting of homonuclear atoms.

Non-empirical treatment of *trans*-butadiene molecule was first undertaken by Parr and Mulliken[1], using the ASMO SCF method, and the wave function for the ground state and the energy levels were calculated. The method of molecular orbitals with configuration interaction has been applied to the study of the π-electronic structure of the molecule by Coulson and Jacobs[2]. Then the influences of the configuration interaction procedure upon the LCAO SCF treatment was investigated by Pullman and Baudet[3].

It does not appear that treatments by the valence bond method have been undertaken. In this paper, the approximate method proposed by us in part I[4] is applied to the calculation of the π-electronic states of the *trans*-butadiene molecule. The wave functions, energy levels, electron densities, and bond orders are evaluated. These results are compared with those, obtained by the molecular orbital method.

Classification of Resonance Structures

The skeleton of the *trans*-butadiene molecule is shown in Fig. 1. Slater $2p_\pi$-orbitals with the effective nuclear charge $Z_C=3.18$ have been

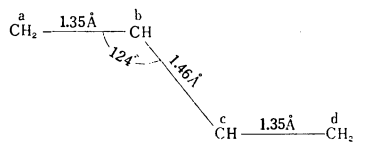


Fig. 1. Skeleton of *trans*-butadiene molecule.

assumed for the atomic orbitals of the carbon atoms. Integrals over atomic orbitals have been taken from Parr and Mulliken[1]. Calculations have been carried out, considering all kinds of overlap, single exchange, and multiple exchange integrals.

Three classes of the canonical structures,

1) R. G. Parr and R. S. Mulliken, *J. Chem. Phys.*, **18**, 1338 (1950).
2) C. A. Coulson and J. Jacobs, *Proc. Roy. Soc.*, **A206**, 287 (1951).
3) A. Pullman and J. Baudet, *Compt. rend.*, **233**, 241 (1954); A. Pullman, *J. chim. phys.*, **51**, 188 (1954).
4) S. Takekiyo, This Bulletin, **35**, 355 (1962).

TABLE I. WAVE FUNCTIONS ASSOCIATED WITH CLASSES AND THE CORRESPONDING ENERGY VALUES

A-Class

$$\phi_1{}^A(^1A_g) = 0.69650\Psi_A + 0.16134(\Psi_{D1}+\Psi_{D2}) + 0.14379(\Psi_{E1}+\Psi_{E2}) + 0.042833(\Psi_{J1}+\Psi_{J2}) + 0.026672\Psi_L + 0.019308\Psi_M \qquad E_1{}^A = -51.009 \text{ eV.}$$

$$\phi_2{}^A(^1B_u) = 0.43857(\Psi_{D1}-\Psi_{D2}) + 0.37715(\Psi_{E1}-\Psi_{E2}) + 0.23695(\Psi_{J1}-\Psi_{J2}) \qquad E_2{}^A = -39.782 \text{ eV.}$$

$$\phi_3{}^A(^1A_g) = -0.077807\Psi_A + 0.47244(\Psi_{D1}+\Psi_{D2}) - 0.43306(\Psi_{E1}+\Psi_{E2}) + 0.0^273967(\Psi_{J1}+\Psi_{J2}) + 0.17201\Psi_L - 0.13351\Psi_M \qquad E_3{}^A = -38.842 \text{ eV.}$$

$$\phi_4{}^A(^1A_g) = 0.93567\Psi_A - 0.29682(\Psi_{D1}+\Psi_{D2}) - 0.36520(\Psi_{E1}+\Psi_{E2}) - 0.29357(\Psi_{J1}+\Psi_{J2}) - 0.12725\Psi_L - 0.13294\Psi_M \qquad E_4{}^A = -35.562 \text{ eV.}$$

$$\phi_5{}^A(^1B_u) = 0.54520(\Psi_{D1}-\Psi_{D2}) - 0.57878(\Psi_{E1}-\Psi_{E2}) - 0.022620(\Psi_{J1}-\Psi_{J2}) \qquad E_5{}^A = -35\cdot463 \text{ eV.}$$

$$\phi_6{}^A(^1A_g) = -0.25850\Psi_A + 0.14459(\Psi_{D1}+\Psi_{D2}) + 0.20197(\Psi_{E1}+\Psi_{E2}) - 0.60574(\Psi_{J1}+\Psi_{J2}) + 0.48110\Psi_L + 0.40945\Psi_M \qquad E_6{}^A = -27.549 \text{ eV.}$$

$$\phi_7{}^A(^1B_u) = 0.44326(\Psi_{D1}-\Psi_{D2}) + 0.45714(\Psi_{E1}-\Psi_{E2}) - 0.79353(\Psi_{J1}-\Psi_{J2}) \qquad E_7{}^A = -25.046 \text{ eV.}$$

$$\phi_8{}^A(^1A_g) = 0.092798\Psi_A - 0.48255(\Psi_{D1}+\Psi_{D2}) + 0.32118(\Psi_{E1}+\Psi_{E2}) + 0.081012(\Psi_{J1}+\Psi_{J2}) + 0.86399\Psi_L - 0.75270\Psi_M \qquad E_8{}^A = -21.918 \text{ eV.}$$

$$\phi_9{}^A(^1A_g) = -0.64760\Psi_A + 0.57117(\Psi_{D1}+\Psi_{D2}) + 0.65752(\Psi_{E1}+\Psi_{E2}) - 0.48308(\Psi_{J1}+\Psi_{J2}) - 0.59975\Psi_L - 0.77956\Psi_M \qquad E_9{}^A = -19.172 \text{ eV.}$$

B-Class

$$\phi_1{}^B(^1A_g) = 0.87202\Psi_B - 0.028051(\Psi_{F1}+\Psi_{F2}) + 0.14073(\Psi_{G1}+\Psi_{G2}) - 0.073901(\Psi_{J1}+\Psi_{J2}) + 0.0^215347(\Psi_{K1}+\Psi_{K2}) \qquad E_1{}^B = -47.593 \text{ eV.}$$

$$\phi_2{}^B(^1B_u) = 0.30402(\Psi_{F1}-\Psi_{F2}) - 0.57044(\Psi_{G1}-\Psi_{G2}) + 0.18725(\Psi_{J1}-\Psi_{J2}) - 0.0^218986(\Psi_{K1}-\Psi_{K2}) \qquad E_2{}^B = -37.334 \text{ eV.}$$

$$\phi_3{}^B(^1A_g) = -0.38216\Psi_B - 0.47364(\Psi_{F1}+\Psi_{F2}) + 0.22006(\Psi_{G1}+\Psi_{G2}) - 0.33059(\Psi_{J1}+\Psi_{J2}) - 0.0^240435(\Psi_{K1}+\Psi_{K2}) \qquad E_3{}^B = -35.532 \text{ eV.}$$

$$\phi_4{}^B(^1B_u) = -0.31915(\Psi_{F1}-\Psi_{F2}) - 0.43752(\Psi_{G1}-\Psi_{G2}) - 0.40064(\Psi_{J1}-\Psi_{J2}) - 0.0^271229(\Psi_{K1}-\Psi_{K2}) \qquad E_4{}^B = -34.700 \text{ eV.}$$

$$\phi_5{}^B(^1A_g) = 0.49807\Psi_B - 0.0^269394(\Psi_{F1}+\Psi_{F2}) - 0.67697(\Psi_{G1}+\Psi_{G2}) - 0.31260(\Psi_{J1}+\Psi_{J2}) - 0.0^237628(\Psi_{K1}+\Psi_{K2}) \qquad E_5{}^B = -34.439 \text{ eV.}$$

$$\phi_6{}^B(^1B_u) = 0.59232(\Psi_{F1}-\Psi_{F2}) + 0.12105(\Psi_{G1}-\Psi_{G2}) - 0.60224(\Psi_{J1}-\Psi_{J2}) + 0.033251(\Psi_{K1}-\Psi_{K2}) \qquad E_6{}^B = -28.715 \text{ eV.}$$

$$\phi_7{}^B(^1A_g) = -0.32135\Psi_B + 0.56549(\Psi_{F1}+\Psi_{F2}) + 0.25634(\Psi_{G1}+\Psi_{G2}) - 0.58847(\Psi_{J1}+\Psi_{J2}) + 0.035068(\Psi_{K1}+\Psi_{K2}) \qquad E_7{}^B = -28.281 \text{ eV.}$$

$$\phi_8{}^B(^1B_u) = -0.28248(\Psi_{F1}-\Psi_{F2}) - 0.022139(\Psi_{G1}-\Psi_{G2}) + 0.064216(\Psi_{J1}-\Psi_{J2}) + 0.74692(\Psi_{K1}-\Psi_{K2}) \qquad E_8{}^B = -13.440 \text{ eV.}$$

$$\phi_9{}^B(^1A_g) = 0.019928\Psi_B - 0.28298(\Psi_{F1}+\Psi_{F2}) - 0.026408(\Psi_{G1}+\Psi_{G2}) + 0.065243(\Psi_{J1}+\Psi_{J2}) + 0.74685(\Psi_{K1}+\Psi_{K2}) \qquad E_9{}^B = -13.438 \text{ eV.}$$

C-Class

$$\phi_1{}^C(^1A_g) = -0.98330\Psi_C + 0.028834(\Psi_{H1}+\Psi_{H2}) + 0.0^386563(\Psi_{I1}+\Psi_{I2}) + 0.0^345712(\Psi_{K1}+\Psi_{K2}) + 0.071200\Psi_L + 0.065556\Psi_M \qquad E_1{}^C = -45.823 \text{ eV.}$$

$$\phi_2{}^C(^1A_g) = -0.082603\Psi_C + 0.38780(\Psi_{H1}+\Psi_{H2}) - 0.51862(\Psi_{I1}+\Psi_{I2}) + 0.033300(\Psi_{K1}+\Psi_{K2}) + 0.21597\Psi_L + 0.090028\Psi_M \qquad E_2{}^C = -36.466 \text{ eV.}$$

$$\phi_3{}^C(^1B_u) = -0.43587(\Psi_{H1}-\Psi_{H2}) + 0.52025(\Psi_{I1}-\Psi_{I2}) - 0.036205(\Psi_{K1}-\Psi_{K2}) \qquad E_3{}^C = -35.808 \text{ eV.}$$

$$\phi_4{}^C(^1A_g) = -0.015013\Psi_C - 0.54691(\Psi_{H1}+\Psi_{H2}) - 0.37571(\Psi_{I1}+\Psi_{I2}) + 0.0^249540(\Psi_{K1}+\Psi_{K2}) + 0.31388\Psi_L - 0.21248\Psi_M \qquad E_4{}^C = -32.938 \text{ eV.}$$

$$\phi_5{}^C(^1B_u) = 0.55945(\Psi_{H1}-\Psi_{H2}) + 0.47970(\Psi_{I1}-\Psi_{I2}) - 0.010689(\Psi_{K1}-\Psi_{K2}) \qquad E_5{}^C = -32.242 \text{ eV.}$$

$$\phi_6{}^C(^1A_g) = 0.16167\Psi_C + 0.069125)\Psi_{H1}+\Psi_{H2}) + 0.29043(\Psi_{I1}+\Psi_{I2}) - 0.019480(\Psi_{K1}+\Psi_{K2}) + 0.92172\Psi_L + 0.15536\Psi_M \qquad E_6{}^C = -28.849 \text{ eV.}$$

$$\phi_7{}^C(^1A_g) = -0.11281\Psi_C + 0.22034(\Psi_{H1}+\Psi_{H2}) + 0.082154(\Psi_{I1}+\Psi_{I2}) + 0.0^242028(\Psi_{K1}+\Psi_{K2}) + 0.10382\Psi_L - 0.96407\Psi_M \qquad E_7{}^C = -28.340 \text{ eV.}$$

$$\phi_8{}^C(^1B_u) = -0.046027(\Psi_{H1}-\Psi_{H2}) + 0.064809(\Psi_{I1}-\Psi_{I2}) + 0.71216(\Psi_{K1}-\Psi_{K2}) \qquad E_8{}^C = -15.538 \text{ eV.}$$

$$\phi_9{}^C(^1Ag) = 0.0^224620\Psi_C - 0.045969(\Psi_{H1}+\Psi_{H2}) + 0.065435(\Psi_{I1}+ + \Psi_{I2}) + 0.70753(\Psi_{K1}+\Psi_{K2}) + 0.013931\Psi_L + 0.0^288951\Psi_M \qquad E_9{}^C = -15.538 \text{ eV.}$$

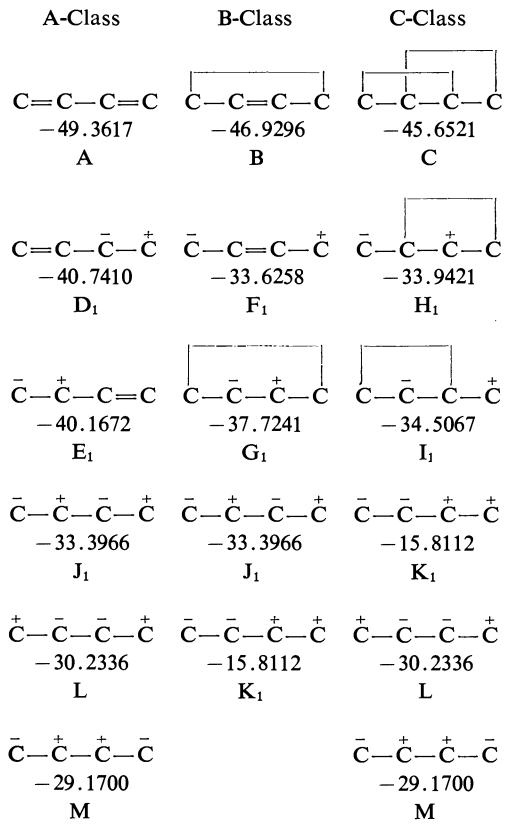


Fig. 2. Classification of resonance structures and the energy values for the structures.

K_2's are given by inversion with respect to the center of molecule from K_1's. Values are in electron volts and are relative to $4W_{2p}$, where W_{2p} is the energy of a $2p_\pi$-electron of a carbon atom in its valence state.

derived from the three covalent structures, and the corresponding energy values are shown in Fig. 2.

Wave functions ϕ_i^K's, associated with class K, and the corresponding energy values E_i^K's are shown in Table I, where Ψ_L is the normalized bond eigenfunction for structure L.

Then, the probability P_L^K of structure L, the π-electrons densities, and the bond orders in class K have been evaluated. Results are shown in Table II and Fig. 3.

A-Class

$$\underset{0.98604}{H_2C} \overset{1.81229}{\text{——}} \underset{1.01396}{CH} \overset{1}{\text{——}} \underset{1.01396}{CH} \overset{1.81229}{\text{——}} \underset{0.98604}{CH_2}$$

B-Class

$$\underset{1}{H_2C} \overset{1}{\text{——}} \underset{1}{CH} \overset{1.85500}{\text{——}} \underset{1}{CH} \overset{1}{\text{——}} \underset{1}{CH_2}$$

C-Class

$$\underset{0.99996}{H_2C} \overset{1}{\text{——}} \underset{1.00004}{CH} \overset{1}{\text{——}} \underset{1.00004}{CH} \overset{1}{\text{——}} \underset{0.99996}{CH_2}$$

Fig. 3. π-Electron densities and bond orders in each class.

Interaction of the Classes

Wave functions, associated with the classes, have been linearly combined, and the wave functions Φ_i's for the molecule and the corresponding energy values E_i's have been calculated These results are shown in Table III.

Probabilities P^K's of class K's are obtained as follows:

$$P^A=0.84750 \quad P^B=0.1243 \quad 7P^C=0.028126$$

TABLE II. PROBABILITIES OF STRUCTURES IN EACH CLASS

A-class

A	D_i	E_i	J_i	L	M
0.65965	0.082133	0.070506	0.011625	0.0^270777	0.0^247473

B-class

B	F_i	G_i	J_i	K_i
0.85038	0.0^223063	0.060866	0.011658	-0.0^423156

C-class

C	H_i	I_i	K_i	L	M
0.97770	0.0^399973	-0.0^577684	0.0^511362	0.010676	0.0^296326

TABLE III. WAVE FUNCTIONS FOR THE MOLECULE AND THE CORRESPONDING ENERGY VALUES

$\Phi_1(^1A_g)=0.85295\phi_1{}^A+0.19279\phi_1{}^B-0.06290\phi_1{}^C$ $E_1=-51.0989$ eV.
$\Phi_2(^1A_g)=0.37406\phi_1{}^A-0.83569\phi_1{}^B-0.37448\phi_1{}^C$ $E_2=-45.2366$ eV.
$\Phi_3(^1B_u)=0.61613\phi_2{}^A+0.35938\phi_2{}^B-0.35463\phi_3{}^C$ $E_3=-41.4287$ eV.
$\Phi_4(^1B_u)=0.86007\phi_2{}^A-0.60375\phi_2{}^B+0.38005\phi_3{}^C$ $E_4=-37.1047$ eV.
$\Phi_5(^1A_g)=3.24187\phi_1{}^A-2.93339\phi_1{}^B+2.97114\phi_1{}^C$ $E_5=-32.8775$ eV.
$\Phi_6(^1B_u)=0.00758\phi_2{}^A-0.95755\phi_2{}^B-1.03260\phi_3{}^C$ $E_6=-26.9595$ eV.

TABLE IV. PROBABILITIES OF RESONANCE STRUCTURES

A	B	D_i	E_i	F_i	G_i
0.57280	0.11951	0.06961	0.05975	0.00029	0.00757
H_i	I_i	J_i	K_i	L	M
0.00003	0.00000	0.01130	0.00000	0.00630	0.00429

From these values, the probabilities P_L's of structure L's, the π-electron densities, and the bond orders in the molecule have been computed. Results are shown in Table IV and Fig. 4.

$$\underset{0.9882}{H_2C} \overset{1.6884}{\text{———}} \underset{1.0118}{CH} \overset{1.1063}{\text{———}} \underset{1.0118}{CH} \overset{1.6884}{\text{———}} \underset{0.9882}{CH_2}$$

Fig. 4. π-Electron densities and bond orders.

Comparison with Other Methods

Calculations have also been performed by the Heitler-London method, including all kinds of overlap, single exchange, and multiple exchange, integrals. The results are as follows:

$$\Phi_1(^1A_g) = 0.90568\Psi_A + 0.15086\Psi_B$$
$$E_1 = -49.4312 \text{ eV}.$$
$$\Phi_2(^1A_g) = 0.81991\Psi_A - 1.21233\Psi_B$$
$$E_2 = -44.8795 \text{ eV}.$$

The probabilities of the two covalent structures are

$$P_A = 0.89875 \qquad P_B = 0.10125$$

and the π-electron densities and the bond orders are given in Fig. 5.

In Fig. 6, the energy levels, obtained above, are shown, together with the results found by the molecular orbital method.

From this figure, it can be seen that the values obtained by our approximate method agree quantitatively with those obtained by the ASMO SCF CI method[5]. The energy value for the ground state computed for the class, derived from the most stable covalent structure, is more satisfactory than that by the Heitler-London method. In the calculation due to that single class. however, it is impossible to obtain the correct order of the levels of the molecule*.

$$\underset{1}{H_2C} \overset{1.89875}{\text{———}} \underset{1}{CH} \overset{1.10125}{\text{———}} \underset{1}{CH} \overset{1.89875}{\text{———}} \underset{1}{CH_2}$$

Fig. 5. π-Electron densities and bond orders (Heitler-London method).

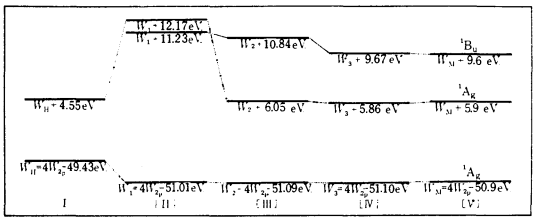


Fig. 6. Comparison of energy levels.
I, The Heitler-London method. II, A-class. III, A-, B-class interaction. IV, A-, B-, C-class interaction. V, The ASMO SCF CI method[5].

The π-electron densities obtained by the ASMO SCF CI method are:

$$D_a = D_d = 0.978 \qquad D_b = D_c = 1.022^{3)}$$

and are in good agreement with our results (Fig. 4).

One of the causes of the success of our method is that the ionic structures are always considered; this point is a difference between our method and the conventional approximate methods.

Summary

An approximate method, proposed in Part I, has been applied to the non-empirical calculation of the π-electronic states of the *trans*-butadiene molecule. All the higher orders of overlap and exchange integrals have been considered. Slater $2p_\pi$-orbitals have been used through out. The values of the energy levels obtained are −51.099 eV. (^1A_g), −45.237 eV. (^1A_g), and −41.429 eV. (^1B_u). The π-electron densities for the ground state are $D_a = D_d = 0.988$, and $D_b = D_c = 1.012$. These results agree quantitatively with those evaluated by the ASMO SCF CI method.

The author wishes to express his sincere gratitude to Professor Kyosuke Omori, Kyushu University, for his helpful criticisms and suggestions. Thanks are also due to Professor Saburo Nagakura, The University of Tokyo for his advice and valuable assistance, and to Professor Eiichi Ishiguro, Ochanomizu University, who has read the manuscript and helped the author to remove obscurities.

Faculty of Liberal Arts
Nagasaki University
Ohashi, Nagasaki

5) Y. Mori, ibid., **28**, 291 (1956).

* In Fig. 6, some of the levels obtained by our mothod are lower than the corresponding levels found by the ASMO SCF CI method. The cause of this appearance seems to be due to intermediate approximations in numerical calculations.

SHORT COMMUNICATIONS

*Presence of a New Species of Titanium-Titanochloroform**

By Isao SHIIHARA, Jun IYODA and Kazuko SUGITA

(Received December 6, 1961)

Titanochloroform or titanium hydrotrichloride[1], $HTiCl_3$, is one of the supposed intermediates in the olefine polymerization by Ziegler and Natta catalysts. Recently Cooper[2] proposed the possibility of the occurrence of titanochloroform as Eq. 1.

$$\text{R-ti} \rightleftarrows \text{Olefine} + \text{H-ti} \quad (\text{ti} = 1/4\ \text{Ti}) \qquad (1)$$

But the actual existence of this compound has not been proved so far. Recently we obtained titanochloroform as a solution and the presence was evidenced by the chemical analysis and the infrared spectrum. Moreover, we could find considerable amount of H-Ti bond remaining in the solid phase of some species of titanium trichloride, especially in the so-called active form prepared by aluminum reduction of titanium tetrachloride in benzene.

Previously, we found that propylene was polymerized by the methylhydropolysiloxane modified Ziegler catalyst system, and gave silicon containing polypropylene[3]. To clarify the process, the reaction of titanium tetrachloride with triethylsilane, triphenylsilane, triethoxysilane, methylhydropolysiloxane, or methylhydrodichlorosilane, were studied and the reaction mechanism was disclosed as Eq. 2.

$$TiCl_4 + R_3SiH \longrightarrow \left[Cl_3Ti \begin{matrix} H \\ \diagup\diagdown \\ Cl \end{matrix} SiR_3 \right] \longrightarrow HTiCl_3 + R_3SiCl \downarrow TiCl_3 + 1/2H_2 \qquad (2)$$

In these experiments, the volatile fraction consisting of titanochloroform and the recovered titanium tetrachloride was obtained in a dry-ice-acetone trap by vacuum distillation of the products at room temperature. In most cases the fraction liberates hydrogen by alcoholic potash which was measured by volume. One typical example, the analysis of the condensate obtained from the reaction of titanium

TABL I. REACTION OF COMMERCIAL TITANIUM HYDRIDE TiH WITH TITANIUM TETRACHLORIDE

TiH g.	$TiCl_4$ g.	Reaction Temp. °C	Reaction Time hr.	Product g.	Analysis[a,b] Ti^{III}	Analysis[a,b] Ti^f	Analysis[a,b] $H(OH^-)$	Analysis[a,b] Cl^f, %	IR absorpn. of H-Ti[c,d] cm^{-1}
5	19	210[e] (5 atm.)	2.5	Brown liq. 5.5					1590[f] m
				Purple sol. 7.0	9.01	12.5	0.068 0.014[f]	24.0	1590 m (1635 s)[g]
3.0	31	135	7	Yellow liq. 30.2		25.4	0.044[f]	74.5	
				Purple sol. 3.1	2.63	6.14	0.044 0.035[f]	11.7	

a) Analysis was performed by the soluble part in 1 N H_2SO_4.
b) Ti: Total titanium, f: about the filtrate
c) In Nujol
d) The starting material TiH has an IR absorption at 1635 cm^{-1} (vw).
e) In 100 cc. autoclave
f) Partially hydrolyzed
g) About the benzene extract of the solid (in benzene)

* Presented at the Symposium on Organosilicon and Organometallic Compounds at Osaka, October, 1961.

1) The name was used in J. W. Melllor, "A Comprehensive Treatise on Inorganic and Theoretical Chemistry", Vol. VII, Longmans, Green and Co., Ltd., London (1927), p. 80.

2) D. Cooper and H. L. Finkbeiner, *Chem. & Eng. News*, 39, No. 37, p. 60 (1961).

3) I. Shiihara, W. Kawai and T. Ichihashi, International Symposium on Macromolecular Chemistry, Montreal, August, 1961.

tetrachloride and triphenylsilane as a benzene solution showed; Ti(total) 4.54, Cl 12.8, H(OH^- active) 0.029, Si 0.10%, and thus Cl/Ti=3.82, H/Ti=0.37. The amount of hydrogen does exist twice as much as that of the amount required from the silicon content, even if the all silicon was assumed to compose silane. This fact affords one evidence that some part of the hydrogen is originated from the volatile H-Ti containing compounds, i. e. titanochloroform in this case.

Moreover, this condensate showed a characteristic infrared absorption at 1610 cm^{-1} (m). It is plausible to consider the absorption is due to H-Ti bond stretching vibration, because the product obtained from the other route by reacting commercial titanium hydride TiH and titanium tetrachloride as Eq. 3 showed the same absorption at about 1600 cm^{-1}. These data are given in Table I.

$$TiH+3TiCl_4 \rightarrow HTiCl_3+3TiCl_3 \qquad (3)$$

The H-Ti bond was also observed in the solid phase of titanium trichloride. Analytical value and infrared data (in Nujol) of some examples are: Titanium trichloride originated from $TiCl_4+Et_3SiH$, Ti^{III} 24.8, Ti 28.7, Cl 64.6, H(OH^- active) 0.092, Si 0.70%, H-Ti absorption, at 1595 cm^{-1} (w); from $TiCl_4+(MeHSiO)_n$, Ti^{III} 10.1, Ti 14.8, H(OH^-) (about the acid extract) 0.038%, H-Ti absorption, at 1602 cm^{-1} (vs); from $TiCl_4$+Al (in benzene)[4], Ti^{III}/Ti> 95%, H-Ti absorption, at 1605 cm^{-1} (m).

This compound in high concentration is unstable liquid, and the blackening, precipitation and then gelation occurred after a few days. The studies on the isolation of titanochloroform and the catalytic action are now undertaken.

Government Industrial Research Institute, Osaka
Oyodo-ku, Osaka

4) Esso Reserch and Engineering Co., Brit. Pat.857181, Dec. 29, 1960.

Effects of Outer Anions on the Recoil Reactions in the Irradiated Hexammine-cobalt(III) Complex Compounds

By Nobufusa SAITO, Takeshi TOMINAGA and Hirotoshi SANO

(Received January 9, 1962)

It was previously reported by the present authors that various ^{60}Co-labeled species were formed through recoil reactions in the irradiated cobalt complex compounds and that among these labeled species were found such substituted products as might be produced by incorporation of outer anions of the target complex into ligands[1]. Though the mechanism of formation of these recoil species has not been fully clarified, such outer anions of the target complex must no doubt play an impotant role during the recoil reactions. In the present work, they have investigated the distribution of recoil species in various hexamminecobalt-(III) complex salts containing different kinds of outer anions in order to elucidate the role of the outer anions in recoil reactions.

Nine kinds of hexamminecobalt(III) complex salts listed in Table I were irradiated in an experimental hole in JRR-1 reactor for one or five hours at ambient temperature. Thermal neutron flux was approximately 3×10^{11} n/cm^2 sec. After bombardments, the ^{60}Co-labeled species present in aqueous solutions of the

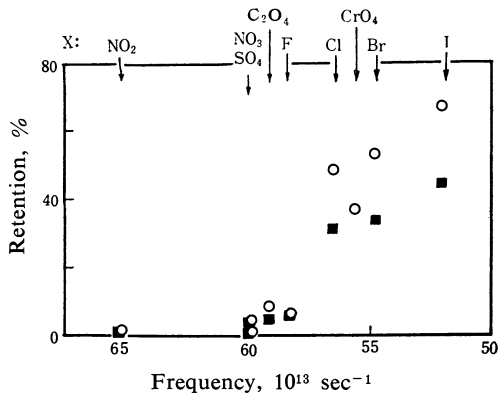


Fig. 1. The relationship between retention and frequency of the maximum in the first absorption band of $Co(NH_3)_5X$.
■ : Irradiated for one hour
○ : Irradiated for five hours

1) N. Saito, T. Tominaga and H. Sano, This Bulletin, 33, 1621 (1960).

TABLE I. PERCENTAGE DISTRIBUTION OF ^{60}Co-LABELED SPECIES IN IRRADIATED HEXAMMINECOBALT(III) COMPLEX SALTS

Target	Time of irradiation hr.	^{60}Co-labeled species, %*					
		CoA_6^{3+}	CoA_5X^{2+}	$CoA_4X_2^{+}$	Co^{2+}	CoA_3X_3	$CoA_2X_4^{-}$
$[Co(NH_3)_6](NO_2)_3$	1	0.8	5.9	20.3	53.2	15.6	4.2
	5	1.4	15.5	34.5	24.7	11.1	12.4
$[Co(NH_3)_6](NO_3)_3$	1	2.8	8.5	20.9	66.7	0.7	0.3
	5	4.4	12.1	25.4	57.8	1.7	0.3
$[Co(NH_3)_6]_2(SO_4)_3 \cdot 5H_2O$	1	0.2		2.1	96.0	1.4	0.3
	5	0.3		0.5	98.2	0.6	0.4
$[Co(NH_3)_6]_2(C_2O_4)_3$	1	3.6			96.4		
	5	≤ 10			≥ 90		
$[Co(NH_3)_6]F_3$	1	6.1	0.6	3.1	87.5	1.8	0.9
	5	6.8		2.4	88.2	1.9	0.5
$[Co(NH_3)_6]Cl_3$	1	33.4	5.2	3	57.5	2.3	—
	5	51.3	4.6	2.9	40.1	1.0	0.1
$[Co(NH_3)_6]_2(CrO_4)_3$	5	≤ 36.8			≥ 63.2		
$[Co(NH_3)_6]Br_3$	1	34.6	3.7	3	54.0	1.5	—
	5	54.2	2.8	1.3	41.0	0.7	—
$[Co(NH_3)_6]I_3$	1	45.0	5.7	5	37.4	1.3	1.2
	5	66.4	4.8	5	21.4	1.1	0.5

* A=NH_3 (or partly H_2O) ; X=NO_2, NO_3, F, Cl, Br, I, etc.

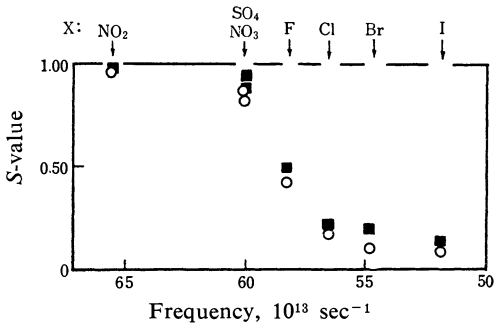


Fig. 2. The relationship between S-value and frequency of the maximum in the first absorption band of $Co(NH_3)_5X$.
■ : Irradiated for one hour
○ : Irradiated for five hours

target salt were separated by procedures involving paper electrophoresis, ion exchange, precipitation, or recrystallization. The results are summarized in Table I.

For the salts shown in Table I, the distribution of ^{60}Co-labeled recoil species was found to vary with the kind of outer anion in the target. The retention (or the percentage of activity as CoA_6^{3+}) tends to increase with the decrease in frequency of the maximum in the first absorption band of CoA_5X (X denotes the outer anion in CoA_6X_3), or the decrease in stability of the outer anion X complexed with cobalt. This relationship is shown in Fig. 1.

For the convenience of discussion on the relative yield of substituted recoil products, a factor, S, was calculated as in the following:

$$S = \frac{\left(\begin{array}{c}\text{Sum of percentages of } ^{60}\text{Co-labeled complexes containing more anionic ligands than the target complex}\end{array}\right)}{\left(\begin{array}{c}\text{Sum of percentages of all } ^{60}\text{Co-labeled complexes}\end{array}\right)}$$

As seen in Fig. 2, the relative yield of substituted products (S) seems to decrease with the decrease in frequency of the maximum in the first absorption band of CoA_5X, or the decrease in stability of the outer anion X complexed with cobalt.

The above relationships indicate together that the facility of incorporation of outer anions into ligands around the hot cobalt atom might mainly depend on the stability of such anions as ligands in cobalt(III) complexes.

It was presumed from these results that chemical processes might mainly contribute to determine the fate of hot cobalt atoms at such stages in recoil reactions as involved energies low enough to distinguish the difference in stabilities of these anions as ligands.

Department of Chemistry
Faculty of Science
The University of Tokyo
Hongo, Tokyo

A Kinetic Study of the Isotopic Exchange of Indium between the Indium Ion and its N-2-Hydroxyethylethylenediamine-N, N', N'-triacetate Complex in an Acid Solution

By Kazuo SAITO and Michiko TSUCHIMOTO (nee TAMURA)

(Received January 24, 1961)

Since tervalent gallium, indium and thallium give co-ordination compounds of a typical d^{10} structure, a kinetic study of the isotopic exchange of these elements, which has been left unchallenged, will provide useful information on the nature of the so-called outer co-ordination compounds. With the aid of a tracer study with indium-114 m, the present authors previously found[1] that exchange of indium proceeds with a measurably slow rate between the indium ion and its *N*-2-hydroxyethylethylenediamine-*N*, *N'*, *N'*-triacetate (written as EDTA-OH henceforth) complex in an acid solution and that the rate depends on the hydrogen ion concentration. The rate is immeasurably small in a neutral solution. It appears to increase in a basic solution of a pH more than 10, where indium remains in the aqueous phase only in the presence of a large amount of a masking agent such as citrate and tartrate. This paper deals with the kinetics of this exchange reaction, especially in a pH range from 2 to 3.5, where the exchange rate is proportional to the hydrogen ion concentration.

Results

According to McKay[2], the exchange constant is expressed by

$$R = -2.303 \cdot \frac{ab}{(a+b)} \cdot \frac{\log (1-F)}{t}$$

where a and b stand for the molar concentration of the indium ion and its EDTA-OH complex respectively, t is the lapse of time, and F the fraction of the reaction. First, the relationship between R, and a and b was examined, the results being shown in Figs. 1 and 2 respectively. It is clearly seen that R is proportional to the concentration of the complex (b), regardless of the presence of a buffer, whereas it is independent of the concentration of the indium ion (a). Hence, the reaction constant k is given by R/b and has a dimension T^{-1}. The pH dependence was tabulated in Table I

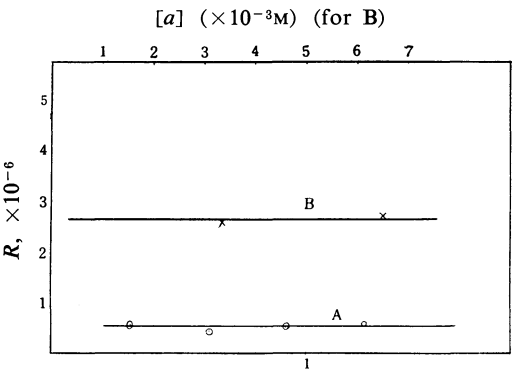


Fig. 1. Relationship between the concn. of In^{3+} and the exchange const. R.
A: ⊙; μ, 0.2 (KNO_3); T, 25°C; pH, 2.93; acetate buffer, 0.043 M; [b], 0.24 ×10⁻³ M
B: ×; μ, 0.2 (KNO_3); T, 25°C; pH, 3.15; citrate buffer, 0.033 M; [b], 0.71 ×10⁻³ M

TABLE I. INFLUENCE OF THE IONIC STRENGTH

μ	pH	$k/[H^+]$ l./mol./sec.
0.042	2.35	1.6×10^{-2}
0.092	2.45	1.7×10^{-2}
0.300	2.63	2.4×10^{-2}

at 25°C; acetate buffer 0.042 M

in Ref. 1 and is also shown in Fig. 3, in which a linear relationship is seen in a pH range from 2.5 to 3.2. In a more acid solution, the exchange proceeds too fast to permit a precise kinetic study, but there appears to be an appreciable deviation from the linear relationship.

It is rather noticeable that the exchange constant R increased by the use of a buffering agent such as citrate and acetate. Especially in the presence of citrate, R increased linearly with an increase in the concentration of the dihydrogen citrate ion, as is shown in Fig. 4. On the other hand, acetate affected the R value to a much less extent.

The temperature dependence of R is shown in Fig. 5, in which $\log k/[H^+]$ is plotted against $1/T$ (T, absolute temperature). The Arrhenius

1) K. Saito and M. Tamura, *J. Inorg. Nucl. Chem.*, **13**, 334 (1960).
2) H. A. C. McKay, *Nature*, **142**, 997 (1938).

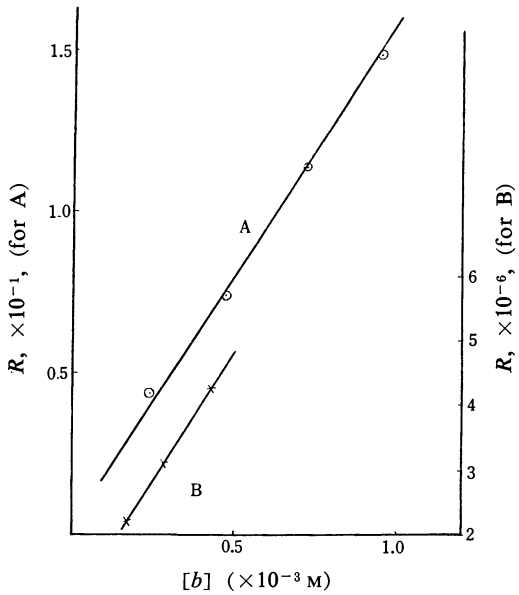


Fig. 2. Relationship between the concn. of In-EDTA-OH and the exchange const. R.
A: ⊙; μ, 0.2 (KNO_3); T, 25°C; pH, 3.05; acetate buffer, 0.05 M; [a], 0.97 ×10⁻³ M
B: ×; μ, 0.2(KNO_3); T, 25°C; pH, 2.91; without buffer; [a], 0.32×10⁻³ M

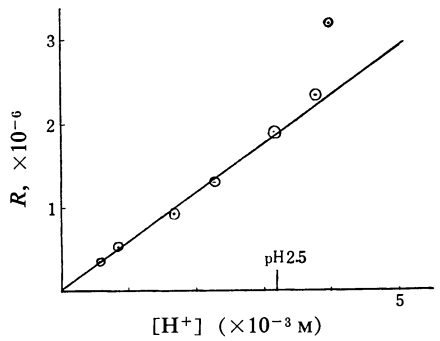


Fig. 3. pH Dependence of the exchange constant.
μ, 0.2 (KNO_3); T, 25°C; without buffer; [a], 1.51×10⁻³ M; [b], 0.55×⁻³ M

TABLE II. INFLUENCE OF THE CHLORIDE ION

Concn. of KNO_3 M	Concn. of KCl M	pH	k/[H⁺] 1./mol./sec.
0.222	0	2.57	0.96×10⁻²
0.218	0.0037	2.68	0.92×10⁻²
0.204	0.0185	2.65	1.24×10⁻²
0	0.222	2.59	6.6 ×10⁻²

[μ, 0.222; 25°C; without buffer]

activation energy was calculated to be 11 kcal. per mole. The influence of the ionic strength is tabulated in Table I, the μ being changed with potassium nitrate. The influence appears

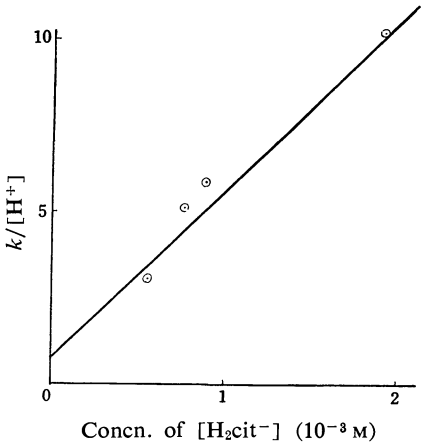


Fig. 4. Effect of the concentration of the citrate ion upon the exchange constant.

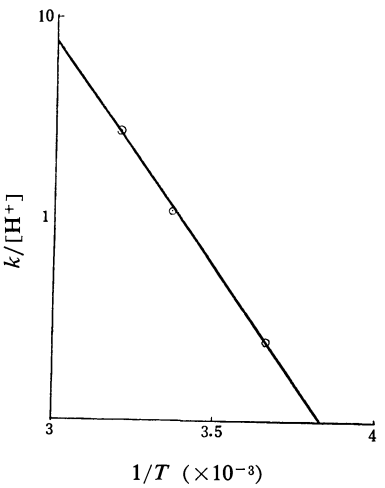


Fig. 5. Temperature dependence of the exchange constant.
μ, 0.2 (KNO_3); pH, 3.01; without buffer; [a], 1.51×10⁻³ M; [b], 0.55×10⁻³ M

to be very small. When potassium chloride was used in place of nitrate, the exchange rate significantly increased, as is seen in Table II.

Discussion

Only a little information is available concerning the mechanism of the isotopic exchange of the co-ordination compounds of EDTA and its analogues, especially of those with tervalent metal ions. Jones and Long[3] reported that the isotopic exchange of iron between the ferric ion and its EDTA complex was dependent on the pH value in a complexed manner in the range from 1 to 2.5 and that at least three separate kinetic terms participated in the exchange. In the case of indium, the kinetic

3) S. S. Jones and F. A. Long, *J. Phys. Chem.*, **56**, 251 (1952).

term appears to be much simpler under the given conditions. The dissociation of the indium EDTA-OH complex must play an important role in determining the exchange rate, because the concentration of the uncomplexed indium does not affect the rate in either the presence or the absence of a buffering agent which is capable of forming complex ions with indium. The pH dependence of the k value suggests that the indium EDTA-OH complex is in a protonated form in the given pH range, and its dissociation appears to be the rate-determining step. (Z, EDTA-OH radical)

$$[{}^*InZ\cdot OH_2] + H^+ \rightleftarrows [{}^*InHZ\cdot OH_2]^+ \quad \text{(Equil.)}$$

$$[{}^*InHZ\cdot OH_2]^+ + In^{3+}\cdot OH_2 \rightleftarrows [InHZ\cdot OH_2]^+ + {}^*In^{3+}\cdot OH_2$$

$$[InHZ\cdot OH_2]^+ \rightleftarrows [InZ\cdot OH_2] + H^+ \quad \text{(Equil.)}$$

The second step can also be written as follows:

$$[{}^*InHZ\cdot OH_2]^+ \xrightarrow{\text{slow}} {}^*In^{3+}\cdot OH_2 + HZ^{2-}$$

$$HZ^{2-} + In^{3+}\cdot OH_2 \xrightarrow{\text{fast}} [InHZ\cdot OH_2]^+$$

The dissociation of the complex $[InHZ\cdot OH_2]^+$ may presumably involve the rupture of one or two of the In-O linkage as the first step, which eventually results in the release of the radioactive indium ion. The free protonated EDTA-OH radical HZ^{2-} could combine with the hydrated indium ion at a greater rate than that of the dissociation. Since neither the equilibrium constant of the protonation nor the rate constant of the rate-determining step is known, further quantitative elucidation must be abundoned. Nevertheless, it is a rather marked fact that the rate is independent of the concentration of one of the components to be exchanged.

When the hydrogen ion concentration is higher, protonation could occur on two acetate radicals of the complex side by side,

$$[{}^*InHZ\cdot OH_2]^+ + H^+ \rightleftarrows [{}^*InH_2Z\cdot OH_2]^{2+} \quad \text{(Equil.)}$$

the diprotonated complex undergoing a similar dissociation at a comparable or a greater rate. Deviation from the linear relationship seen in Fig. 3 could be thus accounted for by taking the participation of the diprotonated complex into consideration. If such a dissociation were regarded as the rate-determining step, it would be rather reasonable to assume that the Arrhenius activation energy is as low as 11 kcal. per mole and that the change in ionic strength affects the rate to a less extent.

Nothing decisive can be stated concerning the role of an acidic radical such as citrate and acetate. It has already been established that the co-ordinated water in an indium EDTA complex can be replaced by an acidic component such as chloride and bromide[4]. It would not be unusual if a similar replacement occurred in an aqueous solution of an indium EDTA-OH complex.

$$[InZ\cdot OH_2] + H_2cit^- \rightleftarrows [InZ\cdot H_2cit]^- + H_2O$$

When it is assumed that the dissociation of the protonated acido complex proceeds faster than that of the aquo complex, the relationship shown in Fig. 4 will be accounted for. Such an explanation expresses, with a little different shade of meaning, the idea that the dissociation of the protonated complex is accelerated in the presence of an organic oxy-acid, which can pull the indium ion to form a complex. The extent to which the dissociation is facilitated depends on the nature and the concentration of the organic compound, citrate exerting a greater influence than acetate. Such an effect must be reflected in the change in Arrhenius activation energy and in the influence of the ionic strength. The accuracy of an isotopic tracer study, however, is not high enough to make such a change clear. The influence of the chloride ion indicated in Table II can be similarly understood. Although the chloride ion forms chloro complexes with indium ions in an acid solution, the formation constant is so small that its effect is appreciable only in the presence of a large amount of the chloride ion.

A gallium complex of EDTA-OH also undergoes isotopic exchange of gallium with the gallium ion in a more acid region[5]. The rate depends on the hydrogen ion concentration to a more marked extent and will be compared with the present result elsewhere.

Experimental

Preparation and Properties of the Complex.— Since this complex is a new compound, its preparation and properties will be described briefly. Indium was dissolved in dilute nitric acid, the hydroxide precipitated with aqueous ammonia solution, centrifuged, washed and boiled with EDTA-OH, slightly less in amount to the equivalent. When the mixture became almost transparent, the solution was filtered to remove the excessive indium hydroxide, evaporated, and treated with ethanol to give prismatic crystals of aquo *N*-2-hydroxyethylethylenediamine-*N*, *N'*, *N'*-triacetato indium monohydrate which lost 8.78% of water at 110°C, corresponding to two moles per mole of the complex (calcd., 8.46%).

Found: N, 6.43; In, 26.78. Calcd. for $C_{10}H_{15}O_7N_2In\cdot 2H_2O$: N, 6.62; In, 26.94%.

When titrated with a sodium hydroxide solution, an aqueous solution of this complex gave a titration curve as shown in Fig. 6, from which the apparent

4) K. Saito and H. Terrey, *J. Chem. Soc.*, **1956**, 4701.
5) K. Saito and M. Tsuchimoto, *J. Inorg. Nucl. Chem.* in press (appear in early issue, 1962).

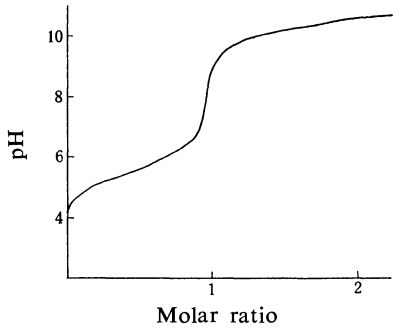


Fig. 6. Titration of $[In \cdot EDTA\text{-}OH \cdot H_2O] \cdot H_2O$ with sodium hydroxyde.
$[InZ \cdot OH_2]H_2O$, 0.2×10^{-4} M; $\mu = 0.05$ (KNO_3); 25°C

dissociation constant was calculated to be approximately 1.5×10^{-6} at 25°C in an ionic strength $\mu = 0.05$. This value is significantly greater than that of the indium EDTA complex (1.6×10^{-9})[4], indicating that the co-ordinated water is bound to indium more firmly than in the latter complex. In an acid solution as used in the present study, the dissociation of the co-ordinated water can be ignored. By the use of an irradiated unit In-114 m, a radioactive indium EDTA-OH comlex of a due specific activity was obtained crystalline.

Procedure for Kinetic Runs.—An aqueous solution (200 ml.) of indium nitrate of a known pH value, containing potassium nitrate and the buffer, was mixed in a thermostat with a radioactive indium EDTA-OH solution (100 ml.) of the same pH value. A 25 ml. portion was taken out at certain intervals and treated with 8-quinolinol in ethanol (0.5%, 1 ml., less than the equivalent amount of indium nitrate), and the pH was adjusted to about 3.2 with brom phenol blue as indicator. The precipitate was filtered off through a sintered glass filter plate No. 4, washed with water, dried at 110°C, weighed and submitted to radioactivity measurement. The molar ratio of 8-quinolinol to indium remained unchanged when the precipitate was formed in the presence of an excess of indium. The separation was satisfactorily effected within 2 min., and no appreciable heterogeneous isotopic exchange was observed between the precipitate and the solute under the given conditions. The zero time exchange was negligible.

Measurement of Radioactivity.—A scintillation spectrometer with a sodium iodide crystal (diameter, 4.8 cm.; thickness, 4.8 cm.) was used with due accessories. The weighed filter plate was covered with cellotape and fixed on a methylmethacryllate plate (thickness, 1 cm.) which absorbed 1.98 MeV. β-rays of ^{114}In. The plate was placed upon the scintillator crystal, and the photo- and the Compton electrons coming from γ-rays of In-114 m were counted, the less distinctive back-scattering peak being biased by a pulse-height analyzer. The overall counting efficiency was about 20%. The integrated counting rate increased linearly with the increase in the amount of radioactive indium, and the specific counting rate of the precipitate was calculated from the weighed amount of the indium 8-oxyquinolinol complex.

All the chemicals were of reagent grade. Indium nitrate was prepared from metallic indum of a purity more than 99.99%. The pH value was measured with a glass electrode, the error being less than 0.02 pH.

Summary

1) The isotopic exchange of indium between the indium ion and its EDTA-OH complex was kinetically studied in an acid solution, indium-114 m being used as tracer.

2) Separation of the indium ion from its EDTA-OH complex was satisfactorily carried out with 8-quinolinol (oxin) at a pH about 3, and no appreciable heterogeneous exchange was observed between the precipitate and the solute.

3) The exchange constant R was proportional to the concentration of the complex, the hydrogen ion and the ions such as dihydrogen citrate, but was independent of the concentration of the indium ion. It was affected by the ionic strength to a less extent, and the Arrhenius activation energy was 11 kcal. per mole.

4) A plausible reaction mechanism was postulated on the basis of the kinetic data. The dissociation of the protonated indium EDTA-OH complex appears to be the rate-determining step.

The authors wish to express their thanks for a grant-in-aid given by the Ministry of Education.

Institute for Nuclear Study
The University of Tokyo
Tanashi, Tokyo

Cationic Polymerization of Isobutene in Liquid Sulfur Dioxide. Role of Water of Cocatalyst[1]

By Niichiro TOKURA, Minoru MATSUDA and Isoo SHIRAI

(Received October 4, 1960)

Cationic polymerization of isobutene in liquid sulfur dioxide has already been proposed by Elwell and Meier[2a], and has been examined by Furuya and Honda[2b], who reported on the formation of high molecular weight polyisobutene when it was polymerized with alminum chloride at low temperature, but no suggestion has been made on the mechanism of the polymerization.

It is widely recognized that when a Friedel-Crafts catalyst was used in a cationic polymerization, a cocatalyst was necessary to initiate the polymerization[3-5]. Among such cocatalysts, water has lately been known as important proton releasing substance[3,4,6].

On the other hand, the solvents used for the polymerization such as alkyl halides or alkylene dihalides[6-8] have often been regarded as useful cocatalysts in cationic polymerization. However, a recent publication[9] is opposing the proposal.

Dainton[10] has carried out polymerization of isobutene in a gas phase at room temperature using boron trifluoride as a catalyst together with D_2O as a cocatalyst. The polymer obtained (DP, 10) was investigated by infrared spectral analysis in order to elucidate the mechanism of the initiation as well as the termination of the polymerization, though no decisive result was obtained concerning the mechanism of the initiation of the polymerization.

Liquid sulfur dioxide has been found to be a peculiar solvent by us and by others[11] in some organic reactions involving polymerization and a small amount of water in it is very difficult to eliminate within the order of 100 p. p. m. by ordinary method[12]. Therefore, water remaining in liquid sulfur dioxide will often act as a cocatalyst. On the other hand, liquid sulfur dioxide is reported to be able to dissociate as follows[13],

$$2SO_2 = SO^{2+} + SO_3^{2-}$$

Thus sulfur dioxide seems likely to play a part as a cocatalyst via the sulfite cation.

This paper aims at the elucidation of the role of water, when the comparable amount of water is present in the cationic polymerization of isobutene in liquid sulfur dioxide by using stannic chloride.

The liquid sulfur dioxide used for the present investigation was dehydrated according to Hata and Asano's method[14] of this Institute, whereby water content in liquid sulfur dioxide was reduced to as low as 30 mg./l., that is calculated from the infrared absorption in 3675 cm^{-1} of the vibration of OH.

The participation of heavy water was examined by adding it to this dried sulfur dioxide in the polymerization of isobutene with stannic chloride as the catalyst.

To obtain polymers having the degree of polymerization (DP) of 2 to 4, an experimental condition has been chosen so as to polymerize the monomer at 35°C and stop at the conversion of 2~3%. The products were examined by their infrared spectral absorptions to determine the possibility of the participation of D_2O or sulfur dioxide as the catalyst in the polymerization reaction.

Experimental

Materials.—Isobutene was prepared by dehydration of *tert*-butyl alcohol with acetic acid anhydride containing a small amount of concentrated sulfuric acid. The purity of the isobutene was analyzed by gas chromatography, no contaminant being found in this material. Commercial stannic chloride was dehydrated with phosphoric acid anhydride

1) Polymerization in Liquid Sulfur Dioxide, Part VII.
2) a) W. E. Elwell and R. L. Meier, U. S. Pat. 442645, *Chem. Abstr.*, **42**, 5655 (1948); b) S. Furuya and M. Honda, *Kobunshikagaku (Chem. High Polymer)*, **16**, 54 (1959).
3) C. G. Overberger, R. J. Ehrig and R. A. Morcus, *J. Am. Chem. Soc.*, **80**, 2456 (1958).
4) A. Lwyn, G. Evans and G. M. Meadows, *Trans. Faraday Soc.*, **46**, 327 (1950).
5) D. C. Pepper, *Quart. Rev.*, **8**, 88 (1954).
6) R. O. Colclough and F. S. Dainton, *Trans. Faraday Soc.*, **54**, 886 (1958).
7) D. C. Pepper, ibid., **45**, 404 (1949).
8) P. H. Plesch, "Cationic Polymerization", Heffer, Cambridge (1953).
9) W. R. Long, P. H. Plesch and P. P. Rutherford, *Proc. Chem. Soc.*, 68 (1960).
10) F. S. Dainton and G. B. B. M. Sutherland, *J. Polym. Sci.*, **4**, 37 (1949).
11) See Ref. 1 and the preceding papers of this series.
12) D. Murakami and N. Tokura, This Bulletin, **33**, 431 (1958).
13) G. Jander and K. Wichert, *Z. phys. Chem.*, **178**, 57 (1937).
14) T. Hata and T. Asano, *Hisuiken Hokoku (Bull. of Inst. of Non-Aqueous Soln.)*, **9**, 79 (1960).

and distilled in dry nitrogen atomosphere. Heavy water of 99.8 mol. per cent, $d_4^{25}=1.1043$, made at the Asahi Kasei Industries Ltd. (Nobeoka) was used.

Sulfur dioxide was dehydrated according to the procedure of Hata and Asano[14]. In a glass pressure vessel, predehydrated sulfur dioxide[12] (200 ml. of liquid sulfur dioxide, which was treated with 30 g. of phosphoric acid anhydride for 24 hr.) was mixed with purified iodine (0.5 g.) and pure pyridine (10 ml.). The mixture was then distilled carefully through a tube packed with copper powders. The water content of the sulfur dioxide thus dehydrated was reported as 30 mg./l.[14]

Polymerization. — A weighed amount of stannic chloride sealed in an ampoule was added to a definite amount of sulfur dioxide in a pressure vessel by breaking the ampoule. This solution after filtration was diluted with a requisite amount of sulfur dioxide to the catalyst of a definite concentration.

The preparation of the normalized D_2O solution of sulfur dioxide was also prepared by a similar manipulation.

The DP of polyisobutene has been reported to be dependent on the temperature of polymerization. If the DP was large, the weak band of C–D stretching vibration derived from the cocatalyst fragment would become difficult to identify by an infrared spectral analysis. The optimum condition to realize the purpose of this project was searched in the ranges, 1.6×10^{-1} to 4.0×10^{-4} mol. per liter for tin(IV) chloride and 1.0×10^{-1} to 9.0×10^{-3} mol. per liter for D_2O respectively and decided as,

$SnCl_4$	3.0×10^{-2} mol./l.
D_2O	6.0×10^{-2} mol./l.

the concentrations being calculated by volume of sulfur dioxide at −10°C. The samples in Figs. 3 and 4 were prepared with catalysts in such concentrations. The specimens in Figs. 1 and 2 were prepared by another recipe, i. e. $SnCl_4$ 7.4×10^{-3} and D_2O 3.3×10^{-2} mol./l., respectively. The polymerization was carried out at 35°C, and the mole ratio of isobutene to liquid sulfur dioxide was 1 to 2. The time for 2∼3% conversion required about 20 min.

To stop the polymerization, liquid sulfur dioxide and isobutene unreacted were evaporated as fast as possible, the temperature of the residue being sustained at −10°C. The polymer produced during this period was so scarce that it should be treated cautiously during the water washing and the separation. The liquid polymer thus obtained, about 1 to 2 g. for each run, was dried with sodium sulfate and fractionated into the respective fractions, dimer (b. p. 104∼105°C)[15], (yield about 50% of the total polymer), trimer (b. p. 181∼183°C)[15] and tetramer (b. p. 120∼121°C/20 mmHg)[15].

The average molecular weight of the liquid polymer obtained was in the range of 138 (DP, 2.5) to 209 (DP, 3.7) which were measured by the cryoscopic method in benzene.

Infrared Spectra. — Infrared spectra were taken by a Perkin-Elmer double beam model 21 spectrometer, the cells being made of sodium chloride of the width, ca. 0.05 to 0.5 mm., respectively.

Results and Discussion

We have obtained a clear evidence to support the participation of water molecule as a cocatalyst in the polymerization. The polymerization in the extremely dried sulfur dioxide did not proceed to an appreciable extent.

As has been pointed out very recently by Kennedy[16], the monomer transfer should be as minimized as possible. So the polymerization was conducted at a higher reaction temperature (35°C) and the reaction was stopped at 2∼3% conversion, thus obtaining the polymer of a lower DP and of a lesser monomer transfer. Another reason for stopping the polymerization at low conversion was to inhibit the further polymerization of the low polymer produced, where the formation of head to head type polymer was expectable.

The C–D bonding of the polymer was observed distinctly by the infrared spectroscopy. The molecular weight of the polymer thus obtained was in the range of 138 (DP, 2.5) to 209 (DP, 3.7) according to the result of cryoscopic measurements in benzene. Figure 1 shows the spectrum of polyisobutene (unfractionated) of DP 2.5.

The solid line 1 in Fig. 2 shows the spectrum of the dimer fraction (cell width, 0.0496 mm.). If sulfur dioxide reacted as the cocatalyst, there should be absorptions corresponding to SO, SO_2H or SO_2 group in the polymer chain. We could not identify SO group absorption (1060∼1040 cm^{-1})[17] in Figs. 1 and 2. Since the polymer obtained was so low in its DP that the presence of any sulfur atom clinging

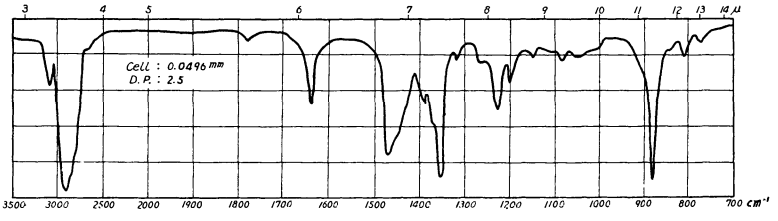


Fig. 1. Infrared spectrum of polyisobutene (DP 2.5).

15) a) H. Adkins, F. F. Diwoky and A. E. Broderick, *J. Am. Chem. Soc.*, **51**, 3422 (1929); b) S. W. Lebedev and G. G. Kobliansky, *Ber.*, **63**, 103 (1930).

16) J. P. Kennedy, *J. Polym. Sci.*, **38**, 263 (1959).

17) L. J. Bellamy, "The Infrared Spectra of Complex Molecules". Methuen, London (1954), p. 280.

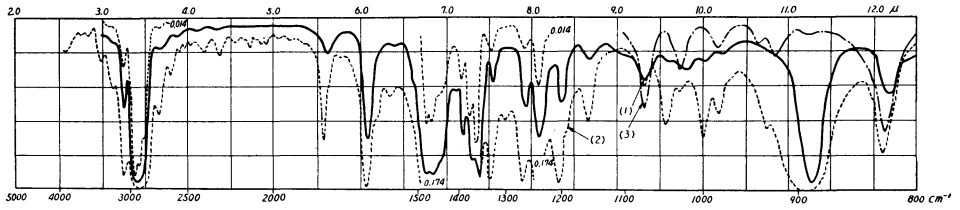


Fig. 2. Infrared spectra of isobutene dimer.

(1) ——— Sample (dimer) (cell, 0.0496 mm.)
(2) ------ 2,4,4-Trimethyl-1-pentene (cell, 0.174 and 0.014 mm.)
(3) —·—· 2,4,4-Trimethyl-2-pentene (cell, 0.013 mm.)

to the polymer chain may be ruled out. The dotted line 2 in Fig. 2 is the infrared spectrum of authentic 2, 4, 4-trimethyl-1-pentene (one of diisobutenes) cited from the Infrared Spectral Data of A. P. I.[18], which is consistent with that of our dimer except only by a small discrepancy in 1100~950 cm^{-1}.

In Fig. 3, line 1 shows a spectrum of the dimer in the range between 3000~1800 cm^{-1}, polymerized with D_2O in liquid sulfur dioxide. Line 2 in Fig. 3 is that of the dimer obtained with water. If water was playing a role as a cocatalyst, the polymer obtained from the polymerization with heavy water added should have a C–D bond at the end of the chain as shown in the following equations:

$$SnCl_4 \cdot D_2O + (CH_3)_2C{=}CH_2 \rightarrow CH_2D{-}\overset{+}{C}(CH_3)_2 + SnCl_4DO^-$$

$$CH_2D{-}\overset{+}{C}(CH_3)_2 + (CH_3)_2 \cdot C{=}CH_2 \rightarrow CH_2D{-}C(CH_3)_2{-}CH_2{-}\overset{+}{C}(CH_3)_2$$

Comparing lines 1 and 2 in Fig. 3, we can recognize a sharp band at 2183 cm^{-1} (C–D stretching frequency) in 1, which evidently proves the participation of water molecule in the polymerization.

The line 3 in Fig. 3 is the spectrum of the dimer fraction obtained at a nearly 100% conversion of the polymerization in the same condition with heavy water. In this spectrum, we can recognize the dilution of the C–D band as the result of transfer reaction during the polymerization.

Figure 4 shows the infrared spectrum of the fraction of trimer and the higher polymer of the same product polymerized with D_2O (line 1). Other lines 2 and 3 are those of trimer and tetramer, respectively, which were derived by polymerization with water. However, the absorptions in the line 1 are overlapping and those at 2130 to 1820 cm^{-1} indicate a slight

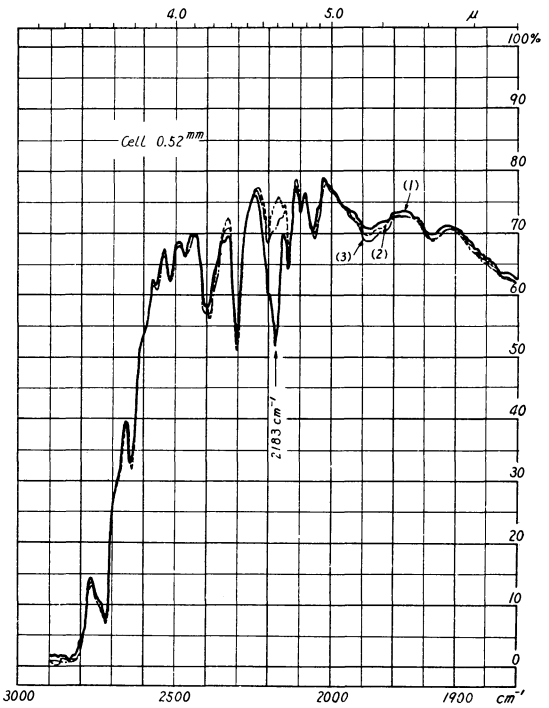


Fig. 3. Infrared spectra of isobutene dimer (3000~1800 cm^{-1}).

(1) ——— with D_2O
(2) ------ with H_2O
(3) —·—· with D_2O (near 100% conversion)

shift, the presence of C–D band is evidenced by a clear peak at 2183 cm^{-1}. From the result above described, it can be concluded that in the cationic polymerization of isobutene with stannic chloride as catalyst in liquid sulfur dioxide, added water may take part in the polymerization as the cocatalyst.

Next, we have to discuss again the spectra in Fig. 3, in which the line 3 is that of authentic 2, 4, 4-trimethyl-2-pentene of A. P. I.[18] The dimer prepared by us had strong absorptions at 1642 and 888 cm^{-1} of terminal double

18) A. P. I., Infrared Spectral Data, I (Pittburgh), No. 276 and 277 (1943—1945).

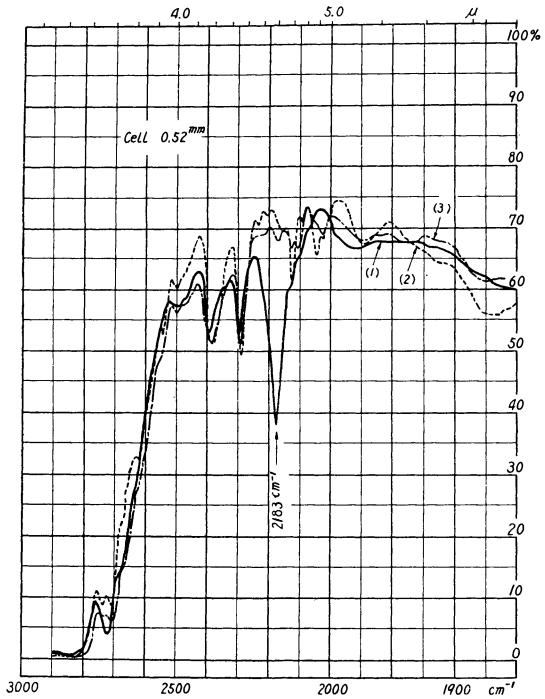


Fig. 4. Infrared spectra of isobutene polymers.
(1) ——— Trimer and higher fraction (with D_2O)
(2) ------ Trimer (with H_2O)
(3) —·—· Tetramer (with H_2O)

bond[19,20] and at 1200 and 1237 cm^{-1} of terminal *tert*-butyl group, respectively, which are almost consistent with 3. But there seem some inaccordances in the range of 1100 to 950 cm^{-1} between the two. The authentic 2, 4, 4-trimethyl-pentene has strong absorptions in its spectrum at 1074, 1034 and 983 cm^{-1}, whereas our dimer has weak bands at 1074 and 1030 cm^{-1}, which may be attributed to the presence of a small amount of 2, 4, 4-trimethyl-2-pentene (cf. line 3 in Fig. 2). Accordingly, in the termination step of the polymerization, reaction 1 may be preferred but reaction 2 may also occur in lower frequency.

$$(CH_3)_3C{-}CH_2{-}\overset{+}{C}(CH_3)_2 + SnCl_4OH^- \rightarrow (CH_3)_3C{-}CH_2{-}\overset{CH_3}{\overset{|}{C}}{=}CH_2 + SnCl_4H_2O \quad (1)$$

$$(CH_3)_3{\cdot}C{-}CH_2{-}\overset{+}{C}{\cdot}(CH_3)_2 + SnCl_4OH^- \rightarrow (CH_3)_3{\cdot}C{-}CH{=}\overset{CH_3}{\overset{|}{C}}{-}CH_3 + SnCl_4H_2O \quad (2)$$

Finally, some comment should be added on the deuterium-hydrogen exchange during the polymerization. If the deuterium hydrogen exchange was proceeding competitively in the polymerization reaction, above conclusion could not be drawn. However, the possible deuterium hydrogen exchange during the polymerization would be rured out by the following reason. The line 3 in Fig. 3, which is the spectrum of the dimer fraction obtained at a nearly 100% conversion of the polymerization with D_2O, shows no strengthening of C–D band absorption as compared with that of 2~3% conversion. On the contrary, there is marked decrease of C–D absorption in 3. Thus, no deuterium hydrogen exchange is conceivable.

This view may be supported by the experiment of Price and Berti[21], who observed no inclusion of deuterium in the polymerization of *cis*-stilben with boron fluoride and heavy water. The discussions on the same subject associated with the reacting species in the cationic reactions with Lewis acid as catalyst will be found abundantly, among which the works of Levy, Taft, Jr. and Hammett[22], Tauber and Eastham[23], and Hart and Levitt[24] are suggestive.

Water can thus be a cocatalyst in a cationic poymerization in liquid sulfur dioxide. However, the conclusion that sulfur dioxide cannot always be a catalyst or a cocatalyst is premature and should be reserved, because the polymerizations described above were undertaken only in a limited condition. The monomers such as vinyl ethers[25] and formaldehyde[26] can be polymerized cationically in liquid and gaseous sulfur dioxide without an acid catalyst.

Summary

Polymerization of isobutene was carried out in liquid sulfur dioxide with stannic chloride as catalyst containing water or heavy water. It was confirmed with the aid of infrared spectrometry that in liquid sulfur dioxide water was playing a part as a cocatalyst when water was present in a comparable amount.

The authors are indebted to Professor Susumu Kinumaki and his associates for carrying out this project, to Messrs. Takeshi Asano and Syuji Aono for infrared spectrometry and to the Befu Chemical Industries for donation of sulfur dioxide.

Research Institute of Non-Aqueous Solutions, Tohoku University
Katahira-cho, Sendai

19) H. W. Thompson and P. Torkington, *Trans. Faraday Soc.*, **41**, 246 (1945).
20) T. A. Kletz and W. C. Price, *J. Chem. Soc.*, **1947**, 265.
21) C. C. Price and G. Berti, *J. Am. Chem. Soc.*, **76**, 1219 (1954).
22) J. B. Levy, R. W. Taft, Jr. and L. P. Hammett, ibid., **75**, 1253 (1953).
23) S. J. Tauber and A. M. Eastham, ibid., **82**, 4888 (1960).
24) H. Hart and G. Levitt, *J. Org. Chem.*, **21**, 921 (1956).
25) W. Reppe, German Pat. 625017, U. S. Pat. 2188778.
26) N. Tokura, to be published.

Studies on the Micro-paraffins. V. X-Ray Investigation of Various Paraffin Waxes

By Kazuo Negoro

(Received February 20, 1961)

Fundamental studies of micro-paraffins performed previously by the present author have revealed that the formation of fine crystal grains of micro-paraffin is not an essential character of micro-paraffin itself[1-3]. It has been found that the existence of a small amount of a certain compound seems to be the cause of the formation of fine crystal grains. In order to verify this point, an X-ray investigation of various paraffins seems to be necessary.

There have been many reports on X-ray diffraction of *n*-paraffin. Müller reported[4] that the cell dimensions of *n*-paraffin (carbon number 29) are $a=7.45$ Å, $b=4.97$ Å, and $c=79.2$ Å. Bunn[5] studied the crystal structure of long-chain normal paraffin hydrocarbons and, in particular, examined the "shape" of $>CH_2$ groups. Furthermore, many data on the X-ray diffraction of *n*-paraffin were introduced by Francis and Piper[6].

The present paper deals with the X-ray diffraction of *n*-dotriacontane (carbon number 32), various paraffin waxes (commercial products), micro-paraffins (commercial products), the micro-paraffin obtained from the tank residue of Aramco crude oil in Saudi-Arabia, and each fraction of micro-paraffin separated by the urea method and chromatography. The chain length, the lengths of a- and b-axes, the cross-sectional area occupied by one paraffin molecule, molecular volume, etc. were determined from the peak in the X-ray diffraction curve. There were a few interesting phenomena and observations on X-ray diffraction when some agents with a O-H group and a benzene ring were added to *n*-dotriacontane.

Experimental

Sample of Paraffin.—The following samples were used as described in the former reports: various paraffin waxes (commercial products), micro-paraffins (commercial products), refined *n*-dotriacontane, the micro-paraffin obtained from the tank residue of Arabian crude oil, and each fraction of micro-paraffin separated by the urea method and chromatography.

Measurement of X-Ray Diffraction.—An X-ray diffractometer (Geiger Flex, manufactured by Rigaku Denki Co.) was used for the measurement of the X-ray diffraction. The sample was placed on a glass plate, melted by heating to 70~75°C (a little higher than its melting point), and kept standing at room temperature (15~20°C), then the solidified sample was placed in the apparatus for the measuremen of the X-ray diffraction. When *n*-dotriacontane, to which substances such as "Santopour", picric acid, *p*-hydroxydiphenyl, asphalt components, etc. had been added, was taken as a sample, it was dissolved in ethyl alcohol and the crystals, formed by cooling gradually to room temperature, were filtered and measured after drying, as in the above operation.

At first, preliminary measurements were made in the range of 0~90° (2θ), in order to fix the range of the diffraction angle where (100) and (200) peaks appeared. Then the diffraction curves were carefully recorded for the range where the main peaks appeared.

The scale of the diffraction angle (2θ) was calibrated by using a standard sample (quartz)[7] and was measured under the conditions shown in Table I.

It was found by preliminary measurement that the peak due to (001) appeared at an angle less than

Table I. Conditions for the measurement on the (110) and (200) peaks

	a_1	b_1
Target	Fe	Cu
Filter	Mn	Ni
Scanning speed (deg./min.)	1/4	1/4
Chart speed (cm./min.)	1	1

Table II. Conditions for the measurement on the (100) peak

	a_2	b_2
Target	Fe	Cu
Filter	Mn	Ni
Scanning speed (deg./min.)	1(1/4)	1
Chart speed (cm./min.)	1	1

1) K. Negoro, *J. Chem. Soc. Japan, Ind. Chem. Sec.* (*Kogyo Kagaku Zasshi*), **64**, 295 (1961).
2) K. Negoro, *J. Chem. Soc. Japan, Pure Chem. Sec.* (*Nippon Kagaku Zasshi*), **82**, 230 (1961).
3) K. Negoro, This Bulletin, **34**, 1366 (1961).
4) A. Müller, *Proc. Roy. Soc.*, **A120**, 455 (1928).
5) C. W. Bunn, *Trans. Faraday Soc.*, **35**, 482 (1939).
6) F. Francis and S. H. Piper, "Science of Petroleum", Vol. II, Ed. by A. E. Dunstan et al., Oxford University Press, London (1938), p. 1203.
7) K. Kubo and S. Kato, "Chemical Analysis by X-Ray Diffraction", Nikkan Kogyo, Tokyo (1955), p. 302.

5°; the measurement of this peak was made under the conditions shown in Table II (Almost all of these experiments were made by using CuK_α radiation). In this case, various paraffin samples, the surfaces of which were cut smooth with a microtome and cut to suitable thickness with a knife, were placed on the glass by means of Scotch tape.

Results and Discussion

The Spacings d_{110} and d_{200}.—From the peak of each X-ray diffraction curve of the various paraffins obtained by FeK_α or CuK_α radiation, the spacings d_{110} and d_{200} were computed by Bragg's equation. The results are shown in Table III.

The results obtained by FeK_α and CuK_α radiation were markedly similar, as is shown in Table III repeatability.

n-Dotriacontane or pure *n*-hydrocarbon (carbon number 32) has the value of 4.15 Å for d_{110} and of 3.77 Å for d_{200}. The crystalline paraffin (m. p. 53.5°C), a mixture of various hydrocarbons, has the value of 4.19 Å for d_{110}; in other words the spacing is increased. Moreover, in the case of micro-paraffin, the product obtained from the tank residue of Aramco crude oil and the commercial one both have the value of 4.16 Å for d_{110}, which is slightly larger than that of *n*-dotriacontane.

Table III. The spacings d_{110} and d_{200} of various paraffins

Name	Radiation	2θ	d_{110}, Å	2θ	d_{200}, Å
n-Dotriacontane	FeK_α	26°58′	4.15	29°48′	3.77
n-Dotriacontane	CuK_α	21°24′	4.15	23°39′	3.76
Crystalline paraffin (m. p. 53.5°C)	FeK_α	26°44′	4.19	29°42′	3.78
Crystalline paraffin (m. p. 53.5°C)	FeK_α	26°42′	4.19	29°41′	3.78
Micro-paraffin	FeK_α	26°56′	4.16	29°59′	3.75
Micro-paraffin (de-asphalted)	FeK_α	26°53′	4.16	29°51′	3.76
Micro-paraffin (de-asphalted)	FeK_α	26°53′	4.16	29°51′	3.76
Micro-paraffin (de-asphalted)	CuK_α	21°18′	4.17	23°39′	3.76
Micro-paraffin (Shell)	FeK_α	26°54′	4.16	29°56′	3.75
Micro-paraffin (Shell)	FeK_α	26°54′	4.16	29°57′	3.75
Micro-paraffin (commercial)	FeK_α	26°56′	4.16	29°59′	3.75
Micro-paraffin urea adducts	FeK_α	26°54′	4.16	29°50′	3.76
Micro-paraffin urea adducts	CuK_α	21°18′	4.17	23°42′	3.75
Micro-paraffin urea rejects	FeK_α	26°39′	4.20	29°35′	3.80
Micro-paraffin urea rejects	CuK_α	21°05′	4.21	23°25′	3.80
Micro-paraffin pentane fraction	FeK_α	26°45′	4.19	29°42′	3.78
Micro-paraffin pentane fraction	CuK_α	21°09′	4.20	23°30′	3.79
Micro-paraffin benzene fraction	FeK_α	26°44′	4.19	29°42′	3.78
Micro-paraffin benzene fraction	CuK_α	21°09′	4.20	23°33′	3.78
Micro-paraffin alcohol fraction	FeK_α	—***	—	—	—
Micro-paraffin alcohol fraction	CuK_α	—	—	—	—
Micro-paraffin (commercial) pentane fraction	FeK_α	26°55′	4.16	29°58′	3.75
Micro-paraffin (commercial) benzene fraction	FeK_α	26°48′	4.18	29°49′	3.77
Micro-paraffin (commercial) alcohol fraction	FeK_α	—	—	—	—
Micro-paraffin adducts pentane fraction	FeK_α	26°57′	4.16	29°56′	3.75
Micro-paraffin adducts pentane fraction	CuK_α	21°23′	4.15	23°37′	3.76
Micro-paraffin adducts benzene fraction	FeK_α	26°48′	4.18	29°49′	3.77
Micro-paraffin adducts benzene fraction	CuK_α	21°16′	4.17	23°34′	3.78
Micro-paraffin adducts alcohol fraction	FeK_α	26°52′	4.17	—	—
Micro-paraffin adducts alcohol fraction	CuK_α	21°17′	4.17	23°39′	3.76
Micro-paraffin rejects pentane fraction	FeK_α	26°43′	4.19	29°42′	3.78
Micro-paraffin rejects pentane fraction	CuK_α	21°08′	4.20	23°27′	3.80
Ar wax*	FeK_α	26°52′	4.17	29°50′	3.76
Amber wax**	FeK_α	26°53′	4·16	29°54′	3.75
Paraffin (PE added) (base crystalline paraffin)	FeK_α	26°45′	4.19	29°44′	3.78
"Santopour" added *n*-dotriacontane	FeK_α	—	—	—	—
Picric acid added *n*-dotriacontane	FeK_α	—	—	—	—
p-Hydroxydiphenyl added *n*-dotriacontane	FeK_α	—	—	—	—
Asphalt added *n*-dotriacontane	FeK_α	—	—	—	—

* Paraffin product to which polyethylene was added.
** Micro-paraffin product to which polybutene was added.
*** — does not show any peak in the X-ray diffraction curve.

It was noticed that the values for d_{110} and d_{200} of the paraffin, about 62% of which formed urea adducts, were vary similar to those of *n*-paraffin when obtained from micro-paraffin by the urea method.

Consequently, though it has been stated that micro-paraffin consists of side-chain paraffins[8] it may be certain from the above results that some straight-chain hydrocarbons are possibly also contained in it.

The value for d_{110} of the remainder of the paraffin forming usea rejects in micro-paraffin was as large as 4.21 Å, and the value for d_{200} increased to 3.80 Å. It seems likely that these parts of micro-paraffin were rich in side-chain hydrocarbons.

When micro-paraffin was directly separated by chromatography, no great difference was observed between the pentane and benzene fractions, and its alcohol fraction was amorphous, for the peak on the X-ray diffraction curve was not observed. However, when micro-paraffin was separated into urea adducts and rejects by the urea method, the fractions of pentane, benzene and alcohol, separated by chromatography, showed remarkable differences.

When substances such as "Santopour", picric acid, *p*-hydroxydiphenyl, asphalt components, etc., were added to *n*-dotriacontane, the peaks (110) and (200) were not clearly observed. Therefore, it appeared that the product became amorphous.

Chain Lengths of Various Paraffins.—From the peak of (001), the chain lengths of carbon of various paraffin samples were computed by Bragg's equation. The results are listed in Table IV. The relation between the chain length and the carbon number of *n*-paraffin is given by the following Eq. 1 obtained by Kurtz and Lipkin[9].

$$\text{Å} = 1.27\, N_1 + 2.0 \qquad (1)$$

where Å is chain lengh in Å and N_1 is carbon number.

Column "a" in Table IV shows the values of N_1 computed by the values of chain length in Eq. 1. If N_1 were calculated by Eq. 1 from the results of the X-ray diffraction of refined *n*-dotriacontane (carbon number 32), its value would be

$$31.7 \fallingdotseq 32$$

Accordingly, it was recognized that the above value nearly agreed with the theoretical one.

In fact, the constant (2.0) in the above equation was in the range of 2.0~3.5 according to the preparation methods of samples as reported by Piper et al.[10] and Müller[11].

It was reported[12] that the lowest value (approximately 2) was obtained when *n*-paraffin, crystallized on a glass plate, was measured by X-ray diffraction. The constant was computed by Eq. 1 at 1.7 from the chain length of *n*-dotriacontane (42.3 Å) and the theoretical value of carbon number (32). Thus, Eq. 1 can be written as follows:

$$\text{Å} = 1.27\, N_1 + 1.7 \qquad (2)$$

TABLE IV. CHAIN LENGTHS OF VARIOUS PARAFFINS

Name	2θ(°)	Chain length Å	Carbon number of chain a	Carbon number of chain b
n-Dotriacontane	2.09	42.3	31.7	32.0
Crystalline paraffin (m. p. 53.5°C)	2.38	37.1	27.7	27.9
Crystalline paraffin (m. p. 60.0°C)	2.08	42.0	31.4	31.7
Crystalline paraffin urea adducts (m. p. 53.5°C)	2.42	36.8	27.4	27.6
Crystalline paraffin urea rejects (m. p. 53.5°C)	2.36	37.8	28.2	28.5
Micro-paraffin	1.20	50.8	38.4	38.6
Micro-paraffin (de-asphalted)	1.48	48.5	36.6	36.8
Micro-paraffin urea adducts	1.70	46.4	34.9	35.2
Micro-paraffin urea rejects	1.21	50.7	38.3	38.5
Micro-paraffin pentane fraction	1.61	47.3	35.6	35.9
Micro-paraffin urea adducts pentane fraction	1.75	45.9	34.5	34.8
Micro-paraffin urea rejects pentane fraction	1.56	47.8	36.1	36.3
Micro-paraffin (commercial)	1.00	53.2	40.3	40.5
Micro-paraffin (Shell)	1.38	49.4	37.3	37.5
Ar wax	2.39	37.0	27.5	27.8
Amber wax	1.18	49.1	37.0	37.3

8) B. T. Brooks, C. E. Board, S. S. Kurtz and L. Schmerling, "The Chemistry of Petroleum Hydrocarbon", Reinhold Publ. Corp., New York (1954).
9) S. S. Kurtz, Jr. and M. R. Lipkin, *Ind. Eng. Chem.*, 33, 779 (1941).
10) S. H. Piper, D. Brown and S. Dwyment, *J. Chem. Soc.*, 127, 2194 (1925).
11) A. Müller and W. B. Saville, ibid., 127, 599 (1925).
12) "Chemistry of Petroleum Hydrocarbons", Vol. II, Kyoritsu Shuppan, Tokyo (1956), p. 2

Table V. Values of constant (k), when those substances which were considered to have micro-crystallization effects were added to n-dotriacontane

Name	2θ(°)	Chain length Å	Constant number k
Base (n-dotriacontane)	2.09	42.3	1.7
n-Dotriacontane (picric acid added)	2.05	43.1	2.5
n-Dotriacontane (" Santopour " added)	2.01	44.0	3.4
n-Dotriacontane (p-hydroxydiphenyl added)	2.05	43.1	2.5
n-Dotriacontane (asphalts added)	2.06	42.9	2.3

Column " b " in Table IV shows the values of the carbon numbers of various paraffins computed by Eq. 2.

As shown in Table IV, it was recognized that the micro-paraffin consisted of long carbon chain hydrocarbons and that the chain length was in the range 47～53 Å, while the value for crystalline paraffin was 36～42 Å.

As for the carbon number of the chain, it was found that the value for micro-paraffin was considerably larger, 37～40, assuming that it was in the fully extended chain state, while the value for crystalline paraffin was 27～32. The straight paraffin obtained from the micro-paraffin by the urea method was C_{35}; therefore, its carbon chain was shorter than that of the base paraffin.

On the contrary, it was recognized that the carbon number of the urea non-adducts was slightly larger than that of the base paraffin, when the value was computed assuming that the paraffin was in the fully extended chain state even though it was actually rich in side chain hydrocarbons.

As reported in the previous paper,[3] when " Santopour ", picric acid, p-hydroxydiphenyl and asphalt components, nemely those compounds which were considered to have micro-crystallization effects, were added to n-dotriacontane, (110) the peak shifted to the smaller angle of 2θ, indicating that the chain length increased compared only with the case of n-dotriacontane of the base paraffin. In this case, the constant (2.0) of Eq. 1 was replaced by k:

$$\text{Å} = 1.27\, N_1 + k \qquad (3)$$

The value of k was computed by replacing $N_1 = 32$ and the observed value of the chain length (Å), the results being shown in Table V.

The larger values of k in Table V suggest that the crystal lattice has a certain disorder, and it was noticed that " Santopour " had the largest effect on the crystal of n-dotriacontane with the largest value of k.

X-Ray Diffraction Pattern of d_{001} and Crystallinity.—The X-ray diffraction curves of typical paraffins are shown in Fig. 1, in which intensity is in ordinate and the diffraction angle (2θ) is in abscissa. As for the crystalline paraffin or n-dotriacontane, various orders of reflections of (001) were observed, but for the micro-paraffin, it was noticed that only the first order appeared. If " Santopour ", picric acid, p-hydroxydiphenyl, etc., or those substances having micro-crystallization effects, were added to n-dotriacontane, it was found that all the higher order reflections disappeared.

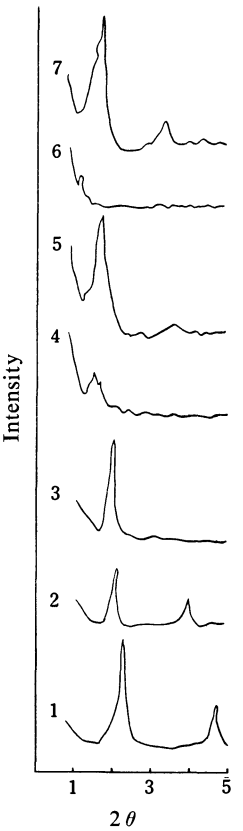


Fig. 1. X-Ray diffraction curve of typical paraffins.
1. Crystalline wax (m. p. 53.5°C)
2. n-Dotriacontane
3. n-Dotriacontane (" Santopour " added)
4. Micro-paraffin
5. Micro-paraffin urea adducts
6. Micro-paraffin urea rejects
7. Micro-paraffin urea adducts pentane fraction

Table VI. Length of a and b axes, cross-sectional area of one molecule (S), and ϕ of various paraffins

Name	a, Å	b, Å	S, cm^2	ϕ
n-Dotriacontane	7.54	5.03	19.0×10^{-16}	67°24′
Crystalline wax (m. p. 53.5°C)	7.56	5.04	19.1×10^{-16}	67°22′
Micro-paraffin	7.50	5.00	18.8×10^{-16}	67°30′
Micro-paraffin (de-asphalted)	7.52	5.00	18.8×10^{-16}	67°14′
Micro-paraffin (Shell)	7.50	5.01	18.8×10^{-16}	67°30′
Micro-paraffin (commercial)	7.50	5.01	18.8×10^{-16}	67°30′
Micro-paraffin urea adducts	7.52	5.00	18.8×10^{-16}	67°14′
Micro-paraffin urea rejects	7.60	5.05	19.2×10^{-16}	67°12′
Micro-paraffin pentane fraction	7.56	5.04	19.0×10^{-16}	67°22′
Micro-paraffin adducts pentane fraction	7.50	5.01	18.8×10^{-16}	67°30′
Micro-paraffin rejects pentane fraction	7.56	5.04	19.0×10^{-16}	67°22′
Ar wax	7.52	5.01	18.8×10^{-16}	67°20′
Amber wax	7.50	5.01	18.8×10^{-16}	67°30′

When micro-paraffin was reacted with urea, the straight paraffin (urea adducts paraffin) thus obtained showed (001) and a very weak (002). However, the pentane fraction, obtained from the urea adducts by chromatography, showed higher order reflections clearly, and it was found that the crystalline state gradually had a resemblance to that of n-paraffin. On the contrary, in the case of urea rejects of paraffin, such peaks did not appear at all. As mentioned above, the appearance of the peaks on X-ray diffraction curves has some relation with the crystallinity of paraffins in actuality, and it is interesting that the details of the X-ray dffraction pattern of micro-paraffin have been made clear, and that the effects of "Santopour" etc., or those compounds with an O–H group and benzene ring, have been observed on the change which occurred in the peaks on the X-ray diffraction curve.

Length of a- and b-Axes and Cross-sectional Area of Various Paraffin Crystals.—Müller[13] studied the X-ray diffraction of n-paraffin, and the cross-section of the unit cell is shown in Fig. 2. It was confirmed that one paraffin chain was in the center of unit cell and that a paraffin chain with a different azimuthal orientation was at each of the four corners of the unit cell.

For the packing of paraffin molecules, no experimental evidence was obtained for any kind of paraffins; however, according to Müller, it would be proper to consider that each crystal had a cross-section as shown in Fig. 2 and a c-axis perpendicular to it. The length of the a- and b-axes, the cross-sectional area occupied by one molecule (S), and ϕ were computed from the values for d_{110} and d_{200} by the following Eqs. 4—7. The calculated values are shown in Table VI, and part of the values which Müller reported on n-paraffins of various carbon numbers are reproduced in Table VII.

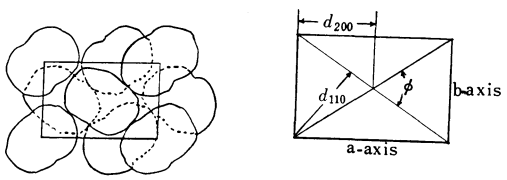


Fig. 2. Cross-section of unit cell.

$$a=2\cdot d_{200} \tag{4}$$

$$b=a\cdot d_{110}/\sqrt{a^2-(d_{110})^2} \tag{5}$$

$$c=a\cdot b/2 \tag{6}$$

$$\tan\phi/2=b/a \tag{7}$$

Table VII. Length of a and b axes, cross-sectional area of one molecule (S), and ϕ of various n-paraffins (Müller)

Number of carbon atoms	a, Å	b, Å	S, cm^2	ϕ
19	7.55	5.01	18.9×10^{-16}	67°10′
24	7.41	4.94	18.3×10^{-16}	67°20′
29	7.42	4.94	18.3×10^{-16}	67°16′
30	7.33	4.92	18.2×10^{-16}	67°44′
31	7.40	4.93	18.2×10^{-16}	67°15′
34	7.40	4.95	18.3×10^{-16}	67°30′
44	7.33	4.93	18.1×10^{-16}	67°52′

The length of the a- and b-axes of n-dotriacontane (n-paraffin of carbon number 32) had slight differences of 0.14 Å and 0.10 Å compared with the values for n-paraffin (carbon number 31) of Müller; it was also recognized that the values for various paraffins were almost similar. As for the cross-sectional area occupied by one molecule, the values for various paraffins were in the range of $(18.8\sim19.2)\times10^{-16}$ cm^2, and it was recognized that no great differences were to be seen among various paraffins, assuming that they were in normal crystal form, though

13) A. Müller, *Proc. Roy. Soc.*, **A128**, 514 (1932).

the urea adducts of paraffins showed somewhat larger values than those of the other paraffins.

Molecular Volume of Various Paraffins. — When the chain length and the cross-sectional area occupied by one molecule have been computed, the molecular volume of various paraffins may be calculated by the following equation, assuming that they are *n*-paraffins:

$$V = d_{001} \cdot ab/2 \qquad (8)$$

Table VIII shows the molecular volume (Å^3/mol.) of various paraffins calculated from Eq. 8.

TABLD VIII. MOLECULAR VOLUME OF VARIOUS PARAFFINS

Name	Molecular volume, Å^3
n-Dotriacontane	804
Crystalline wax (m. p. 53.5°C)	708
Micro-paraffin	955
Micro-paraffin (de-asphalted)	911
Micro-paraffin (Shell)	928
Micro-paraffin (commercial)	998
Micro-paraffin urea adducts	872
Micro-paraffin urea rejects	974
Micro-paraffin pentane fraction	900
Micro-paraffin adducts pentane fraction	867
Micro-paraffin rejects pentane fraction	909
Ar wax	695
Amber wax	923

The molecular volume of *n*-paraffin was computed from carbon number (N_1) by the following equation:

$$V = 23.50\, N_1 + 37.0 \qquad (9)$$

For *n*-dotriacontane the molecular volume, calculated by putting $N_1 = 32$ in Eq. 9, was 789, while that computed from X-ray diffraction data by Eq. 8, was 804. The difference between these two is 15, that is, approximately 2%. As for the micro-paraffin, a mixture of various hydrocarbons, the value of the molecular volume is not accurate, but this might give some clue as to the molecular volume.

Summary

From the X-ray diffraction of *n*-dotriacontane, various paraffin waxes, micro-paraffin, and each fraction of micro-paraffin separated by the urea method and chromatography, the chain length and the spacings (110) and (200) of each crystal have been computed. Furthermore, the carbon number of the chain, the lengths of the a- and b-axes, the cross-sectional area occupied by one molecule, and the molecular volume have been calculated. They have been calculated on the assumption that thay were in normal crystal form, but in order to make it exact, it is necessary to work with a single crystal. The author would like to try further experiments.

The author wishes to express his sincere appreciation to Professor Ryozo Goto and Professor Saburo Yagi, Kyoto University, for their cordial guidance and discussion throughout this research. He is also grateful to Dr. Kenziro Asai and Dr. Tsuneo Seto, Kyoto University, for their cordial guidance in these analyses.

He also thanks Mr. Takashi Matsuoka et al., the personnel of the Central Research Laboratory of Nippon Mining Co., for their cooperation in the measurement of X-ray diffraction.

Central Research Laboratory
Nippon Mining Co.
Kita-adachi-gun
Saitama-ken

Dehydration of Bile Acids and their Derivatives. X. A Study of the Physical Properties of Various 3α-Hydroxycholenates and their Derivatives, with Special Reference to their Optical Rotatory Dispersions

By Ryuzaburo OSAWA

(Received March 13, 1961)

In the previous papers[1,2], the synthesis of methyl 3α-hydroxy-$\Delta^{8(14)}$-cholenate and 3α-hydroxy-Δ^{14}-cholenate was reported. Besides these unsaturated bile acids, various 3α-hydroxycholenic acids of known structure have already been reported. The present paper deals with the study of the correlation of the physical properties with the positions of the double bonds of these 3α-hydroxycholenates and their derivatives, above all, the optical rotatory dispersions of these bile acids are discussed in detail because Djerassi[3] has shown that the rotatory dispersion curve (the RD curve) is an excellent tool for elucidating the structure of steroids.

The ultraviolet absorption spectra of the unsaturated bile acids of various types were studied; their ε values are shown in Table I. The bile acids with exocyclic, tetrasubstituted double bonds ($\Delta^{8(14)}$) give much higher ε values than do unsaturated bile acids of the other types. On the other hand, bile acids with a disubstituted ethylenic linkage, such as 3-keto-Δ^{6}-cholenate, give much lower ε values than those with trisubstituted (Δ^{7}, $\Delta^{9(11)}$, Δ^{14}) or endocyclic, tetrasubstituted (Δ^{8}) double bonds. These results agree fairly well with those reported by Bladon et al.[4]

As Barton[5] has reported, the position of a double bond in the steroid molecule can be deduced by calculating the molecular rotation increment due to the introduction of the double bond. As a supplement to the data in this field, the molecular rotations of various available unsaturated and corresponding saturated bile acids were measured; the calculated M_D contributions of the double bonds are summarized in Table II. It was an interesting finding that the positive sign of the M_D contributions due to the double bonds in ring B or C is strongly inverted when the C_{12}-carbonyl group is simultaneously introduced; e. g., the

TABLE I. ULTRAVIOLET ABSORPTION IN ETHANOL

Unsaturated bile acid	λ_{max}	ε_{max}	ε_{210}	ε_{215}	ε_{220}
Methyl 3α-hydroxy-Δ^{7}-cholenate (I)	210	3000	3000	1930	580
Methyl 3α-acetoxy-Δ^{7}-cholenate (II)	210	2290	2290	1390	650
Methyl 3α-acetoxy-$\Delta^{8(14)}$-cholenate (III)	214	5900	5040	5560	3470
Methyl 3α-hydroxy-Δ^{14}-cholenate (IV)	209	2490	2410	1020	370
Methyl 3-keto-Δ^{4}-cholenate (V)	240	14129	2627	4606	6174
Methyl 3-keto-$\Delta^{7,9(11)}$-choladienate (VI)	245	10920	3030	4190	5610
Methyl 3-keto-Δ^{8}-cholenate (VII)	211	2420	2390	1760	1240
Methyl 3-keto-$\Delta^{8(14)}$-cholenate (VIII)	214	5190	4000	5030	4050
Methyl 3-keto-$\Delta^{9(11)}$-cholenate (IX)	211	2200	2080	1480	880
Methyl 3-keto-Δ^{14}-cholenate (X)	210	1990	1990	980	290
Methyl 3-keto-Δ^{7}-cholenate (XI)	212	2320	2230	2190	1620
Methyl 3-keto-Δ^{6}-cholenate (XII)	214	320	140	300	180
Methyl 3α-acetoxy-12-keto-$\Delta^{9(11)}$-cholenate (XIII)	239	10300	2250	3860	5300
Methyl 3α-acetoxy-12-keto-Δ^{8}-cholenate (XIV)	213	3980	3100	3450	2420
Methyl 3α-acetoxy-12-keto-$\Delta^{8(14)}$-cholenate (XV)	215	5270	3500	5270	4790
Methyl 3, 12-diketo-$\Delta^{8(14)}$-cholenate (XVI)	215	5940	4500	5940	4990
Methyl 3, 12-diketo-Δ^{14}-cholenate (XVII)	210	2140	2140	1090	280

1) R. Osawa and K. Yamasaki, This Bulletin, **32**, 1302 (1959).
2) F. Nakada, R. Osawa and K. Yamasaki, ibid., **34**, 538 (1961).
3) C. Djerassi, "Optical Rotatory Dispersion", McGraw-Hill Book Co., Inc., New York (1960).
4) P. Bladon, H. B. Henbest and G. W. Wood, *J. Chem. Soc.*, **1952**, 2737.
5) D. H. R. Barton, ibid., **1946**, 1116.

TABLE II. MOLECULAR ROTATION DIFFERENCE

Unsaturated bile acid	$(M)_D$ unsaturated	$(M)_D$ saturated	M_D contributions of double bonds
Methyl 3α-hydroxy-Δ^7-cholenate (I)	+207	+ 90	+117
Methyl 3α-acetoxy-Δ^7-cholenate (II)	+370	+194	+176
Methyl 3α-acetoxy-$\Delta^{8(14)}$-cholenate (III)	+241	+194	+ 47
Methyl 3α-hydroxy-Δ^{14}-cholenate (IV)	+213	+ 90	+113
Methyl 3-keto-Δ^4-cholenate (V)	+235	+124	+111
Methyl 3-keto-$\Delta^{7,9(11)}$-choladienate (VI)	+338	+124	+214
Methyl 3-keto-Δ^8-cholenate (VII)	+ 85	+124	− 39
Methyl 3-keto-$\Delta^{8(14)}$-cholenate (VIII)	+263	+124	+139
Methyl 3-keto-$\Delta^{9(11)}$-cholenate (IX)	+127	+124	+ 3
Methyl 3-keto-Δ^{14}-cholenate (X)	+146	+124	+ 22
Methyl 3-keto-Δ^7-cholenate (XI)	+204	+124	+ 80
Methyl 3-keto-Δ^6-cholenate (XII)	−201	+124	− 77
Methyl 3α-acetoxy-12-keto-$\Delta^{9(11)}$-cholenate (XIII)	+489	+692	−203
Methyl 3α-acetoxy-12-keto-Δ^8-cholenate (XIV)	+613	+692	− 79
Methyl 3α-acetoxy-12-keto-$\Delta^{8(14)}$-cholenate (XV)	+244	+692	−448
Methyl 3, 12-diketo-$\Delta^{8(14)}$-cholenate (XVI)	+ 56	+370	−314
Methyl 3, 12-diketo-Δ^{14}-cholenate (XVII)	+208	+370	−168

TABLE III. INFRARED FREQUENCIES FOR BILE ACIDS CONTAINING NUCLEAR DOUBLE BONDS OF VARIOUS TYPES (IN NUJOL)

Unsaturated bile acid	3000∼3100 cm^{-1} (3.3μ)	1620∼1700 cm^{-1} (6μ)	790∼850 cm^{-1} (12μ)
Methyl 3α-hydroxy-Δ^7-cholenate	3018 (sh)*	1640 (st)*	745 (m)*
Methyl 3α-acetoxy-Δ^7-cholenate	3015 (sh)	1678 (sh)	808 (st)
Methyl 3-keto-Δ^7-cholenate	3055 (w) 3012 (sh)	1655 (sh)	795 (w)
Methyl 3-keto-Δ^8-cholenate	3018 (sh)	—	815 (w)
Methyl 3α-acetoxy-Δ^8-cholenate	3045 (sh)	—	840 (w)
Methyl 3-keto-$\Delta^{8(14)}$-cholenate	—	1645 (sh)	770 (w)
Methyl 3α-acetoxy-$\Delta^{8(14)}$-cholenate	—	—	840 (w)
Methyl 3α-hydroxy-Δ^{14}-cholenate	3055 (st)	1648 (m)	793 (m)
Methyl 3α-acetoxy-Δ^{14}-cholenate	3030 (m)	—	770 (m)
Methyl 3-keto-Δ^{14}-cholenate	3055 (m)	1648 (sh)	777 (st)
Methyl 3α-acetoxy-Δ^5-cholenate	—	1680 (sh)	800 (m) 840 (m)
Methyl 3α-hydroxy-Δ^6-cholenate	3040 (m)	—	740 (st)
Methyl 3-keto-Δ^6-cholenate	3040 (m)	1644 (sh)	740 (st)
Methyl 3α-acetoxy-$\Delta^{9(11)}$-cholenate	3020 (sh)	—	775 (w)
Methyl 3-keto-$\Delta^{9(11)}$-cholenate	3018 (sh)	—	825 (w)
Methyl 3α-hydroxy-Δ^4-cholenate	—	1660 (m)	812 (m)
Methyl 3-keto-Δ^4-cholenate	—	1620 (st)	800 (st)
Methyl 3-keto-$\Delta^{7,9(11)}$-cholenate	3020 (sh)	1605 (w)	800 (st)

* sh = shoulder st = strong
w = weak m = moderate

M_D contribution due to the $\Delta^{8(14)}$-bond of methyl 3α-acetoxy-12-keto-$\Delta^{8(14)}$-cholenate is −448, while the corresponding value of 3α-acetoxy-$\Delta^{8(14)}$-cholenate is +47.

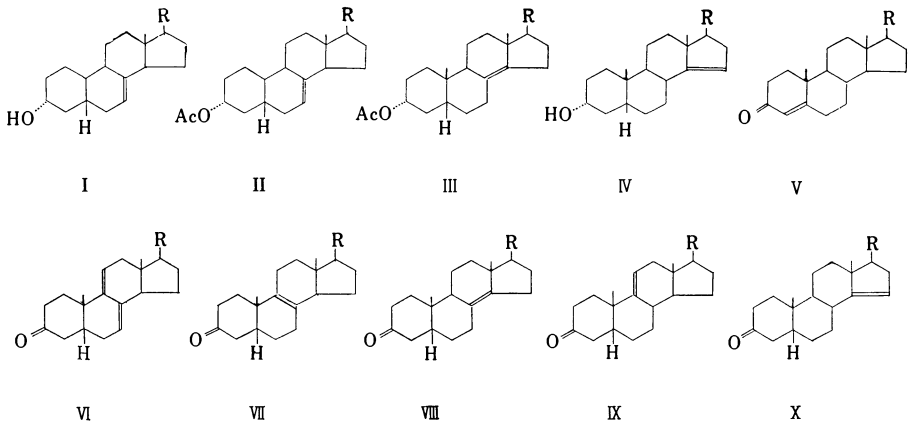
As for the infrared absorption spectra of these unsaturated bile acids (Table III), the trisubstituted ethylenic derivatives (Δ^4, Δ^5, Δ^7 and Δ^{14}) give more or less characteristic absorptions in the regions of 3.3, 6 and 10∼15 μ, as Bladon et al.[7] have pointed out (the $\Delta^{9(11)}$-compounds are exceptions[6]).

While Djerassi et al.[8] have studied the correlation of the isolated ketonic functions in the saturated keto bile acids with the RD curves, the RD curves of unsaturated keto

6) R. N. Jones, P. Humphries, E. Packard and K. Dobriner, *J. Am. Chem. Soc.*, **72**, 86 (1950).

7) P. Bladon, J. M. Fabian, H. B. Henbest, H. P. Koch and G. W. Wood, *J. Chem. Soc.*, **1951**, 2402.

8) C. Djerassi and W. Closson, *J. Am. Chem. Soc.*, **78**, 3761, (1956).



$R = -CH(CH_3)CH_2CH_2COOCH_3$

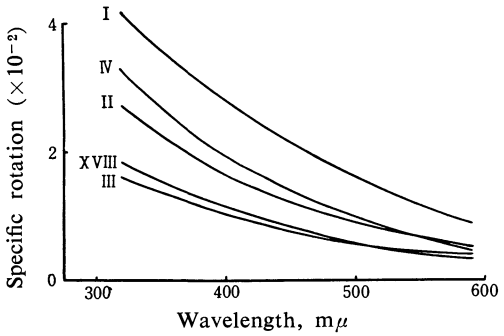


Fig. 1. Rotatory dispersion curves of: methyl 3α-hydroxy-Δ^7-cholenate (I), methyl 3α-acetoxy-Δ^7-cholenate (II), methyl 3α-acetoxy-$\Delta^{8(14)}$-cholenate (III), methyl 3α-hydroxy-Δ^{14}-cholenate (IV) and methyl cholate (XVIII).

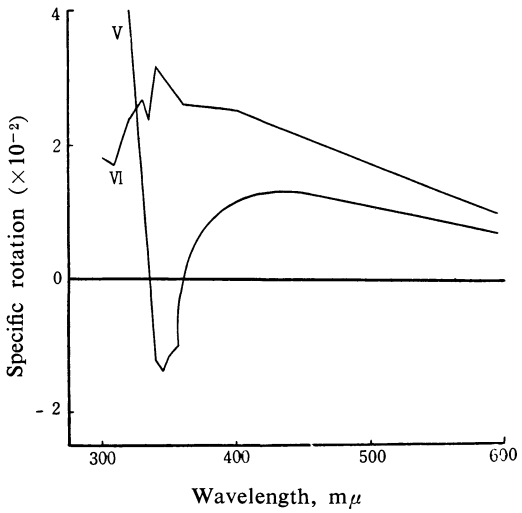


Fig. 2. Rotatory dispersion curves of: methyl 3-keto-Δ^4-cholenate (V) and methyl 3-keto-$\Delta^{7,9(11)}$-choladienate (VI).

bile acids have not yet been covered in the literature. Following Djerassi's report[9], the background rotations of some unsaturated bile acids were measured and compared with that of a saturated bile acid, cholic acid (as methyl ester). As shown in Fig. 1, the unsaturated bile acids (Δ^7, $\Delta^{8(14)}$ and Δ^{14}) (I—IV) give positive plain curves similar to that of cholic acid (XVIII). The background rotations of the above acids, therefore, are not affected by the introduction of these double bonds.

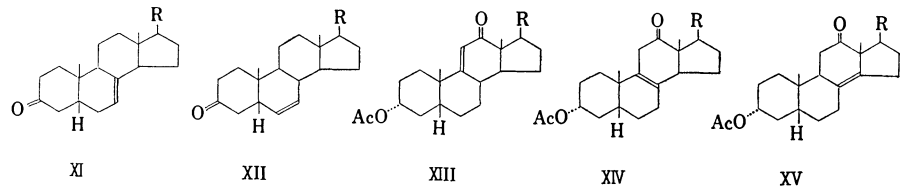
Some kinds of unsaturated keto bile acids with carbonyl groups at C_3 and/or C_{12} were prepared; by measuring their RD curves, the effect of the positions of the double bonds on the RD curves of the parent saturated keto bile acids was studied.

A) Unsaturated 3-Keto Bile Acids.—*A—1) Compounds with Double Bonds in Ring A.*—Methyl 3-keto-Δ^4-cholenate (V) has the same nuclear structure as Δ^4-cholestene-3-one, and, as expected, it gives a multiple negative Cotton-effect RD curve, similar to that of Δ^4-cholestene-3-one[8], as is shown in Fig. 2.

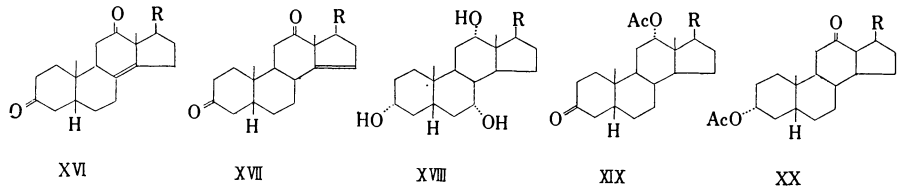
A—2) Compounds with Isolated Double Bonds in Ring C or D.—The unsaturated bile acids VII—X show negative Cotton-effect curves which are not only similar to one another, but also resemble that of methyl 3-keto-12-acetoxycholanate (XIX) (Fig. 3). The result clearly indicates that the introduction of double bonds at positions remote from the carbonyl groups of these bile acids does not exert remarkable effects on the RD curves, though the intensity of the trough in the curves is more or less increased.

A—3) Compounds with Double Bonds in Ring B.—Figure 4 illustrates the RD curves of methyl 3-keto-Δ^7-cholenate (XI) and methyl 3-keto-Δ^6-cholenate (XII). Though the RD curve of

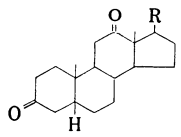
9) C. Djerassi, "Optical Rotatory Dispersion", McGraw-Hill Book Co., Inc., New York (1960), p. 63.



XI XII XIII XIV XV



XVI XVII XVIII XIX XX



XXI

R=-CH(CH$_3$)CH$_2$CH$_2$COOCH$_3$

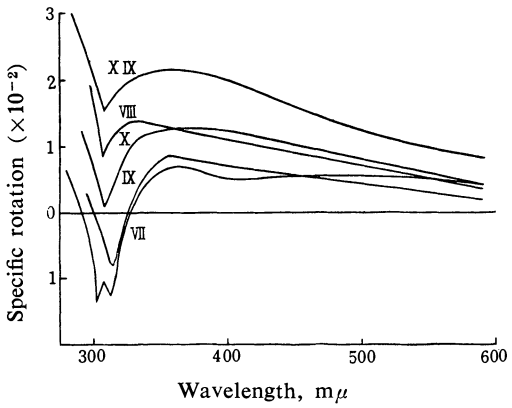


Fig. 3. Rotatory dispersion curves of: methyl 3-keto-Δ^8-cholenate (VII), methyl 3-keto-$\Delta^{8(14)}$-cholenate (VIII), methyl 3-keto-$\Delta^{9(11)}$-cholenate (IX), methyl 3-keto-Δ^{14}-cholenate (X) and methyl 3-keto-12-acetoxycholanate (XIX).

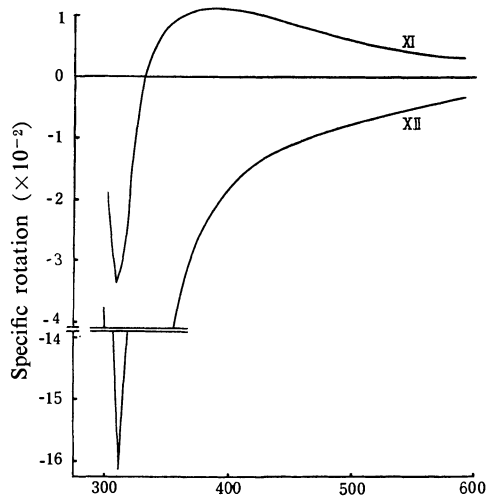


Fig. 4. Rotatory dispersion curves of: methyl 3-keto-Δ^7-cholenate (**XI**) and methyl 3-keto-Δ^6-cholenate (**XII**).

the former XI shows a negative drift greater than those of the above-mentioned compounds with double bonds in ring C or D (A—2), it must be noted that all of these curves are of the same shape. The RD curve of the Δ^6-compound XII is likewise a negative Cotton-effect curve of the same type and, indeed, of a strikingly high intensity (α_{312} −1615°). Since the RD curve of the 3-keto-steroid of the 5α-series with an isolated double bond in ring B hardly differs from that of the corresponding saturated ketone, as Djerassi[9] has pointed out, such a characteristic phenomenon as is given by the above Δ^6-compound XII might be attributable to the cis A/B fusion of this compound and will serve for the diagnosis of the position of the double bond in the unsaturated 3-keto-5β-steroids.

Djerassi et al.[10] reported that the introduction of a second double bond ($\Delta^{9(11)}$) in Δ^7-lanostene-3-one results in a strong positive

10) C. Djerassi and O. Halpern, *J. Am. Chem. Soc.*, **80**, 4001 (1958).

shift of the RD curve. Methyl 3-keto-$\Delta^{7,9(11)}$-choladienate (Fig. 2, VI), which has a structure similar to the lanostadiene derivative, likewise shows a positive, but irregularly shaped, shift of the RD curve of the Δ^{7}-bile acid (XI).

B) Unsaturated 12-Keto Bile Acids. — As reported by Djerassi et al.[8], a series of saturated 12-keto bile acids give positive Cotton-effect curves with peaks on the positive side. The effect of the introduction of double bonds in ring C or D on the RD curves of some 12-keto bile acids was found to be as follows:

B—1) Compounds with α,β-Unsaturated 12-Keto Groups.—The RD curve of methyl 3α-acetoxy-12-keto-$\Delta^{9(11)}$-cholenate (XIII) (Fig. 5) shows a multiple negative Cotton-effect curve quite similar in shape to those of cholestene-3-one and methyl 3-keto-Δ^{4}-cholenate (V) mentioned above (A—1); i. e., the introduction of a double bond conjugated to the keto group resulted in the strong negative shift of the RD curve displayed by the saturated 12-keto bile acid[8]. This phenomenon can be well explained by the fact that the B/C bicyclic system including the $\Delta^{9(11)}$-12-ketone group XIII has quite the same configuration as the A/B bicyclic system with the Δ^{4}-3-ketone group V.

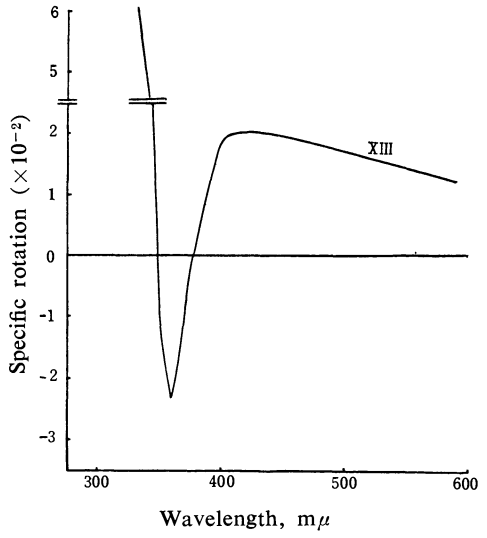


Fig. 5. Rotatory dispersion curves of methyl 3α-acetoxy-12-keto-$\Delta^{9(11)}$-cholenate (XIII).

B—2) Compounds with Isolated Double Bonds in Ring C.—It is very interesting to note that, while the RD curve of methyl 3α-acetoxy-Δ^{8}-cholenate (XIV) gives a positive Cotton-effect curve similar to that of the saturated 12-keto-cholanic acid derivative XX, methyl 3α-acetoxy-12-keto-$\Delta^{8(14)}$-cholenate (XV) shows a very strong negative shift of the RD curve, as is illustrated in Fig. 6. Since methyl 3α-acetoxy-

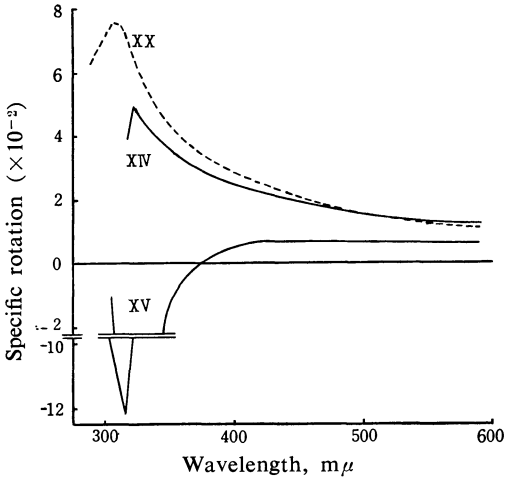


Fig. 6. Rotatory dispersion curves of: methyl 3α-acetoxy-12-keto-Δ^{8}-cholenate (XIV), methyl 3α-acetoxy-12-keto-$\Delta^{8(14)}$-cholenate (XV) and methyl 3α-acetoxy-12-keto-cholanate (XX).

$\Delta^{8(14)}$-cholenate (III) shows a positive background rotation just like the saturated bile acids (Fig. 1), such an inversion of the Cotton-effect as is shown by the $\Delta^{8(14)}$-12-keto bile acid XV might be attributed to a possible fact that the environment surrounding the C_{12}-carbonyl group of the bile acid XX is altered by the introduction of the $\Delta^{8(14)}$-bond so as to result in a strong inversion of the Cotton-effect.

B—3) 3,12-Diketo Bile Acids with Double Bonds in Ring C or D.—Previously Djerassi et al.[8]

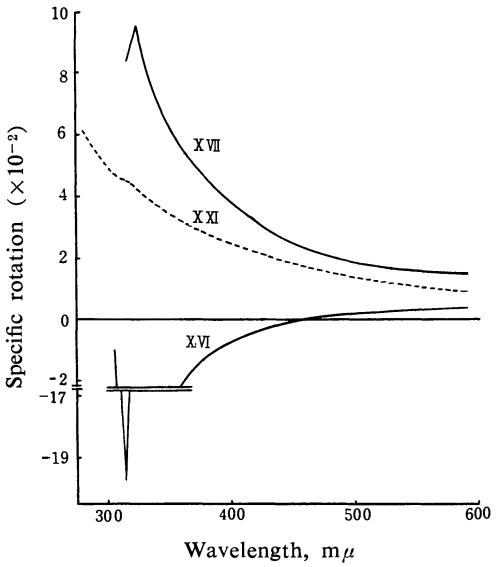


Fig. 7. Rotatory dispersion curves of: methyl 3, 12-dikoto-$\Delta^{8(14)}$-cholenate (XVI), methyl 3, 12-diketo-Δ^{14}-cholenate (XVII) and methyl 3, 12-diketocholanate (XXI).

reported that the RD curves of saturated diketo bile acids, such as 3, 12-diketocholanic acid (XXI), can be calculated by superimposing the RD curve of 3-ketocholanic acid on that of 12-ketocholanic acid. As samples of unsaturated diketo bile acid, methyl 3, 12-diketo-$\Delta^{8(14)}$-cholenate (XVI) and methyl 3, 12-diketo-Δ^{14}-cholenate (XVII) were prepared and their RD curves were determined. The curves are shown in Fig. 7. Such an inversion of the Cotton-effect as is shown above (B—2) is also observed in the RD curve of the $\Delta^{8(14)}$-diketo bile acid (XVI), and the negative Cotton-effect given by methyl 3α-acetoxy-12-keto-$\Delta^{8(14)}$-cholenate (XV) is increased by the introduction of the 3-keto group. The RD curve of the Δ^{14}-diketo bile acid (XVII) shows that the positive Cotton-effect RD curve of the saturated 12-ketocholanic acid XX is superimposed by the curve of methyl 3-keto-Δ^{14}-cholenate (X).

Experimental*

Methyl 3α-Hydroxy-Δ^{7}-cholenate[1] **(I).**—M. p. 108°C, $[\alpha]_D^{24}$ +61° (chf.). IR ν_{max}^{Nujol}; 846 cm^{-1} (=C-H), 1738 cm^{-1} (C=O), 3366 cm^{-1} (OH). RD (Fig. 1); $[\alpha]_{589}^{19.5}$ +85°, $[\alpha]_{400}$ +256°, $[\alpha]_{320}$ +416° (Zr).

Methyl 3α-Acetoxy-Δ^{7}-cholenate[1] **(II).**—M. p. 125°C, $[\alpha]_D^{23}$ +86° (chf.). IR ν_{max}^{Nujol}; 808 cm^{-1} (=C-H), 1241 cm^{-1} (C-O-C), 1745 cm^{-1} (C=O), 1678 cm^{-1} (C=C); RD (Fig. 1); $[\alpha]_{589}^{19.5}$ +45°, $[\alpha]_{400}$ +188°, $[\alpha]_{320}$+322° (Zr).

Methyl 3α-Acetoxy-$\Delta^{8(14)}$-cholenate[2] **(III).**—M. p. 81~83°C, $[\alpha]_D^{18}$ +52° (chf.). IR ν_{max}^{Nujol}; 1200 cm^{-1} (C-O-C), 1740 cm^{-1} (C=O). RD (Fig. 1); $[\alpha]_{589}^{19.5}$ +50°, $[\alpha]_{400}$ +168°, $[\alpha]_{320}$ +286° (Zr).

Methyl 3α-Hydroxy-Δ^{14}-cholenate (IV)[1,2].—M. p. 141°C, $[\alpha]_D^{20}$ +55° (chf.). IR ν_{max}^{Nujol}; 793 cm^{-1} (=C-H), 1743 cm^{-1} (C=O), 3299 cm^{-1} (OH). RD (Fig. 1); $[\alpha]_{589}^{19.5}$ +47°, $[\alpha]_{400}$ +116°, $[\alpha]_{320}$ +164° (Zr).

Methyl 3-Keto-Δ^{4}-cholenate[11] **(V).**—M. p. 125°C, $[\alpha]_D^{21}$ +61° (chf.). IR ν_{max}^{Nujol}; 800 cm^{-1} (=C-H), 1680 cm^{-1} (C=C), 1740 cm^{-1} (C=O). RD (Fig. 2); $[\alpha]_{589}^{23.3}$ +70°, $[\alpha]_{400}$ +117°, $[\alpha]_{350}$ −120°, $[\alpha]_{345}$ −138° (broad trough), $[\alpha]_{340}$ −125° (Zr).

Found: C, 77.43; H, 10.04. Calcd. for $C_{25}H_{38}O_3$ (386.55): C, 77.67; H, 9.91%.

Methyl 3-Keto-$\Delta^{7,9(11)}$-choladienate[12] **(VI).**—M. p. 144°C, $[\alpha]_D^{21}$ +88° (chf.). IR ν_{max}^{Nujol}; 800 cm^{-1} (=C-H), 1709 cm^{-1}, 1738 cm^{-1} (C=O). RD (Fig. 2); $[\alpha]_{589}^{26.7}$ +100°, $[\alpha]_{400}$ +250°, $[\alpha]_{340}$ +315° (peak), $[\alpha]_{335}$ +227° (trough), $[\alpha]_{330}$ +268° (peak), $[\alpha]_{325}$ +259° (Zr).

Found: C, 78.06; H, 9.36. Calcd. for $C_{25}H_{36}O_3$ (384.54): C, 78.08; H, 9.44%.

Methyl 3-Keto-Δ^{8}-cholenate (VII).—3α-Acetoxy-12-keto-Δ^{8}-cholenic acid (m. p. 148°C) (200 mg.), synthesized by the method reported by Fieser et al.[13], was reduced by the Huang-Minlon procedure (hydrazine hydrate, 5 ml. and potassium hydroxide, 5 g.). The resulting free acid (m. p. 173°C) was methylated with diazomethane, and the product was oxidized according to the method of Bladon et al.[3] The oxidation product was chromatographed and recrystallized from methanol. Yield, 68 mg., m.p. 122°C, $[\alpha]_D^{20}$ +22° (chf.). IR ν_{max}^{Nujol}; 1715 cm^{-1}, 1740 cm^{-1} (C=O). RD (Fig. 3); $[\alpha]_{589}^{28.3}$ +18°, $[\alpha]_{400}$ +66°, $[\alpha]_{310}$ −125°, $[\alpha]_{302.5}$ −134° (trough), $[\alpha]_{300}$ −73° (Xe).

Found: C, 77.50; H, 9.84. Calcd. for $C_{25}H_{38}O_3$ (386.55): C, 77.65; H, 9.91%.

Methyl 3-Keto-$\Delta^{8(14)}$-cholenate (VIII).—3α-Hydroxy-$\Delta^{8(14)}$-cholenic acid (m. p. 168°C) (100 mg.), derived from apocholic acid[2], was methylated with diazomethane, and the ester was oxidized according to the method of Bladon et al.[3] Yield, 56 mg., m. p. 104°C, $[\alpha]_D^{19}$ +68° (chf.). IR ν_{max}^{Nujol}; 1710 cm^{-1}, 1730 cm^{-1} (C=O). RD (Fig. 3); $[\alpha]_{589}^{16.4}$ +39°, $[\alpha]_{400}$ +112°, $[\alpha]_{310}$ +105°, $[\alpha]_{307.5}$ +87° (trough), $[\alpha]_{305}$ +115° (Zr.)

Found: C, 77.19; H, 9.80. Calcd. for $C_{25}H_{38}O_3$ (386.55): C, 77.65; H, 9.91%.

Methyl 3-Keto-$\Delta^{9(11)}$-cholenate (IX).—Methyl 3α-acetoxy-12-keto-$\Delta^{9(11)}$-cholenate (200 mg.) obtained by the method reported by Fieser et al.[13], was reduced by the Huang-Minlon method as mentioned above, and the product (its methyl ester) was purified by chromatography. Methyl 3α-hydroxy-$\Delta^{9(11)}$-cholenate (m. p. 103°C) thus obtained was oxidized with a chromic acid-sulfuric acid mixture[3]. The oxidation product was recrystallized from methanol. M. p. 106°C, $[\alpha]_D^{21}$ +33° (chf.). IR ν_{max}^{Nujol}; 825 cm^{-1} (=C-H), 1720 cm^{-1}, 1738 cm^{-1} (C=O); RD (Fig. 3): $[\alpha]_{589}^{21}$ +41°, $[\alpha]_{400}$ +102°, $[\alpha]_{317.5}$ −66°, $[\alpha]_{315}$ −81° (broad trough), $[\alpha]_{312.5}$ −76°.

Found: C, 77.01; H, 9.83. Calcd. for $C_{25}H_{38}O_3$ (386.55): C, 77.67; H, 9.91%.

Methyl 3-Keto-Δ^{14}-cholenate (X)[1].—M. p. 89°C, $[\alpha]_D^{24}$ +38° (chf.). IR ν_{max}^{Nujol}; 777 cm^{-1} (=C-H), 1715 cm^{-1}, 1742 cm^{-1} (C=O). RD (Fig. 3); $[\alpha]_{589}^{19}$ +42°, $[\alpha]_{400}$ +122°, $[\alpha]_{310}$ +14°, $[\alpha]_{307.5}$ +10° (trough), $[\alpha]_{305}$ +24 (Zr).

Methyl 3-Keto-Δ^{7}-cholenate[1] **(XI).**—M. p. 125°C, $[\alpha]_D^{23}$ +62° (chf.). IR ν_{max}^{Nujol}; 795 cm^{-1} (=C-H), 1712 cm^{-1}, 1740 cm^{-1} (C=O). RD (Fig. 4); $[\alpha]_{589}^{20.8}$ +29°, $[\alpha]_{400}$ +110°, $[\alpha]_{310}$ −322°, $[\alpha]_{307.5}$ −334° (trough), $[\alpha]_{305}$ −186° (Zr).

Methyl-3-Keto-Δ^{6}-cholenate (XII).—3α-Hydroxy-Δ^{6}-cholenic acid (m. p. 214°C) prepared according to the method of Schubert et al.[14] was methylated with diazomethane, and the product was oxidized with a chromic acid-sulfuric acid mixture[3]. M. p. 125°C, $[\alpha]_D^{22}$ −52° (chf.). IR ν_{max}^{Nujol}: 740 cm^{-1} (=C-H), 1717 cm^{-1}, 1743 cm^{-1} (C=O). RD (Fig. 4);

* Ultraviolet absorption spectra were measured in ethanol solutions with a Beckman spectrophoto-densitometer (Model DU); rotatory dispersion, in methanol solutions (concentration: 0.1%), with a Rudolph high precision photoelectric polarimeter (Model 200S-80Q) (light source: zirconium lamp (Zr) or xenon arclamp (Xe)).

11) L. F. Fieser and R. Ettorre, *J. Am. Chem. Soc.*, **75**, 1700 (1953).

12) L. F. Fieser, Wei-Yuan, Huang and J. C. Babcock, ibid., **75**, 116 (1953).

13) L. F. Fieser and S. Rajagopalan, E. Wilson and M. Tishler, ibid., **73**, 4133 (1951).

14) A. Schubert and C. Damker, *J. prakt. Chem.* (*4*), **4**, 260 (1957).

$[\alpha]_{589}^{28.2}$ −33°, $[\alpha]_{400}$ −178°, $[\alpha]_{315}$ −1524°, $[\alpha]_{312.5}$ −1615° (trough), $[\alpha]_{310}$ −1485° (Xe and Zr).

Found: C, 77.52; H, 9.85. Calcd. for $C_{25}H_{38}O_3$ (386.55): C, 77.67; H, 9.91%.

Methyl 3α-Acetoxy-12-keto-$\Delta^{9(11)}$-cholenate (XIII). —3α-Hydroxy-12-keto-$\Delta^{9(11)}$-cholenic acid (m. p. 117°C), obtained by Fieser's method[13], was methylated (diazomethane) and then acetylated as usual. M. p. 144°C, $[\alpha]_D^{22}$ +110° (chf.). IR ν_{max}^{Nujol}; 1245 cm^{-1} (C-O-C), 1680 cm^{-1}, 1730 cm^{-1}, 1740 cm^{-1} (C=O). RD (Fig. 5); $[\alpha]_{589}^{22.1}$ +128°, $[\alpha]_{400}$ +185°, $[\alpha]_{365}$ −203°, $[\alpha]_{360}$ −236° (trough), $[\alpha]_{357.5}$ −184° (Xe).

Found: C, 73.06; H, 901 Calcd. for $C_{27}H_{40}O_5$ (444.617): C, 72.94; H, 9.07%.

Methyl 3α-Acetoxy-12-keto-Δ^{8}-cholenate (XIV). —This compound was prepared by the method reported by Fieser et al.[13] M. p. 131°C, $[\alpha]_D^{22}$ +138° (chf.). IR ν_{max}^{Nujol}; 120 cm^{-1}, 1255 cm^{-1} (C-O-C), 1705 cm^{-1}, 1734 cm^{-1} (C=O); RD (Fig. 6); $[\alpha]_{589}^{28}$ +123°, $[\alpha]_{400}$ +263°, $[\alpha]_{325}$ +468, $[\alpha]_{322.5}$ +491° (peak), $[\alpha]_{320}$ +455°.

Found: C, 72.97; H, 8.99. Calcd. for $C_{27}H_{40}O_5$ (444.59): C, 72.94; H, 9.07%.

Methyl 3α-Acetoxy-12-keto-$\Delta^{8(14)}$-cholenate (XV). —3α-Ethoxycarbonyloxy-12-keto-$\Delta^{8(14)}$-cholenate (m. p. 116°C), prepared by the method reported previously[2], was hydrolyzed by boiling over a water bath with 20 ml. of a 3% methanolic potassium hydroxide solution. The free acid obtained was methylated (diazomethane) and then acetylated as usual. M. p. 98°C, $[\alpha]_D^{19}$ +55° (chf.). IR ν_{max}^{Nujol}; 1245 cm^{-1} (C-O-C), 1720 cm^{-1}, 1730 cm^{-1} (C=O); RD (Fig. 6); $[\alpha]_{589}^{22.5}$ +57°, $[\alpha]_{400}$ +52°, $[\alpha]_{317.5}$ −1188°, $[\alpha]_{315}$ −1228° (trough), $[\alpha]_{312.5}$ −1169° (Xe).

Found: C, 73.12; H, 9.08. Calcd. for $C_{27}H_{40}O_5$ (444.59): C, 72.94; H, 9.07%.

Methyl 3, 12-Diketo-$\Delta^{8(14)}$-cholenate (XVI).— Methyl apocholate (m. p. 82°C) was oxidized with a chromic acid-sulfuric acid mixture[3]. M. p. 120°C, $[\alpha]_D^{18}$ +14° (chf.). IR ν_{max}^{Nujol}; 1740 cm^{-1}, 1715 cm^{-1} (C=O). RD (Fig. 7); $[\alpha]_{589}^{28.2}$ +32°, $[\alpha]_{400}$ −67°, $[\alpha]_{320}$ −1384°, $[\alpha]_{317.5}$ −1986° (trough), $[\alpha]_{315}$ −1455° (Xe).

Found: C, 74.59; H. 8.99. Calcd. for $C_{25}H_{36}O_4$ (346.56): C, 74.96; H, 9.06%.

Methyl 3, 12-Diketo-Δ^{14}-cholenate[1].—M. p. 134°C, $[\alpha]_D^{22}$ +60° (chf.). IR ν_{max}^{Nujol}; 780 cm^{-1} (=C-H), 1705 cm^{-1}, 1738 cm^{-1} (C=O). RD (Fig. 7); $[\alpha]_{589}^{20}$ +141°, $[\alpha]_{400}$ +380°, $[\alpha]_{322.5}$ +955° (peak), $[\alpha]_{320}$ +916° (Xe).

Summary

Not only ultraviolet and infrared absorption spectra but also optical rotatory dispersions of various unsaturated bile acids were studied, and most of the data were found to be in good agreement with those hitherto obtained concerning the other steroids. The determination of the rotatory dispersion gave the following results:

1) The background rotation of the saturated bile acid is not affected by the introduction of a double bond in ring B, C or D.

2) The introduction of a double bond in ring C or D does not remarkably affect the RD curve of the saturated 3-keto bile acids, while the negative drift of the RD curve given by 3-keto-Δ^{6}-cholenic acid is so very striking that this phenomenon could be utilized for the diagnosis of Δ^{6}-3-keto bile acids (5β).

3) The positive Cotton-effect RD curve given by a saturated 12-keto bile acid is strongly inverted by the introduction of the $\Delta^{8(14)}$-bond, but not by that of the Δ^{8}-bond.

The author is greatly indebted to Professor Dr. K. Yamasaki, Department of Biochemistry, Tottori University School of Medicine, Yonago, and to Professor Dr. K. Tsuda, Pharmaceutical Institute, the University of Tokyo, for their valuable suggestions and encouragement. He is also heartily thankful to Drs. T. Okuda and S. Susuki, Laboratory of the Tanabe Seiyaku Co., Tokyo; to Mr. F. Nakada, Department of Biochemistry, Tottori University School of Medicine, Yonago; to Miss. F. Tomura and Mr. T. Murata, Laboratory of the Nippon Eiyô Kagaku Co., Tokyo, and to the doctors of the Laboratory for the Applied Microbiology, the University of Tokyo, for their technical assistance.

Department of Biochemistry
Tottori University
School of Medicine, Yonago
and
Laboratory of the Nippon
Eiyô Kagaku Co.
Katsushika-ku, Tokyo

Physicochemical Studies on Cobalt Salts of Higher Fatty Acids. IX. Cobalt Complex Soap

By Hirotaro KAMBE*

(Received March 29, 1961)

It has been certified the cobalt soap is a salt between cobalt ion and fatty acid ion, in Part IV of these studies[1]. In the present paper, the preparation of soaps of cobalt complex ions is presented and some of their properties are investigated.

The reflection spectrum of cobalt complex soap shows that it certainly has color characteristics similar to those of the parent cobalt complex ion. In the infrared absorption spectrum, the existence of carboxylate ion is confirmed, as in simple cobalt soap. The magnetic susceptibility of complex soap verifies that cobalt(III) ion is in a state of an electronic configuration of d^2sp^3 six covalent complex ion. Decomposition at heating was followed by thermogravimetric analysis.

Experimental

Cobalt complex soaps were prepared by metathesis between inorganic cobalt complex salts and potassium soap, as was the simple cobalt soap described in Part I. Luteo-salt, $[Co(III)(NH_3)_6]Cl_3$, and purpureo-salt, $[Co(III)(NH_3)_5Cl]Cl_2$, were used as inorganic salts. Hereafter, these salts are called I and II respectively. Stearates of these complex ions are called I-S and II-S respectively.

Reflection spectrophotometry, infrared absorption spectrophotometry, and the measurement of magnetic susceptibility were carried out as in Parts III and IV. Thermogravimetry was conducted as in Part VI.

Results and Discussion

The reflection spectra of cobalt complex soaps are shown in Fig. 1, with that of inorganic complexes. Their trichromaticity constants were calculated as in Part III and are shown in Table I.

The similarity of the trichromaticity constants, in particular those of the dominant wavelength, of complex soaps to that of the inorganic complex ion suggests the ionic nature of these soaps.

The infrared absorption spectra of these soaps and the parent complexes are shown in Figs. 2 and 3 and in Table II. Since carboxylate absorptions at 1400 and 1540 cm^{-1} are clearly found in them, it is evident that they are truly ionic. Absorptions of ammonia bending appeared as several bands around 1320 cm^{-1}, and as a broad band 1550~1600 cm^{-1}.

The specific magnetic susceptibility of cobalt

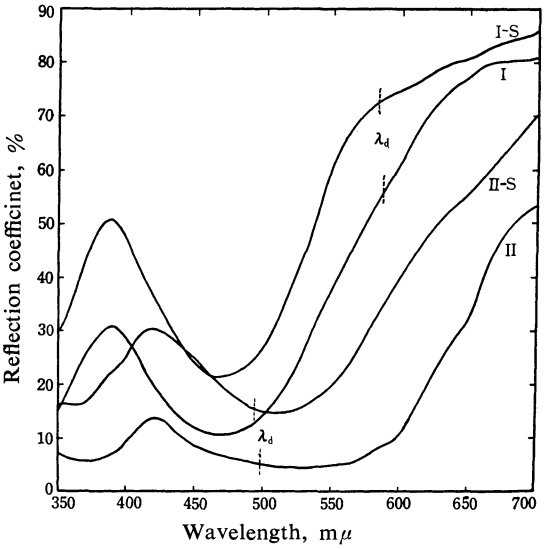


Fig. 1. Reflection spectra of cobalt complexes and cobalt complex soaps.

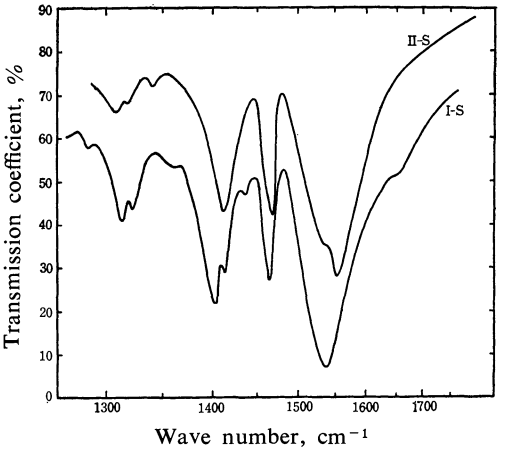


Fig. 2. Infrared absorption spectra of cobalt complex soaps.

* Present address: Aeronautical Research Institute, the University of Tokyo, Meguro-ku, Tokyo.

1) H. Kambe, This Bulletin, 34, 1786, 1790, 1794 (1961); 35, 78, 265, 269 (1962); H. Kambe and I. Mita, ibid., 34, 1797 (1961); H. Kambe, T. Ozawa, M. Onoue and S. Igarashi, ibid., 35, 81 (1962).

TABLE I. TRICHROMATICITY CONSTANTS OF COBALT COMPLEXES AND THEIR STEARATES

System	Tristimulus values			Trichromatic coeff.			Dominant wavelength, purity and brightness		
	X	Y	Z	x	y	z	λ_d	p_c	Y
I, $[Co(NH_3)_6]Cl_3$	48.19	41.46	15.82	0.457	0.393	0.150	587	60	41.46
I-S, $[Co(NH_3)_6]St_3$	61.45	58.01	30.60	0.410	0.386	0.204	583	45	58.01
II, $[Co(NH_3)_5Cl]Cl_2$	12.41	77.69	10.34	0.408	0.253	0.339	499c	44	77.69
II-S, $[Co(NH_3)_5Cl]St_2$	34.04	26.28	27.75	0.387	0.298	0.315	494c	22	26.28

TABLE II. INFRARED ABSORPTION SPECTRA OF COBALT COMPLEXES AND THEIR STEARATES*

	Sym. bend. NH_3		Bend. CH_2			Degener. bend. NH_3		
I, $[Co(NH_3)_6]Cl_3$	s 1326		sh 1356			d,m 1600		
II, $[Co(NH_3)_5Cl]Cl_2$	s 1310		w 1368	sh 1420		d,m 1550		
			sym. str. COO^-			asym. str. COO^-		
I-S, $[Co(NH_3)_6]St_3$	m 1312	sh 1321	s 1398	sh 1443	m 1459	s 1466	s 1542	
II-S, $[Co(NH_3)_5Cl]St_2$	w 1310	sh 1318	w 1340	m 1412		m 1468	sh 1542	s 1557

* s: strong; m: medium; w: weak; sh: shoulder; d: diffuse

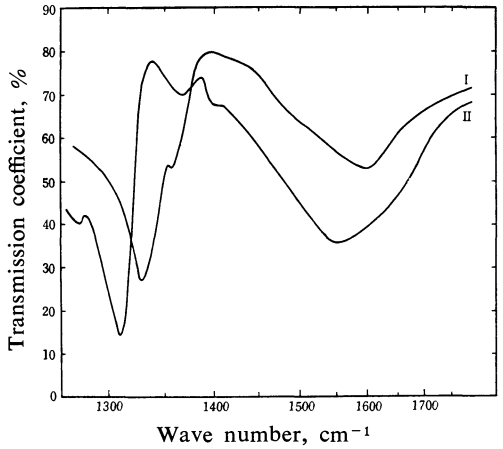


Fig. 3. Infrared absorption spectra of cobalt complexes.

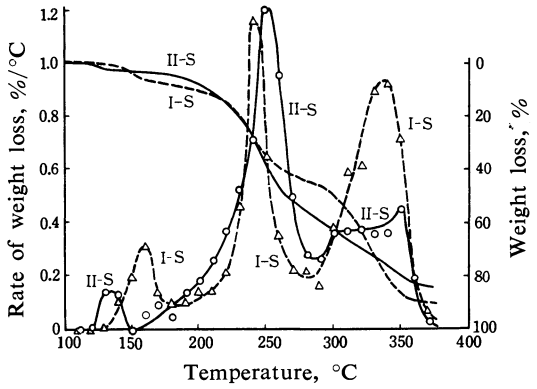


Fig. 4. Thermogravimetric curves of cobalt complex soaps.

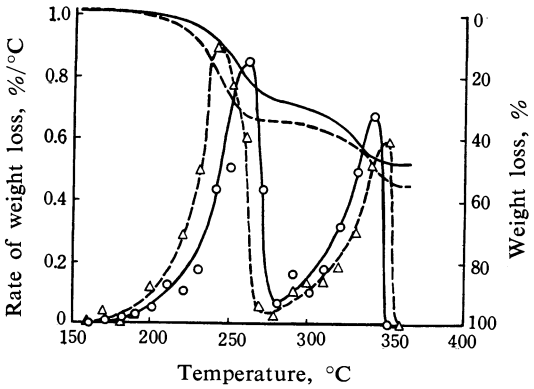


Fig. 5. Thermogravimetric curves of cobalt complexes.

complex soap I-S was measured as -0.58×10^{-6} c. g. s. Its molar susceptibility was calculated as -587.54×10^{-6} c. g. s. As the diamagnetic susceptibility of stearate ion is -209×10^{-6}, and that of cobalt(III) complex ion is -38×10^{-6}, the calculated value of the diamagnetic susceptibility of cobalt complex soap is -665×10^{-6} c. g. s., which is consistent with the observed value. In consequence, cobalt ion in cobalt complex soap is in the octahedral six-covalent electronic configuration, $(3d)^2(4s)(4p)^3$.

The decomposition curves of the cobalt complex soaps are shown in Fig. 4, and that of their parent inorganic complexes in Fig. 5. Inorganic complexes decompose at two stages. The first decomposition begins at 150°C and, through a maximum rate at 230°C for I and at

260°C for II, ends at 280°C. The second decomposition begins at 280°C and ends at 350~360°C, through a maximum rate at 350°C for I and 340°C for II. These peaks correspond to the liberation of ammonia at the first peak and of chlorine at the second peak. The residue is cobalt chloride.

The decomposition curves of cobalt complex soaps show three peaks. At the first peak ammonia is liberated, which is certified by an insertion of litmus paper in it. At the second peak, the white crystal deposits on the inner wall of the glass tube surrounding the reaction chamber, as was also observed in the decomposition of simple cobalt soaps (Part VI). At this stage, about one molecule of stearic acid is liberated as stearone from each soap. The last peak differs greatly between the two soaps. The remainder of stearic acid in the soap must be liberated, but stearone is not observed in this stage. The intermediate reaction products were not confirmed. The residue contains cobalt oxide in both cases.

Summary

Soaps of cobalt complex ions and fatty acid have been prepared and investigated. Reflection spectra and infrared spectra show that these soaps are ionic in nature, as is simple cobalt soap. The magnetic susceptibility of complex soap shows that cobalt ion is in the electronic configuration of octahedral six-covalent cobalt-(III) ion. Thermogravimetric analysis of these soaps shows that they decompose at three stages, but the precise mechanism of these reactions has not yet been determined.

The author expresses his gratitude to Professor Bunnosuke Yamaguchi for his advice throughout these studies, and to Messrs. Itaru Mita and Shoichi Igarashi for their help in the experiments.

Institute for Science and Technology
and Aeronautical Research Institute
The University of Tokyo
Meguro-ku, Tokyo

Electronic Structures of Naphthalenediols. II. β, β′-Naphthalenediols

By Kichisuke NISHIMOTO and Ryoichi FUJISHIRO

(Received April 21, 1961)

To elucidate the molecular properties of naphthalene derivatives with auxochromic substituents, such as methoxy, amino, halogen etc., we have been studying the electronic structures of naphthalenediols. In the previous paper[1], we studied the electronic structures of α, α'-naphthalenediols and pointed out that their molecular properties, such as charge distribution and electronic spectra, depend remarkably upon the type of substitution. These are as follows:

(1) A, A-derivative, in which two hydroxy groups link to the same ring, (A ring in Fig. 1)

(2) A, B-derivatives, in which each hydroxy group bonds with a different ring.

Namely, in the case of 1, 4-diol it is found from the molecular diagram[1] that the substituents have no significant influence upon the B ring, which remains nearly the same as naphthalene, but do produce rather a large effect on the A ring. This fact seems to suggest that the 9—10 bond plays an important role in the conjugation interaction between the ring and the substituents. In the present paper, we will examine this point by calculations based on the perimeter models. It is a well-known fact to organic chemists[2] that the reactivities of naphthalene derivatives with substituents in β-position are peculiar. In the present paper, the theoretical treatment based on the simple MO theory will be applied to the electronic structures of β, β'-naphthalenediols, such as 2, 3-, 2, 6- and 2, 7-diols and

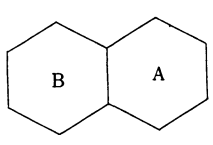


Fig. 1

1) K. Nishimoto and R. Fujishiro, This Bulletin, 32, 445 (1959).

2) a) G. M. Badger, "The Structures and Reactions of the Aromatic Compounds", University Press, Cambridge (1952).

b) L. F. Fieser and M. Fieser, "Textbook of Organic Chemistry", Heath and Company (1950).

we will try to explain the peculiarities in the reactivities of those molecules.

Method of Calculation

The calculation is carried out by means of the simple LCAO MO theory, with only $2p\pi$-electrons considered explicitly. The Coulomb and the resonance integrals used are the same as those in the previous paper[1]. The numbering of the atoms and the symmetry orbitals for the molecules are shown in Fig. 2. The notations of irreducible representations are also the same as those in the previous paper.

Results and Discussion

Vacant MO's and Molecular Diagrams.— The π-MO's of each naphthalenediol are expressed by linear combinations of the twelve $2p\pi$ atomic orbitals. Consequently, there are twelve π-MO's in each diol. According to Pauli's principle, the lowest seven are occupied by fourteen electrons. In the ordinary method

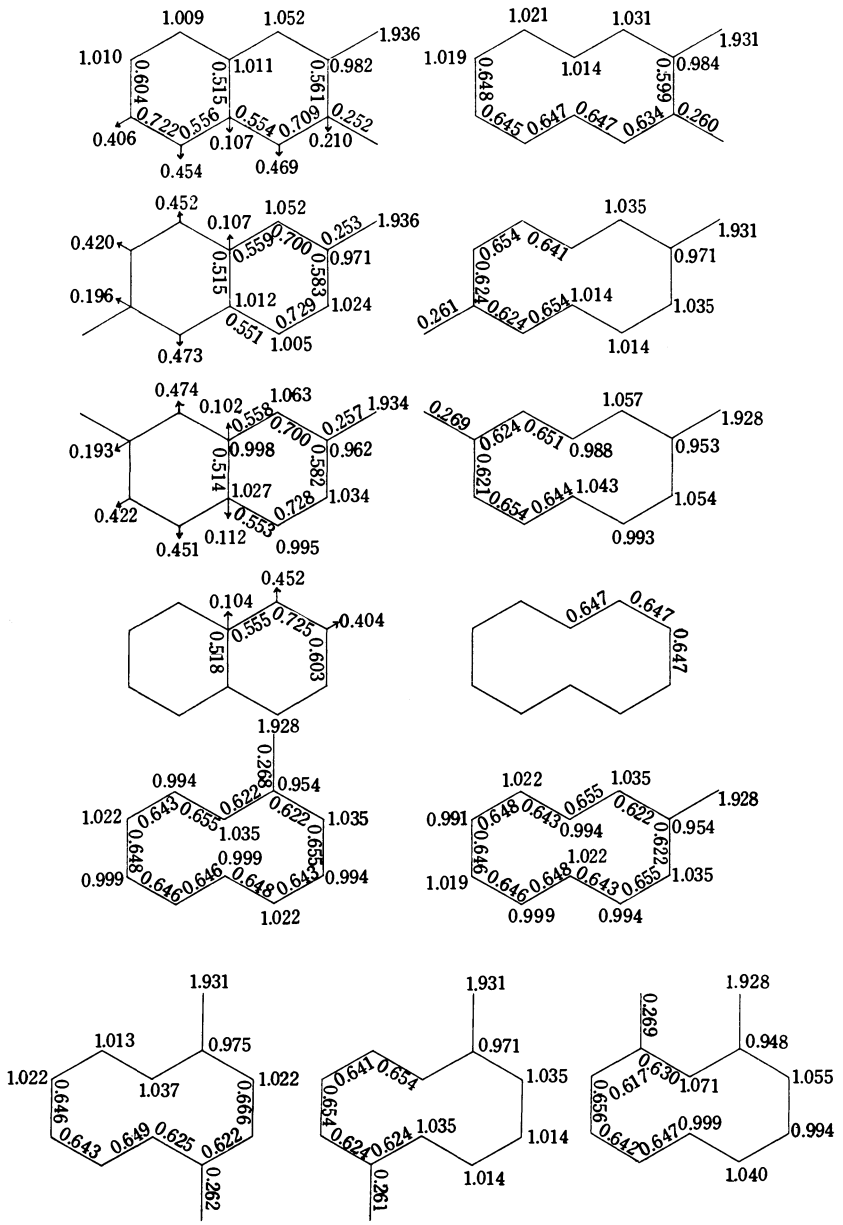


Fig. 2. Molecular diagrams of naphthalene and its hydroxy derivatives.

TABLE I. VACANT MO'S AND MO ENERGIES OF NAPHTHALENEDIOLS

Orbital energy in β	MO
	2,3-Naphthalenediol
−2.3181	$\phi_5^v=0.3063\sigma_7-0.2575\sigma_8+0.2902\sigma_9-0.2202\sigma_{10}-0.4526\sigma_{11}+0.0473\sigma_{12}$
−1.6775	$\phi_4^v=0.2338\sigma_7-0.4468\sigma_8-0.2708\sigma_9+0.3997\sigma_{10}+0.0546\sigma_{11}+0.0984\sigma_{12}$
−1.3143	$\phi_3^v=0.4054\sigma_1-0.1895\sigma_2+0.3891\sigma_3-0.1681\sigma_4-0.3433\sigma_5+0.0473\sigma_6$
−1.0571	$\phi_2^v=-0.0483\sigma_7-0.3589\sigma_8+0.0249\sigma_9-0.4364\sigma_{10}+0.4100\sigma_{11}+0.0983\sigma_{12}$
−0.6518	$\phi_1^v=0.3984\sigma_1-0.2797\sigma_2-0.4315\sigma_3+0.2612\sigma_4+0.0200\sigma_5+0.0908\sigma_5$
	2,6-Naphthalenediol
−2.3173	$\phi_5^v=0.3010\sigma_7-0.2441\sigma_8+0.2332\sigma_9-0.2963\sigma_{10}-0.4535\sigma_{11}+0.0449\sigma_{12}$
−1.6772	$\phi_4^v=0.2761\sigma_1-0.4458\sigma_2+0.4029\sigma_3-0.2299\sigma_4-0.0172\sigma_5+0.0981\sigma_6$
−1.3118	$\phi_3^v=0.3751\sigma_1-0.1485\sigma_2-0.2061\sigma_3+0.4188\sigma_4-0.3435\sigma_5+0.0371\sigma_6$
−1.0686	$\phi_2^v=0.0200\sigma_7-0.4316\sigma_8+0.3589\sigma_9+0.0481\sigma_{10}+0.4103\sigma_{11}+0.1176\sigma_{12}$
−0.6447	$\phi_1^v=0.4075\sigma_7-0.2190\sigma_8-0.3164\sigma_9+0.4230\sigma_{10}-0.0437\sigma_{11}+0.0716\sigma_{12}$
	2,7-Naphthalenediol
−2.3173	$\phi_5^v=0.3020\sigma_1-0.2444\sigma_2+0.2329\sigma_3-0.2953\sigma_4-0.4555\sigma_5+0.4514\sigma_6+0.0449\delta_7$
−1.6766	$\phi_4^v=0.2633\sigma_8-0.4414\sigma_9+0.4086\sigma_{10}-0.2437\sigma_{11}+0.0973\sigma_{12}$
−1.3159	$\phi_3^v=0.3878\sigma_1-0.2151\sigma_2-0.1422\sigma_3-0.4023\sigma_3-0.2952\sigma_5-0.3871\sigma_6+0.0535\sigma_7$
−1.0623	$\phi_2^v=-0.0591\sigma_1-0.3919\sigma_2+0.4005\delta_3-0.0335\sigma_4+0.4547\sigma_5-0.3649\sigma_6+0.1070\sigma_7$
−0.6488	$\phi_1^v=0.3923\sigma_8-0.2545\sigma_9-0.2852\sigma_{10}+0.4395\sigma_{11}+0.0829\sigma_{12}$

it is necessary to use these seven occupied MO's in constructing the molecular diagram. The other five are called "vacant MO's". As we have pointed out in a previous paper[3], the molecular diagram of a diol is obtained from only the five vacant MO's; namely, the π-electron density on the μ-th atom, q_μ, the π-bond order for the μ-ν bond, $p_{\mu\nu}$, and the free valency of the μ-th atom, f_μ, are given by the following relations respectively:

i) $q_\mu=2-2\sum_i^{\text{vac}} C_{\mu i}^2$

ii) $p_{\mu\nu}=-2\sum_i^{\text{vac}} C_{\mu i}C_{\nu i}$

iii) $f_\mu=\sqrt{3}-\sum_\nu p_{\mu\nu}$

(μ and ν are nearest neighbors)

in which $\sum_i^{\text{vac}}$ means the summation over the vacant orbitals and $C_{\mu i}$ is the coefficient of the μ-th $2p\pi$ atomic orbital, ϕ_μ, in the i-th MO, ϕ_i.

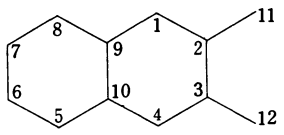
The calculated vacant MO's, ϕ_i^v, are given in Table I, and the molecular diagrams are indicated in Fig. 3. A comparison of these diagrams with those of α,α'-diols[1] makes it possible to say that the introduction of substituents into the α-position leads to increases in the bond orders of the 2—3 and 9—10 bonds and to decreases in those of the 1—2, 1—9 and 3—4 bonds. That is, α-substitutions have a tendency to unify the bond orders along the direction of the short molecular axis. Contrary to this, substitutions in the β-positions cause decreases in the bond orders of the 1—2, 2—3 and 9—10 bonds and an increase in that of the 1—9 bond. The same result is reported in the case of α- and β-naphthylamines[4]. In other words, the substitutions in α-positions cause an increase in the mobilities of π-electrons in the direction of the short molecular axis, whereas those in β-positions lead to decreased π-electron mobilities in this direction and to an increase of mobilities in the direction of the long molecular axis. This is an important difference between the α- and β-derivatives, and this remarkable circumstance may be responsible for the distinction between the α- and β-derivatives in their molecular properties, such as reactivities, etc.

Reactivity.—It is a well-known fact[2a] that in all naphthalene derivatives with substituents in β-positions the 1-position is found to be reactive and the 3-position to be inert, or nearly so in the case of electrophilic substitution reactions.

In the electrophilic substitution reaction, π-electron density at the positions which are attacked by the reagent is a measure of reactivity. From the standpoint of this situation, it may be expected that their 1-positions in any β-substituted naphthalene derivatives are the first point to be attacked by any reagent. In a similar way, the 3-positions in α-derivatives may become less active. It is a well-known fact that the frontier electron

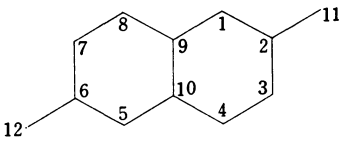
3) K. Nishimoto and R. Fujishiro, This Bulletin, 32, 699 (1959).

4) H. Baba and S. Suzuki, ibid., 34, 82 (1961).



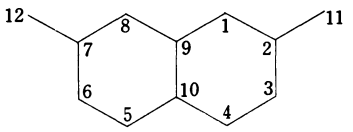
2,3-Naphthalenediol

B_1	$\sigma_1=\phi_1+\phi_4$	A_2	$\sigma_7=\phi_1-\phi_4$
	$\sigma_2=\phi_2+\phi_3$		$\sigma_8=\phi_2-\phi_3$
	$\sigma_3=\phi_8+\phi_5$		$\sigma_9=\phi_8-\phi_5$
	$\sigma_4=\phi_7+\phi_6$		$\sigma_{10}=\phi_7-\phi_6$
	$\sigma_5=\phi_9+\phi_{10}$		$\sigma_{11}=\phi_9-\phi_{10}$
	$\sigma_6=\phi_{11}+\phi_{12}$		$\sigma_{12}=\phi_{11}-\phi_{12}$



2,6-Naphthalenediol

A	$\sigma_1=\phi_1+\phi_5$	B	$\sigma_7=\phi_1-\phi_5$
	$\sigma_2=\phi_2+\phi_6$		$\sigma_8=\phi_2-\phi_6$
	$\sigma_3=\phi_3+\phi_7$		$\sigma_9=\phi_3-\phi_7$
	$\sigma_4=\phi_4+\phi_8$		$\sigma_{10}=\phi_4-\phi_8$
	$\sigma_5=\phi_9+\phi_{10}$		$\sigma_{11}=\phi_9-\phi_{10}$
	$\sigma_6=\phi_{11}+\phi_{12}$		$\sigma_{12}=\phi_{11}-\phi_{11}$



2,7-Naphthalenediol

B_1	$\sigma_1=\phi_1+\phi_8$	A_2	$\sigma_8=\phi_1-\phi_8$
	$\sigma_2=\phi_2+\phi_7$		$\sigma_9=\phi_2-\phi_7$
	$\sigma_3=\phi_3+\phi_6$		$\sigma_{10}=\phi_3-\phi_6$
	$\sigma_4=\phi_4+\phi_5$		$\sigma_{11}=\phi_4-\phi_5$
	$\sigma_5=\phi_9$		$\sigma_{12}=\phi_{11}-\phi_{12}$
	$\sigma_6=\phi_{10}$		
	$\sigma_7=\phi_{11}+\phi_{12}$		

Fig. 3. Numbering of atoms and symmetry orbitals of naphthalenediols.

theory proposed by Fukui et al.[5] provides powerful information for chemical reactions, such as electrophilic, nucleophilic and radical reactions. Frontier electron densities in occupied highest orbitals, which are responsible for electrophilic substitutions, are collected in Table II. As is seen from this table, the 3-positions in any naphthalene derivatives with auxochromic substituents should be inactive for this type of reaction. This expectation is consistent with the experimental facts[2b]. For example, 2, 7-diol couples at positions 1 and 8, but if these positions are blocked by alkyl groups, no coupling occurs. The molecular diagrams of A, A-derivatives show that their A rings are

5) K. Fukui, T. Yonezawa and H. Shingu, *J. Chem. Phys.*, **20**, 722 (1952); K. Fukui, T. Yonezawa, C. Nagata and H. Shingu, ibid, **22**, 1433 (1954).

Table II. Frontier eletron density distributions in the occupied highest orbitals of naphthalenediols

	Position	π-Electron density
1,4-Naphthalenediol	2	0.1784
	7	0.0934
	8	0.1918
1,5-Naphthalenediol	2	0.1682
	3	0.1118
	4	0.3176
1,8-Naphthalenediol	2	0.2156
	3	0.0768
	4	0.3524
2,3-Naphthalenediol	1	0.3196
	7	0.1492
	8	0.3616
2,6-Naphthalenediol	1	0.3596
	3	0.0160
	4	0.2792
2,7-Naphthalenediol	1	0.4468
	3	0.0800
	4	0.2690
Naphthalene	1, 4	0.3618
	2, 3	0.1382

reactive and their B rings less reactive than the A rings. By a simple extension of this result, it would be expected that even in the ecas of α- and β-naphthol the A ring would be more active than the B ring. This expectation has been supported by many experiments in connection with substitution reactions. For example, in α-naphthol the 4-position is the first point of attack, and also in β-naphthol the point of first attack is the activated 1-position. Of course, in the case of A, B-derivatives, the reactivities of the two rings are not different from each other.

Molecular Diagrams based on Perimeter Model.—As mentioned above, the B rings in A, A-derivatives are scarcely influenced by the substitution. This result seems to suggest that the 9—10 bond in the derivatives may play an important role in the motion of the $2p\pi$ electrons in the molecules. When the 9—10 bond in the naphthalene is absent, the reactivity at any position and the bond order of any bond in the molecule may be nearly equivalent. Therefore, the presence of the 9—10 bond may be the main reason for the appreciable difference in the reactivity from one position to another. In order to examine the effect of the 9—10 bond on the electronic structures of the diols, we carried out calculations based on the perimeter model. In this model it is assumed that the π-electrons are moving in the perimeter potential field. Our method of calculation is based on the simple LCAO MO theory. The parameters used were the same as in the above calculation, except

that the 9—10 bond was neglected, that is, the value of resonance integral $\int\phi_9 H\phi_{10}d\tau$ was put at zero. The molecular diagrams obtained on the basis of this model are shown in Fig. 3. We can see from the diagrams that the 9—10 bond has the following effects on the electronic structures of these molecules:

1) It breaks the uniformity of the bond order in the case of naphthalene, which means a decrease in the mobilities of the π-electrons.

2) It suppresses the effect of substituents on the B ring in the case of A, A-derivatives. This circumstance may probably be expected in the cases of mono- and polysubstitution.

3) It restrains the conjugation interactions among the ring and substituents to some extent. We will consider this point in the next section.

4) It makes the distinction of positions, i. e., the α-position or β-position, in naphthalene necessary.

From the above results, the differences among the molecular properties of α-, β-, α, α'-, β, β'-, α, β-, A, A- and A, B-naphthalene derivatives should be attributable to the presence of the 9—10 bond in these molecules.

Extradelocalization Energies.—Extradelocalization energy is defined as the stabilization energy of the molecule due to substitution. By using the VO method[3], the extradelocalization energy, $\Delta\varepsilon$, of a naphthalene derivative with auxochromic substituents can be obtained from five vacant orbital energies, ε_i, using the following equation:

$$\Delta\varepsilon = -2(\sum_i^{\text{vac}}\varepsilon_i - \sum_i^{\text{vac}}\varepsilon_i^\circ)$$

In this equation, the ε_i°'s are those of naphthalene. They are -2.3028, -1.6180, -1.3028, -1.0000 and -0.6180 in β respectively. Therefore, $\sum_i^{\text{vac}}\varepsilon_i^\circ$ amounts to $-6.8416\ \beta$. In the case of the perimeter model, $\sum_i^{\text{vac}}\varepsilon_i^\circ = -6.4720\ \beta$. The calculated $\Delta\varepsilon$'s are given in Table III. The table also contains those values of α- and β-naphthol calculated by using the same parameters as those of the diols.

Table III. Extradelocalization energies of naphthalene hydroxy derivatives

	$\Delta\varepsilon$ in β	
	With 9—10 bond	Without 9—10 bond
α-Naphthol	0.1862	0.1888
β-Naphthol	0.1792	0.1888
1,4-Naphthalenediol	0.3618	0.3720
1,5-Naphthalenediol	0.3700	0.3722
1,8-Naphthalenediol	0.3730	0.3790
2,3-Naphthalenediol	0.3544	0.3706
2,6-Naphthalenediol	0.3560	0.3722
2,7-Naphthalenediol	0.3586	0.3780

From this table we obtain the following results;

1) The α-derivatives are more stable than the β-derivatives.

2) The effect of the insertion of the 9—10 bond in the perimeter model is to decrease the extradelocalization energies. This effect is remarkable in the case of β-, β, β'- and A, A-derivatives, but rather small in that of α-derivatives.

3) The $\Delta\varepsilon$'s of diols are nearly equal to double that of the corresponding naphthol; for example, those of α, α'-diols are nearly equal to twice that of α-naphthol.

Summary

The molecular diagrams and extradelocalization energies of the 2, 3-, 2, 6- and 2, 7-naphthalenediols were calculated by using the LCAO MO method. To elucidate the effect of the 9—10 bond on the molecular properties of naphthalene derivatives, we carried out calculations of the electronic structures of naphthalene hydroxy derivatives based on the perimeter model. These calculations proved that:

1) The 3-position in the naphthalene derivatives in less reative than the other positions.

2) The α-derivatives are more stable than the β-derivatives.

3) The insertion of the 9—10 bond in the perimeter model causes a decrease in the degree of conjugation interactions among the ring and the substituents.

4) In the cases of A, A-derivatives, the substituents have no significant influence on the unsubstituted ring, but produce rather a large effect on the substituted rings.

5) α-Substitutions cause an increase in the mobilities of π-electrons in the direction of the short molecular axis, but the β-substitutions lead to an increase in the direction of the long molecular axis.

The authors wish to express their gratitude to Dr. Noboru Mataga for his helpful discussions.

Department of Chemistry
Faculty of Science
Osaka City University
Kita-ku, Osaka

Anionic Polymerization of Vinylidene Chloride. III. Copolymerization Initiated by n-Butyllithium

By Akio KONISHI

(Received May 10, 1961)

Although plans for the cationic coplymerizations of vinylidene chloride with styrene and with vinyl *n*-butyl ether have been announced by Florin[1] and by Walling[2], reports of their success have yet to be published.

The mechanism of the polymerization of vinyl monomers initiated by *n*-butyllithium has been generally recognized as anionic polymerization. However, there are some questions concerning the mechanism of the polymerization of a monomer such a vinylidene chloride, with a relatively low susceptibility to anionic catalysis.

In order to elucidate the mechanism of the vinylidene chloride polymerization initiated by *n*-butyllithium, a copolymerization study was undertaken because the proof of ionic mechanism can best be accomplished by the relative reactivity ratios in the copolymerization data[3]. Methyl acrylate, styrene and vinyl chloride were chosen as the comonomer for this study because vinylidene chloride is surrounded by the above three monomers in q-ε map[4].

Experimental

The details of the preparation of *n*-butyllithium and of the purification of *n*-hexane and vinylidene chloride were given in a previous report[5]. Methyl acrylate and styrene were dried over calcium hydride and distilled under argon before use. Vinyl chloride produced by the Kureha Kasei Co. was repurified by drying over phosphorus pentoxide, followed by distillation under argon into a polymerization vessel in a closed system.

The polymerization apparatus and procedure were the same as before[5]. The catalyst was added to monomers in the polymerization vessel cooled at -70°C with dry ice-methanol, sealed, and then gradually warmed to the desired polymerization temperature. The polymerization was stopped by adding methanol and the mixture was poured into excess methanol or petroleum ether, and then the polymer was successively filtered, washed and dried to a constant weight in vacuo at 40°C.

All copolymerizations were stopped within a ten per cent conversion. The copolymers formed were repurified as follows: poly(vinylidene chloride *co* methyl acrylate)* was dissolved in acetone, filtered, precipitated by petrolum ether, washed, and dried in vacuo. Poly(vinylidene chloride *co* styrene) is only with difficulty soluble in common solvents and was therefore thoroughly allowed to swell in cyclohexanone and was then reprecipitated by methanol. Poly(vinylidene chloride *co* vinyl chloride) was successively redissolved in tetrahydrofuran, filtered and precipitated by methanol. The compositions of the copolymers were determined by chlorine analysis and some infrared spectroscopic data were added to qualify the copolymer, as is discussed below.

Results

Tables I—III and Figs. 1—6 show details of experiments which were employed to determine the monomer reactivity ratios. The monomer reactivity ratios for the three monomer pairs have been calculated using the intersection

TABLE I. REACTIVITY RATIO DATA FOR THE COPOLYMERIZATION OF VINYLIDENE CHLORIDE (M_1) AND METHYL ACRYLATE (M_2)
(See Figs. 1 and 2)

Total monomers, 1.0 mol.; *n*-BuLi, 0.005 mol.; *n*-hexane, 14.6 cc.; temp., 50°C; time, 3.0 hr.

Number	Charge, M_1 mole fraction	Conversion %	Anal. Cl %
1-1	0.900	2.2	9.09
1-2	0.700	2.1	5.03
1-3	0.500	2.3	2.13
1-4	0.300	3.2	0.892

TABLE II REACTIVITY RATIO DATA FOR THE COPOLYMERIZATION OF VINYLIDENE CHLORIDE (M_1) AND STYRENE (M_2)
(See Figs. 3 and 4)

Total monomers, 1.0 mol.; *n*-BuLi, 0.010 mol.; *n*-hexane, 122 cc.; temp., 26°C; time, 4.0 hr.

Number	Charge, M_1 mole fraction	Conversion %	Anal. Cl %
2-1	0.900	4.1	35.90
2-2	0.700	4.5	21.36
2-3	0.500	6.2	12.54
2-4	0.321	9.0	7.48

1) R. E. Florin, *J. Am. Chem. Soc.*, **71**, 1867 (1949).
2) C. Walling, E. R. Briggs, W. Cummings and F. R. Mayo, ibid., **72**, 48 (1950).
3) C. E. Schildknecht, *Ind. Eng. Chem.*, **50**, 107 (1958).
4) A. Konishi, This Bulletin, **35**, 193 (1962).
5) A. Konishi, ibid., **35**, 197 (1962).

* Poly (A *co* B) means a copolymer between A and B. Cf., *J. Polymer Sci.*, **8**, 227 (1952).

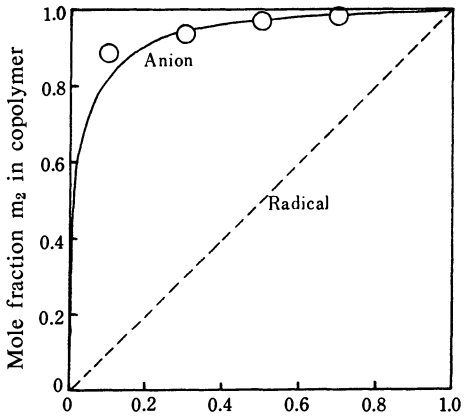


Fig. 1. Copolymer composition curve. Vinylidene chloride (M_1)-methyl acrylate (M_2)

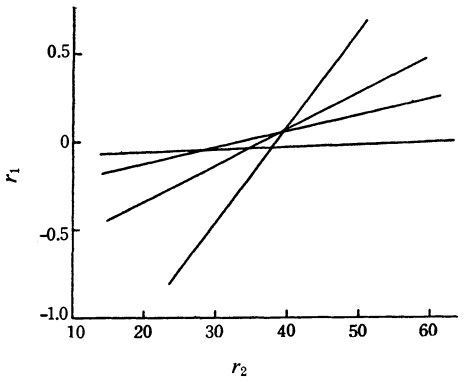


Fig. 2. Reactivity ratio diagram. Vinylidene chloride (M_1)-methyl acrylate (M_2)

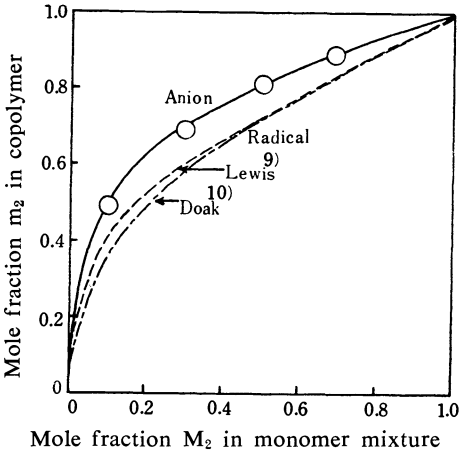


Fig. 3. Copolymer composition curve. Vinylidene chloride (M_1)-styrene (M_2)

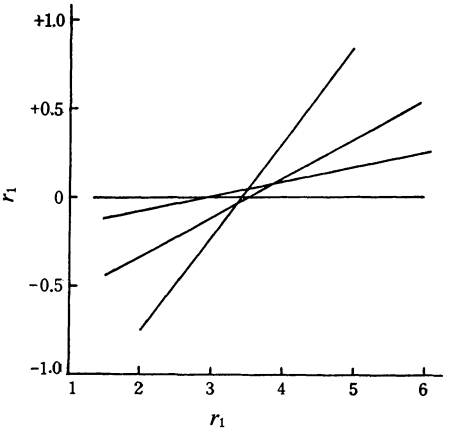


Fig. 4. Reactivity ratio diagram. Vinylidene chloride (M_1)-styrene (M_2)

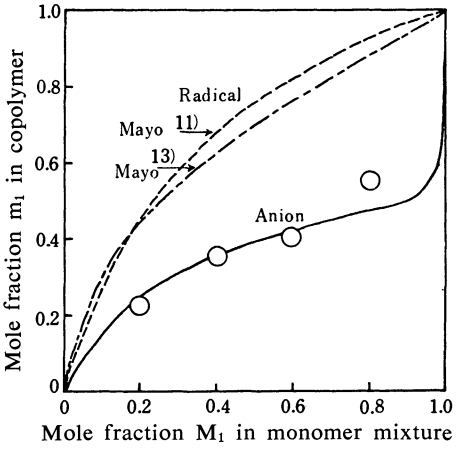


Fig. 5. Copolymer composition curve. Vinylidene chloride (M_1)-vinyl chloride (M_2)

TABLE III. REACTIVITY RATIO DATA FOR THE COPOLYMERIZATION OF VINYLIDENE CHLORIDE (M_1) AND VINYL CHLORIDE (M_2)
(See Figs. 5 and 6)

Total monomers, 1.0 mol.; *n*-BuLi, 0.010 mol.; *n*-hexane, 8.8 cc.; temp., 25°C; time, 1.0 hr.

Number	Charge, M_1 mole fraction	Conversion %	Anal. Cl %
3-1	0.800	3.8	67.50
3-2	0.592	3.6	65.12
3-3	0.400	2.5	64.36
3-4	0.200	4.2	62.87

method of Mayo and Lewis[6]. The r_1 and r_2 values listed in Table V have been determined from Figs. 2, 4 and 6.

The copolymer composition curves are calculated from the values in Tables V and IV.

6) F. R. Mayo and F. M. Lewis, *J. Am. Chem. Soc.*, **66**, 1594 (1944).

Table IV. Literature values for vinylidene chloride reactivity ratios in radical copolymerization

M_1	M_2	r_1	r_2	Temp., °C	Ref.
Vinylidene chloride	Methyl acrylate	1	1	60	7
Vinylidene chloride	Methyl acrylate	1	1	70	7
Vinylidene chloride	Methyl acrylate	0.99	0.84	60	8
Styrene	Vinylidene chloride	2.00	0.14	60	9
Styrene	Vinylidene chloride	1.85	0.085	60	10
Vinylidene chloride	Vinyl chloride	3.2	0.3	60	11
Vinylidene chloride	Vinyl chloride	Large	0.14	68	12
Vinylidene chloride	Vinyl chloride	1.8	0.2	45	13

Table V. Monomer reactivity ratios in the anionic copolymerization of vinylidene chloride

M_1	M_2	r_1	r_2
Vinylidene chloride	Methyl acrylate	0.005	38
Vinylidene chloride	Styrene	0.015	3.4
Vinylidene chloride	Vinyl chloride	0.001	0.5

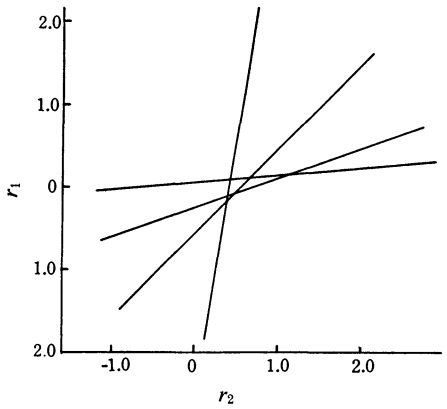


Fig. 6. Reactivity ratio diagram. Vinylidene chloride (M_1)-vinyl chloride (M_2)

The difficulties in determining accurate copolymer compositions arise from the side reaction which is thought to take place during the polymerization reaction and which causes the elimination of chlorine from the copolymer, as has been reported before[5].

In order to confirm the copolymerization and to estimate the copolymer compositions of the copolymers, the infrared spectra given in Figs. 7 and 8 were studied.

The spectra of poly(vinylidene chloride *co* styrene) shown in Fig. 7-a (initiated by *n*-BuLi) and Fig. 7-b (initiated by dibenzoyl peroxide) have common bands at 906 and 842 cm^{-1} whose absorptions increase with an

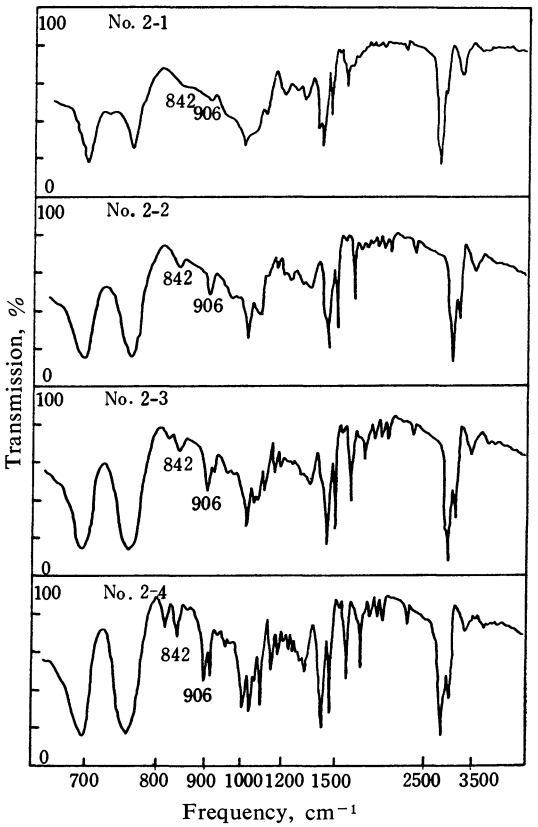


Fig. 7-a. Infrared spectra of poly(vinylidene chloride *co* styrene) initiated by *n*-BuLi.

7) T. Alfrey, Jr., J. J. Bohrer and H. Mark, "Copolymerization", Interscience, New York (1954), p. 34.
8) G. M. Burnett, "Mechanism of Polymer Reactions", Interscience, New York (1954), p. 263.
9) F. M. Lewis, F. R. Mayo and W. F. Hulse, *J. Am. Chem. Soc.*, **67**, 1701 (1945).
10) K. W. Doak, ibid., **70**, 1525 (1948).
11) F. R. Mayo, F. M. Lewis and C. Walling, ibid., **70**, 1529 (1948).
12) P. Agron, T. Alfrey, Jr., J. Bohrer, H. Haas and H. Wechsler, *J. Polymer Sci.*, **3**, 157 (1948).
13) F. R. Mayo and C. Walling, *Chem. Revs.*, **46**, 191 (1950).

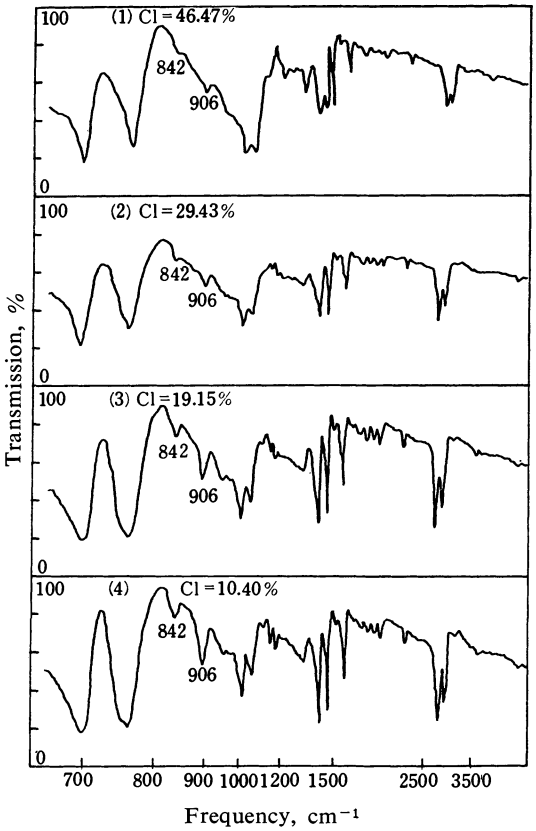


Fig. 7-b. Infrared spectra of poly(vinylidene chloride *co* styrene) initiated by BPO at 60°C.

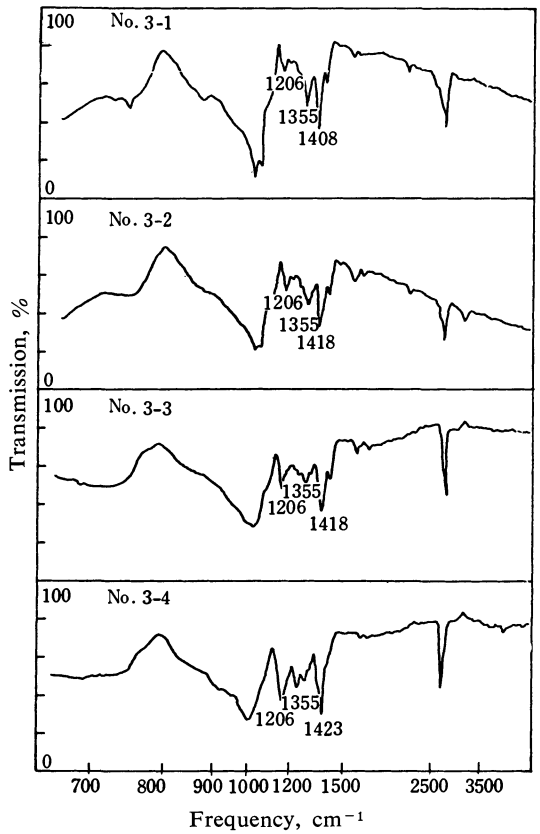


Fig. 8. Infrared spectra of poly(vinylidene chloride *co* vinyl chloride) initiated by *n*-BuLi.

increase in the styrene content; this is thought to be a proof of the copolymerization.

In the spectra of poly(vinylidene chloride *co* vinyl chloride), the shift of the strong CH_2-bending frequency from 1407 to 1428 cm^{-1} and optical density ratio of 1206 to 1355 cm^{-1} have been used for the characterization of the copolymer by Narita[14]. Although the determination of the vinyl chloride fraction in the copolymer is rather difficult in the case of a high vinyl chloride content, the spectra agreed qualitatively with the results obtained from chlorine analysis.

Discussion

The monomer reactivity ratios of all the three monomer pairs initiated by *n*-butyllithium are distinctly different from those initiated by a radical initiator and present a proof of the anionic mechanism of the polymerization of vinylidene chloride initiated by *n*-butyllithium.

The poly(vinylidene chloride *co* styrene) here obtained are only with difficulty soluble, are only partly soluble or are nearly swollen in the common organic solvents, i. e., benzene, acetone, ethyl methyl ketone, tetrahydrofuran and cyclohexanone. On the contrary, the copolymers obtained by radical polymerization are easily soluble in benzene; this suggests that some structural differences may exist between these copolymers.

In Fig. 9 the known copolymer composition curves[15,16] of anionic copolymerizations are shown together with their known radical[7] and cationic copolymerization[15] curves. Comparing them with the curves shown in Figs. 1, 3 and 5, the mutual relationships between the curves obtained in the anionic and in the radical copolymerization of vinylidene chloride-methyl acrylate and vinylidene chloride-styrene pairs can be seen to be similar to the relationships in (2) methyl methacrylate-acrylonitrile, (3) methacrylonitrile-methyl methacrylate and (5) methyl methacrylate-styrene pairs. The curves of vinylidene chloride-vinyl chloride are

14) S. Narita, S. Ichinohe and S. Enomoto, *J. Polymer Sci.*, **36**, 389 (1959).

15) D. C. Pepper, *Quat. Rev.*, **8**, 88 (1954).

16) N. L. Zutty and F. J. Welch, *J. Polymer Sci.*, **43**, 445 (1960).

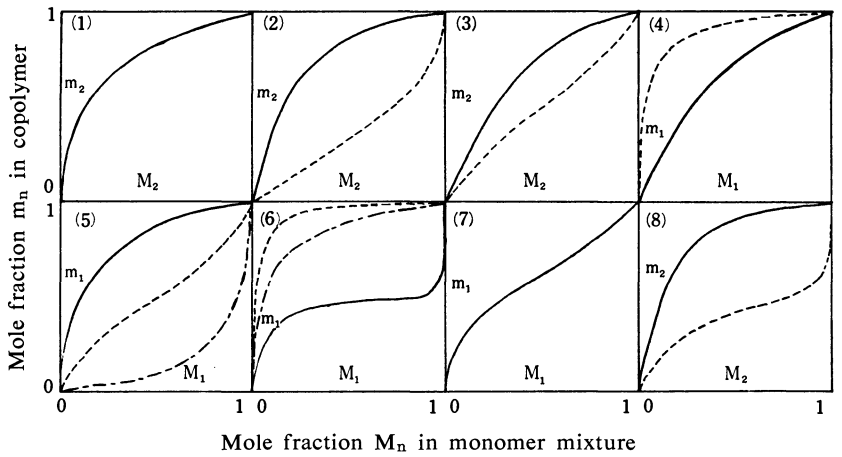


Fig. 9. Copolymer composition curves of known eight pairs; (1) Methyl methacrylate (M_1)-methyl acrylate(M_2), (2) methyl methacrylate(M_1)-acrylonitrile (M_2), (3) methyl methacrylate(M_1)-methacrylonitrile(M_2), (4) methyl methacrylate(M_1)-vinyl acetate(M_2), (5) methyl methacrylate(M_1)-styrene(M_2), (6) styrene(M_1)-vinyl acetate(M_2), (7) acrylonitrile(M_1)-butyl vinyl sulfone(M_2), (8) styrene(M_1)-acrylonitrile(M_2); Anionic ——, Radical ------, Cationic —·—·

similar to those of (4) methyl methacrylate-vinyl acetate and (6) styrene-vinyl acetate pairs.

The experimental results show that the susceptibility of methyl acrylate to anion is larger than that of vinylidene chloride. The copolymer composition curve of styrene-vinyl acetate resembles that of vinylidene chloride-vinyl chloride.

Summary

The copolymerization reaction of vinylidene chloride with methyl acrylate, styrene and vinyl chloride initiated by *n*-butyllithium has been studied. The monomer reactivity ratios have been found to be distinctly different from those of the radical copolymerizations. The results clearly showed that the nature of the polymerization of vinylidene chloride initiated by *n*-butyllithium is anionic, in accordance with the prediction from the q-ε or the Q-e map.

The author wishes to express his sincere thanks to Professor Hiroshi Azumi, Professor Tetuo Nozoe and Professor Shinichiro Fujise of Tohoku University for their kind guidance and encouragement throughout this work. The author is also indebted to Dr. Kanji Mayumi and Dr. Keiichi Numbu of this laboratory for their helpful advice and to the assistance given by Mr. Akira Izuka in conducting these experiments.

Tokyo Laboratory
Kureha Kasei Co., Ltd.
Shinjuku-ku, Tokyo

Rates of Solvolysis of Substituted 4-Biphenylyldimethylcarbinyl Chlorides. A Test of the Free-energy Relationship

By Takashi INUKAI

(Received May 17, 1961)

The general applicability of Hammett Eq. 1 to the correlation of a large number, and a variety of, side-chain reactions and equilibria of aromatic derivatives is well established[1,2]. On the other hand, it has become progressively evident that electrophilic aromatic substitution reactions and some side-chain reactions, involving presumably stronger interactions between the substituent and the electron-deficient reaction center in the transition state do deviate from this equation[3,4].

$$\log k/k_0 = \rho\sigma \qquad (1)$$

Several sets of new substituent constants have thus been proposed by the workers[5-12] to reconcile their own results with the linear free-energy relationship of the type of Eq. 2.

$$\log k/k_0 = \rho\sigma^+ \qquad (2)$$

The fact that the new sets of substituent constants are more or less similar to each other might suggest that those reactions of the type which requires enhanced substituent constants constitute a distinct group on the one hand, as contrasted with the prevailing group of normal reactions on the other hand.

This view was encouraged by the considerable success in correlating a number of appropriate reaction rates by means of the modified substituent constants, σ^+, proposed by Brown and Okamoto[10-12]. There are a few cases of difficulties[13,14], however, which may likely escape the serious attention of proponents of the new treatments. Although the general success of σ^+ is apparent, it is still reasonable to state that the electronic contribution of a substituent could not be represented by a single constant as in Eq. 2, since the resonance contribution by a substituent can vary markedly from reaction to reaction, the very existence of different sets of substituent "constants" showing the non-reality of the "constants"[4,14,15].

In view of the utility of such equations over a wide variety of reactions it is not surprising that Eqs. 1 and 2 have been accepted with tolerance. This situation makes, however, proper evaluation of the linear free-energy relationship considerably complicated: in one case the deviation of a particular series of data may be attributed to a special interaction between the substituent and the solvent molecules or to anything which is convenient for rationalization of the result, in another case the deviation as detected may be thought to be due to experimental errors.

Therefore, it is desired to reexamine the linear free-energy relationship with due care, rather than to explore its utility. The study of the Hammett type relation should be done with the following things in mind; 1) Small deviations from the equation may be neglected in the first approximation. 2) Those deviations or agreements which are observed in the course of a study of a reaction of unknown or ambiguous mechanism do not argue against or for the validity of the relation. 3) The reaction series to be compared in relation to the equation should preferably be closely similar to each other so as to minimize unnecessary complications which may arise otherwise, although this would limit the virtue of the equation as far as its utilities are concerned.

Furthermore, it is anticipated that there will remain some uncertainty or arbitrariness in interpreting the results even if the study

1) L. P. Hammett, "Physical Organic Chemistry", McGraw-Hill Book Co., New York, N. Y. (1940), Chapter 7.
2) H. H. Jaffé, *Chem. Revs.*, **53**, 191 (1953).
3) J. D. Roberts, J. K. Sanford, F. L. J. Sixma, H. Cerfontain and R. Zagt, *J. Am. Chem. Soc.*, **76**, 4525 (1954).
4) P. B. D. de la Mare, *J. Chem. Soc.*, **1954**, 4450.
5) D. E. Pearson, J. F. Baxter and J. C. Martin, *J. Org. Chem.*, **17**, 1511 (1952).
6) N. C. Deno, J. J. Jaruzelski and A. Schriesheim, *J. Am. Chem. Soc.*, **77**, 3044, 3051 (1955).
7) C. W. McGary, Jr., Y. Okamoto and H. C. Brown, ibid., **77**, 3037 (1955).
8) J. Miller, *Aust. J. Chem.*, **9**, 61 (1956).
9) J. K. Kochi and G. S. Hammond, *J. Am. Chem. Soc.*, **75**, 3445 (1953).
10) H. C. Brown and Y. Okamoto, ibid., **79**, 1913 (1957).
11) Y. Okamoto and H. C. Brown, *J. Org. Chem.*, **22**, 485 (1957).
12) H. C. Brown and Y. Okamoto, *J. Am. Chem. Soc.*, **80**, 4979 (1958).
13) H. G. Kuivila and A. R. Hendrickson, ibid., **74**, 5068 (1952); H. G. Kuivila and C. E. Benjamin, ibid., **77**, 4834 (1955).
14) J. K. Kochi and G. S. Hammond, ibid., **75**, 3445 (1953); F. T. Fang, J. K. Kochi and G. S. Hammond, ibid., **80**, 563 (1958).
15) P. B. D. de la Mare and J. H. Ridd, "Aromatic Substitution; Nitration and Halogenation", Butterworths Scientific Publications, London (1959), Chapter 18.

was made under ideal conditions. So far as we remain in the study of simple benzene derivatives, strictly following the original definition of the Hammett equation, such uncertainty always accompanies our interpretation since we have, at present, no basis of estimating how the resonance contribution of a substituent varies depending on the kind of reaction. Therefore it is desirable to find out an obvious case of deviation from the linearity by purposely providing selected conditions for a possible deviation.

In this paper we report the study on the rates of solvolysis of substituted 4-biphenylyldimethylcarbinyl chlorides in 90% acetone and compare them with that of substituted phenyldimethylcarbinyl chlorides[16] under the identical conditions. It is reasonably hoped that the effects of various possible factors on the rate such as solvent interactions with the substituents and/or the reaction center are mostly compensated by comparison of the two series. The only difference is structural, i. e. the effect of the substituent in biphenyl derivatives is transmitted to the reaction center through the biphenyl ring system and that in benzene derivatives through the benzene ring. The two modes of transmission of the substituent effect, inductive and resonance, will play their roles in the biphenyl derivatives in a ratio different from that in the benzenes. Consequently, if these two series deviate from the linear relationship of free-energy of activation we will get an experimental foundation to believe that the deviations can be real and are understandable on the basis of the variance of the relative importance of the resonance and inductive contributions of the substituents.

Results

The substituted 4-biphenylyldimethylcarbinyl chlorides required were synthesized by treating the corresponding tertiary carbinols with dry hydrogen chloride in methylene chloride at 0°C and removing the solvent. Since the tertiary chlorides are unstable and difficult to purify, we were content with preparing pure samples of the tertiary carbinols and using the crude tertiary chloride directly, without further treatment[17].

The tertiary chlorides were dissolved in 90% aqueous acetone and the first order rate constants of solvolysis determined at 0 and 25°C. Since the rates are to be compared with those of the substituted phenyldimethylcarbinyl chlorides by Brown and collaborators[16], the water content of the solvent was adjusted to reproduce the original rate constant for phenyldimethylcarbinyl chloride. The rate constant for 4-biphenylyldimethylcarbinyl chloride was also reproduced quite well in this batch of solvent as it should be. Consequently there is no doubt about the identity of both the expermental conditions. Because of the fast rate exhibited by the 4'-methoxy compound, it was found difficult to obtain its precise rate constant at 25°C. Therefore, the more reliable value was calculated by using the thermodynamical quantities for activation obtained by

Table I. Rate constants for the solvolysis of the aryldimethylcarbinyl chlorides in 90% acetone

Aryl group	Rate constant, $k_1(\text{sec}^{-1}) \times 10^4$			Relative rate at 25°C
	0°C	15°C	25°C	
Phenyl	—	—	1.22	1.00
4-Biphenylyl	—	—	8.05[a] (7.99; 8.12)	6.60
4'-MeO-4-biphenylyl	3.30[b]	17.7[a,b] (17.6; 17.8)	47.5[a,b] (47.7; 47.4)	39.3
4'-Me-4-biphenylyl	1.01	—	16.8[a] (16.8; 16.9)	13.8
4'-Cl-4-biphenylyl	—	—	4.39[a] (4.43; 4.35)	3.60
4'-Br-4-blphenylyl	2.05	—	4.01[a] (4.02; 3.99)	2.29
3'-Cl-4-biphenylyl	1.23	—	2.50[a] (2.49; 2.50)	2.05

a) Mean of the data shown below in parentheses.
b) The least squares treatment of the data, in connection with Eyring equation, leads to 3.32, 17.4 and 48.0 at 0, 15 and 25°C, respectively, which will be adopted in further calculations.

16) a) H. C. Brown and Collaborators, *J. Am. Chem. Soc.*, **79**, 1897, 1906, 1909 (1957); b) H. C. Brown, Y. Okamoto and T. Inukai, ibid., **80**, 4964 (1958).

17) This procedure has been verified by H. C. Brown et al. (Ref. 16a), and by the present author's experience using two samples of phenyldimethylcarbinyl chloride, one vacuum-distilled and one prepared by this procedure.

the least squares treatment of the observed rate constants at 0, 15 and 25°C. The agreement between the observed and the calculated figures was very satisfactory. The rate constants and the derived thermodynamic quantities of activation are presented in Tables I and II, respectively.

TABLE II. THERMODYNAMICAL QUANTITIES OF ACTIVATION FOR THE SOLVOLYSIS OF THE ARYLDIMETHYLCARBINYL CHLORIDES

Aryl group	$\Delta H^{\neq}$ kcal./mol.	$\Delta S^{\neq}$ e. u.
Phenyl	18.8[a]	−12.5[a]
4-Biphenylyl	18.0[a]	−12.2[a]
4'-MeO-4-biphenylyl	16.7	−13.0
4'-Me-4-biphenylyl	18.1	−10.5
4'-Cl-4-biphenylyl	—	—
4'-Br-4-biphenylyl	18.7	−11.5
3'-Cl-4-biphenylyl	18.9	−11.6

a) The value quoted from Ref. 16b

Discussion

The electrophilic subsituent constants, σ^+, for the substituted phenyl groups studied in this investigation, after the definition by Brown and Okamoto[10,12], are presented in Table III. They were calculated by the formula, $\log k/k_H = \rho\sigma^+$, where k_H is the rate constant for the solvolysis of phenyldimethylcarbinyl chloride in 90% acetone at 25°C and ρ is the reaction constant (−4.54)[12]. Hammett's σ values for these groups are also included in the table for ready comparison.

That the σ^+'s are consistently lower (more negative) than σ's is clearly due to the larger resonance contribution of the aryl groups in the solvolysis than the resonance contribution in the dissociation of benzoic acids (such tendency has been remarked in ortho-para directing groups already studied)[12].

TABLE III. SUBSTITUENT CONSTANTS FOR ARYL GROUPS

Group (para)	$\log k/k_H$	σ^+	σ[a]
C_6H_5-	0.819	−0.180	−0.0455
4-MeO-C_6H_4-	1.595	−0.351	−0.114
4-Me-C_6H_4-	1.14	−0.251	−0.0682
4-Cl-C_6H_4-	0.556	−0.122	+0.0985
4-Br-C_6H_4-	0.517	−0.114	+0.0985
3-Cl-C_6H_4-	0.312	−0.0686	(+0.0833)[b]

a) From the dissociation constants of substituted 4-biphenylcarboxylic acids in 50% (by volume) aqueous butyl cellosolve[18]
b) The value for 3-Br-C_6H_4-group (Ref. 18)

18) E. Berliner and L. H. Liu, *J. Am. Chem. Soc.*, **75**, 2417 (1953).

TABLE IV. RELATIVE RATE OF SOLVOLYSIS

X	Relative rate in X-C_6H_4-C_6H_4-CMe_2Cl	$\log k/k_H$	Relative rate in X-C_6H_4-CMe_2Cl	$\log k/k_H$
p-MeO	5.96	0.775	41700.	4.620
p-Me	2.09	0.320	26.0	1.415
H	1.00	0.000	1.00	0.000
p-Cl	0.545	−0.263	0.305	−0.516
p-Br	0.498	−0.303	0.208	−0.682
m-Cl	0.311	−0.508	0.0156	−1.807

In Table IV the effect of substituents on the rate of solvolysis of 4-biphenylyldimethylcarbinyl chlorides are compared with that found for the solvolysis of phenyldimethylcarbinyl chlorides[16]. Figure 1 shows the plot of $\log k/k_H$ for the solvolysis of 4-biphenylyldimethylcarbinyl chlorides versus σ^+, which is numerically equal to $-\log k/k_H \times 1/4.54$, as determined by using the data for the solvolysis of phenyldimethylcarbinyl chlorides.

It is clear in Fig. 1 that there is no simple relation between these two series of reactions. Since the size of the circles shown represents an experimental uncertainty of 3%, the "deviations" from a straight line, if any, are too large to be treated as experimental errors. Therefore, rather than draw a median line through these points, a line was drawn through H and *m*-Cl points in Fig. 1. Since the resonance contribution of the meta substituent is known to be negligible in the benzene series, it should be likewise negligible in biphenyl. This justifies the use of *m*-Cl point to fix an approximate reference line on which

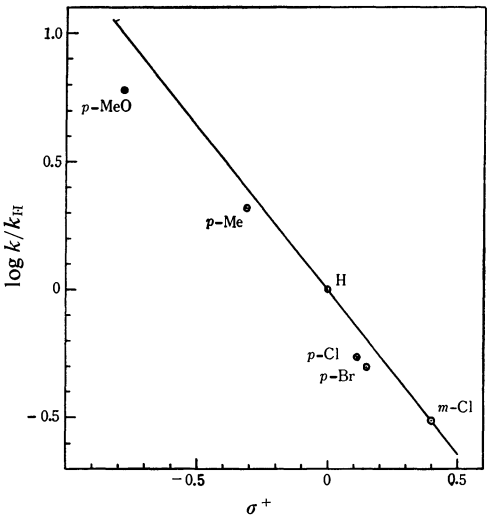


Fig. 1. Plot of $\log k/k_H$ for solvolysis of substituted 4-biphenylyldimethylcarbinyl chlorides versus σ^+.

the para points would lie if the linear free-energy relationship held between these closely related reaction series. Thus the downward displacements from this line exhibited by the four para-substituted compounds correpond to the depression of the resonance contribution by these groups in biphenyl series, compared with the hypothetical resonance contributions expected from the linear free-energy relationship. The depression thus demonstrated agrees with the widely accepted view of the restricted conjugation through the pivot bond of biphenyl.

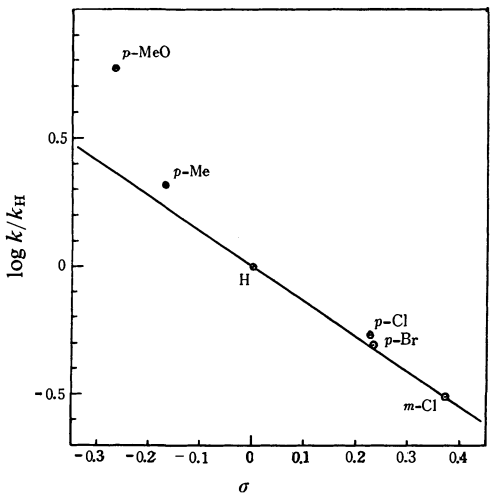


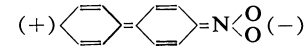
Fig. 2. Plot of $\log k/k_H$ for solvolysis of substituted 4-biphenylyldimethylcarbinyl chlorides versus Hammett's σ.

Figure 2 shows the plot of $\log k/k_H$ for biphenyl series versus the Hammett σ. The plot does not define any straight line either, but a straight line has been drawn through H and *m*-Cl points for the same purpose as above. This line approximately shows the hypothetical rates of reaction for biphenyl derivatives if the effect of the substituent on the rate were such that the linear free-energy relationship holds between the rates of the solvolysis of substituted biphenylyldimethylcarbinyl chlorides on the one hand and the equilibria of substituted benzoic acids on the other hand. The upward displacements of the points for the para substituted compounds from the line shown undoubtedly indicate the incorporation of additional resonance contribution in the solvolysis compared with that in the acid dissociation.

It is clear, from these discussions, that the features of the substituent effects in this solvolysis reactions are intermediate between those which characterize the solvolysis of phenyldimethylcarbinyl chlorides (σ^+-type) and dissociation of benzoic acids (σ-tye).

In searching for some criterion for the applicability of σ^+-values, the following view seems to be fundamentally correct. A resonance interaction or charge delocalization takes place powerfully between the substituent and the electron-deficient reaction center, in the transition state, a view which has been discussed by a number of workers[5-15] in this field and needs no elaboration.

On the basis of this view, the fact that the substituent effects in this solvolysis reactions are intermediate between σ^+-type and σ-type shows that the resonance interaction or charge delocalization which occurs in solvolysis of biphenylyldimethylcarbinyl chlorides is shared by the substituent in lesser degree than in the solvolysis of phenyldimethylcarbinyl chlorides. All chemical data can be explained satisfactorily on the basis of a restricted resonance of the two benzene rings in biphenyl. Thus the orientation in the electrophilic substitution of substiuted biphenyls conforms to the idea that the two rings act independently[19]. For example, Mizuno and Simamura[20] determined the partial rate factors for nitraticn of *o*-, *m*- and *p*-nitrobiphenyl with the results that the resonance formula like I, as would be reasonably suggested by simple application of



I

the electronic theory of organic reaction, is not a predominant factor in determining the reactivity of these compounds. A relative ineffectiveness of the substituent effect in the biphenyl system is also found in a nucleophilic displacement of 2, 4′-dinitro-4-bromobiphenyl[21]. From these chemical evidences it would be concluded that the resonance interactions extending over the biphenyl ring system is in general not influential in determining its chemical reactivities.

This situation only must be responsible for the break-down of the linear free-energy relationship, bipenyl derivatives versus phenyl derivatives, reported in this paper.

Consequently, the deviations from a linear free-energy relationship that have been observed in studies of benzene derivatives[13,14] can be ascribed, in some case and partly at least, to the variance of weight of the resonance contribution from reaction to reaction.

Modified Treatments.—Although the above arguments indicate that it is fundamentally

19) R. L. LeFevre and E. E. Turner, *J. Chem. Soc.*, **1928**, 245; For a discussion of this problem see also Ref. 18.
20) Y. Mizuno and O. Simamura, *J. Chem. Soc*, **1958**, 3875.
21) E. Berliner, B. Newman and T. M. Riaboff, *J. Am. Chem. Soc.*, **77**, 478 (1955).

TABLE V. SUBSTITUENT CONSTANTS

	σ [a]	σ_I [b]	$\sigma_R \equiv \sigma - \sigma_I$	σ^+ [a]	$\Delta\sigma_R^+ \equiv \sigma^+ - \sigma$
H	0.000	0.000	0.000	0.000	0.000
4-MeO	−0.268	+0.23	−0.50	−0.778	−0.510
4-Me	−0.170	−0.05	−0.12	−0.311	−0.141
4-Cl	+0.227	+0.47	−0.24	+0.114	−0.113
4-Br	+0.232	+0.45	−0.22	+0.150	−0.082
3-Cl	+0.373	+0.47	−0.10	+0.399	+0.026

a) Ref. 12, b) Ref. 24

incorrect to assign a single substituent constant to a substituent, it may be still possible to correlate rates by means of a combination of two types of substituent constant, one for the inductive mode and the other for the resonance mode of electronic displacement. Such attempts have been made by Taft[22] (for shielding constants δ^F for fluorine NMR spectra of substituted fluorobenzenes), Corio and Dailey[23] (for proton NMR spectra of substituted benzenes) using σ_I and σ_R[24] and by Yukawa and Tsuno[26,27] for several reaction rate data proposing a formula, $\log k/k_H = \rho \cdot (\sigma + r\Delta\sigma_R^+)$. The substituent constants used for the following computations are tabulated in Table V.

1) Taft's Treatment.—This method in effect treats the substituent effect as a composite of the inductive polar effect (σ_I) and the resonance polar effect (σ_R). Thus the actual formula is,

$$\log k/k_H = \alpha\sigma_I + \beta\sigma_R \qquad (3)$$

Least squares treatment of the present data by means of Eq. 3 leads to expression 4.

$$\log k/k_H = -2.282\sigma_I - 1.650\sigma_R - 0.014 \qquad (4)$$

The plot is shown in Fig. 3. Although this exhibits a satisfactory linearity, the apparent agreement does not prove that this procedure is a correct approach to reality since the introduction of one additional parameter affords a better opportunity of getting a better fit for no other reason but mathematical. The author believes that the success of this procedure suggests rather that the evaluation of σ_I and σ_R by Taft was fairly good.

2) Yukawa's Treatment. — Yukawa and Tsuno[25,26] recently proposed a modified Hammett type Eq. 5 for electrophilic reactions,

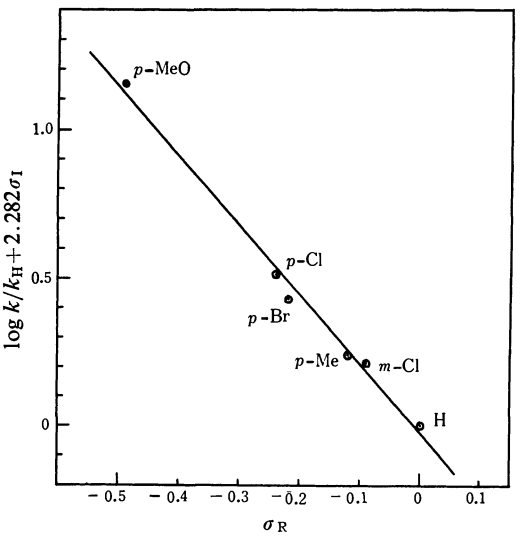


Fig. 3. Plot of $\log k/k_H + 2.282\sigma_I$ versus σ_R; Taft's treatment of the rates of solvolysis of substituted 4-biphenylyldimethylcarbinyl chlorides.

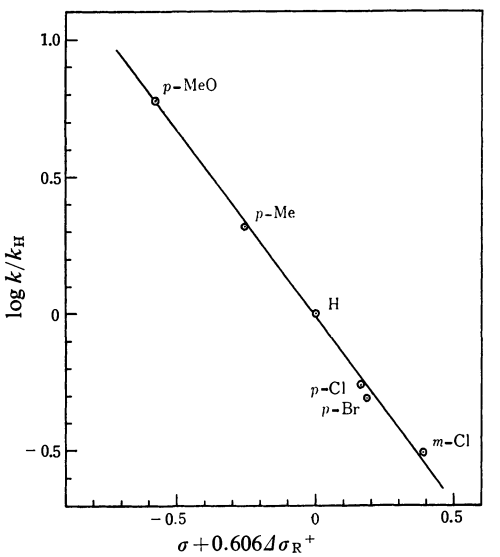


Fig. 4. Plot of $\log k/k_H$ versus $\sigma + 0.606\Delta\sigma_R^+$; Yukawa's treatment of the rates of solvolysis of substituted 4-biphenylyldimethylcarbinyl chlorides.

22) R. W. Taft, Jr., idid., **79**, 1045 (1957).
23) P. L. Corio and B. P. Dailey, ibid., **78**, 3034 (1956).
24) R. W. Taft, Jr., "Steric Effects in Organic Chemistry", John Wiley and Sons, Inc., New York (1956), Chapter 13.
σ_I, Inductive polar effect, σ_R, Resonance polar effect, $\sigma_R \equiv \sigma - \sigma_I$
25) Y. Yukawa and Y. Tsuno, "Yuki Hanno Kiko no Shimpo", Vol. I., Maki Shoten, Tokyo (1958), Chapter 1.
26) Y. Yukawa and Y. Tsuno, This Bulletin **32**, 971 (1959).
27) W. E. Bachmann and R. A. Hoffman, "Organic Reaction", Vol. II, John Wiley and Sons, Inc., New York (1944), p. 224.

$$\log k/k_H = \rho(\sigma + r\Delta\sigma_R^+) \quad (5)$$

where r is a reaction constant describing the degree of resonance stabilization in the transition state, and $\Delta\sigma_R^+$ is a substituent constant suggesting the resonating capacity of the substituent and is defined as $\Delta\sigma_R^+ \equiv \sigma^+ - \sigma$. They demonstrated that Eq. 5 correlates the rate data more satisfactorily than Eq. 2 does, presenting the results of application of Eq. 5 to 35 different reactions. This method, applied to our present rate data, leads to Eq. 6.

$$\log k/k_H = -1.363(\sigma + 0.606\Delta\sigma_R^+) - 0.019 \quad (6)$$

The plot of $\log k/k_H$ versus $\sigma + 0.606\Delta_R^+$, Fig. 4, appears satisfactory.

3) Limitations of Eq. 5.—In view of the success of Eq. 5 in correlating a number of reaction series, it is interesting to see if it can successfully correlate the rates of solvolysis of the benzyl tosylates in 55.6 vol. % aqueous acetone at 25°C[14], which has given the greatest trouble to Brown-Okamoto's treatment[12] (Eq.2). The result of the least squares treatment of the rate data by means of Eq. 5 is expressed by Eq. 7 and has been shown in Fig. 5,

$$\log k/k_H = -2.949\ (\sigma + 2.175\Delta\sigma_R^+) + 0.057 \quad (7)$$

The correlation thus obtained, Fig. 5, is no better than the σ^+-plot shown in Fig. 6. *m*-MeO and *p*-Cl compounds should react faster than the unsubstituted compound according to the correlation line in Fig. 5 or Eq. 7, which is of course contrary to the experimental observations. Such contradiction is also found in correlating the rate data of brominolysis of benzeneboronic acids[13] (see Fig. 9. of Ref. 27).

It is seen that although all the points have been brought closer to a straight line by introduction of a parameter, r, the *m*-MeO and *p*-Cl points thereby moved too far to the left-hand side (in Fig. 5). Consequently, it is difficult to take the r in Eq. 5 for a constant of reaction.

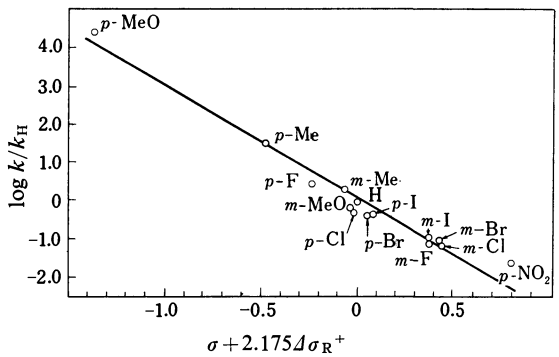


Fig. 5. Plot of $\log k/k_H$ for solvolysis of the benzyl tosylates (Hammond's data) versus $\sigma + 2.175\Delta\sigma_R^+$.

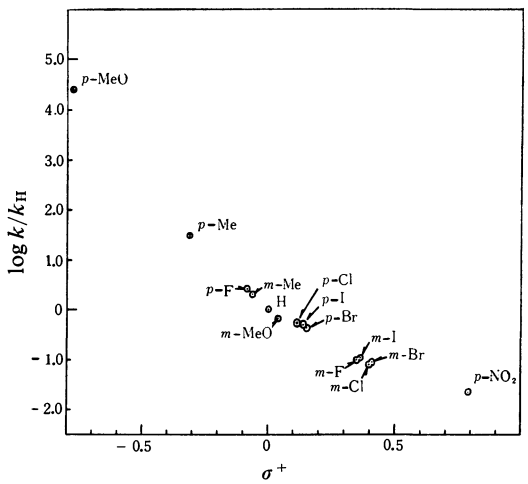


Fig. 6. Plot of $\log k/k_H$ for solvolysis of the benzyl tosylates (Hammond's data) versus σ^+.

Experimental

The following monosubstituted biphenyls were prepared by the Gomberg-Bachmann reaction[27]: *p*-Me, m. p. 48.5~49.5°C (lit.[28] 47.7°C); *p*-Cl, m. p. 78.5~79.5°C (lit.[29] 77.5°C); *p*-Br, m. p. 89.5~90°C (lit.[30] 89.5~90°C); *m*-Cl, b. p. 141~143°/10 mmHg (lit.[31] 150~160°C/6 mmHg). *p*-Methoxybiphenyl was prepared by methylation of commercial *p*-hydroxybiphenyl; m. p. 90~91°C (lit.[32] 90°C).

All the 4-acetylbiphenyls used were prepared by the Friedel-Crafts acetylation of the corresponding biphenyls: 4'-H, m. p. 121~122°C (lit.[33] 121°C); 4'-MeO, m. p. 153~154°C (lit. 153~154°C[34,35], 154.6~155.5°C[36]); 4'-Me, m. p. 122~123°C (lit.[37] 122°C); 4'-Cl, m. p. 102~103°C (lit.[38] 102~103°C); 4'-Br, m. p. 129°C (lit.[39] 131°C).

3'-Chloro-4-acetylbiphenyl.—To a mixture of *m*-chlorobiphenyl (22.5 g., 0.119 mol.), acetyl chloride (12 g., 0.153 mol.) and 100 ml. of dry carbon disulfide was added powdered anhydrous aluminum chloride (21 g., 0.158 mol.) in five portions over a

28) M. Gomberg and J. C. Pernert, *J. Am. Chem. Soc.*, **48**, 1375 (1926).
29) M. Gomberg and W. E. Bachmann, ibid., **49**, 250 (1924).
30) M. Gomberg and W. E. Bachmann, "Organic Syntheses", Coll. Vol. I, (1958), p. 113.
31) J. Elks, J. W. Haworth and D. H. Hey, *J. Chem. Soc.*, **1940**, 1284.
32) A. Werner, *Ann.*, **322**, 167 (1902).
33) L. M. Long and H. R. Henze, *J. Am. Chem. Soc.*, **63**, 1939 (1941).
34) W. S. Johnson, C. D. Gutsche and R. D. Offenhauer, ibid., **68**, 1648 (1946).
35) L. F. Fieser and C. K. Bradsher, ibid., **58**, 1738 (1936).
36) E. Berliner and E. A. Blommers, ibid., **73**, 2479 (1951).
37) N. P. Buu-Hoi, Ng. Hoan and R. Royer, *Bull. soc. chim.* France, (5) **17**, 489 (1951).
38) D. T. Mowry, M. Renoll and W. F. Huber, *J. Am. Chem. Soc.*, **68**, 1105 (1946).
39) B. R. Carpenter and E. E. Turner, *J. Chem. Soc.*, **1934**, 869.

TABLE VI. RATE DATA FOR THE SOLVOLYSIS OF 4-BIPHENYLYLDIMETHYLCARBINYL CHLORIDES AND PHENYLDIMETHYLCARBINYL CHLORIDE IN 90% ACETONE

1) 4-Biphenylyl-, 25°C

t, min.	a, ml.	k_1, $min^{-1} \times 10^2$
0	0.498	—
2	1.185	4.753
4	1.800	4.715
6	2.385	4.774
9	3.167	4.826
12	3.842	4.852
15	4.403	4.830
∞	8.074	—
	Average	4.792

2) 4'-Methoxy-4-biphenylyl-, 0°C

t, min.	a, ml.	k_1, $min^{-1} \times 10^2$
0	0.325	—
2	0.560	(2.052)
3	0.655	(1.937)
5	0.875	1.976
6	0.980	1.981
7.5	1.130	1.975
9	1.285	1.993
10.5	1.425	1.985
∞	6.171	—
	Average	1.982

3) 4'-Methoxy-4-biphenylyl-, 15°C

t, min.	a, ml.	k_1, $min^{-1} \times 10$
0	0.592	—
1	1.080	1.075
2	1.516	1.072
3	1.902	1.065
4	2.254	1.066
∞	5.380	—
	Average	1.070

4) 4'-Methyl-4-biphenylyl-, 25°C

	t, min.	a, ml.	k_1, $min^{-1} \times 10$
#1	0	0.500	—
	1	1.020	1.009
	2	1.490	1.009
	2.667	1.775	1.006
	∞	5.918	—
		Average	1.008
#2	0	0.398	—
	1	0.882	1.002
	2	1.330	1.015
	3	1.735	1.018
	∞	5.473	—
		Average	1.012

5) 4'-Chloro-4-biphenylyl-, 25°C

t, min.	a, ml.	k_1, $min^{-1} \times 10^2$
0	0.305	—
5.1	1.300	2.568
9	1.965	2.546
12	2.485	2.611
14	2.810	2.641
16.25	3.185	2.702
18	3.325	2.590
20	3.595	2.604
∞	8.410	—
	Average	2.609

6) 4'-Bromo-4-biphenylyl-, 0°C

t, min.	a, ml.	k_1, $min^{-1} \times 10^3$
0	0.048	—
65	0.330	1.234
214	0.895	1.230
312	1.212	1.227
341	1.305	1.234
344	1.310	1.230
430	1.554	1.233
∞	3.707	—
	Average	1.231

7) 4'-Bromo-4-biphenylyl, 25°C

t, min.	a, ml.	k_1, $min^{-1} \times 10^2$
0	0.160	—
4	0.350	2.325
7	0.485	2.353
13	0.730	2.382
16	0.847	2.420
20.6	0.998	2.412
24	1.110	2.445
28	1.212	2.416
∞	2.300	—
	Average	2.393

8) 3'-Chloro-4-biphenylyl-, 0°C

t, min.	a, ml.	k_1, $min^{-1} \times 10^4$
0	0.080	—
103	0.635	7.207
241	1.355	7.450
291	1.600	7.493
355	1.882	7.446
372	1.952	7.423
377	1.980	7.451
∞	7.838	—
	Average	7.412

TABLE VI (Continued)

9) 3'-Chloro-4-biphenylyl-, 25°C

t, min.	a, ml.	k_1, $min^{-1} \times 10^2$
0	0.315	—
10	1.080	1.487
14	1.347	1.473
18	1.625	1.500
22	1.870	1.498
26	2.110	1.507
30	2.334	1.512
34	2.532	1.495
∞	5.852	—
	Average	1.496

10) Phenyl-, 25°C

t, min.	a, ml.	k_1, $min^{-1} \times 10^3$
0	0.820	—
13	1.595	7.297
21	2.040	7.320
34	2.710	7.335
42	3.090	7.334
54	3.625	7.350
61	3.950	7.459
∞	9.383	—
	Average	7.349

period of 20 min. without external heating. The mixture was stirred for 10 min. longer and was refluxed for 1/2 hr. Cooled in an iced water bath the complex was decomposed with dilute hydrochloric acid. The carbon disulfide was removed by distillation and the residue recrystallized twice from ethanol; yield 10 g. (36%). Colorless needles, m. p. 57.5~58.5°C. (Found: C, 73.09; H, 4.73. Calcd. for $C_{14}H_{11}OCl$: C, 72.89, H, 4.81%). This material was a sole isolable product from the reaction above. The position of the acetylation is most probably 4' by analogy with the similar acetylation of 3-bromobiphenyl[36].

All the 4-biphenylyldimethylcarbinols used were prepared by the action of methylmagnesium iodide on the corresponding ketones: 4'-H, m. p. 91.5~92.5°C (lit. 92~93°C[40], 91.5~92.5°C[16b]); 4'-MeO, m. p. 137~137.5°C, recrystallized from benzene (Found: C, 79.39; H, 7.31. Calcd. for $C_{16}H_{18}O_2$: C, 79.31; H, 7.49%); 4'-Me, m. p. 116~116.5°C, recrystallized from benzene (Found: C, 84.89; H, 8.09. Calcd. for $C_{16}H_{18}O$: C, 84.91; H, 8.02%); 4'-Cl, m. p. 143.2~144.2°C, recrystallized from benzene (Found: C, 73.16; H, 6.29; Cl, 14.36. Calcd. for $C_{15}H_{15}OCl$: C, 73.02; H, 6.13, Cl, 14.37%); 4'-Br, m. p. 143~145°C, recrystallized from benzene (Found: C, 61.61; H, 5.21; Br, 27.47. Calcd. for $C_{15}H_{15}OBr$: C, 61.87; H, 5.19; Br, 27.45%); 3'-Cl, m. p. 74~75°C, recrystallized from petroleum ether (Found: C, 73.20; H, 6.14; Cl, 14.36. Calcd. for $C_{15}H_{15}OCl$; C, 73.02; H, 6.13; Cl, 14.37%).

Kinetic Measurement.—The solvent, 100 ml., was placed in a long-necked flask and brought to reaction temperature. Approximately 1 g. of the tertiary chloride was dissolved in the solvent and 5 ml. aliquots were removed at appropriate intervals of time. The aliquots were run into 100 ml. of ice-cold dry acetone to stop the reaction and hydrogen chloride was titrated with 0.03 N sodium ethoxide/ethanol using a solution of 3 parts of bromocresol green and 1 part of methyl red in ethanol as an indicator. The reaction mixture was allowed to stand overnight to obtain the aliquots for the "infinity" titer. The first-order rate constants, k_1, were calculated by the formula, $k_1 = [\ln(a_\infty - a_0) - \ln(a_\infty - a_t)]/t$, where a_0, a_t and a_∞ stand for the titer at time 0, t and "infinity", respectively.

Some of the rate data for the solvolysis of 4-biphenylyldimethylcarbinyl chlorides and phenyldimethylcarbinyl chloride in 90% acetone are presented in Table VI.

40) D. T. Mowry, J. Dazzi, M. Renoll and R. W. Shortridge, *J. Am. Chem. Soc.*, **70**, 1916 (1948).

Summary

The rates of solvolysis of 4'-MeO-, 4'-Me-, 4'-H-, 4'-Cl-, 4'-Br- and 3'-Cl-4-biphenylyldimethylcarbinyl chlorides in 90% aqueous acetone have been determined and compared with those of the correspondingly substituted phenyldimethylcarbinyl chlorides. The effect of substituents is very much depressed in biphenyl derivatives as compared with that in phenyl derivatives, and a remarkable deviation from the linear free-enegy relationship was observed between these systems. This is attributed to the difference in the relative importance of the resonance effect and inductive effect of substituents between these two different systems.

Department of Chemistry
Faculty of Science
The University of Tokyo
Hongo, Tokyo

Studies on Fluorene Derivatives. XIII[1]. *The Formation of Tribiphenylenepropane by Self-condensation of Dibiphenyleneethylene*

By Kazuo SUZUKI and Shōji KAJIGAESHI

(Received May 29, 1961)

Certain halides possessing a relatively reactive α-hydrogen such as 9-halogenofluorenes or its derivatives are converted to dimeric olefines by the action of methanolic potassium hydroxide in acetone at room temperature. Thus, 9-bromo-(or chloro)-fluorene[2] gave dibiphenyleneethylene (I). The corresponding substituted I are obtained in good yields from 2-nitro-9-bromofluorene[3], 1-chloro-9-bromofluorene[4], 2,9-dibromofluorene[5], 3,9-dibromofluorene[6a] and 4,9-dibromofluorene[6b].

9-Chlorofluorene[7] and liquid ammonia also interact at room temperature to form I and fluorene.

In regard to the mechanisms[8] involved in the first reaction it has been postulated that a self-alkylation of the halides forms the corresponding dimeric halides which in turn give the dimeric olefines by a β-elimination.

In the present investigation different products were observed when 9-bromofluorene was refluxed for longer periods in methanolic potassium hydroxide-acetone. These were two isomers of tribiphenylenepropane (II)[9,10], m. p. 293°C and m. p. 257°C, dibiphenyleneethane (III)[11], fluorenone, a trace of fluorene, and a small amount of unidentified material, m. p. 90~92°C which analyzed correctly for 9-acetonylfluorene (Chart I).

Under the same conditions 3,9-dibromofluorene and 4,9-dibromofluorene furnished the corresponding 3,3′,3″-tribromotribiphenylenepropane(IV) and 4,4′,4″-tribromotribiphenylenepropane(V), respectively. Both propanes were identical with those obtained previously by the Michael condensation of 3,3′-dibromodibiphenyleneethylene and 3-bromofluorene[5], or 4,4′-dibromodibiphenyleneethylene and 4-bromofluorene[6b], respectively.

However, with 1,9-dibromofluorene and with 2,9-dibromofluorene the methanolic alkali in acetone yielded 1,1′-dibibromodiphenyleneethan (XI) and 2,2′-dibromodibiphenyleneethane (VI)[12], respectively, as reduction products, rather than the substituted tribromotribiphenylenepropanes. With the former compound this could be the result of steric hindrance due to the bromine at the 1-position. The Micheal condensation did not occur either between 1,1′-dibromodibiphenyleneethylene and

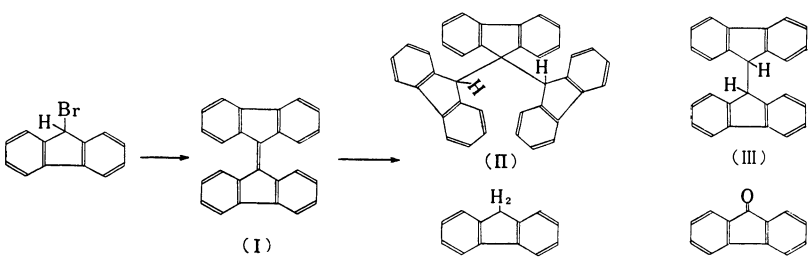


Chart 1.

1) Part XII S. Kajigaeshi, *J. Chem. Soc. Japan, Pure Chem. Soc.* (*Nippon Kagaku Zasshi*), **82**, 1397 (1961).
2) J. Thiele and A. Wansheidt, *Ann.*, **376**, 278 (1910).
3) E. Weisburger et al., *J. Org. Chem.*, **14**, 448 (1948).
4) S. Kajigaeshi, H. Tsuchida and K. Suzuki, *Mem. Fac. Eng. Yamaguchi Univ.*, **9**, 35 (1958).
5) E. Bergmann et al., *Bull. soc. chim. France.* **20**, 78 (1952).
6) a) K. Suzuki, S. Kajigaeshi and M. Sano, *J. Soc. Org. Synth. Chem. Japan* (*Yûki Gôsei Kagaku Kyôkaishi*), **16**, 82 (1958); b) K. Suzuki et al., ibid., **16**, 304 (1958).
7) L. A. Pinck et al., *J. Am. Chem. Soc.*, **68**, 379 (1946).
8) C. R. Hauser et al., ibid., **78**, 1653 (1956).
9) a) L. A. Pinck and G. E. Hilbert, ibid., **57**, 2398 (1935); b) L. A. Pinck and G. E. Hilbert, ibid., **68**, 2014 (1946); K. Suzuki, *J. Chem. Soc. Japan, Pure Chem. Sec.* (*Nippon Kagaku Zasshi*), **70**, 189 (1949); K. Suzuki, *Technol. Repts. Tôhoku Univ.*, XIX, 63 (1955).
10) L. A. Pinck first obtained II (m. p. 300°C, γ-form) by reaction of I and liquid ammonia. Later, in 1949, K. Suzuki also obtaind two kinds of II-isomer (m. p. 275°C, α-form, m. p. 257°C, β-form) by reaction of fluorene and sodium amide. The three compounds were inferred to be restricted free rotation isomers about a single bond and were given the names of α- β-, and γ-form respectively.
11) R. Weissgerber, *Ber.*, **46**, 2913 (1908).
12) J. Schmidt and H. Wagner, *Ann.*, **378**, 155 (1912).

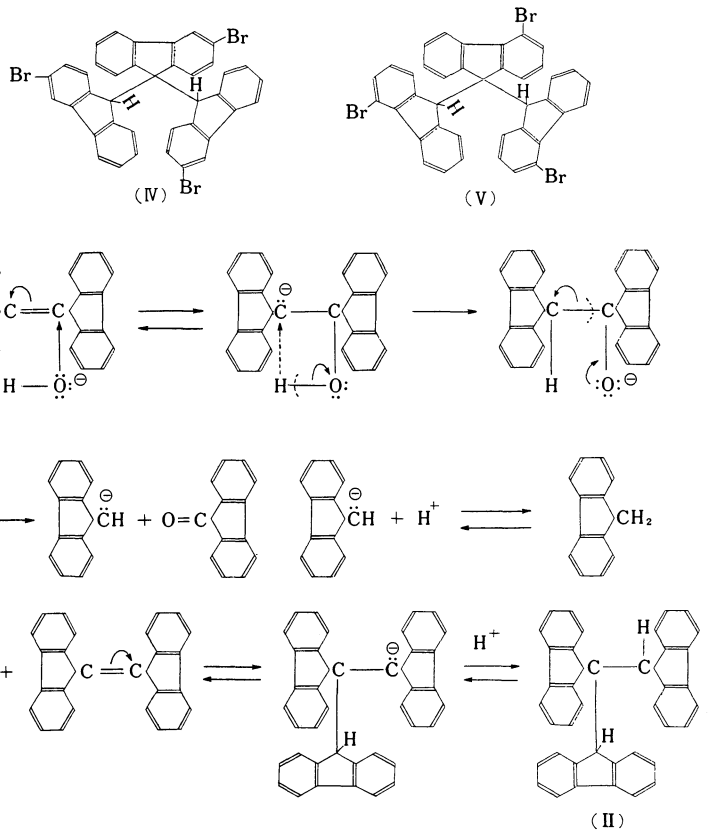


Chart 2.

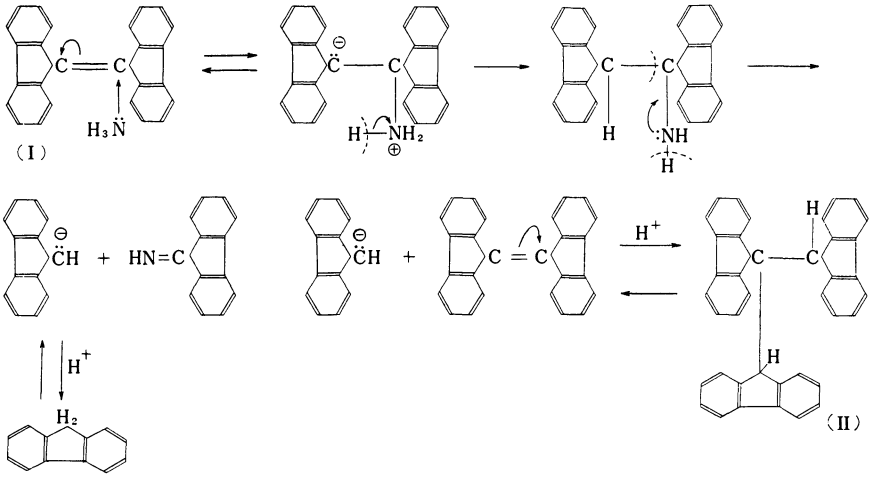


Chart 3.

1-bromofluorene. 2, 9-Dibromofluorene do not give rise to 2, 2′, 2″-tribromotribiphenylenepropane by methanolic alkali in acetone. This reason is not clear; it might be, however, that the formation of VI is the faster rather than the other leading to the 2-substituted propane from 2-substituted ethylene in the two competitive reaction sequences.

In any case, the conversion of 9-bromofluorene to II by the action of methanolic alkali and acetone probably proceeds via the intermediate formation of I. This concept is supported by the fact that practically the same products were obtained (Tables I and II) when the analogous reactions were performed using substituted I as the starting material. Here also,

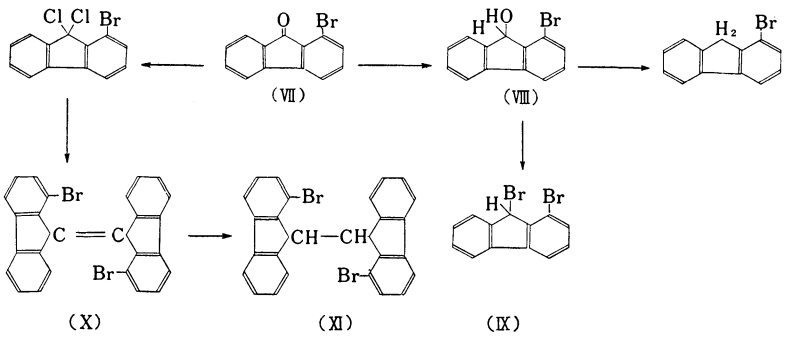


Chart 4.

both isomers of II, III, fluorene and fluorenone were the products.

Central π-electron pairs in I is less firmly held between the two carbon nuclei, and the approach of a negatively charged hydroxyl ion induces a charge separation. This high polarizability is greatly responsible for the reactivity of I for addition reaction.

The reactions accounting for the observed products is illustrated in Chart 2. It may be noted that they are analogous to the production of II from I and liquid ammonia (Chart 3).

The negatively charged fluorenyl ion and fluorenone were formed by addition of hydroxyl ion to I in methanolic alkali in acetone as a preliminary step. I is also reduced to III in the same solution as two competitive reactions. The required proton is obtained by interaction of acetone with alkali; thus these reactions do not proceed in the absence of acetone and alkali.

Moreover, in this case, the fluorenyl ion can not be formed by dissociation of III which is reduced from I in the same alkaline media as suggested by the observations of Weisburger and Grantham[13]. They could not isolate fluorene in any amount when subjecting III to a Wolff-Kischner reduction. On the other hand, they obtained 70% yields of fluorene (and 19% of III) which I as starting material[14].

In another analogous case, Pinck et al.[9a] isolated the γ-form of II, 9-fluorenylidene imine, and fluorene upon treating I with liquid ammonia for 21 days at 60°C. This is a direct addition of ammonia to the unsaturated grouping of I and is also an analogous behavior to that described above. And the mechanism of formation may be proposed as illustrated in Chart 3.

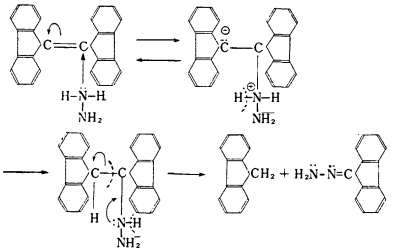
New intermediates required for these studies were prepared by conventional reactions. 1-Bromofluorenone (VII)[15] was obtained from 1-aminofluorenone by a Sandmeyer reaction, a method different from that used by Montagne[16]. The ketone was reduced to 1-bromo-9-fluorenol (VIII) by zinc dust and ammonium hydroxide. VIII was converted to 1, 9-dibromofluorene (IX) by the action of hydrogen bromide in acetic acid, or it was reduced to 1-bromofluorene by hydrogen iodide and red phosphorus. The reaction of phosphorus pentachloride on VII afforded 1-bromofluorene-9, 9-dichloride, which was dehalogenated by powdered copper to 1,1′-dibromodibiphenyleneethylene (X). This compound in turn was reduced to the ethane, XI as illustrated in Chart 4.

Experimental

Formation of Tribiphenylenepropanes.—*Reaction of 9-Bromofluorene and its Bromo-derivatives with Methanolic Potassium Hydroxide in Acetone.*—To a stirred solution of 2.9 g. of potassium hydroxide in 12 cc. of methanol 5 g. of 9-bromofluorene in 23 cc. of acetone was added in small portions at room temperature, and stirring was continued for 20 min. The red I precipitated immediately with heat evolution. The mixture was refluxed gently for 15 hr. during which the color changed from dark red to dark green, and small colorless crystals were deposited after 1/2 hr. The solids were filtered off, washed with water, and extracted with a large volume of ethanol. Colorless needles of III (0.13 g., m.p. and mixed m.p. 243°C) were isolated from the solution.

13) J. H. Weisburger et al., *J. Org. Chem.*, **21**, 1160 (1956).

14) The formation mechanisms of fluorene and hydrazone at the first stage of reaction between I and hydrazine hydrate may be presented as follows.



15) E. H. Huntress, K. Pfister and K. H. T. Pfister, *J. Am. Chem. Soc.*, **64**, 2847 (1942).

16) P. J. Montagne and J. M. Van Charante, *Rec. trav. Chim.*, **32**, 164 (1913); *Chem. Abstr.*, **7**, 3493 (1913).

TABLE I. CONDITIONS AND PRODUCTS WHEN THE SAME REACTIONS WERE PERFORMED ON SUBSTITUTED 9-BROMOFLUOROENES

Dibromo-fluorene g.	Acetone cc.	KOH g.	CH_3OH cc.	Time hr.	Product	Yield, g. (m. p., °C)
1,9-* 2.5	30	3	30	15	XI	0.6 (240~242)
2,9- 9.7	200	16.8	100	2	VI**	2.5 (283~285)
3,9- 0.5	10	0.8	3	7	IV	0.13 (273~275)
4,9- 1.3	20	2.3	10	1	V***	0.1 (254~257)

* 1,1'-Dibromodibiphenyleneethylene did not form at room temperature, but it does by heating.
** Found: Br, 33.08; mol. wt., 720.
*** Found: Br, 32.89; mol. wt., 718. Calcd. for $C_{39}H_{23}Br_3$: Br, 32.78%; mol. wt., 731.

TABLE II. CONDITIONS AND PRODUCTS WHEN THE SAME REACTIONS WERE PERFORMED ON SUBSTITUTED DIBIPHENYLENEETHYLENES

Dibromodibi-phenylene-ethylene, g.	Acetone cc.	KOH g.	CH_3OH cc.	Time hr.	Product	Yield, g. (m. p., °C)
1,1'-, 0.24	4	0.28	1	7	XI	0.04 (242)
2,2'-, 3.4	400	3.9	30	2	VI	0.3 (283)
3,3'-, 0.73	10	0.84	3	7	IV	0.1 (275)
4,4'-, 0.6	10	0.7	3	1	V	0.05 (256)

The ethanol-insoluble residue was fractionally crystallized from benzene to give two isomers of II, colorless tetragonal crystals, m. p. 293°C (decomp.), 0.2 g., and m. p. 257°C (decomp.), 0.25 g.

M. p. 293°C, Found: C, 94.69; H, 5.31; mol. wt., 490; m. p. 257°C, Found: C, 94.70; H, 5.30; mol. wt., 475. Calcd. for $C_{39}H_{26}$: C, 94.69; H, 5.31%; mol. wt., 494.

The mother liquor of the acetone-methanol reaction mixture, above, was steam-distilled. I (0.5 g., m. p. 187°C) was recovered from the brown residual product by crystallization from ethanol. Sublimation of this residue gave 0.01 g. of fluorene and 0.11 g. of fluorenone, m. p. 81°C. Colorless needless, m. p. 90~91°C, 0.1 g., which could be 9-acetonylfluorene were isolated from the mother liquor after removal of I. (Found: C, 86.46; H, 6.14%).

Reaction of I and its Bromoderivatives with Methanolic Potassium Hydroxide in Acetone. — To a solution of 1.8 g. of potassium hydroxide in 7.8 cc. of methanol 3 g. of I in 20 cc. of acetone was added and refluxed gently for 10 hr. The brown color noted during the addition turned dark brown after 1 hr. and dark green after 3 hr. The water-washed precipitate (1.6 g.) was extracted with 300 cc. of boiling ethanol. Colorless needles of III, m. p. 244°C, 0.01 g., crystallized from the solution. The insoluble residue was fractionally crystallized from benzene to yield 0.35 g. of colorless tetragonal II, m. p. 257°C. A further 0.25 g. of II, m. p. 257°C, 0.4 g. of the isomeric II, m. p. 293°C and 0.15 g. of fluorenone, m. p. 81°C were isolated from the mother liquor by chromatography in benzene on alumina.

The mother liquor from the reaction mixture was steam-distilled. The distillate contained 0.15 g. of fluorene, m. p. 113°C. In addition, 0.35 g. of I was recovered from the residue by chromatography in benzene on alumina.

Preparation of Intermediate Products.—*1-Bromofluorenone (VII).*—1-Aminofluorenone (8 g.) in 40 cc. of 40% hydrobromic acid was diazotized with 3 g. of sodium nitrite in 3 cc. of water below 10°C. The diazonium solution was added to a boiling mixture of 10 g. of cuprous bromide in 250 cc. of 40% hydrobromic acid and refluxing continued for 30 min. Upon cooling the product was filtered, washed with sodium hydroxide solution, and recrystallized from ethyl acetate 3 g. (28%), m. p. 132~134°C.

1-Bromo-9-fluorenol (VIII).—A mixture of 2 g. of VII, 6 g. of zinc dust, ammonium hydroxide and 60 cc. of ethanol was refluxed for 1 hr. and filtered hot. VIII (1.5 g., 75%, m. p. 140~141°C, colorless needles from benzene) was isolated upon concentration.

Found: C, 59.56; H, 3.41; Br, 30.38. Calcd. for $C_{13}H_9OBr$: C, 59.79; H, 3.47; Br, 30.61%.

1-Bromofluorene.—A mixture of 0.05 g. VIII, 0.4 g. red phosphorus, 2 cc. of hydroiodic acid (d=1.7) and 10 cc. of acetic acid was refluxed for 9 hr., cooled, filtered and poured into water: Colorless plates (0.39 g., 64%, m. p. 59~60°C from ethanol).

Found: C, 63.73; H, 3.83; Br, 32.76. Calcd. for $C_{13}H_9Br$: C, 63.70; H, 3.70; Br, 32.60%.

1,9-Dibromofluorene (IX).—VIII (2 g.) in 40 cc. of acetic acid and 3 cc. of hydrobromic acid (47%) was heated on a water bath for 3 hr. The crystals isolated upon cooling weighed 1.5 g. (60%), m. p. 137~138°C, from ethanol.

Found: C, 48.13; H, 2.72; Br, 49.51. Calcd. for $C_{13}H_8Br_2$: C, 48.18; H, 2.49; Br, 49.33%.

1,1'-Dibromodibiphenyleneethylene (X).—A mixture of 5 g. of VII and 25 g. of phosphorus pentachloride in a 100 cc. flask was placed in an oil bath preheated to 160°C. The temperature was raised to 185~190°C, and maintained for 1/2 hr. The cool mixture was added to water and the gradually solidifying 9,9-dichloro-1-bromofluorene was filtered: 4.5 g., 74%, m. p. 132~135°C, from benzene.

This material in 70 cc. of absolute xylene was refluxed for 15 hr. with 10 g. of powdered copper. After filtration and concentration, 2 g. (58%) of X (m. p. 230~231°C, dark red from acetone) was obtained.

Found: Br, 32.63; mol. wt., 490. Calcd. for $C_{26}H_{14}Br_2$: Br, 32.87%; mol. wt., 486.

1,1'-Dibromodibiphenyleneethane (XI).—A mixture of 0.5 g. of X in 30 cc. of benzene, 2 g. of zinc dust, and 12 cc. of concentrated ammonium hydroxide was refluxed for 3 hr. After filtration and concentration 0.2 g. (40%) of colorless needles, m. p. 240~242°C from benzene, were isolated.

Found: C, 64.06; H, 3.52; Br, 32.88. Calcd. for $C_{26}H_{16}Br_2$: C, 63.96; H, 3.30; Br, 32.74%.

The authors wish to express their gratitude to Drs. John and Elizabeth Weisburger of National Institutes of Health, U. S. A., for their helpful suggestions.

Department of Chemistry
Faculty of Technology
Yamaguchi University
Tokiwadai, Ube

Studies on Metal Complex Species using an Anion Exchange Resin. III. Uranium(VI)-Nitrate Complex and Zinc-Chloride Complex

By Jun YOSHIMURA, Hirohiko WAKI and Shingo TASHIRO

(Received May 31, 1961)

Kraus and Nelson[1] reported a method to identify the principal metal complex species in the aqueous phase by using an anion exchange resin. This may be applicable when the complex is very stable and when its form in the resin phase is the same as that in the aqueous phase. However, it is also often observed that the complexes in these two phases have different forms. Recently, Marcus and Coryell[2-4] have developed a method for the evaluation of stability constants by taking into consideration an invasion of electrolytes into the resin phase and by using the available data on activity coefficients in equations.

On the other hand, in the previous papers[5-7] of this series two new methods for the determination of the complex form have been derived which are particularly suitable for a study of the relatively unstable complexes.

It is known that uranium(VI) is adsorbed on an anion exchange resin from nitric acid or nitrate solutions[1], but no investigation of its anionic nitrate complex has be undertaken. It is also known that zinc is strongly adsorbed on the same resin from hydrochloric acid or chloride solutions, and thorough studies of its chloride complex have been made by Horne et al.[8,9] by means of anion exchange.

In the present study, the "indifferent electrolyte-adding" method described in the first papers[5,6] of this series was applied to the uranium(VI)-sodium nitrate system and also to the zinc-sodium chloride system in order to examine the applicability of the method to complex species in the aqueous phase. Sodium perchlorate was selected as an additional electrolyte in the uranium(VI)-nitrate system and sodium nitrate in the zinc-chloride system,

1) K. A. Kraus and G. E. Moore, "Anion Exchange Studies of the Fission Products", Peaceful Uses of Atomic Energy, Proceedings of the International Conference in Geneva, Vol. 7, (United Nations) (1955) p. 113.
2) Y. Marcus and C. E. Coryell, *Bull. Res. Council Israel*, **8A**, 1 (1959).
3) Y. Marcus, ibid., **8A**, 17 (1959).
4) Y. Marcus, *J. Inorg. Nucl. Chem.*, **12**, 287 (1960).
5) H. Waki, This Bulletin, **33**, 1469 (1960).
6) H. Waki, **34**, ibid., 829 (1961).
7) H. Waki, **34**, ibid., 1842 (1961).
8) R. A. Horne, *J. Phys. Chem.*, **61**, 1651 (1957).
9) R. A. Horne, R. H. Holm and M. D. Meyers, ibid., **61**, 1655 (1957).

because they have no direct effect on the complex formation in each system.

Experimental

a) Uranium-Nitrate System.—The sodium nitrate solution was prepared from a guaranteed reagent, and the sodium perchlorate solution from a first class reagent. The uranyl nitrate solution was prepared by dissolving the guaranteed reagent $UO_2(NO_3)_2 \cdot 6H_2O$ in dilute nitric acid. Each mixture of these solutions added to the resin had a volume of 10 ml. and contained 0.0347 mmol. of uranium and a series of sodim nitrate and sodium perchlorate mixed in various ratios, although the total concentration was constant within the individual series.

An anion exchanger "Dowex 1-X8" of a nitrate form (100~200 mesh) was swollen in water and then fitered under suction, after which the adhering water was removed with filter paper. Two grams of this resin was promptly put in a stoppered glass vessel. In order to estimate the exchange capacity of this amount of resin, at the same time another 0.5 g. of the resin was converted to chloride form in a small column. Its exchange capacity was then determined by the desorption of the chloride ions with a sodium nitrate solution and by Mohr's titration of them in the effluent. Resin set in this way tends to have a relatively constant value with respect to the exchange capacity and does not suffer an appreciable change in volume when it comes in contact with a nitrate solution.

The batch experiment was carried out with total concentrations of the solutions at 2, 3.2, 3.5, 4 and 6 M, and each series consisted of 4—6 batches of various nitrate concentrations. The resin and the solution were equilibrated at room temperature by being allowed to stand for an hour, with frequent shaking. It was recognized in the preliminary test that a sufficient equilibrium state was attained in about forty minutes. After the equilibrium mixture was filtered through a glass filter under suction without any further washing of the resin, 5 ml. of the filtrate was taken out, and the uranium concentration in the solution phase was determined colorimetrically at 372 mμ by the hydrogen peroxide method, using a Hirama photoelectric colorimeter. The amount of uranium in the resin was estimated from the difference between the total amount given and the amount in the solution phase at equilibrium. The distribution coefficient was calculated as

$$D=\frac{\text{mmol. of U per mequiv. of the resin}}{\text{mmol. of U per ml. of the soln.}}$$

This representation of the ion concentration in the resin phase is suitable in such a system because the density of resin varies with the nitrate-perchlorate exchange. On the other hand, nitrate concentrations were estimated in the following manner: the resin separated from the solution was wrapped in filter paper and pressed in order to remove the solution attached to the surface. About 1 g. of this resin was transferred to a short column, and then the nitrate ions were desorbed by 25 ml. of 2 M perchloric acid. The effluent was diluted to 50 ml., and its absorbance was measured at 300 mμ, using a Shimadzu spectrophotometer QB-50. A correction was made for uranyl ion, which had a little absorption at this wavelength, after the exchange capacity of resin in the column had been determined in the same way as before. The nitrate concentration in the resin phase was represented as millimole of the ion per milliequivalent of the resin.

b) Zinc-Chloride System.—The solutions of sodium chloride, sodium nitrate and zinc chloride were prepared from guaranteed reagents. To the zinc chloride solution a small quantity of hydrochloric acid was added to prevent the hydrolysis of the zinc. "Dowex 1-X8" chloride form (100~200 mesh) of 0.5 g. was set, and at the same time the exchange capacity was determined in the same way as described in a). Each mixture of the solutions added to the resin had a volume of 50 ml. and contained 0.0970 mmol. of zinc and a series of sodium chloride+sodium nitrate mixed in various ratios, although the total concentration was always 0.4 M or 3 M.

The resin and the solution were equilibrated at 25°C for an hour and the zinc and the chloride concentrations in the resin determined by EDTA and Mohr's titration respectively, after the two phases had been separated by a procedure similar to that used in a). The concentrations of these ions in the solution were estimated by subtraction. The distribution coefficient was calculated as:

$$D=\frac{\text{mmol. of Zn per mequiv. of the resin}}{\text{mmol. of Zn per ml. of the soln.}}$$

Results and Discussion

Uranium-Nitrate System. — By the same treatment as in the previous papers, the following equation obtained for the uranyl-nitrate complex:

$$\log D=(n-2)\log[NO_3^-]-(m-2)\log(NO_3^-)+K+G \qquad (1)$$

where (NO_3^-) and $[NO_3^-]$ represent the concentrations of nitrate ion not bound to uranyl ion, and m and n are the numbers of nitrate ions bound to each metal ion of the complex, in the solution and the resin phases respectively. K and G indicate the terms containing equilibrium constants and activity coefficients.

Assuming that a uranyl ion does not form any nitrate complex in the solution ($m=0$) and that at a constant ionic strength the activity coefficient term is kept constant, the following equations may be derived from Eq. 1:

$$\log D-2\log(NO_3^-)=(n-2)\log\{[NO_3]^*-n[U]\}+K+G \qquad (2)$$

and

$$\frac{d\{\log D-2\log(NO_3^-)\}}{d\log\{[NO_3]^*-n[U]\}}=n-2 \qquad (3)$$

where $[NO_3]^*$ is the stoichiometric concentration of all the nitrate ions in the resin, obtained directly by spectrophotometric measurement, and [U] is the concentration of the uranyl-nitrate complex in the resin.

Using the approximate n-value obtained from the gradient of the $\log D-2\log(NO_3^-)$ vs. $\log[NO_3]^*$ curve, $\log D-2\log(NO_3^-)$ was plotted against $\log\{[NO_3]^*-n[U]\}$, i. e., $\log[NO_3^-]$. As shown in Fig. 1, the gradient in the nitrate-rich range was 1.1, 1.4, 1.4, 1.9 and 2.0 for the external concentrations of 2, 3.2, 3.5, 4 and 6 M respectively. The n-values obtained from Eq. 3 in this way are plotted against the external nitrate concentration in Fig. 2. It may be recognized that uranium(VI) exists as $UO_2(NO_3)_3^-$ for the external nitrate concentration of 2 M, as $UO_2(NO_3)_4^{2-}$ for 4~6 M, and as a mixture of $UO_2(NO_3)_3^-$ and $UO_2(NO_3)_4^{2-}$ for the range between 2 M and 4 M.

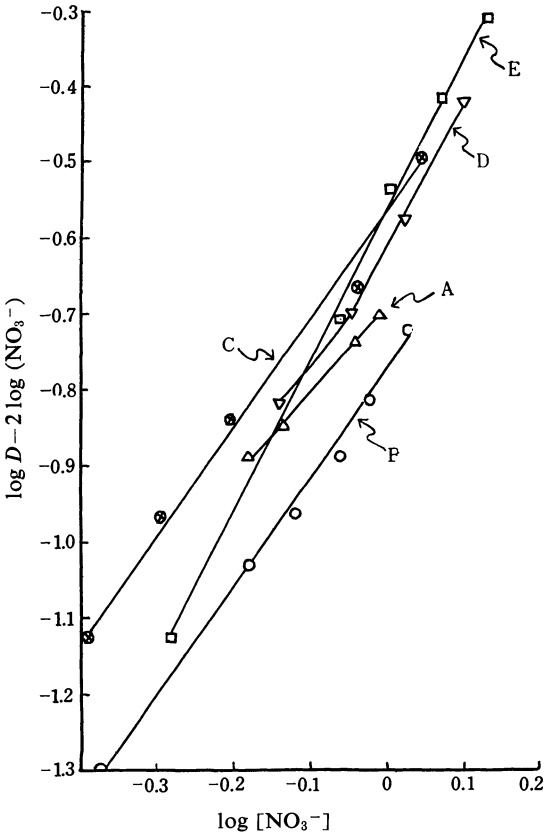


Fig. 1. Determination of n at various total concentration of the external solution in the nitrate-rich range. The rightest point in each curve is one in the absence of perchlorate.

Total external concentration is about; A 2 M, B 3.2 M, C 3.5 M, D 4 M, and E 6 M.

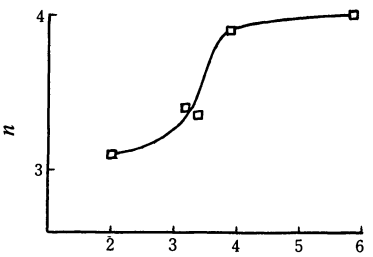


Fig. 2. n-Value of the uranyl-nitrate complex adsorbed from sodium nitrate solutions of various concentrations.

Zinc-Chloride System.—In the same way, the following equation was applied to the zinc-chloride complex:

$$\log D=(n-2)\log[Cl^-]-(m-2)\log(Cl^-)+K+G \qquad (4)$$

where the denotations are the same as those in the uranium-nitrate system. As it is known[9] that zinc is adsorbed as $ZnCl_4^{2-}$ at a 2~7 M chloride concentration, Eq. 4 becomes as follows by substituting $n=4$:

$$\log D-2\log\{[Cl]^*-4[Zn]\}=-(m-2)\log(Cl^-)+K+G \qquad (5)$$

where $[Cl]^*$ and [Zn] are the stoichiometric concentrations of all the chloride ions and zinc ions in the resin, obtained directly by measurement. (Cl^-) has been estimated, without regard to the chloride ions bound to the zinc ions in the solution. When K and G are constant, the following equation is applicable:

$$\frac{d[\log D-2\log\{[Cl]^*-4[Zn]\}]}{d\log(Cl^-)}=-(\bar{m}-2) \qquad (6)$$

where $\bar{m}$ is the mean number of ligands as defined by Bjerrum for the aqueous phase. The $\log D-2\log\{[Cl]^*-4[Zn]\}$ vs. $\log(Cl^-)$ plot at the external ionic strength $\mu=3$ is shown in Fig. 3. As can be seen from the curve, no appreciable change in the composition of complex species took place up to the external chloride concentration of 2 M, and from the gradient $ZnCl^+$ and $ZnCl_2^0$ were presumed to be the predominant species in this region. At a concentration of more than 2 M, anionic complex species were produced, and at the concentration of 3 M where only chloride ion is present, the coexistence of $ZnCl_3^-$ and $ZnCl_4^{2-}$ was presumed from the gradient of about −1.4, i. e., $m=3.4$.

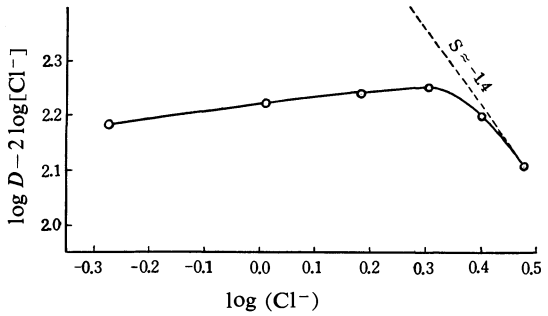


Fig. 3. Variation of distribution coefficient with external chloride concentration at constant ionic strength $\mu=3$.

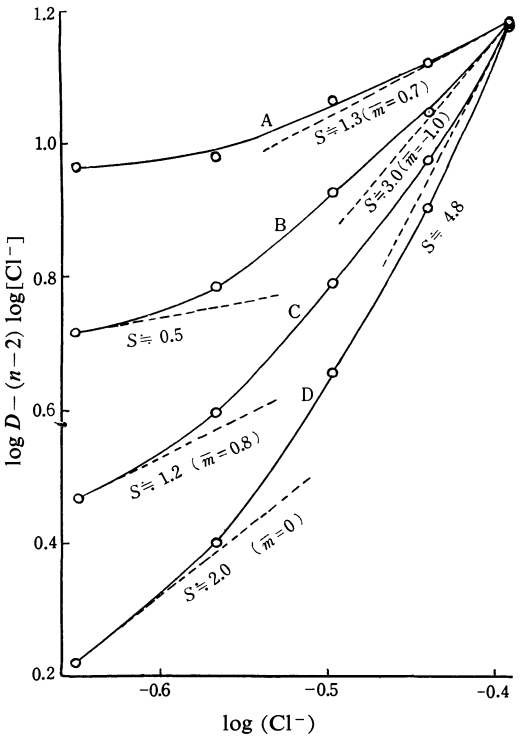


Fig. 4. Distribution coefficient curves when n is arbitrary assumed.

A, $n=4$; B, $n=3.5$; C, $n=3$; D, $n=2.5$

On the other hand, at the ionic strength $\mu=0.4$, the complex in the resin phase does not seem to be limited to one species, this being understood from the fact that the gradient of each curve in Fig. 4 increases with the chloride concentration. Even in such a complicated system, the principal species in the two phases can be identified graphically by introducing a condition $\bar{m}\geqq 0$ and $\bar{n}\leqq 4$. Curves were drawn in Fig. 4 on the assumption that $n=4$, 3.5, 3 and 2.5. At the point designating only the presence of 0.4 M chloride (at the right end of curve), the gradient of the curve was about 1.3 for $n=4$, which corresponded to $\bar{m}=0.7$, and 3.0 for $n=3.5$, which corresponded to $\bar{m}=-1.0$, since the gradient is $-(m-2)$ in Eq. 6. $m=0$ corresponds to $n=3.8$ by interpolation between $n=4.0$ and $n=3.5$. From the fact that $3.8\leqq\bar{n}\leqq 4.0$ corresponds to $0\leqq\bar{m}\leqq 0.7$, it may be considered that $ZnCl_4^{2-}$ is present as a predominant complex in the resin and that Zn^{2+} and $ZnCl^+$ are present in the solution when the aqueous phase is near the 0.4 M chloride solution. For a lower chloride concentration at the same ionic strength, $\bar{m}$ should be less than 0.7. At the chloride concentration of about 0.2 M (at the left end of the curve in Fig. 4), $\bar{m}=0$ corresponded closely to the gradient of the curve D for $n=2.5$ and $\bar{m}=0.7$, nearly to the gradient of the curve C for $n=3.0$ in Fig. 4. Consequently, $ZnCl_3^-$ (more than half) and $ZnCl_2^0$ seemed to be present as principal complexes in the resin phase at this concentration.

Further quantitative relations among the steps of the step-by-step formation of complex species may be estimated only with difficulty unless the stability constants are obtained. The evaluation of these constants requires not only many strict measurements but an extensive knowledge of activity coefficients.

Summary

1) The "indifferent electrolyte-adding" method described in previous papers was applied to the uranyl-nitrate and to the zinc-chloride complexes. A sodium nitrate-sodium perchlorate mixed medium was employed in the former, and a sodium chloride-sodium nitrate mixed medium in the latter.

2) The predominant species of the uranyl-nitrate complex adsorbed from sodium nitrate solutions was $UO_2(NO_3)_3^-$ at the external nitrate concentration of about 2 M and $UO_2(NO_3)_4^{2-}$ at the 4~6 M concentration. The coexistence of the two species may be presumed at 2~4 M.

3) The principal zinc-chloride complex adsorbed on the resin from the chloride solution of 0.4~3 M was simply $ZnCl_4^{2-}$, accompanied by a small quantity of $ZnCl_3^-$ in a low ionic strength. On the other hand, the predominant species in the aqueous phase were $ZnCl_3^-$ and $ZnCl_4^{2-}$ for a sodium chloride concentration of 3 M, and Zn^{2+} and $ZnCl^+$ for a 0.4 M concentration. These results were approximately consistent with those obtained in a hydrochloric acid medium by other investigators.

Department of Chemistry
Faculty of Science
Kyushu University
Hakozaki, Fukuoka

A Systematic Ion Exchange Separation of Metallic Elements. I. Group Separation of Metallic Elements by Anion Exchange with Hydrochloric Acid

By Jun YOSHIMURA and Hirohiko WAKI

(Received July 13, 1961)

A number of systematic separation methods of metallic elements using an ion exchange resin have been reported. Tompkins, Khym and Cohn[1], and Kimura, Minami and Honda[2] have reported systematic procedures for the separation of fission products by means of cation exchange. Minami, Fujimoto and Kakihana proposed a method[3,4] for the analysis of major ionic species in natural water using a cation exchange resin. Takiyama and Suito[5] reported a group separation of cations using anion exchange resins of various forms as precipitants, according to the principle of the usual qualitative analysis. Kraus and his co-workers[6] separated transition metals from each other by anion exchange in a hydrochloric acid medium. They have also carried out an extensive study[7] of the anion exchange adsorption of a number of elements from the same acid and other media. Jentsch and Pawlik[8] have also studied the adsorption from hydrochloric acid. A few years ago, the present authors reported an ion exchange method for silicate analysis[9]. The present authors are now interested in a systematic method for the isolation of all metallic elements in the usual quantity by ion exchange, without any other separatory operation. In systematic separation procedures, it is usual first to separate these elements into several groups, instead of isolating them one by one from the start. For an eluant employed in a group separation as the first stage of systematic procedure by ion exchange, it is necessary that it not produce an insoluble compound with most metals, and that it can be easily removed by heating or other simple operations after elution, since a large excess of eluant may make the subsequent separation troublesome. From this point of view, hydrochloric acid may be considered to be one of the most suitable eluants. In this experiment, the group separation was carried out by elution with various concentrations of hydrochloric acid through an anion exchange column, based on the Kraus' method. Some of the metallic elements which form insoluble or volatile compounds with hydrochloric acid, or which occur rarely in nature, and which form complicated compounds of various oxidation states, were excepted.

1) E. R. Tompkins, J. X. Khym and W. E. Cohn, *J. Am. Chem. Soc.*, **69**, 2769 (1947).
2) K. Kimura, E. Minami and M. Honda, *Japan Analyst*, **3**, 335 (1954).
3) H. Kakihana, *J. Chem. Soc. Japan, Pure Chem. Sec.* (*Nippon Kagaku Zasshi*), **71**, 481 (1950).
4) E. Minami, M. Fujimoto and H. Kakihana, ibid., **74**, 740 (1953).
5) K. Takiyama and E. Suito, *Japan Analyst*, **4**, 8 (1955).
6) K. A. Kraus and G. E. Moore, *J. Am. Chem. Soc.*, **75**, 1460 (1953).
7) K. A. Kraus and F. Nelson, "Anion Exchange Studies of the Fission Products", Peaceful Uses of Atomic Energy, Proceedings of the International Conference in Geneva, Vol. 7, p. 113 (1955) (United Nations).
8) D. Jentsch and I. Pawlik, *Z. anal. Chem.*, **146**, 88 (1955).
9) J. Yoshimura and H. Waki, *Japan Analyst*, **6**, 362 (1957).

Experimental

Resin.—The anion exchanger used in this work was a "Dowex 1-X8". The commercial chloride resin (100~200 mesh) was previously washed with water by means of suspension. The water, together with the resin of the finest mesh, was removed several times by decantation. Ten and forty milliliters columns of this chloride resin were used in the preliminary test and the separation experiment respectively. Each column was washed in turn with concentrated and dilute hydrochloric acids and water, and just before the addition of a sample solution it was treated with 10.5~11 M hydrochloric acid.

Solutions.—Hydrochloric acid as an eluant was of special grade and was used without further purification. Solutions of metal elements were prepared by dissolving their chlorides or oxides in water or hydrochloric acid except in the following cases: solutions of lead, bismuth and uranium were the acidified aqueous solutions of their nitrates: the solution of thallium(III) was prepared by treating thallous nitrate with a mixture of hydrochloric acid and nitric acid and then dissolving it in hydrochloric acid after the volatilization of nitric acid; the solution of arsenic(III) was prepared from arsenous acid, and the solution of arsenic(V) was obtained by oxidizing arseneous acid.

Procedure for Separation Experiments.—Each solution, usually containing about 5~10 mg. of an element, was evaporated to small volume, and concentrated hydrochloric acid was added so that the sample

solution might be adjusted to a volume of 10 ml. and to a hydrochloric acid concentration of 10.5~11 M. This solution was immediately added on the top of the column (Dowex 1, 40 ml., ϕ 1.2 cm.), and at the same time the effluent began to collect. When the sample solution was passed through the resin bed and no liquor was found on the top of the bed, a small volume of 11 M hydrochloric acid was added after washing the inside wall of the vessel used and the glass column, and the elution by 11 M hydrochloric acid was kept continuously by a connection with a separating funnel. When 40 ml. of the effluent was obtained, the elutriant was altered by 6.5 M hydrochloric acid, and the effluent was collected in another vessel. When 80 ml. of the effluent for 6.5 M was obtained, the elutriant was altered by 3 M hydrochloric acid. One hundred milliliters of the effluent for 3 M was collected. The metal elements still remaining in the resin bed after elution with 3 M hydrochloric acid were desorbed with extremely dilute hydrochloric acid below 0.5 M or with other elutriants appropriate for individual cases. The flow rate was 0.5 ml./min. for 11 M and 3 M hydrochloric acids, and 0.8 ml./min. for 6.5 M. All elutions were done at room temperature. In each elution the metal element in each fraction of the effluent was detected or determined, mostly by a usual method. Also, in the preliminary test, a similar procedure was employed, though a smaller column and smaller volumes of sample solution and of elutriant were used.

Results and Discussion

In the preliminary test in which a 10 ml. column was used, results* were obtained as expected from Kraus' experiments. Most metallic elements seemed to be classified experimentally into four groups from their behavior in elution with hydrochloric acid using an anion exchange resin, though each group was not enough separated from the others. The four groups were those not adsorbed even from concentrated hydrochloric acid, those adsorbed from the concentrated hydrochloric acid and desorbed with the 6 M acid, those desorbed by the acid below 6 M to 3 M, and those eluted with difficulty by 3 M hydrochloric acid. Besides, there were also some elements which have behavior intermediate between the first two groups.

The use of a longer column leads to the possibility of the more quantitative separation for these elements, and this may be required when considerable amounts of sample are treated. From this point of view, the column of 40 ml. was employed as well as in the silicate analysis[9]. The second elution was done by preferance with 6.5 M hydrochloric acid, since the use of hydrochloric acid less than 6 M might cause a partial effluence of cobalt into the part of the second group.

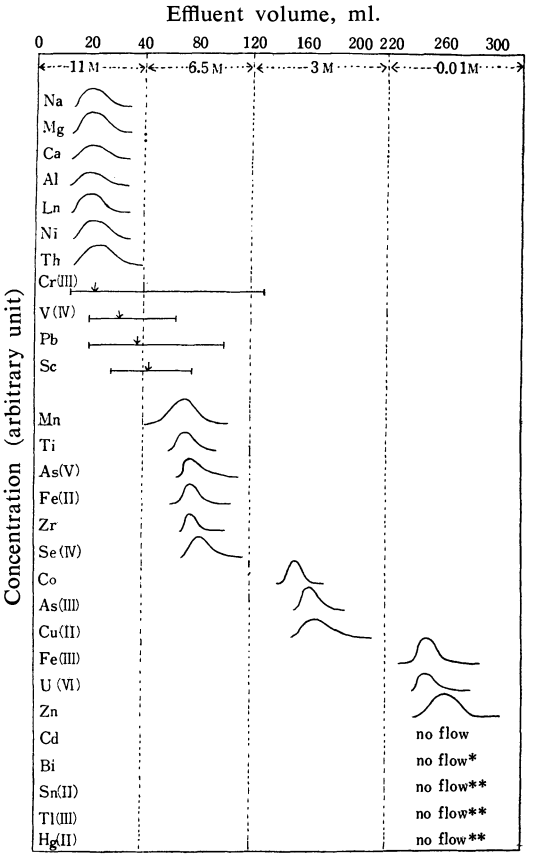


Fig. 1. Elution curves of metallic elements from the 40 ml. column of "Dowex 1-X8" with hydrochloric acid solutions of various concentrations.

|—| : Range where an metal element was detected
↓ : Point of maximum metal concentration in the effluent
* Test by 0.1 M HCl
** Test by 0.5 M HCl

As shown in Fig. 1 which gives an individual elution curve obtained by quantitative or semi-quantitative analysis of the effluent, the metallic elements investigated, except scandium, lead, vanadium(IV) and chromium(III), were quantitatively separated into four groups using the column of 40 ml. Scandium was found in the second section of effluent for the most part, although also in the first section of effluent in some portions. In order to separate it perfectly from non-adsorbed elements, 13 M hydrochloric acid must be employed[10]. But this may be of no practical use as an elutriant. Chromium(III)

* Elution curves have not been shown in this paper to avoid duplication, since they were like in tendency to those in the separation experiment where a 40 ml. column was used.

10) J. Yoshimura, Y. Takashima and H. Waki, *J. Chem. Soc. Japan, Pure Chem. Sec.* (*Nippon Kagaku Zasshi*), 79, 1169 (1958).

TABLE I. CLASSIFICATION OF METALLIC ELEMENTS

Group I			Group II			Group III		Group IV	
Li	Be	Al	Th	Mn	Fe(II)	Se	Co	As(III)	Fe(III)	Zn
Na	Mg	Y			As(V)			Cu(II)	U(VI)	Cd
K	Ca	La–Lu			Ti					Sn(II)
Rb	Sr				Zr					Tl(III)
Cs	Ba				Hf					Hg(II)
	Ni									Bi(III)
	Cr(III)		V(IV)	Sc	Pb					

Group I is eluted by 1 column volume of 11 M HCl.
Group II is eluted by 2 column volume of 6.5 M HCl.
Group III is eluted by 2.5 column volume of 3 M HCl.
Group IV is still held by the resin column after elutions by 11 M, 6.5 M and 3 M HCl.

and vanadium(IV) were found for the most part in the first section of effluent, but some portions of them were in the second one. Chromium can not be concentrated in a small volume of the effluent by hydrochloric acid because, it is considered, chromium has variously stable complex forms in the chloride solution. Lead extended half-and-half over the two sections. The elution favorable for only these elements may, conversely, be unsuitable for the group separation of most other metallic elements.

The classification of metallic elements based on the preliminary test and the separation experiment are tabulated in Table I. Some elements not described in this paper will be added to this table later in further studies. Especially, the assignment of more elements to group IV may be expected from Kraus' distribution data[7].

The use of a longer column and the careful selection of eluting conditions employing more kinds of chloride concentration might permit a further separation of the moderately adsorbable elements (groups II and III). However, much more time and a delicate technique may be required for them. Consequently, other eluants may be preferable for isolation inside these groups. Among the elements in group IV, the separation of Fe, U–Zn–Cd can be done easily using hydrochloric acid of extremely low concentration. However, such an dilute acid must be used prudently, since a number of strongly adsorbable elements tend to be hydrolyzed in dilute acid. The subdividing of this group by more dilute hydrochloric acid can be formalized only with difficulty unless the elution behaviors of these elements are known extensively. For the desorption of group IV in this experiment, hydrochloric acid of an arbitrary concentration below 0.5 M, water, perchloric acid, nitric acid and other elutriants were selected according to individual cases. The use of a smaller column leads to a poor separation between group I and manganese, and at least a near-40 ml. column is needed for a quantitative separation. If a sample contains no manganese, a somewhat smaller column may be used.

These classifications can not be interpreted in terms of the stability constant[11] of a chloro-complex in the solution phase. To explain the adsorbability of a metal ion on an anion exchange resin, the form and the stability of the complex in the resin phase must also be taken into account. Although these are not clear in general at present, the features of the four groups may be given an outline as described below.

Group I contains alkali metals, alkaline earth metals, aluminum, yttrium, lanthanide elements, thorium and nickel. These elements do not form any anionic complex species in either hydrochloric acid solution or resin, and pass through the resin column even with concentrated hydrochloric acid. They are collected in only one column volume of the effluent by 10.5~11 M.

Group II contains manganese, titanium, iron(II), zirconium, arsenic(V), selenium(IV) and also probably hafnium*, which are collected in the next two column volumes of the effluent by 6.5 M. These elements form anionic chloro-complexes in the resin phase for the concentrated hydrochloric acid medium, while they do not form presumably anionic chloro-complexes in any appreciable amount in the solution phase over the whole range of chloride concentration. An exception is arsenic(V), which appears to exist not as a chloro-complex anion but as an arsenate ion. Among non-metallic ions, sulfate and phosphate fall into both groups I and II.

11) J. Bjerrum, G. Schwarzenbach and L. G. Sillén, "Stability Constants, Part II—Inorganic Ligands", London (1958).

* It was confirmed that the adsorption of hafnium was not stronger than that of zirconium, although hafnium was not eluted by 10 M hydrochloric acid.

TABLE II. ANALYSES OF MIXED SOLUTIONS

Sample No.	Element	Taken	Found I	Found II	Found III	Found IV
1	Ni	5.97 mg.	5.94 mg.			
	Mn	2.00 mg.		2.02 mg.		
	Co	0.0840 mmol.			0.1591 mmol.	
	Cu(II)	0.0771 mmol.				
	Fe(III)	9.92 mg.				9.80 mg.
2	Th	7.42 mg.	7.08 mg.			
	Zr	3.97 mg.		3.90 mg.		
	U(VI)	89.4 mg.				89.3 mg.
3	Ni	59.7 mg.	59.5 mg.			
	Cu(II)	49.0 mg.			49.4 mg.	
	Zn	0.0708 mmol.				0.1120 mmol.
	Cd	0.0419 mmol.				

I : Effluent by 11 M HCl
II : Effluent by 6.5 M HCl
III : Effluent by 3 M HCl
IV : Effluent by extremely dilute HCl

Group III contains cobalt, arsenic(III) and copper(II), which are collected in the next two and a half column volumes of the effluent by 3 M. These elements form anionic chloro-complexes not only in the resin phase, but also in the solution phase for the concentrated hydrochloric acid medium.

Group IV contains iron(III), uranium(VI), zinc, cadmium, bismuth, tin(II), mercury(II), thallium, etc., which remain in the column after the elution with 3 M. Most elements in group IV form stable anionic chloro-complexes in both phases, even in a dilute hydrochloric acid medium. Iron(III) and uranium(VI) may be rather like the elements in group III in this point. However, they are conveniently classified in group IV, since their concentration regions of adsorption are as wide as those of other elements in this group.

The separation data on mixed solutions which consist of a few elements are shown in Table II. Sample 1 contains the elements situated in one end of each group with respect to the effluence. Samples 2 and 3 are those which contain a large quantity of special elements. Furthermore, a successful quantitative group separation can be expected in a mixed solution containing more elements in ordinary combination except in the following cases: 1) when an element undergoes a change in valency during the separatory process by reaction with other elements or with hydrochloric acid, 2) when a sample solution contains an element which is apt to produce a volatile compound in hydrochloric acid, 3) when the quantity of metal elements included is beyond a limit permissible from the column exchange capacity, and 4) when a sample solution of 10 ml. of concentrated hydrochloric acid can not be prepared in the case where a metal element of small solubility in the acid is treated in a relatively large amount.

For case 3 or 4, an increase in the resin bed volume and the volume of sample solution may be required.

Summary

1) As the first stage in the systematic separation of metallic elements by ion exchange, a group separation on an ordinary scale was tried using an anion exchanger "Dowex 1-X8", with hydrochloric acid, a method based on Kraus' method.

2) Most metallic elements usually treated in the chemical analysis can be separated into four groups by the elution through a 40 ml. column using 11 M, 6.5 M and 3 M hydrochloric acid as elutriant. Satisfactory results were obtained on analysis for a mixed solution.

3) These classifications may be explained in terms of the formation of a chloro-complex of a metal, not only in the solution phase but also in the resin phase.

The authors wish to thank Mr. Yoshiaki Sota for his assistance in this experiment.

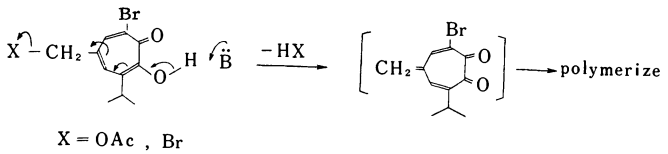
Department of Chemistry
Faculty of Science
Kyushu University
Hakozaki, Fukuoka

The Mannich Base of Troponoid and its Application. VII. The Synthesis of 5-Formyl Derivative of 3-Isopropyltropolone

By Kyozo OGURA

(Received May 30, 1961)

The present author has reported the synthesis of some Mannich bases of 3-isopropyltropolone (α-thujaplicin) and their properties[1]. The present paper describes the synthesis of 5-bromomethyl and 5-formyl derivatives of 3-isopropyltropolone from the Mannich base.



X = OAc , Br

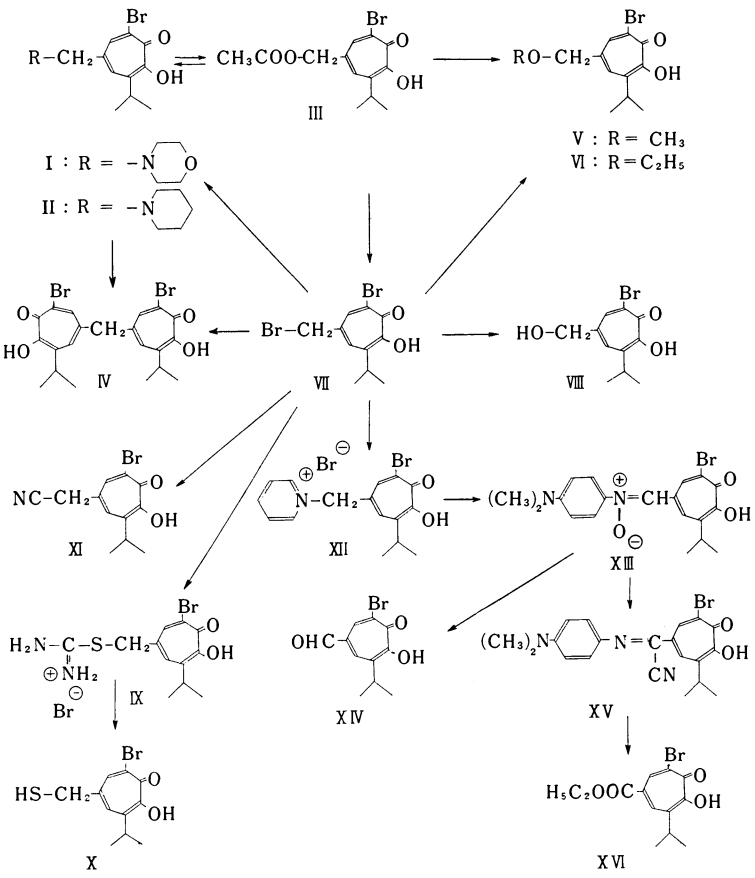
Treatment of 3-isopropyl-5-morpholinomethyl-7-bromotropolone (I) or 3-isopropyl-5-piperidinomethyl-7-bromotropolone (II) with acetic anhydride resulted in cleavage of the C–N bond to give 3-isopropyl-5-acetoxymethyl-7-bromotropolone (III). As in the case of 3, 7-dibromo-5-acetoxymethyltropolone[2], glacial acetic acid could also be used in place of acetic anhydride for the preparation of the acetoxymethyl derivative III, but the yield was lower. In the preparation of 3,7-dibromo-5-acetoxymethyltropolone from 5-morpholinomethyl derivative, bis(3, 7-dibromotropolon-5-yl)methane was produced as a by-product[2], while the reaction of I or II with glacial acetic acid did not give such a by-product; instead the corresponding bis(3-isopropyl-7-bromotropolon-5-yl)methane (IV) was obtained by refluxing II in toluene in the presence of sodium hydroxide. The compound IV forms a ferric complex which is insoluble in both water and organic solvents.

Alcoholysis of III by methanol and ethanol gave 3-isopropyl-5-methoxymethyl-7-bromo- (V) and 3-isopropyl-5-ethoxymethyl-7-bromotropolone (VI) respectively. Treatment of III with morpholine and piperidine, respectively, gave I and II. When III was treated with diluted sodium hydroxide solution, a transitory red color appeared and a resinous substance was formed. When III was heated in hydrobromic acid, 3-isopropyl-5-bromomethyl-7-bromotropolone (VII) was obtained in a good yield. The bromomethyl derivative VII is also very unstable to alkali. The unstability of III and VII to alkali may be due to their tendency to form such a quinonoid structure as follows.

The bromine in the bromomethyl group of VII is very reactive, and it is easily replaced by various anionoid reagents, so that C–O, C–N, C–S and C–C bond can be formed at the end of the methylene in the 5-position of the tropolone ring. Treatment of VII with dimethysulfoxide afforded 3-isopropyl-5-hydroxymethyl-7-bromotropolone (VIII). Alcoholysis of VII gave 5-alkoxymethyl derivatives, V and VI, and aminolysis of VII by morpholine and piperidine gave I and II respectively. The reaction of VII with thiourea gave *S*-(3-isopropyl-7-bromotropolon-5-ylmethyl)isothiouronium bromide (IX), which was converted into 3-isopropyl-5-mercaptomethyl-7-bromotropolone (X) by alkaline hydrolysis. The reaction of VII and potassium cyanide afforded 3-isopropyl-5-cyanomethyl-7-bromotropolone (XI). The reaction of VII with pyridine also easily proceeded in dry benzene at room temperature forming (3-isopropyl-7-bromotropolon-5-ylmethyl)pyridinium bromide (XII) quantitatively, which was soluble in water and formed a water-soluble ferric complex; on the other hand, the reaction of VII with triethylamine resulted in dehydrobromination to give triethylamine hydrobromide and a deep greenish blue substance which was too unstable to be obtained as pure crystals. This substance was decolorized by the action of hydrochloric acid to give IV. The reaction of the pyridinium salt XII with piperidine gave II, and that with sodium acetate afforded III.

Kröhnke's method[3] was applied to XII in order to obtain the 5-formyl derivative. Reaction of XII with *p*-nitroso-*N*, *N*-dimethylaniline

1) K. Ogura, This Bulletin, **34**, 839 (1961).
2) S. Seto and K. Ogura, ibid., **32**, 493 (1959).
3) F. Kröhnke, *Angew. Chem.*, **65**, 605 (1953).



in the presence of sodium hydroxide gave brilliant red crystals of (3-isopropyl-7-bromotropolon-5-yl)-*N*-(*p*-dimethylaminophenyl)nitrone (XIII), which when hydrolyzed with hydrochloric acid afforded 3-isopropyl-5-formyl-7-bromotropolone (XIV). The aldehyde XIV reacts with ordinary ketonic reagents, and its infrared spectrum shows an absorption maxima at 1680 and 2880 cm^{-1} due to its formyl group. When nitrone XIII was treated with potassium cyanide, (3-isopropyl-7-bromotropolon-5-yl)-*N*-(*p*-dimethylaminophenyl)cyanoanile (XV) was obtained as deep wine red prisms, and treating this with alcoholic hydrochloric aicd gave 3-isopropyl-5-ethoxycarbonyl-7-bromotropolone (XVI).

The reaction of the aldehyde will be reported in the near future.

Experimental*

3-Isopropyl-5-acetoxymethyl-7-bromotropolone (III).—a) When II (1 g.) was warmed in acetic anhydride (10 ml.) at 95°C with occasional stirring, the solution turned black in a few minutes, and it was decolorized gradually. After being kept at the same temperature for 1 hr., the solution was filtered to remove a small amount of precipitate, and the filtrate was concentrated under reduced pressure. Colorless needles which separated on being cooled were collected and recrystallized from methanol, m. p. 124~125°C. Yield, 0.6 g.

Found: C, 49.86; H, 4.86. Calcd. for $C_{13}H_{15}O_4Br$: C, 49.52; H, 4.76%.

λ_{max}^{MeOH} mμ(log ε): 262(4.14), 344(3.82), 386(3.65).

b) The solution of I (300 mg.) in glacial acetic acid (3 ml.) was heated at 110~120°C for 3 hr., and colorless needles which separated on being cooled were collected. Evaporation of the filtrate under reduced pressure gave a syrup residue, from which the starting material (100 mg.) was recovered as its hydrochloride by addition of a few drops of 6 N hydrochloric acid.

Bis(3-isopropyl-7-bromotropolon-5-yl)methane (IV).—A suspension of II (150 mg.) and powdered sodium hydroxide (30 mg.) in toluene (1 ml.) was refluxed for 3 hr., and yellow crystals were collected and acidified by 6 N hydrochloric acid to yield colorless powder, which was recrystallized from methanol to afford colorless scales, m. p. 157~158°C. Yield, 50 mg.

Found: C, 50.50; H, 4.46. Calcd. for $C_{21}H_{22}O_4 \cdot Br_2$: C, 50.60; H, 4.42%.

* All melting points are uncorrected. The microanalyses were carried out by Misses Yoko Endo and Yukiko Endo of this Institute, to whom the author is indebted.

λ_{max}^{MeOH} mμ(log ε) : 260(4.74), 340(4.24), 420(3.70).

3-Isopropyl-5-methoxymethyl-7-bromotropolone (V).—A solution of III (50 mg.) in methanol (0.5 ml.) was refluxed for 1 hr., and the removal of methanol left an oily residue, which solidified by addition of a few drops of water. The solid was collected and recrystallized from petroleum ether to give colorless needles, m. p. 60~61°C. Yield, 10 mg.

Found: C, 50.34; H, 5.33. Calcd. for $C_{12}H_{15}O_3 \cdot Br$: C, 50.17; H, 5.22%.

3-Isopropyl-5-ethoxymethyl-7-bromotropolone (VI).—A solution of III (50 mg.) in ethanol (0.5 ml.) was refluxed for 1 hr., and colorless needles of VI were obtained in the same manner as in the case of V. The ethoxymethyl derivative VI was also obtained by refluxing 5-bromomethyl derivative Vll in ethanol, m. p. 60~61°C. Yield ca. 10 mg.

Found: C, 51.89; H, 5.71. Calcd. for $C_{13}H_{17}O_3 \cdot Br$: C, 51.83; H, 5.65%.

3-Isopropyl-5-bromomethyl-7-bromotropolone (VII).—When III (1 g.) was heated in 4 ml. of hydrobromic acid (*d*, 1.4) at 95~100°C with occasional swirling for 40 min., yellow oil separated which was solidified on being cooled. The solid was collected, washed with water and dried well. Recrystallization from petroleum ether gave colorless prisms, m. p. 87~90°C. Yield, 0.95 g.

Found: C, 39.66; H, 3.55. Calcd. for $C_{11}H_{12}O_2 \cdot Br$: C, 39.29; H, 3.67%.

$\lambda_{max}^{isooctane}$ mμ(log ε) : 258(4.48), 330(3.94), 375(3.74).

3-Isopropyl-5-hydroxymethyl-7-bromotropolone (VIII).—After a solution of VII (50 mg.) in dimethylsulfoxide (0.2 ml.) was kept at room temperature for 14 hr., cracked ice (ca. 2 g.) was added to the solution. The solid, which was formed by scratching the wall of the vessel, was collected and recrystallized from benzene-petroleum ether, affording colorless needles, m. p. 84~87°C. Yield, 20 mg.

Found: C, 48.88; H, 5.13. Calcd. for $C_{11}H_{13}O_3 \cdot Br$: C, 48.35; H, 4.76%.

λ_{max}^{MeOH} mμ(log ε) : 260(4.42), 338(3.73), 380(3.65).

***S*-(3-Isopropyl-7-bromotropolon-5-ylmethyl)isothiouronium Bromide (IX).**—When a solution of VII (100 mg.) and thiourea (40 mg.) was warmed in *tert*-butanol (0.7 ml.) on a water bath for 5 min., the colorless crystals separated, which were collected and washed with ethanol, m. p. 217°C (decomp.). Yield, 80 mg.

Found: C, 35.07; H, 3.88; N, 6.08. Calcd. for $C_{12}H_{16}O_2N_2SBr$: C, 35.05; H, 3.97; N, 6.45%.

λ_{max}^{MeOH} mμ(log ε) : 259(4.52), 340(3.96), 395(3.70), 410(3.69).

3-Isopropyl-5-mercaptomethyl-7-bromotropolone (X).—After IX (80 mg.) was warmed in 45% sodium hydroxide (0.7 ml.) on a water bath for a few minutes, the solution was acidified with 6 N hydrochloric acid containing cracked ice (ca. 1 g.). The precipitate was collected, washed with water and recrystallized from methanol, affording 50 mg. of pale yellow needles, m. p. 80~81°C.

Found: C, 46.13; H, 4.73. Calcd. for $C_{11}H_{13}O_2 \cdot SBr$: C, 45.67; H, 4.50%.

λ_{max}^{MeOH} mμ(log ε) : 258(4.49), 333(3.91), 375(3.73).

3-Isopropyl-5-cyanomethyl-7-bromotropolone (XI).—A solution of VII (100 mg.) in dioxane (2 ml.) was added dropwise into a solution of potassium cyanide (100 mg.) in dioxane (3 ml.) and water (0.5 ml.), while being stirred under ice cooling, the drop causing a transitory red color to appear. After completion of addition the mixture was stirred for 1 hr., and the solvent was removed under reduced pressure at room temperature, and the residue was acidified with diluted hydrochloric acid. The precipitate was collected and recrystallized from petroleum ether to colorless needles, m. p. 102~103°C. Yield, 20 mg.

Found: C, 51.27; H, 4.14; N, 5.03. Calcd. for $C_{12}H_{12}O_2NBr$: C, 51.06; H, 4.26; N, 4.97%.

λ_{max}^{MeOH} mμ(log ε) : 260(4.56), 330(3.91), 375(3.79).

(3-Isopropyl-7-bromotropolon-5-ylmethyl)pyridinium Bromide (XII).—When pyridine (350 mg.) was added dropwise into a solution of VII (1.5 g,) dissolved in dry benzene (10 ml.), colorless precipitate appeared immediately. After being allowed to stand for 30 min. with occasional stirring, the precipitate was collected and washed with benzene, m. p. 214~215°C (decomp.). Yield, 1.8 g.

Found: C, 46.70; H, 4.25; N, 3.70. Calcd. for $C_{16}H_{17}O_2NBr$: C, 46.51; H, 4.00; N.3.37%.

λ_{max}^{MeOH} mμ(log ε) : 260(4.53), 340(3.93), 380(3.80).

(3-Isopropyl-7-bromotropolon-5-yl)-*N*-(*p*-dimethylaminophenyl)nitrone (XIII).—To a mixture of XII (1.5 g.), *p*-nitrosodimethylaniline (0.6 g.) and ethanol (14 ml.), 3.9 ml. of sodium hydroxide solution (3.8%) was added, while being stirred under ice cooling. After completion of addition the mixture was stirred at room temperature, and red crystals began to appear in a few minutes. After being stirred for 30 min., the mixture was diluted with water (5 ml.), and the crystals were collected, washed well with water and recrystallized from ethanol, affording brilliant red needles, m. p. 142~143°C (decomp.). Yield, 1.45 g.

Found: C, 55.79; H, 5.55; N, 6.61. Calcd. for $C_{19}H_{21}O_3N_2Br$: C, 55.30; H, 5.18; N, 6.92%.

λ_{max}^{MeOH} mμ(log ε) : 264(4.60), 355(4.17), 427(4.00).

3-Isopropyl-5-formyl-7-bromotropolone (XIV).—When 6 N hydrochloric acid was added to XIII (1 g.), the mixture turned yellow. After being warmed on a water bath for a few minutes, the mixture was allowed to stand at room temperature for 1 hr. with occasional stirring. The precipitate was collected, washed well with water and recrystallized from petroleum ether to give colorless scales, m. p. 102~103°C. Yield, 0.67 g.

Found: C, 48.85; H, 4.22: Calcd. for $C_{11}H_{11}O_3 \cdot Br$: C, 48.81; H, 4.06%.

$\lambda_{max}^{isooctane}$ mμ (log ε) : 277(4.40), 345(4.02).

Oxime.—Yellow prisms, m. p. 143~144°C.

Found: C, 46.80; H, 4.25; N, 4.89. Calcd. for $C_{11}H_{12}O_3NBr$: C, 46.15; H, 3.85; N, 4.90%.

Phenylhydrazone.—Red needles, m. p. 186~191°C.

Found: C, 56.87; H, 4.71; N, 7.74. Calcd. for $C_{17}H_{17}O_2N_2Br$: C, 56.53; H, 4.74; N, 7.76%.

2,4-Dinitrophenylhydrazone.—Red prisms, m. p. 236~237°C.

Found: C, 44.80; H, 3.46; N, 11.99. Calcd. for $C_{17}H_{15}O_6N_4Br$: C, 45.25; H, 3.32; N, 12.41%.

Thiosemicarbazone.—Orange prisms, m. p. 210°C (decomp.).

Found: C, 42.39; H, 3.68; N, 11.12. Calcd. for $C_{12}H_{14}O_2N_3SBr$: C, 41.83; H, 4.07; N, 12.21%.

(3-Isopropyl-7-bromotropolon-5-yl)-*N*-(*p*-dimethylaminophenyl)cyanoanile (XV).—When a mixture of XIII (100 mg.), potassium cyanide (60 mg.) and ethanol (1 ml.) was stirred at room temperature, a yellow precipitate appeared. Addition of a few drops of water to the mixture effected a clear solution, and red crystals separated in a few minutes, which were collected, acidified with 6 N hydrochloric acid and recrystallized from petroleum ether to wine red prisms, m. p. 195~196°C. Yield, 20 mg.

Found: C, 57.22; H, 4.18; N, 9.41. Calcd. for $C_{20}H_{20}O_2N_3Br$: C, 57.97; H, 4.83; N, 10.14%.

λ_{max}^{MeOH} mμ(log ε): 265(4.24), 423(4.22), 500(4.35).

3-Isopropyl-5-ethoxycarbonyl-7-bromotropolone (XVI).—When XV (100 mg.) was heated in 6 N hydrochloric acid (1 ml.) and ethanol (1 ml.) on a water bath, yellow crystals separated, which were collected and recrystallized from petroleum ether to pale yellow needles, m. p. 123~128°C. Yield, 50 mg.

Found: C, 49.48; H, 4.55. Calcd. for $C_{13}H_{15}O_4 \cdot Br$: C, 49.52; H, 4.76%.

λ_{max}^{MeOH} mμ(log ε): 256(4.27), 271(4.21), 370(3.99), 386(4.20).

Summary

3-Isopropyl-5-bromomethyl-7-bromotropolone and 3-isopropyl-5-formyl-7-bromotropolone were synthesized from 3-isopropyl-5-piperidinomethyl-7-bromotropolone, and some 5-substituted 3-isopropyl-7-bromotropolones were derived from the bromomethyl derivative.

The author wishes to express his deep gratitude to Professor Shuichi Seto for his kind guidance and encouragement throughout this work, to Mr. Shuji Aono for infrared spectral measurements and to Mr. Fumio Sato for ultraviolet spectral measurements. A part of the expense for the present work was defrayed by Sankyo Co., Ltd., to whom the author wishes to express his sincere gratitude.

The Chemical Research Institute of Non-Aqueous Solutions
Tohoku University
Katahira-cho, Sendai

Infrared Absorption Spectra of Hydrazides. III. Hydrazides of Aliphatic Acids

By Mitsuo MASHIMA

(Received June 23, 1961)

In a previous paper[1] the amide frequencies characteristic of the hydrazides of aromatic acids were discussed, and for the ion $(RCONHNCOR')^{-}$ [2] amide I, II and III bands were observed within the normal frequency ranges for secondary amides. The present investigation was undertaken to determine the characteristic frequencies of the hydrazides of aliphatic acids. Solid spectra of diformylhydrazine and its *N*-deuterated derivative[3] of diacetylhydrazine, its mono-hydrate, and of their deuterated derivatives[4] have already been published. For the present study, the spectra of dipropionylhydrazine, dibutyrylhydrazine, diisovalerylhydrazine, formyl-acetylhydrazine, and cyanoacetyl-acetylhydrazine were examined in the solid state and in solution. The solution spectrum of diacetylhydrazine was also observed, diformylhydrazine in solution could not, however, be examined because of its sparing solubilities in solvents suitable to observation in infrared spectra.

Experimental

Dipropionylhydrazine was prepared with propionic anhydride and hydrazine hydrate[5] and was purified by recrystallization from benzene, m. p. 136°C. Dibutyrylhydrazine was synthesized by the reaction of butyrylhydrazine with iodine in ethanol[6] and was purified by recrystallization from benzene, m. p. 163°C. Diisovalerylhydrazine was synthesized with isovalerylhydrazine and iodine in ethanol[7] and was purified by recrystallization from benzene, m. p. 180°C. Formyl-acetylhydrazine was synthesized with formylhydrazine and acetic anhydride[8]

1) M. Mashima, This Bulletin, **35**, 338 (1962).
2) M. Mashima, ibid., **35**, 332 (1962).
3) T. Miyazawa, T. Shimanouchi and S. Mizushima, *J. Chem. Phys.*, **24**, 408 (1956); also see T. Miyazawa, *J. Chem. Soc. Japan, Pure Chem. Sec.* (*Nippon Kagaku Zasshi*), **76**, 341 (1955).
4) A. Yamaguchi, ibid., **79**, 880 (1958).
5) T. Curtius and H. Hille, *J. prakt. Chem.*, [2] **64**, 406 (1901).
6) R. Stolle and G. Zinsser, ibid., [2] **69**, 489 (1904).
7) T. Curtius and H. Hille, ibid., [2] **64**, 414 (1901).
8) G. Heller, ibid., [2] **120**, 60 (1929).

and was purified by recrystallization from ethanol, m. p. 96°C. Cyanoacetyl-acetylhydrazine was synthesized with cyanoacetylhydrazine and acetic anhydride[9] and was purified by recrystallization from ethanol, m. p. 171°C. The synthesis of diacetylhydrazine has been described previously[2]. The method of preparation of compounds containing deuterium was similar to that described previously[1]. Solution spectra were obtained in acetonitrile with cells of 0.1 mm. in optical path, and solid spectra were studied in potassium bromide disk with a Hitachi infrared spectrophotometer EPI-2 in the rock salt region.

Results and Discussion

Solid Spectra.—*Symmetric Hydrazides.*—The solid spectra of dipropionylhydrazine (DPH), dibutyrylhydrazine (DBuH), and diisovalerylhydrazine (DIVH) are shown in Fig. 1, in which the solid spectrum of diacetylhydrazine (DAH) is also represented for purposes of comparison. Let us consider mainly the N–H stretching band and the amide I, amide II and amide III bands because they may be characteristic of the hydrazides.

By comparison of the spectra with those of diformylhydrazine (DFH)[3] and DAH[4], the following assignments are possible:

All of these hydrazides have a very intense band near 3200 cm^{-1} which is easily assigned to the N–H stretching vibration ν(N–H) and a rather weak band near 3030 cm^{-1} which is also attributed to ν(N–H). The assignment of the former was confirmed by *N*-deuteration; e. g., *N*-deuterated DPH has a band at 2380 cm^{-1} which corresponds to the 3200 cm^{-1} band of DPH, the ratio ν_H/ν_D being 1.34. The latter disappears from the solution spectra, as is indicated in a following section. Therefore, it is probably also associated with ν(N–H).

The symmetric hydrazides have the most intense band among their absorption bands near 1600 cm^{-1}. The amide I band was found at 1610 cm^{-1} for DFH[3] and at 1598 cm^{-1} for

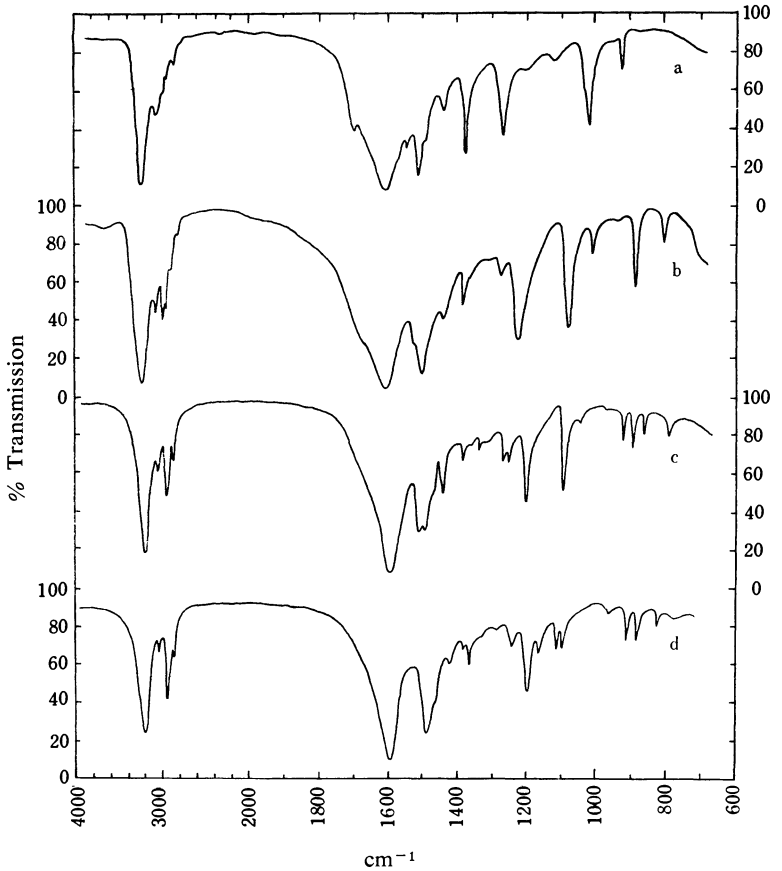


Fig. 1. Infrared spectra of the symmetric hydrazides in KBr disk.
a; DAH, b; DPH, c; DBuH, d; DIVH

9) V. Rothenburg, *Ber.*, **27**, 688 (1894).

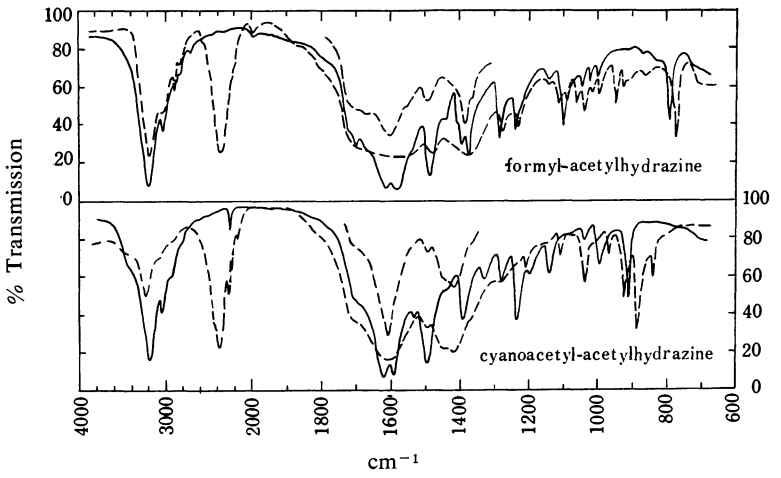


Fig. 2. Infrared spectra of asymmetric hydrazides in KBr disk. Solid curves show the spectra of hydrazides and dashed curves indicate the spectra of *N*-deuterated derivatives.

DAH*. Thus, the band near 1600 cm^{-1} is assigned to the amide I band.

The amide II band is observed near 1500 cm^{-1} for these hydrazides. A corresponding band was found at 1414 cm^{-1} for *N*-deuterated DPH, the ratio ν_H/ν_D being 1492/1414 (1.055). The value is close to 1.106 for DFH[3] and to 1.065 for DAH[4].

For hydrazides of aromatic acids[1] the amide III band was found in the normal range of secondary amides, and it split into two bands. However, no such splitting can be observed for the symmetric hydrazides of aliphatic acids; only a single amide III band is found near 1200 cm^{-1}. For *N*-deuterated DPH a corresponding band is found at 928 cm^{-1}, the ratio ν_H/ν_D being 1217/928 (1.311). The value of ν_H/ν_D is close to 1.248 for DFH[3] and to 1.333 for DAH[4].

Formyl-acetylhydrazine (FAH) and Cyano-acetyl-acetylhydrazine (CAH).—The solid spectra of FAH, CAH, and their *N*-deuterated derivatives are illustrated in Fig. 2. In the 3000 cm^{-1} region a strong band is found at 3200 cm^{-1} for FAH and at 3190 cm^{-1} for CAH. A corresponding band is found at 2380 cm^{-1} for *N*-deuterated FAH and at 2370 cm^{-1} for *N*-deuterated CAH, the values of ν_H/ν_D being 1.344 and 1.346 respectively. These bands are easily assigned to ν(N–H) by comparison of the values of frepuency and ν_H/ν_D with those of the symmetric hydrazides indicated in the foregoing section. The main band near 3200 cm^{-1} is accompanied by several shoulder bands in the spectra of FAH and CAH indicated in Fig. 2 and of DAH indicated in Fig. 1. A well-defined shoulder is found at 3020 cm^{-1} for FAH, at 3050 cm^{-1} for CAH, and at 3060 cm^{-1} for DAH. No corresponding band is found in the solution spectra, as is indicated in a following section. In consequence, the shoulder band near 3050 cm^{-1} is probably due to ν(N–H). Other shoulder bands can probably be ascribed to the C–H stretching vibrations, but we can not assign the individual shoulder band with confidence because of the complexity and the rather weak intensity of the absorption bands.

We will next consider the amide bands. DAH has a very strong band at 1598 cm^{-1} which has been ascribed to the amide I band by Yamaguchi[4], while two corresponding bands are found at 1613 and 1580 cm^{-1} for FAH and at 1623 and 1593 cm^{-1} for CAH. Both bands can undoubtedly be assigned to the amide I because they are in good agreement with the band of DAH in frequency. Yamaguchi[4] observed the solid spectra of diacetylhydrazine monohydrate and ascribed a single band at 1661 cm^{-1} to an amide I band. On the other hand, similar doublets have been observed for hydrazides of aromatic acids[1], and a further consideration will be represented later on. *N*-Deuterated FAH and *N*-deuterated CAH have only a single band at 1604 cm^{-1} and 1607 cm^{-1} respectively, both of which bands correspond to the amide I band.

FAH and CAH have amide II bands at 1483 cm^{-1} and at 1497 cm^{-1} respectively. The values of these frequencies are very close to the 1506 cm^{-1} of DAH and the 1480 cm^{-1} of DFH[3]. The assignments of these bands were confirmed by *N*-deuteration; i. e., *N*-deuterated FAH has a corresponding band at 1383 cm^{-1},

* Yamaguchi (Ref. 4) obtained the band at 1597 cm^{-1} for DAH in Nujol.

the ratio of ν_H/ν_D being 1.072, and *N*-deuterated CAH has a band at 1413 cm^{-1}, the ratio being 1.059. These values of ν_H/ν_D are very close to those of the symmetric hydrazides indicated in the previous section, i. e., 1.106 for DFH, 1.065 for DAH, and 1.055 for DPH.

DAH has only a single amide III band at 1260 cm^{-1}, but FAH has two corresponding bands at 1279 and 1232 cm^{-1} and CAH has two bands at 1281 and 1235 cm^{-1}. The assignment of these two bands is confirmed by the finding of corresponding bands at 946 and 924 cm^{-1} for *N*-deuterated FAH and at 962 and 918 cm^{-1} for *N*-deuterated CAH. The values of the ratio ν_H/ν_D are 1.352, 1.333 for the two bands of FAH and 1.345, 1.342 for CAH.

Vibrations relating to the CH_3, CH_2 and CH groups are also to be associated with bands in the rock salt region. The C–H stretching bands have been discussed already. Bands due to CH_3, CH_2 and CH deformation vibrations are expected to appear in the region 1450~1350 cm^{-1}. DAH has a $\delta_a(CH_3)$ band at 1430 cm^{-1} and a $\delta_s(CH_3)$ band at 1365 cm^{-1}, and DFH[3] has a δ(CH) band at 1368 cm^{-1}. CAH has bands at 1448, 1392, and 1331 cm^{-1}, of which the first band is assigned to $\delta_a(CH_3)$ or $\delta(CH_2)$; the second one can be ascribed to $\delta_a(CH_3)$, while the last band might possibly be due to CH_3 or CH_2 deformation vibration. In this region FAH has three bands at 1441, 1390 and 1372 cm^{-1}, of which the 1441 cm^{-1} band is easily assigned to $\delta_a(CH_3)$, while the other two bands are probably due to either $\delta_s(CH_3)$ or δ(CH). These deformation bands can not be determined in the spectra of *N*-deuterated derivatives of CAH and FAH because of the overlap of the amide II band.

Rocking vibrations of the CH_3 and CH_2 groups can also concern bands which are ordinarily shown in the range of 1200~800 cm^{-1}. DAH has rocking CH_3 bands at 1027 and 1016 cm^{-1} **. CAH has two bands at 1041 and 996 cm^{-1} which can probably be ascribed to the rocking CH_3 or CH_2 vibrations. For *N*-deuterated CAH, corresponding bands are found at 1103 and 1030 cm^{-1}. In this region FAH has a relatively intense band at 1093 cm^{-1} and three weaker bands at 1038, 1018 and 995 cm^{-1}. *N*-Deuterated FAH has six rather weak corresponding bands. C–H out-of-plane deformation vibrations are also to be related to one of them. For sodium diformylhydrazine[2], two bands due to the out-of-plane deformation vibrations have been obtained at 1026 and 974 cm^{-1}. In consequence, the four bands of FAH can not definitely be assigned, but it is sure that they are due to either the CH_3 rocking or the CH out-of-plane deformation vibrations.

An in-plane bending O=C–N band has been obtained at 753 cm^{-1} for DFH[3]. The 784 cm^{-1} band of FAH is also probably due to δ(O=C–N). The corresponding band of *N*-deuterated FAH is observed at 769 cm^{-1}. Further, DFH[3] has the out-of-plane bending N–H band at 770 cm^{-1}, while no band corresponding to it is observed for FAH. In the region examined, neither the δ(O=C–N) nor the π(N–H) is observed for CAH.

On the other hand, DAH has the 921 cm^{-1} band which is to be ascribed to the C–CH_3 stretching vibration[4]. No corresponding band for FAH is observed, while CAH has the 914 cm^{-1} band which is assigned to ν(C–CH_3),

TABLE I. INFRARED FREQUENCIES OF FAH AND CAH IN THE ROCK SALT REGION (in cm^{-1})

Assignment[a]	DFH[b]	DAH[c]	FAH	CAH
ν(N–H)	3100	3210	3200	3190
		3060	3020	3050
ν(C–H)	2900	2980		2970
		2930	2910	
		2860	2860	
			2720	
ν(C≡N)				2270
		1695	1702	1710
			1669	
Amide I	1610	1598	1613	1623
			1580	1593
		1538		1538
Amide II	1480	1506	1483	1497
$\delta_a(CH_3)$		1430	1441	1448
$\delta(CH_2)$				
δ(C–H)	1368		1390	1392
$\delta_s(CH_3)$		1365	1372	1331?
Amide III	1229	1260	1279	1281
			1232	1235
		1195		1200
ν(N–N)			1133	1143
		1112		
r(CH_3)		1027	1093	
r(CH_2)		1016	1038	1041
			1018	996
π(C–H)			995	
ν(C–CH_3)		921		914
π(N–H)	770			
δ(C=O–N)	753		784	

a ν: stretching, δ: deformation, r: rocking, π: out-of-plane deformation, a: asymmetrical, s: symmetrical

b See Ref. 3

c See Footnote 10

** These two bands correspond respectively to the bands at 1029 and 1019 cm^{-1} obtained by Yamaguchi (see Ref. 4).

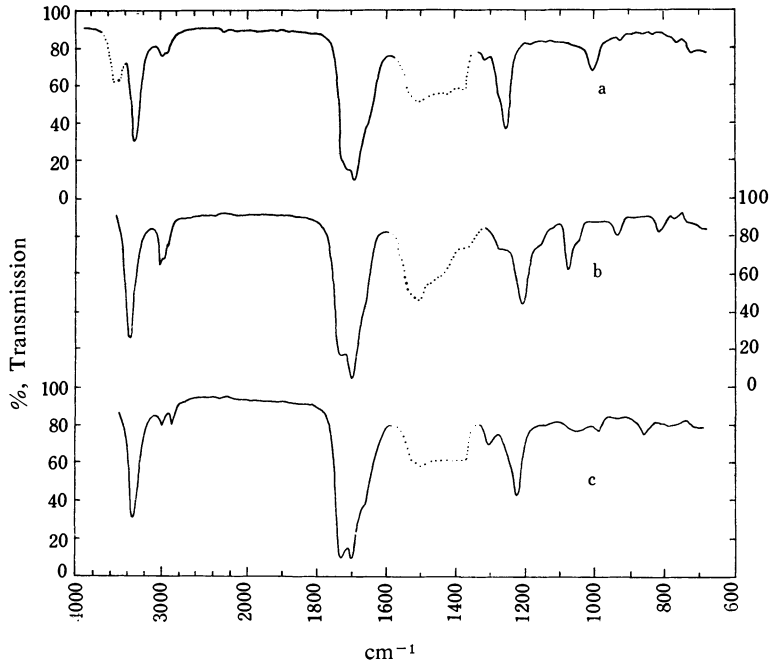


Fig. 3. Infrared spectra of the hydrazides in acetonitrile (0.1 mm. cell). a; DAH (0.1 mol./l.), b; DPH (0.2 mol./l.), c; FAH (0.2 mol./l.)

and the corresponding band of *N*-deuterated CAH is found at 881 cm^{-1}.

CAH has a further band at 2270 cm^{-1} which can possibly be assigned to the stretching C≡N vibration because the frequency hardly changes on *N*-deuteration.

DAH has four bands at 1695, 1538, 1195 and 1112 cm^{-1}, none of which was interpreted by Yamaguchi[4]. The corresponding bands of CAH are found at 1710, 1538, 1200 and 1143 cm^{-1} respectively. Of these four bands, the one near 1700 cm^{-1} is also found for FAH; it may, therefore, be a combination band involving low frequency fundamentals. The 1538, 1195 and 1112 cm^{-1} bands of DAH might also be similar combination bands. However, FAH has a weak band at 1133 cm^{-1} which corresponds to the 1143 cm^{-1} band of CAH. A band at 1100 cm^{-1} of $HCONDNHCOCH_3$[3] and the one at 1165 cm^{-1} of $(CH_3CONH-)_2 \cdot H_2O$[4] were ascribed to the N-N stretching vibration. In consequence, the 1143 cm^{-1} band of CAH and the 1133 cm^{-1} band of FAH may possibly be ν(N-N). A corresponding band of *N*-deuterated CAH is not observed, while for *N*-deuterated FAH a band is found at 1143 cm^{-1}.

The observed frequencies of FAH and CAH and their assignments are summarized, with those of DFH[3] and DAH[10], in Table I.

10) For this compound the values of frequencies are obtained in the present study although their assignments depend on the work by Yamaguchi (see Ref. 2).

Solution Spectra.—The solution spectra of DPH, DAH and FAH are illustrated in Fig. 3 because they are typical.

All the hydrazides examined have a band near 3300 cm^{-1} which is probably due to a monomeric ν(N-H). Further, the hydrazides generally have the amide I band near 1690 cm^{-1} and a well-defined shoulder band on the high-frequency side. However, only FAH has two bands of nearly the same intensity. In spite of this, they are easily assigned to the amide I band, but further consideration will be given to the problem in a following section. The amide II band may not be observed in the solution spectra because of interference by solvent absorption. A band near 1200 cm^{-1} can be assigned to the amide III band because the frequencies are very close to the amide III band of the hydrazides in the solid state.

Characteristic Bands.—The N-H stretching and amide frequencies of the hydrazides of aliphatic acids and *N*-methyl acetamide are summarized in Table II.

In the solid state, simple *N*-mono-substituted amides show a very strong band (amide I) in the range 1680~1630 cm^{-1}, a strong band (amide II) in the range 1570~1515 cm^{-1} and a relatively weaker band (amide III) in the range 1305~1200 cm^{-1} [11]. Sodium hydrazides[2] with only one CONH group showed the amide I band in the normal range of secondary amides. The decrease in the

TABLE II ν(N-H) AND AMIDE FREQUENCIES IN cm^{-1}.

Molecules and State		ν(N-H)	Amide I	Amide II[a]	Amide III
$(HCONH-)_2$	Solid[b]	3100	1605	1480	1229
$(CH_3CONH-)_2$	Solid	3210, 3060	1598	1506	1260
in CH_3CN (ca. 0.1 M)		3320	1699, 1683	—	1234
$(C_2H_5CONH-)_2$	Solid	3200, 3030	1600	1492	1217
in CH_3CN (ca. 0.2 M)		3310	1718, 1690	—	1197
$(C_3H_7CONH-)_2$	Solid	3190, 3040	1593	1499[c]	1202
in CH_3CN (saturated)		3330	1723, 1693	—	—[d]
$(C_4H_9CONH-)_2$	Solid	3210, 3040	1598	1492	1204
in CH_3CN (saturated)		3330	1720, 1691	—	—[d]
$HCONHNHCOCH_3$	Solid	3200, 3020	1613, 1580	1483	1279, 1232
in CH_3CN (ca. 0.2 M)		3310	1731, 1698	—	1222
$CNCH_2CONHNHCOCH_3$	Solid	3190, 3050	1623, 1593	1497	1281, 1235
in CH_3CN (ca. 0.2 M)		3310	1737, 1707	—	—[d]
$CH_3CONHCH_3$	Solid[b]		1653	1566	1301
in CH_3CN (0.47 M)[e]		3398	1676[f]	1547	1286

a) In solutions this band could not be observed because of interference by solvent absorption.
b) See Ref. 2
c) This is a mean value of the frequencies of two peaks at 1507 and 1491 cm^{-1}.
d) These were too weak to detect.
e) See Ref. 12
f) This is the value in a solution of 0.116 mol./l.

frequency of the amide I band may be characteristic of the hydrazides of aliphatic acids since all the hydrazides have this near 1600 cm^{-1} in the solid state. In a dilute solution the secondary amides show the amide I absorption in the range 1700~1670 cm^{-1} [11]. The hydrazides examined here have two amide I bands in acetonitrile. Thus, it may be expected that these two bands come from the coupling of two vibrations which are localized mainly on the C=O groups, as was pointed out for the hydrazides of aromatic acids in a previous paper[1]. Moreover, it is noteworthy that in the solution spectra the amide I band is shown at frequencies higher by ca. 100 cm^{-1} than that in the solid spectra. This fact was not seen for the secondary amides; e. g., *N*-methyl acetamide in an acetonitrile solution has an amide I band higher in frequency by ca. 20 cm^{-1} than that in the solid state.

The amide II band of the hydrazides examined here may also be characteristic. In the solid state the hydrazides have their amide II bands at ca. 1500 cm^{-1}, somewhat lower in frequency than those of secondary amides.

The amide III frequency of the hydrazides in the solid state lies near the lower limit of the normal range of 1305~1200 cm^{-1} for bands of the secondary amides. In the solution spectra the amide III frequency decreases by ca. 20 cm^{-1}. A similar decrease is found with *N*-methyl acetamide, as is indicated in Table II.

All the hydrazides examined in the solid state have N-H stretching bands near 3200 cm^{-1} which are also lower than those of many secondary amides. Miyazawa[3] postulated that the markedly decreased ν(N-H) frequency of diformylhydrazine was due to strong hydrogen bonding in the solid state. The strength of the hydrogen bond will be different from molecule to molecule. However, the hydrazides, with the exception of DFH, have a N-H band the frequency of which is very close to 3200 cm^{-1}. On the other hand, Davies et al.[12] examined the infrared absorption of *N*-methyl acetamide in acetonitrile and obtained a single monomeric ν(N-H) at 3398 cm^{-1}, 80 cm^{-1} lower than that in carbon tetrachloride. Therefore, they concluded that the N-H group was markedly solvated in acetonitrile. The hydrazides in acetonitrile also have an N-H band, the frequency of which is higher by ca. 110 cm^{-1} than that of a main N-H band in the solid spectra of the hydrazides. Further, the ν(N-H) frequency of the hydrazides in acetonitrile is still lower by ca. 90 cm^{-1} than that of *N*-methyl acetamide in the same solvent. The lower value of the ν(N-H) frequency is, therefore, found in both solid spectra and solution spectra of the hydrazides examined here. Such a decrease of the ν(N-H) frequency can not reasonably be explained as the effect of strong hydrogen bonding or solvation only. Thus, the decrease of ν(N-H) in frequency can also be taken as one of the characteristics of the hydrazides examined; namely, there is a coupling between

11) L. J. Bellamy, "The Infrared Spectra of Complex Molecules", Methuen & Co. Ltd., London (1954).

12) M. Davies, J. C. Evans and R. L. Jones, *Trans. Faraday Soc.*, **51**, 761 (1955).

two CONH groups of each hydrazide molecule in the solid state. Probably hydrazide molecules are nonplanar in solution, and the increase of the ν(N–H) frequency in the solution spectra may come from a decrease in the coupling between two CONH groups. In addition to the main 3200 cm^{-1} absorption, the hydrazides have a weak band near 3030 cm^{-1}. Its occurrence is in accordance with that of the band near 3080 cm^{-1} for the secondary amides.

Summary

The infrared absorption spectra of the hydrazides of aliphatic acids have been examined in the rock salt region. The N–H stretching frequencies are found near 3200 and 3030 cm^{-1} in the solid state and near 3320 cm^{-1} in dilute solution. The amide I band is seen near 1600 cm^{-1} in the solid state, while in solution there are two bands, near 1720 and 1690 cm^{-1}. In the solid state the amide II band appears near 1490 cm^{-1}. The amide III band is found near the lower limit of the normal range of 1305$\sim$1200 cm^{-1} for the secondary amides.

The author is grateful to Professor Sunao Imanishi of Kyushu University for his generous permission to use that University's spectrophotometer, and to Dr. Yoshiya Kanda of Kyushu University for his encouragement throughout the work. He is also indebted to the Ministry of Education for financial support.

Department of Literature and Science
Saga University
Saga

*The Chemical Reaction in Silent Electric Discharge. III. The Effect of the Packings on Ozone Formation**

By Kihei MORINAGA and Momotaro SUZUKI

(Received June 26, 1961)

In the previous reports on ozone formation in a silent electric discharge, the relation between the gap length, the electrode area and the pulse current was studied[1,2].

For the present paper, an investigation of the ozone formation from oxygen has been carried out using a special type discharge tube with some adequate fillings to serve as dielectrics.

Experimental

The apparatus and the procedure, except for the packings, are essentially the same as in the previous report[1]. The space between the electrodes was filled with a granular packing of titanous oxide ceramics whose dielectric constant varied in accordance with the percentage composition of the ingredients, such as barium oxide, or tin(IV) oxide. Ordinary soda glass packings with the same geometry were used as a check standard. The packings were made by "one time baking" to an amorphous mass, then by crushing the granules to 0.75~1.00 mm. size mesh, which is an adequate size for filling. The ozonizer was again of a Siemens type, which has a gap length of 2.6 mm. and an effective electrode area of 250 cm^2. The voidage of gap space with the packing was 47% of the total gap volume in each case.

The stoichiometric composition of the ceramics and their dielectric constant, at room temperature and at 1 kc, are given in Table I.

TABLE I

Number of runs	Composition of the packings	Dielectric constant
I	Blank	1
II	Soda glass	6
III	$2MgO/TiO_2$	20
IV	TiO_2	100
V	$BaTiO_3$	1200
VI	$95BaTiO_3/5SnO_2$	5500~6000

The frequency of the electric source for silent discharge was 50 c/sec. The electric circuit that provided a high tension to the discharge tube and the whole flow system with its detecting device for ozone were similar to those described in the previous work[1,2]. Through a packed tube a discharge current can be raised to such a value that eventually damage will occur to the usual ozonizer. For example, in the case of titanous oxide packing, a stable discharge will be established up to around 8 mamp. current, while the maximum ozone concentration will be somewhat over 6.5%. The pulse current

* Presented at the 11th Annual Meeting of the Chemical Society of Japan, Tokyo, April 1958.

1) K. Morinaga and M. Suzuki, This Bulletin, **34**, 157 (1961).

2) K. Morinaga and M. Suzuki, ibid., **35**, 204 (1962).

was measured by the device of the oscillogram with an integral circuit that inserted a series to the earth line of discharge tube. The pulse current will be less than that of an ozonizer of the same type without any packing.

Results

All measurements were carried out with a residence time of the reactant gas of 1.5~80 sec. in the ozonizer.

Figure 1 represents the saturated state ozone concentration under a certain constant total discharge current, and Fig. 2 represents the saturated state ozone concentration under a certain constant pulse current. In both figures, the results are plotted against the value of the dielectric constant of the packing materials, and the location at the value of 1 on the abscissa represents the results that were obtained in a blank discharge tube without any packing fill. Under a constant discharge current, the maximum value of the saturation ozone concentration appears at the packing of titanium(IV)

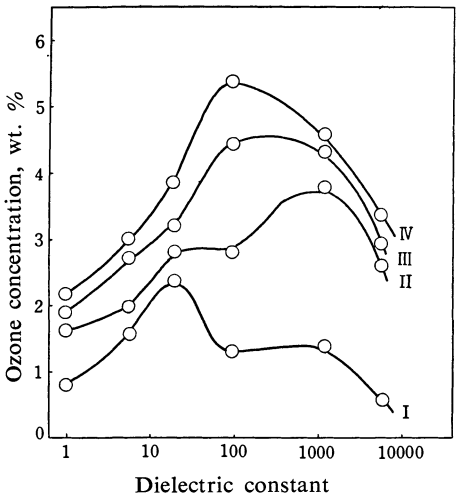


Fig. 1. The saturated state ozone concentration under a given total discharge current, against the dielectric constant of the packing materials.
(I) Total discharge current 1 mA,
(II) 2 mA, (III) 3 mA, (IV) 4 mA

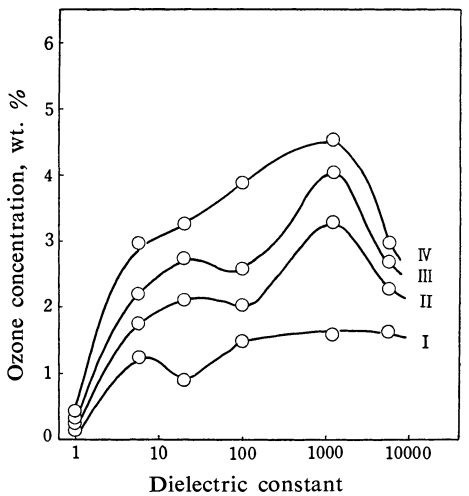


Fig. 2. The saturated state ozone concentration under a given pulse current, against the dielectric constant of packing materials.
(I) Pulse current 7μA, (II) 14 μA,
(III) 21 μA, (IV) 28 μA

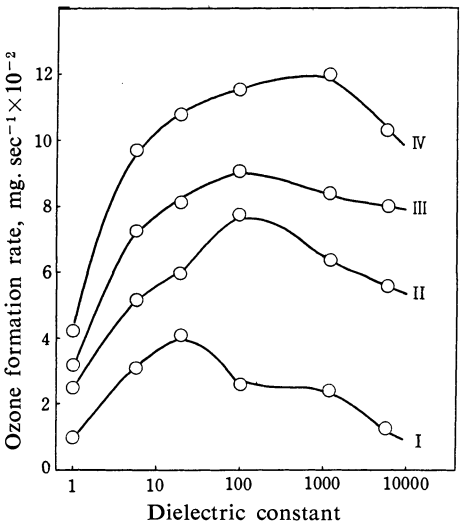


Fig. 3. The ozone formation rate under a given total discharge current, against the dielectric constant of the packing materials.
(I) Total discharge current 1 mA,
(II) 2mA, (III) 3 mA, (IV) 4 mA

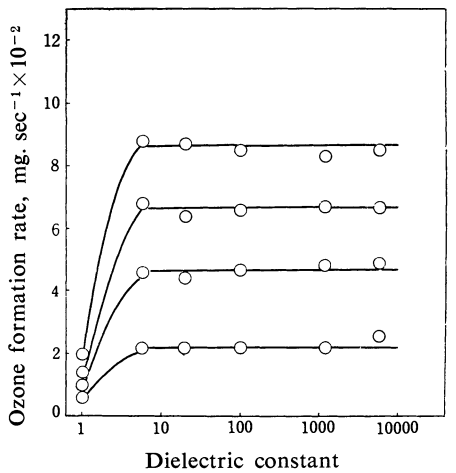


Fig. 4. The ozone formation rate under a given pulse current, against the dielectric constant of the packing materials.
(I) Pulse current 7 μA, (II) 14 μA,
(III) 21 μA, (IV) 28 μA

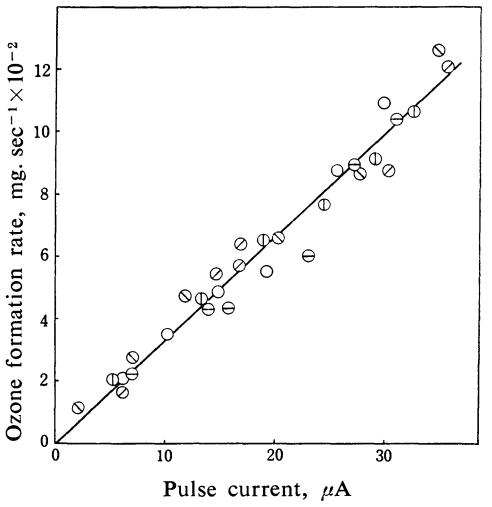


Fig. 5. The rate of ozone formation under various packing against pulse current.
○ Soda glass, ⊕ TiO_2,
⊘ $95BaTiO_3/5SnO_2$,
⊖ $2MgO/TiO_2$, ⊘ $BaTiO_3$

oxide, whose dielectric constant is around 100. In the case of a constant pulse current, the maximum saturation ozone concentration occurs at the dielectric constant value of about 1200 of $BaTiO_3$.

Under the same conditions as in Figs. 1 and 2, the rate (mg./sec.) of ozone formation is plotted in Figs. 3 and 4 against the same abscissa as before. The curves in Fig. 3, where the parameter of each diagram is the discharge current, do not show any regular feature, whereas in Fig. 4, where the parameter is pulse current, the rate of ozone formation at a higher value of dielectric constant is nearly independent of the dielectric constant value of the packing materials. In Fig. 5, the ozone formation rates for various ceramics fillings of different dielectric constants against the pulse current are shown. The rates for each packings, independent of the dielectric constant values, are represented by a straight line whose inclination has a value of 3.3×10^{-3} mg. sec^{-1} μamp^{-1}.

The observed number of hairs of the packing fill ozonizer is more than that of the usual ozonizer without packings where all other conditions are the same.

Discussion

It is highly conceivable that the surface of the dielectric packing is partly electrically conductive. The conductivity will increase in accordance with the higher value of the dielectric constants. At the application of some electric tension between the electrodes, the current will be carried in two ways, one by the discharge current through the gas phase, and the other along the surface leakage. In the oscillogram pattern, the discharge current will manifest itself as pulse current or hair on the base current pattern, where the leakage current is implied together with the basic current.

The presence of the packing is equivalent to the larger value of the electrode area and the small value of gap length, which leads to the conclusion that rate of ozone formation should be higher with a packing-filled ozonizer.

The mean value of the ozone formation rates per unit pulse current for discharge tubes with a filling whose dielectric constant in each case has a different value, was 3.3×10^{-3} mg. sec^{-1} μ amp^{-1}.

In the case of 50 c/sec. discharge and for unit A/d, the corresponding rate is 7.0×10^{-7} mg. sec^{-1} μ amp^{-1} [1], were A is the electrode area and d is the gap length.

The experimental conditions are about the same for both cases, the exception being the packing fill. The rate value should be proportional to the A/d value in both cases. The assumed A/d value for the packed discharge tube is 4.7×10^{3} cm., which means a very large electrode area and/or a very small gap length. In the above pattern of discharge in packed ozonizers, the discharge potential, then, will be appreciably smaller than in the usual ozonizer, which fact accounts for the larger number of hairs and the larger value of the formation rate. The discharge current involves two contributions, the gas discharge and the surface leakage. For a certain fixed value of discharge current, the discharge contribution will increase at first with the increase of ozone formation, because in an ozonizer, absorbed electric energy which is to be proportional to the ozone formation is proportional to the total capacity C, where C is given by

$$1/C=1/C_g+1/C_a$$

in which C_g is the capacity of glass or dielectrics, which is proportional to the value of the dielectric constant, and C_a the capacity of the air gap. On the other hand, the surface leakage effect will increase in company with the increase of the dielectric constant of the fillings, and above a certain value of the ozone formation rate it will begin to decrease according to the increasing leakage current under a certain fixed discharge current, because the leakage current does not benefit the ozone yield. These patterns explain the features of the diagrams in Figs. 1 and 3.

The pulse currents represents only the quantity of discharge electricity through the air gap space, while the base current, in an oscillogram, implies the leakage electricity. For a certain

amount of discharge electricity, or pulse current, the ozone formation should be the same no matter what the value of the dielectric constant of the filled packing, because the rate is referred to the value at zero time of residence and is, therefore, governed solely by the discharge quantity of electricity.

The ozone concentration is the complicated results of reaction under which the gas is exposed for a certain period of residence. It is, therefore, no wonder that the diagram in Fig. 2 does not show any regularity. However, it arouses rather a practical interest that the packing of titanium(IV) oxide under a certain constant total discharge current shows the maximum value. Rummel also uses in his patent** layers of ceramic substances containing titanium(IV) oxide with a dielectric constant of 80 for the preparation of ozone.

In conclusion, the application of the packing in an ozonizer makes two contributions to ozone formation, the one due to the shortening of the gap distance, which is equivalent to the expansion of the electrode area, and the other corresponding to the enhancement of the dielectric constant on the wattage absorbed in the ozonizer and on the leakage current along the surface of the packing. These effects benefit the ozone formation by exempting the adverse effect of leakage current, which will increase according to the increasing value of the dielectric constant.

** T. Rummel, German Pat. 1028544 (April 24, 1958).

Summary

1. The ozone formation rate was increased in a packed discharge tube more than in the same type of ozonizer without packing.

2. The linear relationship, which has been proved before, between the pulse current and the ozone formation rate was also obtained in this case, independent of the dielectric constant value of the packing materials.

3. The ozone concentration shows a maximum value at a certain value of the dielectric constant.

4. The rate of ozone formation is independent of the dielectric constant at the higher values of the dielectric constant.

5. A tentative mechanism which is plausible for the elucidation of the results has been discussed.

Department of Chemistry
Defense Academy
Yokosuka

Studies on Thiophene Compounds. XIX. Syntheses of 2, 3, 4, 5-Tetradehydrobiotin and 2, 3, 4, 5-Tetradehydronorbiotin[1]

By Shoji NISHIMURA and Eiji IMOTO

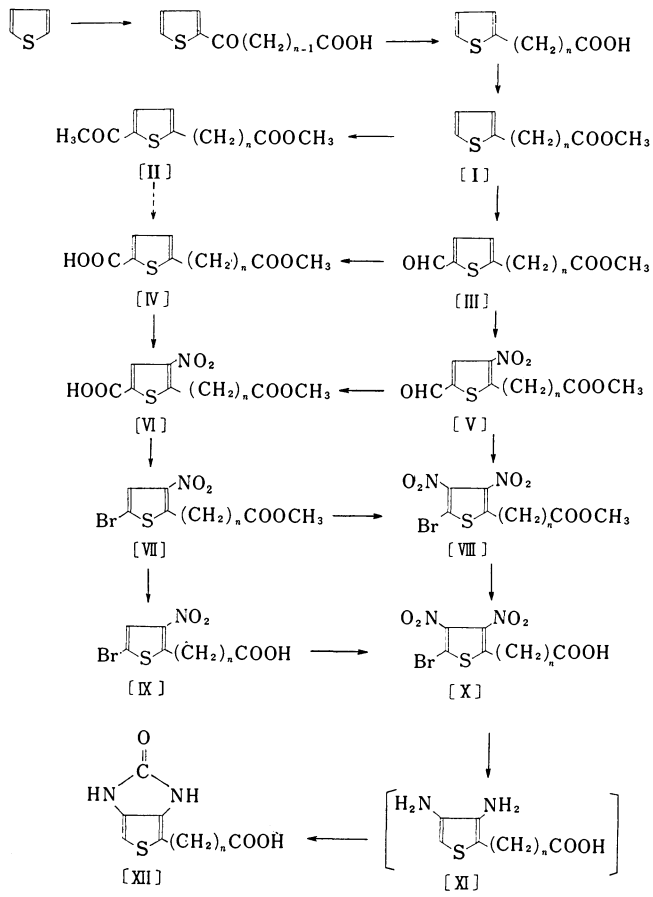
(Received June 30, 1961)

Biotin is a very important growth-promoting factor for yeast and other micro-organisms. Since Harris[2] and his co-workers first synthesized biotin, various methods have been reported by many authors. However, all of the methods proposed required many steps for the synthesis, and consequently the over-all yield was low. According to the patent[3], biotin can be prepared with the hydrogenation of 2, 3, 4, 5-tetradehydrobiotin (or so-called aromatic biotin). In the present paper are reported the syntheses of aromatic biotin and of aromatic norbiotin, which has one less methylene group in the side chain than does aromatic biotin. Both of the compounds were synthesized by starting with thiophene. The following procedures were followed.

Results and Discussion

In the preparation of the aromatic biotin and the aromatic norbiotin, it was most difficult to introduce two amino groups into the 3- and 4-positions of the thiophene nucleus. It has been known that the nitration of 2, 5-dibromo-, 2, 5-dichloro- and 2, 5-dimethyl-thiophene gives the 3, 4-dinitro-derivatives of the respective starting compounds[4-6]. An attempt was thus made to introduce a nitro group into

1) Presented at the Meeting of the Society of Organic Synthetic Chemistry (Japan), Tokyo, Oct., 1959.
2) S. A. Harris et al., *Science*, **97**, 447 (1943).
3) U. S. Pat. 2502422; *Chem. Abstr.*, **44**, 6440 (1950).
4) R. Mozingo et al., *J. Am. Chem. Soc.*, **67**, 2092 (1945).
5) W. Steinkopf et al., *Ann.*, **512**, 136 (1934).
6) W. Steinkopf et al.. ibid., **536**, 128 (1938).



(n=3 or 4)

the vacant 4-position of the thiophene nucleus of 4-(5-bromo-2-thienyl)-butyric acid, but the result was unsuccessful. Nitration under severe conditions caused an oxidative decomposition and gave merely tarry material. No nitrated product was obtained from 5-bromo-2-methylthiophene either. As has been mentioned in another paper[7] of this series, ω-(5-bromo-2-thenoyl)-fatty acid can be nitrated at the 4-position. It must, therefore, be easier to introduce a nitro group into the 4-position if an electron-releasing amino group is placed in the neighboring 3-position. However, the nitration of 3-(3-acetylamino-5-bromo-2-thenoyl)-propionic acid unexpectedly gave 3-acetylamino-5-bromo-2nitro-thiophene, which was produced as the result of the replacement of the succinoyl group by the nitro group in the 2-position. From this experimental result, it could be deduced that the 3-acetylamino group can not promote an electrophilic substitution at the 4-position. As the third method to introduce an amino group into a β-position of the thiophene nucleus, there is the amination of β-halogenothiophenes, in which method the halogene atom is activated by a nitro or a carboxyl group. According to this scheme, an amination of 3-bromo-4-nitro-2-thiophenecarboxylic acid was carried out by the method mentioned in an earlier paper[8] of this series, but no aminated product was obtained. In general, a nitro group can be introduced into the 3-position of the thiophene nucleus when the thiophene nucleus has an electron-releasing group such as chloro or alkyl group in the 2-position and an electron-withdrawing group such as formyl or acetyl group in the 5-position. It is, however, impossible to introduce an additional nitro group to the 4-position after the first nitration has been carried out. As reported in a previous paper[9] of this series, it is necessary to put an electron-releasing group in the 5-position in order to introduce the second nitro group, which has to be

7) S. Nishimura and E. Imoto, *J. Chem. Soc. Japan, Pure Chem. Sec.* (*Nippon Kagaku Zasshi*), **82**, 1413 (1961).

8) S. Nishimura, T. Kitagawa and E. Imoto, ibid., **82**, 1543 (1961).

9) S. Nishimura, A. Sakumoto and E. Imoto, ibid., **82**, 1540 (1961).

neighbored by the first nitro group at the 3-position. The formyl or acetyl group in the 5-position, which is necessary for the introduction of the first nitro group, can be converted to a bromo group by Hunsdiecker's reaction after its oxidation to the carboxylic acid. As the aromatic biotin and the aromatic norbiotin have a ω-caboxybutyl and a ω-carboxypropyl group respectively, the free terminal carboxyl group may simultaneously be replaced by a bromo group by Hunsdiecker's reaction. To avoid this complication, it is necessary to protect the carboxyl group by a method such as esterification. According to this scheme, methyl 4-(5-acety-2-thienyl)-butyrate was oxidized with sodium hypochlorite with the intention of preparing methyl 4-(5-carboxy-2-thienyl)-butyrate, but the oxidation yielded dicarboxylic acid, which was produced by the simultaneous saponification of the terminal methyl ester. Even isopropyl 4-(5-acetyl-2-thienyl)-butyrate, which is expected to resist saponification, was useless for the purpose of oxidation without saponification. This means that alkaline oxidation can not prevent simultaneous saponification. As an alternative method, methyl 4-(5-formy-2-thienyl)-butyrate, prepared by the formylation of methyl 4-(2-thienyl)-butyrate, was oxidized by chromic acid in acetic acid, and thus methyl 4-(5-carboxy-2-thienyl)-butyrate was obtained. Although methyl 4-(5-carboxy-3-nitro-2-thienyl)-butyrate was prepared with the nitration of methyl 4-(5-carboxy-2-thienyl)-butyrate, the oxidation of methyl 4-(5-acetyl-3-nitro-2-thienyl)-butyrate prepared by the nitration of methyl 4-(5-acetyl-2-thienyl)-butyrate gave a more favorable result. Similarly, methyl 5-(5-carboxy-3-nitro-2-thienyl)-valerate was obtained by the oxidation of methyl 5-(5-formyl-3-nitro-2-thienyl)-valerate in acetic acid. The carboxyl group thus obtained was converted to the bromine atom by Hunsdiecker's reaction. Then, 4-(5-bromo-3, 4-dinitro-2-thienyl)-butyric and -valeric acids were derived through the nitration of methyl ω-(5-bromo-3-nitro-2-thienyl)-butyrate and -valerate respectively, followed by the saponification of the terminal methyl ester. When ω-(5-bromo-3, 4-dinitro-2-thienyl)-butyric and -valeric acids were treated with tin and hydrochloric acid, 3, 4-dinitro groups were reduced to 3, 4-diamino groups and the 5-bromo atom was eliminated by reduction. As 3, 4-diaminothiophenes are unstable in an atmosphere of air, the reduced products were not isolated, and the double salts of the diamino-compounds with tin chloride were treated with phosgene after decomposition with an alkaline solution to obtain the aromatic biotin and the aromatic norbiotin respectively. The aromatic biotin obtained here was identical to that obtained by Cheney[10] and his co-workers by another method.

Experimental

4-(5-Bromo-2-thienyl)-butyric Acid.—Into a solution of 4-(2-thienyl)-butyric acid[11] (6 g.) in 50% aqueous acetic acid (65 ml.) was slowly stirred, drop by drop, a solution of bromine (1.85 ml.) in 50% aqueous acetic acid (47 ml.) at $-8\sim-10$°C over a period of 2 hr. After the addition was completed, the reaction mixture was stirred at the same temperature. The crystals which were precipitated from the reaction mixture by the addition of water (100 ml.) were collected by filtration, washed with water and recrystallized from methanol-water. The yield of 4-(5-bromo-2-thienyl)-butyric acid (m. p. 58$\sim$59.5°C) was 56% after recrystallization.

Found: Br, 31.45; Neut. equiv., 250. Calcd. for $C_8H_9O_2BrS$: Br, 32.08%; Neut. equiv., 249.

Nitration of 4-(5-Bromo-2-thienyl)-butyric Acid. — Into a solution of 4-(5-bromo-2-thienyl)-butyric acid (2.5 g.) in acetic anhydride (10 ml.) was slowly stirred mixture of concentrated nitric acid (2 ml.), acetic anhydride (10 ml.) and acetic acid (10 ml.) at $-5\sim-10$°C. The reaction mixture was stirred for 30 min. at the same temperature after the additon and then poured into ice-water. An oily product was separated and solidified after the mixture had been left to stand for several days. The solid collected, m. p. 56$\sim$58°C after recrystallization from methanol-water, did not show a depression of the melting point on mixing with the starting compound. A nitration of 4-(5-bromo-2-thienyl)-butyric acid with a mixed acid consisting of sulfuric acid and nitric acid at 0$\sim$5°C also gave merely a brown tarry matter.

Nitration of 2-Bromo-5-methylthiophene. — A nitration of 2-bromo-5-methylthiophene[12] with a mixed acid consisting of concentrated nitric acid and concentrated sulfuric acid merely gave a brown tarry matter; no crystalline products were separated.

Nitration of 4-Acetylamino-2-bromo-5-thenoyl-propionic Acid.—4-Acetylamino-2-bromo-5-thenoyl-propionic acid[13] (0.32 g.) was stirred into sulfuric acid (2 ml.) which had been greatly cooled by the addition of pieces of dry ice. Into the above viscous solution was stirred dropwise a mixed acid consisting of concentrated nitric acid (0.17 ml.) and concentrated sulfuric acid (0.1 ml.) at a temperature below -20°C. The reaction temperature was kept constant by the frequent addition of small pieces of dry-ice. After adding the mixed acid, the reaction mixture was stirred for one hour and then diluted with iced water. The precipitates were collected by filtration, washed with water and recrystallized from methanol. The pale yellow needles obtained melted at 174$\sim$175°C, produced no 2, 4-dinitrophenylhydrazone, and must be 4-acetylamino-2-bromo-5-nitrothiophene.

10) L. C. Cheney and J. R. Piening, *J. Am. Chem. Soc.*, **67**, 731 (1945).
11) L. F. Fieser and R. G. Kennelly, ibid., **57**, 1611 (1935).
12) K. Dittmer, ibid., **71**, 1201 (1949).
13) R. Motoyama, *J. Chem. Soc. Japan, Pure Chem. Sec.* (*Nippon Kagaku Zasshi*), **78**, 794 (1957).

Found: C, 26.65; H, 2.09; N, 10.11. Calcd. for $C_6H_5O_3BrN_2S$: C, 27.1; H, 1.89; N, 10.05%.

Oxidation of Methyl 4-(5-Acetyl-2-thienyl)-butyrate with Sodium Hypobromite. — A solution of sodium hypobromite was prepared by stirring 5 ml. of bromine into a solution of sodium hydroxide (10 g.) in water (15 ml.) and ice (40 g.) below 0°C. Methyl 4-(5-acetyl-2-thienyl)-butyrate (4 g.) was added to the solution of sodium hypobromite prepaped above and stirred for 5 hr. at 5~10°C. An aqueous solution of sodium bisulfite was added under ice-cooling to the reaction mixture to decompose an excess of sodium hypobromite. After removing the bromoform and carbon tetrabromide by an extraction with ether, the alkaline aqueous layer was acidified. The colorlesss precipitates (1.6 g.) were collected by filtration, washed with water and recrystallized from water, m. p. 192~194°C. The neutralization equivalent of the crystals was 110, which coincided with the calculated value (107) for 4-(5-carboxy-2-thienyl-butyric acid. The mixed melting of the crystals with the authentic sample, which had been synthesized by the oxidation of 4-(5-acetyl-2-thienyl)-butyric acid (m. p. 193~194.5°C), showed no depression.

Isopropyl 4-(2-Thienyl)-butyrate.—A solution of 50 g. of 4-(2-thienyl)-butyric acid in 80 ml. of ether was refluxed, together with 30 ml. of thionyl chloride and few drops of pyridine, for 4 hr. Ether and an excess of thionyl chloride were distilled off in vacuo. The residue was dissolved in a solution of dimethylaniline (40 g.) and isopropyl alcohol (20 g.) and refluxed for 4 hr. After cooling, the reaction mixture was poured into diluted hydrochloric acid and extracted with ether. The ethereal extract was washed successively once each with diluted hydrochloric acid and with an aqueous solution of sodium bicarbonate, and then dried over anhydrous sodium sulfate. After distilling off the ether, the distillation under reduced pressure gave 52 g. of isopropyl 4-(2-thienyl)-butyrate, b. p. 140~149°C.

Found: C, 61.88; H, 7.38. Calcd. for $C_{11}H_{16}O_2S$: C, 62.26; H, 7.55%.

Isopropyl 4-(2-Acetyl-5-thienyl)-butyrate.—Twenty grams of isopropyl 4-(2-thienyl)-butyrate were heated and stirred with acetic anhydride (11 ml.) and phosphoric acid (0.8 ml.) for 4 hr. at 100~110°C. After cooling, the reaction mixture was poured into water, neutralized with powdered sodium carbonate, and extracted with ether. The ether portion was washed with water and dried over anhydrous sodium sulfate. After distilling off the ether, the distillation under reduced pressure gave 20.5 g. of isopropyl 4-(2-acetyl-5-thienyl)-butyrate (b. p. 185~188°C/3.5 mmHg), which solidified after cooling with dry-ice. After the recrystallization from petroleum ether, crystals of m. p. 15~16.5°C were obtained.

Found: C, 61.38; H, 7.10. Calcd. for $C_{13}H_{18}O_3S$: C, 61.42; H, 7.08%.

Oxidation of Isopropyl 4-(2-Acetyl-5-thienyl)-butyrate with Sodium Hypobromite.—To a solution of sodium hypobromite, which had been prepared from sodium hdydroxide (20 g.), water (7 ml.) and bromine (2.4 ml.) by the method similar to that mentioned in the case of (II (n=3)), a solution of isopropyl 4-(2-acetyl-5-thienyl)-butyrate (4 g.) in dioxane (6 ml.) was added and stirred below 10°C for 3 hr. After treating the reaction mixture by a usual method, 1.7 g. of crude acid (m. p. 186~193°C) were obtained and recrystallized from water, m. p. 192~194°C. The mixed melting point with an authentic sample of 4-(2-carboxy-5-thienyl)-butyric acid showed no depression.

Methyl 4-(5-Formyl-2-thienyl)-butyrate (III (n=3)). — A solution of methyl 4-(2-thienyl)-butyrate (4.3 g.) in dimethylformamide (2.5 g.) was slowly combined with oxyphosphorus chloride (2.5 g.) and kept for 2 hr. at 110°C while frequency being shaken. The reaction mixture was poured into water, neutralized with sodium carbonate and extracted with ether. The ethereal extract was washed with water and dried over anhydrous sodium sulfate. After distilling off the ether, the residue was distilled under reduced pressure to obtain methyl 4-(5-formyl-2-thienyl)-butyrate in a yield of 67.5% (3.5 g.), b. p. 172~175°C.

Found: C, 62.18; H, 7.50. Calcd. for $C_{10}H_{12}O_3S$: C, 62.26; H, 7.55%.

Methyl 4-(5-Carboxy-2-thienyl)-butyrate (IV (n=3)).—A mixture of methyl 4-(5-formyl-2-thienyl)-butyrate (III (n=3)) (1.2 g.), acetic acid (10 ml.) and sodium bichromate (1.5 g.) was stirred at 60~70°C for 7 hr. After cooling, cold water and 5 g. of sodium carbonate were added to the reaction mixture to precipitate green crystals. The crystals were extracted with ether. The ether extract was was washed with water and treated with a saturated aqueous solution of sodium bicarbonate. The aqueous portion was acidified with hydrochloric acid, and the colorless precipitates obtained were colleted by filtration and washed with water, m. p. 79.5~81°C. This acid was methyl 4-(5-carboxy-2-thienyl)-butyrate, as is shown in the following analytical results.

Found: Neut. equiv., 226; Sapon. equiv., 112. Calcd. for $C_{10}H_{12}O_4S$: Neut. equiv., 228; Sapon. equiv., 114.

Methyl 4-(5-Formyl-3-nitro-2-thienyl)-butyrate (V(n=3)).—Methyl 4-(5-formyl-2-thienyl)-butyrate (6 g.) was dissolved in ice-cooled concentrated sulfuric acid (30 ml.). Into this solution was slowly stirred the mixed acid consisting of concentrated nitric acid (8.7 ml.) and concentrated sulfuric acid (30 ml.), while the reaction temperature was kept below −5°C by means of the frequent addition of small pieces of dry ice. After this addition, the reaction mixture was stirred for 15 min. at the same temperature and then poured into ice water to afford the precipitations of crude methyl 4-(5-formyl-3-nitro-2-thienyl)-butyrate (7.2 g.). The precipitates obtained were recrystallized from ligroin, m. p. 70.5~72.5°C. Yield, 82%.

Found: N, 5.48. Calcd. for $C_{10}H_{11}O_5NS$: N, 5.44%.

2,4-Dinitrophenylhydrazone: m. p. 202~203.5°C (recrystallized from methanol).

Found: N, 10.49. Calcd. for $C_{16}H_{15}O_8N_3S$: N, 10.27%.

Methyl 4-(5-Carboxy-3-nitro-2-thienyl)-butyrate (VI (n=3)).—A mixture of methyl 4-(5-formyl-3-nitro-2-thienyl)-butyrate (7.5 g.), acetic acid (60 ml.) and sodium bichromate (10 g.) was stirred at 60~

70°C for 6.5 hr. and then poured into iced water to precipitate pale green crystals. After adding 30 g. of sodium carbonate slowly under ice-cooling, the reaction mixture was extracted with ether, and the ether portion was washed with water and shaken with a cold aqueous saturated solution of sodium bicarbonate. Acidification of the alkaline solution afforded a precipitation of methyl 4-(5-carboxy-3-nitro-2-thienyl)-butyrate, m. p. 95~96.5°C. Yield, 4.45 g. (56%).

Found: N, 5.23; Neut. equiv., 276. Calcd. for $C_{10}H_{11}O_6NS$: N, 5.13%; Neut. equiv., 273.

Other Method. — 1) Into a solution of methyl 4-(5-formyl-3-nitro-2-thieny)-butyrate (4 g.) in acetone (200 ml.) was stirred potassium permanganate (4.5 g.) in small portions at 0~5°C. After the addition was completed, stirring was continued at the same temperature for two hours. To the reaction mixture was added 10 ml. of methanol, and it was again stirred for ten minutes. Acetone and methanol were distilled off under reduced pressure, and to the residue was added a cold aqueous saturated solution of sodium bicarbonate. The precipitates were removed by filtration, and the filtrate was acidified with hydrochloric acid under ice-cooling to afford precipitation of crystal (m. p. 92~94°C). The mixed melting point of the crystals with the 4-(5-carboxy-3-nitro-2-thienyl)-butyrate obtained above showed no depresssion. The yield was 55%.

2) A mixed acid consisting of 1.4 ml. of concentrated nitric acid and 5 ml. of concentrated sulfuric acid was slowly stirred at −5~0°C into a soluion of methyl 4-(5-carboxy-2-thienyl)-butyrate (1 g.) in concentrated sulfuric acid (200 ml.). After this addition, the reaction mixture was stirred for 15 min. at the same temperature and then poured into iced water to cause the precipitation of viscous matter. The viscous matter which solidified after standing was dissolved in ether. The ethereal solution was extracted with a cold aqueous saturated solution of sodium bicarbonate; then the alkaline solution was acidified with hydrochloric acid to precipitate crystals of m. p. 92~95°C. The precipitates showed no depression of the melting point on mixing the methyl 4-(5-carboxy-3-nitro-2-thienyl)-butyrate obtained above. The yield was 33%.

Methyl 5-(2-Thienyl)-valerate (I (*n*=4)). — A solution of 5-(2-thienyl)-valeric acid[14] (100 g.) in 500 ml. of methanol was saturated with dry hydrochloric acid and refluxed for 7 hr. After distilling off the methanol, the residue was poured into iced water and then extracted with ether. The ether extract was washed with water and dried over anhydrous sodium sulfate. After distilling off the ether, the residue was distilled under reduced pressure to give methyl 5-(2-thienyl)-valerate in a yield of 85.5% (92 g.), b. p. 139~143°C/13 mmHg.

Found: C, 66.02; H, 7.81. Calcd. for $C_{10}H_{14}O_2S$: C, 66.66; H, 7.77%.

Methyl 5-(5-Formyl-2-thienyl)-valerate (III (*n*=4)).—A formylation of methyl 5-(2-thienyl)-valerate similar to that of methyl 4-(2-thienyl)-butyrate gave methyl 5-(5-formyl-2-thienyl)-valerate in a yield of 79%, b. p. 182~186°C/6 mmHg, m. p. 63~64°C.

Found: C, 58.16; H, 6.15. Calcd. for $C_{11}H_{14}O_3S$: C, 58.41; H, 6.19%.

Methyl 5-(5-Formyl-3-nitro-2-thienyl)-valerate (V (*n*=4)).—A nitration of methyl 5-(5-formyl-2-thienyl)-valerate similar to that of methyl 5-(5-formyl-2-thienyl)-butyrate gave methyl 5-(5-formyl-3-nitro-2-thienyl)-valerate as an oily product in a yield of 91.7%.

Methyl 5-(5-Carboxy-3-nitro-2-thienyl)-valerate (VI (*n*=4)).—This compound was obtained with an oxidation of methyl 5-(5-formyl-3-nitro-2-thienyl)-valerate with sodium bichromate in a yield of 59%, or with potassium permanganate in a yield of 76%, when the treatment was similar to that of methyl 4-(5-formyl-3-nitro-2-thienyl)-butyrate. The melting point of the crystals obtained was 37~38.5°C.

Found: N, 4.84; Neut. equiv., 288. Calcd. for $C_{11}H_{13}O_6NS$: N, 4.88%; Neut. equiv., 287.

Methyl 4-(5-Bromo-3-nitro-2-thienyl)-butyrate (VII (*n*=3)).—To an exactly neutralized solution of methyl 4-(5-carboxy-3-nitro-2-thienyl)-butyrate (2.5 g.) with a 1% aqueous solution of sodium hydroxide was added 1 N silver nitrate to precipitate colorless silver salt. The silver salt was collected by filtration, washed with water, dried at 100~110°C, powdered and then completely dried again over phosphorus pentoxide in a vacuum desiccator. To a refluxing suspension of the silver salt in dry carbon tetrachloride (25 ml.) was slowly added bromine (0.46 g.) in carbon tetrachloride (5 ml.). The addition required 30 min. After the addition, refluxing was continued for 1 hr. The reaction mixtue was filtered while it is hot and the solid obtained was washed twice with 140 ml. of hot carbon tetrachloride. The combined filtrate and washed liquor was washed successively with a solution of sodium bisulfite and a cold solution of sodium bicarbonate and then with water and dried over anhydrous sodium sulfate. Distilling off the carbon tetrachloride yielded a solid material, which was purified by washing with petroleum ether. The yield of methyl 4-(5-bromo-3-nitro-2-thienyl)-butyrate was 82% (2.32 g.). After recrystallization from petroleum ether, the melting point of the crystals was 49~51°C.

Found: N, 4.52. Calcd. for $C_9H_{10}O_4BrNS$: N, 4.54%.

Methyl 5-(5-Bromo-3-nitro-2-thienyl)-valerate (VII (*n*=4)). — Methyl 5-(5-carboxy-3-nitro-2-thienyl)-valerate (5 g.) was treated by the same procedure as described above to prepare methyl 5-(5-bromo-3-nitro-2-thienyl)-valerate (3 g.) in a yield of 53.5%. The product was an oily matter.

5-(5-Bromo-3-nitro-2-thienyl)-valeric Acid (IX (*n*=4)). — A solution of methyl 5-(5-bromo-3-nitro-2-thienyl)-valerate (5 g.) in acetic acid (80 ml.) and concentrated hydrochloric acid 50 ml.) was refluxed for one hour, filtered while hot by adding active charcoal, then diluted with water to precipitate crystals of 5-(5-bromo-3-nitro-2-thienyl)-valeric acid in a yield of 94% (4.5 g.), m. p. 99~102°C. The crystals were recrystallized from acetic acid-water, m. p. 102~103.5°C.

Found: N, 4.56; Neut. equiv., 307. Calcd. for $C_9H_{10}O_4BrNS$: N, 4.54%; Neut. equiv., 308.

14) P. Cagniant and A. Deluzarche, *Compt. rend.*, 222, 1301 (1946).

Methyl 4-(5-Bromo-3, 4-dinitro-2-thienyl)-butyrate (VIII (n=3)).—A mixed acid consisting of concentrated nitric acid (0.21 ml.) and concentrated sulfuric acid (1 ml.) was added slowly to a solution of methyl 4-(5-bromo-3-nitro-2-thienyl)-butyrate (1 g.) in concentrated sulfuric acid (3 ml.) at 5~10°C. After this addition, the reaction mixture was stirred for 30 min., then poured into iced water to precipitate crystals of methyl 5-(5-bromo-3,4-dinitro-2-thienyl)-butyrate. The crystals were collected by filtration and washed with water. The melting point of the crude product was 54~56.5°C, and the yield was 96% (1.1 g.). Recrystallization from ligroin raised the m. p. to 56.5~58°C.

Found: N, 7.96. Calcd. for $C_9H_9O_6BrN_2S$: N, 7.93%.

Methyl 5-(5-Bromo-3, 4-dinitro-2-thienyl)-valerate (VIII (n=4)). — Methyl 5-(5-bromo-3-nitro-2-thienyl)-valerate (5 g.) was treated similarly to the above compound to prepare methyl 5-(5-bromo-3,4-dinitro-2-thienyl)-valerate in a yield of 88% (6 g.) as a crude product, m. p. 57~60.5°C. After recrystallizing from ligroin-benzene, the melting point was 59.5~61.5°C.

Found: N, 7.59. Calcd. for $C_{10}H_{11}O_6BrN_2S$: N, 7.63%.

4-(5-Bromo-3, 4-dinitro-2-thienyl)-butyric Acid (X (n=3)).—A solution of methyl 4-(5-bromo-3,4-dinitro-2-trienyl)-butyrate (0.5 g.) in concentrated hydrochloric acid (15 ml.) was refluxed for 4 hr., then diluted with water after cooling to afford precipitation of crude 4-(5-bromo-3,4-dinitro-2-thienyl)-butyric acid (m. p. 134~136°C) in a yield of 87.5%. After recrystallization from 6 N-AcOH, the m. p. was 135~136.5°C.

Found: N, 8.18; Neut. equiv., 342. Calcd. for $C_8H_7O_6BrN_2S$: N, 8.26%; Neut. equiv., 339.

5-(5-Bromo-3, 4-dinitro-2-thienyl)-valeric Acid (X (n=4)).—A solution of methyl 5-(5-bromo-3,4-dinitro-2-thienyl)-valerate (2.4 g.) in acetic acid (50 ml.) and concentrated hydrochloric acid (50 ml.) was refluxed for one hour, then diluted with water after cooling to afford a precipitate of crude 5-(5-bromo-3,4-dinitro-2-thienyl)-valeric acid in a crude yield of 91% (2.1 g.). After recrystallization from 6 N-AcOH, the m. p. was 132~133°C.

Found: N, 7.90; Neut. equiv., 356. Calcd. for $C_9H_9O_6BrN_2S$: N, 7.93%; Neut. equiv., 353.

When acetic acid was not used as the solvent, tarry matter was produced as a by-product and the yield of the acid was lowered to 35%.

Another Method. — A mixed acid consisting of 0.2 ml. of concentrated nitric acid and 2 ml. of concentrated sulfuric acid was slowly stirred into a solution of 5-(5-bromo-3-nitro-2-thienyl)-valeric acid (0.9 g.) in concentrated sulfuric acid (8 ml.) at 0~5°C. After this addition, the reaction mixture was stirred for 15 min., and the reaction temperature was gradually raised to 10°C while being stirred. The reaction mixture was poured into ice-water. The crystals precipitated were collected by filtration, then washed with water. The yield of crude 5-(5-bromo-3,4-dinitro-2-thienyl)-valeric acid (m. p. 128~132°C) was 87% (0.9 g.). After recrystallization from acetic acid-water, the melting point of the crystals was 132~133°C. No depression of the melting point on mixing them with the compound prepared by the alternative method was observed.

Aromatic-Norbiotin (XII (n=3)).—A suspension of 0.4 g. 4-(5-bromo-3,4-dinitro-2-thienyl)-butyric acid in 10 ml. of concentrated hydrochloric acid was stirred, together with 0.8 g. tin in small pieces, at 25~30°C untill the tin disappeared, then evaporated to dryness in vacuo to obtain colorless tin double salt. The tin double salt was dissolved in 20 ml. of water and a solution of potassium hydroxide while bing cooled by ice; then immediately phosgen was introduced into the solution. The introduction phosgen was continued until the solution became acidic to Congo red paper. The crystals precipitated during the introduction of the phosgen were collected by filtration, washed with water and recrystallized from methanol-water to obtain curde product (m. p. 228~230°C decomp.) in a yield of 0.12 g. (45%). The melting point of the crystals was 244~245°C decomp. after recrystallization from water.

Found: N, 12.46. Calcd. for $C_9H_{10}O_3N_2S$: N, 12.93%.

The absorption maximum (λ_{max}) in a ultraviolet spectrum (solvent: ethanol): 260 mμ.

Aromatic-Biotin (XII (n=4)).—5-(5-Bromo-3,4-dinitro-2-thienyl)-valeric acid (0.4 g.) was similarly treated to obtain crude aromatic-biotin (m. p. 236~238°C decomp.) in a yield of 70% (0.2 g.). After recrystallizing them from water, the melting point of the crystals was 253~254°C decomp. (The meltint point given in the literature was 254~254.5°C decomp.). The λ_{max} (in ethanol as solvent) in ultraviolet spectrum was 260 mμ (coinciding with the value, 260 mμ given in the literature).

Found: N, 11.49. Calcd. for $C_{10}H_{12}O_3N_2S$: N, 11.67%.

Department of Applied Chemistry
College of Engineering
University of Osaka Prefecture
Sakai, Osaka

O→*N*-Acetyl Shift of *O*-Acetylserine and *O*-Acetylthreonine. An Approach to the Separation of Serine and Threonine Fraction from Amino Acid Mixture

By Sadao FUJIWARA, Shigeru MORINAGA and Kozo NARITA

(Received June 30, 1961)

In relation to the modification of proteins, the *N*→*O*-peptidyl shift of serine and threonine residues in proteins through the influence of concentrated sulfuric acid was intensively investigated by Elliott[1-3]. This technique was applied to silk fibroin[1,4], lysozyme[2], wheat proteins[5,6] and clupein[7] in order to split *N*-seryl and *N*-threonyl bonds. Anhydrous formic acid was also shown to be useful as the same purpose of the modification of proteins by Josefsson and Edman[8], but a main reaction of anhydrous formic acid with proteins was demonstrated to be *O*-formylation of serine and threonine residues[9-11].

It was reported that of the β-hydroxy-α-amino acid residues in proteins *N*→*O*-peptidyl shift which resulted with concentrated sulfuric acid or concentrated phosphoric acid, mainly occurred at the serine residues[3,4]. However no experiment on the *N*→*O*-acyl shift has been performed with synthetic *N*-acylthreonine. The kinetic studies on the reverse reaction, *O*→*N*-acyl shift, have been reported for *O*-acetylserine and *O*-acetylserylleucine[8], but that for *O*-acylthreonine or its peptide has not been investigated. In the present communication, the rate of *O*→*N*-acetyl shift of *O*-acetylserine measured by the ninhydrin reaction was compared with that of *O*-acetylthreonine at several pH's, at several temperatures and in the presence and absence of inorganic salts. The present results show that *O*-acetylthreonine is more labile than *O*-acetylserine and that it shifts to the *N*-acetyl derivative even at neutral pH. In addition, an approach to the separation of β-hydroxy-α-amino acids, serine and threonine, from the hydrolyzate of casein is described. The principle of the present method is based on the facts that only serine and threonine react with acetic acid and hydrogen chloride to give their *O*-acetyl derivatives, and that the *N*-acetyl derivatives which were derived from the *O*-acetyl derivatives by the *O*→*N*-acetyl shift can be easily separated from free amino acids by the aid of ion exchange resin.

Experimentals

***O*-Acetyl-L-serine.**—This compound was synthesized by the method of Sheehan and his coworkers[12]. M. p. 167~168°C (with decomp.). Found: C, 40.5; H, 6.22; N, 9.40. Calcd. for $C_5H_9O_4N$: C, 40.8; H, 6.17; N, 9.52%.

***O*-Acetyl-DL-threonine and *O*-Acetyl-D-threonine.**—A solution of 10 g. of DL-threonine in 100 ml. of acetic acid was saturated with hydrogen chloride at 0°C and it was kept overnight at room temperature. The solvent was removed in vacuo and the above procedures were repeated. The residues were crystallized by the addition of ether under scratching the wall of the flask. Upon recrystallization from ethanol-ether, 15 g. of *O*-acetyl-DL-threonine hydrochloride were obtained (78.4%). M. p. 155~157°C (with decomp.). On addition of 3.3 g. of triethylamine into a solution of 6.5 g. of the hydrochloride in 150 ml. of ethanol, *O*-acetyl-DL-threonine was crystallized. It war recrystallized twice from water-ethanol. Yield, 4.7 g. (87.4%). M. p. 144~145°C (with decomp.) (reported m. p.[13] 146~149°C). Found: C, 44.66; H, 6.98; N, 8.59. Calcd. for $C_6H_{11}O_4N$: C, 44.71; H, 6.88; N, 8.69%.

Similarly *O*-acetyl-D-threonine was prepared from D-threonine through its hydrochloride (m. p. 155~156°C, with decomp.) with over-all yield of 68.3%. M. p. 145~146°C (with decomp.). Found; C, 44.68; H, 7.08; N, 8.68%. $[\alpha]_D^{20} = -21.25$ (*c* 2, in 2 N HCl).

***N*-Acetyl-DL-threonine and *N*-Acetyl-D-threonine.**—Both the compounds were prepared by similar

1) D. F. Elliott, *Biochem. J.*, **50**, 542 (1951).
2) D. F. Elliott, "Ciba Foundation Symposium on the Chemical Structure of Proteins", Eds. Wolstenholm and Cameron, J. & A. Churcill Ltd., London, (1953), p. 129.
3) D. F. Elliott, "The Proceedings of the 4th International Congress of Biochemistry, Vol. VIII, Proteins", Eds. Neurath and Tuppy, Pergamon Press Ltd., London, (1960), p. 47.
4) F. Lucas, J. T. B. Shaw and S. G. Smith, *Biochem. J.*, **66**, 468 (1957).
5) L. Wiseblatt, L. Wilson and W. B. McConnell, *Can. J. Chem.*, **33**, 1298 (1955).
6) L. K. Ramachandran and W. B. McConell, ibid., **33**, 1638 (1955).
7) K. Iwai, *J. Chem. Soc. Japan, Pure Chem. Sec.* (*Nippon Kagaku Zasshi*), **81**, 1302 (1960).
8) L. Josefsson and P. Edman, *Biochim. Biophys. Acta*, **25**, 614 (1957).
9) K. Narita, *J. Am. Chem. Soc.*, **81**, 1751 (1959).
10) L. B. Smillie and H. Neurath, *J. Biol. Chem.*, **234**, 355 (1959).
11) J. L. Rabinowitz, *Compt. Rend. des Travaux du Laboratoire Carlsberg*, **31**, 483 (1960).
12) J. C. Sheehan, M. Goodman and G. P. Hess, *J. Am. Chem. Soc.*, **78**, 1367 (1956).
13) W. Sakami and G. Toennies, *J. Biol. Chem.*, **144**, 203 (1942).

methods for the preparation of *N*-acetylserine reported previously[9]. 2.7 g. of *O*-acetyl-DL-threonine were dissolved in 50 ml. of 0.5 N ammonium hydroxide and the solution was kept at room temperature for 3 hr. It was concentrated in vacuo at 60°C and the ammonium salt of *N*-acetyl-DL-threonine was obtained as crystals. The above salt was dissolved in 100 ml. of water. The solution was placed on an acid form of Amberlite IR-120 column (7 $cm^2 \times 10$ cm.) and the column was washed with 150 ml. of water until the effluent became neutral. On concentration of the effluent to a syrup and on addition of ethyl acetate, 2.5 g. of *N*-acetyl-DL-threonine were obtained. 100 ml. of ethyl acetate were added to a solution of the crude material in 4 ml. of ethanol and 2.2 g. (81.5%) of the purified material were obtained as needles. M. p. 130~132°C (reported m. p.[14] 131~133°C). Found: C, 44.62; H, 6.91; N, 8.60. Calcd. for $C_6H_{11}O_4N$: C, 44.71; H, 6.88; N, 8.69%.

N-Acetyl-D-threonine was similarly prepared. M. p. 103~104°C. $[\alpha]_D^{18} = +1.5$ (*c* 2, in water). Found: C, 43.89; H, 6.87; N, 8.34%.

Measurement of the Rate of *O*→*N*-Acetyl Shift. —The *O*-acetyl compound was dissolved in a desired buffer solution with the concentration of 0.1%. One milliliter of the solution was pipetted at scheduled intervals into a 100 ml. of volumetric flask containing 1 ml. of 1 N hydrochloric acid to stop the reaction and filled with water to the mark. The amount of the *O*-acetyl compound that remained was analyzed by the ninhydrin method of Moore and Stein[15] using 1 ml. of the diluted solution.

Isolation of Serine and Threonine from the Acid Hydrolyzate of Casein. — Twenty-five grams of casein (commercial preparation) were hydrolyzed with 250 ml. of 20% hydrochloric acid at 100°C for 24 hr. and it was concentrated to a syrup. The residue was dissolved in 300 ml. of hot water and treated with 5 g. of charcoal. The filtrate was applied to a column of Amberlite IR-120 (acid form, 9 $cm^2 \times 35$ cm.) and the column was washed with 700 ml. of water to remove hydrochloric acid. The adsorbed amino acids were eluted with 500 ml. of 1.5 N ammonium hydroxide from the column and the column was washed with 300 ml. of water. The eluate was evaporated in vacuo and was dried in an evacuated desiccator. Twenty-three grams of acid free hydrolyzate were obtained. The results of amino acid analysis of the hydrolyzate by the Levy's dinitrophenyl technique[16] are listed in Table I. The hydrolyzate was suspended in 250 ml. of acetic acid and saturated with hydrogen chloride at room temperature for 48 hr., acetic acid was removed in vacuo and the above *O*-esterification procedures were repeated. The residues were dried in a desiccator over sodium hydroxide pellet for 24 hr. in vacuo and then it was dissolved in 200 ml. of water. The pH of the solution was adjusted to 8.0 with about 175 ml. of 2 N sodium hydroxide and it was diluted to 500 ml. with water. The solution was kept at room temperature for 4 hr. with an occasional addition of 2 N sodium hydroxide to keep the pH at above 8. Then the reaction mixture was treated with a column of Amberlite IR-120 (acid form, 20 $cm^2 \times$ 32 cm.) and the column was washed with 1.5 l. of water to separate *N*-acetylserine and *N*-acetylthreonine from the other amino acids. The effluent and washings which contained the *N*-acetylamino acids were combined and concentrated to a syrup. It was hydrolyzed with 200 ml. of the boiling 20% hydrochloric acid for 10 hr. The concentrated hydrolyzate was dissolved in 100 ml. of water and treated with a column of Amberlite IR-120 (acid from, 7 $cm^2 \times 15$ cm.) to remove hydrochloric acid as was described previously. The adsorbed amino acids were eluted with 200 ml. of 2 N ammonium hydroxide and the column was washed with 200 ml. of water. The eluate and washings were combined and it was concentrated in vacuo and decolorized with 300 mg. of charcoal. Amino acid analysis of the dried residues which amounted to 2.08 g. (9.0% of the original hydrolyzate) by the Levy's method showed that they contained 0.105 g. of aspartic acid, 0.925 g. of serine (4.0% of the original hydrolyzate), 0.836 g. of threonine (3.6%) and no other amino acids. The recoveries of serine and threonine were 80.5 and 88.8%, respectively. Aspartic acid might have been eluted with the *N*-acetylhydroxyamino acids from the second column, but could be easily removed by the treatment of a weakly basic ion exchange

TABLE I. AMINO ACID ANALYSIS OF THE HYDROLYZATE OF CASEIN

Amino acid	g. amino acid per 100 g. of hydrolyzate
Glycine	1.52
Alanine	2.77
Valine	6.57
Leucine+Isoleucine	15.92
Serine	5.01
Threonine	4.09
Methionine	3.42
Phenylalanine	4.72
Tyrosine*	4.10
Proline	10.19
Histidine**	2.69
Lysine	7.82
Arginine***	2.05
Aspartic acid	8.40
Glutamic acid	19.02
Total	98.29

* Tyrosine was estimated by the 1-nitroso-2-naphthol method[17].
** Histidine was estimated by the Knoop reaction[18].
*** Arginine was estimated by the Sakaguchi reaction[19].

14) Y. Murase, K. Okawa and S. Akabori, This Bulletin, 33, 123 (1960).
15) S. Moore and W. H. Stein, *J. Biol. Chem.*, **176**, 367 (1948).
16) A. L. Levy, "Methods of Biochemical Analysis, Vol. 2", Ed. Glick, Interscience Publishers, New York, (1955) p. 360.
17) S. Udenfriend and J. R. Cooper, *J. Biol. Chem.*, **196** 227 (1952).
18) A. Hunter, ibid., **196**, 589 (1952).
19) S. Sakaguchi, *J. Biochem.* (*Japan*), **37**, 231 (1950).

resin. In another experiment, a mixture of serine and threonine was isolated with the yield of 12.8%. Amino acid analysis of the isolated material showed 83.0% and 88.3% recoveries of serine and threonine, respectively.

Results and Discussion

Stein et al.[20] reported a simple isolation method of serine from the acid hydrolyzate of proteins by the specific precipitating reagent, *p* - hydroxyazobenzene-*p'* - sulfonate. However this reagent also forms sparingly soluble salts with the other amino acids, especially basic ones. Therefore when an attempt is made to isolate serine from usual protein hydrolyzates by the above technique, interfering amino acids have to be removed previously. For this purpose the oxazoline method reported by Elliott[21] is useful. The esters of serine and threonine form the oxazoline derivatives by the action of benziminoethyl ether. However the other amino acids give the aminoether derivatives and the former can be separated from the latter materials by vaccum distillation.

The present method seemed to be simpler than the oxazoline method and was applied to the acid hydrolyzate of casein. Eighty to ninety per cent of serine and threonine were recovered as was described in the experimental part. Sometimes β-hydroxy-α-amino acid fractions thus obtained were contaminated with small amounts of aspartic acid, but the latter amino acid was easily removed by a weak basic ion exchanger such as Amberlite IR-4B.

It is believed that the $O \rightarrow N$-acyl shift of *O*-acetyl - β - hydroxy - α - amino acids proceeds

TABLE II. OPTICAL ROTATION OF SERINE AND THREONINE OBTAINED BY THE $O \rightarrow N$-ACETYL SHIFT OF THE *O*-ACETYL DERIVATIVES*

	Before the reaction	After the reaction	Literature[22]
L-Serine	+15.5	+15.5	+15.1
D-Threonine	+16.5	+16.5	+15.0

* The specific rotation was measured in 2% solution in 2 N HCl at 25°C.

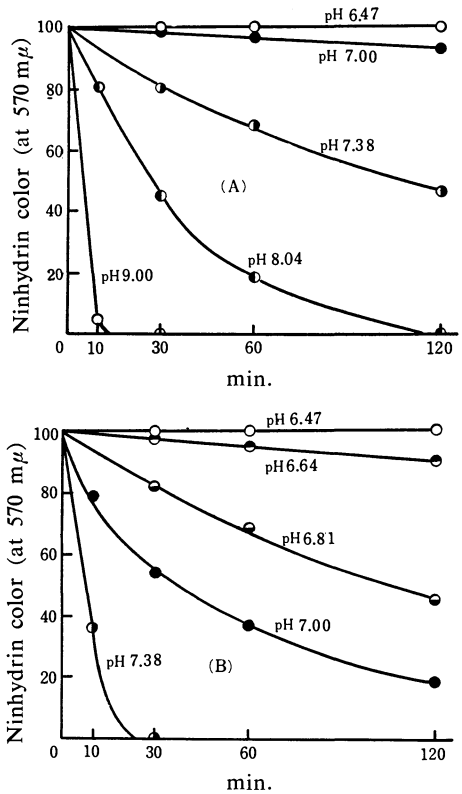


Fig. 1. $O \rightarrow N$-Acetyl shift of *O*-acetyl derivatives of L-serine (A) and DL-threonine (B) in 0.2 M phosphate buffer of various pH's at 20°C.

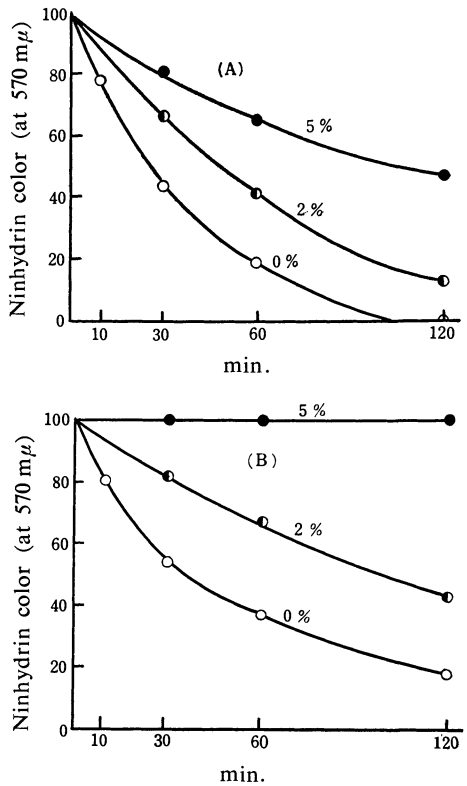


Fig. 2. Effect of sodium chloride on the $O \rightarrow N$-acetyl shift at 20°C. 0.2 M phosphate buffers of pH 8.04 and 7.00 were used for *O*-acetyl-L-serine (A) and -DL-threonine (B) respectively.

20) W. H. Stein, S. Moore, G. S. Stamm, C. Chou and M. Bergmann, *J. Biol. Chem.*, **176**, 367 (1942).
21) D. F. Elliott, *Biochem. J.*, **45**, 429 (1949).
22) J. P. Greenstein, *Advances in Protein Chemistry*, 9, 121 (1954).

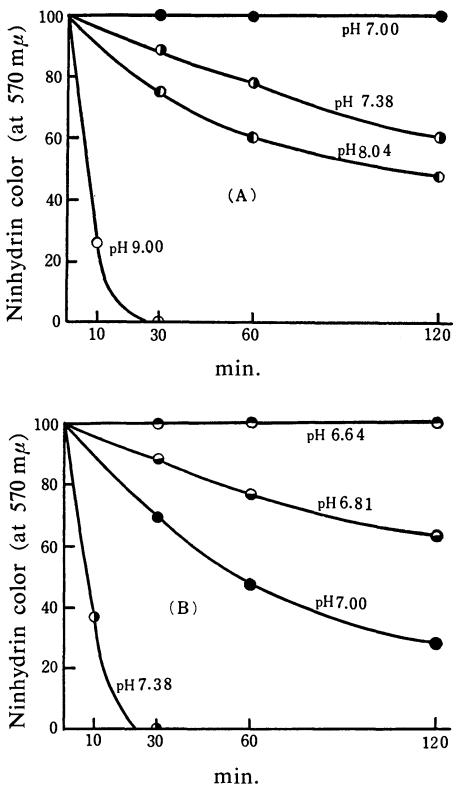


Fig. 3. *O*→*N*-Acetyl shift of *O*-acetyl-L-serine (A) and -DL-threonine (B) in 0.05 M phosphate buffer at 20°C.

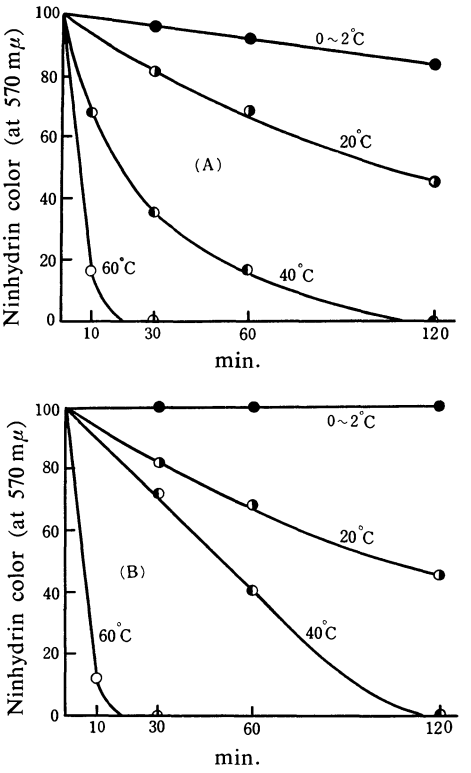


Fig. 4. Effect of temperature on the *O*→*N*-acetyl shift. 0.2 M phosphate buffers of pH 7.38 and 6.81 were used for *O*-acetyl-L-serine (A) and -DL-threonine (B) respectively.

through oxazoline derivatives as intermediates[1,3]. Consequently a possibility of racemization during the reaction must be considered. Synthetic *O*-acetyl-L-serine and -D-threonine were converted to their *N*-acetyl derivatives by incubating them at pH 8 or above, respectively, and then the acetyl group was removed by acid hydrolysis. It is clear from Table II, that no racemization occurred during *O*→*N*-acetyl shift reaction.

If the difference between the rate of the *O*→*N*-acetyl shift of *O*-acetylserine and that of *O*-acetylthreonine were remarkable, both the amino acids might be separable from each other. The rates of *O*→*N*-acetyl shift of *O*-acetylserine and *O*-acetylthreonine at various pH's were measured. As is shown in Fig. 1, the rate of the reaction of *O*-acetylthreonine is greater than that of the serine derivative under the conditions used. The above results seemed to indicate that the mutual separation of serine and threonine would be possible. Therefore a mixture of serine and threonine was treated with acetic acid and hydrogen chloride in order to convert them to their *O*-acetyl derivatives. The hydrochlorides of the *O*-acetyl derivatives thus obtained were incubated at room temperature keeping the pH at 7.0 with sodium hydroxide solution. In this case it was observed that the reaction was quite slow. The difference between the conditions of this reaction and those of model reaction shown in Fig. 1 is the presence of sodium chloride which was formed by the neutralization of the hydrochloride of the *O*-acetylamino acids with sodium hydroxide in the former experiment. Thus the effect of sodium chloride on the shift reaction was examined. As is shown in Fig. 2, sodium chloride inhibits the *O*→*N*-acetyl shift. When Fig. 3, which records the reaction rate of the shift in a low ionic strength of the buffer, 0.05 M phosphate, is compared with Fig. 1, it is clear that the increase of the ionic strength of the buffer has the accelerating effect on the reaction rate contrary to sodium chloride. Temperature increase accelerates the reaction rate and the temperature dependence is remarkable as is shown in Fig. 4. Therefore the mutual separation of serine and threonine from the mixture by the above reaction is affected by the many factors described above. The best conditions could not be found thus far.

In any rate the present experiments demonstrated that *O*-acetylthreonine was more labile than *O*-acetylserine, and even at pH 7 acetyl group of *O*-acetylthreonine migrated to its amino group. Therefore, if the shift reaction occurred at threonine bonds in proteins by the influence of concentrated sulfuric acid, it is difficult to estimate the number of the migrated threonine bond quantitatively, and precautions have to be taken to discuss the results for the modified proteins by this technique.

Summary

The reaction rate of *O*→*N*-acetyl shift of *O*-acetylserine was compared with that of *O*-acetylthreonine, and it was found that the latter was greater than the former. By utilizing the difference of the rates of the reaction of these amino acid derivatives, an attempt to separate serine and threonine from their mixture was unsuccessful owing to the fact that the shift reaction was affected by many factors, i.e., the ionic strength of inorganic salts present, pH of the reaction medium and the reaction temperature. Serine and threonine were isolated from the acid hydrolyzate of casein through their *O*-acetylation and subsequent *O*→*N*-acetyl migration with 80～90% yield.

The Daigo Nutritive Chemicals, Ltd.
Horigamidori, Higashiyodogawa-ku
Osaka
(*S. F. and S. M.*)

Institute for Protein Research
Osaka University, Kita-ku
Osaka
(*K. N.*)

The Infrared Absorption Spectra of 1,3,5-Trichlorobenzene, 1,2,4,5-Tetrachlorobenzene and their Deuterated Derivatives

By Shinnosuke SAËKI

(Received July 19, 1961)

The infrared absorption spectra of 1, 3, 5-trichlorobenzene[1], 1, 3, 5-trichlorobenzene-d_3[1], 1, 2, 4, 5-tetrachlorobenzene[2] and 1, 2, 4, 5-tetrachlorobenzene-d_2[2] have been studied from 4000 to 400 cm^{-1}, and the assignments of the observed bands have previously been proposed by the author. Also, recently the spectra of these substances have been measured in the far infrared region between 400 and 100 cm^{-1} using the cesium bromide prism and the gratings, and the spectra in the sodium chloride region have been reexamined with the aid of the high temperature long path cell described in a previous paper[3]. In this paper, the results of these measurements are reported, and, on the basis of this information, revised assignments for the infrared active normal vibrations of these molecules are proposed.

Experimental

As the method of the measurements was quite identical to that for *p*-dichlorobenzene and *p*-dichlorobenzene-d_4 which has been previously reported[3], any description of the measuring techniques is entirely omitted in this paper. The spectra obtained in the sodium chloride region using the high temperature long path cell were measured at different temperatures below 70°C for trichlorobenzenes and below 90°C for tetrachlorobenzenes, in order to observe the shapes of the bands of various intensities as accurately as possible. When the 85 mm. high temperature cell was used, the measurements were carried out at 240°C for trichlorobenzene and at 280°C for tetrachlorobenzene. The spectra in the far infrared region were measured in a solid state (Nujol mull) at room temperature using the grating spectrophotometer installed at the laboratory of Professor Yoshinaga of Osaka University.

Results

The far infrared absorption spectra of 1, 3, 5-trichlorobenzene and 1, 3, 5-trichlorobenzene-d_3 are shown in Fig. 1. The absorption curves are fragmental below 300 cm^{-1} because of the frequent exchanges of filters and gratings with the decreasing wave number. The spectra in the sodium chloride region measured by using the high temperature long path cell are shown in Fig. 2 for the range where the principal absorption bands appeared. In Figs. 3 and 4 the similar spectra for 1, 2, 4, 5-tetrachlorobenzene

1) S. Saëki, This Bulletin, 33, 1024 (1960).
2) S. Saëki, ibid., 34, 1552 (1961).
3) S. Saëki, ibid., 35, 326 (1962).

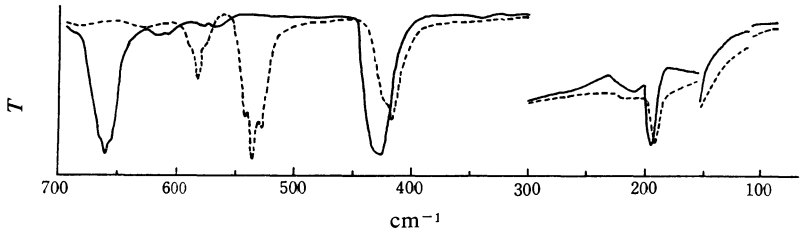


Fig. 1. Infrared absorption spectra of ordinary and deuterated 1,3,5-trichlorobenzenes.
$C_6H_3Cl_3$ ——, $C_6D_3Cl_3$ - - -

TABLE I. INFRARED ABSORPTION BANDS OF 1,3,5-TRICHLOROBENZENE

$C_6H_3Cl_3$			$C_6D_3Cl_3$		
Wave number	Intensity	Type	Wave number	Intensity	Type
1724	3				
1608	1				
1575	15		1560	20	
ca. 1520	0		1543	8	
			1524	0	
1474	5		1396	4	
1412	10		1342	20	
1384	6		1266 1262	8	
			1245	3	
			1211 1208	10	
			1147	4	
			863.2	4	
1105 1101	10		843.2 839.3	12	
1059	5				
859.9 855.4 850.7	10	‖	771.6 767.0 763.5	12	‖
813.7	15		799.2	20	
795.1	6		591.0 583.4 577.4	m	‖
660.9	s	‖	542.0 535.3 527.4	s	‖
623.1	w				
571.4	w		422.8	sh w	
429.7	sb		416.7	s	
194.3	s		193.5	s	

and tetrachlorobenzene-d_2 are shown. The frequencies, the intensities and the types of the observed bands are listed in Tables I and II, in which the intensities are described by a rough visual estimation, and the types are presented only for the bands whose envelopes showed the typical features of any band type.

Comparing the absorption curves shown in Figs. 2 and 4 with those presented in the previous papers[1,2], one can easily see that the absorption bands are separated from each other

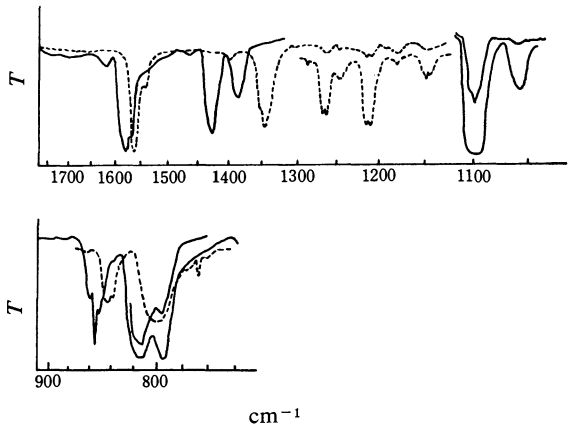


Fig. 2. Infrared absorption spectra of ordinary and deuterated 1,3,5-trichlorobenzenes.
$C_6H_3Cl_3$ ——, $C_6D_3Cl_3$ - - -

TABLE II. INFRARED ABSORPTION BANDS OF 1,2,4,5-TETRACHLOROBENZENE

$C_6H_2Cl_4$			$C_6D_2Cl_4$		
Wave number	Intensity	Type	Wave number	Intensity	Type
			1425	1	
1473	10		1396	20	A ?
1447	20	A	1355	10	A ?
1378	3				
1328	12		1307	9	A
			1243	5	A
1120	15		873.5	10	A
1071 1066	20	B	1060 1054	15	B
			743.6	1	
			738.9	2	
882.4	10	C	726.6	8	C
820.7	3				
767.2	w				
643.1	s		623.1	s	
510.2 504.2	s	B	505.9	s	
444.8 437.5	s		387.9 380.7	s	
140.4	s		140.4	s	

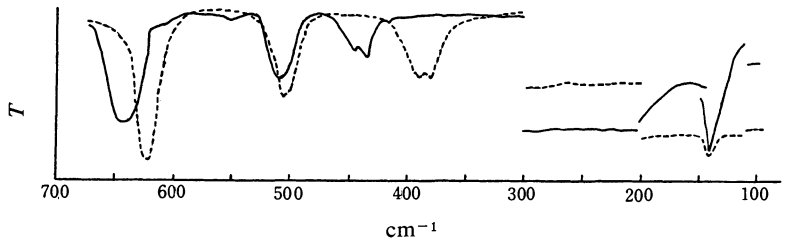


Fig. 3. Infrared absorption spectra of ordinary and deuterated 1,2,4,5-tetrachlorobenzenes.
$C_6H_2Cl_4$ ——, $C_6D_2Cl_4$ - - -

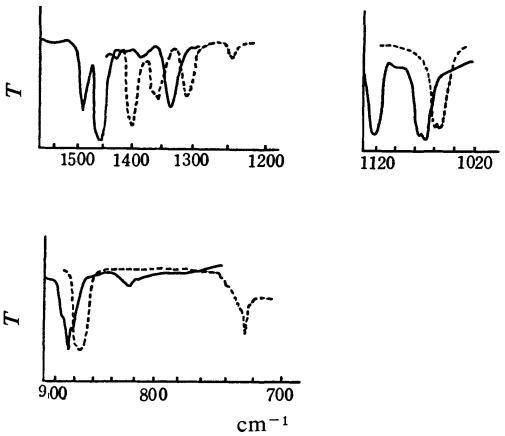


Fig. 4. Infrared absorption spectra of ordinary and deuterated 1,2,4,5-tetrachlorobenzenes.
$C_6H_2Cl_4$ ——, $C_6D_2Cl_4$ - - -

much more distinctly by the use of the high temperature long path cell, and also that the shape of each band can be much more clearly observed by means of this cell.

Band Shapes and Assignment

1, 3, 5-Trichlorobenzene and 1, 3, 5-Trichlorobenzene-d_3. — The vibrations of these molecules, which are active in infrared absorption, belong to species A_2'' or E' because of the high symmetry of the molecule, D_{3h}. Three of the ten infrared active normal vibrations are out-of-plane vibrations belonging to species A_2'', and the other seven are in-plane vibrations belonging to species E'. Furthermore, as the molecule is a symmetric top, the out-of-plane vibrations give parallel bands which show remarkable Q branches under proper resolution of the spectrometer, and the in-plane vibrations are perpendicular, showing less remarkable Q branches.

The bands which actually showed a clear Q branch in the observed spectra were those at 660.9 and 855.4 cm^{-1} of $C_6H_3Cl_3$ and those at 535.3, 583.4 and 767.0 cm^{-1} of $C_6D_3Cl_3$. Of these five bands, the last two were less intense than the first three. The three normal vibrations of species A_2'' are the out-of-plane vibrations of C–H (or C–D), C–Cl and the ring. Therefore, the pair of bands with the highest frequencies, that is, the bands observed at 855.4 and 767.0 cm^{-1}, were assigned to the out-of-plane bending vibrations of C–H and C–D bonds respectively, and the second highest pair of bands, at 660.9 and 535.3 cm^{-1}, were assigned to the ring deformation vibration. To the C–Cl out-of-plane bending vibrations, the pair of bands at 194.3 and 193.5 cm^{-1} which were observed in the grating region were quite confidently assigned. In the above correspondences between the bands of each species of the substance, the bands at 767.0 cm^{-1} of the deuterated substance seems to be too weak to correspond to the band at 855.4 cm^{-1} of the ordinary substance, even if the difference in the concentrations of the sample solutions is taken into account. The explanation for this fact will be seen later. The band at 583 cm^{-1} of the deuterated substance was ruled out from the fundamental bands because it has a relatively low intensity and did not satisfy the product rule.

There is a very noticeable fact in the above-mentioned assignment of the parallel vibrations. According to the above assignment, the band at 855.4 cm^{-1} of the ordinary substance (the out-of-plane bending vibration of the C–H bonds) should show a large frequency shift on the deuteration, and the frequency shift of the band at 660.9 cm^{-1} (the out-of-plane deformation vibration of the ring) should be much smaller than that. But, in practice, the behavior of these bands on the deuteration was quite contrary. While the band at 855.4 cm^{-1} of the ordinary substance shifted to 767.0 cm^{-1} on the deuteration, showing only a 10% decrease in frequency, the band at 660.9 cm^{-1} shifted to the band at 535.3 cm^{-1} on the deuteration, showing a 19% decrease in frequency. However, these experimental results, which appeared to be inconsistent with the assignment, can be explained as follows. As the out-of-plane C–H bending vibration of this molecule has been observed at 855 cm^{-1}, that

TABLE III. THE ASSIGNMENT OF INFRARED ABSORPTION BANDS OF 1,3,5-TRICHLOROBENZENE

Wave number		Assignment	Mode
$C_6H_3Cl_3$	$C_6D_3Cl_3$		
1724		?	
1608		$\nu_{13}(e')+\nu_{20}(e'')$	
1575	1560	$\nu_{12}(e')$	Ring stretching
	1543	$\nu_{14}(e')+\nu_{18}(e'')$	
1520		$\nu_{14}(e')+\nu_{16}(e')$	
1474		$\nu_4(a_1')+\nu_{14}(e')$	
	1396	?	
1412	1342	$\nu_{13}(e')$	Ring stretching
1384	1264	$\nu_8(a_2'')+\nu_{19}(e'')$	
	1245	$\nu_9(a_2'')+\nu_{18}(e'')$	
	1209	$\nu_4(a_1')+\nu_{14}(e')$ or $\nu_{15}(e')+\nu_{16}(e')$	
	1147	$\nu_4(a_1')+\nu_8(a_2'')$	
	863.2	?	
1103	841.3	$\nu_{14}(e')$	C–H or C–D in-plane bending
1059		$\nu_{19}(e'')\times 2$	
855.4	767.0	$\nu_8(a_2'')$	C–H out-of-plane bending / Ring out-of-plane deformation
813.7	799.2	$\nu_{15}(e')$	C–Cl stretching
795.1		$\nu_4(a_1')+\nu_{16}(e')$	
	583.4*	$\nu_4(a_1')+\nu_{10}(a_2'')$ or $\nu_{16}(e')+\nu_{20}(e'')$	
660.9	535.3	$\nu_9(a_2'')$	Ring out-of-plane deformation / C–D out-of-plane bending
623.1		$\nu_{16}(e')+\nu_{20}(e'')$	
571.4		$\nu_4(a_1')+\nu_{10}(a_2'')$	
429.7	416.7	$\nu_{16}(e')$	Ring in-plane deformation
194.3	193.5	$\nu_{10}(a_2'')$	C–Cl out-of-plane bending

* Note in proof: This band may be more confidently assigned to the second overtone of the fundamental at 193.5 cm^{-1} (a_2'', C–Cl out-of-plane bending) which borrows the intensity from the foundamental at 535.3 cm^{-1} of species A_2''. In the case of ordinary trichlorobenzene, this overtone is not observed, because it has no fundamental of the same species in its vicinity.

of the C–D bands can be expected to appear in the vicinity of 650 cm^{-1}. Consequently, in the case of the deuterated molecule, an extreme coupling must be expected between the C–D bending vibration and the ring deformation vibration, and, provided that the proper frequency of the ring deformation vibration exists a little higher than that of a C–D bending vibration, the coupling might push up the former and push down the latter by many wave numbers. The apparently contradictory phenomenon mentioned above is probably brought about in such a way. One can easily see from this consideration that the mode of these vibrations of the deuterated molecule are not simple but an almost fifty-fifty mixture of the C–D bending and the ring deformation modes, and, from the consideration of the intensity shown below, it might be better to assign the band of higher frequency to the ring deformation vibration and the lower to the C–D bending vibration.

This supposition for the vibrational modes appeared to be justified by the inversion of the relative intensities of these bands on the deuteration, that is, the fact that while the band at 855.4 cm^{-1} is stronger than the band at 660.9 cm^{-1} in the case of an ordinary molecule, the band at 767.0 cm^{-1} is weaker than the band at 535.3 cm^{-1} in the case of a deuterated molecule.

Among the seven vibrations belonging to species E′, the C–H (or C–D) stretching vibration (ν_{11}) was not observed, being beyond the high frequency limit of the region of this investigation*, and the C–Cl in-plane bending vibration (ν_{17}) was not found in the observed spectra, in spite of being expected to appear between 200 and 300 cm^{-1}**.

* It has already been reported in our previous paper[1] that this vibration was found at 3089 and 2310 cm^{-1} for the ordinary and deuterated 1,3,5-trichlorobenzene respectively.

** In the grating region, only one absorption band was found and was assigned to ν_{10} of the species A_2'', as has already been mentioned.

The other five vibrations are two stretching vibrations of the ring (ν_{12}, ν_{13}), an in-plane bending vibration of the C–H (or C–D) bonds (ν_{14}), a stretching vibration of the C–Cl bonds (ν_{15}) and an in-plane deformation vibration of the ring (ν_{16}). The observed remarkable absorption bands were unambiguously assigned to these vibrations by taking account of the observed frequencies and intensities, as shown in Table III.

The next step to be done is the applying of the product rule to the assignment determined above. In species E′, although the C–Cl bending vibration (ν_{17}) was observed for neither species of the substance, the ratio of the frequencies of such a low frequency vibration as ν_{17} can well be assumed to be nearly 1. With this assumption, the ratio of the products of the frequencies for each species of the substace was calculated to be 1.956 for species E′. The ratio calculated for species A_2'' was 1.383. As the theoretical values are 1.972 and 1.402 for species E′ and A_2'' respectively, the agreement between the observed and theoretical values are quite satisfactory, verifying the correctness of the proposed assignment.

On the basis of the assignment previously determined for the Raman active normal vibrations[4] and the above-mentioned assignment for the infrared active normal vibrations, the assignment of overtone and combination bands observed in the infrared absorption spectra could be determined. However, since there are three normal vibrations belonging to species A_2' for which there is no way of knowing the frequencies because of the inactivity in both of the Raman effect and infrared absorption, there might unavoidably be some overtone and combination bands for which the determination of assignment is impossible.

Among the observed overtone and combination bands, the three bands of ordinary trichlorobenzene at 1384, 1059 and 795.1 cm^{-1} have unusually high intensities. As an explanation of this fact could be found only in the Fermi resonances with the fundamental bands at 1412, 1103 and 813.7 cm^{-1} respectively, and as all of these fundamental bands belong to species E′, the species of these overtone or combination vibrations should also be E′. On the contrary, the fact that the combination band at 1543 cm^{-1} of the deuterated substance has a relatively low intensity in spite of the close existence of the fundamental band at 1560 cm^{-1} (E′), indicated that the species of this combination band should be A_2''. By taking into account such facts, as well as the frequencies and activities, the assignment of overtone and combination bands was determined as shown in Table III.

1, 2, 4, 5-Tetrachlorobenzene and 1, 2, 4, 5-Tetrachlorobenzene-d_2. — As the symmetry of these molecules is V_h, as in the case of *p*-dichlorobenzene, thirteen of thirty normal vibrations are active in infrared absorption; five of them belong to species B_{1u} (in-plane), five belong to species B_{2u} (in-plane), and three belong to species B_{3u} (out-of-plane)*.

This molecule is an asymmetric top, three moments of the inertia of which are as follows (in physical atomic weight·A^2):

	$C_6H_2Cl_4$	$C_6D_2Cl_4$
I_x:	1470	1482
I_y:	412	423
I_z:	1059	1059

Accordingly, the vibrations belonging to species B_{1u}, B_{2u} and B_{3u} give type B, A and C bands respectively.

The three out-of-plane normal vibrations belonging to species B_{3u} are the C–H (or C–D) and C–Cl bending vibrations and the deformation vibration of the ring. The C–Cl bending vibration appeared at 140.4 cm^{-1} in the grating region. However, since the spectra were measured in a solid state in this region, observation of the band envelope of this vibration was impossible. For the other two vibrations, the observation of the band envelopes was as had been expected. But, in practice, only one band of each substance, that is, the band at 882.4 cm^{-1} of $C_6H_2Cl_4$ and the band at 726.6 cm^{-1} of $C_6D_2Cl_4$, showed the remarkable Q branch which is the feature of the type C band. This pair of bands was assigned to the out-of-plane C–H (or C–D) bending vibration by considering their frequencies. The out-of-plane deformation vibration of the ring was expected to appear between 400 and 600 cm^{-1}. In this region of frequency, three remarkable bands were observed for each substance, that is, the bands at 643.1, 506 and 441 cm^{-1} of ordinary tetrachlorobenzene, and at 623.1, 505.9 and 384 cm^{-1} of the deuterated substance. All of these three pairs of bands have remarkable intensities, but their band envelopes were not clearly observed. Therefore, it was impossible to determine which of these three pairs of bands is to be assigned to the out-of-plane deformation vibration of the ring. However, as the assignment of the other two pairs of normal vibrations of species B_{3u} had already been

4) S. Saëki, This Bulletin, **34**, 1851 (1961).

* In the case of the point group V_h, the notation of the species depends on which of the three principal axes is taken for the x axis, which for the y, and which for the z. In this case, the axis perpendicular to the molecular plane is taken as the x axis, the axis combining two hydrogen (or deuterium) atoms as the z, and the third axis perpendicular to the first two as the y axis.

TABLE IV. THE ASSIGNMENT OF INFRARED ABSORPTION BANDS OF 1,2,4,5-TETRACHLOROBENZENE

Wave number		Assignment	Mode
$C_6H_2Cl_4$	$C_6D_2Cl_4$		
	1425	?	
1473	1396	$\nu_{11}(b_{1u})$	Ring stretching
1447	1355	$\nu_{18}(b_{2u})$	Ring stretching
1378		$\nu_{12}(b_{1u})+\nu_{16}(b_{2g})$	
1328	1307	$\nu_{19}(b_{2u})$	Ring stretching
	1243	$\nu_{12}(b_{1u})+\nu_{16}(b_{2g})$	
1120	873.5	$\nu_{20}(b_{2u})$	C-H or C-D in-plane bending
1069	1057	$\nu_{12}(b_{1u})$	C-Cl stretching
882.4	726.6	$\nu_{28}(b_{3u})$	C-H or C-D out-of-plane bending
820.7		$\nu_{13}(b_{1u})+\nu_{16}(b_{2g})$	
767.2		?	
	743.6	?	
	738.9	?	
643.1	623.1	$\nu_{21}(b_{2u})$	C-Cl stretching
507.2	505.9	$\nu_{13}(b_{1u})$	Ring in-plane deformation
441.2	384.3	$\nu_{29}(b_{3u})$	Ring out-of-plane deformation
140.4	140.4	$\nu_{30}(b_{3u})$	C-Cl out-of-plane bending

determined, the assignment of the third pair could be determined by applying the product rule. Among the observed three pairs of bands, the pair of 441.2 cm^{-1} (of $C_6H_2Cl_4$) and 384.3 cm^{-1} (of $C_6D_2Cl_4$) proved best to satisfy the product rule, and so was assigned to the ring deformation normal vibration, ν_{29}.

The in-plane vibrations of these molecules belong to species B_{1u} or B_{2u}, as was mentioned above. There exist three stretching vibrations of the benzene ring, one of which belongs to species B_{1u}, while the other two belong to species B_{2u}. In the observed spectra, three intense bands were actually found between 1300 and 1500 cm^{-1} for each substance (see Fig. 4 and Table II). Accordingly, these three pairs could apparently be assigned to $\nu_{11}(b_{1u})$, $\nu_{18}(b_{2u})$ and $\nu_{19}(b_{2u})$, and, by analogy to the case of *p*-dichlorobenzene[3], the pair of bands at 1473 and 1396 cm^{-1} was assigned to ν_{11} (b_{1u}) and the other two pairs were assigned to $\nu_{18}(b_{2u})$ and $\nu_{19}(b_{2u})$.

To the C-H and C-D in-plane bending vibration (ν_{20}'s), the bands at 1120 and 873.5 cm^{-1} were assigned respectively. Although, considering the frequency only, the band observed at 1069 cm^{-1} appears to correspond to the C-H in-plane bending vibration better than the band at 1120 cm^{-1}, this pairing must be ruled out, for the band at 1069 cm^{-1} was found to be a type B band showing two clear absorption maxima, as has been shown in Fig. 4 and Table II. As the spectrum of the deuterated substance also shows a type B band at 1057 cm^{-1} which apparently corresponds to the band in question at 1069 cm^{-1} of the ordinary substance, this pair of bands must be considered to originate in vibrations belonging to species B_{1u}. Furthermore, apart from the band envelope, this pair of bands could not be taken for ν_{20} because of the small frequency shift (12 cm^{-1}) on duteration. Thus it was determined that the pair of bands at 1120 and 873.5 cm^{-1} was to be assigned to the C-H (or C-D) in-plane bending vibration, ν_{20}.

The above-mentioned pair of bands at 1069 and 1057 cm^{-1} was assigned to the C-Cl stretching vibrations of species B_{1u}, ν_{13}'s. To the C-Cl stretching vibrations of species B_{2u} (ν_{21}'s), the pair of bands observed at 643.1 623.1 cm^{-1} was assigned. Though the frequency difference between these two pairs of C-Cl stretching vibrations appears to be too large, it is really quite probable considering that the C-Cl stretching vibration has a strong tendency to couple with other vibrations, that is, for example, with a ring deformation vibration or a C-H (or C-D) bending vibration.

The last pair of the observed strong bands, at 507.2 and 505.9 cm^{-1}, was assigned to the deformation vibration of the ring belonging to species B_{1u}.

The remaining two normal vibrations are C-Cl in-plane bending vibrations belonging to species B_{1u} and B_{2u} respectively. Although they were expected to appear around 200 cm^{-1}, no absorption band except the above-mentioned one at 140.4 cm^{-1} was observed in the grating region.

The next step is to prove the assignment determined above by making use of the product rule. The theoretical values of the ratios of the products of frequencies for both species of substance are 1.407 for all three vibrational

species (B_{1u}, B_{2u} and B_{3u}). In the proposed assignment, the frequencies of two C–Cl in-plane bending vibrations of species B_{1u} and B_{2u} are wanted. However, as the ratios of these frequencies could be assumed to be 1 without any serious error, the ratio of the products of the observed frequencies could be calculated based on the proposed assignment as follows:

Species B_{1u}:	1.439
Species B_{2u}:	1.436
Species B_{3u}:	1.394

The calculated values for species B_{1u} and B_{2u} exceeds the theoretical values by about 2%, while that for species B_{3u} is lower than the theoretical value by 1%. The accordances can be said to be satisfactory enough to show the correctness of the assignment.

On the basis of the assignment of the infrared active normal vibrations determined above and the assignment of the Raman active normal vibrations reported previously[5], some of the combination bands observed in the infrared absorption spectra could well be explained. However, since this molecule has two normal vibrations (the out-of-plane vibrations of the C–Cl bonds and the ring) belonging to species A_u which are inactive in both the Raman effect and infrared absorption, and since, even among active normal vibrations, some had not been observed, there were necessarily some combination bands which could not be explained. The assignment of the combination bands is shown in Table IV, together with the assignment of the fundamental bands.

5) S. Sački, This Bulletin, **34**, 1858 (1961).

Summary

The infrared absorption spectra of 1, 3, 5-trichlorobenzene, 1,3,5-trichlorobenzene-d_3, 1,2,4,5-tetrachlorobenzene and 1, 2, 4, 5-tetrachlorobenzene-d_2 were observed in a gaseous state from 700 to 300 cm^{-1} with a cesium bromide prism and in a solid state from 300 to 100 cm^{-1} using a grating spectrometer. Furthermore, the spectra in the sodium chloride region were carefully observed in the ranges where the main absorption bands appear, using a long path (720 cm.) high temperature cell. The obtained accurate frequencies and envelopes of the absorption bands have been reported on.

On the basis of these results, the assignments of the infrared active normal vibrations of these substances have been determined and checked by the product rule.

The assignments of the overtone and combination bands have also been determined using the assigned frequencies and species of infrared active and Raman active fundamental vibrations.

The author wishes to express his appreciation to Professor Hiroshi Yoshinaga and Dr. Akiyoshi Mitzuishi for the use of the far infrared spectrometer, and to Dr. Yoichiro Mashiko for his helpful suggestions.

Government Chemical Industrial Research Institute, Tokyo
Shibuya-ku, Tokyo

Geochemical Investigations of the Volcanoes in Japan. LI. Titanomagnetites in Volcanic Rocks of Nekodake, Aso Volcano***

By Iwaji IWASAKI, Takashi KATSURA and Minoru YOSHIDA

(Received February 8, 1961)

There have been many reports on the magnetochemical or mineralogical properties of titanomagnetites in volcanic rocks[1-4]. Also, many investigations have been made of the titanomagnetites in relation to the chemical or petrological properties of their host rocks. Iwasaki and Katsura[5] have studied the relation between the chemical composition of titanomagnetites in various Japanese volcanic rocks and the stage of magmatic differentiation of their host rocks. Buddington, Fahey, and

* Part L: M. Kamada, *J. Chem. Soc. Japan, Pure Chem. Sec.* (*Nippon Kagaku Zasshi*), **82**, 1346 (1961).

** Presented at the 11th Annual Meeting of the Chemical Society of Japan, Tokyo, April, 1958.

1) S. Akimoto, *J. Geomag. Geoelect.*, **3**, 47 (1951).

2) S. Akimoto, ibid., **6**, 1 (1954).

3) S. Akimoto, *Japan. J. Geophys.*, **1**, No. 2, 1 (1955).

4) R. Chevallier, J. Bolfa and S. Mathieu, *Bull. Soc. Franc. Miner. Crist.*, **78**, 307 (1955).

5) I. Iwasaki and T. Katsura, *Kyûshû. Min. Assoc. J.* (*Kyûshû Kôzan Gakkai-shi*), **18**, 197, 256, 291 (1950).

Vlisidis[6] have reported that the titanium content of magnetite is largely a function of the temperature of its formation. Vincent and Phillips[7] investigated titanomagnetites from the Skaergaard gabbroic intrusion and discussed the variation in content of major and minor constituents in a suite of differentiated gabbros. Recently, Marmo[8] has reported on the correlation of the titanium content of magnetite with certain geological facts. The problems discussed in these papers have, however, been mostly restricted to the variation in the titanium content of titanomagnetite, that is, the changes along the ulvöspinel-magnetite join in the FeO–Fe_2O_3–TiO_2 system.

Recent study by Akimoto and Katsura[9] has shown that the chemical composition of titanomagnetite in volcanic rocks does not always accord with ulvöspinel-magnetite join, but in most cases deviates from this join towards the ilmenite-hematite join side. In other words, some natural titanomagnetites have a more oxidized composition than the solid solutions between ulvöspinel and magnetite. The existence of such an oxidized titanomagnetite is also supported by synthetic investigation[10]. The state of oxidation of that natural titanomagnetite which is represented by the deviation of its chemical composition from ulvöspinel-magnetite join in the FeO–Fe_2O_3–TiO_2 system should be intimately related to the physicochemical history of its host rock.

Vincent and Phillips[7] concluded that the compositions of the magnetite are largely determined by the oxidation-reduction equilibria between ferrous and ferric oxides and oxygen in the crystalizing magma. However, the variation in the degree of oxidation of titanomagnetite dealt with in their report is rather small as compared with those of volcanic rocks. This paper is concerned chiefly with the relation between the state of oxidation of titanomagnetites (free from the ilmenite-hematite series minerals) in volcanic rocks and the chemical and petrological properties of their host rocks.

Materials and Methods

The volcanic rocks of Nekodake, Aso Volcano, from which titanomagnetites were extracted came in through the courtesy of Mr. H. Matsumoto, Institute of Geology, Kumamoto University, who has made geological studies and chemical analyses of these rocks[11]. The localities where these rocks were collected are shown in Table I*. They all belong to andesite (SiO_2 content 52~57%). It is considered that the volcanic activity of Nekodake has been in three stages: that is, the first was an activity of the Old Nekodake, which was followed by the second one forming the chief part of it (Nekodake lava), and then a number of dykes were injected as the last phase of the volcanic activity[11].

Table I. Rocks of Nekodake Aso Volcano from which titanomagnetites have been separated[11]

No.	Rocks*	Locality
1	horn-two-pyr-andesite, D	Tengu-iwa
2	horn-aug-hy-andesite, D	Oshoji-iwa
3	two-pyr-andesite, O	southern part
4	ol-hy-aug-andesite, N	western part
5	ol-hy-aug-andesite, N	western part
6	horn-aug-hy-andesite, D	Jigoku-dani
7	two-pyr-andesite, N	between Tengu-iwa and Higashi-mine
8	hy-aug-andesite, O	northwestern part
9	aug-hy-andesite, N	southeastern part
10	ol-bearing-two-pyr-andesite, N	western part
11	horn-bearing-two-pyr-andesite, D	Tengu-iwa (chilled margine)
12	aug-hy-andesite, O	northern part
13	aug-hy-andesite, O (aggromeratic)	northwestern part
14	two-pyr-andesite, N	southern part
15	aug-hy-andesite, N	Yamaguchi-dani
16	aug-hy-andesite, O	southern part
17	two-pyr-andesite, N	southern part
18	ol-aug-hy-andesite, N	Wakudo-iwa
19	ol-bearing-aug-hy-basaltic andesite, O	southern part

* horn=hornblende
pyr=pyroxene
aug=augite
hy=hypersthene
ol=olivine
D=dike rock
N=Nekodake lava
O=Old Nekodake lava

About 100~300 g. of volcanic rock was crushed by a gunmetal crusher, and the ferromagnetic fraction was separated from silicate minerals by a small permanent magnet. The fraction thus separated was then finely pulverized in an agate

6) A. F. Buddington, J. Fahey and A. Vlisidis, *Am. J. Sci.*, **253**, 497 (1955).
7) E. A. Vincent and R. Phillips, *Geochim. et Cosmochim. Acta*, **6**, 1 (1954).
8) U. Marmo, *Am. J. Sci.*, **257**, 144 (1959).
9) S. Akimoto and T. Katsura, *J. Geomag. Geoelect.*, **11**, 69 (1959).
10) S. Akimoto, T. Katsura and M. Yoshida, ibid., **9**, 165 (1957).
11) H. Matsumoto, Read at the Meeting of the Volcanological Society of Japan, October, (1957). (Abstract, *Bull. Volcanological Soc. Japan* (*Kazan*), 2nd Series, **2**, 95 (1957)).

* The sample numbers used in this paper correspond to those used by H. Matsumoto as follows:
No. 1 : 56062111, No. 2 : 56062301, No. 3 : 56110301,
No. 4 : 56050302, No. 5 : 56050509, No. 6 : 56050605A,
No. 7 : 56050612, No. 8 : 56050703, No. 9 : 56062102,
No. 10 : 56071605, No. 11 : 57100501, No. 12 : 57100502,
No. 13 : 56071603, No. 14 : 56T062111, No. 15 : 56050410,
No. 16 : 56062010, No. 17 : 56062107, No. 18 : 56082004,
No. 19 : 56062108.

TABLE II. CHEMICAL COMPOSITION AND CRYSTALLOGRAPHIC PROPERTIES OF TITANOMAGNETITES CONTAINED IN NEKODAKE VOLCANIC ROCKS

No.	Purity*	Weight %						Formula %			Atomic ratio		Lattice parameter
		FeO	Fe_2O_3	TiO_2	V_2O_3	MnO	CoO	FeO	Fe_2O_3	TiO_2	$32\times(Fe+Ti)/O$	$Fe/(Fe+Ti)$	Å
1	93.7	36.16	45.12	11.37	0.58	0.51	n. d.	54.23	30.44	15.33	23.69	0.883	8.422
2	92.9	33.44	46.72	11.70	0.48	0.53	0.027	51.46	32.35	16.19	23.41	0.878	8.400
3	89.4	22.33	53.89	11.91	0.91	0.37	0.037	38.98	42.32	18.70	22.40	0.869	8.387
4	90.7	32.49	45.16	11.90	0.73	0.46	0.034	51.16	31.99	16.85	23.36	0.872	8.417
5	91.6	36.54	40.37	13.40	0.76	0.51	0.039	54.74	27.21	18.05	23.60	0.858	8.442
6	91.6	35.08	47.40	7.97	0.70	0.42	n. d.	55.18	33.55	11.27	23.96	0.916	8.419
8	80.6	20.34	50.38	8.68	0.80	0.42	n. d.	40.03	44.61	15.36	22.62	0.894	8.391
9	73.1	21.95	43.80	6.93	0.44	n. d.	n. d.	45.84	41.15	13.01	23.13	0.908	n. d.
10	92.5	29.53	49.84	11.95	0.88	0.34	0.039	47.10	35.76	17.14	23.03	0.874	8.408
11	93.3	31.54	52.54	8.26	0.47	0.46	0.033	50.38	37.75	11.87	23.53	0.914	8.408
12	95.9	30.26	52.88	11.78	0.71	0.25	0.022	46.81	36.81	16.38	23.04	0.880	8.391
13	87.6	20.01	62.88	3.44	0.89	0.40	n. d.	38.93	55.04	6.03	22.96	0.961	8.397
14	95.0	33.21	46.82	14.02	0.52	0.46	n. d.	49.65	31.50	18.85	23.14	0.857	8.433
15	93.4	34.28	45.78	12.13	0.73	0.43	n. d.	52.11	31.31	16.58	23.45	0.874	8.421
16	92.8	26.97	52.93	11.66	0.73	0.49	n. d.	44.03	38.86	17.11	22.81	0.877	8.401
17	90.8	34.17	42.33	13.03	0.76	0.50	n. d.	52.62	29.33	18.05	23.42	0.860	8.436
18	91.0	28.64	50.87	10.27	0.74	0.47	n. d.	47.14	37.67	15.19	23.12	0.890	8.398
19	97.6	25.88	55.21	15.32	0.75	0.39	n. d.	40.13	38.51	21.36	22.34	0.846	8.388

* $FeO+Fe_2O_3+TiO_2+V_2O_3+MnO$ (in weight)

motor in the presence of water. The suspension thus prepared was poured into about 100 ml. of water, and the ferromagnetic fraction was attracted by a magnet, the suspension of silicate minerals being abandoned. These procedures were repeated until the purity could hardly be improved by the repetition of these procedures. Titanomagnetites in volcanic rocks are so finely grained that a small amount of silicate, such as olivine, pyroxene, etc., still remained as an impurity in spite of our efforts. As will be seen in Table II, the purity of these specimens mostly exceeds 90% and is sufficient for the present discussion.

X-Ray analysis was carried out for all specimens by means of a wide range X-ray spectrometer "Norelco" with Fe-K radiation. In all these specimens (with only the one exception of No. 13), the amount of the minerals which belonged to the ilmenite-hematite series was less than five percent. The lattice constant of each sample was also measured. In most cases, titanomagnetite lines in the X-ray diffraction diagram showed considerable broadening. This broadening can be attributed to the specimens being not strictly of a single phase which has a definite composition, but rather mixtures of phases with a spinel structure whose chemical composition differ continuously (probably along the oxidation-reduction lines in the FeO-Fe_2O_3-TiO_2 system[9]). Therefore, the chemical and physical properties of these titanomagnetites obtained by several methods will show the average values of such phases and so will involve some ambiguity.

Chemical analyses of titanomagnetite (FeO, Fe_2O_3, TiO_2, V_2O_3 and MnO) have been made by the method devised by Iwasaki et al.[12] The cobalt contents of several specimens were determined by colorimetric methods, using nitroso-R salt[13].

Results and Discussion

The results of the chemical analysis, together with the formular proportions of three oxides (FeO, Fe_2O_3, TiO_2), are given in Table II and are represented in the diagram of the FeO-Fe_2O_3-TiO_2 ternary system (Fig. 1).

The quantity of specimen No. 7 was insufficient for chemical analysis. The atomic ratio Fe/(Fe+Ti) and the atomic proportions of the metals to oxygen calculated on the basis of 32 oxygen atoms $32\times(Fe+Ti)/O$ are also given in Table II. They are used in the report by Akimoto and Katsura[9] in the form of a parameter where the former shows the change along the ulvöspinel-magnetite join, while the latter shows the change along the oxidation-reduction lines in the FeO-Fe_2O_3-TiO_2 system.

As will be seen in Fig. 1, the chemical composition of these titanomagnetites generally

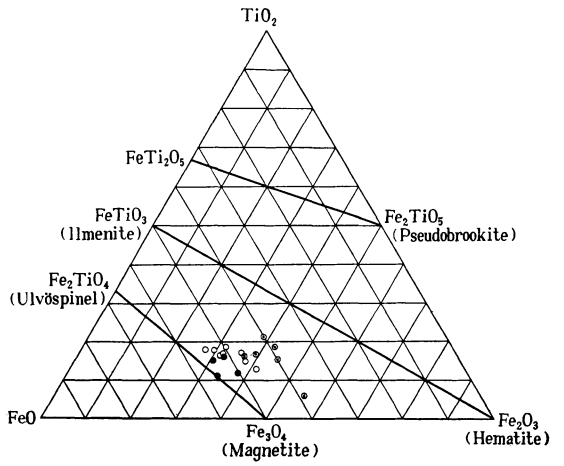


Fig. 1. Chemical composition of analysed titanomagnetites represented on a FeO-Fe_2O_3-TiO_2 system. (Formula %)
● dike rock ○ Nekodake lava
⊙ Old-Nekodake lava

does not accord with the Fe_2TiO_4-Fe_3O_4 solid solution line, but deviates considerably from this join towards the $FeTiO_3$-Fe_2O_3 join side. The TiO_2 contents of these titanomagnetites are confined to a relatively narrow range (Fe/(Fe+Ti)=0.83~0.91), except for No. 13, which contains a fairly large amount of hematite, as has already been mentioned. According to the previous studies[5,9], the titanium content of the titanomagnetite increases (or, Fe/(Fe+Ti) decreases) gradually in the order of the decreasing SiO_2 content of the host rock: rhyolite, dacite, andesite, basalt. The host rocks in this study belong to andesite, and the result agrees satisfactorily with previous reports. It is very convenient for a discussion of the relation between the degree of oxidation of titanomagnetites and other properties that the variation in the TiO_2 contents of these titanomagnetites is small.

Akimoto and Katsura[9] have referred to the titanomagnetite that lies almost precisely on the line of the Fe_3O_4-Fe_2TiO_4 join as "the normal titanomagnetite", to that which lies in the Fe_3O_4-Fe_2TiO_4-$FeTiO_3$ compositional field as "the abnormal titanomagnetite", and to that which lies in the Fe_3O_4-$FeTiO_3$-Fe_2O_3 field as "the very abnormal titanomagnetite". In accordance with this classification, only one specimen (No. 6) of titanomagnetite, can be referred to normal titanomagnetite, eight specimens (including No. 14) to abnormal titanomagnetite, and nine specimens to very abnormal titanomagnetite. As compared with the chemical composition of the already reported titanomagnetites in volcanic rocks[5,9], titanomagnetites in Nekodake volcanic rocks

12) I. Iwasaki, T. Katsura, M. Yoshida and T. Tarutani, *Japan Analyst (Bunseki Kagaku)*, 6, 211 (1957).
13) E. B. Sandell, "Colorimetric Determination of Traces of Metals", 3rd. Ed., Interscience Publishers, New York, London (1959), pp. 415, 429.

have a very oxidized composition (especially those in Old Nekodake lavas). It is also seen in Fig. 1 that titanomagnetites in Old Nekodake lava have the most oxidized composition and that those in dike rocks have the least oxidized composition. The chemical composition of titanomagnetite in Nekodake volcanic rock varies with the periods of volcanic activity.

In order to see the relation between the state of oxidation of titanomagnetite and that of the host rock, the FeO/Fe_2O_3 (by weight) of the titanomagnetites is plotted against the FeO/Fe_2O_3 of their host rocks (Fig. 2). A clear correlation is seen in this figure. It is also seen from the figure that the points which represent the Old Nekodake lavas take positions nearer to the axis of abscissa than do the others. This implies that titanomagnetite in Old Nekodake lava has a more oxidized composition than others in relation to the host rock. No difference seen is between Nekodake lava and dike rock. When the $32\times(Fe+Ti)/O$ value of titanomagnetite is taken in place of the FeO/Fe_2O_3 of titanomagnetite, the result is almost the same as the results obtained by Fig. 2. Some investigators[7,14] have emphasized the importance of the role of the volatile constituent (mainly water) on the state of the oxidation of iron in the rock. The $H_2O(+)$ content of the host rock is plotted against the FeO/Fe_2O_3 ratio of titanomagnetite in Fig. 3. As will be seen in the figure, Old Nekodake lava behaves in a different manner from others.

Apart from the results obtained by the study of titanomagnetites, the properties of Old Nekodake lava are almost same as those

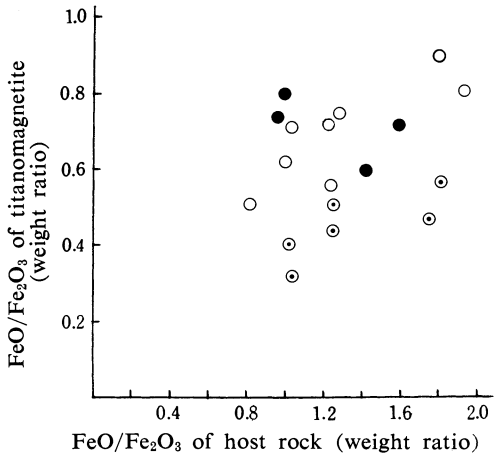


Fig. 2. Relation between FeO/Fe_2O_3 of the titanomagnetite and that of the host rock.
● dike rock ○ Nekodake lava
⊙ Old Nekodake

14) G. C. Kennedy, *Am. J. Sci.*, **246**, 529 (1948).

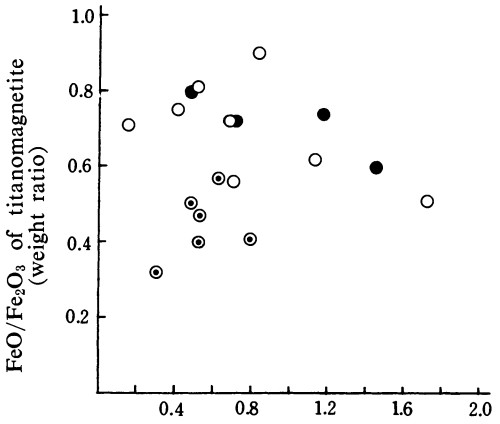


Fig. 3. Relation between FeO/Fe_2O_3 of the titanomagnetite and $H_2O(+)$ of the host rock.
● dike rock ○ Nekodake lava
⊙ Old Nekodake lava

of Nekodake lava. The former can be distinguished from the latter only by the information of the geological field survey[11]. On the other hand, dike rocks are readily distinguished from others by the fact that dike rocks alone bear hornblende as a constituent. Differences between Old Nekodake lava and Nekodake lava in the degree of the oxidation of titanomagnetite might be explained in two ways. First, the Old Nekodake lava may have originally been different from the Nekodake lava in its volatile constituent and the difference may have had an effect on the state of the oxidation of iron ore minerals. Second, the Old Nekodake lava may have been almost the same as the Nekodake lava, but the Old

TABLE III.

No.	Mn % in titanomagnetite	Mn % in host rock	Ratio
1	0.40	0.12	3.3
2	0.41	0.11	3.7
3	0.29	0.12	2.4
4	0.36	0.14	2.6
5	0.40	0.08_5	4.7
6	0.33	0.12	2.7
8	0.33	0.13	2.5
10	0.26	0.12	2.2
11	0.36	0.12	3.0
12	0.19	0.10	1.9
13	0.31	0.12	2.6
14	0.36	0.12	3.0
15	0.33	0.12	2.7
16	0.38	0.12	3.2
17	0.39	0.12	3.2
18	0.36	0.08_5	4.2

Nekodake lava may have suffered strong oxidative actions for some reason (for example, because of secondary heating in the atmospheric conditions). Most of the rocks which contain very abnormal titanomagnetite bear hematite. This fact seems to support the second of these possibilities.

The MnO contents of these titanomagnetites are 0.25~0.53%, and there is no correlation with the oxidation parameter $32\times(Fe+Ti)/O$. Manganese is somewhat concentrated in titanomagnetite. (Mn in titanomagnetite)/(Mn in host rock) are between 1.9 and 4.7 (Table III). The V_2O_3 contents of titanomagnetites are plotted against the oxidation parameter $32\times(Fe+Ti)/O$ in Fig. 4. Generally speaking, the vanadium content increases as the oxidation parameter decreases. Vanadium is considerably concentrated in titanomagnetite, as is shown in Table IV, and this result agrees well with those of previous investigators[5,9,15].

Cobalt is also fairly concentrated in titanomagnetite (Table V). These results agree well with the results of Wager and Mitchell[15].

The lattice constants of these titanomagnetites are plotted against the oxidation parameter. An almost linear relation, in which the lattice constant becomes smaller according as the oxidation proceeds, will be clearly found in Fig. 5. This result is in good accordance with the results obtained by the synthetic experiments[10] and the study on the natural titanomagnetites[9].

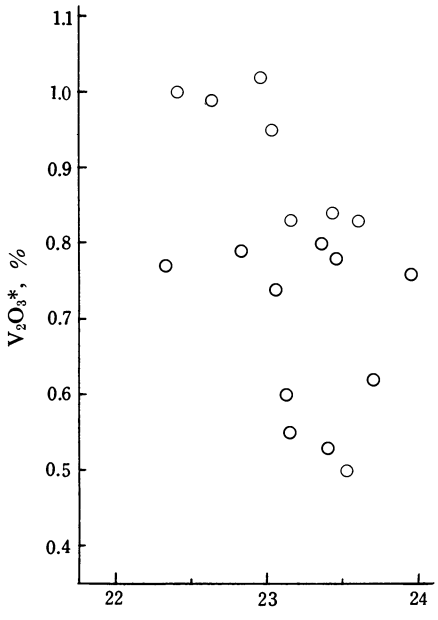


Fig. 4. Relation between V_2O_3 content and oxidation parameter of titanomagnetite
V_2O_3*$=V_2O_3\times100$/purity
purity$=FeO+Fe_2O_3+TiO_2+V_2O_3+MnO$ (weight %)

15) L. R. Wager and R. L. Mitchell, *Geochim. et Cosmochim. Acta*, 1, 129 (1951).

TABLE IV

No.	V % in titanomagnetite	V % in host rock	Ratio
1	0.40	0.023	17
2	0.33	0.008	41
9	0.30	0.009	33
14	0.35	0.022	17
18	0.51	0.026	20

TABLE V

No.	Co % in titanomagnetite	Co % in host rock	Ratio
5	0.031	0.0030	10
11	0.026	0.0027	9.7
12	0.017	0.0033	5.2

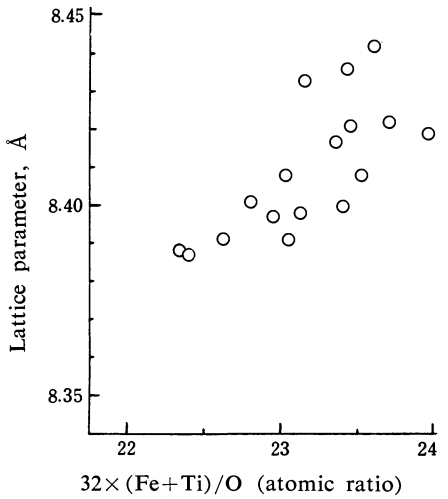


Fig. 5. Relation between lattice parameter and oxidation parameter of titanomagnetite.

Conclusion

The study of the titanomagnetite in volcanic rocks of Nekodake, Aso Volcano, has given the following results:

1. The natural occurrence of titanomagnetite the chemical composition of which lies in the Fe_3O_4–Fe_2O_3–$FeTiO_3$ compositional field, far beyond the Fe_2TiO_4–Fe_3O_4 and $FeTiO_3$–Fe_3O_4 line in the FeO–Fe_2O_3–TiO_2 diagram (" very abnormal titanomagnetite "), is confirmed in these volcanic rocks. About a half of the specimens in this paper are " very abnormal titanomagnetite ", and it may be supposed that " very abnormal titanomagnetite " exists rather commonly in volcanic rocks.

2. The state of the oxidation of titanomagnetite must have an important relation to the physico-chemical history of the host rock.

From the study of the correlation between the state of the oxidation of titanomagnetites and some chemical properties of their host rocks, it becomes possible to distinguish the rock belonging to Old Nekodake lava from that belonging to Nekodake lava or dike rock. However, for the present, the method must be considered valid only for the rocks of Nekodake.

3. Vanadium and cobalt in volcanic rock are considerably concentrated in titanomagnetite, and the vanadium content in titanomagnetite has a correlation to the oxidation parameter $32\times(Fe+Ti)/O$ which represents the state of the oxidation of titanomagnetite.

The authors are much obliged to Mr. Hatao Matsumoto, the Institute of Geology, Kumamoto University, for kindly supplying the specimens of Nekodake volcanic rocks and for many valuable suggestions and discussions from the petrological point of view. They also wish to express their hearty thanks to Dr. Syun-iti Akimoto, Geophysical Institute, the University of Tokyo, both for his great help and valuable advice in X-ray study and for his fruitful discussions throughout the study.

Laboratory of Analytical Chemistry and Geochemistry
Tokyo Institute of Technology
Meguro-ku, Tokyo

Geochemical Investigations of Volcanoes in Japan. LII. Vanadium Content of the Lava Flow in 1950—1951 from Volcano Ō-sima, Izu, Japan***

By Iwaji IWASAKI and Bunji IWASAKI

(Received July 24, 1961)

Since the beginning of the twentieth century, the contents of various elements in volcanic rocks have been determined and these data have been compared with one another. A comparison of these data depends on the assumption that the contents of these elements in one volcanic body, such as one lava flow, are uniform[1]. An experimental approach to these uniformities has not yet been made systematically, but Grout[2] studied the method of selection and preparation of granite and other rock samples without consideration of the error in chemical analysis. Brown et al.[3] found the uniformity of Moune granite G-2 without regard to the selection and preparation of rock samples.

As a part of the geochemical study at our laboratory, an attempt has been made to show whether the contents of various elements in one lava flow are uniform or not, to determine the relation between the contents of these elements and the external appearance of rocks, and to examine the method of selection and preparation of rock samples from a large volcanic body for chemiacl analysis.

In the previous work, Volcano Ō-sima, one of the representative active volcanoes in Japan, was selected for the reasons described below. Volcano Ō-sima has been well studied in the fields of geophysics, geology and geochemistry and is covered with several lava flows, from one of which we can collect rock samples systematically. A systematic collection of the rock samples in the lava flow which erupted in 1950—1951 from Volcano Ō-sima was therefore carried out. From the results of chemical analysis, the major components such as iron[4], titanium[5], manganese[6], sodium[6] and potassium[6] were found to be very uniform in content in spite of the different appearances of the samples. On the other hand, the ratio of ferric

* Cf. Part LI of this series: I. Iwasaki et al., This Bulletin, 35, 448 (1962).

** Read before the Symposium on Geochemistry of the Chemical Society of Japan, Nagoya, 1960.

1) H. S. Washington, "The Chemical Analysis of Rocks" John Wiley & Sons, London (1930), p. 73.

2) F. F. Grout, *Am. J. Sci.*, **24**, 394 (1932).

3) P. E. Brown et al., *Geochim. et Cosmochim. Acta*, **18**, 193 (1960).

4) I. Iwasaki et al., *Bull. Volcanolog. Soc. Japan, Ser. 2*, 5, 9 (1960).

5) I. Iwasaki et al.: Presented at the Symposium on Geochemistry of the Chemical Society of Japan, Fukuoka, 1959.

6) I. Iwasaki et al.: Presented at the 12th Annual Meeting of the Chemical Society of Japan, Kyoto, April, 1959.

oxide to ferrous oxide varied markedly with the degree of oxidation during cooling of the lava flow. This ratio is larger in the samples of red color, porus structure and scoria, or stalactitic structure than in normal compact samples. The vanadium contents of some of the volcanic rocks from Volcano Ō-sima had already been determined by Iwasaki et al.[7]

In this paper, a minor component, vanadium, one of metallic elements, was selected for the determination. A discussion is made of its uniformity, and a comparison of its value with those of volcanic rocks erupted in other ages is made. The relation between the vanadium content and the contents of other elements is also discussed.

Experimental

Selection and Preparation of Rock Samples.— The lava flow, which erupted in 1950—1951, is about 6 m. thick, covers an area of 2.6 km^2, and totals 2×10^{10} kg. in weight. Figure 1 shows the original location of the rock samples collected.

The collection of the rock specimens was carried out as follows. Along the traverse line from Kakō-chaya to Gosinka-chaya, many parallel lines about 150 m. apart were set up. Along these lines, about 2 kg. of single hand specimen or aggregate sample were taken from each place at intervals of about 100 m. Furthermore, three samples were taken from the top, center and base at the particular place where the lave flow was about 13 m. thick. These collected samples were generally normal compact fragments and were often rock specimens of various appearances, such as red color, porus structure, scoria, etc. A total of 171 samples involving 9 samples of Anei lava erupted in 1778 and 3 samples of Meiji-Taisho volcanic rocks erupted in 1912 was collected; in all, 169 samples were analyzed.

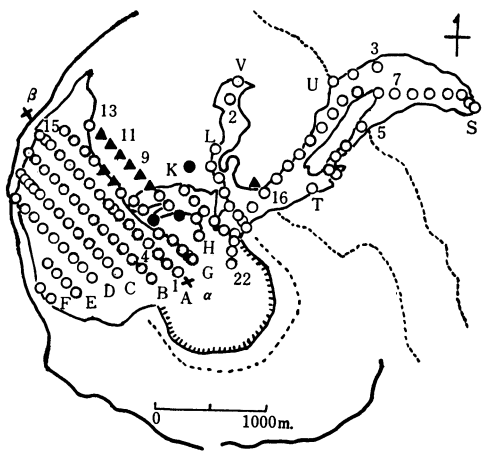


Fig. 1. The location of rock samples.
○ The lava in 1950—1951
● Meiji-Taisho volcanic rock
△ Anei lava
×α Kakō-chaya
×β Gosinka-chaya

About 4 g. of rock specimens, which was found in the previous paper[4] to be sufficient for the determination of the total iron, was crushed in a steel mortar and ground to fineness with an agate mortar and a pestle.

The Colorimetric Method. — About 200 mg. of rock powder was fused with anhydrous sodium carbonate in a platinum crucible, and vanadium was completely extracted with hot water. The colorimetric determination of vanadium in the extract was made directly by the phosphotungstic acid method modified by Katsura[8]. As a test of the reproducibility of this method, the determinations on the samples A-1 were repeated six times. These analyses were carried out on six separate fragments from a single had specimen. The results obtained are presented in Table I.

Table I. The results of repeated determinations

Sample (A-1)	V, %
1	0.046
2	0.046
3	0.047
4	0.047
5	0.048
6	0.046
Mean value	0.0467
Standard deviation	0.00055

By this method, it is possible to ascertain the vanadium contents of rocks with an precision of ±2% when they fall in a range of 0.04 to 0.05%.

Results and Discussion

Vanadium Contents. — Table II shows the contents of vanadium, total iron and ferric iron of 169 rock specimens from Volcano Ō-sima.

The Vanadium contents of 159 rock specimens from the lava flow erupted in 1950—1951 range from 0.043 to 0.048% and average 0.0455% (standard deviation 0.0014%). Even in view of possible error in chemical analysis, these ranges clearly show the differences among them, although they are small.

As a result, the vanadium contents of the lava flow stated above are considered to show a high degree of uniformity.

Figure 2 shows the frequency curve drawn on normal probability paper to test whether this distribution is normal or not.

7) I. Iwasaki et al., *Memoirs Fac. Sci. Kyushu Univ., Sec. Chem.* No. 1, 76 (1950).

8) T. Katsura, "Experimental Chemistry", Vol. 15, Maruzen, Tokyo (1958), p. 142.

TABLE II. THE CONTENTS OF TOTAL IRON, FERRIC IRON AND VANADIUM IN VOLCANIC ROCKS FROM Volcano Ō-sima

Sample	V, %	Fe*, %	Fe**, %		Sample	V, %	Fe*, %	Fe**, %	
A-1	0.047	10.0	2.0	X	C-7	0.043	10.0	1.3	X
A-2-1	0.044	10.0	1.7	X	C-8-1	0.045	10.0	1.5	X
A-2-2	0.046	10.0	1.5	X	C-8-2	0.044	10·0	1.4	X
A-2-3	0.045	10.0	1.8	Z	C-8-3	0.044	10.0	2.0	X
A-3-1	0.046	10.0	1.7	X	C-9-1	0.044	10.1	2.0	X
A-3-2	0.046	10.1	1.7	Z	C-9-2	0.047	10.0	1.6	X
A-4	0.046	10.0	1.7	X	C-10	0.043	10.0	2.3	Y
A-4-1	0.045	10.0	2.1	Y	C-11	0.045	10.0	1.4	X
A-4-2	0.047	10.0	3.1	Y	C-12	0.043	10.0	1.7	X
A-4-3	0.047	10.1	2.5	Y	C-12.3-1	0.045	10.0	1.8	X, R
A-4-4	0.044	10.0	2.4	Y	C-12.3-2	0.043	10.0	0.9	X
A-4-5	0.046	10.0	2.3	Y	C-13	0.043	10.0	1.7	X
A-5-1	0.047	10.1	1.9	X	C-13.4	0.044	9.9	2.0	X
A-5-2	0.048	10.0	1.8	X	C-14-1	0.045	10.0	1.6	X
A-5-3	0.046	10.0	2.0	Z	C-14-2	0.044	10.0	1.7	X
A-6-1	0.047	10.0	1.8	X	D-13-2	0.045	10.0	1.5	X
A-6-2	0.045	10.0	2.8	Z	D-13-1	0.045	10.0	1.5	X
A-6-3	0.045	10.0	2.0	X	D-12	0.045	10.0	1.7	X
A-7	0.046	10.0	1.8	X	D-11-2	0.045	10.0	1.7	X
A-7-1	0.048	10.0	1.8	X	D-11-1	0.044	10.1	1.7	X
A-7-2	0.048	10.1	1.9	X	D-10	0.044	10.0	1.8	X
A-7.5	0.047	10.0	2.0	X	D-9-2	0.043	10.0	1.8	X
A-8	0.048	10.0	1.9	X	D-9-1	0.044	10.0	1.7	X
A-9-1	0.047	10.0	1.7	X	D-8-3	0.045	10.1	2.0	X
A-9-2	0.045	10.0	1.7	X	D-8-2	0.046	10.0	1.7	X
A-10-1	0.048	10.0	1.8	Z	D-8-1	0.045	10.0	2.0	X
A-10-2	0.048	10.0	2.2	Z	D-7	0.045	10.0	1.5	X
A-10-3	0.044	10.0	1.8	X	D-6	0.045	10.0	1.7	Y
A-10-4	0.047	10.0	2.0	X	D-5	0.045	10.1	2.2	X
A-11	0.046	10.0	2.2	X	E-8	0.044	10.1	1.8	Z
A-12-1	0.044	10.0	2.0	X	E-7-6	0.045	10.0	2.4	W
A-12-2	0.047	10.1	1.9	X	E-7-5	0.045	10.0	2.2	X
A-12-3	0.047	10.0	2.4	Y	E-7-4	0.046	9.9	2.7	Y
A-13	0.047	10.0	2.9	Y	E-7-3	0.047	10.0	3.1	Z
A-14	0.047	10.0	2.0	Z	E-7-2	0.046	10.0	2.7	W
A-14.5	0.045	10.0	1.7	X	E-7-1	0.045	10.0	2.4	W
A-15	0.045	10.0	1.7	X	E-6	0.045	10.0	2.6	Z
B-2	0.046	10.0	1.9	X	E-5	0.047	10.0	3.2	Y
B-3	0.047	10.0	1.7	X	F-7-2	0.044	10.0	2.4	Y
B-4	0.045	10.0	1.7	X	F-7-1	0.047	10.0	1.8	X
B-5	0.045	10.0	1.6	X	F-6	0.045	10.0	1.6	Z
B-6	0.044	10.0	1.7	X	G-14	0.046	10.0	1.5	X
B-7	0.045	9.9	2.1	X	G-13	0.046	9.9	1.4	X
B-8	0.046	10.1	1.7	X	G-12	0.046	10.0	2.0	X
B-9	0.043	10.0	1.5	X	G-11	0.047	9.9	1.3	Z
B-10	0.045	10.0	1.7	X	G-10	0.050	10.6	1.9	X
B-11	0.046	10.0	1.5	X	G-9	0.050	10.6	2.0	X
B-12	0.045	10.0	1.6	X	G-8	0.046	10.0	1.7	X
B-13	0.045	10.0	1.5	X	G-7	0.046	10.1	2.0	X
B-14	0.044	10.1	1.5	X	G-6	0.046	10.2	2.0	X
B-15	0.045	10.0	1.5	X	G-5	0.041	8.9	2.0	X
C-4	0.044	10.0	1.3	X	G-4	0.046	10.1	2.6	Z
C-5	0.045	10.0	1.4	X	G-3	0.046	10.0	2.4	Z
C-6-1	0.044	10.0	1.5	X	G-2	0.044	10.0	1.7	X
C-6-2	0.044	10.0	1.4	X	G-1.5	0.045	10.1	2.4	X

TABLE II. (Continued)

Sample	V, %	Fe*, %	Fe**, %		Sample	V, %	Fe*, %	Fe**, %	
G-1	0.045	10.0	4.0	X	S-5	0.048	9.9	2.0	X
H-2	0.046	10.1	1.5	X	S-6	0.046	9.9	1.8	X
H-3	0.047	10.0	1.9	X	S-7	0.045	9.9	2.2	Z
H-4	0.039	8.9	2.0	X	S-8	0.046	10.0	2.6	Z
H-5	0.045	10.0	4.0	Y	S-9	0.046	9.9	1.8	X
H-6	0.046	10.0	2.4	Y	S-10	0.046	10.0	2.1	Z
H-7	0.050	10.8	2.2	X	S-11	0.046	10.0	2.3	Y
H-8	0.050	10.8	2.1	X	S-12	0.047	10.0	2.1	X
H-9	0.051	10.6	2.2	X	T-4	0.045	10.0	2.0	X
H-10	0.052	10.8	2.3	X	S-13	0.045	10.0	2.0	Z
H-11	0.050	10.6	2.1	X	S-14	0.044	10.0	2.0	X
H-12	0.052	10.8	2.2	X	S-15	0.044	10.0	2.0	X
H-13	0.047	10.0	1.7	Z	S-16	0.046	10.0	3.0	Z
K-0	0.047	10.1	2.2	Y	S-17	0.047	10.0	3.1	Z
K-1-1	0.046	10.0	2.2	X	S-18	0.045	10.0	2.4	X
K-1-2	0.045	10.0	2.3	X	S-19	0.044	10.0	2.2	X
K-3	0.047	10.1	1.9	X	S-20	0.045	10.0	2.9	Z
K-4	0.043	10.1	2.0	X	S-21	0.047	10.0	2.4	X
K-5	0.048	10.1	1.9	X	S-22	0.045	10.0	2.2	X
L-6	0.048	10.1	2.4	X	T-1	0.046	10.0	2.9	Z
L-5	0.047	10.1	1.7	X	T-2-1	0.047	10.0	2.3	X
L-4	0.048	10.1	2.2	X	T-2-2	0.044	10.0	2.4	X
L-3	0.047	10.1	1.5	X	T-3	0.045	9.9	2.2	X
L-2	0.047	10.1	2.1	X	T-5	0.045	10.0	2.8	Z
L-1	0.046	10.0	1.9	X	U-1	0.045	9.9	2.2	X
L-0	0.046	10.0	1.5	X	U-2	0.045	10.0	3.1	Y
S-1	0.046	9.9	3.0	Z	U-3	0.044	9.9	2.2	Z
S-2	0.046	10.0	2.9	Y	V-1	0.044	9.9	2.0	X
S-3	0.046	10.0	3.1	Z	V-2	0.044	9.9	2.4	X
S-4	0.045	10.0	2.1	X					

Fe*: Total iron content; Fe**: Ferric iron content
Anei lava: G-10, G-9, H-7, H-8, H-9, H-10, H-11, H-12
Meiji-Taisho volcanic rock: G-5, H-4
Base: A-12-1, D-9-1, Center: A-12-2; Top: A-12-3, D-9-2
X: Normal compact sample; Y: Scoria-like sample
Z: Sample of porus structure; W: Sample of stalactitic structure
R: Sample of red color

This shows almost a normal distribution, although Ahrens[9] has reported that the concentration of a minor element is lognormally distributed in any specific igneous rock.

The vanadium contents of 8 specimens from Anei lava range from 0.050 to 0.052% and average 0.051% (standard deviation 0.0009%), while those of 2 specimens from Meiji-Taisho volcanic rocks average at 0.040%. Consequently, the distinction between the vanadium contents of Anei lava and of Meiji-Taisho volcanic rock is comparatively easy, but it is difficult to distinguish the lava in 1950—1951 from the volcanic rocks of the other ages on the basis of their vanadium contents.

When the vanadium content of Anei lava, the highest value of the three, is compared with those of volcanic rocks in Japan and in the world respectively, it was found to be the highest value of volcanic rocks in Japan, higher than the values (0.015~0.030%) found in gabbroic and basaltic rocks by Goldschmidt[10] which had already been observed by Katsura[11].

As already stated in connection with the total iron content, the vanadium contents of the lava in 1950—1951 are also independent of their appearances as rock specimens.

The Relation between the Vanadium and Ferric Iron Content of the Lava Flow in 1950—1951. —As stated above, the quantities of various elements, such as total iron, titanium, etc., in the lava in 1950—1951 are very uniform. They, therefore, can not be considered to show

9) L. H. Ahrens, *Nature*, **172**, 1148 (1953); *Geochim. et Cosmochim. Acta*, **5**, 49 (1954); **6**, 121 (1954); **11**, 205 (1957).

10) V. M. Goldschmidt, "Geochemistry", Oxford Univ. Press, London (1954), p. 489.

11) T. Katsura, *J. Chem. Soc. Japan, Pure Chem. Sec. (Nippon Kagaku Zasshi)*, **77**, 358, 1076, 1196 (1956).

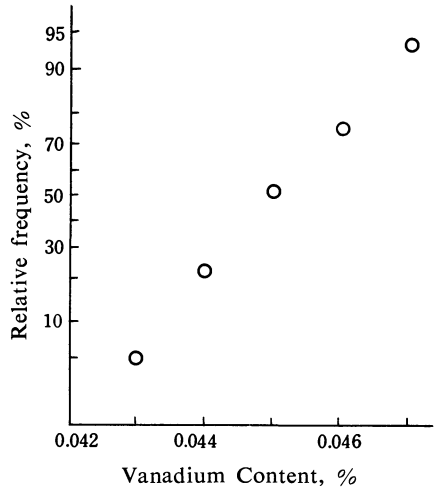


Fig. 2. The frequency curve on normal probability paper.

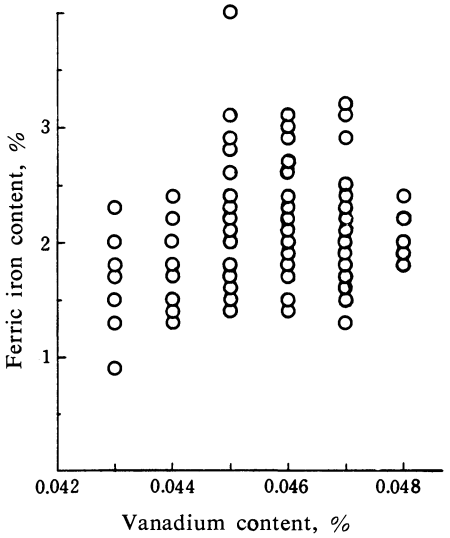


Fig. 3. The relation between vanadium and ferric iron content.

the relationship to the vanadium contents clearly. However, the ferrous iron and ferric iron contents vary markedly. As vanadium is believed to replace ferric iron, the relation between vanadium and ferric iron contents is shown in Fig. 3.

As shown in Fig. 3, there is no distinct, regular relation, although the contents of vanadium appear to become higher with increasing ferric iron contents. This seems to be attributable to the fact that vanadium had no time to replace the ferric iron, which increased rapidly by the oxidation of air and water vapor during the cooling of the lava flow at atmospheric temperature and pressure. In other words, it seems that the distribution of vanadium remains unchanged, but that ferric iron contents vary during the course of solidification and cooling. This consideration also agrees with that of the previous paper[4].

The Relation between the Contents of Vanadium and Other Elements in Volcanic Rocks in Different Ages.—The quantities of various elements[7,12] such as total iron, aluminum, titanium, magnesium and vanadium in volcanic rocks erupted in different ages are shown in Table III.

The number of rock specimens is too small to show the general relation definitely, but the relation may be discussed qualitatively. The positive correlation between the total iron and the vanadium content is shown in Fig. 4.

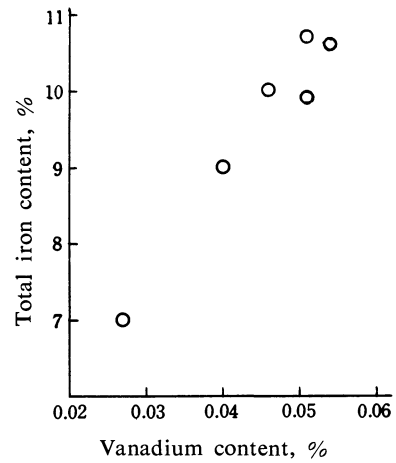


Fig. 4. The relation between vanadium and total iron content.
Regress coefficient, $\gamma=0.86$

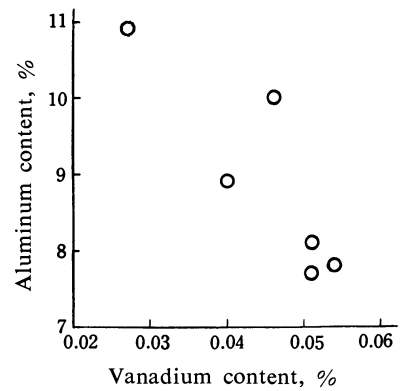


Fig. 5. The relation between vanadium and aluminum content.
Regress coefficient, $\gamma=-0.89$

12) I. Iwasaki, *J. Chem. Soc. Japan (Nippon Kwagaku Kwaishi)*, **56**, 1518 (1935).

Table III. The contents of various elements in volcanic rocks from Volcano Ō-sima

Sample	Fe*, %	Al, %	Mg, %	Ti, %	V, %
Okata volcanic rock	7.0	10.9	3.5	0.47	0.027
Okata volcanic rock	10.6	7.8	3.3	0.49	0.054
Outer Somma lava	9.9	8.1	2.9	0.50	0.051
Anei lava	10.7	7.7	3.0	0.77	0.051
Meiji-Taisho volcanic rock	9.0	8.9	2.7	0.61	0.040
The lava in 1950—1951	10.0	8.0	3.0	0.70	0.046

Fe*: Total iron content.

Vanadium is found to be most concentrated in magnetite among the common rock-forming minerals[7]. Anei lava is 6% magnetite (according to a microscopic analysis by Kuno[13]), with about 0.7% vanadium[14]. This magnetite is not pure magnetite, but involves the glassy ground mass and pyroxene. Thus, the vanadium content in the magnetite corresponds to about 80% ($6\times0.007\times100/0.051$) in rock. If the amounts of magnetite are proportional to the total iron content, the relation under consideration may be understood completely[7].

The negative correlation to aluminum content is presented in Fig. 5.

The main rock-forming mineral involving aluminum in Anei lava is plagioclase (contained in 50% of rock), which generally contains little vanadium. If the amounts of plagioclase decrease along with an increase in the amount of magnetite, this seems to explain this relation.

The contents of vanadium are independent of the titanium and magnesium contents, but the correlation to the contents of total iron plus titanium is shown in Fig. 6.

The magnetite in Anei lava contains 38% total iron plus titanium[14]. If the titanium plus total iron contents are proportional to the amounts of magnetite, this relation seems to be explained well. This relation has also been shown in ultrabasic potassic rocks by Higazy[15].

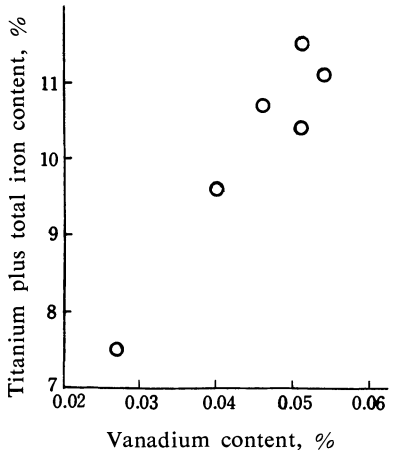


Fig. 6. The relation between vanadium and titanium plus total iron content.
Regress coefficient, $\gamma=0.90$

Conclusion

1) The vanadium contents of the lava flow erupted in 1950—1951 show a high degree of uniformity.

2) The frequency diagram shows an almost normal distribution.

3) It is difficult to distinguish between the lava of 1950—1951 and the volcanic rocks of the other ages in the basis of their vanadium contents.

4) A relation between the vanadium and ferric iron contents of the lava flow in 1950—1951 could not be found.

The expenses of this research were defrayed by a Scientific Research Encouragement Grant from the Ministry of Education, to which the authors wish to express their thanks.

Laboratory of Analytical Chemistry and Geochemistry
Tokyo Institute of Technology
Meguro-ku, Tokyo

13) I. Iwasaki, *Bull. Volcanolog. Soc. Japan, Ser. 2*, 3, 70 (1958).

14) I. Iwasaki et al., *J. Min. Inst. Kyushu*, **18**, 197, 256, 291 (1950).

15) R. A. Higazy, *Bull. Geol. Soc. Am.*, **65**, 39 (1954).

De-localization of Bond Eigenfunctions in π-Electronic Systems. III. Non-Empirical Calculation of the π-Electronic States of the Vinyl Chloride Molecule

By Shozaburo TAKEKIYO

(Received October 21, 1961)

In previous papers[1] an approximate method, in which all the ionic structures are taken into consideration, was applied to the calculation of the π-electronic states of a conjugated homo-nuclear chain compound, and the quantitative agreement of the results with those obtained by the ASMO SCF CI method was achieved.

On the other hand, if that approximate method is applied, in the same way as in part II, to a consideration of the π-electronic states of monosubstituted benzenes, such as chlorobenzene or phenol molecules, almost meaningless results will be obtained. This is because by that method the ionic structures in such molecules, which are obtained by moving one or both of the lone pair of π-electrons in the atom adjacent to the benzene ring in the covalent structure into the ring, are not derived from any covalent structure conceivable at all with respect to those molecules.

In order to apply the approximate method to such molecules, therefore, special treatment will be required.

In this paper, the method is developed in order to be applied to the vinyl chloride molecule, from which chlorobenzene is derived by substituting the benzene nucleus for the vinyl radical. Electronic states of the molecule are calculated, and the results are compared with those obtained by the HLSP standard method.

Derivation of Three Classes of Canonical Structures

A conjugated double bond molecule, having the same number (four) of π-electrons as the vinyl chloride molecule, is supposed, and all the covalent structures conceivable with respect to this molecule are set up (Ref. Fig. 1.).

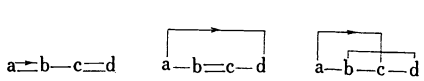


Fig. 1. Resonance structures of the conjugated molecule, consisting of four π-electrons and four atoms.

Then the π-electron, belonging to atom a in each structure, is made to move towards the atom in the direction of the arrow head, and ion a^+ is made to shift to an infinite distance (Ref. Fig. 2.).

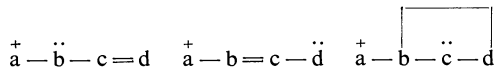


Fig. 2

Atoms b, c and d being substituted for chlorine, carbon and carbon atoms respectively, the resultant structures are the basic forms for the three classes of canonical structures; each class is obtained as in Fig. 3.

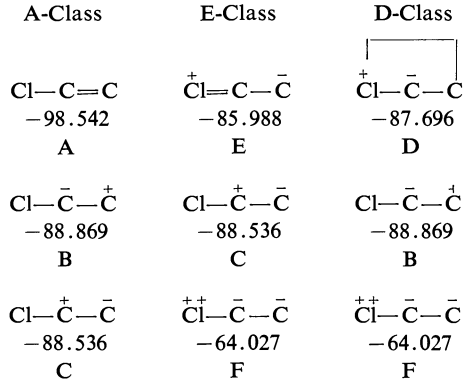


Fig. 3. Three classes of canonical structures and the energy values for the structures. Values are in electron volts.

The skeleton of the molecule is shown in Fig. 4. Slater $2p_\pi$- and $3p_\pi$-orbitals, with $Z_C=3.18$, $Z_{Cl}=6.099$ respectively, have been assumed for the carbon and the chlorine atoms. Numerical values of integrals over the atomic orbitals have been taken from Simonetta et al.[2]

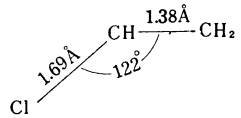


Fig. 4. Skeleton of vinyl chloride molecule.

1) S. Takekiyo, This Bulletin, 35, 355 (1962); 35, 360, (1962).

2) M. Simonetta, G. Favini and S. Carra, *Mol. Phys.*, 1, 181 (1958).

TABLE I. WAVE FUNCTIONS ASSOCIATED WITH CLASSES AND THE CORRESPONDING ENERGY VALUES

A-Class

$\phi_1^A = 0.78468\Psi_A + 0.23865\Psi_B + 0.22923\Psi_C$ $E_1^A = -100.304$ eV.
$\phi_2^A = 0.026821\Psi_A - 0.75119\Psi_B + 0.71540\Psi_C$ $E_2^A = -86.005$ eV.
$\phi_3^A = 0.84357\Psi_A - 0.73278\Psi_B - 0.77065\Psi_C$ $E_3^A = -80.335$ eV.

E-Class

$\phi_1^E = 0.73693\Psi_C + 0.51843\Psi_E + 0.034910\Psi_F$ $E_1^E = -91.061$ eV.
$\phi_2^E = 0.71522\Psi_C - 0.85513\Psi_E - 0.099032\Psi_F$ $E_2^E = -81.517$ eV.
$\phi_3^E = 0.072333\Psi_C - 0.34638\Psi_E + 1.0230\Psi_F$ $E_3^E = -61.593$ eV.

D-Class

$\phi_1^D = 0.81035\Psi_B + 0.55853\Psi_D + 0.024643\Psi_F$ $E_1^D = -89.891$ eV.
$\phi_2^D = 0.58685\Psi_B - 0.82679\Psi_D - 0.041893\Psi_F$ $E_2^D = -86.628$ eV.
$\phi_3^D = 0.0^2 51618\Psi_B - 0.081459\Psi_D + 0.99936\Psi_F$ $E_3^D = -63.870$ eV.

All kinds of overlap, single exchange, and multiple exchange integrals have been considered.

Wave functions ϕ_i^K's for class K's and the corresponding energy values E_i^K's are given in Table I, where Ψ_L is the normalized bond eigenfunction for structure L.

Probabilities of the structures, π-electron densities, and bond orders for each class are shown in Table II and Fig. 5 respectively.

TABLE II. PROBABILITIES OF STRUCTURES IN EACH CLASS

A-Class

A	B	C
0.74923	0.12893	0.12183

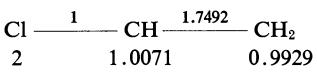
E-Class

C	E	F
0.63234	0.36154	$0.0^2 61249$

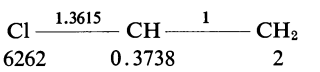
D-Class

B	D	F
0.67160	0.32733	$0.0^2 10717$

A-Class



E-Class



D-Class

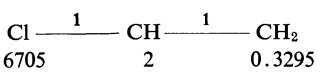


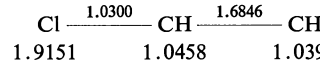
Fig. 5. π-Electron densities and bond orders in each class.

Electronic States of the Molecule

Wave functions for the lowest energy values in the respective classes have been combined linearly, and the wave functions Φ_i's for the molecule and the corresponding enery values E_i's have been calculated. The results are shown in Table III.

Then the probabilities of the structures, the π-electron densities, and the bond orders in the ground state of the molecule have been calculated from the results of Table II and Fig. 5. The results are shown in Table IV and Fig. 6, together with those obtained by the exact method.

HLSP method



Approximate method

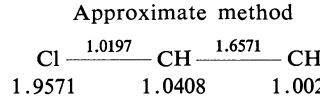


Fig. 6. Comparison of π-electron densities and bond orders.

Discussion

The value of the energy level for the ground state of the molecule, obtained by the exact HLSP method[3], is −100.91 eV. The difference of this value from the one obtained by the approximate method (Table III) is 0.35 eV., so the approximate method constitutes a good approach.

On the other hand, the excitation energy from the ground state to the first excited state is 11.41 eV. in the HLSP method. The approximate method, in which 12.98 eV. is obtained as in Table III, does not show a good agreement.

Finally, the wave function for the ground state has been transformed to represent the bond eigenfunctions explicitly. The result is:

3) S. Takekiyo, This Bulletin, 34, 1466 (1961).

TABLE III. WAVE FUNCTIONS FOR THE MOLECULE AND THE CORRESPONDING ENERGY VALUES

$\Phi_1 = 0.88437\phi_1^A + 0.10501\phi_1^E + 0.11540\phi_1^D$	$E_1 = -100.5590$ eV.
$\Phi_2 = 0.51913\phi_1^A - 1.10164\phi_1^E + 0.09376\phi_1^D$	$E_2 = -87.5810$ eV.
$\Phi_3 = 0.80471\phi_1^A - 0.19716\phi_1^E - 1.17076\phi_1^D$	$E_3 = -83.8402$ eV.

TABLE IV. COMPARISON OF THE PROBABILITIES OF RESONANCE STRUCTURES

HLSP method

A	B	C	D	E	F
0.68460	0.11099	0.11979	0.05429	0.03000	0.00033

Approximate method

A	B	C	D	E	F
0.65709	0.15915	0.14124	0.02245	0.01966	0.00041

$$\Phi_1 = 0.6939\Psi_A + 0.3046\Psi_B + 0.2801\Psi_C + 0.0644\Psi_D + 0.0544\Psi_E + 0.0065\Psi_F$$

while the result obtained by the HLSP method is

$$\Phi_G = 0.7359\Psi_A + 0.2184\Psi_B + 0.2213\Psi_C + 0.1616\Psi_D + 0.1152\Psi_E + 0.0067\Psi_F$$

From these results, it can be noticed that the migration percentage of the π-electrons in the chlorine atom to the vinyl radical in the approximate method is smaller than that in the other method.

One of the causes for such unsatisfactory results seems to be the neglect of the lower excited states in each class, which are at energy states close to the corresponding ground state, in the interaction of the classes (Ref. Table I).

Summary

The π-electronic energy levels, wave functions, π-electron densities, and bond orders of the vinyl chloride molecule have been calculated by the approximate method proposed in part I. Slater orbitals have been employed for the atomic orbitals of the carbon and chlorine atoms. All kinds of overlap, single exchange, and multiple exchange integrals have been considered. The calculated values of the energies for the ground state and the first excited state are -100.56 and -87.58 eV. The values obtained by the HLSP method are -100.91 and -89.50 eV. π-Electron densities are Cl $=1.957$, C (in the center of the molecule) $=1.041$, and C (in the edge of the molecule) $=1.002$. These values, based on the HLSP method, are 1.915, 1.046 and 1.039 respectively. Bond orders between the neighboring carbon and chlorine atoms are 1.02 and 1.03 in the respective methods.

The author wishes to express his sincere gratitude to Professor Kyosuke Omori, Kyushu University, for his helpful criticisms and suggestions. Thanks are also due to Professor Saburo Nagakura, the University of Tokyo, for his advice and valuable assistance, and to Professor Eiichi Ishiguro, Ochanomizu University, who has read the manuscript and helped the author to remove obscurities.

Faculty of Liberal Arts
Nagasaki University
Ohashi, Nagasaki

De-localization of Bond Eigenfunctions in π-Electronic Systems. IV. Non-Empirical Calculation of the π-Electronic States of the Cyclobutadiene Molecule

By Shozaburo TAKEKIYO

(Received October 21, 1960)

In part I[1] of this series an approximate method for the calculation of the π-electronic states of molecules was proposed, and in part II[2], where the method was applied to the consideration of a conjugated homo-nuclear chain compound, *trans*-butadiene molecule, the quantitative agreement of the results with those obtained by the ASMO SCF CI method was obtained. Then, in part III[3], that method was extended to the treatment of a hetero-nuclear system, the vinyl chloride molecule, in which a special atom possesses a lone pair of π-electrons; good results were obtained.

In this paper, the theory is applied to the calculation of the π-electronic states of a molecule, the cyclobutadiene molecule, belonging to the conjugated cyclic systems. Calculations of the probabilities of the resonance structures, the wave functions and the corresponding energy levels are made non-empirically, using the non-orthogonal atomic orbitals. The higher orders of overlap and exchange integrals are taken into account. These results are compared with the values obtained by the HLSP method.

The orthogonalized rather than the non-orthogonal (cf. Ref., part I) atomic orbitals[4] are usually employed for the quantitative considerations of polyatomic molecules, since it is very difficult to consider fully the higher order permutations of the electrons[5]. Therefore, calculations based on the orthogonalized atomic orbitals are also attempted, and the adaptability of the approximate method in this scheme is investigated.

Classification of the Resonance Structures

Cyclobutadiene has been assumed to be a square molecule, with the neighboring carbon nuclear distance $R_{C-C}=1.40$ Å.

Core integrals have been evaluated by the method of Parr and Mulliken[6], and the numerical values of the electron repulsion integrals have been taken from Craig[7].

The three classes of canonical structures are given in Fig. 1, in which energies are relative to $4W_{2p}$, where W_{2p} is the energy of a $2p_\pi$-electron of a carbon atom in its valence state.

Relations between bond eigenfunctions Ψ_L's and functions Ψ_i's which are the bases for

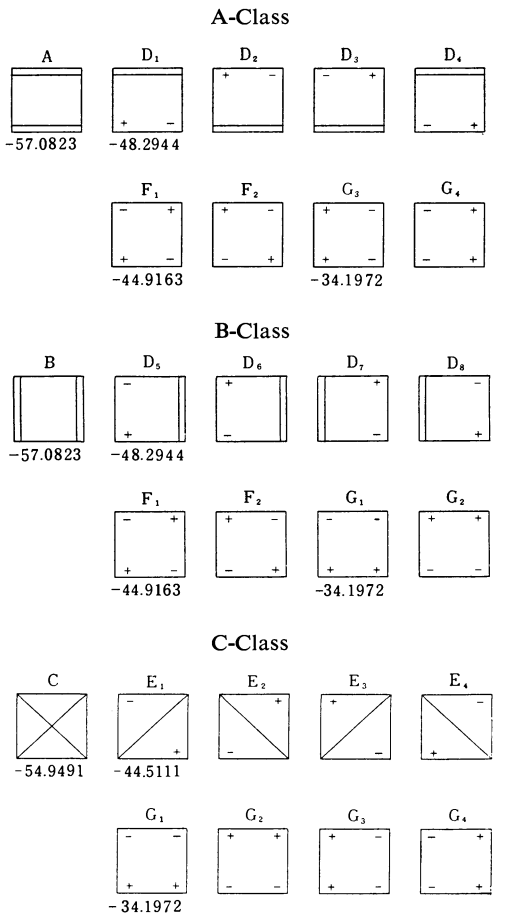


Fig. 1. Classification of resonance structures and the energies for the structures. Values are in electron volts.

1) S. Takekiyo, This Bulletin, **35**, 355 (1962).
2) S. Takekiyo, ibid., **35**, 360 (1962).
3) S. Takekiyo, ibid., **35**, 460 (1962).
4) P. O. Löwdin, *J. Chem. Phys.*, **18**, 365 (1950); **21**, 496 (1953).
5) R. McWeeny, *Proc. Roy. Soc.*, **A227**, 288 (1955); Ref. 4.
6) R. G. Parr and R. S. Mulliken, *J. Chem. Phys.*, **18**, 1338 (1950).
7) D. P. Craig, *Proc. Roy. Soc.*, **A202**, 498 (1950).

TABLE I. WAVE FUNCTIONS ASSOCIATED WITH THE CLASSES AND THE CORRESPONDING ENERGY VALUES

Based on non-orthogonal atomic orbitals

AB-Class

$\phi_1^{AB}(^1B_{2g}) = 0.80023\Psi_9 + 0.26085\Psi_{10} - 0.011107\Psi_{11}$	$E_1^{AB} = -58.352$ eV.
$\phi_2^{AB}(^1A_{1g}) = 0.75713\Psi_1 + 0.33830\Psi_2 + 0.097642\Psi_4 + 0.0^388699\Psi_5$	$E_2^{AB} = -56.182$ eV.
$\phi_3^{AB}(^1B_{1g}) = 0.83604\Psi_6 + 0.23707\Psi_8$	$E_3^{AB} = -51.950$ eV.
$\phi_4^{AB}(^1A_{1g}) = 0.75628\Psi_1 - 0.69019\Psi_2 - 0.40701\Psi_4 - 0.038294\Psi_5$	$E_4^{AB} = -47.316$ eV.
$\phi_5^{AB}(^1B_{2g}) = 1.0579\Psi_9 - 1.2077\Psi_{10} + 0.19836\Psi_{11}$	$E_5^{AB} = -40.215$ eV.
$\phi_6^{AB}(^1B_{1g}) = 0.95809\Psi_6 - 1.2493\Psi_8$	$E_6^{AB} = -35.695$ eV.
$\phi_7^{AB}(^1A_{1g}) = 0.27432\Psi_1 - 0.74924\Psi_2 + 1.0071\Psi_4 - 0.48722\Psi_5$	$E_7^{AB} = -35.170$ eV.
$\phi_8^{AB}(^1B_{2g}) = 0.41455\Psi_9 - 0.88445\Psi_{10} - 1.1124\Psi_{11}$	$E_8^{AB} = -28.912$ eV.
$\phi_9^{AB}(^1A_{1g}) = 0.34795\Psi_1 - 1.2239\Psi_2 + 0.73688\Psi_4 + 1.0501\Psi_5$	$E_9^{AB} = -26.484$ eV.

C-Class

$\phi_1^{C}(^1A_{1g}) = 0.13626\Psi_3 - 0.046463\Psi_5 + 0.97403\Psi_{12}$	$E_1^{C} = -55.268$ eV.
$\phi_2^{C}(^1B_{1g}) = \Psi_7$	$E_2^{C} = -44.354$ eV.
$\phi_3^{C}(^1A_{1g}) = 0.93597\Psi_3 + 0.27181\Psi_5 - 0.15022\Psi_{12}$	$E_3^{C} = -41.995$ eV.
$\phi_4^{C}(^1B_{2g}) = \Psi_{11}$	$E_4^{C} = -34.372$ eV.
$\phi_5^{C}(^1A_{1g}) = 0.35148\Psi_3 - 0.97158\Psi_5 - 0.22506\Psi_{12}$	$E_5^{C} = -32.558$ eV.

Based on orthogonalized atomic orbitals

AB-Class

$\bar{\phi}_1^{AB}(^1B_{2g}) = 0.82284\bar{\Psi}_9 + 0.55729\bar{\Psi}_{10} - 0.11117\bar{\Psi}_{11}$	$\bar{E}_1^{AB} = +41.877$ eV.
$\bar{\phi}_2^{AB}(^1A_{1g}) = 0.78598\bar{\Psi}_1 + 0.55209\bar{\Psi}_2 + 0.25299\bar{\Psi}_4 + 0.11590\bar{\Psi}_5$	$\bar{E}_2^{AB} = +44.029$ eV.
$\bar{\phi}_3^{AB}(^1B_{1g}) = 0.79951\bar{\Psi}_6 + 0.60066\bar{\Psi}_8$	$\bar{E}_3^{AB} = +50.622$ eV.
$\bar{\phi}_4^{AB}(^1A_{1g}) = 0.59540\bar{\Psi}_1 - 0.55874\bar{\Psi}_2 - 0.54996\bar{\Psi}_4 - 0.17564\bar{\Psi}_5$	$\bar{E}_4^{AB} = +53.231$ eV.
$\bar{\phi}_5^{AB}(^1B_{2g}) = 0.54136\bar{\Psi}_9 - 0.70925\bar{\Psi}_{10} + 0.45155\bar{\Psi}_{11}$	$\bar{E}_5^{AB} = +61.182$ eV.
$\bar{\phi}_6^{AB}(^1A_{1g}) = 0.13052\bar{\Psi}_1 - 0.40438\bar{\Psi}_2 + 0.72518\bar{\Psi}_4 - 0.53052\bar{\Psi}_5$	$\bar{E}_6^{AB} = +65.343$ eV.
$\bar{\phi}_7^{AB}(^1B_{1g}) = 0.60066\bar{\Psi}_6 - 0.79951\bar{\Psi}_8$	$\bar{E}_7^{AB} = +67.136$ eV.
$\bar{\phi}_8^{AB}(^1B_{2g}) = 0.17280\bar{\Psi}_9 - 0.43174\bar{\Psi}_{10} - 0.88529\bar{\Psi}_{11}$	$\bar{E}_8^{AB} = +72.725$ eV.
$\bar{\phi}_9^{AB}(^1A_{1g}) = 0.10348\bar{\Psi}_1 - 0.46849\bar{\Psi}_2 + 0.32811\bar{\Psi}_4 + 0.81373\bar{\Psi}_5$	$\bar{E}_9^{AB} = +73.358$ eV.

C-Class

$\bar{\phi}_1^{C}(^1A_{1g}) = 0.0^224190\bar{\Psi}_3 + 0.0^528596\bar{\Psi}_5 + 1.00000\bar{\Psi}_{12}$	$\bar{E}_1^{C} = +48.456$ eV.
$\bar{\phi}_2^{C}(^1B_{1g}) = \bar{\Psi}_7$	$\bar{E}_2^{C} = +58.979$ eV.
$\bar{\phi}_3^{C}(^1A_{1g}) = 0.99999\bar{\Psi}_3 + 0.0^223119\bar{\Psi}_5 - 0.0^224190\bar{\Psi}_{12}$	$\bar{E}_3^{C} = +58.979$ eV.
$\bar{\phi}_4^{C}(^1A_{1g}) = 0.0^373113\bar{\Psi}_3 + 0.31623\bar{\Psi}_5 - 0.0^686422\bar{\Psi}_{12}$	$\bar{E}_4^{C} = +69.990$ eV.
$\bar{\phi}_5^{C}(^1B_{2g}) = \bar{\Psi}_{11}$	$\bar{E}_5^{C} = +69.990$ eV.

Note: $\bar{\phi}_i^{K}$'s, $\bar{\Psi}_i$'s and $\bar{E}_i^{K}$'s are based on the orthogonalized atomic orbitals $\bar{k}(i)$'s. Values of energies $\bar{E}_i^{K}$'s are relative to $4\bar{\alpha}$, where $\bar{\alpha}$ is $\int \bar{k}(i) H_{core}(i) \bar{k}(i) d\nu_i$.

TABLE II. WAVE FUNCTIONS FOR THE MOLECULE AND THE CORRESPONDING ENERGY VALUES

Based on non-orthogonal atomic orbitals

$\Phi_1(^1B_{2g}) = 0.80023\Psi_9 + 0.26085\Psi_{10} - 0.01111\Psi_{11}$	$E_1 = 4W_{2p} - 58.352$ eV.
$\Phi_2(^1A_{1g}) = 0.80081\Psi_1 + 0.28561\Psi_2 - 0.02261\Psi_3 + 0.08243\Psi_4 + 0.00846\Psi_5$	$E_2 = 4W_{2p} - 56.218$ eV.
$\Phi_3(^1B_{1g}) = 0.70008\Psi_6 + 0.24344\Psi_7 + 0.19852\Psi_8$	$E_3 = 4W_{2p} - 52.647$ eV.

Based on orthogonalized atomic orbitals

$\bar{\Phi}_1(^1B_{2g}) = 0.82284\bar{\Psi}_9 + 0.55729\bar{\Psi}_{10} - 0.11117\bar{\Psi}_{11}$	$\bar{E}_1 = 4\bar{\alpha} + 41.877$ eV.
$\bar{\Phi}_2(^1A_{1g}) = 0.74643\bar{\Psi}_1 + 0.59424\bar{\Psi}_2 + 0.00024\bar{\Psi}_3 + 0.27231\bar{\Psi}_4 + 0.12475\Psi_5$	$\bar{E}_2 = 4\bar{\alpha} + 43.991$ eV.
$\bar{\Phi}_3(^1B_{1g}) = 0.70390\bar{\Psi}_6 + 0.47420\bar{\Psi}_7 + 0.52883\bar{\Psi}_8$	$\bar{E}_3 = 4\bar{\alpha} + 47.206$ eV.

TABLE III. WAVE FUNCTIONS FOR THE MOLECULE AND THE CORRESPONDING ENERGY VALUES (the HLSP method)

Based on non-orthogonal atomic orbitals

$\Phi_1(^1B_{2g}) = 0.80023\Psi_9 + 0.26085\Psi_{10} - 0.01111\Psi_{11}$ $E_1 = 4W_{2p} - 58.352$ eV.
$\Phi_2(^1A_{1g}) = 0.75393\Psi_1 + 0.32697\Psi_2 - 0.11784\Psi_3 + 0.09264\Psi_4 - 0.00386\Psi_5$ $E_2 = 4W_{2p} - 56.363$ eV.
$\Phi_3(^1B_{1g}) = 0.68396\Psi_6 + 0.24527\Psi_7 + 0.21925\Psi_8$ $E_3 = 4W_{2p} - 52.652$ eV.

Based on orthogonalized atomic orbitals

$\overline{\Phi}_1(^1B_{2g}) = 0.82284\overline{\Psi}_9 + 0.55729\overline{\Psi}_{10} - 0.11117\overline{\Psi}_{11}$ $\overline{E}_1 = 4\overline{\alpha} + 41.877$ eV.
$\overline{\Phi}_2(^1A_{1g}) = 0.78562\overline{\Psi}_1 + 0.55233\overline{\Psi}_2 - 0.01629\overline{\Psi}_3 + 0.25304\overline{\Psi}_4 + 0.11591\overline{\Psi}_5$ $\overline{E}_2 = 4\overline{\alpha} + 44.025$ eV.
$\overline{\Phi}_3(^1B_{1g}) = 0.75721\overline{\Psi}_6 + 0.49877\overline{\Psi}_7 + 0.42174\overline{\Psi}_8$ $\overline{E}_3 = 4\overline{\alpha} + 46.939$ eV.

the irreducible representations of the D_{4h} group, are shown in the Appendix.

A- and B-classes are incorporated to form one class, AB-class, due to the symmetry of the molecule. Wave functions for each class and the corresponding energy values are given in Table I.

Interaction of the Classes

Wave functions for the lowest energies, belonging to the same symmetry, have been picked up from the two classes, AB- and C-classes, and have been linearly combined.

The resulting wave functions for the molecule and the corresponding energy values are given in Table II.

TABLE IV. WAVE FUNCTIONS FOR THE MOLECULE AND THE CORRESPONDING ENERGY VALUES (the Heitler-London method)

Based on non-orthogonal atomic orbitals

$\Phi_1(^1B_{2g}) = \Psi_A - \Psi_B$ $E_1 = 4W_{2p} - 57.653$ eV.
$\Phi_2(^1A_{1g}) = \Psi_A + \Psi_B$ $E_2 = 4W_{2p} - 54.949$ eV.

Based on orthogonalized atomic orbitals

$\overline{\Phi}_1(^1A_{1g}) = \overline{\Psi}_A + \overline{\Psi}_B$ $\overline{E}_1 = 4\overline{\alpha} + 47.968$ eV.
$\overline{\Phi}_2(^1B_{2g}) = \overline{\Psi}_A - \overline{\Psi}_B$ $\overline{E}_2 = 4\overline{\alpha} + 48.456$ eV.

TABLE V. PROBABILITIES OF THE RESONANCE STRUCTURES IN EACH CLASS

Based on non-orthogonal atomic orbitals

AB-Class

A=B	D_i	F_i	G_i
0.35204	0.031682	0.021115	0.0^458862

C-Class

C	E_i	G_i
0.96449	0.0^270862	0.0^217902

Based on orthogonalized atomic orbitals

AB-Class

A=B	D_i	F_i	G_i
0.30888	0.038101	0.032002	0.0^233580

C-Class

C	E_i	G_i
0.99999	0.0^514629	$0.0^{12}20443$

In Tables III and IV, results based on the usual HLSP method and on the Heitler-London method respectively are shown.

The probabilities of the resonance structures in the first excited $^1A_{1g}$-state have next been calculated*. The results are shown in Tables V and VI.

TABLE VI. COMPARISON OF THE PROBABILITIES OF RESONANCE STRUCTURES

Based on non-orthogonal atomic orbitals

Approximate method

A=B	D_i	E_i	F_i	G_i
0.37253	0.02670	0.00112	0.01779	0.00033

HLSP method

A=B	D_i	E_i	F_i	G_i
0.35027	0.02999	0.00542	0.01941	−0.00024

Based on orthogonalized atomic orbitals

Approximate method

A=B	D_i	E_i	F_i	G_i
0.25752	0.04093	−0.00000	0.03438	0.00361

HLSP method

A=B	D_i	E_i	F_i	G_i
0.30860	0.03813	0.00007	0.03201	0.00336

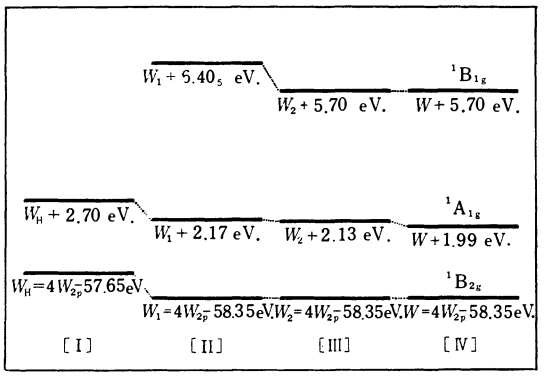
Discussion

In Fig. 2, the energy levels of the cyclobutadiene molecule, which have been found by the various methods, are shown.

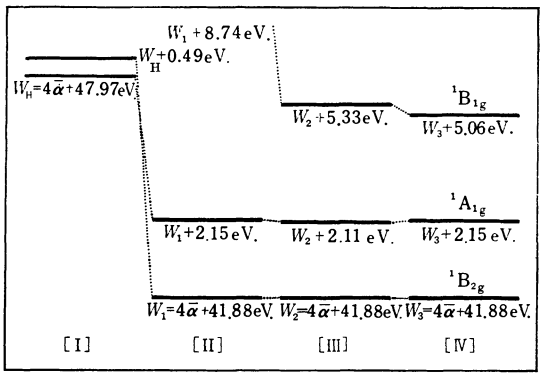
From the figure, it can be noticed that the approximate method gives successful results to the calculations of the electronic states of a conjugated cyclic system, as it did to that of a conjugated chain system investigated in part II.

Good agreements of the energy levels are also seen in the case of the evaluation for only the AB-class, which originates from the most stable covalent structures. From such agreements we can expect that, for molecules with high symmetry, the quantitative calculations of the energy levels may be performed

* For the ground $^1B_{2g}$-state, the approximate and the usual method are theoretically identical.



Based on non-orthogonal atomic orbitals



Based on orthogonalized atomic orbitals

Fig. 2. Comparison of energy levels.
I) Heitler-London method. II) AB-class. III) AB-, C-class interaction. IV) HLSP method (S. Takekiyo, This Bulletin, **34**, 1686 (1961)).

with a good result by a simplified process in the valence bond method.

It is recognized that, for the calculations of the energy levels, the approximate method gives quantitative agreements with the usual method, even if we use the orthogonalized instead of the non-orthogonal atomic orbitals.

Good agreements of the approximate method with the usual method are also seen for the values of the probabilities of the resonance structures (Tables V and VI).

In the cases of complex molecules, the valence bond method has, hitherto, been used only for the object of the qualitative considerations. But in view of the success in trials over parts I–IV, such deadlocks can probably be overcome to some extent by the application of our approximate method.

Summary

Calculations of the π-electronic energy levels, the wave functions, and the probabilities of the resonance structures of cyclobutadiene molecule have been made by an approximate method, proposed in part I, using the non-orthogonal Slater orbitals. Results have agreed quantitatively with the values calculated by the usual HLSP method.

Calculations have also been made using the orthogonalized atomic orbitals. Agreement of the results with those obtained by the usual method has been recognized.

The author wishes to express his sincere gratitude to Professor Kyosuke Omori, Kyushu University, for his helpful criticisms and suggestions. Thanks are also due to Professor Saburo Nagakura, the University of Tokyo, for his advice and valuable assistance, and to Professor Eiichi Ishiguro, Ochanomizu University, who has read the manuscript and helped him to remove obscurities.

Faculty of Liberal Arts
Nagasaki University
Ohashi, Nagasaki

Appendix

AB-Class

$^1A_{1g}$
$$\Psi_1=(1/N_1)(\Psi_A+\Psi_B)$$
$$\Psi_2=(1/N_2)(\Psi_{D1}+\Psi_{D2}+\Psi_{D3}+\Psi_{D4}+\Psi_{D5}+\Psi_{D6}+\Psi_{D7}+\Psi_{D8})$$
$$\Psi_4=(1/N_4)(\Psi_{F1}+\Psi_{F2})$$
$$\Psi_5=(1/N_5)(\Psi_{G1}+\Psi_{G2}+\Psi_{G3}+\Psi_{G4})$$

$^1B_{1g}$
$$\Psi_6=(1/N_6)(\Psi_{D1}-\Psi_{D2}+\Psi_{D3}-\Psi_{D4}+\Psi_{D5}-\Psi_{D6}+\Psi_{D7}-\Psi_{D8})$$
$$\Psi_8=(1/N_8)(\Psi_{F1}-\Psi_{F2})$$

$^1B_{2g}$
$$\Psi_9=(1/N_9)(\Psi_A-\Psi_B)$$
$$\Psi_{10}=(1/N_{10})(\Psi_{D1}+\Psi_{D2}+\Psi_{D3}+\Psi_{D4}-\Psi_{D5}-\Psi_{D6}-\Psi_{D7}-\Psi_{D8})$$
$$\Psi_{11}=(1/N_{11})(\Psi_{G1}+\Psi_{G2}-\Psi_{G3}-\Psi_{G4})$$

C-Class

$^1A_{1g}$
$$\Psi_{12}=\Psi_C$$
$$\Psi_3=(1/N_3)(\Psi_{E1}+\Psi_{E2}+\Psi_{E3}+\Psi_{E4})$$
$$\Psi_5=(1/N_5)(\Psi_{G1}+\Psi_{G2}+\Psi_{G3}+\Psi_{G4})$$

$^1B_{1g}$
$$\Psi_7=(1/N_7)(\Psi_{E1}-\Psi_{E2}+\Psi_{E3}-\Psi_{E4})$$

$^1B_{2g}$
$$\Psi_{11}=(1/N_{11})(\Psi_{G1}+\Psi_{G2}-\Psi_{G3}-\Psi_{G4})$$

* $1/N_i$ is the normalizing factor.

Studien über D-Glucosamin-derivaten. VII[1]. *Darstellung von 3,4; 5,6-Di-O-isopropyliden-N-acetyl-D-glucosaminsäure über das entsprechende D-Glucosaminol-derivat*

Von Juji YOSHIMURA, Toshio NAKAGAWA und Tetsuo SATO

(Eingegangen am 27. Juli 1961)

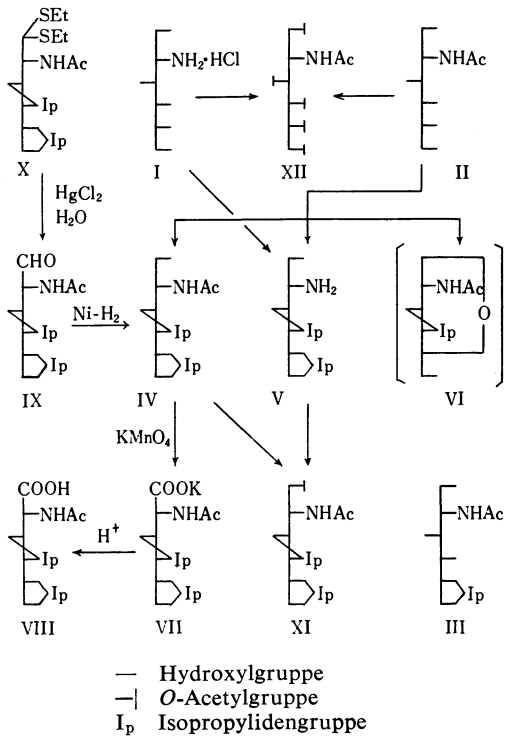
Nach allgemeinen Methoden wird D-Glucosaminsäure nicht acetalisiert, weil die Säure in den organischen Lösungsmitteln schwer löslich ist. Bei Behandlung mit Acetanhydrid und Natriumacetat[2] oder mit Acetanhydrid in Pyridin[3] gibt die Säure nicht das entsprechende Pentaacetat, sondern 2-Acetamino-5-acetoxymethyl-α-pyron. Es ist unerwartet schwer[4], das an den allen Hydroxyl-gruppen blockierten D-Glucosaminsäure-derivat zu erhalten.

Wir haben daher über die Oxydation vom D-Glucosaminol-derivat, in dem nur die Hydroxyl-gruppe am C-1-Stellung frei ist, in das entsprechende D-Glucosaminsäure-derivat versucht. Um die allen andern Hydroxyl-gruppen außer der am C-1-Stellung des D-Glucosaminols oder *N*-Acetyl-D-glucosaminols zu blockieren, muß man eine selektive Reaktion benutzen.

Die Behandlung von Polyhydroxyalkohol mit Aldehyd oder Keton gibt das entsprechende Ringacetal. Dabei ist es bekannt, daß Keton vorzüglich einen α-Ring (5-Ring) gibt und Aldehyd einen β-Ring (6-Ring) gibt[5]. Bei der Acetonisierung von *N*-Acetyl-D-glucosaminol kann man daher die Bildung vom 3,4; 5,6-Di-*O*-isopropyliden-derivat mit einer freien Hydroxyl-gruppe am C-1-Stellung erwarten.

Karrer und Meyer[6] berichteten über die Darstellung von D-Glucosaminol-hydrochlorid (I) und *N*-Acetyl-D-glucosaminol (II) durch katalytische Hydrierung von D-Glucosaminhydrochlorid und *N*-Acetyl-D-glucosamin. Turumi und Yamada[7] stellten 5,6-*O*-Isopropyliden-*N*-acetyl-D-glucosaminol (III) aus II in Aceton in Gegenwart von Kupfersulfat her. Aber andere Derivate des D-Glucosaminols sind noch kaum bekannt.

Nach Behandlung von II in Aceton in Gegenwart von Kupfersulfat und einer kleinen Menge konzentrierter Schwefelsäure, Neutralisierung der Reaktionslösung mit eisgekühlter Alkalilauge, Ausziehung mit Chloroform und Vertreiben des Lösungsmittels haben wir 3,4; 5,6-Di-*O*-isopropyliden-*N*-acetyl-D-glucosaminol (IV) vom Schmp. 158~160°C und $[\alpha]_D^{22}$ −7.8° (in Methanol) gewonnen. Der aus der wäßrigen Schicht beim Eindampfen erhaltene Sirup wurde durch Hochvakuumdestillation in zwei Fraktionen geteilt, d. h. eine kleine Menge Erstdestillates vom Sdp.$_{0.005}$ 105~106°C und eine große Menge Hauptdestillates vom Sdp.$_{0.02}$ 190~192°C. Aus dem Erstdestillat haben wir 3,4; 5,6-Di-*O*-isopropyliden-D-glucosaminol (V) vom Schmp. 65~68°C und $[\alpha]_D^{22}$ +8.5° (in Methanol) erhalten und aus dem Hauptdestillat IV und eine kristalline Verbindung (VI) mit der Formel $C_{11}H_{19}O_5N$ vom Schmp. 170~172°C und $[\alpha]_D^{22}$ −164.1° (in Methanol) erhalten. Die Struktur von VI ist



— Hydroxylgruppe
—| *O*-Acetylgruppe
Ip Isopropylidengruppe

1) VI. Mitt.: J. Yoshimura, Dieses Bulletin, **34**, 8 (1961).
2) M. Bergmann, L. Zervas und E. Silberkweit, *Ber.*, **64**, 2428 (1931).
3) T. Nakagawa, unveröffentlicht.
4) M. L. Wolfrom und M. J. Cron, *J. Am. Chem. Soc.*, **74**, 1715 (1952).
5) a) S. A. Barker und E. J. Bourne, "Advances in Carbohydrate Chemistry", Vol. 7, Academic Press, Inc., New York (1952), S. 137.
b) J. A. Mills, ebenda, Vol. 10, (1955), S. 1.
6) P. Karrer und J. Meyer, *Helv. Chim. Acta*, **20**, 626 (1937).
7) K. Turumi und S. Yamada, *Tohoku J. Exp. Med.*, **62**, 329 (1955).

noch nicht ganz klar, aber weil Zuckeralkohole überhaupt sich mit Hilfe von Säure leicht in die entsprechenden Anhydriden überführen lassen[8], ist die oben gezeigte Konstitutionsformel wahrscheinlich.

Die Oxydation von IV mit alkalischer Kaliumpermanganat-lösung gab das Kaliumsalz (VII) der 3, 4; 5, 6-Di-*O*-isopropyliden-*N*-acetyl-D-glucosaminsäure. Diese Tatsache zeigt, daß es in IV eine freie, primare Hydroxylgruppe gibt. Unter der Wirkung eines kleinen Überschüsses Mineralsäure ließen sich VII in die entsprechende freie Säure (VIII) vom Schmp. 195~196°C und $[\alpha]_D^{22}$ −14.9° (in Methanol) überführen.

3, 4; 5, 6-Di-*O*-isopropyliden-*N*-acetyl-*al*-D-glucosamin (IX), aus dem entsprechenden Diäthylmercaptal[9] (X) dargestellt, konnte unter katalytischer Hydrierung zu IV geführt werden. Die Acetonisierung von I in Gegenwart von konzentrierter Schwefelsäure gab IV, und die Acetylierung von V und IV mit Acetanhydrid in Pyridin dasselbe Diacetat (XI). Daraus folgt, daß die Verknüpfungsstellen von der Isopropylidenresten in IV, V, VII und VIII den in X gleich sind.

Die Acetylierung von I und II mit Acetanhydrid in Pyridin gab auch dasselbe Hexaacetat (XII).

Bescheibung der Versuche

Acetonisierung von *N*-Acetyl-D-glucosaminol (II).—Mit einer Lösung von 260 ccm trocknem Aceton und 4 ccm konz. Schwefelsäure wurden 20 g II und 50 g wasserfreies Kupfersulfat versetzt. Nach 70 stdg. Rühren bei 30~40°C sog man das Unlösliche ab und goß das Filtrat unter kräftigem Rühren tropfenweise ins Eiswasser, das 25 g Natriumhydrogencarbonat enthielt. Nach Vertreiben des Acetons i. Vak. bei 35°C wurde wenig Natriumsulfit zugesetzt und der Niederschlag wurde abgesogen. Dann schüttelte man das Filtrat dreimal mit je 50 ccm Chloroform aus, wusch die Extraktbrühe zweimal mit Wasser, und verdampfte das Lösungsmittel i. Vak. bei 40°C nach Trocknen über Natriumsulfat. Der rückständige Sirup wurde aus Äthanol-Petroläther umkristallisiert. Man erhielt farblose Kristalle des 3, 4; 5, 6-Di-*O*-isopropyliden-*N*-acetyl-D-glucosaminols (IV) vom Schmp. 158~160°C und $[\alpha]_D^{22}$ −7.8° (*c* 0.97, Methanol). Ausb. 6.2 g (23% d. Th.).

$C_{14}H_{25}O_6N$ (303.4) Gef.: C, 55.16; H, 8.48; N, 4.58; Ber.: C, 55.43; H, 8.31; N, 4.62%.

Nach Eindampfen der wäßrigen Schicht i. Vak., Extrahierung des Rückstand mit etwa 100 ccm heißem Äthanol und Vertreiben des Lösungsmittels i. Vak., erhielt man 16.8 g Sirup, welcher durch Hochvakuumdestillation in zwei Fraktionen geteilt wird, d. h. 2.1 g Erstdestillat vom Sdp.$_{0.005}$ 105~106°C und 13.4 g Hauptdestillat vom Sdp.$_{0.02}$ 190~192°C. Das Erstdestillat kristallisierte sich nach einigen Tagen. Nach Umkristallisierung aus Äther-Petroläther erhielt man farblose Kristalle des 3, 4; 5, 6-Di-*O*-isopropyliden-D-glucosaminols (V) vom Schmp. 65~68°C und $[\alpha]_D^{22}$ +8.5° (*c* 0.97, Methanol). Ausb. 1.8 g (7.7% d. Th.).

$C_{12}H_{23}O_5N$ (261.3) Gef.: C, 55.10; H, 8.63; N, 5.33; Ber.: C, 55.15; H, 8.87; N, 5.36%.

Nach Umkristallisierung des Hauptdestillates aus Äther-Petroläther und dann aus Äthylacetat wurden die Kristalle von IV isoliert. Schmp. und Misch-Schmp. 158~160°C. Ausb. 9.5 g (34.9% d. Th.).

Aus der Mutterlauge wurde die zweite Substanz isoliert. Nach Umkristallisierung aus Äthylacetat erhielt man 2.9 g farblose Kristalle (VI), deren Struktur noch nicht ganz klar ist. Schmp. 170~172°C und $[\alpha]_D^{22}$ −164.1° (*c* 0.66, Methanol).

$C_{11}H_{19}O_5N$ (245.3) Gef.: C, 54.52; H, 8.00; N, 6.08; Ber.: C, 53.86; H, 7.81; N, 5.71%.

Acetonisierung von D-Glucosaminol-hydrochlorid (I).—In eine Lösung von 340 ccm trocknem Aceton und 4 ccm konz. Schwefelsäure wurden 15 g I versetzt und etwa 100 Std bei 30~45°C aufgerührt. Nach Abfiltrierung des unreagierten Materials, Neutralisierung des Filtrates mit eiskalter wäßrg. Natriumhydrogencarbonat-lösung und Vertreiben des Acetons i. Vak., schüttelte man den Rückstand dreimal mit je 50 ccm Chloroform aus, aber kein Produkt wurde extraktiert. Aus der wäßrigen Schicht erhielt man 2.2 g Sirup durch die gleiche Behandlung wie in 1) beschrieben. Aus dem Sirup wurden 1.5 g Destillat (105~106°C/0.005 Torr) erhalten und das Destillat kristallisierte sich sofort. Schmp. und Misch-Schmp. mit V aus II 65~68°C und $[\alpha]_D^{22}$ +8.5° (*c* 0.94, Methanol).

Kalium-3, 4; 5, 6-di-*O*-isopropyliden-*N*-acetyl-D-glucosaminat (VII).—Zu einer Lösung von 7 g IV in 50 ccm Wasser ließ man unter Kühlung und Rühren eine wäßrg. Lösung von 6.3 g Kaliumpermanganat und 2.5 g Kaliumhydroxyd langsam zutropfen. Nach 24 stdg. Stehenlassen bei Zimmertemperatur wurde der Niederschlag abgesogt, das Filtrat mit verd. Salzsäure bis auf pH 9.5 neutralisiert und i. Vak. bei 40°C eingedampft. Der Rückstand ließ sich dreimal in je 20 ccm heißem Äthanol aufnehmen. Daraus wurden 7.8 g (95% d. Th.) farblose Nadeln vom Schmp. 203~204°C und $[\alpha]_D^{22}$ −21.7° (*c* 0.69, Methanol) erhalten.

$C_{14}H_{22}O_7NK$ (355.4) Gef. N, 3.73; Ber.: N, 3.94%.

3, 4; 5, 6-Di-*O*-isopropyliden-*N*-acetyl-D-glucosaminsäure (VIII).—Zu einer Lösung von 2 g VII in 20 ccm Wasser ließ man unter Kühlung eine Lösung von 0.6 g konz. Schwefelsäure in 5 ccm Wasser zutropfen und sofort mit 100 ccm Chloroform ausziehen. Nach zweimaligem Waschen mit Wasser und Vertreiben des Lösungsmittls wurden 1.5 g (84% d. Th.) farblose Nadeln erhalten. Schmp. 195~196°C, $[\alpha]_D^{22}$ −14.9° (*c* 0.77, Methanol).

$C_{14}H_{23}O$-N (317.3) Gef.: C, 53.23; H, 7.25; N, 4.61; Ber.: C, 52.99; H, 7.31; N, 4.41%.

Darstellung von IV aus 3, 4; 5, 6-Di-*O*-isopropyliden-*N*-acetyl-D-glucosamindiäthylmercaptal (X).—In eine Lösung von 6 g X[9] in 20 ccm Aceton versetzte man 40 g feuchtes Kadmiumcarbonat

8) L. F. Wiggins, "Advances in Carbohydrate Chemistry", Vol. 5, Academic Press Inc., New York (1950), S. 191.
9) J. Yoshimura und T. Sato, *J. Chem. Soc. Japan, Pure Chem. Sec.* (*Nippon Kagaku Zasshi*), **80**, 1479 (1959).

und dazu ließ unter kräftigem Rühren eine Lösung von 17 g Quecksilberchlorid in 20 ccm Aceton innerhalb einer Stunde bei Zimmertemperatur zutropfen. Nach 24 stdg. Rühren wurde der Niederschlag abgesogen und zweimal mit je 20 ccm Aceton gewaschen. Man vereinigte das Filtrat und die Waschlauge, vertrieb das Aceton i. Vak. bei 40°C und zog den Rückstand dreimal mit je 50 ccm Chloroform aus. Nach Vertreiben des Lösungsmittels i. Vak. wurde der zurückständige Sirup in 50 ccm Äthanol gelöst und im Autoklaven mit Hilfe von Raney-Nickel bei 40°C unter 20 Atm hydriert. Man filtrierte den Katalysatoren ab, vertrieb das Lösungsmittel i. Vak., löste den Rückstand in wenigem Äthanol, versetzte mit Petroläther bis zur Trübung und nach Einimpfen ließ im Eisschrank stehen. Daraus wurden 0.8 g farblose Kristalle erhalten. Schmp. und Misch-Schmp. mit dem früher dargestellten Produkt 158 ~160°C und $[\alpha]_D^{22}$ −7.5° (*c* 0.85, Methanol).

3,4; 5,6-Di-*O*-isopropyliden-di-*N*,*O*-acetyl-D-glucosaminol (XI).—Zwei Gramme V wurden mit 15 ccm Acetanhydrid in 15 ccm Pyridin behandelt und nach 24 Std. in Eiswasser gegossen. Das Gemisch wurde mit Chloroform ausgezogen und das Filtrat mehrmals mit Wasser, dann dreimal mit wäßrg. Natriumhydrogencarbonat-lösung und nochmal mit Wasser ausgeschüttelt. Nach Trocknen über Natrium sulfat verdampfte man das Lösungsmittel i. Vak. und nahm den gelben, öligen Rückstand auf. Das Produkt wurde i. Hochvak. destilliert. Bei 135~136°C unter 0.002 Torr ging hellgelber, viskoser Sirup über, welcher sich nach einigen Tagen kristallisierte. Nach Umkristallisierung aus Äther-Petroläther erhielt man 1.7 g (64% d. Th.) farblose Nadeln vom Schmp. 61~62°C und $[\alpha]_D^{22}$ +6.7° (*c* 1.04, Methanol).

$C_{16}H_{27}O_7N$ (345.4) Gef.: C, 55.85; H, 7.74; N, 4.22; Ber.: C, 55.64; H, 7.88; N, 4.06%.

Nach der gleichen Behandlung, wie oben beschrieben, wurden 1.4 g IV mit 12 ccm Acetanhydrid in 12 ccm Pyridin behandelt. Man erhielt 0.9 g (54% d. Th.) XI von Schmp. und Misch-Schmp. 61~62°C und $[\alpha]_D^{22}$ +6.5° (*c* 0.95, Methanol).

Hexa-*N*,*O*-acetyl-D-glucosaminol (XII). — Nach der gleichen Behandlung wie oben ließ man 3 g I mit 30 ccm Acetanhydrid in 30 ccm Pyridin acetylieren und erhielt 3.6 g hellbraunen Sirup von Sdp.$_{0.02}$ 190~195°C. Nach Umkristallisierung aus Äthanol-Äther erhielt man 3.1 g (52% d. Th.) farblose Nadeln von Schmp. 95~96°C und $[\alpha]_D^{22}$ −3.7° (*c* 1.07, Methanol).

$C_{18}H_{27}O_{11}N$ (433.4) Gef.: C, 49.27; H, 6.61; N, 3.39; Ber.: C, 49.88; H, 6.28; N, 3.23%.

Nach der gleichen Methode wie oben ließen 3 g II sich in die farblose Nadeln von XII von Schmp. und Misch-Schmp. 95~96°C überführen. Ausb. 3.5 g (60% d. Th.).

Zusammenfassung

Nach der Acetonisierung von *N*-Acetyl-D-glucosaminol in Gegenwart von wasserfreiem Kupfersulfat und konzentrierter Schwefelsäure wurden drei kristallisierende Substanzen isoliert: 3,4; 5,6-Di-*O*-isopropyliden-*N*-acetyl-D-glucosaminol (IV), 3,4; 5,6-Di-*O*-isopropyliden-D-glucosaminol (V) und eine kristalline Verbindung (VI) mit der Formel $C_{11}H_{19}O_5N$. Bei der Acetonisierung von D-Glucosaminol-hydrochlorid in Gegenwart von konzentrierter Schwefelsäure wurde nur V erhalten.

Um die Verknüpfungsstellen von der Isopropylidenresten in IV und V zu bestimmen, wurde IV aus 3,4; 5,6-Di-*O*-isopropyliden-*N*-acetyl-D-glucosamindiäthylmercaptal geleitet und wurden IV und V acetyliert.

Die Oxydation von IV mit Kaliumpermanganat gab Kalium-3,4; 5,6-di-*O*-isopropyliden-*N*-acetyl-D-glucosaminat, welches mit der Wirkung eines kleinen Überschüsses Mineralsäure sich zu der entsprechenden freien Säure geführt wurde.

Wir danken Herrn Dr. Asaji Kondo für die Elementaranalysen und auch Herrn Chikao Kikuchi und Herrn Hirokichi Ono für die Mithilfe bei der vorliegenden Versuchung.

Laboratorium für Organische Chemie
Technische Hochschule Tokyo
Meguro-ku, Tokyo

Studies on the Reduction of Phosphorus Trichloride with Copper Powder in Non or Less Polar Solvents

By Masanao NAKAGAWA

(Received June 20, 1961)

It has been reported in former papers[1-3] that chlorides and oxychlorides of arsenic, vanadium and phosphorus can be partially reduced with copper, and that this reduction leads to the formation of compounds of the chlorides with copper, the chlorides or their lower chlorides with cuprous chloride, and of these elements with copper. Recently, arsenic trichloride[4] and vanadium tetrachloride and oxychloride dissolved in titanium tetrachloride[5] have been studied for their reduction with copper. Little knowledge, however, has been obtained on the reduction of the chlorides of the group V element with copper; the behavior of phosphorus trichloride is particularly unclear,

In the present work the reduction of phosphorus trichloride with copper is studied in non or less polar solvents such as carbon tetrachloride, cyclohexane, silicon tetrachloride, chloroform and tetrachloroethane.

Experimental

Materials.—The solvents and the phosphorus trichloride were purified by normal procedure and stored in a desiccator. The water contents of these solvents was less than 1 mg. per 50 ml. Electrolytic copper powder used, of a purity more than 99.5%, was stored in another desiccator. It passed through a standard sieve of 250 mesh.

Procedure.—In a 100 ml. flask, 0.5 ml. of the trichloride was dissolved in 50 ml. of each solvent or dissolved in a mixture of 5 ml. of silicon tetrachloride and 50 ml. of carbon tetrachloride. The solution of the trichloride was refluxed with 10 or 20 g. of copper powder while being stirred. In another case, 10 ml. of the solution was heated with 4 g. of copper powder in an autoclave with a 20 ml. inner tube of "Teflon", while being shaken. After being cooled, a portion of the supernatant, 2 or 5 ml., was pipeted from the resulting solution and hydrolyzed in a conical flask containing 100 ml. of distilled water by cooling with ice water. The aqueous solution thus obtained, without removing the small amount of the organic phase, was half-saturated with sodium chloride and then titrated with a N/10 sodium hydroxide solution, in the presence of methyl orange and phenolphthalein as indicators, to determine the phosphorous acid and hydrochloric acid derived from the phosphorus chlorides. The procedure of the titration is almost the same as that used for the determination of phosphoric acid in the presence of hydrochloric acid. Another analytical method for chlorine, including chloride other than phosphorus chloride, and phosphorus was also used: An aqueous, hydrolyzed solution was treated with an excess of N/10 silver nitrate, the silver chloride precipitated was filtered off, and the filtrate obtained was titrated with N/10 ammonium thiocyanate after the addition of ferric alum solution as an indicator. Another aqueous, hydrolyzed solution was evaporated to nearly dryness in the presence of nitric acid on a water bath, and the residue obtained was dissolved in water and titrated with a N/10 sodium hydroxide solution as described above. In this method the aqueous solution also was subjected to analyses without removing the small amount of the organic phase. The silicon tetrachloride solution also was hydrolyzed, and the resulting solution was heated with hydrofluoric acid in the presence of perchloric acid and evaporated to nearly dryness; then the residue obtained was analyzed for phosphorus by titration with sodium hydroxide solution.

In these experiments the sampling of the trichloride, solvent, etc., was made in a dry box, and precaution was taken to exclude any effect of water vapor.

Results

Figures 1—4 represent the results of the reflux treatment at 20~140°C, where analyses were made only by the titration with sodium hydroxide. The treatment leads to a decrease in the phosphorus content of the solution and of the ratio of Cl/P, which represents the atomic ratio of chlorine to phosphorus in the solution. This reaction is rather rapid even at a lower temperature, as is shown in Figs. 2 and 3, from which it can be observed that the reaction reaches an equilibrium state within one hour. The percentage of decrease in the phosphorus content depended slightly on the preperty of the solvents and on the temperature of the treatment, although its value in every solution was about 40~50%

1) J. W. Mellor, "A Comprehensive Treatise on Inorganic and Theoretical Chemistry", Vol. VIII, (1928), pp. 1016, 1025.
2) Gmelins Handbuch der Anorganischen Chemie, 8. Aufl. Nr. 17, Arsen (1952), p. 378.
3) Ibid,. Nr. 60, Kupfer, Teil B (1958), p. 225.
4) W. Rudorff and J. Gelinek, *Chem. Ber.*, **90**, 2654 (1957).
5) P. Ehrlich and W. Siebert, *Z. anorg. u. allgem. Chem.*, **302**, 275 (1959).

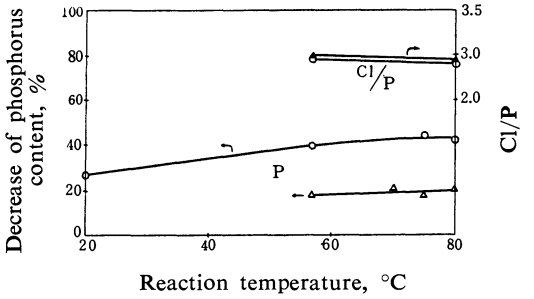


Fig. 1. Temperature dependence of the decrease of the phosphorus content and the value of Cl/P in CCl_4 soln. by the reflux treatment for 1 hr. Reaction temperature represents the temperature of a water bath in which reaction flask is heated.
○ Cu, 20 g. △ Cu, 10 g.

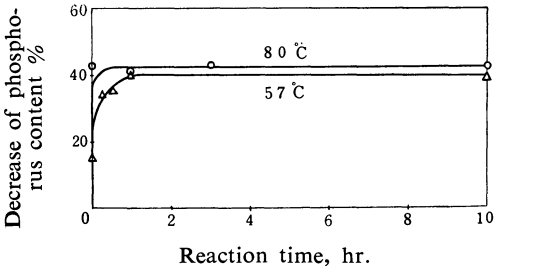


Fig. 2. Reaction time dependence of the decrease of the phosphorus content of CCl_4 soln. by the reflux treatment. Cu, 20 g.

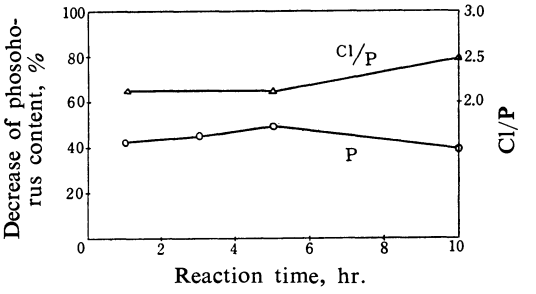


Fig. 3. Reaction time dependence of the decrease of the phosphorus content and the value of Cl/P of $CHCl_3$ soln. by the reflux treatment at 57°C. Cu, 20 g.

under these experimental conditions, whereas the value of Cl/P depended on the property of the solvent, and the values for carbon tetrachloride, chloroform and tetrachloroethane were about 3, 2.2~2.5 and 1.2~1.4 respectively. Cyclohexane, whose graphical representation is omitted, behaved like carbon tetrachloride regarding the percentage of decrease in the phosphorus content and the value of Cl/P, which were 39.6% and 2.96 respectively at 57°C.

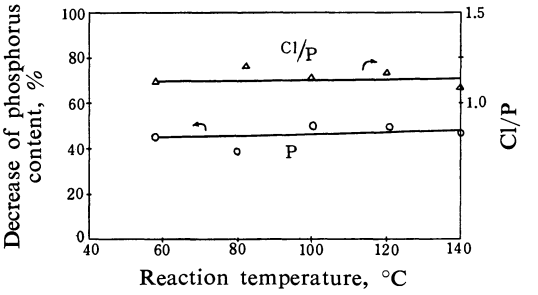


Fig. 4. Temperature dependence of the decrease of phosphorus content and the value of Cl/P of $C_2H_2Cl_4$ soln. by the reflux for 1 hr. Cu, 20 g.

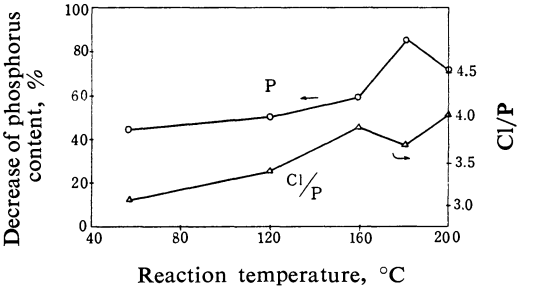


Fig. 5. Temperature dependence of the decrease of the phosphorus content and the ratio of Cl/P of CCl_4 soln. by the autoclave treatment for 1 hr.

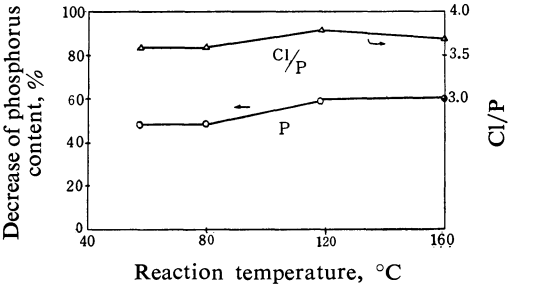


Fig. 6. Temperature dependence of the decrease of the phosphorus content and the ratio of Cl/P of $CHCl_3$ soln. by the autoclave treatment for 1 hr.

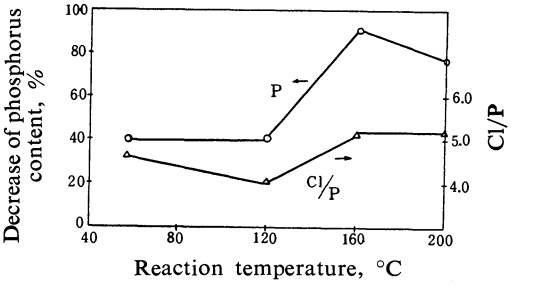


Fig. 7. Temperature dependence of the decrease of the phosphorus content and the ratio of Cl/P of $C_2H_2Cl_4$ soln. by the autoclave treatment for 1 hr.

Figures 5—7 represent the results of the treatment in the autoclave, where analyses were made by titrations with silver nitrate and sodium hydroxide. Although the phosphorus contents of the solutions treated at 56～120°C were comparable to those obtained by the reflux treatment, the ratios of Cl/P of the solution differed from those obtained by the reflux treatment and were more than 3. With an increase in the temperature of the treatment above 160°C, the phosphorus contents decreased and the ratios of Cl/P presented a particular change in every solvent. In the chloroform solutions, the treatment above 160°C gave rise to an obvious change in the quality of the solvent; the copper powder became voluminous and the volume of the liquid phase decreased. Because of this change, the treatment for the chloroform solution was not carried out above 160°C. Some darkening of the surface of copper powder was seen in the treatment at 200°C for the carbon tetrachloride solution and the tetrachloroethane solution. In Fig. 5 or 7, the irregular change in the phosphorus content and the ratio of Cl/P can be observed at 160～200°C, and this change was consistent with the change in the quality of the copper surface at that temperature range. In Figs. 1—7, it can be observed that the percentage of decrease in the phosphorus content in every solution treated by the reflux amounted to nearly the same, 40～50%, whereas the percentage of decrease in the phosphorus content in the carbon tetrachloride solution and the tetrachloroethane solution treated by autoclave at 160 or 180°C amounted to about 85 and 90% respectively, while those treated at 200°C amounted to about 70 and 80% respectively. The value of Cl/P in the former solution treated at 200°C was about 4, and that of the latter solution was about 5.

TABLE I. Cl/P RATIO OF SOLUTION TREATED WITH COPPER FOR ONE HOUR

	Refluxed at 57°C Analyzed by		Autoclaved at 200°C Analyzed by	
Solvent	NaOH	$AgNO_3$, NaOH	NaOH	$AgNO_2$, NaOH
CCl_4	2.97	ca. 3.0	3.30	4.02
$CHCl_3$	.142	3.26	—	3.68[6]
$C_2H_2Cl_4$	1.18	4.75	—	5.15

Table I represents the values of Cl/P in the solutions subjected to the treatments. In Table I it is clear that the values of Cl/P, obtained only by titrations with sodium hydroxide, of the solutions subjected to the reflux treatment were less than 3; this difference afforded a measure of the degree of the reduction, which was higher in more polar solvent. When the estimation of the value of the same solution was made by titration with silver nitrate and sodium hydroxide, the value of every solution became more than 3 and the solution of a more polar solvent took a larger value. The silver nitrate herein used reacts not only with the chloride ion produced by the hydrolysis of phosphorus chloride, but also with cuprous chloride in a solid state and with some others. The Cl/P ratio larger than 3 obtained by this analytical method, therefore, presumably implies the presence of cuprous chloride in the solvent and, in consequence, the reduction of phosphorus trichloride. Such facts were observed for the value of Cl/P in the solutions subjected to the autoclave treatment at 200°C, where the value was larger than 3 even in the case of titration with only sodium hydroxide. In connection with the action of silver nitrate, it also was found qualitatively that the solutions of a more polar solvent subjected to these treatments contained a greater amount of copper compound.

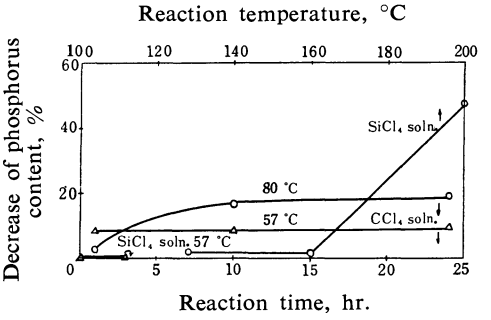


Fig. 8. Effect of $SiCl_4$ on the decrease of phosphorus content. CCl_4 soln. and $SiCl_4$ soln. represents a soln. of PCl_3: $SiCl_4$: CCl_4=1 : 10 : 100 in volume and PCl_3: $SiCl_4$=1 : 100 respectively, Cu, 20 g. in reflux; 4 g. in autoclave.

Figure 8 represents the effect of silicon tetrachloride. A slight decrease in the phosphorus content by the treatment was obtained with the mixed solution of phosphorus trichloride and silicon tetrachloride in carbon tetrachloride. Such facts were observed in the silicon tetrachloride solutions of the trichloride at lower temperatures. Although the phosphorus content presented a marked decrease as a result of the treatment at 200°C, the percentage of decrease was only about 50%, smaller than that in the case of other solvents.

Discussion

From the above results it was considered that the phosphorus trichloride in the solution

6) Representation of the treatment at 160°C.

is primarily decreased by its adsorption on the surface of copper powder; then the trichloride on the surface and in the solution is reduced by another reaction, in which the solvents themselves are dechlorinated[7] with copper and then such dechlorinated products are chlorinated with phosphorus trichloride and with its lower chloride produced by the reduction. This reaction of copper powder yields cuprous chloride, which is insoluble in water and many solvents. The values of Cl/P smaller than 3 were obtained by titration with sodium hydroxide. The values greater than 3, however, were obtained by titration with silver nitrate and sodium hydroxide. These facts suggest that a certain part of the cuprous chloride has been dissolved in the solvents and that this cuprous chloride reacts with silver nitrate. This suggestion contradicts the expectation derived from the solubility of cuprous chloride described above. Thus, it was assumed that cuprous chloride partly reacts with solvents and forms certain complexes, which are soluble in the solvents but only with difficulty soluble in water; such complexes then react with silver nitrate in the aqueous phase in contact with the solvent during analytical procedure. With an increase in the treatment temperature by the autoclave, the compounds of phosphorus trichloride with copper powder are probably transformed into a more reduced form, ultimately into copper phosphides, and this change of the compounds is followed by the darkening of the surface of copper above 140~160°C. Thus, a greater amount of cuprous chloride is produced above this temperature range. The cuprous chloride herein produced is not necessarily in the form of a complex with a solvent, but a part of it may be in the form of another complex which has an ionic property. Such a complex is possibly hydrolyzed during the analytical procedure, thereby leading to the formation of chloride ion and, in consequence, to a greater value of Cl/P, as is shown in the carbon tetrachloride solution at 200°C, in which the value is larger than 3 even in the case of titration only with sodium hydroxide.

Silicon tetrachloride inhibits the reaction of phosphorus trichloride with copper powder. This inhibiting action may be due either to the adsorption of the tetrachloride on the surface of copper powder or to the solvation of phosphorus trichloride with silicon tetrachloride, or it may be due to both the effect of the adsorption and the solvation.

7) Cf. Gmelins Handbuch der Anorganischen Chemie, 8 Aufl. Nr. 60, Kupfer, Teil A (1955), p. 1277.

Summary

A phosphorus trichloride solution in non or less plar solvents was subjected to reaction with copper powder in a flask equipped with a reflux condenser or in an autoclave with an inner tube of "Teflon", and the resulting solution was examined with respect to the phosphorus content and the ratio of Cl/P. By these treatments the phosphorus trichloride was partially reduced with copper powder, and the phosphorus content decreased by the formation of a certain compound of phosphorus trichloride or its lower chloride or phosphorus with copper or cuprous chloride. The degree of the reduction depends on the property of the solvent and on the temperature of the treatment, whereas the decrease in the phosphorus content slightly depends on the property of the solvent. Silicon tetrachloride inhibits the reaction even at 200°C. This action may be due either to the adsorption of silicon tetrachloride on the surface of copper powder or to the solvation of phosphorus trichloride with silicon tetrachloride, or it may be due to the effects of both the adsorption and the solvation.

The author wishes to express his sincere thanks to Mr. Seiichi Ujiie for his helpful co-operation.

Government Chemical Industrial Research Institute, Tokyo
Shibuya-ku, Tokyo

*Studies on Antibiotics and Related Substances. XIV. Synthesis of trans-2-Aminocyclohexyl-D-glucosaminide**

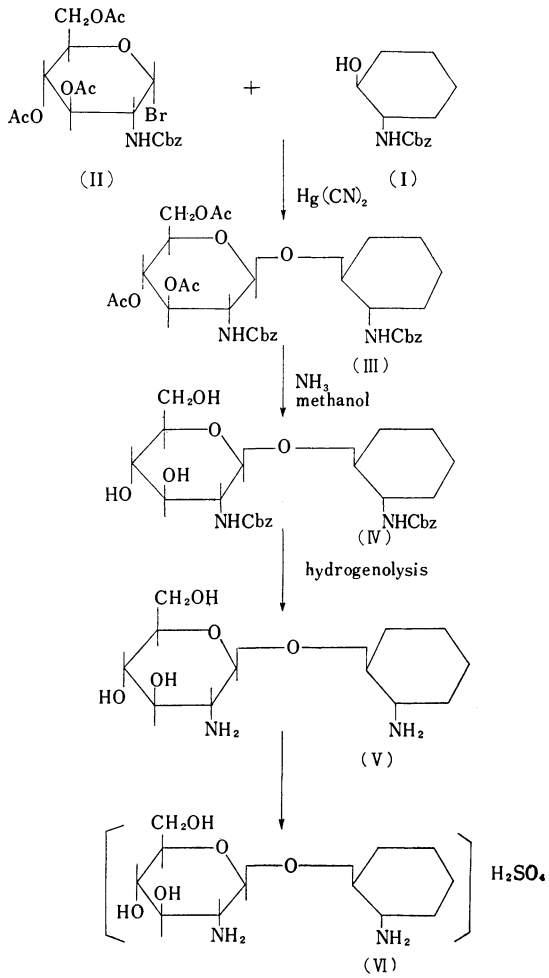
By Tetsuo SUAMI, Seiichiro OGAWA and Sumio UMEZAWA

(Received July 24, 1961)

The interest in inosadiamines and inosamines and inosamines was stimulated by their occurrence in certain antibiotics. Scylloinosadiamine was isolated from streptomycin[1]. Another antibiotics, neomycin[2] and paromomycin[3] contained all-*trans*-2-deoxystreptamine. Pseudoneamine was a glucosaminide of 2-deoxystreptamine[4]. This occurred again in kanamycin[5] in which it linked at C-4 and C-6, respectively, to kanosamine and 6-amino-6-deoxy-D-glucose. Also neosamine-2 was isolated from hygromycin A[6]. So it is desirable to study the relationships between chemical structures and antibiotic activities with model compounds of simpler structure. Besides our interest in this problem has been prompted by the recent development of the structural studies of kanamycin in our laboratory[7].

For this purpose 2-aminocyclohexy-D-glucosaminide is selected. Both cis and trans forms of 2-aminocyclohexanol have been thoroughly characterized[8]. Since the stereochemical studies on streptamine indicate that natural streptamine is the all-trans meso-form[9], *trans*-2-aminocyclohexanol derivatives have been adopted for the present studies.

N-Carbobenzoxy-*d, l-trans*-2-aminocyclohexanol (I) was prepared by carbobenzoxylation



of *d, l-trans*-2-aminocyclohexanol[10] obtained by ammonolysis of 2-chlorocyclohexanol. α-1-Bromo-3, 4, 6-triacetyl-*N*-carbobenzoxy-D-glucosamine (II) was prepared by the method of Irvine et al.[11] and Zervas et al.[12]

The condensation of I and II catalyzed by mercuric cyanide gave β-[*N*-carbobenzoxy-*d, l-trans*-2-aminocyclohexyl]-3, 4, 6-triacetyl-*N*-carbobenzoxy-D-glucosaminide (III) in 19.9% yield.

* This work was reported at the 14th Annual Meeting of the Chemical Society of Japan, Tokyo, April, 1961.

1) H. E. Carter, R. K. Clark, Jr., S. R. Dickman, Y. H. Loo, J. S. Meek, P. S. Skell, W. A. Strong, J. T. Alberi, Q. R. Bartz, S. B. Binkley, H. M. Crooks, Jr., I. R. Hooper and M. C. Rebstock, *Science*, **103**, 53 (1946); M. L. Wolfrom, S. M. Olin and W. J. Polglase, *J. Am. Chem. soc.*, **72**, 1724 (1950).

2) F. A. Kuehl, Jr., M. N. Bishop and K. Folkers, ibid., **73**, 881 (1951).

3) T. H. Haskell, J. C. French and Q. R. Bartz, ibid., **81**, 3480 (1959).

4) M. J. Bartos, *Ann. pharm. franç.*, **16**, 596 (1958).

5) H. Umezawa, M. Ueda, K. Maeda, K. Yagishita, S. Kondo, Y. Okami, R. Utahara, Y. Osato, K. Nitta and T. Takeuchi, *J. Antibiotics, Ser. A*, **10**, 181 (1957); M. J. Cron, O. B. Fordig, D. L. Johnson, D. F. Whitehead, I. R. Hooper and R. U. Lemieux, *J. Am. Chem. Soc.*, **80**, 4115 (1958).

6) J. B. Patrick, R. P. Williams, C. W. Waller and B. L. Hutchings, ibid., **78**, 2652 (1956); R. L. Man and D. O. Wolf, ibid., **79**, 120 (1957).

7) S. Umezawa, Y. Ito and S. Fukatsu, *J. Antibiotics, Ser. A*, **11**, 120 (1958); **11**, 162 (1958); **12**, 187 (1959); S. Umezawa, Y. Ito and S. Fukatsu, This Bulletin, **32**, 81 (1959); S. Umezawa and Y. Ito, ibid., **34**, 69 (1961).

8) G. E. McCasland, R. K. Clark, Jr. and H. E. Carter, *J. Am. Chem. Soc.*, **71**, 637 (1949).

9) S. M. Olin and W. J. Polglase, ibid., **72**, 1724 (1950).

10) A. E. Osterberg and E. C. Kendall, ibid., **42**, 2616 (1920).

11) J. C. Irvine, D. McNicoll and A. Hynd, *J. Chem. Soc.*, **1911**, 250.

12) L. Zervas and S. Konstas, *Chem. Ber.*, **93**, 435 (1960).

The partial hydrolysis of III with absolute methanol saturated with ammonia gave β-[*N*-carbobenzoxy-*d*, *l*-*trans*-2-aminocyclohexyl]-*N*-carbobenzoxy-D-glucosaminide (IV) in 63.1% yield. By the catalytic hydrogenolysis of IV, β-[*d*, *l*-*trans*-2-aminocyclohexyl]-D-glucosaminide (V) was obtained. V was then converted into its sulfate VI by neutralization with dilute sulfuric acid.

Designation of the condensation products as β-anomers is based on their optical rotation and infrared spectra. The optical rotation of V and VI is $[\alpha]_D^{13}$ −71.1° (*c* 1.7, water) and −44.4° (*c* 2, water) respectively. Compared with the optical rotation of kanamycin free base $[\alpha]_D^{13}$ +140° (*c* 1, water)[13] and paromamine free base $[\alpha]_D^{26}$ +114° (*c* 1.35, water)[14] both having α-configurations, that of V and VI are less dextrorotatory and since glucosamine is in D-series, the assignment to V and VI of β-configurations appears to be reasonable. The infrared spectra of III, IV, V and VI show absorption bands at 900, 893, 890 and 891 cm^{-1} respectively, indicating a characteristic absorption band for β-glucoside[15] while kanamycin free base shows absorption bands at 838 and 823 cm^{-1} corresponding to two α-anomeric configurations[16]. So the assignment of β-configuration to III, IV, V and VI will be reasonable.

On the other hand, from the mother liquor of III, a small amount of a crystalline product VII was recovered. Its elemental analysis was identical with that of III, but it showed a sharp and considerably lower melting point. VII was then treated with methanolic ammonia to yield a deacetylated compound VIII. The catalytic hydrogenolysis of VIII gave *d*, *l*-*trans*-2-aminocyclohexyl-D-glucosaminide (IX) but this material was not obtained analytically pure. The optical rotation of IX was $[\alpha]_D^{13}$ +1.8 (*c* 3.9, water).

Considering from the fact that kanamycin and paromamine have strong dextrorotation α-anomer of *d*, *l*-*trans*-2-aminocyclohexyl-D-glucosaminide should have considerably high dextrorotation. Estimating from the molecular rotation of paromamine free base[3], the contribution of the anomeric center to the molecular rotation of *trans*-2-aminocyclohexyl-D-glucosaminide is approximately +30000, and the contribution of the remaining portion is generally about +10000. Thus assuming the β-D-configuration, the molecular rotation of *trans*-2-aminocyclohexyl-D-glucosaminide should be in the order of −20000 and that of α-D-anomer in the order of +40000. So the observed molecular rotation of V (−19600) is in good agreement with the theoretical value for β-D-configuration, but that IX is far below the theoretical value for α-D-configuration. The attempt to obtain pure α-anomer of *trans*-2-aminocyclohexyl-D-glucosaminide by different methods is under way.

13) Ph. D. thesis of K. Maeda, 1958, Keio University.
14) T. H. Haskell, T. C. French and Q. R. Bartz, *J. Am. Chem. Soc.*, **81**, 3481 (1959).
15) S. A. Barker, E. J. Bourne, M. Stacey and D. H. Whiffen, *J. Chem. Soc.*, **1954**, 171; "Methods of Biochemical Analysis", Vol. 3, Interscience (1956), p. 213.
16) M. J. Cron, D. L. Evans, F. M. Palermiti, D. F. Whitehead, I. R. Hooper, Paul Chu and R. U. Lemieux, *J. Am. Chem. Soc.*, **80**, 4741 (1958).

Experimental

α-1-Bromo-3, 4, 6-triacetyl-*N*-carbobenzoxy-D-glucosamine (II).—Starting from commercially available glucosamine hydrochloride, α-1-bromo-3, 4, 6-triacetyl-D-glucosamine hydrobromide was prepared by the method of Irvine et al.[11] in a yield of 20~30%. α-1-Bromo-3, 4, 6-triacetyl-D-glucosamine hydrobromide was introduced with the carbobenzoxyl group by the method of Zervas et al.[12] to give II melting at 97~99°C in a yield of 30% (Found: C, 48.18; H, 4.99; N, 2.89; Br, 15.14%).

***N*-Carbobenzoxy-*d*, *l*-*trans*-2-aminocylohexanol (I).**—A 11.5 g. (0.1 mol.) portion of *d*, *l*-*trans*-2-aminocyclohexanol[9] was dissolved in 50 ml. of water and added with 8.4 g. of sodium bicarbonate. 17.1 g. (0.1 mol.) of carbobenzoxy chloride was added portionwise into the mixture with mechanical agitation. After two hours' agitation at room temperature, the reaction mixture was put in a refrigerator overnight. The precipitate was collected by filtration, washed well with water and dried in vacuo. The colorless crystalline solid weighed 20.5 g. and melted at 94~101°C. The crude product was recrystallized from water-methanol (3:2) to yield 15.8 g. (63.6%) of colorless needles melting at 103~104°C.

Found: C, 67.72; H, 7.67; N, 5.50. Calcd. for $C_{14}H_{19}NO_3$ (249.3): C, 67.44; H, 7.68; N, 5.62%.

β-[*N*-Carbobenzoxy-*d*, *l*-*trans*-2-aminocyclohexyl]-3, 4, 6-triacetyl-*N*-carbobenzoxy-D-glucosaminide (III).—II (2.2 g.), I (1.1 g.) and mercuric cyanide (1.9 g.) were added in 70 ml. of anhydrous benzene and the mixture was refluxed on a boiling water bath for two hours. The reaction mixture was cooled and filtered to remove an insoluble matter. The filtrate was diluted with 180 ml. of chloroform and the solution was washed twice with 100 ml. of 10% sodium chloride solution and three times with cold water. After drying over anhydrous sodium sulfate, the solvent was removed under reduced pressure yielding a pale yellow residue. The residual product was washed with ether to yield 1.55 g. (52.8%) of colorless solid melting at 160~180°C (decomp.).

The product was recrystallized repeatedly from absolute ethanol to yield 0.68 g. (23.2%) of fine needles melting at 201~205°C. $[\alpha]_D^{10}$ +9.6 (*c* 2.7, chloroform).

Found: C, 61.15; H, 6.53; N, 4.35. Calcd. for $C_{34}H_{42}N_2O_{16}$ (670.7): C, 60.88; H, 6.31; N, 4.18%.

β-[*N*-Carbobenzoxy-*d*, *l*-*trans*-2-aminocyclohexyl]-*N*-carbobenzoxy-D-glucosaminide (IV).—Two grams of III was suspended in 100 ml. of absolute methanol saturated with ammonia. After

leaving overnight at room temperature, a clear solution was obtained and evaporated under reduced pressure to yield a colorless residue. The product was washed with warm ethyl acetate to remove acetamide and then recrystallized from isopropanol to yield 1.02 g. (63.0%) of colorless needles melting at 219~221°C (decomp.). A sample further recrystallized for analysis twice from isopropanol melted at 224.5~225°C (decomp.). $[\alpha]_D^{10}$ −31.5° (*c* 2.9, pyridine).

Found: C, 61.94; H, 6.52; N, 4.97. Calcd. for $C_{28}H_{36}N_2O_9$ (544.6): C. 61.75; H, 6.66; N, 5.14%.

β-[*d, l-trans*-2-Aminocyclohexyl]-D-glucosaminide (V).—IV (800 mg.) was suspended in 45 ml. of dioxane-water mixture (1 : 1) and added to a prehydrogenated suspension of 200 mg. of palladium black in 10 ml. of dioxane-water mixture (1 : 1). The reaction mixture was hydrogenated under mechanical shaking at 36~38°C. After four hours, 50 ml. of hydrogen had been absorbed. The reaction mixture was filtered to remove palladium black and the filtrate was evaporated under reduced pressure to yield a colorless syrup. Th product was dissolved in absolute ethanol and added with an hydrous petroleum ether to yield 100 mg. (24.7%) of fine needles melting at 160~161°C (decomp.). $[\alpha]_D^{13}$ −71.1° (*c* 1.7, water).

Found: C, 51.76; H, 8.56; N, 9.99. Calcd. for $C_{12}H_{24}N_2O_5$ (276.3): C, 52.16; H, 8.75; N, 10.14%.

β-[*d, l-trans*-2-Aminocyclohexyl]-D-glucosaminide Sulfate (VI).—The crude free base (470 mg.) was neutralized with 0.1 N sulfuric acid to pH 7 and the solution was filtered to remove a small amount of insoluble matter. Then the filtrate was evaporated under reduced pressure to yield 1 ml. of a residual solution. Addition of absolute ethanol to the residue resulted in precipitation of colorless crystals. After standing for two hours in a refrigerator, the crystals were collected by filtration and washed with absolute ethanol to yield 300 mg. (47.5%) of fine crystals melting at 270~271°C (decomp.). $[\alpha]_D^{13}$ −44.4° (*c* 2, water).

Found: C, 38.07; H, 6.79; N, 7.30. Calcd. for $C_{12}H_{24}N_2O_5 \cdot H_2SO_4$ (374.4): C, 38.49; H, 7.00; N, 7.48%.

***d, l-trans*-2-Aminocyclohexyl-D-glucosaminide (IX).**—After standing the mother liquor of III for five days at room temperature, crystals appeared again and were collected by filtration. The product was recrystallized twice from absolute ethanol to yield 0.15 g. (5.1%) of crystals of *N*-carbobenzoxy-*d, l-trans*-2-aminocyclohexyl-3, 4, 6-triacetyl-*N*-carbobenzoxy-D-glucosaminide (VII) melting at 186~189°C. $[\alpha]_D^{10}$ +16° (*c* 2.6, chloroform). Further recrystallization from absolute ethanol did not raise its optical rotation.

Found: C, 61.01; H, 6.17; N, 4.33. Calcd. for $C_{34}H_{42}N_2O_{12}$ (670.7): C, 60.88; H, 6.31; N, 4.18%.

VII (477 mg.) was suspended in 25 ml. of absolute methanol saturated with ammonia. After standing overnight at room temperature, the solution was evaporated under reduced pressure to dryness. The product was washed with warm ethyl acetate and recrystallized from isopropanol to yield 262 mg. (67.5%) of crystals of *N*-carbobenzoxy-*d, l-trans*-2-aminocyclohexyl-*N*-carbobenzoxy-D-glucosaminide (VIII) melting at 198~199°C. The recrystallization of the product from isopropanol raised the m. p. to 199~200°C. $[\alpha]_D^{15}$ +6.3° (*c* 1.9, pyridine).

Found: C, 61.52; H, 6.55; N, 5.35. Calcd. for $C_{28}H_{36}N_2O_9$ (544.6): C, 61.75; H, 6.66; N, 5.14%.

VIII (189 mg.) was suspended in 10 ml. of dioxane-water mixture (1 : 1) and added to a prehydrogenated suspension of 50 mg. of palladium black in 3 ml. of dioxane-water mixture (1 : 1). After four hours' hydrogenation at 37~39°C, the reaction mixture was filtered to remove palladium black and the filtrate was evaporated under reduced pressure to yield 92 mg. (90.2%) of amorphous solid of IX melting at 190~193°C (decomp.). $[\alpha]_D^{13}$ +1.8° (*c* 3.9, water). The attempt to obtain the product in a crystalline form failed.

Found: C, 49.52; H, 9.01; N, 9.29. Calcd. for $C_{12}H_{24}N_2O_5 \cdot H_2O$ (294.3): C, 48.96; H, 8.90; N, 9.52%.

Chromatography. — No satisfactory chromatographic separation of α- and β-anomer could be accomplished by ascending paper chromatography. Glucosamine hydrochloride, V and IX showed R_f values 0.12, 0.28 and 0.30 respectively in 1-butanol-ethanol-water system (5 : 1 : 4) and 0.12, 0.28 and 0.26 in 1-butanol-acetic acid-water system (4 : 1 : 5). These spots were developed by ninhydrin in pyridine.

Bioassays.—V and IX did not show antimicrobial activity against *E. coli* in a dilution ratio 1 : 1000 by a dilution assay method.

The authors were indebted to Mr. S. Nakada for microanalysis and to Miss S. Fukuyama for bioassays.

Department of Applied Chemistry
Faculty of Engineering
Keio University
Koganei-shi Tokyo

On the Mechanism of Pulp Bleaching. III. Some Properties of Lignosulfonic Acid Treated with Chlorine Water*

By Koichiro SATO and Hiroshi MIKAWA

(Received February 20, 1961)

In part I of this series[1], the present authors reported that when lignosulfonic acid is brought into reaction with chlorine water at 0°C, at least 50% of the sulfonic acid group is split off as sulfuric acid, while the methoxyl group is cleaved as methanol in a yield ca. 80% of the theoretical, when about 4 mol. of chlorine are consumed per methoxyl. As that paper was published in Japanese, the main results of the chlorination of spruce (*Picea jezoensis*) and birch (*Betula Platyphylla*) lignosulfonic acids are cited here again in Figs. 1, 2 and 3. As shown in Figs. 1 and 2, the yield of methanol reaches a maximum at the consumption of about 4 mol. of chlorine and thereafter decreases, probably because of the decomposition of methanol from excess chlorine. The methoxyl content of the residue obtained by evaporation of the solution to dryness after the distillation of methanol decreases very rapidly, as expected, until the yield of methanol reaches a maximum. As is evident from Fig. 2, in which the formation of methanol from birch lignosulfonic acid is shown, the yield of methanol based on the total methoxyl of the lignosulfonic acid is very high, suggesting the formation of methanol not only from guaiacyl but also from syringyl type structural units in a high yield. The amount of sulfuric acid formed during the chlorination is shown in Fig. 3. When about 4 mol. of chlorine are consumed, about 0.5 mol. of SO_4^{2-} are formed per sulfonic acid group in lignin.

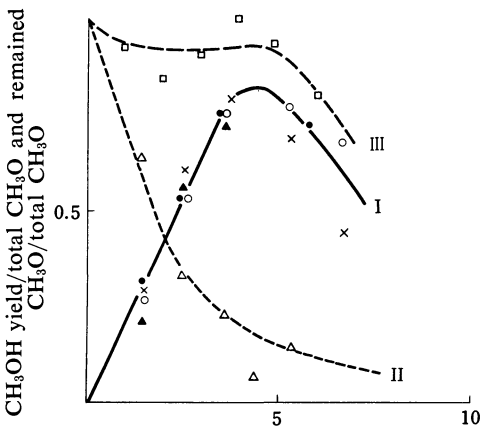


Fig. 1. Formation of methanol from spruce lignosulfonic acid by chlorination. I, mol. ratio of methanol formed to total methoxyl in lignin. II, mol. ratio of methoxyl remaining in the residue after distillation of methanol to total methoxyl in lignin. III, II+I.
[4 g. of Ba-lignosulfonate prepared from spruce (Anal. CH_3O, 11.95%; S in SO_3H form, 4.73%) were dissolved in water, passed through ion exchanger, made up to 100 ml., 20 ml. of this solution were mixed with an appropriate amount of saturated chlorine water at 0°C and analyzed after 16 hr.]

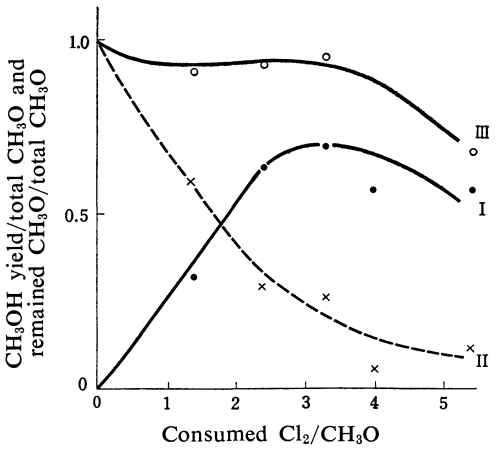


Fig. 2. Formation of methanol from birch lignosulfonic acid by chlorination. I, II and III, same as in Fig. 1. (Experimental conditions are also the same as the case of spruce lignosulfonic acid. Birch lignosulfonic acid, $C_9H_{9.65}O_{2.87}(CH_3O)_{1.40}(SO_3Ba/2)_{0.53}S^{neut}_{0.36}\cdot Ba^{excess}_{0.04}$).

Hibbert[2] assumed that when lignin was treated with chlorine, chlorine atoms were introduced at positions 5 or 6 of the benzene nucleus, the methoxyl group became unstable and the orthoquinone structure was perhaps formed after the cleavage of the methoxyl

* Presented in part at the Second Lignin Symposium of Japan, Tokyo, November, 1957.

1) K. Sato and H. Mikawa, *J. Chem. Soc. Japan, Ind. Chem. Sec.* (*Kogyo Kagaku Zasshi*), **61**, 1090 (1958).

2) H. Schwarz, J. McCarthy and H. Hibbert, *Papar Trade J.*, **113**, 115 (1941).

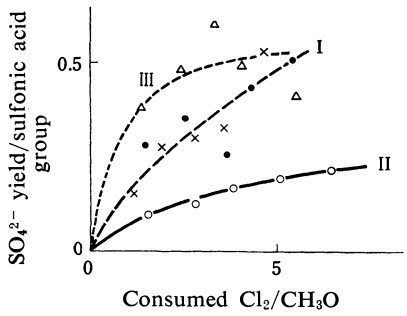


Fig. 3. Formation of SO_4^{2-} from various lignosulfonic acids by chlorination (The conditions of chlorination are the same as those of Figs. 1 and 2).
Curve I, Spruce lignosulfonic acid
Curve II, Methylated spruce lignosulfonic acid
Curve III, Birch lignosulfonic acid

group. Giertz[3] reports that substitution and oxidation reactions may occur when lignin is treated with chlorine water. During the first fifteen minutes the former reaction predominates almost exclusively, while thereafter the latter reaction increases, both reactions being about the same after one hour; after four hours, more than half of the consumed chlorine had been used for the oxidation reaction. Adler[4] has reported recently that the methoxyl groups of the lignin model compounds of the guaiacyl type cleave to give methanol in a good yield when treated with periodate and that guaiacol gives orthobenzoquinone by the same reaction.

It may therefore be expected that carboxyl, carbonyl and/or orthoquinone structures would be formed in the residual lignosulfonic acid in unbleached sulfite pulp when it is treated with chlorine water during the bleaching process. In the present paper, some properties of lignosulfonic acid treated with chlorine water at 0°C were investigated: — 1) the amount of sodium borohydride consumed by the chlorinated lignosulfonic acid, 2) the nature of the weakly acidic group formed by the chlorination, and 3) the change in the ultraviolet and infrared absorption spectra during the chlorination. The main object in the present investigation is, therefore, to see preliminarily the mode of the chemical change of the lignosulfonic acid during its chlorination in aqueous solution at 0°C.

Chlorination of Lignosulfonic Acid

The results obtained when 70, 100, 130 and 160% (by weight) of chlorine were reacted with lignosulfonic acid are shown in Figs. 4, 5, 6 and 7, in which curve I represents the amount of chlorine added, curve II, the chlorine reacted with the lignin, curve III, the amount of carbonyl group estimated from the sodium

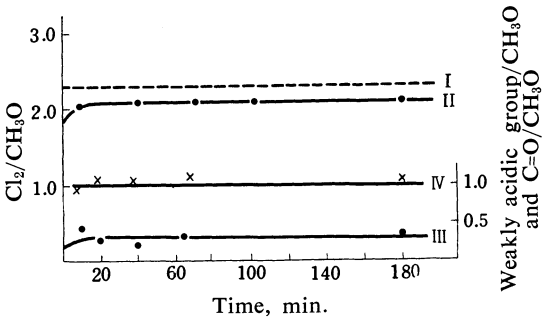


Fig. 4. Chlorination of lignosulfonic acid. 70% of chlorine was added.
I, Chlorine added II Chlorine consumed
III, Carbonyl groups produced IV, Weakly acidic group.

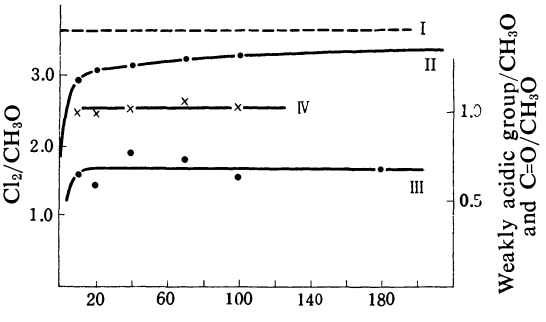


Fig. 5. Chlorination of lignosulfonic acid. 100% of chlorine was added (I, II, III and IV are the same as in Fig. 4).

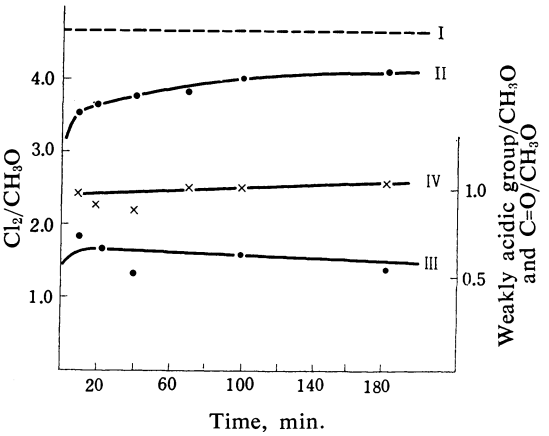


Fig. 6. Chlorination of lignosulfonic acid. 130% of chlorine was added (I, II, III and IV are the same as in Fig. 4).

3) H. W. Giertz, *TAPPI*, **35**, 209 (1951).
4) E. Adler, S. Hernestam and I. Walldén, *Svensk Papperstidn.*, **61**, 641 (1958); E. Adler and R. Magnusson, *Acta, Chem. Scand.*, **13**, 505 (1959).

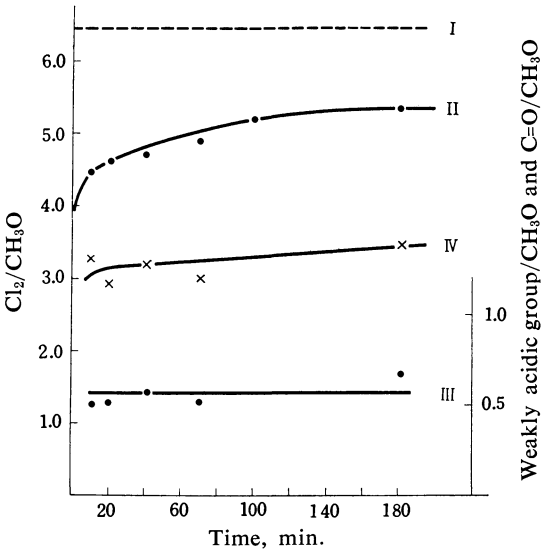


Fig. 7. Chlorination of lignosulfonic acid. 160% of chlorine was added (I, II, III and IV are the same as in Fig. 4).

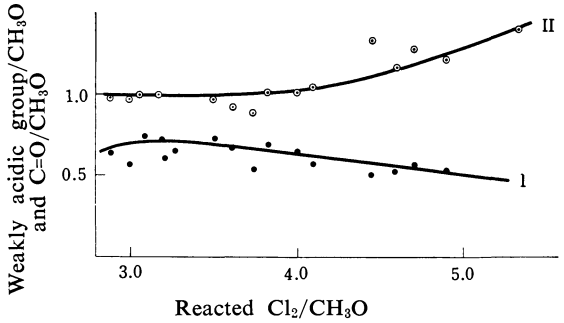


Fig. 8. Formation of weakly acidic groups and carbonyl groups during chlorination.
Curve I, Carbonyl group
Curve II, Weakly acidic group

borohydride consumption, and curve IV, the amount of the weakly acidic group estimated by conductometric titration.

When 70 and 100% of chlorine were used, the amounts of chlorine consumed after twenty minutes were 90 and 85% of the chlorine added respectively. The amount of the consumed chlorine did not exceed 90%, however, even after completion of the reaction.

Curve III in Figs. 4, 5, 6 and 7 shows the amounts of sodium borohydride consumed in the reduction of the reaction mixture with sodium borohydride for various lengths of time, the amounts being expressed for the sake of simplicity as mol. of carbonyl groups equivalent to the sodium borohydride consumed per methoxyl. It must, therefore, be remarked that the carbonyl groups of quinoidal structure, if any, are not calculated as two, because an ordinary carbonyl group consumes two atoms of hydrogen, but quinoidal structure with two carbonyl groups consumes the same amount. Curve IV indicates the amounts of the weakly acidic group. When the amounts of the carbonyl group and of the weakly acidic group of all these figures are plotted against the amount of chlorine consumed, Fig. 8 is obtained. It clearly shows that when the consumed chlorine is lower than 4 mol. per methoxyl, the amount of the weakly acidic group is about 1 equiv./CH_3O, which is distinctly higher than the value of ca. 0.3 equiv./CH_3O of ordinary lignosulfonic acid. After the consumption of about 4 ml. Cl_2/CH_3O, the amount of the weakly acidic group begins to increase, and at the same time the amount of the carbonyl group decreases. This fact might suggest that carbonyl groups, once formed, are oxidized further to give carboxyl groups after the consumption of about 4 mol. of Cl_2/CH_3O.

It must be remarked here that, if no carboxyl groups were formed, the amount of the conductometrically estimated weakly acidic group existing in the solution of chlorination would not exceed one per methoxyl group, insofar as no C_9-building units with more than one phenolic hydroxyl group in a unit—eq. pyrocatechol structure—are formed by chlorination, and only one of the two phenolic hydroxyl groups of the pyrocatechol type structure thus formed is conductometrically titratable.

As shown in Fig. 9, the introduction of chlorine atoms into the nucleus seems to have no influence on the titratability of the carboxyl and phenolic hydroxyl groups (cf. 6-chlorovanillic acid and 5,6-dichlorovanillin), and only one phenolic hydroxyl group of the two phenolic hydroxyl groups of the pyrocatechol structure is conductometrically titratable (cf. protocatechualdehyde and propiocatechon). Moreover, as is evident from Fig. 10, where some hydrochloric acid is added first to the solution of the model compounds almost all of the excess hydrochloric acid was neutralized by adding 3~4 ml. of a 0.1 N sodium hydroxide solution and the remaining excess hydrochloric acid and the phenolic hydroxyl groups were titrated conductometrically, although only one of the two phenolic hydroxyl groups of the pyrocatechol structure is conductometrically titratable, even in the presence of a salt of a strong acid and a base in excess.

The authors will report in a forthcoming paper that some of the pyrocatechol structure may be formed in the chlorination of lignin. As stated above, the maximum amount of the conductometrically estimated weakly acidic group existing in the reaction mixture of chlorination can not exceed one per methoxyl

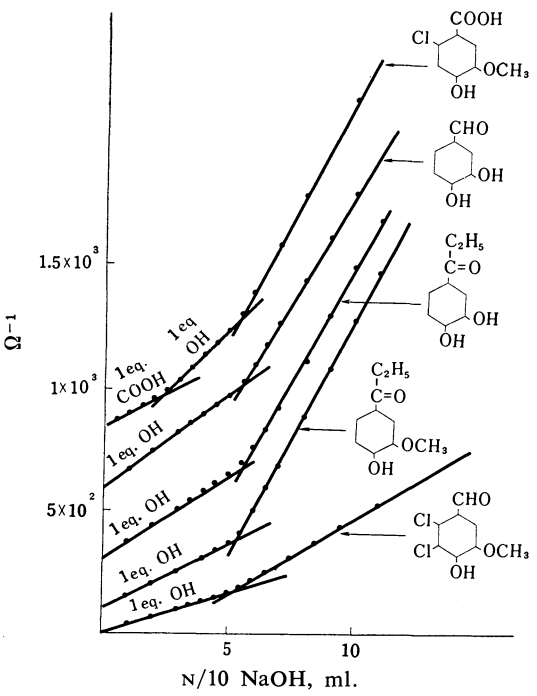


Fig. 9. Conductometric titration curves of some model compounds related to the chlorination of lignosulfonic acid.

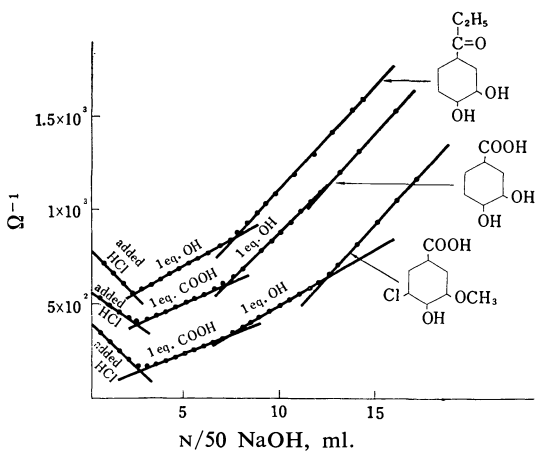


Fig. 10. Conductometric titration curves of some model compounds, titration being performed in the presence of excess hydrochloric acid.

group if no carboxyl group is formed, since it has been proved that only one phenolic hydroxyl of the pyrocatechol structure is conductometrically titratable. Hence it may safely be concluded that at least that part of the weakly acidic group of Fig. 8 exceeding the one-per-methoxyl level may be due to the newly-formed carboxyl group.

The infrared absorption spectra of isolated

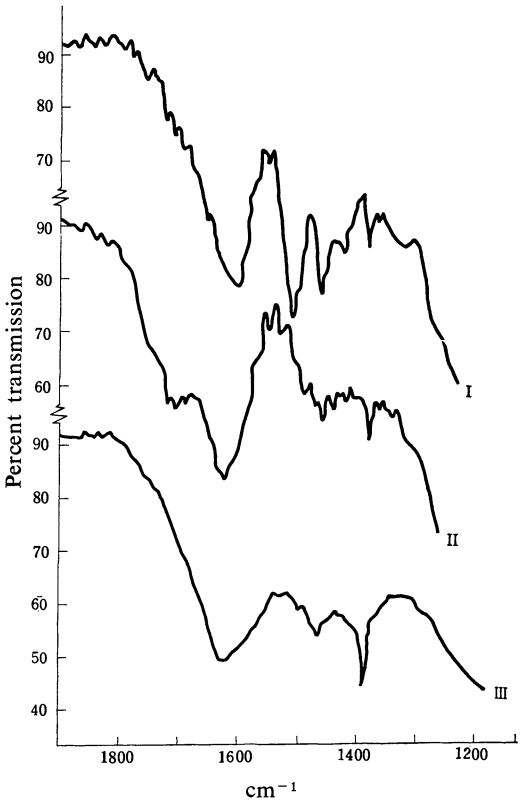


Fig. 11. Infrared absorption spectra of various barium-lignosulfonates. Curve I, Original sulfonate, Curve II, Chlorinated sulfonate; Curve III, Chlorinated sulfonate reduced with $NaBH_4$.

chlorinated barium lignosulfonate also seem to support the theory of the presence of carboxyl groups in it. Figure 11 shows the infrared absorption spectra of ordinary α-lignosulfonic acid (curve I), chlorinated α-lignosulfonic acid (curve II), and chlorinated lignosulfonic acid reduced with sodium borohydride (curve III). Curve II, the absorption spectrum of chlorinated α-lignosulfonic acid, has two absorptions, at 1700 and 1750 cm^{-1}, which do not exist in the case of ordinary α-lignosulfonic acid (curve I). The absorption band at 1700 cm^{-1} disappears after reduction with sodium borohydride, suggesting that this band is due to the carbonyl group. The wave number of this band is somewhat higher than that of the ordinary carbonyl absorption of usual lignin, 1660 cm^{-1} [5]. The wave number of the carbonyl group of lignosulfonic acid seems therefore to shift to the vicinity of 1700 cm^{-1} when chlorine is introduced; similarly, it is known that carbonyl groups of aldehyde, ketone and orthoquinone generally have absorption near 1660 cm^{-1} and

5) H. Sofuye and S. Fukuhara, *J. Chem. Soc. Japan, Ind. Chem. Soc.* (*Kogyo Kagaku Zasshi*), **61**, 1070 (1958).

that this absorption shifts to the 1690 cm^{-1} region when chlorine is introduced into the molecule[6,7].

The absorption at 1751 cm^{-1} seems to be due to the carboxyl group influenced by chlorine, which group is, however, not clear in curve III. There exists, however, anothor, broad absorption at the vicinity of 2610 cm^{-1} which seems to be due to the carboxyl group[7]. It can, therefore, safely be concluded that there exist carbonyl groups and carboxyl groups in chlorinated lignosulfonic acid.

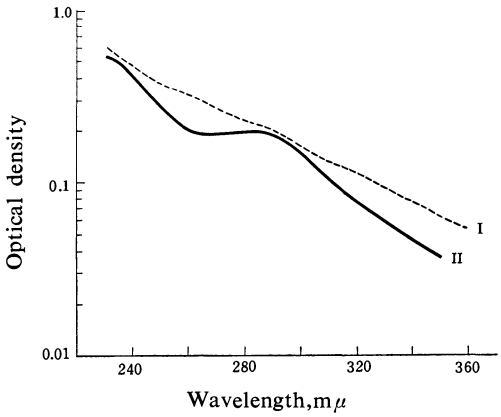


Fig. 12. Ultraviolet absorption curves of the solution of lignosulfonic acid after treatment with chlorine water. Curve I, Reaction mixture not reduced; Curve II, Reaction mixture reduced with sodium borohydride.

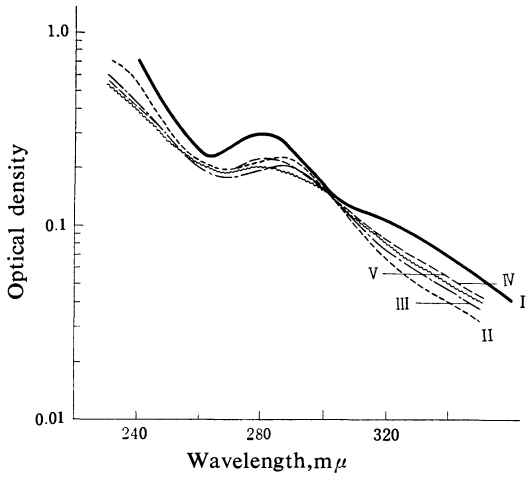


Fig. 13. Ultraviolet absorption curves of lignosulfonic acid at various stages of chlorination. (Spectra were taken after reduction with sodium borohydride.) Curve I, Original; Curve II, $Cl_2/CH_3O=2.09$; Curve III, 3.25; Curve IV, 4.1; Curve V, 5.35.

Figure 12 shows an example of the ultraviolet absorption spectra of lignosulfonic acid both immediately after chlorination and when reduced with sodium borohydride after the chlorination. The former has no minimum and maximum; these reappear only after the reduction. Figure 13 shows the ultraviolet absorption spectra of lignosulfonic acid reduced with sodium borohydride after chlorination to various stages. The minimum and maximum at 263 and 280 mμ in the spectrum of the original lignosulfonic acid shift to 270 and 285 mμ respectively. The fact that the optical density at 285 mμ maximum remains approximately constant might suggest that not very profound structural changes occur when 2 to 5 mol. of chlorine are consumed; i.e., the main part of the benzene ring structure seems not to be destroyed by the chlorination.

Experimental

Barium Lignosulfonate.—Barium lignosulfonate was prepared as usual from spruce (*Picea jezoensis*) sulfite waste liquor by 1-(*N*-piperidinoacetylamino)-naphthalene (PAN)[8], and was analyzed as follows: CH_3O, 11.95; S, 8.07%.

Chlorinated Barium Lignosulfonate.—Barium lignosulfonate (20 g.) was dissolved in a small portion of water and passed through ion-exchange resin in hydrogen form, and an aqueous chlorine solution was added ($Cl_2/CH_3=2.48$). After having been kept at 0°C for 5 min., this was diluted with water, and the chlorinated barium lignosulfonate was precipitated as usual from the above solution by PAN. As it is well known that the chlorine atoms in chlorinated lignin are at least partly unstable to alkali, the separation of the chlorinated lignosulfonic acid from the PAN salt thus obtained was performed as follows: The PAN salt of the chlorinated lignosulfonic acid was suspended in a small amount of water, mixed with ion exchange resin Amberlite IR-120 in hydrogen form, and shaken for about one hour, and then the solution of the chlorinated lignosulfonic acid thus obtained was again passed through ion-exchange resin Amberlite IR-120 in hydrogen form. The solution thus obtained was neutralized with barium carbonate, and the barium salt of the chlorinated lignosulfonic acid was isolated as usual.

Anal. CH_3O, 2.82; Cl, 12.45; Ba, 24.21%.

Chlorination.—Barium lignosulfonate containing 5 mmol. of the methoxyl group was dissolved in a small amount of water, passed through ion exchange resin in hydrogen form, and increased to 30 ml. To the lignin solution thus obtained were added, at 0°C, 190 ml. of an aqueous chlorine solution containing 23.2 mmol. of chlorine (the weight of chlorine is approximately 130% of that of lignin), and the whole was maintained at 0°C while being stirred. At definite periods, 1 ml. of the solution

6) Marie-Louise Josién, N. Fuson and Jeanne-Marie Lebas, *J. Chem. Phys.*, **21**, 331 (1953).

7) L. J. Bellamy, "The Infra-red Spectra of Complex Molecules", Methuen & Co., London (1954).

8) B. Leopold, *Acta Chem. Scand.*, **6**, 64 (1952).

was sucked out and the amount of the chlorine consumed was measured iodometrically as usual. Another 30 ml. of the reaction solution was also sucked out into a graduated flask of 40 ml. capacity, several drops of allyl alcohol were added, the pH adjusted by alkali to 7, and increased to just 40 ml. Half of this solution was used for the sodium borohydride reduction, and the other half for conductometric titration.

Amount of Chlorine Consumed. — The amount was determined iodometrically as usual. No correction is applied for the orthoquinone structure which might be formed during the chlorination and thus exist in the solution. As is known, the orthoquinone structure is able to isolate iodine[9] from the iodide solution.

Reduction with Sodium Borohydride.—The above-mentioned solution (20 ml.) from the chlorination was reduced with sodium borohydride for one hour according to the method of Lindberg[10]. As a control experiment, vanillin, 5-chlorovanillin, acetoguaiacon, propioguaiacon, camphorquinone and β-naphthoquinone were reduced by this method. The amount of the consumed borohydride were 100, 102, 97, 104, 96.6 and 104% of the theoreticals

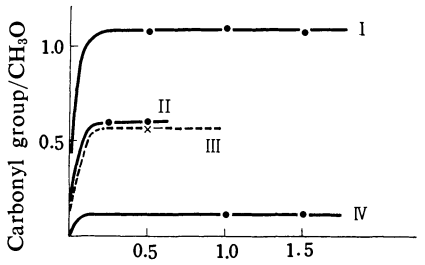


Fig. 14. $NaBH_4$ reduction of several lignin samples. Curve I, Chlorinated thiolignin ($Cl_2/CH_3O=4.58$); Curve II, Chlorinated hydrochloric acid lignin ($Cl_2/CHO_3=2.26$); Curve III, Chlorinated barium lignosulfonate; Curve IV, Thiolignin.

respectively. The chlorinated lignosulfonic acid isolated from the chlorination solution was also reduced. As is evident from Fig. 14, one hour is sufficient for complete reduction.

Conductometric Titration.—Four milliliters of the above-mentioned neutral solution (40 ml.) prepared from the chlorination solution were eluted through ion exchange resin in hydrogen form and were neutralized with 4~5 ml. of a 0.1 N sodium hydroxide solution in order to neutralize a part of the hydrochloric acid. The solution thus obtained was titrated conductometrically with a 0.02 N sodium hydroxide solution. The amount of the weakly acidic group and/or weakly acidic substances were determined from the difference in the titers of the second and the first "breaks".

Ultraviolet Absorption Spectra. — The solution obtained after the above-mentioned reduction with sodium borohydride contains reaction products in reduced form. One milliliter of this solution was diluted to 50 ml. with water, and the ultraviolet absorption spectra were measured and shown directly as the optical density of the solution.

Infrared Absorption Spectra. — The infrared absorption spectra of barium lignosulfonate and chlorinated barium lignosulfonate were measured by the potassium bromide method using a Koken D 101 type infrared spectrophotometer (Japan).

Syntheses of the Model Compounds for the Conductometric Titration. — 5-Chlorovanillic acid was obtained by the oxidation of 5-chlorovanillin with silver oxide[11]; propiocatechon and propioguaiacon, by the condensation of propionic acid with catechol and guaiacol, according to the method of Nakazawa[12], and 5,6-dichlorovanillin, according to the method of Laiford[13].

The authors wish to express their sincere thanks to Professor Yoshikazu Hachihama of Osaka University, for his unfailing kindness in encouraging this work and to Kokusaku Pulp Co. for its permission to publish this paper.

Research Laboratory of the Kokusaku Pulp Ind. Co., Ltd. Shinjuku-ku, Tokyo

9) H. Meyer, "Analyse und Konstitutionsermittlung Organischer Verbindungen", 5. Aufl.), Verlag von Julius Springer, Berlin (1931), p. 628.
10) B. Lindberg and A. Misiorny, *Svensk Papperstidn.*, 55, 13 (1952); B. Lindberg and J. Pajv. *Svensk Kem. Tidskr.*, 65, 9 (1953).
11) I. A. Pearl, *J. Am. Chem. Soc.*, 68, 1100 (1946).
12) K. Nakazawa, *J. Pharm. Soc. Japan* (*Yukagaku Zasshi*), 54, 836 (1954).
13) L. C. Raiford and J. G. Lichty, *J. Am. Chem. Soc.*, 52, 4576 (1930).

On the Mechanism of Pulp Bleaching. IV. Extracts from Unbleached Sulfite Pulp with Dimethyl Sulfoxide*

By Koichiro SATO, Akio KOBAYASHI and Hiroshi MIKAWA

(Received February 20, 1961)

As already reported, a part of the residual lignosulfonic acid in unbleached sulfite pulp can be dissolved by beating the pulp in water violently[1]. This lignin seems to have existed between fibrils. The chemical nature of this residual lignosulfonic acid was also investigated briefly. About 75~80% of the residual lignosulfonic acid remained, however, undissolved in the beaten pulp. It is therefore attempted, in the present communication, to isolate and investigate this residual lignosulfonic acid remaining in the beaten pulp.

Recently Björkman succeeded in extracting the so-called lignin-carbohydrate complex (LCC) with a solvent like acetic acid, dimethyl formamide or dimethyl sulfoxide, after having extracted the so-called milled wood lignin (MWL) from the finely milled wood powder with aqueous dioxane[2].

Lindgren[3] separated this LCC into a pure carbohydrate component consisting of carbohydrate and lignin chemically combined in a one to one ratio by using the technique of electrophoresis on glass fiber paper. Kawamura and Higuchi[4] isolated lignin preparation from beech wood by several different methods and recognized paper-chromatographically that a part of the lignin is chemically combined with xylose and xylobiose. In his investigation of the biosynthesis of lignin, Freudenberg obtained a compound consisting of both carbohydrate and coniferyl alcohol chemically combined[5]. A recent accumulation of experimental results seems to have confirmed almost definitely, the existence of a chemical combination of both the components in wood, although the mode of the combination remains to be investigated as yet.

It has, therefore, been attempted to dissolve the lignin, carbohydrate and lignin-carbohydrate complex, if any, from the unbleached sulfite pulp, which has already been beaten in water and extracted exhaustively with water, with dimethyl sulfoxide, to see if such materials can be extracted with this solvent and, if so, to investigate the chemical nature of the extracted materials.

Already extracted beaten pulp was repeatedly extracted further with dimethyl sulfoxide, and a grayish white powder was obtained. The yield was of the order of 10% of the pulp. The material contains about 6% methoxyl group, has ultraviolet absorption spectra characteristic of lignin, and gives a sugar mixture on hydrolyzation of the material. It is therefore evident that the materials contains both lignin and carbohydrate. In order to know whether the carbohydrate component and the lignin component exist independently or whether they are combined chemically in the material, the material was separated electrophoretically on a filter paper; it was found that there exists no chemical combination between the two components. The carbohydrate component and the lignin component were next separated by zone electrophoresis on cellulose powder, and both the components were investigated separately.

Preparation of the Dimethyl Sulfoxide (DMSO) Extract.—Unbleached sulfite paper pulp from spruce (*Picea jezoensis*, 1615 g.) was beaten in water until no more water-soluble residual lignosulfonic acid dissolved out, and then the beaten pulp was dried, crushed with a disk refiner, and respectively extracted with absolute dimethyl sulfoxide at room temperature (total amount of dimethyl sulfoxide: 50 l.). Figure 1 shows the ultraviolet absorption curves of DMSO extracts from spruce pulp. The dimethyl sulfoxide solution thus obtained was concentrated in vacuo and poured into alcohol, and the precipitate was dissolved in water and reprecipitated with alcohol. The yield of the water-soluble grayish-white "dimethyl sulfoxide extract" thus obtained was 18 g.

Dimethyl Sulfoxide Extract.—As no sugars are found in the extract by paper chromatography, the carbohydrate portion of the extract must be water soluble hemicellulose. The amount of hemicellulose in the extract and the component sugars were determined by hydrolyzing the extract (50 mg.) with 4% sulfuric acid (4 ml.) in an ampoule at 100°C for 8 hr.

* Presented at the 4th Lignin Symposium of Japan, Kyoto, November, 1959.

1) K. Sato and H. Mikawa, This Bulletin, 35, 477 (1962).
2) A. Björkman, *Svensk Papperstidn.*, 60, 243 (1957).
3) B. O. Lindgren, *Acta Chem. Scand.*, 12, 447 (1958).
4) I. Kawamura and T. Higuchi, *J. Soc. Tex. Cell. Ind., Japan*, 7, 269 (1951).
5) K. Freudenberg and G. Grion, *Chem. Ber.*, 92, 1355 (1959).

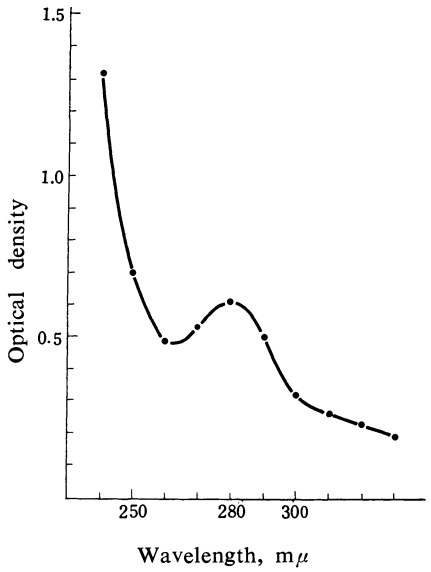


Fig. 1. Ultraviolet absorption curve of the "dimethyl sulfoxide extract" obtained by extracting the beaten unbleached sulfite pulp by dimethyl sulfoxide (52.0 mg. in 300 ml. water).

The total amount of the sugars was determined by Somogyi's method, and the component sugars, by paper chromatography[6]. The amount of the lignin in the extract was estimated from the ultraviolet absorption, the methoxyl content of lignin being assumed as 10.83% and the molar extinction at 280 mμ, as 2870 per CH_3O. The values obtained for the residual lignosulfonic acid in the previous paper[1] were used. The results are shown in Table I. It will be seen from the table that the carbohydrate component consists almost exclusively of xylose.

In order to know the nature of the lignosulfonic acid existing in the dimethyl sulfoxide extract, the extract was titrated conductometrically (Fig. 2). Assuming that all of the strong acid is attached to lignin as a sulfonic acid group, SO_3H/CH_3O was calculated as 0.32, which is considerably lower than that (0.5～0.6) of the ordinary lignosulfonic acid, and the presence of a weakly acidic group is not clear. To make clearer the nature of the residual lignosulfonic acid in the dimethyl sulfoxide extract, the isolation of it free from carbohydrate was attempted.

TABLE I. ANALYSES OF THE "DIMETHYL SULFOXIDE EXTRACT"

Lignin		35.1%	96.9%
carbohydrate		61.8%	
Component sugars	Xylose	94.6%	
	Arabinose*	1.6%	
	Mannose		
	Glucose	2.4%	
	Galactose	1.4%	
CH_3O		5.33%	

* As arabinose shows the same R_f as that of mannose by paper chromatography, it was calculated as mannose.

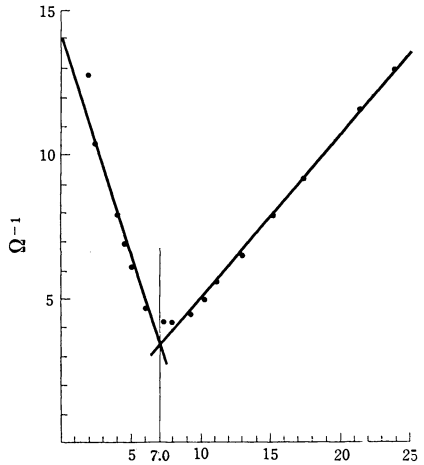


Fig. 2. Conductometric titration of the "dimethyl sulfoxide extract" obtained from the beaten pulp.

The simplest way to isolate the lignin in its sulfonated form, free from carbohydrate, is to sulfonate "the extract" in an acidic condition in order to hydrolyze the linkage between lignin and carbohydrate, if any, and to isolate the lignin in the form of lignosulfonic acid. The extract (4.73 g.) was dissolved in an ampoule in a cooking acid (100 ml. pH 4.2) prepared from 5% sodium hydroxide and sulfur dioxide and cooked at 135°C for 5 hr. The lignosulfonic acid was separated with 1-(*N*-piperidinoacetylamino)-naphthalene as usual. The analytical values of the lignosulfonic acid

TABLE II. ANALYSES OF THE DIMETHYL SULFOXIDE EXTRACT AND THE LIGNOSULFONIC ACID PREPARED FROM THE EXTRACT BY SULFONATION

	Dimethyl sulfoxide extract	Lignosulfonic acid prepared from the extract
CH_3O	5.33%	11.84%
S in SO_3H form	1.77%	4.54%
SO_3H/CH_3O	0.32	0.37
Phenolic OH/CH_3O	—	0.21～0.26
Type I OH/ Type II OH		1 : 4

6) H. Toda and T. Hamada, *J. Jap. Tech. Ass. Pulp. Paper Ind.*, **11**, 429 (1957).

thus prepared and that of the dimethyl sulfoxide extract are shown in Table II.

From the conductometric titration and the spectrum change during the titration[7], the ratio between the type I and the type II phenolic hydroxyl group was found to be ca. 1/4, which is a little lower than that between residual lignosulfonic acid dissolved by beating (1/3～1/4) and ordinary soft wood α-lignosulfonic acid (1/3).

On the Non-existence of the Linkage between Lignosulfonic Acid and Carbohydrate in the Dimethyl Sulfoxide Extract.—As it was thought to be highly possible that the lignin and carbohydrate in the dimethyl sulfoxide extract are chemically combined, the possibility of any linkage between the components was investigated by paper electrophoresis.

An aqueous solution of dimethyl sulfoxide extract was applied quantitatively (1.1 mg. in 0.05 ml.) on the cathodic side of a paper strip (Toyo Roshi Co., No. 50., 2×40 cm.) soaked with a 0.05 N sodium hydroxide solution and developed electrophoretically for 2.5～3 hr., the current density being maintained at 3 mA per paper strip. The paper strip was cut into pieces 2 cm. in length, and every piece was separately eluted with definite amount of water. The eluates were examined spectroscopically. As shown in Fig. 3, the absorption curves are characteristic of lignin. The lignin content of the eluates was therefore calculated from optical density at 280 mμ. For the carbohydrate assay, another paper strip developed similarly at the same time was eluted in just the same manner as in the case of lignin with 1 N sodium hydroxide. Carbohydrate was difficult to elute with water, but with sodium hydroxide it could be eluted very easily. Although the elution was repeated three times, the first elution was almost enough to extract all of the carbohydrate. The carbohydrate thus obtained was estimated as xylose by Somogyi's method.

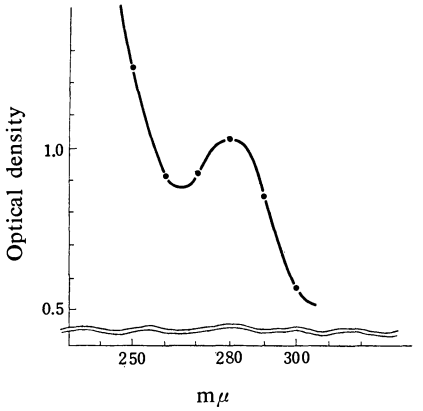


Fig. 3. Ultraviolet absorption curve of the solution of residual lignosulfonic acid obtained by developing electrophoretically the dimethyl sulfoxide extract on a paper strip and eluting the lignosulfonic acid from the strip.

7) H. Mikawa, K. Sato, C. Takasaki and K. Ebisawa This Bulletin, **28**, 653 (1955).

The distribution of the lignin and the carbohydrate over the paper strip thus discovered is shown in Fig. 4. The values are corrected for the blank values due to the impurities coming from the paper, which were not very large. The total amount of the lignin and the carbohydrate thus recovered from the developed paper strip was nearly 100%, as is shown in Table III.

As is evident from the figure, carbohydrate and lignin migrate almost independently. As it does not seem very probable that some linkage between the components existed before the electrophoresis and that this linkage was ruptured during the electrophoresis, the existence of any chemical linkage may not be expected between lignin and carbohydrate in dimethyl sulfoxide extract, just as in the case

Table III.

Carbohydrate eluted	64.4%*
Lignin eluted	40.2%
Total	104.6%

* % based on the materials applied.

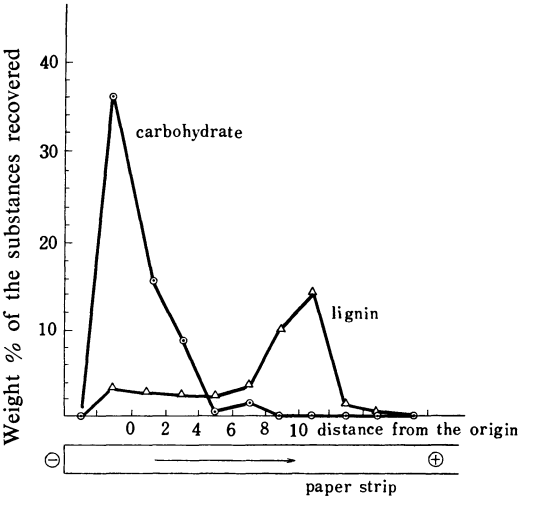


Fig. 4. Distribution of residual lignosulfonic acid and carbohydrate component of dimethyl sulfoxide extract after the development by electrophoresis on a paper strip. The ordinate means the weight percent of the substances obtained by eluting pieces of paper strip cut into 2 cm. length against the total amount of lignin or carbohydrate in the material applied to the origin.

of the residual lignosulfonic acid isolated by beating.

Lignosulfonic Acid in Dimethyl Sulfoxide Extract Separated by Zone Electrophoresis.— In order to investigate the lignin in the extract in detail, the isolation of it free from carbohydrate was attempted. As it was found that electrophoresis is suited for this purpose, zone electrophoresis was applied to the extract. Cellulose powder (Schleicher u. Schüll), which had been exhaustively extracted with 0.05 N sodium hydroxide until the washings no longer showed any absorption at 280 mμ, was used together with 0.05 N sodium hydroxide as the carrier. Five hundred milligrams of DMSO extract was dissolved in a small portion of water, mixed with warm dilute agar-agar solution, and poured into a hole made in the slurry of cellulose powder at the origin of the cathodic side. After the agar-agar solution solidified, the extract was developed with a constant current density of 80 mA per 10 cm^2. This procedure was repeated six times, and then all the carbohydrate-free lignin portions were mixed and eluted with water, and the lignin was separated as barium salt using 1-(*N*-piperidinoacetylamino)-naphthalene as usual. The total yield was 0.557 g. The ultraviolet absorption curve of the lignosulfonic acid thus obtained is characteristic of lignin; the analytical values are listed in Table IV. It may be seen that the degree of sulfonation is low and that the ratio of type II phenolic hydroxyl group to the total phenolic hydroxyl groups is high. This lignosulfonic acid prepared by zone electrophoresis is otherwise not very different from the lignosulfonic acid reported previously, which had been obtained by a drastic beating of pulp.

Table IV. Analyses of the barium salt of the residual lignosulfonic acid extracted from beaten unbleached sulfite pulp by dimethyl sulfoxide and purified by electrophoresis

CH_3O	11.01%
SO_3H/CH_3O	0.34
Total phenolic OH/CH_3O	0.17~0.21
Type I phenolic OH/CH_3O	0.04
Type II phenolic OH/CH_3O	0.13~0.17
Type I OH/type II OH	1 : 3~4
$COOH/CH_3O$	0.15~0.16
Diffussion coefficient of McCarthy's method[8]	9.25 cm^2/day

The authors wish to express their sincere thanks to Professor Yoshikazu Hachihama of Osaka University for his unfailing kindness in encouraging this work, and to Kokusaku Pulp Co. for their permission to publish this paper.

Research Laboratory of the Kokusaku Pulp Co., Ltd. Shinjuku-ku, Tokyo

8) V. F. Felicetta, A. E. Markham, Q. P. Peniston and J. L. McCarthy, *J. Am. Chem. Soc.*, **71**, 2879 (1951).

*Studies on Solid Carbons. I. The Formation of Solid Carbons**

By Masakazu SAKAGUCHI**

(Received June 20, 1961)

The physical and chemical properties of solid carbons are markedly affected by differences in manufacturing methods and starting material.

Many works[1-15] have reported findings by a number of researchers on the reaction kinetics of carbon formation by the pyrolysis of hydrocarbons and on the properties of the

* The main part of this work was presented at the 13th Annual Meeting of the Chemical Society of Japan, Tokyo April, 1960.

** Present address: Department of Chemistry, Faculty of Engineering, Niigata University, Nagaoka City.

1) J. E. Zanetti and G. Egloff, *Ind. Eng. Chem.*, **9**, 350 (1917).
2) L. S. Kassel, *J. Am. Chem. Soc.*, **54**, 3949 (1932).
3) C. R. Kinney and E. DelBel, *Ind. Eng. Chem.*, **46**, 548 (1954).
4) H. Leidheiser, Jr. and A. T. Gwathmey, *J. Am. Chem. Soc.*, **70**, 1206 (1948).
5) W. G. Parker and H. G. Wolfhard, *J. Chem. Soc.*, **1950**, 2038.
6) G. Porter, "Fourth Symposium (International) on Combustion", The Williams and Wilkins Co., Baltimore, Md. (1953), p. 248.
7) L. J. E. Hofer, E. Sterling and J. T. McCartney, *J. Phys. Chem.*, **59**, 1153 (1955).
8) C. W. Sweitzer and G. L. Heller, *Rubber World*, (September), 855 (1956).
9) C. R. Kinney, "Proceedings of the First and Second Conferences on Carbon", Waverly Press, Inc., Baltimore, Maryland (1956), p. 83.
10) R. E. Ferguson, *Combustion and Flame*, **1**, 431 (1957).
11) M. E. Miberg, *J. Phys. Chem.*, **63**, 578 (1959).
12) P. L. Walker, Jr., J. F. Rakszawski and G. R. Imperial, ibid., **63**, 133 (1959).
13) R. G. Haldeman and M. C. Botty, ibid., **63**, 489 (1959).
14) W. R. Smith, ibid., **63**, 173 (1959).
15) M. N. Plooster and T. B. Reed, *J. Chem. Phys.*, **31**, 66 (1959).

carbons produced, but much remains unexplored.

In this report, we are presenting the physical properties of carbons produced by the pyrolysis of hydrocarbons, which have been studied by means of electron microscopy, X-ray diffraction the B. E. T. method and the Kelvin method.

Experimental

Materials.—The applied hydrocarbons, benzene, toluene naphthalene and *n*-hexane were "extra pure grade" reagents supplied by the Wako Junyaku Co., Ltd. Ethylene was prepared by dehydrating ethyl alcohol with concentrated sulfuric acid; it was then purified by vacuum distillation. Methane was provided by the Nihon Kei Kinzoku Co., Ltd. and was passed through a concentrated potassium hydroxide aqueous solution and a calcium chloride tube. Further, this was distilled in vacuo for purification.

Apparatus and Procedure.—The apparatus used for the reaction, constructed of soda-glass except for the reaction tube, is shown in Fig. 1. In this figure, A_1 is a graduated sample vessel which was used for benzene, toluene or *n*-hexane. A_2 is a gas reservoir for methane or ethylene, and A_3 is a side tube of the reservoir. B is a reaction tube made of transparent quartz 2.5 cm. in diameter and 100 cm. long. In the reaction tube, porcelain insulators 0.5 cm. in diameter and 2.5 cm. long are packed to facilitate the pyrolysis of hydrocarbons.

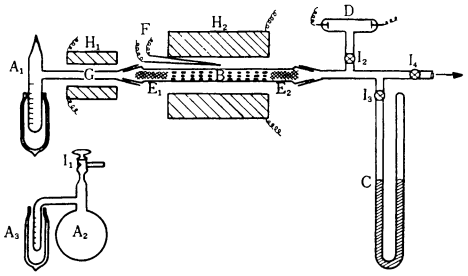


Fig. 1. Apparatus for pyrolysis.

Inside both ends of the tube, glass wool (E_1, E_2) was loosely packed to avoid contamination by the tarry materials produced during the pyrolysis. The tube was connected by a ground glass joint to a vacuum system. H_1 is a pre-heating heater, and H_2 is an electric furnace about 50 cm. long. The temperature of the furnace was controlled (± 1°C) automatically.

In the case of liquid materials, a certain amount (5 cc.) of each material in A_1, kept at the temperature of liquid oxygen (−183°C), was evacuated. The liquid oxygen bath was then removed to melt the frozen material and to draw off any gas involved in it. In order to remove the gas completely, such treatments were repeated three times.

In the cases of methane and ethylene, A_2 was used instead of A_1. The materials (10 cc. of liquid state) were introduced to A_3 by cooling with a liquid oxygen bath (for methane) or with a conical aluminum powder bath, the top of which was immersed in liquid oxygen to maintain the temperature of the bath at −135°C (for ethylene).

In the case of naphthalene, 10 g. of it was loosely packed in an inlet, G.

The pyrolysis was carried out at two temperatures, 800 and 1100°C, and the flow rate of the materials was kept constant at 2.5 cc. per hour, by controlling the opening of tap I_4 and also the temperature of the sample vessel, A_1, A_3 or G. For benzene, toluene and *n*-hexane, the temperatures of the sample vessel were 23, 47 and 12°C respectively, while for methane and ethylene, they were −183 and −135°C respectively. That of naphthalene was 140°C. At these temperatures, the same vapor pressure (83 mmHg) held for all materials. The rates of the consumption of materials were measured with the graduations of the sample vessel. During the pyrolysis, part G was always heated at 200°C (except in the case of naphthalene) to prevent condensation of the materials. After a certain amount of the liquid material had been consumed, A_1 was cooled with a liquid oxygen bath to stop the reaction. In the cases of ethylene and methane, tap I_1 was closed to the stop position. Then tap I_4 was opened completely, and the reaction system was evacuated to remove the tarry substances formed during the reaction; the reaction tube was cooled, it was cut off, and the insulators which had been covered with the carbon produced were taken out. The impurities contained in all the carbon were removed by treating them with aceton and carbone tetrachloride.

The surface areas and the micro-pore size distributions of the carbons were obtained from the adsorption and the desorption of methane gas at the temperature of liquid oxygen (−183°C). The B. E. T. method was applied on the results of the adsorption isotherms to determine the surface areas of the carbons by assuming 18.1 Å^2 as the cross-sectional area of methane; Kelvin's equation was applied to the desorption isotherms to determine the micro-pore size distributions.

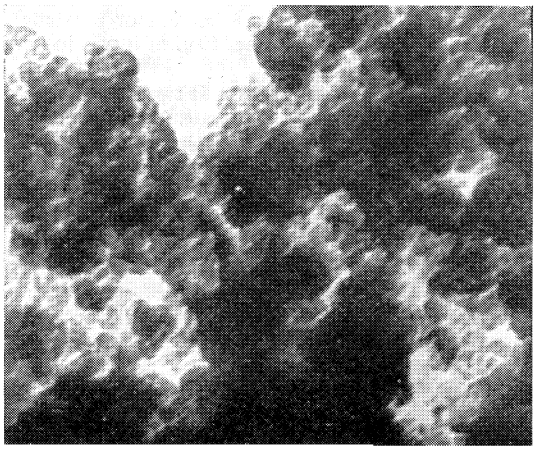
The particle shapes of the carbons were observed with an electron microscope (Type JEM-5G) made by the Japanese Electron Optics Laboratory Co., Ltd. The specimens were prepared by dispersing the carbons in alcohol by an ultrasonic waves apparatus and by scooping them on collodion film supported on a copper mesh.

The degrees of crystallization by X-ray diffraction were measured with a "Geigerflex" made by the Rigaku Denki Co., using Cu(Ni)K_α radiation after the carbons had been pulverized with a mortar.

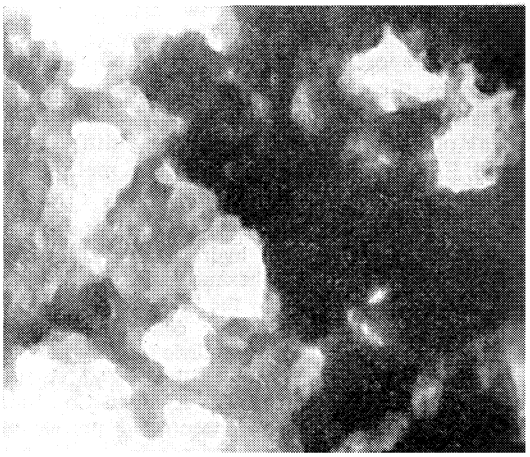
Results and Discussion

The electron micrographs of the carbons are shown in Figs. 2 and 3. The nomenclatures 800BC, 800TC, 800HC, 800EC and 800MC denote the carbons obtained by the pyrolysis of benzene, toluene, *n*-hexane, ethylene and methane respectively at 800°C. Similarly, 1100BC, 1100TC, 1100NC, 1100EC and 1100MC denote those obtained at 1100°C.

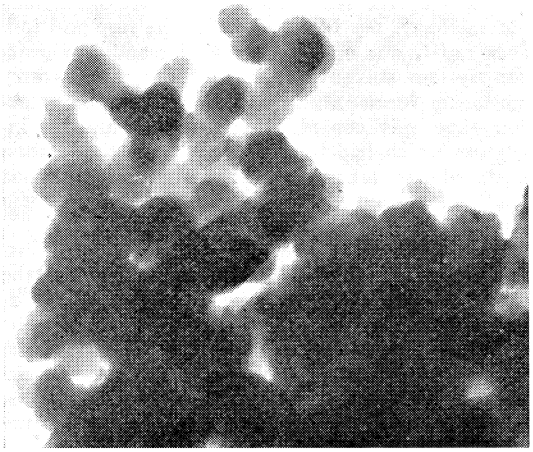
800HC is composed of aggregates of very small particles, the shape of which can not be



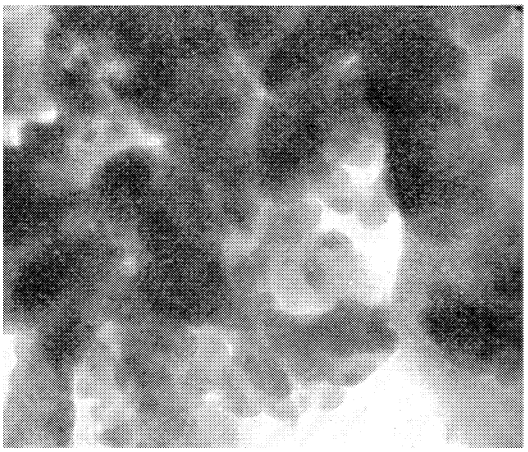
800HC



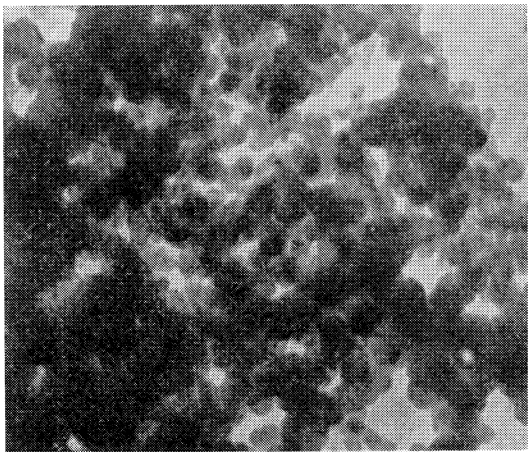
1100HC



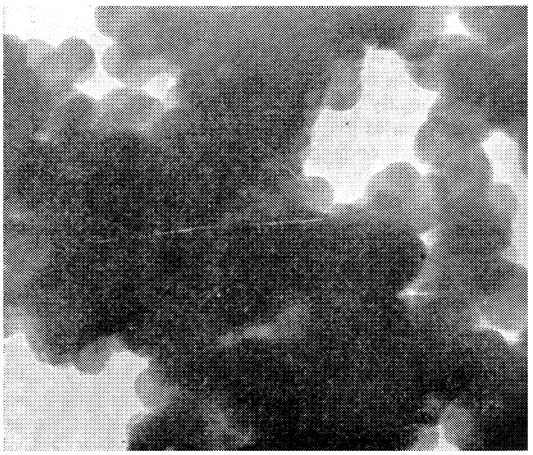
800TC



1100TC

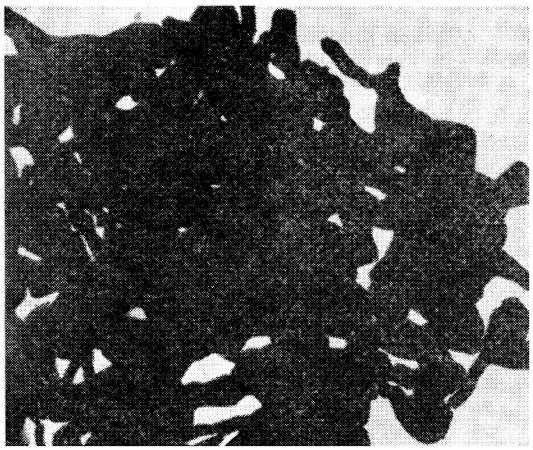


800BC

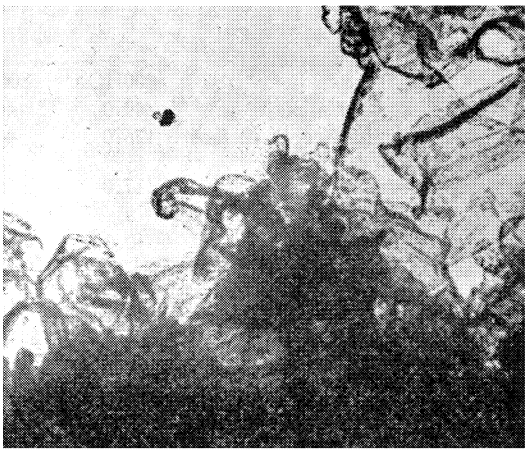


1100BC

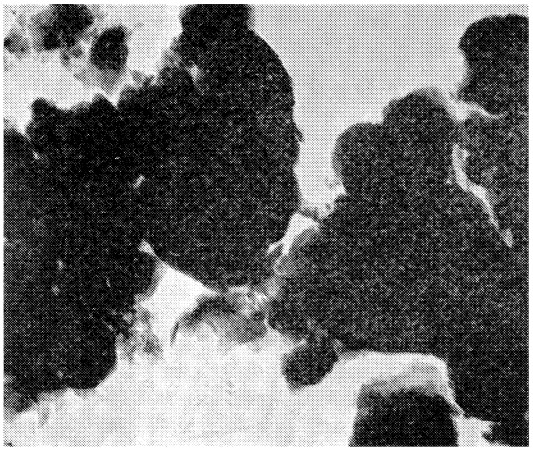
Fig. 2. Electron micrographs of the carbons (×54000).



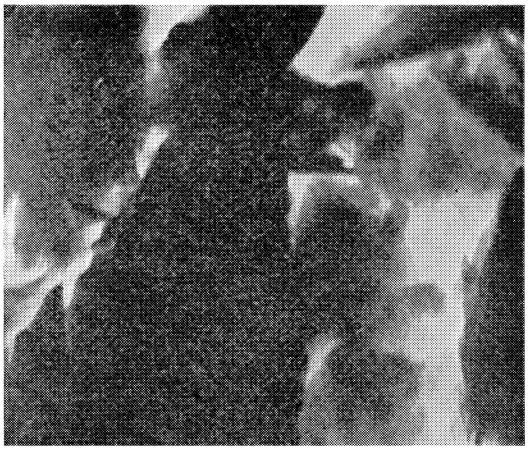
800MC



1100MC



800EC



1100EC



1100NC

Fig. 3. Electron micrographs of the carbons (×54000 .

TABLE I. SURFACE CHARACTERISTICS OF THE CARBONS

Surface character	Carbon produced					
	800HC	800TC	800MC	1100HC	1100TC	1100MC
B.E.T. surface area, $m^2/g.$	49.0	44.0	11.5	4.7	2.9	1.9
Electron microscopic surface area, $m^2/g.$	176.0	40.0	—	—	—	—
Particle diameter, $m\mu$	17.0	75.0	–	–	–	–
Peak micro-pore radius, Å	9	12	18	9	12	18
Micro-pore volume, cc./g.	0.06	0.07	0.03	0.01	0.01	0.01

determined exactly. From the photograph, however, we can estimate their diameters to be about 17 $m\mu$. The samples, 800BC and 800TC, are composed of an aggregation of spherical particles with average diameters of 40 and 75 $m\mu$ respectively. The particle sizes of 800TC are almost equal, but those of 800BC are not equal to one another. 800EC is composed of irregular and thin particles. 800MC has a fiber-like shape; the intensity of its photograph is greater than that of the others, since their state is apparently more compact in the aggregation of the crystallites. The rate of the pyrolysis of naphthalene was very slow at 800°C, and no detectable amounts of carbon could be obtained. When the temperature was raised to 1100°C, the rate increased markedly. This fact accords with the findings of Kinney and DelBel[3].

In the cases of 1100BC, 1100TC and 1100HC, most of the boundaries of the particles become obscure or disappear, causing the formation of uniform plates. However, the diameters of the spherical particles which are found therein do not differ so from those of 800°C. On the other hand, the shape of 1100NC, 1100EC and 1100MC is plate-like, and its uniformity is greater than that of the others. Among them, that of 1100NC is the greatest*.

The results of the surface area measurement are shown in Table I. In the table, the area of 800HC is nearly the same as that of 800TC, while that of 800MC is one-fourth of these carbons; all of them decrease remarkably when the temperature is raised to 1100°C. The electron microscopic area of 800TC calculated by assuming 2.0 as their density (40 $m^2/g.$) coincides with the B.E.T. area (44 $m^2/g.$); however, a great difference was found in 800HC, i. e., 49 $m^2/g.$ for the B.E.T. method and 176 $m^2/g.$ for the electron microscopic method.

X-Ray diffraction patterns of produced carbons are shown in Fig. 4. The results show that the degree of crystallization depends

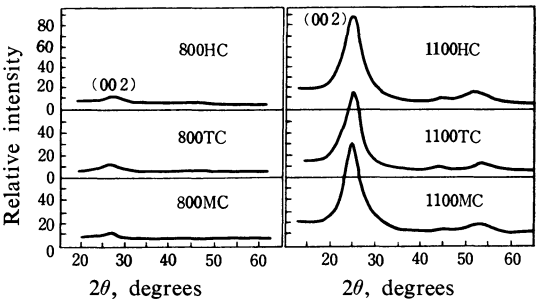


Fig. 4. X-Ray diffraction patterns of the carbons.
Cu(Ni)K_α, 30 kV., 10 mA, 32-0.8-4 sec., $2\,1/2° - 2\,1/2° - 0.2$ mm., 1° − 1 cm./min.

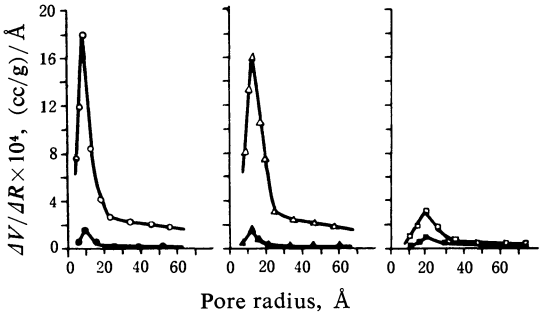


Fig. 5. Micro-pore size distribution curves for the carbons.
○: 800HC, △: 800TC, □: 800MC, ●: 1100HC, ▲: 1100TC, ■: 1100MC.

greatly upon the reaction temperature, but not upon the starting materials, and that the crystallization advances markedly when the temperature is raised from 800 to 1100°C.

The micro-pore size distribution is shown in Fig. 5, and the peak radii and the micro-pore volumes, which were calculated from the figures, are shown in Table I. It should be noted that each carbon kept its inherent peak radii according to the kind of starting material and that their radii did not vary with the change in the reaction temperature. This interesting result is similar to that of the study by Kipling and Wilson[16], who found that the

* To know whether the particle shapes of the carbons produced are affected by the flow rate, an experiment was carried out by changing the flow rate in the range of 0.3 cc./hr. and 10 cc./hr. No obvious change was found in the shape as long as the reaction temperatures were the same.

16) J. J. Kipling and R. B. Wilson, *Trans. Faraday Soc.*, 56, 557 (1960).

pore structure of polymer carbon was controlled by the starting material. However, further studies are required to interpret this phenomena. The micro-pore volume of 800HC was almost the same as that of 800TC, but greater than that of 800MC, and when the reaction temperature was raised to 1100°C, the volume decreased remarkably in every sample and came to be the same as the others.

The significant feature of the electron microscopic observation is as follows: in the cases of benzene, toluene and *n*-hexane, the carbons produced are composed of spherically shape particles, but not, in the cases of ethylene, methane and naphthalene. Those are composed of irregular plate-like or fiber-like shape particles. From this fact, it can be said that the shape of carbons depends upon the starting material; i. e., when the material is liquid (benzene, toluene and *n*-hexane), the shape of the carbons produced is spherical, when it is gas (ethylene and methane) or solid (naphthalene), the sharp is irregular. It can thus be assumed that the liquid material will be pyrolyzed not in the state of gas but in the state of droplets, while the solid material will be pyrolyzed in the state of gas formed by the sublimation.

A great difference in the surface area of 800HC was found between the B.E.T. area and the electron microscopic area. The occurrence of this difference would seem to be due to something about the aggregation of the minute particles; i. e., observation with the electron microscope showed that the aggregation is recognizably very tight. Therefore, it can be considered that the gas used in the observation of the B.E.T. area was not permitted to penetrate the interstices of the minute particles. A very small peak radius was found in the micro-pore size distribution curve of 800HC (see Table I). This result might be ascribed to the fact that this carbon is composed of minute particles aggregated very tightly. Such a supposition agrees well with the observation made about the discrepancy found in both areas. When the reaction temperature was raised to 1100°C, remarkable decreases in the B.E.T. area and in the micro-pore volume of the carbons and a change in the carbon particle shape were observed. This result would be due to the development of the crystallization.

Quantative interpretation of the mechanism of carbon formation will be made in further studies.

Summary

The pyrolysis of six different pure organic compounds (benzene, toluene, naphthalene, ethylene, *n*-hexane and methane) has been studied to discover the relation between the starting materials and the carbon produced. The B.E.T. area, micro-pore size distribution, particle shape, and degree of crystallization have been measured in the carbon produced. The carbonization has been carried out by pyrolyzing the material by means of the flow method at the two temperatures of 800 and 1100°C, keeping the flow rate constant at 2.5 cc./hr. and the vapor pressure at 83 mmHg.

The order of the B.E.T. areas, A, of the carbons produced by pyrolysis is as follows: at 800°C, A(hexane), $49.0 > A$(toluene), $44.0 > A$(methane), 11.5, and at 1100°C, A(hexane), $4.7 > A$(toluene), $2.9 > A$ (methane), 1.9 respectively.

The peak radii, R, of the micro-pore size distribution curves are not changed by the raising of the reaction temperature (800, 1100°C); the order of the radii is R(methane), $18 > R$(toluene), $12 > R$(hexane), 9. Notwithstanding the fact that the peak radii are not changed by the reaction temperature, the micro-pore volumes diminish remarkably.

Electron microscope observation has shown that the shape of the particle is affected by the physical state of the starting material during pyrolysis. If the material is gaseous, plate-like carbon is obtained. If the material is liquid, spherical carbon is obtained.

X-Ray diffraction has shown that the degree of crystallization is not affected by the kind of material. When the temperature of pyrolysis is raised from 800 to 1100°C, the crystallization advances markedly.

The author wishes to express his gratitude to Professor Toyosaburo Takeuchi for his cordial guidance and discussion during this study.

Faculty of Literature and Science
Toyama University, Toyama

*Studies on Solid Carbons. II. The Gas-phase Oxidation of Solid Carbons**

By Masakazu SAKAGUCHI**

(Received June 20, 1961)

The heterogeneous reaction between solid carbon and oxidizing gas is important from both the theoretical and industrial standpoints. In the past, several studies[1-7] have been made of this problem, but there still remain many points unresolved.

It is well known, regarding the oxidation of carbon, that the reactivity diminishes in accordance with the degree of graphitization[8]. The reactivity would be expected to depend primarily upon the physical fine structure (i. e., surface area, micro-pore volume and micro-pore radius) in a case of the same order of graphitization. It appears to be of interest, therefore, to find some correlation between the reaction rate and the surface properties of carbon.

The present work was carried out in order to investigate the gas-phase oxidation with nitrogen dioxide, using five typical carbons which differ in material and in manufacturing method, and also to investigate the characteristics of the rate of reaction under various conditions. The particle shapes and the degrees of the graphitization of carbon samples were observed with an electron microscope and X-ray diffraction. The physical fine surface structure of the composing particles was determined by means of the adsorption and desorption of gas at a low temperature.

Experimental

Apparatus and Procedure. — The reaction apparatus is illustrated in Fig. 1. The reaction vessel H was a modification of that of Takeuchi[9]. The volume of the vessel H up to tap K_4 and K_5 is 123 cc. The carbon sample (2.0 g.) was kept in the vessel H. After it was evacuated under about

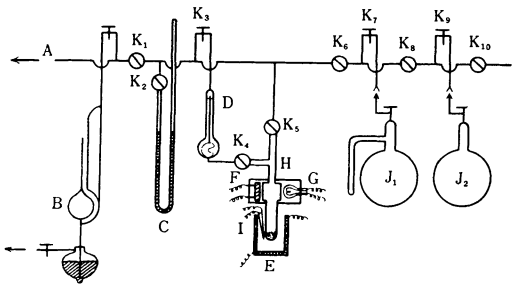


Fig. 1. Apparatus for the reaction between carbons and NO_2.

10^{-5} mmHg at 200°C for several hours, the temperature was lowered to 150°C (reaction temperature). The temperature of the electric furnace E, which contains H, was controlled (±1°C) automatically. A MacLeod gauge B was used for the measurement of the low pressure. J_2 is a reservoir of hydrogen gas used for the "H_2-treatment" of the carbon sample. NO_2 gas was taken from the gas reservoir J_1 into the space between the taps K_1, K_2, K_3, K_5, K_7 and K_8, space with a volume of 277 cc. (not including the volume of the manometer C). The gas was introduced in H by opening K_5 to start the reaction. F is a photo-cell attached closely to H and connected to a micro-ammeter. The intensity of incident light from lamp G was kept constant. The variations of transmittance accompanying the reaction were followed by the photo-cell. The relation between the transmittance and the NO_2 concentration at the temperature range of 120 to 170°C is shown by a curve in Fig. 2. The reaction rate was obtained from this curve. A Bourdon gauge D was used to follow the changes in total pressure.

The surface areas, the micro-pore volumes and the mean micro-pore radii were obtained from

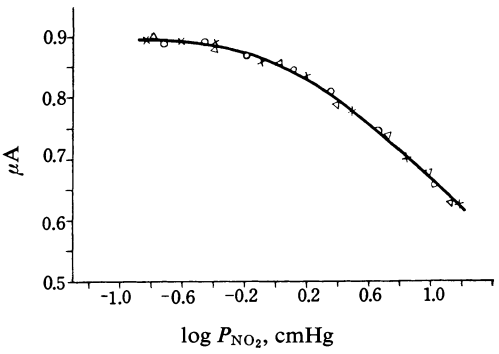


Fig. 2. Calibration curve.
△, 120°C; ○, 150°C; ×, 170°C

* The main part of this work was presented at the 13th Annual Meeting of the Chemical Society of Japan, Tokyo, April, 1960.

** Present address: Department of Chemistry, Faculty of Engineering, Niigata University, Nagaoka.

1) J. D. Lambert, *Trans. Faraday Soc.*, **32**, 452 (1936).
2) W. K. Lewis, E. R. Gilliland and H. Hipkin, *Ind. Eng. Chem.*, **45**, 1697 (1953).
3) P. L. Walker, Jr., R. J. Foresti, Jr. and C. C. Wright, ibid., **45**, 1703 (1953).
4) H. Watts, *Trans. Faraday Soc.*, **53**, 93 (1957).
5) C. N. Spalaris, *J. Phys. Chem.*, **60**, 1480 (1956).
6) A. Turuizumi, *J. Chem. Soc. Japan, Pure Chem. Sec. (Nippon Kagaku Zasshi)*, **79**, 266 (1958).
7) R. N. Smith, J. Swinehart and D. Lesnini, *J. Phys. Chem.*, **63**, 544 (1959).
8) E. g., W. R. Smith and M. H. Polley, ibid., **60**, 689 (1959).
9) T. Takeuchi, *Catalyst*, **7**, 67 (1951).

TABLE I. CHARACTERISTICS OF SAMPLE CARBONS

	Kind of carbons				
	Philblack-I (C_1)	Miike-carbon (C_2)	Artificial graphite (C_3)	Petroleum coke A, (C_4)	Petroleum coke B, (C_5)
Appearance	Spherical particle, ca. 0.5 mm.ϕ	Fine powder, ca. 100-mesh	Scalelike particle, ca. 0.5 mm.ϕ	Fine powder, ca. 200-mesh	Spongelike particle, ca. 2.0 mm.ϕ
Row material	Petroleum modified	Coal gas	Coal coke	—	—
Manufacture method	Imperfect combustion	Thermal decomposition	—	—	—
Degree of agglomeration	Large	Small	—	—	—
Particle diameter (mμ)	29.8	320.0	—	—	—
Surface area (m^2/g.)	101.0	9.4	—	—	—

Fine structure	(C_1)		(C_2)		(C_3)	(C_4)		(C_5)
	C_{orig}	C_{re}	C_{orig}	C_{re}	C_{orig}	C_{orig}	C_{re}	C_{orig} and C_{re}
B. E. T. area (m^2/g.)	104.0	108.0	15.2	12.2	2.1	10.8	8.3	0.9
Micro-pore volume (cc./g.)	0.07	0.06	0.02	0.02	0.01	0.01	0.01	—
Mean micro-pore radius (Å)	13.5	12.1	26.8	32.8	133.4	26.0	33.8	—

adsorption and desorption-isotherms of nitrogen at the temperature of liquid nitrogen (−195°C). The B. E. T. method was applied to the adsorption isotherms to determine the surface areas of the carbon samples assuming 16.1 $Å^2$ as the cross-sectional area of nitrogen, and Kelvin's equation was adopted for the desorption isotherms to determine the micro-pore volumes and the mean micro-pore radii.

The particle shapes of the carbons were observed with an electron microscope (Type JEM-5G, made by the Japan Electron Optics Laboratory Co., Ltd.). The specimens were prepared by dispersing the carbons in alcohol by an ultrasonic wave apparatus (cycle: 7000 kc.; time: 2 min.) and by scooping them on collodion film supported on a copper mesh.

The degrees of crystallization by X-ray diffraction were measured with a "Geigerflex" made by the Rigaku Denki Co., using Cu(Ni)K_α radiation on the specimens packed in an aluminum case after the carbons had been pulverized with a merter.

Materials.—Five carbons produced commercially (Philblack-I (C_1), Miike carbon (C_2), artificial graphite (C_3), petroleum coke-A (C_4) and petroleum coke-B (C_5)) were used, whereas sample C_4 was powder of 200-mesh which had been prepared by the pulverization of sample C_5. The physical properties of these carbons are listed in Table I. Before use, these carbons were washed in boiling water for about one hour and were then dried in the atmosphere.

The "H_2-treatment" of carbon was performed under about 50 cmHg of hydrogen at 500°C for about 30 min. after it had been washed by boiling water. Before use, the temperature of the reaction vessel was lowered to 200°C; the procedure subsequently followed was as mentioned above*.

The treatment of carbon by benzoyl peroxide was performed by Ōkita's method[10].

The following procedure was adopted to regenerate the sample: after the reaction had stopped, the oxidized sample was washed with boiling water for about one hour**.

The nitrogen dioxide gas was prepared by heating of "extra pure grade" lead nitrate (supplied by Wako Junyaku Co., Ltd.) at 470°C. It was purified by vacuum distillation and stored in reservoir J_1.

The nitrogen gas used in the adsorption experiment was of a high purity (99.98%), having been supplied by Nissan Kagaku Co., Ltd.

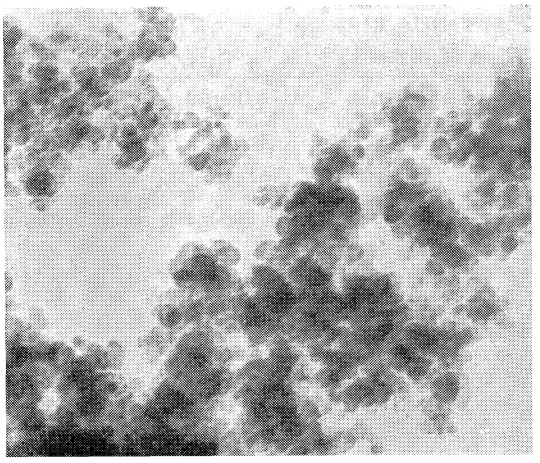
Results

The values of the surface area and of the physical fine structure are shown in Table I, and the results of observation with the electron microscope are shown in Table I and Fig. 3. The sign "C_{orig}" in line 8 of the table denotes the sample washed in boiling water, and the "C_{re}" denotes the sample regenerated by

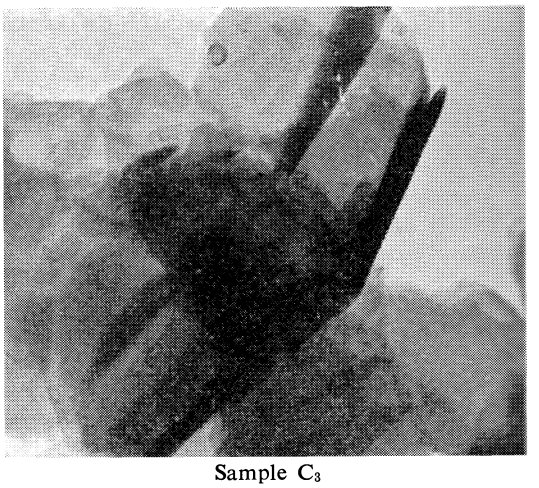
* The hydrogen contents found by elementary analysis of the sample were 0.56% after the "H_2-treatment" and 0.30% for the original sample.

10) K. Ōkita et al., *J. Japan. Rubber Soc.*, **30**, 661 (1957).

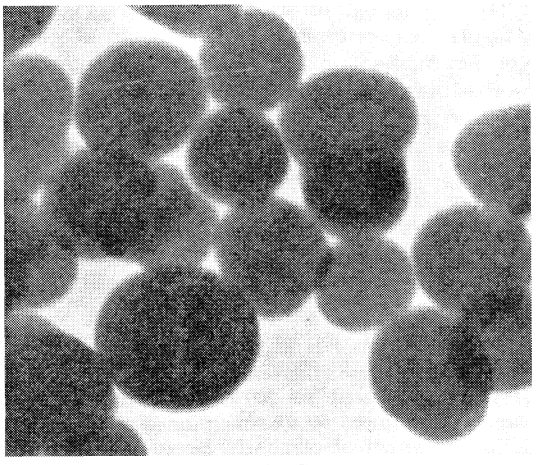
** During this treatment, much dregs-state material rose to the surface of the boiling water.



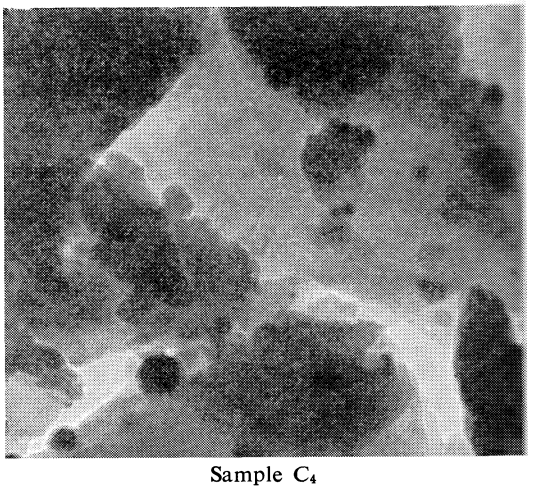
Sample C_1



Sample C_3



Sample C_2



Sample C_4

Fig. 3. Electron micrographs of sample carbons (×54000).

washing with boiling water after it had been used for the reaction with nitrogen dioxide. The electron microscopic areas of samples C_1 and C_2, calculated by assuming 2.0 as their density, are shown in line 7 of the table. The area of sample C_1 coincides with that given by the B. E. T. method, but the area of sample C_2 is smaller by about 40% than the B. E. T. area. From this fact, it can be surmised that the surface of the particles composing C_1 is comparatively smooth. On the other hand, the discrepancy in the areas of sample C_2 found in the two methods can be attributed to the existence of a roughness which could not be recognized with the electron microscope. In Fig. 3, it is also clear that both the samples, C_1 and C_2, are composed of spherical particles of inherent diameters, and that the diameter of C_2 is about 10 times larger than that of sample C_1. The particles of sample C_2 are more dispersed than those of sample C_1, which agglomerate to form secondary particles. Consequently, the physical fine structure of sample C_1 (Table I, lines 10 and 11) is formed of particles which have a smooth surface, while that of C_2 exists on the surface of a composing particle itself. Sample C_3 is composed of irregular thin films, while C_4 is composed of irregular thin films and small spherical particles. Therefore, the roughness in the surfaces can not be estimated as it was in the cases of C_1 and C_2. The electron micrographs suggest also that the degree of graphitization of sample C_3 is higher than those of C_1 and C_2, and that that of sample C_4 is between C_3 and C_1 or C_2, because it is composed of films similar to those found in C_3 and of particles similar to those found in C_1 or C_2.

X-ray diffraction patterns of sample carbons are shown in Fig. 4. The results show that the degrees of graphitization of samples C_1 and C_2 are quite low and indicate the characteristics of typical carbon black. The patterns of both samples, C_3 and C_4, indicate that their degrees

of graphitization are quite high compared with C_1 and C_2 and that that of C_3 is higher than that of C_4. These facts support the conclusion obtained from the results of the electron microscopic observation.

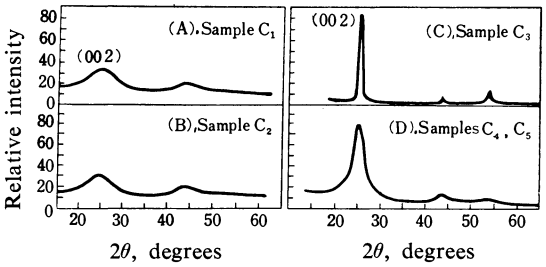


Fig. 4. X-Ray diffraction patterns of sample carbons.
(A) and (B); Cu(Ni)K_α, 35 kV., 15 mA., 32-0.8-4 sec., $2^1/_2°-2^1/_2°-0.2$ mm., 1°−1 cm./min. (C); Cu(Ni)K_α, 30 kV., 10 mA., 64-1-4 sec., 1°−1°−0.1 mm., 1°−1 cm./min. (D); Cu(Ni)K_α, 30 kV., 15 mA., 8-1-4 sec., 1°−1°−0.1 mm., 1°−1 cm./min.

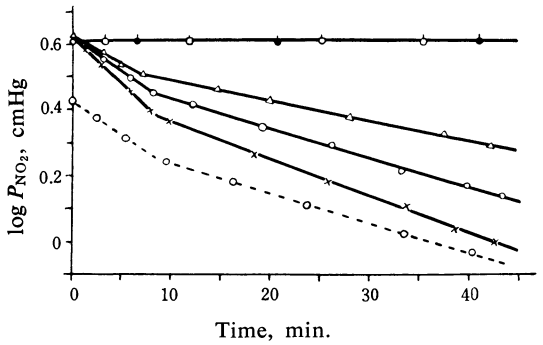


Fig. 5. Changes of NO_2 pressure with time on carbons (per 2 g.) at 150°C. ×, C_1; ○, C_2; ⏚, C_3; △, C_4; ⏚, C_5; --○--, C_2 (at 170°C)

The results of oxidation, which was carried out at 150°C with 4.2 cmHg of initial pressure of nitrogen dioxide, are shown in Fig. 5. The figure shows that the relation of the logarithm of pressure against time can be expressed by bent straight lines which are steep in the the initial stage. The rates of the consumption of nitrogen dioxide obtained from the lines are shown in Table II, where K_1 and K_2 denote the rate constants per unit gram and area respectively. It is noteworthy that the ratio of the rate in the initial stage (k_1) to that in the second stage (k_s) can be given in the range 2.0 to 3.0 for every carbon.

Figure 6 shows the results of the experiments carried out to ascertain the reaction order of

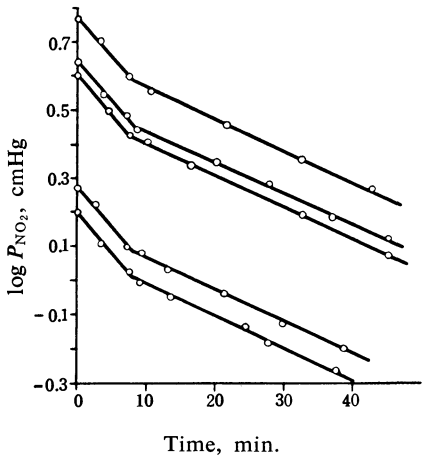


Fig. 6. Effect of initial pressure of NO_2 for the rate of reaction of carbon. Sample carbon: C_2; Reaction temperature: 150°C.

TABLE II. DATA OF THE REACTION BETWEEN CARBONS AND NITROGEN DIOXIDE

Kind of carbon		Rate constant K_1 ($g^{-1}\cdot sec^{-1}$) Initial $k_1\times10^4$	K_1 ($g^{-1}\cdot sec^{-1}$) Second $k_s\times10^4$	K_2, $cm^{-2}\cdot sec^{-1}$ Initial $k_1\times10^9$	K_2, $cm^{-2}\cdot sec^{-1}$ Second $k_s\times10^9$
C_1	C_{orig}	5.56	1.89	0.53	0.18
	C_{re}	5.29	2.00	0.49	0.19
	$C_{no\text{-}re}$*	1.57	1.03	—	—
C_2	C_{orig}	3.84	1.74	2.53	1.14
	C_{re}	2.00	0.89	1.64	0.73
	$C_{no\text{-}re}$*	0.93	0.93	—	—
C_3	C_{orig} and C_{re}	—	—	—	—
C_4	C_{orig}	3.15	1.32	2.92	1.22
	C_{re}	1.68	0.69	2.02	0.83
	$C_{no\text{-}re}$*	0.50	0.50	—	—
C_5	C_{orig} and C_{re}	—	—	—	—

* Sign $C_{no\text{-}re}$ denotes the sample which was outgassed for several hours at 200°C after sample C_{orig} had been oxidized by nitrogen dioxide.

nitrogen dioxide by using sample C_2 under various initial pressures. From the results shown in Figs. 5 and 6, reaction order could be determined to be first. Unexpectedly, in spite of the change of the pressure of nitrogen dioxide in the reaction, no change at all in total pressure was recognized. Figure 5 shows that either the sample C_3 of the highest degree of graphitization or C_5 of a little higher degree did not react with a measurable rate.

It is of particular interest that the pulverization of carbon markedly increased the reaction rate. By pulverization, the rate of C_5 (i. e., that of C_4) became as fast as that of C_2. In the cases of C_1 and C_2, no remarkable difference in the rate K_1 could be found, though a difference exists in their surface areas. Accordingly, the rate K_2 of sample C_2 becomes greater than that of C_1.

The exeriment on sample C_2 at the higher temperature, i. e., 170°C, was carried out to learn the activation energies at the initial and second stages of the reaction. However, no detectable change in the rate could be found. This fact indicates that the activation energies in both stages are very small (< 3 kcal.*), giving thus no difference between the two.

When pre-treated with hydrogen and benzoyl peroxide, the reaction rate of nitrogen dioxide the B. E. T. areas and the electron micrographs showed no detectable change in any sample.

Tables I, II and Fig. 7 show the results of the reaction carried out to observe the effect

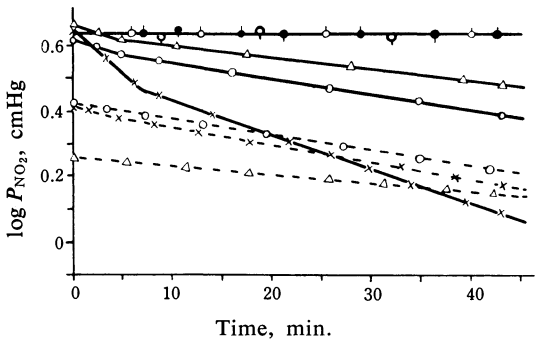


Fig. 7. Changes of NO_2 pressure with time on carbons (per 2 g.) regenerated and not regenerated at 150°C.

—×—; C_1 regenerated
—○—; C_2 regenerated
—♁—; C_3 regenerated
—△—; C_4 regenerated
—●—; C_5 regenerated
--×--; C_1 not regenerated
--○--; C_2 not regenerated
♀ ; C_3 not regenerated
--△--; C_4 not regenerated
● ; C_5 not regenerated

* The value was estimated by the experimental error.

of the regeneration upon the surface structure and the reaction rate of the carbons. In Table II, it can be found that the rate K_1 of the regenerated sample C_1 became markedly greater than that of the not regenerated sample and that it is almost the same as that of fresh carbon. In the cases of C_2 and C_4, the rates also became greater than that of not regenerated samples, while their rates in the initial and second stages of the reaction are about half of those of the fresh carbons. In Table I, it can be found that the change in fine structure of the regenerated sample C_1 is very small, but both samples C_2 and C_4 indicate a decrease in B. E. T. areas and an increase in mean micropore radii. Those facts suggest that the roughness of the composing particles of C_2 and C_4 were diminished to some extent by the regeneration. However, these hypotheses could not be verified by the electron micrographs.

Discussion

The rate of oxidation of carbons can be considered simply to be controlled by the following factors: the degree of graphitization, the physical fine and/or the chemical structures of the surface, though these factors can not be discussed separately.

The well-graphitized carbons, C_3 and C_5, possessed different X-ray diffraction patterns, as is shown in Fig. 4. However, no difference was found in the oxidizing reaction with nitrogen dioxide. This indicates that the progress of graphitization prevents the oxidation by nitrogen dioxide. The samples which are composed from amorphous carbon, i. e., C_1 and C_2 reacted with nitrogen dioxide quickly, but their K_2 rates differed markedly from each other. It can be noticed that the micro-pore volume of sample C_2, which reacted with nitrogen dioxide more rapidly than C_1, is smaller than that of C_1, and that the mean micro-pore radius is greater than that of C_1. If the micropore radius is small, the wall of the capillary will be a much more difficult location for the reaction than a free surface. Therefore, the difference in rates found in the two samples (C_1, C_2) can be attributed to a defference in their physical fine structures. Whether or not the rate of oxidation is affected by the diffusion of gas can be confirmed by plotting the concentration of nitrogen dioxide against square root of time[11]. Figure 8 shows that the relationships are represented by convex curves in the initial stage of the reaction, but, by straight lines in the second stage. This indicates that the rate of the reaction was controlled by the

11) R. M. Barrer and D. W. Riley, *J. Chem. Soc.*, **1948**, 133.

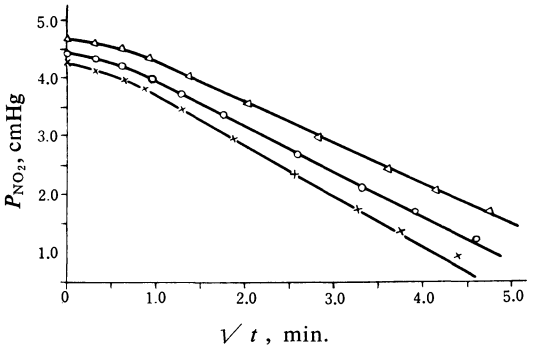


Fig. 8. Changes of NO_2 pressure with square root of time on carbons (per 2 g.) at 150°C. ×: C_1; ○: C_2; △: C_4.

diffusion of gas except in the short initial stage. We can conclude by referring Fig. 5 to Fig. 8 that rate k_1 in Table II concerns only the chemical reaction and that it is the rate of the reaction on the free surface of carbons.

The sites of different reactivities can be considered to exist on the surface of carbon as has been believed in the field of physico-chemical studies on solid surfaces.

To explain exactly the differences in rates k_1 which were not controlled by diffusion, more information about the physical and chemical properties of the free surface, e. g., geometrical arrangement and functional group on the surface, will be required. It is very difficult, however, to make clear the properties mentioned above because of the complexity and the instability of the carbon surface. However, the adaptation of the results in the following two studies can be ascribed to the relation between the rate of reaction and the nature of the surface.

The number of edge atoms in C_5 must be increased by pulverization. The increase in the reaction rate in C_4 should correlate with the increase in edge atoms because the edge atoms of microcrystalline of carbons may be considered to be more susceptible to chemical attack than the atoms in the center of the basal plane. Such a view accords with that of Long and Sykes[12], who studied the oxidation of carbon with steam.

Recently, Smith and his co-workers[7] have reported that the oxidation of carbon by nitrogen monoxide was greatly retarded by pretreatment with hydrogen at 1000°C for 15 min. In this study, the oxidation of carbon was not affected by hydrogen. In both reactions, the adsorption of oxidizer (nitrogen dioxide or nitrogen monoxide) occurs on carbon prior to oxidation. In this case, the number of sites to be occupied by the oxidizer would be decreased by the occupation of pre-treated hydrogen. Accordingly, the rate of oxidation is expected to decrease. The result of the reaction with nitrogen monoxide reveals either that the hydrogen on carbons is not readily attacked by the adsorbed nitrogen monoxide or that the reaction products (or groups) of hydrogen and oxygen given by nitrogen monoxide have a nature which is hard to distinguish from the carbon. However, in the case of nitrogen dioxide the result indicated that because of the nature of the strong oxidizer, the hydrogen was readily released into the gas-phase after it had been attacked by nitrogen dioxide.

In short, the oxidation of carbon by nitrogen dioxide is greatly affected by the physical fine structure but not by the chemical structure of the carbon surface.

12) F. J. Long and K. W. Sykes, *Proc. Roy. Soc.*, A 193, 377 (1948).

Summary

The gas-phase oxidation of five sorts of carbons with nitrogen dioxide has been measured under a pressure range from 2.4 to 9.0 cmHg at 150°C by a static method, in order to determine, primarily, the relation between the reaction rate and the physical properties of carbons (B. E. T. area, degree of graphitization, particle shape, micro-pore volume and mean micro-pore radius).

The rate of consumption of nitrogen dioxide has been determined photometrically.

The well-graphitized carbons did not react with nitrogen dioxide, while the rate curves obtained on the amorphous carbons showed as bent straight lines, the inclination of which is steep at the initial stage, followed by a slow second stage. The activation energy in the reaction is very small (< 3 kcal.).

The explanation of the results is as follows: the consumption of nitrogen dioxide in the initial stage relates mainly to chemical reaction on the free surface of the carbon, and the rate is controlled by the free surface area and the concentration of the edge atoms of the surface. The rate of the second stage relates to the diffusion process the micro-pore of carbon particles, and it is controlled by the physical fine structure of the surface.

The author wishes to express his gratitude to Professor Toyosaburo Takeuchi for his cordial guidance and discussion on this study.

Faculty of Literature and Science
Toyama University, Toyama

Long-chain Phosphates. II. Reactions of Crystalline Sodium Metaphosphates with Solutions of Various Metal Salts

By Shigeru OHASHI and Takashi NAKAMURA

(Received July 17, 1961)

Four modifications of crystalline sodium metaphosphate are known. They are designated as $NaPO_3$-I, $NaPO_3$-II, $NaPO_3$-III and $NaPO_3$-IV. As $NaPO_3$-I is sodium trimetaphosphate, $(NaPO_3)_3$, it is out of the scope of this investigation. $NaPO_3$-II, $NaPO_3$-III and $NaPO_3$-IV are long-chain phosphates. $NaPO_3$-II is called sodium Maddrell salt of high temperature form, $NaPO_3$-III, sodium Maddrell salt of low temperature form, and $NaPO_3$-IV, sodium Kurrol salt.

In the previous paper[1] it was found by Ohashi and Yamagishi that the reaction of crystalline potassium Kurrol salt with a solution of nickel sulfate is a kind of cation-exchange reaction. They investigated also the cation-exchange reactions of crystalline potassium Kurrol salt with various metal ions other than the nickel ion. The present authors have investigated the cation-exchange reactions of the crystalline sodium metaphosphates having long-chain structures with aqueous solutions of various metal salts.

Experimental

Preparation of $NaPO_3$-II.—$NaPO_3$-II is usually prepared by dehydrating sodium dihydrogen orthophoshate at a relatively high temperature in a humid atmosphere[2]. In a platinum dish 100~150 g. of sodium dihydrogen orthophosphate dihydrate was dehydrated by the use of an electric furnace. After the temperature of the furnace reached about 160°C, aqueous steam was introduced over the sample. Then the temperature of the furnace was gradually raised to 400°C. After being kept at 400°C for 3 hr., the sample was removed from the furnace and chilled by holding the lower part of the dish in water. A white powdery product was obtained. The small amount of soluble phosphate remaining in the product was removed by washing it with distilled water. An X-ray diffraction pattern of the sample was identical with that of the ASTM cards.

Preparation of $NaPO_3$-III.—It is very difficult to prepare $NaPO_3$-III in a pure state and in a high yield. The dehydration of sodium dihydrogen orthophosphate should be carried out at a relatively low temperature in a dry atmosphere[3]. When the temperature is too high, $NaPO_3$-II is also produced. When the temperature is too low, a large amount of disodium dihydrogen pyrophosphate remains and the yield of $NaPO_3$-III becomes very low. In a porcelain dish 20~40 g. of sodium dihydrogen orthophosphate dihydrate was gradually dehydrated. The temperature of the furnace was raised from room temperature to 260°C in 5~6 hr. and kept at 260°C for 2.5 hr. A white powdery product was obtained. The product was washed with distilled water to remove the pyrophosphate. Although the X-ray diffraction pattern of the sample was identical with that of the ASTM cards, the yield was only 0.3%. $NaPO_3$-III supplied by Dr. T. P. Kickline of the Monsanto Chemical Co. was used in the present investigation on the cation-exchange reactions. 82% of the sample was composed of $NaPO_3$-III and 18% of $NaPO_3$-II.

Preparation of $NaPO_3$-IV.—$NaPO_3$-IV was prepared by Griffith's method[4]. In a platinum dish about 150 g. of sodium dihydrogen orthophosphate dihydrate was dehydrated at a relatively low temperature and melted at 800°C for 2~3 hr. in an electric furnace. Then the platinum dish was removed from the furnace and transferred to another furnace, which had been previously controlled at 550°C. The temperature of the second furnace was raised to 580°C by introducing the hot dish but fell back to 550°C within 15 min. Seed crystals of $NaPO_3$-IV, supplied by Dr. E. J. Griffith of the Monsanto Chemical Co., were then added to the sample. After being kept at 550°C for 2 hr., the sample was removed from the furnace and chilled by holding the lower part of the dish in water. In order to remove Graham salt and sodium trimetaphosphate, the sample was crushed and washed with distilled water. Although there is no available data on the X-ray diffraction pattern of $NaPO_3$-IV, the pattern of the sample obtained was quite different from those of $NaPO_3$-II and $NaPO_3$-III. Moreover, the appearance of the sample was asbestos-like and quite similar to that of potassium Kurrol salt. The sample was doubtless $NaPO_3$-IV.

The experimental conditions for the cation-exchange reactions and the analytical methods for the determination of phosphate and metal ions were essentially the same as those used in the previous investigation[1].

1) S. Ohashi and K. Yamagishi, This Bulletin, 33, 1431 (1960).

2) J. R. Van Wazer, "Phosphorus and its Compounds", Vol. I, Interscience Publishers, New York (1958), pp. 668—669.

3) Private communication from Dr. T. P. Kickline of the Monsanto Chemical Co.

4) Private communication from Dr. E. J. Griffith of the Monsanto Chemical Co.

Results and Discussion

When any one of the sodium metaphosphates was added to a solution of nickel sulfate, the white crystalline sodium metaphosphate was gradually converted into a green gummy substance. The adsorption of the nickel ion was investigated in the following manner. At the bottom of an Erlenmeyer flask of 300 ml., 1 g. of the ground sodium metaphosphate was placed flat, and then 200 ml. of a 0.1 M solution of nickel sulfate was added to it. The mixture was kept at 20°C without agitation. The variation in the amount of the nickel ion adsorbed as time went on was determined by measuring the decrease in the nickel ion concentration in the solution. As shown in Fig. 1, after about 24 hr. the reaction reached equilibrium in every case of the three sodium metaphosphates. The reaction of $NaPO_3$-IV with a solution of cobalt sulfate also reached equilibrium after about 24 hr., as is shown in Fig. 2.

The cation exchange reactions between the sodium ions in the solid sodium metaphosphates and various metal ions in their solutions were investigated as follows. In an Erlenmeyer flask of 100 ml., about 250 mg. of each crystalline sodium metaphosphate was placed, and then 50 ml. of an about 0.1 M solution of a metal salt was added to it. After being kept at 20°C for 24 hr. without agitation, an aliquot of the solution was taken and analyzed for the metal ion remaining in the solution and for the phosphate dissolved into the solution. From these data a percentage of the sample dissolved, an amount of the sample remaining as a solid phase, and a percentage

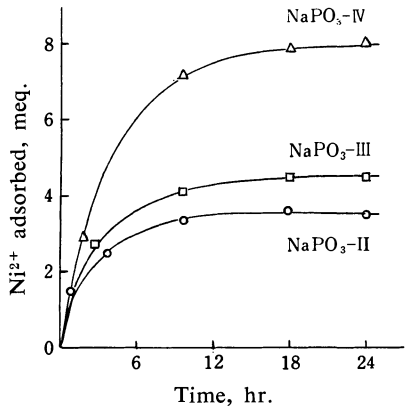


Fig. 1. The variation of the amounts of nickel ion adsorbed with time.

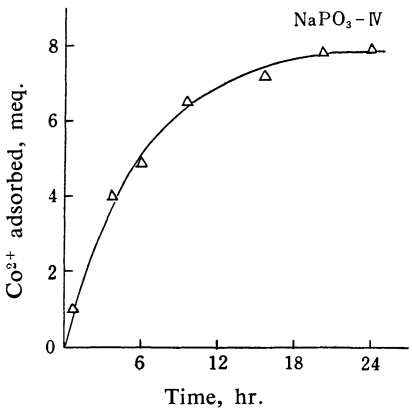


Fig. 2. The variation of the amounts of cobalt ion adsorbed with time.

TABLE I. CATION-EXCHANGE REACTIONS BETWEEN SODIUM METAPHOSPHATE AND SOLUTIONS OF VARIOUS METAL SALTS

Metal salt, initial concn. and pH	Form of $NaPO_3$	Sample added meq.	Sample dissolved %	Sample remaining meq.	Sodium exchanged %	Final pH
$CaCl_2$ 0.0990 M pH 6.15	II	2.48	0.4	2.46	40.7	4.85
	III	2.45	2.0	2.40	82.8	3.86
	IV	2.48	0.4	2.47	98.4	4.85
$MgCl_2$ 0.1029 M pH 5.85	II	2.48	0.4	2.47	23.5	4.70
	III	2.45	1.6	2.41	80.5	3.60
	IV	2.47	0.4	2.46	87.8	4.70
$FeSO_4$ 0.1020 M pH 3.60	II	2.46	0.8	2.44	13.9	3.56
	III	2.47	2.4	2.40	70.7	3.08
	IV	2.46	2.4	2.40	80.8	3.40
$CoCl_2$ 0.1024 M pH 4.40	II	2.53	0.4	2.52	23.0	4.20
	III	2.46	2.1	2.41	78.0	3.24
	IV	2.46	0.4	2.45	85.7	4.14
$NiSO_4$ 0.1074 M pH 5.60	II	2.46	0.9	2.44	37.7	4.70
	III	2.45	4.3	2.23	72.7	4.32
	IV	2.45	2.0	2.40	95.0	4.55
$CuSO_4$ 0.1030 M pH 4.30	II	2.50	39.8	1.50	5.3	3.28
	III	2.46	58.1	1.03	36.9	2.90
	IV	2.50	26.4	1.84	34.8	3.20

of the sodium ion exchanged by the metal ion at the end of the reaction were calculated. Before and after the reaction, the pH values of the solution were measured. The results are summarized in Table I.

The percentages of the cation exchange in the cases of magnesium, calcium, iron(II), cobalt(II) and nickel(II) ions were in the range of 14 to 41 for $NaPO_3$-II, 70 to 83 for $NaPO_3$-III, and 81 to 98 for $NaPO_3$-IV. The tendency of the cation exchange of the sodium metaphosphates for these metal ions decreases in the order:

$$NaPO_3\text{-IV} \gtrsim NaPO_3\text{-III} > NaPO_3\text{-II}$$

In the case of potassium Kurrol salt, the percentages of the cation exchange for these cations were in the range of 82 to 94, as mentioned in the previous paper[1].

The following facts in regard to the dissolution of the sodium metaphophates in water were described by Van Wazer[2]. $NaPO_3$-II is dissolved in water at a very slow rate, 1.8×10^{-2} %/hr., and $NaPO_3$-III is also dissolved in water at a slow rate, 0.34%/hr. $NaPO_3$-IV appears to be dissolved more rapid; it forms a gel-like substance when it is kept in water for a long time. These facts may indicate that the tendency toward hydration of the sodium metaphosphates decreases in the following order:

$$NaPO_3\text{-IV} > NaPO_3\text{-III} > NaPO_3\text{-II}$$

which coincides with the order of the tendency of the cation exchange of the sodium metaphosphates. Therefore, in the course of the cation exchange of the sodium metaphosphates, the process of the hydration may play an important role.

The percentages of the phosphates dissolved during the cation exchange reactions were in the range of 0.4 to 4 for almost all of the bivalent metal ions tested in the present investigation. However, only in the case of copper(II) ion were large amounts of the phosphates, which ranged from 26 to 58%, dissolved in the course of the reactions. In the reaction of potassium Kurrol salt with the copper(II) ion, 32% of the phosphate was dissolved. It is a well-known fact that potassium Kurrol salt is not easily soluble in pure water, but it is soluble in dilute solutions of salts of alkali metals other than potassium; furthermore, crystalline sodium metaphosphates with long-chain structures are also not easily soluble in pure water, but they are soluble in dilute solutions of salts of alkali metals other than sodium. In regard to the reactions with the long-chain phosphates, the copper(II) ion has an intermediate property between alkali metals and bivalent metals such as magnesium, calcium and so on.

In all cases the pH of the solutions of the metal salts decreased in the course of the reactions. The decrease in pH may be due to the dissolution and the hydrolysis of the sodium metaphosphates. Actually, in the case of $NaPO_3$-III, both the percentages of the phosphate dissolved and of the decrease in pH were larger than in the case of the other metaphosphates. As indicated by Wieker and Thilo[5], the hydrolysis of the metaphosphates may be accelerated by the catalytic actions of the metal ions.

Summary

Three kinds of crystalline sodium metaphosphates with a long-chain structure, $NaPO_3$-II, $NaPO_3$-III and $NaPO_3$-IV, were prepared, and the cation exchange reactions of the solid sodium metaphosphates with aqueous solutions of bivalent metal salts, calcium, magnesium, iron(II), cobalt(II), nickel(II) and copper(II), were investigated. The tendency of the cation exchange of the sodium metaphosphates for these metal ions, except for copper(II), decreases in the order:

$$NaPO_3\text{-IV} \gtrsim NaPO_3\text{-III} > NaPO_3\text{-II}$$

which coincides with the order of the tendency of the hydration of the sodium metaphosphates. Only in the case of copper(II) ion were large amounts of the sodium metaphosphates dissolved in the course of the reactions.

The authors are indebted to Dr. Thomas P. Kickline and Dr. Edward J. Griffith for sending them samples of $NaPO_3$-III and $NaPO_3$-IV and for giving them information on the preparation of $NaPO_3$-III and $NaPO_3$-IV.

Department of Chemistry
Faculty of Science
Kyushu University
Fukuoka

5) W. Wieker and E. Thilo, *Z. anorg. u. allgem. Chem.*, **306**, 48 (1960).

Condensed Vanadate-Phosphates

By Shigeru OHASHI and Tadashi MATSUMURA

(Received July 24, 1961)

It is well known that the structural frameworks of condensed phosphates are composed of P–O–P linkages. Some attempts to prepare condensed phosphates containing anions other than phosphate have been made. Thilo and his coworkers[1] have succeeded in making glasses and crystals of sodium or potassium arsenate-phosphates, which are composed of P–O–P and P–O–As linkages. Some experiments have been made on glasses of sulfate-phosphates[2] and silicate-phosphates[3]. The purpose of the present investigation is to prepare glasses and crystals of sodium vanadate-phosphates, which have P–O–V linkages.

Both the glasses and the crystals of alkali arsenate-phosphates, when dissolved in water, decompose by the scission of P–O–As linkages to give arsenate and mixtures of condensed phosphates[1]. As is the case with alkali arsenate-phosphates, sodium vanadate-phosphates, it is assumed, decompose by the scission of P–O–V linkages, when dissolved in water, to give vanadate and mixtures of condensed phosphates.

The present authors have made glasses and crystals of sodium vanadate-phosphates with various P/V ratios and have also obtained some information on the structures of the glasses and the crystals from paper chromatographic analyses of their aqueous solutions.

In the course of the present investigation it was found that vanadium(V) is partially reduced to vanadium(IV) when the starting materials, i.e., sodium metaphosphate, vanadium(V) oxide and sodium carbonate, are melted together to form the glasses or the crystals. Munakata et al.[4] found that a considerable amount of low valency vanadium, probably vanadium(IV), is produced when glasses of the V_2O_5-P_2O_5-BaO system are prepared.

Experimental

Vanadium(V) Oxide.—Ammonium metavanadate was recrystallized at least twice from its hot aqueous solution by adding ammonium chloride. The purified ammonium metavanadate was converted to vanadium(V) oxide by heating it at 350°C in a porcelain dish. The lower oxides of vanadium produced, together with vanadium(V) oxide, were oxidized by heating them with a small amount of nitric acid. The vanadium(V) oxide thus obtained was melted in a platinum crucible and crystallized by pouring out the melt on a copper plate.

Glasses of Sodium Vanadate-Phosphates.—Glasses of sodium vanadate-phosphates with various P/V ratios were prepared by melting mixtures of sodium metaphosphate (Graham salt), vanadium(V) oxide and sodium carbonate.

$$2x\mathrm{NaPO_3}+y\mathrm{V_2O_5}+y\mathrm{Na_2CO_3} = 2x\mathrm{NaPO_3}\cdot 2y\mathrm{NaVO_3}+y\mathrm{CO_2} \quad (1)$$

or

$$= (x+y)\mathrm{Na_2O}\cdot x\mathrm{P_2O_5}\cdot y\mathrm{V_2O_5}+y\mathrm{CO_2} \quad (2)$$

However, a part of the vanadium(V) oxide was reduced to vanadium(IV) oxide formally.

$$y\mathrm{V_2O_5} = (y-z)\mathrm{V_2O_5}+z\mathrm{V_2O_4}+z/2\mathrm{O_2} \quad (3)$$

In a platinum crucible a certain amount (15~30 g.) of monosodium dihydrogen orthophosphate dihydrate was dehydrated and melted by heating and converted into a glass of sodium metaphosphate by cooling the melt in the platinum crucible. After the weight of the glass was measured, calculated amounts of vanadium(V) oxide and sodium carbonate were taken on the glass in the crucible. Then the mixture of these three materials was melted at 900°C for 1 hr. The melt was quenched by pouring it on a copper plate and by pressing it with another copper plate. By this procedure glasses of sodium vanadate-phosphates with P/V ratios (x/y in Eq. 1) of 1, 2, 3, 4, 7, 10, 50, 100 and 200 were prepared. The glasses had colors ranging from dark brown toward yellow with the increasing P/V ratio.

Crystals of Sodium Vanadate-Phosphates.—A melt obtained from a mixture of sodium metaphosphate, vanadium(V) oxide and sodium carbonate was crystallized by keeping it at 450~500°C for 24 hr. By this treatment crystals of sodium vanadate-phosphates with P/V ratios of 7, 10 and 50 were prepared. All of the crystals are yellowish-green. By a similar treatment, the melts with P/V ratios of 3 and 4 were only partially crystallized.

Determination of Percentages of Vanadium(IV) in Relation to Total Vanadium.—An appropriate amount of sodium vanadate-phosphate was dissolved in 2 N sulfuric acid and titrated with 0.03 N potassium permanganate while being warmed on a water bath. After the titration with permanganate, the sample solution was titrated with 0.03 N ammonium iron(II) sulfate by the use of a few

1) E. Thilo and L. Koditz, *Z. anorg. u. allgem. Chem.*, **278**, 122 (1955); E. Thilo and K. Dostal, ibid., **298**, 100 (1958); I. Grunze, K. Dostal and E. Thilo, ibid., **302**, 221 (1959).

2) L. F. Audrieth, J. R. Mills and L. E. Netherton, *J. Phys. Chem.*, **58**, 482 (1954).

3) R. Jary, *Ann. chim.* (Paris) [13], **2**, 58 (1957).

4) M. Munakata, S. Kawamura, J. Asahara and M. Iwamoto, *J. Ceram. Assoc. Japan* (*Yogyo Kyokai-shi*), **67**, 344 (1959).

drops of a diphenylamine solution as an indicator, which solution was made by dissolving about 0.5 g. of diphenylamine in 50 ml. of 85% phosphoric acid. Before the second titration, 3 ml. of 85% phosphoric acid should be added to each 100 ml. of the sample solution in order to mask the iron(III). The first titration corresponds to the amount of vanadium-(IV), and the second, to the total amount of vanadium. From these titrations the percentages of vanadium(IV) in relation to the total vanadium ($z/y \cdot 100$ in Eq. 3) were calculated.

Paper Chromatography.—The paper chromatographic method of Karl-Kroupa[5] was used for samples containing short-chain phosphates and trimetaphosphate, while that of Smith[6] was used for samples containing relatively long-chain phosphates. The acid solvent was made by mixing 735 ml. of isopropyl alcohol, a solution of 50 g. of trichloroacetic acid in 265 ml. of water, and 2.5 ml. of concentrated aqueous ammonia. The basic solvent was made by mixing 387 ml. of isopropyl alcohol, 200 ml. of isobutyl alcohol, 408 ml. of water, and 5 ml. of concentrated aqueous ammonia. Toyo No. 51A filter papers were used. The colorimetric determination of orthophosphate was done by Nakamura's method[7].

A paper area for each phosphate species was cut into pieces and transferred to a small glass-filter connected to a suction bottle. Then 3~4 ml. of 1 N aqueous ammonia was added to the glass filter; after a few minutes it was filtered into a volumetric flask of 25 ml. by the use of a suction pump. This procedure was repeated four times, and a total of 15 ml. of 1 N aqueous ammonia was used. To the solution in the flask, 3.88 ml. of 8 N sulfuric acid was added, and the flask was placed in a boiling water bath for 20 min. in order to hydrolyze all the condensed phosphates to orthophosphate. After the flask was cooled, 3.3 ml. of amidol reagent[7] and 1.7 ml. of molybdate reagent[7] were added. Then the volume was brought up to the 25 ml. mark with distilled water. After the flask had been kept at 20°C for 10 min., the absorbance of blue color was measured against a reagent blank at 750 mμ.

Results and Discussion

When a mixture of sodium metaphosphate, vanadium(V) oxide and sodium carbonate is melted, carbon dioxide and then another kind of gas are evolved. It was qualitatively confirmed that the gas is oxygen. On the other hand, solutions of the glasses or the crystals of vanadate-phosphates are green and discolor a dilute solution of potassium permanganate acidified with sulfuric acid. These facts indicate that a part of the vanadium(V) in the melt is reduced to vanadium(IV) by the evolution of oxygen.

When a melt of vanadate-phosphates with a P/V ratio of 3 is heated at 900°C for 1, 2, 3 or 4 hr., the resulting glasses contain about 19% of vanadium(IV) in relation to the total vanadium in all cases, as is shown in Table I. This fact means that a heating of 1 hr. is sufficient to achieve an equilibrium between vanadium(V) and vanadium(IV) at 900°C.

Table I. Percentages of vanadium(IV) in relation to the total vanadium in the glasses with P/V ratio of 3, prepared by heating for 1~4 hr. at 900°C

Heating time, hr.	V(IV), %
1	18.9
2	18.7
3	18.8
4	18.9

The percentages of vanadium(IV) in relation to the total vanadium in the glasses of vanadate-phosphates with various P/V ratios are shown in Table II. With an increasing P/V ratio, i. e., with a decrease in the absolute amount of vanadium, the percentages of vanadium(IV) increase and reach an almost nearly constant value, 37~38%, when the P/V ratio is larger than 50.

Table II. Percentages of vanadium(IV) in relation to the total vanadium in the glasses having various P/V ratios

P/V ratio	V(IV), %
1	4.5
2	11.4
3	18.9
4	22.8
7	30.1
10	33.8
50	37.4
100	38.0
200	37.8

The percentages of vanadium(IV) in relation to the total vanadium in the crystals of vanadate-phosphates with P/V ratios of 7, 10 and 50, which are shown in Table III, are always a little smaller than those of vanadium-(IV) in the glasses with the same P/V ratios.

Table III. Percentages of vanadium(IV) in relation to the total vanadium in the crystals having various P/V ratios

P/V ratio	V(IV), %
7	27.1
10	32.0
50	34.1

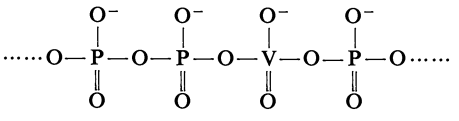
5) E. Karl-Kroupa, *Anal. Chem.*, **28**, 1091 (1956) and her private publication.
6) M. J. Smith, *Ontario Research Foundation, Report* 5703 (1957).
7) M. Nakamura, *J. Agr. Chem. Soc. Japan (Nippon Nogeikagaku Kaishi)*, **24**, 1 (1950).

TABLE IV. PHOSPHATE SPECIES FOUND IN THE AQUEOUS SOLUTIONS OF VARIOUS SODIUM VANADATE-PHOSPHATES

P/V	P, %								
	Ortho	Pyro	Tripoly	Tetra-poly	Penta-poly	Hexa-poly	Hepta-poly	Heigher poly	Tri-meta
Glasses									
1	89	11	0	0	0	0	0	0	0
2	19	65	15	0	0	0	0	0	0
3	12	63	22	4	0	0	0	0	0
4	8	33	9	15	11	9	0	14	0
7	2	15	9	8	1	8	8	48	0
10	3	11	5	3	2	7	10	59	0
Crystals									
7	6	23	8	4		5	5	0	50
10	3	17	7	2		3	2	7	60
50	2	4	0	0		0	0	0	94

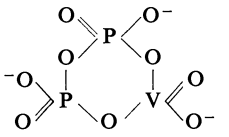
The results of the paper chromatography for the determination of phosphate species in the aqueous solutions of the glasses and the crystals of vanadate-phosphates are summarized in Table IV. Almost all of these data were obtained by the paper chromatography with an acid solvent. Although by the use of the acid solvent trimetaphosphate can not be completely separated from tetrapoly- or pentapolyphosphate, two-dimensional paper chromatograms for the aqueous solutions of the glasses with P/V ratios of 1~10 did not indicate the presence of ring phosphates such as trimeta- or tetrametaphosphate. Since the aqueous solutions of the crystals, on the contrary, contained trimetaphosphate, the total amount of tetrapoly-, pentapoly- and trimetaphosphate was determined by the use of the acid solvent, and the amount of trimetaphosphate was separately determined by the use of the basic solvent. The sum of tetrapoly- and pentapolyphosphate was calculated as the difference between these two figures.

The data for the glasses in Table IV indicate that the contents of the longer chain phosphates increase with an increasing P/V ratio. If it is assumed that P–O–V linkages in the solid substances are hydrolyzed as soon as dissolved in water, it may be presumed that the glasses are composed of chain structures such as



where vanadium(V) atoms are inserted into the phosphate chain.

Since a melt having a composition of sodium metaphosphate is crystallized as sodium trimetaphosphate under the same conditions as those used for the preparation of the crystals of sodium vanadate-phosphates, it is easy to surmise that crystals with P/V ratios of 7, 10 and 50 are mainly composed of trimetaphosphate, as is shown in Table IV. With an decreasing P/V ratio, i.e., with an increase in the absolute amount of vanadium, the amounts of trimetaphosphate decrease and those of pyrophosphate increase. Moreover, the pyrophosphate found in the solutions of the crystals are predominant in comparison with the other chain phosphates. These facts indicate that the pyrophosphate is probably derived from the hydrolysis of the following vanadate-phosphate ring:



At the present stage of investigation, it is not possible to determine, however, whether the chain phosphates other than the pyrophosphate are derived from amorphous substances mixed in the crystals.

The data in Table IV show that the main component in the case of the glass with a P/V ratio of 1 is orthophosphate. This fact may indicate that the glass is composed of a chain structure of alternate P–O and V–O linkages. The aqueous solutions of the glasses with P/V ratios of 2~10 contain predominant amounts of pyrophosphate in comparison with the other short-chain phosphates. From the fact it seems probable that the trimeta-vanadate-phosphate ring described in the case of the crystals is present also in the glasses.

In the aqueous solutions of the glasses, the number of chain phosphates longer than octapolyphosphate increases with an increasing P/V ratio. Although the aqueous solutions of the glasses with P/V ratios of 50, 100 and 200

could not be analyzed quantitatively by paper chromatography, almost all of the phosphorus were found as non-moving spots in their paper chromatograms developed with the acid solvent.

The role of vanadium(IV) in the glasses and the crystals has not been clear. However, from the fact that vanadyl ions VO^{2+} are most stable in crystals and solutions of vanadium(IV) salts, the vanadium(IV) in the vanadate-phosphates may also be present as vanadyl ions and may play a role as a cation like sodium ions.

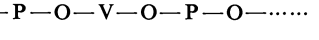
An X-ray diffraction pattern of the crystal with a P/V ratio of 50 is identical with that of sodium trimetaphosphate. This means that the presence of the vanadate, which is a minor constituent in this case, has not a great effect on the pattern of sodium trimetaphosphate. On the contary, X-ray patterns of crystals with P/V ratios of 7 and 10 are quite different from those of both sodium trimetaphosphate and sodium metavanadate.

Summary

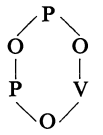
Glasses of sodium vanadate-phosphates with P/V ratios of 1∼200 were prepared from mixtures of sodium metaphosphate, vanadium(V) oxide and sodium carbonate. Crystals of sodium vanadate-phosphates with P/V ratios of 7, 10 and 50 were also prepared.

During the preparation of the glasses and the crystals, a part of the vanadium(V) is reduced to vanadium(IV). The percentages of vanadium(IV) in relation to the total vanadium increase with an increasing P/V ratio.

From the paper chromatographic analyses of the aqueous solutions of the glasses and the crystals, it may be presumed that the glasses are mainly composed of chain structures such as



and that the crystals contain considerable amounts of a vanadate-phosphate ring as follows:



Department of Chemistry
Faculty of Science
Kyushu University
Fukuoka

*Syntheses of γ-Ionone Analogues. IV. An Attempted Approach to 4-(2′-Methylene-3′, 4′, 5′-trimethylcyclohexyl)-but-3-en-2-one from 6-Benzyloxymethyl-2, 3, 4-trimethyl-3-cyclohexenylmethanal, and Investigation on Some Derivatives Thereby**

By Atsuaki ARAI and Iwao ICHIKIZAKI

(Received May 15, 1961)

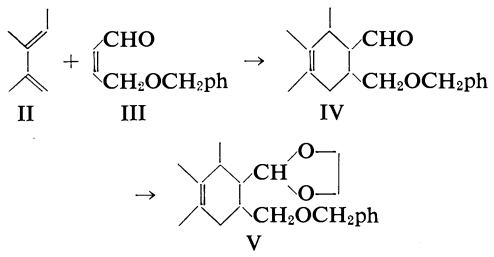
In the present work we have researched a synthetical route for the preparation of 4-(2′-methylene-3′, 4′, 5′-trimethylcyclohexyl)-but-3-en-2-one, an analogue of γ-ionone, from 6-benzyloxymethyl-2, 3, 4-trimethyl-3-cyclohexenylmethanal (IV). During the course of investigation we have studied on the hydrogenolysis products of 6-benzyloxymethyl-2, 3, 4-trimethyl-3-cyclohexenylmethanal ethylene acetal (V), and, moreover, investigated *p*-benzyloxybenzaldehyde as a new hydrogen acceptor for the modified Oppenauer oxidation.

A diene mixture[1] containing 37.5% 3, 4-dimethyl-1, 3-pentadiene (I) and 62.5% 2, 3-dimethyl-1, 3-pentadiene (II) underwent the Diels-Alder reaction with 4-benzyloxy-2-buten-1-al (III). This resulted in the selective addition of III to II in the presence of a small amount of hydroquinone at 140 to 150°C to produce a pale yellow adduct, $C_{18}H_{24}O_2$, which was proved extremely homogeneous after careful redistillation. From the experimental result[1] with regard to the direction of addition of 4-benzyloxy-2-butyn-1-al, $C_6H_5CH_2OCH_2C{\equiv}CCHO$, or of crotonaldehyde to II, the structure IV was assigned for the adduct obtained above. This

* This paper involves the partial correction regarding a short communication reported by one of the authors in *J. Chem. Soc. Japan, Pure Chem. Sec.* (*Nippon Kagaku Zasshi*), **80**, 451 (1959).

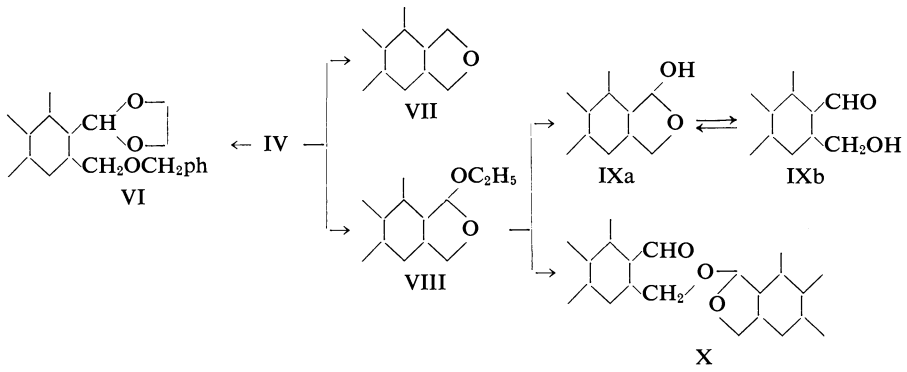
1) A. Arai and I. Ichikizaki, This Bulletin, **35**, 45 (1962).

compound readily reacted with ethylene glycol in the presence of *p*-toluenesulfonic acid in benzene to afford its ethylene acetal V in an 80% yield. No elimination of benzyl alcohol was then observed, although in the analogous treatment of 2-benzyloxymethyl-4,5,6-trimethylcyclohexa-1, 4-dienylmethanal, a doubly unsaturated analogue of IV, a remarkable aromaticization with removal of benzyl alcohol had been observed[1].



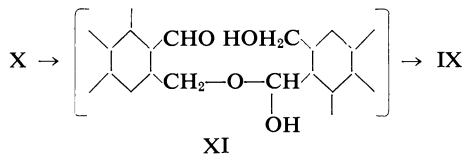
Hydrogenation of V in the presence of a palladium-on-charcoal catalyst in ethanol afforded in a 90% yield 6-benzyloxymethyl-2, 3, 4-trimethylcyclohexylmethanal ethylene acetal (VI), after a little more than one mole of hydrogen had been absorbed. In the presence of a more active catalyst, V afforded on hydrogenation a low-boiling oil, $C_{11}H_{20}O$, and a high-boiling liquid, $C_{13}H_{24}O_2$, in a 25.4 and 69% yield respectively, while ethylene glycol was then also obtained in a 86.5% yield. The low-boiling oil had a strong menthol-like odor, and has been proved to be 8, 9-*cis*-4, 5, 6-trimethyloctahydroisobenzofuran (VII), a full description on whose structure and some reactions will be given in a following paper. The infrared spectrum of the higher boiling oil clearly indicated the presence of a C–O–C–O–C group[2], while, the presence of neither carbonyl nor hydroxyl group was shown. On treatment with the Brady reagent, the oil gave a yellow 2,4-dinitrophenylhydrazone. This crystalline derivative was also obtained from the compound, $C_{11}H_{20}O_2$, which had been given by treating the oil with diluted sulfuric acid and showed a weak absorption band at 1721 cm^{-1} indicative of a carbonyl group in addition to marked absorption band characteristic of a hydroxyl and a C–O–C–O group in the infrared spectrum. From considering the fact[3,4] that α-alkoxytetrahydrofurans are readily converted with aqueous mineral acid into the corresponding γ-hydroxyaldehydes, which generally exist in an equilibrium between an acyclic and a cyclic form, we assigned 3-ethoxy-4, 5, 6-trimethyloctahydroisobenzofuran (VIII) and a tautomeric mixture of 6-hydroxymethyl-2, 3, 4-trimethylcyclohexylmethanal (IXb) and the cyclic hemiacetal IXa for the higher boiling oil and its hydrolyzed product respectively. By comparing the intensity at the carbonyl maximum in the infrared region of the equilibrium mixture with that of 4, 5-dimethyl-2-methoxymethylcyclohexylmethanal[5] which was adopted as a standard compound, it was suggested that the cyclic form IXa exists predominantly and the open free hydroxyaldehyde IXb in only 8.3%.

On hydrolysis of VIII a high-boiling viscous oil, $C_{22}H_{38}O_3$, besides IX was also obtained in a 12.4% yield. This compound reduced Tollens' reagent and its infrared spectrum showed the presence of a carbonyl group but no hydroxyl group, while almost all characteristic absorption bands in the finger print region, especially those at 1460 to 900 cm^{-1}, showed close resemblance to those of IX. With the Brady reagent this compound afforded the same 2, 4-dinitrophenylhydrazone as that from IX. It was obvious, therefore, that the ether linkage of this compound is readily cleaved by the action of acid to yield IX. Consequently, for this compound (3,4,5-trimethyl-2-formylcyclohexylmethyl-4′, 5′, 6′-trimethyloctahydroisobenzofuryl-3′)-ether (X) was assigned. It can be



2) M. Stoll and M. Hinder, *Helv. Chim. Acta*, **36**, 1948 (1953).
3) L. E. Schniepp and H. H. Geller, *J. Am. Chem. Soc.*, **68**, 1646 (1946).
4) C. D. Hurd and W. H. Saunders, Jr., ibid., **74**, 5324 (1952).
5) A. Arai and I. Ichikizaki, This Bulletin, **34**, 1571 (1961).

considered that on hydrolysis this compound, through the fission of the tetrahydrofuran ring, was converted into IX via a temporary intermediate XI.



XI

On reductive alkylation of dimethylamine with IX in the presence of a Raney nickel catalyst in ethanol, *N, N*-dimethyl-6-hydroxymethyl - 2, 3, 4 - trimethylcyclohexylmethylamine (XII) was obtained in a yield of 66% accompanying by an appreciable amount of 1, 2-dihydroxymethyl - 3, 4, 5 - trimethylcyclohexane (XIII) which was proved identical with that prepared by hydrogenating the compound IV. In an attempt to prepare XII in one step, IV and dimethylamine were catalytically hydrogenated at 200°C and then was obtained the expected aminoalcohol XII in a 30% yield and a considerable amount of neutral product consisting mainly of XIII and a small amount of IX was also isolated. From the above results, it is presumed for sure that the initial addition of dimethylamine to a carbonyl group of the compound IV has been markedly hindered by a benzyloxymethyl group.

Oxidation of XII to the corresponding *N*-oxide XIV, followed by thermal decomposition of the latter in the same manner as described for *N,N*-dimethyl-2-hydroxymethyl-4,5-dimethylcyclohexylmethylamine[5] afforded in a 67% yield *N, N*-dimethylhydroxylamine which was characterized as hydrochloride and in a 58% yield 2-methylene-3, 4, 5-trimethylcyclohexylmethanol (XV), b. p. 122~124°C/14 mmHg, n_D^{15} 1.4925, whose infrared spectrum (Fig. 1) showed the presence of both hydroxyl (3333 and 1050 and exocyclic methylene group (3096, 1645 and 889 cm^{-1}). The compound XV was further characterized as allophanate, m. p. 152~153°C.

The amino alcohol XII was oxidized to yield

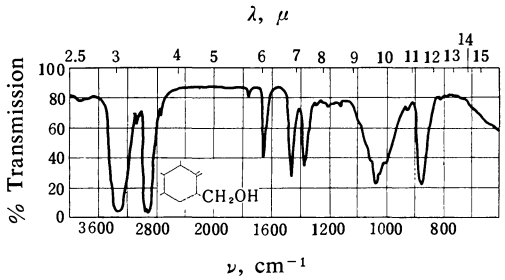
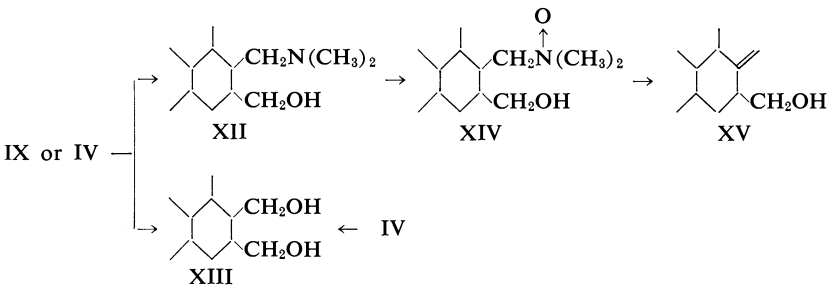


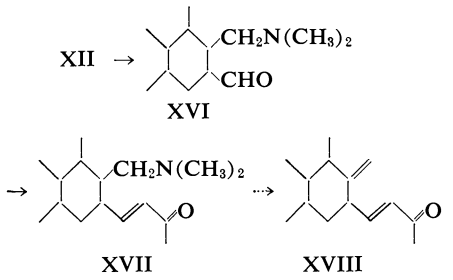
Fig. 1. Infrared spectrum of 2-methylene-3, 4, 5-trimethylcyclohexylmethanol (XV). (liquid film)

N, N-dimethyl-2, 3, 4 - trimethyl - 6 - formylcyclohexylmethylamine (XVI) in a yield of 88% by a modified Oppenauer procedure which involved *p*-benzyloxybenzaldehyde as the hydrogen accepter. For the oxidation of alicyclic primary alcohols to prepare the corresponding aldehydes some modified Oppenauer procedures have been employed successfully, in which cinnamaldehyde[6,7], anisaldehyde[6,8,9] and piperonal[6] as the hydrogen acceptors have hitherto been used. The use of these hydrogen acceptors is particularly advantageous when the desired aldehyde boils at below ca. 100°C/15 mmHg, because an efficient isolation of the resulted aldehyde by continuous distillation can be readily attained. However, in the case of high-boiling material no fruitful result can be expected on account of increasing hazardousness in separation. In this point of view, it was found that only *p*-benzyloxybenzaldehyde is a satisfactory hydrogen acceptor for the oxidation of XII, and that it can be superior in all respects for the case in which the resulted aldehyde boils at below ca. 110°C/1.0 mmHg.

Condensation of the amino aldehyde XVI with acetone in the presence of sodium hydride afforded in a 70% yield the amino ketone XVII, which was fully identified by the infrared absorption spectrum. Several attempts were made in an effort to obtain 4-(2′-methylene-3′, 4′, 5′-trimethylcyclohexyl)-but - 3 - en - 2 - one



6) A. Lachenauer and H. Schinz, *Helv. Chim. Acta*, **32**, 1265 (1949).
7) H. Favre and H. Schinz, ibid., **41**, 1368 (1958).
8) A. Brenner and H. Schinz, ibid., **35**, 1615 (1952).
9) R. Vonderwahl and H. Schinz, ibid., **35**, 1997 (1952).



(XVIII) through the thermal decomposition of the *N*-oxide of XVII, however, a fruitful result has not yet been obtained.

Experimental[10]

Mixed Dimethyl-1, 3-pentadienes.—The same mixed diene (b. p. 107.5~108°C/753 mmHg, n_D^{20} 1.4664) which is a mixture of 37.5% 3, 4-dimethyl-1, 3-pentadiene (I) and 62.5% 2, 3-dimethyl-1, 3-pentadiene (II) as used in the previous paper[1] was employed.

4-Benzyloxy-2-buten-1-al (III).—4-Benzyloxy-2-buten-1-al (III) was prepared in the manner described previously[5] and had b. p. 122~123°C/2.8 mmHg and $n_D^{18.5}$ 1.5310.

6-Benzyloxymethyl-2, 3, 4-trimethyl-3-cyclohexenylmethanal (IV).—A mixture of III (27.5 g.), the mixed diene (16.5 g.) described above and benzene (35 ml.) was heated with a small amount of hydroquinone at 140~150°C for 14 hr. under nitrogen. The reaction product was fractionated through a short column to yield a pale yellow viscous oil (24.0 g.), b. p. 127~129°C/3×10^{-3} mmHg, n_D^{17} 1.5298. The analytical sample obtained by redistillation exhibited b. p. 129°C/3×10^{-3} mmHg and n_D^{17} 1.5299. ν_{max}^{film} 1720 (C=O), 1098 (C-O-C), 3030, 1502, 742 and 704 cm^{-1} (mono-substituted phenyl group).

Found: C, 78.60; H, 8.87. Calcd. for $C_{18}H_{24}O_2$: C, 79.37; H, 8.88%.

The thiosemicarbazone crystallized from ethanol in needles, m. p. 127~127.5°C. λ_{max}^{EtOH} 271 mμ (ε, 37400).

Found: N, 12.13. Calcd. for $C_{19}H_{27}ON_3S$: N, 12.17%.

The phenylsemicarbazone crystallized from ethanol in needles, m. p. 145~146°C. λ_{max}^{EtOH} 248.5 mμ (ε, 29700).

Found: C, 74.18; H, 7.75. Calcd. for $C_{25}H_{31}O_2N_3$: C, 74.04; H, 7.71%.

The 2, 4-dinitrophenylhydrazone crystallized from ethanol in orange-yellow needles, m. p. 108~109°C.

Found: C, 63.68; H, 6.21. Calcd. for $C_{24}H_{28}O_5N_4$: C, 63.70; H, 6.24%.

6-Benzyloxymethyl-2, 3, 4-trimethyl-3-cyclohexenylmethanal Ethylene Acetal (V).—A mixture of the aldehyde IV (45 g.), ethylene glycol (22 g., 100% excess), benzene (50 ml.) and *p*-toluenesulfonic acid (70 mg.) was heated under reflux at a bath temperature of 120~130°C for 4.7 hr. with an azeotroper. The cooled reaction mixture was neutralized with a 5% aqueous sodium carbonate solution and the benzene layer was separated. The aqueous ethylene glycol layer was thoroughly extracted with benzene. The combianed benzene layers were washed with saturated aqueous salt solution and with water, dried over sodium sulfate and evaporated. Distillation of the residue gave the acetal V (42 g., 80%) as a pale yellow viscous oil, b. p. 132~135°C/3×10^{-3} mmHg, n_D^{16} 1.5281.

Found: C, 75.82; H, 9.01. Calcd. for $C_{20}H_{28}O_3$: C, 75.91; H, 8.92%.

6-Benzyloxymethyl-2, 3, 4-trimethylcyclohexylmethanal Ethylene Acetal (VI).—The unsaturated acetal V (20.0 g.) in ethanol (30 ml.) was hydrogenated in the presence of a palladium-on-charcoal catalyst (2.5% Pd, 0.8 g.) for 5.5 hr. at 130°C and 60 kg./cm^2 in a 100 ml. stainless steel autoclave. Removal of the catalyst and solvent, followed by distillation of the residue gave the acetal VI (18.3 g., 91%) as a colorless viscous oil, b. p. 167~170°C/1.0 mmHg, n_D^{21} 1.5150.

Found: C, 75.05; H, 9.70. Calcd. for $C_{20}H_{30}O_3$: C, 75.43; H, 9.50%.

Hydrogenation and Hydrogenolysis of 6-Benzyloxymethyl-2, 3, 4-trimethyl-3-cyclohexenylmethanal Ethylene Acetal (V).—The acetal V (40 g.) in ethanol (40 ml.) was hydrogenated in the presence of a palladium-on-charcoal catalyst (5% Pd, 3.0 g.) at 110 kg./cm^2. A vigorous absorption of hydrogen began at 60°C and the decrease of inner pressure was finished when the temperature reached to 122°C during 7 hr. After the catalyst was removed the filtrate was evaporated under reduced pressure through a 20 cm. Vigreux column to obtain two clear layers. The lower layer was extracted repeatedly with ether and the ether extracts were combined with the upper layer. The combined ethereal solution was washed with water, dried over sodium sulfate and evaporated. The remaining oil was fractionated through a 10 cm. Vigreux column to give two distinct fractions, b. p. 66~70°C/2.0 mmHg, n_D^{12} 1.4761 and b. p. 85~100°C/2.0 mmHg, n_D^{15} 1.4719. The former was redistilled through a short column to afford 8, 9-*cis*-4, 5, 6-trimethyloctahydroisobenzofuran (VII) (5.4 g., 25.4%) having a strong menthol-like odor, b. p. 67°C/2.0 mmHg, $n_D^{13.5}$ 1.4750. ν_{max}^{film} 1457 (CH_2), 1383 (CH_3), 1053 (C-O-C), 1104, 905 and 886 cm^{-1} (tetrahydrofuran ring).

Found: C, 78.18; H, 11.43. Calcd. for $C_{11}H_{20}O$: C, 78.51; H, 11.98%.

The latter on redistillation gave 3-ethoxy-4, 5, 6-trimethyloctahydroisobenzofuran (VIII) (18.5 g., 69%), b. p. 90~100°C/2.0 mmHg, $n_D^{15.5}$ 1.4719, which showed the presence of a C-O-C-O-C group (1108, 995, 920 and 890 cm^{-1}), while the presence of neither carbonyl nor hydroxyl group was indicated in its infrared absorption spectrum.

Found: C, 73.55; H, 11.28. Calcd. for $C_{13}H_{24}O_2$: C,73.53; H, 11.39%.

Treatment with the Brady reagent gave in an excellent yield 6-hydroxymethyl-2, 3, 4-trimethylcyclohexylmethanal 2, 4-dinitrophenylhydrazone which had m. p. 177°C after crystallization from methanol.

10) All m. p. are uncorrected. The ultraviolet spectra were determined with a Hitachi model EPU-2A spectrophotometer and the infrared spectra were obtained with a Nippon Bunkō model IR-S and a Kōken model DS-301 recording spectrophotometers using sodium chloride prisms.

Found: C, 56.32; H, 6.50. Calcd. for $C_{17}H_{24}O_5 \cdot N_4$: C, 56.03; H, 6.64%.

From the residue leaving after being extracted the lower layer with ether, ethylene glycol (5.1 g., 86.5%) could be obtained.

Acid Hydrolysis of 3-Ethoxy-4, 5, 6-trimethyloctahydroisobenzofuran (VIII).—A mixture of VIII (18 g.), tetrahydrofuran (80 ml.) and 2 N sulfuric acid (80 ml.) was heated under reflux at 70~80°C for 7 hr. The resultant mixture was cooled and neutralized with a 10% aqueous sodium carbonate solution. After the bulk of the solvent was removed under reduced pressure, the remaining oil was extracted with ether and the ether extract was washed with a saturated aqueous salt solution and dried over sodium sulfate. Removal of the solvent, followed by distillation of the residue yielded a colorless oil (11 g.), b. p. 112~118°C/2.0 mmHg, n_D^{20} 1.4852 and a colorless viscous oil (2.6 g.), b. p. 188~195°C/2.5 mmHg, n_D^{16} 1.4977.

The former on redistillation gave the tautomeric mixture of 3-hydroxy-4, 5, 6-trimethyloctahydroisobenzofuran (IXa) and 6-hydroxymethyl-2, 3, 4-trimethylcyclohexylmethanal (IXb) (10.3 g., 64%), b. p. 113~116°C/2.0 mmHg, n_D^{17} 1.4875, whose infrared spectrum (liquid film) showed characteristic absorption bands at 3414, 1103 (OH), 998, 935, 910 cm^{-1} (C-O-C-O) and a weak band at 1721 cm^{-1} indicative of a carbonyl group. $\lambda_{max}^{70\% \text{ aq. dioxane}}$ 224 mμ (ε,102), 290 (9.6).

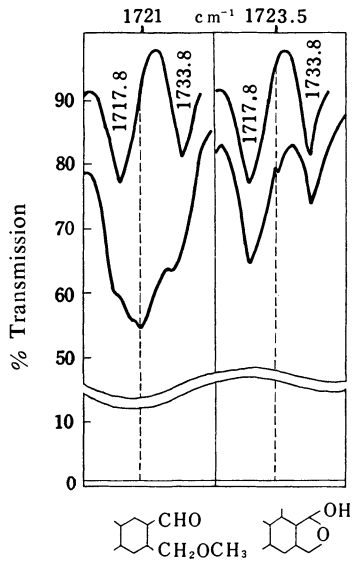


Fig. 2. Determination of the free aldehyde IXb in the tautomeric mixture of IXa and IXb.

(in carbon disulfide solution, 0.125 mm.)		
c (mol./l.)	0.0430	0.176
D	0.2516	0.0853
ε	5.85	0.485

Content of IXb: ca. 8.3%
(Perkin-Elmer model 112 spectrophotometer, NaCl prisms)

Found: C, 71.92; H, 10.98. Calcd. for $C_{11}H_{20} \cdot O_2$: C, 71.69; H, 10.94%.

The proportion of the free aldehyde IXb in the tautomeric mixture was ascertained, as shown in Fig. 2, by comparing the transmittance of the mixture at 1723.5 cm^{-1} with that of 4, 5-dimethyl-2-methoxymethylcyclohexylmethanal[5] at 1721 cm^{-1} in carbon disulfide at 20°C.

The 2, 4-dinitrophenylhydrazone prepared from the tautomeric mixture above was crystallized from ethanol to give yellow leaflets, m. p. 176~177°C, which was undepressed on admixture with that obtained directly from VIII.

After two redistillations the latter, high-boiling fraction afforded (3, 4, 5-trimethyl-2-formylcyclohexylmethyl-4′, 5′, 6′-trimethyloctahydroisobenzofuryl-3′)-ether (X), an intermolecular dehydration product of IX, b. p. 171~172°C, n_D^{19} 1.5017 (1.9 g., 12.4%), which showed a positive Tollens' test. Its infrared spectrum showed a strong carbonyl band at 1721 cm^{-1}, but no hydroxyl band. Moreover, almost all absorption bands indicated in the region of 1460 to 900 cm^{-1} agreed closely with those of IX. $\lambda_{max}^{75\% \text{ aq. dioxane}}$ 224 mμ (ε, 367), 295 (67).

Found: C, 75.48; H, 11.02. Calcd. for $C_{22}H_{38} \cdot O_3$: C, 75.38; H, 10.93%.

Treatment with the Brady reagent X gave in an excelient yield, a yellow 2, 4-dinitrophenylhydrazone which had m. p. 176~177°C after crystallization from ethanol and was identical with that prepared from IX. An attempt to prepare the semicarbazone of this compound in the usual manner has however been unsuccessful.

***N, N*-Dimethyl-6-hydroxymethyl-2, 3, 4-trimethylcyclohexylmethylamine (XII).** — *Reductive Condensation of Dimethylamine and 3-Hydroxy-4, 5, 6-trimethyloctahydroisobenzofuran (IX).*—A solution of IX (10.5 g.) and dimethylamine (4.3 g.) in ethanol (50 ml.) was hydrogenated with a Raney nickel catalyst (1.5 g.) for 2 hr. at 195~200°C and 109 kg./cm^2. After removal of the catalyst and solvent, the remaining colorless oil was dissolved in ether (80 ml.) and then extracted with 2 N hydrochloric acid (20 ml. × 3). The aqueous layer was made, after being washed once with ether, to strongly alkaline with a 10% aqueous sodium hydroxide solution under cooling. The regenerated organic base was taken up in ether and washed with water and dried over potassium carbonate. Removal of the solvent, followed by distillation of the residue yielded *N, N*-dimethyl-6-hydroxymethyl-2, 3, 4-trimethylcyclohexylmethylamine (XII) (8.2 g., 67.5%) as a colorless oil, b. p. 96~97°C/0.6 mmHg, n_D^{12} 1.4880. ν_{max}^{film} 2842, 2790, 2748 (*tert*-amino group), 3380, 1040 (OH), 837 cm^{-1} (unassigned).

Found: C,73.86; H, 12.67; N, 6.54. Calcd. for $C_{13}H_{27}ON$: C, 73.18; H, 12.76; N, 6.57%.

The methiodide crystallized from ethanol-ethyl acetate in leaflets, m. p. 204~206°C.

Found: C, 47.60; H, 8.33; N, 4.15. Calcd. for $C_{14}H_{30}ONI$: C, 47.30; H, 8.50; N, 3.95%.

The ether layer containing the neutral substance was washed with water, dried over sodium sulfate and evaporated. Distillation of the residue gave 1, 2-dihydroxymethyl-3, 4, 5-trimethylcyclohexane (XIII) (1.7 g., 16%) as a viscous oil, b. p. 140~

141.5°C/2.0 mmHg, n_D^{29} 1.4874. ν_{max}^{film} 3320, 1058 cm^{-1} (OH).

Found: C, 71.38; H, 11.90. Calcd. for $C_{11}H_{22}O_2$: C, 70.92; H, 11.90%.

The bis-*p*-nitrobenzoate crystallized from methanol in prisms, m. p. 161~162°C, which gave no melting point depression on admixture with that obtained by the other routes as described below.

Reductive Condensation of Dimethylamine and 6-Benzyloxymethyl-2, 3, 4-trimethyl-3-cyclohexenylmethanal (IV).—A solution of IV (3.5 g.) and anhydrous dimethylamine (1.2 g.) in ethanol (30 ml.) was hydrogenated over Raney nickel (1.0 g.) for 5 hr. at 200°C and 150 kg./cm^2. On similar treatment of the hydrogenated products to the manner in a), the basic fraction (0.85 g.) which had b. p. 97~99°C/0.5 mmHg and showed identical infrared spectrum with XII and the neutral fraction (1.4 g.), b. p. 110~140°C/2.0 mmHg, which was indicated to be mainly the diol XIII contaminated with a small amount of IX by its infrared spectrum, were obtained.

The basic fraction wats treated with methyl iodide to give in a good yield the methiodide of XII as leaflets, m. p. 206~207°C, which gave no melting point depression on admixture with that of the authentic XII and an appreciable amount of what is believed to be the methiodide of *N, N*-dimethyl-6-hydroxy-methyl-2, 3, 4-trimethyl-3-cyclohexenylmethylamine, which exhibited m. p. 258°C (decomp.) after being crystallized from ethanol-ethyl acetate.

Found: C, 47.78; H, 8.20. Calcd. for $C_{14}H_{28}ONI$: C, 47.65; H, 8.01%.

The neutral fraction was fractionated through a short Vigreux column to give the diol XIII (1.1 g., 46%), b. p. 140~142.5°C/2.0 mmHg, n_D^{20} 1.4905, which afforded the bis-*p*-nitrobenzoate, m. p. 162°C, after crystallization from methanol, identified by mixed melting point with an authentic sample.

Preparation of 1, 2-Dihydroxymethyl-3, 4, 5-trimethylcyclohexane (XIII) by Hydrogenation of IV.—The aldehyde IV (3.5 g.) in ethanol (25 ml.) was hydrogenated over Raney nickel (3.5 g.) for 5 hr. at 210~225°C and 190 kg./cm^2. Removal of the catalyst and solvent, followed by distillation of the residue gave a small fore-run and the diol XIII (1.95 g., 81.5%), b. p. 137°C/1.8 mmHg, n_D^{30} 1.4900.

Found: C, 71.11; H, 11.95. Calcd. for $C_{11}H_{22}O_2$: C, 70.92; H, 11.90%.

The bis-*p*-nitrobenzoate crystallized from methanol in leaflets, m. p. 162°C.

Found: C, 61.92; H, 5.96. Calcd. for $C_{25}H_{28}O_8N_2$: C, 61.97; H, 5.83%.

2-Methylene-3, 4, 5-trimethylcyclohexylmethanol (XV).—A mixture of the amino alcohol XII (1.2 g.), methanol (6 ml.) and 30% aqueous hydrogen peroxide (3 ml.) was stirred for 24 hr. at room temperature and allowed to stand for additional 48 hr. with occasional stirring, at which time it gave a negative spot test for the amine with phenolphthalein. Excess hydrogen peroxide was decomposed by stirring the solution with a platinum foil (0.8 g.) for 2 days at room temperature. The solution, after being removed the platinum foil, was concentrated under reduced pressure at a bath temperature of 30~40°C and the residual syrup was diluted with absolute ethanol (7 ml.) and reconcentrated. After the process was repeated five times to remove as much water as possible, *N, N*-dimethyl-6-hydroxymethyl-2, 3, 4-trimethylcyclohexylmethylamine oxide (XIV) was obtained as a colorless syrup.

A 30 ml. Claisen flask fitted with a 10 cm. Vigreux column containing the *N*-oxide XIV prepared as above was connected to a condenser, which led to two receivers in series, first cooled in a freezing mixture and second in a liquid nitrogen respectively. Decomposition of the *N*-oxide and distillation of the product began at 130°C and was complete at 140°C after 1 hr., at which time practically no material remained in the flask. The distillate was dissolved in ether (40 ml.) and washed with cold 5% hydrochloric acid and with water and dried over magnesium sulfate. Removal of the solvent, followed by distillation of the residue under nitrogen afforded 2-methylene-3, 4, 5-tri-methylcyclohexylmethanol (XV) (0.55 g., 58% based on XII) as a colorless oil, b. p. 122~124°C/14 mmHg, n_D^{15} 1.4925. The infrared spectrum of this compound was shown in the theoretical part.

Found: C, 78.12; H, 11.60. Calcd. for $C_{11}H_{20}O$: C, 78.51; H, 11.98%.

The allophanate crystallized from methanol, m. p. 152~153°C.

Found: C, 61.60; H, 8.65. Calcd. for $C_{13}H_{22}O_3N_2$: C, 61.39; H, 8.72%.

The combined washings containing hydrochloric acid were evaporated to dryness. The residue was diluted with absolute ethanol, reconcentrated under reduced pressure and the process was repeated 4 times to remove as much water as possible. The crystalline solid that remained was crystallized from absolute ethanol, after treatment with active charcoal, to afford *N, N*-dimethylhydroxylamine hydrochloride (0.37 g., 67%) as colorless needles, m. p. 105°C, which gave no melting point depression on admixture with an authentic sample.

***p*-Benzyloxybenzaldehyde.**—A solution of *p*-hydroxybenzaldehyde (24.4 g.) in ethanol (40 ml.) was added with cooling to sodium ethylate (prepared from 4.6 g. of sodium) in ethanol (70 ml.). Benzylchloride (25.3 g.) was then added slowly and the mixture was heated in a 300 ml. glass bomb at 130~140°C for 1.5 hr. when sodium chloride was precipitated completely. The reaction mixture was filtered and the precipitate was washed with a small amount of hot benzene. The filtrates were combined and concentrated under reduced pressure. The orange residue was dissolved in a mixture of benzene (200 ml.) and ether (200 ml.), washed with 10% aqueous sodium carbonate and with water, dried over sodium sulfate and evaporated. The residue was distilled under nitrogen or, more conveniently, crystallized from ethanol to give *p*-benzyloxybenzaldehyde (38.0 g., 89.5%), b. p. 187~189°C/5 mmHg, b. p. 155~156°C/1.1 mmHg, m. p. 73.5~74°C (lit.[11] m. p. 72°C).

Found: C, 79.36; H, 5.96. Calcd. for $C_{14}H_{12}O_2$: C, 79.22; H, 5.70%.

11) E. Wörner, *Ber.*, **29**, 142 (1896).

When the reaction was carried out at a temperature of 150~160°C, yield of the product decreased to ca. 60~70%.

p-Benzyloxybenzaldehyde is stable even when it was heated for several hours at 240~250°C under a nitrogen atomosphere.

The semicarbazone crystallized from ethanol in needles, m. p. 201~202°C.

Found: N, 15.75. Calcd. for $C_{15}H_{15}O_2N_3$: N, 15.61%.

The 2, 4-dinitrophenylhydrazone crystallized from ethanol-ethyl acetate in orange needles, m. p. 231~232°C.

Found: N, 14.05. Calcd. for $C_{20}H_{16}O_5N_4$: N, 14.28%.

***N*, *N*-Dimethyl-6-formyl-2, 3, 4-trimethylcyclohexylmethylamine (XVI).**—Aluminum isopropoxide (1.3 g., 120%) was added to the amino alcohol XII (3.4 g.) in a 15 ml. pear-shaped Claisen flask equipped with a 10 cm. Vigreux column. The isopropanol formed was removed over the course of 1.5 hr. at a bath temperature of 70~80°C and 10~12 mmHg pressure. To the XII-aluminate was then added *p*-benzyloxybenzaldehyde (5.6 g., 160%) in one portion, and the mixture was warmed at 80°C for a few minutes to make it homogeneous and distilled slowly by raising the bath temperature from 120 to 180°C. (1.0 mmHg pressure) during 40 min. under nitrogen. Fractionation of the distillate afforded the amino aldehyde XVI (2.95 g., 88%), b. p. 90~92°C/1.2 mmHg, n_D^{18} 1.4833, whose infrared spectrum indicated the presence of a carbonyl (1706) and a *tert*-amino group (2840, 2800 and 2745 cm^{-1}), but no hydroxyl group.

Found: C, 73.86; H, 11.95; N, 6.96. Calcd. for $C_{13}H_{25}ON$: C, 73.88; H, 11.92; N, 6.63%.

An attempt to prepare the 2, 4-dinitrophenylhydrazone of XVI using the Brady reagent gave instead the sulfate of the desiredder ivative. Basifying an aqueous solution of this salt with 10% aqueous sodium hydroxide yielded the free 2, 4-dinitrophenylhydrazone, which was chromatographed from benzene-petroleum ether (1 : 1) on alumina and crystallized from methanol to give orange-yellow needles, m. p. 189~190°C.

Found: N, 17.30. Calcd. for $C_{19}H_{29}O_4N_5$: N, 17.89%.

4-(2'-*N*, *N*-Dimethylaminomethyl-3', 4', 5'-trimethylcyclohexyl)-but-3-en-2-one (XVII). — The amino aldehyde XVI (2.8 g.) in acetone (15 ml.) was added to a solution of sodium hydride (100 mg.) in acetone (25 ml., freshly distilled after being treated with potassium permanganate) and the stirring was continued for 4.5 hr. at room temperature under nitrogen. After removal of the solvent, the residual oil was dissolved in ether and extracted with 10% hydrochloric acid. The aqueous layer was washed once with petroleum ether, basified with 10% aqueous sodium hydroxide and the free base regenerated was taken up in ether. The combined ether extracts were washed with water, dried over sodium sulfate and evaporated. Distillation of the residue gave the amino ketone XVII (2.4 g., 70%) as a pale yellow oil, b. p. 122~123°C/0.6 mmHg, $n_D^{25.5}$ 1.4898. ν_{max}^{film} 1678 (C=O, conju.), 1620 (C=C, conju.), 983 (-CH=CH-, trans), 2836, 2790, 2750 (*tert*-amino group), 1256 (=CH-CO-), 1380 (CH_3), 1361 cm^{-1} (CH_3CO).

Found C, 75.00; H, 11.89. Calcd. for $C_{16}H_{29}ON$: C, 76.44; H, 11.63%.

We wish to thank Dr. Asaji Kondo of the Tokyo Institute of Technology for microanalyses and Dr. Kenji Kuratani of the Aeronautical Institute of the University of Tokyo and Dr. Tadashi Satō of the Waseda University for infrared spectroscopy.

Laboratory of Organic Chemistry
Kobayasi Institute of Physical Research
Kokubunji, Tokyo

Syntheses of γ-Ionone Analogues. V. 8, 9-cis-4, 5, 6-Trimethyloctahydroisobenzofuran and its Derivatives[1]

By Atsuaki ARAI and Iwao ICHIKIZAKI

(Received July 6, 1961)

In the preceding paper[2] we briefly described an oil, $C_{11}H_{20}O$, which was obtained as one of the hydrogenolysis products of the ethylene acetal of 6-benzyloxymethyl-2, 3, 4-trimethyl-3-cyclohexenylmethanal (V). The infrared spectrum and some properties of this compound resembled those of octahydroisobenzofuran[3] and it showed bands in the infrared region (Fig. 1) at 905 and 886 cm^{-1} characteristic of a tetrahydrofuran ring and at 1053 cm^{-1} indicative of an ether group. M^me^ Mousseron-Canet and her co-laborators[4] have pointed out

1) Presented partly before the Meeting of Hokkaido district of the Chemical Society of Japan, Sapporo, July, 1960.

2) A. Arai and I. Ichikizaki, This Bulletin, 35, 504 (1962).

3) J. Entel, C. H. Ruof and H. C. Howard, *J. Am. Chem. Soc.*, 74, 441 (1952).

4) M. Mousseron-Canet and M. Granier, *Bull. soc. chim.*, 1959, 473; M^me^ Mousseron, M. Mousseron and M. Granier, ibid., 1960, 1418.

in their study on the infrared spectra of the octahydroisobenzofuran series that the absorption band of a C–O–C group at 1000 to 1100 cm^{-1} offers an available information to determine the conformation of cyclic oxide, and they have shown by pertinent comparison with the two stereoisomers of tricyclic oxide which are derivatives of the gem. dimethyloctaline that the cis isomer indicates a characteristic band at 1056 to 1060 cm^{-1}, whereas the trans shows a band at 1020 cm^{-1}. Thus, the structure of 8, 9-*cis*-4, 5, 6 - trimethyloctahydroisobenzofuran (I) was assigned for the oil and it was supported also by the succeeding experimental evidences as described below.

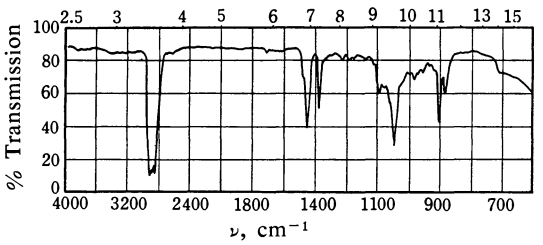


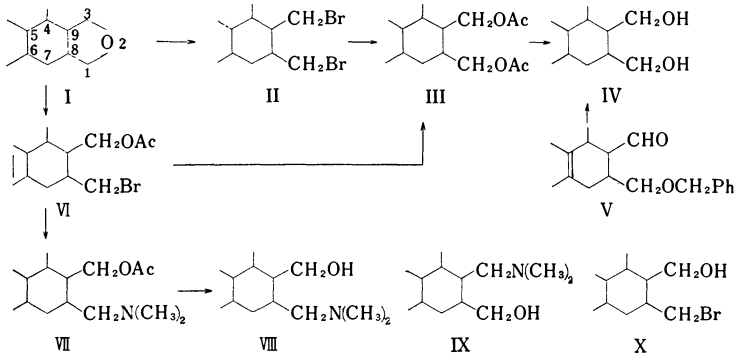
Fig. 1. Infrared spectrum of 8,9-*cis*-4,5,6-trimethyloctahydroisobenzofuran (I).

The compound I reacted with hydrogen bromide in glacial acetic acid at 100°C to give a mixture of dibromide II and a small amount of any acetoxy compounds which showed an infrared absorption band with ν_{max} 1737 cm^{-1}. The mixture could be mostly converted into 1, 2-diacetoxymethyl-3, 4, 5-trimethylcyclohexane (III) on being heated under reflux in glacial acetic acid containing potassium acetate and acetic anhyride and simultaneously gave a considerable amount of I. On alkaline hydrolysis III afforded a high yield of 1, 2-dihydroxymethyl-3, 4, 5-trimethylcyclohexane (IV) which was identical with the hydrogenation product[2] of the compound V. On the other hand, with acetyl bromide in the presence of zinc chloride I reacted to give a bromo acetate, $C_{13}H_{23}O_2Br$, in an expellent yield, which upon further acetylation followed by saponification yielded the diol IV. Although it has been well-known that tetrahydro-furans and -pyrans are generally cleaved by hydrogen halides[5-8] or acid halides[8-10] to give the corresponding dihalides or haloesters, no study on the cleavage of the asymmetric oxide ring as in I has been reported. Now it becomes interesting for us whether the cleavage takes place at the C(1)–O or it does at the C(3)–O linkage.

On treatment with an excess of anhydrous dimethylamine in absolute methanol the bromo acetate obtained above afforded 30% yield of an amino acetate, $C_{15}H_{29}O_2N$, and 35% yield of the parent oxide I, while the starting substance was also recovered in part. Alkaline hydrolysis of this amino acetate gave a high yield of the corresponding amino alcohol, $C_{13}H_{27}ON$, whose infrared absorption bands in almost all regions have close resemblance to those of *N*, *N*-dimethyl-6-hydroxymethyl-2, 3, 4-trimethylcyclohexylmethylamine (IX)[2]. Its methiodide, m. p. 202~203°C, resembled that of IX melted at 204~206°C in many respects, but the mixture melting point showed a marked depression. It is, therefore, no doubt that the amino alcohol is to be a structural isomer of IX and that in it the hydroxymethyl and the *N*, *N*-dimethylaminomethyl groups are reversely located as compared with IX. Thus, we assigned *N*, *N*-dimethyl-2-hydroxymethyl-3, 4, 5-trimethylcyclohexylmethylamine (VIII) for this compound. *N*, *N*-Dimethyl-2-acetoxymethyl-3, 4, 5 - trimethylcyclohexylmethylamine (VII) and 2-acetoxymethyl-1-bromomethyl-3, 4, 5-trimethylcyclohexane (VI) were accordingly assigned for the amino acetate and the bromo acetate, respectively. Furthermore, it became clear that the fission of the tetrahydrofuran ring in I with acetyl bromide occurs essentially in the 1, 2-position. And in the course of reaction involving the ring fission and the reverse cyclization it has been proved that the configuration of oxide I is completely retained still in the derivatives as stated for octahydroisobenzofuran[8]. The compound V is believed to have a 1, 6-*cis* conformation according to the Alders' rule authorized by a number of investigators[11,12]. The 8, 9-*cis* conformation previously proposed for the oxide by its infrared spectral analysis, therefore, received further support from the fact that I as well as V gives the same diol IV.

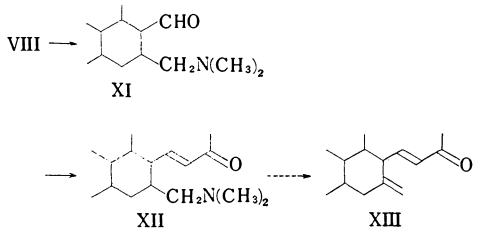
The formation of I in the course of amination of the bromo acetate VI may be conveniently explained by considering the bromo alcohol X as an intermediate, which would be formed readily by the interaction of the acetoxyl group and dimethylamine and converted into oxide I by the base promoted elimination of hydrogen bromide, since such

5) S. Fried and R. D. Kleene, *J. Am. Chem. Soc.*, **62**, 3258 (1940); **63**, 2691 (1941).
6) A. Lüttringhaus and A. Brechlin, *Ber.*, **92**, 2271 (1959).
7) S. F. Birch, R. A. Dean and E. V. Whitehead, *J. Org. Chem.*, **19**, 1449 (1954).
8) G. A. Haggis and L. N. Owen, *J. Chem. Soc.*, **1953**, 389, 408.
9) G. Sieber, *Ann.*, **631**, 180 (1960).
10) J. B. Cloke and F. J. Pilgrim, *J. Am. Chem. Soc.*, **61**, 2667 (1939).
11) M. C. Kloetzel, "Organic Reactions", Vol. IV, John Wiley and Sons, Inc., New York (1948), p. 1.
12) G. Stork and I. J. Borowitz, *J. Am. Chem. Soc.*, **82**, 4307 (1960).



halo alcohols have been commonly used for the most effective preparation of the oxides in this series[8].

The amino alcohol VIII was oxidized by a modified Oppenauer procedure with *p*-benzyloxybenzaldehyde as a hydrogen acceptor[2] to give a high yield of *N*, *N*-dimethyl-2-formyl-3, 4, 5-trimethylcyclohexylmethylamine (XI), which afforded on condensation with acetone in the presence of sodium hydride 4-(6′-*N*, *N*-dimethylaminomethyl-2′, 3′, 4′-trimethylcyclohexyl)-but-3-en-2-one (XII) in 59% yield. Two compounds XI and XII were fully identified by the infrared spectrum. The latter compound would seem to be an intermediate to 4-(6′-methylene-2′, 3′, 4′-trimethylcyclohexyl)-but-3-en-2-one (XIII), an analogue of γ-irone, but further investigation has not been performed.



Experimental[13]

8, 9-*cis*-4, 5, 6-Trimethyloctahydroisobenzofuran (I).—Compound I was previously obtained[2] as one of the hydrogenolysis products of the ethylene acetal of 6-benzyloxymethyl-2, 3, 4-trimethyl-3-cyclohexenylmethanal (V). A sample having b. p. 66～68°C/1.8 mmHg and n_D^{27} 1.4739 was used for the next experiments. Its infrared spectrum is shown in the theoretical part.

1, 2-Dibromomethyl-3, 4, 5-trimethylcyclohexane (II).—A mixture of oxide I (6.7 g.) and acetic acid (20 ml.) containing anhydrous hydrogen bromide (9.0 g.) was heated for 5 hr. at 100°C in a 50 ml. glass bomb. Hydrogen bromide and acetic acid were distilled off and the remaining oil was dissolved in chloroform (15 ml.). The chloroform solution was washed with 20% aqueous sodium bicarbonate and with water and dried over sodium sulfate. The solvent was removed and the residue was distilled to give a colorless pleasant smelling liquid (7.5 g.), b. p. 106～107.5°C/0.8 mmHg, n_D^{11} 1.5248, whose infrared spectrum showed the presence of an acetate group (1737 cm^{-1}) and no hydroxyl group.

Found: C, 46.46; H, 7.20. Calcd. for $C_{11}H_{20}Br_2$ (II): C, 42.31; H, 6.41%.

From the above infrared spectrum and elemental analysis it was believed that the product consists of 1, 2-dibromomethyl-3, 4, 5-trimethylcyclohexane (II) and a considerable amount of any acetoxy derivative.

1, 2-Diacetoxymethyl-3, 4, 5-trimethylcyclohexane (III).—The crude dibromide (4.3 g.) obtained above was heated under reflux with acetic acid (60 ml.) containing potassium acetate (15 g.) and acetic anhydride (3 ml.) for 37 hr. After the bulk of acetic acid was removed under reduced pressure, the residue was extracted with ether and the ether extract was washed with a 20% aqueous sodium carbonate solution and with water, dried over sodium sulfate and evaporated. Distillation of the residue gave a fore-run (0.9 g.) consisting largely of the oxide I, b. p. 65～67°C/1.65 mmHg, and a high-boiling oil (1.8 g.) had b. p. 105～107°C/0.6 mmHg and n_D^{15} 1.4760, which gave on redistillation through a 10 cm. Vigreux column the diacetate III, b. p. 108°C/0.75 mmHg, n_D^{18} 1.4740. ν_{max} (liquid film) 1737 (ester, C=O), 1237 (ester, C-O-C) and 1035 cm^{-1} (C-O).

Found: C, 66.45; H, 9.76. Calcd. for $C_{15}H_{26}O_4$: C, 66.63; H, 9.69%.

2-Acetoxymethyl-1-bromomethyl-3, 4, 5-trimethylcyclohexane (VI).—A mixture of I (4.4 g.), freshly distilled acetyl bromide (4.0 g., 125%), and zinc chloride (0.2 g.) was heated under reflux for 1.5 hr. in which time boiling had ceased. The dark-brown reaction mixture was dissolved in chloroform and the chloroform solution was washed with aqueous sodium bicarbonate and with water, dried and evaporated. The remaining oil was distilled to afford the bromo acetate VI (5.4 g., 71%) as a pale yellow, pleasant smelling oil, b. p. 102～105°C/

13) All melting points and boiling points are uncorrected. Infrared spectra were measured with a Nippon Bunkō model IR-S double-beam recording spectrophotometer with sodium chloride optics.

0.65 mmHg, n_D^{11} 1.5032. For analysis a sample was redistilled through a 8 cm. Vigreux column; b. p. 104～104.5°C/0.5 mmHg, 121～122°C/1.2 mmHg, n_D^{12} 1.5090. ν_{max} (liquid film) 1738 (ester, C=O), 1234 (ester, C-O-C), 1034 (C-O) and 1384, 1372 cm^{-1} (doublet, CH_3 and O-$COCH_3$ groups).

Found: C, 53.38; H, 7.85. Calcd. for $C_{13}H_{23}O_2 \cdot Br$: C, 53.60; H, 7.92%.

1,2-Dihydroxymethyl-3,4,5-trimethylcyclohexane (IV).—*a) Alkaline Hydrolysis of III.*—A solution of the diacetate III (0.55 g.) and potassium hydroxide (0.3 g.) in methanol (7 ml.) was allowed to stand for 41 hr. at room temperature. The reaction mixture was neutralized with 2 N sulfuric acid under cooling and then extracted, after the removal of the bulk of methanol, with ether. The ether extract was washed with water and dried over sodium sulfate. Removal of the solvent followed by distillation of the residue and yielded diol IV (0.35 g., 92.5%) as a viscous oil, b. p. 128～130°C/0.65 mmHg, n_D^5 1.4925. ν_{max} (liquid film) ～3300 and ～1045 cm^{-1} (OH).

Found: C, 70.99; H, 11.76. Calcd. for $C_{11}H_{22}O_2$: C, 70.92; H, 11.90%.

The bis-*p*-nitrobenzoate crystallized from methanol in needles, m. p. 161～162°C, which gave no melting point depression on admixture with that of the diol obtained previously[2] from 6-benzyloxymethyl-2,3,4-trimethyl-3-cyclohexenylmethanal (V).

Found: C, 61.88; H, 5.96. Calcd. for $C_{25}H_{28} \cdot O_8N_2$: C, 61.97; H, 5.83%.

b) Further Acetylation Followed by Alkaline Hydrolysis of VI.—A mixture of the bromo acetate VI (2.2 g.), acetic acid (25 ml.), potassium acetate (10 g.) and acetic anhydride (1.8 ml.) was heated under reflux for 20 hr. The bulk of acetic acid and acetic anhydride was removed under reduced pressure, and the orange-brown residue was dissolved in solution of potassium hydroxide (3.0 g.) in 90% methanol (15 ml.) and the solution was set aside for 24 hr. at room temperature. The reaction mixture was treated with the same method as described for a) to afford VI (0.8 g., 56.8%), b. p. 140～142°C/2.1 mmHg, n_D^{29} 1.4870, whose infrared spectrum and solid derivative were identical with those of the diol IV prepared in the method of a).

Reaction of the Bromo Acetate VI with Dimethylamine.—A solution of the bromo acetate VI (3.4 g.) and anhydrous dimethylamine (6.5 g., 10 times of the theoretical amounts) in absolute ethanol (17 ml.) was allowed to stand for 10 days at room temperature in a 50 ml. amber glass bomb. After removal of the solvent and dimethylamine under reduced pressure, the residue was dissolved in ether (30 ml.). The ethereal solution was extracted with three 10 ml. portions of 2 N hydrochloric acid and the combined extracts were washed once with light petroleum and then made to basic with 10% aqueous alkali under cooling. The organic base regenerated was taken up in ether and the ether layer was washed with an aqueous saturated salt solution, dried over sodium sulfate and evaporated. Distillation of the residue to give a slightly yellow oil (0.75 g.), b. p. 90～91°C/0.5 mmHg, n_D^{16} 1.4808, whose infrared spectrum showed characteristic absorptions of the acetyl group at 1739 and 1240 cm^{-1} and *tert*-amino group at 2846, 2800 and 2755 cm^{-1}, and weak bands the hydroxyl group at of ～3390 and ～3200 cm^{-1}.

Found: C, 70.88; H, 11.36; N, 5.62. Calcd. for $C_{15}H_{29}O_2N$: C, 70.54; H, 11.45; N, 5.48%.

It is believed, therefore, that above oil consists of *N,N*-dimethyl-2-acetoxymethyl-3,4,5-trimethylcyclohexylmethylamine (VII) contaminated with a small amount of its hydrolyzed product VIII.

The ethereal solution remained was washed with water, dried over sodium sulfate and evaporated. The residue was distilled to give the oxide I (0.7 g., 35%), b. p. 51～52°C/0.5 mmHg, n_D^{12} 1.4803, (Found: C, 78.61; H, 11.82%), and to recover the unchanged VI (0.5 g., 14.7%), b. p. 104～105°C/0.5 mmHg.

***N,N*-Dimethyl-2-hydroxymethyl-3,4,5-trimethylcyclohexylmethylamine (VIII).**—A solution of the amino acetate VII (0.3 g.) and potassium hydroxide (0.3 g.) in methanol (5 ml.) was kept for 40 hr. at room temperature. Ether (50 ml.) was added to the reaction mixture and the resultant solution was washed with a saturated aqueous salt solution, dried over potassium carbonate and evaporated. Distillation gave the amino alcohol VIII (0.24 g.) as a colorless liquid, b. p. 87～89°C/0.5 mmHg, n_D^{10} 1.4852. ν_{max} (liquid film) 3395, 3200, 1041 (OH); 2840, 2790, 2750 (-$N(CH_3)_2$); 848, 833 cm^{-1} (unassigned).

Found: C, 73.17; H, 12.82; N, 6.62. Calcd. for $C_{13}H_{27}ON$: C, 73.18; H, 12.76; N, 6.57%.

In a separate preparation from VI without isolation of the amino acetate VII, 35% over-all yield of VIII was obtained.

The methiodide crystallized from methanol-ethyl acetate in leaflets, m. p. 202～203°C, which showed a marked depression in the mixed melting point determination with that of *N,N*-dimethyl-6-hydroxylmethyl-2,3,4-trimethylcyclohexylmethylamine (IX) melted at 204～206°C.

Found: C, 47.28; H, 8.74; N, 3.83. Calcd. for $C_{14}H_{30}ONI$: C, 47.30; H, 8.50; N, 3.95%.

***N,N*-Dimethyl-2-formyl-3,4,5-trimethylcyclohexylmethylamine (XI).**—To the amino alcohol aluminate prepared from IX (1.5 g.) and aluminum isopropoxide (0.55 g., 115%) *p*-benzyloxybenzaldehyde (2.4 g., 160%) was added and the resultant mixture was distilled under nitrogen with the same method as described for the oxidation of the isomeric amino alcohol IX[2] to give an oil (1.23 g.), redistillation of which through an 8 cm. Vigreux column afforded the aminoaldehyde XI (1.05 g., 81%) as a colorless oil, b. p. 87～89°C/0.85 mmHg, n_D^{20} 1.4744, whose infrared spectrum showed the presence of C=O (1711), -$N(CH_3)_2$ (2844, 2798, 2753), and no hydroxyl group.

Found: C, 73.52; H, 11.98; N, 6.61. Calcd. for $C_{13}H_{25}ON$: C, 73.88; H, 11.92; N, 6.63%.

Treatment of this oil with picric or picrolonic acids gave an orange-red oil which could not be induced to crystallize. An attempt to prepare the analytical sample of the 2,4-dinitrophenylhydrazone of XI was unsuccessful.

4-(6'-*N,N*-Dimethylaminomethyl-2',3',4'-trimethylcyclohexyl)-but-3-en-2-one (XII).—The amino aldehyde XI (1.0 g.) in freshly distilled acetone

(5 ml.) was added to a cold solution of sodium hydride (30 mg.) in acetone (15 ml.) with vigorous stirring under a nitrogen atmosphere. The resultant mixture was stirred for additional 3 hr. at room temperature, and evaporated under reduced pressure to remove the bulk of acetone. The residue was dissolved in ether and the ethereal solution was extracted twice with 10% hydrochloric acid. The combined extracts were basified with 10% aqueous alkali, after being washed once with light petroleum, to regenerate the organic base which was taken up in ether. The ethereal solution was washed with water, dried over potassium carbonate and concentrated. Distillation gave the amino ketone XII (0.7 g., 59%) as a pale yellow oil, b. p. 122~125°C/0.7 mmHg, n_D^{23} 1.4842. For analysis a sample was redistilled; b. p. 122~125°C/0.65 mmHg, n_D^{25} 1.4852.

ν_{max} (liquid film) 1680 (C=O, conju.); 1622 (C=C, conju.); 984 (-CH=CH-, trans); 2839, 2800, 2752 ($-N(CH_3)_2$); 1259 (=C-CO-); 1381 (CH_2); 1361 ($COCH_3$); 840 cm^{-1} (unassigned).

Found: C, 76.22; H, 11.78. Calcd. for $C_{16}H_{29}ON$: C, 76.44; H, 11.63%.

An attempt to prepare the 2,4-dinitrophenylhydrazone of this compound was unsuccessful.

The authors are indebted to Dr. Asaji Kondo of the Tokyo Institute of Technology for the microanalyses.

Laboratory of Organic Chemistry
Kobayasi Institute of Physical Research
Kokubunji, Tokyo

Note on the Solvent Extraction of Some Metals by Tri-n-octyl Phosphine Oxide

By Hideo SAISHO

(Received July 27, 1961)

Tri-*n*-octyl phosphine oxide (TOPO) is one of the alkyl phosphine oxides and has been employed as a solvent extraction reagent for many elements[1,2]. The detailed investigation of the extraction behavior with this reagent has been carried out for a few metals[2]. This paper presents the extraction behavior of zirconium, hafnium, niobium and tantalum in the system of TOPO-cyclohexane and hydrochloric or nitric acid.

TOPO was dissolved in cyclohexane without further purification. The distribution ratio, K_d, was determined radiochemically using the radionuclides Zr-95, Hf-181, Nb-95 and Ta-182. Activities in the aliquots of the two phases were measured with a gamma-ray scintillation counter. The aqueous solution containing a radionuclide such as the metallic ions was shaken vigorously with an organic solution for thirty minutes in a thermostat kept at 25±0.5°C.

Figure 1 shows the variation of the K_d values of zirconium and hafnium in the range of 1×10^{-3} to 1×10^{-2} M TOPO concentration in the organic phase, keeping the acidity of the aqueous phase constant. The plots of $\log K_d$ vs. logarithmic TOPO concentration

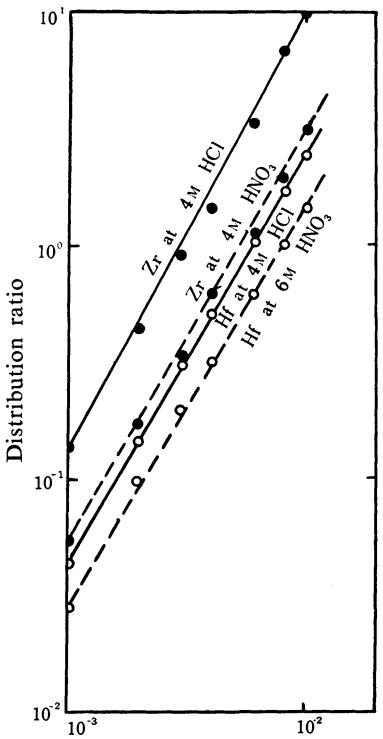


Fig. 1. Power dependence of distribution ratio on TOPO concentration.

1) J. C. White, U. S. AEC Rep., TID-7555, "Analytical Chemistry in Nuclear Reactor Technology", (1957), p. 240.
2) J. C. White, "Symposium on Solvent Extraction in the Analysis of Metals", American Society for Testing Materials, Philadelphia (1958), p. 27.

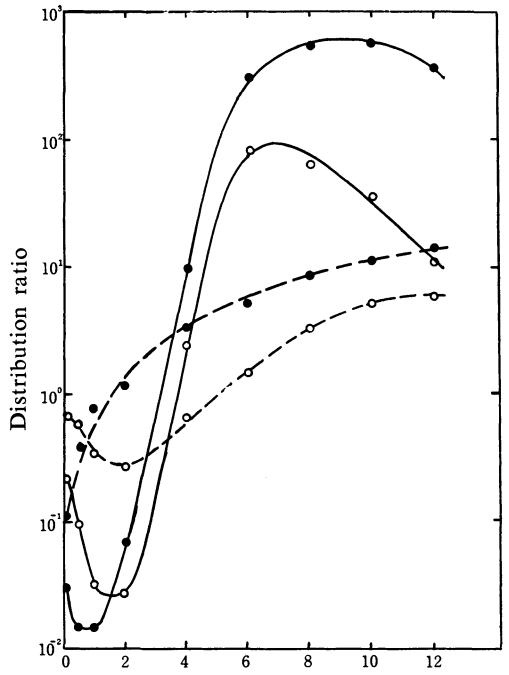


Fig. 2. Distribution ratio of zirconium and hafnium.

——: Hydrochloric acid ----: Nitric acid
● : Zirconium ○ : Hafnium

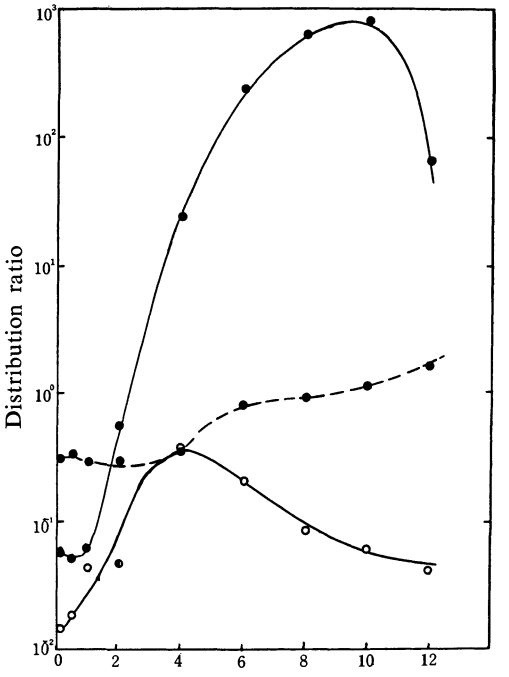


Fig. 3. Distribution ratio of niobium and tantalum.

——: Hydrochloric acid ----: Nitric acid
● : Niobium ○ : Tantalum

show a constant slope of about 2 in all cases. The second power dependence of the K_d values on the TOPO concentration suggests an extracted species that has a value of two for the moles of TOPO per mole of zirconium or hafnium.

Figures 2 and 3 show the K_d values of zirconium, hafnium, niobium and tantalum in the range of hydrochloric or nitric acid concentration from 0.1 to 12 M, keeping the TOPO concentration 1×10^{-2} M except in the case of tantalum in nitric acid. The K_d values for tantalum in nitric acid could not be determined exactly, because the activities extracted into the organic phase were very low. As shown in these figures, the K_d values greatly depend on the kind of acid and on its concentration. Zirconium can be separated from hafnium in the high acidity region, and also from niobium in nitric acid. A mutual separation of niobium and tantalum can be carried out more completely than that of zirconium and hafnium in hydrochloric acid.

Engineerig & Research Laboratory
Mitsubishi Atomic Power Industries, Inc.
Ohmiya, Saitama-ken

Spectrophotometric Determination of Magnesium with Pontachrome Azure Blue B.

By Katsuya UESUGI, Yukiteru KATSUBE and John H. YOE

(Received January 16, 1962)

A new spectrophotometric method for the determination of traces of magnesium has been developed. It is based upon the stable reddish-violet magnesium complex of sodium 2″, 6″-dichloro-4′-hydroxy-3, 3′-dimethylfuchsone-5, 5′-dicarboxylate (Pontachrome Azure Blue B).

Details of this compound have been published in our recent paper[1].

Absorption spectra of the reagent solution (Fig. 1. curve I) and of its magnesium complex (Fig. 1. curve II) indicate the analytical usefulness of this color reaction. At pH 11, the maximum absorbance is at 570 mμ. The complex is formed by adding a small amount of magnesium to the mixture of 5.0 ml. of ammonium chloride-ammonia buffer solution and 2.0 ml. of 0.2% reagent solution in a 25 ml. volumetric flask. The solution is diluted to the mark with distilled water and thoroughly mixed. As seen in Fig. 2, magnesium complex has a maximum absorbance in the pH range 10.8 to 11.4 (λ_{max} 570 mμ). Full color developes within ten minutes and its stability is quite adequate for the determination of magnesium.

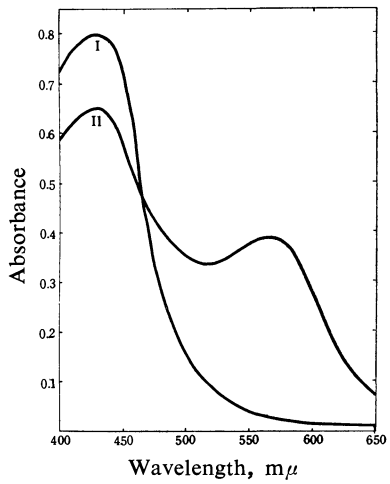


Fig. 1. Absorption spectra of the reagent solution and of its magnesium complex. pH 11.0
I: Reagent 40 p.p.m.
II: Reagent (40 p.p.m.)+Mg(10 p.p.m.)

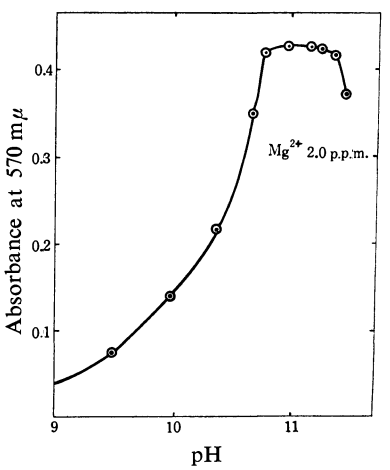


Fig. 2. Effect of pH on the magnesium complex.

1) Y. Katsube, K. Uesugi and J. H. Yoe, This Bulletin, 34, 72 (1961).

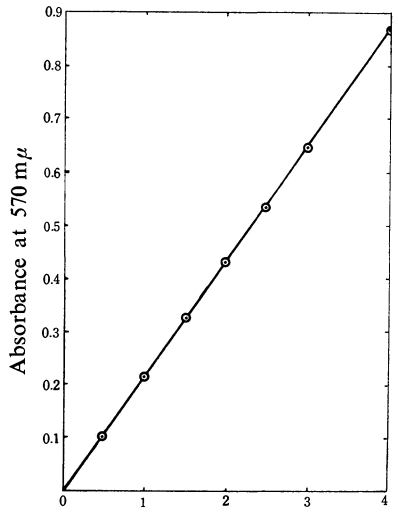


Fig. 3. Beer's law curve. pH 11.0.

TABLE I. LIMITING CONCENTRATION OF INTERFERING IONS FOR DETERMINATION OF MAGNESIUM

Ion	Added as	Limiting concn.* p. p. m.
Be^{2+}	Chloride	0.5
UO_2^{2+}	Nitrate	2.0
Fe^{3+}	Sulfate	0.5
Fe^{2+}	Mohr's salt	0.4
Cu^{2+}	Sulfate	0.1
Ca^{2+}	Chloride	0.7
Co^{2+}	Nitrate	0.9

* The limiting concentration was taken to be one that causes a deviation of more than 0.01 unit in the absorbance of a solution containing 2.5 p.p.m. of magnesium.

Beer's law is obeyed up to a magnesium concentration of at least 4 p.p.m. (Fig. 3). The sensitivity of the color reaction is 0.004 μg. Mg/cm^3 for $\log(I_0/I)=0.001$. The limiting concentrations of the common cations are given in Table I. It will be seen that many metal ions must be removed or masked before the determination.

The presence of these interfering metal ions gives the smaller absorbance at 570 mμ. For example, in the presence of 2 p. p. m. of calcium the absorbance is decreased about 50%.

Himeji Technical Institute
Idei-600 Himeji
(K. U. and Y. K.)
John Lee Pratt Trace Analysis Laboratory
University of Virginia
Charlottesville, Va.
U. S. A.
(J. H. Y.)

Nuclear Quadrupole Resonance of Chlorine in Hexachloroplatinic(IV) Acid Hexahydrate and Sodium Hexachloroplatinate(IV) Hexahydrate

By Koji Ito, Kazuo Ito, Daiyu Nakamura and Masaji Kubo

(Received January 16, 1962)

The pure quadrupole resonance of ^{35}Cl in hexachloroplatinic(IV) acid hexahydrate $H_2PtCl_6 \cdot 6H_2O$ and sodium hexachloroplatinate(IV) hexahydrate $Na_2PtCl_6 \cdot 6H_2O$ was observed at room temperature using a spectrometer previously described[1]. The observed frequencies are shown in Table I. in which that of potassium hexachloroplatinate(IV)[1] at room temperature is included for comparison.

Table I. Pure quadrupole resonance frequencies of ^{35}Cl in hexachloroplatinic(IV) acid hexahydrate and related compounds

Compound	Temp. °C	Frequency Mc./sec.
$H_2PtCl_6 \cdot 6H_2O$	25.0	26.55 ±0.05
$Na_2PtCl_6 \cdot 6H_2O$	23.5	25.730±0.005 26.470±0.005 27.040±0.005
K_2PtCl_6	23.5	25.813±0.001

At dry ice and liquid nitrogen temperatures, these compounds gave rise to a number of weak signals appearing in the frequency range of 28~35 Mc. and 20~30 Mc., respectively. These signals were attributable to piezoelectricity arising from lattice deformations formed in crystals on cooling[2]. The pure quadrupole resonance lines escaped detection either because they were masked by the piezoelectric signals or because the signal-to-noise ratio was small.

The single resonance line observed for hexachloroplatinic(IV) acid might suggest that all chlorine atoms in the crystals are mutually equivalent. However, it is probable that additional resonance lines escaped observation owing to their small signal-to-noise ratios. In fact, the single line was barely detectable. Sodium hexachloroplatinate(IV) yielded three resonance lines of approximately the same signal-to-noise ratio equal to about 3, indicating the presence of at least three kinds of crystallographically nonequivalent chlorine atoms in the crystals.

No X-ray analysis has ever been performed on the crystals of these two compounds. It is reported[3] that sodium hexachloroplatinate(IV) hexahydrate forms triclinic pinacoidal crystals. In order to obtain some information on the crystal structure of these compounds, powder patterns were taken by means of a Norelco X-ray diffractometer. Since the crystals were deliquescent, high-speed scanning was carried out. The recorded powder patterns of these two compounds were quite different from each other. Unlike potassium hexachloroplatinate(IV), which forms cubic crystals, two compounds under investigation gave powder patterns suggesting lower symmetry than the tetragonal symmetry. Evidently, the crystal structures of these three compounds are of quite different type. It is noteworthy that despite the difference in crystal structures, the observed resonance frequencies of these three compounds are nearly the same, the deviations being within several percent. This indicates that the pure quadrupole resonance frequency of chlorine in $[PtCl_6]^{2-}$ is determined primarily by the electronic distribution in the complex ion without being affected greatly by neighboring cations and complex ions[4].

The present authors have already determined the pure quadrupole resonance of halogens in a number of metal complexes[5,6]. The results have been analyzed through the Townes-Dailey procedure[7] to discuss the covalent character of metal-ligand bonds in complex ions, ignoring the effect of neighboring ions on the pure quadrupole resonance frequencies. The present results confirm the adequacy of the analysis.

Chemistry Department
Faculty of Science
Nagoya University
Chikusa-ku, Nagoya

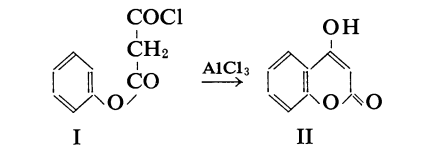
1) D. Nakamura, Y. Kurita, K. Ito and M. Kubo, *J. Am. Chem. Soc.*, **82**, 5783 (1960).
2) S. Kojima, K. Tsukada, S. Ogawa, A. Shimauchi and N. Matsumiya, *J. Phys. Soc. Japan*, **10**, 265 (1955); Y. Yokozawa and I. Tatsuzaki, ibid., **11**, 85 (1956); J. Duchesne and A. Monfils, *J. Chem. Phys.*, **23**, 762 (1955); Y. Kurita, D. Nakamura and N. Hayakawa, *J. Chem. Soc. Japan, Pure Chem. Sec.* (*Nippon Kagaku Zasshi*), **79**, 1093 (1958).
3) P. Groth, "Chemische Krystallographie", Vol. 1, Verlag von Wilhelm Engelmann, Leipzig (1906), p. 542.
4) R. M. Sternheimer and H. M. Foley, *Phys. Rev.*, **102**, 731 (1956).
5) K. Ito, D. Nakamura, Y. Kurita, K. Ito and M. Kubo, *J. Am. Chem. Soc.*, **83**, 4526 (1961).
6) D. Nakamura, K. Ito and M. Kubo, ibid., in press.
7) C. H. Townes and B. P. Dailey, *J. Chem. Phys.*, **17**, 782 (1949).

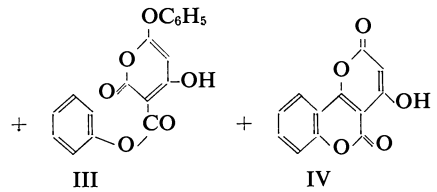
The Reactions of Ester with Acyl Chloride in the Presence of Aluminum Chloride. III. Formation of Dibenzoylmethane and Ethyl Dibenzoylacetate

By Hiroo KANEYUKI

(Received June 7, 1961)

Nakata has reported that acetonetricarboxylic acid derivative III and 3-acyl-4-hydroxycoumarin derivative IV were obtained as by-products in the synthesis[1] of 4-hydroxycoumarin (II) by the action of aluminum chloride on the acid chloride of monophenyl malonate (I) as follows[2]:





The formation of III and IV suggests that the active methylene group of I can be acylated with acid chloride in the presence of aluminum chloride. The acylation of the active methylene group is usually accomplished with a basic reagent such as metallic sodium or sodium alcoholate. With reference to the acylation of the active methylene group in the presence of an acidic reagent, only the synthesis of β-diketones by the acetylation of ketones with acetic anhydride in the presence of boron trifluoride has been studied by Meerwein and Vossen[3] and by Hauser and Adams[4]. Recently, Azatyan[5] has reported that some aromatic ketones were prepared by heating aromatic hydrocarbon and acid chloride in the presence of a small amount of metallic aluminum, and that under similar condition diethyl benzoylmalonate was obtained from diethyl malonate and benzoyl chloride.

The present paper describes the study of the reactions of diethyl malonate with one molecular equivalent of benzoyl chloride, *p*-chlorobenzoyl chloride, *p*-nitrobenzoyl chloride and acetylsalicylic acid chloride in the presence of different amounts of aluminum chloride.

Acylation of Diethyl Malonate with Benzoyl Chloride.—The treatment of diethyl malonate with one molecular equivalent of benzoyl chloride and of aluminum chloride afforded diethyl benzoylmalonate (V) and dibenzoylmethane (VII). When three molecular equivalents of aluminum chloride were used, VII and ethyl dibenzoylacetate (VI) were obtained. It was found that carbon dioxide and ethyl chloride are evolved in the course of the reactions. In these reactions, aluminum chloride reacts not only to give benzoyl derivatives, but also to accelerate the decarbethoxylation of the ester.

$$CH_2(COOC_2H_5)_2 + C_6H_5COCl \xrightarrow{AlCl_3} C_6H_5COCH(COOC_2H_5)_2 + (C_6H_5CO)_2CHCOOC_2H_5 + (C_6H_5CO)_2CH_2$$

Acylation of Diethyl Malonate with *p*-Chlorobenzoyl Chloride.—The products of the reactions of diethyl malonate with *p*-chlorobenzoyl chloride were diethyl *p*-chlorobenzoylmalonate (VIII), ethyl di-*p*-chlorobenzoylacetate (IX) and di-*p*-chlorobenzoylmethane (X). The relation between amounts of aluminum chloride and reaction products was similar to that of the acylation with benzoyl chloride.

Acylation of Diethyl Malonate with *p*-Nitrobenzoyl Chloride.—When one molecular equivalent of *p*-nitrobenzoyl chloride was used as an acylating agent, *p*-nitroacetophenone (XI) and ethyl *p*-nitrobenzoylacetate (XII) were obtained. By the use of three molecular equivalents of aluminum chloride at a higher reaction temperature, di-*p*-nitrobenzoylmethane (XIII) was obtained as the main product.

$$CH_2(COOC_2H_5)_2 + NO_2C_6H_4COCl \xrightarrow{AlCl_3} NO_2C_6H_4COCH_3 + NO_2C_6H_4COCH_2COOC_2H_5$$

$$NO_2C_6H_4COCH_2COOC_2H_5 + NO_2C_6H_4COCl \xrightarrow{AlCl_3} (NO_2C_6H_4CO)_2CH_2$$

1) K. Matsui and M. Ota, *J. Chem. Soc. Japan, Pure Chem. Sec.* (*Nippon Kagaku Zasshi*), **78**, 517 (1957).
2) T. Nakata, ibid., **78**, 1780 (1957).
3) H. Meerwein and D. Vossen, *J. prakt. Chem.*, **141**, 149 (1934).
4) R. Hauser and T. Adams, *J. Am. Chem. Soc.*, **66**, 345 (1944).
5) V. D. Azatyan, *Daklady Akad. Nauk Armyan. S. S. R.*, **29**, No. 3, 111 (1959); *Chem. Abstr.*, **54**, 12044 (1960).

TABLE I. ACYLATION OF DIETHYL MALONATE WITH BENZOYL CHLORIDE AND *p*-SUBSTITUTED BENZOYL CHLORIDES

Reaction condition: 65°C, * 90°C; 8 hr. Solvent: Nitrobenzene 15 ml.

Substituent X	Reactant: X-C_6H_4COCl mol.×10^2	Reactant: $CH_2(COOC_2H_5)_2$ mol.×10^2	Reactant: $AlCl_3$ mol.×10^2	Product and yield: X-BME[a] %	X-DBA[b] %	X-DBM[c] %	X-AP[d] %	X-BAE[e] %	X-C_6H_4COOH %
H	2.1	2.1	2.1	59		8			15
	2.1	2.1	6.3		31	16			23
Cl	1.7	1.7	1.7	59					19
	1.7	1.7	5.1		4	33			43
NO_2	1.6	1.6	1.6				26	10	56
	1.6	1.6	3.2			31	29	8	28
	1.6	1.6	4.8			47	14	8	28
	1.6	1.6	1.6*			58	7	26	7
	1.6	1.6	4.8*			74	7	3	14

Yield: Calculated from X-C_6H_4COCl (X=H, Cl, NO_2).

a) X-BME (V, VIII); X-$C_6H_4COCH(COOC_2H_5)_2$

b) X-DBA (VI, IX); $(X\text{-}C_6H_4CO)_2CHCOOC_2H_5$

c) X-DBM (VII, X, XIII); $(X\text{-}C_6H_4CO)_2CH_2$

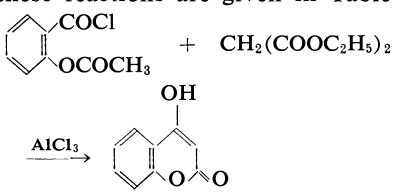
d) X-AP (XI); X-$C_6H_4COCH_3$

e) X-BAE (XII); X-$C_6H_4COCH_2COOC_2H_5$

It can be deduced that the formation of XI and XIII in good yields results in the facilitation of decarbethoxylation by the driving force of the nitro group in the *p*-position.

The reaction conditions and the products of these acylation reactions are summarized in Table I.

Acylation of Diethyl Malonate with Acetylsalicylic Acid Chloride.—Reactions carried out with different amount of aluminum chloride all gave only 4-hydroxycoumarin (II), which may have been formed by decarbethoxylation and intramolecular condensation. The results of these reactions are given in Table II.



The aromatic acids, which should be derived from unreacted acid chlorides, were obtained, and their yields generally increased with the amount of aluminum chloride used.

TABLE II. ACYLATION OF DIETHYL MALONATE WITH ACETYLSALICYLIC ACID CHLORIDE

Solvent: Nitrobenzene 25 ml.

Reaction condition: 95~100°C, 8 hr.

Reactant: Acetylsalicylic acid mol.×10^2	Reactant: Diethyl malonate mol.×10^2	Reactant: $AlCl_3$ mol.×10^2	Product and yield: II %	Salicylic acid %
1.7	3.3	1.7	56	13
1.7	1.7	1.7	52	17
1.7	1.7	5.1	7	57

Yield: Calculated from acetylsalicylic acid.

Experimental*

Materials.—Benzoyl chloride[6] (b. p. 192°C), *p*-chlorobenzoyl chloride[7] (b. p. 112°C/23 mmHg) and *p*-nitrobenzoyl chloride[8] (b. p. 160°C/26 mmHg) were prepared from benzoic acid, *p*-chlorobenzoic acid and *p*-nitrobenzoic acid with phosphorus pentachloride respectively in 65, 96 and 92% yields. Acetylsalicylic acid[9] was prepared from salicylic acid and acetic anhydride, m. p. 137~138°C., 82% theoretical yield. Anhydrous aluminum chloride[10] was prepared by passing a stream of dry hydrogen chloride over aluminum (99.99%) heated in a furnace. The diethyl malonate used was a commercial product purified by distillation.

Acylation of Diethyl Malonate with Benzoyl Chloride.—Diethyl malonte was added to benzoyl chloride and aluminum chloride dissolved in nitrobenzene, and the reaction mixture was kept at 65°C for 8 hr. After cooling, the reaction mixture was poured into crushed ice and extracted with ether. The ethereal solution was successively extracted with a saturated sodium bicarbonate solution, with a sodium hydroxide solution (15%) and then with water. After the aqueous layer, which contained aluminum chloride, was heated on a water bath and left for a few days, solid VII was produced. A precipitate was obtained by acidifying the sodium bicarbonate solution with hydrochloric acid and was identified as benzoic acid by the mixed melting point method (m. p. 118~121°C). The sodium hydroxide solution and the water extract were acidified to give solid VI and oil V respectively. The ether solution was evaporated and the residual solution

* The boiling and melting points are uncorrected.

6) J. B. Cohen, "Practical Organic Chemistry", Macmillan and Co., Ltd., London (1926), p. 254

7) "Organic Syntheses", Coll. Vol. 3 (1955), p. 29.

8) Ibid., Coll. Vol. 1 (1948), p. 394.

9) L. F. Fieser, "Experiments in Organic Chemistry", D. C. Heath & Co., Boston (1955), p. 204.

10) L. Gattermann, "Laboratory Method of Organic Chemistry", Macmillan and Co., Ltd., London (1952), p. 342.

subjected to distillation with water under reduced pressure in order to remove nitrobenzene. Residue VIIa was obtained.

Diethyl Benzoylmalonate (V).—The ethereal solution of the oil V was shaken with a copper acetate solution. The solid obtained on evaporating the ether was crystallized from ethanol as green needles, 3.8 g. (3.3 g. as V), m. p. 180~181°C.

Found: C, 56.90; H, 5.00; Cu, 10.52. Calcd. for $C_{28}H_{30}O_{10}Cu$: C, 56.99; H, 5.12; Cu, 10.76%.

No depression of the melting point was observed on the admixture of this crystalline with copper chelate of diethyl benzoylmalonate (m. p. 180°C) prepared by the method of the literature[11].

Ethyl Dibenzoylacetate (VI).—The solid VI crystallized from ethanol as colorless needles, m. p. 108~111°C, reported m. p. 112°C[12].

Found: C, 72.86; H, 5.52. Calcd. for $C_{18}H_{16}O_4$: C, 72.96; H, 5.44%.

This substance gave copper chelate, which was crystallized from ethanol in the form of light green needles, m. p. 218~220°C, reported m. p. 221°C[12]. The product obtained by boiling the solid VI (0.3 g.) with sulfuric acid (15%) for 15 hr. crystallized from methanol to give light yellow needles, 0.1 g., m. p. 78~79°C. Melting point and mixed melting point with dibenzoylmethane proved the identity of this material.

Dibenzoylmethane (VII).—The solid VII crystallized from methanol as light yellow needles, m. p. 78~79°C. A mixed melting point with dibenzoylmethane prepared by the method of the literature[13] showed no depression.

Found: C, 80.37; H, 5.54. Calcd. for $C_{15}H_{12}O_2$: C, 80.34; H, 5.39%.

This crystalline (0.2 g.) was boiled with semicarbazide hydrochloride (0.2 g.) in methanol (10 ml.) for 4 hr. Water was added to the methanol solution, and the separated crystal was crystallized from ethanol to give colorless plates, 0.19 g., m. p. 199.5 ~200.5°C. The recorded melting point for 3,5-diphenylpyrazol is 200°C[14]. A few drops of concentrated hydrochloric acid was added to the solid VIIa (0.1 g., m. p. above 270°) dissolved in a small amount of tetrahydrofuran, and the solution was kept at room temperature for 1 hr. The precipitated crystal was washed with water and crystallized from methanol, 0.09 g., m. p. 77~78°C. This substance was identified as VII by the mixed melting point method. The yields of products were listed in Table I.

Carbon Dioxide and Ethyl Chloride.—The gas evolved during the reaction was absorbed by a potassium hydroxide solution (30%) and toluene cooled with ice. The alkali solution was analyzed by differential titration with a standard acid solution to determine the amount of carbon dioxide evolved. The obtained value was about 70% of the amount of carbon dioxide which was estimated from the yields of VI and VII. The gas absorbed in toluene was distilled into aniline cooled with ice. The aniline placed in a sealed tube was heated for 7 hr. at 130°C, and then the reaction product was treated with *p*-toluenesulfonyl chloride by the Hinsberg method. The resulting product was crystallized from ethanol to give colorless crystals, m. p. 68~69°C, which agreed with the melting point in the literature[15] for *N*-ethyl-*N*-phenyl-*p*-toluenesulfonamide. The melting point was not depressed on admixture with an authentic sample prepared by the method of the literature.

Acylation of Diethyl Malonate with *p*-Chlorobenzoyl Chloride.—The reaction conditions and treatments of reaction mixture are quite the same as that described for acylation with benzoyl chloride. When the aqueous layer which contained aluminum chloride was heated on a water bath and left to stand for a few days, a solid precipitated. When this solid was collected, washed with water, and extracted with hot ethanol, insoluble solid Xa remained. On cooling the ethanol solution, solid X was obtained. The sodium bicarbonate solution was acidified to give a crystalline substance which gave no depression of melting point on mixture with *p*-chlorobenzoic acid. Nothing was obtained when the sodium hydroxide solution was acidified. The water extract was acidified to give solid IX. The removal of ether and nitrobenzene gave solid Xb. In the experiment used, one molecular equivalent of aluminum chloride, solid VIII, was obtained from the aqueous layer and the water extract.

Diethyl *p*-Chlorobenzoylmalonate (VIII).—The solid VIII crystallized from ethanol in the form of colorless needles, m. p. 52.5~53°C.

Found: C, 56.30; H, 5.05; Cl, 11.73. Calcd. for $C_{14}H_{15}O_5Cl$: C, 56.29; H, 5.06; Cl, 11.87%.

A suspension of the solid VIII in sulfuric acid (30%) was refluxed for 6 hr. The oily substance produced solidified on cooling and crystallized from ethanol as colorless needles, m. p. 20.5~21°C. A mixed melting point with *p*-chloroacetophenone prepared according to the literature[16] showed no depression.

Ethyl Di-*p*-chlorobenzoylacetate (IX).—The solid IX crystallized from ethanol in the form of colorless leaflets, m. p. 127.5~128.5°C.

Found: C, 59.12; H, 3.90; Cl, 19.30. Calcd. for $C_{18}H_{14}O_4Cl_2$: C, 59.20; H, 3.80; Cl, 19.42%.

A suspension of the solid IX (1 g.) in sulfuric acid (30%, 20 ml.) was refluxed for 4 hr., and the resulting product was crystallized from ethanol to give colorless needles, 0.6 g., m. p. 160~160.5°C. This product gave no depression of melting point on mixture with di-*p*-chlorobenzoylmethane.

Di-*p*-chlorobenzoylmethane (X).—The solid X crystallized from ethanol in the form of colorless leaflets, m. p. 160~160.5°C. The literature values for di-*p*-chlorobenzoylmethane are: m. p. 159°C[17], 160~161°C[18].

Found: C, 61.34; H, 3.51; Cl, 24.08. Calcd. for $C_{15}H_{10}O_2Cl$: C, 61.46; H, 3.44; Cl, 24.19%.

A suspension of the solid X (0.5 g.) in a mixture of sulfuric acid (60%, 50 ml.) and ethanol (5 ml.)

11) C. Bülow and E. Hailen, *Ber.*, **35**, 934 (1902).
12) "Beilsteins Handbuch der organischen Chemie", H., **10**, 830 (1927).
13) "Organic Syntheses", Coll. Vol. 1 (1948), p. 199.
14) T. Posner, *Ber.*, **34**, 3984 (1901).
15) "Beilsteins Handbuch der organischen Chemie", Z., **12**, 306 (1950).
16) "Organic Syntheses", Coll. Vol. 1 (1948), p. 105.
17) A. Sieglitz and O. Horn, *Ber.*, **84**, 607 (1951).
18) G. S. Hammond et al., *J. Am. Chem. Soc.*, **81**, 7682 (1959).

was heated under reflux for 15 hr., and the resulting solution was extracted with ether. The ethereal solution was further extracted with a sodium hydroxide solution. With removal of the ether, an oily product (0.2 g.) was obtained. Semicarbazone prepared from this oily product melted at 202～203°C, which was not depressed on admixture with an authentic sample of semicarbazone[19] prepared from *p*-chloroacetophenone. The sodium hydroxide solution was acidified with hydrochloric acid to give a crystalline, 0.2 g., m. p. 236～237°C, which showed no depression on admixture with *p*-chlorobenzoic acid. The solid Xa (0.2 g., m. p. above 270°C) treated by the same merhod as described in the case of solid VIIa gave X, 0.19 g., m. p. 16°C. The solid Xb crystallized from ethanol to afford a crystalline, m. p. 160°C, and was identified as X by the mixed melting point method. The yields of products have been listed in Table I.

Acylation of Diethyl Malonate with *p*-Nitrobenzoyl Chloride.—The reaction conditions and treatments of reaction mixture are quite the same as that described above. The orange-red colored crystalline mass formed when the ethereal solution extracted with a sodium hydroxide solution was collected and washed with ether. The aqueous layer which contained aluminum chloride was heated on a water bath to form a precipitate. The precipitate was collected, washed with water and extracted with hot ethanol and then with cold ethanol-tetrahydrofuran (1 : 2) ; an insoluble solid XIII remained. On cooling the ethanol solution, solid XI precipitated. Upon evaporating the ethanol-tetrahydrofuran solution, solid XIIIa was obtained. The sodium bicarbonate solution was acidified to give a crystalline substance, which was crystallized from ethanol as yellowish white colored crystals and was identified as *p*-nitrobenzoic acid by the mixed melting point method. Nothing was obtained when the sodium hydroxide solution was acidified. When the above-mentioned orange-red colored crystalline was treated with hydrochloric acid and washed with water, it turned into yellow-colored crystalline XIIIb. The water extract was acidified to give solid XII. When the ethereal solution was evaporated and then distilled with water under reduced pressure, solid XIIa was obtained.

***p*-Nitroacetophenone (XI).**—The solid XI crystallized from ethanol in the form of light yellow prisms, m. p. 80～81°C.

Found : C, 58.25 ; H, 4.21 ; N, 8.40. Calcd. for $C_8H_7O_3N$: C, 58.15 ; H, 4.28 ; N, 8.48%.

Phenylhydrazone prepared from the solid XI (0.2 g.) crystallized from ethanol in the form of red needles, 0.2 g., m. p. 133.5～134.5°C.

Found : N, 16.48. Calcd. for $C_{14}H_{13}O_2N_3$: N, 16.46%.

The recorded melting point[20] for *p*-nitroacetophenone and its phenylhydrazone are 80～81°C and 132°C respectively.

Ethyl *p*-Nitrobenzoylacetate (XII).—The solid XII crystallized from ethanol in the form of yellow needles, m. p. 69～72°C. Perkin and Bellenot[21] gave a m. p. of 74～76°C for ethyl *p*-nitrobenzoylacetate.

Found : C, 56.00 ; H, 4.89 ; N, 6.06. Calcd. for $C_{11}H_{11}O_5N$: C, 55.69 ; H, 4.67 ; N, 5.90%.

The solid XII (0.3 g.) was boiled with sulfuric acid (30%) for 8 hr. The separated crystal was crystallized from ethanol as light yellow prisms, 0.1 g., m. p. 80～81°C, and was identified as XI by the mixed melting point method. The solid XIIa which was crystallized from ethanol was determined to be identical with XII by the melting point and mixed melting point, m. p. 69～72°C.

Di-*p*-nitrobenzoylmethane (XIII).—The solid XIII crystallized from ethyl acetate in the form of yellow needles, m. p. 240～243°C, reported m. p. 241～242°C[17].

Found : C, 57.27 ; H, 3.18 ; N, 8.96. Calcd. for $C_{15}H_{10}O_6N_2$: C, 57.33 ; H, 3.21 ; N, 8.91%.

A suspension of the solid XIII (0.4 g.) in a mixture of sulfuric acid (60%, 50 ml.) and glacial acetic acid (4 ml.) was heated at reflux for 17 hr. The reaction mixture diluted with water was extracted with ether. The ethereal solution was extracted with sodium hydroxide solution. Removal of the ether gave a crystalline mass, 0.2 g., m. p. 79～80°C, which showed no depression on admixture with XI. The sodium hydroxide extract was acidified to yield a crystalline substance, 0.2 g., m. p. 234～235°C This substance was identified as *p*-nitrobenzoic acid by the mixed melting point method. XIII was obtained from the solid XIIIa (1 g., m. p. above 270°C) by the same method as has been described in the case of the solid VIIa, 0.97 g., m. p. 240～243°C. The solid XIIIb crystallized from ethyl acetate as yellow needles. The melting point was not depressed on admixture with XIII. The yields of products have been listed in Table I.

Acylation of Diethyl Malonate with Acetylsalicylic Acid Chloride.—Phosphorus pentachloride was added to a solution of acetylsalicylic acid in nitrobenzene, and the solution was warmed at 50～55°C for 3 hr. On cooling, aluminum chloride was added to the solution and dissolved, and then diethyl malonate was added. This solution was kept at 95～100°C for 8 hr. The reaction mixture was poured into crushed ice, and an excess of sodium hydroxide solution (15%) was added until the liquid had a alkaline reaction. The solution was extracted with ether to remove nitrobenzene and stirred into a hydrochloric acid solution (15%). The resulting crystals were crystallized from aqueous ethanol, m. p. 209～210°C. The melting point was not depressed on admixture with an authentic sample of 4-hydroxycoumarin (II)[1]. The filtrate separated from II was extracted with ether. Removal of the solvent from the ether extract gave a crystal. After recrystallization from aqueous ethanol, colorless needles were obtained, m. p. 158～159°C, which showed no depression of melting point on mixture with salicylic acid. The yields of products have been listed in Table II.

19) "Beilsteins Handbuch der organischen Chemie", Z., 7, 219 (1948).

20) I. Heilbron and H. M. Bunburg, "Dictionary of Organic Compounds", Vol. 3, Eyre & Spottiswoode, Ltd., London (1953), p. 608.

21) H. Perkin and G. Bellenot, *J. Chem. Soc.*, **49**, 447 (1887).

The author wishes to express his hearty thanks to Professor Kiyotada Matsui for his kind guidance and encouragement, and to Professor Ryozo Goto, Kyoto University, for his many valuable suggestions. He also wishes to thank Mr. Terutaka Nakata for his help during the experiment.

Department of Industrial Chemistry
Faculty of Technology
Kanazawa University
Uenohonmachi, Kanazawa

The Reactions of Ester with Acyl Chloride in the Presence of Aluminum Chloride. IV. Formation of Tribenzoylmethane

By Hiroo KANEYUKI

(Received June 15, 1961)

The previous paper[1] reported that monoacylated compounds were obtained when diethyl malonate was acylated with equimolecular amounts of benzoyl chloride or *p*-substituted benzoyl chlorides in the presence of equimolecular amounts of aluminum chloride, while a large quantity of catalyst led to decarbethoxylated diacyl compounds.

In this paper, the results of analysis of products obtained by the reactions of diethyl malonate with more than two molecular equivalents of acid chloride in the presence of three molecular amounts of aluminum chloride are reported on.

Acylation of Diethyl Malonate with Benzoyl Chloride.—Ethyl dibenzoylacetate (I), dibenzoylmethane (II), tribenzoylmethane (III) and tribenzoylmethane-*O*-benzoate (IV) were obtained by this reaction. The high-melting substance mentioned in the previous paper was also obtained; it was confirmed by analysis that this substance was aluminum chelate of dibenzoylmethane (IIa). The reaction conditions and the products of these acylation reactions are given in Table I. What differs from the experimental results of the previous paper[1] is the formation of III, IV and II in good yields. From these differences, it can be seen that benzoylation and decarbethoxylation reactions have proceeded further in this case.

$$(C_6H_5CO)_2CHCOOC_2H_5 \text{ or } (C_6H_5CO)_2CH_2 \xrightarrow[C_6H_5COCl]{AlCl_3} (C_6H_5CO)_3CH + (C_6H_5CO)_2C{=}CC_6H_5 \quad (OCOC_6H_5)$$

Acylation of Diethyl Malonate with *p*-Chlorobenzoyl Chloride.—Diethyl *p*-chlorobenzoylmalonate (V), ethyl di-*p*-chlorobenzoylacetate (VI), di-*p*-chlorobenzoylmethane (VII) and tri-*p*-chlorobenzoylmethane (VIII) were obtained by this reaction. Besides these, aluminum chelate of di-*p*-chlorobenzoylmethane (VIIa) of a high melting point was also obtained. These reaction products are given in Table I. From this table, it can be seen that V, VI, VII and VIIa are obtained when two molecular equivalents of *p*-chlorobenzoyl chloride are used, but ester V and VI disappear with the increase in the combined yield of VII and VIIa by the use of three molecular equivalents of *p*-chlorobenzoyl chloride. What differs from the experimental results in the previous paper[1] is the formation of VIII, an increase in the yield of VI accompanied with V, and an increase in the combined yield of VII and VIIa.

Acylation of Diethyl Malonate with *p*-Nitrobenzoyl Chloride.—*p*-Nitroacetophenone (IX), ethyl *p*-nitrobenzoylacetate (X), di-*p*-nitrobenzoylmethane (XI) and its aluminum chelate (XIa) were obtained by this reaction, but tri-*p*-nitrobenzoylmethane was not obtained. These reaction products are given in Table I. From this table, it can be seen that the yield of ester X is decreased, while the combined yield of XI and XIa is increased, when a large quantity of *p*-nitrobenzoyl chloride is used. A good yield of XI and XIa alone is obtained at a high reaction temperature. The species of reaction products are the same as in the case of the previous paper[1], in which equimolecular amounts of *p*-nitrobenzoyl chloride were used. The difference is the increase in the combined yield of XI and XIa.

1) H. Kaneyuki, This Bulletin, 35, 519 (1962).

TABLE I. ACYLATION OF DIETHYL MALONATE WITH BENZOYL CHLORIDE AND *p*-SUBSTITUTED BENZOYL CHLORIDES

Reaction condition: 65°C, *** 90°C; 8 hr. Solvent: Nitrobenzene 8 ml., ** 15 ml.

Substituent X	Reactant			Product and yield							
	$X\text{-}C_6H_4COCl$ mol.$\times 10^2$	$CH_2(COOC_2H_5)_2$ mol.$\times 10^2$	$AlCl_3$ mol.$\times 10^2$	X-BME[a] %	X-DBA[b] %	X-DBM[c] %	X-DBM-Al[d] %	X-TBM[e] %	X-TBM-*O*-B[f] %	X-AP[g] %	X-BAE[h] %	$X\text{-}C_6H_4COOH$ %
H	3.6	1.8	5.4**		1.9	47.0	4.8	12.8	2.6			16.1
	5.4	1.8	5.4**		2.8*	51.8*	11.9*	24.0	5.2			27.7
Cl	1.1	0.5	1.7	16.8*	10.0	40.7	10.5	3.7				15.1
	1.7	0.5	1.7			40.7*	23.3*	trace				50.0
NO_2	1.1	0.5	1.6			26.6*	6.6*			22.6*	9.0*	49.0
	1.6	0.5	1.6			16.4*	41.3*			16.7*	trace	50.0
	1.6	0.5	1.6***			70.0*	22.6*				traec	31.4

Yield: Calculated from $X\text{-}C_6H_4COCl$ (X=H, Cl, NO_2).

* Calculated from $CH_2(COOC_2H_5)_2$.

a) X-BME(V); $X\text{-}C_6H_4COCH(COOC_2H_5)_2$
b) X-DBA(I, VI); $(X\text{-}C_6H_4CO)_2CHCOOC_2H_5$
c) X-DBM(II, VII, XI); $(X\text{-}C_6H_4CO)_2CH_2$
d) X-DBM-Al(IIa, VIIa, XIa); $[(X\text{-}C_6H_4CO)_2CH]_3Al$
e) X-TBM(III, VIII); $(X\text{-}C_6H_4CO)_3CH$
f) X-TBM-*O*-B(IV); $(X\text{-}C_6H_4CO)_2C\cdot C(OCOC_6H_4\text{-}X)C_6H_5$
g) X-AP(IX); $X\text{-}C_6H_4COCH_3$
h) X-BAE(X); $X\text{-}C_6H_4COCH_2COOC_2H_5$

Experimental*

Materials and reaction method were the same as in the previous paper[1]. The reaction conditions are shown in the above table. The treatment of the reaction mixture was also the same; that is, the product was separated into the aqueous layer containing aluminum chloride, sodium bicarbonate extract, sodium hydroxide extract, water extract and residual solution.

Acylation of Diethyl Malonate with Benzoyl Chloride.—Precipitates were separated after the aqueous layer containing aluminum chloride was heated and left standing. These precipitates were recrystallized from methanol to yield II. Benzoic acid was obtained when the sodium bicarbonate extract was acidified. The sodium hydroxide extract was acidified to give I, which recrystallized from ethanol. By acidifying the water extract, solid A was obtained. By distilling off the ether and the nitrobenzene, together witht he water, under reduced pressure from the residual solution, a residue was obtained. This was separated into an ether soluble substance B and an ether insoluble substance C. Yields of the various products are shown in Table I.

Tribenzoylmethane (III).—The solid A was recrystallized from a large quantity of ethanol to afford colorless needles, m. p. 223~240°C. The melting point was not depressed when melted together with tribenzoylmethane which had been prepared by the method of the literature[2]. The infrared spectrum of this compound was identical with that of an authentic specimen.

Found: C, 80.72; H, 5.19. Calcd. for $C_{22}H_{16}O_3$: C, 80.47; H, 4.91%.

Tribenzoylmethane-*O*-benzoate (IV).—The solid B was recrystallized from ethyl acetate-petroleum ether to give colorless granular crystals, m. p. 125~126°C. When recrystallized from ethanol, however, the same product gave colorless plates, m. p. 112~113.5°C. Tribenzoylmethane-*O*-benzoate prepared according to the method of the literature[3] (m. p. 121~123°C, ethyl acetate-ligroin) gave the same kinds of crystals.

Found: C, 80.26; H, 4.74. Calcd. for $C_{29}H_{20}O_4$: C, 80.54; H, 4.66%.

Tris-(1, 3-diphenyl-1, 3-propanediono) - aluminum (IIa).—A small quantity of concentrated hydrochloric acid was added to a tetrahydrofuran solution of the ether insoluble substance C (0.5 g., m. p. above 270°C). The solution was allowed to stand for an hour, and then water was added until preciptation was complete. The precipitate was filtered and recrystallized from methanol to give needle crystals, 0.44 g., m. p. 76.5~78°C. The melting point and mixed melting point with dibenzoylmethane proved the identity of this material. A colloidal precipitate of aluminum hydroxide was produced on the addition of aqueous ammonia to the acidic filtrate.

* Confirmation of compounds which were confirmed in the previous paper[1] is omitted here. Melting points are uncorrected values.

2) "Beilsteins Handbuch der organischen Chemie", H., 7, 877 (1925).

3) Ibid., H., 9, 158 (1926).

Found: C, 77.52; H, 4.90; Al, 3.90. Calcd. for $C_{45}H_{33}O_6Al$: C, 77.57; H, 4.77; Al, 3.87%.

Acylation of Diethyl Malonate with *p*-Chlorobenzoyl Chloride.—Precipitates obtained from the aqueous layer containing aluminum chloride were separated into ether insoluble D and ether soluble substances. This ether soluble substance was recrystallized from ethanol to yield VII. *p*-Chlorobenzoic acid was obtained by acidifying the sodium bicarbonate extract. A precipitate was not obtained by acidifying the sodium hydroxide extract. Crystals obtained by acidifying the water extract were treated with ether, and ether insoluble substance E was separated. After the removal of the ether, the residue was separated to V and VI by fractional crystallization with ethanol. The residue, which was obtained after removing nitrobenzene from the residual solution of extraction, was recrystallized from ethanol to afford VII. The products and yields are shown in Table I.

Tris-(1, 3-dichloro-diphenyl-1, 3-propanediono)-aluminum (VIIa).—The tetrahydrofuran solution of the solid D (0.18 g., m. p. above 270°C) was treated with hydrochloric acid as has been mentioned above. The resulting precipitate was recrystallized from ethanol as colorless plates, 0.17 g., m. p. 159~160°C. The melting point and mixed melting point with di-*p*-chlorobenzoylmethane proved the identity of this material.

Found: C, 60.20; H, 3.29. Calcd. for $C_{45}H_{27}O_6 \cdot Cl_6Al$: C, 59.83; H, 3.01%.

Tri-*p*-chlorobenzoylmethane (VIII).—The solid E was recrystallized from a large quantity of ethanol to yield colorless long needles, m. p. 225~239°C.

Found: C, 61.59; H, 3.13; Cl, 24.58. Calcd. for $C_{22}H_{13}O_3Cl_3$: C, 61.21; H, 3.03; Cl, 24.64%.

Acylation of Diethyl Malonate with *p*-Nitrobenzoyl Chloride.—Precipitates obtained from the aqueous layer containing aluminum chloride were washed with water, and extracted with hot ethanol and then with a mixed solution of ethanol-tetrahydrofuran (1 : 2). The solid obtained by the evaporation of the ethanol extract was recrystallized from ethanol to give IX. By evaporating the ethanol-tetrahydrofuran solution, solid I was obtained. The residue, insoluble in an ethanol-tetrahydrofuran solution, was recrystallized from ethyl acetate to give XI. *p*-Nitrobenzoic acid was obtained when sodium bicarbonate extract was acidified. The reddish orange precipitate produced during sodium hydroxide extraction was filtered, washed with ether and hydrochloric acid, and then recrystallized from ethyl acetate to give XI. The water extract was acidified, and the resulting precipitate was recrystallized from ethanol to afford X.

Tris-(1, 3-dinitro-diphenyl-1, 3-propanediono)-aluminum (XIa).—The tetrahydrofuran solution of the solid F (0.75 g., m. p. above 270°C) was treated with hydrochloric acid, as has been mentioned above. The resulting precipitate was recrystallized from ethyl acetate to afford yellow needles, 0.70 g., m. p. 238~243°C. The melting point and mixed melting point with di-*p*-nitrobenzoyl methane proved the identity of this material.

The author wishes to express his gratitude to Professor Kiyotada Matsui for his helpful guidance throughout the course of this work, and to Professor Ryozo Goto, Kyoto University, for his unfailing encouragement. He also wishes to thank Mr. Minoru Ota for his help.

Department of Industrial Chemistry
Faculty of Technology
Kanazawa University
Uenohonmachi, Kanazawa

Kinetic Studies on Solvolysis. VIII. Phenolysis of Optically Active α-Phenethyl Chloride in Phenol-Benzene Solvent—Three-stage Mechanism in the S_N1-Type Solvolysis*

By Kunio Okamoto, Ken-ichi Takeuchi and Haruo Shingu

(Received June 23, 1961)

The mechanism of phenolysis of α-phenethyl chloride has been extensively investigated by Hart and his co-workers[1]. These authors[1b] carried out the phenolysis in the absence of basic substances and noted that the near identity of rate constants for the racemization of α-phenethyl chloride and for the nuclear alkylation of phenol in various mixtures of phenols and aromatic hydrocarbons. Although they suggested that a common rate-determining step for both reactions would be the ionization step of the halide, they did not refer to the solvolytic

* Presented at the 14th Annual Meeting of the Chemical Society of Japan, Tokyo, April, 1961. Part VII. of this series: K. Okamoto, K. Takeuchi and H. Shingu, This Bulletin, **34**, 1137 (1961).

1) a) H. Hart, W. L. Spliethoff and H. S. Eleuterio, *J. Am. Chem. Soc.*, **76**, 4547 (1954); b) H. Hart and W. L. Spliethoff, ibid., **77**, 833 (1955).

nature of the reaction and presented a second-order rate equation with some additional terms for explaining the rate data. In Part V of this series[2] we have illustrated how a reliable criterion of the S_N1 (first-order) two-step mechanism may be established for the phenolysis of *tert*-butyl halides by examination of the rate dependence on initial concentrations of the added base and also on solvent compositions. In addition, we have suggested the applicability of the first-order mechanism to the aralkyl system. Some doubt, therefore, arises about the validity of the second-order mechanism suggested by Hart[1b] for this phenolysis.

One of the purposes of this study was to re-investigate the previous work[1b] in the presence of a base, especially at lower initial concentrations of the chloride, and to substantiate the applicability of S_N1 mechanism on the phenolysis of α-phenethyl system.

Another purpose was to clarify the details of kinetic nature of the intermediates of this phenolysis, and to examine the concept of Winstein's ion-pair intermediates[3].

First-order Nature of the Polarimetric and Titrimetric Rate Constants.—We have previously[2] shown that the titrimetric rate of the phenolysis of α-phenethyl chloride obeys good first-order kinetics in a phenol-nitrobenzene mixture both in the presence of and in the absence of sodium phenolate. In this study anilinium phenolate was used as a base, because in the phenolysis with sodium phenolate crystalline precipitate of sodium chloride makes the polarimetric measurement impossible.

The polarimetric rate constants, k_α, were measured in phenol-benzene (1 : 1 by weight) at 25°C, and satisfactory first-order behavior was observed in the decrease of optical activity, irrespective of presence or absence of the added base, this being illustrated graphically in Fig. 1. The observed rate constants are summarized in Table I.

Titrimetric rate constants, k_t, were also measured for comparison with the corresponding polarimetric values. Decrease of anilinium phenolate or increase of hydrogen chloride associated with the phenolysis obeyed good first-order kinetics, this being illustrated graphically in Fig. 2. The observed titrimetric rate constants are summarized also in Table I.

From these results it is clear, as previously anticipated[2], that the S_N1-type solvolytic mechanism is the only reasonable one for the phenolysis, at least in the range of lower concentrations of the chloride.

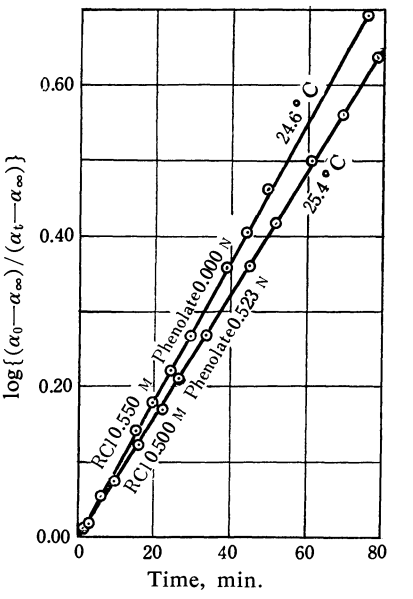


Fig. 1. Polarimetric rate of phenolysis at 25°C of (−)-α-phenethyl chloride in 50 wt.% phenol-benzene.

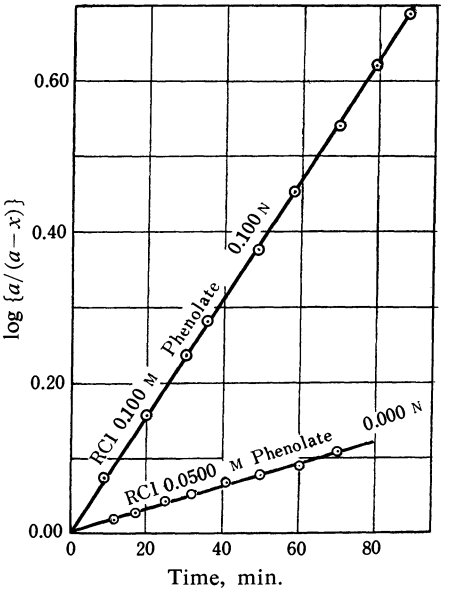


Fig. 2. Titrimetric rate of phenolysis at 25.0±0.1°C of α-phenethyl chloride in 50 wt.% phenol-benzene.

Relationships between the Rate Constants and the Initial Concentrations of the Added Base.—As illustrated graphically in Fig. 3, in the range of the initial anilinium phenolate concentrations from 0 to 0.5 M, the titrimetric rate constant rises very steeply with the phenolate concentration, reaches a maximum value and then decreases gradually. On the other hand,

2) H. Shingu and K. Okamoto, *J. Chem. Soc. Japan, Pure Chem. Sec.* (*Nippon Kagaku Zasshi*), **81**, 111 (1960).
3) S. Winstein, A. H. Fainberg and G. C. Robinson, *Chem. & Ind.*, **1954**, 664.

TABLE I. SUMMARY OF TITRIMETRIC AND POLARIMETRIC RATE CONSTANTS FOR THE PHENOLYSIS OF α-PHENETHYL CHLORIDE IN 50 WT. % PHENOL-BENZENE AT 25.0±0.1°C.

RCl M	Anilinium phenolate N	Me_4NCl N	Method	Initial α°	Final α°	10^2k_1 min^{-1}	Conversion %
0.0500			Tit.			0.357	27
0.0500	0.0049		Tit.			1.38	5.8
0.0500	0.0095		Tit.			1.69	13.6
0.0500	0.0200		Tit.			1.81	33.6
0.0500	0.0500		Tit.			1.82	81.5
0.100			Tit.			0.411	26.0
0.100	0.0402		Tit.			1.82	38.2
0.100	0.100		Tit.			1.76	79.5
0.100	0.104		Tit.			1.84	77.5
0.100	0.265		Tit.			1.70	73.6
0.550			Pol.[a]	−4.84	0.00[a]	2.09	100
0.550	0.470		Pol.[b]	−4.77	+0.89[b]	1.92	100
0.500	0.523		Pol.[c]	−4.18	+1.20[c]	1.92	100
0.495	0.513		Pol.[d]	−4.51	+1.24[d]	1.87	100
0.400	0.513		Pol.[e]	+1.57	−0.47[e]	1.96	100
0.100		0.107	Tit.			0.640	40.5
0.100	0.107	0.107	Tit.			2.26	85.0
0.100	0.109	0.107	Tit.			2.26	81.3
0.100	0.109	0.054	Tit.			2.14	79.8

a 24.6°C, b 25.4°C, c 25.4°C, d 25.3°C, e 25.2°C
a—e Errors of reading of rotations, ±0.02~0.03°

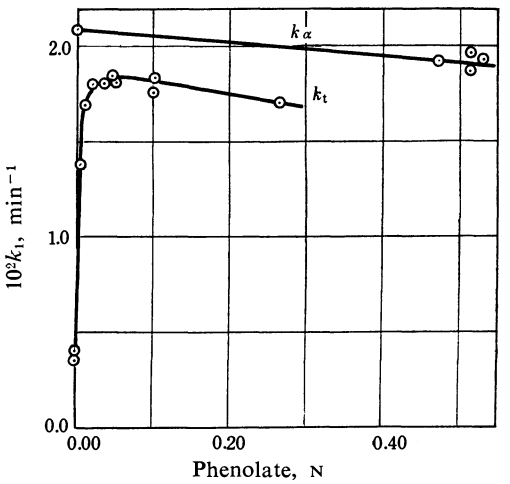


Fig. 3. Effect of initial concentration of anilinium phenolate on phenolysis of α-phenethyl chloride in 50 wt.% phenol-benzene at 25°C.

the polarimetric rate constants exceed the titrimetric values in the whole investigated range of the initial concentrations of the phenolate. The discrepancy between k_α and k_t seems to be definite even in the higher phenolate concentrations. The k_α's may be regarded as fairly constant, because the minor decrease with phenolate concentrations would be explained as originating from the decrease of the net phenol concentration due to the added base.

This result, i. e., the existence of constant gap between k_α and k_t, appears to be similar to the one which Winstein and Robinson[4] found for acetolysis of *threo*-3-*p*-anisyl-2-butyl system. These authors[4] claimed their results as the experimental bases of their "ion-pair" multi-step mechanism. However, the following results of product analysis and of analysis of the steric course for this phenolysis enforced us to consider about the other type of intermediates and mechanism.

Product Analysis and Steric Course of the Phenolysis.—When the reactions were carried out in the presence of anilinium phenolate, it was found that the isolated products were α-phenethyl phenyl ether and a minor amount of α-phenethylphenols. On the other hand, as previously found by Hart and his coworkers[1a], in the absence of the phenolate the only reaction product at a comparable reaction time was a minor amount of α-phenethylphenols. Furthermore, the hydrogen chloride cleavage of α-phenethyl phenyl ether into α-phenethyl chloride and phenol was quite rapid (half-life time, 1~2 min.) in comparison with the phenolysis. In view of these analytical results and the rate-relation, it is clear that the consumption of hydrogen chloride by the anilinium phenolate eliminates the reverse

4) S. Winstein and G. C. Robinson, *J. Am. Chem. Soc.*, **80**, 169 (1958).

formation of α-phenethyl chloride, whereas in the absence of the phenolate the rapid reverse reaction interrupts formation of the phenyl ether.

The establishment of the steric course for this phenolysis made the mechanistic situation clearer. When optically active α-phenethyl chloride was phenolyzed in the absence of anilinium phenolate, the polarimetric measurement showed that almost completely racemic α-phenethylphenols were produced, this being shown in Table I. However, in the presence of anilinium phenolate partially optically active α-phenethyl phenyl ether with retained configuration was obtained along with a minor amount of almost (more than 99%) racemic α-phenethylphenols. It is evident that these optically active products should be derived from an optically active intermediate. This rules out the Winstein's "ion-pair" mechanism[3] which postulates racemic intermediates.

Absence of the Common-ion Effect. — As mentioned above the titrimetric rate constants showed good first-order behavior. This indicates that there is no rate suppression by anilinium hydrochloride produced during the reaction. Furthermore, for the reaction carried out in the presence of tetramethylammonium chloride (0.05~0.100 N) the titrimetric rate constants showed also good first-order kinetics and their values were a little higher than those in the absence of the chloride, probably owing to some ionic strength effects (cf. Table I). These results indicate that there is no common-ion depression for the phenolysis rate of α-phenethyl chloride.

In the case of phenolysis for *tert*-butyl chloride[2], it was found that tetramethylammonium chloride showed extraordinarily marked common-ion depression, and it was concluded that the ion-pair intermediate reacted with the chloride ion, giving the starting chloride through exchange of chloride ion of the intermediate. On the basis of this mechanism the absence of common-ion effect in α-phenethyl system may be explained by the relatively large stability of the ion-pair intermediate. This stability is reflected in the solvolysis rate in α-phenethyl system and may be the cause of the existence of two kinds of intermediates for this system.

Thus it may be concluded that the ion-pair intermediate in this case has no exchangeability for the chloride ion because of the more dipole-like nature of the ion-pair associate or the tightness of the solvation shell around the ion-pair.

Mechanism of the Phenolysis of α-Phenethyl Chloride. — In general the existence of the discrepancy between k_α and k_t merely indicates that the racemization (or ionization) process should preceed the product-formation stage. However, if the discrepancy vanishes at higher concentrations of the base or, in other words, if the rate of product-formation becomes equal to that of racemization (or ionization), it indicates that both of the processes should be connected with the same intermediate and the reaction should obey the two-stage mechanism. This can easily be illustrated by total rate expression for the common S_Ni-type two-stage mechanism. A pertinent example for this is found in the comparison of the ionization rate constants and product-formation rate constants for the acetolysis in 2-*p*-anisylpropyl system[5], although the authors[5] postulated a three-stage mechanism with two species of the intermediate, i. e., "intimate" and "solvent separated" ion-pair.

On the other hand, if the increase of the base concentration dose not lessen the gap between k_α and k_t even at the higher concentrations and the preponderance of k_α over k_t is definitely observed, any rate expression derived from the two-stage mechanism would fail to explain this gap. Therefore, it is suggested that there should be certain, i. e., kinetically distinct, process intervening between the racemization and the product-formation process; in other words, two species of intermediates would be required between these processes, at least. These inferences, of course, are drawn irrespective of the structures of the intermediates and also irrespective of the details of the mechanism for each stage.

From these considerations we are led to postulate the following three-stage (two-intermediate) mechanism for the phenolysis of α-phenethyl chloride. Since the intermediates involved in this reaction should have optical activities, it is required to divide the three-stage mechanism into two parallel series of three-stage reactions of the optically antipodal chlorides, (+)-RCl and (−)-RCl. Thus, each of the series of the reactions involves two species of antipodal intermediates, I_1 and I_2, and the racemization must take place by way of an equilibration between the first antipodal intermediates, i. e., (+)-I_1 and (−)-I_1. If the racemization is caused by an equilibration between the second antipodal intermediates, the coincidence of k_α and k_t at higher phenolate concentrations would result; the process could then be represented by a two-stage mechanism and the kinetical discrimination of I_1 and I_2 would be impossible. The postulated mechanism is illustrated in the following kinetic scheme.

5) S. Winstein and A. H. Fainberg, ibid., **80**, 459 (1958).

$$(+)\text{-RCl} \underset{k_{-1}}{\overset{k_1}{\rightleftarrows}} (+)\text{-I}_1 \underset{k_{-2}}{\overset{k_2}{\rightleftarrows}} (+)\text{-I}_2 \xrightarrow{k_3} (+)\text{-RY}$$
$$\qquad\qquad k_4 \downarrow\uparrow k_4$$
$$(-)\text{-RCl} \underset{k_{-1}}{\overset{k_1}{\rightleftarrows}} (-)\text{-I}_1 \underset{k_{-2}}{\overset{k_2}{\rightleftarrows}} (-)\text{-I}_2 \xrightarrow{k_3} (-)\text{-RY}$$

In this scheme k_3 represents the ove-all rate constant for the product formation stage and actually means the sum of two terms, namely, the rate constant, k_3', for the solvent phenol molecule (YH) and the rate constant, $k_3'' \times [Y]$, for the phenolate (Y).

Using steady-state conditions for the concentrations of these intermediates, we obtain the rate expressions for k_α and k_t in Eqs. 1 and 2, respectively.

$$k_\alpha = \frac{k_1}{1+\dfrac{k_{-1}}{2k_4+\{k_2k_3/(k_3+k_{-2})\}}} \qquad (1)$$

$$k_t = \frac{k_1}{1+\dfrac{k_{-1}}{k_2k_3/(k_3+k_{-2})}} \qquad (2)$$

Since the first intermediate, I_1, is considered as an ion-pair (see the next section), k_1 represents an ionization rate constant. Thus it is clear from Eq. 1 that the observed racemization rate constant, k_α, is not always equal to the ionization rate constant, k_1, except at a limiting condition, $k_4 \gg k_{-1}$. This condition is, of course, unapplicable to this reaction.

From Eq. 1, the independency of k_α on the initial concentration of the phenolate is explained by the limiting condition, $k_4 \gg k_2$, this being shown in Eq. 3.

$$k_\alpha = k_1/\{1+(k_{-1}/2k_4)\} \qquad (3)$$

The constancy of k_t as the first-order rate constant is also explained by the limiting condition, $k_3 \gg k_{-2}$, this being shown in Eq. 4.

$$k_t = k_1/\{1+(k_{-1}/k_2)\} \qquad (4)$$

Thus the constant gap between k_α and k_t observed for higher phenolate concentrations can be explained by comparing the above two equations, 3 and 4.

With diminution of the phenolate concentrations, however, the value of k_3 decreases, and reaches finally, in the absence of the phenolate, the value of k_3', i. e., the rate constant for the solvent phenol. This explains a sudden decrease of k_t in the vicinity of zero-concentration of the phenolate (cf. Fig. 3).

Discussion on the Structures of the Intermediates.— In consideration of the existence of the equilibration between the antipodes (−)-I_1 and (+) -I_1 and of the lack of common-ion depression, the intermediate I_1 may be assumed to be an ion-pair surrounded by a solvation shell, and in the shell the carbonium cation may rotate or invert over a difintie but small potential barrier with a relatively large rate constant k_4, giving another antipodal intermediate, I_1. From the predominant retention of configuration in the product, the second intermediate I_2 may be assumed to be a kind of quadrupolar associate consisting of an α-phenethyl chloride ion-pair and a molecule of phenol or of anilinium phenolate originated from one of the members of the solvation shell. At the third stage, i. e., product-formation step, these quadrupoles may collapse to the products with mostly retained configuration. This stage may proceed similarly to the intramolecular reaction of S_Ni-type[6].

As to structure of the intermediates, a short comment about Winstein's "intimate" and "solvent separated" ion-pair mechanism[3] seems to deserve mention here. It has already been stated that Winstein's three-stage mechanism was not necessary for explaining the acetolysis in 2-*p*-anisyl-1-propyl system[5] but that the common two-stage mechanism was applicable to this system. In contrast to 2-*p*-anisyl-1-propyl system, however, for the *threo*-3-*p*-anisyl-2-butyl system[4] Winstein and Robinson found that the gap between the k_α line and the k_t line in acetolysis actually widened as the concentration of the added lithium perchlorate increased. It is evident from our conclusion in the previous section that the definite discrepancy between k_α and k_t for this system requires two discrete intermediates in the formulation of mechanism. In regard to the structures of the intermediates, however, Winstein's two kinds of ion-pairs, namely "intimate" and "solvent separated", do not seem to be kinetically distinguishable as discrete intermediates, because such ion-pairs should be quite rapidly interchanged among them and their stabilities would be closely the same. Therefore, Winstein's discrimination between the ion-pair structures does not seem chemically well founded, and is inapplicable not only to this system but also to any other system which requires two kinds of intermediates.

For the first intermediate in this *threo*-3-*p*-anisyl-2-butyl system an internally compensated phenonium ion-pair structure, just as postulated by Winstein and Robinson[4], may be regarded as kinetically stable and discrete. The second intermediate which should also be a stable species, would be formulated as chemically different from the first one. In analogy with the second intermediate in the phenolysis of α-phenethyl chloride, it seems reasonable to postulate some stable species, such as a new

6) W. A. Cowdrey, E. D. Hughes, C. K. Ingold, S. Masterman and A. D. Scott, *J. Chem. Soc.*, **1937**, 1252.

phenonium ion-pair involving an acetate ion instead of the arylsulfonate ion involved in the first intermediate, or a quadrupolar associate between the first phenonium ion-pair and a molecule of acetic acid.

Unlike in the phenolysis of active α-phenthyl chloride, the racemization rate in the acetolysis for this system is equalized to the ionization rate owing to the formation of internally compensated phenonium ion-pair. This is interpreted by the kinetic Eq. 1 presented for the polarimetric rate constant of the phenolysis, because, in such a specific case where the interconversion rate between the first antipodal intermediates, k_4, is quite rapid, the equation becomes

$$k_\alpha = k_1 \qquad (5)$$

In addition, the discrepancy between k_α and k_t for this system may also be accounted for by application of Eq. 4. Thus, it is clear that the kinetic characteristics of this *threo*-3-*p*-anisyl-2-butyl system are interpreted by the same mechanism as presented for the phenolysis of α-phenetyl chloride.

Experimental[7]

Materials.—The preparation of racemic and of optically active α-phenethyl chloride followed previous practice[8]; b. p. 68.0°C/16 mmHg. for racemic chloride; b. p. 55.0°C/11 mmHg., $[\alpha]_D^{24.4}+17.76\pm 0.03°$, *l* 1 dm., homogeneous, and b. p. 59.0°C/12 mmHg, $[\alpha]_D^{31}$ −36.5°, *l* 1 dm., homogeneous. Aniline, phenol and benzene (reagent grade for each) were dried and purified by fractional distillation; b. p. 42.0~43.0°C/1 mmHg, 179.0~181.0°C and 80.0~81.0°C, respectively. Reagent grade tetramethylammonium chloride was dried to constant weight in a tarred flask at 120~130°C in vacuo.

Kinetic Measurements. — The phenolyses were carried out by the usual method[8], the diminution of anilinium phenolate (or the development of hydrogen chloride) being followed by titration of aliquots (1.000 cc.) with standard perchloric acid (or sodium acetate) in acetic acid. Each run was followed to 60~70% completion.

For the polarimetric rate measurements with Zeiss-Winckel "Kreispolarimeter 0.01°", the reaction mixtures, prepared at the reaction temperature, were immediately placed into a jacketed 2 dm. polarimeter tube maintained at the reaction temperature by circulation of water from a constant temperature bath.

Phenolyses of Racemic and Optically Active α-Phenethyl Chloride in 50 wt.% Phenol-Benzene in the Presence of Anilinium Phenolate.—A solution of (±)-α-phenethyl chloride (5.02 g.) in 0.52 N anilinium phenolate (70 cc.), prepared from desired weights of aniline and 50 wt.% phenol-benzene at 25.0°C, was kept at 25.0°C for 4 hr. (ca. six half-lives). The phenolysis mixture was then washed twice with 30 cc. portions of water and extracted with four 50 cc. portions of 10% aqueous sodium hydroxide and three 30 cc. portions of 20% aqueous sodium hydroxide. After acidification of the alkaline extract, the liberated phenols were extracted with benzene. The benzene solution was dried, and after distillation of the benzene vacuum distillation of the residual material gave phenol (16.8 g., b. p. 69.0°C/7 mmHg) and mixture of *o*- and *p*-α-phenethylphenols (0.50 g., b. p. 140~155°C/3 mmHg; lit.[1a] 165~180°C/5~6 mmHg). After the alkaline extraction of the phenolysis mixture the remaining benzene layer was washed with water and dried with anhydrous sodium sulfate. Distillation of the benzene afforded an oily material which was distilled in vacuo to give α-phenethyl phenyl ether (4.5 g., b. p. 123~128°C/4 mmHg, m. p. 35.0~36.0°C; lit.[9] 143~145°C/10 mmHg, m. p. 38~39°C) and a mixture of *o*- and *p*-α-phenethylphenols (0.50 g., b. p. 140~145°C/5 mmHg). No attempt was made to determine the ortho-para ratio of the phenol mixture. There was not found any styrene fraction before the α-phenethyl phenyl ether fraction, and the recovered benzene did not give any styrene peak in gas-liquid partition chromatographical analysis.

The phenolysis of (−)-α-phenethyl chloride (α_D, see materials section) was carried out polarimetrically and then the product analysis of the reaction mixture was made. A solution of (−)-α-phenethyl chloride (5.220 g.) in 0.550 N anilinium phenolate (70.0 cc.) was kept at 25.0°C for 22 hr. (ca. 44 half-lives). Part of the solution was used for the polarimetric run at 25°C. The combined reaction mixtures, similarly treated to the run with the racemic chloride, gave (+)-α-phenethyl phenyl ether (4.16 g., b. p, 111.0~113.0°C/2 mmHg, yield 56.5%, $[\alpha]_D^{34}+2.29°$, *l* 1 dm., homogeneous; Found: C, 84.68; H, 7.14. Calcd. for $C_{14}H_{14}O$: C, 84.81; H, 7.12%) and (−)-α-phenethylphenols (a mixture of *o*- and *p*-derivatives, b. p. 150~165°C/7 mmHg, yield 13.6%, $[\alpha]_D^{34}-0.42°$, *l* 1 dm., *c* 23.8, benzene).

The second run carried out under the same conditions with (+)-α-phenethyl chloride (3.525 g., α_D see materials section) solution (50.0 cc.) of 0.552 N anilinium phenolate afforded 3.0 g. of (−)-α-phenethyl phenyl ether (b. p. 133~135°C/5 mmHg, n_D^{25} 1.5665, yield 60.0%, $\alpha_D^{24.7}+1.21°$, *l* 1 dm., homogeneous; Found: C, 84.93; H, 7.20%).

Phenolysis of (±)-α-Phenethyl Chloride in 50 wt.% Phenol-Benzene in the Absence of Anilinium Phenolate.—A solution of (±)-α-phenethyl chloride (4.92 g.) in 50 wt.% phenol-benzene (62.8 g.) was kept at 20~25°C for 22 hr., and then at 50.0°C for 7 hr. After similar treatment to the run in the presence of anilinium phenolate, the benzene layer after alkaline extraction gave 0.10 g. of α-phenethylphenols (b. p. 132~133°C/2 mmHg) and from the alkaline extract 3.5 g. of α-phenethylphenols (140~156°C/4 mmHg) was isolated.

Hydrogen Chloride Cleavage of α-Phenethyl Phenyl Ether in 50 wt.% Phenol-Benzene.—The cleavage was followed titrimetrically. In a 20 cc.

7) Microanalyses by Microanalytical Center, Kyoto University.

8) K. Okamoto, K. Takeuchi and H. Shingu, This Bulletin, **34**, 1132 (1961).

9) H. Hart and H. S. Eleuterio, *J. Am. Chem. Soc.*, **76**, 519 (1954).

volumetric flask, α-phenethyl phenyl ether (137 mg.) solution of 0.045 N hydrogen chloride was made at 25°C. The reaction percentage was estimated to be 74.0% at two minutes after mixing. The diminution of hydrogen chloride reached a minimum value (84.7% of conversion for ether), then the gradual increase of hydrogen chloride concentration, due to the slow phenolysis of α-phenethyl chloride produced, was observed.

Summary

1. Titrimetric and polarimetric rate constants (k_t and k_α) for phenolysis of α-phenethyl chloride in 50 wt.% phenol-benzene at 25°C were measured, and satisfactory first-order behavior was observed irrespective of presence or absence of anilinium phenolate. From this the S_N1-characteristics of this phenolysis was concluded.

2. The values of k_α's were fairly constant at any phenolate concentrations (0.0~0.6 N). The k_t's were also fairly constant at higher phenolate concentrations. However, the k_t's gave smaller values than the k_α's, and showed a sudden decrease in the vicinity of zero phenolate concentration. The gap between the k_α line and k_t line was not diminished and remained fairly constant as the phenolate concentration increased.

3. In the presence of anilinium phenolate the main product was α-phenethyl phenyl ether with predominantly retained configuration, whereas in the absence of the phenolate only a minor amount of α-phenethylphenol was obtained.

4. From the constant gap observed between k_α and k_t it was generally concluded that the phenolysis should proceed by way of a two-intermediate (I_1 and I_2) three-stage mechanism. In view of the predominant retention of configuration in the product, it was postulated that the intermediates should be optically active. Hence the mechanism was divided into parallel series of the three-stage processes for the optically antipodal chlorides and intermediates, namely,

$$(+)RCl \rightleftarrows (+)I_1 \rightleftarrows (+)I_2 \rightarrow (+)RY$$

and

$$(-)RCl \rightleftarrows (-)I_1 \rightleftarrows (-)I_2 \rightarrow (-)RY$$

These parallel series of the processes were connected with each other by fairly rapid equilibration between the first antipodal intermediates ($-I_1$ and $+I_1$). For the first intermediate was suggested an ion-pair surrounded by a solvation shell and for the second a kind of quadrupolar associates which consist of the ion-pair and the reactant dipole (phenol or anilinium phenolate).

5. It was pointed out that a necessary condition for the existence of three-stage mechanism is a kinetically-definite stabilization of the two kinds of intermediates. This stabilization was verified by the absence of common-ion depression for this phenolysis rate. It was also pointed out that unstable ion-pair intermediates, like "solvent separated" and "intimate" ion-pair, could not be kinetically distinguished among themselves, and that in this case any three-stage formulation actually converged to two-stage treatment. This was shown in the case of acetolysis in 2-*p*-anisylpropyl system to which Winstein and Fainberg[5] assumed their three-stage mechanism to be applicable.

6. It was shown that Winstein's three-stage mechanism with the "intimate" and "solvent separated" ion-pairs is generally unapplicable to any cases where a three-stage is required, e.g., not only to this phenolysis but also to the acetolysis in *threo*-2-*p*-anisyl-3-butyl system[4]. For the latter a three-stage mechanism similar to the one suggested for this phenolysis in α-phenethyl system was presented. Fairly stable, two discrete intermediates, namely, a phenonium ion-pair for the first intermediate and a quadrupolar associate between the first intermediate and acetic acid molecule for the second were suggested.

Department of Fuel Chemistry
Faculty of Engineering
Kyoto University
Sakyo-ku, Kyoto

Preparation and Properties of Alkyl Trifluorovinyl Ethers and Related Compounds[1]

By Kunio OKUHARA, Hajime BABA and Rimpei KOJIMA

(Received June 1, 1961)

Since 1946[2], many fluoroethers have been synthesized by the addition of alcohols to fluoroölefins under alkali catalysis, and a mechanism has also been presented[3]. These fluoroethers are usually saturated addition products, and some fluoroethers easily split off hydrogen fluoride to give vinyl ethers[4-6]. According to previous reports[5,6], it can be inferred that the larger the number of fluorine attached to the olefin carbons, the higher the stability of the resulting fluoroether. It was for this reason that the dehydrofluorination of methyl 1, 1, 2-trifluoro-2-chloroethyl ether was found to require a prolonged refluxing over solid potassium hydroxide[7].

Another procedure for preparing fluorovinyl ether has been presented by Meier and Böhler[8]. They synthesized ethyl 1, 2-difluoro-2-chlorovinyl ether directly by the reaction of trifluorochloroethylene with alcohol-free sodium ethylate.

By using the same method, trifluorovinyl, methyl, ethyl, isopropyl and *tert*-butyl ethers were prepared, the first of which has already been described by Dixon[9]. In our experiment the accompanying formation of the corresponding saturated tetrafluoroethyl ethers could not be avoided because highly alcohol-free sodium alcoholates were not available.

$$CF_2=CF_2+NaOR\rightarrow CF_2=CFOR+NaF$$

$$CF_2=CF_2+HOR\rightarrow CF_2HCF_2OR$$

R ; CH_3, C_2H_5, $CH(CH_3)_2$, $C(CH_3)_3$

The apparent reactivity of the alcoholates toward tetrafluoroethylene increased in the following order: methyl, ethyl < isopropyl, *tert*-butyl.

In the alkyl trifluorovinyl ethers, the absorption peak of C=C occurs within the range 5.46～5.50 μ (1832～1818 cm^{-1}). This position seems exceptionally short for C=C, but it is reasonably correlated with those of reference compounds, as is shown in Table II.

Trifluorovinyl and 1, 2-difluoro-2-chlorovinyl ethyl ethers give chlorine and bromine addition products. They are easily hydrolyzed to the corresponding esters according to the method that was used for the hydrolysis of α, α-difluoroethers by Tarrant and Young[10]. The adducts and esters are given in Table III. The adducts are so reactive that crude adducts from the

TABLE I. REACTION OF TETRAFLUOROETHYLENE AND SODIUM ALCOHOLATES

Alcoholate	Temp. °C	Time hr.	Yield[a] %	Product	B. p., °C Found	B. p., °C Reported	Fluorine, % Found	Fluorine, % Calcd.
Methyl	20～40	145	28	$CF_2=CFOCH_3$	12	10.5～12.5[9]	50.0	50.9
			7	$CF_2HCF_2OCH_3$	36	36.5[3]		
Ethyl	40	120	53	$CF_2=CFOC_2H_5$	38.5		44.1	45.2
			4	$CF_2HCF_2OC_2H_5$	57	57.5[2]		
Isopropyl	10	96	26	$CF_2=CFOCH(CH_3)_2$	58.5		38.5	40.7
			20	$CF_2HCF_2OCH(CH_3)_2$	70		45.3	47.5
tert-Butyl	10	27		$CF_2=CFOC(CH_3)_3$	56/375 mmHg			
				$CF_2HCF_2OC(CH_3)_3$	73/375 mmHg	87[11]		

a) Based upon the charged alcoholate.

1) Presented at the 12th Annual Meeting of the Chemical Society of Japan, Kyoto, April, 1959.
2) W. E. Hanford and G. W. Rigby, U. S. Pat. 2409274 (1946).
3) W. T. Miller, Jr., E. W. Fager and P. H. Griswold, *J. Am. Chem. Soc.*, **70**, 431 (1948).
4) J. T. Barr, K. E. Rapp, R. L. Pruett, C. T. Bahner, J. D. Gibson and R. H. Lafferty, Jr., ibid., **72**, 4480 (1950).
5) P. Tarrant and H. C. Brown, ibid., **73**, 1781 (1951).
6) J. D. Park, W, M. Sweeney, S. L. Hopwood, Jr. and J. R. Lacher, ibid., **78**, 1685 (1956).
7) R. S. Corley, J. Lal and M. W. Kane, idid., **78**, 3489 (1956).
8) R. Meier and F. Böhler, *Chem. Ber.*, **90**, 2342 (1957).
9) During the course of our investigation, Dixon has prepared a number of trifluorovinyl ethers of the type $RCH_2OCF=CF_2$ by the same method, and has stated that they can be converted into high molecular weight polymers; U. S. Pat. 2917548 (1959).
10) J. A. Young and P. Tarrant, *J. Am. Chem. Soc.*, **71**, 2432 (1949).

Table II. Absorption peak of C=C in trifluorovinyl alkyl ethers and reference compounds

	Wavelength, μ[a]
$CF_2=CF_2$	5.34[b,c]
$CF_2=CFOCH_3$	5.46[b]
$CF_2=CFOC_2H_5$	5.46
$CF_2=CFOCH(CH_3)_2$	5.48
$CF_2=CFOC(CH_3)_3$	5.50
$CFCl=CF_2$	5.55[b]
$CFCl=CFOC_2H_5$	5.70

a) Liquid unless otherwise mentioned.
b) Gas
c) Raman spectrum data: J. R. Nielsen and H. H. Claassen, *J. Chem. Phys.*, **18**, 812 (1950).

reaction mixtures were always accompanied by the corresponding esters. Furthermore, in the absence of potassium carbonate, some decomposition to acyl fluoride and alkyl halide could not be avoided during the fractional distillation the crude reaction product.

Methyl trifluorovinyl ether polymerized, even when stored in a refrigerator, to give a white solid deposit. Ethyl trifluorovinyl ether became viscous upon standing in a sealed tube at room temperature, and was polymerized with common free-radical initiators to give a balsam-like mass. Propyl trifluorovinyl ether could not be polymerized. These facts are interesting when compared with the facts[12] that the high polymers of vinyl methyl, ethyl and other alkyl ethers can be obtained only by cationic polymerization, and that isopropyl vinyl ether is also capable of forming a polymer.

tert-Butyl trifluorovinyl ether was very unstable and decomposed, upon standing, to the acyl fluoride and isobutene. This is analogous to the decomposition of 1, 1, 2, 2-tetrafluoro- and 1, 1, 2-trifluoro-2-chloroethyl *tert*-butyl ethers[5,11]. It is noteworthy that the vinyl ether decomposed as easily as the saturated ether.

Postulated Carbonium Ion of the Type $-O-\overset{F}{\overset{|}{\underset{+}{C}}}-$.—The high reactivity of the fluoroethers prepared, and of other α-haloethers, seems to be explained by assuming the formation of a carbonium ion* of the type $-O-\overset{|}{\underset{+}{C}}-$. Tiers postulated carbonium-oxonium ion in the transformation of α-fluoroethers with aluminum trichloride to the corresponding α-chloroethers[13].

With this group of compounds, not only the halogen exchange and the hydrolysis to esters, but also the decomposition to alkyl and acyl halides, are subject to acid catalysis. The operation of acid catalysis is supported by the facts that *tert*-butyl 1, 1, 2-trifluoro-2-chloroethyl ether from which hydrogen fluoride had been removed by adsorption was fairly stable[4], and that potassium carbonate is effective as the stabilizer of the ethers prepared in this experiment. The three reactions, decomposition, halogen exchange and hydrolysis, are thought to proceed through the same intermediate, carbonium-oxonium ion.

As this type of compound is relatively stable when acids are removed, an intramolecular reaction through a cyclic transition state[7] is not sufficient to explain the decomposition. It rather seems to be an intermolecular reaction and to proceed by a chain mechanism. With the compound of the type $-O-\overset{F}{\overset{|}{\underset{X}{C}}}-$ (where

Table III. Ethers and esters derived from trifluorovinyl and difluorochlorovinyl ethyl ethers

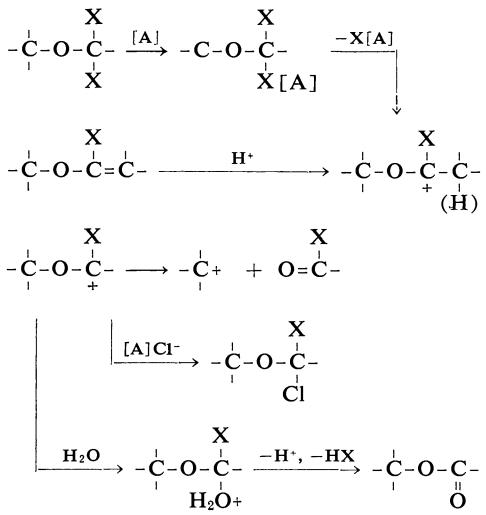
	B. p., °C	Halogen, %		Fluorine, %	
		Found	Calcd.	Found	Calcd.
$C_2H_5OCFBrCFClBr$	170			12.5	12.6
$C_2H_5OCOCFClBr$	145[a]				
$C_2H_5OCFBrCF_2Br$	135.5	55.5	55.9	19.7	19.9
$C_2H_5OCOCF_2Br$	113	39.7	39.4	18.6	18.7
$C_2H_5OCFClCFCl_2$	134	49.9	49.8	17.7	17.8
$C_2H_5OCFClCF_2Cl$	ca. 95[b]				
$CH_3CHClOCFClCFCl_2$	157	56.8	57.2	15.3	15.3
$CH_3CHClOCFClCF_2Cl$	121	45.4	46.0	24.3	24.6

a) F. Swarts, *Bull. soc. chim. France*, [3], **15**, 1135 (1896), reports b. p. 151°C.
b) Impure. See the last part of Experimental.

11) D. E. England, L. R. Melby, M. A. Dietrich and R. V. Lindsey, Jr., ibid., **82**, 5116 (1960).
12) C. E. Schildknecht, "Vinyl and Related Polymers", John Wiley and Sons, Inc., New York (1952), pp. 593, 599.

* For simplicity, the carbonium ion of the type $-O-\overset{|}{\underset{+}{C}}-$ stabilized by carbonium-oxonium resonance will be called carbonium-oxonium ion in the following discussions.
13) G. V. D. Tiers, *J. Am. Chem. Soc.*, **77**, 4837, 6703 (1955).

Chart I. Formation of carbonium-oxonium ion and its secondary transformations.



[A]=H^+ or other acid such as $AlCl_3$
X =F or other halogen

X is Cl or Br), X^- is preferentially removed and fluorocarbonium-oxonium ion is formed, judging from the decomposition products of 1, 2-difluoro-2-chloro-1, 2-dibromoethyl- and 1, 2-difluoro-1, 2, 2-trichloroethyl ethyl ethers.

$$C_2H_5OCFCFClBr \xrightarrow{H^+} C_2H_5OCFCFClBr \xrightarrow{-HBr}$$

$$C_2H_5OCFCFClBr \longrightarrow C_2H_5^+ + O{=}CCFClBr$$

$$C_2H_5OCFCFClBr \xrightarrow{C_2H_5^+} C_2H_5OCFCFClBr + C_2H_5Br$$

$$C_2H_5^+ \longrightarrow CH_2{=}CH_2 + H^+$$

Compounds which are capable of forming carbonium-oxonium ion and thus undergoing a similar decomposition (rearrangement, in the case of cyclic ethers) are not only α-halo and vinyl ethers, but also α-carboxy ethers[14], haloformates[15], etc.

In the hydrolysis of α, α-difluoroethers to the esters, it is inconsistent with experimental findings to assume that the reaction proceeds through the oxonium ion in which a proton is attached to the oxygen of the ether[10]. A route through carbonium-oxonium ion could explain the hydrolysis of both α, α-difluoroethers and α-fluorovinyl ethers[8].

Reactions that could be interpreted as electrophilic aromatic substitution involving carbonium-oxonium ion have also been reported[16].

Experimental

Ethyl Trifluorovinyl Ether.—A mixture of 164 g. of sodium ethylate and 450 ml. of dioxane was placed in a 2 l. autoclave. After moderate evacuation, the autoclave was charged with about 200 g. of tetrafluoroethylene at one time and shaken until the pressure was constant. The pressure readings during the shaking were 30 kg./cm² (initial), 23 kg./cm² (1 hr.), 13 kg./cm² (22 hr.), and 5 kg./cm² (120 hr.; final). The liquid products were separated by centrifiguration or suction filtration from the solid products and the liquid remaining on the solid was evaporated under reduced pressure and collected in cold traps. The rectification of the combined dioxane solution over potassium carbonate under nitrogen atmosphere gave ethyl trifluorovinyl ether (161 g., 53% yield), boiling at 38.5°C, and 1, 1, 2, 2-tetrafluoroethyl ether (15 g., 4% yield), boiling at 57°C.

Methyl trifluorovinyl ether was prepared in a similar fashion, but in one experiment a violent explosion of the charged tetrafluoroethylene occurred.

In the preparation of isopropyl trifluorovinyl ether, the first portion (69 g., 15 kg./cm²) of tetrafluoroethylene was taken up completely by 250 g. of sodium isopropylate within 15 min. at 10°C and considerable heat was generated.

***tert*-Butyl Trifluorovinyl Ether.**—Both trifluorovinyl and 1, 1, 2, 2-tetrafluoroethyl *tert*-butyl ethers were unstable and decomposed to form two layers on storage in a sealed tube at room temperature. The decomposition products were not thoroughly examined, but their infrared spectra showed that the upper layers from both compounds are polyisobutene, the lower layer from the vinyl ether is an acyl fluoride, while the one from the tetrafluoroether is a mixture of a carboxylic acid and a small amount of the acyl fluoride. Based upon similar dicomposition[4,5,11], the acyl fluoride is assumed to be difluoroacetyl fluoride and the acid to be difluoroacetic acid.

$$(CH_3)_3COCF{=}CF_2 \longrightarrow (CH_3)_2C{=}CH_2 + O{=}CCF_2H$$

$$(CH_3)_3COCF_2CF_2H \longrightarrow (CH_3)_2C{=}CH_2 + HF + O{=}CCF_2H$$

In the latter case, the hydrogen fluoride and the acyl fluoride may have reacted with the glass wall to yield the carboxylic acid.

$$\begin{cases} SiO_2 + 4HF \longrightarrow SiF_4 + 2H_2O \\ Na_2SiO_3 + 6HF \longrightarrow Na_2SiF_6 + 3H_2O \end{cases}$$

$$O{=}CCF_2H + H_2O \longrightarrow O{=}CCF_2H + HF$$

14) J. Meinwald, H. Hwang, D. Cristman and A. P. Wolf, ibid., 82, 483 (1960).
15) S. Nakanishi, T. Myers and E. V. Jensen, ibid., 77, 5033 (1955).
16) A. Rieche, H. Gross and E. Hoft, *Chem. Ber.*, 93, 88 (1960); C. T. Mason and L. A. Gist, Jr., *J. Am. Chem. Soc.*, 73, 4644 (1951).

Bromine Derivatives of 1, 2-Difluoro-2-chlorovinyl Ethyl Ether.—Difluorochlorovinyl ethyl ether[8] (26.0 g.) in chloroform (11 g.) was added dropwise to a solution of bromine (29.7 g.) in chloroform (60 g.) with stirring and cooling. The resultant solution was washed with aqueous potassium carbonate-sodium thiosulfate, dried over sodium sulfate, and fractionated. After the chloroform was distilled, the temperature at the head of the column suddenly dropped and fluctuated between 41 and 48°C, showing the occurrence of a decomposition. The liquid decomposition product (37.1 g.) was shown to be a mixture of an acyl fluoride (5.35 μ) and ethyl bromide (reported b. p. 38.4°C) by its infrared spectra. The fluoride is most likely to be fluorochlorobromoacetyl fluoride. (Ref. a of Table III reports b. p. 51°C.) Ethylene was also noted in the gaseous decomposition product by its characteristic multiplet around 10.5 μ.

In order to prevent decomposition, potassium carbonate was added to the still-pot, and the distillation was successfully carried out. A duplicate run, but with distillation over potassium carbonate, gave 1, 2-difluoro-2-chloro-1, 2-dibromoethyl ethyl ether (33.7 g., 61% yield), boiling at 170°C. Sodium carbonate was not so effective as potassium carbonate in preventing such decompositions.

The bromoether (17.8 g.) was treated with 98% sulfuric acid (70 g.) for 50 min. without cooling, poured into ice-water, extracted with chloroform, washed with aqueous potassium carbonate and dried over sodium sulfate. Distillation of the resultant solution gave ethyl fluorochlorobromoacetate (6.7 g. 53% yield), boiling at 145°C.

Chlorine Derivatives of 1, 2-Difluoro-2-chlorovinyl Ethyl Ether.—Chlorine was bubbled through a solution of difluorochlorovinyl ethyl ether (22.0 g.) in chloroform (83 g.) until the solution turned yellow from an excess of chlorine under ice-salt cooling. The resultant solution was washed with aqueous potassium carbonate, dried over sodium sulfate and distilled. A saturated ether (15.4 g., 39% yield) boiling at 157°C was obtained. The elementary analysis showed that three chlorines were introduced during the chlorination. The ether was tentatively identified as 1-chloroethyl 1, 2-difluoro-1, 2, 2-trichloroethyl ether by its infrared spectrum (6.75 μ, 6.90 μ and 7.27 μ), compared with that of 1, 2-difluoro-1, 2, 2-trichloroethyl ethyl ether (6.91 μ, 7.20 μ).

Dioxane was found to be a suitable solvent to stop the reaction at the stage of chlorine addition. Thus, chlorine was bubbled through a solution of difluorochlorovinyl ethyl ether (15 g.) in dioxane (30 g.) until the solution turned yellow from an excess of chlorine. The resultant dioxane solution was poured into aqueous potassium carbonate, and the lower layer was separated, dried over sodium sulfate and distilled over potassium carbonate. 1, 2-Difluoro-1, 2, 2-trichloroethyl ethyl ether (10.4 g., 46% yield), boiling at 134°C, was obtained. A duplicate distillation without potassium carbonate gave no difluorotrichloroethyl ethyl ether. However, ethyl chloride and ethylene, but no ethyl fluoride, were noted in the gaseous decomposition product.

The ethers and ester from ethyl trifluorovinyl ether were obtained like those from 1, 2-difluoro-2-chlorovinyl ethyl ether; their boiling points and analytical data are given in Table III. However, ethyl 1, 2, 2-trifluoro-1, 2-dichloroethyl ether could not be obtained in a pure state, being contaminated with the corresponding ester, ethyl difluorochloroacetate (reported[17] b. p. 97°C).

summary

Trifluorovinyl methyl, ethyl, isopropyl and *tert*-butyl ethers have been prepared. These trifluorovinyl ethers show C=C absorption at such a short wavelength as 5.46~5.50 μ. The methyl and ethyl ethers can be polymerized by free-radical initiators. Halogen addition products of trifluorovinyl- and 1, 2-difluoro-2-chlorovinyl ethers have also been prepared. With α-halo or vinyl ethers, the reactions that are catalyzed by acids, including decomposition, are best interpreted as proceeding through the carbonium ion stabilized by carbonium-oxonium resonance.

Government Industrial Research Institute, Nagoya
Kita-ku, Nagoya

17) F. Swarts, *Rec. trav. chim.*, **27**, 128 (1908).

Studies on D-Glucosamine Derivatives. VIII[1]. *1-C-Substituted-1-anilino-1-deoxy-D-arabitols**

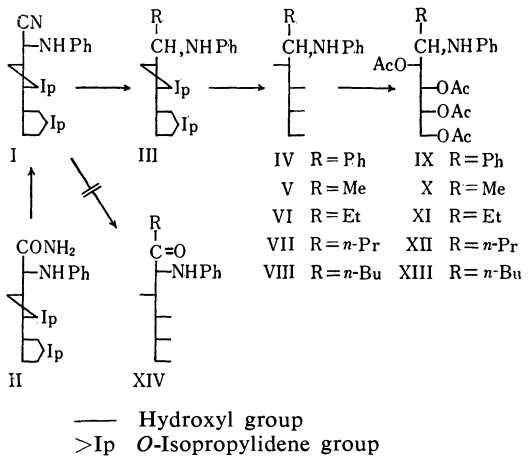
By Juji YOSHIMURA

(Received August 3, 1961)

In a previous paper[2], syntheses of 3, 4; 5, 6-di-*O*-isopropylidene-*N*-phenyl-D-glucosaminonitrile (I) and of 3, 4; 5, 6-di-*O*-isopropylidene-*N*-phenyl-D-glucosaminic acidamide (II) have been described. In the present study, the additon of Grignard reagents or alkyl lithiums to the unsaturated function of these compounds is examined, in expectation of obtaining the corresponding 1-*C*-substituted-1-keto-D-glucosamine derivatives (XIV).

Compound I reacted exothermally with Grignard reagents in ether to yield sirupy materials, which on hydrolysis with mineral acid and extraction of the neutrallized hydrolyzate with ethyl acetate gave crystalline materials. These crude crystals were separated into the two diastereoisomers by fractional crystallization from ethyl acetate, of which the one was a dextro-rotating minor product and the other a levo-rotating major product in every case. (In this report, the former is temporarily represented as A-compound and the latter as B-compound.)

The analytical data of these crystals were, however, not consistent with that of XIV. The infrared spectra shown in Fig. 1 indicated the presence of NH and anilino bands at 3300 and 1600 cm^{-1}, but the absence of CN and -CO- bands. It is worthy to note that a few differences between A- and B-compounds in their absorption bands were generally found in the region from 850 to 1050 cm^{-1}. Moreover, the substitution of alkyls to the C-2 of I was deduced from the fact that the diastereoisomers (IV-A and IV-B) obtained from I and phenylmagnesium bromide gave benzoic acid in 70% yield by alkalline permanganate oxidation. The structures of these crystals were, therefore, assigned to the 1-*C*-substituted-1-anilino-1-deoxy-D-arabitols (IV-VIII).



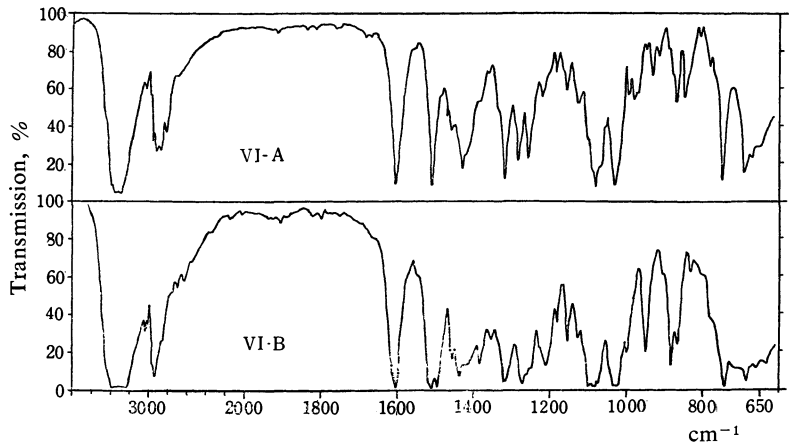


Fig. 1.

* A part of this was presented at the 13th Annual Meeting of the Chemical Society of Japan, Tokyo, 1960.

1) Part VII of this series, This Bulletin, 35, 467 (1962).
2) J. Yoshimura, ibid., 33, 1404 (1960).

These arabitols were converted to the corresponding tetraacetates (IX–XIII) by treating with acetic anhydride in dry pyridine. The melting points, rotation values and analytical data of these diastereoisomeric arabitols and the acetates are listed in Tables I and II.

The reaction products between I and alkyl lithiums were also syrupy, except for 1-*C*-phenyl-1-anilino-1-deoxy-3, 4; 5, 6-di-*O*-isopropylidene-D-arabitol (III; R=phenyl) obtained from I and phenyl lithium, and each crude syrup was hydrolyzed to the two corresponding diastereoisomers, in a manner similar to that in the case of the Grignard reactions. However, the minor products were the B-compounds and the major, the A in this case. A comparison of the yields of both the A- and B-compounds is made in Table III.

To pursue the whereabouts of the nitrile group in I, the cyano ions in the reaction mixture of I and alkyl lithiums, after having been decomposed with water and extracted with ether, were examined qualitatively and quantitatively. It was found that the water layer showed the positive blue coloration of cyano ions with cupric acetate and benzidine, and that the amount were determined, by volumetric titration using silver nitrate, to correspond to the yields of the arabitols (about 60%) in every case.

The above results indicate that the reaction of I with the Grignard reagents or alkyl lithiums gives rise to the replacement of the nitrile group by the alkyls of these reagents instead of the addition to its unsaturated bond. Although this type of reactions has not been

Table I. 1-*C*-Substituted-1-anilino-1-deoxy-D-arabitols

Compound	Formula (mol. wt.)	M. p., °C	$[\alpha]_D$ in methanol	Carbon, %		Hydrogen, %		Nitrogen, %	
				Found	Calcd.	Found	Calcd.	Found	Calcd.
IV-A	$C_{17}H_{21}O_4N$ (303.3)	191~192	+ 2.7	67.34	67.31	7.17	6.98	4.50	4.62
IV-B	$C_{17}H_{21}O_4N$ (303.3)	164~165	− 4.5	67.57	67.31	7.22	6.98	4.55	4.62
V-A	$C_{12}H_{19}O_4N$ (241.3)	128~129	+84.1	59.52	59.73	7.97	7.94	6.00	5.81
V-B	$C_{12}H_{19}O_4N$ (241.3)	160~161	−41.2	59.83	59.73	8.16	7.94	5.98	5.81
VI-A	$C_{13}H_{21}O_4N$ (255.3)	131~132	+76.9	61.49	61.15	8.39	8.29	5.55	5.49
VI-B	$C_{13}H_{21}O_4N$ (255.3)	161~161.5	−38.5	61.08	61.15	8.39	8.29	5.40	5.49
VII-A	$C_{14}H_{23}O_4N$ (269.3)	134~136	+67.6	62.61	62.43	8.81	8.61	5.17	5.20
VII-B	$C_{14}H_{23}O_4N$ (269.3)	160~161	−18.7	62.24	62.43	8.78	8.61	5.05	5.20
VIII-A	$C_{15}H_{25}O_4N$ (283.4)	126~128	+72.5	63.14	63.58	8.63	8.89	5.06	4.94
VIII-B	$C_{15}H_{25}O_4N$ (283.4)	154~155	−13.0	63.57	63.58	9.14	8.89	4.88	4.94

Table II. 1-*C*-Substituted-1-anilino-1-deoxy-2, 3, 4, 5-tetra-*O*-acetyl-D-arabitols

Compound	Formula (mol. wt.)	M. p., °C	$[\alpha]_D$ in methanol	Carbon, %		Hydrogen, %		Nitrogen, %	
				Found	Calcd.	Found	Calcd.	Found	Calcd.
IX-A	$C_{25}H_{29}O_8N$ (471.5)	56~57	+80.5	63.51	63.68	6.35	6.20	2.80	2.97
IX-B	$C_{25}H_{29}O_8N$ (471.5)	Sirup	+44.6	63.44	63.68	6.47	6.20	2.72	2.97
X-A	$C_{20}H_{27}O_8N$ (409.5)	83~85	+60.3	58.34	58.67	6.92	6.65	3.48	3.42
X-B	$C_{20}H_{27}O_8N$ (409.5)	96~98	+21.7	58.59	58.67	6.53	6.65	3.65	3.42
XI-A	$C_{21}H_{29}O_8N$ (423.5)	81~82	+84.0	59.25	59.56	6.77	6.90	3.35	3.31
XI-B	$C_{21}H_{29}O_8N$ (423.5)	86~87	+42.0	59.61	59.56	6.88	6.90	3.18	3.31
XII-B	$C_{22}H_{31}O_8N$ (437.5)	52~53	+10.2	60.62	60.40	7.31	7.14	3.14	3.20
XIII-B	$C_{23}H_{33}O_8N$ (451.5)	Sirup	+14.0	61.32	61.18	7.30	7.39	3.11	3.10

Table III. Yield (%) of the A- and B-compounds in Grignard and alkyl lithium reactions

1-*C*-Substituted group	Grignard reagent		Alkyl lithium	
	A-Compd.	B-Compd.	A-Compd.	B-Compd.
Phenyl	2.7	51.7	63.0	0
Methyl	3.5	48.2	53.7	3.4
Ethyl	3.8	51.8	58.5	5.6
n-Propyl	4.2	50.2	55.2	4.8
n-Butyl	4.2	52.6	60.5	5.1

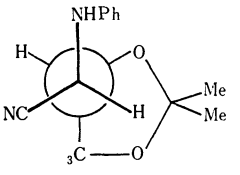
exhaustively investigated, it appears to be fairly general for α, α-disubstituted cyanohydrins[3] and α-aminonitriles[4], among which is I. Kharasch[5] assumed that in all these cases the bond between the nitrile group and the others has a rather high degree of ionic character, with the negative end of the dipole at the cyano group, but the radicals attached to the cyano group are rather weakly electronegative.

On the other hand, the reaction of I with the Grignard reagents led mainly to B-compounds, while alkyl lithiums lead to the A. Although a few examples[6] have been known in which organomagnesium and organolithium compounds showed sterically different behavior, no reports relating to such a characteristic in asymmetric induction has appeared up to the present.

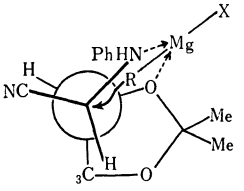
The absolute configuration at C-1 of the diastereoisomers must be determined by another method. However, it seems likely that A-compounds have a glucosamino-structure and the B-compounds a mannosamino-structure, as the former has the same dextro-rotatory character as I. Bonner[7] has already proved that the more dextro-rotatory one of the two diastereoisomers of 1-*C*-phenyl-D-pentitol obtained from 3, 4; 5, 6-diisopropylidene-D-glucosamine and phenylmagnesium bromide, possesses a glucostructure, and the other a manno-structure.

The most stable configuration (XV) of the reaction center of I shown by Newman's representation[8] suggests that it is very reasonable to assume the rigid complex model (XVI) in the transition state, as proposed by Cram et al.[9] as a result of extensive studies on asymmetric induction. Thus, it is concluded that rather polar Grignard reagents reacted smoothly, accompanying Walden inversion[10], to afford a mannosamino-structure.

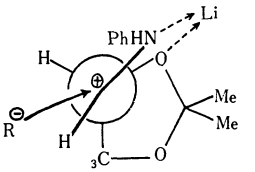
If the nitrile group is eliminated initially through either ionic or free radical mechanism, the alkyl group will predominantly attack from the direction of the previously existing nitrile group on the transition state (XVII), to afford



XV



XVI



XVII

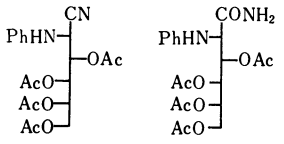
a glucosamino-structure. This mechanism is very suitable to explain the fact that the reaction of I and alkyl lithiums afforded the glucosamino-structure, but the reason for the distinctly different behavior between organomagnesium and organolithium compounds in the reaction described in this paper remains ambiguous. The rather covalent character of the simple organolithium compound, however, has been provided by the non-conductance of solutions of ethyl lithium in benzene[11] and low dipole moment of butyl lithium[12]. This character seems likely to prevent the Walden inversion through the formation of XVI.

The reaction of II with Grignard reagents or alkyl lithiums in ether afforded unchanged II over 80%. Even though the reaction was performed in benzene at 100°C for four hours, 50~56% of II was recovered, and the mother liquor produced a small amount of the D-arabitols when treated in the usual manner. It is interesting that the B-compounds were obtained in the former case and the A-compounds in the latter. From this fact, it can be deduced that the amide II was initially dehydrated to the nitrile[13].

As expected XIV was not obtained in the above-mentioned methods, Hoesch's method[14]

3) T. Asahina et al., *J. Pharm. Soc. Japan*, **494**, 19 (1923); J. Guerden, *Bull. acad. roy. Belg. Classe sci.*, (5), **11**, 701 (1925).
4) P. Bruylants, ibid., (5), **11**. 261 (1925); M. Velghe, ibid., (5), **11**, 301 (1925); A. Christian, *Bull. soc. chim. Belg.*, **33**, 483, (1924); T. S. Stevens et al., *J. Chem. Soc.*, **1931**, 2568; **1932**, 2607; H. M. Taylor and C. R. Hauser, *J. Am. Chem. Soc.*, **82**, 1 (1960).
5) M. S. Kharasch and O. Reinmuth, "Grignard Reactions of Nonmetallic Substances", Prentice-Hall, New York (1954).
6) E. P. Kohler, *Am. Chem. J.*, **31**, 655 (1904); **38**, 511 (1907); A. Luttringhaus, *Ber.*, **67**, 1062 (1934).
7) W. A. Bonner, *J. Am. Chem. Soc.*, **73**, 3126 (1951).
8) M. S. Newman, *J. Chem. Educ.*, **32**, 344 (1955).
9) D. J. Cram and K. R. Kopecky, *J. Am. Chem. Soc.*, **80**, 2737, 2748 (1959).
10) C. G. Swain and H. B. Boyles, ibid., **73**, 870 (1951).
11) F. Hein et al., *Z. anorg. u. allgem. Chem.*, **141**, 161 (1924).
12) M. T. Rogers and A. Young, *J. Am. Chem. Soc.*, **68**, 2748 (1946).
13) Ramart-Lucas et al., *Compt rend.*, **185**, 282 (1927); (Mme) Bruzau, *Ann. Chim.*, (11), I, 257 (1934).
14) K. Hoesch, *Ber.*, **60**, 389, 2537 (1927).

for the synthesis of ketones by condensation of a nitrile with phenols was examined with regard to 3, 4, 5, 6-tetra-*O*-acetyl-*N*-phenyl-L-glucosaminonitrile (XVIII)[2]. The mixed solution of XV, fused zinc chloride in chloroform and phenol or catechol in ether was saturated with hydrogen chloride at 0°C and left to stand 2 weeeks in a refrigerator. However, the product obtained was the corresponding acidamide (XIX). This result indicates that the aminonitrile XVIII has a very weak function as a nitrile.



XVIII XIX

Experimental

General Procedure for the Reaction of 3, 4; 5, 6-Di-*O*-isopropylidene-*N*-phenyl-D-glucosaminonitrile (I) with Organometallic Compounds.—To an ice-cold ether solution of the desired Grignard reagents or alkyl lithiums prepared from 0.045 mol. of the corresponding halides and 0.045 mol. of magnesium ribbon or 0.09 mol. of metal lithium was added 5 g. (0.015 mol.) of I in three portions with stirring. After refluxing on a water bath for 3 hr., the cold reaction mixture was cautiously ponred into ice-water, and precipitates were dissolved by the addition of 2 N hydrochloric acid in the case of Grignard reactions.

The aqueous layer was separated from the ether layer and extracted three times with 30 ml. of ether. The combined ether solution was washed with water, dried over anhydrous sodium sulfate, and concentrated in vacuo. The resultant sirup was hydrolyzed in 50% ethanol containing 2 N hydrochloric acid at 60°C for 40 min. and then concentrated in vacuo. The hydrolysis of the isopropylidene group was also accomplished with a small amount of concentrated hydrochloric acid at room temperature for 20 min.

The sirup obtained from acid hydrolyzate was dissolved in water; the small amount of brown oily substance remained was then filtered off through active carbon on filter paper, and the pH of the filtrate was adjusted to 10 with ammonia. The alkaline solution was extracted three times with 50 ml. of ethyl acetate, and the extracts were washed with water and dried with anhydrous sodium sulfate. After evaporation of the solvent under reduced pressure, the crude 1-*C*-substituted-1-anilino-1-deoxy-D-arabitols obtained (IV—VIII) were fractionally crystallized from ethanol or ethyl acetate.

In general, the crude crystals obtained by the Grignard reactions afford the pure B-compound as plates after one recrystallization in ethyl acetate. After repeated separation of the B-compound, a small amount of the A-compound was obtained as needles. In the case of alkyl lithiums, the crude material were dissolved in a suitable amount of hot ethanol, and a small amount of the B-compound was slowly deposited by leaving it to stand at room temperature.

The amounts of A- and B-compounds in the small amount of remaining crystals were determined from its rotational values and were added to each weight of the separated pure substances.

The physical constants of the arabitols are listed in Table I, and a comparison of the yields of the both diastereoisomers is made in Table III.

1-*C*-Phenyl-1-anilino-1-deoxy-2, 3; 4, 5-Di-*O*-isopropylidene-D-arabitol (III, R=Phenyl).—To an ice-cold ether solution of phenyl lithium prepared from 3.9 ml. of bromobenzene was added 4.2 g. of I with stirring. After refluxing 3 hr. on a water bath, the cooled reaction mixture was poured into ice water. The aqueous layer was then separated from the ether layer and extracted with ether. The volumetric titration of cyano ions in the water layer with 5% silver nitrate was shown to be 62.5% of the theoretical value.

The combined ether solution was washed twice with water, dried over anhydrous sodium sulfate and concentrated in vacuo to dryness. The residual sirup (4.7 g.) afforded colorless needless from ethanol-petroleum ether. Yield, 2.0 g., m. p. 88~89°C.

Found: C, 71.60; H, 7.52; N, 3.73. Calcd. for $C_{23}H_{29}O_4N$ (383.5): C, 72.03; H, 7.62; N, 3.65%.

One gram of the above crystal was dissolved in 2 ml. of concentrated hydrochloric acid and diluted with 30 ml. of water after having been left to stand for 20 min. at room temperature. The resultant clear solution was neutralized with an excess amount of ammonia, and the crystalline materials separated were collected and recrystallized from methanol to afford 0.72 g. of pure 1-*C*-phenyl-1-anilino-1-deoxy-D-arabitol (IV-A), m. p. 191~192°C.

The sirup obtained from the mother liquor of III (R=phenyl) was treated in exactly the same manner as described in the general procedure, and afforded 1.1 g. of IV-A (total yield, 63.0%).

Acetylation of 1-*C*-Substituted-1-anilino-1-deoxy-D-arabitols.—A mixture of 2 g. of each arabitol, 10 ml. of acetic anhydride and 10 ml. of dry pyridine was left to stand overnight at room temperature and then poured into ice-water. The solution was extracted with chloroform in the usual manner. The sirup obtained by evaporation of the solvent was crystallized from ethanol-petroleum ether.

The yield was generally 85~90% of the theoretical value. The physical constants of these tetraacetates are presented in Table II.

Reaction of 3, 4; 5, 6-Di-*O*-isopropylidene-*N*-phenyl-D-glucosaminoamide (II) and Organometallic Compounds.—i) To an ice-cold ether solution of ethylmagnesium bromide prepared from 3.5 ml. of ethyl bromide was added 5 g. of II with stirring. After removing the solvent, 50 ml. of dry benzene was added, and the mixture was refluxed for 3 hr. in an oil-bath at 100°C. The cooled reation mixture was poured into ice-water and treated in the usual manner. The sirup obtained was dissolved into a small amount of ethanol,

and light petroleum ether was added just before clouding took place. After keeping it in a refrigerator overnight, the unchanged II (3.0 g.) was filtered off. The mother liquor was concentrated in vacuo, and the residual sirup afforded crystals of VI-B, m. p. 160°C, 150 mg., after treatment in the manner described in the general procedure. These showed no depression on admixture with authentic samples.

ii) A mixture of II (5.0 g.) and phenyl lithium prepared from 5 ml. of bromobenzene in ether was refluxed for 4 hr. on a water-bath and treated in the same manner as has been described above. Four grams of unchanged II and 60 mg. of IV-A, m. p. 190~191°C, were obtained, and the latter showed no depression on admixture with an authentic sample.

iii) A mixture of 2.5 g. of 3,4; 5,6-di-*O*-isopropylidene-*N*-phenyl-L-glucosaminoamide[2] (L-form of II) and phenylmagnesium bromide prepared from 2.4 ml. of bromobenzene in benzene was refluxed on an oil-bath for 3 hr. and then treated in the usual manner. 1.3 g. of unchanged starting material was filtered off, and the residual sirup obtained from the liquor was re-dissolved in dry benzene, and hydrogen chloride passed into it. The resulted precipitates, when treated in the usual manner, afforded crystalline 1-*C*-phenyl-1-anilino-1-deoxy-L-arabitol, (L-form of IV-B), m. p. 163~165°C, 38 mg., $[\alpha]_D^{25}+3.5°$ (*c* 0.55, methanol) and several milligrams of its diastereoisomer, m. p. 189~191°C.

Found of the former: C, 67.02; H, 7.11; N, 4.66. Found of the latter: C, 66.62; H, 7.29; N, 4.69. Calcd. for $C_{17}H_{21}O_4N$: C, 67.31; H, 6.98; N, 4.62%.

An Attempt at Using the Hoesch Synthesis on 3, 4, 5, 6-Tetra-*O*-acetyl-*N*-phenyl-L-glucosaminonitrile (XVIII) and Catechol. — A clear mixed solution of 2.4 g. of XVIII, 0.65 g. of catechol in 10 ml. of chloroform and 0.7 g. of anhydrous zinc chloride in 20 ml. of ether was saturated with hydrogen chloride at 0°C and stored in a refrigerator. The white sirupy materials separated were gradually crystallized. After being left to stand for two weeks, the supernatant liquid was decanted, and the crystals were rinsed twice with ether, then dissolved in chloroform. The chloroform solution was washed with a small amount of diluted ammonia and water and then concentrated to dryness in vacuo. The remaining material was crystallized from ethanol. Yield 1.5 g., m. p. 160~162°C, $[\alpha]_D^{27}$ −18.5° (*c* 0.67, chloroform).

Found: C, 54.42; H, 6.07; N, 6.43. Calcd. for XIX, $C_{20}H_{26}O_9N_2$ (438.4): C, 54.79; H, 5.98; N, 6.39%.

Summary

In the reaction of 3, 4; 5, 6-di-*O*-isopropylidene-*N*-phenyl-D-glucosaminonitrile and Grignard reagents or alkyl lithiums, the nitrile group was substituted for alkyls to yield each pair of diastereoisomers of the 1-*C*-substituted-1-ailino-1-deoxy-D-arabitols. The levo-rotating diastereoisomer was, moreover, exclusively predominant in the former case, and the dextro-rotating one in the latter.

The reaction mechanism for the above asymmetric induction was discussed.

The author is indebted to Professor Tetsuo Sato for his encouragement throughout this work and to Mr. Hirokichi Ono for his conscientious help during the experiments.

Laboratory of Organic Chemistry
Tokyo Institute of Technology
Meguro-ku, Tokyo

Infrared Spectra and Normal Vibrations of N-Methylformamides $HCONHCH_3$, $HCONDCH_3$, $DCONHCH_3$ and $DCONDCH_3$

By Isao SUZUKI

(Received July 19, 1961)

A number of investigations have been made of the molecular structure and the vibrational spectra of the *N*-methylformaide, $HCONHCH_3$[1-5], which is the simplest molecule containing an NH–CO group. It has been shown that the Raman and infrared spectra of *N*-methylformamide and *N*-deuterated *N*-methylformamide in the liquid state can be interpreted solely in terms of the trans planar model for the molecule[1-4]. The vibrational assignments for the observed frequencies proposed by various

1) T. Miyazawa, *J. Chem. Soc. Japan, Pure Chem. Sec.* (*Nippon Kagaku Zasshi*), **77**, 121, 321, 529, 619 (1956).
2) T. Miyazawa, T. Shimanouchi and S. Mizushima, *J. Chem. Phys.*, **24**, 408 (1956).
3) D. E. DeGraaf and G. B. B. M. Sutherland, ibid., **26**, 408 (1957).
4) R. L. Jones, *J. Mol. Spectroscopy*, **2**, 581 (1958).
5) R. A. Rusell and H. W. Thompson, *Spectrochim. Acta*, **8**, 138 (1956).

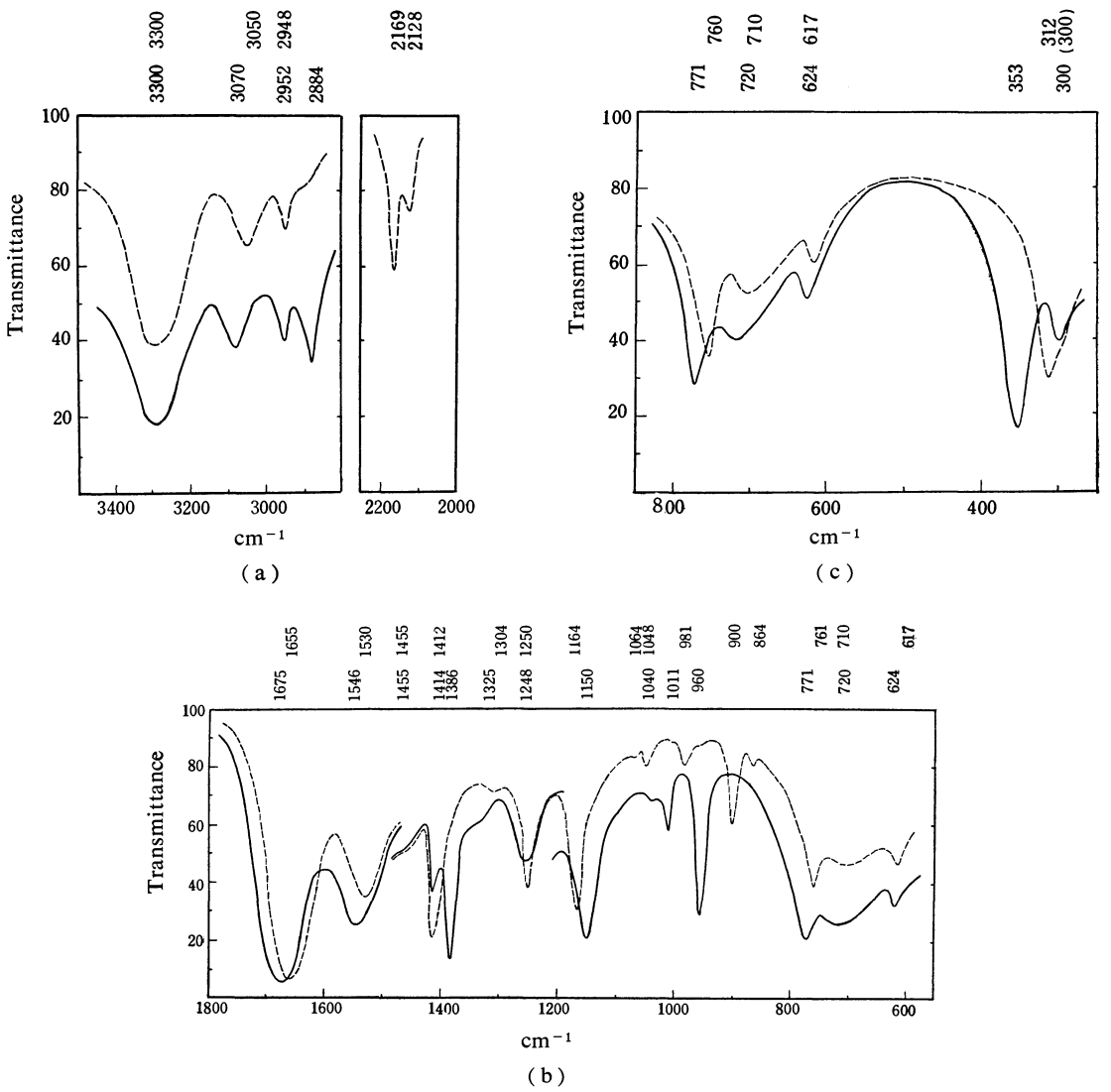


Fig. 1. Infrared spectra of $HCONHCH_3$ and $DCONHCH_3$ in the liquid state; (a) 3500～2000 cm^{-1}, (b) 1800～550 cm^{-1}, (c) 850～250 cm^{-1}, —— $HCONHCH_3$, ---- $DCONHCH_3$.

authors differ somewhat, particularly for the bands found in the region below 1100 cm^{-1}.

In order to eliminate ambiguities in the vibrational assignment and to make a detailed analysis of the nature of the normal vibrations of this molecule, the present author has prepared three other deuterated *N*-methylformamides, i. e., $HCONDCH_3$, $DCONHCH_3$ and $DCONDCH_3$, as well as $HCONHCH_3$, and has measured the infrared spectra of these compounds in the region from 3600 to 260 cm^{-1}. Furthermore, the in-plane and out-of-plane normal vibrations of this molecule have been calculated for all of the isotopic species as a nine-body problem, assuming the trans planar configuration (C_s). The Urey-Bradley force field has been employed in the calculation of the in-plane vibrations[6]. To compute the out-of-plane vibrations, this field has been modified by introducing six other force constants associated with the CH and NH out-of-plane and the torsional coordinates. Twenty-seven force constants have been determined, so that all the observed frequencies (sixty-four in number, excepting the hydrogen stretching vibrations) are explained. With these force constants, the vibrational mode and the potential energy distribution among the symmetry coordinates have been calculated for each normal vibration.

From his analysis of the band contours of

6) T. Shimanouchi, *J. Chem. Phys.*, **17**, 245, 734, 848 (1949).

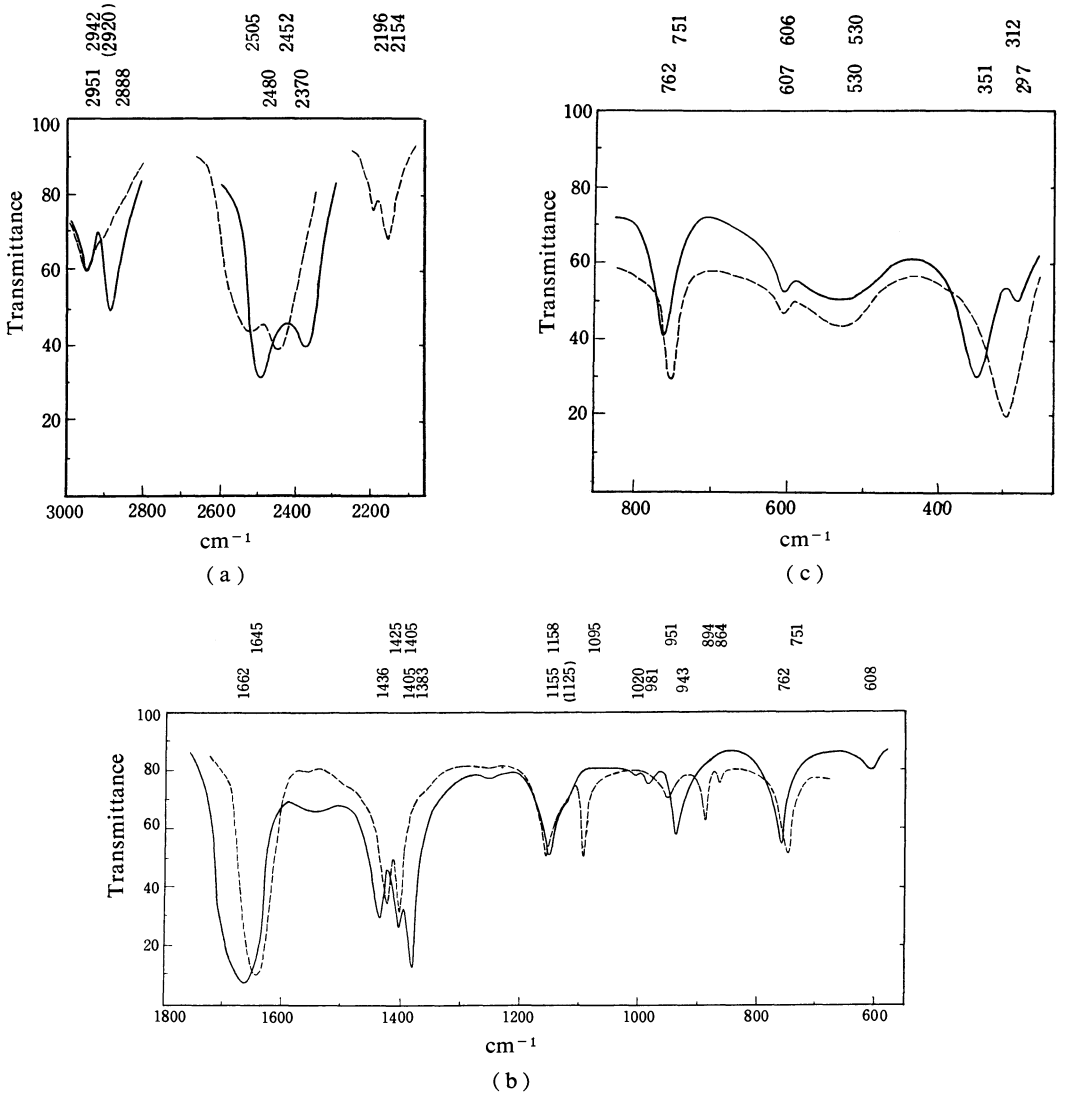


Fig. 2. Infrared spectra of $HCONDCH_3$ and $DCONDCH_3$ in the liquid state; (a) 3000～2000 cm^{-1}, (b) 1800～550 cm^{-1}, (c) 850～250 cm^{-1}, ——$HCONDCH_3$, ----, $DCONDCH_3$.

N-methylformamide in the vapor phase, Jones reached the conclusion that this molecule takes the cis form in the vapor phase[4]*1. It is, therefore, interesting to calculate the normal vibrations of the cis form and to see how each normal mode changes in these two isomeric forms. Such a calculation has been made for the in-plane vibrations of the cis form; the values of the force constants are taken to be the same as those of the trans form.

The present paper contains the results of these measurements and calculations and a detailed discussion of the nature of the normal vibrations of the molecule. The transferability of the values of the force constants between related molecules is also discussed.

*1 The structure is still a subject of controversy. Miyazawa has pointed out that the spectra in the vapor phase may be explained by assuming the molecule to be predominantly in the trans form[7].

7) T. Miyazawa, *J. Mol. Spectroscopy*, **4**, 155 (1960).

Experimental

***N*-Methylformamide $HCONHCH_3$.** — This compound was prepared by the reaction of methylformate and methylamine dissolved in methanol, and it was purified by distillation several times under reduced pressure. B. p. 61°C/3.5 mmHg.

***C*-Deuterated *N*-Methylformamide $DCONHCH_3$.** —This compound was prepared from $DCOOCH_3$ and methylamine dissolved in methanol. $DCOOCH_3$ was obtained from heavy formic acid and methanol by the method shown in Ref. 8.

8) R. F. Curl, Jr., *J. Chem. Phys.*, **30**, 1529 (1959).

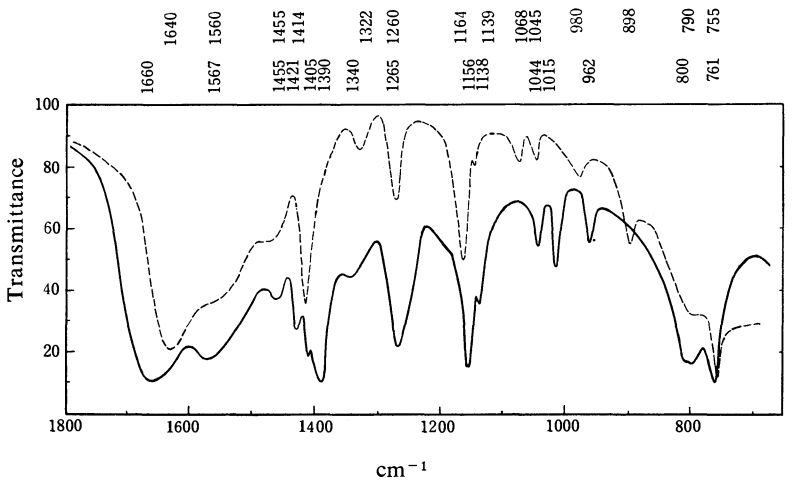


Fig. 3. Infrared spectra of $HCONHCH_3$ and $DCONHCH_3$ in the solid state; —— $HCONHCH_3$, ---- $DCONHCH_3$.

The exchange reaction with deuterium oxide was used to replace the amide hydrogen atom by deuterium.

Infrared Spectra. — The infrared spectra in the liquid state were measured in the region from 3600 to 525 cm^{-1} with a Perkin-Elmer grating spectrophotometer model 112G equipped with a potassium bromide foreprism[9], and in the region from 800 to 260 cm^{-1} with a Nippon Bunko grating spectrophotometer equipped with a cesium bromide foreprism. The spectra of $HCONHCH_3$ and $DCONHCH_3$ in the solid state were obtained with a low temperature cell[10] at the temperature of liquid nitrogen and were recorded in the region from 1800 to 650 cm^{-1} by a Hitachi EPI infrared spectrophotometer with sodium chloride optics.

Infrared Spectra

The infrared spectra of $HCONHCH_3$ and $DCONHCH_3$ in the liquid state are shown in Figs. 1(a)-(c), and those of $HCONDCH_3$ and $DCONDCH_3$, in Figs. 2(a)-(c). The infrared spectra of $HCONHCH_3$ and $DCONHCH_3$ in the solid state are shown in Fig. 3. The values of the observed frequencies for $HCONHCH_3$ and $HCONDCH_3$ agree within a few wave numbers with those give previously by the other authors. In this section, the effects of the *C*-deuteration on the spectra are mainly described. As seen from Figs. 1 and 2, the bands at 2884 and 1386 cm^{-1} of $HCONHCH_3$, which are assigned to the CH stretching and in-plane deformation vibrations ν(CH) and δ(CH) respectively, disappear on *C*-deuteration, and a new band corresponding to the CD stretching vibration is found at 2169 cm^{-1}. It is not easy to identify the band chiefly associated with the CD in-plane deformation vibration. The bands found in the region 1100~900 cm^{-1} are more or less affected by the *C*-deuteration; this fact suggests that the CD deformation motion takes part in each normal mode appearing in this region. In $DCONDCH_3$, the amide III′ band also falls in this region. The nature of these bands will be described more quantitatively in the following section on the basis of the results of the calculation of the normal vibrations.

It is of interest to determine which band is associated chiefly with the CH out-of-plane motion. The 771 cm^{-1} band of $HCONHCH_3$ was assigned to the CH out-of-plane vibration by DeGraaf and Sutherland[3] and by Jones[4], while Miyazawa[1,2] assigned this band to the amide IV (NCO bending) vibration. The fact that the 771 cm^{-1} band of $HCONHCH_3$ is insensitive to the *C*-deuteration excludes the possibility of assigning this band to the CH out-of-plane mode. Considering that the CH out-of-plane vibrations occurs at 1056 cm^{-1} in $HCONH_2$[11], at 1083 cm^{-1} in HCOOH[12], and at 1069 cm^{-1} in $HCOO^-$ [13], it seems reasonable to assign the 1011 cm^{-1} band of $HCONHCH_3$ to this mode. (In $HCONDCH_3$ it is found at 1021 cm^{-1}.) At 864 cm^{-1}, a band with a comparatively weak intensity is found both in $DCONHCH_3$ and $DCONDCH_3$. Since no vibrational mode other than the CD out-of-plane mode, is expected to occur in this region, the 864 cm^{-1} band is assigned to the CD out-of-plane vibration. This assignment is consistent

9) S. Mizushima et al., A Report on the Perkin-Elmer Grating Spectrophotometer Model 112G, The Perkin-Elmer Corp. (1959).
10) T. Miyazawa, *J. Chem. Soc. Japan, Pure Chem. Sec.* (*Nippon Kagaku Zasshi*), **76**, 821 (1955).
11) I. Suzuki, This Bulletin, **33**, 1359 (1960).
12) T. Miyazawa and K. S. Pitzer, *J. Chem. Phys.*, **30**, 1076 (1959).
13) O. Thomas, *Discussions Faraday Soc.*, **9**, 339 (1950).

with the above assignment of the CH out-of-plane vibration.

A band with a strong intensity is found at 353 cm^{-1} in $DCONHCH_3$; this band is hardly affected by the *N*-deuteration. On the *C*-deuteration, on the other hand, the band is shifted by 41 cm^{-1} to a lower frequency. The rather large shift due to the *C*-deuteration shows that this band does not arise from one of the skeletal deformation vibrations, but from the torsional vibration about the C–N bond. This assignment is in agreement with that given by DeGraaf and Sutherland[3].

Calculation of Normal Vibrations

The calculation of the normal vibration was made according to Wilson's method[14]. It was assumed that the molecule is planar (point group C_s) except for two hydrogen atoms attached to the methyl carbon atom (see Fig. 4). Thus, the normal vibrations can be classified into 14 in-plane (A′) and 7 out-of-plane (A″) vibrations. The structural parameters used in this calculation are shown in Table I*[2].

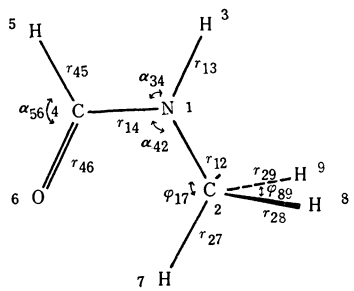


Fig. 4. Molecular structure and internal coordinates of *N*-methylformamide; the H_8 and H_9 atoms lie respectively, above and below the plane determined by the peptide group.

TABLE I. STRUCTURE PARAMETERS*

$r_{C-H}=r_{C'-H}=1.07$ Å	$r_{C'-N}=1.47$ Å
$r_{N-H}=1.04$ Å	$r_{C=O}=1.21$ Å
$r_{C-N}=1.32$ Å	

$\alpha_{ij}^0=120°$ (Bond angles around the C and N atoms)

$\varphi_{ij}^0=109°28'$ (Bond angles around the C′ atom)

* Since no structural analysis has yet been reported for $HCONHCH_3$, the values of the bond lengths are taken from those of $HCONH_2$ [15,16] and $CH_3CONHCH_3$[7].

In-plane Vibrations.—The potential function employed in the calculation is of the Urey-Bradley type[6]:

$$2V=\sum K_i(\Delta r_i)^2+\sum H_{ij}r_i^0r_j^0(\Delta\alpha_{ij})^2+\sum F_{ij}(\Delta q_{ij})^2+\text{linear terms}$$

where r_i and r_j are bond lengths with equilibrium values of r_i^0 and r_j^0, α_{ij}'s are bond angles, and q_{ij}'s, distances between nonbonded atoms. K, H and F are stretching, bending and repulsive force constants respectively. In addition, the intramolecular tension, κ, appears in the elements of the $\boldsymbol{F}$ matrix when the linear terms are eliminated by a redundancy condition[6].

To simplify the computation, the lower frequencies are separated from the four higher frequencies in the region from 3000 to 2000 cm^{-1} [14]. The symmetry coordinates used in the calculation are shown in Table II (a).

The values of the force constants were transferred from formamide[11] and methylamine molecules[18] and were slightly modified so as to obtain a better frequency agreement. The final set of the values of the force constants are given in Table III (a).

Out-of-plane Vibrations. — The type of the internal coordinates associated with the $N-CH_3$ part of the molecule, as well as the form of the potential function, is the same as that used for the calculation of the in-plane vibrations. Besides these six internal coordinates, Ω_1, Ω_4, τ_{25}, τ_{26}, τ_{35} and τ_{36} are introduced for the complete description of the out-of-plane modes, where Ω_i is $(\rho_{ij}\sin\alpha_{kil}+\rho_{ik}\sin\alpha_{lij}+\rho_{il}\sin\alpha_{jik})$ times the distance between the central atom i and the plane of atoms j, k and l, which surround the atom i, $(\rho_{ij}=1/r_{ij})$, and τ_{ij} is $\sin\alpha_{i14}\sin\alpha_{14j}$ times the dihedral angle (θ_{ij}) between the planes determined by atoms $i, 1, 4$ and $1, 4, j$ respectively[12]. Six symmetry coordinates, three of which are redundant, are obtained by the linear combinations of these internal coordinates; these are given in Table II(b). The potential function of the out-of-plane vibrations as a whole is in the following form:

$$2V=\text{Urey-Bradley type for } S_1', S_2' \text{ and } S_3'+f_{44}S_4'^2+f_{55}S_5'^2+f_{66}S_6'^2+2f_{56}S_5'S_6'+2f_{46}S_4'S_6'+2f_{45}S_4'S_5'$$

The values of the Urey-Bradley type force constants are taken to be the same as those used in the in-plane vibrations. Since few data are available for the out-of-plane and torsional force constants, f_{44}, f_{45}, etc., they are determined from the observed frequencies by

14) E. B. Wilson, *J. Chem. Phys.*, **7**, 1047 (1939); **9**, 76, (1941).

*2 C and C′ denote carbonyl and methyl carbon atoms respectively.

15) C. Post and J. Ladell, *Acta Cryst.*, **7**, 559 (1954).

16) R. A. Krombrout and G. B. Mohlton, *J. Chem. Phys.*, **25**, 35 (1956).

17) M. Kimura and M. Aoki, This Bulletin, **26**, 429 (1953).

18) A. Yamaguchi, *J. Chem. Soc. Japan, Pure Chem. Sec.* (*Nippon Kagaku Zasshi*), **80**, 1105 (1959).

TABLE II. SYMMETRY COORDINATES

(a) In-plane vibrations

	Symmetry coordinate	Vibrational mode	Abbr.
S_1	Δr_{46}	C=O Stretching	ν(C=O)
S_2	Δr_{14}	C–N Stretching	ν(CN)
S_3	Δr_{12}	C′–N Stretching	ν(C′N)
S_4	$(\Delta\alpha_{23}-\Delta\alpha_{34})/\sqrt{2}$	NH Deformation	δ(NH)
S_5	$(\Delta\alpha_{15}-\Delta\alpha_{56})/\sqrt{2}$	CH Deformation	δ(CH)
S_6	$(2\Delta\alpha_{42}-\Delta\alpha_{23}-\Delta\alpha_{34})/\sqrt{6}$	CNC′ Deformation	δ(CNC′)
S_7	$(2\Delta\alpha_{61}-\Delta\alpha_{15}-\Delta\alpha_{56})/\sqrt{6}$	NCO Deformation	δ(NCO)
S_8	$(\Delta\varphi_{17}+\Delta\varphi_{18}+\Delta\varphi_{19}-\Delta\varphi_{78}-\Delta\varphi_{79}-\Delta\varphi_{89})/\sqrt{6}$	CH_3 Sym. deformation	$\delta_s(CH_3)$
S_9	$(2\Delta\varphi_{17}-\Delta\varphi_{18}-\Delta\varphi_{19})/\sqrt{6}$	CH_3 Rocking	$r(CH_3)_I$
S_{10}	$(2\Delta\varphi_{89}-\Delta\varphi_{78}-\Delta\varphi_{79})/\sqrt{6}$	CH_3 Asym. deformation	$\delta_a(CH_3)_I$
S_R	$(\Delta\alpha_{42}+\Delta\alpha_{23}+\Delta\alpha_{34})/\sqrt{3}$	Redundant	
$S_{R'}$	$(\Delta\alpha_{15}+\Delta\alpha_{56}+\Delta\alpha_{61})/\sqrt{3}$	Redundant	
$S_{R''}$	$(\Delta\varphi_{17}+\Delta\varphi_{18}+\Delta\varphi_{19}+\Delta\varphi_{78}+\Delta\varphi_{79}+\Delta\varphi_{89})/\sqrt{6}$	Redundant	

(b) Out-of-plane vibrations

	Symmetry coordinate	Vibrational mode	Abbr.
S_1	$(\Delta r_{28}-\Delta r_{29})/\sqrt{2}$	CH_3 Anti. stretching	$\nu_a(CH_3)_O$
S_2	$(\Delta\varphi_{18}-\Delta\varphi_{19})/\sqrt{2}$	CH_3 Rocking	$r(CH_3)_O$
S_3	$(\Delta\varphi_{79}-\Delta\varphi_{78})/\sqrt{2}$	CH_3 Asym. deformation	$\delta_a(CH_3)_O$
S_4	$(\Delta\tau_{25}+\Delta\tau_{26}+\Delta\tau_{35}+\Delta\tau_{36})/2$	CN Torsion	τ(CN)
S_5	$(2\Delta\Omega_1-\Delta\tau_{25}-\Delta\tau_{26}+\Delta\tau_{35}+\Delta\tau_{36})/\sqrt{8}$	NH Out-of-plane	π(NH)
S_6	$(2\Delta\Omega_4-\Delta\tau_{25}+\Delta\tau_{26}-\Delta\tau_{35}+\Delta\tau_{36})/\sqrt{8}$	CH Out-of-plane	π(CH)
S_r	$(-\Delta\tau_{25}+\Delta\tau_{26}+\Delta\tau_{35}-\Delta\tau_{36})/2$	Redundant	
$S_{r'}$	$(\Delta\Omega_1+\Delta\Omega_4+\Delta\tau_{25}-\Delta\tau_{36})/2$	Redundant	
$S_{r''}$	$(\Delta\Omega_1-\Delta\Omega_4+\Delta\tau_{26}-\Delta\tau_{35})/2$	Redundant	

TABLE III. VALUES OF FORCE CONSTANTS

(a) Urey-Bradley type (in md./A)

$K_{C=O}$	8.80	$H_{CNC'}$	0.35	$F_{C\cdots C'}$	0.30
K_{CN}	6.15	$H_{HNC'}$	0.25	$F_{H\cdots C'}$	0.36
$K_{C'N}$	3.15	H_{HNC}	0.30	$F_{H\cdots C}$	0.46
		H_{NCH}	0.18	$F_{N\cdots H}$	0.72
		H_{HCO}	0.20	$F_{H\cdots O}$	0.92
		H_{NCO}	0.37	$F_{N\cdots O}$	1.50
		$H_{NC'H}$	0.28	$F_{N(C')H}$	0.52
		$H_{HC'H}$	0.43	$F_{H\cdots H}$	0.03

$\kappa_{(CH_3)}=-0.04$ (md.·A)
$F'=-0.1F$

(b) General quadratic type for A″ species (md.·A)

f_{44}	0.169	f_{55}	0.106	f_{66}	0.290
f_{45}	0	f_{46}	0.052_3	f_{56}	0.005

the method of least squares[19,20]. The final values of these force constants are given in Table III(b). The methyl torsional vibration lies beyond the limit of the present measurements and is omitted from the calculation.

Results of Calculations. — With the aforementioned force constants given in Tables III (a) and (b), the normal vibrations have been calculated. In Tables IV (a)–(d), the observed and calculated frequencies, percent deviations, the potential energy distributions among the symmetry coordinates for each normal mode, and the signs of the corresponding ***L***-matrix elements are given for the in-plane normal vibrations. In Tables V (a)–(d), those for the out-of-plane vibrations are given.

To visualize the feature of a given normal mode, it is preferable to compute the atomic displacement vectors, which can be obtained

19) T. Miyazawa, ibid., **76**, 1132 (1955).
20) W. T. King, I. M. Mills and B. C. Crawford, *J. Chem. Phys.*, **27**, 455 (1957).

TABLE IV. THE OBSERVED AND CALCULATED FREQUENCIES IN cm^{-1} AND POTENTIAL ENERGY DISTRIBUTIONS $(F_{ii}L_{is}^2/\lambda_s)\times 100$

(a) $HCONHCH_3$

Q	ν_{obs}	ν_{calcd}	Δ	S_1	S_2	S_3	S_4	S_5	S_6	S_7	S_8	S_9	S_{10}
ν_1	1675	1675	0	72	27*	0	22	1	2	1*	0	1*	0*
ν_2	1546	1547	−0.1	2	32	8*	0	60	4*	0	0*	4	1
ν_3	1455	1462	−0.5	1	0*	0	0	0	4*	0	0	13	80
ν_4	1414	1417	−0.2	0	0	9*	0	0	0	0*	104	0	0*
ν_5	1384	1392	−0.6	16*	1*	0*	75	0	0*	2	0*	0	0
ν_6	1248	1246	+0.2	10*	33*	5	4*	36	0*	4	0	0*	2
ν_7	1150	1115	+3.0	1	0	18	0	0*	10*	6	0	54	13*
ν_8	960	960	0	1	12	54	1	0*	2*	0	0	22*	4
ν_9	771	739	+4.1	2	0*	11*	0*	0	18*	60	0*	5*	1
ν_{10}	297	288	+3.0	0*	1	0	0*	0*	67	27	0	1	0*

(b) $DCONHCH_3$

Q	ν_{obs}	ν_{calcd}	Δ	S_1	S_2	S_3	S_4	S_5	S_6	S_7	S_8	S_9	S_{10}
ν_1	1655	1660	−0.3	76	32*	0	10	0	2	0*	0	1*	0*
ν_2	1530	1539	−0.6	4	26	7*	0	63	0	4*	1*	3	1
ν_3	—	1463	—	0	0*	0	0	4*	0	0	0	13	80
ν_4	1412	1416	−0.3	0	0	9*	0	1	0	0*	104	0	0*
ν_5	1250	1252	−0.2	19*	33*	2	3	30	0*	5	0	0*	2
ν_6	1164	1122	+3.6	1	0*	30	6*	1	10*	4	0	39	9*
ν_7	1048	1059	−1.0	1*	0*	12*	52	3*	0*	1	0*	25	5*
ν_8	900	914	−1.5	0	12	32	29	0	2*	2	0	13*	2
ν_9	761	727	+4.4	1	0*	13*	2*	0	17*	59	0*	4*	0
ν_{10}	(297)	288	+3.0	0*	1	0	0*	0*	68	26	0	1	0*

(c) $HCONDCH_3$

Q	ν_{obs}	ν_{calcd}	Δ	S_1	S_2	S_3	S_4	S_5	S_6	S_7	S_8	S_9	S_{10}
ν_1	1662	1671	−0.5	72	31*	0	21	0	2	0*	0	1*	0*
ν_2	—	1476	—	6	16	4*	1	6	0	3*	1*	16	49
ν_3	1436	1434	+0.1	5*	31*	6	0*	14*	0*	6	8	1	32
ν_4	1405	1416	−0.8	0	4	13*	0	1	0	1*	96	0	1*
ν_5	1383	1392	−0.7	14*	0*	1*	77	0	0*	1	0*	0	0
ν_6	1155	1106	+4.3	1	0	15	0	0*	9*	4	0	58	13*
ν_7	981	998	−1.7	5*	23*	14*	3*	43	0	0	0	7	1*
ν_8	943	923	+2.2	0*	1	42	0	35	1*	0	0	11*	2
ν_9	762	735	+3.5	2	0	10*	0*	1	18*	61	0*	5*	1
ν_{10}	297	283	+4.7	0*	1	0	0*	0*	70	27	0	1	0*

(d) $DCONDCH_3$

Q	ν_{obs}	ν_{calcd}	Δ	S_1	S_2	S_3	S_4	S_5	S_6	S_7	S_8	S_9	S_{10}
ν_1	1645	1658	−0.8	76	34*	0	10	0*	2	0*	0	1*	0*
ν_2	—	1472	—	6	9	2*	0	4	0	2*	0*	16	60
ν_3	1425	1434	−0.6	7*	25*	2	0*	13*	0*	4	32	0	18
ν_4	1405	1414	−0.7	3	13	18*	0	6	0	2*	73	0	5*
ν_5	1158	1123	+3.0	7	3	27	22*	5*	6*	1	0	22	6*
ν_6	1095	1087	+0.7	2*	5*	0*	28	8	3*	5	0	43	8*
ν_7	951	941	+1.1	2*	7*	3	20*	61	0	0*	0	0*	0
ν_8	891	908	−1.9	0	9	42	20	4	2*	1	0	13*	2
ν_9	751	723	+3.7	1	0*	11*	2*	1	18*	61	0*	4*	1
ν_{10}	(297)	283	+4.7	0*	1	1	0*	0	69	27	0	1	0*

$$\Delta = [(\nu_{obs}-\nu_{calcd})/\nu_{obs}]\times 100$$

* The asterisk means that the corresponding $\boldsymbol{L}$-matrix element is negative.

TABLE V. THE OBSERVED AND CALCULATED FREQUENCIES IN cm^{-1} AND POTENTIAL ENERGY DISTRIBUTIONS FOR THE OUT-OF-PLANE VIBRATIONS

(a) $HCONHCH_3$

Q	ν_{obs}	ν_{calcd}	Δ	S_1	S_2	S_3	S_4	S_5	S_6
ν_1	2952	2954	−0.1	100	0*	0	0	0*	0*
ν_2	1455	1459	−0.3	1*	15	81	0	0	0*
ν_3	—	1082	—	0*	70	16*	1	4	15*
ν_4	1011	1019	−0.7	0*	15	2*	14*	2*	85
ν_5	720	706	+2.0	0	0*	0	34	54	5
ν_6	353	353	0	0*	1	0*	57	42*	0

(b) $DCONHCH_3$

Q	ν_{obs}	ν_{calcd}	Δ	S_1	S_2	S_3	S_4	S_5	S_6
ν_1	2948	2954	−0.2	100	0*	0	0	0*	0*
ν_2	1455	1459	−0.3	1*	15	81	0	0	0*
ν_3	—	1076	—	0*	82	18*	0*	3	2*
ν_4	864	865	−0.1	0*	3	0*	11*	8*	95
ν_5	710	709	+0.1	0	0*	0	33	50	8
ν_6	312	314	−0.6	0*	1	0*	63	38*	1*

(c) $HCONHCH_3$

Q	ν_{obs}	ν_{calcd}	Δ	S_1	S_2	S_3	S_4	S_5	S_6
ν_1	2951	2954	−0.1	100	0*	0	0	0*	0*
ν_2	—	1459	—	1*	15	81	0	0	0*
ν_3	—	1080	—	0*	73	16*	1	3	13*
ν_4	1020	1015	+0.5	0*	12	2*	12*	1*	90
ν_5	530	535	−1.0	0	0*	0	34	58	4
ν_6	351	356	−1.4	0*	1	0*	59	38*	0

(d) $DCONDCH_3$

Q	ν_{obs}	ν_{calcd}	Δ	S_1	S_2	S_3	S_4	S_5	S_6
ν_1	2942	2954	−0.1	100	0*	0	0	0*	0*
ν_2	—	1459	—	1*	15	81	0	0	0*
ν_3	—	1074	—	0*	83	18*	0*	2	1*
ν_4	864	859	−0.6	0*	2	0*	7*	4*	100
ν_5	530	536	−1.2	0	0*	0	34	58	3
ν_6	312	312	0	0*	1	0*	66	36*	1*

$$\Delta = [(\nu_{obs} - \nu_{calcd})/\nu_{obs}] \times 100$$

* The asterisk means that the corresponding L-matrix element is negative.

from the L^x matrix defined, in matrix expression, as

$$X = L^x Q$$

where X is the column vector of the Cartesian coordinates of the atoms involved. The L^x matrix was computed for the out-of-plane normal modes, for which vibrational features are somewhat difficult to deduce from the P. E. D. matrices. The results are shown schematically in Figs. 5 (a) and (b).

As mentioned above, the in-plane vibrations of the cis configuration have also been calculated with the values of the force constants given in Table III (a); the results are summarized in Tables VI (a)–(d).

The notations used throughout this paper are the same as those used for the previous paper[11]. All the numerical computations were carried out with a parametron computer PC-1, the routines and the method of calculation are given in detail in the Ref. 21 and so are not discussed here.

Discussion

The Nature of the Observed Bands. — Based on the calculated values of vibrational amplitudes and potential energy distributions shown in Tables IV and V, the nature of the observed bands will be discussed*3.

21) T. Shimanouchi and I. Suzuki, *J. Mol. Spectroscopy*, **6**, 277 (1961).

*3 In this and the following sections, one of the abbreviations given in the final columns of Tables II (a) and (b) is used to refer to a given vibrational mode. For instance, $\delta_a(CH_3)_I$ is used instead of " in-plane CH_3 asymmetric deformation vibration ".

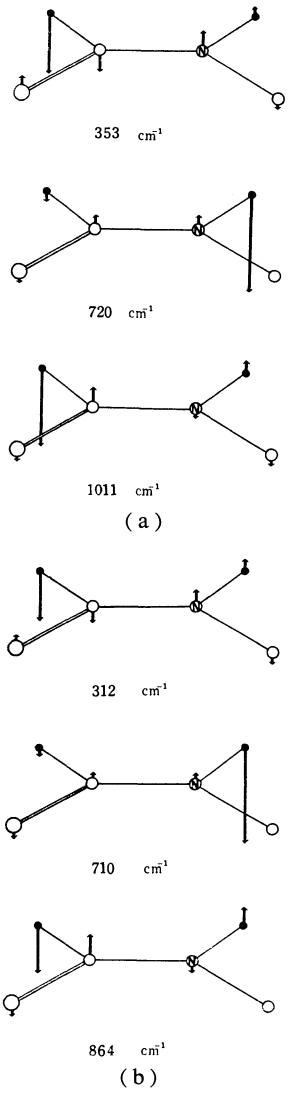


Fig. 5. Schematic representation of vibration features of the out-of-plane normal modes (a) $HCONHCH_3$, (b) $DCONHCH_3$; the movements of hydrogen atoms attached to the C' atom are neglected; ●, ○, Ⓝ and =○ denote hydrogen, carbon, nitrogen and oxygen atoms respectively.

In the Region from 3500 to 2000 cm^{-1}. — The bands chiefly associated with the NH stretching vibration are found in the region from 3500 to 3000 cm^{-1} and those associated with the ND motion, in the region from 2500 to 2400 cm^{-1}. The cause of the doublings of these bands has been discussed in detail by earlier workers[22,23] and so is not discussed here. The bands associated with the various CH stretching vibrations are found around 2900 cm^{-1}. The

22) M. Beer, H. D. Kessler and G. B. B. M. Sutherland, *J. Chem. Phys.*, **29**, 1097 (1958).
23) T. Miyazawa, *J. Mol. Spectroscopy*, **4**, 168 (1960).

TABLE VI. THE CALCULATED FREQUENCIES IN cm^{-1} AND P. E. D. FOR THE IN-PLANE VIBRATIONS OF THE CIS CONFIGURATIONS

(a) $HCONHCH_3$

ν_{calcd}	P. E. D.*
1687	ν(C=O) 60, ν(CN) 34, δ(CH) 19, δ(NH) 12
1459	$\delta_a(CH_3)$ 50, δ(NH) 33
1441	δ(NH) 26, $\delta_a(CH_3)$ 26, ν(C=O) 18, $r(CH_3)$ 13
1416	$\delta_s(CH_3)$ 100
1402	δ(CH) 58, ν(C=O) 16
1328	ν(CN) 41, δ(CH) 18, δ(NH) 18
1108	ν(C'N) 46, $r(CH_3)$ 30
1009	$r(CH_3)$ 45, ν(C'N) 25
595	δ(NCO) 58, ν(C'N) 19
360	δ(C'NC) 79, δ(NCO) 18

(b) $DCONHCH_3$

ν_{calcd}	P. E. D.*
1675	ν(C=O) 62, ν(CN) 36, δ(NH) 14
1475	$\delta_a(CH_3)$ 32, ν(C=O) 21, $r(CH_3)$ 14
1460	$\delta_a(CH_3)$ 45, δ(NH) 35
1416	$\delta_s(CH_3)$ 101
1335	ν(CN) 49, δ(NH) 22, δ(NCO) 11
1120	ν(C'N) 35, $r(CH_3)$ 33
1030	δ(CD) 40, ν(C'N) 30
988	δ(CD) 41, $r(CH_3)$ 35
595	δ(NCO) 58, ν(C'N) 19
351	δ(C'NC) 78, δ(NCO) 19

(c) $HCONDCH_3$

ν_{calcd}	P. E. D.*
1675	ν(C=O) 68, ν(CH) 33, δ(CH) 21
1470	$\delta_a(CH_3)$ 68, $r(CH_3)$ 18
1419	$\delta_s(CH_3)$ 90
1413	ν(C=O) 24, ν(CN) 24, δ(CH) 18
1374	δ(CH) 61, ν(CN) 17
1169	ν(C'N) 35, δ(ND) 28
1060	$r(CH_3)$ 64, $\delta_a(CH_3)$ 12, δ(ND) 11
924	δ(ND) 43, ν(C'N) 34
580	δ(NCO) 56, ν(C'N) 16
355	δ(C'NC) 78, δ(NCO) 19

(d) $DCONDCH_3$

ν_{calcd}	P. E. D.*
1662	ν(C=O) 71, ν(CN) 36, δ(CD) 10
1468	$\delta_a(CH_3)$ 70, $r(CH_3)$ 18
1418	$\delta_s(CH_3)$ 103
1394	ν(CH) 42, $\delta_a((CH_3)$ 13, ν(C'N) 12
1165	ν(C'N) 34, δ(NCO) 20
1093	$r(CH_3)$ 45, δ(CD) 27
991	δ(CD) 62, $r(CH_3)$ 20
923	δ(ND) 44, ν(C'N) 35
583	δ(NCO) 86, δ(C'NC) 15
345	δ(C'NC) 77, δ(NCO) 19

* Only the important terms are given in this table.

CD stretching vibrations occur at about 2150 cm^{-1}.

In the Region from 1700 to 1200 cm^{-1}.—Three characteristic bands of monosubstituted amides are found in this region. They are termed the amide I, II and III bands and are found at 1675, 1546 and 1248 cm^{-1} respectively in *N*-methylformamide. The nature of these bands has been discussed in detail for *N*-methylacetamide[24], and the present calculation gives similar results for these bands; i. e., the amide I band is chiefly associated with the ν(C=O) motion, and the amide II and III bands are chiefly due to the mixed vibrations of the ν(CN) and δ(NH). In addition, there are considerable contributions from the ν(CN) and δ(CH) vibrations to the amide I band, which may be the cause of the lowering of this band by 20 cm^{-1} by the *C*-deuteration.

Three CH_3 and CH deformation vibrations occur also in this region. In the undeuterated species, the bands at 1455, 1414 and 1384 cm^{-1} correspond to almost pure $\delta_a(CH_3)$, $\delta_s(CH_3)$ and δ(CH) vibrations respectively. In *N*-deuterated species, a band is found at about 1430 cm^{-1} and is termed the amide II′ band; the present calculations show that this band is rather complicated in its nature. Both $\nu_a(CH_3)_I$ and ν(CN) vibrations are associated with this normal mode, and in addition, the contributions of the δ(ND) and the skeletal deformation [δ(NCO) and δ(CNC′)] vibrations are not negligible. In other words, this normal vibration is not localized in the peptide linkage. On *N*-deuteration, the bands assigned to the $\delta_s(CH_3)$ and δ(CH) modes are hardly affected; they are found at 1405 and 1383 cm^{-1} respectively.

In the Region from 1200 to 850 cm^{-1}. — In $HCONHCH_3$, the ν(C′N), $r(CH_3)$ and π(CH) vibrations are expected to occur in this region. In fact, the bands at 1150 and 960 cm^{-1} can be assigned to the $r(CH_3)_I$ and ν(C′N) modes respectively, although there are also certain contributions from other vibrational modes. In deuterated species, the δ(CD) and/or δ(ND) vibrations couple with the aforementioned vibrations, and the nature of the bands thus becomes much more complex. As seen in Table IV (b) the 1048 cm^{-1} band of $DCONHCH_3$ is a mixed vibration of δ(CD), $r(CH_3)$ and ν(C′N), and the 900 cm^{-1} band is a mixed vibration of ν(C′N), δ(CD), $r(CH_3)_I$ and ν(CN).

A band named the amide III′ band appears at 981 cm^{-1} in $HCONDCH_3$; the δ(ND) and ν(CN) as well as ν(C′N) vibrations play an important role in this normal mode. In $DCONDCH_3$, the $r(CH_3)_I$, δ(CD), δ(ND) and ν(C′N) vibrational modes interact with each other, and this gives rise to four observed bands at 1158, 1095, 951 and 891 cm^{-1}. The present calculation yields the result that the δ(CD) vibration occurs in each of these normal modes in approximately the same amount, although it predominates in none of these modes.

Two types of the methyl rocking modes must be considered; one belongs to the A′ species; $r(CH_3)_I$, and the other to the A″ species, $r(CH_3)_O$, and they are expected to give different frequencies, because the way of coupling with vibrational modes is different in each symmetry species. A weak band found at 1040 cm^{-1} in $NCONHCH_3$ and at 1064 cm^{-1} in $DCONHCH_3$ may tentatively be assigned to the $r(CH_3)_O$ mode, but this is not certain because the present calculation shows that the average splitting of the $r(CH_3)_I$ and $r(CH_3)_O$ frequencies is about 40 cm^{-1} *4.

As has been mentioned earlier in this paper, the π(CH) and π(CD) vibrations also occur in this region. The features of these modes are illustrated in Fig. 5.

In the Region from 850 to 260 cm^{-1}. — The bands associated with two skeletal deformation vibrations, δ(NCO) and δ(CNC′), are expected to appear in this region. Present calculation shows that an interaction occurs between the δ(NCO) and δ(CNC′) vibrations and that this gives rise to two observed bands at 771 and 297 cm^{-1} of $HCONHCH_3$. For the 771 cm^{-1} band, the energy associated with the δ(NCO) vibration is 60% of the total and that associated with the δ(CNC′) is 20%, while for the 297 cm^{-1} band the energy associated with the δ(NCO) mode is 30% and that associated with the δ(CNC′) is 70%*5. The way of coupling of the δ(NCO) and δ(CNC′) motions seems to be unaffected by deuteration.

In Fig. 5, the features of the normal modes of the bands found at 720 and 353 cm^{-1} are shown. It is clear that the 720 cm^{-1} band corresponds to almost pure π(NH) vibration, while the vibrational coupling occuring between the π(CH) and τ(CN) modes makes the 353 cm^{-1} band complex in its nature.

Force Constants.—*Urey-Bradley Type.* — The Urey-Bradley type of force constants have been classified into three groups after their values

24) T. Miyazawa, T. Shimanouchi and S. Mizushima, *J. Chem. Phys.*, **29**, 611 (1958).

*4 If we adopt this assignment, the observed splitting is about three times larger than the calculated. Such a deviation is rather large even though the splitting of the frequencies depends on the type of force field employed in the calculation.

*5 This may also be the cause of the rather high frequency of the amide IV band, as compared with other amides; the value of the force constants chiefly concerned with this vibrational mode, namely H_{NCO} and $F_{N\cdots O}$, are practically unchanged from those used for the evaluation of the $HCONH_2$[11] molecule, which gives the δ (NCO) vibration at about 600 cm^1.

had first been chosen by the following procedure:

(I) The force constants associated with the HCONH- part of the molecule, i. e. K_{CO}, K_{CN}, H_{NCH}, H_{HCO}, H_{NCO}, H_{HNC}, $F_{N\cdots H}$, $F_{H\cdots C}$, $F_{N\cdots O}$ and $F_{H\cdots C}$.—The values of the force constants belonging to group I were first transferred from the formamide molecule, for which the values of the constants had been definitely determined by an analysis of its normal vibrations[11].

(II) The force constants associated with the N–CH_3 part of the molecules, i. e. $K_{C'N}$, $H_{NC'H}$, $H_{HC'H}$, $F_{N(C')H}$, $F_{H\cdots H}$ and κ.—Their values were primarily transferred from the methylamine molecule[18]; in addition, the results of the recent investigation on methyl halides were also taken into account when the initial values of these constants were selected.

(III) The other force constants, i. e. $H_{CNC'}$, $H_{HNC'}$, $F_{C\cdots C}$ and $F_{H\cdots C'}$. — Their values were primarily transferred from *N*-methylacetamide[24], but slightly modified values were used as initial guesses because in that calculation the methyl group was approximated as a dynamic unit.

In order to obtain a better frequency agreement, the values of the force constants were refined as indicated by the elements of the Jacobian matrix $(\Delta\lambda_i/\Delta K_j)$[19,20]. Thus the final set of force constants given in Table III(a) was obtained. The force constants in group I remain almost unchanged, and an analogous result was obtained for the constants belonging to group II, the maximum change from the initial values being only 0.05 (in md./A). The constants involving hydrogen and carbon atoms only, i. e. $H_{HC'H}$, $F_{H\cdots H}$ and κ, are similar to values found for methyl halides[21]. As for the constants in group III, the deviations from the original are found to be comparatively large for some of the force constants.

The above results indicate that the Urey-Bradley type force constants, if determined carefully for a given molecule, can be used for the calculation of the normal vibrations for related molecules, even when they are relatively complicated and large in size.

General Quadratic Type for the A'' Vibrations.—As an initial set of force constants, the following values were taken: $f_{44}=0.051$, $f_{55}=0.136$, $f_{66}=0.271$, and zero for all the cross terms. The method of least squares was applied to refine these constants, and five repetitions of interaction processes give the values shown in Table III(b). The cross terms, f_{45} and f_{56}, are found to be small, while f_{46}, the cross term between the τ(CN) and π(CH) coordinates, is comparatively large. This implies that an interaction takes place between the τ(CN) and π(CH) vibrations to some degree and is quite consistent with the result of the infrared measurements; i. e., the 351 cm^{-1} band of $HCONHCH_3$ is sensitive to the *C*-deuteration while it is not to the *N*-deuteration.

The force constant, f_{44}, can be related to the barrier to internal rotation about the C–N bond[12]. This constant can be written as:

$$f_{44}=4(2V_2+\Delta E/2)/9 \quad (1)$$

if we assume the sinusiodal potential curve of the following form:

$$V(\theta)=\Delta E(1-\cos\theta)/2+V_2(1-\cos 2\theta)/2 \quad (2)$$

where θ is the angle of internal rotation ($\theta=0$ for the trans form) and ΔE is the energy difference between the cis and trans isomers. If we make use of the relations[12,25] $\Delta\theta=\Delta(\theta_{25}+\theta_{26}+\theta_{35}+\theta_{36})/4=2S_4/3$, and $2V(\theta)=(2V_2+\Delta E/2)(\Delta\theta)^2$ for small $\Delta\theta$, the Eq. 1 can be obtained. From the values of f_{44}, the barrier height, $V_0\fallingdotseq V_2+\Delta E/2$, is estimated as 28.5~28.0 kcal./mol. (ΔE is assumed to be 3~1 kcal./mol.). Since the height of the barrier depends on the type of the potential function used for the calculation, the value itself is not important. However, present calculation shows that the barrier height is considerable and that the internal rotation of the molecule about the C–N bond is severely restricted.

The Vibrational Modes of the cis Isomers.—The calculated frequencies and potential energy distributions, shown in Tables VI(a)–(d), were evaluated with the force constants given in Table III(a). They give the features of the normal vibrations for the cis amide; the results are summarized as follows:

(1) The amide I band is not much affected by the change in structure.

(2) In the cis amide, the δ(NH) vibration interacts with the $\delta_a(CH_3)$ rather than with the ν(CN) vibration. This interaction gives rise to two frequencies around 1450 cm^{-1} and may be a cause of the difficulty in finding the corresponding bands in some lactams[26], in which the NH–CO groups take the cis configuration.

(3) The bands associated with the δ(CH) and $\delta_s(CH_3)$ motions are not sensitive to the change in structure.

(4) The vibration chiefly associated with the ν(CN) vibration occurs around 1330 cm^{-1} in $HCONHCH_3$ and $DCONHCH_3$, and around 1400 cm^{-1} in the *N*-deuterated species. There are small contributions from the δ(CH) or δ(NH) vibration to this normal mode.

(5) In the region from 1200 to 900 cm^{-1},

25) T. Miyazawa, This Bulletin, **34**, 691 (1961).
26) L. J. Bellamy, "The Infrared Spectra of Complex Molecules", Methuen & Co., Ltd., London (1958), p. 216.

two bands which are associated with $r(CH_3)$ and $\nu(C'N)$ modes are expected to occur, and in addition, the $\delta(CD)$ and $\delta(ND)$ modes are also found in the deuterated species. The way of coupling between these vibrational modes is different from that in the trans form. This gives a frequency somewhat different from that in the trans form for each normal vibration.

(6) It is well known that skeletal deformation vibrations are quite sensitive to the structure of a given molecule. Such is also the case for *N*-methylfomamide, and the present calculation gives a value of 595 cm^{-1} to a band chiefly associated with the $\delta(NCO)$ motion (amide IV band) and a value of 360 cm^{-1} to that associated with the $\delta(CNC')$ motion. To the former vibration, there is practically no contribution from the $\delta(CNC')$ mode as there is in the trans configuration; this may be a reason for the comparatively low frequency of the vibration. To the latter band, the contribution from the $\delta(NCO)$ motion is less compared to that in the trans form. The amide IV band can be used to check the molecular configuration in the vapor phase. Miyazawa et al. showed that the amide IV band hardly moves with the change of state[2]. Thus, if the molecule of *N*-methylformamide takes the trans configuration in the vapor phase, the position of the amide IV band scarcely moves, while it is expected to shift towards a lower frequency if the molecule takes the cis form, as concluded by Jones[4]. In the spectrum of *N*-methylformamide in the vapor phase, the amide IV band is found at 785 cm^{-1}; this seems to indicate that the molecule is predominantly in the trans form, although there are some bands found in the spectrum due to the cis isomer[7] coexisting as a less stable one.

(7) Although all the fundamental frequencies are correlated with the observed band, there remained a few unassigned bands for each isotopically substituted species, i. e., 1325, (1040), and 624 cm^{-1} for $HCONHCH_3$, 1304, (1064), 981 and 617 cm^{-1} for $DCONHCH_3$, 1125 and 607 cm^{-1} for $NCONDCH_3$, and (1125) and 606 cm^{-1} for $DCONDCH_3$. They may be interpreted as overtones and combination tones of the fundamentals, but there are some difficulties in assigning these bands to certain overtones and combination tones systematically throughout the four isotopic species of the molecule. In addition, it should be noted that their frequencies are in good agreement with the calculated values of the cis characteristic bands; i. e., the band around 1320 cm^{-1} for the NH species corresponds to the $\nu(CN)$ vibration*6, the band around 1120 cm^{-1} for the ND species, to the mixed vibration of the $\delta(ND)$ and $\nu(C'N)$ modes, the band at 980 cm^{-1} of $DCONHCH_3$, to the mixed one of the $\delta(CD)$ and $r(CH_3)$ and the band around 600 cm^{-1}, to the $\delta(NCO)$ motion (see Table VI). However, objections may arise in assigning these bands as those of the cis isomer, since they persist in the solid phase. This fact does not exclude the possibility of the coexistence of the cis isomer as mixed crystals because of the very high barrier hindering internal rotation, as has been described in the preceding section. Therefore, while it is not possible to give an unequivocal answer to this question at present, it is probable that these bands are arising from the cis isomer of the molecule.

The present author expresses his sincere thanks to Professor Takehiko Shimanouchi for his guidance throughout this work, and to Dr. Tatsuo Miyazawa for his valuable discussions. His thanks are also due to Professor Hidetoshi Takahashi for the use of a PC-1 computer.

Department of Chemistry
Faculty of Science
The University of Tokyo
Hongo, Tokyo

*6 The shift of the band about 20 cm^{-1} with solidification is also consistent with the above assignments.

A Study of the Adsorption of Detergents at a Solution-Air Interface by the Radiotracer Method. V. The Effect of Inorganic Salts on the Surface Behavior of the Dodecyl Sulfate Ion

By Ryohei MATUURA, Hideo KIMIZUKA, Akira MATSUBARA, Kenji MATSUNOBU and Tadashi MATSUDA

(Received July 20, 1961)

It has been known that certain inorganic salts promote the detergent action of soaps. These substances are known as builders. In studying the detergent action it is of importance to see the nature of the effect of these builders on the adsorption of the detergent. In the preceding paper[1], the effect of the cationic valencies of excess salts and the concentration of sodium chloride on the adsorption of dodecyl sulfate ion (DS^-) at the solution-air interface was measured; it was found that the presence of excess salt increases the rate and the amount of the adsorption of DS^- and that the adsorption takes place in accordance with the Gibbs adsorption isotherm. However, the effect of the anion on the adsorption has not yet been studied systematically. Therefore, we have attempted the measurement of the adsorption of DS^- in the presence of excess sodium salt with an anion of a different valency. The discussions of the surface behavior of DS^- are given for the results obtained in the present study as well as for those in the preceding paper[1].

Experimental

Dodecyl alcohol was distilled through a rectifying column of 65 plates using a reflux ratio of 15, the fraction distilling at 139°C/10 mmHg being collected. The melting point of dodecyl alcohol was 25.0°C. ^{35}S-labeled sodium dodecyl sulfate (SDS) was synthesized as described earlier[2]. To remove the unsulfated alcohol, the crystals of SDS were washed with ether for 50 hr. by using a Soxhlet apparatus.

Of the inorganic salts used, those of a guaranteed grade were used without purification, while those of an extra pure grade were purified by recrystallization.

The procedures used for the experiments were the same as described in the preceding paper[1,2], and the experiments were carried out at temperature 30±1°C.

Results and Discussion

The adsorption of DS^- and the surface tension were measured in the presence of excess (0.1 N) sodium salt of an anion of varying valency. In Fig. 1, the surface tension data are plotted against the logarithmic concentration of SDS. As seen in this figure, the surface tension vs. logarithmic concentration

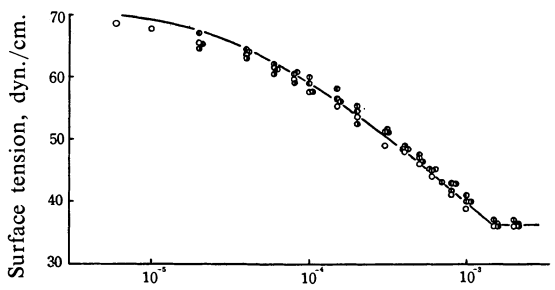


Fig. 1. Effect of excess (0.1 N) electrolyte on the surface tension of SDS solution, 30±1°C. Full line represents relationship calculated with Eq. 2.
○; NaCl ⊕; Na_2SO_4 ◐; $Na_3Fe(CN)_6$
◑; $Na_4Fe(CN)_6$

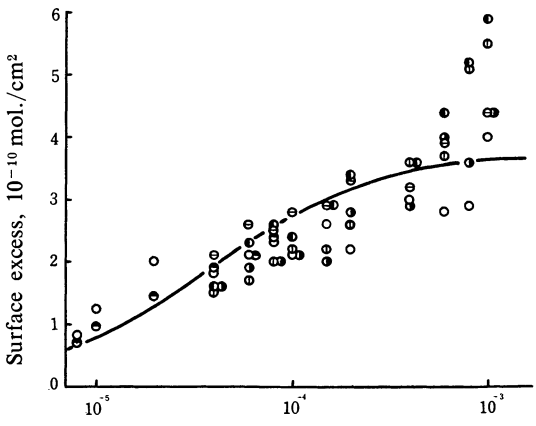


Fig. 2. Adsorption of DS^- from SDS solution containing excess (0.1 N) salt. Full line represents relationship calculated with Eq. 6.
○; NaCl ⊕; Na_2SO_4 ⊖; Na_2CO_3
◐; $Na_2Fe(CN)_6$ ◑; $Na_4Fe(CN)_6$
◓; $NaNO_3$

1) R. Matuura, H. Kimizuka and K. Yatsunami, This Bulletin, 32, 646 (1959).
2) R. Matuura, H. Kimizuka, S. Miyamoto and R. Shimozawa, ibid., 31, 532 (1958).

curves of the detergent solutions containing 0.1 N sodium salts are almost independent of the valencies of the anions of salts. This is true also for the relation between the amount of adsorption of DS^- and the concentration of the detergent solution, as is shown in Fig. 2, although the measured values scatter randomly to some extent in this case.

In Fig. 3, the surface tension of SDS solutions containing excess salt of chlorine with a cation of varying valency, together with the case of sodium chloride of varying concentrations, is plotted against the logarithmic concentration of SDS. It is clear from this figure that the surface tension of the SDS solution decreases with an increase in the valency of the cation of the same normal concentration and decreases in the presence of the same salt (sodium chloride) with an increase in the concentration of the salt.

From the results of Figs. 1 and 3, it may be said that the surface tension lowering of the SDS solution due to the excess salt is governed

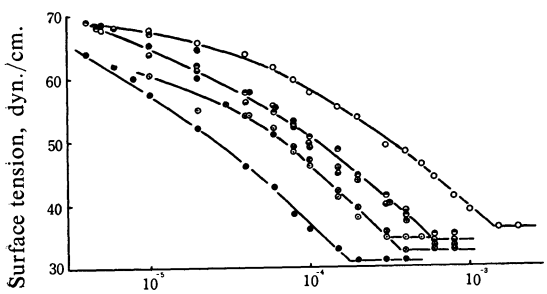


Fig. 3. Effect of excess electrolyte on the surface tension of SDS solution, 29.5± 1.5°C. ○; 0.1 N NaCl ⊕; 0.3 N NaCl ⊗; 0.5 N NaCl ●; 1 N NaCl ◓; 0.1 N $MgCl_2$ ◒; 0.1 N $MnCl_2$ ⊙; 0.1 N $AlCl_3$

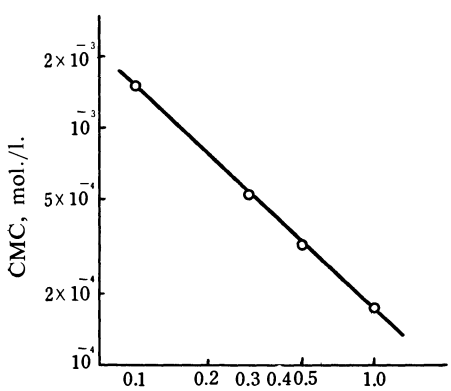


Fig. 4. Effect of concentration of sodium chloride on the CMC of SDS, 29±1°C.

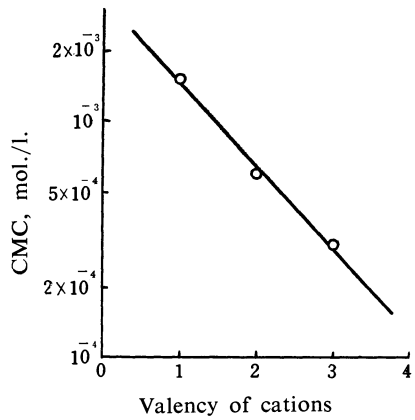


Fig. 5. Effect of added electrolyte on the CMC of SDS, 29±1°C. Concentrations of sodium chloride, magnesium chloride, manganous chloride and aluminum chloride are all 0.1 N.

not by the ionic strength, but by the normality when the sodium salts are used; it is also very much affected by the valency of cation when the various metal salts are used even with the same normality.

The change in the value of critical micelle concentration (CMC), C_m, with the concentration of sodium chloride is shown in Fig. 4 and that with the valency of cation, in Fig. 5. As shown in Fig. 4, log C_m is linear against the logarithmic concentration of sodium chloride; this is a relation similar to that obtained by Corrin and Harkins[3]. In Fig. 5, log C_m is linear against the valency of the cation. This does not agree with the theory of Shinoda, who expected linearity between log C_m and the reciprocal of valency[4]. Though the effect of a high valent cation on the CMC of SDS solution was studied by Lange[5], he did not find this relation. It must, however, be noted here that the pH of the solution depends on the kind of electrolyte, so that the dependence of CMC upon the valency will require more detailed investigation. In Fig. 6, the surface pressure, π_m, at CMC is plotted against the concentration of salt as well as the valency of cation. This figure shows an increase in π_m with the concentration of sodium chloride, but at the normal concentration the valency of the anion has little effect on the value of π_m and the effect of the valency of the cation is not so appreciable.

Now we can put the reduced quantities as:

$$\phi=\pi/\pi_m, \quad X=C/C_m \tag{1}$$

where π denotes a surface pressure of the

3) M. L. Corrin and W. D. Harkins, *J. Am. Chem. Soc.*, **69**, 682 (1947).
4) K. Shinoda, This Bulletin, **28**, 340 (1955).
5) H. Lange, *Kolloid-Z.*, **121**, 66 (1951).

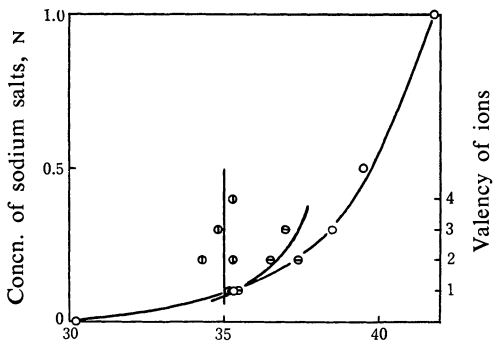


Fig. 6. Effects of salt concentration and of valency of cation on surface pressure of solution at CMC.
○ ; Effect of concentration of sodium chloride
⊖ ; Valency effect of cations
ⓘ ; Valency effect of anions

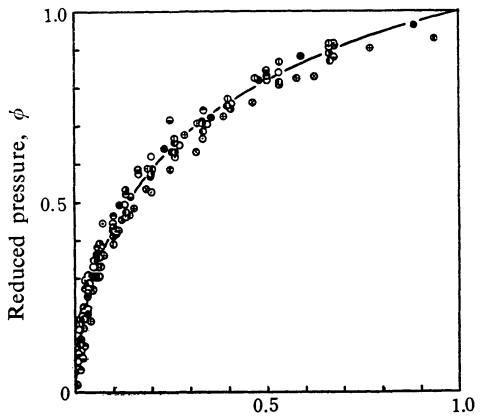


Fig. 7. Reduced pressure vs. reduced concentration.

○ ; 0.1 N NaCl	⊕ ; 0.3 N NaCl
⊗ ; 0.5 N NaCl	● ; 1 N NaCl
◓ ; 0.1 N $MgCl_2$	◒ ; 0.1 N $MnCl_2$
⊙ ; 0.1 N $AlCl_3$	ⓘ ; 0.1 N Na_2SO_4
◐ ; 0.1 N $Na_3Fe(CN)_6$	◑ ; 0.1 N $Na_4Fe(CN)_6$

solution of concentration, C. The ϕ vs. X curves are plotted as shown in Fig. 7. This figure indicates that the surface tension vs. concentration curves can be reduced approximately to the same one, regardless both of the concentration of the excess salt and of the type of salt when we use reduced quantities.

The full line in Fig. 7 shows the calculated relation by using the equation

$$\phi = (1/b)\cdot\ln\{1+(e^b-1)X\} \qquad (2)$$

where b is a constant. The value of b is 3.7 in the present case. Belton and Evans[6] considered the ideal mixture in which the surface tensions of the solution, solvent and solute are γ, γ_A and γ_B respectively; they derived a relation between the surface tension and the mole fraction of solute x:

$$\exp(-\gamma\omega/\boldsymbol{kT}) = (1-x)\exp(-\gamma_A\omega/\boldsymbol{kT}) + x\exp(-\gamma_B\omega/\boldsymbol{kT}) \qquad (3)$$

where ω denotes the occupied area per molecule and $\boldsymbol{k}$ and T are Boltzmann constant and absolute temperature respectively. Equation 3 can be reduced to Eq. 2 by putting $x=X$ and

$$b = (\gamma_A-\gamma_B)\omega/\boldsymbol{kT}$$
$$\phi = (\gamma_A-\gamma)/(\gamma_A-\gamma_B) \qquad (4)$$

It may, therefore, be pointed out that the solution of SDS containing excess salt behaves approximately as if it were the ideal mixture consisting of the salt solution, regarded as a solvent, and the detergent solution at CMC containing a given concentration of salt, regarded as a solute. Thus it may be supposed that the reduced quantities are the suitable expressions in studying the detergent solution.

The Gibbs equation is expressed by:

$$\Gamma = (1/\boldsymbol{nRT})\cdot(\partial\pi/\partial\ln C) \qquad (5)$$

where Γ is the surface excess, $\boldsymbol{R}$, gas constant, and $\boldsymbol{n}$ is put unity in the case of excess salts. Differentiating Eq. 2 and combining it with Eq. 5, we obtain a reduced adsorption isotherm

$$\boldsymbol{RT}\Gamma/\pi_m = (e^b-1)X/b\{1+(e^b-1)X\} \qquad (6)$$

The full lines in Figs. 1 and 2 show calculated relations by using Eqs. 2 and 6 respectively. Agreements between observed and calculated values are satisfactory.

Summary

The adsorption of ^{35}S-labeled dodecyl sulfate ion in the presence of excess sodium salts with anions of various valencies was measured directly by the radiotracer method. The anions of the excess salts were chloride, nitrate, carbonate, ferricyanide and ferrocyanide ions, and the concentrations of the excess salts were all 0.1 N. It was found that the adsorption of dodecyl sulfate ion increased remarkably due to the presence of the excess salt and that the surface tension curves and the adsorption isotherms were almost independent of the type of anions.

The behavior of dodecyl sulfate ion was discussed by using the result of the present study together with the previous one, in which the effect of cationic valency and the salt concentration was studied. The logarithmic value of CMC was found to be linear against the logarithmic concentration of excess sodium

6) J. W. Belton and H. G. Evans, *Trans. Faraday Soc.*, **41**, 1 (1945).

chloride and against the valency of cation when the concentrations were all 0.1 N.

The reduced surface pressure and the reduced concentration referred to CMC were proposed, and it was found that the surface tension data of the solutions of sodium dodecyl sulfate containing various kinds of salts and varying concentration of sodium salts were correlated approximately to one curve regardless both of the types and the concentrations of the excess salts. The curve was well expressed by the reduced equation for the surface pressure as a function of the reduced concentration. By combining the reduced equation with the Gibbs equation of $n=1$, the reduced adsorption isotherm was derived.

It was shown that these reduced equations enable us to reproduce the surface tension and adsorption data of the solutions of sodium dodecyl sulfate in the presence of sodium salts with varying valencies of anions.

Department of Chemistry
Faculty of Science
Kyushu University
Hakozaki, Fukuoka

Effect of Non-hydrogen Bonding Solvents on the Electronic Spectra of Aromatic N-Oxides

By Tanekazu KUBOTA and Masumi YAMAKAWA

(Received July 21, 1961)

In previous papers, the effect of solvents, including active hydrogen atoms, which can form a hydrogen bond, on the electronic absorption spectra of many aromatic *N*-oxides has been reported by us[1-4]. As a result it has been concluded that the absorption spectra of the above compounds show a remarkable blue shift with the increasing polarity of the solvents and that the hydrogen bonding, such as $\gg$N—O···H (solvents), plays an important role in the blue shift phenomena. The effects of non-hydrogen bonding solvents on the absorption spectra of *N*-oxides, however, have hardly been investigated at all. For the present paper, particular interest has been taken in the case of solute-non-hydrogen bonding solvents interactions, and the results have quantitatively been analyzed on the basis of McRae's theory of the solute-solvent interaction[5]. The results thus obtained are compared with the previous results of the solvent effects due to hydrogen bonding polar solvents and the molecular orbital calculations which were carried out by one (T. K.) of the authors to elucidate the electronic structures of heterocyclic *N*-oxides.

Experimental

Ultraviolet absorption spectra were recorded by means of a Hitachi model EPS automatic recording spectrophotometer at room temperature(~25°C), at a scale expansion of 2 (which is just twice as expansible as the normal procedure), at a slow scanning speed (about ten minutes), and using a quartz cell of 1 cm. light path. Measurements of fluorescence spectra were made with a Beckman model DU spectrophotometer which was modified to record fluorescence spectra with good sensitivity[1]. Solvents were purified by the methods recommended by Weissberger and Proskauer[6], and special care was taken to remove contaminating water. Samples used here are pyridine *N*-oxide, 4-nitropyridine *N*-oxide, acridine *N*-oxide and *N*-methylbenzaldoxime. Pyridine *N*-oxide and acridine *N*-oxide were prepared and purified by the usual method[7,18]. 4-Nitro-pyridine *N*-oxide and *N*-methylbenzaldoxime were prepared by Tokuyama of our research laboratory and by Mori of Osaka University respectively. The physical properties and the purification method of the above samples are shown in Table I. The refractive index at the sodium D line (n_D) and the static dielectric constant of solvents used are shown in Table II. These data have been quoted from Ref. 6.

1) T. Kubota, *J. Chem. Soc. Japan, Pure Chem. Sec.* (*Nippon Kagaku Zasshi*), **79**, 916, 930 (1958).
2) T. Kubota, *J. Pharm. Soc. Japan* (*Nippon Yakugaku Zasshi*), **75**, 1540 (1955).
3) T. Kubota, ibid., **74**, 831 (1954), and the other papers.
4) T. Kubota and H. Miyazaki, *Chem. Pharm. Bull.*, **9**, 948 (1961).
5) E. G. McRae, *J. Phys. Chem.*, **61**, 562 (1957).
6) A. Weissberger and E. Proskauer, "Organic Solvent", 2nd Ed. Interscience Pub., Inc., New York (1956).
7) E. Ochiai, *J. Org. Chem.*, **18**, 534 (1953); A. Kliegl and A. Brösamle, *Ber.*, **69**, 197 (1936).

TABLE I. COMPOUNDS USED AND THEIR PHYSICAL PROPERTIES AND PURIFICATION METHODS

Compound	Physical properties	Purification
Pyridine *N*-oxide	B. p. = 105°C/1.5 mmHg	Redistilled three times in vacuo
4-Nitropyridine *N*-oxide	M. p. = 162.5°C	Recrystallized several times from acetone
Acridine *N*-oxide	Decomp. p. = 169.8°C	Recrystallized twice from heptane-chloroform and twice from water-ethanol
N-Methylbenzaldoxime	M. p. = 83.5°C	Recrystallized from benzene-petroleum ether

TABLE II. THE VALUES[6] OF THE REFRACTIVE INDEX AT THE Na-D LINE AND THE STATIC DIELECTRIC CONSTANT OF THE SOLVENTS USED

No.	Solvent	n_D	D
1	*n*-Heptane	1.388	1.924
2	Cyclohexane	1.426	2.023
3	Methylcyclohexane	1.423	2.020
4	Carbon tetrachloride	1.463	2.238
5	Carbon disulfide	1.632	2.641
6	Dioxane	1.424	2.209
7	Benzene	1.501	2.284
8	Toluene	1.494	2.379
9	Acetonitrile	1.344	37.5
10	Nitromethane	1.379	35.87
11	Benzonitrile	1.527	25.20
12	Acetone	1.356	20.70
13	Methyl acetate	1.362	6.68
14	Ethyl acetate	1.370	6.02
15	*n*-Butyl acetate	1.394	5.01
16	Isoamyl acetate	1.405	4.63
17	Diethyl oxalate	1.410	8.1
18	Ethyl ether	1.353	4.335
19	*n*-Butyl ether	1.397	3.06
20	Isoamyl ether	1.409	2.82

Results and Discussion

Theoretical Equation for the Solvent Effect of Absorption Spectra. — Theoretical investigation of solvent-solute interaction on electronic spectra have recently been made by Ooshika[8], by McRae[5] and by Longuet-Higgins and Pople[9] on the basis of applying the perturbation theory. As to the physical meaning, these authors obtained almost the same general expressions for the frequency shift. In this paper we shall use McRae's formula (Eq. 14 in the original paper) in order to analyze the experimental results, since this formula is well arranged for individual solute-solvent interaction terms such as the dispersion force, the solute dipole-solvent dipole thereby induced, the solute dipole-solvent dipole and the quadratic Stark effect. Nevertheless, the original formula is considerably complex and can not be applied to analyze the experimental data. The following simplifications, which are similar to those used by McRae to interpret the solvent effect of phenol blue[5], have been made with the aid of several assumptions. Firstly, the refractive index of the solvent at all frequencies involving the zero frequency has been replaced by the value at the Na-D line*1. Secondly, the quadratic Stark term representing the contribution from the interactions between the permanent dipoles of solvent molecules and the solute dipoles thereby induced has been neglected, since this term is small compared with the other contributions[5], especially for the relatively low polarity of most solvents used here. Lastly, the weighted mean wavelength (L_o) of the solvent introduced by McRae has been conveniently taken to be constant for all the solvents used, because L_o values of most solvents may exist approximately in the far ultraviolet region (about 100~125 mμ) and show considerable separation from the π-π^* absorption bands of *N*-oxide compounds*2. Thus we obtained

$$\tilde{\nu}_{abs} = \tilde{\nu}^g{}_{abs} + (A+B)\frac{n_D^2-1}{2n_D^2+1} + C\left[\frac{D-1}{D+2} - \frac{n_D^2-1}{n_D^2+2}\right] \quad (1)$$

where $\tilde{\nu}^g{}_{abs}$ is the band position at vapor state, and A, B and C are constants which are independent of the characters of the solvents, as is understood from Eqs. 2, 3 and 4 derived by McRae.

$$A = 1.07\times10^{-14}\cdot\frac{1}{a^3}\left[L_o\left\{-2f^u_{io} + \sum_{j\neq o,i}\left(f^u_{ji}-f^u_{jo}\right)\right\} + \sum_{j\neq o,i}\left(\frac{f^u_{jo}}{\tilde{\nu}^u_{jo}} - \frac{f^u_{ji}}{\tilde{\nu}^u_{ji}}\right)\right] \quad (2)$$

$$B = \frac{1}{hc}\left[\frac{(M^u_{oo})^2-(M^u_{ii})^2}{a^3}\right] \quad (3)$$

$$C = \frac{2}{hc}\left[\frac{\vec{M}^u_{oo}(\vec{M}^u_{oo}-\vec{M}^u_{ii})}{a^3}\right] \quad (4)$$

In these equations, the notations and their meaning are the same as those in McRae's

8) Y. Ooshika, *J. Phys. Soc. Japan*, **9**, 594 (1954).
9) H. C. Longuet-Higgins and J. A. Pople, *J. Chem. Phys.*, **27**, 192 (1957).

*1 n_D ordinarily differs little from n for infinite wavelengths except for special solvents (water, etc.).
*2 In practice, it is difficult to estimate L_o for all the solvents used because of a lack of their spectral data.

TABLE III. ABSORPTION MAXIMA OF THE COMPOUNDS USED IN VARIOUS SOLVENTS

Solvent	Pyridine *N*-oxide cm^{-1}	4-Nitro-pyridine *N*-oxide cm^{-1}	*N*-Methyl-benzaldoxime cm^{-1}	Acridine *N*-oxide (ν^{I}) cm^{-1}	Acridine *N*-oxide (ν^{II}) cm^{-1}
n-Heptane	35400	28770	33550	23390	21990
Cyclohexane	35370	28690	33490	23340	21940
Methylcyclohexane	35320	28680	33540	23360	21950
Carbon tetrachloride	35160	28800	33250	23300	21920
Carbon disulfide	—	—	—	22900	21550
Dioxane	35780	28570	33580	23370	22020
Benzene	—	28380	33410	23300	21940
Toluene	—	28340	33410	23270	21920
Acetonitrile	36300	28970	33840	23570	22240
Nitromethane	—	—	—	23580	22250
Benzonitrile	—	28390	33190	23280	21990
Acetone	—	28790	—	23490	22180
Methyl acetate	36060	28780	33760	23510	22190
Ethyl acetate	35840	28740	33700	23470	22130
n-Butyl acetate	35780	28610	33630	23400	22080
Isoamyl acetate	35840	28650	33640	23410	22040
Diethyl oxalate	—	28610	—	23450	22100
Ethyl ether	35600	28750	33670	23440	22050
n-Butyl ether	35560	28680	33540	23370	21990
Isoamyl ether	—	28680	33550	23360	21990

paper[5]. It was possible to explain, within the range of experimental error, the experimental results by using Eq. 1*[3].

Effect of Solvents on Absorption Spectra.— The absorption spectra of pyridine *N*-oxide, 4-nitropyridine *N*-oxide, acridine *N*-oxide and *N*-methylbenzaldoxime in *n*-heptane are shown in Fig. 1, and the π-π^* absorption bands under consideration are shown by arrows. The maxima of the π-π^* bands of the above compounds in various solvents are given in Table III. $\tilde{\nu}^{I}_{abs}$ and $\tilde{\nu}^{II}_{abs}$ of acridine *N*-oxide denote the band maxima (vibrational components of the π-π^* $-{}^1L_A$-band) at 427.5 mμ and at 454.8 mμ in *n*-heptane solution respectively. Thus $\tilde{\nu}^{g}_{abs}$, $A+B$ and C of Eq. 1 have been determined by applying the least square method to the data of Tables II and III*[4]. The numerical values of Eq. 1 thus obtained are given in Table IV. The relations of the calculated (these values were calculated from Eq. 1 using the values in Table IV) vs. the observed frequency shifts in the π-π^* bands of the above compounds are shown in Figs. 2—6. From the values in Table IV, it should be

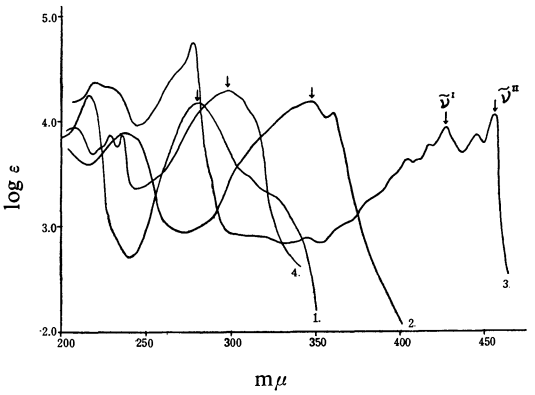


Fig. 1. The absorption spectra of the compounds in *n*-heptane. The absorption bands under consideration are shown by arrows.
1 Pyridine *N*-oxide
2 4-Nitropyridine *N*-oxide
3 Acridine *N*-oxide
4 *N*-Methylbenzaldoxime
Solvent: *n*-Heptane

TABLE IV. $\tilde{\nu}^{g}_{abs}$, $A+B$ AND C VALUES OBTAINED FROM EQ. 1 BY APPLYING THE LEAST SQUARE METHOD

Compound	$\tilde{\nu}^{g}_{abs}$ cm^{-1}	$A+B$ cm^{-1}	C cm^{-1}
Pyridine *N*-oxide	35980	−3260	1280
4-Nitropyridine *N*-oxide	30380	−8760	10
Acridine *N*-oxide	24410	−5290	130
	22900	−4660	250
N-Methylbenzaldoxime	35130	−8000	90

*[3] What differs from the solvent effect of the weak $n\rightarrow\pi^*$ transitions, which were investigated recently by Ito et al.[10], is that the dispersion term can hardly be considered independent of the solvents in the case of the strong π-π^* band of *N*-oxide compounds.

10) M. Ito, K. Inuzuka and S. Imanishi, *J. Am. Chem. Soc.*, **82**, 1317 (1960).

*[4] As is seen in Figs. 2—6, solvents showing a distinct discrepancy from a linear relation between the calculated and the observed values have been removed from the calculations by means of the least square method.

pointed out for all the *N*-oxide compounds that dispersion and dipole-dipole interaction terms cause a red shift and a blue shift respectively. Now let us consider how appropriate are the values of Table IV and Figs. 2—6. All the points, with the exception of anomalous solvents, fit a full straight line with a root mean square deviation of 90 cm^{-1} and 50 cm^{-1} for pyridine *N*-oxide and the other *N*-oxide compounds respectively, which is of the same order of magnitude as the experimental error in the determination of band frequency in solution spectra. Therefore it may be considered that Eq. 1 satisfactorily explains the experimental results. Moreover, it is also worth pointing out the following facts: Firstly, the *C*-value of 4-nitropyridine *N*-oxide is considerably small, 13 cm^{-1}; this result is reasonable because the dipole moment of this

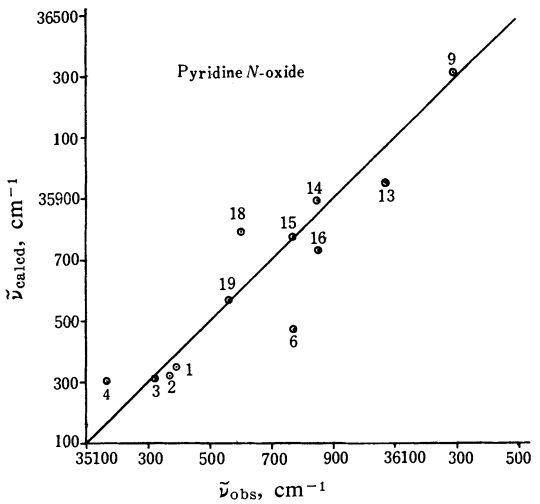


Fig. 2. Relation between $\tilde{\nu}_{obs}$ and $\tilde{\nu}_{calcd}$ for pyridine *N*-oxide.

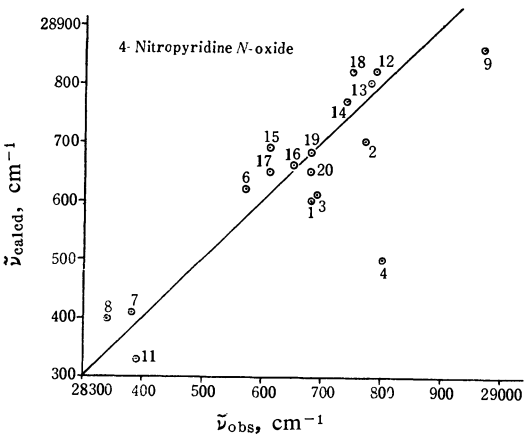


Fig. 3. Relation between $\tilde{\nu}_{obs}$ and $\tilde{\nu}_{calcd}$ for 4-nitropyridine *N*-oxide.

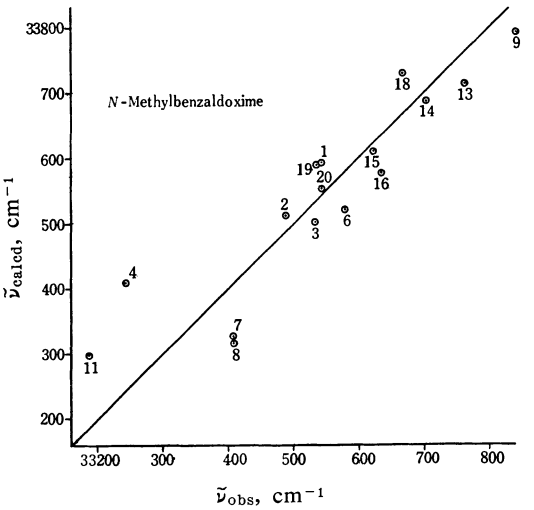


Fig. 4. Relation between $\tilde{\nu}_{obs}$ and $\tilde{\nu}_{calcd}$ for *N*-methylbenzaldoxime.

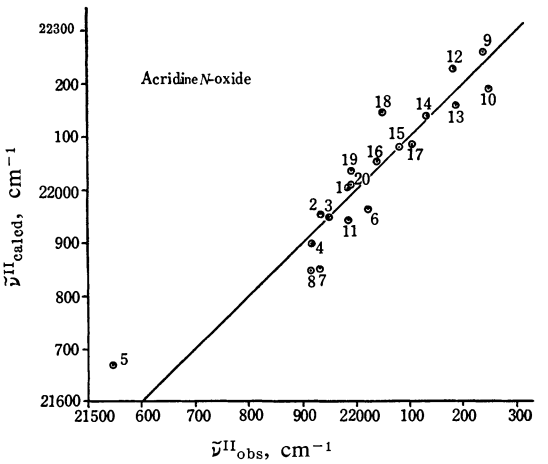


Fig. 5. Relation between $\tilde{\nu}^{II}_{obs}$ and $\tilde{\nu}^{II}_{calcd}$ for acridine *N*-oxide.

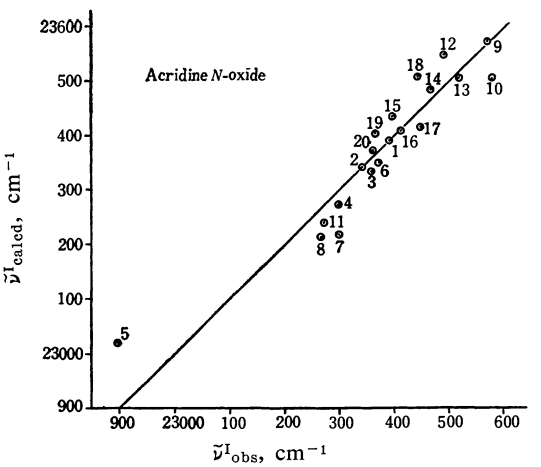


Fig. 6. Relation between $\tilde{\nu}^{I}_{obs}$ and $\tilde{\nu}^{I}_{calcd}$ for acridine *N*-oxide.

compound in the ground state is nearly zero[16]. Secondly, $\tilde{\nu}^{g}_{abs}$ of pyridine *N*-oxide obtained from Eq. 1 is 35980 cm^{-1}; this value agrees well with the experimental value of 36080 cm^{-1} which was measured both by us and by Ito and Hata[11],*5. On the other hand, calculated and observed frequencies frequently do not agree when dioxane and carbon tetrachloride have been used as a solvent; the former is especially irregular for substances having a large *C* value, and the latter, for those having a large $A+B$ value. The abnormal behavior of solvent dioxane is well known[5,10,12]. It is also common that carbon tetrachloride sometimes shows an anomalous behavior owing to short range intermolecular interactions such as molecular complex formation[13]. This fact may be regarded as one of the reasons why carbon tetrachloride shows an anomalous behavior, and some correlation may exist between such anomalous properties and $A+B$ values.

Dipole Moment in the Excited State of Pyridine *N*-Oxide and Acridine *N*-Oxide.—Now it may be possible in principle to evaluate the dipole moment in an excited state from Eq. 4, but practically it is difficult (especially for the absolute $\vec{M}^{u}_{ii}$ value) because the appropriate "a" values ("a" is Onsager's reaction radius of the solute molecule) can not be easily determined and because the molecular symmetries in the ground and the excited states are, in general, not the same. In addition, various assumptions have been made to derive Eq. 4. Taking tentatively "a"=3.5~4 Å with reference to the reports of other authors[5,10,12,14] and assuming that $\vec{M}^{u}_{oo}$ and $\vec{M}^{u}_{ii}$ are parallel, the excited state dipole moments of pyridine *N*-oxide and acridine *N*-oxide are calculated to be 1.9~1.3 D and 0.22~1.5 D, ($\tilde{\nu}^{I}_{abs}$) and 0.3~0.4 D ($\tilde{\nu}^{II}_{abs}$) respectively smaller than those of the ground state. It may be regarded in the first order approximation that such a decrease in excited state dipole moment is based on the change of the π-electron moment (π-moment) arising from an electronic excitation. It has been determined by Linton[15], by Katritzky, Bax et al.[16,17] and by Acheson et al.[18] that the dipole moments of pyridine *N*-oxide and acridine *N*-oxide in the ground state are 4.24 D and 3.90 D respectively and that the total moment ($\sigma+\pi$) is directed very closely from the ring to the oxygen atom along a C_2-axis, while the π-moment vector is in the opposite direction. Therefore, the above experimental fact clearly indicates that the π-electron transfer from the oxygen atom to the ring is much greater in the excited state than in the ground state. Assuming that "a" is taken to be 3.5 Å and 4 Å for pyridine *N*-oxide and acridine *N*-oxide respectively, and making a comparison of the degree of dipole moment decrease in the excited π-π^* state, the degree of pyridine *N*-oxide is 3.2~5.9 times as great as that of acridine *N*-oxide. In the previous papers, one (T. K.) of the authors reported on the electronic structure of various heterocyclic *N*-oxides on the basis of various molecular orbital calculations[19,20]. It was then most reasonable to conclude that the π-π^* bands, that are the subject of discussion, belong to the group species $^1A_1$ and consist of a very large contribution of the single configuration which corresponds to one electronic excitation from the highest occupied orbital to the lowest empty orbital*6. The square values of the above two MO's coefficients are shown schematically in Figs. 7 and 8 for pyridine *N*-oxide and acridine *N*-oxide respectively. As is well understood from Figs. 7 and 8, the degree of the electron transfer from the oxygen atom to the ring of acridine *N*-oxide by an electron excitation is much smaller than that of pyridine *N*-oxide. Therefore, this fact shows a good correspondence with the above estimated values of the π-moment change by an electronic excitation for pyridine *N*-oxide and acridine *N*-oxide.

11) M. Ito and N. Hata, This Bulletin, **28**, 260 (1955).

*5 In this case, however, the reason why $\tilde{\nu}^{g}_{abs}$ and $\tilde{\nu}^{max}_{abs}$ (in vapor state) experimentally determined must rigorously agree can not be found, owing to the several assumptions described above. Moreover, $\tilde{\nu}^{max}_{abs}$ in a vapor state of the other compounds could not be recorded because of the low vapor pressure.

12) E. Lippert, *Z. Naturforsch.*, **10a**, 541 (1955); *Z. für Elektrochem.*, **61**, 962 (1957).

13) A. Kuboyama, Symposium on Electronic States (in Japan), **9**, 13 (1954).

14) K. Mataga, Y. Kaifu and M. Koizumi, This Bulletin, **29**, 465 (1956).

15) E. P. Linton, *J. Am. Chem. Soc.*, **62**, 1945 (1940).

16) A. R. Katritzky, E. W. Randall and L. E. Sutton, *J. Chem. Soc.*, **1957**, 1769.

17) C. M. Bax, A. R. Katritzky and L. E. Sutton, ibid., **1958**, 1258.

18) R. M. Acheson, B. Adcock, G. M. Glover and L. E. Sutton, ibid., **1960**, 3367.

19) T. Kubota, *J. Chem. Soc. Japan, Pure Chem. Sec.* (*Nippon Kagaku Zasshi*), **79**, 916 (1958).

20) T. Kubota, This Bulletin, to be published.

*6 In these calculations the values of SMO parameters are chosen so as to reproduce, by using Jaffé's relation[21], the electronic densities obtained from the experimentally determined Hammett's σ values of the *N*-oxide group in non-polar solvents[22]. The parameters obtained are equal to $k_N=1.6\beta$, $k_O=0.595\beta$ and inductive effect $=(1/3)^n k_N$ respectively. $k_O=0.595\beta$, however, is relatively small to interpret various physico-chemical properties, and $k_O=0.8$ is the best value to reproduce the observed dipole moment, etc. The relative change of π-moments from pyridine *N*-oxide to acridine *N*-oxide will be almost independent of the selection of the k_O-values, either 0.595 or 0.8. In this paper we have used $k_O=0.595$ for discussion, since all the MO calculations for parameter 0.8 are not complete at present.

21) H. H. Jaffé, *J. Chem. Phys.*, **20**, 279, 778, 1554 (1952).

22) H. Shindo, *Chem. & Pharm. Bull.*, **6**, 117 (1958).

TABLE V. CALCULATED RESULTS OF THE π-MOMENT IN THE GROUND AND THE EXCITED π^* STATES AND THE π-MOMENT CHANGE DURING π—π^* ONE ELECTRON TRANSITIONS SHOWN IN FIGS. 7 AND 8

Compound	${}^{\pi}\vec{M}^{u}_{ii}$	${}^{\pi}\vec{M}^{u}_{oo}$	${}^{\pi}\vec{M}^{u}_{ii}-{}^{\pi}\vec{M}^{u}_{oo}$	
	Calcd. value, D	Calcd. value, D	Calcd. value	Calcd. value[19,20]/1.6
Pyridine *N*-oxide	5.58	1.88	3.70	2.31
Acridine *N*-oxide	4.24	3.01	1.23	0.77

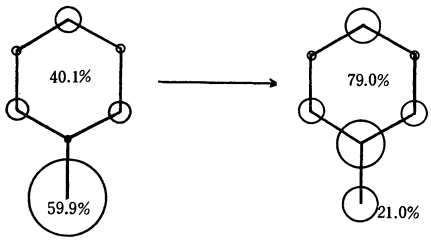


Fig. 7. Distribution of an electron in the highest occupied orbital and the lowest empty orbital of pyridine *N*-oxide.

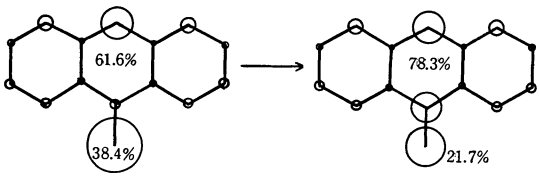


Fig. 8. Distribution of an electron in the highest occupied orbital and the lowest empty orbital of acridine *N*-oxide.

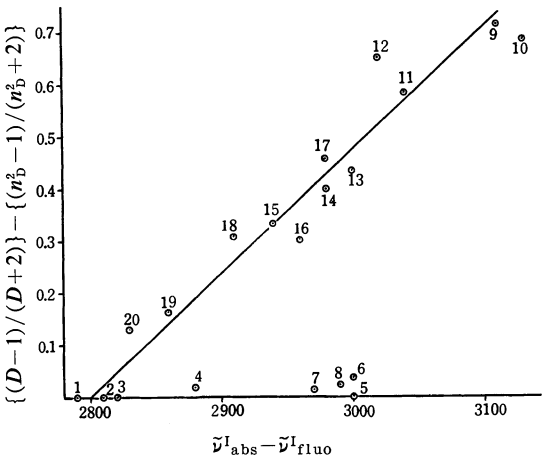


Fig. 9. Relation between $(\tilde{\nu}^{I}_{abs}-\tilde{\nu}^{I}_{fluo})$ and $\{(D-1)/(D+2)\}-\{(n_D^2-1)/(n_D^2+2)\}$ for acridine *N*-oxide.

Making the calculation of the π-moment change between the ground state and the excited π-π^* state shown in Figs. 7 and 8 by applying the molecular orbitals reported in previous papers[19,20], the results in Table V

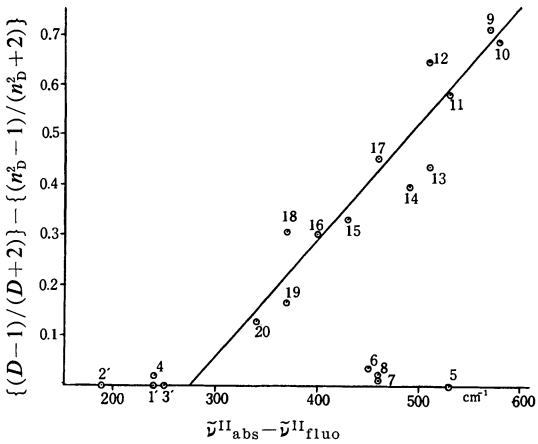


Fig. 10. Relation between $(\tilde{\nu}^{II}_{obs}-\tilde{\nu}^{II}_{fluo})$ and $\{(D-1)/(D+2)\}-\{(n_D^2-1)/(n_D^2+2)\}$ for acridine *N*-oxide.

are obtained*7. As is seen from Table V, the absolute values $({}^{\pi}\vec{M}^{u}_{ii}-{}^{\pi}\vec{M}^{u}_{oo})$ do not show a good agreement with those estimated from the *C* value, this discrepancy being based on the reason described in the beginning of this section. However, comparing the value $({}^{\pi}\vec{M}^{u}_{ii}-{}^{\pi}\vec{M}^{u}_{oo})$ of pyridine *N*-oxide with that of acridine *N*-oxide, the former is 2.93~3.50 times as great as that of the latter; this result agrees well with the experimental value*7,*8.

Effects of Hydrogen Bonding. — As stated above, the electronic spectra of aromatic *N*-oxide compounds show a remarkable blue

*7 In this calculation it has been assumed that the shape of these molecules is a condensed regular hexagon, the bond distance of which is 1.395 Å, and the N—O distance is taken to be equal to 1.28 Å. However, the ratio of the value $({}^{\pi}\vec{M}^{u}_{ii}-{}^{\pi}\vec{M}^{u}_{oo})$ of pridine *N*-oxide to that of acridine *N*-oxide is almost insensitive in the selection of the N→O bond distance (1.28~1.40 Å). According to recent investigations of the crystal structure of phenazine mono-*N*-oxide and 4-nitropyridine *N*-oxide, the N—O distance is 1.24 Å and 1.26 Å for the former and the latter respectively[23,24].

23) R. Curti, V. Riganti and S. Locchi, *Acta Cryst.*, **14**, 133 (1961).

24) E. L. Eichhorn, idid., **9**, 787 (1956).

*8 The nature in the excited and the ground states of *N*-methylbenzaldoxime can not be discussed, since the molecular structure (cis or trans) and the electronic state of this compound have not been investigated as yet. At present we are investigating the electronic structures and the spectroscopic behaviors of nitron type compounds.

TABLE VI. VALUES OF ABNORMAL BLUE SHIFT (cm^{-1}) DUE TO THE HYDROGEN BONDING EFFECT APPROXIMATELY ESTIMATED BY USING EQ. 1 AND OBSERVED VALUES IN WATER AND ETHANOL

Compound	Solvent		
	Water (Obs. value)	Ethanol (Obs. value)	Water/Ethanol
Pyridine *N*-oxide	4860 (39440)	1410 (37660)	3.4
4-Nitropyridine *N*-oxide	5430 (31690)	1200 (30010)	4.5
N-Methylbenzaldoxime	3620 (34990)	940 (34290)	3.9
Acridine *N*-oxide ν^{I}	2270 (24200)	700 (23980)	3.2
Acridine *N*-oxide ν^{II}	2260 (22980)	750 (22730)	3.0

shift in hydrogen bonding solvents, such as alcohol and water. This abnormal blue shift can not be explained by Eq. 1 and is mainly based on the hydrogen bonding complexes such as N→O·····H. The contribution of the normal solvent effect to the frequency shift can be evaluated approximately from Eq. 1 by using n_D and D of the above solvents. The values thus obtained are small, and the remaining portion ($\tilde{\nu}_{hyd}$) of the total frequency shift may mainly be owing to the hydrogen bonding effect, the calculated values being shown in Table VI. The value $\tilde{\nu}_{hyd}$ of water is 3∼4 times as great as that of ethanol in all the compounds used here. It may be considered from the above fact that the hydrogen bonding power of water is about 3∼4 times as great as that of ethanol.

Relation between the Solvent-induced Frequency Shift of the Absorption and the Fluorescence Spectra of Acridine *N*-Oxide.—The difference in solvent effect on the maxima of the absorption and fluorescence spectra was given by Lippert[12], by Mataga et al.[14] and by McRae[5] as in Eq. 5. Here K is approximately constant.

$$\tilde{\nu}_{abs}-\tilde{\nu}_{fluo}=\frac{2}{hc}\cdot\frac{[\vec{M}^{u}_{oo}-\vec{M}^{u}_{ii}]^2}{a^3}\times\left[\frac{D-1}{D+2}-\frac{n_D^2-1}{n_D^2+2}\right]+K \quad (5)$$

As was reported in the previous paper, the fluorescence spectra of acridine *N*-oxide show a good mirror image relative to the absorption band (^1L_a)[1].

The values ($\tilde{\nu}_{abs}-\tilde{\nu}_{fluo}$) in various solvents are given in Table VII. Here $\tilde{\nu}^{I}_{fluo}$ and $\tilde{\nu}^{II}_{fluo}$ correspond to $\tilde{\nu}^{I}_{abs}$ and $\tilde{\nu}^{II}_{abs}$ respectively. Thus the coefficients of Eq. 5 have been determined by means of the least square method by using the above data, and Eqs. 6 and 7 have thereby been obtained*9.

$$\tilde{\nu}^{I}_{abs}-\tilde{\nu}^{I}_{fluo}=2800+420\left[\frac{D-1}{D+2}-\frac{n_D^2-1}{n_D^2+2}\right] \quad (6)$$

$$\tilde{\nu}^{II}_{abs}-\tilde{\nu}^{II}_{fluo}=270+430\left[\frac{D-1}{D+2}-\frac{n_D^2-1}{n_D^2+2}\right] \quad (7)$$

In Figs. 9 and 10, the values $\left(\frac{D-1}{D+2}-\frac{n_D^2-1}{n_D^2+2}\right)$ are plotted against the values ($\tilde{\nu}_{abs}-\tilde{\nu}_{fluo}$) of the $\tilde{\nu}^{I}$ and $\tilde{\nu}^{II}$ bands, and it is found that a good linear relation comes into existence between the above two values, but solvents such as dioxane, toluene and benzene cause a large deviation from the linear relation. The abnormal behavior of dioxane is owing to the same reason as that described in the previous section. The exceptional behavior of benzene and toluene (which in main arises

TABLE VII. EXPERIMENTAL VALUES OF $\tilde{\nu}_{abs}-\tilde{\nu}_{fluo}$ OF ACRIDINE *N*-OXIDE IN VARIOUS SOLVENTS

Solvent	$\tilde{\nu}^{I}_{abs}-\tilde{\nu}^{I}_{fluo}$ cm^{-1}	$\tilde{\nu}^{II}_{abs}-\tilde{\nu}^{II}_{fluo}$ cm^{-1}
n-Heptane	2790	(240)*9
Cyclohexane	2810	(190)*9
Methylcyclohexane	2820	(250)*9
Carbon tetrachloride	2880	240
Carbon disulfide	3000	530
Dioxane	3000	450
Benzene	2970	460
Toluene	2990	460
Acetonitrile	3110	570
Nitromethane	3130	580
Benzonitrile	3040	530
Acetone	3020	510
Methyl acetate	3000	510
Ethyl acetate	2980	490
n-Butyl acetate	2940	430
Isoamyl acetate	2960	400
Diethyl oxalate	2980	460
Ethyl ether	2910	370
n-Butyl ether	2860	370
Isoamyl ether	2830	340

*9 In solvents 1, 2 and 3, $\tilde{\nu}^{II}_{fluo}$ has a tendency to be divided into doublets, but not so in the other solvents. To correct this difference, we used the weighted mean wave number given by the following equation for the determination of $\tilde{\nu}^{II}_{fluo}$ in solvents 1, 2 and 3. The values thus obtained were used to obtain Eq. 7 and are indicated by 1′, 2′ and 3′ in Fig. 10.

$$\tilde{\nu}_{max}=\left[\int\varepsilon\cdot\tilde{\nu}\cdot d\tilde{\nu}\Big/\int\varepsilon\cdot d\tilde{\nu}\right]\fallingdotseq\left[\sum_i\varepsilon_i\cdot\tilde{\nu}_i\Big/\sum_i\varepsilon_i\right]$$

from the abnormal frequency shift in the fluorescence spectra) is caused by mutual short-range interaction between the solute molecules and the π-electrons of the aromatic solvents and coincides with the analogous result that was found previously in the experiment concerning the fluorescence quenching of acridine *N*-oxide[1]. Making the same assumption as that described in the previous section and using the coefficients of Eqs. 6 and 7, the value $(^{\pi}\vec{M}^{u}_{ii} - {}^{\pi}\vec{M}^{u}_{oo})$ can be evaluated to be 1.6~1.8 D. This value, however, does not agree well with the data obtained from the analysis of the absorption spectra. It may reasonably be inferred that this is because the solute-solvent interaction of various types in the excited state differs in some measure from that of the ground state. Therefore, considering the Franck-Condon principle, the frequency shifts of absorption and fluorescence bands do not agree well[12]. In our case, $(\vec{M}^{u}_{oo} > \vec{M}^{u}_{ii})$, the shift of the latter is smaller than that of the former[12]. Indeed, $\tilde{\nu}^{I}_{fluo}$ and $\tilde{\nu}^{II}_{fluo}$ show almost the same wave number in the polar solvents used here, although $\tilde{\nu}^{I}_{abs}$ and $\tilde{\nu}^{II}_{abs}$ do not*10. As a result, some simplifications concerning the treatment of the second term of Eq. 1 have been made, but such simplifications are unnecessary in Eq. 5. Moreover, the character in the excited π-π^* state generally may be considered to be locally more polar than in the ground state, as is understood from the general character of molecular orbitals. The special solute-solvent interactions, which are negligible in the ground state, may be expected in some measure in the excited state, since fluorescence is emitted from the equilibrium state in the excited π-π^* state.

*10 In a hydrogen bonding effect previously investigated[1], such phenomena were frequently found; they have also been discussed by Pimentell[25].

Summary

The strong π-π^* absorption bands of pyridine *N*-oxide, 4-nitropyridine *N*-oxide, acridine *N*-oxide and *N*-methylbenzaldoxime were measured in various solvents, and the frequency shifts induced by solvents were quantitatively analyzed by applying the McRae's theory of the solvent effect. On the other hand, the fluorescence spectra of acridine *N*-oxide have also been recorded in various solvents, and the solvent effect has been discussed in connection with that of the absorption spectra. The results show that the π-electron transfer from the oxygen atom to the ring is much greater in the excited state than in the ground state.

The authors wish to thank Professor Saburo Nagakura of the Institute for Solid State Physics, the University of Tokyo, for valuable discussions and for reading the manuscript; Dr. Noboru Mataga of Osaka Municipal University for valuable discussions; Dr. Kanzi Tokuyama of our research laboratory for supplying a sample of 4-nitropyridine *N*-oxide; and Dr. Yasushi Mori of Osaka University for supplying a sample of *N*-methylbenzaldoxime.

Research Laboratory
Shionogi & Co., Ltd.
Fukushima-ku, Osaka

25) G. C. Pimentel, *J. Am. Chem. Soc.*, **79**, 3323 (1957).

Studies on Lactone Formation in Vapor Phase. II. Synthesis of ε-Caprolactone

By Shinzaburo OKA

(Received July 25, 1961)

The results obtained in a previous study[1] of the dehydrogenation of 1, 4-butanediol to γ-butyrolactone prompted this further investigation on ε-caprolactone.

Dehydrogenation of 1, 4-diols or 1, 5-diols with copper chromite catalyst had been studied by several investigators[2-7] to give γ-lactones or δ-lactones, respectively, in good yields.

1) S. Oka, This Bulletin, **34**, 12 (1961).
2) W. Reppe et al., German Pat. 699945 (1940); *Chem. Abstr.*, **35**, 6977 (1941).
3) L. P. Kyrides et al., *J. Am. Chem. Soc.*, **68**, 1385 (1946).
4) L. E. Schniepp et al., ibid., **69**, 1545 (1947).
5) Y. Hachihama et al., *Chem. High Polymers (Kobunshi Kagaku)*, **8**, 75 (1951).
6) R. I. Longley et al., *J. Am. Chem. Soc.*, **74**, 2012 (1952).
7) W. Reppe et al., *Ann.*, **596**, 180 (1955).

Studies on dehydrogenation of 1, 6-diols to ε-lactones are surprisingly few. Carothers[8] showed that ε-caprolactone was isolated as a by-product from hydrogenation products of ethyl adipate with copper chromite catalyst. Reppe[7] claimed that ε-caprolactone and its polymer were obtained by liquid phase dehydrogenation of 1, 6-hexanediol with a copper catalyst. No details on preparation of the catalyst were described. Suitable catalysts for the dehydrogenation of 1, 6-diols to ε-lactones are not found in the literature.

Attempts to dehydrogenate 1, 6-hexanediol to ε-caprolactone with copper-zinc oxide or copper-magnesium oxide catalyst which gave γ-butyrolactone and δ-valerolactone in good yields, were unsuccessful. Apparently the formation of a seven-membered ring is more difficult as compared with that of the five- or six-membered ring. Examinations of numerous mixed catalysts have resulted in finding a new catalyst, copper chromite-zinc oxide, which gives ε-caprolactone in good yields. The dehydrogenation with this catalyst in vapor phase has an advantage over the liquid phase method which produces the undesirable polymer.

Preparation of 1, 6-hexanediol, the starting material for ε-caprolactone, was performed as follows:

(1) $CH{\equiv}CH + HCHO \rightarrow CH{\equiv}CCH_2OH$

(2) $2CH{\equiv}CCH_2OH + 1/2\ O_2 \rightarrow HOCH_2C{\equiv}CC{\equiv}CCH_2OH + H_2O$

(3) $HOCH_2C{\equiv}CC{\equiv}CCH_2OH + 4H_2 \rightarrow HO(CH_2)_6OH$

Since the ethinylation reaction was found by Reppe[9], several investigations[10-12] including the reaction of acetylene with aqueous formaldehyde have been reported. Propargyl alcohol, the initial reaction product, reacts with a second molecule of formaldehyde to give butynediol, which is usually the main product. Murahashi[11] reported the favorable conditions for the propargyl alcohol formation in an aqueous solution. But so far as aqueous formaldehyde is used, isolation of propargyl alcohol from the dilute aqueous reaction mixture is complicated and time-consuming owing to the formation of an azeotropic mixture. It may be, therefore, favorable to carry out the reaction under non-aqueous conditions. For the purpose of raising the yield of propargyl alcohol, it may be preferable to maintain the high concentration of acetylene by using a suitable solvent. Thus, the author studied the reaction of acetylene with anhydrous paraformaldehyde in various solvents.

8) W. H. Carothers et al., *J. Am. Chem. Soc.*, **56**, 455 (1934).
9) W. Peppe, Brit. Pat. 508062 (1939); *Chem. Abstr.*, **34**, 447 (1940).
10) S. Murahashi et al., *J. Soc., Chem. Japan, Ind. Chem. Sec.* (*Kogyo Kagaku Zasshi*), **55**, 525 (1952).
11) S. Murahashi et al., ibid., **55**, 567 (1952).
12) K. Yamamoto et al., This Bulletin, **27**, 386 (1954).

Experimental

Propargyl Alcohol and Butynediol.—According to Murahashi's procedure[10], a copper acetylide catalyst was prepared from 30 g. of cupric oxide which was obtained by heating basic copper carbonate at 300~350°C. One third of the catalyst was used in each experiment. The reaction was carried out batchwise in a shaking stainless steel autoclave of 300 ml. capacity. The autoclave was charged with paraformaldehyde, solvent and the catalyst. Acetylene was compressed at room temperature. The amount of acetylene compressed was estimated by the pressure drop of the compressor's oil separator which supplied acetylene. After the reaction, the reaction mixture was filtered and about 1 g. of the filtrate was supplied to analytical determination of propargyl alcohol according to Reppe's directions[13]. After removal of the solvent and the propargyl alcohol, the filtrate gave butynediol, b. p. 115~117°C/3 mmHg, m. p. 56~57°C (lit.[10] 57°C).

Hexadiynediol—A shaking stainless steel autoclave of 300 ml. capacity was charged with 56 g. of propargyl alcohol, 6 g. of cuprous chloride, 19 g. of ammonium chloride, and 60 g. of water. Oxygen was filled to 20 kg./cm². The autoclave was heated 55~60°C for one hour. When the pressure fell to 5 kg./cm², oxygen was again changed to 20 kg./cm². The reaction mixture was filtered, and the solid was washed with a minimum amount of water and recrystallized from methanol to yield 51 g. of hexadiynediol, m. p. 112°C (lit.[14] 112°C).

1, 6-Hexanediol.—Hexadiynediol (20 g.) in 180 ml. of methanol was hydrogenated under the initial hydrogen pressure of 50 kg./cm² with 2 g. of Raney nickel W-6 at 50~60°C for two hours. The catalyst was filtered off, and the filtrate, after removal of the solvent, was distilled to yield 20 g. of 1, 6-hexanediol, b. p. 125°C/3 mmHg, m. p. 40~41°C (lit.[15] 41.5°C).

ε-Caprolactone.—A typical catalyst for the dehydrogenation of 1, 6-hexanediol to ε-caprolactone was prepared as follows.

Two solutions, one solution (350 ml.) containing 56 g. of zinc nitrate hexahydrate and 92 g. of cupric nitrate trihydrate, and one solution (350 ml.) containing 24 g. of ammonium dichromate and 56 g. of 28% solution of ammonium hydroxide, were added dropwise into 300 ml. of water with stirring. The orange yellow precipitate formed was filtered and sucked as dry as possible, and dried at 70~80°C for twelve hours. The product was decomposed in a silica tube heated at 260~280°C for

13) W. Reppe et al., *Ann.*, **596**, 34 (1955).
14) J. W. Copenhaver and M. H. Bigelow, "Acetylene and Carbon Monoxide Chemistry", Reinhold Publishing Corp. (1949), p. 123.
15) W. Reppe et al., *Ann.*, **596**, 71 (1955).

three hours. The resulting product was washed with fifteen 2 l. portions of water, and dried at 70~80°C for twelve hours. The composition of the catalyst so obtained was about: 50% cupric oxide, 25% chromium oxide and 25% zinc oxide by weight (mol. ratio=2 : 0.5 : 1).

The apparatus and the procedure for the dehydrogenation were essentially the same as those previously described[1]. The dehydrogenation tube (60 cm.×15 mm.) was packed with 50 ml. of tablets of the above catalyst. After activation of the catalyst with hydrogen at 280~300°C, the pressure in the reaction system was reduced to 5~10 mmHg and 1,6-hexanediol (15 g.) was passed in by vacuum distillation in a period of four hours. The reaction temperature was maintained at 210~220°C. The product was fractionated to yield 0.5 g. of forerun, b. p. 50~65°C/2 mmHg, 7.6 g. of ε-caprolactone, b. p. 78~85°C/2 mmHg and 3.4 g. of unreacted hexanediol, b. p. 110~120°C/2 mmHg. Refractionation gave a sample of b. p. 80°C/2 mmHg, n_D^{25} 1.4615, d_4^{25} 1.071, MR_D: Found, 29.3; Calcd., 29.3.

Found: C, 63.22; H, 8.86. Calcd. for $C_6H_{10}O_2$: C, 63.13; H, 8.83%.

ε-Caprolactone gave a hydrazide melting at 115°C (lit.[8] 115°C).

Found: C, 49.16; H, 9.68. Calcd. for $C_6H_{14}O_2 \cdot N_2$: C, 49.30; H, 9.65%.

From the forerun, a 2,4-dinitrophenylhydrazone of 1-cyclopentene-1-carboxaldehyde was obtained, m. p. 209~210°C (lit.[16] 210~211°C), which showed no depression when mixed with an authentic sample.

Found: C, 52.40; H, 4.44. Calcd. for $C_{12}H_{12} \cdot O_4N_4$: C, 52.17; H, 4.38%.

Cyclopentyl Carbinol.—Copper-magnesium oxide tablets (50 ml.) containing 20% copper were used. After activation of the catalyst with hydrogen at 280~300°C, 1,6-hexanediol (17 g.) was passed in with 20 l./hr. of hydrogen at 270°C in a period of three hours. The products consisted of two layers; the upper water-insoluble layer weighed 11 g. and the lower aqueous layer weighed 2 g. By fractionation of the upper layer, 3.5 g. of forerun, b. p. 50~60°C/22 mmHg and 4 g. of cyclopentyl carbinol, b. p. 73~78°C/22 mmHg were obtained. Refractionation gave a sample of b. p. 74°C/20 mmHg, n_D^{20} 1.4540, d_D^{22} 0.926 (lit.[17] b. p. 161~163°C, n_D^{20} 1.4552, d_4^{20} 0.926), MR_D Found, 29.2, Calcd., 29.2.

Found: C, 71,77; H, 12.14. Calcd. for $C_6H_{12}O$: C, 71.95; H, 12.08%.

Cyclopentyl carbinol gave a phenylurethane melting at 108°C (lit.[18] 110°C).

Found: C, 71.30; H, 7.82. Calcd. for $C_{13}H_{17} \cdot O_2N$: C, 71.20; H, 7.82%.

From the forerun, a 2,4-dinitrophenylhydrazone of cyclopentanecarboxaldehyde was obtained, m. p. 149~152°C. (lit.[19] 158°C).

Found: C, 51.63; H, 5.01. Calcd. for $C_{12}H_{14} \cdot O_4N_4$: C, 51.79; H, 5.01%.

16) M. S. Kharash et al., *J. Org. Chem.*, **16**, 150 (1951).
17) N. Turkiewicz, *Ber.*, **72**, 1060 (1939).
18) N. Zelinsky, ibid., **41**, 2628 (1908).
19) H. M. Fales, *J. Am. Chem. Soc.*, **77**, 5118 (1955).

Results and Discussion

Reaction of Paraformaldehyde with Acetylene under Pressure.—The results obtained in various solvents are shown in Table I. Acetylene was compressed to about 15 kg./cm² at room temperature and the amount of acetylene compressed was about 26 g., except in the case of water (35 kg./cm², 14 g.). Obviously chemical structure of the solvent has effects on the relative yields of propargyl alcohol and butynediol to some extents. Methanol, tetrahydrofuran and acetone were suitable solvents for propargyl alcohol formation and benzene for butynediol.

Effects of the reaction temperature are shown in Table II. The relative yields were hardly

Table I. Effects of solvents

Solvent	Reaction pressure kg./cm²	Yield of PA* %	Yield of BD** %
Water	50~33	30	51
Methanol	48~42	52	30
Tetrahydrofuran	47~40	41	38
Acetone	45~40	47	42
Methyl acetate	40~33	36	47
Benzene	45~40	31	60

* Propargyl alcohol ** Butynediol
Reaction temperature: 110°C
Reaction time: 8 hr.
Paraformaldehyde (15 g.) and 100 g. of solvent were used.

Table II. Effects of the reaction temperature

Reaction temp. °C	Reaction pressure kg./cm²	Yield of PA* %	Yield of BD** %
90~100	42~23	28	31
100~110	40~25	32	45
110~120	40~22	36	49

* Propargyl alcohol ** Butynediol
Reaction time: 8 hr.
Paraformaldehyde (20 g.) and 100 g. of methanol were used.

Table III. Effects of reaction pressure

Amount of acetylene charged g.	Reaction pressure kg./cm²	Yield of PA* %	Yield of BD** %
28	40~25	41	37
14	26~15	32	43
8	15~ 2	10	62

* Propargyl alcohol ** Butynediol
Reaction temperature: 110~120°C
Reaction time: 6 hr.
Paraformaldehyde (20 g.) and 100 g. of methanol were used.

affected by the reaction temperature. Under 100°C, the conversion was low.

Results under various pressure are shown in Table III. Similar to the case of aqueous formaldehyde, the distribution of the products depended upon the reaction pressure—the higher the reaction pressure, the higher the yield of propargyl alcohol.

Table IV. Effects of paraformaldehyde concentration

Concn.	Reaction pressure	Yield of PA*	Yield of BD**
%	kg./cm²	%	%
10	50～44	56	26
20	45～35	41	37
30	43～22	32	45
50	50～30	24	52

* Propargyl alcohol ** Butynediol
Reaction temperature: 110～120°C
Reaction time: 8 hr.
A mixture (100 g.) of paraformaldehyde and methanol was used.

Table V. Oxydative coupling of propargyl alcohol

Reaction temp.	Reaction time	PA* : CuCl	Yield of hexadiynediol
°C	hr.	mol. ratio	%
20～25	8	2～4 : 1**	75
25～25	8	16 : 1	58
50～60	1	16 : 1	93
60～70	1	16 : 1	80
75～80	1	32 : 1	71

* Propargyl alcohol
CuCl (6 g.), NH_4Cl (19 g.), H_2O (60 ml.) and propargyl alcohol (56 g.) were used.
** The molar ratio of propargyl alcohol to cuprous chloride was maintained at ratio of 2～4 : 1 by adding propargyl alcohol at intervals.

The effects of paraformaldehyde concentration are shown in Table IV. With increase of the concentration of paraformaldehyde, the relative yield of propargyl alcohol decreased, but the effect was not so noticeable as in the case of aqueous formaldehyde. Therefore, for the purpose of preparing propargyl alcohol batchwise in the laboratory, it is advisable to increase the concentration of paraformaldehyde.

Oxydative Coupling of Propargyl Alcohol.—Hexadiynediol was prepared by the method using air and cuprous chloride catalyst. Reppe[20] described that the molar ratio of propargyl alcohol to cuprous chloride should be maintained at the most favorable ratio of 2 : 1 to 4 : 1 by adding propargyl alcohol at intervals.

The results in Table V show that even at the ratio of 16 : 1, hexadiynediol was easily obtained in a high yield by elevating the reaction temperature to 50～60°C.

Hydrogenation of Hexadiynediol.—Hydrogenation of hexadiynediol in the presence of Raney nickel W-6 proceeded smoothly in methanol solution to give 93% yield of 1, 6-hexanediol. If an unpurified sample containing copper ions is used, a small amount of zinc dust should be added to prevent deactivation of the catalyst.

Dehydrogenation of 1, 6-Hexanediol.—Some of the results obtained in dehydrogenation of 1, 6-hexanediol with numerous mixed catalysts are shown in Table VI. Similar to the previous study[1], a sample was passed in with a steady current of hydrogen. The yields of ε-caprolactone were based upon the amounts of hexanediol consumed. With all the catalysts, the reaction was very slow as compared with that of 1, 4-diols or 1, 5-diols. With the elevation of the reaction temperature, the amount of the forerun increased and the product decreased. With copper-magnesium oxide, it was ascertained

Table VI. Dehydrogenation of 1, 6-hexanediol with mixed catalysts

Catalyst	Reaction temp.	Sample	Product	Forerun	Yield of lactone	Sample recovered	Conversion
	°C	g.	g.	g.	g.	g.	%
Cu-MgO	280	17	11	7.5	0.5	3.0	82
Cu-ZnO	280	12	9	1.2	—	7.0	42
$CuCrO_2$	280	14	10	4.5	2.2	1.0	93
	230	12	10	3.2	2.7	2.3	79
$CuCrO_2$-Al_2O_3	230	14	11	2.5	4.5	3.8	80
$CuCrO_2$-Fe_2O_3	230	12	11	2.0	2.0	5.0	58
$CuCrO_2$-CdO	230	12	9	3.7	0.8	3.0	75
$CuCrO_2$-ZnO	280	14	11	3.0	4.5	2.0	86
	230	13	12	2.3	5.4	3.2	75

Reaction time: 3 hr.

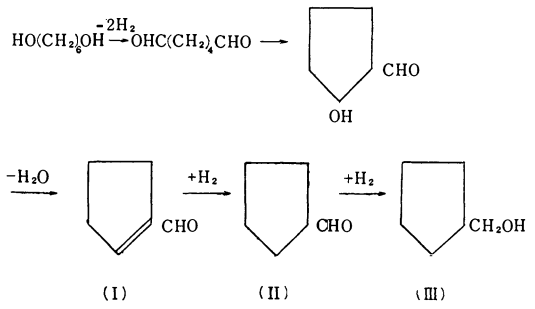
20) W. Reppe et al., *Ann.*, **596**, 51 (1955).

TABLE VII. EFFECTS OF CATALYST COMPOSITION

Catalyst composition (mol. ratio)			Yield of lactone	Sample recovered	Conversion
CuO	Cr_2O_3	ZnO	g.	g.	%
1	0.5	0.5	7.4	2.8	83
1	0.5	1	6.8	4.5	70
1	0.5	2	6.3	4.5	70
1	0.5	3	6.2	3.5	78
2	0.5	1	7.6	3.4	77
3	0.5	1	3.8	4.5	70
1	1	1	Inactive		
1	0.25	1	7.0	4.2	72
1	0.25	2	4.5	5.0	67

The sample (15 g.) was used in each experiment.

that the forerun contained cyclopentyl carbinol (III) and a small amount of cyclopentane carboxyaldehyde (II). This fact suggested the occurrence of the following side reactions.



Copper-chromite catalyst, which had been used for preparing γ-lactones or δ-lactones in the literatures, gave ε-caprolactone in 30% yield in the present work. It was observed that zinc oxide improved the selectivity of copper chromite for the ε-lactone formation.

The relationship between catalytic activity or selectivity and the composition of copper chromite-zinc oxide catalyst was shown in Table VII. In these experiments, the pressure in the reaction system was kept at 5~10 mmHg and the sample was passed in by vacuum distillation. The reaction temperature was maintained at 210~220°C and the reaction time was four hours. The catalysts were prepared by a modification of the procedure for preparing Adkins' copper chromite. The composition of the catalyst has considerable effects on the yield and conversion. The most favorable catalyst giving ε-caprolactone in a 68% yield and in a 78% conversion, had the composition of $CuO : Cr_2O_3 : ZnO = 2 : 0.5 : 1$. The catalysts which contained one of the components excessively lowered both the activity and selectivity. It was also ascertained that the forerun in these experiments contained 1-cyclopentene-1-carboxaldehyde (I).

The author wishes to express his sincere thanks to Professor Sango Kunichika of Kyoto University, for his invaluable advices and discussions. He also thanks Mrs. Chieko Tsuda for the elementary analyses.

Institute for Chemical Research
Kyoto University
Takatsuki, Osaka

Rotatory Dispersion of Metallic Co-ordination Compounds. III. Absorption Spectra and Rotatory Dispersion of Cobalt(III) Complexes of the $[CoN_2O_4]^-$ Type

By Jinsai HIDAKA, Yoichi SHIMURA and Ryutaro TSUCHIDA

(Received July 29, 1961)

In a former paper of this series[1], the relation between the absorption band and the optical rotatory dispersion of D-[Co edta]$^-$ was discussed. In consequence of this study, the splitting of the first absorption band was considered to be of importance for analyses of the so-called "anomalous" rotatory dispersion curve. In order to study the above problem in more detail, the present paper deals with the absorption spectra and optical rotatory dispersion of the cobalt(III) complex ion which belongs to the general type $[Co\ N_2O_4]^-$, where N and O represent respectively a nitrogen and an oxygen atom of ligands attached directly to the central cobalt(III) ion.

There have been a few reports[2] concerning the preparations and the absorption spectra of the complexes of this type, besides some reports concerning Co(III)-EDTA complexes. The trend of splitting of the first absorption band of those complexes, however, has not completely been clarified up to the present. In the present paper, therefore, the absorption spectra of *cis*(N)-K[Co(ada)$_2$]·2.5 H_2O, *trans*-(N)-K[Co(ada)$_2$]·2H_2O and *cis*(N)-K[Co(ata)·gly]·2 H_2O, which were newly synthesized, will be discussed, mainly in relation to the geometrical struture of the complex ions*.

Furthermore, the absorption spectra and the optical rotatory dispersion of Na[Co en ox$_2$]·H_2O and K[Co en malo$_2$]·H_2O, which were recently resolved by Dwyer et al.[3], will be studies in the same way as was done in a former paper[1].

The absorption spectra of the complexes employed will also be considered for spin-forbidden transition bands, i. e., the so-called "A band" and "B band", in the near-infrared region.

1) J. Hidaka, Y. Shimura and R. Tsuchida, This Bulletin, 33, 847 (1960).

2) M. Mori, M. Shibata, E. Kyuno and T. Adachi, ibid., 29, 883 (1956); 31, 296 (1958).

* The sign ada represents a divalent ammoniadiacetate anion $NH(CH_2COO)_2^{2-}$ and ata, a trivalent ammoniatriacetate anion $N(CH_2COO)_3^{3-}$.

3) F. P. Dwyer, I. K. Reid and F. L. Garvan, *J. Am. Chem. Soc.*, 83, 1285 (1961).

Experimental

Preparation. — *cis(N)-K[Co(ada)$_2$]·2.5 H_2O.* — In a solution of 7 g. adaH_2 in 40 ml. of water containing 5.5 g. of potassium hydroxide, 5 g. of cobalt chloride hexahydrate was dissolved. The mixture was cooled in an ice bath, and 15 ml. of 15% hydrogen peroxide was added drop by drop to the mixture. To complete the reaction the mixture was stirred and the desired complex gradually separated out. After being kept for several hours in a refrigerator, the reddish violet crystals deposited were separated by suction and recrystallized from a little water by the usual procedure. The crude product was contaminated by yellowish brown crystals, the solubility of which is comparatively smaller than that of the reddish violet crystals. Therefore, recrystallization was repeated to obtain the pure product.

After washing with a little ice water, ethanol and finally ether, the product was dried in the air.

Found: C, 26.40; H, 2.94; N, 7.74; H_2O, 11.15. Calcd. for K[Co($C_4H_5O_4N$)$_2$]·2.5 H_2O: C, 26.67: H, 2.79; N, 7.77; H_2O, 11.11%.

trans(N)-K[Co(ada)$_2$]·2 H_2O. — In a solution of 3.5 g.of adaH_2 and 3 g. of potassium hydroxide in 40 ml. of water, 2 g. of cobalt chloride hexahydrate was completely dissolved. The mixture was warmed at about 80°C on a water bath and oxidized with 1 ml. of 30% hydrogen peroxide. A yellowish brown crystalline solid was then gradually deposited. The reaction mixture was cooled to room temperature and filtered by suction. An additional crude product was also obtained by boiling the filtrate on a water bath for half an hour. The yield, in total, was almost quantitative. The crude product was recrystallized from hot water and washed with ethanol and ether.

Found: C, 25.93; H, 2.83; N, 7.65; H_2O, 8.75. calcd. for K[Co($C_4H_5O_4N$)$_2$]·2 H_2O: C, 26.67; H, 2.79; N, 7.77; H_2O, 9.09%.

cis(N)-K[Co(ata)gly]·2 H_2O. — Three grams of potassium acetate and 3 g. of glycine were dissolved in 30 ml. of warm water. To this solution 15 g. of β-K[Co(ata) (OH) (OH_2)]·3 H_2O[4] was added. The solution was warmed for about 20 min. on a water bath. After removal of the insoluble substance by filtration, the reddish violet solution was allowed to cool. A large amount of ethanol was added to

4) M. Mori, M. Shibata, E. Kyuno and Y. Okubo, This Bulletin, 31, 940 (1958).

it, and the solution was kept overnight in a refrigerator.

The reddish violet crystals deposited were collected and recrystallized from the cooled solution by the addition of ethanol. The final product was washed with ethanol and ether.

Found: C, 26.66; H, 2.84; N, 7.77; H_2O, 9.09. Calcd. for $K[Co(C_6H_6O_6N)(C_2H_4O_2N)]\cdot 2H_2O$: C, 26.67; H, 2.79; N, 7.77; H_2O, 9.12%.

Sodium dioxalato-ethylenediamine-cobaltate(III) monohydrate, Na[Co en ox_2]·H_2O, and potassium dimalonato-ethylenediamine-cobaltate(III) monohydrate, K[Co en $malo_2$]·H_2O, were prepared in violet crystals and resolved by the method of Dwyer and his co-workers[3]. The optical active complex of the former was precipitated as a more sparingly soluble salt with D-$[Co\ en_2(NO_2)_2]^+$, and the latter, with L-$[Co\ en_2(NO_2)_2]^+$.

The optically active dinitro bis-ethylenediamine-cobalt(III) ion, which gives a positive value of optical rotation for green lines of mercury, has been denoted as a D-isomer. Potassium dicarbonato-diammine-cobaltate(III) monohydrate, $K[Co(NH_3)_2\cdot(CO_3)_2]\cdot H_2O$ was prepared by the method of Mori and his co-workers[2].

Measurements.—The visible and ultraviolet absorption measurements were made by a Beckman DU spectrophotometer in aqueous solutions. The infrared spectra were obtained with a Parkin-Elmer model 21 (double beams) and a Hilger H-800 infrared spectrophotometer with sodium chloride prisms. The potassium bromide disk method was employed. The rotatory dispersion measurements were carried out in aqueous solutions with a Rudolph photoelectric spectropolarimeter, model 200 S-80. The concentration of the solution was 5.0×10^{-2} g. complex ion per liter.

All the measurements were made at room temperature.

Results and Discussion

Absorption Spectra.—The visible and ultraviolet absorption curves of the violet form and the brown form of bis-ammoniadiacetato-cobaltate(III) are shown in Fig. 1, in which the curve of Na[Co edta][5] is also plotted for comparison. The frequencies of the absorption maxima are summarized in Table I with other numerical data. As is seen in Fig. 1, the absorption curves of the violet form and of Na[Co edta] are similar on the whole. On the contrary, the absorption curve of the brown form differs distinctly; namely, the first absorption band I remarkably splits into two components Ia and Ib, and the second band II is shifted towards a shorter wavelength than those of the other two complexes. As will be seen in the figure, the main difference between the curves of the two isomers occurs in the region of the first band. In the absorption curve of the violet form, a component

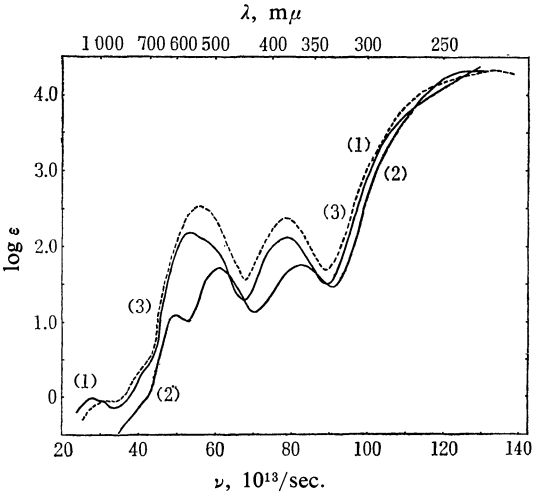


Fig. 1. Absorption spectra of:
1, *cis*(N)-K[Co(ada)$_2$]·2H_2O (violet form)
2, *trans*(N)-K[Co(ada)$_2$]·2H_2O (brown form)
3, Na[Co edta]·4H_2O (dotted curve)

band which is smaller in intensity is recognized in the shorter wavelength side of the first band maximum, at about 58×10^{13}/sec.

Judging from the symmetry of the complex ion, it can reasonably be considered that its first absorption band also splits into two components, Ia and Ib. This fact coincides with the conclusion of the analysis of the optical rotatory dispersion curve of D-K[Co edta][1] in the first absorption band. In the absorption curve of the brown form, the absorption component of the longer wavelength side is smaller in intensity than the component of the shorter wavelength side, and the difference is remarkable. From these trends in the splittings in the first absorption band, therefore, it is concluded that the violet form has one configuration in which the two nitrogen atoms occupy the cis-positions of a coordination octahedron, while the brown form has another configuration in which the two nitrogen atoms occupy trans-positions.

Some similar cases were reported by Linhard and Weigel[6]. Such assignments are also supported by Yamatera from semi-empirical molecular orbital calculations[7].

Three geometrical isomers are possible for the complex ion, $[Co(ada)_2]^-$, as shown in Fig. 2. Two isomers of the trans(N)-form, II and III, are possible. Judging from the bond angles of a nitrogen atom of the ligand, the type suitable for the brown form may be assigned to the structure II.

5) Y. Shimura, J. Fujita and R. Tsuchida, presented at the Symposium on Co-ordination Compounds, Fukuoka, October, 1959.

6) M. Linhard and M. Weigel, *Z anorg. Chem.*, **264**, 321 (1951).

7) H. Yamatera, This Bulletin, **31**, 95 (1958).

TABLE I. ABSORPTION DATA OF Co(III) COMPLEXES $[Co\,N_2O_4]^-$ TYPE

Complex	A band ν_{max} 10^{13}/sec. (log ε_{max})	B band ν_{max} 10^{13}/sec. (log ε_{max})	I band* ν_{max} 10^{13}/sec. (log ε_{max})	II band ν_{max} 10^{13}/sec. (log ε_{max})	Spec. band ν_{max} 10^{13}/sec. (log ε_{max})	Ref.
Na[Co edta]·4 H_2O	30.8($\bar{1}$.96)	ca. 43(0.4)	55.9(2.51)	78.1(2.36)	133(4.33)	5)
cis(N)-K[Co(ada)$_2$]·2.5 H_2O	28.4(0.00)*3	ca. 41(0.2)	53.4(2.18)	79.0(2.13)		
trans(N)-K[Co(ada)$_2$]·2 H_2O			Ia : 61.2(1.72) Ib : 50.0(1.06)	83.3(1.75)		
cis(N)-K[Co(ata)gly]·2 H_2O	27.3(0.07)	ca. 40(0.3)	53.0(2.35)	78.2(2.23)		
cis(N)-K[Co$(NH_3)_2(CO_3)_2$]·3 H_2O*2	27.3(0.64)	ca. 40(0.9)	52.2(2.24)	76.0(2.41)		
cis(N)-NH_4[Co$(NH_3)_2$ ox$_2$]·H_2O	31.2(0.02)	ca. 42(0.3)	54.0(2.04)	78.2(2.30)	128.8(4.26)	5)
Na[Co en ox$_2$]·H_2O	33.3($\bar{1}$.91)	ca. 44(0.2)	55.6(1.93)	77.9(2.12)	127.1(4.19)	
K[Co en malo$_2$]·H_2O	33.3(0.02)	ca. 43(0.2)	55.6(1.96)	77.9(2.08)		

*1 Expressed by the value of (Ia+Ib) except in the case of a trans(N)-form.
*2 Measured in saturated aq. soln. of ammonium carbonate.
*3 A sub-maximum was recognized in the shorter wavelength side : ca. 31($\bar{1}$.95).

TABLE II. ABSORPTION MAXIMUM AND INVERSIVE ROTATORY DISPERSION

Complex	ν_{abs} 10^{13}/sec. (log ε_{max})	ν_{rot} 10^{13}/sec.	Sign of Cotton effect	Degree of rotation*
Na[Co en ox$_2$]	55.6(1.93)	52	(−)	4500°
		60	(−)	1500°
K[Co en malo$_2$]	55.6(1.96)	50	(−)	4500°
		56	(+)	6000°

ν_{abs} : Absorption maximum
ν_{rot} : Center of inversive rotatory dispersion
* The difference between the maximum and the minimum value of the partial inversive rotatory dispersion was halved.

The absorption curves of ptassium glycinato-ammoniatriacetato-cobaltate(III) and potassium dicarbonato-diammine-cobaltate(III) are shown in Fig. 3.

As is seen in Figs. 1 and 3 and in Table I, the absorption spectra are quite similar in appearance to the absorption spectrum of the violet form of the bis-ammoniadiacetate-cobaltate(III) ion mentioned above and have a shoulder in the shorter wavelength side of the first band maximum. It is concluded, therefore, that probably these complexes also have a cis-structure involving the two nitrogen atoms of the ligands.

In Figs. 4 and 5, the absorption curves of sodium dioxalato-ethylenediamine-cobaltate(III) and potassium dimalonato-ethylenediamine-cobaltate(III) are shown with the optical rotatory dispersion curves of these complexes. The absorption curves of both the complexes are quite similar to that of Na[Co edta]. The oxalato complex involves two 5-membered chelate rings involving oxygen atoms of the ligands, while the malonato complex contains two 6-membered rings. This difference in structure was not reflected in the appearance of the absorption spectra. However, since the malonato complex is less stable than the oxalato complex in aqueous solution, no absorption spectra of the former were measured in the far ultraviolet region. As will be seen in Figs.

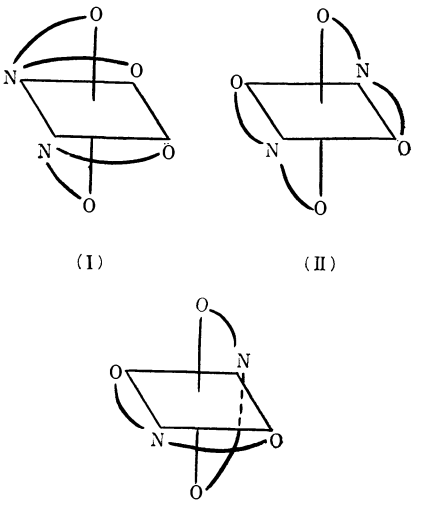


Fig. 2. The possible three geometrical isomers of $[Co(ada)_2]^-$.

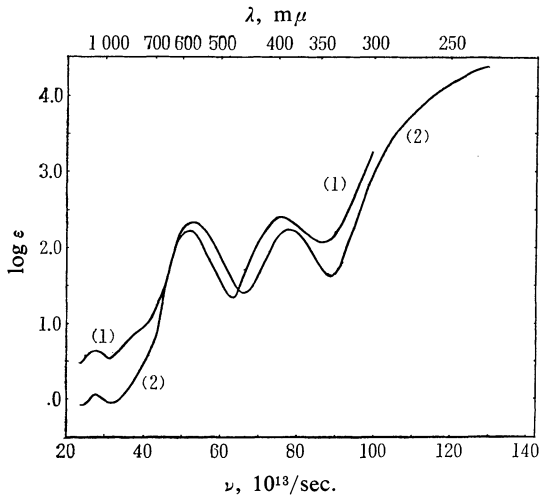


Fig. 3. Absorption spectra of:
1, *cis*(N)-K[Co$(NH_3)_2(CO_3)_2$]·3 H_2O
2, *cis*(N)-K[Co(ata)gly]·2 H_2O

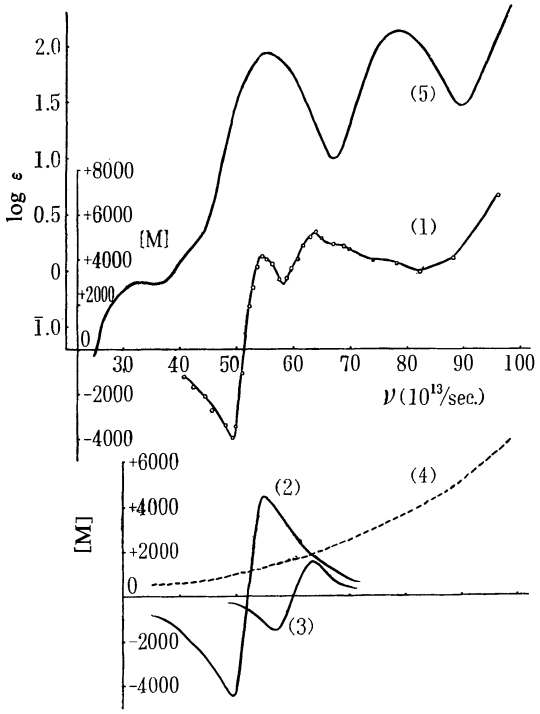


Fig. 4. Rotatory dispersion and absorption of Na[Co en ox_2]:
1, Rotatory dispersion curve; 2—4, Curve analyses of the rotatory dispersion curve; 5, Absorption curve.

1, 3, 4 and 5 and in Table I in the present work, spin-forbidden transition bands are observed in the near-infrared region. After Linhard's notation[8], they can be described as

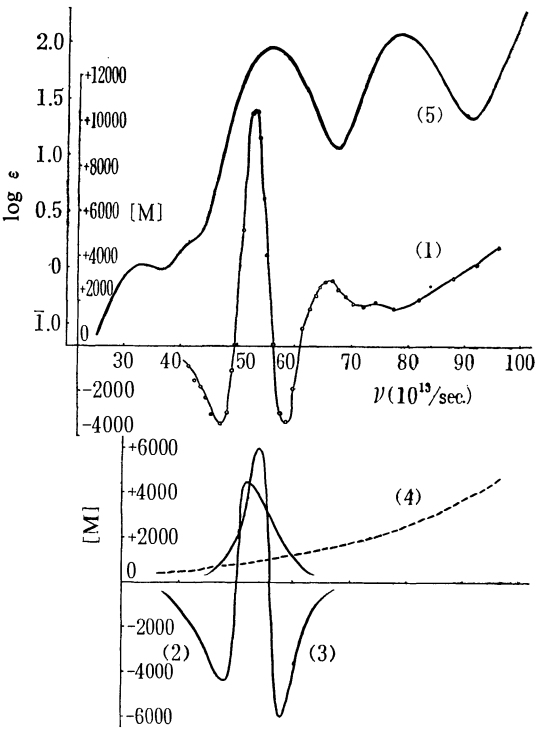


Fig. 5. Rotatory dispersion and absorption of K[Co en $malo_2$]:
1, Rotatory dispersion curve; 2—4, Curve analyses of the rotatory dispersion curve; 5, Absorption curve.

follows: the band in the longer wavelength is the "A bond", and the one in the shorter wavelength, the "B band".

The intensity of the A or B band is found to be about hundredth as weak as that of the first band. The appearance and behavior of the A band are closely related to those of the first band[5]. Frequency differences between the first and the A bands show almost a constant value.

The shape of the A band may suggest that the band splits into some component bands, as does the first band.

The optical resolution of the potassium *cis*(N)-bis-ammoniadiacetato-cobaltate(III) complex was not studied in this work. Further studies will be carried out in the future.

Infrared Absorption Spectra. — Infrared absorption spectra of the three new complexes were measured to confirm that the carboxylate groups were coordinated. It is well known that the carboxylate group in general exhibits strong split bands in the region between 1550 and 1750 cm^{-1} for the free acids. All the spectra of the complexes studied show bands at 1625 and 1660 cm^{-1}.

It is obvious that these bands are due to

8) M. Linhard and M. Weigel, *Z. physik. Chem., N F.*, **11**, 308 (1957).

coordinated carboxylate groups. Similar assignments have been established for some EDTA-complexes by Bush and Bailar[9].

Rotatory Dispersion.—The rotatory dispersion curves and the absorption curves of D-Na[Co en ox_2] and D-K[Co en $malo_2$] are shown in Figs. 4 and 5 and in Table II. The observed curves were analyzed on the basis of the following consideration: It is assumed that the observed curve is the superposition of several partial inversive dispersions[10] and a tail of normal dispersion which has its characteristic frequency in the ultraviolet region.

As is seen in the figures, both the observed curves are apparently displaced to the positive sign. Therefore, the positive tail of the normal dispersion has been presumed to be present. The rotatory dispersion behavior of D-[Co en ox_2]$^-$ in its first absorption band suggests that an overlapping of two inversive dispersions occurs. As a result of curve analyses, it has been shown that the observed curve I is reproduced by the overlap of curves 2, 3 and 4.

Thus, it is concluded that the first absorption band of this complex shows two inversive dispersions and that these two inversive dispersions have the negative signs of the Cotton effect equally. As was described in the preceding section, it is expected that the first absorption band of this complex splits into two components, Ia and Ib.

The two inversive dispersions above obtained, therefore, probably correspond to the two components. There is a small hump at about 75~84(10^{13}/sec.) in the rotatory dispersion.

This is similar to the hump in the second absorption band of an active trioxalato cobalt(III) complex ion which was reported by Kuhn and Bein[11]. It may be considered, therefore, that an inversive dispersion which belongs to the second absorption band also contributes to the observed rotatory dispersion.

The complex ion, D-[Co en $malo_2$]$^-$, also shows two inversive dispersions in the region of the first absorption band, as is seen in Fig. 5. In this case, however, two inversive dispersions which correspond to the two absorption components have different signs of the Cotton effect. The one in the longer wavelength has a negative sign, and the other in the shorter wavelength, a positive one, although the magnitude of these two partial dispersions has been found to be of the same order. The degree of rotation is greater in the malonato complex than in the oxalato complex.

The reason for this difference is unknown, but it may be due to the difference between the 5-membered chelate ring of a dioxalato complex ion and the 6-membered ring of a dimalonato complex ion, although no evidence for this is observed in the absorption curves. The behavior of the dispersion curve in the region of the second absorption band is similar to that of the dioxalato complex ion, and a small hump probably belongs to the second absorption band.

Summary

Three new complexes, *cis*(N)-K[Co(ada)$_2$]·2.5 H_2O, *trans*(N)-K[Co(ada)$_2$]·2 H_2O and *cis*(N)-K[Co(ata)gly]·H_2O, have been synthesized. The visible and the ultraviolet absorption spectra of these complexes have been measured and discussed in relation to the geometrical structures of the complex ions compared with other complexes of the [Co N_2O_4]$^-$ type. Rotatory dispersion measurements have also been made for D-Na[Co en ox_2] and D-K[Co en $malo_2$].

It has been shown that the so-called anomalous rotatory dispersions of these complexes are explicable by assuming the overlap of the two inversive dispersions in their first absorption bands. The slight inversive dispersions are also observed in their second absorption band.

Department of Chemistry
Faculty of Science
Osaka University
Nakanoshima, Osaka

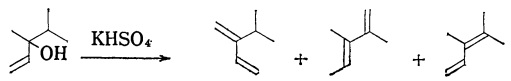
9) D. H. Bush and J. C. Bailar, Jr., *J. Am. Chem. Soc.*, **75**, 4574 (1953); **78**, 716 (1956).
10) J.-P. Mathieu, *Compt. rend.*, **199**, 278 (1934); J.-P. Mathieu, ibid., **201**, 1183 (1935); J.-P. Mathieu, *Bull. soc. chim. France*, [5], **3**, 476 (1936).
11) W. Kuhn and K. Bein, *Z. anorg. Chem.*, **216**, 321 (1934).

Isolation of 3, 4-Dimethylpenta-1, 3-diene

By Toshiaki NISHIDA, Atsuaki ARAI and Iwao ICHIKIZAKI

(Received July 29, 1961)

In an attempt[1] to prepare 3, 4-dimethylpenta-1, 3-diene (I) by dehydrating 3, 4-dimethylpent-1-en-3-ol with potassium hydrogen sulfate, it was noticed that the major products were three isomeric dienes, i. e., 2-isopropylbutadiene (II) (53%), 2, 3-dimethylpenta-1, 3-diene (III) (21%) and I (18%). Although the latter two compounds had not yet been isolated in pure forms, each structure was assigned by chemical transformation of the enriched sample.



II III I

Since the separation of I and III was not sufficiently achieved by fractional distillation, gas chromatography (Carbowax 6000 on firebrick) was successfully employed for the complete fractionation of these two isomers, whose structures were confirmed on the basis of spectral evidences.

The compound (n_D^{20} 1.4625), with a shorter retention time, was a colorless liquid, and its ultraviolet absorption maximum at 232 mμ (ε=22900 in hexane) was in agreement with the calculated value of a trisubstituted butadiene[2]. Infrared absorption bands at 1640 and 1610 cm^{-1} exhibited the presence of cojugated diene, and strong bands at 880 and 830 cm^{-1} were indicative of unsym-disubstituted and trisubstituted double bonds respectively. Therefore, this compound must be 2, 3-dimethylpenta-1, 3-diene (III). Independent confirmation of this was provided by the NMR spectrum[3] (Fig. 1), which displayed a quartet centered at δ=5.62 p. p. m. (J=6.10 c. p. s.) attributable to an olefinic proton having been split by an adjacent methyl group[4]. Two peaks of almost equal intensity at 4.77 and 4.65 p. p. m. were assigned to the two non-equivalent protons of a terminal methylene group. Two peaks at 1.72 and 1.62 p. p. m. can be associated with two methyl groups on double bond, while a doublet (one of which was overlapping on the peak at 1.62 p. p. m.) centered at 1.57 p. p. m. was due to the methyl group having been split by the adjacent olefinic proton.

Another one (n_D^{20} 1.4729), with a longer retention time, was a colorless liquid and had a

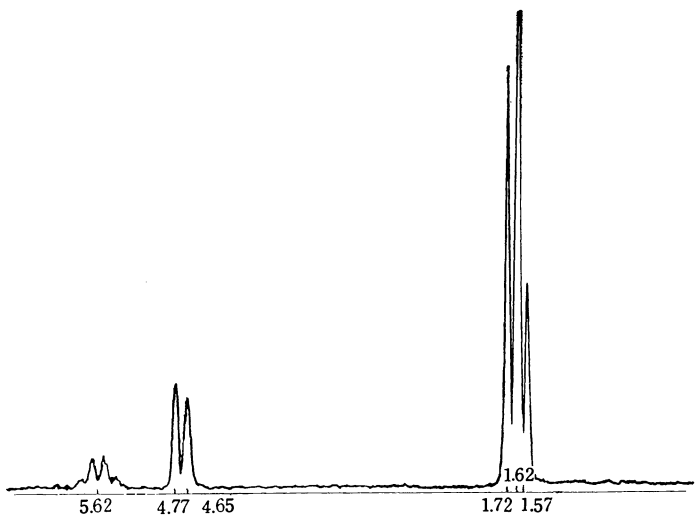


Fig. 1. NMR Spectrum of III.

1) A. Arai and I. Ichikizaki, This Bulletin, 35, 45 (1962).
2) R. B. Woodward, *J. Am. Chem. Soc.*, 64, 72 (1942).
3) NMR Spectra were determined at 60 Mc. using CCl_4 as solvent and siloxane (δ=0.10 p. p. m.) as an internal standard. The chemical shifts were recorded in δ-values (C. Djerassi, T. Nakano, A. N. James, L. H. Zalkow, E. J. Eisenbraun and J. N. Shoolery, *J. Org. Chem.*, 26, 1192 (1961)).
4) L. M. Jackman, "Application of Nuclear Magnetic Resonance Spectroscopy in Organic Chemistry", Pergamon, London (1959), p. 85.

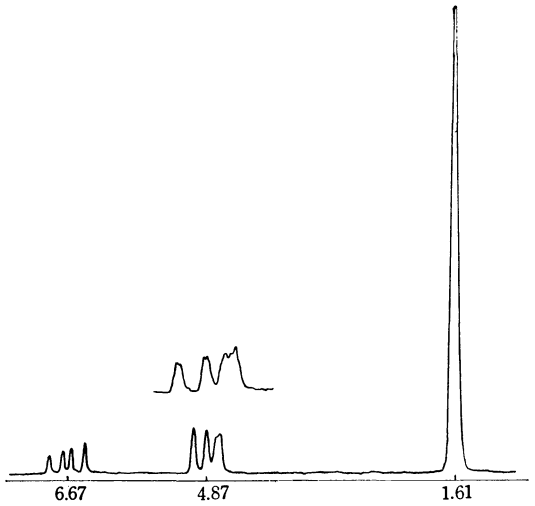


Fig. 2. NMR Spectrum of I.

tendency to polymerize rapidly on standing. Although the ultraviolet absorption spectrum exhibited a bathochromic shift of about 7 mμ[5] (λ_{max} 239 mμ; ε=27700 in hexane) from the calculated value[2], the infrared spectrum showed conjugated diene absorption bands at 1635 and 1605 cm^{-1} and characteristic bands of the vinyl group at 982 and 888 cm^{-1}. Therefore, these pieces of evidence strongly supported the theory that this compound was 3, 4-dimethylpenta-1, 3-diene (I). Finally, the NMR spectrum provided an elegant confirmation of the structure. The spectrum (Fig. 2) showed a typical ABC pattern[6] attributable to the grouping $-CH=CH_2$ with a quartet centered at 6.67 and eight uncompletely resolved lines centered at 4.87 p. p. m. The protons of the methyl groups showed a single peak at 1.61 p. p. m.

As to the mixture of I and III, there was observed a linear relationship between the refractive index and the relative concentration, and the value (1.4729) of our purest sample I was in good agreement with that for I obtained by graphical extrapolation. Although Nazarov and Mavrov[7] have reported the value (1.4691) for the refractive index of I, graphical estimation of their value shows that their hydrocarbon undoubtedly contains a large amount of III and/or other substances. Furthermore, it is noteworthy that, contrary to some claims[7,8], pure diene I did not afford a Diels-Alder adduct with crotonaldehyde even under conditions so drastic as to cause polymerization or isomerization of the diene. The details of this work will be reported elsewhere.

The authors wish to thank Drs. Yoichiro Mashiko, Kenkichi Nukada and Akio Suzuki of Government Chemical Industrial Research Institute of Tokyo for their measurement of the NMR spectra.

Laboratory of Organic Chemistry
Kobayasi Institute of Physical Research
Kokubunji, Tokyo

5) Although it is at present unexplained, this effect can be expected by comparison with the similar bathochromic shift reported in the spectrum of 4-methylpenta-1, 3-diene (λ_{max} 234 mμ in hexane) (I. N. Nazarov and M. V. Mavrov, *Izvest. Akad. Nauk. S. S. S. R., Otdel. Khim. Nauk.*, **1959**, 472).

6) J. A. Pople, W. G. Schneider and H. J. Bernstein, "High-resolution Nuclear Magnetic Resonance", McGraw-Hill, New York (1959), p. 241.

7) I. N. Nazarov and M. V. Mavrov, *Zhur. Obshchei Khim.*, **29**, 1158 (1959).

8) Y. R. Naves and P. Ardizio, *Helv. Chim. Acta*, **31**, 2252 (1948).

Reactions of Active Methylene Compounds. VII. Synthesis of Benzofuro[3′, 2′ : 3, 4]coumarins and 2-Phenylbenzo[b]-furans

By Yoshiyuki KAWASE

(Received August 1, 1961)

In previous papers[1] was reported the action of hydrohalogenic acids, of aluminum chloride and of pyridine hydrochloride on 2-methoxybenzoyl-phenylacetonitriles and related esters. The present paper describes the action of the same reagents on 2-methoxybenzoyl-2-methoxyphenylacetonitriles (Ia, b) and related esters (IIa, b) to give 2-hydroxyphenyl 2-methoxybenzyl ketones (IIIa, b), benzofuro[3′, 2′ 3, 4]-coumarins (IVa, b, b′) and 2-phenylbenzo[*b*]-furans (Va, b′, IX).

1) Y. Kawase, This Bulletin, **31**, 390, 440 (1958); **32**, 9, 11 (1959); *Experientia*, **14**, 435 (1958).

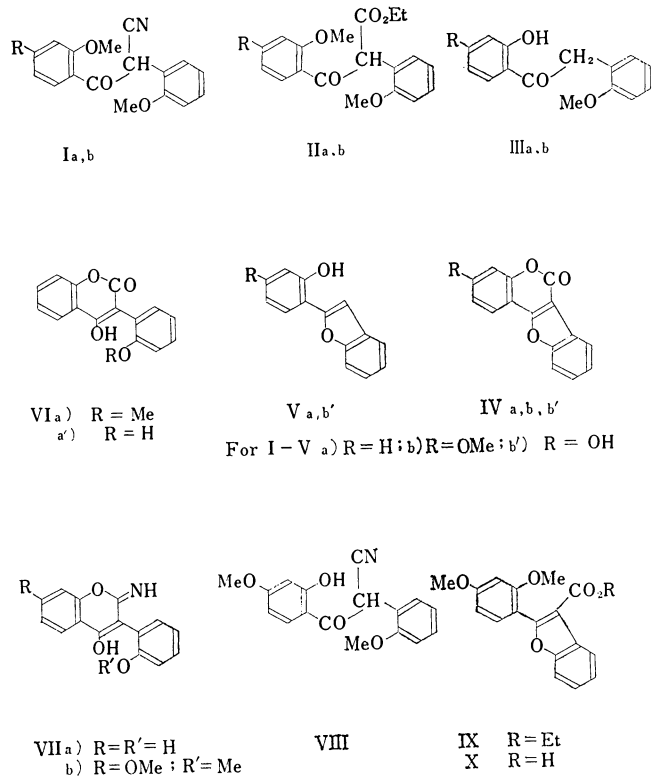


Chart 1

Recently, four derivatives of benzofurocoumarin (wedelolactone[2], coumestrol[3], erosnin[4] and psoralidin[5]) have been isolated from natural sources, and the synthesis of benzofurocoumarins has already been carried out by the action of hydrohalogenic acid, of pyridine hydrochloride, or of aniline hydrochloride on 3-(2-methoxyphenyl)-4-hydroxycoumarins[6] and on 2-methoxybenzoyl-2-methoxyphenylacetonitriles[7]. Also, the formation of 2-phenylbenzofurans has been achieved by the ring closure of 2'-methoxydeoxybenzoins[8] or ω-phenoxyacetophenones[9] and by the interaction of 2-hydroxybenzaldehyde with ethyl α-bromophenylacetates[10].

In the present experiments, benzofurocoumarins (IVa, b, b') were obtained from nitriles Ia, b by the action of hydrobromic or hydroiodic acid in acetic acid or of pyridine hydrochloride, and from esters IIa, b by the action of hydroiodic acid as the main product. It seems that in these cases the reagents cause first a cleavage of the methoxy group ortho to the carbonyl before that cleavage of the nitrile or ester group which forms the coumarin-ring. On the other hand, the action of hydrochloric acid on nitriles Ia, b or esters IIa, b gave deoxybenzoin derivatives, (IIIa, b), while that of hydrobromic acid or pyridine hydrochloride on esters IIa, b gave 2-phenylbenzofurans (Va, b'). In these cases the reagents cause first a cleavage of the nitrile or ester group, followed by that of the methoxy group, furnishing IIIa, b and Va, b' respectively. The action of aluminum chloride on nitrile Ia or ester IIa gave benzofurocoumarin (IVa) through each intermediate, 4-hydroxycoumarin-2-imide derivative (VIIa) or 4-hydroxycoumarin derivative (VIa), but that on nitrile Ib or ester IIb gave only partialy demethylated products,

2) T. R. Govindachari et al., *J. Chem. Soc.*, **1956**, 629; **1957**, 545.
3) E. M. Bickoff et al., *J. Am. Chem. Soc.*, **80**, 3969 (1958).
4) J. Eisenbeiss and H. Schmid, *Helv. Chim. Acta*, **42**, 61 (1959).
5) P. C. Duttagupta et al., *Chem. and Ind.*, **1960**, 937.
6) W. J. Bowyer et al., *J. Chem. Soc.*, **1957**, 542; T. R. Govindachari et al., ibid., **1957**, 548; O. H. Emerson and E. M. Bicoff, *J. Am. Chem. Soc.*, **80**, 4381 (1958); C. Deschamps-Vallet and C. Mentzer, *Compt. rend.*, **251**, 736 (1960).
7) J. N. Chatterjea and S. K. Roy, *J. Indian Chem. Soc.*, **34**, 98 (1957); J. N. Chatterjea, ibid., **36**, 256 (1959); Y. Kawase, This Bulletin, **32**, 690 (1959).
8) F. B. LaForge, *J. Am. Chem. Soc.*, **55**, 3040 (1933); W. B. Whalley and G. L. Lhoyd, *J. Chem. Soc.*, **1956**, 3213; M. Miyano and M. Matsui, *Chem. Ber.*, **91**, 2052 (1958); O. Dann et al., *Ann.*, **631**, 116 (1960).
9) W. Davies and S. Middleton, *J. Chem. Soc.*, **1958**, 822.
10) S. Kawai et al., *Ber.*, **72**, 1146 (1939).

TABLE I THE REACTION PRODUCTS

Reagent	Starting			
	Ia	Ib	IIa	IIb
HCl-AcOH	IIIa	IIIb	IIIa	IIIb
HBr-AcOH	IVa+IIIa	IVb+Vb'	Va	Vb'
HI-AcOH	IVa+VIa'	IVb'	IVa	IVb'
Pyridine-HCl	IVa+VIa'	IVb'	Va	Vb'
$AlCl_3$-$PhNO_2$	VIIa	VIII+VIIb	IVa+VIa	IX

2-hydroxy analog (VIII) of Ib and its ring-closed isomer 4-hydroxycoumarin-2-imide derivative (VIIb) or benzofuran-carboxylic ester derivative (IX) respectively, as is shown in Table I. The structures of VIa, a' and VIIa, b seem to be chromone derivatives, namely 2-hydroxy- and 2-amino-isoflavones respectively; the wave number of the carbonyl band is smaller than that of 4-hydroxycoumarins[1], e. g., IVa.

Experimental*

Preparation of the Starting Materials.—*2-Methoxybenzoyl-2-methoxyphenylacetonitrile (Ia).*—To a solution of methyl 2-methoxybenzoate (4 g.) and 2-methoxyphenylacetonitrile (3.5 g.) in anhydrous benzene (50 ml.) was added sodium hydride (1 g. or 1.7 mol.), and the mixture was refluxed for 4 hr. on an oil-bath (95~100°C), most of the benzene having been distilled off in the meantime. The well-cooled mixture was treated with a little ethanol and then with water, and was extracted with ether. The aqueous layer was acidified, and the solid product formed was collected, washed with aqueous sodium bicarbonate and recrystallized from ethanol as colorless prisms, m. p. 107~108°C; yield 2.8 g. or 42%, IR 2247 (CN), 1681 cm^{-1} (CO). Reported m. p. is 112°C[7].

Found: C, 72.92; H, 5.71; N, 5.11. Calcd. for $C_{17}H_{15}O_3N$: C, 72.58; H, 5.37; N, 4.98%.

Ethyl 2-Methoxybenzoyl-2-methoxyphenylacetate (IIa).—A solution of Ia (3.3 g.) in ethanol (50 ml.) containing one mole of water was saturated with dry hydrogen chloride, and was left at room temperature for 3 days. Water was added to the solution, and ethanol was removed in vacuo. The gummy product separated was dissolved in ethyl acetate, washed with aqueous sodium hydroxide, and then crystallized from dilute ethanol; m. p. 76~77°C, yield 2.2 g. or 57%, IR 1739 (ester), 1695 cm^{-1} (CO).

Found: C, 69.59; H, 6.42. Calcd. for $C_{19}H_{20}O_5$: C, 69.50; H, 6.14%.

The prerparation of nitrile Ib and ester IIb has been described in a previous paper[1].

Reaction with Hydrochloric Acid.—*Nitrile Ia to Give 2-Hydroxyphenyl 2-Methoxybenzyl Ketone (IIIa).*—A solution of Ia (0.5 g.) in acetic acid (10 ml.) containing concentrated hydrochloric acid (5 ml.) was heated on a steam-bath for 15 hr. The cooled solution was made alkaline with aqueous sodium hydroxide and was then extracted with ether. The residual product from the ether solution was distilled to give IIIa as colorless oil, b. p. 140~150°C/0.004 mmHg; yield 0.2 g. 2, 4-Dinitrophenylhydrazone, m. p. 188~189°C (from ethanol).

Found (for 2,4-dinitrophenylhydrazone): C, 59.82; H, 4.26; N, 13.18. Calcd. for $C_{21}H_{18}O_6N_4$: C, 59.71; H, 4.30; N, 13.27%.

Ester IIa to Give IIIa.—A similar treatment of IIa (0.5 g.) in acetic acid (10 ml.) with hydrochloric acid (5 ml.) gave 0.2 g. of IIIa; 2, 4-dinitrophenylhydrazone, m. p. 187~188°C.

Reaction with Hydrobromic Acid.—*Nitrile Ia to Give Benzofuro[3',2' : 3,4]coumarin (IVa) and IIIa.*—A solution of Ia (0.5 g.) in acetic acid (5 ml.) containing 48% hydrobromic acid (5 ml.) was refluxed on an oil-bath (140°C) for 3 hr. The cooled solution was diluted with water, made alkaline with aqueous sodium hydroxide, and then extracted with ether. The residual product from the ether solution was crystallized from methanol to give IVa as colorless needles, m. p. 180~180.5°C; yield 0.05 g., IR 1730 cm^{-1} (α-pyrone). Reported m. p. is 180~181°C[7] or 181~182°C[6].

Found: C, 76.29; H, 3.32. Calcd. for $C_{15}H_8O_3$: C, 76.27; H, 3.41%.

From the mother solution in the above-mentioned crystallization, 2, 4-dinitrophenylhydrazone of IIIa was obtained by the action of dinitrophenylhydrazine sulfate; m. p. 190~191°C.

Nitrile Ib to Give 3-Methoxybenzofuro[3',2' : 3,4]-coumarin (IVb) and 2-(2,4-Dihydroxyphenyl)-benzo[b]furan (Vb').—A similar treatment of Ib (0.5 g.) in acetic acid (5 ml.) with hydrobromic acid (5 ml.) gave IVb as slightly brown-colored needles, m. p. 192~193°C, 0.05g., from an alkali insoluble part through crystallization from ethanol.

Found: C, 72.32; H, 4.23. Calcd. for $C_{16}H_{10}O_4$: C, 72.18; H, 3.79%.

From a sodium hydroxide soluble part a small amount of Vb', m. p. 133~135°C (from benzene), was obtained through distillation; b. p. 180~200°C/0.004 mmHg, identical with the other sample.

Ester IIa to Give 2-(2-Hydroxyphenyl)-benzo[b]furan (Va).—A similar treatment of IIa (0.4 g.) in acetic acid (5 ml.) with hydrobromic acid (5 ml.) furnished Va, m. p. 93~94°C (form benzene), from an alkali insoluble part; yield 0.1 g. Reported m. p. is 95°C[7], 95~98°C[8] or 96~99°C[8].

Found: C, 79.96; H, 4.87. Calcd. for $C_{14}H_{10}O_2$: C, 79.98; H, 4.79%.

Ester IIb to Give Vb'.—A similar treatment of IIb (0.4 g.) in acetic acid (5 ml.) with hydrobromic acid (5 ml.) furnished Vb' as colorless needles,

* Melting and boiling points are uncorrected, and infrared spectra are measured in Nujol.

m. p. 136~138°C (from benzene), from a sodium hydroxyde soluble part through distillation in vacuo, b. p. 180~210°C/0.004 mmHg, identical with the other sample; yield 0.1 g.

Reaction with Hydroiodic Acid.—*Nitrile Ia to Give IVa and 3-(2-Hydroxyphenyl)-4-hydroxycoumarin (VIa').*—A mixture of Ia (0.5 g.), acetic acid (5 ml.), hydroiodic acid (d=1.7, 10 ml.) and acetic anhydride (5 ml.) was refluxed for 30 min. on an oil-bath (160°C) in a carbon dioxide atmosphere. The cooled solution was diluted with aqueous sodium bisulfite, made alkaline with aqueous sodium hydroxide, and then extracted with ether. From the ether extract, IVa (0.05 g.) was obtained; m. p. 176~177°C (from ethanol).

By acidifying the aqueous alkaline solution of the above-mentioned extraction, a small amount of VIa' was obtained; m. p. 250°C (from dilute ethanol), identical with the other sample.

Nitrile Ib to Give 3-Hydroxybenzofuro[3', 2', : 3, 4]-coumarin (IVb').—A similar treatment of Ib (1 g.) with hydroiodic acid (15 ml.) in acetic acid (7.5 ml.) and acetic anhydride (7.5 ml.) furnished IVb' as slightly brown-colored microcrystals (from ethanol) from a sodium hydroxide soluble part; m. p. 273~274°C, identical with the other sample. Acetate, colorless needles (from ethyl acetate), m. p. 210~211°C, identical with the other sample.

Ester IIa to Give IVa.—A similar treatment of IIa (0.5 g.) with hydroiodic acid (10 ml.) in acetic acid (5 ml.) and acetic anhydride (5 ml.) furnished IVa, m. p. 177~178°C (from ethanol), from an alkali insoluble part; yield 0.1 g.

Ester IIb to Give IVb'.—A similar treatment of IIb (0.5 g.) furnished IVb' as slightly brown-colored microcrystals, m. p. 274~275°C (from ethanol), identical with the other sample; yield 0.1 g.

Reaction with Pyridine Hydrochloride.—*Nitrile Ia to give IVa and VIa'.*—A mixture of Ia (0.5 g.) and anhydrous pyridine hydrochloride (2.5 g.) was refluxed for 40 min. on an oil-bath (220~230°C). Dilute hydrochloric acid was added to the cooled mixture, and the solution was warmed for several minutes on a steam-bath. The crystalline product formed on cooling was collected, washed with aqueous sodium hydroxide, and recrystallized from ethanol to give IVa, m. p. 176~177°C; yield 0.2 g.

By acidifying the alkaline solution in the above-mentioned washing, 0.1 g. of VIa' was obtained as colorless microcrystals, m. p. 261~262°C (decomp.) (from ethanol), IR 3390, 3205 (OH), 1664 cm^{-1} (γ-pyrone). The reported m. p. is 253°C[6]

Found: C, 70.63; H, 4.17. Calcd. for $C_{15}H_{10}O_4$: C, 70.86; H, 3.96%.

This VIa' was converted into IVa, m. p. 179~180°C, by heating at 280°C for 2 hr. following the method of Govindachari's report[6].

Nitrile Ib to Give IVb'.—A similar treatment of Ib (0.5 g.) furnished IVb' as slightly brown-colored microcrystals, m. p. 276~277°C (from ethanol); yield 0.2 g.

Found: C, 71.22; H, 3.34. Calcd. for $C_{15}H_8O_4$: C, 71.43; H, 3.20%.

Acetate was prepared by the pyridine-acetic anhydride method; colorless needles, m. p. 211~212°C (from ethyl acetate).

Found: C, 69.04; H, 3.17. Calcd. for $C_{17}H_{10}O_5$: C, 69.39; H, 3.43%.

Ester IIa to Give Va.—A similar treatment of IIa (0.4 g.) with pyridine hydrochloride (2 g.) furnished Va, m. p. 94~95°C (from benzene), from an alkali soluble part; yield 0.1 g.

Ester IIb to Give Vb'.—A similar treatment of IIb (0.4 g.) furnished Vb' as colorless needles, m. p. 137~139°C (from benzene); yield 0.1 g.

Found: C, 73.95; H, 4.51. Calcd. for $C_{14}H_{10}O_3$: C, 74.33; H, 4.46%.

Reaction with Aluminum Chloride.—*Nitrile Ia to Give 3-(2-Hydroyxphenyl)-4-hydroxycoumarin-2-imide (VIIa).*—A mixture of Ia (0.5 g.) and anhydrous aluminum chloride (0.5 g. or 2.1 mol.) in anhydrous nitrobenzene (5 ml.) was heated for 1 hr. on a steam-bath. The cooled solution was treated with water, and the nitrobenzene was removed by steam-distillation. The residual semi-solid product was taken up in ethyl acetate and washed with aqueous sodium carbonate and with aqueous sodium hydroxide. The product obtained from the ethyl acetate solution was crystallized from ethanol to give VIIa as colorless microcrystals, m. p. 230°C (decomp.), soluble in dilute hydrochloric acid; yield 0.1 g., IR 3571, 3333, 3077 (NH_2, OH), 1613 cm^{-1} (γ-pyrone).

Found: C, 70.92; H, 4.67; N, 5.43. Calcd. for $C_{15}H_{11}O_3N$: C, 71.15; H, 4.34; N, 5.53%.

This VIIa was converted into IVa, m. p. 178~179°C, by hydrolysis with dilute hydrochloric acid.

Nitrile Ib to Give 2-Hydroxy-4-methoxybenzoyl-2-methoxyphenylacetonitrile (VIII) and 3-(2-Methoxyphenyl)-7-methoxy-4-hydroxycoumarin-2-imide (VIIb).—A similar treatment of Ib (0.4 g.) with aluminum chloride (0.7 g. or 4 mol.) furnished VIII, m. p. 168~169°C (from ethanol), from a sodium hydroxide soluble part; yield 0.05 g., with a red ferric chloride reaction, IR 2247 (CN), 1608 cm^{-1} (CO).

Found: C, 68.50; H, 5.17. Calcd. for $C_{17}H_{15}O_4N$: C, 68.67; H, 5.08%.

From an alkali insoluble part was obtained VIIb, m. p. 180~182°C (from dilute ethanol), soluble in dilute hydrochloric acid, with a negative ferric chloride reaction; IR 3450, 3250, 3120 (NH_2), 1655 cm^{-1} (γ-pyrone).

Found: C, 68.53; H, 4.82; N, 4.51. Calcd. for $C_{17}H_{15}O_4N$: C, 68.67; H, 5.08; N, 4.71%.

This VIIb was also obtained from VIII by warming it with dilute aqueous sodium hydroxide for a while.

Ester IIa to Give IVa and 3-(2-Methoxyphenyl)-4-hydroxycoumarin (VIa).—A similar treatment of IIa (0.4 g.) with aluminum chloride (0.7 g. or 4 mol.) in nitrobenzene (5 ml.) furnished 0.1 g. of IVa, m. p. 175~176°C, from an alkali insoluble part, and 0.05 g. of VIa, m. p. 171~172°C (from ethanol), from a sodium carbonate soluble part. The reported melting point of VIa is 176°C[6].

Found (for VIa): C, 71.77; H, 4.91. Calcd. for $C_{16}H_{12}O_4$: C, 71.63; H, 4.51%.

Ester IIb to Give Ethyl 2-(2, 4-Dimethoxyphenyl)-benzo[b]furan-3-carboxylate (IX).—A similar treatment of IIb (0.4 g.) with aluminum chloride (0.6 g. or 4 mol.) in nitrobenzene (5 ml.) furnished 0.1 g. of IX, m. p. 80~81°C (from ethanol), from an alkali insoluble part; IR 1718 cm^{-1} (ester).

Found: C, 70.01; H, 5.89. Calcd. for $C_{19}H_{18}O_5$: C, 69.93; H, 5.56%.

This IX was converted into 2-(2, 4-dimethoxyphenyl)-benzofuran-3-carboxylic acid (X) by hydrolysis with aqueous sodium hydroxide; m. p. 214~216°C (decomp.) (from dilute ethanol), IR 1669 cm^{-1} (CO_2H).

Found: C, 68.05; H, 5.05. Calcd. for $C_{17}H_{14}O_5$: C, 68.45; H, 4.73%.

This acid X was identical with the sample, m. p. 213~214°C (decomp.), prepared from IVb' by methylation with dimethylsulfate and sodium hydroxide, followed by hydrolysis.

The author is grateful to the members of the Institute of Agricultural Chemistry of Kyoto University for microanalysis and to the members of the Faculty of Science of Osaka City University for infrared spectroscopy.

Faculty of Literature and Science
Toyama University, Gofuku, Toyama

Activations by Anions in the Oxy-acid Phosphors. I. General Consideration and Preliminary Experiments

By Yoshihide KOTERA, Michiko YONEMURA and Tadao SEKINE

(Received August 10, 1961)

Activations by Anions in the Phosphors.—In the case of sulfide phosphors, it has been said that an anion of, for examaple, halogen, oxygen, phosphorus or arsenic ion, may act as an activator. Kroeger and Hellingman[1] showed for first time that the ions Cl^-, Br^- and I^- play an essential part in the blue centers of ZnS phosphors. They introduced the orbital energy diagram for zinc sulfide with blue centers and attributed the blue emission to the electron transition between the conduction band and the activator level which is introduced by the blue centers. They assumed the following three possibilities for the configurations giving rise to the localized activator level, viz., A^+X^-, A^+ or X^-, together with their respective surroundings, where A^+ stands for metallic ion and X^- for halogen. Also they[2] determined chemically the chlorine present in phosphors and claimed that this finding would support their assumption of a blue centers. Further, Kroeger and Dikhoff[3] investigated the activation by the oxygen ion in zinc sulfide matrix. They established that the incorporation of zinc oxide in zinc sulfide causes the appearance both of a new absorption band and, in the presence of activators, of new fluorescence bands displaced about 150 Å toward long wavelengths with respect to the original bands. They explained these effects by the assumption of local oxygen levels and of new centers consisting of associated pairs of oxygen and activator ions. In addition, Bube, Riehl and several other researchers[4] have also studied the action of halogen and oxygen ions. Subsequently McKeag and Ranby[5] reported the activation of zinc sulfide by phosphorus and Prener[6], its activation by arsenic; both phosphors were proposed for use as a single white screen for television and also for the preparation of transparent luminescent screens. Besides zinc sulfide, the activation by polysulfide ions in the matrix of sulfides and sulfates of alkali and alkali earth was found by Gobrecht and Hahn[7]. They assumed that in all cases the polysulfide compound was formed and that the red emission in these phosphors is to be attributed to the polysulfide formation, concluding that these emissions are the same as those occurring in pure tungstate or uranyl compounds. Meanwhile, Thomson[8] assumed that the emission of pure zinc oxide required the presence of sulfide ion; Kroeger and Dikhoff[3], however, denied this assumption on the basis of their investigations.

1) F. A. Kroeger and J. E. Hellingman, *Trans. Electrochem. Soc.*, **93**, 156 (1948).
2) F. A. Kroeger and J. E. Hellingman, ibid., **95**, 68 (1949).
3) F. A. Kroeger and J. A. M. Dikhoff, *J. Electrochem. Soc.*, **99**, 144 (1952).
4) R. H. Bube, *Phys. Rev.*, **80**, 655, 764 (1950); **90**, 70 (1953); *J. Chem. Phys.*, **19**, 985 (1951); **20**, 708 (1952); F. A. Kroeger, *Physica*, **16**, 297 (1950); H. A. Klasens, *J. Electrochem. Soc.*, **100**, 72 (1953); N. Riehl and H. Ortmann, *J. phys. radium*, **17**, 620 (1956); N. T. Melamed, *J. Phys. Chem. Solids*, **7**, 146 (1958).
5) A. H. McKeag and P. W. Ranby, *Trans. Electrochem. Soc.*, **96**, 85 (1949).
6) J. S. Prener, *J. Electrochem. Soc.*, **98**, 406 (1951).
7) H. Gobrecht and D. Hahn, *Z. Physik*, **132**, 111 (1952); **135**, 523 (1953).
8) S. T. Thomson, *J. Chem. Phys.*, **18**, 770 (1950).

Activations by Anions in the Oxy-acid Phosphors.—It has not yet been reported that activation by anions occurs in the oxy-acid phosphors. We can, however, find in the literature some experimental results which might be explained by assuming this activation, although the authors have not expressed this idea. One of them was described above; that is, Gobrecht and Hahn[7] found the activation by polysulfide ion in alkali earth sulfates. We suppose that the effect of the existence of sulfur upon the emission of aluminosilicate, which was reported by Kirk[9], might be the same activation as that reported by Gobrecht and Hahn. Tungstate, molybdate, vanadate and uranyl ions act as activators in the oxy-acid phosphors, and we could find some corroborative findings, one of which is that presented by Gobrecht and Weiss[10] regarding alkali earth tungstate and molybdate activated by the uranium compound, and another of which is reported for calcium borate[11] or halophosphate[12] activated by the tungstate compound. Further, we would like to propose that titanium or manganese ion in higher valency acts as an activator[13] which should be thought of as an anion. This idea might be partially supported by the fact that titanium in higher valency acts as an activator only when the matrix makes an eutectic compound with the titanate compound (Kroeger[13]). Also, we might explain the effect of the phosphorus[14] or arsenic[15] ion upon the emission of zinc silicate activated by manganese as the occurrence of anionic activation by the phosphorus or arsenic ion.

It is, however, very difficult to conclude the anionic activation from these results because of the lack of reliable experimental facts for the occurrence of this activation. We thought that anions might be able to give localized levels between the filled and conduction bands in those matrices, and so act as activators, when they have a smaller electron affinity than that of the oxy-anions which compose the host crystal. We have prepared various oxy-acid phosphors activated by anions and have obtained some remarkable results[16].

9) R. D. Kirk, *J. Electrochem. Soc.*, **101**, 461 (1954).
10) H. Gobrecht and H. Weiss, *Z. Physik*, **140**, 139 (1955).
11) Y. Uehara, I. Masuda and Y. Kobuke, 2nd Symposium on Photochemistry, Tokyo, September, 1954.
12) N. Ohtani and Y. Yokota, 8th Annual Meeting of the Chemical Society of Japan, Tokyo, April, 1955.
13) F. A. Kroeger, "Some Aspects of the Luminescence of Solids", Elsevier Pub. Co., Inc., Amsterdam (1948), pp. 57, 158.
14) P. Zalm and H. A. Klasens, *Philips Res. Repts.*, **8**, 386 (1953).
15) H. C. Froelich and G. R. Fonda, *J. Chem. Phys.*, **46**, 1 (1942).
16) Y. Kotera et al., ibid., **23**, 219 (1955); *J. Electrochem. Soc.*, **108**, 540 (1961).

Experimental

Selection of Matrices and Activators.—First, it was necessary to determine what kind of matrices and activators should be selected. Two types of matrices were used, the sulfates of alkali earth metals and magnesium, and the silicates of alkali earth metals, magnesium and zinc. It was thought that these anions might have a greater electron affinity; also, they were not expected to decompose during firing at relatively high temperatures. For the electron affinity of oxy-anions there are few data, but we presumed that, if two salts were prepared from two anions with a common metal ion and if the fundamental absorption of one salt has an edge at a shorter wavelength than the second, then the former would have a greater electron affinity than the latter. From this idea we supposed that a sulfate or silicate ion would have the greater electron affinity among the oxy-acid anions. As to decomposition during the firing, the facts that calcium[17] or magnesium[18] sulfate decompose partially above 1000°C and that strontium or barium sulfate behaves similarly, would be overcome by lowering their firing temperatures.

As activators, silicate, phosphate, borate, carbonate and sulfide were used, because they surely exist in the matrix as anions. Also tungstate, molybdate, vanadate and germanate ions were tried, as they probably exist in the matrix as anions; further, arsenate, antimonate[19] and aluminate[20] ions were tried, because they are anionic components of the phosphor matrix.

Preparation of Phosphors.—Sulfates of alkali earth metals were precipitated by mixing a purified ammonium sulfate solution with a purified solution of alkali earth salts. In the purification, precaution was taken, by the addition of distilled hydrogen chloride, that the residue of sulfide used for the purification was thoroughly decomposed. In the precipitation, the sulfate solution was poured into the metallic solution and the precipitation was stopped, when the latter solution was slightly in excess, in order to obtain a precipitate with an excess of cations. The silicate matrices were prepared by a well-known process. Magnesium sulfate was prepared by solid-state reaction between purified magnesium oxide and ammonium sulfate. The purity of raw materials was ascertained spectroscopically.

As activators, the following salts were used: $SiO_2 \cdot nH_2O$, $(NH_4)_2HPO_4$, H_3BO_3, metallic carbonate, metallic sulfide, $WO_3 \cdot nH_2O$ or metallic tungstate, MoO_3, NH_4VO_3, GeO_2, As_2O_3, Sb_2O_3 and $Al(OH)_3$. They were purified by a well-known process or by the process previously reported[19,20]. Metallic sulfides were prepared by the reaction between the metallic sulfate and a reducing agent, the details being described in the following report.

In general the amount of activators was optimum at 0.01 to 0.1 mol. per 1 mol. of sulfate and

17) J. Zawadzki, *Z. anorg. u. allgem. Chem.*, **205**, 180 (1932).
18) G. Grube and M. Staesche, *Z. phys. Chem.*, **A204**, 265 (1955).
19) Y. Kotera, T. Sekine and M. Yonemura, *J. Electrochem. Soc.*, **102**, 390 (1955); This Bulletin, **29**, 743 (1956).
20) Y. Kotera and T. Sekine, ibid., **28**, 129 (1955).

0.001 to 0.05 mol. for silicate. Some results were obtained in which emission colors were different among samples activated by different amounts of activator.

We could not obtain conclusive results for the form of activator. In the following tables we have used the form which is commonly found for an anion.

Flux was seldom used, and it was found in the following experiments that it has little effect.

Firing was done in air, except for special cases, for 2 to 4 hr. at 1100°C. For the activation of calcium sulfate by vanadate or carbonate ion, firing was done at 500°C, and for barium sulfate activated by carbonate ion, at 900°C, while the firing for the preparation of magnesium sulfate phosphors was carried out at 1000°C.

Results

The reselts are shown in Tables I and II for two kinds of matrices. Most of these emissions are excited both by 2537 and 3650 Å; some of them have the emissions only under 2537 Å excitation, whereas magnesium silicate activated by antimonate ion has emission only for the excitation by 3650 Å. In general, the emission under 2537 Å is stronger than that under 3650 Å.

Discussion

It was confirmed that in oxy-acid phosphors anionic centers are present, though their luminescence is weak in most cases. From the results obtained we suggest that anionic activators are to be divided into two group as follows:

1. The first group might be called "intra-ionic activation". They have emissions almost identical with those found in the matrices whose anion is identical with the activating one. The luminescence originates in this group from the electronic transition in the anions. The activations by tungstate and molybdate ions are typical examples of this group, and that by vanadate may belong to it too.

2. The other group might be called "inter-ionic activation". Their emissions have various colors, depending upon the matrices, even for the same activator. This activation occurs when the electron affinity of the activating anions is smaller than that of the host crystal anions. Some ions of this group show a tendency for the emission color to shift to a longer wavelength in the order of calcium, strontium and barium. Phosphate, germanate,

Table I. Emissions of sulfates activated by anions

Matrix	Activator											
	WO_4^{2-}		MoO_4^{2-}		$V_2O_7^{4-}$		PO_4^{3-}		AsO_4^{3-}		$Sb_2O_7^{4-}$		GeO_4^{2-}	
$CaSO_4$	Blue	s	Yellowish green		None		White	f	Yellow	f	Red	m	Greenish white	f
$SrSO_4$	Bluish white	m	Yellow	m	None		White	ff	White	ff	Pink	ff	White	ff
$BaSO_4$	None		None		None		Yellow	f	Blue	ff	Blue	ff	Red	m
$MgSO_4$	Bluish white	s	—		Yellow	m	Red	f	Red	f	—		Red	f

Matrix	Activator											
	SiO_4^{2-}		CO_3^{2-}		BO_3^{3-}		AlO_2^{-}		S^{2-}		SO_3^{2-}	
$CaSO_4$	Greenish white	f	Blue	ff	White	ff	Blue	ff	Blue	m	Bluish white	
$SrSO_4$	White	ff	Yellow	ff	White	ff	White	ff	Bluish white	f	Yellow	f
$BaSO_4$	Blue	f	None		White	f	White	f	Orange	m	Orange	f
$MgSO_4$	Yellow	f	—		None		Blue	f	—		—	

Table II. Emissions of silicates activated by anions

Matrix	Activator											
	$V_2O_7^{4-}$		PO_4^{3-}		AsO_4^{3-}		$Sb_2O_7^{4-}$		GeO_4^{4-}		BO_3^{3-}	
$CaSiO_3$	Yellow	ff	None		None		None		None		Yellow	ff
Ca_2SiO_4	None		Red	m	Red	m	Red	ff	Red	m	Red	m
$BaSi_2O_5$	Yellow	f	Yellow	f	Yellow	f	Bluish white	f	Yellow	f	Bluish white	f
$Ba_2Si_3O_8$	Yellow	m	Yellow	f	Yellow	f	Yellow	f	Yellow	f	Yellow	f
$MgSiO_3$	Yellow	m	Yellow	ff	Red	f	Yellow	ff	Yellow	ff	None	
Zn_2SiO_4	Yellow	f	Yellow	f	Yellow	f	Yellow	f	Yellowish white		Yellow	f

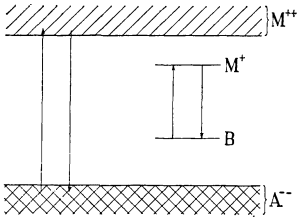


Fig. 1 Energy band model for intraionic activation.

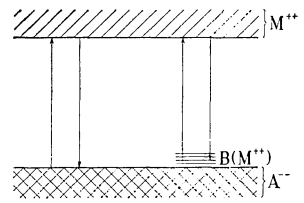


Fig. 2. Energy band model for interionic activation.

aluminate, sulfide and sulfite ions tend to show this tendency.

Phosphors with intraionic activation have a rather strong emission and it might be found that such activation occurs in phosphors which have been studied by other researchers who have assumed them to be activated by other sources[11,12] We assume an energy band model for this group like the one in Fig. 1. This activation may correspond to the activation by divalent manganese or rare earth ions in the case of cationic activation.

In interionic activation, it is difficult to find the relation between the emission and the composition of phosphors because of the weak emission intensity. However, in some cases the regularity is found according to the ionization potential of the cations which compose the matrices. In many cases the emission of this group shows a wide distribution. Such an activation has rarely been found before, the sulfide activation being the only case in this group, but it is not clear whether the sulfide activation belongs to this group or not. We assume an energy band model for the interionic activation as in Fig. 2. Because of the complex structure of the activating anions, their energy levels may be complicated, in turn causing the broadening of the spectral distribution of emission.

Compared to cationic activation, it was found that the amount of activators is considerably large in anionic activation; this may be due to the more complex structure of the anions.

The authors wish to express their thanks to Professor S. Makishima for his general discussions on the subject and on some of their experimental work.

Government Chemical Industrial Research Institute, Tokyo
Sibuya-ku, Tokyo

Activations by Anions in the Oxy-acid Phosphors. II. Activations by the Tungstate Ion

By Yoshihide KOTERA, Michiko YONEMURA and Tadao SEKINE

(Received August 10, 1961)

In the previous paper[1] it was found that anionic centers are present in oxy-acid phosphors and that the activation by tungstate ion is a typical example of "intraionic activation", the luminescence originating from the electron transitions in tungstate ion and being rather strong. The activation by the tungstate ion has been reported by several researchers[2], for example, for calcium borate[3] or halophosphate[4], though the activation is assumed to be caused by the tungsten ion. In these cases it has been found that the brightness of phosphors increases with the increase in the added amount of tungsten, but the highest brightness is only equal to or lower than that of calcium tungstate. It is desirable to obtain phosphors which have a higher brightness and,

1) Y. Kotera, M. Yonemura and T. Sekine, This Bulletin, 35, 577 (1962).
2) F. A. Kroeger, "Some Aspects of the Luminescence of Solids", Elsevier Pub. Co., Inc., Amsterdam (1948), p. 107.
3) Y. Uehara et al., The 2nd Symposium on Photochemistry, Tokyo, September, 1954.
4) N. Ohtani et al., 8th Annual Meeting of the Chemical Society of Japan, Tokyo, April, 1955.

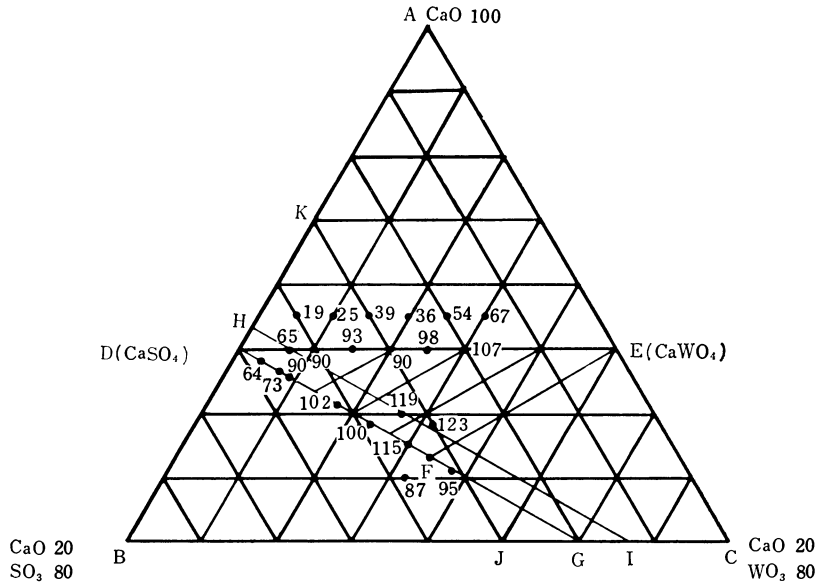


Fig. 1. Relation between the brightness of calcium sulfate activated by tungstate ion and the mixing ratio of batch component.
A: CaO; B: CaO 20, SO_3 80; C: CaO 20, WO_3 80; D: $CaSO_4$, E: $CaWO_4$ (under 2537 Å excitation).

if possible, a cost cheaper than calcium tungstate, if calcium salts are to be activated by tungstate ion. In the various kinds of matrices discussed, it was expected that sulfate salts would satisfy this desire because of the similarity in crystal structure[5] between sulfate and tungstate salts. Among calcium salts the crystal structure of calcium sulfate is most like that of tungstate, the former being orthorombic with $a_0=6.21$, $b_0=6.95$ and $c_0=6.96$, whereas the latter is tetragonal with $a_0=5.24$ and $c_0=11.38$. Likewise, magnesium sulfate has an orthorhombic structure with $a_0=4.82$ $b_0=6.72$ and $c_0=8.35$, while magnesium tungstate is monoclinic, with $a_0=4.67$, $b_0=5.66$, $c_0=4.92$ and $\theta=89°35'$. An American patent[6] makes an interesting relevant suggestion. It is proposed by this patent that the brightness of calcium tungstate increases when sulfuric acid, in amounts corresponding to the excess calcium oxide in the tungstate, is added on firing for the purpose of preventing the formation of calcium oxide. Accordingly we have prepared various sulfate phosphors activated by tungstate ion and have so achieved some remarkable results.

The Experiments and their Results

The starting materials are $CaSO_4$, $CaCO_3$, $WO_3 \cdot nH_2O$, $CaWO_4$, MgO, $(NH_4)_2SO_4$, ZnO, $CdCO_3$, $PbSO_4$, $BaSO_4$ and MoO_3, which had been purified by the process previously reported[7]. They were mixed in a dry state and fired in air for 4 hr., at 1100°C for calcium sulfate and at 1000°C for magnesium sulfate. The spectral distribution was measured by means of a spectroradiometer[8], and the brightness, by a photocell.

Relation between the Brightness of $CaSO_4$: WO_4 and the Mixing Ratio.—The relation is

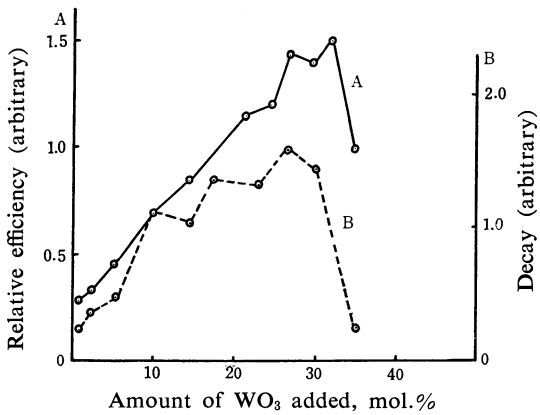


Fig. 2. Brightness and decay characteristics as the function of amount of WO_3 added to calcium sulfate (X-ray excitation). A, Brightness B, Decay

5) R. W. G. Wyckoff, "Crystal Structures", Interscience Publishers, New York (1948).
6) W. A. Roberts, U. S. Pat. 2312267 (1943).
7) Y. Kotera, T. Sekine and M. Yonemura, This Bulletin, 27, 13 (1954).
8) Y. Kotera, *Rept. Govn. Chem. Ind. Research Institute, Tokyo*, 50, 398 (1955).

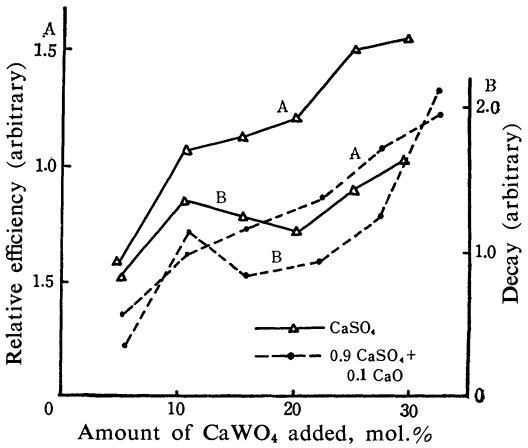


Fig. 3. Brightness and decay characteristics as the function of amount of $CaWO_4$ added to calcium sulfate and (0.9 $CaSO_4$ +0.1 CaO) (X-ray excitation).
A, Brightness B, Decay

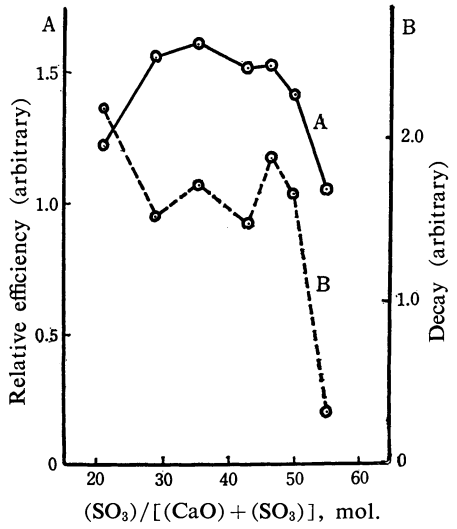


Fig. 4. Brightness and decay characteristics as the function of molar ratio of SO_3 to $CaSO_4$ (X-ray excitation).
A, Brightness B, Decay

shown in Fig. 1 between the brightness of the fired products under 2537Å excitation and the mixing ratio of $CaSO_4$, $CaCO_3$ and $WO_3 \cdot nH_2O$. The brightness and the decay characteristies of these products under X-ray excitation are shown in Figs. 2, 3 and 4.

In Fig. 1 the value of 100 corresponds to the brightness of the commercial product of calcium tungstate phosphor, while the brightness and decay characteristics under X-ray excitation were determined by the blackening of the photographic plate. The commercial product shows a brightness value of 1.40 for those prepared by the precipitation and the firing of calcium tungstate or 1.80 for those prepared by the solid-state reaction between calcium compound and tungsten trioxide, and 1.20 for the decay value.

In Fig. 2 the samples are selected for the mixing ratio from points on the straight line DG in Fig. 1, while in Fig. 3 the mixing ratios of samples are located on DE (A) and on the straight line parallel to DE (B), and in Fig. 4, on JK.

In these preparations it is probable that the reaction

$$CaSO_4 + H_2WO_4 \rightarrow CaWO_4 + H_2SO_4$$

proceeds; that this is the case is confirmed by the formation of white fume, which is presumed to be sulfur trioxide, and by the decrease in the weight of the samples. Then it has to be assumed that, for mixtures of compositions below the line DE (Fig. 1), the composition changes during the firing, along the straight line EF or parallel to EF, the reaction ending when the composition reaches line DE. The spectral distributions are shown in Fig. 5.

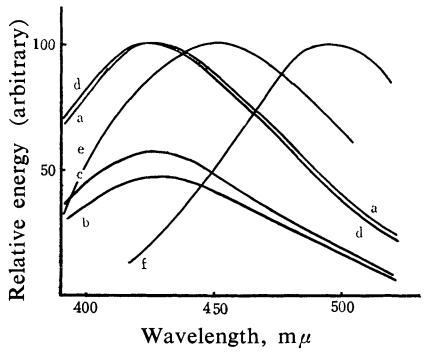


Fig. 5. Spectral distributions of calcium tungstate and calcium sulfate activated by tungstate ion.
a, $CaWO_4$; b, c, d, $CaWO_4$ activated by tungstate ion ($CaSO_4$: H_2SO_4 (molar ratio) = 99 : 1 (b), 9 : 1 (c), 7 : 3 (d)); e, $CaSO_4$ activated by tungstate ion with the addition of lead salt; f, $CaSO_4$ activated by tungstate ion with the addition of magnesium salt.

The Effect of the Addition of other Components than Calcium and Tungstate Compound to Calcium Sulfate Activated by a Tungstate Ion.—By the addition of lead salt to calcium sulfate activated by a tungstate ion, it might be supposed that the product would be about the same as that of calcium tungstate activated by lead. Actually, this is the case. The change in the spectral distribution by the addition of lead occurs in $CaSO_4$: WO_4 as in the case of calcium tungstate; in this case it was also found that the brightness of the

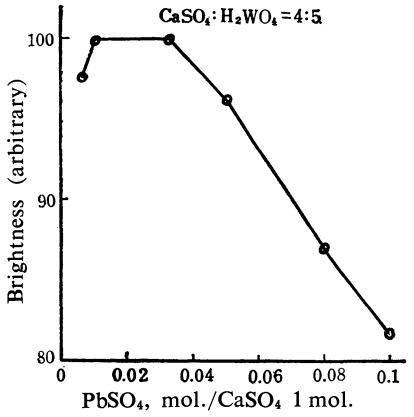


Fig. 6. Brightness as the function of amount of lead salt added to calcium sulfate activated by tungstate ion.

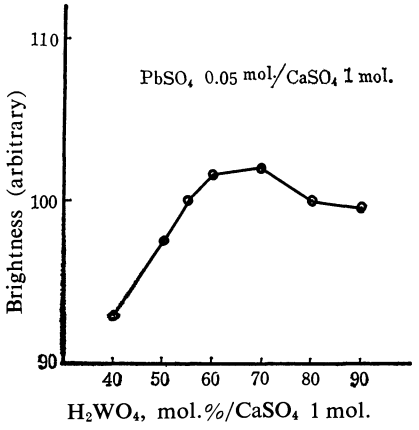


Fig. 7. Brightness as the function of amount of WO_3 added to calcium sulfate activated by tungstate ion with the addition of lead salt.

TABLE I. BRIGHTNESS AND DECAY CHARACTERISTICS OF CALCIUM SULFATE ACTIVATED BY TUNGSTATE ION WITH THE ADDITION OF BARIUM SULFATE (X-RAY EXCITATION)

No.	Mixing ratio, g.			Brightness*2	Decay*2
	$CaSO_4$*1	H_2WO_4	$BaSO_4$		
1	4.0	4.0	0.8	67.0	52.3
2	4.0	4.0	1.6	48.6	41.1
3	4.0	4.0	3.2	34.6	54.4
4	4.0	4.0	5.3	23.8	2.4
5*3	4.0	4.0	0.8	46.2	90.1
6	4.0	5.8	—	100	100
7	4.0	5.8	1.0	85.1	44.4
$CaWO_4$(Commercial material)				135	37.2

*1 $CaSO_4$ contains 1.02 H_2O.
*2 Relative value to that of No. 6.
*3 0.44 g. of $PbSO_4$ was added.

products is considerably higher than that of calcium tungstate activated by lead. In Figs. 6 and 7 the brightness of the samples under 2537 Å excitation is shown; the value of 100 means the brightness of commercial calcium tungstate activated by lead. The spectral distribution is shown in Fig. 5.

By the addition of barium sulfate, it might be presumed that the absorption of the X-ray increase and barium tungstate, which has no emission at room temperature, would be produced. The brightness and the decay characteristics of the products under X-ray excitation are shown in Table I. Under 2537 Å excitation the spectral distribution is almost the same as that of calcium tungstate, and the brightness decreases proportionally with the amount of the addition.

By the addition of magnesium oxide the products show an emission almost the same as that of magnesium tungstate, when the firing

TABLE II. BRIGHTNESS OF CALCIUM SULFATE ACTIVATED BY TUNGSTATE ION WITH THE ADDITION OF MAGNESIUM OXIDE

No.	Mixing ratio, g.			Brightness*2
	$CaSO_4$*1	H_2WO_4	MgO	
1	4.0	5.2	1.1	100
2	4.0	5.2	1.2	93
3	4.0	5.2	1.3	96
4	4.0	5.8	1.1	93
5	4.0	5.8	1.2	93
6	4.0	5.8	1.3	93

*1 $CaSO_4$ contains 1.02 H_2O.
*2 Relative value to that of magnesium tungstate.

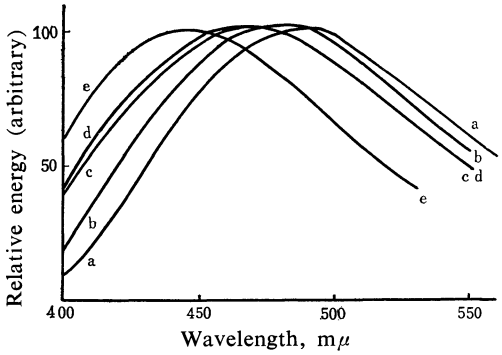


Fig. 8. Spectral distributions of calcium sulfate activated by tungstate ion with the addition of zinc oxide.

	$CaSO_4$ g.	H_2WO_4 g.	ZnO g.
a	0	4.8	1.9
b	4.0	4.8	1.6
c	4.0	4.8	1.2
d	4.0	4.8	0.8
e	4.0	4.8	0.4

temperature is below 1000°C. (See Fig. 5. Above 1100°C the emission is the same as for calcium tungstate, and the firing temperature between 1000 and 1100°C gives their mixture.) Also in this case the brightness is higher than that of an ordinary preparation, the results being tabulated in Table II.

By the addition of zinc or cadmium oxide, the spectral distribution shifts to a longer wavelength, which is shown in Figs. 8 and 9. Molybdenum oxide causes the same shift, which is shown in Fig. 10. This result is like that of Kroeger[2], but the details are not in accordance. The brightness of these samples under 2537Å is considerably high when compared with other commercial phosphors.

The Effect of the Precipitating Condition or Firing Condition.—Preliminary tests were carried out for the production of calcium sulfate activated by tungstate ion. Twelve kinds of samples were prepared as follows:

1. Pure calcium chloride ($CaCl_2 \cdot 2H_2O$ 80 g./l.) was mixed with a pure ammonium sulfate solution ($(NH_4)_2SO_4$ 80 g./l.), and precipitated calcium sulfate was mixed with tungstic acid.

The batch obtained was fired at different temperatures, viz., 1000, 1050 and 1100°C.

2. The same process as 1, except that the concentration of the ammonium sulfate solution was 40 g./l.

3. The same process as 1, except that tungstic acid was re-purified from the one use d in process 1.

4. After the preparation by the process 1, the products were re-fired at 1100°C for 4 hr.

The relation between the relative brightness of these samples and the preparative condition

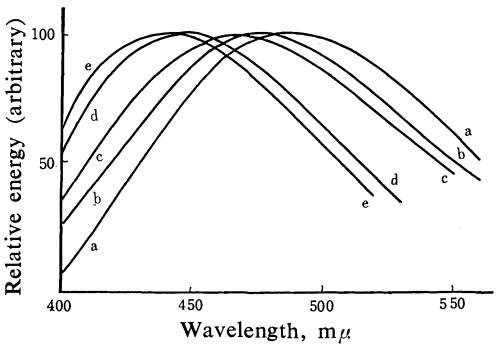


Fig. 9. Spectral distributions of calcium sulfate activated by tungstate ion with the addition of cadmium oxide.

	$CaSO_4$	H_2WO_4	CdO
	g.	g.	g.
a	0	4.8	4.0
b	4.0	4.8	3.4
c	4.0	4.8	3.0
d	4.0	4.8	2.0
e	4.0	4.8	1.0

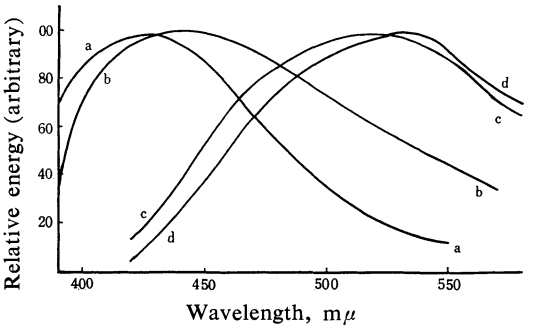


Fig. 10. Spectral distributions of calcium sulfate activated by tungstate ion with the addition of molybdenum oxide.

	H_2WO_4	H_2MoO_4	MoO_3/WO_3 (mol.)
	g.	g.	%
a	0.732	0.0005	0.1
b	0.726	0.0053	1
c	0.696	0.0265	5
d	0.670	0.0530	10

$CaSO_4$: 4.0 g. (a—d)

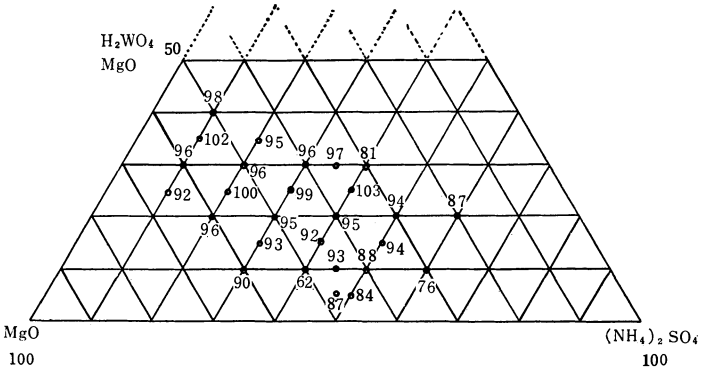


Fig. 11. Relation between the brightness of magnesium sulfate activated by tungstate ion and the mixing ratio of batch component (under 2537 Å excitation).

Table III. Relation between the brightness of calcium sulfate activated by tungstate ion and the precipitating or firing condition

Firing temp. °C	Processes (1)	(2)	(3)	(4)
1000	85	87	90	84
1050	87	90	95	89
1100	88	90	93	87

is shown in Table III.

From these results we tried to investigate the effect of the precipitating condition of calcium sulfate and of the prefiring condition on the brightness of the products. The precipitation of calcium sulfate was carried out under the following conditions:

i. A calcium chloride solution (80 g./l.) was poured into an ammonium sulfate solution (80 g./l.).

ii. A calcium chloride solution (40 g./l.) was poured into an ammonium sulfate solution (160 g./l.).

iii. An ammonium sulfate solution (40 g./l.) was poured into a calcium chloride solution (160 g./l.).

iv. An ammonium sulfate solution (80 g./l.) was poured into a calcium chloride solution (80 g./l.).

Half a portion of precipitated calcium sulfate was prefired at 800°C for 2 hr., while the other half was not prefired. The batches were prepared with these eight calcium sulfate samples, the ratio of calcium and tungsten being the same. The relative brightness of these phosphors is shown in Table IV.

Table IV. Effect of precipitating condition and prefiring upon the brightness of calcium sulfate activated by tungstate ion

Prefiring	Precipitating conditions (i)	(ii)	(iii)	(iv)
Unfired	95	95	97	97
Prefired	98	100	100	101

It can be concluded from these experiments that the brightness becomes greater by the purification of tungstic acid or the prefiring of calcium sulfate, but that other factors are not so important as the former.

Relation between the Brightness of $MgSO_4$: WO_4 and the Mixing Ratio.—The relation is shown in Fig. 11 between the brightness of fired products under 2537 Å excitation and the mixing ratio of MgO, $(NH_4)_2SO_4$ and $WO_3 \cdot nH_2O$. The same is shown in Fig. 12, the brightness change being expressed as the function of tungstic acid proportion.

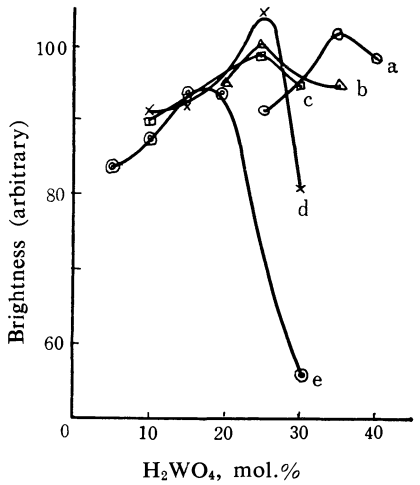


Fig. 12. Brightness of magnesium sulfate activated by tungstate ion as the function of ammount of WO_3 added to magnesium sulfate (under 2537 Å excitation).

Discussion

In his brief studies on the luminescence of tungstates and molybdates, Kroeger[2] presumed from the absorption data of the molybdates that the absorption would be of the characteristic type caused by electronic transitions in the molybdate groups and that the same would be applied to the tungstates. He also assumed from his experiments the absorption and excitation bands on the one hand and the emission band on the other hand must be closely connected, both probably originating in one and the same atomic configuration, which might be tungsten and molybdenum with adjacent oxygen ions. In this case it was not determined whether any tungstate or molybdate group could give rise to an emission or not.

On the other hand, a few reports have been published on the emission of phosphors activated by tungsten or molybdenum. Calcium borate[3] or calcium halophosphate[4] activated by tungsten have been studied, but their details are uncertain, except that it has been explained that the emissions might be the same as those of calcium tungstate and that the brightness increases with the increasing amount of tungsten, its maximum value being the one which is obtained for calcium tungstate. Aluminum oxide activated by tungsten emits an orange light, while activation by molybdenum causes a blue emission[9]; zinc silicate emits a green color when activated by tungsten[10]. These reports are also uncertain but for the last case, where it is obvious that

9) S. Izawa, *Sci. Pap. Inst. Phys. Chem. Res.*, **20**, 163 (1933).
10) Y. Uehara and U. Umekawa, *J. Chem. Soc. Japan* (Nippon Kwagaku Kwaishi), **61**, 107 (1940).

the emission corresponds to that of zinc tungstate. Meanwhile, Robert[6] has found that the brightness of calcium tungstate would increase when sulfuric acid, in amounts corresponding to the excess calcium oxide in the tungstate, is added on firing. This addition of sulfuric acid might cause the formation of calcium sulfate, reducing the amount of calcium oxide, which seems to cause the afterglow in calcium tungstate[11].

It is found that calcium sulfate is activated by the tungstate ion and that the brightness of this phosphor under 2537Å excitation is higher than that of pure calcium tungstate. The spectral distribution of this emission is almost the same as that of calcium tungstate, although a small shift was found in some cases. However, as already stated, the reaction between calcium sulfate and tungstic acid might occur during the firing of their mixture. Further, it was found by us that the addition of ammonium persulfate to calcium tungstate causes its brightness to increase[12]. Thus the results might be explained by the findings of Robert and our above-written finding, that the addition of sulfate ion is favorable for the preparation of calcium tungstate phosphor.

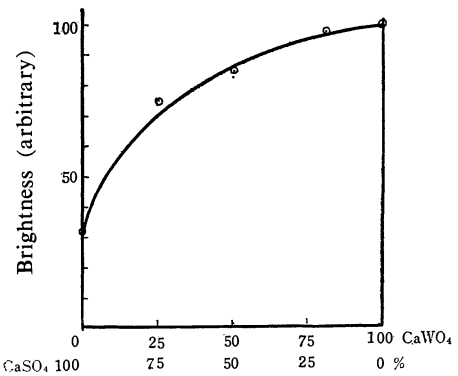


Fig. 13. Relation between the brightness and the mixing ratio of mechanical mixture of calcium sulfate and calcium tungstate.

For these problems it is proposed that, at low contents of tungstic acid, calcium sulfate is being activated by the tungstate ion, because the brightness is much higher than that obtained from a mixture of calcium sulfate and calcium tungstate, whose brightness is increased by the addition of sulfate. However, when the content of tungstic acid is high, a reaction with calcium sulfate occurs to produce calcium tungstae, while the activation by tungstate occurs simultaneously to increase the brightness of the product. In Fig. 13 the brightness of mechanical mixtures of calcium sulfate and calcium tungstate under 2537Å excitation is shown; this clarifies the activation by the tungstate ion compared with Fig. 1. Some qualitative results which might clarify this assumption were obtained from crystallographic analysis by means of a recording X-ray diffractometer. In the phosphor, which was prepared by the firing of a mixture of 1 mol. calcium sulfate and 0.2 mol. tungstic acid, the patterns of both calcium sulfate and tungstate were found, while the pattern of the phosphor from the mixture of 1 mol. calcium sulfate and 0.05 mol. tungstate was almost the same as that of calcium sulfate. Because of this crystallographic similarity, it is quite difficult to determine the content of the constituent. On the other hand, absorption measurements were carried out to compare the spectra of pure calcium sulfate and that activated by tungstate ion, but the special peak was not found until 2800Å, and the measurements at shorter wavelengths were disturbed by the emission which is excited by the light in this region. The final decision as to the occurrence of tungstate activation in the case of calcium sulfate phosphors must be based on measurements of excitation spectra.

Thus, these results may be applied to the preparation of calcium tungstate phosphors. This phosphor is new prepared by two processes, one featuring the solid-state reaction between calcium carbonate or nitrate and tungstic acid, and the other consisting of the precipitation of calcium tungstate in an aqueous solution and its calcination. The former is now applied to the preparation of those phosphors which are used for fluorescent lamps, because they have good characteristics for 2537Å excitation. In this case it might be claimed that better results might be obtained if calcium sulfate were used as a starting material for calcium salt. The advantages of this proposal may be summarized as follows:

1) Compared with the process in which calcium carbonate or nitrate is used as starting material, not so much calcium oxide remains after the firing, though the ratio ($CaO : WO_3$) is large enough, because calcium sulfate decomposes very slowly at 1000°C. (The vapor pressure of sulfur trioxide on calcium sulfate is a few millimeters at 1000°C[13].)

2) The calcium sulfate which might remain after the firing increases the brightness of the prepared phosphor as it is activated by tungstate.

11) T. Nishikawa et al., *J. Chem. Soc. Japan, Ind. Chem. Sec.* (*Kogyo Kagaku Zasshi*), **57**, 890 (1954); **58**, 256 (1955); **61**, 266 (1958).

12) Y. Kotera and T. Sekine, ibid., **54**, 625 (1951).

13) J. Zawadzki, *Z. anorg. u. allgem. Chem.*, **205**, 180 (1932).

3) The phosphor prepared by this procedure is in the form of very fine powder, the size being hardly measurable by an ordinary microscope.

These are advantages for 2537 Å excitation, but for X-ray excitation different considerations are necessary. Under X-ray excitation it is necessary for the phosphor to absorb the X-ray, and it is clear that calcium sulfate has a smaller absorption coefficient than tungstate. From Figs. 2, 3 and 4 it is seen that calcium sulfate activated by tungstate has a weak emission when the amount of tungstate is small. However, advantage 1) mentioned above may, also be important in the case of X-ray excitation, because Nishikawa et al.[11] showed that the decay characteristic depends upon the residual amount of calcium oxide, while advantage 3) may be effective for the preparation of fine phosphor, which is used for X-ray intensifying paper with high resolution.

The effect of the addition of lead or magnesium may be considered for the preparation of calcium tungstate activated by lead or magnesium tungstate. In either case the results show that better phosphors could be prepared than by the ordinary process. It is remarkable that, when magnesium oxide is added to the mixture of calcium sulfate and tungstic acid, the firing temperature determines the characteristic of the product. It might be considered that a solid-state reaction between magnesium tungstate and calcium sulfate occurs. Similar results are obtained in the cases of zinc oxide and cadmium oxide, but in these cases the characteristic are determined by the mixing ratio, and these results could be explained by the formation of a solid solution between the products. The addition of molybdenum oxide causes a somewhat similar effect; the explanation for this case might be given by a combination of that one proposed by Kroeger[2] for the case of mixed crystals $CaWO_4 \cdot CaMoO_4$ and that other which may be concluded from the velocity difference between the solid-state reaction of calcium sulfate and tungstic acid and that of calcium sulfate and molybdenum oxide. It was unsuccessful to attempt to increase the sensitivity for X-ray excitation by the addition of barium sulfate.

The precipitating condition of calcium sulfate or the firing conditions has little influence upon the brightness, and it is shown that the repeated purification of tungstic acid or prefiring makes the brightness higher.

Magnesium sulfate, when activated by tungstate, shows the same characteristic as calcium sulfate. In this case it is necessary to lower the firing temperature, because magnesium sulfate decomposes thermally at a relatively lower temperature (the vapor pressure of sulfur trioxide on magnesium sulfate is reported to be 760 mmHg at 1213°C[14]), and so the firing must be done below 1100°C. It was possible to obtain a phosphor which has a higher brightness than that prepared by the ordinary process.

The authors wish to express their thanks to Dai-Nippon-Toryo Co. for the measurement of phosphor brightness under X-ray excitation.

Government Chemical Industrial Research Institute, Tokyo
Shibuya-ku, Tokyo

14) H. J. Knopf and H. Staude, *Z. physik. Chem.*, **A204**, 265 (1955).

Spectral Response of Photoconductivity in Polycyclic Aromatic Compounds

By Mizuka Sano and Hideo Akamatu

(Received August 14, 1961)

The photoconductive behaviors of polycyclic aromatic hydrocarbons have been investigated in the previous paper[1]. Concerning the nature of conducting electrons in these organic solids, it is interesting to investigate the spectral response of photoconductivity. In the previous reports[2,3] from our laboratory, it was noted

1) M. Sano, This Bulletin, **34**, 1668 (1961).

2) H. Akamatu and H. Inokuchi, *J. Chem. Phys.*, **20**, 1481 (1952).

3) H. Inokuchi, This Bulletin, **27**, 22 (1954).

that the optical threshold energies for photoconduction were nearly in accord with the long-wavelength edges of the optical absorption spectra of crystals, and also in agreement with the values of the energy gaps which were estimated from the temperature dependence for electrical resistivity. From these observations, it was concluded that the semiconductive properties of polycyclic aromatic compounds are intrinsic.

Meanwhile, a number of investigations have been reported on photoconduction in organic solids. Most of them have been concerned with simple compounds, especially with anthracene crystal. Carswell and Lyons[4] found, by employing a surface-type photocell, that the spectral response curve of photoconduction reproduced quite well the absorption spectrum of anthracene crystal. A similar result was observed by Rosenberg[5], who employed a sandwich-type photocell with conducting glass electrodes. Kommandeur and Schneider[6] have found a more complex behavior by employing a sandwich cell with silver electrodes; e. g., the peaks on the response curve of the photocurrent correspond to the minima of the absorption spectrum.

On the other hand, Kallmann and Pope[7] and Moore and Silver[8] have indicated the extrinsic nature of photoconduction in anthracene; i. e., the injection of holes or electrons from metal electrodes, rather than the generation of charge carriers in the bulk of the crystal, is predominant. This might be due to the high-insulating nature of the materials. At any rate, both effects concerning the carrier generation make the photoconductive behaviors complicated.

Thus, it might be anticipated that polycyclic aromatic compounds, poor insulators or semiconductive materials, would show much simpler behaviors in photoconduction. In this paper, the spectral response of the photoconductivity of polycyclic aromatic compounds is investigated in relation to the optical absorption spectra and the thermal energy gaps.

Experimental

Procedures in the photoconductivity measurements are similar to those described in the previous report[1]. For the investigation of the spectral response of the photocurrent, a single monochromator with the normal Wadsworth arrangement was used, associated with a 1000-watt tungsten lamp as the light source. The calibration for the monochromator was made by referring to emission lines from mercury (435.8 mμ, 546.1 mμ, 579.1 mμ), sodium (589 mμ), lithium (670.8 mμ) and potassium (770 mμ) vapors, and to absorption lines of liquid chloroform (1411 mμ, 1694 mμ, 1861 mμ) and of liquid 1, 2, 4-trichlorobenzene (1660 mμ). All of these spectra were detected by a thermopile or a PbS photocell, which was placed in front of the output slit. The spectrum from the monochromator extends from about 370 mμ to 2500 mμ, with the maximum intensity of 2×10^{16} photons/sec. cm^2 at 1415 mμ.

The surface-type photocell was employed; hence the image of the output slit of the monochromator was directed onto the cell perpendicularly to the direction of the electric field. Aromatic films were about 0.5 μ in thickness.

Absorption spectra, in ultraviolet and visible regions, of aromatics, both in thin films and dissolved in benzene, were recorded at room temperature using a Cary Model 14 spectrophotometer. The films, of a suitable thickness, about one micron or less, were prepared on pyrex plates by the sublimation method. The concentration of the solution was adjusted into the order of 10^{-5} mol./l. Measurements of the absorption spectra of solid phases were not easy because their surfaces were not completely flat. It was necessary, consequently, to take account of the light loss due to scattering at the surface and in the bulk, as well as the reflection loss at the surface. Confusion was avoided by inserting a "diffuser" (a pair of opal glass plates) in front of the photoreceiver of the spectrometer.

Fluorescence spectra excited by 365 mμ ultraviolet irradiation from a mercury discharge lamp were determined with the aid of the spectrophotometer. The irradiation was applied to the surface of film which faced the input slit of the spectrophotometer.

Measurement of the electrical resistivity as a function of temperature was made similarly to that method described by Inokuchi[9].

Results

Absorption Spectra.—The optical absorption spectrum of polycrystalline film was noted to resemble closely that of the solution of the same compound, excepting some broadening and shift of peaks. In consequence, assignments of the bands were made easily, according to Clar's notation[10], to the p-, α- and β-bands. The values of the shift for each transition induced by the phase change from solution to polycrystalline film are given in Table I. The red-shifts of the p-bands are in the order of from 1050 cm^{-1} (0.13 eV.) to 2260 cm^{-1} (0.28 eV.) throughout the series of compounds; the larger molecules show greater shifts. On the

4) D. J. Carswell and L. E. Lyons, *J. Chem. Soc.*, **1955**, 1734.
5) B. Rosenberg, *J. Chem. Phys.*, **29**, 1108 (1958).
6) J. Kommandeur and W. G. Schneider, ibid., **28**, 582 (1958).
7) H. Kallmann and M. Pope, ibid., **32**, 300 (1960).
8) W. Moore and M. Silver, ibid., **33**, 1671 (1960).
9) H. Inokuchi, This Bulletin, **24**, 222 (1951).
10) E. Clar, "Aromatische Kohlenwasserstoffe", Springer Verlag, Berlin (1952).

Table I. The red-shift of the absorption peak induced by the change of phase from solution to polycrystalline film

	Peak on the spectrum of solution		Peak on the spectrum of film		Red-shift	
	p-Band	α-Band	p-Band	α-Band	p-Band	α-Band
Anthracene	3.32 eV.	eV.	3.16 eV.	eV.	0.16 eV.	eV.
Chrysene	3.89	3.46	3.73	3.39	0.16	0.07
Pyrene	3.72	3.35	3.56	3.31	0.16	0.04
Perylene	2.87	3.68	2.67	3.61	0.20	0.07
Anthanthrene	2.87		2.71		0.16	
1, 12-Benzperylene	3.21		3.02		0.19	
2, 3, 7, 8-Dibenzpyrene	2.76		2.63		0.13	
Coronene	3.64		3.44		0.20	
Pyranthrene	2.69		2.41		0.28	
Violanthrene	2.53		2.29		0.24	
Ovalene	2.68		2.44		0.24	

other hand, the shift of the α-band remains nearly constant at a magnitude of about 400 cm^{-1} (0.05 eV.). However, there is the possibility that the weak α-band underlies the intense p-band; therefore, it is difficult to detect the α-band from the spectrum, especially when it is a broad one. The vibrational structure was seen in the p-band, which possessed a spacing of about 1450 cm^{-1} (0.18 eV.). This value was noted to be nearly constant for the series of compounds studied in polycrystalline film as well as in solution. This mode of vibration which couples with the electronic excitation might be the stretching of the aromatic skeleton.

No variation was found in the spectra by pumping out the ambient air of the film specimen. In general, the absorption curve of film possesses a considerably long tail extending to long-wavelength range. For instance, the absorption spectrum of pyranthrene film extends its tail as long as to 2.6 μ, the long-wavelength limit of the spectrophotometer. This leads to difficulty in specifying a unique absorption edge. In relation to the spectral response of photoconductivity which will be discussed in the later section, careful observation was made on the absorption in the long-wavelength region outside the main absorption region.

In some cases, a band, weak but comparable in sharpness with p-band, was observed on the tail of the film spectrum. Pyranthrene exhibited the maximum at 1.53 μ, and violanthrene at 1.40 μ. These bands possess no vibrational structure. When a thicker film was employed, the band was quite well developed without any change in the position of the maximum. This is shown in Fig. 1 for violanthrene film. Concerning the origin of these weak absorption bands, it is unlikely that the absorption is caused by an inclusion of impure molecules, for an incorporated impurity usually exhibits a much sharper absorption band. It is also unlikely that the absorption is due to a transition between vibrational levels. Polycyclic aromatic hydrocarbons exhibit specific infrared absorption bands in the wavelength region longer than 3.33 μ[11]. All these absorption bands appear out of the wavelength region concerned. However, there remains the possibility that overtone or combination bands of these fundamental vibrations would appear in the region which is

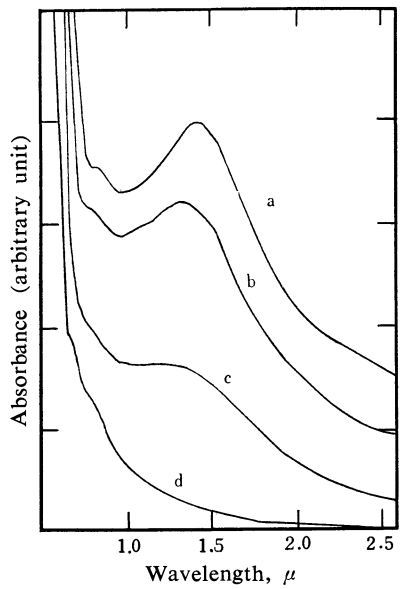


Fig. 1. The optical absorption spectrum of violanthrene film of various thickness in the near infrared region. The thickness of film: a>b>c>d.

11) H. W. Thompson, E. E. Vago, M. C. Cornfield and S. F. D. Orr, *J. Chem. Soc.*, **1950**, 214.

concerned. It was attempted to record the absorption spectra in thick single crystals of pyrene and perylene. Seventeen narrow bands were separated in the region from 2.05 to 2.60 μ (0.13 eV. in interval), of which the most intense band showed a band-width of the order of 0.005 eV. In addition, pyrene exhibited another narrow absorption band at 1.68 μ, 0.01 eV. in width, which was accompanied by a less pronounced peak with the maximum at 1.64 μ. (Fig. 2). In comparison with the bands concerned, these vibrational bands are much sharper in band-width. Other possibilities such as the molecular exciton band or the intermolecular charge transfer band must be kept in mind; however, these have not been clarified at present.

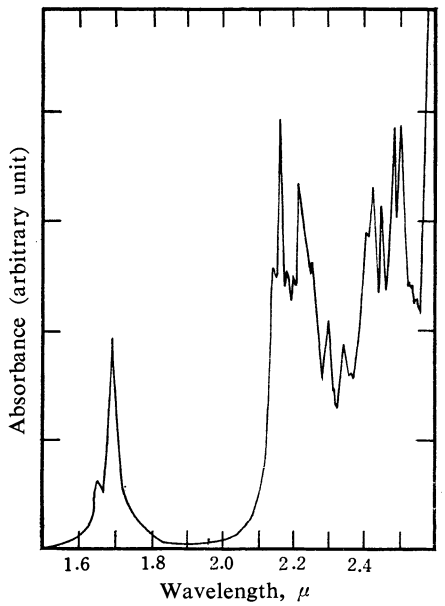


Fig. 2. The optical absorption spectrum of pyrene single crystal in the near infrared region.

Spectral Response of Photoconductivity.— Photocurrent arises whenever light falls in an electronic absorption region of a compound. The magnitudes of the photocurrents were usually in the range of $10^{-9}\sim10^{-14}$ amp. in vacuo (10^{-3} mmHg). A preliminary experiment showed, however, that exposure to air enhanced the photocurrent for most of the specimens. To preclude the oxygen effect, the spectral response of photoconductivity was observed in vacuo, with surface-type cells. The measurements of photocurrent with varying intensity of the incident light indicated that the current observed was almost proportional to the light intensity in the region lower than 10^{16} photons/sec. cm^2. This was true with the different wavelengths[1]. Therefore, in order to normalize the photocurrent to the same input intensity of illumination, the observed photocurrent was divided by the incident light intensity for each wavelength.

The photoconduction spectra of pyranthrene, violanthrene, perylene, violanthrone, anthanthrone and indanthrazine are illustrated in Figs. 3—8. The optical absorption spectra of these films are also shown in the same figures. The photoconduction spectrum resembles the

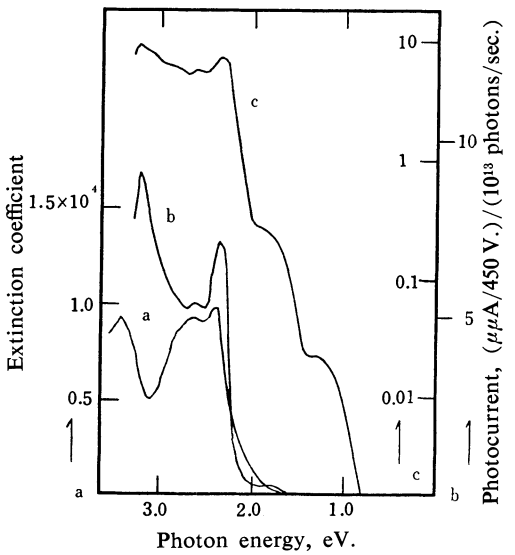


Fig. 3. The spectral responses of (a) extinction coefficient and (b), (c) photocurrent for pyranthrene film.

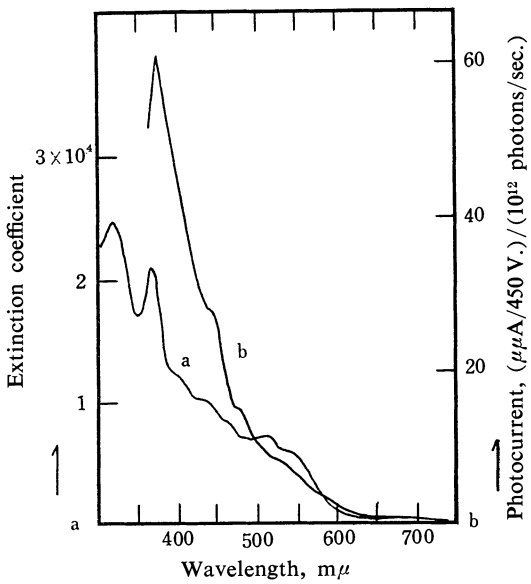


Fig. 4. The spectral responses of (a) extinction coefficient and (b) photocurrent for violanthrene film.

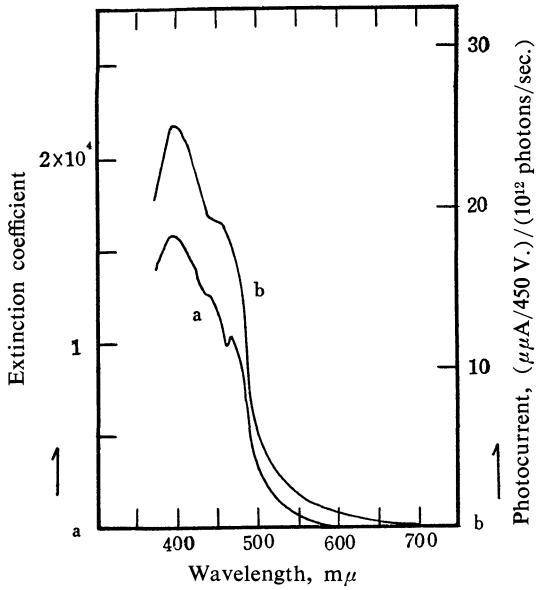


Fig. 5. The spectral responses of (a) extinction coefficient and (b) photocurrent for perylene film.

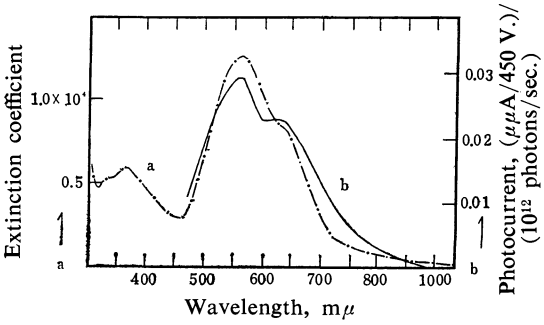


Fig. 6. The spectral responses of (a) extinction coefficient and (b) photocurrent for violanthrone film.

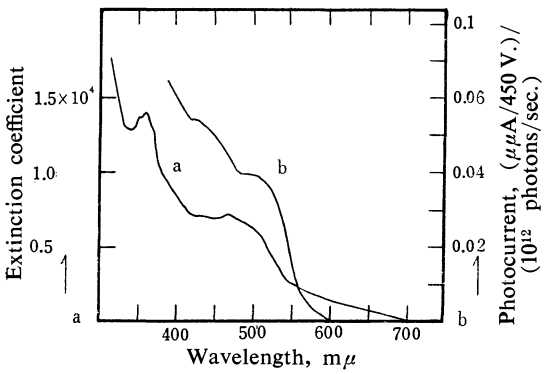


Fig. 7. The spectral responses of (a) extinction coefficient and (b) photocurrent for anthanthrone film.

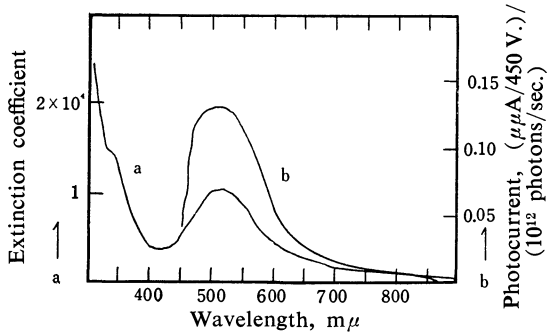


Fig. 8. The spectral responses of (a) extinction coefficient and (b) photocurrent for indanthrazine film.

TABLE II. THE PEAK ON THE SPECTRAL RESPONSE CURVE OF PHOTOCONDUCTION

	Peak of photoconduction spectrum	Peak of absorption spectrum	Assignment
Perylene	25300 cm^{-1}	25700 cm^{-1}	p
		24300	p
		22900	p
	21200	21500	p
Pyranthrene	25800	28000	β
		23400	p
	21300	21400	p
	19000	19400	p
Violanthrene	26400	27100	β
		24300	
	22700	22900	p
		21600	p
	20900	20700	p
		19600	p
	18000	18500	p
Indanthrazine	19400	19550	
Anthanthrone		27700	
	23300	23150	
	19600	21200	
Violanthrone		22750	
	18000	17900	
	15900	15800	

absorption spectrum of the same film, and a good correspondency was found between peaks on the response curve and peaks on the absorption curve, concerning both position and intensity. (Table II). Consequently, assignments could be made for peaks on the response curve by referring to the p- or β-band on the absorption spectrum.

It is concluded that the photoconduction spectrum reproduces the absorption spectrum essentially and, in consequence, that the photocurrent is produced by the light energy which is absorbed into the bulk of the organic solid.

Out of the region of the principal absorption band, the sensitivity of photoconduction

TABLE III. THE THRESHOLD OF THE PHOTOCONDUCTION

	Practical threshold value	$\lambda_{1/2}$ point of the longest wavelength p-band on the photoconduction spectrum	Thermal energy gap ε
Violanthrene	0.70 eV.	2.11 eV.	0.89 eV.
Violanthrone	0.99	1.75	0.78*
Pyranthrene	0.64	2.24	1.11
Indanthrazine	0.80	2.11	0.66**
Anthanthrone	1.91	2.27	1.70*
Perylene	0.94	2.52	2.2***
Anthracene	2.2	3.10	2.7****

* Ref. 9.
** H. Inokuchi, This Bulletin, **25**, 28 (1952).
*** M. Sano and H. Akamatu, **34**, 1569 (1961).
**** H. Inokuchi, ibid., **29**, 131 (1956).

TABLE IV. THE X-BAND IN THE PHOTOCONDUCTION SPECTRUM

	Pyranthrene	Violanthrene	Perylene
X-Band	1.28 eV.	1.09 eV.	2.05 eV.
$\lambda_{1/2}$ point of X-band	1.05	0.87	1.95
Thermal energy gap (ε)	1.11	0.89	2.2
Triplet level presumed	1.29	1.12	1.57*

* G. G. Hall, *Proc. Roy. Soc.*, **A213**, 113 (1952).

decreased more or less exponentially with the increasing wavelength and continued to extend over the infrared region. This makes it difficult to specify the threshold value. The attempt was made, nevertheless, to find a threshold beyond which the photocurrent could not be detected practically. The practical threshold values are compared with the thermal energy gaps for semiconduction for a series of compounds in Table III. It is to be noted that these values are not coincident with each other and that in some cases a rather large discrepancy was found. In the same table, the photon energies at the $\lambda_{1/2}$ point, where the photoconductive sensitivity falls to half its maximum value (the peak of the p-band), are also shown.

In the cases of pyranthrene, violanthrene and perylene, weak maxima were observed on the response curve in the wavelength region longer than the main peaks. These maxima, which are named here as the X-band and the Y-band respectively, were found at 10300 cm^{-1} and 13900 cm^{-1} for pyranthrene (Fig. 3), at 8800 cm^{-1} and 13400 cm^{-1} for violanthrene, and at 16500 cm^{-1} for perylene. These weak bands (X and Y) were detected by a sandwich-type cell as well as by a surface-type cell. Variation in applied electric field and in temperature (from room temperature to $-100°C$), or opening the film to the air, did not change the shape of these extra bands, in spite of the variation in their magnitudes.

An attempt was made to measure photoconduction under an ambient illumination. The pyranthrene surface-type cell was placed under the illumination (ambient) of a monochromatized light, and the same surface was irradiated with a second monochromatized light. The spectral response curve (of the second irradiation) was found to be unchanged from the response curve which was observed in the absence of the ambient light, independently of its wavelength. This was the case for the extra weak bands also; such a behavior as the infrared quenching of the photocurrent could not be observed. The result implied that the X- and Y- bands could not be distinguished in their natures from the main bands and were not produced by trapped electrons.

Discussion

From comparing our results with those of others[4-6], it can be concluded that the photoconduction spectra of aromatic crystals reproduce the optical absorption spectra. With the surface-type cell, when the irradiation is made normally on the film surface, the greatest variation in electrical conductivity (i. e., photocurrent) will be produced in the uppermost layer of the film, because the photons are absorbed most prominently according to Lambert's law; furthermore, the flux of the electric field is concentrated along the uppermost layer to which the electrodes are attached. If it is assumed that the photoconductivity is of the intrinsic nature of the compound and

that the charge carriers are produced in the bulk of the compound, then the number of carriers will be proportional to the number of photons absorbed into the bulk, with a definite coefficient of quantum yield.

The number of photons (L) absorbed by the film with the thickness d is given by the formula

$$L=L_0(1-10^{-Kd})$$

where L_0 is the incident light intensity and K is the extinction coefficient. As K is the order of $10^4\,cm^{-1}$ for the principal bands, a film 0.5 μ in thickness absorbs nearly 70 per cent of the incident light. When Kd is small enough for its higher powers, L will be proportional to Kd. Thus the photocurrent can be anticipated to be proportional to K when the film thickness is slight. Furthermore, when it is assumed that the quantum yield of photoconduction is constant independently of the wavelength of the illumination, the response curve will reproduce the absorption curve. This is the case we have observed. The principal bands of the absorption spectra consist of the singlet-singlet transitions; thus, all of these excited states are equally responsible for the electronic conduction, but with a probability depending on each transition moment.

Outside the principal bands, a long tail is generally observed on the response curve. No reliable interpretation has been offered for the photosensitivity in the long wavelength region. This makes it difficult to specify the threshold of photoconductivity. The practical threshold value is dependent on the sensitivity of the equipment; thus, the concept becomes rather a vague one. For the intrinsic photoconductors, Moss[12] has proposed a convenient characteristic wavelength at which the photosensitivity falls to half its maximum value (the $\lambda_{1/2}$ point). In the cases of perylene and anthracene, the coincidence of the energy values between the thermal energy gap and the $\lambda_{1/2}$ point is not so bad, but in other cases large discrepancies are noted. (Table III). Similar discrepancies were pointed out by Vartanyan and Karpovich[13] for violanthrone and pyranthrone.

In connection with this, the extra peaks which were found on the tail of the main bands of photoconduction spectra are of interest. Similar extra peaks were found for anthracene by Rosenberg[5], and for pyrene by Kommandeur, Korinek and Schneider[14]. In the latter case, it was reported that the extra bands were observable in crystal possessing a rather considerable thickness. In the present case, however, the film was as thin as 0.5 μ in thickness, and the bands are of the same nature as the main bands, as was mentioned in the previous section. The most characteristic fact for the extra bands is that one of them (the X-band) is located at the energy which corresponds to the thermal energy gap. Thus, the $\lambda_{1/2}$ point of the X-band is in fairly good agreement with the value of the thermal energy gap. This is shown in Table IV.

A number of possible explanations for the extra bands are conceivable; some of them were pointed out by Kommandeur et al.[14], while Rosenberg[5] assumed the electron transfer through the triplet state for anthracene.

The location of the X-band is far below the singlet-singlet transition. Concerning the lowest excited singlet state, the fluorescence spectrum is suggestive. For instance, the p-band of the pyranthrene film ranged from around 400 mμ to 650 mμ, with the maximum at 516 mμ, while the fluorescence band ranged from 496 mμ to 734 mμ, with the maximum at 648 mμ (1.92 eV.) (Fig. 9). The peak-peak separation between the absorption and the fluorescence bands is generally found to be in the order of a few thousands cm^{-1} for polycyclic aromatic compounds in a crystalline state. This might be due to the molecular interaction in the excited state. However, it is clear that the lowest excited singlet level

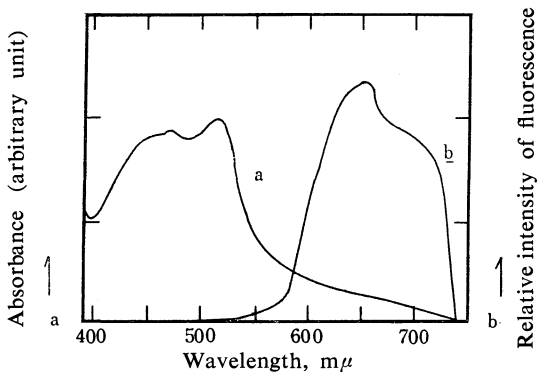


Fig. 9. (a) Absorption and (b) fluorescence spectra of pyranthrene film.

lies above 1.92 eV. for pyranthrene film, while the X-band is located at 1.28 eV. It is known[15] that the lowest triplet state (^3L) is 2.32 eV. below the p-band (^1L_a) in benzene and 1.71 eV. below in naphthalene, while the $^1L_a-{}^3L$ separation is around 1.4 eV. in the larger aromatic

12) T. S. Moss, "Photoconductivity in the Elements", Butterworths Publ., London (1952).
13) A. T. Vartanyan and I. A. Karpovich, *Doklady Akad. Nauk. S. S. S. R.*, **113**, 1020 (1957).
14) J. Kommandeur, G. J. Korinek and W. G. Schneider, *Can. J. Chem.*, **36**, 607 (1958).

molecules. If it is true for pyranthrene and violanthrene and if the triplet level in the crystalline state is not far from the molecular level, it follows that the bands concerned may be assigned to the lowest triplet state (Table IV).

The weak absorption band which was found at 1.40 μ (0.89 eV.) for violanthrene is not far from its X-band, but 1.53 μ (0.81 eV.) for pyranthrene is not in coincidence with the X-band.

From the above discussion, it may be concluded that the photoconduction takes place by associating with the lowest excited state of molecules in the aromatic crystals. The semiconduction also occurs in the same excited state, or even with smaller energy. It has been frequently presumed[16] that the photoconduction band should be located near the ionization level of the molecule, but that the lowest excited state could not be responsible for the electrical conduction, even though the dipole-dipole interaction between excited states results in developing the molecular exciton band. But this is not coincident with observed results. Recently, Lyons and Morris[17] have attempted ultraviolet irradiation in the vacuum region onto anthracene crystal; however, no photoconductivity distinguishable from the usual one could be found.

Concerning the mechanism for photoconduction in the lowest excited state, there are three possible schemes at least. (1) There might be a sufficient intermolecular orbital overlap which results in developing the true conduction band even in the lowest excited state. (2) If it is not the case, the electrons or the positive holes might be exchangeable between neighboring molecules through the vibrational levels in the lowest excited state during the life time of the excited state ($\sim 10^{-8}$ sec.), which is long enough compared with the vibrational period ($\sim 10^{14}$ sec.). This would result in the hopping conduction. (3) The electron transfer may take place via the triplet state much more easily than via the excited singlet state, because of its long life time; the singlet-triplet transition through the intersystem crossing is well known.

Lyons and Morris[18] have found that the photo-emission of electrons from aromatic crystals can occur at a potential which is lower by 1~2 eV. than the ionization potential of the molecules. However, the ionization continuum in the crystal is still much higher than the energy level of the lowest excited state.

With regard to the second and the third scheme, the temperature dependence for photoconductivity is of interest. As reported in the previous paper[1], the activation energy of photoconduction is 0.18 eV. for pyranthrene; nearly the same value was found for anthracene (0.17 eV.) by Rosenberg[5], and for pyranthrone (0.2 eV.) and for violanthrone (0.2 eV.) by Vartanyan[13]. Thus, this value is apparently quite general for polycyclic aromatics and is coincident with the vibrational energy of the skeletal stretching of aromatics. Some reason might be expected for the fact that such a mode of vibration is the most favorable for the coupling with the electronic excitation as well as for the intersystem crossing.

The photosensitivity which was found in the region of the triplet state supports the possibility of the third scheme. Moreover, it has been confirmed[19] that the electron spin resonance absorption in aromatic crystals under irradiation is due to the triplet state. Thus, the scheme for electron transfer via the triplet state is an attractive one.

Summary

The spectral responses of the photoconductivity of perylene, pyranthrene, violanthrene, anthanthrone, violanthrone and indanthrazine, as well as the optical absorption spectra of these aromatic solids, have been investigated. Associated with the surface-type cells, when the aromatic films are thin enough, the response curves reproduce the absorption spectra. It has been concluded from this that the photoconductivity is the intrinsic property of the compound and that the lowest excited states are responsible for the electrical conduction.

The thresholds for photoconductivity are rather vague. In some cases, however, extra bands are found in the photoconduction spectra outside the main bands. These extra bands locate in the energy regions which correspond to the triplet states of the molecules and are coincident with the thermal energy gaps for the semiconduction.

The cost of this study was defrayed by a grant of the Ministry of Education, to which the authors' thanks are due.

Department of Chemistry
Faculty of Science
The University of Tokyo
Hongo, Tokyo

15) H. B. Klevens and J. R. Platt, *J. Chem. Phys.*, **17**, 470 (1949).
16) M. Kasha, *Rev. Mod. Phys.*, **31**, 162 (1959).
17) L. E. Lyons and G. C. Morris, *J. Chem. Soc.*, **1960**, 5200.
18) L. E. Lyons and G. C. Morris, ibid., **1960**, 5192.
19) C. A. Hutchison, Jr. and B. W. Mangum, *J. Chem. Phys.*, **34**, 908 (1961).

Studies on Solvent Extraction using Radioactive Isotope. X[1]. Solvent Extraction of Zirconium-95 and Niobium-95 with Acetylacetone

By Nobuo SUZUKI and Takashi OMORI

(Received August 15, 1961)

The solvent extraction method has been successfully applied to the separation of zirconium-hafnium[2,3] and niobium-tantalum[4,5]. There have been a few reports on the separation of ^{95}Zr (^{95}Nb) from other fission products[6-8]. The present authors have previously reported that ^{144}Ce is nearly perfectly extracted with acetylacetone and that the extraction of ^{95}Zr (^{95}Nb) with the same reagent is possible. According to the literature, the percentage extraction of zirconium from aqueous phases of pH values ranging from 0.9 to 2.3 are 10~70, but the details are inaccessible[9]. Moreover, no study on niobium exists in the literature. In the present wark the extraction behaviors of zirconium and niobium are investigated, and the results of the extraction separation of ^{95}Zr and ^{95}Nb from each other are presented.

Experimental

Reagents.—*Stock Solutions of ^{95}Zr and ^{95}Nb.*—^{95}Zr and ^{95}Nb were separated, by means of the ordinary anion exchange separation procedure[10], from ^{95}Zr-^{95}Nb equilibrium mixture imported from the Oak Ridge National Lab., U. S. A., by an ion-exchange resin Dowex 2-X8 using a 0.1 M hydrochloric acid-0.01 M oxalic acid mixture as an eluant. The respective effluents were evaporated to fumes with sulfuric and nitric acids to give stock solutions. The acidity of the stock solutions was 9 N for ^{95}Zr and concentrated sulfuric acid for ^{95}Nb. As for ^{95}Zr, a solution less than 2 days old was used to eliminate the error due to the contamination of the ^{95}Nb daughter growth. The stock solutions prepared by potassium hydrogen sulfate fusion gave nearly the same results, but the results of ^{95}Nb were slightly less reproducible. For this paper, therefore, the stock solution prepared by the acid treatment was used.

Acetylacetone.—A commercial reagent was further purified by washing with ammonia water (1 : 10) and was distilled twice. The distillation fraction of 138°C was used.

Organic Solvents.—E. P. grade greagents were distilled twice.

Other Chemicals.—Guaranteed grade chemicals were used without further purification.

General procedure.—An acetate buffer solution containing ^{95}Zr and ^{95}Nb was shaken with an acetylacetone-chlorofrom mixture in a vessel for a suitable period. ^{95}Zr or ^{95}Nb was added just before shaking. The pH of the aqueous phase was adjusted with dilute nitric acid or sodium hydroxide, the ionic strength being kept at 0.6 with component salts. After separation of the layers, the radioactivity was measured* with a well-type scintillation counter made by the Kobe Kogyo Co., and the pH value was measured with a M-3 type glass-electrode pH meter made by the Horiba Instrument Co.

Concentration Effect of Acetylacetone.—To examine the effect of the concentration of acetylacetone, the extractions were carried out with acetylacetone-chloroform mixtures of various concentrations, the volume percentages of acetylacetone being 5, 10, 20, 30, 40, 50 and 100. To obtain the data for ^{95}Zr, the aqueous phase of pH 4.9 was shaken for two minutes. As is shown in Fig. 1, the extraction ratio is nearly constant above ca. 10% of acetylacetone in chloroform, but it drops in the case of pure acetylacetone. The lowering of the extractability in the case of pure acetylacetone

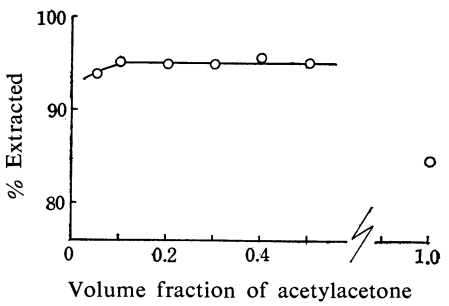


Fig. 1. Extraction of ^{95}Zr as function of volume fraction of acetylacetone in chloroform.

1) Part IX of this series: N. Suzuki and S. Oki, This Bulletin, **35**, 237 (1962).
2) E. H. Huffman and C. J. Blaufait, *J. Am. Chem. Soc.*, **71**, 3179 (1949).
3) W. Fischer, W. Chalybaeus and C. Zumbusch, *Z. anorg. Chem.*, **255**, 277 (1948).
4) J. Y. Ellenburg, G. W. Leddicote and F. L. Moore, *Anal. Chem.*, **26**, 1045 (1954).
5) M. L. Theodore, ibid., **30**, 465 (1958).
6) F. L. Moore, ibid., **28**, 997 (1956).
7) C. G. Hardy and D. Scargill, *J. Inorg. Nucl. Chem.*, **9**, 322 (1959).
8) E. D. Scadden and N. E. Ballou, *Anal. Chem.*, **25**, 1602 (1953).
9) J. P. McKaveney and H. Freiser, ibid., **29**, 290 (1957).
10) K. E. Wacker, *ORLN-638* (1950).

* A correction for the difference in the counting efficiency between the two phases was made by multiplying the counting rate of counting rate of the organic phase by the factor 1.027.

is presumed to be due to the decrease in the partition of the chelated compounds between the two phases. Based on these results, a 20% acetylacetone solution was chosen for further experiments.

Effect of Shaking Time.—The effect of the shaking time on the extraction of ^{95}Zr and ^{95}Nb using a 20 per cent acetylacetone solution was studied. The results are shown in Fig. 2,

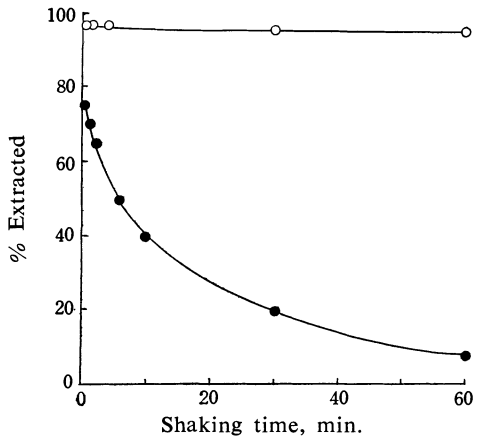


Fig. 2. Extraction of ^{95}Zr and ^{95}Nb with 20% acetylacetone in chloroform as function of shaking time.
-○- ^{95}Zr at pH 5.6
-●- ^{95}Nb at pH 5.7

where no perceptible change in the extraction ratio of ^{95}Zr is seen by the extension of the shaking time up to an hour. On contrary, the the extraction ratio of ^{95}Nb from the aqueous phase having the same pH value of 5.7 decreases remarkably with the length of the shaking time. The lowering of the extractability of ^{95}Nb can be accounted for by hydrolysis, as will be seen in the results of an extraction curve given later. The lowering of the pH value will prevent the hydrolysis, and, in fact, the effect of the shaking time was not appreciable when the pH value was reduced to 3. Based on these results, the shaking time was chosen to be two minutes for ^{95}Zr and one minute for ^{95}Nb for further studies.

Extraction Curve.—To examine the relation between the pH value of the agueous phase and the extractability of ^{95}Zr and ^{95}Nb, extraction with 20% acetylacetone in chloroform was carried out. The extraction curves are shown in Fig. 3, where it is .seen that 98% of the ^{95}Zr was extracted at a pH range of from 3 to 8, and 92% of ^{95}Nb was extracted at a pH range of from 2 to 5 by a single extraction. Thus, the optimum pH range for ^{95}Nb is slightly narrower than that for ^{95}Zr because of hydrolysis. It is doubtful, however,

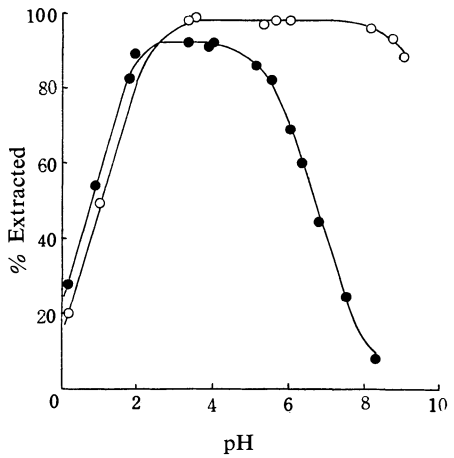


Fig. 3. Extraction of ^{95}Zr and ^{95}Nb with 20% acetylacetone in chloroform as function of pH.
-○- ^{95}Zr -●- ^{95}Nb

that these extraction curves represent the true equilibrium state over the entire pH range examined; the pH range is at least partially in such an unstable condition that hydrolysis is probably occuring.

Extraction by Various Solvents. — Acetylacetone can be used both as a solvent and as an extractant, and in a number of cases various organic solvents are used as a diluent. For example, carbon tetrachloride[1], chloroform[9], and benzene[11-13] were used as a diluent. In the preceding chapter it was reported that an acetylacetone-chloroform mixture showed a higher extractability than pure acetylacetone. The results of the extractions using 20 vol.% solutions of acetylacetone in various solvents are shown in Table I, were the pH values

TABLE I. EXTRACTION OF ^{95}Zr AND ^{95}Nb WITH VARIOUS SOLVENTS

Solvent	% Extracted	
	^{95}Zr	^{95}Nb
Benzene	88.6	61.5
Xylene	—	55.8
Carbon tetrachloride	88.5	37.6
Chloroform	97.7	89.8
Methylene chloride	96.5	79.9
Isopropyl ether	51.5	1.0
Methyl isobutyl ketone	65.4	4.2
Ethyl acetate	71.6	44.3
Isoamyl acetate	64.8	49.0
Tri-*n*-butyl phosphate	64.3	53.5
Kerosene	13.9	10.0

11) N. Suzuki and S. Ohi, This Bulletin, 35, 233 (1962).
12) A. G. Maddock and G. L. Milles, *J. Chem. Soc.*, **1949**, 248.
13) B. G. Harvey, H. G. Heal, A. G. Maddock and E. L. Rowley, ibid., **1947**, 1010.

after the extraction covered the range from 5.7 to 5.8 for ^{95}Zr and from 4.2 to 4.3 for ^{95}Nb. Chloroform showed the highest extractability for both ^{95}Zr and ^{95}Nb, and methylene chloride came next.

Effect of Coexisting Salts.—The coexisting salts show a considerable influence upon the extraction of ^{95}Zr and ^{95}Nb. The results in the presence of a substance such as sodium chloride, sodium nitrate, ammonium sulfate, sodium hydrogenphosphate, potassium thiocyanate, sodium acetate, hydrogen peroxide, hydroxylamine, oxalic acid, citric acid and disodium ethylenediaminetetraacetate (EDTA) are shown in Table II, where the concentrations in the

Table II. Effect of coexisting substances

Substance	Concn. in aq. phase M	% Extracted ^{95}Zr	% Extracted ^{95}Nb
$NaNO_3$	2	97.0(8.3)	79.0(3.7)
NaCl	2	97.6(8.5)	81.7(3.7)
$(NH_4)_2SO_4$	2	98.1(6.3)	69.6(4.1)
Na_2HPO_4	0.2	1·1(—)	1.7(4.7)
KSCN	1	94.3(4.5)	80.0(4.3)
CH_3CO_2Na	0.75	98.2(7.0)	90.9(3.4)
H_2O_2	2%	78.1(5.0)	0.3(5.1)
NH_2OH-HCl	1	96.0(4.6)	59.2(3.8)
	0.1	96.2(8.1)	61.7(3.8)
Oxalic acid	0.04	4.7(4.2)	4.5(5.0)
Citric acid	0.2	3.9(4.0)	0.3(4.6)
EDTA	0.001	2.1(4.4)	6.3(5.0)

Parentheses show the pH of aqueous phase at equilibrium with organic phase.

table denote those of the substances present in the aqueous phase. No effect was observed when the concentration of sodium acetate used as a buffer component was raised to 0.75 M. The extractions of both ^{95}Zr and ^{95}Nb were remarkably interfered with sodium hydrogenphosphate, oxalic and citric acids. In general, ^{95}Nb is more sensitive to the interference from coexisting salts. The use of hydrogen peroxide or hydroxylamine as a masking agent has been found in the literature[6,8]. As is seen in the present results, the extraction ratio of ^{95}Zr was reduced only slightly in the presence of

Table III. Effect of hydrogen peroxide

Concn. of H_2O_2 %	% Extracted ^{95}Zr	% Extracted ^{95}Nb
0	98.0(99.5)	91.4
0.004	93.5(97.7)	0.5
0.2	87.3	0.3
2	78.1(94.6)	0.3

Parentheses show total percentage of two-successive extraction.

hydrogen peroxide, whereas ^{95}Nb was perfectly masked by it. In Table III, the extraction ratios obtained in the presence of hydrogen peroxide in various concentrations at pH 5 are given. ^{95}Nb is not extracted under coexistence with hydrogen peroxide, while the extraction ratio of ^{95}Zr increases with the decreasing concentration of hydrogen peroxide. ^{95}Zr could be extracted as high as 98% by successive extraction from the aqueous phase containing a considerable amount of hydrogen peroxide, but it is not practical to extract ^{95}Nb from the residual aqueous layer because 2% of the ^{95}Zr is still left in the aqueous layer.

Back Extraction.—The following experiments were carried out to find the optimum condition for the back extraction of ^{95}Zr and ^{95}Nb from the solvent phase. A 20% acetylacetone-chloroform solution containing ^{95}Zr or ^{95}Nb-acetylacetonate complex was prepared by the standard method, and an aliquot of this solution was shaken with various concentrations of nitric, hydrochloric, and sulfuric acids and hydrogen peroxide solution. The results are shown in Table IV. Sulfuric acid was most effective for the back extraction, both ^{95}Zr and ^{95}Nb being nearly perfectly stripped into the aqueous phase. Nitric and hydrochloric acids were not so effective. ^{95}Nb was more easily

Table IV. Back extraction with various aqueous solutions

Stripping soln.	Shaking time, min.	% Back-extracted ^{95}Zr	% Back-extracted ^{95}Nb
0.1 N HNO_3	1	50.9	17.9
	10	43.5	61.1
1 N HNO_3	1	67.4	35.6
	10	69.6	83.9
2.5 N HNO_3	1	77.4	51.3
	10	78.2	68.1
5 N HNO_3	1	71.6	46.3
	10	69.8	27.6
10 N HNO_3	1	28.3	12.4
	10	—	12.8
0.1 N HCl	1	72.3	21.2
	10	81.0	55.3
1 N HCl	1	96.3	62.9
	10	99.0	89.2
6 N HCl	1	97.2	34.6
	10	97.3	35.7
1 N H_2SO_4	1	98.3	81.6
	10	99.0	91.3
5 N H_2SO_4	1	98.4	87.9
	10	99.5	96.1
9 N H_2SO_4	10	99.8	—
0.3% H_2O_2*	1	0.6	33.7
	10	4.0	66.5

* pH 4.9 acetate buffer

stripped than ^{95}Zr in the pesence of hydrogn peroxide. However, the back extraction ratio of ^{95}Nb was still as high as 66.5% after being shaken for ten minutes. This fact shows that the acetylacetonate complex formed is rather stable.

Mutual Separation of ^{95}Zr and ^{95}Nb.—The experimental results mentioned above suggest two methods for the separation of ^{95}Zr and ^{95}Nb from each other, one being based on the different behavior of ^{95}Zr and ^{95}Nb at a suitable pH value, and the other on the masking of ^{95}Nb with hydrogen peroxide. In the former method, the intention is to make use of the facts that at a high pH value ^{95}Nb is not extracted and that an extension of the shaking time diminishes its extraction ratio. It was not practical, however, to separate ^{95}Zr perfectly by this method, because a small percentage of ^{95}Nb is always accompanied with ^{95}Zr.

Practically, pure ^{95}Zr, free from ^{95}Nb, can be prepared by the latter method. An oxalic acid solution of ^{95}Zr-^{95}Nb was treated with sulfuric and nitric acids, or by potassium hydrogensulfate fusion. The pH value was adjusted to about 5, and hydrogen peroxide was added until the concentration come to 0.2%. Then the solution was repeatedly shaken with a 20% acetylacetone-chloroform mixture. After washing the organic phase with a dilute hydrogen peroxide solution, the aqueous phase was discarded and the organic phase was shaken with 9 N sulfuric acid for ten minutes to strip ^{95}Zr. The acid solution was then washed with chloroform to remove the acetylacetone. The yield was about 96%. The ^{95}Zr obtained was proved to be radiochemically pure by taking a β-ray absorption curve, which showed normal chemical behavior.

Summary

The extraction of ^{95}Zr and ^{95}Nb with an acetylaceton-echloroform mixture was investigated. The percentage extraction of ^{95}Zr with a 20% acetylacetone solution was 98% at pH valves ranging from 3 to 8, and that of ^{95}Nb was 90% at pH values from 2 to 5. The extraction ratio of ^{95}Nb was lowered by the extension of the shaking time. As an diluent, chloroform and methylene chloride were recommended. Phosphate, oxalic acid, citric acid and EDTA interfered remarkably. Sulfuric acid was most efficient for the back extraction. A high purity of ^{95}Zr was obtained by using hydrogen peroxide as a masking agent. The yield was satisfactorily high.

The authors wish to express their hearty thanks to Professor Kunio Seto for his kindly suggestions in the course of this work.

Department of Chemistry
Faculty of Science
Tohoku University
Katahira-cho, Sendai

*The Effect of Dissolved Paramagnetic Ion on the ESR Spectra of Diphenyl Nitric Oxide**

By Yasuo DEGUCHI**

(Received August 16, 1961)

In the preceding two papers[1,2], the author has reported on the study of the ESR spectra of diphenyl nitric oxide (DPNO) in crystalline states and in liquid solutions respectively.

During the course of the study, we noticed that dissolved oxygen[3] in solvents played a remarkable negative role in diminishing the proton hyperfine lines.

As will be shown in the succeeding section, the effect on the proton hyperfine lines of the presence of dissolved oxygen or other paramagnetic ions in solutions is to be explained not by chemical reaction but by magnetic dipole-dipole interaction.

* This work was supported by the U. S. Air Force through the Air Force Office of Scientific Research of Air Research and Development Command under contract. Reproduction in whole or in part is permitted for any purpose of the U. S. Government.

** Present address: Department of Chemistry, Kyoto University, Kyoto.

1) Y. Deguchi, This Bulletin, **34**, 910 (1961).

2) Y. Deguchi, ibid., **35**, 260 (1962).

3) Y. Deguchi, *J. Chem. Phys.*, **32**, 1584 (1960).

The same effect has already been recognized in the NMR experiments[4,5].

Experimental

All samples have been prepared by the same process as described in the preceding paper[3]. In order to investigate the dissolved oxygen effect, a valve with a tapered ground connector has been attached at one end of a sample tube connected to the vacuum line so that one can introduce air into the sample tube and remove air from it.

For the experiment of the foreign paramagnetic ion effect, a graduated cylinder containing a known volume of it with a certain concentration has been connected to the sample tube so that one can add each known amount of foreign paramagnetic ion to the sample successively. Here we used copper tetraphenyl porphyrin (CuTPP) as the foreign paramagnetic ion.

Results

With Dissolved Oxygen.—Figure 1 shows the effect of dissolved oxygen in solution on the ESR spectra of DPNO. Figure 1a is the spectrum of the degassed sample treated as in reference[3]. We can see the well-resolved proton hyperfine spectra in it. Figure 1b is the spectrum taken after opening the vacuum valve to introduce air into the sample tube. The proton hyperfine lines are all broadened, and only the nitrogen hyperfine lines remain. Again outgassing the sample, one can obtain the same well-resolved proton hyperfine lines in Fig. 1c as in Fig. 1a,

With Copper Tetraphenyl Porphyrin (CuTPP).—In the case of oxygen, it is difficult to control the concentration of oxygen in solution. Therefore, we here employed CuTPP as a foreign paramagnetic ion dissolved in solution.

Figure 2a is the spectrum of the degassed DPNO solution where no foreign paramagnetic ion coexists.

By the addition of 2/11 mg. of CuTPP to the solution, almost all the weak proton hyperfine lines disappear, as in Fig. 2b. Then by dissolving each known amount of CuTPP into the solution successively, as shown in Figs. 2c, 2d and 2e, the proton hyperfine lines become broader and broader until only the broad nitrogen splitting lines can be observed and all the proton hyperfine lines disappear.

Discussion

From the aforementioned experiments, we can conclude that this effect is caused by the magnetic dipole-dipole interaction of DPNO with dissolved oxygen or paramagnetic ions in the solutions.

By this interaction, the spin-lattice relaxation time (T_1) of DPNO will become shorter than when no dissolved paramagnetic ion is present in the solution. Thus, we can follow the theory of Bloembergen, Purcell and Pound[5] (BPP). In their case, the spin orientation of protons is relaxed by the dissolved paramagnetic ions, but in the present case the spin orientation of the unpaired electrons of the free radical will be relaxed by the dissolved paramagnetic ions.

Thus, instead of Eq. 54 in BPP's paper, we will obtain:

$$1/T_1 = 12\pi^2\gamma_e^2\eta N_{\text{ion}}\mu_{\text{eff}}^2/5kT$$

where

γ_e: the gyromagnetic ratio of an electron,
η: the viscosity of the solvent at the temperature T°K,
N_{ion}: the number of dissolved paramagnetic ions per cm^3,
μ_{eff}: the magnetic moment of the dissolved paramagnetic ion in the Bohr magneton number,
k: the Boltzmann constant,
T: the absolute temperature of the experiment.

In the case of dissolved oxygen, knowing that the solubility of oxygen, into ethyl alcohol is

$$143\times10^{-3}\text{ cc. per 1 cc. of ethyl alcohol,}$$

we know that the N_{ion} for this case will be

$$3.844\times10^{18}\text{ cm}^{-3}$$

Also the η for ethyl alcohol at 20°C is 1.20×10^{-2} poise, and the μ_{eff} for oxygen in the Bohr magneton number is 2.83.

Then we shall have

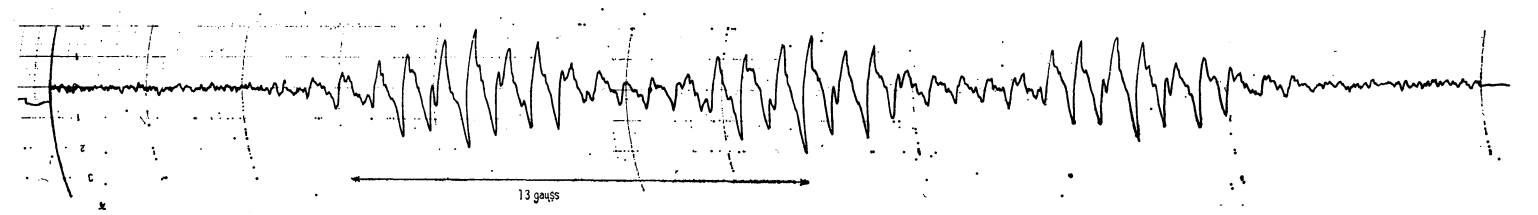
$$1/T_1 = 0.327\text{ gauss}$$

Thus, it turns out that each proton hyperfine line of DPNO in degassed solutions will be broadened further by the amount of 0.327 gauss because of the presence of the dissolved oxygen. As stated, in the preceding papers[2,3], the separation between two successive proton hyperfine lines is about 0.98 gauss, and the half-widths of the sharpest lines in each group of the spectrum are of the order of 0.1 gauss. Thus, not every hyperfine lines will be reserved, and only the broad nitrogen hyperfine lines will be observed.

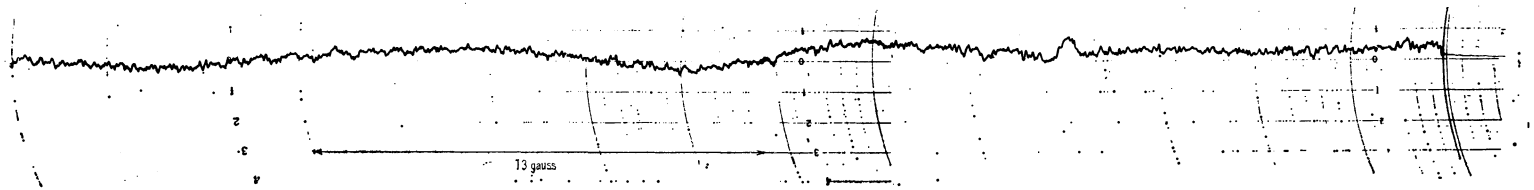
In the same way, foreign paramagnetic ion effect on the proton hyperfine lines can be explained. These results are tabulated in Table I.

There are other spin-lattice relaxation mechanisms such as the exchange interaction[6], the

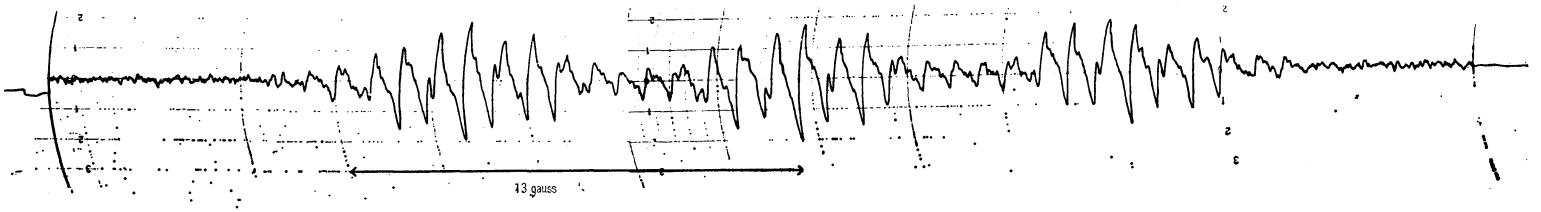
4) F. Bloch, W. W. Hansen and M. Packard, *Phys. Rev.*, **70**, 474 (1946).
5) N. Bloembergen, E. M. Purcell and R. V. Pound, ibid., **73**, 679 (1948).
6) N. Bloembergen, *J. Chem. Phys.*, **72**, 572 (1957).



1a

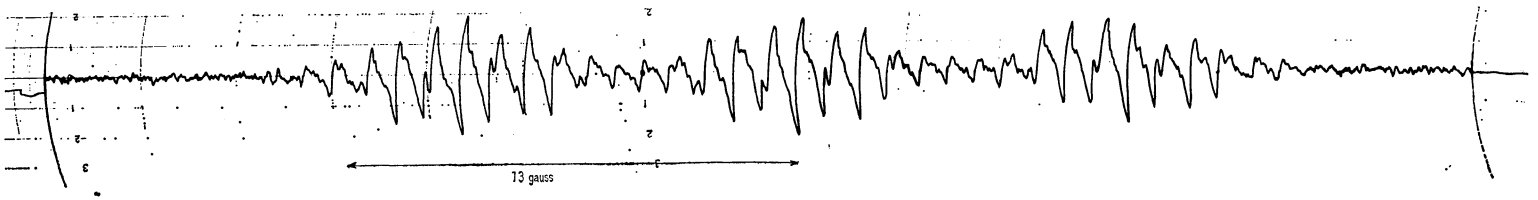


1b



1c

Fig. 1. Dissolved oxygen effect on the ESR spectra of DPNO. 1a: the spectrum of the degassed sample. 1b: the spectrum of the air introduced one. 1c: the spectrum of the again degassed one.



2a

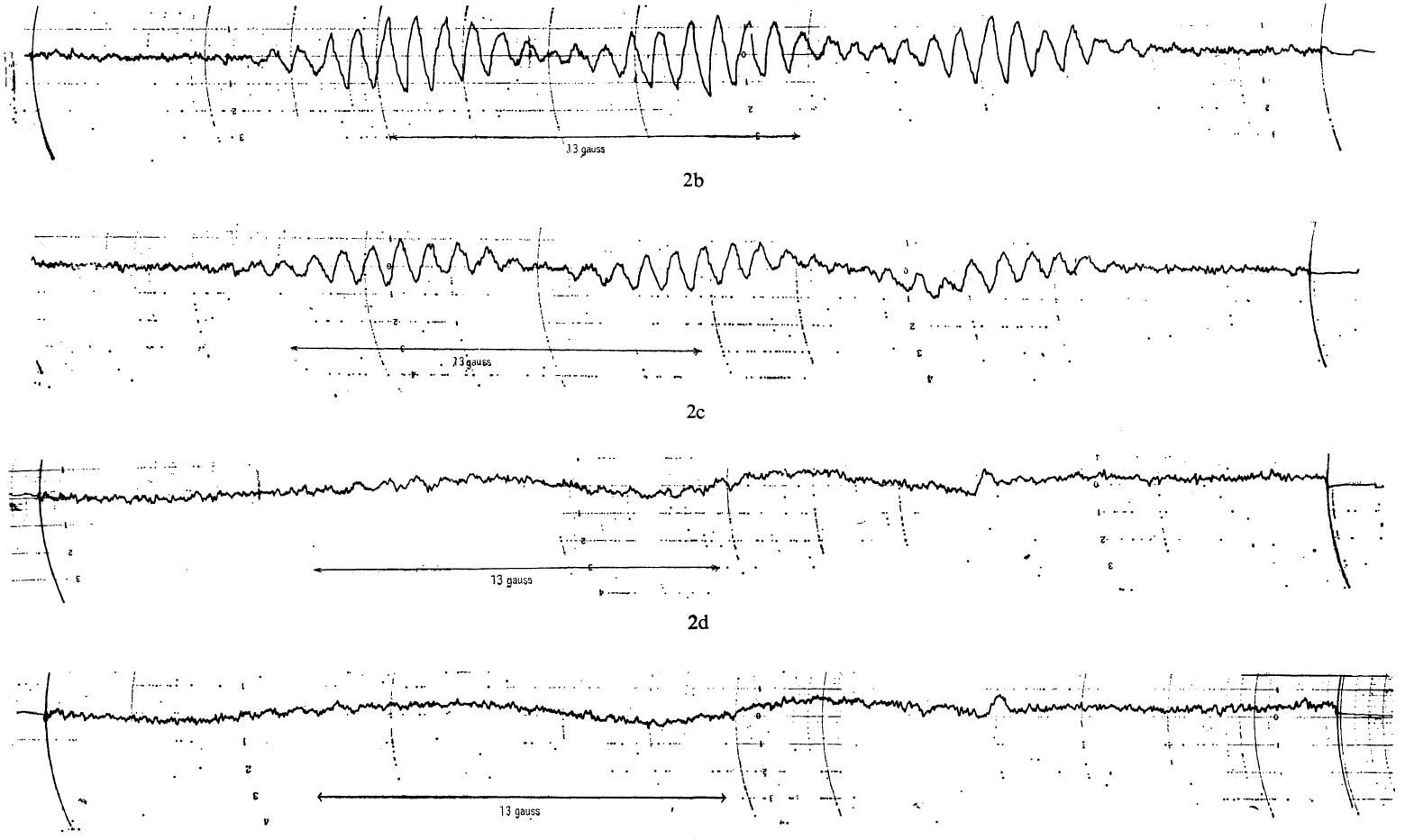


Fig. 2. Dissolved paramagnetic ion effect on the ESR spectra of DPNO. 2a: no dissolved CuTPP presents. 2b, 2c, 2d and 2e: 2/11 mg., 6/11 mg., 10/11 mg. and 52/22 mg. of CuTTP are added into the DPNO sample successively.

Table I

Amounts of added CuTPP to the soln. of DPNO, mg.	No. of CuTPP molecules in the soln. per cc.	Increment of a half-width due to addition of CuTPP, gauss	Resulted half-width for the sharpest hf. line, gauss	Illustration of the spectra
0	0	0	0.1	Normal hf. lines appears.
2/11	0.211×10^{18}	0.055	0.1055	Almost all weak hf. lines disappear and the rest are broader.
6/11	0.632×10^{18}	0.165	0.265	Main hf. lines remain but are more broader.
10/11	1.054×10^{18}	0.274	0.374	Only 2 or 3 broad hf. lines remain but broad nitrogen hf. lines can be clearly observed.
52/22	1.097×10^{18}	0.286	0.386	All proton hf. lines disappear and only nitrogen hf. lines are left.

spin-orbit interaction[7], etc. but in the case of organic free radicals one can neglect these interactions.

From the above discussion, then, one can conclude that dissolved oxygen or other paramagnetic ions in the solutions play an important role in the broadening of the proton hyperfine lines in the ESR spectra of organic free radicals through the spin-lattice relaxation.

Summary

The broadening effect of dissolved oxygen and foreign paramagnetic ions on the ESR spectra of the DPNO solution has been discussed. Using the BPP theory, it is explained that this effect is mainly caused by the magnetic dipole-dipole interaction of an electron with with a proton nuclear spin.

The author wishes to express his appreciation and indebtedness to Professor S. I. Weissman for his helpful discussion and suggestion and to Professor J. Townsend for offering him the chance to use the ESR apparatus which he had constructed. He also wishes to thank Professor K. Tomita and Dr. T. Hashi for their helpful discussions.

Department of Chemistry
Washington University
St. Louis, MO., U. S. A.

7) N. Bloembergen and L. O. Morgan, ibid., **34**, 842 (1961).

Inductive Effects in Some Chlorinated Carbonyl Compounds and their Nuclear Quadrupole Resonance Frequencies

By Shinhachiro SAITO*

(Received March 28, 1961)

It is well known that the chlorine nuclear quadrupole resonance (NQR) frequency increases with the increasing number of chlorine atoms attached to the same carbon atom, and that the frequency increase depends upon the electronic state of the molecule containing the chlorine atom. In the study of the NQR spectra of molecular crystals, Allen[1] suggested that the electron withdrawal abilities of carbonyl groups from the $-CH_2Cl$ and $-CCl_3$

* Present address: The Research Institute for Iron, Steel and Other Metals, Tohoku Uuiversity, Sendai.

1) H. C. Allen, Jr., *J. Am. Chem. Soc.*, **74**, 6074 (1952); *J. Phys. Chem.*, **57**, 501 (1953).

groups are different depending on the type of carbonyl group, and that it is useful to compare the quadrupole coupling constants with the shifts in the carbonyl frequencies in the infrared spectra of these compounds. This discussion has hitherto, however, been only qualitative because C=O stretching frequencies had been measured only for mono-chlorinated carbonyl compounds.

In this paper, the relationships between the nuclear quadrupole coupling constant and the C=O stretching frequency in the infrared spectra are investigated for chlorinated acetylchlorides, chlorinated acetic acids, and chlorinated acetamides.

Experimental

A Perkin-Elmer 112 spectrometer with a calcium fluride prism mounted was used to study the C=O stretching bands. Mono-, di- and tri-chloroacetylchloride and mono-, di- and tri-chloroacetic acids were purchased from Tokyo Kasei Kogyo Co., Ltd. and purified by fractionating prior to measurement. The measurement of the 0.1 mol./l. carbon tetrachloride solutions was done at room temperature.

Results and Discussion

The experimental results are listed in Table I, together with the NQR frequencies observed by Allen[1], Bray[2], and McCall and Gutowsky[3]. They show that the C=O stretching frequencies increase with the increase in NQR frequencies, which is accompanied by the progressive introduction of chlorine atoms into the methyl group, though the process is not so obvious for the acetylchlorides. Therefore, let us consider this fact from the viewpoint of the molecular orbital theory.

For a molecule in which the hydrogen atoms of a methyl group adjacent to a π-electron conjugated system are successively replaced by chlorine atoms (Fig. 1), we shall represent a one-electron molecular π orbital Ψ_i as a linear combination of atomic π orbitals in this conjugated system as follows:

$$\Psi_i = \sum_r C_{ri}\phi_r$$

where r is taken over all the atoms with $2p\pi$ or $3p\pi$ electrons in this system. In order to calculate the secular equation, the values for the Coulomb integrals, $\alpha_r = \int \phi_r H \phi_r d\tau$, the resonance integrals, $\beta_{st} = \int \phi_s H \phi_t d\tau$, and the overlap integrals, $S_{st} = \int \phi_s \phi_t d\tau$, are required. From the calculation of the secular equation, we obtain the bond-atom polarizability (denoted by $\pi_{st,r}$). It has been shown by Coulson and Longuet-Higgins[4] that when the Coulomb integral α_r of the r atom in the conjugated system is slightly changed, the π bond-order (P_{st}) in the s−t bond is also changed, and that the change of the π bond-order is represented by the bond-atom polarizability $\pi_{st,r} = (\partial P_{st}/\partial \alpha_r)$ as follows:

$$\delta P_{st} = (\partial P_{st}/\partial \alpha_r)\delta \alpha_r \qquad (1)$$

When the hydrogen atoms in the methyl group are progressively replaced by chlorine atoms, the ionic characters of the C–Cl bonds decrease in the sequence $-CH_2Cl > -CHCl_2 > -CCl_3$. Livingston[5] has shown this to be true in the case of chloromethanes and chloroethanes. The same may be true for a chlorinated methyl group adjacent to a conjugated system. The NQR frequencies of some compounds with such

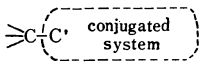
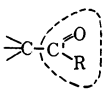


Fig. 1.



R : Cl, OH, and NH_2

Fig. 2.

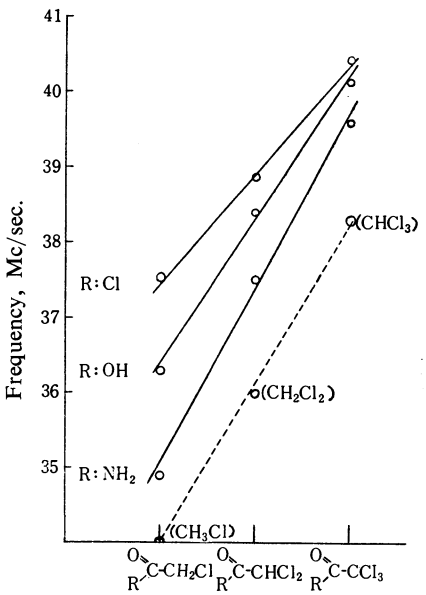


Fig. 3. The ^{35}Cl NQR frequencies were cited from Refs. 1, 2 and 3.

2) P. J. Bray, *J. Chem., Phys.*, 23, 703 (1955).
3) D. W. McCall and H. S. Gutowsky, *J. Chem. Phys.*, 21, 1300 (1953).
4) C. A. Coulson and H. C. Longuet-Higgins, *Proc. Roy. Soc.*, A191, 39 (1947).
5) R. Livingston, *J. Phys. Chem.*, 57, 496 (1953).

TABLE I. C=O STRETCHING AND ^{35}Cl NQR FREQUENCIES IN SOME CHLORINATED CARBONYL COMPOUNDS

Compound	C=O Stretching frequency, cm^{-1}	^{35}Cl NQR Frequency*** (Mc/sec.) at 77°K
Monochloroacetylchloride	1783 (sh w) 1818.8(vs)	37.517
Dichloroacetylchloride	1779.1(vs) 1808.7(vs)	38.862(av)
Trichloroacetylchloride	1800.9(vs)	40.406(av)
Monochloroacetic acid	1736.3(vs) (1736)*	36.280(av)
Dichloroacetic acid	1743.4(vs) (1751)*	38.393(av)
Trichloroacetic acid	1749.4(vs) 1785 (sh w) (1764)*	40.124(av)
Monochloroacetamide	1695**	34.882
Dichloroacetamide	1716**	37.494(av)
Trichloroacetamide	1732**	39.569(av)

sh, shoulder; w, weak; vs, very strog; av, average.

* R. H. Gillette, *J. Am. Chem. Soc.*, **58**, 1143 (1936). His measurements were made for 0.025 mol./l. CCl_4 solutions at 25°C.

** See Ref. 15.

*** See Refs. 1, 2 and 3.

chlorinated methyl groups are plotted in Fig. 3, together with those (the dotted line in Fig. 3) of chloromethanes for comparison. In this figure, it can be seen that the frequency changes of these conjugated compounds are similar to those of chloromethanes[5]. In the conjugated compounds shown in Table I and Fig. 3, the ionic character of the C–Cl bond in dichloroderivatives is smaller than that of a C–Cl bond in monochloroderivatives. According to Townes and Dailey's rule[6], however, the amount of the ionic character of the C–Cl bond in dichloroderivatives is larger than one-half of that in monochloroderivatives. Similarly, the amount of the ionic character of the C–Cl bond in trichloroderivatives is larger than two-thirds of that in dichloroderivatives. From these considerations, it is supposed that the positive formal charge of the carbon atom in the chlorinated methyl group becomes larger in the order, $-CH_2Cl < -CHCl_2 < -CCl_3$. The increase in the positive formal charge of this carbon atom may be responsible for the inductive effect in the C–C′ bond connecting the methyl group and the conjugated system (see Fig. 2). This effect may increase also in the order of mono-, di- and tri-chloroderivatives. This effect will result in a slight increase in the electronegativity of the C′ atom adjacent to the methyl group, and in the electron withdrawal by the C′ atom from the other atom in the conjugated system. Therefore, the absolute value of the Coulomb integral of the C′ atom may be expected to increase slightly in the order of $-CH_2Cl$, $-CHCl_2$ and $-CCl_3$. On the other hand, it is well known that the C=O stretching vibration is one of the characteristic vibrations which are scarcely perturbed by the coupling with other parts of the molecule. Therefore, the frequency change originates mainly from the change in the force constant, which may be associated with the change in the bond order δP_{st} in the present case. In the C=O bond, however, both π and σ bonds contribute to the force constant. If the influence of the inductive effect due to the introduction of chlorine atoms into the methyl group is much smaller in the σ bond than in the π bond, the $\delta P_{c=o}$ given by Eq. 1 would be connected to the displacements of the C=O stretching frequencies*. Consequently, the NQR frequencies and the C=O stretching frequencies can be correlated through the Coulomb integral of the C′ atom.

For the practical investigation of this correlation by using Eq. 1, it is necessary to evaluate

6) C. H. Townes and B. P. Dailey, *J. Chem. Phys.*, **17**, 782 (1949); ibid., **23**, 118 (1955).

* For Eq. 1, a more discreet expression would require the total differential form:

$$\delta P_{c=o}=\frac{\partial P_{c=o}}{\partial \alpha_c}\delta\alpha_c+\frac{\partial P_{c=o}}{\partial \alpha_o}\delta\alpha_o+\frac{\partial P_{c=o}}{\partial \alpha_R}\delta\alpha_R \quad (1')$$

where R is Cl, (OH) and (NH_2). What we are estimating, however, are the relative differences among the $\delta P_{c=o}$'s of the three groups of chloroderivatives. Therefore, we consider that the first term in the right-hand side of Eq. 1′, which is directly affected by the introduction of chlorine atoms into the methyl group, is most important and that the last two terms are less important.

the bond-atom polarizabilities. Such evaluations are, however, beset by the difficulty of estimating suitable parameters for the hetero atoms. Nevertheless, in order to make a rough guess as to what might be observed, a computation was made for the three derivatives which are shown in Fig. 2. For the Coulomb integrals of the hetero atoms, Coulson's prescription[7]

$$\alpha_r - \alpha_c = (X_r - X_c)\beta_{cc}$$

was used, where X_r, X_c are the electronegativities of the r atom and the C atom respectively. For the resonance integrals between the s atom and the t atom, Wheland's expression[8]

$$\beta_{st} = (S_{st}/S_{cc})\beta_{cc}$$

was adopted. In the above expression, α_c, β_{cc} and S_{cc} were taken to be equal to the corresponding values for benzene. Electronegativity values were used for various atoms where $X_c = 2.5$, $X_o = 3.5$ and $X_{Cl} = 3.0$. The conception of group electronegativity[9] was introduced for the (OH) and (NH_2) groups, and the values 3.72 and 3.36 were used for the two groups. In order to evalute the magnitude of β_{st}, the overlap integrals were calculated by interpolation from the published table[10], using the electron diffraction values of 1.77 Å for the C–Cl bond[11], 1.22 Å for the C=O bond of acetylchlorides[11] or acetamides[12], 1.24 Å for the C=O bond of acetic acids, 1.43 Å for the C–O bond[13], and 1.36 Å for the C–N bond[12]. The order of the obtained bond-atom polarizabilities for the three derivatives is:

$$\left(\frac{\partial P_{c=o}}{\partial \alpha_c}\right)_{O=C-Cl} < \left(\frac{\partial P_{c=o}}{\partial \alpha_c}\right)_{O=C-NH_2} < \left(\frac{\partial P_{c=o}}{\partial \alpha_c}\right)_{O=C-OH} \quad (2)$$

Now for hypothetical equal changes of α_c in the three chloroderivatives, the incured displacements of the C=O frequencies for chlorinated acetic acids or chlorinated acetamides should be larger than that for chlorinated acetylchlorids. Moreover, it is seen in Table I that the rise in the NQR frequencies due to the progressive introduction of chlorine atoms into the methyl group is larger in chlorinated acetic acids or chlorinated acetamides than in chlorinated acetylchlorides. As has been explained above, these changes in the NQR frequencies indicate that the changes of the inductive effect for the former are larger than that for the latter. Therefore, the $\delta\alpha_c$ for chlorinated acetylchlorides, which rise in the sequence mono- to tri-chloroderivatives, is smaller than that for chlorinated acetic acids or chlorinated acetamides. Consequently, the shifts of the C=O frequencies can be expected to be larger for chlorinated acetic acids or chlorinated acetamides than for chlorinated acetylchlorides, as witnessed by the observed C=O frequencies listed in Table I. Although the comparison of these C=O frequencies is beset by splittings of these absorption bands resulting from rotational isomerism or other interplay of several factors[14], close investigation of the relation between wave numbers and the intensities of these bands undoubtedly shows that the increase in wave numbers from mono- to tri-chloroacetic acid (or from mono- to tri-chloroacetamide) is larger than that from mono- to tri-chloroacetylchloride.

For the series of chloroacetamides and chloroacetic acids, the bond-atom polarizability of the former is smaller than that of the latter, as is shown in Eq. 2. On the other hand, on can see in Table I and Fig. 3 that the changes in the NQR frequencies for the former are larger than that for the latter; namely, $\delta\alpha_{c(O=C-NH_2)} > \delta\alpha_{c(O=C-OH)}$ is supposed. The obstruction comes in the estimation of the relative difference of the $\delta P_{c=o}$'s by the product of $\delta\alpha_c$ and $(\partial P_{c=o}/\partial\alpha_c)$, viz. Eq. 1. In the experimental data shown in Table I, the changes in C=O frequencies for the former are slightly larger than that for the latter. It seems that the second term in Eq. 1′ (see footnote p. 604) can fairly easily be altered to $\delta P_{c=o}$, because of the large resonance integral for C–N bond. (β_{C-N} is 0.82 β_{cc}, while β_{C-Cl} and β_{C-OH} are equal to 0.56~0.57 β_{cc}).

The author wishes to express his thanks to Professor Kunio Kozima of Tokyo Institute of Tecknology for his kind guidance. He is also grateful to Dr. Tunéo Yosino of Toyo Rayon Co., Ltd. and Professor Siro Maéda of the Defense Academy for their helpful discussions.

Department of Chemistry
Defense Academy
Yokosuka

7) C. A. Coulson, "Valence", Oxford University Press, London (1952), p. 242.
8) G. W. Wheland, *J. Am. Chem. Soc.*, **64**, 900 (1942).
9) J. K. Wilmshurst, *J. Chem. Phys.*, **28**, 733 (1958).
10) R. S. Mulliken, C. A. Rieke, D. Orloff and H. Orloff, ibid., **17**, 1248 (1949).
11) Y. Morino, K. Kuchitsu, M. Iwasaki, H. Arakawa and A. Takahashi, *J. Chem. Soc. Japan, Pure Chem. Sec. (Nippon Kagaku Zasshi)*, **75**, 674 (1954).
12) M. Kimura and M. Aoki, This Bulletin, **26**, 429 (1953).
13) J. Karle and L. O. Brokway, *J. Am. Chem. Soc.*, **66**, 572 (1944).
14) R. N. Jones and C. Sandorfy, "Chemical Applications of Spectroscopy", Vol. IX, Technique of Organic Chemistry (1956), Chap. IV.
15) T. L. Brown, J. F. Regan, R. D. Schuetz and J. C. Sternberg, *J. Phys. Chem.*, **63**, 1312 (1959).

Colloid Chemical Studies on Starching Materials. IV. Viscoelasticity and Structure Change of Starch Solutions

By Masayuki NAKAGAKI

(Received August 21, 1961)

Structural viscosity, that is, the apparent viscosity decreasing with an increasing velocity gradient, is due to the dispersion of highly associated colloidal particles or polymer molecules into smaller aggregates by the effect of the velocity gradient[1]. A structure change like this should obviously affect the dynamic viscosity and the dynamic rigidity of high polymer solutions. The viscoelastic properties of high polymer solutions have been discussed by Rouse[2]. Rouse's theory is satisfactory to the extent that the theory gives the value (−1/2) to the gradient of the relaxation spectra of high polymer solutions[3], but the actual behavior of high polymer solutions is much more complicated than the theory expects. Moreover, Rouse's theory cannot predict the existence of structural viscosity because the theory does not take into account any structure change in the solution.

In the preceding paper of this series[4], experimental data of dynamic viscosity and dynamic rigidity, obtained by using a top-drive coaxial rheometer, have been reported for 3 and 5% potato starch, 5% sweet potato starch and 5% rice starch solutions. Examination of the data, too, has been made on the basis of the modified Rouse equations:

$$\eta=\eta_0 f_1(\tau\omega) \tag{1}$$

$$G=G_0+(6/\pi^2)(\eta_0/\tau)f_2(\tau\omega) \tag{2}$$

where

$$\left.\begin{aligned} f_1&=(6/\pi^2)\sum_{p=1}^{N}[p^2/(p^4+\tau^2\omega^2)] \\ f_2&=\sum_{p=1}^{N}[\tau^2\omega^2/(p^4+\tau^2\omega^2)] \end{aligned}\right\} \tag{3}$$

Here, η is the dynamic viscosity, G is the dynamic rigidity, ω is the angular frequency, p is an integer, and η_0, G_0 and τ are constants. It has been suggested, in the same paper, that the experimental data can be explained satisfactorily if one assumes that there are in the starch solutions large aggregates of polymer molecules with large values of η_0 and G_0 when the frequency is small and that the aggregates change to smaller ones of smaller η_0 and G_0 with the increase of the frequency. In the present paper, the idea described in the preceding paper has been formulated and applied to the experimental data.

Theoretical

According to Rouse's theory, the parameters η_0 and τ in Eqs. 1 and 2 depend on the number N of segments (submolecules) contained in a high polymer molecule as follows:

$$\left.\begin{aligned} \eta_0&=(\pi^2/6)n\boldsymbol{k}T\tau \\ \tau&=\sigma^2N^2/6\pi^2\boldsymbol{B}\boldsymbol{k}T \end{aligned}\right\} \tag{4}$$

where n is the number of molecules in a unit volume of the solution, τ is the longest relaxation time of the polymer molecule (τ_1 in Rouse's original paper), σ is the length of the segment, and B is the mobility of the end of a segment. Therefore, by introducing three parameters α, β and F, defined by:

$$\left.\begin{aligned} \alpha(\tau\omega)&=(2\sqrt{2}/\pi)\sqrt{\tau\omega}\times\sum_{p=1}^{\infty}[p^2/(p^4+\tau^2\omega^2)] \\ \beta(\tau\omega)&=[(2\sqrt{2}/\pi)/\sqrt{\tau\omega}]\times\sum_{p=1}^{\infty}[\tau^2\omega^2/(p^4+\tau^2\omega^2)] \end{aligned}\right\} \tag{5}$$

and

$$F=nN\sigma\sqrt{\boldsymbol{k}T}/4\sqrt{3}\sqrt{B} \tag{6}$$

the modified Rouse equations 1 and 2 can be rewritten into the following equations:

$$\left.\begin{aligned} \eta&=(F/\sqrt{\omega})\alpha(\tau\omega) \\ G&=G_0+F\sqrt{\omega}\beta(\tau\omega) \end{aligned}\right\} \tag{7}$$

The points to be emphasized here are as follows: First, the parameter F is proportional to nN, that is, the total number of segments in a unit volume of the solution, or to the weight concentration, irrespective of the degree of molecular association. Second, the parameters α and β are functions of $(\tau\omega)$ only and have the values cited in Table I. Both α and β approach zero when $(\tau\omega)$ is small and

1) M. Nakagaki and S. Sakata, This Bulletin, **27**, 548 (1954).
2) P. E. Rouse, *J. Chem. Phys.*, **21**, 1272 (1953).
3) M. Yamamoto, *Chem. and Chem. Ind.* (*Kagaku to Kogyo*), **12**, 534 (1959).
4) M. Nakagaki and K. Muragishi, This Bulletin, **34**, 316 (1961).

Table I. Theoretical values of α and β

$\tau\omega$	α	β	$\tau\omega$	α	β
0.0001	0.01480	0	0.5	0.9165	0.2807
0.0002	0.02093	0	1	1.0000	0.5211
0.0005	0.03310	0.00001	2	1.0000	0.6855
0.001	0.04682	0.00003	5	1.0000	0.7986
0.002	0.06620	0.00009	10	1.0000	0.8577
0.005	0.1047	0.00034	20	1.0000	0.8993
0.01	0.1480	0.00097	50	1.0000	0.9362
0.02	0.2093	0.00275	100	1.0000	0.9550
0.05	0.3310	0.01085	200	1.0000	0.9681
0.1	0.4649	0.03055	500	1.0000	0.9799
0.2	0.6459	0.08386	1000	1.0000	0.9858

approach unity when $(\tau\omega)$ is large. However, the manners of approach of α and β to these limiting values are widely different. Under a 1% allowance, α is equal to zero when $(\tau\omega)$ is smaller than 0.0001, but β is already zero when $(\tau\omega)$ is smaller than 0.05; α is already equal to unity when $(\tau\omega)$ is larger than 1, but β is equal to unity when $(\tau\omega)$ is as large as 1000.

In order to consider a mixture of highly associated molecules of N_1 segments and less associated (or not associated) molecules of N_2 segments ($N_2<N_1$), the dynamic viscosity η and dynamic rigidity G of the mixture may be assumed to be:

$$\left.\begin{aligned}\eta&=(x_1\alpha_1+x_2\alpha_2)F/\sqrt{\omega}\\ G&=x_1G_0+(x_1\beta_1+x_2\beta_2)F\sqrt{\omega}\end{aligned}\right\} \quad (9)$$

where x_1 and x_2 are the weight fractions of respective components ($x_2=1-x_1$). α_1 and β_1 are the values of α and β for $(\tau_1\omega)$, and α_2 and β_2 are the values for $(\tau_2\omega)$, where the value of τ_1 is much larger than the value of τ_2 because the suffix 1 designates highly associated, and the suffix 2 less associated, molecules. The G_0 values of the less associated molecules are assumed to be zero.

In order to apply Eq. 9 to experimental values of η and G and to obtain an experimental $x_1-\omega$ relationship, the values of the four parameters F, G_0, τ_1 and τ_2 should be estimated. The choice of the four parameter values is not as arbitrary as it looks, because of the character of the ω dependency of the functions α and β, especially because α_1 should be equal to unity except when ω is very small, and β_2 should be equal to zero except when ω is very large. As a result, the relative value of x_1 (calculated by assuming that the value of x_1 is equal to unity for the smallest ω value used in the experiment) can be obtained without any arbitrariness. The results obtained for starch solutions will be shown later.

By way of application of Eq. 9, it has been recognized that the choice of the values of τ_1 and τ_2 does not affect the final $\log\eta-\log\omega$ relationship and $\log G-\log\omega$ relationship too much. Therefore, an approximate method is also used by assuming $\tau_1\gg1$ and $\tau_2\ll1$, or

$$\alpha_1=1,\quad \beta_1=1,\quad \alpha_2=0,\quad \beta_2=0 \quad (10)$$

In this case, Eq. 9 can be simplified to:

$$\left.\begin{aligned}\eta&=x_1F/\sqrt{\omega}\\ G&=x_1(G_0+F\sqrt{\omega})\end{aligned}\right\} \quad (11)$$

This equation was also applied to starch solutions.

Discussion of Experimental Data

By using either Eq. 9 or 11, the variation of x_1 with the circular frequency ω was calculated for starch solutions, the dynamic viscosity and the dynamic rigidity experimental values of which have been reported in the preceding paper[4]. Results for the 3% potato starch solution are shown in Fig. 1, the 5% potato starch solution in Fig. 2, the 5% sweet potato solution in Fig. 3, and the 5% rice starch solution in Fig. 4. In these figures, the experimental values of $\log\eta$ (○), $\log G$ (●) and x_1 (both values obtained by Eq. 9 (□) and by Eq. 11 (△) are shown) are plotted. The values of the parameters adopted to calculate the values of x_1 are cited in Table II. The values of x_1 thus obtained are linear to $\log\omega$ for potato starch and sweet potato starch solutions, as is

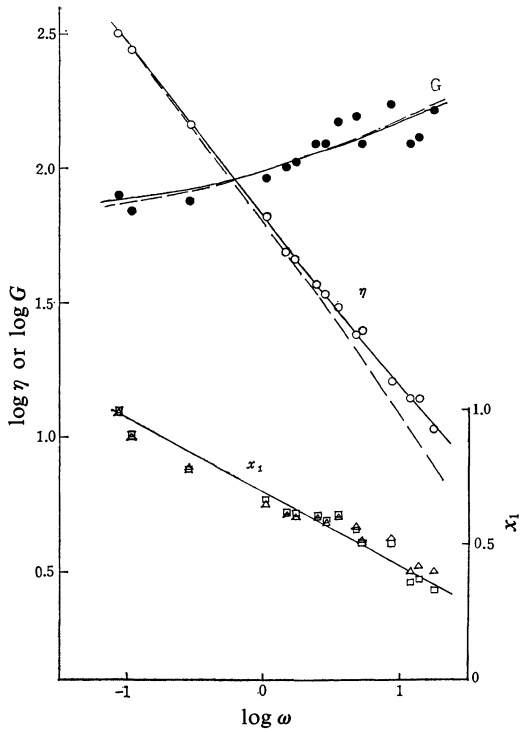


Fig. 1. $\log\eta$ (○), $\log G$ (●), and x_1 by Eq. 9 (□) and Eq. 11 (△) of 3% potato starch solution.

shown by the straight lines in Figs. 1—3. By using x_1 values corresponding to these straight lines, and also by using the parameter values cited in Table II, values of η and G were calculated and shown in these figures by solid lines

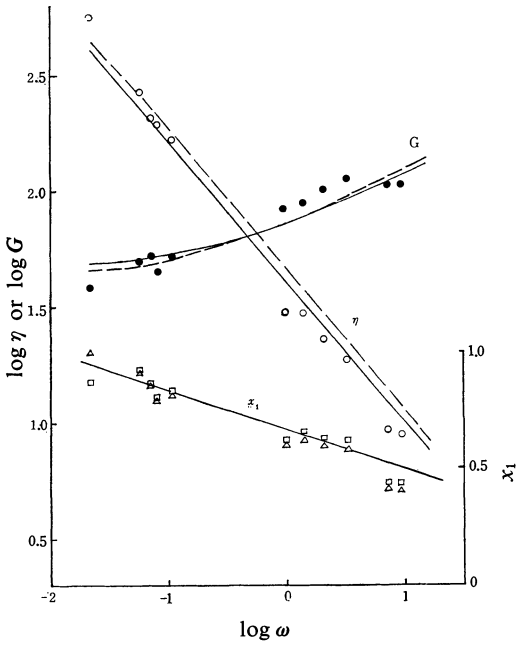


Fig. 2. $\log\eta$ (○), $\log G$ (●), and x_1 by Eq. 9 (□) and Eq. 11 (△) of 5% potato starch solution.

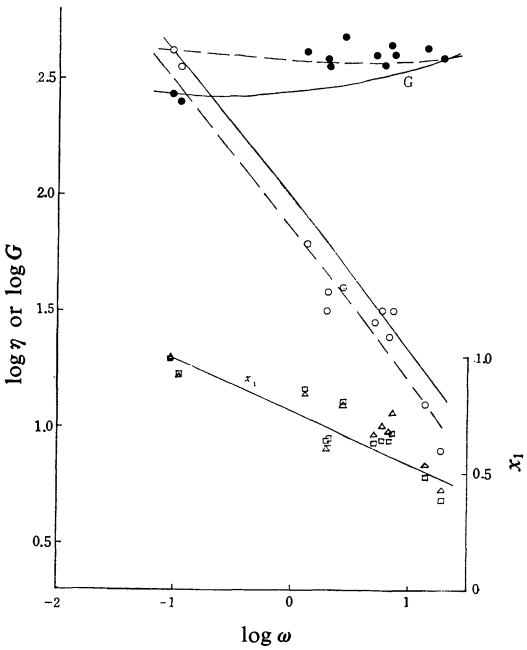


Fig. 3. $\log\eta$ (○), $\log G$ (●), and x_1 by Eq. 9 (□) and Eq. 11 (△) of 5% sweet potato starch solution.

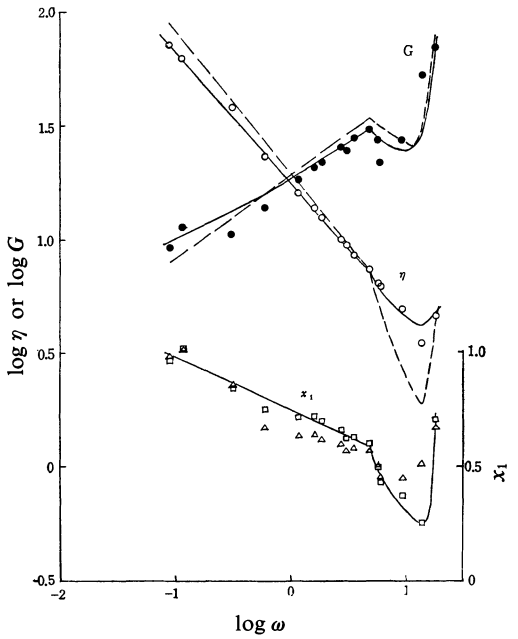


Fig. 4. $\log\eta$ (○), $\log G$ (●), and x_1 by Eq. 9 (□) and Eq. 11 (△) of 5% rice starch solution.

TABLE II. PARAMETERS OF EQS. 9 AND 11 (in c. g. s. units)

Starch	Concn. %	Eq.	F	G_0	τ_1	τ_2
Potato	3	9	93.1	50.9	$\gg 1$	0.0016
		11	99.5	44.1	$\gg 1$	$\ll 1$
Potato	5	9	63.5	47.8	37.2	$\ll 1$
		11	69.7	37.7	$\gg 1$	$\ll 1$
Sweet potato	5	9	127.3	231	$\gg 1$	$\ll 1$
		11	93.4	394	$\gg 1$	$\ll 1$
Rice	5	9	21.3	4.15	190	0.0135
		11	26.6	0	$\gg 1$	$\ll 1$

for Eq. 9 and by broken lines for Eq. 11. Agreements between the experimental plots and the calculated curves are satisfactory for the potato starch solutions (Figs. 1 and 2). In the case of the sweet potato starch solution (Fig. 3), the analysis based on Eq. 9 gave the result that $\tau_1 \gg 1$ and $\tau_2 \ll 1$, so that Eq. 9 turned out to be the same as Eq. 11. The values of the parameter F (and G_0) for Eq. 9 and for Eq. 11 differ because in the case of Eq. 9 the experimental data at about $\log\omega = -1$ were respected highly, while in the case of Eq. 11 they were neglected. It is obvious that a better agreement can be obtained if one adopts for F and G_0 some values between those for Eqs. 9 and 11, if one discards the expectation to the linearity of x_1 to $\log\omega$ and if one adopts more suitable values for x_1 for each $\log\omega$ value. In the case of the rice starch solution (Fig. 4), the value of x_1 decreases linearly as far as

$\log \omega = 0.7$. However, if one attaches importance to the minimum of $\log \eta$ and $\log G$ at about $\log \omega = 1.1$, one should assume a minimum for x_1, too. The rapid increase of x_1 (and consequently of η and G) at high ω values might correspond to the entanglement of rice starch molecules due to mechanical work, a phenomenon familiar to Japanese people in the process of rice-cake making.

Summary

Modified Rouse's equations were applied to solutions consisting of a mixture of highly aggregated and less aggregated polymer molecules. The fraction of higher aggregates, x_1, was calculated for 3 and 5% potato starch solutions, a 5% sweet potato starch solution, and a 5% rice starch solution. The value of x_1 decreased linearly with the increase of $\log \omega$, except for the rice starch. The x_1 value of the latter increased rapidly when the $\log \omega$ became very large.

Faculty of Pharmacy
Kyoto University
Sakyo-ku, Kyoto

Solvent Extractive Fractionation of Ziegler Polystyrene

By Akira YAMADA, Yoshio YAMAMURO and Masaya YANAGITA

(Received December 24, 1960)

In the preceding paper[1], one of the authors pointed out the possibility of the extractive fractionation of Alfin Polystyrene with solvents other than acetone[2], ethyl methyl ketone[2,3] and benzene[4]. In the present paper, the authors wish to report that the polystyrene samples polymerized by the Ziegler catalyst were separated into two parts, i. e., crystalline and amorphous, by extractive fractionation with several solvents.

The solvents have been selected on the basis of the results of the solubility-test and the solvent extractive fractionation in the previous work[1]. The densities and the ratios of the intensities of the infrared spectra (D_{984}/D_{1028}) of the extractive residues were measured in order to check the extractive fractional ability; the molecular weights and melting points of the residues were also measured.

One of the authors has reported previously that the infrared intensity (D_{984}) was proportional to the X-ray crystalline content[5]. However, as shown in Fig. 1, the X-ray crystallinity percentage with a vibration of densities between 1.05 to 1.08 did not vary in proportion to the infrared ratio. Accordingly, X-ray diagrams have not been used in the present studies.

The physical properties measured are summarized in Table I.

It is seen that of the densities of the extractive residues resulting from the hot solvent treatment, the lowest is for ethyl methyl ketone. The decreasing order in the case of hot extraction is; tetrahydrofuran, ethyl acetate, dioxane, cyclohexanone and ethyl methyl ketone. In the cold extraction, however, the highest value was obtained by using ethyl methyl ketone, and this was followed by benzene, toluene, ethyl acetate and tetrahydrofuran.

The ratio of the infrared intensities (D_{984}/D_{1028}) is linearly proportional with the density between 1.05 to 1.08, as is shown in Fig. 1. It is considered that these infrared ratios show the difference in crystallinity (or tacticity) of each residue. The decreasing order of the ratio in the hot extraction was as follows: dioxane, tetrahydrofuran, ethyl acetate and cyclohexanone. In the cold extraction, the order was benzene, ethyl methyl ketone, ethyl acetate, toluene, tetrahydrofuran and ether.

The relation of the molecular weight to the fractional weight percentage of residue is shown in Fig. 2.

The dotted line and the curved line (from right to left in Fig. 2) show the over-all process of the extraction. In the initial step, it is observed that the average molecular weight

1) A. Yamada, *J. Chem. Soc. Japan, Ind. Chem. Sec.* (*Kogyo Kagaku Zasshi*), **64**, 2204 (1961).
2) G. Natta, *Makromol. Chem.*, **16**, 213 (1955).
3) F. Danusso and G. Moraglio, *J. Polymer Sci.*, **24**, 161 (1957).
4) N. Yamazaki, *Chem. High Polymers* (*Kobunshi Kagaku*), **15**, 49 (1958).
5) M. Takeda, K. Iimura, A. Yamada and Y. Imamura, This Bulletin, **33**, 1219 (1960).

TABLE I. PHYSICAL PROPERTIES OF THE EXTRACTIVE RESIDUES; DENSITY, MOLECULAR WEIGHT (mol. wt.) AND MELTING POINT (m. p.)

Extraction type	Solvent	Extractive hr./g.	Extractive fractional wt. % of residue	Density	IR ratio[a] %	Mol. wt. $\times 10^{-4}$	M. p. °C
	Ethyl methyl ketone	5	84	1.078	63	204	240
	Cyclohexanone	7	27	1.078	50	176	245
Hot	Tetrahydrofuran	15	17	1.085	64	—	230
	Dioxan	5	61	1.081	66	189	235
	Ethyl acetate	5	91	1.082	57	232	240
	Ethyl methyl ketone	20	93	1.081	55	220	240
	Ether	21	93	?	31	230	240
Cold	Tetrahydrofuran	20	5	1.073	46	—	240
	Ethyl acetate	20	92	1.075	53	214	240
	Benzene	20	40	1.080	56	257	240
	Toluene	20	91	1.078	51	227	240

a) The IR ratio for atactic polystyrene had been presented as 16.

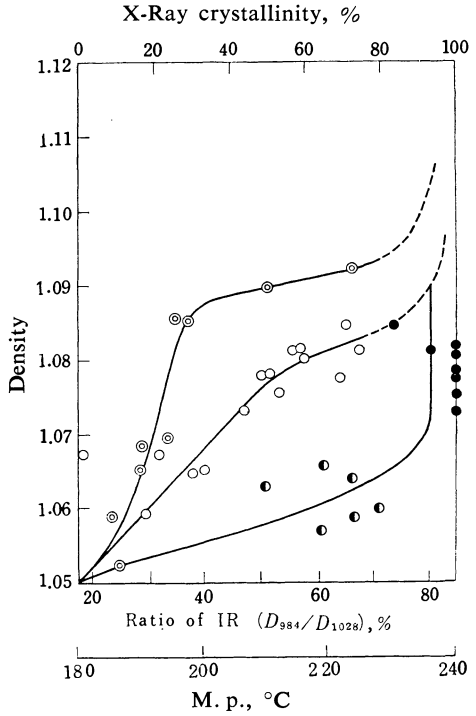


Fig. 1. Relationship between density and X-ray crystallinity, IR ratio and/or melting point.
◎ X-Ray crystallinity previously reported[5].
○ IR ratio in this paper.
● Melting point in this paper.
◐ Melting point of Alfin polystyrene (A. Yamada, *J. Chem. Soc. Japan, Ind. Chem. Sec. (Kogyo Kagaku Zasshi)*, **64**, 2208 (1961).

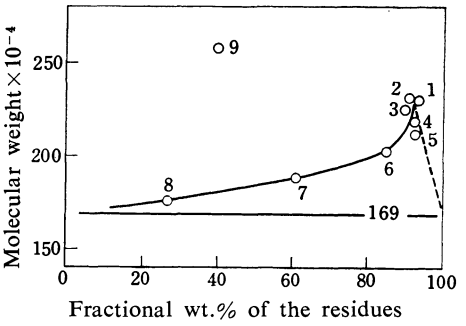


Fig. 2. Relationship between molecular weights and extractive fractional wt. % of residues. Molecular weight of the original sample is 169×10^4. The number in the figure shows hot(h) or cold(c) solvent extraction respectively;

1 c-ether	2 h-ethyl acetate
3 c-toluene	4 c-ethyl methyl ketone
5 c-ethyl acetate	6 h-ethyl methyl ketone
7 h-dioxan	8 h-cyclohexanone
9 c-benzene	

of the residue increases because the lower molecular weight portion was extracted, but thereafter the molecular weight gradually decreases on account of the atactic, higher molecular weight portion that is subsequently extracted. The several extractive types 1 to 6 in Fig. 2 seem to resemble closely those of the hot or cold ethyl methyl ketone extraction. Cold benzene extraction especially, as is seen in Fig. 2, differs from the other in respect to the dependency of the molecular weight on the solvent extractive fractionation.

The residues have a higher melting point, and no information is offered to account for the differences in residues (see Table I).

From the above-described results, it may be considered that the solvent extractive ability in hot extraction decreases in the order: tetrahydrofuran dioxan, ethyl methyl ketone and ethyl acetate. In the cold extraction the

order is: benzene, ethyl methyl ketone, ethyl acetate and toluene. Cold benzene extraction, however, was an exception case.

Experimental

Ziegler Polystyrene. — A four-necked flask with a mechanical stirrer was filled with dried nitrogen. Then 200 ml. of dried isooctane, 13 ml. of titanium tetrachloride and 25 ml. of triethyl aluminum (Al/Ti=3.1) were poured through medical syringes. While the temperature was maintained at 80°C, 500 ml. of freshly distilled styrene monomer diluted with 500 ml. of dried benzene was added dropwise over a six-hour period. After heating the mixture for 18 hr. at 80°C while stirring it, ethanolic hydrogen chloride was poured into the flask at 0°C. The dried crude polymer was obtained in a yield of 88%. The lower molecular weight portion was discarded by hot acetone extraction. After filtration of the small amount of residue, the filtrate was reprecipitated with methanol. The fine polymer was obtained in a yield of 11%.

Treatment with *n*-Heptane[6].—Before extraction, the sample was treated with boiling *n*-heptane for five hours and then cooled gradually to room temperature.

Extraction.—In the hot extraction, a Soxhlet apparatus was used at a temperature several degrees below the boiling point of the solvent. In the cold extraction, a Soxhlet-type apparatus equipped with a drying tower was used at room temperature (15~20°C).

Density. — A floatation method with a sodium chloride aqueous solution was used for the measurement of the density at 25°C. The measurement error is ±0.0005. The sample used was the same as that used for infrared measurement.

Measurement of Infrared Spectra.—Film specimen 0.05 mm. in thickness were prepared by casting on a mercury surface a chloroform solution that had been prepared by heating it in a sealed tube at 100°C. Before the measurement, the films were annealed at 200°C. The infrared spectra were measured in the region of 3500~700 cm^{-1} using a Nippon Bunko DS-201 spectrophotometer.

Molecular Weight. — The molecular weight was determined from viscosity measurements in benzene solution (concentration (C) ; 0.4 g./100 ml.) at 25°C. The molecular weight (M) ; was computed using the two following equations, 1[7] and 2[8]:

$$[\eta]=3(\eta_r^{1/3}-1)/C \quad (1)$$

$$[\eta]=1.06\times10^{-4}M^{0.735} \quad (2)$$

where η_r is the relative viscosity and $[\eta]$ is the intrinsic viscosity.

Melting Point.—Determined as the point of clearance or initial flow using a Shimadzu melting point apparatus.

Materials.—The solvents were purified by the usual methods. The boiling points are shown in parentheses: ethyl methyl ketone (79.6~79.8), cyclohexanone (154.5~156.2), tetrahydrofurane (66), dioxane (100.5~101.2), ethyl acetate (76.9~77.1), ether (34.5), benzene (79.5~79.8) and toluene (110.2~110.5).

Summary

The solvent extractive fractional ability has been described, using Ziegler polystyrene as sample. The order in hot extraction is tetrahydrofuran > dioxane > ethyl methyl ketone ≧ ethyl acetate, while that in cold extraction is benzene ≫ ethyl methyl ketone ≧ ethyl acetate = toluene.

The authors wish to express their sincere thanks to Mr. Toshihide Ishikawa for his help in this experiment and also to Mitsui Chemical Ind. Co. for the supply for triethyl aluminum.

Department of Polymer Chemistry
The Institute of Physical and Chemical Research
Komagome, Bunkyo-ku, Tokyo

6) J. L. R. Williams, W. J. Dunkam, J. V. DenBergh and K. Dulmage, *J. Am. Chem. Soc.*, **78**, 1260 (1956).

7) I. Sakurada, *Chem. High Polymers (Kobunshi Kagaku)*, **2**, 260 (1945).

8) F. Danusso and G. Moraglio, *J. Polymer Sci.*, **24**, 161 (1957).

*Vibrational Spectra of Methyl Ether. I. Assignment of the Spectra**

By Yôko KANAZAWA and Kenkichi NUKADA

(Received August 19, 1961)

In a series of aliphatic ethers, methyl ether has significance for the study of molecular spectra in this homologues because of its simplest structure.

A number of investigations on the vibrational spectra of the molecule have been reported. Herzberg[1] gave an assignment of the vibrational bands using the data published previously[2]. By Ryskina[3] and Siebert[4] the calculation of the normal vibration and assignments were given. Although assignments based on the more detailed measurements of infrared and Raman spectra have been given by Hadni[5] and by Taylor and Vidale[6], there still remains some arbitrariness in their results because they studied the spectra of only one isotopic compound. Therefore, it is desirable to measure the spectra of deuterated compounds in order to obtain more reliable results.

The results of the measurement of the infrared and Raman spectra of methyl ether ($(CH_3)_2O$) and of methyl ether-d_6 ($(CD_3)_2O$) and an assignment of the spectra, referring to that of dimethoxy methane and its deuterated compounds[8], are reported here.

Experimental

Samples. — Methyl ether was prepared from methanol and sulfuric acid. Crude gaseous ether was passed through a concentrated aqueous solution of sodium hydroxide and trapped first with ice-salt and finally with acetone-dry ice. Then it was purified by distillation over metallic sodium. Purification was repeated until no change in the infrared spectrum was observed. A sufficiently pure sample for infrared measurement was obtained, but a shoulder near 1050 cm^{-1} still remained in the Raman spectrum after the final purification. It was considered, therefore, that a very small amount of methanol remained in the sample.

Deuterated ether was prepared from deuterated methanol (CD_3OH or CD_3OD) and deuterated sulfuric acid in the same way as non-deuterated ether. The concentration of deuterium in the sample was analyzed by means of proton magnetic resonance and found to be about 99%.

Measurement of Spectra.—Raman spectra were obtained in the liquid state by a Cary 81 spectrophotometer (3500～250 cm^{-1}, 35～38°C). The degree of depolarization was measured with polarizers around the Raman tube. In the case of non-deuterated methyl ether, a Raman tube for a 5 ml. sample was used, and for the deuterated compound, 0.2 and 0.4 ml. Raman tubes were employed, so the measurement of weak bands was difficult in the latter case.

Infrared spectra (3500～280 cm^{-1}) were obtained by using the following spectrophotometers: Perkin-Elmer 12C (LiF prism), 112G (3500～2000 cm^{-1}), 21 and 321 (NaCl and CsBr prisms), and Nippon-Bunko DS 301 (NaCl prism, 1000～1200 cm^{-1}). Measurement was carried out in the gaseous state over the whole range of the spectrum and also, in the carbon tetrachloride solution, in the sodium chloride and lithiam fluoride prism regions. The obtained spectra are shown in Fig. 1.

Assignment and Discussion

The structure of methyl ether was determined from electron diffraction[10] and microwave spectroscopy[11] to be approximately C_{2v} symmetry. If the molecule belongs to point group C_{2v}, vibrational bands can be classified into four species: $\Gamma = 7A_1 + 4A_2 + 6B_1 + 4B_2$. The vibrations belonging to A_2 are infrared inactive. The envelope of infrared absorption bands of a gaseous substance is of the B type for species A_1, A type for B_1, and C type for B_2. Raman lines which belong to species A_1 are polarized. These characteristics are referred to in the assignment of the bands.

Since the number of observed bands is less than the number of normal vibrations, some overlapping of bands is expected. Therefore, it is not always possible to determine definitely the species of bands by observation of the envelope of infrared absorption bands or by the measurement of the degree of depolarization in the Raman spectra.

* The present paper is an extension of a series of studies on aliphatic ethers[7], dimethoxy methanes, ethylidene dialkyl ethers and related compounds[8].

1) G. Herzberg, "Molecular Spectra and Molecular Structure II. Infrared and Raman Spectra of Polyatomic Molecules", Van Nostrand, New York (1945), p. 353.
2) K. W. F. Koglrausch, *Z. phsik. Chem.*, **B30**, 305 (1935); R. Ananthakrishnan, *Proc. Ind. Acad. Sci.*, **5A**, 285 (1937); B. L. Crawford and L. Joyce, *J. Chem. Phys.*, **7**, 307 (1939); K. S. Pitzer, ibid., **10**, 605 (1942).
3) S. J. Ryskina, *J. Phys. Chem.* (*U.S.S.R.*), **22**, 21 (1948).
4) H. Siebert, *Z. anorg. u. allgem. Chem*, **271**, 65 (1953).
5) A. Hadni, *Compt. rend.*, **229**, 349 (1954).
6) R. C. Taylor and G. L. Vidale, *J. Chem. Phys.*, **26**, 122 (1957).
7) Y. Mashiko, *J. Chem. Soc. Japan, Pure Chem. Sec.* (*Nippon Kagaku Zasshi*), **79**, 470 (1958); **80**, 593 (1959).
8) K. Nukada, *Spectrochim. Acta*, to be published.
9) K. Nukada, This Bulletin, **35**, 3 (1962).
10) K. Kimura and M. Kubo, *J. Chem. Phys.*, **30**, 151 (1959).
11) P. H. Kasai and R. J. Myers, ibid., **30**, 1096 (1959).

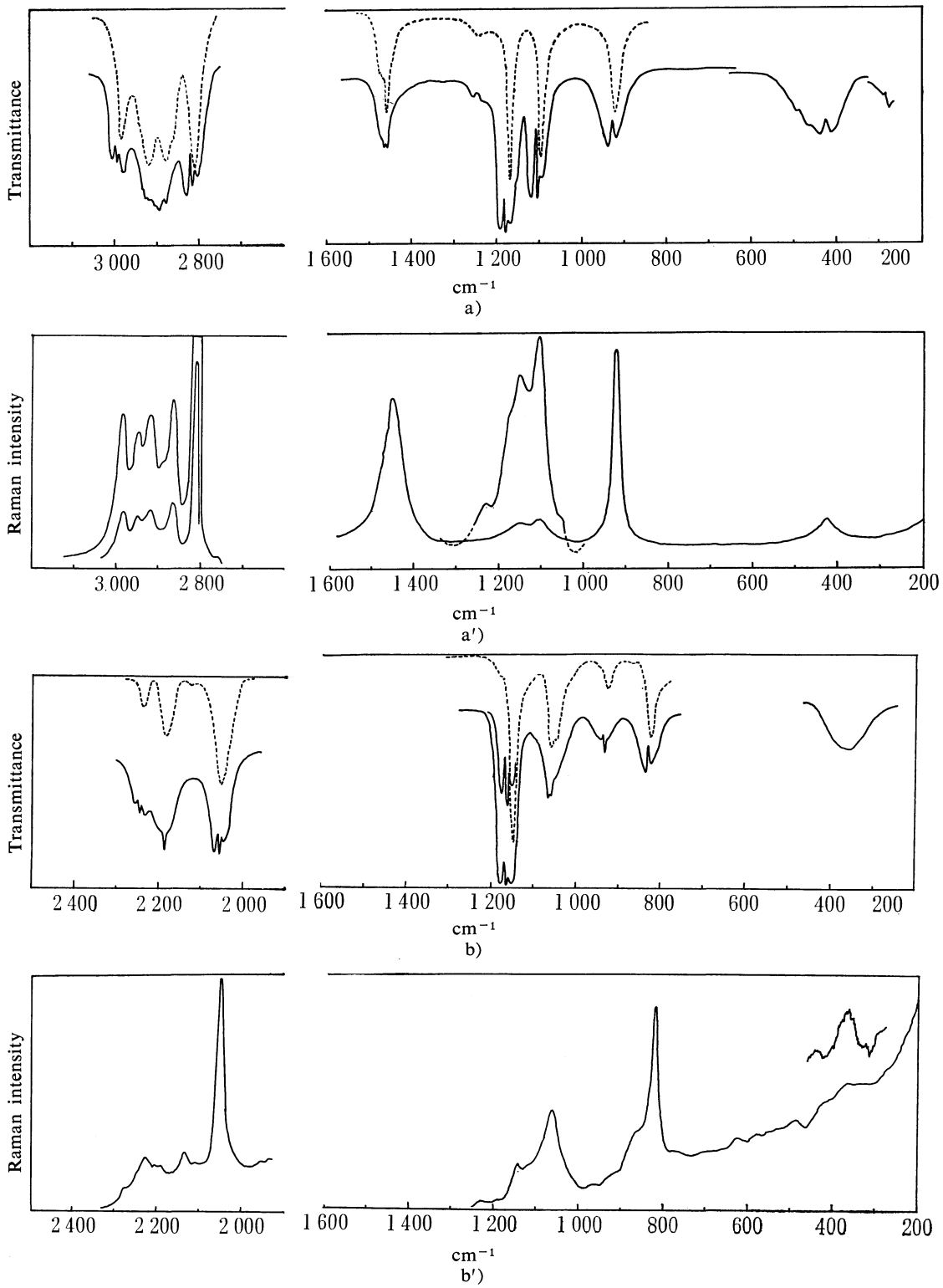


Fig. 1. Infrared and Raman spectra of CH_3OCH_3 and CD_3OCD_3.

a) Infrared spectra of CH_3OCH_3 } —— gas
b) Infrared spectra of CD_3OCD_3 } --- CCl solution, concentration; undetermined
a') Raman spectrum of CH_3OCH_3 } pure liquid
b') Raman spectrum of CD_3OCD_3 }

TABLE I. ASSIGNMENT OF CH_3OCH_3 (IN cm^{-1})

		Herzberg[1]	Ryskina[3]	Siebert[4]	Hadni[5]	Taylor & Vidale[6]	Mashiko[7]
	ν_1 C-H asym. str.	2986	2915	—	2900	2997 ?	2985
	ν_2 C-H sym. str.	2812	2810	—	2900	2821 ?	2845
	ν_3 CH_3 asym. def.	1466	1466	1450	1466	1457*3	1464
A_1	ν_4 CH_3 sym. def.	1466	—	1450	1466	1242	1451
	ν_5 CH_3 rocking	1180	1180	— ?	1135	1053	1142
	ν_6 C-O sym. str.	930*1	940 ?	920	932	929	929
	ν_7 COC deformation	414	440	413	412	413	414
	ν_8 C-H asym. str.	—	2915	—	2900	2889 ?	2865
A_2	ν_9 CH_3 asym. def.	1466	1466	1450	1466	1457*3	1451
	ν_{10} CH_3 rocking	1180	1102	— ?	918	1291, 1167, 1147 ?	1105
	ν_{11} CH_3 torsion	160 ?	—	—	160	—	170*4
	ν_{12} C-H asym. str.	2916	2915	—	2900	2889 ?	2980
	ν_{13} C-H sym. str.	2916	2863	—	2900	2889 ?	2900
B_1	ν_{14} CH_3 asym. def.	1466	1466	1450	1466	1457*3	1464
	ν_{15} CH_3 sym. def.	1466	—	1450	1466	1457*3	1451
	ν_{16} CH_3 rocking	1180	1122	1155	1177	1291, 1167, 1147 ?	1115
	ν_{17} C-O antisym. str.	1112*2	1102	1102	1103	1122	1169
	ν_{18} C-H asym. str.	2916	2915	—	2900	2889 ?	2845
B_2	ν_{19} CH_3 asym. def.	1466	1466	1450	1466	1457*3	1464
	ν_{20} CH_3 rocking	1180	1102	— ?	940	1291, 1167, 1147 ?	1098
	ν_{21} CH_3 torsion	300 ?	—	—	270	—	265*4

*1 and *2 The averaged value between two observed frequencies
*3 The averaged value among three observed frequencies
*4 Y. Mashiko and K. S. Pitzer, *J. Phys. Chem.*, **62**, 367 (1958).

Before making the assignment of vibrational spectra of the molecule, the authors would like to examine the results of other authors as shown in Table I. In the assignment given by Herzberg[1], a point in question is that he assigned a band at 1180 cm^{-1} to the methyl rocking vibrations belonging to four species. Coincidence of the wave numbers of the four bands would be impossible because two of them (A_1, B_1) are the in-plane methyl rocking, and others (A_2, B_2) are the out-of-plane methyl rocking, vibrations. Moreover, since the band at 1179 cm^{-1} measured in the present experiment has a clear envelope of the A or C type, it is difficult to consider it as the overlapping of four bands.

Ryskina[3] assigned a band at 1122 cm^{-1} to the methyl rocking vibration of species B_1, but we consider it to be a branch of the band at 1102 cm^{-1}. In her assignment, the band at 1102 cm^{-1} was assigned to the overlapping of three bands, the species of which was A_2, B_1 and B_2, but this assignment is also questionable for a reason similar to that mentioned above.

Siebert[4] studied the molecular vibration of methyl sulfide ($(CH_3)_2S$) and of methyl selenide ($(CH_3)_2Se$) as well as of methyl ether, but the bands which he assigned were so few that the present authors will not refer to his results.

Hadni[5] considered that there were three fundamental bands at 940, 932 and 918 cm^{-1}. In the present experiment, however, the asymmetric feature of the R branch of the infrared band is not so marked enough to be the basis of such a conclusion, and, in addition, the infrared spectrum in solution shows a single band at 920 cm^{-1}. Therefore, the bands observed at 940 and 916 cm^{-1} should be considered as branches of a B-type band.

The Raman spectra of the molecule in both gaseous and liquid states were measured by Taylor and Vidale[6]. New bands were observed at 1291 (gas) 1242 (gas and liquid), 1167 (liquid) and 1053 cm^{-1} (gas and liquid). Among these, 1291 cm^{-1} had not been observed by other authors. As suggested by the following fact, this band is due to contaminated carbon dioxide. In the synthesis of the sample, carbon dioxide from dry ice used for the trap or from the reacting mixture could be absorbed in ether to some extent. In fact, the same band was observed in the prepared sample in the present experiment if no care was taken to remove it.

The band at 1053 cm^{-1}, which was also observed in the present Raman measurement as a very weak shoulder, might originate from the strongest band of methanol being included as a trace.

C-H and C-D Stretching Vibrations.—Of the observed bands two bands at 2996 and 2817 cm^{-1}

are characteristic bands of aliphatic methoxyl groups[8,9]. These two bands are assigned respectively to overlapping asymmetric and symmetric stretchings of species A_1 and B_1. The fact that both of them show A or C-type band envelopes instead of the B-type for A_1 species may suggest these overlappings. The band at 2952 cm^{-1} observed only in the Raman measurement is assigned to the asymmetric stretching vibration of the infrared inactive species A_2. Of two bands at 2925 and 2887 cm^{-1} which have strong infrared intensities, the one at 2925 cm^{-1} is assumed to be a B_2 band because to the B_2 species belongs an asymmetric C–H stretching vibration whose frequency should not lie far from the A_1 and B_1 asymmetric stretching vibrations. Detailed discussions of the C–H stretching vibrations of methyl ether have not been given in previous papers, but the assignment given here does not contradict that of homologue which have methoxy groups[8,9]. The strong Raman band at 2869 cm^{-1} and the infrared band at 2887 cm^{-1} are to be assigned to an overtone or combination tone of methyl deformation virations.

Deuterated methyl ether shows clearer envelopes of absorption bands in the C–D stretching region than non-deuterated ether does in the C–H stretching region. This can be explained because the ratio of rotational constants B/A increases as the molecule changes from methyl ether to methyl ether-d_6. The bands at 2248 and 2054 cm^{-1} are of the A type, and the band at 2184 cm^{-1} is of the C type. As in the case of C–H stretching vibrations, the band with the highest frequency (2248 cm^{-1}) is assigned to the overlapping asymmetric stretchings and that with the lowest (2054 cm^{-1}), to the overlapping symmetric stretching vibrations of species A_1 and B_1. Then the C-type band at 2184 cm^{-1} (strong in infrared and weak in Raman) is assigned to the vibration of species B_2. The Raman band at 2202 cm^{-1} is assigned to the asymmetric stretching vibration of species A_2. Though the Raman bands at 2285, 2137 and 2100 cm^{-1} also have no corresponding infrared bands, by referring to the assignment of non-deuterated methyl ether it is reasonable to assume that a band nearer to that of species B_2 is to be assigned to species A_2. The strongly polarized band at 2137 cm^{-1} which has a medium intensity is possibly an overtone or combination band of CD_3 deformation vibrations.

Methyl Deformation Vibrations. — In the region of methyl deformation vibrations, infrared and Raman bands are observed only around 1460 cm^{-1}. The infrared spectrum of gaseous ether shows two sharp absorptions at 1464 and 1456 cm^{-1} which can not be considered as branches of a band both bacause the separation of 8 cm^{-1} between them is too small and because the appearance of the doublet does not seem to be that of any type of band envelopes. Furthermore, the infrared spectrum in solution still shows three bands at 1470, 1464 and 1454 cm^{-1}. Therefore, it is suitable to regard them as the superposition of some bands.

Taylor and Vidale[6] assigned the band at 1242 cm^{-1} to a methyl symmetric deformation. This might seem possible because the band is always observed in this region in molecules having a methoxyl group or groups[8,9]. This assignment, however, is denied by the following facts. The first objection stems from the relationship between the vibrational frequencies of methyl symmetric deformation and methyl rocking given by Wilmshurst[12]. Applying it to the observed frequencies, if the frequency of methyl symmetric deformation is assumed to be 1244 cm^{-1}, that of the rocking vibration should be obtained about 900 cm^{-1} or lower where no bands are observed actually; however, both methyl deformation and rocking vibrations prove to appear in the higher frequency region. The second objection stems from the fact that, as Sheppard[13] mentioned, in CH_3X type molecules with various kinds of atoms or group X, the methyl symmetric deformation of methoxyl groups appeared at about 1460 cm^{-1}.

Nukada observed methyl deformation vibrations of dimethoxy methane and dimethoxy methane-d_2 ($CH_3OCD_2OCH_3$) only near 1460 cm^{-1} and not below. From the relative intensity of the infrared and Raman spectra and the degree of polarization, he assigned the bands at 1460 and 1455 cm^{-1} to the symmetric and asymmetric deformations respectively[8]. Considering these, it seems reasonable to assume that all the methyl deformations of methyl ether lie in the range of 1470~1450 cm^{-1}, though at present it is impossible to assign the observed bands to six normal vibrations individually.

CD_3 deformation vibrations are expected to appear around the region of $\nu_{\delta CH_3}/\sqrt{2}$ cm^{-1} or higher. Corresponding to those of non-deuterated ether, infrared bands of a similar complicated shape and a strong Raman band are observed at 1062 and 1056 cm^{-1} and at 1062 cm^{-1} respectively. The assignment is made, as in the case of methyl ether, by treating the six bands together.

Skeletal Vibrations.—There are three skeletal vibrations: a C–O symmetric stretching

12) J. K. Wilmshurst, ibid., **26**, 426 (1957).
13) N. Sheppard, *Trans. Faraday Soc.*, **51**, 1465 (1955).

TABLE II. OBSERVED BANDS OF CH_3OCH_3 AND CD_3OCD_3 (IN cm^{-1})

Infrared			Raman	
Gas	Type of the band	Solution	Liquid	Degree of depolarization
a) CH_3OCH_3				
2996 { 3008 2996 s 2980	A or C	2985 s	2989 s	?
			2952 s	?
2925 { 2935 2925 s 2918	?	2918 s	2922 s	?
2887 { 2893 2887 s 2876	?	2880 s	2893 sh	D
		2864 sh	2869 s	P
2817 { 2831 2817 s 2803	A or C	2813 s	2815 vs	SP
		1470 w		
1464 m		1464 w	1452 s	D
1456 m		1454 m		
1244 { 1255 1235 w	B	1240 w		
			1227 w	D
1179 { 1192 1179 vs 1170	C or A	1167 vs	1170 sh	
(1153 vw)			1150 m	D
1102 { 1116 1102 vs 1090	A or C	1094 vs	1104 m	D
928 { 938 918 s	B	920 s	922 s	SP
470 { 484 457 sh	B			
418 { 425 412 m	B		428 m	P
b) CD_3OCD_3				
		2280 w	2285 w	P
2248 { 2258 2248 s 2235	A	2239 s	2230 m	D
			2202 w	
2184 { 2193 2184 s 2173	C	2182 s	2185 w	
		2138 vvw	2137 m	SP
		2126 vw		
		2109 vvw	~2100 w	
2054 { 2067 2054 s 2042	A	2051 s	2053 vs	SP
1162 { 1173 1162 vs 1149	A	1146 vs	1142 m	?
1062 m		1058 m	1062 s	D
1056 m		1048 m		
1033 sh				

TABLE II. (Continued)

Infrared			Solution	Raman	
Gas		Type of the band		Liquid	Degree of depolarization
931	939 931 m 920	C	926 m		
			(895)		
	872 sh		(864)	865 sh	D
			(847)		
			(836)		
827	834 820 s	B	824 s	821 vs	P
	362 m			365 w	P

TABLE III. ASSIGNMENT OF CH_3OCH_3 AND CD_3OCD_3

		CH_3OCH_3	CD_3OCD_3	Vibrational modes of CH_3OCH_3 (CD_3OCD_3)
	ν_1	2996	2248	C-H (C-D) asym. str.
	ν_2	2817	2054	C-H (C-D) sym. str.
	ν_3	1470～1456	1062～1056	CH_3 (CD_3) deformation
A_1	ν_4	1470～1456	1062～1056	CH_3 (CD_3) deformation
	ν_5	1244	1033	CH_3 (CD_3) rocking
	ν_6	928	827	C-O sym. str.
	ν_7	418	362	COC deformation
	ν_8	2952	2202	C-H (C-D) asym. str.
A_2	ν_9	1470～1456	1062～1056	CH_3 (CD_3) deformation
	ν_{10}	1150	—	CH_3 (CD_3) rocking
	ν_{11}			Torsion
	ν_{12}	2996	2248	C-H (C-D) asym. str.
	ν_{13}	2817	2054	C-H (C-D) sym. str.
B_1	ν_{14}	1470～1456	1162	CH_3 deformation, (C-O antisym. str.)
	ν_{15}	1470～1456	1062～1056	CH_3 (CD_3) deformation
	ν_{16}	1227	1062～1056	CH_3 rocking, (CD_3 deformation)
	ν_{17}	1102	872	C-O antisym. str., (CD_3 rocking)
	ν_{18}	2925	2184	C-H (C-D) asym. str.
B_2	ν_{19}	1470～1456	1062～1056	CH_3 (CD_3) deformation
	ν_{20}	1179	931	CH_3 (CD_3) rocking
	ν_{21}			Torsion

(species A_1), a C–O antisymmetric stretching (B_1), and a COC deformation (A_1).

As can be seen in Table I, the bands at 920 and 420 cm^{-1} have been assigned to the skeletal vibrations of species A_1 by all authors. In the present experiment, strong B-type infrared bands and polarized Raman bands are observed at 928 at 418 cm^{-1} and and are assigned to A_1 bands.

The band of methyl ether-d_6 at 827 cm^{-1} has characteristics corresponding to those of a band at 928 cm^{-1} of methyl ether, so it is assigned to the C–O symmetric stretching vibration. Similarly, the Raman band observed at 365 cm^{-1} is assigned to the COC deformation vibration the measurement of the degree of depolarization, although the corresponding infrared band at 362 cm^{-1} does not show the shape of the B type but a broad singlet structure.

To the assignment of the C–O antisymmetric stretching vibration some consideration should be given. For this vibration an A type infrared band and a depolarized Raman band ether band are to be expected. Methyl ether-d_6 has the very strong A-type infrared band at 1162 cm^{-1} (in the liquid phase the frequency shifts to 1146 cm^{-1}) and no further similar bands in the region, and it also has a Raman band of medium intensity at 1142 cm^{-1}, so the band can be assigned to the C–O antisymmetric stretching vibration.

In the case of methyl ether, one of the two strong infrared bands at 1179 and 1102 cm^{-1} (A or C type) has to be assigned to the C–O antisymmetric stretching vibration of species B_1. Formerly Mashiko[7] observed two pairs of

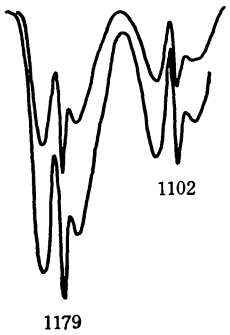


Fig. 2. Infrared spectrum of CH_3OCH_3 (gas) spectral slit width; 1 cm^{-1}.

bands, at 1169 and 1142 cm^{-1} and at 1105 and 1098 cm^{-1}, which had the appearance of B type, but in the present measurement, they proved to be triplet bands having P, Q and R branches. As the matter of fact, only two remarkable bands are observed in this region in the infrared spectrum in solution. The two infrared bands in a geseous state show a similar shape, so it is difficult to decide which one is the antisymmetric skeletal stretching vibration. The infrared spectrum in a gaseous state, measured under various pressures with a constant spectral slit width (1 cm^{-1}, Nippon Bunko DS-301), is shown in Fig. 2. Since the intensity ratios of the Q branch to the P and R branches at 1179 cm^{-1} are larger than those at 1102 cm^{-1}, the two bands could be of different species. If one band is assigned to a C–O antisymmetric stretching vibration, the other should be a methyl rocking vibration of species B_2 because of its strong intensity and shape in the infrared spectrum. As will be shown in a following paper[14], from the calculation of normal vibrations it has been concluded that the band at 1102 cm^{-1} is the C–O stretching vibration and that the one at 1179 cm^{-1} is the methyl rocking vibration.

Methyl Out-of-plane Rocking Vibrations. — Of the two methyl out-of-plane rocking vibrations, one belongs to species A_2 and the other to B_2. As stated above, the infrared band at 1179 cm^{-1} is assigned to the rocking vibration of methyl ether belonging to species B_2 (the corresponding Raman band may be a weak shoulder near 1170 cm^{-1}). In the case of methyl ether-d_6, the band at 931 cm^{-1} surely corresponds to this vibration, which shows a C-type band shape. The corresponding Raman band could not be observed distinctly.

It should be possible to determine the assignment of the methyl rocking vibration of species A_2 from only the Raman spectrum if the molecule belongs to symmetry C_{2v}. Thus, the Raman band at 1150 cm^{-1} is assigned to this vibration, and the fact that the frequency 1150 cm^{-1} is not so far from 1179 cm^{-1} of the B_2 rocking vibration supports the assignment. In deuterated ether, no suitable band could be detected, perhaps because the band is masked by other strong bands or because it has too weak an intensity to be observed in the specta.

Methyl In-plane Rocking Vibrations. — To species A_1 and B_1 belongs one rocking vibration each. In methyl ether, the B-type band is observed at 1244 cm^{-1}, and, from the preceding interpretation, this could not be a methyl deformation vibration. Moreover, the fact that in a molecule including methoxy groups a band was always observed near 1230 cm^{-1} [8,9] suggests that the band is, though weak, a fundamental. This band is therefore assigned to the A_1 methyl rocking vibration.

The depolarized Raman band is observed at 1227 cm^{-1}. In the paper of Tailor and Vidale, the Raman band observed by them at 1242 cm^{-1} was strongly polarized, but the present authors determined the band at 1227 cm^{-1} to be certainly depolarized. Therefore, it is unreasonable to regard the Raman band as corresponding to the infrared band at 1244 cm^{-1}. Therefore, it is assigned to the B_1 methyl rocking vibration.

In methyl ether-d_6, no infrared band with the band shape typical of methyl ether is observed. A shoulder at 1033 cm^{-1} is assigned to the A_1 methyl rocking vibration, and the weak band at 872 cm^{-1} in the Raman and infrared spectrum is assigned to the B_1 band. Applying the product rule to these frequencies, we get the following results which support the assignments.

	A_1	B_1
Theor.	0.1880	0.2150
Calcd.	0.1810	0.2117

The authors wish to express their sincere thanks to Dr. Yo-ichiro Mashiko and Dr. Shinnosuke Saëki of this Institute for their valuable discussions. Also, they wish to thank Dr. Junko Nakamura of The University of Tokyo, who kindly recorded a few of the spectra with a P. E. 112G spectrometer, and Professor Kôji Nakanishi of Tokyo University of Education, who allowed them to use that institution's Nippon Bunko DS-301 spectrometer.

Government Chemical Industrial Research Institute, Tokyo
Shibuya-ku, Tokyo

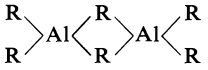
14) Y. Kanazawa et al., to be published.

Raman Spectra of Diethyl Aluminum Monohalogenides

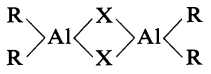
By Osamu YAMAMOTO

(Received August 21, 1961)

It has been established that some lower members of trialkyl aluminum have the molecular structure of the dimeric bridged form represented by



in which the plane containing two terminal alkyl groups and an aluminum atom is perpendicular to the bridge plane[1,2]. These compounds have been defined as "electron deficient compounds", and according to Rundle[3] the bondings between the aluminum and bridging alkyl groups are formed by two "half bonds". Monohalogen derivatives of trialkyl aluminum also exist as dimers, and the following structural formulae can be considered for them.



(A)



(B_1) (B_2)

Formula A with symmetry D_{2h} has a halogen bridge which would be formed by the coordination of lone pair electrons in halogen atoms to aluminum. Formula B_1 with symmetry C_{2h} corresponds to the "trans" form, in which two halogen atoms are present on opposite sides of the bridge plane, while formula B_2 with symmetry C_{2v} corresponds to the "cis" form where the halogen atoms are on the same side of the bridge plane. In the latter two, the alkyl bridge would be formed by the half bonds, as in the case of trimethyl aluminum.

There have been several papers reporting on the structure of dimethyl aluminum monohalogenides. Van der Kelen and Herman[4] suggested after a study of the Raman spectra, that these compounds would have the structure B_2, while Growenewege proposed structure A for dimethyl aluminum chloride as a result of Raman[5] and proton nuclear magnetic resonance spectroscopy[6]. Electron diffraction study[7] by Brockway and Davidson also indicated that the compound would have the structure A. Recently Hoffmann[8] reported Raman and infrared spectral data on some members of trialkyl aluminum and dimethyl and diethyl aluminum chlorides, but his work was mainly concerned with CH deformations and little consideration was given to the structure of the diethyl aluminum monohalogenides.

In this paper, the Raman spectra of diethyl aluminum monohalogenides (except fluoride) as well as of triethyl aluminum have been reached from these spectra as to the structure studied, and some conclusions have been of diethyl aluminum monohalogenides.

Experimental

Materials.—All the materials except diethyl aluminum chloride were prepared by Gross and Mavity's methods[9]; diethyl aluminum bromide and iodide were prepared by the reduction of corresponding aluminum sesquihalides with sodium. Diethyl aluminum chloride was provided by the Meguro Laboratory of Mitsui Chemical Industry Co., Ltd. All the samples were distilled into Raman tubes, which were sealed off under reduced pressure to prevent contamination with air and moisture.

Raman Spectra.—The Raman spectra were obtained with a Cary 81 spectrophotometer. Qualitative polarization factor measurements were also made for the purpose of the tentative assignments.

Results and Discussion

The results are shown in Table I. It can be found from this table that the Raman lines are divided into three groups: 0～700 cm^{-1}, 900～1500 cm^{-1}, and 2700～3000 cm^{-1}, which represent skeletal vibrations, CH deformation vibrations and CH stretching vibrations respectively.

Of these three kinds of vibrations, the CH deformations and stretching vibrations are not so important as far as the molecular structure

1) K. W. F. Kohlrausch und J. Wagner, *Z. physik. Chem.*, **B52**, 185 (1942).
2) P. H. Lewis and R. E. Rundle, *J. Chem. Phys.*, **21**, 986 (1953).
3) R. E. Rundle, ibid., **17**, 671 (1949).
4) C. P. Van der Kelen and M. A. Herman, *Bull. soc. chim. Belges*, **65**, 362 (1956).
5) M. P. Growenewege, *Z. physik. Chem.*, [*N. F.*], **18**, 147 (1958).
6) M. P. Growenewege, J. Smidt and H. de Vries, *J. Am. Chem. Soc.*, **82**, 4425 (1960).
7) L. O. Brockway and N. R. Davidson, ibid., **63**, 3287 (1941).
8) E. G. Hoffmann, *Z. Elektrochem.*, **64**, 616 (1960).
9) A. V. Gross and J. M. Mavity, *J. Org. Chem.*, **5**, 106 (1940).

TABLE I. RAMAN SPECTRA OF TRIETHYL ALUMINUM AND DIETHYL ALUMINUM MONOHALOGENIDES

$[Al(C_2H_5)_3]_2$		$[Al(C_2H_5)_2Cl]_2$		$[Al(C_2H_5)_2Br]_2$		$[Al(C_2H_5)_2I]_2$	
$\Delta\nu$, cm^{-1}	I	$\Delta\nu$, cm^{-1}	I	$\Delta\nu$, cm^{-1}	I	$\Delta\nu$, cm^{-1}	I
119	30 dp	114	44 dp	95	66 dp	81	100 dp
196	sh dp	164	3 dp	183	sh dp	170	85 p
269	91 dp	239	27 dp	197	100 p	202	25 p
362	18 p	263	19 p	236	11 dp	268	20 p
430	100 p	339	56 p	266	26 p	321	25 p
560	66 p	480	5 p	319	23 p	544	100 p
640	30 dp	556	100 p	547	100 p	664	34 dp
		670	27 dp	664	27 dp		
922	8 dp	922	5 dp	921	3 dp	921	3 p
955	12 p	957	10 p	954	12 p	956	8 p
979	41 dp	990	45 dp	988	24 dp	987	19 dp
1190	62 p	1107	1 p	1074	3 p	1098	3 p
1384	1 dp	1197	74 p	1132	3 p	1132	3 p
1404	19 dp	1379	1 dp	1190	84 p	1189	154 p
1460	36 dp	1406	23 dp	1377	2 dp	1381	5 dp
		1463	46 dp	1402	15 dp	1404	11 dp
				1459	25 dp	1462	22 dp
2724	9 p	2732	17 p	2733	8 p	2731	6 p
2792	18 p	2786	14 p	2789	22 p	2790	24 p
2827	54 p	2870	420 p	2866	300 p	2867	360 p
2864	565 p	2904	115 dp	2900	73 dp	2901	33 dp
2896	153 dp	2943	230 dp	2939	160 dp	2940	78 dp
2938	260 dp						

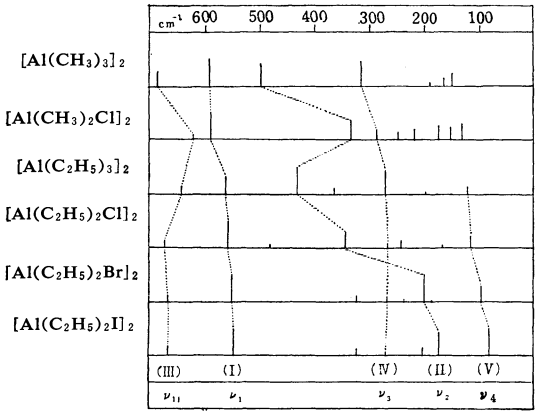


Fig. 1. Schematic representation of Raman spectra in 0~700 cm^{-1} region of diethyl aluminum halogenides and related compounds.

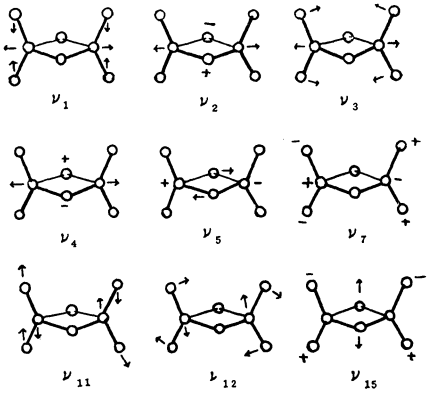


Fig. 2. Normal modes of Raman active vibrations of A_2B_6 type molecule.
ν_1, outer stretching; ν_2, bridge stretching; ν_3, outer bending; ν_4, bridge bending; ν_6, bridge stretching; ν_7, outer wagging; ν_{11}, outer stretching; ν_{12}, outer rocking; ν_{15}, outer twisting.

is concerned. Furthermore, the CH deformations were discussed in some detail by Hoffmann[8], and it appears that there is nothing to be added to his paper. Therefore, the author was interested mainly in the skeletal vibrations and left the CH stretching vibrations to be assigned in the near future.

Tentative assignments for the skeletal vibrations were obtained by comparison with the known spectra of aluminum trihalogenides[10,11], trimethyl aluminum[1], and dimethyl aluminum chloride[5], for which the bridged structure has been firmly established by many authors. The skeletal vibration lines

10) R. P. Bell and H. C. Longuest-Higgins, *Proc. Roy. Soc.*, **A183**, 357 (1945).
11) W. Klemperer, *J. Chem. Phys.*, **24**, 353 (1956).

obtained of the compounds in question are schematically drawn in Fig. 1, in which the notation for the frequencies of Bell and Longuet-Higgins[10] is used. The modes of vibrations of A_2B_6 type molecules are reproduced in Fig. 2 only for Raman active vibrations, symmetry species and polarization characters of which are shown in Table II.

Table II. Symmetry species and polarization characters of the Raman active normal vibrations in Fig. 2

D_{2h}	A_{1g} (p)	ν_1, ν_2, ν_3, ν_4
	B_{1g} (dp)	ν_6, ν_7
	B_{2g} (dp)	ν_{11}, ν_{12}
	B_{3g} (dp)	ν_{15}

Seven to eight Raman lines are observed in the region of the skeletal vibrations of the monohalogenides. In the case of the C_{2h} symmetry model, structure B_2, all of the 18 possible skeletal vibrations are Raman active, while only nine of the vibrations are Raman active for the D_{2h} or C_{2h} symmetry model. It is probable, therefore, that diethyl aluminum monohalogenide has a D_{2h} or C_{2h} symmetry, although this does not appear to be conclusive. Futhermore, in the 400~700 cm^{-1} region of diethly aluminum chloride four infrared absorption bands were observed[8], at 673, 628, 544 and 438 cm^{-1}, which, except for 673 cm^{-1}, do not accord with the Raman lines in Table I. If 673 cm^{-1} in the infrared and 670 cm^{-1} in the Raman spectra can be assigned to each different vibration, and if it is noted that no other infrared band agrees with any of the Raman lines in frequency, it can be considered that the rule of mutual exclusion holds; this fact assures the presence of the center of symmetry in the molecule. Unfortunately, there is no infrared data on diethyl aluminum monobromide and iodide, but the possibility of C_{2v} symmetry can be eliminated with considerable certainty.

In the Raman spectra of trietyl aluminum and diethyl aluminum monohalogenides the following two series of strong lines are observed:

X of $[Al(C_2H_5)_2X]_2$	Series I cm^{-1}	Series II cm^{-1}
Et	560	430
Cl	556	339
Br	547	197
I	544	170

Since both series of lines are polarized, these must be either ν_1, ν_2, ν_3, or ν_4 for D_{2h} symmetry. Furthermore, it is reasonable to assume that series I and II are assigned to either ν_1 or ν_2 by comparison with the assignment of the spectrum of trimethyl aluminum.

Now if the halogen bridge model A with symmetry D_{2h} is acceptable, series II must be assigned to ν_2, the bridge stretching vibration, because it varies in frequency with the increase in the atomic weight of substituents while series I does not. The frequencies of the bridge stretching vibration, ν_2, of aluminum trihalogenides are 340, 204 and 146 cm^{-1} for chloride, bromide and iodide respectively, as is shown in Table III, in which the Raman lines in the skeletal regions of trimethyl aluminum, dimethyl aluminum chloride and aluminum trihalogenides are listed with the normal vibrations to which they are assigned. Thus, it can be found that there is a close relationship in ν_2 between the trihalogenides and diethyl aluminum monohalogenides. When series II is assigned to ν_2, series I is naturally assigned to ν_1, the outer stretching vibration.

If the halogen bridge model A is assumed, the remaining outer vibrations ν_3, ν_7, ν_{11} and ν_{12} must not vary in frequency with the increase in the atomic weight of the substituents. Thus, the series III, 640(Et), 670(Cl), 664(Br) and 664(I) cm^{-1} is assigned to the outer stretching vibration ν_{11} by comparison with methyl compounds and by a consideration of polarization factors. Series IV, 269(Et), 263(Cl), 266(Br) and 268(I) cm^{-} may be assigned to the outer bending vibration ν_3. The depolarized series V, 119(Et), 114(Cl),

Table III. Raman lines in the region of 0~700 cm^{-1} of trimethyl aluminum, dimethyl aluminum chloride and aluminum trihalogenides

	$[Al(CH_3)_3]_2$[1]	$[Al(CH_3)_2Cl]_2$[5]	Al_2Cl_6[10]	Al_2Cl_6[11]	Al_2Br_6[10]	Al_2I_6[10]
ν_1	590 (10 p)	588 (10)	606 ($2^1/_2$ p)	506	491 (3)	406 (3)
ν_2	452 (8 p)	332 (7)	340 (10 p)	340	204 (10)	146 (10)
ν_3	314 (9 p)	286 (4)	217 (5 p)	217	140 (5)	94 (6)
ν_4	148 (5)	131 (6)	112 (6 dp ?)	112	73 (6)	53 (6)
ν_{11}	682 (5 dp)	620 (2)	506 (3 p)	606	407 (2)	344 ($2^1/_2$)
ν_{12}	188 (1)	173 (5)	164 (3 dp)	164	112 (3)	—
ν_6	563 (00)	247 (3)	438 ($^1/_2$ dp ?)	438	(291 ?)	(195 ?)
ν_7	164 (3)	152 (5)	284 (2 dp)	164	176 (2)	—
ν_{15}	—	217 (4)	—	(160)	—	—

95(Br), and 81(I) cm^{-1} might be ν_4 by intensity consideration, although ν_4 has to be a polarized vibration.

So far the assignments have been performed with the halogen bridge model. If the alkyl bridge model, B_1 with symmetry C_{2h} (trans form), is adopted, series which does not vary in frequency is the bridge vibration, so that polarized series I should be a bridge vibration. But even in this case triethyl aluminum must belong to the same symmetry class D_{2h} as trimethyl aluminum, so that, for example, 560 cm^{-1} of triethyl aluminum in series I should be assigned to ν_1, the outer vibration, by comparison with ν_1 and ν_2 of trimethyl aluminum. With the model B, all of the monohalogenides have the alkyl bridge. Then strong lines at approximately 430 cm^{-1} should also be observed as the bridge stretching vibration in the spectra of the monohalogenides as in the case of triethyl aluminum. Actually it is not the case, however. Furthermore, it is impossible to interpret the marked correlation of frequencies between the triethyl aluminum and the diethyl aluminum monohalogenides obtained in Table I.

Accordingly, the results of this study indicate that the Raman spectra of diethyl aluminum chloride, bromide and iodide are consistent with a dimeric bridge structure over the halogen atoms with symmetry D_{2h}.

The author wishes to express his gratitute to Drs. Yoichiro Mashiko and Kenkichi Nukada of the Government Chemical Industrial Research Institute, Tokyo, for their kind encouragement and valuable suggestions given throughout this study. He is also indebted to Misses Michiko Matsushima and Yuriko Matsubayashi of the same Institute for their help in the measurement of the Raman spectra, and to Mr. Ichiro Endo for his experimental assistance.

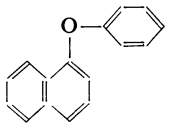
Government Chemical Industrial Research Institute, Tokyo
Shibuya-ku, Tokyo

Synthesis of Naphthyl p-Tolyl Ethers

By Hajime SUZUMURA

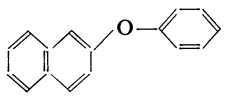
(Received April 26, 1961)

The physical properties of α- and β-naphthyl phenyl ethers (structural formulas I and II) were reported in the literature[1].



(I)

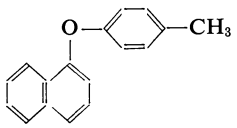
m. p. 54°C
b. p. 349.5°C
(753 mmHg)



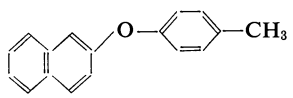
(II)

m. p. 45°C
b. p. 335.5°C
(753 mmHg)

In order to examine the physical properties and the thermal stability of aromatic ethers which have a methyl side chain, the author newly synthesized naphthyl *p*-tolyl ethers (formulas III and IV).



(III)



(IV)

1) F. Ullmann et al., *Ann.*, **350**, 90 (1906).
2) C. Paal et al., *Ber.*, **30**, 884 (1897).

TABLE I

Isomer	α-	β-	
Appearance	Colorless plates	Colorless needles	Calcd.
B. p., °C	184~185 (3 mmHg)	187~188 (3 mmHg)	
M. p., °C	38~39	41~42.3	
Elementary analysis			
C, %	86.96	87.22	87.15
H, %	5.71	6.00	6.02

The properties of purified specimens are shown in Table I.

Paal[2] synthesized the β-isomer by a reaction of β-naphthol and potassium nitroso-*p*-tolylsulfamate in benzene and he reported that the compound was red and melted at 135°C. However, the β-isomer which the present author prepared is a white needle and melted at 41~42.3°C. The melting point of the Paal's compound seems to be too high for the β-isomer in comparison with those of phenoxynaphthalenes and also the red color seems unlikely for a naphthyl tolyl ether structure and it probably be due to some impurities. The

TABLE II. α-NAPHTHYL *p*-TOLYL ETHER

p-Cresol	KOH	α-Bromonaphthalene	Copper	Condition		Main fraction	Crude crystal		
				Temp.	Time		Amount	M. p.	Yield[a]
g.	g.	g.	g.	°C	hr.	g.	g.	°C	%
16.5	6	20.4	1.0	160～173	4	7.5	4.4	35～38	19
15.8	6	20.7	1.0	220～240	2½	9.2	4.6	37～38	20

a) The yield based on α-bromonaphthalene

TABLE III. β-NAPHTHYL *p*-TOLYL ETHER

β-Naphthol	*p*-Bromotoluene	KOH	Copper	Condition		Crude crystal		
				Temp.	Time	Amount	M. p.	Yield
g.	g.	g.	g.	°C	hr.	g.	°C	%
20	17.5	5.6	2.0	144～150	7	4.55	—	19
14.4	17.1	5.6	2.0	180～200	7	9.25	38～41	39
7.2	9.0	3.0	0.7	200～210	6	4.32	35～39.5	37

physical properties and absorption spectra afford evidence in favor of the compound prepared by the author as the correct β-isomer. In the present experiment, the ethers were synthesized by the Ullmann reaction, that is, the α-isomer from α-bromonaphthalene and *p*-cresol, and the β-isomer from β-naphthol and *p*-bromotoluene.

Experimental

Materials. — *p-Cresol*[3]. — B. p. 200°C (uncorr.), m. p. 32°C.

α-Bromonaphthalene[4].—It was synthesized from naphthalene and bromine in the same manner as described in the literature.

Copper Powder.—It was precipitated from an aqueous solution of cupric sulfate by addition of zinc granules and washed with water, dilute hydrochloric acid and finally with ethanol.

β-Naphthol.—Commercial reagent, m. p. 120～121°C (uncorr.).

p-Bromotoluene.—Commercial reagent was redistilled, m. p. 25.2°C.

Synthesis of α-Naphthyl *p*-Tolyl Ether.—*p*-Cresol was dissolved in an aqueous solution of potassium hydroxide and water was evaporated from the resulting solution in vacuo and to the dried residue were added α-bromonaphthalene and copper powder and the mixture was heated in an oil bath. The cooled mixture was first treated with 20% aqueous solution of potassium hydroxide to dissolve unreacted *p*-cresol and then extracted with benzene. The extract was concentrated and distilled in vacuo. The main fraction was at first pale yellow and viscous which gradually solidified to a white mass by cooling and seeding. This solid was recrystallized once from ethanol to give needles which melted at 36～39°C. The experimental results are shown in Table II.

The crude ether was recrystallized twice from ethanol to give colorless plates which melted at 38～39°C.

Found: C, 86.96; H, 5.71; mol. wt. 234. Calcd. for $C_{17}H_{14}O$: C, 87.15; H, 6.02%; mol. wt. 234.

Solubility.—It is readily soluble in toluene, benzene, chloroform, moderately soluble in cold ethanol and insoluble in water.

Trinitrobenzene Complex.—It was prepared from ether (189 mg.) and trinitrobenzene (182 mg.) in ethanol. Three recrystallizations from ethanol yielded 192 mg. of pale yellow crystals, m. p. 72～73°C.

Found: N, 9.20. Calcd. for $C_{23}H_{17}O_7N_3$: N, 9.40%.

The picrate could not be prepared by the usual method.

Infrared Spectrum. — The spectrum in carbon disulfide is shown in Fig. 1. To make the analysis of the spectrum easier, a comparison with that of the α-phenyl ether is shown in Fig. 2. A band appearing at 13 μ(769 cm^{-1}) and 3 strong bands in the range of 9～10 μ correspond to a 1,2,3-substitution in the benzene ring. This means a substitution in 1-position of naphthalene which may be regarded as a substituted benzene. A band at

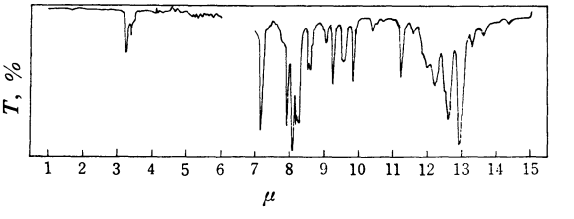


Fig. 1. α-Naphthyl *p*-tolyl ether.

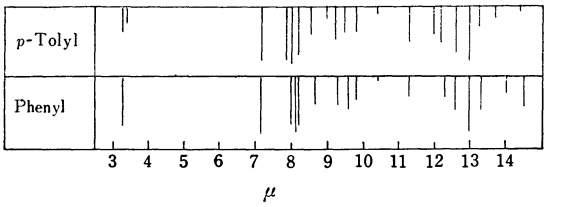


Fig. 2. Aryl α-naphthyl ether.

3) I. Heilbron, "Dictionary of Organic Compounds", Vol. I, Oxford University Press, New York (1953), p. 613.
4) "Organic Syntheses", Collective Vol. I, Second Edition, John Wiley & Sons, Inc., New York (1956), p. 121.

8.1 μ(1235 cm^{-1}) corresponds to an ether linkage and a band at 3.45 μ(2899 cm^{-1}) to aliphatic C-H. As a band at 12.2 μ(820 cm^{-1}) indicates the presence of a para-substitution in the benzene ring, the methyl group is at para position of the phenoxyl bonding. An absorption band at 12.6 μ(794 cm^{-1}) shows 3 adjacent hydrogen atoms in the benzene ring.

Synthesis of β-Naphthyl *p*-Tolyl Ether.—β-Naphthyl ether was synthesized in the same ways as those for α-napththyl ether. The experimental results are shown in Table III.

The crude ether (9.25 g.) was recrystallized from ethanol to give 3.17 g. of short needles, m. p. 41~42°C. This purified specimen distilled at 187~188°C (3 mmHg).

Found: C, 87.22; H, 6.00; mol. wt. 233. Calcd. for $C_{17}H_{14}O$: C, 87.15; H, 6.02%; mol. wt. 234.

Solubility.—It is readily soluble in benzene, toluene and chloroform, moderately soluble in cold ethanol and insoluble in water.

Trinitrobenzene Complex.—It was prepared from the ether and trinitrobenzene in ethanol.—Recrystallized twice from ethanol, pale yellow leaflets were obtained; m. p. 93~94°C. This seems to be unstable.

Infrared Spectrum. — The spectrum in carbon disulfide is shown in Fig. 3 and the comparison with that of the β-phenyl ether is shown in Fig. 4. In this spectrum a band is absent at 14.5 μ. A strong band at 12.2 μ(820 cm^{-1}) shows a para-substitution in the benzene ring, thus indicating the presence of the methyl group at para position. A band at 13.4 μ(746 cm^{-1}) corresponds to the presence of 4 adjacent hydrogen atoms in the benzene ring.

Ultraviolet Spectra. — The spectra of α- and β-isomers of *p*-tolyl ethers and phenyl ethers in cyclohexane are shown in Figs. 5 and 6. Compared with the adsorption maxima of the corresponding phenyl ethers, those of *p*-tolyl ethers are at nearly the same wavelengths.

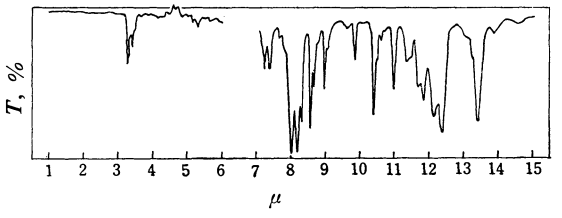


Fig. 3. β-Naphthyl *p*-tolyl ether.

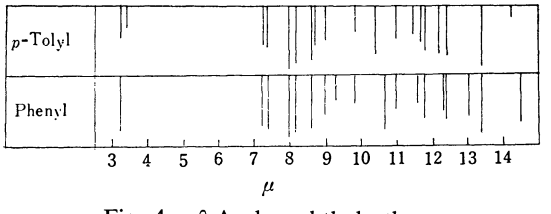


Fig. 4. β-Aryl naphthyl ether.

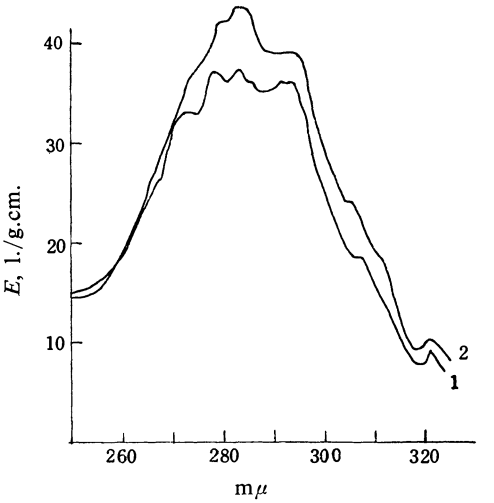


Fig. 5. α-Naphthyl ethers: 1, Phenyl; 2, *p*-Tolyl.

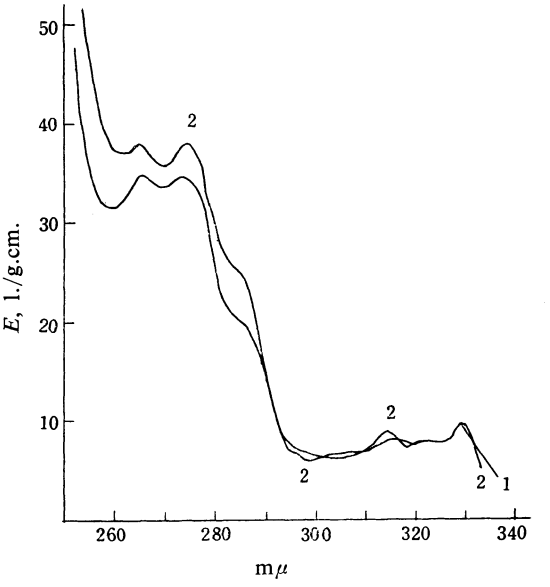


Fig. 6. β-Naphthyl ethers; 1, Phenyl; 2, *p*-Tolyl.

The author is indebted to Professor Ryozo Goto of Kyoto University for helpful discussions and criticisms of this work and to Professor Sakujiro Kimura for his advice and encouragement.

Tokyo Laboratory of Research Center
Yawata Chemical Industry Co.
Chuo-ku, Tokyo

The Reaction of Hydrogen and Oxygen through a Silent Electric Discharge. II. The Effect of Packings on a Peroxide Formation

By Kihei MORINAGA

(Received August 21, 1961)

The formation of ozone in a discharge tube containing various fillings has been previously reported[1]. To complement this report, similar investigations were carried out on the hydrogen-oxygen reaction. The hydrogen-oxygen reaction is generally known to be influenced by the chemical composition and the nature of the material constituting the surface of the reaction vessel[2-5]. Further, it is conceivable that the reaction through silent discharge may be considerably affected by the composition of the fillings employed in the discharge gap. The results were satisfactory from the viewpoint of confirming this hypothesis.

Experimental

The apparatus used and the procedures followed, were similar to the previously reported work[6]; however, the packing fill of the discharge tube was varied. The reactant gas, consisting of 4.5% oxygen by volume, was sent from a reservoir through the discharge tube after passing through the drying column. After passing through the discharge tube, the reactant gas was immediately cooled in a condensation trap, where the hydrogen peroxide and water produced were caught by freezing. The packing materials consisted of several kinds of ceramics containing titanium(IV) oxide, soda glass, boric oxide and orthoboric acid. Except for boric acid, the granular size of the packing materials was 0.7~1.0 mm. sieve mesh, while for boric acid it was between 0.5~0.85 mm. Thus, the void of the packed discharge tube was 45% in the former case and 38% in the latter case. The discharge tube made of hard glass (Hario glass) had a gap length and electrode area of 2 mm. and 200 cm^2 respectively. The electric source frequency for the silent discharge was 1000 c./sec. and the pulse current was measured in a way similar to that of the previous work[1].

Results

In every discharge tube the experiment was carried out under a constant flow rate so that the resident time was between 3.9 to 4.1 sec. Table I shows the peroxide concentration and the overall conversion rate of the reactant oxygen gas to peroxide and water at a certain fixed pulse current of 100 μ amp.

TABLE I.

No.	Composition of the packings	Dielectric constant	Peroxide concn. %	Overall conversion rate, %
1	Blank	1	46.0	2.4
2	Soda glass	6	4.5	3.7
3	$2\,MgO/TiO_2$	20	1.2	3.3
4	TiO_2	100	1.7	3.6
5	$BaTiO_3$	1200	2.5	3.5
6	$95\,BaTiO_3/5\,SnO_2$	5500~6000	0.7	3.2
7	B_2O_3		45.5	3.1
8	H_3BO_3		42.1	2.5

Discharge tube: Hario glass, $A=200\,cm^2$, $d=2$ mm.
Pulse current: 100 μ amp.
Residence time: 3.9~4.1 sec.

When the packing consisted of soda glass, and especially when the packing consisted of ceramics, the peroxide concentration was appreciably lowered. However, when the packing consisted of boric oxide or boric acid, the peroxide concentration was nearly the same as that resulting from a void discharge tube. The overall conversion rate to peroxide and water is larger when the discharge tube has a packing fill than when the tube is empty. This partly agrees with the finding of the investigation of ozone formation in a packed discharge tube[1].

Concerning the boric oxide packing, a kind of aging phenomena was observed. That is, the fresh boric oxide packing initially gave a high concentration of peroxide and a low conversion rate. After repeated use, the above values approached saturation values. In Fig. 1, the results of the aging phenomena are shown. Each point represents the concentration of the conversion rate of the product in one hour of continuous dicharge. Both the concentration and the conversion rate seem to settle to steady values after a few hours of discharge.

Discussion

In an ordinary discharge tube without packing fill, the overall conversion rate to peroxide and

1) K. Morinaga and M. Suzuki, This Bulletin, **35**, 429 (1962).
2) A. H. Willbourn and C. N. Hinshelwood, *Proc. Roy. Soc.*, **A185**, 353, 369, 376 (1946).
3) B. Lewis and G. von Elbe, *J. Chem. Phys.*, **10**, 366 (1942).
4) R. R. Baldwin and R. F. Simmons, *Trans. Faraday Soc.*, **51**, 680 (1955).
5) R. R. Baldwin et al., ibid., **56**, 80, 93, 103 (1960).
6) K. Morinaga, This Bulletin, **35**, 345 (1962).

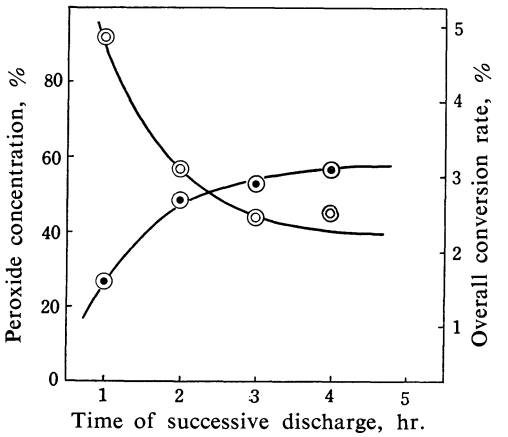


Fig. 1. The peroxide concentration and the overall conversion rate against time of successive dischage.
◎ Peroxide concentration
⊙ Overall conversion rate

water was larger when a smaller gap length was used[6]. This agrees with the results obtained in the investigation of the ozone formation[7]. In a silent discharge with a packing-filled discharge tube, the ozone formation rate and ozone concentration were improved appreciably[1]. This was ascribed to the fact that the shortening of the gap length, which was due to the packing fill, will improve the ozone yield.

In this experiment, however, though the overall conversion rate to peroxide and water was larger in the packing-filled discharge tube, the final product of the reaction was greatly affected by the packing materials employed in the discharge gap. This was not the case in the previously studied formation of ozone. The difference in the peroxide concentration can be seen in Table I. These differences can be ascribed to the effect of the surface of the filling material on the reaction, similar to the case pointed out in the previous paper[6].

Hinshelwood et al.[2] suggested that, in the second explosion limit of hydrogen and oxygen gas, the surface destruction of the HO_2 radical was dominant in halide-coated or in silica vessels. On the other hand, the boric acid-coated vessel does not provide enough reaction for the surface destruction of both HO_2 and H_2O_2; thus, the HO_2 radicals form H_2O_2 either by the surface or the gas phase process. Baldwin et al.[5] showed that the gas phase binary reaction of HO_2 to form H_2O_2 and O_2 was more predominant than the surface process of HO_2 to form $1/2\,H_2O_2$ and $1/2\,O_2$. In the reports[5] it was also concluded that the formation of peroxide from HO_2 and H_2 was preponderant over the formation of water from the same species.

7) K. Morinaga and M. Suzuki, ibid., **34**, 157 (1961).

The peroxide formation resulting from a silent discharge is first assumed to be a gas phase reaction accompanied by the other elementary process of water formation. In the course of the catalytic decomposition of H_2O_2 on the surface of the discharge tube or the packing granules, the quantity of water increased, consequently lowering the peroxide concentration in the product. This tendency will be more preponderant when there is a shorter gap length or when a discharge tube with other than boric oxide and boric acid fillings is used.

Walsh[8] has evidence which has lead him to believe that the anti-knock effect of lead tetra-ethyl is due to the destruction of HO_2 and H_2O_2 on the lead(II) oxide surfaces. In the present case, the ceramics which contained titanium(IV) oxide and other metallic oxides will behave similarly to those described above. Soda glass may be similar to the halide-coated or silica surfaces. On the surface of boric oxide and boric acid, the destruction of HO_2 and H_2O_2 will be suppressed and the concentration of peroxide will be increased.

The overall conversion rate in the packing-filled discharge tube will be increased with the improvement of the discharge efficiency which arises from the packing fill[1,7].

In the case of boric oxide fillings, the water molecules will reside on the fresh surfaces of the granules. After the saturation-like adsorption of water molecules, the surface activity seems to be lowered.

Summary

By applying several packings in the discharge gap space, the peroxide formation through a silent discharge was studied. The peroxide concentration was higher in a void discharge tube or in a boric acid (boric oxide) packing-filled discharge tube and lower in the case of the soda glass and the ceramic packing containing titanium(IV) oxide. This was explained by the insufficient destruction of HO_2 and H_2O_2 on the boric acid surface, and by the great destruction on the surface of the packing consisting of soda glass and ceramics. A kind of aging phenomena observed in the boric oxide packing was tentatively explained.

The author would like to express his great appreciation to Professor Momotaro Suzuki of the Defense Academy for his encouragement and helpful advice throughout this investigation.

Department of Chemistry
Defense Academy
Yokosuka

8) A. D. Walsh et al., *Proc. Roy. Soc.*, **A215**, 175, 454 (1952).

The Reaction of Hydrogen and Oxygen through a Silent Electric Discharge. III. The Ignition of the Hydrogen-Oxygen Gas by Silent Electric Discharge

By Kihei MORINAGA

(Received, September 11, 1961)

The ignition of a detonative gas mixture can be actuated by an electric spark with sufficient strength[1,2]. Usually there is a threshold value of the strength above which the initiation of the detonation is realizable. Very few investigations have, however, been reported on the silent electric discharge which is involved in the initiation of the detonation.

In the present paper, the problem of the initiation of the detonation of a hydrogen-oxygen mixture is dealt with mainly from the view-point of the electrical energy necessary to cause any detonation. The electrical energy is expressed as pulse current estimated from an oscillogram pattern.

Experimental

The oxygen and hydrogen gases taken from each cylinder were dried over calcium chloride and silica gel and then stored in the desired composition for several hours before use.

The electrical circuit system of the silent discharge and a brief diagram of the detonation bomb are shown in Fig. 1. The cylindrical bomb, made of mild steel, has an inside diameter of 6 cm. and a depth of 9 cm. A kind of safety diaphragm to prevent a dangerous pressure rise is attached to the bomb. A silent discharge electrode, composed of ordinary glass plates 5×6 cm. and 1 mm. thick, was mounted in the center of the bomb. The area of the electrode and the gap length are 7.5 cm^2 and 2 mm. respectively. The whole system is air-tight, and the measuring gas can be introduced through a tap just before each measurement. Direct current is supplied from a system of storage batteries of 120 V. and 250 amp. hr. As can be seen in Fig. 1, the voltage of direct current from the storage batteries was potentiometrically regulated and was supplied to the transformer via the throwing switch S. In the secondary coil of the transformer, an inductive high tension is induced according as the switch S is "on" or "off". In the present experiment, the shock current which is induced by the "on" position was used exclusively.

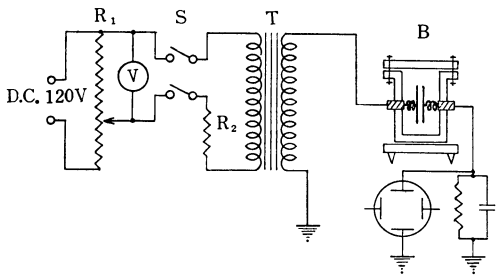


Fig. 1. The electrical circuit system of silent discharge.
R_1, R_2: Resistor
V: Voltmeter
S: Throwing switch
T: Transformer
B: Test bomb

The pulses of the silent electric discharge were observed by an oscilloscope synchronized with the switch S. The time constant of the C-R circuit for observing the pulse current was 5.2×10^{-6} sec.

Whether or not the gas is ignited can easily be detected by a distinct cracking noise of the safety bursting diaphragm, or by the sudden fall of the pressure gauge.

Several shots of the oscillographic pattern of the explosion just above the explosion limit of the primary voltage and of the non-explosion just under the limit were taken. In the experiments the scope of the primary voltage of the explosion and non-explosion patterns could be set within 2.5 V. or, in the worst case, within 5 V.

The composition of the gas mixture covers a range of 8.5~75% oxygen. The ignition is actually observed in gas mixtures of more than 9.9% oxygen.

Results

An oscillographic pattern of the induced high tension which appeared in the secondary coil simultaneously with the primary circuit being closed by switch S is shown in Fig. 2.

With applying the above high tension to the discharge electrode, a kind of one-shot silent discharge was obtained. Figure 3 shows the current diagram of a discharge in a hydrogen and oxygen gas mixture which did not provoke any ignition. The fringe-like figure indicates the pulse current during the silent electric

1) B. Lewis and G. von Elbe, "Combustion, Flames and Explosion of Gases", Academic Press, Inc., New York (1951), pp. 390–425.

2) M. V. Blanc, P. G. Guest, G. von Elbe and B. Lewis, "Third Symposium on Combustion and Flame and Explosion Phenomena", Williams and Wilkins Co., Baltimore (1949), p. 363.

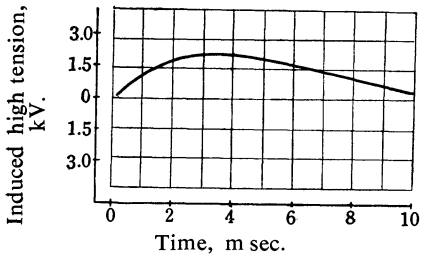


Fig. 2. Induced high tension in the secondary circuit. Dummy load 750 kΩ, primary voltage 60 V.

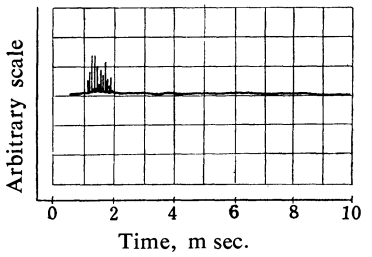


Fig. 3. Current diagram of silent electric discharge in hydrogen and oxygen gas mixture without provoking any ignition. O_2 content 33.5%; total pressure 298 mmHg; primary voltage 60V.

discharge[3-6], and the thick line shows the basic current in the secondary circuit.

In Fig. 4, some types of the oscillogram pattern accompanying the gas ignition are shown. In type A the discharge current flows for some time t_1, and then an ignition which is indicated by rather high and irregular pulse current comes in at the heel of the discharge current. In type B, there is some time delay t_2-t_1 from the quenching of the discharge current to the beginning of the ignition. Types C and D make their appearance when the condition is most contiguous to the threshold of the ignition and are very difficult to observe. The features are virtually the same as those of A and B.

In these patterns in Fig. 4, the base current or the low frequency discharge current in the gap space was appreciably elevated over the pattern of non-ignition in Fig. 3. These elevations on the current diagram could be ascribed to the ionization of the gases, which is accompanied with the inflamation or explosion of the gas[7].

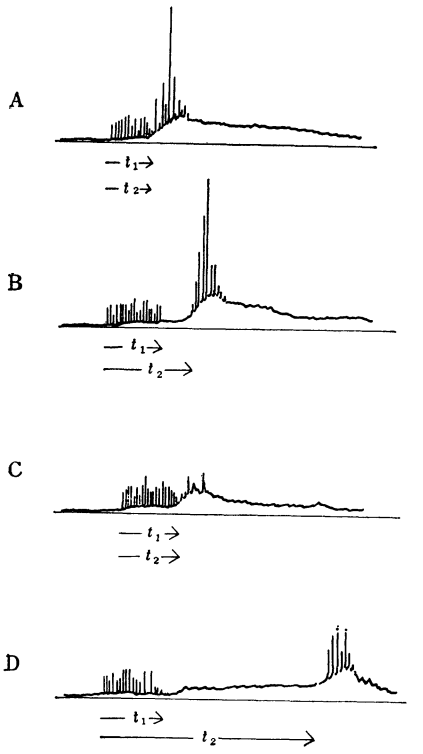


Fig. 4. Current diagram of silent electric discharge accompanied with the gas ignition.
A : O_2 content 23.5%, P=362 mmHg, t_1=1.04 m sec.
B : O_2 content 23.5%, P=226 mmHg, t_1=1.25 m sec.
C : O_2 content 15.0%, P=225 mmHg, t_1=1.33 m sec.
D : O_2 content 15.0%, P=189 mmHg, t_1=1.41 m sec.

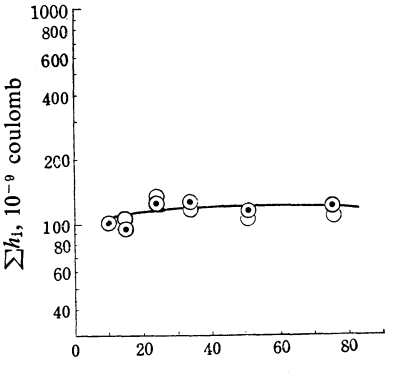


Fig. 5. Threshold value of $\sum h_1$ against oxygen content. P=200 mmHg.
○ $\sum h_1$ value obtained from ignition pattern just above the threshold condition.
◉ $\sum h_1$ value obtained from non-ignition pattern just under the threshold condition.

3) M. Suzuki, *Proc. Japan Acad.*, **26**, 20 (1950).
4) M. Suzuki and Y. Naito, ibid., **28**, 469 (1952).
5) M. Suzuki, S. Okazaki and T. Yamamoto, *Am. Chem. Soc., Adv. Chem. Ser.*, No. **26**, 331 (1957).
6) K. Honda and Y. Naito, *J. Phys. Soc. Japan*, **10**, 1007 (1955).
7) S. Basu and J. A. Fay, "7th Symposium on Combustion", Butterworth Sci. Publications, London (1959), p. 277.

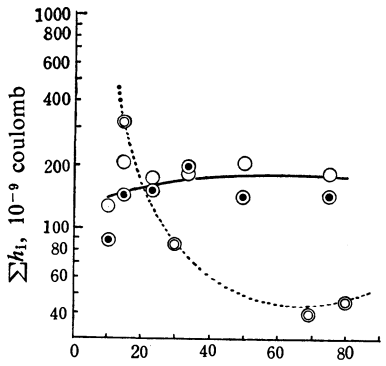


Fig. 6. Threshold value of $\sum hi$ against oxygen content. $P=300$ mmHg.
- ○ $\sum h_1$ value obtained from ignition pattern just above the threshold condition.
- ◉ $\sum h_1$ value obtained from non-ignition pattern just under the threshold condition.
- ◎ modified result of Lewis and von Elbe in the condenser spark ignition.

In Figs. 5 and 6, the total pulse current carried through the electrode for a period of the time t_1 or $\sum h_1$, where the h_1 is the height of a single pulse cuurrent appearing in an oscillogram pattern, was plotted versus the oxygen content of the detonating gas mixture. In these figures, the open circle represents the value of $\sum h_1$, obtained from the oscillographic pattern of discharge, which takes place just above the threshold primary voltage, and the dotted circle represents that of $\sum h_1$ from the pattern just under the threshold primary voltage. The real threshold condition will be in between the two plots, and a little increasing trend is observable. The double circle in Fig. 5 represents the modified result of Lewis and von Elbe in the condenser spark ignition of hydrogen and oxygen gas at 0.33 atm. The numerical value of coulomb is obtained from the C and V values cited in their data[1].

The quantities of electricity are independent of the composition of the detonating mixture, or, in other words, a fixed amount of electricity through a silent discharge is always required to initiate the ignition, no matter what the composition of the detonating gas is.

If the $\sum h_1$ is plotted against the pressure of the detonating gas mixture of a certain definite composition, then a series of straight lines is obtained (Fig. 7). The slope of the straight lines increases as the oxygen content is richer. The quantity of electricity, therefore, which is necessary to initiate a detonation in a gas mixture of a fixed pressure will be more as the oxygen content is richer.

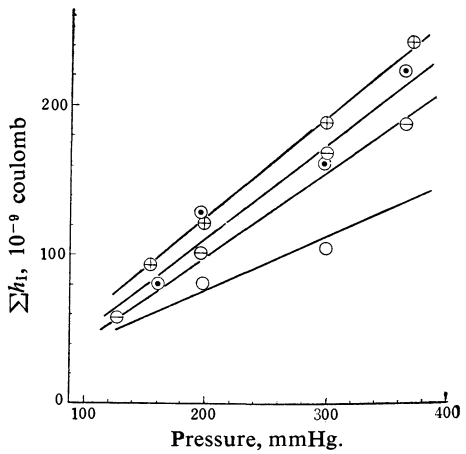


Fig. 7. The relation between $\sum h_1$ and the reactant gas pressure.
O_2 content; ○ 9.9% ⊖ 15.0%
◉ 23.5% ⊕ 33.5%

Discussion

The fact that the quantity of electricity needed for the initiation of the ignition of a hydrogen and oxygen mixture under fixed pressure is independent of the composition of the gas mixture, implies that a certain amount of chemical entity is essential to initate the ignition. Furthermore, the amount of this chemical entity is constant for the gas composition range used in this measurement.

The chemical entity is tentatively presumed to be a OH radical, which may be concluded according to the chain branching mechanism learned from explosion limit studies[8,9];

$$H+O_2 \rightarrow OH+O \qquad (1)$$

Even then, in some cases in our experiment a ignition delay was observed. The accumulation of the necessary concentration of this radical may then be achieved through any possible secondary decade which will proceed during the delay time.

The fixed amount of electricity provides, shall we say, at first a H radical of enough concentration by which reaction 1 will be initiated. The rate of secondary decades providing a OH radical sufficient for an ignition will be very rapid without an ignition delay, or otherwise, it may not be so rapid some delay time is required to attain the sufficient concentration. The alternatives will be decided by the strength of discharge current and/or by the composition of the gas mixture.

The quantity of electricity incresses linearly

8) R. R. Baldwin and A. D. Walsh, *Discussions Faraday Soc.*, **17**, 96 (1954).
9) D. R. Warren, *Proc. Roy. Soc.*, **A211**, 106 (1952).

with the pressure of the gas mixture, which indicates that the primary radical, or the H radical in this case, which is necessary to initiate the reaction 1 and then the ignition, increases in the gas mixture while keeping a linear relationship with the pressure of the gas mixture. The reaction pattern is very much like that of the ozone formation in silent electric discharge[10], where the O radical is produced by a collision process between an electron and an oxygen molecule. The same reasoning discussed there can be applied here, and the mechanism of this reaction pattern and the above relationship will then be understood without any further explanation. The study of the electric ignition of the detonative gas mixture greatly contributes to the exploration of the chain ignition mechanism, though further extensive study will be required to elucidate the actual features in more detail.

10) J. C. Devins, *J. Electrochem. Soc.*, **103**, 460 (1956).

Summary

The ignition of a hydrogen and oxygen gas mixture by a silent electric discharge was investigated.

The quantity of electricity which must be carried in the course of the discharge before a detonation will take place is almost independent of the composition of the gas mixture. Furthermore, for a gas mixture of fixed composition,the quantity of electricity increases along with the increasing pressure of detonative gas. A tentative view of the possible mechanism of the initiation of the detonation was briefly discussed.

The author would like to express his grateful appreciation to Professor Momotaro Suzuki of the Defense Academy for his encouragement and helpful guidance throughout this investigation.

Department of Chemistry
Defense Academy
Yokosuka

Dimensions of Vinylidene Chloride-Alkyl Acrylate Copolymers in Flory Theta Solvents

By Mitsuo ASAHINA, Masaki SATO and Takashi KOBAYASHI

(Received August 17, 1961)

The effects of the length of the pendant side chain on the dimensions of polymer molecules in solution have as yet not been fully elucidated. Recent studies by Chinai[1] et al. on poly(alkyl methacrylates) and by Manson[2] et al. on poly(vinyl alkyl ethers) have shown reversals of the polymer chain extension with an increase in side chain length, but no explanation of these reversals has been given. In the present study we determined the unperturbed dimensions of four copolymers of vinylidene chloride and alkyl acrylates in the hope of obtaining experimental material which might aid in clarifying how the dimensions of a polymer molecule in solution are affected by the length of its pendant side chain.

Experimental

Preparation of Copolymers.—For the purpose of the present study, we prepared four vinylidene chloride-alkyl acrylate copolymers. The alkyl acrylates chosen were ethyl acrylate, *n*-butyl acrylate, *n*-hexyl acrylate and *n*-octyl acrylate. Commercial materials of these alkyl acrylates were distilled and, after small amounts of hydroquinone had been added, stored in a nitrogen atmosphere. Immediately before use, they were washed with a dilute aqueous solution of sodium hydroxide and sodium carbonate to remove the hydroquinone added.

For the preparation of each copolymer the following recipe was used: 100 parts of monomers with the molar ratio of vinylidene chloride to alkyl acrylate being 85/15; 200 parts of 0.1 wt.% aqueous solution of methyl cellulose (Metocell. 100 c. p. s.); and lauryl peroxide 0.1 wt.% to monomers. The polymerization was carried out for 15 hr. at 50°C, with the yield ranging from 30 to 40% of charged monomers. The polymers produced were separated by filtration, dissolved immediately in ethyl methyl ketone, and then precipitated by an addition of excess methanol. The precipitate was isolated by filtration and dried in vacuo to a constant weight. The dry material was again dissolved in ethyl methyl ketone and fractionally precipitated at 30 to 40°C, using methanol as a nonsolvent. Both to check the distribution of two monomer units and to evaluate the average fundamental molecular weight, M_0, of the copolymer, the chlorine contents

1) S. N. Chinai et al., *J. Polymer Sci.*, **41**, 475 (1959).
2) J. A. Manson et al., *Makromol. Chem.*, **37**, 187 (1960).

Table I. Refractive index increments for copolymers in methyl ethyl ketone

Polymer	$\partial n/\partial c$ (λ=4358 Å, at room temperature)
Poly(vinylidene chloride co ethyl acrylate)	0.135
Poly(vinylidene chloride co *n*-butyl acrylate)	0.142
Poly(vinylidene chloride co *n*-hexyl acrylate)	0.130
Poly(vinylidene chloride co *n*-octyl acrylate)	0.130

of the resulting fractions were determined by using the Carius method.

Phase Equilibria.—After a number of preliminary experiments, we found that ethyl acetoacetate is a relevant theta solvent for poly(vinylidene chloride co ethyl acrylate) and that benzyl alcohol is relevant for the remaining copolymers. Given amounts of either of these solvents and a given copolymer were placed in a test tube, 0.8 cm. in diameter, 20 cm. long, and fitted with a ground glass stopper. After the polymer had been dissolved by heating 70 to 80°C for 2 hr., the test tube was immersed in a thermostated water bath. Phase separation occurred when the temperature of the bath was gradually lowered; the rate of cooling used was 0.1°C per min. The temperature at which the separation commenced, T_p, was determined visually with the reproducibility of ± 0.1°C. For each given fraction this temperature was determined as a function of the polymer concentration, and then the critical solution temperature, T_c, of the fraction was found from the maximum of the T_p vs. concentration curve so obtained. By repeating a similar procedure for other fractions with different molecular weights, data for T_c as a function of molecular weight were derived. The desired theta temperature, i. e., the value of T_p for infinite molecular weight, can be deiermined by treating these data in the manner described by Flory[3].

Light Scattering and Viscosity Measurements.—In this work, besides studying the four copolymers in their respective theta conditions, we also measured their dilute solution properties in ethyl methyl ketone for the sake of comparison.

The light-scattering behavior of given solutions was studied by means of a photometer of the Brice type manufactured by Shimadzu Seisakusho, Kyoto. Scattered intensities were measured at 45, 90 and 135°C to the incident beam, and the data obtained were analyzed in terms of the usual procedure[4], assuming a polydisperse random coil for the solute polymer molecule. Dust was removed from the test solutions by centrifugation at 20000 g. for 1.5 hr. Light-scattering measurements were carried out at room temperature. The refractive index increments of the ethyl methyl ketone solution of these copolymers were measured by a Debye-type differential refractometer manufactured by Shimadzu Seisakusho, Kyoto; the values obtained are listed in Table I. The viscosity measurements were performed at 30°C for ethyl methyl ketone solutions and at respective theta temperatures for ethyl acetoacetate or benzyl alcohol solutions.

The viscosities of ethyl methyl ketone solutions of the four copolymers were measured in an Ostwald viscometer; the flow time for ethyl methyl ketone at 30°C was 99.6 sec. Kinetic energy corrections were applied to the measured flow times. Use was made of Ubbelohde dilution viscometers for the study under theta conditions. These viscometers were designed so that their flow times for the theta solvents at the theta temperatures were relatively large; thus no kinetic energy correction was necessary.

Results and Discussion

Composition of Copolymers and Average Fundamental Molecular Weight M_0.—The chlorine contents of fractions of the four copolymers studied are listed in Tables II, III,

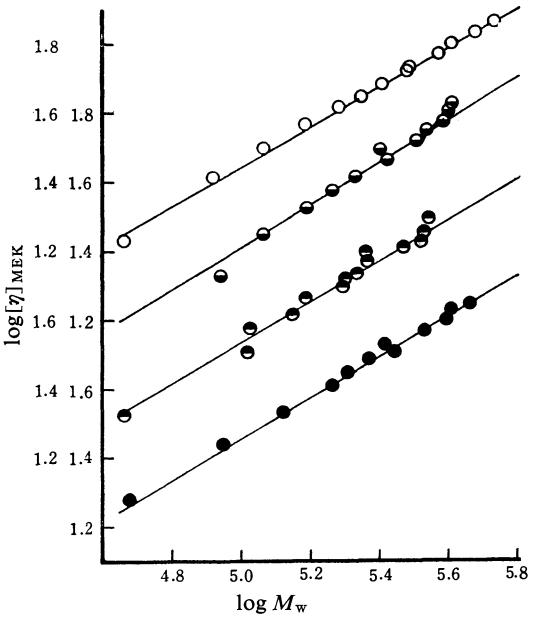


Fig. 1. Logarithmic plot of limiting viscosity number for fractions of copolymers in ethyl methyl ketone against molecular weight.
- ○ Poly(vinylidene chloride co *n*-octyl acrylate)
- ◒ Poly(vinylidene chloride co *n*-hexyl acrylate)
- ◓ Poly(vinylidene chloride co *n*-butyl acrylate)
- ● Poly(vinylidene chloride co ethyl acrylate)

3) P. J. Flory, "Principles of Polymer Chemistry", Cornell Univ. Press, Ithaca (1953).
4) P. Doty et al., *J. Chem. Phys.*, **18**, 1211 (1950).

TABLE II. LIGHT SCATTERING AND VISCOSITY DATA FOR POLY(VINYLIDENE CHLORIDE CO ETHYL ACRYLATE)

Fraction	Cl	$[\eta]_{MEK}$ at 30°C	$[\eta]_\theta$	$M_w \times 10^{-5}$	$\langle r^2 \rangle_w^{1/2} \times 10^6$	$\Phi \times 10^{-21}$
	%	100 cc./g.	100 cc./g.		cm.	
F-1	62.3	0.710	0.420	4.63	4.93	2.74
F-2	61.9	0.685	0.403	4.08	4.63	2.81
F-3	61.9	0.640	0.393	3.97	4.82	2.27
F-4	61.7	0.590	0.405	3.41	4.26	2.60
F-5	62.2	0.545	0.365	2.61	3.60	3.06
F-6	61.9	0.510	0.345	2.80	3.52	3.26
F-7	61.9	0.490	0.335	2.35	3.37	3.00
F-8	62.3	0.445	0.300	2.03	3.06	3.15
F-9	62.1	0.410	0.280	1.84	3.06	2.63
F-10	62.1	0.340	0.245	1.33	2.96	1.74
F-11	62.3	0.275	0.212	0.89	—	—
F-12	61.3	0.190	0.145	0.48	—	—
	av. 62.0					av. 2.73

TABLE III. LIGHT SCATTERING AND VISCOSITY DATA FOR POLY(VINYLIDENE CHLORIDE CO *n*-BUTYL ACRYLATE)

Fraction	Cl	$[\eta]_{MEK}$ at 30°C	$[\eta]_\theta$	$M_w \times 10^{-5}$	$\langle r^2 \rangle_w^{1/2} \times 10^6$	$\Phi \times 10^{-21}$
	%	100 cc./g.	100 cc./g.		cm.	
F-1	58.1	0.795	0.405	3.51	4.93	2.33
F-2	58.1	0.720	0.403	3.37	3.97	3.89
F-3	57.8	0.680	0.400	3.35	3.82	4.09
F-4	58.2	0.665	0.395	2.98	4.41	2.27
F-5	57.7	0.630	0.385	2.32	3.67	2.95
F-6	58.0	0.590	0.365	2.32	3.67	2.77
F-7	58.2	0.545	0.340	2.18	3.52	2.72
F-8	58.2	0.525	0.335	2.02	3.52	2.42
F-9	58.0	0.495	0.323	1.98	3.45	2.39
F-10	57.8	0.460	0.305	1.54	2.96	2.72
F-11	58.3	0.410	0.280	1.42	2.77	2.73
F-12	58.0	0.375	0.267	1.08	2.49	2.63
F-13	57.7	0.320	0.230	1.05	—	—
F-14	57.1	0.210	0.165	0.46	—	—
	av. 57.9					av. 2.83

TABLE IV. LIGHT SCATTERING AND VISCOSITY DATA FOR POLY(VINYLIDENE CHLORIDE CO *n*-HEXYL ACRYLATE)

Fraction	Cl	$[\eta]_{MEK}$ at 30°C	$[\eta]_\theta$	$M_w \times 10^{-5}$	$\langle r^2 \rangle_w^{1/2} \times 10^6$	$\Phi \times 10^{-21}$
	%	100 cc./g.	100 cc./g.		cm.	
F-1	57.2	0.685	0.365	4.08	4.71	2.68
F-2	57.3	0.655	0.350	4.02	4.26	3.40
F-3	57.7	0.610	0.333	3.86	4.11	3.38
F-4	57.6	0.575	0.325	3.48	3.97	3.21
F-5	57.7	0.535	0.310	3.23	3.67	3.49
F-6	58.0	0.505	0.302	2.54	3.52	2.93
F-7	57.6	0.470	0.290	2.66	3.52	2.86
F-8	57.5	0.420	0.268	2.16	3.37	2.36
F-9	57.3	0.380	0.240	1.84	3.37	1.82
F-10	57.8	0.340	0.218	1.55	3.06	1.84
F-11	56.8	0.285	0.185	1.16	2.68	1.72
F-12	57.4	0.215	0.140	0.88	—	—
	av. 57.5					av. 2.61

Table V. Light scattering and viscosity data for poly(vinylidene chloride co *n*-octyl acrylate)

Fraction	Cl	$[\eta]_{MEK}$ at 30°C	$[\eta]_\theta$	$M_w \times 10^{-5}$	$\langle r^2 \rangle_w^{1/2} \times 10^6$	$\Phi \times 10^{-21}$
	%	100 cc./g.	100 cc./g.		cm.	
F-1	54.2	0.740	0.405	5.41	4.82	3.58
F-2	54.1	0.690	0.390	4.75	4.41	3.82
F-3	54.9	0.640	0.375	4.10	3.82	4.71
F-4	55.2	0.595	0.360	3.77	3.37	5.85
F-5	54.3	0.545	0.347	3.09	2.87	7.12
F-6	53.9	0.530	0.313	3.06	2.68	8.43
F-7	53.7	0.485	0.295	2.56	2.68	6.41
F-8	54.6	0.445	0.273	2.23	2.68	5.16
F-9	54.4	0.415	0.265	1.93	2.49	5.20
F-10	54.4	0.370	0.235	1.54	2.11	6.11
F-11	54.4	0.315	0.212	1.16	1.92	5.21
F-12	54.6	0.260	0.175	0.84	—	—
F-13	52.3	0.170	0.117	0.44	—	—
	av. 54.2					av. 5.14

Table VI. Composition and fundamental molecular weight, M_0, of copolymers

Polymer	Composition (mol. % of acrylate)	M_0
Poly(vinylidene chloride co ethyl acrylate)	14.9	97.5
Poly(vinylidene chloride co *n*-butyl acrylate)	16.7	102.2
Poly(vinylidene chloride co *n*-hexyl acrylate)	14.5	105.6
Poly(vinylidene chloride co *n*-octyl acrylate)	15.6	110.6

IV and V. Table VI gives the data for the composition and the fundamental average molecular weight, M_0, in each copolymer computed from these chlorine content values. The molar compositions of the four copolymers are not exactly the same, but the differences among them are small. Hence, if we take into consideration the experimental errors in determining the chlorine content, one may assume that these copolymers are uniform in molar composition.

Relation between Limiting Viscosity Number and Molecular Weight for Ethyl Methyl Ketone Solutions. — Tables II, III, IV and V list the limiting viscosity numbers of fractions of respective copolymers in ethyl methyl ketone at 30°C. and the weight-average molecular weights, M_w, of those fractions. Log-log plots for the limiting viscosity number against M_w prepared from these data are shown in Fig. 1 and yield the following relations:

Poly(vinyldene chloride co ethyl acrylate)

$$[\eta]_{MEK} = 2.88 \times 10^{-4} M_w^{0.60}$$

Poly(vinylidene chloride co *n*-butyl acrylate)

$$[\eta]_{MEK} = 3.43 \times 10^{-4} M_w^{0.60}$$

Poly(vinylidene chloride co *n*-hexyl acrylate)

$$[\eta]_{MEK} = 2.07 \times 10^{-4} M_w^{0.62}$$

Poly(vinylidene chloride co *n*-octyl acrylate)

$$[\eta]_{MEK} = 3.55 \times 10^{-4} M_w^{0.58}$$

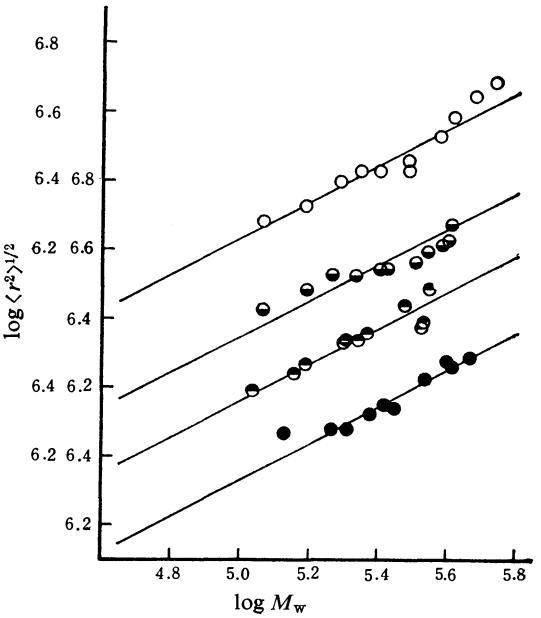


Fig. 2. Logarithmic plot for root mean square end-to-end distance of fractions of copolymers against molecular weight.
○ Poly(vinylidene chloride co *n*-octyl acrylate)
◒ Poly(vinylidene chloride co *n*-hexyl acrylate)
◓ Poly(vinylidene chloride co *n*-butyl acrylate)
● Poly(vinylidene chloride co ethyl acrylate)

It is interesting that the exponent to the weight-average molecular weight is almost identical for the four copolymers, suggesting that the chain flexibilities of these polymers are similar.

Relation between Molecular Dimension in Ethyl Methyl Ketone and Molecular Weight.— Tables II to V also contain values for the weight-average mean square end-to-end distance of the solute molecule, $\langle r^2\rangle_w^{1/2}$, evaluated from dissymmetry data. The log-log plots for $\langle r^2\rangle_w^{1/2}$ against M_w shown in Fig. 2 give the following relations:

Poly(vinylidene chloride co ethyl acrylate)

$$\langle r^2\rangle_w^{1/2}=4.90\times10^{-9}M_w^{0.53}$$

Poly(vinylidene chloride co *n*-butyl acrylate)

$$\langle r^2\rangle_w^{1/2}=5.29\times10^{-9}M_w^{0.53}$$

Poly(vinylidene chloride co *n*-hexyl acrylate)

$$\langle r^2\rangle_w^{1/2}=5.01\times10^{-9}M_w^{0.53}$$

Poly(vinylidene chloride co *n*-octyl acrylate)

$$\langle r^2\rangle_w^{1/2}=3.89\times10^{-9}M_w^{0.53}$$

In order to see the effect of length of the pendant side chain, it is convenient to write these relations in the form in which M_w is replaced by P_w, the weight-average degree of polymerization. The result is

Poly(vinylidene chloride co ethyl acrylate)

$$\langle r^2\rangle_w^{1/2}=5.55\times10^{-8}P_w^{0.53}$$

Poly(vinylidene chloride co *n*-butyl acrylate)

$$\langle r^2\rangle_w^{1/2}=6.14\times10^{-8}P_w^{0.53}$$

Poly(vinylidene chloride co *n*-hexyl acrylate)

$$\langle r^2\rangle_w^{1/2}=5.92\times10^{-8}P_w^{0.53}$$

Poly(vinylidene chloride co *n*-octyl acrylate)

$$\langle r^2\rangle_w^{1/2}=4.71\times10^{-8}P_w^{0.53}$$

The expressions indicate that the difference in the length of the pendant alkyl group has a relatively minor influence on the dimension of the vinylidene chloride-alkyl acrylate copolymer molecule in ethyl methyl ketone (a relatively good solvent for polymer) if the molar ratio of alkyl acrylate is as small as of the order of 0.15.

Theta Temperatures. — Figure 3 illustrates plots for T_p against the polymer concentration of poly(vinylidene chloride co *n*-octyl acrylate) in benzyl alcohol; the data for the other copolymers studied are similar in nature. From the maximum of each cure curve, the value of T_c for each fraction can be determined without ambiguity. According to the theory developed by Flory[3], T_c is related to the molecular weight M by the equation:

$$1/T_c=1/\theta(1+b/M^{1/2}) \qquad (1)$$

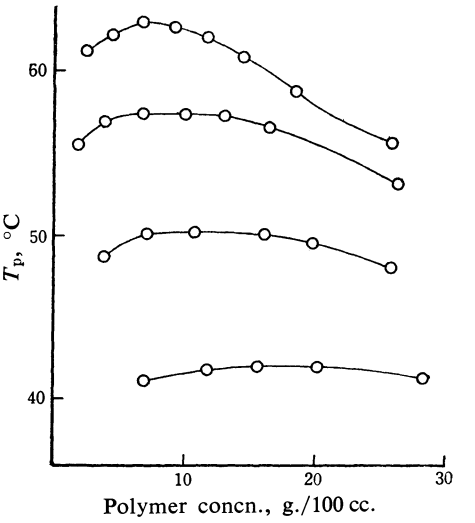


Fig. 3. Phase separation temperature, T_p, of four fractions of poly(vinylidene chloride co *n*-octyl acrylate) as a function of polymer concentration.

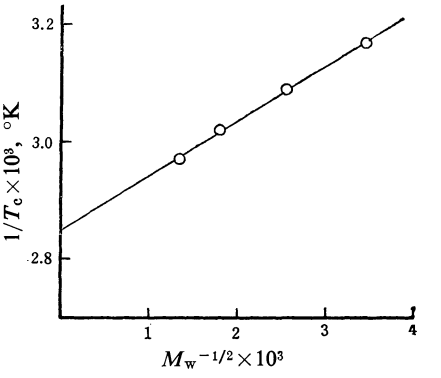


Fig. 4. Reciprocal critical solution temperature, T_c, against reciprocal square root of molecular weight of four fractions of poly(vinylidene chloride co *n*-octyl acrylate).

where b is a constant characteristic of a given polymer-solvent system. The so-called theta temperature θ, i.e., the critical solution temperature for a polymer of infinite chain length, can be determined by plotting $1/T_c$ against $1/M^{1/2}$ and then extrapolating the resulting plot to infiite molecular weight. Figure 4 shows this plot for poly(vinylidene chloride co *n*-octyl acrylate); similar linear plots were obtained for the remaining copolymers. The values of θ found in this way for poly (vinylidene chloride co *n*-butyl acrylate), poly (vinylidene chloride co *n*-hexyl acrylate), and poly(vinylidene chloride co *n*-octyl acrylate), all in benzyl alcohol, were 44.0, 56.8 and 77.9°C respectively, while that for poly(vinylidene

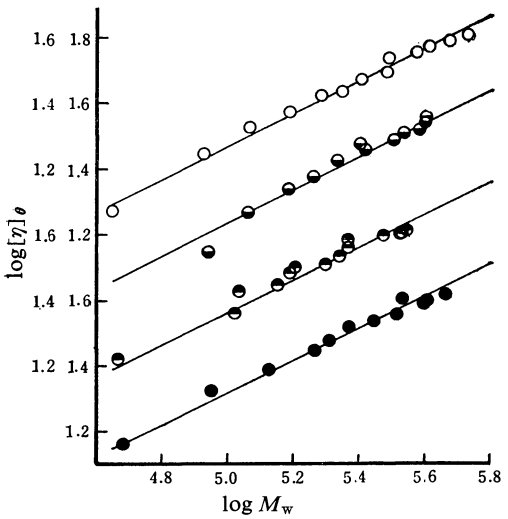


Fig. 5. Logarithmic plot for limiting viscosity number at θ temperature against molecular weight of fractions of copolymers.
- ○ Poly(vinylidene chloride co *n*-octyl acrylate)
- ◒ Poly(vinylidene chloride co *n*-hexyl acrylate)
- ◓ Poly(vinylidene chloride co *n*-butyl acrylate)
- ● Poly(vinylidene chloride co ethyl acrylate)

chloride co ethyl acrylate) in ethyl acetoacetate was 49.6°C.

Relation between Limiting Viscosity Number at Theta Temperature and Molecular Weight.—In Tables II to V are given the limiting viscosity numbers of fractions of the four copolymers in respective theta solvents. These values, $[\eta]_\theta$, are logarithmically plotted against M_w (determined above from light scattering data on ethyl methyl ketone solutions) in Fig. 5. The plots in the figure yield the following relations:

Poly(vinylidene chloride co ethyl acrylate)

$$[\eta]_\theta = 6.64\times10^{-4} M_w^{1/2}$$

(in ethyl acetoacetate)

Poly(vinylidene chloride co *n*-butyl acrylate)

$$[\eta]_\theta = 7.30\times10^{-4} M_w^{1/2}$$

(in benzyl alcohol)

Poly(vinylidene chlorride co *n*-hexyl acrylate)

$$[\eta]_\theta = 5.50\times10^{-4} M_w^{1/2}$$

(in benzyl alcohol)

Poly(vinylidene chloride co *n*-octyl acrylate)

$$[\eta]_\theta = 5.87\times10^{-4} M_w^{1/2}$$

(in benzyl alcohol)

In all case the values of $[\eta]_\theta$ increase in proportion to one half the power of M_w, in conformity with the current theories of dilute polymer solutions.

Dimensions of the Copolymers in Theta Solvents.—The values of the parameter Φ characterizing Flory's theory of dilute polymer solution have been calculated by substituting the data for $[\eta]$, $\langle r^2\rangle_w^{1/2}$ and M_w obtained with ethyl methyl ketone solutions into the equations:

$$[\eta] = k(M_w)^{\alpha} \quad (2)$$

$$K = \Phi\langle r^2\rangle_w^3/(M_w)^{3/2} \quad (3)$$

The results are shown in Tables II to V. It is seen that the Φ values so obtained for poly(vinylidene chloride co ethyl acrylate), poly(vinylidene chloride co *n*-buthyl acrylate), and poly(vinylidene chloride co *n*-hexyl acrylate) agree fairly well with each another and are not very different from the generally accepted value, 2.1×10^{-21}. However, the values for poly(vinylidene chloride co *n*-octyl acrylate) are unusually high. The reason for this is not clear to us but is probably due to the experimental errors involved in $\langle r^2\rangle_w$.

Equations 2 and 3 may be used to calculate the weight-average root mean square end-to-end distance, $\langle r_0^2\rangle_w^{1/2}$, of the polymer molecule in the theta solvent from the measured values of $[\eta]_\theta$ and M_w if the value of the parameter Φ is given, since α is equal to 1/2 under theta conditions. We have made this calculation, assuming $\Phi = 2.1\times10^{-21}$, for all the copolymers studied here. The results are:

Poly(vinylidene chloride co ethyl acrylate)

$$\langle r_0^2\rangle_w^{1/2} = 6.81\times10^{-9} M_w^{1/2} \quad (49.6°C)$$

Poly(vinylidene chloride co *n*-butyl acrylate)

$$\langle r_0^2\rangle_w^{1/2} = 7.03\times10^{-9} M_w^{1/2} \quad (44.0°C)$$

Poly(vinylidene chloride co *n*-hexyl acrylate)

$$\langle r_0^2\rangle_w^{1/2} = 6.04\times10^{-9} M_w^{1/2} \quad (56.8°C)$$

Poly(vinylidene chloride co *n*-octyl acrylate)

$$\langle r_0^2\rangle_w^{1/2} = 6.53\times10^{-9} M_w^{1/2} \quad (77.9°C)$$

In terms of P_w these relations may be written:

Poly(vinylidene chloride co ethyl acrylate)

$$\langle r_0^2\rangle_w^{1/2} = 6.72\times10^{-8} P_w^{1/2} \quad (49.6°C)$$

Poly(vinylidene chloride co *n*-butyl acrylate)

$$\langle r_0^2\rangle_w^{1/2} = 7.11\times10^{-8} P_w^{1/2} \quad (44.0°C)$$

Poly(vinylidene chloride co *n*-hexyl acrylate)

$$\langle r_0^2\rangle_w^{1/2} = 6.58\times10^{-8} P_w^{1/2} \quad (56.8°C)$$

Poly(vinylidene chloride co *n*-octyl acrylate)

$$\langle r_0^2\rangle_w^{1/2} = 6.87\times10^{-8} P_w^{1/2} \quad (77.9°C)$$

TABLE VII. COMPARISON OF UNPERTURBED MOLECULAR PARAMETERS ON VARIOUS POLYMERS

Polymer	θ °C	$(\langle r_0^2\rangle/P)^{1/2}$ $\times 10^8$	$(\langle r_0^2\rangle/\langle r_{0f}^2\rangle)^{1/2}$	$M_0[\eta]_\theta/P^{1/2}$	Ref.
Poly(vinylidene chloride co ethyl acrylate)	49.6	6.72	2.18	0.63	
Poly(vinylidene chloride co *n*-butyl acrylate)	44.0	7.11	2.31	0.74	
Poly(vinylidene chloride co *n*-hexyl acrylate)	56.8	6.58	2.14	0.61	
Poly(vinylidene chloride co *n*-octyl acrylate)	77.9	6.87	2.23	0.68	
Poly(methyl methacrylate)	25.0	4.88	2.24	0.59	1
Poly(ethyl methacrylate)	23.0	4.20	1.94	0.57	1
Poly(*n*-butyl methacrylate)	21.5	4.52	2.09	0.50	1
Poly(*n*-hexyl methacrylate)	32.6	5.33	2.44	0.95	1
Poly(*n*-octyl methacrylate)	16.8	4.99	2.32	0.75	1
Poly(*n*-lauryl methacrylate)	13.0	7.80	3.58	1.30	1
Poly(styrene)	25.0	6.81	2.14	0.89	5
Poly(isobutylene)	24.0	5.95	1.93	0.45	6
Poly(vinyl acetate)	26.5	7.01	2.28	0.73	7
Poly(cyclohexyl methacrylate)	23.0	7.05	2.29	0.73	8
Poly(vinyl benzoate)	32.5	8.15	2.65	1.14	9

The quantity $(\langle r_0^2\rangle_w/P_w)^{1/2}$ provides a measure of the extension of a polymer chain, and it is seen that the values of this quantity for all four copolymers are almost the same. If we take into account the fact that the unperturbed dimension of a polymer molecule may decrease with increasing temperature (due to the enhanced rotation of each chain element), it is likely that, when a comparison is made at a fixed temperature, the values of this quantity for the four copolymers will become closer. We can therefore conclude that if the molar ratio of alkyl acrylate component is relatively small, the unperturbed dimension of vinylidene chloride-acrylate copolymer is hardly affected by the length of the pendant alkyl group.

Table VII summarizes the values of some basic parameters characterizing chain dimensions, such as $(\langle r_0^2\rangle/P)^{1/2}$, $(\langle r_0^2\rangle/\langle r_{0f}^2\rangle)^{1/2}$, and $M_0\ [\eta]_\theta/P^{1/2}$, for the four copolymers studied here, together with those for several other polymers[1,5-9]. Here $\langle r_{0f}^2\rangle^{1/2}$ denotes the root mean square end-to-end distance in the unperturbed state of a polymer molecule in which no hindrance to the rotation of each element is present. Its value has been calculated assuming a value of 1.54Å for the distance between neighboring carbon atoms and a value of 109.5° for the valency angle between successive bonds. The parameter $M_0\ [\eta]_\theta/P^{1/2}$ has been proposed by Chinai and associates.

The authors wish to expresses their grateful appreciation to Professor Shunsuke Murahashi and Professor Hiroshi Fujita of Osaka University and to Professor Akira Kotera of Tokyo University of Education for their encouragement and thoughtful suggestions throughout the course of this study, to Dr. K. Mayumi and to Kureha Kasei Co., Ltd. for their permission to publish this paper.

Kureha Kasei Tokyo Laboratory
Shinjuku-ku, Tokyo

5) W. R. Krigbaum, *J. Polymer Sci.*, **9**, 381 (1951).
6) J. J. Fox, *J. Am. Chem. Soc.*, **73**, 1909 (1951).
7) R. Naito, *Chem. High Polymers* (*Kōbunshi Kagaku*), **16**, 7 (1959).
8) J. Hakozaki, *J. Chem. Soc. Japan, Pure Chem. Sec.* (*Nippon Kagaku Zasshi*), **82**, 159 (1961).
9) I. Sakurada et al., *Chem. High Polymers* (*Kōbunshi Kagaku*), **17**, 227 (1960).

Dilute Solution Properties of Low-temperature Polymerized Polyvinyl Chloride. I. Effects of Dissolution Temperature and Time

By Takashi KOBAYASHI

(Received August 17, 1961)

Asahina and his coworkers have reported[1-3] that the physical properties of the solid state of polyvinyl chloride depend upon the temperature at which the sample is polymerized. The purpose of the study presented in this paper is to examine if there is any difference in the dilute solution properties of polyvinyl chloride polymerized at different temperatures. Our preliminary experiment had indicated that the samples polymerized at low-temperatures were more difficult to dissolve in tetrahydrofuran than commercially available materials usually polymerized at 50~60°C. In this study we measured the viscosity, osmotic pressure and light scattering of tetrahydrofuran solutions of polyvinyl chlorides polymerized at three different temperatures and the changes with time of these properties when left standing; we aimed at establishing the conditions required for the preparation of a solution of this polymer stable enough to use for the evaluation of its physical behavior.

Experimental

Materials.—Three samples of polyvinyl chloride were studied. They were obtained in the following manner:

S-796—A whole polymer suspension polymerized at 58°C. The 43 wt. % lower molecular weight portion was removed, and the remaining portion was designated as S-796-M.

S0968—This was a whole polymer suspension polymerized at 48°C.

F-5-M—The 3 wt. % higher molecular weight portion and the 29 wt. % lower molecular weight portion of a polymer bulk polymerized at −15°C were removed by fractional precipitation, and the remaining portion was designated as F-5-M.

The solvent used was tetrahydrofuran. After the material purchased in a 20 l. can had been dried for about one week over sodium hydroxide pellets, it was distilled, and the fractions between 65.8~66.2°C were collected.

Preparation of Solutions.—An accurately weighed sample was mixed in an ampoule with the required amount of solvent; after the air in it had been replaced by nitrogen, the ampoule was sealed and heated and occasionaly shaken in an oil bath for two hours at the desired temperature. Then it was transferred into a thermostat regulated at 30°C and kept for fifteen minutes. The ampoul was then cut off, and the solution was ready to use.

The concentration of the solution so obtained was calculated from the amounts of polymer and solvent weighed before mixing for the purpose of plotting viscosity and osmotic pressure data. For the light-scattering study it was determined gravimetrically by drying up an aliquot of the solution.

Viscosity Measurements.—Capillary viscometers of the Ostwald type were used throughout the present study. For example, one of them had the following characteristics: bore diameter=0.037 cm., capillary length=10.4 cm., volume of the upper bulb=1.99 cc., and efflux time for tetrahydrofuran of 30°C=167.7 sec. The kinetic energy correction was applied to all flow times measured. Flow times were determined at four concentrations between 3×10^{-3} and 8×10^{-3} g./ml., and the limiting viscosity number was estimated by graphical extrapolation of the plots for viscosity number against concentration (in g./ml.).

Osmotic Pressure Measurements.—A modified Zimm-Meyerson osmometer fitted with gelcellophane was used. The measurements were made at 30°C using the dynamic method. Data were taken at four concentrations between 3×10^{-3} and 8×10^{-3} g./ml.

Light Scattering Measurements.—Use was made of a photometer of the Brice type manufactured by Shimadzu Seisakusho, Kyoto. The calibration was made by referring to the literatures value[4] for the Rayleigh ration, R_{90}, of pure benzene. Measurements were made in a cylindrical cell over the range of scattered angle from 40 to 140° and at three polymer concentrations, using both unpolarized blue light, $\lambda=4360$ Å, and green light, $\lambda=5460$ Å, emitted from a mercury lamp. The depolarization correction was not applied. Dust was removed from the given solution by centrifuging it at 2×10^4 times gravity for one and a half hours immediately before use. All measurements were performed at room temperature, without any specific temperature-controlling device fixed to the instrument. No marked temperature variation occurred during any series of measurements.

The refractive index increment of this system of polymer and solvent was measured by means of a differential refractometer of the Debye type manufactured by Shimadzu Seisakusho, Kyoto. The values obtained were 0.115 and 0.110 for the lights

1) M. Asahina et al., *J. Chem. Soc. Japan, Pure Chem. Sec.* (*Nippon Kagaku Zasshi*), **81**, 1011 (1960).
2) M. Aahina et al., *Chem. High Polymers* (*Kōbunshi Kagaku*), **17**, 612 (1960).
3) M. Asahina et al., ibid., **17**, 325 (1960).
4) S. H. Maron et al., *J. Polymer Sci.*, **14**, 273 (1954).

of $\lambda=4360$ Å and $\lambda=5460$ Å respectively, in good agreement with the literature's, value[5].

The procedure developed by Zimm[6] was followed to evaluate results from these light-scattering experiments.

Results and Discussion

Effect of Dissolution Temperature. — It is generally accepted that polyvinyl chloride samples polymerized at low-temperatures are less soluble than those prepared at higher temperatures. In order to examine this point in a qualitative manner, we measured viscosities, osmotic pressures, and turbidities of solutions of S-796 and of F-5-M prepared at different temperatures. Table I gives viscosity data for S-796 dissolved in tetrahydrofuran at 60, 100 and 140°C. It can be seen that the viscosity values of sample S-796 in tetrahydrofuran are practically independent of the dissolution temperature in the range above 60°C; this is in accordance with Kuroiwa's results[7]. Similar conclusions were derived also from osmotic pressure and turbidity measurements on this sample.

TABLE I. VISCOSITY DATA ON SOLUTIONS OF S-796 PREPARED AT DIFFERENT TEMPERATURES

Concn. g./ml. $\times 10^3$	η_{sp}/c of solution prepared at, 60°C ml./g.	100°C ml./g.	140°C ml./g.
3.000	110	110	110
4.000	113	114	112
6.000	120	120	120
8.000	128	127	127
$[\eta]$ ml./g.	99.0	99.0	99.0
k' *	0.36	0.36	0.35

* k': Huggins' constant

Figure 1 shows η_{sp}/c (viscosity number) for sample F-5-M in tetrahydrofuran as a function of the temperature at which the solution was made. As has been mentioned above, the polymer was dissolved in the solvent by heating at a given temperature for two hours. It was found that a more prolonged heating did not give rise to any detectable change in the viscosity values. Thus, the results shown in Fig. 1 should be free from the effects of the time used to dissolve the sample polymer. The data for osmotic pressure and for light scattering corresponding to Fig. 1 are given in Figs. 2 and 3 respectively. These figures indicate that, contrary to the case of sample S-796, the viscosity, osmotic pressure and light-scattering

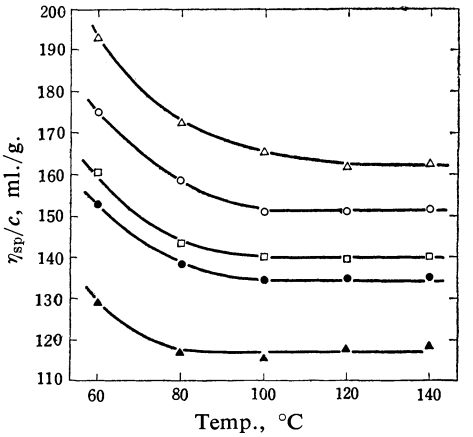


Fig. 1. Viscosity of F-5-M solutions prepared at different temperatures. △ 8.0×10^{-3} g./ml.; ○ 6.0×10^{-3} g./ml.; □ 4.0×10^{-3} g./ml.; ● 3.0×10^{-3} g./ml.; ▲ Limiting viscosity number.

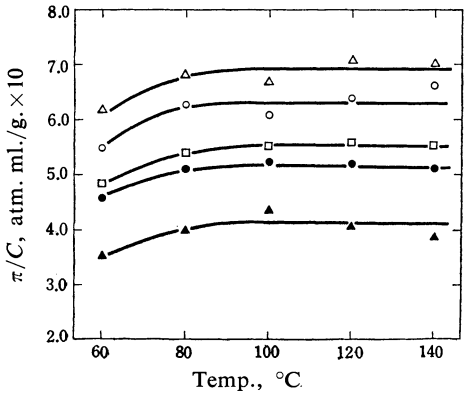


Fig. 2. Osmotic pressure of F-5-M solutions prepared at different temperatures. △ 8.0×10^{-3} g./ml.; ○ 6.0×10^{-3} g./ml.; □ 4.0×10^{-3} g./ml.; ● 3.0×10^{-3} g./ml.; ▲ $(\pi/C)_{C\to0}$.

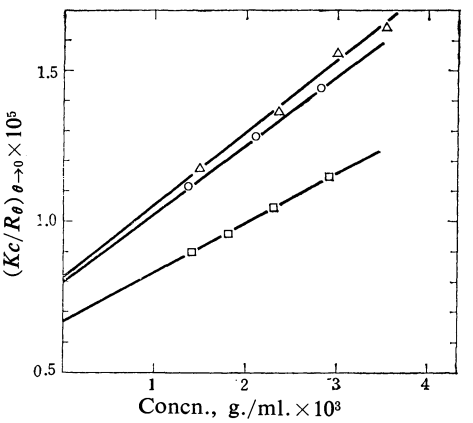


Fig. 3. Light scattering of solutions of F-5-M prepared at different temperatures. △ Solution prepared at 140°C; ○ at 100°C; □ at 80°C.

5) D. Laker, ibid., **25**, 122 (1957).
6) B. H. Zimm, *J. Chem. Phys.*, **16**, 1066, 1093 (1948).
7) T. Kuroiwa and K. Kawahara, *J. Chem. Soc. Japan, Pure Chem. Sec.* (*Nippon Kagaku Zasshi*), **73**, 563 (1952).

properties of F-5-M all become practically independent of the dissolution temperature only in the region above 100°C or more. In the light-scattering plots shown in Fig. 3, there still exists a distinct, though quite small, difference between the data for 100°C and those for 140°C. One may consider this difference to be negligible or else within the limits of accuracy of the light-scattering measurements. However, since we have checked similar differences by repeated measurements, it is believed that even such a small difference is significant.

The interpretation of these differences in solution properties between S-796 and F-5-M cannot be certain, but the most obvious conclusion is that the intermolecular interaction in polyvinyl chloride becomes stronger as the polymerization temperature is lowered. In order to obtain relevant data on tetrahydrofuran solutions of a polyvinyl chloride polymerized at a temperature much lower than that used for commercially available material, the solute must be dissolved in the solvent at a temperature at least higher than 100°C and the mixture must be kept at least for two hours at that temperature. However, use should not be made of too high a dissolution temperature, since that is likely to induce thermal decomposition of the polymer.

Effect of Standing Time. — It has been reported that dilute solutions of ordinary polyvinyl chloride remain stable for several days[8]. In Table II are given viscosity data for S-796-M solutions in tetrahydrofuran as a function of the time for which the solution was allowed to stand after it had been prepared. Figure 4 shows the Zimm plots for S0968 solutions in tetrahydrofuran allowed to stand for different intervals of time. Apparently these solutions remained stable over the time intervals examined. The data for viscosity, osmotic pressure

Table II. Time effect on the viscosity of solutions of S-796-M

Concn. g./ml. $\times 10^3$	η_{sp}/c, ml./g. 0.5* hr.	5.0* hr.	50.0* hr.	100.0* hr.
3.000	138	139	139	139
4.000	144	145	145	144
6.000	155	157	156	156
8.000	167	168	168	167
$[\eta]$ ml./g.	126	126	126	126
k' **	0.36	0.37	0.37	0.36

* Time in hour after the solution was prepared.
** Huggins' constant.

8) A. Nakajima, *Chem. High Polymers (Kobunshi Kagaku)*, 7, 309 (1950).

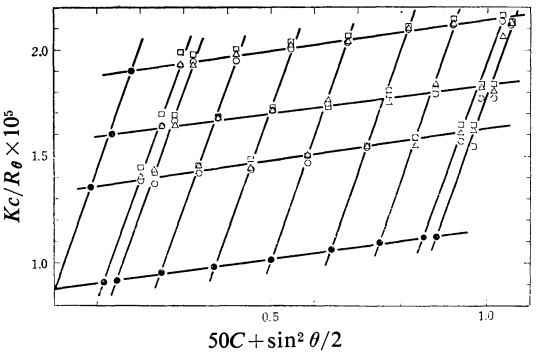


Fig. 4. Time effect on Zimm plots for light scattering of solutions of S0968. △ 5.0 hr. after the completion of heating; ○ 28 hr.; □ 76 hr.

Table III. Time effect on the viscosity of solution of F-5-M

Concn. g./ml. $\times 10^3$	η_{sp}/c, ml./g. 0.5* hr.	5.0* hr.	50.0* hr.	100.0* hr.
3.000	135	136	136	137
4.000	141	142	142	142
6.000	152	154	154	155
8.000	164	166	167	169
$[\eta]$ ml./g.	118	118	118	118
k' **	0.42	0.44	0.44	0.45

* Time in hour after the solution was prepared.
** Huggins' constant.

Table IV. Time effect on the osmotic pressure of solutions of F-5-M

Concn. g./ml. $\times 10^3$	π/C, atm. ml./g. $\times 10$ 3.0* hr.	20.0* hr.	50.0* hr.	100.0* hr.
3.000	5.36	5.34	5.43	5.43
4.000	5.59	5.64	5.53	5.44
6.000	6.63	6.56	6.53	6.47
8.000	7.26	6.99	6.85	6.78
$(\pi/C)_{C\to 0}$	4.00	4.25	4.25	4.25
$A_2 \times 10^3$	1.69	1.45	1.39	1.37

* Time in hour after the solution was prepared.

and light-scattering in tetrahydrofuran solutions of F-5-M as functions of the standing time are given in Tables III, and IV, and Fig. 5 respectively. It can be seen that the dilute solution properties of this sample, especially those at higher concentrations, chaneg to a considerable extent with time. This appears to be due to the gradual association of solute molecules taking place during the course of standing.

A straightforward support to this idea is the marked decrease in $Kc/R_{\theta\to 0}$ on prolonged

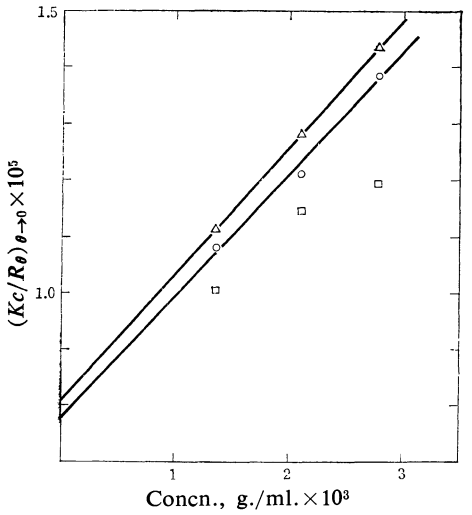


Fig. 5. The time effect on light scattering of solutions of F-5-M. △ 3.5 hr. after the completion of heating; ○ 24.5 hr.; □ 76 hr.

standing, as indicated in Fig. 5, which indicates the formation of increasingly large solute particles by association. It is worth pointing out that the association, if any, had only a minor influence on the viscosity of the solution.

Doty et al.[9] have demonstrated the occurrence of the association of polyvinyl chloride molecules in relatively poor solvents. Since the time effects observed here for tetrahydrofuran solutions of F-5-M are similar to those reported by Doty et al., it appears that tetrahydrofuran, though being though of as a good solvent for ordinary polyvinyl chloride, is a relatively poor solvent for this polymer polymerized at as low a temperature as that employed for the preparation of sample F-5-M.

The author wishes to express his appreciation to Professor Shunsuke Murahashi, Professor Hiroshi Fujita of Osaka University and Professor Akira Kotera of Tokyo University of Education for their encouragement and thoughtful suggestion throughout the course of the study reported in this paper, to Dr. K. Mayumi and Kureha Kasei Co., Ltd., for permission to publish thir paper, and to Mr. M. Sato, Mr. Y. Koshiishi and Mr. S. Aoyagi for their very helpful cooperation in carrying out the experimental work.

Kureha Kasei Tokyo Laboratory
Shinjuku-ku, Tokyo

9) P. Doty et al., *J. Phys. & Colloid Chem.*, **51**, 32 (1947).

Formation Constants of Some Metal Formate Complexes, and the Use of Formate Buffer Solution as an Elutriant for Cation-exchange Chromatography

By Hiroyuki TSUBOTA

(Received August 19, 1961)

Many studies of the elutriants for the ion-exchange separation of mixed fission products have been made over the part several years. Ammonium citrate[1], ammonium butyrate[2] and ammonium α-hydroxy isobutyrate[3] are used as elutriants for the separation of fission products and for the purification of rare earth elements. They have good separability, but some difficulties are encountered in the preparation and preservation of the elutriants and in further treatment of the eluates for analysis.

Honda has shown that ammonium acetate[4,5] or ethylenediaminetetraacetic acid[6] could be effectively used for separating alkaline earth elements and other elements. He has pointed out that ammonium acetate is easily sublimed. Tsubota and Kitano have shown that a new

* A part of this work was done at Kobe University, Kobe. The new elutriant, the formate buffer solution, was first reported on by the present author at the 10th Annual Meeting of the Chemical Society of Japan, Tokyo, April, 1957.

1) E. R. Tompkins, J. X. Khym and W. E. Cohn, *J. Am. Chem. Soc.*, **69**, 2769 (1954).

2) J. G. Cuninghame, M. L. Sigeland, H. H. Willis, J. Eakins and E. R. Mercer, *J. Inorg. Nuclear Chem.*, **1**, 163 (1955).

3) G. R. Choppin and R. J. Silva, ibid., **3**, 153 (1956).

4) M. Honda, *Japan Analyst (Bunseki Kagaku)*, **3**, 132 (1954).

5) E. Minami, M. Honda and Y. Sasaki, This Bulletin, **31**, 372 (1958).

6) M. Honda, *Japan Analyst (Bunseki Kagaku)*, **4**, 240 (1955).

elutriant, a mixture of ammonium formate and formic acid, is a good elutriant for analyzing fission products[7] and alkali or alkaline earth elements[8].

A good elutriant will have the following characteristics: 1) To separate various metal ions with cation-exchange resin, it is desirable that the formation constants between the anion of the elutriant and the metal ions to be separated should differ considerably from each other.

2) It is necessary that the reagent used as the elutriant does not interfere with the later procedures of the analysis. For this purpose, it is desirable that the formation constants should not be too large, or that the reagent should be easily removable from the eluates, e. g., by heating.

3) As the separation is done by changing the concentration of the complexing ion in the elutriant, it is desirable that the concentration of the complexing ion be capable of being varied by varying the pH and by keeping the total concentration of the elutriant constant. Therefore, the reagent used as the elutriant should have a buffer action. The reagent used as the elutriant of high quality must be obtainable at low cost, and one must be able to make solutions of various concentrations and pH's without difficulty. As ammonium formate can be vaporized most easily and completely, a formate solution would be the best elutriant if the formation constants of the metal ions to be separated are suitable.

Therefore, determination of the formation constants of these systems was undertaken as follows.

The Formation Constants of Some Metal Formate Complexes

Except for the system of alkaline earth elements[9], the formation constants of the formate complex systems have not yet been measured. In this work, the formation constants of formate are measured for iron, aluminium, rare earth (Ce) and manganese. These elements are essential portions of an analysis of natural waters, rocks and mixed fission products*.

The determination was done by the ion-exchange method[10,11].

Chemicals used.—

Resin: Dowex 50-X8, 60~80 mesh, Na^+-form, air-dried.

Fe^{3+}-solution: perchlorate prepared from $FeCl_3 \cdot 6H_2O$, reagent grade of Merck.

Al^{3+}-solution: perchlorate prepared from pure aluminum plate (99.99%).

Ce^{3+}-solution: perchlorate prepared from $Ce(SO_4)_2 \cdot 4H_2O$, reagent grade of Merck.

Mn^{2+}-solution: perchlorate prepared from $MnCl_2 \cdot 4H_2O$, reagent grade of Wako-Junyaku.

All other chemicals used were of reagent grade.

Analysical Methods.—Ferric ion was titrated with EDTA, using variamine blue B as an indicator. The Al^{3+} was determined by colorimetry of aluminum oxinate in chloroform at a wavelength of 390 mμ. The determination of Ce^{3+} was made both by colorimetry of Ce^{4+} after oxidizing it with ammonium persulfate and by employing the β-counting method with ^{144}Ce; a good coincidence was obtained. Mn^{2+} was colorimetrically analyzed as potassium permanganate after oxidizing it with potassium periodate.

Measurements.—The complex solutions were prepared by mixing the following two solutions in various proportions:

Solution-1

a mol. $M^{n+}(ClO_4)_n$

$(1-na)$ mol. $NaClO_4$

where M^{n+} is a metal ion, and a is kept constant, $1 \sim 5 \times 10^{-3}$ mol., in each series of experiments.

Solution-2

$(1-b)$ mol. HCOOH

b mol. HCOONa

where b is kept constant, 0.2~0.5 mol., in the series of experiments on each metal ion.

Twenty-five milliliters of the mixed solutions were shaken for 24 hr. with 1.000 g. of the dried ion-exchange resin in a thermostat at 25°C. After an exchange equilibrium had been reached, the solution was rapidly separated from resin with glass filter and the metal concentration of the solution phase was measured.

The relative volume decrease of the solution caused by the swelling of the ion exchanger was estimated by the quotient between the initial and equilibrium ion concentrations of the solution. A cation exchanger column in the hydrogen form was used to convert all cations in the solution to H^+. The H^+ was titrated with a 0.1 N sodium hydroxide standard solution, using phenolphthalein as an indicator, to give the initial and equilibrium ion concentrations. The values of these quotients, constant within each series of experiments, were between 0.99 and 0.97.

7) H. Tsubota and Y. Kitano, This Bulletin, 33, 765 (1960).
8) H. Tsubota and Y. Kitano, ibid., 33, 770 (1960).
9) G. H. Nancollas, *J. Chem. Soc.*, **1956**, 744.
* Titanium was not measured because titanium is hydrolyzed in such a solution.
10) J. Schubert, *J. Phys. & Colloid Chem.*, **52**, 340 (1948).
11) S. Fronæus, *Acta Chem. Scand.*, **5**, 859 (1951).

Calculations.—The following notations are used.

$(M)_T$, $(A)_T$= initial total concentrations of metal ion and anion in the outer solution respectively [mol./l.].

(M), (A)=total concentrations in the outer solution at ion-exchange equilibrium [mol./l.].

$(M)_r$=equilibrium total concentrations of the metal ion in the resin phase [mol./g.].

k_d=distribution coefficient of the total metal ion between the outer solution and the resin phase [l./g.].

$k_d^0=k_d$ at $(A)_T=0$.

K=formation constant.

δ=relative volume decrease of solutions caused by the swelling of the ion exchanger, or $=v/v_1=C_i/C$

When the eqilibrium

$$M+nA \rightleftarrows MA_n \quad (1)$$

exists in the solution, the formation constant can be expressed as

$$K=(MA_n)/(M)(A)^n \quad (2)$$

To obtain the value of the formation constant from the distribution constant k_d and anion concentration (A), the equation derived by Schubert can be used. From the equation

$$\log(k_d^0/k_d-1)=n\log(A)+\log K \quad (3)$$

the formation constant K can be obtained.

The k_d-values are calculated from the relation

$$k_d=(M)_r/(M) \quad (4)$$

The total metal concentration in the resin phase at equilibrium, $(M)_r$, can be calculated from the relation

$$(M)_r=\{(M)_T-(M)/\delta\}\times 25/1000 \quad (5)$$

As the $(M)_T$ was always kept very low, the formate ion concentration of the outer solution was influenced only by the swelling of the resin, not appreciably by the sorption of the complexes. Therefore, (A) was obtained from the relation

$$(A)\cdot\delta=(A)_T \quad (6)$$

Since the values of k_d vary with the $(M)_r$, 3 different values of k_d for 3 different values of $(M)_r$ were estimated for each metal ion, and the corresponding k_d-values were obtained as a function of (A) by interpolation or extrapolation.

Results and Discussions.—The measured data are rearranged and shown in Fig. 1 in order to calculate the formation constants from Eq. 3. As is seen in the figure, the straight lines, the solpes of which are nearly equal to 1, are obtained for Al^{3+}-, Ce^{3+}- and Mn^{2+}-formate ion systems. For Fe^{3+}-formate ion systems, not a straight line, but rather a curve is observed. The straight lines indicate that Al^{3+}, Ce^{3+} and Mn^{2+} mostly form a first order complex with formate ion; even if there were the higher orders, they would exist only slightly. But from the curve for the Fe^{3+}-formate system, it can be concluded that the complex ions between Fe^{3+} and formate ion include the complex ions of higher orders.

TABLE I. FORMATION CONSTANT OF THE SYSTEM OF FERRIC ION AND FORMATE ION

Formation constant			
$K_1(=\beta_1)$	70 ± 5	M^{-1}	
$K_1(=\beta_2)$	4100 ± 500	M^{-2}	K_2 60
$K_1(=\beta_3)$	9000 ± 3000	M^{-3}	K_3 2.5
$K_4(=\beta_4)$	250000 ± 120000	M^{-4}	K_4 28

where

$\beta_n=[Fe(HCOO)_n^{3-n}]/[Fe^{3+}][HCOO^-]^n$

$K_n=\beta/\beta_{n-1}$

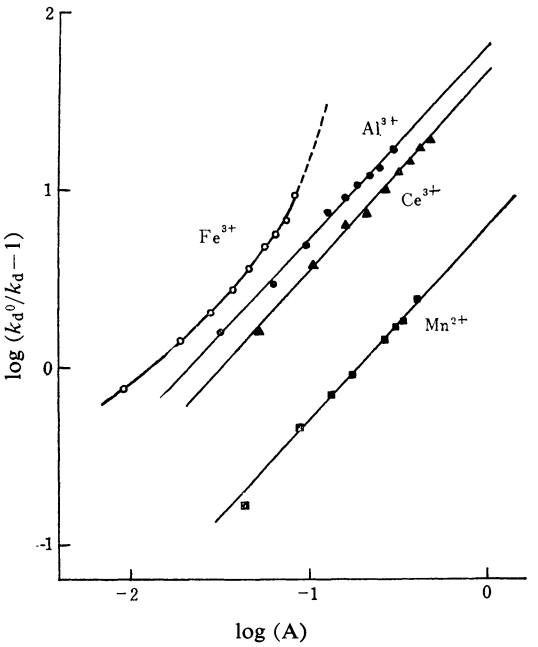


Fig. 1. Relations between log(A) and $\log(k_d^0/k_d-1)$ for Fe^{3+}, Al^{3+}, Ce^{3+}, and Mn^{2+}.

The formation constants for the system between Fe^{3+} and formate ion, therefore, were calculated by the Fronæus method[12],*. The results of the calculations gave four possible complex ions, as shown in Table I. Experiments using an anion exchange column were performed to confirm whether the complex anion, the 4th complex ion, exists or not. Thirty milliliters of the mixed solution of 1 M

* The Fronæus-method was also used to calculate the formation constants for Al, Ce and Mn, but the results were not conclusive because of too small values for the 2nd formation constants compared with the experimental errors.

TABLE II. FORMATION CONSTANT BETWEEN METAL IONS AND FORMATE ION

Metal ion	Codition of measurement (μ=ionic strength)	Method of measurement	Formation constant	Literature
Fe^{3+}	25°C, $\mu=1$	Ion-exchange method	$K_1=70\pm5$	This work
Al^{3+}	25°C, $\mu=1$	Ion-exchange method	61 ± 5	This work
Ce^{3+}	25°C, $\mu=1$	Ion-exchange method	45 ± 5	This work
Mn^{2+}	25°C, $\mu=1$	Ion-exchange method	6.3 ± 0.7	This work
Mg^{2+}	25°C, $\mu=0$	Potentiometry	27.0	10)
Ca^{2+}	25°C, $\mu=0$	Potentiometry	27.0	10)
Sr^{2+}	25°C, $\mu=0$	Potentiometry	24.4	10)
Ba^{2+}	25°C, $\mu=0$	Potentiometry	24.2	10)

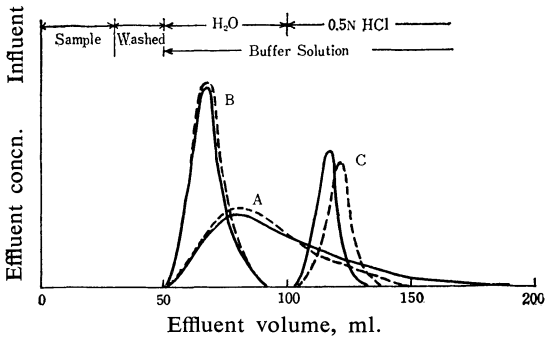


Fig. 2. Adsorption and elution of Fe^{3+} using anion-exchange column.
Curve——pH 3.2} 30 ml. of sample solution and 20 ml. of buffer solution washed
Curve----pH 3.6}
Peak A: eluted with buffer solution
B: washed with water (50 ml.)
C: eluted with 0.5 N HCl after washing with water (Peak B)

formic acid and 1 M ammonium formate containing 3 meq. of Fe^{3+} was passed through a 1.1×10 cm. column of Dowex 1-X4 (50~100 mesh) of formate form and then washed twice with 10 ml. of the mixed solution. Then, the complex ion was eluted with the same mixed solution or water, followed by 0.5 N hydrochloric acid. The results, which are shown in Fig. 2, seem to verify the presence of the anionic, the 4th complex ion.

The values of the formation constants between metal ions and formate ion measured by the author are shown in Table II, together, with the values reported by the other researcher[9]. The elution order from the cation exchanger expected from the table is

$$\text{Fe, Al, R. E. (Ce), Mn,} \quad (7)$$

and

$$\text{R. E., \{Mg, Ca\}, Sr, Ba} \quad (8)$$

To verify the conclusion mentioned above, a sample solution containing 6 meq. of iron(III) and 6 meq. of cerium(III) ions was passed through a 1.1×10 cm. column of Dowex 50-X8 (100~150 mesh) of a hydrogen form. After adsorption and washing, the ferric ion was eluted with 100 ml. of a mixed solution of pH 3.2 prepared from 7 parts of 1 M formic acid and 3 parts of 1 M ammonium formate. The cerous ion was eluted with 100 ml. of another mixed solution of pH 4.0 prepared from 3 parts of 1 M formic acid and 7 parts of 1 M ammonium formate. By this procedure, cerium free from iron was easily obtained, as had been expected.

As an example of separation with anion-exchange resin, the removal of iron(III) from rare earth and alkaline earth elements was carried out. Thirty milliliters of a mixed solution of 1 part of 1 M formic acid and 1 part of 1 M ammonium formate (pH about 3.6) containing 3 meq. of strontium and yttrium (labelled with ^{90}Sr-^{90}Y) was passed through a 1.1×10 cm. column of Dowex 1-X4*(50~100 mesh) of $HCOO^-$ from resin. After the sample solution had passed through, the column was washed twice, with 10 ml. of the buffer solution of the same pH and washed with 20 ml. of water; finally the column was regenerated with 0.5 N hydrochloric acid. The radioactivity of each portion was counted with a GM counter. The results are shown in Table III. It can be seen that only iron was adsorbed on the column, while cerium, yttrium and strontium were not. Thus, it was confirmed that iron could be easily removed from these samples.

As has been previously reported, mixed fission products were completely separated

TABLE III. REMOVAL OF IRON WITH ANION-EXCHANGE RESIN

Influent	Metals in effluent		
	Ce	Sr+Y	Fe
Sample	87.6%	85.7%	0
Washing solution 1	12.3	14.3	0
Washing solution 2	0.03	0.04	0
Washing solution and regenerating hydrochloric acid	0.01	0.01	100

* It is difficult to elute iron from ion-exchange resin of a high D.V.B. content.

using mixed solutions of formic acid and ammonium formate as elutriants[7], and alkaline earth elaments were completely separated by a similar solution[8] of a different pH.

The order of elution of several cations can be predicted by the values of the formation constants between the metal ions to be separated and the anion of the elutriant (cf. (7) and (8)).

However, the other experiments[12] gave slightly different results from those expected:

Fe, Al, Mn, R. E. (Ce), Mg, Ca, Sr, Ba

The elution of Mn and Mg earlier than expected from the formation constant may be attributed to the very small affinity of Mn^{2+} and Mg^{2+} to the resin[13].

From the results mentioned above, it was confirmed that the elution order can be predicted mainly on the basis of the values of the formation constants between the metal ions to be separated and the anion of the elutriant. The separation is easily effected when the difference in formation constants is large, but the separation is due both to formation constants and to affinities between the metal ions and the resin when the difference in formation constants is not large.

The author wishes to express his sincere appreciation to Professor Yasuo Miyake of Tokyo University of Education, Professor Hidetake Kakihana of Tokyo Institute of Technology, Dr. Yasushi Kitano of Nagoya University, and Mr. Masami Izawa of the National Institute of Radiological Sciences for their helpful advice and encouragement throughout his work.

National Institute of Radiological Sciences
Kurosuna-machi, Chiba

12) H. Tsubota, *J. Chem. Soc. Japan, Pure Chem. Sec.* (*Nippon Kagaku Zasshi*), **81**, 927 (1960).
13) O. D. Bonner and L. L. Smith, *J. Phys. Chem.*, **61**, 326 (1957).

Syntheses of Some Amino Acids and Amino Aldehydes. IV. (+)-4-Amino-2, 3-dihydroxybutyric Acid

By Akira Yokoo and Susumu Akutagawa

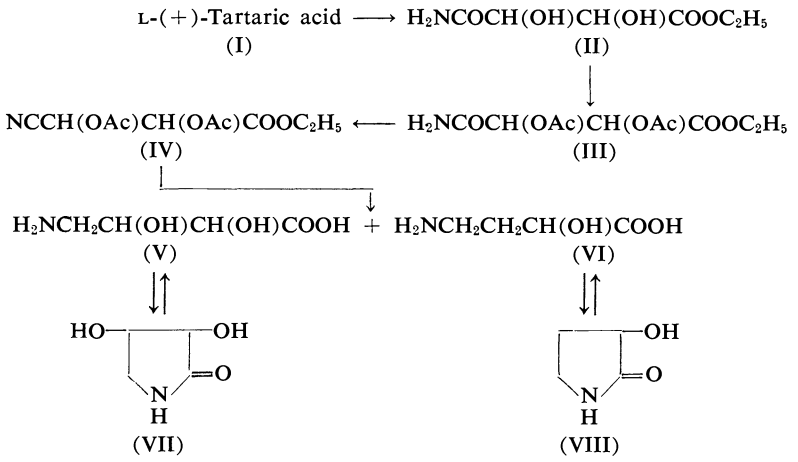
(Received August 28, 1961)

The present authors have synthesized (+)-4-amino-2, 3-dihydroxybutyric acid from L-(+)-tartaric acid (I), which failed in crystallization, as reported in the first paper[1] of this series. Ethyl 3-aminocarbonyl-2, 3-dihydroxypropionate (II), obtained from commercial L-(+)-tartaric acid (I) by Weermann's method[2], was acetylated to give ethyl 3-aminocarbonyl-2, 3-diacetyloxypropionate (III). Dehydration of III yielded ethyl 3-cyano-2, 3-diacetyloxypropionate (IV), which was subjected to catalytic reduction over a platinum oxide catalyst in an acetic acid solution containing sulfuric acid to afford (+)-4-amino-2, 3-dihydroxybutyric acid (4-amino-4-desoxy-L-threonic acid) (V), m. p. 221~222°C (decomp.) (picrolonate, m. p. 198~200°C (decomp.)) and a compound of m. p. 195~196°C (decomp.) (picrolonate, m. p. 182~182.5°C (decomp.); phenylhydrazine salt, m. p. 128~129°C), was assumed to be 4-amino-2-hydroxybutyric acid acid (VI)[3]. On being heating above the melting point, V changed into 3,4-dihydroxy-2-oxopyrrolidine (VII), m. p. 139~142°C, which reformed into V by hydrolysis. In the same way, VI gave 3-hydroxy-2-oxopyrrolidine (VIII), b. p. 159~160°C/1 mmHg, and this reformed into VI.

Experimental

Ethyl 3-Aminocarbonyl-2, 3-dihydroxypropionate (II).—A solution of 200 g. of diethyl L-(+)-tartarate in 400 g. of absolute ethanol was saturated with dry ammonia at 0~3°C for less than 2 hr. After having been left standing for 2 hr. at 10°C, the solvent was removed at as low a temperature as possible under reduced pressure. The crystals formed were collected, washed with ethanol and then with ether. The crystals were heated with a smaller amount of absolute ethanol, and the insoluble diamide was filtered off. The ethanolic solution, on standing, gave 95 g. of crystals, m. p. 134~137°C.

1) A. Yokoo, *Bull. Tokyo Inst. Technol.*, **13**, 13 (1948), (*Chem. Abstr.*, **45**, 553).
2) R. A. Weermann, *Rec. trav. chim.*, **37**, 46 (1918).
3) E. Fischer, *Ber.*, **42**, 4880 (1909), **43**, 3272 (1910); A. Mori, *J. Biochem. (Japan)*, **46**, 59 (1959).



Ethyl 3-Aminocarbonyl-2,3-diacetyloxypropionate (III).—To a solution of 43 g. of II in 60 cc. of pyridine was added 70 g. of acetic anhydride. After having been left standing overnight, the pyridine was removed under reduced pressure and ether was added. The crystals formed were collected and washed with ether. The crystals were heated with 80 cc. of absolute ethanol, and some insoluble materials were removed by filtration. To the ethanolic solution was added twice the volume of ether, and any insoluble material was filtered off. The solution was concentrated to a smaller volume under reduced pressure. The crystals formed on standing were filtered and washed with a small amount of ethanol to yield 33 g. of III, m. p. 95~96°C.

Found: N, 4.47. Calcd. for $C_{10}H_{15}O_7N \cdot C_2H_5OH$: N, 4.56%.

After being heated for 2 hr. at 150°C, the nitrogen content was 5.17% (calcd. for $C_{10}H_{15}O_7N$: N, 5.36%).

Ethyl 3-Cyano-2, 3-diacetyloxypropionate (IV).—To 20 g. of cooling III was gradually added 80 g. of phosphorous oxychloride. After the resulting mixture had been heated for 30 min. on a water bath, the remaining oxychloride was removed almost completely under reduced pressure. Ice was added to cool the residue, which was then extracted with ether. The ethereal solution was washed with a sodium carbonate solution and dried over anhydrous sodium sulfate. The ether was removed, and vacuum distillation gave 11 g. of a colorless viscous oil, b. p. 172~174°C/21 mmHg.

Found: N, 5.48. Calcd. for $C_{10}H_{13}O_6N$: N, 5.76%.

(+)-4-Amino-2, 3-dihydroxybutyric Acid (V) and 4-Amino-2-hydroxybutyric Acid (VI).—A solution of 10 g. of IV in 60 cc. of gacial acetic acid containing 2 g. of concentrated sulfuric acid was reduced for 2 hr. at 60°C in an autoclave in the presence of 1 g. of platinum oxide at an initial pressure of hydrogen 62 atm. The catalyst was filtered off and the acetic acid was removed under reduced pressure. After dilution of the residue with 130 cc. of water, 15 g. of lead acetate was added and the mixture was heated and filtered. The filtrate was treated with hydrogen sulfide, filtered and concentrated to a syrup under reduced pressure. The syrup was refluxed with 100 cc. of 6 N hydrochloric acid for 6 hr. and evaporated to dryness under reduced pressure. Water was added to the residue, which was then treated hot with silver oxide and filtered. The filtrate was again treated with hydrogen sulfide and evaporated to dryness as before. The residue was dissolved in a small amount of water and left to stand in order to deposit crystalline V. This was collected and recrystallized from water to yield 0.8 g. of colorless crystals, m. p. 221~222°C (decomp.), $[\alpha]_D^{27} = +42°$ (water).

Found: C, 35.35; H, 6.77; N, 10.13. Calcd. for $C_4H_9O_4N$: C, 35.55; H, 6.71; N, 10.37%.

Picrolonate of V.—A solution of V and picrolonic acid in water was heated and left to stand. The crystals formed were recrystallized from dilute ethanol to give orange yellow crystals, m. p. 198~200°C (decomp.).

Found: N, 16.50. Calcd. for $C_4H_9O_4N \cdot C_{10}H_8O_5N_4 \cdot H_2O$: N, 16.78%.

The mother liquor of V was evaporated to dryness under reduced pressure, and the residue was dissolved in a small amount of water. Ethanol was added until turbidity took place. The crystals deposited on standing were collected and dissolved in a small amount of water. Methanol was added while hot until the solution became turbid, and the solution was then left to stand. The solution, together with the formed crystals, was warmed for a while, the insoluble crystals of V were filtered off, and again the solution was left to stand. The crystals finally formed were recrystallized from dilute methanol to give 1.05 g. of VI, m. p. 195~196°C (decomp.).

Found: C, 40.20; H, 7.67; N, 12.02. Calcd. for $C_4H_9O_3N$: C, 40.33; H, 7.62; N, 11.76%.

Picrolonate of VI. was obtained, as in the case of V, and recrystallized from water in the form of orange yellow crystals, m. p. 182~182.5°C (decomp.).

Found: N, 18.53. Calcd. for $C_4H_9O_3N \cdot C_{10}H_8O_5N_4$: N, 18.27%.

The picrolonates have shown a melting point depression on admixture with 4-amino-3-hydroxybutyric acid prepared by Tomita's method[4].

4) M. Tomita, *Z. physiol. Chem.*, **124**, 253 (1923).

3,4-Dihydroxy-2-oxopyrrolidine (VII).—After heating 0.7 g. of V in an oil bath at 230°C for 30 min. under diminished pressure (water pump), water was added, treated with decolorizing carbon and evaporated to dryness under reduced pressure. The residue was taken up in ethanol, and a little ether was added. The crystals formed were recrystallized from ethanol to give 0.25 g. of VII, m. p. 139~142°C.

Found: C, 40.99; H, 6.27; N, 12.19. Calcd. for $C_4H_7O_3N$: C, 41.02; H, 6.03; N, 11.96%.

2,4-Dinitrophenylhydrazone of VII.—The crude 2,4-dinitrophenylhydrazone of VII was recrystallized from ethanol to give orange plates, m. p. 163~165°C.

Found: N, 23.95. Calcd. for $C_{10}H_{11}O_6N_5$: N, 23.56%.

Hydrolysis of VII.—A mixture of 0.2 g. of VII and 5 cc. of 6 N hydrochloric acid was refluxed for 2 hr. and evaporated to dryness under reduced pressure. The residue was dissolved in water, treated with silver oxide and then with hydrogen sulfide. The filtrate was evaporated to dryness and dissolved in a small amount of water. A little methanol was added, and the solution was left to stand to deposit crystals, which were recrystallized as before. The crystals, m. p. 219~220°C (decomp.), did not depress the melting point on mixed fusion with V.

3-Hydroxy-2-oxopyrrolidine (VIII).—After 0.5 g. of VI had been heated in a tiny Claisen flask at 215~220°C for 20 min., vacuum distillation gave 0.25 g. of VIII, b. p. 159~160°C/1 mmHg, which on standing solidified as strongly hygroscopic crystals.

Found: N, 13.89. Calcd. for $C_4H_7O_2N$: N, 13.86%.

VIII did not give 2,4-dinitrophenylhydrazone.

Phenylhydrazine Salt of VI.—A mixture of 0.1 g. of VIII, 0.3 g. of phenylhydrazine and 0.3 g. of commercial glacial acetic acid was heated at 130~135°C for 30 min. The crystals deposited on standing were recrystallized from ethanol to form colorless crystals, m. p. 128~129°C.

Found: N, 18.56. Calcd. for $C_4H_9O_3N \cdot C_6H_8N_2$: N, 18.49%.

This salt did not depress the melting point on admixture with that derived from VI.

The authors take this opportunity to express their sincere gratitude to the Ministry of Education for its grant-in-aid for Scientific Research and also to Dr. A. Kondo (the Department of Organic Chemistry of Tokyo Institute of Technology) for carrying out the carbon and hydrogen microanalyses.

Chemical institute
Faculty of Science
Okayama University
Tsushima, Okayama

Effects of Nonelectrolytes on the Temperature of the Maximum Density of Water. I. Alcohols

By Goro WADA and Saburo UMEDA*

(Received April 17, 1961)

The well-known fact that water exhibits its maximum density at 3.98°C under an atmospheric pressure has been discussed by one of the present authors in the previous paper[1] from the viewpoint of the two-state model stating that water holds a chemical equilibrium between the icy and the closely packed states. It may be an interesting problem how the temperature of the maximum density of water varies when a minute quantity of a foreign substance is dissolved in it. The effects of some simple electrolytes on the temperature of the maximum density have already been measured[2], and, so far as is known, electrolytes lower the temperature of the maximum density of water at a rate nearly proportional to the concentrations of electrolytes in dilute solutions, obeying the so-called Despretz's rule[3]. However, nothing is yet known about the effects of nonelectrolytes upon the temperature of the maximum density of water. The authors, therefore, intend in the present paper to find the correlation between the change in the temperature of the maximum density of water and the chemical constitution of some added organic substances, especially of various uni- and polyvalent alcohols.

Experimental

Apparatus and Procedure.—The dilatometer used for the measurement of the volume change of

* Present address: Toppan Printing Co., Ltd., Fukushima-ku, Osaka.

1) G. Wada, This Bulletin, **34**, 955 (1961).

2) R. Wright, *J. Chem. Soc.*, **115**, 119 (1919); N. G. Wilson and R. Wright, *J. Phys. Chem.*, **35**, 624 (1934); "International Critical Tables", Vol. III, p. 107.

3) Despretz, *Ann. chim. phys.*, [ii] **70**, 49 (1839); ibid., **73**, 296 (1840).

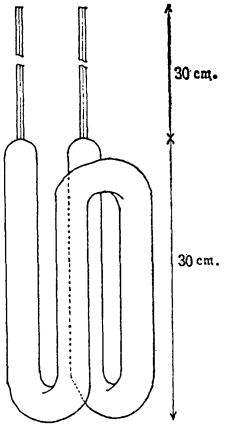


Fig. 1. Dilatometer.

aqueous solutions with temperature is shown in Fig. 1. Its shape as a whole was of a twisted-W type with a capacity of about 300 cc., to which was attached at either end a vertical capillary 0.6 mm. in inside diameter. This enabled us to detect a volume change in a solution as small as 3×10^{-5}% by observing the movement of the liquid surface in the capillary tubes as the temperature was varied. In order to fill the dilatometer with a sample solution, one of the ends of the capillaries was connected with the reservoir of a solution and the other with an aspirator. On working the aspirator, it had been verified preliminarily that no appreciable change in concentration owing to the fractional evaporation of the individual volatile components of the solution occurred during the transfer of the solution from the reservoir to the dilatometer. The height of the surface of the solution which had been introduced was adjusted to be nearly at the center of each capillary by the advance use of a thin injector.

The temperature of the thermostat was regulated within ±0.005°C. The dilatometer attained thermal equilibrium with the thermostat in half an hour. The change in volume was observed in the temperature range covering ±2°C of the temperature of the maximum density of the solution at intervals of about 0.5°C. The apparent volume of a solution does not show a minimum at its true temperature of the maximum density owing to the thermal expansion of the dilatometer itself. The changes in the casese of pure water and aqueous solutions, in the height of the liquid surface with a change in temperature near the respective temperatures of the maximum density, however, were found to be quite similar in type to each other, irrespective of the nature of the solution as long as the solution was very dilute. The temperature of the maximum density of the sample could, therefore be determined, graphically by comparing the apparent volume change of pure water with that of the sample. This method was very accurate, with a maximum error of ±0.02°C*.

Materials.—Sixteen alcohols, including uni- and polyvalent ones, were used for the experiments; these alcohols were purified by usual methods and were ascertained to be pure enough for the present purpose as judged from boiling points, melting points, densities and refractive indices. Pure water was prepared by passing distilled water obtained from an alkaline permanganate solution, through columns of ion-exchange resin.

* The maximum errors ever reported in cases of electrolyte solutions were as large as ±0.2°C.

Results

The elevation of the temperature of the maximum density ΔT is defined as

$$\Delta T = T_m - T_{m_0} \qquad (1)$$

where T_{m_0} represents the temperature of the maximum density of pure water and T_m that of a sample solution of mole fraction x of alcohol respectively. The observed values of ΔT at various concentrations of various alcohols are shown in Table I.

As examples of ternary systems, a mixture of ethyl alcohol, *tert*-butyl alcohol and water and one of *tert*-butyl alcohol, potassium chloride and water were adopted, the concentration of *tert*-butyl alcohol being kept constant at 0.10×10^{-2} mol./H_2O-mol. in the former and that of potassium chloride at 0.11×10^{-2} and 0.20×10^{-2} mol./H_2O-mol. in the latter. The results are pictured in Figs. 2 and 3.

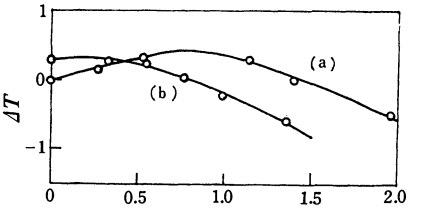


Fig. 2. The ternary system of ethyl alcohol, *tert*-butyl alcohol and water. (a) *tert*-butyl alcohol: none, (b) *tert*-butyl alcohol: 0.10×10^{-2} mol./H_2O-mol.

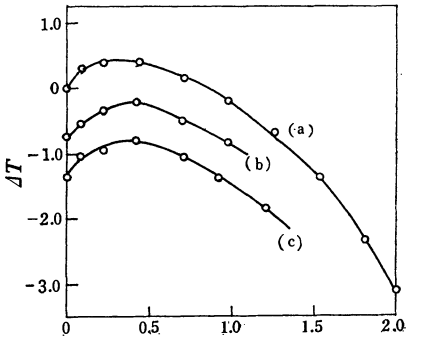


Fig. 3. The ternary system of *tert*-butyl alcohol, potassium chloride and water. (a) KCl: none, (b) KCl: 0.11×10^{-2} mol./H_2O-mol., (c) KCl: 0.20×10^{-2} mol./H_2O-mol.

TABLE I. THE ELEVATION OF THE TEMPERATURE OF MAXIMUM DENSITY OF WATER BY VARIOUS ALCOHOLS

Substance	$x\times10^2$	ΔT	$\Delta T'$
Methyl alcohol			
	0.68	0.02	1.12
	1.00	−0.04	1.59
	1.48	−0.20	2.24
	2.05	−0.48	2.90
	2.59	−0.80	3.48
	3.17	−1.28	4.00
	3.67	−1.64	4.53
	4.21	−2.33	4.77
	4.45	−2.46	5.07
	5.26	−3.54	5.43
Ethyl alcohol			
	0.27	0.16	0.78
	0.53	0.32	1.49
	1.13	0.29	2.73
	1.38	0.00	2.97
	1.92	−0.50	3.70
	2.35	−1.13	4.03
	2.92	−1.93	4.54
	3.40	−2.94	4.60
	3.89	−4.14	4.53
n-Propyl alcohol			
	0.24	0.07	0.71
	0.48	−0.14	1.13
	0.74	−0.24	1.72
	1.00	−0.60	2.04
	1.01	−0.62	2.05
	1.48	−1.50	2.44
	1.98	−2.94	2.35
	2.48	−4.34	2.30
Isopropyl alcohol			
	0.44	0.20	1.38
	0.47	0.16	1.42
	0.56	0.32	1.78
	0.99	0.20	2.89
	1.62	−0.48	3.96
	2.15	−1.30	4.63
n-Butyl alcohol			
	0.21	−0.18	0.41
	0.41	−0.33	0.80
	0.62	−0.85	0.87
	0.84	−1.24	1.08
	1.00	−1.94	0.81
	1.24	−2.52	0.89
	1.51	−3.56	0.60
Isobutyl alcohol			
	0.21	−0.08	0.54
	0.42	−0.38	0.85
	0.71	−0.92	1.20
	0.90	−1.42	1.28
	1.24	−2.33	1.45
	1.52	−3.56	1.04
sec-Butyl alcohol			
	0.21	0.04	0.71
	0.49	−0.11	1.49
	0.76	−0.54	1.92
	1.01	−1.13	2.16
	1.25	−1.62	2.44
	1.52	−2.54	2.42
	1.79	−3.46	2.41
tert-Butyl alcohol			
	0.09	0.30	0.70
	0.22	0.40	1.36
	0.43	0.41	2.26
	0.70	0.16	3.14
	0.97	−0.20	3.96
	1.24	−0.68	4.66
	1.52	−1.36	5.17
	1.78	−2.33	5.34
	1.97	−3.11	5.39
Ethylene chlorohydrin			
	0.22	−0.37	0.04
	0.40	−0.85	−0.02
	0.65	−1.40	−0.06
	0.90	−2.04	−0.17
	1.15	−2.62	−0.23
	1.40	−3.44	−0.50
Phenol			
	0.18	−0.56	−0.15
	0.33	−1.13	−0.37
	0.49	−1.80	−0.65
	0.72	−2.92	−1.23
	0.94	−4.08	−1.88
	1.03	−4.47	−2.06
p-Nitrophenol			
	0.021	−0.23	—
	0.038	−0.37	—
	0.057	−0.49	—
Ethylene glycol			
	0.22	−0.45	−0.21
	0.43	−0.79	−0.41
	0.66	−1.23	−0.65
	0.92	−1.80	−0.95
	1.16	−2.27	−1.20
	1.44	−2.87	−1.55
	1.74	−3.54	−1.93
Propylene glycol			
	0.14	−0.05	0.21
	0.28	−0.12	0.39
	0.48	−0.35	0.51
	0.68	−0.73	0.51
	0.88	−1.17	0.45
	1.09	−1.58	0.44
	1.27	−2.17	0.18
	1.37	−2.39	0.15
	1.54	−2.76	0.07
Glycerin			
	0.18	−0.37	−0.17
	0.39	−0.95	−0.51
	0.53	−1.39	−0.78
	0.76	−1.95	−1.09
	0.92	−2.47	−1.43
	1.04	−2.97	−1.79
Saccharose			
	0.03	−0.29	—
	0.06	−0.52	—
	0.09	−0.70	—
	0.12	−1.03	—
	0.14	−1.29	—
	0.17	−1.47	—
	0.19	−1.78	—
	0.24	−2.19	—
	0.28	−2.51	—
Polyvinyl alcohol*			
	0.044	−0.00	—
	0.085	−0.13	—
	0.127	−0.10	—
	0.167	−0.10	—
	0.212	−0.16	—
	0.256	−0.27	—

* In case of polyvinyl alcohol, x represents the fraction of OH groups. The experimental errors are somewhat larger than in the case of other alcohols, caused by the special properties of its solution. The authors thank Dr. T. Mochizuki of Kurashiki Rayon Co. Ltd. for the supply of polyvinyl alcohol.

Discussion

Preliminary Considerations. — It should be pointed out with reference to Table I that although no substance which elevates the temperature of the maximum density of water has hitherto been known, methyl alcohol, ethyl alcohol, *n*-propyl alcohol, isopropyl alcohol, *sec*-butyl alcohol and *tert*-butyl alcohol are now found for the first time to be surely such substances, at least in dilute concentrations. It is especially worth attention that the ΔT of a *tert*-butyl alcohol solution reaches as high as 0.41°C at the concentration $x=0.0043$. Except for the cases mentioned above, ΔT's are usually negative, similar to those of all electrolyte solutions. Instead of obeying Despretz's rule, which states that the ΔT is proportional to the concentration, they fall off more rapidly than the change in concentration.

If a small quantity of liquid substance dissolves in water with neither an increase nor a decrease in the total volume, the resulting volume V of the aqueous solution at θ°C is expressed by

$$V=xV_s+(1-x)V_w \tag{2}$$

where V_s and V_w are the molar volumes of the solute and water respectively at θ°C. Since it is reasonably accepted that V_s increases linearly with temperature over a small temperature range of 0~5°C, while V_w is satisfactorily expressed by a parabolic function of the temperature in the vicinity of its minimum, namely the maximum density of water, the following relations can be given:

$$V_s=V_{s_o}(1+\alpha\theta) \tag{3}$$

$$V_w=V_{w_m}\{1+\beta(\theta-3.98)^2\} \tag{4}$$

in which V_{s_o} and V_{w_m} represent V_s at 0°C and V_w at 3.98°C respectively, and α and β are coefficients relating to the thermal expansion of the respective substances. From the condition $dV/d\theta=0$ at the temperature of the maximum density of the solution, we obtain

$$T_m'=-\frac{x}{1-x}\cdot\frac{\alpha}{2\beta}\cdot\frac{V_{s_o}}{V_{w_m}}+3.98 \tag{5}$$

where T_m' signifies the imaginary temperature of the maximum density of a solution if the solution were an ideal mixture without any appreciable interaction between the solute and water. The imaginary elevation of the temperature of the maximum density ΔT_n is, therefore, as follows:

$$\Delta T_n=T_m'-T_{m_o}=-\frac{x}{1-x}\cdot\frac{\alpha}{2\beta}\cdot\frac{V_{s_o}}{V_{w_m}} \tag{6}$$

According to Eq. 6, ΔT_n should always be negative in ideal systems and should be approximately proportional to the solute concentration as long as the concentration is very low. Therefore, the elevation of the temperature of the maximum density of real solutions owing to mutual interaction between the solute and water, $\Delta T'$, can be defined as follows:

$$\Delta T'=\Delta T-\Delta T_n \tag{7}$$

The necessary values to estimate ΔT_n are the following: $\beta=7.80\times10^{-6}$ deg^{-2}, $V_{w_m}=18.016$ cc./mol., and α's and V_{s_o}'s for various alcohols as listed in Table II. The values of $\Delta T'$ thus obtained are shown in Table I, together with those of ΔT, the former also being approximately represented by an empirical equation of the second order with respect to the concentration

$$\Delta T'=ax+bx^2 \tag{8}$$

because $\Delta T'/x$ versus x is represented by a straight line, as are some examples shown in

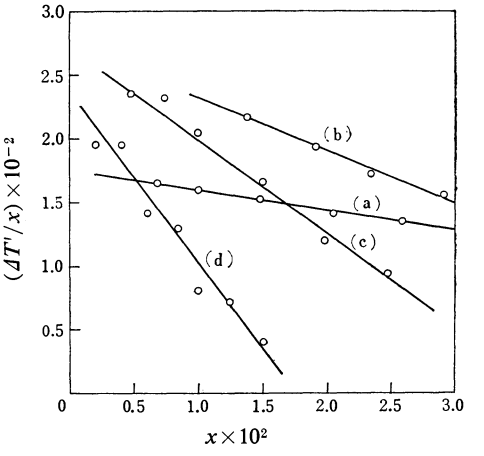


Fig. 4. Linearity of $\Delta T'/x$ against x. (a) Methyl alcohol, (b) ethyl alcohol, (c) *n*-propyl alcohol, (d) *n*-butyl alcohol.

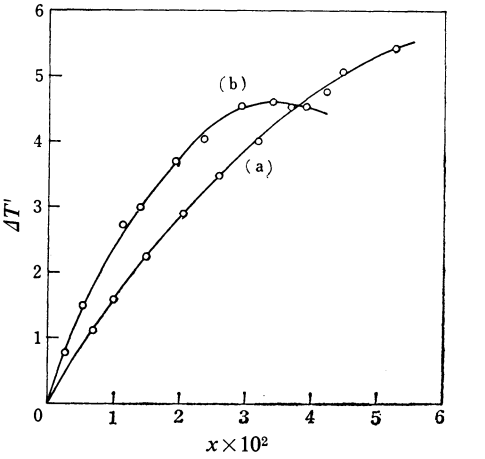


Fig. 5. Variation of $\Delta T'$ with the concentration of (a) methyl alcohol and (b) ethyl alcohol.

TABLE II. COEFFICIENTS OF THERMAL EXPANSION, MOLAR VOLUMES AND PARAMETERS a AND b FOR VARIOUS ALCOHOLS

Substance	$\alpha\times10^{3}$ deg^{-1}	V_{so} cc. mol^{-1}	$a\times10^{-1}$ deg.	$b\times10^{-3}$ deg.
Methyl alcohol	1.148	39.556	17.3	− 1.5
Ethyl alcohol	1.053	57.141	27.3	− 4.1
n-Propyl alcohol	1.002	73.283	26.3	− 6.4
Isopropyl alcohol	1.01	74.993	34.1	− 5.7
n-Butyl alcohol	0.851	89.962	23.7	−13.5
Isobutyl alcohol	0.923	90.733	27.7	−14.0
sec-Butyl alcohol	1.00	90.03	36.5	−14.6
tert-Butyl alcohol	1.295	91.83	60.5	−26.2
Ethylene chlorohydrin	0.878	65.82	0.3	− 2.1
Phenol	0.752	86.181	− 5.4	−15.6
Ethylene glycol	0.464	55.139	− 8.9	− 1.3
Propylene glycol	0.70	73.33	16.3	−11.6
Glycerin	0.43	72.373	− 8.5	− 8.3

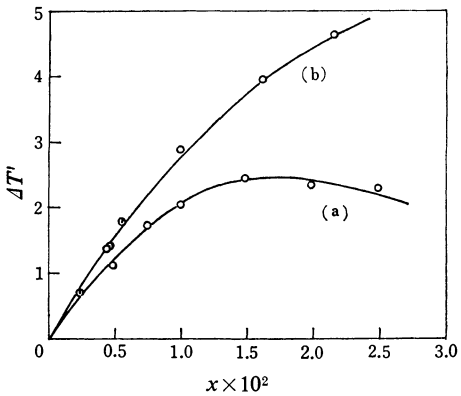


Fig. 6. Variation of $\Delta T'$ with the concentration of (a) *n*-propyl alcohol and (b) isopropyl alcohol.

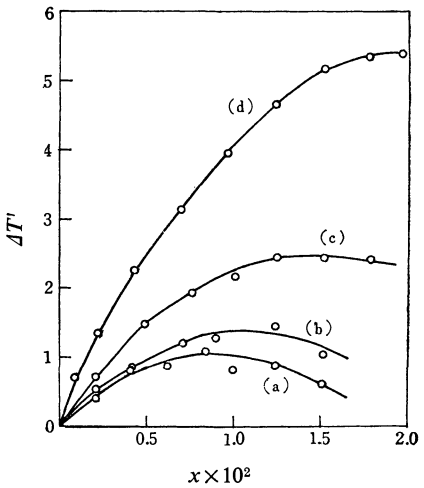


Fig. 7. Variation of $\Delta T'$ with the concentration of (a) *n*-butyl alcohol, (b) isobutyl alcohol, (c) *sec*-butyl alcohol and (d) *tert*-butyl alcohol.

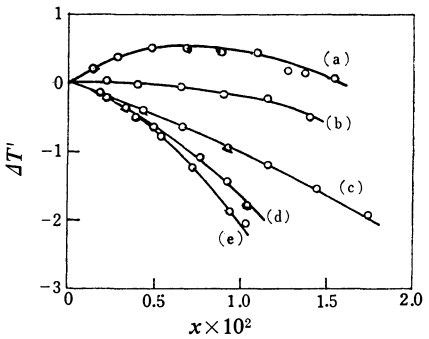


Fig. 8. Variation of $\Delta T'$ with the concentration of (a) propylene glycol, (b) ethylene chlorohydrin, (c) ethylene glycol, (d) glycerin and (e) phenol.

Fig. 4*. Parameters a and b obtained graphically for respective alcohols are also shown in Table II.

The General Tendency of $\Delta T'$, a and b.—In order to discuss the mutual interactions between alcohols and water, it is rather convenient to pay attention to the relationships of $\Delta T'$, instead of ΔT, with the concentration; these relationships are reproduced in Figs. 5—8. Generally speaking, the values of $\Delta T'$ for univalent alkyl alcohols are always positive, while those for polyvalent alcohols show a trend toward being negative. In the cases of propyl alcohols and butyl alcohols, the branching of the alkyl radicals is found to have a clear enhancing effect on $\Delta T'$. Moreover, it should be pointed out in Table II that a's are positive only for all univalent alcohols, while b's are negative for all alcohols adopted here, and that the absolute values of both a and b

* In Fig. 4, the plots of $\Delta T'/x$ at very low concentrations of alcohols are omitted because they are subject to larger errors.

increase as the volumes of alkyl radical become larger.

Nature of a. — On mixing the solute and water, if there were no interaction between the two species, $\Delta T'$ should be zero. In reality, however, interaction occurs to some extent, so that α and V_{s_0} vary as much as $\Delta\alpha$ and ΔV_{s_0} respectively; therefore, $\Delta T'$ can be expressed as follows:

$$\Delta T' = -\frac{x}{1-x} \cdot k(\alpha \Delta V_{s_0} + V_{s_0} \Delta\alpha) \qquad (9)$$

Moreover, from Eqs. 8 and 9 one obtains the next relation:

$$a \equiv \lim_{x \to 0} \left(-\frac{\mathrm{d}\Delta T'}{\mathrm{d}x} \right) = -k(\alpha \Delta V_{s_0} + V_{s_0} \Delta\alpha) \qquad (10)$$

where $k = 1/2\beta V_{w_m}$. In these expressions, ΔV_{s_0} and $\Delta\alpha$ are assumed to include the total changes in volume and in the coefficients of the thermal expansion not only of the solute itself but also of the hydration sheaths formed round the solute molecules where the interaction wholly takes place, β and V_{w_m} being regarded as constant.

Univalent alcohol is taken to exist in the form of hydrogen-bonded chains in a pure liquid state[4] but when it is dissolved in water, there occurs the breaking of the hydrogen bondings between alcohol molecules and, succeedingly, the hydration of the water molecules surrounding them. Since the energies of the hydration are higher than those of hydrogen-bond formation in case of univalent alcohols, the contraction of the volume owing to the compression by hydration exceeds the expansion owing to the breaking of hydrogen bondings and, consequently perhaps, $\Delta V_{s_0} < 0$. Moreover, since water undergoes a transition from the free state (an equilibrating mixture of the icy state and the packed state[1]) to another state similar to the packed state when water hydrates to the solute molecules, $\Delta\alpha$ must be positive, because the coefficients of the thermal expansion of water of the icy state and the packed state are 1.52×10^{-4} and 1.013×10^{-3} deg^{-1} respectively[1]. Accordingly, the first term in the parenthesis in the right-hand side of Eq. 10 should be negative, while the second term is positive. In Table II, since the a's for all univalent alcohols except phenol are positive, the absolute value of the first term must be larger than that of the second term in every alcohol*. Especially, the fact that the magnitude of a for *tert*-butyl alcohol is extraordinarily large may be attributed to the greatness of α itself.

Owing to the intramolecular hydrogen bondings of ethylene chlorohydrin, ethylene glycol, propylene glycol and glycerin, and owing to the intermolecular association of phenol, they are greatly contracted by a strong cohesive force and show a relatively small V_{s_0} compared with those of non-substituted corresponding univalent alcohols in a pure state**. Consequently, ΔV_{s_0} may be nearly equal to zero or rather positive when they are dissolved in water. In such cases, the a's may be smaller than those of univalent alcohols and at last negative in certain instances, as can be seen in Table II.

Tendency of b. — Since b is, on the other hand, the parameter of the second-order term with respect to the concentration in Eq. 8, it may be related to the mutual interaction between the solute molecules themselves. However, the tendencies for b to be negative for all substances so far as have been observed and for the absolute value of b to become larger as the molecular volume of the substance is larger can not be interpreted at the present stage of investigation.

Ternary Systems. — Figure 2 illustrates the variation of ΔT with x of ethyl alcohol in curve a as a binary system and in curve b as a ternary one, *tert*-butyl alcohol being kept at a constant concentration of 0.10×10^{-2} mol./H_2O-mol. as a third substance. ΔT in the ternary system is found to be always smaller than the sum of the ΔT's which ethyl alcohol and *tert*-butyl alcohol will exhibit independently in binary systems. This fact shows that there exists a mutual interaction between the molecules of the different alcohols to disturb their individual behavior.

The situation is, on the contrary, quite different in Fig. 3. Curve a is true for *tert*-butyl alcohol only, while curves b and c correspond to the cases when potassium chloride is added to it as a third substance at 0.11×10^{-2} and 0.20×10^{-2} mol./H_2O-mol. respectively. When curve a is moved down parallel to the axis as far as -0.74 and -1.34°C, it just falls on curves b and c respectively. These distances

4) G. Oster and J. G. Kirkwood, *J. Chem. Phys.*, **11**, 175 (1943); R. H. Cole and W. Dannhauser, ibid., **23**, 1762 (1955); J. B. Hasted and G. W. Roderick, ibid., **29**, 17 (1958); G. P. Pimentel and A. L. McClellan, "The Hydrogen Bond", Freeman Co., San Francisco (1960).

* The fact that a tends to become larger when the alkyl chain of univalent alcohol is longer, as is seen in Table II, can be understood from the observed thermochemical data that the energy of the dissolution of $-CH_2-$ from paraffin into water is about 0.8 kcal./mol.[5] and that the longer the alkyl radical of univalent alcohol, the larger its hydration energy[6].

5) K. Kinoshita, H. Ishikawa and K. Shinoda, This Bulletin, **31**, 1081 (1958).

6) S. Seki and K. Suzuki, ibid., **26**, 63 (1953).

** For instance, ethylene chlorohydrin and ethylene glycol should be compared with ethyl alcohol, the former being derivatives of the latter by substituting H by Cl and OH respectively.

between the curves agree well with the ΔT's which potassium chloride exhibits when it exists alone in water at those respective concentrations. This fact indicates that *tert*-butyl alcohol and potassium chloride do not greatly influence one another in such dilute solutions.

As to the phenomena of the solvation of ions, it is known that only the hydration is overwhelmingly predominant when the concentration of alcohol is less than 10 mol. %, since water molecules are attracted to ions far more preferentially than alcohol molecules at the solvation equilibrium in ternary systems of lithium chloride-ethyl alcohol-water[7], of lithium fluoride-methyl alcohol-water[8] and of lithium fluoride-ethyl alcohol-water[8]. Considering all these facts, nonelectrolytic molecules and electrolytic ions may exhibit independent behavior in dilute aqueous solutions.

Summary

The effects of various kinds of alcohol on the temperature of the maximum density of water were observed. The results revealed are as follows:

1) The change in the temperature of the maximum density due to alcohols, ΔT, is not proportional to the solute concentration, disobeying Despretz's rule and in contrast with ordinary electrolytes.

2) The ΔT for univalent aliphatic alcohols at low concentrations is generally positive; that for *tert*-butyl alcohol is the largest. The ΔT is likely to become high as the number of carbon atoms and the degree of branching in alkyl radicals increase.

3) The elevation of the temperature of the maximum density due to the interaction of alcohol and water, $\Delta T'$, depends upon the weakness of the cohesion of alcohol and the strength of the hydration of the hydrophilic molecules.

4) As the concentration of alcohol increases, there occurs a lowering of ΔT as a result of interaction between the solute molecules themselves. Similar interactions are seen between different alcohol molecules in ternary systems, but can not be seen between alcohol and electrolytic ions, where the solutes behave independently of each other. In the last case, the additivity of ΔT is realized fairly well.

Department of Chemistry
Faculty of Science
Kobe University
Mikage, Kobe

7) G. Wada, *J. Chem. Soc. Japan, Pure Chem. Sec.* (*Nippon Kagaku Zasshi*), **77**, 391 (1956).
8) G. Wada, C. Ito and K. Horie, *J. Electrochem. Soc. Japan*, **28**, 58, E32 (1960).

Studies of the Cage Effect of Solvent. I. Photolysis of Azomethane in n-Hexane

By Sukeya KODAMA

(Received August 31, 1961)

The concept of the cage effect of solvent molecules given in 1936 by Frank, Rabinowitch and Wood[1] has since then frequently been used to explain such experimental findings as the low quantum yield in a photochemical reaction in solution. The presence of the cage effect has been reported in a number of thermal, photochemical or radiation-induced decomposition reactions of the following substances: iodine[2], acetyl peroxide[3], butyryl peroxide[4], α, α'-azobisisobutyronitrile[5], halides[6], etc. To date, however, reliable quantitative studies of the cage effect have been meagre.

It has been found by the present author that the photolysis of azomethane in solution

1) J. Frank and E. Rabinowitch, *Trans. Faraday Soc.*, **32**, 138 (1936); E. Rabinowitch and W. C. Wood, ibid., **32**, 547 (1936).

2) R. M. Noyes et al., *J. Chem. Phys.*, **18**, 658, 999 (1950); *J. Am. Chem. Soc.*, **76**, 2140 (1954); R. L. Strong and J. E. Willard, ibid., **79**, 2098 (1957).

3) M. Szwarc et al., ibid., **76**, 5981 (1954); ibid., **77**, 3486 (1955); *J. Chem. Phys.*, **23**, 1978 (1955); J. R. Nash, W. H. Hamill and R. R. Williams, *J. Phys. Chem.*, **60**, 823 (1956).

4) J. Smid, A. Rembaum and M. Szwarc, *J. Am. Chem. Soc.*, **78**, 3315 (1956).

5) G. S. Hammond et al., ibid., **77**, 3244 (1955); ibid., **81**, 4878 (1959); ibid., **82**, 5394 (1960); J. C. Roy, J. R. Nash, R. R. Williams and W. H. Hamill, ibid., **78**, 519 (1956); C. E. H. Bawn and D. Verdin, *Trans. Faraday Soc.*, **56**, 815 (1960).

6) J. E. Willard, *J. Am. Chem. Soc.*, **73**, 2271 (1951); ibid., **74**, 318 (1952); M. S. Fox and W. F. Libby, *J. Chem. Phys.*, **20**, 487 (1952); J. C. Roy, W. H. Hamill and R. R. Williams, *J. Am. Chem. Soc.*, **77**, 2593 (1955).

exhibits a large cage effect; photolysis has therefore been investigated in various solvents. This paper reports on the study in *n*-hexane solution. The results obtained in other solvents will be reported in a later paper.

Experimental

Materials. — Azomethane was prepared by the thermal decomposition[7] of azomethane-cuprous chloride[8] produced from dimethyl hydrazine dihydrochloride[9], purified by removing water and carbon dioxide with calcium chloride and soda lime respectively and by several-times-repeated distillation from a dry ice-acetone trap to a liquid nitrogen trap in vacuo, and stored in a reservoir protected from light. *n*-Hexane was purified as follows: the commercial hexane of a chemically pure grade was repeatedly washed with chlorosulfonic acid for about a month, stirred with alkaline and acid potasium permanganate solutions, washed with sodium carbonate and water, dried over phosphorus pentoxide, and distilled; the fraction 68 to 69°C was then collected. The hexane thus purified showed no absorption in the wavelength range above 250 mμ. Styrene was used as a scavenger of methyl radicals because of its large methyl affinity[10]. It was also purified by vacuum distillation.

Apparatus.—The photolysis was carried out with 366 and 313 mμ obtained from an ultra-high pressure mercury lamp of 100 Watt (Mazda, SHL-100UV). The filter used for 366 mμ was UV-D1 (Mazda). The transmission ratios of 334 and 390 mμ to 366 mμ were about 6 and 1% respectively. For 313 mμ a 1.8 M solution of nickel sulfate 1 cm. in thickness was used, with a glass plate to cut off the light of shorter wavelengths than 290 mμ. The transmission ratios of 334 and 300 mμ to 313 mμ were roughly 29 and 22% respectively.

The reaction cell used for the photolysis below room temperature was a glass cylinder 3.6 cm. in diameter and 1.0 cm. in length, with a capacity of 10 ml. It was connected to the other parts of the apparatus by a mercury cut-off. For the experiments above room temperature, a cell of the same size but with two side tubes was used. One of these side tubes was made of capillary tubing, and was sealed off after the introduction of the reactants, and the other had a breakable seal for analysis of the products. All the side tubes were made of brown-colored glass to prevent the decomposition of azomethane vapor in those parts. A non-plated Dewar vessel was used as a bath in the experiments with 366 mμ, but for those with 313 mμ a copper-made bath equipped with a quartz window was used.

The Procedure.—Before use hexane was subjected to thrice-repeated bulb-to-bulb distillation using dry ice-acetone and was introduced into the reaction cell. When styrene was used as a scavenger, it was introduced into the cell in a similar way. Azomethane was also purified each time before use by condensation and evacuation at −160°C; it was then introduced into the reaction cell cooled with liquid nitrogen. After closing the mercury cut-off or sealing off the capillary tubing, the cell was warmed to room temperature to get a complete mixing of azomethane with hexane. The cell was then immersed in the bath at the experimental temperature and the photolysis started. The mercury cut-off was used also as a manometer, to measure both pressures of hexane and azomethane and the increase in pressure due to the photolysis.

The reaction cell was cooled with dry ice-acetone after the irradiation was over, and it was connected to the analytical system by the mercury cut-off or by the breakable seal. The cell contained hexane, undecomposed azomethane, nitrogen, methane, ethane, various by-products, and styrene if used. The gaseous components were separated by twice-repeated bulb-to-bulb distillation at the dry ice-acetone temperature and cooled to −160°C to condense azomethane, hexane vapor and by-products. Ethane was then condensed at the liquid nitrogen temperature. Nitrogen and methane that were not condensed were collected in a Toepler gauge, and the sum of their amounts were determined. The mixture was then sent into a platinum combustion tube, where the methane was burnt to carbon dioxide and water. By removing the water by condensation, the amount of carbon dioxide was determined; this gave in turn the amount of methane and, accordingly, that of nitrogen. Ethane condensed in the liquid nitrogen trap was evaporated, collected in the Toepler gauge, and its quantity determined.

Results

Table I shows the results obtained at 0°C. V is the volume of the solution at the reaction temperature. CH_4/N_2 and C_2H_6/N_2 represent respectively the yields of methane and ethane referred to nitrogen. The material balance for nitrogen, methane and ethane is represented by $((1/2)CH_4+C_2H_6)/N_2$, since two

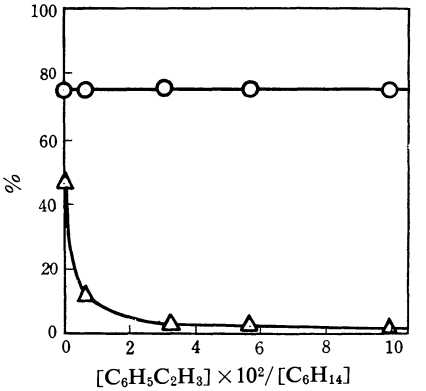


Fig. 1. Effect of styrene on yields of methane and ethane at 0°C.
○, C_2H_6/N_2; △, CH_4/N_2

7) F. P. Jahn, ibid., **59**, 1761 (1937).
8) O. Diels and W. Koll, *Ann.*, **443**, 262 (1925).
9) H. H. Hatt, "Organic Syntheses", Vol. XVI (1936), p. 18.
10) F. Leavitt, M. Levy, M. Szwarc and V. Stannett, *J. Am. Chem. Soc.*, **77**, 5493 (1955); M. Feld and M. Szwarc, ibid., **82**, 3791 (1960).

TABLE I. PHOTOLYSIS OF AZOMETHANE IN *n*-HEXANE AT 0°C

Run No.	Wave-length mμ	*V* cc.	$[(CH_3)_2N_2]\times10^2$ mol./l.	$\frac{[C_6H_5C_2H_3]}{[C_6H_{14}]}$ %	Time of irradiation min.	Rate of formation $\times10^{11}$ mol. cc^{-1} sec^{-1} R_{N_2}	R_{CH_4}	$R_{C_2H_6}$	$\frac{CH_4}{N_2}$ %	$\frac{C_2H_6}{N_2}$ %	$\frac{\frac{1}{2}CH_4+C_2H_6}{N_2}$ %
1[a]	366	13.4	0.852	0	90	11.7	0.448	11.0	3.83	94.1	96.0
2[a]	366	13.4	0.993	0	90	13.8	0.607	12.7	4.40	91.8	94.0
3	366	13.4	0.826	0	198	7.40	3.48	5.57	47.0	75.3	98.8
4	366	13.4	0.898	0	162	7.85	3.64	5.94	46.4	75.7	98.9
5	366	11.2	1.13	0	84	15.5	7.35	11.6	47.5	75.2	99.0
6	366	11.2	1.17	0	66	21.8	10.3	16.4	47.4	75.0	98.7
7	366	10.5	3.23	0	60	49.6	23.2	37.4	46.7	75.5	98.9
8	366	9.9	3.30	0	60	37.1	17.0	28.0	45.8	75.8	98.3
9	366	11.2	4.20	0	48	30.6	14.2	23.1	46.3	75.5	98.6
10	313	10.8	2.70	0	90	13.3	6.25	10.0	47.0	75.4	98.9
11	313	10.6	2.78	0	90	19.0	9.04	14.3	47.6	75.2	99.0
12	>300	9.9	3.50	0	24	108.0	50.3	81.5	46.6	75.4	98.7
13	366	11.3	4.12	0.612	54	32.7	3.80	24.5	11.6	74.9	
14	366	11.1	3.06	3.16	42	45.6	1.37	34.5	3.0	75.7	
15	366	10.6	2.80	5.65	42	43.3	1.08	32.5	2.5	75.2	
16	366	12.5	3.55	9.92	60	28.3	0.44	21.2	1.6	75.0	

a) Runs 1 and 2 are the results obtained with azomethane vapor.

TABLE II. PHOTOLYSIS OF AZOMETHANE IN *n*-HEXANE AT VARIOUS TEMPERATURES

Run No.	Temp. °C	*V* cc.	$\frac{[C_6H_5C_2H_3]}{[C_6H_{14}]}$ %	Time of irradiation min.	Rate of formation $\times10^{11}$ mol. cc^{-1} sec^{-1} R_{N_2}	R_{CH_4}	$R_{C_2H_6}$	$\frac{CH_4}{N_2}$ %	$\frac{C_2H_6}{N_2}$ %	$\frac{\frac{1}{2}CH_4+C_2H_6}{N_2}$ %
17	80	12.2	0	48	22.0	16.3	13.2	74.0	60.0	97.0
18	75	11.3	3.48	60	39.4	5.36	24.1	13.6	61.2	
19	50	11.3	0	42	34.1	22.5	21.8	63.8	65.9	97.8
20	50	10.9	3.47	72	40.2	3.54	26.3	8.81	66.0	
21	25	10.5	3.47	72	36.0	1.90	25.8	5.29	71.6	
22	20	10.8	0	54	31.6	22.9	17.0	53.8	72.6	99.5
23	−31	9.5	0	60	38.6	13.8	31.2	35.8	80.9	98.8
24	−31	10.6	3.18	42	38.2	0.69	30.6	1.80	80.2	
25	−50	11.3	0	60	29.6	9.24	24.8	31.2	83.9	99.5
26	−50	10.3	3.18	42	32.7	0.46	27.3	1.43	83.5	
27	−75	10.3	0	240	4.82	1.02	4.27	21.2	88.7	99.3
28	−75	9.0	0	42	32.0	6.72	28.3	21.0	88.5	99.0
29	−75	10.3	0	90	35.4	7.72	31.3	21.8	88.3	99.2
30	−75	10.2	0.607	120	21.5	0.71	18.5	3.30	86.3	
31	−75	9.9	3.20	42	26.8	0.30	23.4	1.14	87.5	
32	−75	10.5	10.7	72	10.4	0.13	8.99	1.26	86.8	

methyl radicals and a nitrogen molecule are obtained from an azomethane molecule. The extent of conversion was less than 6% in all the runs except in Runs 3 and 4, where it was nearly 10%.

Runs 1 and 2 show the results of the photolysis of azomethane vapor carried out in comparison with those in solution. Figure 1 shows the variation in yields of methane and ethane with the concentration of styrene in the series of Runs 13−16.

Table II shows the effect of temperature on the photolysis with 366 mμ. The concentration of azomethane in each run was about 3×10^{-2} mol./l. The conversion in each run was again less than 6%. Figure 2 summarizes the results given in Tables I and II, $(CH_4/N_2)_s$ and $(C_2H_6/N_2)_s$ denoting respectively the yields of methane and ethane in the presence of styrene of 3.16 to 3.48 mol. %.

Figure 3 shows the effect of temperature on the quantum yield of photolysis determined as follows: Runs 1—4 show that the ratio of the quantum yield in solution against that in

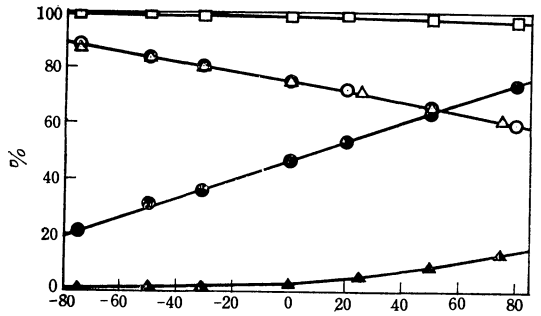


Fig. 2. Effect of temperature on yields of methane and ethane, and material balance.
□, $((1/2)CH_4+C_2H_6)/N_2$
○, C_2H_6/N_2; △, $(C_2H_6/N_2)_s$
●, CH_4/N_2; ▲, $(CH_4/N_2)_s$

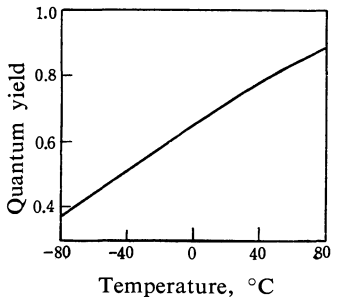


Fig. 3. Dependence of quantum yield on temperature.

the vapor phase is 0.65; since in the vapor phase the quantum yield is reported to be unity[11], those in solution at various temperatures are obtained by comparing rates of the formation of nitrogen. However, in view of various uncertainties involved, the quantum yields thus determined have to be taken only as apparent values.

Discussion

The photolysis of azomethane has been studied in the gas phase by a number of workers[11,12] The mechanism that accounts for the main products, i. e., methane, ethane and nitrogen, is relatively simple and can be represented as

$$(CH_3)_2N_2+h\nu \rightarrow 2CH_3+N_2$$
$$CH_3+(CH_3)_2N_2 \rightarrow CH_4+CH_3N_2CH_2$$
$$CH_3+CH_3 \rightarrow C_2H_6$$

The following addition reactions of methyl radicals have also been proposed to explain the fate of methyl radicals that are not accounted for by methane and ethane:

$$CH_3+(CH_3)_2N_2 \rightarrow (CH_3)_3N_2$$
$$CH_3+(CH_3)_3N_2 \rightarrow (CH_3)_4N_2$$
$$CH_3+CH_2N_2CH_3 \rightarrow C_2H_5N_2CH_3$$

The possibility of the direct formation of ethane by the primary process has been excluded by the experiments carried out with a scavenger such as nitric oxide[12a] and butadiene[12b]. The decomposition into three fragments in the primary act may actually take place in two stages, i. e.,

$$(CH_3)_2N_2+h\nu \rightarrow CH_3N_2+CH_3$$
$$\text{and } CH_3N_2 \rightarrow CH_3+N_2$$

However, since the radical CH_3N_2 is very short-lived[13], such a two-stage decomposition cannot be discriminated from that given above so far as subsequent reactions are concerned.

On the basis of the mechanism thus established in the gas phase, the possible reactions in *n*-hexane solution may be supposed as follows:

$$(CH_3)_2N_2+h\nu \rightarrow [2CH_3+N_2] \quad (1)$$
$$[2CH_3+N_2] \rightarrow C_2H_6+N_2 \quad (2)$$
$$\rightarrow CH_3+N_2+CH_3 \quad (3)$$
$$[2CH_3+N_2]C_6H_{14} \rightarrow CH_4+C_6H_{13}+N_2+CH_3 \quad (4)$$
$$[2CH_3+N_2]C_6H_5C_2H_3 \rightarrow C_6H_5C_3H_6+N_2+CH_3 \quad (5)$$
$$CH_3+C_6H_{14} \rightarrow CH_4+C_6H_{13} \quad (6)$$
$$CH_3+CH_3 \rightarrow C_2H_6 \quad (7)$$
$$CH_3+(CH_3)_2N_2 \rightarrow CH_4+CH_2N_2CH_3 \quad (8)$$
$$\rightarrow (CH_3)_3N_2 \quad (9)$$
$$CH_3+C_6H_{13} \rightarrow C_6H_{13}CH_3 \quad (10)$$
$$CH_3+C_6H_5C_2H_3 \rightarrow C_6H_5C_3H_6 \quad (11)$$
$$C_6H_{13}+C_6H_{13} \rightarrow C_{12}H_{26} \quad (12)$$
$$\rightarrow C_6H_{14}+C_6H_{12} \quad (13)$$

The parenthesis in the primary process denotes that two methyl radicals and a nitrogen molecule are formed together in a solvent cage. Reactions 2 and 3 represent respectively the ethane formation in the solvent cage and the separation of the two methyl radicals from each other by diffusion. Reaction 4 is the hydrogen atom abstraction by one of the

11) M. H. Jones and E. W. R. Steacie, *J. Chem. Phys.*, **21**, 1018 (1953).
12) a) T. W. Davis, F. P. Jahn and M. Burton, *J. Am. Chem. Soc.*, 60, 10 (1938); b) S. Kodama and O. Toyama, to be published; c) W. C. Seppy and J. G. Calvert, *J. Am. Chem. Soc.*, **81**, 769 (1959); d) P. Ausloos and E. W. R. Steacie, *Can. J. Chem.*, **33**, 39 (1955); e) S. Toby and K. O. Kutschke, ibid., **37**, 672 (1959); f) S. Toby, *J. Am. Chem. Soc.*, **82**, 3822 (1960).
13) The decomposition of the CH_3N_2 radical is exothermic by some 29 kcal./mol. (Ref. 14). Sleppy and Calvert (Ref. 12) failed to detect the radical spectroscopically in a flash photolysis of azomethane.
14) C. Steel and A. F. Trotman-Dickenson, *J. Chem. Soc.*, **1959**, 975.

methyl radicals from a solvent molecule constituting the cage, and reaction 5 is an analogue in the case where a styrene molecule participates in constituting the cage. Reactions 6—10 represent various possibilities for methyl radicals distributed at random in the solution. Reaction 11 shows the scavenger action of styrene. Reactions 12 and 13 give possible fates other than reaction 10 for hexyl radicals formed by reaction 6.

The sequence of reactions given above is only a crude picture, but the results obtained in the present work may be discussed by referring to these reactions. The reactions that explain the formation of ethane are those numbered from 2 and 7. As shown in Tables I and II and in Fig. 1, the addition of styrene in an increasing amount reduces the yield of methane nearly to zero, whereas that of ethane remains unaffected, indicating that ethane is formed exclusively by reaction 2 or by the combination of methyl radicals in the solvent cage. Even in the absence of styrene, the results obtained lead to the same conclusion: If ethane is formed by reaction 7, its rate should be proportional to the second power of the steady concentration of methyl radicals, while the rate for methane would be simply proportional to its first power, Runs 3—9, given in Table I, show, however, that the yields of methane and ethane are not affected by increasing the concentration of azomethane, i. e., by increasing the amount of azomethane decomposed per unit time.

As to the formation of methane, the most important process may be supposed to be reaction 6. The effect of styrene shown in Tables I and II and in Fig. 1 is consistent with what is expected for this reaction. Reaction 8 cannot be important, since the mole ratio of azomethane (to *n*-hexane) is (of the order) of 10^{-3} in the present work and the rate constants for reactions 6 and 8 may be of the same order of magnitude[15]. The contribution of reaction 4 is also negligible. If this reaction were important, reaction 5 should also be important; otherwise, the nearly complete suppression of methane formation by styrene could not be explained. However, if reaction 5 were important, the yield of ethane should be reduced in the presence of styrene, which contradicts what was actually found to be true.

The quantum yield of photolysis is, as has been already described, less than unity in *n*-hexane solution, and Fig. 3 shows that it decreases markedly with the lowering of the temperature. In general, a low quantum yield less than unity may be accounted for either by the deactivation of excited substrate molecules or by the recombination of the primary products in the solvent cage, provided that no substrate molecules are regenerated by secondary reactions. Studies of the yield of fluorescence in solution show, however, that quenching by deactivation usually increases with the rise in temperature[16]. The observed falling off of the quantum yield with the lowering of the temperature seems, therefore, to have resulted from the recombination of the initially formed radicals CH_3N_2 and CH_3 in the solvent cage, though the former radical is short-lived, as has been described above, and may not take part in subsequent reactions.

The decomposition of the azomethane molecule into two metyl radicals and a nitrogen molecule requires an energy of 22 kcal./mol[14]. Hence, the photolysis with 366 mμ produces an excess energy of 56 kcal./mol. Though how this excess energy is distributed among the three fragments formed is not clear, there is a possibility that hot methyl radicals are thus formed. In fact, Sleppy and Calvert[12c] concluded, in a flash photolysis of azomethane vapor, the formation of hot methyl radicals from the effect of wavelengths on the yield ratio CH_4/C_2H_6 and from the effect of the addition of C_2F_6. In ordinary photolysis of azomethane, however, no indication of their existence has been reported. Also, in this work, as is shown in Table I, the irradiation with 313 mμ gave almost the same result as that for 366 mμ, although the energy difference between the two mercury lines is not very large (13 kcal./mol.).

As is shown in Fig. 4, the dependence of the yield of ethane on the temperature is approximately represented by

$$1-C_2H_6/N_2=A\exp(-E/RT)$$

with $A=2.08$ and $E=1.17$ kcal./mol. Though the energy value found here probably has some correlation with the diffusion energy of methyl radicals in *n*-hexane, the latter quantity cannot be computed directly from such an energy value since the formula given above is merely an empirical one[17].

15) The rate constants in the gas phase are $k_6=10^{11.1}\exp(-8100/RT)$ and $k_8=10^{11.1}\exp(-7600/RT)$ mol^{-1} cc. sec^{-1}. (A. F. Trotman-Dickenson, "Gas Kinetics", Butterworths, London (1955), p. 200.)

16) For example, E. J. Bowen and J. Sahn, "Photochemistry in the Liquid and Solid States", Ed. by F. Daniels, John Wiley and Sons, Inc., New York and London (1960), p. 55.

17) A simple treatment of reactions 6 and 7 leads to an expression

$$C_2H_6/N_2=k_6/(k_6+k_7)$$

or

$$[1-(C_2H_6/N_2)]/(C_2H_6/N_2)=k_7/k_6$$

where k_6 and k_7 are respective rate constants. If, therefore, k_6 is assumed to be independent of temperature, the Arrhenius plot of the quantity on the left-hand side of the latter equation can be expected to yield the diffusion energy of methyl radicals. The results given in Table II, however, do not give a linear plot, indicating that such a treatment is too crude.

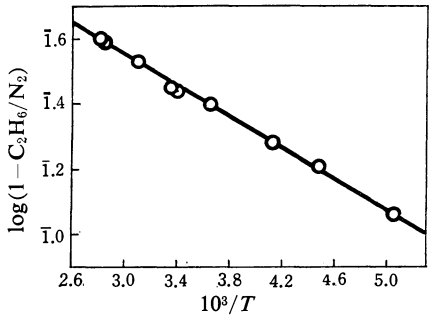


Fig. 4. Arrhenius plot of $1-C_2H_6/N_2$.

As seen in Table II and Fig. 2, the material balance referring to methane and ethane, $((1/2)CH_4+C_2H_6)/N_2$, is nearly 100% below room temperature but slightly falls off at higher temperatures. As has been proposed in the gas phase, the loss in the material balance may be ascribed to addition reactions of methyl radicals such as reactions 9 and 11.

There have been found a number of compounds similar to azomethane in that three fragments are formed by the decomposition of a substrate molecule. Some examples are acetone[18], ethyl methyl ketone[19], diethyl ketone[19], acetyl peroxide[3], butyryl peroxide[4] and dimethyl mercury[20]. None of them, however, have been reported to show such a large cage effect as has been found in the present work. The reason why azomethane behaves exceptionally probably comes from the way in which it decomposes. As has been already described, in the case of azomethane two methyl radicals and a nitrogen molecule are formed almost simultaneously, while in other cases, the decomposition of a substrate molecule probably occurs more clearly in two stages:

$$XYZ \rightarrow XY+Z$$
$$XY \rightarrow X+Y$$

If, therefore, the lifetime of the XY radical is sufficiently large[21], it will become separated from the radical Z before decomposition, and the cage combination $X+Z \rightarrow XZ$ will not be observed. It may still be expected in this case that the recombination $XY+Z \rightarrow XYZ$ takes place in the solvent cage and that this will result in a lowering of the quantum yield, as has been found in the present work. However, such a cage recombination cannot be estimated from quantum yields unless the deactivation of excited substrate molecules is proven to be absent.

18) R. Pieck and E. W. R. Steacie, *Can. J. Chem.*, 33, 1304 (1955); D. B. Peterson and C. J. Mains, *J. Am. Chem. Soc.*, 81, 3510 (1959).
19) P. Ausloos, *Can. J. Chem.*, 36, 400 (1958).
20) D. H. Derbyshire and E. W. R. Steacie, ibid., 32, 457 (1954).
21) It takes a time of the order of 10^{-11} sec. at ordinary temperatures for the two solute molecules enclosed together in a solvent cage to become separated from each other, provided that they do not react with each other (R. M. Noyes, *J. Am. Chem. Soc.*, 77, 2042 (1955)).

Summary

Azomethane in *n*-hexane solution has been decomposed by irradiation of 366 mμ over the temperature range -75 to 80°C, in order to study the effect of the solvent cage on the photolysis. The main products have been found to be nitrogen, methane and ethane. The yield of methane increases, but that of ethane, which amounts to 88% of nitrogen at -75°C, decreases with the rise in temperature. The addition of styrene as a scavenger for methyl radicals in an increasing amount suppresses the formation of methane almost completely, while that of ethane is not affected, indicating that ethane is exclusively formed by the cage combination of an azomethane molecule. The formation of methane is explained by the abstraction of the hydrogen atom from a solvent molecule by methyl radicals that have escaped the original cage. The material balance represented as $((1/2)CH_4+C_2H_6)/N_2$ is nearly 100% below room temperature, but it falls off slightly at higher temperatures; this may be ascribed to addition reactions of methyl radicals. The quantum yield of photolysis is apparently smaller than unity and falls off with a lowering of the temperature; this probably arises from the cage recombination of the initially formed pair of radicals CH_3N_2 and CH_3, though the former radical is very short-lived.

The present author is particularly indebted to Professor Osamu Toyama of the College of Engineering for his discussions and encouragement during this investigation. The author wishes also to thank Mr. Yoshiaki Nishimoto for his assistance.

Department of Applied Chemistry
College of Engineering
University of Osaka Prefecture
Sakai, Osaka

Studies of the Cage Effect of Solvent. II. Photolysis of Azomethane in Various Solvents

By Sukeya KODAMA

(Received August 31, 1961)

It has been reported in a previous paper[1] that ethane, a major product in the photolysis of azomethane in *n*-hexane, is formed exclusively by the combination of a pair of methyl radicals resulting from the substrate molecule in the solvent cage. The photolysis of azomethane in solution thus provides a good example of the cage effect that can be studied quantitatively.

This paper reports the results of a series of experiments carried out to investigate the dependence of the above cage combination of methyl radicals on the nature of the solvent. The solvents selected were *n*-octane, ethanol, ethyl acetate and toluene. They are widely different from each other in molecular structure and in property, and all of them are transparent to the 366 mμ used for the photolysis.

Experimental

The preparation, purification and storage of azomethane have previously been described[1]. *n*-Octane was prepared from *n*-butyl bromide by the Wurts reaction and purified in a way similar to that described for *n*-hexane. Ethanol, ethyl acetate and styrene, used as a scavenger of methyl radicals, were all taken from commercial samples of a special high grade and were used without further purification. Toluene, also obtained from a commercial sample, was boiled with anhydrous aluminium chloride, washed with water, repeatedly shaken with concentrated sulfuric acid until the latter was not colored, washed with a solution of sodium carbonate and with water, dried over calcium chloride and phosphorus pentoxide, and distilled. All the solvents thus obtained were subjected to thrice repeated vacuum distillation each time before use.

The apparatus and procedure were similar to those previously described[1]. A mercury line of 366 mμ was used for the photolysis throughout the whole series of experiments. The extent of conversion in each run was usually less than 4%. In the experiments with toluene it was less than 7%. The concentration of azomethane in each run was fixed at about 3×10^{-2} mol./l., because the previous study showed little dependence of yields of products on the substrate concentration. The volume of the solution in each experiment was adjusted so that it just filled the reaction cell of ca. 10 ml. capacity at the experimental temperature.

1) S. Kodama, This Bulletin, 35, 652 (1962).

Results

Tables I—IV and Figs. 1 and 2 show the results obtained. CH_4/N_2 and C_2H_6/N_2 represent the yields of methane and ethane respectively, since the number of moles of nitrogen formed is equal to that of the azomethane decomposed. $((1/2)CH_4+C_2H_6)/N_2$ gives the material balance referring to methane and ethane.

Figure 3 shows the apparent quantum yields obtained by comparing the rate of formation of nitrogen in a given solution with that in *n*-hexane solution, for which the apparent quantum yield is already known[1].

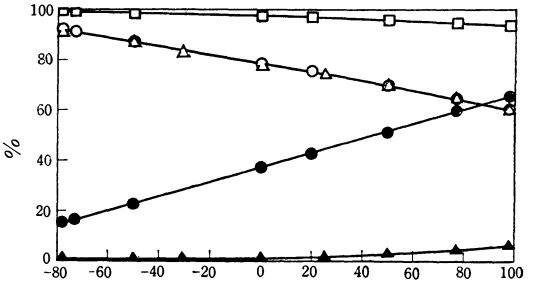


Fig. 1. Effect of temperature on yields of methane and ethane, and material balance in ethyl acetate. ○, C_2H_6/N_2; △, $(C_2H_6/N_2)_S$; ●, CH_4/N_2; ▲, $(CH_4/N_2)_S$; □, $((1/2)CH_4+C_2H_6)/N_2$

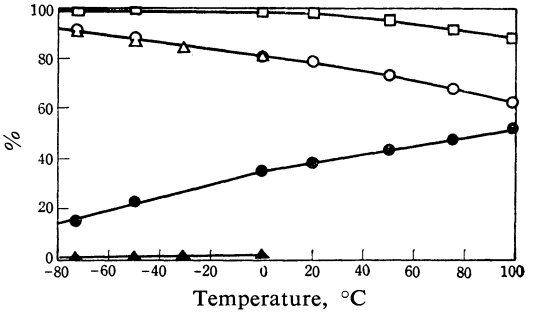


Fig. 2. Effect of temperature on yields of methane and ethane, and material balance in toluene. ○, C_2H_6/N_2; △, $(C_2H_6/N_2)_S$; ●, CH_4/N_2; ▲, $(CH_4/N_2)_S$; □, $((1/2)\cdot CH_4+C_2H_6)/N_2$

TABLE I. PHOTOLYSIS OF AZOMETHANE IN ETHYL ACETATE

Temp. °C	$[C_6H_5C_2H_3]/[CH_3COOC_2H_5]$ %	Time of irradiation min.	Rate of formation $\times 10^{10}$ mol. sec^{-1}			CH_4/N_2 %	C_2H_6/N_2 %	$(1/2)CH_4+C_2H_6/N_2$ %
			R_{N_2}	R_{CH_4}	$R_{C_2H_6}$			
98	0	60	35.0	23.0	21.3	65.8	60.7	93.9
98	2.42	60	32.1	2.00	19.4	6.22	60.6	
77	0	54	31.8	19.0	20.6	59.8	64.8	94.7
77	2.42	72	35.4	1.52	22.9	4.30	64.7	
50	0	60	22.8	11.7	15.9	51.2	69.8	95.9
50	2.42	78	26.0	0.69	18.2	2.65	70.0	
25	2.42	72	19.6	0.29	14.7	1.50	74.8	
20	0	60	17.2	7.37	13.0	42.8	75.7	97.1
0	0	60	27.0	10.2	21.3	37.6	78.8	97.6
0	2.42	72	28.3	0.28	22.0	1.0	77.8	
−31	2.42	78	18.2	0.15	15.1	0.8	83.0	
−50	0	90	15.1	3.41	13.1	22.6	87.0	98.3
−50	2.42	90	13.3	0.09	11.5	0.7	86.6	
−73	0	120	2.42	0.40	2.20	16.4	91.0	99.2
−78	0	120	9.04	1.36	8.31	15.1	92.0	99.6
−78	2.42	120	9.55	0.07	8.65	0.7	90.6	

TABLE II. PHOTOLYSIS OF AZOMETHANE IN ETHANOL

Temp. °C	$[C_6H_5C_2H_3]/[C_2H_5OH]$ %	Time of irradiation min.	Rate of formation $\times 10^{10}$ mol. sec^{-1}			CH_4/N_2 %	C_2H_6/N_2 %	$(1/2)CH_4+C_2H_6/N_2$ %
			R_{N_2}	R_{CH_4}	$R_{C_2H_6}$			
78	0	72	16.2	9.05	11.3	55.8	70.0	97.9
50	0	90	15.9	7.83	11.8	49.2	74.1	98.7
20	0	120	12.5	5.05	9.88	40.4	79.0	99.2
0	0	60	17.7	6.38	14.4	36.0	81.5	99.5
0	1.42	108	17.1	0.58	13.9	3.4	81.2	
−31	1.42	102	11.3	0.23	9.68	2.0	85.7	
−50	0	60	8.93	2.09	7.88	23.4	88.2	99.9
−50	1.42	108	9.02	0.17	8.00	1.9	88.7	
−68	1.42	66	7.07	0.12	6.41	1.7	90.7	
−73	0	120	7.92	1.44	7.20	18.2	90.8	99.9

TABLE III. PHOTOLYSIS OF AZOMETHANE IN TOLUENE

Temp. °C	$[C_6H_5C_2H_3]/[C_6H_5CH_3]$ %	Time of irradiation min.	Rate of formation $\times 10^{10}$ mol. sec^{-1}			CH_4/N_2 %	C_2H_6/N_2 %	$(1/2)CH_4+C_2H_6/N_2$ %
			R_{N_2}	R_{CH_4}	$R_{C_2H_6}$			
98.5	0	48	37.0	19.3	23.1	52.2	62.5	88.6
75	0	48	32.1	15.4	21.8	47.9	67.9	91.9
50	0	54	29.9	13.1	22.0	43.9	73.5	95.5
20	0	54	25.8	9.96	20.4	38.6	79.0	98.3
0	0	60	42.9	15.2	34.7	35.4	81.0	98.7
0	2.55	60	41.2	0.86	33.1	2.1	80.3	
−31	2.55	60	30.2	0.42	25.4	1.4	84.0	
−50	0	60	23.3	5.36	20.6	23.0	88.4	99.9
−50	2.55	60	23.3	0.28	20.0	1.2	86.4	
−73	0	180	21.6	3.26	19.8	15.1	91.6	99.2
−73	2.55	90	17.2	0.21	15.6	1.2	90.8	

TABLE IV. PHOTOLYSIS OF AZOMETHANE IN *n*-OCTANE

Temp. °C	Time of irradiation min.	Rate of formation $\times 10^{10}$ mol. sec^{-1}			$\frac{CH_4}{N_2}$	$\frac{C_2H_6}{N_2}$	$\frac{(1/2)CH_4+C_2H_6}{N_2}$
		R_{N_2}	R_{CH_4}	$R_{C_2H_6}$	%	%	%
98	42	45.8	32.1	26.7	70.2	58.3	93.4
75	42	42.2	26.5	26.8	62.8	63.5	95.0
50	48	39.7	21.5	27.5	54.2	69.3	96.5
25	48	33.4	15.4	25.1	46.0	75.1	98.1
0	60	27.9	10.0	22.3	36.0	80.1	98.6
−25	60	27.9	8.13	23.6	29.1	84.5	99.0
−50	72	25.7	5.14	22.9	20.0	89.2	99.2

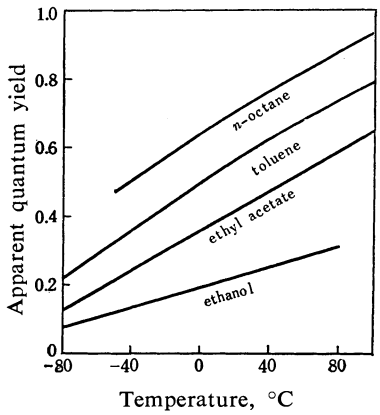


Fig. 3. Dependence of apparent quantum yield on temperature in various solvents.

Discussion

A comparison of the results given in Tables I—IV and Figs. 1 and 2 with those obtained with *n*-hexane[1] shows that the main feature of the photolysis is not affected by the nature of the solvent. Hence, on similar grounds to those previously given, the formation of the main products, i. e., nitrogen, methane and ethane, may be represented as:

$$(CH_3)_2N_2+h\nu \rightarrow [2\,CH_3+N_2] \quad (1)$$

$$[2\,CH_3+N_2] \rightarrow C_2H_6+N_2 \quad (2)$$

$$\rightarrow CH_3+N_2+CH_3 \quad (3)$$

$$CH_3+HR \rightarrow CH_4+R \quad (4)$$

where the parenthesis denotes the solvent cage and HR, the solvent. The hydrogen atom abstraction from azomethane molecules by methyl radicals may be far less important compared to reaction 4. Again, the loss in the material balance, $1-((1/2)CH_4+C_2H_6)/N_2$, may be ascribed to addition reactions such as

$$CH_3+(CH_3)_2N_2 \rightarrow (CH_3)_3N_2 \quad (5)$$

$$CH_3+R \rightarrow CH_3R \quad (6)$$

and the suppression of the formation of methane by styrene to

$$CH_3+S \rightarrow CH_3S \quad (7)$$

where S represents styrene.

As seen in Fig. 3, the quantum yield falls off with a lowering of the temperature in all the solvents investigated; this phenomenon may be ascribed to the recombination of a pair of initially formed radicals, CH_3N_2 and CH_3, in the solvent cage, as previously inferred for the *n*-hexane solution. What the different apparent values of the quantum yield shown in the figure have resulted from cannot be answered for the present. It may be that the absorption curve of azomethane in solution is different from solvent to solvent, but measurements of this have not yet been reported. It may, however, be noted that these apparent quantum yields have some correlation with the dipole moments of the solvents. The latter values are 0(*n*-octane), 0.4(toluene), 1.70 (ethanol) and 1.74 *D*(ethyl acetate); in Fig. 3 the apparent quantum yield increases in reverse order, except for ethanol. The apparent quantum yields in *n*-hexane[1], *n*-octane and cyclohexane[2], whose dipole moments are all zero, have been found to be almost identical at all the temperatures investigated. Ethanol, which apparently gives an exceptionally low quantum yield, is well-known by its tendency to form the hydrogen bond. A comparison of the results given in Tables I—IV with those previously obtained with *n*-hexane shows that the yield of ethane and its dependence on the temperature are rather insensitive to the nature of the solvent. As shown in Fig. 4, the results obtained with various solvents can all be represented by an empirical formula

$$1-C_2H_6/N_2=A\exp(-E/RT)$$

which has been previously found to be applicable to the results obtained with *n*-hexane. The values of the constants *A* and *E* determined from these plots are given in Table V, together with those for *n*-hexane[3]. It is seen that the

2) S. Kodama, ibid., to be published.

3) Although the quantity $1-C_2H_6/N_2$ represents the fraction of methyl radicals that escaped the solvent cage, the constant *E* cannot be taken as the diffusion energy of methyl radicals in solution, as was pointed out in the previous paper.

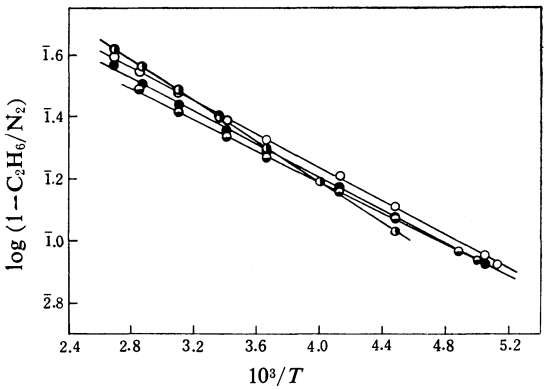


Fig. 4. Arrhenius plots of $1-C_2H_6/N_2$. ○, ethyl acetate; ◒, ethanol; ●, toluene; ◑, *n*-octane.

TABLE V. VALUES OF ARRHENIUS CONSTANTS OBTAINED FROM FIG. 4

Solvent	A	E kcal./mol.
Ethyl acetate	2.22	1.29
Ethanol	1.48	1.12
Toluene	1.90	1.24
n-Octane	2.40	1.51
n-Hexane	2.08	1.17

dependence of the constants A and E on the nature of the solvent is rather small, as has been stated above.

The yield of methane shows a somewhat greater dependence on the nature of the solvent. As has already been described, the values of the material balance $((1/2)CH_4+C_2H_6)/N_2$ show that a small fraction of the methyl radicals is probably lost by addition reactions. Consequently, the greater the number of methyl radicals lost in this way, the lower is the yield of methane. Table III and Fig. 2 show that the relatively low yield of methane above room temperature in the case of toluene arises from a relatively large loss of methyl radicals, which loss may be ascribed to the contribution of the addition of methyl radicals to toluene molecules taking place in this case in addition to those already given. On the other hand, the relatively low yields of methane found with ethanol result from relatively high yields of ethane and not from enhanced addition reactions.

In the presence of styrene as a scavenger, it competes with the solvent for methyl radicals. Accordingly, it follows in the steady state that

$$k_7/k_4=R_{CH_3S}/R_{CH_4}\cdot[HR]/[S]$$

where R's denote respective rates and k's, rate constants. The ratio R_{CH_3S}/R_{CH_4} is obtained by

$$R_{CH_3S}/R_{CH_4}=[(CH_4/N_2)_0-(CH_4/N_2)_S]/(CH_4/N_2)_S$$

where $(CH_4/N_2)_S$ represents the yield of methane in the presence of styrene and $(CH_4/N_2)_0$, that in its absence. Consequently,

$$k_7/k_4=[(CH_4/N_2)_0-(CH_4/N_2)_S]/(CH_4/N_2)_S\cdot[HR]/[S]$$

If, therefore, the rate constant k_4 is known, k_7 is obtained from the observed values of $(CH_4/N_2)_0$ and $(CH_4/N_2)_S$. This is the same principle as that applied by Szwarc[4] to determine the methyl affinities of various compounds in the thermal decomposition of acetyl peroxide.

For the solvents here investigated, exact Arrhenius expressions of k_4 are unknown, but they are expected to have similar activation energies. Figure 5 shows the Arrhenius plots of k_7/k_4 for the results obtained with ethyl acetate and with *n*-hexane[1]. The two plots are parallel to each other and, accordingly, give the same value of 3.2 kcal./mol. for E_4-E_7. The value of E_4 for *n*-hexane is reported as 8.1 kcal./mol.[5] E_7 is therefore obtained as 4.9 kcal./mol.

Figure 5 shows that the frequency factor of the hydrogen atom abstraction from *n*-hexane molecules by methyl radicals is about four times as great as that for ethyl acetate. This can be explained if secondary hydrogen atoms are preferentially abstracted, since the ratio of the number of secondary hydrogen atoms in the two kinds of molecule is just four[6].

The value of 3.2 kcal./mol. found above for

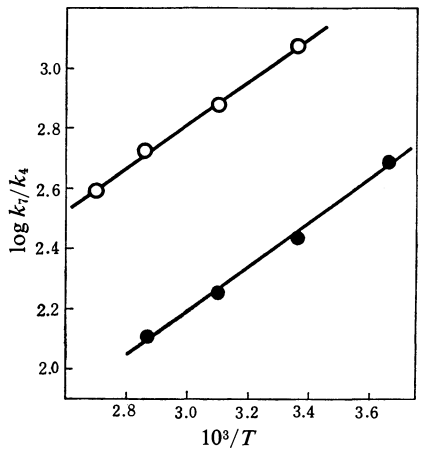


Fig. 5. Arrhenius plots of k_7/k_4 for the results obtained with ethyl acetate and *n*-hexane. ○, ethyl acetate; ●, *n*-hexane.

4) M. Levy and M. Szwarc, *J. Chem. Phys.*, **22**, 1621 (1954); *J. Am. Chem. Soc.*, **77**, 1949 (1955).

5) A. F. Trotman-Dickenson, J. R. Birchard and E. W. R. Steacie, *J. Chem. Phys.*, **19**, 163 (1951).

6) It has been found that the rate of hydrogen atom abstraction by methyl radicals depends on the nature of the hydrogen atom abstracted, and, in general, the order of the reactivity of hydrogen atoms is tertiary>secondary >primary (R. K. Brinton, *Can. J. Chem.*, **38**, 1339 (1960)).

E_4—E_7 is in good agreement with the result obtained by Szwarc[7] with isooctane. However, the reported values of the ratio of rate constants k_7/k_4 in the latter case are higher than those for ethyl acetate shown in Fig. 5. This is contrary to what would be expected, since the isooctane molecule has a tertiary hydrogen atom in addition to as many secondary hydrogen atoms as the ethyl acetate molecule. The reason for this discrepancy is not clear.

Summary

The photolysis of azomethane in *n*-octane, toluene, ethyl acetate and ethanol has been investigated over the temperature range from about −80 to 100°C. The results obtained are very similar to those previously obtained with *n*-hexane and show that, also in these solvents, the ethane, one of the main products, exclusively results from the combination in the solvent cage of a pair of methyl radicals formed from an azomethane molecule. For all the solvents investigated, the temperature dependence of the yield of ethane referred to nitrogen formed, C_2H_6/N_2, can be represented by an empirical expression, $1-C_2H_6/N_2 = A\exp(-E/RT)$, with constants A and E, whose values are rather insensitive to the nature of the solvent. From the reduction of the yield of methane in the presence of styrene, the activation energy of the addition of methyl radicals to styrene molecules is estimated as 4.9 kcal./mol. Apparent quantum yields obtained by comparing the rates of formation of nitrogen fall off with a lowering of the temperature in all the solvents investigated.

The present author is particularly indebted to Professor Osamu Toyama of the College of Engineering for his discussions and encouragement during this investigation. The author wishes also to thank Mr. Katsuji Makino for his assistance.

Department of Applied Chemistry
College of Engineering
University of Osaka Prefecture
Sakai, Osaka

7) M. Feld and M. Szwarc, *J. Am. Chem. Soc.*, **82**, 3791 (1960).

On the Mechanism of Pulp Bleaching. V. Further Investigations on the Residual Lignosulfonic Acid in Unbleached Sulfite Pulp*

By Koichiro SATO, Akio KOBAYASHI and Hiroshi MIKAWA

(Received February 20, 1961)

The residual lignosulfonic acid in unbleached spruce (*Picea jezoensis*) sulfite pulp has previously been partly dissolved out by intensive beating of the fiber in water[1]. Nearly 20% of the total amount of the residual lignosulfonic acid was thus isolated as barium salt in a pure state and analyzed. The material was isolated from the beating water obtained after beating the fiber until no lignin dissolved. In the present communication the beating of the fiber is described step by step. The paper also tells how the residual lignosulfonic acids dissolved during each step were isolated separately and analyzed to see if any differences exist between these fractions.

As has been reported previously[1], the residual lignosulfonic acid remaining undissolved in the beaten pulp was extracted further by dimethyl sulfoxide together with carbohydrate. It was confirmed that no chemical linkages exist between the two components. This residual lignosulfonic acid was prepared in a pure state and analyzed. Nitrobenzene oxidation of the residual lignosulfonic acids obtained by beating and by dimethyl sulfoxide extraction is described in the present communication, and the yields of vanillin obtained both from these residual lignosulfonic acids and from ordinary α-lignosulfonic acid separated from waste liquor are compared.

The authors also attempt to compare the amount of lignin extracted by beating and by dimethylsulfoxide with the amount of lignin remaining in the pulp undissolved by these processes.

* Presented in part at the Third Lignin Symposium of Japan, November, 1958.

1) K. Sato and H. Mikawa, This Bulletin, **35**, 477 (1962); ibid., **31**, 660 (1958); K. Sato, A. Kobayashi and H. Mikawa, ibid., **35**, 483 (1962).

Step by Step Dissolution of Residual Lignin from Soft Wood Unbleached Sulfite Pulp

Emerton reported[2] that the fibrillation of the fiber begins at the so-called P and S_1 layers when the pulp is beaten by an ordinary beater, and proceeds gradually to the inner layer of the fiber. The fiber is fibrillated first to fibrils and then to microfibrils. It is therefore expected that the residual lignosulfonic acid dissolved in the early stage of the beating comes more or less from the outer layer of the fiber cell wall, perhaps from the P and S_1 layers, and from the rather coarse fibrils; on the other hand, that dissolved in the later stage of the beating is from the S_2 and S_3 layers or from fine fibrils.

Unbleached sulfite pulp prepared from *Picea jezoensis* and *Abies mariana* (3 : 1, 1500 g.) was beaten, just as has been reported previously, changing the beating water at appropriate intervals, and six fractions of the residual lignosulfonic acid were prepared (Table I). The first four fractions thus obtained were analyzed for sulfur, sulfonic acid sulfur, and methoxyl. The total amount of the phenolic hydroxyl group was estimated by the so-called $\Delta\varepsilon$-method[3]. Types I and II phenolic hydroxyl groups and carboxyl group were estimated as usual by a combination of conductometric titration and the ultraviolet absorption spectra[4]; the results of the analyses are shown in Table II. Here, the values of the functional groups are shown on a methoxyl basis, as it is already clear from the previous communication[1] that the number of methoxyl groups per C_9-unit is approximately one. Not much variation was observed throughout these fractions. The average of the analytical values shown in the lower part of the table is calculated from the analytical values and the yield of the fractions.

Table I. Yields of the fractions of the residual lignosulfonic acid prepared by step by step beating of the unbleached sulfite pulp from spruce and fir

Fract. No.	SR values of beaten pulp and beating time.	Optical density of beating water at 280 mμ*	Yield of barium lignosulfonate g.
1	50	1.10	2.8
2	70	—	3.5
3	92	1.30	4.5
4	5 hr. more	0.80	3.2
5	5 hr. more	0.34	—**

* Without any dilution.
** Lignin was not separated.

Nitrobenzene Oxidation of the Residual Lignosulfonic Acid Isolated from Unbleached Sulfite Pulp

Among the many reactions of lignin which are used to discover differences in the structure of lignins, ethanolysis and nitrobenzene oxidation are very well studied and are very often used. As has been already reported[1], the amount of the type I phenolic hydroxyl group of the residual lignosulfonic acid is lower than that of ordinary α-lignosulfonic acid separated from the waste liquor, suggesting the existence of some difference in nuclear structure between these two lignosulfonic acid preparations.

Table II. Analyses of the fractions of the residual lignosulfonic acid prepared by step by step beating of the unbleached sulfite pulp from spruce and fir

Fract. No.	Total S %	SO_3H S %	CH_3O %	$\frac{SO_3H}{CH_3O}$	$\frac{\text{weak acid}}{CH_3O}$	$\frac{OH^*}{CH_3O}$	$\frac{\text{Type I } OH^*}{CH_3O}$	$\frac{\text{Type II } OH^*}{CH_3O}$	$\frac{COOH}{CH_3O}$	Type I OH* / Type II OH*
1	4.37	3.7	11.4	0.32	0.17	0.21 −0.17	0.04 −0.03	0.17 −0.14	0.14 −0.13	1/4
2	3.54	3.8	11.3	0.32	0.21	0.24 −0.19	0.07 −0.05	0.17 −0.14	0.16 −0.14	1/2.5
3	3.67	3.4	11.8	0.29	0.14	0.22 −0.16	0.04 −0.03	0.18 −0.13	0.11 −0.10	1/4
4	3.78	3.6	11.7	0.31	0.12	0.21 −0.17	0.04 −0.03	0.17 −0.14	0.09 −0.08	1/4
Aver.			11.5	0.31		0.22 −0.17	0.05 −0.04	0.18 −0.12	0.12 −0.11	1/3

Percentage is for barium salt.

2) H. W. Emerton, *TAPPI*, **40**, 542 (1957).
3) G. A. Erdtman, *Svensk Papperstidn.*, **55**, 745 (1952).
4) H. Mikawa, K. Sato, T. Takasaki and K. Ebisawa, This Bulletin, **28**, 653 (1955).

The authors have therefore attempted to see if any difference can be observed in vanillin yields when nitrobenzene oxidation is applied to ordinary α-lignosulfonic acid (from sulfite waste liquor), to residual lignosulfonic acid separated from the unbleached sulfite pulp (by beating), and to that separated by dimethyl sulfoxide extraction of the beaten sulfite unbleached pulp. The nitrobenzene oxidation of the lignin was performed according to Stone's micro method[5]; the results are shown in Table III.

TABLE III. YIELDS OF VANILLIN OBTAINED BY NITROBENZENE OXIDATION OF ORDINARY α-LIGNOSULFONIC ACID, OF RESIDUAL LIGNOSULFONIC ACIDS EXTRACTED BY BEATING AND OF THAT EXTRACTED WITH DIMETHYL SULFOXIDE

	CH_3O% (Ba-salt)	Yield of vanillin % (methoxyl basis)	Aver.
α-Lignosulfonic acid	11.4	26.4 25.8	26.1
Residual lignosulfonic acid (beating)	10.8	28.6 24.0	26.3
Residual lignosulfonic acid (dimethyl sulfoxide)	11.8	26.2 24.8	25.5

As can be seen from Table III, there is not much difference in the yields of vanillin from these lignin preparations. It is well known that ether linkages in lignin at position 4 are cleaved by nitrobenzene oxidation. Leopold[6] reports that acetoguaiacyl-dihydrodehydro-di-isoeugenol and octahydro-tri-(acetoguaiacyl)-acetoguaiacon methyl ether give vanillin by nitrobenzene oxidation in a yield of 60~80% of the theoretical. Purves[7] and Pew[8] recognized the formation of a considerable amount of vanillin from a veratryl type structure.

Probably not such a large difference exists between the etherified structural units of the lignosulfonic acids separated from the waste liquor and from unbleached sulfite pulp to give different vanillin yields, although the amount of the type I phenolic hydroxyl group in the former acid is a little higher than that in the latter acid, as has been stated previously.

5) J. E. Stone and M. J. Blundell, *Anal. Chem.*, **23**, 771 (1951).
6) B. Leopold, *Acta Chem. Scand.*, **4**, 1523 (1950).
7) W. J. Brickman and C. B. Purves, *J. Am. Chem. Soc.*, **75**, 4336 (1953).
8) J. C. Pew, ibid., **77**, 2831 (1952).
9) P. Q. Bethge, G. Gran and K. E. Ohlsson, *Svensk Papperstidn.*, **55**, 44 (1952).

On the Lignin Balance in the Beating and Extraction with Dimethyl Sulfoxide of Unbleached Sulfite Pulp

The lignin balance in the beating of unbleached sulfite pulp in water and its extraction with dimethyl sulfoxide was determined by measuring the amount of the residual lignosulfonic acid remaining unextracted in the pulp. Twenty-seven grams of unbleached sulfite pulp (*Picea jezoensis*+*Abies mariana* 3:1) were beaten in a Lampen mill for about 40 hr. with 800 ml. of water. A small amount of beaten pulp was, with a little water, taken out from the mill six times during the beating. The pulp was filtered, and the water was diluted twelvefold and measured for ultraviolet absorption at 280 mμ, from which the amount of the dissolved lignosulfonic acid was calculated (Fig. 1). The pulp was suspended in alcohol and filtered with a fine glass filter to make an extremely thin paper. Ten milligrams of the thin paper thus prepared were shaken with 25 ml. of 85% phosphoric acid (free from ultraviolet absorption near 280 mμ) for 12 hr. in a 50 ml. glass tube[9], and the ultraviolet absorption of the solution thus obtained was measured at 280 mμ (Fig. 2). As can be seen in Figs. 1 and 2, the absorption curves are typical for lignosulfonic acid, having a maximum and minimum at 280 and 260 mμ respectively. The values of the maximum optical density at 280 mμ of Figs. 1 and 2 are plotted in Fig. 3 against the duration

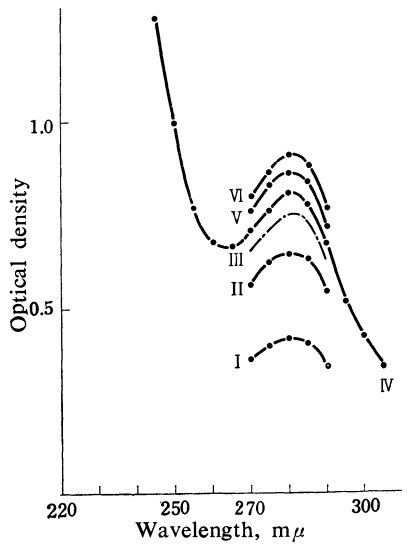


Fig. 1. Ultraviolet absorption curves of beating water obtained at various stages of beating. Curve I, absorption after beating 6 5/6 hr.; II, 20 1/3 hr; III, 25 2/3 hr.; IV, 30 2/3 hr.; V, 35 55/60 hr.; VI, 40 55/60 hr.

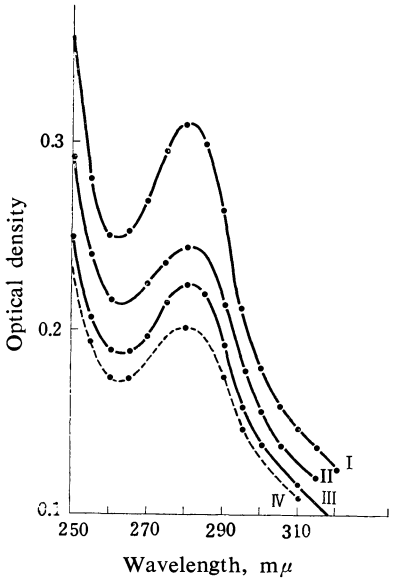


Fig. 2. Ultraviolet absorption curves of phosphoric acid solutions of beaten pulps. Curve I, original pulp; II, pulp beaten for 20 1/3 hr.; III, pulp beaten for 30 55/60 hr.; IV, pulp beaten for 30 55/60 hr. and extracted with dimethyl sulfoxide.

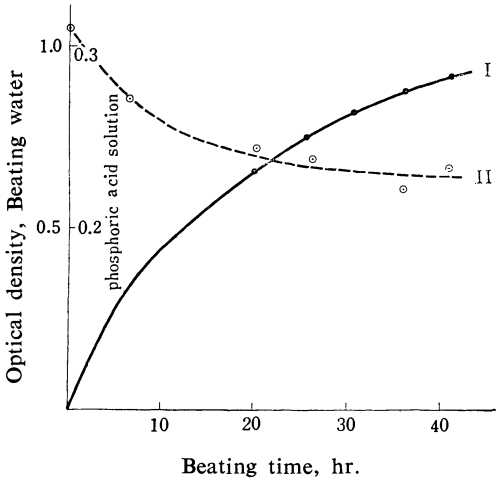


Fig. 3. Optical density at 280 mμ of beating water and phosphoric acid solution of beaten pulp at various stages of beating. Curve I; Beating water, measured after twelvefold dilution. Curve II; Phosphoric acid solution of beaten pulp. (10 mg. of the pulp in 25 ml. of 85% H_3PO_4)

of the beating. Curve I, the optical density of the beating water, continues to increase even after 40 hr., showing that the lignosulfonic acid continues to dissolve even after this time, although the rate of dissolution is small at this time. Curve II, showing the decrease of the ultraviolet absorption of the phosphoric

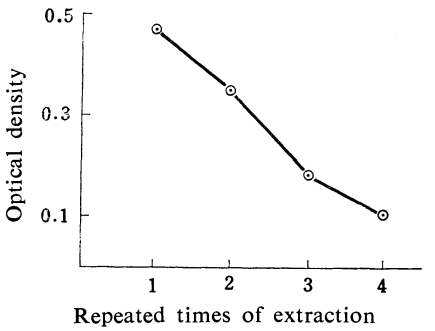


Fig. 4. Decrease of optical density at 280 mμ of dimethyl sulfoxide solutions from the first to fourth extractions of beaten pulp.

TABLE IV. LIGNIN BALANCE IN THE EXTRACTION OF UNBLEACHED SULFITE PULP BY BEATING AND BY DIMETHYL SULFOXIDE

	mmol. of CH_3O estimated by UV-absorption		%
	Remaining in pulp*1	Dissolved in solution*2	
Unbleached sulfite pulp used	6.52	—	100
Beating water*3	—	2.73	42
Beaten pulp	4.17	—	64
Dimethyl sulfoxide*4 solution	—	1.13	17
Extracted pulp*5	3.13	—	48

*1 Estimated from the ultraviolet absorption of the phosphoric acid solution of the pulp at 280 mμ.

*2 Estimated from the ultraviolet absorption of the solutions at 280 mμ.

*3 The yield of the residual lignosulfonic acid in this solution is 416 mg. when 27 g. of unbleached pulp are used.

*4 The yield of the dimethyl sulfoxide extract (residual lignosulfonic acid+carbohydrate) in this solution is 353 mg. when 27 g. of unbleached pulp are used.

*5 The mechanical loss of the pulp is about 8%.

acid solution, demonstrates that the rate of decrease of the residual lignosulfonic acid in the beaten pulp is very small after about 40 hr. Assuming the molar absorption coefficient of lignosulfonic acid per methoxyl group as 3200, the amounts of the residual lignosulfonic acid both dissolved and remaining undissolved in the pulp are calculated and listed in Table IV.

The pulp residue remaining after having been beaten for 40 hr. was separated by a centrifuge, washed successively with alcohol, ether and petroleum ether, and dried. The bone dry pulp thus obtained was defibrated by a Bauer

disk refiner and extracted with dimethyl sulfoxide (700 ml.) for 48 hr. with occasional shaking, centrifuged and extracted with the same amount of fresh dimethyl sulfoxide three times more. The ultraviolet absorption spectrum of the dimethyl sulfoxide solution thus obtained is characteristic of lignosulfonic acid, having a maximum and minimum at 280 and 265 mμ respectively; the values of maximum absorption at 280 mμ decrease as shown in Fig. 4 from the first extract to the fourth extract. The amount of the residual lignosulfonic acid in the combined dimethyl sulfoxide extract was estimated from the ultraviolet absorption, assuming the molar absorption coefficient of the lignin at 280 mμ as 3200 per methoxyl, and the residual lignosulfonic acid remaining in the pulp after dimethyl sulfoxide extraction was estimated from the ultraviolet absorption of the phosphoric acid solution of the pulp in just the same manner as has been described above. The results are summarized in Table IV, where the amounts of lignosulfonic acid are expressed in methoxyl group units.

As can be seen from the table, the amount of the residual lignosulfonic acid dissolved by beating is 42%, and the residual lignosulfonic acid remaining in the beaten pulp is 64% of the total amount of residual lignosulfonic acid which existed in the pulp. The amount dissolved by beating, calculated from the lignin remaining in pulp, 100−64=36%, is in good agreement with 42%. The total amount of residual lignosulfonic acid dissolved by beating and by dimethyl sulfoxide extraction is 42+17=59% of the total lignin which existed in the pulp, which is in good agreement with the dissolved amount calculated from the amount remaining undissolved in the extracted pulp, 100−48=52%.

Summary

1) By beating unbleached sulfite pulp step by step and changing the beating water, four fractions of residual lignosulfonic acids were obtained. Analytically not very distinct differences were observed between these fractions.

2) The residual lignosulfonic acids isolated by beating and by dimethyl sulfoxide were oxidized with nitrobenzene, and the yields of vanillin obtained from these lignin preparations were comparad with that from ordinary lignosulfonic acid separated from waste liquor. Almost no difference was observed.

3) The amounts of residual lignosulfonic acid dissolved by beating and by dimethyl sulfoxide extraction were in good agreement with those calculated from the amount of the residual lignosulfonic acid remaining in the pulp, thus proving the accuracy of the estimation. Approximately 40 and 20% of the total lignin in unbleached sulfite pulp were dissolved by beating and by dimethyl sulfoxide extraction respectively.

The authors wish to express their thanks to Professor Yoshikazu Hachihama for his encouragement, and also to the Kokusaku Pulp Ind. Co., Ltd., for permission to publish this paper.

Research Laboratory of the Kokusaku Pulp Ind. Co., Ltd.
Shinjuku-ku, Tokyo

*Thermodynamic Studies on Cobalt Complexes. X. Chemical Equilibrium between Aquopentamminecobalt(III) Complex and Oxalate Ion**

By Ryokichi TSUCHIYA

(Received August 7, 1961)

It was found in the preceding paper[1] of this series that, when the oxalate ion in the mixed solution of oxalic acid and potassium oxalate reacted with the diaquotetramminecobalt(III) ion, the oxalate ion coordinated as a bidentate ligand, producing an oxalatotetrammine cobalt-(III) ion. On the other hand, when ammonium oxalate reacted with the diaquotetramminecobalt(III) ion, an oxalatopentamminecobalt-(III) ion containing an oxalate inon as a unidentate ligand was produced. As is thus shown, the oxalate ion coordinates as a bidentate ligand in some cases and as a unidentate ligand in others.

* Read at the Symposium on Coordination Compounds of the Chemical Society of Japan, Sendai, September, 1960.

1) M. Mori, R. Tsuchiya and E. Matsuda, This Bulletin, **34**, 1761 (1961).

An oxalatopentamminecobalt(III) ion was also produced when the oxalate ion in the mixed solution of oxalic acid and potassium oxalate reacted with the aquopentamminecobalt-(III) ion.

In the present study, the chemical equilibrium between aquopentamminecobalt(III) and oxalate ions is examined spectrophotometrically, just as in the preceding paper[1], to find the thermodynamic properties of the oxalatopentamminecobalt(III) complex. By combining this result of the equilibrium with that between the diaquotetramminecobalt(III) and oxalate ions, the difference in the thermodynamic properties between the oxalatotetramminecobalt(III) and oxalatopentamminecobalt(III) ions, the former containing an oxalate ion as bidentate ligand and the latter as a unidentate ligand, is discussed.

Experimental

Aquopentamminecobalt(III) perchlorate was prepared by the method of Jörgensen[2]. When the buffer solution, consisting of oxalic acid and potassium oxalate, was added to the aqueous solution of aquopentamminecobalt(III) perchlorate at room temperature, the reaction did not take place, but it proceeded when the solution was heated to 65°C. It was found, as is shown below, by spectral and electric conductivity measurements that the reaction product was an oxalatopentamminecobalt(III) complex, in which the hydrogenoxalate ion was contained as a unidentate ligand.

The electric conductivity of the oxalatopentamminecobalt(III) complex in an aqueous solution was measured by a Yanagimoto Conductivity Outfit Model MY-7. The measurement of the equilibrium was made spectrophotometrically by using a Hitachi EPU 2-type spectrophotometer in the same way as in the case of the reaction between a diaquo-complex and an oxalate. The maximum of the first absorption band of aquopentamminecobalt(III) ion is at $\nu=61.6$ ($\log\varepsilon=1.62$)[3], while that of the oxalatopentamminecobalt(III) ion produced is at $\nu=59.2$ ($\log\varepsilon=1.87$)[4]. Since the equilibrium was shifted toward the aquo-complex, the measurement of the absorbancy was made at 490 mμ. A brown flask was used as the reaction vessel to prevent photodecomposition. The measurement of the pH of the solution at equilibrium was carried out with a Horiba HRL Model M pH meter.

Results

Figure 1 shows the absorption spectra of the solution at the equilibria of the reaction of aquopentamminecobalt(III) perchlorate at different concentrations with the buffer solution consisting of oxalic acid and potassium oxalate at different concentrations. The absorption spectra of aquopentamminecobalt(III) and oxalatopentamminecobalt(III) ions are also shown in this figure. It is presumed from this figure that the reaction product between aquopentamminecobalt(III) and oxalate ions is an oxalatopentamminecobalt(III) ion.

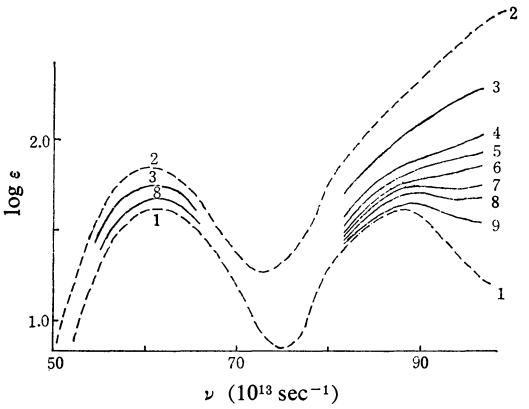


Fig. 1. The absorption spectra of the solution containing aquopentamminecobalt(III) perchlorate reacted with oxalate ion.
1. Aquopentamminecobalt(III) perchlorate only.
2. Oxalatopentamminecobalt(III) ion produced from the above reaction.

Initial concentration of cobalt(III) aquo-complex and that of oxalate ion are as follows respectively:
3. 1/500 F/*l*, 1/5 F/*l*
4. 1/200 F/*l*, 1/10 E/*l*
5. 1/300 F/*l*, 1/20 F/*l*
6. 1/300 F/*l*, 1/40 F/*l*
7. 1/300 F/*l*, 1/80 F/*l*
8. 1/300 F/*l*, 1/160 F/*l*
9. 1/600 F/*l*, 1/320 F/*l*

TABLE I. MOLECULAR CONDUCTANCES OF OXALATOPENTAMMINECOBALT(III) OXALATE AT DIFFERENT CONCENTRATIONS IN AN AQUEOUS SOLUTION AT 25°C

Values calcd. as $[Co(NH_3)_5HC_2O_4]C_2O_4$	Values calcd. as $[Co(NH_3)_5C_2O_4]_2C_2O_4$
$\Lambda_{200}=236.12$	$\Lambda'_{200}=472.24$
$\Lambda_{250}=247.84$	$\Lambda'_{250}=495.68$
$\Lambda_{500}=261.77$	$\Lambda'_{500}=523.54$
$\Lambda_{1000}=259.21$	$\Lambda'_{1000}=518.42$
$\Lambda_{2000}=274.28$	$\Lambda'_{2000}=548.56$

The number of the suffix in Λ and Λ' is the dilution, i.e., the volume of solution containing one gram molecule of solute.

In order to obtain information about the oxalatopentamminecobalt(III) complex, the electric conductivity of the complex oxalate solution was measured. The molecular conductances obtained are listed in Table I.

In this table, the values Λ and Λ' were

2) S. M. Jörgensen, *Z. anorg. Chem.*, **17**, 461 (1898).
3) Y. Shimura and R. Tsuchida, This Bulletin, **29**, 312 (1956).
4) R. Tsuchida, ibid., **13**, 388, 436 (1938).

calculated on the assumption that the oxalatopentamminecobalt(III) oxalate was formulated by $[Co(NH_3)_5HC_2O_4]C_2O_4$ and $[Co(NH_3)_5 \cdot C_2O_4]_2C_2O_4$ respectively. The former formula is reasonable for oxalatopentamminecobalt(III) oxalate, but the latter should be excluded, since A' is too large to be applied to the formula $[Co(NH_3)_5C_2O_4]_2C_2O_4$. Therefore, the reaction between the aquopentamminecobalt-(III) complex and the oxalate buffer is expressed by

$$[Co(NH_3)_5OH_2]^{3+}(aq.) + HC_2O_4^- = [CO(NH_3)_5HC_2O_4]^{2+}(aq.) + H_2O\ (l) \quad (1)$$

There also exist the following ionization equilibria in the solution:

$$H_2C_2O_2 \rightleftarrows H^+ + HC_2O_4^- \quad (2)$$

$$HC_2O_4^- \rightleftarrows H^+ + C_2O_4^{2-} \quad (3)$$

$$K_2C_2O_4 \rightleftarrows 2K^+ + C_2O_4^{2-} \quad (4)$$

The first and second dissociation constants of oxalic acid, K_1 and K_2, are given a follows:

$$K_1 = \frac{C_{H^+} \cdot C_{HC_2O_4^-}}{C_{H_2C_2O_4}} \quad (5)$$

$$K_2 = \frac{C_{H^+} \cdot C_{C_2O_4^{2-}}}{C_{HC_2O_4^-}} \quad (6)$$

where $C_{H_2C_2O_4}$, $C_{HC_2O_4^-}$, $C_{C_2O_4^{2-}}$ and C_{H^+} are respectively the concentrations of oxalic acid, the hydrogenoxalate ion, the oxalate ion and the hydrogen ion at equilibrium.

When the initial concentrations of oxalic acid and potassium oxalate are expressed by $C^\circ_{H_2C_2O_4}$ anc $C^\circ_{K_2C_2O_4}$, they are given by the sum of the concentration of the oxalatopentamminecobalt(III) ion, C_2, which is equal to the concentration of the hydrogenoxalate ion consumed by the aquo-complex and the concentrations of unionized oxalic acid, the hydrogenoxalate ion and the oxalate ion at equilibrium of reactions 1, 2, 3 and 4:

$$C^\circ_{H_2C_2O_4} + C^\circ_{K_2C_2O_4} = C_2 + C_{H_2C_2O_4} + C_{HC_2O_4^-} + C_{C_2O_4^{2-}} \quad (7)$$

By removing $C_{H_2C_2O_4}$ and $C_{C_2O_4^-}$ from Eqs. 5 and 6 respectively as below,

$$C_{H_2C_2O_4} = \frac{C_{H^+} \cdot C_{HC_2O_4^-}}{K_1}$$

and

$$C_{C_2O_4^{2-}} = \frac{K_2 \cdot C_{HC_2O_4^-}}{C_{H^+}}$$

by inserting them into Eq. 7, and by rearranging it, the following equation is obtained for the concentration of the hydrogenoxalate ion at equilibrium:

$$C_{HC_2O_4^-} = \frac{K_1 C_{H^+}(C^\circ_{H_2C_2O_4} + C^\circ_{K_2C_2O_4} - C_2)}{K_1 C_{H^+} + K_1K_2 + C^2_{H^+}} \quad (8)$$

If the concentrations of aquopentamminecobalt-(III) and water at equilibrium are expressed by C_1 and C_{H_2O} respectively, the equilibrium constant of reaction 1 is given as:

$$K_C = \frac{C_2 \cdot C_{H_2O}}{C_1 \cdot C_{HC_2O_4}} \quad (9)$$

The concentrations of the aquo-complex and the oxalato-complex, C_1 and C_2, at equilibrium are obtained by the observed absorbancy of the solution and the known molar extinction coefficients of the above two complexes[3,4] in the same way as in the preceding paper[1]. The dissociation constants are reported as $K_1 = 5.9 \times 10^{-2}$ [5] and $K_2 = 6.4 \times 10^{-5}$ [5]. By using these values in Eqs. 8 and 9, the apparent equilibrium constant, K_C, is calculated. The concentrations and the ionic strengths of each ion at equilibrium are given as follows:

	Concentration	Ionic strength
$[Co(NH_3)_5OH_2]^{3+}$	C_1	$9C_1/2$
$[Co(NH_3)_5HC_2O_4]^{2+}$	C_2	$4C_2/2$
$3\,ClO_4^-$	$3(C_1+C_2)$	$3(C_1+C_2)/2$
$HC_2O_4^-$	$C_{HC_2O_4^-}$	$C_{HC_2O_4^-}/2$
$C_2O_4^{2-}$	$K_2C_{HC_2O_4^-}/C_{H^+}$	$K_2 \cdot C_{HC_2O_4^-}/2\,C_{H^+}$
K^+	$2C^\circ_{K_2C_2O_4}$	$C^\circ_{K_2C_2O_4}$
H^+	C_{H^+}	$C_{H^+}/2$

The total ionic strength, μ, in the solution is calculated by

$$\mu = 6\,C_1 + 7\,C_2/2 + C_{HC_2O_4^-}/2 + K_2 \cdot C_{HC_2O_4^-}/2\,C_{H^+} + C^\circ_{K_2C_2O_4} + C_{H^+}/2 \quad (10)$$

The value obtained by pH measurement is not that of the hydrogen ion concentration, C_{H^+}, but that of the activity of hydrogen ion. Therefore, the calculations of Eqs. 8 and 10 were at first made by using this activity in place of the hydrogen ion concentration. The hydrogen ion concentration can be obtained by finding the activity coefficient[6] of the hydrogen ion in each ionic strength in the solution calculated by Eq. 10. The recalculations of Eqs. 8 and 10 were carried out by using the hydrogen ion concentration obtained above, and the apparent equilibrium constant, K_C, was calculated.

The results of the measurements and calculations are summarized in Table II.

The logarithm of the apparent equilibrium constant, K_C, is plotted against the aquare root of the ionic strength, μ, in Fig. 2. If it is assumed that this plotting gives a quadratic curve, the equation is calculated as:

$$\log K_C = 3.790\,\mu - 3.954\sqrt{\mu} + 3.428$$

The value of $\log K_C$ obtained by extrapolating this curve up to $\sqrt{\mu} = 0$ is given as:

$$\log K = 3.4$$

5) R. Gane and C. K. Ingold, *J. Chem. Soc.*, **1931**, 2153.
6) J. Kielland, *J. Am. Chem. Soc.*, **59**, 1675 (1937).

TABLE II. EQUILIBRIUM OF $[Co(NH_3)_5OH_2]^{3+}+HC_2O_4^-=[Co(NH_3)_5HC_2O_4]^{2+}+H_2O$, AT 25°C
MEASUREMENT OF EXTINCTION COEFFICIENT WAS MADE AT 490 mμ

Initial concn. of $[Co(NH_3)_5\cdot OH_2](C_2O_4)_3$ $C\times10^3$ F/l	Initial concn. of $H_2C_2O_4$ $C^\circ_{H_2C_2O_4}$ $\times10^2$ F/l	Initial concn. of $K_2C_2O_4$ $C^\circ_{K_2C_2O_4}$ $\times10^2$ F/l	ε*	$C_1\times10^3$ F/l	$C_2\times10^3$ F/l	pH	$K_C\times10^{-2}$	log K_C	$\mu\times10^2$	$\sqrt{\mu}$
1.667	0.250	0.250	43.8	1.532	0.135	3.32	11.350	3.055	1.484	0.1218
1.667	0.313	0.313	43.8	1.532	0.135	3.27	8.918	2.950	1.612	0.1270
1.667	0.417	0.417	44.6	1.480	0.187	3.20	9.482	2.977	1.809	0.1345
1.667	0.417	0.417	44.4	1.493	0.174	3.20	8.732	2.941	1.813	0.1347
1.667	0.500	0.500	45.0	1.454	0.212	3.18	9.083	2.958	1.968	0.1403
1.667	1.250	1.250	46.8	1.338	0.328	2.89	5.891	2.770	3.447	0.1857
3.333	1.250	1.250	47.4	2.600	0.734	2.68	6.893	2.838	4.355	0.2087
3.333	1.250	1.250	46.5	2.716	0.618	2.68	5.530	2.743	4.390	0.2095
1.667	2.500	2.500	49.2	1.184	0.483	2.79	4.874	2.688	5.876	0.2424
3.333	2.500	2.500	48.6	2.445	0.888	2.54	4.419	2.645	6.772	0.2602
1.667	5.00	5.00	51.0	1.068	0.598	2.66	3.343	2.524	10.744	0.3278
5.00	5.00	5.00	51.0	3.204	1.796	2.52	3.421	2.534	12.362	0.3516
5.00	10.00	10.00	53.0	2.819	2.181	2.44	2.366	2.374	21.883	0.4678
5.00	10.00	10.00	53.6	2.703	2.298	2.44	2.601	2.415	21.849	0.4728

* ε is the value corresponding to the molar extinction coefficient of the solution observed at equilibrium.

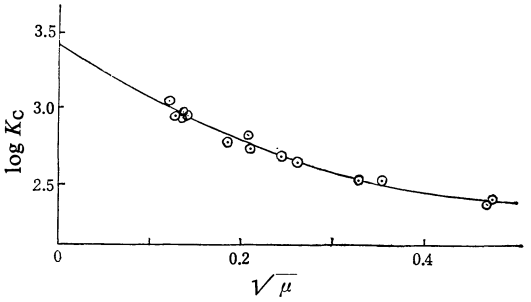


Fig. 2. The relationship between the logarithm of the equilibrium constant of the reaction of aquopentamminecobalt(III) complex with hydrogenoxalate ion, log K_C and the square root of the ionic strength of the solution, $\sqrt{\mu}$.

This is the thermodynamic equilibrium constant of the reaction between the aquopentamminecobalt(III) and hydrogenoxalate ions. The free energy change of the reaction is obtained as:

$$\Delta G^\circ_{298}=-4640 \text{ cal.}$$

Since the free energies of the formation of the aquopentamminecobalt(III) ion, the hydrogenoxalate ion and water in unit activity are known as −104.5 kcal.[7], −167.1 kcal.[8], and −56.69 kcal.[9] respectively, the free energy of the formation of the hydrogenoxalatopentamminecobalt(III) ion in unit activity is calculated as $\Delta G^\circ_{f298}=-219.6$ kcal.

7) A. B. Lamb and A. T. Larson, ibid., 42, 2038 (1920).
8) F. D. Rossini et al., "Selected Values of Chemical Thermodynamic Properties", United States Government Printing Office, Washington (1952), p. 120.
9) F. D. Rossini et al., ibid., p. 9.

Discussion

By using the free energies of the formation of the hydrogenoxalatopentamminecobalt(III) ion obtained above, and the oxalatotetramminecobalt(III) ion[1] and hexamminecobalt(III) ion[5] obtained in previous papers, the free energies of the following two reactions are calculated as:

$$[Co(NH_3)_6]^{3+}+HC_2O_4^- = [Co(NH_3)_5HC_2O_4]^{2+}+NH_3(aq.)$$
$$\Delta G^\circ_{298}=-4.37 \text{ kcal.}$$
$$[Co(NH_3)_5HC_2O_4]^{2+} = [Co(NH_3)_4C_2O_4]^{+}+NH_3(aq.)+H^+$$
$$\Delta G^\circ_{298}=-0.77 \text{ kcal.}$$

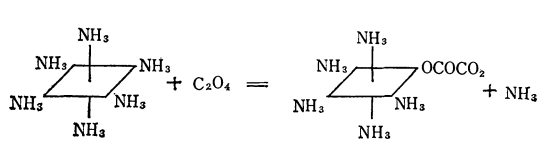
If it is assumed that the free energy required to drive off the hydrogen ion from the hydrogenoxalatopentamminecobalt(III) ion,

$$[Co(NH_3)_5HC_2O_4]^{2+}=[Co(NH_3)_5C_2O_4]^{+}+H^+$$

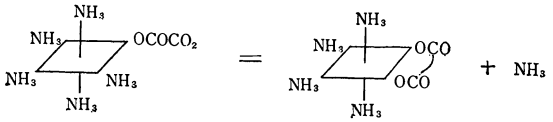
is approximately equal to the free energy change of the second dissociation constant of oxalic acid,

$$HC_2O_4^-=H^++C_2O_4^{2-} \qquad \Delta G^\circ_{298}=5.8 \text{ kcal.}$$

then the free energy and entropy changes of the following two reactions are obtained as below:



$\Delta G^\circ_{298}=-4.37$ kcal. $\Delta S^\circ=37.5$ e. u.



$\Delta G^{\circ}_{298} = -6.57$ kcal. $\Delta S^{\circ} = 44.9$ e. u.

The difference in the free energy changes between the two reactions, $\Delta = -2.2$ kcal., corresponds to the difference in those between the change when an oxalate ion coordinates as a unidentate ligand and that when the unidentate oxalate ion undergoes change to a bidentate. It gives a depression of the free energy owing to the formation of a chelate ring. In the same way, the difference in the entropy changes between the two reactions, $\Delta = 7.5$ e. u., gives the entropy effect in the formation of a chelate ring. It is concluded that the chelate effect, having hitherto been interpreted by the entropy effect, can also be applied to the formation of the chelate ring by an oxalate ion.

Summary

It was confirmed by absorption spectral and electric conductivity measurements that the product of the reaction of the aquopentamminecobalt(III) complex with an oxalate ion was a hydrogenoxalatopentamminecobalt(III) complex in which the oxalate ion was coordinated as a unidentate ligand. The equilibrium of the reaction,

$$[Co(NH_3)_5OH_2]^{3+} + HC_2O_4^- = [Co(NH_3)_5HC_2O_4]^{2+} + H_2O$$

was measured spectrophotometrically, by which method the free energy of formation of the hydrogenoxalatopentamminecobalt(III) ion was calculated.

On the basis of this value and the free energy of the formation of the oxalatotetramminecobalt(III) ion obtained in the preceding paper, the differences in free energy and entropy changes between the bidentate and unidentate oxalate ions were calculated. It was verified that the chelate effect of the oxalate ion was due to the entropy effect.

Department of Chemistry
Faculty of Science
Kanazawa University
Kanazawa

Oxidation Products of Hydroxylycoctonam

By Shozo YAMADA

(Received September 2, 1961)

In a previous paper[1], the author and others reported at length on some oxidation reactions of lycoctonine, but only brief descriptions were reported on the oxidation of hydroxylycoctonam (I), $C_{25}H_{39}O_9N$, with chromic acid. The present communication presents a further consideration of the structures of these oxidation products.

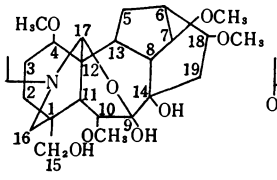
Recently Valenta[2] and, independently, Edwards et al.[3] have proposed the same α-ketol hemiketal structure (II) for hydroxylycoctonine on the basis of several items of experimental evidence.

When I was treated with alkali, there was produced a neutral product, hydroxyisolycoctonam (III), m. p. 185~188°C, $[\alpha]_D^{27}$ −18°, ν_{max}^{Nujol} 3425 (hydroxyl), 1717 (ketone), 1674 cm^{-1} (lactam) (Found: C, 60.62; H, 7.90. Calcd. for $C_{25}H_{39}O_9N$: C, 60.35; H, 7.90%.), and an acid (IV), m. p. 220~222°C, $[\alpha]_D^{34}$ −34°, ν_{max}^{Nujol} 3378, 2551 (hydroxyl), 1715, 1653 (carboxyl), 1587, 1567 cm^{-1} (lactam) (Found: C, 58.12; H, 8.12; OCH_3, 22.93. Calcd. for $C_{25}H_{41}O_{10}N$: C, 58.24; H, 8.01; 4 OCH_3, 24.08%). III was converted into IV by further treatment with alkali. As I has a tertiary α-ketol hemiketal system, the rearragement (I→III) could be expected to proceed in a manner analogous to that of the alkali isomerization of the cevine or germine series[4]. I, however, did not react with sodium bismuthate in acetic acid at room temperature, and when heated at 100°C it gave only a corresponding acetyl derivative. This inertness may be due to its tertiary α-ketol character under steric restriction. IV was proved to be a monocarboxylic acid, but it

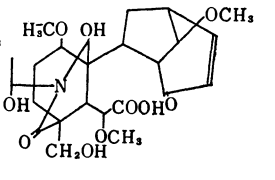
1) H. Suginome et al., This Bulletin, 32, 819 (1959).
2) Z. Valenta, *Chem. & Ind.*, 1959, 633.
3) O. E. Edwards et al., *Can. J. Chem.*, 37, 1996 (1959).
4) S. M. Kupchan et al., *J. Am. Chem. Soc.*, 75, 5519 (1953); S. W. Pelletier and W. A. Jacobs, ibid., 75, 3248 (1953); L. F. Fieser et al., ibid., 76, 1200 (1954).

was not proved to have a ketone group or to lack any methoxyl group. It must be considered, therefore, that a cleavage would have proceeded at a bond either between C_9 and C_{14} or between C_9 and C_{10} without the formation of a ketone group. The author preferred to take the former for IV in view of the absence of ready lactonization, the retention of hyxroxyl bands (3448 and 3390 cm^{-1}) in the infrared spectrum of its acetyl derivative (amorphous), and the consumption of a mole of lead tetraacetate (both at 1.5 and at 15 hr.).

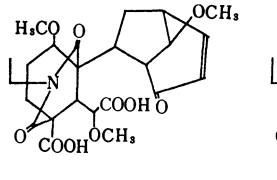
Oxidation of I with chromic acid in the same way as described in the previous paper[1] afforded two acids. One of these was Y-acid (V), m. p. 203~205°C decomp.*, $[\alpha]_D^{27}$ −7.5°, λ_{max}^{EtOH} 225 (ε 7180), 315 (ε 50), λ_{min} 280 mμ (ε 35), ν_{max}^{Nujol} 3333, 2740~2597 (hydroxyl), 1709 (broad, carboxyl), 1669 (α,β-unsaturated ketone), 1580 cm^{-1} (lactam) (Found: C, 57.24; H, 7.09; OCH_3, 17.17. Calcd. for $C_{24}H_{35}O_{10}N\cdot{}^1/_2H_2O$: C, 57.36; H, 7.22; 3 OCH_3,



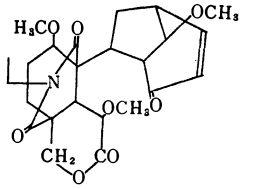
II



V



VI



VII

18.53%.). The other was C_1-acid (VI), m. p. 222~223°C decomp.*, $[\alpha]_D^{28}$ −6°, λ_{max}^{EtOH} 220 (ε 14600), 310 (ε 54), λ_{min} 290 mμ (ε 50), λ_{max}^{Nujol} 1754, 1739 (carboxyls), 1661 (α,β-unsaturated ketone), 1709 (shoulder), 1623 (imide), 675 cm^{-1} (cis-substituted double bond) (Found: C, 58.85; H, 6.45; OCH_3, 17.17. Calcd. for $C_{24}H_{31}O_{10}N$: C, 58.41; H, 6.35; 3 OCH_3, 18.86%.). Also produced was a neutral compound Z (VII), m. p. 236~240°C decomp.*, $[\alpha]_D^{29}$ −102°, λ_{max}^{EtOH} 218 (ε 10300), "shoulder" 300 mμ (ε 45), ν_{max}^{Nujol} 1751 (lactone), 1718 (imide), 1678 cm^{-1} (α,β-unsaturated ketone and imide) (Found: C, 61.83; H, 6.76; OCH_3, 16.35. Calcd. for $C_{24}H_{31}O_8N$: C, 62.46; H, 6.77; 3 OCH_3, 20.17%.). In the present case another neutral compound, Y, was not obtained. Each of these three compounds showed both in their infrared and ultraviolet spectra the absorption band attributed to an α,β-unsaturated ketone group. This accorded with the results of the determinations of their methoxyl groups. Thus it was found that the oxidation of I with chromic acid proceeded in the same way as that of I with lead tetraacetate[5]; namely, the α-ketol bond in I was cleaved, followed by the elimination of a molecule of methanol. However, no compound was secured identical with the oxidation products obtained by Edwards et al.[5] from I on oxidation with lead tetraacetate.

On the basis of the empirical formula and the infrared spectral data above, although an attempts to cleave the imide bond in VII and in VI with alkali or sulfuric acid failed, the structure VII can be assigned to Z.

VI was confirmed as a dicarboxylic acid. When VI was heated over its melting point, under effervescence it gave an acid. m. p. 275~280°C, $[\alpha]_D^{27}$ −49°, ν_{max}^{Nujol} 1739 (carboxyl), 1672 (α,β-unsaturated ketone), 1701, 1631 cm^{-1} (imide) (Found: C, 61.60; H, 6.97; OCH_3, 19.77. Calcd. for $C_{23}H_{31}O_8N$: C, 61.45; H, 6.95; 3 OCH_3, 20.71%.). This decarboxylation can be readily interpreted in the same way as that observed in lycoctonamic acid[6]. In view of the above experimental evidence, the structure of C_1-acid can be represented as VI.

V was proved to be a monocarboxylic acid, and its infrared spectrum showed strong hydrogen bonded bands near the 3 and 6μ regions. V was recovered unchanged after treatment with ethereal diazomethane solution. This perhaps indicates the presence of a lactone group in V. In addition, V was acetylated with acetic anhydride and pyridine to give a reversible acetyl derivative (amorphous), $[\alpha]_D^{10}$ −32°, (Found: C, 59.35; H, 6.78. Calcd. for $C_{28}H_{37}O_{11}N$: C, 59.67; H, 6.62%.), the infrared spectrum of which showed no hydroxyl band. Since V showed acid properties, the lactone group in question, if it was present, should be easily hydrolyzable. From a consideration of the above results, one of the most likely structures for Y-acid was shown to be V.

The author wishes now to formally propose names for the above compounds as follows: desmethanol secolycoctimide ketodicarboxylic acid for C_1-acid, desmethanol des-(oxymethylene) secolycoctimide keto monocarboxylic acid for the decarboxylated C_1-acid, and desmethanol secolycoctimde ketolactone for Z.

* Previously melting points at 193~195, 220~222 and 226~227°C were reported for V, VI and VII respectively[1].

5) O. E. Edwards et al., *Can. J. Chem.*, **34**, 1315 (1956).
6) O. E. Edwards and L. Marion, ibid., **30**, 627 (1952).

Grateful acknowledgment is made to Professor Harusada Suginome, Professor Toshi Irie and Prefessor Shichiro Kakimoto of Hokkaido University, and to Dr. Kunio Okahara and Dr. Yoshio Kurayuki of this laboratory, for their interest and encouragement throughout the progress of this work. The author is furthermore indebted to Dr. Minoru Fukuda and Miss Miyoko Suzuki of the Pharmaceutical Faculty, Osaka University, for the analyses and for the infrared spectra respectively.

Osaka Municipal Hygienic Laboratory
Kita-ku, Osaka

Reaction of 7-Substituted 2-Halotropones with Ethyl Sodiocyanoacetate

By Shingo MATSUMURA

(Received July 27, 1961)

In a previous paper, the formation of α-benzopyran, as well as of azulene derivatives, by the condensation of 2-chlorotropone and ethyl sodiocyanoacetate was reported[1]. In the present paper, the reaction of 2-halotropone derivatives and ethyl sodiocyanoacetate is examined and the results obtained are reported on.

The reaction of 2, 7-dibromotropone (I) and ethyl sodiocyanoacetate (II) in a mixed solvent of dioxane and ethanol affords colorless crystals of m. p. 117°C (III), $C_{17}H_{17}O_5N_2Br$, and of m. p. 150°C (IV), $C_{12}H_9O_4Br$. Under the same conditions, 2, 7-dichlorotropone (V) affords colorless crystals of m. p. 123°C (VI), $C_{17}H_{17}O_5N_2Cl$, and of m. p. 146°C (VII), $C_{12}H_9O_4Cl$, and orange-red crystals of m. p. 152°C (VIII), $C_{22}H_{22}O_8N_2$. The same reaction of 2-chloro-7-bromotropone (IX) gives colorless crystals of m. p. 223°C (X), $C_{10}H_5O_4Br$, besides VI and VII.

The reaction of 2-methoxy-7-bromotropone (XI) in ethanol affords colorless crystals of m. p. 125°C (XII), $C_{18}H_{20}O_6N_2$, and a compound corresponding to VIII, while that of 2-methoxy-3, 7-dibromotropone (XIII) gives colorless crystals of m. p. 115°C (XIV), $C_{13}H_{11}O_5Br$. The same reaction of 2-methoxy-3, 5, 7-tribromotropone (XV) gives colorless crystals of m. p. 146°C (XVI), $C_{18}H_{18}O_6N_2Br_2$, and of m. p. 217°C (XVII), $C_{11}H_5O_3NBr_2$.

The ultraviolet absorption spectra*1 of III, VI, XII and XVI (Fig. 1) are similar to that of 2-amino-2-(cyano-ethoxycarbonylmethyl)-3-ethoxycarbonyl-α-benzopyran (XVIII) reported on in a previous paper[1]. The infrared absorption spectra[2] of these compounds showed the presence of amino, cyano and ester carbonyl groups and of an ester carbonyl group conjugated with an unsaturated bond. On the basis of these spectral data, it is assumed that III is the 8-bromo derivative, that VI is the 8-chloro derivative, that XII is the 8-methoxy derivative, and that XVI is the 5, 7-dibromo-8-methoxy derivative of XVIII.

Condensation of 3-bromosalicylaldehyde (XIX) and ethyl cyanoacetate in the presence of piperidine had given III, and the same reaction with 3-chlorosalicylaldehyde (XX) gave VI. These facts clearly indicate that III, VI, XII and XVI are all α-benzopyran derivatives.

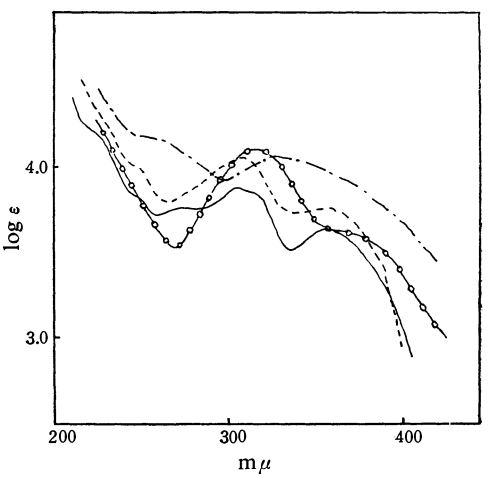


Fig. 1. Ultraviolet absorption spectra of III, VI, XII and XVI in methanol.
—— III : Y=log ε+0 ; ---- VI : Y=log ε +0.2 ; -○- XII : Y=log ε+0 ; - · - XVI : Y=log ε+0.

1) S. Matsumura, This Bulletin, **34**, 995 (1961).
2) S. Matsumura, *Bull. Chem. Research Inst., Non-Aq. Solns., Tohoku Univ.*, **10**, 223 (1961).
*1 The ultraviolet spectra were measured with a Hitachi EPU-2A spectrophotometer by Mr. H. Sato of this Institute, to whom the author is deeply indebted.

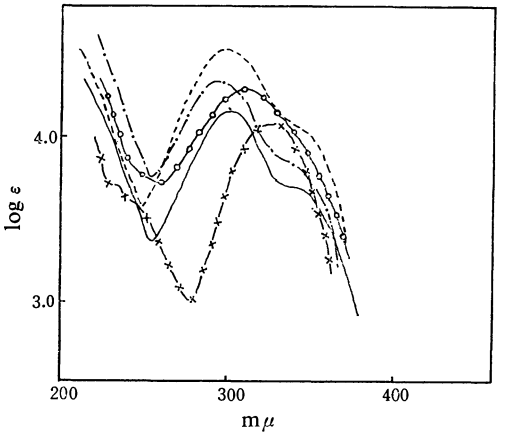


Fig. 2. Ultaviolet absorption spectra of IV, VII, X, XIV and XVII in methanol.
—— IV : Y=log ε+0 ; - · - VII : Y=log ε +0.2 ; ------ X : Y=log ε+0.4 ; -○- XIV : Y=log ε+0 ; -×- XVII : Y=log ε+0.

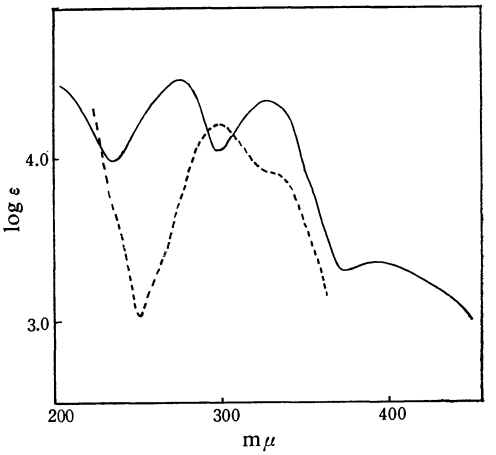


Fig. 3. Ultraviolet absorption spectra of VIII and XXIII in methanol.
—— VIII, ---- XXIII

The ultraviolet absorption spectra of IV, VII, X, XIV and XVII (Fig. 2) are similar to those coumarin derivatives. These compounds all have absorption bands in the region of 1760~1735 cm^{-1} due to the unsaturated δ-lactonic carbonyl group in the coumarin ring. There is an absorption band due to the ester carbonyl group conjugated with an unsaturated bond in the region of 1710~1690 cm^{-1} in IV, VII and XIV, while an absorption band of a carboxyl group is present at 2750 cm^{-1} in X, and that of a cyano group conjugated with an unsaturated bond at 2215 cm^{-1}, in XVII. These spectral evidences show that IV, VII and XIV are 8-bromo, 8-chloro, and 7-bromo-3-methoxy derivatives of 3-ethoxycarbonylcoumarin respectively, while X is 3-carboxy-8-bromocoumarin and XVII is 3-cyano-5, 7-dibromo-8-methoxycoumarin.

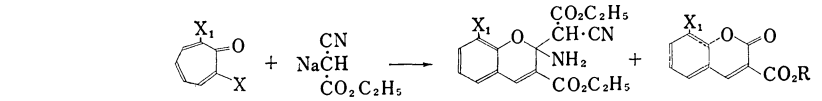
The heating of III with dilute hydrochloric acid for a short time converts it to IV, and a similar reaction of VI gives VII. The treatment of XII with hydrochloric acid gives 3-carboxy-8-methoxycoumarin (XXI), m. p. 172°C, while the treatment of XVI with hydrochloric acid affords 3-ethoxycarbonyl-5, 7-dibromo-8-methoxycoumarin (XXII), m. p. 187°C. XXII is also obtained by the treatment of XVII with absolute ethanol containing hydrochloric acid. On the basis of the ultraviolet spectrum of VIII (Fig. 3), this compound is assumed to be a coumarin derivative. The infrared spectrum of VIII indicates the presence of absorptions due to cyano- and carbonyl groups conjugated with an unsaturated bond and to a carbonyl group not conjugated with an unsaturated bond.

The hydrolysis of VIII with 6N hydrochloric acid gives a compound XXIII, m. p. 215°C, corresponding to the molecular formula of $C_{12}H_8O_6$. The ultraviolet spectrum of XXIII, as shown in Fig. 3, shows an absorption curve similar to that of 3-carboxycoumarin. The infrared spectrum of XXIII indicates the presence of a carboxyl and of a methylene group (1465 cm^{-1}). This spectral evidence shows that XXIII is 3-carboxy-8-carboxymethylcoumarin.

On the basis of the formation of 3-carboxy-8-carboxymethylcoumarin from VIII and the infrared absorption spectrum of VIII, VIII is assumed to be ethyl α-cyano-β-amino-γ-(3-ethoxycarbonylcoumarin-8-yl)-glutaconate.

Recently, the condensation reaction between 2, 4, 7-tribromotropone (XXIV) and II has been examined[3], and seven kinds of structurally unidentified compounds have been obtained; colorless crystals (XXV) of m. p. 177°C, yellow crystals (XXVI) of m. p. 214°C, brown crystals (XXVII) of m. p. 178°C, colorless crystals (XXVIII) of m. p. 155°C, yellow crystals (XXIX) of m. p. 141°C, pale yellow crystals (XXX) of m. p. 181°C, and orange crystals (XXXI) of m. p. above 340°C. From their analytical values, the molecular formula of $C_{17}H_{15}O_5N_2Br$ was given for XXVI, $C_{12}H_9O_3NBr_2$ for XXVII and XXX, and $C_{12}H_8O_3NBr_2Na$ for XXXI. Re-examination of these analytical values showed that the molecular formula of $C_{22}H_{21}O_8N_2Br$ would be more appropriate for XXVI than $C_{17}H_{15}O_5N_2Br$. No molecular formulae were given for XXV and XXVIII, but, from their analytical values, the formula of $C_{12}H_8O_4Br_2$ is now suggested for XXV and $C_{17}H_{16}O_5N_2Br_2$ for XXVIII. The ultraviolet absorption spectra[2] of XXVIII and XXIX are similar

3) H. Akino and S. Matsue, *Sci. Rep. Hirosaki Univ.*, 6, 34 (1959).



I: X=X1=Br
V: X=X1=Cl
IX: X=Br, X1=Cl
XI: X=Br, X1=OCH3

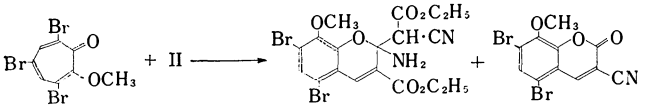
III: X1=Br
VI: X1=Cl
XII: X1=OCH3

IV: R=C2H5, X1=Br
VII: R=C2H5, X1=Cl
X: R=H, X1=Br

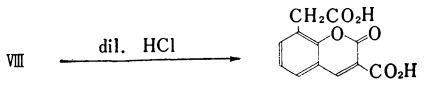
VIII: R=C2H5, X1=C(CN)(CO2C2H5)=C(NH2)-CH-CO2C2H5



XIII XIV

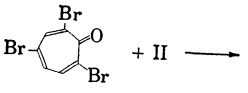


XV XIV XVII

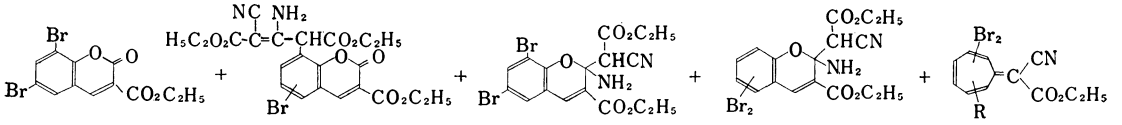


XXIII

Scheme 1.



XXIV



XXV XXVI XXVIII XXIX XXX: R=OH XXXI: R=ONa

Scheme 2.

to those of III and VI. The infrared spectra[3] of XXVIII and XXIX indicate the presence of cyano and ester carbonyl groups not conjugated with unsaturated bonds and of an ester carbonyl group conjugated with an unsaturated bond. This spectral evidence suggests that XXVIII and XXIX are α-benzopyran derivatives.

The condensation of 3, 5-dibromosalicylaldehyde (XXXII), obtained by the bromination of XIX, with ethyl cyanoacetate in the presence of piperidine affords XXVIII; this indicates that XXVIII is 6, 8-dibromo-2-amino-2-(cyano-ethoxycarbonylmethyl)-3-ethoxycarbonyl-α-benzopyran. The ultraviolet spectrum of XXV is similar to those of IV and VII. XXV is obtained by treatment of XXVIII with hydrochloric acid in ethanol. These facts show that XXV is 6,8-dibromo-3-ethoxycarbonylcoumarin.

The ultraviolet spectrum of XXVI is very similar to that of VIII, and the infrared spectrum of XXVI indicates the presence of amino and cyano, lactonic carbonyl, groups and of ester carbonyl groups conjugated with an unsaturated bond. Therefore, XXVI should be a 5- or 6-bromo derivative of VIII.

On the basis of a consideration of the ultraviolet and infrared absorption spectra, it is assumed that XXX and XXXI are heptafulvene derivatives. These reaction sequences are illustrated in Scheme 2.

Condensation of 2-halotropones substituted in the 7-position and II failed to indicate the

formation of an azulene derivative; only rearrangement products were obtained.

Experimental*2

Reaction of 2,7-Dibromotropone (I) and Ethyl Sodiocyanoacetate (II).—A solution of 500 mg. of I dissolved in 20 ml. of dioxane was stirred into II, prepared from 90 mg. of metallic sodium, 3 ml. of absolute ethanol, and 500 mg. of ethyl cyanoacetate, under ice-cooling, the solution thereby became orange-red, and the colorless sodio compound changed into an orange-red precipitate. After the mixture was allowed to stand overnight at room temperature, the precipitate was collected by filtration and washed with ethanol, and the 400 mg. of colorless crystals that remained was recrystallized from ethanol. The easily soluble portion afforded 120 mg. of III as colorless prisms, m. p. 115~117°C.

Found: C, 50.13; H, 4.06; N, 6.65. Calcd. for $C_{17}H_{17}O_5N_2Br$: C, 49.87; H, 4.15; N, 6.84%.

UV λ_{max}^{MeOH} mμ (log ε): 307 (3.84), 360 (3.56).

The sparingly soluble portion afforded 80 mg. of IV as colorless scales, m. p. 149~150°C.

Found: C, 48.56; H, 3.21. Calcd. for $C_{12}H_9O_4Br$: C, 48.48; H, 3.03%.

UV λ_{max}^{MeOH} mμ (log ε): 300 (4.14), 340 (3.68).

Formation of IV from III.—A solution of 50 mg. of III dissolved in 0.5 ml. of ethanol and with 0.2 ml. of 6 N hydrochloric acid added was heated on a water bath for 5 min., the solid thereby dissolved at once, and sparingly soluble needle crystals then separated out. Recrystallization of these crystals from ethanol gave 20 mg. of IV as colorless needles of m. p. 149~150°C.

Reaction of 2,7-Dichlorotropone (V) and II.—A solution of 500 mg. of V dissolved in 20 ml. of dehydrated dioxane was stirred, while being cooled by ice, into II, prepared from 140 mg. of sodium, 3 ml. of absolute ethanol, and 700 mg. of ethyl cyanoacetate, and the mixture was allowed to stand overnight at room temperature. The dioxane-ethanol mixture was evaporated at a reduced pressure, ethanol was added to the residue, and the precipitated orange-red crystals were repeatedly recrystallized from ethanol. The easily soluble portion afforded 160 mg. of VI as colorless scales, m. p. 122~123°C.

Found: C, 56.18; H, 4.56; N, 7.83. Calcd. for $C_{17}H_{17}O_5N_2Cl$: C, 56.03; H, 4.67; 7.69%.

UV λ_{max}^{MeOH} mμ (log ε): 305 (3.53), 355 (3.31).

The sparingly soluble portion afforded 80 mg. of VII as colorless needles, m. p. 145~146°C.

Found: C, 57.36; H, 3.28. Calcd. for $C_{12}H_9O_4Cl$: C, 57.14; H, 3.57%.

UV λ_{max}^{MeOH} mμ (log ε): 296 (4.13), 340 (3.65).

The sparingly soluble portion also afforded 30 mg. of VIII as orange prisms, m. p. 151~152°C.

Found: C, 59.83; H, 5.29; N, 7.01. Calcd. for $C_{22}H_{22}O_8N_2$: C, 59.72; H, 5.01; N, 6.33%.

UV λ_{max}^{MeOH} mμ (log ε): 275 (4.48), 327 (4.35), 395 (3.35).

*2 All the melting points are uncorrected.

Formation of VII from VI.—A solution of 50 mg. of VI dissolved in 0.5 ml. of ethanol and with 0.2 ml. of 6 N hydrochloric acid added was warmed on a water bath for 5 min., and the colorless needle crystals that separated out were recrystallized from ethanol to give VII, m. p. 145~146°C.

Reaction of 2-Chloro-7-bromotropone (IX) and II.—A solution of 500 mg. of IX dissolved in 20 ml. of dioxane was stirred, while being cooled by ice, into II, prepared from 110 mg. of sodium, 3 ml. of absolute ethanol, and 550 mg. of ethyl cyanoacetate, and the mixture was treated as in the case of the reaction of V and II, affording 40 mg. of VI and 60 mg. of VII. The filtrate obtained after isolation of VI and VII was concentrated, the residue was dissolved in water, and the solution was neutralized with dilute nitric acid, from which 50 mg. of brown precipitate was obtained. Recrystallization of this precipitate from ethanol afforded 20 mg. of X as colorless crystals, m. p. 222~223°C (decomp.).

Found: C, 44.83; H, 1.89. Calcd. for $C_{10}H_5O_4Br$: C, 44.60; H, 1.89%.

UV λ_{max}^{MeOH} mμ (log ε): 300 (4.13).

Reaction of 2-Methoxy-7-bromotropone (XI) and II.—A solution of 500 mg. of XI dissolved in 10 ml. of absolute ethanol was stirred, while being cooled by ice, into II, prepared from 100 mg. of sodium, 4 ml. of absolute ethanol, and 600 mg. of ethyl cyanoacetate; as a result the reaction started at once and the solution became reddish and clear. After the mixture had been left to stand overnight, the mixture was filtered and the filtrate was concentrated under reduced pressure. The tarry substance hereby formed was dissolved in benzene, the solvent was evaporated, and ethanol was added to the oily residue. The crystallized solid was recrystallized from ethanol, and 40 mg. of VIII, m. p. 151~152°C, was obtained. The recrystallization of the mother liquor afforded 340 mg. of XII as colorless prisms, m. p. 124~125°C.

Found (for XII): C, 60.57; H, 5.42; N, 7.83. Calcd. for $C_{18}H_{20}O_6N_2$: C, 59.99; H, 5.59; N, 7.77%.

UV λ_{max}^{MeOH} mμ (log ε): 316 (4.11), 360 (3.65).

Reaction of 2-Methoxy-3,7-Dibromotropone (XIII) and II.—A solution of 600 mg. of XIII dissolved in 15 ml. of dehydrated benzene was stirred, while being cooled by ice, into II, prepared from 100 mg. of sodium, 3 ml. of absolute ethanol, and 600 mg. of ethyl cyanoacetate, and the mixture was allowed to stand overnight at room temperature. The precipitate formed was collected and dissolved in 80 ml. of water, and the solution was neutralized with dilute nitric acid, producing 360 mg. of a greyish white precipitate. This precipitate was recrystallized first from benzene and then from ethanol to produce 260 mg. of XIV as colorless scales, m. p. 115~116°C.

Found: C, 47.34; H, 3.56. Calcd. for $C_{13}H_{11}O_5Br$: C, 47.70; H, 3.33%.

UV λ_{max}^{MeOH} mμ (log ε): 311 (4.29).

Reaction of 2-Methoxy-3,5,7-tribromotropone (XV) and II.—A solution of 500 mg. of XV dissolved in 10 ml. of absolute ethanol was stirred, while being cooled by ice, into II, prepared from 80 mg. of sodium, 3 ml. of absolute ethanol, and 400 mg. of ethyl cyanoacetate, and the mixture

was allowed to stand overnight at room temperature. The orange-red precipitate thereby formed was collected by filtration and recrystallized from ethanol to give 100 mg. of XVI as colorless scales, m. p. 146~147°C.

Found: C, 42.03; H, 3.61; N, 5.86. Calcd. for $C_{15}H_{18}O_6N_2Br_2$: C, 41.69; H, 3.47; N, 5.43%.

UV λ_{max}^{MeOH} mμ (log ε): 266 (4.16), 333 (4.04).

Concentration of the filtrate precipitated colorless crystals which recrystallized from ethanol to produce 60 mg. of XVII as colorless prisms, m. p. 216~217°C.

Found: C, 37.04; H, 1.36; N, 4.25. Calcd. for $C_{11}H_5O_3NBr_2$: C, 36.76; H, 1.39; N, 3.90%.

UV λ_{max}^{MeOH} mμ (log ε): 330 (4.07).

Synthesis of III.—One drop of piperidine was added to the solution of 100 mg. of 3-bromosalicylaldehyde (XIX) and 100 mg. of ethyl cyanoacetate dissolved in 0.2 ml. absolute ethanol; the solution here upon immediately became orange-yellow and prismatic crystals began to separate out. The crystals were collected and recrystallized from ethanol to give 120 mg. of III, m. p. 115~117°C.

Synthesis of VI.—One drop of piperidine was added to a solution of 100 mg. of 3-chlorosalicylaldehyde (XX) and 100 mg. of ethyl cyanoacetate dissolved in 0.2 ml. of absolute ethanol; 150 mg. of VI, m. p. 122~123°C, was obtained.

Reaction of XII with an Acid.—A solution of 100 mg. of XII dissolved in 1 ml. of ethanol and with 0.2 ml. of 6 N hydrochloric acid added was heated for 50 min., and the colorless crystals that separated out were recrystallized from ethanol to give 50 mg. of XXI, m. p. 171~172°C.

Found: C, 60.31; H, 4.24. Calcd. for $C_{11}H_8O_5$: C, 60.00; H, 3.66%.

UV λ_{max}^{MeOH} mμ (log ε): 252 (3.89), 305 (4.15).

3-Ethoxycarbonyl-5,7-dibromo-8-methoxycoumarin (XXII).—a) A solution of 100 mg. of XVI dissolved in 2 ml. of ethanol and with 0.3 ml. of 6 N hydrochloric acid added was heated on a water bath for 20 min.; the colorless crystals that separated out were recrystallized from ethanol to give 40 mg. of XXII, m. p. 186~187°C.

Found: C, 38.20; H, 3.09. Calcd. for $C_{13}H_{10}O_5Br_2$: C, 38.42; H, 2.46%.

b) Hydrogen chloride gas was passed through the solution of 100 mg. of XVII dissolved in 3 ml. of absolute ethanol, and the solution was heated on a water bath for 5 hr. Ethanol was evaporated from the solution and the residual crystals were recrystallized from ethanol to give 80 mg. of XXII.

Reaction of VIII and an Acid.—A solution of 100 mg. of VIII dissolved in 6 ml. of ethanol and with 3 ml. of 3 N hydrochloric acid added was heated at 100~120°C for 5 hr. Ethanol was evaporated from this solution, and the residual crystals were recrystallized from ethanol to give 40 mg. of XXIII as colorless crystals, m. p. 214~215°C (decomp.).

Found: C, 57.27; H, 3.85. Calcd. for $C_{12}H_8O_6$: C, 58.07; H, 3.25%.

UV λ_{max}^{MeOH} mμ (log ε): 297 (4.12).

Reaction of 3,5-Dibromosalicylaldehyde (XXXII) and Ethyl Cyanoacetate.—One drop of piperidine was added to a solution of 50 mg. of XXXII and 50 mg. of ethyl cyanoacetate dissolved in 0.2 ml. of absolute ethanol. The solution thereby immediately colored orange-red. After the solution had been allowed to stand overnight, the colorless crystals that precipitated out were collected and recrystallized from ethanol to give 60 mg. of XXVIII as colorless prisms, m. p. 155~156°C.

Found: C, 42.03; H, 3.56; N, 5.68. Calcd. for $C_{17}H_{16}O_5N_2Br_2$: C, 41.80; H, 3.28; N, 5.71%.

3-Ethoxycarbonyl-6,8-dibromocoumarin (XXV).—A solution of 100 mg. of XXVIII dissolved in 5 ml. of ethanol and with 0.3 ml. of 6 N hydrochloric acid added was heated on a water bath for 20 min., and the colorless crystals that separated out were recrystallized from ethanol to give 40 mg. of XXV, m. p. 176~177°C.

Found: C, 38.49; H, 2.51. Calcd. for $C_{12}H_8O_4 \cdot Br_2$: C, 38.30; H, 2.13%.

The author wishes to express his deep gratitude to Professor Tetsuo Nozoe and Professor Shuichi Seto for their unfailing guidance. Also, the author wishes to thank Mr. S. Ohyama and Miss Y. Endo for their microanalyses and Mr. S. Aono for his infrared spectral measurements.

The Chemical Research Institute of Non-Aqueous Solutions
Tohoku University
Katahira-cho, Sendai

Condensation Reaction of Troponoids with Ethyl α-Cyano-β-aminoglutaconate. II. Reaction of Alkyl Derivatives of 2-Chlorotropone with Ethyl α-Cyano-β-aminoglutaconate

By Shingo MATSUMURA

(Received July 27, 1961)

It has already been found[1] that the condensation of 2-chlorotropone (I) with ethyl α-cyano-β-aminoglutaconate (II) results in the formation of 2-(cyano-ethoxycarbonylmethylene)-3-ethoxycarbonyl-1-azaazulane (III) and α-amino-α-(1-oxaazulan-2-on-3-yl)-β-cyano-β-ethoxycarbonylethylene (IV).

It has also often been found that the substitution occurs in the 7-position and not in the position previously occupied by the halogen in the amination of 2-halotropones with ammonia[2], and the same sort of abnormal substitution was also observed in the formation of 1-oxaazulan-2-one derivatives by reaction with acetoacetic ester or malonic ester[3], and in the formation of azulene or 1-azaazulan-2-one derivatives by reaction with cyanoacetic ester[4] or cyanoacetamide[5].

In order to determine whether or not such an abnormal reaction took place in the condensation reaction of 2-halotropones with II, the present series of experiments was carried out.

The reaction of 2-chloro-4-isopropyltropone (V) with II in benzene, in the presence of triethylamine, affords red crystals (VI) of m. p. 147°C and orange crystals (VII) of m. p. 184°C. A similar condensation of 2-chloro-6-isopropyltropone (VIII) gives a reddish oily product (IX), while the reaction with 2-chloro-4-methyltropone (X) gives red crystals (XI) of m. p. 190°C and orange crystals (XII) of m. p. 250°C. The same reaction of 2-chloro-6-methyltropone (XIII) affords an orange oily product (XIV).

The ultraviolet absorption spectra*1 of VI and XI (Fig. 1) are similar to that of the 2-methylene-1-azaazulane derivative[1]. The analytical values of VI correspond to those of the isopropyl derivative of III, and those of

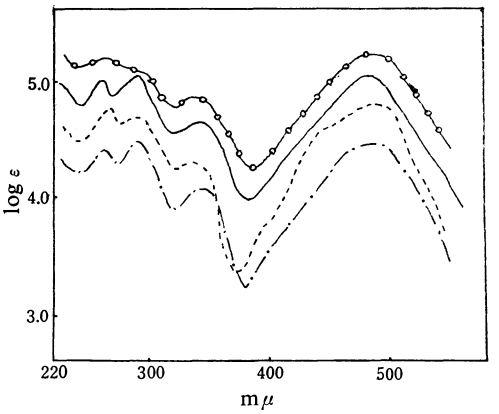


Fig. 1. UV absorption spectra of VI, XI, XVII and XX in methanol.
------ VI: $Y=\log\varepsilon+0.3$
——— XVII: $Y=\log\varepsilon+0.6$
—○— XI: $Y=\log\varepsilon+0.7$
—·—· XX: $Y=\log\varepsilon+0$

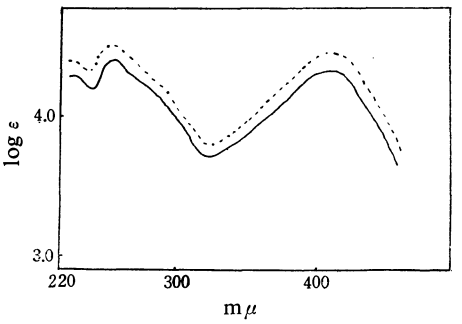
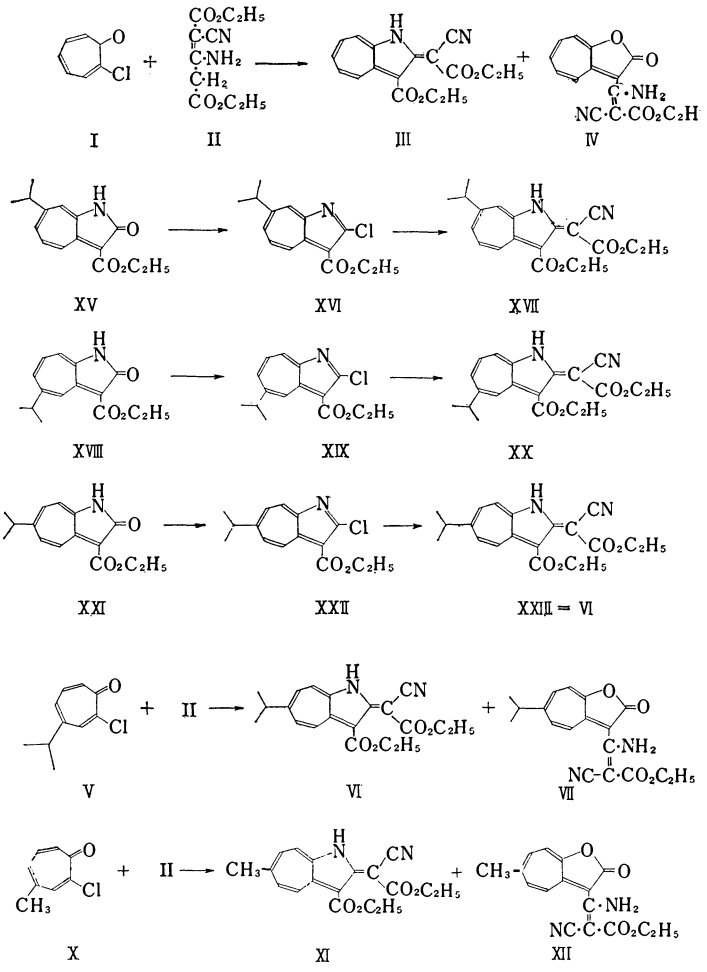


Fig. 2. UV absorption spectra of VII and XII in methanol.
——— VII: $Y=\log\varepsilon+0$
------ XII: $Y=\log\varepsilon+0.1$

XI, to those of the methyl derivative of III.

The ultraviolet absorption spectra of VII and XII (Fig. 2) are similar to that of the 1-oxa-azulan-2-one derivative. The analytical values of VII correspond to those of the isopropyl derivative of IV, and those of XII, to those of the methyl derivative of IV. The ultraviolet spectra of IX and XIV (Fig. 3) are similar to that of the starting 2-chlorotropone derivative except for the absorption at around

1) S. Matsumura, This Bulletin, **34**, 1361 (1961).
2) T. Sato, *J. Chem. Soc. Japan, Pure Chem. Sec.* (*Nippon Kagaku Zasshi*), **80**, 1056, 1173 (1959).
3) T. Sato, ibid., **80**, 1342 (1959).
4) T. Nozoe, S. Seto, S. Matsumura and T. Asano, *Proc. Japan Acad.*, **32**, 339 (1956).
5) T. Nozoe, S. Seto and S. Nozoe, ibid., **32**, 479 (1956); S. Seto and S. Nozoe, ibid., **32**, 765 (1956).
*1 The ultraviolet absorption spectra were measured with a Hitachi EPS-2 Type recording spectrophotometer.



280 mμ. These facts suggest that IX and XIV are tropone derivatives, but their structure still remains undetermined.

In order to determine the position of the isopropyl group in VI, the following experiment was carried out. The application of phosphoryl chloride to 3-ethoxycarbonyl-7-isopropyl-1-azaazulan-2-one (XV) gives 2-chloro-3-ethoxycarbonyl-7-isopropyl-1-azaazulene (XVI), m. p. 79°C, and the condensation of XVI with ethyl sodiocyanoacetate affords 2-(cyano-ethoxycarbonylmethylene)-3-ethoxycarbonyl-7-isopropyl-1-azaazulane (XVII), m. p. 134°C. The ultraviolet absorption spectrum of XVII is shown in Fig. 1.

The application of phosphoryl chloride to 3-ethoxycarbonyl-5-isopropyl-1-azaazulan-2-one (XVIII) affords 2-chloro-3-ethoxycarbonyl-5-isopropyl-1-azaazulene (XIX), m. p. 101°C, whose condensation with ethyl sodiocyanoacetate gives 2-(cyano-ethoxycarbonylmethylene)-3-ethoxycarbonyl-5-isopropyl-1-azaazulane (XX), m. p. 84°C. The ultraviolet absorption spectrum of XX is given in Fig. 1.

The treatment of 3-ethoxycarbonyl-6-isopropyl-1-azaazulan-2-one (XXI) with phosphoryl chloride gives an orange-yellow oily product (XXII) whose condensation with ethyl sodiocyanoacetate affords 2-(cyano-ethoxycarbonylmethylene)-3-ethoxycarbonyl-6-isopropyl-1-azaazulane (XXIII), m. p. 147°C. The mixed fusion of XXIII and VI failed to show any depression of the melting point, and the ultraviolet absorption spectra of these two substances were identical.

As will be clear from the infrared spectra*2 of VI and XI (Fig. 4), the absorptions in the region of the C–H out-of-plane deformation vibrations are very similar in these two compounds, so the position of methyl substitution in XI should be the 6-position.

The absorption band due to the C–H out-of-plane deformation vibration appears at 850 cm^{-1} in VII, while this absorption is present

*2 The infrared spectra were measured with a Perkin-Elmer Model 21 double beam spectrophotometer by Mr. S. Aono of this Institute; the author is deeply indebted to Mr. S. Aono.

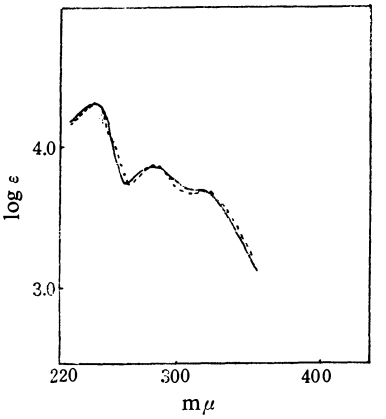


Fig. 3. UV absorption spectra of IX and XIV in methanol.
—— IX ---- XIV

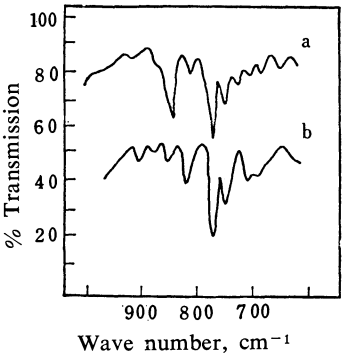
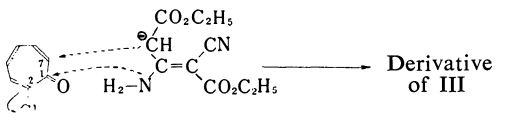


Fig. 4. IR absorption spectra of VI and XI.
a: VI b: XI

at 834 cm^{-1} in XII. These wave numbers agree with that of the 6-substituted derivatives of 1-oxaazulan-2-one[6]. This evidence shows that VII is a 6-isopropyl derivative of IV and that XII is its 6-methyl derivative.

It has become clear from these experiments that an abnormal reaction occurred also in the condensation reaction of 2-halotropones with II. In this reaction, the carbanion formed from II attacks the 7-position in the tropone ring, and this is followed by a dehydrative cyclization reaction between the amino group and the carbonyl in the 1-position to form a 2-methylene-1-azaazulane derivative.



This is the same mode of reaction as that reported already by Seto and others[5] for the formation of 1-azaazulan-2-one derivatives by the condensation of 2-halotropones with cyanoacetamide.

Experimental*3

Reaction of 2-Chloro-4-isopropyltropone (V) and Ethyl α-Cyano-β-aminoglutaconate (II). — To a solution of 260 mg. of V and 350 mg. of II dissolved in 2 ml. of dehydrated benzene, 200 mg. of triethylamine was added dropwise at room temperature; the solution thereby turned red and a precipitate was gradually deposited. After the mixture had been allowed to stand for 5 hr., the precipitate was collected by filtration, washed thoroughly with water, and recrystallized from acetone to give 250 mg. of VII as orange needles, m. p. 183~184°C.

Found: C, 66.51; H, 5.38; N, 8.67. Calcd. for $C_{18}H_{18}O_4N_2$: C, 66.24; H, 5.56; N, 8.53%.

UV λ_{max}^{MeOH} mμ (log ε): 230 (4.29), 254 (4.44), 410 (4.32).

The reaction solution, separated from the precipitate, was washed thoroughly with water, the benzene was evaporated, and the residue was purified by passage through an alumina column. The reddish crystals thereby obtained were recrystallized from ethanol to afford 120 mg. of VI as red needles, m. p. 145~147°C.

Found: C, 67.84; H, 6.15; N, 7.62. Calcd. for $C_{20}H_{22}O_4N_2$: C, 67.78; H, 6.26; N, 7.91%.

UV λ_{max}^{MeOH} mμ (log ε): 263 (4.46), 290 (4.39), 338 (3.98), 489 (4.48).

Reaction of 2-Chloro-6-isopropyltropone (VIII) and II. — A solution of 730 mg. of VIII and 890 mg. of II dissolved in 4 ml. of dehydrated benzene, with 400 mg. of triethylamine added, was allowed to stand for 2 days at room temperature; colorless needle crystals, easily soluble in water, thereby separated out. The benzene solution was washed with water, dried, and concentrated. The residue was purified by passage through an alumina column, and the column was eluted with benzene. The evaporation of the solvent from the effluent afforded 960 mg. of IX as a reddish oil.

Reaction of 2-Chloro-4-methyltropone (X) and II.—A solution of 320 mg. of X and 470 mg. of II dissolved in 2 ml. of dehydrated benzene, with 240 mg. of triethylamine added, was allowed to stand at room temperature for 5 hr. The precipitate thereby formed was collected by filtration and recrystallized from acetone to give 240 mg. of XII as orange-needles, m. p. 250°C (decomp.).

Found: C, 64.51; H, 4.85; N, 9.56. Calcd. for $C_{16}H_{14}O_4N_2$: C, 64.42; H, 4.73; N, 9.39%.

UV λ_{max}^{MeOH} mμ (log ε): 230 (4.35), 254 (4.46), 410 (4.36).

The solvent was evaporated from the filtrate, and the residue was purified by passage through an alumina column. The crystals thereby obtained were recrystallized from ethanol to afford 60 mg. of XI as red needles, m. p. 189~190°C.

Found: C, 66.52; H, 5.53; N, 8.46. Calcd. for $C_{18}H_{18}O_4N_2$: C, 66.28; H, 5.56; N, 8.58%.

UV λ_{max}^{MeOH} mμ (log ε): 264 (4.48), 289 (4.37), 340 (4.12), 490 (4.53).

6) T. Sato, *Bull. Chem. Research Inst. Non-Aq. Soln., Tohoku Univ.*, 8, 47 (1959).

*3 All melting points are uncorrected.

Reaction of 2-Chloro-6-methyltropone (XIII) and II.—A solution of 160 mg. of XIII and 240 mg. of II dissolved in 1 ml. of dehydrated benzene and with 120 mg. of triethylamine added was allowed to stand at room temperature for 2 days, and the reaction mixture was treated as in the reaction of VIII and II; 200 mg. of XIV was thereby obtained as an orange oil.

2-Chloro-3-ethoxycarbonyl-7-isopropyl-1-azaazulene (XVI). — A solution of 200 mg. of 3-ethoxycarbonyl-7-isopropyl-1-azaazulan-2-one (XV) dissolved in 1.5 ml. of phosphoryl chloride was sealed in a glass tube and heated at 150~160°C for 5 hr. The phosphoryl chloride was removed from the reaction mixture, water was added to decompose the residual phosphoryl chloride, and the mixture was neutralized with sodium hydrogencarbonate. This was extracted with benzene, and the extract was dried and passed through a column of alumina. The product thereby obtained was recrystallized from petroleum ether to give 110 mg. of XVI as orange-yellow prisms, m. p. 77~79°C.

Found: C, 64.81; H, 5.75; N, 5.32. Calcd. for $C_{15}H_{16}O_2NCl$: C, 64.98; H, 5.77; N, 5.05%.

2-Chloro-3-ethoxycarbonyl-5-isopropyl-1-azaazulene (XIX). — A mixture of 500 mg. of 3-ethoxycarbonyl-5-isopropyl-1-azaazulan-2-one (XVIII) and 5 ml. of phosphoryl chloride was treated as in the preceding case; 350 mg. of XIX was obtained thereby as orange prisms, m. p. 99~101°C.

Found: C, 64.76; H, 5.38; N, 5.13. Calcd. for $C_{15}H_{16}O_2NCl$: C, 64.98; H, 5.77; N, 5.05%.

2-Chloro-3-ethoxycarbonyl-6-isopropyl-1-azaazulene (XXII). — A mixture of 200 mg. of 3-ethoxycarbonyl-6-isopropyl-1-azaazulan-2-one (XXI) and 1 ml. of phosphoryl chloride was treated as in the preceding cases, obtaining XXII as an orange oil.

2-(Cyano-ethoxycarbonylmethylene)-3-ethoxycarbonyl-7-isopropyl-1-azaazulane (XVII). — To the sodio compound prepared from 30 mg. of sodium granulated in dehydrated dioxane and heated with 260 mg. of ethyl cyanoacetate, 150 mg. of XVI was added and the mixture was heated at 90°C for 1 hr.; an orange-red precipitate thereby gradually formed. The dioxane was evaporated from the mixture, and the residue was dissolved in water, neutralized with dilute acetic acid, and extracted with benzene. The extract solution was dried and passed through a column of alumina. The reddish oily product so obtained solidified when allowed to stand after petroleum ether (b. p. 50~60°C) had been added; the product was then recrystallized from the benzene-petroleum ether mixture to give 80 mg. of XVII as red needles, m. p. 132~134°C.

Found: C, 67.65; H, 6.59; N, 7.84. Calcd. for $C_{20}H_{22}O_4N_2$: C, 67.78; H, 6.26; N, 7.91%.

UV λ_{max}^{MeOH} mμ (log ε): 260 (4.41), 290 (4.45), 340 (4.02), 489 (4.43).

2-(Cyano-ethoxycarbonylmethylene)-3-ethoxycarbonyl-5-isopropyl-1-azaazulane (XX). — Treatment of 30 mg. of sodium, 200 mg. of XIX, as in the preceding case, afforded 120 mg. of XX as red needles, m. p. 82~84°C.

Found: C, 67.53; H, 6.12; N, 8.05. Calcd. for $C_{20}H_{22}O_4N_2$: C, 67.78; H, 6.26; N, 7.91%.

UV λ_{max}^{MeOH} mμ (log ε): 262 (4.41), 290 (4.48), 334 (4.05), 489 (4.44).

2-(Cyano-ethoxycarbonylmethylene)-3-ethoxycarbonyl-6-isopropyl-1-azaazulane (XXIII=VI). — A mixture of 30 mg. of sodium, 200 mg. of ethyl cyanoacetate, and 200 mg. of XXII was treated as in the preparation of XVII; 100 mg. of XXIII was thereby obtained as red needles, m. p. 145~147°C. Mixed fusion of XXIII with VI failed to show any depression of the melting point.

The author wishes to express his deep gratituted to Professor Tetsuo Nozoe and Professor Shuichi Seto for their kind and unfailing guidance throughout the course of the present work. The author is also indebted to Mr. Humio Sato for his cooperation in carrying out the experiments, and to Miss Yoko Endo and Mr. Shinichi Ohyama for their elemental analyses.

The Chemical Research Institute of Non-Aqueous Solutions
Tohoku University
Katahira-cho, Sendai

Acid-catalyzed Hydrogen-Deuterium Exchange Reactions of Deuterated Anisole, Thioanisole and Benzene

By Shigeru OAE, Atuyoshi OHNO and Waichiro TAGAKI

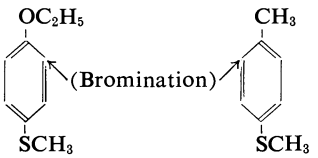
(Received August 30, 1961)

There have been many reports of the electron-pair releasing conjugative ability of divalent sulfides vs. that of the oxygen analogs. The dissociation constants of substituted benzoic acids[1], phenols[2] and anilines[2,3], the dipole moments of substituted benzenes[4], and the dimerization rates of *p*-substituted isopropenyl[5] benzene and a few other examples[6] have all pointed out that the electron-pair releasing conjugative effect of the sulfide function is smaller than that of the oxygen-analog. In both S_N1[7] and S_N2[8] reactions, chloromethyl alkyl ether has been shown to react substantially faster than the sulfur analog. The theoretical considerations, based on molecular orbital treatments, indicate that 3p-π-bonds are less stable than 2p-π-bonds[9].

Baddeley[10] has also shown that the orders of the ratio of the packing radius vs. the single-bond radius are $F > Cl > Br > I$ and $O > S > Se > Te$.

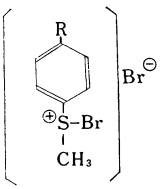
In seeking better evidence of electrophilic aromatic substitution with which one can compare the relative activating and orienting effects of sulfide groups vs. those of oxygen analogs, we have come across only two examples in the literature; namely, the bromination has been shown to take place meta to the methylthio group in both *p*-ethoxyphenyl sulfide[11] and *p*-tolyl methyl sulfide[12].

Although, these data show that the methylthio group has much less activating ability than the methoxyl or even the methyl group, these



examples are not very adequate, because the initial reaction of bromination should be the attack of bromine on the sulfur atom of the methylthio group, instead of on the benzene nucleus, leading to the formation of an intermediate complex I, which then further reacts to give the final product.

Neither the nitration[13] nor sulfonation[14] reaction is desirable, because the initial attack takes place on the sulfur atom, eventually oxidizing the sulfide group.



(I)

Mercuration is also not desirable for the same reason. The other possible electrophilic substitution reactions are the chloromethylation and hydrogen exchange reactions; we have chosen the latter. The acid-catalyzed hydrogen deuterium exchange reaction has been extensively studied by previous workers[15] and has thus been known to give a rate sequence of aromatic substituents identical with that of such well-studied reactions as nitration. Thus, we have studied the acid-catalyzed hydrogen-deuterium exchange reactions of *p*-deuterated anisole, thioanisole and mono-deuterated benzene as a reference compound, in acetic acid containing sulfuric acid as catalyst.

1) a) J. W. Baker, G. F. Barrett and W. T. Tweed, *J. Chem. Soc.*, **1952**, 2831; b) G. Bordwell and P. J. Boutan, *J. Am. Chem. Soc.*, **78**, 854 (1956).
2) F. G. Bordwell and C. C. Cooper, ibid., **74**, 1058 (1952).
3) N. F. Hall and M. R. Sprinkle, ibid., **54**, 3469 (1932).
4) a) L. Chiercici, H. Lumbroso and R. Passerini, *Bull. soc. chim. France*, **V22**, 686 (1955); b) H. Lumbroso and C. Marschalk, *J. chim. phys.*, **49**, 385 (1952).
5) J. M. van der Zauden, J. Nieuwenhuis and H. J. T. Bos, *Rec. trav. chim.*, **76**, 669 (1957).
6) C. C. Price and S. Oae, "Sulfur Bonding", Chap. II, Ronald Press, forthecming.
7) a) F. G. Bordwell, G. D. Cooper and H. Morita, *J. Am. Chem. Soc.*, **79**, 376 (1957); b) H. Boehme, *Ber.*, **74**, 248 (1941); c) H. Boehme and K. Sell, ibid., **81**, 123 (1948).
8) M. Murakami and S. Oae, *J. Chem. Soc. Japan, Pure Chem. Sec. (Nippon Kagaku Zasshi)*, **72**, 598 (1951); *Proc. Japan Acad.*, **25**, No. **11**, 12 (1949).
9) See references, Introduction, in Ref. 6.
10) G. Baddeley, *J. Chem. Soc.*, **1953**, 663.
11) T. van Hone, *Bull. acad. belg.*, (5) **37**, 98 (1928).
12) Th. Zincke and W. Frohneberg, *Ber.*, **43**, 837 (1909).
13) F. G. Bordwell and R. J. Boutan, *J. Am. Chem. Soc.*, **79**, 717 (1957).
14) R. J. Gillespie and R. C. Passerini, *J. Chem. Soc.*, **1956**, 3850.
15) a) C. K. Ingold, C. G. Raisin and C. L. Wilson, *Nature*, **134**, 734 (1934); *J. Chem. Soc.*, **1936**, 915; b) A. P. Best and C. L. Wilson, ibid., **1938**, 28; c) V. Gold and D. P. N. Satchell, ibid., **1955**, 3609, 3619, 3622; d) D. P. N. Satchell, ibid., **1956**, 3911; **1958**, 1927; e) V. Gold, R. W. Lambert and D. P. N. Satchell, ibid., **1960**, 2461; f) W. M. Lauer and J. T. Day, *J. Am. Chem. Soc.*, **77**, 1904 (1955).

Deuteration was accomplished by the Grignard reaction of the corresponding bromo-compounds, while *p*-bromothioanisole was made[16] by resting sodium methylmercaptide with diazotized *p*-bromoaniline.

The kinetic results, obtained through analyzing the compounds with a mass-spectrometer, are shown in Table I.

TABLE I. FIRST ORDER RATE CONSTANTS, k_1, AND ENTHALPIES AND ENTROPIES OF ACTIVATION OF THE HYDROGEN-DEUTERIUM EXCHANGE REACTIONS

Compound	Temp. °C	k_1, sec^{-1}	$H^{\neq}$, kcal./mol.	$S^{\neq}$ e. u.
Benzene-d_1	100.0	1.63×10^{-8}		
p-Deutero-anisole	60.8	3.61×10^{-6}		
	79.9	3.55×10^{-5}	26.30	−4.44
	96.6	1.89×10^{-4}		
p-Deuterothio-anisole	80.0	7.68×10^{-7}		
	99.3	6.35×10^{-6}	27.60	−8.37
	119.9	4.36×10^{-5}		

It has previously been established that the relative affinity for a proton is stronger for anisole than for thioanisole. This means that anisole is in a less favorable condition than thioanisole in using its lone electron pair for conjugation, while the electron-withdrawing inductive effect is also stronger for the methoxyl group than for the methylthio group. Yet one finds that the methoxyl group activates the benzene nucleus substantially more than the sulfur counterpart; i. e., anisole reacts thirty to forty times faster than the thioanisole, while both the enthalpy and entropy of the activation of the sulfur compound are larger than those of the oxygen analog by 1.5 kcal./mol. and 4 e. u. respectively.

This result is another support for the well-accepted concept that the electron-releasing conjugative effects decrease with the increasing atomic number of any periodic group.

It is interesting to note that thioanisole reacts fifty times faster than benzene. This means that the methylthio group, in spite of its small value ($\sigma=-0.047$)[17], actually activates the benzene ring in an electrophilic aromatic substitution. In fact, several previous workers have pointed out the strong electron-releasing conjugative effect of the methylthio group in electron-demanding reaction[1a,7,9,18].

Experimental

***p*-Deuteration.** — *p*-Deuteration was carried out by quenching with D_2O the Grignard reagents of *p*-bromoanisole, *p*-bromothioanisole and bromobenzene prepared in anhydrous ether. The boiling points of the deuterated compounds are as follows: anisole, 155.5°C/760 mmHg; thioanisole, 81~81.5°C/18 mmHg; benzene, 81°C/760 mmHg.

Successful deuteration was confirmed by their infrared spectra, near 2200 cm^{-1} and 835 cm^{-1} for deuterated anisole and thioanisole and near 2200 cm^{-1} for benzene-d_1.

Kinetics. — In 10 ml. of acetic acid containing sulfuric acid (molar ratio, $CH_3COOH : H_2SO_4 = 50 : 1$) was dissolved 0.008 mol. of a deuterated compound, and aliquots (1 ml.) of this solution were reacted in ampoules at the desired temperature. At suitable time intervals the contents of the ampoule were poured into 10 ml. of an aqueous 4 N sodium hydroxide solution under cooling with an ice-salt mixture and were extracted with 5 ml. of ether except for benzene-d_1.

After being washed with 2 ml. of water, the ether layer was placed in a mass spectrometer-sample tube and the ether was removed by suction. Without further treatment, the residue was analyzed directly with a mass spectrometer (Atlas CH-3 type).

For benzene-d_1, quenched alkaline solutions were used directly for the analysis. The amount of *p*-deuteroanisole remaining in the reaction mixture (*p*-deuteroanisole plus anisole) was calculated by comparing the peak height of 109 plus 1/8 of that of 107 against that of 108 plus 7/8 of that of 107, assuming that both hydrogen and deuterium split off indiscriminately, giving the peak of 107. This assumption does not seem to be a terribly absurd one in view of the rather small difference in preference for the loss of hydrogen[19]. *p*-Deuterothioanisole gave its main mass peaks at 125,

TABLE II. SOME DATA OF DEUTERIUM ANALYSES

p-Deuteroanisole

Time, min.	$k_1=3.55\times10^{-5}$ sec^{-1}: $D/(D+H)$[a]	Half-life 325 min.: $\frac{D/(D+H)t}{D/(D+H)t_0}\times100$	Temp. 79.9°C., $k_1(\times10^5)$, sec^{-1}
0	0.7570	100	—
20	0.7280	95.8	3.65
40	0.6992	91.5	3.74
70	0.6655	86.6	3.40
180	0.5467	69.3	3.41

p-Deuterothioanisole

Time, min.	$k_1=4.36\times10^{-5}$ sec^{-1}: $D/(D+H)$[a]	Half-life 264 min.: $\frac{D/(D+H)t}{D/(D+H)t_0}\times100$	Temp. 119.9°C., $k_1(\times10^5)$, sec^{-1}
0	0.6820	100	—
55	0.5830	85.5	4.29
105	0.5169	75.8	4.38
180	0.4241	62.2	4.39
300	0.3105	45.5	4.37

a) *D* and *H* indicate deuterated and ordinary compounds respectively.

16) S. Oae and C. C. Price, ibid., **80**, 3425 (1958).
17) L. P. Hammett, "Physical Organic Chemistry", p. 188.
18) H. C. Brown, Y. Okamoto and T. Inukai, *J. Am. Chem. Soc.*, **80**, 4964 (1958).
19) a) S. Meyerson, P. N. Rylander, E. L. Eliel and J. D. McCollum, *J. Am. Chem. Soc.*, **81**, 2606 (1959); b) S. Meyerson and P. N. Rylander, ibid., **83**, 2481 (1961).

124 and 123, wile deuterobenzene gave its at 79, 78 and 77. Similar treatments were carried out for both compounds for estimating the reaction rates.

The typical kinetic runs are shown in Table II, and the derived first-order kinetic constants are recorded in Table I.

The authors are grateful to Mr. Seiichi Mima, of the Osaka Industrial Research Institute, who generously carried out the mass-spectrometric analyses.

Department of Chemistry
Radiation Center of Osaka Prefecture
Sakai, Osaka

*Electronic Spectra of Substituted Aromatic Hydrocarbons. III. Anthrols**

By Hiroaki BABA and Satoshi SUZUKI

(Received August 30, 1961)

Analysis of the electronic spectra of the polyacene series has been successfully made from both experimental[1-3] and theoretical[4-6] viewpoints. The correlation diagram of Klevens and Platt[1] for the energy levels of the polyacenes predicted that in anthracene a weak $^1A_g \rightarrow {}^1B_{3u}^-$ ($^1A \rightarrow {}^1L_b$ in Platt's notation[4]) transition is hidden under the stronger $^1A_g \rightarrow {}^1B_{2u}$ ($^1A \rightarrow {}^1L_a$) transition. (Here the group theoretical notation is the same as that used in the preceding paper[7] of this series.) The above prediction was supported by Pariser's calculations[6]. On the other hand, experimental attempts[3,8] to obtain direct evidence for the existence of the hidden transition have failed. It seems impossible at the present time to detect the hidden transition in the spectrum of anthracene itself.

The situation may be different in the case of substitution products of anthracene. When a substituent group is introduced into anthracene, the two transitions in question, $^1A \rightarrow {}^1L_b$ and $^1A \rightarrow {}^1L_a$, undergo changes different both in location and in intensity, on account of differences in their symmetry types. As a result, it is possible that the $^1A \rightarrow {}^1L_b$ transition may emerge from the $^1A \rightarrow {}^1L_a$ transition. With this in mind, the electronic spectra of α- and β-anthrol have been investigated in the present study. It has been proved that the $^1A \rightarrow {}^1L_b$ transition does appear in the spectrum of β-anthrol.

Experimental

Materials.—α-Anthrol was prepared by fusing potassium anthracene-α-sulfonate with potassium hydroxide[9]; it was recrystallized several times from aqueous ethyl alcohol; m. p. 151°C (literature, 152 ~152.5°C[10]). β-Anthrol was prepared by fusion of sodium anthracene-β-sulfonate with potassium hydroxide[11], and it was repeatedly recrystallized from benzene; m. p. 264~266°C under reduced pressure in a sealed tube (literature, 254~256°C[10]). Isooctane (2,2,4-trimethylpentane; Enjay Co., Inc., U. S. A.) was purified by distillation over phosphorus pentoxide.

Apparatus and Procedure.—Absorption spectra were obtained at 20°C in the same manner as in the preceding paper[7], with a Hitachi photo-electric spectrophotometer of the EPU-2A type.

Fluorescence spectra were measured at room temperature by attaching a Hitachi fluorescence accessory of the L-3 type to the spectrophotometer. The 365 mμ line of a mercury lamp was used as an exciting light; the slit width was fixed at 0.2 mm. It was found that while a solution of α- or β-anthrol was being illuminated by the exciting light, the intensity of the fluorescence was considerably reduced. This difficulty was overcome by using a light of an extremely low intensity and by measuring the fluorescence quickly.

For the calibration of the spectral energy of the fluorescence, a standard tungsten filament lamp was used. The brightness temperature of the filament was measured with an optical pyrometer, and the true temperature was determined to be 2350°K in the usual way. From the spectral energy distribution (based on Planck's law) of a black body at this temperature and the spectral emissivity of tungsten, the spectral energy distribution of the

* Presented at the Symposium on Electronic States in Molecules, held by the Chemical Society of Japan, at Hokkaido University, August, 1960 (see abstract of the Symposium, p. 1).

1) H. B. Klevens and J. R. Platt, *J. Chem. Phys.*, **17**, 470 (1949).
2) D. S. McClure, ibid., **22**, 1668 (1954).
3) J. W. Sidman, ibid., **25**, 115 (1956).
4) J. R. Platt, ibid., **17**, 484 (1949).
5) W. Moffitt, ibid., **22**, 320 (1954).
6) R. Pariser, ibid., **24**, 250 (1956).
7) H. Baba and S. Suzuki, This Bulletin, **34**, 82 (1961).
8) E. Clar, *Spectrochim. Acta*, **4**, 116 (1950).
9) R. E. Schmidt, *Ber.*, **37**, 66 (1904).
10) K. Lauer, ibid., **70**, 1127 (1937).
11) K. Lagodzinski, *Ann.*, **342**, 59 (1905).

standard lamp was obtained. The transmittance of the envelope of the lamp was assumed to be constant over the range from 380 to 600 mμ. The observed fluorescence spectra were thus corrected to quantum fluorescence spectra by following the procedure of Melhuish[12]. Allowance was made for the reabsorption of fluorescence in the region where fluorescence and absorption overlap.

Results and Discussion

The absorption spectra of α- and β-anthrol in an isooctane solution are shown in Fig. 1, where the spectrum of the parent hydrocarbon, anthracene, is also given for the sake of comparison. Each of the spectra can be divided into two distinguishable parts, with the boundary at about 35000 cm^{-1}. In this paper, particular attention will be devoted to the electronic transitions situated in the low frequency region (<35000 cm^{-1}).

As is seen in the figure, anthracene shows in the low frequency region a single electronic absorption band with a sharp vibrational structure. This band has been conclusively assigned to the $^1A \rightarrow {}^1L_a$ transition[3]. (For brevity this will hereafter be called the ^1L_a transition.)

The transition of α-anthrol in the low frequency region is undoubtedly analogous to the ^1L_a transition of anthracene, though it is shifted as a whole to the red and its vibrational structure is less sharp. It appears at first sight that the spectrum of β-anthrol involves, in the same region, only one electronic band corresponding to the above-mentioned transition of α-anthrol. However, as will be described below, detailed examination of the β-anthrol spectrum reveals that there exist two different transitions in the frequency region under consideration.

Vibrational Analysis.—The ^1L_a transition of anthracene has a prominent progression whose members are the vibrational components P, Q, etc. shown in Fig. 1, where P is the 0–0 transition. The spacings of these components are almost constant (about 1400 cm^{-1}) and are related to a totally symmetric carbon stretching vibration[3,13].

The frequencies of the principal vibrational components for the absorption bands of α- and β-anthrol are given in Table I, together with their differences. The vibrational components P, Q, etc. in α-anthrol are almost equally spaced; they are considered to correspond, respectively, to the components P, Q, etc. in the parent molecule. Thus, the α-anthrol transition, to which the components P, Q, etc. belong, must be of the ^1L_a type.

There are five main vibrational components, A, B, P, Q and R, in the β-anthrol spectrum. Of the intervals of these components, the one between B and P is exceptionally large, so that it is not possible to regard all five components as members of a single progression. One may thus reasonably assume that there are two different overlapping transitions and that the

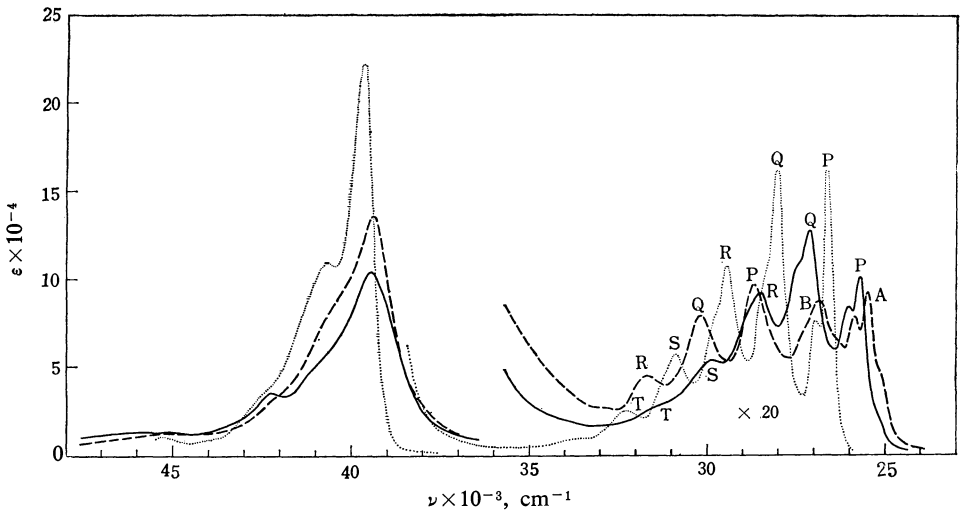


Fig. 1. Absorption spectra of α-anthrol (——), β-anthrol (- - -) and anthracene (·····) in isooctane.
The spectrum of anthracene is taken from American Petroleum Institute Research Project 44, Ultraviolet Spectral Data, Serial No. 170.

12) W. H. Melhuish, *J. Phys. Chem.*, **64**, 762 (1960).

13) S. Sambursky and G. Wolfsohn, *Trans. Faraday Soc.* **36**, 427 (1940).

TABLE I. VIBRATIONAL COMPONENTS OF ABSORPTION BANDS FOR ANTHROLS

		α-Anthrol			β-Anthrol			β-Anthrol negative ion		
			cm^{-1}	cm^{-1}		cm^{-1}	cm^{-1}		cm^{-1}	cm^{-1}
^1L_b	A	(0–0)			A (0–0)	25480				
				1390			1390	ν_{max}	24210	
	B	(0–1)			B (0–1)	26870				
							(1840)			
^1L_a	P	(0–0)	25730		P (0–0)	28710		P (0–0)	28380	
				1410			1490			1430
	Q	(0–1)	27140		Q (0–1)	30200		Q (0–1)	29810	
				1400			1500			1470
	R	(0–2)	28540		R (0–2)	31700		R (0–2)	31280	
				1360						
	S	(0–3)	29900							
				1400						
	T	(0–4)	31300							

components A and B belong to one transition and P, Q and R to the other. These two transitions will be referred to as I and II respectively.

Relation between Fluorescence and Absorption. —The fluorescence spectra of α- and β-anthrol in isooctane solution are shown in Figs. 2 and 3, where $F_Q(\nu)$ denotes the relative fluorescence quantum yield per unit frequency interval at frequency ν. In the figures, the absorption spectra are also given for ready comparison.

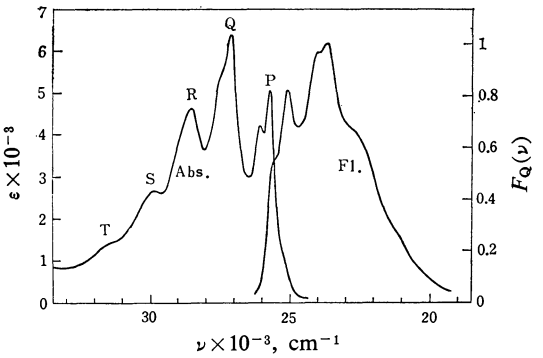


Fig. 2. Fluorescence and absorption spectra of α-anthrol in isooctane. The solute concentration for fluorescence: 5.22×10^{-5} mol./l.

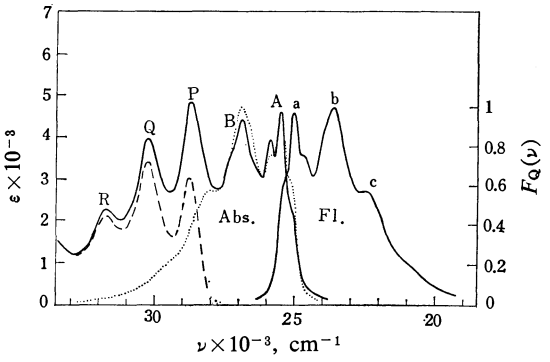


Fig. 3. Fluorescence and absorption spectra of β-anthrol in isooctane. The solute concentration for fluorescence: 4.16×10^{-5} mol./l. See the text for the dotted and broken line curves.

The fluorescence of anthracene is known to be due to the $^1B_{2u} \rightarrow {}^1A_g$ transition[3], which corresponds to the absorption transition of the ^1L_a type. A mirror symmetry has been found between the fluorescence and absorption spectra for anthracene[14]. As is seen in Fig. 2, the fluorescence of α-anthrol has an approximate mirror image relation with the absorption that has been assigned to the ^1L_a transition.

Apparently no such relation exists between the fluorescence and absorption spectra of β-anthrol. In attempting to explain this anomalous fact, let it be assumed, as before, that the low frequency absorption of β-anthrol is due to two overlapping electronic transitions, I and II. It is generally postulated that fluorescence originates in a single electronic transition, which corresponds in most cases to the lowest energy transition. Accordingly, the fluorescence of β-anthrol should be related to that part of the absorption which corresponds to the lower energy transition, I, of the two overlapping transitions.

The above situation can be understood on inspection of the dotted line curve in Fig. 3 which represents the mirror image of the fluorescence spectrum. It is seen that the vibrational peaks a and b of the fluorescence correspond to the absorption peaks A and B respectively. There is another peak, c, in the fluorescence; the corresponding peak cannot be found in the absorption spectrum, probably because it is masked by the absorption due to the higher energy transition, II.

If one is allowed to approximate the absorption due to transition I by the mirror image of the fluorescence, the absorption due to transition II alone may be determined. The latter absorption is depicted in Fig. 3 as a

14) G. Kortüm and B. Finckh, *Z. physik. Chem.*, **B52**, 263 (1942).

broken line curve, wihch is obtained by subtracting the absorption of transition I (dotted curve) from the total absorption (solid curve).

Spectral Changes Accompanying Dissociation of Proton.—The foregoing arguments suggest that two absorption bands due to different electronic transitions appear in the low frequency region when a hydroxyl group is introduced into anthracene at the β-position. This phenomenon is presumably caused by the electron-donating character of that group. It is then to be expected that such a phenomenon will be more distinctly observed in the negative ion of β-anthrol, since the $-O^-$ group is of a more electron-releasing nature than the $-OH$ group. Measurements have therefore been made of the absorption and fluorescence spectra of β-anthrol in a 0.4% aqueous solution of sodium hydroxide[15]. The results are shown in Fig. 4; the frequencies of the absorption maxima are recorded in Table I.

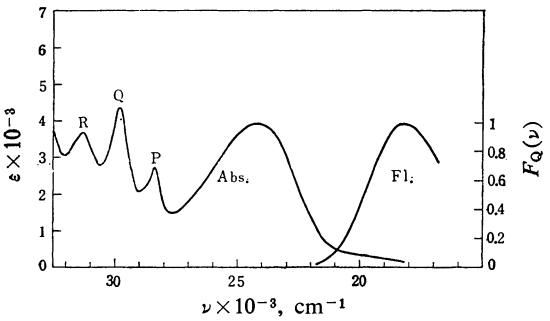


Fig. 4. Fluorescence and absorption spectra of β-anthrol in 0.4% sodium hydroxide solution. The solute concentration for fluorescence: 9.78×10^{-5} mol./l.

As was expected, the negative ion gives two electronic absorption bands at about 24000 cm^{-1} and 30000 cm^{-1}, with a clear minimum between them. Comparison of the absorption spectra for the neutral molecule and the negative ion of β-anthrol shows that, upon dissociation of the proton, transition I is markedly displaced to the red and its vibrational structure is smoothed out, while transition II is shifted only slightly to the red. As a result, the two transitions are separated from each other in the negative ion. The fluorescence of the ion is seen to correspond to the absorption at 24000 cm^{-1}.

Assignment.—It has already been stated that the low frequency absorption of α-anthrol is to be assigned to the ^1L_a transition.

As to the absorption spectrum of β-anthrol in the low frequency region, the results of the present experiments indicate that, in all probability, it consists of two different electronic transitions. It is then natural to consider that the ^1L_b transition, which is believed to be hidden under the ^1L_a transition in the parent molecule, emerges owing to the perturbation of the hydroxyl group at the β-position. If this is the case, the next problem is to decide which of the two transitions, I or II, is of the ^1L_b type.

In order to get a clue to this problem, reference will be made to the absorption spectra of α- and β-naphthol. According to the experimental results reported in the preceding paper[7], substitution of a hydroxyl group into naphthalene at the α-position gives rise to a red shift in both the ^1L_a and ^1L_b transitions. On the other hand, when the substitution is made at the β-position, the ^1L_b transition is noticeably shifted to the red and intensified, whereas the ^1L_a transition is slightly displaced to the blue with a reduction in intensity.

Now, let it be assumed that similar spectral changes take place in the ^1L_a and ^1L_b transitions in going from anthracene to the anthrols. Then the ^1L_b transition is to be expected to appear in β-anthrol on the lower frequency side of the ^1L_a transition, while it remains under the ^1L_a transition in the case of the α-isomer. Transitions I and II of β-anthrol may thus be assigned to the ^1L_b and ^1L_a transitions respectively. The same assignment applies to the transitions of the negative ion of β-anthrol.

It is seen from the observed spectral data that the above assignment in turn leads to the following conclusion: The ^1L_b transition is situated at lower frequencies and is of a higher intensity in β-anthrol (or its negative ion) than in anthracene, while the reverse is true of the ^1L_a transition. The assignment and the interpretation of the individual vibrational peaks are given in Table I for α-anthrol and for the neutral molecule and the ion of β-anthrol.

The effect of substitution on electronic transitions was discussed for anthracene by Jones[16] in terms of the resonance theory. It was suggested that the shift of a transition due to substitution should depend both upon the direction of the electric moment associated with the transition and upon the position of the substitution. Since the ^1L_b and ^1L_a transitions are polarized along the long and short molecular axes respectively, it may be said that the present assignment of the transitions for α- and β-anthrol is compatible with the view of Jones.

15) The absorption spectrum of α-anthrol in the same solution was found to be subject to change during the measurement, so that it is not reported on here.

16) R. N. Jones, *Chem. Revs.*, **41**, 353 (1947).

Mention should also be made of the high frequency transitions. The strong absorption of anthracene at 40000 cm^{-1} has been assigned to a $^1A_g \rightarrow {}^1B_{3u}{}^+$ ($^1A \rightarrow {}^1B_b$) transition[4,6]. It is seen in Fig. 1 that this absorption does not undergo a substantial change when passing from the parent molecule to the anthrols, although a red shift and a change of intensity are seen to occur. Apparently the anthrols have one or two other transitions in the higher frequency region. Discussion of these transitions will be undertaken in a later paper[17].

Summary and Conclusion

The present study of the absorption and fluorescence spectra of α- and β-anthrol has made it possible to explain in a satisfactory manner the origins of their lower electronic transitions. The absorption of α-anthrol in the low frequency region is due to a single electronic transition, which can be assigned to the ^1L_a transition. It is concluded on the basis of vibrational analysis, relation between fluorescence and absorption, and spectral changes accompanying dissociation of the proton that the corresponding absorption in β-anthrol consists of two overlapping electronic bands; this conclusion is further supported by an investigation of spectral changes accompanying the formation of a hydrogen bond between β-anthrol and dioxane[17]. Of the two overlapping bands, the one at the lower frequencies is reasonably assigned to the ^1L_b transition, which has not been found in the spectrum of anthracene, and the other to the ^1L_a transition.

It is of interest to apply to other anthracene derivatives the idea that substitution at the β-position causes the hidden ^1L_b transition of anthracene to appear at lower frequencies. In this connection it is worthy of note that the absorption spectra of β-aminoanthracene and β-acetylanthracene exhibit abnormal features in the lowest frequency region[16]. This fact may perhaps be best explained in the light of the present interpretation of the spectrum of β-anthrol.

The authors wish to express their great gratitude to Dr. Yuichi Kanaoka and Mr. Tetsuya Takeda for preparation of the materials.

Research Institute of Applied Electricity
Hokkaido University, Sapporo

17) S. Suzuki and H. Baba, to be published in *J. Chem. Phys.*

Reactions of Iminocarbonates with Acids

By Teruaki MUKAIYAMA, Tamotsu FUJISAWA and Teruo HYUGAJI

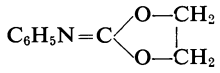
(Received September 2, 1961)

Intramolecular dehydrations of primary nitroparaffins[1,2], aldoximes[3,4,5] and hydroxamic acids[6] into nitrile oxides, nitriles and isocyanates respectively, by means of unsaturated organic reagents, such as isocyanates, carbodiimides, acetylenic ethers, ketene acetals and vinyl ethers, have been described in preceding papers. Further study has now been carried out on the reactions of iminocarbonates, which are considered to be the acetals of isocyanates, with a view to extending the scope of the organic dehydrating reagents.

In the first place, diethyl *N*-phenyl iminocarbonate (I) was chosen. This compound has been reported to be stable towards alkalies and water, but to be split by dilute hydrochloric acid, even while cold, into aniline and diethyl carbonate[7]. Contrary to the cases of isocyanates, however, the reaction of I with benzaldoxime could hardly be observed even at 100°C or in the presence of basic or acidic catalysts, such as triethyl amine or boron trifluoride, and most of the starting materials could be recovered. In the presence of hydrogen chloride, a protonic acid, as a catalyst, the reaction gave the expected ethyl *N*-phenyl carbamate, but the dehydration of benzaldoxime did not take place and the aldoxime was recovered.

1) T. Mukaiyama and T. Hoshino, *J. Am. Chem. Soc.*, **82**, 5339 (1960).
2) T. Mukaiyama and T. Hata, This Bulletin, **33**, 1382 (1960).
3) T. Mukaiyama and T. Hata, ibid., **33**, 1712 (1960).
4) T. Mukaiyama and T. Hata, ibid., **34**, 99 (1961).
5) T. Mukaiyama, K. Tonooka and K. Inoue, *J. Org. Chem.*, **26**, 2202 (1961).
6) T. Mukaiyama and H. Nohira, ibid., **26**, 782 (1961).
7) W. R. Smith, *Am. Chem. J.*, **16**, 372 (1894).

When hydrogen chloride was passed into a solution of I in dry benzene, a violent reaction occurred, forming ethyl *N*-phenyl carbamate in a quantitative yield. This reaction is of the same type as that of diethyl iminocarbonate with hydrogen chloride by which Sandmeyer[8] obtained ethyl chloride and ethyl carbamate. Ethylene *N*-phenyl iminocarbonate (II), which was prepared from phenyl imidophosgene and sodium salt of ethylene glycol, also reacted with hydrogen chloride, giving β-chloroethyl *N*-phenyl carbamate in a 63% yield.

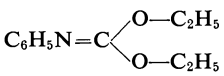


(II)

$$\rightarrow C_6H_5NHCOOCH_2CH_2Cl$$

Since it was found that dehydration did not take place in the reaction with the iminocarbonates and that they were readily decomposed by hydrogen chloride, their reactions with carboxylic and with phosphoric acids studied further.

The reaction of I with acetic acid did not take place at room temperature, but it did proceed well after they had been heated on a water bath at 100°C for 1 hr., giving ethyl *N*-phenyl carbamate and ethyl acetate in high yields. Similarly, I reacted with benzoic acid, giving ethyl *N*-phenyl carbamate and ethyl benzoate, when they had been refluxed in dry benzene for 1 hr.



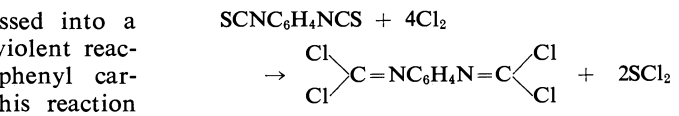
(I)

$$\rightarrow C_6H_5NHCOOC_2H_5 + RCOOC_2H_5$$

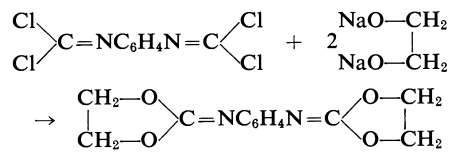
Treatments of II with acetic and benzoic acids also afforded the corresponding β-acyloxyethyl *N*-phenyl carbamate in high yields when refluxed in dry benzene for 2 hr.

$$II + RCOOH \rightarrow C_6H_5NHCOOCH_2CH_2OCOR$$

Next, in order to apply these reactions to the field of polymer chemistry, a compound containing two iminocarbonate groups was treated with acids. As the bifunctional iminocarbonate has not been reported on so far, the preparation of *N*, *N'*-*p*-phenylene bis(ethylene iminocarbonate) (III) was tried by a procedure similar to that for II. *p*-Phenylene diimidophosgene was produced by passing dry chlorine through a solution of *p*-phenylene diisothiocyanate in chloroform instead of the carbon tetrachloride which had been used as a solvent in the case of phenyl imidophosgene.



The use of chloroform is better than that of carbon tetrachloride because the latter leads to the decomposition of the reaction products, giving a dark-stained thick oil. *p*-Phenylene diimidophosgene is unstable towards moisture and is subject to decomposition into *p*-phenylene diamine hydrochloride; it is also desirable to keep it in a vacuum desiccator. One mole of *p*-phenylene diimidophosgene and 2 mol. of sodium salt of ethylene glycol gave III in a 25% yield when refluxed in dry benzene for 5 hr.



(III)

$$+ 4NaCl$$

When a solution of 1 mol. of III and 2 mol. of benzoic acid in dry benzene was refluxed for 2 hr., *p*-phenylene bis(benzoyloxyethyl carbamate) was obtained in a good yield.

$$III + 2C_6H_5COOH \rightarrow C_6H_5COOCH_2\cdot CH_2OCONHC_6H_4NHCOOCH_2CH_2OCOC_6H_5$$

Further, the reactions of III with dicarboxylic acids, such as adipic and terephthalic acids, in dry dimethyl formamide were tried, producing substances with alternating ester and urethan linkages.

$$III + HOCORCOOH \rightarrow [—OCORCOOCH_2\cdot CH_2OCONHC_6H_4NHCOOCH_2CH_2—]_n$$

Finally, when the reaction of I with diethyl phosphate was tried, ethyl *N*-phenyl carbamate and triethyl phosphate were obtained in about 85% yields.

$$I + (C_2H_5O)_2POOH \rightarrow C_6H_5NHCOOC_2H_5 + PO(OC_2H_5)_3$$

This type of reaction of iminocarbonates with acids resembles the so-called Pinner decomposition[9], which involves the reactions of imidoesters with acids to form the amides and esters of the corresponding acids; the reactions seem to proceed through an initial formation of intermediate IV, which in turn decomposes to give urethans and esters of the corresponding acids.

8) T. Sandmeyer, *Ber.*, **19**, 862 (1886).

9) F. Cramer, K. Pawelzik and F. W. Lichtenthaler, *Chem. Ber.*, **91**, 1555 (1958).

$$R'N=C\begin{matrix}OR\\OR\end{matrix} + HX \rightarrow \left[R'\overset{+}{N}H=C\begin{matrix}OR\\OR\end{matrix}\right]X^- \quad (IV)$$

$$\rightarrow R'NHCOOR + RX$$

The initial formation of salt by the interaction of acids because of the strongly basic character attributed to their two alkoxyl groups leads to the formation of ester and urethan, in contrast with the reaction of isocyanates with acids, which yields addition compounds.

Experimental

Diethyl *N*-Phenyl Iminocarbonate (I).—This compound was prepared from phenyl imidophosgene and sodium ethylate following the procedure of Smith[7].

Phenyl Imidophosgene.—This was prepared from phenyl isothiocyanate and chlorine according to the procedure of Bly, Perkins and Lewis[10].

Reaction of I with Hydrogen Chloride.—Into a solution of 3.9 g. (0.02 mol.) of I in 10 ml. of dry benzene was passed dry hydrogen chloride. An evolution of heat was noticeable, and when it was over, the mixture was heated on a water bath at 100°C for half an hour in order to complete the reaction. Then the benzene was removed, and ethyl *N*-phenyl carbamate was obtained and was recrystallized from petroleum ether. Yield 3.3 g. (100%); m. p. 49~51°C, while the mixed melting point with the authentic sample was the same.

Ethylene *N*-Phenyl Iminocarbonate (II).—Into 5.3 g. (0.05 mol.) of sodium salt of ethylene glycol suspended in 30 ml. of dry benzene was added, vigorously stirred, over a period of 10 min., 20 ml. of dry benzene, dissolving 8.0 g. (0.05 mol.) of phenyl imidophosgene. Then the reaction mixture was refluxed on a water bath for 2 hr. while the stirring was continued. It was then poured into water and extracted with benzene, and the benzene solution was washed twice with water. The solution was dried with calcium chloride, and the benzene was removed completely in vacuo. II was solidified and was recrystallized from ether to give needles; yield 6.0 g. (80%); m. p. 73~75°C.

Found: C, 66.03; H, 5.72; N, 8.74. Calcd. for $C_9H_9O_2N$ (II): C, 66.24; H, 5.56; N, 8.58%.

Reaction of II with Hydrogen Chloride.—Dry hydrogen chloride was saturated into a solution of 1.3 g. (0.008 mol.) of II in 40 ml. of dry benzene by warming on a water bath for 1 hr. On evaporation of the benzene, crude β-chloroethyl *N*-phenyl carbamate was obtained and was recrystallized from ether-cyclohexane, yield 1 g. (63%); m. p. 49~51°C.

Reaction of I with Acetic Acid.—A mixture of 7.7 g. (0.04 mol.) of I and 2.4 g. (0.04 mol.) of acetic acid was heated on a water bath at 100°C for 1 hr. Then 2.8 g. (80% yield) of ethyl acetate was obtained by distillation at 78~80°C at ordinary pressure. After the residue had been cooled, ethyl *N*-phenyl carbamate was obtained and was recrystallized from petroleum ether; yield 5.8 g. (88%); m. p. and mixed m. p. 49~51°C.

Reaction of I with Benzoic Acid.—A mixture of 7.7 g. (0.04 mol.) of I and 4.9 g. (0.04 mol.) of benzoic acid in 20 ml. of dry benzene was refluxed on a water bath for 1 hr., and then the benzene was removed. Distillation gave 5.7 g. (95% yield) of ethyl benzoate at 88~90°C/12 mmHg. When the residue was cooled, ethyl *N*-phenyl carbamate was solidified and was recrystallized from petroleum ether; yield 5.8 g. (88%); m. p. and mixed m. p. 49~51°C.

Reaction of II with Acetic Acid.—A solution of 4.0 g. (0.025 mol.) of II and 1.5 g. (0.025 mol.) of acetic acid in 20 ml. of dry benzene was refluxed on a water bath for 2 hr. When the benzene had been removed and the brown oily residue kept standing for three weeks, then there were obtained colorless chunky prisms of β-acetoxyethyl *N*-phenyl carbamate which could not be recrystallized from any solvent; yield 2.3 g. (42%); m. p. 43~45°C.

Found: C, 59.06; H, 6.29; N, 6.33. Calcd. for $C_{11}H_{13}O_4N$: C, 59.18; H, 5.87; N, 6.28%.

Reaction of II with Benzoic Acid.—A mixture of 1.6 g. (0.01 mol.) of II and 1.2 g. (0.01 mol.) of benzoic acid in 20 ml. of dry benzene was refluxed on a water bath for 1 hr. After the removal of the benzene, β-benzoxyethyl *N*-phenyl carbamate was obtained and was recrystallized from benzene to give needles; yield 2.3 g. (81%); m. p. 115~116°C.

Found: C, 67.27; H, 5.46; N, 5.03. Calcd. for $C_{16}H_{15}O_4N$: C, 67.36; H, 5.30; N, 4.91.

***p*-Phenylene Diimidophosgene.**—A solution in 100 ml. of chloroform of 19.2 g. (0.1 mol.) of *p*-phenylene diisothiocyanate, which had been prepared according to the procedure of van der Kerk, Pluygers and de Vries[11] and which had been recrystallized from petroleum ether[12], was saturated with dry chloride. As an evolution of heat was noticeable during the reaction, the solution was cooled in ice-water. The color of the reaction mixture gradually became red. After the chloroform and sulfur chloride had been partially removed by distillation, the resulting crude *p*-phenylene diimidophosgene was kept standing in vacuo in order to remove them completely. Recrystallization from ether afforded pale yellow needles; yield 23.0 g. (85%); m. p. 94~96°C.

Found: C, 35.87; H, 1.58; N, 10.45. Calcd. for $C_8H_4N_2Cl_4$: C, 35.55; H, 1.48; N, 10.37%.

***N,N'*-*p*-Phenylene Bis(ethylene iminocarbonate) (III).**—To 8.7 g. (0.04 mol.) of sodium salt of ethylene glycol suspended in 200 ml. of dry benzene was added dropwise, by vigorous stirring and refluxing on a water bath, a solution of 5.4 g. (0.02 mol.) of *p*-phenylene diimidophosgene in 200 ml. of dry benzene at such a rate that the addition was completed in about 1 hr., while the stirring and the refluxing were continued for an additional 4 hr. Then the reaction mixture was filtered while still hot, and from the filtrate about two-thirds of the benzene was distilled off. When it was cooled, III

10) R. S. Bly, G. A. Perkins and W. L. Lewis, *J. Am. Chem. Soc.*, **44**, 2896 (1922).

11) G. J. M. van der Kerk, C. W. Pluygers and G. de Vries, *Rec. trav. chem.*, **74**, 1262 (1955).

12) This compound, which was recrystallized from glacial acetic acid, did not give a good result.

was obtained as a white precipitate. By extracting the filtered mass with hot benzene, a considerable increase in the yield was observed. Several recrystallizations from acetone afforded a white solid; yield 1.3 g. (25%); m. p. 188~190°C.

Found: C, 58.13; H, 5.13; N, 11.45. Calcd. for $C_{12}H_{12}O_4N_2$ (III): C, 58.06; H, 4.87; N, 11.29%.

Reaction of III with Benzoic Acid.—A mixture of 0.62 g. (0.0025 mol.) of III and 0.61 g. (0.005 mol.) of benzoic acid in 50 ml. of dry benzene was refluxed on a water bath while being stirred for 2 hr. After the removal of the benzene, *p*-phenylene bis(benzoyloxyethyl carbamate) was obtained and recrystallized from methanol many times to give a white solid; yield 1.0 g. (81%); m. p. 180~182°C.

Found: C, 62.62; H, 5.19; N, 5.69. Calcd. for $C_{26}H_{24}O_8N_2$: C, 63.41; H, 4.91; N, 5.68%.

Reaction of III with Adipic Acid.—A mixture of 0.62 g. (0.0025 mol.) of III and 0.37 g. (0.0025 mol.) of adipic acid in 10 ml. of dry dimethyl formamide was heated and stirred on a water bath at 85°C for 2 hr. and was then vigorously stirred into water to precipitate a polymer, alternating poly(adipate/*p*-phenylene bis(ethylene carbamate)), which separated as a brown solid. The polymer was filtered off and washed several times by stirring with water and dried in vacuo overnight; yield 0.81 g. (81%); m. p. 140°C.

Found: N, 7.59. Calcd. for $(C_{18}H_{22}O_8N_2)_n$: N, 7.10%.

Reaction of III with Terephthalic Acid.—A mixture of 0.62 g. (0.0025 mol.) of III and 0.42 g. (0.0025 mol) of terephthalic acid in 15 ml. of dry dimethyl formamide was heated and stirred on a water bath at 85°C for 2 hr. and then filtered. The clear solution was vigorously stirred into water to precipitate a polymer, alternating poly(terephthalate/*p*-phenylene bis(ethylene carbamate)), which separated as a white solid. The polymer was filtered off and washed several times by stirring with water and dried in vacuo overnight; yield 1.01 g. (97%); m. p. 236°C.

Found: N, 7.44. Calcd. for $(C_{20}H_{18}O_8N_2)_n$: N, 6.76%.

Reaction of I with Diethyl Phosphate.—A solution of 3.1 g. (0.02 mol.) of diethyl phosphate and 3.9 g. (0.02 mol.) of I in 10 ml. of dry benzene was refluxed on a water bath for 3 hr. After the benzene had been removed, distillation gave 3.1 g. (86% yield) of triethyl phosphate at 96~98°C/13 mmHg (Found: P, 16.98%).

When the residue was cooled, ethyl *N*-phenyl carbamate was obtained and was recrystallized from petroleum ether; yield 2.6 g. (87%); m. p. and mixed m. p. 49~51°C.

Summary

Iminocarbonates, whose chemical properties have been little investigated, were prepared from sodium alkoxides and corresponding imidophosgene.

Diethyl *N*-phenyl iminocarbonate gave urethan and esters by reaction with acids, such as hydrogen chloride, carboxylic acids and diethyl phosphate. β-Acyloxyethyl *N*-phenyl cabamates were prepared from the reactions of ethylene *N*-phenyl iminocarbonate with carboxylic acids.

These reactions were applied to the syntheses of polymers, and the alternating poly(urethan/ester)s were obtained.

The authors wish to express their hearty thanks to Mr. Keiji Naruse for his microanalyses.

Laboratory of Organic Chemistry
Tokyo Institute of Technology
Meguro-ku, Tokyo

Molecular Polarisability. The Molar Kerr Constant and Conformation of Diphenyl Ether as a Solute in Benzene

By R. J. W. Le Fèvre, A. Sundaram and K. M. S. Sundaram

(Received August 14, 1961)

Attention has recently[1] been drawn to the problem of assigning a space-formula to diphenyl ether. Both in conversations at Princeton and in Ref. 1, p. 30, Professor K. Higasi has indicated that the Sydney group might provide helpful evidence on the matter. Accordingly we have measured the molar Kerr constant of diphenyl ether at infinite dilution in benzene and now desire to record and discuss our results.

Experimental and Computational Methods.— For brevity we omit details of apparatus and

1) K. Higasi, "Dielectric Relaxation and Molecular Structure", *Monograph Series of the Research Institute of Applied Electricity*, No. 9, Hokkaido University, Sapporo, Japan, 1961.

technique since they are described in detail elsewhere[2,3]. Dielectric constants, ε, densities, d, refractive indexes, n, and Kerr constants, B, of solutions containing weight fractions, w, of diphenyl ether in benzene at 25° are listed in Table I; the n's and B's were measured with Na-light. Suffixes 1, 2, and 12 indicate respectively a property of the solvent, solute, or solution; the prefix Δ denotes a difference between solution and solvent, e. g. $\Delta\varepsilon=\varepsilon_{12}-\varepsilon_1$, $\Delta d=d_{12}-d_1$, $\Delta n=n_{12}-n_1$, and $\Delta B=B_{12}-B_1$. The symbols α, β, γ, and δ are from the equations, $\varepsilon_{12}=\varepsilon_1(1+\alpha w_2)$, $d_{12}=d_1((1+\beta w_2)$, $n_{12}=n_1(1+\gamma w_2)$, and $B_{12}=B_1(1+\delta w_2)$, which are assumed to apply at low w_2's and to be usable whenever Δ(property) appears rectilinear with w_2; γ' refers to the square of the refractive index, $n^2_{12}=n^2_1(1+\gamma' w_2)$. Molar Kerr constants, total polarisations, etc., extrapolated to infinite dilution are written ${}_\infty({}_mK_2)$, ${}_\infty P_2$, etc.; calculations of these are via specific quantities, e. g. ${}_sK_2$, p_2, and r_2, which when $w_2=0$ are given by relations 1, 2, and 3:

$$ {}_\infty({}_sK_2)={}_sK_1(1-\beta+\gamma+\delta-H\gamma-J\alpha\varepsilon_1) \quad (1) $$

where ${}_sK_1=6\lambda n_1B_1/(n^2_1+2)^2(\varepsilon_1+2)^2d_1$

$H=4n^2_1/(n^2_1+2)$

and $J=2/(\varepsilon_1+2)$;

$$ {}_\infty p_2=p_1(1-\beta)+3\alpha\varepsilon_1/d_1(\varepsilon_1+2)^2 \quad (2) $$

where $p_1=(\varepsilon_1-1)/d_1(\varepsilon_1+2)$;

$$ {}_\infty r_2=r_1(1-\beta)+3\gamma' n^2_1/d_1(n^2_1+2)^2 \quad (3) $$

where $r_1=(n^2_1-1)/d_1(n^2_1+2)$

Derivations of Eqs. 1, 2, and 3 may be found in Refs. 2 and 3. Benzene used as solvent was purified as described in Ref. 3, p. 45.

Observations and Quantities Deduced Therefrom.—These are set out in Table I. When $w_2=0$ (i. e. for the pure solvent) the following apply at 25°: $n_1=1.4973$, $n^2_1=2.24191$, $\varepsilon_1=2.2725$, $d_1=0.87378$, and $B=0.410\times10^{-7}$.

TABLE I. DIPHENYL ETHER IN BENZENE AT 25°

10^5w_2	1035	2249	3432	6853	10985	14557	18137
$10^4\Delta n$	7	15	22	46	74	102	131
$10^4\Delta n^2$	20	44	64	135	218	301	387
$10^4\Delta\varepsilon$	114	240	372	737	1165	1551	1805
$10^5\Delta d$	173	373	575	1168	1892	2515	3157
$10^{11}\Delta B$	61	132	210	410	681	870	1120

whence $\sum\Delta n/\sum w_2=0.069$

$\sum\Delta n^2/\sum w_2=0.204$

$\sum\Delta\varepsilon/\sum w_2=1.04_6$

$\Delta d=0.1672w_2+0.0340w^2_2$

$\sum\Delta B/\sum w_2=0.606\times10^{-7}$

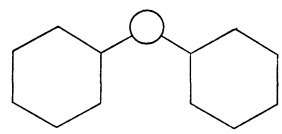
From these data we have: ${}_\infty P_2=80.29$ cc., $R_D=52.68$ cc., ${}_DP=1.05R_D=55.31$ cc., $\mu=1.10_5$D., and ${}_\infty({}_mK_2)=22.4\times10^{-12}$.

Wesson[4] lists two earlier determinations of the dipole moment of diphenyl ether in benzene (viz. 1.02 and 1.13 D.) with neither of which is the new value of 1.10_5 D. in serious disharmony. The Kerr effect of diphenyl ether has never been examined before, either as a pure liquid or as a solute.

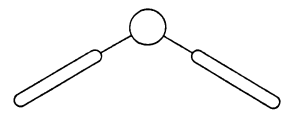
Discussion.—The molar Kerr constant of a substance depends upon the principal axes, b_1, b_2, and b_3, of the appropriate polarisability ellipsoid, together with the direction of action of the resultant dipole moment and its magnitude. For a given molecular model, these axes can be calculated from the longitudinal, transverse, and "vertical" polarisabilities of the constituent bonds and groups. (Examples of such operations are given in Refs. 2 or 5.) In the present case only the C–O link[6] and the phenyl-group[7] are concerned:

		C–O	C_6H_5
Longitudinal polarisability	$b_L\times10^{23}$	0.081	1.056
Transverse 〃	$b_T\times10^{23}$	0.039	1.056
"Vertical" 〃	$b_V\times10^{23}$	0.039	0.671

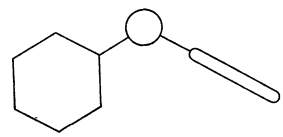
Four models will now be considered, A, B, C and D; only the first three are illustrated here:



A



B



C

2) C. G. Le Fèvre and R. J. W. Le Fèvre, *J. Chem. Soc.*, **1953**, 4041; **1954**, 1577; *Rev. Pure and Appl. Chem.*, 5, 261 (1955); Chap. XXXVI in Physical Method of "Organic Chemistry", Ed. Weissberger, Interscience Pub., New York, London, 3rd edn., Vol. 1, p. 2459.

3) R. J. W. Le Fèvre, "Dipole Moments", Methuen, London, 3rd edn. (1953), Chap. II.

4) L. G. Wesson, "Tables of Electric Dipole Moments", Technology Press, Massachusetts Institute of Technology (1948).

5) R. J. W. Le Fèvre, "Applications in Chemistry of Properties Involving Molecular Polarisability", Liversidge Research Lecture, *J. Proc. Roy. Soc. N. S. W.*, **95**, 1 (1961).

6) C. G. Le Fèvre and R. J. W. Le Fèvre, *J. Chem. Soc.*, **1956**, 3549.

7) M. Aroney and R. J. W. Le Fèvre, ibid., **1960**, 3600.

Table II. Principal polarisabilities and molar Kerr constants calculated for models A to D

Model*	$10^{23}b_1$	$10^{23}b_3$	$10^{23}b_3$	$10^{12}{}_{\mathrm{m}}K_2$ calcd.
A	2.212	2.253	1.420	+84.1
B	1.635	2.060	2.190	−54.1
C	1.836_5	2.243_5	1.805	−16.6
D	2.003	2.246	1.636	+22.6

* The direction in which b_1 is measured bisects the C_1–O–$C_{1'}$ angle, that for b_2 is parallel to the C_1·····$C_{1'}$ line, and that for b_3 is perpendicular to the C_1–O–$C_{1'}$ triangle.

The molecule is planar in A; in B both phenyl-rings are at 90° to the plane of A; C is Morino's conformation[1] with one ring as in A and one as in B; D is generated from A by twisting each phenyl group by 37° about its O–C_1–C_4 line. In all cases $\mu_{\text{resultant}}$ is taken as acting along the bisector of the C–O–C angle, which—following Higasi[1]—is adopted as 120°. Calculations are summarised in Table II.

Since the molar Kerr constant obtained by experiment is 22.4×10^{-12}, it appears that neither A nor B nor C *alone* represents the diphenyl ether molecule in benzene. It is of course possible to devise mixtures of A and B, or of A with B and C, for which the expected ${}_{\mathrm{m}}K$ would equal that observed, yet there seems to be no recorded evidence against the view that the ether exists as a *single* form, in which case one of type D is indicated.

The angle of twist of 37° was selected by trial and error and is advanced as an "order of magnitude" estimate only (because the data for C–O and phenyl are drawn from paraldehyde[6] and benzene[7] respectively and may not be quite appropriate for diphenyl ether, in which some conjugation effects must also be present). Nevertheless it is interesting that Higasi (Ref. 1, p. 26) calculates that the twist angles for the configuration of minimum energy are 32.5°, and later in the same work (pp. 112—113) explicitly mentions the possibility of a form such as D, which *inter alia* would satisfy Katayama's X-ray study of *o*, *o'*-diiododiphenyl ether (in which the I·····I distance was found to be 5.28±0.07 Å) if the twist angles in this substituted molecule had the values 17.5°.

Finally it is relevant to mention that, via the Kerr effect, Aroney and Le Fèvre[7] concluded that the phenyls in triphenylamine were twisted 65∼70° from the positions in which the three-fold axis of symmetry is parallel to the planes of the Ar-rings, while via electron diffraction, Sasaki, Kimura, and Kubo[8] found angles of 47±5°. By similar arguments to those used with NPh_3, Aroney and Le Fèvre[7] have deduced angles of ca. 45° for triphenylmethane, and unpublished measurements and calculations for benzophenone suggest that twists of about 45° are satisfactory for this molecule also.

Grateful acknowledgement is made to the University of Sydney of the award of an H. B. and F. M. Gritton Research Scholarship to K. M. S. and of the F. A. Q. Stephens Research Fellewship to A. S.

Chemistry School
University of Sydney
N. S. W., Australia

8) Y. Sasaki, K. Kimura and M. Kubo, *J. Chem. Phys.*, **11**, 477 (1959).

Molecular Configuration of Diphenyl Ether as Revealed by Dielectric Relaxation Times and Molar Kerr Constants

By Keniti HIGASI

(Received September 28, 1961)

Mesomeric Moments in Morino's Structure

Professor Morino[1,2] of the University of Tokyo proposed a space model of a diphenyl ether molecule in 1938. It is easy to see that steric conditions prevent two rings in diphenyl ether from being fully coplanar. Indeed, the nearest non-bonding hydrogen atoms are the small distance of 0.5 Å apart in a coplanar structure. After calculating the repulsive energies between these atoms for a variety of configurations, Morino reached the conclusion that the rings in diphenyl ether tend to be on planes perpendicular to each other. Later, this view

1) Y. Morino, first cited in Ref. 3 and later fully treated in Ref. 2.
2) K. Higasi, "Dielectric Relaxation and Molecular Structure", Research. Inst. Appl. Elec., Hokkaido Univ., (1961).

was found to be in good agreement with experimental results obtained by measurements of the dipole moments of diphenyl ether derivatives[3] and by electron diffraction studies of *p, p'*-dihalogenodiphenyl ethers[4].

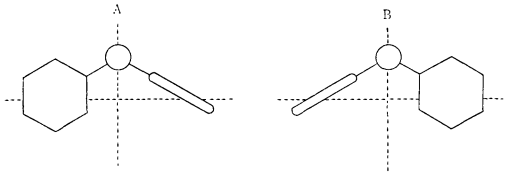


Fig. 1. Two important structures, A and B.

In these earlier studies, however, little attention was paid to the existence of mesomeric moments; Morino's structure in the literature[3] must, therefore, be improved in view of this effect. In order to make this point clearer, two structures, A and B, will be considered, both structures fulfilling Morino's condition: *the two rings are in planes at right angles to each other.* In structure A the ring on the left side of the oxygen atom is taken in the plane of the C–O–C triangle, while the other ring on the right side is perpendicular to the plane of this triangle. In structure B the right ring is in the triangle plane, while the left ring is perpendicular to it.

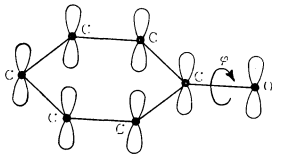


Fig. 2. Overlap of p-orbitals.

Among the atomic orbitals of the oxygen atom, attention will be directed to a pure p orbital which is occupied by two electrons and has its maximum electron density in the direction perpendicular to the C–O–C plane. When the C–O–C triangle is in the plane of a benzene ring, that is, when $\varphi=0$ in Fig. 2, all the p orbitals in the picture are parallel to each other (see Fig. 2). Consequently, in structure A the p orbital of oxygen has a great interaction with the p orbitals of the benzene ring on the left side. On the other hand however, the same orbital has no overlap with the p orbitals belonging to the right ring. It may be said that the oxygen atom is conjugated with the left ring but not with the right ring. According to the molecular orbital theory, π-electrons move freely in the domain of the conjugated part and a fraction of the electrons migrate from the oxygen to the side of the left ring, while no such electron-migration is possible towards the right ring. The so-called "mesomeric moment" is produced only in one direction, that is, towards the left ring in structure A and towards the right ring in structure B.

If the above mesomeric moment had a small magnitude, it seemed that one could usually ignore its effects. However, this seems to have been erroneous. A search in the literature[5] will reveal that the OCH_3 group substituted in benzene is reported to have a mesomeric moment of considerable value, 0.8~0.96 D. If the OCH_3 group lies in the plane of the benzene ring, the mesomeric moment will have a maximum value. Very likely the OCH_3 group has some freedom of rotation. Rotation from the coplanar position will always lower the value of the mesomeric moment; for a twist angle φ mesomeric moment, μ_m, will be expressed by[6]

$$\mu_m = \mu_{max} \cos^2\varphi \qquad (1)$$

The observed values of mesomeric moments show an average value of μ_m for all possible states of rotation, while the mesomeric moment in structure A or structure B corresponds to μ_{max}. Consequently, the latter magnitude must be larger than the former. One may consider that *the moment 0.8~0.96 D will represent the lowest limit of this kind of mesomeric moment in diphenyl ether.*

By a change from structure A to structure B, the region of conjugation is changed and the direction of the mesomeric moment is altered by 120°. Further, such a structural change can be brought about by internal rotation; Morino[1] noticed that the barrier to this sort of internal rotation has an insignificant height. This point was later verified more fully[2].

Dielectric Relaxation Times

According to Debye[7] the dielectric relaxation time of a polar liquid is largely determined both by the size of the polar molecule and by the viscosity of the surrounding medium. Diphenyl ether and benzophenone, both having almost the same molecular size, are expected to have a relaxation time of nearly the same magnitude under the same set of conditions.

3) K. Higasi and S. Uyeo, ibid., **14**, 87 (1939); S. Uyeo and K. Higasi, *J. Chem. Soc. Japan (Nippon Kwagaku Kwaishi)*, **60**, 199 (1939); K. Higasi and Uyeo, ibid., **60**, 204 (1939).

4) K. Higasi, S. Uyeo and S. Yamaguchi, *Bull. Inst. Phys. Chem. Research, Tokyo*, **23**, 788 (1947).

5) L. E. Sutton, "Dipole Moments", p. 373, in E. A. Braude and F. C. Nachod, "Determination of Organic Structures by Physical Methods", Academic Press Inc., New York (1955); A. R. Katritzky, E. W. Randall and L. E. Sutton, *J. Chem. Soc.*, **1957**, 1769.

6) E. G. McRae and L. Goodman, *J. Chem. Phys.*, **29**, 334 (1958).

7) P. Debye, "Polar Molecules", The Chemical Catalogue Co., New York (1929).

However, this is not what is actually observed. The relaxation time of diphenyl ether in benzene at 25°C, 4.1×10^{-12} sec., is only 22% of that of benzophenone, 18.7×10^{-12} sec.[8] Since the magnitude of the latter substance has been regarded as normal in the light of the Debye theory, the relaxation time of diphenyl ether must be considered anomalous.

Let it be assumed, for the sake of simplicity, that diphenyl ether consists of a mixture of molecules which have structure A or structure B. By application of the electric field, the proportions of the mixture will be changed according to Maxwell's distribution law; hence dielectric polarization will be produced[9]. If an alternating field is applied, dielectric dispersion will occur in the range of a certain critical frequency; the latter is largely determined by the activation energy necessary for the change from structure A to structure B, or vice versa. This predicts a new mechanism of dielectric absorption. It must be entirely different from that proposed by Debye, in whose conception rigid spherical dipoles rotate in the viscous medium. Further, by reason of the low barrier to internal rotation which makes structural change from A to B or from B to A feasible, one will expect that the relaxation time of this mechanism will be small—perhaps smaller than usual. The unusually short relaxation time of diphenyl ether, 4.1×10^{-12} sec., has been explained thus[2,10].

Recently Dr. Vaughan and Prof. Smyth[11] of Princeton University discovered that diphenyl ether has two absorption peaks of unequal height, the smaller one being located at a frequency very near to that of benzophenone. This observation is extremely interesting, because one can estimate the magnitudes of the two dipole moments associated with the two absorption peaks. If μ_1 and μ_2 represent the effective moments of the two peaks which one may consider as arising from overall rotation and internal rotation respectively, then $\mu_1=0.60$ D and $\mu_2=0.97$ D. The smaller peak was detected only on data at 40°C, while data at 60°C closely fit a Cole-Cole arc. Consequently, some might be skeptical as to the existence of the small absorption. If no such absorption exists at all, the magnitude of μ_2 should become identical with that of the molecular dipole moment itself[12]. For this reason one may estimate

$$0.97\text{ D}\simeq\mu_2\leqslant1.14\text{ D} \tag{2}$$

Further we may assume

$$\mu_2=\mu_{\max}\sin\theta/2 \tag{3}$$

in which θ is the oxygen valence angle[2]. If $\theta=120°$, $\mu_{\max}$ will have a magnitude

$$1.12\text{ D}\simeq\mu_{\max}\leqslant1.32\text{ D} \tag{4}$$

The above estimate is considered to be of the right order of magnitude in spite of the fact that it is based on a tentative assumption.

Molar Kerr Constant

Prof. R. S. W. Le Fèvre and his co-workers[13] at the University of Sydney were the first to determine the molar Kerr constant of diphenyl ether in benzene solution. They reached the conclusion that the space formula of Morino does not represent the molecular configuration of diphenyl ether, because K_m calculated for this structure has a negative value of -16.6×10^{-12} while the observed value is a positive $K_m=+22.4\times10^{-12}$. However, there is a point here which is worthy of discussion: they assumed the molecular dipole moment to be acting along the bisector of the C–O–C angle.

We shall define three components of the molecular dipole as follows: the direction of μ_1 bisects the angle C_1–O–C_1, that for μ_2 is parallel to the $C_1\cdots\cdots C_1$ line, and that for μ_3 is perpendicular to the C_1–O–C_1 triangle. The assumption employed by Le Fèvre et al.[13] is:

$$\mu_1=1.105\text{ D}\qquad\mu_2=\mu_3=0.0\text{ D} \tag{5}$$

Indeed, this is essentially the same assumption as that used in 1939 by Higasi and Uyeo[3]. However, this assumption will be valid only for certain configurations if a mesomeric moment of an appreciable magnitude exists on account of the conjugation of the oxygen and some ring or rings.

From the analysis of relaxation times two effective moments μ_1 and μ_2 have been obtained in the previous section. One can use these values here with a certain amount of justification[2,10].

$$\mu_1=0.60\text{ D},\quad\mu_2=0.97\text{ D}\quad\text{and}\quad\mu_3=0.0\text{ D} \tag{6}$$

The molar Kerr constant can be calculated with the use of the above values, resulting in $K_m=45\times10^{-12}$. It is to be noted that the calculated value is no longer a negative quantity. In this calculation three principal polarizabilities, b_1, b_2 and b_3, are taken from Le Fèvre's above-mentioned article[13] as 1.8365, 2.2435 and 1.805×10^{-23} respectively*.

8) J. Schneider, *J. Chem. Phys.*, **32**, 665 (1960).
9) H. Fröhlich, "Theory of Dielectrics", Oxford University Press (1949), pp. 15—21.
10) K. Higasi and C. P. Smyth, *J. Am. Chem. Soc.*, **82**, 4759 (1960).
11) W. E. Vaughan and C. P. Smyth, *J. Phys. Chem.*, **65**, 98 (1961).
12) L. G. Wesson, "Tables of Electrical Dipole Moments", Massachusetts Institute of Technology Press (1948).
13) R. J. W. Le Fèvre, (Mrs.) A. Sundaram and K. M. S. Sundaram, This Bulletin, **35**, 690 (1962).

* This is a crude assumption because, as Prof. Le Fèvre remarked, the "longitudinal" polarizability of a partially quinoid phenyl would be greater than the value for ordinary phenyl.

Alternatively we may employ the values of μ_1 and μ_2 given by Higasi and Smyth[10] from an analysis of mesomeric moments,

$$\mu_1=0.54\,\mathrm{D},\quad \mu_2=0.87\,\mathrm{D}\quad \text{and}\quad \mu_3=0.0\,\mathrm{D} \qquad (7)$$

As a result of the use of these values, the molar Kerr constant will become slightly smaller for the above—$K_m=38\times10^{-12}$.

As can be seen from the two examples, one can approach the observed value $K_m=22.4\times10^{-12}$ indefinitely by choosing a larger value for μ_1 and a smaller value for μ_2. However, the writer believes that one might better consider this problem in the following way:

So far the argument has been stated as if a diphenyl ether molecule had a rigid structure shown by structure A or B. On the contrary, the molecule must be non-rigid, with a restricted freedom of rotation around the C–O bonds.

For the purpose of making a little better approximation, a particular type of rotation will be considered, such as satisfying the condition that the two rings are always in planes at right angles to each other. This condition implies that when the left ring in structure A rotates by an angle φ, the right ring must rotate in the same direction by the same amount of angle.

It can be shown by a little calculation[2] that the two components of the molecular dipole, μ_1 and μ_2, will be changed by the above-mentioned rotation in the followlng way:

$$\mu_1=m_0-\frac{1}{2}\mu_{max}$$

$$\mu_2=0.866\,\mu_{max}(\cos^2\varphi-\sin^2\varphi) \qquad (8)$$

in which the valence angle of oxygen is taken as 120°. An estimate of μ_{max} has been given above in Eq. 4. It will be seen that μ_2 is zero only when $\varphi=\pm45°$, $\pm135°$, etc. Consequently, as far as the Morino structure is concerned, one might better consider that the molecular dipole moment is *not* acting along the bisector of the C–O–C angle.

Suppose μ_{max} has quite a large value, 1.4 D, and a magnitude, 0.92 D, for m_0, which represents a dipole arising from two C–O links; we shall obtain for $\varphi=0$

$$\mu_1=0.22\,\mathrm{D}\qquad \mu_2=1.21\,\mathrm{D} \qquad (9)$$

Since μ_2 has a large value while μ_1 is extremely small, K_m for Eq. 9 must have a large magnitude —in fact $K_m=76\times10^{-12}$. This would be the highest possible value for K_m. By use of Eq. 8 one can estimate the variation of K_m with a change in the twist angle φ (see the upper curve* in Fig. 3). It will be seen that if the contribution of rotation to K_m is taken into consideration, the average value of K_m will decrease. The observed value $K_m+22.4\times10^{-12}$ may possibly be accounted for in this manner. The variation of K_m with the twist angle φ when using Eqs. 7 and 8 is shown in the lower curve* of Fig. 3.

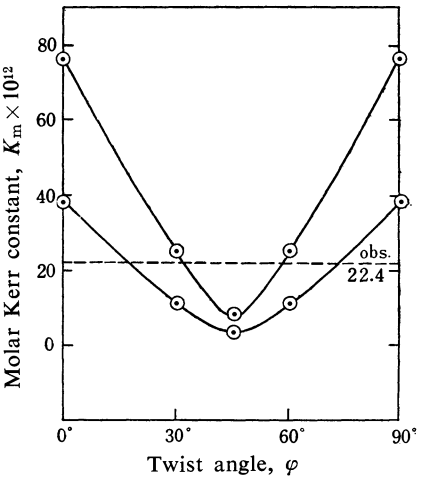


Fig. 3. Variation of the molar Kerr constant of diphenyl ether (Morino) with the twist angle.

It was once suggested by the present writer[2] that the study of the Kerr constant of diphenyl ether might eventually play a decisive role in determining the structure of this molecule. Grateful acknowledgement must be made to Professor Le Fèvre and his group for satisfying this request by carrying out valuable measurements. The analysis of their results has contributed greatly to making many points clearer. However, the magnitude of the molar Kerr constant alone does not appear to be unequivocal evidence *for* or *against* the Morino structure.

Lastly, a few words must be added regarding the dipole moment of diphenyl ether. The dipole moment μ at a twist angle φ is determined by

$$\mu^2=\mu_1^2+\mu_2^2 \qquad (10)$$

in which μ_1 and μ_2 are given by Eqs. 8. Again we shall assume that $\mu_{max}=1.4$ D; then $\mu=1.23$ D, for $\varphi=0$. If free rotation occurs, $\mu=0.88$ D. The observed value, 1.14 D[12], is between the two calculated values.

The above example will suggest that the observed dipole moment and the molar Kerr constant of a non-rigid molecule, diphenyl ether being included, represent average values of various magnitudes corresponding to a great number of possible configurations. The dielectric relaxation time provides two effective dipole moments which are other sorts of

* The estimated values are of only qualitative significance because the three principal polarizabilities are tentatively assumed to be independent of rotation.

average quantities. Possibly the latter is closely associated with the former. However, there is an essential difference: a dipole moment determined from dielectric constant measurements represents a static property of the molecule, while effective moments from dielectric relaxation time analysis are associated with the dynamic nature of the molecule.

The writer wishes to thank Professor R. J. W. Le Fèvre for providing much valuable information. Thanks are also due to Professor C. P. Smyth and Professor Yonezo Morino for their interest in this work.

Research Institute of Applied Electricity
Hokkaido University, Sapporo

SHORT COMMUNICATIONS

Identification of Polyphenyls Formed in the Radiolysis of Biphenyl by Reverse Isotope Dilution Analysis

By Hiroaki KŌYAMA*, Gen-ichi TSUCHIHASHI and Akibumi DANNO

(Received January 22, 1962)

The radiolysis of polyphenyls has been studied by many workers[1-4] in order to elucidate the decomposition mechanism of organic coolant-moderator, however no datailed study on the identification of radiolytic products of high molecular weight has hitherto been carried out. The present work aimed to obtain a precise information concerning the radiolytic mechanism for biphenyl, the simplest polyphenyl. Here, reverse isotope dilution analysis by using ^{14}C-labeled compound was applied to determine the yields of terphenyls and quaterphenyls produced by the radiolysis of biphenyl.

Biphenyl-(phenyl-^{14}C) (33.2 mc/mol.)[5,6] was irradiated at 100±5°C in vacuum by gamma-rays (2.60×10^5 r/hr., 150 hr.)[7]. After the compound was irradiated, each carrier component was added to the irradiated sample and was homogeneously mixed using anisole as a homogenizer. Unchanged biphenyl-(phenyl-^{14}C) was removed by sublimation. Each compound was isolated by liquid elution chromatography on activated alumina with petroleum ether and then recrystallized from a suitable solvent several times to give a constant specific activity. Radioactivity of the purified product was determined using a Tri-Carb liquid scintillation spectrometer or an ionization chamber-vibrating reed electrometer.

TABLE I. *G*-VALUES FOR THE FORMATION OF POLYPHENYLS IN THE RADIOLYSIS OF BIPHENYL

Product	Number of recryst.	Specific activity μc/mol.	*G*-Value	Ratio of *G*-value
o-Terphenyl	5	1.62	0.0063	7.6
	6	1.58		
m-Terphenyl	7	0.109	0.0012	1.4
	8	0.108		
p-Terphenyl	4	0.0194	0.00083	1.0
	5	0.0200		
o,o'-Quaterphenyl	4	0.348	0.0049	5.9
	5	0.350		
m,m'-Quaterphenyl	4	0.576	0.0051	6.1
	5	0.576		
p,p'-Quaterphenyl	4	1.30	0.0104	12.5
	5	1.60		

Table I shows *G*-values for formation of polyphenyls in the radiolysis of biphenyl. The following are a few interesting features drawn from the present results:

1) The formation of polyphenyl in the

* Present address: Central Research Institute of Electric Power Industry, Komae-cho, Kitatama-gun, Tokyo.

1) W. G. Burns, W. Wild and T. F. Williams, "Proceedings of the Second United Nations International Conference on the Peaceful Uses of Atomic Energy", **29**, 266 (1958).

2) K. L. Hall and F. A. Elden, *J. Chem. Phys.*, **31**, 1420 (1959).

3) R. A. Boxter and R. T. Keen, NAA-SR-3154 (1959).

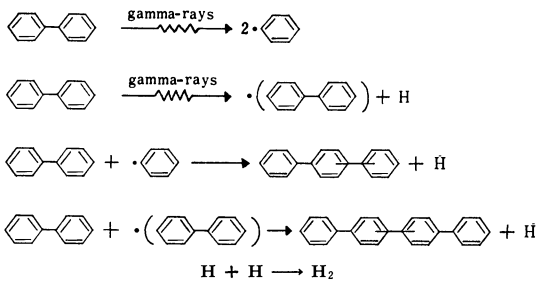
4) W. W. West, AECU-4699 (1960).

5) H. Kōyama, N. Morikawa, T. Migita, R. Itō and G. Tsuchihashi, *Radioisotopes*, **9**, 113 (1960).

6) H. Kōyama, N. Morikawa and G. Tsuchihashi, ibid., in press.

7) A. Danno et al., The 7th Hot Laboratories and Equipment Conference, Cleveland, p. 399 (1959).

radiolysis of biphenyl is assumed to occur according to the following equations:



Each molecule of terphenyl or quaterphenyl is presumed to be formed by the attach of a phenyl radical (ion) or a biphenyl radical (ion), respectively on biphenyl while radicals (ions) are undoubtedly produced directly in the primary process of the irradiation. Although we did not determine *G*-values for the formation of the three remaining unsymmetrical quaterphenyls, they would probably be of the same magnitude as those for the symmetrical ones. Then, the sum of *G*-values for quaterphenyl formation becomes several times as large as that for terphenyl. Therefore, the number of C–H bond ruptures becomes about ten times as large as that of C–C (phenyl-phenyl) bond ruptures. The ratio of these numbers agrees with that of the numbers of C–H and of C–C (phenyl-phenyl) bonds in biphenyl. Consequently, the rate of the rupture C–H bond in biphenyl by gamma-rays is of the same magnitude as that of C–C (phenyl-phenyl) bond.

2) If it is assumed that (1) the radical formation by gamma-rays and the following substitution reaction with these radicals take place at all the positions of biphenyl with equal ease and (2) *o*, *o'*-quaterphenyl can exist only as trans form due to steric hindrance, one would expect that the ratios of *G*-values of *o*-, *m*-, *p*-terphenyl and *o*, *o'*-, *m*, *m'*-, *p*, *p'*-quaterphenyl should be 2 : 2 : 1 and 2 : 4 : 1. However this was not the case. Accordingly, it seems that there is an orientation effect in the substitution reaction of biphenyl with these radicals which were produced initially by the irradiation and then thermalized. We are currently investigating the significance of this large *G*-value for *p*, *p'*-quaterphenyl formation.

Details of this study will be published later.

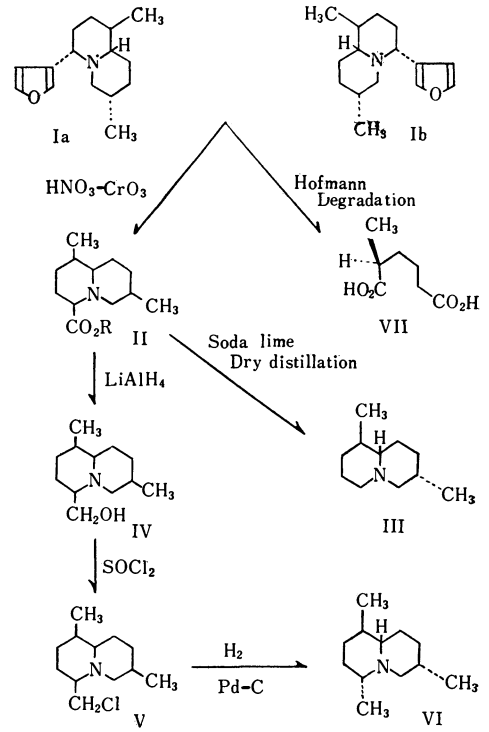
Radiation Application Division
Japan Atomic Energy Research Institute
Tokai, Ibaraki-ken

Absolute Configuration of Deoxynupharidine[1]

By Ichiro KAWASAKI and Takeo KANEKO

(Received February 19, 1962)

Recentry, the determination of the conformation of methylquinolizidine by means of the NMR spectrum was reported briefly[2]. Independently, we have prepared 1-, 3- and 4-methylquinolizidine having a definite conformation and their NMR spectra were compared in order to determine the configuration of deoxynupharidine[3,4] with those of 1, 7-dimethyl (III) and 1, 4, 7-trimethylquinolizidine (VI) which were derived from deoxynupharidine by the degragation according to the following schema:



The doublet of 350~354 c. p. s. and the other doublet of 327~333 c. p. s. in the spectrum of III were attributed to a 1-equatorial and a 3-axial methyl group, respectively. The doublet

1) A part of this work was presented at the 5th Meeting on Natural Organic Compounds of the Chemical Society of Japan, Sendai, October, 1961.

2) T. M. Moynehan, K. Schofield, R. A. Y. Jones and A. R. Katritzky, *Proc. Chem. Soc.*, **1961**, 218.

3) M. Kotake, S. Kusumoto and T. Ohara, *Ann.*, **606**, 148 (1957).

4) M. Kotake, I. Kawasaki, T. Okamoto, S. Kusumoto and T. Kaneko, ibid., **636**, 158 (1960).

of 337~344 c. p. s. in the spectrum of VI was assigned to a 4-equatorial methyl group, since the intensity of the peak at 337 c. p. s. was found to be twice that of the peak at 354 c. p. s.

The absolute configuration of deoxynuphridine can thus be shown as either Ia and Ib. Since the configuration of (−)-α-methyladipic acid (VII) obtained from Hofmann degradation of deoxynupharidine was found to have the S(−) configuration[5], we reached to the conclusion that the absolute configuration of deoxynupharidine should be represented by the

TABLE OF NMR SPECTRA

Compound		c. p. s.*	
1 (equat.)-Methyl-quinolizidine	a		351~356
1 (axial)-Me-	b	329~334	
3 (e)-Me-	c		353~359
3 (a)-Me-	d	329~336	
4 (e)-Me-	e	340~346	
4 (a)-Me-	f		348~354
III		327~333	350~354
VI		330~337~344	354

m. p. of picrate; a: 162~164°C, b: 185~188°C, c: 183~185°C, d: 151~153°C, e: 193~196°C, f: 187~190°C.

* These values were measured in benzene solution at 56.4 Mc/sec. using a Varian Associates 4300 C instrument, calculated from benzene side band.

formula Ib. Compound (IIa R: CH_3), $[\alpha]_D$ −76.25° in EtOH. (IIb R: H), HCl salt, $[\alpha]_D$ −40.3° in EtOH, (III) obtained from IIb, (40%), b. p. 65°C/15 mmHg, $[\alpha]_D$ −34.3° in EtOH, picrate, m. p. 124~125°C, picrolonate, m. p. 200~204°C. (IV) obtained from IIa, (90%), b. p. 88°C/0.6 mmHg, $[\alpha]_D$ −37.1° in EtOH, methiodide, m. p. 173~174°C. (V), (90%), b. p. 91~93°C/1 mmHg, $[\alpha]_D$ −69.4° in EtOH. (VI), (76%), b. p. 95~98°C/12 mmHg, $[\alpha]_D$ −47.8° in EtOH, picrolonate, m. p. 180~184°C, methiodide, m. p. 189~191°C. (VII), $[\alpha]_D$ −12.0° in EtOH.

Department of Chemistry
Faculty of Science
Osaka University
Nakanoshima, Osaka

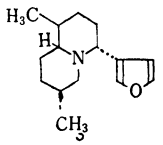
5) T. Kaneko, K. Wakabayashi and H. Katsura, This Bulletin, to be published.

Resolution of dl-Deoxynupharidine; The Total Synthesis of Nupharidine

By Munio KOTAKE, Ichiro KAWASAKI, Shigeru MATSUTANI, Shiro KUSUMOTO and Takeo KANEKO

(Received March 1, 1962)

Recently we have suggested the absolute configuration of deoxynupharidine should be represented as the formula I on the bases of NMR spectroscopic evidences[1]. A chromatography of the diastereoisomeric mixtures of



I

deoxynupharidine (42 g.)[2] on alumina resulted in the separation of the fraction which showed the same infrared and NMR spectra with those of natural deoxynupharidine (10 g., eluted by peterolum-ether)[3]. This fraction was converted to *N*-oxide (hydrochloride, m. p. 193~196°C, Found: C, 62.85; H, 8.29; N, 4.98. Calcd. for $C_{15}E_{23}O_2N$–HCl: C, 63.03; H, 8.46; N, 4.90%, infrared spectrum was found to be identical with that of nupharidine hydrochloride in Nujol), and then reduced with Pd–C to give *dl*-deoxynupharidine. Infrared spectrum of its hydrochloride (m. p. 224~225°C, Found: C, 66.69; H, 8.84. Calcd. for $C_{15}H_{23}ON$–HCl; C, 66.77; H, 8.97; N, 5.19%) in Nujol and free base (liquid) were identical with that of natural deoxynupharidine. The treatment of *dl*-deoxynupharidine (1.5 g.) with *l*-tartaric acid afforded *l*-deoxynupharidine *l*-tartrate (0.6 g., m. p. 142~144°C), which was recrystallized several times from ethyl methyl ketone, yielded 0.2 g., Found: C, 59.30; H, 7.64; N, 3.58. Calcd. for $C_{19}H_{29}O_7N$: C, 59.51; H, 7.62; N, 3.65%, $[\alpha]_D$ −11.54° (*c* 1.00 in EtOH), m. p. 152~153°C and mixed m. p. 152~154°C with *l*-tartrate of natural *l*-deoxynupharidine (m. p. 154~155°C,

1) Previous communication, This Bulletin, **35**, 697 (1962), presented at the 5th Meeting on Natural Organic Compounds of the Chemical Society of Japan, Sendai, October, 1961.

2) M. Kotake, I. Kawasaki, T. Okamoto, S. Kusumoto and T. Kaneko, *Ann.*, **636**, 158 (1960).

3) In the course of this resolution, we found the contribution of F. Bohlmann, E. Winterfeld, P. Studt, H. Laurent, G. Boroschewoki and K. M. Kleine, *Chem. Ber.*, **94**, 3151 (1961).

$[\alpha]_D$ −14.65° (*c* 1.11 in EtOH)), and regenerated *l*-deoxynupharidine showed $[\alpha]_D$ −68.82° (*c* 1.01, in EtOH), its hydrochloride, m. p. 258~260°C, $[\alpha]_D$ −17.03°, (*c* 1.02 in 1 N HCl), Found: C, 66.82; H, 8.96; N, 5.03%, (natural deoxynupharidine had $[\alpha]_D$ −93.5° (*c* 2.03 in EtOH), hydrochloride, m. p. 261~263°C, $[\alpha]_D$ −21.4° (*c* 0.98 in 1 N HCl)). Oxidation of *l*-deoxynupharidine (65 mg.) with hydrogenperoxide yielded *d*-nupharidine (68 mg.), which recrystallized from acetone yielding as white plates, m. p. 212°C (decomp.), $[\alpha]_D$ +13.00° (*c* 0.38 in EtOH), Found: C, 71.81; H, 9.57. Calcd. for $C_{15}H_{23}O_2N$: C, 72.25; H, 9.30%, was identical with natural *d*-nupharidine, ($[\alpha]_D$ +17.2° (*c* 1.10 in EtOH)).

Department of Chemistry
Faculty of Science
Osaka University
Nakanoshima, Osaka

Molecular Weight Measurement of Polystyrene by Archibald Method

By Akira KOTERA, Naomichi ISO, Katsumi UMEZAWA and Yuji MIYAZAWA

(Received February 3, 1962)

Archibald[1] and others[2-9] have reported a method of determining molecular weight by ultracentrifuge during approach to sedimentation equilibrium. Application of this method to synthetic high polymer has been studied in this experiment.

Polystyrene which was used as the common sample by the research group of light scattering measurement in Japan was centrifuged with two kinds of ultracentrifuge, the magnetically suspended free running type ultracentrifuge with a Rayleigh interference optical system and a Spinco Model E ultracentrifuge with a schlieren optical system. All this experiments were done in butanone solution.

Weight average molecular weight, M_w, in this method is determined by obtaining the quantity δ_w at the point a and b, the boundary surface of solution and the bottom of cell, according to the following equation.

$$\delta_w = (1/xC)(dC/dx) = (1-\bar{v}\rho)\omega^2 M_w/RT \quad (1)$$

where x is the distance from the center of rotation, C the concentration of solution, $\bar{v}$ the partial specific volume of solute, ρ the density of solution, R the gas constant, T the absolute temperature, and ω the angular velocity of rotation.

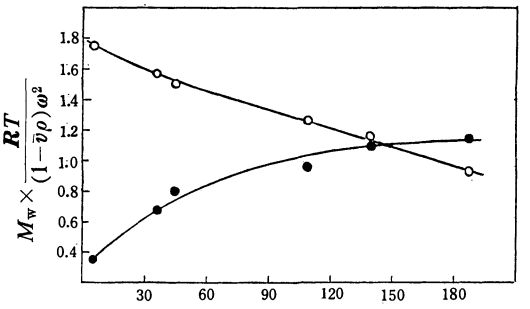


Fig. 1. Time dependencies of the apparent average molecular weights, M_{wb} and M_{wa}, calculated by Archibald's equation.
$C_0=0.243$ RPM$=7.6\times10^3$
● δ_{wa} ○ δ_{wb}

The values of δ_{wa} and δ_{wb} calculated by Eq. 1 vary with time as shown in Fig. 1. In Archbald's expectation, the curve of δ_{wb} will be higher than that of δ_{wa} and both curves should meet when extrapolated to zero time. To the contrary of expectation, however, δ_{wa}'s are larger than δ_{wb}'s at the initial stage of sedimentation. Thereafter δ_{wa}'s decrease and δ_{wb}'s increase gradually with time and both curves become crossing together after some minutes.

Comparing the results of the free running type ultracentrifuge experiments and those of Spinco ultracentrifuge, this crossing point, t_c, seems to be dependent on the time consumed during driving the rotor to experimental speed. On the other hand, in the results obtained by the later experiment it shows that the other experimental conditions, concentratin of solution and the rotor speed, have the effects on t_c. Trautman plot[8] was also examined.

But the both plots corresponding to the boundary surface of solution and the bottom of cell have curvatures indicating the molecular weight heterogeneity and thermodynamical non-ideality of the solution, and they do not meet at zero time.

1) W. J. Archibald, *J. Phys. Chem.*, **51**, 1204 (1947).
2) H. Gutfreund and A. G. Ogston, *Biochem. J.*, **44**, 163 (1949).
3) R. A. Brown et al., *J. Am. Chem. Soc.*, **76**, 3342 (1954).
4) A. Ginsburg, P. Appel and H. K. Schachman, *Arch. Biochem. Biophys.*, **65**, 545 (1956).
5) R. L. Baldwin, *Biochem. J.*, **55**, 644 (1953).
6) H. G. Elias, *Angew. Chem.*, **73**, 209 (1961).
7) H. Fujita et al., *J. Phys. Chem.*, **66**, 4 (1962).
8) R. Trautman, ibid., **60**, 1211 (1956).
9) G. Kegeles et al., ibid., **61**, 1286 (1957).

TABLE I. RESULTS WITH FREE RUNNING TYPE U. C. at 30°C

C_0 g./100 ml.	RPM $\times 10^{-3}$	t_c min.	M_w^{app} $\times 10^{-4}$	M_w^{app}* $\times 10^{-4}$
0.120	5.4	135	29.6	23.0
0.222	5.8	285	23.1	19.5
0.411	5.7	225	20.9	17.8
0.694	5.8	195	19.3	15.8
$C_0 \rightarrow 0$	—	—	31.2	26.4

* The results obtained by sedimentation equilibrium.

TABLE II. RESULTS WITH SPINCO MODEL E U. C. at 20°C

C_0 g./100 ml.	RPM $\times 10^{-3}$	t_c min.	M_w^{app} $\times 10^{-4}$
0.137	10.5	7	20.5
0.209	10.5	12	17.7
0.384	10.5	13	15.4
0.242	8.7	15	17.9
0.242	7.2	18	17.6
0.242	5.1	32	17.0
$C_0 \rightarrow 0$	—	—	23.0

This abnormality is resulted in all our experiments. Then we assumed the values at t_c as δ_w's of the whole solute, and calculated the hypothetical apparent weight average molecular weight, M_w^{app}. The reciprocals of these M_w^{app}'s were plotted against concentration and extrapolated to infinite dilution. The results obtained are shown in Tables I and II with the values obtained by sedimentation equilibrium.

It may be concluded from the results that the Archibald method is a rapid and useful technique in molecular weight measurement but it has some ambiguities in the determination of the average molecular weight of the whole solute which has a molecular weight distribution.

Department of Chemistry
Faculty of Science
Tokyo University of Education
Otsuka, Tokyo

On the Relationship between Electronic State of Molecules and their Biological Actions. I. The Nicotinic Action of Choline Phenyl Ether and the Enzymatic Decomposition of Phenyl Acetate

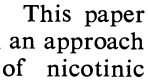
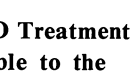
By Akira INOUYE and Yoshiya SHINAGAWA

(Received September 15, 1960)

Several attempts have been made in the quantum-chemical approach for explaining the carcinogenic activity of hydrocarbon molecules since Schmidt's earlier work[1], and some indices correlating the electronic configuration of these molecules with their carcinogenic activity were proposed by these investigators[2-4]. Because of complexities in biological processes involved, however, there remain certain ambiguities concerning their legitimacy from the biochemical point of view, even though their apparent usefulness was established. Indeed, there have been some disputes as to which quantum-chemical index is most effective in predicting the carcinogenic activity of hydrocarbon molecules[5]. It seems rather appropriate at present, therefore, that such a quantum-chemical approach is made in the biological research field on the pharmacological actions or on enzymatic reactions, for their mechanism is simpler and can be analyzed further in detail. But such an attempt has not yet appeared. This paper is principally concerned with such an approach of explaining the effectiveness of nicotinic action of choline phenyl ether derivatives and the substrate specificity of choline esterases by applying the frontier electron method of Fukui et al.[6] A preliminary account of some of their results has already been reported[7].

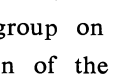
A Perturbation Theory in the LCAO Treatment of Conjugated Molecules Applicable to the Active Center of Enzyme or Receptor

The perturbation theory in the simple LCAO-MO method has been extensively developed by several investigators (Wheland[8], Coulson and Longuet-Higgins[9], Dewar[10], Mulliken and his co-workers[11], and Fukui et al.[6]) and has been applied successfully to the problem of chemical reactivity of molecules containing π-electrons. Long since, some physiologists and pharmacologists assumed tacitly that the drugs combined with so-called "receptors" of living organism as substrates did with active sites of an enzyme. Provided that the substrate or drug molecules contain π-electrons, it seems highly probable that such a complex formation is due to hyperconjugation of the π-part of the active site of enzyme or receptor to that of substrate or drug molecules.

On the other hand, recent developments in MO theoretical treatment of chemical reactivity in conjugated molecules have made a great contribution to the study of the mechanism of aromatic substitutions. One of these analyses was a theoretical treatment of hyperconjugation by Mulliken et al.[11] which occurred with the CH_2 group on $C_6H_7^+$ ion  . In this ion, the H_2 group was considered to be an atom (pseudo-atom) that has a (ls-ls) π-type orbital (quasi-π orbital). Such a treatment was also applied to a transition state of aromatic substitution by Fukui et al.[6] These workers pointed out an importance of hyperconjugation which occurs with the CBX group on  and derived an effective reactivity index, "superdelocalizability", from the stabilization energy due to this hyperconjugation. These treatments appear to be applicable to analysis of the transition state of enzyme-substrate or drug-receptor complex, to some extent at least. Adopting the method of perturbation theory proposed by Fukui et al.[6], therefore, the present authors attempted in this section a general formulation of the effect of conjugated molecules on the perturbation energy of their separating the properly assumed mesomeric group, its applicability to some biological

1) O. Schmidt, *Z. physik. Chem.*, **42**, 88 (1939).
2) A. Pullman and B. Pullman, *Rev. Sci.*, **84**, 145 (1946); "Concerisation par les Substances chimiques et Structure moleculaire" Mass on et Cel, Paris (1955).
3) C. A. Coulson, *Adv. Cancer Research*, **1**, 1 (1953).
4) C. Nagata, K. Fukui, T. Yonezawa and Y. Tagashira, *Cancer. Res.*, **15**, 233 (1955).
5) K. Fukui, T. Yonezawa and C. Nagata, *J. Chem. Phys.*, **31**, 550 (1959).
6) K. Fukui, T. Yonezawa and C. Nagata, This Bulletin, **27**, 423 (1954); *J. Chem. Phys.* **27**, 1247 (1957).
7) Y. Shinagawa and A. Inouye, *Kagaku*, **29**, 608 (1959); Y. Shinagawa, A. Inouye and T. Ban, ibid., **29**, 659 (1959).
8) G. W. Wheland, *J. Am. Chem. Soc.*, **64**, 900 (1940).
9) C. A. Coulson and H. C. Longuet-Higgins, *Proc. Roy. Soc.*, **A191**, 39 (1947).
10) M. J. S. Dewar, *J. Am. Chem. Soc.*, **74**, 3355 (1952).
11) L. W. Pickett, N. Muller and R. S. Mulliken, *J. Chem. Phys.*, **21**, 1400 (1953).

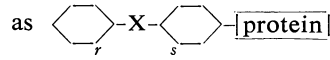
reactions being demonstrated in the following section.

Consider a certain atom X in an active center of enzyme or receptor approaching to the rth atom in the π-part of a substrate molecule. Provided that a hyperconjugation such as the CHX group on  occurs, the secular equation of the π-part of the total system containing the quasi-π orbital is, in a simple LCAO-MO treatment, written as

$$D_1(\lambda)=(h-\lambda)\Delta_1(\lambda)-\gamma_1^2\Delta_{1rr}(\lambda)=0 \qquad (1)$$

where

$$\Delta_1(\lambda)=\begin{vmatrix} a_{11}-\lambda & a_{12} \cdots\cdots a_{1n} \\ a_{21} & a_{22}-\lambda \ \ldots a_{2n} \\ a_{n1} \cdots\cdots\cdots\cdots & a_{nn}-\lambda \end{vmatrix}$$

and $\Delta_{1rr}(\lambda)$ is the minor of $\Delta_1(\lambda)$ corresponding to the element $a_{rr}-\lambda$, a_{ii} and $a_{ij}(i\neq j)$ are the well-known Coulomb and resonance integrals respectively, h and γ_1 are the Coulomb integrals of a properly assumed pseudo-atom and the resonance integral between this pseudo-atom and the rth atom of the substrate molecule respectively. All the quantities which represent energy are expressed in units of $(-\beta)$, all the overlap integrals being neglected. As stated above, however, the hyperconjugation of the π-part in the receptor or enzyme should be further taken into consideration. Assuming that the π-part of enzyme or receptor, whose secular determinant is $\Delta_2(\lambda)=0$, conjugates with the X-atom at its sth atom in such a manner as  , we can write the perturbation determinant as follows:

$$D(\lambda)=(h-\lambda)\Delta_1(\lambda)\Delta_2(\lambda)-\gamma_1^2\Delta_{1rr}(\lambda)\Delta_2(\lambda) -\gamma_2^2\Delta_1(\lambda)\Delta_{2ss}(\lambda)=0 \qquad (2)$$

where γ_2 is the resonance integral between the X-atom and the sth carbon atom in the active center. Considering the resonance integrals, γ_1 and γ_2 to be small perturbation terms, we can obtain the perturbation energy, ΔE.

When h is equal to λ_l, the highest occupied orbital of substrate, the perturbation energy is obtained as follows:

$$\Delta E=2\sqrt{-\frac{\Delta_{1rr}(\lambda_l)}{\Delta_1'(\lambda_l)}}\cdot\gamma_1+O(\gamma_1^2,\gamma_2^2)$$

and

$$-2\frac{\Delta_{1rr}(\lambda_l)}{\Delta'(\lambda_l)}=f_r^{(E)}$$

thence $\Delta E\simeq\sqrt{2}\,(f_r^{(E)})^{1/2}\cdot\gamma_1$

As shown in the following section, pharmacological potency or susceptibility to an enzymatic hydrolysis of homologous compounds has a fairly good parallelism to their f_r at a definite position, which is supposed, from the physiological point of view, to be involved in their reaction processes. The above relation might be said, therefore, to provide a quantum-chemical ground for such a supposition, suggesting a possibility that f_r is a fairly good index for estimating the magnitude of ΔE under a certain condition. On the other hand, superdelocalizability, which was considered by Fukui et al.[6] as one of the most useful index for the reactivity of π-electrons in a molecule was defiined as

$$S_r=\sum_{occ}\frac{2(C_r^{(i)})^2}{\lambda_i}$$

In the limit of $h\to 0$ and $\gamma_2\to 0$, therefore, it is apparent that ΔE is proportional to S_r. Thus the perturbation energy of complex formation is expected under a certain condition to vary nearly parallel to the superdelocalizablility of frontier electron in the substrate molecules.

It is obvious from the above discussions that, the larger the frontier electron density or superdelocalizability of the substrate or drug molecules, the larger the perturbation energy ΔE. Thence it would be expected that the susceptibility of homologous compounds to a certain enzyme or their pharmacological activity runs parallel with their frontier electron density or superdelocalizabillity. It will be shown in the following section, that the indices f_r or S_r have a correlation with the magnitude of drug actions or the rate of enzymatic hydrolysis.

Applications of the Frontier Electron Method

Electronic Structure of Choline Phenyl Ether and their Nicotinic Action.—Taking into account the above-mentioned results, the nicotinic action of choline ether derivatives was analyzed from the view-point of their electronic structure. From the pharmacological point of view, the group of $(CH_3)_3N\cdot CH_2\cdot CH_2-$ of these compounds is considered to react with anionic sites of chemoreceptor protein, while the difference in their potency would chiefly originate from the conjugated groups X-  -O- which is assumed to react with esteratic sites of the receptor[14,15]. Some workers suggested that the potency of these drugs in the depressant action was principally determined by electrostatic

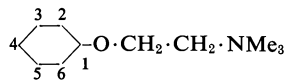
12) H. H. Jaffe, ibid., **20**, 279 (1952).
13) K. Fukui, C. Nagata and T. Yonezawa, *J. Am. Chem. Soc.*, **80**, 2267 (1958).
14) D. Nachmansohn, "Chemical Mechanism of Nerve Activity" in "Modern Trends in Physiology", Ed. by E. S. G. Barron, Academic Press, New York (1952); "Chemical and Molecular Basis of Nerve Activity", Academic Press, New York (1959).
15) R. B. Barlow, "Chemical Pharmacology", Methuen, London (1955).

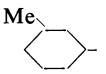
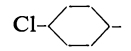
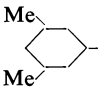
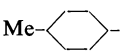
TABLE I

	Ester O	I	Br	Cl	CH_3	MeO	NO_2	N^+Me_3
k	2	1.5	1.8	2	3	1.8	$k_N=1$, $k_O=1$	0
δ	0	0.3	0.4	0.5	−0.1	0	0.2	−0.1
ρ	1	0.5	0.7	0.8	1	0.9	1	0

$\alpha_i=\alpha+k_i\beta$, $\alpha_\delta=\alpha+\delta\beta$, $\beta_{i,j}=\rho_{i,j}\cdot\beta$; $\lambda=(E-\alpha)/\beta$

TABLE II. NICOTIN-LIKE ACTIVITY OF ETHERS OF CHOLINE



	Activity* Suprarenals intact	Activity* Suprarenals ligated	$f_1^{(1)}+f_1^{(2)}$	$f_4^{(1)}+f_4^{(2)}$
	337	268	0.629	0.613
	370	258	0.628	0.538
	220	192	0.570	0.596
	100	100	0.605	0.608
	13.1	13.5	0.542	0.729
	10.4	10.1	0.522	0.522
	5.2	5.2	0.410	0.907
	0.4	0.47	0.513	0.440

* Relative activity (molar) on blood-pressure of cats after atropin.

bonding between the negative charge on the atom of 1-position adjacent to the ether *O*-atom and the positive charge on the esteratic site[16]. As the present treatment of first approximation, therefore, the conjugated group X-  -O- alone was considered.

The value of integrals concerning the hetero-atom is given in Table I, in which the parameters k, ρ and δ are defined as follows:

$$\alpha_O=\alpha+k_O\beta,\ \alpha_{Cl}=\alpha+k_{Cl}\beta,\ \alpha_\delta=\alpha+\delta\beta$$

$$\beta_O=\rho_O\beta \quad \text{and} \quad \beta_{Cl}=\rho_{Cl}\beta$$

These values used for calculation do not differ much from those of other authors, which have lead to reasonable results in some other problems[12,13]. The Coulomb integral of an oxygen atom in an ether bond is taken as $\alpha+3\beta$, that of carbon atom attached to it being $\alpha+0.3\beta$. Solving the secular equations, the electron densities of the first and second highest occupied levels, $f_r^{(1)}$ and $f_r^{(2)}$, and the approximate superdelocalizability, $S'_r=f_r^{(1)}/\lambda_1+f_r^{(2)}/\lambda_2$, are calculated. These two levels are very close to each other.

The calculated electron densities of two highest occupied levels of the positions 1 and 4, ($f_1^{(1)}+f_1^{(2)}$, $f_4^{(1)}+f_4^{(2)}$) are given in Table II, which demonstrates evidently that $f_1^{(1)}+f_1^{(2)}$ shows a distinct parallelism with the magnitude of activtiy of choline ethers observed on blood pressure of cats (Hey[16]). But the parallelism between $f_4^{(1)}+f_4^{(2)}$ and their activity is somewhat slighter, while neither $f_{(r)}^{(1)}+f_{(r)}^{(2)}$ at other positions nor their S'_r have such a correlation with their potency of nicotinic action. On the other hand, Imamura[17] has

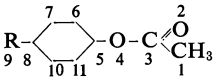
16) P. Hey, *Brit. J. Pharmacol.*, 7, 117 (1952).

17) A. Imamura, personal communication.

TABLE III. SUBSTRATE SPECIFICITY OF BUTYROCHOLINESTERASE

R	Rate*	$f_5^{(E)}$	q_5	$s_5^{(E)}$	$s_3^{(N)}$	q_4
Me_3N^-	95	0.498	0.949	0.821		1.724
H	91	0.495	0.946	0.973	1.608	1.762
Me	65	0.459	0.984	0.944	1.520	1.764
MeO	51	0.454	0.987	0.955	1.521	1.764
NO_2	36	0.426	0.886	0.671	1.720	1.756
Cl	28	0.442	0.927	0.757	1.553	1.760
Br	28	0.440	0.932	0.770	1.539	1.760
I	28	0.437	0.932	0.765	1.539	1.766
tert-Bu	15	0.419				

* Percent maximum rate of hydrolysis of Ach.



recently made calculation of S_r on these compounds and found a fairly good parallelism between S_4 and their activity, a fact which suggests that the approximation of S'_r is not so satisfactory.

The results appear, however, to suggest that ethers of choline form weak bondings with the active sites of the receptor at 1- and 4-position, this process being rate-determinant. In this case, the energy level of substrate's frontier electron would be considered to be close to that of the active center in the receptor. The correlation of f_1 with their potency is not a so unexpected one, for this position corresponds to that of acetylcholine which is bound to the esteratic site of Nachmansohn's acetylcholinesterase model. On the other hand, the correlation of f_4 or S_4, though somewhat less than that of f_1, may be considered to provide support to Hey's view[16].

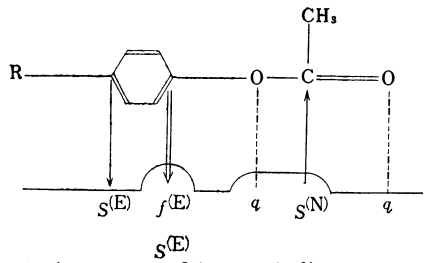
The quantity f_r, as well as S_r, are considered as an index for discussing the reactivity in electrophilic reaction. But, as stated above, the condition for f_r to correlate with ΔE differs from that for S_r. Taking Imamura's results into account, it might be said, therefore, that the two positions of drug molecules would be attached to two positions of the receptor different from each other in their nature. Such a speculation does not conflict with the suggested concept of the esteratic site of the receptor.

Electronic Structure of Phenyl Esters and Substrate Specificity of Cholinesterase.—The electronic structure of choline phenyl ethers has a similarity to that of phenyl acetate, a substrate of cholinesterase, and so we calculated them by the method of LCAO. As indices of reactivity, electron density q_r, frontier electron density f_r and superdelocalizability S_r are calculated by solving the secular equations crresponding to Eq. 1. The values of indices and the rate of hydrolysis by butyrocholinesterase partially purified from human plasma (Whittaker[18]) are given in Table III. A distinct parallelism between frontier electron density f_5 and the magnitude of rate of hydrolysis is clearly seen, only an exception is the case on nitrophenol ester. S_5 shows a slighter correlation with their rate of hydrolysis, while neither f_r nor $S'_r=f_r^{(1)}/\lambda_1$ at any other position in the molecules have such a correlation with their substrate specificity of butyrocholinesterase. In this caes, approximate superdelocalizability S_r' was also found to vary not always parallel to S_r so that their appoximation can said to be not so satisfactory as already suggested in the section above. In view of their similarity to the choline ether derivatives in the molecular structure and pharmacological nature, the position 5 of these compounds corresponds to the position 1 of the latter and so the correlation found on f_5 is not a so unexpected one. The possible sites of an ester molecule making bond with the active center of butyrocholinesterase would be probably such as illustrated in Fig. 1, which can be referred to Nachmansohn's model of true cholinesterase. In this case, the position which should be considered at first as rate-determinant would be position 5.

On the other hand, parallelism was not so striking between the magnitude of rate of hydrolysis of phenyl acetates by acetylcholinesterase and the indices of their electronic structure as in the case of butyrocholinesterase. It is found, however, that the rate of hydrolysis have a slight correlation with indices on the position 8 (except the NO_2-derivative), whose distance to ether oxygen atom is close to that of quarternary nitrogen atom in Ach. This fact seems concordant with Nachmansohn's model of acetylcholinesterase, in which the distance between nitrogen atom and ether oxygen atom can affect the rate of enzymatic hydrolysis. Nevertheless the bonding between the active center and the position 8 in phenyl acetate may

18) L. A. Mounter and V. P. Whittaker, *Biochem. J.*, **54**, 551 (1953).

Phenyl acetates



Active center of butyrocholinesterase

Fig. 1a. The possible sites of ester molecule masking bond with active center of butyrocholinesterase.

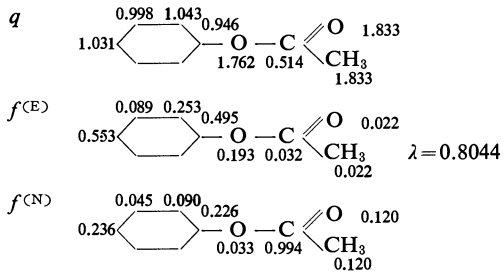
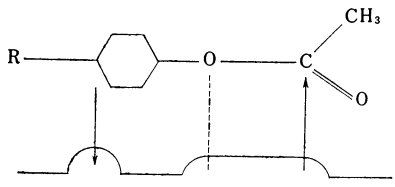


Fig. 1b. Molecular diagram of phenyl acetate.

TABLE IV. ACETOCHOLINESTERASE

R	% rate of hydrolysis	$S_8^{(E)}$	$f_8^{(E)}$	$S_8^{(N)}$	$S_3^{(N)}$
H	60	0.962	0.552	0.781	1.536
I	48	0.948	0.486	0.756	1.539
MeO	47	0.928	0.431	0.755	1.521
Me	45	0.938	0.492	0.765	1.520
NO_2	40	0.827	0.475	0.654	1.720
Cl	18	0.909	0.492	0.754	1.541
Br	15	0.916	0.488	0.752	1.539



Active center

be not so simple as that of Nachmansohn's model. Based on Wilson's results, Nachmansohn maintained that Coulomb force between quarternary nitrogen and active center is one of the essential factors on the bonding of enzyme-substrate complex, but in our results electron density q_8 has no clearer parallelism to the rate of reaction.

Wilson[19] employed the Michaelis-Menten constant as the basis of estimating contribution of electrostatic energy to enzyme-substrate (or -inhibitor) complex formation. As pointed out elsewhere[20], however, use of this constant involves a certain risk of erring in calculation of free energy change of such a complex catalytic reaction by a factor of ν (ν is the stoichiometric number in the rate-determinant process). It is a well-known classical theorem that $\vec{k}/\overleftarrow{k}=K$, where $\vec{k}$ and $\overleftarrow{k}$ are the forward and backward rate constants and K is the equilibrium constant. This theorem has been applied hitherto to the Michaelis-Menten relation of enzyme reaction,

$$E+S \underset{\overleftarrow{k}}{\overset{\vec{k}}{\rightleftarrows}} ES \xrightarrow{k} E+P$$

(E enzyme, S substrate, ES enzyme-substrate complex)

The Michaelis-Menten constant given by $K_m=\vec{k}/\overleftarrow{k}$ was used to calculate the free energy change of this reaction by Wilson as $-\Delta F=\boldsymbol{RT}\ln K_m$. It was already clearly demonstrated by Horiuti[21], that a theorem $(\vec{k}/\overleftarrow{k})^{\nu}=K$ was valid for any reaction having the stoichiometric number ν. Enzymatic reactions should have such complex rate processes that use of the Michaelis-Menten constant is allowable only for a special case of $\nu=1$. Hence, Wilson's results could not be regarded as a sufficient evidence for electrostatic bonding, other bonds such as hydrogen bonding being also allowable. Furthermore, γ-dimethylbutylacetate, which has no positive charge on the corresponding position, is hydrolyzed by acetylcholinesterase at almost the same rate as acetylcholine[15], a fact which seems also unfavorable to Nachmansohn's view. The difference of substrate specificity found between butyro- and acetylcholinesterase suggests that the quantum-chemical process involved in their reactions are different ones. The bonding mechanism of the latter complex seems to be more complex than the former one. The mechanism of enzymatic reaction proposed in the previous section may not be a rate-determinant in this case. It seems worthy to note here, however, that $S_8^{(N)}$ has better correlation with a rate of hydrolysis than other indices (Table IV), and so the negative charge on the position 8 should be considered at least to affect bonding of the complex.

19) I. B. Wilson, "The Mechanism of Enzyme Action", Ed. by W. D. McElroy and B. Glass, Johns Hopkin's Press, Baltimore, Maryland (1954).

20) A. Inouye and Y. Shinagawa, *Kagaku*, **30**, 481 (1960).

21) J. Horiuti, This Bulletin, **13**, 210 (1938); *Z. physik. Chem., N. F.*, **11**, 358 (1957).

Comment

Fukui and his co-workers introduced the frontier electron method and have obtained hitherto many fruitful results in their studies on reaction mechanism of aromatic hydrocarbons. As shown above, a fairly good correlation could be also proved between the π-electron density or its superdelocalizability of a certain position calculated by this method and nicotinic action of phenyl ether derivatives of choline or rate of enzymatic hydrolysis of phenyl acetate derivatives. The position, which was found to have such a correlation, is also expected from a pharmacological and chemical point of view. A possibility of such a correlation is demonstrated theoretically under an assumption that the active site of the receptor (or enzyme) has also π-electron system and a complex is formed between active sites and durgs by hyperconjugation through the π-electron system, their highest occupied level being very close to each other. This assumption is rather bold, but seems not so unreasonable: enzyme substrate complex or receptor-drug combination has been widely assumed in enzymological or pharmacological studies, and in the complex assumed, it is only required that π-electron can be transfered and hence its bonding is not needed to be a covalent one, hydrogen bonding being also allowable. In view of these facts the present invetigative approach might be said to demonstrate a possibility of explaining the drug actions at the molecular level. At least, the results suggest that the electronic configuration of molecules is important in quantitative interpretation of drug actions or substrate specificity of enzyme action and qualitative electronic explanation in these fields would be replaced by its systematic computation by an adequate quantum-chemical treatment in future.

Summary

1. Applying the frontier electron method of Fukui et al., it was attempted to explain the effectiveness of nicotinic action of some choline phenyl ether derivatives and the substrate specificity of some phenyl acetates in the enzymatic hydrolysis.

2. A fairly good correlation could be proved between the frontier electron density (f_r) or its superdelocalizability (S_r) of a certain position of these compounds and their potency or susceptibility to hydrolysis.

3. Assuming that the active site of receptor (or enzyme) has also π-electron systems and a drug-receptor (or -enzyme) complex is formed by hyperconjugation through π-electron systems, a general formulation of the effect of such a hyperconjugation on the perturbation energy of their system was attempted. It was demonstrated, qualitatively at least, by our calculations, that the larger the f_r of drug molecules or their S_r the larger the perturbation energy and so a possibility of above-mentioned correlation was predicted to some extent from the quantum-chemical basis.

Authors' thanks are due to Dr. Chikayoshi Nagata of Faculty of Engineering and Dr. Takashi Ban of Pharmacological Department, Faculty of Medicine, Kyoto University for their kind advise.

Department of Physiology
Faculty of Medicine
Kyoto University
Sakyo-ku, Kyoto

The Energy of the Intermolecular Interaction between the Proton of the OH Group and the π Electron of Some Compounds

By Shozo WADA

(Received March 18, 1961)

The OH infrared absorption bands of both inter- and intra-molecular interactions between the π electron and the proton of the OH group have been observed by many workers[1]. The energies of the intramolecular interaction between the π electron and the proton have also been measured for some typical compounds by Ōki and Iwamura[2]. However, so far little is known of the energy of the intermolecular interaction between the π electron and the proton.

It does not seem correct to calculate the intermolecular interaction energy simply from the frequency shift of the OH band by the use of Badger's postulation[3], in the same manner as Goldman and Crisler[4] tried in the case of intramolecular interaction. Since certain differences may exist between the inter- and intra-molecular interactions in the factors which contribute to the interaction energy of the proton and the π electron, that is, steric factors between the two interacting groups, the direction character of the π electrons, etc., it seems unreasonable to estimate the energy of the intermolecular interaction simply from the frequency shift relationship which is obtained in the case of intramolecular interaction.

In a series of previous papers[5] it has been shown that lignin is a very good reinforcer for some types of synthetic rubbers, and the mechanism of the interaction between these polymers has also been reported. The main object of the present study is to estimate the interaction energy between the π electron in synthetic rubbers (styrene-butadiene copolymer, SBR, and acrylonitrile-butadiene copolymer, NBR) and the proton of the OH groups in lignin. Since it is difficult to measure the interaction energy between these large molecules, simple molecules with similar chemical structures were chosen as model compounds. As the proton donor, phenol, catechol, vanillin and 3-phenylpropanol were used, and as the proton acceptor, isopropylbenzene, cyclohexene and isobutyronitrile were used.

The intermolecular interaction energies between the OH groups and the π-electrons of these model compounds were estimated from the variation with the temperature of the intensities of the OH absorption bands. Infrared absorption spectra were measured for the ternary system of the proton donor, the proton acceptor and the solvent (carbon tetrachloride).

Experimental

Measurement.—A Perkin-Elmer model 13 infrared spectrophotometer was used, with a lithium fluoride prism. The concentration of the proton donor in carbon tetrachloride was 0.015 mol./l. An absorption cell with potassium bromide windows was placed in an asbestos block equipped with a heating coil, and the temperature of the contents was kept at an appropriate temperature (within ± 1°C) by controlling the electric current in the coil. The temperature was read by a thermometer inserted in a hole in the potassium bromide cell wall. Measurements of the infrared absorption of OH group were made at 25, 40 and 60°C.

Materials. — Phenol and 3-phenylpropanol were distilled in a vacuum. Vanillin was purified by sublimation, and catechol was purified by recrystallization.

Cyclohexane, isopropylbenzene and isobutyronitrile were dried and distilled through a short helix-packed column. Carbon tetrachloride, free of hydroxylic or other basic impurities, was dried and distilled before use.

Calculation.—In the calculation of the energy, it has been assumed that one proton donor molecule forms the hydrogen bond with one proton acceptor molecule and that the following equilibrium is maintained:

$$\text{Donor} + \text{Acceptor} \rightleftarrows \text{Complex}$$

$$K = [\text{C}]/([\text{D}] \cdot [\text{A}])$$

where, [D], [A] and [C] are the concentrations of donor, acceptor and complex, respectively, and K is the equillibrium constant. In order to simplify the calculation, the following assumptions were made:

a) $[\text{A}] \gg [\text{C}]$. Hence, [A] is almost constant and equal to $[\text{A}_0]$, the initial concentration of the acceptor.

b) [D] and [C] are proportional to the area intensities (S_D and S_C) of the free and bonded OH

1) R. West, *J. Am. Chem. Soc.*, **81**, 1615 (1958); P. R. Shleyler, O. S. Trifan and R. Bacskai, ibid., **80**, 6691 (1958). See also references cited there.
2) M. Ōki and H. Iwamura, This Bulletin, **33**, 717 (1960).
3) R. M. Badger, *J. Chem. Phys.*, **8**, 288 (1940).
4) I. M. Goldman and R. O. Crisler, *J. Org. Chem.*, **23**, 751 (1958).
5) S. Wada, *Chem. High Polymer* (*Kobunshi Kagaku*), **18**, 541 (1961); S. Wada, ibid., in press.

absorption bands respectively, and the proportional constants are defined as K_D and K_C. As an alternate assumption, [D] and [C] are proportional to the peak values of the molecular absorption coefficients (κ_D and κ_C) of the free and bonded OH absorption bands respectively, the proportional constants being K_D' and K_C'.

c) The changes of entropy and enthalpy in the formation of the bond remain constant throughout the temperature range of the measurement.

From these assumptions, it follows that

$$K=K_C\cdot S_C/K_D\cdot S_D\cdot[A] \quad (2)$$

As
$$-\boldsymbol{R}T\ln K=\Delta H-T\Delta S \quad (3)$$

$$\ln K_{T_1}-\ln K_{T_2}=\ln(S_C/S_D)_{T_1}-\ln(S_C/S_D)_{T_2}$$
$$=-\Delta H/\boldsymbol{R}(1/T_1-1/T_2) \quad (4)$$

Or,
$$K=K_C'\cdot\kappa_C/K_D'\cdot\kappa_D\cdot[A] \quad (2')$$

$$\ln K_{T_1}-\ln K_{T_2}=\ln(\kappa_C/\kappa_D)_{T_1}-\ln(\kappa_C/\kappa_D)_{T_2}$$
$$=-\Delta H/\boldsymbol{R}(1/T_1-1/T_2) \quad (4')$$

Therfore, the enthalpy change ΔH is calculated from the slope of the line obtained by plotting $\ln(S_C/S_D)$ or $\ln(\kappa_C/\kappa_D)$ versus $1/T$. The entropy change ΔS is calculated by Eq. 3, using the values of ΔH and K. In the previous studies[5], the value of the equilibrium constant, K, was obtained from the variation of the molecular absorption coefficient of the free OH band with the concentration of the acceptor.

When the bonded and the free OH absorption bands overlap, as is shown in Fig. 1, the areas of the two bands were estimated as follows: As shown in Fig. 1, the slope of the free OH absorption curve is assumed to be symmetric, and the area of the curve ABCDE is taken for that of the free OH band. The area of the curve EDCF is taken for that of the bonded OH band.

In the case of catechol, another OH absorption band, due to the intramolecular hydrogen bond, appears. However, its intensity remains almost unchanged throughout the temperature range of the measurement and remains almost unaffected even when mixed with the proton acceptor.

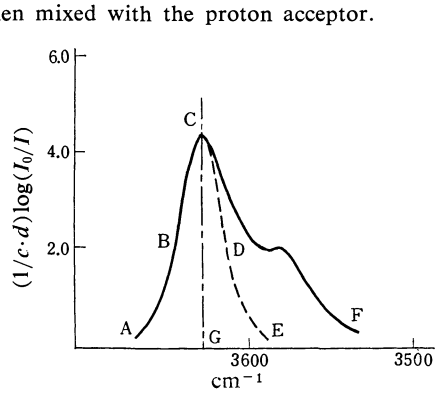


Fig. 1. The infrared absorption spectrum of OH group of 3-phenylpropanol (0.030 mol./l.) in the coexistence of cyclohexene (2.27 mol./l.) in CCl_4. The free OH band and intermolecularly bonded OH band are separated from each other by an extrapolated curve CDE.

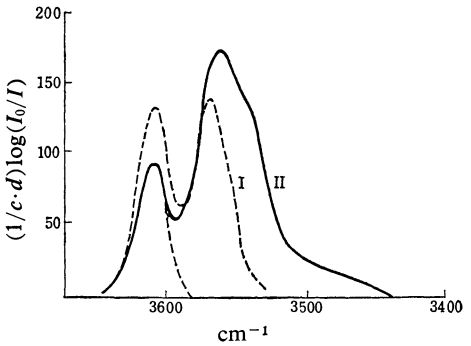


Fig. 2. The infrared absorption spectrum of OH group of catechol. I, 0.015 mol./l. in CCl_4; II, 0.015 mol./l. in CCl_4 in the coexistence of isopropylbenzene (1.80 mol./l.). The area of the intermolecularly bonded OH absorption band is estimated by subtracting the intramolecularly bonded OH absorption I from the absorption curve II.

The intensity ratio of the intramolecularly bonded and the free OH absorption bands is independent of the temperature, being 1.17 at 25°C and 1.12 at 60°C. Moreover, the intensity of the intramolecularly bonded OH absorption band remained almost unaffected even when the amount of free OH decreased very much under the coexistence of isobutyronitrile, the strongest proton acceptor in the present investigation. So, when the inter- and intra-molecularly bonded bands are overlapped, they were separated from each other in a manner similar to that described above by drawing the same intramolecularly bonded absorption curve as in the absence of the acceptor (Fig. 2).

Results and Discussion

The enthalpy change, ΔH, obtained from the slope of the line of the plot of $\ln(S_C/S_D)$ or $\ln(\kappa_C/\kappa_D)$ versus $1/T$, and the entropy change, ΔS, calculated by substituting the values of K and ΔH in Eq. 3, are tabulated in Table I. Generally, when isopropylbenzene is used as an acceptor, the frequency shifts, $-\Delta H$ and $-\Delta S$, are all lower than when cyclohexene is used. This is considered to result from the fact that in isopropylbenzene the degree of localization of the π electrons is lower due to the conjugation in benzene ring and the fact that the proton accepting field is larger, so that the degree of freedom of the complex is greater. When cyclohexene and isobutyronitrile are used as acceptors, $-\Delta S$ are approximately equal to the normal value, 13 e. u., for the ordinary intermolecular hydrogen bond[6,7], while when isopropylbenzene is used, the $-\Delta S$ are generally smaller, as has been stated above, and they amount to as small values as

6) H. Tsubomura, *J. Chem. Phys.*, **23**, 2130 (1955).
7) H. H. Jaffé, *J. Am. Chem. Soc.*, **79**, 2373 (1957).

TABLE I. SOME THERMODYNAMIC VALUES OF THE INTERMOLECULAR HYDROGEN BOND BETWEEN PROTON AND π ELECTRON

Donor	Acceptor	$\Delta\nu$ cm^{-1}	K l./mol.		25°C	40°C	60°C	$-\Delta H$ kcal./mol.	$-\Delta S$ e. u.
Phenol (0.015 mol./l.)	Cyclohexene (2.27 mol./l.)	97	0.230	κ_C/κ_D	0.377	0.332	0.243	2.83	12.8
				S_C/S_D	1.51	1.13	0.819	3.40	14.9
Phenol (0.015 mol./l.)	Isopropylbenzene (3.60 mol./l.)	57	0.320	κ_C/κ_D	1.98	1.57	1.32	2.60	10.9
				S_C/S_D	2.65	2.40	2.07	1.40	7.02
Catechol (0.015 mol./l.)	Cyclohexene (2.27 mol./l.)	129	0.232	κ_C/κ_D	0.825	0.587	0.521	2.96	12.9
				S_C/S_D	0.825	0.570	0.40	3.80	15.8
Catechol (0.015 mol./l.)	Isopropylbenzene (1.80 mol./l.)	72	0.100	κ_C/κ_D	1.378	1.08	0.851	2.68	11.1
				S_C/S_D	2.402	2.16	1.81	1.60	7.82
Catechol (0.015 mol./l.)	Isobutyronitrile (0.15 mol./l.)	194	9.10	κ_C/κ_D	2.44	1.71	1.08	4.82	12.0
				S_C/S_D	11.43	7.16	5.14	4.60	11.1
Vanillin (0.015 mol./l.)	Cyclohexene (2.27 mol./l.)	50	0.076	κ_C/κ_D	0.116	0.10	0.097	1.74	11.2
				S_C/S_D	0.34	0.295	0.256	1.56	10.8
Vanillin (0.015 mol./l.)	Isopropylbenzene (3.60 mol./l.)	33	0.105	κ_C/κ_D	0.383	0.365	0.337	0.62	6.72
				S_C/S_D	0.367	0.308	0.277	1.40	9.34
Vanillin (0.015 mol./l.)	Isobutyronitrile (2.40 mol./l.)	143	0.87	κ_C/κ_D	0.776	0.577	0.444	3.50	12.3
				S_C/S_D	—	—	—	—	—
3-Phenylpropanol (0.030 mol./l.)	Cyclohexene (2.27 mol./l.)	48	0.083	κ_C/κ_D	0.830	0.767	0.687	1.2	9.15
				S_C/S_D	0.950	0.830	0.764	1.2	9.12
3-Phenylpropanol (0.030 mol./l.)	Isopropylbenzene (1.80 mol./l.)	30	0.138	κ_C/κ_D	0.765	0.705	0.654	0.8	6.75
				S_C/S_D	0.785	0.726	0.650	1.0	7.31
3-Phenylpropanol (0.030 mol./l.)	Isobutyronitrile (0.60 mol./l.)	82	0.79	κ_C/κ_D	1.56	1.13	0.90	3.2	11.6
				S_C/S_D	4.064	2.86	1.97	3.2	11.6

6~7 e. u. Such small values are also observed in some weak hydrogen bonds, such as those existing in the combinations of *o*-chlorophenol-methyl acetate[7] or chloroform-acetone[9].

Considering from the values of ΔH and ΔS for vanillin, the guaiacyl OH group seems to be able to form a stronger hydrogen bond with the π electron when a carbonyl group is present at the para position. Such a characteristic difference between a simple guaiacyl OH group and that having a carbonyl group in its para position for the hydrogen bond formation, has been observed by Lindberg[9] in a similar case of the interaction of various guaiacyl compounds and dioxane. The ability of the free OH group of catechol to form a hydrogen bond with the π electron is much larger than that of simple phenol, which is quite parallel to the case of the formation of an ordinary hydrogen bond.

The values of $-\Delta H$ for the intermolecular hydrogen bond between the OH groups and the π electron obtained in our present investigation are larger than those obtained by Ōki and Iwamura[2] for intramolecular hydrogen bonds. This may be explained by considering that the steric stress may influence the formation of the intramolecular hydrogen bond. For example, in *o*-allylphenol, the direction of the π electron orbital of an allyl group seems to be difficult to orient towards the favorable direction for the interaction with the phenolic OH group in its ortho position, probably because in being compelled to be oriented parallel to the direction of the π electron of the benzene ring, they repulse each other. Consequently, it is to be expected that the steric condition for the formation of the bond

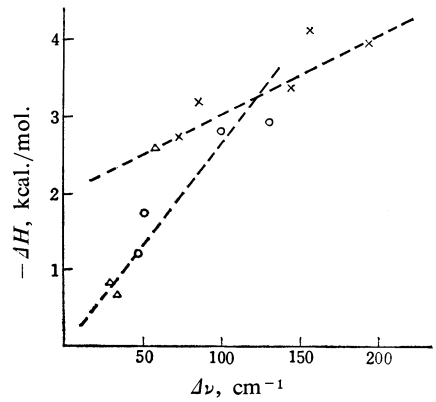


Fig. 3. The relation between $\Delta\nu$ and $-\Delta H$ (1), being used $-\Delta H$ values obtained from the slope of the line $\ln(\kappa_C/\kappa_D)$ versus $1/T$.
× : In the case of isobutyronitrile as acceptor.
○ : In the case of cyclohexene as acceptor.
△ : In the case of isopropylbenzene as acceptor.

8) S. Nagakura, ibid., **76**, 3070 (1954).
9) C. M. Huggins and G. C. Pimentel, *J. Chem. Phys.*, **23**, 1244 (1955).
10) J. J. Lindberg, *Societas Scientiarum Fennica, Commentationes Physico-Mathematicae XX*, 1 (1957).

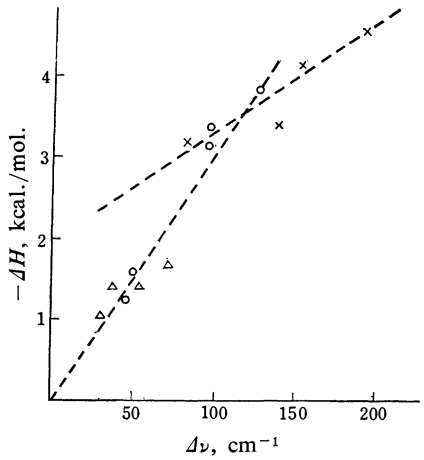


Fig. 4. The relation between $\Delta\nu$ and $-\Delta H$, being used $-\Delta H$ values obtained from the slope of the line $\ln(S_C/S_D)$ versus $1/T$.
×: In the case of isobutyronitrile as accepter.
○: In the case of cyclohexene as acceptor.
△: In the case of isopropylbenzene as acceptor.

is more favorable in the intermolecular interaction than in the intramolecular interaction.

When two acceptors, isobutyronitrile and cyclohexene, are compared, there is no great difference in $-\Delta H$. This is approximately 1 kcal./mol. Therefore, the proton-accepting character of the nitrile group is not always attributable only to the electronegativity of the nitrogen atom, but also rather reasonably to that of the π electron of the triple bond in the nitrile group.

In Figs. 3 and 4 are shown the relations between $-\Delta H$ and the frequency shift $\Delta\nu$. The $-\Delta H$ values in Figs. 3 and 4 are calculated from κ_C/κ_D and S_C/S_D respectively. As seen from these figures, the relations between these two quantities are not linear, which is contrary to Badger's postulation. It seems to be more reasonable to divide the curves into two linear portions:

for $\Delta\nu<100\,\mathrm{cm}^{-1}$;

$$-\Delta H \fallingdotseq \Delta\nu/30 \text{ kcal./mol.}$$

and for $\Delta\nu>100\,\mathrm{cm}^{-1}$;

$$-\Delta H \fallingdotseq 2.0+\Delta\nu/70 \text{ kcal./mol.}$$

The slope in the region of $\Delta\nu<100\,\mathrm{cm}^{-1}$ is considerably greater than that obtained by Badger[2] for ordinary hydrogen bonds.

The author wishes to express his thanks to Professors Takehiko Shimanouchi and Masamichi Tsuboi of the University of Tokyo and to the Kokusaku Pulp Ind. Co. for their permission to publish this work.

The Research Laboratory
The Kokusaku Pulp Ind. Co., Ltd.
Shinjuku-ku, Tokyo

The Interaction between the Proton of the Carboxyl Group and the π Electron of Some Compounds

By Shozo WADA

(Received June 14, 1961)

The hydrogen bond between the proton and the π electron has been studied mainly by investigating the variation of the infrared absorption of the OH or NH group due to the interaction between the proton of these groups and the π electron. The frequency shift of the OH absorption band increases in proportion to the proton-donating power of these groups, as was observed by West[1]. The author[2] has established that the larger the frequency shift, the stronger the hydrogen bond in the intermolecular interaction between the proton and the π electron is; this was established by using compounds having an OH group such as phenol, vanillin, catechol, 3-phenylpropanol as proton donors and some compounds having π electrons such as cyclohexene, isopropylbenzene, isobutyronitrile as proton acceptors. Therefore, the formation of the stronger hydrogen bond may be expected between the π electron and the proton of the carboxyl group, because the proton-donating power of this group is much larger than that of the other ordinary proton donor groups such as OH or NH. So far, however, no investigation on the interaction between the π electron and the proton of a carboxyl group has been made.

1) R. West, *J. Am. Chem. Soc.*, **81**, 1615 (1958).
2) S. Wada, This Bulletin, **35**, 707 (1962).

In the present report, therefore, the interaction between the proton of the carboxyl group of benzoic acid or cinnamic acid, and the π electron of squalene, toluene, or acetonitrile, has been investigated by measurement of the infrared spectra. The main purpose of this investigation is, in connection with the previous one[2], to learn the nature of the secondary bond of the π electron of some synthetic rubbers (such as styrene-butadiene copolymer, SBR, and acrylonitrile-butadiene copolymer, NBR) and the proton of the carboxyl group of thiolignin, which is a good reinforcer for these rubbers.

Experimental

The infrared absorption spectra were measured with a Perkin-Elmer model 13 spectrophotometer with a lithium fluoride prism. The slit width was 70 μ. The absorptions of the solutions of binary systems (a) of acid and carbon tetrachloride and of ternary systems (b) of acid, carbon tetrachloride and a proton-accepting compound (squalene, toluene or acetonitrile) were measured, together with those of the corresponding solvents. The sample solution was placed in a quartz cell 10 mm. in length. The absorbance, $\log I_0/I$, of acid was obtained by subtracting the absorbance of the solvent from that of the solution containing acid. The concentrations of acids are 0.003 and 0.007 mol./l. The two absorption curves, a and b, thus obtained were compared, and the frequency shift of the OH band by hydrogen bonding was estimated from the position of the OH band in the carboxyl group of the acid monomer molecule.

The chemicals used were purified according to the usual methods; their phyical constants were as follows: Benzoic acid, m.p. 121~122°C; cinnamic acid, m.p. 135~136°C; squalene, b.p. 238~240°C/2 mmHg; toluene, b.p. 110.5°C; acetonitrile, b.p. 81.6°C.

Results

The absorption spectra of benzoic acid in the mixture of carbon tetrachloride and a proton-accepting compound in the region of the OH absorption of the carboxyl group of monomeric acid molecule are shown in Figs. 1—3, together with those in pure carbon tetrachloride. Similar absorption spectra were obtained in the case of cinnamic acid. The absorption was measured also towards the region of the OH frequency of the dimeric acid molecule as far as 2400 cm^{-1}, but the difference between binary (a) and ternary (b) systems could not but be ambiguous because of the presence of the intense C–H band in the region of the OH absorption of the dimeric acid. However, in the case of acetonitrile, which is more powerful in proton-accepting power compared with the other two, squalene

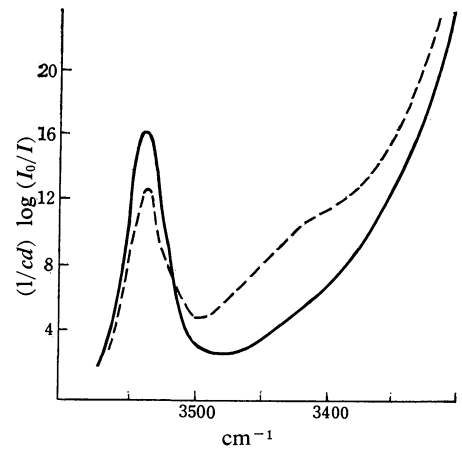


Fig. 1. Infrared absorption spectra of benzoic acid (0.007 mol./l.): a, in CCl_4; b, in the mixture of squalene and CCl_4. (The concentration of squalene is 0.5 mol./l.)
Note: $(1/cd)\log(I_0/I)$, molecular absorption coefficients. (c, concentrations in mol./l.; d, path length in cm.).
—— a ····· b

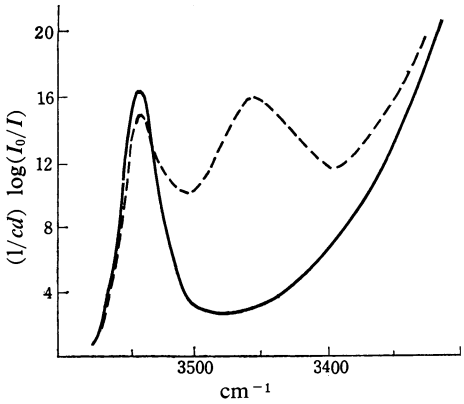


Fig. 2. Infrared absorption spectra of benzoic acid (0.007 mol./l.): a, in CCl_4; b, in the mixture of $C_6H_5CH_3$ and CCl_4. (The concentration of $C_6H_5CH_3$ is 3 mol./l.)
—— a, ····· b

and toluene, this difference was observed, as is shown in Fig. 4.

The frequency shifts of the OH band of carboxyl groups due to the formation of the hydrogen bond with the π etectron are shown in Table I, with reference to those of some phenolic hydroxyl groups as proton donors, reported on in the previous paper[2]. The frequency shifts are much larger in the case of acid than in the case of phenol and even catechol, although the same proton acceptor was not used in both cases.

The maximum of the OH absoption curve when squalene is used as a proton acceptor is not so clear as in the case of the other two

TABLE I. THE ENERGY OF THE HYDROGEN BOND BETWEEN PROTON AND π ELECTRON (kcal./mol.)

Acceptor		Donor: Vanillin	Catechol	Benzoic acid	Cinnamic acid
ν_0		3538	3610	3542	3545
Cyclohexene	$\Delta\nu$	50	129		
	ΔE	1.56*	3.80*		
Squalene	$\Delta\nu$	60	150	217	215
	ΔE	2.08	4.2	5.0	5.0
Isopropylbenzene	$\Delta\nu$	33	72		
	ΔE	1.40*	2.68*		
Toluene	$\Delta\nu$			92	82
	ΔE			3.3	3.2
Isobutyronitrile	$\Delta\nu$	143	192		
	ΔE	3.50*	4.6*		
Acetonitrile	$\Delta\nu$	140		267	255
	ΔE	3.50		5.8	5.6

ΔE*, actually measured values, in the previous investigation[2].

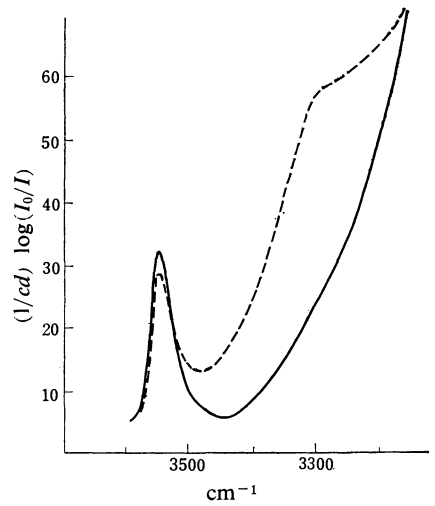


Fig. 3. Infrared absorption spectra of benzoic acid (0.003 mol./l.) : a, in CCl_4 ; b, in the mixture of CH_3CN and CCl_4. (The concentration of CH_3CN is 0.3 mol./l.)
—— a, ····· b

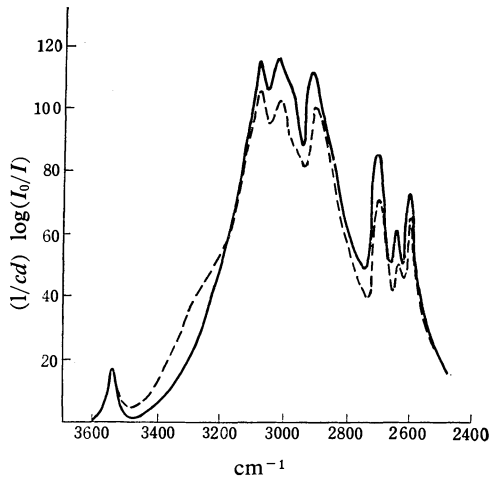


Fig. 4. Infrared absorption spectra of benzoic acid (0.007 mol./l.) : a, in CCl_4 ; b, in the mixture of CH_3CN and CCl_4. (The concentration of CH_3CN is 0.3 mol./l.)
—— a, ····· b

proton acceptors, toluene (Fig. 2) and acetonitrile (Fig. 3). This may mean that the proton-accepting character of the π electron in each double bond of the squalene molecule, which has five double bonds, is not always the same. Such a tendency may be much greater when the proton acceptor molecule is so large as a rubber molecule.

Even when the concentration of the acid in carbon tetrachloride is so dilute as 0.003 mol./l. or 0.007 mol./l., most parts of the acid exist in the state of dimer, and when a proton-accepting compound is added to this carbon tetrachloride solution of acid, the concentrations of both monomer and dimer change, because they are affected by the formation of the hydrogen bond between the proton of the carboxyl group and the π electron of the proton acceptor and by the increase of the dielectric constant of the medium around the acid molecule. Therefore, both the equilibrium constant of the formation of the hydrogen bond and the energy of the hydrogen bond are difficult to determine. However, the energy may be expected to be considerably large, in view of the fact that the frequency shift of the OH absorption of the carboxyl group is larger than that of catechol and that, consequently, its free OH group forms a stronger hydrogen bond with the π electron, as is shown in Table I.

In row ΔE of this table there are presented the energies of the hydrogen bond between the proton of the carboxyl group and the π electron calculated from the frequency shift

on the assumption that the following linear relationship between the frequency shift ($\Delta\nu$) of the OH group and the hydrogen bond energy (ΔE), that relationship reported in the previous paper[2], is also applicable in the present case:

$$\Delta E = 2.0 + \Delta\nu/70 \quad \text{kcal./mol.}$$

From the above result, it is concluded that there is a possibility of interaction between the π electron in a rubber molecule and the proton of a carboxyl group existing in a free state at the surface of a lignin particle in a lignin-rubber (SBR or NBR) compound. Therefore this interaction seems to contribute greatly to the secondary bond between lignin and rubber. The fact that the air-oxidated thiolignin, having a larger number of carboxyl groups, has a much higher reinforcing power on synthetic rubbers than ordinary untreated thiolignin may also be explained by the enhancement of the interaction between the π electron in synthetic rubbers and the carboxyl groups in oxidized thiolignin.

The author wishes to express his thanks to Professor Takehiko Shimanouchi and Professor Masamichi Tsuboi of the University of Tokyo and to the Kokusaku Pulp Ind. Co. for their permission to publish this work.

The Research Laboratory
The Kokusaku Pulp Ind. Co., Ltd.
Shinjuku-ku, Tokyo

3) R. A. V. Raff and O. H. Tomlinson, *Rubber Age*, **64**, 197 (1948); U. S. Pat. 2610954 (1952).

The Reactions of Ester with Acyl Chloride in the Presence of Aluminum Chloride. V. Reaction Mechanism of the Benzoylation of Diethyl Malonate

By Hiroo KANEYUKI

(Received June 28, 1961)

In a previous paper[1] it was reported that triacylated methanes were obtained in addition to diacylated compounds when diethyl malonate was treated with two or three molecular equivalents of benzoyl chloride or *p*-substituted benzoyl chlorides in the presence of three molecular equivalents of aluminum chloride. This paper describes attempts to achieve a more fundamental understanding of the reaction mechanism of the benzoylation of diethyl malonate.

Reaction of Ethyl Dibenzoylacetate with Aluminum Chloride.—These reactions resulted in the formation of acetophenone, dibenzoylmethane, aluminum chelate of dibenzoylmethane, tribenzoylmethane and benzoic acid (Table I). In every reaction, an appreciable amount of dibenzoylmethane was obtained with tribenzoylmethane. This fact shows that ethyl dibenzoylacetate gives dibenzoylmethane by decarbethoxylation and simultaneously decomposes to benzoyl chloride and ethyl benzoylacetate, which converts into acetophenone. On the other hand, tribenzoylmethane is formed by the benzoylation of the dibenzoylmethane which is formed.

$$(C_6H_5CO)_2CHCOOC_2H_5 \rightarrow C_6H_5COCH_2COOC_2H_5 + C_6H_5COCl + (C_6H_5CO)_2CH_2$$

$$(C_6H_5CO)_2CH_2 + C_6H_5COCl \rightarrow (C_6H_5CO)_3CH$$

$$C_6H_5COCH_2COOC_2H_5 \rightarrow C_6H_5COCH_3 + C_2H_5Cl + CO_2$$

Reactions of Dibenzoylmethane-*O*-benzoate with Aluminum Chloride.—The products of these reactions (Table I) were dibenzoylmethane, tribenzoylmethane and benzoic acid. From this table, it can be noted that dibenzoylmethane-*O*-benzoate is fairly stable in the presence of a small amount of aluminum chloride, but is decomposed to dibenzoylmethane in the presence of a large amount of aluminum chloride.

Reactions of Tribenzoylmethane with Aluminum Chloride.—In every case (Table I) tribenzoylmethane is decomposed to dibenzoylmethane, but it is difficult to decompose it to dibenzoylmethane with only a small amount of aluminum chloride.

1) H. Kaneyuki, This Bulletin, 35, 523 (1962).

TABLE I. REACTIONS OF ALUMINUM CHLORIDE WITH ACYLATED COMPOUNDS

Solvent: Nitrobenzene 8 ml.**, 4 ml.

	Reactant		Reaction condition		Product and yield							
	mol. $\times 10^{-2}$	$AlCl_3$ mol. $\times 10^{-2}$	°C	hr.	AP[a] %	DBM[b] %	DBM-Al[c] %	TBM[d] %	TBM-*O*-B[e] %	DBA[f] %	DBM-*O*-B[g] %	BA[h] %
DBA	0.33	0.49	60	8	12.5	46.0	2.1	Trace		4.6*		24.3
	0.33	0.67	30	5	12.5	37.0	16.5	1.3		2.5*		24.3
DBM-*O*-B	0.30	0.30	30	5		20.6	42.5	4.0				54.0
	0.30	0.04	45	26		Trace	32.4	3.5			50.0*	13.5
TBM	0.30	0.7	45	5		44.0	28.1	10.0*				67.6
	0.30	0.3	45	5		20.6	37.8	22.0*				57.0
	0.30	0.1	30	90		20.6		71.0*				26.0
TMB-*O*-B	0.23	0.22	45	5		9.0	40.7	33.0	6.0*			58.4
DBM**	0.22	0.22	65	8		22.0*	75.0					

* Recovered material.

a) AP; Acetophenone
b) DBM; Dibenzoylmethane
c) DBM-Al; Aluminum chelate of dibenzoylmethane
d) TBM; Tribenzoylmethane
e) TBM-*O*-B; Tribenzoylmethane-*O*-benzoate
f) DBA; Ethyl dibenzoylacetate
g) DBM-*O*-B; Dibenzoylmethane-*O*-benzoate
h) BA; Benzoic acid

Reaction of Tribenzoylmethane-*O*-benzoate with Aluminum Chloride.—It is to be noted that tribenzoylmethane-*O*-benzoate is easily converted into tribenzoylmethane and then further decomposed to dibenzoylmethane (Table I).

Reaction of Dibenzoylmethane with Aluminum Chloride.—Dibenzoylmethane seemed to be stable in the presence of aluminum chloride, for it is recovered in substantial quantities with its aluminum chelate (Table I).

Benzoylation of Ethyl Dibenzoylacetate.—In these reactions (Table II), the yield of dibenzoylmethane is good at a higher temperature, but the yield of tribenzoylmethane is good when a larger amount of aluminum chloride is used. It is fairly difficult to benzoylate ethyl dibenzoylacetate; a considerable amount of this material is recovered unchanged.

Benzoylation of Dibenzoylmethane and its Aluminum Chelate.—In these reactions (Table II), the yield of tribenzoylmethane is small when one molecular equivalent of aluminum chloride is used and is lower at a higher reaction temperature. Using 0.1 molecular equivalent of aluminum chloride, the yield of tribenzoylmethane is much increased. In the absence of aluminum chloride, the yield of tribenzoylmethane is very good, however, aluminum chelate of dibenzoylmethane gives it in a 12% yield. Therefore, it can be seen that the formation of tribenzoylmethane by the benzoylation of dibenzoylmethane is hindered to some extent by the presence of aluminum chloride.

Benzoylation of Tribenzoylmethane.—In every case (Table II), the yield of tribenzoylmethane-*O*-benzoate is low and the decomposition of tribenzoylmethane is greatest at a high temperature.

Benzoylation of Diethyl Malonate in the Presence of a Small Amount of Aluminum Chloride.—After diethyl malonate was warmed at 70°C with 1/3 molecular equivalent of aluminum chloride for 2 hr., one molecular equivalent of benzoyl chloride was added to the reaction mass, and then the mixture was kept at 70°C. When the reaction time is 8 hr., diethyl benzoylmalonate is the only product, but after a reaction of 24 hr., its yield is decreased, and instead small amounts of ethyl benzoylacetate, ethyl dibenzoylacetate and traces of acetophenone, dibenzoylmethane are obtained (Table III). In considering these results, diethyl benzoylmalonate seems to be converted slowly by decarbethoxylation into ethyl benzoylacetate, which is partly changed to acetophenone and ethyl dibenzoylacetate. Therefore, the following reaction sequences may be considered:

$$C_6H_5COCH(COOC_2H_5)_2 \rightarrow C_6H_5COCH_2COOC_2H_5$$

$$C_6H_5COCH_2COOC_2H_5 \rightarrow (C_6H_5CO)_2CHCOOC_2H_5$$

$$\downarrow \qquad\qquad\qquad \downarrow$$

$$C_6H_5COCH_3 \qquad\qquad (C_6H_5CO)_2CH_2$$

It can be concluded that the isolation of ethyl

TABLE II. BENZOYLATION OF SOME ACYLATED COMPOUNDS

Solvent: Nitrobenzene 8 ml., **25 ml.

Reactant				Reaction condition		Product*** and yield				
	mol. $\times10^{-2}$	C_6H_5COCl mol. $\times10^{-2}$	$AlCl_3$ mol. $\times10^{-2}$	°C	hr.	DBM[a] %	DBM-Al[b] %	TBM[c] %	TBM-*O*-B[d] %	DBA[e] %
DBA	0.33	0.35	0.67	60	5	43.7	17.8	21.6	2.0	4.0*
			0.37	60	5	14.5	51.0	2.7	Trace	25.0*
			0.37	30	5	20.0	6.3	3.6		54.0*
			0.06	30	56		3.8			95.0*
DBM	0.45	0.43	0.45	70	5	13.0*	75.0	2.4	2.6	
			0.45	30	5	25.0*	62.5	6.5	4.5	
			0.04	30	93	Trace*	23.0	71.5	0.5	
			0	30	90	17.5*		78.0		
DBM-Al**	0.04	0.21	0	30	90	24.2	63.4*	11.8		
TBM	0.30	0.64	0.60	70	8	56.0	8.9	9.5*	6.0	
		0.35	0.37	45	5	40.0	Trace	32.0*	5.7	

* Recovered material.
*** Benzoic acid was obtained in each case.
a) DBM; Dibenzoylmethane
b) DBM-Al; Aluminum chelate of dibenzoylmethane
c) TBM; Tribenzoylmethane
d) TBM-*O*-B; Tribenzoylmethane-*O*-benzoate
e) DBA; Ethyl dibenzoylacetate

TABLE III. BENZOYLATION OF DIETHYL MALONATE WITH BENZOYL CHLORIDE

Reactant: Diethyl malonate 3.1×10^{-2} mol., benzoyl chloride 3.1×10^{-2} mol., $AlCl_3$ 1.0×10^{-2} mol.
Reaction temp.: 70°C. Solvent: Nitrobenzene 16 ml.

Reaction time	Product and yield					
	BME[a]	BAE[b]	AP[c]	DBA[d]	DBM[e]	BA[f] recovered
hr.	%	%	%	%	%	%
8	52					21
24	25	4	Trace	5	Trace	16

Yield: Calculated from benzoyl chloride.
a) BME; Ethyl benzoylmalonate
b) BAF; Ethyl benzoylacetate
c) AP; Acetophenone
d) DBA; Ethyl dibenzoylacetate
e) DBM; Dibenzoylmethane
f) BA; Benzoic acid

benzoylacetate is due to the difficulty of the benzoylation of itself because of the small amount of aluminum chloride. Like these reaction products, ethyl *p*-nitrobenzoylacetate and *p*-nitroacetophenone were also obtained when diethyl malonate was treated with *p*-nitrobenzoyl chloride[1].

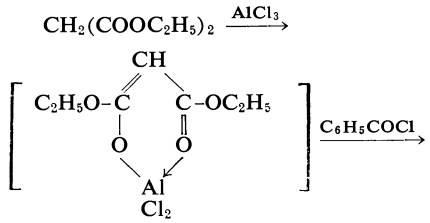
Discussion

The acylation of an active methylene group with acid chloride has been generally accomplished by means of a basic reagent. On the other hand, using an acidic reagent boron trifluoride, Meerwein[2] and Hauser[3] prepared β-diketone by the acylation of ketone with acid anhydride. Hauser has suggested that the acylation of ketone probably involves the conversion, by boron trifluoride, of both the anhydride and the ketone to reactive intermediates which condense. Therefore, the anhydride is presumably converted into carbonium ion, and the ketone is apparently converted into an enol form.

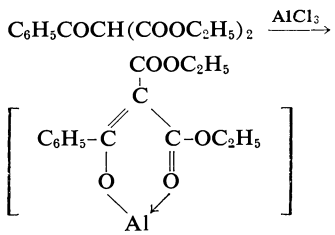
As shown in the experimental part of this paper, by treating diethyl malonate with benzoyl chloride in the absence of a catalyst, only a 4% yield of diethyl benzoylmalonate was obtained. Consequently, it may be considered that in the presence of a proper amount of aluminum chloride, diethyl malonate and β-keto-ester are activated much more effectively than acid chloride. From this standpoint, the

2) H. Meerwein and D. Vossen, *J. prakt. Chem.*, **141**, 149 (1934).
3) R. Hauser and T. Adams, *J. Am. Chem. Soc.*, **66**, 345 (1944).

following mechanism is postulated for the benzoylation of diethyl malonate in the presence of aluminum chloride: Diethyl malonate reacts with aluminum chloride to give the aluminum chloride complex (I). The reaction of I with benzoyl chloride leads to diethyl benzoylmalonate which soon becomes an aluminum chloride complex of diethyl benzoylmalonate (II).

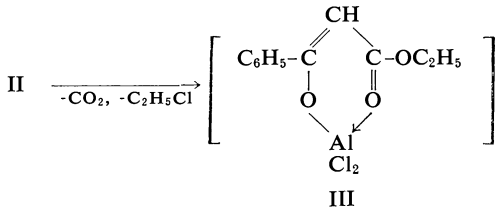


I

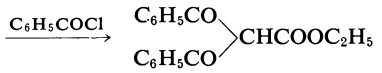


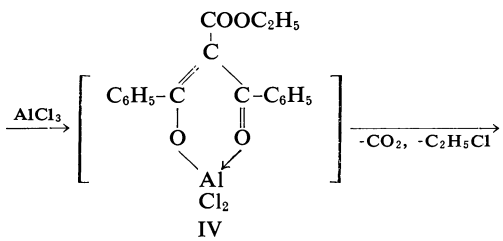
II

II is converted into an aluminum chloride complex of ethyl benzoylacetate (III) by decarbethoxylation. III will react immediately with benzoyl chloride to give ethyl dibenzoylacetate, which soon becomes an aluminum complex of ethyl dibenzoylacetate (IV). By slow decarbethoxylation, IV would be converted into an aluminum chloride complex of dibenzoylmethane (V).

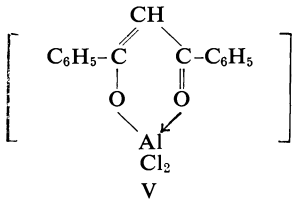


III



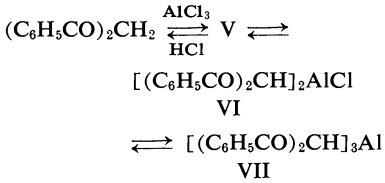


IV



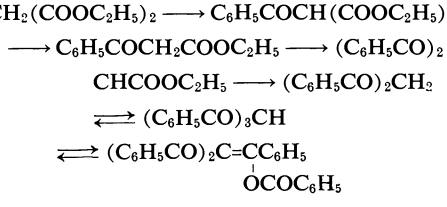
V

The fact that water-insoluble dibenzoylmethane is precipitated from the clear aqueous layer containing aluminum chloride by heating, as has been described in the experimental part of this paper, may show that dibenzoylmethane exists as V or VI in the presence of aluminum chloride. Because dibenzoylmethane and VII were always obtained in any of these experiments, it may be considered that dibenzoylmethane, V, VI and VII are in equilibrium.



When tribenzoylmethane was treated with aluminum chloride only, 22% of tribenzoylmethane was recovered, while dibenzoylmethane-*O*-benzoate gave a small amount of tribenzoylmethane under similar conditions (Table I). Therefore, the formation of tribenzoylmethane is not due to the isomerization of dibenzoylmethane-*O*-benzoate, but to the benzoylation of dibenzoylmethane or such complexes as V, VI and VII. As a similar example with the above reactions, it has been known that a copper complex of β-diketone reacts with *p*-nitrobenzoyl chloride to give copper chelate of triketone[4]. Moreover, in the presence of a large amount of aluminum chloride (Table II), the direct conversion of ethyl dibenzoylacetate into tribenzoylmethane may occur. Besides benzoylation, the reactions of aluminum chloride are complicated by such side reactions as decarbethoxylation, debenzoylation and the cleavage of ester linkage, as shown in Table I.

Owing to the above considerations, the following sequence has to be postulated:



4) W. J. Barry, *J. Chem. Soc.*, **1960**, 670.

Experimental

Reaction methods were the same as in the previous paper[1]. The treatment of the reaction mixture was also the same; that is, it was separated into the aqueous layer containing aluminum chloride, sodium bicarbonate extract, sodium hydroxide extract, water extract and residual solution. Descriptions overlapping with those of the previous paper are omitted here. Reaction conditions are shown in the above tables.

Reaction of Ethyl Dibenzoylacetate with Aluminum Chloride.—Precipitates were deposited with a small amount of an oily substance when the aqueous layer containing aluminum chloride was warmed and allowed to stand. The precipitates were collected, washed with petroleum ether and recrystallized from methanol to afford dibenzoylmethane. 2, 4-Dinitrophenylhydrazone derived from the petroleum ether soluble substance was recrystallized from ethanol to yield crystals, m. p. 245~248°C, which showed no depression of melting point on admixture with 2, 4-dinitrophenylhydrazone of acetophenone.

Reaction of Dibenzoylmethane-*O*-benzoate with Aluminum Chloride.—Dibenzoylmethane-*O*-benzoate was prepared according to the procedure of the literature[5]. By removing the solvent from the residual solution separated from the reaction mixture, dibenzoylmethane-*O*-benzoate was recovered.

Benzoylation of Diethyl Malonate with Benzoyl Chloride in the Presence of a Small Amount of Aluminum Chloride.—An oily substance was precipitated with some solid from the aqueous layer containing aluminum chloride, as has been described above. The solid was collected by filtering, washed with water and recrystallized from methanol to afford dibenzoylmethane. The filtrate was extracted with ether, and the ethereal extract was shaken with a copper acetate solution. A small amount of the yellowish green precipitate formed was filtered. By treating this precipitate with hydrochloric acid, dibenzoylmethane was obtained. After removal of ether from the ethereal solution, a green semi-solid I was obtained. The semi-solid was filtered and washed with ethanol. The ethanol wash was concentrated to yield crystals of copper chelate of diethyl benzoylmalonate. The mother liquor was subjected to steam distillation, and from the distillate 2, 4-dinitrophenylhydrazone was prepared and identified as that of acetophenone by the mixed melting point method. The sodium hydroxide extract was acidified and extracted with ether. After concentrating the ether extract, crystallized ethyl dibenzoylacetate was filtered off. From the ethereal filtrate, copper chelate of diethyl benzoylmalonate was prepared, as has been mentioned above.

Copper Chelate of Ethyl Benzoylacetate.—The solid I was recrystallized from benzene as light green needles, 0.35 g., m. p. 178~184°C, reported m. p. 180°C, 182~183°C[6].

Found: C, 59.53; H, 4.87. Calcd. for $C_{22}H_{22}O_6Cu$: C, 59.25; H, 4.97%.

Reaction of Diethyl Malonate with Benzoyl Chloride.—Diethyl malonate (3.4 g., 0.021 mol.) and benzoyl chloride (3.0 g., 0.021 mol.) were dissolved in nitrobenzene (15 ml.) and kept at 65°C for 8 hr. The treatment of the reaction mixture was the same as has been mentioned above. Benzoic acid (2.3 g.) was obtained on acidifying the sodium bicarbonate extract. The oily substance obtained by acidification of the sodium hydroxide extract and water extract was converted into copper chelate, 0.25 g., m. p. 178~179°C; this was identified as copper chelate of diethyl benzoylmalonate by the mixed melting point method.

The author wishes to express his hearty thanks to Professor Kiyotada Matsui for his kind guidance and encouragement, and to Professor Ryozo Goto, Kyoto University, for his many valuable suggestions.

Department of Industrial Chemistry
Faculty of Technology
Kanazawa University
Uenohonmachi, Kanazawa

5) L. Claisen and E. Hasse, *Ber.*, **36**, 3674 (1903).

6) "Beilsteins Handbuch der Organischen Chemie", H., **10**, 678 (1927).

Activations by Anions in the Oxy-acid Phosphors. III. Activations by the Vanadate Ion

By Yoshihide KOTERA and Michiko YONEMURA

(Received August 10, 1961)

In previous papers[1] it was found that anionic centers are present in the oxy-acid phosphors and that the activation by vanadate might be one of "intraionic activation", then the luminescence would originate from the electron transitions in the vanadate ion. The activation by vanadate ions has been reported by a few researchers[2,3], but in most cases the activation has been assumed to be caused by vanadium ions[2]. We have prepared some magnesium compounds activated by vanadate ions and have obtained some remarkable results.

The Experiments and their Results

Preparation of Phosphors and the Measurements of their Characteristics.—The starting materials were MgO, $(NH_4)_2SO_4$, $SiO_2 \cdot nH_2O$, $(NH_4)_2HPO_4$, NH_4VO_3, As_2O_3, Sb_2O_3, H_3BO_3 and H_2WO_4, which had been purified by the process previously reported[3]. They were mixed in a dry state and fired in air. The spectral distribution was measured by means of a spectroradiometer[4], the brightness was measured by a photocell, and the crystal structure was determined by an X-ray diffractometer.

Activation of Magnesium Compounds by Vanadate Ions.—Magnesium sulfate, silicate or pyrophosphate, was prepared by the reaction between magnesium oxide and oxy-acidic compound. Other phosphates (orthophosphate or halophosphate) or silicates were proved to be worse than those described above. Their spectral distributions are almost the same as that of magnesium vanadate, and their brightnesses are shown in Table I, while their X-ray patterns are shown in Fig. 1.

Effect of the Addition of other Components to Magnesium Silicate Activated by Vanadate Ions.—Magnesium silicate was activated by two ions among the vanadate, phosphate, arsenate, antimonate, germanate and borate ions. Magnesium oxide and amorphous silica were mixed in the molar ratio of 1 : 1.1, and two

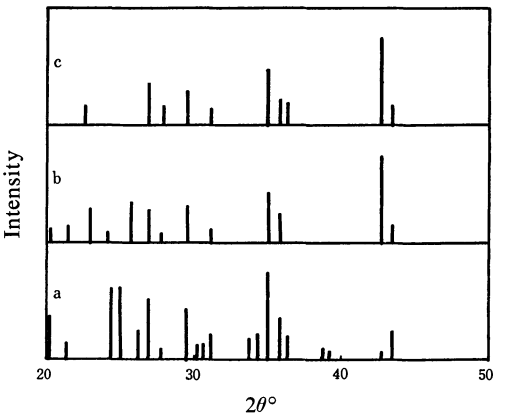


Fig. 1. X-Ray diffraction patterns of magnesium compounds activated by vanadate ions.

	g.		g.		g.
(a)	MgO 1.0	$(NH_4)_2SO_4$	0.7	NH_4VO_3	0.3
(c)	MgO 2.0	$(NH_4)_2HPO_4$	0.4	NH_4VO_3	0.3
(b)	MgO 1.5	SiO_2	0.7	NH_4VO_3	0.3

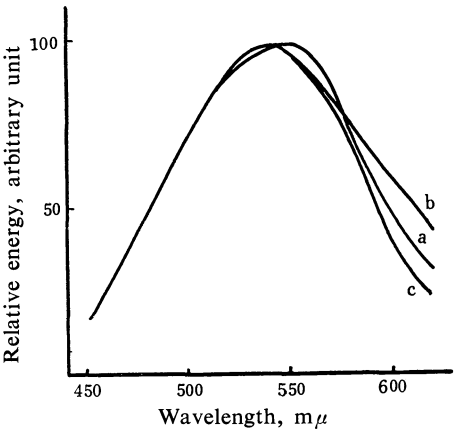


Fig. 2. Spectral distributions of magnesium silicate activated by vanadate and other ions.
(a) Activation by vanadate ions
(b) Activation by vanadate and phosphate ions
(c) Activation by vanadate and arsenate ions

1) Y. Kotera, M. Yonemura and T. Sekine, This Bulletin, **35**, 577 (1962).
2) H. Gobrecht and G. Heinsohn, *Z. Physik*, **147**, 350 (1957).
3) R. Robl, *Z. angew. Chem.*, **39**, 608 (1926); A. Schloemer, *J. prakt. Chem.*, **133**, 51 (1932); Y. Kotera and T. Sekine, This Bulletin, **27**, 13 (1954); S. Rothschild, *Brit. J. Appl. Phys.*, 1955, Supplement No. 4, S. 32.
4) Y. Kotera, *Rept. Gov. Chem. Ind. Research Institute, Tokyo*, **50**, 398 (1955).

Table I. Optimum conditions for preparation of magnesium compounds activated by vanadate ions and their brightness

Matrix	Optimum mixing ratio mol.			Firing temp. °C	Relative brightness*
Mg silicate	MgO 1.5	SiO_2 0.7	NH_4VO_3 0.3	1050	70
Mg phosphate	MgO 2.0	$(NH_4)_2HPO_4$ 0.5	NH_4VO_3 0.2	1050	85
Mg sulfate	MgO 1.0	$(NH_4)_2SO_4$ 0.8	NH_4VO_3 0.2	1000	160

* The value of 100 corresponds to the brightness of a magnesium pyrovanadate phosphor.

Table II. Emissions of magnesium silicate activated by two kinds of anions

	$V_2O_7^{4-}$	PO_4^{3-}	AsO_4^{3-}	$Sb_2O_7^{4-}$	GeO_4^{4-}	BO_3^{3-}
$V_2O_7^{4-}$	Yellow m*1	Yellow m (11)*2	Yellow m (15)	Yellow m (10)	Yellow m (10)	Yellow m (9)
PO_4^{3-}		Yellow ff*1	None	Pink ff	None	None
AsO_4^{3-}			Red f*1	Pink ff	White ff	Red f
$Sb_2O_7^{4-}$				Yellow ff*1	White ff	None
GeO_4^{4-}					Yellow ff*1	None
BO_3^{3-}						None*1

*1 Activated by one kind of anions.
*2 Relative brightness under 2537Å excitation.

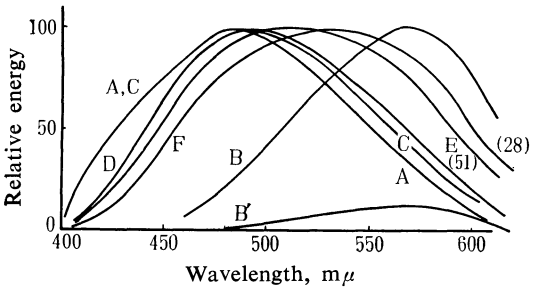


Fig. 3. Spectral distributions of the system of $MgWO_4$-$Mg_2V_2O_7$: A, $MgWO_4$; B, $Mg_2V_2O_7$; C, Calculated from A and B for the mixture of A and B with equivalent molar ratio; D, $MgWO_4$ 0.95+ $Mg_2V_2O_7$ 0.05 (mol.); E, $MgWO_4$ 0.7+ $Mg_2V_2O_7$ 0.3 (mol.); F, $MgWO_4$ 0.5+ $Mg_2V_2O_7$ 0.5 (mol.); B', Relative value of B to A.

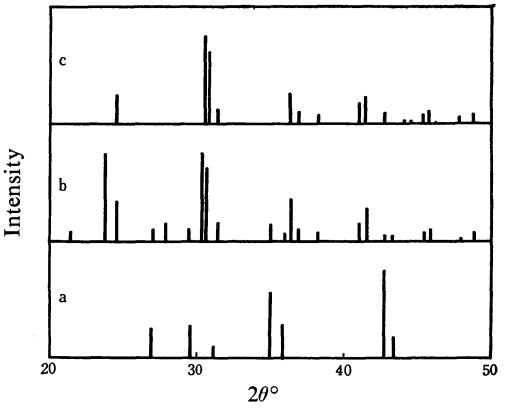


Fig. 4. X-Ray diffraction patterns of the system of $MgWO_4$-$Mg_2V_2O_7$.
(a) $Mg_2V_2O_7$
(b) $Mg_2V_2O_7$ 0.5+$MgWO_4$ 0.5
(c) $Mg_2V_2O_7$ 0.05+$MgWO_4$ 0.95

ions were added to it, each amount being 0.005 mol. per 1 mol. magnesium oxide. They were fired at 1100°C for 4 hr.; the spectral distributions measured are shown in Fig. 2, and the brightness of some of them, in Table II. The color of emission is tabulated in Table II.

The Spectral Distributions of Mixed Crystal $MgWO_4$-$Mg_2V_2O_7$.—The system of $MgWO_4$-$Mg_2V_2O_7$ was examined to clarify the activation effect of the vanadate ion. Mixtures of magnesium oxide, tungstic acid and ammonium vanadate were fired at 1050°C for 2 hr. The spectral distributions of these phosphors are shown in Fig. 3, in which the numbers attached to the curves represent the relative height at their peaks. The X-ray patterns of some products are shown in Fig. 4.

Discussion

The activation by the vanadate ion in alkali or alkali earth vanadate has been studied by us and by others[2,3], but for other compounds few patents[5] have been found. We prepared various magnesium compounds activated by the vanadate ion, and, when a large amount of vanadate compound was added to them, some of these compounds had a higher brightness than that of pure magnesium metavanadate. In the latter case, it might be concluded from a consideration of the case of the calcium sulfate-calcium tungstate system[6], in which the content of tungstic acid is high, that a

5) W. A. Roberts, U. S. Pat. 2312265; French Pat. 869448.
6) Y. Kotera, T. Sekine and M. Yonemura, This Bulletin, 35, 580 (1962).

part of the product is activated by the vanadate ion. The formation of magnesium metavanadate was proved crystallographically in Fig. 1, in contrast to the calcium sulfate-calcium tungstate system, while it was difficult in the latter case to prove the formation of tungstate by means of X-ray analysis because of the structural similarity of the components.

The effect of the addition of other anions to magnesium silicate is relatively small, but it may be concluded that other anions cause the variation in brightness and a small shift in the spectral distribution of the emission.

The system of $MgWO_4$-$Mg_2V_2O_7$ shows almost the same characteristics as the results obtained when zinc or cadmium oxide is added to calcium sulfate activated by a tungstate ion[6]. Those results might be explained by the formation of a solid solution between the constituents, but it was difficult to know its formation from the X-ray pattern shown in Fig. 4.

Government Chemical Industrial Research Institute, Tokyo
Shibuya-ku, Tokyo

Activations by Anions in the Oxy-acid Phosphors. IV. Activations by Sulfide and Sulfo-oxide Ions

By Yoshihide KOTERA and Tadao SEKINE

(Received August 10, 1961)

It was found in previous papers[1] that activation by sulfide occurs in alkali earth sulfate phosphors. Meanwhile, Gobrecht et al.[2] reported activation by polysulfide in alkali earth sulfides and alkali sulfides, and Kirk[3] reported the effect of sulfur in natural sodalite. We have prepared alkali earth sulfate activated by a sulfide ion or a sulfo-oxide ion and have obtained some remarkable results.

The Experiments and their Results

Preparation of Phosphors.—The alkali earth sulfides were prepared by the reaction between purified alkali earth sulfate and a reducing agent, for example, cane sugar, while the alkali earth sulfites were precipitated by the addition of a purified sulfite solution to a purified alkali earth salt solution. The optimum conditions for preparing the phosphors are shown in Table I; it was necessary to maintain the firing atmosphere in a neutral condition because oxidizing or reducing atmosphere causes a variation in the characteristics of the products.

Spectral Distribution of the Emissions of the Phosphors.—The spectral distributions are shown in Fig. 1. It was difficult to obtain accurate distributions for calcium and barium sulfate activated by sulfite ion because of their weak emission, while that of strontium sulfate activated by sulfite is somewhat inaccurate. However, it was ascertained that activation by a sulfite ion gave a different product than that by a sulfide ion.

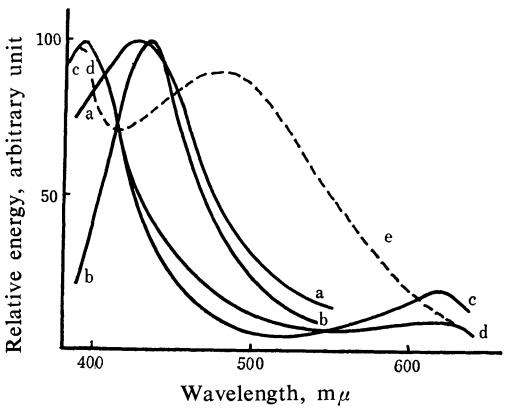


Fig. 1. Spectral distributions of alkali earth sulfate activated by sulfide and sulfite.
a: 0.01 g. $CaS/CaSO_4$ 1 g.
b: 0.1 g. $CaS/CaSO_4$ 1 g.
c: 0.035 g. $BaS/BaSO_4$ 1 g.
d: c+NaCl flux
e: 0.01 g. $SrSO_3/SrSO_4$ 1 g.

It is remarkable that the weak afterglow was detectable in the case of calcium sulfate activated by a sulfide ion.

1) Y. Kotera, M. Yonemura and T. Sekine, This Bulletin, 35, 577 (1962).
2) H. Gobrecht and D. Hahn, *Z. Physik*, 132, 111 (1952); 135, 523 (1953).
3) R. D. Kirk, *J. Electrochem. Soc.*, 101, 461 (1954).

TABLE I. OPTIMUM CONDITIONS FOR PREPARATION OF SULFATE COMPOUNDS ACTIVATED BY SULFIDE AND SULFITE IONS

	Mixing ratio, mol.			Flux	Firing conditions
$CaSO_4$: S	$CaSO_4$ 1	CaS	0.01	Na salt	1100°C, 4 hr. in N_2
$SrSO_4$: S	$SrSO_4$ 1	SrS	0.01	—	
$BaSO_4$: S	$BaSO_4$ 1	BaS	0.035	NaCl 10 mol. %	
$CaSO_4$: SO_3	$CaSO_4$ 1	$CaSO_3$	0.01	—	
$SrSO_4$: SO_3	$SrSO_4$ 1	$SrSO_3$	0.01	—	
$BaSO_4$: SO_3	$BaSO_4$ 1	$BaSO_3$	0.1	NaF 10 mol. %	

Discussion

The spectral distribution of the emission of calcium, strontium or barium sulfate activated by a sulfide ion may differ from that of polysulfide, which was reported by Gobrecht et al.[2], but it is impossible to compare our results with theirs because they concluded that preparation by the reduction of sulfate salts is unsuitable for the preparation of their phosphors. Barium sulfate activated by a sulfide ion has an emission like that of barium polysulfide, but it is probable that barium sulfate is produced during the firing of barium polysulfide. Such comparisons are related to the fact the control of the atmosphere is important during the firing of sulfate salt phosphors. In our experiments it was possible to separate the activations by the sulfide ion and by the sulfite ion by precise control of the atmosphere.

Interesting facts were found in the phosphors activated by the sulfide ion; the flux has some effect on the intensity of the prepared phosphor, and the decay of some samples is relatively long. These facts show that the oxy-acid phosphors activated by the sulfide ion may be the intermediates between sulfide and oxy-acid phosphors. The fact that barium sulfate or calcium sulfate activated by sulfide ion emits, under the excitation of 3650Å, a light of almost the same characteristics as when under 2537Å, supports this idea. The excitation spectrum may be considerably longer than those of the oxy-acid phosphors, but it has not yet been measured precisely. It would be interesting to study the other matrices activated by the sulfide ion in relation to the studies by Gobrecht et al.[2], by Kirk[3] and by Thomson[4].

Government Chemical Industrial Research Institute, Tokyo
Shibuya-ku, Tokyo

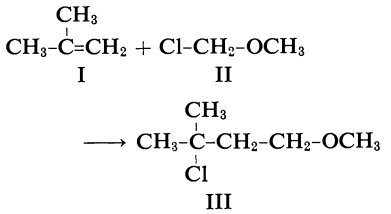
4) S. M. Thomson, *J. Chem. Phys.*, **18**, 770 (1950).

The Reaction of Isobutene with Chloromethyl Methyl Ether in Liquid Sulfur Dioxide

By Niichiro TOKURA, Isoo SHIRAI and Katsuo SHIINA

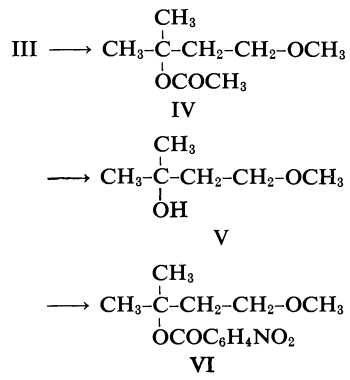
(Received August 7, 1961)

Isobutene (I) reacts with chloromethyl methylether (II) in liquid sulfur dioxide to give 2-chloro-4-methyl-2-methylbutane (III). Straus and Thiel[1] have reported that the formation of III from I and II requires a catalyst such as mercuric chloride, while the present reaction in liquid sulfur dioxide is very rapid and is practically accomplished in a few minutes without any catalyst and at room temperature.



Structure III was confirmed by preparing some derivatives as follows:

1) F. Straus and W. Thiel, *Ann.*, **525**, 151 (1936).



III was treated with sodium acetate to afford 2-acetoxy-4-methoxy-2-methylbutane (IV). IV was hydrolyzed with alkali to 4-methoxy-2-methyl-2-butanol (V), which gave a *p*-nitrobenzoate (VI), m. p. 74.0°C.

Such cross-linking or jointing by the methylene group as has been seen elsewhere[2] was not observed in the present experiment. The yield of III was depressed by the use of a catalyst such as stannic chloride owing to the predominating self-polymerization of isobutene.

Experimental

Reaction of Isobutene (I) with Chloromethyl Methyl Ether (II) in Liquid Sulfur Dioxide.—To 110 ml. of liquid sulfur dioxide was added 21.5 g. (0.38 mol.) of I, and 38.6 g. (0.48 mol.) of II was then dropped into the mixture. The mixture was allowed to stand at room temperature for ten minutes and then mixed with ice water, and the liquid sulfur dioxide was evaporated. The residue was washed with sodium sulfate and distilled in vacuo. The transparent oil, b. p. 60~66°C 100 mmHg, was redistilled under ordinary pressure to yield 7.8 g. of pure 2-chloro-4-methoxy-2-methylbutane (III), b. p. 141~145°C (lit.[1], b. p. 136°C/751 mmHg. Found: C, 52.74; H, 9.51, Calcd. for $C_6H_{13}OCl$: C, 52.71; H, 9.57%, mol. wt., Found: 143 (benzene), Calcd.: 136.5. IR ν_{max}^{liq} 1295 cm^{-1} (methoxy), no absorption at 1600 cm^{-1} (C=C).

2-Acetoxy-4-methoxy-2-methylbutane (IV).—III was treated with anhydrous sodium acetate by a general procedure to give IV, b. p. 34.8~40.0°C/14 mmHg.

4-Methoxy-2-methyl-2-butanol (V).—IV was hydrolyzed with a 1 N potassium hydroxide solution to 4-methoxy-2-methyl-2-butanol (V), b. p. 54~55.5°C 20 mmHg. V gave a *p*-nitrobenzoate (VI), m. p. 74.0°C. Found: C, 58.38; H: 6.24: N, 5.36. Calcd. for $C_{13}H_{17}O_4N$: C, 58.18; H, 6.63: N, 5.21%.

The present investigation was supported by a grant from the Ministry of Education. The liquid sulfur dioxide was supplied by the Befu Chemical Industries, Ltd. The authors are grateful to all of them.

The Chemical Research Institute of Non-Aqueous Solutions
Tohoku University
Katahira-cho, Sendai

2) R. Asami, T. Shiohata and N. Tokura, *Bull. Chem. Res. Inst. Non-Aqu. Soln.* (*Hisuiken-Hokoku*), **10**, 99 (1961).

The Reactions of 1, 2-Cyclopentanedione Dioxime and of 1, 2, 3-and 1,3,5-Cyclohexanetrione Trioximes in Liquid Sulfur Dioxide[1]

By Niichiro TOKURA, Isoo SHIRAI and Tokuji SUGAHARA

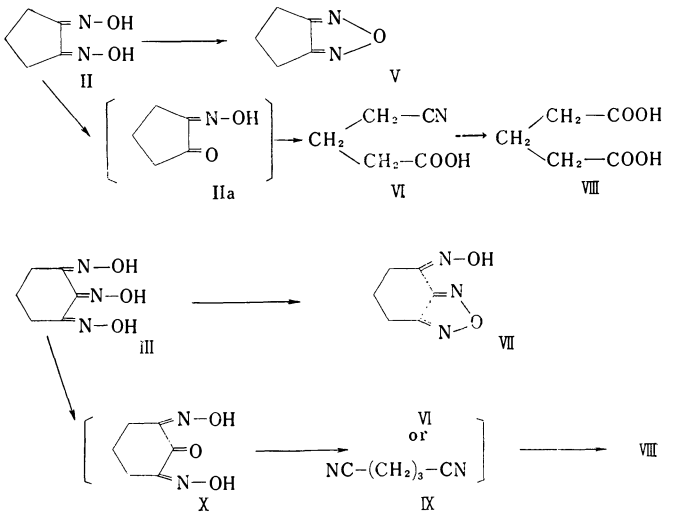
(Received October 12, 1961)

As has been reported in the preceding papers of this series[2,3], 1, 2-cyclohexanedione dioxime, when subjected to Beckmann rearrangement in liquid sulfur dioxide, gives different products according to the reagents applied. Thus, thionyl chloride yielded an oxadiazole (furazan) derivative by condensation of the two neighboring hydroximino groups; bromine yielded a rearranged product, and sulfur trioxide afforded δ-cyanovaleric acid, a product of ring cleavage. The causes of such various reactions have also been discussed.

The result has prompted the present authors to investigate similar reactions with 1, 2-cyclopentanedione dioxime and 1, 2, 3- and 1, 3, 5-cyclohexanetrione trioximes.

1, 2-Cyclopentanedione dioxime (II) was prepared by the method of Belcher et al.[2,4]

1) The Beckmann Rearrangement in Liquid Sulfur Dioxide, Part IX.
2) N. Tokura, R. Tada and K. Yokoyama, This Bulletin, **34**, 270 (1961).
3) N. Tokura, R. Tada and K. Yokoyama, ibid., **34**, 1812 (1961).
4) R. Belcher, W. Hoyl and T. S. West, *J. Chem. Soc.*, **1958**, 2743.



Namely, 2-bromocyclopentanone (I) was converted into 1, 2-cyclopentanedione dioxime by hydroxylamine, but in a low yield, as in the case of 1, 2-cyclohexanedione dioxime[2]. 1, 2, 3-Cyclohexanetrione trioxime (III) was prepared via 1, 2, 3-cyclohexanetrione 1, 3-dioxime by the method of Donald, Batesky and Moon[5]. 1, 3, 5-Cyclohexanetrione trioxime (IV) was prepared from phloroglucinol by the method of Baeyer[6].

In general, the oximes were not completely soluble in liquid sulfur dioxide at first, but they were immediately dissolved to transparent and homogeneous solutions on the addition of the rearranging reagents; the reactions were carried out at room temperature (10~18°C). Because of the unusual instability of the trione trioximes, the addition of the reagents often led to explosive reactions. Therefore, the reactions were sometimes performed at temperature below 0°C. Furthermore, the reactions were accompanied by the formation of large amounts of resinous matters, which has made the quantitative treatment and the discussion of the results difficult.

The reaction of II with thionyl chloride in liquid sulfur dioxide afforded a low melting substance, m. p. 41°C, which was identified as 5, 6-dihydro-4-cyclopenta [*c*] furazan[7] (V) both by analogy with the results disclosed in a preceding paper[2] and from the results of elementary and infrared spectrometric analyses.

The reaction of bromine with II in liquid sulfur dioxide produced only a large amount of a tarry matter, failed to give a product which could be characterized.

The reaction of sulfur trioxide with II in liquid sulfur dioxide afforded the expected γ-cyanobutyric acid (VI) as a product of ring cleavage. However, the yield was very low because of the violent carbonizing and resinifying action of sulfur trioxide. Hydrolysis of VI with aqueous hydrochloric acid gave glutaric acid (VIII). It seems likely that VI was derived through the incipient intermediate (IIa), as has been demonstrated in a preceding paper[2].

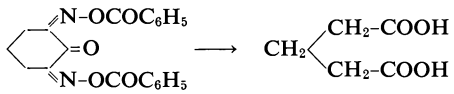
When III reacted with thionyl chloride in liquid sulfur dioxide, a product, m. p. 167~167.5°C, was obtained in a good yield. This was proved to be a cyclodehydrated product like V, and the structure of 7-hydroximino-4, 5, 6, 7-tetrahydrobenzo[*c*]furazan (VII) was assigned to it on the basis of elementary and infrared analyses. The presence of one free hydroximino group and of a furazan ring was deduced from the absorption at 1659 cm^{-1} and from the absorptions at 1622 and 1583 cm^{-1} respectively. The reaction of bromine with III yielded only a small amount of VII with a majority of a resinous matter.

The reaction of sulfur trioxide with III was expected to be of interest, but it turned out to be complicated as well. A small amount of VII was found in the reaction mixture. The residual solution, refluxed with 2 N hydrochloric acid, produced glutaric acid (VIII), but no glutaric acid dinitrile (IX), VI or any other intermediate that would produce VIII by acid hydrolysis, was isolated by extraction of the residual solution with ether.

The only product in the residual solution was apparently a mono-deoximated product,

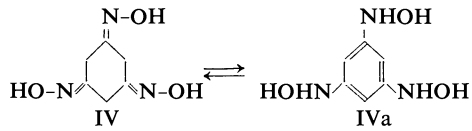
5) D. Donald, C. Batesky and N. S. Moon, *J. Org. Chem.*, **24**, 1694 (1959).
6) A. Baeyer, *Ber.*, **19**, 159 (1886).
7) Definitive Rules for Nomenclature of Org. Chem. (IUPAC, 1957), *J. Am. Chem. Soc.*, **82**, 5545 (1960).
In the preceding papers[2,3], "1, 3, 5-oxadiazole" was used for "furazan".

probably cyclohexanetrione 1, 3-dioxime and not 1, 2-dioxime, for it produced no pink coloration with nickel nitrate solution. One plausible explanation is, therefore, that trioxime III was deoximated to trione 1, 3-dioxime X and the latter was then cleaved to dinitrile IX or to mononitrile VI to be hydrolyzed to VIII. The cleavage of the dibenzoyl derivative (XI) of the 1, 3-dioxime (X) with alkali to glutaric acid has already been reported by Treibs and Kuhn[8].



XI

The reactions of IV with thionyl chloride, with bromine and with sulfur trioxide, all ended in the formation of black nitrogen containing tarry materials, which were not extractable with any organic solvent. Since the following tautomerism in IV may be considered, the formation of a large amount of resinous product from IV may be accounted for by the presence of the reactive tautomer (IVa).



IV IVa

Experimental

Materials.—Commercial sulfur dioxide was dried with concentrated sulfuric acid and distilled. Thionyl chloride and sulfur trioxide were each distilled once. Bromine was dehydrated with sulfuric acid and distilled.

Apparatus and General Procedure.—The procedure and manipulation for the reactions were the same as have been described previously[1,2].

2-Bromocyclopentanone (I)[9].—Bromine (19 ml.) was added to a mixture of cyclopentanone (25 g.), glacial acetic acid (15 ml.) and water (60 ml.) at 55~60°C, and the whole was stirred at this temperature for a while. The reaction mixture was then neutralized with sodium carbonate. The orange oil separated was washed with water. The crude 2-bromocyclopentanone (I) (yield, 34 g.) was oximated without further purification.

1, 2-Cyclopentanedione Dioxime (II).—I (34 g.) was stirred into in small portions to a solution of hydroxylamine hydrochloride (42 g.) and sodium acetate (83 g.) in water (160 ml.), and the mixture was then refluxed for half an hour. After the mixture had been refluxed for twenty minutes more, it was treated with active carbon and filtered while hot. The filtrate was cooled to yield crude crystals of 1, 2-cyclopentanedione dioxime (II), which were then washed with water, thoroughly dried and extracted with 99% ethanol. The crystals obtained on evaporation of ethanol were recrystallized from 50% ethanol, m. p. 205~210°C (lit.: 202~212°C[4]), yield 9.0 g. Found: C, 46.68; H, 5.84; N, 21.66. Calcd. for $C_5H_8O_2N_2$: C, 46.87; H, 6.29; N, 21.87%.

1, 2, 3-Cyclohexanetrione Trioxime (III).—Essentially the method of Donald et al.[5] was employed. 1, 2, 3-Cyclohexantrione 1, 3-dioxime, m. p. 196~197°C, was prepared from cyclohexanone (184 g.), concentrated hydrochloric acid (7.5 ml.) and isoamyl nitrite (250 g.) at −5°C (yield 95 g.). The trione dioxime (31.3 g.) in 50% ethanol was oximated with hydroxylamine hydrochloride (17.4 g.) and sodium carbonate (12.9 g.) to give the 1, 2, 3-trione trioxime (III) (20 g.), m. p. 169.5~170°C (recrystallized from dioxane). Found: C, 42.40; H, 4.50; N, 24.02, Calcd. for $C_6H_9O_3N_3$: C, 42.10; H, 5.30; N, 24.55%.

1, 3, 5-Cyclohexanetrione Trioxime (IV).[6]—Potassium carbonate (3.2 g.) was added to a stirred solution of phloroglucinol dihydrate (25 g.) and hydroxylamine hydrochloride (32.2 g.) in water (1130 ml.). The mixture was allowed to stand overnight. The greyish white crystals were collected, washed with water and then with acetone, and dried under reduced pressure, m.p. 150°C (decomp.). Found: C, 42.53; H, 5.20; N, 23.51. Calcd. for $C_6H_9O_3N_3$: C, 42.10; H, 5.30; N, 23.15%.

Reaction of 1, 2-Cyclopentanonedione Dioxime (II) with Thionyl Chloride in Liquid Sulfur Dioxide.—Thionyl chloride (4.0 g.) in liquid sulfur dioxide (20 ml.) was added to a suspension of II (3.0 g.) in liquid sulfur dioxide (80 ml.). The oxime dissolved instantly. The mixture was allowed to stand at room temperature for two hours. The reaction mixture was then poured into ice water, sulfur dioxide was allowed to evaporate, and the residue was extracted with ether. The ethereal solution was washed with dilute sodium hydroxide solution and then with water and dried. Evaporation of this solution gave an oily substance, which turned to crystals on cooling, m. p. 40.5~41°C (recrystallized from ether) (yield 2.5 g.). By analogy with the previous experiment[2], and by infrared and elementary analyses, the substance was identified as 5, 6-dihydro-4*H*-cyclopenta[*c*]-furazan (V). Found: C, 54.26; H, 4.91; N, 25.29. Calcd. for $C_5H_6ON_2$: C, 54.54; H, 5.49; N, 25.44%. IR, 1585 (s) cm^{-1} (KBr).

Neutralization of the alkaline extract from the ethereal solution gave no acid product.

Reaction of II with Bromine in Liquid Sulfur Dioxide.—Bromine (12.0 g.) in liquid sulfur dioxide (20 ml.) was added to dioxime II (3.0 g.) in liquid sulfur dioxide (80 ml.). The dioxime dissolved gradually in the solution. The mixture was allowed to stand at room temperature for two hours. No product except a tarry matter was extracted with ether from the reaction mixture.

Reaction of II with Sulfur Trioxide in Liquid Sulfur Dioxide.—Sulfur trioxide (1.5 g.) in liquid sulfur dioxide (20 ml.) was added to dioxime II (3.0 g.) in liquid sulfur dioxide (80 ml.). The oxime dissolved immediately. The mixture was allowed to stand at room temperature for two

8) A. Treibs and A. Kuhn, *Ber.*, **90**, 1691 (1957).
9) R. M. Acheson, *J. Chem. Soc.*, **1956**, 4232.

hours. The reaction mixture was treated as above and extracted with ether. The ethereal solution was washed with water and dried. Evaporation of the ethereal solution afforded an orange oil, which turned to crystals, m. p. 37.5~38°C, on cooling (yield 0.5 g.). The substance thus obtained was proved to be γ-cyanobutyric acid (VI) by elementary analysis and hydrolysis to glutaric acid (VIII). Found: C, 52.88; H, 5.88; N, 12.60. Calcd. for $C_5H_7O_2N$: C, 53.09; H, 6.24; N, 12.38%.

Hydrolysis of γ-Cyanobutyric Acid (VI).—VI (0.3 g.) was refluxed with 5 N hydrochloric acid for one hour. Then the mixture was extracted with ether. On condensing the ethereal solution, colorless crystals, m. p. 96.5°C, were obtained (yield 0.15 g.). The specimen recrystallized from ethanol showed m. p. 96.5~97.5°C alone and in admixture with authentic glutaric acid (VIII). Found: C, 46.28; H, 5.68. Calcd. for $C_5H_8O_4$: C, 45.45; H, 6.10%.

Reaction of 1, 2, 3-Cyclohexanetrione Trioxime (III) with Thionyl Chloride in Liquid Sulfur Dioxide.—Thionyl chloride (3.4 g.) in liquid sulfur dioxide (40 ml.) was added to trioxime III (5.0 g.) in liquid sulfur dioxide (100 ml.). The dioxime appeared to dissolve into the solution at room temperature in two hours. The reaction mixture was then treated with ice water, and the sulfur dioxide was allowed to evaporate. The residual solution was treated as above. On condensing the ethereal solution, a light yellow substance was obtained. The product, recrystallized from ethanol showed an m. p. of 167~167.5°C (yield 2.4 g.). The melting point was depressed to 156~158°C on admixture with the starting trioxime (III) (m. p. 170°C).

By analogy with the previous experiment[2], and by infrared and elementary analyses, the product was identified as 7-hydroximino-4, 5, 6, 7-tetrahydrobenzo[*c*]furazan (VII).

Found: C, 45.57; H, 4.20; N, 27.20, Calcd. for $C_6H_7O_2N_3$: C, 47.05; H, 4.61; N, 27.44%. Mol. wt., Found: 156 (benzene), Calcd.: 153. IR ν_{max}^{KBr}, 1622(w) and 1583(s) (furazan), 1659 (=NOH) cm^{-1}.

The alkaline solution was neutralized with an acid, but extraction with ether gave nothing.

Reaction of III with Bromine in Liquid Sulfur Dioxide.—Bromine (14.0 g.) in liquid sulfur dioxide (40 ml.) was added to trioxime III (5.0 g.) in liquid sulfur dioxide (100 ml.), and the mixture was allowed to stand at room temperature for two hours. The mixture, containing a large amount of a tarry matter, was treated as above. From the ethereal extract of the residual reaction mixture, a small quantity (1.3 g.) of crystals was obtained, m. p. 166~167°C (recrystallized from ether). The product showed no melting point depression on admixture with the VII described previously. Found: C, 47.20; H, 4.35; N, 26.72. Calcd. for $C_6H_7O_2N_3$: C, 47.05; H, 4.61; N, 27.44%.

Reaction of III with Sulfur Trioxide in Liquid Sulfur Dioxide.—Sulfur trioxide (1.4 g.) in liquid sulfur dioxide (20 ml.) was added to trioxime III (3.0 g.) in liquid sulfur dioxide (80 ml.), and the mixture was kept at −5~−7°C for one hour. The mixture was then treated and extracted as described above. VII (0.3 g.) was obtained from the ethereal solution, m. p. and mixed m. p. 165~166°C. Found: C, 47.78; H, 4.40; N, 27.04. Calcd. for $C_6H_7O_2N_3$: 47.05; H, 4.61: N, 27.44%. The residual solution was again triturated with three times the ether used at first, and the ethereal solution was washed with water, dried and evaporated. The orange substance thus obtained was analyzed, but the specimen was too small to reward further examination. Found: C, 45.48; H, 5.34. Calcd. for $C_6H_5O_3N_2$ (a trione dioxime): C, 46.15; H, 5.16%. There was positive color reaction with nickel nitrate solution.

The residual solution was then refluxed with 2 N hydrochloric acid for five hours. The solution was extracted with ether. Colorless crystals were obtained and recrystallized from ethanol, m. p. 95~96°C (yield 0.4 g.). No melting point depression was observed when the substance was mixed with authentic acid (VIII). Found: C, 46.68; H, 6.03, Calcd. for $C_5H_8O_4$; C, 45.45; H, 6.10%. IR ν_{max}^{KBr}, 2940 (s), (-OH), 1705 (-COOH) cm^{-1}.

Reaction of 1, 3, 5-Cyclohexanetrione Trioxime (IV) in Liquid Sulfur Dioxide.—Thionyl chloride (4.2 g.), bromine (5.7 g.) and sulfur trioxide (1.7 g.) in liquid sulfur dioxide (20 ml.) were added in turn to trioxime IV (3.0 g.) in liquid sulfur dioxide (80 ml.), but only dark and insoluble resinous matters were produced in all cases.

Summary

1, 2-Cyclopentanedione dioxime (II), 1, 2, 3-cyclohexanetrione trioxime (III) and 1, 3, 5-cyclohexanetrione trioxime (IV) were treated with reagents and exhibited different and characteristic behaviors in liquid sulfur dioxide. The formation of 5, 6-dihydro-4*H*-cyclopenta-[*c*]furazan (V) from II with thionyl chloride by a condensation reaction and of γ-cyanobutyric acid (VI) from II with sulfur trioxide by a cleavage reaction were observed. 7-Hydroximino-4, 5, 6, 7-tetrahydrobenzo[*c*]furazan (VII) was found in the the reaction mixtures from III and thionyl chloride and from III and bromine, accompanied by large amounts of resinous matter.

Mono-deoximation by sulfur trioxide was suggested. 1, 3, 5-Cyclohexanetrione trioxime (IV) gave only black tarry matter, which may be attributable to the instability of IV.

The authors are indebted to the Befu Chemical Industries, Ltd., for the donation of liquid sulfur dioxide.

The Chemical Research Institute
of Non-Aqueous Solution
Tohoku University
Katahira-cho, Sendai

Dilute Solution Properties of Low-temperature Polymerized Polyvinyl Chloride. II. Fractionation and Properties of Fractions

By Takashi KOBAYASHI

(Received August 17, 1961)

In a previous paper of this series (hereafter referred to as Part I) we have shown that the solution behavior of a sample of polyvinyl chloride prepared at −15°C differed significantly from that of samples polymerized at higher temperatures. In order to seek the causes of this difference, we have dermined the molecular weight distributions in some samples of this polymer polymerized at different temperatures and have measured representative solution properties of the fractions of these samples. The present paper is intended to describe the results of this study and to discuss their molecular implications.

Experimental

Materials.—Five samples of polyvinyl chloride were studied. They were as follows:

SO968—A whole polymer suspension-polymerized at 48°C.

XF-13—A whole polymer emulsion-polymerized at 5°C.

F-2 — A whole polymer bulk-polymerized at −15°C.

F-5* — A whole polymer bulk-polymerized at −15°C under conditions similar to those used for F-2.

F-5-M—A middle cut of F-5; the 3 wt.% higher molecular weight portion and the 29 wt.% lower molecular weight portion of F-5 were removed by fractional precipitation.

Of the five samples, SO968 and F-5-M were materials treated also in Part I of this series.

As before, tetrahydrofuran was chosen as the solvent; its preparation has been described in Part I.

Density Measurement. — The film of a given polymer sample cast from its 3% tetrahydrofuran solution was soaked in carbon disulfide and then dried in vacuo. Its density was measured at 30°C in a density gradient tube using carbon tetrachloride and *n*-heptane as the density-forming liquids.

Fractionation. — The polymer was dissolved in tetrahydrofuran by refluxing for three hours at the boiling point of the solvent. At 30°C the precipitant, water in the present case, was vigorously stirred into the polymer solution of 0.625~0.75% until it became turbid. By raising the temperature of the solution to the boiling point of the solvent, again while being vigorously stirred, the once-developed precipitate disappeard. Then the solution was gradually cooled to 30°C and maintained at this temperature until the supernatant became transparent. The precipitate formed was separated and dissolved in tetrahydrofuran. The polymer was recovered from this solution by the addition of excess methanol, and then dried in vacuo to constant weight. This gave the first fraction. The second fraction was obtained by applying the same procedure to the supernatant solution. By repeating this process the desired successive fractions were obtained.

Viscosity, Osmotic Pressure and Light-scattering Measurements. — Details for these measurements were described previously.

Results and Discussion

Fractionation.—For a successful fractionation of a polymeric material, the choice of a solvent and non-solvent is of primary importance. A survey of the literature[1,2] and also our own experience showed that the combination of tetrahydrofuran and water was one of the best for polyvinyl chloride. Preliminary experiments with monohydric alcohols (such as methanol, *n*-propanol and *n*-butanol) as precipitants gave precipitates which were too fine to be separated easily. Therefore, we adopted the system of tetrahydrofuran and water for the present purpose.

Fractionation was made on samples SO968, XF-13, F-2 and F-5; Table I records some related data. For SO968, F-2 and F-5, the fraction number stands for the order in which the precipitates were separated. However, in the case of XF-13, the amount of fraction 4 was so large that it was refractionated into three fractions 4-1, 4-2 and 4-3; moreover,

TABLE I. RELATED DATA OF FRACTIONATION

Sample	Initial concn.	Temp.* °C	Number of fractions	Yield of recovery %
SO968	15 g./2 l.	30	8	93.5
XF-13	25 g./4 l.	30	10	92.5
F-2	30 g./4 l.	20	12	99.7
F-5	50 g./7 l.	20	13	97.1

* Temperature at which precipitate was separated.

* This was prepared later because the sample F-2 had been exhausted in the early stages of this investigation.

1) M. Imoto and T. Ōtsu, *J. Chem. Soc. Japan, Ind. Chem. Sec.* (*Kogyo Kagaku Zasshi*), **57**, 245 (1954).
2) J. Mencik, *J. Polymer Sci.*, **17**, 147 (1955).

Table II. Properties of fractions of SO968

Fraction	Wt.%	$[\eta]$ ml./g.	M_n $\times 10^{-3}$	M_w* $\times 10^{-3}$	A_2 $\times 10^3$	$\langle r^2\rangle_z^{1/2}$ Å	$\langle r^2\rangle_w^{1/2}$ Å	M_w/M_n
Whole	—	118	46.3	105.6	1.24	462	368	2.44
F-1	8.1	197	85.6	321.2	0.95	778	598	3.75
F-2	14.3	164	93.8	171.0	1.17	515	426	1.83
F-3	23.7	142	64.4	154.2	1.29	484	380	2.40
F-4	7.4	119	62.2	110.0	1.40	324	266	1.77
F-5	13.0	100	55.3	79.5	1.35	283	233	1.44
F-6	16.1	79	48.8	63.4	1.45	207	186	1.30
F-7	13.8	55	33.1	35.3	1.54	125	121	1.07
F-8	3.8	28	—	(7.7)	—	—	—	—

* M_w in bracket is calculated value.

Table III. Properties of fractions of XF-13

Fraction	Wt.%	$[\eta]$ ml./g.	M_n $\times 10^{-3}$	M_w* $\times 10^{-3}$	A_2 $\times 10^3$	$\langle r^2\rangle_z^{1/2}$ Å	$\langle r^2\rangle_w^{1/2}$ Å	M_w/M_n
Whole	—	111	45.0	119.6	0.88	650	510	2.67
F-1	10.5	173	65.6	277.0	1.18	725	534	4.23
F-2	6.5	167	—	277.0	1.05	684	—	—
F-3	15.3	165	68.1	211.2	1.34	680	525	3.10
F-4-1-1	9.9	148	75.6	178.3	1.07	548	436	2.36
F-4-1-2	9.8	124	56.3	125.0	0.97	470	377	2.22
F-4-2	7.9	113	48.4	(104.0)	—	—	—	—
F-4-3	4.6	84	42.5	(56.9)	—	—	—	—
F-5	15.6	80	48.1	61.3	1.18	316	280	1.27
F-6	10.7	55	35.0	(27.8)	—	—	—	—
F-7	9.4	31	—	(9.7)	—	—	—	—

* M_w's in brackets are calculated values.

Table IV. Properties of fractions of F-2

Fraction	Wt.%	$[\eta]$ ml./g.	M_n $\times 10^{-3}$	M_w* $\times 10^{-3}$	A_2 $\times 10^3$	$\langle r^2\rangle_z^{1/2}$ Å	$\langle r^2\rangle_w^{1/2}$ Å	M_w/M_n
Whole	—	108	45.0	84.3	1.22	591	488	1.88
F-1	5.8	132	—	(139.0)	—	—	—	—
F-2	11.8	141	105.6	196.7	0.84	765	632	1.86
F-3	15.5	142	—	(161.0)	—	—	—	—
F-4	13.1	138	93.8	152.6	0.76	535	455	1.63
F-5	4.6	133	—	(142.5)	—	—	—	—
F-6	12.3	120	71.3	105.2	1.22	356	309	1.48
F-7	3.4	86	—	(63.5)	—	—	—	—
F-8	12.9	82	59.4	54.4	1.33	212	—	—
F-9	8.2	53	—	(26.0)	—	—	—	—
F-10	6.3	36	35.6	(12.3)	—	—	—	—
F-11	3.1	24	—	(5.8)	—	—	—	—
F-12	3.1	18	—	(3.3)	—	—	—	—

* M_w's in brackets are calculated values.

fraction 4-1 was separated further into 4-1-1 and 4-1-2. The relative weight and limiting viscosity number, $[\eta]$, in tetrahydrofuran at 30°C of each fraction of these four samples of polyvinyl chloride are listed in Tables II, III, IV and V.

For XF-13, F-2 and F-5, the fractions appearing in the initial stage of fractionation (fractions 1 and 2 for XF-13; up to fraction 4 for F-2; up to fraction 5 for F-5) were obtained in the form of fine powder, in contrast to the case of commercial polyvinyl chloride, where gel-like precipitates are usually obtained. Since such powder-like fractions were difficult to separate in the usual manner, these were specifically precipitated at 20°C (not at 30°C)

TABLE V. PROPERTIES OF FRACTIONS OF F-5

Fraction	Wt.%	$[\eta]$, ml./g.	d_{30}
Whole	—	102	1.405_6
F-1	2.1	122	—
F-2	6.3	126	1.409_0
F-3	6.1	135	1.406_5
F-4	10.1	141	1.406_8
F-5	9.6	139	1.408_8
F-6	11.1	136	1.404_9
F-7	5.3	128	1.404_3
F-8	8.3	123	—
F-9	7.8	97	1.404_1
F-10	10.0	76	1.403_0
F-11	7.8	57	1.402_8
F-12	5.8	45	1.401_5
F-13	9.8	26	—

and separated by centrifugation at room temperature (which did not differ significantly from 20°C). It was found that the formation of powder-like precipitates in the initial stage of fractionation was characteristic of low-temperature polymerized polyvinyl chloride. Tables IV and V show that, contrary to what is generally observed, the $[\eta]$ of fractions of these low-temperature polymerized polyvinyl chloride increases with the increase of the fraction number in the initial stage of fractionation, comes to a maximum value, and then decreases in the usual manner. From the results reported in Part I, it was apparent that it would have been desirable to dissolve polymer at as high a temperature as 100°C, but because of the lack of a suitable vessel the original solutions for these fractionations had been prepared at the boiling point of tetrahydrofuran; under these conditions associated particles, or undissociated particles, were present in the solutions of XF-13, F-2 and F-5. Anomalous fractionation data on polyvinyl chloride similar to this have been reported by Mencik[2], who attributed the phenomenon to the association of molecules before the phase separation took place. However, the reason why powder precipitates developed is not clear.

Molecular Weight Distribution.—Figures 1—3 give the integral distributions of (weight average) molecular weight, M_w, for samples SO968, XF-13 and F-2 respectively; the values of M_w for fractions whose M_w were not determined experimentally have been estimated by using the viscosity vs. molecular weight relation described below. The two-stage feature appearing in the data for XF-13 and F-2 seems to be characteristic of polyvinyl chloride polymerized at low temperature. Although any definite conclusion must be left for future work, this feature is likely to be due to the presence of undissociated molecules in the original solution and also to the occurrence of molecular association during the fractionation procedure.

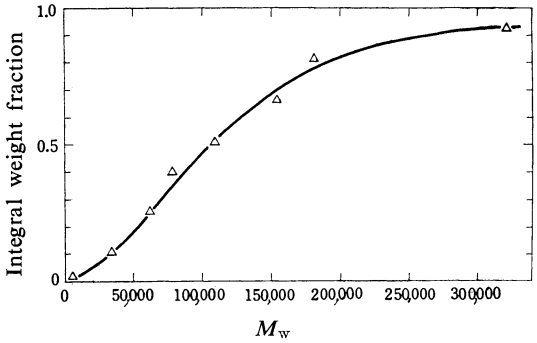


Fig. 1. Molecular weight distribution of SO968.

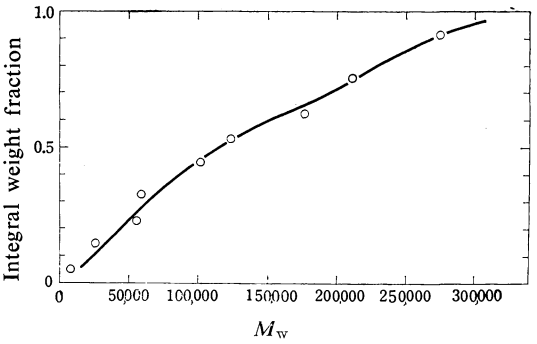


Fig. 2. Molecular weight distribution of XF-13.

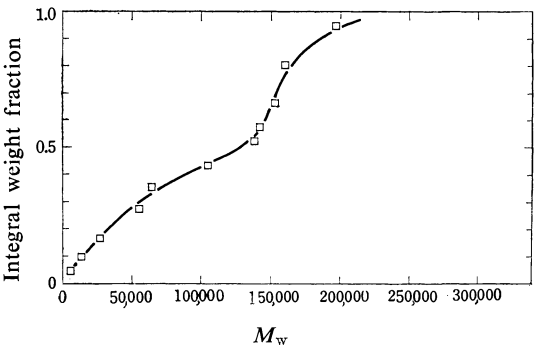


Fig. 3. Molecular weigt distribution of F-2.

Some Physical Properties of Fractions of F-5.—Table V, which gives the densities of successive fractions of F-5, indicates a systematic decrease of the density with the increase of the fraction number. This suggests that the crystallinity or chain regularity is higher for earlier fractions than for later fractions. When the density of each fraction is plotted against its limiting viscosity number in tetrahydrofuran at 30°C, the data for fractions whose fraction numbers are higher than 6 are seen to form a certain order, while those for the remaining

fractions are out of this order. Infrared studies[3-5] on polyvinyl chloride indicate that the ratio of the optical density for absorption at 635 cm^{-1}, which is assigned to the crystalline part, to that for absorption at 690 cm^{-1}, which is assigned to the amorphous part, can be taken as a measure of the crystallinity of a given sample. We measured infrared spectra of several fractions of samples SO968 and F-5 by using a Perkin-Elmer model 13 infrared spectrophotometer; the results obtained are listed in Table VI. One can see that the degree of crystallinity of samples F-5, which was polymerized at −15°C, is higher than that of sample SO968 polymerized at 48°C. Table VI also reveals that, although the values of $[\eta]$ for fractions 1 and 8 of sample F-5 are quite similar, the former fraction is more crystalline than the latter; incidentally, this is in conformity with the preceding suggestion from the density data that the later fractions of F-5 are less crystalline than the earlier fractions. From these results one may consider that white powderlike precipitates of polyvinyl chloride will develop in the tetrahydrofuran-water system when the degree of crystallinity or chain regularity of the polymer is higher than a certain limiting value. If this is the case, it is quite likely that the fractionation of samples XF-13, F-2 and F-5 proceeded in accordance not only with the molecular weight but also with the chain regularity. Previous X-ray[6] and also infrared[3-5] studies showed that the chain regularity of polyvinyl chloride increased as the polymerization temperature was lowered, and this was attributed to the increase in the syndiotactic portion[7] of the polymer.

TABLE VI. CRYSTALLINITY OF FRACTIONS OF SO968 AND F-5

SO968

Fraction	$[\eta]$, ml./g.	D_{635}/D_{690}
F-1	197	1.82
F-3	142	1.75
F-6	79	1.77

F-5

Fraction	$[\eta]$, ml./g.	D_{635}/D_{690}
F-1	122	2.29
F-3	135	2.23
F-8	123	2.10

Relations between Limiting Viscosity Number and Average Molecular Weights. — The values of the limiting viscosity number $[\eta]$ (in tetrahydrofuran at 30°C), number-average molecular weight M_n, obtained from osmotic pressure measurements, and the weight-average molecular weight M_w, determined from light-scattering measurements, for fractions of SO968, XF-13 and F-2 are summarized in Tables II, III and IV. Figure 4 illustrates Zimm plots for fraction 4 of F-2. When these data for $[\eta]$ and M_n are combined on a log-log plot, the points, though quite scattered, fall within the range of the literature's data[8-11]. The corresponding plots for $[\eta]$ vs. M_w are given in Fig. 5, which shows that even if the polymerization temperature is different, the relation between $[\eta]$ and M_w for polyvinyl chloride in tetrahydrofuran remains practically the same.

The relation between the limiting viscosity number and the molecular weight, M, of a polymer generally obeys an empirical equation of the form:

$$[\eta] = KM^{\alpha} \qquad (1)$$

where K and α are constants characteristic of

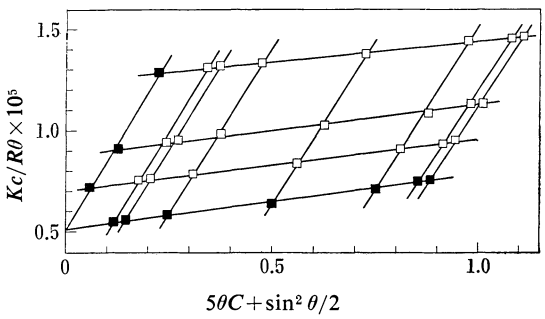


Fig. 4. Zimm plot for fraction 4 of F-2.

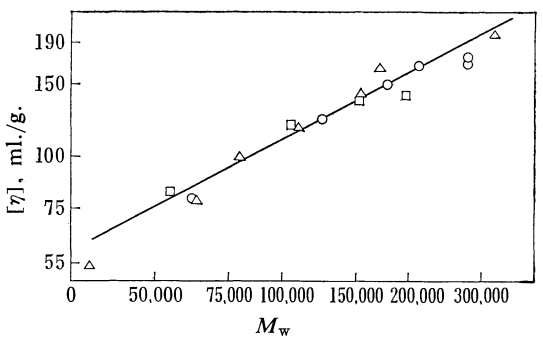


Fig. 5. Relation between limiting viscosity number and M_w.

△ Fraction of SO968; ○ XF-13; □ F-2

3) S. Krimm, *Chem. & Ind.*, **1959**, 433.
4) T. Shimanouchi et al., *High Polymers (Kobunshi)*, **8**, 202 (1959); *J. Chem. Phys.*, **30**, 1365 (1959).
5) M. Asahina et al., *J. Chem. Soc. Japan, Pure Chem. Sec. (Nippon Kagaku Zasshi)*, **81**, 1011 (1960); *Chem. High Polym. (Kobunshi Kagaku)*, **17**, 612 (1960).
6) M. Asahina et al., ibid., **17**, 441, 612 (1960).
7) G. Natta, *J. Polymer Sci.*, **20**, 251 (1956).
8) H. Staudinger et al., *Liebigs Ann. Chem.*, **541**, 151 (1939).
9) J. W. Breitenbach, *Kolloid Z.*, **127**, 1 (1951).
10) H. Staudinger, *Makromol. Chem.*, **9**, 35 (1952).
11) R. M. Fuoss, *J. Phys. Chem.*, **47**, 59 (1943).

the given polymer solvent system. This equation holds not only for a polymer of uniform molecular weight but also for a polymer with a molecular weight distribution, although with the latter polymer M must be replaced by some average molecular weight. For both the monodisperse and polydisperse samples of the same polymer species in the same solvent, the parameter α remains the same although the values of K are different. If α is given and the form of molecular weight distribution is specified, it is possible to examine by calculation the variation of K with the ratio of M_w/M_n. The results of this calculation[12] with logarithmic[13] and exponential[14] distribution functions show that when M_n is substituted for M in Eq. 1, K varies appreciably with the ratio M_w/M_n, but when $[\eta]$ is plotted against M_w, K is almost independent of M_w/M_n. This affords the advantage of using M_w over M_n when we wish to establish a relation between the limiting viscosity number and the molecular weight for a given polymeric substance.

The straight line in Fig. 5, determined by the least square procedure, yields

$$[\eta] = 2.19 \times 10^{-1} M_w^{0.54}$$

or

$$[\eta] = 2.05 \times P_w^{0.54}$$

where P_w denotes the weight-average degree of polymerization. The value 0.54 obtained for the exponent to M_w suggests that the molecules of polyvinyl chloride in tetrahydrofuran assume a random coil form. Ciampa[15], who obtained the value of unity for this exponent, suggested a worm-like form for the molecule of this polymer in cyclohexanone. The lack of non-Newtonian behavior of the solution of F-5-M illustrated in Fig. 6 appears to lend some support to the pertinence of our value for the exponent in the viscosity vs. molecular weight relation.

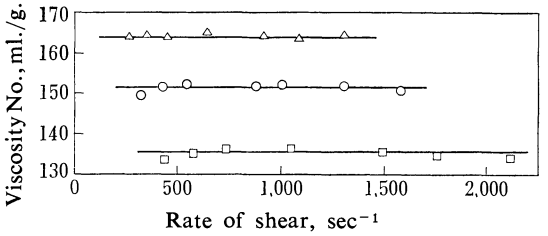


Fig. 6. Shear rate dependency of viscosity of solutions of F-5-M.

△ 8.0×10^{-3} g./ml.; ○ 6.0×10^{-3} g./ml.; □ 3.0×10^{-3} g./ml.

Weight-average Root Mean Square End-to-end Distance, $\langle r^2\rangle_w^{1/2}$ and Light-scattering Second Virial Coefficient, A_2.—The values of $\langle r^2\rangle_w^{1/2}$ and A_2 for fractions of samples SO968, XF-13 and F-2 determined from light-scattering data are listed in Tables II, III and IV. In converting the directly-obtained $\langle r^2\rangle_z^{1/2}$, the z-average root mean square end-to-end distance, to $\langle r^2\rangle_w^{1/2}$ following relations were assumed between the average molecular weights and the average dimensions of the solute molecule:

$$M_n/l+1 = M_w/l+2 = M_z/l+3 \quad (2)$$

$$M_n/\langle r^2\rangle_n^{1/2} = M_w/\langle r^2\rangle_w^{1/2} = M_z/\langle r^2\rangle_z^{1/2} \quad (3)$$

which are valid for the exponential molecular weight distribution[13]. Figure 7 plots A_2 against

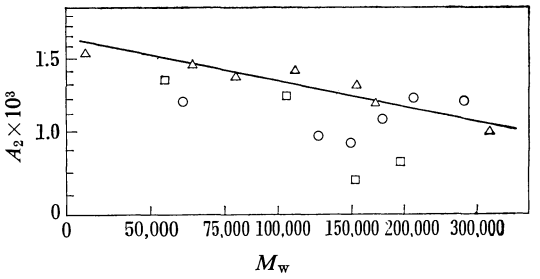


Fig. 7. Relation between A_2 and M_w.

△ Fractions of SO968; ○ XF-13; □ F-2
Full line is for SO968.

M_w on a log-log graph paper. The straight line, which was drawn to fit the data for sample SO968, has a slope of -0.21, comparable to the reported values on polyvinyl acetate[16-18] in butanone and polystyrene[19] in toluene at 30°C. The A_2 values for XF-13 and F-2 are generally smaller than those for SO968 when a comparison is made with the same values of M_w. This fact suggests that the thermodynamic interaction between solute and solvent molecules becomes weaker as the polymerization temperature is lowered. In other words, tetrahyhrofuran acts as a poorer solvent for a polyvinyl chloride sample which has been polymerized at a lower temperature. It is interesting that this difference is in line with the differences in solution properties observed in the study described in Part I of this series.

Figure 8 shows a log-log plot for $\langle r^2\rangle_w^{1/2}$ against P_w, together with that for polystyrene in butanone at 25 and 20°C reported by Outer,

12) Private communication from Dr. K. Takamizawa of Tokyo University of Education. His calculation agreed well with the data on polypropylene. The results will be published soon.

13) a) G. V. Schulz, *Z. physik. Chem.*, **B43**, 25 (1939); b) F. W. Billmeyer and W. H. Stockmeyer, *J. Polymer Sci.*, **5**, 121 (1950).

14) H. Wesslau, *Makromol. Chem.*, **20**, 111 (1956).

15) G. Ciampa, ibid., **21**, 169 (1956).

16) S. N. Chinai et al., *J. Polymer Sci.*, **17**, 117 (1955).

17) A. R. Shultz, *J. Am. Chem. Soc.*, **76**, 3422 (1954).

18) M. Matsumoto et al., *J. Polymer Sci.*, **46**, 441 (1960).

19) F. Dannuso et al., ibid. **24**, 161 (1957).

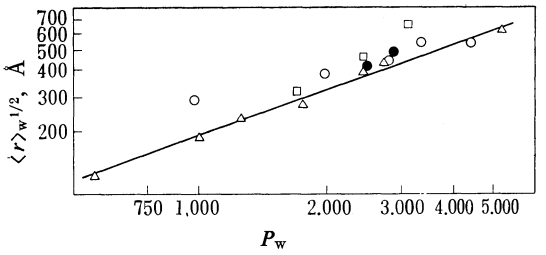


Fig. 8. Relation between dimension of molecules and P_w.

△ Fractions of SO968; ○ XF-13; □ F-2; ● Polystyrene reported by Zimm[20].
Full line is for SO968.

Carr and Zimm[20]. From the straight line drawn, which fits best for SO968, one finds that the weight-average root mean square end-to-end distance of SO968 increases in proportion to the 0.73 power of the weight-average degree of polymerization. One also finds that the average dimension of polyvinyl chloride in tetrahydrofuran increases as the polymerization temperature is lowered. Finally, it is of interest to note that polyvinyl chloride in this solvent has a dimension similar to that of polystyrene in butanone when the degree of polymerization of both polymers are comparable.

Doty et al.[21] pointed out that the polyvinyl chloride molecule has a tendency to become partially syndiotactic, that its chain flexibility is relatively low, and, moreover, that the syndiotactic portions interact with each other through their dipoles, thus limiting its possible configurations in solution. This affords a reasonable explanation for the finding that the molecular dimension of this polymer in solution increases as the polymerization temperature is lowered, since a sample prepared at a lower temperature should be richer in syndiotactic portion. The fact that the relation between the limiting viscosity number and the molecular weight is practically independent of polymerization temperature may be accounted for by the fact that the effect caused by the increase in molecular dimension is cancelled out by the accompanying increase in the permeability of the solute to solvent molecules.

The author wishes to express his appreciation to Professor Shunsuke Murahashi, Professor Hiroshi Fujita of Osaka University and to Professor Akira Kotera of Tokyo University of Education for their encouragement and thoughtful suggestions throughout the course of the study reported in this paper, to Dr. K. Mayumi and Kureha Kasei Co., Ltd., for permission to publish this paper, and to Mr. M. Sato, Mr. Y. Koshiishi and Mr. S. Aoyagi for their cooperation in carrying out the exerimental work.

Tokyo Laboratory
Kureha Kasei Co., Ltd.
Shinjuku-ku, Tokyo

20) P. Outer, C. I. Carr and B. H. Zimm, *J. Chem. Phys.*, **18**, 830 (1950).
21) P. Doty et al., *J. Am. Chem. Soc.*, **69**, 1631 (1947).

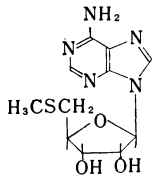
The Syntheses of 5'-Deoxy-5'-methylthioadenine and its Analogues

By Yôko ISHIKURA, Teiichi KANAZAWA and Tetsuo SATO

(Received August 25, 1961)

9β-(5'-Deoxy-5'-methylthio-D-ribofuranosyl)-adenine (I), known as "adenyl thiomethyl pentoside" or "vitamin L_2", was first isolated from yeast by Mandel and Dunhan[1] in 1912. Recently this nucleoside was directly converted into *S*-(5'-deoxyadenosine-5')-methionine[2], "active methionine", which participates in the transmethylation reaction in living cells. Baddiley et al.[3], Makino et al.[4] and Weygand et al.[5] have succeeded independently, in the synthesis of this nucleoside, using adenosine as the starting material. Their synthetic route analogously involved the introduction of a toluene-*p*-sulfonyl group into the 5'-position of 2', 3'-*O*-isopropylidene-adenosine, followed by its replacement by a methylthio group.

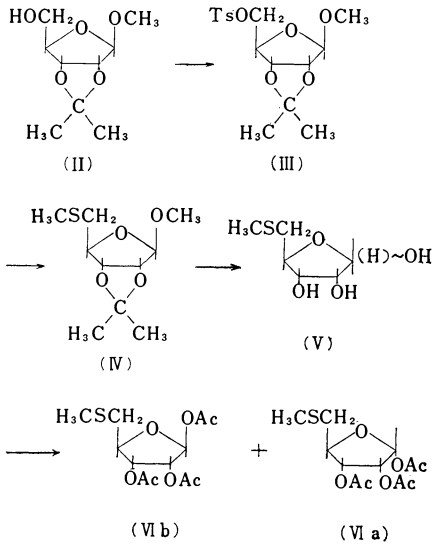
1) I. A. Mandel and E. K. Dunhan, *J. Biol. Chem.*, **11**, 85 (1912).
2) J. Baddiley and G. A. Jamieson, *J. Chem. Soc.*, **1954**, 4280.
3) J. Baddiley, ibid., **1951**, 1343.
4) K. Makino and K. Sato, *Nature*, **167**, 238 (1951).
5) F. Weygand and O. Trauth, *Chem. Ber.*, **84**, 633 (1951).



I

In a previous short communication[6] from this laboratory, a new synthetic method for obtaining compound I was described. In the present paper this new method and the synthesis of its analogues are described in detail.

In the authentic method, considerable difficulty was experienced in the formation of an intramolecular 3-5′-cyclic compound. So, to avoid the formation of this cyclic compound, D-ribose was converted into 5′-deoxy-5′-methylthio derivative and its halide was condensed with a purine base. It was reported by Overend and Parker[7] and by Yoshimura and Sato[8] that methyl 2, 3-*O*-isopropylidene-β-D-ribofuranoside (II) was converted into 5-*O*-toluene-*p*-sulfonyl derivative (III), which reacted with sodium methyl sulfide in acetone to give methyl 2, 3-*O*-isopropylidene-5-deoxy-5-methylthio-D-ribofuranoside (IV). The isolation of this compounds in its pure state was not, however, attempted by these authors.



This reaction was repeated by using anhydrous acetonitrile as a solvent in place of acetone. The yield of the product was increased to 85% by this modification. The solation of the pure product from the reaction mixture was achieved by the use of distillation followed by column chromatography on alumina.

The methyl and isopropylidene residues of IV were removed by heating it in 0.01N sulfuric acid. The resultant syrup (V) could not be crystallized, but gave one spot on paper chromatography (with butanol-acetic acid-water 5 : 1 : 4 v/v). The acetylation of this product with pyridine-acetic anhydride in the usual manner afforded crystals, m. p. 66°C (yield 21%) (VIb), and an oily material (yield 48%) (VIa). Elemental analysis found no difference between these products. It was deduced from the values of the optical rotation of these compounds that VIa and VIb are α- and β-isomer respectively.

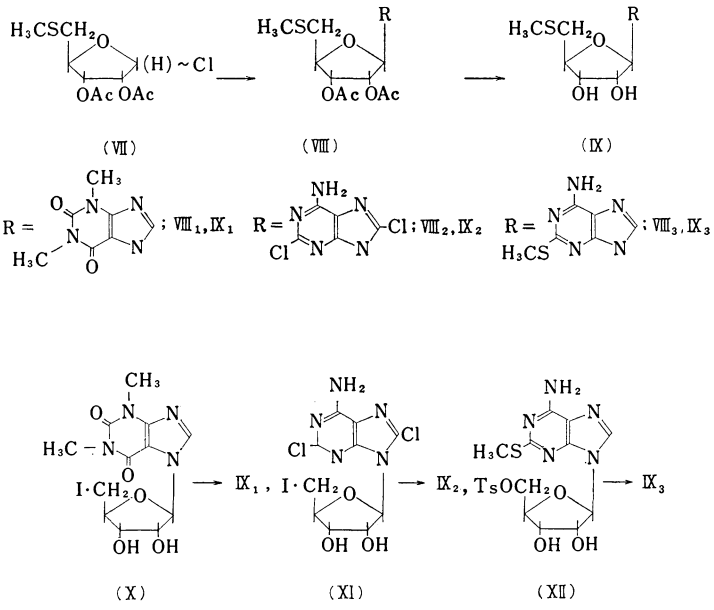
VIb was chlorinated with hydrogen chloride in absolute ether. Freshly prepared 1-chloro derivative (VII) was condensed with the silver salt of theophylline, which is known to react easily with sugar halide in general. The condensation product was deacetylated by methanolic ammonia to give white needles, m. p. 74～76°C (IX_1). The position of the sugar residue at the purine base and the configuration of the glucosidic linkage of this compound were confirmed as follows. The authentic sample of 7β-(5′-deoxy-5′-iodo-D-ribofuranosyl)-theophylline (X) was treated with sodium methyl sulfide to introduce a methylthio group. The product was identical to IX_1. Thus, the structure was confirmed to be 7β-(5′-deoxy-5′-methylthio-D-ribofuranosyl)-theophylline.

Chloromercuri-2, 8-dichloroadenine and chloromercuri-2-methylthioadenine were also condensed with VII, in the manner described above, to give the corresponding derivatives with a methylthio group at position 5′ ($VIII_2$ and $VIII_3$ respectively). $VIII_2$ and $VIII_3$ were deacetylated with methanolic ammonia, and structures of the resultant compounds (IX_2 and IX_3) were confirmed by derivations from XI and XII to be 9β-(5′-deoxy-5′-methylthio-D-ribofuranosyl)-2, 8-dichloroadenine and 9β-(5′-deoxy-5′-methylthio-D-ribofuranosyl)-2-methylthioadenine respectively. Furthermore, the results of elemental analysis, ultraviolet absorption measurement and Fehling's test supported this structure.

Compound I was not obtained from IX_2 or IX_3 by partial reduction in either cases.

It has been reported[9-11] that the yield of

6) T. Kanazawa, *J. Chem. Soc. Japan, Pure Chem. Sec.* (*Nippon Kagaku Zasshi*), **81**, 516 (1960).
7) W. G. Overend and L. E. J. Parker, *Nature*, **167**, 527 (1951).
8) J. Yoshimura and T. Sato, *J. Chem. Soc. Japan, Pure Chem. Sec.* (*Nippon Kagaku Zasshi*), **73**, 350 (1952).
9) J. Davoll and B. A. Lowy, *J. Am. Chem. Soc.*, **73**, 1650 (1951).
10) G. B. Brown and V. S. Weliky, *J. Biol. Chem.*, **204**, 1019 (1953).
11) H. M. Kissman and M. J. Weiss, *J. Org. Chem.*, **21**, 1053 (1956).



adenine with a sugar halide of the condensation reaction of metallic salt is less than 2～3%; 6-acetaminopurine and 6-chloropurine, however, were easily condensed with sugar halides, and the substituents at position 6 were converted into amino groups by treatment with methanolic ammonia. These facts suggest that chloromercuri-6-acetaminopurine and chloromercuri-6-chloropurine might be condensed in a good yield with methylthio sugar derivatives and converted into compound I. The test of the condensation showed that 9β-(2',3'-di-*O*-acetyl-5'-deoxy-5'-methylthio-D-ribofuranosyl)-6-acetaminopurine and 9β-(2',3'-di-*O*-acetyl-5'-deoxy-5'-methylthio-D-ribofuranosy)-6-chloropurine are obtainable in 41% and 63% yields repectively. In either case, the products were treated with methanolic ammonia to afford I, m. p. 205～206°C. (The yields from VIb were 17.5 and 35% respectively.)

The synthetic substance and natural "adenyl thiomethyl pentoside" were proved to be identical by measurement of their melting points and paper chromatography.

Experimental

Methyl 2,3-*O*-Isopropylidene-5-deoxy-5-methylthio-β-D-ribofuranoside (IV).—A mixture of III (30 g., 0.084 mol.) and potassium methyl sulfide (15 g., 0.175 mol.) in dry acetonitrile (150 ml.) was heated in a sealed tube for 7 hr. at 100°C. After the solution had been chilled, the insoluble materials were filtered off and the filtrate was evaporated to dryness. The residue was dissolved in a mixture of ice cold water and chloroform. The chloroform layer was washed with water. After being dried with anhydrous sodium sulfate, it was evaporated under reduced pressure. A colorless syrup (24 g.) was obtained by distillation under 0.03 mmHg (b. $p._{0.03}$ 82°C, b. $p._{0.005}$ 62°C). Yield, 94%. This product (15 g.) was chromatographed on a column of active alumina (150 g.). A colorless syrup (13.7 g., 91%) was obtained when it was eluted with 600 ml. of benzene-petroleum ether (1 : 2).

Found: C, 51.31; H, 7.75; S, 13.99. Calcd. for $C_{10}H_{18}O_4S$ (234.3): C, 51.28; H, 7.69; S, 13.70%. $R_f(a)=0.57$*.

5-Deoxy-5-methylthio-D-ribofuranose (V).—A mixture of IV (13.7 g.), dioxane (80 ml.) and 0.1 N sulfuric acid (200 ml.) was heated at 100°C for 2 hr. The acid was then neutralized with barium carbonate. The insoluble materials were filtered off, and the filtrate was evaporated to dryness. An oily product was obtained. Yield, 9.7 g., 92%.

1,2,3-Tri-*O*-acetyl-5-deoxy-5-methylthio-β-D-ribofuranose (VIb) and its α-Anomer (VIa).—Compound V (6 g.) was acetylated with acetic anhydride in pyridine (50 ml.). By fractional distillation of the acetyl derivatives, the following three fractions were obtained. No. 1: b. p. 114～118°C/0.01 mmHg (2.95 g.); No. 2; b. p. 118～125°C/0.01 mmHg (3.5 g.); No. 3: b. p. 130～134°C/0.01 mmHg (3.2 g.). Ether (2 ml.) was added to fraction No. 3, and the solution was left to stand for 1 day. 1.6 g. of crystals were obtained, m. p. 64～66°C. Yield, 50%. The same crystals (0.1 g.) were obtained from No. 2 (3%). These crystals were collected and recrystallized from ether, m. p. 66°C.

Found: C, 46.95; H, 5.87; S, 10.47. Calcd. for $C_{12}H_{18}O_7S$ (306.32): C, 47.06; H, 5.92; S, 10.45%. $[\alpha]_D$ −26.7° (*c* 0.99, ethanol).

No. 1 and mother liquors of No. 2 and No. 3 (6.3 g.) were dissolved in a mixture of benzene

* Solvent systems of paper chromatography: R_f(a) *n*-Butanol-water (saturated) (upper layer): R_f(b) *n*-Butanol-acetic acid-water, 5 : 2 : 3 (upper layer).

and petroleum ether, and the solution was fractionated on a magnesol-celite column (80 g. of 5 : 1 mixture). The solvents used for elution were mixtures of benzene and petroleum ether with successively increasing concentrations of benzene. The effluents were examined as to the weight of the eluates and their rotation. As is shown in Fig. 1, 0.8 g. of crystals (the β-anomer) and 4.4 g. of the α-anomer were obtained. The α-anomer had $[\alpha]_D$ +26.1° (*c* 1.015, ethanol).

Found: C, 47.15; H, 6.29. Calcd. for $C_{12}H_{18}O_7S$ (306.3): C, 47.05; H, 5.99%.

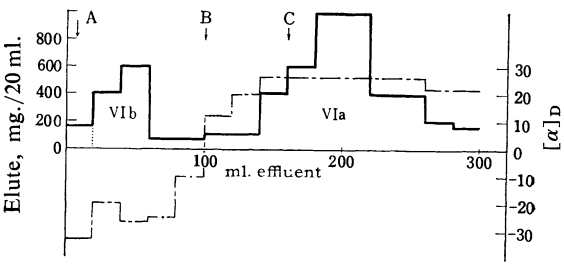


Fig. 1. Chromatographic separation of VI on a magnesol-celite column.
A, B and C are used for elution in which the ratio of benzene to petroleum ether are 0.3, 0.6 and 1 respectively. ——, weight of elute; ———, rotation of elute; VIb, the β anomer; VIa, the α anomer.

2,3-Di-*O*-acetyl-5-deoxy-5-methylthio-D-ribofuranosyl Chloride (VII).—VIb (4 g.) was dissolved in absolute ether (160 ml.), and the solution was saturated with dry hydrogen chloride at −7°C and left to stand for 4 days at 0°C.

7β-(5'-Deoxy-5'-methylthio-D-ribofuranosyl)-theophylline (IX_1).—*From Theophylline Silver.*—A solution of VII, freshly prepared as above from 2.4 g. of VIb in 30 ml. of toluene, was added to an azeotropically-dried suspension of 2.5 g. of theophylline silver in 30 ml. of toluene. The mixture was allowed to reflux for 2 hr. (kept from moisture), and the insoluble materials were filtered off. The filtrate was then evaporated, and the residual syrup was treated with methanolic ammonia. The product (1.4 g.) was recrystallized twice from water, m. p. 66~68°C. Yield, 1.2 g.

Found: C, 45.22; H, 5.30; N, 16.61. Calcd. for $C_{13}H_{18}O_5N_4S$ (342.3): C, 45.61; H, 5.35; N, 16.37%. $R_f(a)=0.66$, $R_f(b)=0.08$. λ_{max}: 275 mμ, $\varepsilon=9300$ (water).

From X.—A mixture of 1 g. of X and 2 g. of dry potassium methyl sulfide was added to 5 ml. of anhydrous dimethylformamide, and the mixture was heated at 100°C for 2 hr. After the solvent had been evaporated in vacuo, the residue was added to water. 0.5 g. of crystals were obtained. This was recrystallized twice from water, m. p. 73~75°C, undepressed on admixture with IX_1.

9β-(2', 3'-Di-*O*-acetyl-5'-deoxy-5'-methylthio-D-ribofuranosyl)-2, 8-dichloroadenine ($VIII_2$).—A solution of sugar halide, prepared as above from 2 g. of VIb in 30 ml. of xylene, was added to chloromercuri-2,8-dichloroadenine on celite (from 2 g. of 2,8-dichloroadenine) in 200 ml. of xylene, and the mixture was allowed to reflux for 2.5 hr. There was obtained 0.9 g. of crystals, m. p. 187~188°C (34% yield).

Found: C, 39.92; H, 3.84; N, 15.37. Calcd. for $C_{15}H_{17}O_5N_5Cl_2S$: C, 40.01; H, 3.78; N, 15.55%. $R_f(a)=0.88$, $R_f(b)=0.92$.

9β-(5'-Deoxy-5'-methylthio-D-ribofuranosyl)-2, 8-dichloroadenine (IX_2).—*From $VIII_2$.*—To a solution of 0.9 g. of $VIII_2$ in 30 ml. of absolute methanol was added 35 ml. of absolute methanol saturated with ammonia at 0°C, and the mixture was left to stand overnight at room temperature. The solution was evaporated in vacuo, and the residual syrup was dissolved in 50 ml. of hot water. After being treated with activated charcoal, the solution was concentrated to 10 ml. and was chilled. White needles were obtained, m. p. 89~92°C. Yield, 0.7 g. 90%. Recrystallization from water, m. p. 94~96°C.

Found: C, 34.61; H, 4.03; N, 18.16. Calcd. for $C_{11}H_{13}O_3N_5S\cdot H_2O$ (313.3): C, 34.39; H, 3.91; N, 18.23%. $R_f(a)=0.79$, $R_f(b)=0.67$. $\lambda_{max}=267$ mμ, $\varepsilon=19500$ (water).

From XI.—A solution of 0.5 g. of XI in 15 ml. of acetonitrile was added to 1 g. of sodium methyl sulfide in a sealed tube at 0°C, and the shaking mixture was kept at 100°C for 7 hr. After the solution had been chilled, the insoluble materials were filtered off and the filtrate was evaporated in vacuo. The residue was dissolved in chloroform and washed with water. The solution was concentrated and dissolved in 30 ml. of hot water and passed through a column of Amberlite IR-120 resin (H form). After washing of the column with 20% alcohol, the product was eluted with a large volume of ammonia (equal parts of water and ammonia of $d=0.880$). The effluent was evaporated to a small volume in vacuo, and the crystalline nucleoside (0.2 g.) was filtered off. Recrystallized from water, m. p. 94~96°C, undepressed on admixture with IX_2.

9β-(2', 3'-Di-*O*-acetyl-5'-deoxy-5'-methylthio-D-ribofuranosyl)-2-methylthioadenine ($VIII_3$).—A mixture of VII (prepared from 1.4 g. of VIb) and chloromercuri-2-methylthioadenine (from 1.8 g. of 2-methylthioadenine) was heated under the reflux condition described above. 0.3 g. of crystals was obtained, m. p. 172~174°C.

Found: C, 44.50; H, 5.10; N, 16.18. Calcd. for $C_{16}H_{21}O_5N_5S_2$ (427.5): C, 44.90; H, 4.95; N, 16.38%. $R_f(a)=0.72$, $R_f(b)=0.78$.

9β-(5'-Deoxy-5'-methylthio-D-ribofuranosyl)-2-methylthioadenine (IX_3)—*From $VIII_3$.*—$VIII_3$ (2 g.) was treated with methanolic ammonia as described in section for IX_2 1.4 g. of crystals, were obtained m. p. 165~166°C.

Found: C, 41.50; H, 5.10; N, 19.86. Calcd. for $C_{12}H_{17}O_3N_5S_2$ (343.4): C, 41.96; H, 4.98; N, 20.39%. $R_f(a)=0.65$, $R_f(b)=0.78$. $\lambda_{max}=235.5$ mμ, $\varepsilon=22900$ and 275 mμ, $\varepsilon=15000$, $\lambda_{min}=250$ mμ, $\varepsilon=8000$ (methanol).

From XII.—A mixture of 0.3 g. of XII and 0.5 g. of potassium methyl sulfide in 12 ml. of dimethylformamide was heated at 100°C for 1.5 hr. and evaporated in vacuo. The residue was dissolved

in chloroform. After the insoluble materials had been filtered off, the solution was washed with water, dried evaporated in vacuo. The obtained syrup was dissolved in 10 ml. of dioxane. 1 N Sulfuric acid (20 ml.) was added, and the solution kept at room temperature for 24 hr. The acid was neutralized with a calculated amount of barium hydroxide solution. Barium sulfate was removed by centrifugation and washed with water, and the combined supernatant liquid and washings were evaporated to dryness in vacuo. The residue was dissolved in 20% ethanol and treated with Amberlite IR-120 as described above. A crystal was obtained m. p. 165~166°C, undepressed on admixture with IX_3.

9β-(5'-Deoxy-5'-methylthio-D-ribofuranosyl)-adenine (I).—*From 6-Acetaminopurine.*—A mixture of chloromercuri-6-acetaminopurine (prepared from 2.1 g. of 6-acetaminopurine) and VII (prepared from 2 g. of VIb) was treated as described above. 9β-(2', 3'-Di-*O*-acetyl-5'-deoxy-5'-methylthio-D-ribofuranosyl)-6-acetaminopurine (1 g.) was obtained. This product was dissolved in 30 ml. of absolute methanol and was added to 35 ml. of methanolic ammonia at 2~4°C. After 24 hr., the solution was evaporated and the residue was dissolved in hot water. After 3 days a crystalline solid was obtained, m. p. 199~201°C. This was recrystallized from water, m. p. 205~206°C, undepressed on admixture with naturally occurring "adenyl thiomethyl pentoside". The mother liquors of the crystallization and recrystallization were purified with Amberlite IR-120; 0.15 g. of the crystals was obtained.

From 6-Chloropurine. — Chloromercuri-6-chloropurine (prepared from 1.5 g. of 6-chloropurine) was condensed with VII (prepared from 1.7 g. of VIb). 1.4 g. of a glass-like material were obtained. Yield from VIb, 63%. This substance was added to 40 ml. of methanol saturated with ammonia at 0°C in a sealed tube, and the mixture was kept at 100°C for 5 hr. The solution was treated as described above. 0.67 g. of the crystals was obtained, m. p. 204~206°C, undepressed on admixture with the natural substance.

Found: C, 44.09; H, 5.29; N, 23.25. Calcd. for $C_{11}H_{15}O_3N_5S$ (297.3): C, 44.43; H, 5.04; N, 23.25%.

Synthetic nucleoside: R_f(a)=0.45, R_f(b)=0.59
Natural nucleoside: R_f(b)=0.42, R_f(b)=0.59.

We are grateful to Dr. Katushi Makino for the gift of a sample of natural "adenyl thiomethyl pentoside".

Laboratory of Organic Chemistry
Tokyo Institute of Technology
Meguro-ku, Tokyo

Studies on Fluorene Derivatives. XV. The Clemmensen Reduction of Fluorenone*

By Kazuo SUZUKI

(Received August 28, 1961)

There have been several investigations of the Clemmensen reduction of fluorenone (I). Harris et al.[1] obtained fluorenol (II), fluorene (III), 10, 10-diphenylene-9-phenanthrone (V), dibiphenylene-ethylene (IX) and -ethane (X) by reduction of I under various conditions in the presence of dilute ethanol.

Bradlow et al.[2] produced III and V in toluene or ethanol, while Ritchie[3] obtained III and X in an ethanolic solution. III was obtained in a fairly good yield in each of these experiments and also in another preparation[4].

However, I has been best reduced to III by the Wolff-Kischner method with or without an alkaline catalyst, as has been observed by Weisburger and Grantham[5].

This is interesting because a great part of I does not normally proceed by way of II in the Clemmensen reduction and also because many related products were obtained by an abnormal reaction. Moreover, some of them do not appear to have been previously reported as direct products from I in this reduction.

* XIV of this series: S. Kajigaeshi, *J. Chem. Soc. Japan, Pure Chem. Sec.* (*Nippon Kagaku Zasshi*), **82**, 1712 (1961).

1) A. S. Harris, E. N. White and D. McNeil, *J. Chem. Soc.*, **1955**, 4216.

2) H. L. Bradlow and C. A. VanderWerf, *J. Am. Chem. Soc.*, **69**, 1254 (1947).

3) E. Ritchie, *J. Proc. Roy. Soc. N. S. W.*, **80**, 33 (1946).

4) H. R. Gutmann and J. H. Peters, *Cancer Res.*, **13**, 415 (1953); F. E. Ray and R. C. Geiser, ibid., **10**, 616 (1950).

5) J. H. Weisburger and P. H. Grantham, *J. Org. Chem.*, **21**, 1169 (1956).

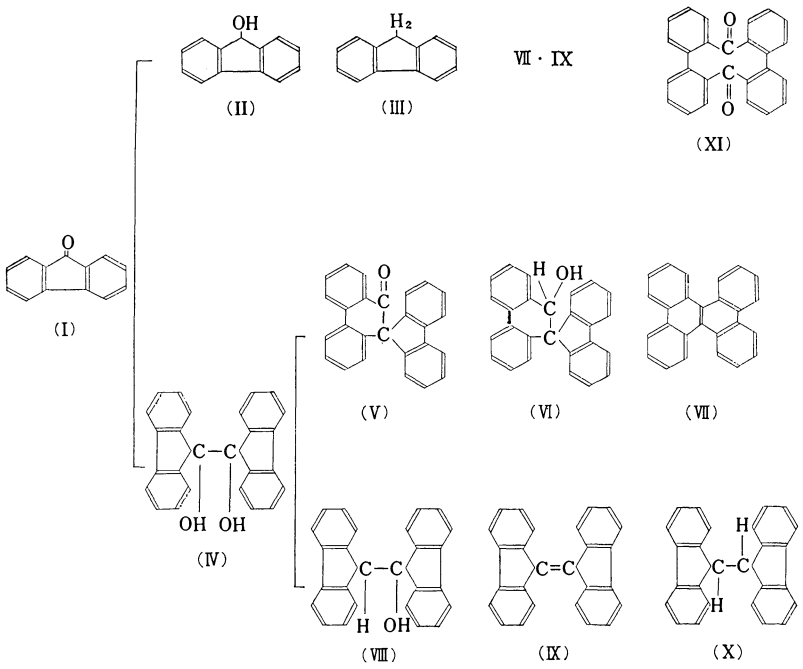


Chart 1

The present author carried out the reduction by the procedure of "Organic Reactions"[6]: I was dissolved in solvents such as toluene, benzene and xylene, which were mixed with the aqueous hydrochloric acid. The mixture was heated under reflux for a period of twenty-four hours, concentrated hydrochloric acid being added at intervals of about six hours. These results are summarized in Table I.

In this work, II, III and dimeric reaction products, namely, 9, 9′-dihydroxy-9, 9′-bifluorenyl (fluorenopinacol) (IV), V, 10, 10-diphenylene-9, 10-dihydro-9-phenanthrol (VI), 9, 10-diphenylene-phenanthrene or tetrabenzonaphthalene (VIII), 9-hydroxy-9, 9′-bifluorenyl (VIII), X and mixed crystals (VII・IX), were isolated by means of a combination of recrystallization and column chromatography. These reaction routes can be outliued as in Chart 1.

Fluorenol (II) and Fluorene (III). — III was obtained in a poor yield by means of steam distillation from the reaction mixture. II was isolated as an intermediate to III in the case of a short reduction period.

In general, it has often been stated heretofore that the carbonyl compound is not reduced to hydrocarbon by way of the corresponding alcohol. However, III was obtained as a normal product from II in a process independent of fluorenopinacol (IV) formation by the Clemmensen reduction.

In another analogous case in this series, 1- and 2-bromo-fluorenone[7] were attacked slowly under the same conditions, whereby substituted fluorenols were also produced, even after twenty-four hours.

III was obtained in an excellent yield and high purity by the reduction of II in a toluene system. In addition, a small amount of 2-(9′-fluorenyl)-fluorene was isolated as an abnormal product. This compound has already been reported by Suzuki et al.[8]

9, 9′-Dihydroxy-9, 9′-bifluorenyl (IV).—IV has been obtained previously by several procedures[9], but not from I by the Clemmensen reduction.

IV exhibits an interesting behavior in the course of the reaction since it reacts further (see Charts 2 and 3). Thus, IV is the main product in the case of a short reduction time such as two hours. Furthermore, the direct reduction of IV was attempted by using the same conditions and leading to other compounds, as are illustrated in Table I.

10, 10-Diphenylene-9-phenanthrone (V).—There have been several reports about V[10,11]. A

6) E. L. Martin, "Organic Reactions", Vol. 1, Chapman and Hall, London (1942), p. 155

7) K. Suzuki, unpublished.

8) A part of this research was presented at the 9th Annual Meeting of the Chemical Society of Japan, Tokyo, April, 1956.

9) M. Gomberg and Bachmann, *J. Am. Chem. Soc.*, **49**, 236 (1927); R. Criegee, *Ann.*, **583**, 11 (1953); M. D. Rausch, *J. Am. Chem. Soc.*, **76**, 3622 (1954).

10) H. Meerwein, *Ann.*, **396**, 212 (1913); C. Graebe and H. Stindt, ibid., **291**, 1 (1896); A. Kliegl, *Ber.*, **43**, 2488 (1910); J. Schmidt et al., ibid., **43**, 1800 (1910); E. Bergmann and J. Hervey, ibid., **62**, 893 (1929).

11) J. Suszko and R. Schillak, *Roczniki Chem.*, **14**, 1216 (1934); *Chem. Abstr.*, **29**, 6231 (1935).

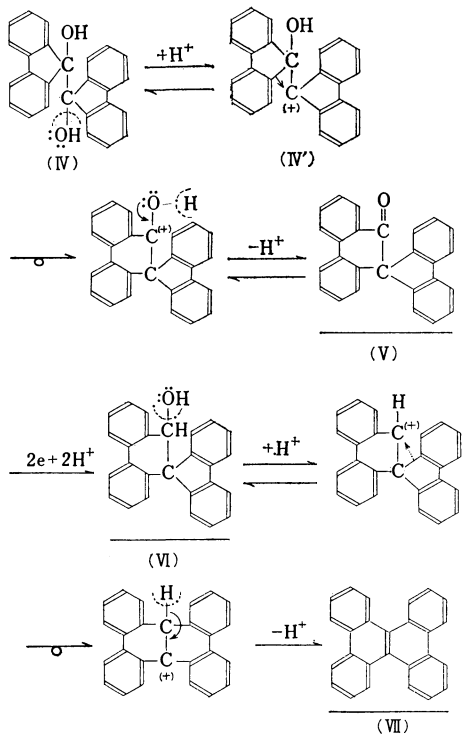
minor part of IV was converted into the β-isomeride of V through the carbonium ion IV′ by a pinacol rearrangement which on further reduction gave VII (10%) as the end-product, as is illustrated in Chart 2 and Table I. V was identical with an authentic specimen prepared by Meerwein's method[10].

9, 10 - Diphenylene - phenanthrene (VII). — VII[11-13] has been reported previously, but it has not been obtained heretofore by the Clemmensen reduction of I. VII would be formed through the intermediate VI. VI[11] was prepared from V by the use of zinc and ammonium hydroxide in an alcoholic solution, and was then converted to VII[cf.14] by treating it under the same conditions as in the Clemmensen reduction but without zinc amalgam.

Furthermore, VII (80%) and intermediate VI (10%) could be isolated by the Clemmensen reduction of V for fifteen hours in the xylene system.

In order to polarize the central double bond, VII was oxidized to tetrabenzocyclodecane-1,6-dione (XI)[11], which was then converted to VII and V by reduction.

The mechanism of the formation of VII via VI from V by the retropinacolone rearrangement involves the intramolecular transfer of the electron pair by formation of a carbonium ion. Thus, the reaction sequences can be written as in Chart 2.



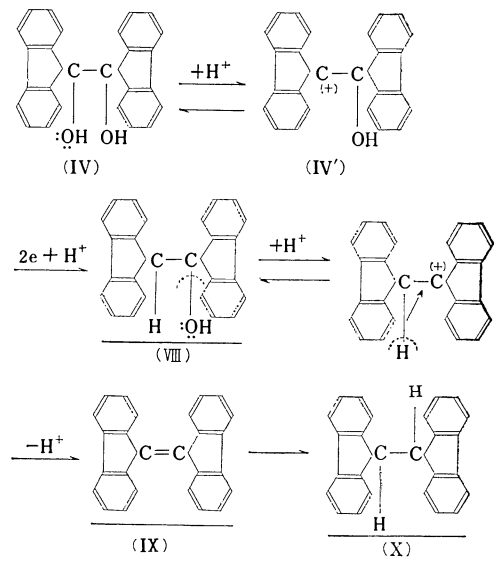
(Underscored compounds were isolated)
Chart 2

Dibiphenylene-ethylene (IX) and -ethane (X). —IX and X were reported by Harpe and Dorp[15] previously. In this reaction, a major part of IV through the IV′ carbonium ion was converted into VIII and then to IX, which on further reduction afforded the end-product X (56%) (see Chart 3 and Table I). VIII was isolated as an intermediate product by short reduction of I (2 hr.) or IV (3 hr). in the toluene solution, as is shown in Table I.

VIII was readily converted to IX[16] by hydrochloric acid in acetic acid. Therefore, IX could be obtained in a better yield by treating VIII under the same conditions as in the Clemmensen reduction but without the amalgamated zinc.

In general, an ethylenic link is reduced easily when it is conjugated with a carbonyl group. In contrast, the reduction of the ethylenic link in IX was extremely slow upon treatment with hydrochloric acid and amalgamated zinc in the toluene solution, and a red color remained even after twenty-four hours.

IX was isolated from the reaction mixture as mixed crystals (red prisms) with VII. However, VII was not obtained by Harris et al.[1] from an alcoholic solution; hence, their product was simply IX.



(Underscored compounds were isolated)
Chart 3

12) E. Bergmann and S. Fujise, *Ann.*, **483**, 80 (1930); A. Werner and A. Grob, *Ber.*, **37**, 2887 (1904); F. Bergmann and H. E. Esckinazi, *J. Am. Chem. Soc.*, **66**, 183 (1944).
13) H. Klinger and C. Lonnes, *Ber.*, **29**, 2152 (1896).
14) W. E. Bachmann, *J. Am. Chem. Soc.*, **55**, 3857 (1933).
15) C. Harpe and W. Dorp, *Ber.*, **8**, 1049 (1875).
16) V. Grignard and C. Courot, *Compt. rend.*, **152**, 272 (1911).

Table I. Reduction of I and IV under various conditions

Red. of g.		Solvent ml.		React. time, hr.	II g.	III g.	IV g.	V g.	VII g.	VII · IX g.	VIII g.	X g.	Recovd. g.
I	10.0	Xylene	20	24		1.3	1.0	0.75	1.3	0.5		2.4	
I	10.0	Toluene	20	24		0.9	0.05	0.11	0.1	1.2		2.9	
I	10.0	Toluene	20	2	0.1	1.1	5.1	0.03		0.05	0.65	0.5	I 0.3
I	10.0	Toluene	20	72		0.8			0.9			5.1	
I	10.0	Benzene	20	24		0.9	1.3	0.1	Trace	0.2		0.3	
IV	2.0	Xylene	6.0	24					0.31			0.3	
IV	2.0	Toluene	6.0	24					0.1	0.25		0.3	IV 0.1
IV	2.0	Toluene	6.0	3				0.01		0.15	0.02	0.1	IV 0.9
IV	2.0	Benzene	6.0	24				0.1		0.06		0.1	IV 1.0

The reaction sequences of IX and X can be visualized as in Chart 3.

Mixed Crystals (VII·IX). — The mixed crystals gave 9,9′-dibromo-9,9′-bifluorenyl[17] and VII (no reaction) by bromination; with the Clemmensen reduction of zinc and ammonium hydroxide, they gave X and VII, and with oxidation, I and XI. Therefore, the mixed crystals can be supposed to consist of VII and IX. Moreover, the ultraviolet spectrum showed maxima in the regions of 220~350 and 450 mμ, as is illustrated in Fig. 1. These maxima were almost identical with those of VII and IX respectively[18,19].

The infrared spectrum also indicated a mixture, and the analytical results were identical with $C_{26}H_{16}$.

The same mixed crystals were produced in nearly a quantitative yield from the solution of VII : IX (0.2 : 1) in acetic ester.

VII is slightly yellow, even when recrystallized several times from different solvents. It is best to purify it by reduction and then by recrystallization.

Effects of the Solvents.—The yields in Table I were slightly different depending on the solvents. In the case of benzene, the reaction went slowly and a large amount of I was recovered, perhaps because of the lower boiling point of benzene as compared with these of toluene and xylene.

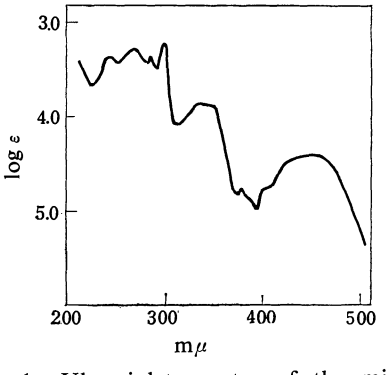


Fig. 1. Ultraviolet spectra of the mixed crystals.

In this study fluorenone was converted to fluorene and the other intermediates, II, IV, V VI, VIII and IX, after a short reduction time (2 hr.) in toluene, as has been described above.

Furthermore, V, VIII and X were increased, but IV was decreased and IV remained almost constant when the reaction was continued for twenty-four hours (red colored toluene). Three kinds of end-products, VII (10%), X (55.6%) and (III, 8.7%) were obtained, as is shown in Chart I and Table I, by extending the refluxing periods for seventy-two hours (almost colorless). VII and X were then obtained in approximately a ratio of 1 : 5.6.

It may, therefore, be assumed that V and VIII were also formed from IV through the positively charged ion IV′ by the action of the acidic medium in the Clemmensen reduction.

In view of these observations, the behavior of each intermediate in the course of the Clemmensen-Martin reduction of fluorenone can be explained. There have also been some other discussions reported recently of the mechanism of the Clemmensen reduction[20].

Experimental*

General Procedure for the Clemmensen Reduction of Fluorenone Materials.—Amalgamated zinc filings were prepared according to Martin's method[6].

A mixture of amalgamated zinc (20 g.), water (15 ml.), xylene (20 ml.), concentrated hydrochloric acid (35 ml.) and fluorenone (10 g.) was refluxed briskly for twenty-four hours in a 500 ml. round-bottomed flask. A 10 ml. portion of concentrated hydrochloric acid was added every six hours during the heating period. The xylene layer turned a bright red color after ten minutes.

The red reaction mixture was cooled to room temperature after 24 hr., and the deposited crystals

17) C. Graebe and B. Mantz, *Ann.*, **290**, 241 ((1896).
18) E. Bergmann and Y. Hirshberg, *Bull. soc. chim. France*, **17**, 1091 (1905).
19) E. Bergmann, E. Fischer and J. Jaffe, *J. Am. Chem. Soc.*, **75**, 3230 (1953).
20) D. Staschewski, *Angew. Chem.*, **71**, 726 (1956); T. Nakabayashi, *J. Am. Chem. Soc.*, **82**, 3900 (1960).
* All the melting points are uncorrected.

in the xylene layer were collected and washed free of acid with a small amount of water and then recrystallized from benzene. Colorless crystalline needless of X (1.6 g.) were obtained. (Part of X coats the surface of the zinc; m. p. and mixed m. p. 224°C). The mother liquor was evaporated to half volume. The deposited crystals were filtered and recrystallized from acetic ester to yield V (0.75 g.) as colorless prisms, m. p. 258°C (Found: C, 90.91; H, 4.86%). This was identical with those of a specimen which was prepared from IV with sulfuric acid in acetic acid following the procedure of Gomberg and Bachmann[9]. Further evaporation of the mother liquor to half volume yielded VII (slightly yellow), which recrystallized several times from benzene as nearly colorless material, (1.3 g.), m. p. 214~215°C.

Found: C, 95.28; H, 5.20. Calcd. for $C_{26}H_{16}$; C, 95.09%; H, 49.1%; Picrate, Found: C, 69.21; H, 3.64 N, 7.60. Calcd. for $C_{32}H_{19}O_7N_3$: C, 68.94; H, 3.44; N, 7.54%.

VII, λ_{max}^{MeOH} mμ (log ε): 265 (4.73), 286 (4.69), 299 (4.84), 335 (4.22), 350 (4.20).

The xylene was separated from the water layer and submitted to steam distillation for one hour to remove both the solvent and the fluorene which was recrystallized from alcohol (1.3 g.), m. p. 113~114°C. This was confirmed by mixed melting point.

The red residue was filtered, dried, and recrystallized from benzene to yield additional X (0.8 g.) (total 2.4 g.), m. p. 243~244°C.

The last benzene mother liquor was evaporated to a small volume, and the deposited red crystals were recrystallized from acetic ester in a red prism to give mixed crystals (0.5 g.), m. p. 185°C.

Found: C, 95.10; H, 5.19. Calcd. for $C_{26}H_{16}$: C, 95.09; 4.91%.

λ_{max}^{MeOH} mμ (log ε): 244 (4.62), 268 (4.71), 286 (4.63), 299 (4.76), 335 (4.15), 348 (4.13) 382 (3.23), 450 (3.60).

Then, IV was isolated from the mother liquor as colorless needles (1.0 g.), m. p. 192°C (Found: C, 86.24; H, 5.14%). The identity of this compound was confirmed by mixed melting point with an authentic sample.

The separation of the reaction products was much simpler when the reduction time was longer (72 hr.). In this reduction, the amalgamated zinc and hydrochloric acid were changed every 24 hr.

In the case of a short reduction period (2 hr.) the first deposited crystals were almost pure IV (m. p. 192°C). II (0.1 g., m. p. 158°C) was extracted by 20% boiling alcohol from the red residue of the steam distillation; furthermore, other compounds were separated by the method described above. The last residual benzene solution was chromatographed on alumina, and two products, VIII (0.65 g., m. p. 192~193°C) and I (0.3 g., m. p. 80°C), were isolated; their identity was confirmed by mixed melting point with authentic samples.

In the case of a short reduction period (3 hr.). of IV, each product was separated by a procedure almost identical to that employed for the reduction products of I.

Oxidation of 9, 10-Diphenylene-phenanthrene (VII).—VII (1 g.) was dissolved in a mixture of acetic acid (25 ml.) and sodium bichromate (5 g.) and refluxed for 2 hr., and the reaction mixture was then poured into cold water. The white amorphous products were filtered, dried, and recrystallized from benzene to yield XI (0.42 g.) as colorless prisms, m. p. 269~271°C[12,13].

Found: C, 86.73; H, 4.38. Calcd. for $C_{26}H_{16}O_2$: C, 86.65; H, 4.48%.

I (0.15 g.), m. p. 80°C, was isolated from the mother solution, as shown by mixed melting point with an authentic sample.

Reduction of Tetrabenzocyclodecane-1,6-dione (XI).—A mixture of XI (0.2 g.), red phosphorus (0.1 g.), hydrogen iodide (3 ml.) and acetic acid (5 ml.) was refluxed for 9 hr. After it had been cooled, the reaction mixture was filtered, and the filtrate was poured into water.

The white deposited product was filtered and recrystallized from benzene, m. p. 256~257°C (0.1 g.). This compound was identical with V, as shown by mixed melting point.

To the benzene mother liquor was added 0.1 g. of picric acid. Dark-red crystalline needles (m. p. 198~200°C) were deposited; this picrate was filtered and decomposed by ammonium hydroxide. The product recrystallized from acetone yielded VII (0.045 g.) as colorless needles, m. p. 214~215°C.

Reactions of the Mixed Crystals.—*Reduction.*—A mixture of amalgamated zinc (4 g.), water (3 ml.), concentrated hydrochloric acid (7 ml.), toluene (8 ml.) and mixed crystals (2 g.) was refluxed for 10 hr. The crude product (1.6 g., m. p. 224~237°C) was isolated from the toluene; from this X (1.1 g., m. p. 242~243°C) and VII (0.2 g., m. p. 212~214°C) were separated by recrystallization. Both X (0.45 g.) and VII (0.08 g.) were also obtained from mixed crystals (0.6 g.) by the use of zinc and ammonium hydroxide in an alcoholic solution; X and VII were confirmed by identity with authentic samples.

Bromination.—To the mixed crystals (0.82 g.) dissolved in carbon tetrachloride (30 ml.) there was added 0.4 g. of bromine in 5 ml. of carbon tetrachloride at room temperature. After the mixture had been let standing for 3 hr., the deposited crystals were filtered and recrystallized from benzene (0.6 g.). This was identical with 9,9'-dibromodibiphenyleneethane (m. p. 235°C) prepared by Graebe and Mantz's method[17]. VII (0.1 g., m. p. 213~214°C) was isolated from the mother solution and did not react with bromine.

Oxidation (1).—Mixed crystals (1.0 g.), acetic acid (25 ml.) and potassium bichromate (5 g.) were refluxed for 2 hr. After being poured into cold water, the light yellow precipitate obtained was recrystallized from benzene to yield XI (0.2 g. m. p. 269.5~271°C); this was confirmed by comparison with an authentic sample. I (0.5 g., m. p. 81°C) was isolated from the mother liquor.

Oxidation (2).—To the mixed crystals (0.5 g.) dissolved in 50 ml. of acetone there were added 2 g. of potassium permanganate during 2 hr. at room temperature. Then, most of the acetone was evaporated by reduced pressure and poured into water.

The deposited material was filtered off and refluxed with 3 ml. of alcohol. I (0.4 g., m. p. 81°C) was obtained from the soluble part, while VII (0.1 g., m. p. 213~214°C) was obtained from the alcohol-insoluble part and was recrystallized from benzene.

Formation of Mixed Crystals.—IX (1.0 g.) and VII (0.2 g.) were dissolved in acetic ester by heating. Upon the cooling of the mixture, bright mixed crystals (red prisms) were deposited and were recrystallized from acetic ester, m. p. 185°C (1.0 g.).

Found: C, 95.10; H, 5.19. Calcd. for $C_{26}H_{16}$: C, 95.11; H, 4.89%.

Reduction of 10, 10-Diphenylene-9-phenanthrone (V) to 9, 10-Diphenylene-phenanthrene (VII).—V (2.0 g.), amalgamated zinc (8 g.), concentrated hydrochloric acid (14 ml.) xylene (40 ml.) and water (6 ml.) were refluxed for 15 hr., a 4 ml. portion of hydrochloric acid being added every 6 hr. After the reaction period, the xylene layer was separated and washed with water, and the xylene was steam-distilled. The white residue was filtered, dried, and then chromatographed in benzene on alumina.

Fractional crystallization yielded VII (1.52 g. m. p. 214~215°C) and VI (0.2 g. m. p. 178~179°C), which were confirmed by mixed melting polnt.

The author wishes to express his gratitude to Drs. John and Elizabeth Weisburger of National Institutes of Health, U. S. A. for their valuable suggestions, and also to Dr. Toshio Mukai for the ultraviolet spectra and to Dr. Yûsaku Ikegami for the infrared spectra, both recorded at Tohoku University.

Department of Chemistry
Faculty of Technology
Yamaguchi University
Tokiwadai, Ube

The Aconite Alkaloids. XXXVI[1]*. Oxidation of Lucaconine and its Derivatives*[2b]

By Takashi AMIYA and Takeo SHIMA[3]

(Received August 8, 1961)

Lucaconine (I) ($C_{24}H_{39}O_7N$) and monoacetyllucaconine (II) ($C_{26}H_{41}O_8N$) have been isolated from *Aconitum luciduscul*um, *Nakai*, and have been subjected to continuous research in this laboratory[4-7].

The present authors have further studied the degradation reactions of compound I and its derivatives; the oxidation reactions of these compounds, mainly with the chromium trioxide-pyridine complex, are reported on this paper (cf. Table I).

The oxidation of compound I with the chromium trioxide-pyridine complex yielded neutral products, oxolucaconine (III) ($C_{24}H_{37}\cdot O_8N\cdot 13/4H_2O$), oxolucaconinone-II(IV) ($C_{24}H_{35}\cdot O_8N$), m. p. 218°C, and oxolucaconinedione (V) ($C_{24}H_{33}O_8N$). Compound IV was a monoketo-lactam and showed absorption bands at 5.83 and 6.15 μ characteristic of a six-membered ring ketone and of a lactam carbonyl group in the infrared spectrum respectively. Its ultraviolet absorption spectrum showed a maximum (λ_{max} 298 mμ, log ε 1.90), indicating the presence of a ketone carbonyl group. Compounds III and V are a lactam and a diketo-lactam respectively; they had been previously obtained by Furusawa through other procedures[7]. Compound III manifested absorption bands in the infrared spectrum at 2.94 and 6.20 μ characteristic of hydroxyl and lactam carboxyl groups respectively. It was also obtained by chromium trioxide-pyridine complex oxidation of diacetyllucaconine (VI) ($C_{28}H_{43}O_9N$)[6], followed by hydrolysis. Compounds III and IV were further oxidized to compound V by the same reagent. The infrared spectrum of compound V manifested absorption bands at 5.72, 5.83 and 6.08 μ characteristic of a five-membered ring ketone, a six-membered ring ketone and a lactam carbonyl group respectively. The reduction of compound III with lithium aluminum hydride gave compound I again.

1) This is one part of a series entitled "The Aconite Alkaloids", by H. Suginome; for Part XXXV, cf. Ref. 2a.

2) a) T. Amiya, This Bulletin, **34**, 898 (1961); b) A preliminary note on part of the matter of this paper appeared in Ref. 4.

3) This paper comprizes part of a dissertation submitted by Takeo Shima, 1959, in partial fulfillment of the requirements for the Degree of Doctor of Science in Hokkaido University. Mr. Shima's present address: Teikoku Rayon Research Laboratory, Iwakuni, Yamaguchi.

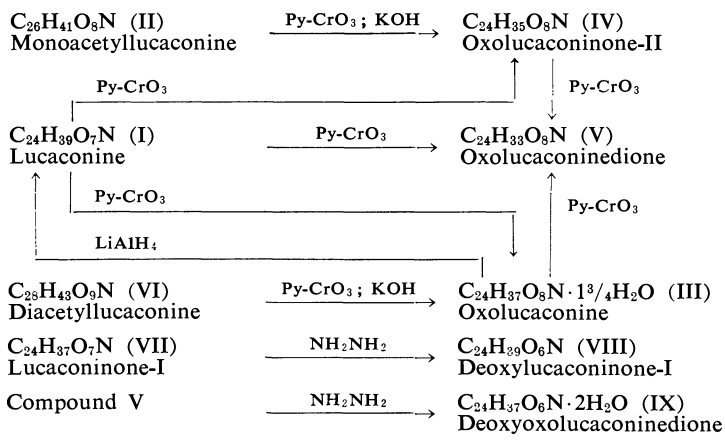
4) T. Amiya and T. Shima, This Bulletin, **31**, 1083 (1958).

5) H. Suginome, S. Kakimoto, J. Sonoda and S. Noguchi, *Proc. Japan Acad.*, **22**, 122 (1946).

6) H. Suginome and S. Furusawa, This Bulletin, **32**, 354 (1959).

7) S. Furusawa, ibid., **32**, 399 (1959).

TABLE I



Lucaconinone-I (VII) ($C_{24}H_{37}O_7N$), a monoketo-base, was prepared from compound I by Furusawa[7]. It showed a band at 5.72 μ in the infrared spectrum due to the presence of a five-membered ring ketone carbonyl group. The ultraviolet absorption spectrum exhibited a maximum (λ_{max} 292 mμ, log ε 1.53). Compound VII was reduced to deoxylucaconinone-I (VIII) ($C_{24}H_{39}O_6N$), m. p. 165°C, by the Wolff-Kishner method. Its infrared spectrum showed no absorption characteristic of a ketone carbonyl group. The ultraviolet spectra of compounds III, VI and VIII showed only end absorptions.

Next, compound II, a naturally occurring base, was oxidized by the chromium trioxide-pyridine complex and subsequently hydrolyzed, giving compound IV. This result shows that an acetylated hydroxyl group in compound II is a secondary one attached to a carbon atom in a five-membered ring.

In view both of the experimental results previously obtained[7] and of those described in this investigation, the partial formula of compounds I and II may be extended as follows:

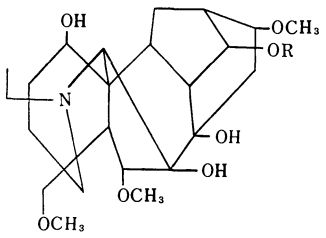
$C_{14}H_{17}$ { $(OCH_3)_3$; $(\rightarrow COH)_2$; $>CHOR$ (five-membered ring); $>CHOH$ (six-membered ring); $-N-C_2H_5$; $-CH_2$ }

I, R=H II, R=Ac

On the other hand, it has been suggested by Stern[8] that lucaconine seems to be identical with delcosine[9]. Since then, several reports concerning delcosine have been published by Marion and his co-workers[10-13]. In those reports a structure of delcosine has been proposed after a revision and the further possibility of identifying delcosine with lucaconine has been considered. Comparison of the physical properties of lucaconine and its derivatives and those of delcosine and its derivatives also leads to the supposition that lucaconine is identical with delcosine. Recently, lucaconine has been found to be identical in melting point and infrared spectrum with Takao base-I[14,15], showing no depression in mixed melting point; therefore, lucaconine must be identical with delcosine, which has already been shown to be identical with Takao base-I[14]. Accordingly, the name "lucaconine", must be revised to "delcosine", and derivatives of compound I should be named as those of delcosine.

According to the structure of delcosine (compound I) proposed by Skaric and Marion[13], compound II, a naturally occurring base, ought to have the structure shown in Scheme A. While oxidation and subsequent hydrolysis of monoacetyldelcosine have given dehydrooxodelcosine[13], compound II has yielded compound IV[4] on the same treatment. As compound IV seems to be identical with dehydrooxodelcosine, compound II is probably identical with monoacetyldelcosine, as has been pointed out by Canadian workers[13].

8) E. S. Stern, "The Alkaloids, Chemistry and Physiology", Vol. 4, Ed. by R. H. F. Manske and H. L. Holmes, Academic Press, Inc., New York (1954), p. 328.
9) L. Marion and O. E. Edwards, *J. Am. Chem. Soc.*, **69**, 2010 (1947).
10) W. I. Taylor, W. E. Walles and L. Marion, *Can. J. Chem.*, **32**, 780 (1954).
11) R. Anet, D. W. Clayton and L. Marion, ibid., **35**, 397 (1957).
12) R. Anet and L. Marion, ibid., **36**, 766 (1958).
13) V. Skaric and L. Marion, *J. Am. Chem. Soc.*, **80**, 4434 (1958); V. Skaric and L. Marion, *Can. J. Chem.*, **38**, 2433 (1960).
14) E. Ochiai, T. Okamoto and M. Kaneko, *Chem. Pharm. Bull.*, **6**, 730 (1958); *Ann. Rept., ITSUU Lab.*, **11**, 21 (1960); ibid., **11**, 29 (1960).
15) The authors are grateful to Professors Ochiai and Okamoto and to Dr. Kaneko, Faculty of Pharmaceutical Science, the University of Tokyo, for kindly supplying sample.



I, R=H II, R=Ac

Scheme A

The Wolff-Kishner reduction of compound V, a diketo-lactam, gave a lactam (IX) ($C_{24}H_{37}O_6N \cdot 2H_2O$), m. p. 80~85°C. It showed no absorption band characteristic of ketone carbonyl in the infrared spectrum. The ultraviolet spectrum of compound IX showed only end absorption. From a consideration of the molecular formula as well as of the spectra of compound IX, it has reasonably been assumed that in this reduction two carbonyl groups of compound V were converted into methylene groups. Oxidation of compound IX, a di-tertiary glycol containing no more than two hydroxyl groups, with periodic acid gave an amorphous material X, the infrared spectrum of which showed bands at 5.70 and 5.92 μ. These bands at 5.70 and 5.92 μ suggest the probable presence of a five-membered and of an α,β-unsaturated six-membered ring ketone carbonyl group respectively, derived from the cleavage of a 1, 2-glycol constituent. This experimental consequence confirms the findings of the Canadian group[11-13], in which compound I has been shown to be a di-tertiary 1, 2-glycol; it also coincides with the result of the oxidation of anhydrohydroxydelcosine with periodic acid[12]. Accordingly, it may be concluded that compound I is not a di-tertiary 1,3-glycol[1].

Thus, the experiments mentioned above, together with the NMR spectrum of compound I[16], strongly support the structure of compound I (Scheme A) suggested by Skaric and Marion[13].

Experimental

Oxidation of Lucaconine (I) with the Chromium Trioxide-Pyridine Complex. — *A) Oxolucaconine (III) and Oxolucaconinone-II (IV).* — A mixture of lucaconine (1 g.) and chromium trioxide (1 g.) in pyridine (20 ml.) that had been allowed to stand at room temperature overnight was evaporated to dryness in vacuo. After the addition of water (100 ml.), the residue was reduced with sulfur dioxide. The excess reagent having been reduced, the acid solution thus obtained was extracted with chloroform three times. After removal of the solvent, the chloroform extract gave a residue which was redissolved in chloroform (13 ml.) and chromatographed on alumina (5 g.). The chromatogram was eluted with chloroform alone (100 ml.), and then with chloroform containing 1% of methanol (100 ml.). From the chloroform portion the residue was obtained. It was crystallized from acetone. On recrystallization from ethanol, it melted at 132°C; yield, 0.05 g. Mixture with oxolucaconine prepared according to the directions of Furusawa[7] did not affect the melting point. The ultraviolet absorption spectrum of this compound in methanol showed end absorption and no maximum. The infrared absorption spectrum in Nujol, identical with that of isooxolucaconine[7], showed the presence of hydroxyl groups (2.94 μ) and of a lactam carbonyl group (6.20 μ).

From the portion of the chloroform containing 1% of methanol of elute, oxolucaconinone-II (0.1 g.) was obtained on evaporation. It crystallized from acetone. On two recrystallizations from ethanol, it melted at 218°C; yield, 0.1 g. The ultraviolet absorption spectrum of this compound in methanol showed λ_{max} 298 mμ, log ε 1.90. The infrared absorption spectrum in Nujol showed the presence of hydroxyl groups (2.87 and 2.98 μ), a ketone carbonyl group (5.83 μ) and a lactam carbonyl group (6.15 μ).

Found: C, 62.31; H, 7.64; OCH_3, 18.22. Calcd. for $C_{24}H_{35}O_8N$: C, 61.92; H, 7.58; $3OCH_3$, 19.99%.

The aqueous liquor described above was made alkaline with sodium carbonate and extracted with chloroform. After removal of the chloroform, a basic substance (0.3 g.) was left. It was crystallized from acetone and further recrystallized from ethanol twice. It melted at 199~200°C either alone or mixed with naturally occurring lucaconine.

B) Oxolucaconinedione (V) and Oxolucaconinone-II (IV). — A mixture of lucaconine (1 g.) and chromium trioxide (2 g.) in pyridine (40 ml.) was allowed to stand at room temperature for two days. It was treated by the same procedure as the above A), and the obtained acid solution was extracted with chloroform three times. The chloroform extract was evaporated. The residue was chromatographed on alumina (5 g.) as in the case of the above A). Evaporation of the chloroform portion (100 ml.) of elute and the subsequent addition of acetone gave a crystalline material, m. p. 203°C. Two recrystallizations from ethanol yielded crystals melting at 209°C, reported[13] m. p. 211~212°C. Mixture with oxolucaconinedione, prepared according to the direction of Furusawa[7], did not alter the melting point. The infrared absorption spectrum of this compound in Nujol showed the presence of hydroxyl groups (2.90 μ), ketone carbonyl groups (5.72 and 5.83 μ), and a lactam carbonyl group (6.08 μ)[7]. It was reported[13] as $\lambda_{max}^{chloroform}$ 3446, 1757, 1720 and 1653 cm^{-1}.

Oxime.—It melted at 248°C and did not depress the melting point of the sample of the oxime prepared by Furusawa[7].

The portion of the chloroform containing 1% of

16) A. Suzuki, T. Amiya and T. Matsumoto, This Bulletin, 34, 455 (1961).

methanol (100 ml.) of elute gave a residue crystallized from acetone. On recrystallization from ethanol it melted at 218°C and did not depress the melting point of the oxolucaconinone-II described above.

In this oxidation reaction from the aqueous liquor, the basic substance was not obtained.

Diacetyllucaconine (VI).—The ultraviolet absorption spectrum of this compound in methanol showed end absorption and no maximum.

Oxolucaconine (III) from Diacetyllucaconine (VI)[13].—A mixture of diacetyllucaconine (0.3 g.), chromium trioxide (0.3 g.) and pyridine (6 ml.) was allowed to stand at room temperature overnight. The chloroform extract, obtained from the acid solution prepared by the same treatment as described above, was evaporated to give a residue (0.3 g.). It was then hydrolyzed with boiling ethanolic potassium hydroxide for 1 hr. After cooling, the solution was evaporated, and the residue neutralized with 1 N hydrochloric acid and extracted with chloroform. After removal of the chloroform, the residue (0.2 g.) was crystallized from acetone. Two recrystallizations from ethanol gave crystals, m. p. 132°C, which did not depress the melting point of the authentic sample (oxolucaconine) described above.

Oxolucaconinedione (V) from Oxolucaconine (III).—A mixture of oxolucaconine (0.3 g.), chromium trioxide (0.3 g.) and pyridine (6 ml.) was allowed to stand at room temperature overnight. The reaction mixture was treated in the above-described manner, and the chloroform extract from the acid solution was evaporated to give a residue, which crystallized from acetone. Two recrystallizations from ethanol yielded 0.2 g. of crystals, m. p. 209°C. It did not alter the melting point of the authentic sample (oxolucaconinedione).

Oxolucaconinedione (V) from Oxolucaconinone-II (IV).—A mixture of oxolucaconinone-II (0.5 g.), chromium trioxide (0.5 g.) and pyridine (10 ml.) was treated in just the above-mentioned manner to give 0.4 g. of oxolucaconinedione, m. p. 209°C. Mixture with the authentic sample did not alter the melting point.

Reduction of Oxolucaconine (III) with Lithium Aluminium Hydride. — Oxolucaconine (0.2 g.) was dissolved in dioxane (5 ml.). An ether solution (3 ml.) of lithium aluminium hydride (0.1 g.) was added and the temperature gradually raised until the ether evaporated. Then the solution was further refluxed for an hour. The excess reagent was destroyed by the use of water, and, after removal of the formed aluminium hydroxide, the solution was evaporated in vacuo. After the addition of water (1 ml.), the residue was extracted with chloroform. Removal of the chloroform left a residue, which was crystallized from acetone. Two recrystallizations from ethanol yielded crystals, m. p. 200°C, which did not depress the melting point of lucaconine.

Lucaconinone-I (VII). — The ultraviolet absorption spectrum of this compound in methanol showed λ_{max} 292 mμ, log ε 1.53. The infrared absorption spectrum in Nujol showed the presence of hydroxyl groups (2.99 μ) and a ketone carbonyl group (5.72 μ)[7]. It was reported as λ_{max}^{Nujol} 1751 cm^{-1} [14] and λ_{max}^{Nujol} 1755 cm^{-1} [11].

Deoxylucaconinone-I (VIII) from Lucaconinone-I (VII).—A solution of lucaconinone-I (40 mg.) in triethylene glycol (1 ml.) and 85% hydrazine hydrate (0.5 ml.) was refluxed for 1 hr. at 130°C. Then potassium hydroxide (80 mg.) was added and the temperature gradually raised to 200°C during an hour, while water and excess hydrazine hydrate were distilled off. After it had been refluxed for an additional 5 hr. at 195~200°C, the solution was cooled, diluted with water, and extracted with chloroform three times. After removal of the chloroform, a residue was obtained. Recrystallization from ethanol gave crystals (30 mg.), m. p. 165°C, $[\alpha]_D$ +64.65° ($CHCl_3$) reported[14] m. p. 170~171°C, $[\alpha]_D$ +51° ($CHCl_3$). The ultraviolet absorption spectrum of this compound showed end absorption and no maximum. The infrared absorption spectrum showed the presence of hydroxyl groups (2.99 μ).

Found: C, 66.16; H, 8.96; OCH_3, 19.25. Calcd. for $C_{24}H_{39}O_6N$: C, 65.87; H, 8.98; $3OCH_3$ 21.27%.

The analysis of this compound has also been reported[14].

Oxolucaconinone-II (VI) from Monoacetyllucaconine (II). — A mixture of monoacetyllucaconine (2 g.), chromium trioxide (2 g.) and pyridine (40 ml.) was allowed to stand at room temperature overnight. The reaction mixture was treated in the same way as in the above-described oxidation. The chloroform extract from the acid solution gave an amorphous residue (2 g.) on evaporation which was hydrolyzed with boiling ethanolic potassium hydroxide for an hour. After cooling, the solution was evaporated. The residue was neutralized with 1 N hydrochloric acid and extracted with chloroform. After removal of the chloroform, the residue was crystallized from acetone. Two recrystallizations from ethanol gave 1.6 g. of crystals, m. p. 218°C, which did not depress the melting point of the authentic sample described above.

Deoxyoxolucaconinedione (IX). — A solution of oxolucaconinedione (730 mg.) in triethylene glycol (10 ml.) and anhydrous hydrazine (3.5 ml.) was refluxed for 3 hr. at 140°C, potassium hydroxide (1 g.) was added, and the temperature was gradually raised to 200°C over the course of an hour without the condenser. After it had been refluxed for an additional 5 hr. at about 200°C, the solution was cooled, diluted with water, and extracted with chloroform five times. The chloroform extract was washed with 1 N hydrochloric acid and evaporated. The residue was redissolved in 5 ml. of chloroform and then chromatographed on alumina (5 g.). The chromatogram was eluted with chloroform (100 ml.). The elute was evaporated. The residue was crystallized from petroleum ether and diethyl ether. Two recrystallizations from aqueous ethanol gave 350 mg. of needle, m. p. 80~85°C. The ultraviolet absorption spectrum of this compound in methanol showed end absorption and no maximum. The infrared absorption spectrum in Nujol showed the presence of hydroxyl groups (2.96 and 2.99 μ) and a lactam carbonyl group (6.19 μ).

Found: C, 60.76; H, 8.71; N, 2.86; OCH_3,

20.15; H_2O, 7.55. Calcd. for $C_{24}H_{37}O_6N \cdot 2H_2O$: C, 61.12; H, 8.76; N, 2.97; $3OCH_3$, 19.74; H_2O, 7.64%.

Cleavage of the Lactam (IX) with Periodic Acid. — To the lactam (IX) (230 mg.) in ethanol (20 ml.), 0.1 N periodic acid (30 ml.) was added, and the mixture was allowed to stand at room temperature for 5 days. After the addition of water (100 ml.), the solution was extracted with chloroform. Evaporation of the chloroform gave a residue. The residue was redissolved in a small quantity of chloroform and chromatographed on alumina (3 g.). The chromatogram was eluted with chloroform (50 ml.). The elute was evaporated to leave 0.15 g. of an amorphous residue. The infrared absorption spectrum in Nujol showed the presence of hydroxyl groups (2.96 μ), a five-membered cyclic ketone (5.70 μ), an α,β-unsaturated six-membered cyclic ketone (5.92 μ) and a lactam carbonyl group (6.11 μ).

The authors are grateful to Professor Harusada Suginome, President of Hokkaido University, for his unfailing kindness in encouraging this work, and to Drs. M. Yamaguchi, Wakayama Prefectural Medical College, and A. Fujino, Faculty of Science, Osaka City University, for their kindness in the determination of the infrared spectra.

Department of Chemistry
Faculty of Science
Hokkaido University
Sapporo

*Hot-atom Reaction in cis- and trans-Dinitrotetrammine Cobalt(III) Nitrate**

By Nobufusa SAITO, Hirotoshi SANO, Takeshi TOMINAGA, Fumitoshi AMBE and Takeo FUJINO

(Received September 9, 1961)

Several models have been proposed to account for the mechanism of the hot-atom reaction in solids[1-4]. It should be possible to check the validity of these models by investigating the hot-atom reaction in compounds exhibiting optical and geometrical specificity. Zuber[5] irradiated dextro-tris(ethylenediamine)cobalt-(III) nitrate and found the yield of ^{60}Co to be 4.5 per cent in the dextro form and 0.5 per cent in the laevo form. Recently, Rausher, Sutin and Miller[6] have studied the Szilard-Chalmers reaction in *cis-* and *trans*-dichloro-bis(ethylenediamine)cobalt(III) nitrate and have found that the yield of ^{60}Co is 3~7 per cent in the parent isomer and 0.1~0.2 per cent in the other isomer, while the corresponding yields of ^{38}Cl in that order are 12~16 per cent and 0.4~0.7 per cent respectively.

We have investigated the chemical effects of the $^{59}Co(n,\gamma)^{60}Co$ reaction in the cis and trans isomers of crystalline dinitrotetrammine cobalt-(III) nitrate, which show a greater stability to aquation than do the dichloro complex salts. Furthermore, the retentions of nitroammine cobalt(III) complex salts are higher than those of the complex salts cited above.

Experimental

Materials.—The complex salts were prepared by the method of Jorgensen[7]. The salts were purified by recrystallization. The purity of the complex salts was checked by taking the absorption spectra of their solutions in distilled water and comparing the molar extinction coefficients and the maximum wavelengths with those reported by Basolo[8].

Neutron Irradiation.—Samples of *cis*-$[Co(NH_3)_4(NO_2)_2]NO_3$ and *trans*-$[Co(NH_3)_4(NO_2)_2]NO_3 \cdot H_2O$ were irradiated at reactor temperature for one to five hours in the thermal column of the JRR-1 reactor. All bombardments were made in the presence of air. The neutron flux at the bombardment site was $(3\sim5)\times10^{11}$ n/cm^2 sec., and the gamma ray flux, approximately 5×10^5 r/hr.

Separation Procedure.—*Ion Exchange Separation.* —Two to five milligrams of the irradiated sample were dissolved in 10 ml. of water. (In preliminary tests, cobalt(II) nitrate, *cis-* or *trans*-dinitrotetrammine nitrate and nitropentammine nitrate were added prior to the dissolution of the sample, but

* Presented in part at the Symposium on Coordination Chemistry, Fukuoka, Japan, Oct., 1959.

1) W. F. Libby, *J. Am. Chem. Soc.*, **69**, 2523 (1947); L. Friedman and W. F. Libby, *J. Chem. Phys.*, **17**, 647 (1949).
2) J. M. Miller and R. W. Dodson, *J. Chem. Phys.*, **18**, 865 (1950).
3) J. E. Willard, *Ann. Rev. Nucl. Sci.*, **3**, 193 (1953).
4) G. Harbottle and N. Sutin, *J. Phys. Chem.*, **62**, 1344 (1958).
5) A. V. Zuber, NYO-6142 (1954).
6) H. E. Rauscher, N. Sutin, J. M. Miller, *J. Inorg. & Nuclear Chem.*, **12**, 378 (1960); ibid., **17**, 31 (1961).
7) S. M. Jörgensen, *Z. anorg. Chem.*, **17**, 470, 473 (1898).
8) F. Basolo, *J. Am. Chem. Soc.*, **72**, 4393 (1950).

no effect on the distribution of ^{60}Co was found.) The solution was passed through a resin column (0.8×17 cm. of Dowex 50W X-8, H-form 100~200 mesh beads). The column was then washed with about 100 ml. of water. The effluent contained anionic and neutral species. Subsequently, 300 to 400 ml. of 1 M sodium chloride solution was passed through the column. Firstly, *trans*-$[Co(NH_3)_4(NO_2)_2]^+$ ions were eluted, and then a mixture of *cis*-$[Co(NH_3)_4(NO_2)_2]^+$ ions and Co(II) species in the next fraction[9]. To the latter fraction were added 10 mg. of cobalt(II) nitrate as a carrier and 10 mg. of *cis*-$[Co(NH_3)_4(NO_2)_2]NO_3$ as a hold-back carrier. The cobalt(II) species were precipitated as hydroxide with a diluted sodium hydroxide solution. After reprecipitation, the precipitates were dissolved in diluted hydrochloric acid.

In another series of experiments, ammonium malonate was used as an eluent instead of sodium chloride. After the sample solution had been passed through a cation exchanger column (under the same condition as mentioned above but kept in ammonium form), the column was washed with about 100 ml. of water. The adsorbed cations were eluted with 300 to 400 ml. of 1/2 M ammonium malonate solution. Anionic and neutral species were collected in the first fraction. The cobalt(II) species was eluted in the second fraction as cobalt(II) malonate*. The *trans*- and *cis*-dinitrotetrammine, and nitropentammine species were eluted in the third, fourth, and fifth fractions respectively.

The non-cationic fraction was poured into an anion exchanger column (Dowex 1 X-8, NO_3-form, 100~200 mesh beads, 0.8×10 cm.). The column was then washed with about 100 ml. of 0.1 M sodium chloride solution. Neutral species were collected in the effluent. The adsorbed anions were eluted with 1 M sodium chloride solution.

All samples were counted as liquids, in a well-type scintillation counter.

Paper Electrophoresis. — Samples of the irradiated compounds were dissolved in a 0.1 M ammonium oxalate solution at a concentration of 1~2 mg./ml. Portions of 20~50 λ were pipetted and placed at a zero-line on electrophoresis paper (Toyo Roshi No. 50). Potentials of the order of 400~600 V. were applied, the useful length of the strips being about 30 cm. The strips were cooled during electrophoresis by immersion in monochlorobenzene. After one to two hours, the voltage was interrupted, the paper dried and cut transversely in 1 cm. strips. These were scintillation-counted in a standard way. It has been known that cis species move faster than trans species toward the cathode[10]. The preliminary tests showed that cobalt(II) species moved toward the anode.

Determination of Cobalt.—Each fraction obtained in the ion exchange separation was dried on a steam bath. After concentrated sulfuric acid and concentrated nitric acid were added, the solution was evaporated almost to dryness. This procedure was repeated until the complexes or malonates were completely decomposed. Then, the amount of cobalt in each fraction was determined spectrophotometrically, using the nitroso-R salt method[11].

Results

It was found that the ion exchange separation using ammonium malonate as an eluting agent was most suitable for our purpose, because those cationic species adsorbed on the resin were eluted chromatographically and, therefore, the precise distribution pattern of ^{60}Co could be obtained. The elution curve of ^{60}Co activity from the cation exchange column is shown in Figs. 1 and 2. Paper electrophoresis was not very effective in the separation of the irradiated cis salts, because the peaks of the trans salt were not sufficiently well-resolved to permit determination.

The percentage distributions of the ^{60}Co activity are summarized in Tables I and II. The most significant result is that there is a considerable amount of ^{60}Co which appears in

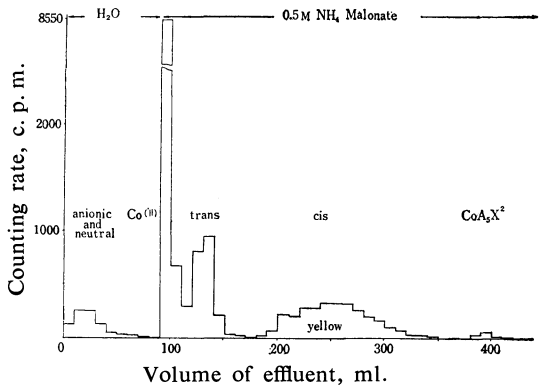


Fig. 1. Elution of ^{60}Co in the 1 hr.-irradiated cis salt.

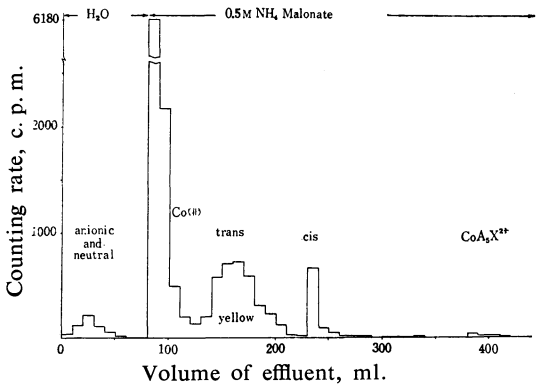


Fig. 2. Elution of ^{60}Co in the 1 hr.-irradiated trans salt.

9) E. L. King and R. R. Walters, ibid., **74**, 1674 (1952).

* From the experiments employing the technique of paper electrophoresis it was found that the species had no charge.

10) M. Maki, *Japan Analyst* (*Bunseki Kagaku*), **4**, 217 (1955).

11) E. B. Sandell, "Colorimetric Determination of Traces of Metals", 3rd Ed., Interscience Publishers, Inc., New York (1959), p. 415.

TABLE I. PERCENTAGE DISTRIBUTION OF ^{60}Co AFTER DISSOLUTION OF IRRADIATED CIS SALT

Irrad. time hr.	Storage time	Percentage distribution of ^{60}Co							Procedure of separation
		Anionic	Neutral	Co(II)	Trans	Cis (retn.)	CoA_5X^{2+}	Resin	
1	0~5 min.	1.2	5.2	58.4	11.9	20.5	1.0	1.7	Ion exchange malonate
1	2 months	4.5		56.4	4.5	29.1	3.9	1.6	Ion exchange malonate
5	2 weeks	1.1	3.2	42.8	4.0	46.5	1.4	0.0	Ion exchange NaCl ; Pptn.
5	5 months	0.3	5.6	39.9	4.1	43.5	6.6	0.0	Ion exchange malonate
5	5 months	6.2		41.1	4.9	45.7	2.1	0.0	Ion exchange malonate
5	12 months	0.0	7.3	42.7	50.0		—	—	Electrophoresis
Enrichment factor		40		340	81	0.46	26	—	

TABLE II. PERCENTAGE DISTRIBUTION OF ^{60}Co AFTER DISSOLUTION OF IRRADIATED TRANS SALT

Irrad. time hr.	Storage time	Percentage distribution of ^{60}Co							Procedure of separation
		Anionic	Neutral	Co(II)	Trans (retn.)	Cis	CoA_5X^{2+}	Resin	
1	0~5 min.	5.0		63.0	23.3	6.7	0.9	1.1	Ion exchange malonate
1	2 months	4.6		48.7	43.2	1.4	1.3	0.8	Ion exchange malonate
5	2 weeks	0.4	3.1	46.1	45.4	4.6	0.4	0.0	Ion exchange NaCl ; Pptn.
5	2 weeks	0.0	4.6	39.1	49.8	2.5	4.0	0.0	Ion exchange malonate
5	5 months	4.6		35.3	57.1	1.3	1.6	0.1	Ion exchange malonate
5	2 days	0.0	3.3	42.9	44.7	9.1	0.0	—	Electrophoresis
5	5 days	0.0	4.7	43.4	45.4	6.5	0.0	—	Electrophoresis
5	6 months	0.0	5.8	41.6	45.8	5.8	0.0	—	Electrophoresis
Enrichment factor		10		380	0.51	23	13	—	

the other isomeric form for either cis or trans targets. Cis isomer was found with an enrichment factor of 23 in the irradiated trans salt, while trans isomer with an enrichment factor of 80 was found in the irradiated cis salt. These results are also shown in Tables I and II.

Discussion

The distribution of ^{60}Co in *cis*-$[Co(NH_3)_4(NO_2)_2]NO_3$ irradiated for one hour is 20.5 per cent in the cis form and 11.9 per cent in the trans form. On storage at room temperature (15~25°C), the retention in the cis form reaches a value of 29.1 per cent, while the distribution of ^{60}Co in the trans form decreases to 4.5 per cent. The distribution of ^{60}Co in *trans*-$[Co(NH_3)_4(NO_2)_2]NO_3 \cdot H_2O$ irradiated for one hour is 23.3 per cent in the trans form and 6.7 per cent in the cis form. On storage at room temperature, the retention in the trans form increases to 43.2 per cent, while the distribution of activity in the cis form decreases to 1.4 per cent. The ratio of isomer formation to retention as parent species is 1/2 to 1/3 in terms of the radioactivity without storage, whereas the ratio decreases to 1/7 to 1/30 after two months storage. It seems important to determine the ratio of isomer formation to retention in a condition where the irradiation is conducted for an extremely short time at solid carbon dioxide temperature, because one-hour irradiation at reactor temperature, as conducted in our experiment, would produce additional annealing, both thermal and radiation.

These facts may indicate that one should prefer a model such as the hot-zone mode[14] to a billiard-ball mode[15], to account for the mechanism of the recoil processes.

It is also worth mentioning that geometric isomerization during recoil processes occurs

more remarkably in cis salts than in trans salts. Although it is too difficult for us at the present stage to give a clear explanation of this, it may be supposed that the cis species yielded in the irradiated trans salts are not so stable to additional annealing processes as the trans species yielded in the irradiated cis salts*.

Summary

The Szilard-Chalmers reaction of cobalt in *cis*- and *trans*-dinitrotetrammine cobalt(III) nitrate have been investigated. After a given isomer was irradiated, ^{60}Co was found in an appreciable amount in the other isomeric form. The distribution of ^{60}Co in *cis*-$[Co(NH_3)_4 \cdot (NO_2)_2]NO_3$ irradiated for one hour is 20.5 per cent in the cis form and 11.9 per cent in the trans form. The distribution in *trans*-$[Co(NH_3)_4(NO_2)_2]NO_3 \cdot H_2O$ is 23.3 per cent in the trans form and 6.7 per cent in the cis form. This observation is consistent with a hot-zone model, where one would except that the original configuration would not be essentially preserved.

Department of Chemistry
Faculty of Science
The University of Tokyo
Hongo, Tokyo

* It has been well-known that radiolysis occurs more easily in cis-isomers than in trans-isomers. For example, Dimotakis and Maddock have reported that *trans*-$[Co(en)_2 \cdot Cl_2]NO_3$ and *trans*-$[Co(en)_2Br_2]NO_3$ show a greater stability to radiolysis than do the corresponding cis salts. (International Symposium on Chemical Effects of Nuclear Transformation, Prague, 1960. CENT/18).

Etude sur le Révélateur Photographique 1-Phényl-3-pyrazolidone. I. Titrage Argentopotentiométrique et Observation à l'Aide de l'Absorption Infrarouge

Par Shinichi KIKUCHI et Hiromi YOSHIDA

(Reçu le 11 Septembre 1961)

Le révélateur, 1-phényl-3-pyrazolidone, qui fut introduit en Angleterre[1] sous le nom commercial de "Phénidone" en 1951 est maintenant un produit populaire et se synthétise même au Japon. Il y a déjà beaucoup de rapports sur les recherches théoriques et les applications de ce produit. Les présents auteurs ont fait un premier rapport concernant l'étude potentiométrique de ce produit en 1957[2] et ont continué leurs recherches pour en éclaircir le mécanisme du développement photographique. Ils ont trouvé que le titrage argentopotentiométrique de la solution aqueuse de la 1-phényl-3-pyrazolidone entre les pH 5 et 11 présente des caractères communs avec le résultat du développement essayé dans ces intervalle de pH[3]. Dans ce présent travail, ils ont voulu savoir quelle était la structure de la forme oxydée par l'ion argent au cours du titrage et extraire la partie organique des produits titrés à chaque pH, pour l'essai au spectre infrarouge. Dans la suite des expériences, la 1-phényl-3-pyrazolidone est oxydée dans diverses conditions et à chaque pH, les produits obtenus dans les phases solide et liquide sont soumis à l'essai des spectres d'absorption infrarouge, visible et ultraviolet.

1) O. Kendall, *Brit. J. Phot.*, **100**, 56 (Jan. 30, 1953).
2) S. Kikuchi et H. Yoshida, Conférence de la Soc. Photo. Sci. Japon, 1957.
3) T. H. James, W. Vanselow, *Phot. Sci. Tech. Série 2*, **1**, 7 (1954).

Expérimental et Résultats

Echantillons. — Comme échantillons, 4 marques commerciales de 1-phényl-3-pyrazolidone (notées dans ce rapport comme 1P, 2P, 3P et 4P) ont été employées. Ils ont été desséchés pendant 2 heures à 100°C et soumis aux mesures suivantes :

1. Absorption infrarouge.
2. Analyse élémentaire.
3. Diffraction aux rayons X.
4. Essai de développement photographique.

Analyses Élémentaires.—Les analyses élémentaires de 4 échantillons sont données dans les tableaux I et II.

D'après les analyses élémentaires, 2P est considéré comme le meilleur.

TABLEAU I. POURCENTAGES DE CARBONE ET D'HYDROGÈNE DES 4 MARQUES

	C calculé %	C observé %	H calculé %	H observé %
1P	66.67	66.87	6.17	6.25
2P	66.67	66.62	6.17	6.14
3P	66.67	66.82	6.17	6.24
4P	66.67	66.74	6.17	6.14

TABLEAU II. POURCENTAGES D'AZOTE ET POINTS DE FUSION

	N calculé %	N observé %	Point de fusion °C
1P	17.28	17.33	119.5
2P	17.28	17.27	120.5
3P	17.28	17.34	117~118
4P	17.28	17.36	119

Absorption Infrarouge[4].—Les 4 marques ont été examinées par analyse infrarouge an moyen du Nujol. Il n'y a pas de grandes différences entre elles, mais en les examinant en détail, il y a tout de même quelques petites différences. 3P possède à 1565 cm^{-1} une absorption qui semble montrer la présence d'impuretés. Comme le produit a une structure en -CH-CH-, l'absorption est compliquée à cause de cette structure du côté des petits nombres d'onde. La vibration d'allongement et de contraction de la liaison C=O s'est fortement déplacée (1690 cm^{-1}) du côté des petits nombres d'onde à cause d'une combinaison d'hydrogène. En jugeant l'ensemble de l'absorption infrarouge,

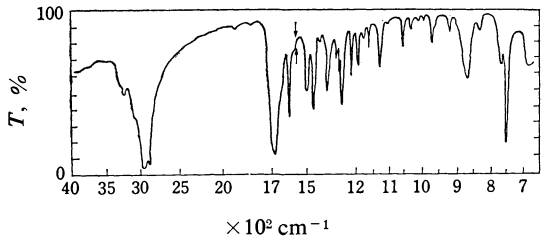


Fig. 1. Spectre d'absorption infrarouge de 1-phényl-3-pyrazolidone (Nujol).

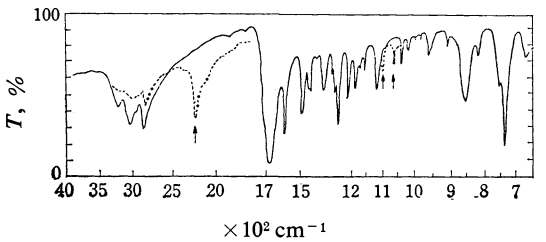


Fig. 2. Spectre d'absorption infrarouge de 1-phényl-3-pyrazolidone (tablette de KBr). Trait interrompu, celle deuterisée.

4) S. Kikuchi et H. Yoshida, Conférence de la Soc. Phot. Sci. Japon, 1959.

la 1-phényl-3-pyrazolidone a une structure de dimère comme la pyridone.

Dans le cas de 2P, les résultats obtenus au moyen du Nujol et au moyen du KBr ne présentent presque pas de différence. La Fig. 1 montre l'absorption de la 1-phényl-3-pyrazolidone obtenue au moyen du Nujol. 3P possède une absorption caractéristique à 1565 cm^{-1}, à l'endroit marqué par la flèche. La Fig. 2 montre celle au moyen du KBr. Dans la même figure la partie de la ligne pointillée montre la différence due à la deutérisation.

Diffraction aux Rayons X.—Les couleurs des cristaux des 4 marques sont: 1P blanc, 2P parfaitement blanc, 3P blanc légèrement rougeâtre, 4P blanc avec un peu de jaune brun clair.

L'ordre de grandeur des grains qui a été observé par diffraction des rayons X (Photo I) est la suivant: 4P < 2P < 1P < 3P

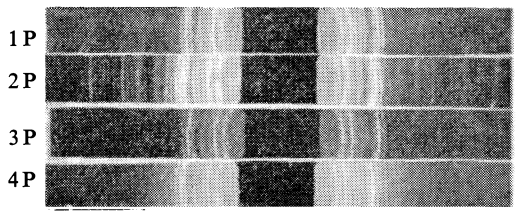


Photo 1. Diffraction aux rayons X des échantillons.

Essai au Développement Photographique.—Le développement du film positif a été fait à 20±0.5°C, soit tout de suite après la préparation, soit 3 jours après la préparation avec le révélateur suivant:

1-Phényl-3-pyrazolide	0.25 g.
Na_2SO_3	25 g.
Hydroquinone	2.5 g.
Na_2CO_3	10 g.
KBr	1 g.
q. s. p. f.	1000 ml.

Les solutions de 1-phényl-3-pyrazolidone et de KBr sont préparées séparément et s'ajoutent au moment de la préparation du révélateur. Les pH des révélateurs préparés avec 4 marques sont mesurés comme l'indique le tableau III dans les 2 cas mentionnés ci-dessus.

Les voiles et les densités maximum des films dans ces conditions de développement sont présentés dans le tableau IV et les courbes

TABLEAU III. pH DES RÉVÉLATEURS

Espèces d'échantillons	1P	2P	3P	4P
Tout de suite après la préparation	10.39	10.39	10.27	10.20
3 Jours après la préparation	10.15	10.20	10.15	10.05

TABLEAU IV. RÉSULTATS DU DÉVELOPPEMENT AVEC LES 4 MARQUES DE PHÉNIDONE

Espèces d'échantillons		Tout de suite après la préparation				3 Jours après la préparation		
		Sans KBr		Avec KBr		Avec KBr		
		5′	12′	5′	12′	5′	10′	15′
Voile	1P	0.09	0.11	0.06	0.10	0.04	0.04	0.04
	2P	0.16	0.29	0.04	0.12	0.04	0.04	0.04
	3P	0.09	0.34	0.08	0.10	0.06	0.04	0.06
	4P	0.08	0.28	0.02	0.10	0.06	0.05	0.08
Densité max.	1P	3.50	3.60	3.36	3.65	3.35	3.45	3.50
	2P	3.35	3.60	3.40	3.60	3.36	3.50	3.54
	3P	3.52	3.70	3.27	3.60	3.25	3.34	3.52
	4P	3.41	3.70	3.35	3.50	3.20	3.40	3.65

caractéristiques du développement avec les 4 marques sont données dans la Fig 3. Même avec le révélateur sans KBr, 1P ne donne pas le voile très fort. Dans ces expériences, on voit que la marque 2P donne le meilleur résultat, et elle est désormais employée pour les expériences principales.

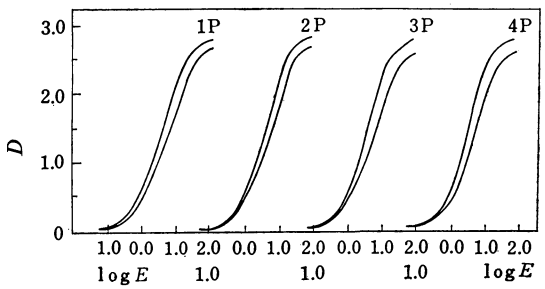


Fig. 3. Essai de développement effectué trois jours après la préparation de solution, 20±0.5°C.
Traits supérieurs, 15 min.
Traits inférieurs, 5 min.

Titrage Argentopotentiométrique.—Au moyen du titrage argentopotentiométrique[5] qui a été souvent utilisé dans le laboratoire des auteurs, une variation de potentiel est automatiquement enregistrée quand l'ion argent est ajouté à la solution de 1-phényl-3-pyrazolidone aux divers pH (Figs. 4 et 5). La vitesse de titrage a été réglée de telle sorte que le temps de versement de l'ion argent correspondant à une mole est de 5 min. A partir du pH 8, la première partie de la courbe de titrage prend un potentiel négatif, de même que le développement donne une grande densité. Le précipité qui se forme dans le mélange de 1-phényl-3-pyrazolidone et d'ion argent, dans le rapport d'un à trois, est filtré; puis le précipité et le filtrat sont extraits du solvant, en éliminant l'argent, et soumis à l'analyse infrarouge. Avec

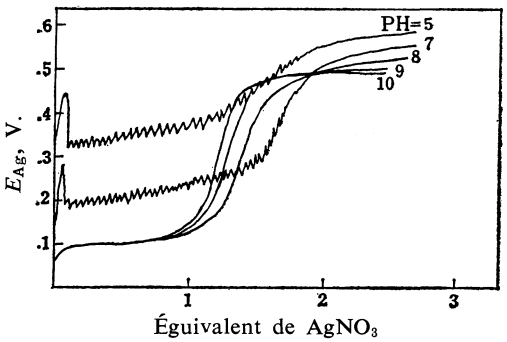


Fig. 4. Courbes de titrage potentiométrique de 1-phényl-3-pyrazolidone pour la solution de $AgNO_3$-potentiels d'électrode d'argent se réfèrent à une électrode normale d'hydrogène.

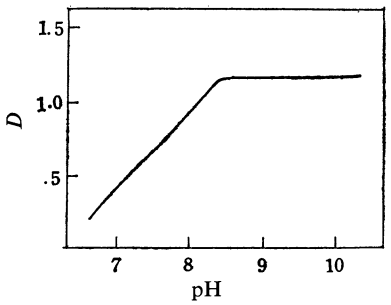


Fig. 5. Densité maximum en fonction du pH de la solution de révélateur.

les courbes de titrage on peut supposer que les produits qui se trouvent dans le mélange de 1-phényl-3-pyrazolidone et d'ion argent, dans le rapport de un à trois, sont exclusivement du type oxydé. (On verra plus tard que celui-ci est la forme oxydée de 1-phényl-3-pyrazolidone.) Quant au mélange de 1-phényl-3-pyrazolidone et d'ion argent dans le rapport 1:1, le précipité et le produit surnageant dans le liquide consistent en oxyde, et l'extrait du filtrat est un mélange de la forme oxydée et du produit original. Ce dernier est la même

5) S. Kikuchi et H. Sakaguchi, *J. Soc. Phot. Sci., Japon*, 12, No 4, 3 (1950).

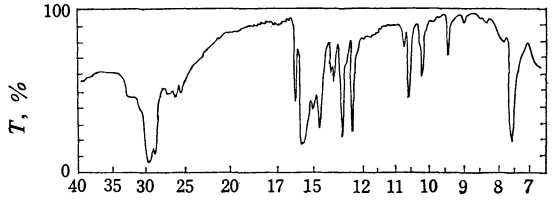


Fig. 6. Spectre d'absorption infrarouge d'un type oxydé de 1-phényl-3-pyrazolidone.

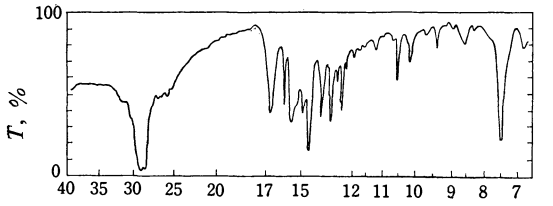


Fig. 7. Spectre d'absorption infrarouge d'un type mélangé.

substance que la 1-phényl-3-pyrazolidone faiblement oxydée par du nitrite de soude. Les produits du mélange dans le rapport 1 : 2 sont aussi examinés en fonction du pH. A partir du pH 7, le mélange est exclusivement la forme oxydée et aux pH 8 et 10, il est identique au produit extrait du filtrat du mélange dans le rapport 1 : 1, c'est-à-dire au mélange de la forme oxydée et du produit original. La Fig. 6 montre l'absorption infrarouge de l'échantillon dans le rapport 1 : 3, la Fig. 7, celle du mélange de l'échantillon avec la forme oxydée et la Fig. 1, celle du produit original.

Forme Oxydée de la 1-Phényl-3-pyrazolidone. —La 1-phényl-3-pyrazolidone et le produit fortement oxydé par l'oxyde de mercure sont soumis à l'analyse infrarouge avec KBr (Fig. 8). Le spectre infrarouge de la forme oxydée est de structure plus simple que celui de la 1-phényl-3-pyrazolidone. La disparition de la vibration de variation d'angle due à chaque CH_2 de structure $-CH_2-CH_2-$ (1230～1150 cm^{-1}), la disparition de la vibration d'allongement et de contraction de la liaison C–N à 1450 et 1365 cm^{-1}, celle de la vibration de variation d'angle de liaison N–H à 862 cm^{-1}, en sont les raisons. Dans la forme oxydée, on peut remarquer une absorption à 2850 cm^{-1} au lieu de 2970 cm^{-1} pour la 1-phényl-3-pyrazolidone et on peut penser que ce changement est dû à la transition de CH_2 de $-C-C-$ à CH de $-C=C-$. D'autre part, de nouvelles absorptions sont dues, vers 2750～2590 cm^{-1} à la vibration d'allongement et de contraction

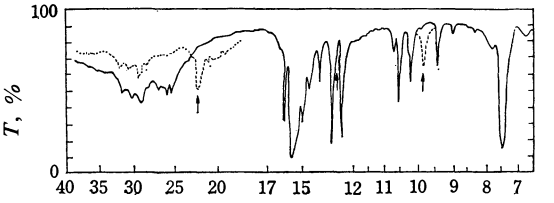


Fig. 8. Spectre d'absorption infrarouge de 1-phényl-3-hydroxypyrazole (tablette de KBr). Trait interrompu, celle deuterisée.

de OH avec forte combinaison d'hydrogène et vers 1570 cm^{-1}, à la vibration d'allongement et de contraction de C=N. La vibration d'allongement et de contraction de C–O à 1325 cm^{-1} et la vibration de variation d'angle à 1266 cm^{-1} apparaissent sensiblement. Les absorptions à 1064, 1025 et 950 cm^{-1} sont aussi les vibrations de variation d'angle qui se trouvent dans le plan ou hors du plan. On peut remarquer cependant que les absorptions à 1602, 1510, 1462 et 755 cm^{-1} dues au radical phényl se trouvent dans la 1-phényl-3-pyrazolidone et dans sa forme oxydée.

Par la suite, la 1-phényl-3-pyrazolidone et sa forme oxydée ont été deutérisées. La première a été obtenue par recristallisation avec la manière habituelle de deutériser. La forme oxydée, peu soluble dans l'eau lourde, ne peut être obtenue de la même façon. Elle a été maintenue dans un mélange de benzène et d'eau lourde à 100°C pendant une heure et desséchée sous vide pour obtenir la forme deutérisée. (L'eau lourde provenait de la Cie. Stuart Oxygen.) L'absorption infrarouge des deux formes deutérisées, a donné les résultats suivants : on a remarqué la vibration d'allongement et de contraction de liaison N–D à 2250 cm^{-1} les vibrations de variation d'angle de liaison N–D à 1137, 1073 cm^{-1} dans la 1-phényl-3-pyrazolidone tandis que dans la forme oxydée, les absorptions dues à la liaison N–D ne sont pas remarquées, mais les vibrations d'allongement et de variation d'angle

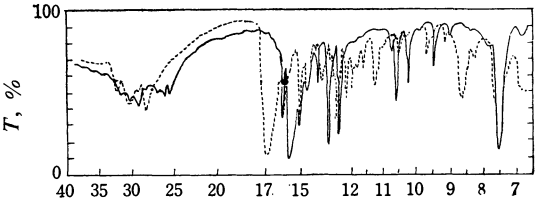


Fig. 9. Spectre d'absorption infrarouge des 1-phényl-3-hydroxypyrazols et 1-phényl-3-pyrazolidone (trait interrompu) (tablette de KBr).

OD[12] à 2260, 1290, 998 cm^{-1} sont observées. D'après les résultats ci-dessus la forme oxydée de la 1-phényl-3-pyrazolidone perd les liaisons C=O, CH_2, C–C, NH et acquiert à nouveau les liaisons C=N, C=C et OH (Fig. 9).

Ce produit oxydé a un point de fusion T_f= 154°C et une composition élémentaire de C= 62.27%, H=5.13%, N=17.14%, qui n'est pas très différente de celle de la 1-phényl-3-pyrazolidone. L'oxydation à l'air de la solution de 1-phényl-3-pyrazolidone au pH 9 et l'extraction par un solvant organique fournissent un produit qui donne la même absorption infrarouge. Le mélange obtenu par le titrage argentopotentiométrique est le simple mélange de 1-phényl-3-pyrazolidone et de sa forme oxydée et il donne la même absorption infrarouge que le produit extrait par le solvant organique de la solution de l'échantillon légèrement oxydé par du nitrite de soude.

Mesure par le Spectre Ultraviolet. — Les spectres ultraviolets de la 1-phényl-3-pyrazolidone et sa forme oxydée ont été mesurés aux pH 5, 7, 9 et 10.8. Les solutions de 1-phényl-3-pyrazolidone et des produits aux pH 5, 7 et 9 avaient un maximum d'absorption à 240 mμ. On a trouvé le point isosbestique aux pH 5~9, mais au pH 10.8, la forme de l'absorption est très différente (Fig. 10). On peut conclure que la forme oxydée a deux formes, une qui se trouve dans la solution aqueuse et à pH 5 a un maximum à 267 mμ et une autre qui se trouve dans la solution de pH supérieur à 7, a un maximum à 292 mμ (Fig. 11). Quand la solution de 1-phényl-3-pyrazolidone à pH 8 est oxydée lentement à l'air, l'absorption à 292 mμ n'aparait pas tout de suite, mais se déplace à 288 mμ. Si l'on ajoute à cette solution un excès d'eau oxygénée, une absorption apparait dès le commencement à 292 mμ (Fig. 12).

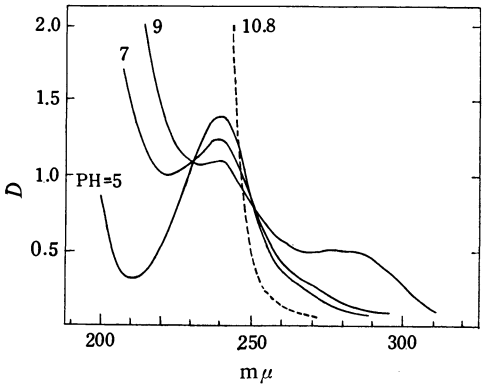


Fig. 10. Spectre d'absorption ultraviolette de 1-phényl-3-pyrazolidone en fonction de pH.

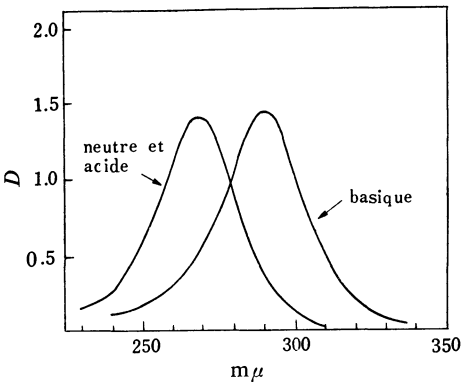


Fig. 11. Spectre d'absorption ultraviolette de 1-phényl-3-hydroxypyrazole en fonction de pH.

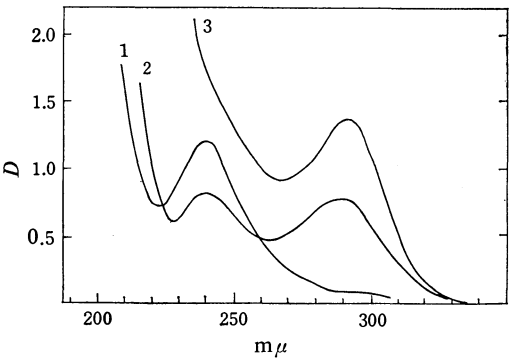
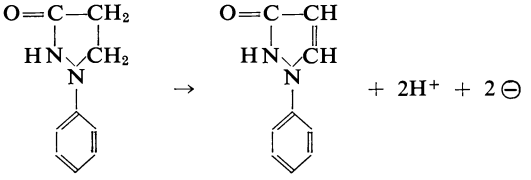


Fig. 12. Influence de l'oxydation à l'air de 1-phényl-3-pyrazolidone.

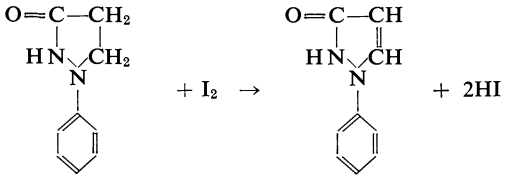
Conclusions

Le fait que γC=O de la 1-phényl-3-pyrazolidone se trouve du côté des nombres d'onde plus petits que le γC=D des substances ordinaires possédant la liaison C=O, fait supposer que ce produit forme une molécule d'association dimère[4]. Kurosaki[6] a montré par l'analyse infrarouge de la phase liquide en faisant varier la concentration et la température, que le produit était un dimère. Axford[7] et ses collaborateurs ont supposé que la forme oxydée de 1-phényl-3-pyrazolidone devait être la suivante :

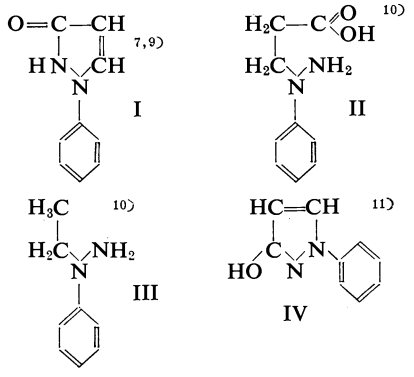


D'autre part, Levenson[8] a dit, d'après l'analyse iodométrique du révélateur usé que la forme oxydée serait la suivante :

6) K. Kurosaki, *J. Chim. Soc. Japon, Pure Chem. Rec. (Nippon Kagaku Zassi)*, **79**, 1339 (1958).
7) A. J. Axford, J. D. Kendall, *J. Phot. Sci.*, **2**, 1 (1954).
8) G. I. T. Levenson, *J. Phot. Sci.*, **7**, 38 (1959).



L'un et l'autre cas supposent que deux électrons sortent de la 1-phényl-3-pyrazolidone. Les présents auteurs pensent, d'après les résultats argentopotentiometriques que cette réaction ne peut se faire qu'en milieu acide ou neutre, mais pas en milieu alcalin. Aux pH 9, 10 et 11, la solution du mélange 1 : 2 ayant le potentiel noble ne peut se développer même s'il reste de la 1-phényl-3-pyrazolidone. Cela montre que du côté alcalin la combinaison entre la 1-phényl-3-pyrazolidone et sa forme oxydée ou entre deux molécules de 1-phényl-3-pyrazolidone peut se former et que ce fait retarde le développement lui-même. Jusqu'ici 4 formes ont été proposées pour la structure de la forme oxydée de la 1-phényl-3-pyrazolidone.



D'parès nos expériences où l'onde d'allongement C=O dans le spectre infrarouge disparait et où les valeurs des pourcentages de C et H sont assez différentes de celles trouvées dans l'analyse élémentaire, on peut dire que les formes I, II et III sont peu probables. Donc la forme IV est la plus probable. L'absorption à 2250 cm^{-1} de la forme deutérisée de la 1-phényl-3-pyrazolidone et à 2260, 1980~2160 cm^{-1} du produit deutérisé de la forme oxydée de la 1-phényl-3-pyrazolidone sont voisines, mais le nombre et la forme des ondes du produit deutérisé de la forme oxydée ressemblent plus à l'onde OD des phénols. La forme deutérisée de la 1-phényl-3-pyrazolidone a des ondes 1137 cm^{-1} et 1073 cm^{-1} de ND, mais ces ondes n'existent pas dans la forme deutérisée de la forme oxydée.

Les auteurs veulent conclure que la forme oxydée de la 1-phényl-3-pyrazolidone est la 1-phényl-3-hydroxypyrazole qui est peu soluble dans l'eau. On peut supposer d'après les résultats de l'absorption infrarouge basée sur la combinason de OH que cette forme oxydée a une forte liaison hydrogène[13,14].

Les auteurs sont spécialement reconnaissants à Messieurs Suzuki de Konishiroku, Iijima de Kawaguchi Chemical Co., et Shindo de Sankyo Pharmaceutical Co., pour leur amabilité d'avoir donné les réactifs qui ont été utilisés dans cette étude.

Institut des Sciences Industrielles
L'Université de Tokyo
Yayoi-cho, Chiba

9) N. Kunimine et S. Uetake, *Konishiroku Review*, **8**, No 2–3, 50 (1957).
10) S. Tojo, K. Kurosaki et M. Ozawa, *J. Soc. Sci. Phot. Japon*, **23**, No 3, 123 (1960).
11) G. F. van Veelen et H. Ruyeschaert, *Phot. Sci. Eng.*, **4**, No. 3, 129 (1960).
12) R. Meck et G. Rossmy, *Z. Elektrochem.*, **59**, No. 9, 866 (1955).
13) D. Heinert et A. E. Martell, *J. Am. Chem. Soc.*, **81**, 3933 (1959).
14) S. F. Manson, *J. Chem. Soc.*, **1957**, 4874.

Thermal Decomposition of Acetaldehyde in the Presence of Hydrogen Sulfide. I. Kinetics of the Reaction

By Naomi IMAI, Yasuo YOSHIDA and Osamu TOYAMA

(Received September 14, 1961)

Hydrogen sulfide was found by Fromherz[1] to exert a catalytic effect on the thermal decomposition of acetaldehyde. Roth and Rollefson[2] studied this catalyzed decomposition and presented an approximate rate equation, but the mechanism of the catalysis was left unexplained. Recently the present authors have investigated the hydrogen-atom abstraction reaction of hydrogen sulfide molecules with methyl radicals[3] and the photolysis of acetaldehyde in the presence of hydrogen sulfide[4].

1) H. Fromherz, *Z. physik. Chem.*, **B25**, 301 (1934).
2) W. L. Roth and G. K. Rollefson, *J. Am. Chem. Soc.*, **64**, 1707 (1942).
3) N. Imai and O. Toyama, This Bulletin, **33**, 652 (1960).
4) N. Imai and O. Toyama, ibid., **33**, 1120 (1960).

These studies have clarified the nature of various elementary reactions taking place in the systems of acetaldehyde and hydrogen sulfide. In this work, we have therefore undertaken to reinvestigate the pyrolysis of acetaldehyde in the presence of hydrogen sulfide in order to elucidate the catalytic effect of the latter. This paper reports on the kinetics of the reaction, and the following paper, Part II, on the effects of various chain-inhibitors on the reaction.

Experimental

Materials.—Acetaldehyde was prepared by distillation of paraldehyde, containing a small quantity of sulfuric acid, and was purified by bulb-to-bulb distillation. Hydrogen sulfide was prepared by dropping water on aluminum sulfide in an evacuated vessel, dried by passing it through a trap at −78°C, and purified by bulb-to-bulb distillation.

Apparatus.—The apparatus used in the present work was similar to that described previously[5]. Three cylindrical vessels were used: A, a quartz vessel of 118 cc., with a ratio of its surface area to its volume of $S/V=1.05\,cm^{-1}$; B, a glass vessel of 137 cc., $S/V=1.20\,cm^{-1}$; C, a glass vessel of 127 cc. packed with glass tubes, $S/V=15.9\,cm^{-1}$.

Procedure.—Required quantities of reactant gases were mixed at room temperature for about 30 min. prior to pyrolysis. They were then introduced into the reaction vessel, which had already been brought to the experimental temperature. In most runs, the change in total pressure with time was followed on a manometer. The products of the decomposition in some runs were analyzed quantitatively in the same way as has been described previously[3]. A Hitachi RMC remodeled mass spectrometer was used to analyze the products in several runs.

Results and Discussion

It has been established by many workers that the products of the thermal decomposition of acetaldehyde are almost exclusively equal quantities of methane and carbon monoxide[6]. Roth and Rollefson[2], analyzing the reaction products in the decomposition of acetaldehyde with added hydrogen sulfide, found that the only appreciable products were about equal amounts of methane and carbon monoxide and that hydrogen sulfide remained unconsumed throughout the course of the reaction. Table I shows the results of the analysis of the reaction products obtained in the present study, together with the pressure changes observed.

Table I. Products of decomposition

Temp. °C	Vessel	Initial press. mmHg		Time min.	Press. of products mmHg			Press. increase mmHg
		CH_3CHO	H_2S		CH_4	CO	C_2H_6	
370	B	69	53.5	10	5.1	5.0		4.9
		128	53.5	10	9.8	9.9		10.5
		154	53.5	10	10.6	10.3		10.8
		215	53.5	10	14.2	14.5		14.1
		247	53.5	10	16.0	16.4		16.6
400	C	69	30	5	6.7	6.7		6.4
		111	30	5	10.1	10.0		9.5
		154	30	5	12.8	12.3		12.2
		245	30	5	20.1	20.4		
		278	30	5	20.4	20.4		20.3
430	C	30	28.5	2	3.8	3.8		
		59	28.5	2	8.3	8.9		
		127	28.5	2	13.8	14.0		13.5
		208	28.5	2	20.4	21.1		
		285	28.5	2	24.6	25.8		23.0
460	B	105	5.7	1.67	0.86	0.87		
		135	5.7	1.67	0.92	0.92		
		183	5.7	1.67	1.07	1.10		
469[a]	A	135	10	1	22.8	25.2	0.007	
		180	10	1	29.1	31.4	0.017	
		183	40	90	173	182	4.7	
		314	44	4.5	200	247	0.78	

a Obtained by mass spectrometric analysis.

5) N. Imai and O. Toyama, ibid., **33**, 1408 (1960).
6) C. N. Hinshelwood and W. K. Hutchson, *Proc. Roy. Soc.*, **A111**, 380 (1926); C. J. M. Fletcher and C. N. Hinshelwood, ibid., **A141**, 41 (1933); C. A. Winkler and C. N. Hinshelwood, ibid., **A149**, 355 (1935); R. V. Seddon and M. W. Travers, ibid:, **A156**, 234 (1936); E. Leifer and H. C. Urey, *J. Am. Chem. Soc.*, **64**, 994 (1942); Ref. 5.

It is seen that the total pressure increase is equal to the pressure of the methane formed as well as to that of carbon monoxide; this is in agreement with the analytical results obtained above by Roth and Rollefson. Mass spectrometric analysis has shown that hydrogen and ethane are also formed in the decomposition, but their amounts are too small to disturb the above relation significantly. These facts indicate that the total pressure increase corresponds to the decrease in acetaldehyde pressure due to decomposition. Accordingly, the initial rate of decomposition is obtained from the initial slope of a total pressure-time curve.

It is generally agreed that the main features of the thermal decomposition of acetaldehyde can be explained by the following mechanism[7]:

$$CH_3CHO = CH_3 + CHO \quad (1)$$

$$CHO = CO + H \quad (2)$$

$$H + CH_3CHO = H_2 + CH_3CO \quad (3)$$

$$CH_3CO = CH_3 + CO \quad (4)$$

$$CH_3 + CH_3CHO = CH_4 + CH_3CO \quad (5)$$

$$CH_3 + CH_3 = C_2H_6 \quad (6)$$

The steady state equations derived from this scheme yield the rate equation

$$-\mathrm{d}[CH_3CHO]/\mathrm{d}t = k_1^{1/2}k_5k_6^{-1/2}[CH_3CHO]^{3/2} \quad (I)$$

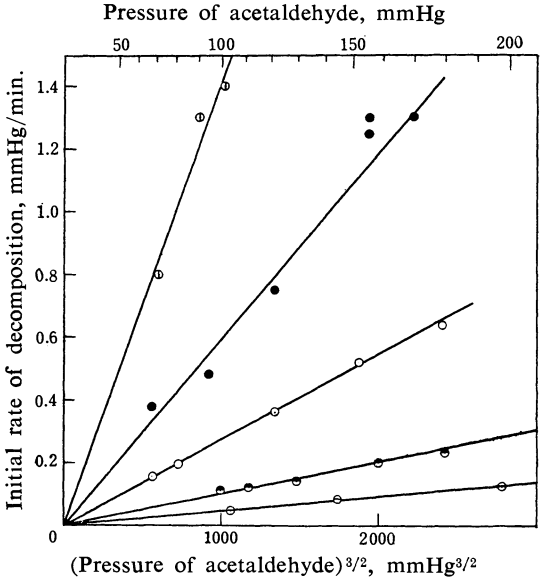


Fig. 1. Rate of decomposition of acetaldehyde alone.
⊖, 380; ◓, 400; ○, 420; ●, 440; ⦶, 460°C

7) F. O. Rice and K. F. Herzfeld, *J. Am. Chem. Soc.*, **56**, 289 (1934); E. W. R. Steacie, "Atomic and Free Radical Reaction", 2nd Ed., Reinhold Publ. Corp., New York (1954), p. 266.

TABLE II. VALUES OF $k_1^{1/2}k_5k_6^{-1/2}$

Temp. °C	$k_1^{1/2}k_5k_6^{-1/2}$ $mol^{-1/2}\,ml^{-1/2}\,sec^{-1}$
380	0.0048
400	0.0105
420	0.030
440	0.067
460	0.18

which is in general agreement with experimental results obtained by various workers. Also in this work, the rate of decomposition was found to be proportional to the 3/2 power of the pressure of acetaldehyde, as is seen in Fig. 1. From the slope of the straight line in the figure, the value of $k_1^{1/2}k_5k_6^{-1/2}$ at each temperature was obtained and listed in Table II.

In the presence of hydrogen sulfide, it was found that the rate of decomposition increases linearly with the pressure of hydrogen sulfide, as is seen in Fig. 2. Although the intercepts of the straight lines on the ordinate are located very close to the point of origin, they are in agreement with the corresponding values in Fig. 1, indicating the great catalytic effect of

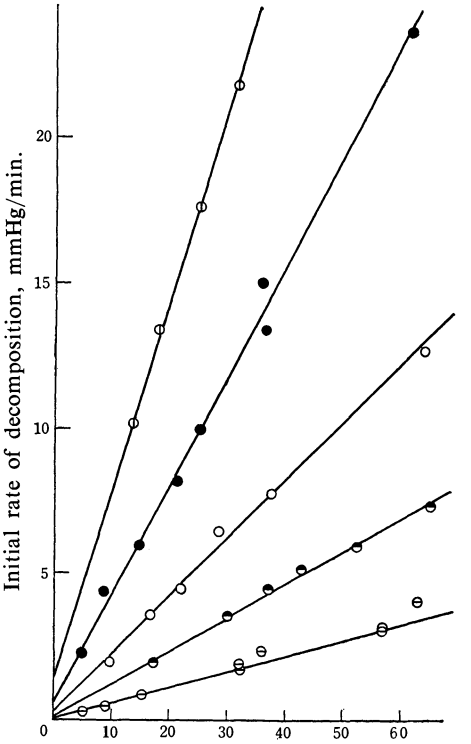


Fig. 2. Dependence of the rate of decomposition of acetaldehyde on the pressure of hydrogen sulfide.
CH_3CHO, 100 mmHg
⊖, 380; ◓, 400; ○, 420; ●, 440; ⦶, 460°C

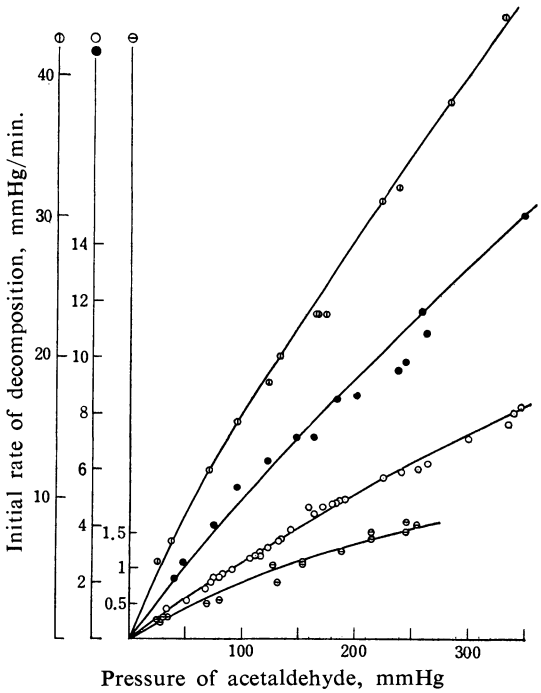


Fig. 3. Dependence of the rate of decomposition of acetaldehyde in the presence of hydrogen sulfide on the pressure of acetaldehyde.
⊖ Series 23, H_2S 28.3 mmHg, 370°C
○ Series 14, H_2S 40 mmHg, 406°C
● Series 7, H_2S 20 mmHg, 431°C
⦶ Series 8, H_2S 20 mmHg, 469°C

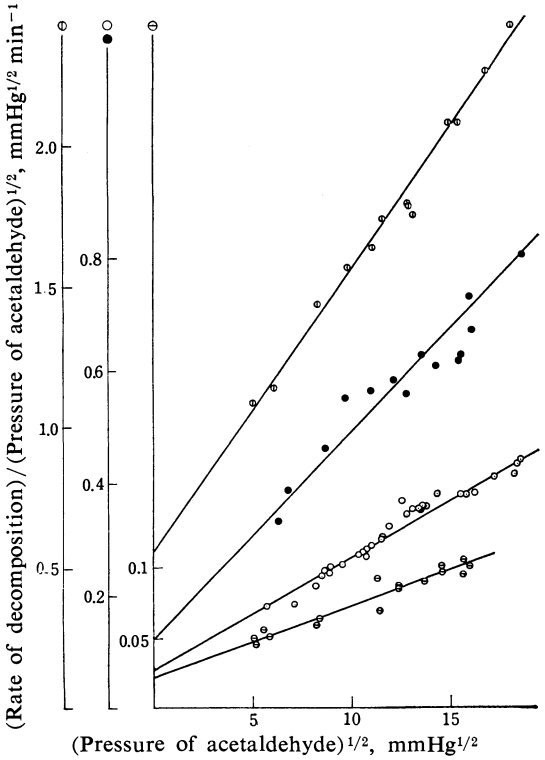


Fig. 4. Plots for Eq. IV.
⊖ Series 23, H_2S 28.3 mmHg, 370°C
○ Series 14, H_2S 40 mmHg, 406°C
● Series 7, H_2S 20 mmHg, 431°C
⦶ Series 8, H_2S 20 mmHg, 469°C

hydrogen sulfide. Several series of runs, where the pressure of acetaldehyde was varied while the pressure of hydrogen sulfide was kept constant, are shown in Fig. 3. As shown below, the results represented by Figs. 2 and 3 conform to the rate equation[8]

$$-\mathrm{d}[CH_3CHO]/\mathrm{d}t = k_0[CH_3CHO]^{3/2} + k[H_2S][CH_3CHO] + k'[H_2S][CH_3CHO]^{1/2} \quad (II)$$

The first term on the right-hand side of the equation, representing the non-catalyzed decomposition, is in most cases much smaller than the other terms and may be neglected. Thus, the rate may be written as

$$-\mathrm{d}[CH_3CHO]/\mathrm{d}t = k[H_2S][CH_3CHO] + k'[H_2S][CH_3CHO]^{1/2} \quad (III)$$

Dividing both sides of Eq. III by $[CH_3CHO]^{1/2}$,

$$(-\mathrm{d}[CH_3CHO]/\mathrm{d}t)/[CH_3CHO]^{1/2} = k[H_2S][CH_3CHO]^{1/2} + k'[H_2S] \quad (IV)$$

Figure 4 shows that Eq. IV and, accordingly, Eq. III fit the results given in Fig. 3. The slope and intercept of the straight line in the figure give the constants k and k'.

In Table III are listed the values of the constants thus determined by various series of experiments in this work. It is seen that the fluctuation in these values is fairly large, apart from the effect of the reaction vessel. The values of the constants were found to be approximately reproducible when the measurements were carried out successively with the same samples of the gases and with the same vessel, whereas a worse reproducibility was obtained with different samples of the gases even in the same vessel. The results obtained by Roth and Rollefson show an even greater fluctuation in the rate. Presumably, minute quantities of an impurity yet unidentified caused these phenomena[9]. The effect of various reaction vessels, with different ratios of surface area to volume is not clearly seen in Table III,

8) Roth and Rollefson proposed the following rate equation
$$-\mathrm{d}[CH_3CHO]/\mathrm{d}t = k_a[H_2S][CH_3CHO] + k_b[H_2S][CH_3CHO]/(1+k_c[CH_3CHO])$$
Their experimental data, however, show too great a fluctuation to justify the rate equation.

9) According to Morris[10], the use of hydroquinone for the purification of acetaldehyde reduces the rate of decomposition of the latter. In this work, however, hydroquinone was not used.

10) J. C. Morris, *J. Am. Chem. Soc.*, 66, 584 (1944).

TABLE III. VALUES OF k AND k'

Temp °C	Series No.	Initial press. of H_2S mmHg	Reaction vessel	k mol^{-1} ml. sec^{-1}	k' $mol^{-1/2}$ $ml^{1/2}$ sec^{-1}
340	18	26.8	C	33	0.043
	22	26.8	B	49	0.046
370	17	28.3	C	120	0.063
	23	28.3	B	130	0.071
380	29	60	B	200	0.12
400	16	30	C	250	0.29
	24	30	B	350	0.27
	27[a]	5.7	B		0.30
406	10	40	A	290	0.38
	14	40	A	360	0.19
430	15	32.5	C	870	0.90
	21	32.5	B	660	0.86
	26[a]	5.7	B		1.00
431	1	20	A	1200	1.8
	4	20	A	1500	1.1
	7	20	A	1300	0.7
	11	40	A	1000	0.7
460	19	35.5	C	2100	3.0
	20	35.5	B	1300	2.8
	25[a]	5.7	B		2.9
469	2	20	A	3100	5.7
	5	20	A	4800	7.5
	8	20	A	3900	3.2
	12	40	A	2300	3.6
494	3	20	A	6600	9.5
	6	20	A	8000	14.6
	9	20	A	5100	11.0
	13	40	A	2600	11.0
	28	20	B	9500	10.2

a Obtained from Fig. 5.

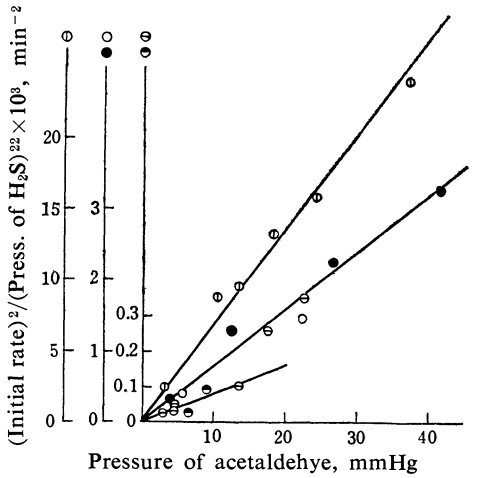


Fig. 5. Plots for Eq. V.
- ⊖ H_2S 5.7 mmHg, 400°C
- ◓ H_2S 11.4 mmHg, 400°C
- ● H_2S 5.7 mmHg, 430°C
- ○ H_2S 11.4 mmHg, 430°C
- ⊕ H_2S 5.7 mmHg, 460°C

being masked by the fluctuation mentioned above. The effect is, however, not greater than the fluctuation, indicating that the reaction is essentially homogeneous, as has been described by Roth and Rollefson.

In Table III are included the values of the constant k' determined in a somewhat different way: when the pressure of hydrogen sulfide is low, the first term of Eq. III may be negligibly small compared to the second, so that

$$(-d[CH_3CHO]/dt)^2/[H_2S]^2 = k'^2[CH_3CHO] \quad (V)$$

Figure 5 shows that Eq. V is applicable to the results of experiments with a low pressure of hydrogen sulfide. As seen in Table III, the values of the constant k' obtained from the slope of the straight line in Fig. 5[11] are in general agreement with those obtained by the use of Eq. IV.

11) In these experiments the rate of decomposition was obtained from an analysis of the products, carbon monoxide and methane, since the pressure could not be followed accurately on a mercury manometer.

As described in Part II, the addition of a sufficient quantity of propylene or isobutylene, both of which are known as chain-inhibitors, completely eliminates the second term of Eq. III, leaving the first term unaffected. This indicates that the decomposition represented by the second term of Eq. III involves a radical-chain mechanism, while the first term probably represents a molecular decomposition catalyzed by hydrogen sulfide.

The radical-chain decomposition represented by the second term of Eq. III is explained on the basis of the previously studied photolysis of acetaldehyde in the presence of hydrogen sulfide[4]. The kinetics of the photolysis showed that, in the presence of not too much hydrogen sulfide, the decomposition takes place through a chain mechanism which involves, in addition to reactions 1—6, the following reactions[12]:

$$CH_3 + H_2S = CH_4 + HS \quad (7)$$

$$HS + CH_3CHO = H_2S + CH_3CO \quad (8)$$

The reaction sequence 1—8, when applied to the thermal decomposition in the presence of hydrogen sulfide, leads to the rate equation

$$(-d[CH_3CHO]/dt)_{chain} = k_1^{1/2}k_5k_6^{-1/2}[CH_3CHO]^{3/2} + k_1^{1/2}k_7k_6^{-1/2}[H_2S][CH_3CHO]^{1/2} \quad (VI)$$

The first term of the right-hand side of the equation corresponds to the first term of Eq. II, which was neglected in Eq. III, and the second term of Eq. VI explains the second term of Eq. III. It follows, therefore, that

$$k' = k_1^{1/2}k_7k_6^{-1/2}$$

The Arrhenius plots of $k_1^{1/2}k_5k_6^{-1/2}$ and $k_1^{1/2}k_7k_6^{-1/2}$ obtained from the results given in Tables II and III are shown in Fig. 6. These yield

$$k_1^{1/2}k_5k_6^{-1/2} = 10^{12.1\pm0.2}\exp(-43300\pm1100/RT) \ mol^{-1/2}\,ml^{1/2}\,sec^{-1} \quad (VII)$$

$$k_1^{1/2}k_7k_6^{-1/2} = 10^{12.8\pm0.2}\exp(-41100\pm1200/RT) \ mol^{-1/2}\,ml^{1/2}\,sec^{-1} \quad (VIII)$$

If E_1(the activation energy of reaction 1) $=75.0$[13], $E_5=6.8$[14] and $E_6=0$ kcal. mol^{-1}, $E_{VII} = 1/2(E_1-E_6)+E_5 = 44.3$ kcal. mol^{-1}. The value of E_{VII} compares satisfactorily with the 43.3 kcal. mol^{-1} found above. Similarly, when E_7 is taken as 2.6 kcal. mol^{-1} [15], $E_{VIII} = 1/2(E_1 - E_6) + E_7 = 40.1$ kcal. mol^{-1}, which is again in agreement with the above experimental value of 41.1 kcal. mol^{-1}.

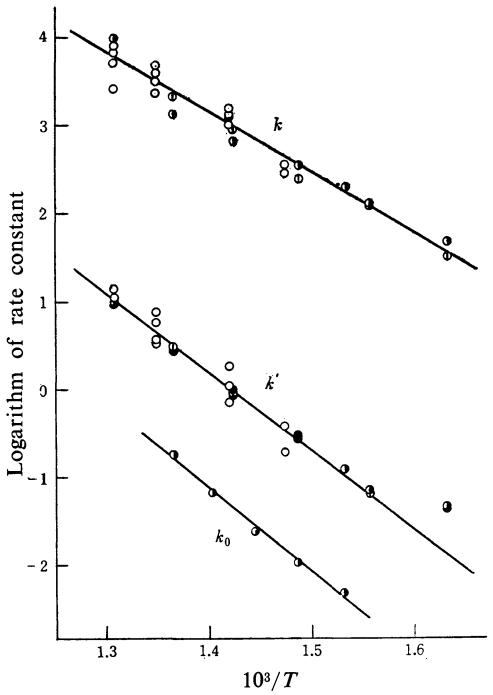


Fig. 6. Arrhenius plots of k_0, k' and k.
○ Vessel A; ◑ Vessel B; ⓘ Vessel C;
● Obtained from Fig. 5.

As has already been described, small quantities of hydrogen and ethane are found among the products of decomposition. Their formation in early stages of the decomposition may be explained by reactions 3 and 6. Their small quantities indicate that the chain length is fairly large.

As has also already been described, the first term of Eq. III probably represents the rate of homogeneous molecular decomposition catalyzed by hydrogen sulfide. Stoichiometrically, the reaction is written as

$$CH_3CHO + H_2S = CH_4 + CO + H_2S \quad (9)$$

since the products obtained in the decomposition are almost exclusively equal amounts of methane and carbon monoxide. The Arrhenius plot of constant k, given in Fig. 6, yields

$$k = 10^{12.7\pm1.0}\exp(-31400\pm3100/RT) \quad (IX)$$

Although this appears to be a reasonable expression for a simple bimolecular process in the gas phase, a detailed mechanism for the catalysis cannot be determined at present from the kinetics alone. It has been known that

12) In the photolysis, the primary step is $CH_3CHO + h\nu = CH_3 + CHO$

13) F. O. Rice and W. R. Johnston, *J. Am. Chem. Soc.*, 56, 214 (1934).

14) P. Ausloos and E. W. R. Steacie, *Can. J. Chem.*, 33, 31 (1655).

15) N. Imai and O. Toyama, This Bulletin, 33, 652 (1960).

the decomposition of acetaldehyde to methane and carbon monoxide is catalyzed by hydrogen chloride and hydrogen bromide in the gas phase[16]. The mechanism of the decomposition is, however, not yet clear in these cases. Recently, Stimson et al.[17] have shown that the hydrogen halides-catalyzed decomposition of alcohols into water and olefins in the gas phase is largely homogeneous and molecular in character in the temperature range 300 to 500°C. Although they present various possible mechanisms for the catalysis, no definite conclusion has yet been obtained. Information from other sources seems necessary to elucidate the mechanism of these reactions.

Summary

The hydrogen sulfide-catalyzed thermal decomposition of acetaldehyde has been investigated over the temperature range 340 to 494°C. The initial rates of decomposition approximately fit the rate equation

$$-\mathrm{d}[CH_3CHO]/\mathrm{d}t = k[H_2S][CH_3CHO] + k'[H_2S][CH_3CHO]^{1/2}$$

where

$$k = 10^{12.7\pm1.0}\exp(-31400\pm3100/RT) \quad \mathrm{mol^{-1}\,ml.\,sec^{-1}}$$

and

$$k' = 10^{12.8\pm0.27}\exp(-41100\pm1200/RT) \quad \mathrm{mol^{-1/2}\,ml^{1/2}\,sec^{-1}}$$

A comparison of the above results with those of the decomposition inhibited by propylene and isobutylene, which will be reported on in the following paper, suggests that the first term of the rate equation probably represents a molecular decomposition catalyzed by hydrogen sulfide, while the second represents a radical-chain decomposition. Combining the chain mechanism generally accepted for the pyrolysis of acetaldehyde alone with the reactions $CH_3+H_2S=CH_4+HS$ and $HS+CH_3CHO=H_2S+CH_3CO$, both of which have been shown to be important in the photolysis of acetaldehyde with added hydrogen sulfide, a rate equation is derived by which the second term of the experimental rate equation and the temperature depedennce of its rate constant k' can be explained.

Department of Applied Chemistry
College of Engineering
University of Osaka Prefecture
Sakai, Osaka

16) R. P. Bell and R. Le G. Burnett, *Trans. Faraday Soc.*, **35**, 474 (1939); K. E. Howlett and D. H. R. Barton, ibid., **45**, 735 (1949).
17) A. Maccoll and V. R. Stimson, *J. Chem. Soc.*, **1960**, 2836; K. G. Lewis and V. R. Stimson, ibid., **1960**, 3087; R. A. Ross and V. R. Stimson, ibid., **1960**, 3090; V. R. Stimson and E. J. Watson, ibid., **1960**, 3920; V. R. Stimson and E. J. Watson, ibid., **1961**, 1392.

Thermal Decomposition of Acetaldehyde in the Presence of Hydrogen Sulfide. II. Effects of Chain-inhibitors

By Naomi IMAI, Yasuo YOSHIDA and Osamu TOYAMA

(Received September 14, 1961)

In the foregoing paper[1], the present authors reported on the kinetics of the thermal decomposition of acetaldehyde in the presence of hydrogen sulfide and suggested that a part of the reaction involves a radical-chain mechanism, while the remaining part is probably molecular in character. Such an interpretation is based upon experiments in which the effects of various chain-inhibitors on the rate of decomposition were investigated. This paper reports on the results of these experiments. Propylene, isobutylene and nitric oxide were used as inhibitors.

Experimental

The preparation and purification of acetaldehyde and hydrogen sulfide were described in the foregoing paper[1]. Propylene was prepared by dehydration of isopropyl alcohol by pyrophosphoric acid supported on granular pumice at 250°C. Isobutylene was prepared from *tert*-butyl alcohol by a similar method. Nitric oxide was produced by the reaction of a concentrated sodium nitrite solution with a hydrochloric acid solution of ferrous chloride, decarbonated by a potassium hydroxide solution and dried by concentrated sulfuric acid and phosphorus

1) N. Imai, Y. Yoshida and O. Toyama, This Bulletin, 35, 752 (1962).

pentoxide. All of these gases were prepared in evacuated vessels and were purified by repeated bulb-to-bulb distillations. The apparatus and procedure were the same as those described in the foregoing paper[1].

Results and Discussion

As has been described in the foregoing paper, when acetaldehyde is decomposed thermally in the presence of hydrogen sulfide, the amount of acetaldehyde consumed is directly indicated by the increase in the total pressure. According to Smith and Hinshelwood[2], the pressure of acetaldehyde thermally decomposed in the presence of propylene also corresponds to the total pressure increase. It was confirmed in this work that such a correspondence between the amount of acetaldehyde decomposed and the total pressure change is retained even in the presence of both hydrogen sulfide and an inhibitor. Accordingly, the rate of decomposition was mostly calculated from the increase in the total pressure, as was the case in the absence of inhibitors.

Figure 1 shows the dependence of the rate of decomposition on the pressure of inhibitors, propylene and isobutylene, at constant pressures of acetaldehyde and hydrogen sulfide. It is seen that the rate decreases with the increasing pressure of the inhibitor until it attains a constant value, and that the rate of the fully inhibited reaction is almost the same for both inhibitors under otherwise constant conditions. Figure 1 shows, moreover, that the rate of fully inhibited reaction may be represented as

$$-\mathrm{d}[CH_3CHO]/\mathrm{d}t = k_1[H_2S][CH_3CHO] \quad (I)$$

since the rate is proportional to the pressure of both hydrogen sulfide and acetaldehyde. Further evidence for Eq. I is given by Figs. 2 and 3, in which the rates of decomposition fully inhibited by propylene and by isobutylene are plotted.

It has been shown in the previous paper[1] that the rate of decomposition of acetaldehyde in the presence of hydrogen sulfide, but in the absence of any inhibitor, can be approximately represented by

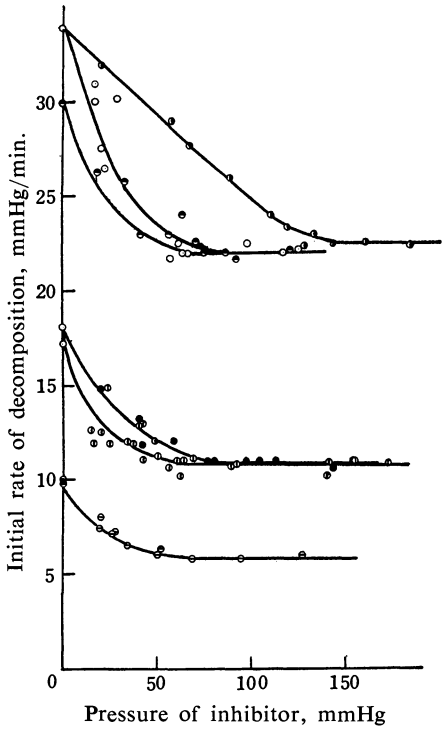


Fig. 1. Inhibition of acetaldehyde decomposition in the presence of hydrogen sulfide by propylene and isobutylene at 469°C.
Propylene: ● CH_3CHO 90 mmHg, H_2S 20 mmHg; ◑ CH_3CHO 50 mmHg, H_2S 40 mmHg; Isobutylene, ⊖ CH_3CHO 90 mmHg, H_2S 10 mmHg; ⦶ CH_3CHO 90 mmHg, H_2S 20 mmHg; ○ CH_3CHO 90 mmHg, H_2S 40 mmHg; ◓ CH_3CHO 180 mmHg, H_2S 20 mmHg

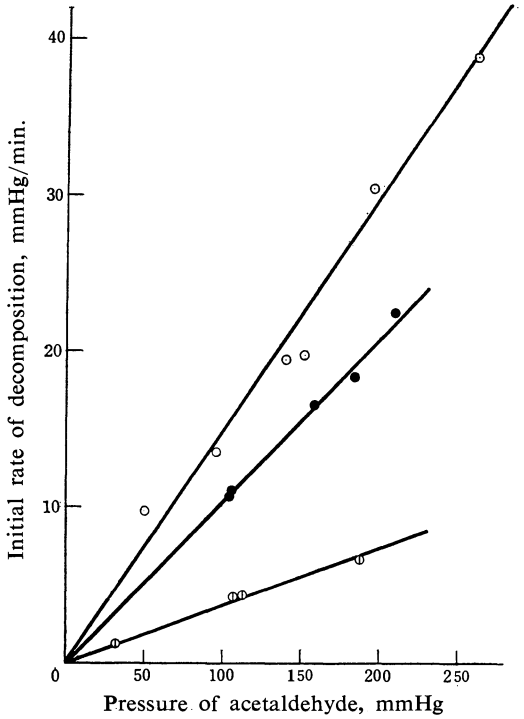


Fig. 2. Dependence on the pressure of acetaldehyde of the rate of isobutylene inhibited decomposition of acetaldehyde in the presence of hydrogen sulfide.
H_2S 20 mmHg, ⦶ 431°C; ● 469°C; ○ 494°C

2) J. R. E. Smith and C. N. Hinshelweed, *Proc. Roy. Soc.*, **A180**, 237 (1942).

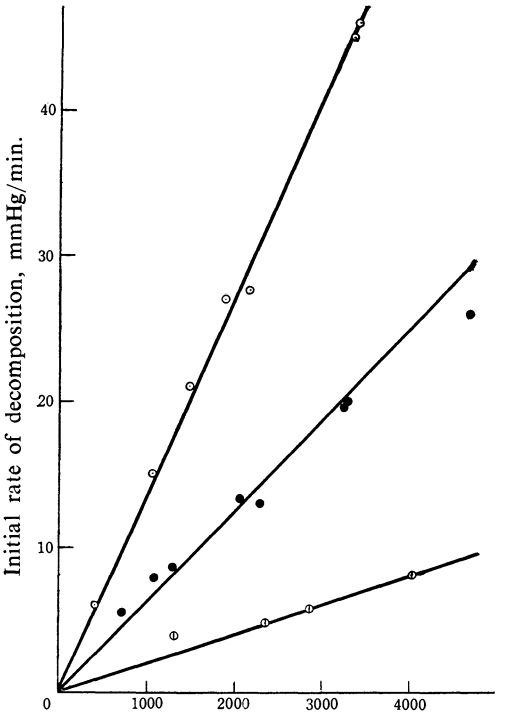


Fig. 3 Dependence of the rate of propylene-inhibited decomposition of acetaldehyde in the presence of hydrogen sulfide on the product of pressures of acetaldehyde and hydrogen sulfide.
ⓘ 431°C; ● 469°C; ○ 494°C

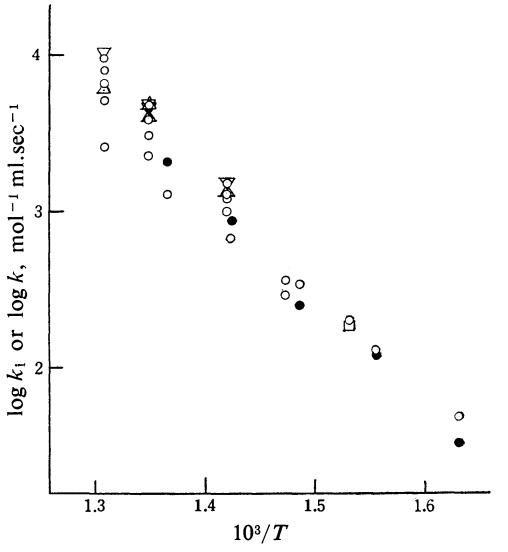


Fig. 4. Arrhenius plot of k_1 and k.
▽ Propylene; △ Isobutylene; □ Nitric oxide; ○ k for the unpacked vessel; ● k for the packed vessel.

$$-d[CH_3CHO]/dt = k[H_2S][CH_3CHO] + k'[H_2S][CH_3CHO]^{1/2} \quad (II)$$

A comparison between Eqs. I and II shows that the former equation is of the same form as the first term of the latter. It is revealed on further examination that they are in fact identical. In Table I are listed the values of constant k_1 in Eq. I obtained from the results given in Figs. 1—3; as seen in Fig. 4, these values are in agreement, within the limit of fluctuation, with those for k given in the preceding paper[1]. It may therefore be concluded that the addition of propylene or of isobutylene, in a sufficient quantity to bring about the maximum inhibition, eliminates the second term of Eq. II, leaving the first unaltered. Although there is much controversy[3] concerning the interpretation that the residual rate of pyrolysis of paraffins maximally inhibited by an inhibitor such as nitric oxide or propylene represents that of a non-chain, molecular decomposition, the results here obtained suggest that the second term of Eq. II represents a radical-chain decomposition, whereas the first term probably represents a hydrogen sulfide-catalyzed molecular decomposition which is not affected by chain-inhibitors.

TABLE I. VALUES OF k_1

Temp. °C	Inhibitor	Method	k_1 mol^{-1} ml.sec^{-1}
380	Nitric oxide	Fig. 5	186
431	Propylene	Fig. 3	1530
	Isobutylene	Fig. 2	1320
469	Propylene	Fig. 1	4760
	Isobutylene	Fig. 1	4800
	Propylene	Fig. 3	4930
	Isobutylene	Fig. 2	4010
494	Propylene	Fig. 3	10700
	Isobutylene	Fig. 2	6000

Additional support for such an interpretation is provided by Fig. 5. The thermal decomposition of dimethyl ether in the presence of hydrogen sulfide, as was found in its absence, is explained entirely by a radical-chain mechanism[4]. When inhibited by nitric oxide, the rate of decomposition falls off to an almost negligible value, as is seen in the figure. The situation with acetaldehyde, on the other hand, is quite different. Here the residual rate of decomposition maximally inhibited by nitric oxide is still about half as large as that when uninhibited, and it yields a value of constant

3) A. Kuppermann and J. G. Larson, *J. Chem. Phys.*, **33**, 1264 (1960); B. W. Wojciechowski and K. J. Laidler, *Can. J. Chem.*, **38**, 1027 (1960); K. J. Laidler and B. W. Wojciechowski, *Proc. Roy. Soc.*, **A259**, 257 (1960); **A260**, 103 (1961).
4) N. Imai and O. Toyama, This Bulletin, **34**, 328 (1961).

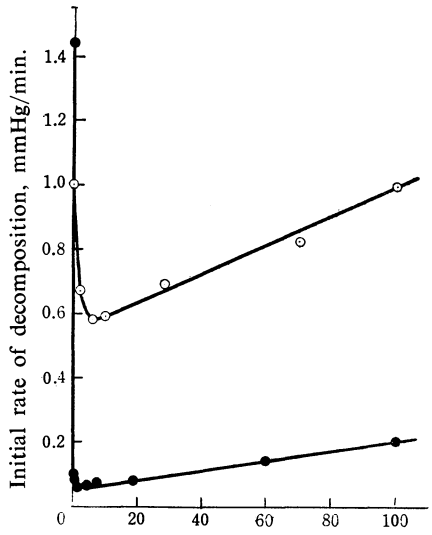


Fig. 5. Inhibition of decomposition of acetaldehyde and dimethyl ether in the presence of hydrogen sulfide by nitric oxide.
○ CH_3CHO 100 mmHg, H_2S 20 mmHg, 380°C; ● CH_3OCH_3 100 mmHg, H_2S 21 mmHg, 440°C

k_1 which is, again, in agreement with that of k as shown in Fig. 4[5].

As is seen in Fig. 5, the rate of decomposition of acetaldehyde as well as of dimethyl ether increases, after passing through a minimum, in proportion to the pressure of nitric oxide added. In view of the complete inhibition of the chain decomposition, as inferred above, these results suggest that nitric oxide catalyzes the molecular decomposition of these compounds[6]. For acetaldehyde in the absence of hydrogen sulfide, a similar behavior of nitric oxide has already been reported by Smith and Hinshelwood[2]. For paraffins, inhibitors such as propylene and isobutylene behave similarly[7]. In the latter case, however, there is serious doubt that the residual decomposition after being maximally inhibited is molecular in character[3].

Jack et al.[7] reported the relative efficiencies of propylene, isobutylene and nitric oxide as inhibitors to be 1 : 1.6 : 11 in the thermal decomposition of *n*-pentane at 560°C. Hinshelwood et al. have shown that nitric oxide is 5 to 100 times as effective as propylene for the inhibition of the decomposition of various organic compounds[2,8]. Figures 1 and 5 show that the results obtained in this work are similar. Rate constants are reported to be $10^{10.8}\exp(-7700/\boldsymbol{RT})$[9], $10^{10.9}\exp(-7300/\boldsymbol{RT})$[9] and $10^{11.1}\,\mathrm{mol}^{-1}\,\mathrm{ml.\,sec}^{-1}$[10] for the reactions between methyl radical and propylene, isobutylene and nitric oxide respectively. Other values of 6.4 and 4.1 kcal. mol^{-1} are reported for the activation energies of the former two reactions respectively[11]. These values are at least qualitatively in agreement with the efficiencies of the three inhibitors.

Summary

The effect of propylene, isobutylene and nitric oxide as inhibitors on the thermal decomposition of acetaldehyde in the presence of hydrogen sulfide has been investigated over the temperature range of 380 to 494°C. Of the three inhibitors, which are all effective in reducing the rate of decomposition, isobutylene is slightly more efficient than propylene, and nitric oxide is far more efficient than the other two. With propylene and isobutylene, the rate of decomposition is reduced with the increasing amount of the inhibitor until a constant rate is reached, while with nitric oxide the rate passes through a minimum value and then increases again in proportion to the pressure of the inhibitor. The residual rate of the maximally inhibited decomposition is almost the same for the three inhibitors and is represented by $-\mathrm{d}[CH_3CHO]/\mathrm{d}t = k_1[H_2S]\,[CH_3\cdot CHO]$. A comparison of the above results with those of the decomposition in the absence of an inhibitor suggests that the residual decomposition remaining after being fully inhibited is a molecular process catalyzed by hydrogen sulfide.

Department of Applied Chemistry
College of Engineering
University of Osaka Prefecture
Sakai, Osaka

5) The value of k_1 in this case was obtained by extrapolation of the linear plot following the minimum in Fig. 5.
6) A further study of the catalytic effect exerted by nitric oxide on the residual decomposition of dimethyl ether after being maximally inhibited is now in progress in our laboratory.
7) J. Jack, F. J. Stubbs and C. N. Hinshelwood, *Proc. Roy. Soc.*, **A224**, 283 (1954).
8) J. R. E. Smith and C. N. Hinshelwood, ibid., **A183**, 33 (1944); F. J. Stubbs and C. N. Hinshelwood, ibid., **A200**, 458 (1950).
9) A. F. Trotman-Dickenson and E. W. R. Steacie, *J. Chem. Phys.*, **19**, 169 (1951).
10) W. A. Bryce and K. U. Ingold, ibid., **23**, 1968 (1955).
11) A. D. Stepukhovich and E. S. Shver, *Zhur. Fiz. Khim.*, **27**, 1013 (1953).

Oxidation of Ferrous Ions in Aqueous Solutions by Cobalt-60 Gamma Rays. III. The Effect of Cupric Ion in Air-free Acidic Solutions

By Hiroshi HOTTA, Shin-ichi OHNO and Nobutake SUZUKI

(Received September 15, 1961)

The effect of cupric ion on the radiolysis of an air-free ferrous acidic solution is usually assumed to be due to the reaction[1]

$$Cu^{2+} + H = Cu^{+} + H^{+} \qquad (10)$$

competing with the reaction

$$Fe^{2+} + H^{+} + H = Fe^{3+} + H_2 \qquad (3)$$

Therefore, the oxidized ferric ion is re-reduced by the reaction

$$Fe^{3+} + Cu^{+} = F^{2+} + Cu^{2+} \qquad (11)$$

On the other hand, it was established in Part II[2] that the reaction

$$Fe^{3+} + H = Fe^{2+} + H^{+} \qquad (4)$$

can not be ignored in some cases. The oxidation rate of the ferrous ion in a mixture of ferrous and ferric ions was evaluated by the equation

$$G(Fe^{III}) = 2G(H_2) + \frac{2G(H)}{1 + \dfrac{k_4(Fe^{III})}{k_3(Fe^{III})}} \qquad (iii)$$

where k is the rate constant of the respective reactions[2,3]. In the present paper, the contribution of reaction 10 in the ferrous-cupric system will be discussed for the analogous equation.

Experimental

Nitrogen-saturated ferrous ammonium sulfate solutions in sulfuric acid, containing some amounts of cupric sulfate, were irradiated by a 10 kc. cobalt-60 gamma ray source, and the amount of ferric ion was measured by optical density at 304 mμ by the usual methods, presented in Part II[2]. All the solutions for Figs. 1 and 3 contained 0.04 M ferrous salt in 0.8 N sulfuric acid. All the solutions for Fig. 4 contained 0.04 M ferrous salt in various concentrations of sulfuric acid. The concentration of cupric sulfate in all the solutions for Fig. 2 was as large as five times that of ferrous salt in 0.8 N sulfuric acid.

Results and Discussion

The Effect of the Cupric Concentration.— The $G(Fe^{III})$ of the 0.04 M ferrous ammonium

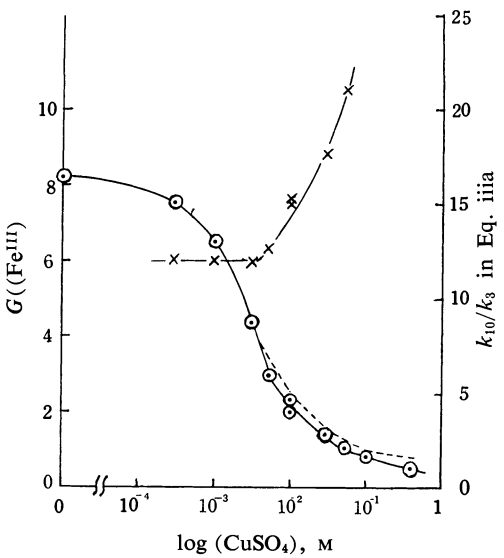


Fig. 1. Effect of cupric sulfate concentration on $G(Fe^{III})$ (⊙) and k_{10}/k_3 in Eq. iiia (×) in air-free 0.04 M ferrous ammonium sulfate solution of 0.8 N sulfuric acid.

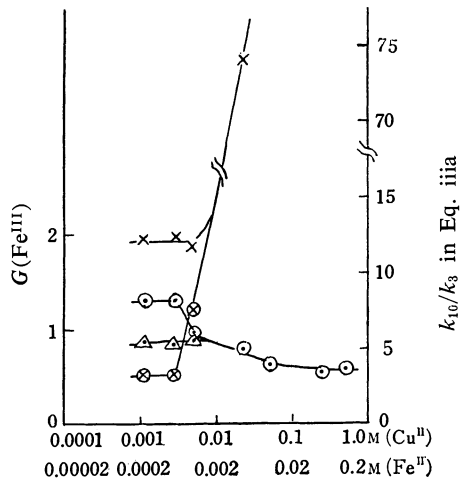


Fig. 2. Effect of concentration of ferrous and cupric sulfate ((Cu^{II})/(Fe^{II})=5) on $G(Fe^{III})$ at initial dose (⊙) and 2×10^5 r (△) and the corresponding k_{10}/k_3 in Eq. iiia (⊗) and (×) respectively, in air-free 0.8 N sulfuric acidic solutions.

1) E. J. Hart, *Radiation Research*, **2**, 33 (1955).
2) H. Hotta and S. Ohno, This Bulletin, **34**, 1640 (1961).
3) W. G. Rothschild and A. O. Allen, *Radiation Research*, **8**, 101 (1958).

sulfate solutions in 0.8 N sulfuric acid is shown by the circles in Fig. 1 as a function of the cupric concentration. Furthermore, in order to confirm the effect of the cupric concentration, the $G(Fe^{III})$ of the 0.8 N sulfuric acidic solutions, containing amounts of cupric sulfate as large as five times that of ferrous ammonium sulfate, was studied, as is shown in Fig. 2. Since the $G(Fe^{III})$ for the dilute solutions in this case decreased above 1×10^5 r, the values at the initial dose and 2×10^5 r were plotted as the circles and triangles respectively in Fig. 2.

When the effect of the cupric ions is assumed as has been mentioned in the introduction, the oxidation rate of the ferrous ions in a mixture of ferrous and cupric ions can be expressed by the equation

$$G(Fe^{III}) = 2G(H_2) + \frac{2G(H)}{1+\dfrac{k_{10}(Cu^{II})}{k_3(Fe^{II})}} \qquad \text{(iiia)}$$

which is like Eq. iii. Therefore, the apparent ratio of the reaction rates, k_{10}/k_3, can be estimated from the observed $G(Fe^{III})$ as is plotted as crosses in Figs. 1 and 2. These ratios increase sharply in the cupric solutions more concentrated than 0.004 M in Fig. 2 as well as in Fig. 1. If this ratio is consistently 12 over the whole range, the $G(Fe^{III})$ can be shown as the dotted line in Fig. 1. This fact shows that the apparent ratio of the reaction rates, k_{10}/k_3, is 12 in the present reaction scheme, and that some reactions must be considered in a concentrated cupric solution in addition to the above scheme. The smaller value of the ratio than 12, corresponding to the initial $G(Fe^{III})$ in Fig. 2, may be due to the effect of the slight residual oxygen.

The smallest $G(Fe^{III})$ for the present reaction scheme should be 0.78 from Eq. iiia. The smaller observed value than 0.78 can be interpreted at first glance by the so-called "track effect", that is, the reaction of the cupric ion with the hydrogen atom, which has the fate of combining with another hydrogen atom or a OH radical outside of the track. Although this may be partially correct in the very concentrated cupric solution, the above cupric concentration, 0.004 M, at which something begins to happen, is too dilute for such a track effect. This suggests that the capture reaction of the cupric ion with the thermerized electron,

$$Cu^{2+} + e = Cu^{+} \qquad (12)$$

must be considered, in addition to reaction 10, in the cupric solution more concentrated than 0.004 M.

All the solutions plotted in Fig. 1 gave the constant $G(Fe^{III})$ up to 1.2×10^6 r, but they were not always constant at higher doses as

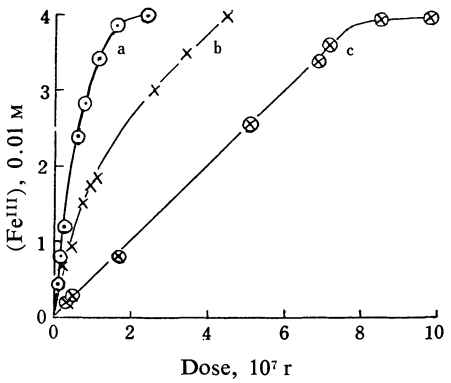


Fig. 3. Oxidation of ferrous ion in air-free 0.04M ferrous ammonium sulfate solutions of 0.8 N sulfuric acid containing a) 0.004 M (⊙), b) 0.04 M (×) and c) 0.4 M (⊗) cupric sulfate.

is shown in Fig. 3, in which the oxidation rate of ferrous ions in 0.04 M ferrous ammonium sulfate solutions of 0.8 N sulfuric acid containing a) 0.004 M, b) 0.04 M and c) 0.4 M cupric sulfate, is shown to be up to 10^8 r. The decrease of the $G(Fe^{III})$ at high doses is expected from Eq. iiia as a result of the decrease in the amount of ferrous ion. Furthermore, at high doses, the reaction between the ferric ions and the thermerized electrons like reaction 12, as has been pointed out by Dobson and Hughes[4], and the effect of the accumulated hydrogen molecules in the system may also be effective. The constancy of $G(Fe^{III})$ (=0.48) for solution c up to 7×10^7 r is due to the complete predominance of reactions 10 and 12 in the highly concentrated cupric solution.

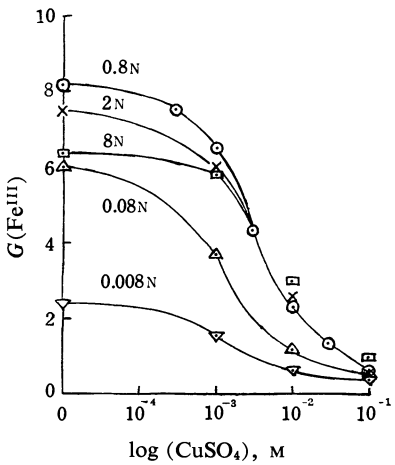


Fig. 4. Effect of concentration of cupric sulfate on $G(Fe^{III})$ for air-free 0.04 M ferrous ammonium sulfate solutions in 0.008 N (▽), 0.08 N (△), 0.8 N (⊙), 2 N (×) and 8 N (⊡) sulfuric acid, respectively.

4) G. Dobson and G. Hughes, *Trans. Faraday Soc.*, 57, 1117 (1961).

TABLE I. k_{10}/k_3 AS A FUNCTION OF H_2SO_4 CONCENTRATION

H_2SO_4 N	Assumed value[3] of $G(H)$	Assumed value[5] of $G(H_2)$	k_{10}/k_3 Apparent from Eq. iiia	k_{10}/k_3 Intrinsic for $(Cu^{2+})/(Fe^{2+})$
0.8	3.7	0.39	12	270
0.08	3.5	0.40	57	200
0.008	3.2	0.44	330	210

TABLE II. k_4/k_3 AS A FUNCTION OF SOLUTE CONCENTRATION

H_2SO_4 N	Initial concentration of ferrous salt M	k_4/k_3 Apparent from Eq. iii	k_4/k_3 Intrinsic for $(Fe^{3+})/(Fe^{II})$
0.01	0.001	7.2[3]	9
0.8	0.001	0.08[3]	11
0.8	0.04	0.67[2]	20

TABLE III. $G(Fe^{III})$ FOR CONCENTRATED SULFURIC ACID SOLUTIONS

Composition, M			$G(Fe^{III})$ for energy absorbed	
H_2SO_4	$Fe(NH_4)_2(SO_4)_2$	$CuSO_4$	by total soln.	by water
0.4	0.04	0	8.20	8.20
1	0.04	0	7.50	8.24
4	0.04	0	6.35	9.32
0.4	0.04	0.001	6.51	6.51
1	0.04	0.001	5.96	6.54
4	0.04	0.001	5.80	8.52

The Effect of the Sulfuric Acid Concentration. —The $G(Fe^{III})$ of the 0.04 M ferrous ammonium sulfate solutions in 0.008, 0.08, 0.8, 2 and 8 N sulfuric acid respectively is shown in Fig. 4 as a function of the cupric sulfate concentration.

When the $G(H)$ and $G(H_2)$ for various sulfuric acidic solutions are assumed as listed in Table I[3,5], the apparent ratios of reaction rates, k_{10}/k_3, for these solutions containing 0.001 M cupric sulfate as evaluated from Eq. iiia depend on the concentrations of sulfuric acid as listed in the same table. On the other hand, the apparent ratio of reaction rates, k_4/k_3, for the 0.001 M ferrous sulfate solution in 0.01 and 0.8 N sulfuric acid (containing no cupric ion), observed by Rothschild and Allen[3], has the same tendency as the present ratio, k_{10}/k_3, and apparently is somewhat at variance with our previous value[2], as listed in Table II. A detailed discussion of these problems will appear in the next section.

In Fig. 4, the $G(Fe^{III})$ in 2 and 8 N sulfuric acid is also smaller for no and 0.001 M cupric solutions than for those of 0.8 N. However, when it is assumed that energy absorbed by sulfuric acid is dissipated without chemical change, the $G(Fe^{III})$ for energy absorbed only by water in 2 N sulfuric acid is quite equal to that in 0.8 N acid, and the same $G(Fe^{III})$ in 8 N acid is larger than in 0.8 N acid, as is shown in Table III. This indicates that the present assumption is not correct in 8 N sulfuric acid. In fact, there was some smell in the irradiated solution in 8 N sulfuric acid.

The Intrinsic Ratio of the Reaction Rates for k_4/k_3 and k_{10}/k_3. — As was mentioned in Part II[2], ions are not always free, but also form many complexes with solutes and solvents in a solution, and the reactivity with hydrogen atom depends on their state. Therefore, in Part II, as a result of the estimation of the concentration for the ith ferric complex, c_i, the relative reduction rate of the respective species by hydrogen atom, k_4^i, to that of reaction 3 was evaluated by the equations

$$\frac{k_4(Fe^{III})}{k_3(Fe^{II})} = \frac{1}{k_3(Fe^{2+})}\sum(c_i)k_4^i \qquad \text{(iv)}$$

and

$$(Fe^{III}) = \sum(c_i) \qquad \text{(vi)}$$

where (Fe^{II}) and (Fe^{III}) represent the total concentration of ferrous and ferric species, and (Fe^{2+}) and (Fe^{3+}), the concentration of their respective free ions, in the present paper. In Eq. iv, the ratio of reaction rates for the respective complexes, k_4^i/k_3, is now defined as the intrinsic ratio.

When the concentration of respective ferric complexes in a solution is estimated on the same assumption as in Part II[2], the intrinsic ratio of the reduction rate of free ferric ion,

5) D. M. Donald and N. Miller, *Radiation Research*, **9**, 487 (1958).

namely, precisely reaction 4 to the oxidation rate of ferrous ion, is evaluated as in Table II for various solutions. In the present evaluation, the perfect dissociation, that is, $(Fe^{II}) = (Fe^{2+})$, is assumed for the ferrous ion. This assumption was not very significant in Part II, for the relative value was discussed in relation to results in solutions containing almost equal amounts of solute (almost the same ionic strength). In the present cases, the dissociation degree of ferrous sulfate should be somewhat different. When the true concentration of the free ferrous ions is put in Eq. iv[6] on the assumption that the undissociated molecules are not reactive with hydrogen atoms, the intrinsic ratio of the reduction rate of the free ferric ions to the oxidation rate of the free ferrous ions by the hydrogen atoms is reduced to 7 from the values in Table II for all the present cases. Therefore, it is concluded that the correction factor for the free ferrous ions in Eq. iv is one-third for the result for the 0.04 ferrous ammonium sulfate solution of 0.8 N sulfuric acid; that is, all the intrinsic ratios for the reduction rates of ferric complexes, as listed in Table IV in Part II[2], should be corrected as in Table IV.

Table IV. Relative rate constants for R+H at room temperature

R	Relative rate constant
Fe^{2+}	1*
Fe^{3+}	7
$(FeCl)^{2+}$	1100
$(FeBr)^{2+}$	1000
$(FeSO_4)^{+}$	<1
$(FeF)^{2+}$	≈ 0
Cu^{2+}	270

* For $Fe^{2+} + H + H^{+} = Fe^{3+} + H_2$

Since the dissociation constant of cupric sulfate is 0.0045 M[7] and the dissociation degree of 0.04 M ferrous sulfate is one-third, as deduced above, the intrinsic ratio of the reduction rate of the free cupric ions to the oxidation rate of the free ferrous ions by the hydrogen atom, k_{10}^{1}/k_3, is evaluated as in Table I, as for ferric ion, from the equation

$$\frac{k_{10}(Cu^{II})}{k_3(Fe^{II})} = \frac{k_{10}^{1}(Cu^{2+})}{k_3(Fe^{2+})} + \frac{k_{10}^{2}(CuSO_4)}{k_3(Fe^{2+})} \qquad \text{(vii)}$$

For the evaluation, k_{10}^{2}/k_3 is almost zero; this means that the undissociated cupric sulfate molecules are not reduced by the hydrogen atoms. The first value in Table I (270) is the most reliable. Therefore, the ratio of the reduction rates of the free cupric ion to the free ferric ion is about 40. The same ratio is obtained as 22 by other investigators[8,9].

As shown in Tables I and II, the apparent ratio can be consolidated by the intrinsic ratio defined by Eqs. iv and vii.

Another possibility for the dependence of the apparent ratio, k_{10}/k_3, on the concentration of cupric sulfate as shown in Figs. 1 and 2 is that it is due to the dependence of its dissociation degree. However, it is easily seen that its dissociation degree is not so sensitive in 0.8 N sulfuric acid.

Although the contribution of reaction 4 in the ferrous-cupric system is ignored in the above discussion, it could be expressed as

$$G(Fe^{III}) = 2G(H_2) + \frac{2G(H)}{1 + \dfrac{k_4(Fe^{III})}{k_3(Fe^{II})} + \dfrac{k_{10}(Cu^{II})}{k_3(Fe^{II})}} \qquad \text{(viii)}$$

However, when the apparent value for k_4/k_3 and k_{10}/k_3 in Tables I and II and the concentration of ferric ions at the initial stage are inserted into this equation, such a disregard is permissible.

Summary

The yield of ferric ions in the air-free ferrous acidic solutions by cobalt-60 gamma rays is reduced in the presence of cupric ion due to their reduction by the hydrogen atoms. The decrement depends on the composition of the solutions. That is, the apparent ratio of this reduction rate to the oxidation rate of the ferrous ions, estimated directly from the observed ferric yield by Eq. iiia increases with the decrease in acidity. On the other hand, the similar ratio for the reduction rate of ferric ions apparently varies according to the composition of the solutions. However, when these apparent ratios are analyzed by a fine composition of the solutions or reduced to the reaction rate for the fine species in solutions, the intrinsic ratios of the reduction rate of the free ferric and cupric ions to the oxidation rate of the free ferrous ions, by the hydrogen atoms, are 7 and 270 respectively and are independent of the composition of the solutions. On the other hand, the direct capture reaction of the cupric ions with the thermerized electrons is effective, in addition to the above reduction reaction with the hydrogen atoms, in the cupric solutions more concentrated than 0.004 M.

Japan Atomic Energy Research Institute
Tokai, Ibaraki-ken

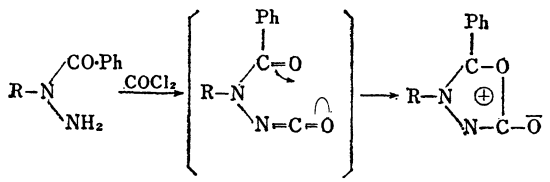
6) "Gmelins Handbuch der Anorganischen Chemie", 59, Fe(B), p. 430.
7) W. D. Bale, E. W. Davies and C. B. Monk, *Trans. Faraday Soc.*, 52, 816 (1956).
8) P. Riesz and E. J. Hart, *J. Phys. Chem.*, 63, 858 (1959).
9) J. H. Baxendale and D. H. Smithies, *Z. physik. Chem.*, 7, 242 (1956).

Studies of Meso-ionic Compounds. XV[1]. *The Preparation of ψ-3, 5-Dihydro-3-methyl-5-keto-1-oxa-2, 3, 4-triazole*

By Mutsuko HASHIMOTO* and Masaki OHTA

(Received September 22, 1961)

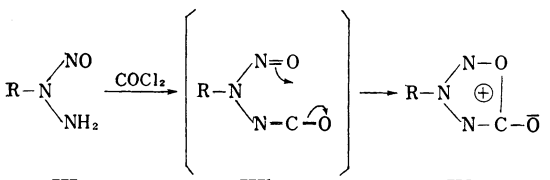
In a previous paper[2], we reported that ψ-oxadiazole (II) was prepared by the action of acyl chloride upon *N*-substituted N-benzoylhydrazine (Ia). The formation of the ψ-oxadiazole ring presumably involves the bond formation between two unsaturated groups of



Ia Ib II

Fig. 1

the intermediate acyl isocyanate (Ib). Thus, it could be expected that replacement of the acyl group of I with a nitroso group gives a new type of meso-ionic compound (IV) having an iso-electronic structure with II.



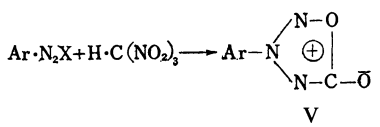
IIIa IIIb IV

R=CH_3

Fig. 2

In the present paper, we report the preparation of compound IV by the action of carbonyl chloride upon *N*-nitroso-*N*-methylhydrazine (IIIa), which is readily accessible.

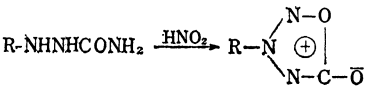
On the other hand, a few analogues of



V

Fig. 3

compound IV have already been obtained by routes different from that described above; Ponzio[3] prepared 3-aryl derivatives (V) by treating nitroform with diazonium salts, and recently Boyer and Canter[4] reported that 1-(2-methylcyclohexyl)- or 1-menthyl-semicarbazides and nitrous acid give the corresponding 3-alkyl derivatives (VI). The latter reaction



VI

R=2-Methylcyclohexyl, menthyl

Fig. 4

apparently proceeds through the intermediate nitroso isocyanate (IIIb; R=2-methylcyclohexyl or menthyl), and therefore the formation mechanisms of IV and VI are perhaps essentially the same.

In the present experiment, *N*-nitroso-*N*-methylhydrazine (IIIa) was subjected to the action of carbonyl chloride in chloroform in the presence of potassium carbonate to give colorless needles, m. p. 11°C, giving a negative test with the Liebermann nitroso reaction. The product can be distilled at 101~101.5°C (3 mmHg) and is unreactive towards hot absolute ethanol, as has been reported by Ponzio and Boyer and Canter. Elemental analysis indicated the product to be the expected meso-ionic compound, ψ-3,5-dihydro-3-methyl-5-keto-1-oxa-2,3,4-triazole** (IV), whose structure was also supported by the infrared spectrum described below. The disappearance of the N-H stretching bands at 3315 and 3220 cm^{-1} observed for the precursor (IIIa) and the lack of a characteristic band for isocyanate in the infrared spectrum of ψ-oxatriazole IV suggest the formation of the meso-ionic ring. The strong absorption band at 1780 cm^{-1} in the spectrum of IV is indicative of the carbonyl group and

1) Part XIV of this series; K. Kishimoto and M. Ohta, This Bulletin, **34**, 1402 (1961).

* Present address: The Textile Research Institute, Yokohama.

2) M. Hashimoto and M. Ohta, This Bulletin, **34**, 668 (1961).

3) G. Ponzio, *Gazz. chim. ital.*, **63**, 471 (1933); *Chem. Abstr.*, **28**, 748 (1934).

4) J. H. Boyer and F. C. Canter, *J. Am. Chem. Soc.*, **77**, 1280 (1955).

** Designated following the systematic nomenclature suggested by W. Baker, W. D. Ollis and V. D. Poole, *J. Chem. Soc.*, **1949**, 311.

is in close agreement with Boyer and Canter's observation (1790 cm^{-1})[4] and the carbonyl band of ψ-oxadiazole II (1755 cm^{-1})[2] having an iso-electronic structure with IV.

Experimental

***N*-Nitroso-*N*-methylhydrazine (IIIa).**—The compound was prepared by Thiele's method[5].

ψ-3, 5-Dihydro-3-methyl-5-keto-1-oxa-2, 3, 4-triazole (IV).—To a solution of IIIa (2 g.) in chloroform (200 ml.) was added finely powdered, anhydrous potassium carbonate (20 g.), and then a violent stream of carbonyl chloride was vigorously stirred in at $-7\sim-8$°C for 10 min. After the mixture had been kept standing at room temperature for 2 days, the precipitates were filtered off, the filtrate was concentrated and the residue was rectified to give 1.8 g. of IV, b. p. 104~106°C/4 mmHg. Redistillation of IV yielded a fraction boiling at 101~101.5°C/3 mmHg, m. p. 11°C, in the form of colorless needles, giving a negative test with the Liebermann nitroso reaction.

Found: C, 24.00; H, 3.00; N, 40.01. Calcd. for $C_2H_3O_2N_4$: C, 23.77; H, 2.99; N, 41.58%.

A solution of IV in absolute ethanol was refluxed for 3 hr. and evaporated under reduced pressure to give colorless needles, m. p. 11°C, giving a negative test with the Liebermann nitroso reaction.

We are indebted to Dr. Asaji Kondo for his microanalyses and to Dr. Tadashi Sato for his infrared spectroscopic work.

Laboratory of Organic Chemistry
Tokyo Institute of Technology
Meguro-ku, Tokyo

5) J. Thiele, *Ann.*, **376**, 244 (1910).

*Reaction of Ferrocene with Acyl Chloride**

By Noboru SUGIYAMA, Hideo SUZUKI, Yoshiaki SHIOURA and Tsutomu TEITEI

(Received September 15, 1961)

The Friedel-Crafts acylation of ferrocene with acetyl chloride was first reported by Woodward and his collaborators[1]. Subsequently the acylation of ferrocene has been reported on by many others. We should like to report briefly on the reactions of ferrocene with succinyl chloride and phenacetyl chloride.

Succinyl chloride is capable of Friedel-Crafts reaction with one or two molecules of aromatic hydrocarbon to give β-aroylpropionic acid or α,β-diaroylethane. The chloride can also react with aromatic hydrocarbons to form γ,γ-diarylbutyrolactone[2]. We found that the chloride reacts with ferrocene to yield β-ferrocenoylpropionic acid (I), γ,γ-diferrocenylbutyrolactone (II) and 1, 2-diferrocenoylethane (III).

$FcCOCH_2CH_2COOH$ (I)

$(Fc)_2CCH_2CH_2$ (II)

$FcCOCH_2CH_2COFc \rightarrow FcCHCH_2CH_2CHFc$ (III) (IV)

IV $\rightarrow$ H_2C——CH_2 / Fc—CH HC—Fc / O (V)

I $\rightarrow$ Fc—$CHCH_2CH_2$ / O——CO (VI)

$FcCOCH_2C_6H_5$ (VII) $FcCHCH_2C_6H_5$ (VIII) $FcCH{=}CHC_6H_5$ (IX)

Fc = Ferrocenyl ; FcCO = Ferrocenoyl**

Diketone III was reduced with lithium aluminum hydride to yield 1, 4-dihydroxy-1, 4-diferrocenylbutane (IV). IV easily gave 2, 5-diferrocenyltetrahydrofuran (V) with acid catalysts. β-Ferrocenoylpropionic acid (I) was readily lactonized by reduction with sodium borohydride in an ethanol solution, giving γ-ferrocenylbutyrolactone (VI). Similarly, phenylacetyl chloride reacts with ferrocene to give benzyl ferrocenyl ketone (VII) in a good yield. VII was reduced with lithium aluminum hydride to yield 1-ferrocenyl-2-phenylethanol (VIII) quantitatively. By treating VIII with

* Presented at the 14th Annual Meeting of the Chemical Society of Japan, Tokyo, April, 1961.

1) R. B. Woodward et al., *J. Am. Chem. Soc.*, **74**, 2125 (1952).

2) V. Migrdichian, "Organic Syntheses", Vol. I, Reinhold Publ. Corp., New York (1957), p. 655.

** According to Chemical Abstracts' Nomenclature.

phosphorus pentachloride, 1-ferrocenyl-2-phenylethylene (IX) was obtained instead of the corresponding chloride.

The infrared spectra of II and VI exhibit strong absorption bands at 1770 and 1780 cm^{-1} (KBr) due to a γ-lactone group, and III and VII, at 1660 and 1665 cm^{-1} (KBr) due to a carbonyl conjugated with a ferrocene nucleus. These bands in III and VII are absent from IV and VIII, and new bands at 3400 and 3480 cm^{-1} (chloroform) due to a hydroxyl group appear in IV and VIII respectively. V shows no bands in the region for either hydroxyl or carbonyl. IX shows bands at 1640 and 960 cm^{-1} (KBr) due to a trans-disubstituted ethylene group (-CH=CH-). All these compounds have absorption bands at 1000 and 1110 cm^{-1} [3].

The visible spectra of II, IV, V, VI and VIII show absorption maxima similar to that of ferrocene itself at 445 (141), 443 (205), 443 (192), 442 (66.7) and 440 mμ (ε 104), and, on the other hand, the conjugate-expanded III and VII have absorption maxima at 458 (958) and at 462 mμ (ε 421) respectively in 95% ethanol which maxima correspond to that of acetylferrocene[4]. Strangely, IX showed also an absorption maximum at 460 mμ (ε 1000) in 95% ethanol.

Experimental

Reaction of Ferrocene with Succinyl Chloride.—To a vigorously stirred solution of ferrocene (10.0 g., 0.054 mol.) and aluminum chloride (7.2 g., 0.054 mol.) in methylene chloride (100 ml.) was slowly added a solution of succinyl chloride (4.2 g., 0.027 mol.) in the same solvent (50 ml.) under an atmosphere of nitrogen. After refluxing for 2 hr., the reaction mixture was cooled and poured onto crushed ice and water (100 ml.). On removal of the aqueous layer, the methylene chloride solution was separated into a neutral and an acidic fraction by extraction with 10% sodium carbonate (100 ml.). The acid fraction, on neutralization with 6 N hydrochloric acid, gave β-ferrocenoylpropionic acid (I, 1.0 g.) in leaflets, m. p. 164~166°C (lit.[5] 166.5~167.5°C). After removal of the solvent, the neutral fraction was dissolved in benzene, chromatographed on alumina and eluted as follows: (1) benzene (first portion) gave unchanged ferrocene (3.3 g.), and (2) benzene (second portion) gave γ-lactone (II) in the form of light orange needles, m. p. 165~165.5°C (from ethyl acetate).

Found: C, 63.47; H, 4.87; Fe, 23.60, 23.86. Calcd. for $C_{24}H_{22}O_2Fe_2$: C, 63.44; H, 4.85; Fe, 24.60%.

(3) Ethyl acetate gave 1,2-diferrocenoylethane (III, 2.1 g.) in the form of orange needles, m. p. 185~186°C (from ethyl acetate).

Found: C, 63.34; H, 4.86. Calcd. for $C_{24}H_{22}O_2Fe_2$: C, 63.44; H, 4.85%.

The oxime of III, prepared with hydroxylamine hydrochloride and sodium acetate in methanol (2 hr. refluxing), m. p. 165~166°C (decomp.) crystallized as needles (from methanol).

Found: N, 5.39. Calcd. for $C_{24}H_{24}O_2N_2Fe_2$: N, 5.74%.

1,4-Dihydroxy-1,4-diferrocenylbutane (IV).—A solution of III (1.0 g.) in anhydrous tetrahydrofuran (50 ml.) was gradually added to a stirred slurry of lithium aluminum hydride (0.5 g.) in the same solvent (50 ml.). The mixture was stirred for 2 hr. at room temperature. The excess of the hydride was destroyed with ethyl acetate. The organic layer was washed with distilled water several times and dried over anhydrous sodium sulfate. After removal of the solvent, the solid was crystallized from ethanol, affording IV (0.9 g.) in the form of yellow needles (from ethanol), m. p. 134~135°C.

Found: C, 62.89; H, 5.93. Calcd. for $C_{24}H_{26}O_2Fe_2$: C, 62.88; H, 5.68%.

2,5-Diferrocenyltetrahydrofuran (V).—After reduction of III with lithium aluminum hydride as above, the tetrahydrofuran solution was shaken first with 10% sulfuric acid and then with water, and dried over anhydrous sodium sulfate. After removal of the solvent, the residue was dissolved in benzene and chromatographed on alumina, and 2,5-diferrocenyltetrahydrofuran (V) was crystallized quantitatively from ethanol, as yellow needles, m. p. 124.5~125°C. The same material was also prepared by refluxing IV in acetic anhydride for 1 hr.

Found: C, 65.23; H, 5.56. Calcd. for $C_{24}H_{24}OFe_2$: C, 65.45; H, 5.45%.

γ-Ferrocenylbutyrolactone (VI).—A solution of β-ferrocenoylpropionic acid (I, 1.0 g.) and sodium borohydride (0.3 g.) in ethanol (50 ml.) was refluxed for 2 hr. After removal of the solvent, the residue was treated with water (30 ml.), acidified with concentrated hydrochloric acid (5 ml.), and warmed for 1 hr. on a water bath. The resulting solid was extracted with ethyl acetate. The extract was crystallized from *n*-pentane to yield γ-ferrocenylbutyrolactone (VI, 0.7 g.) in the form of yellow needles, m. p. 130~131°C.

Found: C, 62.02; H, 5.08. Calcd. for $C_{14}H_{14}O_2Fe$: C, 62.24; H, 5.18%.

Benzyl Ferrocenyl Ketone (VII).—Phenacetyl chloride (8.3 g., 0.054 mol.) solution in methylene chloride (50 ml.) was added during 1 hr. to a stirred solution of ferrocene (10.0 g., 0.054 mol.) and aluminum chloride (7.2 g., 0.054 mol.) in methylene chloride (150 ml.) under an atmosphere of nitrogen. After refluxing for 5 hr., the reaction mixture was cooled and poured onto crushed ice and water (100 ml.). On removal of the aqueous layer, the methylene chloride solution was washed with 3 portions of water (50 ml.) and dried over anhydrous sodium sulfate. After removal of the solvent, the residue was dissolved in benzene and chromatographed on alumina. Elution with benzene and ethyl acetate gave material which crystallized from *n*-hexane. Benzyl ferrocenyl ketone (VII, 12.0 g., 73%) separated as orange-red needles, m. p. 128~129°C.

3) 9-10 Rule, M. Rosenblum, *Chem. & Ind.*, **1958**, 953.
4) K. Schlögel, *Monatsh. Chem.*, **88**, 601 (1957).
5) K. L. Rinehart et al., *J. Am. Chem. Soc.*, **79**, 3423 (1957).

Found: 70.94; H, 5.29. Calcd. for $C_{18}H_{16}OFe$: C, 71.05; H, 5.26%.

The oxime prepared in methanol (2 hr. refluxing), crystallized from methanol in the form of orange-red needles, m. p. 142~143°C (decomp.).

Found: N, 4.32. Calcd. for $C_{18}H_{17}ONFe$: N, 4.38%.

1-Ferrocenyl-2-phenylethanol (VIII).—A solution of benzyl ferrocenyl ketone (VII, 5 g.) in anhydrous tetrahydrofuran (100 ml.) was added to a stirred slurry of lithium aluminum hydride (1 g.) in the same solvent (30 ml.). The mixture was stirred for 1 hr. under reflux after the addition was complete. The excess of the hydride was destroyed by the dropwise addition of moist ether, and the mixture was then acidified with 0.1 N sulfuric acid. The organic layer was washed with water (50 ml.) 3 times. After removal of the solvent, the solid residue was crystallized from *n*-pentane, affording 1-ferrocenyl-2-phenylethanol (VIII, 4.7 g., 93%), m. p. 82~83°C.

Found: C, 70.94; H, 5.29. Calcd. for $C_{18}H_{18}OFe$: C, 70.59; H, 5.88%.

1-Ferrocenyl-2-phenylethylene (IX). — 1-Ferrocenyl-2-phenylethanol (VIII, 1 g.) in anhydrous ether (50 ml.) was stirred under reflux with powdered phosphorus pentachloride (0.7 g.). After 5 hr. of stirring, the ether solution was decanted from the excess of the pentachloride, washed with 3 portions of water (50 ml.), and dried over anhydrous sodium sulfate. After evaporation of the ether, the solid residue was crystallized from *n*-pentane to give 1-ferrocenyl-2-phenylethylene (IX, 0.7 g., 80%) in the form of orange-red needles, m. p. 121~121.5°C.

Found: C, 74.64; H, 5.68. Calcd. for $C_{18}H_{16}Fe$: C, 74.98; H, 5.61%.

Department of Chemistry
Faculty of Science
Tokyo University of Education
Otsuka, Tokyo

The Tubular Structure of Collagen Fibril

By Masao HAISA

(Received September 12, 1961)

According to Arndt and Riley[1], X-ray powder patterns obtained from all sorts of proteins have two characteristic scattering maxima, the principal and the packing peaks. However, the patterns obtained from collagen have, in addition, another peculiar meridional peak which has the 2.86 Å spacing and which seems to be constant whatever the origin of the collagen fibrils. In this case, the equatorial packing peak varies its spacing from 11 to 17 Å with an increase in the water content of the material and it is accompanied with the gradual appearance of streaking[2]. Although it is generally agreed that the collagen molecule consists of a three-stranded helix, it is not always certain whether the fibril is made up of "Collagen II" or of the "Collagen I" proposed by Crick and Rich[3].

On the other hand, small-angle diffraction studies of dry collagen[4,5] have shown that the meridional spacing is about 640 Å and that the layer lines on the meridian exhibit fanning. It was postulated that a particular kind of disordering of the structure produced such a fanning effect. Tomlin and Ericson[6] have shown that the fanning is due to the regular shearing of the fibrils. On inspection of electron micrographs, Schmitt and Gross[7] have found that the axial repeat of 640 Å contains five primary staining levels.

Although it is now permissible to define collagen as any fibrous protein of the collagen group which gives the above features of X-ray wide-angle as well as small-angle patterns[8], there has yet been reached no general agreement about the interpretation of these patterns. An attempt is made in the present paper to elucidate the general features of the X-ray patterns of collagen-class proteins in terms of the helically grooved tubular structure. Some electron-microscopic findings are also given which support this structure.

1) U. W. Arndt and D. P. Riley, *Phil. Trans. Roy. Soc.*, **A247**, 409 (1955).
2) W. T. Astbury and R. Lomax, *J. Chem. Soc.*, 1935, 846.
3) F. H. C. Crick and A. Rich, "Recent Advances in Gelatin and Glue Research", Ed. by G. Stainsby, Pergamon Press, London (1958), p. 20.
4) O. E. A. Bolduan and R. S. Bear, *J. Polymer Sci.*, **5**, 159 (1950).
5) R. S. Bear, *Advances in Protein Chem.*, **7**, 69 (1952).
6) S. G. Tomlin and L. G. Ericson, *Acta Cryst.*, **13**, 359 (1960).
7) F. O. Schmitt and J. Gross, *J. Am. Leather Chemists Assoc.*, **43**, 658 (1948).
8) W. T. Astbury, *Trans. Faraday Soc.*, **34**, 378 (1938).

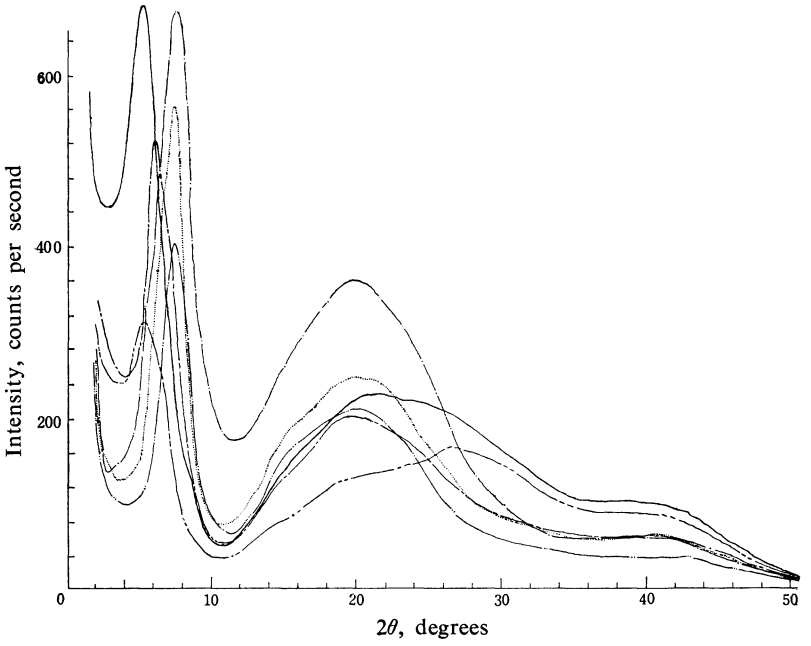


Fig. 1. Wide-angle equatorial spectra of fowl-neck tendon collagen.

——— Native, moist collagen
····· Native, dried collagen
— — — Moist collagen treated with formaldehyde
— · — Dried collagen treated with formaldehyde
———— Moist collagen treated with acetic acid
—··— Dried collagen treated with acetic acid

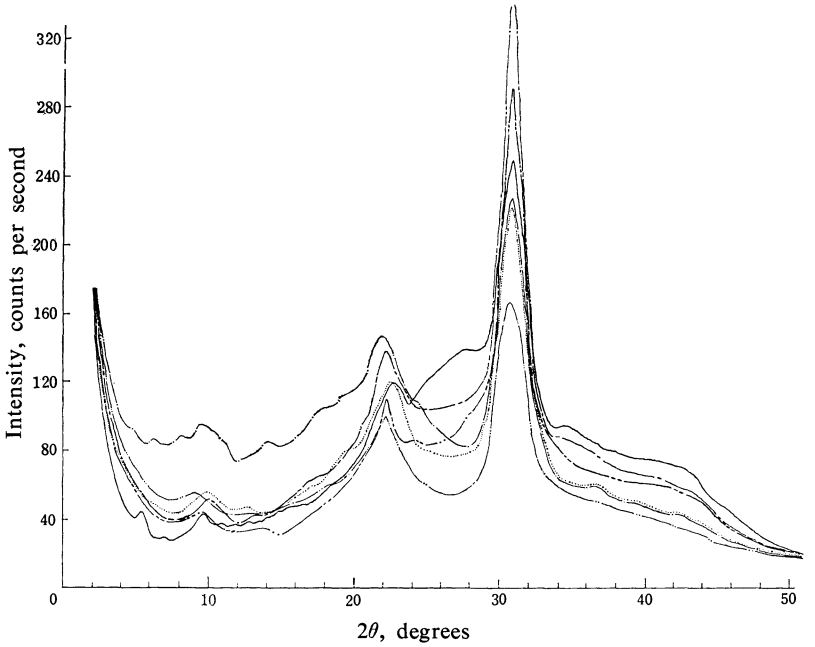


Fig. 2. Wide-angle meridional spectra of fowl-neck tendon collagen. Remarks are shown in Fig. 1.

Wide-angle X-Ray Diffraction

All experiments described in this paper were made on moist and dried fowl-neck tendon collagen, untreated or treated with formaldehyde or acetic acid. Figures 1 and 2 show the equatorial and meridional spectra respectively, obtained by means of a Geiger-counter X-ray diffractometer, "Geigerflex", using Cu radiation filtered by nickel. It will be seen that the meridional peaks are unaffected in either the intensity or the position of the maxima by treatment with formaldehyde or acetic acid, whereas the equatorial peaks are remarkably affected. It should be noted that the principal peak at 4.4Å spacing on the equator is stronger and broader than that at 4.0Å spacing on the meridian and that the water halo is remarkable for moist materials. The streak for moist collagen treated with formaldehyde or acetic acid is weaker than that for untreated collagen. On the assumption of the validity of von Laue's method[9], the linear dimension of the crystalline region along the fiber axis is estimated to be 76Å for the peak at $2\theta=31.3°$.

A closer examination of Figs. 1 and 2 would lead us to suppose that the tanning with formaldehyde provides interchain cross-linking and therefore prevents the intrusion of water molecules and that the swelling by means of acetic acid is caused by breaking the lateral aggregation of polypeptide chains.

Some Fourier Transforms Related to the Small-angle Pattern of Collagen Fibril

The Fourier transform of a uniform helix of infinite length, radius r and pitch P, takes the form

$$J_n(2\pi Rr)\exp[in(\Psi+\pi/2)] \qquad (1)$$

where r, φ and z are the cylindrical coordinates in real space, R, Ψ and Z, those in reciprocal space, and J_n denotes the nth order Bessel function.

In the case of a discontinuous helix with u units per t turns, the orders of the Bessel functions occurring in the lth layer line are given by those values of n satisfying the relation

$$l=tn+um \qquad (2)$$

where the m's are integers[10]. In a fiber diagram, only the cylindrically averaged intensity is relevant; hence, the cross-terms arising from (1) disappear upon this operation. With $t=1$ and $u=5$, for example, we have

$$\left.\begin{array}{lll} \text{when} & l=0,5,\ldots, & J_0^2+2J_5^2+2J_{10}^2+\ldots \\ \text{when} & l=1,4,\ldots, & J_1^2+J_4^2+J_6^2+J_9^2+\ldots \\ \text{when} & l=2,3,\ldots, & J_2^2+J_3^2+J_7^2+J_8^2+\ldots \end{array}\right\} \qquad (3)$$

The transform of a thin disc of radius a is given by[11]

$$\pi a^2\frac{2J_1(2\pi Ra)}{2\pi Ra} \qquad (4)$$

The Fourier transform of a helically grooved rod can be obtained by the convolution of those of disc and helix, and it is integrated by the separation of the coordinates. The integration along the fiber axis z is obtained by considering the disc of thickness fP spaced uniformly in a period of P, f thus being a fraction. This is given by, on the lth layer line,

$$2\pi f\frac{\sin lf\pi}{lf\pi} \qquad (5)$$

The transform of the central core of the rod takes the form 4. For the part of the residual helical ridge with an inner radius a and an outer one $a+b$, b thus being the depth of ridge, the integration with respect to r is given by the form:

$$\int_a^{a+b}J_n(2\pi Rr)r\mathrm{d}r \qquad (6)$$

This can be calculated by using the recurrence formula:

$$\int xJ_n(x)\mathrm{d}x=xJ_{n+1}(x)+n\int J_{n+1}(x)\mathrm{d}x$$

$$xJ_{n+1}(x)+xJ_{n-1}(x)=2nJ_n(x)$$

and the identity:

$$\int J_n(x)\mathrm{d}x=2\sum_{j=0}^{\infty}J_{n+2j+1}(x)$$

where x is the argument of the Bessel function. That is,

$$\int xJ_n(x)\mathrm{d}x=4(n+1)J_{n+2}(x)$$

$$-4\sum_{j=1}^{\infty}[2jJ_{n+4j}(x)-(n+2j+1)J_{n+4j+2}(x)] \qquad (7)$$

The first maxima of the integral 7 lies at (see Appendix)

$$x=n+2+0.81\times\sqrt[3]{n+2}$$

Small-angle X-Ray Diffraction

One of the most striking differences between the small-angle X-ray patterns of moist and dry collagens lies in the fanning effect of the layer lines. Two distinct types of reflection confirmed by the author are depicted schematically in Fig. 3. The first type, which appears

9) M. von Laue, *Z. Krist.*, **64**, 115 (1926).
10) W. Cochran, F. H. C. Crick and V. Vand, *Acta Cryst.*, 5, 581 (1952).
11) R. S. Bear and O. E. A. Bolduan, ibid., 3, 236 (1950).

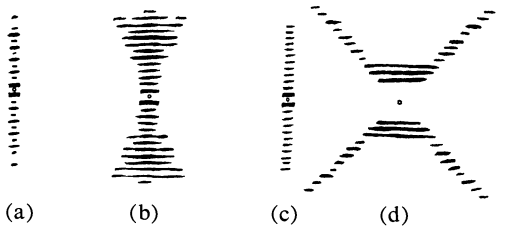


Fig. 3. Schematic illustration of small-angle diffraction patterns from collagen-class proteins. (a) Moist tendon collagen. (b) Dried tendon collagen. (c) Moist elastoidin. (d) Dried elastoidin.

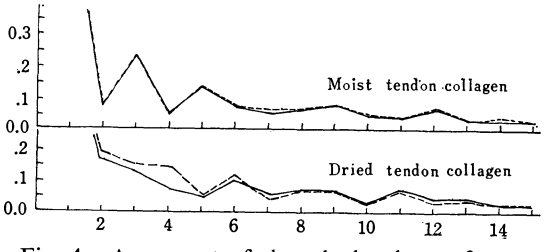


Fig. 4. Agreement of the calculated transform (broken line) and the square root of the observed intensity (full line) for moist and dried fowl-neck tendon collagens.

only on the meridian and is characteristic of moist materials, corresponds to a structure of smooth cylinder scatterers, while the second one, the fanning effect obtained from dry materials, might be attributed to a structure with a helical ridge. As may be readily seen from the theory developed in the foregoing section, the Fourier transform of the former is obtained by the product of (4) times (5). The alteration of intensity with the order of the layer lines may be expressed in excellent agreement with the observation by (5), in which $f=0.47$ (or 0.53) for moist collagen and $f=0.41$ (or 0.59) for dry collagen, as is shown in Fig. 4, (a) and (b) respectively. From a consideration of the transform 6, it is clear that the helical ridge structure is entirely adequate to account for the appearance of fanning and for the phenomenon of complex intensity distribution along the respective layer lines. The point of particular interest is that the intensity distribution of the layer lines is in accord with the transform 3, in which their first maxima occur at the arguments $x=0$, 1.8 and 3.4 respectively.

Electron Micrographs

The possibility of collagen fibrils being of a tubular[12] or a helical[13] structure has been suggested, but there is little conclusive evidence to support such structures. In the present investigation, collagen fibrils obtained from fowl-neck tendon were examined thoroughly. Specimens were picked up on an electron-microscopic grid without use of any supporting film and were shadowed with chromium. Typical electron-micrographs showing the membraneous structure of collagen fibril are reproduced in Figs. 5 to 8. They are cross-striated,

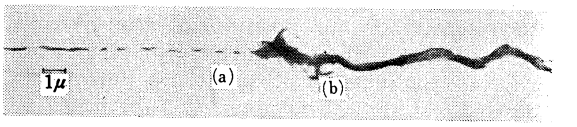


Fig. 5

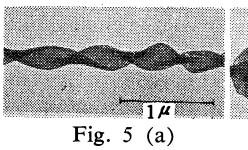


Fig. 5 (a)

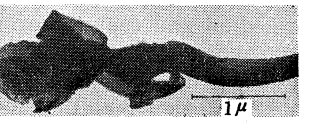


Fig. 5 (b)

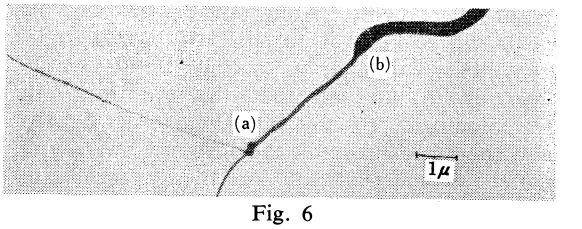


Fig. 6

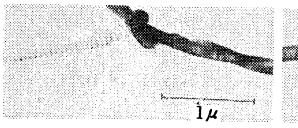


Fig. 6 (a)

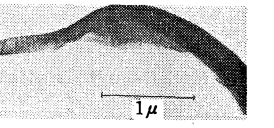


Fig. 6 (b)

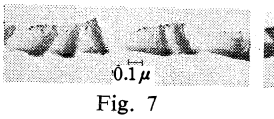


Fig. 7

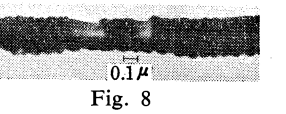


Fig. 8

the period of the striations being of the order of 650Å, i.e., typical of collagen. A feature of interest in relation to this structure is the frequent occurrence of a stepwise transition from an assembly of filaments to a single one. Figs. 5 and 6 show such a transition and higher magnifications of some parts of the specimens. Further evidence for this view is provided by their pronounced tendency to aggregate side to side, with a slight displacement relative to one another, as is shown in Figs. 7 and 8. On the basis of the morphological evidence presented above, the electron-microscopic structure of collagen fibril is considered to be a kind of tubular structure with a circular or flat and coiled cross section.

12) J. J. Kennedy, *Science*, **121**, 673 (1955).
13) R. Reed, M. J. Wood and M. K. Keech, *Nature*, **177**, 697 (1956).

Structure of Collagen

In view of the experimental and theoretical results obtained above, it may be concluded that the collagen fibril consists of two phases alike in quantity, the crystalline phase characteristic of collagen-class and the amorphous phase, which has more hydration sites and, upon drying, loses water molecules to leave the helical groove. These considerations lead us to suppose that the collagen filament may be composed of coiled coils of a large number of polypeptide chains as follows:

$$([-P-P'-M-A-A'-]_4)_n$$

where P and P′ stand for the crystalline part and are rich in sequences of gly-pro-hypro, gly-pro-ala and other similar ones respectively. A and A′ form the amorphous part and are rich in sequences including gly and two other amino-acid residues. M is the transition part, about which the hydration sites are considered to be crowded. The striations are supposed to arise from the periodical occurrence of the P, P′, M, A and A′ parts, of which the distance between successive repeats causes the meridional identity period of 640Å. The fact that the tanning and the swelling do not alter the intrinsic spacing of the wide-angle reflections suggests that they occur outside the P and P′ parts.

Further evidence adduced to support this structure is as follows:

(a) The analytical data[14] provide some evidence that the sequence gly-pro-hypro may be of frequent occurrence in gelatin and collagen. According to Huggins[15], glutamic and aspartic acids can be in the form of condensed rings similar to the pyrrole ring; hence, they can take the place of pro or hypro in the P part. Thus, half of the total amino-acid residues in collagen can form a sequence of the gly-pro-hypro type.

(b) There are some evidence showing that, in collagen fibril, the amino-acid residues occur in groups. For example, Kuhn et al.[16] have stated from electron-microscopic studies that most of the basic residues are crowded in the α- and β-striations. Very likely they correspond to the A and A′ parts.

(c) The effective length of the side chain of pro and hypro is that of the pyrrole rings; hence, they can constitute the crystalline phase. On the other hand, the fully stretched side-chains of the basic residues are fairly long (ca. 8.8Å), whereas that of non-polar residues found in collagen is very short (ca. 3.4Å).

(d) The results obtained by Boedtker and Doty[17] and by Schmitt et al.[18] are in agreement with the view that the collagen molecule can be considered to have a length of the order of 2800Å.

(e) It is likely that the collagen filaments aggregate to each other by means of electrostatic forces, including hydrogen bonding, laterally. The lateral aggregation of the smooth cylinders having like diameters effects the streaking in the X-ray pattern as shown in Fig. 1. This view is supported by the findings that the crystal energy of the collagen fibrils does not always depend on the hydroxyproline content[19] and that the sorbed water is linked by hydrogen bonds to the CO group projecting outwards from and perpendicular to the fiber axis[20].

(f) A plaid pattern observed by Gross[21] perhaps results from a sheet with a helical structure.

Structure of Elastoidin

Elastoidin, a member of the collagen-class proteins obtained from shark fins, gives a small-angle diffraction pattern in which the expansion of the layer lines with an increase in l is outstandingly prevalent, whereas the central region fades out, as shown in Fig. 3(d). This fact may well be interpreted by assuming that a in transform 6 is very small compared with b. This supports the view that the collagen-class proteins have the tubular structure with a helical groove. It has been pointed out that the hydroxyproline content of elastoidin is but two-thirds that of collagen. The X-ray pattern from collagen has the packing peak, whereas elastoidin exhibits no additional bulbous terminal spot of the streak. This is in agreement with the view that elastoidin fibril is short of the regular lateral arrangement of chains because of a relative lack of the crystalline P and P′ parts and that it hence forms a deep groove on drying.

Summary

1. The X-ray scattering has been measured for moist and dry collagens of fowl-neck tendon, untreated or treated with formaldehyde

14) R. E. Schrohenloher, J. D. Ogle and M. A. Logan, *J. Biol. Chem.*, **234**, 58 (1959).
15) M. L. Huggins, *Proc. Natl. Acad. Sci., U. S.*, **43**, 209 (1957).
16) K. Kuhn, U. Hofmann and W. Grassmann, *Naturwissenschaften*, **46**, 512 (1959).
17) H. Boedtker and P. Doty, *J. Am. Chem. Soc.*, **78**, 4267 (1956).
18) F. O. Schmitt, J. Gross and J. H. Highberger, *Symp. Soc. Exptl. Biol.*, **9**, 148 (1955).
19) P. Doty and T. Nishihara, "Recent Advances in Gelatin and Glue Research", Ed. by G. Stainsby, Pergamon, London (1956), p. 92.
20) R. D. B. Fraser and T. P. MacRae, *Nature*, **183**, 179 (1959).
21) J. Gross, *J. Biophys. Biochem. Cytol.*, **2**, Suppl. 261 (1956).

or acetic acid. Some modifications of the collagen fibril were also examined by electron microscope.

2. The wide-angle scattering data are compatible with a structure consisting of crystalline and amorphous parts. The intensity distribution of the small-angle diffraction is interpreted by a helical groove structure. The Fourier transform calculated for this model is shown.

3. The electron micrographs show that collagen fibril has a kind of tubular structure with a circular or flat and coiled cross section.

4. The data are discussed with respect to the assumption that collagen fibril is composed of a woven sheet of polypeptide chains in which the crystalline and amorphous parts occur alternatively.

5. A reasonable assignment of hydration to the helical groove is possible; this gives the fibril an approximately uniform electron density in the moist state.

The author wishes to express his appreciation to Dr. Isamu Nitta, Dr. Masao Kakudo and Dr. Sigeo Hasegawa for their encouragement and for the facilities of their laboratories during the work. This investigation was completed at the Institute for Protein Research of Osaka University. Valuable technical assistance in the electron-microscopic examination was rendered by Mr. Tamotsu Terada.

Department of Chemistry
Faculty of Science
Kwansei Gakuin University
Nishinomiya, Hyogo-ken

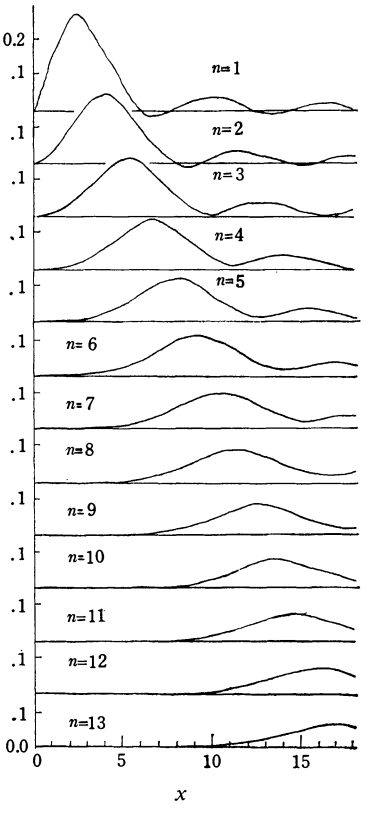
Note added in proof

Reference 3 appeared in complete form:

A. Rich and F. H. C. Crick, *J. Mol. Biol.*, **3**, 483 (1961).

Appendix

$$x^{-2}\int_0^x J_n(x)x\mathrm{d}x$$



The Rate of Formation of Cobalt Hydrocarbonyl under Various Conditions of Oxo Reaction

By Ryoji IWANAGA

(Received July 18, 1961)

It has been previously[1,2] reported that the rate of oxo reaction is inversely proportional to the partial pressure of carbon monoxide. In accordance with this kinetic requirement, several mechanisms have been proposed for this reaction which involve, as a rate-determining step, the displacement of a mole of carbon monoxide by the olefin from the dicobalt octacarbonyl[1,2] added as a catalyst, or from the cobalt hydrocarbonyl[3] presumed to be present in the system. Recently Kirch and Orchin[4] have proposed a mechanism for the

1) G. Natta, R. Ercoli, S. Castellano and P. H. Barbieri, *J. Am. Chem. Soc.*, 76, 4049 (1954).
2) A. R. Martin, *Chem. & Ind.*, **1954**, 1536.
3) G. Natta, R. Ercoli and S. Castellano, *Chim. e. Ind.*, 37, 6 (1953).
4) L. Kirch and M. Orchin, *J. Am. Chem. Soc.*, **81**, 3597 (1959).

oxo reaction which involves the formation and subsequent decomposition of a complex formed from cobalt hydrocarbonyl-olefin-carbon monoxide as follows:

$$2HCo(CO)_4 + RCH{=}CH_2 + CO \rightarrow Complex \quad (1)$$

$$Complex \rightarrow Co_2(CO)_8 + RCH_2CH_2CHO \quad (2)$$

This scheme is based upon the fact that cobalt hydrocarbonyl in hexane reacts with olefin and carbon monoxide to give aldehyde and dicobalt octacarbonyl. They considered that such a complex was formed at the first and rate-determining stage.

We have previously[5] found that the equilibrium concentration of cobalt hydrocarbonyl converted from dicobalt octacarbonyl in benzene is proportional to the rate of the oxo reaction of cyclohexene[1] under various partial pressures of carbon monoxide and hydrogen. From this result it has been considered that the formation of cobalt hydrocarbonyl from dicobalt octacarbonyl may determine the rate of the oxo reaction. However, in order to study the kinetics and mechanism of the oxo reaction it was necessary to determine the rate of formation of cobalt hydrocarbonyl in the system in the course of the oxo reaction.

In the present paper, the rate of formation of cobalt hydrocarbonyl from dicobalt octacarbonyl under various partial pressures of carbon monoxide and hydrogen is presented. In addition, some experimental results concerning the content of cobalt hydrocarbonyl in the system during the oxo reaction of methylacrylate and cyclohexene are presented and discussed.

Experimental

Determination of the Initial Rate of Formation of Cobalt Hydrocarbonyl from Dicobalt Octacarbonyl under Various Partial Pressures of Carbon Monoxide and Hydrogen. — A solution of 0.87 g. (2.55 mmol.) of $Co_2(CO)_8$ in 100 ml. of pure and oxygen-free toluene was placed in a 300 ml. stainless steel rocking autoclave. The autoclave was then sealed, placed in an electrically heated jacket, flushed and pressured with carbon monoxide so as to hold a pressure a little less than the partial pressure of the carbon monoxide to be tested. After the autoclave had been heated to 100°C and the pressure in the autoclave had been adjusted to the partial pressure of the carbon monoxide to be tested, hydrogen was added rapidly from high pressure hydrogen storage up to the mixed gas pressure to be tested, and the autoclave was then maintained at 100°C with rocking. After various periods of time after the addition of hydrogen, about 2 ml. aliquots of the solution were withdrawn directly into a nitrogen atmosphere from the autoclave through a valve and a coil of stainless steel tube of 1 m. in length and 1 mm. inner diameter which was immersed in a bath cooled at −20°C. The cobalt hydrocarbonyl in the aliquot was analyzed by the method described in the preceding paper[6].

Measurement of Cobalt Hydrocarbonyl in the Solution During the Oxo Reaction of Methylacrylate and Cyclohexene. — The apparatus and procedure were the same as has been described above. A solution of 100 ml. toluene containing 0.17 g. of $Co_2(CO)_8$ and 17.2 g. of methylacrylate (98.5% in purity) or 0.22 g. of $Co_2(CO)_8$ and 17.4 g. of cyclohexene (98% in purity) was introduced into a 300 ml. stainless steel rocking autoclave, and the autoclave was then filled with about 75 kg./cm^2 of carbon monoxide. After the autoclave had been heated to 120°C and the pressure had been adjusted to 102 kg./cm^2, hydrogen was added rapidly until the total pressure became 202 kg./cm^2, and the autoclave was then maintained at 120°C with rocking. During the reaction the pressure was maintained at the initial pressure of 202 kg./cm^2 by a continuous addition of the compressed gas mixture of carbon monoxide and hydrogen in a 1 : 1 ratio. The aldehyde in the sample was analyzed by the hydroxylamine hydrochloride method[7].

Results and Discussion

Figures 1 and 2 show plots of the initial rate of the formation of cobalt hydrocarbonyl against the partial pressure of carbon monoxide and hydrogen. From these results, it will be seen that under the constant pressure of carbon monoxide the initial rate increases with the increasing partial pressure of hydrogen, while under the constant pressure of hydrogen, the initial rate inversely decreases with the increasing pressure of carbon monoxide. These effects of partial pressures on the initial rate of formation of cobalt hydrocarbonyl are parallel with the effects of partial pressures on the rate of the oxo reaction reported by Natta[1].

The dotted line in Fig. 1 shows that the rate of formation of hydrocarbonyl is almost constant regardless of the total pressure when the gas mixture consists of equal moles of carbon monoxide and hydrogen. This fact is interesting in connection with Natta's statement[8] that the velocity of the oxo reaction is independent of the pressure of the gas phase of 1 : 1 ratio carbon monoxide and hydrogen.

Although the rate of the oxo reaction determined by Natta et al.[1] decreased with the decreasing pressure of carbon monoxide under

5) R. Iwanaga, T. Fujii and T. Yoshida, presented at the 9th Annual Meeting of the Chemical Society of Japan, Kyoto, April, 1956; R. Iwanaga, T. Fujii, H. Wakamatsu, T. Yoshida and J. Kato, *J. Chem. Soc. Japan, Ind. Chem. Sec.* (*Kogyo Kagaku Zasshi*), **63**, 960 (1960).

6) R. Iwanaga, This Bulletin, **35**, 247 (1962).

7) H. Adkins and G. Krsek, *J. Am. Chem. Soc.*, **71**, 3051 (1949).

8) G. Natta and R. Ercoli, *Chim. e. Ind.*, **34**, 503 (1952).

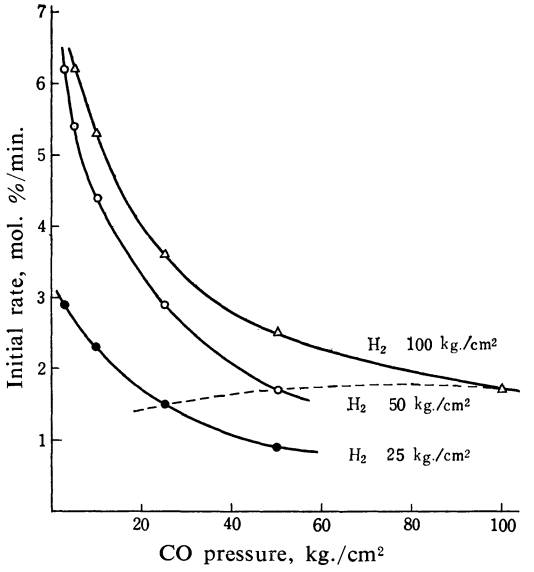


Fig. 1. Initial rate of formation of $HCo(CO)_4$ as a function of partial pressure of CO.

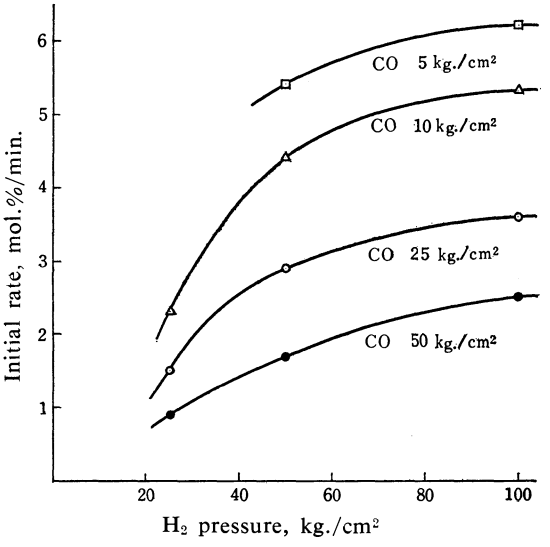


Fig. 2. Initial rate of formation of $HCo(CO)_4$ as a function of partial pressure of H_2.

pressure below about 10 atm., the rate of formation of hydrocarbonyl was observed to increase with the decreasing pressure of carbon monoxide in such a low pressure range. This phenomenon is very interesting for us in spite of the difficulty of explaining the rate of oxo reaction on the basis of the rate of formation of hydrocarbonyl. Under pressures less than 10 atm. of carbon monoxide, the rate of oxo reaction may presumably be influenced by certain other rate-determining stages, a study of which is in progress.

From Fig. 1 it was also induced that the rate is inversely proportional to the logarithm of the partial pressure of carbon monoxide under the constant pressure of hydrogen, but that the rate constant of the rate curve at 25 kg./cm² of carbon monoxide is different from that at 50 and 100 kg./cm². Therefore, no rate equation to fit the results throughout the whole range of the pressure of carbon monoxide and hydrogen could be obtained.

Since the formation of cobalt hydrocarbonyl from dicobalt octacarbonyl seems to take place according to the equation,

$$Co_2(CO)_8 + H_2 \rightarrow 2HCo(CO)_4 \qquad (3)$$

it may be a matter of course that the rate increases with the increasing pressure of hydrogen. However, the inverse effect of carbon monoxide pressure on the rate can not be explained from the above equation. Metlin et al.[9] reported that 1 mol. of carbon monoxide is absorbed per mole of dicobalt octacarbonyl at about 400 atm. and 185°C, and that this is due to the formation of a dicobalt nonacarbonyl complex, $Co_2(CO)_9$.

$$Co_2(CO)_8 + CO \rightarrow Co_2(CO)_9 \qquad (4)$$

If any of the dicobalt octacarbonyl would convert to nonacarbonyl under our experimental conditions, the inverse effect of carbon monoxide pressure might be attributed to the decrease of dicobalt octacarbonyl according to

Table I. Initial rate of formation of $HCo(CO)_4$, from $Co_2(CO)_8$ at 100°C under various partial pressures of carbon monoxide and hydrogen

H_2 Pressure kg./cm²	CO Pressure kg./cm²	Initial rate of formation of $HCo(CO)_4$* mol.%/min.
25	3	2.9
25	5	2.3
25	25	1.5
25	50	0.9
50	3	6.2
50	5	5.4
50	10	4.4
50	25	2.9
50	50	1.7
100	5	6.2
100	10	5.3
100	25	3.6
100	50	2.5
100	100	1.7

* Molar percentage of cobalt hydrocarbonyl formed in a minute against the total cobalt in dicobalt octacarbonyl added.

9) S. Metlin, I. Wender and H. W. Sternberg, *Nature*, **183**, 457 (1959).

TRBLE II. $HCo(CO)_4$ PRESENT IN THE SOLUTION DURING THE OXO REACTION OF METHYLACRYLATE IN TOLUENE AT 120°C AND 200 kg./cm² OF 1 : 1 CO AND H_2

Methylacrylate, 17.2 g./dl.
$Co_2(CO)_8$, 0.17 g./dl.

Reaction time	Aldehyde formed	$HCo(CO)_4$ per added $Co_2(CO)_8$
min.	mol.%	% as Co
0	0	0
10	17.4	0.4
30	48.2	0.7
50	71.9	3.6
70	81.6	19.8
90	82.4	59.4
110	83.0	70.0

TABLE III. $HCo(CO)_4$ PRESENT IN THE SOLUTION DURING THE OXO REACTION OF CYCLOHEXENE IN TOLUENE AT 120°C AND AT 200 kg./cm² OF 1 : 1 CO AND H_2

Cyclohexene, 17.4 g./dl.
$Co_2(CO)_8$, 0.22 g./dl.

Reaction time	Aldehyde formed	$HCo(CO)_4$ per added $Co_2(CO)_8$
min.	mol.%	% as Co
0	0	0
15	8.8	52.1
45	24.6	61.5
75	38.1	65.0
105	47.3	65.7
135	53.7	67.7
180	63.8	70.7
240	70.5	73.6

TABLE IV. FORMATION OF $HCo(CO)_4$ FROM $Co_2(CO)_8$ IN TOLUENE AT THE EQUILIBRIUM STATE AT 100°C

$Co_2(CO)_8$, 0.87 g./dl.

H_2 Pressure	CO Pressure	$HCo(CO)_4$ per added $Co_2(CO)_8$	Time required until equilibrium state
kg./cm²	kg./cm²	% as Co	min.
26	10	23.7	40
27	48	24.8	50
25	96	26.8	70
49	9	33.6	45
47	47	33.9	55
48	94	36.6	65
98	10	41.9	20
95	43	41.8	45
97	97	43.3	45

Eq. 4. To examine the occurrence of this reaction, we have measured the amount of cobalt hydrocarbonyl in the equilibrium state by varying the partial pressures of carbon monoxide at a few fixed pressures of hydrogen. As illustrated in Table IV, the amount of cobalt hydrocarbonyl at the equilibrium state was independent of the partial pressure of carbon monoxide under the constant pressure of hydrogen. Thus, the carbon monoxide pressure affects only the rate of formation of cobalt hydrocarbonyl, not the equilibrium state of reaction 3. Therefore, it is clear that neither reaction 4 nor any other reaction to produce any compound other than cobalt hydrocarbonyl takes place under the experimental conditions employed. Furthermore, it can be noted that the inverse effect of carbon monoxide pressure on the rate is not due to a simple physical interference such as the effect of an inert dissolved gas, because it was observed that an added nitrogen pressure could affect neither the rate nor the equilibrium state of the formation of cobalt hydrocarbonyl under some carbon monoxide and hydrogen pressures. From the above observations it is not easy to explain why the carbon monoxide pressure causes a decrease only in the rate of formation of hydrocarbonyl. However, this phenomenon is an interesting fact for the study of the mechanism of the oxo reaction.

Tables II and III indicate the contents of cobalt hydrocarbonyl and aldehyde in the solutions during the oxo reaction of methylacrylate and cyclohexene in toluene at 120°C. In the former solution, in which the oxo reaction proceeds faster, only a trace of cobalt hydrocarbonyl appears when acrylate is present, while a large amount of it appears after the acrylate is consumed. This phenomenon agrees with the observations by Orchin et al.[10] However, in the latter solution, in which the oxo reaction proceeds more slowly, a large amount of hydrocarbonyl is present even at the beginning of the reaction.

From this result it seems likely that cobalt hydrocarbonyl will react rapidly with acrylate and slowly with cyclohexene. Although it could not be confirmed that cobalt hydrocarbonyl is consumed, whether in a main reaction to produce aldehyde or in some side reaction such as a hydrogenation reaction of double bond of olefin during the oxo reaction, it is significant for the study of the mechanism of the oxo reaction that cobalt hydrocarbonyl reacts rapidly with olefin whose oxo reaction is fast and slowly with that whose oxo reaction is slow.

Summary

By treating a solution of dicobalt octacarbonyl in toluene at 100°C under various partial pressures of carbon monoxide and hydrogen,

10) M. Orchin, L. Kirch and I. Goldfarb, *J. Am. Chem. Soc.*, **78**, 5450 (1956).

and by determining the initial rate of formation of cobalt hydrocarbonyl, we have found that the initial rate increases with the increasing pressure of hydrogen and decreases with the increasing pressure of carbon monoxide. These effects of partial pressures on the initial rate of formation of cobalt hydrocarbonyl are parallel with the effects of partial pressures on the rate of the oxo reaction reported by Natta.

In addition, the amount of cobalt hydrocarbonyl in the system during the oxo reaction of methylacrylate and cyclohexene in toluene at 120°C was determined; it was found that only a trace of cobalt hydrocarbonyl appears when acrylate is present, while a large amount of it is present even when cyclohexene is present in the system.

The author wishes to express his deep thanks to Professor S. Murahashi, Dr. T. Yoshida and Mr. J. Kato for their kind guidance and encouragement throughout this work. The author is also indebted to Mr. T. Fujii for his assistance in this experiment.

Central Research Laboratory
Ajinomoto Co., Inc.
Suzuki-cho, Kawasaki

The Effect of the Partial Pressure of Carbon Monoxide and Hydrogen on the Rate of Oxo Reaction

By Ryoji IWANAGA

(Received July 24, 1961)

It was found by Natta[1] and Martin[2] that the rate of oxo reaction increases with the increasing pressure of hydrogen, but decreases with the increasing pressure of carbon monoxide. These kinetic results led them to propose a mechanism for the oxo reaction which involves the displacement of a mole of carbon monoxide by the olefin from the dicobalt octacarbonyl[1,2] or from the cobalt hydrocarbonyl[3]. Recently Breslow et al.[4] have proposed a mechanism modifying the mechanism postulated by Kirch and Orchin[5]. In Breslow's mechanism the acylcobalt tricarbonyl, $RCH_2CH_2COCo(CO)_3$, produced from cobalt hydrocarbonyl and olefin reacts with hydrogen to give the oxo product and hydrotricarbonyl, $HCo(CO)_3$, or with carbon monoxide to give the unreactive acylcobalt tetracarbonyl, $RCH_2CH_2COCo(CO)_4$, and cobalt hydrotetracarbonyl is regenerated from hydrotricarbonyl.

$$RCH=CH_2+HCo(CO)_4 \rightarrow RCH_2CH_2Co(CO)_4$$

$$RCH_2CH_2Co(CO)_4 \rightarrow RCH_2CH_2COCo(CO)_3$$

$$RCH_2CH_2COCo(CO)_3+CO \rightarrow RCH_2CH_2COCo(CO)_4$$

$$RCH_2CH_2COCo(CO)_3+H_2 \rightarrow HCo(CO)_3+RCH_2CH_2CHO$$

$$HCo(CO)_3+CO \rightarrow HCo(CO)_4$$

The above mechanisms were all based upon the consideration that the cardon monoxide might affect the formation of an intermediate complex of the oxo reaction.

The author established in a preceding paper[6] that the rate of formation of cobalt hydrocarbonyl is increased with the increasing partial pressure of hydrogen but decreased with the increasing partial pressure of carbon monoxide.

To clarify the relationship between this effect of the partial pressure on the rate of formation of cobalt hydrocarbonyl and the effect of the partial pressure on the rate of oxo reaction, the author has studied the initial rate of the oxo reaction of methylacrylate under various partial pressures of carbon monoxide and hydrogen. In this study the reaction was made under the same conditions as have been described in the preceding paper[6], in order that the initial rate of the oxo reaction might be compared directly with that of the formation of cobalt hydrocarbonyl.

1) G. Natta, R. Ercoli, S. Castellano and P. H. Barbieri, *J. Am. Chem. Soc.*, **76**, 4049 (1954).
2) A. R. Martin, *Chem. & Ind.*, **1954**, 1536.
3) G. Natta, R. Ercoli and S. Castellano, *Chim. e. Ind.*, **37**, 6 (1955).
4) D. S. Breslow and R. F. Heck, *Chem. & Ind.*, **1960**, 467.
5) L. Kirch and M. Orchin, *J. Am. Chem. Soc.*, **81**, 3597 (1959).
6) R. Iwanaga, This Bulletin, 35, 774 (1962).

Methylacrylate was chosen for this study because it yielded only one kind of aldehyde, methyl-β-formylbutyrate[7], and reacted rapidly even at about 100°C. If the oxo reaction is carried out at a temperature higher than 100°C, cobalt carbonyl often decomposes under the partial pressure of carbon monoxide less than 10 kg./cm².

Experimental

The methylacrylate and toluene to be used were obtained from commercial sources; they were distilled in a nitrogen atmosphere and were kept in nitrogen before use in order to prevent the decomposition of the dicobalt octacarbonyl added as catalyst. The dicobalt octacarbonyl was also freshly recrystallized from ethyl ether before use. The method described in the preceding paper[6] was followed in general.

Determination of the Initial Rate of the Oxo Reaction of Methylacrylate.—One hundred milliliters of the solution containing 20.3 g. (232 mmol.) of methylacrylate and 0.86 g. (25 mmol.) of dicobalt octacarbonyl in toluene were put into a 300 ml. stainless steel rocking autoclave. After the autoclave had been heated to 100°C and the pressure of carbon monoxide had been adjusted to the pressure to be tested, hydrogen was added for a few seconds to bring it up to the pressure to be tested, and immediately the rocking was started. The temperature was controlled within ±1°C. The initial pressure and the initial ratio of carbon monoxide to hydrogen were maintained by a continuous addition of 1 : 1 synthesis gas throughout the time of the reaction, because about equal amounts of carbon monoxide and hydrogen were absorbed in the oxo reaction of methylacrylate. The initial rate of the oxo reaction was obtained as follows:

Several aliquots of about 2 ml. of the reaction mixture were withdrawn from the autoclave at intervals of 2.5 or 5 min. during the reaction through a high-pressure coil of a stainless tube cooled at −20°C; the amount of aldehyde in an aliquot was determined according to the procedure of Adkins[7]. The aldehyde yield per minute at the initial period of reaction time indicates the initial rate of the oxo reaction.

Results and Discussion

The initial rate of the oxo reaction of methylacrylate in toluene at 100°C under various partial pressures of carbon monoxide and hydrogen are listed in Table I. It shows that under the constant pressure of carbon monoxide, the initial rate increases with the increasing pressure of hydrogen, and under

Table I. Initial rate of the oxo reaction of methylacrylate under various partial pressures of carbon monoxide and hydrogen

Methylacrylate, 232 mmol./dl.
$Co_2(CO)_8$, 2.5 mmol./dl. in toluene at 100°C

H_2 Pressure kg./cm²	CO Pressure kg./cm²	Observed initial rate (aldehyde per acrylate mol.%/min.)	Calculated initial rate (aldehyde per acrylate mol.%/min.)
25	3	1.2	
25	10	2.0	2.0
25	25	0.7	0.8
25	50	0.4	0.4
50	3	4.2	
50	5	5.1	
50	10	5.8	5.6
50	25	2.2	2.2
50	50	1.3	1.1
100	5	9.9	
100	10	15.3	16.0
100	25	5.6	6.4
100	50	3.1	3.2
100	100	1.5	1.6

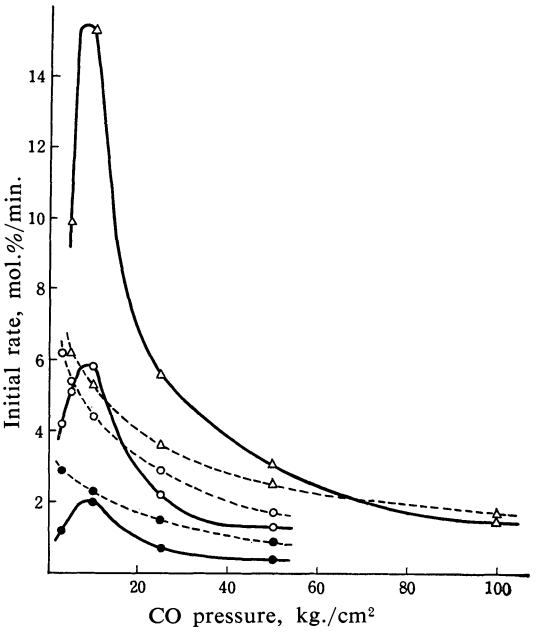


Fig. 1. Initial rate of the oxo reaction of methylacrylate and initial rate of the formation of $HCo(CO)_4$.

—— Initial rate of the reaction
····· Initial rate of the formation of $HCo(CO)_4$
● H_2 25 kg./cm²
○ H_2 50 kg./cm²
△ H_2 100 kg./cm²

7) H. Adkins and G. Krsek reported that ethyl-β-formylbutyrate was obtained by the oxo reaction of ethylacrylate in 74% of the theoretical yield. (*J. Am. Chem. Soc.*, **71**, 3051 (1949).) We have also obtained an aldehyde in an 83% yield from methylacrylate, and the aldehyde was confirmed to be all methyl-β-formylbutyrate through its 2,4-dinitrophenylhydrazone and by infrared analysis in this laboratory.

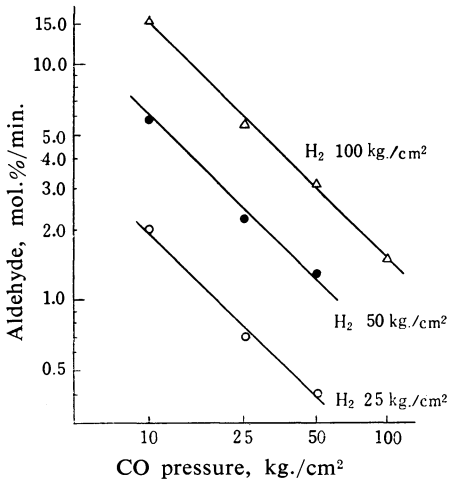


Fig. 2. Initial rate of the oxo reaction of methylacrylate in toluene at 100°C as a function of CO pressure.

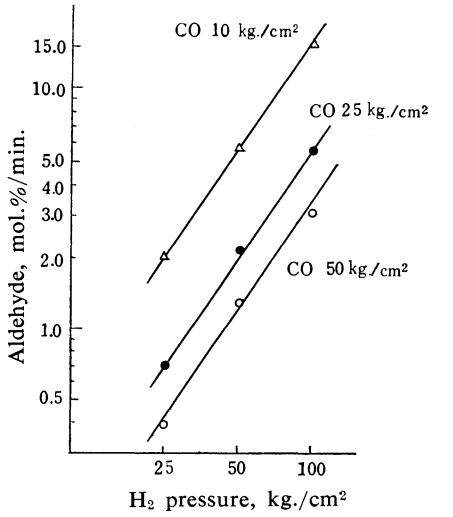


Fig. 3. Initial rate of the oxo reaction of methylacrylate in toluene at 100°C as a function of H_2 pressure.

the constant pressure of hydrogen the initial rate increases with the increasing pressure of carbon monoxide up to about 10 kg./cm^2, but decreases with the increasing pressure in the range of the high pressures of carbon monoxide (refer to Fig. 1). These results are in good agreement with the results obtained by Natta for the oxo reaction of cyclohexene in toluene[1,8]. In the range of the carbon monoxide pressures above 10 kg./cm^2, the plot of the rate against the pressure of carbon monoxide (Fig. 2) and the plot against the pressure of hydrogen (Fig. 3), both in logarithmic graphs, yielded straight lines. Therefore, the initial rate of the oxo reaction of methylacrylate can be represented by the equation:

$$\text{Initial rate} = 0.16\,(P_{H_2})^{1.5}/(P_{CO}) \qquad (1)$$

where P_{H_2} and P_{CO} are partial pressures in kg./cm^2 of hydrogen and carbon monoxide respectively. The data in the fourth column in Table I were calculated by the above equation, and they fit our observations quite well. Martin[2] proposed a rate equation for the case of the oxo reaction of diisobutene,

$$\text{Initial rate} = aP_{H_2}/(bP_{H_2} + cP_{CO}) \cdot [Co_2(CO)_8]\,[C_8H_{16}] \qquad (2)$$

where a, b and c are constants. However, this equation did not fit our observations.

In Fig. 1 the initial rate of the reaction of methylacrylate, together with the initial rate of the formation of cobalt hydrocarbonyl obtained in the preceding paper[6] under identical conditions, are shown. The figure shows that under the pressure of carbon monoxide above 25 kg./cm^2, the former rate is parallel with the latter rate. However, comparing the magnitude of the initial rate of the formation of cobalt hydrocarbonyl from dicobalt octacarbonyl and that of aldehyde from acrylate, it will be seen that the former rate is much lower than the latter rate under identical conditions of partial pressure. For example, it is calculated from the curve in Fig. 1 that when the pressure of carbon monoxide is 25 kg./cm^2 and that of hydrogen is 50 kg./cm^2, the former rate is 0.046 mmol. per minute and the latter rate is 5.1 mmol. per minute. Therefore, assuming that, as Kirch and Orchin described[5], cobalt hydrocarbonyl is the true catalyst of the oxo reaction to combine with olefin, it is impossible to consider that the hydrocarbonyl is formed only from dicobalt octacarbonyl in the oxo reaction. If it is assumed that cobalt hydrocarbonyl is formed from a cobalt carbonyl different from dicobalt octacarbonyl in the oxo reaction and that its rate is very rapid and is affected by the partial pressure, as in the case from dicobalt octacarbonyl, the effect of the partial pressure of carbon monoxide and hydrogen on the rate of the oxo reaction may be attributed to the effect of the partial pressure on the rate of the formation of cobalt hydrocarbonyl from a cobalt carbonyl presumed to be formed in the oxo reaction.

The effect of carbon monoxide pressure on the rate of the oxo reaction under a partial pressure less than 10 kg./cm^2 was observed to be just the opposite to the effect on the rate of the formation of hydrocarbonyl. From this phenomenon, it seems that there may be a certain interaction between carbon monoxide

8) G. Natta, *Brenstoff-Chemie*, **36**, 176 (1955).

and an intermediate complex and that this interaction may determine the rate of the oxo reaction. The author further observed that the color of the solution at an intermediate stage of the oxo reaction under 10 kg./cm^2 of carbon monoxide is light brown, and that at the end of the reaction it turns dark brown, while the color is dark brown throughout the reaction period under the carbon monoxide pressure above 10 kg./cm^2. In addition, analytical work has shown that the ratio of carbon monoxide liberated from the cobalt compound by the addition of iodine to cobalt in the solution is nearly 1.5 : 1 at an intermediate stage of the reaction under less than 10 kg./cm^2 of the carbon monoxide, but that at the end of the reaction the ratio is nearly 4 : 1. On the other hand , at under 10 kg./cm^2 of carbon monoxide, about 4 mol. of carbon monoxide are attached to a mole of cobalt even at the beginning of the reaction (Table II). Although the structure of the above cobalt compound with 1.5 mol. of carbon monoxide to a mole of cobalt could not be confirmed, it is clear that the carbon monoxide pressure significantly affects the structure of the cobalt compound under such a low pressure of carbon monoxide.

Table II. The behavior of cobalt compound during the oxo reaction of methylacrylate in toluene at 100°C

Methylacrylate, 232 mmol./dl.
$Co_2(CO)_8$, 2.16 mmol./dl.

CO pressure	(kg./cm^2)	6	25
H_2 pressure	(kg./cm^2)	50	50
After 10 min. of reaction			
aldehyde formed	(mol.%)	35.0	17.8
acrylate unreacted	(mol.%)	47.7	65.7
Molar ratio of CO : Co		1.55	3.33
After complete reaction			
aldehyde formed	(mol.%)	63.9	
acrylate unreacted	(mol.%)	2.1	
Molar ratio of CO : Co		3.9	

Furthermore, we have observed that at the beginning of the oxo reaction of methylacrylate, cobalt hydrocarbonyl is scarcely found in the reaction solution when the partial pressure of carbon monoxide is higher than 10 kg./cm^2, but that a certain amount of it appears when the partial pressure is lower than 10 kg./cm^2 (Table III). This phenomenon may be accounted for by assuming that in the range of carbon monoxide pressures above 10 kg./cm^2 the velocity of the formation of an intermediate complex from cobalt hydrocarbonyl-olefin-carbon monoxide, the formation of which was proposed by Kirch and Orchin[5], is so rapid that the hydrocarbonyl formed may immediately be consumed, while in the range of carbon monoxide pressures below 10 kg./cm^2 the velocity of the formation of cobalt hydrocarbonyl is so rapid, while the velocity of the formation of the complex is so slow, that some parts of the hydrocarbonyl may appear uncombined.

We have recently observed that in a toluene solution, cobalt hydrocarbonyl, which has been analyzed by the methylene blue method[9], disappears rapidly on the addition of methylacrylate at −20°C in an atmospheric pressure of nitrogen, but disappears slowly on the addition of cyclohexene, and that the molar ratio of the cobalt hydrocarbonyl consumed to the methylacrylate consumed is about 2 : 1. The product of this reaction is now under study. This phenomenon suggests that the effect of olefin structure on the rate of the oxo reaction[10] may be based upon the difference in rate of the combination of olefins with cobalt hydrocarbonyl and that, when the rate of combination is very rapid, as in the case of acrylate, the formation of cobalt hydrocarbonyl may be a rate-determining step in the oxo

Table III. $HCo(CO)_4$ present in the solution during the oxo reaction of methylacrylate in toluene at 100°C

I : Time, min.
II : Mol.% of aldehyde per acrylate added
III : Mol.% of $HCo(CO)_4$ per $Co_2(CO)_4$ added as Co

	CO 25 kg./cm^2 H_2 50 kg./cm^2			CO 10 kg./cm^2 H_2 50 kg./cm^2			CO 5 kg./cm^2 H_2 50 kg./cm^2	
I	II	III	I	II	III	I	II	III
15	9.0	0.3	5	31.0	1.9	5	34.4	4.2
30	20.6	0.3	10	59.3	1.5	10	54.1	5.1
60	38.2	0.5	15	67.5	1.2	15	64.0	—
150	75.5	7.4	30	73.5	3.4	30	67.0	8.1
180	74.6	17.8	65	72.6	15.7	45	66.6	12.1

9) R. Iwanaga, This Bulletin, 35, 247 (1962).

10) I. Wender, S. Metlin, S. Ergun, H. W. Sternberg and H. Greenfield, *J. Am. Chem. Soc.*, 78, 5401 (1956).

reaction. If the intermediate complexes of the oxo reaction could be isolated and the structures could be shown, the mechanism of the oxo reaction could undoubtedly be clarified.

Summary

The initial rates of the oxo reaction of methylacrylate in toluene at 100°C were measured under various partial pressures of carbon monoxide and hydrogen; they were then compared with the initial rate of the formation of cobalt hydrocarbonyl from dicobalt octacarbonyl measured under the same conditions in the preceding paper. The initial rate of the oxo reaction under the carbon monoxide pressure above 10 kg./cm^2 can be represented as follows:

$$\text{Initial rate (mol.\% of aldehyde/acrylate/min.)} = 0.16\ (P_{H_2})^{1.5}/(P_{CO})$$

However, the initial rate decreases with the decreasing partial pressure of carbon monoxide in the range below 10 kg./cm^2 of carbon monoxide. In addition, under the partial pressure of carbon monoxide below 10 kg./cm^2 some behaviors of cobalt carbonyl different from that under the pressure above 10 kg./cm^2 were observed. On the basis of these observations, a possible mechanism of the oxo reaction was discussed.

The author wishes to express his deep thanks to Professor S. Murahashi, Dr. T. Yoshida and Mr. J. Kato for their kind guidance and encouragement throughout this work. The author is also indebted to Mr. T. Fujii for his assistance in this experiment.

Central Research Laboratory
Ajinomoto Co., Inc.
Suzuki-cho, Kawasaki

Sur les Préparations des Complexes Métalliques. I. Les Préparations de Triacetatotriamminechrome(III)

Par Masayoshi NAKAHARA

(Reçu le 22 Août, 1961)

Jusq'ici les complexes non-électrolytes du chrome(III) étaient assez connus, et on savait bien que le trisglycinatochrome(III) et de trispicolinatochrome(III) pouvaient être facilement préparés, mais les complexes non-chelates qui en sont des homotypes n'étaient pas encore obtenus; aussi avons-nous examiné la formation du triacetatotriamminechrome(III) et du triacetatotripyridinechrome(III), et trouvant possibles leur préparations, nous les avons préparés en les comparant avec leur complexes non-chelates qui leur sont très analogues.

Expériences

Préparations.—*1) Diperoxotriamminechrome(III)*, $[Cr(O_2)_2(NH_3)_3]$. —Hofmann et al.[1], Riesenfeld[2], Werner[3] ou Bhatnager et al.[4] les ont déjà préparés; nous avons vu que la manière suivante est la plus simple et la plus profitable. 20 g. d'oxyde de chrome(VI), dissous dans 40 ml. d'eau, ont été ajoutés à 200 ml. de solution faite en diluant 70 ml. de solution concentré d'ammoniaque (28%). Cette solution jaune a été bien refroidie par le mélange réfrigérant et laissée telle quelle jusqu'à ce que la glace cristallise sur la paroi du bécher. Ensuite on y a fait tomber goutte à goutte 40 ml. d'eau oxygénée. Il faut continuer à la refroidir par le mélange réfrigérant pour maintenir la température de la solution au-dessous de −5°C. On a laissé telle quelle toute une heure la solution brun-sombre ainsi obtenue en la refroidissant par le mélange réfrigérant. Alors des quantités considérables de dichromate d'ammonium se sont cristallisés, mais, sans en tenir compte, la solution brun-sombre a été chauffée jusqu'à 50°C; nous avons vu s'échapper grande quantité d'oxygène; 10 min. après ce dégagement la solution a été chauffée, puis filtrée; le filtrat a été refroidi par le mélange réfrigérant jusqu'à 0°C, et laissé tel quel, toute la nuit, dans le réfrigérateur. Les cristaux menus, bruns ont été bien lavés à l'éthanol (95%), puis lavés à l'éthanol absolu et l'éther et aspirés, et conservés dans un dessicateur contenant de la potasse.

Rendement: 3,5～4,0 g.

2) Trichlorotriamminechrome(III), $[CrCl_3(NH_3)_3]$. —Nous avons fait la préparation selon la méthode de Werner[5].

1) K. A. Hofmann et H. Hiendlmaier, *Ber.*, **38**, 3059 (1905).
2) E. H. Riesenfeld, ibid., **38**, 4068 (1905).
3) A. Werner, ibid., **43**, 2286 (1910).
4) S. S. Bhatnager et al., *J. Chem. Soc.*, **1938**, 1432.
5) A. Werner, *Ber.*, **43**, 2290 (1910).

3) Trichlorotripyridinechrome(III), $[CrCl_3(NC_5H_5)_3]$. — Il a été préparé par Pfeiffer[6,7]; si nous pouvons nous procurer le chlorure de chrome(III) anhydre, il sera plus facile de nous en servir. Nous avons su qu'il était très difficile de produire ce composé en grande quantité si nous nous servions du chlorure de dichlorotetraquochrome(III) dihydraté.

4) Triacetatotriamminechrome(III), $[Cr(OCOCH_3)_3(NH_3)_3]$.—2,5 g. de trichlorotriamminechrome-(III) ont été suspendus dans 50 ml. d'éthanol soigneusement desséché; ensuite il a été ajouté 1 g. d'acétate d'argent purifié et soigneusement séché. Ce mélange été doucement chauffé au bain-marie, dans un flacon muni d'un réfrigérant à reflux; dans ce cas, s'il y entre de l'eau, quelque peu que ce soit, l'hydrolyse peut avoir lieu, et la récolte peu être extrémement réduite. La solution, chauffée pendant quelques temps, a été filtrée avant qu'elle ne devienne froide; le filtrat a été refroidi. Les cristaux rouge-violacés ainsi précipités ont été recristallisés par l'éthanol, lavés avec un peu d'éthanol et d'éther, puis séchés à l'air.

Rendement: 2 g.

Calculé: Cr, 18,56; NH_3, 18,23. Trouvé: Cr, 18,92; NH_3, 18,10%.

Cristaux rouge-violacés en forme d'écailles minces. Quand on les cristallise lentement on obtient des cristaux presque violet noirâtre. Solubles dans l'eau, l'éthanol, l'acide acétique recristallisables. En la solution aqueuse, facilement hydrolysables.

5) Triacetatotripyridinechrome(III), $[Cr(OCOCH_3)_3(NC_5H_5)_3]$. — 1 g. de trichlorotripyridine-chrome(III) a été dissous dans 20 ml. de pyridine bien sèche; 2 g. d'acétate d'argent y ont été ajoutés, et le tout a été chauffé sur bain d'huile et dans un flacon muni d'un réfrigérant à reflux. Suffisamment chauffé, on a filtré avant refroidissement, puis refroidi. La solution rouge-violacée ainsi obtenue a été mise dans le dessicateur sous vide avec de l'acide sulfurique concentré. Des cristaux violets noirâtres ont été obtenus. Ils ont été recristallisés par une petite quantité d'éthanol.

Rendement: 0,5 g.

Calculé: Cr, 11,11. Trouvé: Cr, 10,74%.

Cristaux violets noirâtres en forme d'écailles minces. Insolubles dans l'eau. Solubles dans l'éthanol, la pyridine.

6) Trisglycinatochrome(III), $[Cr(NH_2CH_2COO)_3]\cdot 3H_2O$.—Nous l'avons préparé selon la méthode de Ley et al.[8] On peut se servir de sel de chloro-pentamminechrome(III) au lieu du chlorure de dichlorotetraquochrome(III) dihydraté, comme le disaient Ley et al., mais nous avons constaté qu'on pouvait le préparer aussi bien en se servant du sel d'aquopentamminechrome(III), du sel de rhodochrome ou du sel d'erythrochrome.

7) Trispicolinatochrome(III), $[Cr(NC_5H_4COO)_3]\cdot H_2O$.—Nous avons fait la préparation suivante selon méthode de Ley et al.[9].

Les Spectres d'Absorption. — Les spectres d'absorption du triacetatotriamminechrome(III) et du triacetatotripyridinechrome(III), préparés à nouveau, ont été mesurés; ceux du trisglycinatochrome(III) et du trispicolinatochrome(III), qui avaient déjà été préparés, mais dont les spectres d'absorption n'avaient pas encore été mesurés, ont été aussi mesurés. Les spectres d'absorption de l'acétato-complexe obtenus à nouveau, ont été mesurés dans l'éthanol ou la pyridine, parce qu'il était impossible de les mesurer dans la solution aqueuse à cause de l'aquotisation trop rapide. Ensuite les spectres d'absorption des deux chelates susdits ont été mesurés avec la solution d'acide perchlorique à 60%; nous les avons mesurés en nous servant d'une cellule de quartz de 1,0 cm. et de Marque Hitachi EPU Spectrophotomètre photoélectrique. L'éthanol a été purifié selon la méthode de Danner et al.[10]; on l'a fait bouillir avec de l'azotate d'argent on l'a distillé et fait bouillir avec de l'acide sulfurique concentré, puis distillé, enfin l'a déssèché suffisamment par l'oxyde de calcium et distillé. La pyridine a été transformée on oxalate,

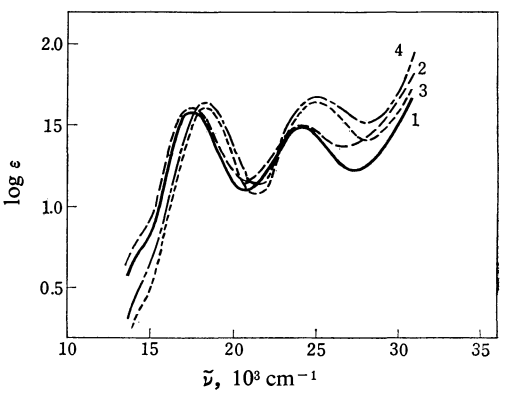


Fig. 1. Spectres d'absorption de:
(1) $[Cr(OCOCH_3)_3(NH_3)_3]$
(2) $[Cr(OCOCH_3)_3(NC_5H_5)_3]$
(3) $[Cr(OCOCH_2NH_2)_3]$
(4) $[Cr(OCOC_5H_4N)_3]$

TABLEAU I. MAXIMA DES BANDES D'ABSORPTION ($\tilde{\nu}$: $10^3\,cm^{-1}$) ET COEFFICIENTS D'EXTINCTION MOLAIRE (ε)

Complexe	La première		La deuxième		Lineaire
	$\tilde{\nu}$	ε	$\tilde{\nu}$	ε	$\tilde{\nu}$
$[Cr(OCOCH_3)_3(NH_3)_3]$	17,7	380	24,0	300	14,5
$[Cr(OCOCH_3)_3(NC_5H_5)_3]$	17,8	410	24,0	300	14,5
$[Cr(OCOCH_2NH_2)_3]$	18,4	400	25,0	450	14,0
$[Cr(OCOC_5H_4N)_3]$	18,4	420	25,0	470	14,5

6) P. Pfeiffer, *Z. anorg. Chem.*, **24**, 278 (1900).
7) P. Pfeiffer, ibid., **55**, 97 (1907).
8) H. Ley et K. Eicken, *Ber.*, **45**, 377 (1912).
9) H. Ley et K. Eichen, ibid., **50**, 1132 (1917).
10) P. S. Danner et J. H. Hildebrand, *J. Am. Chem. Soc.*, **44**, 2824 (1922).

puis décomposée par l'alcali, distillée, sèchée suffisamment par l'oxyde de baryum et distillée[11]. L'acide perchlorique était de qualité spéciale du commerce.

Les résultats sont donnés dans la Fig. 1 et le Tableau I.

Résultats et Discussion

Si l'on regarde les quatre courbes d'absorption montrées dans la Fig. 1, on s'apercevra que leurs formes se ressemblent beaucoup nous avons trouvé, quant au triacetatotriamminechrome(III) et au triacetatotripyridinechrome-(III), que les places de la première et de la deuxième bande d'absorption coïncident presque, ainsi que la valeur du coefficient d'extinction molaire. Seulement, quant au triacetatotripyridinechrome(III), l'augmentation du coefficient d'extinction est remarquable vers 28000 cm^{-1}, dans la région des faibles longueurs d'onde; peut-être est-ce à cause du pied de la bande d'absorption spéciale de la pyridine. Quant au trisglycinatochrome(III) et au trispicolinatochrome(III), nous avons trouvé, de même, que la première et la deuxième bande d'absorption coïncident presque, et que leur coefficient d'extinction sont à peu près égaux; quant au trispicolinatochrome(III), l'augmentation du coefficient d'extinction est plus important autour de 28000 cm^{-1} que pour le trisglycinatochrome(III); ce serait à cause de la bande d'absorption spéciale du noyau de la pyridine de même que pour les acetato-complexes. Ce qui est le plus intéressant—on peut le trouver dans chaque courbe—c'est une petite bande d'absorption autour de 14500 cm^{-1}; nous l'avons classée comme étant celle qui est appelée communément absorption linéaire du chrome[12].

Or l'absorption donnée par deux espèces d'acetato-complexes et celle produite par les complexes chélatés coïncidaient relativement bien entre eux, mais les acetato-complexes et les complexes chélatés nous montrent une absorption assez différente excepté l'absorption linéaire; la première et la deuxième bande d'absorption changent vers les faibles nombres d'onde 700~1000 cm^{-1}. Il semble que l'on ait un grand effet pareil en montrant la différence de structure qui existe entre ces deux matières, mais on n'a pas besoin de tenir compte de ce phénomène qui est l'effet du solvant. Cet effet du solvant sur l'absorption des complexes est présenté dans un mémoire donné par Nakamoto et al.[13] et par nos résultats expérimentaux[14]. On doit penser au changement de la bande d'absorption, suscité par un solvant polaire. On sait bien que la transposition de la première et la deuxième bande d'absorption des complexes chélates apparaît toujours comme étant celle qui se fait vers les courtes longueurs d'onde, à cause de l'effet stabilisateur venant de la chelatisation.

L'absorption linéaire du chrome se trouvant autour de 14500 cm^{-1} ne bouge pas et elle ne subit presque pas l'effet du solvant. Les faits déjà expliqués prouvent avec les effets d'absorption indiqués que l'on peut considérer ces bandes comme étant celles qui sont dues aux complexes homotypes.

Shimura[15] a fait la mesure et la distinction entre les spectres d'absorption de deux isomères (cis-cis- et cis-trans-complexe) du trisglycinatocobalt(III), et Yamatera[16] a déjà donné une thèse sur la séparation de la première bande des complexes de type $[CoX_3Y_3]$. On a constaté que la séparation de cette première bande d'absorption des complexes non-électrolytes se produit à cause de la structure cis-trans. La différence entre la première bande d'absorption des complexes cis-cis et cis-trans est très claire. On peut en conclure facilement que le trisglycinatochrome(III) a la structure cis-cis par analogie avec les complexes du cobalt(III). Il me semble très intéressant, qu'on puisse préparer à la fois les complexes du cobalt(III) cis-cis et cis-trans, alors qu'on ne peut obtenir que les complexes cis-cis du chrome(III), avec les complexes binucléaire di-μ-hydroxo-bis {bisglycinatochrome(III)}. De même, on peut raisonnablement attribuer la forme cis-cis au trispicolinatochrome(III) parce qu'il donne des spectres d'absorption coïncidants presque avec ceux du glycinato-complexe. On peut donc penser que les deux acetato-complexes ayant les spectres d'absorption semblables prennent les structure cis-cis.

Résumé

L'auteur a preparé les deux nouveaux complexes: triacetatotriamminechrome(III) et triacetatotripyridinechrome(III). Il a mesuré les spectres d'absorption de ces deux complexes et il en a conclu que ces complexes obtenus ont tous les deux la structure cis-cis, présentant une coïncidence de spectres d'absorption avec ceux des complexes de genre analogue.

L'auteur exprime ses remerciements sincères à Monsieur le Professeur Taku Uemura pour

11) E. L. Whitford, ibid., **47**, 2934 (1925).
12) C. Joos et H. Schnetzler, *Z. phys. Chem.*, **B20**, 1 (1933).
13) K. Nakamoto, M. Kobayashi et R. Tsuchida, *J. Chem. Phys.*, **22**, 957 (1954).
14) Inédit. Dans l'acétone, les spectres d'absorption du complexe trichlorotripyridinechrome(III), qui est l'homotypes, sont à 16100 cm^{-1} pour la première bande d'absorption, à 21750 cm^{-1} pour la deuxième, mais dans l'acide perchlorique (60%) à 16800 cm^{-1} pour la première, à 23100 cm^{-1} pour la deuxième.
15) Y. Shimura et R. Tsuchida, Ce Bulletin, **29**, 311 (1956).
16) H. Yamatera, ibid., **31**, 95 (1958).

l'intérêt qu'il a porté à ce travail en lui donnant des conseils utiles. Il est particulièrement reconnaissant envers Monsieur le Professeur Yukio Kondo qui a participé à la discussion sur l'interprétation des résultats.

Laboratoire de Chimie Minérale
Faculté des Science
Rikkio Université
Ikebukuro, Tokio

Sur les Préparations des Complexes Métalliques. II[1]. *Les Préparations du Trinitratotriamminechrome(III) et du Trinitritotriamminechrome(III)*

Par Masayoshi NAKAHARA

(Reçu le 12 Septembre, 1961)

Dans les complexes du cobalt(III) le trinitrato- et le trinitrito-triammine complexes étaient bien connus et assez communs, mais les complexes homotypes n'étaient pas encore connus jusqu'ici dans les complexes du chrome(III). En général on ne connaissait que les halogéno- ou les pseudohalogeno-complexes comme complexes triammine-types non-électrolytes et, comme autres, les complexes combinés halogéno et oxalato. Il est très étrange qu'on n'ait pas encore obtenu les complexes de chrome(III) correspondants aux complexes du cobalt(III), de forme si simples. Aussi, avons-nous essayé de préparer les complexes de ce type et de les examiner en les comparant avec les complexes du cobalt(III).

Expérience

Préparations—*1) Trichlorotriamminechrome(III)*, $[CrCl_3(NH_3)_3]$.—Obtenu selon la méthode que nous avons montrée dans la partie I[1].

2) Azotate d'argent, $AgNO_3$.— Purifié selon la méthode de Kolthoff et Lingane[2].

3) Azotite d'argent, $AgNO_2$.—Une solution aqueuse d'azotite de sodium a été ajoutée à une solution aqueuse d'azotate d'argent[3]. Les cristaux jaunes clairs ainsi obtenus ont été dissous dans l'eau chaude et recristallisés. On connaît bien leurs deux formes: la forme α et la forme β. Nous les avons employées, toutes les deux, pour l'essai; les résultats étaient les mêmes.

4) Trinitratotriamminechrome(III), $[Cr(NO_3)_3(NH_3)_3]$.—5,3 g. d'azotate d'argent ont été mis en poudre, bien mélangés avec 2,5 g. de trichlorotriamminechrome(III), mis dans un mortier, et broyés. La couleur bleu du trichlorotriamminechrome(III) est passée immédiatement au rouge, mais nous avons continué à broyer pour que la réaction soit complète. Quand ils étaient bien humidifiés par l'eau ou l'éthanol, la réaction se faisait vite, mais quand ils étaient en trop grande quantité, le rendement n'était pas suffisant. La réaction terminée, une solution froide consistant en 3 g. d'azotate de sodium dissous dans 10 ml. d'eau a été ajoutée au produit de la réaction; puis l'extraction et la filtration ont été faites. Nous avons rapidement rassemblé le filtrat et l'avons longtemps laissé tel quel dans le mélange réfrigérant. Les poudres cristallines rouge-violacées ainsi obtenues ont été aspirées, lavées d'abord avec une petite quantité de solution froide, mélange d'éthanol et d'acide d'azotique dilué, puis à l'éthanol et l'éther, enfin séchées à l'air. Rendement: 0,5 g.

Calculé: Cr, 17,99; NH_3, 17,67. Trouvé: Cr, 16,88; NH_3, 16,14%.

Prisme rouge-violacé. Facilement soluble dans l'eau. Pas déliquescent dans l'air, mais sujet à se mouiller quand on le laisse tel quel; on doit le conserver dans le dessicateur. Stable à la température normale, mais, quand on le chauffe, se décompose en explosant au-dessous de 100°C, et laisse l'oxyde de chrome(III). La solution aqueuse est sujette à l'aquotisation.

5) Trinitritotriamminechrome(III), $[Cr(ONO)_3(NH_3)_3]$.— 5 g. d'azotite d'argent ont été mis en poudre, mêlés avec 2,5 g. de trichlorotriamminechrome(III), mis dans le mortier, et broyés soigneusement. La réaction était un peu plus lente que celle du nitrato-complexe; la couleur des poudres est passée lentement du vert bleuâtre au rouge. Puis, au produit complètement broyé a été ajouté une solution froide consistant en 3 g. d'azotite de sodium dissous dans 10 ml. d'eau. Cela a été filtré et le filtrat violet rougeâtre a été laissé tel quel dans le mélange réfrigérant. Suffisamment refroidie, cette solution a donné des cristaux rouge-violacés. Ces cristaux ont été lavés à l'éthanol et séchés à l'air. Rendement: 0,2 g.

Calculé: Cr, 21,75; NH_3, 21,19. Trouvé: Cr, 20,20; NH_3 20,02%.

Poudre cristalline rouge-violacée. Hydrophile dans l'air. Facilement soluble dans l'eau. Stable à la température normale, mais, quand on la chauffe,

1) Partie I, M. Nakahara, Ce Bulletin, 35, 782 (1962).
2) I. M. Kolthoff et J. J. Lingane, *J. Am. Chem. Soc.*, 57, 2126 (1935).
3) M. C. Sneed et al., "Comprehensive Inorganic Chemistry. II", D. van Nostrand, New York (1954), p 178.

se decompose en explosant au-dessous de 100°C.

6) Trinitratotriamminecobalt(III), $[Co(NO_3)_3(NH_3)_3]$.— Nous l'avons préparé selon la méthode de Jörgensen[4]. Ce composé a été préparé aussi par Mori et al.[5]

7) cis-trans-Trinitrotriamminecobalt(III)[6], *cis-trans*-$[Co(NO_2)_3(NH_3)_3]$.—Nous l'avons préparé selon la méthode de Jörgensen[7].

8) cis-cis-Trinitrotriamminecobalt(III), *cis-cis*-$[Co(NO_2)_3(NH_3)_3]$.—Nous l'avons préparé selon la méthode de Suéda[8] et Mori et al.[5]

Spectres d'Absorption.—Les spectres d'absorption dans l'eau des complexes nouvellement préparés ont été mesurés, mais il a été impossible d'obtenir les spectres d'absorption des composés recherchés, selon la méthode ordinaire, car le changement des spectres d'absorption était remarquable avec le temps. Par exemple, même quand on les mesurait sitôt après la dissolution du spécimen, l'aquotisation se faisait immédiatement, et la bande d'absorption spéciale du nitro et du nitrato qui existait à 26000 ~30000 cm^{-1} diminuait tout d'un coup son coéfficient d'éxtinction. Il a été plus facile, certes, de les mesurer dans le mélange eau-éthanol, l'aquotisation étant un peu plus lente, mais, quand même, nous n'avons pu obtenir des données bien exactes. De toute façon, leurs spectres d'absorption, quelques minutes après, finissaient toujours par coïncider avec ceux du triaquotriamminechrome(III). Nous nous sommes servi de la solution d'acide perchlorique concentré ou de la solution d'acide acétique, mais,

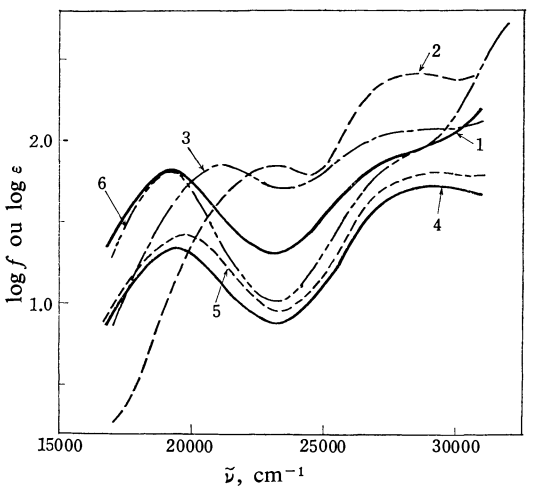


Fig. 1. Spectres d'absorption (de solid) de:
(1) *cis-cis*-$[Co(ONO_2)_3(NH_3)_3]$
(2) *cis-trans*-$[Co(NO_2)_3(NH_3)_3]$
(3) *cis-cis*-$[Co(NO_2)_3(NH_3)_3]$
(4) *cis-cis*-$[Cr(ONO_2)_3(NH_3)_3]$
(5) *cis-cis*-$[Cr(ONO)_3(NH_3)_3]$
(6) *cis-cis*-$[Co(ONO_2)_3(NH_3)_3]$
(en solution; par Shimura[10])

TABLEAU I. LES MAXIMA DES BANDES D'ABSORPTION ($\tilde{\nu}$: 10^3 cm^{-1})

Complexe	La première $\tilde{\nu}$	La deuxième $\tilde{\nu}$
cis-cis-$[Co(ONO_2)_3(NH_3)_3]$	19,0	27,5
cis-trans-$[Co(NO_2)_3(NH_3)_3]$	23,0	
cis-cis-$[Co(NO_2)_3(NH_3)_3]$	20,8	
cis-cis-$[Cr(ONO_2)_3(NH_3)_3]$	19,3	~27,5
cis-cis-$[Cr(ONO)_3(NH_3)_3]$	19,8	~27,5

dans ces deux cas, les résultats n'étaient pas suffisants. Aussi avons-nous renoncé à mesurer les spectres d'absorption en solution, et nous avons décidé de mesurer les spectres d'absorption des solides. Les mesures ont été faites en employant le spectrophotomètre photoélectrique de Marque Hitachi EPU et ses accessoires. L'échantillon a été bien broyé dans un mortier d'agate, et le pouvoir réflecteur R_d a été mesuré. Nous avons obtenu la valeur f en remplacant R_d par sa valeur dans la formule de Kubelka-Munk[9]:

$$f(R_d) \equiv \frac{(1-R_d)^2}{2R_d} = C \cdot \varepsilon$$

On ne peut obtenir la valeur absolue du coefficient d'extinction molaire ε, mais on peut comparer, par la valeur de log f, le coefficient d'extinction molaire avec les chiffres obtenus en solution aqueuse, car la valeur f est théoriquement proportionnelle à ce coefficient d'extinction molaire. La courbe 1 de la Fig. 1, par exemple, qui montre les spectres d'absorption du trinitratotriamminecobalt(III) mesurés selon cette méthode, coïncide bien avec les données de Shimura[10] pour la place de la bande d'absorption, l'intensité relative, la forme etc. Aussi avons-nous mesuré selon cette méthode les autres spectres d'absorption; nous avons montré dans la Fig. 1. les résultats des mesures de 15000 cm^{-1} à 32000 cm^{-1}. Toutefois, on ne peut que comparer l'allure des courbes, car elles sont décalées verticalement.

Résultats et Discussion

Voyant ces résultats, nous avons jugé, que $[Cr(NO_3)_3(NH_3)_3]$ et $[Cr(NO_2)_3(NH_3)_3]$ avaient, tous les deux, des bandes d'absorption très semblables, leurs premières bandes d'absorption autour de 19500 cm^{-1}, et leurs grandes bandes d'absorption au delà de 26000 cm^{-1}. Ordinairement, quand les spectres de réflexion sont mesurés par les poudres, on peut obtenir les spectres d'absorption exacts, si ces poudres sont assez fine grâce de la réflexion diffuse mais si les grains sont gros, le maximum de la bande d'absorption se brisera, sur la bande d'absorption dont le coefficient d'extinction est grand, à cause de la réflexion régulière sur la surface cristalline[11]. En ce cas, les bandes

4) S. M. Jörgensen, *Z. anorg. Chem.*, 5, 185 (1894); E. Birk, ibid., **175**, 409 (1928).
5) M. Mori et al., *J. Chem. Soc. Japan, Pure Chem. Sec. (Nippon Kagaku Zasshi)*, **79**, 1251 (1958).
6) Y. Tanito et al., Ce Bulletin, **26**, 188 (1952).
7) S. M. Jörgensen, *Z. anorg. Chem.*, **17**, 475 (1898).
8) H. Suéda, *J. Chem. Soc. Japan (Nippon Kwagaku Kwaishi)*, **59**, 47 (1938).
9) P. Kubelka et F. Munk, *Z. tech. Physik*, **12**, 593 (1931).
10) Y. Shimura et R. Tsuchida, *J. Chem. Soc. Japan, Pure Chem. Sec. (Nippon Kagaku Zasshi)*, **77**, 734 (1956).
11) G. Kortüm et M. Kortüm-Seiler, *Z. Naturforsch.*, **2a**, 652 (1947); G. Kortüm et H. Schottler, *Z. Elektrochem.*, **57**, 353 (1953); G. Kortüm et P. Hang, *Z. Naturforsch.*, **8a**, 372 (1953); G. Kortüm et G. Schreyer, *Angew. Chem.*, **67**, 694 (1955);

d'absorption de nitrato et nitro sont très larges et doivent apparaître autour de 33000 cm^{-1} et 28000 cm^{-1}; elle prennent alors une forme écrasée comme nous l'avons montré dans la Fig. 1. On ne peut pas considérer comme exacte la valeur autour de 30000 cm^{-1}, du point de vue de la sensibilité de l'appareil de mesure, mais on peut voir du moins qu'il y a une bande d'absorption spéciale[12] au delà de 29000 cm^{-1}, et, au pied de celle-ci, la deuxième bande d'absorption. Or, lorsqu'on observe les spectres d'absorption du trinitratotriamminechrome(III) et du trinitratotriamminecobalt(III), on peut voir que les formes de ces deux premières bandes d'absorption sont très ressemblantes, et, de plus, qu'elles se superposent presque entièrement (19300 cm^{-1} et 19000 cm^{-1}). Les deuxièmes bandes d'absorption se situent autour de 27000 ~27500 cm^{-1}, et il y a, de plus, ce qui serait la bande d'absorption spéciale du nitrato. Nous croyons par là, que le trinitratotriammine-chrome(III) a la même structure cis-cis que celle des complexes du cobalt(III) homotypes. Par la bande d'absorption de $[Cr(NO_2)_3(NH_3)_3]$, on voit un état bien différent de celui des complexes du cobalt(III); la première bande d'absorption de $[Cr(NO_2)_3(NH_3)_3]$ se situe à 19800 cm^{-1}, un peu plus près du côté des faibles longueurs d'onde que celle du trinitratotri-amminechrome(III), qui se situe à 19300 cm^{-1}, quoi qu'il en soit elles sont proches l'une de l'autre. Elle est bien séparée des bandes d'absorption des complexes cis-cis (20800 cm^{-1}) et cis-trans (23000 cm^{-1}) du trinitrotriammine-cobalt(III). On est donc amené à concevoir, pour $[Cr(NO_2)_3(NH_3)_3]$, une structure bien différente de celle du trinitrotriamminecobalt-(III). Il est plus raisonnable de penser à un composé de coordination en nitrito ONO, qui est proche de nitrato ONO_2 dans les séries spectrochimique[10], que de penser à un composé de coordination en nitro NO_2. Voyant que, selon les séries spectrochimiques, dans les séries $[CoX(NH_3)_5]$, NO_2 est à 21800 cm^{-1}, ONO à 20400 cm^{-1}, et ONO_2 à 20000 cm^{-1}, sur la première bande d'absorption, it n'est pas si déraisonnable de formuler une telle conclusion. Nous avons donc jugé que le complexe NO_2-chrome ainsi obtenu est le trinitritotriammine-chrome(III). Or les deux complexes nouvelle-ment obtenus ont leurs spectres d'absorption très ressemblants. Nous avons déduit tout à l'heure la structure cis-cis du trinitratotri-amminechrome(III) par sa ressemblance avec les bandes du trinitratotriamminecobalt(III); nous pouvons déduire, de la même manière, la structure cis-cis du trinitritotriamminechrome-(III). Le trinitritotriamminecobalt(III) n'est pas encorec onnu, mais, comme on le verra dans la Fig. 1, la première bande d'absorption du *cis-cis*-trinitrotriamminecobalt(III) se situe à 20800 cm^{-1}, celle du *cis-trans*-trinitrotriammine-cobalt(III), à 23000 cm^{-1}. Quand on pense à ce fait que la différence entre le maximum du *cis-cis*-trinitratotriamminecobalt(III) et du *cis-cis*-trinitrotriamminecobalt(III) est de 1800 cm^{-1}, et la différence correspondante des $[Co(NO_2)(NH_3)_5]$ et $[Co(NO_3)(NH_3)_5]$ est de 1800 cm^{-1} [10], on doit trouver très remarquable la différence (3200 cm^{-1}) entre le *cis-trans*-trinitrotriamminecobalt(III) et le trinitritotri-amminechrome(III). Le fait que la différence de situation entre la première bande d'absorption du *cis-cis*-trinitratotriamminechrome(III) et celle du trinitritotriamminechrome(III) est telle, prouvera que celui-ci aussi est de structure *cis-cis*; on peut donc considérer les composés nouveaux ainsi obtenus comme le *cis-cis*-trinitratotriamminechrome(III) et le *cis-cis*-trinitritotriamminechrome(III).

Résumé

Les *cis-cis*-trinitratotriamminechrome(III) et *cis-cis*-trinitritotriamminechrome(III), composés nouveaux, ont été préparés. Ils sont tous les deux sujets à être aquotisés dans l'eau, et leurs spectres d'absorption en la solution n'ont pu être mesurés. Nous avons donc obtenu les spectres d'absorption par la méthode de la réflexion sur la poudre. Nous en avons examiné les résultats, et avons conclu, à l'aide des séries spectrochimiques, que les deux complexes étaient les nitrato- et nitrito-complexes combinés par l'oxygène avec le métal central, et qu'ils avaient la structure cis-cis.

L'auteur exprime ses remerciements sincères à Monsieur le Professeur Taku Uemura pour l'intérêt qu'il a porté à ce travail en lui donnant des conseils utiles, et il est particulièrement reconnaissant envers Monsieur le Professeur Yukio Kondo qui a participé à la discussion sur l'interprétation des résultats.

Laboratoire de Chimie Minérale
Faculté des Sciences
Rikkio Université
Ikebukuro, Tokio

12) Y. Shimura et R. Tsuchida, Ce Bulletin, **29**, 311 (1956).

Studies on the Phosphorescence Spectra. I. Phosphorescence Spectra of 1-Naphthol and 2-Naphthol

By Tohru AZUMI

(Received August 15, 1961)

The phosphorescence spectra of aromatic compounds have been studied rather extensively. Lewis and Kasha[1] showed that the phosphorescent state of a molecule is equivalent to the lowest triplet state. McClure[2] measured the lifetime of the phosphorescence of various aromatic compounds and interpreted his results from the standpoint of spin-orbit interaction[3]. The symmetry consideration of the spin-orbit interaction operator has been made by McClure[4], Weissman[5], and Mizushima and Koide[6]. A quantitative calculation of the spin-orbit interaction has been given by Pople and Sidman[7,8] and by Hameka and Oosterhoff[9]. Research into the triplet states in relation to the molecular compounds has been done by Reid[10,11], Platt et al.[12], Czekalla et al.[13] and McGlynn et al.[14-16]. Moreover, the triplet states of aromatic compounds have been considered to play an important role in various phenomena, for example, in the energy transfer between molecules[14-17] and in photoelectric coductivity[18].

The analyses of the triplet states of simple molecules themselves, however, are as yet incomplete. Before dealing with the application of the triplet states a more thorough examination of the phosphorescence spectra is necessary.

In this paper, as a first step toward this goal, the phosphorescence spectra of 1- and 2-naphthols are presented.

Only a little research into the phosphorescence spectra of naphthols has been undertaken so far. In 1944 Lewis and Kasha[1] observed the phosphorescence spectra of 1- and 2-naphthols and reported the 0, 0-band positions in EPA solvent (5 parts diethyl ether, 5 isopentane, and 2 ethanol) at 20500 cm^{-1} and 21100 cm^{-1} respectively. McClure[2] measured the lifetimes of the phosphorescence and gave 1.9 ± 1 sec. for 1-naphthol and 1.3 ± 1 sec. for 2-naphthol.

Experimental

Apparatus. — The apparatus used is similar in principle to that devised by Heckman[19], and is shown schematically in Fig. 1. A xenon short arc lamp (1 kW) (A) provides an exciting light, which is, after passing through slits (B) and a lens (C), reflected from a front surface aluminum mirror (D) and enters a cell through a quartz window. The cell is cooled by liquid nitrogen and has been evacuated to prevent adverse effects from oxygen molecules and from condensation of air. Phosphorescent light emitted from the surface of the rigid sample is reflected by another mirror and is collimated to a Shimadzu quartz spectrograph (G) with a dispersion of 100 cm^{-1}/mm. around, 25000 cm^{-1}. The exciting light and the phosphorescent light are separated by a Bequellel type phosphoroscope (E)[20]. The exposure times ranged from a few minutes to several hours on Neopan SSS film. Spectrograms were calibrated

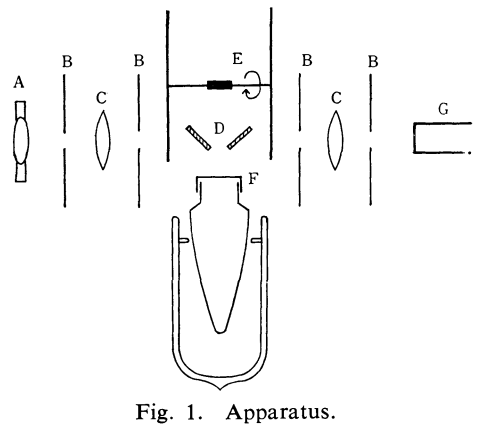


Fig. 1. Apparatus.

1) G. N. Lewis and M. Kasha, *J. Am. Chem. Soc.*, **66**, 2100 (1944).
2) D. S. McClure, *J. Chem. Phys.*, **17**, 905 (1949).
3) D. S. McClure, ibid., **20**, 682 (1952).
4) D. S. McClure, ibid., **17**, 665 (1949).
5) S. I. Weissman, ibid., **18**, 232 (1950).
6) M. Mizushima and S. Koide, ibid., **20**, 765 (1952).
7) J. A. Pople and J. W. Sidman, ibid., **27**, 1270 (1957).
8) J. W. Sidman, ibid., **29**, 644 (1958).
9) H. F. Hameka and K. J. Oosterhoff, *Mol. Phys.*, **1**, 358 (1958).
10) C. Reid, *J. Chem. Phys.*, **20**, 1212, 1214 (1952).
11) M. M. Moodie and C. Reid, ibid., **22**, 252 (1954).
12) H. McConnel, J. S. Ham and J. R. Platt, ibid., **21**, 66 (1953).
13) J. Czekalla, G. Briebleb, W. Herre and H. J. Vahlensieck, *Z. Electrochem.*, **63**, 715 (1959).
14) S. P. McGlynn and J. D. Boggus, *J. Am. Chem. Soc.*, **80**, 5096 (1958).
15) S. P. McGlynn, J. D. Boggus and E. Elder, *J. Chem. Phys.*, **32**, 357 (1960).
16) S. P. McGlynn, *Chem. Revs.*, **58**, 1113 (1958).
17) A. Terenin and V. Ermolaev, *Trans. Faraday Soc.*, **52**, 1042 (1956).
18) D. C. Northrop and D. Simpson, *Proc. Roy. Soc.*, **A234**, 124, 136 (1956).
19) R. C. Heckman, *J. Mol. Spectroscopy*, **2**, 27 (1958).
20) R. J. Deirs, R. K. Brits and W. E. Wentworth, *Anal. Chem.*, **29**, 202 (1957).

with an iron spectrum and were measured with a Riken B-type microphotometer. The maximum precision is believed to be $\pm 5\,cm^{-1}$ for the sharp bands.

Materials. — The solvents used were ethanol, diethyl ether, *n*-hexane, petroleum ether, and carbon tetrachloride. These were purified in the following ways. Ethanol was distilled with sulfuric acid, heated under reflux with potassium hydroxide and silver nitrate, and then distilled. The distillate was dried with activated aluminum amalgam, filtered and distilled. The distillate was further passed through a silica gel-column and was finally distilled. Diethyl ether was shaken with a solution of sodium carbonate, washed with a saturated sodium chloride solution, dried over calcium chloride, distilled over sodium, passed through a silica gel column, and distilled again. *n*-Hexane and petroleum ether were both treated with concentrated sulfuric acid and fuming sulfuric acid, washed with water containing potassium hydroxide, and distilled. Carbon tetrachloride was heated under reflux with potassium hydroxide and distilled. The distillate was again heated with mercury and distilled. The solvents thus purified had no or practically no phosphorescence.

Both 1- and 2-naphthols were recrystallized from ligroin three times. Further purification was made by sublimation under reduced pressure just before measurement.

Results and Discussion

Naphthol exhibits phosphorescence in ethanol and in diethyl ether. The phosphorescence of naphthol in ethanol is more intense than that in ether. In the other solvents used, namely, in *n*-hexane, petroleum ether, and carbon tetrachloride, there is no detectable phosphorescence. When a very small quantity of ethanol, 1% of the total, is added to any of the above solvents, intense phosphorescence can be observed in each case.

The solvent effect upon the intensity of the phosphorescence seems quite complex. The above result resembles that reported by Fernandes and Becker[21], but the same explanation is not possible. Lewis, Lipkin and Magel[22] and Yamamoto[23] have considered that the solvent for the measurement of phosphorescence must have a hydrogen bonding capacity. The above result, however, is not accounted for by their theories. Discussion will be postponed until further experiments have been carried out.

Figures 2 and 3 show the phosphorescence spectra of 1- and 2-naphthols in ethanol, where

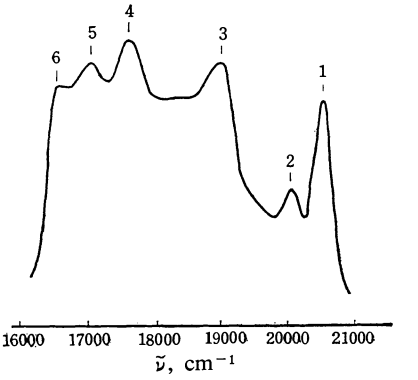


Fig. 2. Phosphorescence spectrum of 1-naphthol.

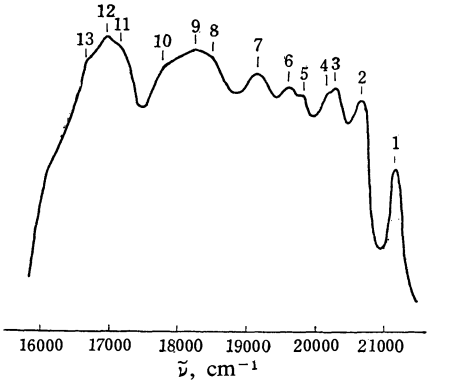


Fig. 3. Phosphorescence spectrum of 2-naphthol.

the ordinates are the plate blackness in arbitrary units. The spectra in ether are almost the same as those in ethanol, except that the latter are less intense.

Vibrational analyses are given in Tables I and II. The infrared and the Raman spectra data determined by the present author are used as a basis of analysis.

A comparison of the spectra of naphthols with the spectrum of naphthalene is of interest. The phosphorescence spectrum of naphthalene was reported by Czekalla et al.[13] As can be seen in Fig. 3, the phosphorescence spectrum of 2-naphthol resembles that of naphthalene in its spectral shape. The spectrum of naphthalene has more vibrational bands than that of 2-naphthol, and every band in the latter, except band 3, has its corresponding band in the former. Both spectra have almost the same progressions. Band 3 at $20325\,cm^{-1}$ in the spectrum of 2-naphthol is quite puzzling. This band is separated by $830\,cm^{-1}$ from the 0, 0-band. Although there is a rather strong band at $842\,cm^{-1}$ in the infrared spectrum, no reasonably matched band is found in the Raman spectrum. Further, there is no corresponding

21) J. Fernandes and R. S. Becker, *J. Chem. Phys.*, **31**, 467 (1959).
22) G. N. Lewis, D. Lipkin and T. T. Magel, *J. Am. Chem. Soc.*, **53**, 3017 (1931).
23) D. Yamamoto and R. Iwaki, *J. Chem. Phys.*, **19**, 662 (1951); D. Yamamoto, *Busseiron Kenkyu*, No. 37, 57; No. 38, 65 (1951); *J. Chem. Soc. Japan, Pure Chem. Sec.* (*Nippon Kagaku Zasshi*), **73**, 739, 794 (1952); **74**, 8 (1953).

TABLE I. PHOSPHORESCENCE SPECTRUM OF 1-NAPHTHOL

Band No.*	Wave number	$\Delta\tilde{\nu}$	Analysis
1	20550		0, 0
2	20060	490	0, 512
3	19075	1475	0, $\left.\begin{matrix}1390\\1584\end{matrix}\right\}=1487$
4	17630	2920	0, 1390+1584=2974
5	17055	3475	0, 512+1390+1584=3486
6	16370	4180	0, 1390×3=4170

* Number as given in Fig. 2.

TABLE II. PHOSPHORESCENCE SPECTRUM OF 2-NAPHTHOL

Band No.*	Wave number	$\Delta\tilde{\nu}$	Analysis
1	21155		0, 0
2	20655	500	0, 519
3	20325	830	
4	20150	1005	0, 519×2=1038
5	19775	1380	0, 1380
6	19590	1565	0, 1587
7	19070	2085	0, 519+1587=2106
8	18400	2755	0, 1380×2=2760
9	18220	2935	0, 1380+1587=2967
10	17710	3445	0, 519+1380+1587=3467
11	17055	4100	0, 1380×3=4140
12	16875	4280	0, 1380+1470×2=4320
13	16640	4515	0, 1470×2+1587=4527

* Number as given in Fig. 3.

band in the phosphorescence spectrum of naphthalene. Therefore, in this paper, this band remains unexplained.

The phosphorescence spectrum of 1-naphthol has even fewer vibrational bands than that of 2-naphthol. Bands 4, 5 and 6 are very wide, and their centers could only with difficulty be determined exactly. Every band except band 3 has its counterpart in the spectrum of 2-naphthol and also in that of naphthalene. Band 3 is separated by 1475 cm^{-1} from the 0, 0-band. There is a strong infrared band at 1460 cm^{-1} and a Raman band at 1458 cm^{-1}. Therefore, band 3 may be ascribed to this vibration. However, through comparison of the spectrum of 2-naphthol with the spectra of 1-naphthol and naphthalene, this band is tentatively ascribed to a superposition of 1390 and 1584 cm^{-1}.

As has been stated above, the spectra of 1- and 2-naphthols resemble the spectrum of naphthalene. Accordingly, the lowest triplet state of naphthol may be considered to be like a perturbed triplet state of naphthalene, not a new type of state, such as a charge-transfer state.

Next, the direction of a transition moment will be discussed. Naphthol has no symmetry, apart from its symmetry with respect to the molecular plane. However, on the basis of what has been mentioned above, consideration of a transition moment may be made by analogy with the case of naphthalene.

The 0, 0-band of naphthalene is shifted toward blue by the introduction of a hydroxyl group, as is seen in an ordinary π-π transition. The amount of blue shift is 750 cm^{-1} for 1-naphthol and 145 cm^{-1} for 2-naphthol. That 1-substitution gives rise to a large shift and 2-substitution, to only a small shift shows that the phosphorescence of naphthol, as well as that of naphthalene, has a moment of a short-axis direction. Williams[24] reached the same conclusion by observing the polarization of the phosphorescence of naphthalene.

The author wishs to express my thanks to Professor Hiroshi Azumi for his advice and encouragement.

Department of Chemistry
Faculty of Science
Tohoku University
Katahira-cho, Sendai

24) R. Williams, *J. Chem. Phys.*, **30**, 233 (1959).

Studies on Foams. IX[1]. *Foaminess and Foam Stability of Polyvinyl Alcohol Solutions*

By Masayuki NAKAGAKI* and Kazu GOTO

(Received September 18, 1961)

Recently polyvinyl alcohol has been used widely as a synthetic protective colloid soluble in water, e. g., as an emulsifier, a dispersing agent and so forth. In this paper, the protective action for gas particles, that is, the foaminess and foam stability of polyvinyl alcohol solutions, will be studied.

Among the various methods for producing foams[2], such as the pneumatic method, agitation and boiling, the shaking method has thus far been used exclusively in the present series, but this method is not suitable for stable foams like that of polyvinyl alcohol solutions, because sometimes a vessel is filled with the foam after shaking. Therefore, instead of the shaking method, the pour method, which has also been used extensively to test the foaming properties of detergents, will be used in this paper.

Experimental

Materials. — As samples of polyvinyl alcohol, six specimens, Gohsenol GH-20, GM-14, GL-05, NH-20, NM-14 and NL-05, were used. These are the same as those used in previous experiments[3]. The symbol G means partially saponified, (the saponification degree is 87.0~87.6%), and N means almost perfectly saponified (98.8~99.3%) specimens, while 20, 14 and 05 indicate polymerization degrees of about 2000, 1400 and 500 respectively.

A specimen of known weight was put into 800 ml. of distilled water in a flask and left alone at room temperature overnight. Then, after placing the flask in a water bath at room temperature, the bath was warmed up to boiling within 15 min. and kept boiling for 30 min. The flask was then taken out of the bath and cooled by dipping it in cold water, and the solution was transferred to a volumetric flask and made up to 1000 ml. From this original solution, solutions of the desired concentration were prepared by dilution.

Pour Test. — The apparatus used for the pour test is that prescribed by JIS (Japanese Industrial Standards)[4] and similar to that used by Ross and Miles[5]. The apparatus consists of a pipet and a long, cylindrical, jacketted glass receiver. Both the pipet and the receiver are held vertically, and the receiver is kept at 30°C by circulating water from a thermostat. The orifice at the lower end of the pipet is made of a glass capillary tube 2.9 mm. in inner diameter, 7 mm. in outer diameter and 10 mm. in length. The content of the pipet is 200 ml. The upper end of the pipet is connected through a valve with a capillary tube to regulate the flow rate so that the 200 ml. solution in the pipet will fall through the orifice within 30 ± 1 sec. To make the pour test, 50 ml. of the solution is placed in the receiver and 200 ml. is run in from the pipet, the orifice of the latter being held exactly 90 cm. above the surface of the solution in the receiver. The height of the foam thus formed is read, as is its change with time, the time being recorded from just the moment when the pouring of the solution finishes.

Results and Discussion

Change of Foam Height with Time. — The height of the foam zone, A (mm.), was measured at various times, t (min.), for various concentrations of six polyvinyl alcohol solutions. For example, the relation between the foam height and concentration at various times is shown in Fig. 1 for GH-20. At first the curve has a very flat maximum at about 0.4 g./100 ml., but, during the destruction of the foam, another maximum appeared at about 0.1 g./100 ml. and the maximum point was shifted to 0.05 g./100 ml. in time. The similar pattern of GM-14 showed that a slight maximum, which had not been observed at first, appeared at about 0.05 g./100 ml. at $t\simeq4$ min. and disappeared at $t\simeq12$ min. Although no maximum was observed in this case at about 0.4 g./100 ml., the foam height at 0.6~1.0 g./100 ml. remained high until $t\simeq9$ min. The behavior of GL-05 was similar to that of GM-14, except that a maximum of foam height appeared at about 0.01 g./100 ml. during the destruction of the foam. The foam formation of NL-05 was poor, but a maximum of foam height appeared at 0.1 g./100 ml. during the destruction of the foam. On the other hand, the foams of NM-14 and NH-20 were very stable, and the foam height scarcely changed within 35 min.

* Present address: Faculty of Pharmacy, Kyoto University, Sakyo-ku, Kyoto.

1) The preceding paper is M. Nakagaki and K. Shinoda, This Bulletin, **27**, 367 (1954).

2) J. J. Bikerman, "Foams", Reinhold Publ. Corp., New York (1953), p. 33.

3) M. Nakagaki and A. Shimazaki, This Bulletin, **29**, 60 (1956).

4) JIS K 3361-1953 and JIS K 3362-1955.

5) J. Ross and G. D. Miles, *Oil and Soap*, **18**, 99 (1941); G. D. Miles and J. Ross, *J. Phys. Chem.*, **48**, 280 (1944).

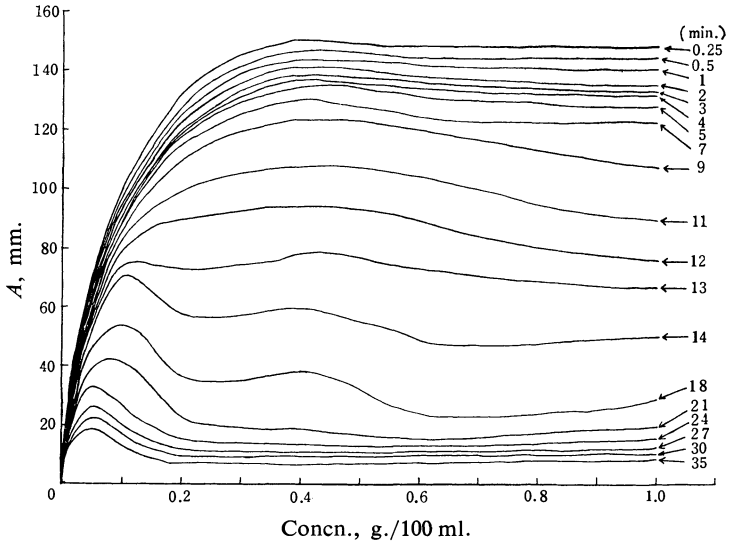


Fig. 1. The relations between foam height and concentration for GH-20 at various times.

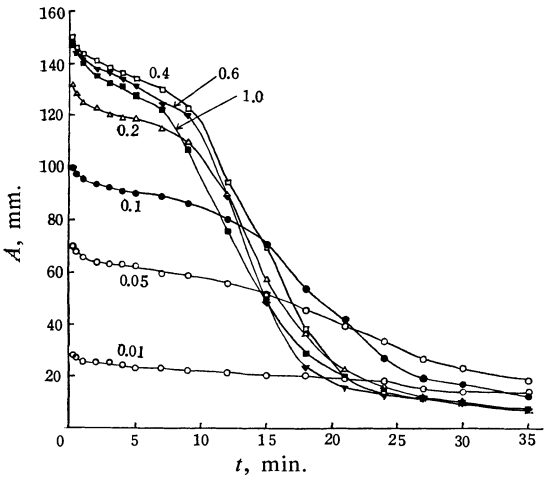


Fig. 2. Time dependence of foam height at various concentrations of GH-20.

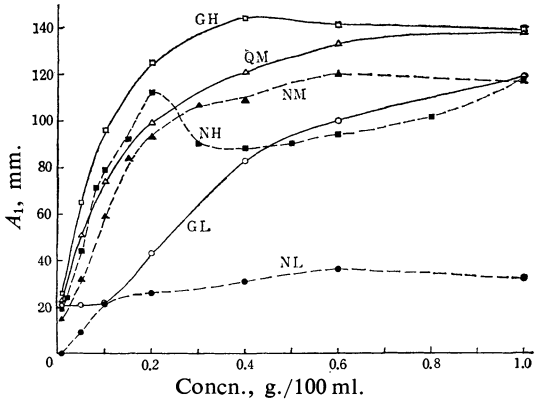


Fig. 3. Relation between foaminess and concentration.

The relationship between the foam height and the time at various concentrations is shown in Fig. 2 for GH-20 as an example. It can be seen that the foam height tends to show a stationary state after about 1 min., and then again rapidly decreases after a certain time. The first rapid decrease of foam height within 1 min. is due to the establishment of a better packing of bubbles in the foam zone, while the second rapid decrease corresponds to the collapse of the foam.

On the basis of these data, the foaminess, lingering fraction and half life of the foam of various polyvinyl alcohol solutions will be discussed.

Foaminess.—In order to show how well the solution foams, the concentration dependence of foaminess is compared in Fig. 3 for six polyvinyl alcohol specimens. As has already been shown above, the foam zone tends to show a steady state at about $t=1$ min., the collapse of foam being not yet serious at that moment. Therefore, the foam height at 1 min., A_1 (mm.), will be of an appropriate quantity to represent the foaminess. The relation between the foaminess, A_1, and the concentration is shown in Fig. 3.

Comparing the partially saponified (G series) and the perfectly saponified (N series) polyvinyl alcohols of the same polymerization degree, the foamer forms better than the latter; that is, GH > NH, GM > NM and GL > NL. Comparing, then, polyvinyl alcohols of the same degree of saponification, the foaminess is the greater, the greater the degree of polymerization; that is, GH > GM > GL and NH > NM > NL, except that NM foams better than NH at the concentration range between 0.26 to

1.0 g./100 ml. It is especially to be noted that the foaminess of NH has a maximum point at about 0.2 g./100 ml.

Lingering Fraction. — In order to compare the stability of foams, the quantity defined by the following equation and called, here, the "lingering fraction" after 35 min., L_{35} (%), is used.

$$L_{35}=(A_{35}/A_1)\times 100 \quad (\%) \qquad (1)$$

where A_{35} is the height of the foam zone remaining after 35 min. The concentration dependencies of the lingering fractions of six polyvinyl alcohol specimens are shown in Fig. 4. At concentrations greater than 0.2 g./100 ml., the foams of partially saponified polyvinyl alcohol solutions are very unstable and mostly collapse within 35 min., while the foams of the perfectly saponified polyvinyl alcohols NM and NH are very stable and practically do not collapse at all within 35 min. The foam of HL is not so stable, but it is still more stable than the partially saponified G specimens. Therefore, the lingering fractions are in the sequence of NH, NM > NL > GH, GM, GL. At concentrations smaller than 0.2%, the lingering fraction of the partially saponified G-series increases with the decrease in the concentration, while the lingering fraction of the perfectly saponified NH and NM decreases with the decrease in the concentration. Therefore, the foams of GH, GM and GL are the less stable, the higher the concentration, while the foams of NH and NM are the more stable, the higher the concentration. On the other hand, the foam of NL has its maximum stability at 0.1 g./100 ml.

Half Life.—Since the decrease in the foam height with time is generally in the manner as shown in Fig. 2, the half life $t_{1/2}$ (min.), defined as the time when the foam height becomes just one half of A_1, is another measure of foam stability. The half lives are shown in Fig. 5, except for NH and NM, the half lives of which can not be determined because the values are greater than 35 min. The curves of unstable GL, GM and GH foams, overlapped

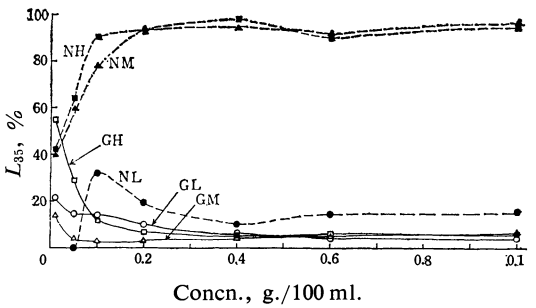


Fig. 4. Relation between lingering fraction and concentration.

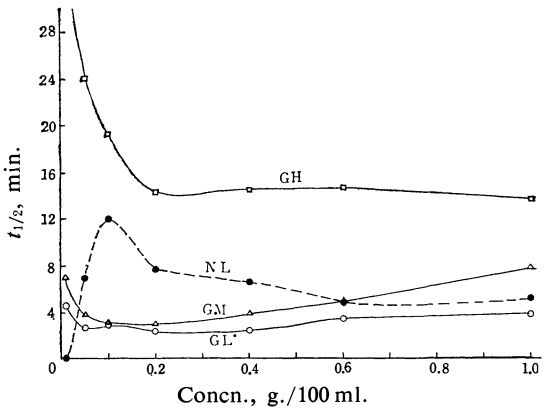


Fig. 5. Relation between half life and concentration. The half lives of NH and NM are not shown here.

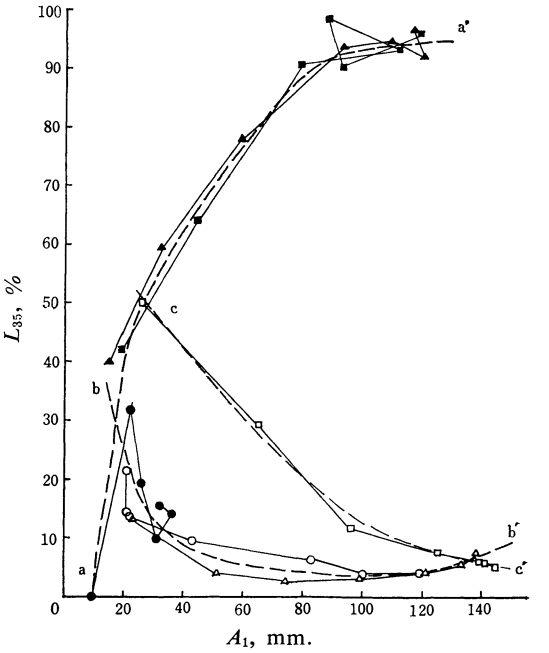


Fig. 6. The relation between A_1 and L_{35} for NH (■), NM (▲), NL (●), GH (□), GM (△) and GL (○).

with each other in Fig. 4, have been separated clearly in Fig. 5. The features observed in both Fig. 4 and Fig. 5 are that the foam stability of GH, GM and GL increases with the decreasing concentration, and that the stability of NL reaches its maximum at about 0.1 g./100 ml. In Fig. 5, however, the points different from Fig. 4 are that half life of GH is greater than that of NL, GM and GL, and that the half life of GM is greater than GL. Consequently, the sequence of half lives is NH, NM > GH > (NL) > GM > GL, although the half life of NL varies greatly with the concentration.

Relation between Foaminess and Foam Stability.—In preceding papers of the present series[6], it has been observed that the foaminess and foam stability are parallel for at least unstable foams formed by shaking. In the case of stable foams of polyvinyl alcohol solutions formed by the pour method, however, the foaminess and foam stability are not always parallel. The relation between the foaminess A_1 and the lingering fraction L_{35} is illustrated in Fig. 6. In this figure, experimental plots are connected with straight lines in the order of concentration. Experimental plots for NH, NM and low concentration solutions of NL are located along a dotted curve, aa′, which indicates that the foam stability is the greater, the greater the foaminess. However, experimental plots for GH, GM, GL and high concentration solutions of NL are located along two dotted curves, bb′ and cc′, which indicates that the foam stability is the greater, the smaller the foaminess, although curve bb′ has a flat minimum and goes up again at high concentrations, at this range the foam stability being the greater, the greater the foaminess. The increase in foam stability at high concentrations of GM and GL has already been shown in Fig. 5.

Summary

The foaminess and foam stability of six polyvinyl alcohol solutions, GH-20, GM-14, GL-05, NH-20, NM-14 and NL-05, were measured by the pour test; the foaminess was represented by the height of the foam zone after 1 min., and the foam stability was represented either by the lingering fraction after 35 min. or by the half life of the foam.

The foaminess of the partially saponified polyvinyl alcohols was greater than that of the perfectly saponified ones of the corresponding molecular weights. Comparing specimens of the same degree of saponification, the foaminess was the greater, the greater the molecular weight. The foaminess was also the greater, the greater the concentration, except for NH, the fomianess of the latter showing a maximum at about 0.2 g./100 ml.

The foam stability of NH and NM was very large, but that of NL was small and showed a maximum at 0.1 g./100 ml. The foam stabilities of GH, GM and GL were small. Comparing the foaminess and the foam stability, these two quantities varied in a parallel manner in the cases of NH, NM, low concentrations of NL, and high concentrations of GM and GL, but in other cases they varied conversely.

The authors wish to thank Nippon Gosei Kagaku Kogyo Co., Ltd., which provided Gohsenols.

Faculty of the Science of Living
Osaka City University
Nishi-ku, Osaka

6) M. Nakagaki, This Bulletin, **21**, 30 (1948); **22**, 21 (1949).

Studies on Antibiotics and Related Substances. XIII. Syntheses of 10-Methylene-11-oxododecanoic Acid and 9-Methylene-10-oxo-undecanoic Acid, Antitumor Substances[1]

By Mitsuhiro KINOSHITA, Saburō NAKADA and Sumio UMEZAWA

(Received May 29, 1961)

In previous papers[2], syntheses and antitumor activities of a series of carboxylic acids containing a terminal methylene-keto group were reported. In the course of synthesizing the above mentioned series of carboxylic acids through the corresponding Mannich bases, we found the formation of two kinds of Mannich base isomers in respect to the active methylene groups at either side of the ketone group, and reported[2] the syntheses of β-methylenelevulinic acid and 4-keto-3-methylenepentane-1-carboxylic acid. The present paper is concerned with an extention of this work and presents the syntheses and antitumor activities of 10-methylene-11-oxododecanoic acid (IVa) and 9-methylene-10-oxoundecanoic acid (IVb). The

1) Presented at the 13th Annual Meeting of the Chemical Society of Japan, Tokyo, April, 1960.

2) M. Kinoshita and S. Umezawa, This Bulletin, 33, 1075 (1960).

syntheses proceeded as shown in the following chart.

$CH_3CO-\underset{\underset{CH_2N(CH_3)_2\cdot HCl}{|}}{CH}-(CH_2)_nCO_2H \rightarrow$

(Ia, Ib)

$CH_3CO-\underset{\underset{CH_2N(CH_3)_3I}{|}}{CH}-(CH_2)_nCO_2CH_3 \rightarrow$

(IIa, IIb)

$CH_3CO-\underset{\underset{CH_2}{||}}{C}-(CH_2)_nCO_2CH_3 \rightarrow$

(IIIa, IIIb)

$CH_3CO-\underset{\underset{CH_2}{||}}{C}-(CH_2)nCO_2H$

(IVa, IVb)

Ia, IIa, IIIa IVa : n=8, Ib, IIb, IIIb : n=7

10-Methylene-11-oxododecanoic Acid (IVa). —10-(Dimethylaminomethyl)-11-oxododecanoic acid hydrochloride (Ia) has been isolated from the mother liquor recovered from the crystallization of the main product[3]. The new Mannich base hydrochloride was esterified, changed into its free base and then converted into a methiodide IIa. Thermal degradation of the methiodide to the desired methylene ester IIIa took place smoothly in a yield of 61%. Hydrolysis of the ester with an aqueous acetone solution of sulfuric acid afforded 10-methylene-11-oxododecanoic acid (IVa).

The ultraviolet absorption spectra of IIIa and IVa in methanol solution showed peaks at 220.5, 319 mμ and 221, 319 mμ, respectively, indicating the presence of α,β-unsaturated ketone group (Fig. 1). The infrared absorption characteristics of IIIa and IVa were just as expected, showing the presence of double

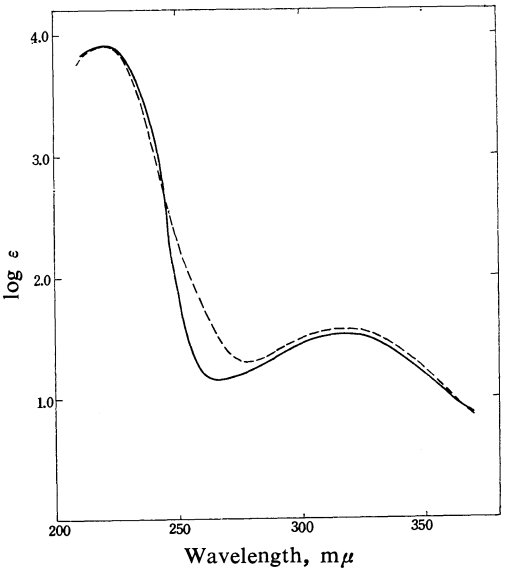


Fig. 1. Ultraviolet absorption spectra of methyl 10-methylene-11-oxododecanoate (IIIa) (------) and 10-methylene-11-oxododecanoic acid (IVa) (——) in methanol.

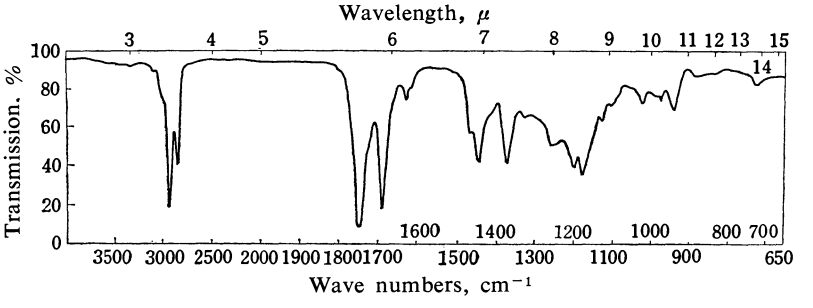


Fig. 2. Infrared absorption spectrum of methyl 10-methylene-11-oxododecanoate (IIIa) (liquid).

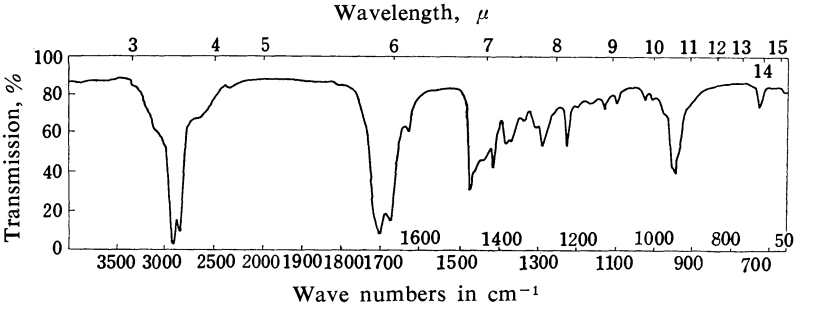


Fig. 3. Infrared absorption spectrum of 10-methylene-11-oxododecanoic acid (IVa) (Nujol).

3) M. Kinoshita and S. Umezawa, ibid., 34, 309 (1961).

bond, conjugated carbonyl and carboxyl groups (Figs. 2 and 3).

9-Methylene-10-oxoundecanoic Acid (IVb). — 9-(Dimethylaminomethyl)-10-oxoundecanoic acid hydrochloride (Ib) has been isolated from the mother liquor recovered from the crystallization of 12-(dimethylamino)-10-oxododecanoic acid[3]. An analogous sequence of reactions as described above in the synthesis of IVa has been applied to afford the title compound.

Both 10-methylene-11-oxododecanoic acid (IVa) and 9-methylene-10-oxoundecanoic acid (IVb) has been found to possess strong antitumor activity in vitro. However, in contrast to 11-oxo-11-dodecenoic acid[2] having the methylene-keto group at the end of straight carbon chain, the activities of both VIa and VIb were unexpectedly weak in vivo tests.

Experimental

10-(Dimethylaminomethyl)-11-oxododecanoic Acid Hydrochloride (Ia).—The mother liquors remaining after filtration of 13-(dimethylamino)-11-oxotridecanoic acid hydrochloride (10.8 g.) previously described[3] were combined and concentrated in vacuo. The oily residue was dissolved in water (25 ml.) and the solution was extracted with four 15 ml. portions of ether to recover the unchanged keto acid (crude 2.5 g.). The aqueous layer was washed with chloroform several times and evaporated to give a yellow oil (15 g.) which, on standing, slowly turned to a crystalline solid intermixed with oil. Trituration with absolute acetone gave 8.5 g. (24.7%) of colorless crystals, m. p. 96～99°C. Three recrystallizations from absolute methanol-ether afforded an analytical sample of 10-(dimethylaminomethyl)-11-oxododecanoic acid hydrochloride (Ia), colorless needles, m. p. 102～103°C. The product gave a positive iodoform reaction.

Found: C, 58.90; H, 9.36; N, 4.55. Calcd. for $C_{15}H_{30}O_3NCl$: C, 58.54; H, 9.83; N, 4.56%.

Methyl 10-(Dimethylaminomethyl)-11-oxododecanoate Methiodide (IIa).—A mixture of Ia (3.5 g.) and absolute methanol (35 ml.) was saturated with dry hydrogen chloride and allowed to stand overnight. The solvent was removed by distillation in vacuo. The resulting viscous orange-yellow oil (4 g.) was dissolved in water (5.2 ml.) and to this solution was added 50% aqueous potassium carbonate solution (8.7 ml.). The separated oil was extracted with three 12 ml. portions of ether. After being dried over fused potassium acetate, the etherial extract was evaporated to give free amine ester as a slightly yellow liquid (2.5 g., 70.7%). To the etherial solution of the product was added methyl iodide (12 g.) to give a crystalline methiodide (IIa), which was collected and washed with ether, yield 3.5 g. (93.3% from free amine ester). Two recrystallizations from methanol-ether gave an analytical sample m. p. 80.5～81.5°C.

Found: C, 47.60; H, 7.70; N, 3.76; I, 29.60. Calcd. for $C_{17}H_{34}O_3NI$: C, 47.79; H, 7.96; N, 3.28; I, 29.69%.

Methyl 10-Methylene-11-oxododecanoate (IIIa). —The above methiodide (IIa) (3.5 g.) was placed in a small distillation flask and heated at 185～200°C in an oil bath under highly reduced pressure (0.05 mmHg). The resulting oil was redistillated to afford a colorless liquid of methyl 10-methylene-11-oxododecanoate (IIIa), yield 1.2 g. (61%), b. p. (bath temp.) 87～93°C/0.002 mmHg, m. p. 20～22°C; λ_{max}^{MeOH} 220.5 (ε 8170) and 319 mμ (ε 35.9); IR, 1748 (ester C=O), 1688 (conjugated C=O), and 1638 cm^{-1} (C=C) (liquid).

Found: C, 70.10; H, 9.82. Calcd. for $C_{14}H_{24}O_3$: C, 69.96; H, 10.0%.

10-Methylene-11-oxododecanoic Acid (IVa).—A solution of the above ester IIIa (1.15 g.) in a mixture (35 ml.) of acetone, water and concentrated sulfuric acid (18 : 15 : 1 by volume) was allowed to stand for 3 days at 20～22°C. The reaction mixture was neutralized with a saturated solution of sodium bicarbonate and evaporated to remove acetone at about 40°C. The residual solution was shaken with ether to remove any unchanged ester. The aqueous layer was adjusted to pH 2.5 with 3 N hydrochloric acid and again extracted with ether. Evaporation of the dried etherial extract afforded crude crystals of 10-methylene-11-oxododecanoic acid (IVa), yield 0.95 g. (87%), m. p. 28～33°C. Recrystallization from ether gave fine needles, m. p. 33～35°C. λ_{max}^{MeOH} 221 (ε 8280) and 319 mμ (ε 33.6); IR, 2700～2500 (carboxyl OH), 1702 (carboxyl C=O), 1675 (conjugated C=O) and 1630 cm^{-1} (C=C) (Nujol).

Found: C, 68.96; H, 9.62. Calcd. for $C_{13}H_{22}O_3$: C, 68.99; H, 9.80%.

Methyl 9-Methylene-10-oxoundecanoate (IIIb).— The mother liquor remaining after filtration of 12-(dimethylamino)-10-oxododecanoic acid (7.7 g.) previously described[3] was processed by the same procedure as employed for the preparation of Ia to afford a hygroscopic crude product of 9-(dimethylaminomethyl)-10-oxoundecanoic acid hydrochloride (Ib), yield 9.9 g., m. p. 74～79°C. The crude hydrochloride (5 g.) was esterified with methanol-hydrogen chloride and the resulting methyl ester hydrochloride was changed to the free amine ester in the same manner as described in preceding paragraph, yield 3.2 g. (crude). To a solution of the free amine (3.2 g.) in benzene (14 ml.) and acetone (9 ml.) was added methyl iodide (16 g.) and the mixture was allowed to stand for 3 days at room temperature. The resulting crystalline solid was the methiodide of methyl 12-(dimethylamino)-10-oxododecanoate and was removed by centrifuging. The supernatant layer was evaporated to afford the desired methiodide IIb as an orange viscous syrup which did not crystallize, yield 4.7 g. To a solution of the crude methiodide in water (11 ml.) was added 10% aqueous potassium bicarbonate solution (23 ml.) and the mixture was allowed to stand for 2 days at 20°C and then extracted with ether. The ether layer was washed with 0.1 N sulfuric acid and with water. After being dried over fused potassium acetate, the etherial extract was evaporated to afford 1.6 g. of crude methyl 9-methylene-10-oxoundecanoate (IIIb) as a slightly yellow liquid. Redistillation of the

crude material gave a pure sample, colorless liquid, yield 1.54 g. (40% based on the crude Mannich base hydrochloride (Ib)), b. p. (bath temp.) 85~87°C/0.005 mmHg., m. p. 8.0~9.1°C, λ_{max}^{MeOH} 220.5 (ε 8720) and 318 mμ (ε 37.1); IR, 1745 (ester C=O), 1686 (conjugated C=O) and 1627 cm^{-1} (C=C) (liquid).

Found: C, 69.11; H, 9.51. Calcd. for $C_{13}H_{22}O_3$: C, 68.99; H, 9.80%.

9-Methylene-10-oxoundecanoic Acid (IVb).—Hydrolysis of IIIb (1.1 g.) by the same procedure as employed for the preparation of IVa gave crude crystals of the title compound, yield 0.9 g. (87.5%), m. p. 37.0~38.2°C. Recrystallization from ether afforded a pure sample, fine prisms, m. p. 38.2~38.7°C; λ_{max}^{MeOH} 220.5 (ε 8350) and 318 mμ (ε 31.8), IR, 2700~2500 (carboxyl OH), 1714 (carboxyl C=O), 1682 (conjugated C=O) and 1632 cm^{-1} (C=C) (Nujol).

Found: C, 67.88; H, 9.22. Calcd. for $C_{12}H_{20}O_3$: C, 67.89; H, 9.50%.

Bioassays[4].—The minimum necessary concentrations of both 10-methylene-11-oxododecanoic acid (IVa) and 9-methylene-10-oxoundecanoic acid (IVb) for the anti-HeLa cell effect were 125 mcg/ml. Against cells of Ehrlich carcinoma, both IVa and IVb had a potency of 1.9 units/mg. (in terms of sarkomycin potency) by cylinder plate method. From these values it seemed that antitumor potencies of IVa and IVb are about the same with those of 11-oxo-12-tridecenoic acid and 10-oxo-11-dodecenoic acid[3] which have the methylene-keto group at the end of straight carbon chain. However, the daily intraperitoneal injections of 300 mcg/mouse were almost ineffective for mice bearing the ascites type of Ehrlich carcinoma by intraperitoneal route. Intravenous acute toxicity test of IVa and IVb in mice indicated the same LD_{50} dose of 670 mcg/mouse.

4) Private communication from Professor H. Umezawa of National Institute of Health, Tokyo.

Summary

1) 10-(Dimethylaminomethyl)-11-oxododecanoic acid hydrochloride (Ia) and 9-(dimethylaminomethyl)-10-oxoundecanoic acid (Ib) have been obtained from the mother liquors remaining after filtration of 13-(dimethylamino)-11-oxotridecanoic acid hydrochloride and 12-(dimethylamino)-10-oxododecanoic acid hydrochloride, respectively.

2) 10-Methylene-11-oxododecanoic acid (IVa) and 9-methylene-10-oxoundecanoic acid (IVb) have been synthesized from the Mannich bases Ia and Ib, respectively.

3) Antitumor activities of IVa and IVb have been described.

The authors are indebted to Professor Hamao Umezawa, National Institute of Health, Tokyo, for antitumor assays. This work has been supported in part by the Cancer Research Grant of the Ministry of Education and by grant from the Research Society of Microbiological Chemistry, to which the authors' thanks are due.

Department of Applied Chemistry
Faculty of Engineering
Keio University
Koganei-Shi, Tokyo

Dipole Moments of Polyethylene Glycol Diethyl Ethers

By Akira KOTERA, Keizo SUZUKI, Kimiyoshi MATSUMURA, Takao NAKANO, Toshiko OYAMA and Utako KAMBAYASHI

(Received September 5, 1961)

The configurations of high polymer molecules can be studied in various ways; the measurement of their dipole moments is considered to be one of the important of these methods.

Studies have been made, therefore, of some high polymer compounds and, particularly, of the high polymer molecules with elementary dipoles along the polymer chain, for the molecules of the lower degree of polymerization are synthesized easily and the relation of their dipole moments with the degree of polymerization thus made manifest. The series of polyoxymethylene dimethyl ethers, polyethylene glycols and polyethylene glycol diethyl ethers have been studied for this purpose.

This report presents a study in detail of the dipole moments of the lower-membered polyethylene glycol diethyl ethers and to decide the configuration of their skeleton.

Experimental

Polyethylene glycol diethyl ethers are generally represented by the formula; C_2H_5-O-$(C_2H_4$-O$)_p$-C_2H_5.

We studied six compounds of which p were 1, 2,

3, 4, 5 and 6 respectively. They were prepared by the condensation reactions as follows: ethylene glycol diethyl ether ($p=1$), b. p. 121°C, from ethyl bromide and sodium salt of ethylene glycol monoethyl ether (cellosolve); diethylene glycol diethyl ether ($p=2$), b. p. 186°C, from ethyl bromide and sodium salt of diethylene glycol monoethyl ether (carbitol); triethylene glycol diethyl ether ($p=3$), b. p. 118°C/10 mmHg, from ethyl bromide and sodium salt of triethylene glycol monoethyl ether; tetraethylene glycol diethyl ether ($p=4$), b. p. 159°C/10 mmHg, from $\beta\beta'$-dichlorodiethyl ether and sodium salt of cellosolve; pentaethylene glycol diethyl ether ($p=5$), b. p. 175°C/3 mmHg, from ethylene glycol $\beta\beta'$-dichlorodiethyl ether and sodium salt of cellosolve; hexaethylene glycol diethyl ether ($p=6$), b. p. 157°C/0.15 mmHg, from $\beta\beta'$-dichlorodiethyl ether and sodium salt of carbitol.

The dielectric constants and the specific volumes of benzene solutions of these compounds were measured at 25°C and at 50°C.

For the calculation of the molecular polarization at infinite dilution, $P_{2\infty}$, the following equations presented by Halverstadt and Kumler[1] were used;

$$P_{2\infty}=M\left\{(v_0+\beta)\frac{\varepsilon_0-1}{\varepsilon_0+2}+\frac{3\alpha v_0}{(\varepsilon_0+2)^2}\right\}$$

$$\alpha=\frac{\varepsilon-\varepsilon_0}{w},\ \beta=\frac{v-v_0}{w}$$

where M is the molecular weight, ε_0 and v_0 are the dielectric constant and the specific volume of solvent, ε and v are those of solution, and w is the weight fraction of the solute.

For the calculation of the dipole moments, we assume that the value of P_A+P_E is $1.1\,MR_D$, since it is so in diethyl ether[2], while P_A and P_E are the atomic polarization and the electronic polarization, and MR_D is the molecular refraction for the D line.

The observed values and the resultant dipole moments are shown in Table I.

Marchal and Benoit[3] measured the dipole moments of diethylene glycol diethyl ether and hexaethylene glycol diethyl ether at 20°C; they obtained 1.99 and 2.93 D respectively. But they used the equation:

$$\mu^2=4.92\times10^{-4}Tv_0M(\alpha-\gamma)/(\varepsilon_0+2)^2$$

where $\gamma=\lim_{w=0}\partial n^2/\partial w$, and n is the refractive index of solution. That is, they assumed that P_A+P_E equals to MR_D. If they had adopted our assumption ($1.1\,MR_D$), they would have obtained 1.93 D and 2.86 D, respectively. These values are in good agreement with our results.

Discussion

Theoretical Treatment.—we define the following notations to examine the observed data, and to calculate the dipole moments for these compounds[4];

$\vec{a}_i$: the unit vector representing the direction of the ith bond of the molecule ($i=0, 1, 2, \cdots 4+3p$). $\vec{a}_{3h}$, $\vec{a}_{3h+1}$ and $\vec{a}_{3h+2}$ represent C–C, C–O and O–C bonds respectively.

μ_i: the dipole moment of the hth bond.

$\vec{\mu}_{3h}=0$, $\vec{\mu}_{3h+1}=-\mu_{CO}\vec{a}_{3h+1}$, $\vec{\mu}_{3h+2}=+\mu_{CO}\vec{a}_{3h+2}$

μ: the total dipole moment of a molecule.

ρ_{ij}: the angle between $\vec{a}_i$ and $\vec{a}_j$. $\rho_{i-1,i}$ is the supplement of the bond angle of the ith atom, and was assumed to be 70.5° in this paper, that is, $\langle\cos\rho_{i-1,i}\rangle=1/3\equiv c$.

φ_i: the rotation angle around the ith bond; $=0$ when $\vec{a}_{i+1}$ is parallel to $\vec{a}_{i-1}$.

b_i: the average value of $\cos\varphi_i$, i. e. $\langle\cos\varphi_i\rangle$;

$b_0=b_3=b_6=\cdots\equiv b_C$ around the C–C bond.

$b_1=b_2=b_4=\cdots\equiv b_O$ around the C–O bond.

TABLE I. THE OBSERVED VALUES OF THE COMPOUNDS

p	Temp. °C	ε_0	v_0 cc./g	α	β	$P_{2\infty}$ cc.	MR_D cc.	μ^* D
1	25	2.273	1.146	2.141	0.058	90.0	33.5	1.61
	50	2.223	1.182	1.855	0.058	86.0	33.5	1.61
2	25	2.273	1.146	2.292	−0.041	124.0	44.5	1.91
	50	2.223	1.182	2.078	−0.061	119.7	44.5	1.94
3	25	2.273	1.146	2.400	−0.088	158.1	55.5	2.18
	50	2.223	1.182	2.187	−0.105	153.8	55.5	2.21
4	25	2.273	1.144	2.464	−0.124	192.0	66.6	2.41
	50	2.223	1.181	2.233	−0.124	187.2	66.6	2.46
5	25	2.273	1.144	2.491	−0.135	226.9	77.7	2.63
	50	2.223	1.180	2.268	−0.151	220.5	77.7	2.67
6	25	2.273	1.144	2.505	−0.141	260.5	88.7	2.82
	50	2.223	1.180	2.313	−0.156	255.8	88.7	2.89

* For the calculations of the dipole moments we assumed that P_A+P_E equals to $1.1\,MR_D$.

1) I. F. Halverstadt and W. D. Kumler, *J. Am. Chem. Soc.*, **64**, 2988 (1942).
2) R. J. W. Le Fèvre, "Dipole Moments", Methuen & Co., London (1953).
3) J. Marchal and H. Benoit, *J. Chim. Phys.*, **52**, 818 (1955); *J. Polymer Sci.*, **23**, 223 (1957).
4) The theory is previously proposed by one of the authors, K. Suzuki, This Bulletin, **20**, 19 (1947).

μ_{CO} was assumed to be 1.04 D, because of the value 1.22 D of diethyl ether in benzene and because of the valency angle of the oxygen atom, 108°.

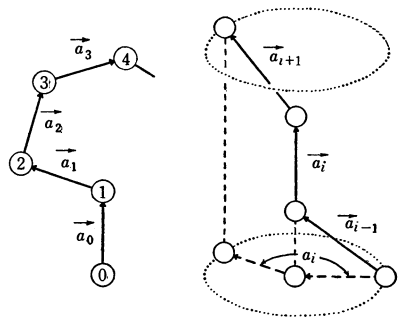


Fig. 1. The feature of the bond vectors.

The total dipole moment of a molecule is expressed by the elementary dipole moments as follows:

$$\langle\mu^2\rangle=\sum_i\mu_i^2+2\sum_{i<j}\sum\mu_i\mu_j\langle\cos\rho_{i,j}\rangle \qquad (1)$$

Assuming that the bond angle of an oxygen atom is equal to that of a carbon atom, i. e.,

$$\langle\cos\rho_{i-1,i}\rangle=c \qquad (2)$$

we have the equations,

$$\langle\cos\rho_{i-2,i}\rangle=c^2(1+b_{i-1})-b_{i-1} \qquad (3)$$

$$\langle\cos\rho_{h,i}\rangle=c(1+b_{i-1})\langle\cos\rho_{h,i-1}\rangle - b_{i-1}\langle\cos\rho_{h,i-2}\rangle \quad \text{for } i\rangle h+2 \qquad (4)$$

Because $\langle\cos\rho_{3i+m,\,3i+m+k}\rangle$ are independent of i (m=0, 1, 2), Eq. 1 leads to

$$\langle\mu^2\rangle=2\mu_{CO}^2\{(p+1)(1-c)+\sum_{i=1}^{p}(p+1-i)(\langle\cos\rho_{1,3i+1}\rangle-\langle\cos\rho_{2,3i+1}\rangle-\langle\cos\rho_{1,3i+2}\rangle+\langle\cos\rho_{2,3i+2}\rangle)\} \qquad (5)$$

in which $\langle\cos\rho_{1,3i+1}\rangle$ etc. can be given by Eq. 4 step by step.

Discussion of Results.—It is well known that the potential minima around each bond in the molecules are close to the trans position (φ=180°, b=−1) or the gauche positions (φ=60° or −60°, b=0.5). Hence, we can assume that the various models having the various trans and gauche forms for each bond in the molecule. The values of the dipole moments of these models, as calculated by Eq. 5, are plotted in Fig. 2.

As shown in Fig. 2, the calculated dipole moments of these compounds do not coincide with the observed ones.

In Fig. 2, when b_C is equal to b_O, it means that the potential values around the C–C bond and the C–O bond are the same; i. e., when $b_C=b_O=-1$, the model of the bonds is a series of trans forms, and similarly, when $b_C=b_O=0.5$ and $b_C=b_O=0$, the models are series of gauche forms and free rotation forms respectively. And in the case $b_C\neq b_O$, the models of the bonds consist of a mixture of the trans, gauche and free rotation forms.

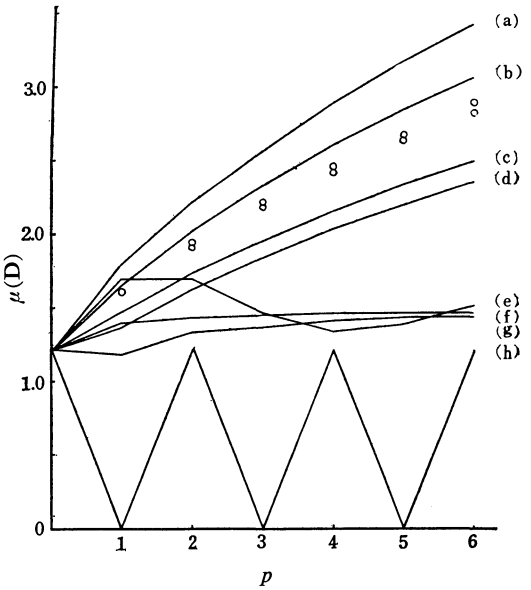


Fig. 2. The calculated moments of the compounds.

(a)	b_C=0.5	b_O=0	(f)	b_C=0	b_O=−1
(b)	0	0		−1	0
(c)	0.5	0.5	(g)	−1	0.5
(d)	0	0.5	(h)	−1	−1
(e)	0.5	−1	○	Observed values	

Furthermore, as shown in Fig. 2, when b_C or b_O is equal to −1, the calculated values of the dipole moments of the models are plotted in a zigzag manner with the increase of p, the degree of polymerization. This fact is in disagreement with the tendency that the observed moments increase in a simple way with the increase of p.

The following hypothesis about the configuration of these polyethylene glycol diethyl ethers may therefore be possible:

1) These compounds consist of a mixture of the various rotational isomers, as shown in Fig. 2. By this hypothesis, the temperature dependence of the observed moments can be explained by the assumption that the mixture ratio of the rotational isomers changes.

In the case of polyoxymethylene dimethyl ethers, it was concluded that their configurations consist of a mixture of various rotational isomers, the predominant ones of which are herical or almost herical structures arising from the gauche minima[5].

5) T. Uchida, Y. Kurita and M. Kubo, *J. Polymer Sci.* 22, 365 (1956).

2) The value of the angle φ in the stable position slightly differs from 180° (trans position), 60° and −60° (gauche positions).

About the configurations of polyethylene glycols, Uchida et al.[6] concluded that these compounds are in a free rotational state in dioxane solutions; on the other hand, about the configurations of polyethylene glycols and polyethylene glycol diethyl ethers in benzene solutions, Marchal and Benoit[3] concluded that the value of b, which is identical with b_C and b_O in this report, is ±0.3. Although Marchal and Benoit do not make any distinction between the value of b_C and that of b_O, these values are generally different. Let us therefore study the relation between the value of b_C and that of b_O to explain the observed dipole moment sufficiently.

When the value of μ in Eq. 5 is taken as the observed value, Fig. 3 can be obtained by plotting the values of b_C and b_O as calculated from Eq. 5.

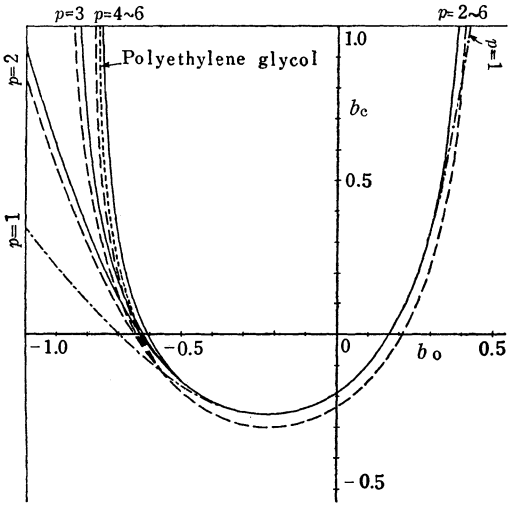


Fig. 3. The relations between the value of b_C and that of b_O.
———; at 25°C (p=2~6)
———; at 50°C (p=2~6)
—·—·; at 25°C and at 50°C (p=1)
------; at 20°C (polyethylene glycol, p=79 and 227)

As shown in Fig. 3, the curve which explains the relation between the value of b_C and that of b_O at 50°C passes the points nearer to the place of origin, where $b_C=b_O=0$, than the curve at 25°C. This fact is considered to show that with the increase in temperature the internal rotations about each bond get more like the free rotation. Moreover, the b_C~b_O curves for the case of p=1 at 25°C are identical with that at 50°C, and this curve for p=1 coincides with the curve for p=2~6 at 50°C.

When p is very large, it is expected that the value of the dipole moment per oxygen atom of polyethylene glycol diethyl ether will be the same as that of polyethylene glycol. Marchal and Benoit[3] measured the value of $\mu^2/p+1$ in a series of polyethylene glycols at 20°C in benzene solutions and got 1.16 when p is 79 and 1.15 when p is 227. They assumed that P_A+P_E is equal to MR_D, but if we assume that P_A+P_E is equal to $1.1MR_D$, the above-mentioned values are 1.11 and 1.10 respectively. The b_C~b_O curve from these values is almost in full agreement with the curve for polyethylene glycol diethyl ethers at 25°C, as is shown in Fig. 3.

In Fig. 3, if we compare the b_C~b_O curves for the compounds, the curves for p=1, 2 and 3 are fairly different from the curves for p=4~6 under the condition $b_O<-0.5$. Therefore, the value of b_O for the compounds should be larger than −0.5, if it is assumed that the degree of the internal rotation around the each bond is independent of the degree of polymerization of the compounds. In fact, under the condition of $b_O<-0.5$, the calculated dipole moments of the compounds are plotted in a zigzag manner when p becomes large. This tendency of the relation between the calculated moments and p disagrees with that of the observed moments and p. Furthermore, as shown in Fig. 3, the value of b_O lies within the range of −0.5~0.4, and in this range we can select a pair of b_C and b_O satisfying the relation between the observed moments and p.

It is considered that the interaction between two C–O dipoles connected with both sides of the C–C bond is fairly large, while the interaction between the C–O dipole and the C–C bond, without the moment, each at one end of the C–O bond, is fairly small. The interactions between the elementary dipoles of each above-mentioned bond make it necessary that the value of b_O be nearer to zero than that of b_C. Taking the above condition, the range of the value of b_O is obtained from Fig. 3; $b_O=-0.3$~0.13 and $b_O>0.28$. However, since the range $b_O=-0.3$~0.13 corresponds to the range $b_C=-0.3$~-0.1 and since these ranges show that each bond takes the positions of the potential maxima, it is considered that these ranges are unreasonable as a basis for explaining the configurations of these compounds, considering the intramolecular potential.

On the other hand, if each bond in the molecule is at the fixed position near the potential minima, the value of b_C should be

6) T. Uchida, Y. Kurita, N. Koizumi and M. Kubo, ibid., 22, 313 (1956).

closer to -1 (trans) or to 0.5 (gauche) than the value of b_O, since interaction between the elementary dipoles exists. The case of $b_C = -1$ cannot then exist, as is shown in Fig. 3; consequently the value of b_C is close to 0.5. Therefore, (1) when the value of b_C is equal to 0.5, the values of b_O are 0.36 (25°C) and 0.33 (50°C), and (2) when the value of b_C is relatively closer to 0.5 than the value of b_O, the range of the value of b_C is 0.3∼0.65.

From what we have seen, it can be concluded that two C–O bonds around the C–C bond approximately take the gauche positions with regard to each other.

Summary

The dipole moments of six lower members of the polyethylene glycol diethyl ethers have been measured, and their configurations have been studied.

As the configurations of these compounds the two models have been considered; one is a mixture of the various rotational isomers, and the other a model in which the positions of the internal rotations of two C–O bonds around the C–C bond approximately take the gauche positions with regard to each other, and the positions of the C–O bond and the C–C bond around the C–O bond take positions similar to those mentioned above with regard to each other.

Department of Chemistry
Faculty of Science
Tokyo University of Education
Otsuka, Tokyo

Dipole Moments of Organosilicon Compounds

By Kimiyoshi MATSUMURA

(Received September 20, 1961)

Although organosilicon chemistry, which has made remarkable progress recently, has produced a large number of new compounds, their molecular configurations remain unknown. The present author has, therefore, been studying them by the determination of their dipole moments, and several of his results will be reported on here.

Experimental

The compounds which have been measured for the present work are:

(I) Methoxytrimethylsilane b.p. 56.1~57.3°C
(II) Dimethoxydimethylsilane b.p. 80.5°C
(III) Trimethoxymethylsilane b.p. 103.5°C
(IV) Tetramethoxysilane b.p. 121.5°C
(V) Tetra-trimethylsiloxy-silane
(VI) Methoxytrichlorosilane
(VII) Dimethoxydichlorosilane
(VIII) Trimethoxychlorosilane.

Of these compounds, tetra-trimethylsiloxy-silane (V) and three methoxychlorosilanes (VI, VII and VIII) were furnished to us by Mr. M. Yokoi of Shinshu University and Mr. H. Murata of Hiroshima University respectively. The others were prepared by the reactions of methyl alcohol upon the corresponding methylhalosilanes[1].

The dielectric constants and the specific volumes of the benzene solutions were measured at 25 and 50°C.

For the calculation of the molecular polarization of the solute at infinite dilution, $P_{2\infty}$, the following equations proposed by Halverstadt and Kumler[2] were used:

$$P_{2\infty}=M\left\{(v_0+\beta)\frac{\varepsilon_0-1}{\varepsilon_0+2}+\frac{3\alpha v_0}{(\varepsilon_0+2)^2}\right\}$$

$$\alpha=\frac{\varepsilon-\varepsilon_0}{w},\quad \beta=\frac{v-v_0}{w}$$

where M is the molecular weight, ε_0 and v_0 are the dielectric constant and the specific volume of the solvent respectively, ε and v are those of the solution, and w is the weight fraction of the solute in the solution.

For the calculation of the dipole moment, (P_A+P_E) is assumed to be 1.1 MR_D, as in the case of hexamethyldisiloxane[3], where P_A and P_E are the atomic polarization and the electronic polarization respectively, and MR_D is the molar refraction for the D line. The results are shown in Table I.

Results and Discussion

Assumed Bond Angles and Bond Moments.—To determine the configurations of the compounds, the bond angles and bond moments

1) Cf., for example, D. F. Peppard, W. G. Brown and W. C. Johnson, *J. Am. Chem. Soc.*, **68**, 73 (1946).

2) I. F. Halverstadt and W. D. Kumler, ibid., **64**, 2988 (1942).

3) Y. Kurita and M. Kondo, This Bulletin, **27**, 160 (1954).

TABLE I. THE OBSERVED VALUES OF THE COMPOUNDS

	Temp. °C	ε_0	v_0 cc./g.	α	β	$P_{2\infty}$ cc.	MR_D cc.	μ D
(I)	25	2.273	1.145	1.108	0.167	62.5	31.0	1.18
(II)	25	2.273	1.145	1.304	0.021	71.2	31.7	1.33
	50	2.223	1.180	1.103	0.022	68.2		1.33
(III)	25	2.273	1.145	1.765	−0.086	88.2	32.4	1.60
	50	2.223	1.181	1.580	−0.096	85.5		1.62
(IV)	25	2.273	1.145	1.986	−0.171	101.1	33.1	1.78
	50	2.223	1.181	1.775	−0.180	97.8		1.80
(V)	25	2.273	1.145	0.146	−0.010	140.7	105.4	1.10
	50	2.223	1.181	0.119	−0.017	138.8		1.10
(VI)	25	2.273	1.146	2.528	−0.390	116.1	29.6	2.02
	50	2.223	1.181	2.252	−0.402	111.4		2.04
(VII)	25	2.273	1.146	2.685	−0.316	121.3	30.8	2.04
	50	2.223	1.181	2.435	−0.327	117.8		2.08
(VIII)	25	2.273	1.146	2.576	−0.264	117.2	32.0	1.97
	50	2.223	1.181	2.364	−0.275	114.7		2.02

used for the calculations of the dipole moments were assumed as follows.

The bond angle of the silicon atom is tetrahedral, and angle SiOC is assumed to be 113° from the results of the electron diffraction study of tetramethoxysilane[4] and methoxytrichlorosilane[5]. Angle SiOSi for tetra-trimethylsiloxy-silane is assumed to be 140° from the results of the electron diffraction study[4].

The CH_3O group moment, 1.15D, is calculated from the dipole moment of methyl ether, 1.29 D[6], and its angle COC, 111.5°[7]. For the group moment of $(CH_3)_3SiO$, Kurita and Kondo obtained 0.95 D[3] from the dipole moment of hexamethyldisiloxane, 0.80D, assuming that angle SiOSi is 130°[4]. However, the $(CH_3)_3SiO$ group moment is assumed to be 1.05D, assuming that angle SiOSi is 135°*. Therefore, 1.65D is obtained for the SiO bond moment and 0.60D for the CH_3Si group moment.

The SiCl bond moment 2.94D is calculated from the dipole moment study of methoxytrichlorosilane in this report, as will be shown below.

Assumed Configurations.—Using the above bond angles and bond moments, the present author calculated the dipole moments of the compounds, assuming the following models:

1) Fundamental Models (trans and gauche Models).—The CH_3 groups of the CH_3O groups and the $(CH_3)_3Si$ groups of the $(CH_3)_3SiO$ groups are at trans or gauche positions with regard to the nonbonding oxygen atoms. The cis models were rejected because of their instability.

The trans and gauche positions are shown in Figs. 1—3; $a_1, b_1, c_1 \cdots\cdots$ are the positions of the CH_3 groups in Figs. 1 and 2, and of the CH_3 groups or $(CH_3)_3Si$ groups in Fig. 3.

2) The Free Rotation Model.—The CH_3 groups and the $(CH_3)_3Si$ groups are rotating around the SiO bonds freely.

The calculated dipole moments for these models, 1) and 2), are shown in Tables II, IV, VI, VIII, X and XII. Moreover, as it has been known that the bond angle of an oxygen atom in organosilicon compounds shows various values, the angles SiOC and SiOSi are calculated from the observed dipole moments which are shown in the third columns of these tables.

3) The Vibration Models and the Staggered Models.—The CH_3–O bonds and the Si–O bonds

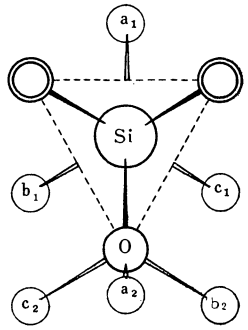


Fig. 1. The trans and gauche positions of the CH_3 groups of the CH_3O groups of dimethoxydimethylsilane and dimethoxydichlorosilane. Two double circles indicate the CH_3 groups or the Cl atoms.

4) M. Yokoi, ibid., **30**, 100 (1957); K. Yamasaki, A. Kotera, M. Yokoi and Y. Ueda, *J. Chem. Phys.*, **18**, 1414 (1950).

5) J. Kakinoki, H. Murata, K. Katayama and K. Shimizu, *Annual Rep. of the Inst. for Fiber Research, Osaka Univ.*, **7**, 14 (1953).

6) R. J. W. Le Fèvre, "Dipole Moments", Methuen & Co., London (1953).

* Mr. M. Yokoi kindly suggests to us in private communication that angle SiOSi may be larger than 130°; C. M. Lucht obtained 137±7°, which figure is yet unpublished.

7) K. Kimura and M. Kubo, *J. Chem. Phys.*, **30**, 151 (1959).

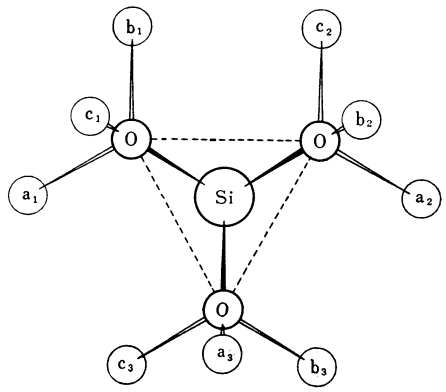


Fig. 2. The trans and gauche positions of the CH_3 groups of the CH_3O groups of trimethoxymethylsilane and trimethoxychlorosilane.

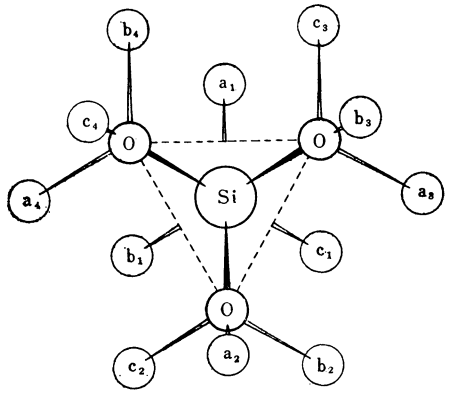


Fig. 3. The trans and gauche positions of the CH_3 groups of tetramethoxysilane, and of the $(CH_3)_3Si$ groups of tetra-trimethylsiloxy-silane.

of $(CH_3)_3SiO$ groups are vibrating about given "equilibrium" positions, trans or gauche positions respectively, or staggering from these positions. The amplitude or the staggered angles are denoted by θ. In the case of the staggered model, if CH_3 or $(CH_3)_3Si$ groups are staggered and situated at θ counterclockwise from the given "equilibrium" positions when viewed from the centered Si atom, these staggered angles may be defined $+\theta$.

The calculated angle θ, giving the observed dipole moments, are shown in Tables III, V, VII, IX, XI and XIII; in every case the "equilibrium" model means that one of the trans and gauche models with the smallest dipole moment.

(I) Methoxytrimethylsilane.—The moment is measured only at 25°C, because of its low boiling point.

The observed value, 1.18D, is in coincidence with the dipole moment of ethoxytrimethylsilane, 1.18D[8]. The observed value is consistent with the calculated value, 1.22D. Hence, the assumed bond angle SiOC, 113°, and the $(CH_3)_3SiO$ group moment, 1.05D, seem reasonable.

As to the molecule of this type, it should be noticed that it is impossible to determine the precise position of the CH_3 group by only the dipole moment data.

(II) Dimethoxydimethylsilane.—The observed value, 1.33D, is also in good agreement with that of diethoxydimethylsilane, 1.36D[8].

The facts that the calculated dipole moments for various models in Table II are not consistent with the observed value, and that the observed dipole moment is independent of the temperature, suggest that the molecule is in the free rotational state.

When it is assumed that the two CH_3 groups rotate with each other freely, the observed moment is well consistent with the calculated moment, provided that angle SiOC is taken

Table II. The calculated moments of dimethoxydimethylsilane (see Fig. 1)

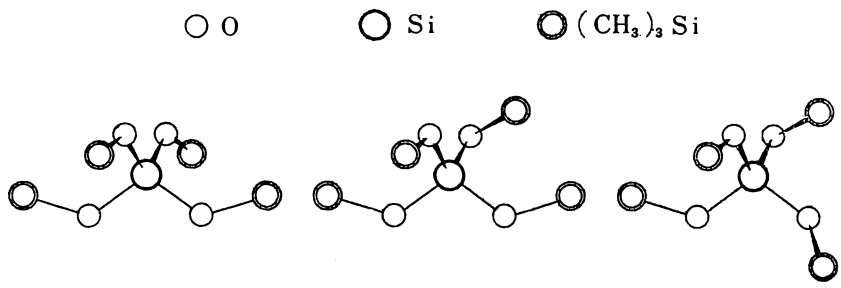
Model	μ (D)	< SiOC
b_1-b_2, c_1-c_2	0.16	
a_1-b_2, a_1-c_2	1.72	129°
b_1-a_2, c_1-a_2	1.72	129°
b_1-c_2, c_1-b_2	1.85	>145°
a_1-a_2	2.40	
Free rotation	1.63	128.5°
(observed 25°C	1.33)	
(observed 50°C	1.33)	

Table III. The vibration model (v) and the staggered model (s) of dimethoxydimethylsilane

θ show the vibrational amplitudes of the C-O bonds of CH_3O groups for (v), and the staggered angles for these bonds for (s), and, + and − are the signs of θ which is positive if the C-O bonds stagger counterclockwise.

	Equilibrium model	θ
	(b_1-b_2)	
(v)		110°
(s)	++	172°
	−−	51°
	+−	60.5°
	−+	60.5°
	(a_1-a_2)	
(v)		>180°
(s)	++	69°
	−−	69°
	+−	150°
	−+	150°

8) H. Freiser, M. V. Eagle and J. Speier, *J. Am. Chem. Soc.*, 75, 2824 (1953).



(a) $a_1-a_2-a_3-a_4$ (b) $a_1-a_2-a_3-b_4$ (c) $a_1-b_2-a_3-c_4$

Fig. 4. The configurations of tetra-trimethylsiloxy-silane.

as 128.5°. In this case the $CH_3\cdots\cdots CH_3$ distance is 2.9Å ; it is a little larger than the sum of the covalent radii of a carbon atom and a hydrogen atom, which makes the free rotation possible.

The value of angle SiOC, 128.5°, is larger than the observed value, 113°, which is obtained by the electron diffraction study of tetramethoxysilane, but it is comparable to the values of angle SiOSi, 130±10° and 137±7° in hexamethyldisiloxane, and 140±5° in tetra-trimethylsiloxy-silane, which values are obtained by electron diffraction studies ; therefore, the value obtained here may not be unreasonable.

Next, in explanation of the observed value, a vibration or fixed staggered model for this molecule, with the b_1-b_2 model as the equilibrium model, was assumed. The calculated results are shown in Table III. In the staggered models two cases are considered ; a) two CH_3 groups are staggering from the given equilibrium positions, b_1 and b_2, in the same direction by angle $+\theta$ or $-\theta$ (++ and −− in Table III), and b) they are staggering in different directions, one by angle $+\theta$ and the other by $-\theta$ (+− and −+ in the same table).

The large amplitude and the staggered angle θ's shown in Table III are difficult to interpret in terms of the intramolecular potential of the molecule. For example, the model with the staggered angle 51° from the b_1-b_2 (gauche) model makes a form almost identical to the cis form. Therefore, it is unsuitable to use these models to explain the experimental results. When the c_1-c_2 model is taken as the equilibrium model, similar relations are obtained.

On the other hand, when the trans (a_1-a_2) model is taken as the equilibrium model, the staggered model, in which one CH_3 group staggers by +150° and the other by −150°, is obtained. This is identical with the case in which the b_1-c_2 model or the c_1-b_2 model is taken as the equilibrium model. That is, for example, if the b_1-c_2 model is chosen as the equilibrium model, the CH_3 group placed at the b_1 position staggers by +30° and the CH_3 group placed at the c_2 position staggers by −30°. This model is considered the most reasonable one, if one ignores the fact that the most stable model, with the smallest dipole moment, is taken as the fundamental equilibrium model.

The third possibility to explain the observed data lies in the consideration of the molecule consisting of a mixture of the various configurations. As there are many configurations which can be mixed with the b_1-b_2 model and the c_1-c_2 model to make the calculated moment fit the observed moment, it is desirable to use the other physical method to determine its details.

(III) Trimethoxymethylsilane.—As is shown in Table IV, these observations can be made about the trans and gauche models and the free rotation model as well as about dimethoxydimethylsilane.

When the $a_1-a_2-a_3$ model or the $a_1-b_2-b_3$ model is chosen as the equilibrium model for

TABLE IV. THE CALCULATED MOMENTS OF TRIMETHOXYMETHYLSILANE (see Fig. 2)

Model type*	μ (D)	<SiOC
$a_1-a_2-a_3$	1.22	<90°
$a_1-b_2-b_3$	1.22	<90°
$a_1-b_2-a_3$	1.39	
$a_1-c_2-b_3$	2.10	128°
$a_1-b_2-c_3$	2.20	136°
$c_1-b_2-a_3$	2.39	148.5°
$a_1-a_2-b_3$	2.79	143°
Free rotation	1.93	128°
(observed 25°C	1.60)	
(observed 50°C	1.62)	

* All of the other trans and gauche models are classified into one of the above models.

Table V. The vibration model (v) and the staggered model (s) similar to Table III but for trimethoxymethylsilane

	Equilibrium model	θ
	$(a_1-a_2-a_3)$	
(v)		80°
(s)	+++	—
	−−−	—
	++−	—
	−−+	—
	+−+	32°
	+−−	32°
	−+−	29°
	−++	29°
	$(a_1-b_2-b_3)$	
(v)		80.5°
(s)	+++	32° 168°
	−−−	29° 110°
	++−	75° 165°
	−−+	15° 104°
	+−+	17° 148°

the vibration model and the staggered models, the calculated angles, θ's, are shown in Table V. The large amplitude, 80°, shows that the vibration model must be rejected upon considering the intramolecular potential. Of all the staggered forms, the models staggering by 15, 17, 29 and 32° from the given equilibrium positions seem reasonable models.

(IV) Tetramethoxysilane.—As is shown in Table VI, of all the trans and gauche models the $a_1-a_2-a_3-b_4$ type models and the $a_1-b_2-a_3-c_4$ type models have the most suitable calculated values to fit the observed dipole moment. Therefore, it is possible to consider that the molecule consists of a mixture of, or one of, these models.

On the other hand, by electron diffraction study[4], the configuration of this molecule is found to be the staggered model in which four CH_3 groups stagger against nonbonding oxygen atoms.

Table VI. The calculated moments of tetramethoxysilane (see Fig. 3)

Model type*	μ (D)	<SiOC
$a_1-a_2-a_3-a_4$	0	
$a_1-b_2-b_3-a_4$	0	
$a_1-a_2-a_3-b_4$	1.83	115°
$a_1-b_2-a_3-c_4$	1.83	115°
$a_1-a_2-b_3-b_4$	2.59	140°
$a_1-a_2-b_3-c_4$	3.18	148.5°
Free rotation	2.12	128.5°
(observed 25°C	1.78)	
(observed 50°C	1.80)	

* All of the other trans and gauche models are classified into one of the above models.

Table VII. The vibration model (v) and the staggered model (s) similar to Table III but for tetramethoxysilane

	Equilibrium model	θ
	$(a_1-a_2-a_3-a_4)$	
(v)		105°
(s)	++++	—
	−−−−	—
	+++−	58°
	+−−−	58°
	+−+−	37°
	++−−	—
	$(a_1-b_2-b_3-a_4)$	
(v)		105°
(s)	++++	37°
	−−−−	37°
	+++−	58°
	++−+	58°
	+++−	58°
	+−+−	58°
	+−−+	—

As is shown in Table VII, of all the staggered models assuming the $a_1-a_2-a_3-a_4$ model or the $a_1-b_2-b_3-a_4$ model as the equilibrium model, the staggered models with the staggered angle of 37° are considered to be most suitable to explain the configuration of the molecule.

Moreover, Asbuzov and Shavsha[9] measured the dipole moment for this molecule and obtained 1.61D, their calculated moment with the free rotation model being 1.7D. From this, they concluded that the free rotation model is reasonable. However, as their report is not available and the details are not known exactly, their results cannot be discussed in the present report.

Configuration of Methoxymethylsilanes and Tetramethoxysilane.—As has been mentioned above, throughout four compounds, three methoxymethylsilanes and tetramethoxysilane, it can be considered first that the configurations for these molecules are in the free rotational state, as the observed dipole moments are independent of temperature, and it has been known in general that organosilicon compounds have a low intramolecular potential barrier as compared with carbon compounds. In methoxytrimethylsilane the observed moment is consistent with the calculated moment, assuming 113° for angle SiOC, while in dimethoxydimethyl-, trimethoxymethyl- and tetramethoxysilane, the angle SiOC must open wider by 15° to make the calculated moments fit the observed moments. These features of the angle may be possible, but it seems difficult

9) B. A. Asbuzov and T. G. Shavsha, *Doklady Akad. Nauk. S. S. S. R.*, **68**, 859 (1949); *Chem. Abstr.*, **44**, 886 (1950).

to accept the free rotation for the configuration of compounds, so long as the bond angles of an oxygen atom are assumed to be the same in these molecules belonging to a series.

As was seen in the conclusion of the electron diffraction study for tetramethoxysilane, some of the staggered models in which the CH_3 groups stagger about each given equilibrium positions seem to be suitable.

The third possibility to explain the configurations of these compounds lies in the assumption that these compounds consist of a mixture of various trans and gauche models. The temperature dependence is expected to appear as more or less in this case.

(V) Tetra-trimethylsiloxy-silane. — The observed moment is independent of temperature. The free rotation model seems preferable. The calculated moment is consistent with the observed moment if angle SiOSi is taken to be 148.5°. This value of the angle is in agreement comparatively with 140±5° according to the results of the electron diffraction study for this compound. But if angle SiOSi is assumed to be 148.5°, the distance between one CH_3 group belonging to one of four $(CH_3)_3Si$ groups and one CH_3 group belonging to another amounts to 1.16Å. The distance between the two above-mentioned CH_3 groups is too small to make the $(CH_3)_3Si$ groups rotate freely, so that the free rotation model is impossible.

TABLE VIII. THE CALCULATED MOMENTS OF TETRA-TRIMETHYLSILOXY-SILANE (see Fig. 3)

Model type*	μ (D)	<SiOSi
$a_1-a_2-a_3-a_4$	0	
$a_1-b_2-b_3-a_4$	0	
$a_1-a_2-a_3-b_4$	1.17	143°
$a_1-b_2-a_3-c_4$	1.17	143°
$a_1-a_2-b_3-b_4$	1.65	154.5°
$a_1-a_2-b_3-c_4$	2.02	159.5°
Free rotation	1.35	148.5°
(observed 25°C	1.10)	
(observed 50°C	1.10)	

* All of the other trans and gauche models are classified into one of the above models.

TABLE IX. THE VIBRATION MODEL (v) AND THE STAGGERED MODEL (s) SIMILAR TO TABLE III BUT FOR TETRA-TRIMETHYLSILOXY-SILANE

	Equilibrium model	θ
	$(a_1-a_2-a_3-a_4)$	
(v)		98°
(s)	++++	—
	----	—
	+++-	54.5°
	+---	54.5°
	+-+-	35°
	++--	—
	$(a_1-b_2-b_3-a_4)$	
(v)		98°
(s)	++++	35°
	----	35°
	+++-	54.5°
	++-+	54.5°
	++--	54.5°
	+-+-	54.5°
	+--+	—

On the other hand, of all the trans and gauche models in Table VIII, the calculated dipole moments of the $a_1-a_2-a_3-b_4$ type models and the $a_1-b_2-a_3-c_4$ type models are most consistent with the observed one. The features of these two models are shown in Figs. 4 (b) and (c). Therefore, it is considered that the configuration of this molecule is identical with one of, or a mixture of, these two types of models.

Considering the resembrance of the structural formula between this molecule and tetramethoxysilane, it is possible that the configuration of the molecule fits any staggered model. For example, when the $a_1-a_2-a_3-a_4$ model or the $a_1-b_2-b_3-a_4$ model is taken as the equilibrium model, the calculated angle of amplitude and the staggered angles are as shown in Table IX. The vibration model is impossible because of its large amplitude, while it seems that, of all the staggered models shown in Table IX, the models having the staggered angle 35° are most suitable as the configuration for the molecule.

According to the conclusion of the electron diffraction study[4], this molecule has a configuration in which two $(CH_3)_3Si$ groups belonging to the different W-shaped chains shown in Fig. 4 (a) are twisted by 60° from each other. The calculated dipole moment of this model is identical with those of the $a_1-a_2-a_3-b_4$ type models and the $a_1-b_2-a_3-c_4$ type models; that is, it is consistent with the observed moment. Little consideration has been given to this model, however, as it is identical with the case in which the two twisted $(CH_3)_3Si$ groups take cis positions against the respective nonbonding oxygen atoms.

(VI) Methoxytrichlorosilane.—The observed dipole moment is independent of temperature.

In order to calculate the dipole moment for this molecule, it is necessary to have the value of the SiCl bond moment. The value, 2.67D, is obtained for the SiCl bond moment from the dipole moment of triethylchlorosilane, 2.07D[10], assuming the SiC_2H_5 group

10) C. Curran, D. M. Witucki and P. A. McCusker, *J. Am. Chem. Soc.*, **72**, 4471 (1950).

moment, 0.60D. Using this bond moment, the calculated moment for this molecule is 1.81D. This value is too small as compared with the observed value.

Using the observed dipole moment, the Cl_3SiO group moment is calculated as 1.29D. From this value, the SiCl bond moment 2.94D is obtained, provided that the SiO bond moment is 1.65D. This SiCl bond moment, 2.94D, is larger than that obtained from the dipole moment study of triethylchlorosilane, 2.67D.

Of this tendency of the SiCl bond moment, the following argument seems to be the most suitable among the various considerations.

It has generally been known that the SiCl bonds in chlorosilane and ethylchlorosilane have the $Cl^+=Si^-$ double bond structure in spite of the fact that the electronegativities of a silicon atom and a chlorine atom are quite different[10,11], and that in many other silane derivatives, such as those containing a phenyl group, there is a so-called "reverse halogen effect" $+\langle\bigcirc\rangle=Si^-$ [12]. In the ClSiO bond of the molecule, it must be considered that the contribution of the structure $Cl^+=Si^--O$ decreases and the contribution of the $Cl^-Si=O^+$ type structure rather increases, leading one to the conclusion that the $Si^-=O^+$ double bond structure contributes appreciably to the normal state of the SiO bond.

Therefore, it is better to assume the SiCl bond moment to be about 2.94D for methoxytrichlorosilane.

The configuration of this molecule cannot be decided only from the dipole moment data, whereas in the results of the electron diffraction study, the CH_3O group is placed at the trans position against one of three chlorine atoms[5].

(VII) Dimethoxydichlorosilane.—Among the fixed trans and gauche models in Table X, the calculated dipole moment of the a_1-b_2 type models is almost consistent with the observed moment. However, the dependence on temperature of the observed moment makes it difficult to select the particular configuration of the molecule.

The next possibility of explaining the observed data lies in the assumption that the molecule consists of a mixture of the various fixed models. That is, the a_1-a_2 model in Table X, where the two CH_3O groups are in the trans position with regard to each other as the most stable configuration, and many other models in Table X which are stable configurations at higher temperatures, are mixed. In this case, it is also expected that the temperature dependence will appear more or less.

According to the electron diffraction study[5], the trans model seems to be the most reasonable one for the molecule, but this conclusion cannot explain the present experimental data.

(VIII) Trimethoxychlorosilane. — The configuration of this molecule is considered to be a mixture of the various trans and gauche models shown in Table XII, similar to the case of dimethoxydichlorosilane.

Configuration of Methoxychlorosilanes. — As has been mentioned above, from the results of the measurement for methoxytrichlorosilane, it is concluded that the SiCl bond moment

TABLE X. THE CALCULATED MOMENTS OF DIMETHOXYDICHLOROSILANE (see Fig. 1)

Model type*	μ (D)
a_1-a_2	0.28
a_1-b_2	2.04
b_1-b_2	2.87
b_1-c_2	3.41
Free rotation	2.51
(observed 25°C	2.04)
(observed 50°C	2.08)

* All of the other trans and gauche models are classified into one of the above models.

TABLE XI. THE VIBRATION MODEL (v) AND THE STAGGERED MODEL (s) SIMILAR TO TABLE III BUT FOR DIMETHOXYDICHLOROSILANE

Equilibrium model		θ	
		25°C	50°C
	(a_1-a_2)		
(v)		132.5°	136°
(s)	++	91°	92.5°
	−−	91°	92.5°
	+−	56°	57°

TABLE XII. THE CALCULATED MOMENTS OF TRIMETHOXYCHLOROSILANE (see Fig. 2)

Model type*	μ (D)
$a_1-c_2-b_3$	0.24
$a_1-a_2-b_3$	1.85
$a_1-a_2-a_3$	2.04
$a_1-b_2-b_3$	2.04
$a_1-b_2-c_3$	2.74
$a_1-b_2-a_3$	3.71
$c_1-b_2-a_3$	4.73
Free rotation	2.53
(observed 25°C	1.97)
(observed 50°C	2.02)

* All of the other trans and gauche models are classified into one of the above models.

11) L. O. Brockway and I. E. Coop, *Trans. Faraday Soc.*, **34**, 1429 (1938); E. L. Reilly, C. Curran and P. A. McCusker, *J. Am. Chem. Soc.*, **76**, 331 (1954).

12) H. Freiser, M. V. Eagle and J. Speier, *J. Am. Chem. Soc.*, **75**, 2821 (1953).

TABLE XIII. THE VIBRATION MODEL (V) AND THE STAGGERED MODEL (S) SIMILAR TO TABLE III BUT FOR TRIMETHOXYCHLOROSILANE

Equilibrium model		θ	
		25°C	50°C
	$(a_1-c_2-b_3)$		
(v)		116.5°	120.5°
(s)	+++	146°	145°
	−−−	26°	25°
	++−	122°	121°
	+−+	122°	121°
	−++	122°	121°
	+−−	64°	61°
	−+−	64°	61°
	−−+	64°	61°

should be 2.94D, which corresponds to the contribution of the $Cl^-Si{=}O^+$ structure to the ClSiO bond.

Of the configurations of dimethoxydichloro- and trimethoxychloro-silane, it seems most suitable to suggest that these compounds consist of a mixture of various trans and gauche models, and not of one particular model, including the free rotation model and the vibration model, on condition that the observed moments depend on temperature.

It is my pleasure to express my gratitude to Mr. Masatoki Yokoi and Mr. Hiroshi Murata for the samples, to Professor Akira Kotera and Professor Keizo Suzuki for their encouragement throughout the experiment, and to Mr. Takao Nakano,Mrs. Toshiko Ooyama and Mrs. Utako Kambayashi for their assistance.

Department of Chemistry
Faculty of Science
Tokyo University of Education
Otsuka, Tokyo

The Mannich Base of Troponoid and its Application. VIII. Reaction of 3-Bromo-5-formyl-7-isopropyltropolone

By Kyozo OGURA

(Received September 28, 1961)

In the preceding paper of this series[1], the synthesis of 3-bromo-5-formyl-7-isopropyltropolone (I) from the Mannich base, 3-bromo-5-piperidinomethyl-7-isopropyltropolone, was described; the present paper concerns the reaction of this aldehyde.

Aldehyde I is highly reactive and is similar to 3, 7-dibromo-5-formyltropolone[2]. It forms an acetal II on merely being warmed in methanol and undergoes a reaction with various amines to form the Schiff base. The reaction of I with aniline, *p*-toluidine, *p*-anisidine and 5-aminotropolone respectively afforded *N*-(3-bromo-7-isopropyltropolon-5-ylmethylene)aniline (III), *N*-(3-bromo-7-isopropyltropolon-5-ylmethylene)-*p*-toluidine (IV), *N*-(3-bromo-7-isopropyltropolon-5-ylmethylene)-*p*-anisidine (V), and *N*-(3′-bromo-7′-isopropyltropolon-5′-ylmethylene)-5-tropolonylamine (VI). The reaction of I and *o*-phenylenediamine afforded 2-(3′-bromo-7′-isopropyltropolon-5′-yl)benzimidazole (VIII) through *N*-(3-bromo-7-isopropyltropolon-5-ylmethylene)-*o*-aminoaniline (VII). The compound VIII was also obtained by the reaction of (3-bromo-7-isopropyltropolon-5-yl)-*N*-(*p*-dimethylaminophenyl)nitrone with *o*-phenylenediamine[1]. The structures of VII and VIII were supported by their ultraviolet spectra. The reaction of I with malononitrile, cyanoacetamide, and ethyl cyanoacetate respectively afforded 3-bromo-5-(β, β-dicyanovinyl)-(IX), 3-bromo-(β-cyano-β-carbamoylvinyl)-(X), and 3-bromo-5-(β-cyano-β-ethoxycarbonylvinyl)-7-isopropyltropolone (XI). The hydrolysis of XI with alkali gave 3-bromo-5-(β-cyano-β-carboxyvinyl)-7-isopropyltropolone (XII). The reaction of I and hippuric acid

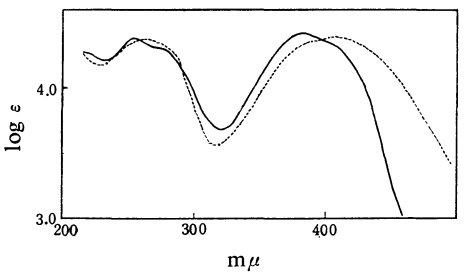
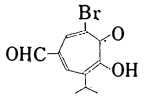
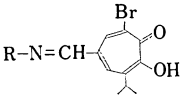


Fig. 1. Ultraviolet spectra of VII(……) and VIII (——) in methanol.

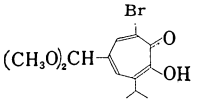
1) K. Ogura, This Bulletin, **34**, 839 (1961).
2) S. Seto and K. Ogura, ibid., **32**, 493 (1959).



I



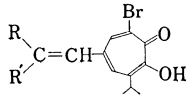
III : R = C_6H_5
IV : R = p-CH_3-C_6H_4
V : R = p-CH_3O-C_6H_4



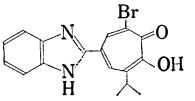
II

VI : R =

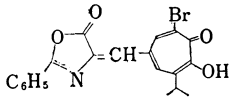
VII : R = o-H_2N-C_6H_4



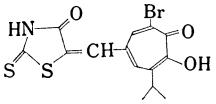
IX : R = R′ = CN
X : R = CN, R′ = $CONH_2$
XI : R = CN, R′ = $COOC_2H_5$
XII : R = CN, R′ = COOH
XIV: R = C_6H_5CONH, R′ = COOH



VIII



XIII



XV

Scheme 1

gave the corresponding azlactone compound (XIII), which was hydrolyzed to 3-bromo-5-(β-benzamido-β-carboxyvinyl)-7-isopropyltropolone (XIV).

The aldehyde I underwent condensation with rhodanine to form 3-bromo-7-isopropyltropolon-5-ylmethylenerhodanine (XV), but its treatment with alkali failed to produce the corresponding thioketocarboxylic acid but afforded colorless crystals (XVI) of m. p. 249°C(decomp.), corresponding to the molecular formula of $C_{13}H_{12}O_4S$, and a small amount of I. The bromination

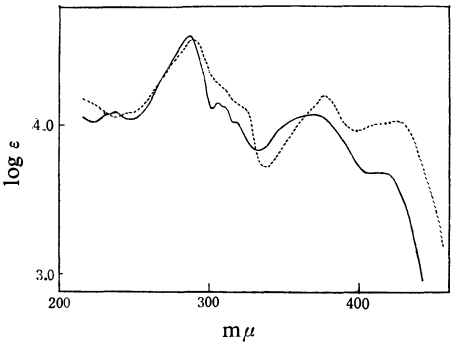
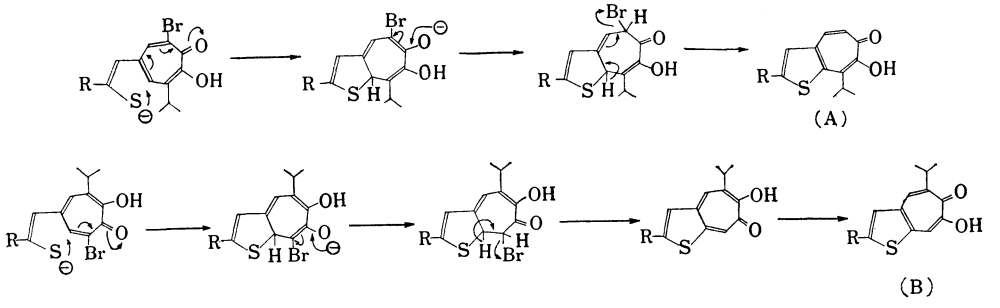


Fig. 2. Ultraviolet spectra of XVI (——) and XVII (·····) in methanol.

of XVI afforded a monobromo compound (XVII) of m. p. 273°C(decomp.). The ultraviolet spectrum of XVI, as indicated in Fig. 2, is not that of a monocyclic tropolone type. The infrared spectrum of XVI showed absorptions for carboxyl group at 2550 and 1672 cm^{-1}. These facts suggest that XVI is a thieno[2, 3-d]tropolone derivative (A or B) formed by the abnormal intramolecular attack of the sulfide anion at the 6- or 4-position of the tropolone ring, with the liberation of the bromide ion from the 3-position.

It may be presumed that the 6-position is sterically hindered by the isopropyl group in 7-position and is liable to be less attacked than the 4-position, so that the product is more likely to be B. Finally, the structure of this product (XVI) was established as 2-carboxy-5-isopropylthieno[2, 3-d]tropolone (B) by the experiments to be described below.

The oxidation of XVI with alkaline potassium permanganate afforded 2, 3, 5-thiophenetricarboxylic acid (XVIII), m. p. 216°C, which formed trimethyl ester XIX, m. p. 83°C with diazomethane. The ester XIX was identified by mixed fusion and through comparison of its ultraviolet and infrared spectra with those of the specimen synthesized by Jones[3]. The



(A)

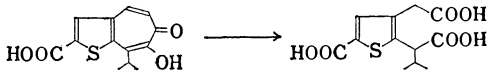
(B)

R = COOH

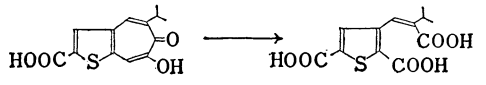
Scheme 2

3) R. G. Jones, *J. Am. Chem. Soc.*, **77**, 4164 (1955).

oxidation of XVI with alkaline hydrogen peroxide afforded a colorless acid substance (XX), m. p. 259°C(decomp.). Elemental analyses of XX gave values corresponding to $C_{12}H_{12}O_6S$, while XX formed a trimethyl ester, (XXI), $C_{15}H_{18}O_6S$, m. p. 86°C, with diazomethane and formed XVIII by oxidation with potassium permanganate. By analogy with the facts known on the oxidation of tropolones with hydrogen peroxide[4-7], it is expected that 8-isopropyl derivative A should afford 2-(α-carboxyisobutyl)-3-carboxymethyl-5-carboxythiophene (A′) and that 5-isopropyl derivative B should give 2, 5-dicarboxy-3-(β-isopropyl-β-carboxyvinyl) thiophene (B′). The ultraviolet spectrum of XX



(A) (A′)



(B) (B′)

Scheme 3

exhibited absorption maxima at 250 mμ(log ε, 4.19) and 280 mμ(log ε, 4.09), while the infrared spectrum of XXI showed absorptions for the carbonyl group of unsaturated ester and for the carbon-carbon double bond at 1715 and 1643 cm^{-1}. The nuclear magnetic resonance spectrum of XXI had absorption corresponding to one ethylenic proton at 222 c. p. s. (with cyclohexane standard). These facts indicate that this oxidation product XX is 2, 5-dicarboxy-3-(β-isopropyl-β-carboxyvinyl)thiophene (B′) and that

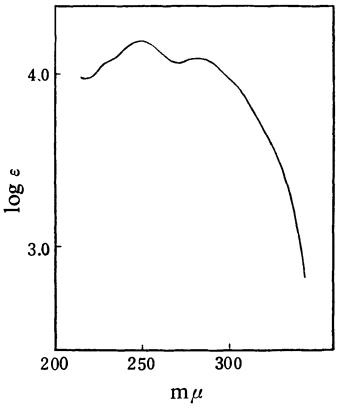


Fig. 3. Ultraviolet spectrum of XX in methanol.

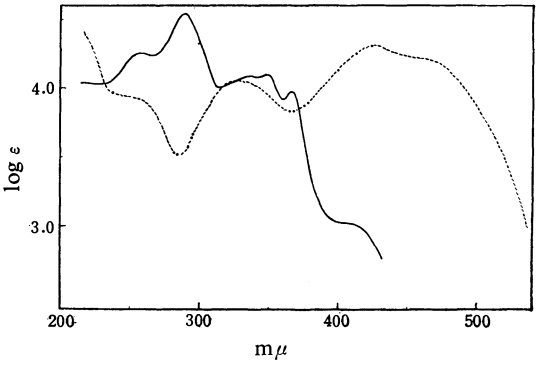
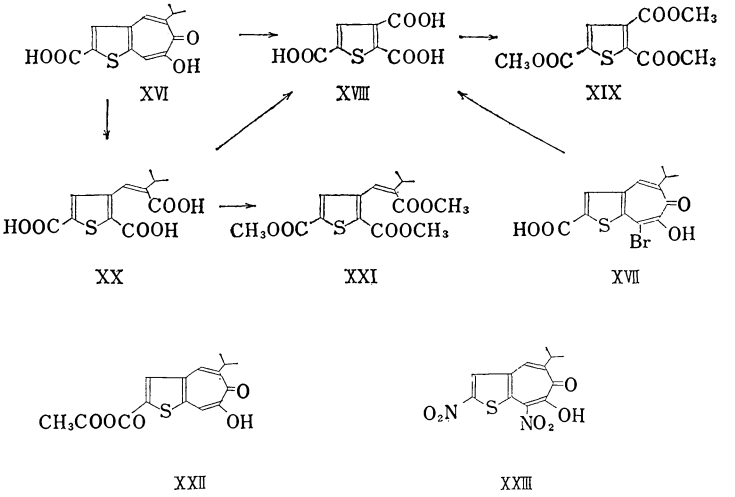


Fig. 4. Ultraviolet spectra of XXII (——) and XXIII (·····) in methanol.



XVI XVIII XIX

XX XXI XVII

XXII XXIII

Scheme 4

4) J. W. Cook et al., *J. Chem. Soc.*, **1951**, 503.
5) T. Nozoe et al., *Proc. Japan Acad.*, **30**, 604 (1954).
6) D. S. Tarbell et al., *J. Am. Chem. Soc.*, **74**, 1234 (1952).
7) H. Fernholz et al., *Ann.*, **576**, 131 (1952).

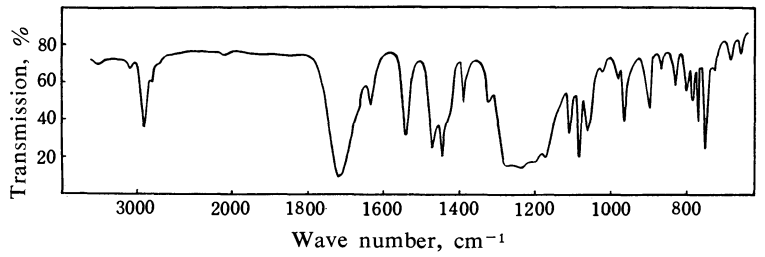


Fig. 5. Infrared spectrum of XXI in KBr disk.

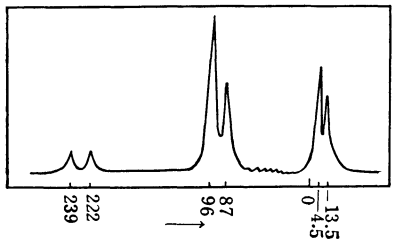
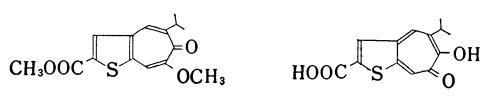


Fig. 6. NMR spectrum of XXI in carbon tetrachloride.

consequently, the position of the isopropyl group in XVI must be 5.

The oxidation of the monobromo compound XVII with potassium permanganate gave 2, 3, 5-thiophenetricarboxylic acid (XVIII), judging from which XVII must be 2-carboxy-5-isopropyl-8-bromothieno [2, 3-d] tropolone. The heating of XVI with acetic anhydride, in the presence of sodium acetate, afforded colorless crystals of m. p. 190°C, $C_{15}H_{14}O_5S$, which showed infrared absorptions of the hydroxyl group at 3160 cm^{-1}, and of the carbonyl group at 1765 and 1730 cm^{-1}. This product was therefore considered to be the anhydride XXII. It reverted to XVI on alkaline hydrolysis. The treatment of XVI with concentrated nitric acid in acetic acid gave yellow needles, of m. p. 185°C, whose elemental analyses and infrared spectrum indicated that this product was 2, 8-dinitro-5-isopropylthieno [2, 3-d] tropolone (XXIII). The ultraviolet spectra of XXII and XXIII are shown in Fig. 4.

The treatment of XVI with diazomethane afforded only one kind of methyl ether XXIV; this is thought to be due to the condensed thiophene ring, as in the case of benzotropolones[6], and there is almost no contribution from the type of XVI′.



XXIV XVI′

Scheme 5

Experimental*

3-Bromo-5-dimethoxymethyl-7-isopropyltropolone (II).—A solution of 20 mg. of I in methanol (1 ml.) was refluxed for 30 min. The evaporation of the methanol left colorless needles. The crystals were collected, with the addition of petroleum ether, and recrystallized from petroleum ether to form colorless rods, m. p. 86~87°C. Yield, 20 mg.

Found: 49.49; H, 5.35. Calcd. for $C_{13}H_{16}O_4Br$: C, 49.38; H, 5.36%.

***N*-(3-Bromo-7-isopropyltropolon-5-ylmethylene)-aniline (III).**—A mixture of I (30 mg.), aniline (15 mg.) and acetic acid (0.1 ml.) was warmed in a water bath, by which the whole first dissolved to form a red solution, but then yellow crystals began to separate out. This mixture was warmed for 30 min., and the crystals were collected and recrystallized from petroleum ether to form yellow scales, m. p. 145~147°C. Yield, 20 mg.

Found: C, 59.71; H, 4.54; N, 3.92. Calcd. for $C_{17}H_{16}O_2NBr$: C, 58.96; H, 4.62; N; 4.05%.

λ_{max}^{MeOH} mμ(log ε): 260(4.50), 340(3.88), 385(4.00).

***N*-(3-Bromo-7-isopropyltropolon-5-ylmethylene)-*p*-toluidine (IV).**—A mixture of I (40 mg.) and *p*-toluidine (20 mg.) in acetic acid (0.1 ml.) was warmed in a water bath for 20 min. and then cooled to room temperature. The crystals that formed were collected and recrystallized from petroleum ether to form yellow needles, m. p. 113~116°C. Yield, 30 mg.

Found: C, 57.71; H, 4.57; N, 3.70; Calcd. for $C_{18}H_{18}O_2NBr.H_2O$: C, 57.15; H, 5.29; N, 3.70%.

λ_{max}^{MeOH} mμ(log ε): 259(4.34), 342(3.78), 390(3.99).

***N*-(3-Bromo-7-isopropyltropolon-5-ylmethylene)-*p*-anisidine (V).**—A mixture of I (20 mg.) and *p*-anisidine (10 mg.) in acetic acid (0.1 ml.) was heated in a water bath for 5 min. and then cooled to room temperature. The crystals that formed were collected and recrystallized from methanol to form yellow needles, m. p. 95~101°C. Yield, 10 mg.

Found: C, 57.39; H, 4.70:, N; 3.91. Calcd. for $C_{18}H_{18}O_3NBr$: C, 57.46; H, 4.79; N, 3.73%.

λ_{max}^{MeOH} mμ(log ε): 259(4.45), 390(4.20).

***N*-(3′-Bromo-7′-isopropyltropolon-5′-ylmethylene)-5-tropolonylamine (VI).**—A mixture of I (20 mg.) and 5-aminotropolone (15 mg.) in acetic acid (0.1 ml.) was heated in a water bath; yellow powder precipitated in 5~6 min. This precipitate was

* All melting points are uncorrected. The microanalyses were carried out by Miss Yoko Endo and Miss Yukiko Endo of this Institute, to whom the author is indebted.

collected and washed with hot methanol and acetic acid, m. p. 203~204°C(decomp.).

Found: C, 55.35; H, 4.06; N, 3.73. Calcd. for $C_{18}H_{16}O_4NBr$: C, 55.40; H, 4.10; N, 3.59%.

λ_{max}^{MeOH} mμ(log ε): 230(4.41), 255(4.52), 420(4.41).

***N*-(3-Bromo-7-isopropyltropolon-5-ylmethylene)-*o*-aminoaniline (VII).**—A mixture of I (40 mg.) and *o*-phenylenediamine (20 mg.) in ethanol (0.1 ml.) was heated in a water bath for a few minutes. The red crystals that precipitated were collected and recrystallized from ethanol to form red prisms, m. p. 104~107°C. Yield, 30 mg.

Found: C, 56.40; H, 4.48; N, 7.55. Calcd. for $C_{17}H_{17}O_2N_2Br$: C, 56.52; H, 4.71; N, 7.75%.

λ_{max}^{MeOH} mμ(log ε): 263(4.37), 406(4.39).

2-(3'-Bromo-7'-isopropyltropolon-5'-yl)benzimidazole (VIII).—A mixture of I (40 mg.) and *o*-phenylenediamine (20 mg.) in 0.1 ml. of acetic acid was heated in a water bath for 5~6 min.; the crystals that formed were collected and recrystallized from methanol to form yellow needles, m. p. 242~243°C(decomp.). Yield, 20 mg.

VIII was also obtained by the use of (3-bromo-7-isopropyltropolon-5-yl)-*N*-(*p*-dimethylaminophenyl) nitrone in place of I and reacted under the same conditions. The compound VII also afforded VIII on being heated in acetic acid.

Found: C, 56.75; H, 3.94; N, 7.68. Calcd. for $C_{17}H_{15}O_2N_2Br$: C, 56.84; H, 4.18; N, 7.81%.

λ_{max}^{MeOH} mμ(log ε): 254(4.39), 383(4.43).

3-Bromo-5-(β, β-dicyanovinyl)-7-isopropyltropolone (IX).—A solution of I (50 mg.), malononitrile (20 mg.), and piperidine (1 drop) dissolved in ethanol (1 ml.) was allowed to stand at room temperature, by which the solution gradually acquired a reddish tint and yellow crystals precipitated out after about 5 hr. After the mixture had been allowed to stand overnight, the crystals were collected, treated with 6 N hydrochloric acid (0.2 ml.), collected on a filter, washed with water, and recrystallized from methanol to form yellow granules, m. p. 145~146°C. Yield, 30 mg.

Found: C, 52.44; H, 3.51; N, 8.30. Calcd. for $C_{14}H_{11}O_2N_2Br$: C, 52.80; H, 3.45; N, 8.78%.

λ_{max}^{MeOH} mμ(log ε): 222(4.20), 280(4.10), 404(4.15), 490(4.70).

3-Bromo-5-(β-cyano-β-carbamoylvinyl)-7-isopropyltropolone (X).—A solution of I (50 mg.), cyanoacetamide (20 mg.), and piperidine (1 drop) dissolved in ethanol (1 ml.) was refluxed for 3 hr., the solvent was distilled off, and the residue was acidified by the addition of 6 N hydrochloric acid. The yellow, powdery precipitate thereby formed was collected and washed thoroughly with water and methanol, m. p. 233°C(decomp.). Yield, 20 mg.

Found: C, 49.14; H, 3.69; N, 7.61. Calcd. for $C_{14}H_{13}O_3N_2Br$: C, 49.87; H, 3.86; N, 8.31%.

λ_{max}^{MeOH} mμ(log ε): 245(4.06), 275(4.14), 466(4.47).

3-Bromo-5-(β-cyano-β-ethoxycarbonylvinyl)-7-isopropyltropolone (XI).—A mixture of I (50 mg.) and ethyl cyanoacetate (30 mg.) dissolved in ethanol (1 ml.) and with one drop of piperidine added was allowed to stand at room temperature for 2 days, and then the ethanol was evaporated. 6N Hydrochloric acid was added to its reddish syrupy residue; the syrup thereby solidified and formed a yellowish powder. This powder was collected and recrystallized from methanol to form yellow needles, m. p. 106~108°C. Yield, 50 mg.

Found: C, 52.71; H, 4.48; N, 3.43. Calcd. for $C_{16}H_{16}O_4NBr$: C, 52.46; H, 4.37; N, 3.83%.

λ_{max}^{MeOH} mμ(log ε): 245(4.04), 276(4.13), 408(4.25), 476(4.57).

3-Bromo-5-(β-cyano-β-carboxyvinyl)-7-isopropyltropolone (XII).—A mixture of XI (60 mg.) and a 20% aqueous solution of sodium hydroxide (0.5 ml.) was heated in a water bath for a few minutes. The mixture formed a red solution and then precipitated out yellow crystals. The mixture was acidified with 6 N hydrochloric acid, and the yellow precipitate thereby formed was collected by filtration. Recrystallization from methanol afforded yellow prisms, m. p. 210~220°C. Yield, 30 mg.

Found: C, 49.67; H, 3.78; N, 3.70. Calcd. for $C_{14}H_{12}O_4NBr$: C, 49.72; H, 3.58; N, 4.14%.

λ_{max}^{MeOH} mμ(log ε): 265(4.28), 290(4.19).

2-Phenyl-4-(3'-bromo-7'-isopropyltropolon-5'-ylmethylene)-5-oxazolone (XIII).—A mixture of I (100 mg.), hippuric acid (80 mg.), freshly fused sodium acetate (40 mg.), and acetic anhydride (0.5 ml). was heated at 80~90°C for 10 min.; the mixture thereby formed a red solution and an orange precipitate separated. The mixture was cooled and diluted with water (0.2 ml.), and the precipitate was collected by filtration. The precipitate was washed thoroughly with water and methanol, m.p. 190~194°C. Yield, 100 mg.

Found: C, 58.29; H, 3.88; N, 2.92. Calcd. for $C_{20}H_{16}O_4NBr$: C, 57.99; H, 3.87; N, 3.38%.

λ_{max}^{MeOH} mμ(log ε): 258(4.28), 320(4.15), 426(4.21); 510(4.43).

3-Bromo-5-(β-benzamido-β-carboxyvinyl)-7-isopropyltropolone (XIV).—A mixture of 100 mg. of azlactone (XIII) and a 10% sodium hydroxide solution (0.5 ml.) in methanol (0.3 ml.) was heated in a water bath for a a few minutes, the methanol was evaporated, and the residual solution was acidified with 6 N hydrochloric acid. The pale yellow precipitate that formed was collected by filtration and recrystallized from methanol to form a yellow powder, m. p. 220°C(decomp.). Yield, 40 mg.

Found: C, 55.98; H, 4.34; N, 3.08. Calcd. for $C_{20}H_{18}O_5NBr$: C, 55.57; H, 4.17; N, 3.24%.

λ_{max}^{MeOH} mμ(log ε): 262(4.42), 375(4.27).

3-Bromo-7-isopropyltropolon-5-ylmethylenerhodanine (XV).—A mixture of I (500 mg.), rhodanine (250 mg.), freshly fused sodium acetate (500 mg.), and acetic acid (3.4 ml.) was heated in a boiling water bath; orange prismatic crystals thereby precipitated out. After the mixture had been heated for 1 hr., water (1 ml.) was added to the mixture, and the crystals were collected and washed with water and methanol. Orange prisms, m. p. 235~240°C. Leaving the filtrate to stand at room temperature further afforded a precipitate of XV. Yield, 700 mg.

Found: C, 44.15; H, 3.10; N, 3.40. Calcd. for $C_{14}H_{12}O_3NS_2Br$; C, 43.55; H, 3.13; N, 3.63%.

λ_{max}^{MeOH} mμ(log ε): 253(4.16), 335(3.96), 430(4.26), 500(4.31).

2-Carboxy-5-isopropylthieno[2, 3-d]tropolone (XVI).—A solution of XV (450 mg.) in a 15% aqueous solution of sodium hydroxide (4 ml.) was heated on a water bath for 1 hr.; the yellow crystals that precipitated out were collected and acidified with 6 N hydrochloric acid, thereby obtaining ca. 20 mg. of I.

The acidification of this filtrate with 6 N hydrochloric acid afforded a colorless precipitate, which was collected after the addition of a small amount of methanol (0.5 ml.). The precipitate was washed with water and methanol and then recrystallized from methanol to form colorless crystals of XVI, m. p. 249°C. Yield, 200 mg.

Found: C, 59.16; H, 4.36. Calcd. for $C_{13}H_{12}O_4S$: C, 59.09; H, 4.58%.

λ_{max}^{MeOH} mμ(log ε); 237(4.09), 287(4.61), 305(4.15), 370(4.08).

2-Carboxy-5-isopropyl-8-bromothieno[2, 3-d]tropolone (XVII).—A solution of bromine (30 mg.) in methanol (0.5 ml.) was added drop by drop into a suspension of XVI (50 mg.) in methanol (2 ml.), while being stirred under ice-cooling, and the whole was stirred at room temperature for 10 min. after the completion of the addition. The crystals that formed were collected and recrystallized from methanol to form pale yellow needles (XVII), m. p. 270~273°C(decomp.). Yield, 20 mg.

Found: C, 45.34; H, 3.30. Calcd. for $C_{13}H_{11}O_4BrS$: C, 45.49; H, 3.21%.

λ_{max}^{MeOH} mμ(log ε): 288(4.58), 377(4.20), 425(4.03).

2, 3, 5-Thiophenetricarboxylic Acid (XVIII).—Into a solution of XVI (100 mg.) dissolved in a 10% sodium hydroxide solution (6.5 ml.), a 5% aqueous solution of potassium permanganate (8 ml.) was stirred drop by drop. After the completion of the addition, the mixture was stirred for 2 hr. and warmed on a water bath for a few min., and the manganese dioxide that had formed was filtered off. The filtrate was concentrated under a reduced pressure to about one-half the original volume, acidified to pH 3~4 by the addition of hydrochloric acid, and extracted three times with ether. The evaporation of ether from the extract left colorless crystals which were collected by filtration, washed with water, and recrystallized from ether to form colorless granular crystals, m. p. 215~216°C. Yield, 30 mg.

Found: C, 38.32; H, 2.40. Calcd. for $C_7H_4O_6S$; C, 38.90; H, 1.87%.

λ_{max}^{MeOH} mμ(log ε): 275(3.97).

Trimethyl 2, 3, 5-thiophenetricarboxylate (XIX).—An excess of diazomethane was added to a solution of XVIII (10 mg.) in ether (1 ml.), and the mixture was allowed to stand in a cold room for 1 hr. The evaporation of the ether left colorless needles which sublimed at 100°C under a reduced pressure. The sublimate afforded colorless needles, m. p. 82~83°C. Yield, 10 mg. This substance showed no depression of melting point on admixture with an authentic sample.

λ_{max}^{MeOH} mμ(log ε): 218(4.11), 274(4.10).

2, 5-Dicarboxy-3-(β-isopropyl-β-carboxyvinyl)-thiophene (XX).—To a solution of XVI (100 mg.) dissolved in 1 N sodium hydroxide (2 ml.), a 35% hydrogen peroxide solution (2 ml.) was added, and the mixture was allowed to stand at room temperature for 2 days. This solution was then acidified (pH 3) with hydrochloric acid and extracted three times with ether, and the extract was concentrated. The colorless crystals that precipitated out were collected and recrystallized form water containing a small amount of ethanol to from colorless prisms, m. p. 256~259°C. Yield 70 mg.

Found: C, 50.39; H, 4.12. Calcd. for $C_{12}H_{12}O_6S$: C, 50.71; H, 4.26%.

λ_{max}^{MeOH} mμ(log ε): 250(4.19), 280(4.09).

2,5-Dimethoxycarbonyl-3-(β-isopropyl-β-methoxycarbonylvinyl)-thiophene (XXI).—An excess of diazomethane was added to a solution of XX (100 mg.) dissolved in ether (5 ml.), and the mixture was allowed to stand at room temperature. The evaporation of the ether left an oily residue which crystallized after being allowed to stand in a cold room with methanol (0.3 ml.). The crystals, m. p. 76~79°C, were collected and sublimed at 100°C under a reduced pressure to form colorless prisms, m. p. 84~86°C. Yield, 60 mg.

Found: C, 54.92; H, 5.58. Calcd. for $C_{15}H_{18}O_6S$: C, 55.21; H, 5.56.

λ_{max}^{MeOH} mμ(log ε): 248(4.21), 282(4.16).

Permanganate Oxidation of XX.—Into a solution of XX (25 mg.) dissolved in a 1 N sodium hydroxide solution (0.5 ml.), a 5% potassium permanganate solution was stirred drop by drop at room temperature, until the color of the permanganate persisted. The manganese dioxide that formed was filtered off, the filtrate was acidified (pH 3) with hydrochloric acid, and the mixture was extracted with ether, by which ca. 5 mg. of XVIII was obtained.

Permanganate Oxidation of XVII.—To a solution of XVII (80 mg.) dissolved in a 5% sodium hydroxide solution (5 ml.), a solution of potassium permanganate (150 mg.) in water (3 ml.) was added drop by drop, and the mixture was stirred until the permanganate color faded. The reaction mixture was treated as in the oxidation of XVI, and XVIII was obtained.

2-Acetoxycarbonyl-5-isopropylthieno[2, 3-d]tropolone (XXII).—A mixture or XVI (20 mg.), freshly fused sodium acetate (10 mg.), and acetic anhydride (0.2 ml.) was heated at 120°C for 30 min. The acetic anhydride was evaporated, water (0.5 ml.) and a drop of 15% sodium hydroxide were added to the residue, and the yellow solution so formed was acidified with hydrochloric acid. The oil that separated crystallized gradually. The crystals were collected by filtration and recrystallized from methanol to form colorless granular crystals, m. p. 186~190°C. Yield, 10 mg.

Found: C, 58.71; H, 4.60. Calcd. for $C_{15}H_{14}O_5S$: C, 58.82; H, 4.61%.

λ_{max}^{MeOH} mμ(log ε): 257(4.25), 289(4.55), 335(4.09), 350(4.10), 367(3.98).

2, 8-Dinitro-5-isopropylthieno[2, 3-d]tropolone (XXIII).—Concentrated nitric acid (0.8 ml.) was added to a solution of XVI (100 mg.) dissolved in acetic acid (16 ml.). After being allowed to stand

at room temperature for 30 min., the mixture was poured into cracked ice. The precipitate that formed was collected, washed with water, and recrystallized from methanol to form yellow needles, m. p. 184~185°C. Yield, 15 mg.

Found: C, 46.19; H, 3.65; N, 9.55. Calcd. for $C_{12}H_{10}O_6N_2S$: C, 46.46; H, 3.25; N, 9.03%.

λ_{max}^{MeOH} mμ(log ε): 328(4.06), 424(4.33).

2-Methoxycarbonyl-5-isopropyl-7-methoxythieno-[2, 3-d]tropone (XXIV).—An excess of an ether solution of diazomethane was added to a solution of XVI dissolved in dioxane (1 ml.) and allowed to stand in a cold room overnight. The colorless crystals that formed were collected and recrystallized from benzene to form colorless needles, m. p. 168~169°C. Yield, 70 mg.

Found: C, 61.94; H, 5.35. Calcd for $C_{15}H_{16}O_4S$: C, 61.64; H, 5.52%.

λ_{max}^{MeOH} mμ(log ε): 230(4.04), 280(4.59), 347(4.21), 375(4.09).

The author wishes to express his deep gratitude to Professor Shuichi Seto for his unfailing guidance throughout this work, and to Dr. Shingo Matsumura and Dr. Yusaku Ikegami for their helpful advice. Also, the author wishes to thank Mr. Kensuke Takahashi for his measurements and advice on NMR spectra, to Mr. Shuji Aono for his infrared spectral measurements, and Mr. Fumio Sato for his ultraviolet spectral measurements. He is also grateful to Dr. R. G. Jones for the gift of the specimen of 2, 3, 5-thiophenetricarboxylic acid and to Sankyo Co., Ltd., which defrayed a part of the expenses for the present research.

The Chemical Research Institute of Non-Aqueous Solutions
Tohoku University
Katahira-cho, Sendai

Diels-Alder Reaction of 2-Isopropyl-1, 3-butadiene with 4-Benzyloxy-2-butyn-1-al and Crotonaldehyde[1]

By Atsuaki ARAI and Iwao ICHIKIZAKI

(Received July 18, 1961)

The formation of two isomeric Diels-Alder adducts may be expected when an asymmetric diene and an asymmetric dienophile interact; however, in most cases the isolation of only one isomer has been reported. Moreover, about certain asymmetric addends of the reaction it has been stated[2] that the substituents in the diene generally produce a high degree of specificity in the direction of addition.

In a research program in this laboratory on the Diels-Alder reactions between asymmetric dienes and asymmetric dienophiles, the direction of the addition of 2-isopropyl-1, 3-butadiene (I) to 4-benzyloxy-2-butyn-1-al (II) as well as to crotonaldehyde (X) has been investigated.

A Diels-Alder reaction carried out by heating I and II at 145~150°C in benzene gave an oily product formulated as $C_{18}H_{22}O_2$, b. p. 132~134°C/3×10^{-3}mmHg, λ_{max}^{EtOH} 236 mμ, ε, 6800, in a 79% yield. This product afforded two red 2, 4-dinitrophenylhydrazones, III′ (m. p. 197~198°C) and IV′ (m. p. 160~161°C), in a ratio of approximately 2 : 3 and proved also to consist of two isomeric adducts. Similarly, it gave, in nearly a quantitative yield, heterogeneous phenylsemicarbazone, recrystallization of which afforded pure fine needles (IV″) with an m. p. of 183~183.5°C and two low-melting fractions, both of which were apparently heterogeneous yet. On treatment with the Brady reagent followed by fractional crystallization, phenylsemicarbazone IV″ gave homogeneous 2, 4-dinitrophenylhydrazone IV′, and one melted at 156.5~158°C of the heterogeneous phenylsemicarbazones gave the 2,4-dinitrophenylhydrazones, III′ and IV′, in a ratio of approximately 2.5 : 1.

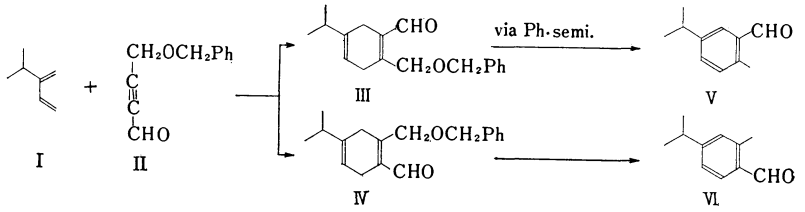
When subjected to a superheated steam distillation over phthalic and sulfuric acids[3,4], the phenylsemicarbazone IV″ was converted into 4-isopropyl-2-methylbenzaldehyde (VI) in a 51% yield, accompanied by the removal of the benzyl alcohol. On similar treatment, the heterogeneous phenylsemicarbazone described above afforded a yellow oily product consisting of 5-isopropyl-2-methylbenzaldehyde (V) and

1) Presented in part at the 13th Annual Meeting of the Cheimcal Society of Japan, Tokyo, April 1960.

2) A. J. Birch, *Ann. Reports on Prog. Chem.*, **47**, 177 (1950).

3) A. Arai and I. Ichikizaki, This Bulletin, **34**, 1571 (1961).

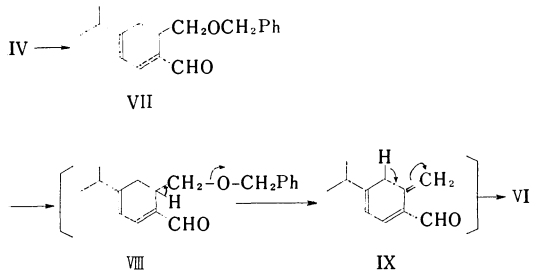
4) A. Arai and I. Ichikizaki, ibid., **35**, 45 (1962).



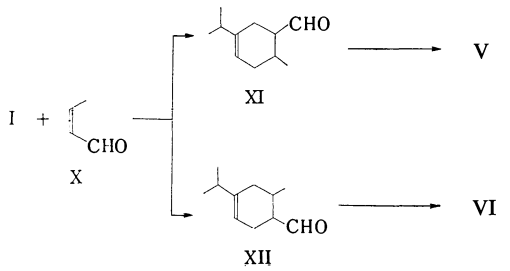
an appreciable amount of VI, both of which were characterized as solid derivatives.

This experimental evidence thus far obtained has made it possible to conclude that the Diels-Alder adduct of I with II consists of 2-benzyloxymethyl - 5 - isopropylcyclohexa - 1, 4-dienylmethanal (III) and 2-benzyloxymethyl-4-isopropylcyclohexa-1, 4-dienylmethanal (IV) in a ratio of approximately 2 : 3.

The original heterogeneous adduct, after being treated with a diluted methanolic sulfuric acid solution at 60°C for 10 min., showed a decrease in the ε_{max} to about 74% of the original value of the light-absorption maximum at 236 mμ; it simultaneously indicated the appearance of a maximum at 308 mμ characteristic of an α, β-γ, δ-unsaturated aldehyde system[5]. On prolonged treatment with acid, the isomerized aldehydes, e. g., VII, were finally aromaticized to the corresponding benzaldehydes, e. g., VI, which were indicated by a new maximum shown at 256 mμ. Such acid-catalyzed aromaticization, remarkable for the 2-benzyloxymethylcyclohexa-1, 4-dienealdehyde series[6], is presumably accelerated by the initial isomerization to the α, β-γ, δ-unsaturated aldehydes, as represented by VII, which readily lose their benzyl alcohol and convert, via labile intermediates, e. g., IX, into the corresponding benzaldehydes.



According to Nazarov and Mavrov[7], the condensation of I with X carried out at 200°C produces a heterogeneous adduct which is concluded to consist of 3-isopropyl-6-methyl-3-cyclohexenylmethanal (XI) and 4-isopropyl-6-methyl-3-cyclohexenylmethanal (XII) from the fact that terephthalic acid and isophthalic acid can be derived therefrom in a ratio of approximately 1 : 3 by successive oxidative treatments. Some modified methods for the identification and determination of the product in the same Diels-Alder reaction were employed by the present authors. The inseparable reaction product obtained under conditions similar to those cited above was treated with sulfur to give the dehydrogenation product which was determined, by being characterized as the 2, 4-dinitrophenylhydrazones, to consist of 3-isopropyl-6-methylbenzaldehyde (V) and 4-isopropyl-6-methylbenzaldehyde (VI), which apparently came from XI and XII respectively. The proportion of XI to XII could be decided directly by gas-liquid chromatography using a Carbowax-4000 on Celite DM-13A as the column packing material; the value of 1/2.5 was thereby obtained. In connection with the direction of the addition of the diene to the dienophile, it should be noted that the proportion of XII to XI markedly increases, as shown in Tables I and II cited in the experimental section, when the condensation was carried out at a lower temperature.



As described above, the Diels-Alder reaction of I with II as well as with X gave both of the two possible adducts in extremely near proportions, although the predominant direction of the addition conforms to the common rule[2]. In the condensation with unsymmetrical addends, it has been generally reported that a β-substituted diene, $CH_2=C(X)-CH=CH_2$, reacts with such a dienophile, R-CH=CH-Y, containing only a negative group Y as crotonaldehyde to give an adduct with X para to Y. As far as we know, such Diels-Alder dienes as

5) J. C. Lunt and F. Sondheimer, *J. Chem. Soc.*, **1950**, 3361.

6) Similar aromaticization in this series was also encountered in the cases of acid-catalyzed acetal formation of 2-benzyloxymethyl-4, 5 - dimethylcyclohexa- 1, 4 -dienylmethanal[3] and 2-benzyloxymethyl-4, 5, 6-trimethylcyclohexa-1, 4-dienylmethanal[4].

7) I. N. Nazarov and M. V. Mavrov, *Zhur. Obshchei Khim.*, **29**, 1158 (1959).

2-isopropyl-1, 3-butadiene (I), effecting a remarkable decrease in specificity[8] in the direction of addition, have rarely been found in the literature.

Experimental[11]

2-Isopropyl-1, 3-butadiene (I).—2-Isopropyl-1, 3-butadiene (I) was obtained by repeated fractionation with a 100 cm. modified Todd fractionating column of the dehydration product of 3,4-dimethyl-1-penten-3-ol[4] and had b. p. 85.5~86.5°C/760 mmHg and n_D^{20} 1.4312 (lit. b. p. 85~85.5°C, n_D^{20} 1.4316[12]; b. p. 86~87°C, n_D^{20} 1.4324[7]).

4-Benzyloxy-2-butyn-1-al (II).—4-Benzyloxy-2-butyn-1-al (II) was prepared by the method described in a previous paper[3,4] and had b. p. 115~118°C/2 mmHg and n_D^{20} 1.5408.

Condensation of I with II.—A mixture of I (13.5 g.), II (22.0 g.) and benzene (4 ml.) was heated with a small amount of hydroquinone for 13 hr. at 145~150°C in a 100 ml. sealed glass tube. Distillation of the reaction product gave an oil (29.0 g.) having b. p. 120~138°C/3×10^{-3} mmHg and n_D^{21} 1.5438~1.5454; on redistillation this oil afforded an inseparable mixture of the adducts III and IV as a pale yellow oil, b. p. 132~134°C/3×10^{-3} mmHg, n_D^{20} 1.5450. λ_{max}^{EtOH} 236 mμ (ε, 6800).

Found: C, 79.96; H, 8.30. Calcd. for $C_{18}H_{22}O_2$: C, 79.96; H, 8.20%.

In order to determine the proportion of III to IV in the original adduct, the aldehyde (0.55 g.) was converted on treatment with the Brady reagent into 2,4-dinitrophenylhydrazone, which was fractionally crystallized from methanol to give red-orange needles, m. p. 197~198°C (III′) (0.27 g.) and red needles, m. p. 160~161°C (IV′) (0.44 g.).

Found: III′: N, 12.36. IV′: N, 12.42. Calcd. for $C_{24}H_{26}O_5N_4$: N, 12.44%.

The aldehyde (20.0 g.) in ethanol (40 ml.) was treated with phenylsemicarbazide (11.0 g.) in the usual manner to afford crude phenylsemicarbazone (28.8 g., 96.6%), which on fractional crystallization from methanol gave colorless fine needles, m. p. 183~183.5°C (IV″) (8.2 g., 28.4% based on the crude crystalline solid), λ_{max}^{EtOH} 235 mμ (ε, 17200), 284 (34200), and two low-melting fractions which melted at 163~169°C (3.8 g., 13.2%) and 156.5~158°C (15 g., 52.0%), λ_{max}^{EtOH} 235 mμ (ε, 11600), 284 (22900), both of which were apparently heterogeneous.

Found: IV″: N, 10.62. The last fraction: N, 10.48. Calcd. for $C_{25}H_{29}O_2N_3$: N, 10.41%.

On treatment with the Brady reagent, the phenylsemicarbazone IV″ gave the homogeneous 2,4-dinitrophenylhydrazone IV′ in an excellent yield, and the heterogeneous one which melted at 156.5~158°C (2.2 g.), afforded the 2,4-dinitrophenylhydrazones III′ (1.5 g.) and IV′ (0.6 g.).

Treatment of the Original Adduct Obtained Above with Methanolic Sulfuric Acid.—The original adduct (2.0 g.), dissolved in 70% aqueous methanol (13.5 ml.) containing concentrated sulfuric acid (1.4 g.), was warmed for 10 min. at 60°C. To the resultant solution a saturated methanolic solution of potassium acetate was added drop by drop while the mixture was being cooled, until the precipitation of potassium sulfate was complete. The cooled reaction mixture was then filtered, and the filtrate was extracted with benzene. Distillation of the dried benzene solution gave a pale yellow oil (1.15 g.), b. p. 145~146°C/1.5×10^{-2} mmHg, n_D^{28} 1.5481, λ_{max}^{EtOH} 236 mμ (ε, 5000), 308 (1100).

Found: C, 79.24; H, 8.20. Calcd. for $C_{18}H_{22}O_2$: C, 79.96; H, 8.20%.

The oil obtained above (1.0 g.) was again treated with a solution of concentrated sulfuric acid (1.0 g.) in 80% aqueous methanol (7 ml.) for 1 hr. at 60°C and successively for 24 hr. at room temperature. The reaction mixture was neutralized with aqueous potassium carbonate, organic material was taken up in ether and the ether layer was washed with water. After removal of the solvent from the dried solution, the residue was distilled to afford a yellow oil (0.6 g.), b. p. 105~135°C/2×10^{-2} mmHg, which showed light-absorption maxima at 236, 256 and 308 mμ in ethanol.

Condensation of I with Crotonaldehyde (X).—A mixture of I (2.5 g.), X (1.09 g.) and an appropriate solvent (10 ml.) was heated with a small amount of hydroquinone under the conditions listed in Table I in a 50 ml. glass bomb tube. Removal of the solvent, followed by distillation of the residue through a 7 cm. Vigreux column under nitrogen, afforded an inseparable mixture of the expected adducts, 3-isopropyl-6-methyl-3-cyclohexenylmethanal (XI) and 4-isopropyl-6-methyl-3-cyclohexenylmethanal (XII); the properties of these adducts, their elemental analyses and their proportions, determined by gas-liquid chromatography using a 0.6×200 cm., 30% Carbowax-4000 on Celite DM-13A as the column-packing material, are summarized in Table II.

4-Isopropyl-2-methylbenzaldehyde (VI).—*a) Steam Distillation of the Phenylsemicarbazone IV″ with Acid.*—A mixture of IV″ (4.4 g.), propylene glycol (60 g.), *o*-phthalic acid (4.4 g.), concentrated sulfuric acid (22.0 g.) and water (80 ml.) was distilled under superheated steam until no more organic material passed over. The distillate (1400 ml.) was then extracted with ether, and the ether extract was washed with 10% aqueous sodium carbonate and with water and dried over sodium sulfate. Removal of the solvent, followed by fractionation of the residue, gave a fore-run consisting mainly of benzyl alcohol and 4-isopropyl-2-methylbenzaldeheyde (VI) (0.9 g., 51%) in the form of a pale yellow oil. A redistilled sample had b. p. 123~124°C/17 mmHg and n_D^{21} 1.5275. λ_{max}^{EtOH} 259 mμ.

The semicarbazone crystallized from methanol in

8) An asymmetric dienophile, such as β-acetyl acrylic acid[9] and 4-methoxy-β-nitrostyrene[10], possessing two negative groups adjacent to the carbon-carbon double bond will, of course, have the same effect on the direction of the addition of a certain asymmetric diene.

9) E. Buchta and G. Satzinger, *Chem. Ber.*, **92**, 449 (1959).

10) W. C. Wildman, R. B. Wildman, W. T. Norton and J. B. Fine, *J. Am. Chem. Soc.*, **75**, 1913 (1953).

11) All melting points were taken on a Kofler hot-stage microscope and are uncorrected. Ultraviolet spectra were measured on a Hitachi model EPU-2A spectrophotometer.

12) C. G. Overberger, A. Fischman, C. W. Roberts, L. A. Arond and J. Lal, *J. Am. Chem. Soc.*, **73**, 2540 (1951).

Table I. Diels-Alder reaction between 2-isopropyl-1,3-butadiene and crotonaldehyde

Exp. no.	Reaction conditions			Total yield of the adduct	
	Temp. °C	Time hr.	Solvent	g.	%
1	125	12	Benzene	1.21	28.0
2	120~125	30	*n*-Hexane	1.20	27.8
3	200	6	Benzene	2.60	60.0
4	200	12	Benzene	2.76	64.0

Table II. Properties and compositions of the adducts listed in Table I

Exp. no.	B. p. °C/mmHg	n_D^T	Found / Calcd. for $C_{11}H_{18}O$ C	H	Composition of the adduct* XI : XII
1	73~74/4	1.4710^{20}	79.65 79.46	10.99 10.92	1 : 8.0
2	70~72/3.5	1.4709^{20}			1 : 8.5
3	75/4	1.4711^{19}	79.71 79.46	11.00 10.92	1 : 2.5
4	74~75/4	1.4710^{20}			1 : 2.6

* The gas-liquid chromatogram of the adduct indicated two peaks, at a retention time of 9.7 and 10.3 min., attributable to the compounds XII and XI respectively and the proportion of XII to XI was calculated from their peak areas column temperature, 200°C; the carrier gas, hydrogen, had a flow rate of 30 ml./min.

needles, m. p. 199~200°C, which yellow rapidly on exposure to the light (lit.[13] m. p. 198~199°C).

Found: N, 19.39. Calcd. for $C_{12}H_{17}ON_3$: N, 19.16%.

The 2,4-dinitrophenylhydrazone crystallized from ethanol-ethyl acetate as red-orange needles, m. p. 184~185°C.

Found: N, 16.42. Calcd. for $C_{17}H_{18}O_4N_4$: N, 16.37%.

b) Sulfur Dehydrogenation of the Adduct Obtained in Exp. 1 Listed in Table I.—The adduct (0.9 g.) was heated under reflux with sulfur (1.3 g.) under a nitrogen atmosphere at 230°C for 45 min. at which time the evolution of hydrogen sulfide ceased. The black reaction mixture was distilled under nitrogen and chromatographed on alumina to give a yellow oil (0.4 g.), which provided only the 2,4-dinitrophenylhydrazone of VI, m. p. 184°C, after two recrystallizations from ethanol-ethyl acetate. No depression was observed in melting point on admixture with the 2,4-dinitrophenylhydrazone prepared in a).

5-Isopropyl-2-methylbenzaldehyde (V).—*a) Steam Distillation of the Heterogeneous Phenylsemicarbazone Melted at 156.5~158°C with Acid.*—A mixture of the phenylsemicarbazone (7.0 g.), propylene glycol (70 ml.), *o*-phthalic acid (7.0 g.), concentrated sulfuric acid (30.0 g.) and water (80 ml.) was distilled in the manner described above. Concentration of the dried ether extract, followed by distillation of the residue under nitrogen, gave a small fore-run, b. p. 90~99°C/16 mmHg, consisting largely of benzyl alcohol and a pale yellow oil (1.8 g.), b. p. 115~118°C/16 mmHg, n_D^{21} 1.5288, which on redistillation through a 10 cm. Vigreux column afforded an oil with b. p. 117~118°C/16 mmHg and n_D^{20} 1.5294.

Found: C, 81.32; H, 8.69. Calcd. for $C_{11}H_{14}O$: C, 81.44; H, 8.70%.

The oil obtained above was treated with semicarbazide acetate in methanol to give, after being crystallized from ethanol, the semicarbazone of V, m. p. 169~170°C (lit.[14] m. p. 170~171°C), and an appreciable amount of that of VI, m.p. 198~199°C; the latter exhibited no melting point depression on admixture with that of authentic VI.

Found (for semicarbazone of V): N, 19.29. Calcd. for $C_{12}H_{17}ON_3$: N, 19.16%.

Treatment of this oil with the Brady reagent afforded, after fractional crystallization from ethanol-ethyl acetate, the 2,4-dinitrophenylhydrazone of V, m. p. 193~194°C (lit.[14] m. p. 190~191°C) as brightly red plates.

Found: N, 16.64. Calcd. for $C_{17}H_{18}O_4N_4$: N, 16.37%.

From the soluble fraction, a small amount of the 2,4-dinitrophenylhydrazone of VI, m. p. 183~184°C, was obtained. It exhibited no melting point depression on admixture with the 2,4-dinitrophenylhydrazone prepared from authentic VI.

b) Sulfur Dehydrogenation of the Adduct Obtained in Exp. 3 Listed in Table I.—The adduct (2.0 g.) was heated under reflux with sulfur (1.5 g.) under the same conditions as have been described for the preparation of 4-isopropyl-2-methylbenzaldehyde (VI). The distillate obtained by simple distillation of the reaction mixture was converted into the crude 2,4-dinitrophenylhydrazone (1.32 g.); this, on fractional crystallization from ethanol-ethyl acetate, afforded the 2,4-dinitrophenylhydrazone of VI (0.45 g.), m. p. 184~185°C, and of V (0.35 g.), m. p. 192~193°C, both of which exhibited no melting point depression on admixture with those prepared from authentic VI and V respectively.

13) P. Chuit and J. Bolle, *Bull. soc. chim.*, **35**, 200 (1924).
14) C. T. Lester, R. E. Donaldson and J. C. Oswald, *J. Am. Chem. Soc.*, **71**, 1502 (1949).

We are indebted to Dr. Asaji Kondo of the Tokyo Institute of Technology for his elemental analyses.

Laboratory of Organic Chemistry
Kobayasi Institute of Physical Research
Kokubunji, Tokyo

Prins Products from 6-Methyl-β-cyclogeraniolene and Synthesis of 6-Methyl-β-cyclolavandulylideneacetone

By Atsuaki ARAI and Iwao ICHIKIZAKI

(Received September 12, 1961)

The condensation of 6-methyl-β-cyclogeraniolene (1, 3, 3, 4-tetramethyl-1-cyclohexene) (II) with formaldehyde has recently been determined[1,2] to afford 6-methyl-α-cyclogeraniol acetate and 6-methyl-γ-cyclogeraniol acetate, both of which are known[3,4] to be important intermediates for the synthesis of irones. The method employed in the reaction has seemed somewhat unusual, however, for the Prins reaction as generally acknowledged.

The present work was undertaken with the object of determining the structures of some cyclic compounds which might be produced when hydrocarbon II was subjected to the usual conditions for the Prins reaction. The starting hydrocarbon in this work was obtained by Wolff-Kishner reduction of 2, 2, 4-trimethyl-3-cyclohexenylmethanal (I)[1,2,5,6], and the structure assigned to II was attained from infrared data in which the bands due to the trisubstituted double bond (1679 and 798 cm^{-1}) were shown, from the results of oxidation with ozone and/or potassium permanganate, which gave β-methylgeronic acid (IV)[7], and moreover, from the nuclear magnetic resonance spectrum[8] (Fig. 1), in which a singlet peak (−0.34 p. p. m.)

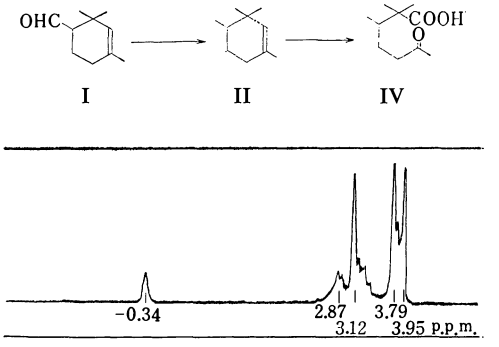


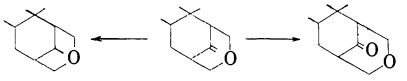
Fig. 1. NMR spectrum of 6-methyl-β-cyclogeraniolene (II).

showed the olefinic proton peculiar to only II of the structures under consideration.

The Prins reaction of II was carried out in a usual manner at −5∼−10°C, and the crude product was divided by fractional distillations into five fractions, as shown in Table I below. The fraction I was demonstrated by gas chromatography and some other means to consist principally of II. From elementary, gas chromatographic and infrared analyses, the principal components of fractions II and IV were revealed to be an unsaturated cyclic oxide and an acetate of unsaturated primary alcohol respectively, while fraction III was also indicated to be a mixture of approximately equal quantities of these two compounds. In order to separate the constituents from each other, the combined fractions of III and IV were treated with alkali and then with boric acid. The oxide was then readily distilled off in vacuo, while the boric ester of the alcoholic component remained in the viscous residue. Redistillation of fraction II combined with the recovered oxide afforded a homogeneous substance, $C_{12}H_{20}O$, whose infrared spectrum showed the presence of a cyclic ether (1111) and an

1) Y. Fujita, *J. Chem. Soc. Japan, Pure Chem. Sec.*, (*Nippon Kagaku Zasshi*), **80**, 452 (1959).
2) Y. Fujita, Dissertation submitted for the doctorate to the Tokyo Institute of Technology, 1959.
3) H. Favre and H. Schinz, *Helv. Chim. Acta*, 35, 1627 (1952).
4) H. Favre and H. Schinz, ibid., **41**, 1374 (1958).
5) O. N. Jitkow and M. T. Bogert, *J. Am. Chem. Soc.*, **63**, 1979 (1941).
6) U. Steiner and H. Schinz, *Helv. Chim. Acta*, **34**, 1176 (1951).
7) P. Bächli and H. Schinz, ibid., **34**, 1174 (1951).
8) The NMR spectra herein recorded were measured with a Varian High Resolution spectrometer, medel V-4300C. All spectra were taken at 56.4 Mc. of a 10% solution of the samples in carbon tetrachloride with an external reference standard of water. All chemical shifts were determined by the side band method. The authors wish to thank Drs. Ichiro Yamaguchi and Naohiro Hayakawa of the Japan Atomic Energy Research Institute for their courtesy in obtaining the spectra.

exocyclic methylene group (3062, 1665, 1414 and 887 cm^{-1}). On catalytic hydrogenation this oxide gave a saturated oxide, $C_{12}H_{22}O$, and on ozonolysis it afforded formaldehyde and a keto-ether, $C_{11}H_{18}O_2$, which was characterized by the presence of bands in the infrared region at 1722 and 1095 cm^{-1}. Thus, the structures of 6, 6, 7-trimethyl-9-methylene-3-oxabicyclo [3, 3, 1] nonane (VII), 6, 6, 7, 9-tetramethyl-3-oxabicyclo [3, 3, 1] nonane (VIII) and 6,6,7-trimethyl-9-oxo-3-oxabicyclo [3, 3, 1] nonane (IX) were assigned respectively for the unsaturated cyclic oxide, the saturated oxide and the keto-ether.



VIII VII IX

The alcohol regenerated from the borate above was found to be an unsaturated primary alcohol, $C_{11}H_{20}O$, and its allophanate, m. p. 167.5°C, was proved to be identical with that of the compound which had been assigned by Fujita[2,9] to 6-methyl-α-cyclogeraniol. Moreover, the alcohol resembled in many respects 6-methyl-α-cyclogeraniol, synthesized by Favre and Schinz[3], to which it had once erroneously been assigned by the present authors[10]. Indeed, the infrared spectrum of the alcohol showed the presence of hydroxyl (3325 and 1041 cm^{-1}) and trisubstituted double bond (1660 and 822 cm^{-1}); however, the nuclear magnetic resonance spectrum failed to conform to the postulated structure. Since the spectrum[8] (Fig. 2) showed for the olefinic proton the singlet peak (−0.52 p. p. m.), which indicates the absence of hydrogen on the carbon atoms adjacent to the olefinic carbon bearing hydrogen, the structure of 6-methyl-α-cyclolavandulol (V) was now furnished to the alcohol. Consequently, it seemed reasonable to consider that the attack of the Prins reagent is extremely difficult on the double bond of II and also that under the reaction conditions II is readily isomerized into 6-methyl-α-cyclogeraniolene (III), which is immediately affected by the reagent to yield V. Examination with the molecular model really showed that the axial approach of the reagent to the double bond in II suffers a large steric hindrance from the gem. dimethyl group and also suggested that III presumably takes the conformation represented as IIIa when it participates in the reaction.

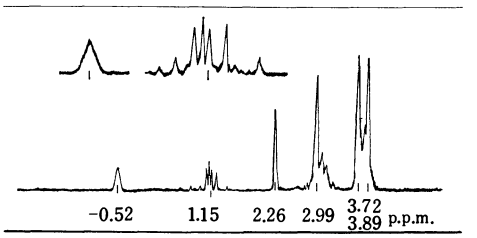
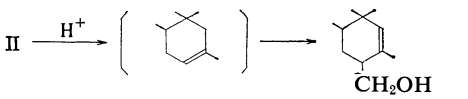
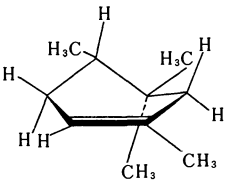


Fig. 2 NMR spectrum of 6-methyl-α-cyclo lavandulol (V).



III V

Va, the acetate



IIIa

Fraction V (Table I) was presumed from the infrared data to contain some acetic esters. An attempted pyrolysis at 350~370°C afforded a small amount of low-boiling liquid which on hydrolysis gave the oxide VII and the alcohol V, whereas most of the high-boiling acetate was recovered unchanged. The latter compound was hydrolyzed to give rise to a glycol which gave a bis-*p*-nitrobenzoate and which was assigned to 3, 3, 4-trimethyl-1-(β-hydroxyethyl)-6-hydroxymethyl-1-cyclohexene (X) by infrared data, in which bands due to a primary hydroxyl (3330 and 1034 cm^{-1}) and to a trisubstituted double bond (1679 and 807 cm^{-1}) were indicated. Thus it was concluded that the fraction V consisted of X-diacetate (Xa) and appreciable amounts of 6,6,7,9-tetramethyl-9-acetoxy-3-oxabicyclo [3,3,1] nonane (XI) and 1, 3, 3, 4-tetramethyl-6-hydroxymethyl-1-cyclohexanol diacetate (XIIa). Although the formation of prim-tert. glycol has been described in many papers[11-16], this is probably the first example in which primary glycol has been isolated.

The mechanism of the Prins reaction has been frequently discussed, and it is generally

9) The authors are indebted to Dr. Yutaka Fujita of the Tokyo Institute of Technology for furnishing a sample of the allophanate, m. p. 166~167°C.

10) Presented by A. Arai and I. Ichikizaki at the 4th Symposium on Perfumery, Terpene and Essential Oil Chemistry, Sapporo, July, 1960 (Abstract, p. 20).

11) A. Brenner, U. Steiner and H. Schinz, *Helv. Chim. Acta*, **35**, 1336 (1952).

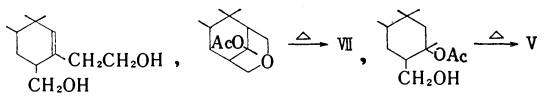
12) A. T. Blomquist and J. Wolinsky, *J. Am. Chem. Soc.*, **79**, 6025 (1957).

13) E. E. Smissman and R. A. Mode, ibid., **79**, 3447 (1957).

14) Y. Matsubara and Y. Watanabe, *J. Chem. Soc. Japan, Pure Chem. Sec. (Nippon Kagaku Zasshi)*, **80**, 651 (1959).

15) J. Colonge and J. Crabalona, *Bull. soc. chim.*, **1959**, 1505.

16) E. E. Smissman and D. T. Witiak, *J. Org. Chem.*, **25**, 471 (1960).

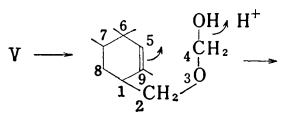


X XI XII

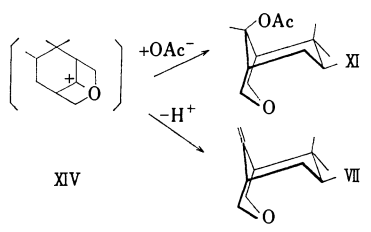
Xa, the diacetate XIIa, the diacetate

accepted[12,13,16] that the first step involves the protonation of a neutral formaldehyde molecule and that the resultant hydroxymethylcarbonium ion carries out an axial attack on a cyclo-olefinic carbon.

The formation of VII and XI offers valuable evidence for the initial axial attachment of the protonated formaldehyde molecule to the double bond in III. These two compounds were plausibly assumed to be produced from an intermediate XIV, which might be provided via the dehydrative cyclization of the hypothetical compound XIII, formed presumably from the interaction between V and another formaldehyde molecule. According to stereochemical considerations, both VII and XI can apparently take up only the 1, 5-diaxial conformation and likely have strainless double-chair forms. If the substituent, $-CH_2OCH_2OH$, in XIII takes the equatrial orientation, the effective approach of C-(4) to C-(5) for cyclization would be obviously impossible; therefore, the hydroxymethylene group in V must have the axial orientation. This was rationally explained independently on the basis of the nuclear magnetic resonance spectrum (Fig. 2), in which the multiplet centering at 1.15 p. p. m. is clearly ascribed to two non-equivalent protons of hydroxymethylene, which is further split by the adjacent ring hydrogen. The non-equivalence of the hydroxymethylene protons is probably due to the restriction of free rotation. Therefore, all the results mentioned above were compatible with the conclusion which involves the initial axial attachment of the hydroxymethylcarbonium ion[12,13,16] to the double bond of cyclic olefins.

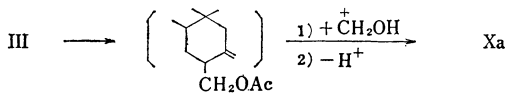


XIII



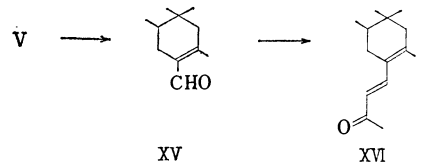
XIV

Additionally, the formation of the primary glycol diacetate Xa might be explained by the attack of another hydroxymethylcarbonium ion on the double bond in the temporarily-formed 6-methylcyclolavandulol acetate (VIa) and the successive elimination of hydrogen.



VIa

Finally, the synthesis of 6-methyl-β-cyclolavandulylideneacetone (XVI) from alcohol V was carried out. Modified Oppenauer oxidation of V with *p*-benzyloxybenzaldehyde as a hydrogen acceptor[17] afforded a high yield of 6-methyl-β-cyclolavandulal (XV), characterized as the semicarbazone whose ultraviolet spectrum revealed the presence of an α, β-unsaturated carbonyl group, while the expected α-isomer was not yielded. Condensation of XV with acetone in the presence of sodium hydride afforded 6-methyl-β-cyclolavandulylideneacetone (XVI)[18], with a strong violet odor, which was authorized by the infrared spectrum and by the light-absorption properties of its solid derivatives.



XV XVI

Experimental[19]

6-Methyl-β-cyclogeraniolene (II). — The Wolff-Kishner reduction of 2,2,4-trimethyl-3-cyclohexenylmethanal (I) was carried out essentially by the method of Fujita[1,2]. Distillation of the reduction product over sodium gave a colorless liquid, b. p. 56~57°C/18 mmHg, whose gas chromatogram, obtained at 196°C with a hydrogen flow of 17.2 ml./min., showed a small peak (about 2% of the total) at a retention time of 3.3 min. and a larger peak (98%) at 3.8 min. The small peak ascribed to an unknown substance disappeared after the sample had been purified by two redistillations with a 40 cm. Vigreux column. The hydrocarbon II had b. p. 60.5~61°C/24 mmHg and $n_D^{18.5}$ 1.4557 (lit.[1] b. p. 59.5~60.5°C/23 mmHg, n_D^{26} 1.4530). IR (film):

17) A. Arai and I. Ichikizaki, This Bulletin, 35, 504 (1962).

18) R. Vonderwahl and H. Schinz, *Helv. Chim. Acta*, 35, 2005 (1952).

19) All melting points were taken on a Kofler-block, and the temperatures are uncorrected. The infrared spectra were determined with a Nippon Bunkō model IR-S spectrophotometer with sodium chloride optics and the ultraviolet spectra, with a Hitachi model EPU-2A spectrophotometer. The gas chromatograms were obtained using a copper column (250 cm.×0.6 cm. ϕ) packed with a Celite DM-13A which was coated with a Carbowax-6000.

1679, 834, 798 (>C=CH-), 1389, 1379, 1362 (CH_3), 854 cm^{-1} (1,3,3,4-tetrasubstituted cyclohexene ring). The NMR spectrum is shown in Fig. 1.

Found: C, 86.76; H, 13.32. Calcd. for $C_{10}H_{18}$: C, 86.88; H, 13.12%.

Oxidation of II.—*a) With Ozone.*—Ozonized oxygen (concentration: 17 g./m^3) was passed through a solution of II (1.2 g.) in carbon tetrachloride (15 ml.) with a flow of 0.5 l./min. over a period of 2.5 hr. The temperature was maintained at −5～−10°C by cooling. Acetic acid (5 ml.) and 30% hydrogen peroxide (1.5 ml.) were added, and the resultant solution was left for 12 hr. at room temperature. After the bulk of the solvent had been removed in vacuo, the residue was made alkaline with 10% aqueous alkali and washed with petroleum ether to remove the neutral substances. The aqueous layer was then made acid with 5% hydrochloric acid and extracted with ether. The ether extract was washed with water, dried over sodium sulfate and evaporated to leave a viscous oil (0.5 g.), which was distilled to give β-methylgeronic acid (IV) (0.35 g.), b. p. 130～135°C/0.8 mmHg, n_D^{21} 1.4564. IR (film): 3060 (broad), ～2680, 1715, 1700, 1472, 1415, 1383, 1369, 1286, 1248, 1167, 1142, 939 cm^{-1} (broad).

The semicarbazone crystallized from methanol in prisms, m. p. 142～143°C (lit.[7] m. p. 141～142°C).

Found: C, 54.38; H, 8.90. Calcd. for $C_{11}H_{21}O_3 \cdot N_3$: C, 54.30; H, 8.70%.

The 2, 4-dinitrophenylhydrazone crystallized from ether-petroleum ether in the form of yellow crystals, m. p. 130～130.5°C (lit.[7] m. p. 130.5～131.5°C).

Found: C, 53.04; H, 6.34. Calcd. for $C_{16}H_{22}O_6 \cdot N_4$: C, 52.45; H, 6.05%.

In this experiment, no formaldehyde was detected in the reaction mixture.

b) With Potassium Permanganate.—A solution of II (1.38 g.) in petroleum ether (b. p. 38～45°C, 30 ml.) was added to an aqueous solution (150 ml.) of potassium permanganate (3.16 g., 3 "O"), and the mixture was stirred vigorously at 5～10°C for 4 hr. Methanol was added, and the resultant mixture was warmed at 60°C for 10 min. to decompose the excess of permanganate and then filtered. The precipitate was repeatedly washed with hot water. The filtrate and washings were combined and concentrated to ca. 30 ml. in vacuo, acidified with 10% hydrochloric acid and extracted with ether. The ether extract was washed with water, dried over sodium sulfate, evaporated and distilled to give an oil (0.3 g.). Its semicarbazone gave no mixed melting point depression with that of IV obtained by the method of a).

Prins Reaction with II.—A solution of II (35 g.) in acetic acid (23 ml.) diluted with ether (8.5 ml.) was added drop by drop over a period of 1 hr. into a mixture of paraformaldehyde (10.3 g.), acetic acid (46 ml.), ether (12.5 ml.) and concentrated sulfuric acid (8.5 ml.), and vigorous stirring was then continued for 7 hr. The temperature was maintained at −5～−10°C by cooling. The reaction mixture was allowed to stand overnight at 0°C, then poured into an ice-cooled 15% aqueous sodium carbonate solution (280 ml.) and extracted with ether. The ether extract was washed with water, dried over magnesium sulfate and evaporated to leave a red-brown oily residue (33.5 g.) which, on repeated fractionations through a 25 cm. Vigreux column, yielded the five representative fractions cited in Table I.

Distillation of fraction I over sodium gave a homogeneous substance (4.3 g.) with a b. p. 51.5°C/14.5 mmHg and $n_D^{18.5}$ 1.4557, which was identified as being the starting hydrocarbon II. Gas chromatogram, infrared and NMR spectra comparisons and ozonolysis showed that II is not subject to isomerization during the reaction.

6-Methyl-α-cyclolavandulol (V).—Combined fractions of III (4.4 g.) and IV (2.9 g.) (Table I) were hydrolyzed by treating them with potassium hydroxide (5.5 g.) in methanol (40 ml.) and water (20 ml.) at room temperature for 44 hr. After removal of the solvent in vacuo, the resulting mixture was neutrallized with 10% hydrochloric acid and extracted with petroleum ether. The petroleum ether extract was washed with water, dried over sodium sulfate and evaporated. The residual oil was heated with boric acid (0.5 g.) at a bath temperature of 160°C and at 500 mmHg for 30 min.; meanwhile, the water formed was distilled off. This work-up was repeated with another boric acid (1.0 g.) to make the esterification of the alcohol complete. The reaction mixture was then distilled gradually until the bath temperature reached 170°C at 0.75 mmHg to give a colorless liquid (2.0 g.), n_D^{25} 1.4833, which was shown by infrared and gas chromatographic analyses to consist mainly of the unsaturated cyclic oxide, and to leave the boric ester as an orange syrup, which was taken up in hot benzene (40 ml.) and hydrolyzed by shaking it with a hot 0.5% aqueous sodium carbonate solution. The

Table I. Fractionation of the reaction mixture

Fraction No.	B. p. °C/mmHg	n_D^T	Fraction wt., g.	Composition C, H %	Infrared maxima cm^{-1}
I	51～51.5/14.5	1.4557^{18}	4.6		
II	70～76/4.0	1.4857^{18}	11.5	79.53	3060m, 1775m, 1661 s, 1418w,
				11.32	1110 s, 887 s, 761m
III	72～75/1.5	1.4782^{20}	4.4	76.11	3062w, 1739 s, 1662m, 1240 s
				10.90	1110 s, 1035m, 888m 866m
IV	62～65/0.75	1.4742^{20}	3.0	75.60	1740 s, 1237 s, 1040 s, 864m,
				11.03	820w
V	100～116/0.75	1.4953^{20}	6.2	69.42	1738 s, 1679w, 1234 s, 1109 s,
				9.92	1029m, 864m, 805w

benzene layer was dried over sodium sulfate, evaporated and distilled to afford 6-methyl-α-cyclolavandulol (V) (3.5 g.) as a colorless oil, b. p. 117～118°C/15 mmHg, n_D^{23} 1.4825. IR (film): 3325, 1041, (OH), 1660, 822 (>C=CH-), 1390, 1379, 1364 (CH_3), 857 cm^{-1} (1, 3, 3, 4, 6-pentasubstituted cyclohexene ring). The NMR spectrum is shown in Fig. 2.

Found: C, 78.50; H, 11.93. Calcd. for $C_{11}H_{20}O$: C, 78.51; H, 11.98%.

The allophanate crystallized from methanol in colorless crystals, m. p. 167.5°C, which gave no mixed melting point depression with that (m. p. 166～167°C) of the so-called 6-methyl-α-cyclogeraniol furnished by Fujita[2,9].

Found: C, 61.44; H, 8.83. Calcd. for $C_{13}H_{22}O_3N_2$: C, 61.39; H, 8.72%.

6, 6, 7-Trimethyl-9-methylene-3-oxabicyclo[3, 3, 1]-nonane (VII).—Fraction II (11.2 g.) (Table I), combined with the above-recovered fraction (2.0 g.) containing oxide, was fractionated over sodium through a 25 cm. Vigreux column to give a fore-run (2.0 g.) with a menthol-like odor, b. p. 96～99.5°C/16.5 mmHg and $n_D^{25.5}$ 1.4828～1.4832, and a colorless oil (8.9 g.), b, p. 100～100.5°C/16.5 mmHg, $n_D^{25.5}$ 1.4852, both of which easily consumed bromine in a carbon tetrachloride solution. Redistillation of the latter afforded 6, 6, 7-trimethyl-9-methylene-3-oxabicyclo[3,3,1]nonane (VII) (8.5 g.) with a strong menthol-like odor, b. p. 72～72.5°C/3.7 mmHg, $n_D^{25.5}$ 1.4853, whose gas chromatogram obtained at 211°C with a hydrogen flow of 28.8 ml./min. showed a single peak at a retention time of 9.3 min.

IR (film): 3062, 1665, 1414, 887 (>C=CH_2), 1775 (over-tone of δ CH (887)), 1111 (ether, C-O-C), 1393, 1380, 1374 (CH_3), 1235, 1198 ($H_3C-\overset{|}{C}-CH_3$), 1009, 760 cm^{-1} (unassigned).

Found: C, 79.60; H, 11.33. Calcd. for $C_{12}H_{20}O$: C, 79.94; H, 11.18%.

From gas chromatography, the fore-run (Found: C, 80.29; H, 11.36%) was shown to consist largely of VII contaminated with ca. 7% of another unknown substance, which appeared as a broad peak at a retention time of 7.6 min. under the same conditions as above; this substance could not be isolated.

6, 6, 7, 9-Tetramethyl-3-oxabicyclo[3, 3, 1]nonane (VIII).—The unsaturated cyclic oxide VII (2.25 g.) in ethyl acetate (20 ml.) was hydrogenated at one atmosphere in the presence of a palladium-calcium carbonate catalyst (5% Pd, 1.0 g.) until one molar equivalent (315 ml. at 21.6°C) of hydrogen had been absorbed. Removal of the catalyst and solvent, followed by distillation of the residue, afforded 6, 6, 7, 9-tetramethyl-3-oxabicyclo[3, 3, 1]nonane (VIII) (1.9 g., 83%) as a colorless liquid with a menthol-like odor, b. p. 110°C/16 mmHg and n_D^{21} 1.4835, which did not decolorize a solution of bromine in carbon tetrachloride. IR (film): 1398, 1386, 1376, 1366 (-CH_3), 1236, 1194 ($H_3C-\overset{|}{C}-CH_3$), 1176, 1134 ($HC-CH_3$), 1088 cm^{-1} (ether, C-O-C).

Found: C, 79.06; H, 12.16. Calcd. for $C_{12}H_{22}O$: C, 79.06; H, 12.16%.

6, 6, 7-Trimethyl-9-oxo-3-oxabicyclo[3, 3, 1]nonane (IX).—The unsaturated cyclic oxide VII (0.5024 g.) in carbon tetrachloride (15 ml.) was ozonized at −10°C for 3 hr., after which time the resultant solution did not consume bromine in a carbon tetrachloride solution. At the end of the apparatus a trap containing water (20 ml.) was equipped to absorb the formaldehyde carried away by the gas stream during the reaction. The reaction mixture was heated under reflux with water (30 ml.) for 2 hr. in a flask fitted with a reflux condenser, the top of which had previously been connected with the water trap. The water in the trap was warmed with a solution of dimedone (0.9 g.) in ethanol (40 ml.) at 60°C for 10 min. to yield the formaldehyde-dimedone condensation product (0.1733 g., 21.2%). The carbon tetrachloride solution was dried over calcium chloride, evaporated in vacuo and distilled to give 6, 6, 7-trimethyl-9-oxo-3-oxabicyclo[3, 3, 1]nonane (IX) (0.25 g., 50%) as a colorless liquid, b. p. 84～84.5°C/1.5 mmHg, n_D^{25} 1.4850. IR (film): 1722 (C=O), 1094 (ether, C-O-C), 1398, 1370 (CH_3), 1220, 1185 ($H_3C-\overset{|}{C}-CH_3$), 861 cm^{-1} (unassigned).

Found: C, 72.06; H, 10.08. Calcd. for $C_{11}H_{18}O_2$: C, 72.49; H, 9.96%.

The semicarbazone crystallized from methanol-ethyl acetate in the form of prisms, m. p. 224～225°C.

Found: C, 60.00; H, 8.99. Calcd. for $C_{12}H_{21}O_2N_3$: C, 60.22; H, 8.85%.

The 2,4-dinitrophenylhydrazone crystallized from methanol-ethyl acetate in the form of yellow needles, m. p. 248～249.5°C.

Found: C, 56.51; H, 6.34. Calcd. for $C_{17}H_{22}O_5N_4$: C, 56.34; H, 6.12%.

Pyrolysis Followed by Alkaline Hydrolysis of the Mixed Acetates (Fraction V in Table I).—Fraction V (6.0 g.) was heated at 350～370°C and 500 mmHg under nitrogen for 4 hr. The pale yellow pyrolyzate (4.9 g.) was taken up in ether and washed with 2% aqueous sodium hydrogencarbonate and with water to remove the acetic acid formed and then dried over sodium sulfate. Removal of the solvent followed by fractionation of the residue gave two fractions, b. p. 74～75°C/2.8 mmHg, $n_D^{21.5}$ 1.4911 (0.5 g.) (Found: C, 80.39; H, 11.32%) and b. p. 100～105°C/0.7 mmHg, $n_D^{21.5}$ 1.4964 (3.9 g.). The low-boiling fraction was hydrolyzed by treating it with potassium hydroxide (0.5 g.) in ethanol (10 ml.) at room temperature for 40 hr. The reaction mixture was neutralized with 10% hydrochloric acid and extracted 5 times with ether. The combined ether extracts were washed with water, dried and evaporated. Distillation of the residue gave a colorless liquid (0.3 g.), b. p. 65～72°C/1.5 mmHg, $n_D^{22.5}$ 1.4858 (Found: C, 79.16; H, 11.57%), which was not yet homogeneous and which showed in the infrared region bands at 3080, 1660, 1413, 891 and 1110 cm^{-1}, attributable to oxide VII, and medium bands at 3350 (broad) and 1041 cm^{-1}, attributable to alcohol V. A small amount of the allophanate of V was obtained, in fact. The high-boiling fraction was hydrolyzed in a similar manner before being used with potassium hydroxide

(1.8 g.) in methanol (20 ml.) to afford 3,3,4-trimethyl-1-(β-hydroxyethyl)-6-hydroxymethyl-1-cyclohexene (X) (1.6 g.) as a viscous liquid, b. p. 123～125°C/0.7 mmHg, n_D^{29} 1.4979. IR (film): 3330, 1034 (OH), 1679, 842, 807 (>C=CH-), 1392, 1378, 1368 (CH_3), 866 cm^{-1} (1,3,3,4,6-pentasubstituted cyclohexene ring).

Found: C, 73.21; H, 11.20. Calcd. for $C_{12}H_{22}O_2$: C, 72.68; H, 11.18%.

The bis-*p*-nitrobenzoate crystallized from ethanol-ethyl acetate in the form of needles, m. p. 131～132°C.

Found: C, 62.41; H, 5.52; N, 5.54. Calcd. for $C_{26}H_{28}O_8N_2$: C, 62.89; H, 5.68; N, 5.64%.

6-Methyl-β-cyclolavandulal (XV).—A mixture of alcohol V (2.0 g.) and aluminum isopropoxide (1.0 g.) was heated at a bath temperature of 70～80°C and at 13 mmHg for 1.5 hr. to form V-aluminate, and then *p*-benzyloxybenzaldehyde (3.78 g., 150%) was added in one portion. The resultant mixture was preheated at a bath temperature of 80°C under ordinary pressure for 2 min. to give the melt, which was subsequently distilled by raising the temperature from 110 to 180°C under nitrogen to afford a product, b. p. 60～101°C/4 mmHg. Redistillation of the product through a 7 cm. Vigreux column afforded 6-methyl-β-cyclolavandulal (XV) (1.35 g., 68.5%), b. p. 93～96°C/13 mmHg, $n_D^{27.5}$ 1.4790.

Found: C, 79.51; H, 10.88. Calcd. for $C_{11}H_{18}O$: C, 79.46; H, 10.92%.

The semicarbazone crystallized from methanol-ethyl acetate in the form of prisms, m. p. 224～225°C (partly decomp.). λ_{max}^{EtOH} 272 mμ (ε, 30300).

Found: C, 64.62; H, 9.69; N, 18.88. Calcd. for $C_{12}H_{21}ON_3$: C, 64.54; H, 9.48; N, 18.82%.

The 2,4-dinitrophenylhydrazone chromatographed on alumina in benzene and crystallized from ethanol-ethyl acetate in the form of red needles, m. p. 207～208°C.

Found: C, 59.04: H, 6.38; N, 16.01. Calcd. for $C_{17}H_{22}O_4N_4$: C, 58.94; H, 6.40; N, 16.18%.

6-Methyl-β-cyclolavandulylideneacetone (XVI).—A solution of XV (1.1 g.) in acetone (10 ml.) was added drop by drop to an acetone solution containing sodium hydride (40 mg.) at room temperature, and the resultant solution was stirred for 6 hr. and then allowed to stand overnight under nitrogen at this temperature. After the solvent had been removed, the residue was taken up in ether, washed with 2 N hydrochloric acid and with water, dried over sodium sulfate and evaporated. Distillation under nitrogen gave a fore-run (0.4 g.), 62～90°C/0.85 mmHg, which consisted largely of unchanged XV and of an oil (0.75 g.), 90～110°C/0.7 mmHg, $n_D^{25.5}$ 1.4940～1.5118. Redistillation of the latter gave the ketone XVI (0.55 g.) as a pale yellow oil with a strong violet odor, b. p. 105～110°C/0.7 mmHg, $n_D^{25.5}$ 1.5118. IR (film): 1675 (C=O, conju.), 1624, 1594 (C=C, conju.), 1382, 1369 (gem. dimethyl), 1268 ($COCH_3$), 970 cm^{-1} (-CH=CH-, *trans*).

Found: C, 81.42; H, 10.94. Calcd. for $C_{14}H_{22}O$: C, 81.50; H, 10.75%.

The 4-phenylsemicarbazone crystallized from methanol-ethyl acetate in the form of fine needles, m. p. 198～199°C, which rapidly turned yellow on exposure to light or air. λ_{max}^{EtOH} 234 mμ (log ε, 4.04), 301 (4.58). (lit.[18] m. p. 196～197°C, λ_{max}^{EtOH} 234 mμ (log ε, 4.70). 307 (4.12)).

Found: C, 74.31; H, 8.66. Calcd. for $C_{21}H_{29}ON_3$: C, 74.30; H, 8.61%.

The 2,4-dinitrophenylhydrazone crystallized from methanol-ethyl acetate in the form of dark-red, silk-like needles, m. p. 209°C. $\lambda_{max}^{CHCl_3}$ 391 mμ (log ε, 4.55). (lit.[18] m. p. 197.5°C, $\lambda_{max}^{CHCl_3}$ 397 mμ (log ε, 4.50)).

Found: C, 62.24; H, 6.76; N, 14.22. Calcd. for $C_{20}H_{26}O_4N_4$: C, 62.16; H, 6.78; N, 14.50%.

The authors wish to express their thanks to Dr. Toshiaki Nishida of this Laboratory for his helpful discussions of the NMR spectra and to Dr. Asaji Kondō of the Tokyo Institute of Technology for his microanalyses. They are also indebted to Mr. Kōsei Tanabe for his technical assistance.

Laboratory of Organic Chemistry
Kobayasi Institute of Physical Research
Kokubunji, Tokyo

Studies of the Cage Effect of Solvent. III. Photolysis of Azomethane in Frozen Solutions

By Sukeya KODAMA

(Received September 4, 1961)

Previous studies of the photolysis of azomethane in *n*-hexane,[1] *n*-octane, toluene, ethyl acetate and ethanol[2] have suggested that a pair of methyl radicals formed by the decomposition of a substrate molecule combine to form an ethane molecule with a high yield in the solvent cage. The yield of ethane has been found to increase with the lowering of the temperature, and it may be expected that still higher yields would be obtained in frozen solutions if the ethane were formed in the way given above.

This paper reports on experiments carried out to investigate the effect of such freezing as well as to obtain additional results in various other solvents than those already studied. The solvents used are cyclohexane, benzene, styrene, *o*-xylene and *tert*-amyl alcohol.

Experimental

The preparation, purification and storage of azomethane have been described previously[1]. Cyclohexane obtained from a commercial sample of a special high grade was boiled with stannous chloride and hydrochloric acid and then distilled. Benzene, styrene, *o*-xylene and *tert*-amyl alcohol were taken from commercial samples of a special high grade without further purification. All these solvents, as well as azomethane, were subjected to vacuum distillation each time befor use.

The apparatus and procedure have been described in a previous paper[1]. The concentration of azomethane was about 3×10^{-2} mol./l. in all the experiments, and the volume of solution was adjusted so that it just filled the reaction cell of ca. 10 ml. capacity at the temperature of photolysis. A mercury line of 366 mμ was used for the photolysis. The extent of conversion in each run was within several percentage points. Nitrogen, methane and ethane, produced by the photolysis, were analyzed in the way that has been described previously[1].

Results and Discussion

The results obtained are shown in Figs. 1—6. As has been described in previous papers[1,2], CH_4/N_2, C_2H_6/N_2 and $[(1/2)CH_4+C_2H_6]/N_2$ represent respectively the yields of methane and ethane and the material balance referring to them. The main feature of the photolysis in the liquid phase is, as seen in the figures, similar to that found previously for a number of other solvents[1,2]. Hence, the mechanism of the photolysis in the liquid solutions here studied may be envisaged as the same as in the previous work. The formation of ethane may thus be ascribed to the cage combination of a pair of methyl radicals resulting from the decomposition of the substrate molecule, and that of methane, mostly to the hydrogen atom abstraction from the solvent molecules by methyl radicals that have escaped the original solvent cage.

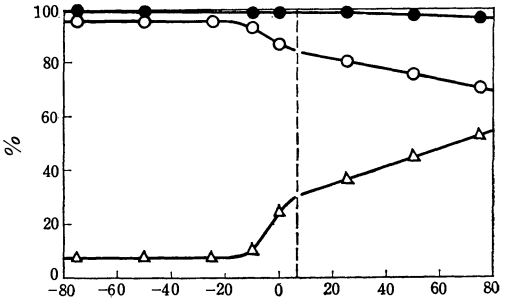


Fig. 1. Effect of freezing on yields of methane and ethane, and material balance in cyclohexane.
△, CH_4/N_2; ○, C_2H_6/N_2;
●, $[(1/2)CH_4+C_2H_6]/N_2$

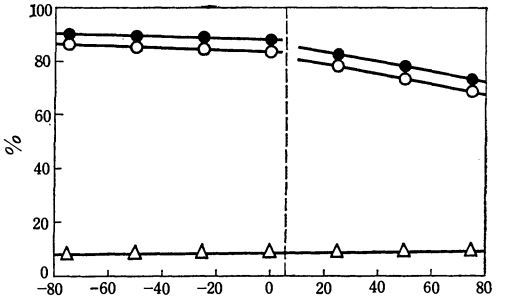


Fig. 1. Effect of freezing on yields of methane and ethane, and material balance in benzene.
△, CH_4/N_2; ○, C_2H_6/N_2;
●, $[(1/2)CH_4+C_2H_6]/N_2$

1) S. Kodama, This Bulletin, 35, 652 (1962).
2) S. Kodama, ibid., 35, 658 (1962).

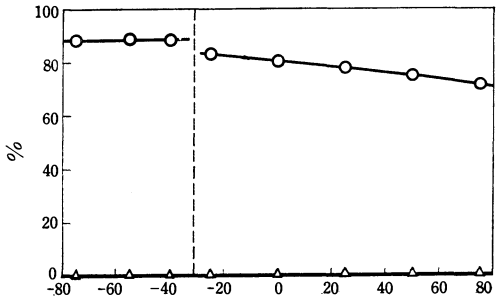


Fig. 3. Effect of freezing on yields of methane and ethane in styrene.
△, CH_4/N_2; ○, C_2H_6/N_2

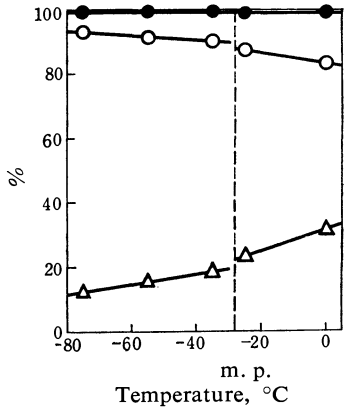


Fig. 4. Effect of freezing on yields of methane and ethane, and material balance in *o*-xylene.
△, CH_4/N_2; ○, C_2H_6/N_2;
●, $[(1/2)CH_4+C_2H_6]/N_2$

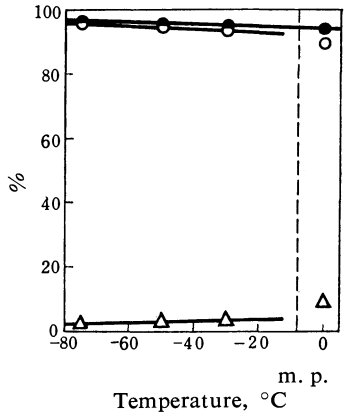


Fig. 5. Effect of freezing on yields of methane and ethane, and material balance in *t*-amyl alcohol.
△, CH_4/N_2; ○, C_2H_6/N_2;
●, $[(1/2)CH_4+C_2H_6]/N_2$

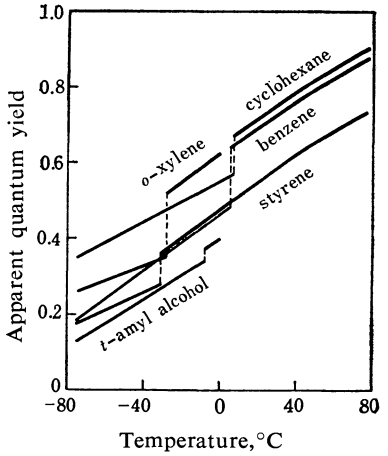


Fig. 6. Apparent quantum yields.

Figures 1—5 show that, on freezing the solution, the yield of ethane is more or less enhanced, while that of methane is mostly reduced. Such a result is in agreement with what is to be expected if the ethane is formed in the way described above, for in the frozen solutions the two methyl radicals formed by the photolysis from an azomethane molecule would not diffuse away from each other with such ease as in liquid solutions.

As the temperature is further lowered, however, the methyl radicals would become more and more immobile, and the yield of ethane would then be determined by the geometrical arrangement of the three fragments produced by the photolysis and by the structure of the environment, rather than by the rate of escaping diffusion of methyl radicals. The small dependence of the yields of ethane and methane in frozen solutions upon temperature as seen in Figs. 1—5 appears to reflect the small variation in the structure of the solid with variations in temperature, as supposed from far smaller expansion coefficients of solids than those of liquids. It seems, however, probable that, in the experiments at very low temperatures, both ethane and methane are partly formed from methyl radicals mobilized on warming up the reaction cell after irradiation.

Frozen solutions are, on the other hand, probably heterogeneous, solute molecules aggregating in boundaries between grains of the frozen solvent. Although it is not feasible to observe the effect of such a heterogeneous structure separately, the variation in the velocity of freezing would lead to different structures and hence, possibly, to different results. Table I shows the results of such experiments carried out with cyclohexane as a solvent. In Runs 1 and 2, the solution was frozen by immersing the cell in liquid nitrogen

TABLE I. PHOTOLYSIS OF AZOMETHANE IN CYCLOHEXANE AT 0°C

Run No.	Time of irradiation min.	Rate of formation $\times 10^{10}$ mol. sec^{-1}			$\frac{CH_4}{N_2}$	$\frac{C_2H_6}{N_2}$	$\frac{\frac{1}{2}CH_4+C_2H_6}{N_2}$
		R_{N_2}	R_{CH_4}	$R_{C_2H_6}$	%	%	%
1	42	22.6	5.33	19.7	23.6	87.2	99.0
2	90	21.3	4.35	18.6	20.4	87.2	97.4
3	66	20.8	4.33	18.1	20.8	87.0	97.4

and in dry ice-acetone respectively, and then warmed to 0°C without melting. In Run 3 the solution was simply cooled from room temperature to 0°C and frozen at the latter temperature. As seen in the table, the yields of ethane in these three runs are identical, though the yield of methane is slightly higher in the solution frozen with liquid nitrogen. The cage combination of methyl radicals thus appears to be rather insensitive to the heterogeneity considered above.

As is seen in Fig. 1, the results obtained with cyclohexane show some anomalies below its melting point; the yields of ethane and methane reflect less sharply the transition from liquid to solid, compared to the other solutions. On inspecting the reaction cell, it was found that the front surface of the frozen solution was melted under irradiation, presumably because of the low heat of the fusion of cyclohexane[3]. It is, therefore, most probable that such partial melting gave rise to the above anomalous behavior in the experiments with cyclohexane.

The results obtained with styrene are of interest in view of its large methyl affinity[4]. In the previous work performed with various solvents, it was used as a scavenger of methyl radicals escaping from the solvent cage. Figures 1—5 show that the yield of ethane in styrene is, in the liquid phase as well as in the solid, of a magnitude comparable to those in the other solvents. This is not an unexpected result, because the scavenging reaction of styrene requires the activation energy of some 5 kcal./mol.[2], while that of the combination of methyl radicals is nearly zero. Figure 3 shows further that the formation of methane is suppressed almost completely in styrene in both the liquid and the solid phases, which may be accounted for by the greater activation energy of the abstraction reaction than that of the addition[5]. The difference $1-C_2H_6/N_2$ in this case may therefore be taken approximately as the fraction of methyl radicals used in the addition to styrene. Such addition may in turn be expected to induce the polymerization of styrene. In the experiments carried out at high temperatures, it has been observed that such polymerization really takes place.

Benzene has also a fairly large methyl affinity[6] owing to its unsaturated structure, and may be expected to show the effect of the addition reaction. The results given in Fig. 2 show that the addition competes with the abstraction, but the effects of temperature on the two reactions suggest that their Arrhenius parameters are appreciably different. By applying the same method as has been described previously[2], the difference in activation energies can be computed as

$$E_{addition} - E_{abstraction} = 1.5 \text{ kcal./mol.}$$

Figure 4 shows that, though *o*-xylene also has double bonds, the contribution of the addition reaction is negligible. On the other hand, Fig. 5 shows a rather large loss in the material balance, though *tert*-amyl alcohol has no double bond. Presumably, impurities in the alcohol have given rise to the loss of methyl radicals in this case.

It has been found in the previous work[1,2] that the variation in the yields of ethane in various solvents can be represented by an empirical equation

$$1-C_2H_6/N_2 = A\exp(-E/RT)$$

wherer A and E are constants. Figure 7 shows that this equation also conforms to the results in the liquid solutions in this work. Table II gives the values of the constants A and E obtained from the figure.

Figure 6 shows the apparent quantum yields obtained by comparing the rates of formation

TABLE II. ARRHENIUS CONSTANTS

	A	E kcal./mol.
Cyclohexane	3.62	1.74
Benzene	2.61	1.48
Styrene	1.06	0.93
o-Xylene	2.10	1.39

3) The heat of fusion of cyclohexane is 0.6398 kcal./mol., which is much lower than the 2.361 kcal./mol. for benzene and the 3.250 kcal./mol. for *o*-xylene. (F. D. Rossini et al., "Selected Values of Physical and Thermodynamic Properties of Hydrocarbons and Related Compounds", Carnegie Press (1953)).

4) F. Leavitt, M. Levy, M. Szwarc and V. Stannett, *J. Am. Chem. Soc.*, **77**, 5493 (1955); M. Feld and M. Szwarc, ibid., **82**, 3791 (1960).

5) Although the activation energy of the hydrogen atom abstraction from styrene molecules by methyl radicals is unknown, most reported values for hydrogen atom abstraction by methyl radicals are greater than 8 kcal./mol.

6) M. Levy and M. Szwarc, *J. Chem. Phys.*, **22**, 1621 (1954); M. Levy, M. Steinberg and M. Szwarc, *J. Am. Chem. Soc.*, **76**, 3439 (1954).

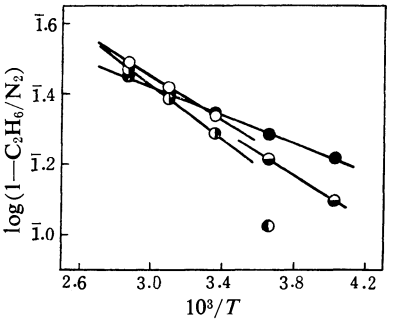


Fig. 7 Arrhenius plots of $1-C_2H_6/N_2$.
◑, Cyclohexane; ○, Benzene;
●, Styrene; ◒, *o*-Xylene;
◐, *tert*-Amyl alcohol

of nitrogen. They all decrease with the lowering of the temperature, as has been found previously[1,2], and are, on freezing the solutions, lowered discontinuously, which may be ascribed to reduced absorption of light by the frozen solution as well as to the increased recombination of a pair of initially formed radicals, CH_3N_2 and CH_3[1]. It has been found in the previous work[2] that the apparent quantum yield is low in polar solvents. Figure 6 shows a similar tendency in this work.

Summary

The photolysis of azomethane has been studied in cyclohexane, benzene, styrene, *o*-xylene and *tert*-amyl alcohol in the temperature range both above and below the freezing point of a given solution. The results obtained in the liquid solutions are essentially similar to those previously obtained with other solvents, except for styrene. The photolysis in the latter differs in that it gives little methane because of the strong scavenging action of styrene. Nevertheless, ethane with a yield comparable to those in the other solvents is formed even in styrene. It has been found with all the solutions investigated that the yield of ethane is more or less enhanced by freezing. All these findings provide additional evidence that the ethane is formed by the cage combination of a pair of methyl radicals resulting from the decomposition of a substrate molecule. For all the solvents investigated, the temperature dependence of the yield of ethane in the liquid phase conforms to the empirical equation previously presented. The apparent quantum yields obtained by comparing the rates of formation of nitrogen decrease with the lowering of the temperature, as was found previously.

The author wishes to thank Professor Osamu Toyama of the College of Engineering for his helpful advice and kind discussions. The author also wishes to thank Mr. Junichiro Shigemasa for his assistance.

Department of Applied Chemistry
College of Engineering
University of Osaka Prefecture
Sakai, Osaka

Studies of the Cage Effect of Solvent. IV. Dependence of the Cage Combination of Methyl Radicals on Solvent and on Temperature

By Sukeya KODAMA

(Received September 15, 1961)

It has been shown in a previous paper[1] that the photolysis of azomethane in *n*-hexane provides a good example of the cage combination of methyl radicals that can be studied quantitatively. This photolysis has further been studied with various other solvents, and the results obtained have subsequently been reported[2,3]. This paper presents a discussion of these results with reference to the dependence of the cage combination of methyl radicals on solvent and on temperature.

Experimental Results

The solvents in which the photolysis of azomethane has been studied are *n*-hexane[1], *n*-octane[2], benzene[3], toluene[2], styrene[3], *o*-xylene[3], cyclohexane[3], ethyl acetate[2], ethanol[2] and *tert*-amyl alcohol[3]. The photolysis was conducted by the irradiation of a mercury line of 366 mμ throughout all the experiments. Some experiments were also carried out with

1) S. Kodama, This Bulletin, 35, 652 (1962).
2) S. Kodama, ibid., 35, 658 (1962).
3) S. Kodama, ibid., 35, 824 (1962).

313 mμ in *n*-hexane[1], but they gave no appreciably different results. The range of the extent of conversion in the runs was usually within several percentage points.

The main products of the photolysis have always been found to be nitrogen, methane and ethane. It has been shown by a scavenger technique using styrene that all the ethane formed by the photolysis can be attributed to the cage combination of a pair of methyl radicals resulting from the decomposition of a substrate molecule[1,2]:

$$(CH_3)_2N_2 + h\nu \rightarrow [2CH_3 + N_2] \quad (1)$$

$$[2CH_3 + N_2] \rightarrow C_2H_6 + N_2 \quad (2)$$

(Here the parentheses denote the solvent cage.) The results obtained with a scavenger show, on the other hand, that the formation of methane is explained by the hydrogen atom abstraction from a solvent molecule by a methyl radical that has escaped the cage:

$$[2CH_3 + N_2] \rightarrow CH_3 + N_2 + CH_3 \quad (3)$$

$$CH_3 + HR \rightarrow CH_4 + R \quad (4)$$

where HR represents a solvent molecule. The material balance referring to nitrogen, methane and ethane, however, indicates that a small fraction of the methyl radicals, increasing in quantity with the temperature, yields other products than methane, presumably by various addition reactions.

Since the rate of photolysis is given by that of the formation of nitrogen, the ratio of the amount of ethane formed to that of nitrogen, C_2H_6/N_2, represents the yield of ethane. According to the mechanism given above, this yield of ethane represents the probability of the cage combination of a pair of methyl radicals produced in the solvent cage. It has been confirmed by experiment that the yield of ethane in a given solvent is affected neither by the rate of photolysis nor by the concentration of substrate, but is dependent only on the temperature. Figure 1 shows the effect of the temperature on the yield of ethane for the various solvents investigated[4]. The figure shows only results obtained in liquid solutions. For some of these solvents, the photolysis in frozen solutions has been studied[3]; the yield of ethane is more or less enhanced on freezing the solution, and the yield in the frozen solution is far less dependent on the temperature than in the liquid. These results are not illustrated here, however, because they have no direct relation to the present discussion.

In this paper viscosity is shown to be an important property of the solvent influencing

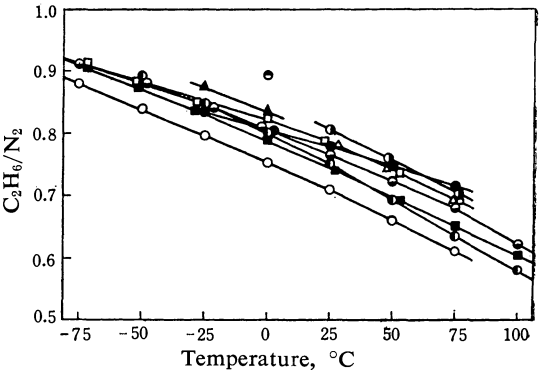


Fig. 1. Yields of ethane obtained with various solvents. ○, *n*-Hexane; ◐, *n*-Octane; ◑, Cyclohexane; ◒, Toluene; ◓, *tert*-Amyl alcohol; ●, Styrene; △, Benzene; ▲, *o*-Xylene; □, Ethanol; ■, Ethyl acetate

the yield of ethane. Table I gives the parameters for the expression $\eta = \eta_0 \exp(E_\eta/RT)$, where η is the viscosity of the solvent. These values were all obtained from Arrhenius plots of the viscosities measured in this work in the temperature range 0 to 60°C, because the solvents used in this work might not always have been pure. For *tert*-amyl alcohol viscosity was measured only at 0°C, with the result that $\eta = 0.1168$ poise. The viscosity values obtained for *n*-octane, ethanol, cyclohexane, benzene, toluene and styrene were in good agreement with those previously reported, while for *o*-xylene, ethyl acetate and *tert*-amyl alcohol somewhat higher values were obtained. *n*-Hexane showed considerably higher values than those in the literature, presumably because the sample used had been prepared from petroleum and so contained higher hydrocarbons, even after purification. All the viscosity values used in the following discussion have been calculated from Table I.

TABLE I. ARRHENIUS PARAMETERS FOR VISCOSITIES OF SOLVENTS

Solvent	$\eta_0 \times 10^5$ poise	E_η cal./mol.
n-Hexane	28.84	1500
n-Octane	14.09	2125
Ethyl acetate	17.23	1920
Ethanol	3.33	3430
Cyclohexane	5.05	3060
Benzene	11.94	2315
Toluene	16.00	2100
o-Xylene	7.18	2720
Styrene	12.82	2380

Discussion

Table II shows the yields of ethane compared with some properties of solvents. The yield

4) The yields of ethane given in the figure for respective temperatures have been obtained from smoothed curves.

Table II. Comparison of yields of ethane with some properties of solvents

Solvent	Mol. wt.	Density at 25°C	Viscosity $\times 10^3$ poise at 25°C	Dipole moment D	C_2H_6/N_2 at 25°C	C_2H_6/N_2 at 0°C
n-Hexane	86.2	0.6545	3.70	0	0.710	0.752
Ethyl acetate	88.1	0.8985	4.43	1.74	0.742	0.787
n-Octane	114.2	0.6984	5.11	0	0.751	0.802
Toluene	92.1	0.8623	5.52	0.4	0.766	0.808
Styrene	104.2	0.9010	7.11	0.15	0.780	0.808
Benzene	78.1	0.8733	5.94	0	0.783	
Ethanol	46.1	0.7847	10.57	1.70	0.787	0.823
o-Xylene	106.2	0.8760	7.22	0.52		0.835
Cyclohexane	84.2	0.7738	8.81	0	0.806	
t-Amyl alcohol	88.2	0.8047	30.9			0.894

Table III. Arrhenius parameters for Eqs. I and II

Solvent	A_I	E_I kcal./mol.	A_{II}	E_{II} kcal./mol.	E_D kcal./mol.
n-Hexane	2.08	1.17	3.42	1.27	2.07
n-Octane	2.40	1.51	6.60	1.78	2.42
Ethyl acetate	2.22	1.29	3.84	1.44	
Ethanol	1.48	1.12	2.30	1.28	4.50
Cyclohexane	3.62	1.74			4.56
Benzene	2.61	1.48			2.00
Toluene	1.90	1.24	2.55	1.29	
o-Xylene	2.10	1.39	4.22	1.66	
Styrene	1.06	0.93	1.42	0.972	

Table IV. β' Values for $a=1.80$ Å

Solvent	β' Lowest temp.	β' 0°C	β' Highest temp.
n-Hexane	0.988 (−75°C)	0.960	0.920 (75°C)
n-Octane	0.990 (−50°C)	0.973	0.915 (100°C)
Ethyl acetate	0.993 (−75°C)	0.968	0.911 (100°C)
Ethanol	0.999 (−75°C)	0.990	0.955 (75°C)
t-Amyl alcohol		0.998	
Cyclohexane	0.977 (25°C)		0.950 (75°C)
Benzene	0.966 (25°C)		0.938 (75°C)
Toluene	0.995 (−75°C)	0.975	0.922 (100°C)
o-Xylene	0.990 (−25°C)	0.982	
Styrene	0.988 (−25°C)	0.980	0.947 (75°C)

appears to depend on the viscosity of the solvent rather than on any other property. However, the differences in the yields are not large, and both the yield and viscosity are dependent on the temperature. No reliable conclusion can, therefore, be drawn from the table.

It has previously been found[1-3] that the variation in the yield of ethane with the temperature, as shown in Fig. 1, conforms to the following equation for all the solvents investigated:

$$C_2H_6/N_2 = 1 - A_I \exp(-E_I/RT) \qquad (I)$$

where A_I and E_I are constants dependent on the nature of the solvent. In Table III are listed the values of these constants determined for various solvents. The constants A_I and E_I thus reflect the specific behavior of each solvent towards the cage combination of methyl radicals and appear at first sight to deserve further discussion. Nevertheless, unfortunately, the equation is merely an empirical one, and hence neither A_I nor E_I is a well defined quantity.

The mechanism of the photolysis represented by reactions 1−4 gives only a crude picture of what would really take place; reactions 2 and 3 would actually involve sequences of complicated diffusive displacements in a system where methyl radicals are surrounded by solvent molecules of complex structure and with variable configurations and orientations. The

situation thus appears to be intractable to any simple theoretical treatment.

The simplest way to interpret the data obtained in this work may be to treat reactions 2 and 3 as though they were elementary processes[1]. This is probably an over-simplification in view of the argument given above, but it may be of some interest to see what is obtained by the application of such a treatment. Reactions 2 and 3 give in the steady state

$$(1-C_2H_6/N_2)/(C_2H_6/N_2)=k_3/k_2 \qquad (II)$$

where k_2 and k_3 are the respective rate constants. It is generally accepted that two methyl radicals in contact with each other require no activation energy to combine. If, therefore, the chance for such a contact in the cage can be assumed to be approximately independent of the temperature, k_3 would be a constant. Then the Arrhenius plot of the quantity on the left-hand side of the above equation would give the activation energy of reaction 3, which may approximately be taken as the diffusion energy of methyl radicals in solution. Figure 2 shows, however, that actually most such plots have bends at about 25°C. It may be expected that the simplified treatment applied here deviates more from reality with a rise in temperature. In Table III are, therefore, listed the Arrhenius parameters A_{II} and E_{II} determined from linear plots in the low temperature range. As seen in the table, these values differ not greatly from those obtained by Eq. I. E_{II} values are lower than the corresponding diffusion energies of solvents given together in the table. The present work gives no evidence to justify the simple treatment applied here, but these low E_{II} values would not necessarily contradict the interpretation that E_{II} represents approximately the diffusion energy of methyl radicals in solution, since the diffusion energies given in the table are those for self-diffusion[5].

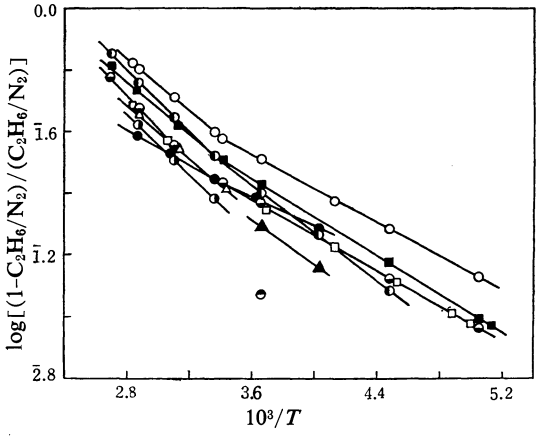


Fig. 2. Arrhenius plots for $(1-C_2H_6/N_2)/(C_2H_6/N_2)$. ○, *n*-Hexane; ◐, *n*-Octane; ◑, Cyclohexane; ◒, Toluene; ◓, *tert*-Amyl alcohol; ●, Styrene; △, Benzene; ▲, *o*-Xylene; □, Ethanol; ■, Ethyl acetate

Another approach to the problem being considered has been given by Noyes[6]. He has derived a theoretical expression for the quantum yield of the photolysis of iodine in solution, assuming that the solvent can be treated as a viscous continuum in which iodine atoms displace by diffusion. The comparison between the theory and experiment has shown that the theory gives rather satisfactory results. The following is an attempt to apply Noyes's theory to the present photolysis, though such a treatment here meets various difficulties.

According to Noyes, if β_0' is the probability that two iodine atoms whose centers were initially separated by a distance s_t will ultimately combine with each other,

$$\beta_0'=2a\beta'/s_t \qquad (III)$$

where a is the radius of the iodine atom and β', the probability that two atoms which were initially in contact with each other will recombine if they separate with an average thermal kinetic energy. The distance of the initial separation s_t is given by

$$s_t=2a+(m\varepsilon)^{1/2}/(3\pi\eta a) \qquad (IV)$$

where m is the mass of an iodine atom, η the viscosity of solvent, and ε the kinetic energy with which two iodine atoms separate in opposite directions. Equations III and IV can be combined to give

$$\beta_0'=\beta'/[1+(m\varepsilon)^{1/2}/(6\pi\eta a^2)] \qquad (V)$$

The expression for β' is obtained in a similar way:

$$\beta'=1/[1+(mkT)^{1/2}/(2\sqrt{6}\,\pi\eta a^2)] \qquad (VI)$$

If ϕ is the quantum yield, β_0' is equal to $1-\phi$. Hence, the quantum yield can be calculated when ε and η are given.

In the photolysis of azomethane, $2a$ in Eq. IV should be replaced by $2s_0$, the distance between the two carbon atoms in an azomethane molecule. Consequently, Eq. V should be written as

$$\beta_0'=a\beta'/s_0[1+(m\varepsilon)^{1/2}/(6\pi\eta a s_0)] \qquad (VII)$$

One of the uncertainties in this case is the magnitude of a, the effective radius of a free methyl radical. Another uncertainty, which

5) Reported values of diffusion energy for free radicals in solution are meagre: Polystyrene radicals (in benzene), 1.9 kcal./mol. (G. M. Burnett, *Trans. Faraday Soc.*, **46**, 772 (1950)); polymethylmethacrylate radicals (in methylmethacrylate), 2.8 kcal./mol. (M. S. Matheson et al., *J. Am. Chem. Soc.*, **71**, 497 (1949); ibid., **73**, 1700 (1951)).

6) a) R. M. Noyes, *J. Chem. Phys.*, **22**, 1349 (1954); b) *J. Am. Chem. Soc.*, **77**, 2042 (1955); c) ibid., **78**, 5486 (1956); d) *Z. Elektrochem.*, **64**, 153 (1960).

gives more difficulty in the evaluation of β_0' is the value of ε. Although an energy of 56 kcal./mol.[1] is liberated in the photolysis with 366 mμ, the share for the methyl radicals is unknown. Moreover, two methyl radicals will not always separate in opposite directions.

On account of these uncertainties, it seems impossible to compute β_0' by Eq. VII in this case. However, approximate values of β' may be estimated, since it has no relation to ε, and, as a first approximation, a may be regarded as equal to s_0, which is known to be 1.80 Å from its molecular structure[7,8]. As seen in Table IV, β' thus calculated is almost unity at low temperatures. It decreases with a rise in temperature, but is still greater than 0.9 at the highest temperature for all the solvents. If, therefore, β' in Eq. VII is put equal to unity,

$$1/\beta_0' = (s_0/a) + (m\varepsilon)^{1/2}/(6\pi a^2)\cdot 1/\eta \quad \text{(VIII)}$$

Since β_0' is equal to the yield of ethane found by experiment, there should be a linear relationship between the ratio N_2/C_2H_6 and the reciprocal viscosity, if Eq. VIII is applicable.

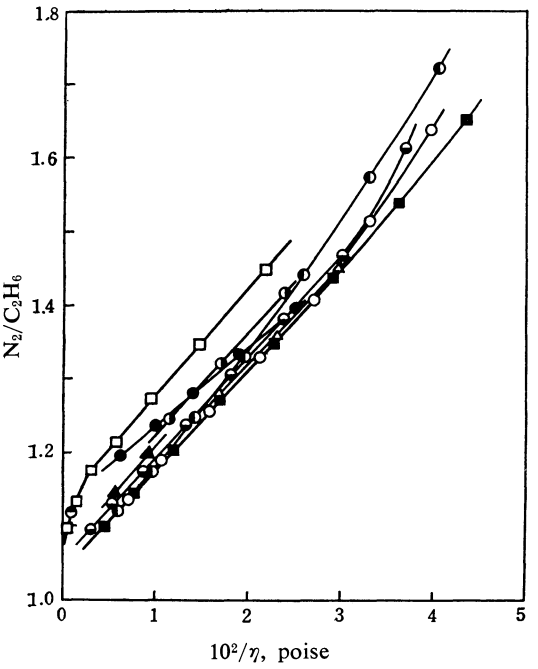


Fig. 3. Plots of N_2/C_2H_6 against reciprocal viscosity. ○, *n*-Hexane; ◐, *n*-Octane; ◑, Cyclohexane; ◒, Toluene; ◓, *tert*-Amyl alcohol; ●, Styrene; △, Benzene; ▲, *o*-Xylene; □, Ethanol; ■, Ethyl acetate

Figure 3 shows that Eq. VIII represents experimental results rather satisfactorily. At high viscosities or at low temperatures, where the equation is expected to be applicable, most plots are linear, run parallel and nearly coincide with each other. The plots for *n*-hexane, *n*-octane and ethyl acetate give identical intercepts on the ordinate, from which a is obtained as 1.73 Å, in approximate agreement with the 1.80 Å assumed above to estimate β'. These plots have almost the same slope at high viscosities, from which ε is obtained as 33.8 kcal./mol. This appears to be not an unreasonable value for the virtual energy separating two methyl radicals in opposite directions to a distance, s_t, in view of the total energy of 56 kcal./mol. liberated in the photolysis. By inserting this ε value into Eq. IV, the distance of initial separation, s_t, is calculated. The values obtained for *n*-hexane, for example, are shown in Table V. These s_t values also appear to be not unreasonable.

Table V. s_t Values for *n*-hexane

Temperature °C	s_t Å	$s_t - 2s_0$ Å
−75	3.93	0.33
0	4.59	0.99
75	5.46	1.86

Figure 3 shows however a general tendency, at low viscosities or at high temperatures, for deviation from the linear plot to appear in the direction of yielding less ethane than would be expected from Eq. VIII. A part of the deviation may be ascribed to the factor β' in Eq. VII, since β' becomes smaller with a rise in temperature, as is shown in Table IV. This effect is, however, by far too small to explain the observed deviations. The deviations seem, therefore, to indicate that the effect of the molecular structure of the medium, which was neglected in the theory, has to be taken into account. A simlar indication has been obtained by Noyes and his coworkers in the photolysis of iodine[6d,9]. As was cited by them in their papers, "Rabinowitch's cage"[10] originated from the idea that if two atoms are separated by only a small distance, the surrounding solvent molecules tend to force the atoms toward each other, while, if the atoms are separated sufficiently enough so that solvent molecules can squeeze between them, solvent molecules will force the atoms farther apart. If, in the present work, the distance of initial separation for a pair of methyl radicals is largely controlled

7) According to H. Boersch (*Sitzungsber. Akad. Wiss. Wien.*, **144**, 1 (1935)), azomethane is of the trans form, with C-N=1.47, N-N=1.24 Å and ∠CNN=110°. s_0 is therefore obtained as 1.80 Å.

8) L. Pauling estimates the van der Waals radius of a methyl radical in a molecule as 2.0 Å. ("The Nature of the Chemical Bond", Third Ed., p. 261. Cornell Univ. Press, Ithaca, N. Y. (1960)).

9) D. Booth and R. M. Noyes, *J. Am. Chem. Soc.*, **82**, 1868 (1960); L. F. Meadows and R. M. Noyes, ibid., **82**, 1872 (1960).

10) E. Rabinowitch and W. C. Wood, *Trans. Faraday Soc.* **32**, 547 (1936).

by the viscosity of the medium, it may be expected from the above behavior of solvent molecules that the experimental yield of ethane will be higher at high viscosities but lower at low viscosities than that predicted by Eq. VII, and that it will approximately conform to the equation in an intermediate range of viscosity. Figure 3 appears to be in general agreement with such an expectation, though the deviation from the linear plot to give a higher yield of ethane is not seen in the range of viscosity studied here except for ethanol.

The plots for the various solvents in Fig. 3 do not completely coincide with each other, which indicates that viscosity is not the only controlling factor. It is probably necessary, for a better description of the matter, to take account of the structure and specific nature of the individual molecules of the solvent. The smaller slope of the plot for styrene seems, however, to have resulted from its polymerization, which has been found to be induced by the photolysis[3]. Since the polymerization increases with the temperature, the viscosity of the medium probably becomes higher than in pure styrene at high temperatures.

Summary

Experimental results for the cage combination of methyl radicals, obtained by the photolysis of azomethane in various solvents, have been discussed with reference to the effects of solvent and temperature. An attempt to interpret the results by treating both the cage combination and the escape of methyl radical from the cage as though they were elementary processes has been found to be not very successful, probably owing to the over-simplification involved in such a treatment. Another attempt to apply Noyes's theory, that assumes diffusion in the viscous continuum, has been found to be rather satisfactory. However, a comparison of the theory with the experimental results indicates that the molecular structure of the medium, as well as the structure and property of individual molecules of the solvent, need to be taken into account for a better description of the matter.

The present author is gratefully indebted to Professor Osamu Toyama of the College of Engineering for his helpful advice and kind discussion during this investigation. The author wishes also to thank Mr. Shin'ichi Fujita for his assistance.

Department of Applied Chemistry
College of Engineering
University of Osaka Prefecture
Sakai, Osaka

The Crystal Structure of D-Tris-ethylenediamine-cobalt(III) Bromide Monohydrate, D-[Co en$_3$]Br$_3$·H$_2$O, and the Absolute Configuration of the D-Tris-ethylenediamine-cobalt(III) Ion, D-[Co en$_3$]$^{3+}$

By Kazumi NAKATSU

(Received October 4, 1961)

The crystal structure of several complex compounds containing $[Co\,en_3]^{3+}$ ions (en: ethylenediamine, NH_2–CH_2–CH_2–NH_2) have been studied to determine the shape and size of the cobalt-ethylenediamine ring[1-3]. The absolute configuration of the complex ion has also been determined[4]. The present work was undertaken to obtain further information on the ion and, at the same time, to confirm the absolute configuration determined for the crystals of D- and L-2 $[Co\,en_3]Cl_3 \cdot NaCl \cdot 6H_2O$.

Since the $[Co\,en_3]^{3+}$ ion is the most familiar and fundamental one in the coordination chemistry and since it exhibits a typical optical isomerism due to the octahedral configuration, the absolute configuration of the complex ion merits further confirmational study. The stability and ease with which this ion can be obtained further favor its use as an internal reference asymmetric center for the determination of the absolute configuration of other

1) K. Nakatsu, Y. Saito and H. Kuroya, This Bulletin, **29**, 428 (1956).
2) K. Nakatsu, M. Shiro, Y. Saito and H. Kuroya, ibid., **30**, 158 (1957).
3) H. Kuroya, Y. Saito, A. Nakahara, Y. Komiyama and K. Nakatsu, *J. Inst. Polytech. Osaka City Univ.*, C5, 1 (1956).
4) Y. Saito, K. Nakatsu, M. Shiro and H. Kuroya, This Bulletin, **30**, 795 (1957); *Acta Cryst.*, **8**, 729 (1955).

optically active compounds[5].

The details of the structure analysis will be given in Part I, while the determination of the absolute structure of the crystal, as well as the absolute configuration of the complex ion, will be described in Part II.

I. The Crystal Structure

Experimental

D-[Co en$_3$]Br$_3$·H$_2$O (which is generally formulated as dihydrate) was prepared by the method described by Werner[6], who concluded that this substance might be dihydrate from the determination of the cobalt as $CoSO_4$. This method of analysis, however, does not seem to be sensitive enough to fix the number of the water of crystallization. The determination of the water of crystallization was made here by direct dehydration. The results are shown in Table I, together with the densities of the crystals. The table supports the monohydrate formula and shows that the results of the chemical analysis are rather dubious; later structure determination verified the monohydrate formula.

TABLE I. DETERMINATION OF THE WATER OF CRYSTALLIZATION

	Calcd. for $C_6H_{24}N_6Co\cdot 2H_2O$	Calcd. for $C_6H_{24}N_6Co\cdot H_2O$	Found
Co	11.42%	11.87%	11.52% for D-crystal[6]
			11.62% for L-crystal[6]
H_2O	6.99%	3.62%	3.12%*
Density (g. cm^{-3})	2.06	1.995	1.971(25°C)[7]
			2.00(30°C)**

* Dehydrated at 3 mmHg, 110°C, until the sameles reached constant weights. The author is very grateful to Mr. J. Gôda of this Faculty for the use of micro-balance.

** Measured by the flotation method.

The crystals are deep orange in color and appear in ditetragonal bipyramidal form, which agrees with Jaeger's description[7]. The crystallographic and physical data obtained were as follows:

D-Tris-ethylenediamine-cobalt(III) bromide monohydrate, D-[Co en$_3$]Br$_3$·H$_2$O, F. W.=497.1

Crystal system: Tetragonal

Unit cell dimensions: $a=9.95\pm0.03$* and $c=16.73\pm0.05$ Å

Axial ratio $a_0 : c_0 = 1 : 0.8399$ obtained by morphology[7], $a : c/2 = 1 : 0.840_7$ obtained by X-rays

Systematic extinction: $(h\,0\,0)$ present only when $h=2n$, and $(0\,0\,l)$ when $l=4n$

Space group: No. 92, $P4_12_12$-D_4^4 or No. 96, $P4_32_12-D_{8}^{4}$, these two are enantiomorphous with each other

Number of the formula units per unit cell: $Z=4$

Volume of the unit cell: 1656 Å^3

Density: Observed 2.00 g. cm^{-3}, 1.971 g. cm^{-3}[7], calculated 1.99$_5$ g. cm^{-3}

Total number of electrons per unit cell: $F(0\,0\,0)=928$

Linear absorption coefficient for Ni K_α rays ($\lambda=1.651$ Å): $\mu=124.1$ cm^{-1}

Using Ni K_α radiation, a complete set of relative intensities for $(h\,k\,0)$ and $(0\,k\,l)$ reflections were obtained by the integrated Weissenberg procedure. For the recording of the weak reflections, a non-integrating procedure was used. The specimens used were obtained by cutting the crystals in a cylindrical form, until μr, where r is the radius of the specimen, became smaller than unity. The radii of the specimens were 0.01 cm. for the a-axis rotation and 0.009 cm. for the c-axis rotation; thus the μr were estimated to be 0.8 and 0.7 respectively.

Intensity measurements were carried out by visual comparison with a calibrated scale prepared by using the same specimen. The multiple film technique was used to correlate strong and weak reflections, ranging in relative intensity from about 5×10^4 to unity. The maximum $\sin\theta$ observed was 0.975. Within this limit, 53 reflections were measured out of 58 possible $(h\,k\,0)$ reflections, and 167 out of 186 possible $(0\,k\,l)$ reflections.

The corrections for polarization and Lorentz factors were made by use of Cochran's chart[8], and that for absorption was made by regarding the specimens as cylinders[9].

Determination of the Structure

Since the number of formula units in a unit cell is four, and since there are four fold special positions, 4(a), and eight fold general positions, 8(b), in the space group[10], it was assumed that 4Co, 4Br (labeled as Br$_1$) out of 12Br and 4O would lie on 4(a), and that the others would lie on 8(b) (labeled as Br$_2$, N$_1$, N$_2$, N$_3$, C$_1$, C$_2$ and C$_3$).

(0 0 1) Projection. — At the outset the Patterson projection $P(UV)$ was evaluated. Although the interpretation of the map was fairly difficult, owing to overlapping of the interatomic vectors, approximate positions of the heavy atoms Co, Br$_1$ and Br$_2$ were derived. An electron density projection $\rho(XY)$ was then calculated, assuming the structure factor to have the same phases as the contributions of the heavy atoms. However, none of the atoms, except Br$_2$, could be resolved owing to the heavy overlapping.

The main problem in interpreting the electron density map thus obtained was to decide where the light atoms should be placed in a composite peak. This was accomplished to

5) A. McL. Mathieson, ibid., **9**, 317 (1956).
6) A. Werner, *Ber.*, **45**, 128 (1912).
7) F. M. Jaeger, *Akad. Amsterdam Versl.*, **23**, 1293 (1914/1915); *Z. Krist.*, **55**, 207 (1919—1920).
* The a-axis was chosen in such a way that well-formed prismatic faces can be assigned for (1 1 0).
8) W. Cochran, *J. Sci. Instruments*, **25**, 253 (1949).
9) "International Tables for X-Ray Crystallography", Vol. II, The Kynoch Press, England (1959).
10) Ibid., Vol. I (1952).

some extent by the use of partial difference syntheses[11], giving the electron density distribution after subtracting the calculated contributions of those atoms whose parameters were fairly accurately known. The coefficients used in these syntheses were $\Delta F=(F_o-F_c')$, where F_c' included only the contributions of the atoms which were to be subtracted, while the same phase as F_c' was given to F_o. These projections gave more information about the positions of the lighter atoms, and at the same time the necessary changes in the coordinates of heavy atoms were found.

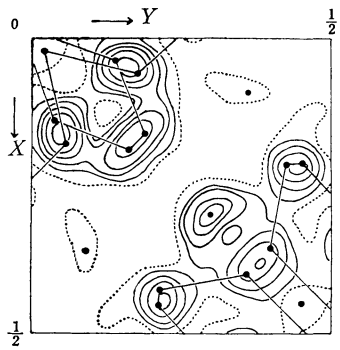


Fig. 1. Electron-density distribution $(\rho_o-\rho_c')$ projected upon (0 0 1) after subtracting the contributions of the cobalt and bromine atoms. Contours are at every 4 e.Å^{-2}, starting at two electron level, whose contours are broken.

Further refinements were made using the ρ_o and ordinary difference syntheses. In some cases difference syntheses using only those reflections with $\sin\theta/\lambda$ larger than 0.35 Å^{-1} were calculated to avoid systematic errors such as the one arising from extinction[12]. A correction for secondary extinction was applied by the method of Pincock et al.[13] Figure 1 shows the result of the partial difference synthesis $(\rho_o-\rho_c')$, where the contributions of heavy atoms were subtracted.

(1 0 0) Projection.—Inspecting $(0\,k\,l)$ reflections, it was found that all the reflections which belong to type $2k+l=4n+2$ were extremely weak intensity compared with the others. The structure factor for this type of reflection can be represented by[10];

$$A=0$$

and

$$B=\sum_j 4f_j \sin 2\pi lz_j(\cos 2\pi ky_j-\cos 2\pi kx_j)$$

where j refers to the jth atom. The values of B will be small only when $\sin 2\pi lz_j$ assumes a small value, because the factor given in parenthesis is not necessarily small, depending on the values of y_j and x_j. This would generally be true for heavier atoms. In order for $\sin 2\pi lz_j$ to become smaller, the z parameters of heavy atoms have to assume 0, 1/4, 1/2 and/or 3/4. Since Co and Br_1 lie on 4(a) and their z parameters take those values, this condition should be imposed for Br_2. If the Br_2 atoms take the z parameters given above, then all the heavy atoms lie on plane (0 0 4), giving rise to a layer structure. The extremely strong intensities of (0 0 l), especially of (0 0 4), also favored this deduction. A Patterson projection $P(VW)$ showed, however, marked peaks which at first seemed to be inconsistent with these parameters. Later it was found that these peaks were due to the multiple overlapping of the interatomic vectors between heavy and light atoms and those between light atoms. Also for the (1 0 0) projection, the refinement procedures were repeated in a similar way. $(\rho_o-\rho_c')$ is given in Fig. 2.

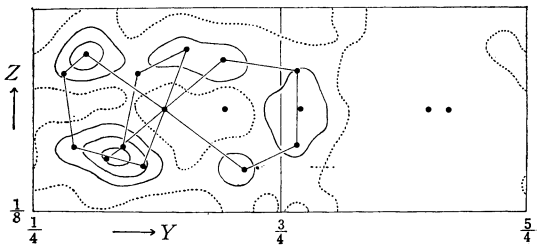


Fig. 2. Electron-density distribution $(\rho_o-\rho_c')$ projected upon (1 0 0). Contours are drawn as same manner as Fig. 1.

TABLE II. ATOMIC COORDINATES

Atom	x/a	y/a	z/c
Co	0.480	0.520	0.250
Br_1	0.550	0.550	0.500
O	0.295	0.295	0.500
Br_2	0.139	0.590	0.500
C_1	0.663	0.313	0.295
C_2	0.218	0.433	0.205
C_3	0.217	0.463	0.295
N_1	0.532	0.360	0.319
N_2	0.362	0.395	0.190
N_3	0.324	0.558	0.322

The final set of atomic coordinates listed in Table II, and the observed and calculated structure factors are given in Table III. In the structure factor calculations, the atomic scattering factors were taken from Thomas and Umeda[14] for cobalt and bromine, and from

11) S. Ooi, Y. Komiyama, Y. Saito and H. Kuroya, This Bulletin, 32, 263 (1959); P. G. Owton, J. M. Partridge and J. M. Rowe, *Acta Cryst.*, 13, 246 (1960).
12) F. Jellinek, ibid., 11, 677 (1958).
13) P. R. Pincock, C. A. Taylor and H. Lipson, ibid., 9, 173 (1956).
14) L. H. Thomas and K. Umeda, *J. Chem. Phys.*, 26, 293 (1957).

TABLE III. OBSERVED AND CALCULATED STRUCTURE FACTORS

h	k	l	$F_o/4$	$F_c/4$	h	k	l	$F_o/4$	$F_c/4$	h	k	l	$F_o/4$	$F_c/4$	h	k	l	$F_o/4$	$F_c/4$
2	0	0	44.2	43.8	0	0	8	41.8	48.8	0	6	14	< 1.0	− 0.5	0	3	14	6.6	7.7
4	0	0	21.0	−18.8	0	0	12	46.0	−44.0	0	6	16	< 0.6	1.4	0	3	16	< 0.9	− 0.1
6	0	0	2.4	− 1.0	0	0	16	32.0	32.5	0	7	1	4.8	1.9	0	3	18	4.8	− 4.3
8	0	0	3.3	− 2.1	0	1	1	5.3	− 5.1	0	7	3	4.5	0.1	0	4	1	33.2	−34.4
10	0	0	< 1.7	− 5.1	0	1	3	4.5	4.8	0	7	5	3.9	− 2.8	0	4	3	24.0	−21.1
1	1	0	32.8	34.3	0	1	5	1.1	1.0	0	7	7	2.5	0.6	0	4	5	31.6	33.2
3	1	0	40.9	40.3	0	1	7	7.0	− 4.0	0	7	9	4.3	3.1	0	4	7	24.4	22.5
5	1	0	27.8	24.4	0	1	9	2.5	− 1.4	0	7	11	3.9	− 3.4	0	4	9	18.1	−15.5
7	1	0	4.4	− 2.0	0	1	11	5.0	2.6	0	7	13	3.5	− 2.3	0	4	11	18.1	−17.6
9	1	0	8.3	− 9.2	0	1	13	< 1.1	3.0	0	7	15	3.4	3.0	0	4	13	10.7	9.0
11	1	0	3.3	− 1.8	0	1	15	< 1.1	− 0.4	0	8	0	3.3	− 2.1	0	4	15	8.9	7.8
2	2	0	21.6	18.3	0	1	17	< 1.0	− 1.2	0	8	2	2.2	− 1.0	0	4	17	7.9	− 7.8
4	2	0	9.7	7.1	0	1	19	0.9	0.2	0	8	4	1.6	1.0	0	5	2	19.5	−14.9
6	2	0	12.9	11.1	0	2	0	44.2	−43.8	0	8	6	2.4	0.6	0	5	4	3.8	− 0.4
8	2	0	7.1	4.5	0	2	2	1.4	− 1.0	0	8	8	2.1	0.9	0	5	6	19.9	15.4
10	2	0	4.1	− 5.7	0	2	4	36.2	35.7	0	8	10	1.4	0.7	0	5	8	< 1.1	− 3.3
3	3	0	22.4	19.7	0	2	6	2.5	1.5	0	8	12	< 0.8	− 0.7	0	5	10	15.9	−12.6
5	3	0	12.3	− 9.8	0	2	8	30.2	−27.8	0	8	14	0.9	− 0.2	0	5	12	1.1	1.1
7	3	0	2.0	− 1.3	0	2	10	4.8	0.0	0	9	1	13.7	−11.3	0	5	14	10.2	7.1
9	3	0	2.8	− 0.4	0	2	12	25.6	21.1	0	9	3	12.4	12.3	0	5	16	2.4	1.9
11	3	0	4.7	1.7	0	2	14	1.9	− 0.8	0	9	5	12.5	11.6	0	6	1	2.3	− 1.9
4	4	0	30.4	32.4	0	2	16	17.5	−11.8	0	9	7	10.1	−11.0	0	6	3	3.3	− 1.2
6	4	0	12.7	10.8	0	2	18	< 0.8	0.0	0	9	9	9.1	7.6	0	6	5	< 0.9	1.0
8	4	0	< 1.9	− 3.5	0	3	1	35.8	−36.6	0	9	11	5.6	6.6	0	6	7	4.5	− 3.6
10	4	0	2.5	− 2.3	0	3	3	18.3	17.3	0	10	0	1.7	5.1	0	6	9	1.6	1.7
5	5	0	< 2.3	0.4	0	3	5	26.4	26.4	0	10	2	0.9	− 1.4	0	6	11	7.6	3.3
7	5	0	6.0	8.0	0	3	7	9.5	−10.0	0	10	4	3.4	− 3.9	0	6	13	4.6	− 3.9
9	5	0	2.1	1.8	0	3	9	10.6	− 7.6	0	10	6	1.5	0.6	0	6	15	3.9	− 0.5
6	6	0	6.9	− 5.2	0	3	11	10.8	10.1	0	10	8	3.7	2.3	0	6	17	< 0.4	1.5
8	6	0	3.9	− 3.6	0	3	13	7.9	4.7	0	10	10	1.4	1.4	0	7	2	36.2	39.7
10	6	0	6.1	6.6	0	3	15	8.6	− 6.9	0	11	1	3.6	3.1	0	7	4	3.0	− 1.5
7	7	0	8.3	11.0	0	3	17	8.4	− 6.0	0	11	3	3.2	− 3.0	0	7	6	25.8	−29.5
9	7	0	1.3	1.5	0	3	19	3.5	4.1	0	11	5	4.7	− 4.2	0	7	8	< 1.1	0.4
8	8	0	1.9	4.0	0	4	0	21.0	−18.8	0	11	7	2.7	2.4	0	7	10	19.5	21.1
2	1	0	< 0.9	0.3	0	4	2	5.0	− 3.5	0	1	2	13.9	−12.4	0	7	12	< 1.0	0.8
4	1	0	8.9	− 7.4	0	4	4	8.4	11.1	0	1	4	2.2	− 0.5	0	7	14	14.0	−15.5
6	1	0	2.1	0.8	0	4	6	1.8	0.5	0	1	6	31.2	−29.5	0	8	1	5.1	− 7.4
8	1	0	10.4	9.4	0	4	8	3.4	− 6.4	0	1	8	1.2	0.7	0	8	3	4.4	− 7.2
10	1	0	6.3	6.0	0	4	10	3.0	− 2.5	0	1	10	19.6	18.3	0	8	5	2.7	5.6
3	2	0	16.3	16.3	0	4	12	3.3	8.1	0	1	12	< 1.1	0.2	0	8	7	2.5	5.2
5	2	0	26.8	26.1	0	4	14	< 1.1	− 1.3	0	1	14	2.2	− 3.1	0	8	9	3.3	− 4.0
7	5	0	12.1	−10.7	0	4	16	2.4	− 6.5	0	1	16	1.1	− 0.3	0	8	11	< 1.0	− 3.2
9	2	0	16.4	−15.1	0	4	18	1.9	1.4	0	1	18	3.4	2.6	0	8	13	4.0	3.1
11	2	0	< 1.3	0.7	0	5	1	26.4	26.7	0	2	1	42.8	42.9	0	9	2	1.5	− 2.1
4	3	0	2.4	1.3	0	5	3	18.1	−19.5	0	2	3	37.3	35.9	0	9	4	< 1.1	− 0.1
6	3	0	10.3	−11.0	0	5	5	21.1	−24.3	0	2	5	45.1	−45.8	0	9	6	6.2	7.3
8	3	0	14.4	13.8	0	5	7	17.9	20.4	0	2	7	34.7	35.9	0	9	8	< 1.0	− 0.4
10	3	0	3.9	1.4	0	5	9	14.0	13.1	0	2	9	36.6	35.3	0	9	10	6.2	− 6.6
5	4	0	25.6	25.8	0	5	11	14.9	−15.9	0	2	11	28.2	30.3	0	9	12	0.8	0.3
7	4	0	12.5	13.3	0	5	13	11.6	−11.0	0	2	13	20.9	−20.6	0	10	1	0.9	1.4
9	4	0	1.7	− 2.5	0	5	15	7.4	7.9	0	2	15	17.4	−17.4	0	10	3	0.9	1.8
11	4	0	2.3	− 2.0	0	5	17	9.9	8.6	0	2	17	10.8	10.7	0	10	5	2.8	3.5
6	5	0	4.7	5.0	0	6	0	2.4	1.0	0	2	19	8.1	7.4	0	10	7	2.8	− 3.8
8	5	0	2.4	− 1.3	0	6	2	1.4	0.1	0	3	2	16.5	−18.3	0	10	9	1.2	1.9
10	5	0	5.7	− 4.3	0	6	4	4.3	− 4.9	0	3	4	2.4	1.3	0	11	2	4.9	− 4.8
7	6	0	7.7	7.3	0	6	6	2.9	− 1.6	0	3	6	5.0	7.4	0	11	4	2.8	2.3
9	6	0	3.5	3.9	0	6	8	5.0	5.5	0	3	8	< 0.8	0.5	0	11	6	3.3	3.7
8	7	0	7.7	− 3.9	0	6	10	1.9	1.0	0	3	10	4.5	− 7.1					
0	0	4	(75.4)*	−118.1	0	6	12	1.5	− 2.3	0	3	12	1.5	− 1.1					

* Extremely large effect of extinction is expected.

Berguis et al.[15] for carbon, nitrogen and oxygen. The correction to be applied to the real part of the atomic structure factor due to the dispersion[16] caused by K-electrons, $\Delta f_K'$, was taken into account for cobalt and bromine. This amounts to -3.5 for cobalt and -1.5 for bromine for Ni K_α rays. No correction was made for the dispersion caused by L-electrons. The isotropic and overall temperature correction was applied in the usual manner. The temperature factor, B, was found to be 3.4Å^2 for $(h\,k\,0)$ and 3.2Å^2 for $(0\,k\,l)$ reflections.

The final reliability indices, $R=\Sigma||F_o|-|F_c||/\Sigma|F_o|$, are 0.128 for $(h\,k\,0)$ and 0.148 for $(0\,k\,l)$ reflections, without the contribution of hydrogen atoms, non-observed reflections being excluded. In the calculation of R, $(0\,0\,l)$ reflections were omitted, because these reflections would be influenced critically by such an effect as extinction.

Description and Discussion of the Structure

The arrangement of the atoms in the unit cell is shown in Figs. 3, 4 and 5, with some interatomic distances. The most striking feature is that the heavy cobalt and bromine atoms and water molecules are in layers, the layers being $c/4$ apart.

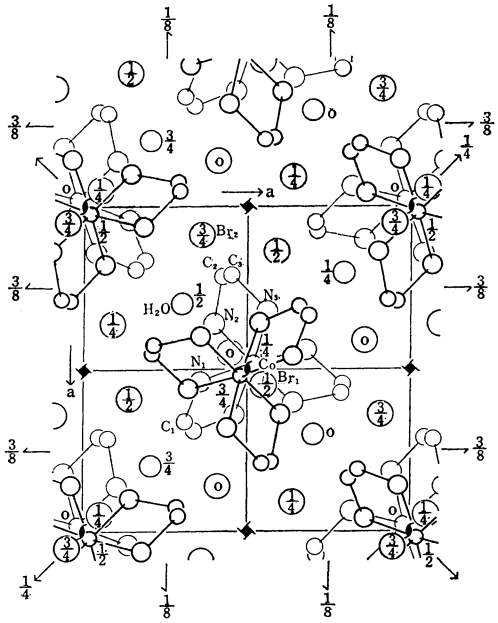


Fig. 3. Projection of the structure upon (0 0 1). The figures in or near the atoms show the z-coordinates of the atoms respectively.

Adopting the absolute configuration of the dextrorotatory complex ion determined previously[4], we can deduce that the present crystal belongs to the space group $P4_32_12$-D_4^8. This choice of space group from the enantiomorphous pair was verified by the anomalous dispersion experiment for the present crystal, as will be shown later.

Since the cobalt atoms lie on the special positions 4(a), having point symmetry 2, the complex ion is required to have a digonal symmetry. This would be compared with the

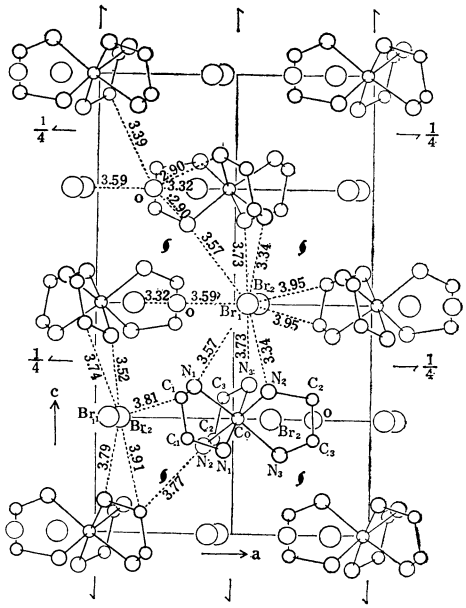


Fig. 4. Projection of the structure upon (1 0 0).

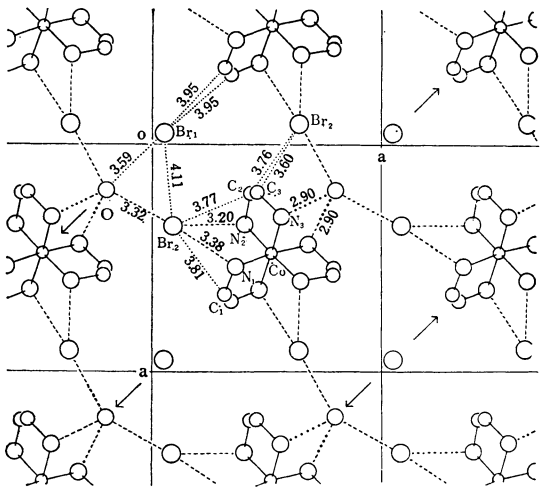


Fig. 5. Atomic arrangements within one layer around $Z=(1/4)C$. The broken lines show the linkages constructing the layer.

15) J. Berguis, I. M. Haanappel, M. Potters, B. O. Loopstra, C. H. MacGillabry and A. L. Veenendaal, *Acta Cryst.*, **8**, 478 (1955).

16) R. W. James, "The Optical Principles of the Diffraction of X-Rays", G. Bell & Sons, London (1948), Appendix.

cases of DL-[Co en]$Cl_3 \cdot 3H_2O$[1] and D- and L-2[Co en$_3$]$Cl_3 \cdot NaCl \cdot 6H_2O$[2], where the cobalt atoms lie on the three-fold symmetry axis because of the requirement of the space group. The ethylenediamine molecules take a nearly "gauche" form, and the six nitrogen atoms form a slightly distorted octahedron around the central cobalt atom. There are four possibilities of the configuration of the three cobalt-ethylenediamine rings. To employ the symbols used by Corey and Bailar[17], they are k k k, k′ k k, k k′ k′ and k′ k′ k′*. The relevant combination in the present case is k k k, designated the "lel" form, which is the most stable one according to Corey and Bailar, and which is the same as that existing in the crystals DL-[Co en$_3$]$Cl_3 \cdot 3H_2O$, D- and L-2[Co en$_3$]$Cl_3 \cdot NaCl \cdot 6H_2O$ and [Ni en$_3$]$(NO_3)_2$[18].

The complex ion, therefore, possesses the symmetry D_3-32 within the precision of the experiment. Bond lengths and bond angles within the complex ion are nearly in agreement with those previously found, as is shown in Table IV. The azimuthal angles between the planes determined by the C–C and C–N bonds are found to be 43 and 52° for the two independent ethylenediamine ligands.

TABLE IV. BOND LENGTHS AND BOND ANGLES WITHIN THE COMPLEX ION

Co–N_1	2.03 Å	$\angle N_1CoN_1$	87.3°
Co–N_2	1.98 Å	$\angle N_1CoN_2$	86.3°, 90.5°
Co–N_3	2.00 Å	$\angle N_1CoN_3$	90.4°
C_1–N_1	1.44 Å	$\angle N_2CoN_3$	87.5°, 93.4°
C_2–N_2	1.50 Å	$\angle N_3CoN_3$	93.8°
C_3–N_3	1.49 Å	$\angle N_1C_1C_1$	110.7°
C_1–C_1	1.54 Å	$\angle N_2C_2C_3$	102.0°
C_2–C_3	1.54 Å	$\angle N_3C_3C_2$	114.3°

The complex ions are located at about 0 0 0, 0 0 1/2, 1/2 1/2 1/4 and 1/2 1/2 3/4, and their three-fold axis is nearly in the *c*-direction. This aspect of the complex ions had also been suggested by the study of the dichroism of the crystals[19].

A complex ion is surrounded by 2Br_1, 2Br_2 and H_2O in close approach to the N atoms. Among them, the 2Br_1 lie above and below the complex ion in the *c*-direction and 3.34, 3.57 and 3.73 Å apart from the N_2, N_1 and N_3 atoms respectively. 2Br_2 and O are in the level of Co and form an isosceles triangle. The $Br_2 \cdots N$ distances are 3.20 and 3.38 Å, and the $N \cdots O$ distances are 2.90 Å, probably forming N–H···O type hydrogen bonds. The water molecule is located between the complex ion and the Br_1 lying on the same level. This scheme of the atomic arrangements within a layer can be most easily seen in Fig. 5, where the arrangement of the atoms in one layer around $Z=(1/4)c$ is illustrated. The role of the water molecules is probably to link the positive and negative ions to form a layer.

The layers are related to each other by the operation of the 4_3 axis, and also of the 2_1 axes at $Z=1/8$ or 3/8. No remarkably close contact between two layers, except that one between Br_1 and N_2 has been found.

II. Absolute Structure

"Absolute Structure" vs. "Absolute Configuration"

"Absolute configuration" is usually used to refer to the spatial arrangement of atoms or atomic groups around an asymmetric carbon atom without any ambiguity which otherwise exists between the two antipodes. The crystal which contains only one of the antipodes always lacks a center of symmetry, and if we could determine its crystal structure, including its handedness, we could consequently fix the "absolute configuration" of the antipode involved. On the other hand, there are many crystals which do not contain any optically active group, and yet the handednesses of which present some problems to be solved.

Thus, "absolute structure" means the unambiguous description of the atomic arrangement in a non-centrosymmetric crystal, while "absolute configuration" is to be used when the atomic arrangement within an optically active molecule, ion or atomic group is described in an absolute way. "Absolute structure" rather than "absolute configuration" would be the adequate term for α-quartz[20], sodium chlorate[21], etc. Takéuchi first used the term "absolute structure" in the study of ullmannite[22].

The Problem of Absolute Structure in the Present Case

Since the absolute configuration of D-tartaric acid was determined in 1951 by Bijvoet et al.[23] using the anomalous dispersion effect of X-rays, many attempts have been made to determine the absolute configuration of various com-

17) E. J. Corey and J. C. Bailar, Jr., *J. Am. Chem. Soc.*, **81**, 2620 (1959).
* In the Refs. 1 and 3, the symbols D_{ddd}, D_{dll}, D_{lld} and D_{lll} were used.
18) L. N. Swink and M. Atoji, *Acta Cryst.*, **13**, 639 (1960).
19) S. Yamada and R. Tsuchida, This Bulletin, **33**, 98 (1960).
20) A. de Vries, *Nature*, **181**, 1193 (1958).
21) G. N. Ramachandran and K. S. Chandrasekaran, *Acta Cryst.*, **10**, 671 (1957).
22) Y. Takéuchi, *Mineral. J.*, **2**, 90 (1957).
23) J. M. Bijvoet, A. F. Peerdeman and A. J. van Bommel, *Nature*, **168**, 271 (1951).

pounds in the similar way[24]. The absolute configuration of optically active complex ion D- or L-$[Co\,en_3]^{3+}$, was determined by Saito, Nakatsu, Shiro and Kuroya[4] from the observation of the Bijvoet inequality, and was examined more quantitatively, using the $P_s(u)$ function, by Saito, Okaya and Pepinsky[25] on the crystals D- and L-2$[Co\,en_3]Cl_3 \cdot NaCl_3 \cdot 6H_2O$.

The problem with the present crystal about the absolute structure or absolute configuration is that the crystal has an enantiomorphous pair of space groups which can not be distinguished by the conventional method; this can be done only by the anomalous dispersion technique. If we could substantiate the true space group and therefore, the absolute structure, we could consequently fix the absolute configuration of D- or L-$[Co\,en_3]^{3+}$.

The phase relation among the reflection pairs which are enantiomorphous with each other and whose intensities are to be compared when the anomalous dispersion takes place, is a rather complicated one, depending on the types of $(h\,k\,l)$ in the present space group. In short, it is possible to classify the types of reflections into two groups:

Group I $h\,k\,l$, $k\,h\,\bar{l}$, $\bar{k}\,h\,l$, $\bar{h}\,k\,\bar{l}$, $\bar{h}\,\bar{k}\,l$, $\bar{k}\,\bar{h}\,\bar{l}$, $k\,\bar{h}\,l$ and $h\,\bar{k}\,\bar{l}$

Group II $h\,k\,\bar{l}$, $k\,h\,l$, $\bar{k}\,h\,\bar{l}$, $\bar{h}\,k\,l$, $\bar{h}\,\bar{k}\,\bar{l}$, $\bar{k}\,\bar{h}\,l$, $k\,\bar{h}\,\bar{l}$ and $h\,\bar{k}\,l$

The structure factor for a reflection of a given index which belongs to Group I can find its complex conjugate or its permuted equivalents in the reflections listed in Group II. For example, if $\alpha(h\,k\,l)$ is the phase angle for $(h\,k\,l)$, then $\alpha(h\,k\,\bar{l}) = \alpha(k\,h\,l) = \pi - \alpha(h\,k\,l)$*, and $\alpha(k\,h\,\bar{l}) = \alpha(h\,k\,l)$. The intensities of all the reflections in groups I and II are mutually equal in the ordinary diffraction experiment. However, when comparing the intensities of pairs of reflections whose indices belong to groups I and II respectively, e.g., $(h\,k\,l)$ and $(h\,k\,\bar{l})$ the failure of Friedel's law due to the anomalous dispersion can be observed and, hence, the absolute structure deduceed. If the reflections considered belong to the same group, then the effect of the anomalous dispersion can not be observed.

Experimental Procedure and Result

Peterson[26] and others[21,27] were successful in measuring the effect of anomalous dispersion, even when the X-rays used are far from the absorption edge of any atom in the crystal. However, it is les difficult to observe the Bijvoet inequality if the radiation whose wavelength is close to the absorption edge is available; the photographic method can be used successfully in this case. Therefore, Cu K_α rays ($\lambda = 1.541$ Å) where used, because they can excite just the K-electrons of cobalt atoms ($\lambda_K = 1.608$ Å), and, in addition, a smaller effect

TABLE V. COMPARISON OF THE OBSERVED INEQUALITIES WITH CALCULATED VALUES

$h\ k\ l$	$\lvert F(hkl)\rvert^2$	$\lvert F(hk\bar{l})\rvert^2$	$\Delta\lvert F\rvert^2$ % *	Observed**
2 1 1	416	401	3.7	?
4 1 1	178	123	36.4	>
6 1 1	334	457	−31.1	<
8 1 1	159	171	− 7.3	<
10 1 1	207	221	35.8	>
3 2 1	65	88	−29.9	<
5 2 1	319	240	28.2	>
7 2 1	899	732	20.5	>
9 2 1	80	52	43.8	>
11 2 1	144	223	−42.6	<
4 3 1	398	311	34.5	>
6 3 1	44	88	−66.7	<
8 3 1	281	336	−17.9	<?
10 3 1	679	609	10.9	>
5 4 1	237	272	−13.7	<?
7 4 1	277	230	18.5	>
9 4 1	430	313	31.4	>
11 4 1	195	136	35.5	>
6 5 1	505	433	15.4	>?
8 5 1	326	394	−18.9	<?
10 5 1	312	300	3.9	?
7 6 1	225	337	−39.9	<
9 6 1	302	221	23.6	>
8 7 1	265	215	20.8	>

* $$\Delta|F|^2(\%) = \frac{|F(h\,k\,l)|^2 - |F(h\,k\,\bar{l})|^2}{\frac{1}{2}\{|F(h\,k\,l)|^2 + |F(h\,k\,\bar{l})|^2\}} \times 100$$

** The inequality sign > or < shows that the observed intensity for $(h\,k\,l)$ is larger or smaller than that for $(h\,k\,\bar{l})$. The sign >? or <? means that the inequality is not so definite as that without the symbol ?. The symbol ? shows that the inequality could not be observed.

24) I. Nitta (Editor), "X-Ray Crystallography" (in Japanese), Vol. II, Maruzen, Tokyo (1961), Chap. IV.

25) Y. Saito, Y. Okaya and R. Pepinsky, *Phys. Rev.*, **100**, 970 (1955); R. Pepinsky, J. M. Robertson and J. C. Speakman (Editors), "Computing Methods and Phase Problem in X-Ray Crystal Analysis", Pergamon Press, Oxford (1961), p. 288.

* In this respect the description in International Tables, Vol. I[10] is not correct. p. 427, 10th and 19th line; p. 430, 6th and 15th line: $-\alpha(h\,k\,l)$ should be $\pi - \alpha(h\,k\,\bar{l})$.

26) S. W. Peterson, *Nature*, **176**, 395 (1955).

27) A. W. Hanson and F. R. Ahmed, *Acta Cryst.*, **11**, 724 (1958); J. M. Bijvoet, ibid., **13**, 1100 (1960); G. Kartha, F. R. Ahmed and W. H. Barnes, ibid., **13**, 1038 (1960); A. F. Peerdeman, ibid., **9**, 824 (1956); S. Raman, *Z. Krist.*, **111**, 301 (1959).

due to the *L*-electrons of the bromine atoms ($\lambda_L = 8$Å) could be expected.

The intensities of $(h\,k\,l)$ and $(h\,k\,\bar{l})$ reflections were compared visually on oscillation photographs taken around the *c*-axis in order to observe the inequalities more conveniently. The specimen used was a small needle about 0.1 mm. in diameter elongated along the *c*-direction. Slight but discernible differences in intensities were found for many pairs of reflections. Large differences were found in some weak reflections. In Table V the observed inequalities are compared with the calculated values. In the calculation of the intensities, the following corrections for atomic scattering amplitude due to anomalous dispersion were used[28] in the form $f = f^0 + \Delta f' + i\Delta f''$, where f^0 is the atomic scattering amplitude for the X-rays far from the absorption edge and $\Delta f'$ and $\Delta f''$ are the corrections for the real and the imaginary parts of the scattering factor respectively:

Atom	$\Delta f'$	$\Delta f''$
Co	−2.2	3.9
Br	−0.9	1.5

The calculated values of the intensities are based on the set of coordinates given in Table II, the space group $P4_32_12$ being assumed. The right-handed coordinate system was used throughout the work.

As a more reliable observation of the effect of dispersion, photometric measurements of intensities for some particular reflections were made. Those reflections were selected which are of moderately low intensity in order to reduce the errors in measurements while reflections of low indices in order to reduce the errors of atomic positions. The results are shown in Table VI, where the observed intensities were measured with a micro-photometer.

The agreement between the observed and calculated inequalities seems to be satisfactory for the present study, and it can be stated with certainty that the atomic positions shown in Table II and Figs. 3 and 4 correspond to the absolute structure of D-[Co en$_3$]Br$_3$·H$_2$O. The absolute configuration of D-[Co en$_3$]$^{3+}$ deduced from the present study thus substantiates the configuration determined previously[4].

Table VI. Comparison of calculated and observed $|F|^2$

	Calculated		Observed	
	$\frac{\overbrace{\lvert F(h\,k\,l)\rvert^2}}{\lvert F(h\,k\,\bar{l})\rvert^2}$	$\overbrace{\Delta\lvert F\rvert^2}$ %	$\frac{\overbrace{\lvert F(h\,k\,l)\rvert^2}}{\lvert F(h\,k\,\bar{l})\rvert^2}$	$\overbrace{\Delta\lvert F\rvert^2}$ %*
(611)	0.731	−31.1	0.813	−20.7
(521)	1.33	28.2	1.22	19.6

* See legend of Table V.

Summary

The absolute crystal structure of D-[Co en$_3$]·Br$_3$·H$_2$O was determined by means of X-rays. The space group is $P4_32_12$-D_4^8, with four formula units in a cell of the dimensions a= 9.95 and c=16.73Å. The complex ion takes the "lel" form designated by Corey and Bailar and is in the same configuration as had been determined previously. The structure can be most easily described as consisting of layers of complex ions, two types of bromine ions and water molecules perpendicular to the *c*-axis. The water molecules link the positive and negative ions to form a layer.

A definition of "absolute structure" and "absolute configuration" was proposed. The absolute structure was determined by means of the X-ray absorption edge technique of Bijvoet. CuK_α rays were used to observe visually the effect of the anomalous dispersion between the reflections $(h\,k\,l)$ and $(h\,k\,\bar{l})$, and quantitative measurements of the effect were attempted for some reflections. The absolute configuration of the complex ion deduced from the absolute structure of the crystal is in agreement with the one previously determined for the crystals D- and L-2[Co en$_3$]Cl$_3$·NaCl·6H$_2$O.

The author wishes to express his sincere thanks to Professor Emeritus Isamu Nitta of Osaka University, Professor Tokunosuké Watanabé of Osaka University, Professor Hisao Kuroya of Osaka City University, Professor Yoshihiko Saito of The University of Tokyo and Professor Akira Shimada of Osaka City University for their encouragement and invaluable advice through out the work. Thanks are also due to Dr. Koji Toyoda of Kyoto University for the use of KDC-1 (electronic computer of Kyoto University) for the calculation of the interatomic distances. This research was partly aided by funds from the Scientific Research Fund of the Ministry of Education and the Nishina Memorial Foundation, to both of which the author's thanks are due.

Department of Chemistry
Faculty of Science
Osaka City University
Kita-ku, Osaka

28) C. H. Dauben and D. H. Templeton, *Acta Cryst.*, **8**, 841 (1955).

Reduction of Organic Compounds with Urushibara Catalysts under High Pressure. X[1]. *Hydrogenation of 2-Butyne-1,4-diol to cis-2-Butene-1,4-diol with Various Urushibara Catalysts*

By Shin-ichi TAIRA

(Received September 25, 1961)

In the previous paper[1] of this series, the catalytic reduction of some carbonyl compounds with various Urushibara catalysts was reported. Since the discovery of the Urushibara nickel catalyst[2], the preparation of the catalyst has been successively modified and some varieties of the nickel catalysts, U-Ni-B[1-5], U-Ni-BA[6,7], U-Ni-NH_3[8], U-Ni-CB[5], U-Ni-A[1,4,5,9,10], U-Ni-AA[11], U-Ni-CA[5] and U-Ni-A(HCl)[1], have been furnished. Besides these nickel catalysts, some Urushibara cobalt and copper catalysts, namely, U-Co-B[5,8,12,13], U-Co-CB[5], U-Co-A[5,13], U-Co-CA[5], U-Cu[5] and U-Cu-C[1,5], have been reported on. As each of them has its own characteristics and proper activity, one can choose a catalyst in accordance with the compound to be reduced.

In the present paper, the hydrogenation of 2-butyne-1,4-diol with some Urushibara catalysts is studied.

Experimental

Apparatus.—Hydrogenation was carried out in an electro-magnetically stirring-type autoclave with a capacity of 100 ml. (Sakashita SE-10).

2-Butyne-1,4-diol.—A commercially available crude sample was recrystallized from benzene, m.p. 58.5°C.

General Procedure for Hydrogenation.—The catalyst was carefully transferred with ethanol into the autoclave. The air in the autoclave was replaced by hydrogen gas four times. Most operations were carried out under the following conditions: (1) sample; 4.3 g. (0.05 mol.) (2) solvent; ethanol (99%) 50 ml. (3) agitation; 40~45 strokes per minute. Agitation was started when the temperature in the autoclave reached the reaction temperature. (4) pressure; Initial pressure was chosen to be above 50 kg./cm^2. Depression of the pressure was observed at intervals of five minutes.

Hydrogenation Products.—*cis-2-Butene-1,4-diol.*—After the hydrogenation was finished, the catalyst was filtered off and washed with ethanol. The major part of the solvent was distilled off from the combined solution, and the residual liquid was distilled under reduced pressure. *cis*-2-Butene-1,4-diol was obtained as a colorless oil, b.p. 125~126°C/12 mmHg. Yield, 70~75% of the theoretical. The dibenzoate crystallized into colorless prisms from ethanol, m.p. 67~68°C.

1,4-Butanediol.—After removal of the catalyst, the product was distilled to give 1,4-butanediol as a colorless oil, b.p. 131~132°C/25 mmHg. Yield, 73% of the theoretical. The dibenzoate crystallized into colorless prisms from ethanol, m.p. 82.5~83.5°C.

Preparation of Catalysts.—The U-Ni-A(s)*(HCl) was prepared by the method described in the reference cited[1]. Some new Urushibara catalysts were prepared by the methods described below. The U-Fe-BA was also prepared from ferric chloride and aluminum grains in the same way as the U-Ni-BA, but it was found to be inactive.

a) Urushibara Iron Prepared from Ferric Chloride, Abbreviated as U-Fe(III).—To a well mixed zinc dust (25 g.) and water (8 ml.) placed in a 50 ml. beaker, 9.68 g. (containing 2 g. of iron) of the crystal of commercially available ferric chloride ($FeCl_3 \cdot 6H_2O$) was added. The mixture was then well stirred with a glass rod. Soon a vigorous exothermic reaction started, but it subsided within about ten seconds. To complete the reaction the mixture was stirred until the color of the ferric ion disappeared. The reaction mixture (precipitated iron) was washed with 400 ml. of cold water, and then the washing was removed by filtration or decantation. The precipitated iron was digested in 330 g. of 15% acetic acid with occasional stirring at 60~70°C for about 20~25 min. At the end of the digestion, the generation of hydrogen gas subsided, and a solid, adsorbing hydrogen gas came up to the surface of the almost colorless solution. The solid was quickly collected on a glass filter and washed with 300 ml. of cold water and then

1) Part IX; S. Taira, This Bulletin, **34**, 1294 (1961).
2) Y. Urushibara, ibid., **25**, 280 (1952).
3) Y. Urushibara and S. Nishimura, ibid., **27**, 480 (1954).
4) Chem. Soc. Japan, ed., "Jikken Kagaku Kōza", Vol. 17, Part 2, Maruzen, Tokyo (1956), p. 311.
5) S. Taira, This Bulletin, **34**, 261 (1961).
6) K. Hata, S. Taira and I. Motoyama, ibid., **31**, 776 (1958).
7) I. Motoyama, ibid., **33**, 232 (1960).
8) S. Nishimura and A. Sugimori, *J. Chem. Soc. Japan, Pure Chem. Soc. (Nippon Kagaku Zasshi)*, **81**, 314 (1960).
9) Y. Urushibara, S. Nishimura and H. Uehara, This Bulletin, **28**, 446 (1955).
10) S. Taira, ibid., **34**, 1072 (1961).
11) K. Hata, K. Watanabe and H. Watanabe, ibid., **32**, 6 (1959).
12) S. Saito, *J. Pharm. Soc. Japan (Yakugaku Zasshi)*, **76**, 351 (1956).
13) Chem. Soc. Japan, ed., "Jikken Kagaku Kōza", Vol. 17, Part 2, Maruzen, Tokyo (1956), p. 334.

* In the present paper the notation (s) temporarily implies the catalysts obtained from the precipitated metals prepared by the simplified method[1].

with 100 ml. of ethanol. In this way a grayish black catalyst, contaminated with a small quantity of zinc, was obtained.

b) Urushibara Iron Prepared from Ferrous Chloride, Abbreviated as U-Fe(II).—To a mixture of zinc dust (20 g.) and water (6 ml.) placed in a 50 ml. beaker, the crystal of commercially available ferrous chloride ($FeCl_2 \cdot nH_2O$) containing 2 g. of iron* was added, and then the mixture was warmed on a boiling water bath and stirred with a glass rod for about 2 min. The reaction mixture (precipitated iron) was washed with 300 ml. of cold water, and then the washing was removed by filtration or decantation. The precipitated iron was treated with occasionl stirring in 300 g. of 15% acetic acid at 60~70°C for about 15~20 min. until the generation of hydrogen gas subsided and a solid came up to the surface of the almost colorless solution. The following operation was similar to that described in a). In this way a bulky brownish black catalyst, containing about 2 g. of iron and a considerable quantity of zinc, was obtained.

c) U-Fe(II)-Ni or U-Fe(III)-Ni.—To the mixture of zinc dust (20 or 25 g.) and water (6 or 8 ml.), 0.2 ml. of an aqueous nickel chloride solution (10 ml. of the solution contains 1 g. of nickel) was added, and then the crystal of ferrous or ferric chloride (containing 2 g. of iron) was added. The following procedure was the same as that described in a) or b).

d) U-Fe(II)-Co or U-Fe(III)-Co.—The procedures for the preparation were the same as those for the U-Fe-Ni, but 0.5 ml. of a cobalt chloride solution (10 ml. of the solution contains 1 g. of cobalt) was used.

e) Urushibara Cobalt A Obtained from the Precipitated Cobalt Prepared by a Simplified Method by Treatment with Hydrochloric Acid, Abbreviated as U-Co-A(s)(HCl).—To a mixture of zinc dust (5 g.) and water (1 ml.), 2.02 g. (containing 0.5 g. of cobalt) of the crystal of commercially available cobalt chloride was added, and then the mixture was well stirred with a glass rod. Soon a weak exothermic reaction occurred and the mixture became slushy after about 5 min. The reaction mixture (precipitated cobalt) was washed with 100 ml. of cold water, and then it was treated with 200 ml. of 0.75 N hydrochloric acid at an ordinary temperature. A vigorous reaction took place, and a black solid came up to the surface of the pink solution within one minute. The solid was quickly collected on a glass filter and washed with 200 ml. of cold water and then with 100 ml. of ethanol.

f) U-Co-B(s).—The precipitated cobalt prepared by the simplified method as described in e) was treated with 80 g. of a 10% aqueous sodium hydroxide solution as in the usual way[5,8,13].

In all procedures, purified water was used for washing except for the preparations of precipitated metals. The U-Ni-A(s)(HCl), U-Co-A(s)(HCl) and U-Co-B(s) were prepared thoroughly with city water. The solid should be protected from contact with air as far as possible after the treatment of the precipitated metals with acid or alkali.

* As the content of iron in commercially available ferrous chloride is usually indefinite, it should previously be determined by analysis.

Results and Discussion

The Urushibara Iron Catalysts.—The problem of the partial hydrogenation of acetylenic compounds to the corresponding ethylenic compounds has attracted many workers. For the partial catalytic hydrogenation of acetylenic compounds in the liquid phase, it it necessary to stop the hydrogenation when one mole of hydrogen has reacted. Palladium has been accepted as a catalyst whose selective action can be utilized for this partial hydrogenation. Campbell and O'Connor[14] reported that Raney nickel exhibits a similar selective property and used it as a catalyst in the preparation of numerous olefins from the corresponding acetylenes. However, both the palladium and the Raney nickel catalyst are unsatisfactory for the partial hydrogenation because they are excellent catalysts also for the hydrogenation of ethylenic bonds, and the hydrogenation must therefore be watched constantly and stopped at a proper moment so as to prevent the saturation of the ethylenic bonds. Therefore, the publication by paul and Hilly on Raney iron catalyst[15], which has been prepared much like Raney nickel but is unable to effect the hydrogenation of ethylenic linkage, is of considerable importance. It is, however, very troublesome to prepare the iron-aluminum alloy in a laboratory. The procedure of preparing such an iron catalyst would be very simple if the iron particles obtained by the Urushibara method had a similar catalytic activity.

As the difference between the standard electrode potentials of iron and zinc is smaller than the difference between those of nickel, cobalt or copper and zinc, a ferric or ferrous chloride solution can only with difficulty be reduced by zinc dust by the ordinary procedure for preparing precipitated metals. Ferric chloride, however, can react vigorously with zinc dust under conditions similar to that described in the preceding paper[1] as a simplified method for the preparation of precipitated nickel, The precipitated iron thus obtained gives a fine, grayish black solid after treatment with acetic acid. As ferrous chloride reacts gently with zinc dust under the same conditions, external heating is advisable to complete the reaction. The precipitated iron obtained from ferrous chloride gives a fine, brownish

14) K. N. Campbell and M. J. O'Connor, *J. Am. Chem. Soc.*, **61**, 2897 (1939).

15) P. Paul and G. Hilly, *Bull. soc. chim. France*, [5] **6**, 218 (1939); A. F. Thompson and S. B. Wyatt, *J. Am. Chem. Soc.*, **62**, 2555 (1940).

TABLE. HYDROGENATION OF 2-BUTYNE-1,4-DIOL

2-Butyne-1,4-diol (4.3 g., 0.05 mol.) was dissolved in 50 ml. of ethanol.

Exp. No.	Catalyst	Weight of catalyst, g.[a]	Initial Press. kg./cm²	Initial temp., °C	Reaction temp., °C	Time[b] min.	Hydrogenation Product
1	U-Fe(III)	2 (2.2)	51	23	23~105[c]	130	*cis*-2-Butene-1,4-diol
2	U-Fe(II)	2 (4.6)	72.5	21	100~105	130	*cis*-2-Butene-1,4-diol
3	U-Fe(III)-BA	2 (1.9)	50.5	28	105~118		None[d]
4[e]	U-Fe(III)	2 (0.65)	56	21	144~154	345	*cis*-2-Butene-1,4-diol
5	U-Fe(III)-Ni	2.02[f](1)	70	21	101~105	60	*cis*-2-Butene-1,4-diol
6	U-Fe(II)-Ni	2.02[f](5.3)	65	24	101~105	70	*cis*-2-Butene-1,4-diol
7	U-Fe(III)-Co	2.05[g](1.6)	78	29	100~103	45	*cis*-2-Butene-1,4-diol
8	U-Fe(II)-Co	2.05[g](5)	62.5	33	100~105	265	*cis*-2-Butene-1,4-diol
9	U-Ni-A(s)(HCl)	0.5 (0.4)	58	24	24~ 36[h]	10	1,4-Butane-diol
10	U-Co-A(s)(HCl)	0.5 (0.6)	60	28	33~ 41[h]	50	*cis*-2-Butene-1,4-diol
11	U-Co-B(s)	0.5 (3)	64	30	31~ 35[h]	70	*cis*-2-Butene-1,4-diol

a) The figures show the net weight of the catalyst metal, which was used as chloride at the beginning of the preparation of the catalyst. The figures shown in the parentheses are the gross weight of dried catalysts after use for hydrogenation.
b) The time required to finish the hydrogenation after hydrogen uptake begins.
c) Agitation was started at room temperature and hydrogen uptake began at about 80°C and the rate increased at about 100°C.
d) Hydrogenation did not get on.
e) 0.1 mol. of the sample in 50 ml. of ethanol was used, and hydrogen gas was charged four times in the course of the operation.
f) Fe 2 g. and Ni 0.02 g.
g) Fe 2 g. and Co 0.05 g.
h) The temperature rose spontaneously by the heat of reaction.

black solid after treatment with acetic acid. Both solids have proved to be active as catalysts. These new catalysts can be named Urushibara iron catalysts, or U-Fe(II) and U-Fe(III) when abbreviated. The figures in parentheses show the original valencies of iron in the chloride. Both U-Fe(II) and U-Fe(III) consist of iron and a quantity of zinc, but the former is somewhat bulkier and contains more zinc than the latter.

In place of zinc dust, aluminum grains are used as a reducing agent for nickel ion in the preparation of the U-Ni-BA[6] or the U-Ni-AA[11]. The diluted ferric chloride solution also reacted vigorously with aluminum grains to give a precipitated iron. However, Urushibara iron BA, similarly obtained by treatment of the precipitated iron with a sodium hydroxide solution, was found to have no catalytic activity.

Partial Hydrogenation of 2-Butyne-1,4-diol. —The partial hydrogenation of 2-butyne-1,4-diol to cis-2-butene-1,4-diol has already been studied by many workers with Raney nickel[16], palladium-calcium carbonate[17], iron[18] or partially poisoned copper, nickel, cobalt and platinum[19] catalysts.

The present author attempted the hydrogenation of 2-butyne-1,4-diol with some Urushibara catalysts and studied the activity of each catalyst. The results are listed in the table. The first experiment was carried out to determine the temperature at which hydrogen uptake begins with the Urushibara iron catalyst. The hydrogen uptake starts at about 80°C, and the rate increased at about 100°C (Exp. No. 1). Accordingly, the following experiments were carried out at about 100°C when the iron catalyst was applied. The result obtained with the U-Fe(II) was similar to that obtained with the U-Fe(III) (Exp. No. 2). No appreciable hydrogen uptake was observed with the U-Fe(III)-BA under similar conditions (Exp. No. 3).

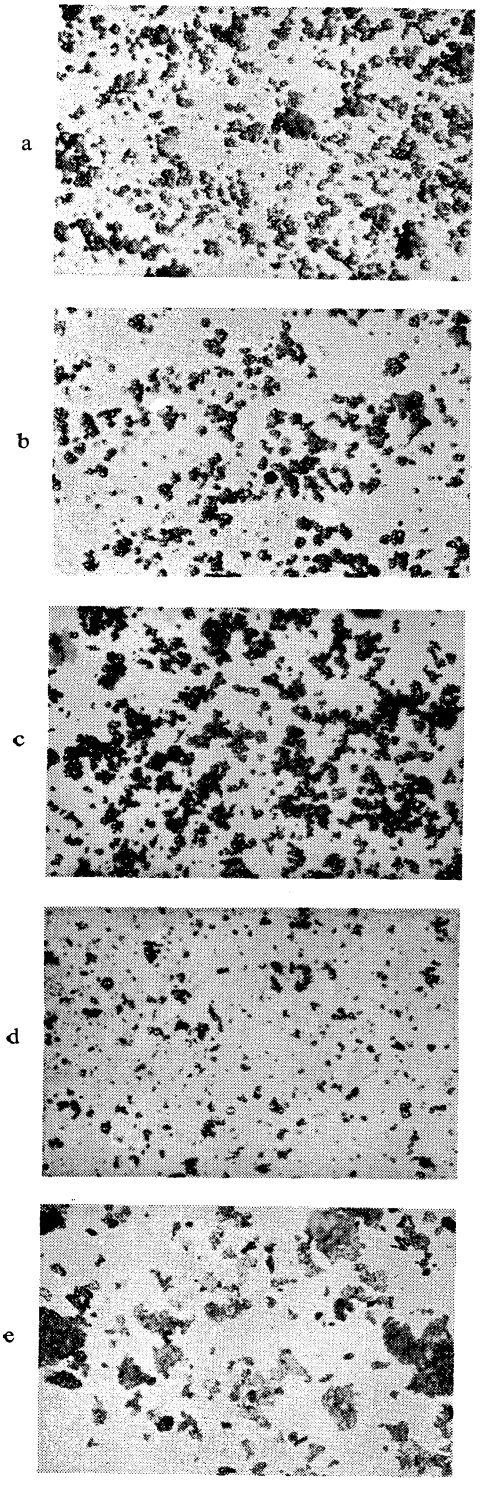
It has been recognized that the increase of the concentration of the substance to be reduced in a solution or the elevation of the reaction temperature exerts a favorable effect on the reduction rate of benzophenone[5].

16) A. Valette, *Ann. chim.*, [12] 3, 667 (1948); C. Prévost and A. Valette, *Compt rend.*, **222**, 327 (1946); N. Lozac'h, *Bull. soc. chim. France*, **1949**, 287; W. Reppe et al., *Ann.*, **596**, 44 (1955); J. Yasumura, *J. Chem. Soc. Japan, Pure Chem. Sec.* (*Nippon Kagaku Zasshi*), **82**, 218 (1961).

17) A. W. Johnson, *J. Chem. Soc.*, **1946**, 1014; T. Fukuda and T. Kusama, This Bulletin, **31**, 339 (1958).

18) Basf. D. B. P. 873, 545 (1941); *Chem. Zentr.* **1953**, 7401; W. Reppe et al., *Ann.*, **596**, 43, 60 (1955).

19) I. G. Farbenind., German Pat. 734312 (1938); German Pat. *Org. Chem.*, **6**, 548; General Aniline and Film Corp. U. S. Pat. 2300598 (1939), *Chem. Abstr.*, **37**, 2018 (1943).



Micro-photographs of Precipitated Irons and Urushibara Iron Catalysts (×75)
(a) Precipitated iron prepared from ferrous chloride. (b) Precipitated iron prepared from ferric chloride (c) U-Fe(II) (d) U-Fe(III) (e) U-Fe(III)-BA

Accordingly, the hydrogenation of 2-butyne-1,4-diol was attempted in a concentrated solution at a higher temperature, but the results were unsatisactory (Exp. No. 4), probably because of an insufficiency of catalyst.

As seen from the table, the gross weight of the U-Fe(II) is much more than that of the U-Fe(III), though they are prepared so as to contain the same quantity of iron and are nearly equal in apparent bulk. The U-Fe(II) probably contains more zinc than the U-Fe(III). The micro-photographs of both iron catalysts show that the grains of zinc dust contaminated in them are covered with iron and that many spherical iron-zinc couples coagulate to form a block. The above-mentioned difference between the state of the U-Fe(II) and U-Fe(III) may be supposed to be due to the difference between the nature of the two precipitated irons, because they are treated with acetic acid under nearly identical conditions to give each U-Fe catalyst. Probably the state of iron may differ in the two precipitated irons. The precipitated iron from ferric chloride is found to be more easily eroded by acetic acid during the digestion. Therefore, quick collection of the U-Fe(III) is necessary after the completion of digestion to prepare the catalyst containing a sufficient quantity of iron.

The author found that a U-Ni-A obtained from zinc dust and the precipitated nickel prepared from a nickel chloride solution, contaminated with a little ferric chloride, is more active than the usual U-Ni-A in the reduction of acetophenone. The iron is considered to act as a promoter. It is similarly expected that the addition of a little nickel to the iron may have a favorable effect on the activity of the iron catalyst in the hydrogenation. Actually, such catalysts, U-Fe(II)-Ni and U-Fe(III)-Ni (Fe 1 : Ni 0.01), were proved to have higher activities than the U-Fe(II) or U-Fe(III) (Exp. Nos. 5 and 6). The activity of the iron catalyst may also be increased by the addition of cobalt. As a cobalt catalyst is generally less active than a nickel catalyst in the catalytic reduction, especially in the hydrogenation of carbon-carbon double bonds, the ratio of cobalt to iron in the catalyst may safely be increased in the hydrogenation of carbon-carbon triple bonds. A good result was obtained with the U-Fe(III)-Co (Fe 1 : Co 0.025) (Exp. No. 7). In contrast with the U-Fe(III)-Co, the U-Fe(II)-Co was strikingly low in activity (Exp. No. 8). The cause of this low activity is obscure except for the wrong dispersability of the U-Fe(II) into a solution by the up and down agitation employed in those experiments.

It has been reported in the preceding paper[1] that the U-Ni-A(s) is somewhat lower in activity than the U-Ni-A prepared by the usual method, and that hydrochloric acid can be used for the digestion of the precipitated nickel to give a less active catalyst, U-Ni-A(HCl). Accordingly it is expected that U-Ni-A(s)(HCl) may be much less active than the usual U-Ni-A, and that the partial hydrogenation of the acetylenic bond to the ethylenic bond may safely be attained with the catalyst. However, the catalyst was unexpectedly still so active that butynediol was rapidly hydrogenated to butanediol (Exp. No. 9). It is not yet hopeless with a cobalt catalyst, and the U-Co-A(s)(HCl) and U-Co-B(s) served the purpose, though the hydrogenation should have been checked at the point where the hydrogen uptake became very slow after the absorption of almost stoichiometric hydrogen gas (Exp. Nos. 10 and 11). In these experiments, hydrogen uptake was not obsered for five to fifteen minutes after stirring was started at room temperature. The reaction started when the temperature in the autoclave exceeded about 31°C, and the temperature then went on rising owing to the heat of the reaction. As the room temperature was near 31°C, it was not clear whether the first time lag was due to an induction period or to an inadequate temperature for starting the reaction.

Summary

The Urushibara iron catalysts were newly developed. Partial hydrogenation of 2-butyne-1,4-diol to cis-2-butene-1,4-diol was successfully attained with the iron catalysts, and some modified Urushibara cobalt catalysts were also found to be applicable.

The author wishes to express his thanks to Professor Kazuo Hata for his continuous encouragement throughout this work.

Department of Chemistry
Faculty of Science
Tokyo Metropolitan University
Setagaya-ku, Tokyo

Studies of the Urushibara Catalysts. I. Some Structural Features Revealed by X-Ray Diffraction

By Shin-ichi TAIRA

(Received September 25, 1961)

Since the discovery of the Urushibara nickel catalyst[1], some modifications in the preparation of the catalyst have been successively performed; thereby several varieties of the catalyst, such as U-Ni-B[2-5], U-Ni-BA[6,7], U-Ni-NH_3[8], U-Ni-CB[4], U-Ni-A[3-5,9,10], U-Ni-AA[11] U-Ni-CA[4] and U-Ni-A(HCl)[5], have been developed. The Urushibara cobalt, copper and iron catalysts, namely, U-Co-B[4,8,12-14], U-Co-CB[4], U-Co-A[4,13], U-Co-A(HCl)[14], U-Cu[4], U-Cu-C[4,5], U-Fe(II)[14] and U-Fe(III)[14], have also been reported on. With these catalysts, various kinds of organic compounds have successfully been reduced, as with the corresponding Raney catalysts.

In the present paper, a brief study of the crystal structures of the Urushibara nickel and iron catalysts by means of X-ray diffraction is presented.

Experimental

Samples.—Newly prepared catalysts or those recovered after use and then stored were used.

X-Ray Diffraction.—The crystal structures of the catalysts were examined by the X-ray powder diffrac-

1) Y. Urushibara, This Bulletin, **25**, 280 (1952).
2) Y. Urushibara and S. Nishimura, ibid., **27**, 480 (1954).
3) Chem. Soc. Japan, ed., "Jikken Kagaku Kōza", Vol. 17, Part 2, Maruzen, Tokyo (1956), p. 311.
4) S. Taira, This Bulletin, **34**, 261 (1961).
5) S. Taira, ibid., **34**, 1294 (1961).
6) K. Hata, S. Taira and I. Motoyama, ibid., **31**, 776 (1958).
7) I. Motoyama, ibid., **33**, 232 (1960).
8) S. Nishimura and A. Sugimori, *J. Chem. Soc. Japan, Pure Chem. Sec.* (*Nippon Kagaku Zasshi*), **81**, 314 (1960).
9) Y. Urushibara, S. Nishimura and H. Uehara, This Bulletin, **28**, 446 (1955).
10) S. Taira, ibid., **34**, 1072 (1961).
11) K. Hata, K. Watanabe and H. Watanabe, ibid., **32**, 6 (1959).
12) S. Saito, *J. Pharm. Soc. Japan* (*Yakugaku Zasshi*), **76**, 351 (1956).
13) Chem. Soc. Japan, ed., "Jikken Kagaku Kōza", Vol. 17, Part 2, Maruzen, Tokyo (1956), p. 334.
14) S. Taira, This Bulletin, **35**, 840 (1962).

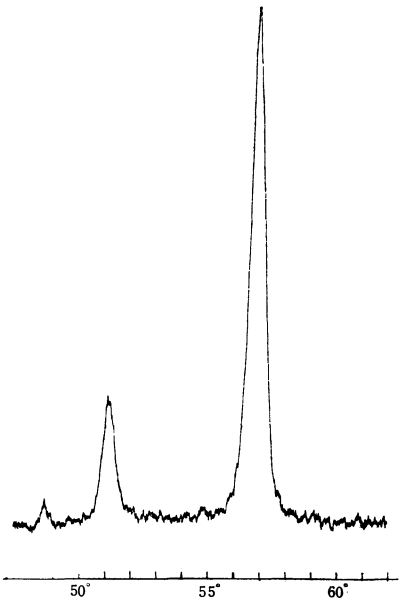


Fig. 1-a

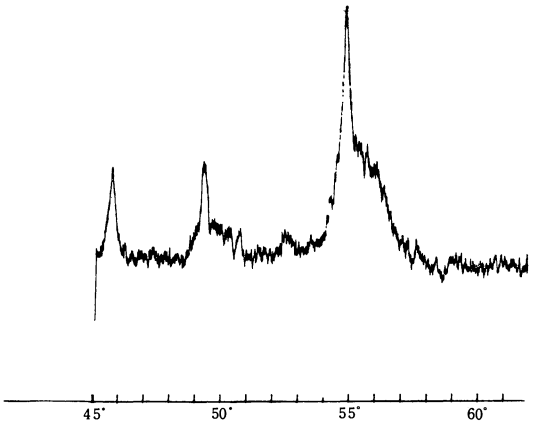


Fig. 1-b

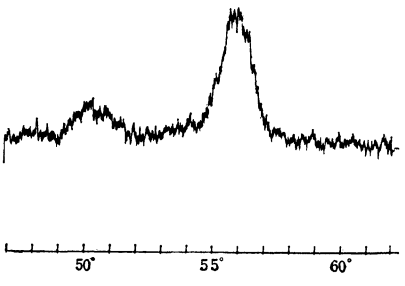


Fig. 1-c

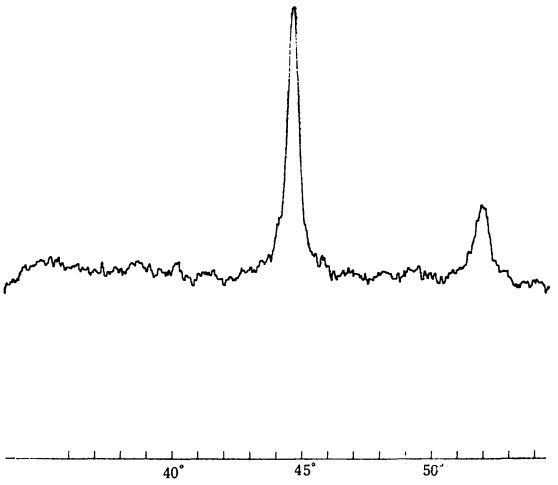


Fig. 1-d

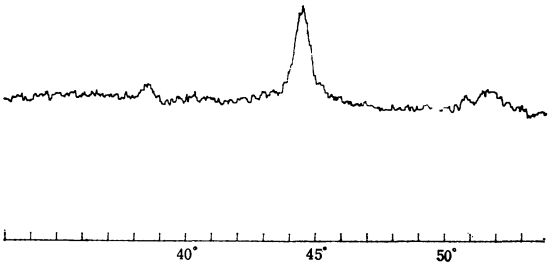


Fig. 1-e

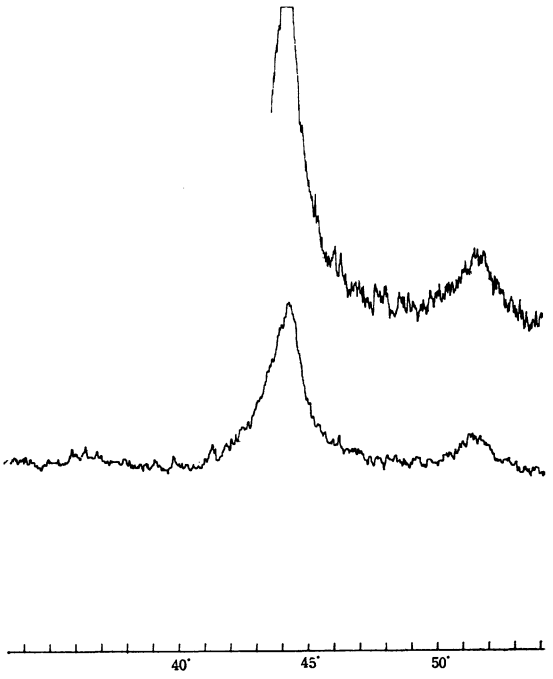


Fig. 1-f

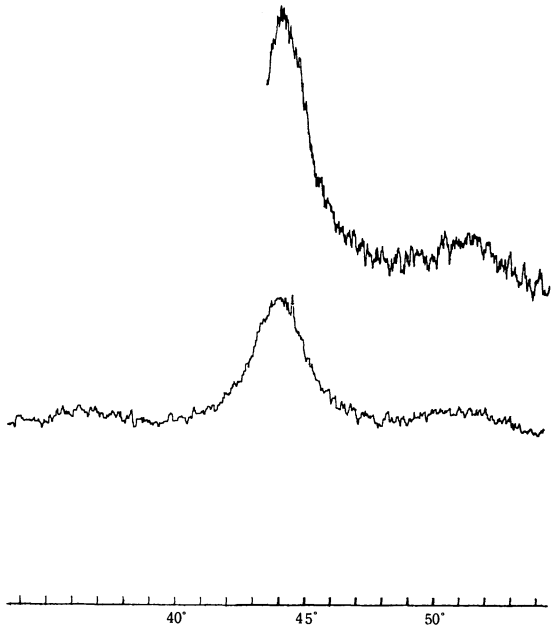


Fig. 1-g

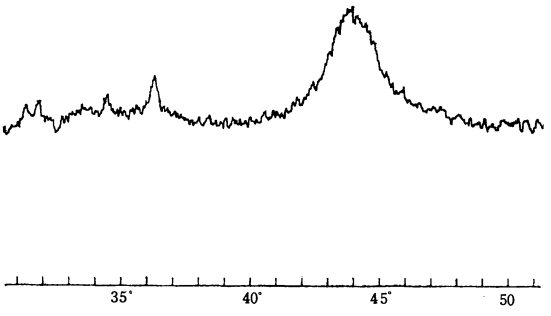


Fig. 1-h

Fig. 1. X-Ray diffraction diagrams of Urushibara nickels and Urushibara irons.
a. U-Fe(III)-BA b. U-Fe(II) c. U-Fe(III)
d. U-Ni-BA e. U-Ni-AA f. U-Ni-A
g. U-Ni-A h. U-Ni-A prepared from nickel acetate.

tion method. Cu-K_α radiation was used for the Urushibara nickel catalysts, and Fe-$K_{\alpha,\beta}$ radiation, for the Urushibara iron catalysts. The diffraction diagrams were obtained by means of a recording X-ray diffractometer.

Results and Discussion

The preparation of the Urushibara catalyst can be divided into two steps, the preparation of precipitated metal and the digestion of it with acid or alkali. Supposing that the relation of the precipitated metal to the Urushibara catalyst is similar to that of the Raney alloy to the Raney catalyst, the method of preparation of the Urushibara catalyst has some resemblance to that of the Raney catalyst. However, the precipitated metal is essentially different from the Raney alloy. For example, the precipitated nickel is obtained by the reduction of the nickel ion with zinc dust, and it is a mixture of zinc grains covered with precipitated nickel metal and some zinc compounds. The treatment of the precipitated nickel with acid removes the zinc compounds and the major part of the zinc grains to give the Urushibara nickel A. The Urushibara method is one way to prepare fine particles of a metal, and the obtained metal particles may be different from the Raney catalyst in nature. It is possible that the particles could be merely fine particles of the metal and have no catalytic activity. In fact, however, these particles of metals obtained by the Urushibara method have been proved to be as active as the Raney catalysts. Accordingly, the particles must have special crystal structures.

In the catalytic hydrogenation of 2-butyne-1,4-diol to 2-butene-1,4-diol with an Urushibara iron catalyst[14], the author has observed that the U-Fe(II) or U-Fe(III) which is prepared from ferrous or ferric chloride and zinc dust has catalytic activity, while the U-Fe(III)-BA, prepared from ferric chloride and aluminum grains in nearly the same manner as that used to prepare the U-Ni-BA, has not.

The reason why the U-Fe(II) and U-Fe(III) have catalytic activities and the U-Fe(III)-BA has not, may be supposed to be due to the difference in their crystal structures. Their X-ray diffraction diagrams are shown in Fig. 1-a, b and c. The diffraction diagram of the U-Fe(III)-BA (Fig. 1-a) shows a good agreement with that of a sample considered to be pure α-iron and the position of the peak shifts only slightly (0.3°) in diffraction angle (2θ: 51.1° and 56.8°, the former is Fe-K_β reflection) from that corresponding to the reflection from the (110) plane in the regular configuration of α-iron (cf. Table I; All peaks in Fig. 1-b and c also show the same shift). In contrast with the diagram of the U-Fe(III)-BA, the U-Fe(II), which is recovered after the hydrogenation of 2-butyne-1,4-diol[14] and which contains much zinc, gives the sharp peaks of zinc in the diffraction diagram (2θ: 45.8°, 49.4° and 54.9°) in addition to the diffused peaks of iron (2θ: about 50° and 55.3°) (Fig. 1-b, cf. Table I). The U-Fe(III), which is also recovered after use, gives the same diffused peaks of iron, but the peaks of zinc can not be observed, probably indicating that the sample contains, if any, but a trace of zinc (Fig. 1-c). Why does the

inactive U-Fe(III)-BA give a regular diffraction diagram of α-iron while the active U-Fe(II) and U-Fe(III) do not ? Further investigation of this problem will give a clue to clarify the substantial feature of the activity of the Urushibara catalysts.

Urushibara et al.[15] have studied the Urushibara nickel catalysts in detail. As the X-ray diffraction of the Urushibara nickels gave only a diffused peak reflected from the plane regarded as (111) of nickel, which has a face-centered cubic structure, they concluded that the development of the crystal lattices in the Urushibara nickels is insufficient and thus that the nickel exists not in a state of crystals, but in a state of crystallites (Table II). The fact was also revealed by electron diffraction[16].

Table I. X-Ray data for nickel (face-centered cubic structure), α-iron (body-centered cubic structure) and zinc (hexagonal closest packed structure)

	$(h\,k\,l)$	Interplanar spacing d Å	Diffraction angle* 2θ (°)	Intensity
Ni	(111)	2.03	44.58(Cu)	1.00
	(200)	1.76	51.9 (Cu)	0.50
	(220)	1.244	76.50(Cu)	0.32
	(311)	1.061	88.05(Cu)	0.32
α-Fe	(110)	2.0268	57.10(Fe)	1.00
	(200)	1.4332	85.0 (Fe)	0.19
	(211)	1.1702	111.7 (Fe)	0.30
Zn	(101)	2.094	43.3 (Cu) 55.2 (Fe)	1.00
	(002)	2.473	36.3 (Cu) 46.1 (Fe)	0.53
	(100)	2.308	39.1 (Cu) 49.7 (Fe)	0.40

* The figures are the values of 2θ derived from the interplanar spacing of each plane by using the value of Cu-K_α or Fe-K_α.

The size of the crystallites can be calculated by means of a modified Scherrer's formula:

$$D_{hkl}=\frac{0.9\,\lambda}{\beta_{1/2}\cos\theta}$$

where D_{hkl} is the mean thickness of the crystallites in the perpendicular direction to the $(h\,k\,l)$ plane (Å) (This value is usually called the size of the crystallites.), λ, the wave length of the applied X-ray (Å), and $\beta_{1/2}$, the half value breadth (rad.). The calculation of the size of the crystallites in the Urushibara nickels prepared under various conditions led the cited authors to the following conclusions[15]: (1) The more vigorously the reaction of nickel chloride solution with zinc dust takes place, the smaller the size of the crystallites becomes. That is, crystallites increase in size in the following order; conc. $NiCl_{2\,aq.sol.}$+Zn dust, 100°C< conc. $NiCl_{2\,aq.sol.}$+Zn dust, room temp.<dil. $NiCl_{2\,aq.sol.}$+Zn dust, 100°C<dil. $NiCl_{2\,aq.sol.}$+Zn dust, room temp. (2) The activity of the nickel catalyst declines as the size of the crystallites increases. Supposing that the crystallites are cubic and that the activity of

Table II. X-Ray diffraction data of U-Ni catalysts (quoted from the report by Urushibara et al.[15])

Sample	Solvent	Concentration of nickel chloride	Temperature of the exchange reaction with zinc dust °C	Reagent for digestion	Temperature of digestion °C	Size of D_{111} Å	Position of peak for (111) plane 2θ (°)
U-Ni-B	H_2O	2 g./10 ml.	100	20% $NaOH_{aq}$	80	41	43.9
U-Ni-B	H_2O	2 g./10 ml.	Room temp.	20% $NaOH_{aq}$	80	48	44.1
U-Ni-B	H_2O	2 g./100 ml.	100	20% $NaOH_{aq}$	80	52	44.0
U-Ni-B	H_2O	2 g./100 ml.	Room temp.	20% $NaOH_{aq}$	80	59	44.1
U-Ni-B	H_2O	2 g./100 ml.	100	20% $NaOH_{aq}$	Room temp.	41	44.0
U-Ni-A	H_2O	2 g./10 ml.	100	10% $AcOH_{aq}$	Room temp.	37	43.8
U-Ni-A	H_2O	2 g./10 ml.	100	10% $AcOH_{aq}$ then 30% $AcOH_{aq}$	Room temp.	44	43.9
U-Ni-A	H_2O	2 g./10 ml.	100	20% $AcOH_{aq}$	55	49.5	44.0
U-Ni-B	C_2H_5OH	2 g./10 ml.	80	20% $NaOH_{aq}$	80	38	43.85
U-Ni-B	C_2H_5OH	2 g./100 ml.	80	20% $NaOH_{aq}$	80	46	44.0
U-Ni-B	C_2H_5OH	2 g./100 ml.	Room temp.	20% $NaOH_{aq}$	80	61	44.3
U-Ni-A	Ethylene glycol	2 g./10 ml.	160	12.5% $AcOH_{aq}$	Room temp.	41	44.0
U-Ni-B	Ethylene glycol	2 g./10 ml.	120	20% $NaOH_{aq}$	80	43	43.9
U-Ni-B	Ethylene glycol	2 g./10 ml.	Room temp.	20% $NaOH_{aq}$	80	42	43.9

15) Y. Urushibara, M. Kobayashi, S. Nishimura and H. Uehara, *Shokubai*, **12**, 107, 160 (1956).

16) Y. Urushibara, S. Yamaguchi and M. Kobayashi, This Bulletin, **29**, 815 (1956).

TABLE III. X-RAY DIFFRACTION DATA OF U-Ni-A

No.[a]	Sample	Concentration of nickel ion[b]	Temperature of the exchange reaction with zinc dust °C	Reagent for digestion	$\beta_{1/2}$(°)	Position of peak 2θ(°)	Size of the crystallites Å[c]
31[d]	U-Ni-A	1 g./14 ml.	100	13% $AcOH_{aq}$	1.5	44.4	57.4
32[d]	U-Ni-A	1 g./14 ml.	100	13% $AcOH_{aq}$	1.6	44.4	53.9
33[d]	U-Ni-A(HCl)	1 g./14 ml.	100	0.75 N HCl	2.0	44.0	43.1
34-a	U-Ni-A	1 g./14 ml.	100	13% $AcOH_{aq}$	2.4	43.8	35.5
34-b	U-Ni-A	1 g./14 ml.	100	13% $AcOH_{aq}$	2.2	43.8	38.7
34-c	U-Ni-A(HCl)	1 g./14 ml.	100	0.75 N HCl	2.4	43.6	35.5
35-a	U-Ni-A	1 g./14 ml.	100	13% $AcOH_{aq}$	2.1	43.9	40.8
35-b	U-Ni-A	1 g./14 ml.	100	13% $AcOH_{aq}$	2.1	43.9	40.8
35-c	U-Ni-A(HCl)	1 g./14 ml.	100	1.5 N HCl	1.7	43.9	50.4
36	U-Ni-A	1 g./14 ml.	100	13% $AcOH_{aq}$	2.0	43.9	42.8
37-a	U-Ni-A	1 g./14 ml.	100	13% $AcOH_{aq}$	2.1	43.7	40.7
37-b	U-Ni-A	1 g./14 ml.	100	20% $AcOH_{aq}$	2.2	43.7	38.9
38	U-Ni-A	1 g./14 ml.	100	20% $AcOH_{aq}$	2.1	43.6	40.6
39	U-Ni-A	1 g./14 ml.	100	20% $AcOH_{aq}$	2.1	43.6	40.6
310	U-Ni-A	1 g./14 ml.	100	20% $AcOH_{aq}$	2.3	44.0	37.2

a) The samples 34-a, b and c are the different catalysts prepared from the same precipitated nickel. The 35-a, b, c and 37-a, b are the similar groups respectively.
b) 1 g. of the nickel ion is supplied by 4.04 g. of nickel chloride ($NiCl_2 \cdot 6H_2O$).
c) The figures were calculated by the modified Scherrer's formula.
d) The sample was prepared about 4 years ago.

TABLE IV. X-RAY DIFFRACTION DATA OF SOME SPECIAL U-Ni-A

No.	Sample	Concentration of nickel ion[a]	Temperature of the exchange reaction with zinc dust °C	Reagent for digestion	$\beta_{1/2}$(°)	Position of peak 2θ(°)	Size of the crystallites Å[b]
41	U-Ni-A(s)	1 g./6 ml.	Room temp. about 60	13% $AcOH_{aq}$	2.2	44.0	39.0
42	U-Ni-A(s)(HCl)	1 g./6 ml.	Room temp. about 60	1 N HCl	2.0	43.8	42.6
43	U-Ni-A(s)	1 g./6 ml.	Room temp. about 60	20% $AcOH_{aq}$	2.3	44.1	37.2
44	U-Ni-A(s)	1 g./6 ml.	Room temp. about 60	20% $AcOH_{aq}$	2.1	44.1	40.8
45	U-Ni-A(s)	1 g./6 ml.	Room temp. about 60	20% $AcOH_{aq}$	2.2	44.0	39.0
46	U-Ni-A(s)	1 g./6 ml.	Room temp. about 60	20% $AcOH_{aq}$	2.3	44.0	37.2
47	U-Ni-A[c]	1 g./31 ml.	100	13% $AcOH_{aq}$	2.2	43.9	38.9
48	U-Ni-A[c]	1 g./31 ml.	100	13% $AcOH_{aq}$	1.8	43.3	47.4
49	U-Ni-A[c]	1 g./31 ml.	100	13% $AcOH_{aq}$	2.0	43.4	42.6
410	U-Ni-A[c]	1 g./31 ml.	100	13% $AcOH_{aq}$	2.0	44.0	43.1
411	U-Ni-A[c]	1 g./31 ml.	100	13% $AcOH_{aq}$	2.0	43.9	42.8
412	U-Ni-CA	1 g./14 ml.	Room temp.	10% $AcOH_{aq}$	1.9	43.7	45.0
413	U-Ni-CA	1 g./14 ml.	Room temp.	10% $AcOH_{aq}$	2.1	43.9	40.8
414	U-Ni-CA	1 g./14 ml.	Room temp.	13% $AcOH_{aq}$	2.0	43.8	42.6
415	U-Ni-CA	1 g./14 ml.	Room temp.	13% $AcOH_{aq}$	2.0	44.0	43.1

a) 1 g. of the nickel ion is supplied by 4.04 g. of nickel chloride ($NiCl_2 \cdot 6H_2O$) or by 4.24 g. of nickel acetate $(CH_3COO)_2Ni \cdot 4H_2O$.
b) The figures were calculated by the modified Scherrer's formula.
c) In place of nickel chloride, nickel acetate was used to prepare the precipitated nickel (sample nos. 47-411).

TABLE V. X-RAY DIFFRACTION DATA OF U-Ni-BA AND U-Ni-AA

No.	Sample	Concentration of nickel ion[a]	Temperature of the exchange reaction with aluminum grains °C	Reagent for digestion	$\beta_{1/2}$(°)	Position of peaks, 2θ(°) (111), (200)	Size of D_{111}, Å[b]
51	U-Ni-BA	1 g./15 ml.	50~70	20% $NaOH_{aq}$	0.6	44.6, 51.9	143.6
52	U-Ni-BA	1 g./15 ml.	50~70	20% $NaOH_{aq}$	0.6	44.6, 52.0	143.6
53	U-Ni-BA	1 g./15 ml.	50~70	20% $NaOH_{aq}$	0.8	44.5, 51.8	107.8
54	U-Ni-BA	1 g./15 ml.	50~70	20% $NaOH_{aq}$	0.5	44.6, 51.9	172.3
55	U-Ni-BA	1 g./15 ml.	50~70	20% $NaOH_{aq}$	0.9	44.5, 51.8	95.7
56	U-Ni-BA	1 g./15 ml.	Room temp.	20% $NaOH_{aq}$	0.7	44.59, 51.9	123.1
57	U-Ni-AA	1 g./15 ml.	50~70	40% $AcOH_{aq}$ and $NaCl_{aq}$.	0.7	44.4, 51.7	123.2

a) 1 g. of the nickel ion is supplied by 4.04 g. of nickel chloride ($NiCl_2 \cdot 6H_2O$).
b) The figures were calculated by the modified Scherrer's formula.

the nickel catalyst is proportional to the total surface area of the crystallites, the following relation may be deduced, as the total surface area of the nickel catalyst of a definite weight may be roughly said to be in inverse proportion to the size of the crystallites:

Activity of catalyst × Size of crystallites = const. This relation was certified by their experiments. (3) The size of the crystallites was not affected by the temperature of digestion and by the kind of digesting reagent.

The results of X-ray diffraction of the various Urushibara nickels obtained by the present author are tabulated in Tables III, IV and V. The size of the crystallites of the U-Ni-A(s)* shown in Table. IV, Nos. 41—46, are generally smaller than that of the U-Ni-A shown in Table III. If the activity of a nickel catalyst is mainly decided by the size of the crystallites, as has been pointed out by the cited authors, the U-Ni-A(s) should be more active than the U-Ni-A. In fact, the U-Ni-A(s) was proved to be somewhat inferior in activity to the U-Ni-A[5]. In the case of catalytic reduction under high pressure, the apparent activity of a catalyst may be considerably affected by the following factors: (1) The presence and amount of the texture necessary for metal particles to be active as a catalyst; (2) Weight of a catalyst; (3) Apparent size of the catalyst grains; (4) Dispersability of a catalyst into a solution (This factor may be decided by the size of the grains of a catalyst and the presence of contaminating substances. It must be noted that the Urushibara nickels B are contaminated by a large quantity of zinc and zinc compounds); (5) Reaction temperature; (6) Pressure of hydrogen gas; (7) Kind and volume of solvent; (8) Method and degree of agitation; and (9) Nature and purity of the sample to be reduced. A proper selection of experimental conditions may control factors 5 to 9. With the Urushibara catalysts, factors 1 to 4 vary with the method of preparation. The weight of the U-Ni-A(s), prepared to contain a definite quantity of nickel, is usually somewhat smaller than that of the U-Ni-A. Supposing that factors 3 and 4 are similar in them, the inferiority of the U-Ni-A(s) to the U-Ni-A in activity may mainly be ascribed to factor 1. Certainly factor 1 plays an important rôle in the actual activity of the catalyst.

The U-Ni-BA, prepared from a nickel chloride solution and aluminum grains, gives two sharp peaks in the X-ray diffraction diagram corresponding to the reflection from the (111) and (200) planes of nickel, and the position of the peaks lies at the regular angle position for nickel (Fig. 1-d, cf. Table. I). On the other hand, the Urushibara nickel A, prepared from either nickel chlorid or nickel acetate soultion and zinc dust, gives only a diffused peak, and the position accepted as a peak shifts from the regular position to a lower angle (Fig. 1-f, g and h) (In Fig. 1-h some peaks of zinc and zinc oxide are also observed). Occasionally, another diffused peak is observed (Fig. 1-f).

In Scherrer's formula, the calculated values of D_{hkl} are greatly affected by small differences in the value of $\beta_{1/2}$, but not so seriously by those in the values of θ. Samples Nos. 34-a, b and c (Table. III) are the Urushibara nickel catalysts prepared from the same precipitated nickel by separate treatment with the same or different acids. Samples Nos. 35-a, b, c and Nos. 37-a, b form respective groups of the same kind. In each group small differences in the value of $\beta_{1/2}$ cause a difference of several Å in the value for D_{hkl}. However, the values of 2θ are nearly equal in each group. The author has paid attention to the 2θ values.

Many workers have pointed out that in an

* The notation(s) implies temporarily the catalyst obtained from the precipitated metal prepared by the simplified method[5].

actual crystal small blocks (crystallites) of 10~0.1μ in sizes are disorderly accumulated into a so-called "mozaic structure". The smallness of the crystallites and the disorder of accumulation cause an enlargement in the breadth of the X-ray diffraction peaks. In the crystallites having a regular lattice arrangement, however, an enlargement in the breadth of the diffraction peaks takes place at the positions of definite angles determined by the interplanar spacing of the substance, and a large shift of the diffraction angle does not take place. Thus, it is conceivable that the (111) and (200) planes of nickel are indeed present in the U-Ni-BA, but there is much less probability of them in the Urushibara nickel A and B. Why is such a curious phenomenon observed only in the Urushibara nickel A and B? To clarify this problem, the process of preparing the precipitated nickel must be taken into account. The situation is considered to be similar to that of the formation of an evaporated film. From studies of evaporated films by means of electron diffraction, the phenomenon of oriented overgrowth or epitaxy has been brought to light[17]. A definite relation exists between the orientation of the crystallites of the deposit and that of the substrate crystals. The crystal structure of the crystallites in a evaporated film is generally in accordance with the structure of the crystal in the macro state. However, some exceptions have been found. Schulz[18] observed that the oriented overgrowth of crystallites occured in the evaporated films of those substances, which usually crystallize in the cesium chloride structure when, they were evaporated on lithium fluoride, sodium chloride, potassium bromide or mica, and that in such evaporated films there were many substances not with the original structure of the cesium chloride type but with the structure of the sodium chloride type. In the case of the formation of the precipitated nickel from a nickel salt solution and zinc dust, such a epitaxy may be possible to happen. Nickel, having a face-centered cubic structure (abbreviated as f. c. c. structure) in the normal state, is known to be possible to have a hexagonal closest packed structure (abbreviated as h. c. p. structure), as the difference in the energies of the two packings may not be so large. Thus, nickel can crystallize into a h.c.p. structure on the surface of zinc which normally has a h. c. p. structure. On this basis, it is presumed that such a epitaxy happens in the preparation of the precipitated nickel, and that the nickel precipitated on the surface of zinc may crystallize in a h. c. p. structure because it may grow larger on the embryo crystallites to some extent. The state in which nickel has a complete h. c. p. structure is temporarily named the ideal h. c. p. state. In this ideal h.c.p. state, the X-ray diffraction diagrams of Urushibara nickel A and B should be composed of sharp peaks and the position of peaks should be located in the diffraction angle very close to those of zinc (cf. Table I). Besides, in this state the crystals of nickel should come to contain many lattice defects, such as vacancies and dislocations, because the lattice constant of nickel is forced to be unusual. This hypothesis is quite successfully applied to interpreting the diffraction diagrams of the Urushibara nickel A and B.

In the actual Urushibara nickel A and B, the diffraction peaks are diffuse, and the position of the peak, which is divided into many small peaks, shifts to an angle higher than the ideal position. This may be caused by the small size of the crystallites and by the deformation of the structure of the crystallites from the ideal h. c. p. structure. If the extent of the shift of a peak from the position for the ideal h. c. p. structure is proportional to the degree of the deformation from the ideal h. c. p. structure to the proper f. c. c. structure, the amount of lattice defects will be in inverse proportion to the extent of the shift in the diffraction angle. The lattice defects may offer proper seats and spaces in which a foreign atom or molecule (for example, H or H_2) may be so loosely locked that it can move freely to some extent. As such places may be active centers of a catalyst, the more the lattice defects and present in the crystallites, the more active the crystal will become as a catalyst.

The author draws the following conclusions from the above considerations:

(1) In the Urushibara nickel A and B, nickel may have a h. c. p. structure which has been somewhat deformed to the f. c. c. structure. On the contrary, in the Urushibara nickel BA, nickel has a normal f. c. c. structure as a whole, for it is prepared from nickel chloride solution and aluminum, which has the f. c. c. structure. Thus, the Urushibara nickel BA is regarded as a catalyst of quite a different type from the Urushibara nickel A and B. Accordingly, it is naturally accepted that the shape of the diffraction diagram and the activity of the Urushibara nickel BA are quite different from those of the Urushibara nickel A and B.

(2) If a nickel catalyst, prepared by any method, gives a diffraction diagram similar to those of the Urushibara nickels, it will possess a similar catalytic activity when other factors are disregarded.

17) D. W. Pashley, *Advances in Physics*, 5, 173 (1956).
18) L. G. Schulz, *Acta Cryst.*, 4, 487 (1951).

(3) In the Urushibara nickel A and B, the higher the catalyst in activity, the smaller the extent of the shift of a peak in the diffraction angle from the ideal position of the peak for the h. c. p. structure of nickel. Thus, the reason why the U-Ni-A(s) is somewhat inferior in activity to the usual U-Ni-A may naturally be understood by comparing the 2θ values of the former with those of the latter. The same relation can be observed between the U-Ni-A (s) and the U-Ni-CA or the U-Ni-A prepared from nickel acetate solution and zinc dust.

(4) If each catalyst has the same crystal structure, the activity of a catalyst will be affected by the size of the crystallites.

The above considerations may also be successfully applied to solving the problems which lie in the Urushibara iron catalysts. Iron exists in the following two allotropic crystal modifications: at the lower temperature, iron crystallizes as α-Fe in a body-centered cubic structure (abbreviated as b. c. c. structure).

$$\underset{\text{(b.c.c.)}}{\alpha\text{-Fe}} \overset{910^\circ\text{C}}{\rightleftarrows} \underset{\text{(f.c.c.)}}{\gamma\text{-Fe}} \overset{1400^\circ\text{C}}{\rightleftarrows} \underset{\text{(b.c.c.)}}{\delta(\alpha)\text{-Fe}}$$

As aluminum has a f. c. c. structure and as there is an intimate relation between the lattice planes in the b. c. c. and the f. c. c. structure*, iron in the U-Fe(III)-BA must crystallize into a b. c. c. structure. This is the reason why the diffraction diagram of the U-Fe(III)-BA coincides with that of the α-Fe.

Iron in the ideal h.c.p. state must be greatly strained as the stable b. c. c. structure at low temperature is forced into the h. c. p. structure. Then it will get catalytic activity. In the actual U-Fe(II) and U-Fe(III), the crystal lattices of iron may be in the relation of coherency to those of zinc, and then there may be many lattice defects in them. Therefore, the reason why the U-Fe(II) and U-Fe(III) have catalytic activity and the U-Fe(III)-BA has not may be ascribed to the difference in their crystal structures.

Naturally the crystal structure of the metal in a Urushibara catalyst is affected to some extent by the temperature and the concentration of the solution to be applied in the preparation of a precipitated metal. The author esteems the effect of concentration as more important than that of temperature. That is, the decreased concentration of a metal ion in a solution may exert the favorable effect upon the crystal structure necessary for the metal to have catalytic activity, in consideration of the values in the Tables II, III and IV. However, further study is required in this area. As it has been widely recognized that special sections in the crystal of a metal are preferentially attacked by an acid, a digesting reagent for the precipitated metals may exert some secondary action on the Urushibara catalyst. The solution of the subject also belongs to the studies of the future.

* $\{110\}_{\text{b.c.c.}} \longleftrightarrow \{100\}_{\text{f.c.c.}}$. A similar relation has been observed in the epitaxial growth of the CsCl type (b. c. c.) into the NaCl type(f. c. c.)[18].

Summary

Some structural features in the Urushibara catalysts were revealed by means of X-ray diffraction, and a hypothesis regarding the activity of the Urushibara catalysts was proposed.

The author wishes to express his thanks to Professor Kazuo Hata for his continuous encouragement throughout this work.

Department of Chemistry
Faculty of Science
Tokyo Metropolitan University
Setagaya-ku, Tokyo

SHORT COMMUNICATION

Mechanism of the Ninhydrin Reaction on a Filter Paper

By Naotomo TOMINAGA*

(Received March 12, 1962)

It is known that color shades of reaction products of amino acids with ninhydrin on a paperchromatogram are different from one amino acid to another and also from one solvent to another used for development in a paperchromatography[1,2]. However, Ruhemann's purple (I, diketohydrindylidene diketohydrindamine) is known as the final product on the

* Present address: Faculty of Literature and Science, Kagoshima University, Kamoike-cho, Kagoshima.

1) R. Consden et al., *Biochem. J.*, **38**, 224 (1944).
2) C. E. Dent, ibid., **43**, 169 (1948).

ninhydrin reaction of usual α-amino acid in aqueous solution[3]. These facts indicates that side reactions must occur on a paper besides a main reaction which gives I.

In a previous publication[4], it was reported that various by-products on the reaction of 11 α-amino acids with ninhydrin on a paper were separated from I by a paperchromatography using methanol-water (1 : 1, v/v). Therefore, different color shades of products on the reaction of various amino acids with ninhydrin on paper seem to be resulted from differences of quality and quantity of the by-products.

In the present communication, a blue pigment derived from phenylalanine by the side reaction is described. The pigment was easily separated by paperchromatography and extracted from the paper with methanol. The extract showed the maximum absorption at 608~610 mμ and decomposed and faded by heating with an excess of ninhydrin. By the addition of acetic acid or diluted hydrochloric acid into methanolic solution of the pigment, it turned to violet color showing its absorption spectrum not identical with that of I, but regained its original blue color by further addition of pyridine or ammonia.

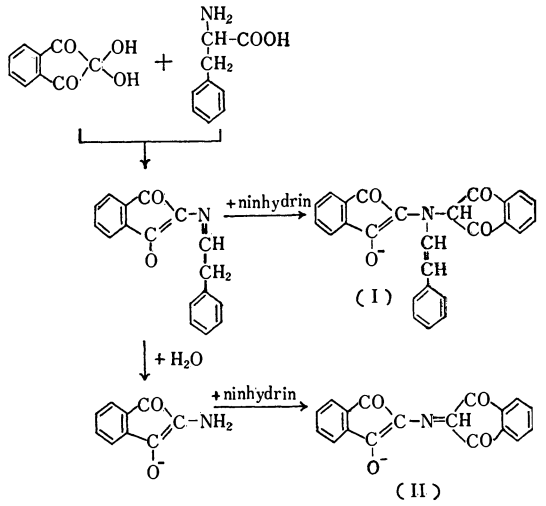
In an aqueous solution, no blue pigment was produced from phenylalanine by the ninhydrin reaction in spite of the presence of a piece of filter paper or air-bubbling into the solution.

When phenylalanine was heated with ninhydrin in absolute ethanol, black-green crystals, methanolic solution of which showed the same absorption spectrum and R_f value as those of the above blue pigment, were obtained. Namely a suspension of 1 g. of L-phenylalanine and 4 g. of ninhydrin in 50 ml. of absolute ethanol was heated at 60~70°C until carbon dioxide was no longer evolved. After the solution was cooled, the black-green crystals were filtered off (480 mg.) and washed with 50% methanol. They were recrystallized form benzene. M. p. (decomp.) 227~232°C. Found: C, 76.91; H, 3.81; N, 2.75. Calcd. for $C_{26}H_{17}O_4N$ (II) : C, 76.65; H, 4.17; N, 3.43%.

When uniformly labeled ^{14}C-phenylalanine was used, 71% of the expected radioactivity was found in the blue pigment II. Consequently II must contain major parts of the skeleton of phenylalanine.

Comparing the infrared spectrum of I with that of II, both substances showed the absorption at 1670 cm^{-1}(carbonyl), 1640 and 1592cm^{-1}(benzene nucleus), and 1443 cm^{-1} (〉C=C〈$_{O-}$) but 1477 cm^{-1}(-N=C〈) was observed only in I. Characteristic absorption for II were at 1522, 1397 and 986 cm^{-1}(-CH=CH-), and 1351 and 1296 cm^{-1}(〉N-CH〈).

Therefore the reaction of ninhydrin with phenylalanine on a paper seems to proceed through the following two routes.



The present reaction mechanism of phenylalanine on a paper may be extended to those of other amino acids.

Institute for Protein Research
Osaka University
Osaka

3) D. J. McCaldin, *Chem. Revs.*, **60**, 39 (1960).
4) N. Tominaga, *Seikagaku*, **33**, 829 (1961).

*Synthesis of Trisubstituted Triptycenes and the Optical Resolution of 7-Carboxy-2, 5-diacetoxytriptycene**

By Akio SONODA, Fumio OGURA and Masazumi NAKAGAWA

(Received October 23, 1961)

Triptycene is a novel type of cage compound which was synthesized by Bartlett and his coworkers[1] by the elaboration of the Diels-Alder type addition product of *p*-benzoquinone with anthracene. The three benzene rings in the molecule are tightly connected at their *o*-positions by the two sp^3-hybridized carbon atoms holding the aromatic rings in the fixed spatial positions. The rigid structure of the molecule has been demonstrated by the inert reactivity for various displacement reactions of the substituent group or atom attached to the central tetrahedral carbon atom[2].

Triptycene derivatives bearing different substituent groups in two of the three benzene rings should be capable of existing in the optically isomeric forms shown in Fig. 1.

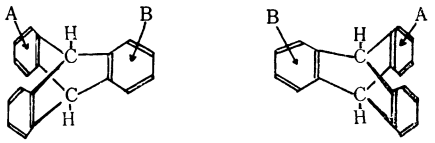
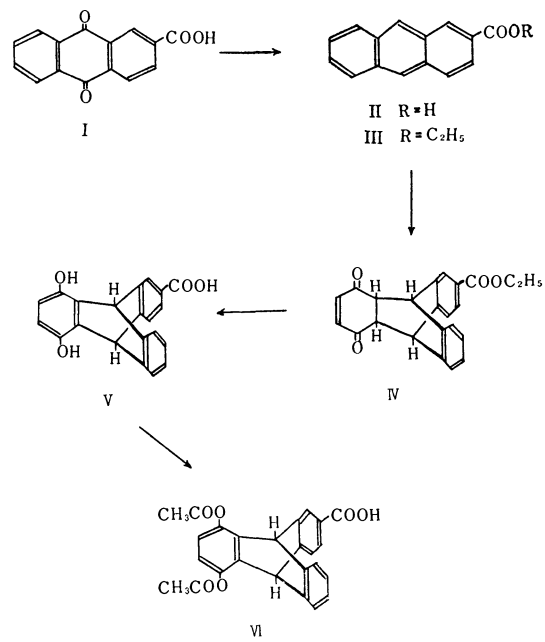


Fig. 1. Optical isomers of substituted triptycene.

Optical active triptycene derivatives may offer best means for studying the dependence of optical activity or rotatory dispersion on the nature of the substituent groups, since the rigid and fixed geometry of the molecule should exclude the influence of the complicated effects arising from the flexibility of the molecule. For the purpose of studying the above-mentioned relationships, the present authors have investigated the synthesis and optical resolution of trisubstituted triptycenes.

2-Methylanthraquinone was prepared according to the well-known procedure starting from toluene and phthalic anhydride[3]. The quinone was oxidized to 2-carboxyanthraquinone (I) by chromium trioxide in acetic acid[4]. This



substance was submitted to the reduction by means of zinc dust in aqueous ammonia[5] to give 2-carboxyanthracene (II). The attempts to condense II with *p*-benzoquinone in various solvents such as ethanol, acetic acid and dioxane gave unsatisfactory results. II was converted into the corresponding ethyl ester III. The ester III was treated with an excess of *p*-benzoquinone in benzene to yield the adduct IV. The structure of IV was inferred from the comparison of the infrared spectrum of IV with that of the adduct of anthracene and *p*-benzoquinone[6]. The adduct was found to be sensitive to a strong alkali and the hydrolysis of IV with aqueous sodium hydroxide to the corresponding free acid resulted in the formation of a resinous material.

Treatment of IV in acetic acid with a small amount of hydrobromic acid yielded 8-carboxy-2, 5-dihydroxytriptycene (V). V was found to be difficult to purify owing to its unstable nature to oxygen. Therefore, the crude V was

* Optically Active Triptycenes. I.

1) P. D. Bartlett, M. J. Ryan and S. G. Cohen, *J. Am. Chem. Soc.*, **62**, 2649 (1942).

2) P. D. Bartlett, S. G. Cohen, J. D. Cotman, Jr. and N. Kornblum, ibid., **72**, 1003 (1950); P. D. Bartlett and E. S. Lusis, ibid., **72**, 1005 (1950); P. D. Bartlett and F. G. Greene, ibid., **76**, 1088 (1954).

3) L. F. Fieser, "Organic Syntheses", Coll. Vol. I (1948), pp. 517, 353.

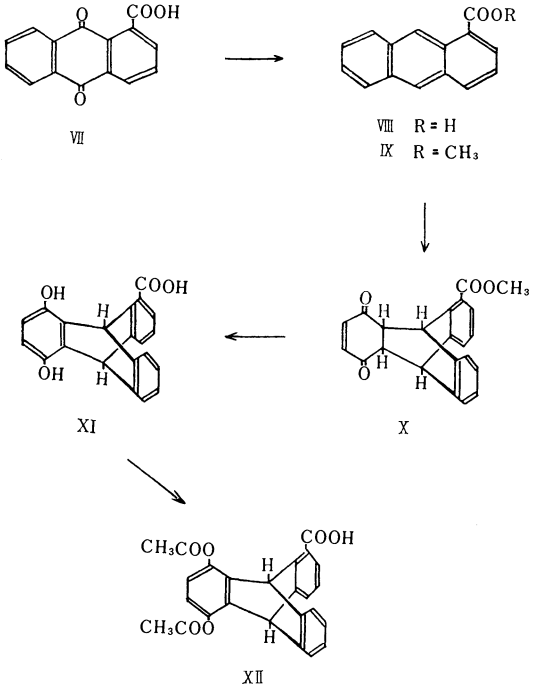
4) C. Liebermann and G. Glock, *Ber.*, **17**, 888 (1884).

5) E. Bornstein, ibid., **26**, 2609 (1883).

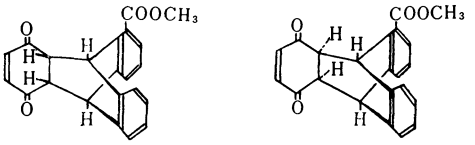
6) Cf., P. D. Bartlett and F. D. Greene, *J. Am. Chem. Soc.*, **76**, 1088 (1954).

converted into the diacetyl derivative VI by treatment with acetic anhydride in the presence of anhydrous sodium acetate. The structure of VI was confirmed by the analytical data and the infrared spectroscopy.

Several unsuccessful attempts were made to resolve the *dl*-VI in its antipodes by using different kind of optical active amines such as quinine, brucine, ephedrine and cinchonine. It was found that the racemic acid VI gives no crystalline salts with these alkaloids. The failure in the optical resolution of VI urged the authors to the synthesis of the isomeric substituted triptycene. 1-Carboxyanthracene (VIII) was derived from 1, 9-benz-10-anthrone by chromic acid oxidation in dilute sulfuric acid[7] followed by the reduction of resulted 1-carboxyanthraquinone (VII) with zinc dust in aqueous ammonia[8]. The reaction of 1-carboxyanthracene (VIII) with *p*-benzoquinone under



various conditions in different solvents resulted in the formation of a polymeric substance with high melting point or in the recovery of the starting materials. Treatment of VIII with absolute methanol in the presence of concentrated sulfuric acid yielded methyl ester IX in good yield. It is to be noted that the esterification of VIII with absolute ethanol under the same condition resulted in the recovery of the acid VIII. Two isomeric adducts X_a (m. p. 190.5°C) and X_b (m. p. 206°C) were obtained from the products of the condensation of *p*-benzoquinone with IX. The infrared spectra of these isomers were found to be almost identical over the entire region of wavelength, but a remarkable depression of the mixed melting point (175°C) was observed. It seems to be reasonable to attribute the formation of the two isomers to the *endo*- and the *exo*- addition of *p*-benzoquinone with regard to the benzene ring bearing methoxycarbonyl group yielding X_a and X_b as illustrated in Fig. 2.



X_a or X_b X_b or X_a

Fig. 2. Possible structures of the isomeric adducts, X_a and X_b.

Both of the isomers gave 7-carboxy-2, 5-dihydroxytriptycene (XI) on treatment with a small amount of hydrobromic acid in acetic acid. XI was converted without further purification into the corresponding diacetyl derivative XII by the reaction with acetic anhydride and anhydrous sodium acetate.

7-Carboxy-2, 5-diacetoxytriptycene (XII) was dissolved in hot absolute ethanol and mixed with half the equivalent of brucine tetrahydrate. Well defined colorless needles were obtained on standing the mixture overnight at room temperature. The crystals were recrystallized five times from absolute ethanol to give an optically pure *d*-salt. The salt was decomposed with acetic acid to give pure *d*-acid, m. p. 269~271°C, $[\alpha]_{5461}^{13} = +96.3°$ (*c* 0.7042, dioxane).

The filtrate was concentrated and treated with acetic acid to remove brucine. The crude *l*-acid thus obtained was converted into the quinine salt. Recrystallization of the salt from 95% ethanol gave the pure quinine salt. The optically pure *l*-acid, $[\alpha]_{5461}^{24} = -93.1°$ (*c* 1.0272, dioxane) was obtained by the decomposition of the pure quinine salt. The infrared spectra of the *d*- and *l*-acid are found to be identical over the entire region of wavelength as recorded in Fig. 3.

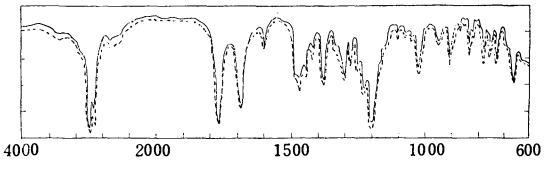


Fig. 3. The infrared spectra of *d*-XII (—) and *l*-XII (- - -) (Nujol mull).

7) E. B. Barnett, J. W. Cook and H. H. Grainger, *Ber.*, **57**, 1775 (1924).
8) C. Graebe and S. Blumenfeld, ibid., **30**, 1115 (1897).

TABLE I. ADDITION OF *p*-BENZOQUINONE TO 2-ETHOXYCARBONYLANTHRACENE (III)

Run	III g.	Quinone g.	Molar ratio III : quinone	Solvent (ml.)	Time hr.	Yield of IV g.	Yield of IV %
1	2.1	1.4	1 : 1.6	Xylene (35)	5	—	Resin
2	2.0	1.1	1 : 1.2	Benzene (20)	10	0.3	10.5
3	4.0	2.5	1 : 2.5	Toluene (15)	15	0.4	7.0
4	1.8	1.1	1 : 1.3	Ligroin (50) + Benzene (10)	15	0.6	23.5
5	5.0	3.1	1 : 1.2	Ligroin (300)	12	—	Recovery
6	4.0	2.1	1 : 1.2	Benzene (20)	31	—	Resin
7	5.0	5.0	1 : 2.3	Benzene (20)	5	2.6	36.6
8	5.9	3.26	1 : 1.3	Benzene (20)	4	2.6	32

The ultraviolet spectrum and the rotatory dispersion of XII will be discussed together with its homologous series in the following paper.

Experimental**

2-Carboxyanthraquinone (I).—Chromium trioxide (60 g.) was added gradually in small portions with constant mechanical stirring to the solution of 2-methylanthraquinone (20 g.) in acetic acid (500 ml.) at 70°C. After all chromium trioxide had been added, the mixture was stirred at 70~80°C for further 5 hr. The reaction mixture changed to dark brown and then the separation of a crystalline precipitate was observed. The reaction mixture was cooled to room temperature and poured into water (3 l.) yielding the crude I. The product was digested repeatedly with a hot diluted aqueous ammonia. Pure 2-carboxyanthraquinone (I), 19.9 g. (88%), m. p. 283~284°C (value in literature, m. p. 284~285°C[4]) was obtained by neutralizing the ammoniacal solution with concentrated hydrochloric acid.

2-Carboxyanthracene (II).—The solution of II (19 g.) in a dilute aqueous ammonia (1 l.) was heated on a boiling water bath, zinc dust (50 g.) was added in small portions to the hot solution under vigorous mechanical stirring. A small amount of 28% aqueous ammonia was added occasionally to the reaction mixture. Development of a blood red color was observed on the addition of zinc dust and faded in accord with the progress of reduction. After 3 to 5 hr., the hot reaction mixture was filtered and the filtrate was acidified with concentrated hydrochloric acid to precipitate the crude II, m. p. 273°C. This was recrystallized from ethanol to yield pure II, 10 g. (60%), m. p. 277~278°C, (value in literature, 275~276°C[5]).

2-Ethoxycarbonylanthracene (III).—The mixture of II (6 g.), 99% ethanol (500 ml.) and concentrated sulfuric acid (6 ml.) was refluxed for 5 hr. Light yellow crystals, 5.4 g., m. p. 139.5~140°C were obtained on standing the reaction mixture at room temperature. The concentration of the filtrate gave the second crop of III, 1.1 g., m. p. 138~139°C. Total yield, 6.5 g. (95%) (value in literature, m. p. 134°C[9]).

Formation of the Adduct (IV).—The results of several experiments on the addition of *p*-benzoquinone to III are summarized in Table I. All the reactions were carried out at the temperature of the boiling point of the particular solvent. The formation of quinhydrone was generally observed throughout these experimental conditions. The experimental condition shown in Run 7 gave the best yield of the adduct. The reaction mixture was cooled to room temperature precipitating yellow crystal mixed with black crystals of quinhydrone. The crystals were filtered, washed with benzene, ethanol and hot water, successively. The crude crystals were digested with light petroleum under reflux to remove the unchaneged III. The yellow powder obtained (2.6 g. (36.5%), m. p. 187.5~188°C) was recrystallized from ethanol to give pure IV, m. p. 188~189°C.

Found: C, 76.71; H, 5.20. Calcd. for $C_{23}H_{18}O_4$: C, 77.08; H, 5.06%.

IR, 1619, 1661 (C=O); 1710 (C=O of ester); 1278 (-C-O-) and 1175 cm^{-1} (-C-O-).

Isomerization and Hydrolysis of IV to V.—IV (3.3 g.) was dissolved in acetic acid (30 ml.) under reflux. Hydrobromic acid (47%, 15 ml.) was added dropwise to the solution and the mixture was refluxed for 5 hr. The reaction mixture was poured into ice-water (350 g.) to precipitate crude V. The precipitate was filtered and washed with water yielding crude V, 2.1 g. (68%), m. p. 210~214°C (decomp.).

Acetylation of V.—The crude V (2.1 g.) was heated on a boiling water bath for 4 hr. with acetic anhydride (40 ml.) in the presence of a small amount of anhydrous sodium acetate. Water (10 ml.) was

** All melting points were not corrected.

9) C. Liebermann and A. Bischof, ibid., 13, 47 (1880).

added to the reaction mixture. After heating for several minutes the mixture was poured into water (400 ml.). The precipitate formed was recrystallized twice from acetic acid yielding pure 8-carboxy-2,5-diacetoxytriptycene (VI), 1.9 g. (49.5% from IV), m. p. 235~237°C.

Found: C, 72.06; H, 4.43. Calcd. for $C_{25}H_{18}O_6$: C, 72.46; H, 4.38%.

IR, 3200~2500 (-COOH); 1690 (C=O of aromatic acid); 1766 (C=O of phenolic acetate) and 1187 cm^{-1} (-C-O- of phenolic acetate).

1-Carboxyanthraquinone (VII).—1, 9-Benz-10-anthrone was oxidized according to the Bernett's procedure with slight modification. M. p. 286~289°C, yield, 68%.

1-Carboxyanthracene (VIII).—Reduction of VII (22 g.) with zinc dust (40 g.) and diluted aqueous ammonia (50 ml. of 28% aqueous ammonia + 600 ml. of water) with occasional addition of 28% aqueous ammonia (60 ml.) in small portions yielded VIII, 11.8 g. (60%), m. p. 235~243°C. Recrystallization of the crude VIII from ethanol gave pure VIII, yellow rods, m. p. 242~244°C (value in literature, m. p. 245°C[8]).

1-Methoxycarbonylanthracene (IX).—The mixture of the crude VIII (5.2 g., m. p. 235~243°C), absolute methanol (150 ml.) and concentrated sulfuric acid (5 ml.) was refluxed for 3 hr. The mixture was kept for several hours at room temperature precipitating IX as yellow plates. The precipitate was filtered and the filtrate was concentrated under reduced pressure yielding second crop of IX. The total yield of the crude IX (m. p. 101~103°C) was found to be 4.2 g. (77%). This was recrystallized from methanol to give pure IX, m. p. 103.5~104°C.

Found: C, 81.40; H, 5.40. Calcd. for $C_{16}H_{12}O_2$: C, 81.34; H, 5.12%.

Formation of the Adduct (X).—IX (17.7 g., 0.075 mol.) and *p*-benzoquinone (8.9 g., 0.083 mol.) was added to anhydrous benzene (100 ml.). Immediate development of red color was observed. The mixture was refluxed for 3 hr. and cooled to room temperature. Yellow crystals deposited were separated, washed with a small amount of benzene and hot water successively, yielding the crude low melting isomer (X_a), 7.8 g. (32.1%), m. p. 181~183°C. This was recrystallized from benzene to yield the pure material, m. p. 190.5°C.

Found: C, 76.38; H, 4.70. Calcd. for $C_{22}H_{16}O_4$: C, 76.73; H, 4.68%.

Rapid stream of steam was passed into the mother liquor to remove the unchanged quinone and the solvent. The dried residue was ground down into fine powder and then refluxed with methanol (80 ml.) to remove the unchanged IX. The yellow powder thus obtained (8.8 g. (36.2%), m. p. 182~186°C, sintering at 175°C) was successively recrystallized from ethyl acetate, acetone and benzene giving the pure high melting isomer (X_b), m. p. 206~206.5°C.

Found: C, 76.48; H, 4.41. Calcd. for $C_{22}H_{16}O_4$: C, 76.73; H, 4.68%.

X_b showed a depression of the melting point on admixture with X_a (mixed melting point, 174~180°C).

IR, X_a: 1667 (C=O of dihydroquinone), 1717 (C=O of ester) and 1283, 1144 cm^{-1} (-C-O- of ester). X_b: 1667 (C=O of dihydroquinone), 1717 (C=O of ester) and 1285, 1137 cm^{-1} (-C-O- of ester).

7-Carboxy-2,5-diacetoxytriptycene (XII.)—Hydrobromic acid (6 ml., 20% aqueous solution) was added to the hot solution of X_a (6.9 g.) in acetic acid (140 ml.). The mixture was heated on a boiling water bath for 5 hr. The solvent was removed under reduced pressure. The residue was washed with water and dried to give the crude XI, 5.9 g., m. p. 305~310°C (decomp.) as a light brown crystalline mass. The mixture of the crude XI (5.9 g.), acetic anhydride (30 ml.) and a small amount of anhydrous sodium acetate was heated on a boiling water bath for 1 hr. Water (40 ml.) was added to the cooled reaction mixture. The crude XII, 7 g. (84.2%), m. p. 220~231°C was obtained on standing the dilute mixture at room temperature for several hours. This substance was recrystallized 4 times from acetic acid to yield the pure XII, 5 g., m. p. 261~263°C. X_b (14.2 g.) was heated with 20% hydrobromic acid (40 ml.) in acetic acid (280 ml.) to yield the crude XI, 14.7 g. (85.9%), m. p. 245~250°C. This substance was acetylated and recrystallized twice from acetic acid to give pure XII, 11.1 g. (65%), m. p. 261~264°C. This substance showed no depression of the melting point on admixture with XII which was derived from X_a. The analytical sample of XII was obtained by sublimation under reduced pressure (220~230°C/1 mmHg).

Found: C, 72.92; H, 4.16. Calcd. for $C_{25}H_{18}O_6$: C, 72.46; H, 4.38%.

IR, 3200~2500 (-COOH), 1758 (C=O of acetate), 1685 (C=O of -COOH) and 1188 cm^{-1} (-C-O- of acetate).

Optical Resolution of *dl*-7-Carboxy-2, 5-diacetoxytriptycene (XII).—*d-XII.*—The racemic XII (5.950 g., 0.0144 mol.) was dissolved in absolute ethanol (160 ml.). Brucine tetrahydrate (3.344 g., 0.00722 mol.) was added at once to the hot solution and the mixture was refluxed for 30 min. The mixture was allowed to stand overnight at room temperature to precipitate well-defined colorless needles. The mother liquor was separated by decantation and the crystals thus obtained was washed several times with a small amount of ethanol. The crystals obtained were dried under reduced pressure yielding the brucine salt, 5.7 g., $[\alpha]_D^{10} = -7.28°$ (*c* 0.906, acetone). The brucine salt was recrystallized 3 times from absolute ethanol yielding a salt with $[\alpha]_D^{10} = +6.2°$ (*c* 1.46, acetone). This salt was recrystallized from ethanol 2 times affording an optically pure salt with a constant specific rotation $[\alpha]_D^{10} = +7.5°$, (*c* 0.69, acetone).

Found: C, 71.83; H, 5.40; N, 3.39. Calcd. for $C_{48}H_{44}O_{10}N_2$: C, 71.28; H, 5.48; N, 3.46%.

Water (24 ml.) was added to the hot solution of the optically pure salt (2.354 g.) in acetic acid (24 ml.) and the white precipitate formed was filtered, washed with water and dried to yield *d*-XII, 1.088 g., m. p. 263~266°C. This was recrystallized from acetic acid to give pure *d*-XII, m. p. 269~271°C, $[\alpha]_{5461}^{13} = +96.3°$, $[\alpha]_{4358}^{13} = +174.8°$ (*c* 0.7042, dioxane).

Found: C, 72.99; H, 4.40. Calcd. for $C_{25}H_{18}O_6$: C, 72.46: H, 4.38%.

l-XII.—The above-mentioned mother liquor which was obtained by decantation of the brucine salt was concentrated under reduced pressure. Treatment of the residue with 25% acetic acid gave the optically impure *l*-XII, m. p. 261~263°C, $[\alpha]_{5461}^{10} = -49.25°$ (*c* 0.873, acetone). Quinine (6.5 g., 0.023 mol.) was added to the hot solution of the crude *l*-XII (9.6 g., 0.023 mol.) in 95% ethanol (120 ml.) and the mixture was refluxed for 30 min. The solution was allowed to stand overnight in a refrigerator. The colorless crystals deposited were filtered, washed with 95% ethanol to yield the crude quinine salt (9.8 g.). This was recrystallized 4 times from 95% ethanol to give optically pure *l*-salt (3.2 g.). This salt showed no definite melting point. Development of yellow color was observed near 140°C and it decomposed gradually at 155~160°C with frothing. The specific rotation of the pure salt was found to be $[\alpha]_{5791}^{19.5} = -109°$, $[\alpha]_{5461}^{19.5} = -139°$ (*c* 1.028, acetone).

Found: C, 71.59; H, 6.33; N, 3.66. Calcd. for $C_{45}H_{42}N_2O_8 \cdot H_2O$: C, 71.40; H, 5.86; N, 3.70%.

The pure quinine salt obtained (3.1 g.) was heated on a water bath with 25% acetic acid (50 ml.) for 30 min. The mixture was kept at room temperature overnight, and the precipitate formed was filtered, washed with 25% acetic acid and water successively, to result in *l*-acid, (1.5 g.), m. p. 252~263°C. The *l*-acid was recrystallized twice from acetic acid yielding the pure *l*-XII, m. p. 269~271°C, $[\alpha]_{5461}^{24} = -93.1°$, $[\alpha]_{4358}^{24} = -168.2°$ (*c* 1.0272, dioxane).

Found: C, 71.76; H, 4.46. Calcd. for $C_{25}H_{18}O_6$: C, 72.46; H, 4.38%.

The infrared spectra of the *d*- and *l*-acid were found to be completely identical over the entire region of wavelength.

The authors are grateful to Mr. Masakazu Okumiya and Miss Kiku Koike for performing the elementary analyses. Part of the cost of this research was defrayed from the grant-in-aid of the Ministry of Education, to which the authors thanks are also due.

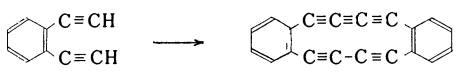
Department of Chemistry
Faculty of Science
Osaka University
Nakanoshima, Osaka

Another Example of the Formation of Highly Strained Cyclic Dimer of o-Diethynyl Compound[1]

By Mamoru MORIMOTO, Shuzo AKIYAMA, Sōichi MISUMI and Masazumi NAKAGAWA

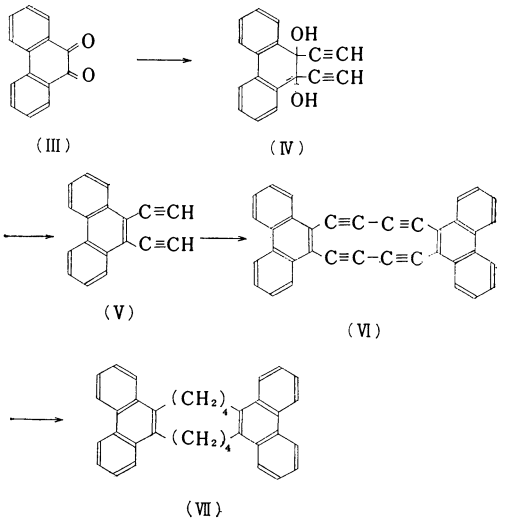
(Received October 23, 1961)

Recently, Raphael, Eglinton and their coworkers have studied the oxidative coupling of *o*-diethynylbenzene (I) by means of cupric acetate in pyridine, and the product was proved unexpectedly to be the highly strained cyclic dimer of I on the basis of chemical and physical evidence[2]. This result is rather surprising, because the starting material I has a rigid geometry favorable for the formation of strainless cyclic trimer[3].



(I) (II)

The present authors have carried out the oxidative coupling of 9, 10-diethynylphenanthrene (V) to confirm whether the forced



(III) (IV) (V) (VI) (VII)

1) This paper is Cyclic Acetylenes VII. For the previous paper in this series see F. Toda and M. Nakagawa, This Bulletin, **34**, 874 (1961).

2) O. M. Behr, G. Eglinton and R. A. Raphael, *Chem. & Ind.*, **1959**, 699; O. M. Behr, G. Eglinton, R. A. Galbraith and R. A. Raphael, *J. Chem. Soc.*, **1960**, 3614.

3) W. Baker, J. F. W. McOmie and W. D. Ollis, ibid., **1951**, 200.

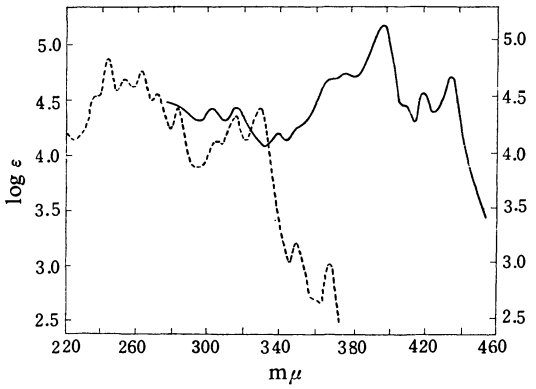


Fig. 1. The ultraviolet spectra of 9,10-diethynylphenanthrene, V (----) and the cyclic dimer, VI (——).

cyclic dimerization of *o*-diethynyl compounds is general or not in the Eglinton's reaction. 9, 10-Diethynylphenanthrene (V), which has a rigid geometry similar to I, was synthesized according to the method of Ried[4] with a slight modification as indicated in the foregoing chart. 9, 10-Diethynyl-9, 10-dihydroxy-9, 10-dihydrophenanthrene (IV) was obtained by the reaction of phenanthrenequinone (III) with sodium acetylide in liquid ammonia. The reductive aromatization of glycol IV afforded 9, 10-diethynylphenanthrene (V) in a reasonable yield. The oxidative coupling of V according to the procedure of Eglinton[2,5] furnished a fairly stable product which is found to be sparingly soluble in common organic solvents. The substance was recrystallized from a large amount of benzene or chlorobenzene yielding orange yellow fine needles. The color of the crystals changed to black on heating to ca. 290°C, but no fusion was observed even at 360°C. The analysis of the crystals suggests that the substance contains 1 mol. of solvent of crystallization. The absence of free ethynyl absorption in the infrared spectrum indicates the cyclic nature of this substance. A remarkable red-shift was observed in the ultraviolet spectrum of this substance as compared with that of V (Fig. 1). After removal of the solvent of crystallization by heating the substance to 110°C in vacuo, the analysis proved the molecular formula of the substance to be $(C_{18}H_8)_n$. The molecular weight of this hydrocarbon could not be determined by Rast's method owing to its poor solubility in camphor or other analogous solvents. Hydrogenation of the orange yellow crystals, $(C_{18}H_8)_n$ in benzene over palladium-on-charcoal furnished a colorless crystalline hydrocarbon, $(C_{18}H_{16})_n$. The determination of the molecular weight of the reduction product revealed the molecular formula of the hydrogenated product to be $(C_{18}H_{16})_2$. The ultraviolet spectra of the reduction product and 9, 10-dimethylphenanthrene[6] resembled closely in their absorption maxima, but the intensities of the former were found to be approximately double the relevant intensities of the latter (Fig. 2). From these observations the structure of VII, diphenanthro [9′, 10′-*a*; 9″, 10″-*g*] cyclododeca-1, 7-diene was given to the reduction product. Therefore, the structure of the parent hydrocarbon, $(C_{18}H_8)_2$, was confirmed to be the highly strained cyclic dimer VI, diphenanthro [9′, 10′-*a*; 9″, 10″-*g*] cyclododeca-1, 7-dien-3, 5, 9, 11-tetrayne.

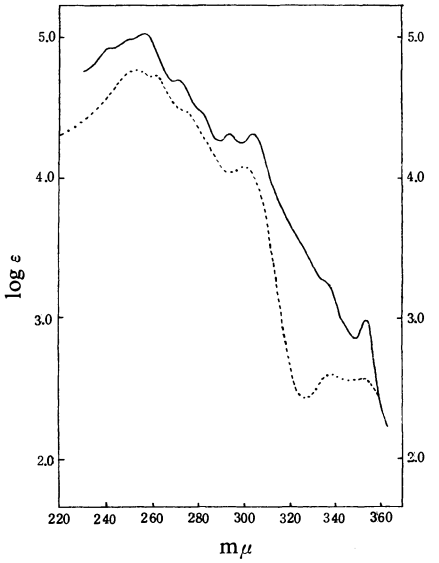


Fig. 2. The ultraviolet spectra of VII (——) and 9,10-dimethylphenanthrene (----).

The above-mentioned result is consistent with that of the oxidative coupling of *o*-diethynylbenzene, and can be regarded as the second example of an unusual cyclic dimerization. On the other hand, it has been reported that the oxidative coupling of aliphatic α, ω-diethynyl compounds under a similar condition results in the formation of the mixture of cyclic di, tri, tetra, penta and hexamer[7]. These facts strongly indicate that some specific cyclization mechanism operates in the Eglinton's coupling reaction of *o*-diethynyl compounds. The mechanism of the forced dimerization or the retardation of the cyclic

4) W. Ried, H. J. Schmidt and A. Urschel, *Chem. Ber.*, **91**, 2472 (1958).
5) G. Eglinton and A. R. Galbraith, *Chem. & Ind.*, **1956**, 737; *J. Chem. Soc.*, **1959**, 886.
6) W. L. Mosby, *J. Org. Chem.*, **19**, 299 (1954).
7) F. Sondheimer, Y. Amiel and R. Wolovsky, *J. Am. Chem. Soc.*, **81**, 4600 (1959).

trimerization in the coupling reaction is not clear, but it seems to be probable to assume the formation of an intermediate copper complex containing *o*-diethynyl compound as ligand, in which the circumstance should be so favorable for the cyclic dimerization of the *o*-diethynyl ligands that the increase of strain energy can be overcome.

Experimental*

9, 10-Diethynylphenanthrene (V).—A hot solution of 9, 10-diethynyl-9, 10-dihydroxy-9, 10-dihydrophenanthrene (IV, 13 g., 0.05 mol.) in methanol (100 ml.) was added under stirring to a solution of stannous chloride dihydrate (22.5 g., 0.1 mol.) in concentrated hydrochloric acid (45 ml.) and water (30 ml.). The mixture was stirred for 1.5 hr. at 60~65°C. After cooling the mixture, the flocculent brown precipitate was filtered, washed with water and dried in vacuo. The brown mass was dissolved in carbon tetrachloride (140 ml.) and the red solution was filtered through a short column of alumina (35 g.). The same solvent (500 ml.) was passed through the column. The colorless filtrate and the washing were combined, and the solvent was removed under reduced pressure at 45°C in an atmosphere of nitrogen to give yellow crystals (3.6 g., 32%). The analytical sample was prepared by recrystallizing the crude crystals from petroleum benzine (b. p. 60~70°C). Pale yellow prisms, m. p. 130°C (decomp.).

Found: C, 95.52; H, 4.46. Calcd. for $C_{18}H_{10}$: C, 95.54; H, 4.46%.

IR, 3260 cm^{-1} (-C≡CH). UV, $\lambda_{max}^{C_2H_5OH}$ 235 mμ (log ε=4.53), 242.5 (4.85), 252.5 (4.64), 261 (4.74), 271 (4.53), 282.5 (4.41), 303 (4.08), 315 (4.33), 328.5 (4.40), 348 (3.18), 366 (3.02).

Diphenanthro[9′, 10′ - *a*; 9″, 10″ - *g*]cyclododeca-1, 7-dien-3, 5, 9, 11-tetrayne (VI). — 9, 10-Diethynylphenanthrene (V, 4.0 g.) was added under stirring to a mixture of cupric acetate monohydrate (60.0 g.) in pyridine (400 ml.). The mixture was stirred at room temperature for 3 hr., and then at 60°C for 4 hr. The green reaction mixture was cooled to room temperature and the stirring was continued for further 10 hr. The precipitate deposited was filtered, washed thoroughly with water to remove cupric acetate and pyridine, and the residue was washed with small amounts of ethanol and benzene, successively. The coupling product thus obtained was recrystallized twice from chlorobenzene or benzene yielding pure VI, tiny orange needles, 1.38 g., (33%). The determination of solvent of crystallization gave the following results. Benzene: 10.1~11.4%; Chlorobenzene: 16.3~18.2%. It was found that the solvent of crystallization can be removed by heating the crystals to 110°C in vacuo.

Found: C, 96.19; H, 3.61. Calcd. for $C_{36}H_{16}$: C, 96.40; H, 3.60%.

UV, $\lambda_{max}^{benzene}$ 300 mμ (log ε=4.42), 315 (4.42), 338 (4.21), 375 (4.72), 396 (5.51), 420 (4.56), 435 (4.70).

The solubility of VI in benzene was estimated to be 6.3 mg./l. at 10°C by a spectroscopic method.

Diphenanthro[9′, 10′ - *a*; 9″, 10″ - *g*]cyclododeca-1,7-diene (VII).—VI (200 mg.) in benzene (600 ml.) was hydrogenated over 5% palladium-on-charcoal (160 mg.) until no change of the ultraviolet spectrum of the solution was observed. During the course of the hydrogenation the yellow color of the solution disappeared. The catalyst was filtered off, and digested with hot benzene (500 ml.). The solvent was removed under reduced pressure from the combined benzene solution to yield yellow solid (120 mg.). The solid was dissolved in benzene (25 ml.) and the solution was filtered through a short column of alumina (15 g.). The alumina layer was washed with benzene (75 ml.). Removal of the solvent from the combined filtrate and washing gave a yellowish solid contaminated with yellow liquid. A colorless solid (55 mg., m. p. 328~333°C (decomp.)) was obtained on addition of a small amount of benzene-petroleum benzine (1 : 1) to the reduction products. This was recrystallized twice from benzene yielding pure crystals, m. p. 339~340.5°C (decomp.).

Found: C, 92.77; H, 6.63. Calcd. for $C_{36}H_{32}$: C, 93.06; H, 6.94%.

Molecular weight determination (Rast's method in camphor): 445, 468, 487. $C_{36}H_{32}$=465.

IR, 2930, 2860 cm^{-1} (-CH_2-) (KBr-disk). UV, $\lambda_{max}^{tetrahydrofuran}$ 241 mμ (log ε=4.92), 256 (5.02), 272 (4.69), 292.5 (4.31), 304 (4.31), 353 (3.01).

The absorption intensity (256 mμ, ε=105800) was found to be approximately double of the relevant intensity of 9, 10-dimethylphenanthrene (253 mμ, ε=58900).

The financial support for this research was granted by the Ministry of Education, to which the authors thanks are due.

Department of Chemistry
Faculty of Science
Osaka University
Nakanoshima, Osaka

* All melting points are not corrected. All ultraviolet and infrared spectra were measured with Hitachi autorecording spectrophotometers, EPS-2 and EPI-2 respectively. The analyses were performed by Mr. M. Okumiya in the Microanalytical Laboratory of Department of Chemistry, Faculty of Science, Osaka University.

Thermal Decomposition of Dimethyl Ether in the Presence of Hydrogen Sulfide and Nitric Oxide

By Naomi IMAI and Osamu TOYAMA

(Received September 28, 1961)

We have recently studied the catalytic effect of hydrogen sulfide on the thermal decomposition of acetaldehyde[1,2] and of dimethyl ether[3]. It has been suggested from the effects of chain inhibitors such as propylene and isobutylene that the hydrogen sulfide-catalyzed decomposition of acetaldehyde involves two mechanisms, i. e., a free radical chain mechanism and a non-chain molecular mechanism, while the hydrogen sulfide-catalyzed decomposition of dimethyl ether has been explained solely by a radical chain mechanism. There is, however, an indication[2] that nitric oxide catalyzes the molecular decompositon of dimethyl ether even though it suppresses the chain decomposition of the ether almost completely. It seems, therefore, possible that the molecular decomposition of dimethyl ether is also catalyzed by hydrogen sulfide. Although the contribution of such a catalysis, if present, must be considered from the results given above to be usually so small that its existence can hardly be recognized, it may be expected that the suppression of the chain decomposition by a suitable inhibitor will enable the hydrogen sulfide-catalyzed molecular decomposition to be measured.

This paper reports such an attempt, carried out with nitric oxide as an inhibitor, which has been found to be the most efficient of the inhibitors investigated.

Experimental

Materials.—Dimethyl ether was prepared by the dehydration of methyl alcohol by concentrated sulfuric acid at 80°C, decarbonated and dried over potassium hydroxide and calcium chloride. Hydrogen sulfide was prepared by dropping water on aluminum sulfide and dried by passing through a trap at −78°C. Nitric oxide was produced by the reaction of a concentrated sodium nitrite solution with a hydrochloric acid solution of ferrous chloride, decarbonated by a potassium hydroxide solution and dried by concentrated sulfuric acid and phosphorus pentoxide. All of these gases were prepared in evacuated vessels and purified by repeated bulb-to-bulb distillation.

Apparatus and Procedure. —The apparatus used was one for ordinary statical experiments similar to that described previously[4]. The rate of decomposition in most cases was followed by measuring the total pressure change, but, in some runs, the major decomposition products uncondensable at −196°C, i. e., methane, carbon monoxide and hydrogen, were analyzed by a Yanagimoto GCG-2 type gas chromatograph.

Results and Discussion

Figure 1 shows the results of a series of experiments in which the time of pyrolysis was varied under otherwise constant conditions. It had previously been found that the rate of formation of carbon monoxide in the uninhibited reaction[3] is approximately equal to that of hydrogen but smaller than that of methane, and that the total pressure-time curve is of a sigmoidal form. These findings have been explained by decomposition in two stages, i. e., by the reaction $CH_3OCH_3 \rightarrow CH_4 + HCHO$, followed by $HCHO \rightarrow H_2 + CO$, though neither of them is a simple reaction; both are radical chain reactions catalyzed by hydrogen sulfide. Figure 1 shows that the rate of the formation of carbon monoxide in the inhibited pyrolysis is lower than that of methane, but it is about ten times as great as that of hydrogen, indicating that formaldehyde does not decom-

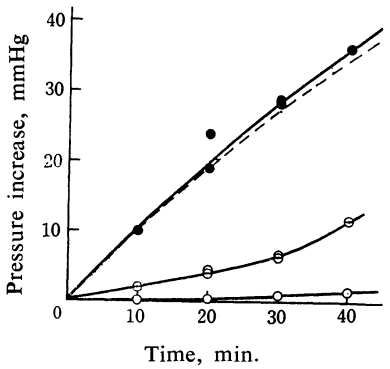


Fig. 1. Dependence of total pressure and pressures of products on reaction time. $CH_3O \cdot CH_3 = 100$ mmHg, $H_2S = 30$ mmHg, $NO = 10$ mmHg, 500°C. ●, CH_4; ⊖, CO; ○, H_2. Dotted line represents total pressure increase.

1) N. Imai, Y. Yoshida and O. Toyama, This Bulletin, 35, 752 (1962).
2) N. Imai, Y. Yoshida and O. Toyama, ibid., 35, 758 (1962).
3) N. Imai and O. Toyama, ibid., 34, 328 (1961).
4) N. Imai and O. Toyama, ibid., 33, 1408 (1960).

TABLE I. RATE OF DECOMPOSITION UNDER VARIOUS CONDITIONS
P, initial pressure (mmHg); R, rate of pressure increase (mmHg min^{-1})

440°C

$P_{CH_3OCH_3}=100$
$P_{H_2S}=20$

P_{NO}	R
0	1.44
0.5	0.10
0.7	0.084
1.5	0.060
1.5	0.060
4.5	0.064
7.5	0.073
19	0.078
35	0.106
60	0.142
100	0.205

480°C

$P_{CH_3OCH_3}=100$
$P_{H_2S}=20$

P_{NO}	R
0	8.6
0.5	1.0
1.0	0.33
3.2	0.30
15	0.40
17	0.40
45	0.60
62	0.71
89	0.91

$P_{CH_3OCH_3}=100$
$P_{H_2S}=0$

P_{NO}	R
0	1.80
0	1.86
3	0.026
22	0.14
51	0.31
93	0.58

500°C

$P_{CH_3OCH_3}=100$
$P_{H_2S}=20$

P_{NO}	R
20	0.88
20	0.90
35	1.03
46	1.20

$P_{CH_3OCH_3}=100$
$P_{H_2S}=0$

P_{NO}	R
0	5.0
0	5.4
2.7	0.075
21	0.26
50	0.58
86	1.04

$P_{H_2S}=30$
$P_{NO}=10$

$P_{CH_3OCH_3}$	R
59	0.66
68	0.73
79	0.80
80	0.82
100	1.02
160	1.58
176	1.50
223	2.02
224	2.28
225	2.20

520°C

$P_{CH_3OCH_3}=100$
$P_{H_2S}=20$

P_{NO}	R
20	1.90
39	2.6
55	2.7

$P_{CH_3OCH_3}=100$
$P_{H_2S}=0$

P_{NO}	R
1.4	0.56
3.5	0.40
20	0.80
20	0.82
77	2.07

$P_{CH_3OCH_3}=100$
$P_{NO}=20$

P_{H_2S}	R
0	0.80
0	0.82
28	1.9
48	3.4
68	4.4
88	5.7

pose according to the stoichiometric equation $HCHO \rightarrow H_2 + CO$ in the presence of nitric oxide. Figure 1 also shows that the total pressure increase is almost identical with that of methane in the initial stage of decomposition. In the experiments described below, the initial rate of total pressure increase was determined as a measure of the initial rate of decomposition. These initial rates of pressure increase may be taken as those for the formation of methane, as is shown above.

Table I shows the initial rates of pressure increase obtained with various gaseous compositions in the temperature range 440~520°C. Figure 2 shows the dependence of the rate on the pressure of nitric oxide in the presence and absence of hydrogen sulfide. Table I and Fig. 2 show that for the ether of 100 mmHg pressure, irrespective of the presence of hydrogen sulfide, the maximum inhibition is attained by about 3 mmHg of nitric oxide, and that the rate of maximally inhibited decomposition is only a fraction of that uninhibited in both the presence and the absence of hydrogen sulfide. As has been shown in the decomposition of acetaldehyde in the presence of hydrogen sulfide[2], the residual decomposition remaining after the maximum inhibition is probably of a molecular character. This, however, does not contradict the previous finding that the uninhibited decomposition of dimethyl ether in the presence or absence of hydrogen sulfide is to be explained solely by a radical chain mechanism[3], since the rate of decomposition maximally inhibited by nitric oxide is only a fraction of that uninhibited, as is shown above.

Figure 2 further shows that, in both the presence and the absence of hydrogen sulfide, the rate of inhibited decomposition increases linearly with the pressure of nitric oxide. This probably indicates that the molecular decomposition of dimethyl ether is catalyzed by nitric oxide, as has already been described in a previous paper[3]. The linear parts of the two plots for the rates in the presence and absence of hydrogen sulfide are parallel, suggesting that the inhibited decomposition of dimethyl ether is catalyzed independently by

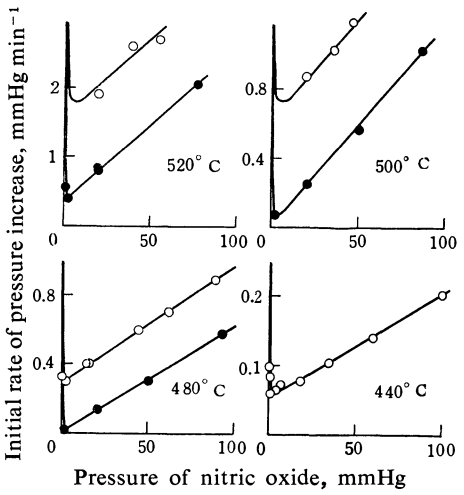


Fig. 2. Dependence of rate of decomposition on pressure of nitric oxide. $CH_3OCH_3=100$ mmHg ●, $H_2S=0$; ○, $H_2=20$ mmHg

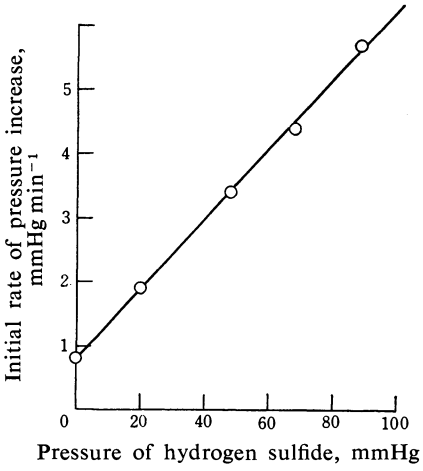


Fig. 3. Dependence of rate of decomposition on pressure of hydrogen sulfide. $CH_3OCH_3=$ 100 mmHg, NO=20 mmHg, 520°C.

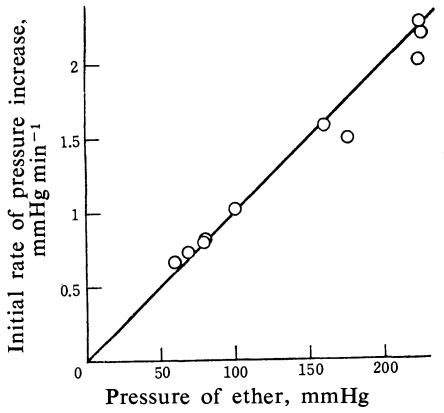


Fig. 4. Dependence of rate of decomposition on pressure of ether. $H_2S=30$ mmHg, NO=10 mmHg, 500°C.

hydrogen sulfide and by nitric oxide. Figures 3 and 4 show that the rate of inhibited decomposition increases linearly with the pressure of hydrogen sulfide and with that of the ether. The results shown in Figs. 2, 3 and 4 may, therefore, be combined to give a general expression for the inhibited rate:

$$-\mathrm{d}[CH_3OCH_3]/\mathrm{d}t = k[H_2S][CH_3OCH_3] + k'[NO][CH_3OCH_3]$$

The constant k can be determined from the intercept given by extrapolating the linear part of the plot obtained with hydrogen sulfide in Fig. 2 or from the slope of the straight line in Fig. 3, and k' from the slope of linear

TABLE II. VALUES OF RATE CONSTANTS

Temp. °C	k, mol^{-1} cc. sec^{-1} (a)	(b)	k', mol^{-1} cc. sec^{-1} (c)	(d)
440	22.1		10.6	
480	106		54	49
500	249		97	95
520	486	449	202	186

(a) From intercept of upper line in Fig. 2
(b) From slope of line in Fig. 3
(c) From slope of upper line in Fig. 2
(d) From slope of lower line in Fig. 2

parts of the plots given in Fig. 2. The results are listed in Table II, where the values of these constants obtained by different methods are in satisfactory agreement with each other. The slope of the straight line in Fig. 4 is 0.0100 min^{-1}, in good agreement with the value of 0.0105 calculated from these values of k and k'. The least square treatments of the values given in Table II yield the following Arrhenius expressions:

$$k = 10^{(14.7\pm0.35)} \exp\{-(43600\pm1200)/\boldsymbol{RT}\} \quad mol^{-1}\,cc.\,sec^{-1}$$

$$k' = 10^{(13.4\pm0.10)} \exp\{-(40500\pm600)/\boldsymbol{RT}\} \quad mol^{-1}\,cc.\,sec^{-1}$$

As has already been described, these reactions are probably molecular decomposition of the ether catalyzed by hydrogen sulfide and by nitric oxide respectively. Both expressions appear to be reasonable for a simple bimolecular process. However, as has been described previously for acetaldehyde[2], information from other sources than kinetics seems necessary to clarify further the detailed mechanisms of these reactions.

The effect of nitric oxide on the thermal decomposition of dimethyl ether has also been studied by Smith and Hinshelwood[5]. Their

5) J. R. E. Smith and C. N. Hinshelwood, *Proc. Roy. Soc.*, **A180**, 237 (1942).

results, however, differ considerably from those obtained in the present work. According to them, the rate of decomposition was reduced by the addition of an increasing amount of nitric oxide, but after a limiting rate was reached the rate remained constant and did not show any increase with the pressure of nitric oxide. The reason for this discrepancy is not yet clear. On the other hand, Freeman[6] studied the effect of nitric oxide on the thermal decomposition of diethyl ether and found a linear increase of the rate with the pressure of nitric oxide similar to the results shown in Fig. 2.

Summary

Dimethyl ether has been decomposed in the presence of hydrogen sulfide and nitric oxide over the temperature range 440~520°C. On increasing the amount of nitric oxide, the rate of decomposition decreases rapidly but after passing through a minimum value it increases linearly with the pressure of nitric oxide. The minimum value of the rate, which is reached in the presence of a small percentage of nitric oxide, is only a fraction of the uninhibited rate, irrespective of the presence of hydrogen sulfide. The rate of decomposition after being maximally inhibited, which is probably molecular in character, is represented by the equation $-\mathrm{d}[CH_3OCH_3]/\mathrm{d}t=k[H_2S][CH_3OCH_3]+k'[NO]\cdot[CH_3OCH_3]$, indicating that the inhibited decomposition is catalyzed by hydrogen sulfide and by nitric oxide independently. Arrhenius expressions $k=10^{14.7}\exp(-43600/\boldsymbol{RT})$ and $k'=10^{13.4}\exp(-40500/\boldsymbol{RT})\,\mathrm{mol}^{-1}\,\mathrm{cc.}\,\mathrm{sec}^{-1}$ have been obtained.

Department of Applied Chemistry
College of Engineering
University of Osaka Prefecture
Sakai, Osaka

6) G. R. Freeman, ibid., **A245**, 49 (1958).

Determination of Deuterium in Organic Compounds

By Nobuo TAMIYA

(Received July 21, 1961)

The method of Graff and Rittenberg[1] is the basis of the commonly applied deuterium analysis. The water obtained by the combustion of an organic sample is reduced with the aid of heated zinc. The resulting gaseous hydrogen is subjected to mass spectrometric analysis.

Several attempts have been reported to improve this method by reducing the memory effect of the apparatus used for the combustion and the reduction[2-6]. The present paper describes a modification by which both combustion and reduction are carried out in small, sealed glass tubes. The new method is simple, and one can analyze more than twenty samples a day without interference by the memory effect.

1) J. Graff and D. Rittenberg, *Anal. Chem.*, **24**, 878 (1952).
2) C. A. Dubbs, ibid., **25**, 828 (1953).
3) F. P. Chinard and T. Enns, ibid., **25**, 1413 (1953).
4) T. Titani, S. Horibe and M. Kobayakawa, *Mass Spectroscopy (Tokyo)*, **No. 6**, 27 (1956).
5) N. Tamiya, *Anal. Chem.*, **32**, 724 (1960).
6) T. Titani, S. Horibe and S. Koda, *J. Chem. Soc. Japan, Pure. Chem. Sec. (Nippon Kagaku Zasshi)*, **81**, 1624 (1960).

Experimental

Apparatus and Procedure.—Figure 1a shows a combustion tube made of Pyrex glass. The tube is dried in an electric furnace at 300°C for 60 min. under vacuum. After dried air is introduced into it, the tube is connected to a magnesium perchlorate tube. An organic sample, which will give about 2.5 mg. (±20%) of water on combustion, is taken into the tube (Fig. 1b). The capillary end of the tube is cut off, and dried oxygen is passed through to replace the air. The tube is then sealed at both ends as shown in Fig. 1c (9 ml. in volume) and placed in an electric furnace of 620°C for 30 min. This is the highest temperature which the glass will stand. When the combustion is completed, the furnace is allowed to cool. The water produced is collected in the capillary end by this procedure (Fig. 1d). One may centrifuge the tube with a vacuum rubber tube as a cap at 1,500 r.p.m. for 5 min. if the water contains bubbles. The water vapor remaining in the main part of the tube must contain less deuterium than the water. The amount of the vapor is, however, too small to affect the results.

Figure 2a shows a reduction tube with a breakable seal on one end. This is essentially similar

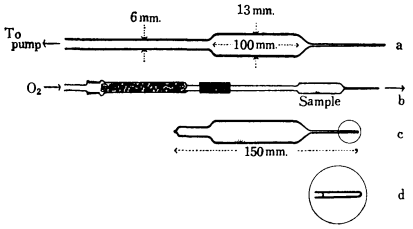


Fig. 1. Combustion tube for organic samples.
a: A combustion tube.
b: A combustion tube with a sample, being flashed with dried oxygen.
c: A sealed combustion tube.
d: The top of a combustion tube with deuterium containing water produced in it.

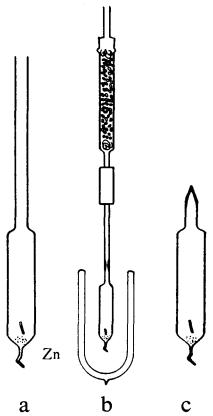


Fig. 2. Reduction tube for water.
a: A reduction tube with zinc granules and a water sample in a capillary in it.
b: A reduction tube chilled with solid carbon dioxide.
c: An evacuated and sealed reduction tube.

to that described by Chinard et al.[3] The tube is dried at 300°C for 60 min. with 0.25 g. of 20~30 mesh zinc granules in it. The capillary end of the combusition tube, which contains the water, is cut off and thrown into the reduction tube. The reduction tube is attached to a magnesium perchlorate tube and made thinner, with a flame at a part of its neck, as shown in Fig. 2b. The tube is then chilled with solid carbon dioxide to freeze the water, evacuated and cut by a flame under vacuum (9 ml. in volume, Fig. 2c). The reduction of the water is carried out at 620°C for 60 min. in an electric furnace. The hydrogen produced is taken out from the breakable seal and subjected to mass spectrometry. A Process and Instruments Model M-60 mass spectrometer was used. The reduction procedure is essentially similar to that described previously[8], except that a larger tube is used and that a higher temperature is applied. The addition of platinum catalyst to zinc, described in the previous paper, is no longer necessary, because the higher temperature is applied.

Results

The results are summarized in Table I. The standard water was prepared by diluting commercially available 99.65 mol.% deuterium oxide.

Table I. Examples of deuterium analysis

Sample		Deuterium found: Atom %	Deuterium found: Atoms per mole
10% (v/v) D_2O	2.5 μl.	9.95 10.01 9.89	
DL-Alanine-2d	3.5 mg.	14.15 14.3 13.5	0.990 1.00 0.945
L-Alanine-2d, $3d_3$	3.5 mg.	54.0	3.78
Glycine-$2d_2$	7.0 mg.	34.8 36.3	1.75 1.82
L-Aspartic acid-2d		14.8	1.04
L-Aspartic acid-3d		13.6	0.95
L-Aspartic acid-2d, 3d		28.9	2.02
DL-Aspartic acid-2d, $3d_2$		39.7	2.78

DL-Alanine-2d was prepared by an electrolytic reduction of pyruvic acid oxime in deuterium oxide in the presence of deuterated sulfuric acid[7]. A rough estimation of the deuterium content at the α- and β-positions of the preparation was made by comparing the infrared absorption peaks at 1308 cm^{-1} (α-CH deformation) and 1451 cm^{-1} ($-CH_3$ degenerating deformation) with that at 1410 cm^{-1} ($-COO^-$ symmetric stretching), which was taken as the standard. According to this estimation, the deuterium content of the α- and β-positions is 90 and 7 atom %, respectively[8,9]. L-Alanine-2d, $3d_3$ was prepared by treating L-alanine with transaminase in deuterium oxide; the infrared absorption spectrum of the preparation showed an almost complete disappearance of the $-CH_3$ and α–CH groups[8,9]. Glycine-$2d_2$ was prepared by treating glycine with salicyl aldehyde and cupric ion in deuterium oxide[10]. The results of the mass spectrometric analysis are in good agreement with the infrared absorption data.

Deuterium derivatives of L-aspartic acid were synthesized enzymically, and their infrared absorption spectra showed that there was almost no contamination of each other[10] and of hydrogen compound.

Summary

A device to simplify the deuterium analysis of organic compounds was described. The

7) S. Suzuki, T. Oshima, N. Tamiya, K. Fukushima, T. Shimanouchi and S. Mizushima, *Spectrochim. Acta*, **11**, 969 (1959).
8) T. Oshima and N. Tamiya, ibid., **17**, 384 (1961).
9) T. Oshima and N. Tamiya, *Biochem. J.*, **78**, 116 (1961).
10) N. Tamiya, *J. Biochem.*, **51**, 78 (1962).

combustion of organic samples and the reduction of deuterium containing the water produced were both carried out in sealed glass tubes. By this procedure one could completely avoid the "memory effect" and get satisfactory results, as shown by the examples of amino acid analysis.

The author is grateful to the Rockefeller Foundation and to Dr. A. E. Mirsky for providing the mass spectrometer.

Tokyo Medical and Dental University
Bunkyo-ku, Tokyo

Effects of Organic Bases on the Rate of the Oxo Reaction of Methylacrylate[1)]

By Ryoji IWANAGA

(Received July 25, 1961)

When cobaltic oxide suspended in benzene is treated with synthesis gas under high pressure at about 100°C in the presence of a small amount of dicobalt octacarbonyl as an initiator, carbon monoxide and hydrogen are readily absorbed and cobalt carbonyl is formed. This reaction is considered to be catalyzed by cobalt hydrocarbonyl, which is produced from dicobalt octacarbonyl and which increases in amount as the reaction proceeds.

We have previously[2)] found that the rate of this reaction is remarkably accelerated by the presence of a small amount of pyridine. Studying the mechanism of this reaction, it has occurred to the author that this effect of pyridine on the rate of the formation of cobalt carbonyl may be applied to the oxo reaction for the purpose of increasing the rate.

We have, therefore, examined the rate of the oxo reaction of methylacrylate in benzene in the presence of an amount of pyridine equimolar to cobalt of dicobalt octacarbonyl added as catalyst. It was consequently found that the rate of this oxo reaction is thereby about doubled.

To obtain information on the mechanism of this pyridine effect, we have studied the rate of the oxo reaction by adding various amounts of pyridine. In addition, the effects of various other aliphatic and aromatic amines on the rate were investigated.

Wender et al. previously[3)] reported that the treatment of a solution of dicobalt octacarbonyl in pyridine with synthesis gas at 120°C and 230 atm. results in the conversion of all of the cobalt to the pyridinium salt of cobalt hydrocarbonyl, $[C_5H_5NH]^+ [Co(CO)_4]^-$, and that the oxo reaction of a mixture of 2, 3-dimethylbutene-1 and -2 at 135°C and 230 atm. of synthesis gas was completely inhibited in the presence of triethylamine. The author has also observed that the oxo reaction of methylacrylate is suppressed in the presence of a large amount of pyridine or other amines.

Thus, the effect of pyridine in increasing the rate of oxo reaction appears only in the presence of a small amount of pyridine. Therefore, in the case of the examination of the effects of other amines, an amount of them equi-molar to the cobalt of dicobalt octacarbonyl added as catalyst was used.

Furthermore, to elucidate the mechanisms of the effects of pyridine and other amines on the rate of oxo reaction, the initial rate of the formation of the cobalt carbonyl anion was measured in this paper.

Experimental

Rate of the Formation of Cobalt Carbonyl from Cobaltic Oxide.—Fine powders of 16.6 g. (100 mmol.) of cobaltic oxide and a 180 ml. benzene solution containing 0.47 g. (6 mmol.) or 0.16 g. (2 mmol.) of pyridine were put into a 600 ml. stainless steel rocking autoclave, and then 20 ml. of a benzene solution containing 1.71 g. (5 mmol.) of dicobalt octacarbonyl were slowly pipetted into the solution. The autoclave was immediately sealed, placed in an electrically heated jacket, flushed and pressured with 1 : 1 synthesis gas to 200 kg./cm^2 at room temperature, and heated. After the temperature had risen to 110°C, the rocking was started, and the temperature was controlled at 110 ± 1°C. The

1) R. Iwanaga, T. Fujii and T. Yoshida, presented in part at the 9th Meeting of the Chemical Society of Japan, Kyoto, April, 1956.
2) T. Yoshida, R. Iwanaga and H. Mori, U. S. Pat. 2848304 (1958).
3) I. Wender, H. W. Sternberg and M. Orchin, *J. Am. Chem. Soc.*, 75, 3041 (1953).

rate of the reaction was estimated by the pressure decrease in the autoclave.

Rates of the Oxo Reaction of Methylacrylate in Benzene in the Presence of Pyridine or Other Amines.—Pyridine and other amines were obtained in the best commercial grades available. These were treated with anhydrous sodium sulfate for 24 hr. and then distilled. The middle fractions consistent with the boiling points described in the literature were then collected in dry flasks, protected from any atmospheric moisture, and were used immediately. Methylacrylate and benzene were treated in the same way.

A solution of 148 ml. benzene containing 30.0 g. (348 mmol.) of methylacrylate and 0.60 g. (1.74 mmol.) of dicobalt octacarbonyl was put into a 300 ml. stainless steel rocking autoclave, and 2 ml. of a benzene solution containing pyridine or other amines to be tested were pipetted slowly into the solution in the autoclave. The autoclave was immediately filled with 1 : 1 synthesis gas to 200kg./cm^2 and heated as described above. After the temperature of the solution had reached a temperature a little lower than the temperature to be tested, the rocking was started and the reaction temperature was controlled at 100 ± 1°C or 120 ± 1°C. The rocking was continued until the pressure decrease stopped.

Rates of the Formation of the Cobalt Carbonyl Anion from Dicobalt Octacarbonyl in the Presence of Amines in the Oxo Condition.—The methods described in the preceding paper[4] were in general followed, except that a crystal of dicobalt octacarbonyl was added to a toluene solution of pyridine or of triethylamine after the pressure and temperature had been raised to the reaction condition. Namely, 100 ml. of a toluene solution containing 198 mg. (2.5 mmol.) of pyridine or 254 mg. (2.5 mmol.) of triethylamine were put into a 300 ml. stainless steel rocking autoclave, and, on the other hand, 0.87 g. of dicobalt octacarbonyl crystal was put into a 10 ml. beaker, which was set rigidly with a stainless steel wire on the inside of the cover of the autoclave in order to keep dicobalt octacarbonyl separate from the pyridine or triethylamine until the pressure and temperature had been raised to the reaction condition. The autoclave was then sealed, flushed and pressured to about 70 kg./cm^2 with 1 : 1 synthesis gas. After the temperature of the system had been raised to 100°C and the pressure had been adjusted to 100 kg./cm^2, the autoclave was turned upside down and the rocking was started immediately so that the dicobalt octacarbonyl crystal could be dissolved into the solution. About 2 ml. aliquots of the reaction solution were withdrawn directly into a nitrogen atmosphere from the autoclave through a high pressure coil of tube in the course of the reaction, and the cobalt hydrocarbonyl in the aliquot was analyzed by the methylene blue method.

Results and Discussion

Figure 1, which illustrates the pressure decrease in the autoclave during the production of cobalt carbonyl from cobaltic oxide in benzene, shows that the rate of gas absorption is much higher in the presence of pyridine than when pyridine is absent. After about 62% of the cobaltic oxide was digested, the gas absorption stopped. The stopping was due to the coagulation of powders of cobaltic oxide in the water which was produced during the reaction in a separated phase from the benzene solution. When about 5 g. of dry kieselguhr were added as a absorbent of the water, this reaction could proceed until the cobaltic oxide had been digested completely.

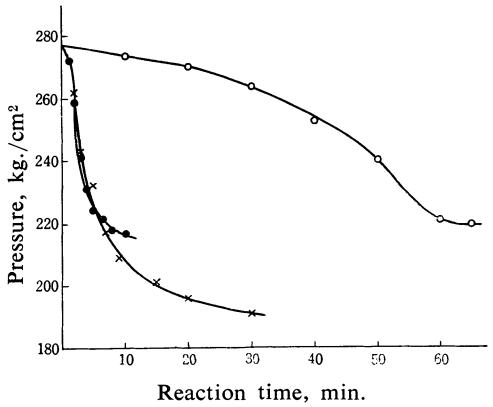


Fig. 1. Effect of pyridine on the rate of formation of cobalt carbonyl from cobaltic oxide.
—○— In absence of pyridine
—●— In presence of pyridine
—×— In presence of pyridine and kieselguhr

In view of the fact that the production of cobalt carbonyl from cobaltic oxide in the absence of cobalt carbonyl under high pressure synthesis gas did not take place until the temperature had been raised to 150°C, whereas in the presence of cobalt carbonyl it took place immediately even at temperatures below 100°C, and the fact the the rate of gas absorption increased with time, as is shown in Fig. 1, it is likely that cobalt carbonyl itself is the catalyst for the production of cobalt carbonyl. Therefore, the author visualizes the reaction as occurring in the following steps:

$$Co_2O_3 + 6HCo(CO)_4 \rightarrow 2Co + 3Co_2(CO)_8 + 3H_2O \quad (1)$$

$$2Co + 8CO \rightarrow Co_2(CO)_8 \quad (2)$$

$$Co_2(CO)_8 + H_2 \rightarrow 2HCo(CO)_4 \quad (3)$$

On the other hand, as illustrated in Table III, the initial rate of the formation of the cobalt carbonyl anion from dicobalt octacarbonyl under a high pressure synthesis gas and at an elevated temperature is greatly increased in the presence of pyridine or triethylamine.

4) R. Iwanaga, This Bulletin, 35, 778 (1962).

In a number of papers it has been shown that Lewis bases react with dicobalt octacarbonyl under mild conditions according to the equation,

$$2xB + 3Co_2(CO)_8 \rightarrow 2[Co(B)_x][Co(CO)_4]_2 + 8CO \quad (4)$$

When B is pyridine or triethylamine, this homomolecular disproportionation occurs similarly. However, under a high pressure of synthesis gas, no carbon monoxide is liberated and all the cobalt in the system is present in the forms of cobalt hydrocarbonyl, cobalt carbonyl anion and dicobalt octacarbonyl, even in the presence of amines. Therefore, it is considered that the effect of pyridine on increasing the rate of the production of cobalt carbonyl may be due to an acceleration of the rate of the reaction (Eq. 3) by a formation of an intermediate complex and a subsequent rapid formation of cobalt hydrocarbonyl from the complex and hydrogen as follows:

$$Co_2(CO)_8 + 2B \rightarrow (CO)_4Co\cdots Co(CO)_4 \quad (5)$$
$$\begin{matrix} \vdots & \vdots \\ B & B \end{matrix}$$
Complex

$$\text{Complex} + H_2 \rightarrow 2HCo(CO)_4 + 2B \quad (6)$$

$$HCo(CO)_4 + B \rightleftarrows [BH]^+[Co(CO)_4]^- \quad (7)$$

However, the amount of free cobalt hydrocarbonyl decreases while the hydrocarbonyl combined with amine, as shown in Eq. 7, increases in amount as the basicity of amine becomes stronger. Therefore, in the oxo reaction the effects of amines must appear in different manners from that in the formation of the anion as shown in Table III.

Plots of $\log\{(P_0-P_f)/(P_t-P_f)\}$ against time in the oxo reaction of methylacrylate in benzene under a 1:1 synthesis gas yielded approximate straight lines (P_0=initial pressure at reaction temperature, P_f=pressure at the end of reaction, P_t=pressure at time t), indicating that the rate of decrease of the pressure was linear with the total pressure drop. Several such plots are given in Fig. 2. The relative rate listed in Tables I and II gives the ratio between the slope of a straight line for the reaction with the amine and that for the reaction without the amine.

As illustrated in Table I, the rate of the oxo reaction of methylacrylate in benzene about doubles in the presence of an amount of pyridine equi-molar to the cobalt of the dicobalt octacarbonyl added as a catalyst, and the rate increases with the increasing amount of pyridine, although the effect becomes smaller, the larger the amount of pyridine is. Although the author did not measure such an amount of pyridine by which the maximum effect could be obtained, the oxo reaction may be rather suppressed or inhibited completely when a large amount of it is present.

The effects of other amines on the rate of the oxo reaction are listed in Table II. The amines listed in Table II are conveniently divided into three structural classifications for the purpose of comparison.

Aromatic Tertiary Amines.—This type of amine shows a completely positive effect on increasing the rate. Like pyridine, pyridine homologues, except 2, 6-lutidine, show the effect to a remarkable extent, but there are small differences in effects. The effect decreases

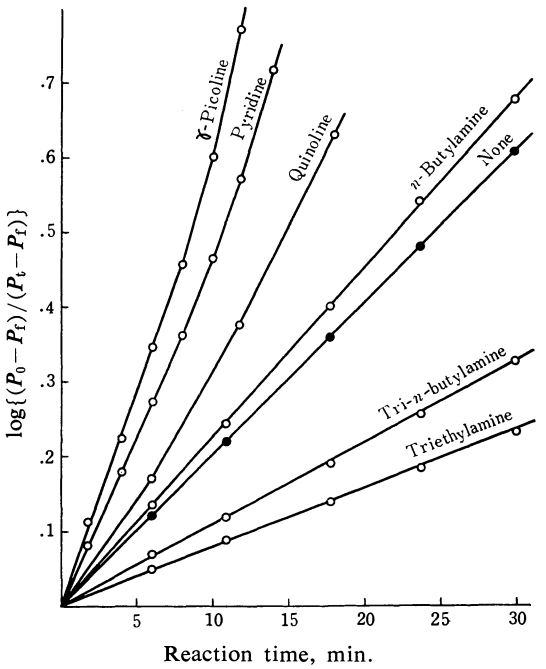


Fig. 2. Effects of amines on the rate of oxo reaction of methylacrylate in toluene at 120°C.

TABLE I. RATE OF OXO REACTION OF METHYLACRYLATE IN THE PRESENCE OF PYRIDINE

Methylacrylate: 232 mmol./dl.;
$Co_2(CO)_8$: 1.16 mmol./dl. as Co, in benzene.

Pyridine mmol./dl.	Reaction temp. °C	Reaction time min.	Relative rate
0	100	305	1.00
0.58	100	175	1.82
1.16	100	130	2.13
11.6	100	120	3.14
0	120	55	1.00
1.16	120	22	2.46
11.6	120	18	4.28

TABLE II. RATE OF OXO REACTION OF METHYLACRYLATE IN THE PRESENCE OF AMINES

Methylacrylate: 232 mmol./dl.; $Co_2(CO)_8$: 1.16 mmol./dl. as Co; Amine: 1.16 mmol./dl., at 120°C, in benzene.

Amine	Reaction time, min.	Relative Rate
None	55	1.00
Pyridine	18	2.46
α-Picoline	24	2.16
β-Picoline	22	2.84
γ-Picoline	20	3.52
2,4-Lutidine	24	2.68
2,6-Lutidine	45	1.11
Quinoline	35	1.58
N,*N*-Diethylaniline	40	1.37
Aniline	47	1.03
Cyclohexylamine	50	1.07
n-Butylamine	70	1.13
N-Methylaniline	57	1.10
N-Ethylaniline	57	1.20
Diethylamine	70	1.03
Di-*n*-butylamine	68	0.95
Triethylamine	>125	0.44
Tri-*n*-butylamine	>120	0.62

TABLE III. INITIAL RATE OF FORMATION OF $[Co(CO)_4]^-$ FROM $Co_2(CO)_8$ IN TOLUENE IN THE PRESENCE OF PYRIDINE OR TRIETHYLAMINE

$Co_2(CO)_8$: 0.87 g./dl.; Pyridine or Triethylamine: 2.5 mmol./dl. at 100°C and at 100 kg./cm² of synthesis gas.

Amine	Initial rate of formation of $[Co(CO)_4]^-$ mol. % as Co per min.
None	1.7
Pyridine	10.0
Triethylamine	21.2

in the order of the decreasing strength of base, as γ-picoline> β-picoline> pyidine. 2,4-Lutidine and α-picoline are stronger than γ- and β-picoline in basicity, but show smaller effects. This may be due to weak steric factors. The far smaller effect of 2,6-lutidine and *N*,*N*-diethylaniline may be explainable in terms of great steric hindrance, probably in complex formation. Quinoline shows a small effect, and this may be due to its weak basicity.

5) It was reported by Sternberg et al.[6] that dimethylformamide is produced from dimethylamine and dicobalt octacarbonyl at 0°C and atmospheric pressure, and that at 220°C and at carbon monoxide pressure of 200 atm. dimethylamine and piperidine are readily carbonylated to the corresponding formamide in the presence of catalytic amounts of dicobalt octacarbonyl.

6) H. W. Sternberg, I. Wender, R. A. Friedel and M. Orchin, *J. Am. Chem. Soc.*, 75, 3148 (1953).

Primary and Secondary Amines.—This type of amine shows little or no effect on increasing or decreasing the rate. The reason may be that these compounds with an NH-group are readily carbonylated with carbon monoxide to the corresponding formamide in the presence of dicobalt octacarbonyl[5], and consequently are weak in basicity.

Aliphatic Tertiary Amines.—Since all aliphatic tertiary amines have a very strong base and can not be carbonylated, they may form stable salts with cobalt hydrocarbonyl. Therefore, the major part of the cobalt added into the system converts to unreactive cobalt carbonyl anions, and the rate of the oxo reaction may be rather decreased as compared with the rate in their absence. The results obtained for them indeed show great negative effects.

Finally, the effect of pyridine and its homologues on increasing the rate of the oxo reaction may be accounted for by comparing the above results for the three types of amines. Namely, pyridine and its homologues have no NH-group to be carbonylated with carbon monoxide and consequently can be kept active for the formation of an intermediate complex with a cobalt carbonyl formed in the course of the oxo reaction and the rapid formation of that cobalt hydrocarbonyl presumed to be the catalyst of the oxo reaction from the complex. This concept may be supported by the small effect of 2,6-lutidine, which is likely hindered from forming the complex by a steric factor. On the other hand, pyridine and its homologues are far weaker in basicity than aliphatic tertiary amines such as triethylamine, and it may be considered that when the amount of pyridine is small in the solution, the free hydrocarbonyl formed reacts as the catalyst of the oxo reaction without forming a salt with pyridine.

Summary

It has been found that the rate of the formation of cobalt carbonyl from cobaltic oxide in benzene with the high pressure of 1:1 synthesis gas at 110°C is remarkably accelerated by the presence of a small amount of pyridine.

When the oxo reaction of methylacrylate in benzene is carried out in the presence of an amount of pyridine equi-molar to the cobalt of dicobalt octacarbonyl added as a catalyst, the rate is about doubled. By examining the oxo reaction in the presence of other organic bases, the following results were obtained: the rates are decreased by aliphatic tertiarx amines such as triethylamine and tributylamine, and are scarcely affected by primary and secondary amines such as aniline and dibutylamine. Pyridine homologues except 2,6-lutidine, are as

effective as pyridine. On the basis of these results, the mechanism of the effects of organic bases on the rate of oxo reaction has been discussed.

The author wishes to express his thanks to Professor Shunosuke Murahashi, Dr. Tôichi Yoshida and Mr. Jiro Kato for their kind guidance and encouragement throughout this work. The author is also indebted to Mr. Takashi Fujii and Mr. Hachiro Wakamatsu for their assistance in this experiment.

Central Research Laboratory
Ajinomoto Co., Inc.
Suzuki-cho, Kawasaki

Effects of Solvents on the Rate of Oxo Reaction of Methylacrylate

By Ryoji IWANAGA

(Received August 2, 1961)

While extensive studies on the effect of the structure of olefin and the partial pressure of carbon monoxide and hydrogen upon the rate of oxo reaction have been carried out, very little work on solvents in this regard has yet been done. Wender et al.[1], however, did study the effects of solvents on the oxo reaction rate of cyclohexene and established that the rate is increased only about 1.5 times in going from a saturated hydrocarbon to methanol; they therefore considered that highly polar intermediates may not be involved in the oxo reaction.

However, we have found that the effect of solvent on the rate of oxo reaction varies widely according to the olefin used[2]. For example, the oxo reaction rate of acrylonitrile in methanol at 120°C is about 6 times that in benzene. In this paper the author has investigated the effects of a variety of organic solvents and mixed solvents on the oxo reaction rate of methylacrylate. In addition, to obtain information on the mechanism of the effects of solvents, the rate of "base reaction" of Lewis base solvents such as methanol and acetone with dicobalt octacarbonyl, and the rate of formation of cobalt hydrocarbonyl from dicobalt octacarbonyl in toluene, methanol and acetone at 100°C and at 100 kg./cm^2 of 1 : 1 carbon monoxide and hydrogen, were measured.

Methylacrylate was chosen as the raw material for this study, because it gives a considerably wide variation in the effects of solvents and yields only one aldehyde, methyl-β-formylbutyrate. In addition, the oxo reaction of methylacrylate proceeds with scarcely any side reactions, because it gives a good yield of the aldehyde in every solvent.

Experimental

All of the solvents used were obtained in the best commercial grades available. These were treated with anhydrous sodium sulfate for 24 hr. and then distilled. The middle fraction consistent with the boiling point described in the literature was then collected in a dry flask, protected from atmospheric moisture. Methylacrylate was treated in the same way; its purity as determined by the morphorine method[3] was 98.5%.

Rates of the Oxo Reactions of Methylacrylate in Various Solvents.—The oxo reactions were carried out in a batch system by the same procedure as described in a preceding paper[4].

Thus, 150 ml. of the solvent containing 30.5 g. (350 mmol.) of methylacrylate and 0.60 g. (1.74 mmol.) of dicobalt octacarbonyl were put into a 300 ml. stainless steel rocking autoclave, and the autoclave was immediately filled with 1 : 1 synthesis gas to 200 kg./cm^2 and heated. After the temperature had risen to 120°C, the rocking was started, and the temperature was controlled at 120±1°C. The rocking was continued until the pressure decrease stopped. The rate constant of the oxo reaction, k_a, was obtained from the following equation:

$$k_a = 2.303 \log \{(P_0 - P_f)/(P_t - P_f)\}/t$$

where P_0 is the initial pressure at the reaction temperature, P_f is the pressure at the end of the reaction, and P_t is the pressure at time t.

1) I. Wender, S. Metlin, S. Ergun, H. W. Sternberg and H. Greenfield, *J. Am. Chem. Soc.*, **78**, 5401 (1956).
2) H. Wakamatsu, R. Iwanaga and J. Kato, reported at the 12th Annual Meeting of the Chemical Society of Japan, Kyoto, April, 1959.
3) F. E. Critchfield, G. L. Funk and J. B. Johnson, *Anal. Chem.*, **28**, 76 (1956).
4) R. Iwanaga, This Bulletin, **35**, 865 (1962).

Rates of "Base Reaction" of Solvents with $Co_2(CO)_8$.—Reactions were carried out at 20°C, and the rates were measured by the same procedure as described in a preceding paper[5]. The rate constants of the base reaction, k_b, were obtained from the following equation;

$$k_b = 2.303 \log \{[A^-]_f/([A^-]_f - [A^-]_t\}/t$$

where $[A^-]_f$ is the final amount of cobalt carbonyl anion, which corresponds to 2/3 mol. of the total cobalt in the $Co_2(CO)_8$ added, and $[A^-]_t$ is the amount of the anion at time t.

Initial Rates of Formation of Cobalt Hydrocarbonyl from $Co_2(CO)_8$ in Methanol and Acetone.—These were measured by the same technique as used in the measurement of the rate of formation of cobalt carbonyl anions from dicobalt octacarbonyl in the presence of amines[4]. Namely, a crystal of 0.87 g. of dicobalt octacarbonyl was added to 100 ml. of methanol or of acetone after the temperature of the system had been raised to 100°C and the pressure of 1 : 1 carbon monoxide and hydrogen had been adjusted at 100 kg./cm², and the amount of cobalt hydrocarbonyl in an aliquot of the reaction solution was analyzed by the methylene blue method.

Results and Discussion

The rates of oxo reaction of methylacrylate in 17 organic solvents at 120°C and at the initial pressure of 260 kg./cm² of 1 : 1 carbon monoxide and hydrogen are listed in Table I, together with their dielectric constants and their rates of "base reaction" with dicobalt octacarbonyl at 20°C. An about eight-fold variation was observed between the fastest and slowest rates. As is illustrated by the data in Table I, no relationship between the rates of oxo reaction and the dielectric constants or the rate of base reaction could be found.

Benzene, toluene, ethylacetate and ethyl ether are considered to be inert in the oxo reaction. Therefore, the value of about 40×10^{-3} min^{-1} may be considered a standard rate constant for the oxo reaction of methylacrylate; a value above it indicates a positive effect of the solvent, and a value below it indicates a negative effect of the solvent.

The rates in alcohols are very great except for the rate in *tert*-butanol. The large effects of alcohols may be explained by the same mechanism as proposed in the effect of pyridine[4], which involves the formation of an intermediate complex with cobalt carbonyl and the consequent rapid formation of cobalt hydrocarbonyl. This consideration agrees well with the observation that the formation of cobalt hydrocarbonyl in methanol is very rapid (cf. Table II).

The small positive effect of *tert*-butanol may be due to a steric hindrance, which may

TABLE I. RATES OF THE OXO REACTION OF METHYLACRYLATE IN VARIOUS SOLVENTS AT 120°C

Solvent	Rate constant $k_a \times 10^3$ min^{-1}	Dielectric constant[a]	°C	Rate const. of base reaction[c] $k_b \times 10^3$ min^{-1}
Benzene	41.8	2.284	20	—
Toluene	43.4	2.379	25	—
Ethylacetate	36.4	6.40	20[b]	9.9
Ethyl ether	41.2	4.335	20	—
Methanol	157	32.63	25	64.5
Ethanol	186	24.30	25	—
n-Butanol	167	17.8	20	13.8
Cyclohexanol	154	15.4	25	—
tert-Butanol	66.2	10.9	30	—
Acetone	59.5	20.7	25	57.5
Ethyl methyl ketone	39.1	15.45	20[b]	52.0
Tetrahydrofuran	57.1			47.2
Dioxane	27.4	2.235	25[b]	7.4
Acetic anhydride	30.2	20.7	19	—
Acetonitrile	77.2	37.5	20	196
Ethylene glycol	—	37.7	25	—
Formamide	—	109	20	—

a) The values were obtained from "American Institute of Physics Handbook", McGraw-Hill Co., New York (1957).
b) The values were obtained from C. Marden, "Solvents Manual", Cleaver-Hume Press Ltd., London (1954).
c) About 0.5 g. of $Co_2(CO)_8$ was reacted with 50 ml. of solvents at 20°C under atmospheric nitrogen.

5) R. Iwanaga, ibid., 35, 247 (1962).

Table II. Initial rates of formation of $HCo(CO)_4$ in toluene, methanol and acetone at 100°C and 100 kg./cm² of 1 : 1 synthesis gas

Solvent	Initial rate	Conversion at equilibrium
	mol. % as Co per min.	%
Toluene	1.5	34
Acetone	3.2	29
Methanol	ca. 40	52

Table III. Analytical data of a solution resulted from treatment of $Co_2(CO)_8$ in ethylene glycol under oxo condition

		Found	Calcd.[a]
Total cobalt	mg./ml.	5.13	
Co in the product	mg./ml.	3.45	
Co(II) ion	mg./ml.	1.70	
Co/total Co	%	67.3	66.7
Co(II)/total Co	%	33.1	33.3

a) Calculated from the formula; $[Co(C_2H_6O_2)_3][Co(CO)_4]_2$

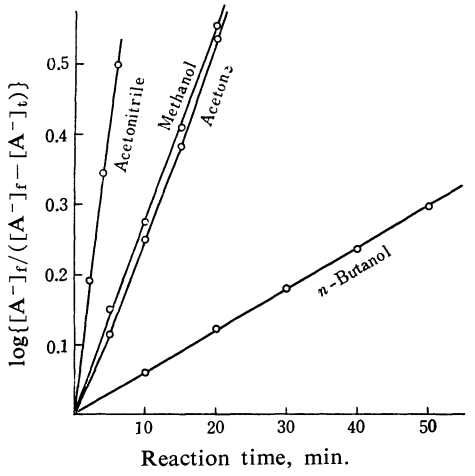


Fig. 1. Rates of the base reaction of dicobalt octacarbonyl with various Lewis bases.

occur in the complex formation with cobalt carbonyl, as described in the effect of 2,6-lutidine on the rate[4].

Acetone shows a moderate effect on the rate. Ethyl methyl ketone has an approximate standard value and is considered to be inert in the oxo reaction on the basis of its presumed steric factors.

In the case of the oxo reaction in acetonitrile, the original dark-brown solution changes to light yellow after the reaction is complete. This is probably due to the formation of amine by some hydrogenation of the nitrile.

In ethylene glycol, the oxo reaction did not take place. As is illustrated by Table III, it was found that dicobalt octacarbonyl reacts with ethylene glycol to form cobalt(II) ions and cobalt carbonyl anions even under the oxo condition, presumably according to Eq. 1.

$$3Co_2(CO)_8 + 6C_2H_6O_2 \rightarrow 2[Co(C_2H_6O_2)_3][Co(CO)_4]_2 + 8CO \quad (1)$$

Because the oxo reaction proceeds with no interference in benzene containing a small amount of ethylene glycol, as is shown in Fig. 2, it will be rather practical to explain the fact that the oxo reaction does not take place in ethylene glycol as follows: the complex salt consisting of a cobalt-ethylene glycol cation and a cobalt carbonyl anion has been produced by the base reaction before the pressure and temperature are raised to the oxo reaction condition, and the salt, once produced, is too stable in a higher polar solvent such as ethylene glycol to be converted to dicobalt octacarbonyl or cobalt hydrocarbonyl. It may be due to the same reason why the oxo reaction does not take place in formamide.

As is illustrated in Fig. 3, the rate is decreased by increasing the amount of water in the methanol. When 15 vol.% or more of water was added to the methanol, the reaction

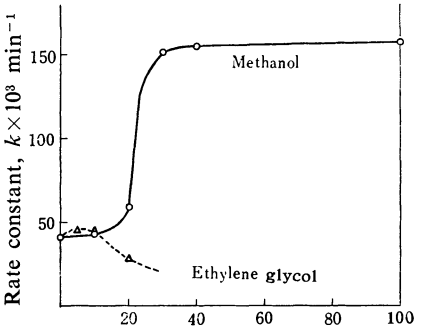


Fig. 2. Rates of the oxo reaction of methylacrylate in mixed solvent of benzene and methanol or ethylene glycol.

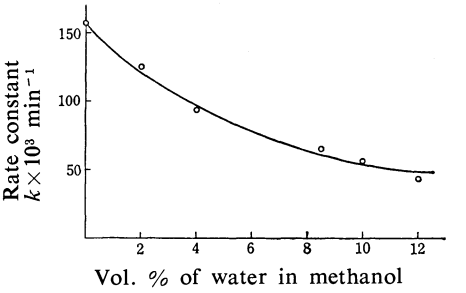


Fig. 3. Effects of water content in methanol as solvent of the oxo reaction of methylacrylate.

did not take place. This negative effect of water may be explained in terms of the dissociation of the cobalt hydrocarbonyl presumed to be a catalyst of the oxo reaction, because it is known that cobalt hydrocarbonyl dissociates completely in water at 26°C[6].

Summary

The rates of methylacrylate oxo reactions in a variety of organic solvents were measured by a batch system at 120°C. In general, the rate varies widely in the following order: alcohols > acetone > toluene; this order did not correspond with the order of their dielectric constants nor with the rates of their "base reactions" with dicobalt octacarbonyl, but it does agree with the order of their rates of formation of cobalt hydrocarbonyl under oxo conditions. *tert*-Butanol shows a positive but small effect on the rate as compared with toluene. When ethylene glycol and formamide having higher dielectric constants were used as solvents, the oxo reaction did not take place. On the bases of these results the mechanisms of the effects of the solvents have been discussed.

The author wishes to express his deep gratitude to Professor Shunsuke Murahashi, Dr. Tôichi Yoshida and Mr. Jiro Kato for their kind guidance and encouragement throughout this work. The author is also indebted to Mr. Takashi Fujii and Mr. Hachiro Wakamatsu for their assistance in this experiment.

Central Research Laboratory
Ajinomoto Co., Inc.
Suzuki-cho, Kawasaki

6) H. W. Sternberg, I. Wender, R. A. Friedel and M. Orchin, *J. Am. Chem. Soc.*, 75, 2717 (1953).

Dendritic Growth of Polyoxymethylene Crystal

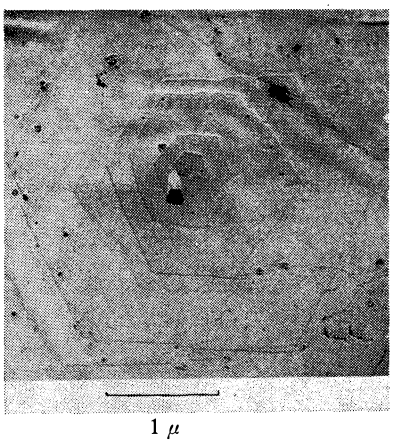
By Nobukazu ISHIHARA, Yasumasa TANI and Hiroshi SAKAI

(Received September 28, 1961)

It has been reported by Geil and others[1-3] that polyoxymethylene (POM) crystallized from a dilute phenol solution or from dimethyl phthalate forms the regular hexagonal plate single crystal*. Figure 1 shows that a fresh single crystal of POM grown from aniline has the same hexagonal form.

However, the dendritic growth of the needle-like crystal of POM was observed in some specimens which had been aged for a month after their preparation. A typical electron-micrograph of the POM dendrite is shown in Fig. 2. The crystal aspect of the dendrite is similar to that of the whisker or the snow crystal. To prevent thermal damage to the crystal by electron beam irradiation, the specimen was cooled in an electron microscope by liquid nitrogen below $-50°C$ during the observation.

Though the hexagonal plate and the dendrite were apparently different in form, however, the same crystal structure was obtained from their electron diffraction patterns in the process of our experiment.



1 μ

Fig. 1. The regular hexagonal single crystal of polyoxymethylene.

Our results suggest that the polymer crystal can grow in other forms than in the thin plate

1) P. H. Geil, N. K. J. Synoms and R. G. Scott, *J. Appl. Phys.*, **30**, 1516 (1959).
2) D. H. Renker and P. H. Geil, ibid., **31**, 1916 (1960).
3) K. Kobayashi, reported at the 17th Annual Meeting of the Society of Electron-microscopy of Japan, May, 1961.
* The six-pointed star-like crystal was also obtained from cyclohexanone[2].



1 μ

Fig. 2. The dendrite of polyoxymethylene.

(lamellar) form which is commonly known. Further experiments are now in progress.

The authors wish to express their thanks to Professor Keinosuke Kobayashi of Kyoto University for his useful suggestions and encouragement, and also to Mr. Zenji Nagao of Marusho Ind. Ltd. Co. for supplying the sample material and valuable information.

Department of Physics
College of Humanities and Sciences
Nihon University
Setagaya-ku, Tokyo

Rapid Microdetermination of Dysprosium in Terbium Oxide by Neutron Activation and γ-Ray Spectrometry

By Minoru OKADA

(Received October 4, 1961)

A neutron activation analysis method has been devised to evaluate the dysprosium content of high-purity terbium-oxide powder. Since the activation cross section for terbium is large (more than 22 barns[1] for thermal neutrons), terbium may interfere with the determination of dysprosium unless the matrix is removed. From the calculation based on the data[2] for thermal neutron activation and γ-ray spectrometry, it is seen that the most abundant γ-ray from 0.1 g. of activated terbium is in the same order as that from 1 μg. or more of activated dysprosium when both elements are irradiated at the same flux density of thermal neutrons. This implies that the non-destructive determination of dysprosium in terbium oxide may be interfered with terbium if the dysprosium content is less than 10 p. p. m. The possible interferences from terbium are γ- and X-rays of ^{160}Tb. The energies in MeV. are: 0.96(35%), 0.88(33%), 0.30(30%), 0.05 (~30%), etc.

Experimental

Varying amounts (7~25 mg.) of the sample to be analyzed were sealed in separate polyethylene capsules (1 cm. in diameter and 2 cm. in length) and placed by turns in the Japan-Research-Reactor-1 for 60 sec. to be irradiated with neutrons at a flux of 3×10^{11} neutrons per cm^2/sec. Then, after a 15-sec. interval, the decay of the activities produced was determined by use of a 2 in. thick, well-type, thallium-activated sodium-iodide crystal attached to a 256-channel pulse-height analyzer. In each successive γ-spectra obtained, the height of the photopeak of 0.108 MeV. γ-ray from ^{165m}Dy was measured, and a decay curve was made by plotting the log peak height vs. the time. Identification was made from the γ-ray energy and the half-life. Dysprosium standards were made so as to contain known amounts of dysprosium ranging from 0.05 to 5 μg.

Results and Discussion

Typical γ-ray spectra obtained are shown in Figs. 1 and 2. It can be seen from these figures that the γ-ray spectra for the irradiated terbium-oxide sample consist mainly of those of ^{165m}Dy; that is, the Compton continuum for the γ-rays of ^{160}Tb is negligible. The half-life of the photopeak which appeared at about 0.108 MeV. in the spectra for the sample was equal to that of the photopeak at the same position in the spectra for the dysprosium standard solution.

Table I shows the results of analyses where nine aliquots have been taken from one unknown sample. Since the observed dysprosium contents are nearly constant in the range of the sample amounts below 24 mg., it can be concluded that the self-shielding effect is negligible in this range. Hence, the average

1) D. J. Hughes and R. B. Schwartz, *U. S. Atomic Energy Comm., BNL-325*, 2nd ed. (1958).
2) M. Okada, Paper presented at the 4th Japan Conference on Radioisotopes, Kyoto, October, 1961.

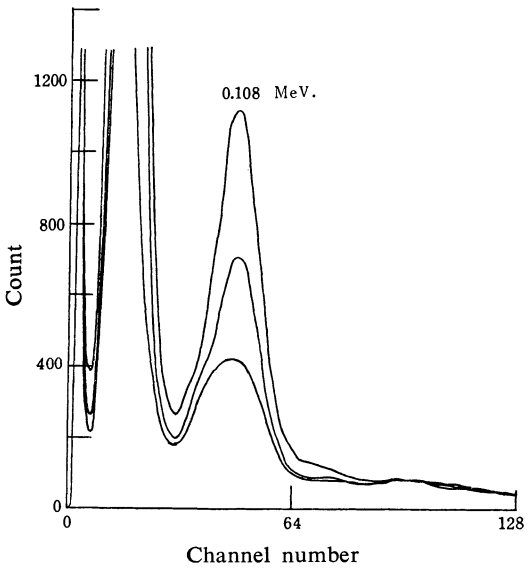


Fig. 1. Spectra for γ-rays of an activated terbium oxide sample (No. 2 in Table I).
Time interval between the 1st (the highest) and the 2nd spectra is 65 sec., and that between the 2nd and the 3rd spectra is 70 sec.

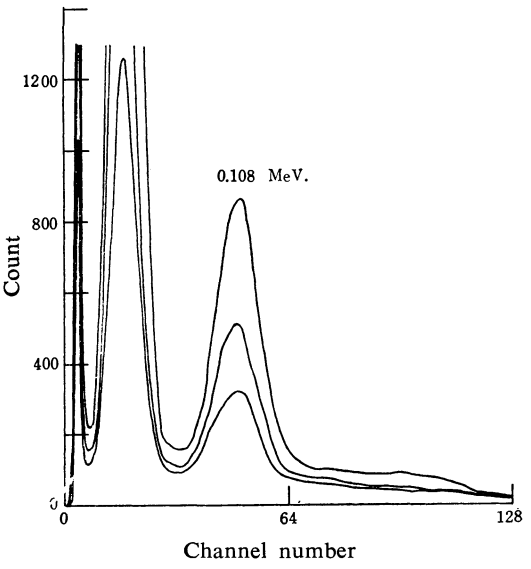


Fig. 2. Spectra for γ-rays of an activated dysprosium standard solution containing 0.22 μg. of dysprosium.
Time intervals are the same as those in Fig. 1.

(48 p. p. m.) can be taken for the dysprosium content. From the five values for "dysprosium found" shown in the lower part of Table I, the coefficient of the variation of single analyses can be estimated at 5.2% for 24.4$_4$ mg. sample.

TABLE I. RESULTS OF ANALYSES OF A TERBIUM OXIDE POWDER SAMPLE

No.	Sample wt. used mg.	Dysprosium found p. p. m.
1	6.96	49
2	11.1	50
3	11.1	45
4	19.4	50
5	24.5	46
6	24.4	52
7	24.5	49
8	24.4	48
9	24.4	45

The production of ^{165m}Dy through ^{165}Ho (n, p) and ^{168}Er(n, α) reactions was neglected in this experiment because their cross sections were expected to be very small and because the amounts of holmium and erbium in the sample were expected to be less than that of the dysprosium.

The radioactive nuclides which were produced by neutron irradiation of the samples and which decay with a γ-ray energy about 0.108 MeV. are ^{183m}W, ^{m}Yb(6 sec.), ^{165m}Dy, ^{161}Gd, ^{79m}Se, ^{151}Nd, ^{188m}Re, ^{155}Sm, ^{149}Nd, ^{165}Dy and ^{153}Sm. The radionuclides which can only slightly be formed upon 60 sec. irradiation with thermal neutrons are omitted. In these eleven nuclides, the ratio of the half-life of ^{165m}Dy to the nearest half-life is 1 : 3.1. Therefore, only a few successive spectra per sample are enough to identify dysprosium so long as the interfering activity of the nearest half-life is negligible. This was true in the sample tested in this work.

It is a good point of this method that the procedures required are simple and can be carried out on a very low-level radioactivity. From Fig. 1, which represents a sample of 48 p. p. m. dysprosium content, it can be deduced that one-tenth of this concentration of dysprosium would produce an adequate size of photopeak. Contamination can hardly become a problem in this method because no chemical procedure is employed for the sample to be analyzed.

Summary

Dysprosium in terbium oxide powder was determined by a simple method involving 1 min. irradiation with pile neutrons of 3×10^{11} neutrons per cm^2/sec. and repeated γ-ray spectrometry using a 2 in. thick sodium-iodide crystal attached to a 256-channel pulse-height analyzer. Both interferences and the self-shielding effect were negligible. The coefficient of variation of single analyses was 5.2% for a 24 mg. sample of 48 p. p. m. dysprosium content.

The author wishes to express his thanks to Professor Shoji Makishima for his keen interest in the work, and to Dr. Toshio Nakai for his permission to use the laboratory facilities.

Government Chemical Industrial Research Institute, Tokyo
Shibuya-ku, Tokyo

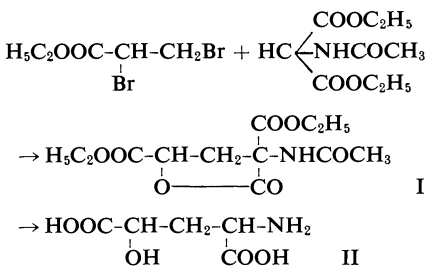
*Syntheses of γ-Hydroxyglutamic Acid**

By Takeo KANEKO, Yong Kyun LEE and Teruko HANAFUSA*1

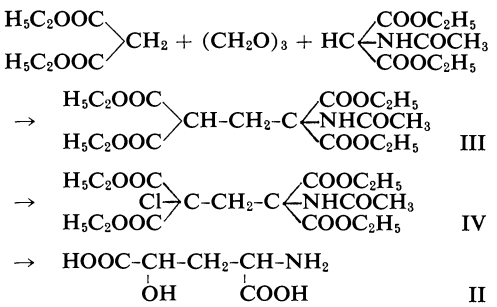
(Received September 14, 1961)

In 1955 Virtanen and Hietala[1] isolated γ-hydroxyglutamic acid from *Phlox decussata*, and Benoiton and Bouthillier[2] synthesized this hydroxyamino acid from ethyl *o*-acetylchlorolactate and ethyl acetamidocyanoacetate. Later, this synthetic method was improved by Benoiton et al.[3], who deduced the configuration of its optical isomers. Since the absolute configuration of the four optical isomers of β-hydroxyglutamic acid was determined in our laboratory[4], it has seemed to us of interest to study some of the properties of the stereo isomers of γ-hydroxyglutamic acid. First, attempts were made for a new synthesis of γ-hydroxyglutamic acid.

The hydroxyamino acid (II) was synthesized by hydrolysis of condensation product I of ethyl dibromopropionate with diethyl acetamidomalonate.



Two racemic diastereomers of II have been separated with procedures similar to those described by Benoiton et al.[3] When a crude hydrolyzate of the synthetic hydroxyamino acid was saturated with hydrogen chloride, one of the diastereomers, DL-γ-hydroxyglutamic acid (A) was precipitated asits lactone hydrochloride, m. p. 230~232°C (decomp.). From the mother liquor, another isomer, DL-γ-hydroxyglutamic acid (B), m. p. 166°C (decomp.), was obtained after treatment with pyridine and ethanol. After treatment of the amino acid A lactone hydrochloride with pyridine or silver carbonate, DL-γ-hydroxyglutamic acid (A) lactone, m. p. 245°C (decomp.), or DL-γ-hydroxyglutamic acid (A), m. p. 172~173°C (decomp.) was obtained*2.



Since the above synthesis, however, did not give a good yield, the next method was attempted. Tetraethyl α-acetamidomethylene-bismalonate (III), obtained by condensation of diethyl acetamido-malonate and diethyl malonate with paraformaldehyde according to the method of Hellmann and Lingens[5], was chlorinated with sulfuryl chloride in acetic acid to give, in a high yield, chlorinated compound IV, which was then hydrolyzed to γ-hydroxyglutamic acid with hydrochloric acid. The two diastereoisomeric DL-γ-hydroxyglutamic acids were isolated from the crude hydrolyzate in the same manner as has been described

* Studies on γ-Hydroxyglutamic Acid. I.

*1 Present address: Research Institute for Microbial Diseases, Osaka Univ., Dojima Nishimachi, Osaka.

1) A. I. Virtanen and P. K. Hietala, *Acta Chem. Scand.*, **9**, 175 (1955).

2) L. Benoiton and L. P. Bouthillier, *Can. J. Chem.*, **33**, 1473 (1955).

3) L. Benoiton, M. Winitz, S. M. Birnbaum and J. P. Greenstein, *J. Am. Chem. Soc.*, **79**, 6192 (1957).

4) T. Kaneko, R. Yoshida and H. Katsura, *J. Chem. Soc. Japan, Pure Chem. Sec.* (*Nippon Kagaku Zasshi*), **80**, 316 (1959).

*2 Presented at the 10th Annual Meeting of the Chemical Society of Japan, Tokyo, April, 1957.

5) H. Hellmann and F. Lingens, *Angew. Chem.*, **66**, 201 (1954).

above. The over-all yield from ethyl acetamidomalonate by this procedure was about 60% of the theoretical yield*3.

The solubility behaviors of the two racemates in hydrochloric acid and the melting points of *N*-benzyloxycarbonyl derivatives of the isomer A lactone and of B and its lactone were in good agreement with those reported by Benoiton et al.[3] It is clear from these facts that the two racemic modifications, A and B, correspond to the epimeric compounds (A and B)*4 obtained by the synthetic method. It failed to yield the hydrochloride of the isomer A because of its liability to form a lactone formation with hydrochloric acid.

Benzyloxycarbonyl-DL-γ-hydroxyglutamic acid (A) lactone was formed either by benzyloxycarbonylation of the lactone[3] or by treatment of benzyloxycarbonyl-DL-γ-hydroxyglutamic acid (A) with hydrochloric acid. The benzyloxycarbonyl-DL-γ-hydroxyglutamic acid (B) lactone was also obtained from the corresponding derivative of hydroxyamino acid B by treatment with hydrochloric acid.

Only benzoyl-amino acid A lactone was obtained after benzoylation of amino acid A, whereas both benzoylamino acid B and its lactone were obtained from amino acid B.

Experimental

Method 1.

α-Acetamido-α, γ-diethoxycarbonyl-γ-butyrolactone (I).—To a solution of 4.6 g. (0.2 mol.) of sodium in absolute ethanol, 43.4 g. (0.2 mol.) of ethyl acetamido-malonate were added. After evaporation of the mixture to dryness in vacuo, the residual sodium salt was suspended in anhydrous benzene, into which 54.6 g. (0.2 mol.) of ethyl dibromopropionate were stirred drop by drop at below 35°C. The reaction mixture was stirred until the solution became neutral, and then the reaction mixture was washed with water and dried. Benzene and unreacted ethyl dibromopropionate were removed by distillation, and diethyl acetamido-malonate was removed by vacuum distillation. By further distillation under 10^{-3} mmHg, an oily substance was distilled as 166~180°C with slight decomposition. Yield 35%.

Found: C, 50.38; H, 5.72; N, 4.85. Calcd. for $C_{12}H_{17}O_7N$: C, 50.17; H, 5.97; N, 4.88%.

Almost the same results were obtained from the reaction using dimethyl formamide in place of benzene.

DL-γ-Hydroxyglutamic Acid (II).—The lactone ester I was hydrolyzed and decarboxylated by boiling it with 6 N hydrochloric acid for several hours. After evaporation to dryness in vacuo, the hydrolyzate was dissolved in a minimal amount of water and the solution was saturated with hydrogen chloride to precipitate DL-γ-hydroxyglutamic acid (A) lactone hydrochloride m. p. 230°C (decomp.).

Found: C, 33.02; H, 4.73; N, 7.58; Cl, 19.74. Calcd. for $C_5H_8O_4NCl$: C, 33.07; H, 4.44; N, 7.75; Cl, 19.53%.

From the mother liquor, DL-γ-hydroxyglutamic acid (B) was obtained after treatment with pyridine and ethanol, m. p. 162~163°C (decomp.). Recrystallization from water gave m. p. 166°C. (decomp.).

Found: C, 36.62; H, 5.37; N, 8.56. Calcd. for $C_5H_9O_5N$: C, 36.81; H, 5.56; N, 8.59%.

The over-all yield from diethyl acetamido-malonate was about 20%.

Method 2.

Tetraethyl-1-acetamidopropane-1, 1, 3, 3-tetracarboxylate (III).—To 150 ml. of dried xylene, 67.2 g. (0.3 mol.) of diethyl acetamidomalonate, 67.2 g. (0.42 mol.) of diethyl malonate, 12.6 g. (0.42 mol.) of paraformaldehyde and 1.5 g. of powdered sodium hydroxide were added, and the mixture was refluxed for 7 hr. After cooling, the supernatant solution was separated from the sedimented residue by decantation, and the residue was washed twice with 20 ml. of ethyl acetate. The supernatant solution, combined with the washings, was evaporated in vacuo, and the residue was dissolved in 30 ml. of ethyl acetate. The ethyl acetate solution was washed with water, 5% sulfuric acid, water, 5% sodium bicarbonate and water in turn, dried with anhydrous sodium sulfate and concentrated in vacuo. The residue was crystallized from 30% ethanol; yield 92 g. (80%), m. p. 50~52°C. A pure sample recrystallized from 70% ethanol for elementary analysis melted at 58~59°C.

Found: C, 51.96; H, 7.14; N, 3.38. Calcd. for $C_{17}H_{27}O_9N$: C, 52.43; H, 6.99; N, 3.60%.

Tetraethyl-1-acetamido-3-chloropropane-1, 1, 3, 3-tetracarboxylate (IV).—Into a solution of 15.6 g. (0.04 mol.) of the tetracarboxylic acid ethyl ester III in 60 ml. of acetic acid, 7 g. (0.052 mol.) of sulfuryl chloride were stirred drop by drop at room temperature. Then the bath temperature was raised gradually, and the reaction mixture was heated for 1 hr. at 75°C. After the mixture had been evaporated to dryness in vacuo, the residue was dissolved in 100 ml. of ethyl acetate, washed several times with 5% aqueous sodium bicarbonate, dried, and concentrated in vacuo.

The residue was crystallized from water and triturated with 4 ml. of 40% ethanol. After standing overnight, the mixture was filtered. Yield 16 g., m. p. 83~85°C. A pure sample was obtained after recrystallization from 10 ml. of 70% ethanol. Yield 15.2 g. (90%), m. p. 91~92°C.

Found: C, 48.17; H, 6.18; N, 3.30; Cl, 8.37. Calcd. for $C_{17}H_{26}O_9NCl$: C, 48.41; H, 6.13; N, 3.03; Cl, 8.40%.

DL-γ-Hydroxyglutamic Acid (II).—The chloro compound (IV, 10 g.) was hydrolyzed and decarboxylated by refluxing with 70 ml. of concentrated hydrochloric acid for 7 hr. The hydrolyzate was evaporated to dryness in vacuo after treatment with charcoal, and the residue was redissolved in 15 ml.

*3 Reported at the 12th Annual Meeting of the Chemical Society of Japan, Kyoto, April, 1959.

*4 α-Amino and γ-hydroxyl groups of the A form have a threo type configuration in the Fischer formulation, while those of the B form have an erythro type configuration[3].

of dilute hydrochloric acid and saturated with hydrogen chloride in the cold. After standing overnight, the precipitate was filtered and washed once with concentrated hydrochloric acid and twice with acetone. Yield 1.8 g., m. p. 228~229°C (decomp.). From the mother liquor, 0.2 g. of the same product was recovered. The total yield was 2.0 g. (46.5%). Pure γ-hydroxyglutamic acid (A) lactone hydrochloride, recrystallized by saturation of the aqueous solution with hydrogen chloride, melted at 230~232°C (decomp.).

Found: C, 33.24; H, 4.67; N. 7.88; Cl, 19.50. Calcd. for $C_5H_8O_4NCl$: C, 33.07; H, 4.44; N, 7.75; Cl, 19.53%.

The amino acid A lactone hydrobromide was obtained in a yield similar to that of the hydrochloride by hydrolysis of the chlorinated compound IV with hydrobromic acid, m. p. 230~232°C (decomp.).

Found: C, 26.49; H, 3.81; N, 6.50; Br, 34.82. Calcd. for $C_5H_8O_4NBr$: C, 26.55; H, 3.54; N, 6.20; Br, 35.36%.

γ-Hydroxyglutamic acid (A) lactone was obtained from the amino acid lactone hydrochloride by treatment with pyridine. It was recrystallized from water, m. p. 245°C (decomp.).

Found: C, 41.23; H, 4.89; N, 9.43. Calcd. for $C_5H_7O_4N$: C, 41.38; H, 4.86; N, 9.65%.

After treatment with silver carbonate, the lactone hydrochloride was converted almost quantitatively to γ-hydroxyglutamic acid (A), which was recrystallized from water and ethanol to give a monohydrate, m. p. 172~173°C (decomp.).

Found: H_2O, 10.5. Calcd. for $C_5H_9O_5N \cdot H_2O$, 9.9%. Found with the anhydrous form: C, 36.78; H, 5.40; N, 8.73. Calcd. for $C_5H_9O_5N$: C, 36.81; H, 5.56; N, 8.59%.

The R_f values were 0.13 (80% phenol) and 0.10 (80% phenol containing a small amount of ammonia). Racemic amino acid A had a weak taste of L-glutamic acid.

The mother liquor, from which γ-hydroxyglutamic acid (A) lactone hydrochloride had been isolated, was evaporated to dryness in vacuo. The addition of water and evaporation to dryness was repeated several times to remove hydrochloric acid. When pyridine and ethanol were gradually added to the residue dissolved in water, a precipitate formed. Yield 1.5 g. (40%), m. p. 158°C (decomp.). A pure sample of γ-hydroxyglutamic acid (B) was obtained by recrystallization from water and ethanol. M. p. 166°C (decomp.).

Found: C, 36.74; H, 5.40; N, 8.57. Calcd. for $C_5H_9O_5N$: C, 36.81; H, 5.56; N, 8.59%.

The R_f values were identical with those of the isomeric amino acid (A). Racemic amino acid B had only an acid taste.

The over-all yield from ethyl acetamidomalonate was about 55~60%.

***N*-Benzyloxycarbonyl-DL-γ-hydroxyglutamic Acid (A) and its Lactone.**—To 36 g. (0.2 mol.) of the amino acid A dissolved in 200 ml. of 2 N sodium hydroxide, 52 g. (0.3 mol.) of benzyloxycarbonyl chloride and 110 ml. of 4 N sodium hydroxide were added simultaneously at 10°C, and the mixture was stirred for 1 hr. Then the reaction mixture was washed three times with ether. The aqueous solution was acidified with 6 N hydrochloric acid, with Congo red paper as an indicator, and extracted ten times with ethyl acetate. When the ethyl acetate extract was dried and concentrated, colorless crystals were obtained. After recrystallization from ethyl acetate, 41.6 g. of benzyloxycarbonyl-DL-γ-hydroxyglutamic acid (A) were obtained. Yield 70%, m. p. 109~110°C.

Found: C, 52.34; H, 5.24; N, 4.57. Calcd. for $C_{13}H_{15}O_7N$: C, 52.52; H, 5.09; N, 4.71%.

When the benzyloxycarbonyl-amino acid (A) was treated with 1 N hydrochloric acid, its lactone was obtained in crystalline form. This melted at 165~166°C after two recrystallizations from 1 N hydrochloric acid. No depression of the melting point was observed when it was mixed with another sample of benzyloxycarbonyl-DL-γ-hydroxyglutamic acid (A) lactone (m. p. 165~166°C; lit.[3] m. p. 168~169°C), which was obtained in a yield of 75% from DL-γ-hydroxyglutamic acid (A) lactone hydrochloride in the same manner as described above, and recrystallized from water and ethanol.

Found: C, 55.95; H, 4.85; N, 4.99. Calcd. for $C_{13}H_{13}O_6N$: C, 55.91; H, 4.70; N, 5.02%.

***N*-Benzyloxycarbonyl-DL-γ-hydroxyglutamic Acid (B) and its Lactone.**—*N*-Benzyloxycarbonyl-DL-γ-hydroxyglutamic acid (B) was obtained in a manner similar to that reported by Benoiton et al.[3] M. p. 132~133°C (decomp.) (lit.[3] 132~133°C).

Found: C, 52.53; H, 5.12; N, 4.58. Calcd. for $C_{13}H_{15}O_7N$: C, 52.52; H, 5.09; N, 4.71%

The above *N*-benzyloxycarbonyl-DL-amino acid (B) was converted to its lactone by recrystallization using 1 N hydrochloric acid, m. p. 152~153.5°C (decomp.) (lit.[3] m. p. 152~153°C).

Found: C, 55.55; H, 4.84; N, 4.89. Calcd. for $C_{13}H_{13}O_6N$: C, 55.91; H, 4.70; N, 5.02%.

Benzoyl-DL-γ-hydroxyglutamic Acid (A) Lactone.—To a solution of 3.6 g. (0.02 mol.) of DL-γ-hydroxyglutamic acid (A) lactone hydrochloride and 10 g. of sodium bicarbonate in 100 ml. of water, 4.2 g. (0.03 mol.) of benzoyl chloride were added drop by drop at 10°C; the reaction mixture was then stirred vigorously for one and a half hours at 10~15°C. Then the solution was acidified slightly with 6 N hydrochloric acid, using Congo red paper, and the benzoic acid which precipitated was filtered off. The filtrate was washed twice with ether, and the aqueous layer was evaporated to dryness in vacuo. To the residue dissolved in 10 ml. of water, 4~5 drops of concentrated hydrochloric acid were added, and the precipitate formed was filtered and washed with water. A crude sample of benzoyl-DL-γ-hydroxyglutamic acid (A) lactone was obtained by recrystallization of the precipitate from ethanol; yield 3.1 g. (62%). For elementary analysis, it was further recrystallized from ethanol. m. p. 230~232°C.

Found: C, 58.03; H, 4.61; N, 5.71. Calcd. for $C_{12}H_{11}O_5N$: C, 57.83; H, 4.45; N, 5.62%.

Benzoyl-DL-γ-hydroxyglutamic Acid (B) and its Lactone.—Benzoylation of DL-γ-hydroxyglutamic acid (B) was carried out in the same manner as described above from 9.8 g. (0.06 mol.) of DL-γ-hydroxyglutamic acid (B), 17 g. (0.12 mol.) of

benzoyl chloride, 35 g. of sodium bicarbonate and 200 ml. of water. A crude sample of the benzoyl-amino acid (B) was recrystallized from water. Yield, 11 g. (68%), m. p. 145°C (decomp.).

Found: C, 53.80; H, 5.02; N, 5.44. Calcd. for $C_{12}H_{13}O_6N$: C, 53.93; H, 4.87; N, 5.24%.

When concentrated hydrochloric acid was added to an aqueous solution of benzoyl-amino acid (B) and heated for a short time, its lactone was deposited. A pure sample of benzoyl-DL-γ-hydroxyglutamic acid (B) lactone was obtained after recrystallization from hot water; m. p. 202~203°C (decomp.).

Found: C, 57.42; H, 4.40; N, 5.49. Calcd. for $C_{12}H_{11}O_5N$: C, 57.83; H, 4.45; N, 5.62%.

The authors wish to express their thanks to Mr. Masakazu Okumiya and Miss Kiku Koike for their microanalyses.

Department of Chemistry
Faculty of Science
Osaka University
Nakanoshima, Osaka

Using Iron Ores of Kalabagh. I. Production of Limonite-Alkali Method

By M. I. ALI*

(Received July 24, 1961)

The ammonium sulfate plant at Daudkhel based on pressure gasification of local coal containing sulfur of about 5.0% faced the problem of hydrogen sulfide removal from the process gas. After much deliberation a method of preferential water-washing under pressure (about 15.0 kg./cm^2) has been adopted to effect the removal of hydrogen sulfide along with some carbon dioxide. The efficiency of water-washing-out process ranges between 92.0 and 96.0% and this quantity of hydrogen sulfide is being utilized for the manufacture of sulfuric acid, 60° Bé (20.0 tons/day on 100.0% basis). The remaining 4.0~8.0% hydrogen sulfide constitute 0.1~0.2% of the process gas which is being removed by limonite in the boxes before and after CO-conversion. During normal run of the factory about 7600 Nm^3 gas per hour is being purified which requires about 600 kg. limonite per day. This calculation is based on 0.1% hydrogen sulfide in the gas and absorption efficiency nearly to maximum. Due consideration was also given to the fact that the spent limonite can be regenerated by air oxidation and used over again until sulfur content reaches over 40.0% in the limonite mass. In practice, the consumption will be slightly more than the mentioned quantity. At present imported limonite from European countries especially Holland and Denmark are in use in the factory at an approximate cost of about U. S. $ 45.00 per 1000 kg. In view of this recurring expenditure, it was felt necessary to exploit our own resources by suitable processing, if possible.

The first attempt was made in this regard to assess the availability of naturally occurring limonite in the country. One report[1] shows that the Yellow Ochre of Khewra has 71.6% hydrogen sulfide absorption capacity at maximum pH with respect to ferric hydroxide but other samples are limited within 40.0%. Further informations are lacking. The observations made in some explanatory experiments with oxide ores of Kalabagh, led to look for a method of processing the material to suit the purpose. From a study of available methods of limonite production, alkali method was chosen to be tried. A short review is presented below:

The general alkali methods[2] described as the fusion of iron ores (FeS, FeS_2, Fe_2S_3 and oxides, etc.) with sodium carbonate or hydroxide[3] to produce ferrite first then its hydrolysis to yield hydrated ferric oxide.

The thermal activation of iron oxide by fuller's earth in conjunction with sodium carbonate has also been recognized[4].

Some other methods recommended the use of ammonia or alcohol[5], steam[6], lime, sodium carbonate[1], etc. on ferric chloride or some other iron salts.

* Present adress: Natural Gas Fertilizer Factory, Fenchuganj, Sylhet, East Pakistan.

1) S. A. H. Jafri, M. Se, Thesis, Punjab University (W. Pakistan) (1956).
2) D. E. Redford, *Natural Gas Bull.*, **11**, No. 5, 13 (1947).
3) Gilbert and Fr. Seil, 776, 903 (1935).
4) R. G. Capall and R. C. Amero, U. S. Pat. 2433426 (1947).
5) Yu A. Klyachke et al., *Zavodskaya Lab.*, **13**, 901 (1947).
6) L. Reeves and Geofrey, Brit. Pat. 677645, 677690 (1952).

One patent[7] claims the use of 25~30% soda lye at 200°C for preparing desulfurizing material using "Boue Rouge" (Bayer process) in aluminum industry.

Another method[8] describes the use of ferric oxide residue from bauxite. Sodium carbonate was reacted upon to form sodium ferrate (Na_2FeO_4) which on subsequent hydrolysis produced hydrated oxide of iron.

Another patent[9] of Metallgesellschaft used the residual mud known as "Lux" or "Lauta" of aluminum industry and also the hydrates of iron in conjunction with 5.0% alkali for desulfurization of gas.

In view of the above facts it was thought to produce the small quantity of limonite to meet the demand in this factory from local iron ore of Kalabagh by alkali method. Sodium hydroxide was considered to be suitable reagent for its possible use on recovery either in carbon dioxide removal plant of this factory or in the proposed soda-ash factory.

Experimental

There are several iron mines of different types of ores in this locality. The iron content of these ores varies within a wide range of 30.0~65.0%. The availability of high grade ore cannot be guaranteed. However, a better quality ore was selected for this purpose to avoid pretreatment and interference of gangue materials during processing. This sample was found to contain 56.5% Fe. A tentative analysis of the sample is given below:

Fe	56.5% (0.6% Fe^{2+})
SiO_2	5.0%
Al_2O_3	1.5%
CaO	2.2%
MgO	0.58%
S	0.32%

The underlying principle of this method was to heat an appropriate mixture of iron oxide ore and sodium hydroxide to produce sodium ferrite and hydrolyze in the subsequent step to obtain hydrated iron oxide along with the recovery of sodium hydroxide used. Alkali used for this purpose was of a commercial grade containing about 96.8% sodium hydroxide and over 2.0% sodium carbonate.

Preparation of Sodium Ferrite.—A known quantity (10 g.) of powdered and sieved (through a sieve of No. 100 French series) sample of iron ore was taken in a stainless steel tank (10×10×2 cm.) with 40.0% solution of sodium hydroxide, having 10.0% excess of the calculated quantity. The whole mass was mixed thoroughly, evaporated to dryness and heated at 200~225°C at least for 3 hr. to complete the reaction:

$$Fe_2O_3+2NaOH \longrightarrow Fe_2O_3,\ Na_2O+H_2O \qquad (1)$$

The reaction proceeded well to completion and resulted a hard mass adhering to the reacting vessel.

Preparation of Limonite.—The mass of sodium ferrite as prepared above was taken out of the vessel, grinded and sieved. The powdered mass (sometimes without crushing) was taken into a beaker, treated with water heated for one hour to effect hydrolysis according to the reaction:

$$Fe_2O_3\cdot Na_2O+H_2O \longrightarrow 2Fe(OH)_3+2NaOH \qquad (2)$$

On settling, the mixture was filtered on a Büchner funnel. The filtrate was the mixture of sodium hydroxide and sodium carbonate (in some cases sodium bicarbonate depending upon the mode of operation). The residue was ferric hydroxide with certain quantity of residual alkali. The mass obtained thus was blended with saw dust (wood shavings or pulp) for proper consistency, humidity (about 30.0%) and bulk density (approx. 0.8). This was then tested for its hydrogen sulfide absorption power* which was found comparable to the imported mass.

Results and Discussion

The progress of the above reactions was found satisfactory for the production of limonite but certain practical difficulties stood on the way e.g.:

1. The mass of sodium ferrite was found to stick to the reacting vessel and was difficult to remove it.
2. The hard mass of sodium ferrite was evassive to hydrolysis if not grinded and was much time consuming.
3. Filtration of hydrolysis product was difficult for its higher alkali concentration and slow rate of sedimentation of the hydrated oxide.
4. Recovery of alkali was incomplete.

However, to find out the optimum condition for the whole process, some experiments were carried out under different conditions of mass-alkali ratio, temperature and time of reaction. Active iron in the hydrolyzed product was the measure of yield. In all cases, grinded mass was hydrolyzed in boiling water for one hour. The results of the above experiments are presented in Table I.

From the results it may be concluded that:

1) The most suitable temperature for reaction 1 was from 200 to 225°C (curve 1 in Fig. 1). Next experiments were carried out at this temperature.

2) Heating for longer time over 3 hr. was found to be useless. Curve 2 in Fig. 1 indicates that the progress of reaction upto 3 hr. was steady but beyond this it was very slow.

3) Further, the effect of mass-alkali ratio

7) H. J. Zhibon, U. S. Pat. 2432071 (1947).
8) S. Doldi, *Chemical Industria*, **29**, 140 (1947).
9) Brit. Pat. 452504 (1943); *Rec. Brev. Belg.*, 871 (1943).

* Activity test is given in Appendix.

TABLE I. PRODUCTION OF LIMONITE UNDER DIFFERENT CONDITIONS

Experiment	Variable		Yield, %	Remark
Fe/NaOH, 1.3 Reaction time, 1 hr.	Temp. °C :	100	48.0	Brown hard mass, easily breakable
		150	70.0	Brown hard mass
		200	82.0	Less brown hard mass
		225	84.5	Less brown hard mass
		250	85.3	Lesser brown harder mass breaks with difficulty
		300	86.0	
Fe/NaOH, 1.3 Temp., 200°C	Reaction time, hr.	2	90.0	Brown hard mass
		3	93.1	Brown hard mass
		3	95.2*	Brown hard mass
		6	94.5	Brown hard mass
		12	94.5	Harder mass
Temp., 225°C Reaction time, 3 hr.	Mass/alkali ratio (Fe/NaOH)	1.40	79.5	Brown hard mass
		0.90	95.5	Brown hard mass
		0.75	96.0	More brown hard mass

* This experiment was done at 225°C.

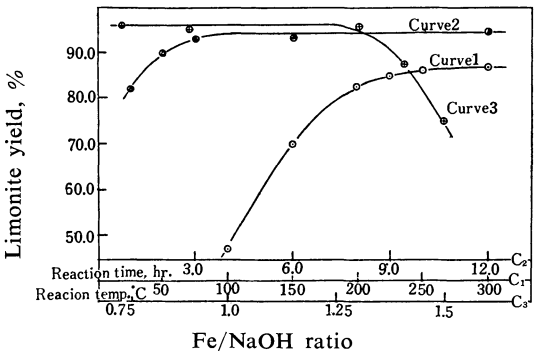


Fig. 1. Yield of limonite under different conditions.
—⊙—⊙— C_1 Temperature-yield
—△—△— C_2 Time-yield
—⊕—⊕— C_3 Fe/NaOH ratio-yield

was distinct arround stoichiometric ratio. The reaction at stoichiometric ratio was 79.5% while with 10.0% excess of alkali it was 95.2%. But with more excess the effect was insignificant (curve 3, Fig. 1).

4) Finally, the optimum condition for this reaction was found to be:

a) Alkali: 10.0% excess of stoichiometric ratio.
b) Temperature: 200~225°C.
c) Reaction time: 3~4 hr.

The first difficulty of adherence of mass to the reacting vessel could somehow be eliminated by stirring thoroughly during evaporation to dryness but the process became laborious. The carbonate (sometimes bicarbonate) content in recovered alkali solution was much high in this case.

Since the reaction[1] was considerably satisfactory, more attention was paid to alkali recovery. To effect maximum alkali recovery without causing deterioration of limonite quality, special stress was given to the hydrolysis under different conditions of temperature and water/mass ratio. Attempt was also made to recover more alkali by passing carbon dioxide in the solution but as it will be seen later, it did not claim any superiority over the others. In all the cases, the recovery reached towards a limiting value upto which it might be economical. However, these results are presented in Tables IIa and IIb.

In view of the difficulties experienced during this work, the macaronies (solid) of 6~10 mm. diameter were prepared from the paste of powdered ore and sodium hydroxide for smooth handling, dried and treated in the same way as those of previous experiments. Some of the results of those experiments are presented in Table III. Some changes in experimental conditions were also tried.

It was interesting to note here that the recovery of alkali as hydroxide was prominent and considerably higher than the recovery with other method tried earlier (cf. Table IIa). This treatment was definitely an improvement over the other in respect of easier handling and slightly better overall recovery (with higher percentage of sodium hydroxide). Limonite quality was more or less the same as prepared otherwise.

Figure 2 presents the curves showing the extent of alkali recovery on hydrolysis of sodium ferrite under different conditions. Curves B, C and D^1 show the influence of

TABLE IIa. RECOVERY OF ALKALI BY HYDROLYSIS OF SODIUM FERRITE

Sample	No. of Washings	Water/mass ratio	Recovery of alkali expressed as Na %				Remark
			NaOH	$NaHCO_3$	Na_2CO_3	Total	
A	1	14	27.9	—	22.7	50.6	Hydrolysis of ferrite at room temperature, 35°C (without grinding)
	2	10	13.0	—	10.4	23.4	
B	1	8	29.0	—	28.8	58.0	Hydrolysis carried out at 85°C after grinding
	2	8	7.6	—	7.3	14.9	
	3	8	2.0	—	1.4	3.4	
	4	8	1.1	—	0.8	1.9	
C	1	8	32.2	—	30.7	62.9	Hydrolysis carried out at 100°C after grinding
	2	8	5.5	—	4.6	10.1	
	3	8	1.7	—	1.4	3.1	
D	1	8	29.4	—	20.9	50.3	First step hydrolysis at room temperature and subsequent washing after passing CO_2 in it (at room temperature) after grinding.
	2	8	—	4.5	13.9	18.4	
	3	8	—	6.18	1.35	7.53	
	4	8	—	3.1	0.38	3.48	

TABLE IIb. EXTENT OF ALKALI RECOVERY WITH VARIED WATER/MASS RATIOS

Water/mass ratio	Recovery of alkali (Na %)				Remark
	A	B	C	D	
8	—	58.0	62.9	50.3	A, B, C and D
14	50.6	—	—	—	represent the
16	—	72.9	73.0	68.7	A, B, C and D of
24	74.0	76.3	76.1	76.23	Table IIa
32	—	78.2	—	79.71	respectively.

TABLE III. RECOVERY OF ALKALI BY HYDROLYSIS OF SODIUM FERRITE MACARONIES (SOLID)

Experiment	No. of washing	water/mass ratio	Recovery of alkali (Na %)			Remark
			NaOH	Na_2CO_3	Total	
1. Ferrite reaction at 200°C for 24 hr.	1	5	47.5	23.2	70.7	These expts. were carried out according to methods D in Table IIa without CO_2. These are represented by curve E in Fig. 2.
	2	5	3.6	5.9	9.5	
	3	5	1.9	1.5	3.4	
		15	53.0	30.6	83.6	
2. Ferrite reaction at 225°C for 24 hr.	1	5	50.8	20.5	71.3	Symbols ⧋, △ and ▲ are for 1, 2 and 3 sets of expts. respectively.
	2	5	5.5	5.0	10.5	
	3	5	0.6	0.8	1.4	
		15	56.9	26.3	83.2	
3. Ferrite reaction at 225°C for 3 hr.	1	5	47.6	21.7	69.3	
	2	5	8.6	4.0	12.6	
	3	5	1.1	1.0	2.1	
		15	57.3	26.7	84.0	

temperature on the progress of hydrolysis. Though at the beginning, higher temperature enhances the hydrolysis but at the later stage with water-mass ratio about 24, all the results tend to reach a limiting value. Beyond this, hydrolysis was very slow. For a recovery of alkali lower than 70.0%, heating has a favorable effect but for higher recovery heating effect is insignificant. From the curve D^2 it was clear that the interaction of carbon dioxide did not offer any improvement.

The curves A and D^1 have shown marked influence of grinding on the progress of hydrolysis at the initial stage. An increase of 13.0% alkali recovery was observed due to grinding at water/mass ratio 16, and thus, the grinding was always preferred before hydrolysis.

Curve E, indicates the better recovery of alkali where procedure D without carbon dioxide was followed. However, the recovery over 80.0% was considered to be uneconomical.

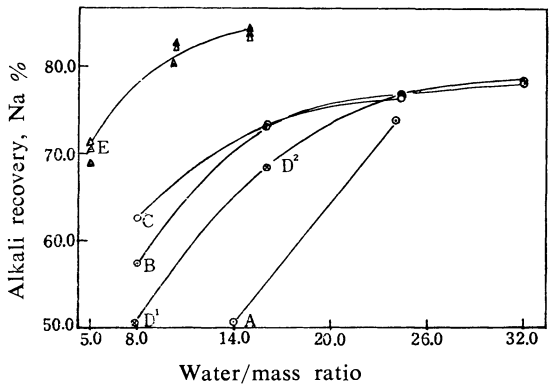


Fig. 2. Extent of alkali recovery on hydrolysis of Na-ferrite.
A Hydrolysis at 35°C (without grinding)
B Hydrolysis at 85°C (with grinding)
C Hydrolysis at 100°C (with grinding)
D^1 Hydrolysis at 35°C (with grinding)
D^2 Further hydrolysis of D^1 after passing CO_2
E Hydrolysis of macaronies (D^1 without CO_2)

Summary

An industrial process of limonite production has been developed in this laboratory using local iron oxide ore of Kalabagh by alkali method. Sodium hydroxide was allowed to react with pulverized ore at 200~225°C to produce sodium ferrite. This product was then hydrolyzed to obtain hydrated ferric oxide (limonite) and alkali in aqueous solution. The method was further modified in the light of some operational difficulties.

Hydrolysis was carried out under varied conditions for maximum recovery of alkali and the recovery upto 80% found to be economical. A graphical representation of this recovery was also given.

The author wishes to express his thanks to Pakistan Industrial Development Corporation for kind permission to publish this paper. He also thanks Mr. G. Courtois for some suggestions during this work.

Pak-American Fertilizer Factory
Daudkhel, West Pakistan

Appendix

Activity of Limonite.—The activity of limonite was determined by its hydrogen sulfide absorption capacity and subsequent liberation of elementary sulfur on regeneration according to overall reaction:

$$Fe_2O_3(H_2O)_x + 3H_2S \rightarrow Fe_2S_3(H_2O)_x + 3H_2O$$

$$Fe_2S_3(H_2O)_x + 3/2O_2 \rightarrow Fe_2O_3(H_2O)_x + 3S$$

In other words, free sulfur liberate on air oxidation was the measure of activity of limonite. The experimental arrangement was as shown in Fig. 3.

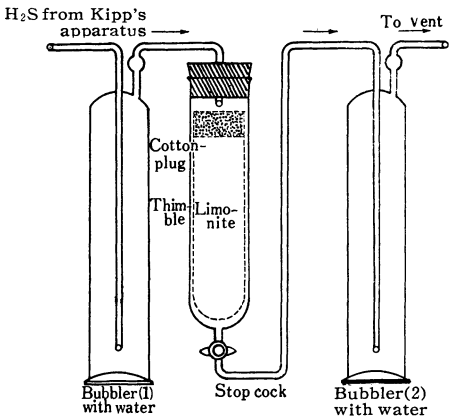


Fig. 3. H_2S absorption system for activity test of limonite.

Procedure.—Ten grams limonite was taken in a thimble and it was moistened thoroughly. A cotton plug was placed at the mouth of the thimble. The thimble was then placed into a cylindrical separating funnel having an internal diameter 16 mm. This was connected to the bubblers containing water according to the diagram. Hydrogen sulfide was generated in a Kipp's apparatus. Moist gas was passed through the limonite bed for a considerable period of time. When the rate of gas flow shown by two bubblers almost the same, the stop-cock was then closed for 3 min. If there was no bubble in bubbler (1) during this period, the hydrogen sulfide absorption by limonite was considered to be complete. The impregnated limonite was then oxidized by passing air through the same system for 12 hr. at the rate of 60 l./hr. using suction pump. The oxidation was complete during this period.

The thimble was taken out and dried at 80°C. The dry mass was then extracted with carbon disulfide (CS_2) in a Soxhlet apparatus. The extracted sulfur was weighed directly.

All the tests were carried out under identical conditions. The activity of natural "Bog ore" (imported from Holland and Denmark) and the limonite produced by the above method was comparative. Ninety-seven per cent iron content of limonite (produced) was found to be active.

Using Iron Ores of Kalabagh. II. Production of Limonite-Acid Method

By M. I. Ali*

(Received July 24, 1961)

Earlier work[1] done in this laboratory on limonite production from local iron oxide ore by alkali method was technically disadvantageous. In view of those results, some other suitable process was looked for. Next attempt was made to utilize acid method. Several acid methods covered under patents acclaimed satisfactory results. A brief review is given below:

A mixture of ferrous and ferric sulfate and chloride on heating produced iron oxide[2] and liberated chlorine which was recycled for production of further chloride.

The oxidation of ferrous sulfate was carried out by passing oxygen or air through the hot solution in presence of zinc or magnesium oxide[3]. Sometimes iron shaving were added and oxidation was carried out under pressure (5 atm.) at 120°C[4].

Another cyclic process[5] utilized iodine as attacking agent to produce iodide which on oxidation liberated free iodine for reuse.

Thermal decomposition of nitrate, oxalate and carbonyls of iron, etc. constituted another method of limonite production[6].

One patent[7] has been claimed the production of limonite and free chlorine by decomposing iron chloride at 1000°C. Chloride was produced by using hydrogen chloride and chorine.

Recently, U. C. B.[7] tried to produce limonite from oxide ores of iron. The ore was first reduced to ferrous oxide (FeO) by using process gas ($CO+H_2=56.0\%$) at 700°C. Ferrous oxide was treated with chlorine or hydrochloric acid to obtain ferric oxide and chloride. This on treating with ammonia yielded hydrated ferric oxide (and ferric hydroxide) i. e. limonite.

Another method[9] described the production of iron sulfate by heating soluble iron salt with ammonium sulfate. This iron sulfate was treated with ammonia in oxidizing medium to obtain hydrated ferric oxide. Ammonium sulfate was being recovered as alum by treating it with bauxite.

None of the above methods was found to suit the purpose. Finally, the use of locally produced dilute sulfuric acid was tried to produce iron sulfate from limonite ore. This proved satisfactory (presenteted in A). Iron sulfate was then treated with ammonia to obtain ferric hydroxide (and hydrated oxide) and ammonium sulfate (in solution). Ferric hydroxide was dried and blended to proper consistency while ammonium sulfate solution was suggested to be sent to sulfatation plant.

Disposal of spent limonite was another problem. Sulfuric acid manufacturing facilities in the country either use elementary sulfur or hydrogen sufide gas. So, the spent material cannot be disposed there. On the other hand, the standard methods of washing out sulfur from spent limonite leaving revivified material ready for further use, could not be practised due to non-availability of cheap solvent. The production of limonite by sulfuric acid method opened up the idea of recovering both limonite and sulfur simultaneously from spent material by following the same procedure. This is presented in B.

A) Production of Limonite from Iron Oxide Ore

(Using Sulfuric Acid)

Considering the scopes and limitations of the above-mentioned methods, none of them was found suitable for the purpose. The use of corrosive chemicals like chlorine, nitric acid and hydrochloric acid, etc. were not desired. The non-availability of the required chemicals in the country was another vital consideration. Finally, it was thought that locally produced sulfuric acid (60° Bé) could be tried for the production of ferric sulfate. This could easily be converted into ferric hydroxide by the action of ammonia. Recovery of by-product ammonium sulfate was also thought to be

* Present address: Natural Gas Fertilizer Factory, Fenchuganj, Sylhet, East Pakistan.

1) M. I. Ali, This Bulletin, 35, 878 (1962).
2) C. Podberg., German Pat. 568239 (1931).
3) J. W. Ayers and G. Plews, U. S. Pat. 2255607 (1941).
4) I. Riskin and G. Pugacheva, *J. Appl. Chem.* (*U. S. S. R.*), **11**, 25 (1934).
5) L. G. Grindin and M. V. Pavlova, *Zhur. Priklad Khim.*, **24**, 1151 (1951).
6) Vereinigte Stahlwerke A. G., German Pat. 581657 (1933).
7) U. E. Bowes, U. S. Pat. 2291206 (1946).
8) Union Chimique Belge (Belgium), private communication (1957).
9) V. Parishat, *Indian.*, **42**, 281 (1951).

feasible. The reactions involved were likely to be as follows:

$$Fe_2O_3 + 3H_2SO_4 \rightarrow Fe_2(SO_4)_3 + 3H_2O \quad (1)$$

$$Fe_2(SO_4)_3 + 6NH_4OH \rightarrow 2Fe(OH)_3 + 3(NH_4)_2SO_4 \quad (2)$$

$$2Fe(OH)_3 \rightarrow Fe_2O_3(H_2O)_x \quad \text{(Partly)} \quad (3)$$

Experimental

A suitable variety of limonite ore was procured from Kalabagh iron mines. The sample was crushed and grinded to 100 mesh (French series) and analyzed[1]. Some exploratory experiments were carried out to ascertain the possibility of the reaction 1 under varied conditions of acid concentration, temperature and reaction time.

The general procedure of the experiments were as follows: 10.0 g. sample was taken in a beaker with requisite quantity of sulfuric acid and it was heated slowly to boiling. This condition was maintained for a desired length of time which was termed "reaction time". On completion of the reaction the whole mass was treated with water, allowed to settle and filtered. After filtration, the filtrate was analyzed for iron content. The results were expressed in percentage (reaction %) on the basis of total iron contents of the sample ore.

The first set of experiments was carried out with varried concentrations of acid. In this case, 40 ml. of sulfuric acid at different concentrations was used. The results are tabulated below in Table I (Fig. 1, curve I)

TABLE I. EFFECT OF SULFURIC ACID CONCENTRATIONS ON THE SAMPLE ORE

Sample, 10.0 g. Sulfuric acid, 40 ml.
Reaction time, 10 min.

Acid. concn. % (by wt.)	Reaction %	Remark (product after reaction)
15.0	9.2	Turbid liquor
30.0	20.0	Turbid liquor
50.0	39.5	Muddy liquor
60.0	51.2	Muddy liquor
70.0	68.0	Thin paste
80.0	68.5	Paste
97.0	70.0	Thick paste

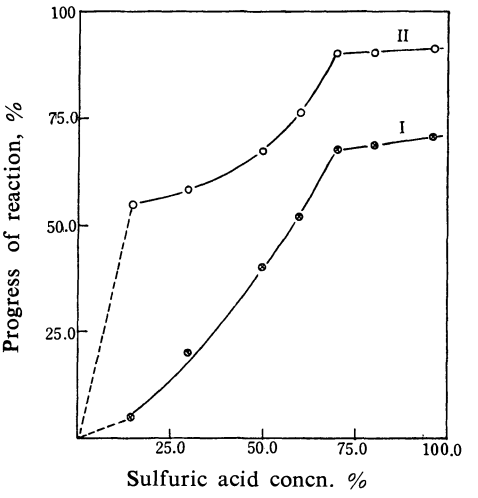


Fig. 1. Progress of reaction with acid concentration.
I, Reaction with ore sample
II, Reaction with spent limonite

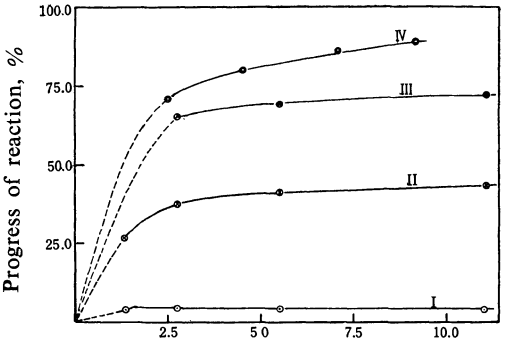


Fig. 2. Progress of reaction with different acid ratio.
I, Reaction with ore sample at 25°C
II, Reaction with ore sample at 98°C
III, Reaction with ore sample at 160~170°C
IV, Reaction with spent limonite at 150~160°C

TABLE II. EFFECT OF TEMPERATURE, REACTION TIME AND ACID/MASS RATIO ON THE PROGRESS OF REACTION 1

Sample taken, 10.0 g. Sulfuric acid concn., 70.0%

Quantity. of acid, ml.	Acid/mass ratio, w/w	Acid ratio (Quantity used / Stoichiometric quantity)	Reaction (%) at room temp. (25°C) for 30 min.	Reaction % at 98°C		Reaction (%) at boiling temp. 160~170°C	
				30 min.	60 min.	10 min.	30 min
13.3	2.12	1.44	4.6	26.0	—	—	—
25.0	4.00	2.70	4.8	38.0	—	65.5	—
50.0	8.07	5.45	5.0	41.0	—	70.0	—
100.0	16.14	10.95	5.0	44.0	66.0	73.5	71.5

Remarks: The reactions at boiling temperature produced a dry pasty mass. So, lengthy reaction time was not possible.

From the above observation 70.0% acid was chosen for further experiments. This time the temperature and reaction time were changed. The results are presented in Table II.

The above results are shown in Fig. 2 (curves I, II and III). It was clear that sulfuric acid needed was much higher than the stoichiometric quantity. The recovery of sulfuric acid as ammonium sulfate was imperative. Some of the experiments were carried out with 1.0 kg. charges each and those were carefully observed to ascertain the prospect of utilizing the method on semi-pilot plant scale. The following observations made thereof are discussed hereunder briefly:

a) Formation of Ferric Oxide Hydrate.—On dilution after sulfuric acid digestion, a fluffy brown precipitate found to remain suspended in the liquid while the undigested material settled at the bottom. This was found to be as active as ferric hydroxide towards hydrogen sulfide and was assumed to be ferric oxide hydrate. It was about 5.0% (as Fe) of the total iron. This was, of course, an addition to the overall yield of limonite.

b) Decantation and Transfer of Ferric Oxide Hydrate.—It was possible to separate undigested mass from the rest (Fe in solution and suspended hydrate) by decantation. Ferric oxide hydrate settled only on long standing. Residue was rejected generally.

c) Ammonia (20~25%) Treatment and Filtration.—Ammonia directly from the purge tank of the ammonia section was used for the purpose. Gelatinous iron hydroxide precipitate was formed, the filtration of which was rather difficult. It was improved to some extent by boiling the whole mass with pulp (or saw dust). Though saw-dust was useful, it could not be recommended due to its resin content, which was apprehended to cause trouble in the evaporator. This warrants further investigation.

d) Drying and Final Removal of Ammonium Sulfate from Residue.—Hot air at about 100°C was passed over the residue after filtration c) till it was half dried. At this stage, the limonite lost its gelatinous character. It was then washed with water to remove ammonium sulfate. The resultant material was dried under shade at a temperature below 50°C by occasional turning.

e) Analytical Results.—Alkaline ammonium sulfate filtrate was analyzed. This was compared with the analysis of ammonium sulfate solution in the neutralization tank of "ammonium sulfate" plant. The results obtained are as follows (Table III):

Table III. Analysis of ammonium sulfate solutions: (1) after ferric hydroxide filtration and (2) solution from neutralization tank

Ingredient	Ammonium sulfate solution	
	After Fe-hydroxide filtration	From neutralization tank
Acidity (H_2SO_4)	—	0.05 g./l.
NH_3 (free)	1.8 g./l.	—
$(NH_4)_2SO_4$	448.0 g./l.	485.0 g./l.
Fe	0.08 mg./l.	0.3 mg./l.
Ca	20.0 mg./l.	540.0 mg./l.
Cl	nil	17.7 mg./l.

f) Recovery of Different Materials.—1) Loss of iron ores ····· about 40% (silicous material over 50.0%). 2) Recovery of sulfuric acid ····· 90~95.0% as free acid and Fe-sulfate. 3) Recovery of ammonia as ammonium sulfate and free ammonia, a) 1st stage filtration ····· 80~83.0%; b) 2nd stage washing out ····· 10~12%.

As a matter of fact, these obesrvations stimulated further investigation to find out some more easily digestible material. In this case, high temperature produced better results but it is feared that the corrosion problem will arise in operating at an elevated temperature. Further one sample of "siderite" (available plenty) was found to be more easily digestible. The nature of reaction was more or less similar to that of oxide ore, the yield was high and could be operated at low temperature.

B) Recovery of Spent Limonite and Sulfur (Using Sulfuric Acid)

The spent limonite containing about 50.0% sulfur could not be utilized for the manufacture of sulfuric acid in the country because of the existing plants are based on either elementary sulfur or hydrogen sulfide. The use of carbon disulfide for sulfur extraction in situ was not practicable due to non-availability of cheap solvent. Its economic disposal was a problem. About 100 tons of sulfur could be recovered every year from the spent limonite. The observations made on limonite production by acid method led to the interesting idea of recovering both limonite and sulfur simultaneously. The reactions involve in limonite purifying process may be represented through a cyclic scheme comprising oxide-sulfide-oxide reactions as follow:

$$Fe_2O_3(H_2O)_x + 3H_2S \rightarrow Fe_2S_3(H_2O)_x + 3H_2O \quad \cdots\cdots \text{(Absorption)} \quad (4)$$

$$2Fe_2S_3(H_2O)_x + 3O_2 \rightarrow 2Fe_2O_3(H_2O)_x + 6S \quad \cdots\cdots \text{(Regeneration)} \quad (5)$$

Non-regenerative FeS_2 and Fe_8S_9 was also reported to form at elevated temperature.

However, sulfuric acid was considered to be useful for the recovery of sulfur. The experimental procedure adopted was more or less the same as with the iron ores. The first step reaction with regenerated material was:

$$[Fe_2O_3(H_2O)_x + S] + H_2SO_4 \rightarrow Fe_2(SO_4)_3 + H_2O + S \quad (6)$$

Experimental

The technical analysis of the raw material (spent limonite) was as follows (Table IV):

TABLE IV. ANALYSIS OF SPENT LIMONITE

Constituent	%
Acidity	Neutral
Humidity	26.9
Ash content	37.4
Iron (Fe)	23.8
Sulfur	
a) As sulfate	2.2
b) Elem. sulfur	45.8
Specific weight	
a) Loose packing	680 g./l.
b) Close packing	900 g./l.

The spent limonite was found to be more reactive with sulfuric acid than the oxide ores. One series of experiments was carried out using different concentrations of acid. The results are presented in Table V and in Fig. 1 (curve II). One sample of unregenerated sample was also tried for the purpose.

From the above results, 70.0% acid was found to be most suitable for the reaction. Another set of experiments was carried out with this acid to ascertain the optimum quantity. Those results are shown in Table VI and also by Fig. 2 (curve IV).

From the above Tables V and VI, 40 ml. sulfuric acid (70%) was found to be the requisite quantity for 10.0 g. spent limonite. Some experiments were also carried out with 5.0 kg. sample. The results were found satisfactory. The similar difficulties of iron hydroxide filtration as with the oxide ores were also encountered here. The advantages in this case were that the reaction temperature was lower while the progress was better. The over-all recovery of limonite was 80.0% by this method (considering the loss during processing).

Recovery of Sulfur.—The residue obtained after digestion of spent limonite with sulfuric acid contained mainly sulfur, iron oxide and little organic matters. The approximate compositions was found to be:

Sulfur	75.0%
Iron oxide	20.0%
Others	5.0%

TABLE V. EFFECT OF SULFURIC ACID CONCENTRATION ON THE PROGRESS OF REACTION WITH THE SPENT LIMONITE

Sample taken, 10.0 g. Quantity of acid used, 40 ml.
Time of reaction, 10 min. Water added for dilution, 100 ml.

Concn. of sulfuric acid, % (by wt.)	Acid ratio (Quantity used / Stoichiometric quantity)	Observed temp., °C		Reaction, %	Remark
		before diln.	after diln.		
15.0	1.06	No remarkable rise of temperature		53.9	—
30.0	2.34	—		58.0	Muddy liquid
50.0	4.47	40	35	68.5	Slurry
60.0	5.75	50	45	76.5	Thin paste
70.0	7.22	65	50	89.0	Thin paste
80.0	8.9	70	60	89.5	Thick paste
97.0	11.4	75	90	90.0	Pasted and charred
70.0†	7.22	65	65	83.5	Thin paste
70.0	7.22	60	55	79.5	Thin paste The sample was not regenerated.

† 100 ml. water was used for dilution in two portions of 50 ml. each.

TABLE VI. EFFECT OF QUANTITY OF ACID ON THE PROGRESS OF REACTION

Sample taken, 10.0 g. Concn. of acid used, 70.0%
Reaction time, 10 min. Water used for dilution, 100 ml.
Temperature, to boiling

Quantity of acid used ml.	Acid ratio (Quantity used / Stoichiometric quantity)	Reaction, %	Remarks on reaction product	
			before dilution	after dilution
14.0	2.52	71.0	Paste	Easily decantable (sp. gr. 1.05)
25.0	4.5	79.5	Paste	Easily decantable
40.0	7.2	87.2	Thin paste	Easily decantable
50.0	9.0	89.0	Pasty liquor	Decantable
100.0	18.0	90.0	Muddy	Decantable with time (sp. gr. 1.19)

The impure sulfur thus recovered was purified to about 90.0% by melting out process. For further purification any standard method could be adopted.

In view of the above observations, it appears fairly agreeable to operate such plant. It is, of course, not free from difficulties. The main difficulty with this method that it is a lengthy process. It is always difficult to realise movement of such type of materials through the process equipments. However, it may be concluded that 80.0% of the spent limonite can be recovered by this method. The rest 20.0% make up limonite may be supplemented by producing it from local iron ores preferably "siderite".

Summary

A method of limonite production has been developed in this laboratory and it was produced from both "Kalabagh iron ores" and "spent limonite" by using local sulfuric acid (60° Bé). Ammonium sulfate, by-product, was also recovered. The process comprised of (i) digestion of the raw materials with 70.0% sulfuric acid, (ii) ammonia treatment of the resultant ferric sulfate solution to produce ferric hydroxide and (iii) careful drying and blending of ferric hydroxide (and oxide) to the desired consistency. The over-all recovery of spent limonite was found to be 80.0%. A material balance sheet is also presented. For the production of 20.0% make-up limonite "siderite" iron ore is suggested to be of use.

The author wishes to express his thanks to Pakistan Industrial Development Corporation for providing facilities to carry out this work.

Pak-American Fertilizer Factory
Daudkhel, West Pakistan

Appendix

Flow Diagram: The material balance of the limonite production (by sulfuric acid method) could be shown by following flow diagram (1.0 kg. iron oxide ore basis).

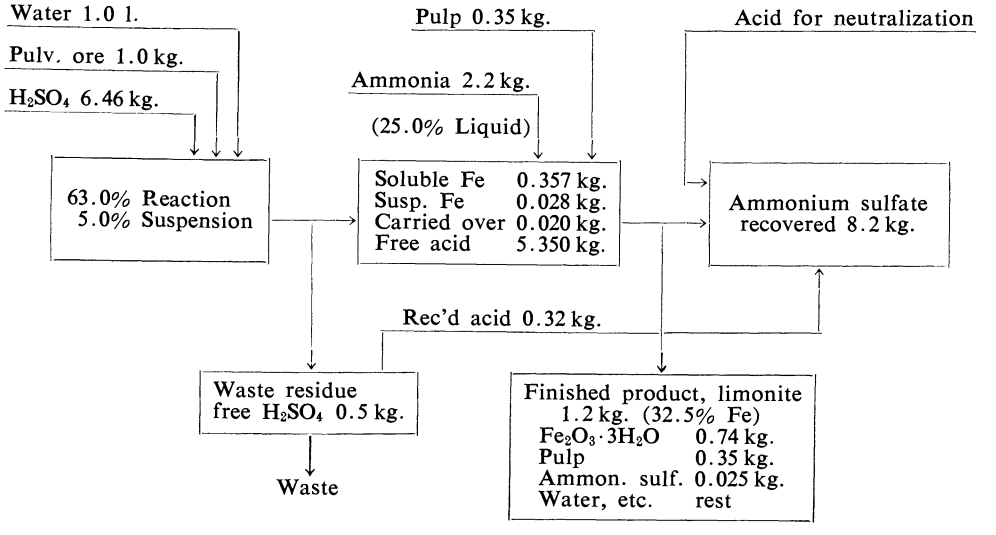


Fig. 3. Material flow diagram of limonite production (acid method).

Regeneration of Spent Limonite using Gasoline. I

By M. I. ALI*

(Received July 24, 1961)

It was observed that the crude gasoline, a by-product in coal gasification process, could dissolve certain quantity of sulfur when hot, from the spent limonite and the dissolved sulfur could easily be crystallized out by cooling. This observation suggested that it could be utilized profitably as a solvent for sulfur. Some important characteristics of this gasoline were studied including the solubility of sulfur in it. On satisfactory preliminary tests, a batch process of regeneration of limonite was tried. It was possible to recover 90.9% sulfur from spent limonite at a regeneration temperature of 85°C using a weight ratio 11.7 : 1 of gasoline and spent limonite respectively.

Next, a continuous flow of hot gasoline through a fixed bed of spent limonite was tried. This had shown some improvement over the batch process mentioned above, 96.0% sulfur was recovered at 86°C with gasoline limonite ratio 12 : 1 (w/w). The main difficulty encountered in this process was the sticking of sulfur crystals on the cooling surface and thereby heat transfer was retarded. This was overcome by direct quenching in cold water. Another problem was to remove the retained gasoline from the regenerated limonite. The removal was effected by passing nitrogen through the limonite bed in suit at regeneration temperature. The exit gas was then washed with oil to recover gasoline. The over-all activity of this regenerated limonite was found to be over 80.0%.

It has already been discussed in part I[1] and part II[2] that the recurring import of fresh limonite and the disposal of spent limonite are problems to this factory. A practical method[2] (cf. part II) for the production of limonite from iron ore has since been developed. Relatively easier method of solvent extraction was also considered but due to non-availability of indigenous solvent it was not tried earlier. In the meantime, the problem of by-product gasoline purification was at hand. The crude gasoline could not be marketed for its high sulfur content in the form of H_2S, mercaptans and other organic sulfur compounds. It has a nauseating odor. Attempt was made to use limonite for gasoline purification. Almost complete removal of sulfide-sulfur was effected by limonite but last trace could not be removed by this. Thus purified gasoline could not stand Doctor's test. The treated gasoline was of rather dark color while the fresh one is of straw color. It may be mentioned here that fresh gasoline on long exposure to atmosphere became dark. Presently, the gasoline is being utilized as fuel in the power station. This is equivalent to twice its weight of coal.

During this experimentation with gasoline and limonite two important observations were made:

1) Hot gasoline dissolved considerable amount of sulfur from spent limonite and the crystalline sulfur could be obtained from rich gasoline on cooling.

2) The gasoline did not wet limonite and the treated limonite could be dried easily. These stimulated to undertake the present work, the extraction of sulfur from spent limonite with gasoline and thereby to regenerate the spent limonite.

Study of Gasoline

First, the study of gasoline was necessary to find out its suitability for the purpose. The characteristics of gasoline are presented in Table I.

TABLE I. CHARACTERISTICS OF CRUDE GASOLINE

1.	Physical appearance	Straw colored liquid
2.	Color on standing	Dark
3.	pH	>7 (slightly alkaline)
4.	Specific gravity	0.79 at 20°C
5.	Viscosity	1.13°E at 20°C
6.	Flash point	<20°C
7.	Calorific value (gross)	11000 cal./g.
8.	Specific heat	0.450 cal./g./°C at 37°C
9.	Sulfide sulfur (H_2S)	0.714g./1.
10.	Sulfate	Trace
11.	Total sulfur	0.770g./1.
12.	Phenol content	3.5 g./1.

Fractionation of Gasoline.—The composition of gasoline was not known. But it was reported[3]

* Present address: Natural Gas Fertilizer Factory, Fenchuganj, Sylhet, East Pakistan.

1) M. I. Ali, This Bulletin, 35, 878 (1962).

2) M. I. Ali, ibid., 35, 883 (1962).

3) A. H. Permantier, Private communication, 1957.

to contain 12.0% benzene. It is understood that higher aromatic hydrocarbons e. g. toluene or xylene are found to be good solvent for sulfur at an elevated temperature. So it was necessary to assess the availability of suitable fraction. The fractionation of gasoline was carried out by using a Vigreux model 800 mm. long fractionating column. The results are presented in Table II. Further, the fractionation of gasoline saturated with sulfur was also carried out, under similar conditions, for comparison.

Table II. Fractionation of crude gasoline and sulfur impregnated gasoline

Temp. °C	Distillate (%) by vol. Crude gasoline	Distillate (%) by vol. Sulfur saturated gasoline	Remark
40	0.6	0.2	1.0 l. samples were used for fractionation.
50	3.2	1.0	
60	6.0	3.0	A thick dark residue was obtained in case of crude gasoline
70	10.0	4.8	
80	18.0	7.6	
90	29.2	18.0	Some carbon particles were also found therein.
100	34.0	32.0	
110	40.0	40.0	
120	50.0	48.0	In case of sulfur impregnated sample residual sulfur became dark plastic mass.
130	55.4	54.0	
140	68.8	63.0	
150	72.0	74.0	
155	79.0	80.0	

From the close study of above results, gasoline fractions may be divided into 4 parts.

1) Fraction below 70°C……10.0% light fraction.
2) Fraction between 70~85°C……18.0% rich in benzene.
3) Fraction between 85~110°C……12.0% rich in toluene.
4) Fraction above 110°C……40.0% heavy fraction containing xylene and others.

The remaining 20.0% polymerized and decomposed at the distilling temperature. The light fraction and benzene fraction are obviously unsuitable for the purpose.

But it was observed that the residue was readily soluble in the light fraction. The solution was, of course, dark. However, for the practical purposes the gasoline fractions may be divided into two parts a) fraction below 85°C lighter fraction (LF) and b) the fraction above 85°C heavy fraction (HF). Heavy fraction was considered to be useful for the purpose. The above study revealed that there was not much influence of dissolved sulfur on fractionation except at the initial stage. The residue obtained was a plastic one, probably due to allotropic modification of sulfur. In view of the above observations, the solubility of sulfur in gasoline was studied only with the heavy fraction (above 85°C).

Solubility of Sulfur in Gasoline.—A sample of sulfur was recovered from the spent limonite by using gasoline. This was purified with LF gasoline and carbon disulfide. It was needle shaped crystalline sulfur of m. p. 114 (±0.5)°C. Optimum contact period for saturation of sulfur in gasoline and its solubility at different temperature were established. Eight minutes contact period at 70°C was found to be sufficient to reach saturation point. Therefore, 10 min. contact period was chosen for further solubility experiments at different temperature from 20 to 112°C. The results are presented in Table III (Fig 1). A depression of melting point of sulfur by 2°C was observed during these experiments. At 112°C excess sulfur formed a molten layer at the bottom.

The melting point of sulfur used in above experiments was 114°C. But in gasoline it melted at 112°C. The depression may be due to the presence of gasoline. Similar effect was also observed previously (melting point of crude

Table III. Solubility of sulfur in gasoline with temperature

Temp. °C	Solubility g./l.	Solubility % by wt.	Remark
20.0	6.5	0.77	(a) At 112°C or above, molten sulfur formed dark layer at the bottom.
50.0	22.7	2.62	
65.0	36.8	4.2	
80.0	51.6	5.74	(b) True solubility at higher temperature above 85°C are different from the presented value. These require correction in the light of evaporation and change of composition of gasoline with the rise of temperature. Since the working temperature will be ultimately 85°C, these value are not so important.
85.0	55.1	6.16	
90.0	62.9	6.96	
100.0	75.2	8.21	
110.0	90.0	9.68	
112.0	Started melting	—	

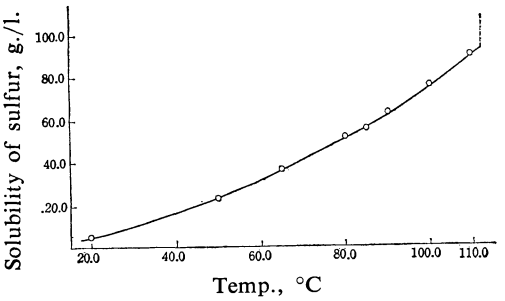


Fig. 1. Solubility of sulfur in gasoline with temperature.

recovered sulfur 111~112°C). However, the solubility of both the sulfur samples, purified in gasoline (LF) and carbon disulfide, were more or less the same. Solubility was expressed with respect to volume of gasoline at 16°C.

Study of Limonites

A sample of spent limonite was collected from the heap and stored in well stoppered cans. The sample was analyzed and found to contain:

Moisture	13.5%
Sulfur (elem.)	45.8%
Limonite etc.	Rest

There are several varieties of limonite $Fe_2O_3 \cdot H_2O$ of which only α and γ varieties are known[4] to be most active towards hydrogen sulfide. The structure and properties of these materials are susceptible to the climatic conditions. Temperature has much influence to that effect. Limonite looses its activity at high temperature. So, to retain the desired activity, the temperature is required to control within 40°C during normal use.

The main object of this work was to regenerate spent limonite and to recover sulfur as secondary product. A series of experiments were performed at different temperatures to find out the optimum regeneration temperature. The activity of each regenerated sample was studied (cf. Appendix I, part I). The results are presented in Table IV; Fig. 2.

It may be concluded from the above results that the activity of limonite decreases with increase of regeneration temperature and remarkably above 80°C. However, considering the solubility of sulfur in gasoline and activity loss of limonite with temperature, 85°C was chosen for further experiments. The loss of activity of limonite, at this regeneration temperature was about 10.0%. In view of above informations, a systematic study of limonite regeneration by gasoline was made with a batch process.

TABLE IV. ACTIVITY OF LIMONITE REGENERATED AT DIFFERENT TEMPERATURES

Regeneration temp. °C	Activity %	Remark
50	98.0	The activity was calculated only on the basis of active iron (Fe) content in regenerated limonite according to the equation: $A\ (\text{activity}) = \frac{X}{Y} \times 100$ where X=active iron (Fe) and Y=total iron present in the limonite.
60	97.0	
70	95.0	
80	92.0	
90	85.0	
100	70.0	

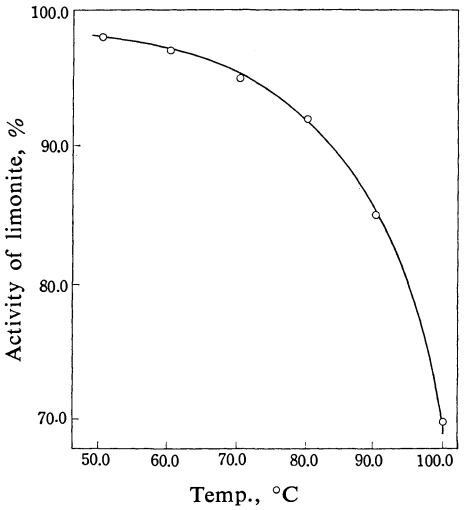


Fig. 2 Activity loss of limonite with temperature.

Regeneration of Spent Limonite

Batch Process.—One hundred grams spent limonite was taken in a separating funnel containing 200 ml. gasoline (HF). The funnel with its content was immersed in a water bath at 85°C and agitated slowly. This was continued for 10 min. The solid-liquid mixture attained the same temperature of bath (85°C) within 3~4 min. Then, gasoline rich in sulfur was drained out and filtered at 85°C. Let this liquid be called "overflow". This was cooled down to 16°C and sulfur crystallized out was measured. Certain quantity of gasoline was retained by limonite mass and this liquid was termed "underflow".

Next, the mass in the separating funnel (including "underflow") was treated with another 200 ml. fresh gasoline in the same way as before. The batch leaching was continued until sulfur concentration in "overflow" became negligibly low.

The results of one set of experiments with 7th batch leaching are presented in Table V.

The progress of extraction falls too low with the increasing number of washings i. e. with the decrease of sulfur concentration in limonite. After sixth washing further treatment was almost useless. This fall of efficiency probably due to the fact that gasoline could not reach into the core of limonite particle to dissolve out sulfur therein entrapped. It is more clear from the extraction of sulfur (Table V), particularly extraction efficiencies there. It means

4) R. H. Griffith and A. R. Morcom, *J. Chem. Soc.*, 1945, 786.

TABLE V. EXTRACTION OF SULFUR FROM SPENT LIMONITE WITH GASOLINE

Temp., 85°C; Contact period, 10 min.

No. of treatment	Gasoline / S. limonite (w/w)	"Overflow" gasoline recovery vol. %	Sulfur extraction wt. %		Extraction efficiency %		Remark
			Separately	Cumulative	Separately	Cumulative	
1	1.68	66.5	14.8	14.8	92.5	92.5	For each washing fresh gasoline was used. Gasoline distilled out with water content of limonite is neglected here.
2	3.36	88.0	19.2	34.0	90.6	91.4	
3	5.04	95.5	20.1	54.1	87.6	90.0	
4	6.72	97.7	18.1	72.2	71.0	84.7	
5	8.40	98.7	9.8	82.0	42.0	73.1	
6	10.08	99.7	5.1	87.0	21.0	65.5	
7	11.76	99.7	1.9	88.9	8.0	56.6	

that a longer contact period is required. To produce the desired effect, it was thought that a modified procedure of continuous liquid flow at 85°C through the fixed bed of limonite would be suitable.

Continuous Liquid Flow Processes.—In view of the above observations, it was thought that a continuous liquid (gasoline) flow through the fixed bed of limonite may be useful. Due consideration was given to temperature condition, gasoline-limonite contact period, the quality of recovered sulfur and the by-products. Provision for direct feeding of crude gasoline was also kept in view.

It was thought that the distillation process would be suitable to effect both extraction of sulfur by reflux and separation of lighter fraction as distillate in the same process and equipments. To achieve this end, a modified equipment had been drawn up. It was also thought that the cyclic regenerative process would be a complementary measure against short supply of gasoline.

First attempt was made to separate lighter fraction of gasoline by distillation and utilize reflux gasoline for leaching the spent

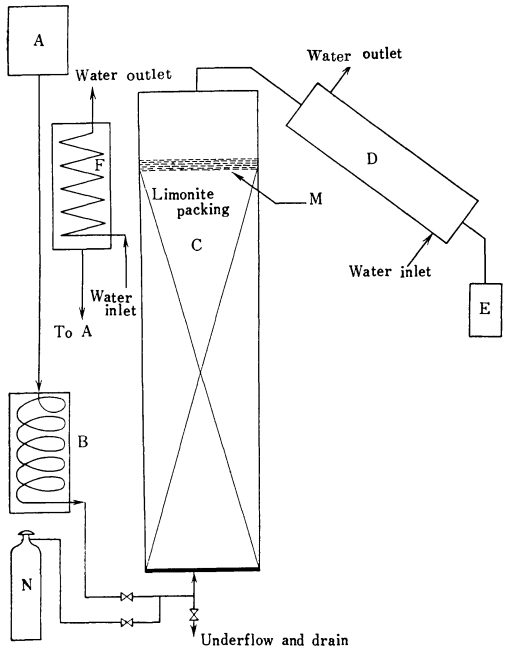


Fig. 3. Hot gasoline flow process.
A Gasoline reservior
B Gasoline heater
C Limonite column
D Condenser
E LF gasoline receiver
F Overflow receiver
N Nitrogen cylinder
M Porous plug filter

TABLE VI. SOME PHYSICAL CONSTANTS OF GASOLINE AND LIMONITE AND THEIR USEFUL RELATIONS

1 Specific gravity of gasoline (HF): 0.84 at 16°C
2 Expansion of gasoline volume with temperature: 10.0% at 85°C on the vol. at 16°C
3 Specific heat of gasoline (HF): 0.545 cal./g./°C at 37°C
4 Latent heat of vaporization: 207 cal./g.
5 Packing density of spent limonite
  a) Loose packing: 725 g./l.
  b) Close packing: 820 g./l.
6 a) Free space in spent limonite packing (loose): 62.0%
  b) Free space in regenerated limonite packing (loose): 68.0%
7 Retention of gasoline
  a) HF by spent limonite: 37.0% (by vol.)
  b) HF by regenerated limonite: 38.0% (by vol.)
  c) LF by regenerated limonite: 36.0% (by vol.)
8 Reduction in volume of limonite on regeneration: 25.0%
9 Specific gravity of regenerated limonite: 0.52 (approx.)

limonite at the same time. But recovered sulfur was dirty while the heat loss was much. Moreover, the process was time-consuming.

In view of these observations it was further modified were hot gasoline at 85°C was passed through the fixed bed of limonite. By this "hot gasoline flow process" recovered sulfur was of 99.0% purity. The process is shown in Fig. 3. Arrangement was also made to dry up regenerated limonite by passing nitrogen gas through it and to recover lighter fraction of gasoline as distillate with steam. For smooth operation of the process, some physical constants of gasoline and limonite and their useful relations have been established. Those are presented in Table VI.

Having the above informations ready at hand to calculate the results under changing conditions, a systematic study of "hot gasoline flow process" was started. This was done

TABLE VII. RECOVERY OF SULFUR AND GASOLINE UNDER DIFFERENT CONDITIONS

Experimental condition	Ratio (w/w) Gasoline / S. limonite	Gasoline recovered* Rich %	Gasoline recovered* Distillate %	Sulfur recovered %	Water removed from limonite %	Remark
I. Temp., 70°C; liquid velocity, 1.84 cm./min.; contact period, 10.9 min.	2.0	89.2	10.8	18.9	66.0	In all cases initially sulfur was slightly dirty but beyond gasoline - limonite ratio 2 it was bright. It tarnished on long standing in gasoline. Overall efficiency, 57.0%
	4.0	91.2	8.8	38.5	72.5	
	5.0	92.1	7.9	48.0	74.3	
	6.0	93.0	7.0	56.0	—	
	8.0	94.2	5.8	68.5	76.8	
	10.0	95.2	4.8	76.8	—	
	12.0	96.0	4.0	81.0	78.0	
	14.0	96.3	3.7	83.5		
II. Temp., 80°C; liquid velocity, 0.8 cm./min.; contact period, 24.7 min.	3.0	89.2	10.8	40.8	74.5	Overall efficiency, 61.5%
	5.0	91.5	8.5	63.5	77.7	
	6.5	92.8	7.2	75.0	78.8	
	8.4	94.2	5.8	83.5	—	
	10.5	95.2	4.8	88.1	79.9	
	12.5	95.9	4.1	90.0	80.0	
III. Temp, 84°C; liquid velocity, 2.3 cm./min.; contact period, 8.8 min.	2.0	—	—	—	75.7	Overall efficiency, 48.8%
	4.0	88.9	11.1	49.0	83.0	
	6.5	91.9	8.1	68.5	84.2	
	8.6	93.6	6.4	78.0	84.6	
	10.8	94.8	5.2	85.0	—	
	13.5	95.7	4.3	87.5	84.8	
IV. Temp., 86°C; liquid velocity, 0.64 cm./min.; contact period, 25.2 min.	2.0	—	—	—	78.0	Overall efficiency, 54.0%
	4.0	87.3	12.7	54.5	86.3	
	5.1	89.4	10.6	70.0	87.0	
	8.0	92.7	7.3	90.5	87.8	
	10.0	94.1	5.9	94.2	—	
	12.0	95.0	5.0	96.0	88.0	
V. Temp., 84°C; liquid velocity, 0.7 cm./min.; contact period, 27.8 min.	2.0	84.0	16.0	26.3	74.0	Overall efficiency, 49.2%
	4.0	89.5	10.5	53.5	80.0	
	5.6	91.4	8.6	74.4	81.5	
	7.3	92.8	7.2	84.0	—	
	10.0	94.6	5.4	91.0	—	
	13.0	95.8	4.2	93.5	82.5	

* In the continuous liquid flow process "underflow" is assumed to be constant which is neglected in gasoline recovery calculations. This should be accounted only at the end of the experiment.

under varied operating conditions. The variables were (a) liquid velocity, (b) contact period of gasoline and (c) gasoline-limonite ratio, etc. The results of one set of experiments are presented in Table VII.

A close study of Table VII revealed that the best result was obtained under the conditions of experiment IV (temp. 86°C). The result of experiment V (temp. 84°C) was also almost equally good. These results are compared with that of batch process. The "hot gasoline flow process" was found to have some superiority over other two processes—"batch process" and "distillation process", with respect to both sulfur recovery and its quality. Moreover, this was much advantageous from operational point of view.

It was interesting to note that the liquid flow and contact period have marked influence at the initial stage up to gasoline/spent limonite ratio 8. Beyond this ratio in all cases, the efficiency of extraction slowed down rapidly. From Table VII, it appears that sulfur extraction never reaches completion within reasonable gasoline/limonite ratio.

During these experiments, the percentage of gasoline escaped as distillate and the quantity of water eliminated from the system (i.e. from limonite) were also accounted.

However, a certain quantity of sulfur and water always remain in regenerated limonite. An average analysis of the same is presented in Table VIII for comparison with that of fresh limonite.

Table VIII. A comparative study of fresh and regenerated limonite

	Particular	Regenerated limonite*	Fresh limonite
1.	Humidity, %	5~10	30~35
2.	Sulfur content, %	6~8	Nil
3.	Iron content, % (dry basis)	34.0	38.0
4.	H_2S absorption (Sulfur % on limonite)	23.0 (against 26.% theor.)	20.5
5.	Efficiency**, %	90.0	Standard

* This analysis was done before conditioning the regenerated limonite.

** This efficiency is on the basis of active iron content only. The presence of 6~8% sulfur reduces the iron content in the bulk and thereby lowers the efficiency. Finally, the overall efficiency of thus regenerated limonite stands at about 85%.

Discussion

Recovery of Sulfur.—Impregnated gasoline on cooling yields crystalline sulfur of different shape and sizes depending upon mode of operation. Under ordinary condition, the crystals used to stick to the cooling surface and thereby retarded the heat transfer in the system. This would cause operation difficult. To make it much easier, direct quenching was tried and found to be satisfactory. The arrangement for the quenching process is shown by Fig. 4.

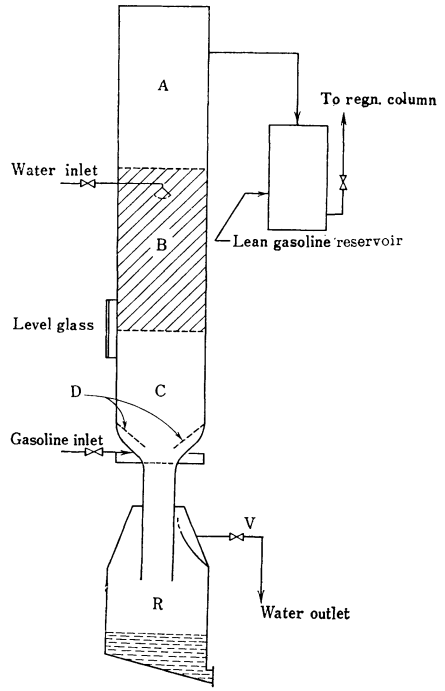


Fig. 4. Quenching column.
A Top zone
B Middle zone
C Bottom zone
D Distributor
R Receiver (sulfur settling)
V Control valve

The quenching apparatus consisted of a quenching column and a receiver for sulfur. Quenching column was a straight one, vertically placed on the receiver R. There were three distinct liquid phases in the column:

A Top zone: lean gasoline
B Middle zone: emulsion of gasoline-water.
C Bottom zone: clear water with bubbling gasoline and falling sulfur crystals.

The column was provided with a gasoline inlet at the bottom (at two points) under the distributor D, and exit at the top (zone A). Water was introduced at the top of middle zone. It was then allowed to flow down through the central clearance of the distributor, carrying sulfur to the receiver. Cryslals of sulfur settled down at the bottom of the receiver while water overflowed through the level controlling valve, V. A level glass would be necessary for this apparatus at the junction of zones B and C.

It is very important to maintain water level in the column and counter current flow ratio of gasoline and water rate. Gasoline flow at low pressure would stop if water flow is much higher. On the other hand increased gasoline flow would cause inefficient separation of sulfur. In short, the efficiency of the process is the function of (1) gasoline-water flow ratio, (2) gasoline-water contact period and (3) temperature of the liquids.

It was necessary to adjust all the variables for optimum condition. It has been observed that a streamline flow is required for effective cooling and separation of sufur. However, the working condition of a small column (30×2.5 cm. ϕ) particularly at maximum flow rates is presented here:

a) Rich gasoline feed 500 ml./min. (445.0 g.)
b) Gasoline pressure 0.1 kg./cm^2
C) Gasoline-water contact period (in bottom zone) 3 sec.
d) Quenching water 579.0 ml
e) Temperatures of inlet and outlet water, −20°C and 50°C respectively
f) Temperatures of inlet and outlet gasoline, −83°C and 23°C respectively

Under this limiting condition the cooling efficiency was found to be 71.6%. A better efficiency could be achieved if the contact period is increased reasonably by increasing the column length and operating under higher gasoline pressure head. A modified column would help bettering stream-line flow of gosoline.

Crystalline sulfur accumulated in the receiver was of sizes arround 60 mesh. Some crystals used to agglomerate to form loose and soft lumps bound by emulsion film of gasoline while others moved freely in quenching water. On long standing bound gasoline in the lumps and emulsion film bubbled up to the surface. Thus settled sulfur became almost pure. It is interesting to note here that there was no appreciable oxidation of sulfur during quenching. Purification of recovered sulfur could be effected by steam treatment.

Drying of Regenerated Limonite.—It has been observed that a considerable quantity of gasoline was retained (underflow) in regenerated

TABLE IX. REMOVAL OF RETAINED GASOLINE BY NITROGEN

Regenerated limonite: 256.0 ml.
Gasoline to be removed: 97.0 ml.
Temperature: 60~80°C

Expt.	N_2/gasoline ratio (v/v) $\times 10^2$	Gasoline recovery wt. %	Remark
I. Gas flow 42 l./hr.; space velocity, 433 cc./cc./hr.; time, 83 min.	2.18	50.0	During drying process, the temperature was lowered as a precaution against activity loss of limonite. Too much lowering of temperature would cause drying inefficient. To maintain the temperature inlet nitrogen might be necessary to heat up occasionally.
	2.93	74.5	
	3.8	86.0	
	4.7	93.0	
	5.65	96.5	
II. Gas flow 12 l./hr.; space velocity, 124 cc./cc./hr.; time, 110 min.	2.25	48.5	
	2.92	75.0	
	3.66	90.0	
	4.46	97·0	
III. Gas flow 87.5 l./hr.; space velocity, 903 cc./cc./hr.; time, 43 min.	2.21	49.5	
	3.0	70.5	
	4.05	81.0	
	5.0	87.5	
	6.0	91.0	
IV. Gas flow 30 l./hr.; space velocity, 310 cc./cc./hr.; time, 114 min.	2.23	49.0	
	2.92	75.0	
	3.71	88.0	
	4.54	96.5	
	5.52	99.0	

Note: (1) Nitrogen/gasoline ratio was calculated on the quantity of gas passed and total quantity of gasoline to be removed. (gas vol./liquid vol.)
(2) Average gas flow is indicated here.

limonite. Removal of this gasoline was important. Open air drying must not be permitted for its hazardous effect. It is inflamamble liquid and forms explosive mixture in air. It is also injurious for health. Its permissible limit[5] in U. S. A. is 1000～1500 p. p. m. and U. S. S. R. is 55～115 p. p. m. After careful consideration locally available nitrogen gas was the choice to be used for the purpose. A study of space velocity of carrier gas on gasoline removal system is presented in Table IX.

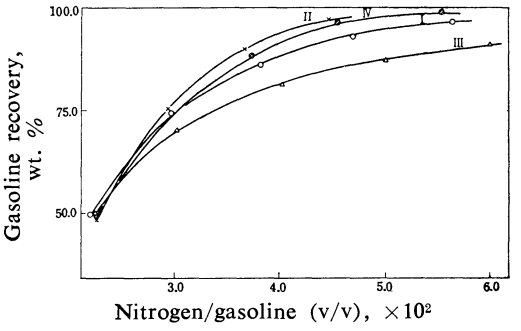


Fig. 5. Removal of retained gasoline by nitrogen.

I	Space velocity	433 cc./cc./hr.
II	Space velocity	124 cc./cc./hr.
III	Space velocity	903 cc./cc./hr.
IV	Space velocity	310 cc./cc./hr.

From above data and curves in Fig. 5 it is clear that gas flow and space velocity have bearing on the removal of gasoline from regenerated limonite. At higher space velocity, the removal of gasoline was relatively low (curve III), while at lower space velocity it was slow. An intermediate space velocity arround 310 cc./cc./hr. was found to be satisfactory.

Arrangements were also made to recover gasoline from the exit gas by oil washing and subsequent rich oil on distillation yields gasoline.

In conclusion, it may be said that the plant should be modified in the light of above observations by replacing the "overflow receiver" (F in Fig. 3) with a quenching column and adding one gasoline recovery unit.

The author extends his thanks to Pakistan Industrial Development Corporation for providing facilities to carry out this work.

Pak-American Fertilizer Factory
Daudkhel, West Pakistan

5) V. J. Altieri, "Gas Analysis and Testing of Gaseous Materials", American Gas Assoc. Inc. (1945).

Regeneration of Spent Limonite using Gasoline. II. Continuous Countercurrent Process

By M. I. ALI*

(Received July 24, 1961)

Earlier, a process of regeneration of limonite using hot gasoline on fixed bed was worked out. This study indicated the possibility of developing a countercurrent process where both gasoline and limonite could move physically in opposite directions. For this purpose, free movement of different limonite particles under gravity in still and flowing gasoline was studied. After careful consideration, regeneration column was designed for further experiments and operated under varied conditions. Optimum liquid velocity and solid-liquid contact period at different limonite velocity were ascertain and discussed. Finally, a modified process flow sheet has been drawn up and presented.

Regeneration of Spent Limonite Continuous Countercurrent Process

In view of earlier observations[1] and data obtained thereof, attempt was made to realize a continuous countercurrent process in which both gasoline and limonite could move physically. The Dorr multideck classifier was the only suitable equipment for this type of closed circuit leaching. But the fact that limonite did not get wet in gasoline and its movement was considerably free, led to think otherwise. It was thought that gravity flow of limonite through gasoline might be feasible. To achieve this end, it was first necessary to study counter-

* Present address: Natural Gas Fertilizer Factory, Fenchuganj, Sylhet, East Pakistan.

1) M. I. ALi, This Bulletin, 35, 888 (1962).

TABLE I. FALLING VELOCITY OF LIMONITE PARTICLES THROUGH GASOLINE UNDER GRAVITY

Specific gravity of gasoline;	0.84 at 16°C
Viscosity of gasoline;	1.13°E at 20°C
Height of the place of experiment above sea level;	200 m. (approx.)
Temperature during experiment;	20°C
Travelling distance of limonite particles;	2.5 m.

Particle size mm.	% of different size particles			Falling velocity of limonite particles in gasoline, cm./sec.								
	Fresh limonite	Spent limonite	Regenerated limonite	Fresh limonite	Spent limonite				Regenerated limonite			
				1	1	2	3	4	1	2	3	4
>5	23.6	3.9	5.1	23.6	23.6	—	—	—	19.7	—	—	—
3.36~5	9.8	10.4	5.7	19.7	19.7	19.7	19.7	19.7	15.7	15.7	15.6	15.6
2~3.36	12.7	26.8	14.5	15.7	16.4	16.4	16.4	16.4	13.1	13.0	13.0	12.9
1~2	14.1	24.5	22.7	9.8	13.4	12.9	12.6	12.5	9.8	9.8	9.7	9.5
0.5~1	11.9	11.7	12.7	6.95	8.1	7.8	7.5	7.3	5.9	5.8	5.5	5.3
0.21~0.5	15.0	11.0	14.8	4.23	4.7	4.8	4.6	4.3	3.6	3.4	3.1	2.8
<0.21	11.5	10.2	23.8	2.62	2.45	2.1	1.8	1.2	1.5	1.0	0.8	0.5
Fine particles	—	—	—	0.98	0.4	0.2	0.1	Station-ary	<0.1	Station-ary	Station-ary	−0.1

Remarks: i) 1, 2, 3 and 4 in this table correspond to the experiments with still gasoline and flowing gasoline of rates 4.9, 9.8 and19.7 ml./cm² min. respectively.
ii) For this short distance movement acceleration of the particles is neglected.
iii) Higher per cent of 5 mm. particles of fresh limonite was due to agglomerated lumps.

current flow of limonite particles through gasoline. The experiments were carried out with different size particles of fresh, spent and regenerated limonite.

Procedure. A long glass tube (2.7 m.× 160 mm.ϕ) was erected vertically. Lower end was closed and gasoline poured into it. In still gasoline the particles of limonite were allowed to fall under gravity. Time taken by individual particle to travel a distance of 2.5 m. was noted. The velocity of the falling particle was then calculated. Next, gasoline was forced to flow upward in the column at a certain velocity and the above experiments were repeated with only regenerated and spent limonite. These results are presented in Table I and Fig. 1.

From the above table and Fig. 1, it appears that the average particles of both spent and regenerated limonite are not affected much by upstream flow of gasoline even at flow rate 19.7 ml./cm² min. Only the fine particles 0.5~1.0% of the mass were affected and some showing negative velocity i. e. the particles were moving upwards with flowing gasoline. If above mentioned gasoline velocity is considered as limiting velocity, then the contemplated regeneration column may be examined by the following way (Fig. 2).

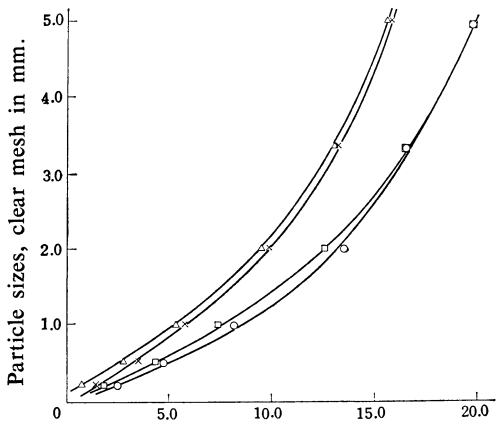


Fig. 1 Change of falling velocity of Limonite in gasoline with particle sizes.
Regenerated limonite particles:
in still gasoline (×); in flowing gasoline, 19 ml./cm² min. (△).
Spent limonite particles:
in still gasoline (○); in flowing gasoline, 19 ml./cm² min. (□).

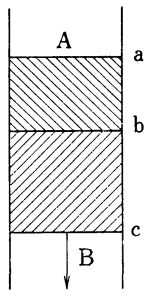


Fig. 2. Upper section of regeneration column.

Let AB is a section of contemplated regeneration column. Rich gasoline leave the column at 'a', limonite particles enter into the column at 'b' while limonite bed starts from 'c' to downwards. Then, ac is liquid zone. If only particle sizes below 0.21 mm. are considered it will be seen that 10.2% in spent limonite and 23.8% in regenerated limonite constitute this fraction. Their spatial distribution in the column may be as follows:

The spent limonite particles would normally be in zone 'bc' and below. These particles from 'b' will, of course, have slow fall and ultimately come down to c-line. At this position there should be some eddy zone e, in Fig. 3, where there is no upward movement of

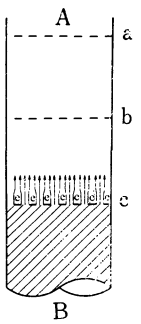


Fig. 3. Upper section of regeneration column. Arrow heads indicate gasoline flow while 'e' indicates 'eddy zones'. Other notations are same as in Fig. 2.

gasoline (rather downward) and even the stationary particles will settle on the limonite bed there. Once it is settled, it will be soon covered by the larger particles which are continuously falling on the bed. Thus covered small particles will have restricted movement and it will move down with other particles. Further, downward movement of fine particles in zone 'bc' will be enhanced by the impact of falling particles.

As regards regenerated limonite, particles below 0.21 mm. is much higher than that of spent limonite. It is due to breakage of particles during processing, and sulfur elimination. These particles are mostly at the bottom of limonite bed where its movement is much restricted. There is a little chance of its being carried by gasoline. However, a filter must be used at 'a' to take care of carried particles, if any.

In view of the above observations, it was deemed fit to realize a continuous counter current process in which both limonite and gasoline would move physically in opposite direction. Finally, a small apparatus was used to regenerate about 10.0 kg. spent limonite per

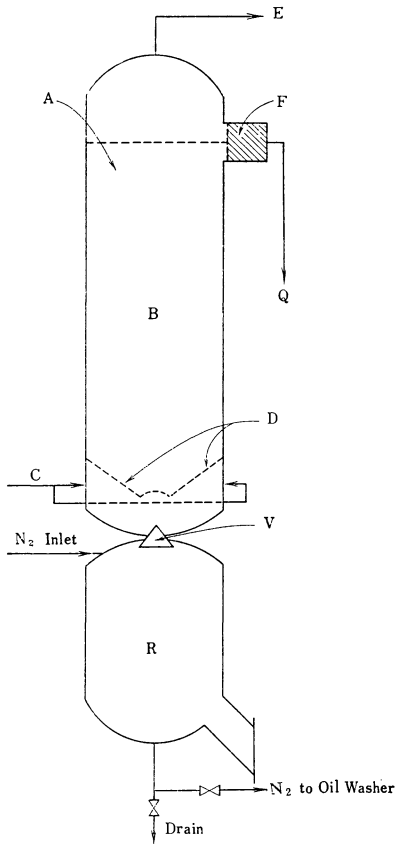


Fig. 4. Regeneration column for counter current process.
A Spent limonite inlet
B Regeneration column
C Gasoline inlet
D Distributor
E Condenser
F Filter
Q Quenching column
R Receiver (Sulfur)
V Cone valve

day. The operation was manual. In this case, other set up remained unchanged as in "hot gasoline flow process" except the regeneration column which was modified. Feeding system was changed. The regeneration column is shown in Fig. 4.

Description of the Equipments and Operation. Spent limonite was introduced into regeneration column B at A, and hot gasoline at C, under the distributor D. Rich gasoline was led to the quenching column through filter F. On opening the cone-valve V. limonite was allowed to fall down slowly to the receiver R, after regeneration. The movement of limonite was regulated by the cone-valve. Valve V was closed when the receiver was almost full. Gasoline was drained out from the receiver and nitrogen was passed for drying the mass.

After drying, the regenerated material was removed from the bottom. During drying of limonite, leaching was stopped. But it could be made continuous by installing one more receiver. The distillate gasoline was passed to the condenser E.

Equipment Specifications.—

Material movement:

a) Limonite particles; 25.0 g./min.

b) Gasoline; 360.0 ml./min.
(gasoline/limonite = 12.0)

A regeneration column (120 cm. × 10 cm. ϕ) was selected. This could operate under conditions of 0.44 cm. limonite velocity with 273 min. contact period and 7.4 cm. gasoline velocity with 16.2 min. contact period. The velocity and contact period of both limonite and gasoline is changeable. The experiments were carried out under varied conditions.

A review of contact periods of limonite in different experiments done earlier could not give any clear indication for its requirement. Therefore, special attention was paid to "contact period of limonite" in subsequent experiments. These results are presented in Table II and Fig. 5.

The above results indicate that contact period of limonite has some bearing on the recovery of sulfur at the final stage. To ascertain the behavior at earlier stages a few experiments were carried out with lower gasoline/limonite ratio. These results are presented in Table III.

From the results in Table III it appears that at the initial stage contact period of limonite has practically no influence on sulfur recovery. As gasoline/limonite ratio increases, the effect of contact period of limonite becomes significant. This may be explained from the fact

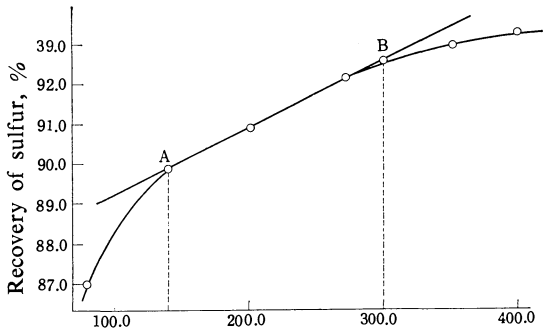


Fig. 5 Progress of sulfur recovery with contact period of limonite.

TABLE II. PROGRESS OF SULFUR RECOVERY WITH CONTACT PERIOD OF LIMONITE

Gasoline/limonite: 12.0; temperature: 85.0°C

Limonite		Gasoline		Sulfur recovery %	Remark
Velocity cm./min.	Contact period min.	Velocity cm./min.	Contact period min.		
* 1.5	80	24.8	4.85	87.0	"Overflow" and "distillate" gasoline are about 95.0% and 5.0% respectively.
0.86	140	14.2	8.45	89.9	
0.60	200	10.0	12.0	90.9	
0.44	273	7.4	16.2	92.2	
0.40	300	6.65	18.0	92.6	
0.34	352	5.7	21.0	93.0	
0.30	400	5.0	24.0	93.3	

* In this experiment some limonite particles were found to be carried over by gasoline.

TABLE III. EFFECT OF CONTACT PERIOD OF LIMONITE AT LOWER GASOLINE/LIMONITE RATIO

Temperature; 85.0°C

Gasoline/limonite ratio	Limonite		Gasoline		Sulfur recovery %	Remark
	Velocity cm./min.	Contact period min.	Volocity. cm./min.	Contact period min.		
3.0	0.86	140	3.60	33.4	49.8	The change of limonite velocity and contact period was effected by regulating the cone valve. Gasoline flow was adjusted according to limonite velocity.
3.0	0.40	300	1.68	71.7	50.4	
6.0	0.86	140	7.20	16.7	68.4	
6.0	0.40	300	3.35	35.7	69.5	
9.0	0.86	140	10.80	11.2	86.5	
9.0	0.40	300	5.00	24.0	88.8	

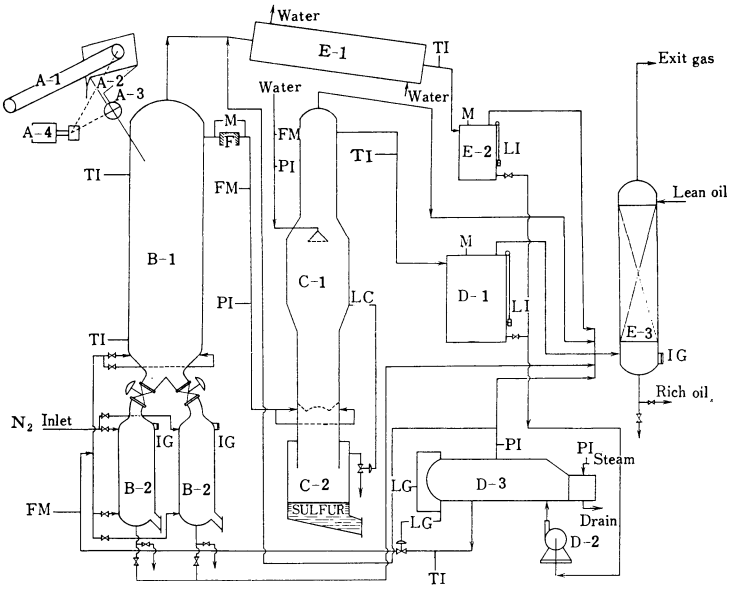


Fig. 6. Equipment flow sheet of limonite regeneration plant with control instrument.

Control instruments

Symbols and Instruments		No. regd.	Symbols and Instruments		No. regd.
FM	Flow meter	3	IG	Inspection glass	2
LC	Level controller	2	TI	Temperature indicator	5
LG	Level glass	2	PI	Pressure indicator	4
LI	Level indicator	2	M	Manometer	3

Equipments

A-1	Belt conveyor	D-1	Gasoline storage tank
A-2	Screen	D-2	Gasoline feed pump
A-3	Rotary valve	D-3	Gasoline reboiler
A-4	Motor for BC and RV	E-1	LF gasoline condenser
B-1	Regeneration column	E-2	LF gasoline storage tank
B-2	Drying vessels	E-3	Off gas scrubber
C-1	Quenching column	F-1	Filter
C-2	Sulfur settling tank		

that sulfur remains entrapped in the particles and does not come in contact with gasoline readily. It takes time. It can be explained easily from the peculiar phenomenon "the migration of iron oxide" during reverse oxidation process[2]. The liberated sulfur does not form film on the surface of the particles. On the contrary, ferric oxide migrates so that sulfur forms the core of each particle. Moreover, caking also occurs frequently due to careless operation at elevated temperature.

The effect of contact period of limonite was found to be uniform and linear between the range of 140~300 min. (AB in Fig 5). Beyond 300 min., the effect of contact period becomes insignificant. But in case of lower contact period yield was found to be low which may be due to insufficient contact period of gasoline (minimum contact period desired 6 min. for saturation (1)).

It is evident that longer contact period is desired for better efficiency. It is possible to regulate the contact period to some extent by controlling the production. It would have been much appreciating if arrangement could be made to pass gasoline through regenerated limonite using a by-pass line for final washing out of sulfur. However, a modified flow sheet for this process is presented in Fig. 6.

The author is indebted to Pakistan Industrial Development Corporation, Professor Dr. Shiro Yoshizawa and Professor Dr. Wataru Funasaka of Kyoto University and extends his thanks to them.

Pak-American Fertilizer Factory
Daudkhel, West Pakistan

2) H. B. Avery, *Chem. & Ind.*, **17**, 171 (1939).

Diphenylcarbazone as an Internal Indicator in Volumetric Analysis. VII. Determination of Mercury

By G. S. DESHMUKH and A. L. J. RAO

(Received December 26, 1960)

While many gravimetric procedures are available for the determination of mercury only a few indirect titrimetric procedures have been reported in the literature. Mercury is determined by the titrimetric precipitation analysis as the thiocyanate using ferric ion as the indicator[1]. An indirect alkalimetric procedure[2] involving the addition of sodium hydroxide and potassium iodide and titrating the liberated alkali with standard acid is also known. Mercury is precipitated as iodate[3] and also as periodate[4] and in both the cases the precipitate is treated with potassium iodide and hydrochloric acid and titrated iodimetrically with standard thiosulfate. It is also precipitated as 2-(*o*-hydroxyphenyl)-benzimidazole[5] and the amount of mercury in the precipitate is determined by the bromate method.

Diphenylcarbazone as an indicator in volumetric analysis was first used by Roberts[6] and mercurimetric determination of thiocyanate using this indicator is already well known. Recent studies[7] in these laboratories have reported the applicability of this indicator to various types of titrimetric procedures. The present work deals with the direct determination of mercury by titrating with potassium iodide in presence of the above indicator.

Experimental

Reagents.—Mercuric nitrate solution was prepared by dissolving Merck's reagent grade sample in appropriate volume of water adding two drops of concentrated nitric acid and was standardized with thiocyanate. Potassium iodide solution contained an accurately weighed pure AR reagent in water and was standardized against potassium iodate. A saturated solution of diphenylcarbazone in alcohol was used as the indicator.

Procedure.—To 10 ml. of iodide solution 4~5 drops of the indicator and 2 ml. of alcohol were added. This was slowly titrated with mercuric nitrate from a burette. The original faint red brown color of the solution (due to the presence of the indicator) faded and the precipitate formed due to the addition of mercuric nitrate redissolved during the initial stage of titration. Towards the end a bright red precipitate of mercuric iodide was obtained. Mercuric nitrate was now added dropwise until the bright red precipitate turned dark. At the end point the precipitate turned reddish violet imparting a bright pink tinge to the supernatant solution. The end point is very easy to detect and there is no risk of over titration. It is, however, possible to rectify the error due to over titration by adding a measured amount of iodide and continuing the titraction in the usual way. Alternatively the reverse titration may also be carried out successfully. The molecular ratio of mercury to iodide calculated from the amount of mercury reacting with iodide at the equivalence

TABLE I

Strength of mercuric nitrate, 0.04359N
Strength of potassium iodide, 0.05107N

Sample number	Volume of iodide solution ml.	Volume of mercuric nitrate solution ml.	Amount of mercury: By KI method g.	Amount of mercury: By KNCS method g.	Difference %
1	20.0	23.25	0.2026	0.2034	0.4
2	10.0	11.60	0.1014	0.1017	0.3
3	9.0	10.50	0.09181	0.09219	0.4
4	6.0	7.00	0.06120	0.06148	0.4
5	4.0	4.70	0.04110	0.04099	0.3
6	3.0	3.50	0.03061	0.03073	0.4

1) A. I. Vogel, "A Text Book of Quantitative Analysis", Longmans Green & Co., p. 265.
2) M. N. Das, *Anal. Chem.*, **25**, 1406 (1953).
3) C. H. R. Gentry and L. G. Sherrington, *Analyst*, **70**, 419 (1945).
4) H. H. Willard and J. J. Thompson, *Ind. End. Chem., Anal. Ed.*, **3**, 398 (1931).
5) J. L. Walter and H. Freiser, *Anal. Chem.*, **25**, 127 (1953).
6) I. Roberts, *Ind. Eng. Chem., Anal. Ed.*, **8**, 365 (1936).
7) G. S. Deshmukh, This Bulletin, **27**, 623 (1954); **29**, 27 449 (1956); *Z. anal. Chem.*, **145**, 251 (1955).

point is 1 : 2 and the composition of the precipitate, therefore, corresponds to mercuric iodide.

The results of a set of typical titrations are given in Table I.

The chief advantage of this procedure is its simplicity, accuracy and the sharpness of the end point. Moreover this is a direct method for the determination which may be readily adopted in the routine analysis of mercury.

Summary

A simple and direct method of estimating mercury by standard potassium iodide with diphenylcarbazone as an indicator has been described. The results are accurate and comparable favorably with the classical procedures.

The authors wish to express their sincere thanks to Professor G. B. Singh for providing the facilities during the above work.

Chemical Laboratory
Banaras Hindu University
Varanasi-5

Sur les Préparations des Complexes Métalliques. III[1]. *Les Préparations des Sels du Diacidobiséthylènediaminecobalt(III) et du Diacidobiséthylènediaminechrome(III)*

Par Masayoshi NAKAHARA

(Reçu le 12 Septembre, 1961)

Dernièrement Linhard et Stirn[2] ont préparé les composés du $[Co\,en_2\,ac_2]ClO_4$ (ac est l'acide monocarboxylique acylique). Ils ont utilisé comme ac, de l'acide formique (nombre de carbones de radical alcoyle: 0) à l'acide caprylique (nombre de carbones de radical alcoyle: 0), et ils ont obtenu, dans tous les cas, les trans-sels et les cis-sels. En les préparant, ils ont toujours obtenu les perchlorates de *trans*-diacidobiséthylènediaminecobalt(III) en se servant comme matières premières du perchlorate de *trans*-dichlorobiséthylènediaminecobalt(III) ou du perchlorate de carbonatobiséthylènediaminecobalt(III), et les perchlorates du *cis*-diacidobiséthylènediaminecobalt(III), en se servant du perchlorate de *cis*-diaquobiséthylènediaminecobalt(III). Mais nous y trouvons une seule exception: ils ont obtenu le perchlorate de *cis*-distearinatobiséthylènediaminecobalt(III) en se servant du perchlorate de *trans*-dichlorobiséthylènediaminecobalt(III). Nous avons essayé, nous intéressant à cette isomerisation trans-cis, d'examiner son mécanisme de réaction, du point de vue du procédé de préparation. Et alors, nous avons fixé notre attention sur la situation où les composés, dont la chaîne carbonée est longue, comme le radical stéarique, se coordinaient au métal, et l'avons comparée avec celle de la coordination des composés dont la chaîne carbonée est courte. Pour cela nous avons fait réagir, dans des conditions constantes, les perchlorate de *trans*- et de *cis*-dichlorobiséthylènediaminecobalt(III) et de *trans*- et de *cis*-dichlorobiséthylènediaminechrome(III) avec le carboxylate de sodium dans l'éthanol, et obtenu de nouveaux sels complexes.

Expériences

Préparations.—*1) Perchlorate de trans-Dichlorobiséthylènediaminecobalt(III), trans-*$[Co\,en_2\,Cl_2]ClO_4$ *(le sel de trans-Co).*—Selon le procédé de Linhard et al.[2]

2) Perchlorate de cis-Dichlorobiséthylènediaminecobalt(III), cis-$[Co\,en_2\,Cl_2]ClO_4\cdot$*(le sel de cis-Co).*—Perchlorate de carbonatobiséthylènediaminecobalt-(III)[2] a été mis dans l'éthanol saturé de chlorure d'hydrogène, et chauffé. On y a vu apparaître du dioxyde de carbone, mais on l'a laissé au bain-marie jusqu'à la fin de cet dégagement. Les poudres violet-bleuâtres ainsi obtenues ont été filtrées, lavées plusieurs fois à l'éthanol, et séchées. Le rendement était très grand, proche de la quantité calculée.

Trouvé: Co, 16.75, N, 8.00. Calculé: Co, 16.87; N, 8.01%.

3) Perchlorate de trans-Dichlorobiséthylènediaminechrome(III), trans-$[Cr\,en_2\,Cl_2]ClO_4$ *(le sel de trans-Cr).*—Selon le procédé de Pfeiffer[3].

1) Partie II, M. Nakahara, *Ce Bulletin*, 35, 785 (1962).
2) M. Linhard et G. Stirn, *Z. anorg. Chem.*, 268, 105 (1952).
3) P. Pfeiffer, P. Koch, G. Lando et A. Trieschmann, *Ber.*, 37, 4255 (1904).

4) Perchlorate de cis-Dichlorobiséthylènediaminechrome(III), cis-[Cr en$_2$ Cl$_2$]ClO$_4$ (le sel de cis-Cr). —Le perchlorate de triséthylènediaminechrome(III) a été mis dans l'acide chlorhydrique concentré, chauffé pendant 6 hr. à 75°C[4]. Les cristaux rouge-violacés ainsi obtenus ont été recristallisés dans une solution de perchlorate de sodium.

5) Purifications des Acides Carboxyliques. — Les acides carboxyliques du commerce été estérifiés selon le procédé habituel, et sont devenus les esters de méthyle. Chaque ester de méthyle a été fractionné au point d'ébullition désigné dans la littérature et purifié[5]. L'ester purifié a été hydrolysé et est devenu le sel de sodium.

6) Perchlorate de trans-Dicaprinatobiséthylènediaminecobalt(III), trans-[Co en$_2$ ($C_9H_{19}COO$)$_2$]ClO$_4$.— 3.5 g. du sel de *trans-* Co ont été suspendus dans 100 ml. d'éthanol; on y a ajouté une solution d'éthanol de 3.5 g. du caprinate de sodium. Cela a été mis dans un flacon muni d'un réfrigérant à reflux et chauffé une heure au bain-marie. La solution rouge a été filtrée avant qu'elle ne devienne froide; le filtrate a été refroidi et les cristaux ont été séparés; ces cristaux ont été recristallisés à l'éthanol, lavés plusieurs fois à l'eau, puis séchés.

Rendement: 5,0 g. (80%).

Trouvé: Co, 9.40; N, 4.50. Calculé: Co, 9.49; N, 4.51%.

Cristaux rouge-violacés luisants en forme d'écailles. Insolubles dans l'eau. Solubles dans l'éthanol et l'acétone.

7) Perchlorate de trans-Dicaprinatobiséthylènediaminechrome(III), trans- [Cr en$_2$($C_9H_{19}COO$)$_2$]ClO$_4$.— Nous nous sommes servis de 3.4 g. du sel de trans-Cr et 3.9 g. de caprinate de sodium, et nous avons opéré de la même façon qu'au 6).

Rendement: 4.3 g. (70%).

Trouvé: Cr, 8.41; N, 4.54. Calculé: Cr, 8.47; N, 4.56%.

Cristaux rouge-violacés sales. Insolubles dans l'eau, solubles dans l'éthanol.

8) Perchlorate de trans-Dilaurinatobiséthylènediaminecobalt(III), trans-[Co en$_2$($C_{11}H_{23}COO$)$_2$]ClO$_4$.— Nous nous sommes servis de 3.5 g. du sel de *trans-* Co et 4 g. de laurinate de sodium, et nous avons opéré comme au 6).

Rendement: 4.5 g. (70%).

Trouvé: Co, 8.65; N, 4.10. Calculé: Co, 8.70; N, 4.14%.

Cristaux rouge-violacés sales en forme d'écailles. Insolubles dans l'eau, solubles dans l'éthanol. Par desséchement donne une poudre rose.

9) Perchlorate de trans-Dilaurinatobiséthylènediaminechrome(III), trans-[Cr en$_2$($C_{11}H_{23}COO$)$_2$]ClO$_4$. —Nous nous sommes servis de 3.4 g. du sel de trans-Cr et 4 g. de laurinate de sodium, et nous avons opéré comme au 6).

Rendement: 4.3 g. (70%).

Trouvé: Cr, 7.68; N, 4.14. Calculé: Cr, 7.76; N, 4.18%.

Cristaux brun-violacés. Insolubles dans l'eau, solubles dans l'éthanol.

10) Perchlorate de cis-Dilaurinatobiséthylènediaminecobalt(III), cis-[Co en$_2$($C_{11}H_{23}COO$)$_2$]ClO$_4$.— Nous nous sommes servis de 3.5 g. du sel de *cis-*Co et 4 g. de laurinate de sodium, et nous avons opéré comme au 6).

Rendement: 3.0 g. (47%).

Trouvé: Co, 8.59; N, 4.01. Calculé: Co, 8.70; N, 4.14%.

Cristaux rouge-violacés luisants. Solubles dans l'éthanol.

11) Perchlorate de cis-Dilaurinatobiséthylènediaminechrome(III), cis-[Cr en$_2$($C_{11}H_{23}COO$)$_2$]ClO$_4$.— Nous nous sommes servis de 3.4 g. du sel de *cis-*Cr et 4.0 g. de laurinate de sodium, et nous avons opéré comme au 6).

Rendement: 2.5 g. (40%).

Trouvé: Cr, 7.70; N, 4.02. Calculé: Cr, 7.76; N, 4.18%.

12) Perchlorate de cis-Dimyristinatobiséthylènediaminecobalt(III), cis-[Co en$_2$($C_{13}H_{27}COO$)$_2$]ClO$_4$. — Nous nous sommes servis de 3.5 g. du sel de *trans-*Co ou *cis-*Co et 5.2 g. de myristate de sodium, et nous opéré comme au 6).

Rendement: 4.5 g. (60%).

Trouvé: Co, 8.14; N, 3.73. Calculé: Co, 8.04; N, 3.82%.

Poudre rose. Insoluble dans l'eau, et soluble dans l'éthanol.

13) Perchlorate de cis-Dimyristinatobiséthylènediaminechrome(III), cis-[Cr en$_2$($C_{13}H_{27}COO$)$_2$]ClO$_4$.— Nous nous sommes servis de 3.4 g. du sel de *trans-*Cr ou *cis-*Cr et 5.2 g. de myristate de sodium, et nous avons opéré comme au 6).

Rendement: 4.5 g. (70%).

Trouvé: Cr, 7.03; N, 3.66. Calculé: Cr, 7.16; N, 3.86%.

Poudre rouge-violacée. Insoluble dans l'eau, soluble dans l'éthanol.

14) Perchlorate de cis-Dipalmitinatobiséthylènediaminecobalt(III), cis-[Co en$_2$($C_{15}H_{31}COO$)$_2$]ClO$_4$.— Nous nous sommes servis de 3.5 g. du sel de *trans-*Co et 5.9 g. de palmitate de sodium, et nous avons opéré comme au 6).

Rendement: 6.8 g. (83%).

Trouvé: Co, 7.49; N, 3.50. Calculé: Co, 7.47; N, 3.55%.

Poudre rose. Insoluble dans l'eau, soluble dans l'éthanol, le propanol et le benzène.

15) Perchlorate de cis-Dipalmitinatobiséthylènediaminechrome(III), cis- [Cr en$_2$($C_{15}H_{31}COO$)$_2$]ClO$_4$.— Nous nous sommes servis de 3.4 g. du sel de *trans-*Cr et 5.9 g. de palmitate de sodium, et nous avons opéré comme au 6).

Rendement: 5.8 g. (71%).

Trouvé: Cr. 6.51; N, 3.60. Calculé: Cr, 6.65; N, 3.58%.

Poudre rouge-violacée. Insoluble dans l'eau, soluble dans l'éthanol et le benzène.

16) Perchlorate de cis-Distéarinatobiséthylènediaminechrome(III), cis-[Cr en$_2$($C_{17}H_{37}COO$)$_2$]ClO$_4$.— Nous nous sommes servis de 3.4 g. du sel de *trans-*Cr ou *cis-*Cr et 5.1 g. de stéarate de sodium, et nous avons opéré comme au 6).

Rendement: 5.5 g. (66%).

Trouvé: Cr, 6.06; N, 3.42. Calculé: Cr, 6.20; N, 3.34%.

4) M. Linhard et M. Weigel, *Z. anorg. Chem.*, **271**, 115 (1952).

5) Haller et Youssoufian, *Compt. rend.*, **143**, 805 (1857).

Poudre rouge-violacée. Insoluble dans l'eau, soluble dans l'éthanol à chaud, et facilement soluble dans benzène à chaud.

Spectres d'Absorption.—Les spectres d'absorption du perchlorate de diacidobiséthylènediaminecobalt-(III) et du perchlorate de diacidobiséthylènediaminechrome(III), nouvellement préparés, ont été mesurés. La mesure a été faite dans une solution d'éthanol. Les résultats obtenus sont montrés dans la Fig. 1. Toutes les courbes d'absorption ont été classées en quatre espèces; toutes coïncidaient presque entièrement.

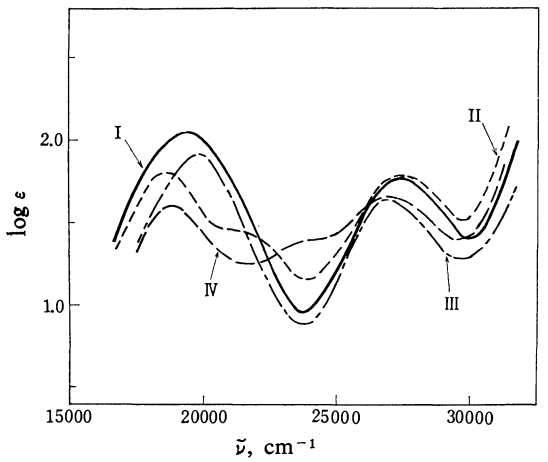


Fig. 1. Spectres d'absorption de:
(I) *cis*-[Co en$_2$ ac$_2$]ClO$_4$
(II) *trans*-[Co en$_2$ ac$_2$]ClO$_4$
(III) *cis*-[Cr en$_2$ ac$_2$]ClO$_4$
(IV) *trans*-[Cr en$_2$ ac$_2$]ClO$_4$

Résultats et Discussion

Quand nous observons chaque courbe d'absorption montrée dans la Fig. 1, nous pouvons facilement voir leur différence de structure. On sait bien, par de nombreux exemples, que la séparation de la première bande d'absorption est suscitée par la structure trans du [Co en$_2$ ac$_2$]$^+$ [6,7]. Et les courbes ainsi obtenues sont tout à fait correspondantes aux courbes d'absorption de l'acetato-complexe, [Co en$_2$(CH$_3$COO)$_2$]$^+$. Par conséquent, la différence de structure du perchlorate de diacidobiséthylènediaminecobalt(III) visible sur les courbes d'absorption de I et II provient du fait que I correspond à la structure trans et II à la structure cis. De même, quant au perchlorate de diacidobiséthylènediaminechrome(III), de la différence qui existe entre les structures trans et cis vient la séparation distincte de la première bande d'absorption; III correspond à la structure trans, IV à celle de cis. Or le Tableau I montre les résultats

Tableau I

Complexes de départ	Radicaux carboxyles	Produits
[M en$_2$ Cl$_2$]ClO$_4$		[M en$_2$ ac$_2$]ClO$_4$
trans-Co	$C_{17}H_{35}COO$	*cis*
trans-Co	$C_{15}H_{31}COO$	*cis*
trans-Co	$C_{13}H_{27}COO$	*cis*
trans-Co	$C_{11}H_{23}COO$	*trans*
trans-Co	$C_9H_{19}COO$	*trans*
cis-Co	$C_{17}H_{25}COO$	*cis*
cis-Co	$C_{13}H_{27}COO$	*cis*
cis-Co	$C_{11}H_{23}COO$	*cis*
trans-Cr	$C_{17}H_{35}COO$	*cis*
trans-Cr	$C_{15}H_{31}COO$	*cis*
trans-Cr	$C_{13}H_{27}COO$	*cis*
trans-Cr	$C_{11}H_{23}COO$	*trans*
trans-Cr	$C_9H_{19}COO$	*trans*
cis-Cr	$C_{17}H_{35}COO$	*cis*
cis-Cr	$C_{13}H_{27}COO$	*cis*
cis-Cr	$C_{11}H_{23}COO$	*cis*

de la réaction de l'isomérisation trans-cis sur les complexes que nous avons ainsi préparés. Lors de la réaction de tous les complexes de départ, avec le stéarate, le palmitate et le myristate, nous avons toujours obtenu les complexes cis comme produits de réaction. Il est donc certain que nous avons vu l'isomérisation à travers la réaction des trans-complexes avec le carboxylate. Il en est de même des complexes du cobalt et du chrome. Mais on obtiendra toujours les trans-complexes par la réaction des trans-complexes du cobalt et du chrome avec le laurate, le caprinate etc., et de même, les cis-complexes par la réaction des cis-complexes avec le carboxylate. De plus, on peut ajouter à cela les résultats de Linhard et al.[2]: par la réaction du perchlorate de carbonatobiséthylènediaminecobalt(III) avec l'acide caprylique, l'acide caproique, l'acide valérique, seront toujour obtenus les trans-complexes, mais, selon le même procédé, on ne pourrait obtenir les cis-complexes (en évaporant et concentrant à la température ordinaire le perchlorate de *cis*-diaquobiséthylènediaminecobalt-(III) et les carboxylate de potassium, on peut obtenir les cis-complexes). De là, lorsque nous examinons ces réactions d'isomérisation trans-cis, il serait le plus naturel que nous cherchions leur cause à la longueur du radical alcoyle. On obtiendra toujours, quels que soient les complexes de départ, les cis-complexes, au delà de l'acide myristique dont le nombre de carbones du radical alcoyle est 13, le radical carboxyle exclus; avec l'acide laurique ou l'acide caprique dont le nombre de carbones est 11 ou 9, les résultats dépendent de la structure des complexes de départ, et, avec des radicaux dont le nombre de carbones

6) M. Linhard et M. Weigel, *Z. anorg. Chem.*, **267**, 121 (1951).
7) Y. Shimura, Ce Bulletin, **25**, 49 (1952).

est inferieur à 7, dans les conditions expérimentales susdites, on pourra toujours obtenir les trans-complexes.

Or, en tenant compte de ces faits, considérons, par exemple, la réaction du *trans*-$[M\,en_2\,Cl_2]\cdot ClO_4$ (M=Co, Cr) avec le radical carboxyle. Au cours de cette réaction, le *trans*-$[M\,en_2\cdot Cl(ac)]\,ClO_4$ sera d'abord obtenu. Ensuite, quand on sera passé au $[M\,en_2\,ac_2]\,ClO_4$, les radicaux alcoyles qui doivent être combinés dans la position trans s'arrangent comme l'indique à la Fig. 2 par attraction entre eux, lorsque la chaîne du carbone est longue, et pour cela ils feront une distorsion vers la

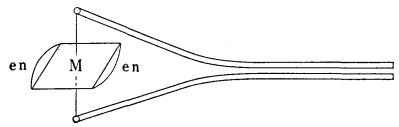


Fig. 2

position coordinée de l'autre coordinat (l'éthylènediamine à cette place-ci), et par conséquent il en resultera l'isomérisation. On obtient la même réaction, que le radical carboxyle qui coordiné en second s'arrange avant la coordination ou après la coordination. On peut considérer ce pouvoir d'attraction comme ressemblant à celui qui est dû aux forces de van der Waals. Et alors à cause du prolongement de la chaîne carbonée, l'attraction par les longs radicaux alcoyles l'effet de la charge du radical carboxyle exclus, devient plus grande que la répulsion par les charges négatives des radicaux carboxyles. Et au contraire, on peut considérer la réaction d'isomérisation cis-trans, où la chaîne carbonée est courte, comme suscitée par le phénomène inverse, et quand l'isomérisation n'a pas lieu, on peut croire que ces pouvoires sont proportionnels. Des faits qui ressemblent beaucoup aux résultats susdits, sont connus par expérimentation sur les agents actifs de surface. Et alors quand on ajoute des agents actifs de surface divers dont les nombres de carbones sont différents, au sol d'hydroxyde de fer(III) la cohésion a toujours lieu. Mais, ensuite, quand on ajoute avec excès un agent actif de surface ayant, par exemple, un nombre de carbones superieur à 12 comme le dodecylsulfate de sodium, cette précipitation se disperse à nouveau ; mais, elle ne se disperse pas entièrement si le nombre de carbones est inferieur à 10[8]. De même, l'action de l'alcoylsulfate sur la cohésion et la dispersion du colorant et de la protéine etc.[9], sera influencée par la longueur de la chaîne. Ces phénomènes sont expliqués par le mécanisme suivante : la charge du sol, du colorant et de la protéine etc., est d'abord neutralisée par l'ion alcoylsulfate et les suspensoïdes précipitent. Si c'est un radical alcoyl long, les chaînes alcoyle de l'ion alcoylesulfate dissous s'arrangent dans la direction contraire à celles des précipitations, et par ces attractions, les précipitations sont dispersées de nouveau.

Il est très intéressant, selon les résultats que nous avons obtenus, que cette distinction ait lieu, de même, autour du nombre du carbone 12, grâce à cela on peut concevoir un mécanisme analogue.

Résumé

Les *trans*- et *cis*-$[M\,en_2\,ac_2]\,ClO_4$ (M=Co, Cr) de plusieurs sortes, composés nouveaux, ont été préparés. Nous avons considéré l'isomérisation lors de la préparation des complexes. Nous avons conclu que l'isomérisation se fait, dans tout les cas, par les attraction des radicaux alcoyles.

L'auteur exprime ses remerciements sincères à Monsieur le professeur Taku Uemura pour l'intérêt qu'il a porté à ce travail et il est particulièrement reconnaissant envers Monsieur le professeur Yukio Kondo qui a participé à la discussion sur l'interprétation des résultats. Il est aussi reconnaissant envers Monsieur Takeo Miyake qui a assisté à la purification des acides carboxyliques.

Laboratoire de Chimie Minérale
Faculté des Sciences
Rikkio Université
Ikebukuro, Tokyo

8) K. Meguro et T. Kondo, *J. Chem. Soc. Japan, Pure Chem. Sec.* (*Nippon Kagaku Zassi*), **76**, 642 (1955).
9) K. Aoki et T. Hori, Ce Bulletin, **29**, 104 (1956).

A Semi-empirical Theory of the π-Electronic Spectra of Aromatic Derivatives

By Kichisuke NISHIMOTO and Ryoichi FUJISHIRO

(Received October 11, 1961)

In a previous paper[1], we have reported a convenient method (VO method) for calculation of the molecular diagrams of aromatic derivatives. In this paper, a semi-empirical theory of the π-electronic spectra of aromatic derivatives based on the antisymmetrized molecular orbital method (ASMO method) is formularized by the use of the results of the VO method and is applied to calculation of the π-electronic spectra of hydroquinone and phloroglucinol.

Theory

The framework of the present theory is similar to that of Pariser[2] and of our previous paper[3]. The procedure of calculation is as follows:

i) MO's are determined by a simple LCAO MO method based on π-electron approximation, using appropriately chosen parameters.

ii) We give each π-electron a molecular spin orbital (MSO) which is given by the product of a MO and spin function α or β.

iii) Configurational wave functions are built up as antisymmetrized products, or Slater determinants, of these MSO's.

iv) Configurational energies are calculated by a semi-empirical procedure based on zero differential approximation.

v) Electronic state functions and their energies are calculated by the method of the linear combinations of these configurational wave functions.

A) Calculation of MO's.—When the molecule contains n 2pπ atomic orbitals (2pπ AO), the MO, ψ_i, is represented by the linear combination of these AO's as follows:

$$\psi_i=\sum_{\mu}C_{i\mu}\phi_\mu \qquad (1)$$

where ϕ_μ is the μ-th 2pπ AO and $C_{i\mu}$ is the coefficient to be determined by the variational method. First of all, from the variational theory we obtain the following equations for the coefficients which form the simultaneous equations of n dimensions:

$$\left.\begin{aligned}&\sum_{\mu=1}^{n}C_{i\mu}\left(\int\phi_1 H\phi_\mu d\nu-E\delta_{1\mu}\right)=0\\&\qquad\vdots\\&\sum_{\mu=1}^{n}C_{i\mu}\left(\int\phi_n H\phi_\mu d\nu-E\delta_{n\mu}\right)=0\end{aligned}\right\} \qquad (2)$$

where H is an effective one-electron Hamiltonian and $\delta_{\mu\nu}=1$ if $\mu=\nu$, $=0$ otherwise. E is orbital energy defined by H and MO. Now, we assume the matrix elements, $H_{\mu\nu}=\int\phi_\mu H\phi_\nu\, d\nu$, as follows:

$$\left.\begin{aligned}&H_{\mu\mu}=\alpha && (\phi_\mu \text{ is carbon 2p}\pi \text{ AO})\\&H_{\mu\mu}=\alpha+\delta_\mu\beta && (\phi_\mu \text{ is heteroatom 2p}\pi \text{ AO})\end{aligned}\right\} \qquad (3)$$

$$\left.\begin{aligned}&H_{\mu\nu}=\beta && (\mu \text{ and } \nu \text{ are nearest neighbor carbon atoms})\\&H_{\mu\nu}=k_{\mu\nu}\beta && (\mu \text{ and } \nu \text{ are nearest neighbors, but one or both of them are heteroatom})\\&H_{\mu\nu}=0 && (\mu \text{ and } \nu \text{ are non-neighbors})\end{aligned}\right\} \qquad (4)$$

where the numerical values of δ_μ and $k_{\mu\nu}$ are determined by a semi-empirical procedure; e. g., for the case of phenol we have determined these values from the experimental ionization potentials of benzene, methanol and phenol[3]. Energies E_i are obtained as the roots of the following secular determinant:

$$\begin{vmatrix}(H_{11}-E) & H_{12} & \cdots\cdots & H_{1n}\\ H_{21} & (H_{22}-E) & \cdots\cdots & H_{2n}\\ \vdots & & & \\ H_{n1} & H_{n2} & \cdots\cdots & (H_{nn}-E)\end{vmatrix}=0$$

which is defined by Eq. 2. From the secular determinant we obtain the n E_i's. If we substitute the lowest energy E_1 into Eq. 2 and use the normalization condition

$$\int\phi_1^2 d\nu=\sum_{\mu=1}^{n}C_{1\mu}^2$$

we obtain the coefficients $C_{1\mu}$'s for the lowest MO, ψ_1. In the same way we obtain the MO's, ψ_2, ψ_3, ……, ψ_n associated with the energies E_2, E_3, ……, E_n respectively. When E is expressed by

1) K. Nishimoto and R. Fujishiro, This Bulletin, **32**, 699 (1959).
2) R. Pariser, *J. Chem. Phys.*, **24**, 250 (1956).
3) K. Nishimoto and R. Fujishiro, This Bulletin, **31**, 1036 (1958).

$$E_i=\alpha-x_i\beta \tag{5}$$

the MO's corresponding to $x_i<0$ are called bonding orbitals, whereas the MO's corresponding to $x_i>0$ are called antibonding orbitals. In the case of a molecule having m π-electrons, the ground state of the molecule is given by the state in which the lower MO's, ψ_1, ψ_2, ……, $\psi_{m/2}$ are used twice. We call the MO's, ψ_1, ψ_2, ……, $\psi_{m/2}$, occupied orbitals, and the other MO's vacant orbitals. Consequently, the π-electron density of the μth atom, q_μ, and π-bond order (or quantity analogous to it) for the $\mu\nu$ atom pair, $p_{\mu\nu}$, in the ground state of the molecule are expressed as follows:

$$\left.\begin{aligned} q_\mu&=2\sum_{i}^{\text{occ.}}C_{i\mu}^2=2-2\sum_{i'}^{\text{vac.}}C_{i'\mu}^2=2-q_\mu^v \\ p_{\mu\nu}&=2\sum_{i}^{\text{occ.}}C_{i\mu}C_{i\nu}=-2\sum_{i'}^{\text{vac.}}C_{i'\mu}C_{i'\nu}=-p_{\mu\nu}^v \end{aligned}\right\} \tag{6}$$

where $\sum_{i}^{\text{occ.}}$ and $\sum_{i'}^{\text{vac.}}$ indicate the sums over occupied orbitals and vacant orbitals respectively. The relations of Eqs. (6) are found in our previous paper[1]. The calculation of q_μ's and $p_{\mu\nu}$'s using vacant orbitals is simple compared with that using occupied orbitals.

B) Reduced Formula for the Calculation of π-Electronic State Energies.—The configurational wave function of the ground state of the molecule, χ_0, is now represented by a Slater determinant having the form of:

$$\chi_0=\frac{1}{\sqrt{m!}}\cdot\begin{vmatrix} (\psi_1\alpha)^1(\psi_1\beta)^1\cdots\cdots(\psi_{m/2}\alpha)^1(\psi_{m/2}\beta)^1 \\ (\psi_1\alpha)^2(\psi_1\beta)^2\cdots\cdots(\psi_{m/2}\alpha)^2(\psi_{m/2}\beta)^2 \\ \vdots \qquad\qquad\qquad\qquad \vdots \\ (\psi_1\alpha)^m(\psi_1\beta)^m\cdots(\psi_{m/2}\alpha)^m(\psi_{m/2}\beta)^m \end{vmatrix}$$

$$\equiv(1\,\bar{1}\,2\,\bar{2}\cdots\cdots\frac{1}{2}m\frac{1}{2}\bar{m})$$

The configurational wave function of the excited state corresponding to the one-electron transition from ψ_i to $\psi_{k'}$, $\chi_{i\to k'}$, is given by:

$$\chi_{i\to k'}^1=2^{-1/2}[(1\,\bar{1}\cdots\cdots i\bar{k}'\cdots\cdots\frac{1}{2}m\frac{1}{2}\bar{m})-(1\,\bar{1}\cdots\cdots k'\bar{i}\cdots\cdots\frac{1}{2}m\frac{1}{2}\bar{m})]$$

$$\chi_{i\to k'}^3=2^{-1/2}[(1\,\bar{1}\cdots\cdots ik'\cdots\cdots\frac{1}{2}m\frac{1}{2}\bar{m})+(1\,\bar{1}\cdots\cdots\bar{i}\bar{k}'\cdots\cdots\frac{1}{2}m\frac{1}{2}\bar{m})]$$

where superscripts 1 and 3 indicate singlet and triplet states, respectively. When we use complete many electron Hamiltonian $\mathscr{H}$ instead of an effective one-electron Hamiltonian, the configurational energies are given by:

$$\mathscr{H}_{i\to k}=\int\chi_{i\to k'}\mathscr{H}\chi_{i\to k'}\,dv$$

$$\mathscr{H}_{00}=\int\chi_0\mathscr{H}\chi_0 dv$$

where

$$\mathscr{H}=\sum_i H_{\text{core}}(i)+\frac{1}{2}\sum_{ij}\frac{e^2}{r_{ij}}$$

where $H_{\text{core}}(i)$ is core Hamiltonian, which consists of the kinetic energy term of the ith π-electron and potential energy terms representing the attraction among the σ-cores and this electron. A rigid core which consists of a nucleus, inner shell electrons and valence electrons except π-electrons, is called a σ-core. Therefore the σ-core of μth atom with q_μ^0 π-electrons in its free state has a q_μ^0 $|e|$ positive charge. According to Pariser[2], the energy $\Delta E_{ik'}$ associated with a one-electron transition from ψ_i to $\psi_{k'}$ is given by

$$\begin{aligned}\Delta E_{ik'}&=\mathscr{H}_{ik'}-\mathscr{H}_{00}\\&=I_{k'k'}-I_{ii}+[ii|k'k']\pm[ik'|ik']\\&\quad-[ii|ii]-\sum_{f\neq i}\{2[ff|ii]-2[ff|k'k']\\&\quad-[fi|fi]+[fk'|fk']\}\end{aligned} \tag{7}$$

where the upper and lower signs are associated with the singlet and triplet configurations respectively. Summation over the index f means that over the occupied MO's in χ_0. The integrals $[ij|kl]$ and I_{ij} are

$$[ij|kl]=\int\psi_i(1)\psi_j(1)\frac{e^2}{r_{12}}\psi_k(2)\psi_l(2)dv$$

$$I_{ij}=\int\psi_i(1)H_{\text{core}}(1)\psi_j(1)dv$$

When we define the following quantities:

$$\mathscr{H}_{\mu\mu}=-I_\mu+\frac{1}{2}q_\mu\gamma_{\mu\mu}+\sum_{\nu\neq\mu}(q_\nu-q_\nu^0)\gamma_{\nu\mu}$$

$$\mathscr{H}_{\mu\nu}=\beta_{\mu\nu}-\frac{1}{2}p_{\mu\nu}\gamma_{\mu\nu}$$

$$\bar{\varepsilon}_i=\sum_{\mu\nu}C_{i\mu}C_{i\nu}\mathscr{H}_{\mu\nu} \tag{8}$$

where

$$\int\phi_\mu^2(1)\frac{e^2}{r_{12}}\phi_\nu^2(2)dv=\gamma_{\mu\nu}$$

$$\int\phi_\mu(1)H_{\text{core}}(1)\phi_\mu(1)dv=I_\mu$$

$$\int\phi_\mu(1)H_{\text{core}}(1)\phi_\nu(1)d\nu=\beta_{\mu\nu}$$

Equation 7 can be rewritten by these quantities as

$$\Delta E_{i\,k'}^{1,3}=\bar{\varepsilon}_{k'}-\bar{\varepsilon}_i+[ik'|ik']-[ii|k'k']\pm[ik'|ik']$$

In many cases we have a number of configurational wave functions χ_i, belonging to the same symmetry. Therefore, the allowed electronic state function Ψ_a must be given by the linear combination of these χ_i's; that is,

$$\Psi_a=\sum d_{ai}\chi_i$$

where d_{ai} is a coefficient to be determined by variational procedure. Energies E associated with allowed electronic states are determined by following secular determinant:

$$\begin{vmatrix} (\mathscr{H}_{00}-E) & \mathscr{H}_{01} & \mathscr{H}_{02}\cdots\cdots \\ \mathscr{H}_{10} & (\mathscr{H}_{11}-E) & \mathscr{H}_{12}\cdots\cdots \\ \vdots & & \end{vmatrix}=0$$

Excitation energy $\Delta E_{0\to a}$ associated with a transition from Ψ_0 to Ψ_a is given by:

$$\Delta E_{0\to a}=E_0-E_a$$

General formulas for interconfigurational matrix elements $\mathscr{H}_{ij}$ were given by Pariser[2]. These can be rewritten as follows:

$$[\chi_0|\chi_i^{1\to k'}]=\int\chi_0\mathscr{H}\chi_i^{1\to k'}dv=\sqrt{2}\sum_{\mu\nu}C_{i\mu}C_{k'\nu}\mathscr{H}_{\mu\nu}$$

$$[\chi_i^{1\to k'}|\chi_j^{1\to l'}]=\int\chi_i^{1\to k'}\mathscr{H}\chi_j^{1\to l'}dv=2[ik'|jl']-[ij|k'l']$$

$$[\chi_i^{1\to k'}|\chi_i^{1\to l'}]=\sum_{\mu\nu}C_{k'\mu}C_{l'\nu}\mathscr{H}_{\mu\nu}+2[ik'|il']-[ii|k'l']$$

$$[\chi_i^{1\to k'}|\chi_j^{1\to k'}]=-\sum_{\mu\nu}C_{i\mu}C_{j\nu}\mathscr{H}_{\mu\nu}+2[ik'|jk']-[ij|k'k']$$

$$[\chi_0|\chi_i^{3\to k'}]=0$$

$$[\chi_i^{3\to k'}|\chi_j^{3\to l'}]=-[ij|k'l']$$

$$[\chi_i^{3\to k'}|\chi_i^{3\to l'}]=[\chi_i^{1\to k'}|\chi_i^{1\to l'}]-2[ik'|il']$$

$$[\chi_i^{3\to k'}|\chi_j^{3\to k'}]=[\chi_i^{1\to k'}|\chi_j^{1\to k'}]-2[ik'|jk']$$

C) Semi-empirical Estimation of Basic Integrals and Semi-empirical Formulation of $\mathscr{H}_{\mu\nu}$ and $\bar{\varepsilon}_i$. — All molecular integrals can be expanded into integrals over AO's which are I_μ, $\beta_{\mu\nu}$ and $\gamma_{\mu\nu}$. These basic integrals are estimated by a semi-empirical procedure. The two-center electron repulsion integral, $\gamma_{\mu\nu}$, is calculated from the expression which we found in the previous paper[4]; that is,

$$\gamma_{\mu\nu}=\frac{e^2}{a_{\mu\nu}+r_{\mu\nu}}$$

where $r_{\mu\nu}$ is the interatomic distance between the μ and ν atoms.

$a_{\mu\nu}$ is a characteristic constant which is given by

$$\frac{e^2}{a_{\mu\nu}}=\frac{I_\mu+I_\nu-A_\mu-A_\nu}{2}$$

where I_μ and A_μ are the valence state ionization potential and the electron affinity of the μ atom respectively. The core integrals, I_μ and $\beta_{\mu\nu}$, are estimated in the following manner:

i) In case both ϕ_μ and ϕ_ν are carbon 2pπ AO's, we assume that:

a) I_μ is the valence state ionization potential of the carbon atom

b) $\beta_{\mu\nu}=\beta_{CC}$ for the $\mu\nu$ bond

c) $\beta_{\mu\nu}=0$, if μ and ν are nonneighbors

In this case, $\mathscr{H}_{\mu\mu}$ and $\mathscr{H}_{\mu\nu}$ can be rewritten as follows:

$$\mathscr{H}_{\mu\mu}=-y_c+\frac{1}{2}(1-q_\mu^\nu)\gamma_{\mu\mu}+\sum_{\nu\neq\mu}(2-q_\nu^0-q_\nu^\nu)\gamma_{\nu\mu}=-y_c+G_{\mu\mu}$$

$$\mathscr{H}_{\mu\nu}=\beta_{cc}+\frac{1}{2}p_{\mu\nu}^\nu\gamma_{\mu\nu}=\beta_{cc}+G_{\mu\nu} \qquad (9)$$

where y_c and q_ν^0 are the valence state electronegativity of the carbon atom and the core charge of the ν atom respectively. By definition,

$$G_{\mu\mu}=\frac{1}{2}(2-q_\mu^0-q_\mu^\nu)\gamma_{\mu\mu}+\sum_{\mu\neq\nu}(2-q_\nu^0-q_\nu^\nu)\gamma_{\nu\mu}$$

$$G_{\mu\nu}=\frac{1}{2}p_{\mu\nu}^\nu\gamma_{\mu\nu}$$

ii) In case either ϕ_μ or ϕ_ν is a heteroatom 2pπ AO, we assume that:

$$\mathscr{H}_{\mu\mu}=-y_c+\delta_\mu\beta_{cc}+\frac{1}{2}(2-q_\mu^0-q_\mu^\nu)\gamma_{\mu\mu}+\sum_{\nu\neq\mu}(2-q_\nu^0-q_\nu^\nu)\gamma_{\nu\mu}=-y_c+\delta_\mu\beta_{cc}+G_{\mu\mu}$$

$$\mathscr{H}_{\mu\nu}=k_{\mu\nu}\beta_{cc}+G_{\mu\nu} \qquad (10)$$

where we assign the same values as in Eqs. 3 and 4 for δ_μ and $k_{\mu\nu}$. $(2-q_\mu^0-q_\mu^\nu)$ gives the net charge of the μ atom. Substituting Eqs. 9 and 10 into Eq. 8, we obtain the following expression:

$$\bar{\varepsilon}_i=-y_c-x_i\beta_{cc}+\sum_{\mu\nu}C_{i\mu}C_{i\nu}G_{\mu\nu}$$

where x_i has the same value as in Eq. 5. The numerical estimation of β_{cc} is carried out by a semi-empirical procedure to fit the observed spectra.

D) Oscillator Strength. — The oscillator strength, f, associated with a one-electron

4) K. Nishimoto and N. Mataga, *Z. physik. Chem.* [*N. F.*), **12**, 335 (1957); N. Mataga and K. Nishimoto, ibid., **13**, 140 (1957).

transition from Ψ_a to Ψ_b is given by Mulliken and Rieke[5] as follows:

$$f=1.085\times10^{11}\tilde{\nu}_{ab}D_{ab}^2$$

where $\tilde{\nu}_{ab}$ is the frequency of the transition in cm^{-1}. D_{ab} is the so-called transition moment which is defined by

$$D_{ab}=\int\Psi_a\sum_i e_i r_i\Psi_b\,dv$$

where e_i and r_i are the charge and the position vector of the ith charged particle respectively. From the calculation of D_{ab}, we can know the direction of the polarization of the transition. The knowledge of the direction of the transition moment is not only useful for the classification of the electronic state, but also plays an important role in the study of intermolecular interaction[6].

Application to the Spectra of Hydroquinone and Phloroglucinol

We have also applied the method to the π-electronic spectra of hydroquinone, phloroglucinol and parent hydrocarbon, benzene. The parameters used are collected in Table I. Many of them are the same as those of phenol[3]. The core structures of the molecules are shown in Fig. 1. The calculated MO's are given in Table II. In the calculation of configuration interaction, the four lowest singly excited singlet configurations, $\chi^1{}_{1\to1'}$, $\chi^1{}_{1\to2'}$, $\chi^1{}_{2\to1'}$ and $\chi^1{}_{2\to2'}$, and the ground state, χ_0, are taken into account. The calculated molecular integrals are collected in Table III. Other kinds of integrals not involved in the table be come to zero. The $\bar{\varepsilon}_i$'s correspond formally to the orbital energies in the sence of the self-consistent field method. Therefore, $\bar{\varepsilon}_1$'s are regarded as the calculated apparent first ionization potentials. With same reason $\bar{\varepsilon}_{1'}$'s are regarded as calculated electron affinities. From the table we expect that the magnitudes of first ionization potentials are in the order; benzene > hydroquinone > phloroglucinol. Similarly, the order of electron affinity should be benzene > hydroquinone > phloroglucinol. Unfortunately, experimental data to be compared with our calculated ones are not available. The calculated electronic state energies E_a and the corresponding electronic state functions Ψ_a are given in Table IV. The results in this table show that the calculated excitation

TABLE I. PARAMETERS AND INTEGRALS OVER AO'S

$\delta_o=1.5$
$k_{co}=0.7$
$\beta_{cc}=-2.388$ eV. (for benzene and hydroquinone)
$\beta_{cc}=-2.621$ eV. (for phloroglucinol)
$a_{cc}=1.328$ Å
$a_{co}=0.889$ Å
$a_{oo}=0.669$ Å
All C-C bond distances are equal to 1.390 Å.
All C-O bond distances are equal to 1.460 Å.
All bond angles are equal to 120°.

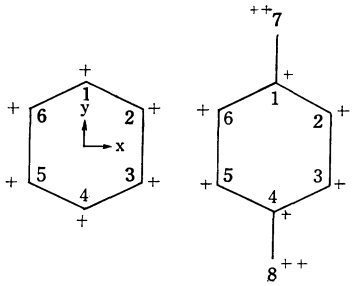
TABLE II. MO'S AND MO ENERGIES

$E-\alpha=-x_1\beta$	MO
	Benzene
-2β	$\psi_{3'}=1/\sqrt{6}\,(\phi_1-\phi_2+\phi_3-\phi_4+\phi_5-\phi_6)$
$-\beta$	$\psi_{2'}=1/2(-\phi_2+\phi_3-\phi_5+\phi_6)$
$-\beta$	$\psi_{1'}=1/\sqrt{12}(2\phi_1-\phi_2-\phi_3+2\phi_4-\phi_5-\phi_6)$
$+\beta$	$\psi_1=1/\sqrt{12}(2\phi_1+\phi_2-\phi_3-2\phi_4-\phi_5+\phi_6)$
$+\beta$	$\psi_2=1/2(\phi_2+\phi_3-\phi_5-\phi_6)$
	Hydroquinone
-2.0475β	$\psi_{3'}=0.4180(\phi_1-\phi_4)-0.3990(\phi_2-\phi_3-\phi_5+\phi_6)-0.0826(\phi_7-\phi_8)$
-1.1269β	$\psi_{2'}=0.5748(\phi_1+\phi_4)-0.2702(\phi_2+\phi_3+\phi_5+\phi_6)-0.1532(\phi_7+\phi_8)$
-1.0000β	$\psi_{1'}=0.5000(-\phi_2+\phi_3-\phi_5+\phi_6)$
$+0.6440\beta$	$\psi_1=0.4556(\phi_1-\phi_4)+0.2771(\phi_2-\phi_3-\phi_5+\phi_6)-0.3726(\phi_7-\phi_8)$
$+1.0000\beta$	$\psi_2=0.5000(\phi_2+\phi_3-\phi_5-\phi_6)$
	Phloroglucinol
-2.0698β	$\psi_{3'}=0.4111(\phi_1+\phi_3+\phi_5)-0.3973(\phi_4+\phi_2+\phi_6)-0.0806(\phi_7+\phi_8+\phi_9)$
-1.0987β	$\psi_{2'}-0.2961(2\phi_1-\phi_3-\phi_5)+0.2695(2\phi_4-\phi_2-\phi_6)-0.0797(2\phi_7-\phi_8-\phi_9)$
-1.0987β	$\psi_{1'}=0.5129(\phi_3-\phi_5)-0.4668(\phi_2-\phi_6)-0.1381(\phi_8-\phi_9)$
$+0.7309\beta$	$\psi_1=0.3676(\phi_3-\phi_5)+0.5029(\phi_2-\phi_6)-0.3347(\phi_8-\phi_9)$
$+0.7309\beta$	$\psi_2=0.2122(2\phi_1-\phi_3-\phi_5)-0.2903(2\phi_4-\phi_2-\phi_6)-0.1932(2\phi_7-\phi_8-\phi_9)$

5) R. S. Mulliken and C. A. Rieke, *Repts. Progr. Phys.*, **8**, 231 (1941).

6) For example, M. A. El-Bayoumi, Thesis, Florida State Univ. (1961).

energies agree satisfactorily with the observed ones. It is natural results that β_{cc}'s have different values for various molecules, because the π-electron distribution varies from molecule to molecule. From the calculation of transition moment, $D_{0\to a}$, we can show that all Ψ_1's given in the table have the polarization in the direction of x axis, whereas all Ψ_2's have the polarization in the direction of y axis. This fact means that the Ψ_1's of hydroquinone and of phloroglucinol may be regarded as modified Ψ_1 of benzene, on the other hand, the Ψ_2's of them may be regarded as modified Ψ_2 of benzene. This situation is shown in Fig. 2.



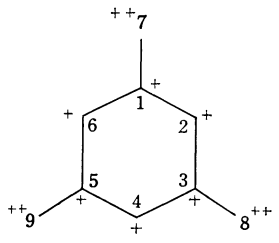


Fig. 1 Numbering of atoms.

Table III. Calculated molecular integrals in eV.

	Benzene	Hydroquinone	Phloroglucinol
$\bar{\varepsilon}_{2'}+y_c$	4.738	5.195	5.488
$\bar{\varepsilon}_{1'}+y_c$	4.738	4.777	5.488
$\bar{\varepsilon}_1+y_c$	−4.738	−3.611	−3.502
$\bar{\varepsilon}_2+y_c$	−4.738	−4.709	−3.502
[11|1'1']	5.874	4.731	5.460
[11|2'2']	5.009	5.393	4.715
[22|1'1']	5.009	5.874	4.715
[22|2'2']	5.874	4.913	5.460
[11'|11']	1.473	0.674	1.221
[12'|12']	0.731	1.196	0.610
[21'|21']	0.731	1.473	0.610
[22'|22']	1.473	0.641	1.221
[11'|22']	0.010	0.657	−0.001
[12'|21']	0.731	−0.004	0.610
[12|1'2']	0.433	0.389	0.370
$[\chi_0\|\chi_{1\to1'}]$	0	0	0.124
$[\chi_0\|\chi_{2\to2'}]$	0	0	0.124

Table IV. Electronic state functions and electronic state energies

Electronic state function	Electronic state energy in eV.	Calculated oscillator strength	Observed excitation energy in eV.	Observed oscillator strength
	Benzene			
$\Psi_0=\chi_0$	0	Ref.	Ref.	Ref.
$\Psi_1=1/\sqrt{2}\,(\chi^1_{1\to2'}-\chi^1_{2\to1'})$	4.900	0	4.9[a]	0
$\Psi_2=1/\sqrt{2}\,(\chi^1_{1\to1'}+\chi^1_{2\to2'})$	6.135	0	6.0[a]	0.1
$\Psi_3=1/\sqrt{2}\,(\chi^1_{1\to1'}-\chi^1_{2\to2'})$ $\Psi_4=1/\sqrt{2}\,(\chi^1_{1\to2'}+\chi^1_{2\to1'})$	6.958	2.353	7.0[a]	0.69
	Hydroquinone			
$\Psi_0=\chi_0$	0	Ref.	Ref.	Ref.
$\Psi_1=0.8847\chi^1_{1\to1'}-0.4893\chi^1_{2\to2'}$	4.518	0.058	4.25[b]	—
$\Psi_2=0.9192\chi^1_{1\to2'}+0.3938\chi^1_{2\to1'}$	5.634	0.250	5.51[b]	—
$\Psi_3=0.3938\chi^1_{1\to2'}-0.9192\chi^1_{2\to1'}$	6.727	1.112	—	—
$\Psi_4=0.4893\chi^1_{1\to1'}+0.8847\chi^1_{2\to2'}$	6.760	0.962	—	—
	Phloroglucinol			
$\Psi_0=0.9995\chi_0-0.0223(\chi^1_{1\to1'}+\chi^1_{2\to2'})$	−0.005	Ref.	Ref.	Ref.
$\Psi_1=1\sqrt{2}\,(\chi^1_{1\to2'}-\chi^1_{2\to1'})$	4.645	0	4.65[c]	—
$\Psi_2=0.7068(\chi^1_{1\to1'}+\chi^1_{2\to2'})+0.0316\chi_0$	5.605	0	5.52[c]	—
$\Psi_3=1/\sqrt{2}\,(\chi^1_{1\to1'}-\chi^1_{2\to2'})$ $\Psi_4=1/\sqrt{2}\,(\chi^1_{1\to2'}+\chi^1_{2\to1'})$	6.351	2.302	—	—

a) R. Pariser and R. G. Parr, *J. Chem. Phys.*, **21**, 767 (1953).
b) R. Adams and J. C. Anderson, *J. Am. Chem. Soc.*, **72**, 5154 (1950).
c) H. Köhler and G. Scheibe, *Z. anorg. u. allgem. Chem.*, **285**, 221 (1956).

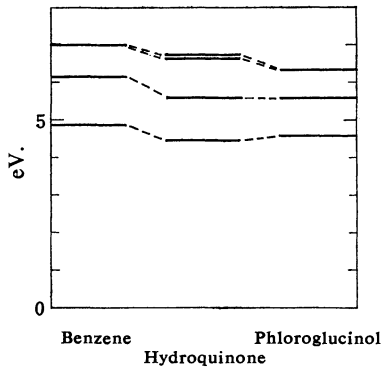


Fig. 2. Electronic state energies of benzene, hydroquinone and phloroglucinol.

Summary

A semi-empirical theory of the π-electronic spectra of aromatic derivatives based on anti-symmetrized molecular orbital method is given and is applied to the calculations of the singlet π-electronic states of hydroquinone and of phloroglucinol. In the theory the core integrals over AO's of heteroatoms are expressed as the functions of the core integrals over carbon atom $2p\pi$ AO's. The calculated excitation energies for these molecules agree satisfactorily with the observed ones. In addition, our calculations give some informations with respect to the nature of their electronic state and their first ionization potentials.

The authors express their gratitude to Dr. Noboru Mataga for his helpful discussion.

Department of Chemistry
Faculty of Science
Osaka City University
Sumiyoshi-ku Osaka

Electronic Structures and Spectra of Non-benzenoid Hydrocarbons: Fulvene, Heptafulvene, Fulvalene, Heptafulvalene and Sesquifulvalene

By Takeshi NAKAJIMA* and Shigeyoshi KATAGIRI

(Received October 11, 1961)

Fulvene, the most fundamental non-benzenoid hydrocarbon, has received considerable attention from both theoretical and experimental points of view. Among previous theoretical treatments[1-4], François and Julg's recent calculations of the dipole moment and spectrum have been in quite satisfactory quantitative agreement with the experimental information. Compared with fulvene, however, its seven-membered analogue, heptafulvene, has been relatively little studied either theoretically or experimentally. Only recently has the attempted synthesis of heptafulvene succeeded[5]. Earlier theoretical treatments of heptafulvene[1,2] have achieved notable success in pointing out the basic causes for its dipole moment and color, but quantitative agreement with the experimental values has not been very satisfactory.

On the other hand, Doering[6] has recently reported the synthesis of the interesting non-benzenoid hydrocarbons, fulvalene and heptafulvalene, together with their ultraviolet-visible spectra. Furthermore, their even more interesting relative, sesquifulvalene, which consists, so to speak, of joined five- and seven-membered rings, has been long exposed to repeated attempts to synthesize it. Earlier theoretical predictions of the spectra of fulvalene[7-9] and heptafulvalene[9] have proved to be far from satisfactory when compared with the now available experimental data.

The aim of this paper is to add, in view of these circumstances, to the understanding of the structures and spectra of heptafulvene and fulvalenes through an attempt to calculate these by a theoretical method within the framework

* Present address: Department of Chemistry, Ibaraki University, Mito.

1) E. D. Bergmann, "Progress in Organic Chemistry", Vol. III, Academic Press, Inc., New York (1955), p. 81.
2) A. Julg and B. Pullman, *J. chim. phys.*, **52**, 481 (1955).
3) H. Kon, *J. Chem. Phys.*, **23**, 1176 (1955).
4) P. François and A. Julg, *J. chim. phys.*, **57**, 490 (1960).
5) W. von Doering and D. W. Wiley, *Tetrahedron*, **11**, 183 (1960).
6) W. von Doering, "Theoretical Organic Chemistry (Kekulé Symposium)", Butterworths Sci. Publ., Ltd., London (1959), p. 35.
7) R. D. Brown, *Trans. Faraday Soc.*, **45**, 296 (1949); **46**, 146 (1950).
8) B. Pullman and G. Berthier, *Compt. rend.*, **229**, 717 (1949).
9) E. D. Bergmann et al., *Bull. soc. chim. France*, **18**, 697 (1951).

of the LCAO MO approximation. The method starts from the Fock self-consistent orbital equations. These are simplified by approximation of the Fock matrix elements; at the same time, special attention will be paid to the marked bond alternation inherent in these molecules. To test the validity of this method, it will be applied first to fulvene.

Method and Procedure

It will be noted at the outset that the fulvenes and fulvalenes that concern us belong to the class of molecules called "classical",[10] a typical example of which is a linear polyene such as butadiene, and therefore that all these molecules are expected to exhibit a bond alternation to almost the same considerable degree as butadiene does. The carbon skeleton structure of fulvene, heptafulvene, fulvalene, heptafulvalene and sesquifulvalene are taken as in Fig. 1, with the lengths of the single and double bonds set equal to 1.48 and 1.34 Å respectively, as in butadiene[11], the rings being assumed to be regular in all cases.

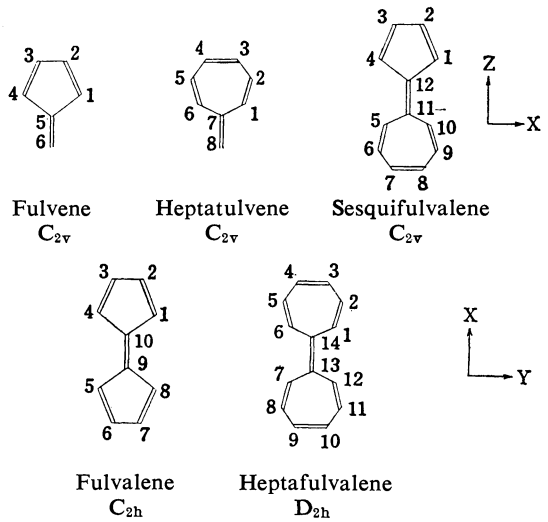


Fig. 1. Carbon skeleton, choice of axes, and numbering of non-benzenoid hydrocarbons.

According to the self-consistent orbital theory[12], the orbital energies of a conjugated hydrocarbon are obtained by solving the Fock secular equation,

$$| F_{pq} - S_{pq}\varepsilon | = 0 \qquad (1)$$

where F_{pq} is the Fock matrix element and S_{pq} the overlap integral between atoms p and q. The simplifying approximations that we make in order to build and solve the Fock equations for conjugated hydrocarbons are as follows: (a) The overlap integral, S_{pq} is neglected unless $p=q$, in which case it is unity. (b) The diagonal Fock elements, F_{pp}, are taken as empirical parameters, α_p^F and the off-diagonal ones, F_{pq}, as parameters, β_{pq}^F for nearest neighbors, and zero otherwise[13]. The Fock secular equations thus reduce to expressions involving empirical parameters analogous to those in the Hückel theory. (c) All the carbon atoms are presumed to have the same α^F. The energy zero is therefore assumed to be such that $\alpha^F=0$, and energies are computed in units of one of the β_{pq}^F in the same manner as in the Hückel theory.

In setting up the Fock equations for the non-benzenoid hydrocarbons that concern us, we introduce, in addition to the above simplifying parameters, the bond alternation parameter defined by

$$\gamma = \beta_{\text{single}}^F / \beta_{\text{double}}^F, \qquad (2)$$

where the subscripts single and double mean the single and double bonds in the Kekulé structures respectively. The value for γ used throughout this paper is so chosen as to reproduce, with the above simplifications of the secular equation, the self-consistent orbitals of butadiene (trans) calculated by using the standard self-consistent field technique. This makes practically unnecessary successive solutions of the Fock equations to find the self-consistent orbitals and so they are not allowed for in this paper. Of the self-consistent orbitals of butadiene so far reported[14-16], we take Lefebvre and Moser's as the reference orbitals to determine the value of γ. The reason for this choice is that in Lefebvre and Moser's procedure, the overlap is neglected, as in the present procedure, and the Coulomb repulsion integrals necessary for the spectral calculations were estimated using the same approximation (Pariser and Parr's) as will be used in this paper (vide infra). The value for γ with which Lefebvre and Moser's orbitals can be reproduced was found to be equal to 0.55[17].

10) A classical molecule is defined as one for which only a single (unexcited) resonance structure can be written.
11) A. Almenningen, O. Bastiansen and M. Troettbery, *Acta Chem. Scand.*, **12**, 1221 (1958).
12) R. Daudel, R. Lefebvre and C. Moser, "Quantum Chemistry", Interscience Publishers, New York (1959), Part II.
13) L. Goodman and H. Shull, *J. Chem. Phys.*, **22**, 1138 (1954).
14) R. G. Parr and R. S. Mulliken, *J. Chem. Phys.*, **18**, 1338 (1950).
15) J. A. Pople, *Trans. Faraday Soc.*, **49**, 1375 (1953).
16) R. Lefebvre and C. M. Moser, *J. chim. phys.*, **53**, 393 (1956).
17) In butadiene, the ratio of the Fock element for the single bond (−3.3 eV.) to that for the double bond (−6.5 eV.) actually proves to be about 0.5, while the ratio of the core resonance integral for the single bond (−2.40 eV.) to that for the double bond (−2.95 eV.) is about 0.8; for the numerical values, see A. Julg, *J. chim. phys.*, **57**, 19 (1960).

The electron transition energies are calculated by the following formula, no configuration interaction being allowed for:

$$\left.\begin{matrix}{}^1E_{ij}\\ {}^3E_{ij}\end{matrix}\right\} - E_N = (\varepsilon_j - \varepsilon_i) - (J_{ij} - K_{ij}) \pm K_{ij} \qquad (3)$$

where E_N, ${}^1E_{ij}$, and ${}^3E_{ij}$ designate the energy of the ground, excited singlet, and excited triplet states respectively, the electronic excitation being from i to j. J_{ij} and K_{ij} are the Coulomb repulsion and exchange repulsion integrals in terms of molecular orbitals. Neglecting differential overlap, these may be rewritten in terms of Coulomb repulsion integrals over atomic orbitals. The integrals of the latter type are evaluated using Pariser and Parr's procedure[18]. Orbital energies are computed in units of β^F_{double}. The value for β^F_{double} was determined so as to reproduce, by application of Eq. 3, the observed energy of the lowest singlet transition ($B_{1u} \leftarrow A_{1g}$), i. e., 5.9 eV. of *trans*-butadiene, and was found equal to -7.0 eV. The oscillator strengths are calculated on the basis of the well-known formula:

$$f = 1.085 \times 10^{11} \nu Q^2 \qquad (4)$$

where Q designates the transition moment.

Results and Discussion

The calculated transition energies and oscillator strengths are summarized and compared with experimental data in Tables I. Tables II, III, IV, V and VI present the molecular orbitals and energies of fulvene, heptafulvene, fulvalene, heptafulvalene and sesquifulvalene respectively. The bond orders and charge densities are also included in these Tables.

Fulvene. — Comparison of the calculated orbitals with those so far obtained by using the SCF technique, among others, Francois and Julg's orbitals, which have been calculated with the same skeleton structure as assumed in this paper, shows that these two sets of orbitals agree well with each other. Further, application of Coulson's formula for bond order vs. bond distance[19] predicts 1.35 Å for the double bonds and 1.47 to 1.48 Å for the single bonds, while the assumed lengths are 1.34 and 1.48 Å respectively, the situation being satisfactorily self-consistent. The calculated dipole moment proves to be 1.14 D, which is in remarkable agreement with the experimental value, 1.1 D.[20] The direction of

TABLE I. TRANSITION ENERGIES AND OSCILLATOR STRENGTHS OF NON-BENZENOID HYDROCARBONS

Molecule	Assignment	Calculated		Experimental	
		Energy (eV.)	f	Energy (eV.)	f
Fulvene	${}^3B_1 \leftarrow {}^1A_1$	2.48			
	${}^1B_1 \leftarrow {}^1A_1$	3.31	0.049	3.32	0.012
	${}^1A_1 \leftarrow {}^1A_1$	5.16	0.92	5.13	0.32
Heptafulvene	${}^3B_1 \leftarrow {}^1A_1$	2.30			
	${}^1B_1 \leftarrow {}^1A_1$	2.96	0.057	2.91	0.02
	${}^1A_1 \leftarrow {}^1A_1$	4.55	0.89	4.43	0.4
Fulvalene	${}^3B_{3u} \leftarrow {}^1A_{1g}$	1.96			
	${}^3B_{1g}$, ${}^3B_{2u} \leftarrow {}^1A_{1g}$	2.03			
	${}^1B_{1g} \leftarrow {}^1A_{1g}$	2.38	forb.		
	${}^1B_{2u} \leftarrow {}^1A_{1g}$	2.47	0.03	2.98	?
	${}^1B_{3u} \leftarrow {}^1A_{1g}$	3.81	1.2	3.95	0.3
Heptafulvalene	${}^3B_{3u} \leftarrow {}^1A_{1g}$	1.64			
	${}^3B_{1g}$, ${}^3B_{2u} \leftarrow {}^1A_{1g}$	2.30			
	${}^1B_{1g} \leftarrow {}^1A_{1g}$	2.54	forb.	1.7—2.8	?
	${}^1B_{2u} \leftarrow {}^1A_{1g}$	2.62	0.02		
	${}^1B_{3u} \leftarrow {}^1A_{1g}$	3.11	1.1	3.42	0.38
Sesquifulvalene	${}^3A_1 \leftarrow {}^1A_1$	1.59			
	${}^3B_1 \leftarrow {}^1A_1$	2.75			
	${}^3B_1 \leftarrow {}^1A_1$	2.94			
	${}^1A_1 \leftarrow {}^1A_1$	3.20	1.0		
	${}^1B_1 \leftarrow {}^1A_1$	3.33	0.05		
	${}^1B_1 \leftarrow {}^1A_1$	3.50	0.02		

18) R. Pariser and R. G. Parr, *J. Chem. Phys.*, **21**, 466, 767 (1953).
19) C. A. Coulson, *Proc. Roy. Soc.*, **A169**, 413 (1939).
20) J. Thiec and J. Wiemann, *Bull. soc. chim. France*, 1956, 177.

TABLE II. FULVENE MOLECULAR ORBITALS, ENERGIES, CHARGE DENSITIES AND BOND ORDERS

MO	Sym	Orbital[a]				Energy[c]	Charge density	Bond order
		$(\chi_1\pm\chi_4)$[b]	$(\chi_2\pm\chi_3)$[b]	(χ_5)	(χ_6)			
1	b_2	0.4198	0.4035	0.4802	0.3020	1.5904	$q_1=1.019$	$p_{1,2}=0.926$
2	b_2	0.1303	0.4033	−0.5265	−0.6030	0.8731	$q_2=1.018$	$p_{1,5}=0.266$
3	a_2	0.5624	0.4286	0.0000	0.0000	0.7621	$q_5=1.016$	$p_{2,3}=0.284$
4	b_2	0.3894	−0.3655	0.3001	−0.5828	−0.5150	$q_6=0.910$	$p_{5,6}=0.925$

a) By definition for the ith MO, $\phi_i=\sum_p C_{pi}\chi_p$. The C_{pi} are listed under the corresponding χ_p.

b) + and − refer to MO's of symmetry b_2 and a_2, respectively.

c) The energies are in units of β^F_{double} (= −7.0 eV.).

TABLE III. HEPTAFULVENE MOLECULAR ORBITALS, ENERGIES, CHARGE DENSITIES AND BOND ORDERS[a]

MO	Sym	Orbital					Energy	Charge density	Bond order
		$(\chi_1\pm\chi_6)$	$(\chi_2\pm\chi_5)$	$(\chi_3\pm\chi_4)$	(χ_7)	(χ_8)			
1	b_2	0.3712	0.3501	0.3314	0.4305	0.2723	1.5801	$q_1=0.994$	$p_{1,2}=0.926$
2	b_2	0.1233	−0.1323	−0.4996	0.4972	0.4340	1.1456	$q_2=0.994$	$p_{1,7}=0.266$
3	a_2	0.4727	0.5084	0.1347	0.0000	0.0000	1.0755	$q_3=0.994$	$p_{2,3}=0.285$
4	b_2	0.3469	0.3137	−0.3453	−0.2547	−0.5091	0.5004	$q_7=0.995$	$p_{3,4}=0.921$
5	a_2	0.4463	−0.2920	−0.4643	0.0000	0.0000	−0.6541	$q_8=1.043$	$p_{7,8}=0.925$
6	b_2	0.2343	−0.4109	0.1296	0.4299	−0.5778	−0.7441		

a) See notes to Table II.

TABLE IV. FULVALENE MOLECULAR ORBITALS, ENERGIES, CHARGE DENSITIES AND BOND ORDERS

MO	Sym	Orbital[a]			Energy	Charge density	Bond order
		$(\chi_1\pm\chi_4)$[b]	$(\chi_2\pm\chi_3)$[b]	$(\chi_9\pm\chi_{10})$[c]			
1	b_{1u}	0.2918	0.2512	0.4511	1.7114	$q_1=1.022$	$p_{1,2}=0.926$
2	b_{2g}	0.3194	0.3707	−0.1457	1.4116	$q_2=1.006$	$p_{1,10}=0.269$
3	b_{1u}	0.0880	0.3444	−0.4973	0.8054	$q_9=0.944$	$p_{2,3}=0.271$
4	a_{1u}	0.3977	0.3031	0.0000	0.7621		$p_{9,10}=0.859$
5	b_{3g}	0.3977	0.3031	0.0000	0.7621		
6	b_{2g}	0.2628	−0.3080	−0.4150	−0.3034		
7	b_{1u}	0.3964	−0.2613	−0.2217	−0.9669		

a) See footnote a to Table II.

b) + refers to MO's of symmetry b_{1u} or b_{2g}, and − refers to those of symmetry a_{1u} or b_{3g}. The C_{pi} corresponding to $(\chi_5\pm\chi_8)$ and $(\chi_6\pm\chi_7)$ are the same as those corresponding to $(\chi_1\pm\chi_4)$ and $(\chi_2\pm\chi_3)$, respectively, for MO's of symmetry b_{1u} and a_{1u} and different in sign from these for MO's of symmetry b_{2g} and b_{3g}.

c) + and − refer to MO's of symmetry b_{1u} and b_{2g}, respectively.

the moment is such that the ring is negative with respect to the methylenic group.

The lowest singlet transition corresponds to a $^1B_1\leftarrow{}^1A_1$ electronic transition, with its moment directed along the short axis, whereas the next singlet corresponds to an $^1A_1\leftarrow{}^1A_1$ transition with its moment directed along the long axis. The predicted energies of these singlet transitions are in remarkably good agreement with the experimental values[20]. The calculated f value for the lowest singlet transition is lower than that for the next one, which is in agreement with the order of magnitude of the experimental f values. However, as is often the case[21], the absolute values of the calculated f values are too high. A correction factor of 0.30 is introduced, which is the ratio of f_{obs} to f_{calcd} for the lowest allowed singlet transition in benzene. It will be seen that the corrected values accord well with the observed ones.

The validity of the present theoretical approach is thus demonstrated by the results for the spectrum as well as for the dipole moment of fulvene.

Heptafulvene.—The bond lengths predicted from the bond orders, 1.48 Å for the single bonds and 1.34 to 1.35 Å for the double bonds, are in satisfactory agreement with the assumed lengths. The dipole moment was calculated to be 0.63 D, reduced considerably from the value, 4.6 D, predicted by the conventional Hückel

21) R. S. Mulliken and C. A. Rieke, *Repts. Progr. Phys.*, **8**, 231 (1941).

TABLE V. HEPTAFULVALENE MOLECULAR ORBITALS, ENERGIES, CHARGE DENSITIES AND BOND ORDERS

MO	Sym	Orbital[a]				Energy	Charge density	Bond order
		$(\chi_1\pm\chi_6)$[b]	$(\chi_2\pm\chi_5)$[b]	$(\chi_3\pm\chi_4)$[b]	$(\chi_{13}\pm\chi_{14})$[c]			
1	b_{1u}	0.2733	0.2196	0.1716	0.4384	1.6857	$q_1=0.991$	$p_{1,2}=0.921$
2	b_{2g}	0.2315	0.2828	0.3333	−0.1033	1.4668	$q_2=1.001$	$p_{2,3}=0.283$
3	b_{1u}	−0.0623	0.1324	0.3980	−0.3747	1.1829	$q_3=0.994$	$p_{3,4}=0.921$
4	b_{3g}	0.3342	0.3595	0.0953	0.0000	1.0755	$q_{13}=1.029$	$p_{1,14}=0.281$
5	a_{1u}	0.3342	0.3595	0.0953	0.0000	1.0755		$p_{13,14}=0.850$
6	b_{2g}	0.3006	0.1354	−0.3524	−0.1849	0.7887		
7	b_{1u}	0.2225	0.2792	−0.2324	−0.3704	0.3392		
8	b_{2g}	−0.1503	0.3394	−0.1146	0.4452	−0.6286		
9	b_{3g}	0.3156	−0.2065	−0.3283	0.0000	−0.6541		
10	a_{1u}	0.3156	−0.2065	−0.3283	0.0000	−0.6541		

a) See footnote a to Table II.
b) + refers to MO's of symmetry b_{1u} or b_{2g}, and − refers to those of symmetry a_{1u} or b_{3g}. The C_{pi} corresponding to $(\chi_7\pm\chi_{12})$, $(\chi_8\pm\chi_{11})$, and $(\chi_9\pm\chi_{10})$ are the same as those corresponding to $(\chi_1\pm\chi_6)$, $(\chi_2\pm\chi_5)$ and $(\chi_3\pm\chi_4)$, respectively, for MO's of symmetry b_{1u} and a_{1u} but different in sign from these for MO's of symmetry b_{2g} and b_{3g}.
c) + and − refer to MO's f symmetry b_{1u} and b_{2g}, respectively.

TABLE VI. SESQUIFULVALENE MOLECULAR ORBITALS, ENERGIES, CHARGE DENSITIES AND BOND ORDERS[a]

MO	Sym	Orbital							Energy	Charge density	Bond order
		$(\chi_1\pm\chi_4)$	$(\chi_2\pm\chi_3)$	$(\chi_5\pm\chi_{10})$	$(\chi_6\pm\chi_9)$	$(\chi_7\pm\chi_8)$	(χ_{11})	(χ_{12})			
1	b_2	0.3010	0.2620	0.2656	0.2098	0.1652	0.4388	0.4532	1.6987	$q_1=1.026$	$p_{1,2}=0.914$
2	b_2	0.2836	0.3162	−0.2403	−0.3122	−0.3843	−0.0645	0.1710	1.4468	$q_2=1.033$	$p_{1,12}=0.295$
3	a_2	0.0000	0.0000	0.4727	0.5084	0.1347	0.0000	0.0000	1.0755	$q_5=0.993$	$p_{2,3}=0.299$
4	b_2	0.1592	0.3149	−0.1958	0.0446	0.4417	−0.4570	−0.2670	1.0556	$q_6=0.973$	$p_{5,6}=0.914$
5	a_2	0.5624	0.4286	0.0000	0.0000	0.0000	0.0000	0.0000	0.7621	$q_7=0.987$	$p_{5,11}=0.294$
6	b_2	−0.0110	0.2553	0.3259	0.2920	−0.3245	−0.2284	−0.4743	0.5070	$q_{11}=0.915$	$p_{6,7}=0.297$
7	b_2	0.3241	−0.3216	−0.0779	0.3110	−0.1174	−0.5007	0.3149	−0.4759	$q_{12}=1.062$	$p_{7,8}=0.914$
8	a_2	0.0000	0.0000	0.4463	−0.2920	−0.4643	0.0000	0.0000	−0.6541		$p_{11,12}=0.866$

a) See footnotes to Table II.

theory[1]. No experimental dipole moment data for heptafulvene are available. However, a comparison may be made with an experimentally estimated moment, e. g., the value of about 0.7 D estimated from the observed moment of tropone[22]. The direction of the moment is such that the ring is positive, contrary to the case of fulvene, with respect to the exocyclic carbon atom. This contradicts the prediction based on the non-empirical SCF theory[1] but accords with the conclusions put forward on the basis of the conventional Hückel[1] and semi-empirical SCF theories[2].

No unambiguous spectral assignment in heptafulvene has been made so far. According to the results of the present calculations, the first long wavelength absorption band, with its maximum at 427 mμ, is assigned to a $^1B_1\leftarrow{}^1A_1$ transition (transverse polarization), and the next band, at 280 mμ, to an $^1A_1\leftarrow{}^1A_1$ transition (symmetry-axis polarization). The expected energies for these two transitions are in good agreement with the experimental values. In addition, the relative order of magnitude of the calculated oscillator strengths for the two transitions is consistent with these assignments. If, further, a correction factor of 0.30 is introduced, the calculated and experimental f values are brought into good agreement in their numerical values.

Fulvalene.—The calculated bond lengths are 1.35 to 1.36 Å for the double bonds and 1.47 to 1.48 Å for the single bonds. These are in fairly good agreement with the assumed lengths.

Brown[7] and Pullman and Berthier[8] have discussed the orbitals and spectrum of fulvalene on the basis of the conventional Hückel theory.

22) Y. Kurita et al., This Bulletin, 26, 272 (1953). See also M. Yamakawa et al., *J. Am. Chem. Soc.*, 82, 5665 (1960). The latter authors have estimated a value of 3.07 D from the observed moment of heptafulvene dinitrile. This unreasonably high value for the moment of heptafulvene is not compatible with the results of the present calculation. On the other hand, one of the present authors and his associates have independently measured the moment in heptafulvene dinitrile and estimated from it the moment of heptafulvene to be from 0.7 D to 1.0 D; S. Katagiri et al., (to be published).

The predicted orbitals and spectrum possess the following curious features: (a) The lowest vacant orbital is bonding in the sense that its energy value is positive in β units. (b) If electron interactions are taken into account using Eq. 3, the first and second excited states of symmetries B_{1g} and B_{2u} respectively prove to be lower in energy than the ground state (A_{1g}), which implies that the lowest energy state is not totally symmetric. (c) If the value $\gamma=23$ k.cm^{-1}*, which was found to be moderately successful in accounting for the spectra of the ring conjugated hydrocarbons[23], the lowest allowed singlet transition, with excitation energy $0.296\,\gamma$ is predicted to appear in the infrared. These are somewhat unexpected, since in no known hydrocarbons have such circumstances been known to occur. The orbitals of fulvalene calculated by using the present procedure show no such unusual features. The lowest vacant orbital is very sensitive to bond alternation and becomes anti-bonding in the sense that its energy value is now negative.

The fulvalene absorption spectrum shows an intense band characterized by a series of comparatively sharp maxima, which is no doubt due to the vibrational fine structures and culminates in a maximum at 314 mμ, and a weak maximum at 416 mμ, followed by long tailing into the visible[6,24]. The calculated transition energies and oscillator strengths are compared with the experimental values in Table I. The longer wavelength weak maximum is assigned to the electronic transition ($^1B_{2u}\leftarrow{}^1A_{1g}$), with its moment directed along the short axis, whereas the shorter wavelength strong maximum is assigned to the transition ($^1B_{3u}\leftarrow{}^1A_{1g}$), with its moment directed along the long axis.

Heptafulvalene.—The predicted bond lengths, 1.35 to 1.36 Å for the double bonds and 1.47 to 1.48 Å for the single bonds, are in fairly good agreement with the assumed lengths.

Heptafulvalene molecular orbitals calculated on the basis of the conventional Hückel theory[9] are similar in their unusual features to the fulvalene Hückel orbitals; that is, the top occupied orbital is anti-bonding in the sense that its energy value is negative in β units, and if electron interactions are taken into account, the lowest energy state loses its total symmetry. Further, the lowest allowed transition is predicted to appear in the infrared, which is not supported by the experimental facts now available.

The top occupied orbital of heptafulvalene is calculated to be bonding in the present procedure. Bond alternation stabilizes it considerably. The absorption spectrum of heptafulvalene shows an intense maximum at 362 mμ ($\log\varepsilon=4.32$), followed by an almost linearly decreasing absorption throughout the visible region[6,24]. According to the results of the present calculations of transition energies and oscillator strengths, it appears that the intense maximum at 362 mμ is to be assigned to an electronic transition ($^1B_{3u}\leftarrow{}^1A_{1g}$), with its moment directed along the long axis, and that the long tail is composed of one singlet-allowed transition ($^1B_{2u}\leftarrow{}^1A_{1g}$), with its moment directed along the short axis, one singlet-forbidden transition ($^1B_{1g}\leftarrow{}^1A_{1g}$), and three triplet transitions.

Sesquifulvalene.—The calculated distribution of bond orders reproduces fairly well the assumed bond lengths. In this connection, it is interesting to note the order of the central bond calculated on the basis of the conventional Hückel theory. The Hückel bond order of this bond is 0.446[9], which is particularly small as an order of double bonds[25]. This is not consistent with the high double bond character of the central bond expected from the fact that only a single Kekulé structure can be written for sesquifulvalene.

The predicted dipole moment is 3.0 D, reduced considerably from the value of about 12 D predicted using the conventional Hückel theory. The direction of the moment is such that the negative pole is directed toward the pentagonal ring. This accords with the expectation based upon the aromatic sextet rule.

Sesquifulvalene Hückel orbitals show no peculiar characteristics such as those seen in fulvalene and heptafulvalene Hückel orbitals. The top occupied orbital is positive, and the lowest vacant orbital is negative in β units. Neither of the orbitals is so sensitive to bond alternation as in fulvalene and heptafulvalene.

As for the predicted spectrum of sesquifulvalene, it should be noted that the lowest singlet transition is expected to correspond to an $^1A_1\leftarrow{}^1A_1$ electronic transition polarized along the long axis*. The electronic transitions ($^1B_1\leftarrow{}^1A_1$) polarized along the short axis are expected to be considerably higher in energy than the corresponding transitions in fulvalene and heptafulvalene.

* For the spectral calculations in the conventional Hückel approximation, orbital energies are corrected for the overlap and written in units of γ instead of β.

23) J. R. Platt, *J. Chem. Phys.*, **18**, 1168 (1950).

24) W. von Doering, private communication.

25) It is noted that the Hückel bond order of the central single bond of butadiene is 0.447.

* *Note added in proof*: Very recently Prinzbach and his associates have reported the synthesis of sesquifulvalene; see Prinzbach et al., *Angew. Chem.*, **73**, 169, 543 (1961). The absorption spectrum of sesquifulvalene shows an intense maximum at 404 mμ ($\log\varepsilon=4.4$) which may be assigned to the lowest singlet transition ($^1A_1\leftarrow{}^1A_1$).

Summary and Conclusion

It appears now well established that in fulvene, heptafulvene, and the fulvalenes that we have dealt with in this paper, there is a remarkable difference in length between the single bonds and the double bonds, the bond alternation being substantially in a degree comparable to that in open chain polyenes. The foregoing calculations show that the assignment of a value of 0.55 to the bond alternation parameter is essential for the theoretical elucidation of the electronic structures and spectra of these molecules. In conclusion, it may be said that although all the above molecules can be shown to be endowed a priori with an aromatic character on the basis of Craig's criterion[26], none of them can, from the viewpoint of bond alternation, be regarded, as a matter of fact, as belonging to the "aromatic" category in a traditional sense. They have, rather, characteristics of the cyclic polyolefins. Indeed, neither fulvene, heptafulvene, fulvalene, nor heptafulvalene has been shown to exhibit the chemical integrity characteristic of the so-called aromatic hydrocarbons[5,6].

The authors would like to thank Professor William von Doering for sending us copies of the ultraviolet spectra of fulvalene and heptafulvalene prior to publication. They are also grateful to Professors Hiroshi Azumi and Yoshio Kitahara for their continued interest during this work.

Department of Chemistry
Faculty of Science
Tohoku University
Katahira-cho, Sendai

26) D. P. Craig, "Theoretical Organic Chemistry (Kekulé Symposium)", Butterworths Scientific Publications Ltd., London (1959), p. 20.

Studies on Micro-paraffin. VI. Properties of the Micro-paraffin

By Kazuo NEGORO

(Received March 22, 1961)

Although micro-paraffin has been reported[1] to consist of side-chain hydrocarbons, the author has considered the problem from different standpoints and has confirmed that micro-paraffin contains a considerable amount of straight-chain compounds and that the carbon number is slightly larger than that of crystalline paraffins[2,3]. When crystalline wax or *n*-dotriacontane was crystallized in the presence of those organic compounds with a hydroxyl group attached to the benzene ring and of a similar molecular structure, it was observed that micro-crystallization occurred[4]. The alcohol-extracted fraction obtained by chromatography from those asphalt components which had been isolated from micro-paraffin was also found to give micro-crystallization effects, and its ultraviolet and infrared spectra revealed that it also had the same hydroxyl groups and benzene ring as other pure organic compounds.

The present paper deals with the properties of the micro-paraffin from the above viewpoints.

Results and Discussion

The Micro-crystallizing Properties of the Micro-paraffin are Caused by Secondary Factors. —Although micro-paraffin has previously been reported to consist mainly of isoparaffin[5,6], about 60% of the micro-paraffins have been found by the present study to be urea-adductible when treated by the urea method. None of these urea-adductible paraffins are *n*-paraffins, because paraffins having few side-chains and long carbon chains are urea-adductible[7]. However, the fraction, which was obtained by treating the urea-adductible paraffins by chromatography with silica gel and then extracting it by pentane, was found to be straight-chain crystalline paraffin. Namely, the micro-paraffin forms micro-crystals, as is shown in Fig. 1, and its

1) B. T. Brooks, C. E. Boord, S. S. Kurtz and L. Schmerling, "The Chemistry of Petroleum Hydrocarbon", Reinhold Publ. Corp., New York (1954).
2) K. Negoro, This Bulletin, **34**, 1366 (1961).
3) K. Negoro, ibid., **35**, 375 (1962).
4) K. Negoro, ibid., **34**, 1374 (1961).
5) A. N. Sachanen, "The Chemical Constituents of Petroleum", Reinhold Publ. Corp., New York (1945), p. 289.
6) W. L. Nelson and L. D. Stwart, *Ind. Eng. Chem.*, **41**, 2231 (1949).
7) W. J. Zimmerschied et al., ibid., **42**, 1300 (1950).

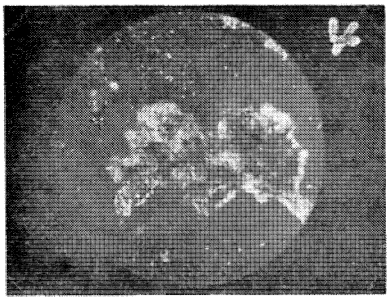


Fig. 1. Micro-crystals of the micro-paraffin.

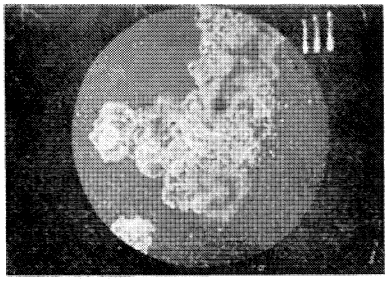


Fig. 2. Crystals of the pentane fraction which had been obtained from the urea-adductible paraffin by chromatography.

X-ray diffraction curve shows that the crystals are imperfect. However, the author recognized that the pentane fraction of the chromatography, with urea-adductible paraffin, formed tabular crystals similar to those of crystalline paraffin and *n*-paraffin[2,8], as is shown in Fig. 2, and that the X-ray diffraction pattern was similar to those of crystalline paraffin and *n*-paraffin[3].

As described above, a considerable amount of *n*-paraffin was clearly contained in micro-paraffin, and so it is not true that the micro-paraffin is essentially micro-crystallized paraffin with side-chains. The ordinary paraffin waxes consist mainly of *n*-paraffin and contain a small quantity of low melting point hydrocarbons and probably side-chain paraffins[9-12].

According to the reports of the compositions of crystalline paraffins obtained by the mass spectrum analysis method[13,14], they consist of 80~95% *n*-paraffin, 5~15% isoparaffin, 1~10% cycloparaffin, and 0~0.9% alkylbenzene, though there are small differences corresponding to the sorts of crude oils. On the contrary, studies of the compositions of micro-paraffins have very seldom been reported; Ridenour et al.[15], however, recently explained that the quantities of urea-adducting material contained in the three sorts of micro-paraffins were 47, 60 and 20% respectively.

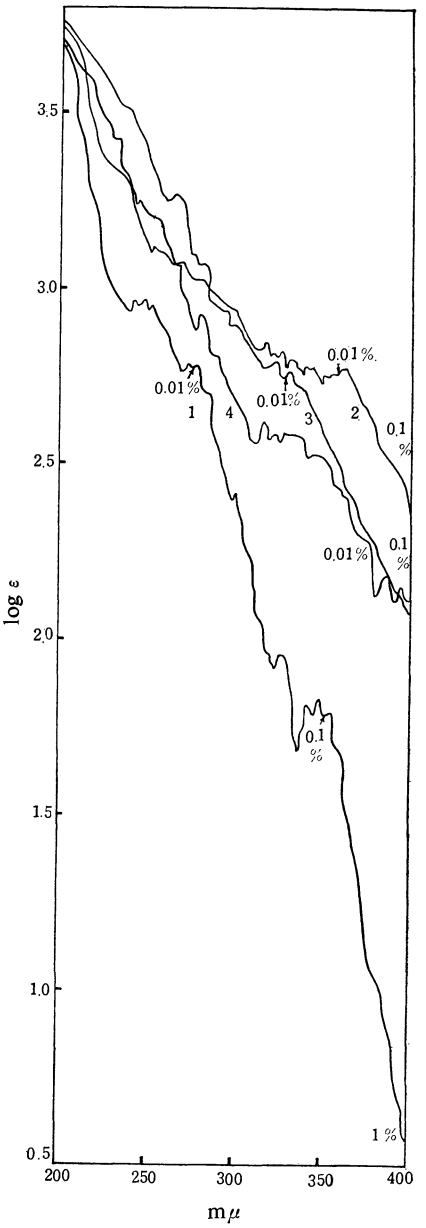


Fig. 5. Ultraviolet spectra of each fraction in asphalt components.
1. Pentane fraction 2. Benzene fraction
3. Alcohol fraction 4. Residue

The micro-paraffin obtained from the tank residue of Aramco crude oil consisted of various components, as is shown in Table I, and the

8) S. Yagi and K. Negoro, *Chem. Ind.* (*Kagaku Kogyo*), **8**, No. 12, 32 (1957).
9) C. C. Buchler and G. D. Groves, *Ind. End. Chem.*, **19**, 718 (1927).
10) S. W. Ferris and H. C. Cowles, ibid., **37**, 1054 (1945).
11) J. A. Carpenter, *J. Inst. Petroleum Tech.*, **12**, 288 (1926).
12) K. Negoro, *Chem.* (*Kagaku*), **15**, 370 (1960).
13) H. J. O'Neal and T. P. Weir, *Anal. Chem.*, **23**, 843 (1951).
14) W. R. Turner, D. S. Brown and D. N. Herrison, *Ind. Eng. Chem.*, **55**, 1219 (1955).
15) W. P. Ridenour, I. J. Spinners and P. N. Templin, *TAPPI*, **41**, No. 6, 257 (1958).

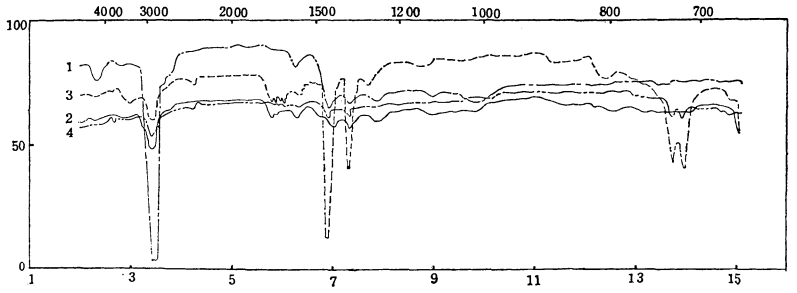


Fig. 4. Infrared spectra of each fraction in asphalt components.
1. Pentanne fraction 2. Benzene fraction
3. Alcohol fraction 4. Residue

TABLE I. COMPONENTS OF MICRO-PARAFFINS AND THEIR PROPERTIES[2,3]

Name	M. p. °C	Refractive index (70°C)	Mean molecular weight	Yield %	Crystal property	Length of carbon chain, Å	Carbon number
Micro-paraffin	73.0	1.4477^{8}	599	—	Micro-crystal	50.8	39
Micro-paraffin (imported)	78.0	1.4442^{85}	581	—	Micro-crystal	53.2	40
Micro-paraffin (de-asphalting)	65.0	1.4406^{75}	583	100.0	Small plate crystal	48.5	37
Micro-paraffin (urea-adducting)	67.0	1.4400	613	61.8	Plate crystal	46.4	35
Micro-paraffin (urea-non-adducting)	54.5	1.4460	620	28.9	Micro-crystal	50.7	39
Urea-adducting micro-paraffin, pentane fraction	65.0	1.4390	607	48.8	Plate crystal	45.9	35
Urea non-adducting micro-paraffin, pentane fraction	54.0	1.4410	636	22.1	Small plate crystal	47.8	36

TABLE II. PROPERTIES OF EACH FRACTION OF THE ASPHALT COMPONENTS

Sample name	Yield, %		Refractive** index	Mean molecular** weight	Crystal property
	vs. Soluble components	vs. Asphalt components			
Pentane fraction	71.8	54.6	1.4685^{70}	593	Plate crystal
Benzene fraction	12.4	9.4	—	564	Amorphous
Alcohol fraction	6.6	5.0	—	571	Amorphous
Residues*	—	24.0	—	599	Amorphous, small plate crystal

* Pentane insoluble matter of asphalt components.
** Measured by the methods described in a previous report[2].

quantity of urea-adductible paraffins which were almost *n*-paraffins was about 60%; furthermore, micro-paraffin showed crystalline properties when isolated by the above treatment.

Clark[16] has described how hydrocarbons (carbon number 26) having alkyl groups, or a naphthene or benzene ring, etc. at any position of the structure, formed crystals as well as *n*-paraffins. From the above facts, it can be deduced that the peculiar micro-crystallization of the micro-paraffin is caused by secondary, not essential, factors.

Micro-crystallizing Substances.—As has been previously described[2], the paraffin formed crystals when asphalt components were removed perfectly from the micro-paraffin by applying the propane de-asphalting method. Therefore, the author considered that original substances for forming fine crystal grains would be present in the asphalt component. Asphalt components form amorphous crystals and are mixtures of various compounds. By chromatography through

16) E. W. Clark, *Ind. Eng. Chem.*, 43, 2526 (1951).

a column packed with alumina gel, the asphalt components were separated into three fractions by being extracted by pentane, benzene and ethyl alcohol. The properties of each fraction were measured, and the results are shown in Table II and in Figs. 3 and 4.

The last absorption band changed to a deep color when the side-chain numbers increased in benzene derivatives. The last absorption band of the asphalt components was 277 mμ, which represented a shift of about 9 mμ from that of the benzene of no side-chains[17], and substances having some side-chains of benzene ring were considered to be present in the asphalt components. Therefore, small amounts of various series of aromatic hydrocarbons besides such benzene derivatives, were also contained in each fraction.

The crystal band was observed at 723~717 cm^{-1} in the infrared spectrum of the pentane fraction of asphalt components (as has also been found in *n*-dotriacontane or crystalline paraffin). This fraction of asphalt components was almost the same as the ordinary paraffin waxes, and if the fraction was added to crystalline paraffin (m. p. 53.5°C, mean carbon number 28) or *n*-dotriacontane (m. p. 69.5°C, carbon number 32), micro-crystallization effects could not be observed, as is shown in Figs. 5 and 6*.

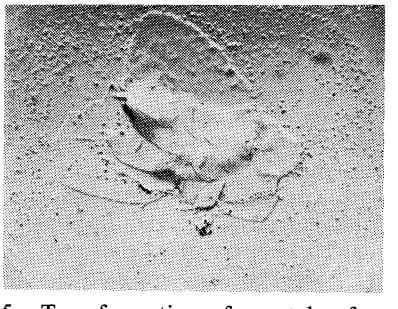


Fig. 5. Transformation of crystals of crystalline paraffin caused by the addition of the pentane fraction of asphalt components (almost no transformation).

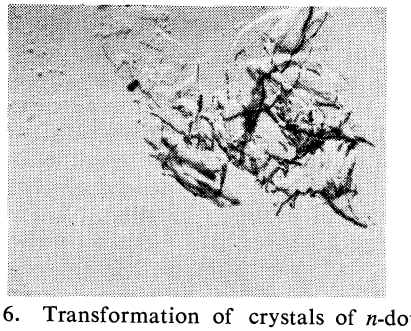


Fig. 6. Transformation of crystals of *n*-dotriacontane caused by the addition of the pentane fraction of asphalt components (almost no transformation).

17) "Hydrocarbon Chemistry (Tankasuiso Kagaku)", Vol. 2, Kyoritsu Shuppan, Tokyo (1956), p. 69.

The crystal band was not seen in the infrared spectrum of the benzene-extracted fraction, and it was shown to be amorphous. Therefore, this fraction caused almost no transformation when added to *n*-paraffin.

In the case of an alcohol-extracted fraction, the author discovered that the addition of a small amount of crystalline paraffin formed fine crystal grains, as is shown in Fig. 7; it was also clearly observed, as is shown in Fig.

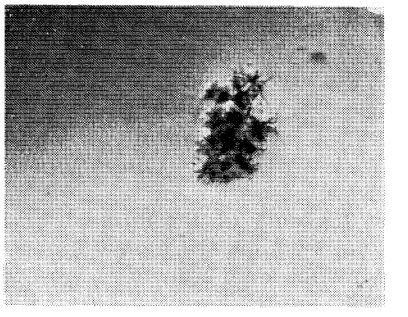


Fig. 7. Transformation of crystals of crystalline paraffin caused by the addition of the alcohol fraction of asphalt components (micro-crystallized).

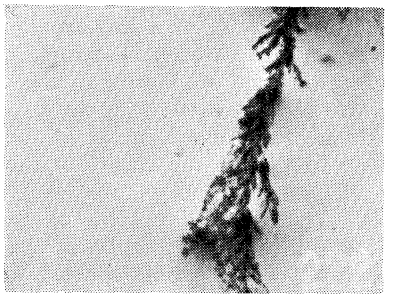


Fig. 8. Transformation of crystals of *n*-dotriacontane caused by the addition of the alcohol fraction of asphalt components (micro-crystallized).

TABLE III. INFRARED SPECTRUM OF THE ALCOHOL FRACTION OF ASPHALT COMPONENTS

Wave number, cm^{-1}	Assignment of vibration
3410	OH Stretching vibration
2980	C-H Stretching vibration
1731	C=O Stretching vibration
1600	Conjugated double bond stretching vibration
1471	deg-CH Bending vibration
1380	sym-CH Bending vibration
1284~1260	Aromatic derivatives vibration

* The experiment was made by the method described in a previous report[4], in which the solvent used was purified ethyl alcohol.

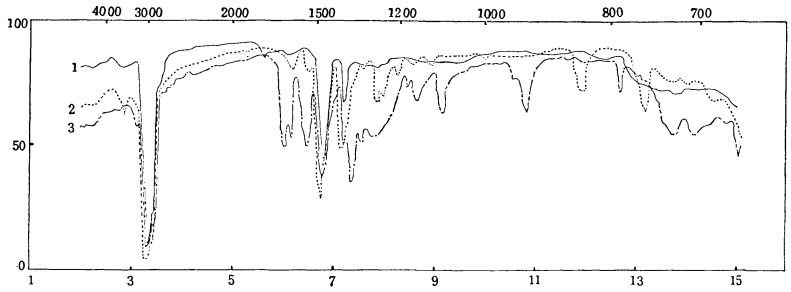


Fig. 9. Infrared spectra of organic compounds.
1. Santopour 2. *p*-Hydroxydiphenyl 3. Picric acid

8, that the fraction caused a remarkable transformation of crystals on *n*-dotriacontane[4], on which the asphalt components themselves had almost no noticeable effects. Therefore, the residues of the asphalt components were recognized as showing small micro-crystallization effects.

From the data of the infrared spectrum of the alcohol fraction, the atomic groups present in the fraction were deduced as shown in Table III.

The absorption band which originated in hydroxyl groups at 3410 cm^{-1} was remarkably attractive. As has previously been described[4], the infrared spectra of Santopour, picric acid, and *p*-hydroxydiphenyl formed fine crystal grains of crystalline paraffin or *n*-dotriacontane, as is shown in Fig. 9. In each spectrum, however, the absorption band originating in the carboxyl groups was seen at 3190~3520 cm^{-1}.

The shape of the above curves of the spectra was very similar to the curves of the spectra of the alcohol fraction of the asphalt components. The infrared spectra of Santopour and those of the alcohol fraction of the asphalt components (in the whole sphere) were very similar, and it was concluded that their structures were similar, too.

Santopour has been reported to be 2, 3, 5, 6-tetraalkylbenzene[18],  and its mean molecular weight was measured to be 265. The alkyl chains at the 4 radicals of the benzene ring were therefore considered to consist of C_4.

If the alcohol-extracted fraction, isolated from the asphalt components, had a structure like Santopour, the length of the methylene chain was presumed to be C_{34}, because its molecular weight was 571. Therefore, the alcohol fraction was considered to have parts of alkyl chains much longer than Santopour.

It is noticeable that the formation of fine crystal grains of paraffin is caused in the presence of the compounds of similar structures having hydroxyl groups and benzene rings.

Crystal Structure of the Micro-paraffin. — Many studies have been made on the crystals of *n*-paraffin[19-23]; its unit cell has been reported to form hexagonal, orthorhombic, monoclinic, or triclinic system, according to the sort of individual hydrocarbons and the temperature. As has been mentioned above[3], the crystal systems of paraffin waxes and micro-paraffins were orthorhombic.

The values of d_{110} and d_{200}, the length of the a and b axis, the cross-sectional area occupied by one molecule, and the molecular volume were calculated; the results are shown in Table IV.

The above values on crystal lattice are mean values, because micro-paraffin is a mixture of various hydrocarbons. The tips of carbon chains are not arranged in order. It seems to be reasonable to consider that its lattice spacings are somewhat larger than those of *n*-paraffin and that its side-chains are seen at some places of the paraffin chains. In particular, the values of both d_{110} and d_{200} of the urea non-adducting paraffins, isolated from the micro-paraffin by the urea method, were so large that it was proved to have many side-chains.

According to Edwards[24], the development of crystal lattice was affected by the molecular weights of hydrocarbons and by the presence of non-*n*-hydrocarbons. The mean carbon chain of micro-paraffins was somewhat longer than that of ordinary crystalline paraffins, and the molecular volume was nearly 20~30% larger than that of ordinary paraffins.

Several peaks of the X-ray diffraction curve of 001, 002, etc. were seen in the case of the crystalline paraffin of *n*-dotriacontane, but the

18) N. Iimure, "Guide-Book of Petroleum Products (Sekiyu Seihin Gaido Bukku)", Sangyo Tosho, Tokyo (1956), p. 162.

19) A. Müller, *Proc. Roy. Soc.*, **A120**, 437 (1928).
20) A. Müller, ibid., **A127**, 417 (1930).
21) A. Müller, ibid., **A138**, 514 (1932).
22) C. W. Bunn, *Trans. Faraday Soc.*, 35, 482 (1939).
23) A. E. Smith, *J. Chem. Phys.*, **21**, 2229 (1953).
24) R. T. Edwards, *TAPPI*, **41**, No. 6, 267 (1958).

TABLE IV. RESULTS OF X-RAY DIFFRACTION FOR VARIOUS PARAFFINS[3]

Sample name	d_{110}, Å	d_{200}, Å	a Axis, Å	b Axis, Å	Cross-sectional area, $\times 10^{-16}$ cm^2	Molecular vol. Å^3/mol.
Crystalline paraffin (m. p. 53.5°C)	4.19	3.78	7.54	5.03	19.0	708
Micro-paraffin	4.16	3.75	7.50	5.01	18.8	955
Micro-paraffin (de-asphalting)	4.16	3.76	7.52	5.00	18.8	911
Micro-paraffin (Shell)	4.16	3.75	7.50	5.01	18.8	928
Micro-paraffin (commercial)	4.16	3.75	7.50	5.01	18.8	998
Micro-paraffin, urea-adducting paraffin	4.16	3.76	7.52	5.00	18.8	872
Micro-paraffin, urea non-adducting paraffin	4.21	3.80	7.60	5.05	19.2	974
Micro-paraffin pentane fraction	4.20	3.79	7.56	5.04	19.0	900
Urea-adducting micro-paraffin, pentane fraction	4.16	3.75	7.50	5.01	18.8	867
Urea non-adducting micro-paraffin, pentane fraction	4.20	3.79	7.56	5.04	19.0	909
n-Dotriacontane	4.15	3.77	7.54	5.03	19.0	804

peak was only one in the case of the micro-paraffin[3]. Moreover, the peaks of less than 002 in the urea-adducting materials of micro-paraffin and its pentane-extracted fraction revealed that their crystal structures resembled those of *n*-paraffin. This presumption was verified by observation of the crystal structure of paraffins traced on a carbon film with an electron microscope by applying the replica method[25,26].

Micro-crystallization Phenomenon. — A few reports have been made on the spiral growth of the crystal of *n*-paraffin[27-29]; it was studied by the present author[8] and also by Jaccordine[30] with a phase-contrasts microscope on paraffin crystals. Asphalts resins or dark color substances, etc. in petroleum inhibited the crystallization of paraffins[31] in the case of ordinary paraffin waxes, and very slight dust particles prevented the grow-step of the crystal growth[29] in the studies of the spiral growth.

The author has already reported several phenomena revealing that the formation of fine crystal grains of micro-paraffin is caused by secondary factors[2-4,32] and has discussed the cause of the micro-crystallization phenomena.

The relation between the concentration of Santopour, picric acid, *p*-hydroxybiphenyl, and the alcohol fraction of asphalt components and log ε at each wavelength are shown in the graphs. Therefore, 10 mg. of each organic compound was added to 100 mg. of the crystalline paraffin or *n*-paraffin to crystallize, and the mother liquor was taken out to measure the log ε, which was plotted in the above graphs for investigation. However, the amount of each organic compound in the liquor was discovered to be not very different from that previously added, even taking into consideration the effects of the presence of paraffin on the log ε. Accordingly, it may be surmised that very few compounds are contained in the crystal lattice of paraffin.

Moreover, the amount of crystallized paraffin was weighed, and the crystal growth of 100 mg. of the crystalline paraffin (m. p. 53.5°C) was inhibited by the presence of such organic compounds; the non-crystallized amounts have been calculated and are shown in Table V.

TABLE V. CHANGE IN AMOUNTS OF THE PARAFFIN CRYSTAL CAUSED BY SOME SORTS OF ORGANIC COMPOUNDS

Name of Compounds	Crystallized amount, mg.	Non-crystallized amount, mg.
—	94.1	5.9
Picric acid	69.9	30.1
Santopour	67.2	32.8
p-Hydroxydiphenyl	66.2	33.8
Alcohol fraction of asphalt components	64.5	35.5

25) K. Negoro, *Science* (*Kagaku*), **31**, 326 (1961).
26) K. Negoro, on application to *J. Japan Petroleum Inst.* (*Sekiyu Gakkaishi*).
27) I. M. Dawson and V. Vand, *Nature*, **167**, 476 (1951).
28) I. M. Dawson and V. Vand, *Proc. Roy. Soc.*, **A206**, 555 (1951).
29) N. G. Anderson and I. M. Dawson, ibid., **A218**, 255 (1953).
30) R. J. Jaccodine, *Nature*, **187**, 498 (1960).
31) N. F. Chemberlin, G. A. Dinouddie and J. L. Franklin, *Ind. Eng. Chem.*, **41**, 566 (1949).
32) K. Negoro, *J. Chem. Soc. Japan, Ind. Chem. Sec.* (*Kogyo Kagaku Zasshi*), **64**, 295 (1961).

It was made clear by those results that the crystallization of the paraffin was fairly much inhibited by the presence of such organic compounds. As has been described previously, micro-paraffin contained more side-chain components than the crystalline paraffin; therefore, its crystal growth was more prevented, and its tendency to inhibit crystallization was larger than that of crystalline paraffin. Accordingly, it seems reasonable to consider that the formation of fine crystal grains of micro-paraffin is made possible by the presence of the alcohol fraction, which has been separated from micro-paraffin materials and which is supposed to have a structure consisting of an alkyl chain and a benzene ring with hydroxyl groups.

The compounds with a similar structure wrap up the paraffin molecules in the crystallization of paraffin and inhibit the formation of the crystal lattices by a continuous arrangement of paraffin molecules to form larger crystals. As a result, the crystallization is partially prevented, and the formation of fine crystal grains occurs. Very small tabular crystals are also rolled up to form needle crystals, by which the direction perpendicular to the 110° side agrees with the length for the smaller surface area and the more stable form before the crystals grow up in the direction of a and b axes.

Experimental

Chromatography. — Fifty grams of an asphalt component isolated from the tank residues of Arabian crude oil (Aramco oil of Saudi-Arabia)[32] was extracted by a Soxhlet extractor at 50~60°C with 1 l. of purified benzine (b. p. 50~60°C) for about 10 hr. The benzine-extracted components were isolated from the insoluble components by filtration. The yields were 39 and 12 g. respectively. The system for chromatography consisted of 5 columns 100 cm. long and 2 cm. in diameter and of 5 columns 75 cm. long and 1.5 cm. in diameter; all the columns were packed with 1.6 kg. of 200 mesh alumina gel (a product for chromatography, manufactured by the Kanto Kagaku Co.). Then, the benzine-extracted-components solution was poured into the top of the first column. The refractive index of the elute solution showed a larger value than that of benzine. Then the solution was poured into the second column. The index was examined successively at each column, and the last index agreed with that of benzine. Then it was extracted by 52 l. of pentane (b. p. 40~50°C), 67 l. of purified benzene (b. p. 80°C), and 42 l. of purified ethyl alcohol (b. p. 78°C), successively and classified into its extracted fractions. In this case, the index of each solvent had been measured previously; as well, each index of each elute solution was examined. It was extracted by the same solvents (pentane, benzene and ethyl alcohol) until the latter value agreed with the former. Then, each extracted fraction was obtained by using the above amounts of the solvents.

X-Ray Diffraction and Absorption Spectra.—A X-ray diffractometer (Geiger flex, manufactured by the Rigaku Denki Co.) was used for the measurement of the X-ray diffraction[33]. The samples were fixed on glass, and the measurements were made in the range of 0°~90° of 2θ (scanning speed, 1 deg./min.) and 25~31° (scanning speed, 1/4 deg./min.) with FeK_α, and in the range of 0~5° (scanning speed, 1 deg./min.) with CuK_α.

As has already been reported[2], the sample solution of purified *n*-hexadecane was prepared by the weighing method, and a photo-electric spectrophotometer of type EPU-2 (manufactured by the Hitachi Mfg. Co.) was used for the measurement of the ultraviolet spectrum. An infrared spectrophotometer (Perkin Elmer Model-21) with a sodium chloride prism was used for the measurement of the infrared spectrum. As has previously been reported[2], each sample of the various paraffins or the asphalt components was applied to the spectrophotometer for measuring. However, organic compounds were measured by the Nujol method with purified liquid paraffin.

Action of Various Organic Compounds (Table V). — 10, 5 and 1 mg. each of Santopour, picric acid, *p*-hydroxydiphenyl, and the alcohol fraction of the asphalt components were weighed out and dissolved in 25 ml. of purified ethyl alcohol, which had been confirmed as suitable for use as a diluent by the measurement of the ultraviolet spectrum in the range of 200~400 mμ.

Each amount was diluted with ethyl alcohol to the constant ratio (*p*-hydroxybiphenyl 0.001 wt. %, and the others 0.01 wt. %), and the absorptions at each wavelength (Santopour, 264 mμ; picric acid, 270 mμ; *p*-hydroxydiphenyl, 256 mμ; the alcohol fraction of asphalt components, 277 mμ), which had been selected according to the results of the ultraviolet spectrum of each organic compound measured previously, were measured to determine ε. The relation between the concentration and ε is shown in the graph. One hundred milligrams of the crystalline paraffin (m. p. 53.5°C; mean carbon number, 28) was weighed in an Erlenmeyer flask with a stopper, and 10 mg. of each of the various organic compounds described above was added to the flask to be treated[4]. The crystallized paraffins were isolated by filtration and dried at below 30°C until reaching a constant weight, which was measured to compute the amount of non-crystallized paraffins. Then, the absorption at respective constant wavelengths was measured to compute for each filtrate, and each content of organic compounds was determined.

Summary

1) The micro-paraffin has longer mean carbon chains than those of ordinary crystalline paraffins, and the content of side-chain hydrocarbons is less than that in ordinary paraffins; its crystals belong to an orthorhombic system, and the formation of fine crystal grains is a result of secondary causes.

2) If the paraffin is recrystallized in ethyl alcohol in the presence of organic compounds of a similar structure which have benzene rings with hydroxyl groups such as Santopour, picric acid, *p*-hydroxybiphenyl, etc., the crystal growth is inhibited and the crystallized amount of the paraffin crystals is reduced, which is the cause of the formation of fine crystal grains.

3) The alcohol-extracted fraction, isolated from the micro-paraffin materials, has a fairly long alkyl chain and benzene rings with the hydroxyl groups. The crystalline or *n*-paraffin is micro-crystallized, the same as the above organic compounds, when a very small amount of the fraction is added to it.

4) The content of *n*-paraffin in the micro-paraffin is less than that in ordinary crystalline paraffin, but the former contains more side-chain components. The paraffin forms fine crystal grains in the presence of compounds such as the alcohol-extracted fraction.

5) As a result of the purification by the urea method and chromatography, X-ray diffraction, etc., a considerable amount of the crystalline *n*-paraffins has clearly been found to be contained in micro-paraffin. Therefore, the micro-paraffin does not consist of side-chain paraffin and is not originally micro-crystallized, as has hitherto been believed.

6) The effects of such additive organic compounds on *n*-dotriacontane, on crystalline paraffins or on a mixture of various hydrocarbons are not the same. In the case of the latter, the tips of the carbon chain in the crystal lattice are arranged in disorder, with a few side-chains; therefore, the crystal growth of the paraffin is believed to be inhibited and then the formation of fine crystal grains occurs.

7) The additive organic compounds wrap up paraffin molecules in the crystallization of paraffin, and the process from the formation of the crystal lattices to the growth of large crystals is so inhibited that the crystal growth is prevented. Crystallization seems to be partially prevented, and micro-crystallization or needle crystallization of small tabular crystals occurs.

The author wishes to express his deep appreciation to Professor Ryozo Goto and Professor Saburo Yagi, Kyoto University, for their cordial guidance and discussion throughout this research; he also is grateful to Dr. Kenziro Asai and Dr. Tsuneo Seto, Kyoto University, for their cordial guidance in the analyses of X-ray diffraction, and to Mr. Kazuo Naito and Mr. Osamu Nanbu, Osaka Ind. Tech. Lab., who co-operated in the infrared spectrum experiments. He also wishes to thank Mr. Takashi Matsuoka and the personnel of the Central Research Lab. of Nippon Mining Co., for their co-operation in the measurement of the X-ray diffraction and to all the other personnel of Nippon Mining Co. for their great kindness throughout this research.

Central Research Laboratory
Nippon Mining Co.
Kitaadachi-gun, Saitama

Quantitative Analysis of Mixtures of L-Glutamic Acid Polymorphs by X-Ray Diffraction

By Hiroshi TAKAHASHI, Tadao TAKENISHI and Nobuya NAGASHIMA

(Received November 1, 1961)

Two polymorphic forms of L-glutamic acid have been reported by a few authors. One form, α, reported by Bernal[1], has an orthorhombic structure, with $a=7.06$, $b=10.3$, $c=8.75$ kX. The other form, β, which has been studied by Hirokawa[2], also has an orthorhombic structure, with $a=5.17$, $b=17.34$, $c=6.95$ Å. The X-ray diffraction patterns of these two polymorphic forms of L-glutamic acid are given in Fig. 1. L-Glutamic acid crystallizes in a mixture consisting of various proportions of the α- and the β-forms, from an aqueous solution under certain conditions. In industrial processes, it is necessary to control the formation of the L-glutamic acid polymorphs. To analyze the two forms quantitatively, usual chemical methods are useless. The X-ray diffraction method does, however, give satisfactory results for this purpose. The application of

1) J. D. Bernal, *Z. Krist.*, **78**, 363 (1931).
2) S. Hirokawa, *Acta Cryst.*, **8**, 637 (1955).

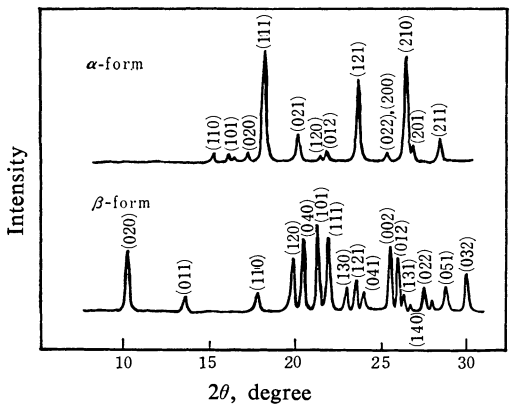


Fig. 1. X-Ray diffraction patterns of L-glutamic acid polymorphs. (CuK_α radiation)

such a diffraction method to the quantitative analysis of crystalline organic systems has been investigated by Christ et al.[3] This paper describes an analytical method for polymorphs of organic crystals using the X-ray diffractometer. Sufficiently accurate results can be obtained within 40 min.

A general theory of quantitative X-ray analysis by the diffractometer has been reported by Klug and Alexander[4] and by Copeland and Bragg[5]. They have shown that the integrated intensity of the $(h\,k\,l)$ line of the jth component in the diffraction pattern is given by

$$I_{(h\,k\,l)j}=K_{(h\,k\,l)j}\ (x_j/\rho_j\mu) \qquad (1)$$

where $K_{(h\,k\,l)j}$ depends upon the nature of the component j and the geometry of the apparatus, x_j is the weight fraction, ρ_j, the density of the jth component, and μ, the total mass absorption coefficient of the sample. In the case of such mixtures of polymorphic forms, μ does not change with the composition. Equation 1 indicates that the intensity is directly proportional to the concentration of the component.

For a binary mixture (α- and β-forms), Eq. 1 can be written:

$$I_{(h\,k\,l)\alpha}=k_{(h\,k\,l)\alpha}x_\alpha,\quad I_{(H\,K\,L)\beta}=k_{(H\,K\,L)\beta}x_\beta \qquad (2)$$

where $k_{(h\,k\,l)\alpha}$ and $k_{(H\,K\,L)\beta}$ are constant. The following selected lines were used:

$I_{(1\,1\,1)\alpha}$: Intensity of the 4.87Å line of the α-form, (1 1 1) reflection.

$I_{(1\,0\,1)\beta}$: Intensity of the 4.17Å line of the β-form, (1 0 1) reflection.

Each $(1\,1\,1)\alpha$, $(1\,0\,1)\beta$ line is the strongest in its respective pattern. Fig. 1 shows that the $(1\,0\,1)\beta$ line is superposed with the (1 2 0) line of the α-form. In practice, Eq. 2 must be modified to:

$$I_{(1\,1\,1)\alpha}=k_{(1\,1\,1)}x_\alpha$$
$$I_{(1\,0\,1)\beta}=k_{(1\,0\,1)\beta}x_\beta+k_{(1\,2\,0)\alpha}x_\alpha \qquad (3)$$

Division of $I_{(1\,0\,1)\beta}$ by $I_{(1\,1\,1)\alpha}$ gives:

$$I_{(1\,0\,1)\beta}/I_{(1\,1\,1)\alpha}=K_1(x_\beta/x_\alpha)+K_2 \qquad (4)$$

where K_1 and K_2 are constant. The plotted values of $I_{(1\,0\,1)\beta}/I_{(1\,1\,1)\alpha}$ vs. x_β/x_α give a straight line having the slope K_1 and the interception K_2. K_1 and K_2 can be obtained experimentally from the synthetic mixtures.

Equation 4 combined with $x_\alpha=1-x_\beta$, on solving for x_β, yields:

$$x_\beta=[K_1\{(I_{(1\,0\,1)\beta}/I_{(1\,1\,1)\alpha})-K_2\}^{-1}+1]^{-1} \qquad (5)$$

Equation 5 gives the relation between the intensity ratio $I_{(1\,0\,1)\beta}/I_{(1\,1\,1)\alpha}$ and the concentration x_β. By this calibration curve, direct analysis is possible.

To analyse the quantities of the α- and the β-forms of L-glutamic acid when these forms are mixed with other substances, the internal standard method should be used.

A known amount of the internal standard is added to the sample. Let the weight fraction of the internal standard be x_s, and let the weight fraction of the component j after adding the internal standard be x_j'. Then the intensity of the jth component $I_{(h\,k\,l)j}$ and that of the internal standard $I_{(H\,K\,L)s}$, are given from Eq. (1):

$$I_{(h\,k\,l)j}=K_{(h\,k\,l)j}(x_j'/\rho_j\mu),$$
$$I_{(H\,K\,L)s}=K_{(H\,K\,L)s}(x_s/\rho_s\mu)$$

Dividing $I_{(h\,k\,l)j}$ by $I_{(H\,K\,L)s}$ gives:

$$I_{(h\,k\,l)j}/I_{(H\,K\,L)s}=K(x_j'/x_s)$$

where K is constant. As an internal standard, sodium chloride was suitable, because of the following properties:

i) Satisfactory purity.
ii) Sharp diffraction lines.
iii) It has a suitable line free from interference and superposition (see Fig. 2).

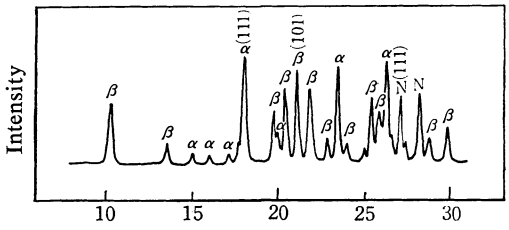


Fig. 2. Diffraction pattern of a sample for the internal standard method.
α: α-form L-glutamic acid, β: β-form L-glutamic acid, N: sodium chloride

3) C. L. Christ, R. B. Barnes and E. F. Williames, *Anal. Chem.*, **20**, 789 (1948).
4) L. Alexander and H. P. Klug, ibid., **20**, 886 (1948).
5) L. E. Copeland and R. H. Bragg, ibid., **30**, 196 (1958).

Calibration curves were prepared by measuring the following intensities:

$I_{(1\,1\,1)\alpha}$: Intensity of the 4.87Å line of the α-form, (1 1 1) reflection.

$I_{(1\,0\,1)\beta}$: Intensity of the 4.17Å line of the β-form, (1 0 1) reflection.

$I_{(1\,1\,1)s}$: Intensity of the 3.26Å line of NaCl, (1 1 1) reflection.

To determine the concentration of the α- or the β-form, Eq. 6 is modified as (the (1 0 1) line of the β-form is superposed with the (1 2 0) line of the α-form),

$$I_{(1\,1\,1)\alpha}/I_{(1\,1\,1)s}=K_\alpha'(x_\alpha'/x_s)$$

$$I_{(1\,0\,1)\beta}/I_{(1\,1\,1)s}=K_{\beta 1}'(x_\beta'/x_s)+K_{\beta 2}'(x_\alpha'/x_s)$$

When x_s is held constant, the weight fractions of the components α and β-forms, in the original sample, x_α and x_β, are given by:

$$x_\alpha=x_\alpha'/(1-x_s)=K_\alpha(I_{(1\,1\,1)\alpha}/I_{(1\,1\,1)s})$$

$$x_\beta=x_\beta'/(1-x_s)=K_{\beta 1}(I_{(1\,0\,1)\beta}/I_{(1\,1\,1)s})-K_{\beta 2}(I_{(1\,1\,1)\alpha}/I_{(1\,1\,1)s}) \quad (7)$$

where K_α, $K_{\beta 1}$, $K_{\beta 2}$ are constant. Thus, when the internal standard is added in a constant proportion, the concentration of the component α or β is a linear function of the intensity ratio $I_{(1\,1\,1)\alpha}/I_{(1\,1\,1)s}$ and $I_{(1\,0\,1)\beta}/I_{(1\,1\,1)s}$.

Experimental

Instrumentation. — The diffractometer used was a "Geigerflex" D-3F type (Rigakudenki Co.) using CuK_α radiation (filtered through Ni). The operating conditions were as follows: CuK_α, 30 kV. 15 mA.; Divergence slit, 1°; Scatter slit, 1°; Receiving slit, 0.2 mm.; Time constant, 2 sec.; Counter speed, 1/2° per minute; Chart speed, 1 cm. per minute.

The intensity ratio was obtained by measuring relative peak heights above their backgrounds. It is essential in accurate work to measure peak areas rather than peak heights, although the latter may be sufficient for simple analysis.

Preparation of Calibration Curves. — The compositions of the mixtures prepared for the calibration curves for the analysis in the binary system and in the multicomponents system are given in Tables I and II respectively. Each sample was ground in an agate mortar to about a 5 μ particle size. The β-form crystal has a tendency to crystallize in various habits. When crystallites were ground, they were frequently oriented in a preferred

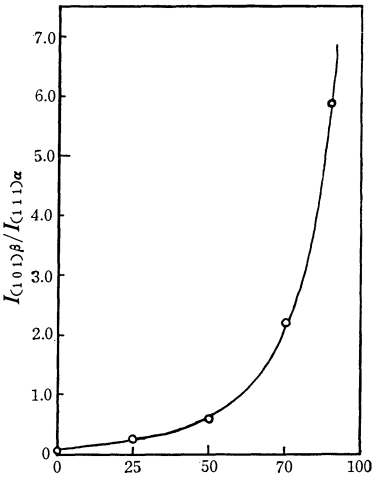


Fig. 3. Calibration curve for the analysis of the β-form concentration by the direct method.

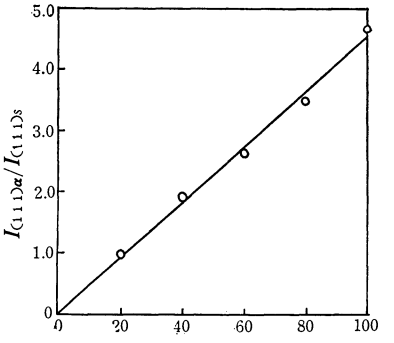


Fig. 4. Calibration curve for the analysis of the α-form concentration by the internal standard method.

Table I. Composition of synthetic mixtures for binary system

Sample	B-1	B-2	B-3	B-4	B-5
α-Form (g.)	1.00	0.753	0.502	0.248	0.101
β-Form (g.)	0	0.249	0.499	0.745	0.902
β-Form (wt.%)	0	25	50	75	90

Table II. Composition of synthetic mixtures for multi-component system

Sample	M-1	M-2	M-3	M-4	M-5	M-6
α-Form (g.)	0	0.201	0.400	0.601	0.801	1.001
β-Form (g.)	0.999	0.800	0.600	0.400	0.201	0
NaCl (g.)	0.500	0.499	0.501	0.500	0.500	0.500
β-Form (wt.%)	100	80	60	40	20	0

direction, and the preferred orientation caused an abnormal increase in the intensity of the $(0\,k\,0)$ lines in the diffraction pattern. However, sufficient grinding reduced this effect, and the intensity of the line (1 0 1) for the analysis in question was scarcely effected by the preferred orientation. The data for the calibration curves are given in Table III. Each value is an average of 7—8 specimens of each sample. From these data, using the method of least squares, the values of K_1 and K_2, and of K_α, $K_{\beta 1}$ and $K_{\beta 2}$ are obtained as follows:

$$K_1=0.673, \quad K_2=0.037$$

$$K_\alpha=21.7, \quad K_{\beta 1}=32.1, \quad K_{\beta 2}=2.08$$

From Eqs. 5 and 7, each combined with these experimental values, the calibration curves can be obtained (Figs. 3 and 4).

Results and Discussion

Three samples of different concentrations were analyzed by the internal standard method and the direct method. These results are given in Table IV. From these data the standard deviations in analytical work were estimated at about 1 wt.% by the direct method. The reproducibility of the analytical results by the internal standard method was generally poorer than by the direct method. This may be due to the lower peak heights caused by the X-ray absorption of sodium chloride and the imperfection of mixing of the standard with the samples. In practice, glutamic acid crystallites have good purity, so polymorphic analysis can be carried out by the method of the binary system. Many experiments suggest that the lower limit of detection of each component in practical samples is about 2%. To obtain more accurate results, it seems necessary to repeat the experiment. Quantitative analysis based on the intensities of two or more selected lines of one component seems to be more accurate, but in organic substances, it is difficult, because of their complex diffraction patterns, to choose lines free from the superposition of other materials. High stabilization of the tube current and voltage is important in obtaining reproducible data.

TABLE III. DATA FOR CALIBRATION CURVES

Sample	B-1	B-2	B-3	B-4	B-5
I_β/I_α	0.0456	0.259	0.557	2.18	5.89
x_β/x_α	0	0.331	0.995	3.00	8.93

Sample	M-1	M-2	M-3	M-4	M-5	M-6
I_α/I_S	0	0.96	1.91	2.62	3.47	4.63
I_β/I_S	3.19	2.45	1.96	1.46	0.91	0.269

TABLE IV. ANALYTICAL RESULTS FOR SAMPLES X, Y AND Z

Sample	Method direct β-Form wt.%	Internal standard method α-Form wt.%	Internal standard method β-Form wt.%
X	90.1	10.1	90.5
	88.3	13.1	98.3
	88.9	10.1	87.7
	90.4	11.0	102
	90.6	9.7	92.1
	S. D.[a] 1.0	1.1	5.9
Y	47.6	55.6	47.8
	47.6	53.4	44.5
	47.4	50.2	49.1
	47.4	58.2	72.3
	45.7	55.8	62.7
	S. D.[a] 0.8	3.1	11.6
Z	10.0	84.7	9.2
	10.1	97.0	10.2
	11.3	119	13.5
	12.0	90.3	9.9
	12.2	78.6	10.9
	S. D.[a] 1.0	15.7	1.6

a Standard deviation

Department of Chemistry
Faculty of Science
The University of Tokyo
Hongo, Tokyo
(H. T.)

Central Research Laboratory
Ajinomoto Co., Inc.
Suzuki-cho, Kawasaki
(T. T. & N. N.)

Synthesis of 1,4-Dihydro-N-[1′ : 3′ : 4′ : 6′-tetraacetylglucosyl-(2′)]-3,5-diacetylpyridine Derivatives

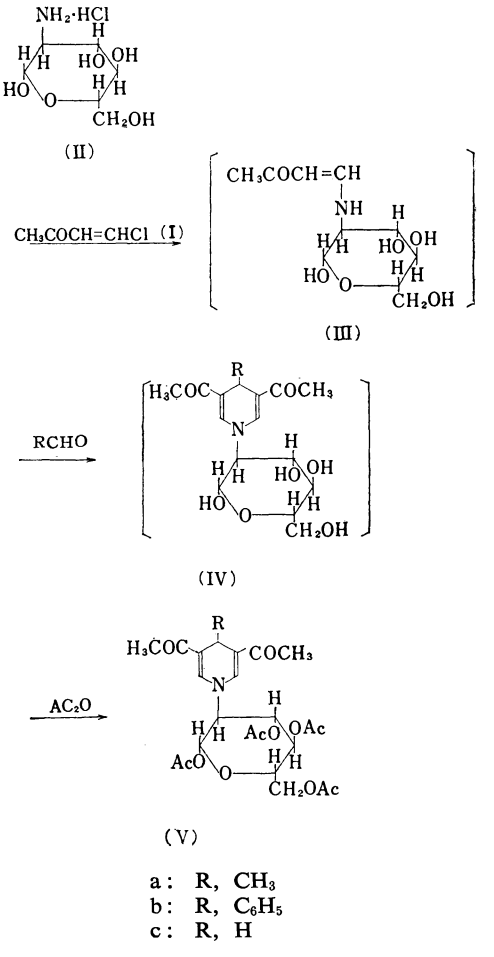
By Noboru SUGIYAMA, Goro INOUYE** and Kimie ITO

(Received October 13, 1961)

Fischer et al.[1] had reported the synthesis of *N*-[tetraacetylglucosyl-(1′)]-pyridinium salts by the condensation of pyridine and tetraacetylglucosyl bromide. As a model compound of DPN*1, Karrer[2] and Todd[3] synthesized various sugar derivatives of nicotinamide by this method. We could not find any other *N*-sugar derivatives of pyridine or pyridine derivatives in the literature.

In his previous papers[4], Inouye has reported that 1,4-dihydro-3,5-diacetylpyridine derivatives are obtained in a good yield by the condensation of aldehydes with methyl β-(*N*-monosubstituted amino)-vinylketone. According to this method, 1,4-dihydro-*N*-[glucosyl-(2′)]-3,5-diacetylpyridine derivatives (IV) will be obtained by the condensation of aldehydes with methyl β-[*N*-glucosyl-(2′)-amino]-vinylketone (III), which, in trun, is prepared from methyl β-chlorovinylketone (I) and glucosamine (II). In fact, we could obtain the expected compound, V. Although the yield of V was not good, similar derivatives with other sugar or substituents can be synthesized by this method. We will report on the results of this experiment.

In the presence of potassium carbonate, aldehyde was added to the condensation products of methyl β-chlorovinylketone (I) with glucosamine hydrochloride (II) in water or ethanol. From the reaction mixture, the expected compounds IV could not be obtained in a crystalline state. However, by acetylation, pure 1,4-dihydro-*N*-[1′ : 3′ : 4′ : 6′-tetraacetylglucosyl-(2′)]-3,5-diacetylpyridine derivatives Va, Vb were obtained. Formaldehyde did not give the corresponding compound, Vc.



a: R, CH_3
b: R, C_6H_5
c: R, H

The structure of Va and Vb were confirmed by a comparison of their spectral data with those of the corresponding 1,4-dihydropyridine derivatives, VI, VII, VIII and IX (Table I). The infrared spectra of 3,5-diacetyldihydropyridine derivatives show a band at 1640 and 1642 cm^{-1} respectively. The absorption maxima of the ultraviolet spectra of Va and Vb (377, 375 mμ) are nearly the same. The same relationships exist between the spectra of VI and VIII or VIII and IX. The shift of λ_{max} on the nitrogen atom by changing substituents seems to be due to the difference in the

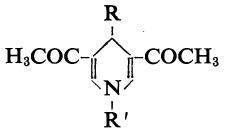
* This paper constitutes Part V of a series entitled "The Synthetic Reaction with Methyl β-Chlorovinylketone". Part IV: G. Inouye, N. Sugiyama and T. Ozawa, *J. Chem. Soc. Japan, Pure Chem. Sec.* (*Nippon Kagaku Zasshi*), **82**, 1272 (1961).

** Present address: The Technical Research Laboratory of Asahi Chemical Industry Co., Ltd., Itabashi-ku, Tokyo.

1) E. Fischer and K. Raske, *Ber.*, **43**, 1750 (1910).
2) P. Karrer and U. Solsmann, *Helv. Chem. Acta.*, **20**, 55 (1937).
3) A. R. Todd and L. J. Haynes, *J. Chem. Soc.*, **1950**, 303.
4) G. Inouye, *J. Chem. Soc. Japan, Pure Chem. Sec.* (*Nippon Kagaku Zasshi*), **79**, 1243 (1958); **80**, 1061 (1959).

*1 Diphosphopyridine nucleotide

TABLE I. ULTRAVIOLET ABSORPTION SPECTRA AND INFRARED ABSORPTION SPECTRA OF 1,4-DIHYDRO-3,5-DIACETYLPYRIDINE DERIVATIVES



	R	R'	λ_{max}, mμ (log ε)	$\nu_{C=O}$, cm^{-1} c)	Fluorescence
Va	CH_3	TAGL[a)]	377[b)] (3.92)	1640	Blue
Vb	C_6H_5	TAGL	375[b)] (3.89)	1642	Blue
VI	CH_3	C_6H_5	386 (3.94)	1640	Blue
VII	C_6H_5	C_6H_5	385 (3.91)	1645	Blue
VIII	CH_3	CH_3	396 (4.00)	1637	Blue
IX	C_6H_5	CH_3	394 (3.98)	1632	Blue

a) Tetraacetylglucosyl-(2')
b) In methanol; all others in ethanol
c) KBr

effects of the methyl, phenyl and tetraacetylglucosyl groups on the nitrogen atom*2.

Experimental

1,4-Dihydro-*N*-[1' : 3' : 4' : 6'-tetraacetylglucosyl-(2')]-4-phenyl-3, 5-diacetylpyridine (Va). — I (10 g.) was stirred drop by drop into an ice-cooled solution of glucosamine hydrochloride (21 g.) and potassium carbonate (30 g.) in water (70 ml.), and the stirring was then continued for 6 hr. Acetaldehyde (5.5 g., 80% aqueous solution) was added to the reaction mixture, and the mixture was left overnight at room temperature. After filtering off the precipitates, concentrated hydrochloric acid (20 ml.) was added to the filtrate. The solution was evaporated to dryness under reduced pressure in an atmosphere of nitrogen. The residue was acetylated by refluxing in acetic anhydride (50 ml.) for an hour. The acetic anhydride was removed under reduced pressure in an atmosphere of nitrogen. After dissolving in ethyl acetate and chromatographing on an alumina column, the residue gave 1,4-dihydro-*N*-[1' : 3' : 4' : 6'-tetraacetylglucosyl-(2')-4-methyl-3, 5-diacetylpyridine (Va) in the form of pale yellow needles (from benzene), m. p. 180°C (decomp.).

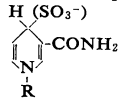
Found: N, 2.43. Calcd. for $C_{24}H_{31}O_{11}N$: N, 2.74%.

1, 4-Dihydro-*N*-[1' : 3' : 4' : 6'-tetraacetylglucosyl-(2')]-4-phenyl-3, 5-diacetylpyridine (Vb).—I (10 g.) was stirred drop by drop into an ice cooled mixture of glucosamine hydrochloride (21 g.), ethanol (50 ml.) and a saturated aqueous solution (50 g.) of potassium carbonate, and the stirring was continued for 6 hr. Benzaldehyde (10 g.) was added to the reaction mixture, and the mixture was left overnight at room temperature. After acidification with concentrated hydrochloric acid, the excess benzaldehyde was removed by steam distillation. The solution was evaporated to dryness under reduced pressure in an atmosphere of nitrogen. The residue was acetylated by refluxing in acetic anhydride (50 ml.) for an hour. After cooling, saturated aqueous solution (50 ml.) of sodium acetate was added to the mixture. 1,4-Dihydro-*N*-[1' : 3' : 4' : 6'-tetraacetylglucosyl(2')]-4-phenyl-3,5-diacetylpyridine (Vb) was separated and crystallized from acetic acid-water in the form of pale yellow needles, m. p. 265°C (decomp.).

Found: C, 60.41; H, 5.74; N, 2.28. Calcd. for $C_{29}H_{33}O_{11}N$: C, 60.94; H, 5.77; N, 2.45%.

Department of Chemistry
Faculty of Science
Tokyo University of Education
Bunkyo-ku, Tokyo

*2 The ultraviolet absorption spectra of similar compounds have been reported as:



R=Methyl, λ_{max} 339 mμ
R=Tetraacetylglucosyl(β) λ_{max} 313 mμ

G. Pfleiderer, E. Soun and A. Stock, *Chem. Ber.*, 93, 3091 (1960).

Effects of Tyrosyl Residue on the Polypeptide Monolayers

By Takuya YAMASHITA and Toshizo ISEMURA

(Received November 21, 1961)

Protein has a definite conformation which is responsible for its biological activity. This conformation is believed to be chiefly maintained by the intramolecular hydrogen bonding. Tyrosyl residue is very specific among other amino acid residues in protein because of the potency of its hydrogen bonding. In our previous investigations[1,2], we have studied the monolayers of poly-L-tyrosine, poly-DL-tyrosine, poly-*o*-benzyl-DL-tyrosine and poly-DL-phenylalanine in terms of the hydrogen bonding of the phenolic hydroxyl group of tyrosyl residue at the air/water and oil/water interfaces.

Poly-*o*-benzyl-DL-tyrosine was found, like most polypeptide films, to be spread in a β-configuration. Poly-L-tyrosine and poly-DL-tyrosine, however, showed solvent effects at the air/water interface owing to their phenolic hydroxyl group. If they were spread from the solution in a mixture of pyridine and isopropyl alcohol, they occupied much less area per residue than polypeptide films such as poly-DL-phenylalanine in a β-configuration. This fact suggests that poly-L-tyrosine might not be spread in an extended monolayer in a strict sense, but in a coiled state probably owing to the hydrogen bonding between the phenolic hydroxyl group and the carbonyl or imino group in a main chain. On the other hand, if poly-L-tyrosine is spread from the solution in a mixture of dichloroacetic acid and benzene, it probably assumes a β-form.

In the present study, we have investigated the effects of the phenolic hydroxyl group of tyrosyl residue on the polypeptide monolyers. For this purpose, the monolayers of poly-L-tyrosine, copoly-1 : 1-(L-tyrosine, L-phenylalanine), copoly-1 : 1 : 2-(L-tyrosine, *o*-benzyl-L-tyrosine, L-phenylalanine) and copoly-1 : 1-(L-tyrosine, glycine) have been investigated. For comparison, the monolayer of poly-DL-phenylalanine was also studied.

Experimental

Materials.—The same samples of poly-L-tyrosine and poly-DL-phenylalanine were used as in the preceding study. Copolypeptides containing tyrosyl residue were kindly supplied by Professor J. Noguchi of Hokkaido University.

As spreading solvents, mixtures of dichloroacetic acid and benzene were used. The ratio of dichloroacetic acid (DCA) to benzene is various for different polypeptides, as can be seen in Table I.

TABLE I. THE RATIOS OF DCA TO BENZENE IN SPREADING SOLUTIONS

Sample	DCA : Benzene (v/v)
Poly-DL-phenylalanine	3 : 7
Poly-L-tyrosine	7 : 3
Copoly-1 : 1-(L-tyrosine, L-phenylalanine)	3 : 7
Copoly-1 : 1 : 2-(L-tyrosine, *o*-benzyl-L-tyrosine, L-phenylalanine)	3 : 7
Copoly-1 : 1-(L-tyrosine, glycine)	1 : 1

Method.—The films were spread at the air/water and oil/water interfaces. The surface pressure and surface potential were measured simultaneously by the Wilhelmy hanging plate method and by the vibrating electrode method respectively. Interfacial pressure was measured by the ring method. At the oil/water interface, the interfacial concentration was changed by the successive injection method, using a micrometer syringe, and was corrected by the Thomas theoretical correction formula[3]. Measurements were carried out five minutes after every injection. The pH value of the subphase was adjusted to any desired value by adding hydrochloric acid or potassium carbonate and was measured with a Horiba M-3 glass electrode pH meter. Petroleum ether with a boiling point of 85~115°C was used as an oil phase. All the experiments were carried out at room temperature without any temperature regulation. However, the change never exceeded more than one degree in the course of the experiment.

The limiting area per residue of the film was obtained from the minimum of its compressibility, $\delta = -dA/Ad\Pi$, and the surface moment, μ, was calculated from the surface potential, ΔV, using the Helmholtz formula, $\mu = \Delta VA/4\pi$.

The average residual weight of copolypeptide was calculated on the basis of its polymerization ratio.

Results

The surface pressure-area (Π-A) and surface moment-area (μ-A) curves of poly-DL-phenylalanine at the air/water interface are shown

1) T. Isemura, S. Ikeda and T. Yamashita, *Mem. Inst. Sci. and Ind. Research, Osaka Univ.*, **15**, 167 (1958).
2) T. Isemura and T. Yamashita, This Bulletin, **32**, 1 (1959).
3) A. G. Thomas, *Nature*, **179**, 776 (1957).

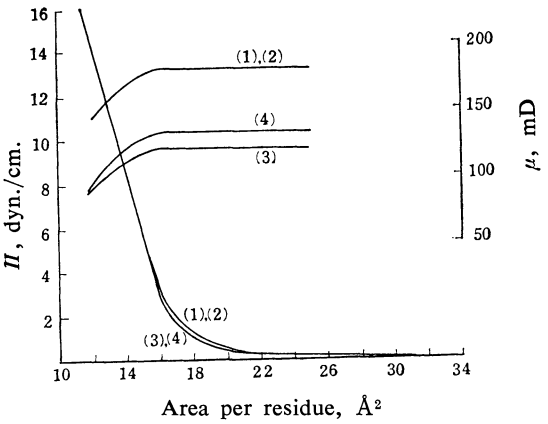


Fig. 1. Surface pressure-area and surface moment-area curves of poly-DL-phenylalanine (24°C): (1), on 0.01 N HCl; (2), on distilled water; (3), on 0.02 N K_2CO_3; (4), on 0.1 N K_2CO_3.

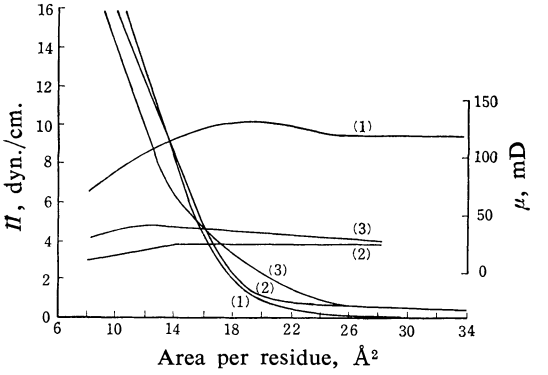


Fig. 2. Surface pressure-area and surface moment-area curves of poly-L-tyrosine (16°C): (1), on distilled water (Ref. 2); (2) on 0.02 N K_2CO_3; (3), on 0.1 N K_2CO_3.

in Fig. 1. The *Π-A* curves were nearly independent of the pH value of the subphases, although the *μ-A* curves were affected. The limiting area per residue was 15.6 Å² irrespective of the pH value of the subphases. On the alkaline subphase, the surface moment is lower by 50~60 mD than on the acid subphase.

The *Π-A* and *μ-A* curves of poly-L-tyrosine spread from a solution in a dichloroacetic acid-benzene mixture at the air/water interface are given in Fig. 2. In a low pressure region the film expands slightly more on 0.02 N potassium carbonate than on distilled water. Among the three subphases the film expands most on 0.1 N potassium carbonate. On the alkaline subphase, the surface moment is lower by 90~100 mD than on distilled water.

The *Π-A* and *μ-A* curves of copoly-1 : 1-(L-tyrosine, L-phenylalanine) and copoly-1 : 1 : 2-

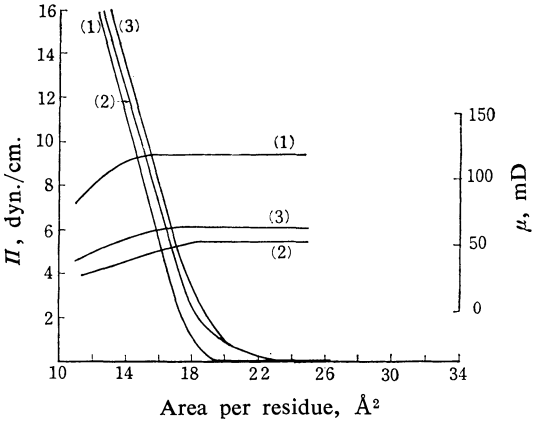


Fig. 3. Surface pressure-area and surface moment-area curves of copoly-1 : 1-(L-tyrosine, L-phenylalanine (19°C): (1), on distilled water; (2), on 0.02 N K_2CO_3; (3), on 0.1 N K_2CO_3.

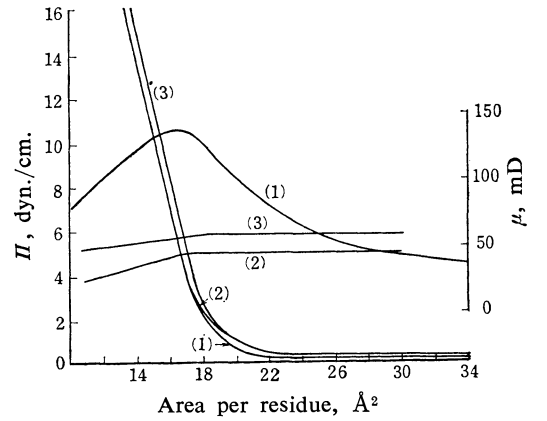


Fig. 4. Surface pressure-area and surface moment-area curves of copoly-1 : 1 : 2-(L-tyrosine, *o*-benzyl-L-tyrosine, L-phenylalanine) (10°C): (1), on distilled water; (2), on 0.02 N K_2CO_3; (3), on 0.1 N K_2CO_3.

(L-tyrosine, *o*-benzyl-L-tyrosine, L-phenylalanine) at the air/water interface are given in Figs. 3 and 4 respectively. The effects of the change in the pH values of the subphases on the *Π-A* relations of these copolypeptides are smaller than in the case of poly-L-tyrosine. The difference between surface moments of copoly-1 : 1-(L-tyrosine, L-phenylalanine) on acid and alkaline subphases is comparable to that between those of poly-DL-phenylalanine. The surface moment of copoly-1 : 1 : 2-(L-tyrosine, *o*-benzyl-L-tyrosine, L-phenylalanine) increased steeply on distilled water, as the film was compressed, as has been found with the film of poly-*o*-benzyl-DL-tyrosine[2]; it reached 137 mD at its maximum.

The Π-A and μ-A curves of copoly-1 : 1-(L-tyrosine, glycine) at the air/water interface are shown in Fig. 5. This copolypeptide occupies much less limiting area per residue in the surface film than those of any other

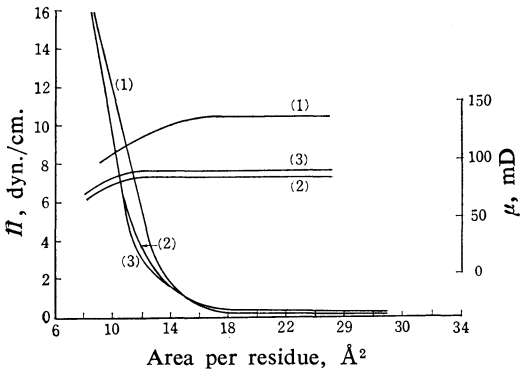


Fig. 5. Surface pressure-area and surface moment-area curves of copoly-1 : 1-(L-tyrosine, glycine) (10°C): (1), on distilled water; (2), on 0.01 N K_2CO_3; (3), on 0.1 N K_2CO_3.

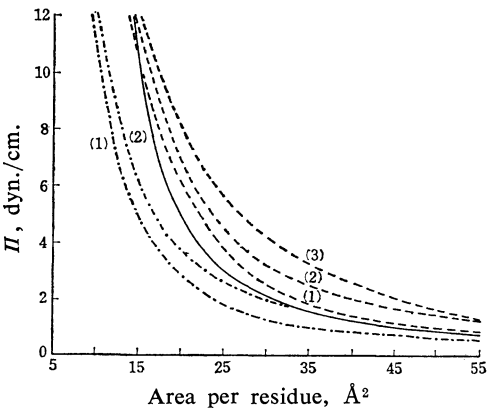


Fig. 6. Interfacial pressure-area curves of various polypeptides (16.5°C).
—— Poly-DL-phenylalanine, on distilled water.
---- Copoly-1 : 1-(L-tyrosine, L-phenylalanine): (1), on 0.01 N HCl; (2), on 0.02 N K_2CO_3; (3), on 0.1 N K_2CO_3.
-·-· Copoly-1 : 1-(L-tyrosine, glycine): (1), on 0.01 N HCl and distilled water; (2), on 0.01 N K_2CO_3 and 0.1 N K_2CO_3.

TABLE II. FILM CHARACTERISTICS OBTAINED FROM Π-A AND μ-A RELATIONS AT AIR/WATER INTERFACE

Polypeptide	Subphase	Temp. °C	A_Π Å²/residue	A_μ Å²/residue	μ_c mD	$\Delta\mu$ mD
Poly-DL-	0.01 N HCl	24	15.6	16.0	182	
phenylalanine	dw	24	15.6	16.0	182	
	0.02 N K_2CO_3	24	15.6	16.0	124	58
	0.1 N K_2CO_3	24	15.6	16.0	134	48
Poly-L-						
tyrosine	dw**	16	15.6	18.8	132*	
	0.02 N K_2CO_3	16	15.7	14.0	26	106
	0.1 N K_2CO_3	16	—	12.4	42*	90
Copoly-1 : 1-						
(L-tyrosine,	dw	19	17.0	15.2	120	
L-phenylalanine)	0.02 N K_2CO_3	19	17.2	18.0	54	66
	0.1 N K_2CO_3	19	17.2	17.0	66	54
Copoly-1 : 1 : 2-						
(L-tyrosine,	dw	10	17.0	17.0	137*	
o-benzyl-L-	0.02 N K_2CO_3	10	17.0	17.2	46	91
tyrosine, L-	0.1 N K_2CO_3	10	17.2	18.2	62	75
phenylalanine)						
Copoly-1 : 1-	dw	10	11.5	16.0	138	
(L-tyrosine,	0.02 N K_2CO_3	10	10.9	12.0	85	53
glycine)	0.1 N K_2CO_3	10	10.9	11.5	90	48

A_Π: Limiting area (area at minimum compressibility)
A_μ: Area at which μ begins to decrease
μ_c: Value of constant surface moment
$\Delta\mu$: Difference between constant (or maximum) values of surface moments on distilled water (or acid subphase) and on alkaline subphase
dw: Distilled water
*: Maximum value
**: Ref. 2

polypeptide mentioned above.

The film characteristics obtained from the *Π-A* and *μ-A* relations are listed in Table II.

The *Π-A* curves of poly-DL-phenylalanine, copoly-1 : 1-(L-tyrosine, L-phenylalanine) and copoly-1 : 1-(L-tyrosine, glycine) at the oil/water interface are shown in Fig. 6. The *Π-A* curve of poly-DL-phenylalanine measured by the ring method was slightly shifted to the left (namely, to the smaller area) in comparison with the curve obtained by the hanging plate method employed in the previous study[2]. This discrepancy is probably caused by the neglect in the previous work of the change in the contact angle of the glass handging plate. At the oil/water interface, the films expanded more than at the air/water interface. The film of copoly-1 : 1-(L-tyrosine, glycine) occupied much less area per residue than any other polypeptides at the oil/water interface as well as at the air/water interface.

Discussion

Effect of Subphase pH on the Surface Potential or Moment.—*Poly-DL-phenylalanine.*—The surface potential or moment of poly-DL-phenylalanine changes considerably in spite of its lack of ionizable side chains. The difference between constant values of the surface moments on the acid and alkaline subphases, $\Delta\mu$, is 50~60 mD. Because the change cannot be attributed to the ionization of the side chain, it must be caused by a change in the main chain. A similar change in surface potential or moment has been found for several synthetic polypeptides with a non-polar side chain, e. g., poly-DL-alanine[4], poly-DL-leucine[5], and poly-α-aminolauric acid[6].

Glazer and Dogan[4] found that the maximum value of the surface potential of poly-DL-alanine decreased with the increase in subphase pH. They attributed the decrease in surface potential with pH to the varying degree of ionization of the carboxyl and amino end groups. However, in the polypeptide of a high degree of polymerization, the ionization effect of end groups on the surface potential or moment might not be so effective.

Davies[5] found that values of the surface moment of poly-DL-leucine at 20 Å^2 per residue were 188 mD on 0.01 N hydrochloric acid, 137 mD on 0.02 N phosphate (pH 6.8), and 113 mD on 0.1 N sodium hydroxide. From this finding, he suggested that on the neutral and alkaline subphases the hydrogen bond between keto-imide groups in neighboring chains was formed and that on the acid subphase the hydrogen bond would be broken. However, his view that the hydrogen bond is maintained on such a strong alkaline subphase as 0.1 N sodium hydroxide is very doubtful, because the protein is unfolded in an alkaine solution, owing to the breaking of the hydrogen bonding as commonly accepted, while the breaking of the hydrogen bonding on the acid subphase is probable, although the effect of the acid seems to appear at a very high acidity.

The probable explanation of the change in surface potential or moment of non-polar synthetic polypeptide with pH seems to be the keto-enol transformation of the peptide bond. According to Pankhurst[7], the keto-imide group of polypeptide chain in gelatin is capable of resonance between the keto and the enol forms as amides, while the addition of a hydrogen ion would prevent the resonance. Schauenstein and Perko observed this effect for 3, 6-dioxo-1, 2, 4-triazine[8] with $HO\cdot C_6H_4\cdot CH_2-$, $C_6H_5\cdot CH_2-$ or CH_3- in the 5 position, and poly-L-tyrosine[9] from the differences in ultraviolet absorption spectra between their acid and alkaline solutions; they called this effect "peptenol effect". Owing to the peptenol effect, the surface moment or potential of the polypeptide monolayer can decrease more on alkaline than on the acid subphase, because most of the keto-imide groups in the main chain are in an enolate form, and the film would be more condensed on the subphase of a high pH, as has been found for the poly-DL-leucine monolayer[10], since the increase in the double bond nature of the peptide bond enhances the rigidity of the film.

Accordingly, the change in the surface moment or the potential of non-polar synthetic polypeptides with the pH might be caused primarily by the keto-enol transformation of peptide bond, i. e., the peptenol effect, although the ionization of the end groups and the breaking of the hydrogen bond on a strong acid solution may be effective to some extent on the change in the surface potential or the moment with pH. The *Π-A* relation of poly-DL-phenylalanine seems not to be affected by the change in the pH value of the subphase because of the effect of its large side chains.

Polypeptides other than Poly-DL-phenylalanine.—The difference between the constant or maximum values of the surface moments on

4) J. Glazer and M. Z. Dogan, *Trans. Faraday Soc.*, **49**, 448 (1953).
5) J. T. Davies, ibid., **49**, 949 (1953).
6) K. Eda and Y. Masuda, This Bulletin, **24**, 140 (1951).
7) K. G. A. Pankhurst, "Surface Chemistry", Butterworth Scientific Publication, London (1949), p. 109.
8) E. Schauenstein and G. M. Perko, *Z. Elektrochem.*, **57**, 927 (1953).
9) E. Schauenstein and G. M. Perko, ibid., **58**, 45 (1954).
10) D. F. Cheesman and J. T. Davies, "Advance in Protein Chemistry", Vol. 9, Academic Press, New York (1954), p. 439.

acid and alkaline subphases, $\Delta\mu$, is about 100 mD for poly-L-tyrosine and higher by 40~50 mD than that for poly-DL-phenylalanine. The abnormally large difference in the surface moment is probably due both to the peptenol effect of the main chain and to the ionization of the phenolic hydroxyl groups of the side chains.

The $\Delta\mu$ value of copoly-1 : 1-(L-tyrosine, L-phenylalanine) is about 60 mD and is comparable to that of poly-DL-phenylalanine. From the fact that the film expands slightly more on the alkaline than on the acid subphase, the decrease in surface moment seems to be due not only to the peptenol effect of the main chain, but also to the partial ionization of the side chains.

The surface moment of copoly-1 : 1 : 2-(L-tyrosine, *o*-benzyl-L-tyrosine, L-phenylalanine) on distilled water steeply increases with the compression of the film, as was found with the film of poly-*o*-benzyl-L-tyrosine[2]. This change is probably caused by reorientation of the large polar side chain of the *o*-benzyl-L-tyrosyl residue. On the other hand, the surface moment is nearly constant on the alkaline subphase. This fact suggets that the remarkable reorientation of the side chain is not accompanied by a compression of the film on the alkaline subphase. The $\Delta\mu$ values of this copolypeptide are 91 mD on 0.02 N potassium carbonate and 75 mD on 0.1 N potassium carbonate. These values are greater than those for copoly-1 : 1-(L-tyrosine, L-phenylalanine) film, although this copolypeptide has much less ionizable groups.

The $\Delta\mu$ value of copoly-1 : 1-(L-tyrosine, glycine) is about 50 mD and is comparable to that of poly-DL-phenylalanine. This finding suggests that the effect of the ionization of the phenolic hydroxyl group is slight in this case.

Effect of Subphase pH on the *II-A* Relation. —*Air/Water Interface.*— The film of poly-L-tyrosine spread from a solution in pyridine-isopropyl alcohol mixture is affected remarkably by the pH of the subphase, as has been previously reported[1,2]. On the other hand, the effect of subphase pH on the *II-A* relation is not so remarkable if it is spread from a solution containing dichloroacetic acid as a component of the solvent, and the limiting area per residue is close to 15 Å^2. Therefore, in this case, there is no hydrogen bonding between the phenolic hydroxyl group and the carbonyl or imino group in the main chain, and poly-Ltyrosine is probably spread in the β-form.

Schauenstein and Perko[9] found the pK value of the phenolic hydroxyl group of poly-L-tyrosine to be 11.0, and Katchalski and Sela[11] found that the spectrophotometric titration curve fitted the theoretical curve computed by assuming the pK_0 to be 9.5. Therefore, on 0.02 N potassium carbonate (pH 10.3), about a half of the side chains may be dissociated. However, the *II-A* relation here is little affected compared with that on distilled water, although the monolayers of poly-L-glutamic acid[12] and copoly-1 : 2 : 1-(L-lysine, L-leucine, L-glutamic acid)[13] are affected remarkably by the pH of the subphase. This is probably due to the peptenol effect of the main chain and to the van der Waals attraction between the large side chains, both of which prevent the expansion of the film. On 0.1 N potassium carbonate (pH 10.7), however, the film rather expands since the side chains dissociate more, and the repulsive force between the ionized side chains can overcome the van der Waals force and the peptenol effect.

The effect of the subphase pH on copoly-1 : 1-(L-tyrosine, L-phenylalanine) is between that on poly-DL-phenylalanine and that on poly-L-tyrosine. Since this copolypeptide consists of equal numbers of ionizable and unionizable side chains, the effect of the pH appears between poly-DL-phenylalanine and poly-L-tyrosine.

The *II-A* relation of copoly-1 : 1 : 2-(L-tyrosine, *o*-benzyl-L-tyrosine, L-phenylalanine) is little affected by the change in the subphase pH because it consists of fewer ionizable side chains (25%) than the tyrosine-polypeptides mentioned above.

The film of copoly-1 : 1-(L-tyrosine, glycine) condenses more on the alkaline subphase than on distilled water, probably because of the peptenol effect. This copolypeptide can condense by peptenol effect because only half of all its residues have side chains and the contraction of the main chain is rather easy owing to the steric effect.

All the polypeptide monolayers mentioned above except copoly-1 : 1-(tyrosine, glycine) seem to be in the β-form because their limiting areas per residue are very close to 15 Å^2.

Oil/Water Interface.—At the oil/water interface, the films of poly-DL-phenylalanine, copoly-1 : 1-(L-tyrosine, L-phenylalanine) and copoly-1 : 1-(L-tyrosine, glycine) expand more than at the air/water interface and change from a condensed type at the air/water interface into an expanded type. These changes are caused by the release of van der Waals force between the side chains due to oil.

11) E. Katchalski and M. Sela, *J. Am. Chem. Soc.*, **75**, 5284 (1953).
12) T. Isemura and K. Hamaguchi, This Bulletin, **27**, 339 (1954).
13) T. Isemura, K. Hamaguchi and S. Ikeda, *J. Polymer Sci.*, **23**, 651 (1957).

The change in the subphase pH appears to be more effective than at the air/water interface. The films of copoly-1 : 1-(L-tyrosine, L-phenylalanine) and copoly-1 : 1-(L-tyrosine, glycine) are more expanded on the alkaline than on the acid subphase, while at the air/water interface, the films of these copolypeptides are slightly affected by the change in pH. At the oil/water interface, the release of the van der Waals force between the side chains causes the expansion of the film by the repulsion among ionized groups.

Effect of Glycyl Residue on Polypeptide Monolayers.—At both the air/water and oil/water interfaces, the film of copoly-1 : 1-(L-tyrosine, glycine) occupies much less area per residue than in any other polypeptide mentioned above.

This copolypeptide contains the same number of tyrosyl and glycyl residues, so both the residues should affects its film properties. However, the tyrosyl residue would not be responsible for a small area per residue of copoly-1 : 1-(L-tyrosine, glycine) because poly-L-tyrosine and tyrosine-copolypeptides without glycyl residue, such as copoly-1 : 1-(L-tyrosine, L-phenylalanine) and copoly-1 : 1 : 2-(L-tyrosine, *o*-benzyl-L-tyrosine, L-phenylalanine), were spread in the β-form. The presence of glycyl residue in polypeptide chain might result in a small limiting area per residue.

Polyglycine (in trifluoroacetic acid) and copoly-1 : 2-(L-tyrosine, glycine) (in a DCA-benzene mixture) could not be spread as a monolayer at the air/water interface[14]. Davies[5] also found polyglycine not to be spread as a monomolecular film. Isemura and Hamaguchi[15] found that at the air/water interface the film of copoly-1 : 1-(glycine, DL-alanine) occupied a very small area per residue. They attributed this fact to the folding of the polypeptide chain due to the presence of the glycyl residue.

From these facts, the reason why copoly-1 : 1-(L-tyrosine, glycine) occupies much less area at both the air/water and oil/water interfaces than any other polypeptides studied here may be attributed to the folded structure caused by strong intrachain hydrogen bonding due to the presence of a glycyl residue which lacks a side chain.

14) T. Yamashita, unpublished results.
15) T. Isemura and K. Hamaguchi, This Bulletin, 27, 339 (1954).

Summary

The monolayers of poly-DL-phenylalanine (I), poly-L-tyrosine (II), copoly-1 : 1-(L-tyrosine, L-phenylalanine) (III), copoly-1 : 1 : 2-(L-tyrosine, *o*-benzyl-L-tyrosine, L-phenylalanine) (IV), and copoly-1 : 1-(L-tyrosine, glycine) (V) have been investigated at the air/water and oil/water interfaces.

The surface moment of I decreased by 50~60 mD more on alkaline than on the acid subphase, probably owing to the keto-enol transformation of the peptide bond. The decrease in the surface moment of II is about 100 mD; this decrease seems to be caused by the ionization of the side chains and by the enolation of the peptide bond.

At the air/water interface, the effects of the dissociation of the tyrosyl residue on the *II-A* relations of II, III, IV and V were not very remarkable, probably because of the peptenol effect and the van der Waals force between side chains. It was found that the monolayers of I, II, III and IV assume a β-configuration. On the other hand, the film of V occupies much less area per residue than those in the β-form, which might be attributed to the folded structure caused by the strong intrachain hydrogen bond due to the glycyl residue.

At the oil/water interface, the films of I, III and V expand more and the change in subphase pH seems to be more effective than at the air/water interface. These facts might be caused by the release of van der Waals force between the side chains.

The authors wish to express their hearty thanks to Professor Junzo Noguchi of Hokkaido University, to Professor Hisaya Tani and Dr. Heimei Yuki of the Faculty of Science, Osaka University, and to Professor Ephraim Katchalski and Dr. Michael Sela of the Weizmann Institute of Science for supplying valuable samples. This work was partly supported by a grant given by the Ministry of Education, to which the authors' thanks are due.

Institute for Protein Research
Osaka University
Kita-ku, Osaka

Absorption Spectra of Dyes. VII[1]. *Some Steric Effects and Auxochrome-Effects on Complex Formation*[*1]

By Teruaki KOBAYASHI[*2], Kenzo SAITO[*2], Yoshié TANIZAKI and Noboru ANDO

(Received October 21, 1961)

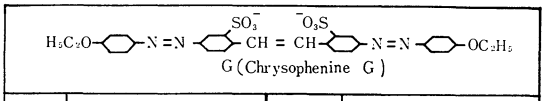
The interaction between molecules of different kinds of dyes in aqueous solutions has been studied extensively[2-4]. This problem is especially interesting because the forces involved in the complex formation are considered to be closely related to those responsible for the combination of dye molecules or ions with cellulose[2,3]. According to the conventional theory of the substantivity of dyes, it is important for substantivity that the molecule be planar so as to maintain a conjugated system between the terminal auxochromes, and that the hydrogen bonding be capable of being formed between such auxochromes and functional groups of cellulose. As for the latter, no direct experimental evidence has yet been obtained, though the possibility of hydrogen bonding between dyes and cellulose seems to be great. Nevertheless, there is no doubt that the auxochromes, by their functional property, play an essntial role in the formation of the complex or in the adsorption on cellulose.

In the present investigation, in order to obtain some preliminary information on how the above two factors, i. e., the steric effect by which the planarity of the dye molecule is hindered and the effect of the auxochromes, are reflected in the 1 : 1 complex formation, we examined the spectral changes of the binary mixtures of dyes described in the preceding paper[1], with Chrysophenine G as the common ingredient.

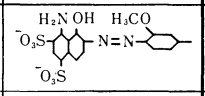
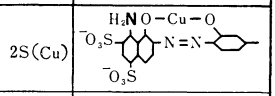
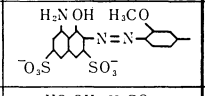
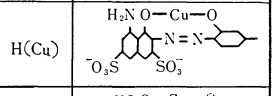
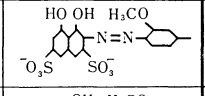
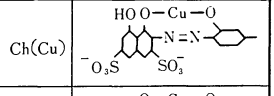
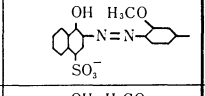
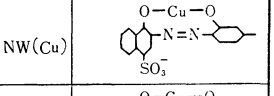
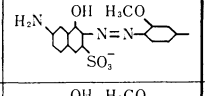
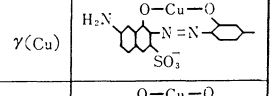
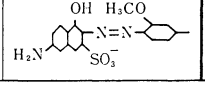
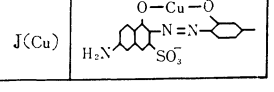
Experimental

Sample.—The dyes used are shown by notations in Table I, with the drawings of their half structures,

TABLE I. THE CHEMICAL STRUCTURE OF CHRYSOPHENINE G AND HALF CHEMICAL STRUCTURES OF DYES USED AND THEIR NOTATIONS



G (Chrysophenine G)

Notation	Half chem. structure	Notation	Half chem. structure
2S		2S(Cu)	
H		H(Cu)	
Ch		Ch(Cu)	
NW		NW(Cu)	
γ		γ(Cu)	
J		J(Cu)	

except for Chrysophenine G, a full-structure drawing is given. Since all the dyes but Chrysophenine G differ only in their coupling components, for convenience let us call them by abbreviations such as 2S or NW taken from the name of the coupling components. Corresponding copper derivatives will also be called 2S(Cu), NW(Cu), etc. The J dye was prepared by coupling diazotized J acid with dianisidine, and J(Cu) was obtained from the J dye and copper sulfate by the usual method[5]. The other dyes were the same as those used before[1].

Absorption Spectra.—Most absorption spectra were measured with a Shimadzu QR-50 spectrophotometer at room temperature (21±3°C); the spectra of only the mixture of J and G (Chrysophenine G) were recorded with a Hitachi EPS-2 recording spectrophotometer. The other experimental procedures followed have already been reported[1,4],*3.

1) Part VI of this series: T. Kobayashi, Y. Tanizaki and N. Ando, This Bulletin, 33, 913 (1960).

*1 Presented at the 13th Annual Meeting of the Chemical Society of Japan, April, 1960.

*2 Present addresses: T. Kobayashi, Hitachi Central Research Laboratory, Kokubunji, Tokyo. K. Saito, Yao Electric Co., Ltd., Suinaga 1116, Kawasaki, Kanagawa-ken.

2) M. N. Inscoe, J. H. Gould, M. E. Corning and W. R. Brode, *J. Research National Bureau of Standards*, 60, 65 (1958).

3) A. N. Derbyshire and R. H. Peters, *J. Soc. Dyers Col.*, 72, 268 (1956).

4) T. Kobayashi, Y. Tanizaki and N. Ando, This Bulletin, 33, 661 (1960).

5) U. S. Pat. 2036159 (1935).

*3 Precautions were taken with light in order to avoid the phototropism of Chrysophenine G.

Results

In the dyes containing no copper a similar change against the G concentration was seen in the difference between the sum of the individual absorption curves and those observed with the mixed system, as seen in 2S (Sky Blue) and G[4]. Examples are illustrated in Figs. 1 and 2 for the mixtures of the Ch dye or of the NW dye and G respectively. Two well-defined isosbestic points appear, indicating the formation of two sorts of complexes, a 1 : 1 and a 1 : 2 complex. As seen from the first isosbestic point shown in Figs. 1 and 2, the molar ratio in the complex formed is 1 : 1 when the amount of G is not over the concentration of the partner dye. An equilibrium constant K for the formation of a 1 : 1 complex can be determined by the method mentioned elsewhere with the condition that the formation of a 1 : 2 complex is extremely small[4]. The K values thus determined for the 1 : 1 complex formation are listed in Table II*[4].

Figure 3 illustrates the absorption spectra (solid lines) in an aqueous solution of nearly equimolar mixtures (ca. 1×10^{-5} mol./l.) of G and second components not containing copper. The broken lines in the figure indicate the results of the individual curves of the components,

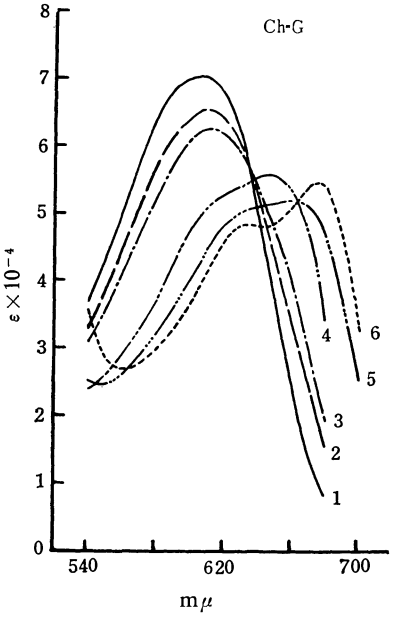


Fig. 1. Absorption spectra of mixture of Ch (chromotropic acid-derivative dye) and G (Chrysophenine G) in aqueous solution at room temperature.
ε : Absorption coefficient for Ch. ; Concentration of Ch : $1.20\sim1.24\times10^{-5}$ mol./l., Concentration ratio G/Ch : Curve 1 : 0, 2 : 0.25, 3 : 0.87, 4 : 8.2, 5 : 20, 6 : 82.4.

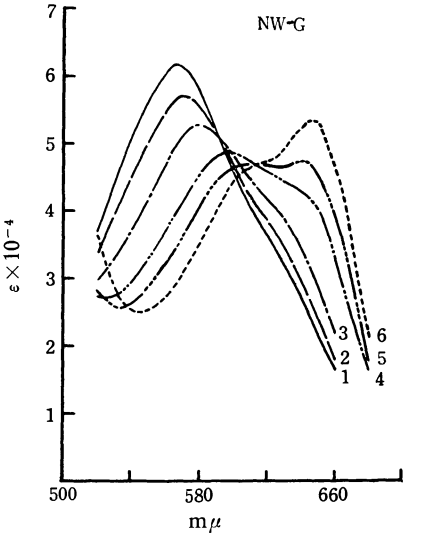


Fig. 2. Absorption spectra of mixture of NW (NW-acid-derivative dye) and G in aqueous solution at room temperature.
ε : Absorption coefficient for NW ; Concentration of NW : $1.00\sim1.04\times10^{-5}$ mol./l., Concentration ratio G/NW : Curve 1 : 0, 2 : 0.63 3 : 1.98, 4 : 4.24, 5 : 7.32, 6 : 19.2

TABLE II. THE CHANGE IN SPECTRA OF MIXTURES OF CHRYSOPHENINE G AND BENZIDINE DISAZO DYES IN AQUEOUS SOLUTION AT ROOM TEMPERATURE

Partner of G dye	Equilibrium constant K for 1 : 1 complex	$\Delta\nu$, cm^{-1} (*1)	$\Delta D/D$, % (*2)	Concn. (mol./l. $\times10^5$) (*3)
2S	6.0×10^5	2200	30	0.996 (1.009)
H	3.5×10^5	1400	19	1.067 (1.035)
NW	9.4×10^4	1600	26	1.060 (1.044)
Ch	7.7×10^4	1600	23	1.010 (1.058)
γ	3.7×10^4	1100	9	1.074 (1.007)
J	1.7×10^4	800	7	0.991 (0.999)

*1) Difference in wave number between maximum positions (around 400 mμ) of the sum and mixture curves, corresponding to the first absorption band of G alone : $(\nu_{sum}-\nu_{mix})$
*2) Decreasing ratio in optical density of the mixed system at the first maximum position (around 600 mμ) of the sum curve : $(D_{sum}-D_{mix})/D_{sum}$, %
*3) The figure in parenthesis indicates the concentration of G dye combined.

*4 Four to seven different concentrations of G were used in each mixture. The relation of the difference in optical density ΔD to G-concentration[4] was fairly well in agreement with the curve calculated with the respective K in Table II.

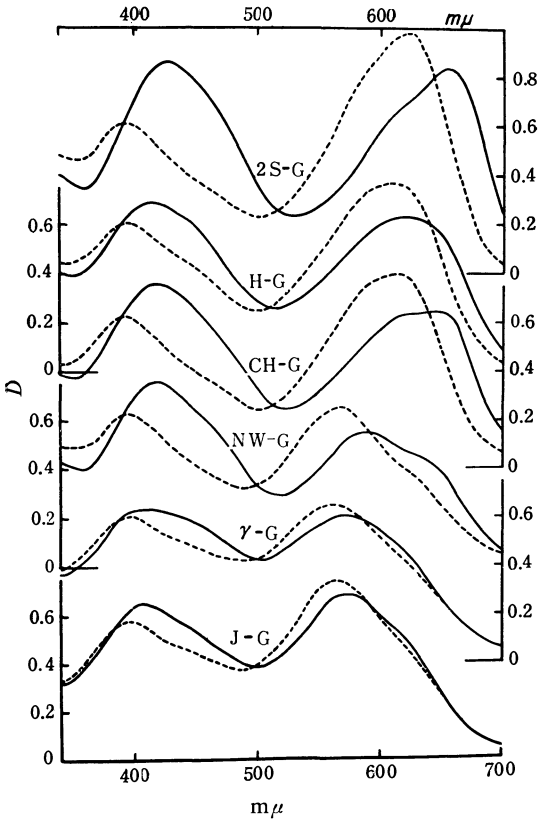


Fig. 3. Absorption spectra in aqueous solution of nearly equimolar mixtures of G and the second components (ca. 1×10^{-5} mol./l. each).
Solid line; observed with the mixture.
Broken line; resultant curve of the individuals of the mixture.

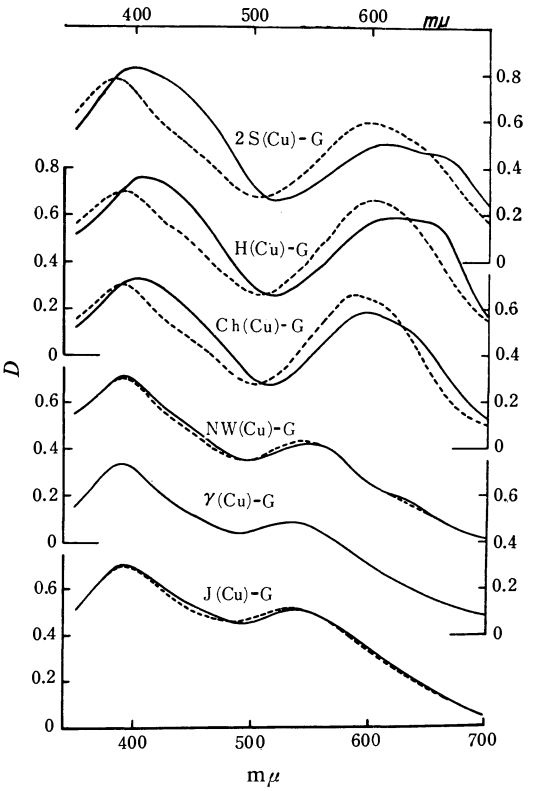


Fig. 4. Absorption spectra of mixtures of copper derivatives and the G dye (ca. 1×10^{-5} mol./l. each).
Solid line; observed with the mixture.
Broken line; resultant curve of the individuals of the mixture.

Table III. The change in spectra of mixtures of Chrysophenine G and copper derivatives in aqueous solution at room temperature

Partner of G dye	$\Delta\nu$, cm^{-1}	$\Delta D/D$, %	Concn. (mol./l. $\times10^5$)	Classification
2S(Cu)	1000	16	1.204 (1.252)	
H(Cu)	1100	13	1.171 (1.257)	First group
Ch(Cu)	900	15	1.183 (1.251)	
NW(Cu)	0	3	1.195 (1.255)	
γ(Cu)	0	0	1.194 (1.256)	Second group
J(Cu)	0	3	1.194 (1.251)	

See the footnotes of Table II.

each observed with the same concentration as in the mixture. The order of magnitude of the difference between the sum (broken line) and the mixture (solid line) curves in Fig. 3 appears to be comparable with that of the equilibrium constants. Indeed, in the present case, comparing the differences of the two curves in the following values, i.e., the difference in wave number, $\Delta\nu$ cm^{-1}, of the two peaks (around 400 mμ) corresponding to the first band of G, and the decreasing ratio in optical density, $\Delta D/D$ %, at the maximum point (around 600 mμ) of the partner dye of G, it is seen that both of the orders of the values thus obtained are approximately parallel to that of K as shown in Table II. These values, therefore, may be taken as a measure for comparing the relative order of the amounts of complex formed.

Figure 4 shows the absorption spectra of mixtures of copper derivatives and the G dye observed in the same way as above. It is noticed in Fig. 4 that the copper dyes are divided into two classes; one is the class in which the dyes reveal apparent spectral differences, the other, the class in which the differences are extremely small. The values of $\Delta\nu$ and $\Delta D/D$ for these dyes are given in Table III, divided into two groups.

Discussion

When the dyes not containing copper are combined with the G dye, judging from the examples shown in Figs. 1 and 2, two sorts of complex 1 : 1 and 1 : 2 are formed. Moreover, the correlation between the first isosbestic point and the mixing ratio of the components indicates that in the region where the G concentration does not exceed that of the partner dye, only a 1 : 1 complex is formed. Accordingly, at the present stage, when only the 1 : 1 complex formation is to be considered, discussion will be possible under the conditions of relative concentration just mentioned. (A detailed investigation, including the 1 : 2 complex formation, will be undertaken in the next paper.) According to Table II, the order of the magnitudes of the equilibrium constant K for the formation of a 1 : 1 complex is approximately parallel to the order of $\Delta\nu$ and $\Delta D/D$ observed with the equimolar mixture. Therefore, at least insofar as the 1 : 1 complex formation is concerned, $\Delta\nu$ and/or $\Delta D/D$ may rather safely be employed instead of K as a relative measure of the extent of the formation of a 1 : 1 complex. Such a comparison by $\Delta\nu$ and $\Delta D/D$ will be made below.

The skeletal structure of dyes used here is sterically restricted by the introduction of copper[1]. Thus, first, the case of the copper derivatives (Table III) in which the steric condition is simplified will be discussed; next, the case of those not containing copper (Table II) will be considered.

According to Table III, the magnitude of $\Delta D/D$ is about 15% for 2S(Cu), H(Cu) and Ch(Cu), but it is zero or almost zero for the rest, NW(Cu), γ(Cu) and J(Cu). These dyes can thus be clearly divided into two groups. A similar separation is even more distinctly revealed concerning the magnitude of the $\Delta\nu$ value; the value for the former group is about 1000 cm^{-1} and for the latter, zero. So the dyes 2S(Cu), H(Cu) and Ch(Cu), which are considered to form a 1 : 1 complex to some extent, will be termed the first group, and the rest, considered to form no complex, the second group.

Since the G dye is the common ingredient of all the combinations used here, it must be considered that the results mentioned above were brought about by certain differences in the nature of the partner dyes. Now, as these dyes are copper derivatives, they are regarded as of sterically similar skeletal structure, as has already been established[1]. Consequently, as dominant factors responsible for the interaction with the G molecule, only two factors may be considered at the present stage, the number and the position of sulfonic groups, and the presence and the position of effective auxochromes (amino, hydroxyl). Discussion of these factors will be undertaken below.

First, let us consider the effect of the sulfonic groups. The nearer the sulfonic groups are to the center of the partner molecule, and the more the number of the groups, the smaller in amount should be the complex produced, because the repulsion of the ionic charges of the sulfonic groups from those in the G molecule probably acts to prevent the complex from being formed*5. According to Table III, however, the difference in position of the sulfonic groups of 2S(Cu) and H(Cu) of the first group is not appreciably revealed in the results. From a comparison of the results of the first and the second categories, it is also clear that those in the first category with more sulfonic groups produce more complexes, while those in the second category produce almost none. For the above reason, it may be said in this case that the ionic charge of the sulfonic group has no great influence in outline on the complex formation.

The other possible factor is the influence of the auxochromes. As has been pointed out before[4], the effect of the auxochromes upon the complex formation with the G dye is such that the complex is stabilized by the occurrence of an intermolecular charge-transfer through the auxochromes, and at the same time the $\Delta\nu$ value grows large. This is reflected in the fact that all the dyes in the first group with large $\Delta\nu$ values have amino or hydroxyl groups which are terminal groups of a conjugated system. On the other hand, in the second group, with zero values of $\Delta\nu$, NW(Cu) especially has no auxochromes of such kinds, and γ(Cu), though it has two amino groups, can also be considerd to have no effective auxochromes because they are not conjugated terminal groups in a usual sense. Thus, the expected effect of the auxochromes and the experimental results show a good correspondence. However, the case of the J(Cu) dye, which has amino groups as its conjugated terminal groups, deviates from the above reasoning; the experimental results indicate that almost no complex is produced. However, whether or not amino groups of J(Cu) exerts a positive effect on the complex formation is obviously connected with its configuration relative to the G dye under the complex formation. Therefore, it is supposed here that the amino groups of J(Cu) could not reveal such a characteristic of auxochromes as seen in the

*5 The model of the complex formed assumes that the molecules overlap each other so as to be parallel longitudinally. See Ref. 4.

first group, owing to some reason, a correlation of geometric configuration, for instance.

Therefore, it may safely be said for the copper derivatives that the presence of the auxochromes as the terminal groups of a conjugated system is the necessary condition, even though not sufficient, to cause a spectral change with the formation of a complex.

Next, let us consider the case of Table II, where no copper is included. In this case, the hydroxyl group becomes free from copper to act as an effective auxochrome, and at the same time some dyes take a more planar structure as a result of being disengaged from the sterical restriction by copper. Namely, the 2S dye and the NW dye become more suitable structures for the complex formation than 2S(Cu) and NW(Cu) respectively, while the rest are left in nearly the same steric structure as the copper derivatives[1]. As mentioned above, the adding of effective auxochromes promotes the forming of a complex. Comparing Table II with Table III, the $\Delta\nu$ and $\Delta D/D$ of H, Ch, γ and J are evidently larger than those of the respective copper derivatives. This indicates the effect of hydroxyl. Moreover, according to the above considerations, 2S and NW ought to exhibit planar effects on their skeletal structures in addition to the effect of hydroxyl. Indeed, these dyes, as compared with 2S(Cu) and NW(Cu), respectively, show a more remarkable increase in $\Delta\nu$ and $\Delta D/D$ than expected from the hydroxyl effect. This indicates that the planar effect promotes the formation of a complex and, moreover, that it is quite large.

According to the qualitative results discussed above from Tables II and III, the disazo dyes must have effective amino or hydroxyl groups as auxochromes and be planar to some extent, in order to produce a complex by combination with G and to show the spectral change with the complex formation. Further, the sulfonic groups attached to the coupling components are important not because of the number of their ionic charges, but rather because of such steric effects as that the sulfonic groups prevent the dye from taking a more planar structure, or in some influence of their configuration relative to those of the G dye.

Thus, at the present time, nothing has been obtained more than a qualitative decision on the respective effects. However, some quantitative estimation of the effects will become possible after the detailed investigation being carried out on the equilibrium constants and their temperature dependence, etc., including the 1 : 2 complex formation.

Summary

1. The absorption spectra of the dyes prepared by coupling disazotized 2S-, H-, chromotropic, NW-, γ- and J- acid with dianisidine, and of their copper derivatives were observed in aqueous solutions of the binary mixture with Chrysophenine G, and were compared with the sum curves of the component absorption spectra.

2. The order of the equilibrium constants for a 1 : 1 complex formed between the dyes not containing copper and Chrysophenine G was parallel to the respective values of the difference in wave number ($\Delta\nu$ cm^{-1}) between maximum positions in the region of 390~420 mμ of the curve simply added and that observed with the equimolar binary mixture of about 1×10^{-5}mol./l.; it was also parallel to those of the decreasing ratio in optical density ($\Delta D/D$) of the mixed system at the first maximum position of the sum curve.

3. Under the same conditions as above, $\Delta\nu$ and $\Delta D/D$ were also determined for the mixture of the copper derivatives and Chrysophenine G. In this case, the copper derivatives of 2S-, H-, and chromotropic acid, in the presence of effective auxochromes, still revealed large values of $\Delta\nu$ (ca. 1000 cm^{-1}) and $\Delta D/D$ (ca. 15%), while the values for the rest of the derivatives were almost zero.

4. Discussing the above results, it was shown that in order to display a spectral change due to the formation of a 1 : 1 complex in a binary mixture with Chrysophenine G, it is necessary that the partner dye has effective auxochromes (amino, hydroxyl) as terminal groups of a conjugated system. It was also shown that the sulfonic groups which are attached to the terminal naphthalene nuclei act on the structure of the dye itself as a steric factor rather than as an electric effect (repulsion) between the ionic charges in the groups and those of Chrysophenine G, and that the more planar structure, resulting in a smaller steric effect, produces more complex.

The authors wish to express their thanks to Mr. Toshihiko Hoshi for his help in the measurement of absorption spectra.

Laboratory of Physical Chemistry
Tokyo Institute of Technology
Meguro-ku, Tokyo

Organoboron Compounds. IV. The Dyeing Property of Polyvinyl n-Butylboronate with Congo Red*

By Seiji KATO, Yoshiko KURANO and Yojiro TSUZUKI

(Received June 22, 1961)

Recently Fujino and Fujimoto reported on the dyeing properties of two kinds of polyvinyl alcohol films[1], one of which had previously been heat-treated and the other, formalized. They showed that the dye sorbed by films decreases in quantity with the extent of formalization. In a previous paper[2], the present authors reported on the reaction of polyvinyl alcohol with *n*-butylboronic acid and on some properties of the products, showing that it is possible to prepare some films with various esterification grades. Generally it is considered that the force binding dye molecules to polyvinyl alcohol is chiefly due to the hydrogen bond and some mechanical retention. If the binding force comes into play by co-ordination, even in the absence of mordants, it will strengthen the bond between the dye molecule and the substrate. The aim of this investigation consists in the point mentioned above. Since it is well known that the boron atom can co-ordinate easily with such negative atoms as oxygen, nitrogen and halogens, the dyeing capacity of polyvinyl boronate is expected to become large. In a previous communication[3] the authors showed that the quantity of the dye sorbed by films increases with the increasing esterification grade and that the apparent diffusion coefficient also corresponds to the esterification grade. The authors have observed some facts regarding the property of polyvinyl *n*-butylboronate films dyed with Congo red, the former containing boron atoms and the latter, nitrogen atoms.

Experimental

Substrates.—Boronate films were prepared, as described in a previous paper[2], by pouring a carbon tetrachloride solution of polyvinyl *n*-butylboronate with different esterification grades on a surface of mercury and then drying it for several days at room temperature. The films were all cut in pieces 1 cm.×2 cm. The thickness was about 0.1 mm. Congo red was purified according to Robinson and Mills' method[4].

Dyeing Procedure.—The films with different esterification grades were immersed into a Congo red solution at various temperatures. Then the sample were taken out one by one at definite intervals, well washed with cold water, and desorbed with a pyridin-water mixture. The amounts of dye sorbed by the samples were measured with a photo-electric colorimeter.

Measurement of the Heat of Sorption by Micro-desorption Method.—The samples having various esterification grades were previously dyed with Congo red and immersed into water kept at 20, 40 and 60°C according to the method which was proposed by Gilbert and Rideal[5]; after reaching equilibria, the desorbed dye was measured by a photo-electric colorimeter.

Results and Discussion

In dyeing experiments, it is generally necessary to record the time needed to reach the equilibrium of sorption. The sorption rate here was always faster than that of the polyvinyl alcohol film prveiously studied by Fujino and Fujimoto[1]. Figure 1 shows the relation between the rate and the temperature obtained with samples of the same esterification grade. Above 60°C the samples swelled for the first 10 hr. and later partially dissolved owing to

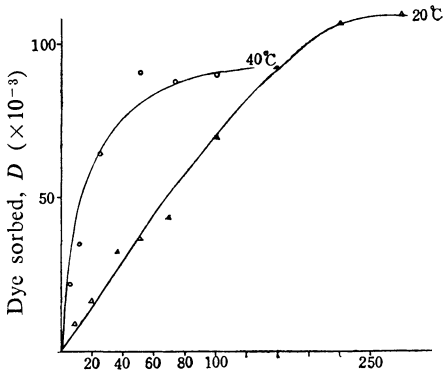


Fig. 1. Dye sorbed and absorption rate.

* I, This Bulletin, **34**, 1107 (1961); II, ibid., **33**, 1741 (1960); III, *Waseda Applied Chem. Soc. Bulletin, (in Japanese)* **28**, No. 5, 28, (1961).

1) K. Fujino and N. Fujimoto, *J. Soc. Textile and Cellulose Industries, Japan*, **15**, 138, 217 (1959).

2) S. Kato, Y. Tsuzuki and S. Kitajima, This Bulletin, **34**, 1107 (1961).

3) S. Kato and Y. Tsuzuki, ibid., **33**, 1741 (1960).

4) C. R. Robinson and H. A. Mills, *Proc. Roy. Soc.*, **A131**, 576 (1931).

5) G. A. Gilbert and E. K. Rideal., ibid., **A182**, 335 (1944).

the hydrolysis of the samples; therefore, the rate curves above 60°C were all neglected.

With samples of different esterification grades (E_g), differences in sorption were also observed. At the same time the quantity of the dye sorbed corresponds to the value of E_g, the data of which are given in Table I.

TABLE I. RELATION BETWEEN THE QUANTITY OF THE DYE SORBED AND ESTERIFICATION GRADE (E_g)

No. of sample	E_g, %	Dye sorbed (g./g. dry film) $\times 10^2$ 20°C	40°C	Activation energy kcal./mol.
B-1	75.4	5.6	4.7	17.4
B-2	80.6	7.9	6.0	16.1
B-3	85.6	10.9	9.2	13.0

Esterification grade (E_g) can be estimated from the boron content of the products by the following equation:

$$E_g = (133.74 \times B\%)/(16.41 - B\%)$$

Heat of Sorption.—In order to learn whether co-ordination takes place or not in this dyeing mechanism, the measurement of the heat of sorption was desirable. In the case of cellulose fiber and Vinylon, the heat of sorption was estimated to be about 10 to 20 kcal./mol.[6] According to Laubengayer and Condike[7], the heat of formation of the complex between trimethylboron and ammonia is 41.3 kcal./mol. This value seems to represent the energy of the B–N bond. The heat of sorption can be measured by means of the microdesorption method, which is quite convenient and can be used smoothly*. The results were shown in Fig. 2.

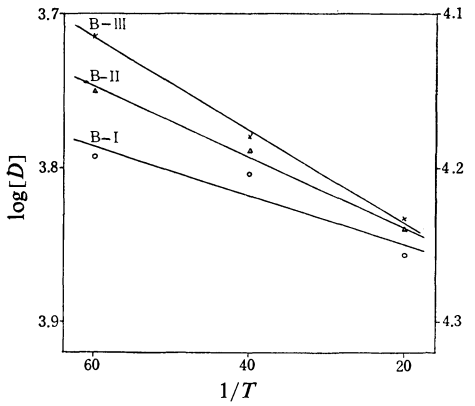


Fig. 2. Temperature dependance of the desorption of dye in equilibrium.

The slopes of the three lines in Fig. 2 represent the heat of sorption. These values apparently correspond to E_g. The values obtained are, however, not so high as those observed with cellulose and Vinylon fibers, as can be seen in Table II.

TABLE II. THE HEAT OF SORPTION AND ESTERIFICATION GRADE

No.	% E_g	Heat of Sorption (HS) kcal./mol.	HS/E_g
B-1	75.4	15.9	0.21
B-2	80.6	22.5	0.23
B-3	85.6	30.1	0.35

In order to study this problem, deeper infrared spectra were taken with dyed as well as undyed films, the data of which are shown in Fig. 3.

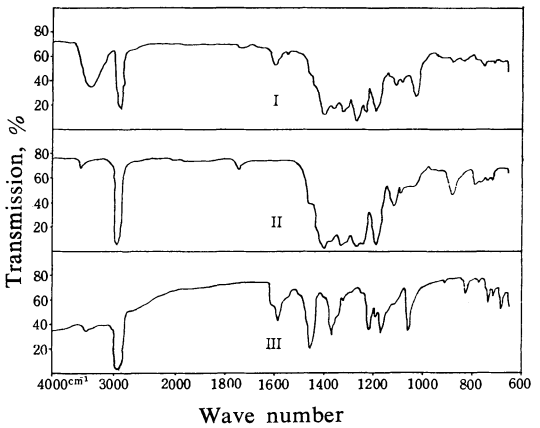


Fig. 3. Infrared spectra.
I Film dyed with Congo red
II Film not dyed
III Congo red in Nujol

The absorption band at 1580 cm^{-1} can be assigned to the azo bond, that at 3420 cm^{-1} to the bonds of amino group, and many bands below 1300 cm^{-1} in III to those of the aromatics[8]. Among the bonds of the boron atom linked with such negative atoms as oxygen, nitrogen and halogens, the B–N bond is the strongest, so bonding can be expected to occur with the azo and amino groups. The weak band at 3510 cm^{-1} may be regarded as due to a free type of hydroxyl group in II, and this absorption peak and that of the amino group at 3420 cm^{-1} shift to a lower frequency after the dyeing with Congo red, while the absorption band of the azo group shifts to a slightly higher frequency. From these results, it is considered that the bonding between the boron

6) T. Vickerstaff, "Physical Chemistry of Dyeing", 2nd. ed, Oliver and Boyd, London (1954), p. 229.
7) A. W. Laubengayer and G. F. Condike, *J. Am. Chem. Soc.*, **70**, 2274 (1954).
* Ref. 4 traced by A. Yabe and A. Uchida, *J. Soc. Org. Synth. (in Japanese)*, **13**, 601 (1955).
8) L. J. Bellamy, "The Infra-red Spectra of Complex Molecules", Methuen & Co., London (1958), p. 272.

atom and the nitrogen atoms may take place, for the most part, at the amino group in the dye molecules. Of course, the hydrogen atom of the amino group in the dye molecule can make a hydrogen bond with the oxygen atom[9] in polyvinyl *n*-butylboronate; hence, the presence of the broad band at 3400 cm^{-1} in the spectrum of I can be ascribed to two factors, one of which is the formation of the hydrogen bond between the amino group of the dye and the oxygen atom of polyvinyl *n*-butylboronate, and the other is the co-ordination of the boron atom to the nitrorgen atom of the amino group. The energy of dyeing should become ca. 40 kcal./mol. if all dye molecules are fixed to polyvinyl *n*-butylboronate by co-ordination, but, in fact, the values of the heat of sorption per E_g are not always equal. This means that the dyeing proceeds not only through co-ordination but also through a hydrogen bond.

Another factor which should be considered regarding the results of the relation between E_g and the dyeing property is the destruction of the dense polyvinyl alcohol structure by the treatment with boronic acid. Sakurada and Okada[10] have studied the reaction of boric acid with polyvinyl alcohol by means of X-ray diffraction; on the basis of the diminished fine structure in the diffraction pattern, they concluded that the crystalline part of polyvinyl alcohol is thereby decreased. In the case of the reaction of *n*-butylboronic acid with polyvinyl alcohol the molecular weight and the size of this acid are larger than those of boric acid, so that the crystalline part of polyvinyl alcohol, will diminish with the increasing esterification grade. The results of the estimation of activation energy suggest this consideration. Thus, experimenial results show that the two factors mentioned above overlap. In order to demonstrate the co-ordination, further experiments with various dyes should be carried out. The effects of various reactants on the spectra of the polyvinyl *n*-butylboronate in solution will be discussed later.

Tokyo College of Science
Shinjuku-ku, Tokyo

9) M. St. C. Flett, *J. Soc. Dyer and Col.*, **68**, 59 (1952).

10) I. Sakurada and A. Okada, *Chem. High Polymers (Kobunshi Kagaku,)* **15**, 491 (1958).

Studies on Sulfabenzothiazoles

By Prithwi Nath BHARGAVA and Suresh Chandra SHARMA

(Received September 15, 1961)

With a view to examining the medicinal and industrial importance of "benzothiazole derivatives", sulfabenzothiazole, sulfa-6-methyl-, -6-chloro-, -6-methoxy-, -6-nitro-benzothiazoles and sulfa-β-naphthothiazole, have been synthesized. As an extension of the previous work on 2-aminobenzothiazole derivatives[1], acetylamino-, benzoylamino-, 2-(2-hydroxy-1-naphthylazo)- and 2,2'-azobisbenzothiazole derivatives from the substituted 2-aminobenzothiazoles have also been prepared.

The starting compound, 2-aminobenzothiazole[2] was obtained by the action of liquid bromine on asymmetrical phenylthiourea in an inert medium like chloroform. Similarly other substituted, 2-amino-4-methyl-[3], -5-methyl-[1], -6-methyl-[4], -5-chloro-, -6-chloro-[4], -4-methoxy-, -6-methoxy-[1], -4-ethoxy-[4], -6-nitro-[1]benzothiazoles and 2-amino-α-naphtho-[1], -β-naphtho-[1]thiazoles have been prepared from the corresponding substituted asymmetrical arylthioureas and the latter were subsequently prepared[5,6] by the interaction of ammonium thiocyanate with the corresponding amine hydrochlorides.

The compound, sulfathiazole[7] was obtained by the condensation of acetylsulfanilyl chloride[8] (ASC) and 2-aminothiazole in pyridine and

1) P. N. Bhargava and B. T. Baliga, *J. Ind. Chem. Soc.*, **35**, 807 (1958).
2) A. Hugershoff, *Ber.*, **36**, 3121 (1903).
3) R. F. Hunter, *J. Chem. Soc.*, **129**, 1385 (1926).
4) P. N. Bhargava and K. A. Jose, *J. Ind. Chem. Soc.*, **37**, 314 (1960).
5) De. Clermont., *J. Chem. Soc.*, **31**, 70 (1877).
6) J. M. Berkebile and A. H. Fries, *J. Chem. Educ.*, **25**, 617 (1948).
7) J. Laudon and B. S. Svensk, *Kem. Tid.*, **52**, 64 (1940), in German.
8) M. L. Moore, C. S. Miller and E. Miller, *J. Am. Chem. Soc.*, **62**, 2097 (1940).

by subsequent alkaline hydrolysis of the condensed product. Following the same procedure all the sulfabenzothiazoles and sulfanaphthothiazoles have been synthesized and tested for bactericidal activity[9]. Further an absorption spectra study of these sulfabenzothiazoles has been made as a physical evidence in confirmation of structure of these compounds.

Experimental

2-(*p*-Aminobenzenesulfonamido)-benzothiazole.—Into a flask 3 g. of 2-aminobenzothiazole, 4.4 g. of acetylsulfanilyl chloride and 18 ml. of pyridine were taken and heated under reflux on a water bath for about two and a half hours. The contents were poured on cooling into water and the solid was filtered and crystallized from dilute ethanol. This intermediate product was heated under reflux on a low flame with 20 ml. of alcoholic 10% sodium hydroxide solution for two hours. The solution of the flask was poured into cold water and the solid substance filtered, dried and finally crystallized from ethanol into a white crystalline form, m. p. 213°C.

Similarly other substituted sulfabenzothiazoles were prepared. Their proprties and analytical data are recorded in Table I. However, with this procedure, the synthesis of sulfabenzothiazoles was not successful with 2-amino-4-methyl-, -5-methyl-, -5-chloro-, -4-methoxy-, -4-ethoxy-benzothiazoles and 2-amino-α-naphthothiazole.

2-Acetylamino-6-methylbenzothiazole.—One gram of 2-amino-6-methylbenzothiazole and 4 ml. of acetic anhydride were heated under reflux for 15 min. and then on cooling poured into cold water. The solid substance was filtered, dried and crystallized from ethanol into a white crystalline form, m. p. 202°C.

Similarly acetylamino derivatives of 2-amino-5-chloro-, -6-chloro-, -4-methoxy-benzothiazoles were prepared and on analysis the number of acetyl group in these derivatives was found to be one. Their properties and analytical data are given in Table II.

2-Benzoylamino-6-methylbenzothiazole. — Into a flask 1 g. of 2-amino-6-methylbenzothiazole was dissolved in 10 ml. of 20% sodium hydroxide solution and then it was treated with 1.5 ml. of benzoyl chloride, small quantity at a time with vigorous shaking and cooling. After the addition of the latter, the flask was warmed on a water bath under reflux to hydrolyze the excess of benzoyl chloride. The solid was cooled, filtered, washed with water, dried and crystallized from ethanol into a colorless crystalline from, m. p. 178°C.

Similarly, 2-benzoylamino derivatives of 5-chloro-, -6-chloro-, -4-methoxy-, -6-methoxy-benzothiazoles were prepared and on analysis the number of benzoyl groups in these derivatives was found to be one. Their properties and analytical data are mentioned in Table III.

6-Methyl-2-(2-hydroxy-1-naphthylazo)-benzothiazole.—Into a flask 20 ml. of dilute hydrochloric acid 1 g. of 2-amino-6-methylbenzothiazole was dissolved and diazotized as usual. The diazotized product was coupled with 0.9 g. of β-naphthol dissolved in 10 ml. of 4% sodium hydroxide solution. The orange brown azo compound on extraction with ether and crystallization in vacuum gave chocolate crystals, m. p. 124°C. It developed rosy red color in glacial acetic acid and gave the original

Table I. 2-(*p*-Aminobenzenesulfonamido)-benzothiazoles

No.	Compound	Yield %	Color	M. p. °C	Molecular formula	S, % Found	S, % Calcd
1	*A-B	61	Colorless	213	$C_{13}H_{11}O_2N_3S_2$	20.75	20.98
2	A-6-methyl-B	63	Colorless	200	$C_{14}H_{13}O_2N_3S_2$	19.66	20.06
3	A-6-chloro-B	67	Colorless	212	$C_{13}H_{10}O_2N_3S_2Cl$	18.98	18.85
4	A-6-nitro-B	48	Yellow	253	$C_{13}H_{10}O_4N_4S_2$	18.41	18.28
5	A-6-methoxy-B	64	Colorless	198	$C_{14}H_{13}O_3N_3S_2$	18.85	19.10
6	A-β-naphothiazole	62	Light grey	above 300	$C_{17}H_{13}O_2N_3S_2$	17.86	18.03

*A : -2-(*p*-aminobenzenesulfonamido)-
B : Benzothiazole

Table II. Acetyl derivatives of substituted 2-aminobenzothiazoles

No.	Compound	Color	M. p. °C	Molecular formula	N, % Found	N, % Calcd.
1	A-6-methyl-B	Colorless	202	$C_{10}H_{10}ON_2S$	13.37	13.59
2	A-5-chloro-B	Colorless	227	$C_9H_7ON_2SCl$	12.43	12.36
3	A-6-chloro-B	Colorless	224	$C_9H_7ON_2SCl$	12.29	12.36
4	A-4-methoxy-B	Colorless	245	$C_{12}H_{10}O_2N_2S$	12.51	12.73

A : 2-Acetylamino B : Benzothiazole

9) A. Mukherji, *Ind. Med. Gaz.*, **31**, 415 (1954).

TABLE III. BENZOYL DERIVATIVES OF SUBSTITUTED 2-AMINOBENZOTHIAZOLES

No.	Compound	Color	M. p. °C	Molecular formula	N, % Found	N, % Calcd.
1	A-6-methyl-B	Colorless	178	$C_{15}H_{12}ON_2S$	10.19	10.41
2	A-5-chloro-B	Colorless	Above 300, changes to black at 218	$C_{14}H_9ON_2SCl$	9.54	9.70
3	A-6-chloro-B	Colorless	Above 300, changes to black at 225	$C_{14}H_9ON_2SCl$	9.57	9.70
4	A-4-methoxy-B	Colorless	174	$C_{15}H_{12}O_2N_2S$	9.98	9.86
5	A-6-methoxy-B	Colorless	202	$C_{15}H_{12}O_2N_2S$	10.02	9.86

A: 2-Benzoylamino B: Benzothiazole

TABLE IV. 2-(2-HYDROXY-1-NAPHTHYLAZO)-BENZOTHIAZOLE DERIVATIVES

No.	Compound	Color	M. p. °C	Color in glacial acetic acid	Molecular formula	N, % Found	N, % Calcd.
1	5-Methyl-A	Dark violet	147	Yellowish pink	$C_{18}H_{13}ON_3S$	12.84	13.17
2	6-Methyl-A	Chocolate	124	Rosy red	$C_{18}H_{13}ON_3S$	12.73	13.17
3	5-Chloro-A	Brown	101	Orange	$C_{17}H_{10}ON_3SCl$	12.12	12.37
4	6-Chloro-A	Dark grey	156	Dirty yellow	$C_{17}H_{10}ON_3SCl$	12.61	12.37
5	6-Nitro-A	Dark brown	133	Pink	$C_{17}H_{10}O_3N_4S$	15.63	15.82
6	4-Methoxy-A	Dark violet	105	Red	$C_{18}H_{13}O_2N_3S$	12.31	12.54
7	6-Methoxy-A	Chocolate	96	Red	$C_{18}H_{13}O_2N_3S$	12.29	12.54

A: 2-(2-Hydroxy-1-naphthylazo)-benzothiazole

TABLE V. 2,2'-AZOBISBENZOTHIAZOL DERIVATIVES FROM SUBSTITUTED 2-AMINOBENZOTHIAZOLES

No.	Compound	Color	M. p. °C	Color in glacial acetic acid	Molecular formula	N, % Found	N, % Calcd.
1	2,2'-Azobis(6-methyl-A)	Dark black	Above 300	Brownish red	$C_{16}H_{12}N_4S_2$	16.82	17.28
2	2,2'-Azobis(5-chloro-A)	Reddish black	Above 300	Yellow	$C_{14}H_6S_2Cl_2N_4$	14.97	15.34
3	2,2'-Azobis(6-chloro-A)	Chocolate	191	Orange yellow	$C_{14}H_6N_4S_2Cl_2$	15.21	15.34
4	2,2'-Azobis(4-methoxy-A)	Dark pink	Above 300	Light chocolate	$C_{16}H_{12}O_2N_4S_2$	15.13	15.73
5	2,2'-Azobis(6-ethyl-A)	Dark violet	Above 300	Pink	$C_{18}H_{16}O_2N_4S_2$	14.33	14.58

A: Benzothiazole

TABLE VI. ULTRAVIOLT ABSORPTION OF SULFABENZOTHIAZOLES

Solvent: Absolute ethanol Concn.: 0.01 g./l.

No.	Compound	1st peak mμ	2nd peak mμ	3rd peak mμ
1	Sulfabenzothiazole	226.00	269.50	—
2	Sulfa-6-methylbenzothiazole	228.75	268.75	—
3	Sulfa-6-chlorobenzothiazole	230.25	268.25	—
4	Sulfa-6-nitrobenzothiazole	224.00	352.00	—
5	Sulfa-6-methoxybenzothiazole	227.50	269.50	—
6	Sulfa-β-naphthothiazole	229.75	257.50	299.50

2-amino-6-methylbenzothiazole on reduction with tin and concentrated hydrochloric acid.

Similarly six more azo-compounds were prepared from different substituted 2-aminobenzothiazoles. Their properties and analytical data are recorded in Table IV.

2,2'-Azobis(6-methylbenzothiazole). — One gram of 2-amino-6-methylbenzothiazole was suspended in 30 ml. of water taken in a beaker and was gradually treated with 50 ml. of 0.3 N solution of sodium hypochlorite and kept for half an hour. The brown solid, after being washed with ether, was extracted with a mixture of chloroform and light petroleum ether (1 : 1). After evaporation of the solvents the products was left as dark brown crystals, m. p. above 300°C. It developed brownish red color in glacial acetic acid and gave the original benzothiazole on reduction with tin and concentrated hydrochloric acid.

Similarly other azobisbenzothiazole derivatives were prepared from 2-amino-5-chloro-, -6-chloro-, -4-methoxy-, -4-ethoxy-benzothiazoles and their properties and analytical data are given in Table V.

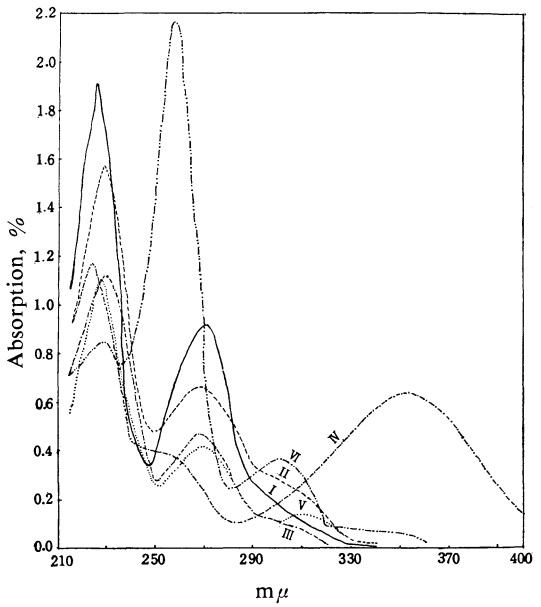


Fig. 1. Ultraviolet absorption curves of sulfabenzothiazoles.

I Sulfabenzothiazole
II Sulfa-6-methylbenzothiazole
III Sulfa-6-chlorobenzothiazole
IV Sulfa-6-nitrobenzothiazole
V Sulfa-6-methoxybenzothiazole
VI Sulfa-β-naphthothiazole

Absorption Spectra Measurements of Sulfabenzothiazoles.—The study of ultraviolet spectra of sulfabenzothiazoles was carried out in spectroscopically pure absolute ethanol on Beckman D. U. spectrophotometer. The values of λ_{max} for different peaks observed from the curves are given in Table VI.

The λ_{max} at 226 mμ in 2-(*p*-aminobenzenesulfonamido)-benzothiazole is due to the presence of benzenesulfonamido nucleus and the second peak at 269.5 mμ is due to the presence of 2-aminobenzothiazole (a shift of λ_{max} from 262 to 269.5 mμ due to the presence of benzenesulfonamido nucleus). Substituents like chlorine atom, methyl and methoxy groups in 2-aminobenzothiazoles at position 6 have little effect on the shift. But in sulfa-6-nitrobenzothiazole a tendency of absorption peak to appear at higher wavelength is observed because of the presence of chromophoric group like nitro group which has pronounced effect to increase absorption from ultraviolet to visible region and thus cause for the appearance of color (yellow). So in this case the second absorption peak appeared at 352 mμ. In the case of sulfa-β-naphthothiazole absorption peaks are found at 229.75, 257.5 and 299.5 mμ, as the latter two are due to the presence of β-naphthothiazole.

Assay of Sulfabenzothiazoles for Bactericidal Activity.—The compounds were tested in Central Drug Research Institute, Lucknow, India, for bactericidal activity according to the method[9] and it was found that sulfa-6-methyl-, -6-chloro-, -6-methoxy-, -6-nitro-benzothiazoles were inactive upto a dilution of 1 : 1000 against Klebsilla pneumonial; Salmonella paratyphi; Salmonella typhi; Escherichia coli; Shigella dysenteriae (Shiga); Micrococcus pyrogenes Var aureus; Acrobactor aerogenes and B. subtillis.

Thanks of the authors are due to Professor Gurbakhsh Singh, head of the Department of Chemistry and other authorities of the Banaras Hindu University for providing necessary facilities and also to Dr. Dashrath Lal Srivastava, Deputy Director C. D. R. I., Lucknow for the assaying of sulfabenzothiazoles.

Department of Chemistry
College of Science
Banaras Hindu University
Varanasi, India

Electronic Spectra and Electronic Structures of Some Basic Heterocyclic N-Oxides

By Tanekazu KUBOTA

(Received January 24, 1961)

In a series of previous papers[1,2], we reported on the electronic spectra and electronic structures of various basic heterocyclic *N*-oxides such as pyridine, quinoline, acridine *N*-oxides, etc. and also on their derivatives. The assignment of ultraviolet absorption bands and the interpretation of other physicochemical properties (such as dipole moments, infrared spectra, molecular diagrams, reactivities, dissociation constants, etc.) of basic heterocyclic *N*-oxides were made from the experimental and theoretical points of view. It was concluded that the strongest band near 280 mμ observed with pyridine *N*-oxide and its simple derivatives can not be assigned to the ^1L_b band whose transition moment is parallel to the x-axis as shown in Fig. 4 and that, on the other hand, it may reasonably be interpreted as a new band (charge transfer band) whose transition is associated with the charge displacement from the oxygen atom to the pyridine nucleus*1.

As to the absorption bands of polyheterocyclic *N*-oxides, however, band assignments by means of Platt's treatment were possible. In the present work, the spectra and the electronic structures of some basic *N*-oxides are reported in a development of our previous work*2. The electronic absorption spectra of pyrazine mono- and di-*N*-oxides and 4-methylpyrimidine *N*-oxide and the electronic structures of pyrazine di-*N*-oxide and some other compounds have been studied and compared with the results in the previous studies.

Experimental

Materials. — Pyrazine mono- (m. p. 108°C) and di- (d. p. 260°C) *N*-oxides were prepared by the oxidation of pyrazine with an equivalent and an excess of hydrogen peroxide respectively, and were purified by sublimation in vacuum. A pure sample of 4-methylpyrimidine *N*-oxide (m. p. 76~79°C) was supplied by Dr. Yamanaka of Tohoku University[7]. Organic solvents such as *n*-heptane, dioxane, alcohol, etc. for spectrophotometric measurements were purified according to the standard method[8].

Measurement. — A Hitachi recording spectrophotometer model EPS-2 and a Beckman spectrophotometer model D. U. were used for the ultraviolet absorption measurements of solutions. Measurements were usually carried out at room temperature (20~25°C), using the quartz cell with a stopper of a 1 cm. light path. For measurements of weak absorption bands, quartz cells of 2, 5 and 10 cm. light path were also used. If necessary, however, the temperature of the absorption cell was kept constant by circulating water of a desired constant temperature through the cell jacket.

Experimental Results

Absorption Spectra of Pyrazine Di-*N*-oxide. — As is shown in Fig. 1, the spectrum in an absolute dioxane solution*3 apparently consists of the three main bands (i. e., 324, ~260 and 223 mμ*4) and of some bands of a lower intensity superposed on the main absorption band near 350~370 mμ. Figure 1 also shows our band analysis based on the method which was used by Stephenson for the interpretation of the $n\rightarrow\pi^*$ and $\pi\rightarrow\pi^*$ bands of pyridine and its simple derivatives[9]. Oscillator strengths of each band obtained by the above analysis were calculated in terms of Eq. 1,

$$f=4.32\times10^{-9}\int\varepsilon d\tilde{\nu} \qquad (1)$$

where the value of the integral, $\int\varepsilon d\tilde{\nu}$, was estimated by the approximate formula, $\int\varepsilon d\tilde{\nu}\fallingdotseq$ [(half wide value in cm^{-1})$\times\varepsilon_{max}$] and the

1) T. Kubota, *J. Chem. Soc. Japan, Pure Chem. Sec. (Nippon Kagaku Zassi)*, **79**, 930 (1958), etc.
2) T. Kubota, ibid., **80**, 578 (1959), etc.
*1 The concept of the intramolecular charge transfer spectra was first introduced by Nagakura and Tanaka[3-5] to interpret the spectra of substituted benzenes.
3) S. Nagakura and J. Tanaka, *J. Chem. Phys.*, **22**, 236 (1954).
4) J. Tanaka and S. Nagakura, ibid., **24**, 1274 (1956).
5) S. Nagakura, *Molecular Physics*, **3**, 152 (1960).
*2 Moreover, many spectra of heterocyclic *N*-oxides with much more complex constitutions have also been recorded, and we have found some general properties on these spectra[6].
6) T. Kubota and H. Miyazaki, *Chem. Pharm. Bull.*, **9**, 948 (1961).
7) Cf. E. Ochiai and H. Yamanaka, *Pharm. Bull.*, **3**, 175 (1955).
8) A. Weissberger and E. Proskauer, "Organic Solvent", 2nd Edition, Interscience Pub., Inc., New York (1956).
*3 Accurate measurement of the spectrum in the *n*-heptane solution could not be carried out because of the much lower solubility.
*4 This value, cited in the previous papers, was obtained in an absolute ethanol solution[2,6].
9) H. P. Stephenson, *J. Chem. Phys.*, **22**, 1077 (1954).

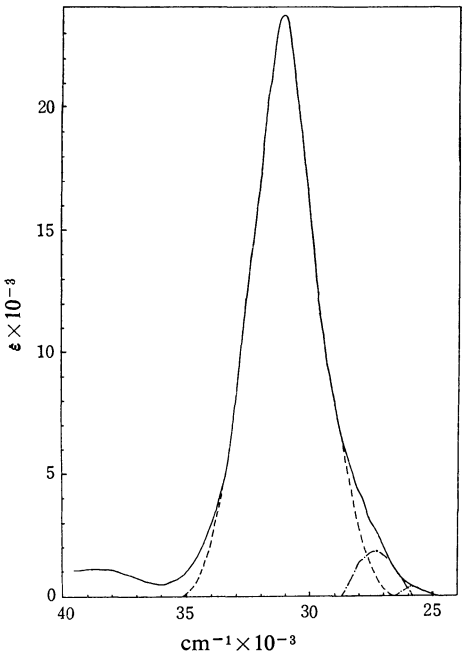


Fig. 1. Absorption spectrum in absolute dioxane solution and band analysis of pyrazine di-*N*-oxide.

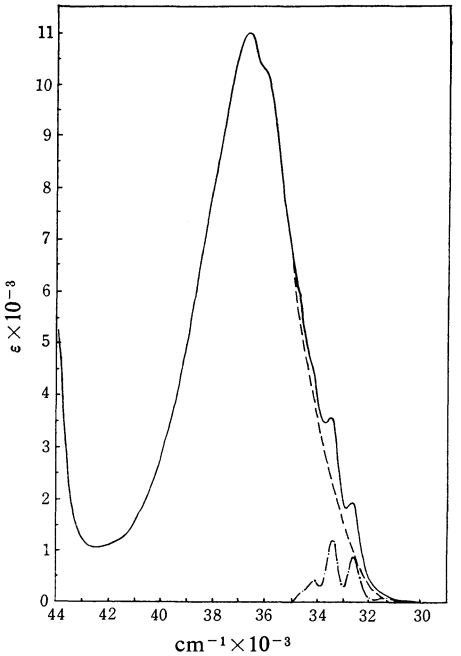


Fig. 2. Absorption spectrum in *n*-heptane solution and band analysis of pyrazine mono-*N*-oxide.

graphic integration for the main band and the weak bands respectively. The results are shown in Table I. In solvents such as alcohol and water, the absorption bands show a blue shift with the increase in solvent polarity. Especially, the weak band which appeared obviously in the longest wavelength region in non-polar solvents could not be observed even by careful measurement using the cell of a 10 cm. light path[6]. It may be possible that the blue shift of the above weak bands due to the change from non-polar to polar solvents is much greater than that of the main $\pi \rightarrow \pi^*$ band*[5], and that therefore we could not find the weak bands in polar solvents, which are hidden below the main $\pi \rightarrow \pi^*$ band.

Absorption Spectra of Pyrazine Mono-*N*-oxide. —As is shown in Fig. 2, the spectrum of this compound in an *n*-heptane solution shows distinct maxima at 275 and 222 mμ*[6] which exhibits three fine structures. The spectrum also shows some fine structures superposed on the long wavelength side of the $\pi \rightarrow \pi^*$ band. Our band analysis of the above spectrum is also shown in Fig. 2. It may be inferred that the above weak band has a fine structure consisting of three peaks. The behavior of the spectra in polar solvents is similar to that of pyrazine di*N*-oxide[6], while the weak band could not be observed in polar solvents. The results of our band analysis are shown in Table I.

Absorption Spectra of 4-Methylpyrimidine *N*-oxide. — The spectra of this compound in *n*-heptane and water solutions are shown in Fig. 3 and in Table I. A distinct difference compared with the above two compounds is that the low intensity band which appears obviously in non-polar solvents at the longest wavelengh region can also be found partly in water. Our band analysis was carried out by the following method. First, the tail of the strong longest wavelength $\pi \rightarrow \pi^*$ band in water was extended as smooth as possible; the $\pi \rightarrow \pi^*$ band thus obtained was symmetrical with respect to the band's center line. This band was then subtracted from the total absorption band. Thus we obtained band I. Second, the same procedure was applied to the spectrum in *n*-heptane, and band II was obtained. Finally, it was assumed that band I had almost the same intensity in *n*-heptane as in water, and band I′ (the absorption band in *n*-heptane corresponding to the band I in water) was subtracted from band II as shown in Fig. 3. This

*5 According to the general rule for the UV spectra of heterocyclic *N*-oxides, these $\pi \rightarrow \pi^*$ bands show a remarkable blue shift with the above-described variation in solvent[1,6]. On the other hand, the hydrogen bonding such as $\rangle N \rightarrow O \cdots\cdots H$ (solvent) is an essential mechanism in such general spectral behavior[10,11].

10) T. Kubota, *J. Pharm. Soc. Japan* (*Yakugaku Zasshi*), **74**, 831 (1954); **75**, 1540 (1955), etc.

11) T. Kubota, *J. Chem. Soc. Japan, Pure Chem. Sec.* (*Nippon Kagaku Zasshi*), **79**, 916 (1958).

*6 This value was taken from the previous papers[2,6].

TABLE I

Substance	Solvent	Weak band ($n\rightarrow\pi^*$) cm^{-1}	Weak band ($n\rightarrow\pi^*$) f-Value	CT band cm^{-1}	CT band f-Value	$f_{n\rightarrow\pi^*}/f_{CT}$	Weak band (^1L_b band) cm^{-1}	Weak band (^1L_b band) f-Value
Pyrazine di-*N*-oxide	1,4-Dioxane	27250 25800	0.001 0.014 (+ 0.015)	30900	0.303	0.050	—	
	Water	—		32670	—	—	—	
Pyrazine mono-*N*-oxide	*n*-Heptane	34050 33350 32520	0.006	36500	0.186	0.033	—	
	Water	—		37880	—	—	—	
4-Methyl-pyrimidine *N*-oxide*3	*n*-Heptane*3		0.011	35970	0.180	0.064	32180	0.020
	Water	—		38820	0.183	—	34750	0.020
Pyridine *N*-oxide*2	*n*-Heptane	~32000	0.012*1	35520	0.173*1	0.079*1	—	

*1 See Ref. 22.
*2 See Ref. 1.
*3 If we should assume that all weak bands in the longest wavelength region are due to $n\rightarrow\pi^*$ transition, the value of $[f_{n\rightarrow\pi^*}/f_{CT}]$ is 0.174. This value, however, is abnormally large.

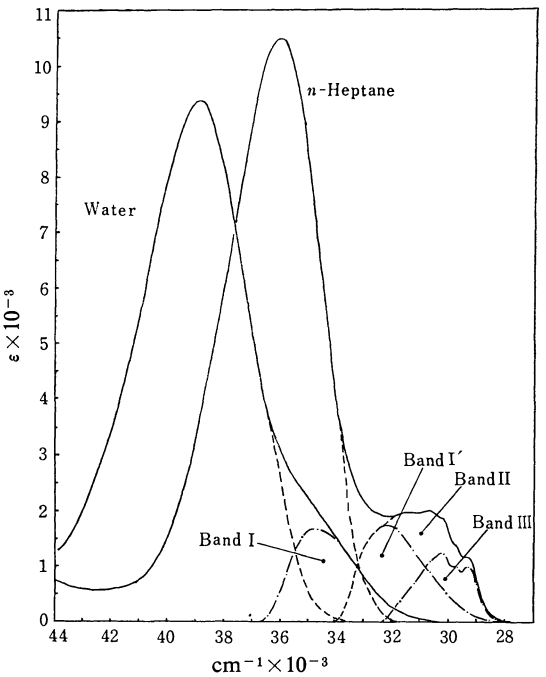


Fig. 3. Absorption spectra in *n*-heptane and water solutions and band analysis of 4-methylpyrimidine *N*-oxide.

way of subtraction would be fairly reasonable. The weak band in *n*-heptane was thus divided into bands I′ and III. The results obtained by the above band analysis are shown in Table I.

Theoretical

Electronic State and Electronic Spectrum of Pyrazine Di-*N*-oxide. — Theoretical calculation based on π-electron approximation, in which electron repulsion terms are taken into account, was carried out on pyrazine di-*N*-oxide. The method is almost the same as that of the previous calculation on pyridine *N*-oxide. Following the procedure of Longuet-Higgins and Murrell, pyrazine di-*N*-oxide is divided into two parts, pyrazine nucleus and two oxygen atoms, and self-consistent field (SCF) calculations for the above two parts are carried out. Then the interaction between the above two parts is calculated. Now, let us explain the procedure in some detail.

SCF Calculation of the Pyrazine Residue.— The electronic structure of pyrazine residue may differ considerably from that of the normal pyrazine molecule, because the N–O bond may be considered to be like a semi-polar bond. In view of the above point[2], a virtual proton model, which was used to calculate the electronic structure of pyridine *N*-oxide, is also adopted in the present calculation. This model is shown in Fig. 4. Hamiltonian calculations for the total π-electrons may be written as:

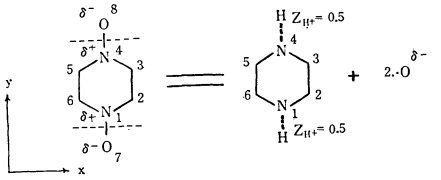


Fig. 4. The model of pyrazine di-*N*-oxide for MO calculation by composite system method. The proton potential, where Z_{H^+} was taken equal to 0.5, should be regarded as representing the core potential due to the formally charged nitrogen atom "$N^{\delta+}$".

$$H=\sum_i\left[H_i^{\text{core}}-\sum_p\frac{Z_{H^+}\cdot e^2}{r_{pi}}\right]+\sum_{i<j}\frac{e^2}{r_{ij}} \quad (2)$$

Here, r_{pi} represents the distance (1.032 Å)[2] between a virtual proton and an ith electron, while $Z_{H^+}\cdot e$ represents the effective charge of the virtual proton, the value being 0.5. We have used here the semiempirical SCF MO method, including zero-differential overlap approximation, as developed by Pople[12]. According to this method, the matrix elements of Fock's Hamiltonian calculation in terms of AO's can be written as follows:

$$F_{\mu\mu}=\alpha_\mu^{\text{core}}+V_\mu^p+\frac{1}{2}p_{\mu\mu}\cdot\gamma_{\mu\mu}+\sum_{k(\neq\mu)}(p_{kk}-1)\gamma_{\mu k} \quad (3)$$

$$F_{\mu\nu}=\beta_{\mu\nu}^{\text{core}}-\frac{1}{2}p_{\mu\nu}\cdot\gamma_{\mu\nu} \quad (4)$$

V_μ^p in Eq. 3 can be written as

$$V_\mu^p=-Z_{H^+}\cdot e^2\int\sum_p(\phi_\mu^2(i)/r_{pi})\mathrm{d}\tau_i \quad (5)$$

where ϕ_μ represents a 2pπ-AO of atom μ. V_μ^p was calculated by Roothaan's formula[13] using Slater type AO for ϕ_μ. As for the molecular dimensions of the pyrazine residue, it was assumed for the sake of simplicity that the pyrazine residue was a regular hexagon of V_h symmetry. The virtual proton potential as shown in Eq. 5 does not necessarily mean the simple electrostatic potential; it can be regarded as representing the modifications of core potentials due to the formally charged nitrogen atom "$N^{\delta+}$" in the pyrazine residue. Z_{H^+} is taken to be 0.5 in view of the fact that, in the previous calculation of pyridine *N*-oxide by the method of the composite system, SCF MO's of the pyridine residue obtained by the virtual proton model*7, where Z_{H^+} was taken to be equal to 0.5, were in nice agreement with the SMO's (simple molecular orbitals) of the pyridine residue obtained by the following procedures*8. The values of parameter k_N and k_O in Eqs. 7 and 8 are chosen so as to reproduce the electron densities obtained from the experimentally-determined Hammett's σ-value of the aromatic *N*-oxide group in non-polar solvents, using Jaffe's relation[2]. In this case

$$\alpha_N=\alpha+k_N\cdot\beta \quad (7)$$

$$\alpha_O=\alpha+k_O\cdot\beta \quad (8)$$

all resonance integrals including β_{NO} are assumed equal to β, and the inductive effect is put at $(1/3)^n\cdot k_N$. The SMO's of the pyridine residue were calculated by using the parameters k_N and $(1/3)^n\cdot k_N$ thus obtained.

The values of the two center electronic repulsion integrals $\gamma_{\mu\nu}$ have been evaluated by Mataga's method[15], where the point-charge model[12] was modified by means of Pariser-Parr's treatment[16]. The values of the integrals α_N^{core}, α_C^{core}, γ_{NN}, γ_{CC}, β_{CC}^{core} and β_{CN}^{core} are taken to be the same as those used in the previous paper[2]. The values of V_N^p and V_C^p are -8.107 and -5.455 eV. respectively.

As for the starting MO in the SCF procedure, the SMO obtained by the use of parameters $k_N=k_1=\alpha+1.6\beta$ and $\alpha_2=\alpha+0.711\beta$ (0.711 is a sum of inductive effects—$(1/3)^n\cdot k_N$—contributed from each nitrogen atom) from the above point of view was used; this SMO is near to the SCF MO's obtained by the iterative calculation of Eq. 9.

$$\sum_\nu F_{\mu\nu}\cdot C_{i\nu}=\varepsilon_i\cdot C_{i\mu} \quad (9)$$

The SCF MO's, eigen-values and symmetries of orbitals obtained in this way are shown in Table II and in Fig. 5. Here, symmetries of the orbitals are the same as those described in the previous paper[2].

Energy Levels of Oxygen Atoms.—The MO's of two oxygen atoms can be written as follows:

$$(b_{2u})\phi_7=1/\sqrt{2}(\phi_7+\phi_8) \quad (10)$$

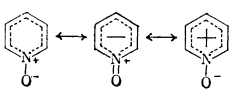
$$(b_{3g})\phi_8=1/\sqrt{2}(\phi_7-\phi_8) \quad (11)$$

Here, ϕ_7 and ϕ_8 represent the 2pπ AO of oxygen atoms 7 and 8 respectively. ϕ_7 and ϕ_8 are nearly degenerate, and the eigen-value for these MO's was evaluated using Eq. 12, were $\overline{F}^c{}_{\mu\mu}$ and $\overline{F}^c{}_{\mu\nu}$ represent the mean value of $F_{\mu\mu}$'s for carbon atoms and that of $F_{\mu\nu}$'s for the nearest neighbor carbon atoms respectively, because the matrix elements ($F_{\mu\mu}$ and $F_{\mu\nu}$) in the SCF MO method correspond reasonably to the matrix elements in the SMO method (for example, Eq. 7 and 8):

$$F_{OO}=\overline{F}^c{}_{\mu\mu}+k_O\cdot\overline{F}^c{}_{\mu\nu} \quad (12)$$

k_O was taken to be 1, since the F_{OO} value obtained from the previous ASMO CI calculation on pyridine *N*-oxide corresponds to the case $k_O=1$[1], and thus $F_{OO}=-15.34$ eV. was obtained.

12) J. A. Pople, *Trans. Faraday Soc.*, **49**, 1375 (1953).
13) C. C. J. Roothaan, *J. Chem. Phys.*, **19**, 1445 (1951).
*7 This treatment for heterocyclic compounds was carried out first by S. Mataga and N. Mataga[14].
14) S. Mataga and N. Mataga, *Z. physik. Chem., N. F.*, **19**, 231 (1959).
*8 $Z_{H^+}=0.5$ may be a reasonable value, since the following resonance formulas can be conceived:



15) N. Mataga and K. Nishimoto, ibid., **13**, 140 (1957).
16) R. Pariser and R. G. Parr, *J. Chem. Phys.*, **21**, 466, 767 (1953).

TABLE II. SCF MO'S, EIGEN-VALUES AND SYMMETRIES OF EACH ORBITAL OF PYRAZINE RESIDUE

Symmetry	SCF MO	Eigen-value
b_{2u}	$\phi_1=0.5207(\phi_1+\phi_4)+0.3383(\phi_2+\phi_3+\phi_5+\phi_6)$	−21.249 eV.
b_{3g}	$\phi_2=0.6318(\phi_1-\phi_4)+0.2245(\phi_2-\phi_3-\phi_5+\phi_6)$	−19.374 eV.
b_{1g}	$\phi_3=1/2(\phi_2+\phi_3-\phi_5-\phi_6)$	−16.322 eV.
b_{2u}	$\phi_4=0.4784(\phi_1+\phi_4)+0.3682(-\phi_2-\phi_3-\phi_5-\phi_6)$	− 8.566 eV.
a_u	$\phi_5=1/2(\phi_2-\phi_3+\phi_5-\phi_6)$	− 6.926 eV.
b_{3g}	$\phi_6=0.3174(\phi_1-\phi_4)+0.4468(-\phi_2+\phi_3+\phi_5-\phi_6)$	− 4.588 eV.

TABLE III. ENERGIES AND EXCITED STATE WAVE FUNCTIONS OF PYRAZINE RESIDUE, AND ENERGIES OF CHARGE TRANSFER CONFIGURATIONS AND INTERCONFIGURATIONAL MATRIX ELEMENTS (Energies are in unit of eV.)

$[{}^1\chi_{3\to4}\,|\,H\,|\,{}^1\chi_{3\to4}]=4.7855$ $(34\,|\,G\,|\,34)=5.3527$, $(34\,|\,G\,|\,43)=1.1911$

$[{}^1\chi_{3\to5}\,|\,H\,|\,{}^1\chi_{3\to5}]=6.4808$ $(35\,|\,G\,|\,35)=5.8662$, $(35\,|\,G\,|\,53)=1.4754$

$[{}^1\chi_{2\to4}\,|\,H\,|\,{}^1\chi_{2\to4}]=7.7151$ $(24\,|\,G\,|\,24)=6.1655$, $(24\,|\,G\,|\,42)=1.5360$

$[{}^1\chi_{2\to5}\,|\,H\,|\,{}^1\chi_{2\to5}]=7.9208$ $(25\,|\,G\,|\,25)=5.4130$, $(25\,|\,G\,|\,52)=0.4426$

$[{}^1\chi_{7\to5}\,|\,H\,|\,{}^1\chi_{7\to5}]=4.8299$ $(75\,|\,G\,|\,75)=3.5887$

$[{}^1\chi_{8\to5}\,|\,H\,|\,{}^1\chi_{8\to5}]=[{}^1\chi_{7\to5}\,|\,H\,|\,{}^1\chi_{7\to5}]$

$[{}^1\chi_{8\to4}\,|\,H\,|\,{}^1\chi_{8\to4}]=2.7922$ $(84\,|\,G\,|\,84)=3.9863$

$[{}^1\chi_{7\to4}\,|\,H\,|\,{}^1\chi_{7\to4}]=[{}^1\chi_{8\to4}\,|\,H\,|\,{}^1\chi_{8\to4}]$

$[{}^1\chi_{7\to4}\,|\,H\,|\,\Psi_0]=\sqrt{2}\cdot[C_{77}\cdot C_{41}\cdot\beta_{71}^{\text{core}}+C_{78}\cdot C_{44}\cdot\beta_{84}^{\text{core}}]=\sqrt{2}\cdot\varepsilon_{74}=-1.9135$

$[{}^1\chi_{3\to4}\,|\,H\,|\,{}^1\chi_{2\to5}]=-1.0221$ $(24\,|\,G\,|\,53)=-0.7261$, $(24\,|\,G\,|\,35)=-0.4301$

$[{}^1\chi_{3\to5}\,|\,H\,|\,{}^1\chi_{2\to4}]=0.3940$ $(25\,|\,G\,|\,43)=-0.0180$, $(25\,|\,G\,|\,34)=-0.4301$

${}^1L_b({}^1B_{3u}:x)=0.9586({}^1\chi_{3\to4})+0.2849({}^1\chi_{2\to5})$: 4.4817

${}^1B_b({}^1B_{3u}:x)=0.2849({}^1\chi_{3\to4})-0.9586({}^1\chi_{2\to5})$: 8.2246

${}^1L_a({}^1B_{1u}:y)=0.9599({}^1\chi_{3\to5})-0.2803({}^1\chi_{2\to4})$: 6.3657

${}^1B_a({}^1B_{1u}:y)=0.2803({}^1\chi_{3\to5})+0.9599({}^1\chi_{2\to4})$: 7.8301

$[{}^1\chi_{8\to4}\,|\,H\,|\,{}^1\chi_{3\to5}]=0$

$[{}^1\chi_{8\to4}\,|\,H\,|\,{}^1\chi_{2\to4}]=-\varepsilon_{28}=1.7871$

$[{}^1L_a\,|\,H\,|\,{}^1\chi_{8\to4}]=-0.5009$

$[{}^1B_a\,|\,H\,|\,{}^1\chi_{8\to4}]=1.7155$

$[{}^1\chi_{8\to5}\,|\,H\,|\,{}^1\chi_{3\to4}]=0$

$[{}^1\chi_{8\to5}\,|\,H\,|\,{}^1\chi_{2\to5}]=-\varepsilon_{82}=1.7871$

$[{}^1L_b\,|\,H\,|\,{}^1\chi_{8\to5}]=0.5091$

$[{}^1B_b\,|\,H\,|\,{}^1\chi_{8\to5}]=-1.7131$

Obtained energy levels are shown in Fig. 5. Now, it may be possible that electronic transitions, as shown by arrows in Fig. 5, make a great contribution to the near-ultraviolet absorption of pyrazine di-*N*-oxide. Therefore, these transitions were taken into account. The calculation of the excitation energies was made as follows. First, the energy values of the locally excited states were calculated on the basis of the results shown in Table II, using the method of configuration interaction. These results are shown in Table III. In this table, for example, ${}^1\chi_{3\to4}$ denotes the configuration produced by one electron transition from ϕ_3 to ϕ_4, and the necessary formulas for transition energies and interaction energies between these configurations are shown in the footnote*9.

The energy values of the charge transfer configurations due to electron transfers from ϕ_7 and ϕ_8 to the orbitals of pyrazine nucleus are also shown in Table III. In this case, it is assumed that r_{NO}, $r_{77}=r_{88}$ and $\beta_{71}^{\text{core}}=\beta_{84}^{\text{core}}$ are equal to 1.27 Å, 14.127 eV. and −2.00 eV. respectively, owing to the same reason as described in a previous paper[2]. The values

*9 $[{}^1\chi_{i\to j}\,|\,H\,|\,{}^1\chi_{i\to j}]=\varepsilon_j-\varepsilon_i+2(ij\,|\,G\,|\,ji)-(ij\,|\,G\,|\,ij)$

$[{}^1\chi_{i\to j}\,|\,H\,|\,{}^1\chi_{k\to l}]=2(kj\,|\,G\,|\,li)-(kj\,|\,G\,|\,il)$

$[{}^1\chi_{i\to j}\,|\,H\,|\,\Psi_0]=\sqrt{2}\,\varepsilon_{ij}$

$[{}^1\chi_{i\to j}\,|\,H\,|\,{}^1\chi_{k\to j}]=-\varepsilon_{ik}+2(kj\,|\,G\,|\,ji)-(kj\,|\,G\,|\,ij)$

$[{}^1\chi_{i\to j}\,|\,H\,|\,{}^1\chi_{i\to l}]\varepsilon_{jl}+2(ij\,|\,G\,|\,li)-(ij\,|\,G\,|\,il)$

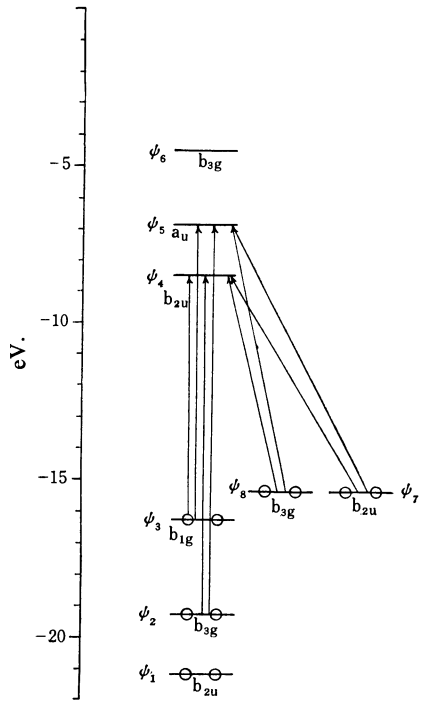


Fig. 5

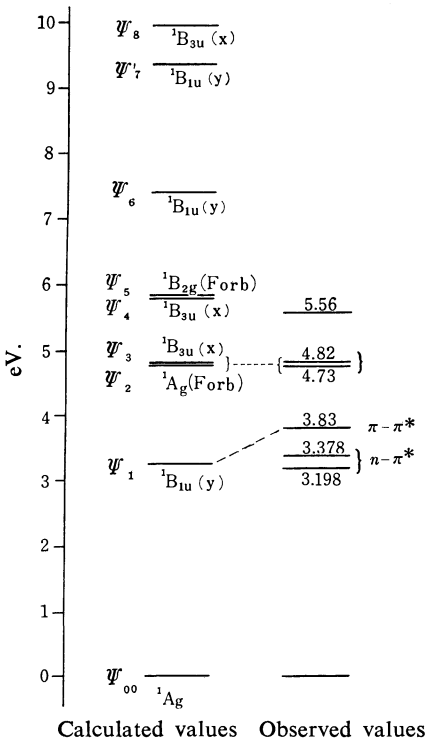


Fig. 6. The calculated energy levels and observed values in dioxane solution of pyrazine di-*N*-oxide.

of $\gamma_{7\mu}$ etc. were evaluated in the same way as that for the pyrazine nucleus. Next, the matrix elements of the interactions between each state of ^1L_b, ^1B_b, ^1L_a and ^1B_a and each state of the above charge transfer configurations were calculated. Therefore, we could obtain the energy levels of pyrazine di-*N*-oxide as solutions of secular equations belonging to the same symmetry, such as Eq. 13 etc. (Eq. 13 is for $^1B_{3u}$ (x)).

$$\begin{vmatrix} {}^1\chi_{8-5} & {}^1L_b & {}^1B_b \\ 4.8299-E & 0.5091 & -1.7131 \\ 0.5091 & 4.4817-E & 0 \\ -1.7131 & 0 & 8.2246-E \end{vmatrix} = 0 \quad (13)$$

The results obtained by the above treatment were shown in Table IV and Fig. 6, together with the experimental results.

The Electronic States of Isoquinoline *N*-Oxide and Acridine *N*-Oxide. — The following values of parameters for SMO can be shown to be suitable for interpreting various physicochemical properties of heterocyclic *N*-oxides[2]. Namely,

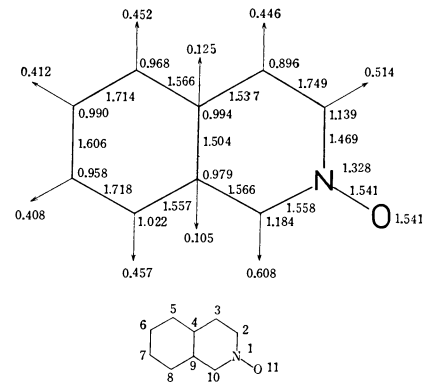


Fig. 7

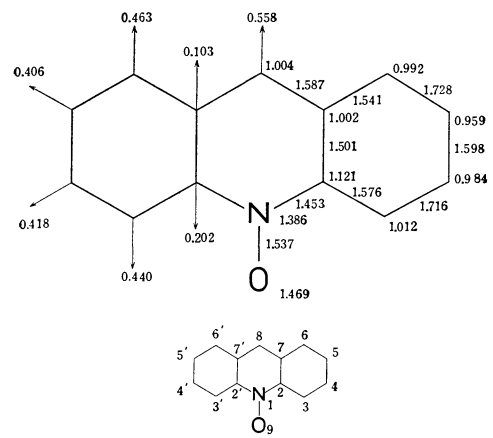
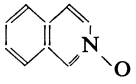
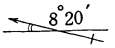
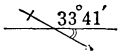
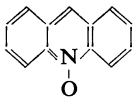
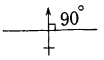
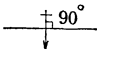


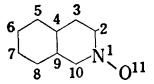
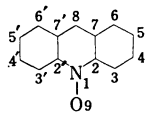
Fig. 8

TABLE IV. GROUND STATE AND EXCITED STATE WAVE FUNCTIONS AND EIGEN VALUES OF PYRAZINE DI-*N*-OXIDE (Energies are in unit of eV.)

$\Psi_{00}(^1A_g)=0.8915(\Psi_0)+0.4531(^1\chi_{7\to4})$	−0.9726
$\Psi_1(^1B_{1u}:y)=0.9502(^1\chi_{8\to4})+0.1145(^1L_a)-0.2899(^1B_a)$	2.2084
$\Psi_2(^1A_g)=0.4531(\Psi_0)-0.8915(^1\chi_{7\to4})$	3.7648
$\Psi_3(^1B_{3u}:x)=0.7747(^1\chi_{8\to5})-0.5671(^1L_b)+0.2969(^1B_b)$	3.7920
$\Psi_4(^1B_{3u}:x)=0.5088(^1\chi_{8\to5})+0.8225(^1L_b)+0.2543(^1B_b)$	4.7967
$\Psi_5(^1B_{2g})=1(^1\chi_{7\to5})$	4.8299
$\Psi_6(^1B_{1u}:y)=0.0872(^1\chi_{8\to4})-0.9906(^1L_a)-0.1053(^1B_a)$	6.4098
$\Psi_7(^1B_{1u}:y)=0.2993(^1\chi_{8\to4})-0.0748(^1L_a)+0.9512(^1B_a)$	8.3699
$\Psi_8(^1B_{3u}:x)=0.3884(^1\chi_{8\to5})+0.0443(^1L_b)-0.9204(^1B_b)$	8.9475

TABLE V. DIPOLE MOMENTS AND REACTIVITIES ESTIMATED FROM SMO CALCULATIONS

Substance	π-Moment (Debye unit)		Total moment (Debye unit)*		
	π/1.6	The angle between x-axis and π-moment	Calculated values	The angle between x-axis and total moment	Observed value
	0.76		4.33		—
	1.88		3.14		3.90[20]

Substance	Electrophilic reaction**	Nucleophilic reaction	Radical reaction
	10≫6≈8>2	10≈3>5≈8	10≫3>8
	8>6>4	8>6>4≈3	8>6>4

* Following Katritzky's analysis[30], total moments were calculated with vector addition between π-moment and observed value (5.02 D) of trimethylamine *N*-oxide.

** Recently, bromination and nitration of acridine *N*-oxide which were investigated by R. M. Acheson et al. gave 8-Br- and 8-NO_2- acridine *N*-oxides[20]. This fact agrees with present theoretical prediction.

k_N, k_O and inductive effects in Eqs. 7 and 8 were set equal to 1.6, 0.595 and $(1/3)^n \cdot k_N$ respectively. We also carried out the SMO calculations on isoquinoline *N*-oxide and acridine *N*-oxide, because the calculations using the above parameters were not carried out on these compounds in the previous paper[2]. Molecular diagrams and MO's obtained in this way are shown in Figs. 7 and 8 and in an appendix respectively, while the calculated dipole moments ($\vec{\mu}$) and active points for electrophylic, nucleophylic and radical reactions are shown in Table V. The π-moments ($\vec{\mu}_\pi$) obtained from the present calculations are considerably larger than those estimated from the observed value. Therefore, by Orgel et al.'s procedure[17], $\vec{\mu}_\pi$ was divided by 1.6.

The geometrical structure of the molecules used to calculated the dipole moments was the same as that described in the previous paper[2]. Namely, it was assumed that the shape of these molecules was a condensed regular hexagon the bond distance of which was 1.395 Å, and r_{NO} was taken to be equal to 1.27~1.28 Å. The prediction of reaction centers was based upon the frontier orbital method as used in previous papers[2,18].

The reaction centers of acridine *N*-oxide obtained from the above calculations are in approximate agreement with those of the

17) L. E. Orgel, T. L. Cottrell, W. Dick and L. E. Sutton, *Trans. Faraday Soc.*, **47**, 113 (1951).

18) K. Fukui, T. Yonezawa and H. Shingu, *J. Chem. Phys.*, **20**, 722 (1952); K. Fukui, T. Yonezawa, C. Nagata and H. Shingu, ibid., **22**, 1433 (1954).

previous calculation in which parameters for *N*-oxide molecules in polar solvents were employed instead of the present ones.

As for isoquinoline *N*-oxide, it is interesting that even if the reaction types are different from one another, the tenth position in Fig. 7 is always the most active position*10).

Moreover, some molecular constants (charge densities and bond orders) obtained by the present calculation on isoquinoline *N*-oxide, and also those of isoquinoline obtained by the use of parameters close to the present ones, are shown in Fig. 9 for the purpose of comparison[21].

As can be well understood from Fig. 9, electron migration from the oxygen atom to ring, which does not include the *N*-oxide group, is quite small. Therefore, it may be reasonable to consider the reactivity for such a ring as almost the same as that of isoquinoline.

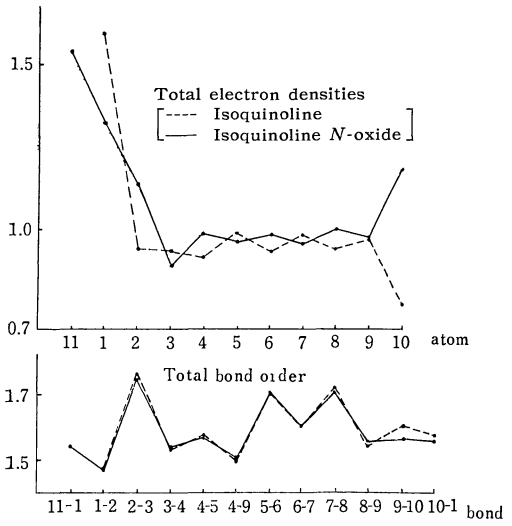


Fig. 9. The comparison of total electron densities and bond orders between isoquinoline *N*-oxide and isoquinoline ($k_N = 2$; $k_{C'} = 0.25$ on isoquinoline)[21].

Discussion

On the Absorption Bands of Pyrazine Mono-*N*-Oxide and 4-Methylpyrimidine *N*-Oxide. — According to our previous investigations[1,2] and those of the other authors[22,23], it is evident that the near ultraviolet absorption of pyridine *N*-oxide and related compounds exhibit three main absorption bands from both experimental and theoretical points of view. These bands are the $n\rightarrow\pi^*$ band (this is due to electron transitions from lone pair orbitals of oxygen to π^*-orbitals), the charge transfer (CT) band and the ^1L_b band (this corresponds to the $^1B_{2u}$ band of benzene). We can make an approximate interpretation of the electronic spectra of pyrazine mono*N*-oxide and 4-methylpyrimidine *N*-oxide based on the previous results of ASMO CI calculation for pyridine *N*-oxide[2] because the effects of the replacement of –CH= by –N= and the substitution for ring hydrogen of methyl on the electronic spectra are rather small and because the intrinsic natures of the absorption bands of the parent compound seem to be scarcely affected by such replacement and substitution*11.

As can be seen in Table I, Fig. 2 and Fig. 3, it would be moderately possible for the weak bands which pyrazine mono-*N*-oxide and 4-methylpyrimidine *N*-oxide show at 300 mμ and at 331 mμ respectively to be assigned to the $n\rightarrow\pi^*$ bands, because these weak bands having fine structures in non-polar solvents shift obviously toward a shorter wavelength with an increase of solvent polarity and can not be found in water or alcohol solutions.

According to Ito's rule[22], obtained from the comparison in oscillator strength (f) between the $n\rightarrow\pi^*$ and $\pi\rightarrow\pi^*$ bands of conjugated compounds, the value of $f(n\rightarrow\pi^*)/f(\pi\rightarrow\pi^*)$ should be about 0.05 and may not exceed $\sim$0.1*12.

*10 Whenever a nitration is tried for isoquinoline *N*-oxide in the usual manner, the nitro group is introduced into a benzene ring[19]. This fact does not agree with the above theoretical prediction. As has been reported in a previous paper as well as in the present paper[2], however, theoretical predictions on pyridine *N*-oxide, quinoline *N*-oxide and acridine *N*-oxide[20] agree with the experimental results. The discrepancy in the case of isoquinoline *N*-oxde may perhaps be due to the so-called ortho effect. Namely, the main reason of this discrepancy between experimental results and theoretical predictions may be attributed to steric effects and to various mutual interactions between *N*-oxide and the nitro groups, which are very polar bulky substituents and occupy the ortho position relative to each other.

19) a) E. Ochiai and Z. Sai, *J. Pharm. Soc. Japan Yakugaku Zasshi*, **65**, 418 (1945). b) E. Ochiai and N. Ikehara, ibid., **73**, 666 (1953). c) E. Ochiai and Y. Kawazoe, *Chem. Pharm. Bull.*, **8**, 24 (1960).

20) R. M. Acheson, B. Adcock, G. M. Glover and L. E. Sutton, *J. Chem. Soc.*, **1960**, 3367,

21) H. C. Longuet-Higgins and C. A. Coulson, *Trans. Faraday Soc.*, **43**, 87 (1947).

22) M. Ito and N. Hata, This Bulletin, **28**, 260 (1955).

23) M. Ito and W. Mizushima, *J. Chem. Phys.*, **23**, 495 (1956).

*11 Recent theoretical investigations on *N*-heterocyclic compounds indicate that the k_N of Eq. 7 is equal to about 0.5 and that the UV spectra of the free base of *N*-heterocyclic compounds can be interpreted on the basis of those of corresponding hydrocarbons[15,24,25].

24) N. Mataga, *Z. physik. Chem., N. F.*, **18**, 516 (1958).

25) H. Tubomura, *J. Chem. Soc. Japan, Pure Chem. Sec. (Nippon Kagaku Zasshi)*, **78**, 293 (1957).

*12 We have examined whether or not Ito's rule is valid for many other compounds. For example, the above ratios on pyridine, 2-pycoline, 3-pycoline, 4-pycoline, 3-fluoro-, 3-chloro- and 3-bromopyridine are 0.073, 0.040, 0.049, 0.072, 0.045, 0.032 and 0.023 respectively[26]. It seems that the rule is approximately applicable to the other compounds.

26) The experimental values of these compounds are cited from Stephenson's paper[9].

Testing the above rule for each band obtained from the band analysis, we can find that the rule is approximately valid for the compounds used here, as is shown in Table I.

The band I′ near 310 mμ in 4-methylpyrimidine *N*-oxide (Fig. 3) can also be found in a water solution and may perhaps be the ^1L_b band which could not be found experimentally in the cases of pyridine *N*-oxide and pyrazine mono-*N*-oxide. It may be considered that the band can be observed in this case because the band has shifted slightly from that of pyridine *N*-oxide owing to the lower symmetry of this compound. A band which may be assigned to the ^1L_b band has also been found on many other compounds, such as 4-aminopyridine *N*-oxide[6,27,28].

The high intensity bands which 4-methylpyrimidine *N*-oxide and pyrazine mono-*N*-oxide show near 278 mμ with $\varepsilon=10480$ and near 274 mμ with $\varepsilon=10980$ respectively can reasonably be assigned to the CT band as it was reported in a previous paper in the case of pyridine *N*-oxide[2].

Absorption Spectra of Pyrazine Di-*N*-oxide.—As shown in Table I, this compound has weak bands in the longest wavelength region. The behavior of these bands is similar to that of the corresponding bands of pyrazine mono-*N*-oxide and 4-methylpyrimidine *N*-oxide, and the bands can conceivably be ascribed to the $n\rightarrow\pi^*$ transition. As can be seen from Fig. 2, they are apparently two $n\rightarrow\pi^*$ bands. We can explain the above two weak bands from two different points of view, but it is difficult to determine which point of view is valid. The one is to ascribe the apparent two weak bands to vibrational structures. The other is as follows. In the case of pyrazine di-*N*-oxide, two group orbitals, whose wave functions are similar to Eqs. 10 and 11, can be obtained from the lone pair orbitals belonging to the O_7 and O_8 atoms as shown in Fig. 4. Consequently, two bands may be expected, owing to the electron transitions from the above two lone pair orbitals to the π^* orbital of the pyrazine nucleus, just as in the case of two $n\rightarrow\pi^*$ bands found on pyrazine[23].

The high intensity $\pi\rightarrow\pi^*$ band near 323.6 mμ of pyrazine di-*N*-oxide can reasonably be assigned to the CT band, the excited state wave function of which has a great contribution from $^1\chi_{8\rightarrow4}$ configuration in view of the results of the calculation described in the Theoretical section, and the direction of the transition moment of this band is expected to be parallel to the y-axis. In the case of these *N*-oxide compounds, however, it may be considered that the character of absorption bands was emphasized by using the method of the composite system adopted here, and that the degree of charge transfer from the oxygen atoms to the ring is smaller than that expected from the present calculation[29]. The calculated energy levels of pyrazine di-*N*-oxide do not give such a nice agreement with the experimental results as in the case of pyridine *N*-oxide. The main reason for this discrepancy may be ascribed to the fact that the various energy integrals are assumed to be the same as those of pyridine *N*-oxide.

The weak band near 260 mμ in Fig. 1 may probably be due to the transition from the ground state to the $^1A_{1g}$ (Ψ_2: forbidden) state or the $^1B_{3u}$ (Ψ_3: x) state in view of the calculated results, as indicated in Table IV. However, it can not be concluded which assignment is more plausible. It is probable that the ^1A_g (Ψ_2) band appears near 260 mμ with a low intensity due to the vibrational interactions.

Moreover, the stabilization energy (0.973 eV.) for the ground state of pyrazine di-*N*-oxide is about twice as large as that (0.437 eV.) of pyridine *N*-oxide[2]. From this fact, it is probable that the electronic structure for the ground state of pyrazine di-*N*-oxide may be represented by a resonance hybrid in which each of two oxygen atoms makes resonance with the pyrazine residue almost independently.

On the Parameter of Oxygen Atoms of Heterocyclic *N*-Oxides.—It has been pointed in a previous paper[2] and in a previous section of this paper that the π-electron densities obtained from the SMO calculation using $\alpha_0=\alpha+0.595\beta$ were an over-estimation of the electron migration from the oxygen atom to the heterocyclic nucleus. For example, about the same values as observed dipole moments were obtained by dividing the π-moments obtained from the above calculation by 1.6. These results are ascribed to the use of a small k_O value in Eq. 8. On the other hand $k_O\approx1$ was derived from the ASMO CI calculation for the ultraviolet spectra of pyridine *N*-oxide. However, the dipole moment calculated by the SMO method using $k_O\approx1$ is somewhat smaller compared to the observed one. To estimate a reasonable k_O value, pyridine *N*-oxide has been selected as a model compound, and SMO calculations have been undertaken under various sets of k_O values. The values of dipole moments obtained by the same treatment as that described in the previous paper[2] are shown by curve 1 in Fig.

27) T. Kato, F. Hamaguchi and T. Oiwa, *Ann. Rept. Tokyo Coll. Pharm.*, **27** (1956).
28) N. Hata, This Bulletin, **29**, 82 (1956).
29) T. Kubota and M. Yamakawa, ibid., **35**, 555 (1962).

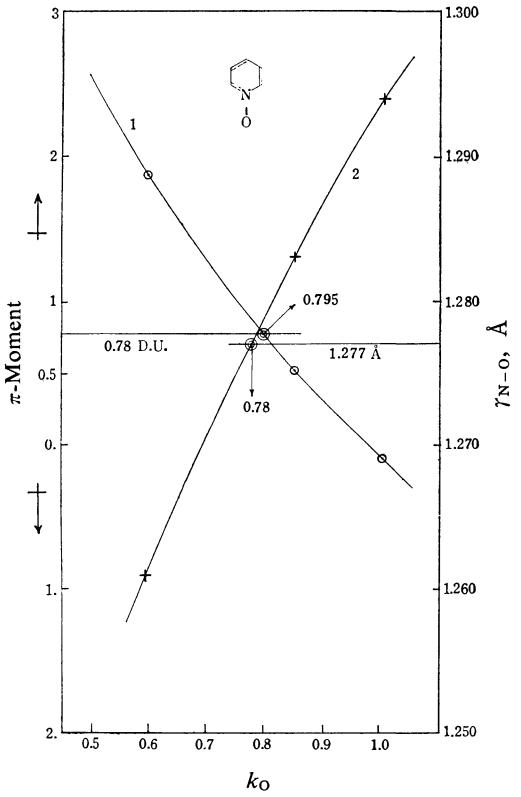


Fig. 10

10*[13]. The value (0.78 Debye unit) of the π-moment estimated from the analysis of the observed total moment was taken from Katritzky's paper[30]. As shown in Fig. 10, $k_O \approx 0.8$ is the best value, and a nice agreement with the observed dipole moment was obtained with this value of k_O. Moreover, as shown by curve 2 in Fig. 10, the N–O distance (this is calculated by the same method as in footnote 13) obtained from the SMO calculation using $k_O \approx 0.8$ is nearly equal to the value (1.277 Å) obtained from an empirical relation between the N–O stretching frequency and the N–O bond length; this fact means that $k_O \approx 0.8$ is reasonable.

13* The bond order of N-O changes somewhat according to the selection of the k_O value. Therefore, the N-O distance may also change to some extent. However, whether or not the change in bond distance estimated from the order-length relation for the N-O bond described in the previous paper[2] is taken into account, the calculated results of dipole moment are almost the same.

30) C. M. Bax, A. R. Katritzky and L. E. Sutton, *J. Chem. Soc.*, **1958**, 1258.

Summary

The ultraviolet absorption spectra of pyrazine mono-*N*-oxide, 4-methylpyrimidine *N*-oxide and pyrazine di-*N*-oxide have been measured under various conditions, and band analyses of those spectra have been carried out. In order to interpret the spectra and other physicochemical properties of pyrazine di-*N*-oxide, semi-empirical LCAO MO calculations including the treaments of configuration interactions, have been undertaken in a manner similar to previous calculations on pyridine *N*-oxide. On the other hand, the spectra of pyrazine mono-*N*-oxide and 4-methylpyrimidine *N*-oxide have been interpreted on the basis of the calculated results on pyridine *N*-oxide described in a previous paper. The high intensity bands (278, 274 and 323.6 mμ for 4-methylpyrimidine *N*-oxide, pyrazine mono- and di-*N*-oxides respectively) can reasonably be assigned to charge transfer bands such as the 282 mμ band of pyridine *N*-oxide.

The above substances also exhibit weak bands in the longest wavelength region in non-polar solvents. These weak bands may possibly be due to the $n \rightarrow \pi^*$ transitions. SMO calculations on isoquinoline *N*-oxide and acridine *N*-oxide have also been carried out with the same parameters as those in the case of pyridine *N*-oxide in non-polar solvents, and various physicochemical properties have been discussed on the basis of these calculations. As has been pointed out in a previous paper, the parameter for the oxygen atom used here is too small. To estimate the most reasonable value, SMO calculations were carried out many times on pyridine *N*-oxide, which was used as a model compound. As a result, it was found that k_O (in Eq. 8) ≈ 0.8 is the best value.

The author wishes to express his deep gratitude to Professor Saburo Nagakura of the Institute for Solid State Physics, The University of Tokyo, for valuable discussions and for reading the manuscript; to Dr. Kenichi Takeda, Director of this Research Laboratory, Dr. Noboru Mataga of Osaka Municipal University and Dr. Mituo Itō of Kyushu University for valuable discussions; to Mr. Masumi Yamakawa of this Research Laboratory for his cooperation in the SMO calculation of isoquinoline *N*-oxide, and to Dr. Hiroshi Yamanaka of Tohoku University for supplying a sample of 4-methylpyrimidine *N*-oxide.

Research Laboratory
Shionogi & Co., Ltd.
Fukushima-ku, Osaka

Appendix

SIMPLE MOLECULAR ORBITALS OF ISOQUINOLINE *N*-OXIDE ($k_N=1.6$; $k_O=0.595$; Ind.$=(1/3)^n\cdot k_N$)

ϕ_i	Eigen value ε_i	C_{i1}	C_{i2}	C_{i3}	C_{i4}	C_{i5}	C_{i6}	C_{i7}	C_{i8}	C_{i9}	C_{i10}	C_{i11}
		+	+	+	+	+	+	+	+	+	+	+
ϕ_1	3.03113	0.72279	0.36183	0.18099	0.15460	0.06238	0.03371	0.03967	0.08605	0.21607	0.37587	0.29669
		+	+	−	−	−	−	−	−	−	−	+
ϕ_2	2.18861	0.30840	0.06799	0.19587	0.46184	0.34676	0.29280	0.29286	0.34455	0.44080	0.07998	0.19353
		+	−	−	−	−	+	+	+	+	+	+
ϕ_3	1.55933	0.09375	0.44456	0.54986	0.31511	0.18154	0.03426	0·23483	0.32902	0.25872	0.34353	0.09721
		+	+	−	−	+	+	+	+	−	−	+
ϕ_4	1.32388	0.15812	0.05882	0.11162	0.18675	0.28609	0.56197	0.45558	0.03554	0.41064	0.31942	0.21694
		+	−	−	+	+	+	−	−	−	+	+
ϕ_5	0.88856	0.07049	0.44659	0.22913	0.28373	0.47937	0.13630	0.35882	0.45071	0.01495	0.15634	0.24010
		−	−	+	+	−	−	−	+	+	−	+
ϕ_6	0.47457	0.08776	0.18298	0.09851	0.21221	0.12440	0.26971	0.00249	0.26856	0.11402	0.44694	0.72868
		−	−	+	−	−	+	+	−	−	+	+
ϕ_7	−0.37522	0.31905	0.16383	0.46789	0.09492	0.32307	0.22013	0.23957	0.31298	0.10359	0.46518	0.32884

$\varepsilon_8=-0.67$ $\varepsilon_9=-1.135$ $\varepsilon_{10}=-1.37$ $\varepsilon_{11}=-2.15$

SIMPLE MOLECULAR ORBITALS OF ACRIDINE *N*-OXIDE ($k_N=1.6$; $k_O=0.595$; Ind.$=(1/3)^n\cdot k_N$)

ϕ_i	Eigen value ε_i	Sym-metry	C_{i1}	C_{i2}	C_{i3}	C_{i4}	C_{i5}	C_{i6}	C_{i7}	C_{i8}	C_{i9}
			+	+	+	+	+	+	+	+	+
ϕ_1	3.15620	b_2	0.67255	0.39201	0.15321	0.06432	0.04597	0.08021	0.20244	0.13074	0.26259
				+	+	+	+	+	+		
ϕ_2	2.19741	a_2	0	0.36769	0.30593	0.25018	0.22899	0.25018	0.30593	0	0
			+	−	−	−	−	−	−	−	+
ϕ_3	2.07512	b_2	0.41223	0.04133	0.10756	0.16275	0.22053	0.29214	0.36839	0.36549	0.27851
			+	−	−	−	−	+	+	+	+
ϕ_4	1.50721	b_2	0.02851	0.01695	0.32246	0.41173	0.27371	0.00257	0.27743	0.38321	0.03126
				+	+	−	−	−	+		
ϕ_5	1.20982	a_2	0	0.39174	0.13250	0.25499	0.42589	0.25499	0.13250	0	0
					+	+		−	−		
ϕ_6	1.12027	a_2	0	0	0.36386	0.34294	0	0.34294	0.36386	0	0
			+	−	−	+	+	+	−	−	+
ϕ_7	1.02660	b_2	0.19434	0.28085	0.30762	0.01974	0.32671	0.31163	0.02526	0.05222	0.45027
			−	−	+	+	−	−	+	+	+
ϕ_8	0.30475	b_2	0.17995	0.19344	0.16901	0.21490	0.11626	0.24890	0.05515	0.44934	0.61997
			−	+	+	−	−	+	+	−	+
ϕ_9	−0.25300	b_2	0.39519	0.13313	0.22312	0.22925	0.15153	0.26946	0.06739	0.43162	0.46603

$C_{i2}=\pm C_{i2'}$; $C_{i3}=\pm C_{i3'}$; $C_{i4}=\pm C_{i4'}$; $C_{i5}=\pm C_{i5'}$; $C_{i6}=\pm C_{i6'}$; $C_{i7}=\pm C_{i7'}$ (+ and − represent b_2 and a_2 orbitals respectively). $\varepsilon_{10}=-0.77215(a_2)$; $\varepsilon_{11}=-0.88324(a_2)$; $\varepsilon_{12}=-1.07(b_2)$. ε_{13}, ε_{14} and ε_{15} were not calculated.

Neutron Irradiation of Acetoxime and Acetaldoxime

By Enzo TACHIKAWA and Gen-ichi TSUCHIHASHI

(Received September 12, 1961)

Previously, the present authors irradiated propionamide[1] with thermal neutrons and found that the yields of methylation products from propionamide, ^{14}C-isobutyramide and ^{14}C-butyramide were proportional to the number of hydrogen atoms which are available for substitution. These results served to indicate that "synthesis"[2] products were mainly formed by the methylation reaction.

In order to understand the mechanism more completely, however, further studies were required. The present authors carried out the neutron irradiation of acetoxime and acetaldoxime and so separated a few "synthesis" products and "re-entry"[2] products.

Particular attention was paid to the relationship between the yields of these products. The Beckmann rearrangement product of acetoxime was also examined. Carbon-14 distributions in the product molecules from acetoxime were determined by a stepwise degradation method.

On the basis of these results, the relationship between "re-entry" and "synthesis" reactions is discussed.

Experimental

Materials. — Acetoxime was synthesized from hydroxylamine hydrochloride and acetone[3]. Acetaldoxime, ethylmethylketoxime and propionaldoxime were synthesized by a method analogous to that for acetoxime. *N*-Methylacetamide was obtained from acetic anhydride and methylamine hydrochloride. These compounds were purfied in a Podbielniak high-temperature distillation apparatus (with a 60-plates heli-grid packing column).

Neutron Irradiation. — About 15 g. of acetoxime was sealed in a polyethylene tube, which was then packed in a polyethylene capsule. Also, 15 g. of pure acetaldoxime was sealed in a quartz tube under a pressure of 10^{-4} mmHg, and then the ampoule was packed in an aluminum capsule. These assemblies were irradiated for 120 hr. in the No. 13 experimental hole of the J. R. R.-1, with an approximate flux of 10^{11} n./cm^2·sec. Samples were cooled for about two weeks after irradiation in order to eliminate short-living activities stemming from impurities in the polyethylene capsule or the aluminum capsule.

Processing of Irradiated Acetoxime.—In order to determine the reaction products, the isotope-dilution method was used. After the irradiated sample was divided into four portions, each portion was distilled in order to remove polymeric substances produced. Before beginning the distillation, known amounts of corresponding carriers were first added to the distillation vessel separately. Gas liquid partition chromatography was employed for the final purification of the desired compounds.

For chromatography, a 6 ft. column, 1/2 inch i. d., packed with 30~80 mesh fire brick coated with polyethylene glycol-600, was used. The column was operated at 100°C, and the flow rate of helium carrier gas was kept about 150 ml./min.

Degradation of ^{14}C-Acetoxime.—After 3 g. of the irradiated sample had been distilled in the usual way, the portion of acetoxime was purified by gas chromatography. ^{14}C-acetoxime purified was divided into two portions. By the usual iodoform reaction[4], one portion of ^{14}C-acetoxime was converted to iodoform, which was then recrystallized until it showed a constant specific activity. The remaining ^{14}C-acetoxime was converted into *N*-methylacetamide by the Beckmann rearrangement and was then hydrolyzed to acetic acid. The acetic acid was treated with benzoyl chloride and ammonia, and the resulting acetamide was recrystallized from methanol-ether.

Degradation of ^{14}C-Ethyl Methyl Ketoxime.—After 4 g. of ethyl methyl ketoxime had been added to 3.99 g. of the irradiated sample as a carrier, the mixture was distilled and the ^{14}C-ethyl methyl ketoxime collected was purified further by gas chromatography. Purified ^{14}C-ethyl methyl ketoxime was also divided into two portions. The first portion was hydrolyzed to ethyl methyl ketone, which was then converted to iodoform by the iodoform reaction. The rest of the ^{14}C-ethyl methyl ketoxime was converted to propionic acid by the bromoform reaction[5]. The propionic acid thus obtained was decarboxylated to ethylamine by Schmidt's method in order to locate the distribution of carbon-14 according to the suggestions of Phares[6]. The ethylamine produced was converted to acetic acid by the method of Phares and was further degraded to methylamine. The methylamine produced was oxidized to carbon dioxide by the same method.

Degradation of ^{14}C-*N*-Methylacetamide. — *N*-Methylacetamide (3.02 g.) was added to the

1) E. Tachikawa and G. Tsuchihashi, This Bulletin, **34**, 770 (1961).
2) A. P. Wolf, *Angew. Chem.*, **71**, 237 (1959).
3) N. D. Cherronis, "Technique of Organic Chemistry, Vol. VI. Micro and Semimicro Method", Interscience Publishers, Inc., New York (1954), p.337.
4) N. D. Cherronis, "Technique of Organic Chemistry, Vol. VI. Micro and Semimicro Method", Interscience Publishers, Inc., New York (1954), p. 284.
5) "Organic Syntheses", Coll. Vol. I (1948), p. 526.
6) E. F. Phares, *Arch. Biochem. Biophys.*, **33**, 173 (1951).

irradiated sample (3.00 g.) as a carrier. The ^{14}C-*N*-methylacetamide separated from the mixture by the same procedure was hydrolyzed by refluxing it for two hours with potassium hydroxide. The acetic acid obtained was fractionated by gas-liquid chromatography, using 50% D. C. 710 silicone plus 10% stearic acid as the liquid phase. The methylamine was oxidized to carbon dioxide.

Processing of Irradiated Acetaldoxime. — The irradiated sample was distilled in order to remove polymeric substances after the sample had been divided into several portions. The acetoxime and propionaldoxime formed by the neutron irradiation of acetaldoxime were identified separately by gas chromatography after suitable amounts of acetoxime or propionaldoxime had been added as a carrier. The separated oximes were further purified by gas chromatography until they showed constant specific activity.

Measurement of Activity. — The purified compounds were converted to carbon dioxide by the Van Slyke-Folch method[7]. The resulting carbon dioxide was converted to barium carbonate by the same method as in the previous paper[1]. About 150 mg. of the barium carbonate suspended in ethyl alcohol was poured into a particular type of counting dishes (0.8 cm.ϕ). Using an infrared lamp, ethyl alcohol was evaporated and barium carbonate was dried up. This barium carbonate was mounted in the dishes in infinite thickness. The specific activity of barium carbonate was measured with an Aloka low-back ground counter (model: BD-1). Barium carbonate of 22.4 d.p.s./mg. was used as a standard sample. These measurements are reproducible to about 3% for samples of the same material and to about 3~4% samples of different compound containing the same labelled group. The absolute accuracy of the assays is probably good to about 7%.

Results and Discussion

The Distribution of Carbon-14 in Neutron Irradiation Products. — As is well known, an ^{14}N(n, p)^{14}C reaction occurs on the nitrogen atom of oxime during neutron irradiation. Because ^{14}C recoil atoms have high energy, they are supposed to undergo various reactions. Among them, "re-entry" and "synthesis" products have been considered in the present study, together with the Beckmann rearrangement product. In the neutron irradiation of acetoxime, the ^{14}C-acetoxime, ^{14}C-ethyl methyl ketoxime and ^{14}C-*N*-methylacetamide produced are here called "re-entry", "synthesis" and rearrangement products respectively. Table I shows the distribution of carbon-14 in each compound.

Analogously, neutron irradiation of acetaldoxime will bring about reactions similar to those for acetoxime. In this reaction, ^{14}C-acetaldoxime is a "re-entry" product. Both ^{14}C-acetoxime and ^{14}C-propionaldoxime are referred to as "synthesis" products.

The comparative yields of these compounds are shown in Table II. Table II shows that the ratio of the yields of ^{14}C-acetoxime and ^{14}C-propionaldoxime is about 1 : 3, which agrees with the ratio of the number of hydrogen atoms available for the substitution in acetaldoxime to give acetoxime or propionaldoxime. This result is in accord with that for the neutron irradiation of propionamide[1].

Carbon-14 Distribution on Molecules. — Recently, many researchers have carried out stepwise degradations of "synthesis" and "re-entry" products[8]. These results have shown that the differences betwen theoretical and experimental values for the distribution of carbon-14 are not so large in "re-entry" products, while the differences become remarkable in "synthesis" product. Especially in the latter case, one finds a considerable number of carbon-14 atoms at positions where carbon-14 could not be found theoretically. In the present study, degradations of ^{14}C-acetoxime,

TABLE I. YIELDS OF RADIOACTIVE SPECIES FROM THE NEUTRON IRRADIATION OF ACETOXIME

Product	Total activity, assay of compd. $\times 10^{-1}$ μc./mol.	Activity relative to total activity in irradiated crude sample, %	Relative ratio
Acetoxime	4.4	2.1	1.0
Ethyl methyl ketoxime	9.9	3.9	1.9
N-Methylacetamide	2.9	1.3	—

TABLE II. YIELDS OF RADIOACTIVE SPECIES FROM THE NEUTRON IRRADIATION OF ACETALDOXIME

Product	Total activity, assay of compd. $\times 10^{-1}$ μc./mol.	Activity relative to total activity in irradiated crude sample, %	Relative ratio
Acetaldoxime	3.0	3.0	1.0
Acetoxime	1.7	1.3	0.4
Propionaldoxime	4.6	3.6	1.2

7) D. D. Van Slyke and H. Folch, *J. Biol. Chem.*, **139**, 509 (1940).

8) R. C. Extermann, "Radioisotopes in Scientific Research", Vol. 2, Pergamon Press, London (1958), p. 114.

Table III. Carbon-14 distribution in "re-entry" product from the neutron irradiation of acetoxime

	Product		
	CH_3	C(NOH)	CH_3
Theoretical	33	33	33
Found	36	28	36

Table IV. Carbon-14 distribution in "synthesis" product from the neutron irradiation of acetoxime

	Product			
	4 CH_3	3 CH_2	2 C(NOH)	1 CH_3
Theoretical	100	0	0	0
Found	69	9	9	13

^{14}C-ethyl methyl ketoxime and ^{14}C-*N*-methylacetamide were carried out in order to discover the distributions of carbon-14 atoms in these molecules. Degradation of ^{14}C-acetoxime showed that 72% of the carbon-14 activity was present in methyl groups. Similar studies on the ^{14}C-ethyl methyl ketoxime showed that 70% of the activity was in the 4-position. Tables III and IV illustrate the observed values together with the theoretical values.

The results in Table III seem to indicate that ^{14}C-acetoxime has resulted from a "knock on" reaction between carbon-14 and carbon-12 in acetoxime. The methyl group is tagged with about 8 per cent more carbon-14 than the central carbon atom. This is perhaps caused by the steric effects of neighboring CH_3 groups that hinder the attack of carbon-14 on the central carbon atom.

As Table IV shows, the 1-, 2- and 3-positions in ethyl methyl ketoxime are all labelled with carbon-14. This result coincides well with those of others[8]. In this compound, the amount of compound, the amount of carbon-14 in the 1-position exceeds that in the 2- or 3-position. This is also caused by the steric effects similar to that in the case of acetoxime.

When an organic molecule reacts with a carbon-14 hot atom, the kinetic energy given to the organic molecule is so high that isomerizations or some other reactions could easily take place. The distribution of carbon-14 in *N*-methylacetamide, the Beckmann rearrangement product of acetoxime, is shown in Table V.

Table V. Carbon-14 distribution in ^{14}C-*N*-methylacetamide produced from the neutron irradiation of acetoxime

	Product		
	CH_3	CONH	CH_3
Theoretical	33	33	33
Found	50		50

From Table V, one finds a higher C-14 distribution in the migrating methyl group than in the other positions. Possibly the mechanism for the formation of ^{14}C-*N*-methylacetamide differs from that of the acid-catalyzed Beckmann rearrangement. In this case, the rearrangement probably takes place for the following reason. When a methyl group in acetoxime is labelled with carbon-14, a high kinetic energy is given to it. An excited acetoxime isomerizes rather easily into *N*-methylacetamide by the migration of the labelled methyl group before the kinetic energy in this methyl group completely diffuses over the molecule.

The Relation between the Yields of "Re-entry" and "Synthesis" Products.—Acetoxime contains three carbon atoms, each of which could be tagged with carbon-14, forming ^{14}C-acetoxime. Also, it contains six hydrogen atoms which are available for methylation, resulting in ^{14}C-ethyl methyl ketoxime. Also, acetaldoxime contains two carbon atoms, three hydrogen atoms attached to carbon atom 2, and one hydrogen atom attached to carbon atom 1, all of which are available for giving ^{14}C-acetaldoxime, ^{14}C-propionaldoxime and ^{14}C-acetoxime respectively. Similarly, propionamide has three carbon atoms, two hydrogen atoms attached to carbon atom 2, and three hydrogen atoms attached to carbon atom 3.

These carbon or hydrogen atoms are capable of being used for the formation of "re-entry" or "synthesis" product. The preceeding paper[1] gave the results of the neutron irradiation of propionamide, results shown in Table VI.

The above results seem to show that some relationship exists between the yields of "re-entry" or "synthesis" products and the number of carbon or hydrogen atoms in the mother compounds. Table VII shows the number of atoms which are available for the formation of "re-entry" or "synthesis" products, together with the ratio of the yields of "synthesis" products to that of "re-entry" products.

Previously, Wolf et al.[9] examined the neutron irradiation of benzene, toluene, aniline, pentane, methanol, acetamide and alanine. Except for pentane and methanol, similar results were observed. In pentane and methanol, hydrogen replacement was found to be favored twofold over carbon replacement.

In Fig. 1, the relative values of activity found in "synthesis" product, divided by that in "re-entry" products, are plotted as a function of the ratio of the number of hydrogen atoms which are available to form "synthesis"

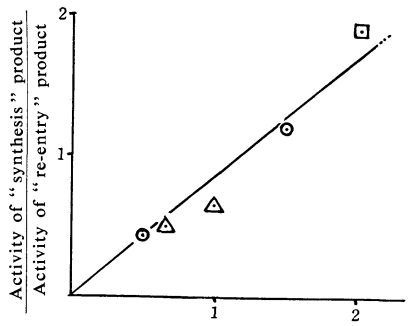
9) A. P. Wolf, BNL, 4891 (1960).

TABLE VI. RESULTS OF NEUTRON IRRADIATION OF PROPIONAMIDE

Product	Total activity, assay of compd. $\times 10^{-1}$ μc./mol.	Activity relative to total activity in irradiated crude sample, %	Relative ratio
Propionamide	6.6	3.3	1.0
Isobutyramide	4.1	1.7	0.5
Butyramide	5.2	2.1	0.6

TABLE VII. FROM THE NEUTRON IRRADIATION ACETOXIME (CH_3-C(=NOH)-CH_3)

Product	No. of atoms available for the substitution	Yield of "synthesis" or "re-entry" products
Acetoxime	3 carbon	—
Ethylmethylketoxime	6 hydrogen	1.88
From the neutron irradiation of acetaldoxime (CH_3-CHNOH)		
Acetaldoxime	2 carbon	—
Acetoxime	1 hydrogen	0.43
Propionaldoxime	3 hydrogen	1.20
From the neutron irradiation propionamide (CH_3-CH_2-$CONH_2$)		
Propionamide	3 carbon	—
Isobutyramide	2 hydrogen	0.50
Butyramide	3 hydrogen	0.64

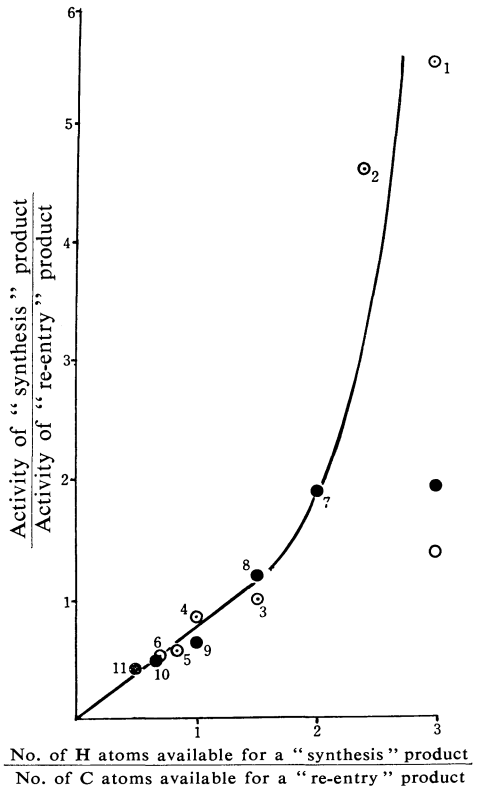


⊡ : From neutron irradiation of acetoxime
⊙ : From neutron irradiation of acetaldoxime
△ : From neutron irradiation of propionamide

Fig. 1.

products to the number of carbon atoms available for the formation of "re-entry" products. This figure is based on the present authors' results, together with results obtained by Wolf et al.

This figure shows that a linearity exists over nearly the range from zero to two of the horizontal values; beyond this range the yields of "synthesis" products increase rapidly.



⊙ Results obtained by Wolf et al.
1 : Ethanol/methanol
2 : *n*-Hexane+2Me-pentane+3Me-pentane/pentane
3 : Propionamide/acetamide
4 : Toluene/benzene
5 : Toluidines/aniline
6 : Xylenes/toluene
● Our results
7 : Ethyl methyl ketoxime/acetoxime
8 : Propionaldoxime/acetaldoxime
9 : Butyramide/propionamide
10 : Isobutyramide/propionamide
11 : Acetoxime/acetaldoxime

Fig. 2.

In the range where the ratios of the number of hydrogen atoms to that of carbon atoms are less than two, it seems that the amount of "synthesis" and of "re-entry" products are proportional to the number of hydrogen and carbon atoms available for the product formation.

Since in the present results, nearly 70% of the activity in the "synthesis" product exists in the methyl group attached to the mother skeleton, the major reaction undoubtedly being the methylation.

The distribution of the activity in ^{14}C-acetoxime is nearly uniform, and the yields of "re-entry" products are proportional to the carbon atoms. These results seem to suggest that the "knock on" and methylation reactions are the main paths for the formation of "re-entry" and "synthesis" products respectively when the two reactions occur simultaneously in a constant ratio as shown in Fig. 1. However, as the ratio of hydrogen to carbon atoms increases, the methylation reaction gradually predominates, as in pentane and methanol.

Summary

The neutron irradiation of acetoxime and acetaldoxime was studied. Degradation of the products obtained from the neutron irradiation of acetoxime shows that the distribution of carbon-14 activity deviates a little from the statistical behavior on account of steric and other effects.

However, the yields of "synthesis" product are found to be proportional to the number of hydrogen atoms available for their formation. Also there seems to be a linear relationship between the yields of "re-entry" or "synthesis" products and the number of atoms available for formation. The present results suggest that the main process forming the "synthesis" products is simple methylation by ^{14}C-methyl or ^{14}C-methylene radicals, while that giving the "re-entry" products is a "knock on" reaction of carbon-12 by carbon-14.

The authors wish to express their thanks to Professor K. Kimura, Dr. A. Danno and Dr. T. Ishimori for their kind encouragement and helpful discussions throughout the present work.

Division of Radiation Applications
Japan Atomic Energy Research Institute
Tokai, Ibaraki-ken

Determination of Small Amounts of Copper and Iron with X-Ray Fluorescent Spectroscopy. Combination with Organometallic Precipitation

By Kichinosuke HIROKAWA and Hidehiro GOTÔ

(Received September 28, 1961)

The determination by X-ray fluorescent spectroscopy[1] of small amounts of copper and iron in metals without separation is difficult. Therefore, the application of organometallic precipitation to X-ray fluorescent spectroscopy has been investigated. In previous determinations of small amounts of metals by X-ray fluorescent spectroscopy, the element to be analyzed has been concentrated on filter paper or on Mylar film or metal foils[2]. The organic precipitate of metals without carriers[3], however, has not been used as a sample for X-ray spectroscopy.

On the other hand, it has been recognized that alizarin blue reacts with copper and iron[4] in acidic solutions. Investigation was therefore carried out, first, to find the optimum conditions for the reaction of alizarin blue with copper and iron and then X-ray fluorescent spectroscopy, combined with this organic precipitation separation, was applied to the determination of small amounts of copper and iron.

1) K. Hirokawa, *J. Japan Inst. Metal (Nippon Kinzoku Gakkaishi)*, **24**, 555 (1960).
2) H. G. Pfiffer, *Nature*, **174**, 397 (1954); R. C. Hirt *Anal. Chem.*, **28**, 1649 (1956); J. F. Fagel, ibid., **29**, 1287 (1957).
3) J. E. Fagel et al., ibid., **29**, 1287 (1957).
4) K. Hirokawa, *J. Japan Inst. Metal (Nippon Kinzoku Gakkaishi)*, **23**, 698 (1959); F. Feigl et al., *Anal. Chim. Acta*, **8**, 339 (1953).

Experimental and Results

Reagents.—*Alizarin Blue Solution.*—Alizarin blue-saturated solution in tetrahydrofran was used.

Standard Solution of Copper.—Copper (0.4~0.5 g.) was dissolved with nitric acid, and a solution containing 5~100 μg. of copper was prepared by dilution with water when needed. A standard solution of iron was also prepared, as well as a copper standard solution. The nitric acid, hydrochloric acid and sulfuric acid used were all analytical grade reagents. A 0.2 M EDTA solution, a 0.1 M glycine solution and a 20% potassium thiocyanate solution were also used in the experiment.

Instruments. — G. E. XRD-5 X-ray spectrometer with AEG50-S tungsten tube, lithium fluoride analyzer, 0.025 cm. solar slit, and 2 SPG detector, was used. The X-ray irradiation area was controlled by the aluminum plate with a round window 1.5 cm. in diameter. A Hitachi spectrophotometer, model EPU-2, with 1 cm. cells was also used.

Condition of Precipitation. — The formation of alizarin blue precipitate with copper or iron in an acid solution has been already reported[4]. In order to determine the optimum conditions for the precipitation, the following experiments were carried out.

From the copper standard solution, 40.4 μg. of copper was placed in a beaker. The acidity of this solution was controlled with hydrochloric acid and ahydr ochloric acid-glycine buffer solution, and the total volume was made up to about 50 ml. After 10 ml. of the alizarin blue solution* had been added, the rest was left to stand for a few minutes; the precipitates formed were then filtered and washed with water a few times. The precipitate and filter paper were together transferred back into the original beaker, and the precipitate was completely decomposed by heating with 5 ml. of sulfuric acid and 10 ml. of nitric acid. After the fuming of the sulfuric acid, the deposited salt was dissolved with 20 ml. of nitric acid (1+2) and cooled. This solution was diluted with water to 100 ml., one-fifth of this solution was taken into a separatory funnel; then the amount of copper in it was determined by the diethyl dithiocarbamate method. From these results, the relation between the pH of the solution and the content of copper in the precipitate was determined, as shown in Fig. 1; it was discovered

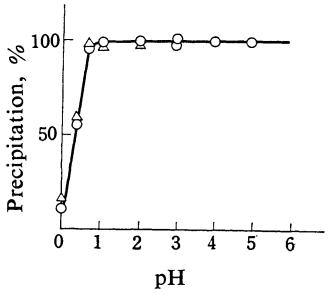


Fig. 1. The precipitation of Cu at various pH.
—○— KSCN not present
—△— KSCN present

that the copper was completely precipitated above a pH of 0.7. Next, the same attempt was carried out for the precipitation at a more acidic range in the presence of 2 ml. of 0.2% potassium thiocyanate, but the presence of potassium thiocyanate did not affect the precipitation. Similarly, 282 μg. of iron was treated with the same procedure as has been previously described. The precipitation of iron with alizarin blue was decomposed, and the amount of

* Five milliliters of the alizarin blue solution was enough to from the precipitate with about 400 μg. of copper; 10 ml. of the alizarin blue solution was used throughout the experiments.

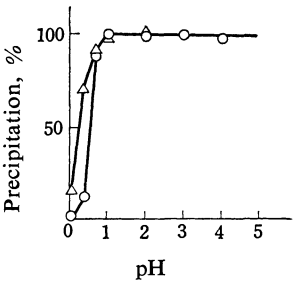


Fig. 2. The precipitation of Fe at various pH.
—○— KSCN not present
—△— KSCN present

iron was determined by the spectrophotometric method using potassium thiocyanate. The relation between precipitation and pH is shown in Fig. 2. In this case, the presence of potassium thiocyatate had no effect on the precipitation of iron. From these results, it was recognized that copper and iron was completely precipitated with alizarin blue at pH values above 1.0.

Precipitation of Calibration Curves of Copper and Iron, and their Interaction.—As has been reported in the previous paragraph, copper and iron were completely precipitated with alizarin blue at pH values above 1; calibration curves for the X-ray spectroscopy of copper and iron can, therefore, be prepared with the following procedure.

Copper (20~100 μg.) were taken into a beaker and made up to 50 ml. of a 0.02~0.1 N hydrochloric acid solution. Ten milliliters of alizarin blue solution was added to it, forming the precipitate. After being left standing for a few minutes, the preci pitate was filtered with the apparatus as shown in Fig. 3. The precipitate on the filter paper was washed a few times with water and stuck with cellophane tape to the filter paper. Iron (20~100 μg.) was treated the same way as the copper. These samples were put in the sample holder and baked with aluminum plate. The fluorescent X-ray intensity of each element in these samples was measured under the conditions shown in Table I. The results are shown in Fig. 4 for copper and in

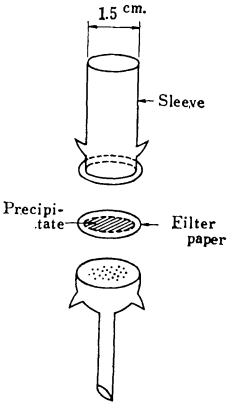


Fig. 3. Schematic diagram of filter.

Fig. 5 for iron. Below 100 μg. of iron or copper, the X-ray intensity is proportional to the amounts of the element in the samples. Using these calibration curves, the effect of iron on copper and of copper on iron could be investigated. The results obtained appear in Tables II and III. The possibility of a simultaneous determination of copper and iron under the same conditions was also recognized. Therefore, this method was applied to the determination of copper and iron in some metals.

TABLE I. OPERATION CONDITIONS FOR THE DETERMINATION OF Cu AND Fe

Excitation soure	40 kV. 15 mA.
Spectral lines (Å)	CuK_α (1.542 Å) 45.02°
$LiF_{2\theta}$°	FeK_α (1.937 Å) 57.50°
Fixed counting	10000 counts
Irradiated area	1.5 cm. in diameter

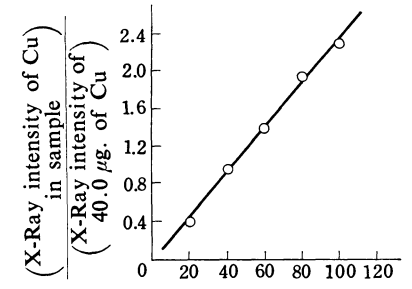


Fig. 4. Calibration curve for Cu.

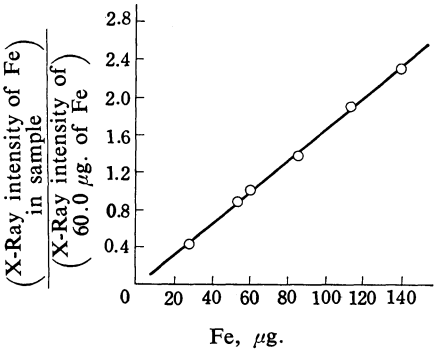


Fig. 5. Calibration curve for Fe.

Simultaneous Determination of Copper and Iron in Nonferrous Metals.—Using the system of measurement described above the determination of coppr and iron in nonferrous metals was undertaken. The nonferrous metals used were aluminum, zinc, manganese and nickel, which do not react with alizarin blue at pH values below 5; the analytical procedure used was as follows.

Procedure. — A definite sample (0.5~1.0 g.) was taken and dissolved with 5~10 ml. of hydrochloric acid or nitric acid, and the sample solution was prepared as a 0.02~0.1 N acid solution of 100 ml. From this solution a one-tenth or one-twentieth solution (containing below about 100 μg. of copper and iron) was taken out, and an alizarin blue solution was added. In accordance with the procedure for the preparation of the calibration curve previously described, copper and iron were analyzed. These results are shown in Table IV. On the basis of these results, small amounts of copper and iron in these metals can be rapidly analyzed with a simple procedure.

TABLE II. THE INFLUENCE OF Fe ON THE DETERMINATION OF 40.4 μg. OF Cu

Fe used μg.	Cu found μg.	Difference μg.
56.4	41.0	+0.6
112.8	40.4	0.0
225.6	40.0	−0.4

TABLE III. THE INFLUENCE OF Cu ON THE DETERMINATION OF 56.4 μg. OF Fe

Cu used μg.	Fe found μg.	Difference μg.
40.4	57.2	+0.8
80.8	57.3	+0.9
161.6	56.4	0.0

TABLE IV. DETERMINATION OF Cu AND Fe IN Al, Zn, Mn AND Ni

Sample	Sample taken g.	Cu added μg.	Cu found μg.	Cu recovered μg.	Fe added μg.	Fe found μg.	Fe recovered μg.
Al	0.044	0.0	0.9	—	0.0	1.5	—
	0.089	0.0	2.0	—	0.0	3.2	—
	0.089	41.8	44.0	42.0	41.8	44.0	40.8
Zn	0.057	—	—	—	0.0	4.2	—
	0.114	0.0	2.2	—	0.0	8.5	—
	0.114	38.3	40.8	38.6	—	—	—
Mn	0.052	0.0	1.2	—	0.0	0.5	—
	0.104	0.0	2.3	—	0.0	0.5	—
	0.104	—	—	—	56.5	55.5	55.5
Ni	0.041	0.0	4.9	—	0.0	3.8	—
	0.041	38.3	42.8	37.9	—	—	—
	0.082	0.0	9.0	—	0.0	8.0	—
	0.082	38.3	47.0	38.0	—	—	—

Discussion

The simultaneous determination of copper and iron in aluminum, zinc, manganese or nickel has been investigated. Copper in zinc, iron in manganese, or copper in nickel is difficult to analyze with a non-destructive method due to the high background of the matrix. Therefore, it is necessary to diminish this matrix effect as much as possible. Examples of spectrograms of iron in manganese, of copper in nickel and of zinc after separation are indicated in Fig. 6; these excitation conditions are similar to those in Table I. In the case of manganese and zinc, the separation was complete, but in the case of nickel, a small amount of it remained. However, as indicated in Table IV, the remaining nickel had little effects on the copper and iron. On the basis of these facts, it was considered that the presence of organic materials decreases the effect of diverse metals, and hence, that the effect of nickel is negligibly small for the X-ray spectroscopic determination of copper. Iron, nickel and copper also exhibited similar behavior regarding X-ray intensity, so the presence of a small amount of nickel has no effect if the total amount of copper and nickel is below three times that of iron.

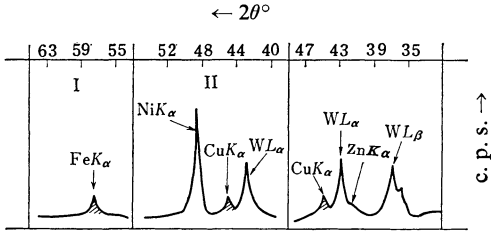


Fig. 6. Examples of spectrograms of Fe in Mn (I), and Cu in Ni (II) and Zn (III) after separation.
I 0.104 g. of Mn was taken, and full scale of the chart was 100 c. p. s.
II 0.082 g. of Ni was taken, and full scale of the chart was 500 c. p. s.
III 0.114 g. of Zn was taken, and full scale of the chart was 500 c. p. s.

Adding these findings to the results of the previous experiments, oxine and other organic reagents may be used for concentration of a small amounts of an element for purposes of fluorescent X-ray spectroscopy. Alizarin blue has the advantages that the precipitation reaction takes place at low pH regions and that it can be treated with a simple procedure. The amounts of silver and molybdenum, which react with alizarin blue under the same conditions[4], can be determined as well as those of copper and iron.

Summary

The simultaneous determination of small amounts of copper and iron with X-ray fluorescent spectroscopy combined with organic precipitation was investigated. Using an alizarin blue solution, which reacts with copper and iron at a low pH value, as the precipitant, satisfactory results were obtained. The amounts of copper and iron in aluminum, zinc, manganese and nickel were rapidly determined with X-ray fluorescent spectroscopy after this separation.

The Research Institute for Iron, Steel and Other Metals
Tohoku University
Katahira-cho, Sendai

Determination of Uranium in Thorium by X-Ray Fluorescent Spectroscopy. The Organometallic Precipitation Method

By Kichinosuke HIROKAWA and Hidehiro GOTÔ

(Received September 28, 1961)

For the determination of a small amount of uranium in thorium, Cheng[1] has suggested the PAN *o*-dichlorobenzene extraction method. This method[2], however, requires complicated procedures. Therefore, X-ray spectroscopy after organic precipitation separation was applied in this analysis. When the amount of uranium in thorium is determined by X-ray fluorescent spectroscopy, the effect of matrix element, thorium, is so great that it is necessary to isolate uranium from thorium. In order to separate them, the solvent extraction

1) K. L. Cheng, *Anal. Chem.*, **30**, 1028 (1958).
2) R. F. Clayton, *Analyst*, **83**, 13 (1948); A. R. Eberle, *Anal. Chem.*, **29**, 1134 (1957); H. Matsuyama, *J. Chem. Soc. Japan, Pure Chem. Sec.* (*Nippon Kagaku Zassi*), **79**, 958 (1958).

method[1,2], accompanied by the precipitation method[3], is investigated here. In this study alizarin blue[4] is used as the precipitant for uranium, and an X-ray fluorescent spectroscopic determination for uranium is proposed.

Experimental and Results

Reagents.—An alizarin solution was prepared by the methed described in a previous report[4]. For the uranium standard solution, 1 g. of uranium nitrate, analytical grade, was dissolved in a 1 N sulfuric acid solution. The uranium content of this solution was determined as 8.5 mg. 1 ml. by the zinc amalgam reduction potassium permanganate titration method. The solution was then diluted to the proper concentration before being used.

For the thorium standard solution, 1.5 g. of thorium nitrate, analytical grade, was dissolved in water; the concentration of thorium in it was determined by weighing the oxide after precipitation with oxalic acid (0.0107 g. 1 ml.). The acetic acid-sodium acetate buffer solution was prepared by mixing 0.2N acetic acid and 0.2N sodium acetate. The glycine buffer solution was prepared by mixing 0.1M glycine solution and 0.1M hydrochloric acid. The hydrochloric, nitric and other acids used were of an analytical grade. A 0.2M EDTA solution, a 0.1% PAN methanol solution, a 1% potassium cyanate solution, and an *o*-dichlorobenzene and buffer solution of pH 10 were also used.

Apparatus. — A G. E. XRD-5 X-ray spectrometer with AEG-50S tungsten tube was used, as described in the previous paper[4].

Conditions for the Formation of Metal Alizarin Blue Precipitate.—Uranium reacts with alizarin blue and forms a red-violet precipitate at once in neutral solutions, while thorium first develops a blue color with alizarin blue and then gradually forms a blue precipitate. In this case, the presence of EDTA prevents the formation of thorium precipitate. On the basis of these facts, the following conditions for precipitation were set up.

One hundred and seventy micrograms of uranium were taken from the uranium standard solution, the pH value of which was controlled with hydrochloric acid, a glycine-hydrochloric acid buffer solution or an acetic acid-sodium acetate solution; then the total volume of the solution was made up to about 50 ml. with water. Ten milliliters of alizarin blue solution was added. After the solution had stood for a few miuntes, the precipitate formed was filtered and repeatedly washed with water. The precipitate was put into the original beaker together with the filter paper. The precipitate and the filter paper were decomposed with 5 ml. of sulfuric acid and 10 ml. or more if necessary, of nitric acid by heating. Then it was diluted to 50 ml. with water, and one-tenth of it was taken for the extraction. The uranium content in this solution was determined by the PAN-*o*-dichlorobenzene extraction method. These results are shown in Fig. 1. From these results, the uranium was precipitated completely with alizarin blue in the pH range of 2~10. The effects of the presence of EDTA at pH values from 2 to 6 were not visible, as is shown in Fig. 1.

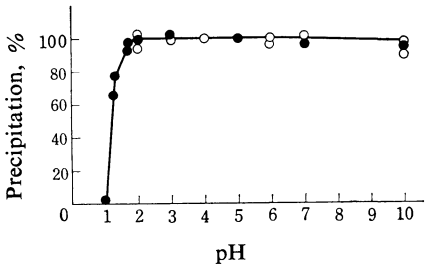


Fig. 1. Precipitation of U at various pH.
-○- 4 ml. of 0.2M EDTA soln. present.
-●- EDTA soln. not present.

Preparation of the Calibration Curve and Separation of Thorium.—In previous investigations, it was established that uranium forms a precipitate with alizarin blue in the presence of EDTA at pH values above 2. Therefore, the calibration curve for uranium was prepared as follows:

Various amounts of uranium, from 15 to 350 μg., were taken, and 4 ml. of a 0.2M EDTA solution and 20 ml. of an acetic acid-sodium acetate buffer solution (4; 6) were added; the pH value of this solution was controlled between 4 and 5, and its total volume was diluted with water to about 50 ml. After the addition of 10 ml. of the alizarin blue solution, the precipitate formed was filtered with the apparatus described in the previous report[4] and washed a few times with water. The precipitate on filter paper was fixed with cellophane tape directly and put in the sample holder with a round irradiation area 1.5 cm. in diameter and with aluminum plate backing. The fluorescent X-ray intensity from it was measured under the conditions of Table I. In Fig. 2, the calibration curves for uranium up to 100 μg. (a) and up to 350 μg. (b) are given. A spectrograph of the sample is shown in Fig. 3. The X-ray intensity of thorium caused by the absence of EDTA or by the unsatisfactory separation of thorium gives its peak at the notch part. According to the previous procedure, thorium below 0.05 g. was completely masked by EDTA and so was not affected. However, when the pH value of the solution was above 10 before the addition of EDTA, the peak of thorium appeared. As this thorium peak seemed to be due to thorium hydroxide, the addition of EDTA should be carried out before the control of the pH value.

Table I. Operating conditions for the determination of U

Excitation source	50 kV. 10 mAp.
Spectral line	
(Å) $LiF_{2\theta}$°	$UL\alpha_1$ (0.911 Å) 26.14°
Fixed counting	10000 counts
Irradiation area	1.5 cm. in diameter

3) Seberka et al, *Chem. Listy*, **47**, 512 (1953).
4) K. Hirokawa, *J. Japan Inst. Metal* (*Nippon Kinzoku Gakkaishi*), **23**, 688 (1959); K. Hirokawa and H. Gotô, This Bulletin, **35**, 961 (1962).

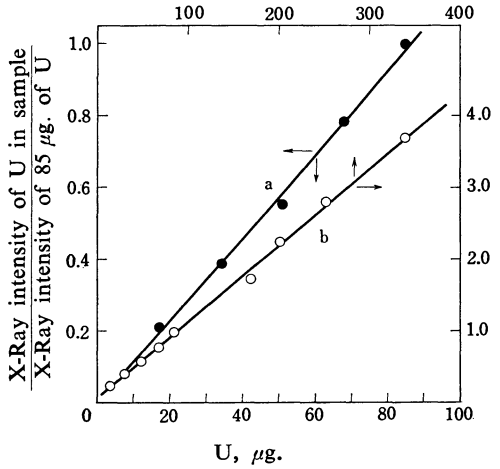


Fig. 2. Calibration curve for U.

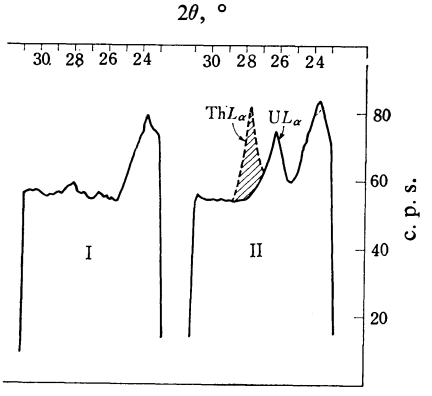


Fig. 3. X-Ray spectrogram of U separated from Th.
I, Blank; II. 68 μg. of U

Determination of Uranium in Thorium. — As in previous studies, a small amount of uranium in thorium was analyzed as follows:

Procedure. — From 0.1 to 0.5 g. of the sample was dissolved with a small amount of nitric acid as well as possible. This solution was diluted to 100 ml. with water, and one-tenth or one-fifth of this solution was put into a beaker. Four milliliters of EDTA solution and 20 ml. of an acetic acid-sodium acetate buffer solution were added to this solution. The pH of this solution was controlled at 4~5, and the total volume of this solution was increased to about 50 ml. The milliliters of an alizarin blue solution was added and the specimen for X-ray was prepared by the method described in the section dealing with the preparation of the calibration curve. The prepared specimen was irradiated with X-ray under the same conditions as listed in Table I, and the uranium content was determined from the intensity ratio of the uranium in the sample against that of the standard sample (85.0 μg. of U in this experiment). The amount of uranium in thorium was determined with this method; the results obtained are shown in Table II. These results agreed well with those obtained by the PAN *o*-dichlorobenzene extraction method.

TABLE II. DETERMINATION OF U IN Th

Sample	Chem. anal., %	X-Ray anal., %
A	0.32	0.30
B	0.44	0.48
C	0.45	0.43
D	0.22	0.23
E	0.17	0.18

Discussion

Various other precipitants for uranium can be considered besides alizarin blue. This alizarin blue solution, however, has the advantage of forming the precipitate over a wide pH range. When this alizarin blue solution is used, copper, iron and silver form precipitates under the same conditions, although these precipitations were masked by the addition of EDTA[4]. When the thorium metal was dendritic and porous, the non-destructive method could not be applied. Therefore, analysis using oxide powder was tried. An X-ray spectrographs of a thorium sample containing 2 and 4% of uranium oxide form were obtained, as is shown in Fig. 4. From this spectrograms, it was considered that uranium content below 1% was difficult to determine without separation because of the high background of X-ray due to thorium near the uranium peak.

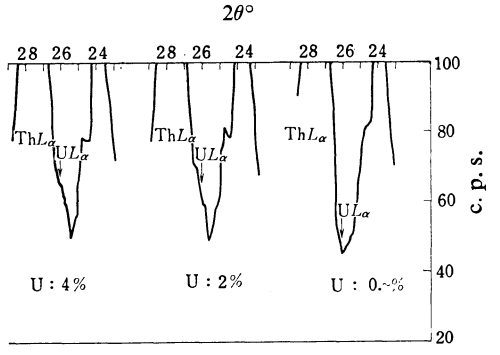


Fig. 4. X-Ray spectrograms of U in Th as oxide without separation.

Summary

A method for the determination of a small amount of uranium in thorium using the separation method with precipitation, combined with X-ray fluorescent spectroscopy, was investigated. About 100 μg. of uranium in thorium could be determined simply and rapidly by using alizarin blue as the precipitant for uranium and EDTA as the masking reagent for thorium.

The Research Institute for Iron, Steel and Other Metals
Tohoku University
Katahira-cho, Sendai

*Infrared Spectra of Troponoid Compounds. IV. Infrared and Raman Spectra of Tropone**

By Yusaku IKEGAMI

(Received August 23, 1961)

Infrared absorption spectrum of tropone (I) has been reported by a number of workers[1-4] but no detailed reports have been made on the assignment of the absorption bands. No work seems to have been done on the measurement of its Raman spectrum. As a part of the studies on the infrared spectra of troponoids, tropone was taken up as a compound having the most fundamental structure of this series. Measurements were made on the infrared spectra in the region of 4000~400 cm^{-1} and on Raman spectrum, and considerations were made on the vibrational assignments for these spectra.

Experimental

Measurement of Infrared Spectra.—Infrared spectra were measured with a Perkin-Elmer model 21 infrared spectrophotometer, using sodium chloride prism for the region of 4000~700 cm^{-1} and potassium bromide prism for the region of 700~400 cm^{-1}. The absorption bands in the region of 4000~1700 cm^{-1} were measured also by using a calcium fluoride prism which has a higher resolution.

Measurement of Raman Spectrum. — Raman spectrum was measured with a Shimadzu automatic grating Raman spectrometer, type GRS-750, using the Hg-e line (4358 Å) from the Toronto type mercury lamp for the exciting line. In this case, a solution containing 0.2 g. of Ethyl Violet and 39 g. of *p*-nitrotoluene in 1.8 l. of denatured alcohol was used as the filter for the light source. This filter solution had a 1 cm. light pass, and the cell was cooled by circulating water to avoid the rise in temperature of the sample cell. Tropone is easily colored on exposure to light, and, in order to avoid this coloration, the sample was preserved in a dark, cool place after purification and caution was taken to shorten the time required for measurement.

Sample. — Tropone used for the measurement was prepared by the known method[5], recrystallized as picrate, and passed through an alumina column to liberate picric acid. The purified tropone was distilled in vacuum more than five times. $n_D^{18}=1.6190$.

Infrared and Raman Spectra of Tropone

Infrared absorption spectrum of liquid tropone is shown in Fig. 1a. This spectrum hardly shows the absorption band at around 3530 cm^{-1} due to the adsorbed moisture always present in the spectra reported to date[2-4]. The spectra of tropone in carbon tetrachloride and carbon disulfide are shown in Fig. 1b. The wave number of absorption bands in these spectra and those in the spectrum measured in a vapor state earlier[4] are listed in Table II.

The Raman spectrum of liquid tropone is shown in Fig. 2, and the wave numbers, their approximate, relative intensities, and depolarization factors are listed in Table II. The relative intensities are given taking the peak intensity of the most intense line at 1520 cm^{-1} as the standard.

Molecular Structure and Vibrational Modes of Tropone

Tropone, C_7H_6O, has the structure of cycloheptatrienone (Ia). Therefore, a structure with all the 14 atoms in the plane and having a symmetric plane including a C=O line perpendicular to that plane can naturally be presumed to be tropone. Under such a presumption, a vibrational spectrum of tropone can be treated as a planar ring structure of C_{2v} symmetry, and, therefore, normal vibrations corresponding to 36 degrees of vibrational freedom can be classified as shown in Table I. In this table, the expected frequency ranges were assigned with reference to the vibrational frequencies of benzene, tropylium cation[6],

* A part of this work was presented at the Tohoku Local Meeting of the Chemical Society of Japan, Sendai, September, 1960.

1) H. J. Dauben and H. J. Ringold, *J. Am. Chem. Soc.*, **73**, 876 (1951); A. P. Ter Borg, R. van Helden, A. F. Bickel, W. Renold and A. S. Dreiding, *Helv. Chem. Acta*, **43**, 457 (1960).

2) W. von E. Doering and F. L. Detert, *J. Am. Chem. Soc.*, **73**, 876 (1951).

3) T. Nozoe, T. Mukai, K. Takase and T. Nagase, *Proc. Japan Acad.*, **28**, 477 (1952); T. Nozoe, T. Mukai and K. Takase, *Sci. Repts. Tohoku Univ.*, **139**, 164 (1956).

4) S. Kinumaki, K. Aida and Y. Ikegami, *Sci. Repts. Research Inst. Tohoku Univ.*, **A8**, 263 (1956).

5) T. Ikemi, T. Nozoe and H. Sugiyama, *Chem. & Ind.*, **1960**, 932.

6) K. Aida, *Sci. Repts. Research Inst. Tohoku Univ.*, **A8**, 361 (1956); W. G. Fateley, B. Curnutte and E. R. Lippincott, *J. Chem. Phys.*, **26**, 1471 (1957).

7) M. V. Evans and R. C. Lord, *J. Am. Chem. Soc.*, **82**, 1876 (1960).

8) G. R. Hunts and I. G. Ross, *J. Mol. Spectroscopy*, **3**, 604 (1959).

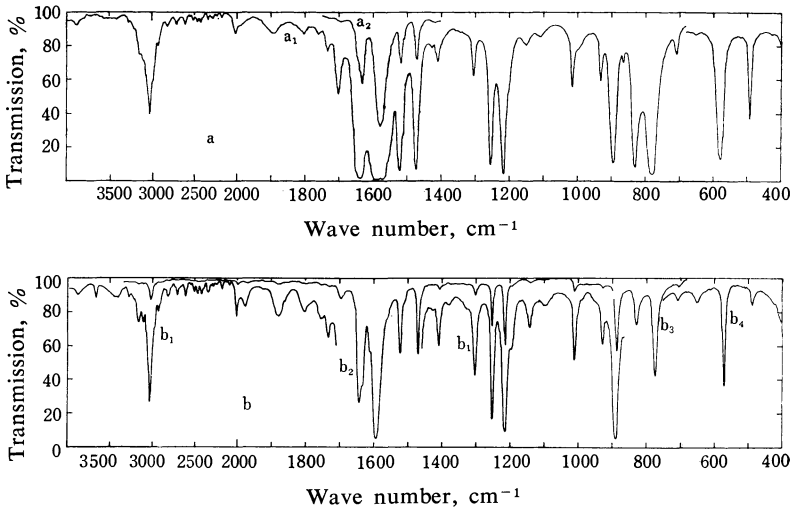


Fig. 1. Infrared spectra of tropone.

a: Pure liquid, a_1; 0.119 mm. thickness, a_2; 0.021 mm.

b: In carbon tetrachloride (4000~880 cm^{-1} range) and in carbon disulfide (900~400 cm^{-1} range), b_1; 6.03% (0.52 mm. thickness), b_2; 2.88% (0.092), b_3; 2.83% (0.092), b_4; 3.86% (0.12).

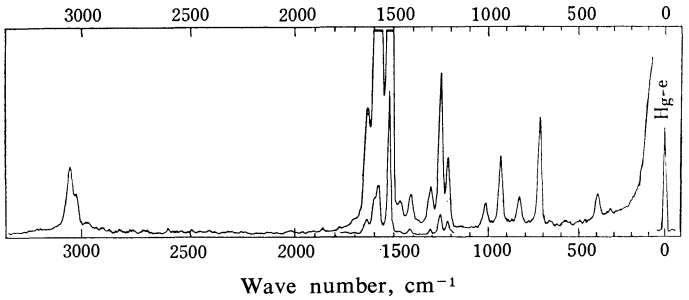


Fig. 2. Raman spectrum of liquid tropone (5100~4340 Å range).

TABLE I. DISTRIBUTION OF VIBRATIONAL FUNDAMENTALS FOR C_{2v} STRUCTURE OF TROPONE

Vibrational mode	Species				Total	Expected range cm^{-1}
	A_1	A_2	B_1	B_2		
In-plane						
CH stretch.	3		3		6	3100~3000
C=O stretch.	1				1	1650~
C=C stretch.	2		1		3	1650~1450
C-C stretch.	2		2		4	1450~ 700
CH bend.	3		3		6	1450~1000
C=O bend.			1		1	1000~?
Ring deform.	2		2		4	900~ 250
Out-of-plane						
CH bend.		3		3	6	1000~ 650
C=O bend.				1	1	1000~?
Ring deform.		2		2	4	700~ 200
Total	13	5	12	6	36	
Activity Infrared	a	ia	a	a		
Activity Raman	p	dp	dp	dp		

TABLE II. OBSERVED FREQUENCIES (cm^{-1}) AND THEIR POSSIBLE ASSIGNMENTS FOR TROPONE

Infrared			Raman			Assignment	
Liquid	Solution	Vapor	Liquid		ρ	Vibrational mode	Species
3205 sh							
3141 sh	3162 w						
3110 sh	3114 w	3100 sh					
3073 sh	3077 sh						
3050 sh	3055 sh		3055	0.5	0.38		A_1
		3048 s				CH stretching	
3024 m	3031 m		3031	0.3	0.61		B_1
2988 sh	3006 sh	3000 sh	2984	vw			
	2975 sh		2972	0.1			
2013 w	2005 w	2011 w				2×1000 ca.	
1980 sh	1973 w						
1892 w	1881 w					1000+893	
1808 w	1807 w	1805 w				934+867 ?	
1763 w	1757 w					934+830 or 893+867	
1737 m	1736 m	1735 sh				2×867	
1702 m	1702 m	1687 sh	1704	w		867+830	
1648 sh						867+779	
1634 vs	1645 vs	1651 vvs	1637	1.0	0.59	C=O and C=C stretch.	A_1
	1636 sh						
	1614 sh						
			1598	sh		C=C stretch.	B_1
1580 vvs	1595 vvs	1613 vvs					
			1580	3.4	0.51	C=C and C=O stretch.	A_1
1521 s	1525 s	1516 s	1520	10.0	0.30	C=C stretch.	A_1
1512 sh	1512 sh					932+577	
1473 s	1473 s	1465 s	1473	0.1	0.7	C-C stretch. ?	B_1
1429 w	1427 vw					779+650 or 2×712	
1411 m	1409 w	1405 w	1412	0.3	0.87	CH bend. (in-plane)	B_1
	1379 vw		1380	w		712+664 ?	
1345 vw							
	1328 sh					2×664	
1305 m	1304 m	1305 m	1309	0.4	0.78	CH bend. (in-plane)	B_1
1253 s	1253 s	1251 m	1254	1.3	0.37	CH bend. (in-plane)	A_1
1216 s	1215 s	1208 s	1217	0.6	0.72	CH bend. (in-plane)	B_1
1204 sh	1200 sh	1185 w				CH bend. (in-plane)	A_1?
1151 w	1142 w	1145 wb				CH bend. (in-plane)	A_1?
1108 w	1100 vw	1086 w				712+396 or 779+329	
1015 m	1013 m	1010 w	1017	0.2	0.79	C-C stretch. ?	B_1
1000 sh	990 sh	999 w	990	sh		CH bend. (out-of-plane)	A_2
932 m	930 m		934	0.6	0.44	CH bend. (out-of-plane) ?	A_2
						C-C stretch.	A_1
893 s	889 s	882 s				CH bend. (out-of-plane)	B_2
867 w						CH bend. (out-of-plane)	A_2
830 s	830 s	827 m	833	0.3	0.56	CH bend. (out-of-plane)	B_2
779 vs	776 vs	767 s				CH bend. (out-of-plane)	B_2
712 w	709 w	703 w	716	0.9	0.29	C-C stretch.	A_1
			664	vw		Skeletal deform.	A_2
650 vw	653 w	650 vw	653	0.1	0.7	Skeletal deform.	B_1
			644	w		Skeletal deform.	A_2
577 s	574 s		576	0.1	0.8	Skeletal deform.	B_2
492 m	490 m		492	0.1	0.8	Skeletal deform.	B_2
402 w	405 m						
			396	0.3	0.72	Skeletal deform.	A_1
			386	sh		Skeletal deform.	B_1?
			329	0.1	0.8	Skeletal deform.	B_1?
			259	vw		Skeletal deform.	?

(vs : very strong, s : strog, m : medium, w : weak, vw : very weak, sh : shoulder)
ρ : Depolarization factor

tropilidene[7], and azulene[8] whose vibrational spectra had already been analyzed.

As can be seen from this table, all the vibrational modes are Raman active, and 31 of them except those of A_2 species are also infrared active. However, the observed spectra show that the number of Raman lines are much smaller than the anticipated number and this is probably due to the non-observation of weak Raman lines by the afore-mentioned defect in the measurement and also to the superposition of adjacent lines.

Vibrational Assignment

From the distribution of vibrational modes and the spectral data, the following considerations were made on the vibrational assignments for tropone. Results are summarized in Table II.

Around 3000 cm^{-1}.—Six vibrations due to the CH stretching mode, active both in the infrared and Raman spectra, can be anticipated in this region, which should not be higher than 3100 cm^{-1} but higher than 3000 cm^{-1}. The observed spectra show the bands assignable to CH stretching vibrations as an absorption of strong intensity with 3~4 shoulders in the infrared spectrum and as two lines at 3055 and 3031 cm^{-1} in the Raman spectrum. These bands are probably the six vibrations overlapped due to the low resolution of the spectrometer. The infrared spectrum using a calcium fluoride prism does not give an excellent separation. It should further be noted that, in this region, the foot of CH stretching absorption bands in the infrared spectra is extended outside the region of 3100~3000 cm^{-1}, with several shoulders, and that a distinct band has been recorded at 2972 cm^{-1} in the Raman spectrum. Such bands, extending outside the expected range, should naturally be explained in most cases, as the combination bands or over-tones of the vibrations in the lower frequency region, especially in the region of 1660~1450 cm^{-1}, where the bands of strong intensity appear in both the infrared and Raman spectra. This Raman line at 2972 cm^{-1} is not improbable as a CH stretching vibration, refering to the assignment of naphthalene spectrum[9], but there is no evidence to support this assignment. A Raman line at 3055 cm^{-1} belongs to A_1 species by its depolarization factor.

Region of 1660~1450 cm^{-1}. — It is noticed that the bands in this region are very strong in both infrared and Raman spectra, as compared with those of tropilidene (II)[7] which has the same C_{2v} symmetry as tropone. Of the stretching vibrations anticipated from the tropone skeleton, the four vibrational modes due to C=O and C=C bonding are expected to appear in a higher side in this region. A most intense, polarized Raman line at 1520 cm^{-1} is assigned to the C=C in-phase stretching vibration belonging to A_1 species, and is analogous to the most intense Raman lines of tropilidene and tropolone (1535[7] and 1473 cm^{-1} [10] respectively). In the higher side than this line, there are three distinct lines in the Raman spectrum, as anticipated, and two absorption bands of strong intensity with several shoulders are observed in the infrared spectrum. The nature and assignment of these bands will be discussed in a later paper[11] with consideration of the infrared spectra measured in various solvents. A Raman line at 1598 cm^{-1} belongs to B_1 species and other two bands in the region of 1651~1580 cm^{-1} are explained as the vibrations whose main components are the C=O and C=C stretching modes.

The shoulder at 1512 cm^{-1} is thought to correspond to the combination band, 932+577 cm^{-1}. Another distinct band at 1473 cm^{-1}, in both infrared and Raman spectra, may be assigned to the C–C stretching vibration belonging to B_1 species, although it locates rather higher, compared to that in tropilidene[7].

Region of 1450~700 cm^{-1}.—Absorptions of CH out-of-plane bending vibrations belonging to B_2 species and present in the region below 1000 cm^{-1} are generally expected to have strong intensity in the infrared spectrum but weak or indistinct in the Raman spectrum. The three bands at 893, 830 and 779 cm^{-1} are assigned to this vibration. The strong lines at 934 and 716 cm^{-1} in Raman spectrum are assigned to the C–C stretching modes belonging to A_1 species because of their depolarization factors. The latter is analogous to the strong Raman line at 744 cm^{-1} in tropolone[10,12].

The CH out-of-plane bending vibration belonging to A_2 species should be weak in the Raman spectrum and only observed as forbidden bands in the infrared spectrum. In accordance with this presumption the band at 867 cm^{-1} is assigned to this bending vibration. The characteristic weak bands in the region of 2000~1600 cm^{-1} in benzenoids, depending on the position of substituents, are explained

9) E. R. Lippincott and E. J. O'Reilly, *J. Chem. Phys.*, 23, 238 (1955); A. L. McClellan and G. Pimentel, ibid., 23, 245 (1955).

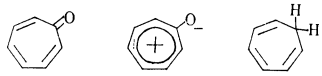
10) Y. Ikegami, unpublished data. The Raman spectra of tropolone and 3- and 4-isopropyltropolones were measured in carbon tetrachloride solution and the spectra showed the most intense Raman lines respectively at 1473, 1489 and 1475 cm^{-1}.

11) Y. Ikegami, Part V, This Bulletin, 35, 972 (1962).

12) S. Imanishi and M. Ito, ibid., 28, 75 (1955); 29, 632 (1956); *J. Chem. Phys.*, 24, 1272 (1956).

as the combination bands or over-tones of CH out-of-plane bending vibrations[13]. If such an interpretation were to apply in the case of planar tropone skeleton, the infrared absorption band at 2013 cm^{-1} would probably by the anticipated over-tone of CH out-of-plane bending vibration at around 1000 cm^{-1}, because, if this band is the combination of two fundamental frequencies, one of these must be higher than the expected frequency range to the CH out-of-plane bendings. This vibration belongs to A_2 species and corresponds to the shoulder of a band at 1017 cm^{-1}. Under such consideration, the probable combination, 934+867 cm^{-1}, is assumed to be a weak band at 1808 cm^{-1}. Accordingly, another CH out-of-plane bending vibration belonging to A_2 species probably exists at around 934 cm^{-1} together with the C–C stretching vibration.

It is noticed that, in this region, the CH out-of-plane bendings of tropone appear at 120~150 cm^{-1} higher than those of tropilidene (II)[7]*.



Ia Ib II

In the region higher than 1000 cm^{-1}, there should be one C–C stretching (B_1 species) and six CH in-plane bending vibrations. Of the observed frequencies, the band at 1253 cm^{-1} can be assigned to the vibration belonging to A_1 species from its depolarization factor. The four bands at 1412, 1309, 1217 and 1017 cm^{-1} are considered to belong to B_1 species, and one of them would be assigned to the C–C stretching vibration. Although there are no definite grounds, the line at 1017 cm^{-1} may probably be assigned to the C–C stretching vibration, since many troponoids show the characteristic absorption band, independent of substituents, in this region[14]. Of the remaining bands, those weak in both infrared and Raman spectra may be assigned as combination bands or over-tones, as indicated in Table II, and distinct bands at 1204 and 1151 cm^{-1} are assumed to belong to A_1 species though indistinct in Raman spectrum.

Region Lower than 700 cm^{-1}.—The bands in this region are assigned to the deformation vibrations of the tropone skeleton. A Raman line at 396 cm^{-1} is assigned to the vibration of A_1 species, similar to that of tropilidene at 420 cm^{-1} and that of tropylium cation at 433 cm^{-1}, although this is doubtful in its depolarization factor. The bands at 576 and 492 cm^{-1} which are strong in the infrared spectrum and weak in the Raman spectrum are assigned to that of B_2 species, and the bands at 644 and 664 cm^{-1}, indistinct in infrared and weak in Raman, are probably assigned to those belonging to the A_2 species. The remaining bands at 653, 386 and 329 cm^{-1} distinct in Raman spectrum were assumed to be assigned to the B_1 species.

Others.—Due to the lack of reliable data, two deformation modes of oxygen atom have been excluded. Of the remaining observed absorption, combination bands or over-tones in the region higher than 1650 cm^{-1} are included in Table II.

The author expresses his deep gratitude to Professor Susumu Kinumaki, Professor Shuichi Seto, and Assistant Professor Koyo Aida for the unfailing guidance throughout the course of the present work. He is also indebted to Mr. Shuji Aono and Miss Hisako Minegishi for their technical cooperation in the spectral measurement.

The Chemical Research Institute of Non-Aqueous Solutions
Tohoku University
Katahira-cho, Sendai

13) Y. Kakiuchi, *J. Chem. Soc. Japan, Pure Chem. Sec.* (*Nippon Kagaku Zassi*), **77**, 1839 (1956); *Kagaku-no-Ryoiki*, Extra No. **38**, 1 (1959).

* The structural difference between tropone and tropilidene is known as the aromatic character of tropone due to some contribution from ionic structure Ib and the quasi-aromatic character of tropilidene due to the conjugation of its three double bonds.

14) Y. Ikegami, unpublished data.

Infrared Spectra of Troponoid Compounds. V. Absorption Bands in the Region of 1700~1530 cm^{-1} of Tropone, 2-Chlorotropone and Tropolone[*1]

By Yusaku IKEGAMI

(Received August 23, 1961)

Infrared absorption bands due to the vibration of tropone skeleton are generally not present in the higher wave number side than 1651 cm^{-1}, and appear as two or more bands in the region of 1651~1530 cm^{-1} [1]. In most reports made to date, the absorption bands with the highest wave number have been treated as that of C=O stretching and the next higher absorption as the C=C stretching mode. Such an assignment, however, has little experimental or evidental basis. Accordingly, it should naturally be considered that $\nu_{C=O}$ might show a lower wave number than $\nu_{C=C}$, as was considered earlier by Kloster-Jensen and others[2] with $\nu_{C=O}$ of 2, 7-polymethylene-4, 5-benzotropones.

As shown in the previous reports[3,4], the infrared spectrum of tropone (I) in this region shows considerable variation of absorption wave numbers according to the condition of measurement, and the relative intensity of Band I[*2] and Band II[*2] is just reverse, according to whether it is observed in a vapor or liquid state. Such a difference in spectrum may be attributed to the association of molecules. Then, as one of the means for obtaining some informations on the assignment of these bands, the variation of the intensity and the shift of the absorption bands accompanying changes in the state and solvent were examined. Discussions are also given on the results obtained by the measurement of infrared spectra in the region of 1700~1500 cm^{-1}, in various solvents. Besides tropone, 2-chlorotropone (II) and tropolone (III) were also examined.

Measurement

The infrared absorption spectra were measured with a Perkin-Elmer model 21 infrared spectrophotometer equipped with a sodium chloride prism. The measurement on solids were made with the potassium bromide disk method and the sample cell with potassium chloride windows was used for the measurement in solution and liquid. Standard absorption lines of water vapor and polystyrene film were used for wave number calibration. The probable error of the wave number in Tables I, II and III is about ± 2 cm^{-1}. Tropone, 2-chlorotropone[5], and tropolone were prepared by known methods and purified. The kind of solvents to be used and the concentration of the solution were selected considering the infrared absorption of solvents themselves and the solubility of samples.

Results and Discussion

Tropone.—The spectra measured on tropone are shown in Fig. 1. The spectrum obtained earlier[4] in the vapor state is also shown in Fig. 1a. The wave number (ν) of absorption bands found, relative wave number shift ($\Delta\nu/\nu_0$), apparent molecular extinction coefficient (ε^a) at each wave number, and apparent half band width ($(\Delta\nu)_{1/2^a}$) are summarized in Table I. The value of $\Delta\nu$ shows the wave number shift ($\nu_0-\nu$) and is given taking the wave number (ν_0) in the vapor state as the standard. The values of ε^a and $(\Delta\nu)_{1/2^a}$ are rough values, because the Bands I and II are often accompanied with shoulders. However, these values will be sufficient in knowing the tendency of spectral variation. As a measure to compare the intensities of Bands I and II, the values of r are taken as shown in Table I. These values show $[\varepsilon^a\times(\Delta\nu)_{1/2^a}]_I/[\varepsilon^a\times(\Delta\nu)_{1/2^a}]_{II}$ and roughly mean the ratio of the area of Band I to that of Band II.

Following features in the spectra are found in Fig. 1 and Table I:

a) The direction of the shift of absorption bands according to changes in the measuring condition is the same in Bands I and II but the magnitude of this shift is greater in Band II (maximum of $\Delta\nu$: 39 cm^{-1}) than in I (maximum of $\Delta\nu$: 18 cm^{-1}). Bellamy and Williams[6] discussed the relation between the

*1 A part of this work was presented at the 13th Annual Meeting of the Chemical Society of Japan, April, 1960.

1) Y. Ikegami, *Kagaku-no-Ryoiki*, Extra No. 38, 33 (1959).

2) E. Kloster-Jensen, N. Tarköy, A. Eschenmoser and E. Heilbronner, *Helv. Chim. Acta*, 39, 786 (1956).

3) Y. Ikegami, This Bulletin, 35, 967 (1962).

4) S. Kinumaki, K. Aida and Y. Ikegami, *Sci. Repts. Research Inst. Tohoku Univ.*, A8, 263 (1956).

*2 Each spectrum, referred to in this report, has two strong absorption bands in the region of 1660~1530 cm^{-1}. Hereinafter this band at higher and at lower wave numbers will be designated respectively as "Band I" and "Band II".

5) T. Nozoe, S. Seto, H. Takeda, S. Morosawa and K. Matsumoto, *Sci. Repts. Tohoku Univ.*, I36, 126 (1952); S. Seto, ibid., 37, 275 (1953).

6) L. J. Bellamy and R. L. Williams, *Trans. Faraday Soc.*, 55, 14 (1959).

TABLE I. COMPARISON OF TWO BANDS (I AND II) OF TROPONE IN VARIOUS STATES

Spectral no. and state (Fig. 1)	Band I				Band II				r
	ν cm^{-1}	$\Delta\nu/\nu_0$ $\times 10^3$	ε^a	$(\Delta\nu)_{1/2}{}^a$	ν cm^{-1}	$\Delta\nu/\nu_0$ $\times 10^3$	ε^a	$(\Delta\nu)_{1/2}{}^a$	
a Vapor	1651				1613				1.19[a]
b In *n*-heptane	1645	3.63	277	14.2	1602	6.82	406	15.0	0.65
c In diisopropyl ether	1645	3.63	217	20.0	1600	8.06	407	19.8	0.54
d In triethylamine	1644	4.24	246	19.3	1598	9.30	470	16.5	0.61
e In carbon tetrachloride	1645	3.63	243	21.5	1595	11.16	513	15.5	0.66
f In 1-chlorobutane	1645	3.63	211	21.5	1595	11.16	458	19.5	0.51
g In carbon disulfide	1644	4.24	290	19.5	1593	12.40			
h In dioxane	1642 1634	5.45	195	23.5	1590	14.26	556	17.5	0.47
i In acetonitrile	1634	10.30	170	22.5	1585	17.36	545	18.5	0.38
j In chloroform	1635	9.69	210	13.0	1582	19.22	515	25.0	0.21
k In ethanol	1633	10.90	209	12.5	1574	24.18	468	31.0	0.18
l Liquid	1634	10.30		25	1580	20.46		32	0.36

$\Delta\nu/\nu_0$; Relative wave number shifts, were estimated in all cases by reference to the wave number in vapor state.
ε^a; Apparent molecular extinction coefficient at absorption maximum (peak height).
$(\Delta\nu)_{1/2}{}^a$; Apparent half band width, cm^{-1}.
$r=[\varepsilon^a\times(\Delta\nu)_{1/2}{}^a]_I/[\varepsilon^a\times(\Delta\nu)_{1/2}{}^a]_{II}$ [a]; $[\varepsilon^a]_I/[\varepsilon^a]_{II}$

TABLE II. COMPARISON OF TWO BANDS (I AND II) OF 2-CHLOROTROPONE IN VARIOUS STATES

Spectral no. and state (Fig. 3)	Band I				Band II				r
	ν cm^{-1}	$\Delta\nu/\nu_0{}^a$ [a] $\times 10^3$	ε^a	$(\Delta\nu)_{1/2}{}^a$	ν cm^{-1}	$\Delta\nu/\nu_0{}^a$ [a] $\times 10^3$	ε^a	$(\Delta\nu)_{1/2}{}^a$	
	(1648)				(1622)				
a In *n*-heptane	1642	3.64		11.5	1611	6.78		20.0	1.37
b In diisopropyl ether	1639	5.46	334	14.5	1609	8.01	281	17.0	1.01
c In triethylamine	1639	5.46	317	13.7	1610	7.40	234	18.0	1.03
d In carbon tetrachloride	1636	7.28	284	14.5	1609	8.01	285	17.3	0.84
e In 1-chlorobutane	1636	7.28	298	13.8	1608	8.63	327	16.3	0.77
f In carbon disulfide	1634	8.50	318	12.0	1606	9.86	296	16.8	0.77
g In dioxane	1634	8.50	271	13.0	1605	10.48	340	14.7	0.71
h In acetonitrile	1632	9.71	218	12.5	1600	13.56	335	19.5	0.42
i In chloroform	1632	9.71	312	13.0	1597	15.41	411	25.5	0.39
j In ethanol	1629	11.53	183	16.5	1590	19.73	287	31.8	0.33
k Solid	1628	12.14		15.4	1591 1583	19.11		30.2	0.26

[a]; Relative wave number shifts were estimated in all cases by reference to the wave number presumed to vapor state.

relative wave number shift for C=O stretching absorption band in various ketones and that of acetophenone in various solvents. According to their method, the values of $\Delta\nu/\nu_0$ of tropone in various solvents are plotted against their values of benzophenone, in Fig. 2*[3]. As is clearly noticed from this figure, an effect, which is similar to that of solvent on the carbonyl group of benzophenone, appears in both Bands I and II of tropone. The effect appeared is smaller in Band I and larger in Band II, than that for the carbonyl group of benzophenone. This effect on Band II is typical as the effect on the usual C=O stretching absorption[6].

b) The Band I is stronger than Band II in a vapor state but Band II is stronger and has wider width in other states.

c) As the Bands I and II shift towards the lower wave number side, the value of ε^a of Band I decreases slightly and that of Band II tends to increase. Consequently, value of r decreases.

d) The spectrum of liquid tropone in this

*[3] Benzophenone was chosen as the standard because two π-electron systems are conjugated with the carbonyl group in a molecule as in tropone. The values of $\Delta\nu/\nu_0$ of tropone in *n*-heptane and in diisopropyl ether corresponded respectively to those of benzophenone in *n*-hexane and in *n*-butyl ether.

region is similar to that of tropone in ethanol or acetonitrile, generally known as a polar solvent.

On the basis of these features, following discussions are built. There is no doubt that the absorption bands in this region are due to the stretching vibrations of C=O and C=C linkages[7]. According to the consideration on the vibrational assignments of tropone spectrum, one C=O stretching (A_1 species) and two C=C stretching (A_1 and B_1 species) vibrations are expected in the region of 1700~1530 cm^{-1}, as discussed in the preceding paper[3]. That of B_1 species was observed

TABLE III. COMPARISON OF TWO BANDS (I AND II) OF TROPOLONE IN VARIOUS STATES

Spectral no. and state (Fig. 5)		Band I				Band II				r
		ν cm^{-1}	$\Delta\nu/\nu_0$ $\times 10^3$	ε^a	$(\Delta\nu)_{1/2}{}^a$	ν cm^{-1}	$\Delta\nu/\nu_0$ $\times 10^3$	ε^a	$(\Delta\nu)_{1/2}{}^a$	
a	Vapor	1628			31.0	1573 1575			40.0	2.03
b	In *n*-heptane	1622	3.69		16.0	1564	5.72		32.0	1.09
c	In diisopropyl ether	1620	4.91	326	19.0	1565	5.09	166	32.7	1.14
d	In carbon tetrachloride	1618	6.14	297	18.0	1555	11.44	158	37.0	0.91
e	In 1-chlorobutane	1618	6.14	308	18.5	1557	10.17	166	33.0	1.04
f	In carbon disulfide	1617	6.76	343	18.8					
g	In dioxane	1617	6.76	389	14.3	1565	5.09	255	30.3	0.72
h	In acetonitrile	1616	7.37	342	15.0	1553	12.71	167	32.5	0.95
i	In chloroform	1615	7.99	349	15.0	1551	13.99	237	23.5	0.94
j	In ethanol	1614	8.60	336	18.3	1547	16.53			
	In pyrrole[a]	1612	9.83		14.0	1548	15.89		26.8	0.69
k	Liquid	1614	8.60		22.5	1553	12.71		40.0	0.69
l	Solid	1613	9.21		22.5	1548	15.89		36.5	1.04

a) Concentration; ca. 2.4 mol./l. (0.018 mm. thickness)

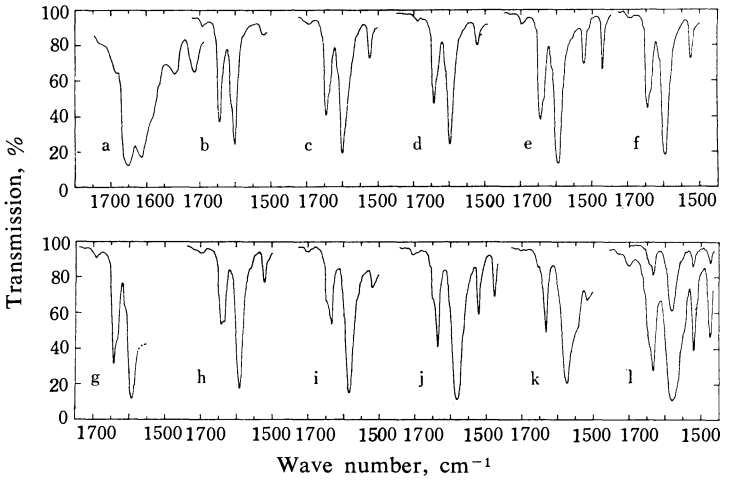


Fig. 1. Infrared spectra of tropone in the states of vapor and liquid, and in various solvents (1700~1500 cm^{-1} range): a; vapor, b; in *n*-heptane, 0.029 mol./l. (0.524 mm. thickness), c; in diisopropyl ether, 0.185 (0.095), d; in triethylamine, 0.141 (0.092), e; in carbon tetrachloride, 0.185 (0.092), f; in 1-chlorobutane, 0.185 (0.095), g; in carbon disulfide, 0.182 (0.092), h; in dioxane, 0.147 (0.092), i; in acetonitrile, 0.160 (0.092), j; in chloroform, 0.185 (0.095), k; in ethanol, 0.153 (0.092), l; liquid.

7) That the $\nu_{C=O}$ in tropone is less than 1651 cm^{-1} is generally explained as follows. The $\nu_{C=O}$ of saturated cycloheptanones is between 1708 and 1698 cm^{-1}, according to many references. When the molecule has a double bond conjugated with a C=O group, the frequency is less than this value by ca. 40 cm^{-1} (for example, eucarbone: 1660 cm^{-1}). Therefore, the $\nu_{C=O}$ of tropone is expected at the lower than 1650 cm^{-1} because tropone has a longer conjugated system and the polar character of Ib type. Moreover, from the the length of C=O bond, which was determined as 1.26 Å by electron diffraction analysis, we can expect the $\nu_{C=O}$ of tropone at around 1610 cm^{-1} because of the relation between the bond length and the frequencies reported by Leyton et al. (Cf. K. Kimura, S. Suzuki, M. Kimura and M. Kubo, This Bulletin, 31, 1051 (1953); E. M. Leyton, R. D. Kross and V. A. Fassel, *J. Chem. Phys.*, 25, 135 (1956).)

distinctly at 1598 cm^{-1} in the Raman spectrum but it is not so clear in the infrared spectra and is probably superposed in Band II. Consequently, Bands I and II both must belong to the A_1 species, as they are also supported from their depolarization factors[3].

It is well known in general that the C=O stretching vibration appears strongly in infrared spectra and the wave number of absorption band and the intensity are easily affected by the internal or external effects[8]. Such properties are found in both of Bands I and II in tropone, although often more in Band II than I, as shown in the foregoing a)—c). On the other hand, it is hardly expected that the out-of-phase C=C stretching vibration of tropone appears strongly, because of the fact that the absorption of tropilidene[9], which has the same C_{2v} symmetry as tropone, is very weak in this region. The wave number 1580 cm^{-1} in the liquid tropone, for example, is too low for pure out-of-phase C=C stretching vibration belonging to A_1 species, compared with that of tropilidene (1609 cm^{-1})[9] and of tropylium cation (1594 cm^{-1})[10].

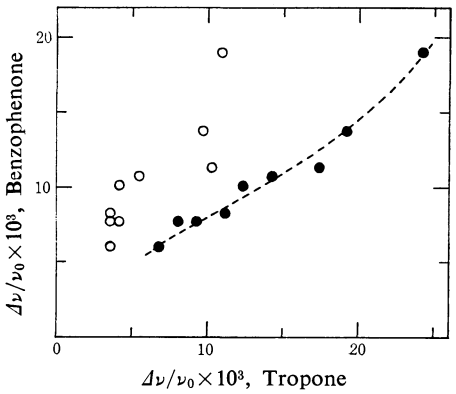


Fig. 2. Relation between the values of $\Delta\nu/\nu_0$ of Bands I and II in tropone and of $\nu_{C=O}$ in benzophenone in various solvents. ○ ; Band I, ● ; Band II

Considering the facts described above, it is natural to assume that both Bands I and II have contributions from the C=O and C=C stretching vibrations, which belong to A_1 species and both are expected at around 1600 cm^{-1}. If such is the case, there would be relative variation in the frequency, intensity, and width of absorptions in both Bands I and II as the C=O bond is polarized by external effects, and the foregoing characteristics a)—c) in spectra should mean that the character of C=O stretching vibration in Band II is greater than that in Band I, except in a vapor state. If the Ib character of a tropone skeleton becomes stronger and the double bond character of C=O bond becomes smaller, it is likely that the $\nu_{C=O}$ appears in a further lower wave number region. For example, Buchanan

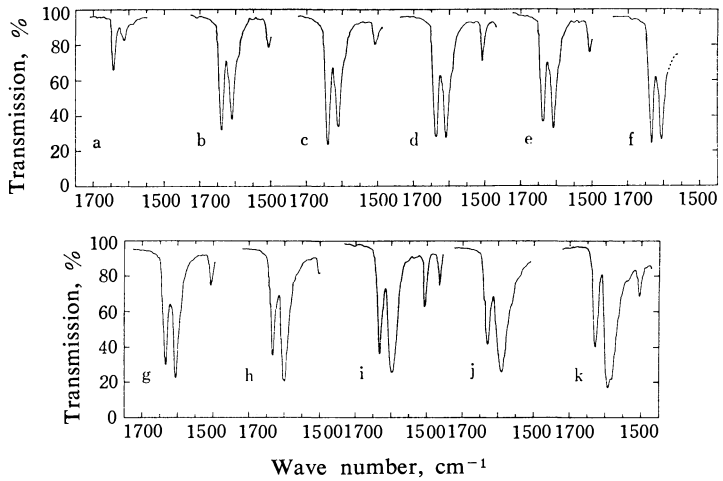


Fig. 3. Infrared spectra of 2-chlorotropone in the state of solid and in various solvents (1700~1500 cm^{-1} range) ; a ; in *n*-heptane, saturated (0.13 mm. thickness), b ; in diisopropyl ether, 0.146 mol./l. (0.10), c ; in triethylamine, 0.149 (0.13), d ; in carbon tetrachloride, 0.146 (0.13), e ; in 1-chlorobutane, 0.146 (0.10), f ; in carbon disulfide, 0.146 (0.13), g ; in dioxane, 0.142 (0.13), h ; in acetonitrile, 0.153 (0.13), i ; in chloroform, 0.149 (0.095), j ; in ethanol, 0.153 (0.13), k ; solid.

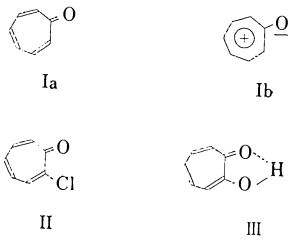
8) R. N. Jones and C. Sandorfy, "Chemical Application of Spectroscopy", Ed. by W. West, Interscience, New York (1956), p. 443.

9) M. V. Evans and R. C. Lord, *J. Am. Chem. Soc.*, **82**, 1876 (1960).

10) W. G. Fateley, B. Curnutte and E. R. Lippincott, *J. Chem. Phys.*, **26**, 1471 (1957).

and others[11] assumed that the strong absorption at 1540~1470 cm^{-1} in associated 4-hydroxy-2, 3-benzotropone is that of the C=O bond, and the same treatment was also made regarding to the band at 1465 cm^{-1} in associated 4-hydroxytropone[1].

Solvation effect on C=O bond in tropone, as far as it appears in $\nu_{C=O}$, is similar to that on the carbonyl group in benzophenone, as clearly noticed in Fig. 2. The fact d) that the spectrum of liquid tropone is similar to that in a polar solvent, which generally has a strong effect on the C=O bond, means that tropone itself is strongly associated with the Ib type polar character. The polar character of tropone is distinctly seen in its large dipole moment (4.17 D)[12].



2-Chlorotropone.—Figure 3 shows the spectra obtained with 2-chlorotropone (II). In the same way as with tropone, the values of ν, $\Delta\nu/\nu_0$, ε^a, $(\Delta\nu)_{1/2}{}^a$, and r are summarized in Table II. The value of ν_0 was presumed from the frequencies in solutions, as it is not known in the vapor state. Plotting of the values of $\Delta\nu/\nu_0$ against those of $\nu_{C=O}$ in benzophenone, Fig. 4 is obtained. The tendency of spectral variation, as observed from these figures and table, is essentially the same as that of tropone, and the assignment of Bands I and II can be discussed by the coupling of $\nu_{C=O}$ and $\nu_{C=C}$ in the same way as in tropone. Further, the followings are clear from the comparison with tropone.

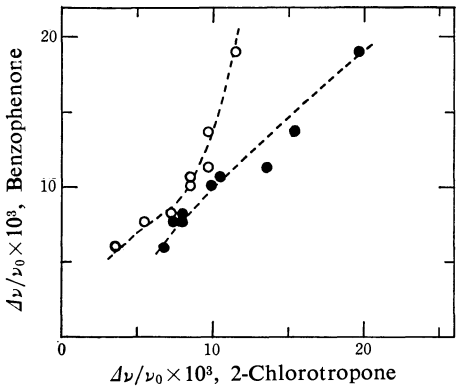


Fig. 4. Relation between the values of $\Delta\nu/\nu_0$ of Bands I and II in 2-chlorotropone and of $\nu_{C=O}$ in benzophenone in various solvents.
○ ; Band I, ● ; Band II

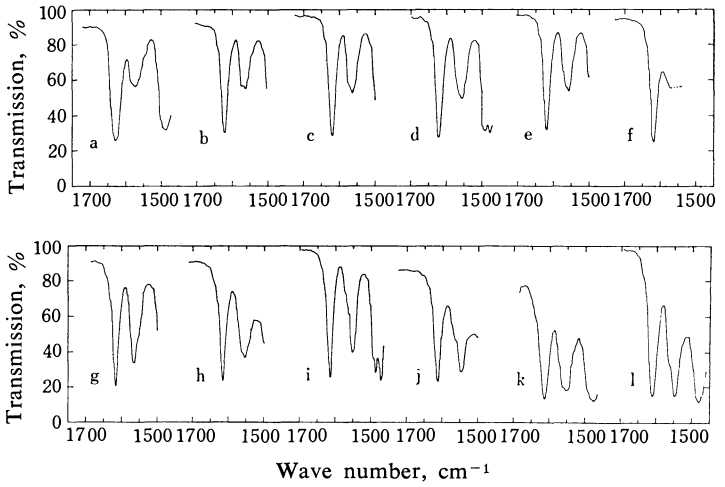


Fig. 5. Infrared spectra of tropolone in the states of vapor, liquid, solid, and in various solvents (1700~1500 cm^{-1} range) : a ; vapor, b ; in *n*-heptane, saturated (0.102 mm. thickness), c ; in diisopropyl ether, 0.172 mol./l. (0.095), d ; in carbon tetrachloride, 0.24 (0.12), e ; in 1-chlorobutane, 0.164 (0.095), f ; in carbon disulfide, 0.164 (0.102), g ; in dioxane, 0.164 (0.102), h ; in acetonitrile, 0.164 (0.102), i ; in chloroform, 0.176 (0.095), j ; in ethanol, 0.164 (0.102), k ; liquid, l ; solid.

11) G. L. Buchanan and J. K. Sutherland, *J. Chem. Soc.*, **1956**, 2620.

12) Y. Kurita, S. Seto, T. Nozoe and M. Kubo, This Bulletin, **26**, 272 (1953).

e) The difference in wave number (27～39 cm^{-1}) in Bands I and II is much less than that in tropone (38～59 cm^{-1}).

f) Band I is stronger than II in non-polar solvents and Band I is weaker than II in polar solvents. The variation of relative intensity is noticeble.

The fact e) suggests that the carbonyl group in 2-chlorotropone is less affected by the external effects than that of tropone. Also, comparing the fact f) with Fig. 4, it is found, that the $\Delta\nu/\nu_0$ values of the two bands are close to each other when the intensities of Bands I and II are nearly equal, but the variation of $\Delta\nu/\nu_0$ is generally larger with a stronger band than with a weaker band. This may be indicated that the one with larger character of C=O stretching vibration shows more variation in wave number.

Tropolone.—In tropolone (III), the carbonyl group is fixed by a intramolecular hydrogen bond. So it is of interest to examine how the effects of solvents appear in the spectra. Figure 5 shows the spectra measured in various states and solvents, as well as in vapor state obtained earlier[4]. The various values obtained from Fig. 5 are shown in Table III, and the relative wave number shifts are given in Fig. 6.

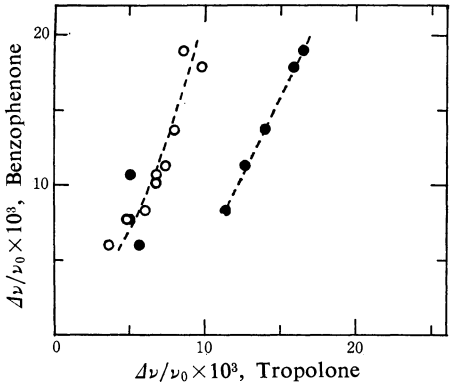


Fig. 6. Relation between the values of $\Delta\nu/\nu_0$ of Bands I and II in tropolone and of $\nu_{C=O}$ in benzophenone in various solvents.
○; Band I, ●; Band II.

From these results the following features are found.

g) In accordance with the results on tropone, the direction of shift is the same for both of Bands I and II and the degree of shift of Band II is larger than that of Band I. However, the peak intensity of Band I is larger than that of II and Band II is broader.

h) The wave numbers of Bands I and II are smaller than those of tropone by 23～21 and 38～27 cm^{-1}, respectively.

i) The values of $\Delta\nu/\nu_0$ of Bands I and II in polar solvents are smaller than those of tropone, 2-chlorotropone, and $\nu_{C=O}$ of benzophenone.

j) ε^a of Band II does not show the tendency to decrease with the shift to the lower wave number side. As is noticed from the values of r, the variation of the intensity of Band II is less than that of tropone, though the values of intensity are not sufficiently reliable because of the absorption of the solvent itself and the broad absorption at around 1490 cm^{-1} due to a C–O–H group[13].

The variation of spectrum is thus the same in tendency as in the cases of tropone and 2-chlorotropone but is very small in its degree. This means that the C=O stretching absorption shifts to the lower side than that of tropone by 23～40 cm^{-1} by the effect of intramolecular hydrogen bond and that, by this hydrogen bond, the carbonyl group is affected little by the external actions at any state of measurement. This effect is comparatively large in polar solvents.

Summary

Infrared absorption spectra of tropone, 2-chlorotropone, and tropolone in the region of 1700～1500 cm^{-1} were measured in various states and in various solvents, and the variation of two strong Bands I and II in the region of 1700～1530 cm^{-1} was investigated. The data are shown in tables and figures. These two bands are explained as the participation of both of the C=O and C=C stretching vibrations in a tropone skeleton. The variation of the spectrum of tropolone with the measuring condition is much smaller than that of tropone. This is because the carbonyl group in tropolone is fixed by the intramolecular hydrogen bond.

Grateful acknowledgement is made to Professor Susumu Kinumaki, Professor Shuichi Seto, and Assistant Professor Koyo Aida who gave valuable guidance to this study and to Mr. Shuji Aono who performed part of the measurement.

The Chemical Research Institute of Non-Aqueous Solutions
Tohoku University
Katahira-cho, Sendai

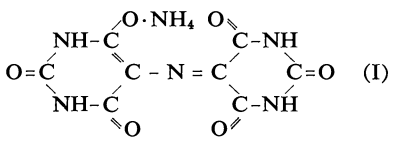
13) Y. Ikegami, ibid., 34, 94 (1961).

Spectrophotometric Studies on the Kinetics of Decomposition of Tetramethylmurexide in Acid Medium

By R. K. CHATURVEDI

(Received August 12, 1961)

Murexide or ammonium purpurate (I) has



(I)

found extensive application in analytical procedures for qualitative detection and quantitative estimation[1-8] of various metal ions. For these purposes murexide is used both in acidic[9] as well as alkaline media[10], but in highly acidic or alkaline solutions this metal ion indicator is quite unstable. A research programme was therefore, undertaken on the kinetics of decomposition of murexide in acidic[11] and alkaline[12] media in order to elucidate the reaction mechanism (s) and to formulate proper conditions for the analytical use of murexide[13]. These kinetic studies are now being extended to various compounds related to murexide. The present communication refers to the study on the kinetics of decomposition of tetramethylmurexide (ammonium tetramethylpurpurate) in acid solutions.

Experimental

Tetramethylmurexide was prepared by the method of Gysling and Schwarzenbach[15] by the action of ammonium carbonate on tetramethylalloxantin. This last named compound was obtained by careful degradation of caffeine following the procedure outlined by Biltz[16]. Repeated recrystallization of ammonium tetramethylpurpurate by salting it out from its aqueous solution[17] by the addition of ammonium chloride gave a sample of satisfactory purity. Hydrochloric acid used was an Analar sample; diluted solutions of this acid were standardized against a standard sodium carbonate solution. Throughout these studies redistilled water was used for preparing the solutions etc. All the spectrophotometric measurements were made with a Beckman DU spectrophotometer using corex cells of 1 cm. width. The temperature of the reaction system was maintained at desired value with an accuracy of ± 0.05°C (or better) by employing a Beckman dual thermospacer set in combination with an externally connected thermostat; this last was operated by a micro relay.

Results and Discussion

Absorption Spectra of Tetramethylmurexide. —Figure 1 gives a typical set of results on the absorption of tetramethylmurexide solution in the visible region; the curve in this figure refers to a concentration of 0.05 mM. It may be noted from Fig. 1 that tetramethylmurexide exhibits an absorption maximum at $\lambda = 530$ mμ.

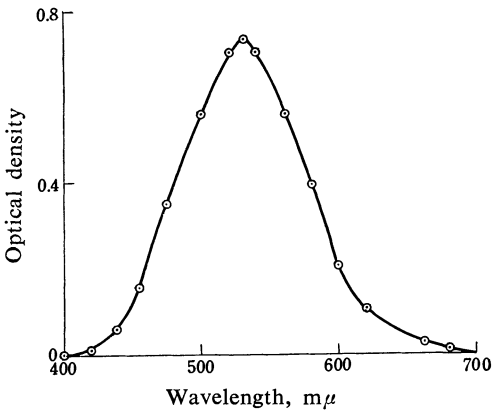


Fig. 1. Absorption spectrum of tetramethylmurexide in the visible region.

1) C. A. Kumins, *Anal. Chim. Acta*, **1**, 69 (1947).
2) H. Ostertag and D. E. Rinck, *Chim. Anal.*, **34**, 108 (1952).
3) W. Th. G. M. Smeets and L. Seekles, *Nature*, **169**, 802 (1952).
4) W. F. Harris and T. Sweet, *Anal. Chem.*, **24**, 1062 (1952).
5) G. Schwarzenbach, W. Biederman and F. Bangerter, *Helv. Chim. Acta*, **29**, 811 (1946).
6) M. G. Williams and J. E. Moser, *Anal. Chem.*, **25**, 1414 (1953).
7) H. Flaschka and F. Huditz, *Z. anal. Chem.*, **197**, 104 (1952).
8) N. A. Ramaiah, Vishnu and R. K. Chaturvedi, *Naturwiss.*, **45**, 290 (1958).
9) S. P. Sangal and A. K. Dey, *Proc., Natl. Acad. Sci. (India), Symposium*, 12 (1961).
10) Cf. Ref. 5.
11) N. A. Ramaiah, S. L. Gupta and Vishnu, *Z. physik. Chem.*, **106**, 254 (1956); R. K. Chaturvedi, ibid., communicated.
12) R. K. Chaturvedi, Doctoral Thesis, Agra University, 1960; R. K. Chaturvedi, *Z. physik. Chem.*, communicated.
13) N. A. Ramaiah and R. K. Chaturvedi, *Curr. Sci.*, **29**, 305 (1960).
14) R. K. Chaturvedi, *Naturwiss.*, **48**, 643 (1961).
15) H. Gysling and G. Schwarzenbach, *Helv. Chim. Acta*, **32**, 1484 (1944).
16) H. Biltz, *Ber.*, **45**, 3674 (1912).
17) See also D. Davidson, *J. Am. Chem. Soc.*, **58**, 1821 (1936).

Further, this wavelength of maximum absorption was unaffected by the change in the concentration or/and pH of the system. Studies on the variation of optical density with concentration of tetramethylmurexide were carried out in the concentration range 0.01～0.08 mM. It is evident from Fig. 2 that the absorption of tetramethylmurexide at $\lambda=530$ mμ is governed by Beer's law; the value of the Beer's constant from the slope corresponds to 1.464×10^4.

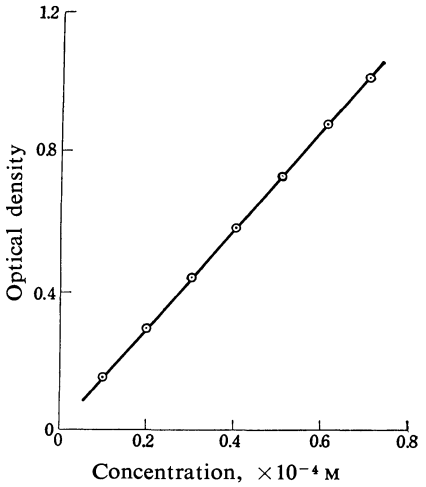


Fig. 2. Application of Beer's law to the absorption of tetramethylmurexide at $\lambda=530$ mμ.

The observations recorded above thus provide a method for following the reaction kinetics by observing the variation with time of the optical density of acidic solution of tetramethyl murexide at $\lambda=530$ mμ. In the experiments reported here the concentration of hydrochloric acid and tetramethyl murexide were 5 and 0.05 mM respectively. Thus the temperature was the only variable parameter in these experiments; the range of temperature investigated in these experiments was from 25～45°C.

Determination of the Rate Constants.—For a first order reaction, we have

$$\ln C=\ln C_0-kt \qquad \text{(i)}$$

Where C_0 is the initial concentration of the substance and C is the concentration after a time interval t. Equation 1 suggests that $\log C$ vs. t plots should be linear with slope being equivalent to $-k/2.303$. Instead of concentration one may also employ a physical property linearly dependent upon C such as optical density (vide supra). Figure 4 gives the plots of log(OD) vs. t for the reaction under investigation; from the slope of these plots, we get the value of the apparent rate constant (in time^{-1})

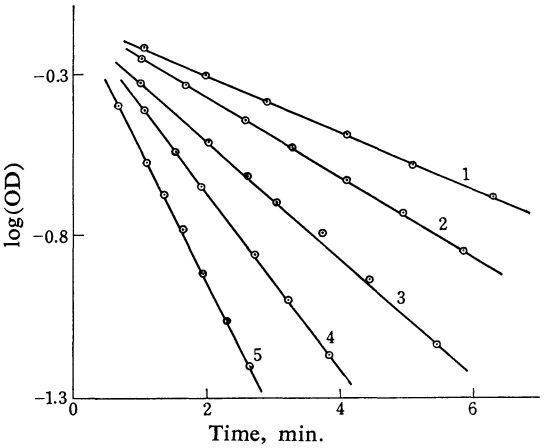


Fig. 3. log(OD) vs. time plots: concentration of HCl, 5 mM; concentration of tetramethylmurexide, 0.05 mM. Temperature: curve 1, 25°C; curve 2, 30°C; curve 3, 35°C; curve 4, 40°C; curve 5, 45°C.

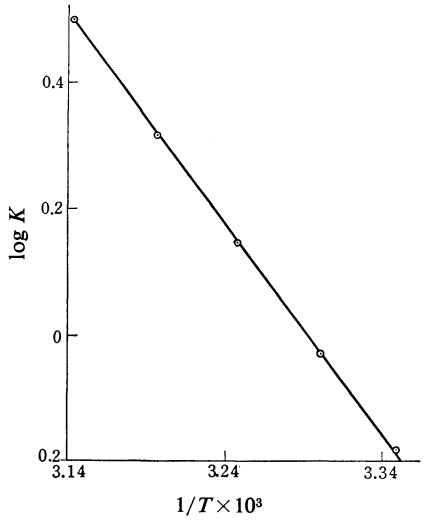


Fig. 4. Arrhenius plot.

for the reaction. As pointed out previously[18], these k values are linearly variant with hydrogen ion concentration $[H^+]$ and refer here to the experimental conditions under which the initial concentration of H^+ is taken in much excess over that of the tetramethylmurexide. The reaction is in fact bimolecular and the rate constant characteristic of the reaction is given by the relationship.

$$k=\frac{2.303\,\Delta\log(\mathrm{OD})}{[H^+]\times\Delta t}$$

which differs from the values obtained from the slope in Fig. 4 by the factor $[H^+]$ which appears in the denominator. These values of k (expressed in sec^{-1} l. mol^{-1}) corresponding to

18) Cf. Ref. 14.

TABLE I. RATE CONSTANTS OF DECOMPOSITION OF TETRAMETHYLMUREXIDE IN ACID SOLUTIONS

Temp., °K	298	303	308	313	318
Rate constant $l.mol^{-1}sec^{-1}$	0.67	0.93	1.39	2.07	3.17

TABLE II. FREQUENCY FACTOR, ENERGY AND THERMODYNAMIC QUANTITIES OF ACTIVATION (25°C)

E	15.49 kcal.
$\log A$	11.18
$\Delta F^{\ddagger}$	17.69 kcal. $deg^{-1}\,mol^{-1}$
$\Delta S^{\ddagger}$	−4.75 e. u.
$\Delta H^{\ddagger}$	16.27 kcal. mol^{-1}

different temperatures are returned in Table I. Thus for example the values of k were 0.937 and 3.17 at 30°C and 45°C respectively.

Determination of Quantities of Activation.—For computation of the energy of activation of the reaction, the well-known Arrhenius equation was applied. Figure 4 gives the linear plot of $\log k$ vs. $1/T$; from the slope of this plot, we get a value of 15.49 kcal. for the energy of activation. This value of E along with the values of k in Table I, gives a value of 11.18 for the Arrhenius frequency factory ($\log A$)[19]. Also presented in this table are the data on the free energy and entropy of activation calculated from the relationship[20]

$$\Delta F^{\ddagger}=2.303\,\boldsymbol{R}T\left(\log\frac{\boldsymbol{R}T}{Nh}-\log k\right) \qquad (1)$$

$$\Delta S^{\ddagger}=2.303\,\boldsymbol{R}\left(\log A-\log e\frac{\boldsymbol{R}T}{Nh}\right) \qquad (2)$$

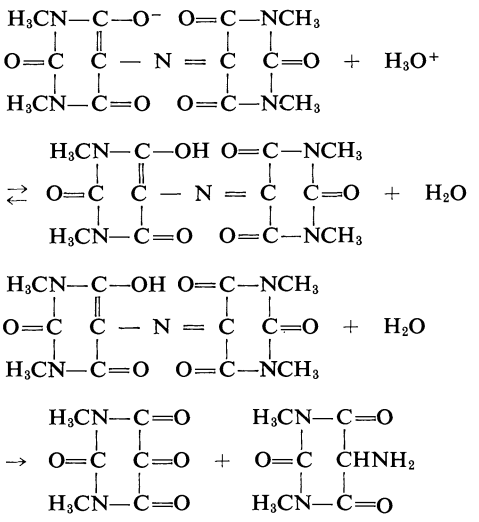
and the value of $\Delta H^{\ddagger}$ obtained from the values of $\Delta F^{\ddagger}$ and $\Delta S^{\ddagger}$.

Comparison with Collision Theory.—From consideration based on the collision theory one can shown that for a biomolecular reaction the kinetic collision frequency is given by[21]

$$Z=\frac{N}{1000}\,\sigma^2\left[8\Pi\boldsymbol{R}T\left\{\frac{1}{M_a}+\frac{1}{M_b}\right\}\right]^{1/2} \qquad (3)$$

where σ is the distance of approach between the reactions for effective collision, M_a and M_b are molecular weights of the reactants and the terms N, Π, $\boldsymbol{R}$ and T have their usual significance. From Eq. 3 we get a value of 11.62 for $\log Z$ in good agreement with a value of 11.18 obtained experimentally for the Arrhenius frequency factor. Similar agreements have been obtained for various reactions in solutions[22] which are free from complications arising out of ionic interactions etc.

Possible Reaction Mechanism.—In view of the above observations and with the knowledge of the reaction products, a possible mechanism of the reaction can be formulated. The problem of the products formed as a result of the decomposition of murexide and substituted murexides in acid solutions has been widely discussed[23]. The presence of alloxan and uramil along with some alloxantin has been detected[24]. In fact it was a controversial point as to whether the alloxan and uramil are primary products or the alloxantin. It was, however, convincingly shown by Davidson[25] that the decomposition of murexide in acid medium gives alloxan and uramil; these compounds then undergo secondary reactions to give alloxantin. For tetramethylmurexide the products of the primary reaction would thus be dimethyl substituted alloxan and uramil. It is suggested that this process takes place according to the following mechanism:



It is of interest to point out here that it has not been so far possible to isolate the free purpuric acid or substituted purpuric acids because of their extreme instability. On the other hand in case of certain compounds related to murexide for which the corresponding acids are stable, the addition of acids to say ammonium salts results in the liberation of free acid[26]. Further the direct interaction of the tetramethylpurpurate ion and the hydronium

19) Calculated from the equation:
$$\log A=\log k+E/2.303\boldsymbol{R}T$$
20) S. Glasstone, K. L. Laidler and A Eyring, "The Theory of Rate Processes", McGraw Hill Book Co., Inc. New York (1941), pp. 195, 199.
21) E. A. Molewyn-Hughes, "The Kinetics of Reaction in Solutions", Macmillan & Co., London (1933), p. 79.
22) Cf. Ref. 21.
23) O. Piloty, *Ann.*, **22**, 333 (1904); B. J. R. Mohlau, *Ber.*, **37**, 2686 (1904); M. D. Slimmer and J. Stieglitz, *Am. Chem. J.*, **31**, 661 (1904).
24) H. E. Wohler and J. Liebig, *Ann.*, **26**, 319 (1838); F. K. Beilstein, ibid., **107**, 176 (1858).
25) D. Davidson and E. Epstein, *J. Org. Chem*, **1**, 305 (1936).
26) Cf. Ref. 15.

ion cannot be the rate determing one, as for such a process the kinetic data should be such as to suggest an ionic interaction. Moreover the tetramethylpurpurate is considered to be in equilibrium with tetramethylpurpuric acid as a result of the ionic combination of the former with the hydronium ion. This process will be governed by an equilibrium constant the reciprocal of which will be, according to the modern concepts[27], the ionization constant of tetramethylpurpuric acid; the ionic combination of tetramethylpurpurate and the hydronium ion cannot be considered to be the rate determing one, as such processes are known to be extremely fast[28]. Thus it appears very likely that the instability of tetramethylpurpuric acid, the formation of which is favored in presence of excess of acid, is responsible for the decomposition of tetramethylmurexide in acid medium and for the observed kinetics of the reaction.

Summary

Kinetics of the decomposition of tetramethylmurexide in acid solutions have been investigated spectrophotometrically by following the absorption at $\lambda=530$ mμ. The optical density of tetramethylmurexide at this wavelength has been shown to obey Beer's law with a value of 1.464×10^4 for the Beer's constant. The change in the optical density with time of tetramethylmurexide solutions in presence of hydrochloric acid has been shown to obey a first order law and from these data the rate constants of the reaction have been computed at different temperatures in the range 25~45°C. These data have been employed to obtain quantities such as energy and entropy of activation etc. and the Arrhenius frequency factor; the comparison of this last has been made with the collision theory. The possible mechanism of the reaction has been discussed.

Author's grateful thanks are due to Dr. H. Trivedi, Principal, for facilities and encouragement and to Dr. J. B. Lal, head of the Chemical Engineering Department, for his kind interest in the work.

Department of Physical Chemistry
H. B. Technological Institute
Kanpur, India

27) R. W. Gurney, "Ionic Processes in Solutlon", McGraw Hill Book Co., Inc., New York (1953); see also M. Mandel and C. Decroly, *Trans. Faraday Soc.*, **56**, 29 (1960).

28) M. Eigen, *Discussions Faraday Soc.*, **17**, 194 (1954); P. Delahay and T. J. Adams, *J. Am. Chem. Soc.*, **74**, 1437 (1954).

Electrical Conduction in the Violanthrene-Iodine System

By Tokiko UCHIDA and Hideo AKAMATU

(Received November 30, 1961)

With relation to the nature of conductive electrons or the mechanism of electrical conduction in organic solids, the intermolecular charge transfer complexes are interesting, because the complex formation results in a remarkably low electrical resistivity compared with that of the constituents[1-5]. However, there is a variety in their electrical properties, which depend on the combination of the electron donor compounds and the acceptor compounds. The complexes which possess a relatively high conductivity are those which belong to the "strong" charge transfer complexes, whereas the "weak" charge transfer complexes possess a relatively high resistivity. The former can be characterized by its strong electron spin resonance absorption at room temperature; a correlation between the charge carriers and the unpaired electrons has even been suggested. The typical examples with which we are concerned here are the complexes between polycyclic aromatic hydrocarbons and halogens. Most of these complexes consist of definite stoichiometic compositions in the solid state, for instance, pyrene-iodine (1 : 1 and 1 : 2), perylene-iodine (2 : 3 and 1 : 3), pyranthrene-iodine (1 : 2), etc. Under X-ray diffraction,

1) H. Akamatu, H. Inokuchi and Y. Matsunaga, *Nature*, **173**, 168 (1954); This Bulletin, **29**, 213 (1956).
2) R. G. Kepler, P. E. Bierstedt and R. E. Merrifield, *Phys. Rev. Letters*, **5**, 503 (1960).
3) M. M. Labes, R. Sehr and M. Bose, *J. Chem. Phys.*, **33**, 868 (1960).
4) J. Komanduer and F. R. Hall, ibid., **34**, 129 (1961).
5) T. Uchida and H. Akamatu, This Bulletin, **34**, 1015 (1961).

these complexes show particular crystal patterns. In contrast to these complexes, violanthrene forms a complex with iodine, which has a non-stoichiometric composition; furthermore, X-ray diffraction indicates that it is completely amorphous. The structure of the violanthrene-iodine complex has been discussed in a previous paper[6], where we concluded that this complex is to be regarded as the solid solution between iodine and violanthrene. From the view point of semiconducting material, a system like this is specially interesting, because iodine molecules (acceptor) can be distributed homogeneously among violanthrene molecules (host matrix) at any concentration. This will result in a semiconducting system which is analogous to an impurity semiconductor or a valence-controlled semiconductor, lithium-nickel oxide, for instance.

Experimental and Results

Preparation.—Violanthrene was prepared from violanthrone by reduction with zinc-dust. After the usual purification, it was carefully purified by repeated sublimation in vacuo. In order to vary the iodine content in the complex widely, the following two procedures were applied according to the iodine concentration.

For High Iodine Content Complex.—Crystalline powder of violanthrene was suspended in a benzene solution of iodine and boiled for about 30 min. using a reflux condenser. After cooling, the black-colored precipitate was filtered off with a glass filter. (When this precipitate was heated, iodine was liberated and the original hydrocarbon could be recovered. This indicates that the black precipitate was not a substitutional product but a molecular additional compound.) The quantity of added iodine was determined from the difference in weight between the original hydrocarbon and the precipitate. The amount of violanthrene dissolved into the benzene solution was disregarded as being too small compared with the total amount of the sample.

For Low Iodine Content Complex.—Finely powdered violanthrene was suspended in a carbon tetrachloride solution of iodine and, being kept at room temperature for more than three days, was shaken from time to time. Then the precipitate was filtered off with a glass filter. The amount of added iodine was determined from the difference between the initial and the final concentration of dissolved iodine, which difference was measured by iodometry with sodium thiosulfate.

In both procedures, the iodine content in the precipitates could be varied by controlling the amounts of dissolved iodine in the initial solutions. The high iodine content complex was black colored, while, as the iodine content decreased, the color approched that of the original hydrocarbon (dark red).

Electrical Resistivity.—The measurement of electrical resistivity was made with a sample packed into an ebonite pipe (3 mm. in diameter), both ends of which were attached to electrodes of platinum or silver-coated copper. At least 116 kg./cm^2 pressure was applied to the sample in order to reduce the contact resistance at the grain boundary. The resistance was read with an ohmmeter for the samples with low resistivity, while it was measured also with a galvanometer for the samples possessing higher values of resistivity. The applied voltage was less than 20 V./cm., at which the electrolysis did not take place.

The resistivities at room temperature are shown in the third column in Table I. The second column denotes the composition of the sample in the mole ratio of iodine to violanthrene.

All the specimens showed a negative temperature coefficient of resistivity and changed in value in accordance with the formula $\rho = \rho_0 \exp(E/kT)$. The observed values for activation energy, E, for the electrical conduction are shown in the fourth column in Table I. The temperature ranges for these observations are indicated in the last column.

The results show that the conductivity is enhanced by the addition of a small quantity of iodine and increases monotonously with the increase in iodine content (Fig. 1), while the activation energy has a nearly constant value in the range of low iodine content. If the iodine molecules are assumed to be distributed homogeneously in the host matrix, they might be separated from each other by 13 molecules of violanthrene (about 100 Å) in the sample with the least iodine content.

Qualitative observation for thermoelectric power was attempted to know the sign of the predominant charge carriers. Both electrodes of the specimen cell, the mole ratio of which was 1.90, were connected to a galvanometer. By heating one side of the electrodes, a minute current flow was observed. The direction of the flow through the galvanometer was from the cold side electrode to the hot side electrode. Namely, the contribution of the positive holes was more predominant than that of the electrons to the conduction in this complex, while the opposite was observed in pure violanthrene.

Hall Effect.—The Hall effect has not been observed in semiconductive simple organic compounds because of their high resistivities. The only report presented has been on a rather special compound, poly-copper-phthalocyanine[7].

6) H. Akamatu, Y. Matsunaga and H. Kuroda, ibid., 30, 618 (1957).

7) A. Epstein and B. S. Wildi, *J. Chem. Phys.*, 32, 324 (1960).

Table I. Electrical resistivity at room temperature and activation energy of violanthrene-iodine

Sample No.	Mole ratio	Resistivity ohm cm.	E eV.	Temp. range °C
1	3.17	127	0.12_5	−180～15
2	1.90	18.0	0.07_5	−180～15
3	1.31	24.0	0.09	−180～15
4	0.118	2.2×10^{2}	0.09	−180～15
5	1.0×10^{-2}	3.1×10^{5}	0.22_5	15～90
6	3.6×10^{-3}	2.8×10^{7}	0.22_5	15～90
7	8×10^{-4}	6.0×10^{8}	—	—
8	5×10^{-4}	1.4×10^{9}	0.22	15～65
	Violanthrene	2.0×10^{14}	0.47	60～200

Table II. Number of spins and charge carriers

Sample No.	Iodine concn. N_{I_2} per cc.	Spin concn. N_{spin} per cc.	Line width gauss	Carrier concn. N^* per cc. (calcd.)	Mobility μ cm²/V. sec. (calcd.)
1	4.48×10^{21}	8.0×10^{19}	18	2.93×10^{19}	1.7×10^{-3}
2	2.63×10^{21}	9.0×10^{19}	14	1.29×10^{20}	2.7×10^{-3}
3	1.79×10^{21}	1.0×10^{20}	11	4.79×10^{19}	5.4×10^{-3}
4	2.27×10^{20}	4×10^{18}	10	6.07×10^{18}	4.7×10^{-3}
5	2.1×10^{19}	$<10^{18}$	—	2.4×10^{15}	8.4×10^{-3}
6	7.4×10^{18}	—	—	8.7×10^{14}	2.6×10^{-4}
7	1.7×10^{18}	—	—	1.9×10^{14}	5.4×10^{-5}
8	1.0×10^{18}	—	—	1.5×10^{14}	3.0×10^{-5}

It was hoped to observe the Hall effect successfully in the halogen-complexes, because they possess low resistivities. The attempt was made with a sample with the mole ratio of 1.90. The specimen powder was pressed into a frame of Bakelite plate with a load of 1000 kg. The dimensions of the specimen were $5\times20\times1.73$ (t) mm. Platinum electrodes and leads were mounted in the frame. The electrical resistance of the specimen was 140 ohm between current leads and 700 ohm between potential leads. This frame was placed between poles of a magnet. The applied electrical current (I) was 8.5 mamp. The magnetic field (H) was 8000 oersted. For the electromotive force measurement, a Leed & Northrup potentiometer was employed in association with a galvanometer (Kaken) possessing the sensitivity of 4.6×10^{-8} V. All the apparatus was carefully insulated from the ground to avoid a slight irregular current.

When the magnetic field was applied, a slight potential difference was recognized between the potential leads. Although the magnitude was very small (about 0.5 mm. movement on the scale of the galvanometer), a quite definite change in direction of the electromotive force was noted following alternation of the direction of the magnetic field or electric current in the specimen. This direction indicated the hole conduction, which was consistent with the results of the thermoelectric power. From this, it might be concluded that a very weak Hall effect was perceived in the violanthrene-iodine complex. However, the Hall voltage was small, restricted by the limits for the sensitivity of the galvanometer, $\Delta V<4.6\times10^{-8}$ V. Thus, the Hall coefficient was $R=10^{8}\cdot\Delta Vt/HI<1.2\times10^{-2}$ cm³/coulomb. If the conduction is assumed to be carried by positive holes, the number of carriers and the mobility might be estimated as:

$$n_h=\frac{3\pi}{8}\frac{1}{Re}>7\times10^{20}\ \mathrm{cm}^{-3}$$

$$\mu_h=\frac{8}{3\pi}R\sigma<1.6\times10^{-3}\ \mathrm{cm}^2/\mathrm{V.\ sec.}$$

This indicates that the mobility possesses a very small value, and this is the reason for the difficulty of Hall effect measurement for these organic compounds. These values quoted the lower limit and the upper limit respectively due to the sensitivity of the galvanometer. However, they are perhaps not far from the real values, which will be discussed in a later section.

ESR Absorption.—The electron spin resonance absorption was observed at room temperature with a Hitachi MPS-1 ESR X-band spectrometer. All the samples showed absorption and, consequently, the existence of unpaired electrons. No fine structure was found in the absorption line.

The g-value was determined by referring to a standard sample of ultramarine ($g=2.028$). The g-value of the violanthrene-iodine system was 2.0035, regardless of the composition, which is very close to the value of the free electron or of organic free radicals. The spin concentration of the samples was determined from the integral areas of absorption lines by comparison with that of a standard sample of diphenylpicrylhydrazyl. The observed values are summarized in Table II. For the samples of lower iodine content, the estimationof spin numbers could not be made quantitatively because of their weak absorptions. Violanthrene usually shows a weak absorption (for a reason unknown at present), and the values quoted in Table II are those for which correction has been made for the absorption of violanthrene (2×10^{18}/g.). Such being the case, a spin concentration of less than 10^{18} per cc. (for sample 5) is not reliable.

Discussion

It has been found that a small amount of iodine added to violanthrene enhances the electrical conduction remarkably, and that the resistivity decreases monotonously with an increase in the iodine concentration until the mole ratio 1:2, where the intermolecular pseudo-compound is formed[6]. This effect of iodine is almost comparable to that of lithium oxide added to nickel(II) oxide. The resistivity of pure oxide nickel is 10^{13} ohm-cm. at room temperature, which is comparable to that of violanthrene, 10^{14} ohm-cm. It is well known[8,9] that the alloying of lithium oxide with nickel(II) oxide in a homogeneous solid solution leads to a semiconducting material (the so-called valence control semiconductor) with a remarkable range of resistivity depending on the lithium concentration. In Fig. 1, the variation of resistivity with the concentration of the impurity is illustrated for the systems of both violanthrene-iodine and nickel(II) oxide-lithium oxide. One can see that the two curves are quite similar to each other. Moreover, a few common characteristics can be noted between these two systems. In the nickel oxide system, the activation energy for electrical conduction is as small as around 0.1 eV. and depends on the lithium content; the conduction is carried by positive holes, and its mobility is so small that the Hall effect could hardly be observed. However, from the Seebeck effect it has been estimated

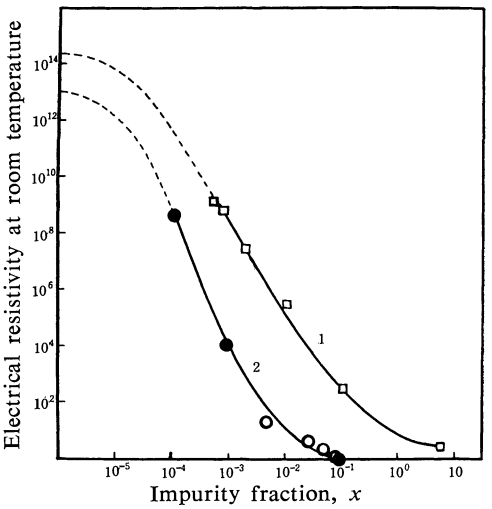


Fig. 1. Electrical resistivity for various impurity content.
Curve 1: Violanthrene-iodine. Curve 2: $Li_xNi_{(1-x)}O$. (After Morin. Ref. 9, p. 622). Impurity content is represented by the fractional number x for both curves.

as 10^{-3} cm^2/V. sec. at room temperature, depending on the lithium content.

The mechanism of electrical conduction in the nickel oxide system has long been discussed as a typical example to which the energy band model could not be applied. Recently, the "hopping" type electrical conduction theory has been proposed and has been quite successful[10]. Thus, it might be interesting to speculate on the conduction mechanism in the violanthrene-iodine system on the analogy of the nickel(II) oxide-lithium oxide system.

In nickel oxide, neighboring Ni^{2+} ions are so far separated from each other that the overlap of 3d wave functions is very small and the 3d charge carriers can be considered to occupy energy levels localized on the cations. In consequence, pure nickel oxide possesses a high resistivity. However, nickel oxide can be made conducting by introducing Ni^{3+} ions into the lattice by the substitution of Li^+ ions for some of the Ni^{2+} ions. The Ni^{3+} ions (holes) are not bound to definite positions in the lattice, but can wander through the crystal by jumping from ion to ion if there is some overlap between hole wave functions localized on neighboring ions. However, the hole tends to be "self-trapped" in the crystal as a result of the polarization of the surrounding lattice, and when the hole can jump, the polarization associated with the hole must jump with it. The jumping process is then

8) E. J. W. Verwey, "Semiconducting Material", Ed. by H. K. Henisch, Butterworths Scientific Publications, London (1951), p. 151.
9) F. J. Morin, "Semiconductors", Ed. by N. B. Hannay, Reinhold Pub. Co., New York (1959), p. 600.
10) J. Yamashita and T. Kurosawa, *J. Chem. Phys. Solids*, 5, 34 (1958).

expected to involve an activation energy associated with the self-trapping of the holes.

In the violanthrene-iodine system, the electron transfer takes place from violanthrene (D) to neighboring iodine (A) through an overlap of molecular orbitals by the quantum mechanical resonance; the dative structure (D^+A^-) will result, in which the violanthrene molecule can be regarded as a positive ion. The dative structure may not be bound to a definite donor molecule, but may wander by the resonance among the neighboring molecules; thus resulting in a positive hole. However, the hole may be localized (trapping) around the acceptor molecule (I_2^-), and an activation energy is then expected to make it the "free" hole, which gives rise to electrical conduction by the jumping process. In transport of this type one may expect low mobility and a low value of activation energy because of the polarization effect, as in the case of nickel oxide.

In such a scheme, as many dative structures will be produced as the number of iodine molecules in the violanthrene matrix, but the number of free holes must be smaller than this. This is characteristic of the charge transfer complexes which possess a relatively high conductivity; i. e., a strong ESR absorption is generally observed. Singer and Kommandeur[11] have found, for the complex of pyrene-iodine and perylene-iodine, that the spin concentration increases with the temperature and that the activation energy for the spin generation is in accordance with that for the electrical conduction. Calvin et at.[12] assumed that the number of charge carriers is the same as the number of unpaired spins in the phthalocyanine-chloranil complex. The origin of the observed spins in the charge transfer complex has not yet been clarified; however, a close relation between these unpaired spins and the charge carriers can be presumed. The observable number of unpaired spins is much less than the number of iodine molecules added to violanthrene, and just a small percentage of it at room temperature. If one can assume that the trapped holes are thermally excited and give rise to the free holes, then the number of free holes N^* might be given by $N_{I_2} \exp(-E/kT)$, where N_{I_2} is the number of iodine molecules and E is the activation energy for electrical conduction. In Table II, the calculated values of N^* are shown. These values are almost comparable with the observed numbers of spins in samples 1, 2, 3 and 4, whose spin concentration could be measured quantitatively.

Further speculation can be made on the mobility of charge carriers, which can be given by $\mu = \sigma/N^*e$. The calculated values for the mobility are shown in the last column of Table II. These values are likely reasonable and consistent with the results of the measurement of the Hall effect. In this speculation, it has been assumed that the unpaired spins are observable only when associated with the free holes, but no spin is observable when the hole is trapped by the acceptor ion. Furthermore, the observed activation energy is assumed to be associated predominantly with the delocalization of the hole, rather than with the polarization effect in the transportation process.

11) L. S. Singer and J. Kommandeur, *J. Chem. Phys.*, **34**, 133 (1961).
12) D. R. Kearns, G. Tollin and M. Calvin, ibid., **32**, 1020 (1960).

Summary

Electrical conduction and ESR absorption in the violanthrene-iodine system have been investigated, varying the iodine content. Observation of the Hall effect has been attempted, but the Hall voltage was so small that the effect could not be determined. It was pointed out that, concerning conductive behaviors, the violanthrene-iodine system is analogous with the nickel(II) oxide-lithium oxide solid solution, and that the hopping model of electrical conduction can be applied. From such a view point, the correlation between the observed unpaired spins and charge carriers has been estimated.

The cost of this research has been defrayed by a grant-in-aid for Fundamental Scientific Research from the Ministry of Education, to which the authors' thanks are due.

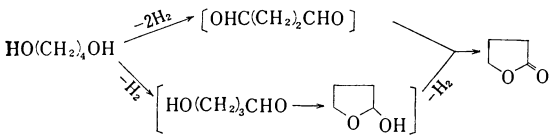
Department of Chemistry
Faculty of Science
The University of Tokyo
Hongo, Tokyo

Studies on Lactone Formation in Vapor Phase. III. Mechanism of Lactone Formation from Diols

By Shinzaburo OKA

(Received September 19, 1961)

In previous papers[1,2], it was clarified that the catalytic dehydrogenation of 1,6-hexanediol to ε-caprolactone was very difficult as compared with those of 1,4-butanediol and 1,5-pentanediol, and that it yielded 1-cyclopentene-1-carboxaldehyde, cyclopentanecarboxaldehyde and cyclopentylcarbinol as by-products. These facts aroused the author's interest in the mechanism of this reaction. Reppe[3] considered that first dialdehyde or oxyaldehyde was formed and that then an intramolecular reaction of the Cannizzaro type or an intramolecular acetalization, followed by a dehydrogenation to lactone, took place. For example, in the case of 1,4-butanediol:



Copenhaver[4] wrote that the latter route seemed more likely in view of the nature of the catalyst. Wagner[5] also supported the latter route on the basis of the fact that δ-valerolactone is readily prepared by air oxydation of the corresponding oxyaldehyde[6].

The reactions of dialdehydes or oxyaldehydes leading to the corresponding lactones have, however, been studied by only a few investigators. Meerwein[7] and Longley[8], for instance, prepared δ-valerolactone derivatives by the action of sodium ethoxide or sodium hydroxyde upon dialdehydes in the liquid phase. Bremmer[6] studied the air oxydation of δ-oxyvaleraldehyde to δ-valerolactone in the presence of a cobalt salt in the liquid phase. But the reaction conditions and the catalysts in their investigations are different from those of the dehydrogenation of diols to lactones with the copper catalysts. A study of the behavior of dialdehydes or oxyaldehydes over the copper catalysts used in the previous studies[1,2] has therefore been made.

Experimental

γ-Oxybutyraldehyde (2-oxytetrahydrofuran).—The oxyaldehyde was obtained by thermal decomposition of butane-1,4-dinitrite in the vapor phase, as has been described by Kuhn[9]. From 50 g. of butanedinitrite (b. p. 62~63°C/23 mmHg, n_D^{25} 1.4049), there was obtained 13 g. of γ-oxybutyraldehyde, b. p. 72°C/18 mmHg, n_D^{25} 1.4400, d_4^{25} 1.0808 (Found: C, 54.47; H, 9.20%). Its infrared spectrum (Fig. 1) showed a strong band due to a hydroxyl group at 2.95 μ and a weak band due to a carbonyl group at 5.80 μ, and it formed a 2,4-dinitrophenylhydrazone, m. p. 116°C (lit.[9] 120°C).

δ-Oxyvaleraldehyde (2-oxytetrahydropyran).—The oxyaldehyde was prepared by hydrolysis of 3,4-dihydro-α-pyran[10], as has been described in "Organic Syntheses"[11]. From 60 g. of dihydropyran (b. p. 85~86°C, n_D^{25} 1.4350, d_4^{25} 0.9072), there was obtained 25 g. (33%) of δ-oxyvaleraldehyde, b. p. 54~55°C/3 mmHg, n_D^{25} 1.4515, d_4^{25} 1.0527 (Found: C, 58.63; H, 9.95%). Its infrared spectrum (Fig. 2) showed a strong band due to a hydroxyl group and a weak band due to a carbonyl group, and it formed a 2,4-dinitrophenylhydrazone, m. p. 106~107°C (lit.[12] 109°C).

1,1,4,4-Tetraethoxybutane.—1,1,4,4-Tetraethoxy-2-butyne[13] (42 g., b. p. 104°C/3 mmHg, n_D^{25} 1.4319) in 100 ml. of ethanol was hydrogenated under 80 kg./cm² of initial hydrogen pressure with 6 g. of Raney nickel W-6 at 50~60°C for 2 hr. The catalyst was filtered off, and the filtrate was distilled to yield 40.5 g. (92%) of tetraethoxybutane, b.p. 92~93°C/4 mmHg, n_D^{25} 1.4150 d_4^{25} 0.9136 (Found: C, 61.45; H, 11.32%).

Succinaldehyde Dioxime.—A mixture of 47 g. of tetraethoxy butane and 100 ml. of 0.2 N sulfuric acid was stirred at 30°C. After the mixture had been stirred for 2 hr. the water-insoluble layer disappeared. After another 2 hr., 34 g. of hydroxylamine chloride was added. Then, 50 g. of anhydrous sodium carbonate was added in small portions. After the mixture had been kept in the refrigerator overnight, the crystals were filtered, washed with

1) S. Oka, This Bulletin, **34**, 12 (1961).
2) S. Oka, ibid., **35**, 562 (1962).
3) W. Reppe et al., *Ann.*, **596**, 159 (1955).
4) J. W. Copenhaver and M. H. Bigelow, "Acetylene and Carbon Monoxide Chemistry", Reinhold Pub. Co., New York (1949), p. 152.
5) R. B. Wagner and H. D. Zook, "Synthetic Organic Chemistry", John Wiley & Sons., New York (1953), p. 536.
6) J. G. M. Bremmer et al., U. S. Pat., 2429799 (1947); *Chem. Abstr.*, **42**, 923 (1948).
7) H. Meerwein, *Ber.*, **53**, 1829 (1920).
8) R. I. Longley et al., *J. Am. Chem. Soc.*, **72**, 3079 (1950).
9) L. P. Kuhn et al., ibid., **78**, 2719 (1956).
10) R. L. Sawyer et al., "Organic Syntheses", **23**, 25 (1943).
11) G. F. Woods, ibid., **27**, 43 (1947).
12) G. F. Woods et al., *J. Am. Chem. Soc.*, **68**, 2111 (1946).
13) A. L. Kranzfelder et al., ibid., **60**, 1714 (1938).

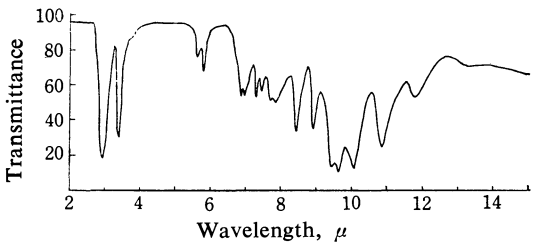


Fig. 1. Infrared spectrum of γ-oxybutyraldehyde.

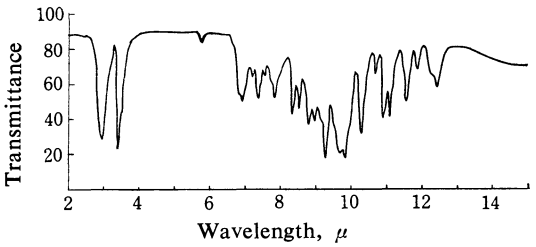


Fig. 2. Infrared spectrum of δ-oxyvaleraldehyde.

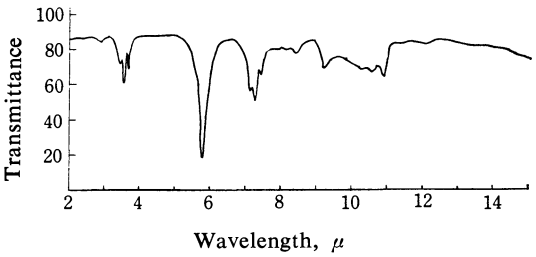


Fig. 3. Infrared spectrum of succinaldehyde.

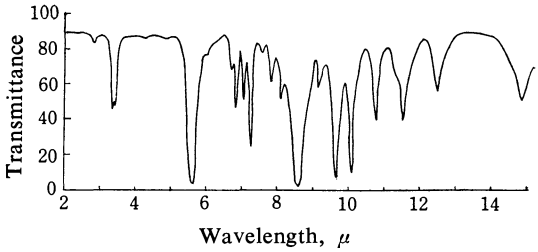


Fig. 4. Infrared spectrum of γ-butyrolactone.

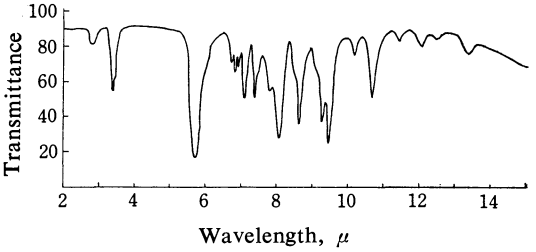


Fig. 5. Infrared spectrum of δ-valerolactone.

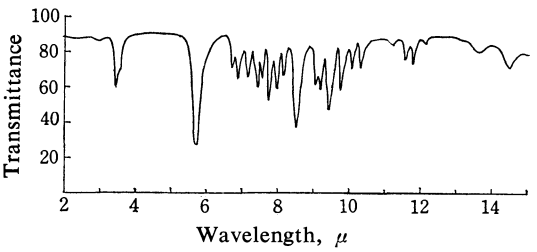


Fig. 6. Infrared spectrum of ε-caprolactone.

water, and dried. The yield of dioxime was 18 g. (74%). Recrystallisation from aqueous ethanol gave a sample melting at 168~169°C (lit.[14] 171~172°C).

Succinaldehyde.—The dialdehyde was obtained by treating its dioxime with sodium nitrite in dilute sulfuric acid, as has been described by Keagle[14]. From 18 g. of the dioxime, there was obtained 6.5 g. (49%) of succinaldehyde, b. p. 78°C/25 mmHg, n_D^{25} 1.4240, d_4^{25} 1.0492 (Found: C, 55.77; H, 7.29%). Its infrared spectrum (Fig. 3) showed a medium band due to C-H group in aldehyde at 3.65 μ and a strong band due to carbonyl group at 5.80 μ.

Glutaraldehyde.—The dialdehyde was prepared by hydrolysis of 2-methoxy-3,4-dihydro-α-pyran, as has been described by Longley[8]. From 30 g. of methoxydihydropyran (b. p. 126~127°C, n_D^{25} 1.4400, d_4^{25} 0.9961), there was obtained 16 g. (61%) of glutaraldehyde, b. p. 53~55°C/3 mmHg, n_D^{25} 1.4280, d_4^{25} 1.0077 (Found: C, 59.14; H, 8.19%). It formed a dioxime, m. p. 164~166°C (Found: C, 46.42; H, 7.83%).

1, 1, 6, 6-Tetraethoxyhexane.— Tetraethoxyhexane was prepared by essentially the same method as that of Kranzfelder[13]. From 150 g. of ethyl orthoformate, 24 g. of magnesium, and 108 g. of tetramethylene bromide, there was obtained 62 g. (47%) of tetraethoxyhexane, b. p. 115~117°C/4 mmHg, n_D^{25} 1.4220, d_4^{25} 0.9085. (Found: C, 64.21; H, 11.40%).

Adipaldehyde.—A mixture of tetraethoxyhexane (52 g.) and 0.4 N sulfuric acid (100 ml.) was stirred at 30°C. After the mixture had been stirred for 3 hr., the water-insoluble layer disappeared. The solution was kept at room temperature for another 4 hr. Then the solution was neutralized with sodium bicarbonate, saturated with sodium chloride and extracted with ether. The dried ether extract gave 14 g. (62%) of adipaldehyde, b. p. 110~112°C/20 mmHg, n_D^{25} 1.4335, d_4^{25} 0.9754 (Found: C, 63.13; H, 9.17%). It formed a dioxime, m. p. 170~171°C (Found: C, 49.96; H, 8.58%).

Vapor Phase Reactions. — The apparatus, procedures, and methods for the preparation of the catalysts were essentially the same as those previously described[1,2]. Tablets of the catalyst (50 ml.) were used. The pressure in the reaction system was reduced to 20~30 mmHg. A sample was passed in by vacuum distillation in a period of one hour. The reaction temperature was maintained at 220~230°C. Some experiments are shown below.

γ-Butyrolactone.—The copper-zinc oxide catalyst was used. γ-Oxybutyraldehyde (15 g.) gave a product (13 g.), b. p. 98~100°C/25 mmHg, n_D^{25} 1.4350, which was identified as γ-butyrolactone. It formed a hydrazide, m. p. 92°C, which gave no depression when mixed with an authentic sample.

14) L. C. Keagle et al., ibid., 68, 1609 (1946).

δ-Valerolactone.—The copper chromite-zinc oxide catalyst was used. δ-Oxyvaleraldehyde (10 g.) gave a product (6.2 g.), b. p. 73~74°C/4 mmHg, n_D^{25} 1.4550, which was identified as δ-valerolactone. It formed a hydrazide, m. p. 105~106°C, which gave no depression when mixed with an authentic sample.

The infrared spectra of the lactones obtained in the present work (Figs. 4—6) showed strong bands due to lactone group at 5.75 and 8.60 μ.

1-Cyclopentene-1-carboxaldehyde. — The copper chromite-zinc oxide catalyst was used. Adipaldehyde (10 g.) gave a product (4.5 g.), b. p. 55~57°C/25 mmHg, n_D^{24} 1.4765, d_4^{25} 0.9522, which was identified as 1-cyclopentene-1-carboxaldehyde (lit.[15] b. p. 57~59°C/27 mmHg, n_D^{20} 1.4866). MR_D Found: 27.1. Calcd.: 27.3.

Found: C, 74.62; H, 8.79. Calcd. for C_6H_8O; C, 74.97; H, 8.39%.

Cyclopentenecarboxaldehyde gave a 2,4-dinitrophenylhydrazone melting at 209~210°C (lit.[16] 210~211°C).

Found: C, 52.16; H, 4.48. Calcd. for $C_{12}H_{12}O_4N_4$: C, 52.17; H, 4.38%.

Cyclopentylcarbinol. — The copper - magnesium oxide catalyst was used. Unlike as in the above experiment, adipaldehyde (10 g.) was passed in with a steady current of hydrogen (20 l./hr.) in a period of one hour. The reaction temperature was maintained at 230~240°C. The product (5.2 g.), b. p. 75~78°C/25 mmHg, n_D^{25} 1.4550, d_4^{25} 0.9309, was identified as cyclopentylcarbinol. It formed a phenylurethan, m. p. 108°C, which gave no depression when mixed with an authentic sample.

Results and Discussion

The results are summarized in Table I. With all the catalysts used, it was ascertained that the oxyaldehydes gave the corresponding lactones as easily as the diols did. On the contrary, the dialdehydes examined gave no lactones, and they were recovered up to 70%

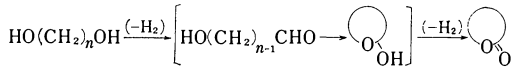
TABLE I. LACTONE FORMATION FROM DIOLS, OXYALDEHYDES AND DIALDEHYDES

Catalyst	Copper-zinc oxide	Copper chromite	Copper chromite-zinc oxide
Sample	Yield of lactone %	Yield of lactone %	Yield of lactone %
1,4-Butanediol	95	53	78
γ-Oxybutyraldehyde	93	53	80
Succinaldehyde	0	0	0
1,5-Pentanediol	84	54	76
δ-Oxyvaleraldehyde	76	55	65
Glutaraldehyde	0	0	0
1,6-Hexanediol	trace	28	68
Adipaldehyde	0	0	0

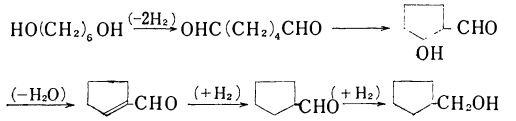
Reaction temperature: 220~230°C. Reaction time: 1 hr.

15) J. English et al., ibid., **71**, 3310 (1949).
16) M. S. Klarash et al., *J. Org. Chem.*, **16**, 150 (1951).

except in the case of adipaldehyde. Adipaldehyde gave 1-cyclopentene-1-carboxaldehyde even in the presence of the copper chromite-zinc oxide catalyst which was the most favorable catalyst for ε-caprolactone formation. Adipaldehyde gave cyclopentylcarbinol as well as 1,6-hexanediol, under a hydrogen stream over the copper-magnesium catalyst. From these experimental results, it is concluded that the dehydrogenation of the diols to the lactones proceeds according to the latter route mentioned above, although the formation of ε-caprolactone from ε-oxycaproaldehyde could not be examined.



The products obtained from adipaldehyde support the occurrence of the side reaction proposed in the previous paper[2].



From a study of the ultraviolet spectra, Hurd et al.[17] concluded that, in aqueous dioxane, γ-oxybutyraldehyde and δ-oxyvaleraldehyde exist predominantly as cyclic lactoles, and that ε-oxycaproaldehyde exists as 85% free aldehyde. The infrared spectra of γ-oxybutyraldehyde and δ-oxyvaleraldehyde in the present work were in accord with the above results.

The difficulty of lactone formation from 1,6-hexanediol can be understood by considering that of seven-membered lactole ring formation from ε-oxycaproaldehyde. The slow lactole formation would cause undesirable dehydrogenation to adipaldehyde, from which 1-cyclopentene-1-carboxaldehyde is formed by intramolecular aldol condensation followed by dehydration. The occurrence of this side reaction was observed especially in the case of the copper-magnesium oxide catalyst. The high selectivity of the copper chromite-zinc oxide catalyst may be attributed to its accelerating effect on the lactole formation.

Ester formation[18,19] in the dehydrogenation of alcohol to aldehyde with coeppr chromite has been believed to be a result of the Tischtschenko reaction:

$$2RCHO \longrightarrow RCOOCH_2R$$

However, the mechanism of lactone formation

17) C. D. Hurd et al., *J. Am. Chem. Soc.*, **74**, 5324 (1952).
18) H. Adkins et al., ibid., **55**, 2714 (1933).
19) R. E. Dunbar, *J. Org. Chem.*, **3**, 242 (1938).

in the present work explains the ester formation more reasonably in the following manner:

$$RCH_2OH \xrightarrow{(-H_2)} RCHO \xrightarrow{(+RCH_2OH)}$$

$$RCH(OH)(OCH_2R) \xrightarrow{(-H_2)} RCOOCH_2R$$

The author wishes to express his thanks to Professor Ryozo Goto and Professor Sango Kunichika of Kyoto University for their invaluable advice and criticisms. He also wishes to thank Mr. Tohru Takenaka for his infrared spectra analyses and Mrs. Toshiko Ikegami for her elementary analyses.

Institute for Chemical Research
Kyoto University
Kosobe, Takatsuki

Study on Nickel Oxide-Silica-Alumina Catalyst for Ethylene Polymerization. I. Catalyst Activity for Ethylene Polymerization and Selectivity in the Formation of Butene-Isomers

By Hiroshi UCHIDA and Hisao IMAI

(Received October 12, 1961)

A number of papers[1-7] have dealt with the catalytic polymerization of olefins over nickel oxide-silica-alumina catalysts, but the catalyst selectivity from the view point of isomer formation has not been described at all. In this paper both the catalyst activity for ethylene polymerization and the selectivity in butene-isomer formation are presented on a series of catalysts with a progressively increasing aluminum content and with a fixed amount of nickel oxide.

Experimental

Catalyst. — Coprecipitated catalysts comprising silica, alumina, and nickel oxide were used in this study. The catalysts contained a fixed amount of nickel oxide, 0.03[8] in terms of the atom ratio Ni/(Ni+Al+Si), while the aluminum content, given by the atom ratio Al/(Al+Si), varied from 0 to 0.5. The precipitation was made by vigorously mixing a sodium silicate solution containing 5 wt. % of silica with another solution of nitrates of aluminum and nickel. Caution was exercised to keep the pH of the resulting hydrogel solution within the small range of 8±0.5. This was achieved either by adding, prior to the mixing, an amount of caustic soda to the sodium silicate solution or an amount of nitric acid to the solution of nitrates, according to whether a greater amount of silica or of alumina was to be contained in the finished catalyst. Moreover, the product concentration[9] was maintained at 0.03 g./cc. The solution was then subjected to a treatment similar to that of Holm et al.[7]: after filtration on a Buchner funnel, the hydrogel was broken up, placed in evaporating dishes under heat lamps, and allowed to dry in this manner for a day, after which it was dried for several hours in an oven at 110°C. The dried catalyst was treated with successive portions of a 5% hot ammonium nitrate solution and then with hot water in order to remove the sodium. After drying, it was heated at 350°C for 4 hr. The compositions of the catalysts prepared in this way (hereafter designated as catalysts A) are shown in Table I.

Besides the catalysts A, two other catalysts, designated as calalyst AI-4 and AII-4, of the same composition as catalyst A-4 but prepared by different methods, were used. In the preparation of

TABLE I. CATALYSTS COMPOSITION

Catalyst[a]	A-1	A-2	A-3	A-4	A-5	A-6
Al/(Al+Si) (atom)	0	0.03	0.05	0.11	0.30	0.50

a) Throughout all the catalysts the nickel oxide content is kept at a fixed Ni/(Ni+Al+Si) ratio of 0.03.

1) Y. Konaka, *J. Soc. Chem. Ind., Japan* (*Kôgyô Kwagaku Zassi*), **39**, 906 (1936).
2) K. Morikawa, ibid., **41**, 694 (1938).
3) M. Koizumi et al., *J. Chem. Soc. Japan* (*Nippon Kwagaku Kwaisi*), **64**, 257, 263, 794 (1943).
4) T. Shiba and A. Ozaki, ibid., **74**, 295 (1953); A. Ozaki, ibid., **75**, 1, 4, 6 (1954); **77**, 888 (1956); *Catalyst* (*Shokubai*), **14**, 65 (1957).
5) S. Kawaguchi and K. Kihara, ibid., **75**, 15 (1954); S. Kawaguchi, *J. Phys. Chem.*, **61**, 394 (1957).
6) J. P. Hogan, R. L. Banks et al., *Ind. End. Chem.*, **47**, 752 (1955).
7) V. C. F. Holm, G. C. Bailey and A. Clark, ibid., **49**, 250 (1957).
8) According to the statement by Holm et al.[7], the catalyst activity for ethylene polymerization was highest in the catalyst with this nickel content.
9) The product concentration was defined by g. NiO+Al_2O_3+SiO_2 contained in 1 cc. of the hydrogel (refer to 10).
10) C. J. Plank and L. C. Drake, *J. Colloid Sci.*, **2**, 389 (1947).

catalyst AI-4, the hydrogel was washed before the drying, while catalyst AII-4 was a sample of aerogel prepared by means of the method of Kistler[11] from the washed hydrogel of catalyst A-4.

The catalyst samples were crushed into granules 1~2 mm. in size and heated at 500°C for 15 hr. in a stream of air, atter which they ware evacuated at the same temperature for 3 hr. under a reduced pressure of 1×10^{-4} mmHg and were used for the polymerization.

Ethylene.—Ethylene was produced by the dehydration of ethanol over an alumina catalyst. It was purified by successive passages through 30% caustic soda solution, 87% sulfuric acid, and finally a trap placed in a bath of dry ice and methanol. After the purification, it was frozen in a trap cooled with a liquid nitrogen bath. The solid ethylene was distilled in vacuo into another trap by replacting the liquid nitrogen bath with a dry ice bath. The distillation was repeated four times to get rid of the last traces of inert gas, and then the gaseous ethylene was introduced into a gas reservoir.

Catalyst Activity.—The apparatus was a circulatory flow system with a total volume of 2.1 l. and a catalyst cell containing 5 cc. of the catalyst. The flow rate throughout was 70 l./hr. at N. T. P., and the initial ethylene pressure was 350 mmHg. Immediately after the catalyst cell there was placed a U-trap which had been cooled in a bath of dry ice and methanol. Since butene at −78°C retains a vapor pressure of 10 mmHg, all the butene produced was circulated throughout the system until the butene formation had proceeded so far as to attain the pressure of 10 mmHg (an earlier stage of the polymerization); as soon as butene attained this pressure, a part of the circulating butene began to condense in the trap in an amount corresponding to the amount produced (a subsequent stage). The pressure decrease in the system within time of polymerization was measured by means of a mercury manometer attached to the system; the decrease at the subsequent stage gave a measure of the catalyst activity.

After the polymerization had proceeded to such an extent that the total pressure of the system was as low as 0.57 times the initial pressure, the catalyst cell was removed by sealing off the glass tube on both sides of the cell. Part of the condensation product in the trap was then evaporated into the system by replacing the dry ice bath with an ice bath. After the evaporation the gaseous product comprised ethylene and butene, while the liquid product comprised hydrocarbons higher than hexene. The liquid product remaining in the trap was weighed. The experiments made in this manner will be denoted as in series A.

On the other hand, another series of experiments (series B) was made with a few modifications in the experimental procedure, using the same apparatus with a smaller catalyst bed of 1 cc. The modifications were that the trap was cooled with ice and that small portions of the exit gas from the cell were withdrawn at frequent intervals. The change in the composition of butene isomers with time was followed by a gas chromatographic analysis of the portions at 32°C by the use of a 5 m. column of benzyl cyanide plus silver nitrate on cellite 408[12]. In this procedure all the butene produced was circulated throughout the system, together with reactant ethylene, while a major part of the product hydrocarbons higher than hexene were condensed in the trap.

Specific Surface Area Pore Volume, Pore Size Distribution and Density.—The specific surface area was obtained by the aid of the BET method applied to the nitrogen adsorption isotherm determined at −196°C. The amount of nitrogen adsorbed at the relative pressure of 0.967 gave the the pore volume, including pores smaller than 300 Å in radius. Furthermore, the desorption isotherm was determined on three kinds of catalysts, A-, AI- and AII-4. On the basis of the isotherm, the pore size distribution was calculated by the aid of Barrett's method[13]. The catalyst density was measured by the helium displacement method[14] at 20°C.

Experimental Results

Catalyst Activity for Ethylene Polymerization.—The data on the pressure decrease in the experiments of series A are found to follow the following rate equation proposed for the ethylene polymerization by Koizumi et al.[3], provided that the reaction does not proceed too far:

$$-dp/dt=kP/(1+b(P_0-P)) \quad (1)$$

or upon integration,

$$(P_0-P)/t=(P_0+1/b)\ln P_0/P-k/b \quad (2)$$

In the equations, P_0 is the initial pressure of ethylene, P is the observed ethylene pressure at time t, k is the rate constant, and b is a

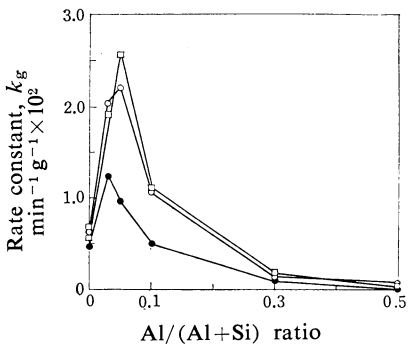


Fig. 1. Dependency of catalyst activity for ethylene polymerization on Al/(Al+Si) ratio.
Reaction temp., °C
—□— 40
—○— 60
—●— 100

11) S. S. Kistler, *J. Phys. Chem.*, **36**, 52 (1932).

12) F. van de Craats, *Anal. Chim. Acta*, **14**, 136 (1956).

13) E. P. Barrett, L. G. Joyner and P. P. Halenda, *J. Am. Chem. Soc.*, **73**, 373 (1951).

14) F. O. Wiig and A. J. Juhola, ibid., **71**, 561 (1949).

TABLE II. CATALYST ACTIVITY, SPECIFIC SURFACE AREA, AND OTHER MATTERS ON CATALYSTS A-, AI- AND AII-5

Catalyst	k_g 40°C	k_g 100°C	F_b 40°C	F_b 100°C	Specific surface area $m^2/g.$	Pore volume cc./g.	Average pore radius Å
	$\times 10^2$ min.$^{-1}$ g.$^{-1}$						
A-4	1.24	0·53	0.72	0.84	278	0.344	24.7
AI-4	1.68	0.37	0.59	0.73	403	0.252	12.5
AII-4	1.41	0.43	0.69	0.79	576	1.500	52.0

constant. In this paper, k_g, which gives the rate constant per gram of the catalyst, is used as a comparative measure of the catalyst activity. It decreases with the increasing temperature (refer to Fig. 1), but the Arrhenius plot of the k_g is not linear.

In Fig. 1, the k_g is plotted against the Al/(Al+Si) ratio, and a maximum is produced in the narrow range from 0.03 to 0.05. On the other hand, the values of k_g for catalysts A-, AI- and AII-4 are listed in Table II, which includes also the data on the specific surface area and the other matters. The k_gs have been found to be almost the same among the three catalysts.

In the ethylene polymerization, a major part of the broduct is usually butene, while a part of the product consists of the trimer and the higher polymers. The fraction of the amount of ethylene converted to butene in the total polymerization product (the fraction is designated as F_b hereafter) is given approximately by $2(P_b+10)/(P_0-P+10)$, where P_b is the pressure rise caused by the evaporation of that butene which has been condensed in the trap during the polymerization, and 10 (mmHg) stands for the vapor pressure of the butene in the circulatory system. The values of F_b at the different reaction temperatures of 40, 60 and 100°C are plotted in Fig. 2 as a function of the Al/(Al+Si) ratio. Comparison of the

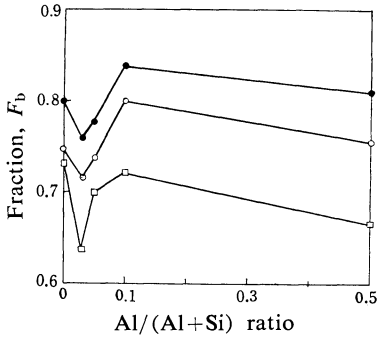


Fig. 2. Dependency of ethylene fraction converted to butene in total ethylene polymerized on Al/(Al+Si) ratio.
Reaction temp., °C
—□— 40
—○— 60
—●— 100

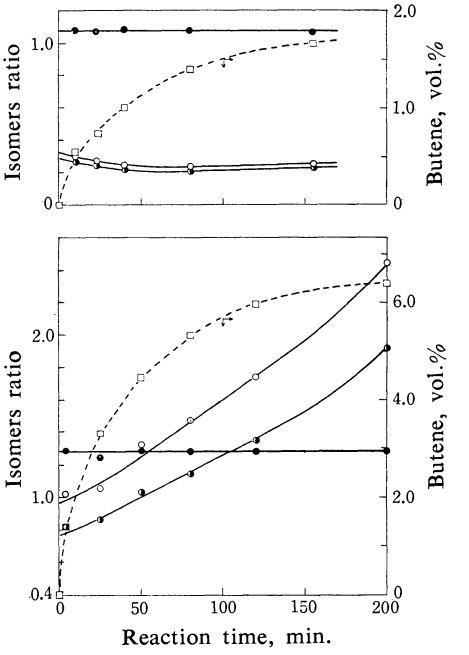


Fig. 3. Change in butene-isomers ratio with progress of polymerization.
Above, results on catalyst A-1. Below, results on catalyst A-3 at 40°C.
Isomers ratio
—◑— *cis*-/1-butene
—○— *trans*-/1-butene
—●— *trans*-/*cis*-
···□··· Amount of butene (vol.%) in circulating gas.

figure with Fig. 1 discloses that F_b is lowest for the catalyst of the highest k_g.

Catalyst Performance in the Selectivity of Isomer Formation.—Additional data from the experiments of series B give information on the distribution of butene isomers but not any on the rates of polymerization. The data are exemplified in Fig. 3, showing the reaction at 40°C on catalyst A-1 with no aluminum and on A-3 with some aluminum[15]. As regards catalyst A-3, both the ratios of *cis*- and *trans*-2-butene to 1-butene tend to increase with the duration of reaction time. This is the case with all the catalysts with aluminum,

15) There has been found hardly any evidence of the presence of isobutene.

more or less pronounced according to the aluminum contents, but it is not the case with the catalysts with no aluminum. Emphasis should be laid on the fact that throughout all the catalysts the ratio between two 2-butene isomers is maintained at values approximate to 1 regardless of the amount of butene formed[16]. Anyhow, the isomer composition at the beginning of the reaction is far removed from the thermodynamical equilibrium composition[19].

Specific Surface Area, Volume and Size of Pore and Density.—Figure 4 shows the specific surface area (S) and the pore volume (V) as respective functions of the Al/(Al+Si) ratio. The S shows a maximum at the ratio of 0.05; as the ratio increases further, it gradually decreases to about a half of the S of catalyst A-1 with no aluminum. The V is largest at catalyst A-1 and decreases, at first rapidly and then more slowly, with the increasing ratio. The average pore radius calculated from the values of S and V is plotted against the ratio and shows a minimum at the ratio corresponding to the maximum of S.

The pore size distribution curves are given in Fig. 5 for catalysts A-, AI- and AII-4.

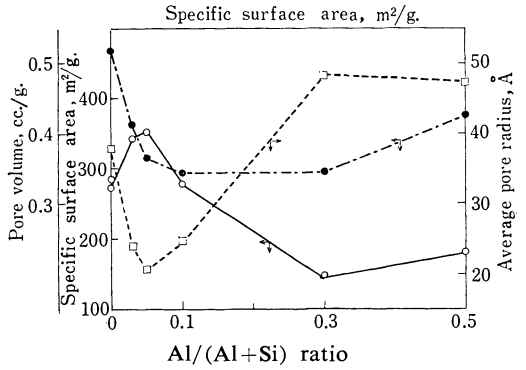


Fig. 4. Specific surface area, pore volume, and average pore radius as a function of Al/(Al+Si) ratio.
—○— Specific surface area
···●··· Pore volume
···□··· Average pore radius

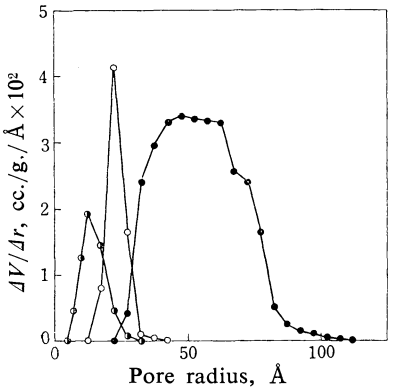


Fig. 5. Pore size distribution curves.
—○— Catalyst A-4
—◑— Catalyst AI-4
—●— Catalyst AII-4

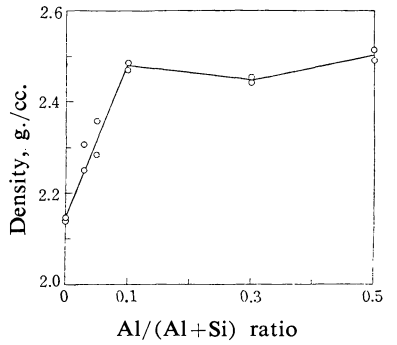


Fig. 6. Density as function of Al/(Al+Si) ratio.

The distribution curves differ markedly from each other, even though the catalysts have the same composition. The pore radii corresponding to the maximum in the curves ($\Delta V/\Delta r_{max}$) are 22.5, 12.5 and 47.5 Å for catalysts A-, AI- and AII-4 respectively.

Figure 6 shows the plot of the density vs. the Al/(Al+Si) ratio. The density at first rises rapidly with the increasing ratio, and it remains nearly constant in the range above 0.1.

Discussion

Specific Activity per Unit Surface Area.—As regards catalysts A-, AI- and AII-4, comparison of the pore size distribution curves (Fig. 5) or of the pore radii at $\Delta V/\Delta r_{max}$ with the k_g (Table II) reveals no direct relationship existing between them. Moreover, catalyst A-3 with the smallest pore radius, gives the highest k_g (compare Fig. 1 with Fig. 4). These facts may lead to the reasonable assumption that the polymerization takes place uniformly along the pore well. Under this assumption, the specific catalyst activity per unit surface area (hereafter denoted by k_s) can be obtained

16) In this connection, Foster et al.[17] stated that, in the isomerization of 1-butene to 2-butene isomers on a clay catalyst, the ratio of trans- to cis-isomer was kept at values approximate to 1 independent of conversion, whereas Lucchesi et al.[18] pointed out that in the isomerization on a silica-alumina catalyst the ratio increased.

17) N. F. Foster and R. J. Cvetanovic, *J. Am. Chem. Soc.*, **82**, 4274 (1960).

18) P. J. Lucchesi, D. L. Baeder and J. P. Longwell, ibid., **81**, 3235 (1959).

19) The thermodynamical equilibrium composition of butene isomers at 40°C has been calculated on the basis of the physical constants given by Kilpatrick et al.[20], as follows: 1-butene, 4.2%: *cis*-2-butene, 13.3%: *trans*-2-butene, 82.5%.

20) J. E. Kilpatrick, E. J. Prosen, K. S. Pitzer and F. D. Rossini, *J. Research Nat. Bur. Standards*, **36**, 559 (1946).

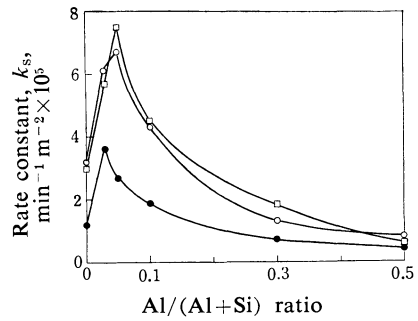


Fig. 7. Rate constant of ethylene polymerization per unit surface surface area given as function of Al/(Al+Si) ratio.
Reaction temp., °C
—□— 40
—○— 60
—●— 100

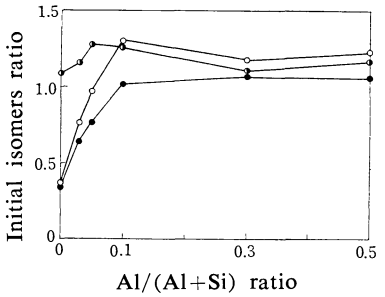


Fig. 8. Dependency of initial ratio of isomers on Al/(Al+Si) ratio.
Initial isomers ratio
—●— *cis*-/1-butene
—○— *trans*-/1-butene
—◑— *trans*-/*cis*-2-butene

by dividing k_g by S, and it is shown in Fig. 7 as a function of the Al/(Al+Si) ratio. The figure shows a maximum of the k_s at the Al/(Al+Si) ratio where the maxima of k_g and S appeared. The high k_g is therefore to be attributed to the high k_s as well as to the large S.

The structures of the catalyst responsible for the high k_s will be described in the next paper[21].

Selectivity in the Formation of Butene-isomers. —The tendency in the ratio of *cis*- or *trans*-2-butene to 1-butene to increase with the reaction time may be due to the increasing amount of 2-butene isomers converted from the 1-butene which has been once present in the gas phase as the desorbed product. Nevertheless, it by no means follows that all the 2-butene isomers are produced by way of the desorbed 1-butene. In this connection, Fig. 3 reveals that the ratio of cis- or trans-isomer to 1-butene is not reduced to zero even at a very short period of the reaction.

Applying the method proposed by Schneider et al.[22] to their study of the catalytic isomerization of *n*-butenes, Foster et al. plotted the ratio of the product isomers (for instance, the ratio of cis- to trans-isomer) against the corresponding per cent conversion of the reactant isomer (for instance, 1-butene), and obtained the ratio between the product isomers at zero conversion by extrapolation of the plot. This procedure is now followed; the extrapolation to $t=0$ of the plots in Fig. 3 results in the initial ratio at zero extent of the polymerization. The initial ratios thus obtained are shown in Fig. 8 as a function of the Al/(Al+Si) ratio. Both the initial ratios of cis- and trans-isomers to 1-butene increase with the increasing aluminum content up to the highest value at the Al/(Al+Si) ratio of 0.1, beyond which they remain almost constant. In contrast, the initial ratio between the two 2-butene isomers remains at about 1 throughout the aluminum content of the present study, except for a slight maximum at the content corresponding to the maximum of the k_g.

The initial isomers ratio thus obtained gives the relative rates for the formation of the two isomers. There are, then, the following relations:

$$r_{01}/r_{02} = [\text{cis-}]/[\text{1-butene}] \quad \text{at } t=0$$
$$r_{03}/r_{01} = [\text{trans-}]/[\text{1-butene}] \quad \text{at } t=0$$
$$\text{and } r_{03}/r_{02} = [\text{trans-}]/[\text{cis-}] \quad \text{at } t=0 \qquad (3)$$

where r_0 is the initial rate of formation, and the subscripts 1, 2 and 3 stand for 1-butene, *cis*- and *trans*-2-butene respectively. On the other hand, the initial rate of ethylene polymerization (r_0) is given by

$$r_0 = r_{01} + r_{02} + r_{03} \qquad (4)^{23}$$

Eq. 3 being combined with Eq. 4, r_{01}, r_{02} and r_{03} can be evaluated, if r_0 is known. In this connection, the initial polymerization rate based on the unit surface area can be calculated with the aid of Eq. 1, in which k_s, in place of k_g, is taken into account[24]. Figure 9 shows the calculated r_{01}, r_{02} and r_{03} based on the unit surface area at a fixed pressure (345 mmHg) and at a fixed temperature (40°C) as a function of the Al/(Al+Si) ratio. The figure reveals that, as the aluminum content is varied, the

21) At present it can at the most be pointed out that the density of the catalyst granule is not directly correlated to the specific activity, as can be seen by a comparison of Fig. 6 with Fig. 7.
22) V. Schneider and P. K. Frolich, *Ind. End. Chem.*, **23**, 1405 (1931).
23) At the beginning of polymerization, all the ethylene polymerized may be assumed to produce butene[6].
24) Since k_g was evaluated from the data at the subsequent stage of the reaction, the calculation is rather uncertain, but the initial rates obtained may be adequate for the comparative discussion in this study.

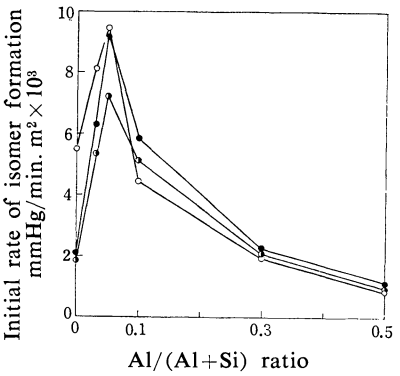


Fig. 9. Dependency of initial rates of isomer formation on Al/(Al+Si) ratio.
—○— Initial rate of 1-butene formation
—◑— Initial rate of *cis*-2-butene formation
—●— Initial rate of *trans*-2-butene formation

initial rates r_{01}, r_{02} and r_{03} change in approximately the same manner as r_0, rising with the increasing aluminum content until a maximum is attained at the Al/(Al+Si) ratio of 0.05 and decreasing with the further-increasing content. However, a closer examination of Figs. 8 and 9 reveals that not all the rates change in exactly the same manner; on the catalyst with the highest r_0, the cis- and trans-isomers are formed about four times as fast as on the catalyst with no aluminum, whereas 1-butene is formed only 1.7 times as fast as the rate on the catalyst with no aluminum.

Effects of Aluminum Addition on Catalytic Activity for Polymerization and Selectivity in Isomer-formation.—All the mechanisms which have been proposed for the hydrocarbon reactions on the acid catalysts, such as the carbonium ion mechanism, the hydrogen transfer mechanism, and the others[25], as well as the mechanism proposed by Horiuchi[26], predict the formation of a chemisorbed species of 1-butene on the catalysts when the mechanisms are applied to the dimerization of ethylene. For instance, the carbonium ion mechanism modified by Lucchesi et al.[18] indicates the following scheme[27];

$$H_2C{=}CH_2 + H^+X^- \rightarrow H_2C\overset{\overset{H}{\cdots+\cdots}}{-}CH_2\ X^-$$

I

$$I + H_2C{=}CH_2 \rightarrow H_3C{-}CH_2{-}C\overset{\overset{H}{\cdots+\cdots}}{-}CH_2\ X^- \qquad (5)$$

II

where H^+X^- represents the acid site. If with no rearrangement, the chemisorbed species II leads to 1-butene as the desorbed product,

$$II \rightarrow 1\text{-Butene} + H^+X^- \qquad (6)$$

while, with rearrangement, it leads to either one of the 2-butene isomers by way of III or IV respectively.

$$II \rightarrow H_3C{-}\overset{H}{C}\overset{\overset{H}{\cdots+\cdots}}{-}\overset{H}{C}{-}CH_3 \rightarrow \textit{cis}\text{-2-Butene} + H^+X^-\ X^-$$

III (7)

$$II \rightarrow \begin{matrix}H_3C\\|\\HC\end{matrix}\overset{\overset{H}{\cdots+\cdots}}{-}\overset{H}{C}{-}CH_3 \rightarrow \textit{trans}\text{-2-Butene} + H^+X^-\ X^-$$

IV (8)

The scheme represented by 5—6 can explain the simultaneous formation of the three isomers as the initial dimerization products and can explain also the constant ratio of about 1 between the two 2-butene isomers regardless of the duration of the reaction time, provided that rearrangement 7 can proceed at a rate equal to that of rearrangement 8 and provided also that the direct rearrangement between III and IV can be excluded at the low temperature.

However, the above scheme can not explain the present experimental facts on the catalyst selectivity related to the aluminum content, as is shown below. According to the above scheme, both the polymerization and the isomerization are to take place on the same site, H^+X^-. The increase in polymerization activity, which comes from the increase in the surface concentration of polymerization sites, can not, therefore, be expected to change the selectivity in initial butene isomer formation, whereas the experimental facts demonstrate that both the polymerization activity and the selectivity are changed by the addition of aluminum, and, moreover, that the changes take place in different manners (cf. Figs. 1 and 8).

The fact thus seems to be too complicated to be explained in terms of the above scheme, in which only one kind of acid site was considered. In this respect, we should like to suggest that, in addition to H^+X^-, another kind of acid site, H^+Y^-, which could serve as the site for the rearrangements II → III and II → IV, might be present on the catalyst and

25) Cf. L. Schmering and V. N. Ipatieff, "Advances in Catalysis and Related Subjects", II, Academic Press Inc., New York (1949), p. 21.

26) J. Horiuchi, *Catalyst (Shokubai)*, **1**, 67 (1948).

27) For convenience, the mechanism is discussed from this point of view.

that H^+X^- and H^+Y^- could be separately increased in number by the addition of aluminum. The experimental facts capable of demonstrating the presence of the two kinds of acid sites will be described in the next paper.

Summary

The activity for the ethylene polymerization per unit mass of the catalyst has been found highest for the catalyst with the Al/(Al+Si) ratio of 0.05. The high activity is ascribed to the high specific activity per unit surface area as well as to the large specific surface area of the catalyst. The pore sizes scarcely produce any effect on the catalyst activity.

Even at a very short reaction time, the three isomers of *n*-butene are produced simultaneously. The ratios both of *cis*- and of *trans*-2-butene to 1-butene increase with the reaction time more or less according to the aluminum content, whereas for all the catalysts the ratio between the two 2-butene isomers is kept at values approximate to 1. At the zero extent of reaction, the former ratios, given as a function of the aluminum content, show an increase with the progressively increasing content up to the highest value at the Al/(Al+Si) ratio of 0.1, while the latter remains nearly constant throughout all the catalysts.

For the sake of a convenient explanation of the change in the selectivity as well as in the activity related to the aluminum content of the present catalysts, two kinds of acid sites are suggested as possibly present.

Government Chemical Industrial Research Institute, Tokyo
Shibuya-ku, Tokyo

Study on Nickel Oxide-Silica-Alumina Catalyst for Ethylene Polymerization. II. Catalyst Structures Related to Catalyst Activity

By Hiroshi UCHIDA and Hisao IMAI

(Received November 2, 1961)

Our preceding paper[1] presented the results concerning the catalyst activity for ethylene polymerization and the selectivity in butene-isomer formation which were obtained for a series of nickel oxide-silica-alumina catalysts. The catalysts contained progressively increasing amounts of alumina with a fixed nickel oxide content. The results showed that both the activity and the selectivity change in a particular manner that is greatly dependent on the alumina content. In the present study, the catalysts were successively treated with hydrogen and carbon monoxide to remove nickel oxide, and the catalyst acidities before and after the treatment have been measured, along with the determinations of the changes in the activity and specific surface area. The valence state of nickel has also been determined. The results may serve for the elucidation of catalyst structure which, in turn, determines the activity.

Experimental

Catalyst Acidity.—The acidity was determined on a separate sample drawn from the same batch as the catalysts used in the activity test in the preceding paper[1]. The procedure of the determination is dependent on the chemisorption measurement of quinoline or ammonia. In this study, the quinoline chemisorption method was adopted, and the data were in some cases supplemented with the ammonia chemisorption method.

The quinoline chemisorption measurement was made by means of the technique developed by Mills et al.[2], using an apparatus of a more simplified design developed by Hara et al.[3] Prior to the chemisorption the catalyst sample was successively heated at 500°C in a stream of dry air for fifteen hours and a stream of purified nitrogen for three hours. The quinoline chemisorption and subsequent flushing of the sample with nitrogen at the flow rate of 300 cc./min. were made at 300°C.

The ammonia chemisorption was pointed out by Tamelle[4], Milliken et al.[5], Webb[6], and Voltz[7] as

1) H. Uchida and H. Imai, This Bulletin, 35, 989 (1962).

2) G. A. Mills, E. R. Boedeker and A. G. Oblad, *J. Am. Chem. Soc.*, 72, 1554 (1950).

3) N. Hara, M. Ikeda and K. Mita, *J. Chem. Soc. Japan, Ind. Chem. Sec.* (*Kogyo Kagaku Zassi*), 56, 377 (1953).

4) M. W. Tamelle, *Discussions Faraday Soc.*, 8, 270 (1950).

5) T. H. Milliken, Jr., G. A. Mills and A. G. Oblad, ibid., 8, 279 (1950).

6) A. N. Webb, *Ind. Eng. Chem.*, 49, 261 (1957).

7) S. E. Voltz and S. W. Weller, *J. Phys. Chem.*, 62, 574 (1958).

serving as a measure for the catalyst acidity. In this study, the method of Voltz was followed, and the chemisorption measurement was conducted in a static system at a fixed ammonia pressure of 35 mmHg at 60°C (the polymerization temperature). Each molecule of quinoline or ammonia chemisorbed was considered to correspond to one acid site, and the acidity data were given in the form of mmole equivalent base (quinoline or ammonia)/g. catalyst.

Removal of Nickel Oxide from Catalyst.—It would be desirable to divide the observed acidity of the catalyst into the individual contributions of the catalyst components. This would be possible if nickel oxide could be removed without causing irreversible changes in the silica-alumina support. In this respect, Schuit et al.[8] developed a very convenient method for removing nickel at a comparatively low temperature. In their study on nickel-on-silica catalysts, nickel was converted to nickel carbonyl by treatment with carbon monoxide at atmospheric pressures to remove it from the catalysts, and then the changes in the specific surface area and average pore radius caused by the removal were investigated. This method of romoval has been followed in this study with some modifications: after having been thoroughly reduced at 450°C under high pressure (50~100 kg./cm^2) of hydrogen for a week, the catalyst was treated with flowing carbon monoxide at high pressure (150 kg./cm^2) at 150°C for a week. Schuit et al.[8] stated that the removal of nickel seldom proceeded quantitatively when the coprecipitated catalysts were treated. It has been proved in the present study, however, that by the treatment at the higher pressure and temperature, more than 99% of the nickel can be removed from the coprecipitated catalysts. The catalyst acidity and the activity as well as the specific surface area were determined, in the same manner as described previously[1], on the catalyst samples thus depleted of nickel oxide (hereafter denoted as catalyst A′).

Valence State of Nickel in Catalyst.—The valence state of nickel was evaluated by precise reduction of the nickel oxide with hydrogen. The reduction was conducted according to the method of Hill et al.[10] in a circulatory flow system similar in construction to that used for the catalyst activity test in the preceding paper[1]. The catalyst sample weighing about 5 g. was placed in a catalyst tube and was pretreated in the same way as for the activity test[1], followed by introduction of hydrogen from an attached gas burette into the system to a pressure of 500 mmHg. Two U-traps were placed in the circulating system and were cooled at −78°C to remove the water vapor formed by reduction. The reduction was made at 540°C in a circulating current of hydrogen maintained at about 500 mmHg by frequent introductions of hydrogen from the gas burette. It was continued until the hydrogen consumption diminished to such a small extent as 0.1 cc. (N. T. P.)/g. catalyst·day. The reduction durations ranged from 7 to 15 days according to the reducibility. After the reduction was completed, the volume of hydrogen necessary for keeping the final pressure of the entire system exactly at 500 mmHg was measured. The system was evacuated again at 540°C for 3 hr., followed by the immediate introduction of hydrogen to the pressure of 500 mmHg. The difference between the volumes of hydrogen introduced before and after the evacuation gave the hydrogen consumption for the reduction of the nickel oxide. The processings of evacuation and the subsequent introduction of hydrogen were done in such a way as to minimize the error of overestimating the hydrogen consumption, which error might result from a considerable amount of hydrogen chemisorption on the reduced catalysts.

Experimental Results

Catalyst Activity after Nickel Oxide Removal.—In the preceding paper[1], the catalyst activity for ethylene polymerization was expressed in terms of the rate constant per gram of catalysts A (k_g). For the sake of a convenient comparison between the k_g and the activity of corresponding catalysts A′ after the nickel oxide removal, the activity of the latter catalysts is given by a rate constant based on the amount of silica-alumina contained in 1 g. of the original catalysts A but not in 1 g. of catalysts A′. The rate constant defined in this manner will be conventionally denoted by k_g of catalysts A′[11]. The results are listed in Table I, which includes the k_g for catalysts A. The table shows that catalysts A′, the silica-alumina residues from catalysts A, give poor activities which are lower than several hundredths of the activities of the corresponding catalysts A, with the exception of catalyst A–6, with a large aluminum content[12]. The ethylene

Table I. Decrease in activity after nickel oxide removal

Catalyst	Al/(Al+Si) ratio	k_g at 40°C $\times 10^2 min^{-1}g^{-1}$	k_g at 40°C after NiO removal $\times 10^2 min^{-1}g^{-1}$
A-1	0	0.68	0.0058
A-2	0.03	2.04	0.028
A-3	0.05	2.57	0.077
A-4	0.11	1.18	0.066
A-5	0.30	0.18	—
A-6	0.50	0.075	0.055

8) G. C. A. Schuit and L. L. van Reijen, "Advances in Catalysis and Related Subjects", X, Academic Press Inc. Publishers, New York and London (1958), p. 243; G. C. A. Schuit and N. H. de Boer, *J. Chim. Phys.*, 51, 482 (1954). Recently, this method was followed by Morikawa et al.[9] for their study of supported nickel catalysts.

9) K. Morikawa and F. Nozaki, *J. Chem. Soc. Japan, Ind. Chem. Sec.* (*Kogyo Kagaku Zasshi*), 64, 1562 (1961).

10) F. N. Hill and P. W. Selwood, *J. Am. Chem. Soc.*, 71, 2522 (1949).

11) The rate constant defined in this way is 0.996 times the value of the rate constant based on 1 g. of catalysts A′.

12) With respect to propylene polymerization, Clark[13] reported that when the oxides of metals in group V and higher of the periodic table were supported on silica-alumina they gave an increase in the activity over silica-alumina alone.

13) A. Clark, *Ind. Eng. Chem.*, 45, 1476 (1953).

polymerization seems to proceed on the active sites on which nickel oxide is acting effectively.

Changes in Specific Surface Area and Pore Volume by Nickel Oxide Removal.—The specific surface area and the pore volume of catalysts A′ are expressed in m^2 and cc. respectively of the silica-alumina contained in 1 g. of catalysts A. The area thus defined, in place of the surface area based on 1 g. of catalysts A′, may lead to an easier understanding of the effect of nickel oxide addition on the change in the catalyst surface area. Figure 1 presents the results as a plot against the Al/(Al+Si) ratio, together with the plot for a series of catalysts A. The former plot lies a little above the latter plot over the whole range of aluminum content examined in this study[14]. The result is the opposite of that of Schuit[8], who stated a decrease in the specific surface area of nickel-on-silica catalysts from which nickel had been driven out.

Definite tendencies in the change of the pore volume have scarcely been found between the catalysts A and corresponding catalysts A′ (refer to Fig. 2).

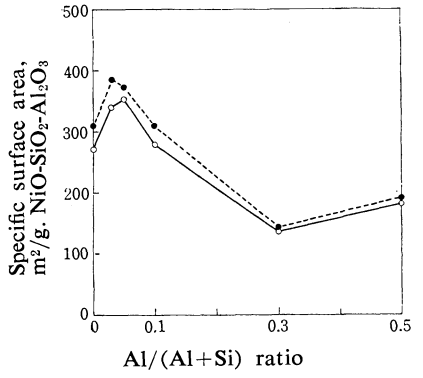


Fig. 1. Change in specific surface area by nickel oxide removal as function of Al/(Al+Si) ratio.
—○— Catalysts A
--●-- Catalysts A′

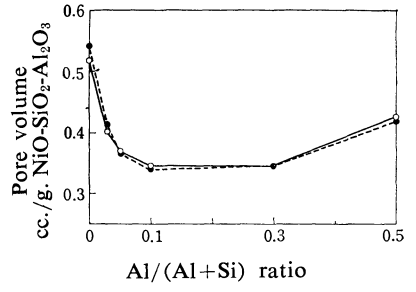


Fig. 2. Change in pore volume by nickel oxide removal as function of Al/(Al+Si) ratio.
—○— Catalysts A
--●-- Catalysts A′

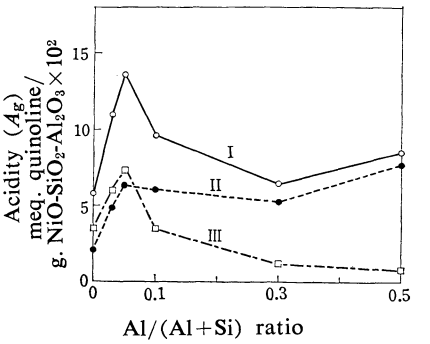


Fig. 3. Catalyst acidities before and after nickel oxide removal as function of Al/(Al+Si) ratio.
—○— Catalysts A
--●-- Catalysts A′
-·-□-·- Difference between acidities of catalysts A and A′

Catalyst Acidity.—Figure 3 shows the acidity (denoted by A_g) determined by the quinoline chemisorption method for the two series of catalysts A and A′, plotted against the Al/(Al+Si) ratio. Again, the acidity for the catalysts A′ for the sake of convenience, is expressed in mmole equivalent (meq.) quinoline chemisorbed on the silica-alumina contained in 1 g. of the original catalysts A. The plot for catalysts A (plot I) tends to rise rapidly, to pass through a maximum at a Al/(Al+Si) ratio of about 0.05, and to fall off gradually with the increasing aluminum content. The plot for catalysts A′ (plot II) lies below plot A, and the difference between the two plots (plot III), which is larger in the range of the higher acidity of catalysts A, is a measure of the acidity resulting from the nickel oxide. A small amount of nickel oxide can in some cases produce a large number of acid sites, besides those of silica-alumina alone[15]. It should be noted, further, that the numbers of acid sites thus produced are greatly dependent on the aluminum content.

Valence State of Nickel in Catalyst.—The result is shown in Fig. 4 as a plot of the atom ratio of hydrogen consumed for reduction to

14) Since the specific surface area of catalyst A-2 decreased by 2.5% of the original area after the catalyst underwent the hydrogen treatment at 450°C and subsequent oxidation at 500°C with air, the increase in the specific surface area can not be ascribed to the treatments other than the nickel oxide removal.

15) The increase in the acidity caused by an addition of metal oxides, such as chromium oxide, copper oxide, and other oxides of the transition metals, to silica-alumina over that of silica-alumina alone has already been pointed out by Clark[13] and Fisher et al.[16]

16) K. A. Fisher and G. Brandes, *Erdoel u. Kohle*, 9, 81 (1956).

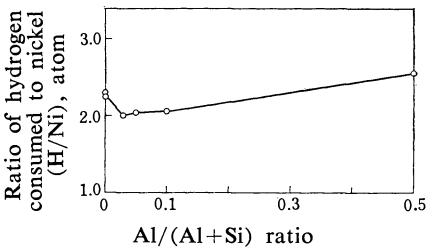


Fig. 4. Hydrogen consumption plotted against Al/(Al+Si) ratio.

nickel vs. the Al/(Al+Si) ratio. Nickel exhibits a normal valence of 2 in the Al/(Al+Si) range from 0.03 to 0.1, while on the sides both of decreasing and increasing aluminum contents valences a little higher than 2 are found. Concerning the valence of nickel in catalysts, Holm et al.[17] reported the normal valence of 2 for series of impregnated and coprecipitated nickel oxide-silica-alumina catalysts containing silica and alumina in the ratio of 9 : 1 with a wide range of nickel oxide contents. The present result is consistent with the result of Holm et al. in the sense that the valence is 2 for the catalysts with relatively small aluminum contents. On the other hand, Selwood[18] obtained a valence higher than 2 for nickel in nickel oxide-on-alumina catalysts. The slight valence increase in the range of higher aluminum content may be explainable in view of Selwood's result, since the larger the aluminum content, the larger the amount of nickel oxide which can be combined with alumina. However, no interpretation of the higher nickel valence for catalyst A-1 with no aluminum is possible.

Discussion

Relationship between Catalyst Activity and Acidity.—Previous papers dealing with the nickel oxide-silica-alumina catalysts indicated no direct relationship between the catalyst activity for olefin polymerization and the catalyst acidity[19,20]. As shown in Fig. 5[21], a simple plot of the activity (k_g) against the acidity (A_g) does not show such a relationship, either. Regarding dual-oxide catalysts, however, it was not infrequently possible to obtain

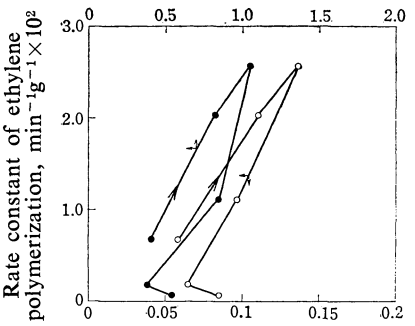


Fig. 5. Plots of catalyst activity vs. acidity.
—○— Acidity by quinoline chemisorption method (300°C)
—●— Acidity by ammonia chemisorption method (60°C)
The arrow on the line indicates the order of increasing aluminum content.

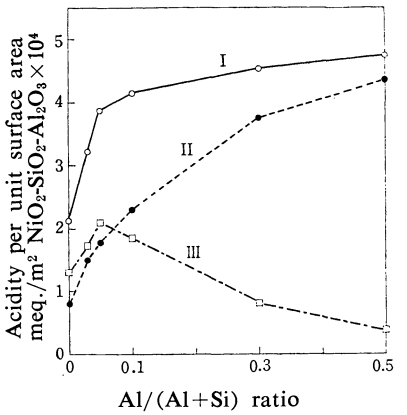


Fig. 6. Plots of acidity per unit surface area vs. Al/(Al+Si) ratio.
—○— Catalysts A
--●-- Catalysts A'
--□-- Difference between acidities of catalysts A and A'

a definite relationship between them[4,22,23], and hence the present data will be treated in further detail.

The preceding paper[1] of this series established that the specific activity per unit surface area of the catalyst and the specific surface area are the major factors determining the catalyst activity for ethylene polymerization on the nickel oxide-silica-alumina catalysts. In the present work, it has been determined that the nickel oxide has no appreciable effect on the surface area of silica-alumina and, therefore, that the increased activity is not due to an increase in the specific surface area. In order

17) V. C. F. Holm, G. C. Bailey and A. Clark, *Ind. Eng. Chem.*, **49**, 250 (1957).
18) P. W. Selwood, "Advances in Catalysis and Related Subjects", III, Academic Press Inc. Publishers, New York and London(1951), p. 28.
19) M. Koizumi, *Chemical Researches (Kagaku no Kenkyu)* **9**, 1 (1951).
20) J. P. Hogan, R. L. Banks, W. C. Lanning and A. Clark, *Ind. Eng. Chem.*, **47**, 752 (1955).
21) The figure is included with the acidity data determined by means of the ammonia chemisorption method, which data are always higher than the corresponding data obtained by the quinoline chemisorption method.
22) O. Johnson, *J. Phys. Chem.*, **59**, 827 (1955).
23) E. Echigoya, *J. Chem. Soc. Japan, Pure. Chem. Sec. (Nippon Kagaku Zassi)*, **76**, 1049 (1955).

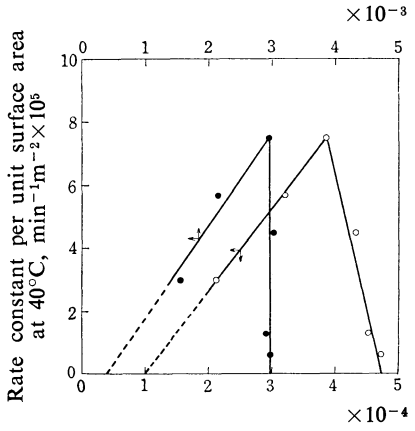


Fig. 7. Relationship of rate constant per unit surface area to acidity per unit surface area.
—○— Quinoline chemisorption method (300°C)
—●— Ammonia chemisorption method (60°C)

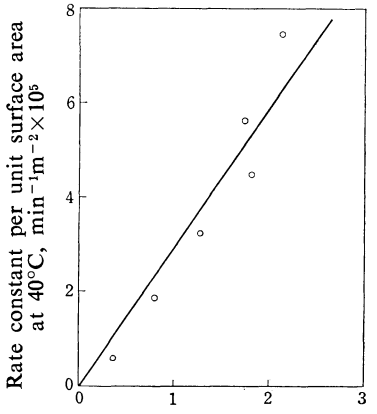


Fig. 8. Rate constant per unit surface area plotted against difference between acidities of catalysts A and A'.

to examine the possible relationship of the specific activity to the acidity, the acidity is likewise considered on the basis of unit surface area (denoted by A_s); namely, the A_g in Fig. 3 is divided by the surface area in Fig. 1 to result in the acidity based on the unit surface area of the catalysts. The A_ss are shown in Fig. 6 with separate plots of I and II for respective series of catalysts A and A' as a function of the Al/(Al+Si) ratio. Plot I rises rapidly in the range of the Al/(Al+Si) ratio from 0 to 0.05 and more slowly in the range of higher ratios with the increasing aluminum content. In contrast to this, plot II rises monotonously with the increasing content, as is usually the case with silica-alumina catalysts[24,25]. Further, the difference between the two plots, which indicates the acidity produced on the unit surface area of the catalysts with nickel oxide (denoted by A_{sNi} hereafter), is shown by plot III as a function of Al/(Al+Si) ratio. Plot III is quite different in tendency from plot I, showing a maximum at the Al/(Al+Si) ratio of 0.05.

The direct relationship of the catalyst activity to the acidity is to be given rather by the plot of k_s against A_s than by that of k_g against A_g. Of the two acidities, namely, A_s with catalysts A, and A_s with nickel oxide (A_{sNi}), only the latter acidity gives an approximate straight line when plotted against the k_s (refer to Figs. 7 and 8). In view of this fact, combined with the extremely low activity of catalysts A' as compared with that of catalysts A, it can be concluded that only the acid sites produced with nickel oxide act effectively for the ethylene polymerization and that the individual acid sites thus produced promote the polymerization to an equal extent, regardless of the aluminum contents.

Acid Site Produced with Nickel Oxide.—If an extension of Thomas' proposal[25] for silica and other binary oxide mixtures, in which he postulates the formation of protons from residual water to satisfy the valence deficiencies associated with the unit cell, is applied conventionally to the present three-component catalysts, two kinds of acid sites, as pictured respectively by models I and II in Fig. 9, may be formed. On the other hand, the preceding paper[1] suggested the existence of two kinds of acid sites, H^+X^- and H^+Y^-, on the catalysts, one of which acts effectively for the ethylene polymerization and the other one of which acts effectively for the isomerization between

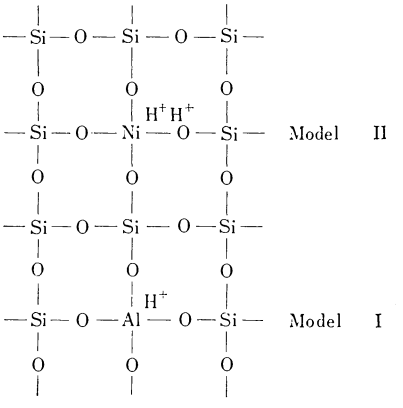


Fig. 9. Structures of acid sites.

24) V. C. F. Holm, G. C. Bailey and A. Clark, *J. Phys. Chem.*, **63**, 129 (1959).
25) C. L. Thomas, *Ind. Eng. Chem.*, **41**, 2564 (1949).

the product butene-isomers. Taking into account the linear relationship observed between the k_s for the polymerization and A_{sNi}, H^+X^- would correspond to the acid site given by the model II.

The model II proposed for the acid site H^+X^- can explain the observed relationship between the A_{sNi} and the aluminum content of the catalysts. The acid site represented by model II is brought about by the condensation of hydroxyls existing at the interface between silica and nickel oxide particles. This suggests that the acid sites could be increased in number according as the particles of nickel oxide and silica are more finely dispersed, consequently according to the increasing specific surface area of the catalyst granules. As for the present series of catalysts containing a fixed amount of nickel oxide with varying amounts of alumina, the specific surface area is greatly dependent on the alumina contents[26], and the plot of the specific surface area against the aluminum content is recognized as running approximately parallel with the same plot of A_{sNi} (compare Fig. 6 with Fig. 1). The fact that nickel in the catalysts of high A_{sNi} is divalent is another support for the model.

Moreover, the decreasing tendencies in the activity and the acidity with the increasing aluminum content in the Al/(Al+Si) range above 0.05 may be partially due to the more frequent formation of the nickel oxide-alumina compound, which gives neither the high activity[19] nor the acidity.

The fact that the initial rates of formation of three *n*-butene isomers and the A_s due to silica-alumina both depend on the aluminum content might lead to the assumption that the acid site H^+Y^- as pictured by model I acts as the site for the isomerization. However, nothing decisive can be established until further experimental data are available with respect to the catalysts with a wide range of the ratio between nickel and aluminum. The matter will be dealt with in one of the succeeding papers of this series.

26) Milligan et al.[27] stated that in the dual-oxide system (e. g. nickel oxide-alumina), one oxide (e. g. alumina) might exhibit a protective action against crystallization, resulting in finer particles of the other oxide.

27) W. O. Milligan and L. Merten, *J. Phys. Chem.*, **50**, 465 (1946); H. B. Weiser, W. O. Milligan and G. A. Mills, ibid., **52**, 942 (1948).

Summary

After nickel oxide is removed from the catalysts consisting of nickel oxide, silica, and alumina, the catalysts usually show a much lower activity than the original catalysts, with a slight increase in the specific surface area.

The acidity of the original catalysts indicates a maximum at the Al/(Al+Si) ratio of 0.05 and diminishes to some extent after the removal of the nickel oxide. The difference between the acidities before and after the removal of nickel oxide, which is a measure of the acidity originating from nickel oxide, is larger in the range of the higher acidity of the original catalysts. The valence state of nickel is found to be 2 in the Al/(Al+Si) range from 0.03 to 0.1, while it is a little higher than 2 with both decreasing and increasing aluminum contents.

Very few definite relationship have been found between the catalyst activity and acidity. However, when both the activity and the acidity originating from nickel oxide are considered on the basis of the unit surface area, an approximately linear relationship is found between them. The structure of the acid site produced by an addition of nickel oxide is discussed from the view point of an extension of Thomas' proposal for silica and other binary oxide mixtures.

Government Chemical Industrial Research Institute, Tokyo
Shibuya-ku, Tokyo

Ultraviolet Spectrophotometric Determination of Vanadium in Silicate Rocks

By Jun YOSHIMURA and Yoshio MURAKAMI

(Received September 19, 1961)

The spectrophotometric determination of a metal using various mineral acids has the advantage of not requiring a special reagent such as organic reagents, besides having the merits of simplicity of operation and of giving comparative accuracy.

Several works have recently reported on the spectrophotometric determination of various metals, such as iron(III), lead and bismuth, in which sulfuric[1], perchloric[2,3], and hydrochloric acid[4-6] were used as reagents respectively. These methods are based on the absorbance measurement at maximum wavelength of the absorption band, which is considered to be due to the complexes formed between metallic ions and anions such as sulfate, hydroxy and chloride ions.

Regarding vanadium, there are a few articles on the spectrophotometric investigation of vanadium species in acidic media[7-9], but nothing on the spectrophotometric determination of vanadium with mineral acid.

Desesa and Rogers[4] have suggested, on the other hand, the possibility of the ultraviolet spectrophotometric determination of vanadium-(V) with hydrochloric acid in their investigation of interference in the spectrophotometric determination of iron with hydrochloric acid.

The present paper is concerned with the investigation of the absorption spectra of vanadium(V) in a hydrochloric acid medium and with the application of their results to the spectrophotometric determination of vanadium(V) in silicate rock.

Experimental

Apparatus.—All absorbance measurements were carried out with a Shimadzu photoelectric spectrophotometer QB-50, with 1 cm. silica cells.

Reagents.—A standard vanadium solution was prepared by dissolving 0.4595 g. of analytical reagent grade ammonium metavanadate in 500 ml. of distilled water. One milliliter of this solution contained 200 μg. of vanadium. The solutions for the absorption spectra measurements were prepared by drying up the aliquots of the stock solution on the water bath and then dissolving the residues in hydrochloric acid solutions of various concentrations. All the other reagents used were of analytical reagent grade.

General Procedure.—Transfer about 2 g. of the rock samples to a platinum crucible and mix with 10 g. of anhydrous sodium carbonate. Fuse the mixture and allow it to cool to room temperature. Transfer the crucible and contents to a 300 ml. beaker and add a few milliliters of distilled water. Heat to boiling in order to loosen the residue in the crucible, and crush any large particles with a flattened stirring rod. Remove the crucible, and wash it sufficiently with water. Add 3 ml. of methyl alcohol to reduce the manganate, warm in the boiling water for 10 min., and filter through filter paper (Toyo-roshi 5B) into a 100 ml. beaker while the solution is hot. Wash the residue 2~3 times with 10 ml. of hot water, and add the washing to the filtrate. After cooling the filtrate, transfer it to a 100 ml. volumetric flask and dilute to the volume with distilled water. Add 25 ml. of this solution to an ion-exchange column containing Dowex-50 Na-form and collect the effluent in a 50 ml. flask. Rinse the column with several portions of water. After neutralizing the effluent, adjust the pH to 4.5~5.2 with acetate buffer and add 0.2 ml. of a 2.5% oxine solution with 2 N acetic acid and 2 ml. chloroform[10]. Shake for 1 min. to extract the vanadium oxinate, transfer the organic phase into a platinum crucible, then repeat the extraction three times and evaporate up to dryness. Add 0.2 g. of anhydrous sodium carbonate to the crucible containing the residue, and fuse it again to convert the vanadium into sodium vanadate. Dissolve the melt in a few milliliters of water. Transfer this solution into a 25 ml. volumetric flask, add 5 ml. of 5 N hydrochloric acid, and dilute to the volume with water. Measure the ultraviolet absorbance at 222 mμ. and obtain the concentration of vanadium from a calibration curve.

Results and Discussion

Absorption Spectra.—A series of complete absorption spectra for vanadium(V) in hydrochloric acid solutions of various concentrations

1) R. Bastian et al., *Anal. Chem.*, **25**, 284 (1957).
2) Y. Yamamoto, *J. Chem. Soc. Japan, Pure Chem. Sec.* (*Nippon Kagaku Zasshi*), **80**, 1256 (1959).
3) M. Ishibashi et al., This Bulletin, **29**, 57 (1956).
4) M. A. Desesa and L. B. Rogers, *Anal. Chim. Acta*, **6**, 534 (1952).
5) M. Ishibashi et al., This Bulletin, **30**, 433 (1957).
6) C. Merritt et al., *Anal. Chem.*, **25**, 572 (1953).
7) F. J. C. Rossotti and H. Rossotti, *Acta Chem. Scand.*, **10**, 957 (1956).
8) Yu. V. Morachevskii and L. I. Belyaeva, *Zhur. analit. Khim.*, **11**, 672 (1956).
9) L. Newman and K. P. Quinlan, *J. Am. Chem. Soc.*, **81**, 547 (1959).
10) E. B. Sandell, *Ind. Eng. Chem., Anal. Ed.*, **8**, 336 (1936).

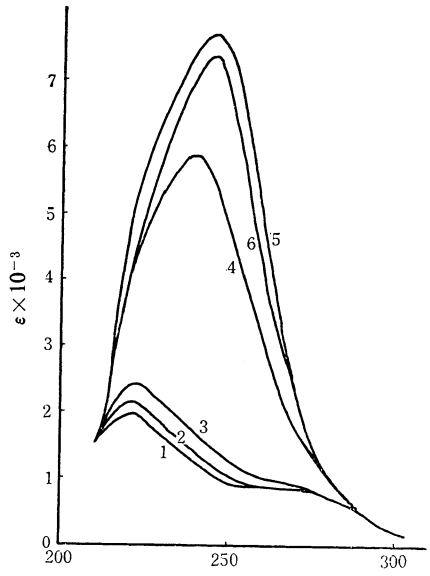


Fig. 1. Absorption spectra of vanadium in HCl.

1:	0.1~2 N HCl	4:	8 N HCl
2:	4 N HCl	5:	10 N HCl
3:	6 N HCl	6:	11.4 N HCl

is shown in Fig. 1. In a 0.1~2 N hydrochloric acid solution, the absorption spectra hardly changed with the acid concentration, but in an acid solution more concentrated than in 4 N, the absorption band shifted to a longer wave length with the increasing acid concentration. The position of the maximum was 222 mμ for a 0.1~2 N, but 246 mμ for an 11.4 N hydrochloric acid solution. In a 0.1~2 N hydrochloric acid solution, vanadium(V) exists in the form of pervanadyl ion, VO_2^+ [7,9]. Moreover, the bathochromic and hyperchromic effects with hydrochloric acid, mentioned above, are presumably due to the formation of the higher complex species. The decrease of absorbance in an 11.4 N hydrochloric acid solution compared with that in a 10 N acid solution is attributed to the reduction of a part of vanadium(V) to vanadium(IV) by hydrochloric acid, because concentrated hydrochloric acid has a reducing power and reduces vanadium(V) slowly to vanadyl(IV) ion, VO^{2+}, which is the sole species of vanadium(IV) in a hydrochloric acid medium[11], and the molar extinction coefficient of vanadium(IV) is smaller than that of vanadium(V) in the near ultraviolet region (Fig. 2). Moreover, it is well known that when vanadium(V) is dissolved in an 11.4 N hydrochloric acid solution, the solution becomes intense brown. The absorption spectra for a

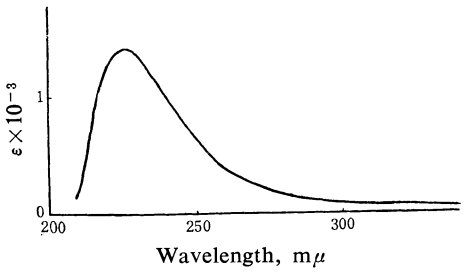


Fig. 2. Absorption spectrum of vanadyl-(IV) ion (VO^{2+}) in 11.4 N HCl.

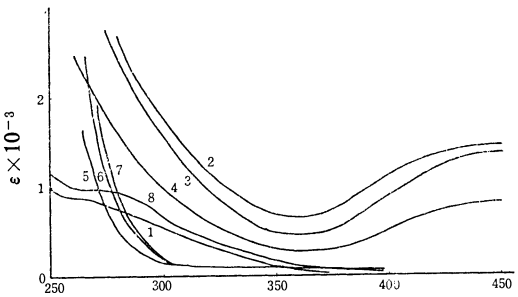


Fig. 3. Absorption spectra of vanadium. $H^+ = 10$ N.

1:	0.0 N Cl^-	5:	4.0 N Cl^-
2:	0.5 N Cl^-	6:	6.0 N Cl^-
3:	1.0 N Cl^-	7:	8.0 N Cl^-
4:	2.0 N Cl^-	8:	2.0 N H^+ 8.0 N Cl^-

series of solutions having a constant 10 N hydronium ion concentration but varying chloride concentrations, obtained by mixing hydrochloric acid and perchloric acid in various ratios are shown in Fig. 3. This red brown species, which has its absorption maximum at 450 mμ, was formed in a high hydronium ion concentration such as in 10 N, but it was not formed in a low concentration even if a solution of 8 N chloride concentration was used (Fig. 3). At a high hydronium ion concentration, with the increasing chloride concentration this species became unstable and was converted into vanadyl(IV) ion. From the facts that this species was formed at a high hydronium ion concentration, reduced to vanadyl ion easily, adsorbed by anion exchange resin[12], and extracted to tributyl phosphate, and that the species extracted to tributyl phosphate from the solution of low acid concentration was considered to be $VOCl_3$[13], this red brown complex seemed to be $VOCl_4^-$. The relation between the absorbance of the vanadium and the hydrochloric acid concentration of the solution

11) H. T. S. Britton and G. Welford, *J. Chem. Soc.*, **1940**, 758.

12) K. A. Kraus et al., *J. Am. Chem. Soc.*, **58**, 11 (1954).

13) S. K. Majumdar and A. K. De, *Anal. Chem.*, **33**, 297 (1961).

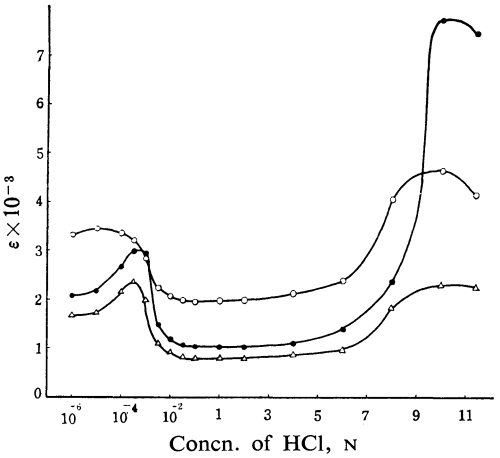


Fig. 4. Relation between the absorbance and the hydrochloric acid concentation.
-○- at 220 mμ -●- at 245 mμ
-△- at 270 mμ

at a specific wavelength is shown in Fig. 4; it is clear from this figure that in the range of hydrochloric acid concentrations from 0.1 to 2 N the effect of the acid concentration on the absorbance was very small and that the absorbance values are nearly equal.

Determination of Vanadium.—On the basis of the above results, a 1 N hydrochloric acid concentration and 222 mμ were chosen as the working conditions for the determination of vanadium making use of the absorption of pervanadyl ion.

Calibration Curve.—Using the standard solution, having the concentration of 200 p. p. m. of vanadium with 1 N hydrochloric acid, a series of 1 N hydrochloric acid solutions having various concentrations of vanadium from 0 to 25 p. p. m. was prepared; then the absorbance was measured at 222 mμ, using a 1N hydrochloric acid solution as reference. As shown in Fig. 5, Beer's law is obeyed up to 25 p. p. m. at 222 mμ.

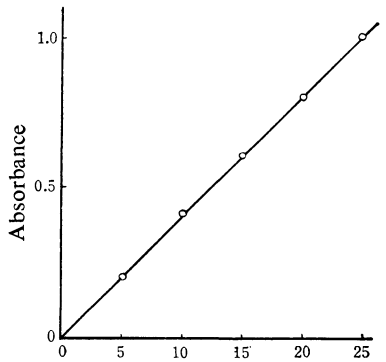


Fig. 5. Calibration curve at 222 mμ.
HCl : 1 N

Stability.—The stability of the system was then investigated for a week; it was found that the absorbance at 222 mμ did not change during this time, as is shown in Fig. 6.

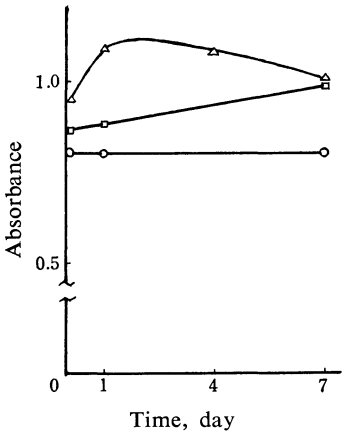


Fig. 6. Stability of absorbance at 222 mμ.
V(V) : 20 p. p. m.
-○- 0.1~2 N HCl -□- 4 N HCl
-△- 6 N HCl

Application of This Method to Silicate Rock Analysis.—After fusion and extraction with water as in the usual method, the sample solution was passed through a column of Dowex-50 Na-form. In the sample solution vanadium existed in the form of vanadate and was not adsorbed by cation exchange resin. However, in this treatment, silicate, phosphate, arsenate, chromate, molybdate and tungstate passed through together with vanadate. Therefore, the absorption spectra of all these elements were observed and are shown in Fig. 7. It is evident from this figure that chromium, molybdenum and tungsten seriously interfered with the determination of vanadium at 222 mμ. Of these three elements, chromium

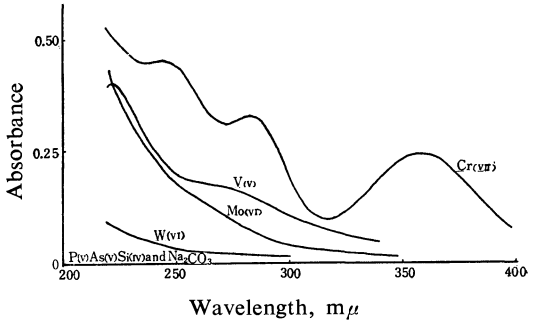


Fig. 7. Absorption spectra of interfering elements in 1N HCl solution.

V(V)	: 10 p. p. m.	P(V)	: 10 p. p. m.
Mo(VI)	: 10 p. p. m.	As(V)	: 10 p. p. m.
Cr(VII)	: 10 p. p. m.	Si(IV)	: 10 p. p. m.
W(VI)	: 10 p. p. m.	Na_2CO_3	: 2 g./50 ml.

Table I. Determination of vanadium in the presence of diverse ions

Vanadium taken, μg.	Diverse ion	Added as	Amt. added	Vanadium found μg.
200	—	—	—	205
200	—	—	—	198
200	Mo(VI)	$(NH_4)_2MoO_4$	50 μg.	240
200	W(VI)	Na_2WO_4	50 μg.	205
200	Cr(VII)	$KCrO_4$	50 μg.	195
200	Si(IV)	SiO_2	15 mg.	190
200	P(V)	K_2HPO_4	2 mg.	200
200	As(V)	Na_3AsO_4	2 mg.	202

could be separated from vanadium by oxine extraction, but the others could not be separated[14]. The results obtained by the general procedure are shown in Table I. Generally, however, these elements present in silicate rocks are very small quantities compared with vanadium, so the interference by these elements is negligible. The analyses of the Sekisonzan Lave of Asama and of the standard rock sample, diabase W-1, by this method gave the values of 0.024% and 0.043% respectively as V_2O_3; these values were consistent with the value of 0.021% obtained by the phosphotungstate method and with the average value of 0.038%[15].

14) E. B. Sandell, "Colorimetric Determination of Traces of Metals", Interscience Publishers, Inc., New York (1950), p. 606.

15) R. M. Mckenzie et al., *Geochim. et Cosmochim. Acta*, **14**, 68 (1958).

Summary

1) The absorption spectra of vanadium(V) in the media of various concentrations of hydrochloric acid were studied.

2) A 1 N hydrochloric acid concentration was recommended as the working medium for the spectrophotometric determination of vanadium(V), because the change in the intensity of the absorbance with the change in the reagent concentration is slight.

3) Beer's law was obeyed up to 25 p. p. m. of the metal, measuring the absorbance at 222 mμ.

4) The analysis of the silicate rocks by this method was studied, and good results were obtained.

The authors wish to express many thanks to the Ministry of Education for its financial support of this study.

Department of Chemistry
Faculty of Science
Kyushu University
Hakozaki, Fukuoka

Catalytic Asymmetric Cyanohydrin Synthesis with Synthetic Optically Active Polymer. I. Synthesis of Benzaldehyde Cyanohydrin

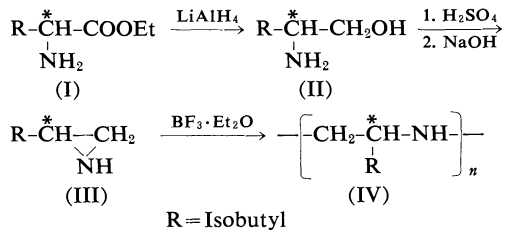
By Sei TSUBOYAMA

(Received November 29, 1961)

Catalytic asymmetric synthesis with optically active substances has been studied by several investigators[1-6], however, no attempts with synthesized polymer. The present author used a synthesized optically active polymer with amino groups as functional group for asymmetric synthesis of benzaldehyde cyanohydrin. This study is of interest for the subject is an enzyme model of biological asymmetric synthesis.

Recently, Minoura et al.[7] reported that, in the polymerization of R- and S-propylenimine, asymmetry of the obtained polymer was well retained. This process was considered available for the synthesis of an optically active polymer with functional groups. In the present work, S-isobutyl-ethylenimine (III), synthesized from L-leucine, was polymerized to an optically active linear polymer IV with ring opening.

1) L. Rosenthaler, *Biochem. Z.*, **14**, 238 (1908); **19**, 186 (1909); **239**, 227 (1931).
2) G. Bredig et al., ibid., **46**, 7 (1912); **249**, 241 (1932); **250**, 414 (1932); **282**, 88 (1935).
3) H. and E. Albers, *Z. Naturforsch.*, **9b**, 122, 133 (1954).
4) V. Prelog and M. Wilhelm, *Helv. Chim. Acta*, **37**, 1634 (1954).
5) H. Pracejus, *Ann.*, **622**, 10 (1959); **634**, 9 (1960).
6) V. K. Krieble and W. A. Wieland, *J. Am. Chem. Soc.*, **43**, 164 (1921).
7) Y. Minoura et al., ibid., **81**, 4689 (1959).



This polymer is solid, softening at about 56°C. Its molecular weight is 4000~6000, and the sign of optical rotation is opposite to that of the monomer, similar to poly-s-propylenimine. An insoluble polymer could not so far be obtained by common cross-linking reagents except tolylene-diisocyanate.

In carrying out the asymmetric cyanohydrin synthesis, styrene-divinylbenzene copolymer containing methyl-D-glucosamide, diethylaminoethyl cellulose, L-leucinol, quinine and Amberlite IR-4B were also employed as catalysts for reference. The results are listed in Table V.

Experimental

Preparation of s-Isobutyl-ethylenimine Polymer (IV, IEI-Polymer).—*L-Leucinol (II).* — The amino alcohol was prepared as described by Karrer[8]. L-Leucine ethyl ester[9] (I) (20 g., 0.125 mol.; b. p. 74°C/7 mmHg, n_D^{20} 1.4289) in ether (150 ml.) was added dropwise with stirring to lithium aluminum hydride (7.6 g., 0.2 mol.) in ether (170 ml.). After the mixture was stirred for 15 min., diluting with ether, water (10 ml.) was added with vigorous stirring. The ether solution was decanted from the precipitate, which was extracted with ether and then with alcohol. These extracts were combined with the first ether solution. The mixture was dried and fractionated under reduced pressure, this gave 10~12 g. (69~82%) of L-leucinol, 78.5°C/2 mmHg, 83°C/4 mmHg, n_D^{27} 1.4470.

S-Isobutyl-ethylenimine (III). — The imine was obtained by a modified procedure of Campbell[10]. A cold mixture of sulfuric acid (11 g., 0.11 mol.) and water (20 ml.) was added with shaking to a solution of L-leucinol (11.7 g., 0.1 mol.) and water (20 ml.). The mixture was distilled at atmospheric pressure until the temperature of the contents reached 115°C. The distillation was continued under reduced pressure while the bath temperature was gradually raised to 180°C. The contents, when solidified, were left as it was for one hour. A cold solution of 40% sodium hydroxide (25 g., 0.25 mol.) was added to the cooled solidified product. The mixture was distilled and the distillate at 94~101°C was collected and saturated with potassium hydroxide. The organic layer formed was separated and was dried with potassium hydroxide pellets and finally with sodium. Distillation gave 4.5 g. (45%) of colorless liquid of ammoniacal odor, b. p. 130~131°C, d_{28}^{28} 0.8123, n_D^{28} 1.4242, $[\alpha]_D^{28}$ −15.39° (original liquid), $[\alpha]_D^{32}$ −24.60° (*c* 1.828 in benzene).

Found: C, 72.58; H, 13.12; N, 13.72%; MR_D, 31.172. Calcd. for $C_6H_{13}N$: C, 72.66; H, 13.21; N, 14.12%; MR_D, 31.307.

The infrared spectrum of the imine III is shown in Fig. 1.

Polymerization of the Imine III.—The polymerization was carried out according to Minoura's procedure. s-Isobutyl-ethylenimine was placed in a dry nitrogen-filled hard glass tube which was

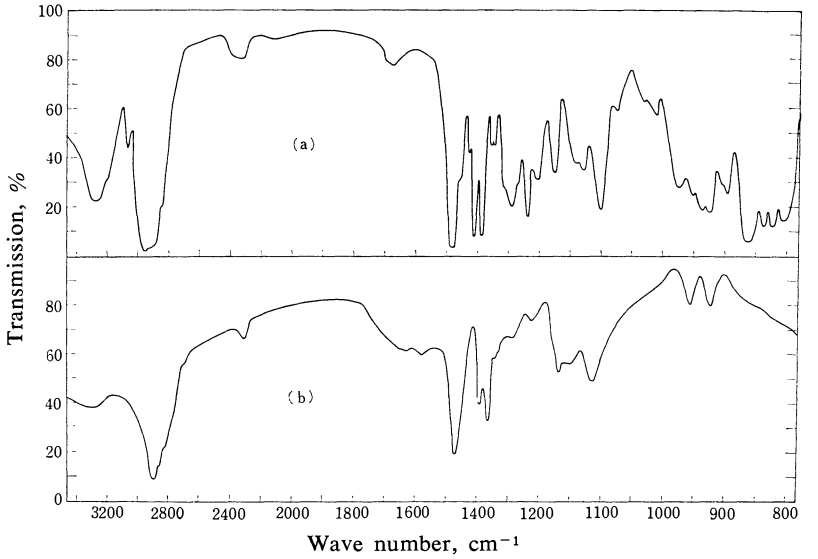


Fig. 1. Infrared absorption spectra of s-isobutyl-ethylenimine (a) and its polymer (b).

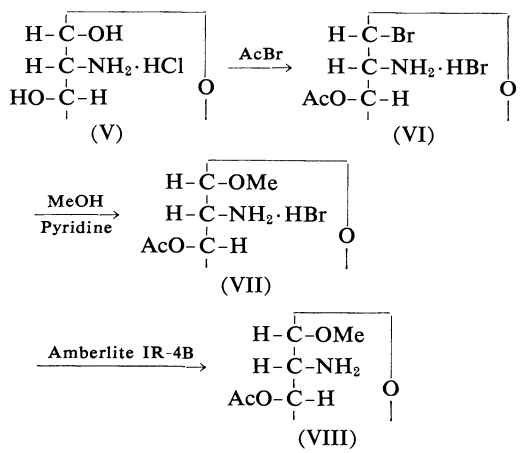
8) P. Karrer et al., *Helv. Chim. Acta*, **31**, 1617 (1948).
9) E. Fischer, *Ber.*, **34**, 442 (1901).
10) K. N. Campbell et al., "Organic Syntheses", Coll. Vol. III (1955), p. 148; T. L. Cairns, *J. Am. Chem. Soc.*, **63**, 871 (1941).

TABLE I. POLYMERIZATION OF S-ISOBUTYL-ETHYLENIMINE*1

Temp. °C	Time hr.	Catalyst		Yield of polymer g.	Mol. wt.	Softening point °C	$[\alpha]_D^{20}$ in C_6H_6	$[\alpha]_D^{20}$ in EtOH
80	20	$BF_3 \cdot Et_2O$	0.2 ml.	2.36			62.6	
80	24	$BF_3 \cdot Et_2O$	0.2 ml.	2.41			66.3	
100	48	$BF_3 \cdot Et_2O$	0.2 ml.	2.40	4000～5000	55	60.6	50.8
25～90*2	53 days	$BF_3 \cdot Et_2O$	0.2 ml.	2.15	4000～6000*3	56	66.7	
150	24	Conc. HCl	0.2 ml.		1020*4			37.5
80	24	Camphor sulfonic acid	0.05 g.			53		

*1 The used imine was 2.5 g.
*2 The temperature was raised gradually.
*3 The polymer was used in the asymmetric synthesis. Found: C, 72.12; H, 12.65; N, 13.69. Calcd. for $(C_6H_{13}N)_n$: C, 72.66; H, 13.22; N, 14.12%.
*4 Found: C, 71.55; H, 12.98; N, 13.34%.

cooled in a dry ice-methanol bath, and when cooled, boron trifluoride-etherate was added to the imine. The tube, after flushed again with nitrogen and sealed, was placed in a constant temperature bath (see Table I). After the required reaction time, the reaction mixture was dissolved in benzene and washed with 10% sodium hydroxide solution to remove the catalyst. The pale yellow benzene solution of the polymer was then washed with deionized water until the washings became neutral and was dried with anhydrous sodium sulfate. The benzene was then removed from the solution in vacuo at room temperature (freez-dry technique was always unsuccessful with this polymer). The obtained polymer was tacky, it solidified when cooled in a dry ice bath. The pale yellow glassy polymer softened at about 56°C. The softened polymer did not vitrify at room temperature unless cooled again in a dry ice bath. The polymer was soluble in common organic solvents, slightly soluble in dimethyl formamide, and insoluble in water. Its molecular weight was measured by cryoscopic method in benzene. For the polymerization, hydrochloric acid and camphor-sulfonic acid were also used as catalysts in place of boron trifluoride as shown in Table I. The infrared spectrum of the linear polymer is given in Fig. 1. From the spectra, it is found that characteristic absorption of ethylenimine, 3070 cm^{-1}, disappeared in spectrum of the polymer.



Polymer Containing Methyl-D-glucosamide (GA-Resin). — Generally, methyl glucoside of amino sugar is said to be very resistant to acid hydrolysis on account of its positive charge of amino group or betain structure, especially, methyl-D-glucosamide is known to be extremely stable to alkali[11,12]. For that reason, methyl-D-glucosamide is available as a functional group for anion exchange resin. Moreover, the amine has many hydroxy groups and many asymmetric carbons. The amine was introduced into chloromethylated styrene-divinylbenzene copolymer.

3,4,6-Triacetyl-methyl-D-glucosamide (VIII). — The amine was prepared from D-glucosamine hydrochloride (V) via bromotriacetyl-D-glucosamine hydrobromide (VI) and triacetyl-methyl-D-glucosamide hydrobromide (VII)[11]. A methanol solution of glucosamide hydrobromide (VII) was passed through a column of free form of Amberlite IR-4B to remove bromine anion. In this procedure, α- and β-methyl-D-glucosamide mixture is supposed to be produced. Recrystallizations from methanol-ether gave free glucosamide (VIII) of m. p. 139～140°C, $[\alpha]_D^{14}$ −20° (*c* 1; methanol).

TABLE II. CAPACITIES OF AcO-GA-RESIN AND GA-RESIN

Amination Temp. °C	Amination Time hr.	Capacities (meq./g.) AcO-GA-Resin HCl	AcO-GA-Resin MA*	GA-Resin HCl	GA-Resin MA*
70	5	1.20	1.84		
85	15	1.83	2.48	2.21	2.68**
90	20	1.60			
100	15	1.55	2.10	1.88	1.96

* MA: Mandelic acid.
** Nitrogen contents: AcO-GA-resin, 2.83; GA-resin, 3.13%. Calculated capacities from the nitrogen contents: AcO-GA-resin, 2.02; GA-resin, 2.24 meq./g. 83% of chlorine in chloromethylated polymer was exchanged by the glucosamide. For the asymmetric synthesis the resin was used.

11) J. C. Irvine et al., *J. Chem. Soc.*, **99**, 250 (1911).
12) R. C. G. Moggridge and A. Neuberger, ibid., **1938**, 745.

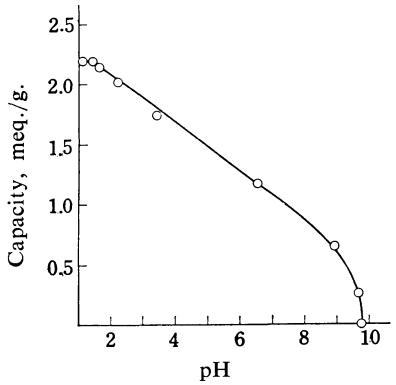


Fig. 2. Titration curve of methyl-D-glucosamide polymer (GA-resin).

Amination.—Styrene-divinylbenzene copolymer (2% crosslinked, 80~100 mesh) was chloromethylated for 48 hr. at 25°C by Pepper's procedure[13]. After the chloromethylated copolymer (10 g.; chlorine content, 16.5%) was allowed to stand overnight in dioxane, the acetylated glucosamide (VIII) (15 g.), dioxane (35 g.), and a trace of methanol were added and the mixture was placed in a bath at constant temperature for appropriate time listed in Table II. The product was washed by cycling with 1 N hydrochloric acid and 1 N sodium hydroxide to remove soluble materials.

The exchange capacity of the resin was fairly high in spite of a bulky group. The resin exhibited an abnormal behavior for adsorption to mandelic acid as shown in Table II. The polymer containing acetyl-glucosamide (VIII) (AcO-GA-resin) was then treated by a barium hydroxide solution for 45 min. to remove the acetyl group. The obtained deacetylated polymer (GA-resin) swelled in alcohol and shrank with acetone and acetic acid. In this respect, acetylated resin was opposite to GA-resin. A titration curve of the resin was typical of weak basic resin.

Diethylaminoethyl Cellulose (DEAE-Cellulose).—This ion-exchange cellulose was prepared from cotton or wood cellulose powder (Toyo Roshi Co., Ltd.) and 2-chlorotriethylamine hydrochloride as described by Peterson and Sober[14]. The exchange capacities of cotton cellulose (nitrogen content, 1.02%) and wood cellulose (nitrogen content, 0.79%) were 0.6 and 0.4 meq./g. respectively.

Asymmetric Synthesis and Analysis of Benzaldehyde Cyanohydrin.—The catalysts used in the cyanohydrin synthesis are very different from one another in chemical, physical and kinetic properties. Since it is essentially difficult to apply the same condition to those catalysts the reaction was carried out under similar conditions as for mole ratio of reagents, reaction time, reaction temperature and solvent.

To a solution of refined benzaldehyde (10.0 ml.) and anhydrous hydrogen cyanide (4.0 ml.), catalyst (0.1~1.0 mmol.) was added and the mixture was made up to 50 ml. with benzene. The solution of benzene was allowed to stand at 20°C for 20 hr. with stirring. The catalyst was filtered off and the filtrate was distilled under reduced pressure to remove unreacted hydrogen cyanide and again was made up to 50 ml. with benzene. Optical rotation of the solution was measured by a polarimeter (Hitachi Ltd.) in 2 dm. tube. A sample of given volume was pipetted from the benzene solution and, after dilution with water, it was treated with 0.1 N potassium hydroxide until pH ca. 11 and was titrated with 0.1 N silver nitrate by means of the potentiometric method[15]. As shown in Fig. 3, the titration curves of benzaldehyde cyanohydrin (fresh distilled, b. p. 118~119°C/0.25 mmHg, 124~126°C/1mmHg[16]), potassium cyanide and several samples from the reaction product mixture were almost of the same form and their end points were very sharp. The titration value of fresh distilled cyanohydrin in benzene

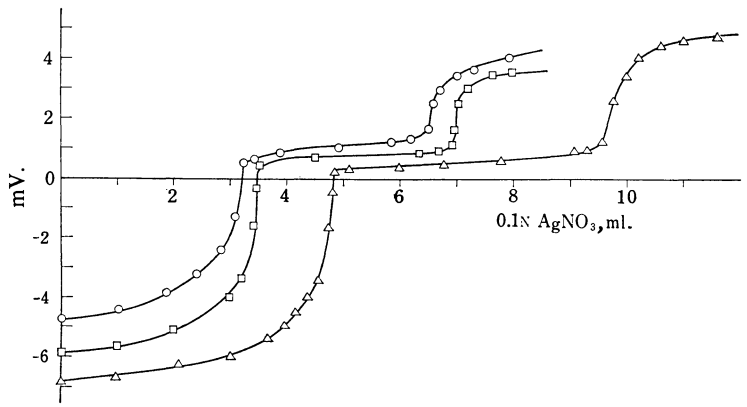


Fig. 3. Titration curve of potassium cyanide and benzaldehyde cyanohydrin.
-○- Reaction mixture
-△- Benzaldehyde cyanohydrin, 0.1302 g. (0.978 mmol.)
-□- 0.07 N KCN, 10 ml.

13) K. W. Pepper et al., ibid., **1953**, 4093.
14) E. A. Peterson and H. S. Sober, *J. Am. Chem. Soc.*, **78**, 751 (1956).
15) J. E. Ricci, *Anal. Chem.*, **25**, 1650 (1953).
16) K. Freudenberg and H. Biller, *Ann.*, **510**, 239 (1934), reported b. p. 115~116°C/0.1 mmHg.

TABLE III. VARIATION OF P% IN EXISTENCE OF CATALYST

	Yield %	α_D	$[\alpha]_D$	P%
When 100 mg. of catalyst was used:				
Containing catalyst	51.5	−2.28	−8.57	19.6
Distilled cyanohydrin*1			−8.20	18.7
When 50 mg. of catalyst was used:				
Containing catalyst	44.5	−1.42	−6.26	14.2
Catalyst removed*2	43.0	−1.30	−5.86	13.3
After a week:				
Containing catalyst	42.7	−1.20	−5.73	13.1
Catalyst removed*2	42.0	−1.20	−5.53	12.6
Distilled cyanohydrin*3			−5.21	11.5

*1 Distilled at 118~119°C/0.25 mmHg under presence of one drop of conc. H_3PO_4. n_D^{20} 1.5308.
*2 Diluted sulfuric acid was used.
*3 Distilled at 123~124°C/1 mmHg, n_D^{25} 1.5221.

TABLE IV. VARIATION OF ROTATION OF IEI-POLYMER UNDER VARIOUS CONDITIONS
(Used: 21.5 mg. of the polymer in 10 ml. of benzene)

	α_D*
IEI-Polymer	+0.14
When D,L-cyanohydrin (37.2 mg.) added	+0.30
In 10 hr.	+0.21
In 20 hr.	+0.13

* Measured with 1 dm. tube.

solution with benzaldehyde agreed throughly with that of equal quantity of the same cyanohydrin used alone. For the calculation of cyanohydrin concentration, the value of the first inflection point in the titration curve was doubled. IEI-polymer, dissolved in benzene solution, may be removed by shaking with sulfuric acid but this process gives rise to various troubles. Furthermore, Amberlite IR-120 or Dowex-50·X-1 (low crosslinked) did not adsorb the polymer even if it is low molecular weight. From Tables III and IV we see that the value of optical rotation of the product with catalyst still in it should be considered satisfactory with the accuracy of 1% or less in error if the correction is made for optical rotation of the polymer itself. Therefore, the optical rotation of cyanohydrin was measured regardless of the polymer content. The optical yield, "P%", expresses the ratio of specific rotation of the product to the absolute value of rotation of optically pure cyanohydrin in benzene, $[\alpha]_D^{25}$ 43.75 (2 dm., c 5.006)[17].

Results and Discussion

As regards P% in the last column of Table V, IEI-polymer gives considerably good results presumably because of steric hindrance of bulky isobutyl group adjacent to a functional group and large influences of structural regularity of optically active polymer on the asymmetric synthesis of cyanohydrin. In the regularity of the polymer, a helical conformation may be existent to some extent in dilute benzene or toluene solution. If we could make an IEI-polymer of higher molecular weight, we could expect a better result because of enhanced stereo-regularity.

With GA-resin, the yield and P% are both poor. The resin hardly swelled in benzene and, therefore, the reaction velocity was very slow. Even if satisfactorily swelled, the aldehyde group could not approach the amino group of the catalyst, for the functional amino group is sandwhiched between the polymer skeleton and the bulky glucoside ring. Furthermore, the resin has no asymmetric carbon in the polymer main chain. In spite of many optically active carbons that are in side chains, reagents may be receiving just a slight chance of steric control in transition state.

Concerning DEAE-celluloses, wood cellulose is inferior to cotton cellulose both in yield and in P%, for which lower crystallinity of original wood cellulose powder and intermingled impurities seem responsible. But, what is most unaccountable about wood cellulose is, that the signs of optical rotations of the two reaction produdts are reversed, notwithstanding the two celluloses, one obtained on the market, the other synthesized in the laboratory, being of the same structure (see Table V). It may have been due to differences of the synthetic methods of the DEAE-celluloses or of their

17) I. A. Smith, *Ber.*, **64**, 427 (1931).

TABLE V. ASYMMETRIC SYNTHESES OF BENZALDEHYDE CYANOHYDRIN WITH OPTICALLY ACTIVE POLYMERS

Catalyst	Cata. mg.	Yield %	α_D	$[\alpha]_D$	P%
IEI-Polymer*1	100	51.5	−2.28	−8.57	19.6
	100*2	40.0	−1.86	−9.13	20.8
	100*3	50.0	−1.81	−7.07	16.1
	50*3	44.5	−1.42	−6.26	14.2
	10	8.8	−0.62	−6.80	15.5
GA-Resin	500	23.4	+0.06	+0.50	1.1
	100	13.9	+0.07	+0.98	2.2
DEAE-Cellulose (Cotton)	500	84.4	−1.29	−2.96	6.8
	1670	80.2	−0.84	−2.25	5.2
DEAE-Cellulose (Wood)	500	48.8	−0.32	−1.01	2.3
	500*4	52.0	+0.17	+0.75	1.7
L-Leucinol	117	6.9	(±)	0	0
Quinine	324	74.3	+0.28	+0.73	1.7
Amberlite IR-4B	500	28.8	0	0	0
	100	11.3	0	0	0

*1 $[\alpha]_D$ are the values corrected for the rotation of the polymer.
*2 Catalyst polymerized with camphor sulfonic acid was used; softening point, 53°C.
*3 Molecular weight of the catalyst, 1020. In other cases, molecular weight is 4000~6000.
*4 DEAE-Cellulose of Type 20 (Brown Co.) was used (nitrogen content, 1.10%; exchange capacity, 0.7 meq./g.).

fine structure of the cellulose part. Previously, Bredig et al.[2] found that when diethylamino cellulose was used in the studies of asymmetric cyanohydrin synthesis, the optical yield of the product was 22% as mandelic acid. In comparison with this, the results shown in Table V are too small, which is attributable to the difference between amination processes and the difference in distance between the cellulose part and the amino group.

L-Leucinol, regarded as monomer of IEI-polymer, did not catalize in the asymmetric cyanohydrin synthesis and the cyanohydrin was obtained in a poor yield.

The result with quinine is similar to the results obtained by other workers[2-4].

Amberlite IR-4B does not swell easily in solvent, hence, the reaction velocity is slow and, as expected, stereo-specific reaction did not occur.

Behavior of IEI-Polymer under Various Conditions.—Rate of cyanohydrin formation with IEI-polymer is shown in Fig. 4 (A mixture of 20 ml. of benzaldehyde, 8 ml. of hydrogen cyanide, and 200 mg. of polymer was made up to 100 ml. with benzene. Five milliliters of this reaction mixture was used for every analysis.). Variation of P% vs. reaction time is similar to that in Bredig's case[2] of diethylamino cellulose; it is accompanied with slow racemization. Specific rotation of the polymer is affected a little by the temperature of toluene solution (Fig. 5). Curve of P% vs. reaction temperature is shown in Fig. 5; it has a

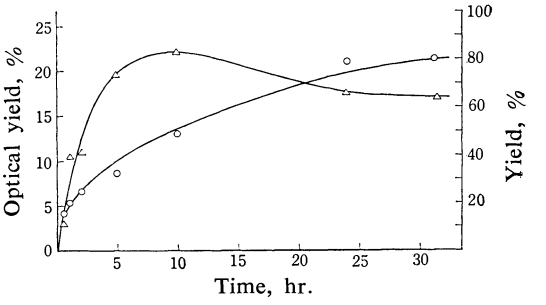


Fig. 4. Time dependence of yield (-○-) and optical yield (-△-) of benzaldehyde cyanohydrin with IEI-polymer.

maximum near −10°C at which temperature the ratio of (−)-cyanohydrin to (+)-isomer is 65:35. It is of interest to note that the existence P% maximum in the range of reaction temperature resembles the enzyme action which becomes powerful within limited ranges of temperature and pH.

In cyanohydrin synthesis, it is well known that carbonium ion of the carbonyl group is more unstable than negatively polarized oxygen, hence, the first step of the reaction is the nucleophilic attack. The reaction is therefore accelerated by the base.

In this asymmetric synthesis, we consider that either the conformation of the transition state is fixed by the steric effect of isobutyl group of the polymer when the carbonyl group approaches the nitrogen of the catalyst or cyanide ion weakly bonded with the amino

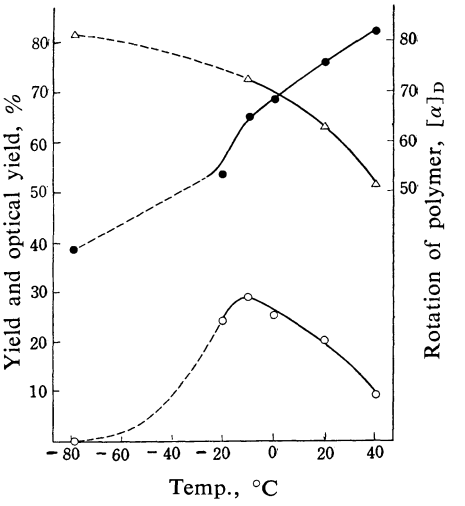


Fig. 5. Temperature dependence of yield (-●-) and optical yield (-○-) of benzaldehyde cyanohydrin and specific rotation (-△-) of IEI-polymer.

group of the polymer attacks the carbonyl group only from a definite direction on account of the isobutyl group. In any case, the spiral structure of the polymer, too, is presumed to give rise to a promoting effect on the asymmetric synthesis.

Summary

Poly-s-isobutyl-ethylenimine was synthesized and with it asymmetric synthesis of benzaldehyde cyanohydrin was carried out with good results: P% is 20%.

This is ascribable to (1) the steric effect of the isobutyl group adjacent to the amino group in the polymer, (2) the stereo-regularity of the polymer, and presence of an asymmetric center and functional group in the main chain of the polymer, and (3) the spiral structure, if it exists, of the polymer enhancing its stereo-regularity effect.

The author wishes to thank Dr. Masaya Yanagita for his many valuable suggestions and constant encouragement throughout the course of this study.

Laboratory of Polymer Chemistry
The Institute of Physical
and Chemical Research
Komagome, Bunkyo-ku, Tokyo

The Reaction of Tropoids and Quinone Derivatives. III. Reaction of Several Tropolones and o-Benzoquinone Dibenzimide

By Shuichi SETO and Yukio NISHIYAMA

(Received November 22, 1961)

In earlier papers of this series, reaction of several tropolones with *p*-benzoquinone-dibenzenesulfonimide[1] and *p*-benzoquinone[2] was reported. The present paper describes the structure of the reaction products of tropolone and its bromo derivatives with *o*-benzoquinone-dibenzimide (I)[3].

A solution of tropolone and I dissolved in a mixture of methanol and chloroform, added with a small quantity of triethylamine, affords colorless crystals (II) when allowed to stand at room temperature. Analytical values of II correspond to the formula $C_{27}H_{20}O_4N_2$ and the presence of a tropolone ring in II is certain from its ultraviolet absorption spectrum and coloration to ferric chloride. II is also obtained by the use of diethylamine in place of triethylamine in the foregoing reaction, and also by the same reaction carried out in an aqueous solution with addition of alkali, though in a poor yield. Heating of II in a sealed tube with concentrated hydrochloric acid gives 2-phenylbenzimidazole derivative III and phenylenediamine derivative IV. Although the latter was not isolated in a pure state, its formation seemed certain from the facile formation of a triazole derivative V by application of sodium nitrite to the mother liquor left after separation of III. III is also obtained on treatment of II with alcoholic potassium hydroxide. Oxidation of III with alkaline potassium permanganate affords 2-phenylbenzimidazole and

1) S. Seto, H. Yamazaki and Y. Nishiyama, This Bulletin, 33, 1081 (1960).
2) S. Seto and H. Sato, ibid., 35, 349 (1962).
3) R. Adams and J. W. Way, *J. Am. Chem. Soc.*, 76, 2763 (1954).

this fact suggests that 2-phenylbenzimidazole and tropolone are bonded through the nitrogen in the imidazole ring in III.

In order to make further confirmation of the structure of III, rearrangement of the tropolone ring in III into benzoic acid was attempted.

Application of diazomethane to III afforded only one kind of methyl ether VI, suggesting that 2-phenylbenzimidazole is bonded to 5-position of the tropolone ring in III. The methyl ether VI was converted into 2-chlorotropone derivative VIII through the hydrazino derivative VII[4].

2-Chlorotropone derivative VIII easily underwent conversion to a benzoic acid derivative when heated with alkali and this derivative was changed to a methyl ester IX with diazomethane. According to the afore-mentioned assumption, this methyl ester IX should be 1-(4′-methoxycarbonylphenyl)-2-phenylbenzimidazole and structurally apparent IX was synthesized by the following route.

2-Amino-4′-methyldiphenylamine[5] was treated with benzoyl chloride in pyridine and the monobenzoyl derivative so formed was treated with acetic anhydride to effect cyclization to 1-(4′-methylphenyl)-2-phenylbenzimidazole, which was oxidized with potassium permanganate to form the benzoic acid derivative.

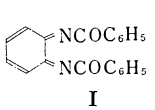
The methyl ester obtained from this acid derivative has the structure of 1-(4′-methoxycarbonylphenyl)-2-phenylbenzimidazole and this was found to be identical with the foregoing IX through mixed fusion test and by comparison of ultraviolet and infrared spectra. The foregoing facts have proved that III is 1-(tropolon-5′-yl)-2-phenylbenzimidazole and II is *N*-(tropolon-5-yl)-*N*, *N*′-dibenzoyl-*o*-phenylenediamine.

3-Bromotropolone also undergoes reaction with I to form a monobromo derivative X, whose structure was determined from its analytical values and formation of II by hydrogenolysis.

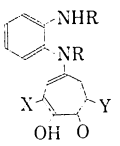
X is also obtained by monobromination of II.

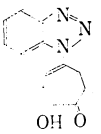
3, 7-Dibromotropolone also affords a dibromo derivative XI by the reaction with I and the structure of XI was also determined from its analytical values and formation of II by hydrogenolysis.

From the similarity of tropolone and phenol, reaction of I with phenol is of interest and examination of this reaction revealed that the product in this case is *N*-(4-hydroxyphenyl)-



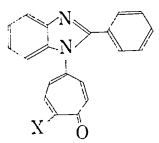
I

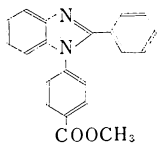




V

II; R=COC_6H_5, X=Y=H
IV; R=X=Y=H
X; R=COC_6H_5, X=Br, Y=H
XI; R=COC_6H_5, X=Y=Br





III; X=OH
VI; X=OCH_3
VII; X=$NHNH_2$
VIII; X=Cl

IX

N, *N*′-dibenzoyl-*o*-phenylenediamine, analogous to II in the case of tropolone[6].

Experimental[7]

***N*-(Tropolon-5-yl)-*N*, *N*′-dibenzoyl-*o*-phenylenediamine (II).**—a) A solution of 1 g. of *o*-benzoquinone-dibenzimide (I) and 770 mg. of tropolone dissolved in 65 ml. of a mixture (3 : 1 by volume) of methanol and chloroform, added with 3 drops of triethylamine, was allowed to stand at room temperature for 4 days. Evaporation of the solvent in a reduced pressure precipitated crystals. The first crop of 470 mg. of crystals melted at 212～213°C. Its mother liquor was further concentrated, the residue was treated with dilute hydrochloric acid, and washed with petroleum ether, affording a second crop of 780 mg. of crystals melting at 199～203°C. The two crops of crystals were combined and recrystallized from a chloroform-ethanol mixture to give 970 mg. of colorless crystals (II), m. p. 220～221°C.

Found: C, 73.55; H, 4.74; N, 6.87. Calcd. for $C_{27}H_{20}O_4N_2$: C, 74.30; H, 4.62; N, 6.42%. λ_{max}^{MeOH} mμ (log ε): 230 (4.62), 352 (4.20).

The petroleum ether layer left after separation of the second crop of crystals was evaporated and the residue was sublimed at 60°C (bath temperature) at 1 mmHg, affording 200 mg. of the recovered tropolone.

Addition of an aqueous solution of ferric chloride to a solution of II in ethyl acetate resulted in coloration of the aqueous layer to green and organic layer, red.

b) A solution of 100 mg. of I and 100 mg. of tropolone dissolved in 16 ml. of a mixture (3 : 1 by volume) of methanol and benzene, added with 3 drops of diethylamine, was allowed to stand for

4) S. Seto, *Sci. Repts. Tohoku Univ.*, **37**, 292 (1953).
5) W. Borsche and M. Feise, *Ber.*, **40**, 383 (1907).
6) S. Seto and Y. Nishiyama, *J. Pharm. Soc. Japan* (*Yakugaku Zasshi*,) **82**, 590 (1962).

7) All melting points are uncorrected. Microanalyses were carried out by Misses Yôko Endô and Yukiko Endô of this Institute. Measurements of ultraviolet spectra were made by a Hitachi EPU-2A type spectrophotometer.

7 days at room temperature. Evaporation of the solvent in a reduced pressure left 40 mg. of crystals, m. p. 217~222°C, which were recrystallized from an ethanol-chloroform mixture to 35 mg. of colorless crystals, m. p. 225°C, undepressed on admixture with the product obtained by the foregoing method a).

c) A mixture of 100 mg. of I with 100 mg. of tropolone, 100 mg. of potassium hydroxide, and 5 ml. of water was stirred for 15 hr. under ice cooling, and *o*-phenylenedibenzamide (40 mg.) that separated from the reaction mixture was filtered off. The filtrate was acidified with dilute hydrochloric acid, the solid that precipitated, was collected, and recrystallized from an ethanol-chloroform mixture to 5 mg. of colorless crystals. This product was found to be identical with the product obtained by the foregoing methods a) and b). The filtrate left after separation of the solid was extracted with chloroform and the extract was sublimed on a water bath at 60°C 1 mmHg, affording 50 mg. of recovered tropolone.

Reaction of II and Concentrated Hydrochloric Acid.—A mixture of II (432 mg.) and concentrated hydrochloric acid (8.8 ml.) was heated in a sealed tube at 120°C for 3 hr. When cooled, the tube was opened and the reaction mixture was extracted with benzene. The benzene extract afforded benzoic acid. Concentration of the aqueous layer in a reduced pressure gave 100 mg. of colorless crystals, m. p. 248~250°C (decomp.), which is the hydrochloride of 1-(tropolone-5′-yl)-2-phenylbenzimidazole (III).

Found: C, 68.08; H, 4.38; N, 7.81. Calcd. for $C_{20}H_{15}O_2N_2Cl$: C, 68.45; H, 4.31; N, 7.99%.

A solution of sodium nitrite (50 mg.) in water (0.5 ml.) was added to the filtrate left after separation of the foregoing crystals and the crystals that separated immediately were recrystallized from an ethanol-chloroform mixture to 10 mg. of 1-(tropolon-5′-yl)-benztriazole (V) as crystals of m. p. 225°C.

Found: C, 64.91; H, 3.75; N, 18.13. Calcd. for $C_{13}H_9O_2N_3$: C, 65.26; H, 3.76; N, 17.57%. λ_{max}^{MeOH} mμ (log ε): 288 (4.41), 345 (4.25).

Reaction of II and Potassium Hydroxide. — A solution of II (1 g.), potassium hydroxide (3 g.), water (10 ml.), and ethanol (15 ml.) was heated at 120°C for 4 hr. and then evaporated to dryness. A small amount of water was added to the residue, insoluble matter was collected, and suspended in water. The mixture was adjusted to pH 4 with acetic acid, the solid (530 mg.) that remained was collected, and recrystallized from an ethanol-chloroform mixture to 340 mg. of 1-(tropolon-5′-yl)-2-phenylbenzimidazole (III) as colorless crystals, m. p. 247~248°C.

Found: C, 75.99; H, 4.03; N, 9.03. Calcd. for $C_{20}H_{14}O_2N_2$: C, 76.42; H, 4.49; N, 8.91%. λ_{max}^{MeOH} mμ (log ε): 227 (4.55), 289 (4.24), 341 (4.19), 405 (3.70).

Oxidation of III with Potassium Permanganate. — A solution of VII (100 mg.) dissolved in 2 N potassium hydroxide (2 ml.), added to 1 ml. of 5% aqueous solution of potassium permanganate and 2 ml. of pyridine, was heated on a water bath for 30 min., cooled, and filtered to remove manganese dioxide. Evaporation of the filtrate left 30 mg. of colorless crystals, m. p. 293°C, undepressed on admixture with an authentic specimen of 2-phenylbenzimidazole.

1-(2′-Methoxytropon-5′-yl)-2-phenylbenzimidazole (VI). — An ether solution of diazomethane was added to a suspension of III (50 mg.) in methanol (10 ml.) and the mixture was allowed to stand over night. The solvent was evaporated from the reaction mixture in a reduced pressure and the residue was recrystallized from ethanol to 20 mg. of colorless crystals, m. p. 161~162°C.

Found: C, 74.67; H, 4.51; N, 8.42. Calcd. for $C_{21}H_{16}O_2N_2$: C, 76.81; H, 4.91; N, 8.53%. λ_{max}^{MeOH} mμ (log ε): 289 (4.29), 325 (4.11).

1-(2′-Hydrazinotropon-5′-yl)-2-phenylbenzimidazole (VII). — A solution of the 2-methoxytropone derivative (VI) (100 mg.) dissolved in methanol (1 ml.), added with 80% hydrazine (20 mg.), was allowed to stand for one hour, during which yellow crystals began to precipitate after a few minutes. The crystals were collected by filtration and 90 mg. of yellow crystals, m. p. 233~235°C (decomp.), was obtained.

Found: C, 71.96; H, 4.26; N, 16.29. Calcd. for $C_{20}H_{16}ON_4$: C, 73.15; H, 4.91; N, 17.06%. λ_{max}^{MeOH} mμ (log ε): 230 (4.47), 255 (4.45), 352 (4.23), 415 (3.98).

1-(2′-Chlorotropon-5′-yl)-2-phenylbenzimidazole (VIII). — A solution of cupric sulfate crystals (1 g.) dissolved in water (1.6 ml.) with warming was maintained at 120°C and a mixture of VII (110 mg.) and concentrated hydrochloric acid (1 ml.) was added with stirring, by which a vigorous evolution of nitrogen was observed. After being maintained at 120°C, the solution was cooled, adjusted to pH 4 by addition of water (10 ml.) and sodium hydrogencarbonate, and shaken thoroughly with chloroform. The mixture was filtered, the chloroform layer was separated from the filtrate, and dried over anhydrous sodium sulfate. The solution was purified through an alumina column and evaporation of the solvent from its effluent afforded 95 mg. of colorless crystals, m. p. 185~186°C.

Found: C, 72.09; H, 3.86; N, 8.36. Calcd. for $C_{20}H_{13}ON_2Cl$: C, 72.18; H, 3.94; N, 8.42%. λ_{max}^{MeOH} mμ (log ε): 237 (4.50), 290 (4.29), 336 (3.97).

Rearrangement Reaction of VIII with Alkali.— A mixture of the chlorotropone derivative (VIII) (90 mg.), 50% methanol (4 ml.), and sodium hydroxide (200 mg.) was heated on a water bath for 30 min., methanol was evaporated, and the solid that separated was collected. This solid was suspended in water and acidified with acetic acid by which 1-(4′-carboxyphenyl)-2-phenylbenzimidazole separated as colorless crystals (50 mg.), m. p. 330°C (decomp.).

Found: C, 74.78; H, 4.00; N, 9.04. Calcd. for $C_{20}H_{14}O_2N_2$: C, 76.42; H, 4.49; N, 8.91%. λ_{max}^{MeOH} mμ (log ε): 272 (4.25).

The carboxylic acid (40 mg.) thereby obtained was suspended in methanol (3 ml.), ether solution of diazomethane was added, and the mixture was allowed to stand over night. The solvent was

evaporated to dryness, the residue was dissolved in ether, and the solution was passed through an alumina column for purification. Evaporation of the solvent from the effluent afforded 20 mg. of the methyl ester as colorless crystals, m. p. 115°C.

Found: C, 74.84; H, 4.61; N, 8.09. Calcd. for $C_{21}H_{16}O_2N_2 \cdot 1/2H_2O$: C, 74.76; H, 5.08; N, 8.30%. λ_{max}^{MeOH} mμ (log ε): 276 (4.31).

This methyl ester showed no depression of the melting point on admixture with 1-(4'-methoxycarbonylphenyl)-2-phenylbenzimidazole (IX), prepared by the method to be described below. The ultraviolet and infrared spectra of the two were also identical.

1-(4'-Methoxycarbonylphenyl)-2-phenylbenzimidazole (IX).—Benzoyl chloride (0.9 ml.) was added to a solution of 2-amino-4'-methyldiphenylamine (1 g.) dissolved in pyridine (5 ml.) while cooling with ice, the mixture was allowed to stand at room temperature for 30 min., and heated at 90°C for 30 min. Ice water was added to the reaction mixture, crystals that precipitated were collected, and recrystallized from ethanol to 1.2 g. of 2-benzamido-4'-methyldiphenylamine, m. p. 145~146°C.

Found: C, 79.63; H, 4.18; N, 9.18. Calcd. for $C_{20}H_{18}O_2N_2$: C, 79.44; H, 6.00; N, 9.27%. λ_{max}^{MeOH} mμ (log ε): 270 (4.23).

A mixture of the diphenylamine derivative (500 mg.) obtained as above and acetic anhydride (4 ml.) was heated at 140°C for 6 hr. Acetic anhydride was evaporated in a reduced pressure from the reaction mixture, water (2 ml.) was added to the residue, and the mixture was allowed to stand to over night. This was extracted with ether, the extract was dried over anhydrous sodium sulfate, and passed through a column of alumina.

Evaporation of ether from the effluent afforded 430 mg. of 1-(4'-methylphenyl)-2-phenylbenzimidazole, m. p. 91~92°C.

Found: C, 83.93; H, 5.34; N, 9.70. Calcd. for $C_{20}H_{16}N_2$: C, 84.48; H, 5.67; N, 9.85%. λ_{max}^{MeOH} mμ (log ε): 289 (4.22).

The benzimidazole derivative (400 mg.) so obtained was dissolved in pyridine (3 ml.), added to a solution of potassium permanganate (450 mg.) in water (6 ml.), and the mixture was heated on a water bath for 1 hr. After cooling, manganese dioxide that separated out was filtered off, a small amount of water was added to the filtrate, and extracted with ether to remove neutral substances. Acidification of the aqueous layer with acetic acid afforded 120 mg. of 1-(4'-carboxyphenyl)-2-phenylbenzimidazole as crystals of m. p. 340°C (decomp.).

The carboxylic acid (110 mg.) thereby obtained was suspended in methanol (6 ml.), ether solution of diazomethane was added to it to effect methylation, and the solvent was evaporated. The residue was dissolved in ether, the solution was passed through a column of alumina, and the solvent was evaporated from the effluent, affording 1-(4'-methoxycarbonylphenyl)-2-phenylbenzimidazole (IX) (60 mg.) as colorless crystals, m. p. 115°C.

***N*-(3-Bromotropolon-5-yl)-*N*, *N'*-dibenzoyl-*o*-phenylenediamine (X).** — A solution of 3-bromotropolone (35 mg.) and I dissolved in a mixture (3 : 1 by volume) of ethanol and chloroform, added with 1 drop of triethylamine, was allowed to stand at room temperature for 3 days. The crystals that separated were collected. Concentration of the filtrate in a reduced pressure afforded a second crop of crystals. The two crops of crystals were combined and recrystallized from an ethanol-chloroform mixture to give pale yellow crystals (30 mg.), m. p. 242~243°C (decomp.).

Found: C, 63.19; H, 3.83; N, 5.36. Calcd. for $C_{27}H_{19}O_4N_2Br$: C, 62.90; H, 3.72; N, 5.44%. λ_{max}^{MeOH} mμ (log ε): 230 (4.54), 240 (4.53), 250 (4.53), 355 (4.23), 420 (3.86).

***N*-(3, 7-Dibromotropolon-5-yl)-*N*, *N'*-dibenzoyl-*o*-phenylenediamine (XI).** — By the same procedure as above, 250 mg. of 3, 7-dibromotropolone and 150 mg. of I afforded 75 mg. of yellow crystals, m. p. 230~231°C (decomp.)

Found: C, 54.35; H, 3.19; N, 4.72. Calcd. for $C_{27}H_{18}O_4N_2Br_2$: C, 54.55; H, 3.05; N, 4.72%. λ_{max}^{MeOH} mμ (log ε): 265 (4.49), 275 (4.49), 360 (4.16), 430 (3.86), 440 (3.87).

Hydrogenolysis of X.—A solution of the monobromo derivative X (90 mg.) dissolved in a solution of potassium hydroxide (20 mg.) in water (1 ml.), to which was added palladium-carbon (50 mg.), was shaken in a hydrogen stream at room temperature. When the absorption of hydrogen had ceased, the catalyst was filtered off, the filtrate was acidified, and the precipitate that appeared was collected. Its recrystallization from an ethanol-chloroform mixture afforded 30 mg. of colorless crystals, m. p. 218~220°C, undepressed on admixture with II. The ultraviolet spectra of the two were identical.

Bromination of II.—A chloroform (1 ml.) solution of bromine (15 mg.) was added to the tropolonyl-*o*-phenylenediamine derivative II (20 mg.) suspended in chloroform (2 ml.) and the mixture was allowed to stand over night at room temperature, by which a resinous substance precipitated. The chloroform layer was separated by decantation, a small quantity of methanol was added to the resinous precipitate, and the crystallized solid was recrystallized from an ethanol-chloroform mixture to 5 mg. of crystals, m. p. 237~240°C undepressed on admixture with X. The ultraviolet spectra of these two substances were identical.

Hydrogenolysis of XI. — A solution of the dibromo derivative XI (200 mg.) in water (20 ml.) and ethanol (10 ml.) containing potassium hydroxide (600 mg.), added with palladium-carbon (400 mg.), was shaken in a hydrogen stream at room temperature. When the absorption of hydrogen had ceased, the catalyst was filtered off, the ethanol was evaporated from the filtrate at a reduced pressure, and the residual solution was acidified with 6 N sulfuric acid. This was extracted with ethyl acetate, the solvent was evaporated from the extract, and the residue was washed with benzene. The benzene-insoluble residue was recrystallized from an ethanol-chloroform mixture to 10 mg. of colorless crystals, m. p. 218~220°C, undepressed on admixture with II. The ultraviolet spectra of these two substances were identical.

Summary

Reaction of tropolone and *o*-benzoquinone dibenzimide was carried out and the structure of its product was determined by deriving it to a 2-phenylbenzimidazole derivative. This revealed that the product is *N*-(tropolon-5-yl)-*N*, *N'*-dibenzoyl-*o*-phenylenediamine. 3-Bromotropolone and 3, 7-dibromotropolone also underwent the same reaction to afford the corresponding bromo derivatives. For the sake of identification, 1-(4'-methoxycarbonylphenyl)-2-phenylbenzimidazole was synthesized from 2-amino-4'-methyldiphenylamine.

A part of the expenses for the present work was supported by a fund from the Sankyo Co., Ltd., which is gratefully acknowledged.

The Chemical Research Institute of
Non-Aqueous Solutions
Tohoku University
Katahira-cho, Sendai

Krypton-85 in the Atmosphere

By Kunihiko KIGOSHI

(Received November 21, 1961)

Measurements of the krypton-85 in atmospheric krypton have been reported by deVries[1] and by Delibrias et al.[2] The atmospheric krypton-85 produced by the fission of uranium or plutonium may possibly serve as a tracer for geophysical circulation problems. This article presents a recent variation in the concentration of atmospheric krypton-85, together with some details on the experimental method.

Experimental

Collection of the Atmospheric Krypton.—The atmospheric krypton of 10~50 ml. was collected in Tokyo from the liquid oxygen obtained from a small-scale nitrogen-liquefier machine after it had run continuously for a day or two. About 5 l. of this liquid oxygen—which is supposed to have more krypton than usual liquid oxygen because the liquid oxygen had been used as a coolant in the nitrogen liquefier—was evaporated in a Dewar vessel until the volume was reduced to about 100 ml. The gas evaporated from the final 100 ml. of liquid oxygen was passed through a trap refrigenated with liquid oxygen. Nearly 50 ml. of the atmospheric krypton gas was obtained from the liquid condensate (20~30 ml.) in the trap by heating the evaporated gas with calcium. Further purifications of the krypton were made by condensation in a trap at 61~65°K and by evaporation at the temperature of liquid oxygen. The purity of the krypton was examined by gas density measurements and by static vapor pressure measurements at the liquid oxygen point.

Radioactivity Measurements.—The radioactivities of the purified krypton samples were measured by using the small-volume Geiger counter shown in Fig. 1. As shown in Fig. 2, the counter worked as an external quenching Geiger counter and had a good characteristic curve for the mixture of the purified krypton of 150~350 mmHg and propane of 2~5 mmHg. The effective volume of the counter was estimated from the geometrical dimensions, and the end effect was measured by the use of the movable teflon rod in the counter, as shown in Fig. 1.

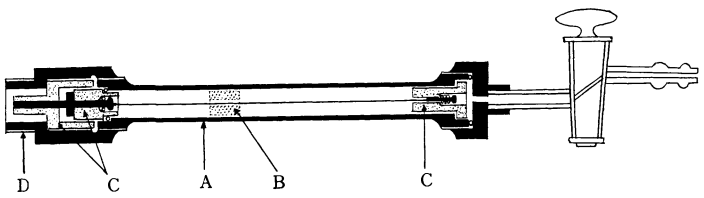


Fig. 1. Small volume counter tube.
A: Copper tubing; D=10.4 mm., L=97.0 mm.
B: Movable teflon rod used for the measurement of effective volume
C: Teflon insulator
D: High voltage supply connector

1) H. deVries, *Appl. Sci. Research*, **B5**, 387 (1956).

2) G. Delibrias and C. Jehanno, *Bulletin d'informations scientifiques et technologiques*, **No. 30**, June, (1959).

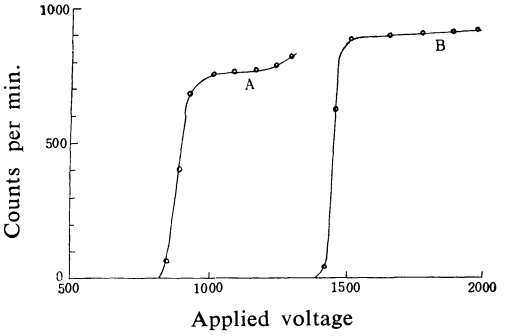


Fig. 2. Characteristic curve for Kr—Propane filled counter.
A: Kr 175 mmHg, C_3H_8 5.5 mmHg
B: Kr 386 mmHg, C_3H_8 5 mmHg

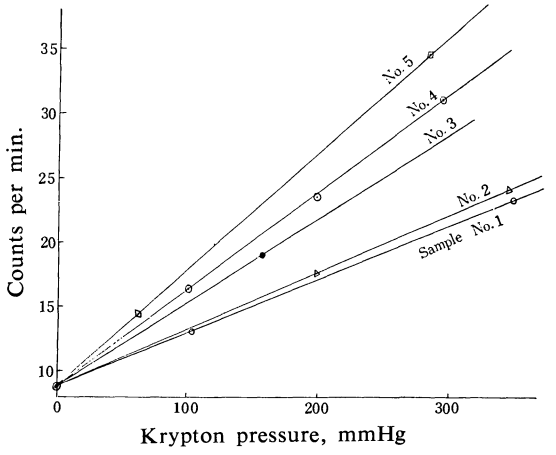


Fig. 3. Measured activities of the atmospheric krypton.

The measured counting rates showed a linear dependence on the amount of krypton in the counter. As shown in Fig. 3, the extrapolated counting rate of every sample at zero pressure met at a background counting rate, which was also checked with the counting with argon and propane. The number of disintegrations per minute was calculated by assuming a counting efficiency of 100% in the measured effective counter volume of 8.25 ml.

Results

The results of the measurements are shown in Table I. Sample 1 was collected from a large-volume liquid oxygen reservoir in an air liquefaction plant in Tokyo. Therefore the exact date of the collection of this sample is unknown. The data shown here and the data by Delibrias et al.[2] (1954; 1.160 d. p. m./ml. Kr; 1958: 4.200 d. p. m./ml. Kr) and by deVries[1] (March 1955: 26000 c.p.m./mol. Kr) show a steady increase in the concentration of atmospheric krypton-85 between 1954 and 1961. The increase in the atmospheric krypton-85 after the end of 1958 gives a maximum possible rate of supply of stratospheric krypton-85 to the troposphere, because the increase arose from the transfer of krypton-85 from the stratosphere to the troposphere and the direct supply to the troposphere by the atomic piles.

TABLE I. VARIATION OF KRYPTON-85 ACTIVITY IN THE ATMOSPHERIC KRYPTON

Sample No.	Collection date	Measured activity d.p.m./ml. Krypton (NTP)
1	Sept.—Nov. 1959	3.90±0.05
2	18—19 May 1960	4.14±0.04
3	9—11 July 1960	5.97±0.05
4	1— 2 Oct. 1960	6.86±0.09
5	10 Jan. 1961	8.32±0.09

The amount of man-made carbon-14 transported into the stratosphere from the troposphere after the biginning of 1959 can be estimated from the annual variation in mean atmospheric carbon-14 concentration. Using the measured variation of carbon-14 in tree rings[3,4] as the variation range of the atmospheric carbon-14, and assuming a mean residence time of 6 years for the carbon atoms in the troposphere before transfer to surface ocean water[5], the amount of injection of carbon-14 into the troposphere is estimated as follows:

$$1959: \quad 8\times10^{26} \text{ atoms/year}$$

$$1960: \quad 4\times10^{26} \text{ atoms/year}$$

The estimated total amount of man-made carbon-14 in the troposphere and ocean water is about 1.3×10^{28} atoms at the end of 1958[6]. Almost the same ratio of the amount injected into the troposphere from the stratosphere to the total amount in the troposphere and in ocean water may hold in the case of man-made carbon-14 and in the case of krypton-85 produced by nuclear tests.

The solubility of krypton in the sea water is so small that we can disregard sea water as a reservoir of krypton-85. When we assume that all the krypton-85 in the atmosphere in 1959 was produced by nuclear tests, the total atmospheric krypton-85 of 2.5×10^{26} atoms at that time corresponds to the carbon-14 of 1.3×10^{28} atoms in the troposphere and in sea water. Using these figures, the amount of krypton-85 injected from the stratosphere to the troposphere is estimated as 6×10^{24} atoms per year in 1959 and 3×10^{24} atoms per year

3) K. Kigoshi and Y. Tomikura, This Bulletin, **33**, 1576 (1960).
4) K. Kigoshi, *Journal of Radiation Research*, **1**—2, 111 (1960).
5) H. Craig, *Tellus*, **9**, 1 (1957).
6) F. Hagemann, J. Gray, L. Machta, Jr. and A. Turkevich, *Science*, **130**, 542 (1959).

in 1960. These figures correspond to the increase in atmospheric krypton activities of 0.24 d. p. m./ml. Kr/year in 1959 and 0.12 d. p. m./ml. Kr/year in 1960. The observed slow increase up to May, 1960, does not contradict the above estimate based on the parallelism between carbon-14 and krypton-85.

The increase after July, 1960, can not be attributed to the transfer of stratospheric krypton-85 to the troposphere. Even if the total fission energy released by nuclear tests between 1953 and 1958 were equivalent to the energy produced by 200 megatons of TNT, the total calculated amount of produced krypton-85 is about 7×10^{25} atoms. This amount is too small to explain the atmospheric krypton-85 after July, 1961, because the krypton activity of 8 d. p. m./ml. Kr corresponds to about 5×10^{26} atoms of krypton-85 in the whole atmosphere. The escape of krypton-85 from the atomic piles and from chemical processing plants for used fuel might be the main sources of the supply of atmospheric krypton-85 after July, 1960.

In the present situation, information on the mixing and movement of the air masses in the troposphere can be obtained when detailed measurements are made on the local distribution and variation in atmospheric krypton.

Summary

The activities of atmospheric krypton-85 were measured on the samples of krypton collected in Tokyo. The observed activities show a remarkable increase after May, 1960, which can not be explained by the production of krypton-85 by nuclear tests. The slow increase before May, 1960, does not contradict an assumed parallelism between the behavior of the man-made carbon-14 in the atmosphere and that of the krypton-85 produced by nuclear tests.

The author wishes to thank Dr. S. Horibe of Tokyo Metropolitan University and members of his laboratory for permission to operate their nitrogen-liquefier machine in order to sample atmospheric krypton.

Department of Physics and Chemistry
Gakushuin University
Mejiro, Toshima-ku
Tokyo

Hydrophile-Lipophile Balance Values for O/W Emulsions Stabilized by Nonionic Surfactants. I. Hydrophile-Lipophile Balance Values of Nonionic Surfactants Determined by Emulsification

By Noriaki OHBA

(Received June 30, 1961)

Concerning the study of emulsifications or emulsions stabilized by any nonionic surfactants, there is the well-known concept of HLB (hydrophile-lipophile balance) suggested by Griffin[1].

Following this concept, Kawakami[2] has presented an equation to calculate the HLB value from the structure of the surfactant molecule, that is,

$$\mathrm{HLB}=7+11.7\log(M_w/M_o) \qquad (1)$$

In this equation, M_w is the molecular weight of the hydrophilic group in the molecule and M_o, that of the lipophilic group.

In 1954, Griffin[3] also proposed another equation for this purpose, which enabled one to calculate the HLB value from both analytical and composition data. His second equation was,

$$\mathrm{HLB}=20(1-S/A) \qquad (2)$$

where S is the saponification number of the ester and A, the acid number of fatty acid used for the preparation of the derivatives of polyhydric alcohols, such as sorbitan, glycerol, etc.* For the surfactants, which involve only the polyoxyethylene chain as a hydrophilic group, the following equation was said to be suitable:

1) W. C. Griffin, *J. Soc. Cosmetic Chemists*, **1**, 311 (1949).
2) Y. Kawakami, *Kagaku*, **23**, 546 (1953).
3) W. C. Griffin, *J. Soc. Cosmetic Chemists*, **5**, 249 (1954).

* The values calculated by Eq. 1 are not materially different from those calculated by Eq. 2; we used the latter equation, together with Eq. 3, in the present experiment.

$$HLB = E/5 \quad (3)$$

where E is the weight percentage of oxyethylene content.

Furtheremore, Griffin assumed that the HLB of the surfactant mixture can be calculated by the following equation:

$$[HLB]_m = [HLB]_a x/100 + [HLB]_b(100-x)/100 \quad (4)$$

where $[HLB]_m$, $[HLB]_a$ and $[HLB]_b$ are the HLB values for the mixture, surfactant "a" and surfactant "b" respectively, and x, the weight percentage of "a" in the mixture. By this equation, the HLB value of any mixture of two surfactants can be predicted.

The concept of HLB, though convenient in practice, still has some difficulties in its applications. Besides, Griffin did not give the details of his emulsification experiments which are required for the HLB calculation. To clarify these points, we took up those O/W emulsions stabilized by nonionic surfactants and studied the system in detail by a method of emulsification experiments similar as those proposed by Griffin.

Experimental

Materials.—*Nonionic Surfactants.*—Sorbitan fatty acid esters and their polyoxyethylene derivatives were selected as typical nonionic surfactants, polyethylene glycol stearates as the ester type, polyoxyethylene-lauryl ethers and -cetyl ethers as the ether type, and polyoxyethylene nonylphenyl ethers as the alkylphenyl ether type, as listed in Tables I to VI.

These were used without further purification, as we needed to know merely the exact HLB value of a given sample. The nonionic surfactants listed in Tables III, IV, V and VI were exclusively prepared in the author's laboratory.

Mineral Oil. — "Carnation white mineral oil", prepared by the Sonneborn Co., U.S.A., was used as the oil to be emulsified, its average viscosity being 70 cp.

Table I. Sorbitan fatty acid esters

Abbr.	Chemical constitution	Trade name*
SML	Monolaurate	Span 20 or SL-10
SMP	Monopalmitate	Span 40 or SP-10
SMS	Monostearate	Arlacel 60 or SS-10
SMO	Monoöleate	Arlacel 80 or SO-10
SSO	Sesquioleate	Arlacel 83 or SO-15
STS	Tristearate	Arlacel 65 or SS-30
STO	Trioleate	Arlacel 85 or SO-30

* In Tables I and II, Spans, Arlacels and Tweens are commercial products of Atlas Powder Co., the others were prepared in our laboratory.

Table II. Polyoxyethylene sorbitan fatty acid esters

Abbr.	Chemical constitution		Trade name*
	Esters	n**	
E-SML-20	SML	20	Tween 20 or TL-10
E-SMP-20	SMP	20	Tween 40 or TP-10
E-SMS-6	SMS	6	Tween 61 or TS-106
E-SMS-20	SMS	20	Tween 60 or TS-10
E-SMO-6	SMO	6	Tween 81 or TO-106
E-SMO-20	SMO	20	Tween 80 or TO-10
E-STS-20	STS	20	Tween 65 or TS-30
E-STO-20	STO	20	Tween 85 or TO-30

Table III. Polyethylene glycol stearates

Abbr.	Chemical constitution n**	Trade name
PEGS-2	2	MYS-2
PEGS-4	4	MYS-4
PEGS-10	10	MYS-10
PEGS-25	25	MYS-25
PEGS-45	45	MYS-45

Table IV. Polyoxyethylene lauryl ethers

Abbr.	Chemical constitution n**	Trade name
POEL-4.2	4.2	BL-4.2
POEL-5	5	BL-5
POEL-10	10	BL-10
POEL-20	20	BL-20
POEL-25	25	BL-25

Table V. Polyoxyethylene cetyl ethers

Abbr.	Chemical constitution n**	Trade name
POEC-2	2	BC-2
POEC-3	3	BC-3
POEC-5.5	5.5	BC-5.5
POEC-7	7	BC-7
POEC-10	10	BC-10
POEC-15	15	BC-15
POEC-20	20	BC-20

Table VI. Polyoxyethylene nonylphenyl ethers

Abbr.	Chemical constitution n**	Trade name
POENP-2	2	NP-2
POENP-7.5	7.5	NP-7.5
POENP-9	9	NP-9
POENP-10	10	NP-10
POENP-20	20	NP-20

** n, Average mol. number of ethylene oxide in molecule.

Emulsification.—In the present series of experiments, an "Emulsification by Inversion"[4], which involves phase inversion as an important process, was utilized to prepare the emulsions.

The standard composition of the emulsion for this series of experiments is shown in Table VII.

TABLE VII. COMPOSITION OF EMULSION

Mineral oil	40.0%
Mixture of emulsifiers	4.0%
Distilled water	56.0%

The emulsifications were carried out by the following procedure. A mixture of mineral oil and mixed surfactants was heated up to about 90°C. Into this mixed oil phase, water which had also been heated to about 90°C was added slowly with stirred. After adding all of the water, stirring was continued until the temperature of the emulsion fell to about 40°C. The emulsions thus obtained were used for studying their properties.

Estimation of the "Required HLB Value" of O/W Emulsion

Griffin suggested the HLB system, but there is no nonionic surfactant to use as the standard of the HLB value.

In our series of experiments, however, Arlacel 60 (HLB=4.7) and Tween 60 (HLB=14.9), i. e., SMS and E-SMS-20 in our case, were used as the standards of the HLB value. These two samples were selected as standard because they are easy to prepare as a series of homologues, they emulsify a wide variety of oils, and they are situated in appropriate positions in the HLB region.

The HLB value of an emulsion or the HLB value for an oil in making an emulsion can be estimated by means of an emulsification test following the concept of HLB. Griffin proposed the term "required HLB" for the oil phase used to emulsify. This required HLB value is considered to be equal to $[HLB]_m$ in Eq. 4, calculated from the composition of a system when the mixture of two surfactants gives the most stable emulsion among a series of emulsions made with a given pair of agents under varying compositions, as is shown in Table VIII.

TABLE VIII. ESTIMATION OF THE HLB VALUE BY EMULSIFICATION TESTS

No.	Composition of emulsifier: SMS %	Composition of emulsifier: E-SMS-20 %	Stability of emulsion
1	52.5	47.5	+
2	50.0	50.0	++
3	47.5	52.5	+++
4	45.0	55.0	+++
5	42.5	57.5	++
6	40.0	60.0	++

We can see in Table VIII that the emulsions of Nos. 3 and 4 are the most stable, and the HLB, $[HLB]_m$, required for a mineral oil to be emulsified with a pair of SMS and E-SMS-20 is estimated as 10.2 by Eq. 4. In later sections, we adopt this value as the standard of the required HLB. Thus, by these experiments, the required HLB of mineral oil may be determined for every pair of emulsifiers. To make the comparison simple, one of the emulsifiers taken as the standard is always kept as a fixed component in any pair of surfactants in the emulsification tests.

Results and Discussion

Applicability of Eq. 4.—The results of sorbitan fatty acid esters and their polyoxyethylene derivatives are shown in Table IX. In this table, the required HLB values of mineral oil, $[HLB]_m$, which are shown in the 4th column, were calculated by Eq. 4, using the HLB value of the combined component surfactant, $[HLB]_{calcd}$, shown in the 2nd column, and the HLB value of the fixed component surfactant.

TABLE IX. HLB VALUES FOR SORBITAN DERIVATIVES

Combined emulsifier	$[HLB]_{calcd}$	Fixed emulsifier	$[HLB]_m$	$[HLB]_a$
SML	8.6	E-SMS-20	11.6	5.8
SMP	6.7	E-SMS-20	11.2	4.4
SMS	4.7	E-SMS-20	10.2	4.7
STS	2.1	E-SMS-20	(7.8)	(6.5)
SMO	4.3	E-SMS-20	9.8	5.1
SSO	3.7	E-SMS-20	9.4	5.2
STO	1.8	E-SMS-20	(4.4)	(9.0)
E-SML-20	16.7	SMS	9.9	17.3
E-SMP-20	15.6	SMS	10.2	15.6
E-SMS-6	9.6	E-SMS-20	10.4	9.4
E-SMS-20	14.9	SMS	10.2	14.9
E-SMO-6	10.0	E-SMS-20	11.0	9.0
E-SMO-20	15.0	SMS	10.2	15.0
E-STS-20	10.5	SMS	10.2	10.5
E-STO-20	11.0	E-SMS-20	11.6	9.3
			Average 10.5 ± 1.1	

The required HLB value of mineral oil is

$$[HLB]_m = 10.5 \pm 1.1 \quad (5)$$

excepting the values for STO and STS, which are not considered to fall into the category of O/W emulsifiers. Within the range of this error, it may be said that the concept of the HLB system is applicable in emulsion systems with nonionic surfactants.

4) Presented at the 12th Symposium of Colloid Chemistry, Hiroshima, 1959.

For the rest of the types of nonionic surfactants, the required HLB values of mineral oil were calculated by the same procedure as in Table IX; the results obtained are:

$$\text{PEGS}, \quad [\text{HLB}]_m = 10.2 \pm 0.3 \qquad (6)$$

$$\text{POEL}, \quad [\text{HLB}]_m = 9.7 \pm 1.6 \qquad (7)$$

$$\text{POEC}, \quad [\text{HLB}]_m = 9.0 \pm 0.6 \qquad (8)$$

$$\text{POENP}, [\text{HLB}]_m = 8.9 \pm 0.8 \qquad (9)$$

From these results, it may be concluded that the allowance of an obtained $[\text{HLB}]_m$ is in the range of ± 1, excepting the case of POEL. However, we must draw attention to the fact that the mean value of the HLB itself fluctuates according to the pair of surfactants used. This fact has a very important implication concerning the concept of the HLB, which becomes the starting point for the further study of these phenomena.

HLB Values of Nonionic Surfactants.—If the additivity expressed in Eq. 4 is assumed to be correct, we can calculate $[\text{HLB}]_a$ from the values of $[\text{HLB}]_m$ and $[\text{HLB}]_b$ according to the following equation:

$$[\text{HLB}]_a = \{[\text{HLB}]_m - [\text{HLB}]_b(100-x)/100\}100/x \qquad (10)$$

Thus, using these $[\text{HLB}]_m$ and $[\text{HLB}]_b$ values;
$[\text{HLB}]_m$: 10.2, determined with the standard emulsifiers, SMS and E-SMS-20,
$[\text{HLB}]_b$: 4.7 for SMS, and 14.9 for E-SMS-20,
x: percentage content of emulsifier "a" in the mixed emulsifier,
the HLB value of any nonionic surfactant can be estimated from the emulsification experiments. The results are shown in the last column of Table IX.

Of course, in this case, it is assumed as an important condition that the required HLB of mineral oil takes a fixed value.

$[\text{HLB}]_{calcd}$ and $[\text{HLB}]_a$. — To make a comparison between the values, $[\text{HLB}]_{calcd}$, calculated by Eq. 2 or 3 and $[\text{HLB}]_a$, those obtained experimentally, $[\text{HLB}]_{calcd}$ vs. $[\text{HLB}]_a$ diagrams are plotted in Figs. 1 and 2 for each type of nonionic surfactant. In these figures we should expect the plot to fall on the bisector of the angle between two coordinate axes.

In Fig. 1, for sorbitan derivatives, ○, an interesting curve is obtained. Their polyoxyethylene derivatives showed a coincidence between two values; however, sorbitan fatty acid esters deviated remarkably from the bisector, and this deviation seemed to follow a definite function of the HLB values. As a result, the values of $[\text{HLB}]_a$ for STO, STS, SSO and SMO are higher than the corresponding $[\text{HLB}]_{calcd}$ drawn from Eq. 2, while those for

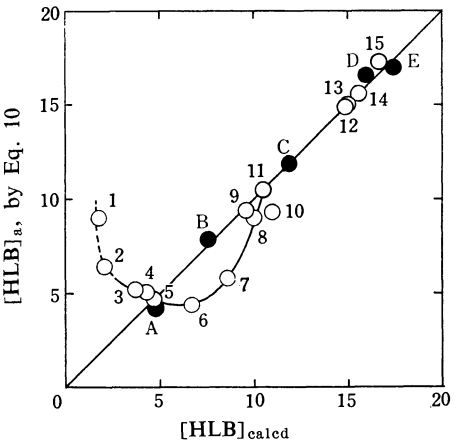


Fig. 1. $[\text{HLB}]_{calcd}$ vs. $[\text{HLB}]_a$ diagram for sorbitan derivatives: ○,
1, STO 2, STS 3, SSO
4, SMO 5, SMS 6, SMP
7, SML 8, E-SMO-6 9, E-SMS-6
10, E-STO-20 11, E-STS-20 12, E-SMS-20
13, E-SMO-20 14, E-SMP-20 15, E-SML-20;
and for polyethylene glycol stearates: ●,
A, PEGS-2 B, PEGS-4 C, PEGS-10
D, PEGS-25 E, PEGS-45

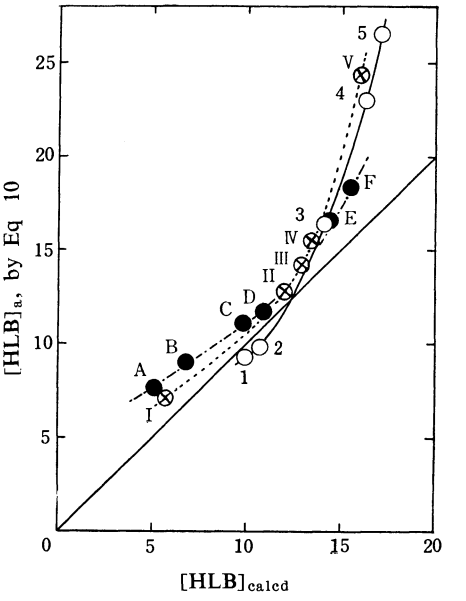


Fig. 2. $[\text{HLB}]_{calcd}$ vs. $[\text{HLB}]_a$ diagram for polyoxyethylene lauryl ethers: ○,
1, POEL-4.2 2, POEL-5 3, POEL-10
4, POEL-20 5, POEL-25;
for polyoxyethylene cetyl ethers: ●,
A, POEC-2 B, POEC-3 C, POEC-5.5
D, POEC-7 E, POEC-15 F, POEC-20
and for polyoxyethylene nonylphenyl ethers: ⊗,
I, POENP-2 II, POENP-7.5 III, POENP-9
IV, POENP-10 V, POENP-20

SMP and SML are lower than the corresponding $[HLB]_{calcd}$.

As the sorbitan group is a complicated hydrophilic group compared with those of polyoxyethylenes, there is some question as to the calculation of the HLB value according to Eq. 2 or 3, which merely involve the percentage content of the hydrophilic group in the molecule.

STS and STO, having little hydrophilic property, show too high a $[HLB]_a$ compared with their $[HLB]_{calcd}$. This means that the amount of emulsifiers, x, necessary for optimum emulsification is larger than that calculated from its $[HLB]_{calcd}$. Further, they do not produce fine emulsions. Thus, the behavior of a poorly hydrophilic emulsifier is quite different from the more hydrophilic one.

Polyethylene glycol stearates, as shown in Fig. 1, ●, showed only a slight deviation in plot from the bisector; i. e., Eqs. 2 and 10 give nearly equal results for this type of nonionic surfactants.

In this case, the emulsifiers used are all stearic acid esters, and an agreement is obtained between the values of $[HLB]_{calcd}$ and $[HLB]_a$. From this fact, together with the fact that the two components of the emulsifier have a stearate radical in common, we are inclined to the opinion that the mutual interaction between hydrophilic emulsifier and oleophilic one is due largely to this oleophilic stearate group in the molecule.

In Fig. 2, POELs, ○, POECs ●, and POENPs ⊗, show remarkable difference between their two values. POENP shows nearly the same deviation as POEL; that is, nonylphenol behaves quite similarly to lauryl alcohol in the emulsification of mineral oil, although the carbon number 15 for nonylphenol is different from the carbon number 12 for lauryl alcohol. As a whole, this difference between their two values is greater at a higher HLB and smaller at a lower HLB range. In other words, the difference between $[HLB]_a$ and $[HLB]_{calcd}$ for these types of nonionic surfactants becomes greater at a higher mole number of the ethylene oxide unit in the molecule, and the difference increases in the following order:

$$PEGS < POEC < POEL \leqslant POENP$$

The difference is due perhaps to the emulsifier having a different oleophilic group.

HLB Value by Emulsifications. — In HLB systems, the additivity of HLB values between two components was assumed as an important basis. Generally, in many cases of the two-component system their physicochemical properties show some deviation from an algebraic additivity as a result of their component properties.

To investigate the value of $[HLB]_m$ in Eq. 4 is merely to discuss its deviation from the value which is calculated by interpolation using two emulsifiers obtained by Eq. 2 or 3.

On the other hand, to examine the values of $[HLB]_a$ in Eq. 10 is to study its deviation, adopting the value calculated by extrapolation using the fixed $[HLB]_m$ and $[HLB]_b$ from $[HLB]_{calcd}$, which is calculated only by the percentage content of the hydrophilic group in the molecule. By this latter procedure, the difference between $[HLB]_{calcd}$ and $[HLB]_a$ naturally becomes larger, and this makes the discussion rather easy.

The above results and discussions lead us to the conclusion that it is possible to illustrate and study more details of the HLB systems or the HLB values for several nonionic surfactants in the emulsifications of mineral oil when we refer them to the properly assigned standards.

Summary

The HLB values of several types of nonionic surfactants were determined by experiments in emulsification according to the concept of HLB suggested by Griffin.

The HLB values required to emulsify the mineral oil do not show a consistent value, although the values are limited within a narrow range.

The HLB values calculated according to the law of the additivity for the surfactant mixture, $[HLB]_a$, and the values calculated by the equations proposed by Griffin, $[HLB]_{calcd}$, were compared. The differences between these two values were most remarkable in the case of sorbitan fatty acid esters and became greater at the higher mole numbers of the ethylene oxide in the molecule, excepting polyoxyethylene sorbitan esters and polyethylene glycol stearates.

Some explanations were attempted for such differences and for the deviations from the assumed additive properties of the HLB system, in connection with the role or behavior of nonionic surfactants in emulsification.

The author wishes to thank Professor Tsunetaka Sasaki of Tokyo Metropolitan University, for his encouragement and advice in this work.

Nihon Surfactants Ind. Co.
Itabashi-ku, Tokyo

Hydrophile-Lipophile Balance Values for O/W Emulsions Stabilized by Nonionic Surfactants. II. "Required Hydrophile-Lipophile Balance Values" of the Oil Mixture

By Noriaki OHBA

(Received June 6, 1961)

In a preceding paper[1], the HLB values of nonionic surfactants were determined by means of emulsification tests conducted according to the HLB concept presented by Griffin[2]. The HLB values thus obtained were compared with the values calculated from their structural data, and the additivities of these values were discussed in connection with the behaviors of these nonionic surfactants in the systems of O/W emulsions.

In the HLB concept, an algebraic additivity of the HLB values in the mixtures of two or more surfactants is assumed as an important basis, which is expressed as follows[3]:

$$[\mathrm{HLB}]_m = [\mathrm{HLB}]_a x/100 + [\mathrm{HLB}]_b(100-x)/100 \quad (1)$$

Here, $[\mathrm{HLB}]_m$, $[\mathrm{HLB}]_a$ and $[\mathrm{HLB}]_b$ are the HLB values of the mixed emulsifier and of the surfactants "a" and "b" respectively, and x, the percentage content of surfactant "a" in the mixture.

Furthermore, the HLB concept is extended to apply in the case of the oil phase of the emulsion, and the term "required HLB value" is adopted for the given oil in a sense similar to that of the HLB value for the emulsifier. It was shown by Griffin that this required HLB value can be determined by means of emulsification tests, and such values obtained for several oils and waxes were presented by him[3].

In a manner similer to that in the case of the HLB values for emulsifier mixtures, he also assumed that the required HLB value for the oil mixture is obtained as an algebraic additivity from those values for the component oils in the mixture; that is,

$$[\mathrm{HLB}]_o = \sum [\mathrm{HLB}]_i R_i/100 \quad (2)$$

where $[\mathrm{HLB}]_o$ is a required HLB value of the oil mixture, and $[\mathrm{HLB}]_i$ and R_i a required HLB value and the percentage content of the ith component oil in the oil mixture respectively.

In this paper, to study the additivity in the HLB system and the characteristics of oil mixtures, the required HLB values of several oil mixtures were determined by means of emulsification tests[1].

Experimental

Materials. — *Nonionic Surfactants.* — Commercial products of sorbitan monostearate, SMS, and polyoxyethylene sorbitan monostearate, E-SMS-20, which were used in a preceding report[1], were also adopted as the standards for nonionic emulsifiers. The HLB values for these materials are 4.7 for SMS and 14.9 for E-SMS-20. When the required HLB of an oil mixture exceeds 14.9, polyoxyethylene cetyl ether, POEC-20, with the HLB value of 18.4, was adopted instead of E-SMS-20.

Oils and Waxes.—"Carnation White Mineral Oil" produced by the Sonneborn Co. was adopted as the fixed component of the oil mxture to be emulsified, its HLB value being 10.2 and its average viscosity, 70 cp.

Several materials were used as the additive component of the oil mixture; these are listed in Tables II to VI.

These additives, which are usually employed in the emulsion technique, were used without further purification.

TABLE I. REQUIRED HLB VALUES FOR ADDITIVES TO OIL PHASES OF O/W EMULSIONS

Oil phase	Required* HLB value	$[\mathrm{HLB}]_i$**
Acid, stearic	17	33.7~38.2
Alcohol, cetyl	13	15.7~16.2
Kerosene	12.5	—
Lanolin, anhydrous	15	10.7~12.2
Oil		
Mineral, heavy	10.5	—
Mineral, light	10	10.2
Silicone	10.5	—
Petrolatum	10.5	—
Wax		
Beeswax	10~16	13.9~16.2
Candelilla	14.5	—
Carnauba	14.5	—
Microcrystalline	9.5	—
Paraffin	9	6.2~8.9

* Values presented by Griffin

** Apparent values of HLB for additives

1) N. Ohba, This Bulletin., 35, 1016 (1962).
2) W. C. Griffin, *J. Soc. Cosmetic Chemists*, 1, 311 (1949).
3) W. C. Griffin, ibid., 5, 249 (1954).

TABLE II. FATTY ACIDS

Abbr.	Substance	Main component
L-Ac	Lauric	90%
S-Ac	Stearic	80%(20% palmitic)
O-Ac	Oleic	95%

TABLE III. ALCOHOLS

Abbr.	Substance	Main component
L-Alc	Lauryl	85%
C-Alc	Cetyl	80%(20% stearyl)
La-Alc	Lanolin	100%(mixture)

TABLE IV. ESTERS

Abbr.	Substance	Main component
IPM	Isopropyl myristate	97%
BS	Butyl stearate	95%
IPLa	Isopropyl lanolate	100%(mixture)

TABLE V. ACETYLATED ESTERS

Abbr.	Substance	Hydroxyl value
AGMS-I	Acetylated glyceryl monostearate	4
AGMS-II	Acetylated glyceryl monostearate	35
AGMS-III	Acetylated glyceryl monostearate	75
AGMS-IV	Acetylated glyceryl monostearate	155
AGML	Acetylated glyceryl monolaurate	30
AGMO	Acetylated glyceryl monoöleate	4
ALa	Acetylated lanolin	1

TABLE VI. OILS AND WAXES

Abbr.	Substance	Main component
CS-O	Cotton seed oil	Glyceryl trioleate
La	Lanolin	
B-W	Beeswax	
C-W	Ceresin Wax	Paraffin

TABLE VII. COMPOSITION OF O/W EMULSION

Oil mixture	40.0%
Emulsifier	
SMS+E-SMS-20	4.0%
Distilled water	56.0%

Emulsification.—Emulsification was carried out by the phase inversion method reported on in a preceding paper[1]. The composition of the emulsion tested in the present series of experiments is shown in Table VII.

In this table, the oil mixture consists of a mineral oil taken as the fixed component and an additive component, the content of which varies from 0 up to 30% in weight.

The required HLB values of the oil mixtures were determined as the value which was calculated by Eq. 1 for the composition of the mixed emulsifier giving the most stable emulsion in the series of emulsification tests, as described in a preceding paper[1].

Results

In Figs. 1—5, $[HLB]_o$ vs. R diagrams are shown. In Table VIII, which selects one example from many calculations, the content (R %) of the additive in the oil mixture is listed in the 2nd column, the required HLB value ($[HLB]_o$) in the 3rd, and the difference (Δ) between the required HLB value of the oil mixture and the required HLB value of mineral oil ($[HLB]_m$), in the 4th column. In the last column, the apparent HLB value of the additive,

$$[HLB]_i = \Delta(100/R) + [HLB]_m$$

calculated from Δ at each concentration, is shown; $[HLB]_m = 10.2$ in the present case. If the additivity in Eq. 2 is valid, $[HLB]_i$ should be constant.

TABLE VIII. REQUIRED HLB VALUES OF MIXTURES OF FATTY ACIDS AND MINERAL OIL

	R, %	$[HLB]_o$	Δ	$[HLB]_i$
L-Ac	0	10.2	—	—
	10	13.4	3.2	42.2
	20	17.2	7.0	45.2
S-Ac	5	11.6	1.4	38.2
	10	12.8	2.6	36.2
	20	14.9	4.7	33.7
O-Ac	5	12.8	2.6	62.2
	7.5	12.8	2.6	44.4
	10	9.8	−0.4	6.2
	20	15.6	5.4	37.2
	30	18.4	8.2	37.5

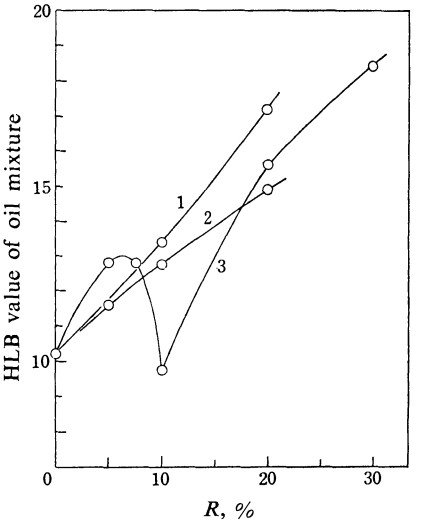


Fig. 1. Required HLB value of oil mixtures, Additives to mineral oil:
1, Lauric acid 2, Stearic acid
3, Oleic acid

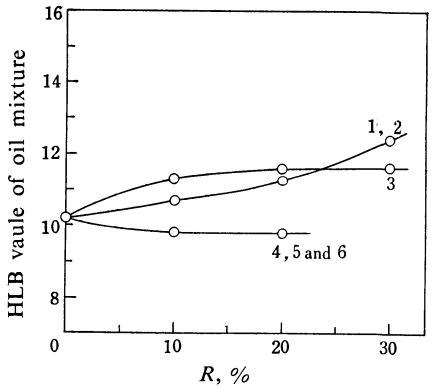


Fig. 2. Required HLB value of oil mixtures.
Additives to mineral oil:
1, Lauryl alcohol 2, Cetyl alcohol
3, Lanolin alcohol 4, Isopropyl myristate
5, Butyl stearate 6, Isopropyl lanolate

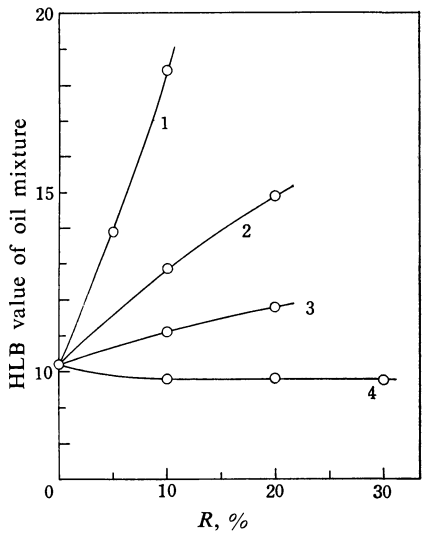


Fig. 3. Required HLB value of oil mixtures.
Additives to mineral oil:
1, AGMS-IV 2, AGMS-III 3, AGMS-II
4, AGMS-I

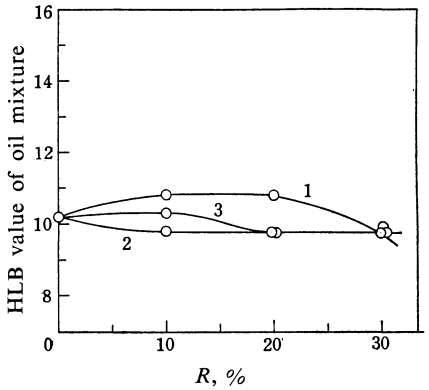


Fig. 4. Required HLB value of oil mixtures.
Additives to mineral oil:
1, AGML 2, AGMO 3, ALa

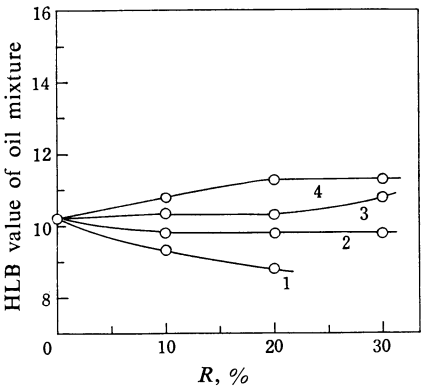


Fig. 5. Required HLB values of oil mixtures.
Additives to mineral oil:
1, CS-O 2, C-W 3, La 4, B-W

Discussion

Fatty Acids.—Among the three fatty acids, lauric acid is the nearest of all to the additivity rule expressed by Eq. 2; however, the observed required HLB values, $[HLB]_i$, 42~45, are remarkably large, even considering the required HLB value for stearic acid listed in Table I. We should like to draw attention to the fact that no HLB value exceeding 20 can be evaluated according to the equation presented by Griffin.

Stearic acid also shows a marked deviation from Griffin's value listed in Table I, and the additive property of the HLB value is not distinct.

In the case of oleic acid, the diagram obtained is complicated in the region of R near 10%, where this curve shows a minimum. In the rest of the region studied, the curve runs similar to the other two acids. The value of $[HLB]_i$ for an R larger than 10% is constant and is nearly the same as those for stearic acid.

The elucidation of the anomalous phenomena mentioned above for oleic acid must await further investigation.

Alcohols.—Lauryl alcohol and cetyl alcohol gave coincident results in the region of R examined, and the obtained values of $[HLB]_i$ were 15~17, which are slightly larger than the corresponding values in Table I.

Though the composition and chemical structure of lanolin alcohol is not so simple as those of lauryl alcohol and cetyl alcohol, the curves for these three alcohols run parallel to each other, excepting the curve for lanolin alcohol in the region of R exceeding 10%, where the $[HLB]_o$ is nearly independent of R. Precisely speaking, therefore, the curve for lanolin alcohol is somewhat different from the other two but is, on the other hand, rather similar to that of waxes, as is shown in Fig. 5.

TABLE IX. ANALYTICAL DATA AND THE VALUES OF $[HLB]_i$

Additives[1]	$[HLB]_i$	COOH[3]	COOR[3]	OH[3]	C=C
AGMS-IV	82.2	4	210	155	N[2]
O-Ac(7.5%)	44.4	200	N	N	94
L-Ac	42.2	278	N	N	N
O-Ac(20%)	37.2	200	N	N	94
AGMS-III	37.2	3	275	75	N
S-Ac	36.2	202	N	N	N
AGMS-II	20.2	3	315	35	N
La-Alc	21.2	—	40	90	—
L-Alc	16.2	N	N	300	N
C-Alc	16.2	N	N	217	N
AGML	16.2	3	370	30	N
B-W	16.2	18	76	20	9
ALa	11.2	N	120	N	—
La	11.2	5	95	30	22
AGMS-I	6.2	2	330	4	N
AGMO	6.2	2	325	4	80
C-W	6.2	N	N	N	N
O-Ac	6.2	200	N	N	94
IPM	6.2	N	207	N	N
BS	6.2	N	168	N	N
IPLa	6.2	N	—	N	—
CS-O	1.2	N	—	N	90

1) Content of additives is 10% unless otherwise stated.
2) Negligible
3) COOH: acid value, COOR: ester value, OH: hydroxyl value, C=C: iodine value.

Acetylated Esters.—The molecules of this group contain a different number of free hydroxyl radicals, as the result of a varying degree of acetylation. This enables us to study the effects of the increase of the OH-radical on emulsification. Indeed, the results obtained show large differences in $[HLB]_o$ values according to the degree of acetylation, as is shown in Figs. 3 and 4.

The values of the $[HLB]_o$ of acetylated esters increases with the increase in the OH content of the molecules, as indicated in the following series:

AGMS-I<AGMS-II<AGMS-III<AGMS-IV

In the case of AGMS-I, which lacks an OH-radical in the molecule due to the nearly perfect acetylation, the curve is somewhat like that for waxes in Fig. 5. The large difference in the inclinations of curves between these esters and those for alcohols suggests the effect of other factors than the OH content, such as ester linkage and the alkyl chain length of their molecules.

Though the values of $[HLB]_i$ do not fluctuate so much with R, its values are too large in the cases of AGMS-III (33.7~37.2) and AGMS-IV (82.2~84.2).

Oils and Waxes.—Though the natural oils and waxes are of a complicated nature in composition, they behave rather simply, as is shown in Fig. 5. $[HLB]_i$ values are also listed in Table I.

The results obtained for esters are somewhat similar to those for oils and waxes, although their structures are more simple than those for oils and waxes, as is shown in Fig. 2.

Structural Effects.—As far as the present experiments are concerned, the additivity of the required HLB values of the oil mixture from its components, as shown by Eq. 2, if any, is recognized to hold to some extent in the cases of saturated fatty, acids, *n*-fatty alcohols and some acetylated esters.

For the rest of the materials examined, the additivity of the required HLB values is hardly valid. Generally, the required HLB values of oil mixtures varied to some extent with the increase of R up to 10%, and they level off with the further increase of R; in certain cases, as in the AGML in Fig. 4, even an inversion of the sign of Δ from positive to negative is observed with the increase of R.

As for the explanation of these results, it is worth while to list the analytical data of these additives in Table IX. They are arranged in

the decreasing order of $[HLB]_i$ at 10% R. From this table, it may be concluded as a whole that the intensity of the structural effects on the value of $[HLB]_i$ decreases in the following order:

$$COOH > OH > COOR$$

As seen from this order, the OH-radical by itself does not increase so markedly the values of $[HLB]_i$ as in the case of alcohols, although it increases the value of $[HLB]_i$ when ester-linkage coexists with the OH-radical in a molecule, as seen, for instance, in the case of AGMS-IV.

Summary

To study the additivity of the HLB values of an oil mixture from its component and the characteristics of the oil mixture forming a component of the emulsion, the required HLB values of several oil mixtures were determined by means of the emulsification tests proposed by Griffin.

The oil mixtures examined in this series of experiments consist of two oils, one being a mineral oil of fixed components and the other an oil to be studied as the additive, which is added in varying ratios to the fixed-component mineral oil.

The additivity of the required HLB values in oil mixtures was shown to hold to some extent for the case of saturated fatty acids, *n*-fatty alcohols, and some acetylated esters. For the rest of the additives, the additivity is not valid.

The required HLB values of these additive oils were remarkably large in the case of fatty acids, alcohols and some acetylated esters, excepting the anomalous value for oleic acid.

The structural effects on the increase of required HLB values seem to be in the following order:

$$COOH > OH > COOR$$

Nihon Surfactant Ind. Co.
Itabashi-ku, Tokyo

Gas Absorption by Cobalt Soaps

By Hideo FUNAKOSHI

(Received September 22, 1961)

Cobalt soaps are of wide industrial application as oxidizing calalysts in organic reactions, such as dryers of paints. It has been known that if the cobalt soaps of unsaturated acids, such as cobalt resinate, are left standing in the air, they change color from red to dark brown and sometimes ignite spontaneously. The mechanism of these characteristic oxidizing actions of cobalt soaps is not, however, known well. Ingle[1] has indeed presented a theory based on the oxidation of a substance by the oxygen carried by cobalt soaps, but direct evidence for this theory has not been offered. In this report the absorptive properties of cobalt oleate and stearate for a few gases are studied. Especially the absorption of oxygen by cobalt oleate is investigated from various points of view.

Experimental

Materials.—Cobalt soaps were prepared by metathesis from alkali soaps and cobaltous salts in ethanol-water solutions at about 50°C. It had previously been established that the composition of cobalt soaps depends perceptibly on the conditions of the preparation[2]. In this experiment the conditions were kept as constant as possible in order to obtain samples of a definite composition. The details are as follows.

Cobalt Oleate.—Oleic acid (15 g.) was dissolved in 95% ethanol (185 ml.) and neutralized by 1 N sodium hydroxide, using phenolphthalein as an indicator. This was diluted dy hot water (400 ml.) (solution A). Cobaltous nitrate (7.6 g.) was dissolved in water (230 ml.) (solution B). Both solutions were warmed at 50°C. Solution B was added to solution A drop by drop. The precipitated cobalt oleate was filtered and washed with ethanol and water. To avoid oxidation, all procedures were carried out in a stream of nitrogen gas. The sample was dried in vacuo at room temperatures and kept by sealing it in a glass bottle. Pink powder.

Found: Co, 12.70; C, 63.56; H, 10.13. Calcd. for $Co_3(C_{18}H_{33}O_2)_4(OH)_2 \cdot 2H_2O$: Co, 12.88; C, 63.00; H, 10.13%.

Cobalt Stearate.—Stearic acid (2 g.) was dissolved in 95% ethanol (100 ml.) and neutralized with 1 N

1) H. Ingle, *J. Soc. Chem. Ind.*, **36**, 319 (1917).

2) Y. Koga and R. Matuura, *Mem. Faculty Sci., Kyushu Univ.*, **C4**, 1 (1961).

sodium hydroxide as above. This mixture was then diluted with hot water (100 ml.) (solution A'). A solution of cobaltous chloride (1.2 g.) in water (50 ml.) (solution B') was added drop by drop at 50°C to solution A'. The precipitate was treated as in the case of cobalt oleate. Blue powder.

Found: Co, 10.26; C, 69.01; H, 11.59. Calcd. for $Co(C_{18}H_{35}O_2)_2$: Co, 9.42; C, 69.02; H, 11.28%.

Oleic acid was obtained from camellia oil by treating it with potassium hydroxide, lead acetate and lithium hydroxide and finally by distilling it at 228.5°C/13 mmHg. M. p. 12.6°C. Stearic acid was recrystallized from commercial samples. M. p. 68.8~69.3°C. Cobaltous nitrate, $Co(NO_3)_2 \cdot 6H_2O$, and chloride, $CoCl_2 \cdot 6H_2O$, were purified by recrystallization. As gases, oxygen, nitrogen and hydrogen were used. They were purified by the usual method.

Procedure.—The gas absorption was measured by using a Warburg manometer at 22~23°C under atmospheric pressure. The weight change accompanying the gas absorption was also measured. X-Ray diffraction patterns and ultraviolet and infrared absorption spectra of oxygenated cobalt oleate were investigated, too. The X-ray patterns were obtained by the Debye-Scherrer method. A Shimadzu QB-50 spectrophotometer was used for the ultraviolet absorption spectra, while for the infrared studies a Hitachi EPI-2 infrared spectrometer was used.

Results and Discussion

Gas Absorption by Cobalt Oleate.—In Fig. 1 the volume of gases (STP) absorbed by one gram of cobalt oleate is plotted against the time required. It is clear that oxygen is absorbed noticeably, while the absorption of nitrogen and hydrogen is very small. For the first hundred minutes the absorption of oxygen

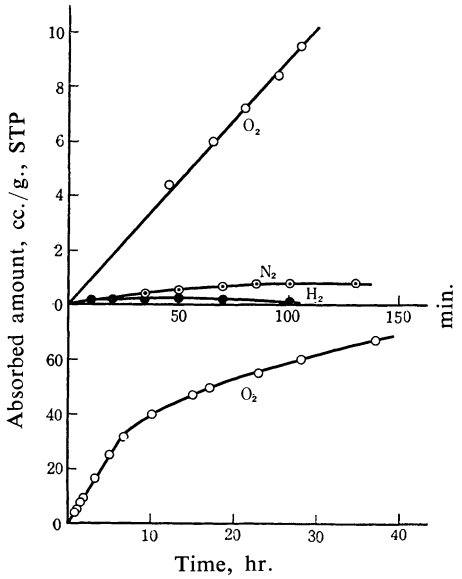


Fig. 1. Absorption of gases by cobalt oleate. 23°C, 1 atm.

by cobalt oleate is almost linear against time, and it was found that a few months are required to reach the absorption equilibrium. At the end of the linear part of the absorption rate curve, the composition of the sample corresponds to $Co_3(C_{18}H_{33}O_2)_4(OH)_2 \cdot 2H_2O \cdot 6O$. After the complete oxygenation of cobalt oleate, the composition was found to be $Co_3(C_{18}H_{33}O_2)_4 \cdot (OH)_2 \cdot 2H_2O \cdot 16O$. The color was changed from pink (original sample) to dark brown (completely oxygenated sample), and the solubility in organic solvents decreased considerably as a result of the absorption of oxygen. When cobalt oleate was in contact with dry air, the results were almost the same in quantity as in the case of oxygen absorption.

The Absorption of Oxygen by Cobalt Stearate and by the Mixture of Cobalt Stearate and Oleic Acid.—From Fig. 2 it is evident that the absorptive power of cobalt stearate for oxygen is negligible compared with that of cobalt oleate. However, the mixture of cobalt stearate and oleic acid absorbs oxygen fairly well compared with the absorption of oxygen by oleic acid alone. It may be said that cobalt

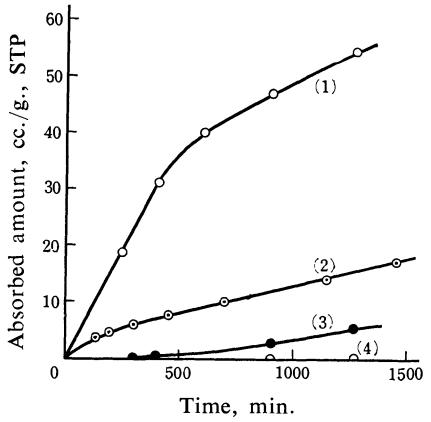


Fig. 2. Absorption of oxygen by (1) cobalt oleate, (2) cobalt stearate+oleic acid (1 : 70), (3) oleic acid, and (4) cobalt stearate.

stearate, although a poor oxygen absorber by itself, is a rather good catalyzer for the oxygenation of oleic acid. At any rate, the absorptive capacity of cobalt oleate for oxygen is by far the most remarkable. Probably the origin of absorption exists both in cobalt atoms and in double bonds, which will be examined below.

Ultraviolet Spectroscopic Investigation of Oxygen Absorption by Cobalt Oleate.—A thin film of cobalt oleate was prepared on the surface of the quartz cell from its benzene solution, and the cell was placed in contact with dry air. The ultraviolet spectra of this film were taken at various intervals of time. The results

are shown in Fig. 3. It is shown that the absorption at 350 mμ increases. It is evident that this increase reveals the absorption of oxygen by cobalt oleate. The relation of the absorption intensity at 350 mμ to time is represented in Fig. 4. The intensity becomes almost constant after about three days in contact with air. No doubt, the absorption at 350 mμ is not due to the oxydation of the double bond of oleate, since there is no absorption near 350 mμ in either the spectrum of oxygenated oleic acid as well or in that of non-oxygenated oleic acid. On the basis of various experimental results by many workers[3], it is concluded that

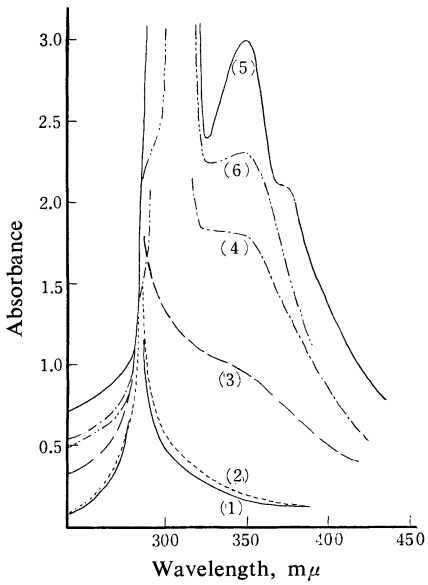


Fig. 3. Ultraviolet absorption spectra of oxygenated cobalt oleate. Oxygenation time: (1) 0, (2) 15, (3) 27, (4) 36, (5) 75 and (6) 175 hr.

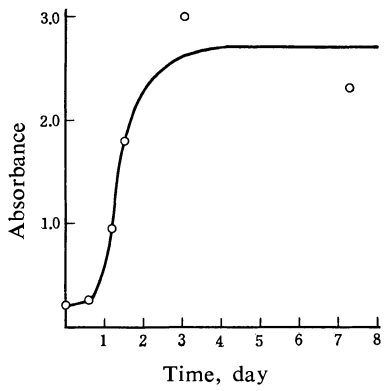


Fig. 4. Absorbance at 350 mμ against time of oxygenation.

3) E. g., R. Tsuchida, This Bulletin, 13, 388, 436 (1938); M. Linhard and M. Weigel, *Z. physik. Chem., N. F.*, 20 (1955).

the absorption at 350 mμ corresponds to the second absorption band, i. e., the absorption of shorter wavelength usually appearing in the spectrum of cobalt coordination compounds. In the process of oxygen absorption by cobalt oleate, therefore, it may be concluded that, at least in the initial stage, oxygen is coordinated to the cobalt atom.

The Infrared Spectra of Oxygenated Cobalt Oleate.—Infrared spectra of the original cobalt oleate and of a few oxygenated cobalt oleates, differing in their degree of oxygenation, were taken by the potassium bromide disk method. In Fig. 5 the infrared absorption spectrum of non-oxygenated cobalt oleate is shown together with a reference spectrum of oleic acid. The essential differences between these spectra are the disappearance of the bands of 2670, 1715 and 935 cm^{-1} and the appearance of the 1565 cm^{-1} band in the spectrum of cobalt oleate. The three bands, 2670, 1715 and 935 cm^{-1}, are ascribed respectively to the stretching vibration of hydroxyl, the stretching vibration of carbonyl and the out-of-plane deformation mode of hydroxyl, all in the carboxyl group of oleic acid. It is known that the bands at 2670 and 935 cm^{-1} vanish on the esterification of the acid. The band at 1565 cm^{-1} is ascribed to the characteristic frequency of carbonyl in the ionized carboxyl group, appearing as a shift of the 1715 cm^{-1} absorption of carbonyl in the unionized carboxyl group. The ionic structure of cobalt oleate is thus clearly indicated. The band at 3031 cm^{-1} is ascribed to the stretching vibration of the =CH- group in unsaturated hydrocarbons.

The infrared absorption spectra of oxygenated cobalt oleates are shown in Fig. 6. The three samples used were different in their oxygenating time, that is, 4 hr., 24 hr. and 150 days. The noticeable effect of the oxygen absorption is the appearance of bands near 1720 and 1178 cm^{-1}, which bands increase in intensity as the oxygenation proceeds, and of a band at 971 cm^{-1}, which again decreases its intensity and

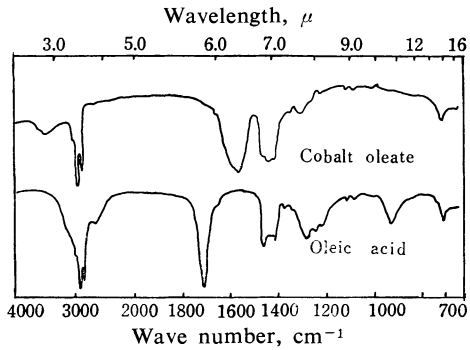


Fig. 5. Infrared absorption spectra of cobalt oleate and oleic acid.

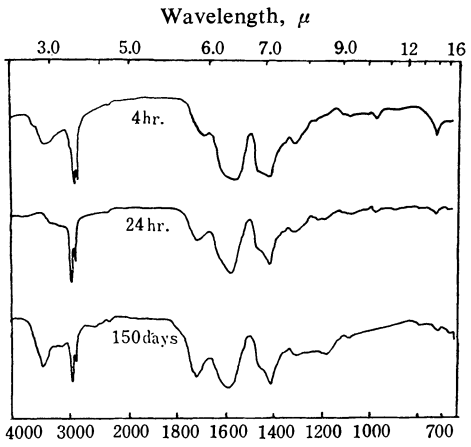
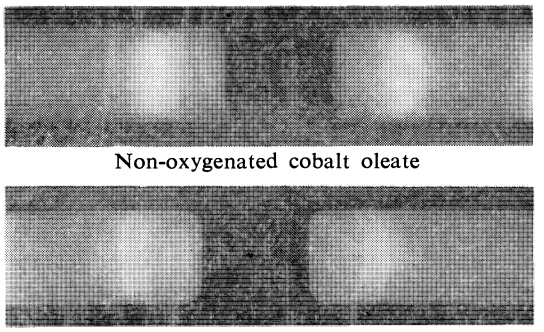


Fig. 6. Infrared absorption spectra of oxygenated cobalt oleates, for the oxygenating time, 4 hr., 24 hr. and 150 days.

finally disappears as a result of the strong oxygenation of cobalt oleate. A band at 3020 cm^{-1} of the original sample also vanishes when the sample is oxygenated strongly. The band at 1720 $^{-1}$ is ascribed to the stretching vibration of carbonyl in the carboxyl group of the acid, as has already been mentioned. The band at 971 cm^{-1} is originally the CH out-of-plane deformation vibration of the -CH=CH- group (trans) which is observed in the spectrum of elaidic acid, a geometrical isomer of oleic acid (cis). Swern et al.[4-5] have reported that the cis-trans isomerization of methyl oleate arises from the oxygenation of oleyl group and that the trans-type hydroperoxide is produced. It is reasonable to ascribe the absorption at 1178 cm^{-1} to the stretching vibration of the

—C—C— group of hydroperoxide produced by the oxygenation of cobalt oleate. The decrease in intensity of a band at 3020 cm^{-1} with oxygenation shows that the double bond structure is destroyed as the oxygenation proceeds. All these results would indicate that, in the oxygenating process of cobalt oleate, the oxygenation of the double bond takes place and that a hydroperoxide structure is formed, together with acid produced by the destruction of the double bond. It is probable that oxygen attacks double bonds as well, as it is coordinated to the cobalt atom, as is shown by the ultraviolet spectroscopy of the oxygenating process.

4) D. Swern et al., *J. Am. Chem. Soc.*, **75**, 3135 (1953).
5) H. B. Knight, C. R. Eddy and D. Swern, *J. Am. Oil Chemists' Soc.*, **28**, 188 (1951).



Non-oxygenated cobalt oleate

Oxygenated cobalt oleate
(about three-month contact with dry air)

Fig. 7. The X-ray diffraction patterns of cobalt oleate.

The X-Ray Diffraction Pattern of Oxygenated Cobalt Oleate.—As shown in Fig. 7, the X-ray diffraction pattern of non-oxygenated cobalt oleate consists of a "halo". This indicates that non-oxygenated cobalt oleate is an amorphous solid. When the sample is completely oxygenated (after about three months contact with air), it is seen that the crystallization is effected to some degree. We have proposed[6] a polymeric structure, loosely bonded through OH groups, for cobalt oleate, which gives rise to an amorphous pattern in an X-ray spectrum. The crystallization by oxygenation may results from the coordination of oxygen to cobalt and the formation of an oxidized product, which gives the rigid crystalline structure to the original cobalt oleate. However, the point must be investigated further.

The Probable Mechanism of the Catalytic Action of Cobalt Soaps.—It may be concluded from the experimental results obtained in the present study that oxygen is coordinated to the cobalt atom and attacks the double bond in the case of cobalt oleate. Cobalt stearate alone does not absorb oxygen, but in the presence of oleic acid considerable absorption of oxygen takes place. This suggests that the oxygen absorption by cobalt soaps takes place when the oxygen acceptor is present at the same time. Oxygen will be coordinated to the cobalt atom and activated, resulting in the oxidation of the unsaturated compounds existing with the soap. This is similar to Ingle's theory[1] on the mechanism of the drying action of metal soaps, but the present study gives a more direct explanation for the mechanism, based on various experimental facts.

Summary

The gas absorption by cobalt oleate and stearate has been studied. It was found that cobalt oleate absorbs oxygen very remarkably,

6) H. Funakoshi, *Bull. Fukuoka Gakugei Univ.*, Part III, **11**, 93 (1961).

but nitrogen and hydrogen, very little. Cobalt stearate absorbs oxygen negligibly, but in the presence of oleic acid the absorption becomes considerable. From the studies of ultraviolet and infrared spectra and X-ray analysis of the oxygen absorption by cobalt oleate, it was found that oxygen is coordinated by the cobalt atom and destroys the double bond structure. The probable mechanism of the catalytic action of cobalt soaps has also been presented.

The author wishes to thank Professor Ryohei Matuura for his kind guidance throughout this study. The author is also deeply grateful to Dr. Hideo Kimizuka for his helpful advice and encouragement, and to Dr. Shigeru Miyamoto for valuable discussions. The author wishes also to thank Professor Sunao Imanishi and Dr. Yoshiya Kanda for their valuable suggestions for using the spectrophotometers, and Dr. Ryoichi Shimada for his recording and for discussions of infrared and ultraviolet absorption spectra. The author is indebted to Professor Atsushi Okazaki for taking Debye-Scherrer photographs, and to Mr. Michio Shito for the elementary analysis of cobalt soaps.

Department of Chemistry
Faculty of Science
Kyushu University
Hakozaki, Fukuoka

Chemical Use of the Absorption of Soft γ-Rays, β-Ray-excited X-Rays and K-Capture X-Rays. II. Application to the Analysis of a Binary Alloy and the Determination of a Heavy Element in a Multi-component System

By Tadashi NOZAKI

(Received December 20, 1960)

The technique described in Part I[1] provides a method of chemical analysis by the use of the absorption phenomenon of the photon-beams. Determination of a heavier element in a given sample was tried by using a single source of a suitable energy and the exponential-absorption law[2]. In applying such a method, the use of a pair of sources appears to be suitable for a greater variety of samples. This is easily to be understood by analogy with the so-called absorption-edge method in X-ray absorptiometry.

The present author has intended to extend this technique by the use of radio-isotopes as the radiation source. Mono-energetic soft X-rays (less than 25 keV.) can be obtained, of course, by the use of an X-ray tube and a proper diffraction crystal. Almost mono-energetic photon-beams of a higher energy, however, are required or preferable when a certain kind of element is to be analyzed or when the absorbance due to the matrix elements is too large for a photon of a lower energy. Radio-isotopes giving soft γ-rays, β-ray-excited X-rays and K-capture X-rays are more useful, and the discussion[3] concerning the comparison of K-capture spectroscopy with ordinary X-ray absorptiometry for sulfur in petroleum appears to hold in other cases.

In this paper, the use of two photon-beam sources with suitable energies is generally discussed, and the application to the analysis of a binary alloy (solder) and of a heavy element in a multi-component system (glass) is proposed.

With a binary system, there are two alternative modes in the choice of the sources: (1) the K absorption edge of one of the two elements, usually of the higher atomic number, is to fall between the energies of the two sources, and (2) both sources are to have higher energies than any of the K absorption edges of the elements, but the absorption coefficients of the two elements for one of the photon-beams are to be markedly different from each other and those for the other photon-beams are to be narly equal (The latter demand is fulfilled by a γ- ray of more than 1 MeV. in energy, to which the photoelectric effect contributes only slightly.). Choice 1 is useful for a sample of this foil, while choice 2 is suitable when the sample is a thick plate or block. The composition of solders without appreciable impurity was determined by using two pairs of sources. (1) U-β and ^{204}Tl, (2) ^{203}Hg and ^{60}Co. (For convinience, M-β is used in this paper for the β-ray-excited X-ray of element M.)

1) T. Naoki, This Bulletin, **34**, 1769 (1961).
2) H. K. Hughes et al., *Anal. Chem.*, **26**, 1889 (1954).
3) W. R. Doughman et al., ibid., **30**, 1924 (1958).

For a plate (either a foil or a block) of a binary alloy consisting of x(g./cm^2) of element A and y(g./cm^2) of element B, there are the following relationships:

$$\left.\begin{aligned}\Phi(E_1\ \mathrm{A})x+\Phi(E_1\ \mathrm{B})y&=-\ln D(E_1)\\ \Phi(E_2\ \mathrm{A})x+\Phi(E_2\ \mathrm{B})y&=-\ln D(E_2)\end{aligned}\right\} \quad (1)$$

$$[\text{Thickness of the plate}]=x+y \quad (2)$$

where Φ (E M) is the total absorption coefficient of element M for a photon-beam of energy E, and $D(E)$ is the transmittance (denoted by a fraction) of a photon-beam of energy E through the plate. Thus, simultaneous determination of the composition and of the plate thickness is possible.

When the element to be determined is in a multi-component system, the situation is slightly more complicated. The use of a number of sources of suitable energies equal to the number of the component elements offers the necessary relationships for determining all the component elements and the plate thickness. Such an argument, however, is only theoretical and impracticable. In practice, the plate thickness must be measured by some other method. Therefore, the measurement of the transmittances of two photon-beams, between the energies of which lies the absorption edge of only the element to be determined, offers a relationship for calculating the content. This relationship (indicated by Eq. 5) is derived as follows:

Eq. 13 in Part I can also be written as

$$\frac{\phi(E_1\ \mathrm{M})}{\phi(E_2\ \mathrm{M})}=(E_1/E_2)^{-\lambda}\quad (8/3<\lambda<7/2) \quad (3)$$

where $\phi(E$ M) is the absorption coefficient (of an element or a material M for a photon-beam of energy E) excluding the contribution of the Compton scattering. When one gram of the sample contains x gram of the element A to be determined and y_m gram of a matrix element M_m, there are the following relationships, where G means the sample (glass):

$$\left.\begin{aligned}\phi(E_1\ \mathrm{A})x+\sum_m[\phi(E_1\ \mathrm{M}_m)y_m]&=\phi(E_1\ \mathrm{G})\\ \phi(E_2\ \mathrm{A})x+\sum_m[\phi(E_2\ \mathrm{M}_m)y_m]&=\phi(E_2\ \mathrm{G})\end{aligned}\right\} \quad (4)$$

On assuming that λ in Eq. 3 remains constant for all elements, Eq.s 3 and 4 offer this relationship for calculating x:

$$x=-\frac{\begin{vmatrix}\phi(E_1\ \mathrm{G}) & 1\\ \phi(E_2\ \mathrm{G}) & (E_1/E_2)^{-\lambda}\end{vmatrix}}{\begin{vmatrix}\phi(E_1\ \mathrm{A}) & 1\\ \phi(E_2\ \mathrm{A}) & (E_1/E_2)^{-\lambda}\end{vmatrix}} \quad (5)$$

For a β-ray-excited X-ray or a K-capture X-ray, the E_1 and E_2 should be the weighed means of the energies of K_{α_1} and K_{α_2}. A source pair consisting of RaD and Ce-β and that of U-β and ^{204}Tl were used for the determination of barium and lead respectively.

The error of results is discussed below.

Experimental

Sample.—Solder containing no appreciable ammount of any elements other than tin and lead was rolled to a plate or a foil. Plates of barium glass and lead glass of uniform thickness (about 2 mm.) were prepared. The barium glass contained sodium, boron, silicon, barium and oxygen, while the lead glass consisted of boron, sodium, aluminum, zinc, lead and oxygen. The thickness (g./cm^2) of the glass plates and of the solder foils was determined by measuring the weihgt and the area, while that of the solder plates was done by measuring the thickness and the specific gravity.

Counting.—In all cases a scintillation counter was used with the geometrical arrangement shown in Fig. 1, Chapter I.

The sources were chosen as described above. The measurement was done by using the techniques in Part I, tin foil and lead foil being used as the auxiliary absorbers for Ce-β and U-β respectively. With ^{60}Co as the source, only the γ-ray of the higher energy was counted. For the analysis of solder, the total count taken in each measurement was over 5×10^4, while for that of glass at least 3×10^3 (when the counting rate was smallest) or 3 minutes' counting (when it is largest) was taken.

Chemical Analysis.—Chemical analyses by ordinary methods were carried out for comparison. Solders were analyzed by determining tin gravimetrically as tin(IV) oxide and lead, electrochemically as lead(IV) oxide. A part of any of the glass samples was decomposed with hydrofluoric and sulfuric acid, and barium was determined gravimetrically as barium sulfate, while lead was converted into lead chromate and determined iodometrically by the standard technique.

Results and Discussion

In Tables I, II, III and IV are shown the results. The values with the sign ± indicate the error due to the standard error of counting. In general, all values are in good agreement with those obtained by ordinary chemical analysis. Moreover, the usefulness of Eq. 5 is proved.

TABLE I. ANALYSIS OF SOLDER BY THE USE OF ^{204}Tl AND U-β

Source	Φ(Sn)	Φ(Pb)
^{204}Tl	4.02	3.06
U-β	1.68	5.51

	Absorption method		Chem. anal.	
	mg./cm^2	%	mg./cm^2	%
Tin	64.6±2.0	42.4±1.5	64.3	42.9
Lead	87.6±1.4	57.6±1.3	85.5	57.1
Solder	152.2±2.5		149.8	

TABLE II. ANALYSIS OF A SOLDER BY THE USE OF ^{60}Co AND ^{203}Hg

Source	Φ(Sn)*	Φ(Pb)*
^{60}Co	0.0464	0.0510
^{203}Hg	0.162	0.431

	Absorption method		Chem. anal.	
	g./cm^2	%	g./cm^2	%
Tin	2.12±0.22	35.7±3.7	2.01	35.0
Lead	3.81±0.19	64.3±3.2	3.73	65.0
Solder	5.93±0.29		5.74	

* Values under the given geometrical arrangement

TABLE III. ANALYSIS OF BARIUM IN GLASS

Sample No.	Barium content, %			
	λ=3/8	λ=2/7	Mean	Chem. anal.
I	25.6	25.6	25.6±0.5	25.6
II	18.3	18.4	18.3±0.4	17.8
III	8.8	9.0	8.9±0.2	9.0
IV	4.5	4.7	4.6±0.1	4.61
V	0.00	0.16	0.08±0.1	0.00

ϕ(Ba) for RaD and for Ce-β are 16.36 and 8.87 respectively.

TABLE IV. ANALYSIS OF LEAD IN GLASS

Sample No.	Lead content, %			
	λ=3/8	λ=2/7	Mean	Chem. anal.
1	−0.4	−0.07	−0.2±0.3	0.00
2	1.78	2.04	1.9±0.3	1.77
3	3.30	3.48	3.4±0.4	3.15
4	8.15	8.43	8.3±0.5	8.2
5	17.7	17.9	17.8±0.6	17.5
6	35.4	35.6	35.5±1.0	34.0
7	54.7	54.9	54.8±1.1	54.6

The error in the final result due to the standard error of counting is calculated as follows: When $\Phi(E\,\mathrm{M})$ in Eq. 1 has been preliminarily determined accurately, the final error in x and y in the same equations depends on that of the determination of $D(E)$. When it is assumed that total counts C is taken during time t without the sample, and C', during t' with the sample, the fractional standard error in $\ln D(E)$, denoted by $\Delta \ln D(E)$, is the standard error in

$$\ln\left[\frac{(C'+\Delta C')/t'}{(C+\Delta C)/t}\right]-\ln\left[\frac{C'/t'}{C/t}\right]$$

where ΔC equals $\pm\sqrt{C}$ and $\Delta C'$, $\pm\sqrt{C'}$. For large values of C and C', for which the approximation

$$\ln\left(1\pm\sqrt{\frac{1}{C}+\frac{1}{C'}}\right)=\pm\sqrt{\frac{1}{C}+\frac{1}{C'}}$$

is valid,

$$\Delta \ln D(E)=\sqrt{\frac{1}{C}+\frac{1}{C'}} \qquad (6)$$

because, the fractional standard error in

$$\frac{C'+\Delta C'}{C'}\Big/\frac{C+\Delta C}{C} \quad \text{is equal to}$$

$$\sqrt{\left(\frac{\Delta C'}{C}\right)^2+\left(\frac{\Delta C}{C}\right)^2} \quad \text{or} \quad \sqrt{\frac{1}{C}+\frac{1}{C'}}$$

The errors in Tables I and II are calculated by Eq. 6. For a multi-component system, when $\phi(E\,\mathrm{A})$ in Eq. 4 and the thickness of the sample have been preliminarily determined with precision, the final error is derived either from the determination of $\phi(E\,\mathrm{G})$ or from the uncertainty of λ in Eqs. 3 and 5. The latter can be regarded as small, as is shown in Part I. By a calculation similar to that for the binary system, the standard error in the final result due to the error of counting for $\Phi(E\,\mathrm{G})$ is obtained and is shown in Tables III and IV. When the optimum determination accuracy within a given counting time is required, the time should be so divided that the determination of $\phi(E\,\mathrm{G})$ for the photon-beam of the higher energy may be done more precisely than for that of the lower energy, owing to the factor of $(E_1/E_2)^{-2}$ in Eq. 5. There are, of course, some uncertainties in $\Phi(E\,\mathrm{A})$, but they can be made insignificantly small when determined once with precision.

The value x in Eq. 5 varies with the value of λ for a given value of $\phi(E\,\mathrm{A})$ and ϕ $(E\,\mathrm{G})$. However, the mean value of x for λ=8/3 and λ=7/2 agrees well with the result of ordinary chemical analysis. This mean value is not significantly different from the value for λ=3.

The physical meaning of the denominator of Eq. 5 is the coefficient of the photoelectric absorption by only the K-shell for a photon-beam of energy E_2 (with a negative sign) with a small contribution of the coherent scatterings. There are several theoretical formulas for the photoelectric absorption cross section by the electrons in the K-shell, (σ_k). The formula obtained by the Born approximation[4] is:

$$\sigma_k=\phi_0\,4\sqrt{2}\,\frac{Z^5}{137^4}\,\frac{(mc^2)^{7/2}}{E} \qquad (7)$$

$$\phi=\frac{8\pi}{3}\,(e^2/mc^2)^2=6.651\times10^{-25}\,\mathrm{cm}^2$$

However, application of the correction factor from the chart[3] to the value of Eq. 7 usually offers a value higher than the experimental result by several per cent, in spite of the contribution of the coherent scatterings to the latter. Other, simpler formulas provide poorer results.

4) E. Segrè, "Experimental Nuclear Physics", Vol 1, John Wiley & Sons, Inc., New York (1953), pp. 310—311.

Summary

The absorption phenomenon of soft γ-rays, β-ray-exited X-rays and K-capture X-rays was applied to the following two kinds of analyses (1) Analysis of solder (simultaneous determination of the composition of a binary system and the sample thickness), and (2) Determination of barium or lead in glasses (determination of an element of high atomic number in a multi-component system). Two photon-beams of energies suitable for each purpose were chosen, and for the latter purpose the relationship between the absorption coefficient of an element and the photon-beam energy was used. The results were in good agreement with those obtained by usual chemical analysis.

The Electrical Communication Laboratory
Musashino, Tokyo

Chemical Use of the Absorption of Soft γ-Rays, β-Ray-excited X-Rays and K-Capture X-Rays. III. Application to Column-chromatographic Separation of Halogen Compounds

By Tadashi NOZAKI

(Received December 20, 1960)

Column-chromatographic separation of colorless compounds always involves a tedious procedure or requires a special instrument[1]. With such a method, usually only frontal analysis is possible, and no information concerning the behavior of each compound in the column is offered. Even where colored compounds are concerned, a small overlap of two adsorption zones is often overlooked and the observation of their behavior in the column is ambiguous. In this paper, the author will indicate that utilization of the absorption phenomenon of soft γ-rays, β-ray-excited X-rays and K-capture X-rays offers a very useful technique for the column-chromatographic separation of iodine-, bromine- or chlorine-containing substances, which are mostly colorless. Frontal analysis is thus made always possible regardless of the use of the solvent consisting of lighter elements than oxygen. With iodine- or bromine-containing compounds, nondestructive determination of the location of each compound in the column is made possible. As shown in Table I, a photon-beam of a suitable energy is absorbed strongly by bromine or iodine, but only slightly by column-wall substances, adsorbents and solvents; these usually consist of elements of a low atomic number. Nondestructive determination of the location of the compounds at a given time is named "in-situ determination".

1) E. g., E. Lederer and M. Lederer, "Chromatography", Elsevier Pub. Co., Amsterdam (1955), p. 41.
2) R. Adams, "Organic Syntheses", Vol. VIII (1928), p. 42.

TABLE I. ABSORPTION COEFFICIENT ($cm^2/g.$)

Source	Substance				
	C	Al	Cl	Br	I
^{55}Fe	4.5	48	ca. 110	>100	>300
Bγ-β	1.3	ca. 15	42	ca. 30	ca. 90
Ce-β	0.23	0.89	ca. 1.5	12	ca. 30
RaD	0.19	0.46	0.68	5.22	14.79
^{204}Tl	0.17	0.24	0.35	1.9	5.17

Outline of the Technique.—Figure 1 shows the measuring device. Useful sources are listed in Table II. (For convenience, the β-ray-excited X-rays of element M are written as M-β in this paper.)

As shown in Table II, the source for the in-situ determination of iodine or bromine must be chosen according to the diameter of the column or the concetration of the solution.

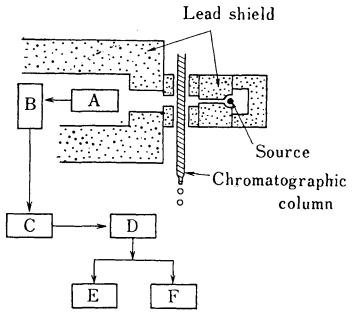


Fig. 1. Measuring device.
A: Detector head B: Preamplifier
C: Linear amplifier
D: Single channel analyzer
E: Scaler F: Automatic recorder

Table II. Useful photon-beam sources

	In-situ determination	Frontal analysis
Chlorine	Unsuccessful	^{55}Fe, Sr-β, Br-β
Bromine	Ce-β[a], Ba-β[a] RaD[b]	Ba-β, Sn-β, Mo-β
Iodine	RaD[c] ^{204}Tl[d] ^{203}Hg[e]	RaD, Ce-β

a) When a small amount of bromine is adsorbed.
b) When a large amount of bromine is adsorbed.
c) When the column diameter is small (less than 3 cm.).
d) When the column diameter is large (3 to 8 cm.).
e) When the column diameter is still larger.

For the in-situ determination of iodine, the following method is useful for a column of a larger diameter: a fine polyethylene tube is placed at a suitable position in the adsorbent along the direction of the tube, so that a point source can be moved in the tube and the absorption of the photon-beam by the material can be measured at a given location in the column. This method is one of the techniques that are made possible only by utilizing a radio-isotope rather than an X-ray generator. For the in-situ determination of bromine of a smaller concentration, Ba-β or Ce-β should be used in spite of the ease with which the photon-beam is absorbed by other materials than the compounds in question. Hence, the column should preferably be made of polyolefine, and, whenever possible, the adsorbent should be charcoal or carbohydrate. When a large amount of bromine compounds is to be separated, it is preferable to carry out, in the first place, both the in-situ determination and the frontal analysis by the use of a small column and of a minor portion of the compounds. The behavior of the compounds in the column, including the retention volumes and the relation between the results of both determinations, are thus made clear. The major portion is then separated on a large scale with the aid of only frontal analysis.

Unfortunately, the in-situ determination of chlorine is very difficult because of the more pronounced absorption of the soure photon-beam by other materials than the compounds in question.

Throughout these cases, the use of an exact exponential absorption curve is not essential, unless an accurate determination of the compound is to be made in the column.

Discussion on the Usefulness of the Technique. —By the use of the in-situ determination, the following important information for column-chromatographic separation can be obtained in the early stage of adsorption (when only a small quantity of the original solution has been treated): (1) the retention volume of each compound, (2) minimum recovery of most weakly adsorbed substance in a pure state without elution, and also without elution tailing, (3) maximum quantity of the original solution which can be treated in one lot for complete separation under the given conditions, (4) the necessary quantity of an eluent for eluting each of the compounds. An almost ideal case (without marked elution tailing) is exemplified by the separation of iodobenzene and 4-iodobiphenyl described below.

When a pronounced elution tailing is observed, complete separation is usually impossible. But a part of the most weakly adsorbed compound is obtained in a pure state, leaving a mixture in the column. For molecules having a similar functional group, it is generally true that the stronger the affinity with an adsorbent, the less the solubility in a given solvent. Thus, for the separation of a binary mixture, a method consisting of the following procedures is useful; (1) the mixture is dissolved in a suitable solvent of a quantity sufficient for complete dissolution of the more soluble compound I; (2) when the less soluble compound II remains undissolved, it is obtained in a pure state by filtration and, whenever necessary, by recrystallization; (3) a part of pure I is obtained chromatographically; (4) the mixture of I and II is completely eluted with a solvent with a strong eluting power; (5) the solvent is removed from this effluent to give a solid mixture, which is submitted to the same process again to give further I and II in a pure state. Step 3, the most important procedure, can be made easier by the use of the photon-beam absorption technique for colorless bromine and iodine compounds. Such a case is exemplified by the preparation of 4-iodobiphenyl and 4, 4′-diiodobiphenyl by direct iodination of biphenyl and their separation (see below).

Column chromatography is also useful for purifying some kinds of material. Crude halogen compounds prepared by the Sandmeyer reaction always contain impurities (e. g., phenols and oxidation products of the amines), which are much more easily adsorbed than the halogen compounds themselves. When the halogen compound is colorless, the photon-beam absorption provides a valuable tool in its chromatographic purification. Such a process is exemplified by the purification of 2-chloro-*p*-terphenyl (see below).

Separation of Iodobenzene and 4-Iodobiphenyl. —Figure 2 shows the behavior of iodobenzene

(A) (724 mg.) and 4-iodobiphenyl (B) (555 mg.) which have been dissolved in petroleum benzine (50 ml.). The column was 13.5 mm. in diameter and contained alumina (38 g.; apparent length: 30 cm.). The adsorption heads of the two substances move at a definite rate according to the volume of both the solution and the eluent (5.0 mm. per ml. for A, 2.0 mm. per ml. for B). Iodobenzene gives some elution tailing, though not pronounced, and 4-iodobiphenyl gives a marked tailing.

When the rate of migration of substance I, which is eluted easier, and that of substance II are denoted by R_I and R_{II} (in cm. per ml.) respectively, and the length of the adsorbent is L (cm.), the retention volumes of the substances V_I and V_{II} (ml.) are:

$$V_I = L/R_I \qquad V_{II} = L/R_{II} \tag{1}$$

In the absence of tailing, there are the following approximate relationships between the maximum treatable quantity of the original solution for complete separation, Q (ml.), and the minimum volume of the eluent necessary for complete elution of I under the given condition, S (ml.):

$$L = (Q+S)R_{II} = SR_I$$

Thus,

$$Q = L/R_{II} - L/R_I = V_{II} - V_I \tag{2}$$

$$S = L/R_I = V_I \tag{3}$$

Since L, R_I and R_{II} are 30, 0.50 and 0.20 respectively, V_I and V_{II} are 60 and 150 respectively; without tailing of I, Q and S should be 90 and 60 respectively. When the elution tailing of I is as in Fig. 2, Q is 70 to 75 and S about 75.

When only the original solution is passed through the column until the adsorption head of II reaches the lower end of the column with the aim of obtaining a part of I in a pure state, the yield, Y, is expressed by:

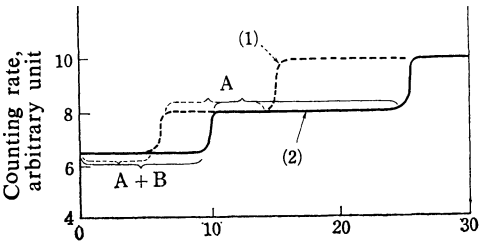
$$Y > (V_{II} - V_I)/V_{II} \tag{4}$$

This is because the concentration of I at the location where only I is adsorbed is higher than that at the location where both I and II are present, owing to the displacement of I by II. Moreover, this relation is always valid regardless of the presence of tailing. When this mixture is submitted to such a treatment,

$$(V_{II} - V_I)/V_{II} = 0.60$$

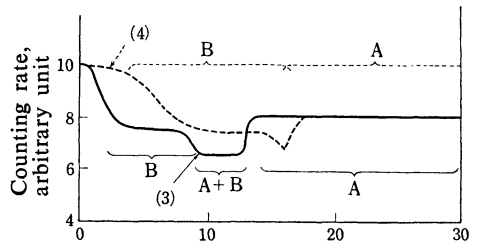
but the true value of Y, which is easily obtainable from Fig. 2 and the quantity of the substances present, should be about 0.75.

When elution is carried out to such a degree that an incomplete separation is caused, an approximate value of Y can be estimated by the use of the in-situ determination.



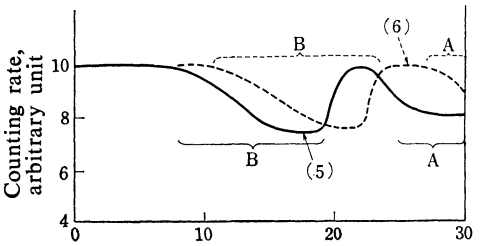
Location, cm. from the upper end

Fig. 2-1. Behavior of iodobenzene (A) and 4-iodobiphenyl (B) in a column.



Location, cm. from the upper end

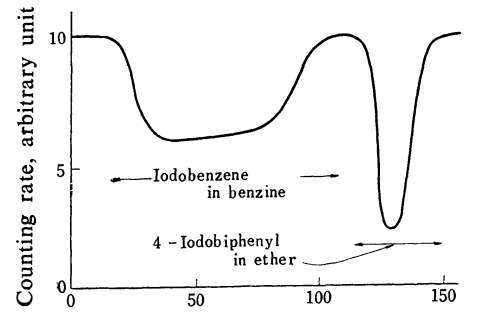
Fig. 2-2. Behavior of iodobenzene (A) and 4-iodobiphenyl (B) in a column.



Location, cm. from the upper end

Fig. 2-3. Behavior of iodobenzene (A) and 4-iodobiphenyl (B) in a column.

(1); 30 ml. adsorption
(2); 50 ml. adsorption
(3); 50 ml. adsorption and 15 ml. elution
(4); 50 ml. adsorption and 30 ml. elution
(5); 50 ml. adsorption and 45 ml. elution
(6); 50 ml. adsorption and 60 ml. elution



Volume of effluent, ml.

Fig. 3. Frontal analysis of iodine.

Frontal analysis was also carried out successfully, the results being shown in Fig. 3. When all of A came out, ether was caused to pass in order to elute B rapidly.

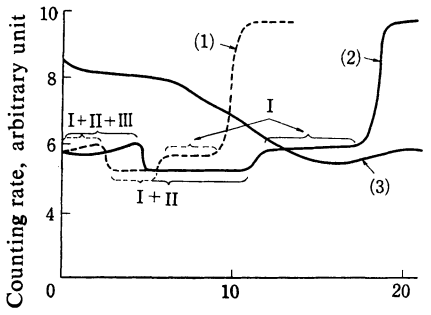
Similar results were obtained with bromobenzene and 4-bromobiphenyl.

Preparation of 4-Iodobiphenyl and Similar Compounds.—4-Iodobiphenyl and 4-bromobiphenyl are useful for the synthesis of polyphenyl compounds. Direct bromination of biphenyl offers 4-bromobiphenyl contaminated with 4, 4′-dibromobiphenyl, which can be only with difficulty removed. Thus, the standard method[2] for the synthesis of pure 4-bromobiphenyl is the reaction of the diazotization product of 4-bromoaniline with benzene in an alkaline medium. 4-Iodobiphenyl is prepared by the Sandmeyer reaction from 4-aminobiphenyl, which must be synthesized from biphenyl.

Direct iodination of biphenyl can be attained easily in acetic acid with the aid of nitric acid. Column-chromatographic separation offers both 4-iodobiphenyl and 4, 4′-diiodobiphenyl in a good yield and with a satisfactory purity.

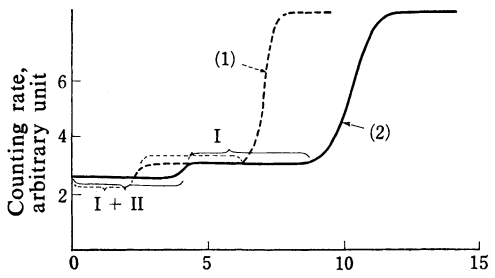
For the bromine compounds, the separation method is less effective, because the adsorbing power of an adsorbent toward 4-bromobiphenyl and 4, 4′-dibromobiphenyl differs less than in the case of corresponding iodo-compounds, and because the in-situ determination of bromine is less easy than that of iodine. For most synthetic purposes, however, the use of 4-iodobiphenyl is preferable to that of 4-bromobiphenyl.

Figure 4 indicates the behavior of 4-iodobiphenyl (I) and 4, 4′-diiodobiphenyl (II) including by-product (III) of the iodination reaction of biphenyl. Both I and II are partly replaced by III, which forms a visible zone. The head of the zone of II becomes less clear with the progress of elution owing to the elution tailing of I. Frontal analysis is useless in such a case.



Location, cm. from the upper end

Fig. 4. Behavior of 4-iodobiphenyl (I), 4,4′-diiodobiphenyl (II) and by-product (III) in a column.
(1); 20 ml. adsorption
(2); 40 ml. adsorption
(3); 40 ml. adsorption and 20 ml. elution



Location, cm. from the upper end

Fig. 5. Adsorption of 4-iodobiphenyl (I) and 4, 4′-diiodobiphenyl (II).
(1); 320 ml. adsorption
(2); 500 ml. adsorption

Figure 5 shows the behavior of the same iodine compounds, from which the by-product has been removed by a preliminary treatment. In this case, all the substances in the column are easily eluted with benzene or, preferably, with ethyl acetate, and the alumina can be reused after heat treatment at 200 to 250°C under a reduced pressure. The impurity in the eluted I appears to consist of a small quantity of remaining biphenyl or, more probably, 2-iodobiphenyl simultaneously formed. The impurity, however, can be removed, by recrystallization and pure I is obtained easily in a good yield. This synthesis of I is definitely superior to the Sandmeyer reaction with 4-aminobiphenyl with respect to the saving of time, labor and expense. The product will contain no trace of II.

Direct iodination of *p*-terphenyl is similarly attained by using a larger amount of the solvent. 4-Iodo-*p*-terphenyl is obtained from the product, by a similar, process, but with a disadvantage due to its lower solubility. Benzene must be used in place of benzine despite the much smaller retention volume, which always decreases the quantity of materials treated in one lot. This method, however, is preferable for preparing a small quantity (less than a few grams) of pure 4-iodo-*p*-terphenyl, which must otherwise be synthesized through many tedious steps[3].

Purification of Mono-halogeno-*p*-terphenyls.—Figure 6 shows the results of the frontal analysis of 2′-chloro-*p*-terphenyl prepared by the Sandmeyer reaction. The size, shape and mode of attachment of the adsorption cell are very important in determining the real concentration of chlorine in the effluent at a given instant. Some other mono-halogeno-*p*-terphenyls prepared by the same reaction were

3) T. Nozaki et al., This Bulletin, 33, 1329 (1960).

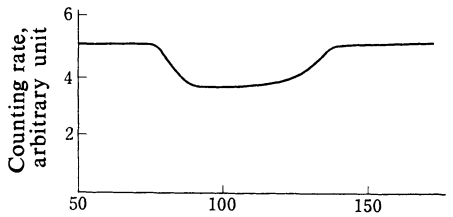


Fig. 6. Frontal analysis of chlorine.

similarly purified with the aid of the absorption technique, and their properities are now under investigation.

The technique was, however, unsatisfactory for the separation of a mixture of 2-, 3- and 4-chloro-*p*-terphenyl, prepared by the decomposition of 4-(*N*-nitrosoacetamido)-biphenyl in chlorobenzene because of the marked elution tailing.

Experimental

Adsorbent and Reagents.—Freshly purchased commercial alumina (Kantō Chem. Co. for chromatographic purpose) was used without further treatment. Too great an activity of alumina sometimes caused a slight decomposition of the iodine compounds. All solvents were of the first grade and were used after having been kept in contact with a small quantity of highly activated alumina for several days. In some cases, extremely purified solvents were also used, but no significant difference in the behavior of the compounds was observed. Other reagents were also of a commercial first grade.

Measurement Device.—For the in-situ determination, a collimated photon-beam was caused to pass along cross-section of the chromatographic column to enter the scintillation crystal or the counter tube (Fig. 1). For the frontal analysis of chlorine, the outlet of the tube was connected to a polypropylene absorption cell of a suitable dimension, while for that of iodine, the alumina near the outlet was replaced by cotton wool. The output pulse of the scintillation head or the counter tube was amplified by a linear amplifier, and the photo-peak was counted by the use of a single channel analyzer and a scaler or an automatic recorder.

For the analysis of chlorine Br-β was adopted and the photon-beam was measured by a xenon-filled proportional counter tube. For other sources a scintillation counter was used.

Preparation of 4-Iodobiphenyl and 4, 4'-Diiodobiphenyl.—A mixture of 20 g. of biphenyl and 20 g. of iodine in acetic acid (150 ml.) containing nitric acid (d=1.38, 25 ml.) was boiled gently under reflux (for about 1.5 hr.) until the color of iodine disappeared. After the mixture had been poured into water, the separated solid was filtered off, washed with an aqueous alkali solution and dried. About 40 g. of a faintly yellowish hydrophobic powder was obtained, which was recrystallized from 200 ml. benzene. On filtration and washing of the precipitate with ethanol, 8 g. of fairly pure 4,4'-diiodobipenyl (II) was obtained (m. p. and mixed m. p. 203~205°C). The mother liquor was caused to pass through a column of alumina (ca. 200 g.) to remove the yellow material, from which a small quantity of 4-nitrobiphenyl was isolated by further purification, including recrystallization. Benzene was then removed from the effluent, aud the colorless residual solid was digested with 600 ml. of petroleum benzine. The insoluble solid offered 2 g. of fairly pure II. Moreover, the mother liquor was submitted to column-chromatographic separation with the aid of the adsorption technique by using a column 6 cm. in diameter containing 300 g. of alumina.

Alter all the solution had been passed through, petroleum benzine was caused to pass through the column for elution until the adsorption head of II reached the lower end of the column. The effluent gave, on removal of the solvent, 20 g. of solid melting at 107~112°C. This gave, however, after a single recrystallization from a small quantity of ethanol, 15 g. of pure 4-iodobiphenyl (I) (m. p. and mixed m. p. 113~114°C). The column was eluted with ethylacetate to offer 6 g. of solid with ease after removal of the solvent. This solid gave, on a treatment similar to that above under a diminished scale, 1 g, of II, 3 g. of I and 2 g. of their mixture. The I obtained at this time was pure enough without recrystallization from ethanol. Thus, from 20 g. of biphenyl and 20 g. of iodine, 18 g. of I and 11 g. of II were obtained in a fairly pure state along with 2 g. of their mixture.

Another experiment which did not involve the removal of the yellow material (nitro-compounds) was also carried out. About 4 g. of the crude iodination mixture was treated with 80 ml. of petroleum benzine, and, after removal of the insoluble II, the solution was submitted to column chromatography. Both the in-situ determination and the frontal analysis were applied.

Purification of 2'-Chloro-*p*-terphenyl.—2'-Nitro-*p*-terphenyl (2 g.) prepared by the reaction of nitrosation product of 3-nitro-4-acetamidobiphenyl with benzene was reduced with tin(II) chloride, and the amine hydrochloride was diazotized and decomposed in concentrated hydrochloric acid with the aid or copper(I) chloride. The product was extracted with a mixture of petroleum benzine (40 ml.) and benzene (40 ml.), caused to pass through a column of alumina (40 g.), and eluted with the same solvent. The chlorine-containing part, which was recognized by frontal analysis, offered, on removal of the solvent, a colorless mass which was recrystallized from ethanol (25 ml.) into transparent square platelets (0.5 g.) [m. p. 101°C].

Summary

The absorption technique of soft γ-rays, β-ray-excited X-rays and K-capture X-rays was successfully applied to column-chromatographic separation and purification of halogen compounds. By this technique, the behavior of the iodine- and bromine-containing compounds

in the column was determined in situ, and important information for column chromatography, including the retention volume, was obtained at an early stage of adsorption. The technique was also satisfactorily applied to the frontal analysis of halogen compounds. An excellent method for the preparation of pure 4-iodobiphenyl by the use of the in-situ determination was provided.

The Electrical Communication Laboratory
Musashino, Tokyo

Radiation-induced Polymerization of α-Methylstyrene. II. Reply to the Criticism of Bates et al.

By Kozo HIROTA and Fukuo TAKEMURA

(Received November 20, 1961)

In radiation-induced polymerization, there are now a number of examples which can be explained by ionic mechanisms. However, these experiments were carried out at much lower temperatures than 0°C, and the monomers irradiated were all, except isobutene, of a solid state[1]. On the other hand, α-methystyrene (αMS) is known to be hardly polymerizable by ordinary peroxide initiators. Therefore, it would be interesting from the point of view of the reaction mechanism to investigate the radiation-induced polymerization of liquid αMS at room temperature[2].

In former reports[3], we came to the conclusion that the mechanism would be a radical one by taking the following experimental facts into consideration: 1) Besides such radical inhibitors as oxygen and *p*-benzoquinone, the reaction was retarded or inhibited by the presence of naphthalene or nitrobenzene respectively, which would make it likely for the polymerization to occur by an ionic mechanism. 2) Radical initiators produced photochemically or by a redox-reagent[4] had the power to polymerize αMS at room temperature. 3) Though the amount of polymerized product increased in proportion to the dose rate, this could be explained if the degradative chain transfer were considered in the reaction scheme, taking the existence of a low ceiling temperature for this monomer (60~70°C) into consideration. 4) The activation energy was found to be 4.1 kcal., which was a reasonable value for radical polymerizations initiated photochemically or by irradiation.

However, Bates et al.[5] recently proposed a cationic mechanism for this reaction based on the fact that its *G* (-monomer) increased up to 10000 from 10 if the monomer was pretreated with silica gel. Their theory is slightly contradictory to ours, because the monomer used in our experiment was dehydrated more severely with evaporated sodium film, while our *G* (-monomer) was smaller (200~600) than that of the Bates experiment. Such being the situation, further experiments were carried out by the use of three different methods of research in order to decide the mechanism.

Experimental and Results

The method of preparation of the samples was quite similar to that used in a former report; i. e., the monomer was deaerated and sealed in a glass ampule. Dehydration was carried out with calcium hydride instead of metallic sodium.

Experiment 1. The Effect of Zinc Oxide.—In order to study the effect of dehydration on the polymerization, the effect of zinc oxide was investigated, according to the suggestion of Bates et al. For the sake of comparison, styrene was irradiated as well as αMS. All the samples in the systems to be compared were irradiated for 18 hr. under the same dose rate. The results are shown in Table I.

In the case of αMS without dehydration, the yield of polymer rather decreased in the presence of zinc oxide, but it increased twofold when αMS was deaerated and dehydrated with calcium hydride. It is noteworthy that no such accelerating effect was observed in the case of styrene, which is a well-known monomer polymerizable by the radical mechanism.

1) E. Collinson, F. S. Dainton and H. A. Gills, *J. Phys. Chem.*, **63**, 909 (1959).
2) K. Hirota, K. Kuwata and K. Makino, *Isotopes and Radiation*, **1**, 104 (1958).
3) K. Hirota, K. Makino, K. Kuwata and G. Meshitsuka, This Bulletin, **33**, 251 (1960).
4) G. G. Lowry, *J. Polymer Sci.*, **31**, 187 (1958).
5) T. H. Bates, J. V. F. Best and T. F. Williams, *Nature*, **188**, 469 (1960).

TABLE I. THE EFFECT OF ZnO ON THE POLYMERIZATION

Run No.	Sample		Monomer used g.	Total dose r	Polymer obtained %	G (-monomer)
3	αMS	ZnO	3.77	1.6×10^5	0.093	50
4		—	1.75	1.6×10^5	0.11	60
1′	αMS	ZnO	3.11	2×10^5	0.16	80
2′	Dehydrated	—	2.34	2×10^5	0.09	50
10	Styrene	ZnO	3.54	3.6×10^4	6.07	1.69×10^3
11	Dehydrated	—	1.74	3.6×10^4	5.58	1.55×10^3

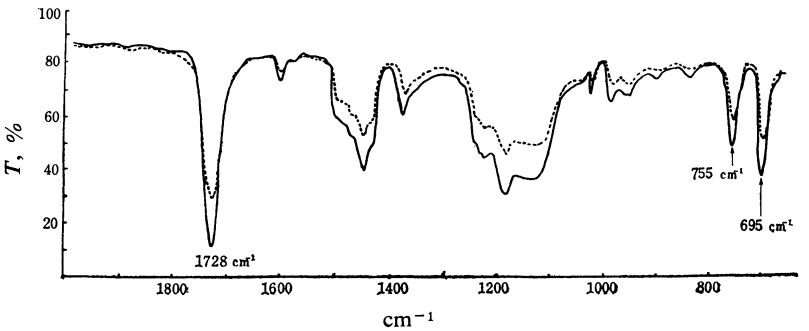


Fig. 1. Infrared spectra of the polymers obtained from the mixture of αMS and MMA.
—— Product polymerized by irradiation
---- Product polymerized by ABIN
1728 cm^{-1} stretching vibration of C=O group
755 and 695 cm^{-1} out-of-plane bending vibrations of CH of C_6H_5 group

Experiment 2. Copolymerization with Methyl Methacrylate.— Six cc. of an equivolume mixture of αMS and MMA (methyl-methacrylate) which was sealed and deaerated in a glass ampule was irradiated with γ-rays for 376 hr. at room temperature. The dose rate was 0.73×10^4 r/hr., the total dose therefore amounting to 2.7×10^6 r. In the infrared spectrum of the polymer thus obtained, characteristic bands corresponding to the carbonyl group at 1728 cm^{-1} and to the phenyl group at 755 cm^{-1} and 695 cm^{-1} appeared, as is shown by the full curve in Fig. 1. Moreover, this spectrum was quite similar to the spectrum (dotted curve) of the product copolymerized from the same mixture of αMS and MMA with azo-bis-isobutylonitril. Therefore, the product obtained by irradiation may be a copolymer of both monomers.

Experiment 3. Turbidometry of the Copolymer. —Strictly speaking, there is yet a possibility in Exp. 2 that the product might be a mixture of poly-αMS and poly-MMA. In order to investigate this possibility, turbidometry was adopted on the product by use of a self-recording apparatus manufactured by Shimadzu. By dropping a mixture of methanol-water (50% : 50%) into the acetone solution (100 cc.) of the polymer, a turbidity-time curve was obtained, as is shown in Fig. 2. It was found by the shape of the curve that the product was composed of two polymers. The major part (90%) of the polymer is established as copolymer, while the remaining, more insoluble part (10%) as poly-αMS, in the following discussion.

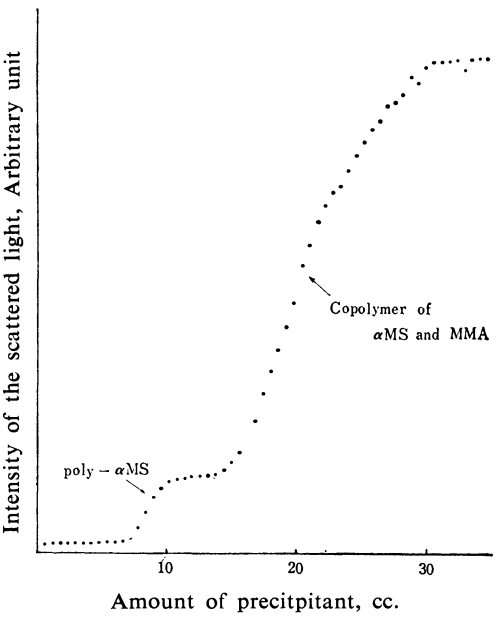


Fig. 2. Turbidity-time curve of the polymer obtained by irradiating the mixture of αMS and MMA.
Sample : 100 cc. of acetone solution (0.01%)
Precipitant : Water-methanol (50% : 50%)
Apparatus : Shimadzu PG-21.

Discussion

Generally, there exists no reliable report on radiation-induced polymerization which is explained by an anionic mechanism, in a case when no solvent is used and the polymerization is carried out at room temperature. The present polymerization, therefore, must be explained by radical or cationic mechanisms, or by both. According to Exp. 2, the polymerization may be explained at least by a radical mechanism for the following reasons. First, MMA is only with difficulty copolymerizable with αMS by a cationic catalyst, such as iodine[6]. Second, it is hardly conceivable that the radical ends of both poly-αMS and poly-MMA coexist in the solution. Therefore, the polymer here obtained must be a copolymer, produced by a radical mechanism.

However, according to Exp. 1, the presence of zinc oxide seems to accelerate the polymerization, though the effect was not so marked. This result can be explained by the cationic mechanism, if zinc oxide plays the role of an electrontrap, which would help the formation of cation, though Bates et al. attributed its dehydrating action to the origin of the accelerating effect. It may therefore be reasonable to conclude that the polymerization did not necessarily always occur according to one and the same mechanism. If this is so, the product of Exp. 2 will include not only the copolymer but also the homopolymer. Such a possibility is actually confirmed by Exp. 3. Now the minor part of the product confirmed by Exp. 3 must be the homopolymer of αMS, considering that it is less soluble than the major part and also that the homopolymer of MMA may not be produced under the present conditions.

In short, the above results teach us that γ-ray-induced polymerization of αMS occurs simultaneously as a result of both radical and cationic initiators produced by irradiation, the fraction of the polymer produced by the radical initiator, however, being much larger. By assuming such a coexistence of two mechanisms during the process of the present polymerization, the data of Bates et al. and those of present authors, regarding this reaction, can be explained without any contradiction.

Summary

Gamma-ray-induced polymerization of α-methylstyrene occurs mostly according to the radical mehanism, as had been concluded by one of the present authors, but simultaneously it occurs to some extent according to the cationic mechanism, as had been asserted by Bates et al.

In conclusion, we wish to express our deep thanks to Dr. Keiji Kuwata and Mr. Junichi Matuura of Osaka University for their discussions and help in the measurement of the turbidometry.

Department of Chemistry
Faculty of Science
Osaka University
Nakanoshima, Osaka

6) K. Hirota, G. Meshitsuka, F. Takemura and T. Tanaka, This Bulletin, 33, 1316 (1960).

7) Cf. K. Hayashi, *Isotopes and Radiation*, 3, 109 (1960).

NOTES

The Electron Spin Resonance Absorption of the Complexes of Aromatic Sulfur Compounds with Lewis Acids

By Minoru KINOSHITA and Hideo AKAMATU

(Received December 14, 1961)

The origin of the unpaired electrons which are responsible for the electron spin resonance (ESR) absorption of the complexes of aromatic compounds with Lewis acids has not been clarified. The ESR absorption of aromatic hydrocarbons, such as tetracene and perylene, in a sulfuric acid solution has been observed. Also, the ESR absorption of the complexes of these hydrocarbons with antimony pentachloride[1,2] and aluminum chloride[3,4] has been investigated, both in solids and in solutions in phosphorus oxychloride or carbon disulfide. In solutions the complexes display hyperfine structures which are similar to those of the corresponding hydrocarbon solutions in sulfuric acid. Thus the same organic radicals are likely responsible for the ESR absorption of the complexes and the sulfuric acid solutions. On the other hand, it is known that the radicals produced from compounds containing sulfur atoms show absorption lines which are characterized by relatively large g-values, because of the localization of unpaired electrons on the sulfur atoms. The ESR absorption of aromatic sulfur compounds, such as thio-phenol, thio-β-naphthol and thianthrene, in a sulfuric acid solution has been reported[3,5,6]. The characteristic features in the absorption of these radicals are large g-values in comparison with those of other organic free radicals and the appearance of two absorption bands[5]. Hence, the similar characteristic features in the ESR absorption of the complexes of aromatic sulfur compounds with Lewis acids can be expected. This short report is concerned with these.

The solid complexes with antimony pentachloride were made by mixing the solutions of sulfur compound and antimony pentachloride in dried chloroform. The solutions of the complexes with aluminium chloride were prepared in the same way by the use of nitrobenzene as a solvent. The concentration of these solutions and of the sulfuric acid solutions of the compounds was about $10^{-2}\sim10^{-3}$ M.

The solid complexes are deeply colored; thio-β-naphthol and 2, 2′-dinaphthyl disulfide give dark green compounds, while thianthrene forms a brownish purple compound. These colorations are identical with the colors of the sulfuric acid solutions of the corresponding compounds. When once dried completely in vacuum, the complexes with antimony pentachloride are very stable even in exposure to the air, but the complex of dibenzothiophene seems to be rather unstable.

The ESR absorption was examined at a frequency of 9.4 kMc./sec. at room temperature with a Hitachi MPS-1 spectrometer. As shown in Table I, the g-values of these complexes, estimated by a comparison with DPPH ($g=2.0036$), were found to be large, coinciding with those of the sulfuric acid solutions of these compounds.

In the sulfuric acid solution, thio-β-naphthol and 2, 2′-dinaphthyl disulfide showed two absorption lines. The peak of the lower field side was very weak. This weak peak was not observed in the dried complexes, but when an excess of antimony pentachloride was added to the complexes, the weak line at the lower field could be detected; on removal of the exceses of the reagent, this peak disappeared.

In the solid complexes with antimony pentachloride, the ESR absorption lines were found to be very broad in contrast to those of the complexes of aromatic hydrocarbons[2]. In Table II, the line widths are shown by the distances between the points of maximum slope. The broadness and the large g-values of the ESR absorption of the radicals containing sulfur atoms can be interpreted by the localization of an unpaired electron on the sulfur atom[7]. In the powdered thianthrene complex with

1) S. I. Weissman, E. deBoer and J. J. Conradi, *J. Chem. Phys.*, **26**, 963 (1957).
2) Y. Matsunaga, This Bulletin, **34**, 893 (1961).
3) J. M. Hirshon, D. M. Gardner and G. K. Fraenkel, *J. Am. Chem. Soc.*, **75**, 4115 (1953).
4) J. J. Rooney and R. C. Pink, *Proc. Chem. Soc.*, **1961**, 142.
5) J. E. Wertz and J. L. Vivo, *J. Chem. Phys.*, **23**, 2193 (1955).
6) A. Fava, P. B. Sogo and M. Calvin, *J. Am. Chem. Soc.*, **79**, 1078 (1957).
7) For example, Y. Kurita and W. Gordy, *J. Chem. Phys.*, **34**, 1285 (1961).

TABLE I. THE OBSERVED g-VALUES OF THE COMPLEXES

Donor	Acceptor		
	$SbCl_5$ (powder)	$AlCl_3$ (solution)	H_2SO_4 (solution)
Thio-β-naphthol	2.0076±0.0002	2.0074±0.0002	2.0074±0.0002 2.0139±0.0002
2,2'-Dinaphthyl disulfide	2.0074±0.0001	2.0076±0.0002	2.0076±0.0001 2.0140±0.0002
Thianthrene	2.0080±0.0001	2.0080±0.0002	2.0083±0.0001
Dibenzothiophene	2.0044±0.0002	—	—

TABLE II. THE OBSERVED LINE WIDTHS[a] OF THE COMPLEXES

Donor	Acceptor		
	$SbCl_5$ (powder)	$AlCl_3$ (solution)	H_2SO_4 (solution)
Thio-β-naphthol	8.5	3.0	2.9
2,2'-Dinaphthyl disulfide	8.2	3.1	3.0
Thianthrene	Three lines[b]	Five lines[c]	Five lines[c]
Dibenzothiophene	4.5	—	—

a) Distance between the points of maximum slope in gauss.
b) Over-all width of about 45 gauss.
c) Over-all width of about 10 gauss.

antimony pentachloride, the absorption was found to consist of three broad lines, which may be ascribed to the anisotropy of g-value. In other complexes studied here, no structure in the ESR absorption was observed, but thio-β-naphthol and 2, 2'-dinaphthyl disulfide seemed to form two kinds of complexes; one of them had a g-value of 2.0076 and 2.0074 respectively and the other 2.0051, for both compounds. When the antimony pentachloride solution was dilute, a complex with a higher g-value was resulted, but if a somewhat concentrated solution was used, a complex with $g=2.0051$ and a line width of 5.6 gauss, or the mixture of these two kinds of complexes, which gave an asymmetric or two absorption lines, was obtained. The presence of two kinds of complexes has been already found in the system of tetracene and antimony pentachloride[2].

The solutions of these compounds as well as of the complexes displayed sharp absorption lines compared with the solid complexes; however, no hyperfine structures were observed other than in the solutions of thianthrene and its complex. For dibenzothiophene we could not obtain any ESR absorption in the dissolved state, but in a fuming sulfuric acid solution it showed a weak and sharp absorption.

Since the thianthrene complex with antimony pentachloride was found to show an interesting behavior in the ESR absorption, we shall describe it in detail shortly.

Department of Chemistry
Faculty of Science
The University of Tokyo
Hongo, Tokyo

Pure Quadrupole Spectra of Propargyl Chloride and its Related Compounds

By Takashi SHIMOZAWA*, Takehiko CHIBA** and Yonezo MORINO

(Received December 19, 1961)

In the preceding papers[1], the molecular structures of propargyl chloride and its related compounds were discussed on the basis of the observed dipole moments. The results obtained so far are listed in Table I. It can readily be seen that the C–Cl bond moment in these compounds is smaller than the average value of the usual C–Cl bond moment of the halogenated saturated hydrocarbons (1.86 D), except in the case of monochlorobutyne-2. The early investigation gave a considerably longer C–Cl distance for the bond which is adjacent to a triple bond[2]. Pauling explained

* Present address: Department of Chemistry, Faculty of Science, Rikkyo University, Ikebukuro, Toshima-ku, Tokyo.

** Present address: Institute for Solid State Physics, The University of Tokyo, Azabu, Minato-ku, Tokyo.

1) Y. Morino, I. Miyagawa, T. Chiba and T. Shimozawa, This Bulletin, **30**, 222 (1957); T. Chiba, T. Shimozawa, I. Miyagawa and Y. Morino, ibid., **30**, 223 (1957).

2) L. Pauling, W. Gordy and J. H. Saylor, *J. Am. Chem. Soc.*, **64**, 1753 (1942).

TABLE I. THE STRUCTURAL PARAMETERS OF PROPARGYL HALIDES AND ITS RELATED COMPOUNDS

$HC{\equiv}C\text{-}CH_2Cl$	Pauling[2] (Electron diffraction)	r(C-Cl)	1.82 A
Propargyl chloride	Morino[1] (Dipole moment)	μ(C-Cl)	1.76 D
$HC{\equiv}C\text{-}CH_2Br$	Rogers[3] (Dipole Moment)	μ(C-Br)	1.62 D
Propargyl bromide			
$ClH_2C\text{-}C{\equiv}C\text{-}CH_2Cl$	Morino[1] (Dipole moment)	μ(C-Cl)	1.57 D
1,4-Dichloro-2-butyne	Kuchitsu[7] (Electron diffraction)	r(C-Cl)	1.79 A
$H_3C\text{-}C{\equiv}C\text{-}CH_2Cl$	Morino[1] (Dipole moment)	μ(app.)	2.17 D
1-Chlorobutyne-2			

TABLE II. NUCLEAR QUADRUPOLE COUPLING CONSTANTS AND APPARENT DIPOLE MOMENT OF PROPARGYL CHLORIDE AND ITS RELATED COMPOUNDS

	at 77°K	(eqQ)	μ(app.)
Propargyl chloride	35.812,3 Mc.	71.6 Mc.	1.65 D
1-Chlorobutyne-2	35.361,8 Mc.	70.7 Mc.	2.17 D
1,4-Dichloro-2-butyne	36.372,8 Mc.	72.6 Mc.	1.47 D

this lengthening of the C-Cl bond in propargyl chloride by assuming that the resonance form II makes a large contribution to the structure. However, the experimental results on the bond moment stated above contradict this explanation. Rogers[3] attributed this small dipole moment to the presence of structure III.

$$\underset{\text{I}}{HC{\equiv}C\text{-}CH_2Cl}, \quad \underset{\text{II}}{HC^+{=}C{=}CH_2Cl^-}$$

$$\underset{\text{III}}{HC^-{=}C{=}CH_2Cl^+}$$

As is well known, the electric quadrupole coupling constant (eqQ) obtained from the pure quadrupole spectra provides us with information on the charge distribution of the chemical bond[4]. If the distribution of the electron is spherically symmetric, as it is in a free Cl-ion, the eqQ constant vanishes, whereas it must be quite large in the case of Cl^+, where two unbalanced p-electrons exist. Therefore, it seemed of interest to measure the pure quadrupole resonance spectra of propargyl chloride and its related compounds to obtain some information about the electronic structure of the C–Cl bond in these compounds. The experimental method used is the same as that reported previously[5]. The results are listed in Table II.

A linear relation was previously pointed out[5] between the nuclear quadrupole coupling constants and the apparent C–Cl bond moment of the halogen derivatives of saturated hydrocarbons, as is shown in Fig. 1. Using the bond moments, 1.65 D, 2.17 D and 1.47 D, derived from the observed dipole moments[1],

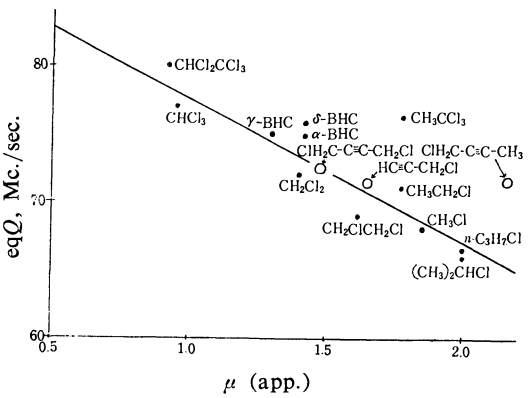


Fig. 1. Relation between eqQ and apparent C–Cl bond moment.

the eqQ constants of the three compounds are plotted on this diagram with white circles. They are in good agreement with the straight-line relation for the saturated hydrocarbons, though in the case of monochlorobutyne-2 a sight discrepancy from the line is apparent. It may be concluded, therefore, that the electronic states of the C–Cl bond in these molecules are nearly the same as those of the halogenated saturated hydrocarbons: the presence of a triple bond in the molecule has no great effect on the local C–Cl bond structure. It should be noted here that recent microwave study of propargyl chloride has confirmed the normal value, 1.78 A, of the C–Cl bond distance of this molecule[6].

Department of Chemistry
Faculty of Science
The University of Tokyo
Hongo, Tokyo

3) M. T. Rogers and M. B. Panish, ibid., **77**, 3684 (1955).
4) W. Gordy, "Microwave Spectroscopy", John Wiley & Sons, Inc., New York (1953) Chap. 7.
5) Y. Morino, I. Miyagawa, T. Chiba and T. Shimozawa, *J. Chem. Phys.*, **25**, 185 (1956).
6) E. Hirota, T. Oka and Y. Morino, ibid., **29**, 444 (1958).
7) K. Kuchitsu, This Bulletin, **30**, 391 (1956).

SHORT COMMUNICATIONS

Liquid Sulfur Dioxide Catalyzed Polymerization of Styrene Derivatives and Formaldehyde

By Niichiro TOKURA, Minoru MATSUDA, Isoo SHIRAI, Katsuo SHIINA, Yasuo OGAWA and Yasuhiko KONDO

(Received March 27, 1962)

It has been recently shown that liquid sulfur dioxide is an excellent medium for cationic polymerization[1] with Lewis acid as catalyst. Moreover, there have been reported several cases where the polymerizations were carried out only by the medium (sulfur dioxide) without any catalyst[2,3]. Vinyl ethers are known as belonging to this class[3].

The present authors have found some additional monomers which are capable of carrying out such a liquid sulfur dioxide catalyzed polymerization. It has been found by the present authors that alkyl substituted styrenes are easily polymerized by liquid sulfur dioxide itself. Especially, *p*-methylstyrene will be mentioned here as an example. *p*-Methylstyrene, b. p. 58.5°C/12 mmHg, was dissolved in liquid sulfur dioxide with a trace of hydroquinone and allowed to stand at 50°C in a thermostat. The polymer obtained was separated and purified by the usual procedure (precipitation by methanol from benzene solution of the polymer). The product (5.67 wt.% conversion at 90 min.) was an amorphous powder and melted at 159~162°C (Found: C, 91.23; H, 8.58. Calcd. for poly-*p*-methylstyrene: C, 91.47; H, 8.35%, $[\eta]_{\text{dl./g.}}$ (in DMF), 0.04).

That the polymerization is of cationic mechanism is proved by the facts (a) the radical polymerization of the *p*-methylstyrene in liquid sulfur dioxide must result in the formation of of polysulfone[4], (b) the polymerization by sulfur dioxide was inhibited by electron-donors such as dimethylformamide (DMF), dioxane or amine into the mixture and (c) the reaction was not inhibited by hydroquinone or else which were recognized as radical inhibitor. When the monomer was subjected to a condition of a radical polymerization at 50°C with azobisisobutyronitrile (AIBN), as a catalyst, the product obtained was a mixture of poly-*p*-methylstyrene and *p*-methylstyrene polysulfone, the constitution of the latter being *p*-methylstyrene : SO_2 = 2 : 1 in its mole ratio. The polymer melted at 149~151°C. Analysis of the polysulfone, (Found: C, 71.30; H, 6.61; S, 10.23. Calcd. for 2 : 1 polysulfone; C, 72.00; H, 6.67; S, 10.67%, $[\eta]_{\text{dl./g.}}$, (DMF), 0.4).

Thus a cationic polymerization arose competitvely in liquid sulfur dioxide with an AIBN catalyzed radical polymerization. The product produced by the simultaneous cationic and radical polymerization could be separated by the extraction of poly-*p*-methylstyrene with cyclohexane in a Soxhlet apparatus, the yield of the poly-*p*-methylstyrene being 13~15% of the total.

α-Methylstyrene was polymerized readily by liquid sulfur dioxide. However, in contrast to the result of *p*-methylstyrene, an attempted radical polymerization with AIBN was not successful and gave only poly-α-methylstyrene as a result of a cationic polymerization. The detail of the simultaneous polymerization will be reported elesewhere in the near future.

The present authors have also observed that formaldehyde was polymerized by liquid sulfur dioxide or by sulfur dioxide vapor to yield polyoxymethylene. When liquid sulfur dioxide was maintained at a constant temperature between −70 to −10°C and formaldehyde vapor was streamed into this medium, semitransparent films were obtained on the surface of the solution or on the wall of the glass vessel. The films produced at −70°C were colorless and melted at 169~172°C, containing no sulfur atom (Found: C, 39.37; H, 6.37. Calcd. for $(-CH_2O-)_n$: C, 40.0; H, 6.67%). $[\eta]_{\text{dl./g.}}$ (acetylated polymer in *p*-chlorophenol with 2% α-pinene) was 0.6. The infrared spectrum of the specimen was in close resemblance to that of polyformaldehyde prepared by Novak et al.[5], at low temperature. IR, 2990

1) R. Asami and N. Tokura, *J. Polymer Sci.*, **42**, 545 (1960).
2) C. E. Schildknecht, "Polymer Process", Interscience Publishers, Inc., New York (1956), p. 201.
3) W. Reppe and E. Kühn, U. S. Pat. 2188778 (1940).
4) a) N. Tokura and M. Matsuda, *J. Chem. Soc. Japan, Ind. Chem. Sec.* (*Kogyo Kagaku Zasshi*), **64**, 501 (1961); b) N. Tokura, M. Matsuda and F. Yazaki, ibid., **64**, 713 (1961); c) N. Tokura, R. Asami, M. Matsuda and H. Negishi, ibid., **64**, 717 (1961).
5) A. Novak and E. Whall, *Trans. Faraday Soc.*, **55**, 1490 (1959).

(m, ν-CH), 1492, 1472, 1435, 1387(m), 1290, 1220, 1240(s), (CH_2 bending), 1100 (v. s. –C–O–) and 910~970(s) (KBr). From the evaporation residue of the sulfur dioxide solution, a powdery polymer was also obtained, which was identified as lower molecular weight polyoxymethylene from elementary analysis, infrared spectrum and viscosity, [η], 0.1, the sulfur test was negative. The total yield of the film and the powder was almost quantitative.

The authors are grateful to the Seitetsu Kagaku K. K. for the donation of liquid sulfur dioxide. Part of this research was supported by the grant-in-aid for Scientific Research from the Ministry of Education.

The Chemical Research Institute
of Non-Aqueous Solutions
Tohoku University
Katahira-cho, Sendai

Thunbergene[1], *a Macrocyclic Diterpene**

By Hiroshi KOBAYASHI and Saburo AKIYOSHI

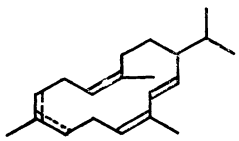
(Received March 29, 1962)

Thunbergene, $C_{20}H_{32}$, m. p. 61°C, $[\alpha]_D$ (benzene) +260°, is a monocyclic diterpene hydrocarbon obtained from several kinds of pine roots. Isolation and some properties of this compound were reported previously by one of the authors (S. A.)[2] and by some other investigators[3-5].

This communication comprises the results of the dehydrogenation and of the ozonolysis of thunbergene, the most probable structure of this interesting compound being proposed.

The dehydrogenation of thunbergene with selenium gave 7-isopropyl-2, 9-dimethylphenanthrene, m. p. 78°C, the picrate melting at 133°C[6] (Found: C, 91.90; H, 8.19. Calcd. for $C_{19}H_{20}$: C, 91.88; H, 8.12%). The structure of the dehydrogenation product was assigned on the basis of the spectroscopic data[7,8] UV λ_{max}^{hexane} 224, 249, 257, 274, 281, 288, 299, 319, 328 and 335 mμ, log ε 4.44, 4.84, 5.00, 4.41, 4.37, 4.19, 4.08, 2.46, 2.40 and 2.45. NMR (in carbon tetrachloride solution with water as an external reference) δ −3.5, −2.5, 3.0 and 4.0 p. p. m., relative intensities 2, 5, 6 and 6 respectively), and was confirmed by infrared spectra and mixed melting point test with an authentic sample synthesized by the standard method from eudalene.

The ozonization at low temperature followed by the oxidative decomposition gave levulinic acid (semicarbazone, m. p. 184°C) and 2-isopropyl-5-oxohexanoic acid, $[\alpha]_D$ ($CHCl_3$) −30° (semicarbazone, m. p. 138~140°C[9]. Found: C, 52.30; H, 8.55; N, 18.14. Calcd. for $C_{10}H_{19}O_3N_3$: C, 52.38; H, 8.35; N, 18.33%). The latter was identified by infrared spectral comparison with a racemic authentic sample. Other fragments on ozonolysis have not been determined yet. As known already, thunbergene has a conjugated diene system which does not undergo the Diels-Alder's addition (UV λ_{max}^{hexane} 240 and 246 mμ, log ε 4.15 both) and octahydrothunbergene is optically inactive. Therefore, the carbon skeleton of thunbergene together with the positions of four double bonds can be reconstructed as shown below with an assistance of the isoprene rule.



According to this formula, thunbergene is hydrogenated to a mixture of eight stereoisomers of octahydrothunbergene; four symmetric isomers and two pairs of enantiomers. The product should be optically inactive as a whole even if the asymmetric center** of thunbergene would be retained.

* Contribution No. 26 from the Department of Organic Synthesis, Faculty of Engineering, Kyushu University.

1) The old name "*d*-Thumbelen" proposed by one of the authors (S. A.) is revised according to the kind suggestion of Professor H. Erdtman, The Royal Institute of Technology, Stockholm, Sweden.

2) S. Akiyoshi, *Rep. Osaka Ind. Res. Inst.*, **17**, No. 10 (1937).

3) Y. Sebe, *J. Chem. Soc. Japan* (*Nippon Kwagaku Kwaishi*), **56**, 1118 (1935).

4) H. Wienhaus, *Nord. Kemistmötet*, (1926) 211; *Chem. Abstr.*, **24**, 1635 (1930).

5) a) A. J. Haagen-Smit, T. H. Wang and N. T. Mirov, *J. Am. Pharm. Assoc.*, **40**, 557 (1951); b) N. T. Mirov and P. M. Iloff, Jr., ibid., **44**, 424 (1955); c) P. M. Iloff, Jr. and N. T. Mirov, ibid., **45**, 77 (1956).

6) This phenanthrene seems to be identical with C_{20}-phenanthrene reported by Sebe, Ref. 3.

7) a) E. Heilbronner, H. U. Däniker and Pl. A. Plattner, *Helv. Chim. Acta*, **32**, 1723 (1949); b) T. Sugasawa, *Chem. Pharm. Bull.* (*Tokyo*), **9**, 889 (1961).

8) J. A. Pople, W. G. Schneider and H. J. Bernstein, "High-Resolution Nuclear Magnetic Resonance" McGraw-Hill, Inc., New York (1959), p. 247.

9) O. Wallach, *Ann.*, **379**, 182 (1911).

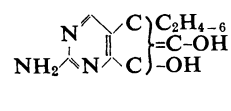
** *Added in proof.*

The absolute configuration at the asymmetric center: (−)-2-isopropyl-5-oxohexanoic acid was oxidized with hypobromite to 2-isopropylglutaric acid, m. p. 94°C, $[\alpha]_D$ −20°, the absolute configuration of which had been confirmed by Fredga (*Acta Chem. Scand.*, **1**, 371 (1947)).

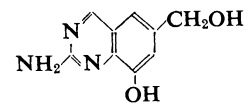
Since the asymmetric center is not affected in the course of degradation, the isopropyl group of thunbergene seems to project up ward from the plane of paper when the ring framework being placed as shown above.

Thunbergene is a hydrocarbon with the fourteen membered macroring. This type of diterpene seems to be very rare. No example could be found in literature. Details will be presented elsewhere in the near future.

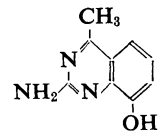
Department of Organic Synthesis
Faculty of Engineering
Kyushu University
Hakozaki, Fukuoka



(I)



(II)



(III)

Structure of the C_9-Base, an Alkaline Degradation Product of Tetrodotoxin

By Toshio GOTO, Yoshito KISHI and Yoshimasa HIRATA

(Received March 29, 1962)

By alkaline degradation of tetrodotoxin, Kawamura[1] obtained a yellow compound (C_9-base), to which he assigned a molecular formula $C_9H_{11}N_3O_2$ and a partial structure (I). 2-Aminopyrimidine moiety of the structure was rigorously established by isolation of 2-aminopyrimidine-4, 5-dicarboxylic acid from the oxidation products of the C_9-base. Tsuda et al.[2] further assumed that the pyrimidine nucleus would be fused with a five-membered ring containing an enol group. From the results reported, however, an alternate possibility that the C_9-base might be a phenol derivative, instead of the enol, can not be excluded. We wish to present a new structure, 2-amino-6-hydroxymethyl-8-hydroxyquinazoline (II), to the C_9-base from the following evidences.

The analytical value of the C_9-base hydrochloride is rather consistent with the formula of $C_9H_9N_3O_2 \cdot HCl$ (Found: C, 47.86; H, 4.47; N, 18.33, 18.09. Calcd.: C, 47.48; H, 4.42; N, 18.46%)[3]. Since one of the two hydroxyl groups in the C_9-base is alcoholic[1], only possible structure having a phenolic hydroxyl group is 2-amino-x-hydroxymethyl-x'-hydroxyquinazoline. For alkyl substituents would not influence much on the ultraviolet spectra of aromatic compounds, 2-amino-4-methyl-8-hydroxyquinazoline (III) was synthesized to compare its ultraviolet spectrum with that of the C_9-base. The quinazoline III, m. p. over 270°C (in sealed tube), was obtained from 2-nitro-3-hydroxyacetophenone by catalytic hydrogenation to 2-amino derivative, m. p. 165~168°C, and then by condensation with cyanamide. Ultraviolet spectra of the synthetic quinazoline III in different pH's almost superimposable, except for slightly hypsochromic shifts of 2~5 mμ, with those of the

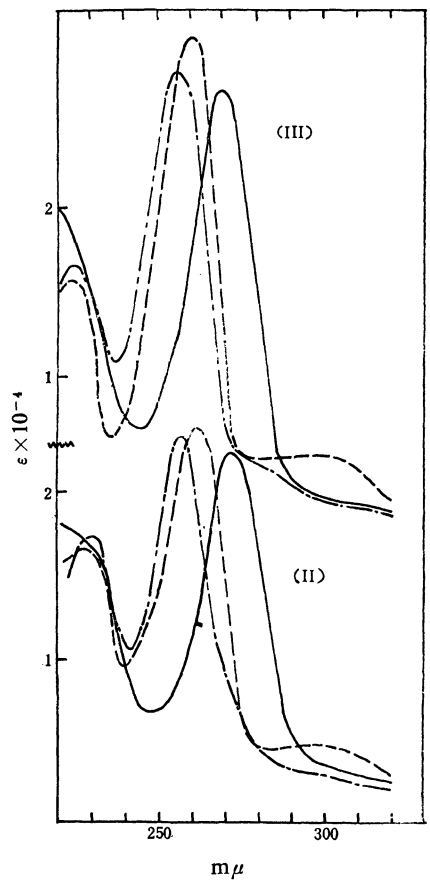


Fig. 1

——— 0.1 N NaOH —·—· H_2O
– – – 0.1 N HCl

1) M. Kawamura, *Chem. Pharm. Bull. (Japan)*, **8**, 262 (1960).
2) K. Tsuda, M. Kawamura and R. Hayatsu, 3rd Symposium of Natural Products, Japan, October, 1959.
3) Analyses of the all derivatives of the C_9-base reported[1] are consistent with this formula.

C_9-base (Fig. 1). It is, therefore, quite reasonable to assume that the C_9-base has a 2-amino-8-hydroxyquinazoline skeleton[4].

NMR spectrum of the C_9-base shows four signals (all singlet) at +26, −48, −65, −113 c. p. s.[5] (area ratio ca. 2 : 1 : 1 : 1), which are assigned to two protons in $-CH_2O-$, two in benzene ring (two signals), and one attached at C_4-position, respectively. Since no coupling is observed between their signals, two aromatic protons are not in adjacent position. Thus the hydroxymethyl group must be attached to the C_6-position. NMR spectrum of the triacetate[1] of C_9-base possesses the following signals which are also consistent with the structure assigned: (τ-values) 8.00 (NH); 7.80, 7.50, 7.30 (three acetyl groups); 4.70 ($-CH_2O-$); 2.40, 2.25 (arom.); 0.68 (proton at C_4); all signals are singlets[6].

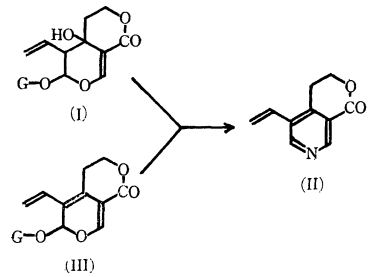
The authors wish to thank Fujisawa Pharmaceutical Co., Ltd. for collecting ovaries of swellfish and to express appreciation to the Public Health Service, National Institutes of Health, for support of this work under Research Grant RG-7969.

Chemical Institute
Faculty of Science
Nagoya University
Chikusa-ku, Nagoya

4) 2-Amino-4-methyl-6-hydroxyquinazoline was also synthesized, but its UV spectrum ($\lambda_{max}^{H_2O}$ 233 mμ; $\lambda_{max}^{0.1N\ NaOH}$ 245 mμ) was quite different from that of the C_9-base.

5) Spectra were taken on a Nihondensi JM (40 Mc) spectrometer using D_2O containing NaOD as solvent, and a signal of DOH as an internal reference (0 c. p. s.).

6) Using $CDCl_3$ as solvent and tetramethylsilane as an internal reference (τ = 10).



G = glucose

reaction was applicable to gentiopicrin[3] (III) also. A solution of gentiopicrin (178 mg.) in ethanol was saturated with ammonia and allowed to stand overnight. The solvent was removed and 1 N hydrochloric acid (20 ml.) was added. The solution was then heated under reflux for 30 min. The acidic solution was made alkaline with ammonium hydroxide and extracted with chloroform. The resinous product (50 mg.) was adsorbed on a silica gel column and eluted with acetone-chloroform (1 : 9). Recrystallization from petroleum ether gave colorless needles (19 mg.), m. p. 83~84°C. This substance was found to be identical with gentianin (II) (mixed melting point and infrared absorption spectrum).

Faculty of Science
Osaka City University
Kita-ku, Osaka

3) Y. Asahina et al., *Ber.*, **69**, 771 (1936); Y. Asahina and Y. Sakurai, ibid., **72**, 1534 (1939); F. Korte, *Chem. Ber.*, **87**, 512, 780 (1954); L. Canonica et al., *Tetrahedron Letters*, **1960**, No. 24, 7.

Derivation of Gentianin from Gentiopicrin

By Takashi KUBOTA and Tadao KAMIKAWA

(Received April 12, 1962)

In a previous communication[1], it was reported that swertiamarin (I)[2], the bitter principle of *Swertia japonica* Makino, was transformed into gentianin (II), a concomitant alkaloid, under mild conditions. It was found that the same

1) T. Kubota and Y. Tomita, This Bulletin, **34**, 1345 (1961).
2) T. Kubota and Y. Tomita, *Chem. & Ind.*, **1958**, 229; *Tetrahedron Letters*, **1961**, No. 5, 176.

Isolation and Characterization of Lunamycin, an Antitumoric Substance from Lampteromyces japonicus

By Haruhisa SHIRAHAMA, Yohei FUKUOKA and Takeshi MATSUMOTO

(Received March 24, 1962)

Lampteromyces japonicus (tsukiyotake) has long been well known in Japan as a poisonous mushroom. However, untill recently, the nature of the active principle has attracted

only little attention. In 1958, Nakai[1] concentrated a toxic material from this fungus and studied its pharmacological action, but could not obtain the toxin in a pure state. More recently, the active constituent of the mushroom has come to attract growing interest, since Komatsu and his coworkers[2] demonstrated a remarkable effect of extracts of the mushroom antagonistic to Ehrlich ascites carcinoma.

The writers wish to report the isolation of an active principle which exhibits antitumoric as well as toxic action[3], $C_{15}H_{22}O_4$, for which the name "Lunamycin" is suggested. Lunamycin was obtained in about 10^{-4}% yield from fresh mushrooms by careful, repeated chromatography through alumina of the ethyl acetate soluble, neutral part of the mushroom as a prismatic crystal, m. p. 122~124°C (Found: C, 67.78; H, 8.20; mol. wt. (micro Rast), 280. Calcd. for $C_{15}H_{22}O_4$: C, 67.64; H, 8.33%; mol. wt. 266. UV spectrum; λ_{max}^{EtOH} 235 mμ (log ε; 4.1), 325 mμ (log ε; 3.5). IR bands at 3500, 3400, 3280, 1692, 1660, 1602, 1107, 1026 cm^{-1}). Treatment of lunamycin with acetic anhydride and pyridine gave a diacetate, m. p. 98~99°C (Found: C, 65.38; H, 7.09; Calcd. for $C_{19}H_{26}O_6$; C, 65.12; H, 7.48%. UV spectrum; λ_{max}^{EtOH} 227 mμ (log ε; 4.1), 317 mμ (log ε; 3.5). IR bands at 3480, 1730, 1695, 1650, 1605, 1230, 1110, 1035 cm^{-1}). Thus lunamycin seems to have one conjugated carbonyl, two acylable hydroxyl and one hindered or tertiary hydroxyl groups. In certain cases a crystal $C_{15}H_{20}O_4$, m. p. 179~181°C (Found: C, 67.84; H, 7.28; mol. wt. (micro Rast), 281. Calcd. for $C_{15}H_{20}O_4$; C, 68.16; H, 7.63%; mol. wt. 264. UV spectrum; λ_{max}^{EtOH} 248 mμ (log ε; 4.3). IR bands at 3430, 3330, 1685 cm^{-1}) was isolated from a fraction eluted just before the most toxic part. This crystal exhibited rather low toxicity; injection of 26 mg. of sample killed a mouse in three days. The compound gave a triacetate, m. p. 110~111°C (Found: C, 64.68; H, 6.76; Calcd. for $C_{21}H_{26}O_7$: C, 64.60; H, 6.71%. UV spectrum λ_{max}^{EtOH} 253 mμ (log ε; 4.3). IR bands at 1730, 1700, 1240 cm^{-1}) upon treatment with pyridine and acetic anhydride. The details of the procedure for isolation of lunamycin will be reported elsewhere.

1) K. Nakai, *Medicine and Biology*, **48**, 33, 103, 211 (1958); **49**, 129 (1958).

2) N. Komatsu, Y. Ogata, S. Nakazawa, I. Yamamoto, M. Hamada, H. Terakawa and T. Yamamoto; Lecture at the 34th Annual Meeting of the Japan Bacteriological Society, April, 1961.

3) Lunamycin kills a mouse in a dosis of 0.6 mg. within 12 hr. Daily administration of 5 γ lunamycin for 4 days completly cures a mouse transplanted with 2.5×10^6 Ehrlich ascites carcinoma cells. The treatment was started one day after the transplantation (private communication from Dr. N. Komatsu).

The authors express their sincere thanks to Drs. Nobuhiko Komatsu, Takehiko Suzuki, Kengo Nakai and Professor Sajiro Makino for tests of biological activity, to Professor Yoshio Ohtani for botanical advice and to Messrs. Shoji Ueno, Hiroshi Yokoyama, Noboru Mikami and Akinori Sugiyama for their great help in collecting and extracting a huge amount of the mushroom.

Department of Chemistry
Faculty of Science
Hokkaido University
Sapporo

Added in proof; Professor Koji Nakanishi of Tokyo University of Education also isolated a toxic material lampterol from the same mushroom. The two samples were proved to be identical by comparison of infrared spectra and m. p. s.

Intramolecular Hydrogen Bonding in o-Aryloxybenzoic Acids

By Michinori Ōki and Minoru Hirota

(Received March 7, 1962)

Although many investigators[1-4] reported the infrared spectra of benzoic acids, most of the measurements were restricted to the O–H stretching absorptions. A report by Brooks, Eglintion and Morman[2] is an exception which reports both ν_{O-H} and $\nu_{C=O}$ absorptions and the higher $\nu_{C=O}$ frequencies with the *ortho* substituted acids are mentioned. In the light of the recent observation[5] of the intramolecular hydrogen bonding in aryloxy- and alkoxyacetic acids, it will be interesting to interprete the data of the ν_{O-H} and $\nu_{C=O}$ absorptions with *o*-aryloxybenzoic acids from the stand point of the cis and trans isomerism (Ia, Ib and II) of the carboxyl group.

---

1) M. M. Davies, "Hydrogen Bonding .... Papers presented at the Symposium on Hydrogen Bonding held at Ljubljana, 29 July-3 August, 1957" (Pergamon Press, 1959) and *J. Chem. Soc.*, **1955**, 132.
2) C. J. W. Brooks, G. Eglinton and J. E. Morman, ibid., **1961**, 106.
3) D. Peltier and A. Pichevin, *Bull. soc. chim. France*, **1960**, 1141.
4) O. H. Wheeler, *Can. J. Chem.*, **39**, 2603 (1961).
5) M. Ōki and M. Hirota, This Bulletin, **34**, 374, 378 (1961).

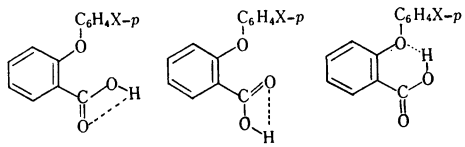
TABLE I. ν_{O-H} ABSORPTION DATA OF p-$XC_6H_4OC_6H_4COOH$-o

X		$\nu_{max}(cm^{-1})$	ε_{max}	$\Delta\nu_{1/2}(cm^{-1})$	$A\times10^{-3}$ (l./mol. cm²)	A_t/A_c
CH_3O	cis	3528.2	22.9	29.7	1.07	13.7
	trans	3391.0	130	53.2	10.86	
		3350.4	44.0	54.5	3.76	
H	cis	3527.8	40.4	29.8	1.89	6.70
	trans	3399.5	120	50.6	9.53	
		3357.9	34.1	58.4	3.13	
Cl	cis	3527.6	59.6	30.1	2.82	2.86
	trans	3411.7	74.7	54.5	6.39	
		3374.8	17.4	61.6	1.68	

TABLE II. $\nu_{C=O}$ ABSORPTION DATA OF p-$XC_6H_4OC_6H_4COOH$-o

X		$\nu_{max}(cm^{-1})$	ε_{max}	$\Delta\nu_{1/2}(cm^{-1})$	$A\times10^{-3}$ (l./mol. cm²)	A_t/A_c
CH_3O	cis	1730	138	15.5	3.36	4.60
	trans	1752.4	863	11.4	15.45	
H	cis	1731	157	14.8	3.65	3.88
	trans	1752.1	785	11.5	14.17	
Cl	cis	1733	188	18.0	5.31	2.21
	trans	1752.1	646	11.6	11.76	

The infrared spectral data* are summarized in Tables I and II. It will be seen that the electronic effect of thes ubstituent is operative to the hydrogen bonding. An electron repelling group at the *para*-position enhances the hydrogen bond formation and causes a larger A_t/A_c ratio, where A_t and A_c represent the integrated intensities due to trans and cis isomers, respectively.



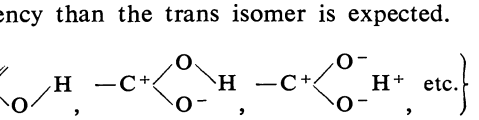
Ia Ib II

In the ν_{O-H} region, the band at the lower frequency (3411~3350 cm^{-1}) is undoubtedly assigned to the trans hydrogen-bonded isomer (II). On the other hand, the assignment of the $\nu_{C=O}$ absorption band is not clearly established and the lower $\nu_{C=O}$ band has been assigned to the trans isomer by several investigators. Quite contrary to the previous assignment, the present authors attribute the higher $\nu_{C=O}$ band (ca. 1752 cm^{-1}) for aryloxybenzoic acids) to the trans isomer from the following reasons.

i) The ratio A_t/A_c increases as the Hammett's σ-constant of the substituent decreases, and this tendency is consistent with the A_t/A_c ratio in the ν_{O-H} region.

ii) Through the intensity measurement at various temperatures with the ν_{O-H} and the $\nu_{C=O}$ bands of o-phenoxybenzoic acid, nearly equal energy difference (ΔH) values (1.90 kcal./mol. with the ν_{O-H} bands and 1.87 kcal./mol. with the $\nu_{C=O}$ bands) for the equilibrium between the cis and the trans isomers were obtained by assuming the assignment in Table II.

iii) Since the resonance forms of the cis isomer illustrated below are possible and the ionic character of the C=O bond may cause the lower C–O bond order, the lower $\nu_{C=O}$ frequency than the trans isomer is expected.



The ultraviolet spectra of these acids were

* The infrared measurement was carried out with a Perkin Elmer 112G spectrophotometer under the condition in which the spectral slit width was less than 1.0 cm^{-1} for the ν_{OH} region and less than 0.7 cm^{-1} for the $\nu_{C=O}$ region. (See Refs. 5 and 6) The samples were dissolved in carbon tetrachloride to make up ca. 0.001 mol./l. solution.

6) M. Ōki and M. Hirota, *Spectrochim. Acta*, **17**, 583 (1961).

also measured and an outstanding hypsochromic shift of B-band[7] was observed when the solvent was changed from heptane to ethanol. (For example, the bands at 287 and 293 mμ of *o*-phenoxybenzoic acid in heptane shift to 274 and 279 mμ.) This phenomenon can be interpreted as support for the existence of an intramolecular hydrogen bonding.

Department of Chemistry
Faculty of Science
The University of Tokyo
Hongo, Tokyo

7) A. E. Gillam and E. S. Stern, "An Introduction to Electronic Absorption Spectroscopy", Edward Arnold Ltd., London (1954), p. 124.

The pH Change with Concentration of Aqueous Solutions of Metal Dodecyl Sulfates

By Ryohei MATUURA, Iwao SATAKE
Ichiro IWAMATSU and Shizuko HOSOKAWA

(Received April 27, 1962)

Lawrence and McDonald[1] reported that the critical micelle concentration (CMC) of aqueous solutions of sodium dodecyl sulfate (SDS) could be determined by pH measurements, showing that the pH vs. concentration curve of SDS solution has a kink point at the CMC. We have made experiments on the concentration dependence of the pH of aqueous solutions of some metal dodecyl sulfates and obtained a result different from theirs for SDS. For some metal dodecyl sulfates, however, for example copper and nickel salts, we have found that the kink point appears in the pH vs. concentration curve at the CMC of each dodecyl sulfate solution.

SDS used in the present experiment was prepared from fractionally distilled pure dodecyl alcohol. It was recrystallized several times from butanol solution and washed with ether for 60 hr. Finally the sample was recrystallized from aqueous solution. Copper dodecyl sulfate tetrahydrate (CuDS) and nickel dodecyl sulfate hexahydrate (NiDS) were prepared from SDS by the method of Lottermoser and Püschel[2]. They were recrystallized several times from aqueous solution. The purity of these samples were confirmed by elementary analysis and surface tension measurements. The pH measurements were performed with a glass electrode pH meter at 25°C. Special precautions were not taken for eliminating carbon dioxide from the solution investigated in order to compare the result with that of Lawrence and McDonald. We suppose, in any way, that the effect of carbon dioxide is not so serious for the solution of anionic detergents as for cationic ones.

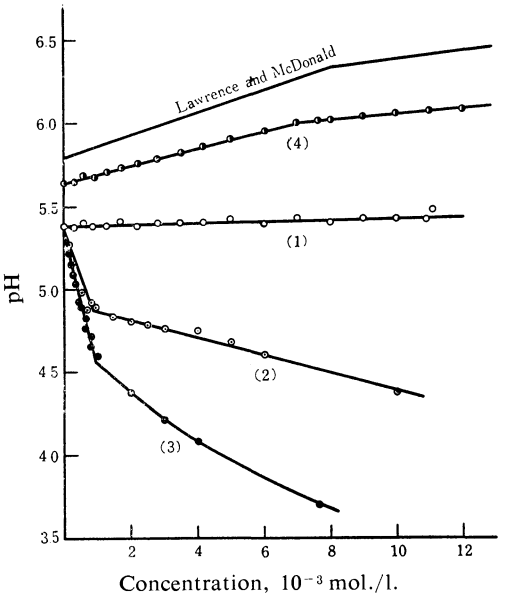


Fig. 1. The pH vs. concentration curves for aqueous solutions of metal dodecyl sulfates.
(1) SDS, (2) CuDS, (3) NiDS, (4) SDS+NaOH ($1:1\times10^{-4}$)

The result is shown in Fig. 1. It is evident that the pH vs. concentration curve for SDS (curve 1) shows no kink point at the CMC ($6\sim8\times10^{-3}$ mol./l.), while the curve for CuDS (curve 2) and for NiDS (curve 3) shows a clear kink at the CMC (both 1×10^{-3} mol./l.[3]). The Lawrence and McDonald's curve for SDS is shown in Fig. 1 for comparison with ours. The difference is remarkable. We do not completely understand the origin of this difference at the present stage, but one reason is supposed to exist in the purity of the sample. We investigated the effect of alkali added to the SDS solution on the pH vs. concentration curve and found that small amounts of alkali

1) A. S. C. Lawrence and M. P. McDonald, Abstract of the 2nd International Congress of Surface Activity, I, 385 (1957).

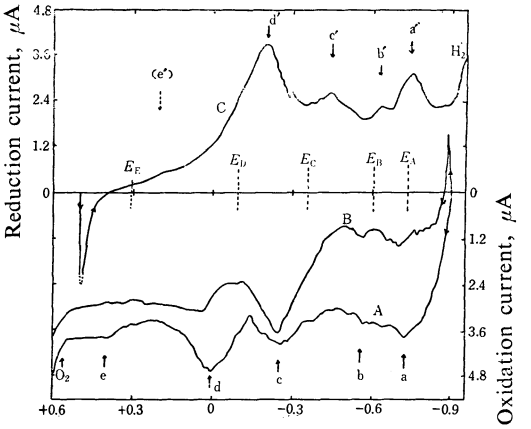
2) A. Lottermoser and F. Püschel, *Kolloid-Z.*, **63**, 175 (1933).

3) S. Miyamoto, This Bulletin, **33**, 375 (1960); I. Satake and R. Matuura, to be published.

caused an appearance of a kink at the CMC of the SDS solution. The curve 4 in Fig. 1 represents this effect. In this case the mole ratio of SDS to sodium hydroxide in the solution was 1 to 1×10^{-4}. It may be inferred that SDS used by Lawrence and McDonald contained alkali as an impurity.

The kink at the CMC of CuDS and NiDS solutions comes undoubtedly from hydrolysis of these detergents. The details of the discussion will be reported in connection with the surface activity of metal dodecyl sulfates in a near future.

Department of Chemistry
Faculty of Science
Kyushu University
Hakozaki, Fukuoka



Potential vs. Hg/HgO (5 M KOH), V.

Fig. 1. Current-potential curves for a platinum electrode in 5 M KOH. A and B: oxidation curves of an electrochemically pre-reduced Pt electrode at the 1st and 3rd trials respectively from −0.9 to +0.6 V. C: reduction curve of a Pt electrode with some platinum oxides and/or hydroxides on it from +0.5 to −0.9 V.

Evidence for a Series of Redox Couples on the Surface of a Platinum Electrode and their Significance

By Akiya KOZAWA*

(Received March 20, 1962)

A series of redox couples on a platinum electrode was found by a voltammetric method as follows. A platinum electrode (approximately 0.6 cm^2 surface area) was placed in one arm of an H-cell containing 5 M potassium hydroxide solution from which air had been expelled by an inert gas. The counter electrode was Hg/HgO. The potential applied to the platinum electrode against the Hg/HgO electrode was scanned at a rate of 0.3 V. per 100 sec. from −0.9 to +0.6 V. or +0.5 to −0.9 V. and the current flow through the platinum electrode was recorded automatically. In Fig. 1 there are shown two oxidation curves for a pre-reduced platinum electrode and a reduction curve for the platinum electrode at which the oxidation curves had been taken. The presence of many peaks on these curves is evident. These peaks may not be attributed to adsorbed oxygen nor hydrogen as repeated experiments with the same electrode produced identical peaks. Peaks a, b, c, d and e on the oxidation curve may indicate the formation of five kinds of platinum oxides and/or hydroxides. The corresponding reduction peaks a', b', c' and d' can be seen on the reduction curve. The potentials (E_A, E_B, etc. in Fig. 1) between a pair of oxidation and reduction peaks can give approximate redox potentials for the redox couples. This has been verified of known redox couples such as $Ni \rightleftharpoons Ni(OH)_2$ and $Ni(OH)_2 \rightleftharpoons NiO_2$. The same experiments at a platinum electrode in 0.05 M potassium hydroxide showed also four to five peaks. The standard redox potentials in alkaline solution for the redox couples on the platinum surface were obtained from the values E_A, E_B, E_C, E_D and E_E in 5 M and 0.05 M potassium hydroxide by making correction for OH^- activity and were −0.67, −0.54, −0.25, +0.05 and (+0.3$_9$) V. vs. N. H. E. respectively.

A platinum electrode has been used to measure redox potential in solution. It is well known that the potential of a platinum electrode placed in a solution containing a redox system follows the Nernst equation. It was assumed that the platinum electrode was inert and served only as a means of transferring electrons. The present finding of a series of oxidation-reduction couples on the surface of a platinum electrode suggests a new interpretation for the behavior of a platinum electrode. When a platinum electrode is placed into a solution containing a redox system, the surface redox couples, which are probably composed of platinum oxides and/or hydroxides, are reduced or oxidized to the redox potential of the system, and the platinum electrode exhibits exactly the redox potential of the system in the solution. As the standard potentials of

* Present address: Department of Chemistry, Western Reserve University, Cleveland 6, Ohio, U. S. A.

the five redox couples on the platinum surface are well distributed between the potentials of hydrogen and oxygen evolution, the potential of the platinum electrode can be kept stable at any potential depending on the redox system involved. Platinum thus can not be considered as an inert electrode as has been traditionally assumed, but rather as an active metal. Recently, existence of oxide film[1] on platinum electrodes and their important role in various electrode reactions at platinum electrode have been reported[2-5] but the redox character of these oxide films was not made clear. In addition to the new interpretation which these redox couples on platinum can give to the behavior of so-called "inert platinum electrodes", these redox couples may play an important role in the explanation of the catalytic activity of platinum in various chemical reactions.

1) F. C. Anson and J. J. Lingane, *J. Am. Chem. Soc.*, **79**, 4901 (1957).
2) F. C. Anson, ibid., **81**, 1554 (1559).
3) J. J. Lingane, *J. Electroanal. Chem.*, **2**, 296 (1961).
4) D. T. Sawyer and L. V. Interrante, ibid., **2**, 310 (1961).
5) F. C. Anson, *Anal. Chem.*, **33**, 934 (1961).

Department of Applied Chemistry
Faculty of Engineering
Nagoya University
Chikusa-ku, Nagoya

Physico-chemical Studies on the Complex of Metals. I. Thermometric Studies on the Composition of Manganese Arsenate Complexes

By Mahendra Singh BHADRAVER and Jifendra Nath GAUR

(Received June 10, 1960)

The composition of so-called manganese arsenate has been studied by the thermometric method involving the thermometric titrations between $MnCl_2 \cdot 4H_2O$ and disodium hydrogen arsenate in aqueous and alcoholic medium. The direct titration curves suggest the formation of $MnHAsO_4$, $MnNa_2(HAsO_4)_2$, and in reverse titrations the formation of $MnHAsO_4$ (ratio of Mn : As is 1 : 1) is indicated. The results of this investigation support the formation of $MnHAsO_4$.

Referance in literature about the elaborate study of the composition of manganese arsenate is scarcely available. Coloriano[1] prepared chestnut brown needles of manganese ortho-arsenate $Mn_3(AsO_4)_2 \cdot H_2O$ by heating sodium ortho-arsenate with an excess of manganese sulfate in a sealed tube at 175°C. Scheele[2] treated manganese salt with alkali-hydro-arsenate and obtained a white gelatinous precipitate, which according to J. H. Debray became crystals when digested for a long time in the mother liquor. Rose[3] said that the precipitate was a mixture of sodium-manganese-ortho-arsenate and manganese-hydro-arsenate $MnHAsO_4 \cdot H_2O$. The monohydrate of the hydro-arsenate, $MnHAsO_4 \cdot H_2O$ was obtained from solutions containing MnO and As_2O_5 in the ratio of 3 : 1 by precipitation with alcoholic solution of arseneous acid. The salt is stable in water at 25°C. Schiefer[4] reported that $Mn(H_2AsO_4)_2$ was obtained from a solution of $MnCO_3$ in theoretical quantity of arseneous acid. Amadori[5] found that $Mn(H_2AsO_4)_2 \cdot H_2O$ was deposited from a solution containing excess of arseneous acid. The composition of manganese arsenate should correspond to the formula $MnHAsO_4$ when manganese chloride is added to disodium hydrogen arsenate. Apart from the above study a number of variable and more complex formula have been reported in literature, e. g., $Mn(H_2AsO_4)_2H_3AsO_4$, $Mn_2As_2O_7$ (Otto), $Mn_5 \cdot As_4O_7 \cdot 2H_2O$ or $Mn_5H_2(AsO_4)_4 \cdot H_2O$ (Coloriano), $MnAsO_4 \cdot H_2O$ (Christensen[6]).

Takahasi and Sasaki[7] during the course of phase rule study of MnO-As_2O_5-H_2O system and heat of formation of $MnHAsO_4$ showed the existence of $Mn_3(AsO_4)_2 \cdot H_2O$, $MnHAsO_4 \cdot H_2O$, $Mn(H_2AsO_4)_2$ and $Mn(H_2AsO_4) \cdot 2H_3AsO_4$. Reference in literature about the study of these complexes by applying other physico-chemical methods i. e., conductometric, potentiometric and thermometric, etc. is scarcely available. In view of the difficulties associated with the analytical work and in the absence of any decisive views on the composition of manganese-arsenate complexes, it was considered worthwhile to undertake the study of these complexes by physico-chemical methods.

With the results of potentiometric, conductometric and amperometric measurements in progress, the results of thermometric titrations are incorporated and discussed in this paper.

Experimental

A.R.E.D.H reagents were used. Solutions of $MnCl_2 \cdot 4H_2O$ and Na_2HAsO_4 were prepared by weighing and the strength of $MnCl_2 \cdot 4H_2O$ was further cheked by estimating manganese as manganese pyrophosphate, Na_2HAsO_4 solution was standardized against sodium thiosulfate of known strength.

The arrangements for the thermometric titrations were the same described by Haldar[9]. Using different concentrations of the two salts in solution, the direct and reverse titrations (i. e., when manganese chloride solution from micro-burette was added to Na_2HAsO_4 solution in the thermos flask and vice versa) were done. Titrations were also carried out in presence of alcohol upto the total concentration of 20% by volume. The conditions for the experiments for the various titrations were maintained the same. The total rise in temperature was then plotted against the titre in cc.

Discussion

The possible reaction between manganese chloride and sodium hydrogen arsenate in reverse titrations i. e., when disodium hydrogen

1) A. Coloriano, *Compt. rend.*, **103**, 273 (1886); *Bull. Soc. Chim.*, (2), **45**, 707, (1886); "Recherches sur quelques arsénates cristallisés", Paris, (1886).
2) C. W. Scheeles, *Svenska Akad. Handl.*, **40**, 316 (1778).
3) H. Rose, *Z. anal. Chem.*, **1**, 414, 425 (1862).
4) F. C. B. Schiefer, *Z. ges. Naturw. Halle*, **23**, 365 (1864).
5) M. Amadori, *Atti Ist. Veneto*, **81**, 603 (1922).
6) O. T. Christensen and J. W. Mellor, "A Comprehensive Treatise on Inorganic and Theoretical Chemistry", Vol. IX, p. 219.
7) T. Takahasi and K. Sasaki, *J. Chem. Soc. Japan, Ind. Chem. Sec.* (*Kōgyō Kagaku Zassi*), **56**, 843 (1953).
8) A. I. Vogel, "Text Book of Quantitative Inorg. Analysis", p. 468.
9) B. C. Haldar, *J. Ind. Chem. Soc.*, **23**, 147 (1946).

TABLE I. SUMMARY OF THERMOMETRIC TITRATIONS-OBSERVATIONS

Curve No.	$MnCl_2$ Concn.	Na_2HAsO_3 Concn.	Points showing breaks: Medium	Calcd.	Obs.	Formula supported	Ratio
Direct titrations (Fig. 1)							
1	M/5	M/20	Aq.	5.0	5.0	$MnHAsO_4$	1 : 1
1	M/5	20 cc.		2.5	2.5	$MnNa_2(HAsO_4)_2$	(1 : 2)
2	M/5	18 cc.	Alc. 10%	4.5	4.5	$MnHAsO_4$	1 : 1
2	M/5	18 cc.	Alc. 10%	2.25	2.2	$MnNa_2(HAsO_4)_2$	1 : 2
3	M/5	16 cc.	Alc. 20%	4.0	4.0	$MnHAsO_4$	1 : 1
3	M/5	16 cc.	Alc. 20%	2.0	2.0	$MnNa_2(HAsO_4)_2$	1 : 2
4	M/5	M/40	Aq.	2.5	2.6	$MnHAsO_4$	1 : 1
4	M/5	20 cc.	Aq.	1.25	1.1	$MnNa_2(HAsO_4)_2$	1 : 2
5	M/5	18 cc.	Alc. 10%	2.25	2.1	$MnHAsO_4$	1 : 1
5	M/5	18 cc.	Alc. 10%	1.125	1.1	$MnNa_2(HAsO_4)_2$	1 : 2
6	M/5	16 cc.	Alc. 20%	2.0	1.0	$MnHAsO_4$	1 : 1
6	M/5	16 cc.	Alc. 20%	1.0	0.95	$MnNa_2(HAsO_4)_2$	1 : 2
Reverse titrations (Fig. 2)							
1	M/40	M/5	Aq.	2.5	2.3	$MnHAsO_4$	1 : 1
	20 cc.						
2	18 cc.	M/5	Alc. 10%	2.25	2.2	$MnHAsO_4$	1 : 1
3	16 cc.	M/5	Alc. 20%	2.0	2.0	$MnHAsO_4$	1 : 1
4	M/20	M/5	Aq.	5.0	5.2	$MnHAsO_4$	1 : 1
	20 cc.						
5	18 cc.	M/5	Alc. 10%	4.5	4.4	$MnHAsO_4$	1 : 1
6	16 cc.	M/5	Alc. 20%	4.0	4.0	$MnHAsO_4$	1 : 1

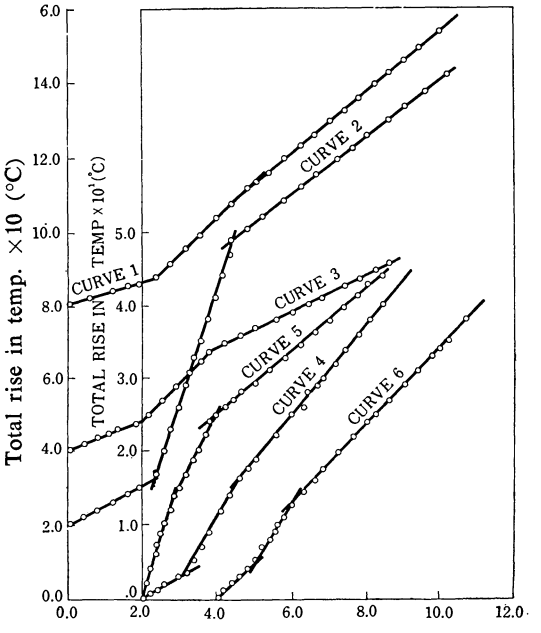


Fig. 1. Direct-thermometric-titrations. Curves 1,2 and 3; M/5 $MnCl_2$ and M/20 Na_2HAsO_4. Curves 4,5 and 6; M/5 $MnCl_2$ and M/40 Na_2HAsO_4.

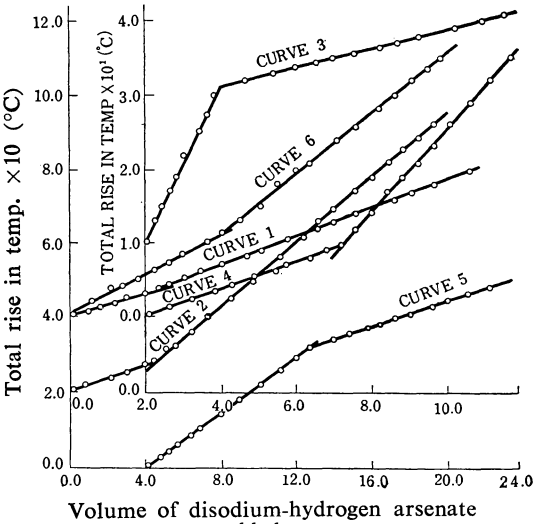


Fig. 2. Reverse thermometric-titrations. Curves 1,2 and 3; M/5 Na_2HAsO_4 and M/40 $MnCl_2$. Curves 4,5 and 3; M/5 Na_2HAO_4 and M/20 $MnCl_2$.

arsenate was added from microburette to manganese chloride contained in thermos flask, can be represented as follows:—

$$Na_2HAsO_4 + MnCl_2 = 2\,NaCl + MnHAsO_4$$

In case of direct titrations the mechanism may be explained as follows:—

$$MnCl_2 + 2\,Na_2HAsO_4 = 2NaCl + MnNa_2(HAsO_4)_2 \quad (1)$$

$$MnCl_2 + Na_2HAsO_4 = 2NaCl + MnHAsO_4 \quad (2)$$

Considering the strength of the solutions of manganese chloride (M/5) and disodium hydrogen arsenate (M/20 and M/40), the theoretical calculated titre values for 20, 18 and 16 cc. of disodium hydrogen arsenate solution for the direct thermometric titrations are 5.0, 2.5, 4.5, 2.25, 4.0, 2.0, 2.5, 1.25, 2.25, 1.125, 2.0 and 1.0 cc. respectively, which are in fair agreement with the observed values in each case respectively, for the formation of the compounds: $MnHAsO_4$ and $MnNa_2(HAsO_4)_2$ (in direct titrations). The formation of only $MnHAsO_4$ is supported in reverse titrations. The theoretical titre values required for the formation of $MnHAsO_4$ (ratio 1 : 1) in reverse titrations can be calculated accordingly. It is observed that the formation of $MnNa_2(HAsO_4)_2$ in the ratio of $Mn : AsO_4$ as 2 : 1 is not proved in the reverse titrations. It is observed from the curves obtained in direct titrations that only two breaks are observed corresponding to the formation of $MnHAsO_4$ and $MnNa_2 \cdot (HAsO_4)_2$ in the ratio of $Mn : AsO_4$ as 1 : 1 and 1 : 2. The reverse titration curves show only one break at the point of equivalence (the ratio of $Mn : AsO_4$ as 1 : 1).

Potentiometric and conductometric studies on the complexes are in progress and the results will shortly follow.

Lohia College
Churu, India

Infrared Absorption Spectra of Water of Crystallization in Aluminum Sulfate Octodecahydrate Crystals

By Itaru GAMO

(Received January 19, 1961)

The study of the vibrational spectra of hydrated aluminum salts seems to be more attractive than that of most of the hydrated salts of other metals, because the water bands of the former present some peculiar features that are not observable in those of the latter. We meet in particular several bands that are not found in other salts. Among aluminum salts, aluminum chloride hexahydrate has already been subject to several fairly detailed infrared[1,2] and Raman[3] studies.

In the present paper the infrared absorption spectra of aluminum sulfate octodecahydrate are compared with those of aluminum chloride hexahydrate, and their characteristic features are analyzed. Attention is mainly focused on the water bands.

Experimental

Preparation.—Commercial aluminum sulfate octodecahydrate of a guaranteed grade was recrystallized from water.

Measurement.—Spectra were obtained by means of a Perkin-Elmer Infracord spectrophotometer with a rock-salt prism. The potassium bromide disk technique was employed.

Results

The spectra are shown in Fig. 1. In the 3μ region, two strong bands are observed at 3330 and 2940 cm^{-1}. The former can be assigned to the antisymmetric, while the latter can be assigned to the symmetric, O–H stretching mode of a water molecule affected by the aluminum-water coördination and by the hydrogen bonding O–H···O[2]. It is interesting that in hydrated salts usually only one peak is observed in this region, while in the present case there are two clearly-separated bands. They seem to correspond to the one broad band which ranges from 3400 to 2900 cm^{-1} in aluminum chloride hexahydrate.

In the 4 μ region, one weak band is observed at 2460 cm^{-1}. This probably corresponds to the band at 2420 cm^{-1} in aluminum chloride hexahydrate and can be assigned to a combination of the bending and a restricted rotation mode of a ligand water molecule. In the 6μ region, the spectrum shows a band of medium intensity at 1640 cm^{-1}, attributable undoubtedly to the bending mode of water. In the 8$\sim$10μ

1) E. Hartert and O. Glemser, *Z. Elektrochem.*, **60**, 746 (1956).
2) I. Gamo, This Bulletin, **34**, 760 (1961).
3) A.-W. Marchand, Thesis (University of Paris). (1957), p. 17.

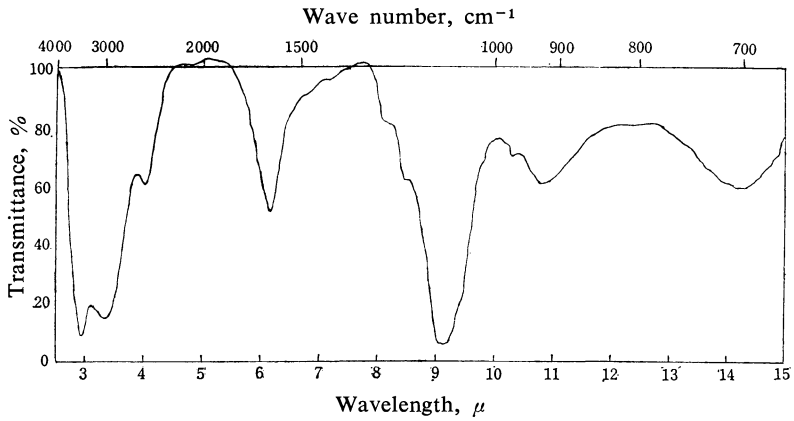


Fig. 1. Absorption bands of $Al_2(SO_4)_3 \cdot 18H_2O$.

region, characteristic bands of inorganic sulfates[4] are observed at 1230, 1190, 1110 and 975 cm^{-1}, all attributable to the stretching vibrations of the sulfate ion and presumably resulting from a distortion of the tetrahedron of the ion caused by some perturbations from outside.

The weak broad band at 920 cm^{-1} can be assigned, from its position and shape, to a restricted rotation mode of water. It is probably due to the rotation of a water molecule about the axis of the smallest moment of inertia (wagging vibration). Similarly, the very broad band at 690 cm^{-1} can be assigned to another restricted rotation, that is, the twisting or the rocking vibration. Since the twisting band is too weak to be observed in ice and in other cases, it seems reasonable to attribute this band to the rocking vibration (rotation about the axis of the greatest moment of inertia). Of course, the difference between the binding states of the water molecules in aluminum salts and in ice must be taken into account; the latter is free from coördination. Judging from its very broad shape, one cannot assign this band to the bending vibration of the sulfate ion (613 cm^{-1} in solution[5]). The very weak band at 1390 cm^{-1} can be tentatively assigned to the first overtone of this band.

Table I summarizes these results.

TABLE I. OBSERVED FREQUENCIES OF $Al_2(SO_4)_3 \cdot 18H_2O$[a]

Wave number, cm^{-1}		Assignment
3330	s	$\nu_3(H_2O)$ antisym. stretch.
2940	s	$\nu_1(H_2O)$ sym. stretch.
2460	w	$\nu_2+\nu_{R'}(H_2O)$
1640	m	$\nu_2(H_2O)$ bend.
1390	vw	$2\nu_{R''}(H_2O)$
1230	w shoulder	$\nu_3(SO_4)$ triply degenerate stretch.
1190	w shoulder	$\nu_3(SO_4)$ triply degenerate stretch.
1100	vs	$\nu_3(SO_4)$ triply degenerate stretch.
975	w	$\nu_1(SO_4)$ totally sym. stretch.
920	w, b	$\nu_{R'}(H_2O)$ wag.
690	m, vb	$\nu_{R''}(H_2O)$ rock.

a) Abbreviations: s, strong; m, medium; w, weak; b, broad; v, very.

Discussion

The results obtained above supply some insight into the binding states of the water molecules in the crystal. As in the previous studies[6], the water frequencies will be assumed to be influenced by the coördination and the hydrogen bonding.

The deviations of the two stretching frequencies from the values of the vapor state (3755.8 and 3651.7 cm^{-1}) are reasonable as compared with the usual cases of hydrated salts. It suggests that at least some of the water molecules are coördinated with an aluminum atom, like the six water molecules in aluminum chloride hexahydrate, and that at the same time they form hydrogen bonds with oxygen atoms of other water molecules or sulfate ions. The clear separation of the symmetric stretching band from the antisymmetric one is probably due to its sharpness and strong intensity. The combination band at 2460 cm^{-1} is also much stronger than usual.

The position of the bending band is the same as in aluminum chloride hexahydrate within the range of experimental error. This indicates that in this mode the total effect of aluminum-water coördination and hydrogen

4) L. J. Bellamy, "The Infrared Spectra of Complex Molecules", Methuen, London (1958), p. 345.

5) K. W. F. Kohlrausch, "Ramanspektren. Hand- und Jahrbuch der chemischen Physik", 9, Part 6 (1943), p. 399.

6) I. Gamo, This Bulletin, 34, 760, 764 (1961).

bonding O–H···O is of the same order as in aluminum chloride hexahydrate.

The 920 cm^{-1} wagging frequency is, on the contrary, about 80 cm^{-1} higher than the corresponding one in aluminum chloride hexahydrate. (In a previous paper[2] the bands in the 11~14 μ region were tentatively assigned to the rocking mode, but it seems better to assign them to the wagging vibration for reasons stated in the preceding section.) Therefore, the total effect mentioned above is somewhat greater in aluminum sulfate octodecahydrate. Furthermore, the value, 920 cm^{-1}, is much higher than in the usual cases of inorganic hydrated salts[2]. This leads one to expect a very high frequency also for the rocking mode, since the two modes are likely to be influenced in a similar manner by the two effects. This seems to provide another reason for the assignment which was proposed in the preceding section for the band at 690 cm^{-1}. The rocking frequency is usually under 650 cm^{-1}.

The discussion hitherto has been based on the assignments described in the preceding section. As an alternative, an assumption of the existence of two kinds of water molecules is possible if the bands at 920 and 690 cm^{-1} are assigned to wagging vibrations, and if the bands at 2940 and 3330 cm^{-1} are regarded as due to the corresponding stretching modes. However, the following discussion suggests the invalidity of such an assumption. First, it will be reasonable in this case to suppose that water molecules of the first kind are coördinated with the aluminum atom, while those of the second kind are almost free from such coördination, since coördination lowers the stretching and increases the wagging frequency. On these suppositions one may try to apply to the 3330 cm^{-1} band the relationship proposed by Glemser[7] between the O–H···O distance and the stretching frequency in inorganic hydrated salts. This relationship seems to be correctly applicable to cases where only the hydrogen bonding effect dominates the frequency. In the present case, the 3330 cm^{-1} band is supposed to be due to the stretching mode affected only by this effect. Hence, the application is suitable, giving 2.66 Å for the O–H···O distance. Then, from the band at 690 cm^{-1}, one may try to estimate this distance by applying the relationship obtained in a previous study[2]. It shows the dependence of the wagging frequency* upon the hydrogen bond distance and the metal-water distance[2]. The aluminum-water distance in the present case must be far greater than 1.88 Å (the value in aluminum chloride hexahydrate[8]), because the water molecules are supposed to be almost free from coördination and 1.88 Å is abnormally short, even for coördination distance. Correspondingly, a value far less than 2.66 Å is obtained for the O–H···O distance by the above-mentioned relationship. After all, the two values estimated from the stretching and from the wagging frequency conflict with each other, while in the original assignments they can be reconciled by proper adjustment. These circumstances seem to favor the original assignments.

Lastly, we have been able to observe an overtone and a very strong combination band of water, just as we observed several in the case of aluminum chloride hexahydrate, because of their great intensity. It may be that some connection exists between this fact and the aluminum-water coördination, because the coördination distance in aluminum chloride hexahydrate (1.88 Å) is anomalously shorter than usual.

Summary

The observed spectra of water of crystallization were compared with those of aluminum chloride hexahydrate and interpreted on the basis of the effects of aluminum-water coördination and hydrogen bonding O–H···O. The wagging and the rocking frequency were both much higher than is usual in water of crystallization. It was proposed that this result, together with other peculiarities, may have some connection with the coördination strength between aluminum and water.

The author wishes to express his thanks to Professor Takehiko Shimanouchi of the University of Tokyo for his helpful guidance.

Institute for Science and Engineering Research
Waseda University
Shinjuku-ku, Tokyo

* Described as the rocking frequency in Ref. 2.

7) O. Glemser and E. Hartert, *Naturwiss.*, **42**, 534 (1955).

8) K. R. Andress and C. Carpenter, *Z. Krist.*, **A87**, 446 (1934).

Infrared Absorption Spectra of Water of Crystallization in Sodium Sulfate Decahydrate Crystals

By Itaru GAMO

(Received January 19, 1961)

Preceding papers[1] have examined the observed spectra of water of crystallization of various salts as they were affected by the coördination of the water molecule on the metal atom and by the hydrogen bonding between the water molecule and the anion.

For the present study, spectra of sodium sulfate decahydrate were investigated. Attempts were made to interpret the results by the effect of hydrogen bonding only, because no coördination exists between the water molecule and the sodium atom. The spectra suggest the existence of at least two kinds of water molecules in the unit cell of the crystal.

Experimental

Preparations.—Commercial sodium sulfate decahydrate of a guaranteed grade was recrystallized from water. Sodium sulfate, used for the reference spectra, was obtained by keeping this purified sodium sulfate decahydrate at 100°C for 30 min.[2]

Measurements.—Spectra were obtained by means of a Perkin-Elmer Infracord spectrophotometer with a rock-salt prism. For the hydrate, the use of the potassium bromide disk was unsuitable because a large amount of water escaped during the vacuum process, resulting in a considerable weakening of the water bands. Therefore, the Nujol and H.C.B. mull techniques were employed. For the anhydride, however, the potassium bromide disk technique was suitable.

Results

The spectra are given in Fig. 1. (For reference, the spectra of sodium sulfate are also given in the figure.) In the 3μ region, one strong band is observed at 3510 cm^{-1}. Is can be assigned to the O–H stretching mode of a water molecule affected by hydrogen bonding. A weak but relatively sharp band is observed at 2940 cm^{-1}. It disappears upon complete dehydration and therefore must be attributde to a water mode. Probably this is due to a stretching vibration much more strongly influenced by hydrogen bonding than that mentioned above. These two bands are too widely separated to be attributed to the antisymmetric and the symmetric O–H stretching mode respectively of one and the same water molecule. In the 5μ region a very weak but clear band is observed at 2170 cm^{-1}. It also disappears upon dehydration and can be assigned to a combination of the bending and the wagging (probably) vibration of a restricted water molecule. A similar band is observed at 2080 cm^{-1}. It does not disappear by the same treatment and therefore can be attributed to a

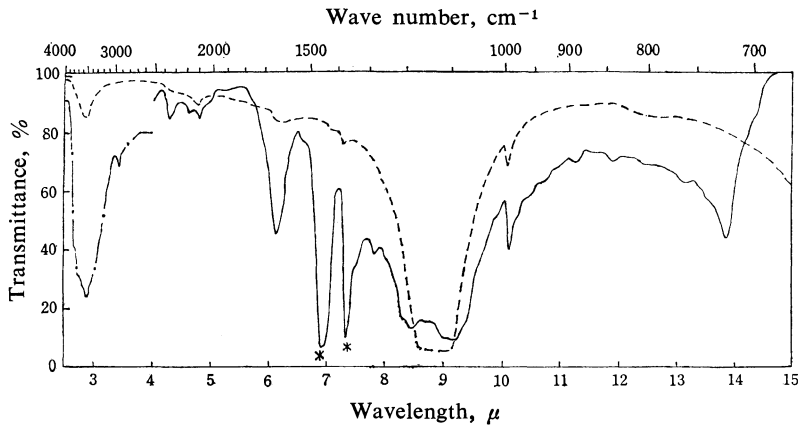


Fig. 1. Absorption bands of $Na_2SO_4 \cdot 10H_2O$ and Na_2SO_4.
—— $Na_2SO_4 \cdot 10H_2O$ (Nujol) -·-· $Na_2SO_4 \cdot 10H_2O$ (H. C. B.)
---- Na_2SO_4 (KBr disk) * Nujol bands

1) I. Gamo, This Bulletin, 34, 760, 764, 1430, 1433 (1961).

2) L. Gmelin, "Handbuch der anorganischen Chemie", Verlag Chemie, Berlin (1928), No. 21, p. 559.

combination of the triply degenerate and the totally symmetric stretching mode of the sulfate ion. In the 6 μ region the spectrum shows a band of medium intensity at 1650 cm^{-1}, attributable undoubtedly to the bending mode of a water molecule. The band of medium intensity at 1290 cm^{-1} disappears upon dehydration. Therefore, it must be attributed to a water mode even though its origin cannot be decided at present. Probably it is due to an overtone of some deformation mode or to a combination of deformation modes. The bands at 1180, 1090 and 988 cm^{-1} can be assigned to the stretching vibrations of the sulfate ion, as in the usual cases of sulfates[3]. The band at 720 cm^{-1} overlaps a Nujol band to some extent. It can be assigned from its position to the wagging vibration[1] of that water molecule which is responsible for the 2940 cm^{-1} stretching band. (The reason is explained later).

Table I summarizes these results.

Table I. Observed frequencies of $Na_2SO_4 \cdot 10H_2O$[a]

Wave number, cm^{-1}		Assignment[b]
3510	s	$\nu(H_2O)$ stretch. of H_2O (I)
2940	w	$\nu(H_2O)$ stretch. of H_2O (II)
2170	vw	$\nu_2+\nu_R(H_2O)$
2080	vw	$\nu_3+\nu_1(SO_4)$
1650	m	$\nu_2(H_2O)$ bend.
1290	m	(H_2O)
1180	s	$\nu_3(SO_4)$ antisym. stretch.
1090	vs, b	$\nu_3(SO_4)$ antisym. stretch.
988	m, sh	$\nu_1(SO_4)$ sym. stretch.
720	m	$\nu_R(H_2O)$ wag. of H_2O (II)

a) Abbreviations: s, strong; m, medium; w, weak; v, very; b, broad; sh, sharp.
b) H_2O (I) and H_2O (II) denote two different kinds of water molecules in the unit cell respectively.

Discussion

The results obtained in the preceding section supply some insight into the binding states of water molecules in the crystal. Since the water molecules in this crystal do not seem to be affected by the coördination, only the influence of hydrogen bonding will be considered. From this standpoint, at least some of the water molecules must form hydrogen bonds with the oxygen atoms of other water molecules or of sulfate ions. Otherwise, it is impossible to explain the observed deviations in the water stretching frequencies from the values of the vapor state.

The 3510 cm^{-1} stretching frequency, which is considerably higher than the values for the water of crystallization in the usual inorganic salts[1], must be due to water molecules which are relatively free. Water molecules which are much more strongly influenced by hydrogen bonding are probably responsible for the band at 2940 cm^{-1}, since, in general, hydrogen bonding lowers the stretching frequency. By an application of Glemser's relationship between the stretching frequency and the O–H···O distance[4], 3.01 and 2.58 Å are obtained for the first and the second water molecule respectively. These values are comparable with those for ice (2.76 Å[5]) and gypsum (2.82 Å[6]), in both of which the water molecules are also free from coördination.

By the aid of the values thus obtained, the origin of the wagging band at 720 cm^{-1} can be deduced as follows. To begin with, this band may tentatively be assumed to be due to that water molecule which is responsible for the stretching band at 3510 cm^{-1}, the corresponding O–H···O distance being 3.01 Å. A previous study[7] shows roughly the dependence of the wagging frequency upon the metal-water distance and the hydrogen bond distance. It follows from this relationship that in the present case the metal-water distance is far less than 1.80 Å. But the distance cannot be less than 2.27 Å, the sum of the ionic radii of sodium and oxygen, since no water molecule seems to be coördinated with the metal atom, the interaction between them being purely electrostatic. The distance is estimated to be about 2.80 Å when this band is correlated with the stretching band at 2940 cm^{-1}. These circumstances seem to favor the assignment of this band described in the preceding section.

Summary

The observed spectra of water of crystallization were interpreted on the basis of the effect of hydrogen bonding. It was proposed that at least two kinds of water molecules exist in the unit cell of the crystal. The corresponding two O–H···O distances were roughly estimated to be 3.01 and 2.58 Å respectively by the use of Glemser's relationship between the stretching frequency and the hydrogen bond distance.

The author wishes to express his thanks to Professor Takehiko Shimanouchi of the University of Tokyo for his helpful guidance.

Institute for Science and Engineering Research
Waseda University
Shinjuku-ku, Tokyo

3) L. J. Bellamy, "Infrared Spectra of Complex Molecules", Methuen, London (1958), p. 345.
4) O. Glemser and E. Hartert, *Naturwiss.*, **42**, 534 (1955).
5) W. H. Barnes, *Proc. Roy. Soc.*, **A125**, 670 (1929).
6) M. Atoji and R. E. Rundle, *J. Chem. Phys.*, **29**, 1306 (1958).
7) I. Gamo, This Bulletin, **34**, 760 (1961). See also the preceding paper as regards the change of assignment from the rocking to the wagging mode.

On the Basicities of the Nitro-derivatives of Benzoanthrones

By Takashi HANDA

(Received February 25, 1961)

Benzene is considered to be a weak base or electron-donor in relation to bromine and iodine owing to the existence of its π-electrons. Its trinitro-derivative, however, behaves as an acid or electron-acceptor in relation to naphthalene, anthracene and other highly condensed aromatic hydrocarbons. This is a result of the strong electron-accepting power of the nitro-group, which is due to the group's inductive and resonance effect. In the nitro-derivatives of aniline, it is observed that the influence of the substituted nitro-group on the lone-pair electrons of the nitrogen atom of the amino-group reduces its proton-affinity or basicity.

The present author has observed that the influence of electron-donating methyl-groups on the basicities of matrix-benzenes in the methyl-derivatives of aromatic compounds can be explained in terms of the amount of decrease in empirical resonance energies among such complexes as solvated ions and original compounds. The influence can be expressed as $\log(N^*/N)$ with the application of Carter's equation by estimating the number of resonance structures of polarized polymethylbenzene, including polarization on methyl-groups, on the assumption that the resonance structures polarized on methyl-groups possess the same weight or maintain a constant ratio (α) of weights to those polarized in a matrix compound. The details of these studies will be submitted elsewhere[1].

In this paper, the influence of the nitro-group on the decrease in basicity of the carbonyl-oxygen atom of the nitro-derivatives of benzoanthrone is explained with reference to the resonance effect.

Experimental Procedures

The measurement of optical absorption was carried out with a Beckman DU-type spectrophotometer according to the method of Hammett and Dingwall[2]. The observed values satisfied Beer's law considerably well in the range of concentration from 10^{-5} to 10^{-6} mol. per liter.

The applied specimens were synthesized in the manner proposed by M. Shioda of the University of Tokyo.[3] These were recrystallized from *o*-dichlorobenzene and further purified by means of sublimation in vacuo of the order of 10^{-3} mmHg. The solutions were prepared by a dilution method from the standard solution with a definite concentration. The chemical structures of the specimens used in this experiment are shown in Table I.

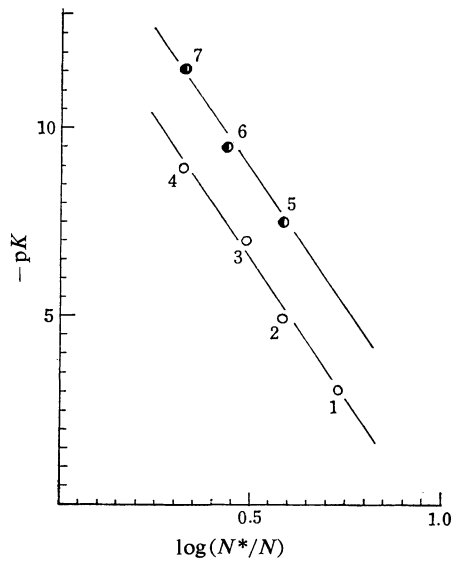


Fig. 1. The correlation of pK with $\log(N^*/N)$ in nitro-derivatives of benzoanthrone and anthraquinone.
(1) Benzoanthrone (Bz), (2) 3-NitroBz, (3) 3,9-DinitroBz, (4) TrinitroBz, (5) Anthraquinone (An), (6) 1-NitroAn, (7) 4,5-DinitroAn.

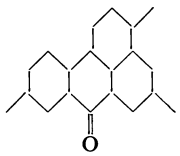
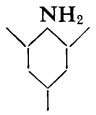
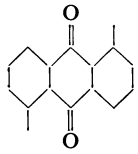
Results and Discussion

The absorption spectra of mono-nitrobenzoanthrone, di-nitrobenzoanthrone and tri-nitrobenzoanthrone in concentrated sulfuric acid of various acidities are shown in Figs. 2–4. From these spectral curves, the pK-value of each compound is obtained as listed in Table I according to the method of Hammett[2]. The substitution of one nitro-group decreases the basicities of benzoanthrone by the amount of two in a pK unit as shown in Table I.

Similar results were obtained in the nitro-substitution of aniline and also of anthraquinone, as illustrated in the table. In order to explain this decrease in basicity by nitro-substitution from the point of view of the change of empirical resonance energy, in such

1) T. Handa, This Bulletin, to be published.
2) L. P. Hammett and J. Dingwall, *J. Am. Chem. Soc.*, **57**, 2103 (1935).
3) M. Shioda and S. Kato, *J. Soc. Org. Synth. Chem., Japan*, **15**, 361 (1957).

TABLE I. THE p*K*-VALUE OF NITRO SUBSTITUTED AROMATICS

Matrix compound	*p*K-Value			
	Unsubstituted	Mono-NO_2	Di-NO_2	Tri-NO_2
	−3.2	−5.1	−7.1	−9.2
	ca. 5.3	*ortho-* −0.16 *para-* 1.4	−4.1	−9.1
	−7.5	−9.5	ca. −12.1	Not measured

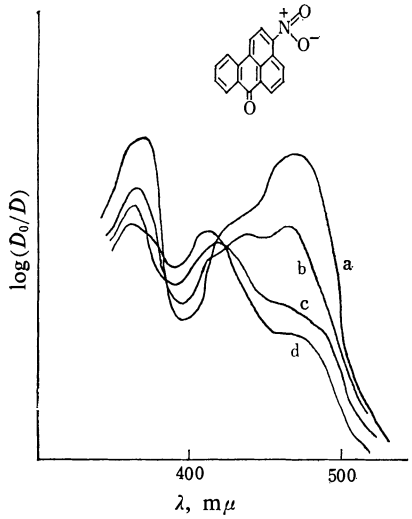


Fig. 2. The spectral response curves of mono-nitrobenzoanthrone in concentrated sulfuric acid.
(a) 90~100% H_2SO_4, (b) 78% H_2SO (c) 70% H_2SO_4, (d) 67% H_2SO_4.

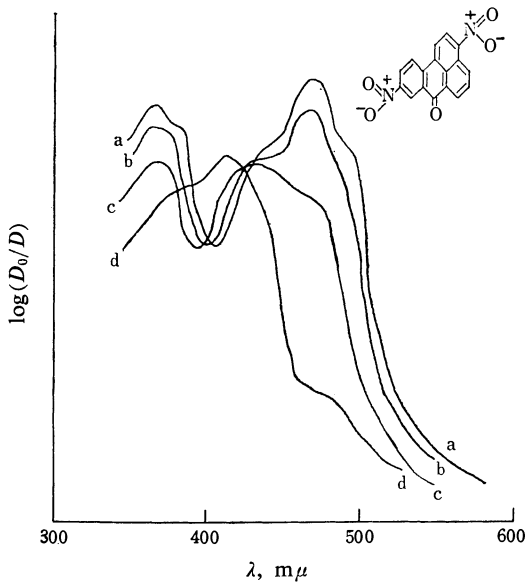


Fig. 3. The spectral response curves of di-nitrobenzoanthrone in 100% (a), 82% (b), 75% (c), and 70% (d) sulfuric acid.

a manner as we have used to explain the basicities of hydrocarbons and their related quinones, it is necessary to estimate the number of Keküle resonance structures in the ground-state of the original compound and those in the ground-state of a complex such as solvated ion protonated at its carbonyl-oxygen atoms.

In the preceding papers[1,4], in the explanation of the basicities of polymethylbenzenes as measured by McCanlay, et al.[6], we estimated structure I due to the resonance in the matrix and structure II due to the resonance of the polarized methyl-group, as shown in Fig. 5 in the previous report[4], equally or with a definite ratio of weights, for the purpose of making a rough estimation of the number of resonance structures, explaining the contribution of methyl-groups to basicity as a change in empirical resonance energy with the use of Carter's empirical equation.

In the case of nitro-derivatives of benzoanthrone, structures I and II are the principal structures, where it is estimated that II possesses a weight equal to that of I, or where the weight of I is in a definite ratio to that of II

4) T. Handa, ibid., **14**, 338, 550 (1956).
5) P. G. Carter, *Trans. Faraday Soc.*, **45**, 597 (1947).
6) D. A. McCanlay and A. P. Lien, *J. Am. Chem. Soc.*, **73**, 2013 (1951); D. A. McCanlay, B. H. Shoemaker and A. P. Lien, *Ind. Eng. Chem.*, **42**, 2103 (1950).

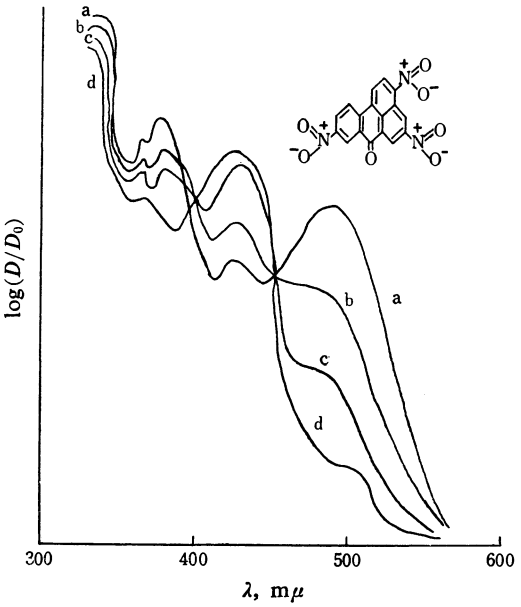


Fig. 4. The spectral response curves of trinitrobenzoanthrone in 100% (a), 95% (b), 90% (c), and 85% (d) sulfuric acid.

in nitrobenzoanthrone, though that ratio may in fact be considerably small.

As for the structures of the protonated nitrobenzoanthrone, structures III and IV belong to the localized non-bonding part, as in the case of the quinones[1,4]*, and structures V and VI belong to the dative part of that complex. The contribution of the VI structures with a double charge in the same molecule may be very small.

In the same manner, for protonated dinitro- and trinitrobenzoanthrone, we assume the contribution of various structures to the resonance energy. Structures X, XI and XII, with weights equal or in a definite ratio (α) to those the former group, are the principal structures belonging to the non-bonding part of the complex, and XV, XVI and XVII are the structures of trinitrobenzoanthrone. Structures XIII and XIV, with weights equal or in a definite ratio (α) to that of XIII, are also principal factors in the dative part of the complexes in the ground-state, while XIX and XX are such factors for trinitrobenzoanthrones.

Therefore, as was explained in the previous reports[1,4], Eq. 1 is derived approximately for the nitro-derivatves of benzoanthrone:

$$\Delta H_G \fallingdotseq \Delta R_G + C' \fallingdotseq R_2 - R_1 + C' = C_0 + C_2^2(R_H^+ - R)\ ^{4)} \quad (1)$$

or $$\Delta R_G \fallingdotseq C + 69\beta^2 \log N_D/N\ ^{1)} \text{ kcal./mol.}$$

where R_H^+ and R represent the resonance energies of the protonated ion and the original compound, and C_2 is the coefficient of the wave function expressing the dative part in the ground-state of the complex-ion. ΔR_G is the change in empirical resonance energy in the ground-state as a result of complex-formation, and β^2 and N_D are the coefficients of the wave function expressing the dipole-oriented state and the number of the resonance structures in this state respectively. The meaning of R_H^+ is taken to be the same in this case as in that of R_D.

In estimating the resonace energy of the nitro-derivatives of benzoanthrone, when we assume that the contribution from the nitro-group (an) can be included in the estimation independently from that of the matrix polarized by the resonance of the charge of the nitro-group, it is expressed in terms of Eq. 2, as was described by Carter for hydrocarbons:

$$R = a_0 + an + bD + c \log N \quad (2)$$

where a_0, a, b and c are constants, n is the number of nitro-groups, D is the number of double bonds, and N is the number of Keküle resonance structures, which are explained above.

When we take α as 1.0**, pK may be plotted versus log (N^*/N) lineary in Fig. 1, as well as in the case of nitroanthraquinones. By the application of Eq. 2, we can roughly estimate the weights of the dipole-oriented structure in the ground-state of the complex from the gradient observed in Fig. 1.

Thus, we are able to explain the decrease in the basicities of benzoanthrone by the nitro-substitution from the resonance effect of the nitro-groups.

When we plot the pK values of the chloro-derivatives of benzoanthrone versus log(N^*/N),

* Basicity which corresponds to the change in the total energy in the ground-state, ΔH_G, between the complex and its matrix is estimated as follows; assuming the term $T\Delta S$ to be constant for a series of compounds:

$$\Delta H_G = C + 69b^2\{\log(N_{Ip}/N) - \beta^2 \log(N_D/N)\} + 69\beta^2 \log(N_D/N) \quad (3)$$

where N_{Ip} is the number of cannonical resonance structures in the ionized-state, N_D is that of those in the dipolar excited state, and b and β are the coefficients of the wave-function expressing the dative part of the ground-state of the complex and the dipole oriented-states respectively. The energy of the dipole-oriented state W_{00} is assumed to be as follows:

$$W_{00} = \alpha^2 W_0 + \beta^2 W_{01} \quad (4)$$

where W_0 is the energy of the original hydrocarbons in the ground-state and W_{01} is that of the perturbed dipole-oriented state. This relation is discussed in detail in another report[1]. In the case of proton-complexes which existed as solvated ions (σ-from), the term $b^2\{\log(N_{Ip}/N) - \beta^2 \log(N_D/N)\}$ becomes very small owing to the greatly increased values of β^2 in strongly acidic media, as compared to the second term in Eq. 3, $69\beta^2 \log(N_D/N)$.

** The real value of α can be estimated by comparing the empirical resonance energies of this series of nitro-compounds with the gradient of 69 kcal./mol. in Carter's equation.

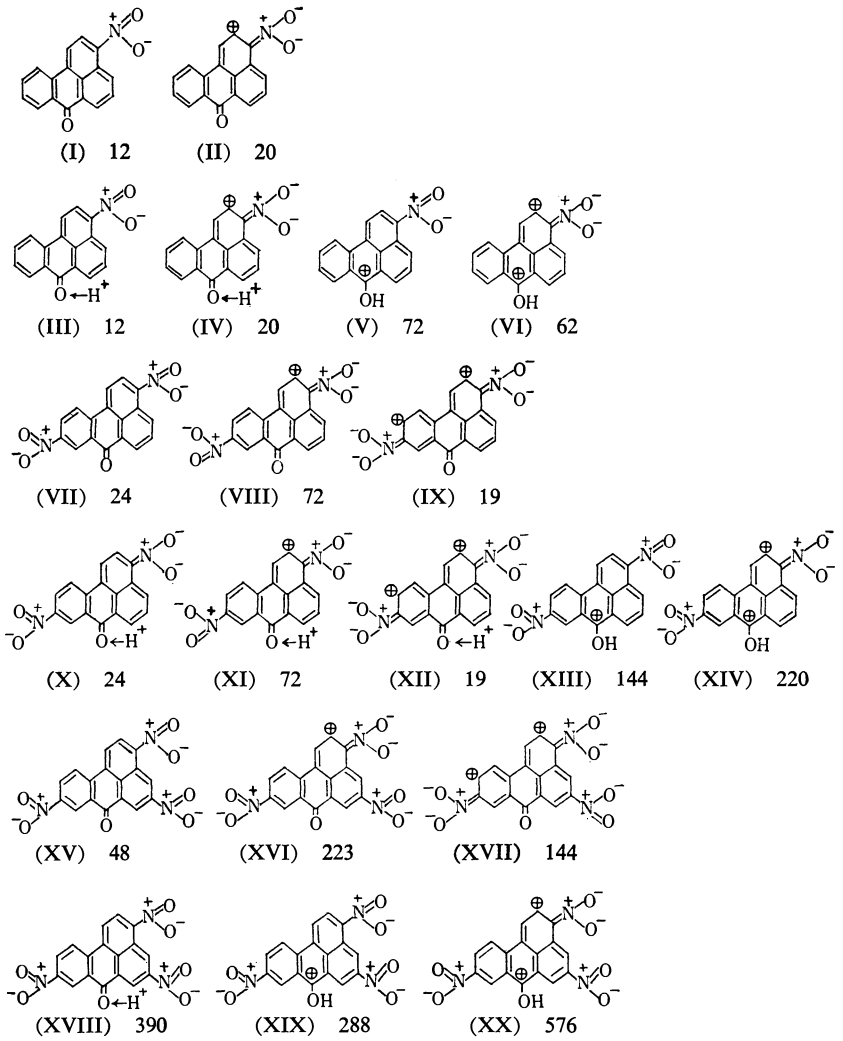


Fig. 5. The resonance srtuctures of nitrobenzoanthrone derivatives.

values which are estimated formally as in the case of nitrobenzoanthrones, they correspond with $\log(N^*/N)$ approximately linearly. In this case, the gradient of the line is smaller than that in the case of the nitro-derivatives. This means that the contribution of the polarized structure in the ground-state is larger in the case of nitro-derivatives than in the case of chloro-derivatives.

Summary

The basicities of the nitro-substituted benzoanthrones were measured. One nitro-substitution decreases the basicity of beazoanthrone by about two pK units, as in the case of nitro-substituted aniline and anthraquinone. This is explained qualitatively not by the inductive effect but by the resonance effect of the nitro groups on the carbonyl group of benzoanthrone in such way as to estimate approximately the change of resonance energies in the cases of both hydrocarbons and their related quinones. The gradient of the straight line of pK plotted versus $\log(N^*/N)$ in the case of nitro-substitution is greater than in the case of chloro-substitution. This means that the contribution of the polarized structure in the ground state to resonance effect is greater in the case of the nitro-derivatives of benzoanthrone than in the case of the chloro-derivatives.

The anthor wishes to extend his hearty thanks to Professor Hideo Akamatu for his kind guidance throughout this study, and to Dr. Hiroo Inokuchi, Dr. Yoshio Matsunaga, and Mr. Hidetsuru Matsushita for their kind advice.

Department of Chemistry
Faculty of Science
The University of Tokyo
Hongo, Tokyo

Chain Transfer to Telomer[1]. *II. In the Case of Catalyzed β-Polymerization*

By Seizo OKAMURA and Keizo KATAGIRI

(Received March 15, 1961)

In the previous report[1] the transfer constants of telomer prepared by the thermal polymerization of styrene in a carbon tetrachloride solution were determined in the thermal β-polymerization[2] of styrene as $C_M=2\times10^{-4}$ and $KC_E=4\times10^{-2}$ (at 100°C) by the method previously suggested by Schulz et al.[3], where C_M and KC_E are the chain transfer constants belonging respectively to the middle part and to the end along the telomer chain. However, at a high rate of conversion of monomer, C_M and KC_E values were lower than the above values. In other words, a somewhat greater degree of polymerization was obtained than that at the lower conversion rate. The present investigation is concerned with this problem.

Moveover, the present report treats the effect of the presence of a catalyst on the apparent degree of polymerization. The contribution of a catalyst in β-polymerization has not been discussed by any other investigators but Hayes[4], who observed the graft efficiency in the emulsion polymerization. Such an observation appears to be a more logical consequence of the chain transfer reaction of a catalyst radical with the α-polymer competing with the usual initiation reaction. Although his findings can not be applied directly to the present homogeneous polymerization, in order to examine the effect of such a catalyst chain transfer reaction experimentally, the following experiments were carried out by polymerizing styrene in the presence of azobisisobutyronitrile (AIBN) as a catalyst and telomer as a α-polymer. The experimental conditions differed from those of the previous report only in the addition of 1 ml. of the catalyst solution to the mixture of styrene (5 ml.) and α-polymer in β-polymerization.

Experimental

Materials.—Styrene was purified by washing it with alkali and water to remove the inhibitor, drying it with calcium chloride, and distilling it twice under reduced pressure. G. R. grade benzene and carbon tetrachloride were distilled before use.

α-Polymer was prepared by uncatalyzed styrene-carbon tetrachloride polymerization at 100°C. Ampoules were thoroughly cleaned with chromic acid, washed with water and then with steam, and dried. α-Polymer was precipitated with methyl alcohol and dried.

The degree of polymerization of β-polymer, P_β, was determined from the relation of $P_n=K[\eta]^a$, (where P_n indicates the degree of polymerization, $[\eta]$, the intrinsic viscosity, and K and a are constants)[5]. The viscosity measurements were done in a benzene solution at 30°C. The fractionation of α-polymer (telomer) was not carried out for the reason stated previously[1].

Procedures.—The catalyst solution consists of AIBN 0.1623 g. in benzene 100 ml. Mixtures of 5 ml. of styrene, various amounts of telomer, and 1 ml. of the catalyst solution were taken in the ampoules, frozen in dry ice, evacuated and sealed. The polymerizing temperature is 100°C, and its time, 1 hr. and 20 min. As the concentrations of the catalyst were in the range of from 1.56 to 1.67×10^{-3} mol./l. in all the experiments, the largest difference in the overall rates between minimum and maximum concentrations of the catalyst is still with in the range of experimental error. Total polymers were precipitated with methyl alcohol and dried.

The total polymer obtained by the above procedures was weighed. (This gives $W+W_\alpha$ according to a definition proposed below.)

The intrinsic viscosities for the total polymer were measured in a benzene solution at 30°C by the use of an Ostwald viscometer.

Results

The experimental results are summarized in Table I, in which the intrinsic viscosity of β-polymer, $[\eta]_\beta$, freshly produced in the presence of α-polymer, was calculated from the relation between the intrinsic viscosities of α-polymer, $[\eta]_\alpha$, and that of the total polymer, $[\bar{\eta}]$, which is expressed by the equation

$$[\bar{\eta}]=W_\alpha[\eta]_\alpha+W_\beta[\eta]_\beta \qquad (1)$$

where, W_α and W_β are the weight fractions of α- and β-polymers respectively. At this

1) Part I of this series, S. Okamura and K. Katagiri, *Makromol. Chem.*, **28**, 177 (1958).

2) β-Polymerization indicates that in the presence of telomer (α-polymer).

3) G. Henrici-Olivé, S. Olivé and G. V. Schulz, *Makromol. Chem.*, **23**, 207 (1957).

4) R. A. Hayes, *J. Polymer Sci.*, **11**, 531 (1953).

5) F. R. Mayo et al., *J. Am. Chem. Soc.*, **73**, 1691 (Eq. VI) (1951).

time the weight fraction of monomer converted, W, is conveniently assumed to be equal to W_β. The values of $[\eta]_\beta$ calculated above will be discussed later on the basis of a consideration of a less abbreviated equation than Eq. 1,

A plot of $1/P_\beta$ against the ratio of the concentration of α-polymer to that of monomer [Poly]/[M] is presented in Fig. 1 with the aid of the data shown in Table I. In the present report, P_β was not corrected for the small change in the rate of polymerization, because of that changes small effect on P_β.

In the previous report the acceleration of the rate at the high concentration and at the high degree of α-polymer was explained by the gelation effect, but this is not true in the present case because of the addition of benzene to the polymerizing system.

Discussion

By comparing our present findings with the previous results, the conversion of monomer in the present experiment is found to be present to the extent given in the previous report. In both cases, W is comparable with W_α. Although in the present reports P_β is lowered by the addition of catalyst, the limiting condition of $[\eta]_\alpha \ll [\eta]_\beta$ holds. As the gelation effect is not observed at present, the very confused features revealed in Fig. 1 seem to come from the presence of a catalyst. Therefore, it seems that the catalyst plays an important role through the reaction discussed below.

An inactive compound X and a telomer radical T·, which afterward becomes a block polymer, are produced as a consequence of the polymer transfer reaction of the radical R· produced from AIBN or a polymer radical M_n· with a telomer T shown below, with the reaction containing β-polymer:

$$R\cdot \text{ (and } M_n\cdot) + T \rightarrow X + T\cdot$$

$$R\cdot \text{ (and } M_n\cdot) + \beta\text{-Polymer} \rightarrow X + \beta\text{-Polymer radical (Catalyzed } \beta\text{-polymer)}$$

The amount of block polymer increases more in the catalyzed β-polymerization than in the thermal polymerization, where the polymer transfer reaction occurs only by:

$$M_n\cdot + T \rightarrow M_n + T\cdot$$

$$M_n\cdot + \beta\text{-Polymer} \rightarrow X + \beta\text{-Polymer radical (Thermal } \beta\text{-polymer)}$$

where M_n is the dead polymer containing n monomer units. The above discussion is also supported by the finding of Henrici-Olivé and Olivé[6] that the ratio of rate constants (k_{tri}/k_{st}) of the following reactions is about 10^{-1}:

$$R\cdot + M \rightarrow k_{st}$$

$$R\cdot + \text{Polystyrene} \rightarrow k_{tri}$$

The above reactions containing catalyst radicals are considered to make W_B and $W_{\beta\beta}$ larger than in the absence of a catalyst, where W_B and $W_{\beta\beta}$ are the weight fractions of the block polymer and the branched β-polymer which is produced from the reaction of β-polymer with the growing or catalyst radicals respectively. Thus, with the same extent of conversion, W_B and $W_{\beta\beta}$ are comparatively larger than those obtained in the previous report.

Accordingly, Eq. 1 used in the calcution of P_β in Table I becomes inadequate when applied to the present case, in which a large amount of block and branched polymer are produced. One must return to the unabbreviated form[1], i. e., to Eq. 2.

If Z is defined by $2[\eta]_\alpha[\eta]_\beta/([\eta]_\alpha + [\eta]_\beta)$ and $[\eta]_{\beta\beta}$ is the intrinsic viscosity of the branched β-polymer, one obtains:

$$[\bar{\eta}] = W_\alpha[\eta]_\alpha + (W - W_{\beta\beta})[\eta]_\beta + W_B Z + W_{\beta\beta}[\eta]_{\beta\beta} \quad (2)$$

And if $[\eta]_{\beta\beta}$ is assumed to be approximately equal to $2[\eta]_\beta$, Eq. 3 can be derived:

$$[\bar{\eta}] = W_\alpha[\eta]_\alpha + W[\eta]_\beta + W_B Z + W_{\beta\beta}[\eta]_\beta \quad (3)$$

It can be seen that the $[\eta]_\beta$ value in Eq. 3 increases if $W_\beta Z + W_{\beta\beta}[\eta]_\beta$ is neglected. By the use of C_M and KC_E values obtained in the previous report, the actual $[\eta]_\beta$ value, which is, for the sake of convenience, defined as $[\eta]_\beta'$ in Table II, is calculated when it is

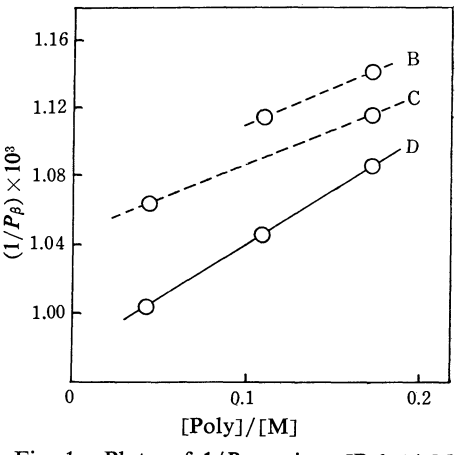


Fig. 1. Plots of $1/P_\beta$ against [Poly]/[M] indexes are to be referred to Table I.

6) G. Henrici-Olivé and S. Olivé, *Makromol. Chem.*, **27**, 166 (1958).

TABLE I. THE DEGREE OF POLYMERIZATION OF β-POLYMER CALCULATED BY EQ. 1.

	α-Polymer g.	β-Polymer g.	$[\bar{\eta}]$ 100 cc./g.	$[\eta]_\beta$ 100 cc./g.	$(1/P_\beta)\times10^5$	[Poly]*/[M]
B1	0.500	0.756	0.466	0.656	111.3	0.110
B2	0.800	0.751	0.408	0.645	114.1	0.176
C1	0.200	0.699	0.562	0.680	106.3	0.044
C2	0.800	0.765	0.399	0.657	111.5	0.176
D1	0.200	0.704	0.555	0.708	100.2	0.044
D2	0.500	0.778	0.426	0.689	104.3	0.110
D3	0.800	0.766	0·339	0.669	108.5	0.176
Without α-polymer	0	0.703	—	0.650	113.0	0

$[\eta]_\alpha$, Values of α-polymers are as follows.

	B	C	D
$[\eta]_\alpha$	0.180	0.151	0.016

* [Poly] indicates the concentration in monomer unit mol./l.

TABLE II. VALUES OF $[\eta]_\beta'$ AND $W_BZ+W_{\beta\beta}[\eta]_\beta'$

P_α		$[\eta]_\beta'$	$W_BZ+W_{\beta\beta}[\sigma]_\beta'$
B1	136	0.652	0.002
B2		0.636	0.004
C1	69	0.672	0.006
C2		0.628	0.014
D1		0.690	0.014
D2	29	0.643	0.028
D3		0.602	0.037

P_α, the degree of α-polymer is calculated by the following equation[7],

$$P_\alpha=(2-x)[M]_0/2C_s[S]_0$$

where $[M]_0$: the initial concentration of monomer
$[S]_0$: the initial concentration of solvent
C_s: the chain transfer constant of solvent
x: the conversion ratio of monomer to polymer

assumed that the intercept of each line at [Poly]/[M] $=0$ in Fig. 1 remains constant. The $W_BZ+W_{\beta\beta}[\eta]_\beta$ value may also be calculated as shown in Table II, which shows that the value increases with the increase in [Poly]/[M] and as it moves from the B to the D group; the somewhat greater degree of polymerization at a high rate of conversion in the previous paper can be explained from the same discussion even for uncatalyzed β-polymerization.

Although $W_{\beta\beta}$ and W_B are not obtainable separately by the present treatment, the kinetical attempt of using the considerable elementary reactions was suggested in the styrene-carbon tetrachloride polymerization[7].

It may be concluded that $W_{\beta\beta}$ and W_B are increased by the reactions between a catalyst radical and a telomer or a β-polymer under the same experimental conditions as those of the previous report except for the presence of a catalyst. Therefore, the apparent degrees of polymerization of β-polymer larger than they actually are.

Summary

Catalyzed styrene polymerization in the presence of azobisisobutyronitrile and telomer has been carried out to investigate the effects of the conversion of monomer and of the addition of catalyst on the degree of polymerization of polymer under the same conditions as in the previous report.

The apparent degree of polymerization of polymer was obtained as a rather larger value than expected. This situation is qualitatively explained by the reactions of a catalyst fragment radical with telomer and with polymer freshly produced.

The authors wish to thank Professor Ichiro Sakurada and Professor Kenichi Fukui for their kind advice, and Professor G. V. Schulz for his valuable discussion.

This report is a part of K. Katagiri's doctorate thesis for Kyoto University.

Faculty of Engineering
Kyoto University
Sakyo-ku, Kyoto

7) S. Okamura and K. Katagiri, *Chem. High Polymers Japan (Kobunshi Kagaku)*, **16**, 173 (1959).

Thermodynamical Studies on Binary Systems Consisting of Polar and Non-polar Liquids. VI. Refined Calculation of the Electrostatic Part of van Laar Coefficients and Comparison with the Experimental Results

By Kazuo AMAYA

(Received June 13, 1961)

In a previous paper, the electrostatic parts of the heat mixing polar and non-polar liquids were calculated on the assumptions that the polar molecule was a sphere with isotropic polarizability and that the dipole was located at the center of the sphere. The comparison of these results with those of the experiment for the group of systems containing non-aromatic non-polar liquid showed qualitative agreements. However quantitative agreements were poor, especially for systems containing polar liquid with a large dipole moment.

To ascertain the reason for these poor quantitative agreements, the electrostatic parts of the van Laar coefficients were calculated for two cases, one where the polar molecule was spherical with anisotropic polarizability and the other where it was an ellipsoid with anisotropic polarizability. The dipole was not located at the center of the ellipsoid. These results were compared with the experimental results.

The Effect of the Anisotropy of the Polar Molecule

First, the effect due only to the anisotropy of the polar molecule will be examined by assuming a spherical molecule. In the previous paper[1], the polarizability of the molecule was assumed to be isotropic, and in the subsequent calculations approximate values of the mean polarizability derived from the refractive index of liquids for the sodium D line were used. However, the reaction field of the surrounding medium is always in a direction parallel to the axis of the dipole; therefore, strictly speaking, the polarizability α in the previous paper[1] should be replaced by α_1 polarizability, parallel to the axis of the dipole, if the anisotropy of the polar molecule is to be taken into consideration.

Actual polar molecules are more or less anisotropic; this effect may be significant for the derivatives of benzene or for those molecules having many anisotropic polar groups, such as C≡N. Mean polarizability $\bar{\alpha}$ is defined as

$$\bar{\alpha}=\frac{1}{3}(\alpha_1+\alpha_2+\alpha_3) \qquad (1)$$

where α_1, α_2 and α_3 are the polarizabilities along each of three principal axes.

Table I. Polarizability of polar molecules in unit of 10^{-25} cc./mol.

Substance	α_1	α_2	α_3
Chlorobenzene	155.1	138.2	74.2
Bromobenzene	168.4	121.3	95.6
Benzonitrile	163.8	121.1	84.9
Nitrobenzene	171.6	141.9	74.1
Diethylketone	100.1	126.4	71.5

The values of α_1, α_2 and α_3 for some of the above polar molecules are taken from the literature and are reproduced in Table I, where α_1 is the polarizability along the direction of the dipole and α_2 and α_3 are those perpendicular to the direction of the dipole.

In the same table, the $n_{21}^2/\bar{n}_2^2$ ratio is shown where n_{21} is the refractive index of the polar molecule along the direction of the dipole and $\bar{n}_2$ is the mean value for three axes, expressed as:

$$\frac{n_{21}^2-1}{n_{21}^2+2}=\frac{4}{3}\pi N\alpha_1, \quad \frac{\bar{n}_2^2-1}{\bar{n}_2^2+2}=\frac{4}{3}\pi N\bar{\alpha} \qquad (2)$$

It can be seen from Table I that the polarizability parallel to the dipole for benzene derivatives is about 30% larger than the mean polarizability.

It is likely that other molecules, not shown in Table I, have a similar tendency. This suggests that the values of n_2^2 in expression (11) of the previous paper[1] must be replaced with values about 30% larger. This would change the values of integrands g and h the expressions (5) and (6) of the previous paper[1] and, accordingly, that of $\alpha_{\text{calcd.}}^{\text{el}}$.

Wilson[2] derived the following expression for the dielectric constant of pure polar liquid and of a solution based on Onsager's model, taking the anisotropy of the polar molecule

1) K. Amaya, This Bulletin, **34**, 1584 (1961).

2) J. N. Wilson, *Chem. Revs.*, **25**, 377 (1939).

into consideration. For a pure liquid he obtained:

$$\frac{\varepsilon_2-1}{\varepsilon_2}-\frac{3(n_2^2-1)}{2\varepsilon_2+n_2^2}=\frac{4\pi N}{9kT}\mu^2\frac{(2\varepsilon_2+1)(n_{21}^2+2)^2}{2\varepsilon_2+n_{21}^2} \tag{3}$$

where n_{21} is the refractive index of the polar molecule along the dipole axis and n_2 is the mean refractive index.

For a binary solution consisting of polar and non-polar molecules,

$$\frac{\varepsilon_{12}-1}{\varepsilon_{12}}=\frac{4\pi N_2}{9kT}\mu^2\frac{(n_{21}^2+2)^2(2\varepsilon_{12}+1)}{(2\varepsilon_{12}+n_{21})^2}+\frac{3v_2(n_2^2-1)}{2\varepsilon_{12}+n_2^2}+\frac{3v_2(n_1^2-1)}{2\varepsilon_{12}+n_1^2} \tag{4}$$

in which the following notations were used;

N_2: the number of the polar molecule in unit volume,

v_2: volume fraction of the polar component,

v_1: volume fraction of the non-polar component,

n_2: mean refractive index of the polar molecule,

n_1: mean refractive index of the non-polar molecule,

n_{21}: refractive index along the dipole axis of the polar molecule,

ε_{12}: dielectric constant of the solution.

Following a procedure similar to that used before, we can express ε_{12} by using values for pure components; the following expression is obtained:

$$\frac{\varepsilon_{12}-1}{\varepsilon_{12}}=v_2\cdot\frac{(2\varepsilon_2+n_{21}^2)^2}{2\varepsilon_2+1}\times\left(\frac{\varepsilon_2-1}{\varepsilon_2}-\frac{3n_2^2-1}{2\varepsilon_2+n_2^2}\right)\cdot\frac{2\varepsilon_{12}+1}{(2\varepsilon_{12}+n_{21}^2)^2}+\frac{3v_2(n_2^2-1)}{2\varepsilon_{12}+n_2^2}+\frac{3(1-v_2)(n_1^2-1)}{2\varepsilon_{12}+n_1^2} \tag{5}$$

where ε_1 and ε_2 are the dielectric constants of non-polar and polar liquids respectively.

By the use of the above expression, the volume fraction of the polar component v_2' for any value of ε_{12} can be determined from the data of the pure liquids. To see how the anisotropy of the polar molecule affects the calculated values of the volume fraction, the values of v_2' * for chlorobenzene-cyclohexane and nitrobenzene-cyclohexane systems were compared with v_2, for which the anisotropy of the polar molecule is not taken into consideration. It was found that the differences were of the order of 0.01.

By using these values of the volume fraction v_2' and by replacing the values of n_2 with those along the dipole axis, n_{21}, van Laar coefficients $\alpha_{\text{calcd}}^{\text{el}'}$ were calculated for the above two systems and are shown in Table II. The $\alpha_{\text{calcd}}^{\text{el}'}/\alpha_{\text{calcd}}^{\text{el}}$ and $\alpha_{\text{calcd}}^{\text{el}'}/\alpha_{\text{obs}}^{\text{el}}$ ratios for $v_2=1$, 0.75, 0.5, 0.25 and 0 are also shown in Table III.

It can be seen from the above results that the introduction of the anisotropy of polarizability makes the calculated values of α^{el} in these two systems larger by 10 to 50%. For other systems, similar changes may be expected. The agreement between the calculated and observed values is not very much improved by consideration of the anisotropy.

* v_2' designates the value of v_2 obtained by taking into consideration the anisotropy of the polar molecules.

TABLE II. THE CALCULATED VALUES OF THE ELECTROSTATIC PART OF VAN LAAR COEFFICIENT, $\alpha^{\text{el}'}$, TAKING THE ANISOTROPY OF POLAR MOLECULES INTO ACCOUNT

System	v_2'	$\alpha^{\text{el}'}$ (joul./cc.)
	1.00	8.50
Chlorobenzene	0.829	8.86
+	0.651	9.68
Cyclohexane	0.461	10.68
	0.251	12.22
	0	13.76
	1.00	20.91
	0.811	24.50
Nitrobenzene	0.622	31.51
+	0.431	43.97
Cyclohexane	0.236	71.10
	0.076	131.84
	0	175.31

TABLE III. RATIO OF THE VALUES OF ELECTROSTATIC PART OF VAN LAAR COEFFICIENTS CALCULATED ACCORDING TO WILSON'S FORMULA TO THAT CALCULATED ACCORDING TO ONSAGER'S FORMULA $\alpha^{\text{el}'}/\alpha^{\text{el}}$

System	Volume fraction of polar component	$\alpha^{\text{el}'}/\alpha^{\text{el}}$
	1.00	1.183
Chlorobenzene	0.75	1.195
+	0.50	1.170
Cyclohexane	0.25	1.175
	0	1.143
	1.00	1.530
Nitrobenzene	0.75	1.511
+	0.50	1.477
Cyclohexane	0.25	1.404
	0	1.242

The Effect of the Position of the Dipole on the Molecule and on Molecular Shape

The calculations were based on the assumptions that the molecule was spherical and that the dipole was located at the center of the

molecule. The deviations in the position of the dipole from the center of the molecule and the deviation in molecular shape from a sphere will be discussed here to see how they affect the results.

First, the deviation in the position of the dipole from the center of the molecule will be considered. Assuming that the radius of the sphere is a, and that the dipole point is located at a distance s from the center of the sphere, Böttcher[3] derived the following expression for the electrostatic free energy, W, of a non-polarizable dipole whose dipole moment is μ, in the dielectric medium as a function of ε, the dielectric constant of the medium, and the ratio s/a:

$$W=-\frac{\varepsilon-1}{2\varepsilon}\frac{\mu^2}{a^3}\times\left[\sum_{l=0}^{\infty}\frac{l^2(l+1)(2\varepsilon+1)}{2(\varepsilon l+\varepsilon+l)}\left(\frac{s}{a}\right)^{2l-2}\right] \quad (6)$$

When the dipole is at the center of the sphere, the value in the bracket become unity; hence, the correction factor for the deviation in the position of the dipole is obtained by evaluating the value in the bracket.

For actual molecules, however, their dipoles are polarizable and their molecular shapes are not spherical. It may be assumed that for the polarizable dipole the correction factor for the deviation in the position of the dipole from the center of the sphere does not differ from that for the non-polarizable dipole; it may also be assumed that for an ellipsoidal molecule the correction factor for the ellipsoid does not differ from that for the sphere. Instead of s/a in the above formula, we may take the ratio s_i/l_i, where s_i is the distance between the center of the ellipsoid and the projection of the center of the dipole on each principal axis i, and l_i is half the length, along the corresponding principal axis i. By using the values for van der Waals' radii and the bonding radii of atoms found in the literature, the length along each principal axes, $2a$, $2b$ and $2c$, of the molecule can be obtained. By assuming that the molecule is an ellipsoid with principal axes $2a$, $2b$ and $2c$ and that the dipole is located at the center of that bond, the results shown in Table IV are obtained.

In some molecules the centers of the dipoles are not on one of their three principal axes and the direction of the dipole does not coincide with that of one of three principal axes. In these cases, the circumstances may be changed, but this problem will not be considered here in detail.

By using the values in Table IV, the correction factors r_p were calculated at eleven or twelve points of the dielectric constants for each system. Only the extreme values ($v_2=1$ and 0) are shown in Table V.

Table IV. Values of a, b, c, s_a/a, s_b/b and s_c/c for the polar molecules ($a>b>c$)

Kind of polar molecule	$2a$ Å	$2b$ Å	$2c$ Å	s_a/a	s_b/b	s_c/c
Chlorobenzene	8.6	6.7	3.7	0.37	0	0
Bromobenzene	8.9	6.7	3.9	0.35	0	0
Benzonitrile	9.3	6.7	3.7	0.54	0	0
Nitrobenzene	8.6	6.7	3.1	0.51	0	0
n-Butyl chloride	9.0	4.5	4.1	0.44	0.02	0
n-Butyl cyanide	9.2	4.8	4.1	0.57	0.25	0
Diethyl ketone	9.1	5.4	4.1	0	0.26	0
Cyclohexanone	7.5	7.1	5.1	0.50	0.24	0
Chlorocyclohexane	8.6	7.1	5.1	0.39	0.03	0
Bromocyclohexane	8.8	7.1	5.1	0.36	0.02	0

It can be seen from these results that the effect of the deviation in the position of the dipole from the center of the molecule is considerable and that the correction factors are always greater than unity and amount to as much as about 4 for *n*-butyl cyanide.

Next, the effect of the deviation in the molecular shape from a sphere will be considered. For an ellipsoid with principal axes $2a$, $2b$ and $2c$, the reaction field factor along the direction of the principal axis a, f_a, in a medium with a dielectric constant ε is expressed as:

$$f_a=\frac{3}{abc}A_a(1-A_a)(\varepsilon-1)/\{\varepsilon+(1-\varepsilon)A_a\}$$

$$A_a=\frac{abc}{2}\int_0^{\infty}\frac{\mathrm{d}x}{(x+a^2)\sqrt{(x+a^2)(x+b^2)(x+c^2)}} \quad (7)$$

For other axes similar expressions were obtained.

For an ellipsoid $a\geqq b\geqq c$, A_a A_b and A_c are expressed as:

$$A_a=\frac{(b/a)\cdot(c/a)}{\{1-(c/a)^2\}^{3/2}}\cdot\frac{1}{k^2}\{F(k,\rho)-E(k,\rho)\} \quad (8)$$

$$A_b=\frac{(b/a)\cdot(c/a)}{\{1-(c/a)^2\}^{3/2}}\cdot\frac{1}{k'^2}\left\{\frac{E(k,\rho)-k'^2F(k,\rho)}{k^2}-\frac{(c/a)\cdot\sqrt{1-(c/a)^2}}{b/a}\right\} \quad (9)$$

$$A_c=\frac{(b/a)\cdot(c/a)}{\{1-(c/a)^2\}^{3/2}}\cdot\frac{1}{k'^2}\left\{\frac{b}{a}\cdot\tan\rho-E(k,\rho)\right\} \quad (10)$$

where

$$k_2=\{1-(b/a)^2\}/\{1-(c/a)^2\}$$

$$k'^2=1-k^2$$

$$\sin^2\rho=1-(c/a)^2$$

$$F(k,\rho)=\int_0^{\rho}\frac{d\theta}{\sqrt{1-k^2\sin^2\theta}}$$

$$E(k,\rho)=\int_0^{\rho}\sqrt{1-k^2\sin^2\theta}\;d\theta$$

For a spherical molecule A becomes 1/3, for elongated molecules, the values of A are smaller than 1/3, and for oblate molecules, they are greater than 1/3. Therefore, the reaction field factor is smaller than that for a shpere when A is smaller than 1/3, and is larger than that of a sphere when A is larger than 1/3.

When the direction of the dipole does not coincide with one of the principal axes, the values of A for the direction of the dipole moment, A_μ, may be approximated as

$$A_\mu=\sum A_i\cos^2\theta_{\mu i} \qquad (11)$$

where $\theta_{\mu i}$ is the angle between the direction of the dipole moment μ and that of the principal axis i. Using the molecular dimensions shown in Table IV, the values of A for each polar molecule have been calculated and are shown in Table VI. If an ellipsoidal model is assumed and if also an anisotropy of the polarizability of the polar molecule is taken into consideration, integrand g in expression (2) in the previous paper[1] must be replaced by g'

$$g'=f_{\mu e}/(1-f_{\mu e}\alpha_\mu) \qquad (12)$$

where $f_{\mu e}$ is the reaction field factor along the direction of the dipole of a non-polarizable ellipsoid and α_μ is the polarizability along the direction of the dipole. α_μ is expressed as

$$\alpha_\mu=\sum_i\alpha_i\cos^2\theta_{\mu i} \qquad (13)$$

where α_i is the polalizability along the principal axis i and $\theta_{\mu i}$ is the same as has been mentioned above.

α_i's are calculated from the bond polarizability and molecular structure when the experimental values are not available; thus the ratio $\alpha_\mu/\bar{\alpha}$ was obtained, where $\bar{\alpha}$ is the mean polarizability, $\bar{\alpha}=(1/3)\cdot\sum_i\alpha_i$.

The ratios of $\alpha_\mu/\bar{\alpha}$ are shown in Table VI.

The correction factor r_s due to the deviation of the shape of the molecule from sphere r_s for integrand g of the expression (2) in the previous paper[1] may be expressed as

$$r=\frac{g'}{g}=\frac{f_\mu/(1-f_{\mu e}\alpha_\mu)}{f_s/(1-f_s\cdot\bar{\alpha})} \qquad (14)$$

where $f_s=\{(2\varepsilon-2)/(2\varepsilon+1)\}\cdot 1/a^2$, and f_s relates to g as $g=f_s/(1-f_s\alpha)$.

By using the above values of $\alpha_\mu/\bar{\alpha}$ and $\bar{\alpha}=(n_D^2-1)/(n_D^2+2)$, and assuming that a^3 in f_s, the reaction field factor for a sphere, is equal to abc in f_e, the values of r_s were calculated at eleven or twelve points of dielectric constant for each system, only extreme values are shown in Table V.

The effect of deviation in molecular shape from a sphere and that of the deviation in the position of the dipole from the center of the molecule is simultaneously represented as a product of both. The products of both correction factor are also represented in Table V.

It may be assumed that the resultant correction factors for h are the same as that for g. In calculating the van Laar coefficient the integrand h for a definite value of ε is multiplied by the resultant correction factor for the corresponding values of ε, and the corrected h is integrated with the volume fraction which is obtained by solving the equation relating volume fraction and ε derived according to the ellipsoidal model. However, as the resultant correction factor obtained above for g varies very little with the concentration, the approximate values of the refined van Laar coefficient

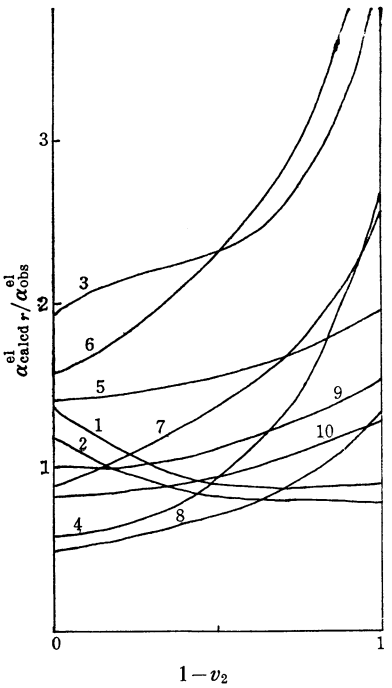


Fig. 1. Ratio of $\alpha^{el}_{calcd\,r}/\alpha^{el}_{obs}$ plotted against volume fraction.

1. Chlorobenzene-Cyclohexane
2. Bromobenzene-Cyclohexane
3. Benzonitrile-Cyclohexane
4. Nitrobenzene-Cyclohexane
5. *n*-Butyl chloride-Cyclohexane
6. *n*-Butyl cyanide-Cyclohexane
7. Cyclohexanone-Cyclohexane
8. Diethyl ketone-Cyclohexane
9. Chlorocyclohexane-Methylcyclohexane
10. Bromocyclohexane-Methylcyclohexane

TABLE V. THE CORRECTION FACTOR DUE TO MOLECULAR SHAPE AND POSITION OF THE DIPOLE OF POLAR MOLECULES FOR THE ELECTROSTATIC ENERGY OF THEIR SOLUTIONS

System	v_2	Correction factor		
		Due to molecular shape, r_s	Due to position of the dipole, r_p	Resultant r_r
Chlorobenzene	1	0.5075	1.7444	0.8852
+				
Cyclohexane	0	0.5748	1.7134	0.9848
				mean 0.9231
Bromobenzene	1	0.5769	1.6405	0.9463
+				
Cyclohexane	0	0.6388	1.6149	1.0316
				mean 0.9797
Benzonitrile	1	0.5586	3.6096	2.0164
+				
Cyclohexane	0	0.6535	3.4128	2.2304
				mean 2.0716
Nitrobenzene	1	0.4705	3.0977	1.4574
+				
Cyclohexane	0	0.5768	2.9399	1.6959
				mean 1.5100
n-Butyl chloride	1	0.7327	2.2435	1.6439
+				
Cyclohexane	0	0.7916	2.1796	1.7254
				mean 1.6712
n-Butyl cyanide	1	0.7025	4.2669	2.9975
+				
Cyclohexane	0	0.7759	4.0187	3.1182
				mean 8.0309
Cyclohexanone	1	0.9789	2.9404	2.8783
+				
Cyclohexane	0	0.9826	2.8046	2.7557
				mean 2.8446
Diethyl ketone	1	1.2048	1.3137	1.5827
+				
Cyclohexane	0	1.1168	1.2959	1.4474
				mean 1.5408
Chlorocyclohexane	1	0.7722	1.8695	1.4437
+				
Methylcyclohexane	0	0.8257	1.8254	1.5071
				mean 1.4653
Bromocyclohexane	1	0.7500	1.6971	1.2728
+				
Methylcyclohexane	0	0.8072	1.6625	1.3420
				mean 1.2967

TABLE VI. VALUES OF A_a, A_b, A_c, A_μ AND $\alpha_\mu/\bar{\alpha}$ FOR THE POLAR MOLECULES

Kind of polar molecule	A_a	A_b	A_c	A_μ	$\alpha_\mu/\bar{\alpha}$
Chlorobenzene	0.1756			0.1756	1.266
Bromobenzene	0.1953			0.1953	1.312
Benzonitrile	0.1993			0.1993	1.328
Nitrobenzene	0.1756			0.1756	1.328
n-Butyl chloride	0.1646	0.4080		0.2486	1.095
n-Butyl cyanide	0.1679	0.3852		0.2430	1.127
Diethyl ketone	0.3875			0.3875	1.007
Cyclohexane	0.2660		0.4315	0.3232	1.057
Chlorocyclohexane	0.2420		0.4506	0.2621	1.095
Bromocyclohxane	0.2343		0.4549	0.2556	1.110

TABLE VII. THE CALCULATED AND THE OBSERVED VALUES OF $d\alpha/dv_2$ AT $v_2=0$

System	$(d\alpha/dv_2)_{v_2=0}$ calcd.	Refined calcd.	Obs.
Chlorobenzene-Cyclohexane	6.688	6.174	7.53
Bromobenzene-Cyclohexane	6.505	6.373	10.02
Benzonitrile-Cyclohexane	392.5	813.1	87.44
Nitrobenzene-Cyclohexane	601.0	907.5	~90
n-Butyl chloride-Cyclohexane	25.58	42.75	13.50
n-Butyl cyanide-Cyclohexane	349.5	1059.3	54.01
Cyclohexanone-Cyclohexane	143.9	409.3	57.44
Diethyl ketone-Cyclohexane	127.2	196.0	60.62
Chlorocyclohexane-Methylcyclohexane	17.95	26.30	17.95
Bromocyclohexane-Methylcyclohexane	16.83	21.82	6.61

may be obtained by multiplying the values formerly calcurated for the spherical model by a constant, that is, the mean values of the resultant correction factors in Table V averaged over the whole concentration, if the difference between v_2 calculated by a spherical model and that calculated by an ellipsoidal model is disregarded as small. By assuming that these approximations are permissible, the refined van Laar coefficients $\alpha^{el}_{calcd\,r}$ are obtained. The ratio $\alpha^{el}_{calcd\,r}/\alpha^{el}_{obs}$ is plotted in Fig. 1.

It will be seen from the results that in general, the agreement between the refined calculation and the experimental results is similar to those of the former calculation for systems of polar liquids of a small dielectric constant, but for systems of polar liquids of a large dielectric constant the agreement is even poorer than before. Since the values of α^{el}_{obs} are correlated to the assumed values of α^{n-el} by the relation $\alpha_{obs}=\alpha^{n-el}+\alpha^{el}_{obs}$, the impropriety of the assumed values of α^{n-el} affect α^{el}_{obs}, and hence $\alpha^{el}_{calcd}/\alpha^{el}_{obs}$. However, the values of $d\alpha^{el}/dv$ are not affected by the assumed values of α^{n-el} whatever they may be, provided that α^{n-el} is independent of the concentration. The calculated values of $d\alpha^{el}/dv_2$ at $v_2=0$ obtained by the former calculation and by the refined calculation are shown in Table VII, together with the experimental values. It can be seen from the table that the agreement is not improved.

It may be concluded that the main sources of the poor agreement of the former theory with the experimental results, especially for solutions of polar liquids with a large dielectric constant, is not the assumption of a spherical molecule with its dipole at the center.

To make clear what is responsible for the poor quantitative agreement between theory and experiment in the heats of mixing a polar liquid (especially one with a large dielectric constant) and a non-polar liquid, the following points have to be considered from a theoretical as well as from an experimental point of view:

(1) To consider the orientational effect of polar molecules in pure liquids and in their concentrated solutions, due to dipole and anisotropy similar to that which is observed for toluene molecules in its solutions with polar molecules and to examine the assumption that the van Laar coefficient due to the non-electrostatic part of the energy is constant over the whole concentration.

(2) To examine the assumption that the microscopic dielectric constant near the polar molecule is the same as the microscopic one.

(3) To employ an extended dipole instead of a point dipole one in deriving the theory.

(4) To eliminate the error caused by using calculated values of the dielectric constant of solutions, by making use of the observed values of dielectric constants and of the temperature dependence of solutions

Summary

The electrostatic parts of van Laar coefficients for binary systems of polar and non-polar liquids were calculated, assuming that (1) the polar molecule is anisotropic in polarizability, (2) that the polar molecule is an ellipsoid, and (3) that the dipole is a point dipole and its position is not at the center of the molecule.

The results were compared with the experimental results.

The agreement between the experimental values and the calculated values based on the refined model cannot be said to have been improved compared with the previous results, in which the calculations were made based on the much simpler model in which the polar molecule was spherical and isotropic, and the dipole was at the center of the sphere.

The author wishes to express his thanks to professor Ryoichi Fujishiro of Osaka City University and to Professor Yonezo Morino of the University of Tokyo for their constant

encouragement and helpful discussions, and also to Professor Masashi Yasumi of the University of Tokyo for his valuable suggestions.

Government Chemical Industrial Research Institute, Tokyo
Shibuya-ku, Tokyo

*Dye-sensitized Photopolymerization of Vinyl Monomers. I. Preliminary Report on the Polymerization of Acrylonitrile by Various Dyes**

By Fukuo TAKEMURA

(Received July 27, 1961)

In the past decade it has been found that vinyl monomers can be polymerized by visible light in the presence of certain dyes[1-10]. The following types of the mechanism of dye-sensitized photopolymerization have been proposed; (1) direct energy transfer from the excited dye to monomer[3], (2) direct interaction between an excited molecule of the dye and the vinyl monomer[5,6,10], and (3) the production of free radicals by the self-decomposition of the excited dye or by the reaction of the excited dye with a third substance involved in the system[4,8].

Ueberreiter and Sorge[3], in their study of the sensitized polymerization of styrene by neutral red, attributed the chain initiation to the transference of energy from the excited dye to the monomer. However, Miyama[7] reported later that the polymerization by neutral red was really accompanied by a decomposition of the dye. Koizumi and Watanabe[6,10] investigated the photopolymerization of styrene induced by excited cyanine dyes. They established that direct interaction between the excited dye and the monomer was responsible for the initiation of polymerization. It was shown by Oster et al.[4,8] that vinyl compounds such as acrylonitrile or acrylamide could be polymerized by using the proper combination of a certain dye and an appropriate reducing agent in the presence of oxygen.

From the photochemical point of view, the first two types, in particular the first type, are interesting and important, but there are few reports on the sensitized polymerization belonging to these types. The present investigation was undertaken to select the dyes capable of sensitizing the polymerization of vinyl monomers even in the absence of a third substance and oxygen; it aimed, namely, at selecting such dyes whose excited state might directly take part in the initiation of polymerization, so as to elucidate the mechanism of polymerization sensitized by an excited dye.

Acrylonitrile was used as a vinyl monomer. One of the reasons for this selection is that aqueous solutions of dyes can be conveniently used, as acrylonitrile is able to some extent to dissolve water in itself. Another reason is that the progress of polymerization can be followed by observing the precipitation of its polymer insoluble to the system. Then acridine yellow, when chosen for a more detailed study, was found to be the most effective as a sensitizing agent.

Experimental

Materials.—Commercial acrylonitrile was purified by successive washings with dilute sulfuric acid, an aqueous solution of sodium carbonate, and water. After drying with calcium chloride, it was twice distilled at atmospheric pressure and stored in a dark room.

The dyes used in these experiments were arbitrarily chosen; most of them were made by E. Merck Co. or by G. Grübler Co. The aqueous solutions of dyes were prepared without further purification, the concentrations being about 10^{-2} mol./l.

Experimental Procedure.—In the preliminary experiments, 3 ml. of acrylonitrile and 2 drops of

* Presented at the 9th Annual Meeting of the Chemical Society of Japan, April, 1956.

1) C. H. Bamford and M. J. S. Dewar, *J. Soc. Dyers Colourists*, **65**, 674 (1949).

2) M. Koizumi, Z. Kuroda and A. Watanabe, *J. Inst. Polytech. Osaka City Univ.*, **2C**, 1 (1951).

3) K. Ueberreiter and G. Sorge, *Z. Elektrochem.*, **57**, 795 (1953).

4) G. Oster, *Photo. Eng.*, **4**, 173 (1953); *Nature*, **173**, 300 (1954).

5) M. Koizumi, A. Watanabe and Z. Kuroda, ibid., **175**, 770 (1955).

6) M. Koizumi and A. Watanabe, This Bulletin, **28**, 136 (1955); A. Watanabe and M. Koizumi, ibid., **28**, 141 (1955).

7) H. Miyama, *J. Chem. Soc. Japan, Pure Chem. Sec. (Nippon Kagaku Zassi)*, **76**, 1013, 1016, 1361 (1955); **77**, 691 (1956).

8) G. Oster and Y. Mizutani, *J. Polymer Sci.*, **22**, 173 (1956); M. Taniyama and G. Oster, This Bulletin, **30**, 856 (1957); G. K. Oster, G. Oster and G. Prati, *J. Am. Chem. Soc.*, **79**, 595 (1957).

9) J. J. Moran and H. J. Stonehill, *J. Chem. Soc.*, **1957**, 788.

10) A. Watanabe, This Bulletin, **32**, 557 (1959).

an aqueous solution of a dye were put into a glass tube (8 mm. in diameter; 15 cm. in length). The tube was attached to the vacuum system (10^{-4} mmHg), degassed three times by successive evacuations and thawings, and then sealed off. All of these procedures were carried out in a dark room. The concentrations of dyes in the reaction systems thus prepared were of the order of 10^{-4} mol./l. These tubes were placed in a thermostat (40°C) and illuminated for 24 hr. with a 500 W. tungsten lamp 1 m. distant from them. The polymers thus obtained were separated by the use of glass filters, washed with water, and dried to a constant weight. When the concentrations of dyes in the reaction system were allowed to change, more diluted aqueous solutions of dyes were used for the above-mentioned procedure instead of the original stock-solutions.

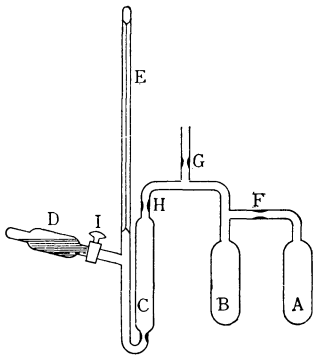


Fig. 1. Dilatometrical apparatus.

A, B : Reservoir for monomer and dye-solution respectively
C : Reaction vessel
D : Reservoir for Hg
E : Capillary tube (30 cm. long)
I : Stopcock

The kinetic experiments were studied dilatometrically, the reaction vessel being suspended in a thermostat (30 or 50°C). Figure 1 shows a schematic representation of the type of dilatometer used in these experiments. This dilatometer was designed to fill its capillary tube with mercury purposely to avoid the precipitation of polymers in it. Definite amounts of the monomer and of the dye solution in *n*-butanol were weighted in storage reservoirs A and B respectively. After a through evacuation as described above, the monomer in A was distilled into B in vacuo and mixed there with the dye solution. Then, the dilatometer was sealed off from reservoir A at F and also from the vacuum system at G. Finally, all of the reactant in reservoir B was allowed to pour into the reaction vessel C by inclining the reservoir. The dilatometer was enclosed at the top of reaction vessel H, turned upside down with caution while keeping the reactant in the reaction vessel, and filled up with mercury through the stopcock I. The meniscus of mercury in the capillary tube being adjusted, the dilatometer was immersed in a thermostat. After thermal equilibrium had been attained, the change in the meniscus was followed by a catheto-meter. The light source was a 500 W. tungsten lamp 50 cm. distant from the thermostat.

The rate of polymerization was calculated from the rate of contraction, assuming that a 23.5% contraction at 30°C and a 25.7% contraction at 50°C correspond to a 100% conversion of the monomer[11].

The viscosities of the solutions of acrylonitrile polymers in dimethylformamide were measured at 30°C in an Ostwald viscosimeter. The molecular weights were calculated by using the following equation quoted by Bamford and Jenkins[11]:

$$[\eta] = 1.75 \times 10^{-3} M^{0.66}$$

where the concentration unit was g./100 ml.

Experimental Results and Discussion

The Sensitizing Effects of Various Dyes on the Polymerization of Acrylonitrile. — Table I shows a series of comparative experiments. Of

TABLE I. SENSITIZED PHOTOPOLYMERIZATION OF ACRYLONITRILE BY VARIOUS DYES

Dye group	C. I. No.	Dye	Sensitization*
Nitroso	1	Resorcin green	+
Monoazo	20	Chrysoidine	−
	77	Palatine scarlet A	−
	142	Methyl orange	+
	143	Trapaeolin OO	−
	148	Trapaeolin O	−
	151	Orange II	−
	176	Fast red A	+
Diazo	238	Anthracene brown	+
	252	Crocein scarlet 3B	−
	370	Congo red	−
Pyrazolone	640	Tartrazine	+
Triphenyl-methane	657	Malachite green	+
	677	Fuchsine	−
	679	Hoffman's violet	++
	680	Methyl violet	++
	684	Methyl green	+
	705	Soluble blue	−
Xanthene	739	Pyronine G	+++
	766	Uranine	++
	768	Eosine	++
	772	Jodeosine	++
Acridine	785	Acridine yellow	+++
	790	Acryflavine	+++
Indamine	820	Toluylene blue	+
Azine	825	Neutral red	+
	841	Saflanine T	++
Thiazine	922	Methylene blue	+

* In this column, (−) points out no polymerization induced and (+), (++) and (+++) indicate that the polymerization have been well accelerated in that order: namely, (+) shows the conversion less than 1% in 24 hr., (++) less than 10%, and (+++) more than 10%.

11) C. H. Bamford and A. D. Jenkins, *Proc. Roy. Soc.* **A216**, 515 (1953).

course, no polymerization was induced by any dye in the dark at 40°C. From Table I, it will be seen that the overall efficiency varies over a very wide range. Of all the dyes tested, acridine dyes are the most effective, followed by xanthene dyes. It was shown by Oster[4] that acrylonitrile in an aqueous solution could be polymerized by eosin and erythrosin (jodeosin) only in the simultaneous presence of a mild reducing agent and of oxygen. However, in the present preliminary experiments, both eosin and erythrosin were shown to be able to induce to some degree the polymerization, even in the absence of a reducing agent and of oxygen.

The concentrations of dyes used in these preliminary experiments were not necessarily the same for all dyes, though they were of the order of 10^{-4} mol./l. Thereupon, the dependence of the rate of polymerization on the concentration of these effective dyes was roughly examined; the results are shown in Fig. 2. For acridine yellow and acryflavine, there appears to be an optimum concentration, probably indicating that they play the role of retarder for polymerization as well as that of sensitizer.

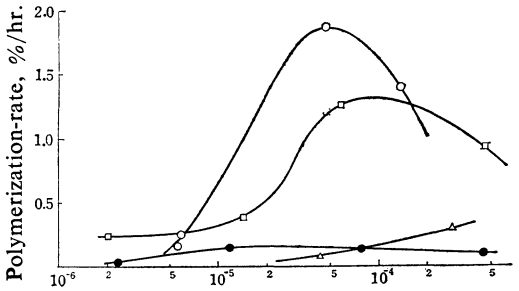


Fig. 2. Dependence of the rate of photopolymerization of acrylonitrile on dye-concentration.
○ Acridine yellow ● Iodeosin
□ Acryflavine △ Pyronine

In view of the fact that acridine yellow is the most effective, this dye was chosen for a more detailed study in these preliminary investigations.

Acridine Yellow-Sensitized Polymerization of Acrylonitrile.—The course of a typical run is shown in Fig. 3, where it will be seen that there is a gradual increase in the rate of contraction and, thus, in the rate of polymerization also, until a steady state is reached. This would appear to mean that the initial stage of polymerization is complicated by the necessity of generating some intermediate product before real sensitization can occur, or by an induction period resulting from the presence of a trace of an inhibitor such as oxygen.

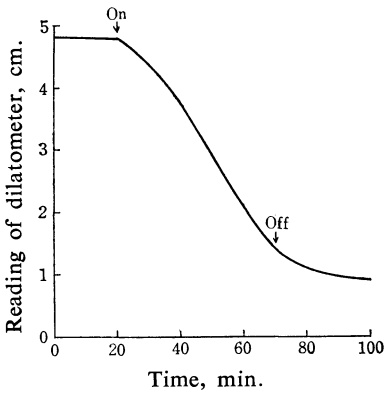


Fig. 3. Course of acridine yellow-sensitized polymerization of acrylonitrile.

When the light was switched off, the reaction did not cease immediately but exhibited a long decay period. This may be caused by the after-effect owing to the presence of trapped radicals in the precipitated polymers. Bamford and Jenkins[11] made a kinetic study of the polymerization of acrylonitrile and found that the reaction showed kinetic features which were different from those of homogeneous vinyl polymerization, e. g., (a) an initial increase in rate with time in the thermal catalyzed- and photo-polymerization, and (b) a photochemical after-effect. The observations in the present study are similar to those made by Bamford and Jenkins.

When the steady rates of polymerization are plotted against the concentration of acridine yellow (Fig. 4), the rate is shown to be proportional to the concentration in the range studied at both temperatures (30 and 50°C). This seems to be different from the usual

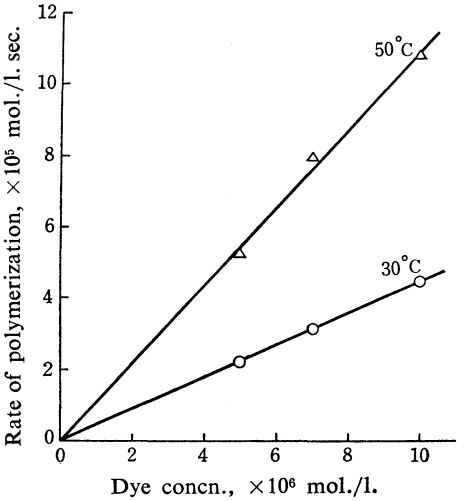


Fig. 4. Dependence of polymerization-rate on dye concentration.

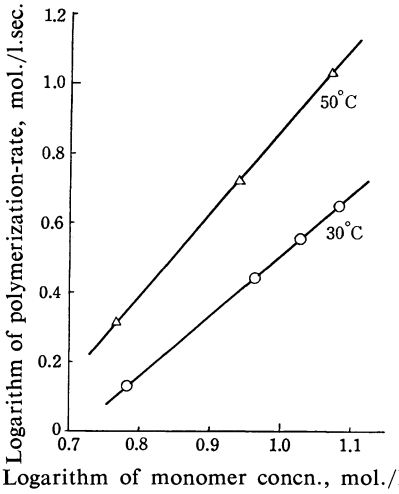


Fig. 5. Dependence of polymerization-rate on acrylonitrile concentration.

cases, in which the rate depends upon the square root of the concentration of the sensitizer, and seems to be characteristic for the polymerization of acrylonitrile in a heterogeneous system, in which Thomas and Pellon[12] have shown a 0.82 power dependence of the rate on the concentration of an initiator (azobisisobutylonitrile).

In Fig. 5 the logarithm of the rate is plotted against the logarithm of the monomer concentration, which was changed by the use of *n*-butanol as a solvent. The experimental points determine a line whose slope is about 1.7 and 2.4 at 30 and 50°C respectively. It is difficult at present to interpret these results satisfactorily, but Nakatsuka[13] has also found a discrepancy in the dependence of the rate on the monomer concentration between at 30°C and at 60°C, i. e., one power and two power dependence at the two temperatures respectively. This discrepancy may be attributed to the heterogeneous condition of the polymerization of acrylonitrile. In view of such a higher power dependence of the rate on the monomer concentration, it seems probable that the monomer plays a part in the initiation process, together with an excited molecule of the dye, and that the interaction between them give rise to the bleaching of the dye.

The dependence of the molecular weight of the polymer thus obtained on the dye and the monomer concentration were also investigated. They are shown in Tables II and III, together with kinetic data. It is worth noticing that the molecular weight of polymer is nearly independent of the dye concentration at 30°C,

12) W. H. Thomas and J. J. Pellon, *J. Polymer Sci.*, **13**, 329 (1954).
13) K. Nakatsuka, *Chem. High Polymers* (*Kobunshi Kagaku*), **14**, 613 (1957).

TABLE II. THE EFFECT OF ACRIDINE YELLOW CONCENTRATION ON THE RATE OF POLYMERIZATION OF ACRYLONITRILE AND ON THE MOLECULAR WEIGHT OF ITS POLYMER

Temp. °C	Concn. of dye $\times 10^{-6}$ mol./l.	Concn. of monomer mol./l.	Rate $\times 10^{-5}$ mol./l.sec.	$\overline{M}$ $\times 10^4$
30	10	12.1	4.46	12.6
	7	12.1	3.12	11.0
	5	12.1	2.22	11.7
50	10	11.7	10.8	9.40
	7	11.7	7.93	—
	5	11.7	5.25	—

TABLE III. THE EFFECT OF MONOMER CONCENTRATION ON THE RATE OF POLYMERIZATION OF ACRYLONITRILE AND ON THE MOLECULAR WEIGHT OF ITS POLYMER

Temp. °C	Concn. of monomer mol./l.	Concn. of solvent mol./l.	Rate $\times 10^{-5}$ mol./l.sec.	$\overline{M}$ $\times 10^4$
30	12.1	2.19	4.46	12.6
	10.6	3.28	3.62	—
	9.15	4.38	2.78	5.85
	6.05	6.56	1.35	2.87
50	11.7	2.1	10.8	9.40
	8.7	4.2	5.3	2.92
	5.8	6.4	2.1	1.60

although the rate is dependent on it. From Table III it is found that the molecular weight decreases with the decrease in the monomer concentration. This may be caused by chain transfer to the solvent and will be discussed below in detail.

The overall activation energy can be roughly estimated from the rates at two temperatures. It is about 8.6 kcal./mol., the value being conceivable for the photochemical reaction.

In short, these results are not concordant with a simple familiar theory on homogeneous free radical polymerizations with respect to the following points: (1) one power dependence of the rate on the sensitizer concentration, (2) a higher power dependence of the rate on the monomer concentration, and (3) the molecular weight of the polymer independent of the sensitizer concentration.

Development of a Kinetic Scheme. — In developing a kinetic scheme to account for these observations, it is assumed that: the polymers obtained in this system, being highly insoluble in the monomer, precipitate as soon as they are formed, so that the propagating free radical chains become occluded in polymer aggregates during polymerization, resulting in a unimolecular termination. As mentioned above, the initiation process seems likely to be an interaction between the excited dye and the

monomer, which leads also to bleaching of the dye. Therefore, the reaction scheme will be as follows:

Absorption	$D \xrightarrow{h\nu} D^*$	I
Deactivation	$D^* \rightarrow D +$ heat or light	
Initiation	$D^* + M \rightarrow R\cdot$	k_i
Propagation	$R\cdot + M \rightarrow R\cdot$	k_p
Transfer to monomer	$R\cdot + M \rightarrow P + R\cdot$	k_{trM}
Transfer to solvent	$R\cdot + S \rightarrow P + S\cdot$	k_{trS}
Reinitiation	$S\cdot + M \rightarrow R\cdot$	k'_{tr}
Termination	$R\cdot \rightarrow P$	k_t

where D, D*, M, S, R·, S· and P indicate dye, excited dye, monomer, solvent, propagating free radical, solvent radical and stable polymer involving an occluded radical respectively. Furthermore, I is the light intensity absorbed, and k_i, k_p, k_{trM}, k_{trS}, k'_{tr} and k_t are the rate constants of initiation, propagation, transfer to monomer, transfer to solvent, reinitiation of solvent radical and termination respectively.

Assuming that most of the excited molecules of the dye are deactivated with the release of energy and also that these concentrations are proportional to the light intensity absorbed or approximately to the dye concentration at the constant light intensity, the following reaction rate, R_p, may be given by the steady-state treatment:

$$R_p = \frac{-d[M]}{dt} = \frac{kk_ik_p}{k_t} I[D][M]^2 \qquad (1)$$

where k is a constant, corresponding to the quantum efficiency for the initiation. The average degree of polymerization of polymer, $\overline{P}$, may be expressed by

$$\overline{P} = \frac{k_p[M]}{k_t + k_{trS}[S]} \qquad (2)$$

if the chain transfer to the monomer is disregarded. In regard to the variation in dye concentration, the experiments support Eq. 1, although the dependence of the rate on the monomer concentration is not necessarily coincident with the experimental results. This may be due to the complications of the heterogeneous system. The experimental finding that the molecular weight of the polymer is independent of the dye concentration at the constant monomer concentration appears to satisfy Eq. 2.

As shown above, the molecular weight of the polymer varied with the concentration of the monomer. Supposing that the proposed kinetic scheme is true, the degree of polymerization must be given by Eq. 2, rewriting it, the following equation is obtained:

$$\frac{[M]}{\overline{P}} = \frac{k_t}{k_p} + \frac{k_{trS}}{k_p}[S] \qquad (3)$$

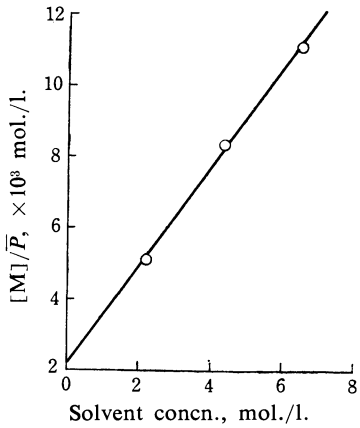


Fig. 6. Plots of $[M]/\overline{P}$ against butanol concentration according to Eq. 3.

Eq. 3 shows that $[M]/\overline{P}$ will vary in a linear relation with the solvent concentration. The data at 30°C fell reasonably close to a straight line, as shown in Fig. 6, though those at 50°C did not do so well. The slope of the line gives a value of k_{trS}/k_p of 13.7×10^{-4}, while the intercept gives a value of k_t/k_p of 22×10^{-4} mol./l.

As described above, the conclusion that the initiation process is the interaction between excited dye and monomer has been obtained only from the kinetic study of the polymerization. However, it will be desirable to confirm it from a absorption-spectrometric investigation of the dye in the reaction system. Such a kind of investigation was abandoned in the present system, due to the disturbance of the insoluble polymers, but it will be taken up in future studies, so as to elucidate the mechanisms of sensitization in detail.

Summary

Among various dyes, the dyes suitable for the sensitization of the polymerization of acrylonitrile have been determined. Acridine and xanthene dyes have been found to be the most effective.

Using acridine yellow, one of the most effective, the dye-sensitized photopolymerization has been investigated in detail; it has been shown that the reaction has several features characteristic of heterogeneous polymerization, e. g., its order is higher than one-and-a-half on monomer concentration.

Assuming the initiation process to be a direct interaction between excited dye and

monomer, and assuming the unimolecular termination by occlusion of the propagating radicals, the kinetic data has been interpreted.

The author wishes to express his hearty thanks to Professor Masao Koizumi, Tohoku University, and to Professor Kozo Hirota, Osaka University, for their encouragement and advice, and also to Mrs. I. Tanaka and Miss K. Yamashita for their assistance in part of this work.

Department of Chemistry
Faculty of Science
Nara Women's University
Nara

*Dye-sensitized Photopolymerization of Vinyl Monomers. II. Photobleaching of Acridine Yellow in Some Vinyl Monomers**

By Fukuo TAKEMURA

(Received July 27, 1961)

In the first paper of this series[1], it was reported that, among the various dyes tested, acridine yellow was the most effective in sensitizing the polymerization of acrylonitrile and that, from the kinetic study of that polymerization using this dye, the initiation of polymerization seemed to be attributable to the direct interaction of the excited molecule of the dye with the monomer. However, no knowledge of the behavior of the dye in the course of polymerization could be obtained, since it was impossible to measure the absorption spectra of the dye in the reaction system because of the precipitation of polymers thereby produced.

Now, in order to account in more detail for the mechanism of such a sensitization by acridine yellow, we have undertaken to examine the bleaching of the dye in some vinyl monomers (vinyl acetate, styrene, α-methylstyrene and methyl methacrylate) besides acrylonitrile, and to discuss the mechanism of sensitization.

Experimental

Materials.—Acrylonitrile was purified by the same method as that employed in the first paper[1]. Vinyl acetate was obtained from the Katayama Kagaku Co. and was distilled three times at atmospheric pressure. It was shown by dilatometrical measurement that, whenever vinyl acetate and a solution of the dye were put together into a reservoir and were degassed in vacuo, the monomer was appreciably polymerized even in the dark, perhaps owing to impurities such as aldehyde. This was overcome by further distillation of the monomer in vacuo. Therefore, not only vinyl acetate but also all of the other monomers were enclosed in reaction vessels by the procedure of distillation in vacuo as described below. Styrene was prepared from β-phenylethyl alcohol by dehydration, heating it with caustic potash. The crude styrene thus obtained was washed with aqueous solutions of caustic soda and sodium bisulfite, dried with calcium chloride, and distilled twice under reduced pressure. α-Methylstyrene was obtained from the Tokyo Kasei Co. and was purified in the same way as styrene. Methyl methacrylate was made by the Fujikura Kagaku Co. It was shaken with an aqueous caustic soda solution to remove the inhibitor, washed with water, dried with potassium carbonate anhydride, and then twice distilled under reduced pressure.

Acridine yellow was added to the reaction systems as a *n*-butanol solution with the exception of the case of acrylonitrile. Azobisisobutylonitrile was twice recrystallized from ethanol. Hydroquinone was used without further purification.

Apparatus.—The thermostat was doubly constructed; the inner bath was regulated within $\pm 0.002°$ at 30°C, and the outer bath, within $\pm 0.02°$ at a slightly lower temperature than 30°C. The cell holder supporting a reaction vessel in the inner bath was the same as that usually used in a spectrophotometer. The light source (a 75V,750W. tungsten projection lamp) in the outer bath was convered with a metallic housing with a window and was supplied by a. c. source controlled at 60 V. by means of a voltage regulator or by means of a slide rheostat and a resistance box. In order to prevent overheating caused by the light source, cold water was forced to flow into the metallic housing during the experiment by a gear pump controlled by a relay connected with a toluene-Hg regulator.

In all of the experiments, a Mazuda color glass filter V-B3$_B$ was inserted between the reaction vessel and the light source. It had its maximum transmission near the maximum (about

* Presented at the 11th Annual Meeting (April, 1958) and at the 12th Annual Meeting (April, 1959) of the Chemical Society of Japan.

1) F. Takemura, This Bulletin, 35, 1073 (1962).

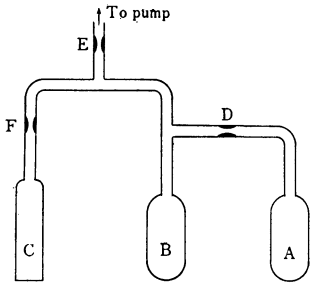


Fig. 1. The glass apparatus for sampling.
A, B; Reservoir
C; Reaction vessel

460 mμ) of the absorption band of acridine yellow. The intensity of light was, if necessary, changed with a blackened metallic net, whose shielding efficiency was 30.5%.

The reaction vessel was the same glass cell, 1 cm. in thickness, used as a absorption cell for a spectrophotometer except that it was provided with an arm, as is shown in Fig. 1.

Experimental Procedure.—In the glass apparatus shown in Fig. 1, definite amounts of monomer and dye-solution were weighted in storage reservoirs A and B respectively. After complete degassing by successive evacuation and thawing, the monomer in A was distilled into B in vacuo and mixed with the dye-solution. Then, having been sealed off from reservoir A at D and from the vacuum system at E, the reaction vessel was filled with the reaction mixture by inclining it and was sealed off at F. The quantity of the reaction mixture was sufficient to fill it up above the edge of the window of a cell holder, and if necessary, it was obtained from the initial quantities of monomer and dye-solution substracted the residual quantity in reservoir B.

Generally the reaction systems in photobleaching experiments were prepared from 1 ml. of an acridine yellow solution in *n*-butanol and 3 ml. of vinyl monomers. The initial concentrations of the dye in the reaction systems were about 2×10^{-5} mol./l. In changing the monomer concentration,the monomer was replaced with appropriate amounts of a suitable solvent, e. g., ethyl acetate instead of vinyl acetate, or benzene or ethylbenzene instead of styrene, α-methylstyrene and methyl methacrylate.

By way of exception, acrylonitrile was diluted with dimethylformamide, which was a good solvent for the polymer of acrylonitrile. Otherwise polyacrylonitrile would be precipitated in the course of the reaction. The dye was, of course, added as a solution in dimethylformamide in this case.

In a run of irradiation, the vessel was taken out of the thermostat at some minutes' intervals, and the absorption spectra were measured with a Hitachi spectrophotometer (model EPU-2).

Results and Discussion

Preliminary Tests of the Photobleaching in Various Solvents.—The bleaching of the dye was preliminarily investigated in such solvents as dimethylformamide, methanol, *n*-butanol, benzene and ethylbenzene. In these experiments one of these solvents (except dimethylformamide) was taken up instead of the monomer in the recipe of the reaction mixture described above. (As the bleaching of the dye in the solution of acrylonitrile in dimethylformamide needed to be compared with that in dimethylformamide alone, the dye was added as a solution in dimethylformamide in this case.)

In all solvents examined, the bleaching of the dye was very slight even in the light, not to mention in the dark, and may be considered negligible as compared with the photobleaching in the presence of monomers. Therefore, the appreciable photobleaching in the presence of monomers described below is undoubtedly due to the interaction of some excited molecules of the dye with the monomers.

No bleaching was observed when a solution of the dye in benzene was heated in the presence of azobisisobutylonitrile at 60°C for 80 min. From this finding, it appears that the dye is not attacked by radicals from azobisisobutylonitrile nor, presumably, by polymer radicals.

Photobleaching in the System of Acrylonitrile.—No shift of the absorption maximum of the dye in this reaction system was observed during irradiation, and the main absorption band in the visible region declined monotonously with irradiation. The relation of the optical density at the absorption maximum (465 mμ) to the irradiation time is simple, with no induction period (Fig. 2).

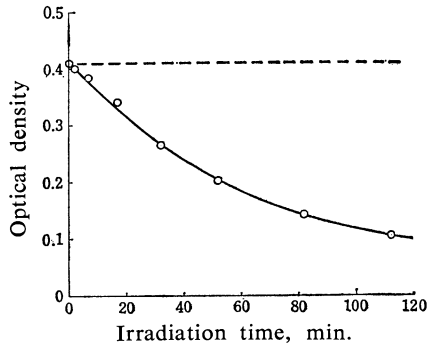


Fig. 2. The variations of optical densities at 460 mμ of the dye in acrylonitrile with irradiation time.
Dotted line; in the presence of KI or in the dark

After the irradiation, the reaction mixture was poured into a large amount of methanol, and the polymer was precipitated. Therefore, the bleaching seems to be accompanied by the polymerization of acrylonitrile.

In the presence of potassium iodide, which was added as a quencher of fluorescence, it

was shown that neither photobleaching nor polymerization occurs. This fact suggests that the singlet-excited dye molecule would otherwise lead to the photobleaching and the polymerization.

Rate Formula of the Bleaching.—According to Imamura[2], such a simple photobleaching curve can be expressed by Eq. 1 under the assumption that the rate of photobleaching depends on and is proportional to only the light absorbed:

$$-\frac{dc}{dt}=k'I_0(1-e^{-\alpha cd}) \quad (1)$$

where c is the concentration of the dye; d, the thickness of the solution, α, the average molar absorption coefficient; I_0, the total light intensity, and k', the overall rate constant.

By integration, Eq. 1 may be transformed into

$$\ln(1-e^{-\alpha c_0 d})-\ln(1-e^{-\alpha cd}) + \alpha d(c_0-c)=\alpha dk'I_0t \quad (2)$$

where c_0 is the initial concentration of the dye.

For the sake of convenience in dealing with the data, Eq. 2 was rewritten in terms of optical density as follows:

$$\log(1-10^{-D_0})-\log(1-10^{-D}) + D_0-D=\varepsilon dk'I_0t \quad (3)$$

where D and D_0 are the optical densities at time $t=t$ and $t=0$, and ε is the average molar extinction coefficient.

Since ε, d, k' and I_0 are constant in each run, the product, $\varepsilon dk'I_0$, is expressed in k and the left side of Eq. 3 is expressed in terms of S for convenience. Therefore, Eq. 3 shows that S would be proportional to t. As is shown in Fig. 3, it seems that these results are consistent with Eq. 3. From the slope of the straight line, the apparent overall rate constant k was found to be 0.0074 min^{-1} in this experimental condition.

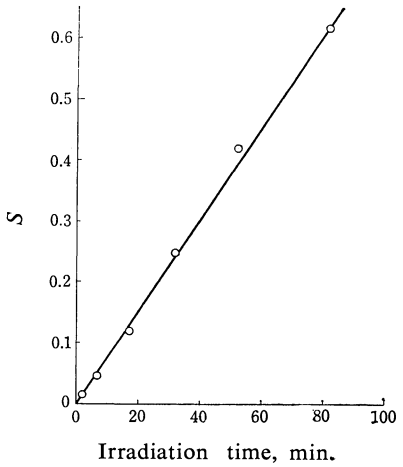


Fig. 3. S vs. irradiation time in acrylonitrile. S is the left side of Eq. 3

In view of the fact that the photobleaching of the dye did not occur in the absence of the monomer but did in its presence, the monomer must play a part in the photobleaching of the dye. However, the relation of the rate of bleaching to the monomer concentration could not be examined, since the monomer concentration was not allowed to increase owing to the precipitation of polymers. Therefore in order to understand more clearly the relationship between photobleaching and polymerization, other vinyl monomers than acrylonitrile were chosen for the following experiments.

Photobleaching in the System of Vinyl Acetate.—The absorption maximum of this system did not shift at various irradiation times, similarly as in the case of acrylonitrile. The optical densities at the maximum wavelength (456 mμ) are plotted against the irradiation time in a series of monomer concentrations in Fig. 4. It has been examined whether or not these photobleachings obey the simple rate formula, Eq. 3. As is seen from Fig. 5, linear relationships between S and t can not be always obtained. However, it may be considered that at the initial stage of irradiation the slopes of these lines correspond to the apparent overall rate constants in various monomer concentrations. Then, these rate constants seem to be roughly proportional to the monomer concentrations. Therefore, it may be concluded that the apparent overall rate constant is also a function of the monomer concentration, and that the photobleaching is not due to the self-decomposition of the dye but to the

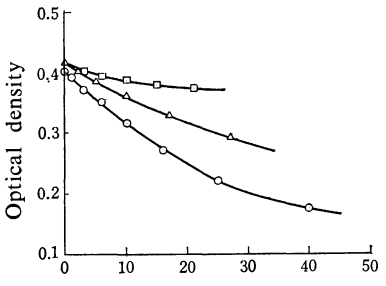


Fig. 4. Variation of optical densities at 456 mμ of the dye in various concentrations of vinyl acetate with irradiation time.
Monomer concn. (mol./l.)
○ 8.13, △ 5.42, □ 2.71

2) M. Imamura and M. Koizumi, ibid., **28**, 117 (1955); M. Imamura, *J. Inst. Polytech. Osaka City Univ.*, **6C**, 85 (1956).

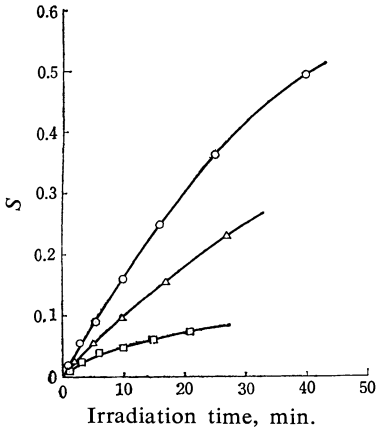


Fig. 5. Variations of S in various concentrations of vinyl acetate with irradiation time.
Monomer concn. (mol./l.)
○ 8.13, △ 5.42, □ 2.71

interaction of the excited dye molecule with the monomer.

Under aerobic conditions, neither photobleaching nor polymerization could be brought about. This might be because oxygen deactivated the excited state of the dye.

Photobleaching in the System of Styrene.— The experiment was further extended to the system involving styrene. In various concentrations of styrene, the change in optical density at the initial absorption maximum (460 mμ) was plotted against time, as is shown in Fig. 6. From the results, it can be seen that the bleaching of the dye was very rapid and that its rate was nearly independent of the styrene concentration if it was higher than about 2 mol./l. When the light intensity was reduced to 30.5% by inserting a blackened

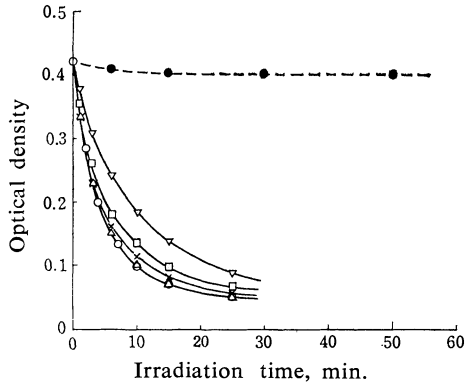


Fig. 6. Variations of optical densities at 460 mμ of the dye in various concentrations of styrene with irradiation time.
Styrene concn. (mol./l.)
○ 6.40 △ 4.24 × 2.13
□ 1.06 ▽ 0.53 ● 0

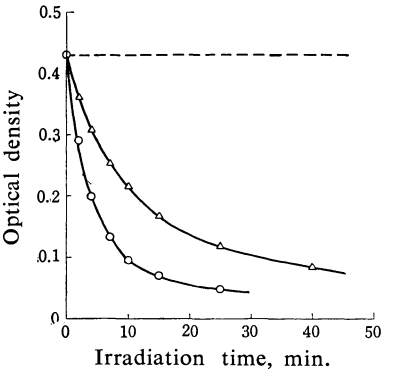


Fig. 7. Variations of optical densities at 460 mμ of the dye under various light-intensities in the system of styrene.
Monomer concn. 6.40 mol./l.
Relative light intensity ○ 1
△ 0.305 --- 0 (dark)

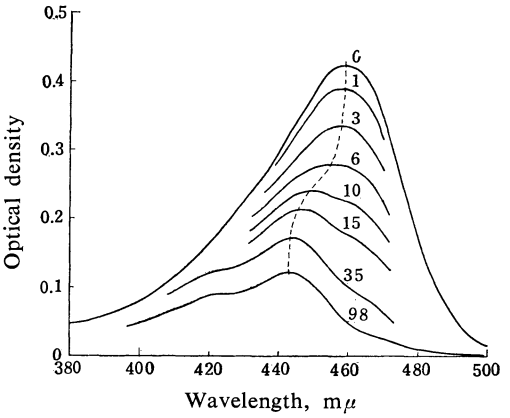


Fig. 8. The change of spectra of acridine yellow in styrene with irradiation time.
Monomer concn. 2.13 mol./l.
Relative light intensity 0.30
Numbers beside curves indicate the irradiation time in minute.

metallic net, the rate of bleaching decreased as compared with that carried out under full intensity, as is shown in Fig. 7.

When the absorption spectra in the range of 400~500 mμ were followed in the order of the irradiation time (Fig. 8), it was unexpectedly found that the optical density decreased rapidly in spite of the reduced intensity of light and that, at the same time, an absorption maximum appeared at the shorter wavelength. This new absorption did not change in the dark, but disappeared only on irradiation. This phenomenon was soon observed whenever both photobleaching and polymerization occurred in these experiments, but it was observed only after a time in the presence of air or hydroquinone, where the polymerization was hardly able to occur. Since it is well

known that hydroquinone can not inhibit polymerization without the coexistence of air and that it is a good quencher for a phosphorescent state, it is clear that the effect of hydroquinone in this case does not result from the inhibition of polymerization but from the quenching of a triplet state of the dye.

The addition of polystyrene to the reaction system in the dark did not lead to the shift in absorption maximum. This result may indicate that the shift does not result from the mere adsorption or binding of the dye on the polymer.

From these reasons, the photobleaching and the shift in the absorption maximum do not always accompany the polymerization of styrene but may be realized prior to it.

Analysis of the Absorption Spectra in the System of Styrene.—Although a gradual shift in the absorption maximum was observed during irradiation in the above system, its limiting position in every case was in the neighborhood of 443 mμ. Since the above results strongly suggest the formation of a coloring product from acridine yellow, identification of the product was attempted from an analysis of absorption spectra. The method is entirely the same as that reported by Imamura[3].

An example of absorption curves obtained for a coloring product by such an analysis is given in Fig. 9, from which it can be seen that the optical density of the product increases with irradiation time, moderately at the initial stage and more slowly at the intermediate stage, and then begins to decrease, though slowly. The absorption band of the coloring product is quite broad and has a maximum at 443 mμ which is not displaced with time.

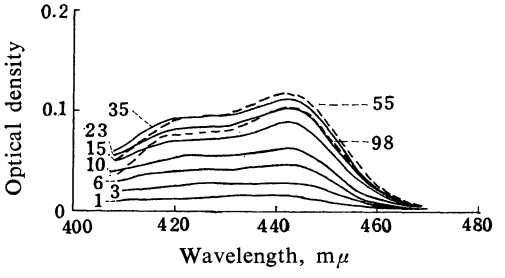


Fig. 9. The change of spectra estimates for a intermediate product in styrene from Fig. 12 with irradiation time

Estimation of the Coloring Product in the System of Styrene.—An attempt was undertaken to decide if the coloring product was a substance produced photochemically by a direct interaction of the excited dye with the styrene monomer. After the reaction system was irradiated for a suitable period, it was poured into a proper amount of methanol. The polystyrene thus precipitated was separated by filtration. The filtrate showed the same spectra, with an absorption maximum at 443 mμ, as that obtained by the above-mentioned analysis. The polystyrene thus obtained had spectra with a broad absorption maximum at ca. 450 mμ in the benzene solution, in spite of the repeated treatment of successive precipitation and dissolution, as is shown in Fig. 10.

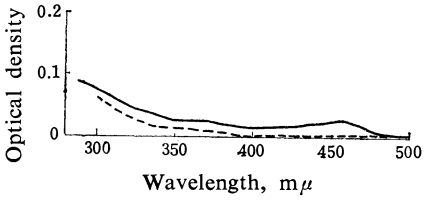


Fig. 10. The absorption spectra of the benzene solutions of the polystyrene obtained photochemically and thermally in the presence of the dye.
Full line; Photochemically
Dotted line; Thermally

On the other hand, when the same reaction system was polymerized thermally in the dark, the filtrate obtained by the same procedure as before showed essentially the same absorption spectra as those of the original reaction system. The polystyrene obtained in this case did not show an absorption maximum near 450 mμ (Fig. 10).

Therfore, it may be concluded that the coloring product was photochemically produced only by a direct interaction of the excited dye with the styrene monomer, and that it was bound to the polymer in the course of the polymerization.

Rate of Photobleaching in the System of Styrene.—It is therefore clear that the optical density at the initial absorption maximum (460 mμ) does not obey Eq. 3, but that on the other hand, at the initial stage of irradiation the decrease in the optical density at 460 mμ may be taken to represent the bleaching of the initial dye. The values of k_{Init} thus obtained correspond to the apparent overall rate constants of the bleaching. By plotting them against the monomer concentration, as in Fig. 11, it is found that k_{Init} increases rapidly with the monomer concentration but is nearly independent of it in the region higher than about 2 mol./l., even though the conditions of irradiation is different. In addition, it is shown that k_{Init} is approximately proportional to the light intensity. These results suggest that the bleaching of the dye is so rapid that the rate of bleaching is

3) M. Imamura and M. Koizumi, This Bulletin, **29**, 913 (1956).

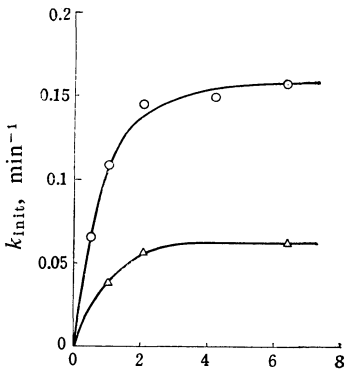


Fig. 11. Dependence of k_{init} on the concentration of styrene.
Relative light intensity
○ 1, △ 0.305

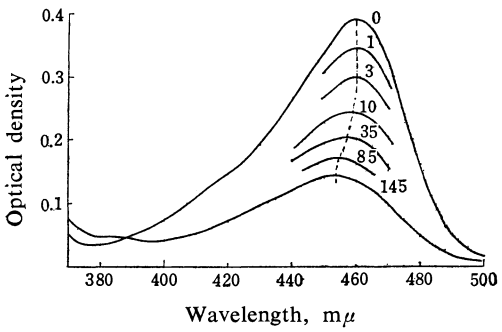


Fig. 12. The change of spectra of acridine yellow in α-MS with irradiation time.

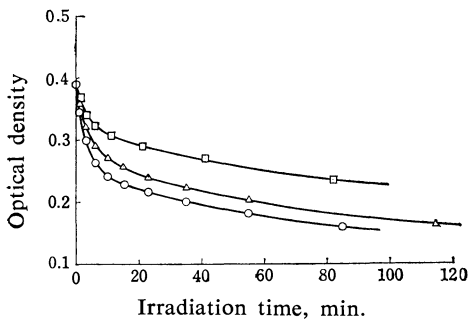


Fig. 13. Variation of optical densities at 460 mμ of the dye in various concentration of α-MS with irradiation time.
Concn. of α-MS (mol./l.)
○ 5.56, △ 3.82, □ 1.96

mainly determined in the case of concentrated monomer concentrations by the intensity absorbed, while it depends both upon the light intensity and upon the monomer concentration in the case of more dilute solutions. Therefore, it may be concluded that the decrease in optical density at the initial absorption maximum (460 mμ) of the dye is attributed to the interaction of the dye molecule, excited to the triplet state, with the monomer to produce a new coloring product which will be destroyed by further irradiation.

Photobleaching in the System of α-Methylstyrene. — The photobleaching in α-methylstyrene (α-MS) was found to closely resemble that in styrene. The absorption curves of a reaction system, as is shown in Fig. 12, shifted towards a shorter wavelength with irradiation time. For the sake of convenience, the optical densities at 460 mμ at various monomer concentrations are plotted against irradiation time in Fig. 13. It can be seen that the rate of bleaching is smaller than that in styrene. On the same assumption as in the case of styrene, the apparent overall rate constants k_{init} were calculated from Eq. 3. The dependence of k_{init} on the monomer concentration appears to be proportional to the square root of the concentration in this region, as is shown in Fig. 14. The efficiencies in polymerizing this monomer were very low. This may be attributable to the low polymerizability of α-MS. It is interesting the features of the photobleaching of acridine yellow are alike in styrene and α-MS. This may be due to the production of coloring products similar in their structure.

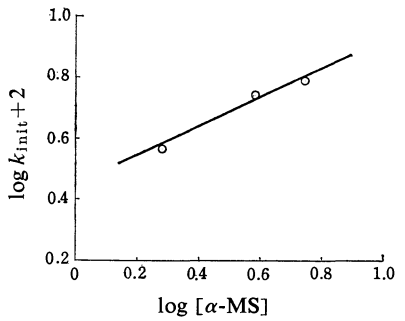


Fig. 14. Logarithm of k_{init} vs. logarithm of the concentration of α-MS.

Photobleaching in the System of Methyl Methacrylate.—In view of the fact that the apparent behaviors of the bleaching of acridine yellow may be differentiated in two groups (acrylonitrile and vinyl acetate; styrene and α-MS), it is attractive to extend the experiments to the system involving methyl methacrylate (MMA), which is one of the most well-known vinyl monomers. Contrary to the author's expectation, it was found that the bleaching ceased after an initial slight photobleaching, the rate of which depended upon the monomer concentration and the extent of which was nearly always in the same ratio to the initial dye concentration even though the concentra-

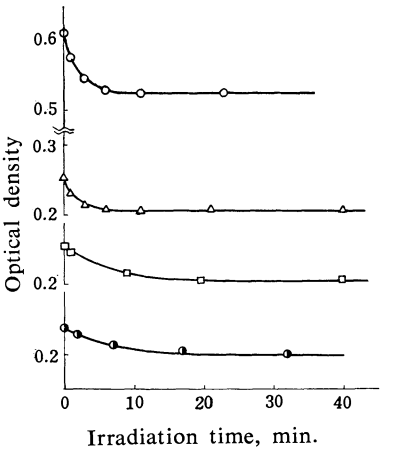


Fig. 15. Variations of optical densities at 457 mμ of the dye in various concentration of methyl methacrylate with irradiation time.
Concn. of MMA (mol./l.) ○, △ 7.01
□ 4.68 ◑ 2.34

tions of the dye and the monomer differed (Fig. 15.), while the monomer continued to polymerize as long as the system was irradiated[4]. In this case, no shift in the absorption maximum of the dye was observed. In the presence of air or hydroquinone, the photobleaching was very slight, without polymerization even in the light; moreover, the optical density of the reaction system could be restored to its initial value after a long period in the dark. This may be evidence for the transient production of a comparatively stable intermediate. Furthermore, the bleaching could not occur in the dark at 30 and 60°C, irrespective of the presence of azobisisobutylonitrile. This leads to the conclusion that acridine yellow can not be attacked by radicals produced thermally from the radical source and, so, perhaps not by polymer radicals.

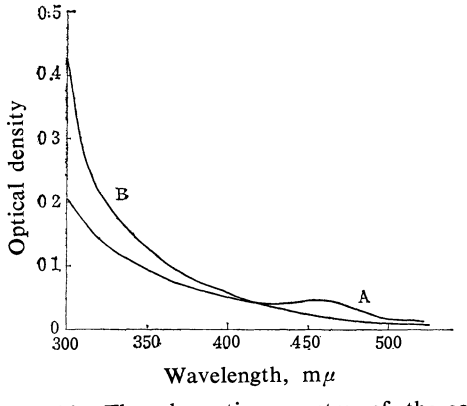


Fig. 16. The absorption spectra of the solution of poly-MMA obtained photochemically (A) and thermally (B) in the presence of the dye.

The absorption spectra of the solution of polymers, which were obtained photochemically in the light and thermally in the dark, are shown in Fig. 16. In spite of the treatment of these polymers by a procedure similar to that described before, the polymers obtained photochemically showed a broad absorption maximum near 460 mμ, while those obtained thermally did not. It is sure that the broad absorption near 460 mμ may be attributed to the dye bound to the polymer and not to the dye merely adsorbed on it, and that the bonding of the dye to the polymer is caused by the action of light in the course of the sensitization of the polymerization.

General Discussion

Acridine dyes are characterized by their resistance to reduction in the dark. Millich and Oster[5] reported that those acridines which had amino groups in both the 3- and 6-positions underwent photoreduction rapidly in the presence of a suitable reducing agent such as allylthiourea. It has now been found that acridine yellow, which was also included in their research, underwent photobleaching in the presence of various vinyl monomers in vacuo without any reducing agent and at the same time, sensitized their polymerizations.

It has been shown that the photobleaching of acridine yellow was apparently different in feature depending on the type of monomer: a) the absorption curves of the dye declined monotonously without any shift in absorption maximum in such monomers as acrylonitrile and vinyl acetate; b) the photobleaching was brought about rapidly with a shift towards shorter wavelengths in both styrene and α-MS, and c) the decreases in its optical density at the absorption maximum with irradiation ceased after a decrease of about 20% from the initial values in the reaction system containing MMA, and even thereafter the polymerization continued as long as irradiation was carried out.

In view of the fact that the intermediate coloring products, which are produced by an interaction of the excited dye with the monomer, seem to be bound to the polymers only in the cases of the photopolymerization of styrene and MMA but not in the dark thermal polymerization, it seems likely that the intermediate products are produced only under the influence of light and play a role in initiating

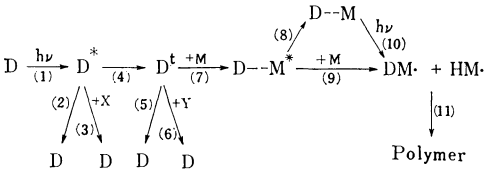
4) The Kinetic experiments involving this sensitize polymerization will be reported on in a forthcoming paper.

5) F. Millich and G. Oster, *J. Am. Chem. Soc.*, **81**, 1357 (1959).

polymerization either for themselves or in the course of their production. The apparent features of the photobleaching of the dye in various monomers may be attributed to such properties of the intermediates as optical properties and their photochemical stabilities. Thus, although the photobleaching in vinyl acetate seemed to be simple, it obeyed Eq. 3 only incompletely. After a long period of irradiation, the absorption curves of the system involving vinyl acetate seem to shift slightly towards shorter wavelengths. In this case, an intermediate coloring product would be gradually produced by irradiation and be rather rapidly lost by further irradiation. Therefore, the polymers thereby obtained did not have an absorption band in visible regions. On the contrary, the poly-MMA obtained photochemically in the presence of the dye had a relatively clear absorption band near the same wavelength as the absorption maximum of the original dye. This shows the intermediate products to have absorption spectra similar to those of the dye itself and probably to be rather stable.

Considering the effects of such quenchers as potassium iodide and hydroquinone, it may be concluded that the first singlet and triplet-excited states of the dye are involed in the course of interaction between the dye and monomers. In the acridine yellow-sensitized polymerization of an aqueous solution of methacrylic acid[6], it has been found that potassium thiocyanate, which is well-known as a quencher for fluorescence, can retard the photosensitized polymerization and that the efficiency of the retardation is of the same magnitude as that of the quenching of fluorescense,

Accordingly, the over-all reaction scheme of the photobleaching of acridine yellow in various monomers and the sensitization of polymerization may be expressed by the following:



(1) absorption of light with excitation to the first excited singlet state; (2) reversion to the ground state by a radiationless transition or by emission of fluorescence; (3) fluorescence quenching by potassium iodide or probably by oxygen; (4) transition to the triplet state; (5) transition from the triplet state to the ground state; (6) quenching of the triplet state by hydroquinone or probably by oxyen; (7) production of an activated intermediate product by the interaction of the triplet state with the monomer; (8) transformation to a stable coloring product; (9) initiation of polymerization; (10) re-absorption of light by the stable coloring product, which may lead to polymerization and to photobleaching of the coloring product; and (11) growth of polymer chains, which may be retarded or inhibited by oxygen. For styrene process (7) seems to be very rapid and process (1), a rate-determining step in the concentration range of more than 2 mol./l. For vinyl acetate, process (7) is the rate-determining step. For MMA the coloring product is so stable that it may induce the polymerization, probably by the energy transfer mechanism, without further bleaching.

Watanabe[7] has discussed, in the sensitized polymerization of styrene, the state activated by the use of cyanine dyes and has estimated that an electon transfer from X^- to D^+ was involved in the process of activation, where D^+ and X^- were a dye cation and a halogen anion respectively. In the present cases, it is difficult to decide whether or not such a electron transfer is involved, but it may be reasonable to assume that the intermediate product, which is produced by the direct interaction of the triplet state of the dye with the monomers, is responsible for the photobleaching and leads to the polymerization.

Summary

The photobleaching of acridine yellow has been studied in various vinyl monomers, such as acrylonitrile, vinyl acetate, styrene, α-methylstyrene and methyl methacrylate.

It has been found that (a) the photobleaching is apparently different in featue depending on the type of monomer; (b) the absorption maximum of the dye in the reaction systems shifted rapidly to a shorter wavelength in the cases of both styrene and α-methylstyrene by the irradiation of light, while it did not in the cases of acrylonitrile, vinyl acetate and methyl methacrylate; (c) a new absorption maximum at a shorter wavelength may result from the production of a relatively stable intermediate from the dye and styrene.

Considering also the effects of such quenchers as potassium iodide and hydroqinone on the photobleaching and the polymerization, it has been concluded that the interaction of the triplet state of the dye molecule with the monomers is responsible for both the bleaching and the polymerization.

6) This will be reported on in a forthcoming paper.

7) A. Watanabe, This Bulletin, 32, 557 (1959).

The anthor wishes to express his hearty thanks to Professor Masao Koizumi, Tohoku University, and Professor Kozo Hirota, Osaka University, for their encouragement and advice, and also to Miss T. Manabe, Mrs. A. Iwasa and Miss S. Hamanaka for their assistance in part of this work. A part of the expense for this research has been defrayed by a grant from the Ministry of Education, to which the author's thanks are also due.

Department of Chemistry
Faculty of Science
Nara Women's University
Nara

Stability of Condensed Phosphate Complexes. I. Alkaline-earth Metal Complexes

By Akira ROPPONGI and Takio KATO

(Received August 23, 1961)

It has been reported that a mixture of soap and a condensed phosphate such as hexametaphosphate is more effective than soap alone for removing radioactive contaminations on surfaces of concrete, glass, various metals and films[1]. It has been further found that EDTA and condensed phosphate are more useful as complexing agents than surface active agents for cleaning cotton goods contaminated with radioactive nuclides[2].

Condensed phosphate has been used as a boiler cleaner. In this case, the addition is very minute compared with the amount necessary to keep metallic ions as soluble complexes in hard water. Thus, the condensed phosphate is thought to have two different functions: complex formation and surface activity.

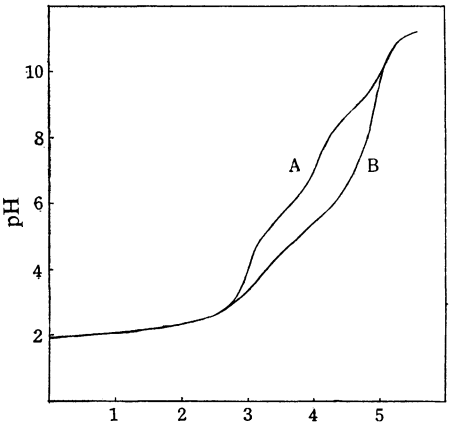
Many investigators have measured the ability of condensed phosphates to make complex formations by using various methods, but the metal elements used were limited to alkali and alkaline-earth metals. Furthermore, the stability constants measured by different methods do not agree with each other[3].

In order to obtain fundamental information about the washing ability of condensed phosphates, as well as about their usefulness as decontaminating agents, the stability constants of the complexes formed between condensed phosphates and metals were measured in this experiment.

Theoretical

The stabilty constants were measured either by acid-base titration using a glass electrode or by the replacement reaction. Schwarzenbach et al.[4] and Watters et al.[5-6] have evaluated the stability constants of magnesium and calcium complexes with triphosphoric acid by method A.

Method A. — If triphosphoric acid in the presence of a relatively large excess of metal ions can be titrated without precipitation, the decrease in pH should be attributed to the complex formation, as is expressed by the reaction:



a: alkali mol./triphosphoric acid mol.

Fig. 1. The effects of metal ion on titration curve of triphosphoric acid with alkali solution.
Curve A: 10^{-3} M triphosphoric acid titrated with 0.1 M KOH solution, Curve B: 10^{-3} M triphosphoric acid containing 10^{-3} M alkaline-earth metal ion titrated with 0.1 M KOH solution.

1) F. D. Snell et al., *Soap sanit. Chemicals*, **1**, Oct. (1953).
2) Y. Tajima and Y. Wadachi, *J. Chem. Soc. Japan, Pure Chem. Sec.* (*Nippon Kagaku Zasshi*), **81**, 891 (1960).
3) J. R. Van Wazer et al., *Chem Revs.*, **58**, 1011 (1958).
4) G. Schwarzenbach et al., *Helv. Chim. Acta*, **38**, 653 (1955).
5) J. I. Watters et al., *J. Am. Chem. Soc.*, **79**, 5606 (1957).
6) J. I. Watters et al., ibid., **81**, 3201 (1959).

$$mM^{+p}+l(H_{n+1}P_3O_{10})^{-(5-n-1)} \rightleftarrows M_m(H_nP_3O_{10})_l^{-((5-n)l-pm)} + lH^+ \quad (1)$$

As the metal ions are present in a large excess and as no pH change is observed in the region $a<3$ in Fig. 1, it is probable that only a 1 to 1 complex exists in the corresponding region, $a>3$. In such a case, the stability constants of the normal complex, K_{ML}, and the acidic complex, K_{MHL}, can be evaluated by Eqs. 2 and 3:

$$K_4'=K_4+K_{MHL}K_4[M] \quad (2)$$

$$K_5'=\frac{K_5+K_{ML}K_6[M]}{1+K_{MHL}[M]} \quad (3)$$

where [M] is the free metal ion concentration, K_n is the dissociation constant of triphosphoric acid, and K_n' is the apparent dissociation constant defined by Eq. 4 or 5.

$$K_4'=\frac{(H)\{[MHP_3O_{10}]+[HP_3O_{10}]\}}{[H_2P_3O_{10}]} \quad (4)$$

$$K_5'=\frac{H\{[MP_3O_{10}]+[P_3O_{10}]\}}{\{[MHP_3O_{10}]+[HP_3O_{10}]\}} \quad (5)$$

As the metal ion is present in a large excess, the free metal ion concentration can be considered to be equal to the total metal concentration. The apparent dissociation constants can be evaluated by Eq. 6 in a way similar to that used for acid-base titration. When the acid is not too dilute, pK_{5-n}' has the same value as the pH at the point where a is $5-(n+0.5)$.

$$K_{5-n}'=\frac{(H)\left[(5-n-a)\cdot C_L-\frac{K_W}{(H)\cdot f}+\frac{(H)}{f}\right]}{\left[(a-4+n)\cdot C_L+\frac{K_W}{(H)\cdot f}-\frac{(H)}{f}\right]} \quad (6)$$

Method B.—In Schwarzenbach's method, the constants are evaluated only in a system in which no precipitate is formed and in which metal ions can exist in a large excess compared with triphosphate ions. In the system of triphosphate and alkaline-earth metal, a precipitate is formed unless the system is kept under such conditions that triphosphate ions are present in an excess over the metal ions. Thus, the number of ligands bound with metal ions will increase to $1, 2, \cdots\cdots, n$, and the complexes of $M(HP_3O_{10})_n$ and $M(P_3O_{10})_m$ may coexist. In the investigation of polyamino complexes, Schwarzenbach[7] proposed general formulae to evaluate stability constants for the case where the ligand is the only one in the presence of an excess of amines.

The present authors tried to evaluate the stability constants of triphosphate complexes formed in a system in which triphosphate is present in an excess as compared with metal ions.

In the $a>3$ region, the total triphosphate concentration is expressed as

$$C_L=[H_2L]+[HL]+[L]+\sum n[M(HL)_n]+\sum m[ML\,m] \quad (7)$$

where L represents the P_3O_{10} ion. The concentration of replaceable hydrogen is given by

$$C_H=2[H_2L]+[HL]+[H]+\sum n[M(HL)_n] \quad (8)$$

Subtracting Eq. 7 from 8 gives

$$C_H-C_L=[H_2L]+[H]-[L]-\sum m[ML\,m] \quad (9)$$

If C_L is greater than C_M and $[H_2L]-[L]$ is much greater than $\sum m[ML\,m]$, we obtain the following approximate expression:

$$C_H-C_L=[H_2L]+[H]-[L] \quad (10)$$

The mean ligand number per metal ion, $\bar{n}$, is expressed by Eq. 11, obtained by combining Eq. 10 with α defined by Eq. 12:

$$\bar{n}=\frac{[MHL]+2[M(HL)_2]+\cdots\cdots+[ML]+2[ML_2]+\cdots}{[M]+[MHL]+[M(HL)_2]+\cdots\cdots+[ML]+[ML_2]+\cdots}=\frac{C_L-\frac{C_H-C_L-[H]}{\alpha}}{C_M} \quad (11)$$

$$\alpha=\frac{[H_2L]-[L]}{[H_2L]+[HL]+[L]} \quad (12)$$

$\bar{n}$ is also expressed in the following way by using successive stability constants:

$$\bar{n}=\frac{k_1\cdot[HL]+2\cdot k_1\cdot k_2\cdot[HL]^2+\cdots+k_1'\cdot[L]+2\cdot k_1'\cdot k_2'\cdot[L]^2+\cdots}{1+k_1\cdot[HL]+k_1\cdot k_2\cdot[HL]^2+\cdots+k_1'\cdot[L]+k_1'\cdot k_2'\cdot[L]+\cdots} \quad (13)$$

where k_n' and k_n are the n-th successive stability constants of the normal and the acidic complexes respectively. The spreading factors of k_n and k_n' being different, Bjerrum's successive approximation method can not be applied. Thus the authors employed the following method. In the $\bar{n}<1$ region, $\bar{n}$ is expressed by

$$\bar{n}=\frac{k_1\cdot[HL]+k_1'\cdot[L]}{1+k_1\cdot[HL]+k_1'\cdot[L]} \quad (14)$$

As both [HL] and [L] are known, k_1 and k_1' are calculated at the same time. In the $1<\bar{n}<2$ region, $\bar{n}$ is expressed by

$$\bar{n}=\frac{k_1\cdot[HL]+2\cdot k_1\cdot k_2\cdot[HL]^2+k_1'\cdot[L]+2\cdot k_1'\cdot k_2'\cdot[L]}{1+k_1\cdot[HL]+k_1\cdot k_2\cdot[HL]^2+k_1'\cdot[L]+k_1'\cdot k_2'\cdot[L]} \quad (15)$$

7) G. Schwarzenbach et al., *Helv. Chim. Acta*, 33, 985 (1950).

Using the values of k_1 and k_1' calculated from Eq. 14, k_2 and k_2' can also be evaluated. Repeating the above calculation allows the determination of k_n and k_n'.

Method C.—In method B, the existence of ML is neglected in the calculation of $\bar{n}$. Therefore, the error become naturally greater with the increasing ML concentration. In the present calculation, $\bar{n}$ was found in the following manner.

In the $a>3$ region, if the complexes are formed according to reaction 16, the difference in the amounts of alkali required for the titrations of the triphosphate solution and of the solution containing metal ions and triphosphate ions is equal to the amount of triphosphate combined with the metal.

$$\begin{aligned} &M+nH_2L \rightleftarrows M(HL)n+nH \\ &M+mHL \rightleftarrows MLm+mH \end{aligned} \qquad (16)$$

$\bar{n}$ is then expressed as

$$\bar{n}=\frac{C_L\cdot \Delta a}{C_M} \qquad (17)$$

where Δa is the difference in the amounts ot alkali explained above. Furthermore, k_n and k_n' are calculated in a way similar to method B.

The dissociation of the acidic complexes may be considered as

$$M(HL)_n \rightleftarrows M(HL)_pL_q+qH \qquad (18)$$

where p, $q>0$ and $p+q=n$.

In such a case, $\bar{n}$ will become greater than the true value, and mixed complexes are formed. If the formation of such mixed complexes is considered, it is not so easy to evaluate the stability constants of the acidic, normal and mixed complexes.

Method D.—*Replacement Reaction Method.*—The equilibrium constant between two kinds of ligands and a metal is given by Eq. 19:

$$K=\frac{[ML_2]\cdot[L_1]}{[L_2]\cdot[ML_1]} \qquad (19)$$

The constant is further expressed as the ratio of the stability constant of each complex.

$$K=\frac{K_2}{K_1} \qquad (20)$$

In the case where one ligand is a dye such as a metal indicator and the other is condensed phosphate, the concentration of ligands and complexes can be measured spectrophotometrically; therefore, K can be calculated. From K and the stability constant of the dye complex, the stability constant of the condensed phosphate complex is evaluated.

Experimental

Recrystallization of commercial anhydrous sodium triphosphate, Nippori, with ethanol was carried out three times according to the procedure described by Quimby[8]. The purified triphosphate, when tested by the X-ray diffraction method, showed only patterns of sodium triphosphate hexahydrate.

Trimetaphosphate was prepared from monosodium di-hydrogen orthophosphate by heating it for 5 hr. at 530°C[9] and recrystallizing it three times with ethanol. The dehydrated salt showed the X-ray patterns of anhydrous trimetaphosphate.

Tetrametaphosphate was prepared as follows[10]. Diphosphorous pentoxide, 100 g., was dissolved in 600 ml. of water at 15°C, and the solution was neutralized with sodium hydroxide. After ethanol was added to 50 v/o, the precipitated salt was filtered and redissolved in water. Repeating these procedures three times yielded crystalline tetrametaphosphate tetrahydrate, whose X-ray diffraction patterns showed no evidence of the existence of any other substances except tetrametaphosphate tetrahydrate.

EBT and Phthalein Complexon, obtained from the Dozin Yakukagaku Research Institute, were used as metal indicators for the replacement reaction.

A solution of triphosphoric acid was prepared by passing a solution of sodium triphosphate through an ion exchange column filled with an Amberlite IR-120 H-form. To avoid the effect of the complex formation of alkali metal with triphosphate, Watters used tetramethyl ammonium hydroxide and chloride. The stability constants obtained by Schwarzenbach in the titration of the triphosphate complex with potassium hydroxide in the presence of potassium chloride were not greatly different from Watters' values. Therefore, 20 ml. of the eluate from the column was mixed with 10 ml. of the metal standard solution and 3.3 ml. of 1 M potassium chloride solution, and the solution was finally titrated with a standard potassium hydroxide solution. The pH measurements were made by using a Hitachi EHP-1 pH meter with a glass electrode. The concentration of triphosphoric acid was determined by tiration prior to the experiment. Solutions of magnesium and calcium were prepared by dissolving magnesium bicarbonate and calcium carbonate in hydrochloric acid and by removing the free acid respectively. Solutions of strontium and barium were further prepared by dissolving their chloride salts in distilled water.

Replacement reactions were performed as follows. The dissociation constant of EBT was evaluated from the change in the absorbance of the EBT solution with a pH value at the maximum absorption in the visible range of the spectrum; the molar extinction coefficient was also evaluated from the change in concentration. The stability constants of phosphate complexes were found from the equilibrium constants and the stability constants

8) O. T. Quimby, *J. Phys. Chem.*, **58**, 603 (1954).
9) L. F. Audrieth, "Inorganic Syntheses", Vol. 3, (1950), p. 104.
10) R. N. Bell et al., *Ind. Eng. Chem.*, **44**, 568 (1952).

of the dye complexes. On calcium, strontium and barium, the measurements of the constants were performed in replacement reactions of phosphate with Phthalein Complexon in a way similar to that used for the EBT-magnesium system, since the stability of EBT complexes with the metals is too low and the complexes are not formed in a concentration suitable for the replacement reaction. The measurements were performed at an ionic strength of 0.1 with a buffer solution consisting of ammonium hydroxide and chloride.

Results

Though the results obtained by Watters show that the M_2L-type complex is present in the system of triphosphate and magnesium, the following experimental results make it seem probable that the main species of soluble complexes is a 1 to 1 complex. That is, the relations of the pH value and the volume of the 0.01 M sodium triphosphate solution which was added to 10 ml. of 0.01 M alkaline-earth metal solution are as shown in Fig. 2. As

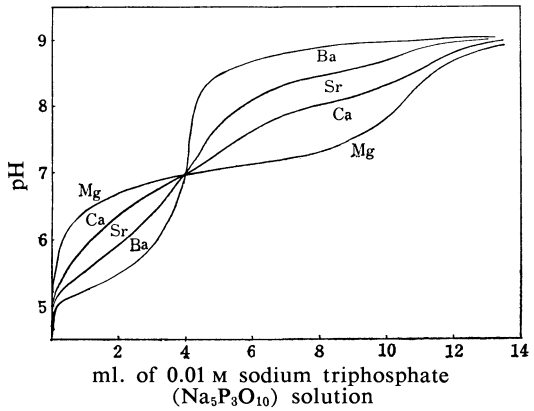


Fig. 2. The titration curves of 10 ml. of 0.01 M alkaline-earth metal solutions with 0.01 M sodium triphosphate solution.

can be seen in Fig. 2, the precipitated salt is normal salt ($P_3O_{10}/M=2/5$), and it redissolves in the form of a 1 to 1 complex in a higher region of the ratio of L/M than 2/5.

The stability constants calculated by method A, as given in Table I, are found at various

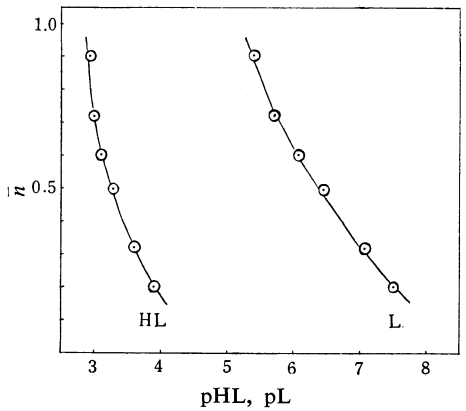


Fig. 3. Correlation of $\bar{n}$ with pHL and pL for Mg.

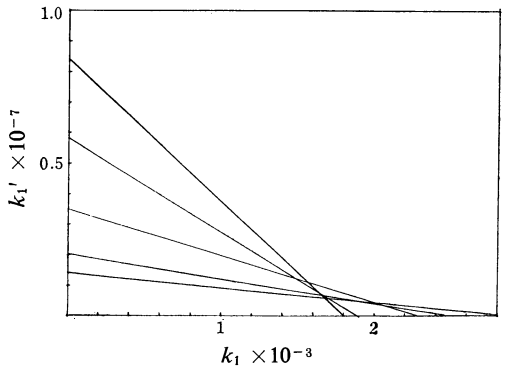


Fig. 4. Graphical solution of k_1 and k_1' for Mg.

Table I. Stability constants calculated by method A

	$C_L \times 10^3$ M	$C_M \times 10^3$ M	log K_{MHL}	$C_L \times 10^3$ M	$C_M \times 10^3$ M	log K_{ML}
Mg	4.53	2.78	3.23	4.34	2.66	4.83
		5.55	3.37		5.32	5.36
		11.1	3.33		10.6	5.36
		22.2	3.23		21.6	5.80
	3.78	64.7	3.00	3.62	62.0	5.92
Ca	4.53	1.29	2.74	4.34	1.24	3.55
		2.59	2.91		2.48	4.18
		3.89	2.97		3.72	4.47
Sr	4.03	0.35	2.18	3.88	0.34	3.02
		0.58	2.33		0.57	3.09
		1.16	2.45		1.12	3.19
		1.74	2.53		1.67	3.51
		2.32	2.57		2.23	3.63
Ba	4.51	0.42	2.47	4.32	0.40	2.85
		0.70	2.47		0.67	2.98
		1.41	2·59			

metal concentrations at which no precipitation occurs. The results on magnesium obtained by method B are plotted in Fig. 3, in which the relation between $\bar{n}$, pHL and pL is illustratrated. In the range where $\bar{n}$ is less than unity, both k_1 and k_1' are found graphically from the intersection of the lines corresponding to Eq. 21, as is seen in Fig. 4.

$$\left.\begin{aligned}
0.191 &= 0.809\times 1.28\times 10^{-4}\times k_1 \\
&\quad + 0.809\times 2.81\times 10^{-8}\times k_1' \\
0.319 &= 0.681\times 2.48\times 10^{-4}\times k_1 \\
&\quad + 0.681\times 7.86\times 10^{-8}\times k_1' \\
0.517 &= 0.483\times 4.59\times 10^{-4}\times k_1 \\
&\quad + 0.483\times 2.96\times 10^{-7}\times k_1' \\
0.601 &= 0.399\times 7.28\times 10^{-4}\times k_1 \\
&\quad + 0.399\times 8.37\times 10^{-7}\times k_1' \\
0.731 &= 0.269\times 9.91\times 10^{-4}\times k_1 \\
&\quad + 0.269\times 1.76\times 10^{-6}\times k_1'
\end{aligned}\right\} \quad (21)$$

The mean values of k_1 and k_1' are 3.24 and 5.69 respectively.

The results obtained by method C with magnesium, calcium, strontium and barium are plotted in Fig. 5. In the region where $\bar{n}$ is below unity, the k_1 and k_1' of magnesium are evaluated as mentioned above; their logarithms were found to be 3.63 and 5.41 respectively. In the case of calcium, strontium and barium, k_1' in Eq. 14 becomes zero, indicating that the concentration of ML is negligible compared with that of MHL.

Table II. Stability constants of acidic complexes calculated by method C

	Mg	Ca	Sr	Ba
$\log k_1$	3.63	3.29	2.95	2.69
$\log k_1'$	5.41			

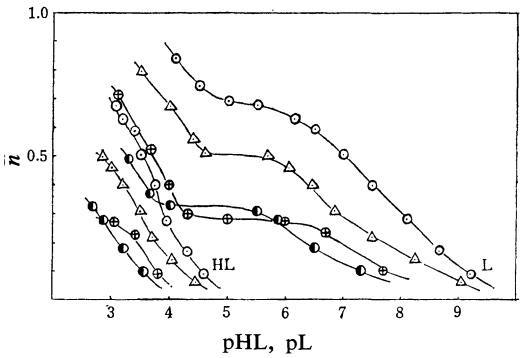


Fig. 5. Correlation of $\bar{n}$ with pHL and pL.
⊙: Mg, △: Ca, ⊕: Sr, ◐: Ba

Therefore, in the region where $\bar{n}$ is below unity, Eq. 22 gives the relation between $\bar{n}$, k_1 and HL. The values of k_1 are listed in Table II.

$$\bar{n} = \frac{k_1\cdot[\mathrm{HL}]}{1+k_1\cdot[\mathrm{HL}]} \quad (22)$$

As ring phosphoric acids are comparatively strong acids, the stability constants of the complexes between alkaline-earth metals and ring phosphoric acids cannot be evaluated by the usual titration method. In place of the titration method, the replacement reaction was utilized in the present experiments. The stability constants of magnesium complexes of ring phosphate and triphosphate are given in Table III.

The dissociation constants of phthalein complexon (H_6F) and the stability constants of the dye complexes with calcium and barium were reported by Schwarzenbach[11]. According to his data, the ratio of the concentration of CaF and CaHF is 0.01 at pH 9. At this pH,

Table III. Stability constants of ring phosphates and triphosphate complexes with magnesium

	pH	$C_{L1}\times 10^5$ M	$C_M\times 10^5$ M	$C_{L2}\times 10^3$ M	$\log K_{ML}$
Trimetaphosphate	9.31	2.28	1.16	2.30	2.84
	9.31	2.28	1.56	2.30	2.73
	9.31	2.28	1.94	2.30	2.64
					2.74
	pH	$C_{L1}\times 10^5$ M	$C_M\times 10^5$ M	$C_{L2}\times 10^5$ M	$\log K_{ML}$
Tetrametaphosphate	9.29	2.27	1.16	1.87	4.57
	9.28	2.27	1.56	2.80	4.51
	9.27	2.27	1.94	3.74	4.41
					4.51
	pH	$C_{L1}\times 10^5$ M	$C_M\times 10^5$ M	$C_{L2}\times 10^5$ M	$\log K_{ML}$
Triphosphate	9.32	1.60	1.56	1.06	5.69
	9.28	2.00	1.56	1.06	5.95
	9.27	2.40	1.56	1.06	6.12
					5.92

L_1: EBT, L_2: Phosphate

11) G. Schwarzenbach et al., *Helv. Chim. Acta*, **37**, 113 (1954).

only the acidic complex can exist. As both the complexes and HF exhibit the maximum absorption at the same wavelength, 570 mμ, the concentration of MHF was determined after correction for the absorption due to HF. The stability constants thus obtained are listed in Table IV.

Table IV. Stablity constants of ring phosphates and triphosphate complexes obtained by method D

	$\log K_{ML}$		
	Ca	Sr	Ba
Trimetaphosphate	1.68	0.62	0.08
Tetrametaphosphate	3.77	1.46	1.00
Triphosphate	4.59		

Discussion

Because of the formation of precipitate at high pH values, the stability constants of triphosphate complexes cannot be evaluated by method A. The logarithmic values of the stability constants reported by Schwarzenbach and his coworkers are 3.7 and 3.1 respectively for magnesium and calcium acidic complexes MHL, and 5.80 and 4.85 for magnesium and calcium complexes ML. The values obtained by Watters are 3.34 and 3.01 respectively for magnesium and calcium acidic complexes, and 5.83 and 5.44 for magnesium and calcium complexes at an ionic strength of 0.1. With calcium, however, titration cannot be continued up to the alkaline region without causing precipitation. Therefore, the values for calcium complexes reported by them do not seem reasonable. However, if the stability of the complex is low, the amount of metal present in the form of the complex is negligible compared with the total concentration of metal ion, even if the latter is smaller than the concentration of acid.

In method B, the error becomes greater with the increasing concentration of ML, as can be seen from Eq. 9. In method C, the value of $\bar{n}$ becomes greater with the increasing dissociation of MHL as acid, as is evident from Eq. 18.

Our values found by methods B and C indicate that the dissociation of MHL is not very great; therefore, the assumption involved in the above methods is considered to be quite reasonable. The values obtained by the replacement reactions are consistent with the results found by using methods B and C. Further, the values evaluated at the largest metal concentration in the measurements by method A are nearly equal to those evaluated by the other methods, and the values summarized in Table V seem to be near to the true values.

Figure 6 shows the relation of the stability constants of the complexes to the ratio of the square of the charge of metal ions to the

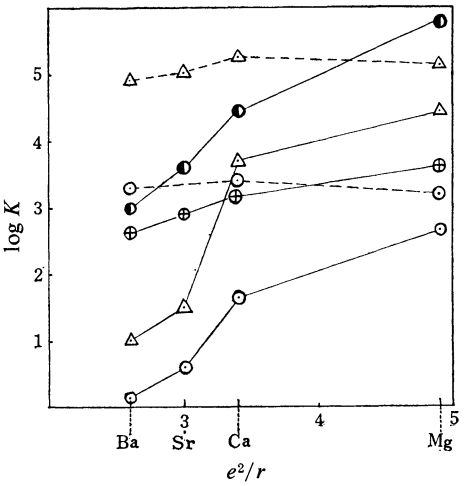


Fig. 6. Correlation of stability constants of condensed phosphate complexes of alkaline-earth metals with e^2/r of metals.
⊙ : Trimetaphosphate
△ : Tetrametaphosphate
◐ : Triphosphate (ML)
⊕ : Triphosphate (MHL)
——: Measured values
- - -: Reported values by Monk et al.

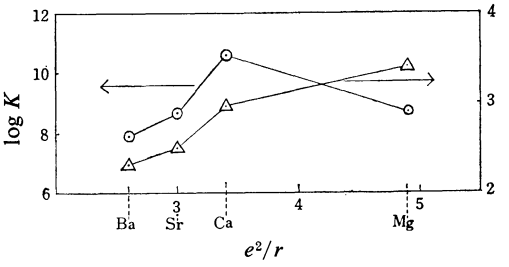


Fig. 7. Correlation of stability constants of alkaline-earth metal complex of EDTA or oxalic acid with e^2/r of metals.
⊙: EDTA, △: Oxalic acid

Table V. Stability constants of alkaline-earth metals with triphosphate and ring phosphates

	$\log K_{ML}$	$\log K_{MHL}$	$\log K_{ML}$	$\log K_{MHL}$	$\log K_{ML}$	$\log K_{MHL}$	$\log K_{ML}$	$\log K_{MHL}$	Method
Trimetaphosphate	2.74		1.68		0.62		0.08		D
Tetrametraphosphate	4.52		3.77		1.46		1.00		D
Triphosphate	5.8	3.6	4.6	3.3	3.6	3.0	3.0	2.7	A,B,C,D

ionic radius. The stability of principally ionic complexes of alkali and alkaline-earth metals is affected by both the charge and the ionic radius of the metal ions. Figure 7 shows the relation between $\log K$ and e^2/r for the series of alkaline-earth metal complexes. The two different trends are also observed with other ligands[12]. One group of ligands exhibits a maximum stability with calcium, while the stability of complexes with the other group of ligands increases monotonously from barium to magnesium. Ligands belonging to the former group possess a greater number of functional groups and form a greater number of chelate rings (e. g., EDTA) than do those belonging to the latter group.

As the stability of the condensed phosphate complexes increases monotonously from barium to magnesium, they do not seem to form complicated rings.

In Fig. 6, the values measured by electroconductivity and solubility methods by Monk et al.[13] are also included. The curves show a maximum at calcium, but there are no significant differences between the metals. Our data are different from theirs, and the values of Monk have already been criticized as too great by Gross[14].

It is already known that the complexes with ring phosphate are less stable than the chain phosphate complexes. This difference is attributed to the steric hindrance, which acts against the formation of chlelate rings, and to the stronger acidity of ring phosphate than chain phosphate. The results obtained by us also show that ring phosphate complexes are less stable than chain phosphates.

Department of Applied Chemistry
Faculty of Engineering
Tohoku University
Sakurakoji, Sendai

12) A. E. Martell and M. Calvin, "Chemistry of the Metal Chelate Compounds", Prentice-Hall Inc., Englewood Cliffs, New York (1952), p. 160.

13) C. B. Monk et al., *J. Chem. Soc.*, **1949**, 413.

14) R. J. Gross et al., *J. Am. Chem. Soc.*, **77**, 3695 (1955).

Stability of Condensed Phosphate Complexes. II. Rare-earth Metal Complexes

By Akira ROPPONGI and Takio KATO

(Received January 22, 1962)

Condensed chain phosphate has become an important commercial product since it has been known that its chemical properties, based on complex formation and surface activity, are useful in many fields of chemical industry.

Its ability of complex formation has been investigated by various methods, but the metal elements studied have been limited to alkali and alkaline-earth metals because of the precipitate formation of heavy metals with condensed chain phosphates over a wide range of pH values.

In order to investigate fundamentally the washing ability of chain phosphate, the present authors evaluated the stability constants of soluble complexes with various metals. As has been reported previously[1], triphosphate forms a precipitate in the presence of an excess of alkaline-earth metal ions except when magnesium is over the phosphate. On rare-earth metals, too, precipitate formation is observed in the presence of excess metal ions[2,3].

Therefore, the authors evaluated the stability constants of triphosphate complexes with the rare-earth metals by a new method to be described in the later part of this paper.

The ratio of triphosphate to metal in the complex was estimated by the following experiment: the change in the pH value of 10 ml. of a 0.01 M metal solution due to the addition of a triphosphate solution was measured by a glass electrode pH meter; the relation of the pH value to the ratio of the phosphate concentration to the metal concentration for several rare-earth metals is shown in Fig. 1. The abrupt change in pH value at the point where C_L/C_M is 3/5 means that the precipitate is normal salt and begins to dissolve as the concentration ratio of the phosphate to the metal becomes greater. The pH value of the solution increases again at the point where

1) A. Roppongi and T. Kato, This Bulletin, 35, 1086 (1962).

2) E. Giesbecht et al., *J. Inorg. Nuclear Chem.*, 6, 308 (1958).

3) E. Giesbecht, ibid., 15, 265 (1960).

C_L/C_M is 2/1; this means that the greatest number of the phosphates bound with the metal is equal to 2. Between 3/5 and 2/1 of C_L/C_M, 1 to 1 and 2 to 1 complexes may form successively; therefore, the precipitate dissolves in the presence of an excess of triphosphate.

Theoretical

A solution containing triphosphoric acid and rare-earth metal corresponding to one-fourth of the triphosphate concentration can be titrated with an alkaline hydroxide solution without precipitation up to an alkaline region; the pH value of the solution is lower than that of the solution which contains triphosphate only at a certain value in the region between 5 and 3 of *a*, which is the molar ratio of the added alkali per triphosphate. The decrease in pH value may be attributed to the complex formation of triphosphate with metal.

It is assumed that the species of complexes are only acidic, MHL and $M(HL)_2$, in the low pH region.

The equilibrium constants which are expressed by Eqs. 1 and 2:

$$k_1=\frac{[MHL]\cdot[H]}{[M]\cdot[H_2L]} \tag{1}$$

$$k_2=\frac{[M(HL)_2]\cdot[H]^2}{[M]\cdot[H_2L]^2} \tag{2}$$

are related to known values, that is, the total concentrations of the phosphate, and the metal, the dissociation constants of triphosphoric acid and the hydrogen ion concentration as follows:

The total concentration of triphosphate, C_L, and the replaceable hydrogen ion concentration, C_H, are:

$$C_L=[H_3L]+[H_2L]+[HL]+[MHL]+2[M(HL)_2] \tag{3}$$

$$C_H=3[H_3L]+2[H_2L]+[HL]+[H]+[MHL]+2[M(HL)_2] \tag{4}$$

and C_L is four times as large as the total metal ion concentration, C_M. The free phosphate ion concentration is expressed by

$$[H_3L]+[H_2L]+[HL]=\frac{C_H-C_L-[H]}{\frac{2[H]}{K_3}+1}\times\left(\frac{[H]}{K_3}+1+\frac{K_4}{[H]}\right) \tag{5}$$

where K_3 and K_4 are the third and the fourth dissociation constants of triphosphoric acid. The concentration of triphosphate combined with metal is

$$[MHL]+2[M(HL)_2]=[MHL]\times\left(1+\frac{2k_2}{k_1}\cdot\frac{\frac{C_H-C_L-[H]}{\frac{2[H]}{K_3}+1}}{[H]}\right) \tag{6}$$

Therefore, the concentration of MHL is

$$[MHL]=\frac{C_L-\frac{C_H-C_L-[H]}{\frac{2[H]}{K_3}+1}\cdot\left(\frac{[H]}{K_3}+1+\frac{K_4}{[H]}\right)}{1+\frac{2k_2}{k_1}\cdot\frac{\frac{C_H-C_L-[H]}{\frac{2[H]}{K_3}+1}}{[H]}} \tag{7}$$

By combining the condition that C_L is equal to $4\times C_M$ with Eqs. 5—7, the free metal concentration may be expressed by Eq. 8:

$$[M]=\frac{1}{4}\left[\left\{\frac{2(C_H-C_L-[H])}{\frac{2[H]}{K_3}+1}\times\left(\frac{[H]}{K_3}+1+\frac{K_4}{[H]}\right)-C_L\right\}-2\left\{\frac{C_L-\frac{C_H-C_L-[H]}{\frac{2[H]}{K_3}+1}\cdot\left(\frac{[H]}{K_3}+1+\frac{K_4}{[H]}\right)}{\frac{2k_2}{k_1}\cdot\frac{(C_H-C_L-[H])}{\frac{2[H]}{K_3}+1}\cdot[H]}\right\}\right] \tag{8}$$

By substituting Eqs. 5—8 into Eq. 1, Eq. 9 is obtained; it is then transformed into Eq. 10, in which k_1 is the tangent of the straight line and k_2 is the intercept in the y-axis.

$$k_1=\frac{C_L-\frac{C_H-C_L-[H]}{\frac{2[H]}{K_3}+1}\cdot\left(\frac{[H]}{K_3}+1+\frac{K_4}{[H]}\right)}{1+\frac{2k_2}{k_1}\cdot\frac{(C_H-C_L-[H])}{\frac{2[H]}{K_3}+1}\cdot[H]}\cdot[H]\Bigg/\frac{1}{4}\left[\left\{\frac{2(C_H-C_L-[H])}{\frac{2[H]}{K_3}+1}\cdot\left(\frac{[H]}{K_3}+1+\frac{K_4}{[H]}\right)-C_L\right\}-2\left\{\frac{C_L-\frac{C_H-C_L-[H]}{\frac{2[H]}{K_3}+1}\cdot\left(\frac{[H]}{K_3}+1+\frac{K_4}{[H]}\right)}{1+\frac{2k_2}{k_1}\cdot\frac{(C_H-C_L-[H])}{\frac{2[H]}{K_3}+1}\cdot[H]}\right\}\right]\times\frac{C_H-C_L-[H]}{\frac{2[H]}{K_3}+1} \tag{9}$$

$$k_1\cdot\frac{A}{B}\cdot D+k_2=\frac{C}{B}\cdot D^2 \tag{10}$$

where

$$A=1-\frac{3}{4}\cdot\frac{C_L}{\frac{C_H-C_L-[H]}{\frac{2[H]}{K_3}+1}\cdot\left(\frac{[H]}{K_3}+1+\frac{K_4}{[H]}\right)}$$

$$B=1-\frac{1}{2}\cdot\frac{C_L}{\frac{C_H-C_L-[H]}{\frac{2[H]}{K_3}+1}\cdot\left(\frac{[H]}{K_3}+1+\frac{K_4}{[H]}\right)}$$

$$C=\frac{C_L}{\frac{C_H-C_L-[H]}{\frac{2[H]}{K_3}+1}\cdot\left(\frac{[H]}{K_3}+1+\frac{K_4}{[H]}\right)}-1$$

$$D=\frac{[H]}{\frac{C_H-C_L-[H]}{\frac{2[H]}{K_3}+1}}$$

Both k_1 and k_2 can be evaluated graphically from the plot of $(A/B)\cdot D$ against $(C/B)\cdot D^2$. The stability constants are calculated from the equilibrium constants and the dissociation constants of triphosphoric acid. With an increase in the pH value of the solution, normal complexes such as ML and ML_2 may coexist, and the plot for Eq. 10 will deviate from a linear relation. In such a region, the stability constants of ML and ML_2 are obtained as follows by using the stability constants of the acidic complexes calculated above.

The constants are calculated on the assumption that the concentration of MHL is much greater than that of ML, since the main species of normal complexes is ML_2, as is seen in Fig. 1.

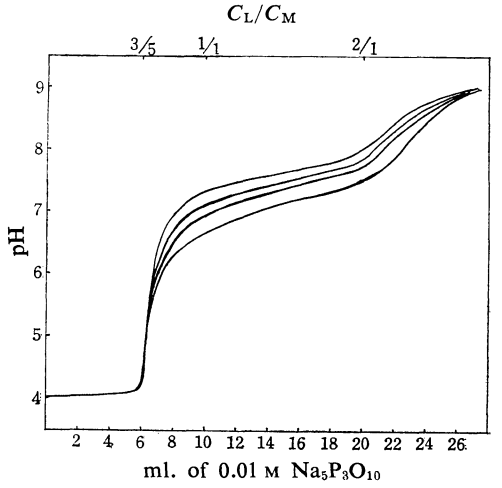


Fig. 1. The titration curves of 10 ml. of 0.01 M rare-earth metal solutions with 0.01 M sodium triphosphate ($Na_5P_3O_{10}$) solution.

Based on this assumption, the free metal ion concentration is derived from Eq. 11, where K_1^* is the stability constant of MHL.

$$4[M]+4[MHL]+4[ML]+4[M(HL)_2]+4[ML_2]=[H_2L]+[HL]+[L]+[MHL]+[ML]+2[M(HL)_2]+2[ML_2] \quad (11)$$

$$[M]=\frac{[H_2L]+[HL]+[L]-\frac{C_L}{2}}{K_1^*\cdot[HL]+2} \quad (12)$$

The total phosphate concentration, C_L, and the replaceable hydrogen concentration, C_H, are expressed as:

$$C_L=[H_2L]+[HL]+[L]+[MHL]+[ML]+2[M(HL)_2]+2[ML_2] \quad (13)$$

$$C_H=2[H_2L]+[HL]+[H]+[MHL]+2[M(HL)_2] \quad (14)$$

Combining Eqs. 12 and 14, Eq. 15, containing the stability constants of the acidic complexes, K_1^* and K_2^*, is induced.

$$C_H-[H]=\left(\frac{2[H]^2}{K_4\cdot K_5}+\frac{[H]}{K_5}\right)\cdot[L]+\frac{\left(\frac{[H]^2}{K_4\cdot K_5}+\frac{[H]}{K_5}+1\right)[L]-\frac{C_L}{2}}{K_1^*\cdot\frac{[H]}{K_5}\cdot[L]+2}\times\left(K_1^*\cdot\frac{[H]}{K_5}\cdot[L]+2K_2^*\cdot\left(\frac{[H]}{K_5}\right)^2\cdot[L]^2\right) \quad (15)$$

Equation 15 is then transformed to Eq. 16, which is the third order equation of [L] and can be solved graphically at a certain pH value.

$$2K_2^*\cdot\left(\frac{[H]}{K_5}\right)^2\cdot\left(\frac{[H]^2}{K_4\cdot K_5}+\frac{[H]}{K_5}+1\right)\cdot[L]^3+\left\{K_1^*\cdot\frac{[H]}{K_5}\cdot\left(\frac{3[H]^2}{K_4\cdot K_5}+\frac{2[H]}{K_5}+1\right)-K_2^*\cdot C_L\times\left(\frac{[H]}{K_5}\right)^2\right\}\cdot[L]^2+\left\{2\left(\frac{2[H]^2}{K_4\cdot K_5}+\frac{[H]}{K_5}\right)-K_1^*\cdot\frac{[H]}{K_5}\cdot\left(\frac{C_L}{2}+C_H-[H]\right)\right\}\cdot[L]-2(C_H-[H])=0 \quad (16)$$

Without neglecting the existence of ML, the concentration of ML_2 is expressed as:

$$[ML_2]=\frac{C_L-C_H+2[H]+[H_2L]-[L]}{\frac{K_1'}{K_2'}\cdot\frac{1}{[L]}+2} \quad (17)$$

and the concentration of M is:

$$[M]=\frac{[H_2L]+[HL]+[L]-\frac{C_L}{2}}{2+K_1^*\cdot[HL]+K_1'\cdot[L]} \quad (18)$$

where

$$K_1' = \frac{[ML]}{[M]\cdot[L]} \tag{19}$$

$$K_2' = \frac{[ML_2]}{[M]\cdot[L]^2} \tag{20}$$

Substituting Eqs. 17 and 18 into Eq. 20, K_2' is expressed as:

$$K_2' = \frac{\dfrac{C_L - C_H + 2[H] + [H_2L] - [L]}{\dfrac{K_1'}{K_2'}\cdot\dfrac{1}{[L]} + 2}}{\left(\dfrac{[H_2L] + [HL] + [L] - \dfrac{C_L}{2}}{2 + K_1^*\cdot[HL] + K_1'\cdot[L]}\right)\cdot[L]^2} \tag{21}$$

Equation 21 is transformed into the first order equation for K_1' and K_2', and the constants are evaluated by the plot of variables possible to be calculated from the concentration of L obtained graphically and the pH value measured.

$$\frac{2K_5 + K_1^*\cdot[L]\cdot[H]}{K_5\cdot[L]} \times \frac{C_L - C_H + [H] + \left(\dfrac{[H]^2}{K_4\cdot K_5} - 1\right)\cdot[L]}{C_H - \dfrac{3}{2}C_L - [H] + \left(\dfrac{[H]}{K_5} + 2\right)\cdot[L]} = K_1' + 2K_2'\cdot[L]\cdot\frac{\left(\dfrac{[H]^2}{K_4\cdot K_5} + \dfrac{[H]}{K_5} + 1\right)\cdot[L] - \dfrac{C_L}{2}}{C_H - \dfrac{3}{2}C_L - [H] + \left(\dfrac{[H]}{K_5} + 2\right)\cdot[L]} \tag{22}$$

If this assumption is reasonable, the plots should be on a linear line. In a high pH value region, complexes containing a hydroxyl group may be formed, and the difference in pH value for different rare-earth metals decreases. Therefore, it is reasonable that the estimation of the stability constants in the lower pH value region is better.

Experimental

In the case where the triphosphate concentration was twice as much as that of metal, a precipitate was slightly formed in the range of low pH values, approximately in the vicinity of 4. Thus the experiment were performed when the triphosphate concentration was four times the metal concentration.

Rare-earth metal solutions were prepared by dissolving 99.9% oxide in hydrochloric acid and removing the free acid completely by evaporation; the concentration was thus finally kept to 0.005 M.

A solution of 0.02 M sodium triphosphate was prepared by dissolving the recrystallized salt in distilled water; it contained 0.2 M of sodium perchlorate.

After mixing 10 ml. of a metal solution with a sodium triphosphate solution, the resulting solution was titrated with a 0.05 M perchloric acid solution containing 0.1 M sodium perchlorate.

The pH value was measured by a Hitachi pH meter EHP-1 type with a 0.02 unit.

Results and Discussion

The values of the variables in Eq. 10 were calculated by using the dissociation constants of triphosphoric acid, and the hydrogen ion concentration was obtained by dividing the pH values by Kieland's activity coefficient at the ionic strength, $\mu = 0.1$.

The dissociation constants are $10^{-2.15}$, $10^{-6.00}$ and $10^{-8.73}$ for K_3, K_4 and K_5 respectively.

The values of the variables in Eq. 10 for lanthanum are shown in Table I, while the values calculated for various rare-earth metals are plotted in Fig. 2. The stability constants for MHL and $M(HL)_2$ obtained from the lines in Fig. 2 are tabulated in Table II. In order to evaluate the stability constants of normal complexes, the values of [L] at various pH values were obtained from Eq. 16 by using the stability constants of acidic complexes obtained above. By substituting the values of [L] into Eq. 22, the variables were calculated. The values for lanthanum are tabulated in Table III. Further, the values of the left term and the right term in Eq. 22 for various rare-earth metals are plotted in Fig. 3. From the inclination and the intercept of the straight lines giving the relation between K_1' and K_2' for the rare-earth metals, the stability constants of ML and ML_2 were obtained; these results are shown in Table IV.

In Fig. 2, the deviation from linearity in variables of a smaller value may be attributed to the formation of the normal complexes. As the calculated values have a linear relation MHL and $M(HL)_2$ coexist, and neither ML nor

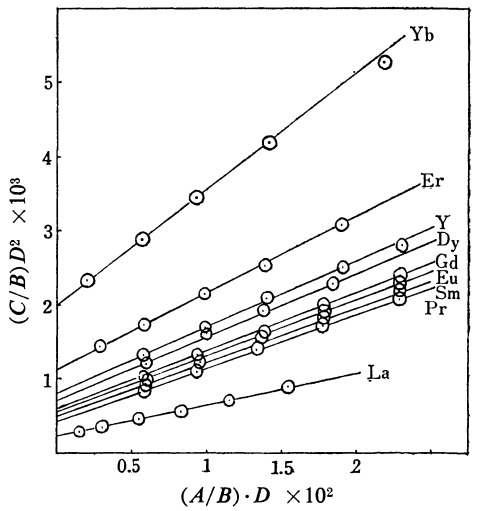


Fig. 2. The relations between $(A/B)\cdot D$ and $(C/B)\cdot D^2$ in Eq. 10 for rare-earth metals.

Table I. The values of the variables in Eq. 10 for lanthanum

pH	$HClO_4$, ml.	$C_L \times 10^3$ M	$C_H \times 10^3$ M	$(A/B)\cdot D$	$(C/B)\cdot D^2$
3.41	6.70	7.49	14.9	2.57×10^{-2}	1.45×10^{-3}
3.49	6.60	7.52	14.8	2.02×10^{-2}	1.14×10^{-3}
3.58	6.50	7.55	14.6	1.54×10^{-2}	8.62×10^{-4}
3.66	6.40	7.58	14.4	1.16×10^{-2}	7.17×10^{-4}
3.75	6.30	7.61	14.3	8.31×10^{-3}	5.70×10^{-4}
3.85	6.20	7.63	14.1	5.48×10^{-3}	4.31×10^{-4}

Table II. The stability constants of the acidic complexes with rare-earth metals

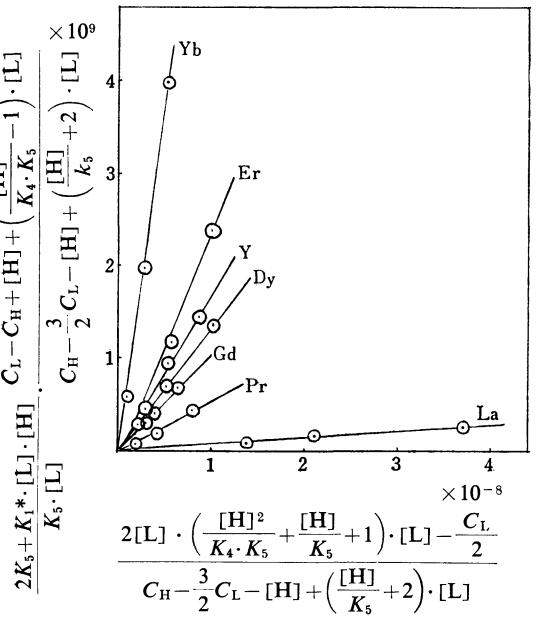
	La	Pr	Sm	Eu	Gd	Dy	Er	Yb	Y
$\log K_{MHL}$	4.63	4.86	4.89	4.90	4.91	4.94	5.00	5.20	4.97
$\log K_{M(CHL)_2}$	8.32	8.64	8.66	8.68	8.72	8.84	9.05	9.29	8.87

Table III. The values of the variables in Eq. 22 for lanthanum

pH	$HClO_4$, ml.	$C_L \times 10^3$ M	$C_M \times 10^3$ M	[L]	Values of left term	Values of right term
4.41	5.70	7.78	13.2	6.40×10^{-9}	9.51×10^{7}	1.37×10^{-8}
4.50	5.60	7.81	13.0	9.54×10^{-9}	1.86×10^{8}	2.25×10^{-8}
4.58	5.50	7.84	12.8	1.36×10^{-8}	2.68×10^{8}	3.66×10^{-8}
4.66	5.40	7.87	12.7	1.95×10^{-8}	5.73×10^{8}	8.57×10^{-8}

Table IV. The stability constants of the normal complexes with rare-earth metals

	La	Pr	Sm	Eu	Gd	Dy	Er	Yb	Y
$\log K_{ML_2}$	15.81	16.95	16.98	16.91	16.92	17.12	17.41	17.95	17.21



$$\frac{2K_5+K_1^*\cdot[L]\cdot[H]}{K_5\cdot[L]}\cdot\frac{C_L-C_H+[H]+\left(\frac{[H]^2}{K_4\cdot K_5}-1\right)\cdot[L]}{C_H-\frac{3}{2}C_L-[H]+\left(\frac{[H]}{K_5}+2\right)\cdot[L]}$$

$$\frac{2[L]\cdot\left(\frac{[H]^2}{K_4\cdot K_5}+\frac{[H]}{K_5}+1\right)\cdot[L]-\frac{C_L}{2}}{C_H-\frac{3}{2}C_L-[H]+\left(\frac{[H]}{K_5}+2\right)\cdot[L]}$$

Fig. 3. The relations of K_1' and K_2' in Eq. 22 for rare-earth metals.

ML_2 exist appreciably in the pH range in which calculations were made.

ML and ML_2 may form successively as the value of pH becomes greater. However, as is seen in Fig. 3, the intercepts in the y-axis of the lines are nearly zero for all the metals measured. This shows that the main species of normal complexes is ML_2 under the conditions for which the measurements were made.

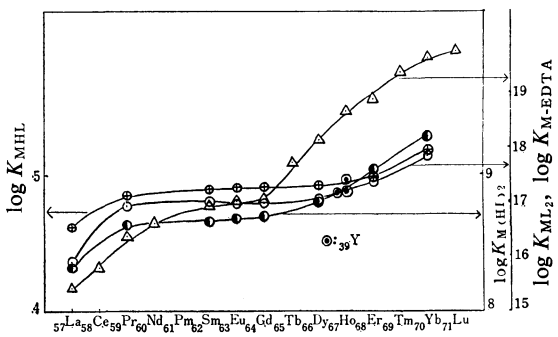


Fig. 4. The relations of the stability constant with the atomic number of rare-earth metals.
⊕ : $\log K_{MHL}$, ◐ : $\log K_{M(CHL)_2}$,
⊙ : $\log K_{ML_2}$, △ : $\log K$ for EDTA complex

Thus, the assumption made for the calculation seems to be reasonable.

The relation between the stability constants and the atomic number of the rare-earth metals is shown in Fig. 4; the tendency is the same as that of the EDTA complex[4].

Triphosphate can keep the rare-earth metal in solution over a wide range of pH values if it exists in a large excess over the metal.

Department of Applied Chemistry
Faculty of Engineering
Tohoku University
Sakurakoji, Sendai

4) J. E. Powell et al., AL-119, Ames Lab. AEC.

Ultraviolet Spectrophotometric Determination of Boron Using Tiron as a New Reagent

By Kazuo HIIRO*

(Received September 6, 1961)

Previous publications have described how many kinds of colorimetric reagents, such as oxyanthraquinones, flavone compounds, curcumin, etc., have been examined photometrically for boron. In the case of oxyanthraquinones, the colored complexes are formed in a concentrated sulfuric acid medium, while in the case of flavones or curcumin, sample solution should be evaporated with the reagent solution under conditions carefully controlled for color development. Since these procedures are very tedious and time-consuming, it would seem advantageous if the color development could be achieved simply and rapidly in an aqueous medium.

Tiron, disodium 1, 2-dihydroxybenzene-3, 5-disulfonate, was initially proposed as a photometric reagent for iron by Yoe and Jones[1]; thereafter this reagent has been utilized for the determination of titanium[2-7], iron[3,6], cerium[8-10], molybdenum[11,12], uranium[13] and niobium[14] in many kinds of samples.

This compound is expected to be a useful reagent of boron, because it has vicinal hydroxy groups which may be functional groups for boron. As a result of preliminary experiments based upon the above expectation, it was found that tiron could be applicable to the photometric determination of boron. The new photometric method is very convenient and advantageous, because the procedure is carried out rapidly in an aqueous medium and the boron-tiron complex formed is very stable under controlled conditions.

In this paper, the application of the reagent to the new spectrophotometric method for boron is described. The absorption spectra of dilute tiron solutions with various pH values were taken, and the existence of four isosbestic points, at 230, 243, 279 and 293 mμ, was confirmed. Then the absorption curves of mixed solutions of boron and tiron with various pH values against tiron solution as a reference were taken, and the optimum pH value and wavelengths for measurements were found. The effects of the concentrations of a tiron and buffer solution, of diverse salts and of the temperature were examined. It was found that the boron-tiron complex had a mole ratio of 1 : 1 under the proposed conditions, and that Beer's law was obeyed in the range from 0.40 to 3.20 p. p. m. of boron at the wavelengths of both 252 and 306 mμ.

Experimental

Apparatus. — Spectrophotometric measurements were made with a Shimadzu quartz spectrophotometer, model QB-50, using 1.000 cm. quartz transmission cells. A Horiba glass electrode pH meter, model H-3, was used for all pH measurements.

Materials.—*Standard Boron Solutions.*—Dissolve 0.5716 g. of reagent grade boric acid in 1000.0 ml. of water. This solution corresponds to 100.0 p.p.m. of boron. Dilute an aliquot of the solution with water, and prepare 10.0 p. p. m. of a standard boron solution.

Tiron Solution.—Dissolve 3.1422 g. of tiron (Dotite-Tiron) in 1000.0 ml. of water and prepare a 10^{-2}M solution.

Buffer Solution.—Prepare a buffer solution of the Michaelis type by mixing 4 parts of a 0.5 M disodium hydrogen phosphate solution and 1 part of a 0.5 M potassium dihydrogen phosphate solution, and adjust the pH to 7.40~7.50. Various other salt solutions were prepared from the reagents of an analytical grade.

Procedure.—Pipet an aliquot of the boron solution into a 25.0 ml. measuring flask, and add to it 2.0 ml. of a 10^{-2} M tiron solution and 1.0 ml.

* Present address: Osaka Industrial Research Institute, Nishi-2-chome, Oyodo-ku, Osaka.

1) J. H. Yoe and A. L. Jones, *Ind. Eng. Chem., Anal. Ed.*, **16**, 111 (1944).
2) J. H. Yoe and A. R. Armstrong, *Anal. Chem.*, **19**, 100 (1947).
3) *A. S. T. M. Proc.* **52**, 163 (1952); *Anal. Abstr.*, **1**, 2100 (1954).
4) K. Hagiwara, H. Suzuki and I. Muraki, *Bull. Osaka Ind. Res. Inst.*, **11**, 200 (1960).
5) L. Shapiro and W. W. Brannock, *Econ. Geol.*, **48**, 282 (1953); *Anal. Abstr.*, **1**, 2072 (1954).
6) G. V. Potter and C. E. Armstrong, *Anal. Chem.*, 20, 1208 (1948).
7) P. N. R. Nichols, *Analyst*, **85**, 452 (1960).
8) B. Sarma, *J. Sci. Ind. Res. (India)*, **14B**, 538 (1955); *Anal. Abstr.*, 3, 1657 (1956).
9) R. Püschel, *Mikrochim. Acta*, 344 (1960).
10) B. Sarma, *J. Sci. Ind. Res. (India)*, **15B**, 696 (1956); *Chem. Abstr.*, **51**, 17572 (1957).
11) F. Will, *Dissert. Abstr.*, **14**, 761 (1954); *Anal. Abstr.*, **2**, 69 (1955).
12) B. Sarma, *J. Sci. Ind. Res. (India)*, **16B**, 478 (1957); *Chem. Abstr.*, **52**, 5203 (1958).
13) B. Sarma and C. P. Savariar, *J. Sci. Ind. Res. (India)*, **16B**, 80 (1957); *Chem. Abstr.*, **51**, 11168 (1957).
14) H. Flaschka and E. Lassner, *Mikrochim. Acta*, 778 (1956).

of a buffer solution of pH 7.40~7.50, and dilute it to the mark with water. Mix thoroughly and measure the absorption of the solution at 252 or 306 mμ against a reagent blank.

In order to study the effect of diverse salts, color developments were made using 30.0 μg. of boron in the presence of varying amounts of 2.0% salt solutions.

To ascertain the stability of the color, absorbances of the solution were measured at proper time intervals after color development.

Measurements of the absorption spectra of the dilute tiron solution at various pH values are made as follows: Into a 50.0 ml. measuring flask, pipet 2.0 ml. of a 10^{-3} M tiron solution, and add 5.0 ml. of a buffer solution of 0.5 M disodium hydrogen phosphate-potassium dihydrogen phosphate, 1 M sodium acetate-acetic acid, and or 1 M aqueous ammonia-ammonium chloride to the flask and dilute it to the mark with water. The absorption spectra of these solutions were measured at 5 mμ intervals of wavelength against water as a reference.

Results

Absorption Spectra of Tiron Solution.—As shown in Fig. 1, when the pH of the solution increases, two absorption maxima (260 and 305 mμ) appear, while when the pH decreases, absorbance at the absorption maximum (290 mμ) increases. There are four isosbestic points, at 230, 243, 279 and 293 mμ.

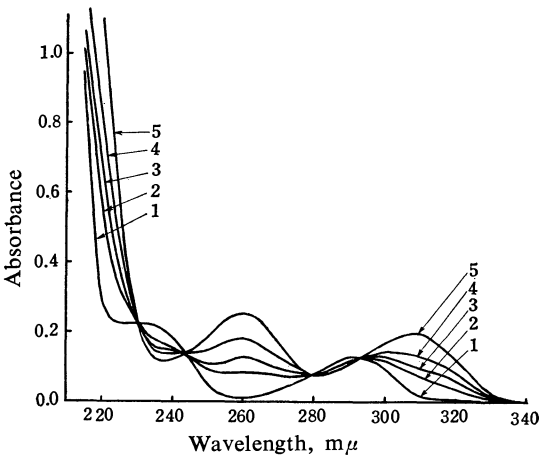


Fig. 1. Absorption spectra of tiron solutions.

Tiron; 4×10^{-5} M
Buffer soln.; 5.0 ml./50.0 ml.
Reference; Water

1 pH=6.00 2 pH=7.51 3 pH=7.85
4 pH=8.01 5 pH=9.52

Absorption Spectra of Boron-Tiron Complex.—Figure 2 shows the absorption curves of boron-tiron solutions. There are two absorption bands in the ultraviolet region, both of which are affected by the pH value of the solution.

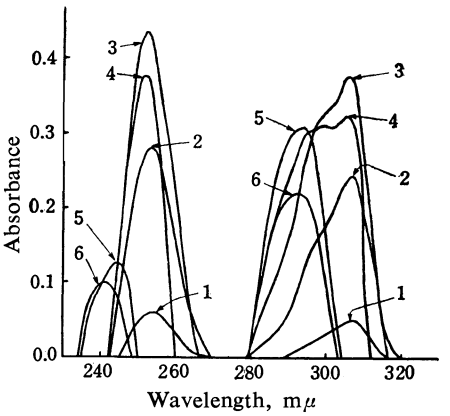


Fig. 2. Absorption spectra of boron-tiron complex.

Boron; 4×10^{-4} M
Tiron; 4×10^{-4} M
Buffer soln.; 5.0 ml./50.0 ml.
References; Blank solns.

1 pH=5.89 2 pH=6.79
3 pH=7.49 4 pH=7.59
5 pH=8.51 6 pH=9.80

Effect of pH.—In Fig. 3, the absorbances at the absorption maxima are plotted against the pH values. It was found that the maximum absorptions were obtained over the pH range of 7.40~7.50. For the photometric measurements, it is advantageous to select the wavelengths of maximum absorption, at 252 and 306 mμ, as is shown in Fig. 4, in which graphs are plotted of the maximum wavelengths against the pH values.

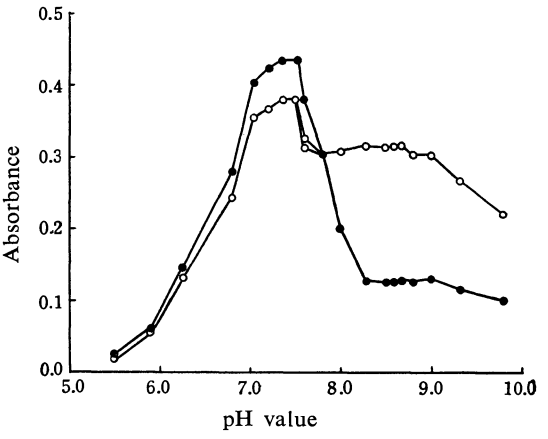


Fig. 3. Relation between absorbances at the absorption maxima and pH values.

Boron; 4×10^{-4} M
Tiron; 4×10^{-4} M
Buffer soln.; 5.0 ml./50.0 ml.
References; Blank solns.

—●— Obtained at 252 mμ
—○— Obtained at 306 mμ

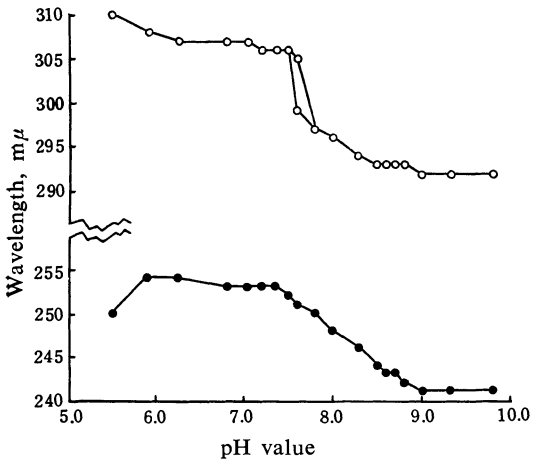


Fig. 4. Relation between wavelengths of maximum absorption and pH values.
Boron ; 4×10^{-4} M
Tiron ; 4×10^{-4} M
Buffer soln. ; 5.0 ml./50.0 ml.
References ; Blank solns.

Reagent Concentration.—In order to find a proper concentration of tiron, the measurement of the absorbances of a series of solutions containing 2.00 or 4.00 p. p. m. of boron with varying amounts of the reagent was undertaken, using the reagent blanks of the same concentration as references. As is shown in Fig. 5, 2.0 ml. of a 10^{-2} M tiron solution in 25.0 ml. is the optimum amount.

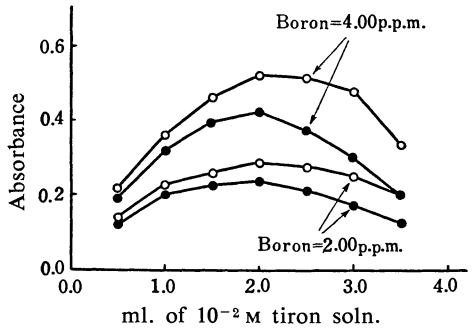


Fig. 5. Effect of concentration of tiron.
Boron ; 4.00 p. p. m. or 2.00 p. p. m.
Buffer soln. ; 1.0 ml./25.0 ml.
References ; Blank solns.
—○— Obtained at 252 mμ
—●— Obtained at 306 mμ

Effect of the Buffer Solution.—The effect of the buffer solution was tested with varying amounts of a 0.5 M disodium hydrogen phosphate-potassium dihydrogen phosphate buffer solution. 1.0~2.0 ml. of the buffer solution is favorable, as is shown in Fig. 6. The addition of 1.0 ml. of the buffer solution is thus adopted in the following experiments.

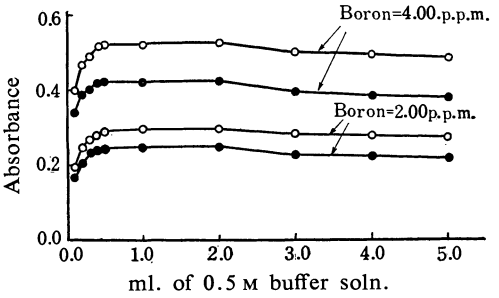


Fig. 6. Effect of concentration of buffer solution.
Boron ; 4.00 p. p. m. or 2.00 p. p. m.
Tiron ; 8×10^{-4} M
References ; Blank solns.
—○— Obtained at 252 mμ
—●— Obtained at 306 mμ

TABLE. I. EFFECT OF DIVERSE SALTS

Boron : 2.00 p. p. m.
Tiron : 8×10^{-4} M
Buffer soln. : 1.0 ml./25.0 ml.
Reference : Blank soln.

Salt	Added mg.	Absorbance at 252 mμ	Absorbance at 306 mμ
—	—	0.285	0.236
NaF	5	0.289	0.239
	10	0.303	0.249
	20	0.312	0.260
	50	0.371	0.306
	100	0.439	0.369
NaCl	5	0.297	0.244
	10	0.300	0.245
	20	0.293	0.236
	50	0.341	0.274
	100	0·360	0.291
Na_2SO_4	5	0.283	0.235
	10	0.284	0.237
	20	0.285	0.236
	50	0.311	0.256
	100	0.329	0.270
Na_2SO_3	5	0.387	0.301
	10	0.478	0.347
	20	0.619	0.436
	50	1.01	0.631
	100	1.37	0.812
$CH_3COONa\cdot3H_2O$	5	0.284	0.238
	10	0.290	0.242
	20	0.294	0.244
	50	0.317	0.257
	100	0.333	0.275
KNO_3	5	0.290	0.241
	10	0.308	0.264
	20	0.340	0.291
	50	0.408	0.365
	100	0.517	0.479

Stability of Absorbance.— The absorbances of the solution of a boron-tiron complex show no appreciable change during about 20 hr., although they decrease slightly after 3 days.

Effect of Temperature.—It is observed that the absorbances are affected by the temperature of the solution; that is, the values of absorbance increase as the temperature falls. The temperature coefficients are 0.00159~0.00176/°C at 252 mμ and 0.00161~0.00176/°C at 306 mμ for 1.00 p. p. m. of boron.

Effect of Diverse Salts.— As is shown in Table I, it is found that sodium sulfate and sodium acetate do not interfere when they are present 20 mg. per 25.0 ml. However, sodium sulfite interferes seriously at a concentration of 10 mg. per 25.0 ml.

Mole Ratio of Boron to Tiron in Solution.— In order to confirm the mole ratio of the boron-tiron complex, two methods were employed, the continuous variation and the slope ratio methods. In the first method, the measurement of the absorbances of a series of solution containing a varying mole per cent of 10^{-2} M boron and 10^{-2} M tiron was undertaken, using as references the reagent blanks of the same concentrations. As is shown in Fig. 7, the maximum absorbance of the complex was obtained when the mole ratio of boron to tiron is 1 to 1.

In the second method, two series of solutions were prepared: one with a varying concentration of boron in the presence of a large, constant amount of tiron, and the other with a varying concentration of tiron in the presence of a large, constant amount of boron. The absorbances of each series of solutions were also measured. Two linear absobance-concentration curves with the same tangential value of the slope were obtained, as is shown in Fig. 8. From the results of these experiments, it is confirmed that the mole ratio of boron to tiron in the complex formed is 1 to 1.

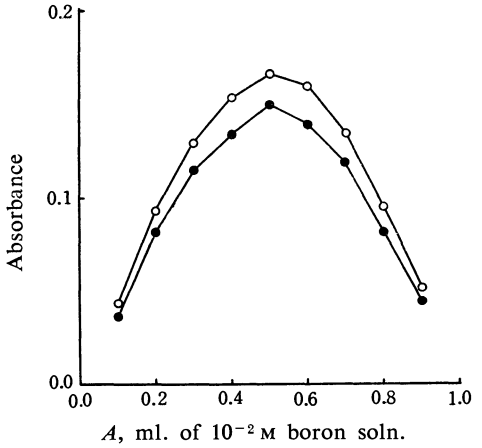


Fig. 7. Determination of mole ratio of boron to tiron by the method of continuous variations.

Boron; 10^{-2} M soln., A ml.
Tiron; 10^{-2} M soln., $(1.0-A)$ ml.
Buffer soln.; 1.0 ml./25.0 ml.
References; Blank solns.

—○— Obtained at 252 mμ
—●— Obtained at 306 mμ

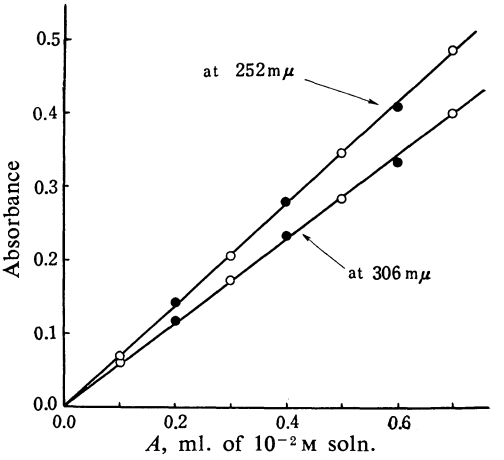


Fig. 8. Determination of mole ratio of boron to tiron by the method of slope ratios.

—●— Boron; A ml. Tiron; 2.0 ml.
—○— Boron; 2.0 ml. Tiron; A ml.

Calibration Curves.—To establish calibration curves, measurements of absorbance readings were made with a number of the boron-tiron solutions containing different amounts of boron; they were plotted against boron content. The results show that Beer's law is obeyed over the range from 0.40 to 3.20 p. p. m. of boron at the wavelengths of both 252 and 306 mμ,

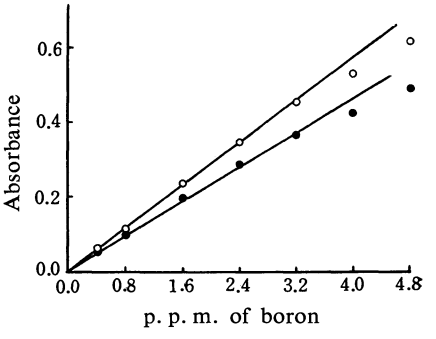


Fig. 9. Calibration curves.

Tiron; 8×10^{-4} M
Buffer soln.; 1.0 ml./25.0 ml.
Reference; Blank soln.
Temperature; 18°C

—○— Obtained at 252 mμ
—●— Obtained at 306 mμ

as in Fig. 9. The sensitivities of this method are 0.17/cm^2 and 0.20/cm^2, and the molar extinction coefficients are 1620 and 1370 at 252 and 306 mμ respectively.

Discussion

The proposed new photometric method for the determination of boron with tiron as a color reagent is more simple and rapid than other methods. As is shown in Figs. 7 and 8, the constitution of the boron-tiron complex has the mole ratio of 1 : 1. Because the measurements of absorbance are made in the ultraviolet region, some obvious interferences with diverse metal ions are to be expected. Therefore, for the determination of boron in many kinds of practical samples, a proper separation of boron is desired. In this procedure, absorbance is affected by the temperature, so the absorption measurements must be done under as constant temperature as possible. Fortunately, the effect of temperature difference can be eliminated, provided that the calibration curves are made simultaneously with the sample analysis. Determination of the boron content of many samples is now proceeding in this laboratory. In this procedure, however, absorbance is very stable for about 20 hr.; this is advantageous for the spectrophotometric measurements.

The author is indebted to Dr. Yuroku Yamamoto, Hiroshima University, for his guidance, and to Dr. Isao Muraki, Chief o the 5th Department of our Institute, for his useful suggestions.

Osaka Industrial Research Institute
Oyodo-ku, Osaka

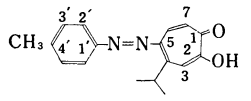
*The Bromination Product of 2-(p-Tolyl)-hinopurpurin**

By Seiji EBINE

(Received September 14, 1961)

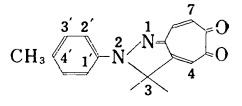
As has been previously reported by Nozoe et al., hinokitiol, i.e., 4-isopropyltropolone, couples with diazotized amines to yield azo-hinokitiols, which, on heating in an acetic acid solution or in an ethanolic solution in the presence of *p*-benzoquinone, bring about its transformation into so-called hinopurpurins[1]. It has recently been found that 2-phenyl-hinopurpurin is brominated to yield 2-phenyl-4, 7-dibromohinopurpurin[2]. This paper reports on similar experiment undertaken in order to determine the position of bromine atoms of dibromo-2-(*p*-tolyl)-hinopurpurin (A).

The dibromo compound A was obtained by bromination of 2-(*p*-tolyl)-hinopurpurin (I)[3] and also by bromination of 2-(*p*-tolyl)-7-bromohinopurpurin (II). The ultraviolet spectrum of A was closely analogous to that of I. These facts indicate that A is not a bromine-addition product but a bromine-substitution product of I, and that one of its two bromine atoms is situated at the 7-position in the tropoquinone ring. An ortho directing effect exerted by methyl and nitrogen substituents and an electromeric effect (shown by Ia) suggest that the substitution reaction of I with bromine may take place at the 2′- or 3′-position in the benzene ring, or at the 4- or 7-position in the tropoquinone ring. Accordingly, it can be presumed that A is either a 7, 2′-, 7, 3′- or 4, 7-dibromo derivative of I. An attempt, therefore, was made to synthesize these dibromo derivatives of I as well as some other bromo derivatives of 5-(*p*-tolylazo)-hinokitiol.



5-(*p*-Tolylazo)-hinokitiols

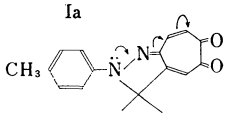
III : 2′-Bromo-
IV : 3′-Bromo-
VII : 7, 2′-Dibromo-
IX : 7, 3′-Dibromo-
XI : 3, 7-Dibromo-



2-(*p*-Tolyl)-hinopurpurins

II : 7-Bromo-
V : 2′-Bromo-
VI : 3′-Bromo-
VIII : 7, 2′-Dibromo-
X : 7, 3′-Dibromo-
XII : 4, 7-Dibromo-
XIII : 4, 7, 2′-Tribromo-
XIV : 4, 7, 3′-Tribromo-

Ia



* Presented before the 11th Annual Meeting of the Chemical Society of Japan, Tokyo, April, 1958.

1) T. Nozoe, E. Sebe, Y. Kitahara and H. Fujii, *Sci. Repts. Tohoku Univ.*, **136**, 290 (1952); T. Nozoe, T. Ikemi and T. Ozeki, *Proc. Japan Acad.*, **31**, 455 (1955).

2) T. Ikemi, to be published.

3) T. Nozoe, S. Ebine, S. Ito and I. Takasu, *Proc. Japan Acad.*, **27**, 197 (1951).

Hinokitiol was coupled with diazotized 2- and 3-bromo-4-methylanilines to yield 5-(2′-bromo-4′-methylphenylazo)- and 5-(3′-bromo-4′-methylphenylazo)-hinokitiols (III and IV), which, on heating with *p*-benzoquinone in an ethanolic solution, were then transformed into the corresponding 2-(2′-bromo-4′-methylphenyl)- and 2-(3′-bromo-4′-methylphenyl)-hinopurpurins (V and VI) respectively. The bromination of V and VI gave 2-(2′-bromo-4′-methylphenyl)- and 2-(3′-bromo-4′-methylphenyl)-*x*,*x*-dibromohinopurpurins. The coupling of 7-bromohinokitiol with diazotized 2-bromo-4-methylaniline afforded 5-(2′-bromo-4′-methylphenylazo)-7-bromohinokitiol (VII), which was subsequently transformed into 2-(2′-bromo-4′-methylphenyl)-7-bromohinopurpurin (VIII). Although 5-(*p*-tolylazo)-hinokitiol is brominated to its 7-bromo derivative[3], bromination of III did not give VII but, rather, yielded a tribromo hinopurpurin identical with a bromination product of V. The coupling of 7-bromohinokitiol with diazotized 3-bromo-4-methylaniline afforded 5-(3′-bromo-4′-methylphenylazo)-7-bromohinokitiol (IX), which was also prepared by bromination of IV. The transformation of IX into 2-(3′-bromo-4′-methylphenyl)-7-bromohinopurpurin (X) was effected in the usual manner. Neither of the dibromohinopurpurins, VIII or X, was identical with A. The coupling of 3, 7-dibromohinokitiol with diazotized *p*-toluidine failed to occur in an alkaline solution, but it did take place in a pyridine solution to yield 5-(*p*-tolylazo)-3, 7-dibromohinokitiol (XI). XI was somewhat stable towards hinopurpurin-transformation and recovered unchanged when its acetic acid solution was heated on a water bath for 3 hr. However, when heated with *p*-benzoquinone in an ethanolic solution under reflux for 5 hr., XI underwent transformation, accompanied by the elimination of one of its bromine atoms, to yield II. Thus it was impossible to prepare 2-(*p*-tolyl)-4, 7-dibromohinopurpurin (XII) from XI, which had its bromine atoms at known positions. Nevertheless, it has now become evident that XII is the only possible structure for A because neither VIII nor X proved to be identical with A, as has been described above. Therefore, it is furthermore presumed that the above-mentioned bromination products of V and VI are 2-(2′-bromo-4′-methylphenyl)- and 2-(3′-bromo-4′-methylphenyl)-4, 7-dibromohinopurpurins (XIII and XIV) respectively.

It is of interest to note that 2′-brominated 2-(*p*-tolyl)-hinopurpurins, such as V, VIII and XIII, are light red-colored compounds, while all other hinopurpurins are dark purple or deep blue. The light color of 2′-brominated 2-(*p*-tolyl)-hinopurpurins may be ascribed to the steric hindrance of the 2′-bromine atoms which rotate the benzene rings, out of the plane of the hinopurpurin molecules.

Experimental

Monobromo-5-(*p*-tolylazo)-hinokitiols.—*5-(2′-Bromo-4′-methylphenylazo)-hinokitiol (III).*—2-Bromo-4-methylaniline hydrochloride (1.5 g.), dissolved in 8 ml. of 1.2 N hydrochloric acid, was diazotized with a solution of 0.42 g. of sodium nitrite in 4 ml. of water. The diazotized solution was added drop by drop to a solution of 1 g. of hinokitiol and 1.2 g. of potassium hydroxide in 30 ml. of water. The product which separated out on acidification with dilute hydrochloric acid was collected, washed with water, dried and crystallized from benzene to yield 1.65 g. (75%) of III, in the form of orange needles, m. p. 147.5°C.

Found: C, 56.47; H, 4.94; N, 7.85. Calcd. for $C_{17}H_{17}O_2N_2Br$: C, 56.52; H, 4.74; N, 7.75%.

5-(3′-Bromo-4′-methylphenylazo)-hinokitiol (IV).—This was prepared by the coupling of hionkitiol with diazotized 3-bromo-4-methylaniline in the same way as described above. Yield, 77% in the form of reddish orange needles (from benzene), m. p. 147°C.

Found: C, 56.28; H, 4.96; N, 7.88. Calcd. for $C_{17}H_{17}O_2N_2Br$: C, 56.52; H, 4.74; N, 7.75%.

Dibromo-5-(*p*-tolylazo)-hinokitiols.—*5-(2′-Bromo-4′-methylphenylazo)-7-bromohinokitiol (VII).*—A solution of 0.5 g. of 7-bromohinokitiol[4] and 0.4 g. of potassium hydroxide in 50 ml. of water was coupled with a diazotized solution prepared from 0.5 g. of 2-bromo-4-methylaniline hydrochloride, 0.14 g. of sodium nitrite and 2.7 ml. of 1.2 N hydrochloric acid. The crude product obtained was crystallized from acetone to yield 0.6 g. (66%) of VII, as reddish orange needles, m. p. 132.5°C.

Found: C, 46.53; H, 3.55; N, 6.65. Calcd. for $C_{17}H_{16}O_2N_2Br_2$: C, 46.39; H, 3.66; N, 6.35%.

5-(3′-Bromo-4′-methylphenylazo)-7-bromohinokitiol (IX).—a) It was prepared by the coupling of 7-bromohinokitiol with diazotized 3-bromo-4-methylaniline in the same way as cited above. b) To a solution of 0.5 g. of IV in 70 ml. of acetic acid was added, drop by drop, 0.35 g. of bromine dissolved in 3.5 ml. of acetic acid. After the mixture had been left standing for 30 min., the precipitate was collected by filtration. The product obtained was an addition compound which, on crystallization from acetone, regenerated IV with the liberation of bromine. The addition compound was dissolved in pyridine, and the solution was warmed at 80°C for 10 min., and diluted with water. The precipitate formed was recrystallized from acetone to yield 0.32 g. (52%) of IX, in the form of orange needles, m. p. 168~169°C.

Found: C, 46.58; H, 3.75; N, 6.55. Calcd. for $C_{17}H_{16}O_2N_2Br_2$: C, 46.39; H, 3.66; N, 6.35%.

5-(p-Tolylazo)-3,7-dibromohinokitiol (XI).—3, 7-Dibromohinokitiol[4] (500 mg.) dissolved in 50 ml. of pyridine was coupled with a diazotized solution prepared from 185 mg. of *p*-toluidine, 107 mg. of

4) T. Nozoe, E. Sebe, S. Mayama and S. Iwamoto, *Sci. Repts. Tohoku Univ.*, I, 36, 184 (1952).

sodium nitrite and 3.4 ml. of 1.2 N hydrochloric acid. After the mixture had been left standing overnight in an ice-chest, the pyridine was removed in vacuo below 30°C and the residue was treated with boiling ligroin. The ligroin solution gave a crystalline precipitate on cooling, which precipitate was collected and recrystallized from methanol or acetone to yield 110 mg. (16%) of XI, as orange needles, m. p. 167°C.

Found: C, 46.26; H, 3.56; N, 6.14. Calcd. for $C_{17}H_{16}O_2N_2Br_2$: C, 46.39; H, 3.66; N, 6.35%.

Monobromo-2-(*p*-tolyl)-hinopurpurins.—An ethanolic solution consisting of monobromo-5-(*p*-tolylazo)-hinokitiols and of a 1 mol. equiv. of *p*-benzoquinone was refluxed for 5 hr. The ethanol was then evaporated, and the residue was recrystallized from ethanol or acetic acid to yield the corresponding hinopurpurins.

2-(2'-Bromo-4'-methylphenyl)-hinopurpurin (V).—A solution of 200 mg. of III and 60 mg. of *p*-benzoquinone in 10 ml. of ethanol was refluxed for 5 hr. to yield 150 mg. (75%) of V, in the form of orange, prismatic needles, m. p. 222~223°C.

Found: C, 56.79; H, 4.31; N, 7.91. Calcd. for $C_{17}H_{15}O_2N_2Br$: C, 56.84; H, 4.21; N, 7.80%.

2-(3'-Bromo-4'-methylphenyl)-hinopurpurin (VI).—IV (200 mg.) and 60 mg. of *p*-benzoquinone dissolved in 10 ml. of ethanol gave 140 mg. (70%) of VI, as dark blue crystals with a greenish luster, m. p. 241°C.

Found: C, 57.12; H, 4.38; N, 7.55. Calcd. for $C_{17}H_{15}O_2N_2Br$: C, 56.84; H, 4.21; N, 7.80%.

2-(p-Tolyl)-7-bromohinopurpurin (II).—A solution of 200 mg. of XI and 60 mg. of *p*-benzoquinone in 80 ml. of ethanol was refluxed for 5 hr. to give 100 mg. (61%) of II, in the form of steel-blue prisms, m. p. 222°C (Found: C, 57.18; H, 4.01; N, 7.86. Calcd. for $C_{17}H_{15}O_2N_2Br$: C, 56.84; H, 4.21; N, 7.80%), the melting point of which was not depressed on admixture with an authentic sample[5] prepared by the transformation of 5-(*p*-tolylazo)-7-bromohinokitiol.

The same tranformation was effected when an acetic acid solution of XI was refluxed for 5 hr. Dilution of the reaction mixture with water gave II in a 55% yield, and an addition of silver nitrate to the filtrate caused the precipitation of a quantitative amount of silver bromide.

Dibromo-2-(*p*-tolyl)-hinopurpurins.—*2-(p-Tolyl)-4,7-dibromohinopurpurin (XII).*—a) To a solution of 200 mg. of I in 160 ml. of acetic acid was added 250 mg. (2.2 mol. equiv.) of bromine dissolved in 3 ml. of acetic acid. A crystalline product began to separate immediately. After the solution had been left standing for 30 min., the product was collected and recrystallized from acetic acid to yield 220 mg. (70%) of XII, m. p. 227°C. XII dissolves in boiling acetic acid, forming a deep purple solution, from which on cooling it separates in the form of golden yellow scales with a metallic luster. XII showed a marked melting point depression on admixture with VIII and X, as is described below.

Found: C, 46.32; H, 3.56; N, 6.58. Calcd. for $C_{17}H_{14}O_2N_2Br_2$: C, 46.60; H, 3.22; N, 6.39%. Treatment of I with a 1 mol. equiv. of bromine again gave XII, the corresponding monobromo derivative not being formed. b) Bromination of 100 mg. of II with 75 mg. of bromine in 110 ml. of acetic acid gave 90 mg. (74%) of XII.

2-(2'-Bromo-4'-methylphenyl)-7-bromohinopurpurin (VIII).—A solution of 70 mg. of VII and 35 mg. of *p*-benzoquinone in 30 ml. of ethanol was refluxed for 3 hr.; the ethanol was then evaporated, and the residue was recrystallized from ethanol to give 45 mg. (64%) of VIII, in the form of reddish orange crystals, m. p. 207.5~208°C.

Found: C, 46.39; H, 3.20; N, 6.20. Calcd. for $C_{17}H_{14}O_2N_2Br_2$: C, 46.60; H, 3.22; N, 6.39%.

2-(3'-Bromo-4'-methylphenyl)-7-bromohinopurpurin (X).—A solution of 100 mg. of IX in 5 ml. of acetic acid was heated at 100°C for 3 hr. The product which separated on cooling was crystallized from acetic acid to afford 55 mg. (55%) of X, as dark violet prisms, m. p. 248~249°C.

Found: C, 46.58; H, 3.33; N, 6.15. Calcd. for $C_{17}H_{14}O_2N_2Br_2$: C, 46.60; H, 3.22; N, 6.39%.

Tribromo-2-(*p*-tolyl)-hinopurpurins.—*2-(2'-Bromo-4'-methylphenyl)-4,7-dibromohinopurpurin (XIII).*—To a solution of 100 mg. of III in 15 ml. of acetic acid at 60°C was added 100 mg. of bromine. The solution was allowed to stand for 30 min. at the same temperature. Dilution with 5 ml. of water gave a precipitate, which was collected and crystallized from ethanol. Yield, 85 mg. (59%), in the form of reddish orange prisms, m. p. 179°C.

Found: C, 39.65; H, 2.72; N, 5.25. Calcd. for $C_{17}H_{13}O_2N_2Br_3$: C, 39.49; H, 2.54; N, 5.42%.

XIII was reduced with alkaline hydrosulfite to a leuco compound which regained its original red color on exposure to air and which gave a quinoxaline derivative of red plates melting at 189°C.

Found: C, 47.19; H, 2.86; N, 9.18. Calcd. for $C_{23}H_{17}N_4Br_3$: C, 46.89; H, 2.91; N, 9.51%.

2-(3'-Bromo-4'-methylphenyl)-4,7-dibromohinopurpurin (XIV).—Bromine (200 mg.) dissolved in 2 ml. of acetic acid was added to a solution of 100 mg. of VI in 300 ml. of acetic acid; the resulting solution was allowed to stand for 30 min. Dilution with water gave the product, which was collected and recrystallized from acetic acid. Yield, 90 mg. (62%) in the form of scales with a golden metallic luster, m. p. 246°C.

Found: C, 39.22; H, 2.67; N, 5.70. Calcd. for $C_{17}H_{13}O_2N_2Br_3$: C, 39.49; H, 2.54; N, 5.42%.

The author takes this opportunity to express his gratitude to Professor Tetsuo Nozoe of Tohoku University for his encouragement. The author is also indebted to Mrs. Kuniko Kodaira of Tohoku University for her microanalyses.

Department of Chemistry
Saitama University
Urawa, Saitama-ken

5) T. Nozoe, E. Sebe and S. Ebine, *Proc. Japan Acad.*, 26(8), 24 (1950).

Dehydration Reactions of Benzaldoxime by Means of Compounds Having a Nitrogen-Carbon Double Bond

By Teruaki MUKAIYAMA, Tamotsu FUJISAWA and Ohyo MITSUNOBU

(Received October 14, 1961)

Preceding papers of this series have shown that acetylenic ethers, vinyl ethers, vinyl acetate, ketene acetals, isocyanates and carbodiimides dehydrate aldoximes, primary nitroparaffins and hydroxamic acids, giving nitriles, nitrile oxides and isocyanates respectively[1-6]. These results lead to the conclusion that compounds having either a cumulate double bond or a multiple bond, with alkoxyl or acyloxyl groups, are effective as dehydrating reagents. This paper reports a further study of the dehydration reactions of benzaldoxime by means of phenylimidophosgene, ethyl *N*-phenyliminochloroformate and ethyl *N*-phenylformimidate. These substances are nitrogen-carbon double bond compounds which have halogen(s) and/or an alkoxyl group as substituents attached to the carbon atom.

First, when 1 mol. of phenylimidophosgene was treated with 1 mol. of benzaldoxime in dry benzene under stirring, an evolution of heat was noticeable, and phenyl isocyanate and benzonitrile were obtained in good yields, along with hydrogen chloride and a small amount of aniline hydrochloride (Eq. 1).

$$\begin{aligned} &C_6H_5N{=}C\begin{matrix}Cl\\Cl\end{matrix} + HON{=}CHC_6H_5 \\ &\longrightarrow \underset{\text{(I)}}{\left[C_6H_5N{=}\overset{Cl}{C}ON{=}CHC_6H_5\right]} + HCl \\ &[C_6H_5NHCOCl] + C_6H_5C{\equiv}N \longleftarrow \text{(I)} \\ &[C_6H_5NHCOCl] \longrightarrow C_6H_5N{=}C{=}O + HCl \end{aligned} \quad (1)$$

It is reasonable to postulate that the reaction proceeds through the intermediate I, which in turn decomposes to give benzonitrile and *N*-phenylcarbamyl chloride. The latter subsequently decomposes to produce phenyl isocyanate and hydrogen chloride. The formation of aniline hydrochloride may be attributed to the decomposition of adduct II of phenyl isocyanate and benzaldoxime by hydrogen chloride, as is shown in the following equation:

$$\begin{aligned} &C_6H_5N{=}C{=}O + HON{=}CHC_6H_5 \\ &\longrightarrow \underset{\text{(II)}}{C_6H_5NHCOON{=}CHC_6H_5} \\ &\longrightarrow C_6H_5NH_2 + C_6H_5C{\equiv}N + CO_2 \\ &\quad \xrightarrow[HCl]{} C_6H_5NH_2HCl \end{aligned} \quad (2)$$

In order to confirm the above assumption, the reaction of 2 mol. of benzaldoxime with 1 mol. of phenylimidophosgene was tested. When they were allowed to react in dry benzene at room temperature under vigorous stirring for a while, a violent reaction suddenly took place and aniline hydrochloride and benzonitrile were obtained in good yields, along with the evolution of hydrogen chloride and carbon dioxide. The results show that the violent reaction is initiated by the hydrogen chloride initially formed.

Secondly, the treatment of ethyl *N*-phenyliminochloroformate with benzaldoxime was attempted. When they reacted in dry benzene, the evolution of hydrogen chloride and carbon dioxide was observed, and ethyl *N*-phenylcarbamate and benzonitrile were produced in good yields, along with a small amount of aniline hydrochloride and *sym*-diphenylurea (Eq. 3).

$$\begin{aligned} &C_6H_5N{=}\overset{Cl}{C}OC_2H_5 + HON{=}CHC_6H_5 \\ &\longrightarrow \underset{\text{(III)}}{\left[C_6H_5N{=}\overset{OC_2H_5}{C}ON{=}CHC_6H_5\right]} + HCl \\ &C_6H_5NHCOOC_2H_5 + C_6H_5C{\equiv}N \longleftarrow \text{(III)} \end{aligned} \quad (3)$$

Analogous to the case of phenyl imidophosgene, the reaction can be explained by assuming the existence of the intermediate III, which is the condensation product of ethyl *N*-phenyliminochloroformate and benzaldoxime. This readily decomposes to give ethyl *N*-phenylcarbamate and benzonitrile. Further, since ethyl *N*-phenyliminochloroformate is decomposed with hydrogen chloride or at temperatures over 100°C, yielding phenyl isocyanate and ethyl chloride (Eq. 4), the formation of

1) T. Mukaiyama and T. Hoshino, *J. Am. Chem. Soc.*, **82**, 5339 (1960).
2) T. Mukaiyama and T. Hata, This Bulletin, **33**, 1382 (1960).
3) T. Mukaiyama and T. Hata, ibid., **33**, 1712 (1960).
4) T. Mukaiyama and T. Hata, ibid., **34**, 99 (1961).
5) T. Mukaiyama and H. Nohira, *J. Org. Chem.*, **26**, 782 (1961).
6) T. Mukaiyama, K. Tonooka and K. Inoue, ibid., **26**, 2202 (1961).

aniline hydrochloride and *sym*-diphenylurea is attributed to the reactions of the isocyanate with benzaldoxime (Eq. 2) and with aniline (Eq. 5) respectively.

$$C_6H_5N{=}\underset{\underset{Cl}{|}}{C}OC_2H_5 \rightarrow C_6H_5N{=}C{=}O + C_2H_5Cl \qquad (4)$$

$$C_6H_5N{=}C{=}O + C_6H_5NH_2 \rightarrow (C_6H_5NH)_2CO \qquad (5)$$

On the other hand, it is noteworthy that diethyl *N*-phenyliminocarbonate, which has two alkoxyl groups to the carbon atom of the nitrogen-carbon double bond, hardly reacted with benzaldoxime, even in the presence of basic or acidic catalyst, such as triethylamine or boron trifluoride, and most of the starting materials were recovered[7].

Finally, the reaction of ethyl *N*-phenylformidate with benzaldoxime gave benzonitrile and formanilide, in 83 and 66% yields respectively, when refluxed in dry benzene with boron trifluoride and yellow mercuric oxide as catalysts (Eq. 6).

$$C_6H_5N{=}CHOC_2H_5 + HON{=}CHC_6H_5 \xrightarrow[BF_3\cdot HgO]{} \underset{(V)}{\left[\begin{array}{c} C_6H_5NHCHOC_2H_5 \\ | \\ O \\ | \\ N{=}CHC_6H_5 \end{array}\right]} \longrightarrow C_6H_5C{\equiv}N + C_6H_5NHCHO + C_2H_5OH \qquad (6)$$

This reaction can be represented by the above scheme, which involves the initial formation of the intermediate V, the adduct of ethyl *N*-phenylformimidate and benzaldoxime, analogous to the explanation proposed for the dehydrations of aldoxime with vinyl ethers[3]. The V subsequently decomposes to give benzonitrile, formanilide and alcohol.

Experimental

Phenylimidophosgene.—This compound was prepared from phenyl isothiocyanate and chlorine according to the procedure of Bly, Perkins and Lewis; b. p., 102~104°C/28 mmHg[8].

Reaction of Phenylimidophosgene with Benzaldoxime (1 : 1).—When a solution of phenylimidophosgene (3.5 g. 0.02 mol.) and benzaldoxime (2.4 g. 0.02 mol.) in dry benzene (20 ml.) was stirred vigorously, an evolution of heat was noticeable and aniline hydrochloride precipitated. Then the reaction mixture was refluxed for an hour. The hydrochloride was filtered and was recrystallized from ethanol; yield, 0.3 g. (11%); m. p. and mixed m. p., 195~197°C. Benzene was removed from the filtrate, and the residual materials were fractionated. Two grams (84% yield) of phenyl isocyanate (b. p., 48~50°C/10 mmHg) and 1.5 g. (72% yield) of benzonitrile (b. p., 70~72°C/10 mmHg) were obtained.

Reaction of Phenylimidophosgene with Benzaldoxime (1 : 2).—A solution of phenylimidophosgene (3.5g., 0.02 mol.) and benzaldoxime (4.8g., 0.04 mol.) in dry benzene (20 ml.) was stirred. After a while, a violent reaction suddenly took place and aniline hydrochloride precipitated. By the same procedure as described above, the hydrochloride (yield, 2.3 g., 92%; m. p. and mixed m. p., 195~197°C) and benzonitrile (yield, 3.1 g., 75%; b. p., 66~68°C/10 mmHg) were obtained.

Ethyl *N*-Phenyliminochloroformate.—This compound was prepared from phenylimidophosgene and sodium ethylate according to the procedure of Smith; b. p., 114~116°C/12 mmHg[9].

Reaction of Ethyl *N*-Phenyliminochloroformate with Benzaldoxime.—Into an ice cold solution of ethyl *N*-phenyliminochloroformate (3.7 g. 0.02 mol.) in dry benzene (20 ml.) was vigorously stirred, drop by drop, a solution of benzaldoxime (2.4 g., 0.02 mol.) in dry benzene (20 ml.). The reaction mixture was refluxed for an hour, and the precipitated aniline hydrochloride was filtered; yield, 0.2 g. (8%); m. p. and mixed m. p., 197~199°C. After the removal of the benzene from the filtrate, 1.6 g. (78% yield) of benzonitrile (b. p., 85~87°C/25 mmHg) and 2.5 g. (76% yield) of ethyl *N*-phenylcarbamate (b. p., 106~115°C/2 mmHg) were obtained by distillation. The latter solidified on cooling and was recrystallized from petroleum ether; m. p. and mixed m. p., 48~50°C. *sym*-Diphenylurea remained in a distillation flask and was recrystallized from acetic acid; yield, 0.6 g. (14%); m. p. and mixed m. p., 234~236°C.

Decomposition of Ethyl *N*-Phenyliminochloroformate with Hydrogen Chloride.—Into a solution of ethyl *N*-phenyliminochloroformate (1.8 g., 0.01 mol.) in dry benzene (20 ml.) was passed dry hydrogen chloride, with refluxing for an hour. After the removal of the benzene, phenyl isocyanate was distilled; yield, 0.8 g. (66%); b. p., 58~60°C/15 mmHg.

Ethyl *N*-Phenylformimidate.—This compound was prepared from aniline and ethyl orthoformate according to the procedure of Roberts and Vogt; b. p., 117~118°C/40 mmHg.[10]

Reaction of Ethyl *N*-Phenylformimidate with Benzaldoxime.—A solution of ethyl *N*-phenylformimidate (3.0 g., 0.02 mol.), benzaldoxime (2.4 g., 0.02 mol.), boron trifluoride etherate (5 drops) and a catalytic amount of mercuric oxide in dry benzene (5 ml.) was refluxed for 5 hr. and was then filtered. The benzene was removed from the clear filtrate, and 1.7 g. (85% yield) of benzonitrile (b. p., 76~78°C/18 mmHg) and 1.6 g. (67% yield) of formanilide (b. p., 108~112°C/0.35 mmHg) were obtained by distillation. The latter solidified on cooling; m. p., 40~44°C.

Summary

The dehydration reactions of benzaldoxime with such nitrogen-carbon double bond compounds having halogen and alkoxyl groups as

7) T. Mukaiyama, T. Fujisawa and T. Hyugaji, This Bulletin, **95**, 687 (1962).
8) R. S. Bly, G. A. Perkins and W. L. Lewis, *J. Am. Chem. Soc.*, **44**, 2896 (1922).
9) W. R. Smith, *Am. Chem. J.*, **16**, 372 (1894).
10) R. M. Roberts and P. J. Vogt, *Org. Syn.*, **35**, 65 (1955).

phenylimidophosgen, ethyl *N*-phenyliminochloroformate and ethyl *N*-phenylformidate were studied.

One mole of phenyl imidophosgene, when reacted with 1 mol. of benzaldoxime, gave phenyl isocyanate and benzonitrile as main products. On the other hand, with 2 mol. of the aldoxime, aniline hydrochloride and benzonitrile were obtained in good yields. The aldoxime was also dehydrated effectively by ethyl *N*-phenyliminochloroformate to give, among other byproducts, the nitrile and ethyl *N*-phenylcarbamate. The nitrile and formanilide were obtained by the reaction of the aldoxime with ethyl *N*-phenylformimidate.

The authors wish to express their hearty thanks to Mr. Kohichi Awano for his help in the course of this experiment. Thanks are also due to Mr. Keiji Naruse for his microanalyses.

Laboratory of Organic Chemistry
Tokyo Institute of Technology
Meguro-ku, Tokyo

A Selective Phosphorylation by Means of α-Bromocyanoacetamides and Trialkyl Phosphites

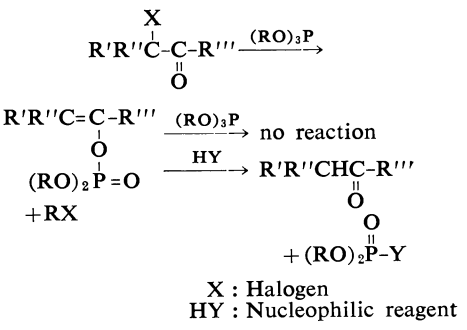
By Tsujiaki HATA and Teruaki MUKAIYAMA

(Received October 17, 1961)

Phosphorylation by means of ketene dimer, ethyl vinyl ether, tetraethyl pyrophosphite and diethylphosphorochloridite has been described in a preceding paper[1].

The well-known methods of phosphorylation by means of dehydrating reagents mostly consist of the initial formation of enol-phosphate by the addition of a monohydrogen or a dihydrogen phosphate to the organic dehydrating reagents with a triple or a cummulated double bond, such as carbodiimides[2], acetylenic ethers[3] and trichloroacetonitrile[4], followed by alcoholysis or phosphorolysis. However, except in the case of trichloroacetonitrile, the isolation of an intermediate adduct, enol-phosphate, was not possible, with the result that the coupling of two different phosphates invariably produced a mixture of the two symmetrical pyrophosphates, together with the unsymmetrical product. The formation of undesirable symmetrical pyrophosphates is attributed to the fact that phosphates used in the phosphorylation react more rapidly with the enol-phosphates than with the dehydrating reagent, thereby causing the formation of symmetrical pyrophosphates. Therefore, the enol-phosphate must be isolated in advance if a selective phosphorylation is to take place.

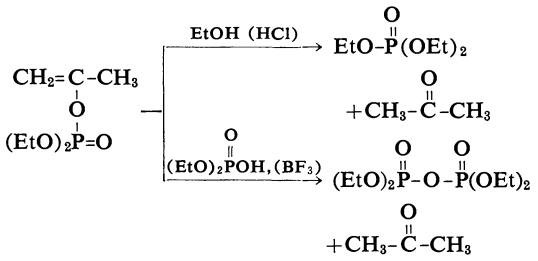
The preparation of the intermediates, the enol-phosphates, by the Perkow reaction from trialkyl phosphites and α-haloketones or α-haloaldehydes involves the oxydation of phosphite to phosphate. Since the enol-phosphate thus formed does not further react with the trialkyl phosphite but reacts exclusively with nucleophilic reagents, such as alcohols, monohydrogen phophates and amines, a selective phosphorylation can be effected successfully without isolating the enol-phosphate.



Most of the enol-phosphates obtained by the Perkow reaction[5], however, are not suitable for the purpose of phosphorylation because they are prepared under severe conditions or are sluggish toward nucleophilic reagents, except in the case of a ketene acylal reported by Cramer[6]. The low reactivity of enol-phosphates

1) T. Mukaiyama, T. Hata and O. Mitsunobu, *J. Org. Chem.* **27**, 1815 (1962).
2) H. G. Khorana and A. R. Todd, *J. Chem. Soc.*, **1953**, 2257.
3) J. F. Arens and T. Doornbos, *Rec. trav. chim.*, **74**, 79 (1955)
4) F. Cramer and G. Weimann, *Chem. & Ind.*, **1960**, 46.
5) J. F. Allen and O. H. Johnson, *J. Am. Chem. Soc.*, **77**, 2871 (1955).
6) F. Cramer and K. G. Gärtner, *Chem. Ber.*, **91**, 704 (1958).

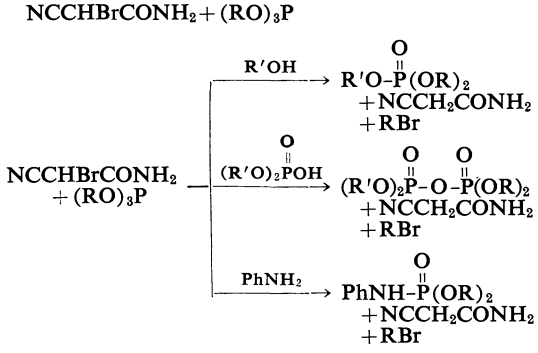
toward alcohols and monohydrogen phosphates has been demonstrated. The reaction of diethyl isopropenyl phosphate, an example of enol-phosphates, with ethanol could not be observed even when they were heated for 2 hr. at 150°C. However, when they were treated in the presence of a catalytic amount of hydrogen chloride for 12 hr. at 100°C, they gave a 55% yield of triethyl phosphate. Similarly, a 55% yield of tetraethyl pyrophosphate was obtained by heating the above enol-phosphate with diethyl hydrogen phosphate in the presence of a catalytic amount of boron trifluoride for an hour at 100°C.



However, one of the enol-phosphates which are reactive toward nucleophilic reagents can be prepared from monobromocyanoacetamide and trialkyl phosphites, as will be described below.

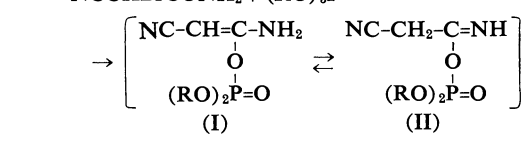
When a solution of 1 mol. of monobromocyanoacetamide and 1 mol. of either an alcohol, a monohydrogen phosphate or aniline in ether was treated with a solution of 1 mol. of trialkyl phophite at −50°C, the reaction started instantly, cyanoacetamide soon separated from the solution, and the corresponding phosphate, pyrophosphate or phosphoramidate was obtained in a high yield, along with an alkyl bromide, as is shown in the following:

$NCCHBrCONH_2 + (RO)_3P$



The reactions seem to proceed through the initial formation of the enol-phosphate as a result of the interaction of monobromocyanoacetamide with trialkyl phosphite, followed by the attack of nucleophilic reagents to form phosphates, pyrophosphates and phosphoramidate.

$NCCHBrCONH_2 + (RO)_3P$



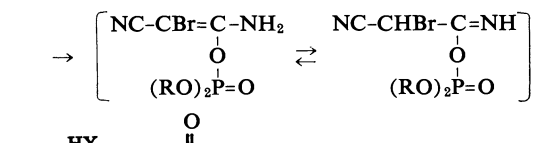
$\xrightarrow{HY}$ $Y\text{-}P(O)(OR)_2 + NCCH_2CONH_2 + RBr$

HY : Alcohol, monohydrogen phosphate or aniline

It is reasonable to postulate that the enol-phosphate (I), which possesses an amino group attached to its carbon-carbon double bond, is capable of existing in both the amine I and imine II forms. The phosphorylation probably proceeds as a result of the contribution of the imine form II rather than the amine form I which existed in equilibrium. It has been shown that when *N, N*-diethyl monobromocyanoacetamide, which does not exist as the imine form, was treated with triethyl phosphite and ethanol, not triethyl phosphate but a tar product was produced. As phosphorylation proceeds, the imine II is continually removed from the equilibrium by an irreversible phosphorylation, and eventually the amine I is transformed through the imine intermediate II into cyanoacetamide.

Similarly, when a solution of 0.5 mol. of dibromocyanoacetamide was used in place of the 1 mol. of monobromocyanoacetamide, the corresponding phosphates, pyrophosphate and phosphoramidate were obtained in good yields.

$NCCBr_2CONH_2 + (RO)_3P$



$\xrightarrow{HY}$ $Y\text{-}P(O)(OR)_2 + NCCHBrCONH_2{}^{*} + RBr$

HY : Alcohol, monohydrogen phosphate or aniline

* Monobromocyanoacetamide further reacts with trialkyl phosphite through the former equation.

In addition, a new method for the preparation of monobromocyanoacetamide was found. When a solution of dibromocyanoacetamide and cyanoacetamide was treated in the presence of a catalytic amount of boron trifluoride, monobromocyanoacetamide was obtained in a yield 74% of the theoretical one. This is a simpler treatment and produces a higher yield than those hitherto reported in the literature[7].

$NCCBr_2CONH_2 + NCCH_2CONH_2 \xrightarrow{BF_3} 2\,NCCHBrCONH_2$

7) B. M. Gupta and J. F. Thorpe, *J. Chem. Soc.*, **121**, 1902 (1922).

Experimental

Reaction of Diethyl Isopropenyl Phosphate with Ethanol.—A mixture of diethyl isopropenyl phosphate (1.94 g.), ethanol (0.55 g.) and 2 drops of concentrated hydrochloric acid was heated for 12 hr. at 100°C. The mixture was then distilled under reduced pressure to give triethyl phosphate (1.0 g., 55%), b. p., 67~69°C/1.2 mmHg., along with acetone and ethyl bromide.

Reaction of Diethyl Isopropenyl Phosphate with Diethyl Hydrogen Phosphate.—A mixture of diethyl isopropenyl phosphate (1.94 g.), diethyl hydrogen phosphate (1.54 g.) and 2 drops of boron trifluoride etherate was heated at 100°C for an hour. Diethyl isopropenyl phosphate (1.0 g.) was recovered, and tetraethyl pyrophosphate (1.6 g., 55%), b. p., 132~~135°C/0.8 mmHg., was obtained.

Monobromocyanoacetamide.—A solution of dibromocyanoacetamide (24.2 g.) and cyanoacetamide (8.4 g.) in 150 ml. of ethanol, in the presence of 10 drops of boron trifluoride etherate was refluxed for 5 hr. After removal of the ethanol, a large amount of white precipitate was separated, washed with benzene, and recrystallized from benzene; monobromocyanoacetamide (24 g., 74%), m. p., 116 117°C, was obtained.

Reactions of Alcohols, Phenol or Diethyl Hydrogen Phosphate with Monobromocyanoacetamide and Trialkyl Phosphites.—*Ethanol.*—To a solution of ethanol (0.28 g.) and monobromocyanoacetamide (1.0 g.) in dry ether (90 ml.) was added, drop by drop a solution of triethyl phosphite (1.0 g.) in dry ether (10 ml.) at −50°C. A white precipitate, cyanoacetamide, soon separated; the solution was kept for an additional hour at room temperature and was then filtered. After removal of the ether and ethyl bromide, triethyl phosphate (1.0 g., 91%), b. p., 65~67°C/1 mmHg., was obtained.

In a similar fashion, other alcohols, phenol and diethyl hydrogen phosphate gave the corresponding phosphates or pyrophosphates. The results of the phosphorylation of alcohols, phenol and diethyl hydrogen phosphate by means of monobromocyanoacetamide and trialkyl phosphites are summarized in Tables I and II.

Reactions of Ethanol, Phenol or Diethyl Hydrogen Phoshate with Dibromocyanoacetamide and Triethyl Phosphite.—*Ethanol.*—To a solution of ethanol (0.9 g.) and dibromocyanoacetamide (2.4 g.) in dry ether (30 ml.) was added, drop by drop a solution of triethyl phosphite (3.3 g.) in dry ether (10 ml.) at −50°C. A white precipitate, cyanoacetamide, soon separated; the solution was kept for

TABLE I. PHOSPHORYLATION OF ALCOHOLS AND PHENOL BY MEANS OF MONOBROMOCYANOACETAMIDE AND TRIETHYL PHOSPHITE

Alcohol	Charge g.	Product: Phosphate	Yield %	B. p. °C/mmHg	Cyanoacetamide Yield %
Methanol	2.20	Methyl diethyl-	77	102~104/25	93
Ethanol	0.28	Triethyl-	91	65~67/1	88
n-Propanol	0.37	*n*-Propyl diethyl-	85	73~74/0.8	82
Phenol	0.58	Phenyl diethyl-	72	103~120/1	94

TABLE II. PHOSPHORYLATION OF DIETHYL HYDROGEN PHOSPHATE BY MEANS OF MONOBROMOCYANOACETAMIDE AND TRIALKYL PHOSPHITES

Phosphite	Charge g.	Product: Pyrophosphate	Yield %	B. p. °C/mmHg	Cyanoacetamide Yield %
Trimethyl-	0.76	*unsym*-Dimethyl diethyl-	92	100~106/0.004	87
Triethyl-	0.93	Tetraethyl-	94	135~136/1	98
Tri-*n*-butyl-	1.55	*unsym*-Diethyl di-*n*-butyl-	96	114~118/0.02	85

TABLE III. PHOSPHORYLATION OF ETHANOL, PHENOL AND DIETHYL HYDROGEN PHOSPHATE BY MEANS OF DIBROMOCYANOACETAMIDE AND TRIETHYL PHOSPHITE

Reagent	Charge g.	Product: Phosphate	Yield %	B. p. °C/mmHg	Cyanoacetamide Yield %
Ethanol	0.90	Triethyl-	72	94~95/11~12	96
Phenol	1.88	Phenyl diethyl-	57	103~123/1	94
Diethyl hydrogen phosphate	3.08	Tetraethyl pyro-	60	134~136/1	84

an additional 2 hr. and was then worked up in the usual manner, producing cyanoacetamide (0.5 g., 96%), m. p., 120°C, and triethyl phosphate (2.6 g., 72%), b. p., 94~95°C/11~12 mmHg.

In a similar fashion, phenol and diethyl hydrogen phosphate gave phenyl diethyl phosphate and tetraethyl pyrophosphate respectively. The results of the phosphorylation of these compounds are summarized in Table III.

Reactions of Mono- or Dibromocyanocetamide with Aniline and Triethyl Phosphite.—*Monobromocyanoacetamide.*—To a solution of monobromocyanoacetamide (1.0 g.) in dry ether (90 ml.) was added, drop by drop, a solution of aniline (0.57 g.) and triethyl phosphite (1.0 g.) in dry ether (10 ml.) at −50°C. A white precipitate, cyanoacetamide, (0.51 g., 98%) was filtered off. After removal of the ether and ethyl bromide, diethyl *N*-phenylphosphoramidate (1.3 g., 93%) was obtained and recrystallized from benzene, m. p. and mixed m. p., 94~96°C.

Dibromocyanoacetamide.—When dibromocyanoacetamide (1.5 g.) was used in place of monobromocyanoacetamide (1.0 g.), diethyl *N*-phenylphosphoramidate (1.3 g., 93%) was obtained.

Summary

A method of selective phosphorylation by means of α-bromocyanoacetamides and trialkyl phosphites was devised. In this method, various phosphates, pyrophosphates and phosphoramidate were obtained in excellent yields under mild conditions without isolating the intermediate, enol-phosphate.

The use of dibromocyanoacetamide in place of monobromocyanoacetamide produced the same results, the yields being, however, less.

A new method for the preparation of monobromocyanoacetamide was also described.

The authors wish to express their hearty thanks to Mr. Ohyo Mitsunobu for his kind advice, and to Mr. Isao Kuwajima and Mr Kowa Tasaka for their assistance during the course of this experiment.

Laboratory of Organic Chemistry
Tokyo Institute of Technology
Meguro-ku, Tokyo

Rotational Isomers of Vinyl Ethers. Studies of the Vibrational Spectra and Dipole Moments of cis- and trans-β-Chlorovinyl Methyl Ethers

By Yukio MIKAWA, Shiro MORITA and Sukenari TSUNAKAWA

(Received November 1, 1961)

In the course of organic studies for the synthesis of β-chlorovinyl methyl ether in our laboratory, two kinds of compounds with the same chemical composition, C_3H_5OCl, were obtained. The first was distilled out at 85～86°C, and the second, at 105～106°C. These two compounds were considered to be the *trans-* and *cis-β*-chlorovinyl methyl ethers. Though the one having the lower boiling point has been supposed to be the trans compound and the other the cis compound, no real evidence has been given for deciding which is the cis or the trans compound. This study was initiated with the aim of identifying the cis and trans compounds in the light of the structural chemistry. First the infrared spectra of these compounds were recorded. The results, however, were not simple enough to enable us to decide confidently which was the cis or the trans compound. Especially, the spectrum of the compound having the lower boiling point proved complex. It seemed to be difficult to explain the complexity of the spectrum in the usual ways, and to be necessary for us to take internal rotation into account. In order to make clear the cis-trans isomerism, the dipole moments were also measured. As the result of these experiments, not only has the compound having the lower boiling point been identified with the trans compound and the other with the cis compound, but also some interesting imformation in connection with the rotational isomerism have been obtained.

The vinyl ether, CH_2=CH–O–R, has a freedom of internal rotation about the axis of the C–O bond adjacent to the double bond.

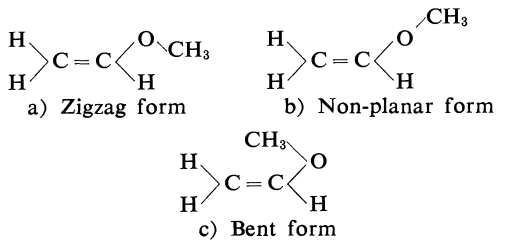


Fig. 1. Rotational isomers of vinyl ether.

Therefore, three types of spacial configuration are possible with regard to the position of alkyl group R: i.e., the zigzag, non-planar and bent forms, which are indicated in Fig. 1.

In a previous study[1] the infrared spectra of several vinyl ethers were investigated, and the observed spectra were assigned in conformity with the assumption that the molecule had the zigzag (planar) configuration. Davison and Bates[2] investigated the infrared spectra of several vinyl ethers and discussed some of the characteristic absorption bands. Kirrman and Chancel[3] also published an elaborate study of the Raman and infrared spectra of vinyl ethers, paying particular attention to the doublets which appeared around 1630 cm^{-1} in most of the spectra investigated, and suggested that the doublets were due to rotational isomers. Since the doublets can also be explained in terms of Fermi resonance[1], uncertainty about the existence of rotational isomers will remain until further experimental evidence is offered.

In the present paper, from the investigation of the Raman and infrared spectra and measurements of the dipole moments of the two compounds, in addition to identifying the cis and trans compounds, we will show that the cis compound* having the higher boiling point consists of a single molecular species which has a non-planar configuration and that the trans compound* having the lower boiling point consists of two rotational isomers, both of which have planar configurations.

Experimental

Preparation of the Samples.—Both *cis*- and *trans*-β-chlorovinyl methyl ethers were prepared by workers in this laboratory. The samples were purified by fractional distillation. The boiling points of the cis and trans compounds were 105~106°C and 85~86°C respectively. Although a small amount of the cis compound had not been perfectly removed from the trans compound, it did not disturb the interpretation of the spectra to a large extent.

Infrared Absorption Spectra.—Infrared spectra were obtained by a Perkin-Elmer model 21 spectrometer equipped with sodium chloride, calcium fluoride and potassium bromide prisms. Vapor spectra were recorded at 130~150°C using a heated 5 cm. cell[4]. For the trans compound, the spectra in the solid state were also measured, using a low temperature cell[4] constructed in our laboratory. The spectra are reproduced in Figs. 2 and 3, and the data are tabulated in Tables I and II. Since the solvent effect was not found in any appreciable amount, the spectra in solutions are not reproduced here.

Raman Spectra.—Raman spectra were obtained using 4358 Å excitation with a three-prism spectrograph (17 Å/mm. at 4358 Å) constructed in this laboratory. A low-pressure mercury arc lamp was used. A double layer composed of a sodium nitrate solution (40 g./100 g. solution) and a Rhodamine 6G dilute solution was used as a liquid filter. Exposure was for from one to six hours. The data are tabulated in the first columns of Tables I and II. Approximate line intensities on the photographic plates are indicated by the numbers in parentheses.

Dipole Moments.—The dielectric constants of the benzene solution of the compounds were observed in several dilutions at 20~60°C. Densities were also measured by a pycnometer. From those values, the dipole moments were calculated by the conventional way; 2.53 D was obtained for the cis compound, and 1.6 D for the trans compound, at 25°C. It was also found that, as to the trans compound, its dipole moment did not depend on the temperature in the range 20~60°C.

Discussion

Rotational Isomers.—As can be seen in Figs. 2b and 3b, the spectrum of the trans compound in the liquid state is very complicated compared with that of the cis compound. Thirteen absorption bands are theoretically expected in the 600~1700 cm^{-1} region for this compound. Nevertheless, nineteen bands are observed for the trans compound in liquid. Since most of the bands have fairly strong intensities and their intensities did not change through repeated purifications of the samples, those bands are believed to be inherent to the molecule and not to come from impurities. Furthermore, the fact that some bands disappeared on the solidification of the sample (see Fig. 3c), is strong evidence for the presence of rotational isomers in the liquid. The number of bands in the solid spectra is in accordance with the theoretical expectations. That means the trans compound in the liquid state is a mixture of two or more rotational isomers, and that, in the course of solidification, every molecule takes on an unique configuration suitable for the low temperature by rotating the methoxy group around the C–O bond axis. On the other hand, the liquid spectrum of the cis compound is very simple, and the numbers of bands is so few that it seems possible that only one molecular species seems to exist.

Dipole Moments.—The dipole moments are estimated for both the trans and cis compounds on the basis of the vector model shown in

1) Y. Mikawa, This Bulletin, **29**, 110 (1956).
2) W. H. T. Davison and G. R. Bates, *J. Chem. Soc.*, **1953**, 2607.
3) A. Kirrman and P. Chancel, *Bull. soc. chim. France* **1954**, 1338.
* In the following sections, for convenience, the terms "the cis and trans compounds" will be used for denoting the compounds having the higher and lower boiling points respectively.
4) S. Mizushima, "Structure of Molecules and Internal Rotation", Acad. Press, New York (1954).

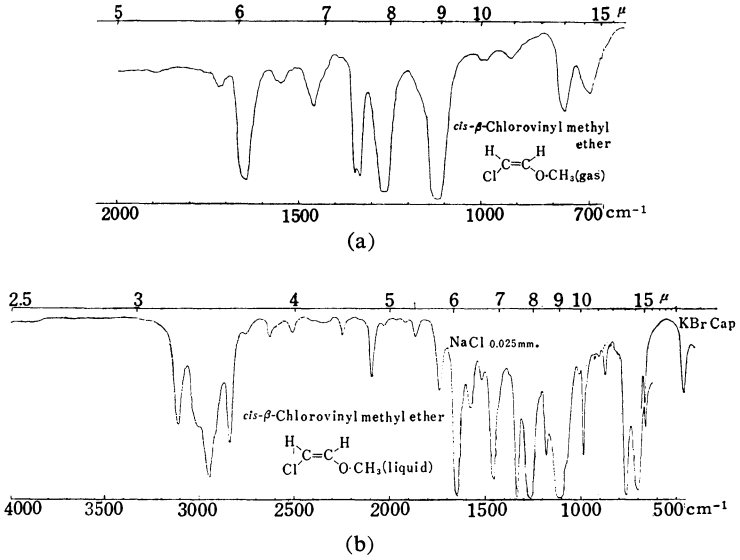


Fig. 2. Infrared absorption spectra of *cis*-chlorovinyl methyl ether. (a) Vapor at ca. 130°C; (b) Liquid film at the room temperature.

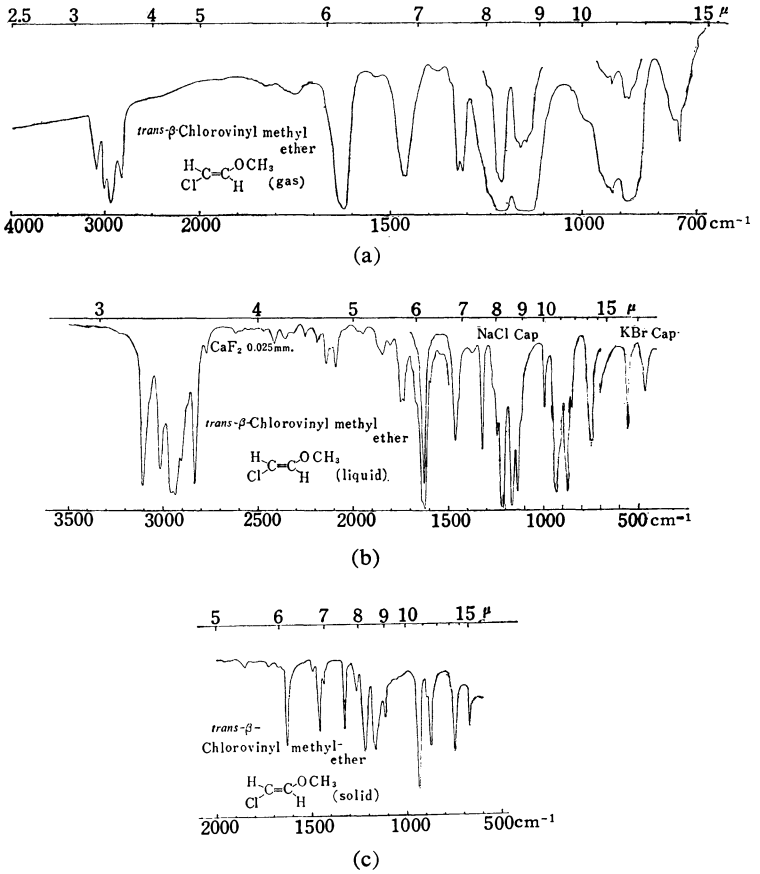


Fig. 3. Infrared absorption spectra of *trans*-chlorovinyl methyl ether. (a) Vapor at ca. 130°C; (b) Liquid film at the room temperature; (c) Solid at ca. −190°C.

TABLE I. THE VIBRATIONAL SPECTRA OF *cis*-β-CHLOROVINYL METHYL ETHER

Raman data Liquid	Infrared data Vapor		Liquid	Assignment
173 (5)				
359 (4)				
466 (6)			460m	Skeletal vibration
667 (5)			662w	
707 (0)	700w		703vs	=CH out-of-plane bend.
763 (7)	768w		763vs	C-Cl stretch.
879 (5)			873w	=CH out-of-plane bend.
918 (0)	918w		908vw	
	985, 988	w	998m	C-O-C sym. stretch.
			1010w	
			1050sh	
1080 (2)			1070sh	CH_3 wag.
	1118vs		1110vs	C-O-C anti-sym. stretch.
1185 (4)	1175sh		1181m	CH_3 rock.
1265 (6)	1260, 1268	vs	1261vs	=CH in-plane bend.
1337 (4)	1333, 1345	m	1331 s	=CH in-plane bend.
			1430sh	CH_3 asym. deformation
1463 (5)	1459w		1452 s	CH_3 sym. deformation
			1520vw	
	1552w			
			1578vw	
1655 (10)	1647, 1665	m	1650 s	C=C stretch.
	1713, 1720	w	1740w	
			1870vw	
			2098w	
			2250w	
			2510vw	
			2630vw	
2842 (6)			2842m	CH_3 sym. stretch.
2950 (9)			2947 s	CH_3 asym. stretch.
3050			3000sh	CH sym. stretch.
3100			3112m	CH asym. stretch.

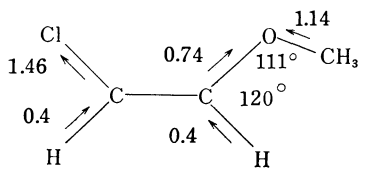


Fig. 4. Bond moments of chlorovinyl methyl ether.

Fig. 4*. It should be noted that the estimated values for the trans compound did not depend upon the angle of internal rotation. The estimated value, 1.55 D, is in good agreement with the observed value, 1.6 D. The fact that the observed values remained constant within the temperature range of 20~60°C does not contradict the presumption of rotational isomers, because even if the ratio of the number of the two rotational isomers varies with the temperature of the system, the dipole moment of the whole system should not change.

As for the cis compound, the estimated dipole moments are 3.08, 2.55 and 1.75 D as the angle of rotation, τ, increases from 0° to 90° and 180° (corresponding to the zigzag, the non-planar and the bent form respectively). Since the observed value was 2.53, the results of the calculation indicate that, as far as the bond moments approximation is valid, the molecule in the solution at 25°C takes on a non-planar configuration with an angle of internal rotation of about 90°.

At any rate, there is no doubt that the "trans compound" having a lower boiling point has a trans configuration and that the "cis compound" has a cis configuration.

* In Fig. 4. the figure for the cis molecule is given. The same bond moments are used for the trans molecule.

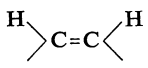
TABLE II. THE VIBRATIONAL SPECTRA OF *trans*-β-CHLOROVINYL METHYL ETHER

Raman data Liquid	Infrared data Vapor	Infrared data Liquid	Infrared data Solid	Assignment
142 (4)				Skeletal vibration
220 (0)				
327 (6)				
415 (3)				
457 (0)				
553 (2)				
			668w	Impurity
742 (4)	746m	745m	746 s	C-Cl stretch.
757 (2)	760sh	765sh		L.
	855sh, 866sh	850m		L.
	879m, 890m	872 s	874m	=CH out-of-plane bend.
		910sh		
932 (5)	924m	928 s	932 s	C-O-C sym. stretch.
	935sh	940sh		
987 (2)	985sh	992m		L.
		1110sh	1111m	
	1135sh, 1146 s	1133 s		L.
1161 (1)	1162 s, 1170sh	1160 s	1162 s	=CH in-plane bend.
1210 (2)	1212vs	1210 s	1214 s	C-O-C anti-sym. stretch.
1248 (5)	1250sh	1240m		
		1260sh	1261m	CH_3 rock.
1316 (7)	1314m, 1325m	1320 s	1322 s	=CH in-plane bend.
	1377w	1370w		
1445 (4)		1445sh	1436w	CH_3 asym. deformation
1450 (4b)	1462 s	1460 s	1454 s	CH_3 sym. deformation
			1490w	
1623 (9)	1623 s	1623 s	1630 s	C=C stretch.
1637 (6)	1635sh	1640sh		L.
		1732w		
		1750w		
		1806vw		
		1845w		
		1950vw		
		1973vw		
		2090w		
		2116vw		
		2140w		
		2190vw		
		2251vw		
		2310vw		
		2360vw		
		2416vw		
		2772vw		
2830 (6)	2835 s	2832 s		CH_3 sym. stretch.
		2902sh		
2946 (9)	2945 s	2934, 2956 s		CH_3 asym. stretch.
3012 (5)	3005 s	3010 s		CH sym. stretch.
3100 (4)	3090 s	3103 s		CH asym. stretch.

s=strong, m=medium, w=weak, vw=very weak, sh=shoulder
L=Bands arising from the less stable form of the molecule

Vibrational Spectra.—*cis-Chlorovinyl Methyl Ether.*—It can be seen from Table I that most of the Raman bands are also observed in the infrared spectra and that, except for the rotational structure of the vapor spectra, no essential difference between the infrared absorption frequencies measured in the liquid and vapor states is found. Furthermore, the number of the absorption bands is in accordance with the expectations. These facts exclude the possibility of the existence of the rotational isomers in the liquid or the vapor state. This exhibits a contrast to the trans compound, which will be mentioned later.

The observed frequencies can be interpreted as a superposition of the characteristic frequencies of vinyl and ether compounds. For instance, the bands at 1655, 1337, 1265 and 879 cm^{-1} correspond to those at 1601, 1360, 1271 and 908 cm^{-1} [5] of vinyl chloride. The fact that C=C stretching and =CH out-of-plane frequencies appear at 1655 and 707 cm^{-1} respectively gives strong spectroscopic evidence for the cis configuration, because the compound having the group



has, in general, two distinct characteristic bands in the regions 1635~1675 and 665~730 cm^{-1} [6]. The bands, at 466, 988 and 1118 cm^{-1} are due to the ether linkage, corresponding to those of dimethyl ether at 418, 929 and 1115 cm^{-1}, which were assigned[7] to the COC bending, symmetric and anti-symmetric stretching vibration respectively.

As was discussed in the previous study[1], methyl vinyl ether and other alkyl vinyl ethers have characteristic frequencies which distinctly differ from compounds having a vinyl group alone or an ether group alone, and the spectra of vinyl ethers can be interpreted on the assumption of a planar configuration. The reason why the cis compound concerned does not have the characteristic frequencies of vinyl ether can be explained only by rejecting the assumption of a planar configuration, i. e., by assming instead that the molecule of the cis compound takes on a non-planar configuration. In this case no resonance effect is taken into consideration, and consequently, the force constant of -C=C- or -C-O- keeps its original value. Therefore, some of the bands characteristic of vinyl compounds and ethers can be expected in the cis compound.

Though the angle of internal rotation cannot be predicted from the spectroscopic data, the conclusion is in conformity with that deduced from dipole moment measurement.

trans-Chlorovinyl Methyl Ether.—Several bands of the liquid spectra disappeared in the solid spectra. The bands which remain in the solid spectra are considered to be the spectra arising from the stable form of the rotational isomers. From this point of view, the liquid spectra as well as the vapor spectra were interpreted as superposed spectra of two or more configurational isomers, and the bands belonging to the stable form were tentatively assigned on the basis of an assumed model.

In the vapor spectrum (see Fig 3a), the band at 1322 cm^{-1} shows a very distinctive band shape. As will be seen later, this band is assigned to the =CH in-plane bending mode. The C=C stretching mode is expected around 1650 cm^{-1}, and it is known that the frequency of the trans compound usually appears at a higher frequency range than of the corresponding cis compound. However, in the present case, a strong band to be assigned to C=C stretching mode appears at 1623 cm^{-1}, or on the lower frequency side of the corresponding band of the cis compound. Furthermore, the general features of the spectra of this compound have a strong resemblance to those of methyl vinyl ether. The correlation between the two compounds is given in Table III. Based on these considerations, the molecular configuration of the stable form of the trans compound is supposed to be planar in form, probably the zigzag form, which had been shown to be plausible in the case of methyl vinyl ether. Thus, the assignment for most of bands was performed by reference to methyl vinyl ether. Though conclusive assignments are not possible at this stage, tentative assignment are shown in Table II.

TABLE III. CORRELATION BETWEEN THE BANDS OF *trans*-CHLOROVINYL METHYL ETHER AND THOSE OF VINYL METHYL ETHER

Vinyl methyl ether cm^{-1}	*trans*-Chlorovinyl methyl ether, cm^{-1}
1618	1623
1325	1320
1225	1212
1140	1166
965	924
886	885

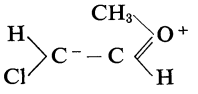
In the liquid and vapor spectra, there exist several bands which vanish in the solid state. These bands presumably belong to another rotational isomer existing in the liquid or vapor. Though the configuration of the

5) Landolt-Börnstein, "Zahlenwerte und Funktionen" 6, Anflage, I. Band, 2. Teil, Springer-Verlag, (1951).
6) A. D. Cross, "An Introduction to Practical Infrared Spectroscopy", Butterworth, London (1960).
7) Y. Mashiko, *J. Chem. Soc. Japan, Pure Chem. Sec.* (*Nippon Kagaku Zassi*), **79**, 470 (1958).

TABLE IV. MOMENTS OF INERTIA OF *trans*-CHLOROVINYL METHYL ETHER AND THEIR DIRECTION COSINES

$\tau=0$ (Zigzag form)			
	I_A	I_B	I_C
Moment of inertia ($\times10^{-40}$ g. cm^2)	601.2	573.0	33.28
Direction cosine l	0	0.545	0.838
m	0	−0.838	0.545
n	1	0	0
$\tau=180°$ (Bent form)			
	I_A	I_B	I_C
Moment of inertia ($\times10^{-40}$ g. cm^2)	516.7	469.1	52.74
Direction cosine l	0	0.608	0.794
m	0	−0.794	0.608
n	1	0	0

unstable form cannot be decided on, it may be supposed to be a planar-bent form which is stabilized by the contribution of the resonance structure

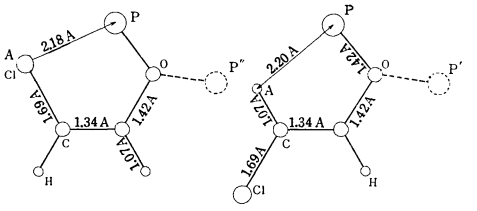


for the C=C frequency at 1635 cm^{-1} is still lower than that of the cis compound.

The Band Shape.—The moments of inertia and the direction cosines of the three principal axes of the trans molecule (in the zigzag form) are listed in Table IV. The bond lengths and the bond angles adopted in the calculation are shown in Fig. 5b. The calculation was carried out for every 30° from 0 to 180° of τ, and it was found that the symmetric top model could be approximately applied in every case. The degree of separation between the P and R branches of the parallel bands was estimated by the Gerhard-Dennison method[8], being found within the values 11.25 and 12.17 cm^{-1} at 400°K for any value of τ. The observed separation, 12 cm^{-1}, at the 1322 cm^{-1} band is in good agreement with the predicted value.

The exact modes of the normal vibrations can be pictured only by the normal coordinate treatment of the molecule. However, if the C–H in-plane bending vibration is localized in C–H bonds and there is on mixing with the other mode, the direction of the change of dipole moment can be decided upon. Therefore, it is easy to calculate the angle between one of the principal axes of the moment of inertia and the direction of the change of the bond moment of the C–H in-plane vibration. The calculated values for the zigzag and the bent forms of the trans compounds were 3°30′ and 7° respectively; i. e. the bands, in both cases, should exhibit an almost pure parallel type. Thus, for the C–H in-plane vibration, it is predicted that the band shape and the frequency do not change appreciably no matter what value the angle of internal rotation takes. This is why the band at 1322 cm^{-1} is assigned to the C–H in plane mode.

Many bands beside 1322 cm^{-1} show very complex band shapes. The band features of these bands are interpreted as the overlapping of two bands. For instance, the band at 1130～1170 cm^{-1} is composed of two doublets; the one is of 1135 cm^{-1} and 1146 cm^{-1}, and the other is of 1162 cm^{-1} and 1170 cm^{-1}. Similarly, the band at 850～890 cm^{-1} is composed of the doublets of 855 cm^{-1} and 865 cm^{-1}, and of 881 cm^{-1} and 891 cm^{-1}. These doublets are separated by 8～11 cm^{-1}, a separation compatible with the calculated value within the margins of experimental error.



(a) *cis*-Chlorovinyl methyl ether (b) *trans*-Chlorovinyl methyl ether

Fig. 5. The molecular configurations of chlorovinyl methyl ethers.

Internal Potential.—In the preceding sections, it was concluded that the cis compound takes just one non-planar configuration, while the trans compound in the liquid or vapor states two types of configuration, both of which are considered to be planar. It is of interest to discuss the internal forces which determine the stable configuration of the rotational isomers.

Three main factors are taken into consideration:

8) S. L. Gerhard and D. M. Dennison, *Phys. Rev.*, **43**, 197 (1933).

TABLE V. DIPOLE INTERACTION ENERGY (kcal./mol.)

Angle of internal rotation	Cis-compound			Trans-compound
	$\rho=0.4$	$\rho=0.5$	$\rho=0.7$	$\rho=0.5$
0° (zigzag)	0.55	0.96	1.30	1.17
90° (non-planar)	0.14	0.37	0.28	0.92
180° (bent)	−1.49	−1.28	−1.13	1.17

i) The steric repulsion
ii) The contribution of the resonance structure, $C^--C=O^+$
iii) The electrostatic force

First, the steric repulsion of the non-bonded atom in the molecule must be considered. Interatomic distances are shown in Fig. 5. If the methyl group is situated at P (Fig. 5), the interaction between the group at P and the atom at A becomes prominent. Especially for the cis compound, the distance between A and P is 2.18Å, much less than the sum of the van der Waals radii of the chlorine atom and the methyl group. Consequently, the methyl group cannot be situated at P on the plane of the vinyl group. Thus, the bent form is excluded from consideration for the cis compounds. Secondly, the resonance effect has to be considered. From the infrared study[1], it was concluded that in vinyl ether there was an appreciable single bond-double bond resonance. Therefore, the resonance effect would be of considerable importance for the chlorovinyl ethers concerned. If there is no other predominant factor than the resonance effect, the planar configurations, both the bent and the zigzag forms, become the stable forms. Such is the case with the trans compound. As has deen described before, the infrared spectra and the observed dipole moment are compatible with this model. However, as to the cis compound, the other effect seems to dominate over the resonance effect. The electrostatic interaction plays a significant role in this case, as will be shown below.

The interaction energy between two dipoles, μ_1 and μ_2, can be evaluated by the equation:

$$\mu_1\mu_2(\cos\theta-3\cos\alpha\cdot\cos\beta)/R \qquad (4)$$

where R is the distance between the dipoles, θ denotes the angle betwee μ_1 and μ_2, and α or β denotes the angle between one of the dipoles and the line connecting the two. On the base of the bond moments as shown in Fig. 4, the interaction energy of the dipoles was calculated with several values of τ, varying from 0 to 180°. Some of the results are listed in Table V, where the ρ value, which is a parameter which decides the apparent position of a dipole on the line connecting the atoms cencerned, is assumed to be 0.4, 0.5, or 0.7 for the cis compound. From Table V it can be seen that the difference between the values at $\tau=0°$ and $\tau=180°$ does not seriously depend upon the choice of the ρ value. In the cis compound, the bent form is more stable by 2.2±0.2 kcal, than the zigzag form. As to the trans compound, the dipole-dipole interaction seems to be minor; the zigzag, the non-planar and the bent forms have almost the same energy in so far as the electrostatic forces are concerned.

Form the consideration of these three factors, it is concluded that the trans compound takes the zigzag form as the most stable configuration, and that if the resonance energy overcomes the steric repulsion, the bent form also becomes stable. The non-planar configuration is unfavorable in all respects. On the other hand, as to the cis compound, the zigzag form is not always the most stable because it can have a higher energy than the non-planar form; i. e., if the amount of resonance energy is quite small in comparison with the dipole-dipole interaction, the zigzag form is less stable than the non-planar form. Although many other factors beside the three mentioned above could be considered in connection with the internal rotation, and although the estimation of the dipole-dipole interaction was made only roughly, it is sure that the dipole-dipole interaction plays a significant role in the cis compound which takes the non-planar configuration.

Summary

Raman and infrared spectra of *cis*- and *trans*-β-chlorovinyl methyl ethers ($ClCHCHOCH_3$) were measured in the vapor and liquid states, and the infrared spectra in the solid state were also measured for the trans compound. The dipole moments were measured for both of the compounds in a benzene solution. From the observed value of the dipole moments, it was decided that the compound having the lower boiling point had a trans configuration and the other, a cis configuration.

On the basis of these configuration, interpretation of the vibrational spectra of both compounds was undertaken. As for the trans compound, the existence of the rotational isomers arising from the internal rotation around the C–O axis was verified by the fact that some of the infrared bands disappeared on solidification of the samples. The spectra

in the liquid and vapor states were interpreted as a mixture of those of two rotational isomers, and tentative assignments were given for one of the isomers by reference to the spectra of methyl vinyl ether. The most probable form of the molecule was supposed as the planar zigzag form.

On the contrary, it was established that there existed no rotational isomer in the cis compound in any state. The spectra of the cis compound did not resemble those of the trans compound or the methyl vinyl ether and were interpreted as a superposition of group frequencies of the ether linkage and of the -CH=CH- group. Consequently, a non-planar model was proposed, and the angle of internal rotation was determined to be about 90° from the observed value of the dipole moment. In order to explain the difference in the spacial configuration between the cis and the trans compounds, the electrostatic effect, in addition to the resonance effect and the steric repulsion, was considered. From the results of the calculation of the dipole-dipole interaction, it was shown that this electrostatic force played a very significant role in the internal rotation.

The authors wish to express their thanks to Professor Takehiko Shimanouchi of the University of Tokyo for his valuable advice and to Mr. Saburo Hattori, who prepared the samples for this work.

Central Research Laboratory
Mitsubishi Chemical Industries Limitea
Kawasaki-shi, Kanagawa-ken

Stereospecificity and Dipole Moment of Polymers. I. Dielectric Property of Polyvinyl Chloride Solution

By Akira KOTERA, Mikiko SHIMA, Noriko FUJISAKI and Takeshi KOBAYASHI*

(Received November 8, 1961)

The properties of polyvinyl chloride (PVC) vary according to the temperature at which it is polymerized. Studies of the infrared absorption spectrum reveal that low-temperature polymerized PVC, compared with commercial PVC[1], is rich in syndiotactic portion. Owing to their high crystallinity, however, most of the studies of stereospecific polymers have been limited to a consideration of their solid state properties, such as X-ray diffraction, infrared absorption spectrum and melting point. It is expected that molecules of isotactic, syndiotactic and atactic polymers, which are stereoisomers of each other, may take different shapes in solution and, therefore, give their solutions different porperties. However, not many reports on studies of the solutions of stereospecific polymers have yet been published. Danusso and his coworkers[2,3] pointed out that the second virial coefficients of a toluene solution of isotactic polystyrene obtained from osmotic pressure measurements are different from that of atactic polystyrene. Differences in Flory temperature and in entropy parameter between isotactic and atactic polystyrene were reported by Wessling et al.[4] New approaches in this field seem to be found in the study of tacticity through the measurement of the nuclear magnetic resonance absorption spectra of isotactic and syndiotactic polymethyl methacrylates in a chloroform solution[5] and in the estimation of the tacticity of polyalkyl methacrylate from the reaction velocity of hydrolysis[6].

The dipole moment of polar vinyl polymer is related to the orientation of monomer units carrying polar groups, and the observed moment is the statistical average over the molecular conformations. Its theoretical treatment was originally developed by Eyring[7] and by Suzuki[8] et al., and has been recently extended by Volkenstein[9], Nagai[10] and Suzuki[11].

* Kureha Kasei Co., Ltd., Tokyo Laboratory, Shinjuku-ku, Tokyo.

1) T. Shimanouchi, S. Tsuchiya and S. Mizushima, *J. Chem. Phys.*, **30**, 1365 (1959).
2) F. Danusso and G. Moraglio, *J. Polymer Sci.*, **24**, 161 (1957).
3) F. Ang, ibid., **25**, 126 (1957).
4) J. B. Kinsinger and R. A. Wessling, *J. Am. Chem. Soc.*, **81**, 2908 (1959).
5) A. Nishioka, H. Watanabe, I. Yamaguchi and H. Shimizu, *J. Polymer Sci.*, **45**, 232 (1960).
6) G. Smetz and W. De Laecker, ibid., **45**, 461 (1960).
7) H. E. Eyring, *Phys. Rev.*, **39**, 746 (1932).
8) Y. Suzuki and K. Suzuki, *Studies on Phys. Prop. (Bussei-ron Kenkyu)*, **9**, 39 (1947).
9) M. V. Volkenstein, *J. Polymer Sci.*, **29**, 441 (1958).
10) K. Nagai, *J. Chem. Phys.*, **31**, 1169 (1959).
11) Y. Suzuki, ibid., **34**, 79 (1961).

Recently Pohl[12] et al. measured the dipole moments of isotactic, syndiotactic and atactic polymethyl methacrylates and found that their values differ.

With low-temperature polymerized PVC, one of the authors measured the viscosity, osmotic pressure and light scattering of a tetrahydrofuran solution and found that both the solvent-solute interaction parameter and the extension of the molecule are somewhat larger than those of commercial PVC[13].

For this report, the dielectric properties of both low-temperature polymerized and commercial PVC solutions were measured in order to discuss the relation between the dipole moment values and the tacticity of polymers.

Experimental

Samples.—Sample I is PVC obtained by radical polymerization carried out at −15°C, and sample II is commercial PVC obtained by radical polymerization at 58°C. Both samples were purified by being dissolved in tetrahydrofuran, precipitated by the addition of a large amount of methanol, and dried in vacuo to a constant weight.

Measurement of Dielectric Polarization and Method of Calculation. — The dielectric constants and densities of tetrahydrofuran solutions of samples I and II were measured and the average dipole moment per monomer unit was determined according to the generally accepted procedure[14].

$$p_2 = p_1\{3\alpha/(\varepsilon_1-1)(\varepsilon_1+2) - \beta/d_1 + 1\} \quad (1)$$

$$\mu = 0.0128\sqrt{(P_2 - [MR]_D)T}\ \text{D} \quad (2)$$

where $[MR]_D$ is the molcular refraction of the molecular unit.

The specific polarization p_2, determined by formula 1, proposed by Halverstadt-Kumler[15], multiplied by the molecular weight M of the monomer unit gives the molecular polarization, $P_2(=M\times p_2)$. Orientation polarization was obtained by subtracting $[MR]_D$ from P_2, and the dipole moment, μ, per monomer unit of polymer was determined by formula 2.

α and β in formula 1 are increments of the dielectric constant and the density of the solution respectively. When ε_1, ε_{12} and d_1, d_{12} denote the dielectric constants and the densities of the solvent and solution respectively, and w denotes the weight fraction of the solute, α and β will be given by:

$$\alpha = \{(\varepsilon_{12}-\varepsilon_1)/w\}_{Av}$$

$$\beta = \{d_{12}-d_1)/w\}_{Av}$$

P_1 in formula 1 is the specific polarization of the solvent given by

$$P_1 = (\varepsilon_1-1)/(\varepsilon_1+2)d_1$$

The dielectric moment measurements were made at 500 kc/sec. by the heterodyne beat method. Details of the apparatus were given in a previous report[16].

The cell is composed of three concentric cylindrical platinum electrodes, the first and the third of which are earthed. The three-electrode system makes the shielding better and the capacity larger;

TABLE I. DIELECTRIC PROPERTY OF TETRAHYDROFURAN SOLUTION OF LOW-TEMPERATURE POLYMERIZED POLYVINYL CHLORIDE (SAMPLE I)

w	20°C		40°C	
	ε_{12}	d_{12}	ε_{12}	d_{12}
0.06144	8.153	0.9082	7.402	0.8877
0.04658	7.989	0.9028	7.295	0.8816
0.03730	7.850	0.8999	7.159	0.8782
0.02412	7.650	0.8926	7.008	0.8736
0	7.474(=ε_1)	0.8863(=d_1)	6.882(=ε_1)	0.8650(=d_1)

TABLE II. DIELECTRIC PROPERTY OF TETRAHYDROFURAN SOLUTION OF COMMERCIAL POLYVINYL CHLORIDE (SAMPLE II)

w	20°C		40°C	
	ε_{12}	d_{12}	ε_{12}	d_{12}
0.06778	8.123	0.9109	7.371	0.8897
0.05295	7.972	0.9064	7.265	0.8848
0.04190	7.856	0.9015	7.186	0.8802
0.02714	7.718	0.8962	7.064	0.8746
0	7.474(=ε_1)	0.8863(=d_1)	6.882(=ε_1)	0.8650(=d_1)

w: Weight fraction of polymer, ε_{12}: Dielectric constant of solution, d_{12}: Density of solution, ε_1: Dielectric constant of solvent, d_1: Density of solvent

12) R. Bacskai and H. A. Pohl, *J. Polymer Sci.*, **42**, 151 (1960).
13) T. Kobayashi, submitted to this Bulletin for publication.
14) A. Kotera, *High Polymers* (*Kobunshi*), **1**, 1 (1944).
15) I. F. Halverstadt and W. D. Kumler, *J. Am. Chem. Soc.*, **64**, 2988 (1942).
16) M. Shima, *J. Polymer Sci.*, **56**, 213 (1962).

it is approroximately 75 $\mu\mu$F. Density was determined by means of a density bottle of a flask shape, the volume of which was approximately 10ml.

Meaurements were carried out at four concentrations between 2~7% for each sample at 20 and 40°C. Each solution was prepared by heating polymer and tetrahydrofran in a sealed glass ampoule for two hours at 100°C immediately before the measurement. The results are listed in Tables I, II and III. The errors in μ-values are estimated to be $\pm$0.02D.

Results and Discussion

Dipole Moment of Stereospecific Polymer.— The results in Table III show that the dipole moment per monomer unit of sample I is 1.39 D, and that of sample II is 1.31 D, both independent of the measurement temperature. This 6% decrease may be attributed to the decrease in the syndiotactic portion, although the values are apparent ones, affected by the interaction between the polymer and the polar solvent, tetrahydrofuran.

TABLE III. DIPOLE MOMENT OF POLYVINYL CHLORIDE IN TETRAHYDROFURAN

	Low-temperature polymerized PVC (sample I)		Commercial PVC (sample II)	
	20°C	40°C	20°C	40°C
p_1	0.7710	0.7655	0.7710	0.7655
α	10.839	8.503	9.329	7.140
β	0.358	0.354	0.369	0.362
p_2	0.8684	0.8260	0.8021	0.7588
P_2 (cc.)	54.28	51.63	50.13	47.43
μ (D)	1.39	1.39	1.31_5	1.31

p_1: Specific polarization of solvent (tetrahydrofuran)
p_2: Specific polarization of polymer
P_2: Molecular polarization per monomer unit of polymer
μ: Dipole moment per monomer unit of polymer

$\alpha=\{(\varepsilon_{12}-\varepsilon_1)/w_2\}_{Av}$, $\beta=\{(d_{12}-d_1)/w_2\}_{Av}$

$[MR]_D=14.11$ cc.

The dipole moments of stereospecific polymers were reported by Pohl et al. for isotactic and syndiotactic polymethyl methacrylates[12], by Krigbaum et al. for isotactic polystyrene in toluene[17], and recently by Imamura et al. for isotactic polyvinyl isobutyl ether[18].

The values reported in these papers are listed in Table IV. Isotactic polymers have larger moments than atactic polymers in all cases. With polymethyl methacrylates the values are of the order of iso. > atac. > syn. In this experiment the inverse tendency, syn. > atac., was observed with PVC.

Some of the theories shown above derived the formulae to express the values of the dipole moment per monomer unit of polar vinyl polymers, and concluded that generally the values for isotactic and syndiotactic chains are not the same. However, it can not be concluded either that isotactic polymers always have larger dipole moment values than syndiotactic polymers or the inverse. The formula should contain many factors in order to give an exact numerical value of the dipole moment.

Under the present circumstances, it is impossible to explain the inverse tendency obtained here.

However, it may be said that the stereospecificity of the chain can be related to the dipole moment value, and that it will be possible to determine the magnitude of the stereospecificity of the polar vinyl polymer through the measurement of the dipole moment.

TABLE IV. DIPOLE MOMENTS OF STEREOSPECIFIC POLYMERS

Polymer		Dipole moment D	Solvent	Temp. °C
Polystyrene[17]	isotactic	0.435	Toluene	38.4
	atactic	0.36	Toluene	38.4
Polymethyl methacrylate[12]				
	isotactic	1.43	Benzene	30
	atactic	1.35	Benzene	30
	syndiotactic	1.27	Benzene	30
Polyvinyl isobutyl ether[18]				
	isotactic	1.16	Benzene	25
	atactic	1.07	Benzene	25
Polyvinyl chloride				
Sample II,	atactic	1.31	Tetrahydrofuran	20
Sample I,	rich in syndiotactic	1.39	Tetrahydrofuran	20

17) W. R. Krigbaum and A. Roig, *J. Chem. Phys.*, 31, 544 (1959).

18) Y. Imamura, M. Takeda, S. Okamura and T. Higashimura, ibid., 33, 631 (1960).

Effect of the Solvent on the Conformation of Polymer Molecules.—The dipole moment measurements so far mentioned were carried out with a polar solvent, tetrahydrofuran, because low-temperature polymerized PVC is insoluble in any nonpolar solvent. The effect of polar solvent should be discussed.

The total dipole moment of N-mer, μ_T, is expressed by

$$\langle \mu_T^2 \rangle / N = \mu^2 = \mu_0^2 \phi$$

where μ_0 is the moment of the individual dipole and ϕ is the interaction parameter.

Marchal and Benoit[19] explained that ϕ is independent of N when $N \to \infty$ under the conditions; (1) the dipole of each monomer unit is on a bisector of the valence angle of skeleton chain, and (2) the mean square end-to-end distance of the chain is proportional to N^α, where $\alpha < 2$.

The first condition can be easily modified: it is on the bisecting plane. Then both conditions seem to be satisfied by polyvinyl chloride. In such a case ϕ becomes the function only of the short-range conformations, such as valence angles, internal rotations etc., and long-range ones can be neglected.

Taking μ_0 to be the dipole moment of the reference substance close in the structure to the monomer unit, we can determine ϕ from the measurement of μ_0 and μ. In this way the solvent effect upon short-range conformation can be estimated.

Of course, the values of μ_0 and μ are affected by the choice of solvent, owing to the change in electrostatic interaction, but when the values of ϕ determined from μ_0 and μ in polar and nonpolar solvents coincide, one may assume that the short-range conformation of the molecules is not affected appreciably by the interaction between the solvent and polymer molecules.

Marchal et al. showed that the value of ϕ is almost independent of the polarity of solvents with polymethyl methacrylate[19,20]. In order to see if the same situation holds with PVC, *sec*-butyl chloride was selected as the reference substance; its dipole moment and that of commercial PVC were measured in dioxane and in tetrahydrofuran by the use of the same apparatus at the same temperatures as above. ϕ values were determined from the observed dipole moments and are listed in Table V.

TABLE V. INTERACTION BETWEEN POLYVINYL CHLORIDE AND SOLVENT

Temp. °C	Solvent	μ_0, D	μ, D	ϕ
20	Dioxane	2.12	1.61	0.59
20	Tetrahydrofuran	1.64	1.31_5	0.64
40	Dioxane	2.12	1.62	0.59
40	Tetrahydrofuran	1.66	1.31	0.62

μ : Dipole moment per monomer unit of PVC
μ_0: Dipole moment of *sec*-butyl chloride

TABLE VI. INTERACTION BETWEEN POLYMETHYL METHACRYLATE AND SOLVENT[19,20]

Temp. °C	Solvent	μ_0^2	μ^2	ϕ	ϕ_{MB}
25	Benzene	2.99	1.87	0.62	—
25	Dioxane	2.96	1.82	0.61	0.65
25	Chloroform	1.98	1.22	0.61	0.62
25	Butyl acetate	0.34	0.20	0.60	0.58

μ : Dipole moment per monomer unit of polymethyl methacrylate
μ_0: Dipole moment of methyl propionate

They proved to be 0.63 (tetrahydrofuran) and 0.59 (dioxane) and do not differ appreciably. The results reported by Marchal et al. with polymethyl methacrylate are listed in Table VI for purposes of reference, where ϕ_{MB} is the value of ϕ reported in the older report.

As in the case with polymethyl methacrylate, it can be said that the interaction between the molecules of the polymer and the solvent seems to have no significant effect on the short-range conformation of the PVC molecules in tetrahydrofuran and that the determination of the apparent dipole moment in polar solvent will serve for purposes of relative comparison.

The authors wish to express their thanks to Professor Keizo Suzuki for his discussions concerning the interpretation of the theories.

Department of Chemistry
Faculty of Science
Tokyo University of Education
Otsuka, Tokyo

19) J. Marchal and H. Benoit, *J. Polymer Sci.*, **23**, 223 (1957).
20) J. Marchal and C. Lapp, *J. Polymer Sci.*, **27**, 571 (1958).

The Reaction of Carbon Monoxide with Organometallic Compounds. VI. Synthesis of Symmetrical Ketones by the Reaction of Carbon Monoxide with Organolithium Compounds*

By Membo RYANG and Shigeru TSUTSUMI

(Received November 22, 1961)

In the last previous paper[1] of this series, the present authors reported that carbon monoxide reacted with an organolithium compound in an ether solution at −10°C, producing various products. The formation of these products could be interpreted in terms of an ionic reaction mechanism from the results of the reaction of carbon monoxide with organomagnesium halides[2].

The reaction of an organolithium compound with carbon monoxide occurs violently, so it seems desirable to control the reaction on applying this reaction to a synthetic method.

In this regard, we have undertaken a study of the reaction of carbon monoxide with phenyllithium in an ether solution at −70°C.

Phenyllithium[3] was prepared from bromobenzene and metallic lithium in anhydrous ether, and then dry, pure carbon monoxide was bubbled into the solution at −70°C.

The above reaction gave benzophenone in a 55% yield, instead of the benzoin which was expected on the basis of the previous results[2,3].

The symmetrical ketones were prepared by various methods. For example, Marvel[4] prepared benzophenone from benzene and carbon tetrachloride in the presence of aluminum chloride, but this method was not used for preparing other ketones. Sommelet[5] obtained 4, 4′-ditolyl ketone from *p*-toluic acid chloride and toluene in a poor yield.

Furthermore, the preparations of di-*n*-butyl ketone[6], di-*n*-amyl ketone[7] and diisopropyl ketone[8] by earlier methods are not satisfactory in yield and involve complicated starting materials.

We have found that the new method is simple and can be extended to similar reactions in good yields.

The symmetrical ketones prepared by this new method are as follows: benzophenone (55%), 4, 4′-ditolyl ketone (50%), di-*n*-amyl ketone (28%), di-*n*-butyl ketone (40%) and diisopropyl ketone (30%).

Results and Discussion

The results of the synthesis of various ketones according to our new method are summarized in Table I.

Although the mechanism of this reaction is still open to question, two probable reaction paths may be considered.

In the first, the carbon monoxide adducts (A), mentioned in previous papers, react with organic halides (Wurz-Fitting type reaction) to produce ketones (Eq. 1).

$$R\text{-}\overset{\overset{O}{\|}}{C}\text{-}Li + R\text{-}X \longrightarrow R\text{-}\overset{\overset{O}{\|}}{C}\text{-}R + LiX \qquad (1)$$

In the second, carbon monoxide attacks organolithium compounds and abstracts lithium as lithium carbonyl, producing ketone (Eq. 2). The stoichiometric equation is shown as follows:

$$2R\text{-}Li + 3CO \longrightarrow R\text{-}\overset{\overset{O}{\|}}{C}\text{-}R + 2LiCO \qquad (2)$$

The reaction path of Eq. 1 may be considered to be improbable for the following reasons: 1) The carbonation of organolithium compounds by solid carbon dioxide gave acids in good yields, and the number of organic halides was found to be very small[9]. 2) The yields of ketones in this reaction are parallel with those of organolithium compounds (C_6H_5–Li 97.5%[10], *p*-$CH_3C_6H_4$–Li 95.6%[10], *n*-Bu–Li 85%[11], *n*-Am–Li 85%[11], *iso*-Pr–Li 75%[11]) and, in the case of phenyllithium, the further addition of equimol bromobenzene did not increase the yield of benzophenone. 3) The Wurz-Fittig type reaction would not be expected at such a low temperature.

* Part V, This Bulletin, **34**, 1341 (1961).

1) M. Ryang and S. Tsutsumi, *J. Chem. Soc. Japan, Pure Chem. Sec.* (*Nippon Kagaku Zasshi*), **82**, 880 (1961).

2) M. Ryang and S. Tsutsumi, ibid., **82**, 878 (1961).

3) "Organic, Syntheses" Coll. Vol. II (1948), p. 518.

4) C. S. Marvel and W. M. Sperry, "Organic Syntheses" Coll. Vol. I (1956), p. 95.

5) M. Sommelet, *Compt. rend.*, **180**, 1350 (1925).

6) J. V. Brawn, *Ber.*, **67**, 221 (1934); R. R. Briese and S. M. McElvain, *J. Am. Chem. Soc.*, **55**, 1697 (1933).

7) J. C. Sauer, "Organic Syntheses", Vol. 31 (1951), p. 68.

8) C. R. Hauser and W. B. Renfrow, *J. Am. Chem. Soc.*, **59**, 1862 (1937).

9) H. Gilman, ibid., **55**, 1258 (1933).

10) H. Gilman, E. A. Zoellner and W. W. Selby, ibid., **55**, 1252 (1933).

11) H. Gilman, F. W. Moore and O. Baine, ibid., **63**, 2479 (1941).

TABLE I

Starting material	Solvent	Temp., °C	Ketone	Yield*, %
Bromobenzene	Ether	−70	Benzophenone	55
p-Tolyl bromide	Ether	−70	4,4'-Ditolyl ketone	50
n-Amyl chloride	Ether and petroleum ether	−70	Di-*n*-amyl ketone	28
n-Butyl chloride	Ether	−70	Di-*n*-butyl ketone	40
Isopropyl chloride	Petroleum ether	−70	Diisopropyl ketone	30

* The calculations of yields are based on the number of the organic halides used.

The above consideration indicates that the unreacted organic halides do not react with (A) in Eq. 1.

If the reaction path of Eq. 1 is improbable for the above reasons, the ketones must be formed by the reaction path of Eq. 2.

Although there is no experimental evidence for the formation of lithium carbonyl in these reaction systems, several workers have reported that ionized alkali metals react easily with carbon monoxide, producing alkali metal carbonyls.

For example, Liebig[12] obtained potassium carbonyl by passing carbon monoxide over heated potassium, and Joannis[13] more easily prepared alkali metal compound corresponding to the formulas, KCO and NaCO, by the action of carbon monoxide on alkali metals in a liquid ammonia solution.

Pearson[14] also prepared the carbonyls of lithium, rubidium and calcium by passing carbon monoxide into the solution of the metals in liquid ammonia at −60°C.

Although there are various opinions about the behavior of alkali metals in a liquid ammonia solution, it is generally believed that the metals exist in a positively charged state[15].

The above facts seem to suggest that carbon monoxide can react more easily with an ionized alkali metal than with an alkali metal itself.

As the carbon-lithium bond in an organolithium compound has a 43% ionic character, it seems probable that the nucleophilic attack of carbon monoxide on positively charged lithium gives lithium carbonyl and ketone.

Furthermore, the authors carried out the reaction of iron pentacarbonyl with phenyllithium in an ether solution at −70°C. It is improbable to suppose the formation of lithium carbonyl by the reaction of iron pentacarbonyl with the organolithium compound, because the carbon monoxide in iron pentacarbonyl is coordinated to the iron atom and has not the ability to abstract lithium as lithium carbonyl.

For the above reasons, benzophenone was not obtained in this reaction; benzoin (25%) was the main product, the formation of which was explained by an ionic reaction mechanism, as has already been discussed.

Experimental

Materials.—*Bromobenzene.*—Commercial bromobenzene was purified by fractional distillation; b. p. 150°C, n_D^{15} 1.5625. *p*-Bromotoluene was prepared by the Sandmeyer reaction of *p*-toluidine[16]; b. p. 185°C, m. p. 25~26°C.

n-Amyl chloride was prepared from *n*-amyl alcohol by reaction with thionyl chloride[17]; b. p. 106°C, n_D^{20} 1.4122.

n-Butyl Chloride. — Commercial *n*-butyl chloride was purified by fractional distillation; b. p. 78°C, n_D^{20} 1.4022.

Isopropyl Chloride.—Commercial isopropyl chloride was purified by fractional distillation; b. p. 36°C.

Carbon monoxide was prepared by the reaction of formic acid with concentrated sulfuric acid, was washed with a 10% sodium hydroxide solution, and dried with calcium chloride and phosphorus pentoxide.

Synthesis of Symmetrical Ketones. — *Benzophenone.*—Into a 500 ml. four-necked flask equipped with a mechanical stirrer, a low temperature thermometer, a reflux condenser protected from moisture, a gas bubbler and a dropping funnel, were placed 50 ml. of anhydrous ether (dried over sodium) and, after sweeping the apparatus with dry oxygen-free nitrogen, 4.9 g. (0.7 g. atom) of lithium in the form of small pieces of thin coil. A solution of 47.1 g. (0.3 mol.) of bromobenzene in 200 ml. of anhydrous ether stirred in from the dropping funnel over a period of 2 hr., while the internal temperature was maintained at 35°C. After the addition was completed, the stirring was continued for a further 2 hr., after which the reaction mixture was cooled to −70°C with a dry ice-methanol bath kept at −78°C.

Dry pure carbon monoxide was next introduced from the gas bubbler at a rate of 0.5 l/min. for 2 hr.

The reaction mixture was then decomposed with 50 ml. of 95% ethanol and further with 100 ml. of 4 N hydrochloric acid. The separated organic layer was treated with three succesive 100 ml. portions of saturated aqueous potassium carbonate and then with three succesive 100 ml. portions of 5% aqueous sodium hydroxide and divided into (1) the organic layer, (2) potassium carbonate solution and (3)

12) J. Liebig, *Ann.*, **11**, 182 (1834).
13) A. Joannis, *Compt. rend.*, **158**, 874 (1914).
14) T. G. Pearson, *Nature*, **131**, 166 (1933).
15) M. C. R. Symons, *Quart. Rev.*, **8**, 99 (1959).
16) "Organic Syntheses", Coll. Vol. I (1956), p. 136.
17) F. C. Whitmore, F. A. Karnatz and A. H. Popkin, *J. Am. Chem. Soc.*, **80**, 2541 (1938).

sodium hydroxide solution. The organic layer containing neutral compounds was washed with water and dried over anhydrous sodium sulfate. The brownish residual oil obtained after removal of the solvent was distilled under reduced pressure to give the following fractions: (1) b. p. 70~120°C/4 mmHg 3.5 g., (2) b. p. 120~125°C/4 mmHg 15 g., (3) b. p. 130~140°C/2 mmHg 2.4 g., (4) b. p. 190~210°C/2 mmHg 3.3 g. and a dark orange residue.

Fraction 1 was assumed to be mainly diphenyl and was identified by mixed melting point measurement.

Fraction 2 was identified as benzophenone by mixed melting point measurement of its 2,4-dinitrophenylhydrazone (m. p. 236°C, recrystallized from ethyl acetate) or its semicarbazone (m. p. 165°C, recrystallized from ligroin and benzene) (theoretical yield: 55%).

Fraction 3 was recrystallized from benzene and ligroin to give colorless crystals, m. p. 87~88°C, while fraction 4 gave white crystals by recrystallization from benzene, m. p. 201~202°C. The structures of the above two compounds have not yet been determined.

The acidic and phenolic compounds which were involved in the potassium carbonate solution and the sodium hydroxide solution respectively were confirmed to be the same as those of a previous report[1].

4,4'-Ditolyl Ketone.—The procedure employed here was identical to that described above. The ether solution of *p*-tolyllithium was prepared by using 34.2 g. (0.2 mol.) of *p*-bromotoluene, 3.5 g. (0.5 g. atom) of lithium and 250 ml. of anhydrous ether, and the introduction of carbon monoxide into the solution was carried out at −70°C. The organic layer, separated after the decomposition of the reaction mixture, was divided into a neutral part, an acidic part and a phenolic part by means of the above-mentioned method. The neutral part was distilled under reduced pressure to give the following fractions: (1) b. p. 115~140°C/9 mmHg 1.8 g., (2) b. p. 175~185°C/9 mmHg 10.4 g., (3) b. p. 180~215°C/1 mmHg 4.6 g. and a dark, brownish residue. Fraction 1 was identified as 4,4'-ditolyl by its mixed melting point measurement (m. p. 121°C, recrystallized from ethanol).

Found: C, 92.36; H, 7.67. Calcd. for $C_{14}H_{14}$: C, 92.26; H, 7.74%.

Fraction 2 was recrystallized from ethanol to give 4,4'-ditolyl ketone as colorless prisms, m. p. 95~95.5°C (theoretical yield: 50%).

Found: C, 86.03; H. 6.71. Calcd. for $C_{15}H_{14}O$: C, 85.68; H, 6.71%.

Fraction 3 solidified on standing and was recrystallized from ligroin to give yellow crystals, m. p. 109~110°C, the structure of which has not yet been determined.

Found: C, 84.02; H, 6.30%.

The acidic and phenolic parts were not examined.

Di-n-butyl Ketone.—Dry pure carbon monoxide was introduced into an ether solution, cooled to −70°C, of *n*-butyllithium prepared from 27.75 g. (0.3 mol.) of *n*-butyl chloride, 4.9 g. (0.7 g. atom) of lithium and 300 ml. of anhydrous ether at the rate of 0.51/min. for 2 hr. The reaction mixture was decomposed immediately and divided into a neutral part and an acidic part. The neutral part was distilled under reduced pressure to give the following fractions: (1) b. p. 105~115°C/50 mmHg 9.3 g. and (2) b. p. 147~150°C/35 mmHg 2.2 g.

The infrared absorption spectra measurement showed the presence of a carbonyl group in fraction 1 and that the semicarbazone of fraction 1 had an identical melting point with that of di-*n*-butyl ketone (m. p. 90°C, recrystallized from ligroin).

Found: C, 60.38; H, 10.59. Calcd. for $C_{10}H_{21}ON_3$: C, 60.26, H, 10.62%.

The results of gas chromatographic analysis showed that fraction 1 was mainly di-*n*-butyl ketone and that about 10% of impurities was included. (Column-SiDC 550 2 m.; column temperature, 167°C; carrier gas, H_2; gas pressure, 0.3 kg./cm²; retension time of di-*n*-butyl ketone, 14~15 min.) (theoretical yield: 40%). Pure di-*n*-butyl ketone was obtained by purification of fraction 1 using preparative gas chromatography (column-SiDC 550; column temperature, 170°C; carrier gas, N_2; gas pressure, 1 kg./cm²). B. p. 111~112°C/70 mmHg, n_D^{15} 1.4210.

Found: C, 75.60; H, 12.86. Calcd. for $C_9H_{18}O$: C, 75.99; H, 12.76%.

Fraction 2 and the acidic part were not examined.

Di-n-amyl Ketone.—Carbon monoxide was introduced at −70°C, into an ether solution of *n*-amyllithium prepared by using 32 g. (0.3 mol.) of *n*-amyl chloride, 4.9 g. (0.7 g. atom) of lithium, 150 ml. of ether and 150 ml. of petroleum ether (b. p. 40~50°C). The distillation of the neutral part, obtained from the reaction mixture, under reduced pressure gave the following fractions: (1) b. p. 100~120°C/37 mmHg 2 g., (2) b. p. 123~133°C/37 mmHg 7.5 g., and high boiling fractions. Fraction 2 was purified by preparative gas chromatography. (Column-SiDC; column temperature, 160°C; carrier gas, N_2; gas pressure, 1 kg./cm²). The colorless liquid, thus obtained 6.9 g., was confirmed to be di-*n*-amyl ketone. B. p. 110~111°C/19 mmHg, n_D^{15} 1.4301.

Found: C, 77.50; H, 12.97, Calcd. for $C_{11}H_{22}O$; C, 77.58; H, 13.02%.

Diisopropyl Ketone.—Carbon monoxide was introduced at −70°C into a solution of isopropyllithium prepared from 23.7 g. (0.3 mol.) of isopropyl chloride, 4.9 g. (0.7 g. atom) of lithium and 200 ml. of petroleum ether. The distillation of the neutral part, obtained from the reaction mixture, gave 5 g. of an oily product, boiling at 120~127°C/760 mmHg. This was identified as diisopropyl ketone from the results of infrared absorption spectra measurement and a mixed melting point test of its semicarbazone (m. p. 144~145°C, recrystallized from ligroin and benzene) (theoretical yield: 30%).

Found: C, 56.37; H, 9.93. Calcd. for $C_8H_{17}ON_3$: C, 56.11; H, 10.01%.

The other high boiling products were not identified.

The Reaction of Iron Pentacarbonyl with Phenyllithium.—To an ether solution of phenyllithium, prepared from 31.4 g. (0.2 mol.) of bromobenzene, 3.5 g. (0.5 g. atom) of lithium and 250 ml.

of anhydrous ether, was added 9.4 g. (0.048 mol.) of iron pentacarbonyl in 100 ml. of anhydrous ether at −70°C over a period of 30 min. The reaction mixture was decomposed with ethanol and dilute hydrochloric acid, and the organic layer was divided into neutral, acidic and phenolic parts. The distillation of the neutral part under reduced pressure gave the following fractions: (1) b. p. 80~100°C/2 mmHg 2.9 g., (2) b. p. 144~147°C/3mmHg 5.2 g., (3) b. p. 150~170°C/3 mmHg 0.9 g. and a dark brownish residue.

Fraction 1 was identified as diphenyl. Fraction 2 solidified on standing and was recrystallized from ethanol to give white crystals, m. p. 132~133°C, which were identified as benzoin by a mixed melting point test (yield: 25%).

Found: C, 79.14; H, 5.61. Calcd. for $C_{14}H_{12}O_2$: C, 79.22; H, 5.70%.

Fraction 3 was recrystallized from ethanol to give triphenylmethane, m. p. 93°C (yield: 5.6%).

Found: C, 93.34; H, 6.66. Calcd. for $C_{19}H_{16}$: C, 93.40; H, 6.60%.

Summary

The reaction of carbon monoxide with an organolithium compound at −70°C yielded symmetrical ketones.

Benzophenone (55%), 4, 4′-ditolyl ketone (50%), di-*n*-butyl ketone (40%), di-*n*-amyl ketone (28%) and diisopropyl ketone (30%) were prepared by this new method.

A reaction path for the formation of ketones was discussed.

Department of Chemical Technology
Faculty of Engineering
Osaka University
Miyakojima-ku, Osaka

Organoboron Compounds. On the Reaction of Phenylboronic Acid with Diols and Diamines

By Seiji KATO, Moriyasu WADA and Yojiro TSUZUKI

(Received November 28, 1961)

In previous papers[1] the present authors showed that when polyvinylalcohol (PVA) is treated with phenylboronic acid, it is readily converted into polyvinylboronic ester, which is characterized by being soluble in some organic solvents, insoluble in water, and capable of being transformed into colorless strong films or fibers with a water resistance superior to that of PVA itself. The dyeing property of PVA can be improved by this esterification in some respects[2].

From these facts, it can be expected that by introducing boron into polymeric substances, remarkable specialities will appear in its properties. However, relatively little is known of polymeric substances which contain boron, especially in the main chain of polymers. It is the main object of this experiment to devise a method of preparing such polymeric substances, containing boron atoms bonded directly to a nitrogen or carbon atom in the main chain of polymers. In order to prepare these substances, phenylboronic acid was heated at 120~200°C with organic reagents containing a reactive hydrogen atom until any water or hydrogen chloride formed as a by-product was eliminated. In general, it is preferable to use bifunctional organic reagents such as glycol and diamines with at least one hydrogen atom on each terminal carbon or nitrogen atom, since the acid reacts with them to give linear polymers. Beside these reactants, organosilane compounds such as diphenylsilanediol and dichlorodiphenylsilane were used.

Experimental

Preparation of Phenylboronic Acid[3].—From bromobenzene and methylborate, phenylboronate was prepared, and after hydrolysis phenylboronic acid was obtained. Yield, 82%; m. p., 214°C.

Preparation of Phenylboronic Anhydride.—Phenylboronic acid can easily be converted to the anhydride by azeotropic distillation of water with toluene.

Preparation of Phenylboronic Dichloride.—A mixture of phenylboronic anhydride (32 g., 0.31 mol.) and phosphorus pentachloride (74 g., 0.36 mol.) was melted at 160°C and heated under reflux at 120~130°C for 24 hr. Subsequent distillation gave phosphorus oxychloride as a forerun. The main fraction, after redistillation, consisted of

1) S. Kato, Y. Tsuzuki and S. Kitajima, This Bulletin, **34**, 1107 (1961); S. Kato, *Waseda Applied Chem. Soc. Bulletin*, **28**, 28 No. 5, (1961).

2) S. Kato and Y. Tsuzuki, This Bulletin, **33**, 1741 (1960).

3) "Organic Syntheses", Vol. 39 (1959), p. 3.

phenylboronic dichloride. Yield, 4.9 g. (11%); b. p., 48~50°C/5 mmHg.

Preparation of Diphenylsilanediol. — Into a heterogeneous mixture of 26 ml. of toluene, 54 ml. of *tert*-amyl alcohol and 220 ml. of water was stirred drop by drop 67 g. of diphenyldichlorosilane dissolved in 26 ml. of toluene. The solution was maintained at 25°C with a cooling bath. About one-half hour was required for the addition of the chloride, after which the solution was stirred for ten minutes. The solution was then filtered by suction. The crystals obtained were washed with water until they became free of acid, and were then dried in air and recrystallized from warm ethyl methyl ketone. Yield, 49 g.; (90%) m. p., 143°C.

Reaction of Phenylboronic Acid with Diamines. —All the following reactions were carried out in an atmosphere of dry oxygen-free nitrogen.

a-1) With Ethylenediamine. — Ethylenediamine (1.34 ml., 1.2 g., 0.02 mol.), together with a 5% excess of phenylboronic acid, was placed in a 50 ml. three-necked Claisen flask with a receiver, a thermometer, and an inlet for dry oxygen-free nitrogen. Reaction took place spontaneously with the evolution of heat. The flask was heated in a silicone oil-bath. At about 140°C (bath temperature), reaction set in. Water distilled off freely during the first hour and very slowly during the succeeding two hours at 120°C (inner temperature). The flask was provided with a very fine capillary, and heating was continued in vacuum (5 mmHg) for about half an hour, the temperature of the bath being raised to 160~170°C. During this period a little distillate was collected. The residue, which was a glassy, granular, slightly brown substance, was readily soluble in hot water, absolute methyl and ethyl alcohol, but insoluble in carbon tetrachloride, chloroform, dimethylformamide, ethyl ether, benzene, xylene, aceton and dioxane. This polymer-like substance melts at 80°C and can be drawn out into thread at that temperature, but it seems to be readily hydrolyzed by atmospheric moisture. Analysis indicates that this crude substance contains 23.52% nitrogen, 38.20% carbon and 7.20% hydrogen.

a-2) About 2.8 g. (ca. 002 mol.) of phenylboronic acid and 1.34 ml. (0.02 mol.) of ethylenediamine were simultaneously added to 40 ml. of toluene. Reaction took place spontaneously with evolution of heat. The mixture was then refluxed for an hour. The water formed in this reaction was distilled by means of water-toluene azeotropic distillation. After removal of the residual toluene at 5 mm., no further distillation took place up to the bath temperature of 180°C. The residue showed the same properties as were found in a-1).

b) With Trimethylenediamine. — In a two-necked flask equipped with a condenser and a nitrogen inlet were placed about 2.8 g. (ca. 0.02 mol.) of phenylboronic acid and 1.48 g. (1.67 ml., 0.02 mol.) of trimethylenediamine (b. p. 135~136°C/738 mmHg). The flask was thoroughly swept with dry nitrogen and was heated first at 130~150°C for 13 hr., and then at 150~190°C for the succeeding two hours under 5 mmHg. During the heating at 140~160°C, water was distilled, and the viscosity of the reaction mixture increased greatly. When this viscous liquid was heated under 5 mmHg, there remained a bright brittle material in the bottom of the flask. The appearance and solubility were the same as with a). Analysis showed that this crude substance contained 12.27% nitrogen, 30.67% carbon and 6.21% hydrogen.

c) With Hexamethylenediamine.—A mixture of 2.8 g. (ca. 0.02 mol.) of phenylboronic acid and 2.4 g. (0.02 mol.) of hexamethylenediamine was heated to 190~195°C under atmospheric pressure for six hours and then for two and one-half hours at 210°C under 5 mmHg. About 3.2 g. of microcrystalline powder were obtained.

d) With p-Phenylenediamine.—In a mortar 3.8 g. (0.03 mol.) of phenylboronic acid and 3.3 g. (0.03 mol.) of *p*-phenylenediamine (m. p. 145~147°C) were triturated. This mixture was placed in a flask filled with dry nitrogen and heated to 210°C for twenty minutes. At about 150°C reaction set in; water distilled off during this period. Heating was continued for an additional ten minutes under reduced pressure. The final residue, which was a light brown, resinous mass, was soluble in hot water and alcohols, but insoluble in warm benzene, carbon tetrachloride and chloroform. This substance became dark brown on standing in the air.

Esterification of Phenylboronic Acid with Glycols. — *a) With Ethylene Glycol.*—An attempt to condense phenylboronic acid with ethylene glycol was unsuccessful.

b) With Tetramethylene Glycol. — Phenylboronic acid (2.5 g., ca. 0.02 mol.) and tetramethylene glycol (1.8 ml., ca. 0.02 mol.) were heated together in a nitrogen atmosphere from 120°C to 130°C for ten hours. Additional heating was continued below 140°C under reduced pressure for an hour. The final residue was a brittle, transparent solid which could be drawn out into thread from a molten condition. This thread seemed to be easily hydrolyzed by moisture in the air. Analysis indicated that this substance contained 64.7% carbon and 8.13% hydrogen.

c) With Pentamethylene Glycol.—About 2.5 g. of phenylboronic acid and 2.08 ml. (0.02 mol.) of pentamethylene glycol was added to 50 ml. of toluene. This mixture was refluxed for an hour, followed by removal of the water as a ternary azeotrope. The product showed the same properties as were found in b) above.

d) With Diphenylsilanediol.—A mixture of 4.32 g. (0.02 mol.) of diphenylsilanediol and 2.6 g. of phenylboronic acid was heated in a reaction flask equipped with a condenser, a thermometer and an inlet for dry oxygen-free nitrogen. The mixture was heated for 24 hr. at 190~200°C and for a further hour at 200°C under a pressure of 6 mmHg. The resulting resinous substance was a light yellow, glassy solid melting at about 90°C. This substance is soluble in benzene, ethyl methyl ketone, alcohol, etc., slightly soluble in carbon tetrachloride, and insoluble in water. When molten, this material can be drawn out into elastic threads. A flame

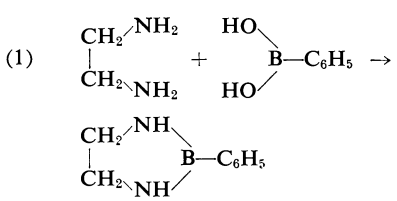
test showed that this substance contains boron.

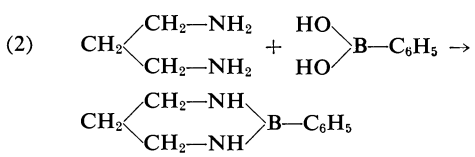
e) With Dichlorodiphenylsilane.—To a reaction vessel equipped with a thermometer, a nitrogen inlet tube extending to the bottom of the flask, and a glass tube leading to an 1 N sodium hydroxide solution, were added 3.8 g. (0.03 mol.) of phenylboronic acid and 6.7 g. (0.03 mol.) of dichlorodiphenylsilane. The reaction mass was heated in an atmosphere of nitrogen for 20 hr. at 190~200°C and then for an hour at 210°C under a pressure of 5 mmHg. The hydrogen chloride evolved during the reaction hours was absorbed in 100 ml. of an 1 N sodium hydroxide solution. Titration of the sodium hydroxide solution with a 1.011 N hydrochloric acid solution indicated that this reaction proceeded to the extent of 70% of the theoretical. About eight grams of the resinous mass were obtained. This residue showed the same properties as observed in experiment d).

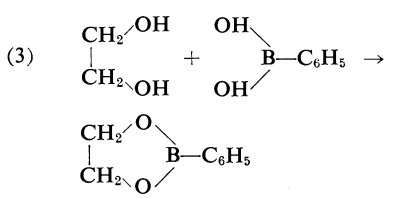
f) An attempt to get phenylboron dichloride to react with bifunctional substances by way of interfacial polycondensation was unsuccessful.

Discussion

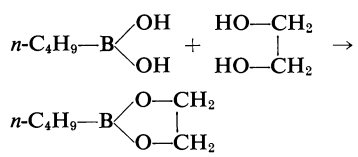
It is a well-known fact that if a 5- or 6-ring can be formed by esterification, the intramolecular reaction usually prevails over the inter-molecular reaction; in the case of 6- and 7-membered rings, both a monomolecular ring and linear polymers of a medium molecular weight are produced. It follows from this well-established fact that three of the reagents used, i. e., ethylenediamine, trimethylenediamine and ethylene glycol, might react with phenylboronic acid to give reaction products of the intra-molecular type:







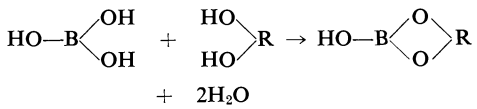
However, two of these three cyclic structures, 1 and 2, do not appear to have the indicated structures, since they could be drawn out into threads. Lestinger and Skoog[4] obtained the ethylene glycol ester of *n*-butylboronic acid by the addition of ethylene glycol and toluene to a concentrated aqueous solution of *n*-butylboronic acid, followed by removal of the water as a ternary azeotrope.



On the other hand, the ethylene glycol ester of phenylboronic acid could not be obtained by the same method. The reason for this is partly that phenylboronic acid is more easily deboronated by heating with water[5]:

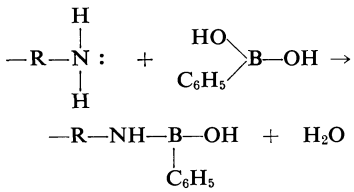
$$C_6H_5B(OH)_2 + H_2O \rightarrow C_6H_6 + B(OH)_3$$

Therefore, the following side reaction seems to accompany the main reaction:



Thus, the reaction product between phenylboronic acid and glycols must be a mixture of products of the linear and cyclic types.

The reaction of phenylboronic acid with diamines can be formulated as follows:



In this reaction the nitrogen atom of the diamine donates a pair of electrons to the boron atom. This results in a partial polarization of each atom, and the positive charge on the nitrogen atom will facilitate the removal of hydrogen atom as a proton. On the other hand, the negative charge on the boron atom promotes the removal of the hydroxyl group as a hydroxyl ion. Thus, the reaction proceeds with the formation of water, and the nitrogen-boron bond may be produced as a covalent bond.

Becher and his co-workers[6] investigated the Raman and ultraviolet spectra of methylamino- and diethylaminoboron and showed that the boron-nitrogen bond has a considerable double bond character. The infrared absorption

4) R. L. Lestinger and I. H. Skoog, *J. Am. Chem. Soc.*, **76**, 4176 (1955).
5) A. D. Ainley and F. Challenger, *J. Chem. Soc.*, **1930**, 219.
6) H. J. Becher et al., *Z. anorg. u. allgem. Chem.*, **286**, 133 (1952).

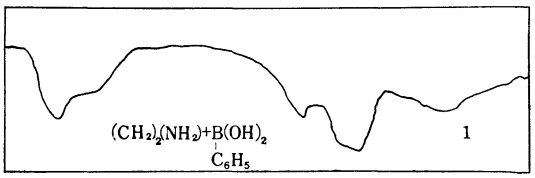


Fig. 1

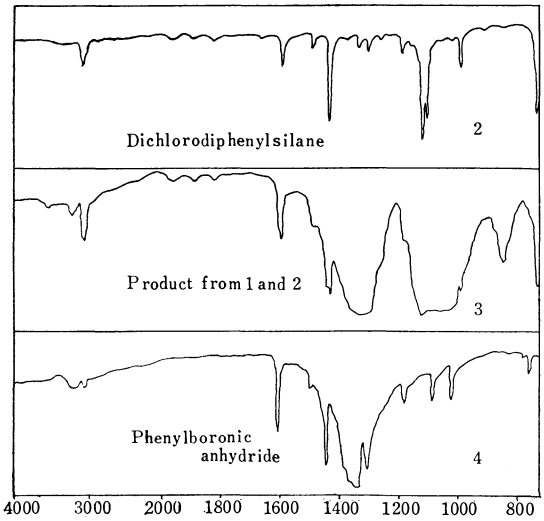


Fig. 2

spectra of the derivatives of phenylboronic acid condensed with a diamine as well as with an organo-silicone are shown in Figs. 1—4. As regards the compounds formed from phenylboronic acid and ethylenediamine (Fig. 1), perhaps the most striking feature in the generally, weak absorption spectrum is a broad band in the region of 1300～1400 cm^{-1}. The same absorption band occurred with *N, N, N*-trimethylborazol[7]. It seems certain that the band is associated with the B–N group (1330～1380 cm^{-1}) and the B–O group (1330～1390 cm^{-1}). Figure 2 shows the absorption spectrum of dichlorodiphenylsilane, while Fig. 4 is that of phenylboronic anhydride. Figure 3 is also the spectrum of the compound formed from these two. The three bands at 850, 1000～1100 and 1300～1350 cm^{-1} seen in Fig. 3 are characteristic of this condensed compound. The band at 850 cm^{-1}, which can not be found in either of the parent spectra, suggests the formation of some new bond during the reaction. Moreover, the broad and strong band in the 1000～1100 cm^{-1} region is probably connected with the stretching vibration of the Si–O–B bond, the band of which casually comes near the 1100 cm^{-1} absorption due to the ether linkage C–O–C. In conclusion, the most notable feature observed in this spectrum is that the polymer formed from phenylboronic acid and dichlorodiphenylsilane shows a very strong band in the 1000～1100 cm^{-1} range; this band is probably due to Si–O–B absorption, and therefore the product must be polyborosiloxane.

Tokyo College of Science
Shinjuku-ku, Tokyo

7) Sadtler, Standard Spectra, No. 11868.

Hot-Atom Chemistry of Arsenates.—Effect of Cation, Water of Crystallization and Irradiation Temperature on the Retention of Radioarsenic in Neutron-irradiated Solid Arsenates

By Nobufusa SAITO and Isao TOMITA

(Received December 1, 1961)

On the retention of radioarsenic as arsenate after neutron irradiation of arsenic acid or sodium arsenates in a solid state or in an aqueous solution, several investigators have obtained various results[1-5]. Typical results given by these workers are shown in Table I.

In the present investigation, the effect of cation, water of crystallization in molecules, irradiation temperature and storage time have been studied. The nuclide under investigation is 26.8 h ^{76}As, a hard-beta-emitter (E_{max}= 2.965 MeV.) with accompanying gamma rays.

Experimental

Arsenates of lithium, ammonium, sodium, potassium, cobalt(II) and barium were used as target materials for neutron irradiation. Irradiation of

1) W. F. Libby, *J. Am. Chem. Soc.*, **62**, 1930 (1940).
2) P. Süe, *J. Chim. Phys.*, **45**, 177 (1948).
3) H. Müller and E. Broda, *Monath.*, **82**, 48 (1951).
4) J. Malý and R. Šimáňová, *Chem. listy*, **49**, 814 (1955).
5) H. Kawahara and G. Harbottle, *J. Inorg. Nuclear Chem.*, **9**, 240 (1959).

TABLE I. TYPICAL RESULTS OBTAINED BY EARLIER WORKERS ON THE HOT-ATOM CHEMISTRY OF ARSENATES

Investigator	Investigated As(V) compound	Retention %	Note
W. F. Libby	H_3AsO_4 (solid)	93±10	Dissolved in H_2O
	H_3AsO_4 (soln.)	100±3	
	H_3AsO_4 (solid)	75±15	Dissolved in 6 N H_2SO_4
	H_3AsO_4 (solid)	75±15	Dissolved in 6 N NaOH
P. Süe	Na_2HAsO_4 (solid)	55~62	
	Na_2HAsO_4 (soln.)	38~59	
H. Müller and E. Broda	Na_2HAsO_4 (soln.)	14.4~16.3	Independent on concn., pH value and temperature
	Na_2HAsO_4 (solid)	65	Slow neutron irradiation
	Na_2HAsO_4 (solid)	74.5	Fast neutron irradiation
J. Malý and R. Simánová	$Na_2HAsO_4 \cdot 7H_2O$ (solid)	67	
G. Harbottle and H. Kawahara	As_2O_5 (solid)	46.8±1.7	Irradiated at room temperature
	As_2O_5 (solid)	40.8±1.6	Irradiated at dry-ice temperature
	Na_2HAsO_4 (solid)	55.9±0.3	Irradiated at dry-ice temperature

these salts was carried out for 2.5 to 3 hr. with neutrons produced by Be-D reaction. Deuterons were accelerated by the cyclotron of the Institute of Physical and Chemical Research, Tokyo. The flux was approximately $10^7 n/cm^2 \cdot sec$. Neutrons were thermalized through a paraffin block or through water. In some cases, they were slowed down through ethanol. The temperatures of the bombardment site were −196°C (liquid nitrogen), −72°C (mixture of dry ice and ethanol), and room temperature.

After irradiation, each of the irradiated samples was dissolved in water containing an arsenic(III) carrier (arsenite solution). To this solution were added magnesia mixture and ammonia water to precipitate ammonium magnesium arsenate, $NH_4 \cdot MgAsO_4 \cdot 6H_2O$. The precipitate was dissolved in hydrochloric acid, hold-back carrier of arsenic(III) was added, and then precipitation was repeated by adding ammonia and an excess of a magnesia mixture. Hydrogen peroxide was added to the combined filtrate to oxidize arsenic(III). The precipitate formed contained radioarsenic, which was originally in the valence state of III as a result of the recoil process or a subsequent reaction. The precipitate was again dissolved in hydrochloric acid and diluted to 25 ml. The β-activity of each fraction was measured with a dipping counter. Finally, the retention value of radioarsenic as arsenate was calculated on each salt as follows:

$$R = \frac{I(\mathrm{AsV})}{I(\mathrm{AsIII}) + I(\mathrm{AsV})} \times 100 \ (\%)$$

were I is the intensity of radioactivity.

Results

First, the effect of irradiation temperature and storage time on retention was investigated. The irradiated sample was principally sodium

TABLE II. EFFECT OF IRRADIATION TEMPERATURE, STORAGE TEMPERATURE AND STORAGE TIME ON RETENTION OF NEUTRON-IRRADIATED $Na_2HAsO_4 \cdot 7H_2O$

Run No.	Irrad. temp. °C	Storage temp. °C	Storage time hr.	Retention %
1	−196	−196	1	48.3
2	−196	−196	1	47.8
3	−196	−196	16.5	50.0
4	−72	−72	1	50.0
5	−72	−72	1	48.7
6	−72	−72	17	51.4
7	−72	−72	18	51.1
8	−72	−72	18	52.7
9	Room	Room	0.5	64.6
10	Room	Room	1	65.1
11	Room	Room	18	67.8
12	Room	Room	18.5	69.0
13	Room	Room	119	72.6
14	−196	Room	3.5	59.8
15	−196	Room	18.5	60.9
16	−72	Room	1	55.5
17	−72	Room	18.5	64.3
18	150~100	Room	1	68.2
19	150~100	Room	18	69.0
20	Room	Room	0.5	60.9
21	Room	Room	0.5	60.6
22	Room	Room	3.5	63.4
23	Room	Room	22	66.1
24	Room	Room	25	67.2

1—19 Irradiated for 2.5~3.0 hr.
20—24 Irradiated for 1.0 hr.

arsenate, $Na_2HAsO_4 \cdot 7H_2O$, of an especially pure grade obtained from the Merck Co. The crystal size was not uniform but was roughly within the range of 1~3 mm. in diameter. The results are given in Table II. In the case of irradiation at 150~100°C, the state of the target crystals differed from that at room temperature. Having a large amount of water of crystallization, the crystal melted at these high temperatures, and then the water was evaporated. The target had probably been partly changed into $Na_4As_2O_7$.

The results of the irradiation of Li_3AsO_4 and $H_4As_2O_7$ at low or room temperatures are shown in Table III. Further, the dependence of retention upon storage time was investigated for several kinds of arsenates, the results being given in Table IV.

Table III. Effect of irradiation temperature, storage temperature and storage time on retention of irradiated Li_3AsO_4 and $H_4As_2O_7$

Compound	Irrad. temp. °C	Storage temp. °C	Storage time hr.	Retention %
Li_3AsO_4	−196	−196	1	36.2
Li_3AsO_4	−196	−196	4	36.2
Li_3AsO_4	Room	Room	1	40.6
$H_4As_2O_7$	−72	−72	1	45.4
$H_4As_2O_7$	Room	Room	1	55.2

Table IV. Dependence of retention upon storage time

Compound	Storage time hr.	Retention %
Li_3AsO_4	1.0	40.6
Li_3AsO_4	4.0	44.0
Li_3AsO_4	21.0	44.0
Li_3AsO_4	24.5	46.4
$Na_3AsO_4 \cdot 12H_2O$	1.0	39.5
$Na_3AsO_4 \cdot 12H_2O$	42.5	40.9
$Na_2HAsO_4 \cdot 7H_2O$	0.5	64.6
$Na_2HAsO_4 \cdot 7H_2O$	1.0	65.1
$Na_2HAsO_4 \cdot 7H_2O$	18.0	67.8
$Na_2HAsO_4 \cdot 7H_2O$	119	72.6
$NaH_2AsO_4 \cdot 2H_2O$	1.0	46.9
$NaH_2AsO_4 \cdot 2H_2O$	42.5	54.0
$KH_2AsO_4 \cdot H_2O$	1	54.9
$KH_2AsO_4 \cdot H_2O$	23.0	59.5
$BaHAsO_4$	1.0	49.4
$BaHAsO_4$	24.5	51.5
$Co_3(AsO_4)_2 \cdot 8H_2O$	1.0	21.1
$Co_3(AsO_4)_2 \cdot 8H_2O$	24.5	50.5

Irradiated salts were stored at room temperature.

In general, the results show a gradual increase in retention values, i. e., an increase in the arsenic(V) fraction, when the irradiated salts are stored at room temperature.

Table V. Retentions in irradiated crystalline arsenates

Arsenate	Retention %
Li_3AsO_4	40.6±1.1
$(NH_4)_3AsO_4 \cdot 3H_2O$	41.0±0.5
$Na_3AsO_4 \cdot 12H_2O$	39.5±0.1
$(NH_4)_2HAsO_4$	46.8±0.4
$Na_2HAsO_4 \cdot 7H_2O$	65.1±0.5
$Co_3(AsO_4)_2 \cdot 8H_2O$	21.1±0.6
NaH_2AsO_4	52.7±1.0
$NaH_2AsO_4 \cdot 2H_2O$	46.9±0.3
$KH_2AsO_4 \cdot H_2O$	54.9±0.1
$BaHAsO_4$	51.8±2.4
$BaHAsO_4 \cdot H_2O$	49.6±0.2

Fluctuation of obtained retention value was shown after mean value in the form such as 41.0±0.5.

In Table V, the results of the irradiation of various kinds of crystalline arsenates are shown; here the effects of cation atom and of water of crystallization can be observed. The given values have been obtained for the irradiation at room temperature and for the storage for one hour. It was found that each salt had its characteristic retention value and that the value for $Na_2HAsO_4 \cdot 7H_2O$, 65%, agreed with the results of Müller and Broda, and also agreed roughly with those by Malý and Šimáňová, who had obtained the value of 67%.

Discussion

It is clear from the data of the retention values of irradiated $Na_2HAsO_4 \cdot 7H_2O$ after one hour's storage that the values at the two lower temperatures are nearly the same, about 50%, and that they show a fairly large difference from the value, 65%, obtained for the irradiation at room temperature. When the irradiated crystals were stored for 17~18 hr. at liquid nitrogen or dry ice-ethanol temperature, the retention values increased very little, while the storage of radioactive crystals at room temperature resulted in a gradual increase in the radioactivity of the 'arsenate' fraction, and the retention values increased. It is considered that, in these cases, the recoil process and subsequent reactions in solids play an important role in the observed retention. The lower values obtained at lower irradiation- and storage temperatures suggest that, after the recoil process, very slow or no subsequent reaction occurred to produce radioarsenic atoms in an oxidation state higher than III.

In the preliminary experiment, solutions containing arsenate or arsenic acid at various pH's were irradiated and the retention values,

15~21%, were obtained, independent of the pH of the solution*.

Considering the above results, it is quite probable that the chances for recombination or other reactions of the recoil species with collision fragments or with parent molecules may be larger in the solid phase than in the liquid phase because of the large cage energy and the longer lifetime of the 'hot zone'[6]. For example, the following speculation may be true: a recoil fragment containing ^{76}As, which otherwise can oxidize the water upon solution of the irradiated target, may be able to react with oxygen ions or parent species in the neighborhood in the crystal to form a new fragment which is liable to hydrate to arsenate ion when dissolved. This reaction would result in the high initial retention and the gradual increase in its value during storage of irradiated arsenate crystals**.

Low temperatures at the bombardment site would affect the reaction period or the lifetime of the 'hot zone', thus resulting in lower retention than in the case of bombardments at room or higher temperatures. A few experimental data in Table I support the above statement; that is, when target salts which had been irradiated at -196 or $-72°C$ were stored at room temperature, the retention increased rather rapidly with lengthening storage time. It can be thought that the thermal- or radiation annealing effect and storage effect are so remarkable even at room temperature that the slight difference in experimental conditions affects the reproducibility of the experimental results. In fact, when the crystals were irradiated at room temperature for 1 hr. instead of 3 hr., the resulting retention was 60.9% after the storage of the irradiated salts for 0.5 hr. This value is lower than that for 3 hr's irradiation, 64.6%.

The dependence of retention upon irradiation temperature is also observed for arsenates other then sodium arsenate (Table III). It seems that these phenomena are caused by the reaction mechanism described above, although the absolute values of retention are very specific for each salt.

Similar results were obtained from the experiment to investigate the dependence of retention upon storage time of radioactive crystals (Table IV). An increase in retention with storage at room temperature is considered a general tendency for all irradiated arsenated salts, since the activation energy barrier opposing the recombination reaction of recoil arsenic ions with oxygen is assumed to be rather small.

In Table V are shown the retentions in various crystalline arsenates. No regularity can be found in the obtained values with regard to the mass of cation which has collided with a recoil atom, and a model which is based upon elastic-collision between them cannot account for the experimental data, which are common to the studies of the Szilard-Chalmers process in oxyanion salts. Harbottle and Sutin[8] suggested that ammonium ion and water of crystallization would act as reducing agents in the 'hot zone' and would result in low retentions in case of the irradiation of the salts containing them. Our results, although not so remarkable, do not contradict their suggestion. For example, low retentions for $Na_3AsO_4 \cdot 12H_2O$ and $Co_3(AsO_4)_2 \cdot 8H_2O$ are assumed to be due to their high content of water of crystallization; ammonium salts such as $(NH_4)_3AsO_4 \cdot 3H_2O$ and $(NH_4)_2HAsO_4$ also have rather low retentions as compared with those of salts of alkali metals except lithium salts. Further, the retentions of hydrate and anhydrous form of one compound such as $NaH_2AsO_4 \cdot 2H_2O$ and NaH_2AsO_4 can be compared in some cases, and lower values are obtained for hydrate crystals.

The presence of elementary radioarsenic, which has been suggested by Harbottle and Kawahara, could not be confirmed because only the precipitation method was adopted in the present experiment. Perhaps, parallel experiments using several kinds of separation methods would be valuable in studying the behavior of radioarsenic in the state of oxidation number of zero, or in intermediate valency states in the solid phase.

Department of Chemistry
Faculty of Science
The University of Tokyo
Hongo, Tokyo

* Very concentrated arsenic acid solution (2 g. $H_4As_2O_7$/ml.) gives the retention, 37%.

6) G. Harbottle and N. Sutin, *J. Phys. Chem.*, **62**, 1344 (1958).

** A similar argument has been made, with respect to the recombination of the fragments produced by neutron capture in potassium chromate, by Maddock et al.[7]

7) M. M. de Maine, A. G. Maddock and K. Taūgbŏl, *Discuss. Faraday Soc.*, **1957**, 211.

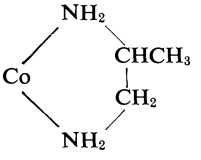
8) G. Harbottle and N. Sutin, "Advances in Inorganic Chemistry and Radiochemistry", Vol. 1, Academic Press, New York (1960). p. 267.

*The Crystal Structure of trans-Dichloro-bis-l-propylenediamine Cobalt(III) Chloride Hydrochloride Dihydrate and the Absolute Configuration of the Complex Ion, [Co l-pn_2Cl_2]$^+$**

By Yoshihiko SAITO and Hitoshi IWASAKI

(Received December 5, 1961)

During the past several years the crystal structures of various cobalt-ethylenediamine complexes have been determined by one of the present authors (Y. S.), Kuroya et al.[1-4] and Becker et al.[5] The puckered form of the cobalt-ethylenediamine ring has thus been established. In connection with this, the present investigation was initiated in order to determine the configuration of the cobalt-propylenediamine ring;



with special interest in the orientation of the substituted methyl group. Corey and Bailar[6] have recently discussed the geometry of various metal-chelate rings. Their conclusion for the metal-propylenediamine ring agrees quite well with the results obtained here. The absolute configuration of the complex ion [Co l-pn_2Cl_2]$^+$ has also been determined by the usual absorption edge technique.

Experimental

Crystals of [Co l-pn_2Cl_2]Cl.HCl.$2H_2O$ were prepared by the method of Werner and Fröhlich[7]**. They are well-developed dark green tablets, showing predominant (100) faces. In polarized light, they exhibit a marked dichroism similar to that observed for [Co en_2Cl_2]Cl.HCl.$2H_2O$. This fact suggest that the structure is closely related to those of the ethylenediamine-analogues.

As the crystals of [Co l-pn_2Cl_2]Cl.HCl.$2H_2O$ decompose gradually when exposed to air, special precautions had to be taken to preserve the crystals. It was found that adequate protection was afforded by a thin layer of grease. Specimens treated with grease were preserved intact for several weeks.

From measurements made by using an X-ray diffractometer with Cu$K\alpha$ radiation ($\lambda=1.5418$ Å), the unit cell is found to be monoclinic, with

$$a=22.092\pm0.004\text{ Å}$$
$$b=8.406\pm0.002\text{ Å}$$
$$c=9.373\pm0.004\text{ Å}$$

and $$\beta=99°39'\pm7'$$

The cell contains four formula units of [Co l-pn_2Cl_2]Cl.HCl.$2H_2O$ (density, calculated 1.494 g./cc.; found 1.495 g./cc. at 26°C). The space group was found to be $C2/m$, Cm or $C2$ from Weissenberg photographs taken with Fe$K\alpha$ radiation. The former two space group estimates can be excluded since it is certain that the compound is optically active and cannot have a center or a plane of symmetry in the arrangement in the crystals.

The structure determination was based on analysis of the ($h0l$) and ($hk0$) reflections, which could be carried out in quite a straightforward fashion.

Intensity data for the ($h0l$) and ($hk0$) reflections were recorded on zero level Weissenberg films about the b- and c-axes by the multiple-film technique. Fe$K\alpha$ radiation was used ($\lambda=1.937$ Å). The intensities of the reflections were measured by visual comparison with an intensity scale. They were corrected for absorption, Lorentz and polarization factors. Observed structure amplitudes were brought to an absolute scale afterwards by scaling them against the calculated values, the maximum $\sin\theta/\lambda$ observed being 0.514.

Patterson functions could be solved without difficulty by comparison with those of the ethylenediamine-analogues, yielding approximate positions not only for the heavy atoms but also for lighter atoms. Thus, Fourier syntheses of the electron density projections along [001] and [010] could be computed.

Fourier refinements were repeated as usual. Final projections of the electron density along [010] and [001] are shown in Figs. 1 and 2 respectively. They can be interpreted in terms of Figs. 3 and 4 respectively. The final set of parameter values is

* Part of this paper is taken from the paper of the same title by the same authors, from "Advances in the Chemistry of the Coordination Compounds", © Stanley Kirschner, 1961, and published by the Macmillan Company, New York.

** Optically active propylenediamine was kindly prepared by Prof. H. Kuroya of Osaka City University, to whom the authors' thanks are due.

1) A. Nakahara, Y. Saito and H. Kuroya, This Bulletin, **25**, 331 (1953).
2) S. Ooi, Y. Komiyama, Y. Saito and H. Kuroya, ibid., **32**, 263 (1959).
3) K. Nakatsu, Y. Saito and H. Kuroya, ibid., **29**, 428 (1956).
4) K. Nakatsu, M. Shiro, Y. Saito and H. Kuroya, ibid., **30**, 158 (1958).
5) K. A. Becker, G. Grosse and K. Plieth, *Z. Krist.*, **112**, 375 (1959).
6) E. J. Corey and J. C. Bailar, Jr., *J. Am. Chem. Soc.*, **81**, 2620 (1959).
7) A. Werner and A. Fröhlich, *Ber.*, **40**, 2228 (1907).

TABLE I. ATOMIC PARAMETERS

		x	y	z	B(Å^2)
Co		0.250	0	0.250	3.4
Cl	(1)	0.392	0.365	0.171	3.2
	(2)	0.109	0.681	0.327	3.2
	(3)	0.267	0.022	0.017	3.0
	(4)	0.232	−0.022	0.483	3.0
N	(1)	0.268	−0.232	0.251	3.2
	(2)	0.338	0.036	0.320	3.2
	(1′)	0.231	0.235	0.255	3.2
	(2′)	0.164	−0.039	0.175	3.2
C	(1)	0.334	−0.250	0.261	6.0
	(2)	0.365	−0.119	0.355	6.0
	(3)	0.434	−0.117	0.345	6.0
	(1′)	0.168	0.246	0.167	6.0
	(2′)	0.136	0.109	0.211	6.0
	(3′)	0.067	0.117	0.154	6.0
O	(1)	0.441	0.488	0.473	3.4
	(2)	0.059	0.509	0.029	3.4

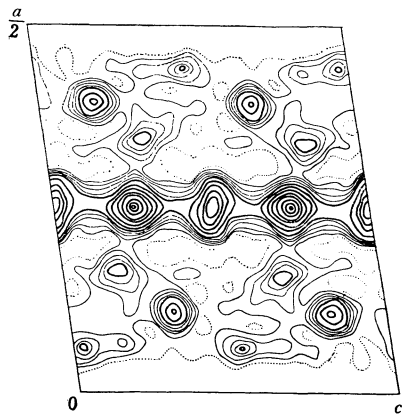
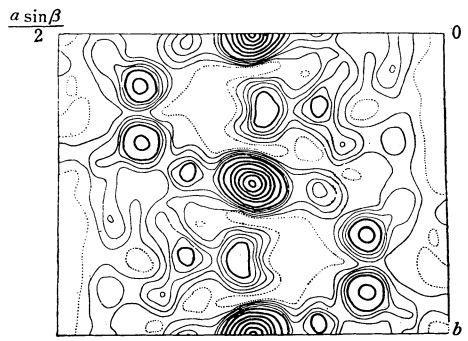


Fig. 1. Electron-density projection along [010]. Contours are drawn at intervals of $2e.\,A^{-2}$. Contours above $10e.\,A^{-2}$ are drawn at $5e.\,A^{-2}$ with thick lines. Zero contours are broken.



Electron density projection

Fig. 2. Electron-density projection along [001]. Contours are drawn at intervals of $2e.\,A^{-2}$. Thick contours are at intervals of $10e.\,A^{-2}$. Zero contours are broken.

listed in Table I. This gives the reliability index $R=\sum \big|\,|F_o|-|F_c|\,\big|/\sum |F_o|$ of 0.14 and 0.15 for ($h0l$) and ($hk0$) respectively, non-observed reflections being excluded. The contributions of hydrogen atoms were neglected. The agreement between the observed and calculated structure factors is shown in Table II.

Calculation of the structure factors as well as of the electron density projections was carried out with a PC-1 parametron computer in the Faculty of Science of this University. In the calculation of the structure factors, the atomic scattering factors were taken from the paper of Vand, Eiland and Pepinsky[8]. Different isotropic temperature factors were applied for each atoms; these are listed in the last column of Table I.

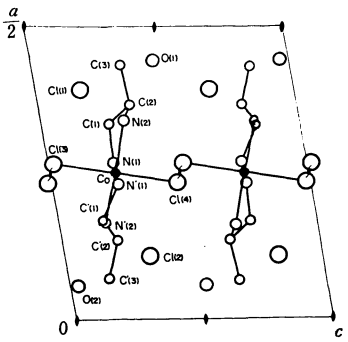


Fig. 3. Projection of the atomic arrangement on (010).

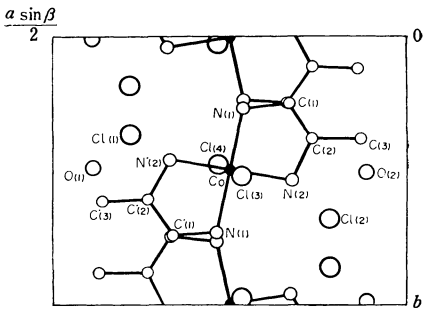


Fig. 4. Projection of the atomic arrangement on (001).

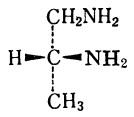
Determination of the Absolute Configuration

The absolute configuration of *l*-propylenediamine has been chemically related to D-alanine by modification of COOH in the latter to CH_2NH_2 of the former[9]. Since the absolute configuration of D-alanine is already known, *l*-propylenediamine must possess the absolute configuration shown by I:

8) V. Vand, P. F. Eiland and R. Pepinsky, *Acta Cryst.*, **10**, 303 (1957).
9) H. Reihlen, E. Weinbrenner and G. V. Hessling, *Ann.*, **494**, 143 (1932).

TABLE II. OBSERVED AND CALCULATED STRUCTURE FACTORS

h 0 *l*	$\lvert F_o\rvert/4$	$F_c/4$	*h* 0 *l*	$\lvert F_o\rvert/4$	$F_c/4$	*h* 0 *l*	$\lvert F_o\rvert/4$	$F_c/4$	*h k* 0	$\lvert F_o\rvert/4$	$\lvert F_c\rvert/4$
0 0 1	2.2	+ 0.5	8	11.0	− 8.5	4	17.0	−17.3	19	7.2	7.8
2	33.0	−33.2	9	2.6	+ 0.9	5	0	− 1.5	21	1.1	1.3
3	3.4	− 1.7	8 0 0	35.0	+34.5	6	4.8	− 6.5	0 2 0	44.0	43.8
4	35.0	+35.3	1	3.5	− 1.9	7	3.1	− 1.7	2	36.5	28.6
5	0	+ 0.8	2	40.5	−43.0	8	6.7	− 5.9	4	39.7	40.0
6	15.4	+17.1	3	0	+ 1.7	16 0 0	8.0	+ 8.8	6	23.4	28.8
7	0	+ 0.1	4	23.3	+26.3	1	4.6	− 0.3	8	12.4	9.7
8	14.4	+ 7.9	5	2.9	+ 2.1	2	14.0	−14.0	10	25.1	32.2
9	1.5	− 0.9	6	10.6	−10.1	3	0	− 2.5	12	14.1	15.9
2 0 0	58.8	−59.3	7	0	− 1.7	4	7.4	+ 9.3	14	7.3	3.6
1	0	− 1.2	8	2.0	− 2.2	5	0	− 1.0	16	7.0	9.8
2	14.1	+14.5	$\bar{8}$ 0 1	0.6	− 2.0	$\overline{16}$ 0 1	0	− 0.2	18	5.5	5.0
3	1.1	+ 1.4	2	3.7	+ 2.2	2	4.5	+ 4.9	20	2.3	3.3
4	41.0	−41.2	3	3.4	+ 4.5	3	4.5	+ 0.3	1 3 0	13.3	4.5
5	0	+ 0.3	4	9.0	+ 6.4	4	4.2	+ 2.9	3	13.3	14.7
6	6.1	+ 7.9	5	0	− 1.4	5	0	+ 2.3	5	13.0	13.4
7	2.2	− 2.2	6	7.5	+ 7.2	6	6.3	− 1.7	7	5.3	6.0
8	8.5	−11.2	7	0	+ 0.1	7	3.0	− 1.9	9	2.2	5.4
9	2.2	+ 1.5	8	16.8	+18.3	18 0 0	9.2	+12.3	11	2.3	4.2
$\bar{2}$ 0 1	1.1	− 0.3	9	1.4	+ 0.7	1	1.7	+ 1.2	13	7.7	8.6
2	23.8	+23.7	10 0 0	32.3	−30.9	2	3.6	− 4.3	15	11.0	13.8
3	2.3	− 0.2	1	6.3	− 0.9	3	0	− 0.4	17	5.6	7.2
4	34.3	−34.5	2	16.4	+18.3	4	0	+ 0.3	19	1.5	0.5
5	0	− 0.3	3	3.5	+ 2.0	$\overline{18}$ 0 1	0	+ 1.2	0 4 0	33.9	34.3
6	9.1	+ 9.2	4	21.2	−26.2	2	8.8	+ 7.3	2	43.7	37.1
7	1.4	+ 0.8	5	3.6	− 2.7	3	5.0	− 1.4	4	40.5	40.7
8	19.2	−18.7	6	15.9	+16.2	4	9.8	+ 8.9	6	16.8	18.1
9	0	− 0.7	7	0	− 0.7	5	0	− 2.1	8	9.7	9.5
4 0 0	12.0	+13.2	$\overline{10}$ 0 1	2.7	+ 1.2	6	8.1	+12.8	10	26.2	27.5
1	1.2	+ 1.2	2	11.3	−17.4	20 0 0	4.9	+ 3.1	12	18.2	17.8
2	19.2	+21.8	3	5.7	− 4.8	1	0	+ 0.4	14	7.9	6.1
3	0	+ 2.3	4	22.0	−22.1	2	7.8	− 7.3	16	2.3	4.7
4	21.1	+22.4	5	3.5	+ 2.7	$\overline{20}$ 0 1	0	+ 0.9	18	4.6	3.7
5	0	− 3.8	6	2.9	+ 0.8	2	8.3	−11.2	1 5 0	5.8	7.4
6	19.8	−20.8	7	2.0	− 0.0	3	4.0	+ 0.9	3	2.8	4.5
7	0	+ 2.2	8	26.1	−25.3	4	5.2	+ 8.1	5	9.5	12.8
8	16.8	+16.2	9	0	− 0.7	5	0	− 0.6	7	1.9	4.1
9	0	− 0.4	12 0 0	18.0	+17.9	$\overline{22}$ 0 0	6.1	− 6.2	9	7.3	10.3
$\bar{4}$ 0 1	0	− 0.0	1	4.9	+ 2.3	$\overline{22}$ 0 1	0	− 1.2	11	7.5	7.9
2	8.8	+12.1	2	4.6	+ 2.2	2	7.1	+ 7.8	13	9.2	11.9
3	0	− 1.2	3	0	− 2.1	3	0	− 0.9	15	4.4	3.5
4	65.5	+67.5	4	1.9	− 1.6				17	2.4	2.8
5	2.2	+ 1.2	5	1.4	+ 0.8	*h k* 0	$\lvert F_o\rvert/4$	$\lvert F_c\rvert/4$	0 6 0	24.8	24.0
6	15.9	−15.6	6	9.3	− 7.5	2 0 0	58.8	59.3	2	17.9	9.8
7	0	− 0.6	7	0	− 1.4	4	11.3	13.2	4	10.2	11.8
8	26.7	+25.1	$\overline{12}$ 0 1	0	+ 2.4	6	56.7	56.4	6	20.1	19.6
9	0	− 0.2	2	32.3	−29.7	8	46.8	34.5	8	15.2	13.7
6 0 0	56.7	−56.4	3	5.5	− 1.5	10	32.4	30.9	10	5.9	8.3
1	0	+ 1.0	4	24.3	+31.1	12	20.4	17.9	12	6.5	5.0
2	10.8	−13.2	5	0	− 0.6	14	18.4	19.0	14	8.3	10.8
3	3.8	− 4.4	6	3.3	− 6.7	16	8.3	8.8	1 7 0	4.8	9.3
4	13.6	−16.5	7	2.3	+ 2.1	18	8.7	12.3	3	9.0	8.7
5	0	+ 2.1	8	5.5	+ 5.1	20	4.4	3.1	5	4.2	4.8
6	2.9	− 0.2	14 0 0	15.7	−19.0	22	4.8	6.2	7	3.2	4.6
7	0	− 0.1	1	4.7	− 0.2	1 1 0	10.0	5.8	9	3.4	6.3
8	13.5	−13.4	2	21.3	+17.2	3	9.1	3.2	11	5.1	7.1
$\bar{6}$ 0 1	0	+ 0.3	3	0	− 1.0	5	22.1	23.6	0 8 0	17.9	14.3
2	11.8	−13.1	4	3.6	+ 4.9	7	2.4	3.7	2	13.6	8.6
3	2.6	+ 2.3	5	0	+ 1.0	9	16.7	16.4	4	10.9	9.4
4	43.1	−42.3	6	3.7	+ 4.3	11	11.5	8.6	6	11.1	10.1
5	0	− 0.8	$\overline{14}$ 0 1	3.1	− 3.0	13	11.4	14.3	8	8.1	5.3
6	2.6	− 0.8	2	16.1	+18.4	15	6.2	5.8			
7	1.0	− 0.3	3	4.4	+ 2.8	17	2.6	2.8			



(I)

On the basis of the principles of stereochemical analysis developed by Corey and Bailar, it is possible to correlate the absolute configurations of various complex ions, for instance, those of L-$[Co\ en_3]^{3+}$, L-$[Co\ l\text{-}pn_3]^{3+}$ and *l*-pn. The result of the assignment of the absolute configuration of L-$[Co\ en_3]^{3+}$ based on that of *l*-propylenediamine agrees with the absolute configuration found for L-$[Co\ en_3]^{3+}$ by X-ray analysis[10]. Nevertheless, it was thought worthwhile to check the absolute configuration of the *l*-propylenediamine molecule, since so much stereo-specificity depends upon this chemical assignment of *l*-propylenediamine, and also, this will add support to our previous findings on the absolute configuration of L-$[Co\ en_3]^{3+}$.

The absorption edge of the K electrons of cobalt is 1.608 Å. Since Cu$K\alpha$ radiation (λ= 1.542 Å) has a wavelength a little shorter than the absorption edge of cobalt, it can excite the K electrons, and it was found that $\Delta f' = -2.2$ and $\Delta f'' = 3.9$[11]. Corrections for chlorine atoms due to the anomalous dispersion caused by K-electrons were also taken into account. They were: $\Delta f' = +0.2$ and $\Delta f'' = +0.7$ (calculated from the Table in James' book[12]).

Intensities were calculated for the structure model which corresponds to the *l*-configuration shown by I. In Table III experimental and calculated relations between I_{hkl} and $I_{h\bar{k}l}$ are compared, the latter being equal to $I_{\bar{h}k\bar{l}}$ by symmetry. Visual estimations of the last column have been made, on a series of oscillation photographs taken around the b-axis, by several people independently. It is seen that the configuration is in agreement with the chemical convention.

TABLE III. DETERMINATION OF THE ABSOLUTE CONFIGURATION

	Calculated		Observed	
h k l	I_{hkl}	$I_{h\bar{k}l}$	I_{hkl}	$I_{h\bar{k}l}$
5 1 1	1240	1550		<
3 1 3	524	669		<
7 1 3	309	163		>
1 1 5	1065	981		>
11 1 5	361	460		<
5 1 $\bar{3}$	243	303		<
15 1 $\bar{1}$	124	81		>
13 1 $\bar{3}$	913	1054		<
7 1 $\bar{5}$	470	369		>
13 1 $\bar{7}$	416	510		<

10) Y. Saito, K. Nakatsu, M. Shiro and H. Kuroya, This Bulletin, 30, 795 (1957).
11) C. H. Dauben and C. F. Templeton, *Acta Cryst.*, 8, 841 (1955).
12) R. W. James, "The Optical Principles of the Diffraction of X-Rays", G. Bell and Sons Ltd., London (1958), p. 608.

Description of the Structure and Discussion

The determined structure seems most easily understood with the aid of the projection upon (010) shwon in Fig. 3. The interatomic distances and bond angles are given in Table IV.

The estimated errors of interatomic distances are; ± 0.01 Å for Co–Cl, ±0.04 Å for O–Cl, N–Cl, and Co–N, and ±0.06 Å for other interatomic distances between lighter atoms.

The structure is essentially ionic and consists of the complexes, [Co *l*-pn_2Cl_2]$^+$ and [H_2O. H. H_2O]$^+$ and the Cl^- ion. Figure 5 shows a perspective drawing of the [Co *l*-pn_2Cl_2]$^+$ ion. Two chlorine atoms are coordinated, at

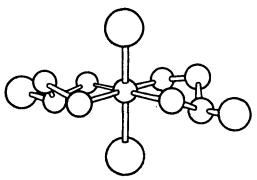


Fig. 5. A perspective drawing of the complex ion [Co *l*-pn_2Cl_2]$^+$.

a distance of 2.29 Å, to a cobalt atom in trans positions. A line joining them is approximately perpendicular to the plane in which the four nitrogen atoms of the two propylenediamine molecules were found to lie. Within the range of experimental error, these ligand atoms (4N and 2Cl) form a distorted octahedron around a cobalt atom. The bond length found for Co–Cl agrees with those found in [Co en_2Cl_2]·Cl.HCl.$2H_2O$[1] and [$Co(NH_3)_3H_2OCl_2$]Cl[13]. However, it is significantly longer than the value of 2.22 Å found in the crystals of anhydrous [Co en_2Cl_2]Cl[5]*. The chelating molecule assumes a gauche configuration with an azimuthal angle of 55° between the planes determined by the C–C and C–N bonds. The azimuthal angles between the planes determined by the C–C and C–N bonds and that determined by the Co–N and C–N bonds are, on the average, 38°. Consequently, the configuration of the five membered cobalt propylenediamine ring can be assigned as gauche-gauche-gauche with respect to the N–C, C–C and C–N bonds.

The shape and size of this five-membered ring agree well with those of the cobalt-ethylenediamine rings found in [Co en_2Cl_2]$^+$, and [Co

* This big difference might have some relation to the difference in stability between [Co en_2Cl_2]Cl.HCl.$2H_2O$ and [Co en_2Cl_2]Cl.

13) Y. Komiyama, Y. Saito and H. Kuroya, This Bulletin, 25, 328 (1952).

TABLE IV. INTERATOMIC DISTANCES AND BOND ANGLES

Co	Cl(3)	2.29 Å	O(1)	O(1)	2.57 A
	Cl(4)	2.29	O(2)	O(2)	2.57
	N (1)	1.99			
	N (2)	1.97	O(1)	Cl(1)	3.04
	N'(1)	2.02		Cl(2)	3.48
	N'(2)	1.94			
			O(2)	Cl(1)	3.78
N(1)	C(1)	1.46		Cl(2)	3.17
N(2)	C(2)	1.45			
C(1)	C(2)	1.50	C (3)	C (3)	3.76
C(2)	C(3)	1.51	C'(3)	C'(3)	3.77
N'(1)	C'(1)	1.49	∠CoN(1)C(1)		107.4°
N'(2)	C'(2)	1.46	∠N(1)C(1)C(2)		108.3°
C'(1)	C'(2)	1.45	∠C(1)C(2)N(2)		113.4°
C'(2)	C'(3)	1.53	∠C(2)N(2)Co		106.5°
			∠C(1)C(2)C(3)		111.0°
N (2)	Cl(1)	3.40	∠N(2)C(2)C(3)		112.3°
	Cl(2)	3.54	∠N(1)CoN(2)		87.9°
N'(2)	Cl(1)	3.37			
	Cl(2)	3.10	∠CoN'(1)C'(1)		103.1°
			∠N'(1)C'(1)C'(2)		104.3°
N (1)	Cl(3)	3.31	∠C'(1)C'(2)N'(2)		111.5°
N'(1)	Cl(4)	3.19	∠C'(2)N'(2)Co		101.5°
			∠C'(1)C'(2)C'(3)		111.7°
C (3)	O(1)	3.53	∠N'(2)C'(2)C'(3)		113.1°
C'(3)	O(2)	3.49	∠N'(1)CoN'(2)		88.8°

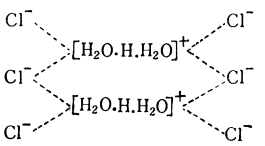
$en_3]^{3+}$. The same type of puckered rings is also found in other metal-ethylenediamine complexes, such as [Cr $en_2Cl_2]^{+}$ [14], [Ni $en_3]^{2+}$ [15] and [Cu $en_2]^{2+}$ [16].

The presence of a substituted methyl group on the carbon of the ethylenediamine molecule does not disturb the essential features of the five-membered ring.

The complex ion possesses approximate two-fold symmetry around the Cl–Co–Cl bond. Therefore, this complex ion assumes the *kk* form; that is, the two cobalt propylenediamine rings take the same configuration. The complex ions [Co $en_2Cl_2]^{+}$ and [Co *dl*-$pn_2Cl_2]^{+}$ [17], however, are found to take the *kk'* configuration; namely, two kinds of ligand molecules, the one being the mirror image of the other, are coordinated to the central atom in such a way that one is related by the operation of a center of symmetry to the other. According to Corey and Bailar, the *kk* form is intrinsically more stable than the *kk'* form. The reason why the *kk'* form often occurs in crystals of various complex compounds may be that the *kk'* form is favored by specific intermolecular forces in the solid state.

Since the five-membered ring is puckered, there are two possibilities of the orientation of the C–CH_3 group, namely, axial and equatorial types with respect to the Cl–Co–Cl bond. It was found that the bond is equatorial in the complex ion [Co *l*-$pn_2Cl_2]^{+}$, in agreement with the conclusion of Corey and Bailar that the equatorial orientation is of a lower energy than the axial one.

Since the structure is closely related to that of the en-analogue, a similar consideration of the arrangement of chlorine ions around the two water molecules leads us to locate a proton midway between the water molecules. The O–O distances were found to be 2.57 Å. A molecule of H_2O possesses two Cl^- ions as the nearest neighbor anions, the $Cl^-\cdots O$ distance being shown in Table II. Thus, every [H_2O.$H.H_2O]^{+}$ group is surrounded by four Cl^- ions. The complexes [$H_2O.H.H_2O]^{+}$ form a chain of the composition:



this chain runs parallel to the c-axis.

Such complexes have been found in crystals of Co-en analogues[1,2] and in a Cr-en analogue[14]

14) S. Ooi, Y. Komiyama and H. Kuroya, ibid., 33, 354 (1960).
15) L. N. Swink and M. Atoji, *Acta Cryst.*, 13, 639 (1960).
16) Private communication from Dr. Y. Komiyama.
17) Y. Komiyama and Y. Saito, to be published.

with an average O–O distance of 2.60 Å. The existence of the complex $[H_2O.H.H_2O]^+$ was suggested by Huggins[18] and was indeed verified by our investigations of these coordination compounds.

As in the case of the en-analogues, the complex ions form a layer parallel to the plane (100). The Cl–Co–Cl bond is inclined to the plane (010) at an angle of 5°, and the projection of this direction upon (010) makes an angle of 9.5°C with the c-axis.

In the case of the en-analogues, these angles are 14.5° and 10°. The closest distance of approach between the complex ions in the layer was found to be about 3.19 Å, between the coordinated Cl atom of one complex ion and the N atom of the adjacent. Thus, the complex ions are held together in layers by these Cl···N bonds. One complex $[Co\ l\text{-}pn_2Cl_2]^+$ ion has four nearest Cl^- ions. The closest approach of a complex ion and Cl^- ion is between N′(2) and Cl(2), the Cl···N distance being 3.10 Å. Other Cl^-···N distances are 3.37, 3.40 and 3.54 Å. These values may be compared with those found in crystals of the en-analogues.

Between the layers of the complex $[Co\ l\text{-}pn_2Cl_2]^+$ ions are arranged the complexes $[H_2O\cdot H\cdot H_2O]^+$ and Cl^- ions. These general features of the structure are quite similar to those of the ethylenediamine analogues. This fact can be more easily seen if an alternative a-axis is taken along one of the face diagonals. Then the propylenediamine ligands lie approximately on the new (001) plane. This new unit cell is very similar to that of the en-analogues in projection. However, the packing of the chlorine ions and water molecules is different from those in the en-analogues because of the methyl groups attached to the cobalt ethylenediamine ring. Thus, there is a twofold axis of rotation midway between the water molecules instead of a center of symmetry. This situation leads to a doubling of the a-spacing in the case of the present propylenediamine analogue.

Thin tabular crystals extended on (010) appear blue when the electric vector is parallel to the c-axis, while they appear yellowish green when the light is polarized along the b-axis. Such a striking dichroism may be reasonable, since there is a large component of the Cl–Co–Cl bond along the c-axis. This dichroism is quite similar to that of the en-analogues. The dichroism of the latter crystals have been extensively measured by Yamada et al.[19]

The absolute configuration of the *l*-propylenediamine molecule is found to be given by I and to agree with the chemical convention. The absolute configuration of $[Co\ l\text{-}pn_2Cl_2]^+$ corresponds to the drawing given in Fig. 5. Accordingly, on the basis of the principles of Corey and Bailar, the absolute configuration of the complex ion $[Co\ en_3]^{3+}$ can be shown to agree with our previous results, directly obtained by X-ray techniques.

In conclusion, the stereochemical principles and the method for correlation of absolute configuration developed by Bailar et al. have been proved to be reliable and useful.

Part of the cost of this investigation was defrayed by the Scientific Research Expenditure of the Ministry of Education and by The Nishina Memorial Foundation, to which the authors' thanks are due. They are also indebted to Professor R. Sadanaga and his colleagues for their aid in calculations on the PC-1 Parametron Computor.

The Institute for Solid State Physics
The University of Tokyo
Minato-ku, Tokyo

18) M. L. Huggins, *J. Phys. Chem.*, **40**, 723 (1936).

19) S. Yamada, A. Nakahara, Y. Shimura and R. Tsuchida, This Bulletin, **28**, 222 (1955).

The Electron Spin Resonance Absorption of the Complex of Thianthrene with Antimony Pentachloride

By Minoru KINOSHITA

(Received January 22, 1962)

In a previous note[1] we presented some preliminary results of the ESR absorption study of the complexes of some aromatic sulfur compounds with strong Lewis acids, in both the solid and dissolved states. In the course of the study it was found that thianthrene, when treated with antimony pentachloride, formed a very stable complex which showed a very strong ESR absorption. Its absorption consists of three broad lines in the powdered state, while in the dissolved state the complex shows the hyperfine structure which has been known to be characteristic of the sulfuric acid solution of thianthrene[2,3]. In the case of aromatic hydrocarbons such as anthracene, tetracene and perylene, it has been observed that a complex with antimony pentachloride[4] or aluminum chloride[5] shows the hyperfine structure in the dissolved state similar to that of the sulfuric acid solution of the corresponding hydrocarbon; meanwhile, in the solid state the absorption is only a single sharp line[6]. In this report, the system of thianthrene and antimony pentachloride is investigated; the results will be discussed with reference to the case of aromatic hydrocarbons.

Experimental

Preparation and Composition of the Complex.—Similarly to the case of aromatic hydrocarbon[6,7], the complex of thianthrene with antimony pentachloride was prepared by mixing the dilute solutions of both the components in dried chloroform. When the solutions were mixed, a brownish purple precipitate was formed immediately. This precipitate was filtered, washed with dried chloroform, and then dried in a vacuum for about 30 min. The dried complex is very stable and has a definite melting point of 152~153°C. For the determination of the composition, it was decomposed in boiling water, and the concentration of the free chlorine ion was determined by titration with silver nitrate solution. It was estimated that the complex consists of one mole of thianthrene and 0.93 mol. of antimony pentachloride. The complexes of thianthrene with aluminum chloride and titanium tetrachloride were prepared in a similar way. These complexes were not so stable as the complex with antimony pentachloride. Stannic chloride did not seem to form any solid complex with thianthrene in a dried condition.

Measurements.—The ESR absorption spectra of the complexes were examined at 9.4 kMc./sec. by the use of a Hitachi MPS-1 spectrometer. The unpaired spin concentration and the *g*-value of the complex were estimated by comparison with a standard piece of diphenylpicrylhydrazyl, for which the *g*-value of 2.0036 had been decided upon.

The magnetic susceptibilities of thianthrene and its complex were measured by the Gouy method, and the electronic absorption spectra were obtained in association with a Cary model-11 spectrophotometer. All the mesurements in this work were carried out at room temperature.

Results

The complex formed by the reaction of thianthrene with antimony pentachloride was a brownish purple powder. When examined by an X-ray diffractometer, it gave a sharp crystalline pattern which was quite different from that of thianthrene itself. The complex remained unchanged after being exposed to the air for about one year, but when boiled with water, it decomposed completely, leaving thianthrene.

The ESR Absorption Spectra. — The ESR absorption spectrum of the complex in its powdered state was found to consist of three broad lines which were distributed asymmetrically (Fig. 1). The separations between the three lines increased in proportion to the resonance frequency (Fig. 1b). The *g*-value for the main center line was found to be 2.0080 ± 0.0001, and the spin population was estimated as 1.3×10^{21} per gram, with an error of about 10%. Similar ESR absorption patterns were obtained for the complexes with aluminum chloride and titanium tetrachloride, but, as they were very weak, they were not investigated further.

In the nitrobenzene solution, the complex showed, in contrast to the spectrum of the

1) M. Kinoshita and H. Akamatu, This Bulletin, **35**, 1040 (1962).
2) J. E. Wertz and J. L. Vivo, *J. Chem. Phys.*, **23**, 2193 (1955).
3) A. Fava, P. B. Sogo and M. Calvin, *J. Am. Chem. Soc.*, **79**, 1078 (1957).
4) S. I. Weissman, E. deBoer and J. J. Conradi, *J. Chem. Phys.*, **26**, 963 (1957).
5) J. J. Rooney and R. C. Pink, *Proc. Chem. Soc.*, **1961**, 142.
6) Y. Matsunaga, This Bulletin, **34**, 893 (1961).
7) K. Brass and E. Tengler, *Ber.*, **64**, 1650 (1931); K. Brass and K. Fanta, ibid., **69**, 1 (1936).

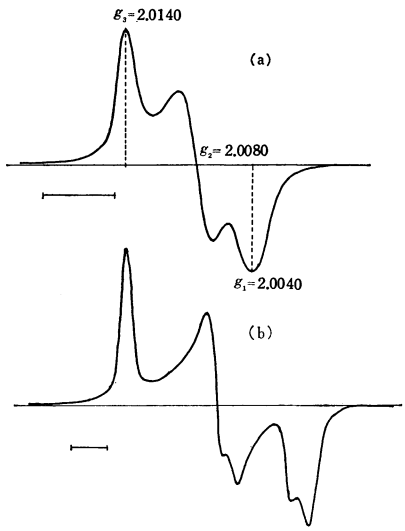


Fig. 1. The derivative curves of the ESR absorption for the powdered complex of thianthrene-$SbCl_5$, at the frequencies of 9.4 kMc./sec. (a), and of 23 kMc./sec. (b). The scale (10 gauss) is indicated in the spectra. The magnetic field increases from left to right.

solid, a hyperfine structure consisting of five equally spaced lines with an intensity ratio of about 1 : 4 : 6 : 4 : 1 (Fig. 2a). This hyperfine structure is identical with that of thianthrene or thianthrene disulfoxide in a concentrated sulfuric acid solution (Fig. 2b and c), which has been investigated by previous workers[3]. The g-value for the center of the structure was found to be $g=2.0080\pm0.0001$, while the spacing of the five lines was about 1.2 gauss.

The Electronic Absorption Spectra. — The solutions of the complex in nitrobenzene and in *o*-dichlorobenzene displayed identical spectra, characterized by an absorption band with a maximum at 547 mμ, which was in coincidence with the band at 546 mμ observed in the sulfuric acid solution of thianthrene[3]. In these solutions the complex decomposed slowly. The spectrum of the complex in the solid state was obtained by the KBr-disk method. This spectrum was similar to that of the solution, but the absorption band was shifted by about 30 mμ to the longer wavelength side. In the KBr-disk, the complex was also unstable.

The Magnetic Susceptibilities.—The observed susceptibilities are as follows:

Thianthrene: $\chi_g=-0.601\times10^{-6}$ per gram, or $\chi_M=-129.8\times10^{-6}$ per mole.

This molar susceptibility is in good agreement with the value of -129.3×10^{-6} reported by Banerjee[8].

The complex of thianthrene with antimony pentachloride: $\chi_g=1.74\times10^{-6}$ per gram, or $\chi_M=897\times10^{-6}$ per mole.

The molar susceptibility of the complex was calculated assuming the composition to be one to one in mole ratio.

Discussion

The facts that identical ESR patterns can be observed in the powdered complexes of thianthrene with antimony pentachloride, with aluminum chloride and with titanium tetrachloride, and that in solution the complex with antimony pentachloride shows the hyperfine structure which has been found in the sulfuric acid solution of thianthrene suggest that the paramagnetism of these complexes originates from thianthrene, presumably its monopositive ion, and not from the chlorides. From this investigation only, the form of these chlorides in complexes can not be deduced. However, it has been suggested, in the case of the complexes of diphenylamine derivatives

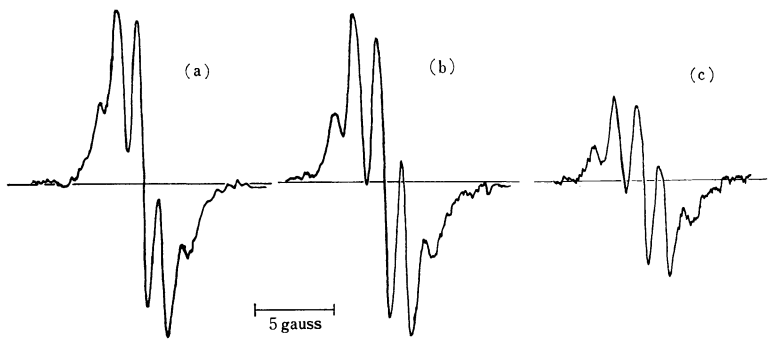


Fig. 2. The ESR hyperfine structures of the solutions of (a) the complex of thianthrene with $SbCl_5$ in nitrobenzene, (b) thianthrene in conc. H_2SO_4, and (c) thianthrene disulfoxide in conc. H_2SO_4.

8) S. Banerjee, *Z. Krist.*, **100**, 316 (1939).

with antimony pentachloride, that the diamagnetic form of $(SbCl_6^- + SbCl_4^-)/2$ might result[9].

The three absorption lines may be attributed to the g-factor anisotropy because of the proportionality of their spacing change to the microwave frequency. Such an anisotropy has been found in some organic free-radicals, e. g., the irradiated proteins[10] and amino acids[11] containing sulfur. In the case of the organic free-radicals containing sulfur atoms, the anisotropy is often observed very clearly, but it can only with difficulty be obtained so clearly in many other free-radicals in powdered or glassy states. This fact has been interpreted qualitatively by the localization of an unpaired electron on the sulfur atom, which can be expected because of the large g-values and broad absorptions in free radicals containing sulfur. Recently this explanation has been confirmed to be valid in the quantitative treatment of the γ-irradiated single crystal of thiodiglycolic acid[12]. The principal g-values, g_1, g_2 and g_3, of the complex with antimony pentachloride, shown in Fig. 1a, are obtained by the method described by Kneubühl[13], who has made a theoretical treatment of line shapes for the powdered samples. This method has given results agreeing well with the single crystal work when applied to copper chloride powder which shows very broad anisotropic lines.

Another explanation for the three absorption lines is that they might be due to the coexistence of three kinds of paramagnetic species. In the case of the mixture of tetracene and antimony pentachloride, it has been shown that there are two kinds of paramagnetic compounds which give the two ESR absorption lines in its powdered state, the intensity ratio of which is dependent on the amount of antimony pentachloride[6]. Also, the presence of two kinds of paramagnetic species has been suggested in the systems of thio-β-naphthol and 2, 2'-dinaphthyl disulfide with the same reagent[1]. In the present complex, it was found that the absorption line shape was not changed by repeated evacuations, but the addition of a small amount of the chloride to the dried complex generated new lines at the near position of the peak with $g=2.0040$.

Although the possibility of the presence of some kinds of compounds could not be excluded completely, the suggestion of the g-factor anisotropy for the dried complex may be supported by the facts that the isotropic hyperfine structure, which is characteristic of the sulfuric acid solution of thianthrene, can be observed in a nitrobenzene solution of the complex, and that the optical absorption spectra for both solid and solution are identical (that is, the same species is responsible for the paramagnetism in both the solid and dissolved states). In the case of some polycyclic aromatic hydrocarbons, it has been shown that the same species is formed in the complex with antimony pentachloride and in the sulfuric acid solution, and identical ESR hyperfine structures[4] and optical absorption spectra[14,15] can be observed. This seems to hold in the present case also.

The concentration of 1.3×10^{21} spins/g. obtained from the ESR absorption intensity indicates that there are 6.7×10^{23} unpaired electrons in one mole of the complex, assuming that the complex is formed by each mole of thianthrene and antimony pentachloride. Since the measurements of the ESR absorption intensities have errors of about 10%, it may be considered likely that each thianthrene molecule has one unpaired electron in the complex. If so, the paramagnetic part of the molar susceptibility of this system can be calculated as about 1250×10^{-6} at room temperature. On the other hand, the observed magnetic susceptibility of the complex is 897×10^{-6}. This leads to 1150×10^{-6} as the paramagnetic part of the susceptibility after the diamagnetic correction is made, assuming that the susceptibility of thianthrene is not altered in the course of the complex formation and that antimony pentachloride takes the diamagnetic form mentioned above, for which the susceptibility is estimated as -124×10^{-6} [9]. The paramagnetic part derived from the susceptibility measurement shows a somewhat large depression below that of the ESR method. This may be ascribed to the unsuitable diamagnetic correction, the experimental error, or other elements such as the Weiss constant, if any. Among these factors, the diamagnetic correction of thianthrene is of especial interest.

In the thianthrene molecule there may be no π-electron conjugation between the two benzenoid rings through the lone pair electrons on sulfur atoms, because of the non-planarity of the molecule. This can be demonstrated from the magnetic susceptibility of thianthrene. From the values of the molar susceptibilities of thianthrene and benzene, $\chi_M = -129.8\times10^{-6}$

9) H. Kainer and K. H. Hausser, *Chem. Ber.*, **86**, 1563 (1953).
10) G. McCormick and W. Gordy, *J. Phys. Chem.*, **62**, 783 (1958).
11) H. Shields and W. Gordy, ibid., **62**, 789 (1958).
12) Y. Kurita and W. Gordy, *J. Chem. Phys.*, **34**, 1285 (1961).
13) F. K. Kneubühl, ibid., **33**, 1074 (1960).
14) W. Ij Aalbersberg, G. J. Hoijtink, E. L. Mackor and W. P. Weijland, *J. Chem. Soc.*, **1959**, 3049, 3055.
15) M. Das and S. Basu, *Spectrochim. Acta*, **17**, 897 (1961).

and $\chi(\text{Benz.}) = -55.6 \times 10^{-6}$ respectively, and the atomic susceptibility of hydrogen, $\chi(\text{H}) = -2.93 \times 10^{-6}$, the atomic susceptibility of sulfur, $\chi(\text{S})$, can be calculated as:

$$\chi_{\text{M}} = 2\chi(\text{Benz.}) - 4\chi(\text{H}) + 2\chi(\text{S})$$
$$\chi(\text{S}) = -15.2 \times 10^{-6}$$

This value agrees with Pascal's constant, $\chi(\text{S}) = -15.0 \times 10^{-6}$, within the range of experimental error. If the conjugation can cover the whole molecule of thianthrene, the atomic susceptibility of sulfur must become more diamagnetic by the above treatment. In the complex, however, it may be suggested that the thianthrene molecule, which is presumably presented as a monopositive ion, may be capable of taking a more diamagnetic planar (or nearly planar) form and that the diamagnetism may be increased by π-electron conjugation over the whole molecule. This suggestion is supported by the stability of the complex and by the ESR hyperfine structure which can be assigned to the four equivalent protons.

The author would like to express his appreciation to Professor Hideo Akamatu, Dr. Hiroo Inokuchi and Dr. Yoshio Matsunaga for their valuable advice and discussion, and to Professor Eitaro Abe, of the Institute of the Solid State Physics, for his work of ESR measurement at 23 kMc./sec.

Department of Chemistry
Faculty of Science
The University of Tokyo
Hongo, Tokyo

Polyterpenes. IV[1]. *The Oxidation Products of Thujopsene*[*1, *2]

By Shizuo NAGAHAMA, Hiroshi KOBAYASHI and Saburo AKIYOSHI

(Received December 22, 1961)

As a result of a recent investigation by Erdtman and Norin[2], the sesquiterpene hydrocarbon thujopsene has been shown to possess structure I. In a previous communication[3] we described the isolation of the keto acid, together with four other degradation products of thujopsene formed by permanganate oxidation. Now using sodium bichromate these same products were again isolated. On the basis of structure I for thujopsene, we now wish to propose structures for these degradation products (II, III, IV and V)[4].

Acid II, $C_{15}H_{22}O_4$, on further permanganate oxidation, afforded IV, $C_{14}H_{22}O_3$[5], which was oxidized by sodium hypobromite to the known C_{13}-dicarboxylic acid VI[1]. The structure of the latter was established by Erdtman and Norin[2].

Acid II did not show the ultraviolet absorption expected of an α-keto acid; furthermore, its infrared spectrum exhibited a hydroxyl band at 3300 cm^{-1}. However, on esterification a methyl ester was obtained which showed ultraviolet and infrared absorptions consistent with the structure VII (R=Me). It therefore appears that, in the solid state, diketo acid II exists in a lactone form. This confirmed by the presence of a band at 1761 cm^{-1} in its infrared spectrum. The compound is therefore formulated as VIII; the alternative structure of IX may be ruled out on the basis of the ultraviolet evidence.

Keto acid IV, on the basis of spectral evidence, exists as a pseudo acid and may therefore be formulated as X. This was confirmed by its dehydration to the enol lactone XI, which on subsequent hydrolysis regenerated the original compound X. The methyl ester of this pseudo acid showed spectral bands in agreement with the structure XII (R=Me).

The treatment of II with alkali gave a further acid III, also isolated by the direct oxidation of thujopsene; the assignment of structure III is based on the following reactions. Chromic acid oxidation of III gave the β-diketone XIII, which on further oxidation

1) Part III of this series: H. Kobayashi, S. Nagahama and S. Akiyoshi, This Bulletin, **34**, 1123 (1961).

*1 Contribution No. 24 from the Department of Organic Synthesis, Faculty of Engineering, Kyushu University, Fukuoka.

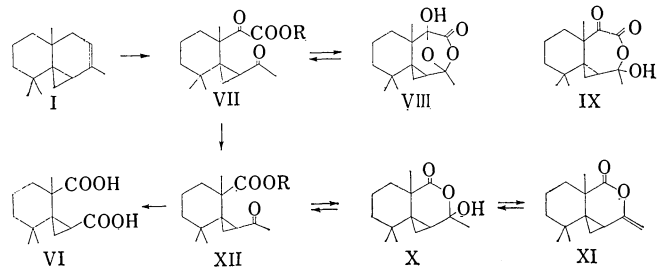
*2 The essential part of this paper was presented before the 13th Annual Meeting of the Chemical Society of Japan, Tokyo, April, 1960.

2) H. Erdtman and T. Norin, *Chem. & Ind.*, **1960**, 622; T. Norin, *Acta Chem. Scand.*, **15**, 1676 (1961).

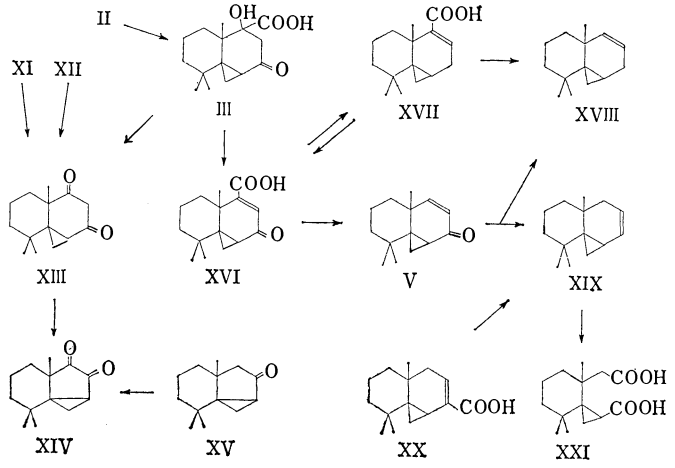
3) S. Akiyoshi and S. Nagahama, This Bulletin, **30**, 886 (1957).

4) These correspond to II, III, IV and V respectively in Part I[3]. The same results for II, III and V have been reported by T. Nozoe et al., *Chem. Pharm. Bulletin*, **8**, 936 (1960).

5) Previously described as an oxyacid $C_{12}H_{14}O_3$ in Ref. 3.



Scheme 1

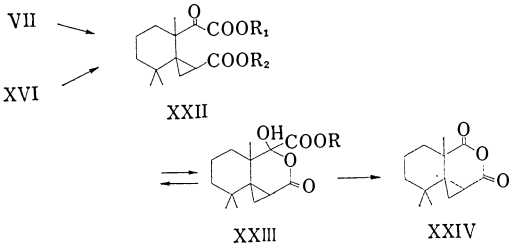


Scheme 2

afforded the yellow α-diketone XIV previously obtained from cycloketone XV[1]. The β-diketone XIII was also obtained by treatment of the enol lactone XI or methyl ester XII (R=Me), with methanolic potassium hydroxide. The dehydration of III gave unsaturated keto acid XVI, $C_{15}H_{20}O_3$[3], which on Huang-Minlon reduction gave the unsaturated acid XVII. XVII could be reoxidized back to XVI. The decarboxylation of XVI, using copper and quinoline, afforded the unsaturated ketone V[6], which was also obtained by direct oxidation of thujopsene. The Huang-Minlon reduction of V gave a mixture of the two hydrocarbons XVIII and XIX. Compound XVIII was also obtained by the decarboxylation of XVII, whereas hydrocarbon XIX was formed by the decarboxylation of hinokiic acid XX. The oxidation of XVIII with potassium permanganate gave C_{13}-dicarboxylic acid VI, and that of XIX, the known C_{14}-dicarboxylic acid XXII.

Acid II and methyl ester VII (R=Me), on oxidation with sodium hypobromite, gave a dicarboxylic acid formulated as XXII (R_1=R_2=H). Different samples of the latter compound, however, exhibited different infrared spectra; this may perhaps be attributed to varying proportions of a lactonoid form such as XXIII (R=H). On methylation, these samples all gave the same dimethyl ester XXII, (R_1=R_2=Me).

The acid XXII, (R=H) was also obtained by the ozonolysis of XV and, on chromic acid oxidation, it gave anhydride XXIV corresponding to C_{13}-acid VI.



Scheme 3

The bichromate oxidation of ester VII (R=Me) gave an acid product $C_{15}H_{22}O_5$, m. p. 190°C. Its infrared spectrum showed bands at 3322, 1762 and 1712 cm^{-1}. Therefore, it might be represented by XXIII (R=Me), rather than by XXII (R_1=Me, R_2=H). Attempted chromic

6) This derivation was first reported by T. Ozeki, S. Seto and T. Nozoe, at the First Symposium on Perfumary, Terpene and Essential Oil Chemistry, Osaka, November, 1957.

acid oxidation of the dimethyl ester XXII ($R_1=R_2=Me$) gave the same product.

Experimental

Permanganate Oxidation of Thujopsene. — An ice-cooled mixture of thujopsene (100 g.) and acetone (400 cc.) was oxidized with finely powdered permanganate (250 g.).

Separation of Acid Products.—The acid part was obtained as an oil or semisolid. When benzene was added to it, acid III, if produced during separation, was precipitated. The benzene extract was concentrated and ketonic acid was crystallized on cooling. The mother liquor was diluted with petroleum ether and cooled in a refrigerator for several weeks or more, giving acids II and IV. After the second or third crop was obtained, the remaining acid II was converted to acid III, which was easily separable, by treating it with alkali for two or three days.

Separation of Neutral Products. — About 750 g. of the neutral part was obtained by several runs; it was separated in 5 fractions by distillation. (The yields in this paragraph are shown as percentage of the whole neutral part.) Fraction 1 (b. p.~119°C/11 mmHg, n_D^{23} 1.5030~1.5050 28.4%) was mainly unreacted thujopsene containing a small number of isomerized hydrocarbons. Fraction 2 (b. p. 119~130°C/11 mmHg, n_D^{23} 1.5057~1.5090, 5.9%) was redistilled, and the fraction of maximum refractive index (b. p. 95~100°C/6 mmHg, n_D^{23} 1.5097, 1.6%) was chromatographed on an alumina column. Petroleum ether eluate was hydrocarbon (0.9%), n_D^{30} 1.5111, d_4^{30} 0.9245, $[\alpha]_D^{30}$ +40.4°, IR, 1515, 812 cm^{-1}. From a benzene eluate, cycloketone XV was obtained. Fraction 3 (b. p. 130~143°C/11 mmHg, n_D^{23} 1.5018~1.5030, 5.8%) was redistilled, and the fraction of minimum refractive index (b. p. 125°C/6 mmHg, n_D^{23} 1.4987, 1.5%) was chromatographed. The petroleum ether eluate was a mixture of ketones; one of them was separated as semicarbazone, m. p. 205~206°C (decomp.).

Found: C, 69.21; H, 9.80; N, 15.40. Calcd. for $C_{16}H_{27}ON_3$: C, 69.27; H, 9.81; N, 15.15%.

Another impure semicarbazone, m. p. 201.5~202.5°C (decomp.), was obtained from the mother liquor. Cycloketone XV was obtained successively, and benzene eluate gave a crystalline alcohol, $C_{15}H_{26}O$ m. p. 85.5~86°C, which was identified as cedrol by infrared spectrum and mixed melting point tests with an authentic specimen[7]. When petroleum ether was added to the ethyl acetate eluate and the mixture was cooled, it was partly crystallized. This was filtered quickly and recrystallized from petroleum ether, giving crystals of m. p. 116~117.5°C IR, 3330 and 1740 cm^{-1}.

Found: C, 76.27; H, 10.28. Calcd. for $C_{15}H_{24}O_2$: C, 76.22; H, 10.24%.

A similar treatment of fraction 4 (b. p. 143~165°C/10 mmHg, n_D^{20} 1.5060~1.5100, 18.2%) gave 0.4% of V from petroleum ether and benzene eluate. Ethyl acetate eluate gave an oxyketone, m. p. 68~70.5°C, (0.5%) IR, 3384, 3195 and 1702 cm^{-1} (Nujol).

Found: C, 76.15; H, 10.46. Calcd. for $C_{15}H_{24}O_2$: C, 76.22; H, 10.24%.

Semicarbazone of the oxyketone, m. p. 214°C (decomp.).

Found: C, 65.31, 65.37; H, 9.29, 9.24; N, 14.23, 14.31. Calcd. for $C_{16}H_{27}O_2N_3$: C, 65.49; H, 9.28; N, 14.32%.

Methanol eluate gave a lactone, m. p. 81.5~82.5°C (1.4%) IR, 1795 cm^{-1}.

Found: C, 72.13; H, 8.87. Calcd. for $C_{15}H_{22}O_3$: C, 71.97; H, 8.86%.

Fraction 5 (b. p. 165~180°C/10 mmHg n_D^{18} 1.5178, 3.3%) gave only ketone V (0.7%) as a crystalline substance.

Bichromate Oxidation of Thujopsene. — Into a mixture of thujopsene (100 g.) and acetic acid (200 g.), a solution of sodium bichromate (250 g.) in acetic acid (750 g.) was stirred drop by drop over a period of nine hours, and the temperature was kept at 50~70°C. After the solution had been left standing overnight, about 250 g. of acetic acid was distilled. The remainder was poured into water (3 l.) and extracted with benzene. The acid part was separated and treated as above. Benzene was removed, and the residue was distilled in vacuo. The fraction of b. p. 140~146°C/11 mmHg (28 g.) deposited crystals which were identified as ketone V (4.1 g.). The mother liquor was chromatographed on an alumina column, giving ketone V (4.0 g.) and oxyketone (0.2 g.). The results are summarized in Table I.

Oxidation of Acid II. — An acetone solution of II (280 mg. in 15 cc.) was treated with potassium permanganate (420 mg.) in acetone (40 cc.) below 50°C. The reaction mixture was treated in the usual manner, and the product was recrystallized from benzene-petroleum ether or ethanol-water; melting point and mixed melting point with IV, 154.5~156°C.

Bichromate Oxidation of Acid IV.—IV (270 mg.) was dissolved in acetic acid (5 cc.), and a solution of sodium bichromate (500 mg.) in acetic acid (5 cc.) was added. The mixture, after being left overnight, showed no color change. Diluted sulfuric acid (5 cc.) was added, and the mixture was left for 2 days. The excess bichromate was decomposed with ethanol, the mixture was diluted with water, and the product was taken into an ether phase. The residue remaining after evaporation of the ether was triturated with benzene, affording a benzene insoluble product (45 mg.) which was identified as C_{13}-dicarboxylic acid VI m. p. 183~185°C (decomp.).

Found: C, 64.94; H, 8.40. Calcd. for $C_{13}H_{18}O_4$: C, 64.98; H, 8.39%.

From the benzene solution, the unchanged IV was recovered.

Hypobromite Oxidation of Acid IV. — IV (500 mg.) was treated with a hypobromite solution, and carbon tetrabromide (400 mg.) was isolated. Working up of the acid products afforded C_{13}-diacid VI (100 mg.).

Methyl Ester of Acid II (VII, R=Me) and its Saponification. — The methyl ester of II was prepared with diazomethane, m. p. 85~87° (from petroleum ether). $[\alpha]_D^{17}$ −187° (*c* 0.593, ethanol).

7) The authors are indebted to Ogawa Perfumary Co., Osaka, for an authentic sample of cedrol.

TABLE I

Substance	Formula	M. p. °C	$[\alpha]_D$	Yield (g. from 100 g. of thujopsene) $KMnO_4$ oxid.	Yield (g. from 100 g. of thujopsene) $Na_2Cr_2O_7$ oxid.
Acid part					
Keto acid	$C_{15}H_{24}O_3$	165	−120°	10	0.2
II	$C_{15}H_{22}O_4$	124	− 28.0°	3.5	2.0
III	$C_{15}H_{22}O_4$	193(d)	+ 21.6°	4.9	0.4
IV	$C_{14}H_{22}O_3$	156	− 85.5°	0.3	4.0
Neutral part					
V	$C_{14}H_{20}O$	77	+193.5°	0.6	8.1
Oxyketone	$C_{15}H_{24}O_2$	70.5		0.2	0.2
Lactone	$C_{15}H_{22}O_3$	82.5		0.7	
XV	$C_{13}H_{20}O$	121		Trace	
Ketone	$C_{15}H_{24}O_2$	117.5		Trace	

Found: C, 68.41; H, 8.85. Calcd. for $C_{16}H_{24}O_4$: C, 68.54; H, 8.63%.

When the ester was treated with methanolic potassium hydroxide, acid III was obtained.

Isomerization of Acid II to Acid III. — A solution of II in a 5% sodium hydroxide solution was left at room temperature overnight. Acidification and working up in the usual manner gave III. From ethanol or ether solution of II containing hydrogen chloride, only the starting material was recovered.

Huang-Minlon Reduction of Acid XVI.—A mixture made from XVI (2.55 g.), hydrazine hydrate (2 cc.), potassium hydroxide (2.5 g.), and diethylene glycol (25 cc.) was refluxed for 4 hr. The reaction mixture was diluted with water and acidified, giving precipitates (XVII, 1.54 g.) which were recrystallized three times from ethanol, m. p. 171～172°, $[\alpha]_D^{30}$ −21.2° (*c* 1.19 chloroform).

Found: C, 76.82; H, 9.53. Calcd. for $C_{15}H_{22}O_2$: C, 76.88; H, 9.46%.

This shows a marked melting point depression when mixed with hinokiic acid (XX).

Permanganate Oxidation of Acid XVII. — To a solution of XVII (186 mg.) in a 3% potassium hydroxide solution (4 cc.), a 2% potassium permanganate solution (10 cc.) was added. The mixture was stirred for 1.5 hr. and was then treated with sodium bisulfite after acidification. The precipitate was recrystallized from ethanol-water, giving acid XVI, melting point and mixed m. p. 206°C and superimposable infrared spectra.

Found: C, 72.59; H, 8.14. Calcd. for $C_{15}H_{20}O_3$: C, 72.55; H, 8.12%.

Permanganate Oxidation of Hinokiic Acid (XX). —Hinokiic acid (2.4 g.) was dissolved in acetone (20 cc.) and treated with permanganate (5.0 g.) in acetone for 1.5 hr. The acetone was removed, and the remainder was dissolved in ether and extracted with a sodium bicarbonate solution. The neutral part crystallized (120 mg.) was identified as C_{13}-anhydride XXIV. From the acid part, C_{14}-diacid XXI (200 mg.), m. p. 206～211°C, was separated. The mother liquor was treated with diazomethane, giving a product (1.03 g.) which was absorbed onto an alumina column. Elution with petroleum ether-benzene (1 : 1) afforded C_{13}-diacid dimethyl ester (165 mg.).

Decarboxylation of Hinokiic Acid (XX), Acid XVII and Acid XVI.—A mixture of hinokiic acid (1.05 g.), copper powder (1.05 g.) and quinoline (10 cc.) was heated in a distillation flask at 230～250°C for 2 hr. The copper was removed and the filtrate, combined with the distillate, was diluted with ether and extracted with hydrochloric acid. The ether layer was washed with a sodium bicarbonate solution and water, and, after it was dried over potassium carbonate the ether was removed. The solid residue (320 mg.) was distilled in vacuo, and the distillate was recrystallized from methanol three times, m. p. 47°C, $[\alpha]_D^{33}$ −135° (*c* 0.933 ethanol) (XIX).

One gram of acid XVII was treated similarly and afforded an oily product (XVIII), n_D^{17} 1.5042, $[\alpha]_D^{30}$ −114° (*c* 0.957 ethanol), which solidified on cooling, m. p. 12～14°C.

Treatment of acid XVI in a similar manner gave ketone V.

Huang-Minlon Reduction of Ketone V.—Ketone V (5 g.) was reduced with a mixture of hydrazine hydrate (3.3 cc.), potassium hydroxide (4.8 g.), and diethylene glycol (50 cc.). The waxy product was recrystallized several times from methanol, using a methanol-dry ice mixture as a cooling agent, m. p. 33～35°C, (2.85 g.). This was shown to be a mixture of XVIII and XIX by the infrared spectrum.

Permanganate Oxidation of Hydrocarbon XVIII and XIX. — To a solution of XIX (550 mg.) in acetone (10 cc.), a solution of permanganate (2 g.) in acetone (50 cc.) was added; the mixture was then stirred for 1.5 hr. below 40°C. After being left overnight, it was worked up as usual. The product was recrystallized from ethanol-water, m. p. 210～211.5°C, (60 mg.). Admixture with authentic C_{14}-diacid (XXI, m. p, 209.5～210.5°C) showed m. p. 210～211°C.

A similar treatment of XVIII (710 mg.) gave C_{13}-diacid VI, (170 mg.).

Permanganate Oxidation of Acid XVI. — XVI (290 mg.) was oxidized in an alkaline permanganate solution in the usual manner. From the neutral part, C_{13}-anhydride XXIV (76 mg.) was obtained and recrystallized three times from petroleum ether, m. p. 211～212°C.

Found: C, 70.42; H, 8.59. Calcd. for $C_{13}H_{18}O_3$: C, 70.24; H, 8.16%.

Permanganate Oxidation of Ketone V. — To ketone V a solution of permanganate (4.27 g.) in water (100 cc.) was added. The oxidation was allowed to proceed for 2.5 hr. below 70°C, and the product was then treated as usual. The acid part contained C_{13}-diacid VI (90 mg.), and the neutral part, the corresponding anhydride (XXIV) m. p. 206~207°C (165 mg.).

Bichromate Oxidation of Acid III. — To a mixture of III (30 g.) and acetic acid (450 cc.) (not a complete solution) a solution composed of sodium bichromate (12 g.) and acetic acid (50 cc.) was added; the mixture was left at room temperature for one week. The insoluble material (7.84 g.) was identified to be the starting material, m. p. 205.5~207°C (decomp.). The filtrate was concentrated to about 1/3 of the original volume and was poured into water (1 l.). The precipitate filtered and triturated with hot benzene gave an insoluble product which was recrystallized from ethanol to give XIII, m. p. 218~221°C (4.0 g.), $[\alpha]_D^{14}$ +272° (*c* 0.93, ethanol).

Found: C, 75.91; H, 9.12. Calcd. for $C_{14}H_{20}O_2$: C, 76.32; H, 9.15%.

The benzene extract contains a mixture of yellow diketone XVI and C_{13}-diacid anhydride XXIV. From the acid part, C_{13}-diacid VI (440 mg.) was obtained. The amount of sodium bichromate (20 g.) relative to III (15 g.) was increased and the yield of XIII was diminished, but a larger amount (8 g.) of a mixture of XIV and XXIV was obtained.

Bichromate Oxidation of Diketone XIII.—XIII (1.34 g.) was dissolved in acetic acid (40 cc.), and a solution of sodium bichromate (1.75 g.) in acetic acid (10 cc.) was added. The mixture was kept below 50°C for 5 hr., and then concentrated to 1/2 volume. The yellow precipitates obtained upon dilution with water were dissolved in benzene and freed from acids. Recrystallization from methanol-water gave yellow crystals of diketone XIV, m. p. 175~180°C (960 mg.). Chromatography on an alumina column gave a sample, m. p. 179.5~180°C and mixed melting point with XIV prepared from cycloketone XV[1], 181~182.5°C.

Methyl Ester XII (R=Me) and its Saponification. — Treatment of acid IV with diazomethane gave crystals, m. p. 69~71°C. $[\alpha]_D$ −211° (*c* 0.78, ethanol).

Found: C, 71.40; H, 9.80. Calcd. for $C_{15}H_{24}O_3$: C, 71.39; H, 9.59%.

The product (140 mg.) was refluxed with 5% methanolic sodium hydroxide for 2 hr. and then poured into water and acidified. The precipitates, on trituration with petroleum ether, were crystallized. Recrystallization from ethanol-water gave β-diketone XIII (5 mg.) as the first crop, m. p. 219~220°C (decomp.). From the second crop, acid IV was obtained.

Enol Lactone XI and its Saponification.—Treatment of acid IV with acetic anhydride in pyridine gave the anhydroderivative XI, m. p. 80.5~83°C (from ethanol).

Found: C, 76.29; H, 9.39. Calcd. for $C_{14}H_{20}O_2$: C, 76.32; H, 9.15%.

Saponification. a) XI (46 mg.) in a 5% sodium hydroxide solution (5 cc.) was refluxed for an hour; 12 mg. of acid IV was isolated. b) XI (85 mg.) in a methanolic potassium hydroxide solution was refluxed for two hours, and about a half of the methanol was removed. The remainder was poured into water, and the precipitates were purified, giving the ester XII (R=Me). The filtrate was acidified and a small amount of β-diketone XIII was obtained. Both were identified by their infrared spectra.

Hypobromite Oxidation of Ester XII (R=Me). —A solution of XII (R=Me) (450 mg.) in dioxane (22 cc.) was treated with a hypobromite solution (20 cc.) for 30 min. Water (30 cc.) was added and extracted with ether. The acid product was recrystallized from aqueous methanol, giving C_{13}-diacid monomethyl ester (168 mg.) m. p. 139~141°C. The infrared spectrum was identical with an authentic sample[1].

Hypobromite Oxidation of II.—Fine crystals of II (680 mg.) were added to a hypobromite solution (20 cc.) and left for 2.5 hr. When sodium bisulfite and hydrochloric acid were added, the whole solution became a gel. A crude material obtained from air-dried gel showed infrared bands at 3390 and 1690 cm^{-1} (broad). The gel was shaken with ether. Evaporation of ether left fine needles, which were recrystallized from a mixture of ether-petroleum ether, m. p. 178~180°C (decomp.). IR, 3378, 1745 and 1667 cm^{-1}.

Found: C, 62.49; H, 7.66. Calcd. for $C_{14}H_{20}O_5$: C, 62.67; H, 7.51%.

Alternatively the gel-product was treated with an alkaline hydrogen peroxide solution overnight and then acidified. The precipitates were dissolved in methanol-water. An oil separated and solidified on standing, then needles were crystallized from the solution. The needles, m. p. 178~180°C, show infrared bands at 3408, 3155 and 1721 cm^{-1}. The solidified oil shows infrared bands at 3333, 1727 and 1675 cm^{-1} (Nujol). With diazomethane both of them gave the same dimethyl ester (XXII, R=Me) m. p. 80.5~82.5°C, which was identical with the dimethyl ester obtained from the gel without hydrogen peroxide treatment.

Found: C, 64.91; H, 8.39. Calcd. for $C_{16}H_{24}O_5$: C, 64.84; H, 8.16%.

Ozonolysis of Acid XVI.—To a solution of XVI (1.1 g.) in a carbon tetrachloride-chloroform mixture (1 : 1, 80 cc.), ozone was passed for three hours while the solution was cooled in an ice-bath. The solvent was removed, and the residue was taken up in ether, from which the acid product was extracted. The product (air-dried gel) was identified as acid XXIII by infrared spectral comparison.

Chromic Acid Oxidation of Acid XXIII.—XXIII (90 mg.) was dissolved in acetic acid (3 cc.), and a solution composed of chromic acid (200 mg.) and concentrated sulfuric acid (3 drops) was added. The mixture was kept for 24 hr. and diluted with water. C_{13}-anhydride XXIV (20 mg.) m. p. 208°C was obtained.

Bichromate Oxidation of Ester VII ($R=M_e$).— To an acetic acid solution (2 cc.) of VII (500 mg.), a solution of sodium bichromate (2.0 g.) in acetic acid (3 cc.) was added. Four drops of concentrated sulfuric acid was added, and the mixture was left

for a few minutes. The precipitates occurring were recrystallized from a benzene-petroleum ether mixture and sublimed under reduced pressure, giving XXIII (R=Me), m. p. 188~190°C.

Found: C, 64.03; H, 8.03. Calcd. for $C_{15}H_{22}O_5$: C, 63.81; H, 7.85%.

Attempted Oxidation of Ester XXII ($R_1=R_2=$ Me).—The ester was treated with chromic acid in a mixture of acetic and sulfuric acid for 1.5 hr. Water was added, and the resulting precipitates were filtered. They contain mostly the starting material, besides a small amount of a petroleum ether-insoluble material, which was recrystallized from benzene, m. p. 187~190°C, and was shown to be identical with the XXIII (R=Me) obtained from VII (R=Me).

The authors wish to express their gratitude to Dr Peter J. L. Daniels and Dr. Yuan-Lang Chow of the Royal Institute of Technology, Stockholm, Sweden, for revising the language of the manuscript. They are also indebted to Mr. Michio Shido for his elementary analyses.

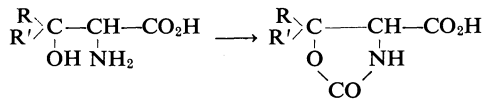
Department of Organic Synthesis
Faculty of Engineering
Kyushu University
Hakozaki, Fukuoka

*Oxazolidone Derivatives of Hydroxyamino Acids. III. Inversion of the erythro- to the threo-Form of Threonine via Oxazolidone Ester**

By Takeo KANEKO and Toshishige INUI

(Received December 5, 1961)

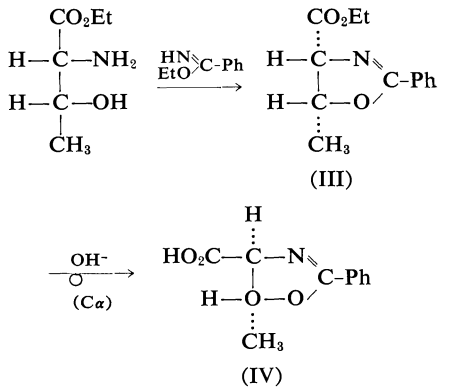
In a previous paper of this series[1], it was shown that α-amino-β-hydroxylic acids (I) in an alkaline solution cyclised to oxazolidone derivatives (II) under the action of phosgene. During this reaction the configuration at both



(I) (II)

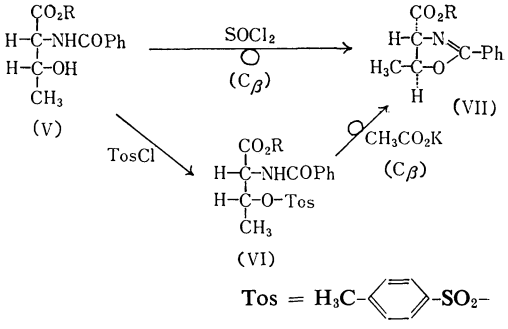
the asymmetric centers remains unchanged, and DL-*trans*- and DL-*cis*-5-methyl-2-oxo-oxazolidine-4-carboxylic acids (II; R=H, R′=CH_3) are easily obtained from DL-threonine and DL-allothreonine respectively.

Oxazoline derivatives, as is well known, are important intermediates for the configurational transformation of allothreonine into threonine, and this conversion has been achieved by epimerization at either the α- or the β-carbon position. According to the first method, the less stable *cis*-oxazoline-ester (III) derived from allothreonine ester is transformed into the more stable trans-configuration IV with epimerization at the α-carbon atom and with



(III) (IV)

the simultaneous hydrolysis of the ester group[2,3] under the action of aqueous alkali. According to the second method, on the other hand, *N*-benzoyl-allothreonine ester (V) or its *O*-tosyl derivative (VI) is converted into the *trans*-oxazoline ester (VII), with the inversion



(V) (VII) (VI)

* This work was partly presented at the 11th and 13th Annual Meetings of the Chemical Society of Japan, Tokyo, April, 1958, and April, 1960.

1) T. Kaneko and T. Inui, *J. Chem. Soc. Japan, Pure Chem. Sec.* (*Nippon Kagaku Zasshi*), **82**, 1075 (1961).

2) D. F. Elliott, *Nature*, **162**, 657 (1948); *J. Chem. Soc.*, **1949**, 589.

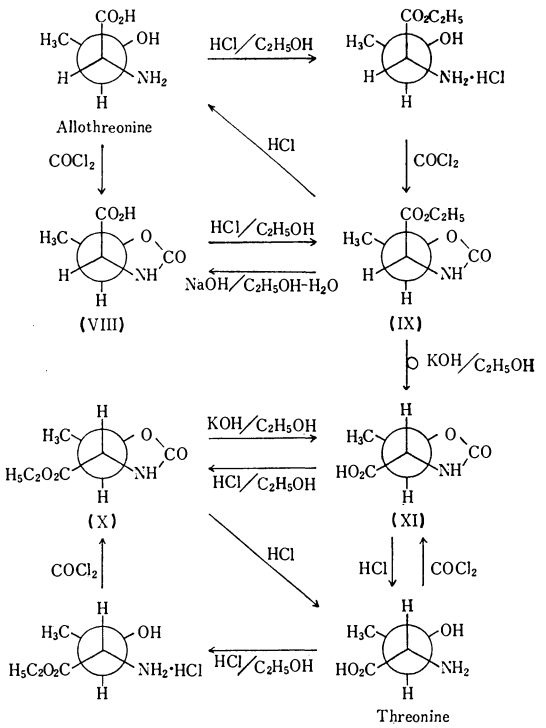
3) D. F. Elliott, *J. Chem. Soc.*, **1950**, 62.

of the configuration at the β-carbon atom, by the action of thionyl chloride[4,5] or potassium acetate[5] respectively. In both cases, the resulting *trans*-oxazoline derivatives (IV and VII) give threonine on acid hydrolysis.

These facts suggest that the *cis*-oxazolidone derivative derived from allothreonine by the present authors may be similarly converted into the stable trans-configuration, because of the expected instability of the cis-configuration of oxazolidone ester. In the present paper, it is reported that *cis*-oxazolidone-carboxylic ester converts into *trans*-carboxylic acid on alkaline hydrolysis.

Upon treatment with hydrogen chloride in absolute alcohol, DL-*cis*-5-methyl-2-oxo-oxazolidine-4-carboxylic acid (VIII)[1] derived from DL-allothreonine yielded DL-*cis*-4-ethoxycarbonyl-5-methyl-2-oxo-oxazolidine (IX), b. p. 126~128 °C/10^{-3} mmHg. without any detectable change in the configuration. The configuration assigned was confirmed by isolating pure DL-allothreonine from the acid-hydrolyzate of this oxazolidone-carboxylic ester (IX). The same ester IX was also obtained by the reaction of DL-allothreonine ethyl ester hydrochloride with phosgene in aqueous potassium carbonate. In a similar way, DL-threonine ethyl ester hydrochloride gave DL-*trans*-4-ethoxycarbonyl-5-methyl-2-oxo-oxazolidine (X), b. p. 115~118°C/10^{-3} mmHg. The configuration of this ester X was also assigned by hydrolyzing it with hydrochloric acid and by isolating the resulting pure DL-threonine.

When DL-*cis*-ester IX was heated with one equivalent of alcoholic aqueous sodium hydroxide according to the method employed by Elliott[3], only the hydrolysis of the ester group took place, without any inversion; on the other hand, if the same ester IX was treated with a slightly excessive amount of 0.4 N alcoholic potassium hydroxide, both the conversion and the hydrolysis of ester took place. The resulting product possessed an infrared spectrum similar to that of DL-*trans*-5-methyl-2-oxo-oxazolidine-4-carboxylic acid (XI) derived from DL-threonine, but its melting point (120~122°C) was somewhat lower than that of XI (127~128°C). On the other hand, DL-*trans*-ester X gave DL-*trans*-carboxylic acid XI with the retention of configurations under the same conditions, and the infrared spectrum of the product was identical with that of an authentic sample. Therefore, it may be supposed that the less stable DL-*cis*-ester IX converted to the more stable DL-*trans*-form XI but not from

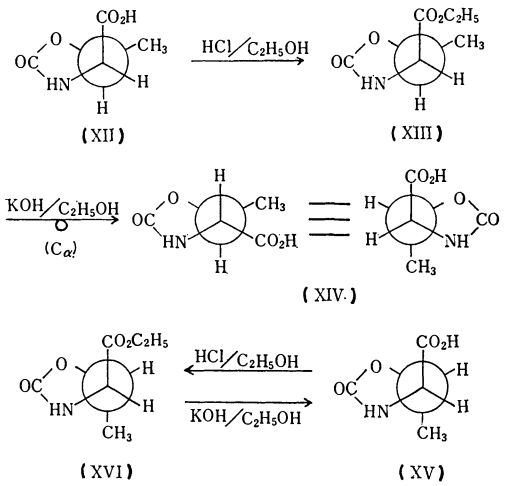


trans to cis, under the conditions used. The compound obtained from DL-*cis*-ester IX seemed to be impure DL-*trans*-carboxylic acid XI contaminated with DL-*cis*-carboxylic acid VIII, as the hydrolysis of this compound with hydrochloric acid gave DL-threonine, together with a small quantity of DL-allothreonine, both of which were identified by paper chromatographic analysis[6]. Recently, chromatographic separation and determination of a synthetic mixture of *N*-2,4-dinitrophenylated threonine and allothreonine were carried out by Seki using a column of carboxylic type resin, Amberlite IRC-50[7]. By the use of this method, the ratio of DL-threonine to DL-allothreonine in the acid-hydrolyzate was estimated to be 6.1. From these results, it was presumed that the conversion was due to epimerization at the asymmetric center corresponding to the α-carbon atom of the original amino acid molecules.

In order to prove this presumption exactly, this conversion should be applied to optically active material. Thus, the conversion at the α-carbon atom should result in the conversion of L-*cis*-ester to D-*trans*-carboxylic acid. To obtain L(−)-*cis*-ester XIII, the DL-*cis*-carboxylic acid VIII was resolved by means of brucine[8], and the resulting L(−)-*cis*-carboxylic acid (XII)

4) K. Pfister, C. A. Robinson, A. C. Shabica and M. Tishler, *J. Am. Chem. Soc.*, **70**, 2297 (1948); **71**, 1101 (1949).
5) J. Attenburrow and D. F. Elliott, *J. Chem. Soc.*, **1948**, 310.
6) K. N. F. Shaw and S. W. Fox, *J. Am. Chem. Soc.*, **75**, 3421 (1953).
7) T. Seki, *J. Biochem. Japan*, **47**, 253 (1960).
8) T. Inui and T. Kaneko, *J. Chem. Soc. Japan, Pure Chem. Sec.* (*Nippon Kagaku Zasshi*), **82**, 1078 (1961).

was treated with hydrogen chloride in absolute alcohol. Hydrolysis of this ester XIII with hydrochloric acid yielded pure L(+)-allothreonine, confirming the configuration assigned. Upon the treatment of this L(−)-*cis*-ester XIII with alcoholic potassium hydroxide, an optically active acid XIV, m. p. 131~133.5°C, $[\alpha]_D$ −37.7°, was obtained. Hydrolysis with hydrochloric acid yielded a mixture of D(+)-threonine and L(+)-allothreonine. Chromatographic analysis of this mixture as the dinitrophenyl derivative[7] showed that the ratio of D(+)-threonine to L(+)-allothreonine was identical with that of the optically inactive case mentioned already. As a comparison, L(+)-*trans*-carboxylic acid XV was obtained by the reaction of L(−)-threonine with phosgene in the presence of potassium hydroxide[8]. The infrared spectrum of the compound XIV was similar to that of L(+)-*trans*-carboxylic acid XV. As a result, it was proved that this levorotatry acid XIV was D(−)-*trans*-carboxylic acid contaminated with L(−)-*cis*-carboxylic acid XII. The L(+)-*trans*-ester XVI derived from L(+)-*trans*-carboxylic acid XV gave pure L(−)-threonine upon hydrolysis with hydrochloric acid. Moreover, the treatment with alcoholic potassium hydroxide resulted only in the hydrolysis of ester group, yielding L(+)-*trans*-carboxylic acid XV without any configurational change.



From the results of this investigation, it was concluded that this conversion of the cis- to trans-form was the result of epimerization at the asymmetric center corresponding to the α-carbon atom in the original amino acid molecules.

Experimental**

DL-*cis*-Ethoxycarbonyl-5-methyl-2-oxo-oxazolidine (IX). *Method A. By Esterification of DL-cis-5-Methyl-2-oxo-oxazolidine-4-carboxylic Acid (VIII).*—a) A suspension of DL-*cis*-carboxylic acid[1] VIII (8.0 g., 0.055 mol.) in 100 ml. of absolute alcohol was saturated with hydrogen chloride by passing the dry gas as a vigorous stream at 0°C. The solution, after being left standing overnight at room temperature, was evaporated to dryness under reduced pressure. The residue was dissolved in water and extracted with four 60 ml. portions of ethyl acetate. The combined extract was dried over sodium sulfate, and the solvent was removed by distillation. The residue, on distillation under reduced pressure, yielded 8.0 g. (84%) of DL-*cis*-ester IX, b.p., 126~128°C/10^{-3} mmHg, n_D^{20} 1.46376.

IR, 3300 (amide), 1760 (cyclic amide and ester) cm^{-1} (liquid film).

Found: C, 48.41; H, 6.39; N, 7.87. Calcd. for $C_7H_{11}O_4N$: C, 48.55; H, 6.40; N, 8.09%.

b) A suspension of the above DL-*cis*-carboxylic acid[1] VIII (3.6 g., 0.025 mol.) in 80 ml. of ether was treated with an excess of diazoethane dissolved in ether. After the evaporation of the solvent and the reagent, the residue was distilled under reduced pressure. Yield, 2.7 g. (63%); b. p., 138~140°C/10^{-2} mmHg. The infrared spectrum was identical with that of the ester obtained by a).

Method B. By Cyclization of DL-Allothreonine Ethyl Ester Hydrochloride.—Crude DL-allothreonine ethyl ester hydrochloride[2] obtained from DL-allothreonine (7.2 g., 0.06 mol.) was dissolved in 200 ml. of water, and the solution was covered with 105 ml. of toluene. To the mixture, after it was cooled to 3°C, 1 N potassium hydroxide (70 ml., 0.07 mol.) and 26.0 g. (0.18 mol.) of anhydrous potassium carbonate were added, and then a solution of 14.6 g. (0.147 mol.) of phosgene in toluene (45 ml.) was stirred in drop by drop over a 40 min. period. After being stirred for an additional hour, the aqueous layer separated from the toluene layer was acidified with concentrated hydrochloric acid and extracted with four 60 ml. portions of ethyl acetate. The combined extract was dried over sodium sulfate, the solvent was removed by distillation, and the residue was distilled under reduced pressure. Yield, 4.1 g. (39% for DL-allothreonine); b. p., 122~124°C/10^{-3} mmHg., n_D^{20} 1.46420. All properties of this sample were identical with those of the product obtained by the above method A.

The aqueous layer remaining after the extraction with ethyl acetate was evaporated under reduced pressure, and the residue was extracted with four 50 ml. portions of ethyl acetate while hot. The extract was concentrated under reduced pressure. On scratching of the side of the vessel, DL-*cis*-carboxylic acid VIII crystallized out. Yield, 2.0 g. (23% for DL-allothreonine); m. p., 193~195°C (decomp.). All properties of this sample were identical with those of an authentic sample[1].

DL-Allothreonine.—A solution of 0.99 g. (0.0057 mol.) of DL-*cis*-ester IX in 20 ml. of 1 : 1 hydrochloric acid was refluxed for 8 hr. After being cooled at room temperature, the reaction mixture was extracted with ethyl acetate, and the aqueous

** All melting points and boiling points are uncorrected. Infrared spectra were recorded with a Hitachi EPI-2 type infrared spectrophotometer, and refractive indices were determined with a Bausch and Lomb precision refractometer.

solution was evaporated to dryness under reduced pressure. The residue was dissolved in 17 ml. of 94% alcohol, and pyridine (3 ml.) was added. DL-Allothreonine crystallized out. Yield, 0.5 g. (86%); m. p., 241~242°C (decomp.). On recrystallization from water and alcohol, its melting point rose to 246~247°C (decomp.). All properties of this sample were identical with those of an authentic sample.

DL-*cis*-5-Methyl-2-oxo-oxazolidne-4-carboxylic Acid (VIII).—*By Hydrolysis of DL-cis-Ester IX with Aqueous Alcoholic Sodium Hydroxide.*—To a solution of 0.74 g. (0.00428 mol.) of DL-*cis*-ester IX in 40 ml. of 94% alcohol, 3.9 ml. (0.00426 mol.) of 1.09 N sodium hydroxide was added. The mixture was heated under reflux for 20 min. After being cooled, the solvent was evaporated in vacuo, and the residue was dissolved in water. The aqueous solution was extracted with ethyl acetate, acidified with concentrated hydrochloric acid, and then evaporated in vacuo to dryness. The residue was extracted with three 40 ml. portions of ethyl acetate. When the combined extract was evaporated in vacuo, DL-*cis*-carboxylic acid VIII crystallized out. Yield, 0.42 g. (68%); m. p., 193~195°C (decomp.). The melting point could be raised to 196~197°C (decomp.) by recrystallization. All properties of this sample were identical with those of an authentic sample[1].

DL-*trans*-4-Ethoxycarbonyl-5-methyl-2-oxo-oxazolidine (X).—According to the same method as used in the synthesis of DL-*cis*-ester IX by method B, DL-threonine ethyl ester hydrochloride[2] obtained from DL-threonine (4.8 g., 0.04 mol.) was cyclized to DL-*trans*-ester X with phosgene (11.8 g., 0.119 mol.) in the presence of potassium carbonate. Yield, 3.4 g. (49%); b. p., 115~118°C/10^{-3} mmHg., n_D^{20} 1.46105.

IR, 3300 (amide), 1765 (cyclic amide and ester) cm^{-1} (liquid film).

Found: C, 48.17; H, 6.32; N, 7.81. Calcd. for $C_7H_{11}O_4N$: C, 48.55; H, 6.40; N, 8.09%.

DL-*trans*-Carboxylic acid XI could not be obtained from the remaining aqueous solution.

Treatment of DL-*trans*-carboxylic acid XI with hydrogen chloride in absolute alcohol also yielded the same ester X.

DL-*trans*-5-Methyl-2-oxo-oxazolidine-4-carboxylic Acid (XI).—*A) By Hydrolysis of DL-cis-Ester IX with Alcoholic-Potassium Hydroxide.*—To a solution of 1.16 g. (0.00670 mol.) of DL-*cis*-ester IX in 7.5 ml. of absolute alcohol, 7.5 ml. (0.00677 mol.) of 0.89 N alcoholic potassium hydroxide was added, and the mixture was refluxed for 15 min. After the mixture had been cooled, 15 ml. of water was added, and the solution was acidified with concentrated hydrochloric acid. The aqueous solution was evaporated to dryness under reduced pressure. The residue was extracted with 3 times with 30 ml. of ethyl acetate. The combined extract was evaporated in vacuo to a syrup, which was crystallized on scratching of the side of the vessel. Yield, 0.57 g. (77%); m. p., 119~121.8°C. The melting point could be raised to 121~123°C by recrystallization. Its infrared spectrum was similar to that of DL-*trans*-carboxylic acid XI[1], m. p. 127~128°C.

B) By Hydrolysis of DL-trans-Ester X.—In a similar way, DL-*trans*-ester X (1.72 g, 0.010 mol.) was hydrolyzed with 0.40 N alcoholic potassium hydroxide (25 ml., 0.010 mol.). Yield, 1.07 g. (74%); m. p., 125~126.5°C. The melting point could be raised to 126.5~127.5°C by recrystallization, and it was undepressed on admixture with a pure authentic sample[1]. All properties of both compounds were identical.

DL-Threonine.—*A) By Hydrolysis of DL-trans-Carboxylic Acid XI Derived from DL-cis-Ester IX.*—The substance XI (6.06 g., 0.035 mol.) was refluxed with 120 ml. of 1 : 1 hydrochloric acid. From the hydrolyzate, DL-threonine containing a small quantity of DL-allothreonine was obtained by the usual method. Yield, 3.71 g. (73%); m. p., 230.5~231.5°C (decomp.). Its infrared spectrum was similar to that of pure DL-threonine. The proportion of DL-threonine (R_f 0.16) to DL-allothreonine (R_f 0.12) present was determined by paper chromatography using the upper layer from a mixture of *n*-butanol-acetone-concentrated aqueous ammonia-water (8 : 1 : 1 : 6 by volume)[6] as the developer. The ratio of DL-threonine to DL-allothreonine was about 5. Chromatographic analysis of the dinitrophenylated sample[7] showed that the ratio was 6.1. On recrystallization from water and alcohol, its melting point rose to 231~232°C (decomp.). Chromatographic analysis of this sample showed that the ratio was 10.1.

B) By Hydrolysis of DL-trans-Ester X.—One gram (0.0058 mol.) of DL-*trans*-ester X was hydrolyzed with hydrochloric acid (1 : 1; 16 ml.) in the usual way. Yield, 0.46 g. (67%); m. p., 232.5.~233.5°C (decomp.). The melting point could be raised to 236~237°C (decomp.) by recrystallization. All properties of this sample were identical with those of an authentic sample.

L(−)-*cis*-Ethoxycarbonyl-5-methyl-2-oxo-oxazolidine (XIII).—Four grams (0.0376 mol.) of L(−)-*cis*-carboxylic acid XII[8], m. p., 169.5~170.5°C, $[\alpha]_D$ −19.2±0.5°C (H_2O), were esterified with hydrogen chloride in absolute alcohol. Yield, 4.1g. (86%); m. p., 71~73°C. After recrystallization from ethyl acetate and petroleum ether, it melted at 72~73°C. $[\alpha]_D^{27}$ −3.6°C (*c* 3.29, 99% EtOH).

IR, 3290 (amide), 1760, 1750, 1730 (cyclic amide and ester) cm^{-1} (Nujol).

Found: C, 48.75; H, 6.39; N, 8.16. Calcd. for $C_7H_{11}O_4N$: C, 48.55; H, 6.40; N, 8.09%.

L(+)-Allothreonine.—L(−)-*cis*-Ester XIII (0.79 g., 0.00456 mol.) was hydrolyzed with hydrochloric acid (1 : 1; 20 ml.) in the usual way. Yield, 0.47g. (89%); m. p., 273.5~275°C (decomp.), $[\alpha]_D^{29}$ +9.1° (*c* 2.97, H_2O). All properties of this sample were identical with those of an authentic sample[2].

L(+)-*trans*-4-Ethoxycarbonyl-5-methyl-2-oxo-oxazolidine (XVI).—Four and a half grams (0.031 mol.) of L(+)-*trans*-carboxylic acid XV[8], m. p., 139.5~140.5°C, $[\alpha]_D$ +41.2±0.5° (H_2O), were esterified with hydrogen chloride in absolute alcohol. Yield, 4.0 g. (75%); b. p., 123~125°C/10^{-3} mmHg; m. p., 63~65°C. On recrystallization from small amounts of ethyl acetate and petroleum ether, its melting point rose to 64~66°C. $[\alpha]_D^{28}$ +37.4° (*c* 3.50, 99% EtOH).

IR, 3260 (amide), 1750, 1715 (cyclic amide and ester) cm^{-1} (Nujol).

Found: C, 48.53; H, 6.12; N, 7.98. Calcd. for $C_7H_{11}O_4N$: C, 48.55; H, 6.40; H, 8.09%.

L(−)-Threonine.—In the usual way, 0.84 g. (0.00485 mol.) of L(+)-*trans*-ester XVI was hydrolyzed with 20 ml. of hydrochloric acid (1 : 1). Yield, 0.51 g. (89%); m. p., 261~262°C (decomp.), $[\alpha]_D^{28}$ −28.4° (*c* 2.81, H_2O). All properties of this sample were identical with those of an authentic sample[8].

L(+)-*trans*-5-Methyl-2-oxo-oxazolidine-4-carboxylic Acid (XV).—To a solution of 1.14 g. (0.00658 mol.) of L(+)-*trans*-ester XVI in 8.0 ml. of absolute alcohol, 7.6 ml. (0.00661 mol.) of 0.87 N alcoholic potassium hydroxide was added. After the mixture bad been lett standing for 1.5 hr. at room temperature, 20 ml. of water was added. The solution was acidified with concentrated hydrochloric acid and evaporated in vacuo to dryness. The residue was extracted 3 times with 40 ml. of hot ethyl acetate. When the extract was evaporated under reduced pressure, L(+)-*trans*-carboxylic acid XV crystallized out. Yield, 0.8 g. (85%); m. p., 139.8~140.2°C, $[\alpha]_D^{29.8}$ +41.8°(*c* 2.70, H_2O). All properties of this sample were identical with those of an authentic sample[8].

D(−)-*trans*-5-Methyl-2-oxo-oxazolidine-4-carboxylic Acid (XIV).—*Conversion of L(−)-cis-Ester XIII.*—In a similar way, 1.57 g. (0.00907 mol.) of L(−)-*cis*-ester XIII were hydrolyzed with 21.2 ml. (0.00915 mol.) of 0.43 N alcoholic potassium hydroxide. Yield, 1.10 g. (84%); m. p., 131~133.5 °C, $[\alpha]_D^{27}$ −37.7° (*c* 2.71, H_2O). Its infrared spectrum was similar to that of L(+)-*trans*-carboxylic acid XV.

D(+)-Threonine.—In the usual way, 0.54 g. (0.00454 mol.) of D(−)-*trans*-carboxylic acid XIV obtained from L(−)-*cis*-ester XIII was hydrolyzed with 20 ml. of hydrochloric acid (1 : 1). Yield, 0.37 g. (83%); m. p., 251~253.5°C (decomp.), $[\alpha]_D^{29}$ +24.8° (*c* 2.82, H_2O). Chromatographic analysis of the dinitrophenylated sample[7] showed that the ratio of D(+)-threonine to L(+)-allothreonine was 5.7.

The authors wish to express their thanks to Dr. Tokuichiro Seki for his assistance in carrying the chromatographic analysis and to the Ajinomoto Co., Inc., for its gift of amino acids. Thanks are also due to Mr. M. Okumiya and Miss. K. Koike for micro analyses.

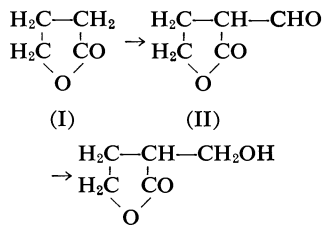
Department of Chemistry
Faculty of Science
Osaka University
Nakanoshima, Osaka

*The Absolute Configuration of α-Methyladipic Acid**

By Takeo KANEKO, Ken-ichi WAKABAYASHI** and Hakuji KATSURA

(Recieved December 11, 1961)

Recently, determinations of the stereostructures of terpenoids, alkaloids and antibiotics have become important. In order to obtain clear sterostructures of key-substances, absolute configurations of a few compounds containing branched alkyl groups have been determined[1]. The absolute configuration of α-methyladipic acid, obtained as an oxidation product of an alkaloid nupharidine[2], has however, never been determined. The present paper deals with the chemical determination of the absolute configuration of α-methyladipic acid by the establishment of the configurational correlation between this acid and methylsuccinic acid, the absolute configuration of which is already known[3].



(I) (II) (III)

α-Formyl-γ-butyrolactone (II) was synthesized from γ-butyrolactone (I) by the modified methods described by Korte[4] and McGraw[5]. DL-α-Hydroxymethyl-γ-butyrolactone (III) was obtained from formyl derivative II in a high

* Presented at the 14th Annual Meeting of the Chemical Society of Japan, Tokyo, April, 1961.

** Present address: Central Research Laboratory, Mitsubishi Chemical Industries, Ltd., Kawasaki-shi.

1) Cf. K. Freudenberg, "Stereochemie", Franz Deutcke, Leipzig (1933), p. 679; W. Klyne, "Progress in Stereochemistry", Vol. I, Butterworths Scientific Publication, London (1954), p. 188.

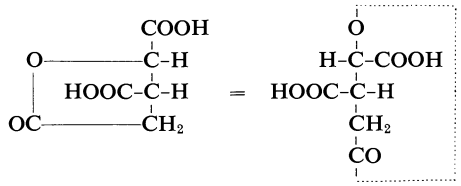
2) M. Kotake, S. Kusumoto and T. Ohara, *Ann.*, **606**, 148 (1957).

3) A. Fregda, *The Svedberg-Festschrift, Uppsala*, **1944**, 261; *Acta Chem. Scand.*, **1**, 371 (1944).

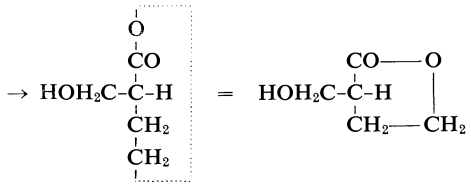
4) F. Korte and H. Machleidt, *Chem. Ber.*, **88**, 136, 1684 (1955).

5) Wm. J. McGraw, U. S. Pat. 2624723 (1953); *Chem. Abstr.*, **47**, 11232g (1953).

yield by catalytic reduction according to the method of McGraw[5]. An optical resolution of hydroxymethylbutyrolactone (III) was attempted, but no optically pure substances were obtained. Then, optically active (+)-α-hydroxymethyl-γ-butyrolactone (+III) ([α]D+10.4°) was prepared from (+)-alloisocitric lactone

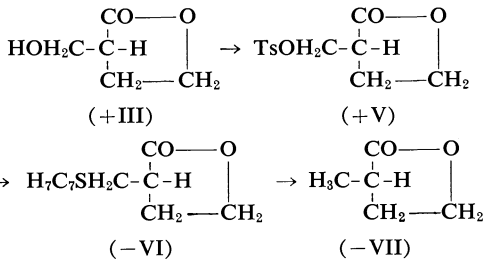


(+IV)



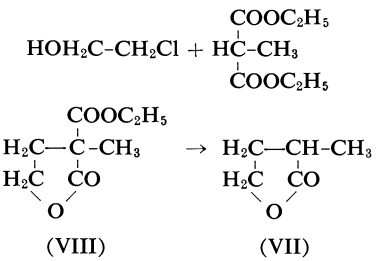
(+III)

(+IV) by the methods described earlier[6]. (−)-Benzyl thioether (−VI), which was derived from the (+)-tosylate (+V) of +III by the action of benzylmercaptan, was converted into (−)-α-methyl-γ-butyrolactone([α]D −0.2°(*c* 23,



Ts=*p*-CH_3-C_6H_4-SO_2-
C_7H_7=C_6H_5-CH_2-

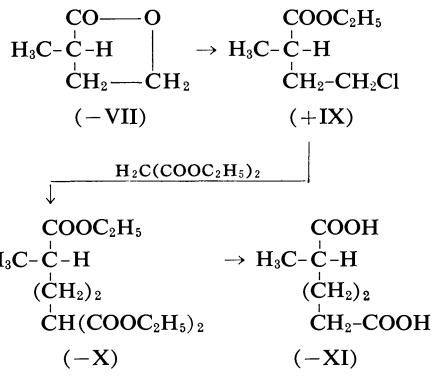
l=2 dm., absolute ethanol))(−VII) by treatment with a Raney-nickel catalyst. In another



(VIII) (VII)

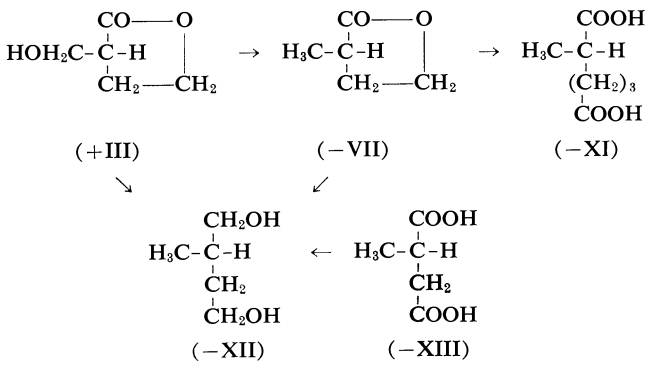
way, DL-α-methyl-γ-butyrolactone (VII) was synthesized from lactone-ester VIII, the condensation product of diethyl methylmalonate with ethylene chlorohydrin, by hydrolysis followed by decarboxylation. Its enatiomers were obtained in an almost optically pure state([α]D −21.5°, +11.9°) by methods of optical resolution.

Optically active α-methyladipic acid([α]D −1.4°)(−XV) was obtained by means of saponification and decarboxylation of triester −X, which was formed by condensation of diethyl malonate with ethyl (+)-γ-chloro-α-methylbutyrate (+IX), derived from (−)-α-methyl-γ-butyrolactone ([α]D−21.5°)(−VII).



(−VII) (+IX) (−X) (−XI)

As the correlations of (+)-α-hydroxymethyl-γ-butyrolactone (+III) and (−)-2-methyl-1,4-butanediol (−XII) with La-(−)-methylsuccinic acid (−XIII) have previously been shown by



(+III) (−VII) (−XI) (−XII) (−XIII)

6) T. Kaneko, H. Katsura, H. Asano and K. Wakabayashi, *Chem. & Ind.*, **1960**, 1187; H. Katsura, *J. Chem. Soc. Japan, Pure Chem. Sec.* (*Nippon Kagaku Zasshi*), **82**, 91 (1961).

us[6], it is clear that the configuration of (−)-α-methyl-γ-butyrolactone (−VII) is the same as that of L$_a$-(−)-methylsuccinic acid (−XIII) and is to be represented by L$_a$ or s.

Because the absolute value of the optical rotation of the (−)-α-methyl-γ-butyrolactone-(−VII) obtained from (+)-α-hydroxymethyl-γ-butyrolactone (+III) was small, (−)-2-methyl-1, 4-butanediol (−XII) was derived from (−)-α-methyl-γ-butyrolactone (−VII) obtained by resolution, using lithium aluminum hydride reduction to confirm the latter configuration. From the above results, it was concluded that (−)-α-methyl-γ-butyrolactone has the s-configuration, or belongs to the L$_a$-series, while (+)-α-methyl-γ-butyrolactone has the R-configuration, or belongs to the D$_a$-series, as (−)-2-methyl-1, 4-butanediol (−XII) is related to L$_a$-(−)-methylsuccinic acid (−XIII). (−)-α-Methyladipic acid had the s-configuration (L$_a$-series), as it is related to L$_a$-(−)-α-methyl-γ-butyrolactone, while (+)-α-methyladipic acid has the R-configuration (D$_a$-series).

Experimental

DL-α-Hydroxymethyl-γ-butyrolactone (III).—To prepare α-formyl-γ-butyrolactone (II), γ-butyrolactone (I) was condensed with ethyl formate, as described by Korte[4], except that the extraction of the reaction mixture with ethyl acetate instead of with ether was employed.

Yield, 55%; b. p., 93∼100°C/3 mmHg (lit., b. p. 68°C/0.03 mmHg[4], 83∼85°C/1 mmHg[5]).

This formyl derivative was reduced with a Raney-nickel catalyst to give III, following the procedures of McGraw[5]:

Yield, 76%; b. p. 105∼112°C/1 mmHg. Found: C, 52.02; H, 6.98. Calcd. for $C_5H_8O_3$: C, 51.72; H, 6.94%.

Resolution of α-Hydroxymethyl-γ-butyrolactone (III).—To a solution of 18.0 g. of barium hydroxide octahydrate in 100 ml. of water, 11.6 g. of DL-α-hydroxymethyl-γ-butyrolactone (III) was added, and the solution was heated to 90°C over a 2-hr. period. After the solution had cooled, 10% sulfuric acid was added, and the precipitated barium sulfate was removed by filtration. To the filtrate, 36.0 g. of quinine was added, and the mixture was heated at 90°C to make a clear solution. After standing over night, the solution was concentrated under reduced pressure, and the residue was recrystallized from acetone-methanol six to ten times. From a purified, less soluble quinine salt, optically impure α-hydroxymethyl-γ-butyrolactone (yield 0.5 g., b. p. 105∼107°C/1 mmHg, $[\alpha]_D^{14}$ −4.1°(*c* 12.2, ethanol)) was obtained, while the maximum value of its specific rotation was +10.4°.

(+)-α-Hydroxymethyl-γ-butyrolactone (+III).—It was obtained from (+)-alloisocitric lactone (+IV), as has been previously described[6].

Yield, 19%; b. p., 103∼107°C/0.5∼1 mmHg, $[\alpha]_D$ +10.4°(*c* 5.6, ethanol). Found: C, 51.83; H, 6.94. Calcd. for $C_5H_8C_3$: C, 51.72; H, 6.94%.

Tosylate (V) of α-Hydroxymethyl-γ-butyrolactone (III).—To an ice-cold solution of 11.9 g. of DL-α-hydroxymethyl-γ-butyrolactone (III) in 5 ml. of anhydrous pyridine, a solution of 21.5 g. *p*-toluenesulfonyl chloride in 45 ml. of anhydrous pyridine was added drop by drop during the course of 30 min., and the solution was then stirred continuously in an ice bath for another 3 hr. The reaction mixture was stirred into 3 N hydrochloric acid containing ice, and the separated crystalline substances were recrystallized from 94% ethanol.

Yield, 16 g. (60%); m. p., 86°C. Found: C, 53.26; H, 5.27; S, 11.53. Calcd. for $C_{12}H_{14}O_5S$: C, 53.32; H, 5.22; S, 11.86%.

From 7.0 g. of (+)-α-hydroxymethyl-γ-butyrolactone ($[\alpha]_D$+10.4°), (+)-tosylate (+V) was obtained in the manner described above.

Yield, 8.9 g. (54.6%); m. p., 97°C, $[\alpha]_D^{10}$ +3.0° (*c* 3.6, acetone). Found: C, 53.52; H, 5.16; S, 11.81%.

α-Benzylthiomethyl-γ-butyrolactone (VI).—To a boiling sodium ethoxide solution (4.2 g. of metallic sodium in 100 ml. of absolute ethanol), 22.0 g. of benzylmercaptan was added drop by drop over a half-hour period, and to this mixture, a solution of DL-tosylate (V) in 250 ml. of hot absolute ethanol was added at once. Crystals of sodium *p*-toluenesulfonate began to separate immediately. After the reaction mixture had been heated and stirred for 3 hr., the crystals were removed by filtration and the filtrate was evaporated under reduced pressure. The residue obtained was dissolved in water, and after acidifying with concentrated hydrochloric acid, the solution was extracted with benzene. After the benzene layer had been dried and the solvent removed by distillation, the residue was distilled to give DL-benzylthiomethyl-γ-butyrolactone.

Yield, 12.9 g. (58%); b. p., 145∼152°C/1 mmHg. Found: C, 64.95; H, 6.29. Calcd. for $C_{12}H_{14}O_2S$: C, 64.85; H, 6.35%.

From 8.9 g. of (+)-tosylate (+V), (−)-benzyl thioether (Yield, 4.4 g. (59.4%); b. p., 163°C/0.05 mmHg, $[\alpha]_D$−0.46°(*c* 8.0, benzene)) (−VI) was obtained in the manner described above.

Found: C, 65.28; H, 6.46; S, 14.21. Calcd. for $C_{12}H_{14}O_2S$: C, 64.85; H, 6.35; S, 14.42%.

α-Methyl-γ-butyrolactone (VII) from Benzyl Thioether (VI).—To a solution of 12.9 g. of benzyl thioether (VI) in 400 ml. of absolute ethanol, Raney-nickel (developed from 100 g. of alloy) was added and refluxed for 12 hr. The insoluble materials were removed by centrifugation, and the alcohol was removed carefully by rectification using a 50 cm. column. DL-α-Methyl-γ-butyrolactone (yield, 2.5 g. (55%); b. p., 92.5°C/20 mmHg) (VII) was obtained on distillation of the residual oil.

Found: C, 60.21; H, 7.96. Calcd. for $C_5H_8O_2$: C, 59.98; H, 8.05%.

From 4.4 g. of (−)-benzyl thioether (−VI), (−)-α-methyl-γ-butyrolactone (b. p., 94∼95°C/20 mmHg, $[\alpha]_D^{10}$ −0.2°(*c* 23, l=2 dm., absolute ethanol)) (−VII) was obtained in the manner described above.

Found: C, 60.45; H, 8.28%.

DL-α-Methyl-γ-butyrolactone (VII) from Diethyl Methylmalonate.—To a warm sodium ethoxide

solution (50°C) (9.5 g. of sodium in 120 ml. of absolute ethanol), 140 g. of diethyl methylmalonate was added drop by drop; the solution was then heated under reflux for 30 min. To this solution, 32 g. of ethylene chlorohydrin was added drop by drop and after the solution had been refluxed for 3 hr., the ethanol was removed by distillation. The residue was dissolved in water and extracted with ether. After the solvent was removed by distillation from the extract, α-carbethoxy-α-methyl-β-butyrolactone (yield, 43.5 g. (63.3%); b. p., 130~131°C/10 mmHg) (VIII) was obtained by fractional distillation of the residue.

Found: C, 55.74; H, 7.07. Calcd. for $C_8H_{12}O_4$: C, 55.80; H, 7.03%.

A mixture of 33 g. of this ester VIII and 350 ml. of 3 N hydrochoric acid was refluxed for about 20 hr. until hydrolysis and decarboxylation were complete. The reaction mixture was evaporated under reduced pressure, and the residue was dissolved in ether. After the ether extract had been dried over anhydrous sodium sulfate and the solvent removed, DL-α-methyl-γ-butyrolactone (yield, 13.1 g. (70%); b. p., 95~98°C/21mm Hg) (VII) was obtained by distillation of the residue.

Found: C, 59.77; H, 8.29. Calcd. for $C_5H_8O_2$: C, 59.98; H, 8.05%.

Optical Resolution of DL-α-Methyl-γ-butyrolactone (VII).—To a solution of 15 g. of barium hydroxide octahydrate in 100 ml. of water, 8.4 g. of DL-α-methyl-γ-butyrolactone was added. After the solution had been heated at 90°C for 2 hr., it was neutralized by the addition of 10% sulfuric acid; the barium sulfate precipitated was removed by filtration. To this filtrate, 35 g. of quinine was added; it was then heated at 90°C until dissolution was complete. After standing overnight, the reaction mixture was evaporated under reduced pressure, and the residue was dissolved in 85 ml. of acetone. After the solution had stood overnight in a refrigerator, the less soluble quinine salt precipitated was collected and recrystallized 3 times from acetone-methanol (9 : 1). (−)-α-Methyl-γ-butyrolactone (yield, 1.5 g.; b. p., 92.5°C/20 mmHg, $[\alpha]_D^{15}$ −21.5°C (*c* 5.5, absolute ethanol)) was obtained from this purified, less soluble quinine salt by the usual manner.

Found: C, 59.69; H, 7.98. Calcd. for $C_5H_8O_2$: C, 59.98; H, 8.05%.

From the mother liquor, after removing less soluble salt, (+)-α-methyl-γ-butyrolactone (yield, 1.2 g.; b. p., 93~95°C/22 mmHg, $[\alpha]_D^{15}$ +11.9° (*c* 6.9, absolute ethanol)) was obtained.

Ethyl γ-Chloro-α-methylbutyrate (IX).—A solution of 20 g. of DL-α-methyl-γ-butyrolactone (VII) in 150 ml. of absolute ethanol was saturated with dry hydrogen chloride under cooling with ice-water. After standing for 48 hr., the reaction mixture was poured into ice-water to give an oily layer, which was separated. The aqueous layer was extracted with chloroform. The oily layer and the chloroform extract were then combined, washed with water and aqueous sodium hydrogen carbonate solution, and dried over anhydrous sodium sulfate. After the solvent was removed, ethyl DL-γ-chloro-α-methylbutyrate (yield, 29.5 g. (90%); b. p., 92~95°C/25 mmHg) was obtained by means of fractional distillation of the residual oil under reduced pressure.

Found: C, 50.93; H, 7.82. Calcd. for $C_7H_{13}O_2Cl$: C, 51.06; H, 7.96%.

From 1.5 g. of (−)-α-methyl-γbutyrolactone ($[\alpha]_D$ −21.5°), ethyl (+)-γ-chloro-α-methylbutyrate (yield, 1.9 g. (77%); b. p., 90.7°C/23 mmHg, $[\alpha]_D^{15}$ +26.7° (*c* 14.9, absolute ethanol)) was obtained in the manner described above.

Found: C, 50.98; H, 7.80%.

Diethyl α-Methyl-α'-carbethoxyadipate (X).—Seventy three milliliters of absolute ethanol, 1.8 g. of sodium and 3.1 g. of sodium iodide were dissolved. Into this solution, 21.0 g. ethyl malonate was stirred at 80°C, and the mixture was refluxed for 30 min. To the reaction mixture 11.0 g. of ethyl DL-γ-chloro-α-methylbutyrate was added over a 1 hr. period, and the solution was refluxed for 20 hr. After reaction had ceased, the solvent was removed by distillation in vacuo, and the residue was acidified by the addition of 5 ml. of glacial acetic acid. After water was added to the mixture, the solution was extracted with benzene; the extract was washed with water and aqueous sodium hydrogen carbonate solution, and then dried with anhydrous magnesium sulfate. After the solvent was removed, diethyl DL-α-methyl-α'-carbethoxyadipate (yield, 11.3 g. (60%); b. p. 111~114°C/1 mmHg) (X) was obtained on distillation of the oily residue.

Found: C, 58.32; H, 8.44. Calcd. for $C_{14}H_{24}O_6$: C, 58.31; H, 8.39%.

From 1.9 g. of ethyl (+)-γ-chloro-α-methylbutyrate ($[\alpha]_D$+26.7°C), diethyl (−)-α-methyl-α'-carbethoxyadipate (yield, 2.0 g. (60.6%); b. p., 115~116°C/1 mmHg, $[\alpha]_D^{15}$ −0.64° (*c* 11, ethanol)) was obtained in the manner described above.

Found: C, 58.37; H, 8.25%.

α-Methyladipic Acid (XI).—A mixture of 38.7 g. of ethyl DL-α-methyl-α'-carbethoxyadipate (X) and 400 ml. of 3 N hydrochloric acid was refluxed for 18 hr. After hydrolysis and decarboxylation were ended, the reaction mixture was treated with active charcoal and condensed under reduced pressure. On distillation of the residue in vacuo, a fraction, b. p., 150~155°C/1 mmHg, was obtained, which formed waxy crystals immediately. It was recrystallized from benzene, m. p., 59~60°C. This sample showed no depression of melting point on admixture with an authentic sample and its infrared spectra were identical with that of the authentic sample.

From 1.9 g. of diethyl (−)-α-methyl-α'-carbethoxyadipate ($[\alpha]_D$ −0.64°), (−)-α-methyladipic acid (m. p. 53~54°C, $[\alpha]_D$ −1.4° (*c* 4, ethanol)) was obtained in the manner described above.

Found: C, 52.07; H, 7.51. Calcd. for $C_7H_{12}O_4$: C, 52.49; H, 7.55%.

2-Methyl-1, 4-butanediol (XII) from α-Methyl-γ-butyrolactone (VII) via its Acetate.—DL-2-Methyl-1, 4-diacetoxybutane (b. p. 115~117°C/16 mmHg) was obtained from 5 g. of DL-α-methyl-γ-butyrolactone (VII) by lithium aluminum hydride reduction, followed by acetylation with acetic anhydride.

Yield, 3.0 g. (32%). Found: C, 57.22; H, 8.53. Calcd. for $C_9H_{16}O_4$: C, 57.43; H, 8.57%.

The diacetate (2.2 g.) was hydrolyzed with barium hydroxide to give 2-methyl-1, 4-butanediol (b. p., 112°C/6 mmHg). Yield, 0.8 g. (77%).

From 2.2 g. of (+)-α-methyl-γ-butyrolactone ($[\alpha]_D$ +11.9°), (+)-2-methyl-1, 4-diacetoxybutane (yield, 1.0 g.; b. p., 118°C/15 mmHg, $[\alpha]_D^{15}$ +0.41°(*c* 21, acetone)) was obtained.

Found: C, 57.21; H, 8.69. Calcd. for $C_9H_{16}O_4$: C, 57.43; H, 8.57%.

The above (+)-diacetate gave (+)-2-methyl-1, 4-butanediol ($[\alpha]_D^{17}$ +2.3°(*c* 4.2, acetone)) in the manner described above.

(−)-2-Methyl-1, 4-butanediol (−XII) from (−)-α-Methyl-γ-butyrolactone (−VII) by Means of Ether Extraction.—To a suspended mixture of 0.5 g. of lithium aluminum hydride in 25 ml. of absolute ether, a solution of 1.2 g. of (−)-α-methyl-γ-butyrolactone ($[\alpha]_D$−7.5°) in 15 ml. of absolute ether was added and refluxed for 3 hr. The reaction mixture was decomposed by the addition of water, acidified with 10% sulfuric acid, and extracted repeatedly with ether. The extract was washed with an aqueous sodium hydrogen carbonate solution and dried over anhydrous magnesium sulfate. After the solvent had been removed, the residual oil was distilled under reduced pressure.

Yield, 0.5 g.; b. p,, 110~112°C/6 mmHg, $[\alpha]_D^{14}$ −2.1°(*c* 10, acetone). Diphenylurethane, m. p., 123°C. Found: C, 66.55; H, 6.47; N, 8.20. Calcd. for $C_{19}H_{22}O_4N_2$: C, 66.65; H, 6.48; N, 8.18%.

The authors wish to express their thanks to Kyowa Fermentation Ind. Co., Ltd., for its gift of (+)-alloisocitric lactone.

Department of Chemistry
Faculty of Science
Osaka University
Nakanoshima, Osaka

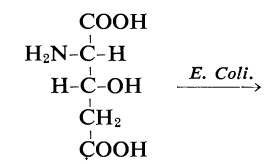
On the Absolute Configuration of l-Carnitine (Vitamin B_T)[*1]

By Takeo KANEKO and Ryonosuke YOSHIDA[*2]

(Received January 9, 1962)

The chemical structure of (−)-carnitine[1] or vitamin B_T[2,3] has been conclusively established by Tomita et al.[4] as (−)-γ-trimethyl-β-hydroxybutyrobetaine by synthesizing natural (−)-carnitine through the methylation of (−)-β-hydroxy-γ-aminobutyric acid, which was obtained by resolution of its racemic modification. The configuration of the β-asymmetric carbon atoms of (−)-β-hydroxy-γ-aminobutyric acid and (−)-carnitine, however, has not yet been established. In this paper the determination of these configurations by a chemical method is reported.

It has been known that the racemic modification of β-hydroxyglutamic acid could be decarboxylated by the action of decarboxylase and that the rate of the decarboxylation of the threo isomer is higher than that of the erythro isomer[5-7]. Recently, we resolved two racemic modifications of β-hydroxyglutamic acid to four optical isomers and determined their configurations[7]. One of the optical isomers, *threo*-β-hydroxy-L(+)-glutamic acid hydrochloride ($[\alpha]_D$ +9.5° in water), which was represented by the configurational formula I, was treated with glutamic acid decarboxylase of *E. Coli.*, and (−)-γ-amino-β-hydroxybutyric acid was isolated as the decarboxylated product of I by means of ion exchange chromatography, using Dowex 50. The melting points, specific rotations, R_f values and infrared spectra of the isolated γ-amino-β-hydroxybutyric acid and its benzoyl derivative were identical with those of the authentic specimens[*3], as is shown in Table I, and no depressions of melting point were observed.



(I)

threo-β-Hydroxy-L(+)-glutamic acid
or R(+)-Hydroxy-S-glutamic acid

[*1] Presented at the 14th Annual Meeting of the Chemical Society of Japan, Tokyo, April, 1961.

[*2] Present address: Central Institute of Ajinomoto Co., Inc., Kawasaki-shi.

1) W. L. Gulewitsch and R. Krimberg, *Z. physiol. Chem.*, **45**, 326 (1905).

2) G. Fraenkel, M. Blewet and M. Coles, *Nature*, **161**, 981 (1948).

3) E. Carter, P. K. Bhattacharyya, R. Weidmen and G. Fraenkel, *Arch. Biochem. Biophys.*, **38**, 405 (1952).

4) M. Tomita and Y. Sendju, *Z. physiol. Chem.*, **169**, 263 (1927).

5) S. Akabori, T. Kaneko, S. Sakurai and Y. Izumi, *J, Chem. Soc. Japan, Pure Chem. Sec. (Nippon Kagaku Zassi)*, **75**, 942 (1954).

6) W. W. Umbreit and P. Heneage, *J. Biol. Chem.*, **201**, 15 (1953).

7) T. Kaneko, R. Yoshida and H. Katsura, *J. Chem. Soc. Japan. Pure Chem. Sec. (Nippon Kagaku Zasshi)*, **80**, 316 (1957).

[*3] The standard samples of (−)-γ-amino-β-hydroxybutyric acid and its benzoyl derivative were supplied by Dr. Y. Hirose and Mr. K. Nishimura.

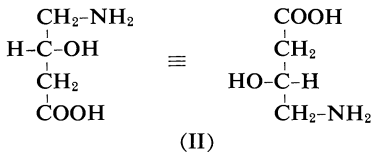
TABLE I. PHYSICAL PROPERTIES OF (−)-γ-AMINO-β-HYDROXYBUTYRIC ACID AND ITS BENZOYL DERIVATIVE

(−)-γ-Amino-β-hydroxybutyric acid	Decarboxylated product	Synthetic*3 sample	Cited in the literature[4]
M. p., °C (decomp.)	216~217	216~217	212
$[\alpha]_D$ (water)	−20.7°	−20.8°	−21.06°
R_f value			
80% phenol	0.43	0.43	
Butanol : acetic acid : water (4 : 1 : 1)	0.21	0.21	
N-Benzoyl derivative			
M. p., °C	112~113	111~112	114
$[\alpha]_D$ (water)	−11.2°	−11.9°	−11.84°

TABLE II. PHYSICAL PROPERTIES OF CARNITINE

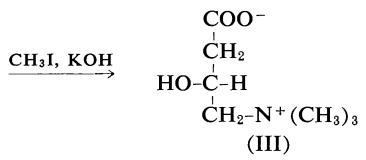
	Carnitine	a)	b)	c)
M. p., °C (decomp.)	197~198		196~198	210~212
$[\alpha]_D$ (water)	−23.9°	−20.98°	−21.5°	−30.9°
M. p., °C (decomp.)				
Chloroaurate	153~155	155	153~155	157
Chloroplatinate	228	220	216~219	

a) M. Tomita et al., *Z. physiol. Chem.*, **169**, 263 (1927).
b) H. E. Carter et al., *Arch. Biochem.*, **38**, 405 (1952).
c) E. Strack et al. *Z.*, *physiol. Chem.*, **318**, 129 (1960).



(II)

Ls(−)-γ-Amino-β-hydroxybutyric acid
or 2,4-Didesoxy-4-amino-Lg-threonic acid
or R(−)-γ-amino-β-hydroxybutyric acid



Vitamin B_T
or Ls(−)-Carnitine
or R(−)-Carnitine

Scheme 1

Consequently, the configuration of the asymmetric carbon atom of (−)-γ-amino-β-hydroxybutyric acid must be the same as that of the β-asymmetric carbon atom of *threo*-β-hydroxy-L(+)-glutamic acid. Although the β-asymmetric carbon atom of the latter has a Ds configuration[7], a Ls or Lg configuration II to be assigned to that of (−)-γ-amino-β-hydroxybutyric acid, since the carboxyl group of (−)-γ-amino-β-hydroxybutyric acid corresponded to the γ-carboxyl group of *threo*-β-hydroxy-L(+)-glutamic acid. Strictly speaking, it should be designated as the R configuration according to the nomenclature of absolute configuration presented by Cahn, Ingold and Prelog[8].

(−)-γ-Amino-β-hydroxybutyric acid was methylated to its betaine with some modifications by Carter's method[9], which was applied to racemic amino acid. The properties of the betaine and its obtained salts were consistent

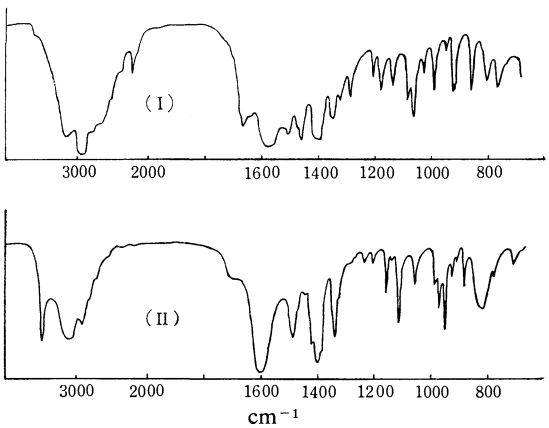


Fig. 1. Infrared spectrum of (I) R(−)-γ-amino-β-hydroxybutyric acid (Nujol), (II) R(−)-carnitine (KBr disk).

8) R. S. Cahn and C. K. Ingold, *J. Chem. Soc.*, **1951**, 612; R. S. Cahn, C. K. Ingold and V. Prelog, *Experientia*, **12**, 81 (1956).
9) H. E. Carter and P. K. Bhattacharyya, *J. Am. Chem. Soc.*, **75**, 2503 (1953).

with that of natural (−)-carnitine, as is shown in Table II.

As it is clear from these results that (−)-carnitine and (−)-γ-amino-β-hydroxybutyric acid have the same configuration, the natural (−)-carnitine may be designated as R(−)-carnitine.

Experimental*4

Decarboxylation of *threo*-β-Hydroxy-L(+)-glutamic Acid.—To 630 mg. of *threo*-β-hydroxy-L(+)-glutamic acid hydrochloride ($[\alpha]_D$ +9.5° (water)), 0.1 N sodium hydroxide was added until a pH of 5.0 was reached. To this solution, 4.5 g. of dry, powdered E. Coli. and 50 ml. of phosphate buffer (pH 5) were added, and the suspension was shaken mechanically at 37°C for 3 hr. until the theoretical amount of carbon dioxide was evolved. The reaction mixture was centrifuged, and the sediment was mixed with water and centrifuged again. The combined supernatant liquid was treated with charcoal under warming and filtered.

In another experiment, 731 mg. of *threo*-β-hydroxy-L(+)-glutamic acid hydrochloride was treated as mentioned above. The combined filtrate was passed through a column (4×50 cm.) of Dowex 2-X8 (50~100 mesh, H form), which was then washed thoroughly with water. The elution of the amino acid from the column was carried out first with 1800 ml. of 0.05 N acetic acid and then with 2000 ml. of 0.1 N acetic acid, using a 15 ml. fraction collector. An aliquot of each fraction was subjected to paper chromatography to test it for the presence of the amino acid. The combined solution of tubes number 237 to 258, which contained γ-amino-β-hydroxybutyric acid, was concentrated in vacuo, and the residue was crystallized by adding ethyl alcohol; m. p., 208~209°C (decomp.); yield, 600 mg. The product was recrystallized from water and ethyl alcohol repeatedly to give 236 mg. of pure crystals; m. p. 216~217°C (decomp.), $[\alpha]_D^{20}$ −20.7° (*c* 1.83, water). The melting point was not depressed on admixture with the authentic specimen. The R_f values of the sample were 0.43 and 0.21, using 80% phenol and *n*-butanol: acetic acid: water (4 : 1 : 1) as the solvents. Its infrared spectrum and other properties were identical with those of the authentic specimen.

Found: C, 40.17; H, 7.66; N, 11.67. Calcd. for $C_4H_9O_3N$: C, 40.33; H, 7.62; N, 11.76%.

***N*-Benzoyl-(−)-γ-amino-β-hydroxybutyric Acid.** Two hundred and eighty eight milligrams of (−)-γ-amino-β-hydroxybutyric acid and 0.5 g. of sodium carbonate were dissolved in 8 ml. of water, and the solution was cooled in an ice bath. To this solution 0.4 g. of benzoyl chloride was added, and the mixture was vigorously stirred for 2 hr. The solution was extracted with ether to remove the benzoic acid; then the aqueous layer was concentrated. (−)-*N*-Benzoyl-γ-amino-β-hydroxybutyric acid separated out as a solid which was removed by filtration; after recrystallization from water, 0.2 g. of monohydrate was obtained; m. p., 70~85°C. The anhydrous crystals were obtained by recrystallization from ethyl acetate; m. p. 112~113°C, $[\alpha]_D^{23}$ −11.2° (*c* 1.43, water), p*K*a' 4.45. The melting point was not depressed on admixture with the authentic specimen. The infrared spectrum was also identical with that of the authentic specimen.

Found: C, 59.17; H, 5.96; N, 6.39. Calcd. for $C_{11}H_{13}O_4N$: C, 59.18; H, 5.87; N, 6.28%.

The optically pure (−)-γ-amino-β-hydroxybutyric acid could be recovered by refluxing the *N*-benzoyl-derivative with 48% hydrogen bromide for 4 hr.

(−)-Carnitine.—A solution of 5.8 g. of methyl iodide in 60 ml. of methanol was added to a solution of 1.2 g. of (−)-γ-amino-β-hydroxybutyric acid ($[\alpha]_D$ −20.3° (water)) and 2.2 g. of potassium hydroxide in 10 ml. of water. After standing overnight at room temperature, the mixture was concentrated in vacuo and the residue was dissolved in 50 ml. of water. The solution was extracted four times with 50 ml. of 80% phenol[9]. After the combined phenol extract had been washed with 20 ml. of water, 600 ml. of ether was added. The aqueous layer was separated, and the ether-phenol layer was extracted four times with 50 ml. of water. The combined aqueous layer was washed with 150 ml. of ether and passed through an anion exchanger column (IR4B, 3×25 cm.), which was then washed with 500 ml. of distilled water. The alkaline fraction of the effluent was concentrated in vacuo to a syrupy residue, which crystallized on standing in a desiccator. It was filtered using ethyl alcohol-acetone (2 : 3); yield, 1.0 g. After recrystallization two times from the same mixed solvent, 0.5 g. of hygroscopic crystals were obtained. M. p., 197~198°C (decomp.) $[\alpha]_D^{30}$ −23.9° (*c* 0.86, water).

Found: C, 52.17; H, 9.59; N, 9.08. Calcd. for $C_7H_{15}O_3N$: C, 52.15; H, 9.38; N, 8.69%.

(−)-Carnitine chloroaurate was obtained by the usual method[4]. M. p. 153~155°C (decomp.)

Found: C. 17.02; H, 3.28; N, 2.62. Calcd. for $C_7H_{16}O_3N \cdot AuCl_4$: C, 16.77; H, 3.22; N, 2.79%.

(−)-Carnitine chloroplatinate was also obtained[4]. M. p., 228°C (decomp.)

All properties of the synthetic product were practically identical with those of natural (−)-carnitine as cited in the literature.

The authors wish to express their deep thanks to Dr. Yoshio Hirose and Mr. Kiichi Nishimura of the Research Institute for Food Chemistry, Foundational Juridical Persons, for their kind gift of authentic samples of (−)-γ-amino-β-hydroxybutyric acid and its benzoyl derivative; Dr. Setsuji Sakurai, Central Institute of Ajinomoto Co., Inc., for his kind gift of the enzyme, and Dr. Kazuo Okunuki for his advice and for affording facilities for carrying out the decarboxylation experiments. Thanks are also due to Messrs. Masakazu Okumiya and Kenzi Yoshimura for their microanalysis.

Department of Chemistry
Faculty of Science
Osaka University
Nakanoshima, Osaka

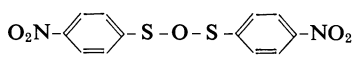
*4 All melting points are uncorrected.

The Structures of Zincke's So-called o- and p-Nitrobenzenesulfenic Anhydrides

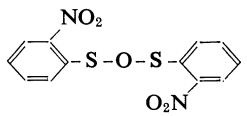
By Shigeru OAE and Shunichi KAWAMURA

(Received December 22, 1961)

Zincke[1,2], in the neutral hydrolysis of *o*- and *p*-nitrobenzenesulfenyl chlorides, obtained compounds corresponding to $C_{12}H_8N_2S_2O_5$ and he then assumed these compounds to be the sulfenic anhydrides, I and II, respectively.



I



II

Much later Kharasch[3] has cited five more examples of similar anhydrides and presumed that they arise in the following fashion:

$$ArSCl \xrightarrow{HOH} [ArSOH] \xrightarrow{ArSCl} ArSOSAr$$

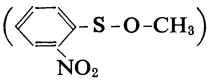
All these compounds are known to darken or sinter before melting or decomposing.

We have interested in Zincke's so-called *o*- and *p*-nitrobenzenesulfenic anhydrides, since we thought these would be the ideal compounds for the determination of the bond length of sulfur-oxygen single bond which has hitherto been unknown. However, somewhat unexpected patterns of the ultraviolet and infrared spectra of both compounds have led us to suspect the authenticities of the structures of these compounds hitherto accepted.

The compound, obtained from the hydrolysis of *p*-nitrobenzenesulfenyl chloride, when recrystallized from benzene[1], has a distinct band in infrared region, i. e., 1145 cm^{-1} which corresponds either to sulfoxide or sulfone. Meanwhile, the compound corresponding to I, would display a strong band below 1000 cm^{-1} in view of other examples shown in Table I which indicates that the characteristic bands of Si–O–Si and of P–O–P are both similar or shifted slightly toward longer wavelengths as those of Si–O–C and of P–O–C.

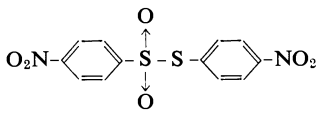
Since the oxygen exchange is known to take place in sulfuric acid with the sulfoxide but not with the sulfone[5] and also we found that nitrobenzene does not exchange oxygen in the same medium, we carried out the oxygen exchange experiment with the ^{18}O-enriched Zincke's compound in sulfuric acid. However, the compound recovered by diluting in water did not lose any excess of ^{18}O.

TABLE I*. CHARACTERISTIC BANDS OF ETHER LINKAGES OF SECONDS-ROW ELEMENTS

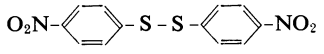
		cm^{-1}
Si–O–C		1090～1020 (s)
Si–O–Si	(ring)	1090～1020 (s)
Si–O–Si	(chain)	1090～1010 (s)
P–O–C	(aliphatic)	1050～1030 (s)
P–O–C	(aromatic)	1240～1190 (s) 1160 (w)
P–O–P		970～910 (s)
S–O–C		990 (s)

* About the spectra of six compounds except for the last methyl ether, for instance see the Ref. 4.

Infrared spectra of *p*-nitrophenyl *p*-nitrobenzenethiolsulfonate (III) and *p,p'*-dinitrodiphenyl disulfide (IV) were then taken.



III



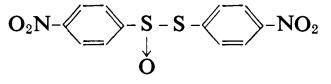
IV

When these spectra were compared with that of recrystallized Zincke's compound, we could find virtually all the bands of III and IV in Zincke's compound. When an equimolar mixture of III and IV was recrystallized from benzene, the resulting mixture, which could not be separated by ordinary recrystallization,

1) T. Zincke and S. Lenhardt, *Ann.*, **400**, 1 (1913).
2) T. Zincke and F. Farr, ibid., **391**, 55 (1912).
3) N. Kharasch, S. J. Potempa and H. L. Wehrmeister, *Chem. Revs.*, **1947**, 327.
4) L. J. Bellamy, "The Infra-red Spectra of Complex Molecules", 2nd Ed., Methuen, London (1958).
5) S. Oae, T. Kitao and Y. Kitaoka, *Chem. & Ind.*, **1961**, 291.

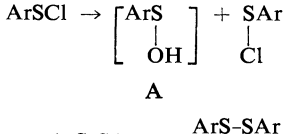
gave completely identical infrared and ultraviolet spectra with those of Zincke's compound. These results point to the fact that Zincke's so-called *p*-nitrobenzenesulfenic anhydride is actually an equimolar mixture of *p*-nitrophenyl *p*-nitrobenzenethiolsulfonate (III) and *p*, *p*'-dinitrodiphenyl disulfide (IV).

In searching a possible intermediate in the hydrolysis of *p*-nitrobenzenesulfenyl chloride, we carried out the oxidation of *p*, *p*'-dinitrodiphenyl disulfide by perbenzoic acid, following the method of Backer[6] and Small[7], hoping to obtain *p*-nitrophenyl *p*-nitrobenzenethiolsulfinate (V). However, what we obtained was also an equimolar mixture of *p*-nitrophenyl *p*-nitrobenzenethiolsulfonate (III) and *p*, *p*'-dinitrodiphenyl disulfide (IV).

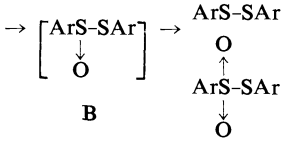


V

In the meantime, fresh hydrolysis product of *p*-nitrobenzenesulfenyl chloride, when only washed with ether and quickly dried, gave a very strong band at 1118 cm^{-1} and darkened at about 123°C. When this fresh product was subjected to heating in vacuo, storing for a long time or recrystallization, it gradually ceased darkening before melting and lost the band at 1118 cm^{-1} while changing its ultraviolet spectrum. This band at 1118 cm^{-1} is close to that of *p*-tolyl *p*-toluenethiolsulfinate, 1094 cm^{-1} [8] and is likely to be that of thiolsulfinate but is shifted toward shorter wavelength on account of strong electron-attracting nitro groups. This means that the fresh hydrolysis product is likely to be *p*-nitrophenyl *p*-nitrobenzenethiolsulfinate (V), which subsequently disproportion to *p*-nitrophenyl *p*-nitrobenzenethiolsulfonate (III) and *p*, *p*'-dinitrodiphenyl disulfide (IV) when the fresh product is recrystallized or kept standing for a while.



A



B

The consideration of *p*-nitrophenyl *p*-nitrobenzenethiolsulfinate (V) as an intermediate* is quite likely in view of the facts that many known thiolsulfinates are very unstable and disproportion easily to corresponding thiolsulfonates and disulfides[6] and also that the sulfur atom of A, being more nucleophilic than oxygen atom, would attack sulfenyl chloride in the second step of the hydrolysis giving B rather than the anhydride, I.

o-Nitrobenzenesulfenyl chloride, when hydrolyzed following Zincke's procedure[2] gave the product which was claimed to be the sulfenic anhydride. The fresh product had a strong band at 1108 cm^{-1}, corresponding to the thiolsulfinate band of *p*-isomer and also a medium band at 1145 cm^{-1} corresponing to that of thiolsulfonate. These bands subsisted even after repeated recrystallizations from benzene or heating in vacuo for a few hours, while the darkening point fluctuated up and down around 70°C on each batch. We tried similar oxidation of *o*, *o*'-dinitrodiphenyl disulfide with perbenzoic acid[6,7], hoping to obtain the thiolsulfinate. The reaction was very sluggish even under irradiating with ultraviolet light[9], and the only compound we could isolate was a small amount of the thiolsulfonate, recovering most of the starting material. We tried a few other attempts to synthesize the authentic *o*-nitrophenyl *o*-nitrobenzenethiolsulfinate in vain. When an equimolar mixture of *o*-nitrophenyl *o*-nitrobenzenethiolsulfonate and *o*, *o*'-dinitrodiphenyl disulfide was recrystallized from benzene and this mixture was compared with Zincke's compound, we found some small discrepancies in both ultraviolet and infrared spectra, while the melting point also did not show identity. However, we found that Zincke's compound has all the infrared bands of the equimolar mixture of *o*-nitrophenyl *o*-nitrobenzenethiolsulfonate and *o*, *o*'-dinitrodiphenyl disulfide in addition to the characteristic band at 1108 cm^{-1}. This seems to indicate that Zincke's so-called *o*-nitrobenzenesulfenic anhydride is the mixture of *o*, *o*'-dinitrodiphenyl disulfide, *o*-nitrophenyl *o*-nitrobenzenethiolsulfinate and *o*-nitrophenyl *o*-nitrobenzenethiolsulfonate. Since we could not obtain the thiolsulfinate, there is no way to estimate in what ratio these three compounds are mixed to make up Zincke's ortho compound.

A question still remains why the *o*-nitrothiolsulfinate does not disproportion so readily as compared to the *p*-isomer. We cannot offer

6) H. J. Backer and H. Kloosterziel, *Rec. trav. chim.*, **73**, 129 (1954).
7) L. D. Small, J. H. Bailey and C. J. Cavallito, *J. Am. Chem. Soc.*, **69**, 1710 (1947).
8) H. Bredereck, A. Wagner, H. Beck and R. -J. Klein, *Ber.*, **93**, 2736 (1960).

* After this work was completed in our laboratory, we learned that Vinkler has also suggested the similar intermediate in their kinetic study of hydrolysis of various sulfenyl chlorides: E. Vinkler, *Acta Chim. Hung.*, **11**, 15 (1957); **22**, 345 (1960).
9) C. J. Cavallito, La Verre and L. D. Small, *Chem. Abstr.*, **44**, 9977 (1950).

any satisfactory answer with our present knowledge. Probably the steric arrangement of ortho groups has some role in stabilizing the thiolsulfinate. In this connection, it is interesting to note that *o*-nitrobenzenesulfenyl methyl ether was easily obtained when *o*-nitrobenzenesulfenyl chloride was reacted with sodium methoxide[2] and is quite stable while the *p*-isomer could not be obtained in pure form. We could not reproduce the same result when we followed Zincke's procedure[1], or slightly modified ways. Everytime, we found that the product was mixed with *p*-nitrophenyl *p*-nitrobenzenethiolsulfonate and *p*, *p'*-dinitrodiphenyl disulfide.

Experimental

So-called Zincke's *p*-nitrobenzenesulfenic anhydride was prepared by hydrolyzing the corresponding sulfenyl chloride[1]. Zincke reported this compound darkened at 126°C and melted with decomposition at 160°C. After repeated recrystallization from benzene, it lost the darkening point and melted with decomposition at 151~153°C. Fractional crystallization was tried using benzene as solvent, always obtaining the same compound.

Found: C, 44.69; H, 2.63. Calcd. for $C_{12}H_8N_2O_5S_2$: C, 44.44; H, 2.49%.

UV λ_{max} mμ (log ε): 270 (4.15), 303 (4.17).

IR characteristic band: 1145 cm^{-1} (s).

***o*-Nitrobenzenesulfenic anhydride** was also prepared in the same way[2]. The darkening point of this compound fluctuated around 70°C, melted at 181~196°C (darkened at 92~93°C., fused and did not melt until heated abov 180°C)[2].

Found: C, 44.31; H, 2.60%. Calcd. the same to *p*-isomes.

UV λ_{max} mμ (log ε): 234 (4.37), 326 (3.88).

IR characteristic band: 1108 (s), 1145 cm^{-1} (m).

***p*-Nitrophenyl *p*-nitrobenzenethiolsulfonate and ortho analog** were both prepared from the reaction of the silver salts of sulfinic acids and sulfenyl chlorides[1,2], m. p. 182~183°C and 145~145.5°C respectively.

UV spectrum for *p*-nitrophenyl *p*-nitrobenzenethiolsulfonate: λ_{max} mμ (log ε): 262 (4.29), 290 (4.00) and IR characteristic band: 1145 cm^{-1} (s).

UV spectrum for ortho analog: λ_{max} mμ (log ε): 231 (4.30) and IR characteristic bands: 1360 (s), 1145 cm^{-1} (s).

***o*-Nitrobenzenesulfenyl methyl ether** was prepared from the reaction of *o*-nitrobenzenesulfenyl chloride and sodium methoxide[2], m. p. 51~52°C.

***p*-Nitrobenzenesulfenyl methyl ether** was obtained following the procedure by Zincke[1]. The compound darkened at 125~135°C and melted with decomposition around 151~156°C. The reaction was also carried out in hexane as solvent, cooling with ice or shortening the reaction time always attaining the same result.

Found: C, 44.96; H, 2.64. Calcd. for $C_7H_7NO_3S$: C, 45.40; H, 3.70%.

UV λ_{max} mμ (log ε): 270, 312 (3.99).

IR characteristic band: 1145 cm^{-1} (s).

Oxidation of *p*, *p'*-Dinitrodiphenyl Disulfide.—To 10 g. of *p*, *p'*-dinitrodiphenyl disulfide dissolved in 450 cc. of chloroform was added for 40 min. an equivalent amount of perbenzoic acid in chloroform with vigorous stirring and cooling in an ice-bath[6,7]. Stirring was continued to next day at room temperature. When the disulfide was completely dissolved, the solution was neutralized with sodium bicarbonate solution, washed with water and dried over sodium sulfate. Chloroform was evaporated at room temperature and the precipitate was collected fractionwise after separated off the starting material. The second crop was recrystallized from benzene. This crystals gradually got dark and melted at 148~151°C with decomposition, giving 2 g. of pale yellow crystals.

Found (for the second crop): C, 44.94; H, 2.55. Calcd. for $C_{12}H_8N_2O_5S_2$: C, 44.44; H, 2.49%.

UV spectrum for the second crop; λ_{max} mμ (log ε): 271 (4.14), 305 (4.18).

IR characteristic band of the second crop: 1145 cm^{-1} (s).

IR characteristic bands of the third crop: 1145 cm^{-1} (s), 1118 cm^{-1} (s).

Oxidation of *o*, *o'*-Dinitrodiphenyl Disulfide.—*o*, *o'*-Dinitrodiphenyl disulfide was oxidized similarly with perbenzoic acid under irradiating with ultraviolet light[9], obtaining a small amount of product which darkened at about 100°C and decomposed at 128~130°C. When recrystallized from petroleum ether-benzene mixture, white and yellow crystals formed. Both crystals were mechanically separated. The white crystals were recognized by infrared spectra to be corresponding to the thiolsulfonate and the yellow to the disulfide, respectively.

Identification of the Equimolar Mixture.—When an equimolar mixture of authentic *p*-nitrophenyl *p*-nitrobenzenethiolsulfonate and *p*, *p'*-dinitrodiphenyl disulfide was recrystallized from benzene, the resulting crystals melted at 152.5~153.5°C. Ultraviolet and infrared spectra of the crystals coincided well with those of the corresponding alleged sulfenic anhydride I.

UV λ_{max} mμ (log ε): 270 (4.15), 302 (4.16).

IR characteristic band: 1145 cm^{-1} (s).

The crystals, recrystallized from an equimolar mixture of *o*-nitrophenyl *o*-nitrobenzenethiolsulfonate and *o*, *o'*-dinitrodiphenyl disulfide melted gradually from 136°C to 157°C with decomposition and had bands at 1360 and 1145 cm^{-1}, but had no band at 1108 cm^{-1}.

^{18}O Exchange Reactions.—Nitrobenzene, 0.7 g., was dissolved in 10 cc. of ^{18}O-enriched 98% sulfuric acid (0.5 atom % ^{18}O) at 0°C for 10 min., then was diluted with ice-water. The nitrobenzene recovered was distilled once, obtaining 0.5 g., and was subjected to ^{18}O analysis[10].

^{18}O for $C_6H_5NO_2$	0.209%
^{18}O for tank CO_2	0.210%

^{18}O Enriched Zincke's So-called *p*-nitrobenzenesulfenic anhydride was prepared from the hydrolysis of *p*-nitrobenzenesulfenyl chloride with equimolar amount of $H_2{}^{18}O$ (1.5 atom % ^{18}O) in glacial acetic acid.

10) D. R. Christman and S. Oae, *Chem. & Ind.*, 1959, 1251.

TABLE II

Treatment	Darkening point	Melting point, °C	The ratio of intensity ($-\log T$) at 270 mμ and 303 mμ
Only washed with ether, quickly dried	~123°C	145~155	1 : 0.885
Heated at 72~73°C for 3 hr. in vacuo	Obscure	148~150	1 : 0.948
Heated at 72~73°C for 6 hr. in vacuo	Almost indistinct	149~151	1 : 1.032
Repeated recrystallization, well dried in vacuo	Did not occur	151~153	1 : 1.017

^{18}O for p,p'-$O_2NC_6H_4S^{18}OSC_6H_4NO_2$ 0.46%
^{18}O for tank CO_2 0.210%

One gram of this compound was dissolved into 98% H_2SO_4 at 0°C, and was kept standing for 15 min., then filtered and the filtrate was poured into ice-water. The precipitate formed was collected, washed with a sufficient amount of water, repeatedly, dried, and recrystallized from benzene, m. p. 156~168°C, 0.25 g.

^{18}O for p,p'-$O_2NC_6H_4S^{18}OSC_6H_4NO_2$ 0.44%
^{18}O for tank CO_2 0.210%

In the case of ortho compound, the starting material could not be recovered.

The Variation of Melting Point and Ultraviolet Spectrum of *p*-Nitrobenzene-sulfenic Anhydride only Washed with Ether. — Fresh *p*-nitrobenzene-sulfenic anhydride only washed with ether and quickly dried was treated under various conditions, and melting points and the ultraviolet spectra taken with the corresponding changes are as shown in Table II.

Ultraviolet Spectra.—All spectra were taken on Shimadzu model RS-27 auto-recording spectrophotometer using the solutions of the compounds dissolved in purified dioxane.

Infrared Spectra. — In all spectrophotometries potassium bromide disks were used.

Department of Chemistry
Radiation Center of Osaka Prefecture
Sakai, Osaka

The Radiation-Induced Oxidation of Stannous Chloride in Aqueous Hydrochloric Acid

By Ken'ichi SUGIMOTO and Shigeru OAE

(Received January 5, 1962)

Numerous investigators[1-6] in recent years have suggested a radical diffusion model for various radiation-induced chemical reactions in aqueous media. According to this model radiation-induced chemical reactions in aqueous solutions are initiated by radicals generated from water as a result of energy degradation processes. In fact, a few supporting evidences[7-9] have been presented in the study of the effect of gamma irradiation from cobalt-60 on ferrous sulfate in 0.8 N sulfuric acid.

For this model investigations of the radiation-induced oxidations or reductions of other inorganic compounds in aqueous media have been studied by many workers[10-14]. Solutions of oxidizing agents are reduced by gamma irradiation usually in a yield of about 2.3 atom-equivalents per 100 eV. While, these of common reducing agents are oxidized in the same yield as that of hydrogen gas formed, the radiation-induced oxidation of stannous to stannic ion was also investigated as one of these reactions and could be used for chemical dosimetry.

Aqueous hydrochloric acid solution of stannous ion, exposed to the gamma irradiation

1) A. O. Allen, *Radiation Research*, **1**, 85 (1954).
2) C. J. Hochanadel, *J. Phys. Chem.*, **56**, 587 (1952).
3) H. A. Dewhurst, A. H. Samuel and J. L. Magee, *Radiation Research*, **1**, 63 (1954).
4) J. Weiss, *Nature*, **165**, 728 (1950).
5) E. J. Hart, *Radiation Research*, **1**, 53 (1954).
6) N. F. Barr and C. G. King, *J. Am. Chem. Soc.*, **78**, 303 (1956).
7) R. M. Lazo, H. A. Dewhurst and M. Burton, *J. Chem. Phys.*, **22**, 1370 (1954).
8) R. H. Schuler and A. O. Allen, ibid., **24**, 56 (1956).
9) C. J. Hochanadel and J. A. Ghormley, ibid., **21**, 880 (1953).
10) M. Lefort, *J. chim. phys.*, **54**, 782 (1957).
11) H. A. Schwarz and A. O. Allen, *J. Am. Chem. Soc.*, **77**, 1324 (1955).
12) H. A. Schwarz and A. J. Salzman, *Radiation Research*, **9**, 502 (1958).
13) M. Haissinsky and M. Lefort, *J. chim. phys.*, **48**, 429 (1951).
14) M. Daniels and J. Weiss, *J. Chem. Soc.*, **1958**, 2467.

from cobalt-60, yields stannic ion and hydrogen gas as the products. This system is of particular interest because of the transfer of two electrons is involved in the oxidation of stannous to stannic ion. Since stannous ion is powerful reducing agent in aqueous solutions, it could be used as a scavenger for radicals produced in the irradiation of aqueous solution, and also as a chemical dosimeter.

Boyle, Weiner and Hochanadel[15] have studied the irradiation of stannous ion in aqueous sulfuric acid and mixtures of stannous ion with ferrous and ferric ion. All their experiments were carried out in 0.8 N sulfuric acid. Amell[16] studied the irradiation of stannous chloride in aqueous hydrochloric acid, but his study has to be extend further in detail in order to use this reaction for chemical dosimetry. Therefore, we have undertaken this investigation.

Experimental

Irradiations.—Cylindrical and basket style sources of cobalt-60 gamma rays, which have 1000 and 3800 curies respectively, were used. Energy absorption in solutions was determined with the Fricke ferrous sulfate dosimeter taking G as 15.6[9]. Initial dose rate values for the two sources are shown in Table I. The dose rates were corrected for decay. All the irradiations were carried out at ambient temperature between 27 and 32°C.

For continuous measurements, a dropping mercury apparatus with mercury pool electrolysis cell was placed in the irradiation room, while lead wires were led outside from the room, and were connected with a polarographic recorder. The measurements of polarogram were taken periodically during the irradiations.

TABLE I. DOSE RATES ON THE VARIOUS POSITIONS AT THE IRRADIATION FACILITIES

Co-60 source curies	Distance from source to sample cm.	Dose rate $\times 10^{19}$ eV./l. min.
3800	15	10.3
3800	20	6.8
1000	12	3.7
1000	20.5	2.0

Preparation of Solutions.—Water used was prepared by at first distillation over acid permanganate, then over alkaline permanganate, and finally by ordinary distillation. This water was used throughout this experiment. Solutions used for irradiation were made oxygen free. Because of rapid air oxidation of stannous ion it was necessary to avoid oxygen during preparation, irradiation and analysis of the solution. Stock solution of stannous chloride was prepared by dissolving reagent grade stannous chloride in concentrated hydrochloric acid and diluting with water to the final desired concentrations for both stannous ion and the acid. These solutions were stored in nitrogen atmosphere to minimize the oxidation of the stannous ion by oxygen.

Standard solutions of stannic ion were prepared by dissolving reagent grade stannic chloride. The concentration of stannic ion was determined gravimetrically as stannic oxide.

Deaerated solutions of the stannous chloride (0.5~3 mM) in 6 N hydrochloric acid were used in most cases. The solutions were then irradiated and analyzed in the following method.

Analytical Methods.—The stannous and stannic ion were determined polarographically, using a Yanagimoto PA-101 polarography with the temperature controlled at 30±1°C. The reduction of stannic to stannous ion produces wave suitable for this analytical purpose when the supporting electrolyte was 6 N hydrochloric acid. This wave is diffusion controlled and occurring at a half-wave potential of −0.25 V. vs. S. C. E. The measurements were taken in mercury pool electrolysis cell. The diffusion constant for stannic ion used in this study were taken by $I=i_d/m^{2/3}t^{1/6}c=4.77$ μA/mM.

Dissolved oxygen was removed satisfactorily by bubbling nitrogen through the solution for 10 min. before each polarographic determination. The nitrogen stream was purified by bubbling through alkaline pyrogallol solution and distilled water.

The polarographic measurements were made both by the ordinary method and continuous measurement method. The former determined diffusion current difference between non-irradiated sample and irradiated sample. This difference corresponds to conversion value from stannous to stannic ion. Analyses generally were made within half an hour after taking out the sample from the irradiation room. Continuous measurements were taken during the irradiations, where variation of measurements appeared to have no effect on diffusion current.

Results and Discussion

The effects of irradiation time, initial stannous ion concentration, stannic ion concentration and dissolved oxygen on the yield were investigated.

Irradiation Time.—Figure 1 shows a fews plots of stannic ion formed against irradiation time. The amount of stannic ion formed from stannous ion in hydrochloric acid is proportional to that of energy absorbed up to at least 5×10^{22} eV./l. and is essentially independent of dose rate. The G-values obtained from stannic ion formation are shown in Table II. The continuous measurement method gave a variety of formation curves of stannic ion. A few typical curves for stannic ion formation are shown in Fig. 2. However, in most cases we obtained curve similar to B, which indicate that the rate of oxidation is a linear function of irradiation time over the range we studied.

15) J. W. Boyle, S. Weiner and C. J. Hochanadel, *J. Phys. Chem.*, **63**, 892 (1959).
16) A. R. Amell, ibid., **64**, 1277 (1960).

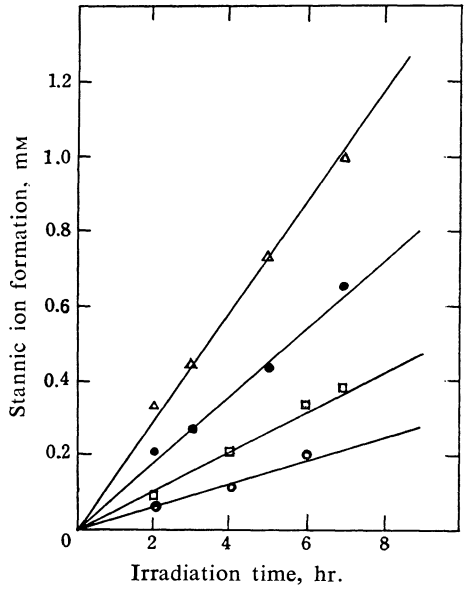


Fig. 1. Formation of stannic ion in deaerated solution of 6 N hydrochloric acid.
Initial stannous chloride concentration; 0.5 ~3×10^{-3} M
Dose rate; △ 10.3×10^{19} eV./l. min.
● 6.8×10^{19} eV./l. min.
□ 3.7×10^{19} eV./l. min.
○ 2.0×10^{19} eV./l. min.

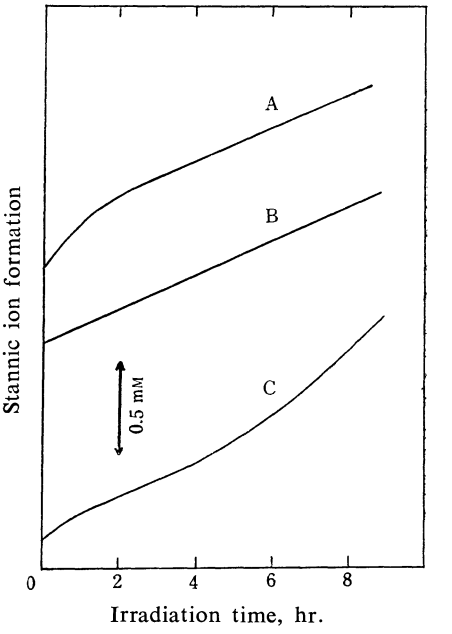


Fig. 2. Various formation curves of stannic ion on continuous measurement method.
Initial concentration;
A Sn(II) 2.87 mM, Sn(IV) 0.43 mM
B Sn(II) 2.16 mM, Sn(IV) 0.14 mM
C Sn(II) 1.57 mM, Sn(IV) 1.03 mM
Dose rate; 6.8×10^{19} eV./l. min.

TABLE II. THE *G*-VALUES FOR STANNIC ION FORMATION

Deaerated solutions of the stannous chloride in 6 N hydrochloric acid were irradiated.

Dose rate $\times10^{19}$ eV./l. min.	Oxidation rate mM/hr.	*G*-value
10.3	0.146	1.4_1
6.8	0.091	1.3_5
3.7	0.052	1.4_1
2.0	0.031	1.5_7
2.0	0.021	1.0_1[a]

a) In 0.8 N hydrochloric acid

Fricke and Hart[17,18] irradiated with X-rays air-free solutions of a number of common reducing agents. The pH for the most of these solutions was varied over a wide range from 2 to 11. In most cases the amounts of reducing agents oxidized are equivalent to $G_{H_2}=0.5=G_{H_2O_2}-(G_H-G_{OH})/2$. While in air-free ferrous sulfate solutions ferrous ion is oxidized in a yield of $G(Fe(III))=8.2=G_H+G_{OH}+2G_{H_2O_2}$[7-9]. Boyle et al.[15] reported that the yield of $G(Sn(IV))=0.49$ is equivalent to G_{H_2} in 0.8 N sulfuric acid solutions by the gamma irradiation, indicating that oxidation is done by H_2O_2 and OH and reduction by H.

In aqueous hydrochloric acid the yield $G(Sn(IV))=1.50$ was shown by Amell[16]. It is interesting to note the marked difference of *G*-values between 0.8 N sulfuric acid and hydrochloric acid. This difference was explained by Amell that stannous ion forms many different complex ions with chloride ion as the concentration is changed, thus be changing the reacting species which have both different oxidation potentials and different rates of reaction.

Using the values for the individual radical and molecular yield generated from water, the following sequence should give rise to the *G*-value.

$$H_2O \text{ -W-> } H + OH + H_2O_2 + H_2 \quad (1)$$

$$Sn(II) + OH \rightarrow Sn(III) + OH^- \quad (2)$$

$$Sn(III) + OH \rightarrow Sn(IV) + OH^- \quad (3)$$

$$2\,Sn(III) \rightarrow Sn(II) + Sn(IV) \quad (4)$$

The results can be interpreted to mean that the tin is being oxidized by OH only while H does not react with anything, but merely combine with itself to forms H_2. In view of the abundant evidences for the general high reactivity of H and OH, it seems quite unlikely that these radicals can wait around to

17) H. Fricke and E. J. Hart, *J. Chem. Phys.*, 3, 365 (1935).
18) H. Fricke and E. J. Hart, ibid., 3, 596 (1935).

combine with one another in the presence of such chemically reactive species as stannous chloride. More likely, the H atoms can reduce Sn(II) to Sn(I), and can also oxidize Sn(II) to Sn(III) as follows.

$$Sn(II) + H \rightarrow Sn(I) + H^+ \quad (5)$$

$$Sn(II) + H + H^+ \rightarrow Sn(III) + H_2 \quad (6)$$

$$Sn(I) + Sn(III) \rightarrow 2\,Sn(II) \quad (7)$$

The oxidation-reduction potential calls for all of these stannous ions to be oxidized by hydrogen peroxide. Nevertheless, the reaction between stannous ion and hydrogen peroxide is apparently slow, and $G(Sn(IV))$ to be equal to $G_{OH}/2+G_{H_2O_2}$ if this reaction is occurring.

Hydrochloric acid in contrast to sulfuric acid, is relatively less stable to irradiation. Chloride ion does not react effectively with OH in neutral solutions, probably because of the reaction

$$Cl^- + OH \rightarrow OH^- + Cl \quad (8)$$

is endothermic. However, the reaction

$$Cl^- + OH + H^+ \rightarrow H_2O + Cl \quad (9)$$

is exothermic and chloride ion does react with OH in acid solution. The rate of reaction of Cl^- with OH would therefore be expected to increase with acid concentration and in fact, it is found that chloride ion changes as chlorine radical and the radical reacts with stannous ion the higher acid concentration.

On the other hand, the increase of G-value at higher acid concentrations is probably due to the direct deposition of energy by irradiation into the chloride ion. This becomes important at higher concentrations of hydrochloric acid, and leads to oxidation in a higher yield over that of the formation of radicals from water alone.

$$Cl^- \text{-}\!\!\sim\!\!\rightarrow Cl \quad (10)$$

$$Sn(II) + Cl \rightarrow Sn(III) + Cl^- \quad (11)$$

$$Sn(III) + Cl \rightarrow Sn(IV) + Cl^- \quad (12)$$

Effect of Initial Stannic Ion Concentration.—To determine the effect of the initial concentration of stannous ion on the oxidation, various solutions were prepared for irradiation. These solutions differed only in stannous ion concentration. The results of these concentration are shown in Fig. 1. Within these concentrations (0.5~3 mM) there is no effect of stannous ion concentration on the oxidation.

Effect of Stannic Ion Concentration.—The concentration of stannic ion was varied to determine this effect. After the stannous ion is half depleted, stannous ion is oxidized at the rate which depends on stannic ion as shown by Fig. 2-C curve. The G-value as a function of stannic ion is given in Fig. 3.

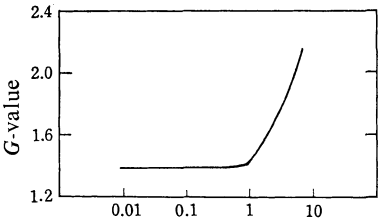


Fig. 3. Effect of stannic ion concentration.
Sn(II)+Sn(IV); 1.57×10^{-3} M in 6 N HCl
Dose rate; 3.7×10^{19} eV./l. min.

The G-value from the radiation-induced oxidation of stannous and stannic ion mixtures is significantly higher than that obtained by stannous ion alone. Although we can offer no statisfactory explanation for this difference, it is probably due to the catalytic effect of stannic ion in the reaction of stannous ion with hydrogen peroxide.

Dissolved Oxygen.—Various experiments showed that the oxidation of stannous ion by irradiation is greatly increased when oxygen or air is present. This is seen in Fig. 2-A. After oxygen is depleted, formation curve shows linearity. Thoroughly bubbled solution by purified nitrogen gas does not show any increase of oxidation.

Application for Dosimetry

The good reproducible data obtained on the determinations of stannic ion suggest that this system can be used as a dosimeter for higher doses of irradiation. The analysis of stannous or stannic ion can be performed conveniently. However, it should be pointed out that even though the oxidation of stannous ion is pre-

TABLE III. REPRODUCIBLE RESULTS OF CHEMICAL DOSIMETRY

Irradiation dose	Conversion value	Reproducibility	
		Range	Standard deviation
$\times10^5$ r.	mM	mM	mM
4.20	0.66 0.59 0.58 0.57	0.09	0.04
2.79	0.42 0.36 0.34 0.37	0.08	0.03
1.51	0.18 0.21 0.22 0.22	0.04	0.02
0.82	0.14 0.11 0.13 0.13	0.03	0.01

sented to be the reaction only with OH radical, the quantities of products involved are still quite small. Consequently, for doses less than 10^4 r., microtechniques would have to be employed. By irradiating 1 cc. of 6 N hydrochloric acid solution of stannous ion one would expect only 1.4×10^{-5} mmol. of stannic ion to be produced by 10^4 r.

Summary

The radiation-induced oxidation of stannous to stannic ion in aqueous hydrochloric acid has been studied and that this system is proposed as a chemical dosimeter for higher doses.

The amount of oxidation is proportional to the energy absorbed and the yield of stannic ion is independent of dose rate and initial stannous chloride concentration over a wide range studied, but increases when stannic conconcentration is high or oxygen is present. Mechanism for this oxidation based on *G*-values is discussed in terms of the primary decomposition products of water radiolysis. The results can be interpreted to mean that the stannic ion is oxidized only by OH radical. This system could be used for a chemical dosimeter having 8% reproducibility.

Department of Chemistry
Radiation Center of Osaka Prefecture
Sakai, Osaka

Studies of the Drawing of Polyamide Fibers. I. Dependence of Some Physical Properties on the Draw Ratio

By Hiroshi HATTORI, Yasuo TAKAGI and Tatsuro KAWAGUCHI

(Received January 5, 1962)

It is well-known that an oriented fiber is obtained from synthetic linear high polymer by drawing it to several hundred per cents of its original length, and that various properties of the fiber are changed by this drawing.

The relation between the draw ratio and some physical properties of nylon 6 monofilament—especially the tensile strength and the shrinkage in boiling water—has been studied in order to elucidate the process of the change in polymer structure during the course of the drawing.

A curious relation was discovered between the draw ratio and the tensile strength; that is, the tensile strength becomes the smallest at a draw ratio near two.

Experimental

Samples.—*Group I.*—An undrawn monofilament of nylon 6 (1300 denier), which had been meltspun and quenched in water, was drawn immediately after spinning in hot water at 90°C to various draw ratios, from 1 to 5.2, at intervals of 0.3. The feeding speed of the undrawn sample at the drawing was 26 m./min.

Group II.—The same undrawn monofilament as that in group I was drawn 53 days after it had been meltspun. The feeding speed of the undrawn sample at the drawing was 5 m./min., and the temperature of the water bath was 95°C.

Measurement.—Tensile tests of these samples were carried out with an Instron tensile tester at 20°C and at 65% RH. From the load-elongation curves thus obtained, the tensile strength and Young's modulus were measured. The shrinkage was measured by treating the samples in boiling water for 30 min. without tension. Birefringence was measured as follows: The sample was cut obliquely, and its wedge-shaped end was laid between crossed Nichol's prisms of a polarization microscope. From the number of the interference fringes which were observed on the wedge portion of the sample when the monochromatic light of a sodium lamp was used as the light source, the birefringence was determined according to the following equation:

$$\Delta n = N\lambda/d \qquad (1)$$

where Δn is the birefringence, N, the number of interference fringes, λ, the wevelength of the light, and d, the diameter of the sample.

Results

Change of Tensile Strength by Drawing.—In many kinds of fibers made from synthetic linear high polymers, the tensile strength of a filament changes with the draw ratio[1-4]. Generally, the strength of a filament from such

1) T. Yoshida, *J. Soc. Textile and Cellulose Ind. Japan*, **11**, 230 (1955).
2) J. Furukawa, K. Muramatsu and S. Ohya, *J. Japan Soc. Testing Materials*, **8**, 320 (1959).
3) R. Suda, *J. Soc. Textile and Cellulose Ind. Japan*, **8**, 272 (1952).
4) A. R. Urquart, *J. Appl. Chem.*, **4**, 195 (1954).

a polymer, whose crystallinity increases with orientation, tends to increase with the draw ratio. Polyamide filaments also become stronger as the degree of orientation increases, when the draw ratio is high enough.

The present authors investigated the change in tensile strength of nylon 6 monofilaments over a wide range of draw ratios. Figure 1 is the plot of the tensile strength against the draw ratio. This figure shows that the strength decreases, reaches a minimum and then increases again as the draw ratio increases, though the draw ratio and the decrease in strength at the minimum point differ between group I and group II. In group I, a 90%-drawn sample is 60% weaker than the undrawn sample, but in group II a 150%-drawn sample (the weakest one) is 35% weaker than the undrawn sample.

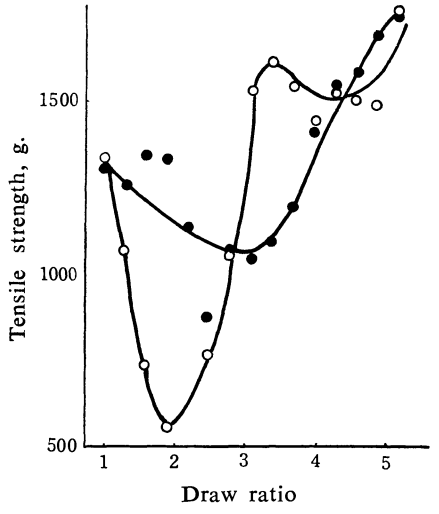


Fig. 1. Dependence of tensile strength on the draw ratio. ○, Group I ●, Group II

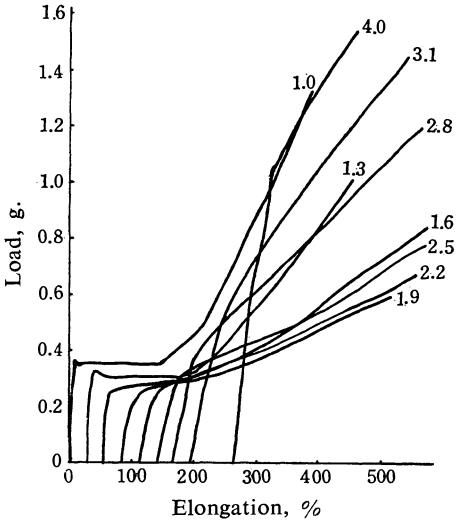


Fig. 2. Load-elongation curves for group I.

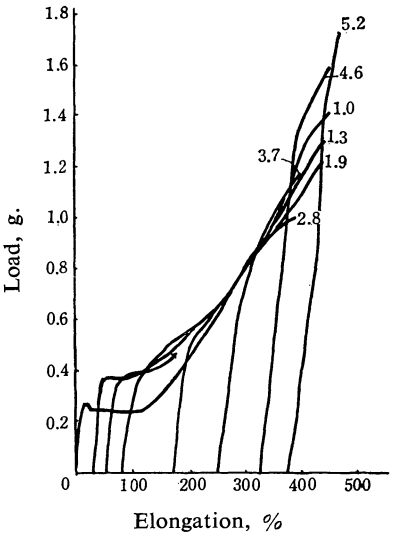


Fig. 3. Load-elongation curves for Group II.

These differences may result from some change in the structure of the undrawn filament during the lapse after spinning.

The load-elongation curves of these samples were shown in Figs. 2 and 3.

There is a contrast between the groups of curves of these two groups. In the case of group I, the yield value and the slope at the higher elongation of the load-elongation curve become smaller and reach a minimum at a draw ratio near 2; then the yield value increases, and the slope becomes steeper as the draw ratio increases.

The curves of group II do not show such tendencies, but they nearly overlap one another in the range of high elongation percentages.

Young's modulus obtained from the initial slope of the load-elongation curve was plotted against the draw ratio of the sample in Fig. 4. Young's modulus is nearly constant in the range of draw ratio from 1 to ca. 2, and then it increases with the draw ratio. This behavior suggests that the mechanism of drawing in the

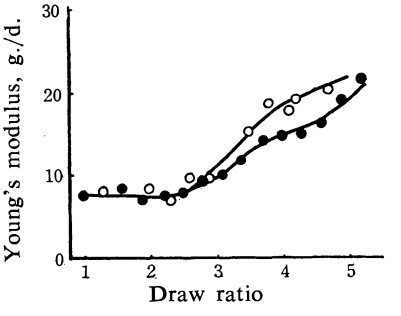


Fig. 4. Plot of Young's modulus against draw ratio. ○, Group I ●, Group II

range of lower draw ratio differs from that in the higher draw ratio.

Other polyamides (nylon 66, 69 and 610) exhibited behavior similar to that of nylon 6.

Shrinkage in Boiling Water.—The shrinkage of group I in boiling water, as shown in Fig. 5, is kept nearly constant in the range of draw ratio lower than ca. 2, increases rapidly in the range of draw ratio from ca. 2 to ca. 3.5, and gradually approaches to a saturation point as the draw ratio increases.

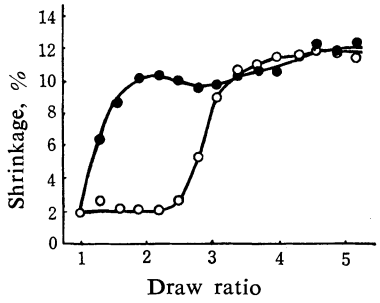


Fig. 5. Relation between draw ratio and shrinkage in boiling water.
○, Group I ●, Group II

Such behavior seems to be related to the existence of a minimum strength point near draw ratio 2, but, as is shown in Fig. 5, the dependence of the shrinkage of group II on the draw ratio differs from that of group I. In this case, the shrinkage increases quite rapidly in the first stage of drawing and then nearly saturates near the draw ratio of 2.

This difference between I and II seems to be a proof that the difference in the inner structure of the undrawn samples influences the mechanism of drawing.

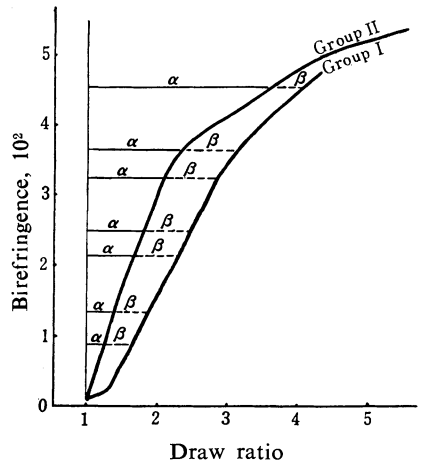


Fig. 6. Change of birefringence with draw ratio.

Birefringence.—Figure 6, a plot of the birefringence against the draw ratio, also shows a difference between groups I and II.

The rate of increace in birefringence at a low draw ratio is less in group I than in group II. This means that the degree of orientation does not always correspond to the draw ratio, but depends on the history of the undrawn sample.

Discussion

These curious relations between the draw ratio and some physical properties of polyamide filament seem to be due to one cause, that is, the process of the change of polymer structure during the drawing changes near the draw ratio of 2.

At first, the flow phenomenon during drawing was considered to be the cause. This phenomenon is known to occur when an amorphous undrawn polymer, such as polyethylene terephthalate, is drawn under a controlling condition; it is called "super drawing" [5]. In an extreme case of flow, orientation does not occur at all and the fiber becomes weaker. In the case of polyamide monofilament, it is probable that the flow phenomenon occurs because the polyamide melt was quenched in water, with the result that the crystallinity of the undrawn filament is low (the crystallinity of the undrawn sample of group I is less than 10%, and that of group II is 14%).

The fact that the decrease in strength at the minimum is more striking in the case of group I (lower crystallinity) than in the case of group II (higher crystallinity) also suggests the possibility of the flow.

In order to give a more quantitative explanation of this, the authors assume, as the first approximation, (a) that during the process of the drawing of group II, no flow phenomenon occurs at all, and (b) that unless flow occurs when group I is drawn, its birefringence is quite the same as that of group II at a same draw ratio.

According to these assumptions, α in Fig. 6 corresponds to an effective drawing accompanying real orientation, and β is a deformation due to the flow. Figure 7 is the drawing of a model in which α and β are shematically distinguished from each other. Now we suppose that an undrawn filament of a unit length is "effectively" drawn $(1+\alpha)$ times and then elongated further $(1+\gamma)$ times by flow deformation, where $\gamma=\beta/(1+\alpha)$, the final length being $(1+\alpha+\beta)$. So, $(1+\gamma)$ or $((1+\alpha+\beta)/(1+\alpha))$ is the draw ratio due to the flow only.

5) A. B. Thompson, *J. Polymer Sci.*, 34, 741 (1959).
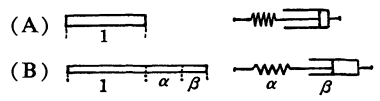


Fig. 7. Model of deformation.
(A) undrawn sample; (B) drawn sample

The values of α, β and $(1+\gamma)$ are listed in Table I.

If the monofilament did not become thinner because of the flow, the strength would be equal to the measured strength multiplied by the factor $(1+\gamma)$. The right column of Table II is the result of this multiplication. Although the magnitude of strength-decrease becomes smaller by this correction, the value is still the smallest at the draw ratio of 1.82 and becomes extraordinarily large near the draw ratio 3.

TABLE I. CALCULATION OF THE RATIO OF FLOW DEFORMATION

Draw ratio[a]	α	β	$1+\alpha$	$\frac{1+\alpha+\beta}{1+\alpha}$
1.00	0.00	0.00	1.00	1.00
1.28	0.03	0.25	1.03	1.24
1.54	0.21	0.33	1.21	1.27
1.82	0.35	0.47	1.35	1.35
2.09	0.58	0.51	1.58	1.32
2.38	0.71	0.67	1.71	1.39
2.66	0.99	0.67	1.99	1.34
2.94	1.20	0.74	2.20	1.34
3.78	2.36	0.42	3.36	1.12

[a]Actual draw ratio: (denier on undrawn filament) ÷ (denier of drawn filament)

TABLE II. CORRECTED TENSILE STRENGTH

Draw ratio	Measured strength s, g.	Corrected strength $s\times\frac{1+\alpha+\beta}{1+\alpha}$, g.
1.00	1340	1340
1.28	1063	1320
1.54	735	933
1.82	558	754
2.09	765	1010
2.38	1050	1390
2.66	1538	2060
2.94	1620	2170
3.78	1450	1620

Therefore, we cannot give a satisfactory explanation of the phenomenon of minimum strength by considering only the flow as the cause, though this seems to contribute partly to the phenomenon, because the assumptions mentioned above are not always correct.

Another possible cause of the phenomenon is a change in the mechanism of drawing in the intermediate stage of drawing. It is known that the crystal form of nylon 6 changes from α form to β form when it is drawn about 150%[6]. Therefore, it may be reasonable to consider that the phenomenon of minimum strength is related to the transition of crystal form. However, as the crystallinity of the undrawn samples is rather low and as the strength of a sample seems to depend chiefly on the state of the amorphous part and not on the crystal form, the transition of the crystal form itself has no direct influence on the change in strength. Therefore, it is more natural to consider that on the intermediate stage of drawing, where the transition of crystal form can occur, the structure of the polymer becomes most unstable, as the result of which the strength reaches a minimum, though the authors are not sure how or why the structure becomes most unstable.

As to the difference in the changes of some properties between groups I and II, the authors have considered the influence of the history of the sample from spinning to drawing. The decrease in tensile strength of group II is less than that of group I, and the shrinkage of group II increases more rapidly in the first stage of drawing than that of group I.

Therefore, we suppose (1) that sufficient time is necessary for a network structure in the polymer to be completed, and (2) that, if a structure is once completed, it does not completly disappear but partly remains after the sample has been deformed.

Thus, when a sample is drawn immediately after spinning (before the structure of the undrawn filament is formed), it becomes either stronger or weaker, depending on the draw ratio, becoming the weakest near the draw ratio of 2. On the contrary, when the sample is drawn after the structure of undrawn filament is completed (group II), the structure of the undrawn sample remains in the drawn one, and, as a result, the strength decrease at the minimum becomes less than that of group I.

The difference in birefringence-shrinkage relationship, shown in Fig. 8, between groups I and II can be explained to some extent by these assumptions. The sample drawn before the structure of the undrawn filament is formed retains less residual internal stress than the sample in which the structure of undrawn filament has not disappeared; therefore, the shrinkage of group II increases rapidly with the draw ratio from the first stage of drawing, while that of group I does not.

As the phenomenon of minimum strength near the draw ratio of 2 is observed not only in the case of monofilaments drawn in hot

6) K. Fuchino and A. Okada, *Sci. Rep. Toyo Rayon Co.*, 4, 163 (1949).

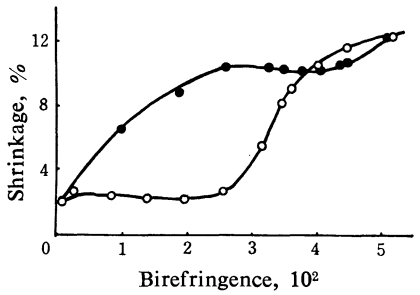


Fig. 8. Relation between birefringence and shrinkage in boiling water.
○, Group I ●, Group II.

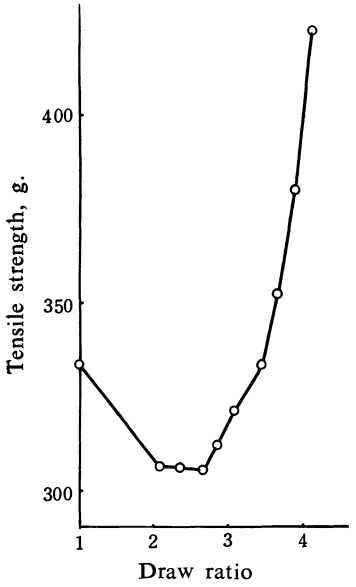


Fig. 9. Change of tensile strength of nylon filament yarn with draw ratio.

water, but also in the case of multifilament yarns cold-drawn with an ordinary draw-twister (Fig. 9), this phenomenon seems to be peculiar to polyamide fibers, irrespective of the way of drawing.

Further efforts will be made in order to explain the change in physical properties by drawing more systematically and quantitatively in the experiments to be described in later papers of this series.

Conclusion

From some peculiar behaviors of nylon 6 monofilament concerning the change in physical properties with the change in draw ratio, the authors have discussed the change in the molecular structure of the polymer during drawing.

Although no definite conclusions were obtained, the following assumptions seem to fit the observed phenomena:

(a) The flow of the polymer occurs during drawing to some extent.

(b) The structure of polyamide filament becomes most unstable near the draw ratio of 2.

(c) Sufficient time is necessary for a network structure in the polymer to be completed.

(d) If a structure is once completed, it does not completely disappear but partly remains even after the polymer has been deformed.

Summary

The relation between the draw ratio and some physical properties of nylon 6 fibers was investigated, using monofilament drawn in hot water to various draw ratios. The tensile strength decreases, passes through a minimum at a draw ratio near 2, and then increases as the draw ratio becomes higher. The decrease in strength at the minimum in the sample drawn immediately after spinning amounts to 60% of the strength of the undrawn sample. The shrinkage in boiling water of the sample drawn immediately after spinning is nearly zero in the range of a low draw ratio, increases in the range of the ratio from ca. 2 to ca. 3.5, and gradually approaches a saturating value, but that of the samples drawn many days after spinning increases most rapidly in the range of the ratio from 1 to ca. 2 and then gradually approaches to a saturating value with the draw ratio. On the first stage of drawing, the rate of increase in birefringence with the draw ratio of the sample drawn immediately after spinning is smaller than that of the sample drawn many days after spinning. On the basis of these results, the authors discussed the mechanism of the drawing of polyamide filaments.

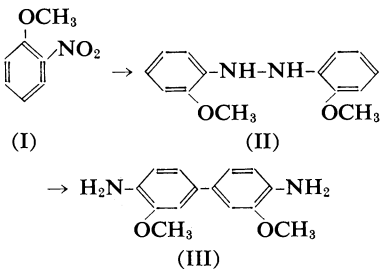
Nagoya Laboratory
Research Department
Toyo Rayon Co., Ltd.
Minato-ku, Nagoya

Electrolytic Process for the Preparation of Dianisidine Using Rotating Cathode Cell for the Reduction of o-Nitroanisole to Hydrazoanisole

By K. S. UDUPA, G. S. SUBRAMANIAN and H. V. K. UDUPA

(Received June 28, 1961)

Dianisidine is largely employed as a dye intermediate in the production of direct cotton colors and the same to the extent of 573 Cwts. was imported into this country in 1959. An electrochemical method for the process would therefore be of interest to meet the immediate requirements of the country. Hydrazoanisole (II) is generally prepared[1] by the reduction of



(I) (II)

(III)

o-nitroanisole (I) with zinc and sodium hydroxide in alcoholic or benzene solution. The hydrazoanisole thus obtained is rearranged to dianisidine (III) by reaction with acids.

Chemical Methods of Reduction.—Pellegrini[2] studied the reduction of *o*-nitroanisole by means of sodium amalgam and found that hydrazoanisole is formed when solvents like alcohol and pyridine are used without which the nitro group is reduced to the amine. In this reduction he concluded that the initial concentration of sodium hydroxide is of great importance, the formation of primary amines as a by-product being greater, the smaller the amount of alkali present initially. Gandry and Keirstead[3] have used dextrose and sodium arsenite as a reducing agent for the reduction. Reduced nickel prepared from nickel nitrate mixed with a compound containing sulfur or chlorine as a reducing agent for the reduction has been suggested by Rikagaku[4]. Recently Iida and Konishi[5] have studied the reduction by using a ferrosilicon alloy and found that the best condition for the reduction are obtained by using 10 g. of *o*-nitroanisole with 6～9 g. of ferrosilicon (Si content 15%) in 15～30 g. of 13～18% sodium hydroxide solution containing 7.9 g. of calcium hydroxide at 100°C for 2～6 hr.

Electrolytic Methods of Reduction.—The first electrolytic reduction of *o*-nitroanisole has been reported by Haussermann[6] by reducing *o*-nitroanisole in alcoholic solution. Elbs[7] and Brand[8] have also reported the electrolytic reduction of *o*-nitroanisole. McKee and Gerapostolou[9] have extensively studied the reduction of *o*-nitroanisole in concentrated solution mixtures of sodium and potassium xylene sulfonates at different pH and reported that hydrazo compounds are formed only under alkaline pH. Dey and co-workers[10] have also studied the electrolytic reduction of an alkaline emulsion of *o*-nitroanisole, employing stationary cathode and low current densities of the order of 2 amp./dm^2 to obtain an yield of 67.7% of hydrazoanisole.

The use of rotating cathode technique in the reduction of nitro compounds in acid medium was reported from this laboratory earlier[13,14]. The reduction of nitrobenzene and *o*-chloronitrobenzene in alkaline emulsion using the same technique was reported in subsequent studies by the authors[11,12] and the application of this technique in the reduction of other substituted nitro compounds has led us to the present investigation.

Experimental

Electrolytic Cell.—The cell (Fig. 1) consisted of a 600 cc. Pyrex beaker (A) without spout, and

1) V. O. Lukashevich, *J. Gen. Chem.* (*U. S. S. R.*), **5**, 103 (1935); *Chem. Abstr.*, **29**, 4745 (1935).
2) G. Pellegrini, *Giorn. chim. ind. applicata*, **8**, 175 (1926); *Chem. Abstr.*, **21**, 376 (1927).
3) R. Gandry and K. F. Keirstead: *Can. J. Research*, **27B**, 890 (1949); *Chem. Abstr.*, **44**, 3927 (1950).
4) K. Yoshikawa and B. Kubota, Japanese Pat. 101254 (1933).
5) H. Iida, T. Shibano and K. Konishi, *J. Chem. Soc. Japan, Ind. Chem. Soc.* (*Kogyo Kagaku Zassi*), **57**, 830 (1954); *Chem. Abstr.*, **49**, 10873 (1955).
6) C. Haussermann, *Chem. Ztg.*, **17**, 209 (1893).
7) K. Elbs, *Z. Elektrochem.*, **5**, 108 (1898); **7**, 145 (1900).
8) K. Brand, *J. prakt. Chem.*, [2] **67**, 156 (1903).
9) R. H. McKee and B. G. Gerapostolou, *Trans. Electrochem. Soc.*, **68**, 329 (1935).
10) B. B. Dey, T. R. Govindachari and S. C. Rajagopalan, *J. Sci. Ind. Research* (*India*), **4**, 642 (1946).
11) K. S. Udupa, G. S. Subramanian and H. V. K. Udupa, *J. Electrochem. Soc.*, **108**, 373 (1961).
12) K. S. Udupa, G. S. Subramanian and H. V. K. Udupa, *Bull. acad. polon. sci.*, IX, 419 (1961).
13) G. S. Krishnamurthi, H. V. K. Udupa and B. B. Dey, *J. Sci. Ind. Research* (*India*), **15B**, 47 (1956).
14) G. S. Subramanian, H. V. K. Udupa and B. B. Dey, Proc. of the Symp. "Electrolytic-cells" CECRI, Karaikudi-3, S. Rly (1962), p. 188.

was fitted with a cement asbestos sheet cover having the necessary openings for the introduction of cathode (B), diaphragm (D), condenser (F) and thermometer (T). The cathode (B) was of a mild steel disk type each disk being 2.5 cm. diameter and with a spacing of 1.25 cm. There are 5 such disks and the cathode is rotated at about 1800 r. p. m. by means of a fractional H. P. motor. The catholyte was 200 cc. of 10% soduim hydroxide (Commercial grade) containing 2 g. of commercial grade litharge (yellow) PbO. The anolyte was 25% sodium hydroxide. *o*-Nitroanisole (L. R. grade B. D. H.) was used in the ratio of 1 : 4 (1 g. of nitro compound per 4 cc. of the catholyte). The diaphragm was of asbestos cloth wound on a nickel plated mild steel cage — 2.5 cm. diameter ×12.5 cm. height — and the anode was a strip of stainless steel plate (C) — 1.25 cm. breadth ×15 cm. height ×0.16 mm. thick. A cathode current density of 30 amp./dm² was employed.

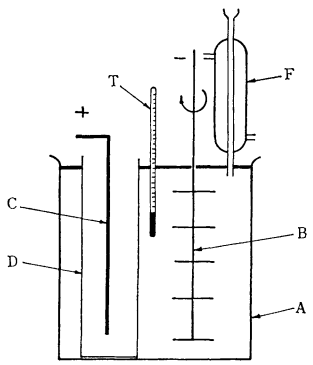


Fig. 1. Cell diagram using a rotating disk-type cathode.
A, Cell container; B, Rotating cathode; C, Anode; D, Diaphragm; T, Thermometer; F, Condenser

Procedure.—After the lead had been deposited on the rotating cathode by pre-electrolysis, with a current of 8 amp., 50 g. of *o*-nitroanisole was added to the hot electrolyte (85°C) and theoretical current for reduction to hydrazoanisole passed from a selenium rectifier. After 90% of the current was passed, xylene (50 ml.) was added into catholyte to keep the solid hydrazoanisole in solution and to favor further reduction of azoanisole and any nitroanisole trapped in the solid.

Conversion to Dianisidine and Isolation of the Product.—The xylene layer from the electrolyte was separated and poured into a mixture of ice and 19 cc. of sulfuric acid (specific gravity 1.84) and stirred for 5 hr. in the cold condition after which the temperature was raised to 90°C. The dianisidine free base was liberated by basifying the crude sulfate and the ansidine is separated by steam distillation and dianisidine was then filtered after cooling and estimated as free base. The xylene layer was steam-distilled and the *o*-azoanisole remaining in the still was cooled, filtered, dried and weighed.

Results

The results of the investigation are given in Table I. It may be seen that *o*-azoanisole is a fairly poor depolarizer, because by passing nearly 10% excess current, the dianisidine yield could be increased only by about 2%.

Cathode Potential Studies.—The measurement of cathode potentials was carried out with a view to study the nature of the reduction process. For this purpose, a cylindrical iron cathode was used and the potential measured

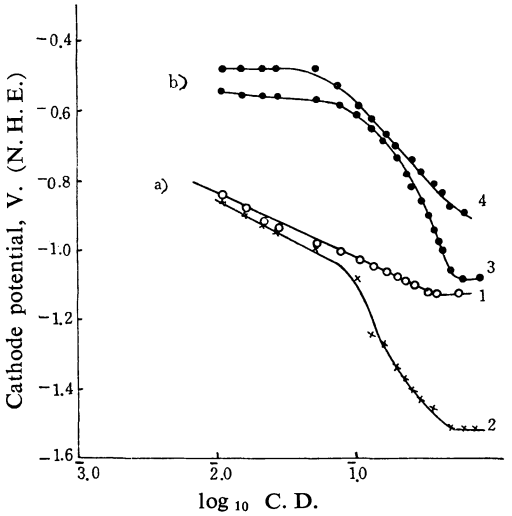


Fig. 2. Plot of cathode potential vs. log C. D. (amp./dm²).
a) Without addition of *o*-nitroanisole
1, Stationary cathode
2, Rotating cathode
b) With addition of *o*-nitroanisole
3, Stationary cathode
4, Rotating cathode

TABLE I. RESULTS OF ELECTROLYTIC REDUCTION OF *o*-NITROANISOLE

Conditions: Catholyte, 200 cc. of 10% NaOH; Anolyte, 50 cc. of 25% NaOH; PbO, 2 g; Temperature, 85±2°C; Weight of *o*-nitroanisole taken, 50 g.; Cell voltage, 3.5 to 4.5 V.

Expt. No.	Current passed (amp.·hr.)	Current density (amp./dm²)	Per cent yield		
			Dianisidine	*o*-Azoanisole	Anisidine
1	44	30	70.2	19.7	7.8
2	44	30	74.5	20.5	5.8
3	48.4 (10% excess)	30	76.5	17.1	4.9

Energy consumption: 9.0 kwh./kg.

against Hg/HgO/N NaOH reference electrode and a calibrated Heathkit vacuum tube voltmeter.

The influence of current density on the cathode potential was studied for the cathode that was plated rotating as well as that plated stationary. Graphs 1 and 2 in Fig. 2 show the polarization under stationary and rotating conditions of the respective cathodes plated under stationary and rotating conditions. It is necessary to indicate here that the lead deposit is spongy and not adherent when deposited on a stationary cathode and hence cannot be rotated after deposition without dropping out the deposit. Hence only the cathode on which lead was deposited while rotating can alone be used in the reduction of nitroanisole with rotation. These results clearly indicate the advantages of rotation of the cathode while depositing lead. The deposit though somewhat spongy, is quite adherent, and does not peel off during the reduction of nitroanisole so that the cathode can be used several times without having to redeposit lead. The rotating cathode is polarized to a greater extent because the deposit is less spongy. The cathode potential was also measured at different current densities after adding *o*-nitroanisole. Graphs 3 and 4 in Fig. 2 show considerable lowering of the cathode polarization on addition of *o*-nitroanisole.

A study of the cathode polarization curves shows that *o*-nitroanisole is a good depolarizer. A maximum displacement of 0.39 V. in the case of stationary cathode and of 0.64 V. in the case of rotating cathode in the positive direction was observed. This displacement is observed at a particular depolarizer ratio of 1 : 4

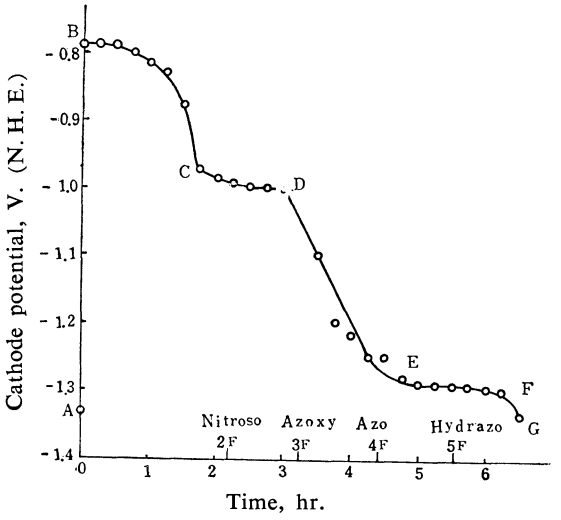


Fig. 3. Plot of cathode potential vs. duration on electrolysis using rotating cathode.

and at a temperature of 80~85°C. The maximum displacement in the cathode polarization occured at a current density of 7.8 amp./dm^2 in the case of stationary and at 23.4 amp./dm^2 for the rotating cathodes respectively. Figure 3 shows the change of cathodic polarization during the actual course of reduction of *o*-nitroanisole in alkaline emulsion at a rotating cathode with a deposit of lead at a current density of 25 amp./dm^2. The curve indicates the combined effects of the depolarizing action of different compounds which are likely to be formed at various periods during the course of reduction of the nitro compound. The first steep fall (A to B) is probably due to the depolarization of *o*-nitroanisole and the portion (B to C) represents the reduction to the nitroso stage and the fairly steady state (C to D) is probably due to the combined action of reduction of the nitro and nitroso to the azoxy stage. The steep fall (D to E) points to the reduction to the azo and/or hydrazo stage and thereafter the steady portion E to F probably represents the reduction of azo to hydrazo only and the potential slowly approaches the hydrogen evolution potential.

Summary

The technique of using rotating cathodes for electrolytic reduction of nitro compounds developed in this Institute earlier has now been extended to the study of the reduction of *o*-nitroanisole in an alkaline emulsion to obtain hydrazoanisole, which is subsequently converted to dianisidine by reaction with acid. The various chemical methods of obtaining hydrazoanisole as well as the previous attempts for obtaining the same by electrolytic reduction of *o*-nitroanisole are briefly reviewed.

The experimental technique adopted, the isolation of the product and the subsequent conversion of the hydrazoanisole to dianisidine are described.

Cathode potential has been measured at different current densities using lead deposited iron cathode under stationary and rotating condition of the cathode without the addition of nitro compound. The effect of the nitro compound addition on the cathode potential at different current densities has also been studied. The potential of a rotating cathode measured during the course of an experiment is graphically presented and the results discussed.

The authors sincerely thank Professor K. S. G. Doss, Director of the Institute, for his keen interest in this investigation.

Central Electrochemical Research Institute, Karaikudi-3, S. Rly., India

Viscosities of O/W Emulsions Stabilized by Nonionic Surfactants. I. Characteristics of Nonionic Surfactants in Emulsion Viscosities

By Noriaki OHBA

(Received June 30, 1961)

Numerous reports are available on the viscosities of emulsions stabilized by the ionic emulsifiers. Viscosity has been discussed in detail in relation to the several factors affecting viscosity, such as the phase-volume ratio, the particle size distribution, the role of the interfacial films or of the stabilizers, the electroviscous effect, etc.[1]

On the other hand, there are relatively few data on and discussions of the viscosity of emulsions stabilized by the nonionic surfactants. Therefore, we have studied the behavior of nonionic surfactants towards the viscosity of emulsions. We first made the experiments on the emulsifications of mineral oil, using several types of nonionic surfactants; then we measured the viscosities of the emulsions thus obtained with a "MacMichael type" rotating-cup viscometer[2]. From these experiments, we have obtained a conclusion with relation to the HLB concept proposed by Griffin[3] on the nature of nonionic surfactants.

Experimental

Mineral Oil.—"Carnation White Mineral Oil" produced by Sonneborn Co., USA, was used as the oil phase in the emulsification, its average viscosity being 70 cp.

Nonionic Surfactants.—To examine the relative effects of nonionic surfactants on the emulsion viscosity, several samples differing in molecular constitution were selected for use; part of these were the same as those listed in the preceding report[4], and the other samples are listed in Table I.

TABLE I. GLYCERYL MONOSTEARATES

Abbr.	Type[a]	MG, %[b]	
MGS-I	N	45	Free glycerol <10%
MGS-II	N	55	Free glycerol <2%
MGS-III	S	—	MGS-I + K-soap
MGS-IV	S	—	MGS-II + K-soap
MGS-V	S	—	MGS-II + Nonionic surfactant

a : N, Noneself-emulsifying type
S, Self-emulsifying type
b : Monoglyceride content (%) determined with periodate.

Viscosity Measurements.—The viscometer employed in the present experiments was a "MacMichael type" rotating-cup viscometer equipped with a heating device to control the temperature of the emulsions measured. The angular velocity (Ω) of this viscometer can be varied from 25 to 100 r. p. m., and the values of the deflection angle (θ) at 50 r. p. m. were used for comparisons of the relative viscosity.

Results and Discussion

Emulsions of mineral oil were prepared by means of emulsification by inversion[5]. A composition of these emulsions is shown in Table II.

TABLE II. COMPOSITION OF EMULSION

Mineral oil	40.0%
Emulsifier	8.0%
Distilled water	52.0%

The process of emulsification is as follows; Into a mixture of mineral oil and emulsifier, which has been kept at about 90°C, water, which has also been kept at about the same temperature, is gradually added with an adequate stirring. This stirring is continued until the temperature of the emulsion decreases to about 40°C. After the emulsion has been left standing for about 20 hr., the viscosities of these emulsions are measured, at 25°C.

The HLB Method and the Viscosity of the Emulsion.—In the case of emulsifications using nonionic surfactants as stabilizers, there is the well-known HLB method to obtain the most stable emulsion[3]. To study the relations between the stabilities and viscosities of emulsions, sorbitan monostearate (SMS; HLB=4.7) and polyoxyethylene sorbitan monostearate (E-SMS -20; HLB=14.9) were adopted as standards for the emulsifiers[4]. To simplify comparison, one of these two standards was kept as a fixed component in any pair of surfactants in the emulsion studies. In this way, it was possible to study the relative effect of the nonionic surfactant upon the viscosity.

1) W. Clayton, "Theory of Emulsions", 4th Ed., The Blakiston Co., Philadelphia (1943); P. Becher, "Emulsions: Theory and Practice", Rheinhold Pub. Corp., New York (1957); etc.
2) Shimadzu Seisakusho, Kyoto, Japan.
3) W. C. Griffin, *J. Soc. Cosmetic Chemists*, **1**, 311 (1949).
4) N. Ohba, This Bulletin, **35**, 1016 (1962).
5) N. Ohba, K. Meguro and T. Kondo, Presented at the 12th Symposium of Colloid Chemistry, Hiroshima University, October, 1959.

In Table III, an example of the HLB values for mixtures composed of two emulsifiers, SMS and E-SMS-20, is shown.

To measure the relative viscosity, the resultant angle of deflection (θ) was plotted against the angular velocity (Ω), as is shown in Fig. 1.

TABLE III. HLB VALUES FOR MIXED EMULSIFIERS, θ AT 50 r. p. m., AND STABILITIES OF EMULSIONS

No.	Emulsifier composition (g.)		HLB (Eq.1)	θ at 50 r. p. m.	Stability
	SMS	E-SMS-20			
1	3.4	4.6	10.55	214	+
2	3.5	4.5	10.43	320	++
3	3.6	4.4	10.30	366	++
4	3.7	4.3	10.18	335	++
5	3.8	4.2	10.05	445	++
6	3.9	4.1	9.80	298	++

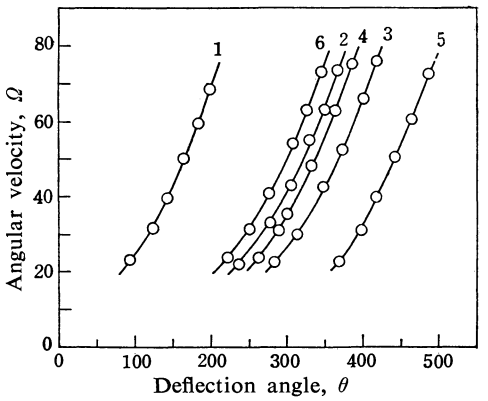


Fig. 1. The relations between deflection angle and angular velocity of viscometer.

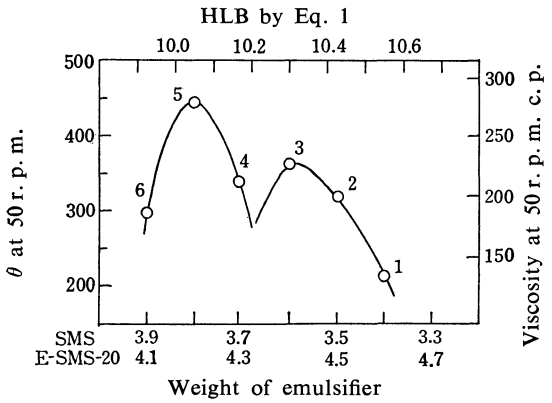


Fig. 2. The relations between the viscosity, the composition of emulsifier, and HLB.

On the basis of this figure, to show the effect of emulsifier composition on the relative viscosities of these emulsions, the values of θ at 50 r. p. m., which is an intermediate value of angular velocity, were listed in the 5th column of Table III and were plotted against the composition of the mxied emulsifiers, as is shown in Fig. 2.

At the top of this figure, a scale of the HLB values for the mixture is shown, calculated from the assumption of the weighed mean of HLB values of their components, using Eq. 1[6].

$$[\mathrm{HLB}] = [\mathrm{HLB}]_a x/100 + [\mathrm{HLB}]_b(100-x)/100 \quad (1)$$

where [HLB], $[\mathrm{HLB}]_a$ and $[\mathrm{HLB}]_b$ are the HLB values of the mixed emulsifier, surfactant "a" and "b" respectively, and x is the percentage content of surfactant "a" in the mixture.

In the case of SMS and E-SMS-20, $[\mathrm{HLB}]_a$ is 4.7, $[\mathrm{HLB}]_b$, 14.9, and

$$x = (\text{weight of SMS}) \times 100/8$$

This scale enables us to follow the $\theta \sim x$ relation with respect to the HLB of the mixed emulsifier.

Following the concept of HLB, it is assumed that the most stable state of emulsions results when the suitable HLB value is attained.

In the case of the series of emulsions shown in Table III, the following relations were found to exist among the HLB values, the particle size by a visual observation, the stability against creaming, and the relative viscosity of these emulsions:

1) The particle size of these emulsions first becomes smaller with the decrease in the HLB value for the emulsions numbered from 1 to 3, and then it becomes larger again with the further decrease in the HLB value for those of 5 and 6:

$$1 > 2 > 3 \geqslant 4 \leqslant 5 < 6$$

2) The stability of these emulsions varied with the decrease in the HLB value as shown in the last column of Table III; that is:

$$1 < 2 < 3 \approx 4 \approx 5 > 6$$

3) The relative viscosity of these emulsions has two maxima with respect to the HLB of the mixed emulsifier, as is shown in Fig. 2. As a whole, the relative viscosity of these emulsions shows two maxima as the HLB decreases with the change in composition of the mixed emulsifiers. Between these two maxima of viscosity, we can observe a deep or flat minima according to the nature of mixed surfactants, as is shown in Fig. 3.

In the case of ionic emulsifiers, it was reported by Richardson[7] that the apparent viscosity of emulsions having the same concen-

6) W. C. Griffin, *J. Soc. Cosmetic Chemists*, **5**, 249 (1954).
7) E. G. Richardson, *J. Colloid Sci.*, **5**, 404 (1950); **8**, 367 (1953).

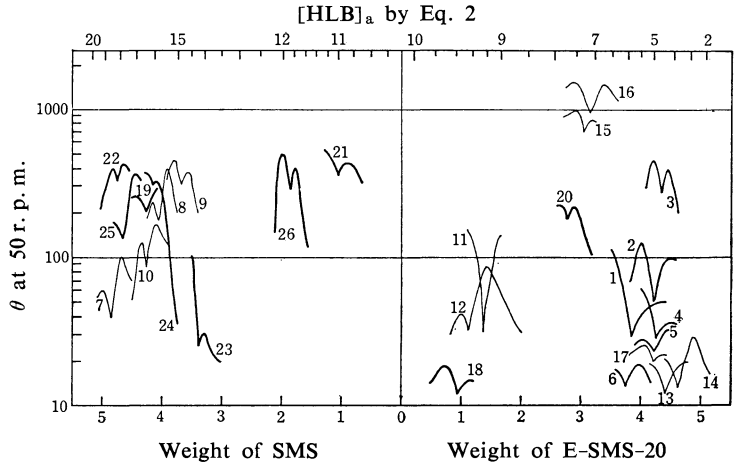


Fig. 3. The relations between the relative viscosity and the composition of mixed emulsifiers.

1, SML	2, SMP	3, SMS	4, SMO	5, SSO
6, STS	7, E-SML-20	8, E-SMP-20	9, E-SMS-20	10, E-SMO-20
11, E-SMS-6	12, E-SMO-6	13, GMS-I	14, GMS-II	15, GMS-III
16, GMS-IV	17, GMS-V	18, POEL-5	19, POEL-10	20, POEC-2
21, POEC-5.5	22, POEC-20	23, POENP-9	24, POENP-10	25, POEOP-10
26, PEGS-10				

tration and a similar type of particle size distribution is inversely proportional to their mean grobule diameter. Applying his opinion to our case of the series of emulsions in Table III, the relation between the particle size, the stability and the relative viscosity of these emulsions can reasonably be understood, excepting for the region between the two maxima. To discuss the phenomena occuring in this region, further detailed studies must be made.

Sorbitan Fatty Acid Esters.—In Fig. 3, the cases of sorbitan fatty acid esters, curves 1—6, which were used with E-SMS-20 as the mixed emulsifiers, are shown.

All of the curves have two maxima in relative viscosities, like those shown in Fig. 2. In this figure, the relative viscosities, as a whole, are shown to decrease in the following order:

SMS > SMP > SML > SMO > SSO > STS

We can see, as a whole, that this order is in agreement with the increasing order of carbon numbers in the fatty acid radicals for saturated fatty acid monoesters and with the melting points of these acids, involving unsaturated acid monoesters. In the case of STS, the emulsions obtained were coarse and gave low relative viscosities.

Polyoxyethylene Sorbitan Fatty Acid Esters. —Derivatives having about 20 and 6 mol. of ethoxy-units in a molecule are used as component emulsifiers, and the results, curves 7—12, are shown in Fig. 3. These curves also gave two maxima, except for the case of E-SMS-6, the magnitude of relative viscosities (and of melting point) being in the following order:

E-SMS-20 > E-SMP-20 > E-SMO-20 > E-SML-20

We can also see that this order is in agreement with the order of the carbon numbers of the saturated fatty acid esters. Thus we can confirm that the melting points of these varying components run parallel with the above series. However, if we consider the melting point of the fixed emulsifier component, the situation is not so simple. For instance, in the case of mixed emulsifiers consisting of SMS and polyoxyethylene fatty acid esters containing 20 mol. of ethoxy-unit in a molecule, SMS has a higher melting point than the rest of these polyoxyethylene derivatives, while the amounts in the emulsifier mixture required for optimum emulsification increase with the decrease in the relative viscosities. These relations are contrary to what can be expected from simple reasoning based upon the fact that the higher melting component increases the viscosity of the emulsion at its optimum composition.

Glyceryl Monostearates. — In Fig. 3, the results obtained, curves 13—17 are shown; all of these curves show two maxima, like the preceding examples. GMS-I and II gave levels of relative viscosities similar to those of the sorbitan esters. However, in the case of the so-called "self-emulsifying types", GMS-IV and III gave the considerably high levels compared with the rest of the cases examined, although those for GMS-V were in an order of magnitude comparable with that of the other nonionic surfactants.

The relative viscosities of this group decreased

TABLE IV. HLB VALUES BY EMULSIFICATION TEST, (A), VISCOSITY TESTS, (B) AND ASSIGNED, (C)

	(A)	(B)	(C)		(A)	(B)	(C)
SML	5.8	6.0	8.6	E-SML-20	17.3	18.5	16.7
SMP	4.4	5.0	6.7	E-SMP-20	15.6	16.0	15.6
SMS	4.7	4.7	4.7	E-SMS-20	14.9	14.9	14.9
SMO	5.1	5.0	4.3	E-SMO-20	15.0	16.5	15.0
SSO	5.2	5.1	3.7	E-SMS-6	9.4	9.3	9.6
STS	6.5	6.2	2.1	E-SMO-6	9.0	9.5	10.6
POEL-5	9.7	9.6	10.8	MGS-I	4.4	4.5	—
POEL-10	16.4	16.4	14.1	MGS-II	3.7	3.8	—
POEC-2	7.6	7.7	5.1	MGS-III	7.4	7.4	—
POEC-5.5	11.1	11.1	9.8	MGS-IV	7.1	7.2	—
POEC-20	18.4	18.1	15.5	MGS-V	5.5	5.1	—
POENP-9	14.2	14.2	12.9	PEGS-10	11.9	11.9	11.9
POENP-10	15.5	16.1	13.4	POEOP-10	—	17.8	13.6

in the following order:

$$\text{GMS-IV} > \text{GMS-III} \gg \text{GMS-V} > \text{GMS-II} > \text{GMS-I}$$

The anomalous large values of relative viscosity observed for GMS-III and IV are probably due to the presence of K-soap in these self-emulsifying types, that is, to the effects of the ionic surfactants. On the other hand, the relative viscosity observed for GMS-V, which involves nonionic surfactants alone as a component to make the self-emulsifying type, differs from those for those others involving K-soap.

Other Nonionic Surfactants.—For most of this group, two maxima in the curves of relative viscosities were also observed, as is shown in Fig. 3. (curves 18—26). The magnitudes of the relative viscosities did not show a considerable difference or a systematic variation among them, except for the case of POEL-5, which has a lower viscosity level.

HLB and Viscosities of O/W Emulsions.—In Fig. 3, the top scale $[HLB]_a$ of these figures is of the virtual values of HLB for varying components of the surfactant mixture calculated from the following equations, based upon reasoning similar to that leading to Eq. 1:

$$[HLB]_a = \{[HLB]_m - [HLB]_b x/100\}100/(100-x) \quad (2)$$

where $[HLB]_m$ indicates the HLB value of standard mineral oil, 10.2[4], $[HLB]_b$ is the HLB value for the fixed component, 4.7 for SMS and 14.9 for E-SMS-20, and x is the percentage of the fixed component in the emulsifier mixture. Therefore, when SMS is combined with any other surfactants, Eq. 2 becomes

$$[HLB]_a = (10.2-4.7x/100)100/(100-x) \quad (3)$$

while in the case of E-SMS-20, we have

$$[HLB]_a = (10.2-14.9x/100)100/(100-x) \quad (4)$$

Now, from these virtual values of $[HLB]_a$, we can determine the most probable value of the HLB of the component emulsifier in question from the value of x, which gives the most stable emulsions corresponding to the minima between the two maxima of the $[HLB]_a$ vs. θ curve. The HLB values thus obtained from the relative viscosities of emulsions can be directly compared with the HLB values of nonionic surfactants determined by emulsification tests by visual observation. In our recent paper[3], the HLB values of several nonionic surfactants by emulsification tests were reported. Although the water-oil-emulsifier ratio in the tests differed from that of the present systems, and this makes comparison somewhat difficult, the HLB values reported and the values corresponding to the viscosity minimum between two maxima as listed in Table IV show a good agreement for all nonionic surfactants. However, these experimental values do not always agree with the values calculated from the structural or analytical data of nonionic surfactants, C in Table IV.

Shapes of the Two Maxima and the Distances between Them.—The shapes of the two maxima and the distance between them may be an important measure to specify the characters of a given nonionic surfactant in emulsifications. Throughout these emulsification tests, it can generally be confirmed that the more distant are the two maxima separated in the viscosity curve, the more insensitive becomes the stability of the emulsion towards its surfactant composition. For this reason, we may introduce the term, "Viscosity Spectra of the Nonionic Surfactant".

Summary

O/W emulsions of mineral oil were prepared, using several types of nonionic surfactants, and their relative viscosities were measured with

a rotating-cup viscometer, together with microscopic and visual observation of the emulsions.

It was found that there are two maxima in the curve of the relative viscosity vs. the ratio of the two surfactants in the mixed emulsifier employed. From these figures, the relative effects of the nonionic surfactants on the emulsion viscosities were discussed.

It was confirmed that the emulsion viscosity at the optimum composition decreases in the following order:

for sorbitan fatty acid esters,

$$SMS > SMP > SML > SMO > SSO > STS$$

for polyoxyethylene sorbitan fatty acid esters,

$$E\text{–}SMS\text{–}20 > E\text{–}SMP\text{–}20 > E\text{–}SMO\text{–}20 > E\text{–}SML\text{–}20$$

for glyceryl monostearates,

$$GMS\text{–}IV > GMS\text{–}III \gg GMS\text{–}V > GMS\text{–}II > GMS\text{–}I$$

For the other types the order of the series was not distinct. In the former two series, the orders of the arrangements are parallel with those of the decreasing carbon atom numbers in the molecule in the case of saturated fatty acid derivatives.

The soap effect is considered to appear in the case of glyceryl monostearates, the so-called self-emulsifying types of the emulsifier.

Using the scale of viscosity vs. virtual HLB value, we can determine by means of emulsification the most probable HLB value of the nonionic surfactants.

Good agreements are seen between the HLB values determined by viscosity minimum and those determined by the emulsification test reported on in the preceding paper.

The author wishes to thank Professor Tsunetaka Sasaki, of Tokyo Metropolitan University, for his encouragement and advice in this work.

Nihon Surfactants Ind. Co.
Itabashi-ku, Tokyo

Viscosities of O/W Emulsions Stabilized by Nonionic Surfactants. II. Effects of Oil Mixtures on the Emulsion Viscosities

By Noriaki OHBA

(Received August, 28, 1961)

In a preceding paper[1], the effects of nonionic surfactants on the emulsion viscosities were measured, and the relations between the structures of nonionic surfactants and the viscosities of emulsions stabilized by them were studied. In another paper[2], the effects of the substances added to the oil on the HLB values of the mixtures thus obtained were determined, according to the concept of HLB suggested by Griffin[3], as being equal to the HLB value of that mixed surfactant which gives the most stable emulsion. Thus we studied the relations between the HLB values and the nature of the materials added to the mineral oil.

Several factors which influence the viscosities of the emulsion have been discussed by several workers[4] in connection with the properties of the oil phase of O/W emulsions. In the practice of emulsion techniques, a certain "thickener" is added to increase the viscosity of a given emulsion. Certain waxes and higher fatty alcohols, such as beeswax, cetyl alcohol and stearyl alcohol, are such examples.

Concerning thses problems, several oil mixtures were selected and were emulsified with nonionic surfactant mixtures of a fixed constituency. The viscosities of the emulsions thus obtained were measured and discussed in relation to the properties of the components of the oil mixture.

Experimental

Nonionic Surfactants.—To make comparison simple, sorbitan monostearate (SMS) and polyoxyethylene sorbitan monostearate (E-SMS-20) were adopted as standards of the nonionic emulsifiers, as has been described in the preceding paper[2]. The HLB values adopted for these materials are 4.7 for SMS and 14.9 for E-SMS-20. When the required HLB of an oil mixture is over 14.9, polyoxyethylene

1) N. Ohba, This Bulletin, 35, 1171 (1962).
2) N. Ohba, ibid., 35, 1021 (1962).
3) W. C. Griffin, *J. Soc. Cosmetic Chemists*, 1, 311 (1949).
4) W. Clayton, "Emulsions and their Technical Treatment", 4th Ed., J. and A. Churchill Ltd. (1947); P. Becher, "Emulsions. Theory and Practice", Rheinhold Pub. Corp., New York (1957); etc.

cetyl ether (POEC-20), having the HLB value of 18.4, was adopted in place of E-SMS-20.

Oil and Waxes.—"Carnation White Mineral Oil" produced by the Sonneborn Co., USA, was used as the fixed component of the oil mixture to be emulsified, its HLB value being 10.2 and its average viscosity, 70 cp.

Several materials were used as the varying component of the oil mixture. They were selected from those described in the foregoing paper[2]; in this paper we distinguish acetylated glyceryl mono-oleate into two, i. e.,

AGMO-I Acetylated mono-oleate (OH. V.=4)
AGMO-II Acetylated mono-oleate and mono-stearate (OH. V.=4).

These materials were used in a varying ratio to the fixed component of mineral oil.

Viscosity Measurements.—The emulsions used in the present experiment were prepared by the same method as has been described in a preceding paper[5], i. e., that method involving phase inversion. The HLB values of these emulsions were also determined by the same method as presented in another paper[2].

TABLE I. COMPOSITION OF O/W EMULSIONS

Oil mixture	40.0%
Emulsifiers	
SMS+E-SMS-20	4.0%
Distilled water	56.0%

The compositions of these emulsions are shown in Table I. After these emulsions had been left standing for about 20 hr., their viscosities were measured, by a "MacMichael type" rotating-cup viscometer which indicates the values of strain θ as the deflection angle of inner cylinder, for varying angular velocities, Ω, of the cup. For convenience, the values of strain θ at 50 r.p.m. were adopted as the relative viscosities of the emulsions.

Results and Discussion

Viscosity and Composition Diagrams.—The results obtained are illustrated in Figs. 1—4.

In Fig. 1 we can see that the viscosities of S-Ac/mineral oil mixtures increase steeply when the S-Ac content exceeds 10% of the oil mixture. On the other hand, in the case of L-Ac, such an increase was observed in the concentration ranges beyond 15%.

In the case of fatty alcohols, as shown in Fig. 2, the effects of C-Alc were remarkably greater than those of La-Alc and L-Alc. A sudden increase in this viscosity vs. the composition diagram for C-Alc was observed at a 5% content of C-Alc in the oil mixture, while for the cases of the other two alcohols a similar increase was observed at a 20% content.

We can see from these results that, among these fatty acids and alcohols, C-Alc is the most effective additive to the oil phase to increase the emulsion viscosity, both with respect to the amount required and to the degree of viscosity increase. Such an effect of C-Alc can be succcssfully applied in certain fields of emulsion technique.

In Fig. 3, viscosity vs. composition diagrams for acetylated esters are shown. In this figure, it can be seen that AGMS-I, -III and -IV have a greater effect on the viscosities of emulsions than AGMO-I and II. Among these three stearates, AGMS-IV shows a remarkably large effect on the emulsion viscosity, its magnitude being comparable to that of C-Alc. It is also used for the similar purpose of increasing viscosity. AGMS-III and I are effective to the same extent.

The viscosities of emulsions containing AGMO-I and II are considerably different

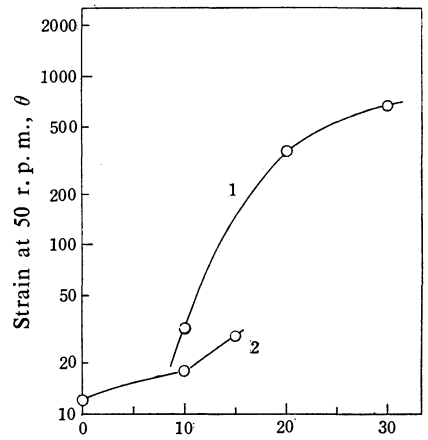


Fig. 1. Viscosity of emulsion.
Oil phase: 1, Mineral oil~stearic acid
2, Mineral oil~lauric acid

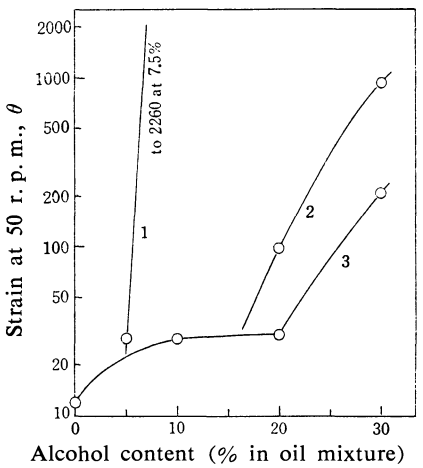
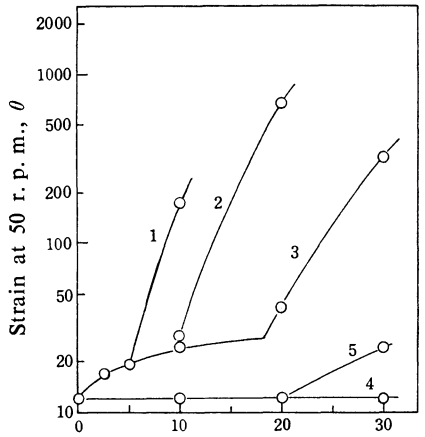


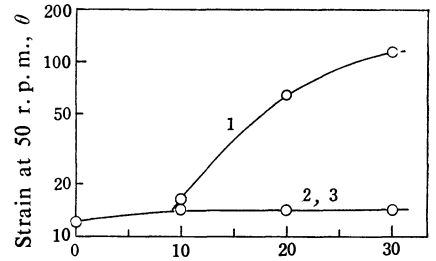
Fig. 2. Viscosity of emulsion.
Oil phase: 1, Mineral oil~cetyl alcohol
2, Mineral oil~lanolin alcohol
3, Mineral oil~lauryl alcohol

5) N. Ohba, This Bulletin, 35, 1016 (1962).



Acetylated ester content (% in oil mixture)

Fig. 3. Viscosity of emulsion.
Oil phase: Mixtures of mineral oil and
1, AGMS-IV 2, AGMS-III 3, AGMS-I
4, AGMO-I 5, AGMO-II



Wax content (% in oil mixture)

Fig. 4. Viscosity of emulsion.
Oil phase: Mixtures of mineral oil and
1, beeswax 2, ceresin wax 3, lanolin

from that of AGMS-I in the range of concentration studied. As to AGMO-I and -II, the former being oleic acid ester and the latter being a mixture of oleic and stearic acid ester, as can be confirmed from the analytical data, AGMO-II shows a slight effect in increasing the emulsion viscosity, while AGMO-I does not, in the region beyond a 20% content in the oil.

Figure 4 shows the results of viscosity measurements for waxes. B-W had a fairly large effect in increasing the emulsion viscosity, while La and C-W showed little influence over the whole range of concentration examined.

The sudden increase in the emulsion viscosity by B-W occurs at a certain content of B-W within the region from 10 to 20% of the oil mixture, as in the case of C-Alc, AGMS-IV, etc., but the increase is smaller for B-W.

As a whole, we can see in Figs. 1—4 that the magnitudes of the effects of these additives on the increasing emulsion viscosity are in the following order, with respect both to the amount required for the sudden increase in viscosity and to the rate of its increase:

C-Alc, AGMS-IV > S-Ac, AGMS-III > La-Alc > AGMS-I, L-Ac, L-Alc > B-W > AGMO-II, AGMO-I, C-W, La

Factors Affecting the Emulsion Viscosities.— It was reported in a preceding paper[2] that the effects of additives on the required HLB values of the oil mixtutres vary both with the nature and the amount of the additives in the oil mixture.

Concerning the emulsion viscosities, Toms[6] and Sherman[7] reported that the emulsion viscosity is affected greatly by the chemical nature of the internal phase, while the viscosity of the internal phase is of no consequence.

To make sure of the factors affecting the emulsion viscosities, several data were measured and are listed in Table II; the substances are arranged in the decreasing order of influence on the emulsion viscosities shown above. In this table, the following abbreviations are used:

A: Amount of additive required to increase the emulsion viscosity ten times as much as that of the mineral oil emulsion without any additives; these amounts are determined from the results shown in Figs. 1—4.

Δ: The increase in the required HLB value of the mixture from that of mineral oil[2] at the additive contents corresponding to A.

Figure 5 shows graphically the correlations between "A" and other factors. From these figures we cannot deduce any simple correlation between these factors which may be used to find an effective additive for increasing emulsion viscosity. However, we can safely say that in order to be effective as an additive in increasing emulsion viscosity, a substance's iodine value should be small, while an ineffective additive always shows a low Δ as well as a low hydroxyl value. The melting point of an additive has, on the whole, no correlation with the power of increasing emulsion viscosity. The acid value also shows no correlation with the viscosity of the emulsion formed.

These general tendencies may sometimes become useful guides for the selection of additives to increase emulsion viscosity.

Critical Phenomena. — Throughout all the experiments shown in Figs. 1—4, we can see a fairly distinct critical phenomenon. That is, the viscosities of these O/W emulsions increase steeply beyond a certain critical content of the

6) B. A. Toms, *J. Chem. Soc.*, **1941**, 542.
7) P. Sherman, *Mfg. Chemist*, **26**, 306 (1955); *Kolloid-Z.*, **6**, 141 (1955).

TABLE II. VISCOSITY INCREASE AND CHEMICAL NATURE OF THE ADDITIVES

	A	Δ	COOH*	OH*	C=C*	M. p., °C
C-Alc	5.7	6	N	217	N	50
AGMS-IV	9	74	4	155	N	54
S-Ac	14	28	202	N	N	62
AGMS-III	14	27	3	75	N	39
La-Alc	21	7	N	90	—	—
AGMS-I	25	− 2	4	4	N	31
L-Ac	15∼25	35	278	N	N	38
L-Alc	27	6	N	300	N	22
B-W	30	4	18	20	9	62
AGMO-II	>30	− 1	2	4	40	—
AGMO-I	>30	− 1	2	4	80	—
C-W	>30	− 1	N	N	N	66
La	>30	2	5	30	22	(30)

N: Negligible

* COOH: acid value, OH: hydroxyl value and C=C: iodine value

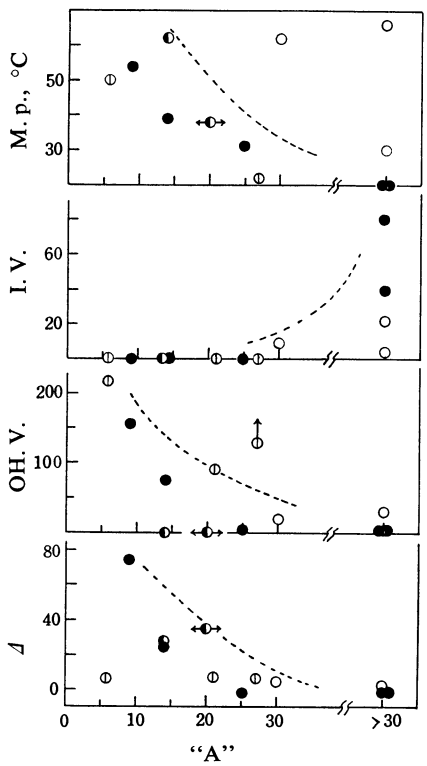


Fig. 5. Correlations between "A" and other factors.
Additives: ◑, Fatty acids; ⓘ, Fatty alcohols; ●, Acetylated esters; ○, Waxes

additives, and these critical contents form characteristics of each material. The critical contents determined for the substances are listed, though roughly, in Table III. In this table, the substances are arranged in the decreasing order of their critical contents, which order agrees as a whole with that shown in Table II. That is, a substance having a lower

TABLE III. CRITICAL CONTENTS OF SUBSTANCES

	Critical content, %		Critical content, %
C-Alc	5	L-Ac	10∼20
AGMS-IV	5∼10	L-Alc	20∼30
S-Ac	5∼10	AGMO-II	20∼30
AGMS-III	10	AGMO-I	>30
B-W	10	C-W	>30
La-Alc	10∼20	La	>30
AGMS-I	10∼20		

critical content shows a stronger tendency to increase the emulsion viscosity than a substance having a higher critical content.

We may also notice that the additive shows no effect in increasing emulsion viscosity when it does not contain any polar group other than ester linkage.

Besides the critical point, the inclination of viscosity vs. additive content diagrams beyond the critical point also offers some measure of the efficiency of additives in increasing emulsion viscosity, with some exceptions, as in the case of B-W, where the small critical content does not always correspond to the steep inclination of the viscosity vs. content diagram beyond the critical point. Precisely speaking, therefore, we should take account of both the critical point and the inclination of the steeper part of the diagram in estimating the efficiency of an additive in increasing emulsion viscosity.

Although many studies on the emulsion viscosities have been carried out by several workers[4,6,7], none of them is entirely satisfactory in explaining the phenomena. At least, the chemical structure of the additives, and the change in the viscosity of the external phase produced by the solubilization of the oil component into micelles of the emulsifier which is considered to exist in the external

phase, are considered to be important in elucidating the phenomena. For the further elucidation of these critical phenomena, however, more details must be studied.

Summary

To study the effects on the viscosities of O/W emulsions of the addition of several materials to the oil phase, oil mixtures were emulsified and the viscosities of the emulsions so obtained were measured with a rotating-cup viscometer,

The effects of these additives in increasing emulsion viscosity are in the following order, with respect both to the amounts required to give a specified increase in viscosity and to the minimum amount required for a sudden increase in viscosity:

C-Alc, AGMS-IV > S-Ac, AGMS-III > La-Alc > AGMS-I, L-Ac, L-Alc > B-W > AGMO-II, AGMO-I, C-W, La

It was confirmed that in order to be effective as an additive in increasing emulsion viscosity, the iodine value should be small, while an ineffective additive always shows a low Δ as well as a low hydroxyl value. The melting point of an additive has, on the whole, no correlation with the power of increasing the emulsion viscosity. The acid value also shows no correlation with the viscosity of the emulsion formed.

A sudden increase in emulsion viscosity was observed beyond a certain amount characteristic of each additive.

The author wishes to express his deep gratitude to the members of his laboratory for their close cooperation in this work.

Nihon Surfactants Ind. Co.
Itabashi-ku, Tokyo

The Synthesis of Azulene Derivatives from Troponoids[*1]

By Tetsuo NOZOE, Shuichi SETO[*2], Shingo MATSUMURA[*2] and Yasuhiro MURASE[*3]

(Received January 9, 1962)

Various methods for the synthesis of azulene derivatives have in the past been reported by numerous organic chemists. Almost all of these methods required a dehydrogenation reaction in the final stage, and, although many improvements have been effected, these have resulted generally in a poor yield[1].

The present authors have recently found that the condensation of troponoids, such as 2-halo- and 2-methoxytropone derivatives, with ethyl cyanoacetate or malononitrile, in the presence of a base, afforded 2-amino- and 2-hydroxyazulene derivatives in one step and in a fairly good yield. Although short summaries of this work have already been published[2], a detailed description of the new synthetic method has not yet been given.

In this paper, the authors wish to describe this synthetic procedure in full detail. The reaction of 2-chlorotropone (Ia) with two molar equivalents of ethyl cyanoacetate in absolute ethanol, in the presence of two molar equivalents of sodium ethoxide, was allowed to stand at room temperature; a sparingly soluble sodium salt, from which an acid substance (II) (m. p. 188~189°C), was liberated by treatment with mineral acid, and orange crystals (III), $C_{16}H_{17}O_4N$ (m. p. 93~94°C) precipitated out. The mother liquor from these precipitates afforded a small amount of colorless crystals (IV), m. p. 135~137°C. The main product III was obtained in about a 70% yield. Under the same conditions, the condensation of 2-bromotropone (Ib) with ethyl cynoacetate

*1 Presented at the 8th Annual Meeting of the Chemical Society of Japan, Tokyo, April, 1955.

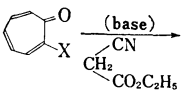
*2 Present address: The Chemical Research Institute of Non-Aqueous Solutions, Tohoku University, Sendai.

*3 Present address: Takamine Research Laboratory, Sankyo Pharmaceutical Co., Ltd., Shinagawa-ku, Tokyo.

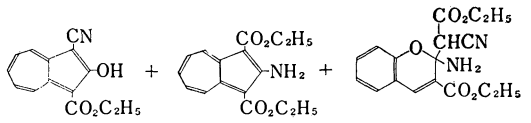
1) a) M. Gordon, *Chem. Revs.*, **50**, 127 (1952); b) W. Keller-Schierlein and E. Heilbronner, "Non-Benzenoid Aromatic Compounds", Ed. by D. Ginsburg, Interscience, New York (1959), p. 277; c) T. Nozoe and T. Asao, "Dai Yuki Kagaku" (Comprehensive Organic Chemistry), Ed. by M. Kotake, Vol. 13, Asakura Shoten, Tokyo (1960), p. 535.

2) a) T. Nozoe, S. Matsumura, Y. Murase and S. Seto, *Chem. & Ind.*, **1955**, 1257; b) T. Nozoe, S. Seto, S. Matsumura and T. Asano, *Proc. Japan Acad.*, **32**, 339 (1956); c) T. Nozoe, S. Seto and S. Matsumura, *Chem. & Ind.*, **1961**, 1715.

gave III in about a 60% yield. The reaction of Ia with two molar equivalents of ethyl sodiocyanoacetate in dehydrated benzene yielded II and III, but not IV.

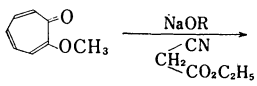


Ia: X=Cl
Ib: X=Br

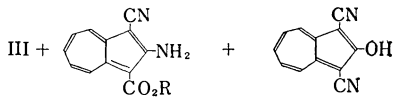


II III IV

The use of tertiary amine in place of alkoxide as the condensation agent resulted in the formation of III in a 35% yield and of a small amount of orange crystals (V) (m. p. above 300°C), sparingly soluble in organic solvents. The reaction of 2-methoxytropone (Ic) with two molar equivalents of ethyl cyanoacetate, in the presence of two molar equivalents of sodium ethoxide, afforded III in a 5% yield and a 7% yield of orange crystals (VI), $C_{14}H_{12}O_2N_2$, of m. p. 167~168°C. The remainder



Ic



VI: R=C_2H_5 VII
XX: R=CH_3

(about 75%) was an acid substance (VII), m. p. above 300°C, sparingly soluble in organic solvents. The application of one molar equivalent of alkoxide to Ic afforded III in over a 70% yield, while the yields of VI and VII were very poor.

It was interesting that the ratio of these products differed markedly according to the amount of alkoxide[3].

The ultraviolet absorption spectra[4] (Fig. 1) of II, III and VII are very similar to each other, and these compounds are assumed to have a common skeletal structure.

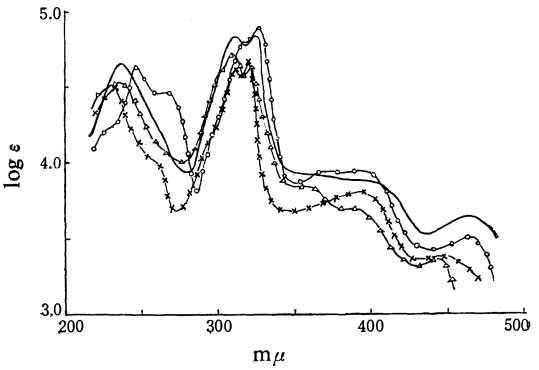


Fig. 1. UV absorption spectra of II, III, VII and XXI in methanol.
——— II, —○— III, —△— VII, —×— XXI

The main product III easily formed picrate melting at 125°C and styphnate melting at 150°C. The passage of dry hydrogen chloride gas through a dehydrated benzene solution of III formed reddish orange crystals assumed to be the hydrochloride of III, but the free compound III was easily liberated when the salt was left in the air.

The infrared absorption spectrum[5] of III,

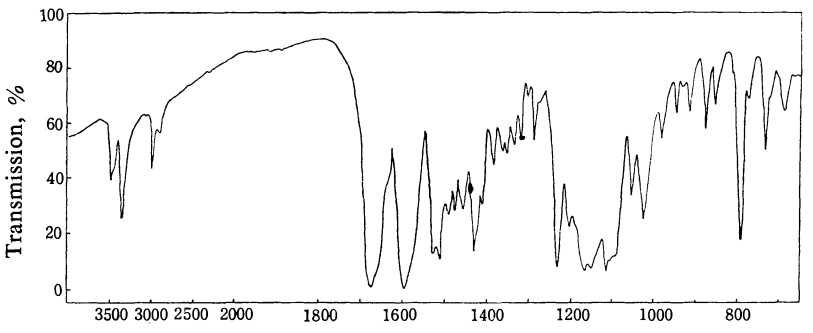
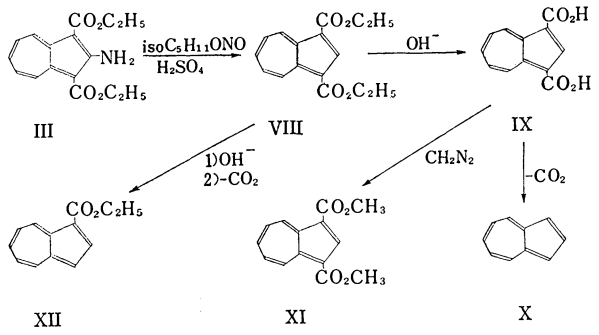


Fig. 2. IR absorption spectrum of III in KBr disk.

3) A similar phenomenon has also been observed in the cases of the reaction of tropolone methyl ether (2-methoxytropone) derivatives, such as hinokitiol methyl ether and 4-methyltropolone methyl ether etc., with ethyl cyanoacetate (T. Nozoe et al., to be published).

4) Ultraviolet spectra were measured with a Beckman Model DU spectrophotometer.

5) Infrared spectra were measured with a Perkin-Elmer Model 21 double-beam spectrophotometer.



as indicated in Fig. 2, exhibits absorption bands at 3500 and 3310 cm^{-1} for the primary amino group, and at 1660 and 1225 cm^{-1} for the ester group conjugated with the unsaturated bond. The attempted acetylation of III with acetic anhydride containing one drop of pyridine failed to give its acetate. The attempted deamination of the compound III with isoamyl nitrite in its ethanolic solution, in the presence of concentrated sulfuric acid, resulted in changing the color from orange to brownish red, and gave reddish violet crystals (VIII), $C_{16}H_{16}O_4$, of m. p. 120~121°C. The hydrolysis of VIII with an ethanol-aqueous solution of potassium hydroxide afforded a crystalline dicarboxylic acid IX, m. p. 270°C (decomp.), very sparingly soluble in organic solvents.

The thermal decomposition of IX produced blue crystals X, m. p. 98~99°C, with an odor of naphthalene. The ultraviolet (Fig. 3), visible[6], and infrared absorption spectra of compound X and its melting point are identical with those of azulene; by mixed fusion it was confirmed that X was azulene.

The position of the principal maximum (513 mμ) in the visible spectrum of compound VIII (Fig. 3) was found to be in excellent agreement with that of dimethyl azulene-1, 3-dicarboxylate (511 mμ), first synthesized by Anderson et al.[7] The action of diazomethane on IX afforded red crystals XI, m. p. 170~171°C. The melting point of XI was in good agreement with that of dimethyl azulene-1, 3-dicarboxylate reported in the literature.

Consequently, compound VIII was diethyl azulene-1, 3-dicarboxylate, and IX was its free dicarboxylic acid, azulene-1, 3-dicarboxylic acid. The maximum absorption of compound III (465 mμ) in the visible region causes a shift toward a shorter wavelength (48 mμ) than that of VIII. The additivity of the spectral shifts in the visible region caused by alkyl groups on the different positions of azulene ring was first found by Plattner et al.[1a] Not only alkyl groups, but also other *o, p*-directing groups are found to cause a hypsochromic shift of the absorption bands when substituted at the even-numbered positions in the azulene nucleus[8,9]. These considerations supported the view that compound III was diethyl 2-aminoazulene-1, 3-dicarboxylate. The hydrolysis of VIII with one molar equivalent of potassium hydroxide gave a red crystalline carboxylic acid sparingly soluble in organic solvents, and its decarboxylation by heating at 240~250°C under a partially reduced pressure afforded, in addition to azulene, ethyl azulene-1-carboxylate (XII) as a reddish violet oil which formed a picrate of m. p. 124°C.

The infrared absorption spectrum of compound VI exhibits the absorption bands due to the primary amino group and to the cyano and ester carbonyl groups conjugated with an unsaturated bond. From these spectral data and from the molecular formula, it was assumed compound (VI) was ethyl 2-amino-3-cyano-azulene-1-carboxylate[10]. The hydrolysis of III with an ethanol-aqueous solution of potassium hydroxide afforded 2-aminoazulene-1, 3-dicarboxylic acid (XIII), m. p. 158~160°C (decomp.), sparingly soluble in organic solvents. Its decarboxylation by heating at 125~130°C in pyridine or heating at 170~175°C under a reduced pressure gave, in a good yield, 2-aminoazulene (XIV) as red crystals, m. p. 93~94°C, the acetylation of which with acetic anhydride afforded 2-acetamidoazulene (XV) as violet crystals, m. p. 168~169°C. Compound XIV easily formed an unstable picrate of m. p. 145°C (decomp.). 2-Aminoazulene appears more stable than the 1-aminoazulene prepared

6) Visible absorption spectra were measured with a Beckman DK spectrophotometer.

7) A. G. Anderson, Jr., R. Scotoni, Jr., E. J. Cowles and C. G. Fritz, *J. Org. Chem.*, **22**, 1193 (1957).

8) E. J. Cowles, *J. Am. Chem. Soc.*, **79**, 1095 (1957).

9) T. Nozoe, S. Seto, S. Matsumura and A. Sato, This Bulletin, in press.

10) The present authors have previously given an erroneous structure of ethyl 2-amino-3-cyano-azulene-1-carboxylate for compound A of m. p. 135~137°C[1b]. Re-examination of the structure of the compound A has shown that A is not an ethyl ester but a methyl ester converted from compound VI by ester exchange reaction.

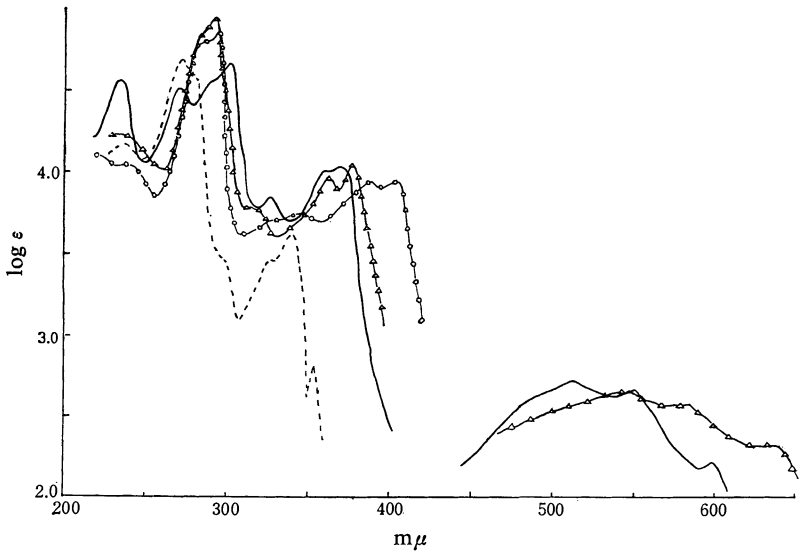
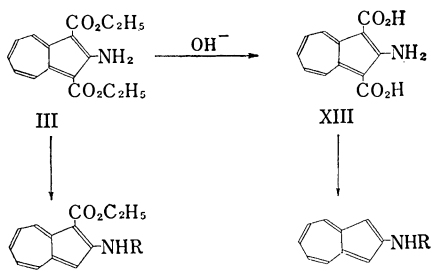


Fig. 3. UV absorption spectra of VIII, X, XIV and XV in methanol.
——— VIII, ------ X, —○— XIV, —△— XV

by Schulze and Heilbronner[11]. However, 2-aminoazulene also becomes a brownish black substance on exposure to air and light for a few days. The hydrolysis of III with one molar equivalent of potassium hydroxide yielded a crystalline carboxylic acid, and its decarboxylation by heating in pyridine afforded ethyl 2-aminoazulene-1-carboxylate (XVI) as red crystals, m. p. 68~70°C. The acetylation of XVI with acetic anhydride gave ethyl 2-acetamidoazulene-1-carboxylate (XVII) as red crystals, m. p. 140~141.5°C.



XVI : R=H
XVII : R=Ac

XIV : R=H
XV : R=Ac

The ultraviolet and visible absorption spectra of XIV and XV are shown in Fig. 3. The application of nitrous acid to XIV resulted in a change of color from green to dark brown, and no pure product could be isolated.

Although compounds II and VII are acid substances, these compounds do not dissolve in an aqueous solution of sodium hydrogencarbonate, but exhibit a dark brown coloration with ferric chloride in ethanol. There are absorption bands for the unsaturated ester carbonyl group at 1655 cm^{-1}, for the unsaturated cyano group at 2200 cm^{-1}, and for the hydroxyl group at 3100 cm^{-1} in compound II, while absorption bands due to unsaturated cyano and hydroxyl groups are present at 2200 and 3100 cm^{-1} respectively in compound VII. The heating of II with an excess of acetic anhydride containing pyridine gave its acetate XVIII as red crystals, m. p. 142°C. Under the same conditions, VII afforded its acetate XIX as red crystals, m. p. 192°C. The infrared absorption band due to the carbonyl group at 1655 cm^{-1} in compound II is displaced to the higher frequency region of 1702 cm^{-1} in compound XVIII. It would be rational to attribute this shift to an intramolecular hydrogen bonding between the carbonyl and hydroxyl groups in compound II. From these facts, it was assumed that compound II was ethyl 3-cyano-2-hydroxyazulene-1-carboxylate and that compound VII was 1, 3-dicyano-2-hydroxyazulene (1, 3-dicyanoazulen-2-ol).

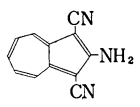
The reaction of Ic with ethyl cyanoacetate, in the presence of two molar equivalents of sodium methoxide in place of sodium ethoxide, afforded methyl 2-amino-3-cyanoazulene-1-carboxylate[10] (XX) as orange crystals, m. p. 135~137°C, in a poor yield, besides III, VI and VII. The condensation of 2-chlorotropone (Ia) with malononitrile, in the presence of sodium ethoxide or tributylamine, afforded, in a quantitative yield, very sparingly soluble orange

11) J. Schulze and H. Heilbronner, *Helv. Chim. Acta*, **41**, 1492 (1958).

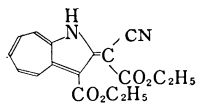
crystals (XXI), m. p. above 300°C. The ultraviolet absorption spectrum of compound XXI, as indicated in Fig. 1, is very similar to that of III; moreover, there are absorption bands for amino and unsaturated cyano groups in the infrared spectrum of compound XXI. Consequently, these observations support the view that compound (XXI) is 2-amino-1, 3-dicyanoazulene(1,3-dicyano-2-azulenamine). The hydrolysis of the cyano group of II, VII and XXI by acid or alkali was unsuccessful.

The formation of 2-amino-1, 3-dicyanoazulene (XXI) is explained by the reaction of two moles of malononitrile with one mole of 2-chlorotropone; even when one mole of malononitrile was reacted with one mole of 2-chlorotropone the same azulene derivative XXI was formed. The same result was found in the reaction of 2-chloro- or 2-methoxytropone with ethyl cyanoacetate. The use of one mole of the dimer of ethyl cyanoacetate, i. e. ethyl α-cyano-β-aminoglutaconate (XXII), instead of two moles of ethyl cyanoacetate, however, failed to give any azulene; the products were the heterocyclic azulenoid compounds XXIII and XXIV[12].

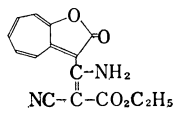
From the foregoing experimental facts, it is considered that the first intermediate XXV



XXI

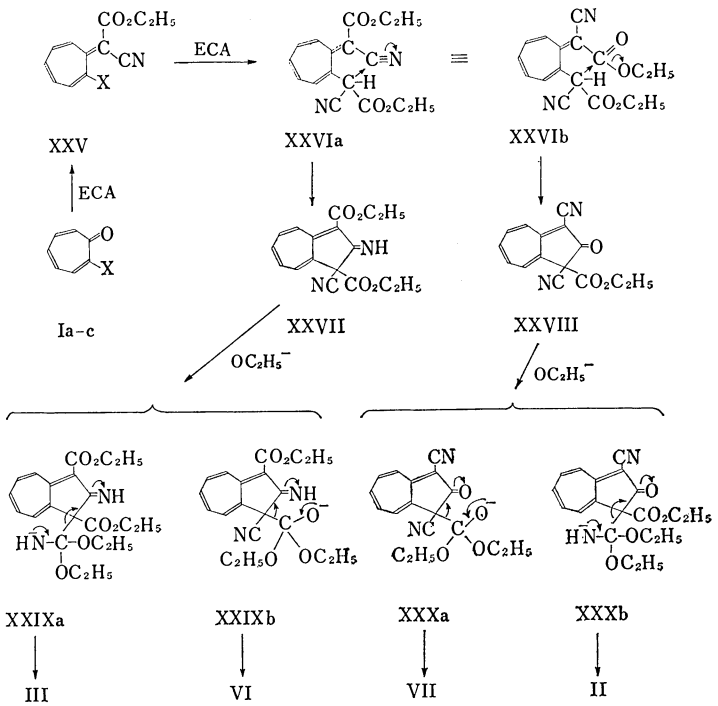


XXIII



XXIV

formed by the reaction of both ethyl cyanoacetate and 2-halo- or 2-methoxytropone is much more reactive than the original troponoids Ia–c and immediately reacts with the second mole of the reagent to form second intermediates such as XXVIa and XXVIb, whose Ziegler-type condensation, forming a five-membered ring, would give a bicyclic intermediate XXVII and XXVIII. By the polarizing effect of the carbonyl or imino group in the 2-position, and the attack on the ethoxycarbonyl or cyano group by the base (alkoxide anion), the intermediate suffers a cleavage of the C–C bond[13] through the third intermediates, XXIXa–b and

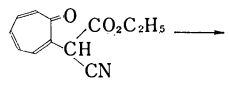


ECA=Ethyl cyanoacetate

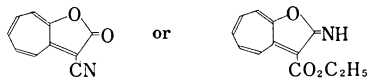
Scheme 1

12) S. Matsumura, This Bulletin, 34, 1361 (1961).
13) A. C. Cope, "Organic Reactions", Ed. by R. Adams, Band IX, John Wiley & Sons, Inc., New York (1957), p. 107.

XXXa–b, and forms the final azulenoid products II, III, VI and VII, as is shown in Scheme 1. More recently, it has been found that an application of malononitrile to tropone itself[14], or ethyl cyanoacetate or malononitrile to 8, 8-disubstituted heptafulvenes[15] (e.g. XXV: X=H), also gives the afore-mentioned azulene. The structure of the first intermediate might also be tropone derivative XXXI or its cyclization product XXXIIa or b, rather than the afore-mentioned heptafulvene derivative XXV.



XXXI



XXXIIa XXXIIb

In this connection, it is interesting to note that the compound of the XXXIIa type also gave azulene derivatives in its reaction with ethyl cyanoacetate in the presence of an excess of sodium alkoxide[16]. All this evidence seem to confirm the general correctness of our proposed mechanism of this novel azulene synthesis starting with the troponoids.

After the completion of this study[2a], Ziegler and Hafner very interestingly reported a practical synthetic method of azulenes; they also found that the alkylation and arylation of the 4- and 8-positions could be effected by the application of organometallic compound to azulenes[17]. However, this method would have some disadvantages for the synthesis of special azulene derivatives possessing versatile groups, such as hydroxyl, amino, hydrazino and mercapto groups, on the five or seven-membered ring. In our method, the azulenes first formed always have a versatile functional group, i.e., amino or hydroxyl in the 2-position, which may be easily substituted afterwards by various groups; moreover, such groups may be easily introduced in the seven-membered ring while in the troponoid stage used for this synthesis. Accordingly, our process would complement the Ziegler-Hafner method for azulene synthesis.

As a simpler and more useful process has recently been found in several laboratories for the synthesis of tropone and tropolone[18], the novel process for the synthesis of azulene derivatives elaborated by us would have a very great significance. Thus, a large number of new azulene derivatives produced by the application of this process are now continuously being synthesized in the authors' laboratory[15b].

The yield of compound V is so very poor that further examination of this product was not made. Compound IV is identical with the product obtained by the condensation of salicylaldehyde with ethyl cyanoacetate, and the structure of compound IV was established to be 2-amino-2-(cyano-ethoxycarbonylmethyl)-3-ethoxycarbonyl-α-benzopyran[19].

Experimental[20]

Reaction of 2-Chlorotropone (Ia) and Ethyl Cyanoacetate.—a) To a suspension of ethyl sodiocyanoacetate prepared from 5 g. of metallic sodium, 27 g. of ethyl cyanoacetate and 100 ml. of absolute ethanol, a solution of 15 g. of Ia dissolved in 100 ml. of absolute ethanol was added drop dy drop under ice-cooling, and the mixture was stirred thoroughly. Immediately the color of the solution changed from yellow to orange. The mixture was allowed to stand at room temperature for 4 hr., and the orange crystals that separated out were then collected by filtration. The collected crystals were dissolved in benzene to be separated into benzene-insoluble and soluble portions. The addition of water to the benzene-insoluble portion precipitated 900 mg. of orange-yellow crystals insoluble in water. This substance was extremely sparingly soluble in various organic solvents. Its recrystallization from a large quantity of ethanol afforded the orange-yellow sodium salt of II, m.p. above 300°C.

Found: N, 4.98. Calcd. for $C_{14}H_{10}O_3NNa$: N, 5.34%.

A mixture of sodium salt of II and 5 ml. of 6 N hydrochloric acid was warmed on a water bath for 1 hr. The orange crystals that separated out were recrystallized from benzene, and 370 mg. of orange needles II, m.p. 188~189°C, was obtained.

Found: C, 69.78; H, 4.63; N, 5.92. Calcd. for $C_{14}H_{11}O_3N$: C, 69.70; H, 4.59; N, 5.80%.

UV λ_{max}^{MeOH} mμ (log ε): 235 (4.53), 311 (4.72), 325 (4.49), 355 (3.77), 470 (3.34).

The evaporation of the solvent of the benzene-soluble portion left orange crystals, m.p. 80~83°C. Repeated recrystallization from ethanol afforded 19 g. of orange prisms III, m.p. 93~94°C.

Found: C, 66.93; H, 6.26; N, 4.82. Calcd. for $C_{16}H_{17}O_4N$: C, 66.88; H, 5.96; N, 4.88%.

14) Y. Kitahara and K. Doi, to be published.
15) a) T. Nozoe and T. Mukai et al., to be published; b) T. Nozoe and S. Ito, *Fortsch. Chem. org. Naturestoffe*, **19**, 32 (1961).
16) T. Nozoe and K. Takase et al., to be published.
17) a) K. Ziegler and K. Hafner, *Angew. Chem.*, **67**, 301 (1955); K. Hafner, *Ann.*, **606**, 69 (1957); b) K. Hafner and H. Weldes, ibid., **606**, 90 (1957); c) K. Hafner, *Angew. Chem.*, **69**, 393 (1957); K. Hafner and H. Kaiser, *Ann.*, **618**, 140 (1958).
18) a) A. P. Ter. Borg, R. van, Helden, A. F. Bickel, W. Renold and A. S. Dreiding, *Helv. Chim. Acta*, **43**, 457 (1960); b) T. Ikemi, T. Nozoe and H. Sugiyama, *Chem. & Ind.*, **1960**, 932.
19) S. Matsumura, This Bulletin, **34**, 995 (1961).
20) All melting points are uncorrected. The microanalyses were carried out by Mr. S. Ohyama, Mr. S. Azumi and Miss. A. Iwanaga, to whom the authors are deeply indebted.

UV λ_{max}^{MeOH} mμ (log ε): 245 (4.42), 265 (4.36), 315 (4.77), 326 (4.69), 380 (3.84), 465 (3.41).

The mother liquor, after the separation of the above products, was evaporated under a reduced pressure, the residue was dissolved in benzene, and the solution was washed with water. After being dried over anhydrous sodium sulfate, the solvent was evaporated. The orange crystalline residue thereby obtained was recrystallized from ethanol and 5 g. of colorless prisms IV, m. p. 135~137°C, was obtained.

Found: C, 61.37; H, 5.25; N, 8.42. Calcd. for $C_{17}H_{18}O_5N_2$: C, 61.81; H, 5.49; N, 8.49%.

UV λ_{max}^{MeOH} mμ (log ε): 296 (3.72), 305 (3.69), 357 (3.60).

The recrystallization of the mother liquor afforded 2.5 g. of III.

b) To a sodium ethoxide solution prepared from 1 g. of metallic sodium and 20 ml. of absolute ethanol, 5.4 g. of ethyl cyanoacetate was added to form its sodio compound, and the ethanol was evaporated completely. The sodio compound was suspended in 30 ml. of dehydrated benzene, and the solution of 3 g. of Ia dissolved in 50 ml. of dehydrated benzene was stirred into it, by which process the solution became a dark reddish orange and an orange precipitate began to separate out. The orange precipitates were collected by filtration, and the addition of water afforded 200 mg. of sodium salt of II. The reaction mixture left after the removal of the above substance was washed with water. After being dried over anhydrous sodium sulfate, the solution was passed through a column of alumina. The column was eluted with benzene, and the solvent of the effluent was evaporated. The crystalline residue was recrystallized from ethanol to afford 1.2 g. of III.

c) To a solution of 500 mg. of Ia and 2.7 g. of ethyl cyanoacetate dissolved in 10 ml. of absolute ethanol, 1.7 g. of tributylamine was added; the color of the solution gradually changed from yellow to orange. The reaction mixture was allowed to stand overnight at room temperature, and the solvent was evaporated. The orange residue was dissolved in benzene, and the solution was washed with dilute nitric acid and water. After being dried over anhydrous sodium sulfate, the solution was passed through a column of alumina. The column was eluted with benzene, and 350 mg. of III was obtained. Further elution of the column with ethyl acetate afforded ca. 10 mg. of orange crystals. Recrystallization from acetone gave orange scales V, m. p. above 300°C.

Picrate of III.—Found: C, 51.25; H, 3.63; N, 10.64. Calcd. for $C_{22}H_{20}O_{11}N_4$: C, 51.16; H, 3.90; N, 10.85%. Reddish orange needles, m. p. 125~126°C, as recrystallized from ethanol. The solution of picrate-dissolved ethanol was passed through a column of alumina. The column was eluted with benzene, and III was easily regenerated.

Styphnate of III.—Found: N, 10.15. Calcd. for $C_{22}H_{20}O_{12}N_4$: N, 10.52%. Orange scales, m. p. 147~150°C, as recrystallized from ethanol.

Hydrochloride of III.—Dry hydrogen chloride gas was passed through a solution of III dissolved in dehydrated benzene, and the reddish orange prisms that separated out were collected by filtration. The product underwent a change to the starting material by atmospheric moisture.

Action of Acetic Anhydride on III.—A solution of 100 mg. of III dissolved in 1 ml. of acetic anhydride, in the presence of one drop of pyridine, was heated at 120~130°C for 3 hr. The excess acetic anhydride was evaporated under a reduced pressure, and the residues were recrystallized from ethanol, by which 80 mg. of III was recovered.

Reaction of 2-Bromotropone (Ib) with Ethyl Cyanoacetate.—To a suspension of ethyl sodiocyanoacetate prepared from 780 mg. of metallic sodium, 4 g. of ethyl cyanoacetate and 10 ml. of absolute ethanol, a solution of 3 g. of Ib dissolved in 7 ml. of absolute ethanol was added and the mixture was stirred thoroughly. Immediately the color of the solution changed from yellow to a dark reddish orange. After the solution had stood overnight at room temperature, the orange crystals that separated out were collected by filtration. The collected crystals were dissolved in benzene, and the solution was passed through a column of alumina. The column was eluted with benzene, and the solvent was evaporated. The crystallized residue was recrystallized from ethanol, and 2.6 g. of III was obtained. The mother liquor, after the separation of the above crystals, was concentrated, and the residue thereby obtained was dissolved in benzene. The solution was passed through a column of alumina, and the column was eluted with benzene. Evaporation of the solvent from the effluent afforded 400 mg. of III.

Reaction of 2-Methoxytropone (Tropolone Methyl Ether) (Ic) with Ethyl Cyanoacetate.—a) Into a suspension of ethyl sodiocyanoacetate prepared from 600 mg. ($2.6/10^2$ mol.) of metallic sodium, 3.0 g. ($2.67/10^2$ mol.) of ethyl cyanoacetate and 10 ml. of absolute ethanol, a solution of 1.8 g. ($1.3/10^2$ mol.) of Ic dissolved in 10 ml. of absolute ethanol was stirred under ice-cooling. After allowing the solution to stand overnight at room temperature, a large amount of precipitate separated out and was collected by filtration. The collected precipitate was dissolved in benzene to be separated into benzene-soluble (A) and benzene-insoluble (B) portions. Evaporation of the solvent of A portion left orange crystals, m. p. 160~164°C. Four recrystallizations from ethanol afforded 210 mg. of orange scales VI, m. p. 167~168°C.

Found: C, 69.41; H, 4.88; N, 11.82. Calcd. for $C_{14}H_{12}O_2N_2$: C, 69.99; H, 5.03; N, 11.66%.

UV λ_{max}^{MeOH} mμ (log ε): 238 (4.06), 310 (4.75), 322 (4.78), 368 (3.81), 445 (3.04).

The benzene-insoluble portion was dissolved in water, and the solution was neutralized with dilute sulfuric, acid, from which 2.1 g. of a brown precipitate was obtained. This substance was sparingly soluble in organic solvents. Its recrystallization from a large quantity of acetone afforded 1.92 g. of orange-yellow scales VII, m. p. above 300°C.

Found: C, 73.98; H, 3.42; N, 14.06. Calcd. for $C_{12}H_6ON_2$: C, 74.22; H, 3.11; N, 14.43%.

UV λ_{max}^{MeOH} mμ (log ε): 233 (4.35), 311 (4.72), 322 (4.62), 362 (3.86), 448 (3.50).

The mother liquor, after the separation of the

above products, was evaporated under reduced pressure. The orange residue thereby obtained was dissolved in benzene; the evaporation of the benzene left an oily substance. The residue was repeatedly digested with hot petroleum ether (b. p. 60~70°C) to be separated into petroleum ether-soluble and insoluble portions. The solvent of the petroleum ether-soluble portion was evaporated. The orange crystalline residue hereby produced was recrystallized from ethanol to give 190 mg. of III. Recrystallization of the petroleum ether-insoluble portion from the ethanol-benzene mixture afforded ca. 10 mg. of VI.

b) To a suspension of ethyl sodiocyanoacetate prepared from 600 mg. ($2.59/10^2$ mol.) of metallic sodium, 6.04 g. ($5.34/10^2$ mol.) of ethyl cyanoacetate and 10 ml. of absolute ethanol, 3.64 g. ($2.74/10^2$ mol.) of Ic was added, drop by drop under ice-cooling, and the mixture was stirred thoroughly. When the reaction mixture was treated as in the foregoing case, 5.5 g. of III, 100 mg. of VI and 500 mg. of VII were obtained.

c) To a suspension of ethyl sodiocyanoacetate prepared from 1.42 g. of sodium methoxide, 3.02 g. of ethyl cyanoacetate and 5 ml. of absolute ethanol, a solution of 1.8 g. of Ic dissolved in 10 ml. of absolute ethanol was added, and the mixture was treated as in the foregoing cases. The orange crystals were separated out from the benzene-soluble portion, besides 200 mg. of III, and 120 mg. of VI. The orange crystals were recrystallized from ethanol to afford 40 mg. of orange scales XX, m. p. 135~137°C.

Found: C, 68.98; H, 4.36; N, 12.56. Calcd. for $C_{13}H_{10}O_2N_2$: C, 69.01; H, 4.46; N, 12.38%.

UV λ_{max}^{MeOH} mμ (log ε): 238 (4.05), 310 (4.73), 322 (4.77), 368 (3.79), 445 (3.03).

The benzene-insoluble portion was acidified with dilute sulfuric acid, from which 2 g. of VII was obtained.

Diethyl Azulene-1, 3-dicarboxylate (VIII). — To a solution of 1 g. of III dissolved in 100 ml. of ethanol containing 500 mg. of concentrated sulfuric acid, 500 mg. of isoamyl nitrite was added. The reaction mixture was allowed to stand overnight at room temperature. The color of the solution gradually changed from an orange, reddish green, to a brownish red. The ethanol was then evaporated under reduced pressure. The dark red residue was suspended in water, and the suspension was neutralized with an aqueous solution of sodium carbonate. The residue thereby formed was extracted with benzene and the extract was dried over anhydrous sodium sulfate. The solution was passed through a column of alumina, and the column was eluted with benzene, by which 450 mg. of red crystals was obtained. Recrystallization from ethanol afforded 400 mg. of reddish violet prisms VIII, m. p. 120~121°C.

Found: C, 70.88; H, 5.71. Calcd. for $C_{16}H_{16}O_4$: C, 70.57; H, 5.92%.

UV λ_{max}^{MeOH} mμ (log ε): 234 (4.56), 271 (4.50), 302 (4.67), 326 (3.83), 365 (3.99), 371 (4.03), [513 (2.71), 550 (2.65), 604 (2.21) in cyclohexane].

Azulene-1, 3-dicarboxylic Acid (IX).—A solution of 1 g. of VIII dissolved in 10 ml. of a 10% ethanol-water (4:1) solution of potassium hydroxide was warmed on a water bath for 30 min. The color of the solution changed from red to violet. After being cooled, the solution was acidified with 6 N hydrochloric acid. The precipitate thereby formed was collected by filtration and repeatedly washed with water, by which 800 mg. of a sparingly soluble red substance IX, m. p. 270°C (decomp.), was obtained.

Azulene (X).—The low-pressure (200 mmHg) sublimation of 500 mg. of IX by heating at 270~280°C produced blue crystals. The crystals were dissolved in petroleum ether (b. p. 50~60°C), and the solution was passed through a column of alumina. The column was eluted with petroleum ether, and the solvent was cautiously removed. The crystalline residue was recrystallized from a methanol-water (4:1) mixture to afford 250 mg. of X as blue leaflets, m. p. 98~99°C, which showed no depression on admixture with an authentic specimen of azulene.

UV λ_{max}^{MeOH} mμ (log ε): 238 (4.17), 273 (4.68), 279 (4.64), 295 (3.55), 326 (3.45), 341 (3.60), 352 (2.70), 580 (2.50), 633 (2.41), 700 (1.98).

Dimethyl Azulene-1, 3-carboxylate (XI). — An ether solution of diazomethane was added to 100 mg. of IX suspended in 10 ml. of methanol, and the mixture was allowed to stand overnight. The solvent was evaporated, and the residue was dissolved in benzene. The solution was passed through a column of alumina. The column was eluted with benzene, and the solvent was distilled off. The crystallized residue was recrystallized from methanol to give 80 mg. of reddish violet scales XI, m. p. 171~172°C.

Found: C, 68.64; H, 4.86. Calcd. for $C_{14}H_{12}O_4$: C, 68.84; H, 4.95%.

Ethyl Azulene-1-carboxylate (XII).—To a solution of 100 mg. of potassium hydroxide dissolved in 5 ml. of an ethanol-water (4:1) mixture, 500 mg. of VIII was added; the mixture was then warmed on a water bath for 15 min. After being cooled, the solution was acidified with 6 N hydrochloric acid. The precipitate thereby formed was collected by filtration and repeatedly washed with water, by which 60 mg. of crystalline carboxylic acid was obtained. The low-pressure (100 mmHg) sublimation of the carboxylic acid by heating at 240~250°C produced a violet oil. The oil was dissolved in petroleum ether (b. p. 60~70°C) and chromatographically purified through an alumina column. The product separated into blue and reddish violet bands. The elution of the blue band with petroleum ether afforded ca. 10 mg. of X. The further elution of the reddish violet oil produced XII.

UV $\lambda_{max}^{Cyclohexane}$ mμ (log ε): 234 (4.30), 291 (4.61), 296 (4.65), 351 (3.76), 365 (3.95), 545 (2.65), 588 (3.60), 645 (2.23).

Picrate of XII.—Found: C, 53.41; H, 5.48; N, 9.81. Calcd. for $C_{19}H_{15}O_9N_3$: C, 53.15; H, 3.52; N, 9.79%. Red needles, m. p. 123~124°C, as recrystallized from ethanol.

2-Aminoazulene-1, 3-dicarboxylic Acid (XIII).—To a solution of 200 mg. of potassium hydroxide in 5 ml. of an ethanol-water (4:1) mixture, 500 mg. of III was added; the mixture was then refluxed in a water bath for 3 hr., by which the solution clearly colored orange-yellow. The solution was

acidified with 6 N hydrochloric acid. The precipitate hereby formed was collected by filtration and repeatedly washed with water; 350 mg. of crude 2-aminoazulene-1,3-dicarboxylic acid (XIII), m. p. 158~160°C (decomp.), sparingly soluble in organic solvents, was obtained.

2-Aminoazulene (XIV).—a) A suspension of 400 mg. of XIII in 2 ml. of pyridine was heated at 125~130°C for 15 min. to effect decarboxylation. The residue obtained by evaporation of the excess pyridine was dissolved in benzene, and the solution was passed through a column of alumina. The column was eluted with benzene. Evaporation of the solvent from the effluent afforded red crystals. Recrystallization from benzene-cyclohexane mixture gave 200 mg. of red needles (XIV), m. p. 93~94°C.

Found: C, 83.31; H, 6.44; N, 9.40. Calcd. for $C_{10}H_9N$: C, 83.88; H, 6.34; N, 9.78%.

UV λ_{max}^{MeOH} mμ (log ε): 218 (4.10), 240 (4.08), 284 (4.80), 294 (4.89), 345 (3.74), 387 (3.92), 403 (3.83).

b) The low-pressure (2 mmHg) sublimation of 60 mg. of XIII by heating at 170~175°C afforded red crystals. Their recrystallization from the benzene-cyclohexane mixture gave 20 mg. of XIV.

2-Acetamidoazulene (XV).—When 2-aminoazulene (200 mg.) was added to 0.2 ml. of acetic anhydride, the mixture colored violet immediately. After allowing the mixture to stand at room temperature for 2 hr., the violet crystals that separated out were collected by filtration; recrystallization from benzene afforded 200 mg. of violet needles XV, m. p. 168~169°C.

Found: C, 77.49; H, 5.80; N, 7.49. Calcd. for $C_{12}H_{11}ON$: C, 77.81; H, 5.99; N, 7.56%.

UV λ_{max}^{MeOH} mμ (log ε): 240 (4.23), 285 (4.84), 294 (4.97), 345 (3.73), 363 (3.94), 379 (4.06), 548 (2.64), 584 (2.57), 640 (2.31).

Ethyl 2-Aminoazulene-1-carboxylate (XVI).—To a solution of 250 mg. of potassium hydroxide dissolved in 4 ml. of an ethanol-water (4 : 1) mixture, 1.3 g. of III was added, and the mixture was refluxed in a water bath for 3 hr. The solution was acidified with 6 N hydrochloric acid. The precipitate thereby obtained was collected by filtration and washed with water. After being dried, the precipitate was suspended in 2 ml. of pyridine, and the suspension was heated at 120~130°C to effect decarboxylation. The residue produced by evaporation of the excess pyridine was dissolved in benzene, and the solution was passed through a column of alumina, by which the products were separated into red, reddish-orange and orange bands. Elution of the red band with benzene gave a small amount of XIV. Elution of the reddish orange band with benzene afforded a reddish orange oil which was crystallized from cyclohexane to crystals of m. p. 60~65°C. Recrystallization from cyclohexane afforded 400 mg. of reddish orange needles (XVI), m. p. 68~70°C.

Found: C, 72.48; H, 5.97; N, 6.67. Calcd. for $C_{13}H_{13}O_2N$: C, 72.54; H, 6.09; N, 6.51%.

UV λ_{max}^{MeOH} mμ (log ε): 304 (4.76), 314 (4.93), 358 (3.96), 378 (3.86).

Ethyl 2-Acetamidoazulene-1-carboxylate (XVII).—A mixture of 200 mg. of XVI and 2 ml. of acetic anhydride was treated as in the preparation of XV, and 200 mg. of XVII as red leaflets, m. p. 140~141.5°C, was obtained.

Found: C, 69.96; H, 5.85; N, 5.15. Calcd. for $C_{15}H_{15}O_3N$: C, 70.02; H, 5.88; N, 5.44%.

UV λ_{max}^{MeOH} mμ (log ε): 246 (4.32), 304 (4.82), 314 (4.97), 356 (3.96), 371 (3.96), 503 (2.55).

Ethyl 2-Acetoxy-3-cyanoazulene-1-carboxylate (XVIII).—A mixture of 50 mg. of II and 0.2 ml. of acetic anhydride containing one drop of pyridine was heated at 120~130°C for 3 hr., by which the II dissolved completely. The mixture was evaporated under reduced pressure, and the crystalline residue was recrystallized from ethanol to give 40 mg. of XVIII as reddish orange needles, m. p. 141~142°C.

Found: C, 67.74; H, 4.61; N, 4.81. Calcd. for $C_{16}H_{13}O_4N$: C, 67.84; H, 4.63; N, 4.95%.

2-Acetoxy-1,3-dicyanoazulene (XIX).—A mixture of 50 mg. of VII and 1 ml. of acetic anhydride was treated as in the foregoing case, and 30 mg. of reddish orange scales XIX, m. p. 191~192°C, was obtained.

Found: C, 70.97; H, 3.67; N, 11.63. Calcd. for $C_{14}H_8O_2N_2$: C, 71.18; H, 3.41; N, 11.86%.

Reaction of 2-Chlorotropone (Ia) with Malononitrile.—a) Into a suspension of sodiomalononitrile prepared from 320 mg. ($1.4/10^2$ mol.) of metallic sodium, 920 mg. ($1.4/10^2$ mol.) of malononitrile and 10 ml. of absolute ethanol, a solution of 1 g. ($7/10^3$ mol.) of Ia dissolved in 8 ml. of absolute ethanol was stirred, drop by drop, ice-cooling. The mixture was allowed to stand at room temperature for 1 hr., by which the solution became clearly a green color and orange crystals began to separate out. The crystals were collected by filtration and washed with water. Their recrystallization from a large quantity of acetone afforded 1.2 g. of orange needles XXI, m. p. above 300°C.

Found: C, 74.83; H, 3.41; N, 21.62. Calcd. for $C_{12}H_7N_3$: C, 74.60; H, 3.65; N, 21.75%.

UV λ_{max}^{MeOH} mμ (log ε): 231 (4.50), 309 (4.58), 322 (4.64), 393 (3.75), 445 (2.90).

b) To a solution of 500 mg. ($3.5/10^3$ mol.) of Ia and 460 mg. ($7/10^3$ mol.) of malononitrile dissolved in 10 ml. of absolute ethanol or dehydrated benzene was added 1.3 g. ($7/10^3$ mol.) of tributylamine, by which the solution immediately turned reddish-orange and a precipitate gradually deposited. The precipitate was collected by filtration and recrystallized from acetone to give 700 mg. of XXI.

c) When a solution of 500 mg. ($3.5/10^3$ mol.) of Ia, 230 mg. $3.5/10^3$ mol.) of malononitrile and 650 mg. ($3.5/10^3$ mol.) of tributylamine dissolved in 5 ml. of absolute ethanol was treated as in the foregoing cases, 300 mg. of XXI was obtained.

The authors wish to take this opportunity to express their gratitude for the donation of a grant-in-aid for Scientific Research from the Ministry of Education and for financial assistance from the Sankyo Pharmaceutical Co., Ltd. The authors gratefully acknowledge

their debt to Dr. Y. Ikegami for his infrared spectral measurements and to Mr. A. Sato for his co-operation in carrying out the experiments.

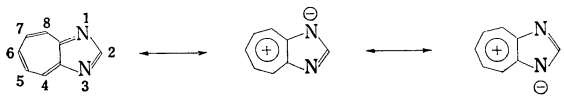
Department of Chemistry
Faculty of Science
Tohoku University
Katahira-cho, Sendai

*Synthesis and Reactions of 2, 6-Disubstituted 1, 3-Diazaazulene**

By Tetsuo NOZOE, Toshio MUKAI and Toyonobu ASAO

(Received January 16, 1962)

Since 1, 3-diazaazulene derivatives have been synthesized by the reaction of 2-methoxytropones with guanidine or thiourea[1-3], and also by the reaction of 2, 5-diaminotroponimine with formic or acetic acid[4], widespread theoretical interest in this series of compounds has been aroused among physical chemists, and calculations by the molecular orbital method have been carried out by Kon[5].



According to him, the electron densities of the 1- and 3-positions are much higher than those of the 2-, 4(8)-, 5(7)- and 6-positions of 1, 3-diazaazulene. In fact, as has been reported[6], 1, 3-diazaazulene has a large dipole moment, such as 4.03D in a benzene solution at 25°C. Furthermore, it has been reported that the substituents in the 2-position[2,3,7] can be easily replaced by nucleophilic reagents, as can those in the 4-[8], 5-[5] and 6-positions[10].

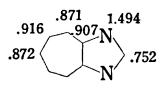
Since the findings concerning the electron density of 1, 3-diazaazulene as calculated by the MO method varied according to the manner of correction**, it is difficult to anticipate which substituent of the 2- or 6-position of 2, 6-disubstituted 1, 3-diazaazulene is most easily replaced by nucleophilic reagents.

The present series of experiments was undertaken to clarify this respect experimentally. First, several kinds of 2, 6-disubstituted 1, 3-diazaazulene were synthesized. By the condensation reaction with guanidine, tropolone methyl ethers with a nitro group[11], a bromine[12] or a chlorine[13] atom at the 5-position afforded 6-nitro (I), 6-bromo (II) and 6-chloro derivatives (III) of 2-amino-1, 3-diazaazulene respectively. I is soluble in an alkaline solution and shows a bathochromic shift in its ultraviolet spectrum in an alkaline medium compared with that in methanol (Fig. 1). This is due to the formation of an aci-form (Ia). The heating of 2-amino-6-nitro-1, 3-diazaazulene (I) with concentrated hydrochloric acid in a sealed tube at 130°C gives 2-amino-6-hydroxy-1, 3-diazaazulene (IV), while the more severe condition, heating at 200°C, affords 2, 6-dihydroxy-1, 3-diazaazulene (V). IV and V are soluble in acid

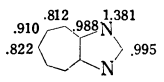
* Presented at the 8th Annual Meeting of the Chemical Society of Japan, Tokyo, April, 1955.

1) T. Nozoe, T. Mukai, K. Takase, I. Murata and K. Matsumoto, *Proc. Japan Acad.*, **29**, 452 (1953).
2) T. Nozoe, T. Mukai and I. Murata, *J. Am. Chem. Soc.*, **76**, 3352 (1954).
3) T. Nozoe, T. Mukai and I. Murata, *Proc. Japan Acad.*, **30**, 482 (1954).
4) T. Nozoe, M. Sato, S. Ito, K. Matsui and T. Matsuda, ibid., **29**, 565 (1953).
5) H. Kon, *Sci. Repts., Tohoku Univ., I*, **38**, 67 (1954).
6) Y. Kurita and S. Kubo, *J. Am. Chem. Soc.*, **79**, 5460 (1957).
7) I. Murata, This Bulletin, **33**, 56, 1367 (1960).
8) K. Matsumoto, Master's Thesis, Tohoku Univ., 1955.
9) I. Murata, This Bulletin, **34**, 580 (1961).
10) T. Nozoe, S. Ito, K. Matsui and S. Suzuki, unpublished data.

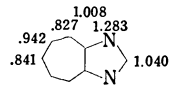
** The calculated results by three different corrections for the hetero-atomic Coulomb integral and the induction effect are as follows[5]:



Correction I



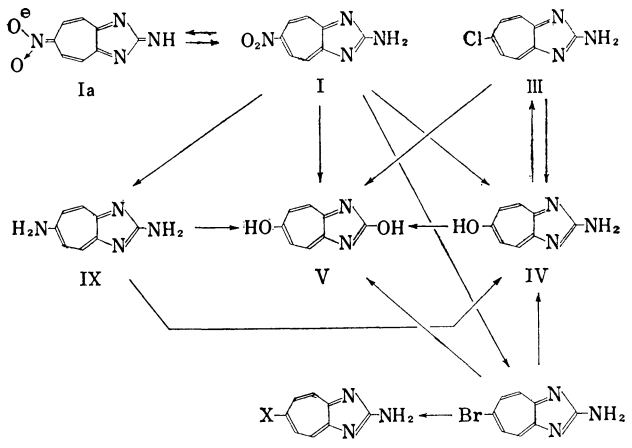
Correction II



Correction III

Correction I; $\delta\alpha$ Naza $=\beta$, no correction for induction.
Correction II; $\delta\alpha$ Naza $=\beta$, correction for induction effect on the two carbon atoms adjacent to an aza-nitrogen atom $=0.3\beta$.
Correction III; $\delta\alpha$ Naza $=0.5\beta$, correction for induction effect $\fallingdotseq 1/3\cdot\delta\alpha$ Naza.

11) T. Nozoe, Y. Kitahara, T. Ando and E. Kunioka, *Proc. Japan Acad.*, **27**, 231 (1951).
12) T. Nozoe, S. Seto, T. Ikemi and T. Arai, ibid., **27**, 102 (1951).
13) T. Sato, *J, Chem. Soc. Japan, Pure Chem. Sec.* (*Nippon Kagaku Zasshi*), **80**, 1171 (1959).



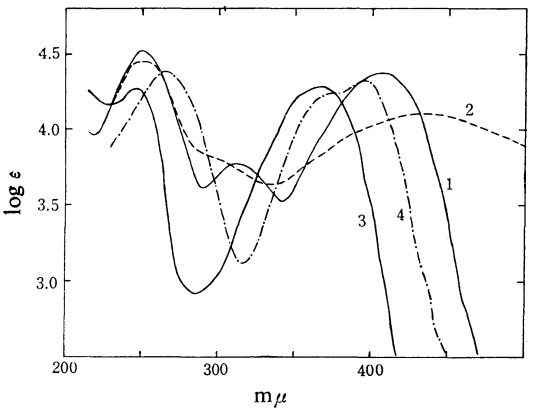


Fig. 1. Ultraviolet absorption spectra.
1, 2-Amino-6-nitro-1,3-diazaazulene (I) in methanol
2, I in 1 N NaOH
3, 2,6-Dihydroxy-1,3-diazaazulene (V) in methanol
4, V in 1 N NaOH

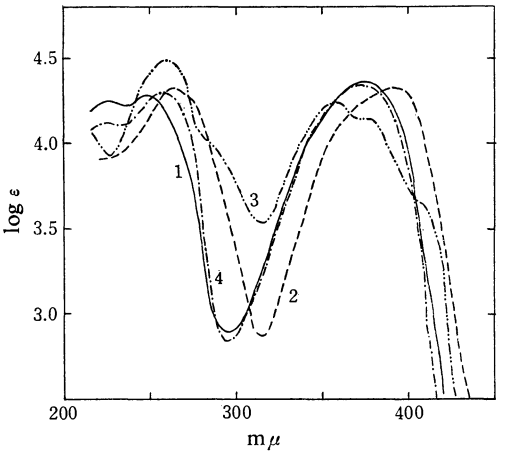


Fig. 2. Ultraviolet absorption spectra.
1, 2-Amino-6-hydroxy-1,3-diazaazulene (IV) in methanol
2, IV in 1 N NaOH
3, 2-Amino-6-methoxy-1,3-diazaazulene (VI) in methanol
4, 2-Amino-1-methylimidazolo[4, 5-d]-tropone (XV) in methanol.

and alkali, and their ultraviolet spectra shift to a longer wavelength region in an alkaline medium compared with those in methanol (Figs. 1 and 2). V does not form a picrate, but IV and the methylated compound of V do form picrates. I also gives 2-amino-6-bromo-1, 3-diazaazulene (II), although the yield is rather low, on heating with acetic acid saturated with hydrogen bromide in a sealed tube. The reaction of IV and phosphoryl chloride in the presence of pyridine affords 2-amino-6-chloro-1, 3-diazaazulene (III). Structural proof of both the halogenated products is given by their identification with the condensed products of 5-bromo- and 5-chloro-tropolone methyl ether and guanidine respectively. On refluxing in 6 N hydrochloric acid, II and III give a 2-amino-6-hydroxy compound IV, and heating both in concentrated hydrochloric acid in a sealed tube gives 2, 6-dihydroxy-1, 3-diaza-azulene (V). The bromine atom of II was replaced with methoxide, methylamine and dimethylamine, giving 6-methoxy (VI), 6-methylamino (VII) and 6-dimethylamino derivatives (VIII) of 2-amino-1, 3-diazaazulene respectively. VI is identical with one of the products obtained from the reaction of IV with diazomethane, as will be described later.

From these results, it is clear that the substituents in the 2- and 6-positions of 1, 3-diazaazulene suffer from the attach of nucleophilic reagents.

To establish the order of the reactivity to nucleophilic reagents of the substituents of the 2- or 6-position, however, it is neccessary to experiment by using 2, 6-disubstituted 1, 3-diazaazulene having the same substituents in the 2- and 6-positions. While any attempted synthesis of 2, 6-diamino-1, 3-diazaazulene by the reaction of II or III with ethanolic ammonia or liquid ammonia results only in the recovery of the starting material, the catalytic reduction of the 2-amino-6-nitro compound I in acetic acid using Pd-C as a catalyst is successful in giving 2, 6-diamino-1, 3-diazaazulene (IX). The heating of IX with concentrated hydrochloric acid in a sealed tube affords V, whereas the refluxing of IX in 6 N hydrochloric acid gives IV, in which the 6-amino group is only hydrolyzed.

2, 6-Dichloro-1, 3-diazaazulene (X) is obtained from 2, 6-dihydroxy-1, 3-diazaazulene (V) by treatment with phosphoryl chloride in the presence of pyridine, accompanying monochloro monohydroxy 1, 3-diazaazulene (XI). The same treatment of XI gives X. X and XI can also be converted to V by heating with concentrated hydrochloric acid, but the heating of X with 2 N acetic acid affords monochloro monohydroxy 1, 3-diazaazulene (XII), which is different from XI. Similarly, the reaction of X and methanolic ammonia gives, in a good yield, monoamino monochloro 1, 3-diazaazulene (XIII), which is different from 2-amino-6-chloro-1, 3-diazaazulene (III).

The structures of XI and XII are examined by comparing their ultraviolet spectra with those of 2-[3] and 6-hydroxy-1, 3-diazaazulene[10] respectively. There are some differences between the absorption curves of 2- and 6-hydroxy-1, 3-diazaazulene, as is shown in Fig. 3. The similarity of XI in the ultraviolet spectrum to that of the 2-hydroxy compound and the similarity of XII to the 6-hydroxy compound indicates that XI would be 6-chloro-2-hydroxy-1, 3-diazaazulene and XII, 2-chloro-6-hydroxy-1, 3-diazaazulene. In the same manner, XIII is ascertained to be 6-amino-2-chloro-1, 3-diazaazulene. In Fig. 4, the ultraviolet spectra of III, XIII and 2-[1] and 6-amino-1, 3-diazaazulene[4] are shown; the spectrum of XIII is more similar to that of the 6-amino compound than to that of the 2-amino compound. Incidentally, isomeric 2-amino-6-chloro-1, 3-diazaazulene (III) has an absorption curve similar to that of the 2-amino compound.

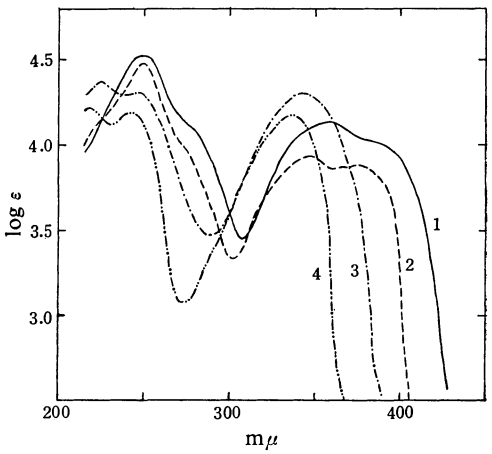
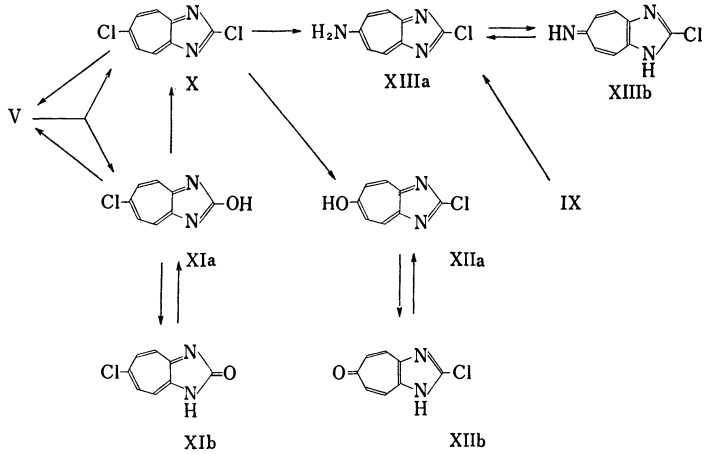


Fig. 3. Ultraviolet absorption spectra in methanol.
1, 6-Chloro-2-hydroxy-1, 3-diazaazulene (XI)
2, 2-Hydroxy-1, 3-diazaazulene
3, 2-Chloro-6-hydroxy-1, 3-diazaazulene (XII)
4, 6-Hydroxy-1, 3-diazaazulene

From this series of experiments, it is clear



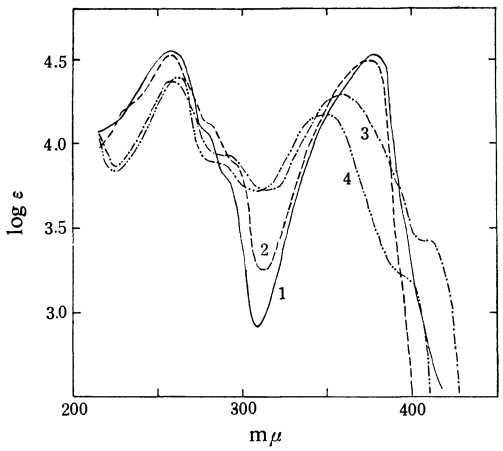


Fig. 4. Ultraviolet absorption spectra in methanol.
1, 6-Amino-2-chloro-1,3-diazaazulene (XIII)
2, 9-Amino-1, 3-diazaazulene
3, 2-Amino-6-chloro-1,3-diazaazulene (III)
4, 2-Amino-1,3-diazaazulene

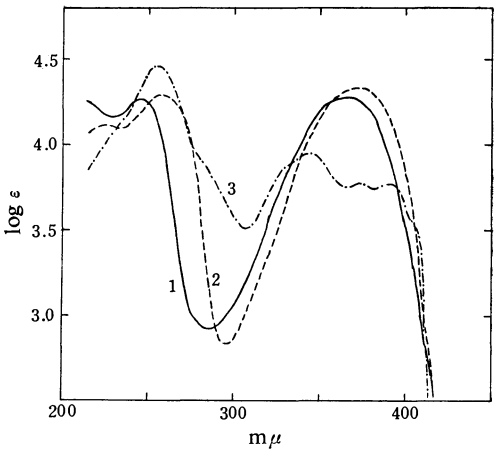
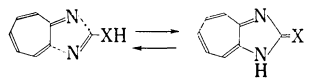


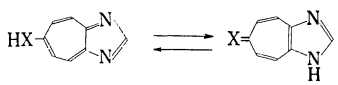
Fig. 5. Ultraviolet absorption spectra in methanol.
1, 2,6-Dihyroxy-1,3-diazaazulene (V)
2, 2-Amino-1-methylimidazolo[4,5-d]-tropone (XV)
3, 1-Methylcycloheptimidazol-2-one (XVI)

that nucleophilic substitution occurs preferentially at the 6-position rather than at the 2-position in 2, 6-disubstituted 1, 3-diazaazulene. In other words, the electron density at the 6-position is less than that at the 2-position of 2, 6-disubstituted 1, 3-diazaazulene.

Furthermore, it has been reported[3,5,10,14] that 2- or 6-hydroxy-1, 3-diazaazulene are present in the so-called lactim-lactam or keto-enol tautomerisms (A and B type: X=O) and that its tautomeric equilibrium tends towards the lactam or keto form (B type: X=O). It has also been reported that there are similar tautomerisms (A and B type: X=NH) in 2- and 6-amino-1,3-diazaazulene and that the imino form (B: X=NH) is preferred to the amino form (A: X=NH). Consequently, the ultraviolet spectra of XI, XII and XIII in Figs. 3 and 4 supported that their equilibrium tends to XIb, XIIb and XIIIb rather than to XIa, XIIa and XIIIa.



A type B type

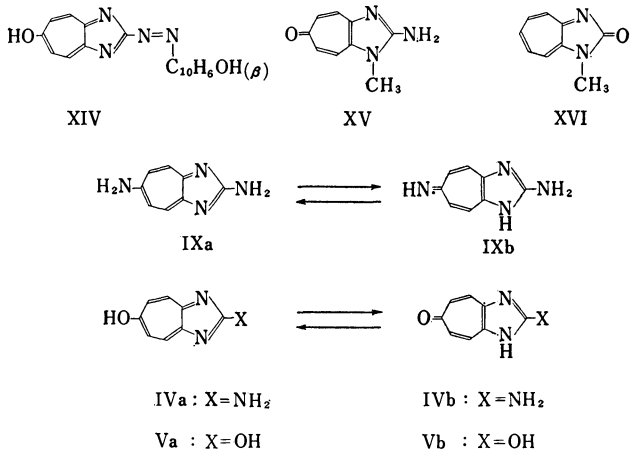


A type B type

It is also interesting to discuss the tautomerism of IV, V and IX. Although 2- or 6-amino-1, 3-diazaazulene is not diazotized[1,4], 2-amino-6-hydroxy-1, 3-diazaazulene (IV) and 2, 6-diamino-1, 3-diazaazulene (IX) are diazotized. The diazonium salt of IV couples with β-naphthol to give an azo-compound XIV. IX consumes only one equivalent of nitrous acid, while the Sandmeyer reaction of its diazonium salt gives 6-amino-2-chloro-1, 3-diazaazulene (XIII). Preferential diazotization of the 2-amino group of IX is also compatible with the fact that the electron density at the 2-position is higher than at the 6-position. This means that the tautomeric equilibrium of IX seems to be tend towards IXb rather than IXa.

Methylation of 2-amino-6-hydroxy-1, 3-diazaazulene (IV) with diazomethane affords two compounds, 6-methoxy-2-amino-1, 3-diazaazulene (VI) and 2-amino-1-methylimidazolo[4, 5-d]tropone (XV), in approximately a 1 : 4 ratio. The ultraviolet spectra of IV, VI and XV are shown in Fig. 2. The spectrum of IV is very similar to that of XV or 6-hydroxy-1, 3-diazaazulene, but it is different from that of VI. The infrared spectrum of XV exhibits a carbonyl band at 1663 cm^{-1}, and that of IV, at 1660 cm^{-1}. In Fig. 5, the ultraviolet spectra of 2, 6-dihydroxy-1, 3-diazaazulene (V), XV and 1-methylcycloheptimidazol-2-one[3] (XVI) are shown. The absorption curve of V is similar to that of XV rather than to that of XVI, and the infrared spectrum of V exhibits a carbonyl band at 1686 cm^{-1}. From these facts, the tautomeric equilibrium of IV and V seems to tend towards IVb and Vb respectively rather than towards IVa and Va.

14) I. Murata, *Sci. Rep. RITU*,. A-12, 271 (1960).



Experimental*

2-Amino-6-nitro-1, 3-diazaazulene (I). — To a suspension of 1 g. of 5-nitrotropolone methyl ether in 100 ml. of ethanol, a solution of 0.33 g. of potassium hydroxide (or 0.13 g. of sodium) and 0.56 g. of guanidine hydrochloride in 50 ml. of ethanol was added, and the mixture was refluxed for about 3 hr. The yellowish brown prisms which precipitated out were collected by filtration and recrystallized from acetic acid, giving 0.75 g. (75%) of I as yellow needles, m. p. over 300°C.

Found: C, 50.45; H, 2.92; N, 29.56. Calcd. for $C_8H_6O_2N_4$: C, 50.53; H, 3.18; N, 29.42%.

Picrate.—Organge prisms, turned to black from around 240°C.

Found: C, 39.42; H, 2.56; N, 23.82. Calcd. for $C_{14}H_9O_9N_7$: C, 39.82; H, 2.86; N, 23.39%.

2-Amino-6-bromo-1, 3-diazaazulene (II).—a) To a solution of 420 mg. of 5-bromotropolone methyl ether in 10 ml. of ethanol, a solution of 250 mg. of guanidine hydrochloride and 130 mg. of potassium hydroxide dissolved in 10 ml. of ethanol was added, and the mixture was refluxed for 2 hr. The yellow crystals which precipitated out were collected by filtration, washed with water and recrystallized from ethanol, affording 320 mg. of II as yellow prisms, which slowly changed to black from around 240°C.

Found: C, 43.28; H, 2.55; N, 18.45. Calcd. for $C_8H_6N_3Br$: C, 42.90; H, 2.70; N, 18.75%.

Picrate.—Orange yellow prisms, m. p. 262~263°C (decomp.).

Found: N, 18.58. Calcd. for $C_{14}H_9O_7N_6Br$: N, 18.54%.

b) After heating 50 mg. of I with 3 ml. of acetic acid saturated with hydrogen bromide in a sealed tube for 5 hr. at 90°C, the solid which precipitated out was dissolved in water. Neutralization of the solution with sodium hydrogen carbonate gave crystals, which were recrystallized from ethanol, giving II as yellow prisms, which slowly changed to black from around 240°C. The infrared spectrum of these crystals showed the same maxima as that of the sample obtained by method a).

2-Amino-6-chloro-1, 3-diazaazulene (III) — a) 2.5 g. of III was obtained from 2.8 g. of 5-chlorotropolone methyl ether by method a), by which II was obtained. Yellow prisms, gradually changing to black from around 247°C.

Found: C, 53.24; H, 3.68; N, 22.90. Calcd. for $C_8H_6N_3Cl$: C, 53.60; H, 3.36; N, 23.40%.

Picrate.—Yellow powder, slowly changing to black from around 280°C.

Found: N, 20.78. Calcd. for $C_{14}H_9O_7N_6Cl$: N, 20.56%.

b) A mixture of 90 mg. of 2-amino-6-hydroxy-1,3-diazaazulene (IV), 3 ml. of phosphoryl chloride and 0.15 ml. of pyridine was heated at 105°C for 2.5 hr. while being stirred. After the excess of phosphoryl chloride had been distilled off, the residue was poured onto ice. Yellow crystals soon separated out. The crude crystals were dissolved in diluted hydrochloric acid, treated with charcoal and neutralized with sodium hydrogen carbonate, giving 60 mg. of yellow micro needles. Recrystallization of these crystals from ethanol gave II as yellow prisms, which changed to black from around 247°C.

2-Amino-6-hydroxy-1, 3-diazaazulene (IV).—After heating 0.5 g. of I with 2 ml. of concentrated hydrochloric acid in a sealed tube for 12 hr. at 130°C, the mixture was evaporated to dryness on a steam bath. The residue was dissolved in a small amount of water and treated with charcoal. Neutralization of this solution with sodium hydrogen carbonate gave 330 mg. of yellow needles. Recrystallization from water afforded IV as yellow needles, which slowly changed to black from around 240°C.

Found: C, 53.20; H, 4.72; N, 23.27. Calcd. for $C_8H_7ON_3 \cdot H_2O$: C, 53.62; H, 5.06; N, 23.45%.

Picrate. — Yellow powder, slowly changing to black from around 250°C.

Found: C, 42.71; H, 3.40. Calcd. for $C_{14}H_{10} \cdot O_8N_6$: C, 43.08; H, 2.58%.

Reaction of IV with Phenylhydrazine.—A solution of IV and phenylhydrazine in ethanol was refluxed for 5 hr. in the presence of a small amount of acetic acid. After removing the solvent, the

* All melting points are uncorrected. The microanalyses were carried out by Mr. S. Ohyama and Miss A. Iwanaga, to whom the author's sincere gratitude is hereby extended.

residue was recrystallized from ethanol, affording red micro meedles, m. p. over 280°C.

Found: C, 67.03; H, 4.45. Calcd. for $C_{14}H_{13}N_5$: C, 66.91; H, 5.21%. Calcd. for $C_{14}H_{11}N_5$: C, 67.45; H, 4.45%.

Ultraviolet; λ_{max}^{MeOH} mμ (log ε): 250 (4.38), 300~315 (4.17), 416 (4.42).

2,6-Dihydroxy-1,3-diazaazulene (V).—A solution of 0.5 g. of I in 3 ml. of concentrated hydrochloric acid was heated in a sealed tube for 24 hr. at 200°C. The black material which separated out was removed by filtration, and the filtrate was evaporated to dryness. Recrystallization of the residue from water afforded 300 mg. of V as yellow needles, m. p. over 300°C.

Found: C, 52.98; H, 4.84; N, 15.74. Calcd. for $C_8H_6O_2N_2 \cdot H_2O$: C, 53.33; H, 4.48; N, 15.55%.

Diacetate.—Pale yellow needles, m. p. over 300°C.

Found: N, 12.67. Calcd. for $C_{12}H_{10}O_4N_2$: N, 12.61%.

Dimethyl Derivative.—V was methylated with diazomethane in the mixture of methanol and ether, giving a dimethyl derivative as yellow needles, m. p. 254~255°C (decomp.).

Found: N, 14.74. Calcd. for $C_{10}H_{10}O_2N_2$: N, 14.68%.

Picrate of Dimethyl Derivative.—Yellow needles, m. p. 240~241°C (decomp.).

Found: N, 16.70. Calcd. for $C_{16}H_{13}O_9N_5$: N, 16.63%.

2-Amino-6-methoxy-1,3-diazaazulene (VI).—A mixture of 150 mg. of II and 80 mg. of sodium methoxide in 20 ml. of absolute methanol was refluxed for 6 hr. After the mixture had been cooled, 50 mg. of II was recovered by filtration, was and the filtrate passed through an alumina column. Crystals obtained from the effluent were recrystallized from ethanol, giving VI as yellow needles, m. p. 237~238°C (decomp.).

Found: C, 61.68; H, 5.24; N, 23.90. Calcd. for $C_9H_9ON_3$: C, 61.70; H, 5.18; N, 23.99%.

Picrate.—Yellow powder, m. p. 266~267°C. (decomp.).

Found: N, 20.22. Calcd. for $C_{15}H_{12}O_8N_6$: N, 20.79%.

2-Amino-6-methylamino-1,3-diazaazulene (VII). After heating a mixture of 100 mg. of II, 40 mg. of methylamine hydrochloride, 30 mg. of sodium methoxide and 1.5 ml. of absolute methanol in a sealed tube at 160°C for 6 hr., an orange solid was obtained by evaporating the solvent. This solid was dissolved in methanol and passed through a column of ion-exchange resin (Amberite IRA-410). 40 mg. of VII was obtained as orange yellow prisms, m. p. 264~265°C (decomp.) (from ethanol).

Found: C, 56.24; H, 6.24; N, 29.31. Calcd. for $C_9H_{10}N_4 \cdot H_2O$: C, 56.23; H, 6.29; N, 29.15%.

2-Amino-6-dimethylamino-1,3-diazaazulene(VIII).—The reaction of II with dimethylamine gave VIII as orange yellow prisms, which slowly changed to black from around 240°C (from water).

Found: C, 63.28; H, 6.20; N, 29.89. Calcd. for $C_{10}H_{12}N_4$: C, 63.81; H, 6.43; N, 29.77%.

2,6-Diamino-1,3-diazaazulene (IX).—A solution of 500 mg. of I dissolved in 20 ml. of acetic acid was submitted to hydrogenation in the presence of 200 mg. of 5% Pd-C. 180 ml. of hydrogen was absorbed. The solvent was distilled off under reduced pressure, and the resulting reddish crystalline was dissolved in ethanol and passed through a column of ion-exchange resin (Amberlite IR-4B). The ethanol was evaporated off from the elute, and the residue was sublimed under reduced pressure. Recrystallization of the sublimate from water afforded 170 mg. of IX as yellow silky needles, m. p. over 300°C.

Found: C, 59.99; H, 5.05; N, 34.56. Calcd. for $C_8H_8N_4$: C, 59.98; H, 5.03; N, 34.98%.

Bis-picrate.—Yellow powder, m. p. over 300°C.

Found: N, 22.71. Calcd. for $C_{20}H_{14}O_{14}N_{10}$: N, 22.65%.

Dihydrochloride.—Pale yellow prisms, m.p. over 300°C.

Found: N, 24.26. Calcd. for $C_8H_8N_4 \cdot 2HCl$: N, 24.04%.

2,6-Dichloro-1,3-diazaazulene (X) and 6-Chioro-2-hydroxy-1,3-diazaazulene (XI).—A mixture of 270 mg. of V, 7 ml. of phosphoryl chloride and 0.9 ml. of pyridine was stirred for 3 hr. at 110°C. The excess of phosphoryl chloride was distilled off under reduced pressure, and the residue was poured onto ice. The solution was adjusted to a slightly acidic state with sodium hydrogencarbonate and extracted with chloroform. The chloroform was then removed, the residue was redissolved in benzene, and the benzene solution was passed through an alumina column. The benzene was distilled off from the eluate, and the residue was recrystallized from benzene, affording 110 mg. of 2,6-dichloro-1,3-diazaazulene (X) as colorless needles, m. p. 226~227°C (decomp.).

Found: C, 48,97; H, 2.36; N, 14.38. Calcd. for $C_8H_4N_2Cl_2$: C, 48.27; H, 2.03; N, 14.08%.

After the chloroform extraction, the water layer was adjusted to a slightly alkaline state with sodium hydrogen carbonate, affording yellow needles. Recrystallization of the crystals from water gave 80 mg. of 6-chloro-2-hydroxy-1,3-diazaazulene (XI), which gradually changed to black from around 240°C.

Found: C, 53.12; H, 3.21; N, 15.71. Calcd. for $C_8H_5ON_2Cl$: C, 53.21; H, 2.79; N, 15.51%.

2-Chloro-6-hydroxy-1,3-diazaazulene (XII).—A mixture of 50 mg. of X, 4 ml. of 2 N acetic acid and 1 ml. of ethanol was refluxed for 1.5 hr. Thirty milligrams of colorless needles were obtained by cooling the reaction mixture in an ice box. Recrystallization of the crystals from water gave XII as colorless needles, m. p. 237~237.5°C (decomp.).

Found: C, 52.79; H, 3.21; N, 15.52. Calcd. for $C_8H_5ON_2Cl$: C, 53.21; H, 2.79; N, 15.51%.

6-Amino-2-chloro-1,3-diazaazulene (XIII).—a) The heating of 40 mg. of X in 2 ml. of methanol saturated with ammonia in a sealed tube at 100°C for 1 hr. afforded 35 mg. of yellow crystals. The crystals were dissolved in dilute hydrochloric acid and neutralized with a sodium hydrogencarbonate solution, giving XIII as yellow needles, m. p. over 300°C.

Found: C, 53.46; H, 3.34; N, 23.47. Calcd. for $C_8H_6N_3Cl$: C, 53.60; H, 3.36; N, 23.40%.

b) Fifty milligrams of IX dissolved in 0.6 ml. of

acetic acid was diazotized with sodium nitrate, and the reaction mixture was poured into a solution of 50 mg. of cuprous chloride in 0.3 ml. of concentrated hydrochloric acid. The mixture was adjusted to a slightly alkaline state with sodium hydrogencarbonate, affording a brown solid. The solid was extracted with ethanol continuously, and yellow crystals were obtained. Recrystallization of the crystals from ethanol gave yellow needles, m. p. over 290°C. The ultraviolet and infrared spectra of these crystals completely agreed with those of XIII obtained by procedure a).

6-Hydroxy-2-(2-hydroxy-1-naphthyl)-azo-1, 3-diazaazulene (XIV).—One hundred milligrams of IV dissolved in 2 ml. of 6 N hydrochloric acid were diazotized with a solution of 50 mg. of sodium nitrate dissolved in 0.4 ml. of water. The reaction mixture was slowly poured into a solution of 90 mg. of β-naphthol dissolved in 3 ml. of a 3 N sodium hydroxide solution. The color of the mixture immediately turned to violet, and a deep-colored solid was salted out. The solid was then dissolved in water and neutralized with dilute hydrochloric acid, giving 60 mg. of violet crystals. Recrystallization of these crystals from pyridine afforded XIV as brownish violet needles, m. p. over 300°C.

Found: C, 68.13; H, 3.70. Calcd. for $C_{18}H_{12}O_2N_4$: C, 68.35; H, 3.82%.

Ultraviolet: λ_{max}^{MeOH} mμ (log ε): 225 (4.71), 290 (4.20), 355 (418), 510 (4.59).

Reaction of IV with Diazomethane.—To a solution of 300 mg. of IV dissolved in 6 ml. of methanol, 25 ml. of diazomethane ether solution prepared from 2.5 g. of *N*-nitrosomethylurea was added and left to stand overnight. The crystals which precipitated out were filtered and washed with benzene, affording 190 mg. of crystals. Recrystallization of the crude crystals from ethanol afforded XV as yellow prisms, which gradually changed to black from around 290°C.

Found: C, 55.92; H, 5.73; N, 21.37. Calcd. for $C_9H_9ON_3 \cdot H_2O$: C, 55.95; H, 5.74; N, 21.75%.

Picrate.—Yellow needles, gradually changing to black from around 240°C.

Found: C, 44.78; H, 2.74; N, 21.18. Calcd. for $C_{15}H_{12}O_8N_6$: C, 44.56; H, 2.99; N, 20.79%.

The solvent was distilled off from the original reaction filtrate, and the residue was dissolved in benzene and passed through an alumina column. Benzene was removed from the eluate, leaving 50 mg. of crystals. Recrystallization of these crystals from ethanol afforded yellow needles, m. p. 236°C (decomp.), which showed no depression of melting point on admixture with VI.

The authors gratefully acknowledge the financial help from the Ministry of Education of a grant-in-aid for scientific research and from the Sankyo Co., Ltd., for part of the expenses of the present work. The authors also thank Dr. I. Murata for much helpful discussions.

Department of Chemistry
Faculty of Science
Tohoku University
Katahira-cho, Sendai

Condensation of the Triad System with Carbonyl Compounds. I. Condensation of Ethyl Itaconate with Ketones[*1]

By Chiaki KATSUTA[*2] and Noboru SUGIYAMA

(Received September 16, 1961)

Although the chemical behavior of itaconic acid has already been studied in detail, there has yet been no report on the condensation of its active methylene group with carbonyl compounds other than the classical paper by Fittig and Bock[1]; this lack is a result of the isomerisation of the ester in a strongly basic media to a mixture of its isomers[2].

From the close structural resemblance of the acid to succinic acid and alkylidenesuccinic acid (A) the ethyl ester of itaconic acid(I) was

$$(R_1R_2)C{=}C(H_2C{-}COOH){-}COOH \qquad (R_1R_2)C{=}C(H_2C{-}COOH){-}COOH$$

(A) (B)

expected to condense with carbonyl compounds by Stobbe condensation[3] and to afford new fulgenic acids (B). However, Fittig et al. obtained, by condensation of I (a molecule) with benzaldehyde (two molecules) in the presence of

*1 This paper is a part of a doctoral thesis and was partly presented at the Symposium of the Organic Reaction Mechanism, Shirahama, October, 1960.

*2 Present Address: Department of Agricultural Chemistry, Tokyo University of Education, Meguro-ku, Tokyo.

1) R. Fittig, *Ann.*, **331**, 151 (1904); R. Fittig and K. Bock, ibid., **331**, 174 (1904).

2) E. R. Alexander, "Principles of Ionic Organic Reactions", John Wiley & Sons, Inc., New York (1950), p. 286.

3) W. S. Johnson and C. H. Daub, "Organic Reactions", **6**, 1 (1951).

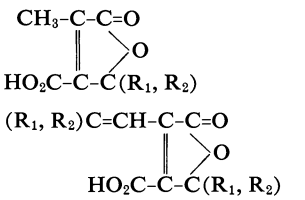
sodium ethoxide, two isomeric heptenedilactones which can not be explained by Stobbe condensation in a straightforward manner. Their findings supported the possibility of the condensation of I with other carbonyl compounds and suggested that I behaves quite differently from ethyl alkylidenesuccinats (A).

In this paper, the novel reactions of I with ketones are described.

Resuits and Discussion

The condensation of I with acetone was conducted in the presence of alcohol-free sodium ethoxide in an ice bath or an ice-salt bath. In the ice bath, the condensation reaction afforded two acidic products, II (R_1=R_2=CH_3) and III(R_1=R_2=CH_3), while in the ice-salt bath the reaction gave only III(R_1=R_2=CH_3).

I also condensed with cyclohexanone. The reaction afforded an acid, II [R_1, R_2=$-(CH_2)_5-$], in the ice bath, and, in the ice-salt bath, two acidic products, II [R_1, R_2=$-(CH_2)_5-$] and III [R_1, R_2=$-(CH_2)_5-$].



II

III

The yields, properties and analytical data of these products are shown in Tables IV, V and VI.

The II products were monobasic acids and gave methyl esters and anilides by ordinary procedures.

Structures.—The structures of the II products were determined to be as follows:

i) The analytical data (Table VII) showed that they were condensation products of I(C_5)

Table I. Infrared absorption spectra (in KBr)

Compound	γ-Lactone C=O	Carboxyl C=O	C=C
α, γ, γ-Trimethylaconic acid (II, R_1=R_2=CH_3)	1725	1700(sh)	1650
Methyl α, γ, γ-trimethylaconate	1765	1720[a]	1650
Anilide of α, γ, γ-trimethylaconic acid	1755	1693[b] 1540	1664
α-Methyl-γ, γ-pentamethyleneaconic acid (II, R_1, R_2=$-(CH_2)_5-$)	1725	1690(sh)	1650
Methyl α-methyl-γ, γ-pentamethyleneaconate	1745	1706[a]	1640
Anilide of α-methyl-γ, γ-pentamethyleneaconic acid	1750	1690[b] 1550	1660
Aconic acid	1723	1706(sh)	1640
Lichesterinic acid*	1740	1705(sh)	1650

(sh) Shoulder, a) Ester C=O band, b) Amide bands

Table II. Ultraviolet absorption (in EtOH)

Compound	log ε/mμ 210	220	230	240
α, γ, γ-Trimethylaconic acid (II, R_1=R_2=CH_3)	3.93	4.04	4.03	3.85
Methyl α, γ, γ-trimethylaconate	—	4.05	4.12	4.00
α-Methyl-γ, γ-pentamethyleneaconic acid (II, R_1, R_2=$-(CH_2)_5-$)	3.93	4.04	4.07	3.99
Methyl α-methyl-γ, γ-pentamethyleneaconic acid	—	4.06	4.14	4.11
Lichesterinic acid[5] (II, R_1=H, R_2=n-$C_{13}H_{27}$)	3.82	4.02	4.07	3.80
Methyl α-methylaconate (II, R_1=R_2=H)	3.87	4.01	4.04	3.88

* The Sample was given by Professor Shoji Shibata. The authors want to appreciate him.

Table III. Infrared spectra of α-alkylidenemethylaconic acids (III) (cm^{-1})

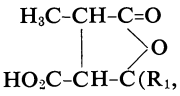
Compound	γ-Lactone C=C	COOH C=O	C=C
α-Isopropylidenemethyl-γ, γ-dimethylaconic acid (in KBr)	1720	—	1660 1610
α-Isopropylidenemethyl-γ, γ-dimethylaconic acid (chloroform solution)	1753	1690	1650 1610
α-Cyclohexylidenemethyl-γ, γ-pentamethyleneaconic acid (in KBr)	1772	1710	1685 1620

with molecules of acetone and cyclohexanone respectively.

ii) The infrared spectrum of these methyl esters and anilides indicated the presence of C=C and of α,β-unsaturated γ-lactone C=O bands (Table I). In free acids, II showed broad bands with a shoulder near 1725 cm^{-1}, bands which were attributable to α,β-unsaturated γ-lactone C=O[4] and carboxyl C=O.

iii) The close resemblance of ultraviolet spectrum of II and of their methyl esters to those of metaconic acid, aconic acid,and more especially, lichesterinic acid (II, R_1=H, R_2=*n*-$C_{13}H_{27}$)[5] and ethyl ester of α-methylaconic acid (II, R_1=R_2=H)[5] tended to confirm the presence of a substituted O=C-C=C-C=O (trans) conjugated system (Table II).

iv) II [R_1=R_2=CH_3 and R_1, R_2=-$(CH_2)_5$-] afforded a corresponding paraconic acid(IV) by reduction with a sodium amalgam. The infrared spectrum of IV [R_1=R_2=CH_3 and R_1, R_2=-$(CH_2)_5$-] well agreed with those of γ,γ-dimethyl paraconic acid and γ,γ-pentamethyleneparaconic acid.



IV

v) The NMR spectrum of the methyl ester of II(R_1=R_2=CH_3) showed three peaks, corresponding to $COOCH_3$, =C-CH_3 and $C(CH_3)_2$[6] (Fig. 1).

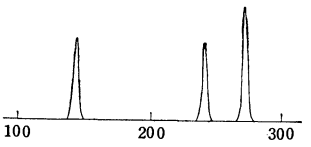


Fig. 1. NMR of methyl α,γ,γ-trimethylaconate.

From the following evidence, the structures of the III products were determined:

i) The analytical data of the III products [R_1=R_2=-CH_3 and R_1, R_2=-$(CH_2)_5$-] showed that I condensed with two molecules of the corresponding ketone.

ii) The infrared spectrum of the III products suggested that they were conjugated dienoic acid, which has an α,β-unsaturated γ-lactone ring (Table III).

iii) The ultraviolet spectrum of the III products showed end absorption and broad bands near 277 mμ (both log ε = 3.67). This suggested

TABLE IV. CONDENSATION REACTIONS

Exp.	Ester, g.	Ketone, g.	Cooling media	Time[a]
a	I, 13.6	Acetone, 8.8	Ice bath	Overnight
b	V, 13.6	Acetone, 8.8	Ice bath	Overnight
c	VI, 13.6	Acetone, 8.8	Ice bath	Overnight
d	I, 18.6	Acetone, 11.6	Ice-salt bath	Overnight
e	I, 18.6	Cyclohexanone, 19.6	Ice-bath	Overnight
f	I, 18.6	Cyclohexanone, 22.5	Ice-salt bath	Overnight[b]

a) Times for keeping at room temperature.
b) The reaction mixture was allowed to stand overnight in ice-salt bath.

TABLE V. CONDENSATION PRODUCTS

Exp.	Products	Yields, %	M. p., °C	Properties
a	II	65.6	231~232	Colorless acid, sublimable
	III	23.0	131~132	Colorless acid, sublimable
b	II	9.7		
c	II	13.7		
d	III	62.0		
e	II	47.2	276 (decomp.)	Colorless acid, sublimable
f	II	40.1		
	III	11.9	137~138	Colorless acid

4) The C=O bands of saturated or α,β-unsaturated γ-lactone β-carboxylic acids were of exceptionally lower frequencies than those acids in the normal saturated or α,β-unsaturated γ-lactone C=O region. This spectral behavior may be attributed to intermolecular hydrogen bonding between carboxyl OH and lactone C=O (cf. L. J. Haynes and J. R. Plimmer, *Quart. Revs.*, 14, 307 (1960); Y. Hirata, *J. Japan. Chem.* (*Kagaku-no-Ryoiki*), Supplement, 42, 76 (1961).

5) E. E. Van Tamelen, C. E. Osborne and S. R. Bach, *J. Am. Chem. Soc.*, 77, 4625 (1955).

6) N. F. Chemberlain, *Anal. Chem.*, 31, 56 (1959).

7) The normal frequencies of the lactone C=O(1772 cm^{-1}) of III[R_1, R_2=-$(CH_2)_5$-] suggested the absence of intermolecular hydrogen bonding between carboxyl OH and lactone C=O by bulky substituents.

TABLE VI. ANALYTICAL DATA*

Compound	Formula	Found, % C	Found, % H	Calcd., % C	Calcd., % H
II, R_1=R_2=CH_3	$C_8H_{10}O_4$	56.52	5.94	56.47	5.88
Methyl ester of II	$C_9H_{12}O_4$	58.85	6.55	58.69	6.57
Anilide of II	$C_{14}H_{15}O_3N$	68.53	6.04	58.55	6.16
		N 5.70		N 5.71	
III, R_1=R_2=CH_3	$C_{11}H_{14}O_4$	62.80	6.54	62.84	6.71
II, R_1, R_2=$-(CH_2)_5-$	$C_{11}H_{14}O_4$	62.65	6.68	62.84	6.71
Methyl ester of II	$C_{12}H_{16}O_4$	64.22	7.01	64.27	7.19
Anilide of II	$C_{17}H_{19}O_3N$	N 4.91		N 4.91	
III, R_1, R_2=$-(CH_2)_5-$	$C_{17}H_{22}O_4$	70.19	7.56	70.32	7.64

* We are indebted to Dr. Haruo Homma of the Institute of Physical and Chemical Research for these analyses.

that they were mostly substituted conjugated dienoic acids[8].

iv) The NMR spectrum of III [R_1=R_2=CH_3] showed the presence of COOH, $C(CH_3)_2$ and $CH{=}C(CH_3)_2$[9] (Fig. 2).

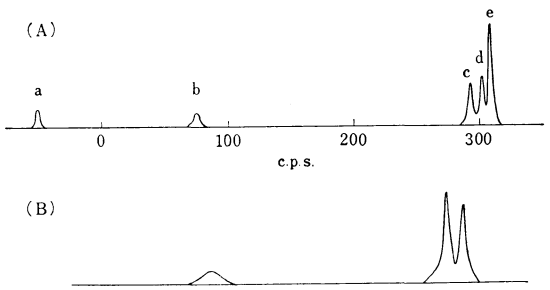
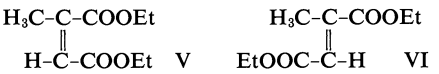


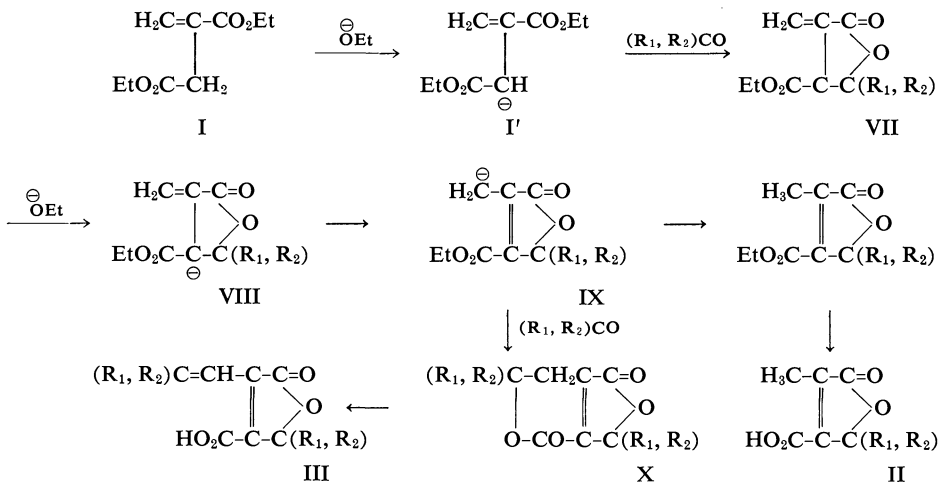
Fig. 2. NMR spectrum

(A) α-Isopropylidenemethyl-γ, γ-dimethylaconic acid (III)
(B) β-Methylcrotonic acid

Reaction Mechanism.—However, I condensed readily with the ketones, its isomerides, ethyl citraconate (V) and ethyl mesaconate (VI), which were expected to be produced from I by a prototropic change of its triad system (CH–C=CH) in the reaction condition; it also dully condensed with acetone and afforded II(R_1=R_2=CH_3) in poor yields. From this fact and the structure of II, it is clear that I condensed with ketones at its active methylene group and that the isomerisation of I to the isomerides is negligible under the reaction conditions.



The formation of II and III can not simply be explained by Stobbe condensation but only by the following mechanism:



8) K. Hirayama, "Jikken Kagaku Koza", Vol. I-1, Ed. by Chem. Soc. of Japan, Maruzen Co., Tokyo, (1957) p. 125.

9) L. M. Jackman, "Application of Nuclear Magnetic Resonance Spectroscopy in Organic Chemistry", Pergamon Press, London (1959), p. 120. From the resemblance of this NMR to that of β-crotonic acid [S. Fujiwara et al., This Bulletin, 33, 428 (1960)], the peaks b(broad), c and d are attributed to protons of =CH-, cis-methyl and trans-methyl of $=C-CH=C(CH_3)_2$ respectively.

In this process, the formation of II is explained by a mechanism similar to that employed by Stacy et al.[10] to account for the condensation of ethyl oxaloacetate with carbonyl compounds. The change of anion VIII to anion IX is a tautomerism of the triad system. Moreover, the formation of III was explained by the extended Stobbe condensation[11] of anion IX with the ketones.

By this reaction mechanism, the formation of Fittig's heptenedilactones may be explained. The dilactone X and Fittig's heptenedilactone will be reported on in the near future.

Experiments

Ethyl Itaconate (I).—I was prepared by the conventional procedure from itaconic acid, using hydroquinone as a polymerisation inhibitor without isomerisation[12]; b. p., 118°C/20 mmHg and n_D^{20}= 1.4383 (b.p. 117.5°C/20 mmHg, and n_D^{20}=1.4377[12]).

Ethyl Citraconate (V).—V was prepared from citraconic anhydride[13] by the ordinary procedure without isomerisation; b. p., 121°C/20 mmHg and n_D^{20}=1.4440 (b. p. 122°C/20 mmHg, and n_D^{20}=1.4442[12]).

Ethyl Mesaconate (VI).—VI was prepared from mesaconic acid[14] by the ordinary procedure without isomerisation; b. p., 118°C/20 mmHg and n_D^{20}=1.4485 (b.p. 118°C/20 mmHg, and n_D^{20}=1.4488[12]).

Condensation of the Esters with Ketone. General Procedure.—Alcohol-free sodium ethoxide was prepared by Fittig's method[15] in a 300 ml. three-necked flask. The flask was fitted with a dropping funnel and a reflux condenser, each protected by calcium chloride tubes, and with a mercury-sealed mechanical stirrer. The molar ratio of the sodium ethoxide, the ester and the ketone was 2 : 1 : 2. The flask was cooled in an ice or ice-salt bath. The mixture of the ester and the ketone was dropped from the funnel into the stirred suspension of sodium ethoxide in ether over a period of one hour. After the addition of the mixture and an additional two hours' cooling, the flask was allowed to stand overnight at room temperature. The reaction mixture was dissolved in water (150 ml.), and the resulting aqueous solution was extracted with ether (50 ml.) several times. The aqueous layer was acidified with excess hydrochloric acid (1 : 1); then the condensation products, which separated as an oil or slurry, were extracted by ether and purified according to the usual procedure. The details of these reactions, products and analytical data are shown in Tables 4, 5 and 6.

Aconic Acid.—Aconic acid was prepared from itaconic acid by the method of Champbell[16].

Methyl α,γ,γ-Trimethylaconate.—α,γ,γ-Trimethylaconic acid (II, R_1=R_2=CH_3) 1.70 g. was esterified by diazomethane[17], and the ester was obtained in the form of colorless prisms (1.45 g.) (from light petroleum); m. p., 30~31°C.

Methyl α-Methyl-γ,γ-pentamethyleneaconate.—The ester was prepared from α-methyl-γ,γ-pentamethyleneaconic acid (II, R_1, R_2=$-(CH_2)_5-$) 0.51 g. and diazomethane, in the form of colorless prisms (from light petroleum), 0.45 g., m. p., 93~94°C.

Anilide of α,γ,γ-Trimethyl Aconic Acid.—The acid (1.05 g.) was converted to the anilide by the ordinary procedure. Colorless prisms (from ethanol), 0.92 g.; m. p., 187~188°C.

Anilide of α-Methyl-γ,γ-pentamethyleneaconic Acid.—From the acid (1.00 g.), the anilide (0.73 g.) was obtained in the form of colorless prisms (from ethanol); m. p., 182~183°C.

α,γ,γ-Trimethylparaconic Acid (IV, R_1=R_2=CH_3).—α,γ,γ-Trimethylaconic acid (1.54 g.) was suspended in water (20 ml.), dissolved by neutralization with a 10% sodium hydroxide solution, and then stirred with a 1% sodium amalgam (53 g.) for 10 hr. at room temperature. The aqueous layer was separated and was acidified with cold 1 : 1 hydrochloric acid in ice bath, and then extracted with three portions (10 ml.) of ether. The acidic products were thoroughly extracted with a saturated sodium bicarbonate solution. After careful acidification, extraction with ether yielded the acid as a colorless solid (0.77 g.) (m. p., 186~189°C) that crystallized from acetonitrile as colorless scales; m. p., 191~192°C.

α-Methyl-γ,γ-pentamethyleneparaconic Acid.—This acid was obtained by reduction of α-methyl-γ,γ-pentamethyleneaconic acid (II) (0.52 g.) as above; 0.38 g.; in the form of colorless scales (from ethyl acetate); m. p., 196~197°C.

γ,γ-Dimethylparaconic acid.—This acid was prepared by the lactonization[18] of teraconic acid, obtained by Stobbe condensation of ethyl succinate and acetone[19]. Colorless scales (from acetonitrile); m. p., 173~174°C.

γ,γ-Pentamethyleneparaconic acid.—This acid was prepared by the method of Robinson[20] from the Stobbe condensation of ethyl succinate with cyclohexanone. Colorless scales (from acetonitrile); m. p., 184~185°C.

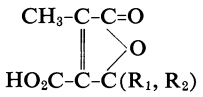
Measurements.—The ultraviolet spectra were determined with a Hitachi ESP-2 spectrophotometer. Infrared measurements were made with a Nihon Bunko IR-S and a 301 spectrophotometer. NMR measurements were made with a Varian V 4300 spectrometer (56.4 Mc) using a 10% chloroform solution with toluene as the internal standard.

Summary

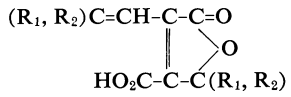
In the presence of sodium ethoxide, ethyl itaconate condensed with ketones (acetone and cyclohexanone) at the terminal carbon atoms of its triad system without any appreciable

10) G. W. Stacy et al., *J. Am. Chem. Soc.*, **74**, 999 (1952); **79**, 1451 (1957).
11) H. J. F. Loewenthal and R. Pappo, *J. Chem. Soc.*, **1952**, 4799.
12) E. H. Coulson and G. A. R. Kon, ibid., **1932**, 2568.
13) "Organic Syntheses", Col. Vol., 2, (1948), p. 140.
14) Ibid., Col. Vol. 2 (1948), p. 382.
15) R. Fittig and N. Petkow, *Ber.*, **35**, 4322 (1909).
16) N. R. Champbell and J. H. Hunt, *J. Chem. Soc.*, **1947**, 1176.
17) "Organic Syntheses", Vol. 36, (1956), p. 16.
18) R. Fittig and B. Frost, *Ann.*, **226**, 365 (1884).
19) W. Rose, ibid., **220**, 254 (1883).
20) R. Robinson et al., *J. Chem. Soc.*, **1941**, 582.

isomerisation and afforded novel compounds, α-methyl-γ, γ-disubstituted aconic acids (C) and α-alkylidenemethyl - γ, γ - disubstituted aconic acids (D).



C



D

The chemical structures of C and D were determined by ultraviolet, infrared, NMR spectra etc.

A reaction mechanism has been proposed (p. 1197).

The authors wish to express their thanks to Professor Koji Nakanishi for his helpful advice; to Professor Tatsuyoshi Kobayashi, who kindly provided itaconic acid for the writers' use, and to Mr. Takashi Kubota, who helped in part of this work.

Department of Chemistry
Tokyo University of Education
Otsuka, Tokyo

Dielectric Behavior of Hydrated Crystals. IV. Cupric Formate Tetrahydrate, $Cu(HCO_2)_2 \cdot 4H_2O$

By Hideko KIRIYAMA (née IBAMOTO)

(Received January 20, 1962)

As part of the studies of the dielectric properties of salt hydrate crystals[1], a single crystal of cupric formate tetrahydrate, $Cu(HCO_2)_2 \cdot 4H_2O$, has now been examined. The crystal has a predominant layer structure[2] in which two non-equivalent water molecules are sandwiched between $\{Cu(HCO_2)_2\}_\infty$ layers. One kind of water molecule coordinates to a copper atom directly, but the other does not. The results of the structure analysis by X-rays suggest that the two kinds of water molecules are linked together by weak hydrogen bonds. It was considered that the crystal might have characteristic dielectric properties with a large anisotropy because of the peculiar arrangement of the water molecules.

This substance undergoes a solid phase transition at $-36°C$ which is accompanied by a sudden change in the permittivity. The large dielectric dispersion and absorption observed above the transition temperature can be ascribed to the dipole orientation of the water molecules within the crystal lattice. A further absorption at much lower frequencies is also found for one particular direction of the single crystal. It may be suggested that this low frequency absorption is associated with lattice imperfections in the hydrogen-bonded systems.

In respect to the motion of the water molecules, definite information can be obtained from the results of proton magnetic resonance studies[3].

Experimental

The material was prepared by dissolving basic cupric carbonate in a dilute formic acid solution which had been made from cupric chloride and potassium carbonate, while the pure polycrystalline salt was obtained by several recrystallizations from cold aqueous water solution. A large single crystal was grown from a seed crystal in a silightly acidic solution. The crystal was cut into sections about 1.5 mm. thick and $1.5 \times 1.5\ cm^2$ in area; the main faces of the two square plates were parallel to (0 1 0) and (0 0 1) respectively, and the other was 11°5′ (i.e. the monoclinic angle β, 101°5′, minus 90°) out of (1 0 0). Considerable care in cutting and grinding the crystal was necessary because of the perfect cleavage parallel to (0 0 1).

The specimen was inserted directly between the platinum-coated electrodes of a parallel-plate condenser. The condenser was mounted in a cylindrical glass container placed in an acetone bath or liquid nitrogen bath of a large Dewar flask. By the careful addition of powdered dry ice into the acetone bath or by controlling the electric current of a heater wound around the cell, the temperature was kept constant within 0.2°C. Since the crystal was efflorescent, the specimens were usually kept in diffusion pump oil, and on measurements the crystal grains were spead on the bottom of the glass container to obtain the equilibrium water vapor pressure.

1) Part III: R. Kiriyama and H. Ibamoto, This Bulletin, **27**, 323 (1954).
2) R. Kiriyama, H. Ibamoto and K. Matsuo, *Acta Cryst.*, **7**, 482 (1954).
3) H. Kiriyama, This Bulletin, **35**, 1205 (1962).

The frequency range from 30 c./sec. to 10 Mc./sec. was covered. In the audio and radio frequency regions, a wide-range conductance-capacitance bridge (Ando Elec. Co. Type TR-1B), and at the highest frequency of measurement, a commercial Q-meter (Yokogawa Elec. Co.), were used. The value of the permittivity was determined from the ratio of the capacity of the specimen to that of a rock salt plate with the same thickness; a standard value of 5.62 for rock salt was used throughout the measurements.

Results

Permittivities and Dielectric Losses at Room Temperature.—The permittivities ε' and corresponding loss factors ε'' of this monoclinic crystal at 20°C are shown in Table I. The complex dielectric constant ε, $(\varepsilon=\varepsilon'+i\varepsilon'')$, is denoted as follows: ε_a and ε_b mean those with the electric field along the *a*- and the *b*-axis respectively, while ε_c is that with the external field perpendicular to the *c* plane, the cleavage plane. As indicated in Table I, there was a marked dielectric anisotropy, the values of ε_a and ε_b being much larger than that of ε_c. In addition, remarkable dielectric dispersions and absorptions were observed for both the *a* and *b* directions.

TABLE I. PERMITTIVITIES AND LOSS FACTORS AT 20°C AS A FUNCTION OF FREQUENCY

	3 Mc./sec.		3 kc./sec.		0.3 kc./sec.	
	ε'	ε''	ε'	ε''	ε'	ε''
ε_a	6.5	2.2	18.7	7.5	28.0	8.5
ε_b	7.0	3.5	31.6	2.5	33.5	2.8
ε_c	4.8	0.0	6.3	0.3	7.3	1.0

Temperature Dependence of Dielectric Properties. — Figure 1 shows the temperature dependence of the permittivities and ratios $\varepsilon''/\varepsilon'$ $(=\tan\delta)$ for various directions of the applied electric field in the audio frequency range. At the lowest temperature of measurement, −170°C, the value of permittivity was about 4.5 in every direction, a magnitude usually found in ionic solid dielectrics. There was no evidence of dielectric loss at low temperatures, and the permittivity increased slightly with an increase in temperature. When a temperature of −36°C was reached, a distinct change in dielectric character occurred, and remarkable dielectric relaxation phenomena were observed above this temperature. Such discontinuity suggests that this crystal undergoes a phase transition. The measurement of specific heat[4] has shown that the transition of the first order occurs at −36°C. Above the transition temperature, T_{tr}, there were great differences in

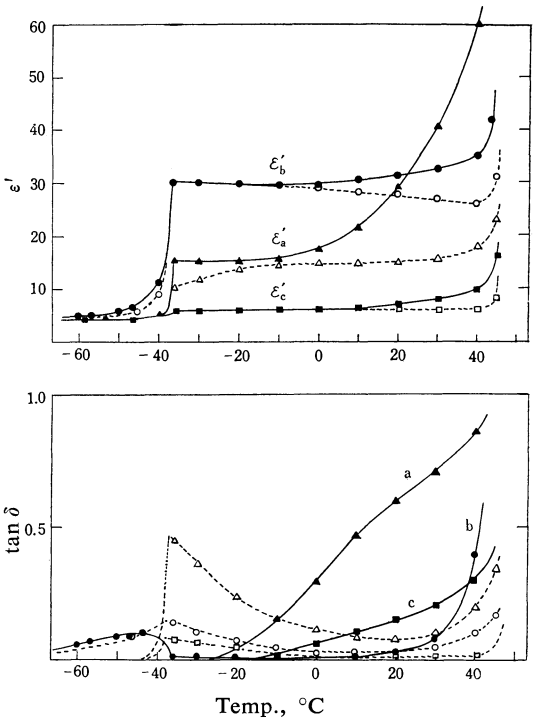


Fig. 1. Temperature dependence of the permittivity and dielectric loss angle at audio frequencies. Hollow symbols represent values obtained at 10 kc. and filled symbols at 0.1 kc.

dielectric properties in the three directions. Thus, just above T_{tr} ε'_b had the largest value among them, ε'_a, about half the value of ε'_b and ε'_c, only 6 at 0.1 kc. Moreover, at higher temperatures another type of dielectric absorption began to appear in different fashions, dependent on the direction of the applied electric field. In the *a* direction, ε'_a and also $\tan\delta_a$ rapidly increased again above about −20°C with a rise in temperature, and an apparent loss maximum was frequently observed at the lowest frequency of measurement, whereas in the *b* direction no such high dielectric losses were observed, while both ε'_b and $\tan\delta_b$ gradually increased up to 30°C. The shapes of the ε'_c-*T* and $\tan\delta_c$-*T* curves were rather similar to those in the *b* direction, but the dielectric absorption and dispersion in the former direction were quite small compared with those in the latter.

At the dehydration temperature of 46°C, a sudden increase in the permittivities and corresponding losses were observed in all three directions. Similar phenomenon was always observed in the dielectric measurements for a hydrated crystal when dehydration took place. This may be, therefore, a result of a d.c. conduction in the adsorbed layers of dehydrated water molecules on the crystal surface.

4) The thermal measurement was kindly carried out by Dr. Hiroshi Suga of the Faculty of Science, Osaka University.

Frequency Dependence of Dielectric Constants. —As is shown in Fig. 1, audio frequencies could not cover the dispersion region sufficiently. To obtain full information about the relaxation process, further measurements were made over a wide range from 30 c./sec. to 10 Mc./sec. at several fixed temperatures above the transition point. Representative results of these measurements with the electric field along the *a*- and *b*-axis are shown in Figs. 2 and 3 respectively, in which figures the permittivity and the loss factor are plotted against frequency. The absorption feature with the external field perpendicular to the cleavage plane was similar to that in the *b*-axis direction. In every direction, the absorption in the radio frequency region behaved as a typical relaxational one, and the absorption maxima gradually shifted to higher frequencies as the temperature was increased. The absorption curve in every set of measurements was a little wider than a Debye curve, indicating a spread in relaxation times. Consequently, the experimental maximum value of the loss factor, ε''_{max}, was lower than the value obtained from the term $(1/2)(\varepsilon'_0-\varepsilon'_\infty)$[5] in the Debye expression, where ε'_0 and ε'_∞ were the permittivities respectively below and above the absorption region. According to the method of Cole and Cole[6], ε'' was plotted against ε' in Fig. 4. The plots in the *a*- and the *b*-axis directions at 0°C were circular arcs, the diameters of which made angles of $0.09(\pi/2)$ and $0.16(\pi/2)$ respectively with the ε' axis. These values were rather small as compared with those obtained for a number of solid dielectrics.

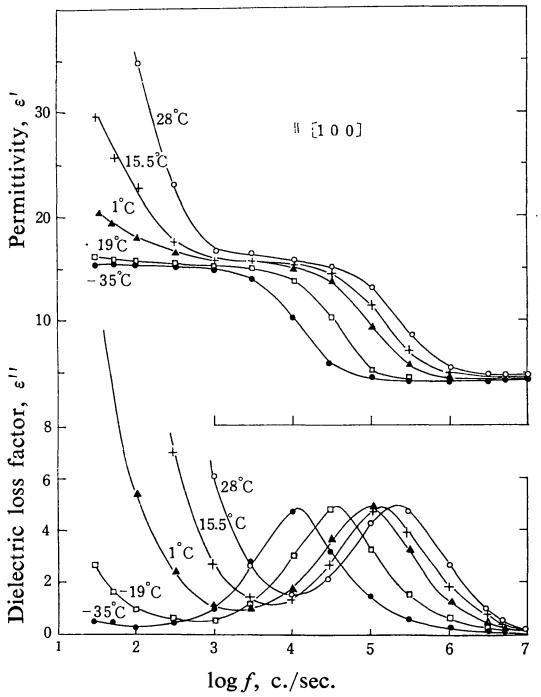


Fig. 2. Dielectric dispersion and absorption with electric field along the *a*-axis at various temperatures above T_{tr}.

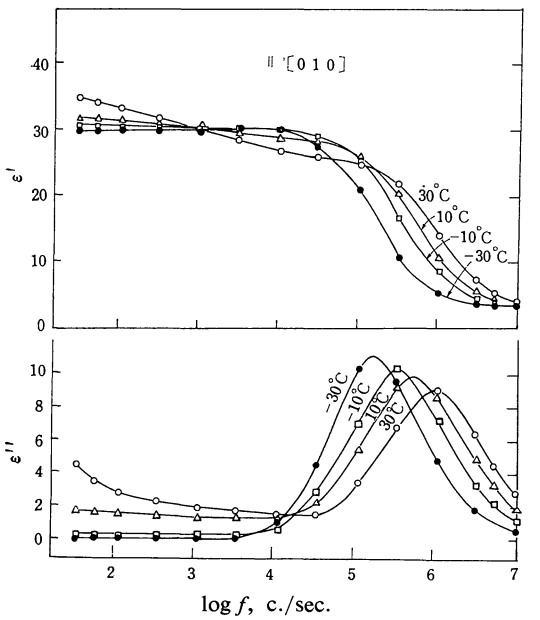


Fig. 3. Dielectric dispersion and absorption with electric field along the *b*-axis above T_{tr}.

The dielectric absorption observed at radio frequencies was ascribed to the dipole orientation resulting from the transition of the dipole from one equilibrium position to another over an energy barrier. The characteristic relaxation time for dipole orientation, τ, was obtained from the frequency of the maximum absorption, f_{max}, according to the relation:

$$\tau=1/(2\pi f_{max})$$

Then the height H of the energy barrier could be determined from the temperature dependence

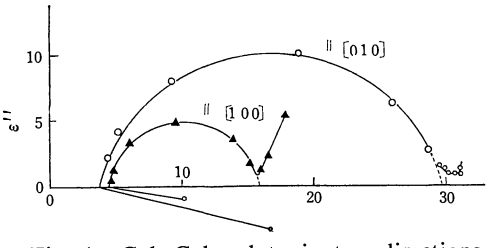


Fig. 4. Cole-Cole plots in two directions of the single crystal at 0°C.

5) For example, see H. Fröhlich, "Theory of Dielectrics", Oxford University Press, London (1949), p. 74.
6) K. S. Cole and R. H. Cole, *J. Chem. Phys.*, **9**, 341 (1941).

of the relaxation time by means of the usual rate law:

$$\log \tau = -\log A + H/(2.3\,RT)$$

where R was the gas constant, T the absolute temperature, and A the frequency factor. Figure 5 shows the variation of $\log \tau$ with $1/T$ for the three cases, and the values of the energy barrier, H, and the frequency factor, A, are listed in Table II.

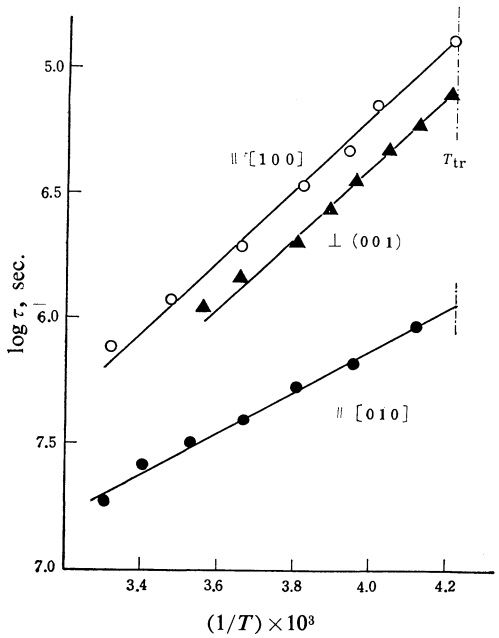


Fig. 5. Plots of $\log \tau$ (sec.) for the high frequency dispersion against reciprocal temperature (°K).

TABLE II. THE VALUES OE THE ENERGY BARRIER AND THE FREQUENCY FACTOR DESCRIBING THE OBSERVED DISPERSIONS

Direction of electric field	A sec^{-1}	H kcal./mol.
∥ [1 0 0]	1×10^{11}	6.7
∥ [0 1 0]	8×10^{9}	4.5
⊥ (0 0 1)	7×10^{10}	6.3

It can be seen in Fig. 2 that a further absorption region, in which the dielectric loss continues to increase with a decrease in frequency, is present at much lower frequencies. This type of absorption was prominent when the electric field was applied along the a-axis as mentioned above. However, the magnitudes of permittivity ε'_a and loss factor ε''_a for the low frequency absorption were somewhat variable from one sample to another, and the values obtained initially for a particular sample could not be reproduced after cooling it to the low-temperature phase and then rewarming it, whereas the results for the radio frequency absorption were quite reproducible in different runs. It would appear that in each run the loss factors of the low frequency absorption do finally attain a region where ε''_a is proportional to $1/f$, this being the evidence of d. c. conductivity.

The Atomic Arrangement in the Crystal Lattice

The crystal structure of the high temperature modification has already been determined by X-rays[2]. The structure projected on the (0 1 0)

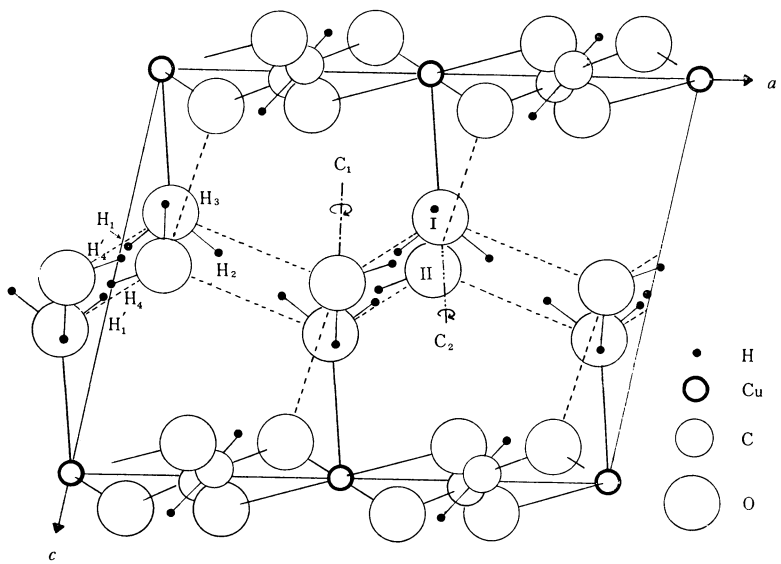


Fig. 6. Projection of the crystal structure on (0 1 0). —— Chemical bonds, ---- Possible hydrogen bonds. C_1 and C_2 represent axes of reorientation of the water molecules.

plane is represented in Fig. 6. A distinct layer structure is formed parallel to the (0 0 1) plane, in which one formate ion is coordinated to two copper atoms and each copper atom is surrounded by four oxygen atoms of four different formate ions in an approximately square configuration. Two non-equivalent water molecules are sandwiched between these layers. One kind of water molecule (H_2O-I) is coordinated to a copper atom with a far longer Cu–O distance, 2.36Å, than the ordinary covalent Cu–O distance of about 2.0Å. Another kind of water molecule (H_2O-II) is not linked to any copper atom, but to one oxygen atom of the formated ion and two oxygens of the first kind of water molecule with hydrogen bond distances of 2.82, 2.78 and 2.74Å respectively.

This crystal has a transition point at −36°C, as has already been mentioned. Though the crystal structure of the low temperature modification has not yet been available, there is no evidence of any significant change in the atomic arrangement above or below the transition point. First, even if the crystal was gradually cooled to the temperature of liquid nitrogen through the transition point, it did not collapse, and the dielectric behavior in the radio frequency region was almost reproducible after such treatment. Moreover, no visible change in optical properties in the neighborhood of T_{tr} was disclosed under a polarizing microscope. Secondly, the heat capacity and volume expansion of the crystal have already been measured by Suga[4], who found that the slight discountinuity at −36°C was due to a transition of the first order. The enthalpy, entropy and volume changes associated with the transition were estimated as follows: $\Delta H=$ 206 cal./mol., $\Delta S=0.87$ e. u., $\Delta V=0.22$ ml./mol. These values are too small to account for a structural change in the transition. Thirdly, a preliminary X-ray study made by superimposing Weissenberg photographs taken at −95°C on the 25°C photographs revealed that the low temperature crystal structure was almost the same as that of room temperature except for a little contraction of about 0.1Å in *c*.

On the basis of this evidence, the hydrogen atoms of water molecules have been located by the proton magnetic resonance experiment[3]; these results are also included in Fig. 6. Two protons (H_1 and H_2) of the water molecule H_2O-I contribute to form bent hydrogen bonds between the oxygen of its own water molecule and the two nearest oxygens of H_2O-II, whereas one proton (H_3) of H_2O-II makes a rather close approach to one oxygen of the formate ion, where a weak hydrogen bond is also predicted from the X-ray method and the remaining proton (H_4) is free from any hydrogen bond. It should be noted that two folding chains of hydrogen bonds run along the *a*-axis direction. Furthermore, with respect to packing in the *b*-axis direction, some of the hydrogen atoms, H_1', H_4, H_4', H_1, neighbor each other with H–H distances of 1.9∼2.3Å, these values being smaller than twice the van der Waals radius of 1.2Å.

Discussion

In the temperature range between −170°C and about −80°C, the permittivities in the three directions are almost independent of the frequencies, and those temperature coefficients which are present are positive and have values found in usual ionic crystals. Above about −80°C, the permittivity with the applied electric field parallel to the *b*-axis increases gradually up to the transition point, and the corresponding dielectric loss appears to be distinctly measurable, while in both directions of the *c*- and the *a*-axis no such dielectric anomalies are observed. It is, therefore, evident that the molecular motion of water within the crystal lattice is almost frozen below the transition point; this is consistent with the result of the proton magnetic resonance experiment. The gradual increase in permittivity in the *b* direction, however, indicates that some sort of reorientational motion of the water molecules has already been excited at several tens of degrees below T_{tr}.

When a temperature of −36°C is reached, the crystal undergoes a phase transition, a process which is associated with a slight volume expansion but without any significant structural change. The transition is also accompanied by a large increase in the permittivities parallel to the cleavage plane and a little increase perpendicular to it. These results indicate that the phase transition does involve freezing and releasing processes of electric dipoles. Thus, the large dielectric absorption and dispersion above T_{tr} must be due to the onset of the rotation of water molecules; this is confirmed by the proton magnetic resonance spectra. Hitherto, we have encountered difficulty in distinguishing the dipole orientation of water molecules from apparent dispersions due to cationic conduction in some hydrated salts, especially in zeolite crystals, for instance, analcite[7] and synthetic zeolites[8]. In the present case, however, there is no possibility of ionic conduction due to the cupric ions

7) R. Kiriyama, H. Ibamoto, M. Koizumi and R. Kitagaki, *Min. J.*, 1, 313 (1955).
8) R. Kiriyama, H. Kawai and W. Murayama, to be published.

present, referring to the crystal structure and the bond nature. It may, therefore, be inferred that the slight expansion along the *c* direction at T_{tr}, with a little change in the crystalline field but any without fundamental alternation in the structure, is able to give sufficient freedom to the water molecules to permit their reorientation in the external field. The second order transition caused by such sorts of the orientational motion of water molecules was also found in hydrated chromic sulfate, $Cr_2(SO_4)_3 \cdot 18H_2O$[9].

Dielectric absorptions due to the reorientation of water molecules have previously been observed in a number of hydrated crystals, such as $MgPt(CN)_4 \cdot 7H_2O$, $Y_2Pt_3(CN)_{12} \cdot 21H_2O$[10], $(NH_4)Cr(SO_4)_2 \cdot 12H_2O$[11], $Na_2HPO_4 \cdot 12H_2O$, $Na_2SO_4 \cdot 10H_2O$, $Na_2CO_3 \cdot 10H_2O$[12] and pinacol hydrate[13]. The dispersion phenomena in some of these crystals have been explained on the assumption that the water molecules are grouped together in the crystal to form a hydrogen-bonded system similar to that of ice, but from a lack of detailed knowledge of the crystal structure, except for that of alum, definite information about the molecular mechanism of the rate process has not yet been given. For the present case, the atomic arrangements, including also the proton positions, are available; therefore, the large dielectric anisotropy can be elucidated qualitatively on the basis of the individual motion of two kinds of water molecules with different neighbors.

The results of proton magnetic resonance[3] reveal that the axial rotations of both kinds of water molecules are excited in the high temperature phase. If the motion of every water molecule is possible only around the molecular dipole axis, this being a unique two-fold axis C_2 for water molecule, the dielectric properties should then be unaffected by this type of motion. Therefore, to explain the observed dielectric relaxation, the possibility of dipole orientation caused by another type of motion must be considered. In respect to H_2O-I, however, such a type of motion is rather unlikely because of the electrostatic interaction between the cupric ion and the water dipole. The dipole moment of H_2O-II may be easily oriented to the external field, in contrast to that of H_2O-I, because of the weak interactions between it and its surroundings. The permittivity values at a frequency of 30 c./sec. just above T_{tr} were 30, 15 and 6 when the electric field was, respectively, parallel to the *b*- and the *a*-axis and perpendicular to the *c* plane. The remarkable dielectric anisotropy means that the axes about which the water dipoles can rotate are closely bunched around an axis nearly perpendicular to the cleavage plane (referred to as the C_1 axis). Under these circumstances, it is suggested that H_2O-II may rotate about the C_1-axis, whereas H_2O-I rotates most probably about the Cu–O bond; consequently, the effective orientational polarization is mainly due to the dipole orientation of H_2O-II.

The activation energies associated with the dielectric relaxation in the radio frequency absorption are found to be 6.7 for the *a*-direction and 4.5 kcal./mol. along the *b*-axis. These values are much smaller than the values for ice[14] and also for crystalline *n*-primary alcohol[15] and pinacole hydrate[13], in which the dielectric absorptions are associated with the hydrogen bondings of hydroxyl groups. The low energy barrier and the high value of critical frequency suggest that the mechanism of the dielectric relaxation for cupric formate tetrahydrate is of a different nature from those proposed for ice and the others. On the basis of the atomic arrangement in the crystal, it seems that the C_1 axis around which the water molecule H_2O-II can rotate corresponds to the O–H···O bond between H_2O-II and the nearest formate oxygen. A characteristic feature of the arrangement of water molecules is the presence of an isolated hydroxyl group, i.e., $O–H_4$ of H_2O-II. Because of this and the consequent absence of hydrogen bonding, the $O–H_4$ group can easily rotate about the C_1-axis, giving the large dielectric absorption and dispersion with the marked anisotropy. The small distribution of relaxation times may support the proposed mechanism involving the rotation of the hydroxyl group.

The data for the absorption at much lower frequencies are somewhat divergent from sample to sample and also depend on their thermal histories. These structurally sensitive characters suggest that the low frequency absorption is associated with lattice imperfections or ionic impurities. For instance, the origin of hydronium impurity may be considered to be as follows: To obtain a good single crystal, it was necessary to add a few drops of formic acid to the salt solution. In view of this, the crystals used in the present experiments might contain a minute amount of hydronium ions (H_3O^+) replacing water molecules in normal sites. If

9) H. Grayson-Smith and R. F. Sturrock, *Can. J. Phys.*, **30**, 687 (1952).
10) J. Errera and H. Sack, *Trans. Faraday Soc.*, **30**, 687 (1934).
11) R. Guillin, *Compt. rend.*, **213**, 791 (1941).
12) R. Kiriyama and Y. Saito, This Bulletin, **26**, 531 (1953).
13) J. S. Cook and R. J. Meakins, *Trans. Faraday Soc.*, **51**, 1483 (1955).
14) R. Auty and R. H. Cole, *J. Chem. Phys.*, **20**, 1309 (1952).
15) J. S. Dryden, *Australian J. Sci. Res.*, **5**, 661 (1952).

proton conduction starts from such a impurity center, the ionic state can move under the influence of the external field from one molecule to another by the successive transfer of protons along the hydrogen bond. The fact that the conducting effect is predominant only in the *a*-direction may be the most favorable evidence for the proposed mechanism.

Summary

The dielectric properties of single crystals of cupric formate tetrahydrate have been investigated over the range 30 c./sec. to 10 Mc./sec. from the liquid nitrogen temperature to the dehydration point, 46°C. This crystal undergoes a phase transition at −36°C, indicated by a sudden change in the dielectric properties. Above the transition point, large dielectric dispersion and absorptions are present when the applied electric field is along the crystallographic *a*- and *b*-axes, whereas along the normal to (0 0 1) plane, the variations in permittivity and the loss factor with temperature and frequency are quite small.

The results for the radio frequency absorption can be explained on the basis of a molecular mechanism involving the axial reorientation of two water dipoles in the formula unit of $Cu(HCO_2)_2 \cdot 4H_2O$. The energy barrier H(kcal./mol.) and the frequency factor $A(sec^{-1})$ associated with the dipole orientation have been obtained as follows: along the *a*-axis $A=1\times10^{11}$, $H=6.7$; along the *b*-axis $A=8\times10^{9}$, $H=4.5$; and in the direction normal to (0 0 1) $A=7\times10^{10}$, $H=6.3$.

A further absorption at much lower frequencies is remarkable only in the *a*-axis direction. The observed high dielectric loss suggests the possibility of proton transfer in the hydrogen-bonded chains found in this crystal structure.

The author wishes to express her sincere thanks to Professor Isamu Nitta and Professor Ryôiti Kiriyama for their helpful discussions and encouragement.

The Institute of Scientific and Industrial Research
Osaka University
Sakai, Osaka

Proton Magnetic Resonance in Cupric Formate Tetrahydrate, $Cu(HCO_2)_2 \cdot 4H_2O$

By Hideko KIRIYAMA (née IBAMOTO)

(Received January 20, 1962)

In the preceding paper[1] the results of the dielectric measurement of a single crystal of cupric formate tetrahydrate, $Cu(HCO_2)_2 \cdot 4H_2O$, have been described. This substance undergoes a phase transition of the first order at 237°K. The transition is characterized by a sudden increase in the dielectric constant as it passes through the transition region towards higher temperatures. Above the transition point, the crystal exhibits marked dielectric dispersions and absorptions with a large anisotropy. The atomic arrangement in the crystal lattice at room temperature has been determined by X-rays[2], except for that of the hydrogen atom. On these bases, it has been concluded that certain types of the orientational motion of the water molecule should occur above the transition temperature.

For the purpose of locating the protons of the water molecules in this crystal below the temperature of the phase transition, and also in order to ascertain the motion of water molecules above that, the proton magnetic resonance (PMR) spectra have been studied as a function of the orientation and the temperature in both single crystal and polycrystalline samples. Some results of the proton magnetic resonance experiment will give additional information on the nature of the transition.

It is to be noted that this crystal contains paramagnetic Cu^{2+} ions which in principle cause the resonance spectra to be broad at very low temperatures. Bloembergen has already examined the proton resonance in a single crystal of cupric sulfate pentahydrate, $CuSO_4 \cdot 5H_2O$, both theoretically and experimentally[3]. With this work in mind, we have

1) H. Kiriyama, This Bulletin, **35**, 3146 (1962).
2) R. Kiriyama, H. Ibamoto and K. Matsuo, *Acta Cryst.*, **7**, 482 (1954).
3) N. Bloembergen, *Physica*, **16**, 95 (1950).

made an experiment above the temperature of liquid air and at a quite low field of about 1300 gauss. Under these conditions, the expected paramagnetic effect could be almost ignored and the problem could be treated by Pake's method[4] for the water molecule in gypsum, $CaSO_4 \cdot 2H_2O$.

Experimental

The experimental method and the apparatus were almost the same as have already been reported[5]. A Pound-Watkins r. f. spectrometer was used to observe the first derivative of the resonance line. All the experiments herein reported were made at a fixed frequency of about 5.5 Mc./sec., and the magnetic field was slowly swept by a resistance network. The applied magnetic field was modulated with a small amplitude at 60 c./sec., and the derivative of the resonance line was plotted as a function of the applied field by a recording milliammeter, preceded by a phase-sensitive detector and a narrow-band amplifier. The absorption curve was obtained by graphical integration of the derivative.

The powdered sample was prepared by dissolving basic cupric carbonate in formic acid, and the single crystal was grown from the aqueous solution by slow cooling. The single crystal sample used was a cylinder, 8 mm. in diameter and 25 mm. long, cut from large crystals. The axes of three sorts of cylindrical samples were chosen to be parallel to [010], to the normal of (001) and to that of (100) respectively. The crystal was rotated around a given axis perpendicular to the external magnetic field H_0, and the spectra were observed at regular intervals.

The temperature was varied from 110 up to 310°K. Liquid air or dry ice was used as the cooling material, and a heating coil was wound on the probe to obtain a temperature higher than that achieved with the given refrigerant. Temperatures were measured with a copper-constantan thermocouple set close to the sample. Recording was always taken after a steady condition had been reached for a time far longer than the observed time lag.

Preliminary Remarks

The Crystal Structure.—The crystal structure[2] of $Cu(HCO_2)_2 \cdot 4H_2O$ has been studied at room temperature. The crystal is monoclinic holohedral, and the corresponding space group is $C_{2h}^5 - p2_1/a$. The unit cell contains two formula units, and its dimensions are $a=8.18$, $b=8.15$, $c=6.35$ Å, $\beta=101°5'$. The water molecules are sandwiched between layers in which two copper ions are bridged by one formate ion to form two-dimensional networks parallel to (001). Each copper ion is surrounded by four oxygen atoms of four formate ions ($Cu-O = 2.00$ and 2.01 Å) in a nearly square configuration and by two water molecules (H_2O-I) above and bolow this planar CuO_4 at a greater distance (2.36 Å). Another water molecule (H_2O-II) is linked not to the copper ion, but to an oxygen atom of formate ion and two oxygens of water molecules (H_2O-I) with hydrogen bond distances of 2.82, 2.78 and 2.74 Å respectively. It is an interesting structural problem that there are four available protons as against three O-O lines capable of forming hydrogen bonds.

Though the crystal structure below the transition temperature has not yet been refined by X-ray studies, as has already been mentioned in the preceding paper[1], some experimental evidence indicates that the low temperature crystal structure is almost the same as the room temperature one, except, of course, for the positions of the hydrogen atoms. Only a small contraction of about 0.1 Å in c, and no appreciable changes in either a or b are found by superimposing Weissenberg photographs taken at 180° on the 300°K photograph.

It is easy to locate the proton of the formate ion in the lattice because the direction and the distance of the C–H bond are known approximately, but this is outside our problem. Therefore, our interest will be confined to the protons of the water molecule.

The Effect of Paramagnetic Ion.—The paramagnetic resonance absorption for a single crystal of this substance was investigated by Shimada et al.[6] in a millimeter wave region. Their conclusion was that there is an exchange interaction between the cupric ions; only one absorption line is observed in every direction, whereas two non-equivalent ions are contained in the unit cell. More recently, Martin and Waterman[7] have measured the temperature variation of the magnetic susceptibility between 80 and 300°K on the polycrystalline sample. According to them, this crystal obeys the Curie-Weiss law of the form $\chi \propto (T-\theta)^{-1}$ where θ, the Weiss constant, has the large value of $-175°$. Although the exchange energy is not known accurately, these results indicate that the exchange interaction between the non-equivalent cupric ions in this crystal is fairly strong. Consequently, the broadening action of cupric ions may be considerably reduced by exchange interaction between them.

The time-averaged magnetic moment μ_c of the cupric ion is given in order of magnitude by Curie's law:

$$\bar{\mu}_c = (\mu_c^2/3kT)H_0 \qquad (1)$$

4) G. E. Pake, *J. Chem. Phys.*, **16**, 327 (1948).
5) T. Yukitoshi, H. Suga, S. Seki and J. Itoh, *J. Phys. Soc. Japan*, **12**, 506 (1957).
6) J. Shimada, H. Abe and K. Ono, ibid., **11**, 137 (1956).
7) R. L. Martin and H. Waterman, *J. Chem. Soc.*, **1959**. 1359.

where μ_c is the magnetic moment of the cupric ion. In an applied field of 1300 gauss at 110°K, which is the lowest temperature of our measurements, the value of $\bar{\mu}_c$ given by Eq. 1 is very small, of the order of 1 nuclear magneton, and it is much smaller still at higher temperatures. The average local field due to cupric ions, therefore, will not produce any further splitting in the proton resonance lines under consideration. The only effect of the paramagnetic ions is a slight shift of the center of the absorption line from the resonance field of liquid water, a shift which amounts to about 0.5 gauss or less, according to the formula of Bloembergen[3].

Results and Discussion

Proton Resonance below the Transition Temperature.—The experiment at liquid air temperature was made with the single crystal mounted in such a way that it could be rotated about the *b*-axis, which was perpendicular to the applied magnetic field, H_o. The derivative curve was recorded at 10° intervals as the crystal was rotated thruogh 180°. Typical traces and the corresponding integral curves are shown in Fig. 1. The absorption curves were almost symmetrical about the center of line, and no distortion due to cupric ions was disclosed within the range of experimental error. Furthermore, the resonance pattern in every orientation remained unchanged from 110° up to about 230°K. These experimental results have given a direct confirmation of the expectation discussed in the previous section. It is, therefore, evident that the fine structure observed in the present study is not to be attributed to the copper-proton interaction but to the proton-proton interaction in each water molecule.

If a proton pair exhibits only dipole-dipole interaction, the displacement of component lines, ΔH in gauss, from the field strength corresponding to free protons is related to the orientation of crystal by the formula given by Pake[4]:

$$\Delta H = \pm\alpha\,[3\cos^2(\phi-\phi_o)\cos^2\delta - 1] \qquad (2)$$

Here $\alpha = (3/2)\mu r^{-3}$, in which μ is the proton magnetic moment and r is the pair separation. ϕ is the angle between the external magnetic field, H_o, and a reference axis attached to the crystal that is in the plane of crystal rotation. ϕ_o is the angle between the projection of the p-p line (let p-p indicate proton-proton) onto the plane of rotation and the reference axis in the crystal, and δ is the angle between the p-p line and the plane of rotation. The effect of the paramagnetic cupric ions should be added to expression 2, but it is very small in this case, less than 0.5 gauss.

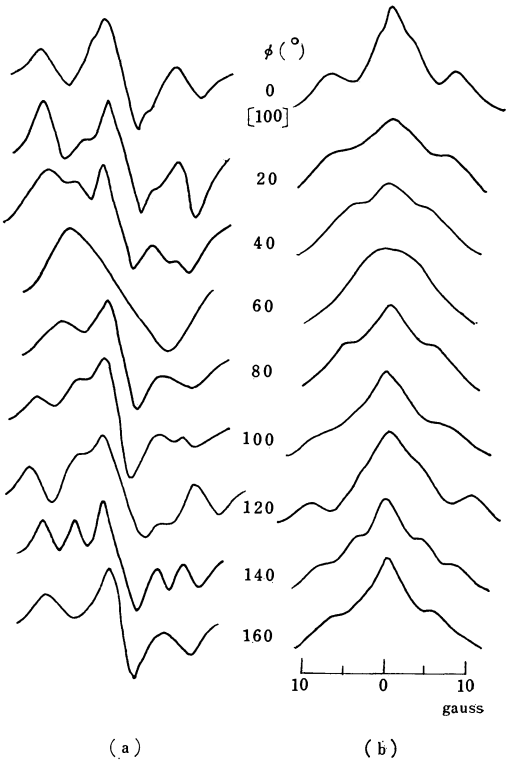


Fig. 1. Resonance patterns with various directions of H_o in the *ac*-plane at 110°K, (a) derivatives, (b) integrals.

When the crystal is turned about the two-fold axis *b*, two resonance doublets and, in addition, a central peak may be expected, because the unit cell would contain only two types of proton pairs of two non-equivalent water molecules and isolated protons of formate ions. At some orientations, the experimental derivative curves obviously displayed up to three peaks on either side of the center. However, owing to the broadening effect of the cupric ions, and also to the interaction between the proton pairs, each component line was quite broad; the overlap of the peaks was serious over part of the range, and the values of the peak displacements had to be derived by a decomposition procedure described later. As may be seen in Fig. 1, near $\phi = 0°$ and 120° the outermost peaks of the absorption curves were fairly well (though not completely) resolved. The measured peak displacements, ΔH (after correction for the effect of the paramagnetic ions), are shown as closed symbols in Fig. 2 against ϕ, which is, herein, the angle of H_o measured from the *a*-axis in the monoclinic angle β chosen above.

If, however, the shape of each component

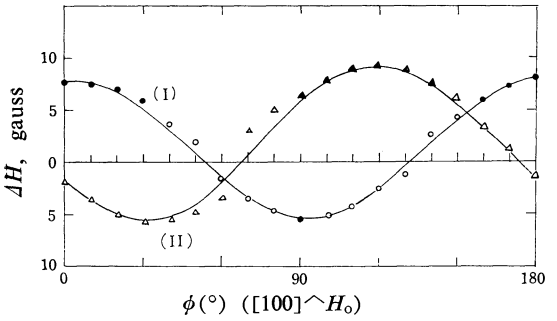


Fig. 2. Angular variation of the peak displacement ΔH in the *ac*-plane at 110°K. Closed symbols represent experimental points and open symbols denote decomposition procedure (see text). Calculated curves: I, $\phi_0=3°$, $\delta=25°$, $\alpha=5.4$ g.; II, $\phi_0=120°$, $\delta=20°$, $\alpha=5.4$ g.

line is assumed to be symmetrical, the area of the outermost peaks on the experimental absorption curves near $\phi=120°$ would amount to roughly half as much as that of the outermost peaks near $\phi=0°$. Thus, near $\phi=0°$ the ratio of the area under these peaks to that under the rest of the curve is close to 2 : 3, whereas near $\phi=120°$ the area ratio is only about 1 : 4 rather than the expected 2 : 3. Such a difference in peak height was an essential feature, because different samples behaved in the same manner because relaxation measurements confirmed that the PMR signals were unsaturated. The near-Gaussian form of the resolved outermost peaks near both $\phi=0°$ and $\phi=120°$, and also the approximate correlation between the areas, suggested the presence of residual proton pairs, but the derivative curves at no setting provided any evidence for it. Instead, it was more plausible that dipole-dipole interaction between the proton and the next nearest protons gave rise to further splitting in the resonance lines; consequently, the shape of the peak might not be symmetrical with respect to its maximum. On this supposition, we tried to resolve the absorption curves. To do this, mean absorption half curves were constructed from at least four experimental half-traces. On each of these, a standard curve, derived from the outer peak at $\phi=0°$, was superimposed at the appropriate peak displacement, and another standard curve, derived from the outer peaks at $\phi=120°$, was shifted along the field axis until the sum of the two standard curves yielded a close approximation to the outer part of the averaged experimental curve; substraction from the total curve left a residue corresponding to the protons of formate ions. The less reliable peak displacements derived from such a decomposition procedure are shown as open symbols in Fig. 2. By fitting the angular variation of the peak displacements to Eq. 2, ϕ_0 was measured to be 3° for one p-p line and 120° for the other, and the δ values were estimated to be about 25° and 20° respectively. Curves I and II in the figure are those calculated from Eq. 2, assuming $2\alpha=10.8$ gauss for all proton pairs.

In order to ascertain the p-p orientations given above, two other axes of rotation were examined. Figure 3 shows representative experimental absorption patterns for the various directions of H_0 in the *ab*-plane at 110°K. The angle ϕ between H_0 and the *a*-axis is stated with each spectrum. The angular dependence of the peak displacement ΔH is given in Fig. 4. As expected from the symmetry of the crystal, the resonance pattern at an angle $-\phi$ was just the same as one for $+\phi$; namely, two orientations of ϕ_0 and $-\phi_0$ for each group of proton pairs were allowed. The Pake curves in the *ab*-plane were calculated from Eq. 2 using the angular dispositions just determined from the peak displacements in the *ac*-plane and are presented in Fig. 4 as curves I (I_1 and I_2) and II (II_1 and II_2) for each of two non-equivalent proton pairs respectively. Since nine component lines were expected usually, a complete analysis of the resonance patterns was more difficult than that in the *ac*-plane.

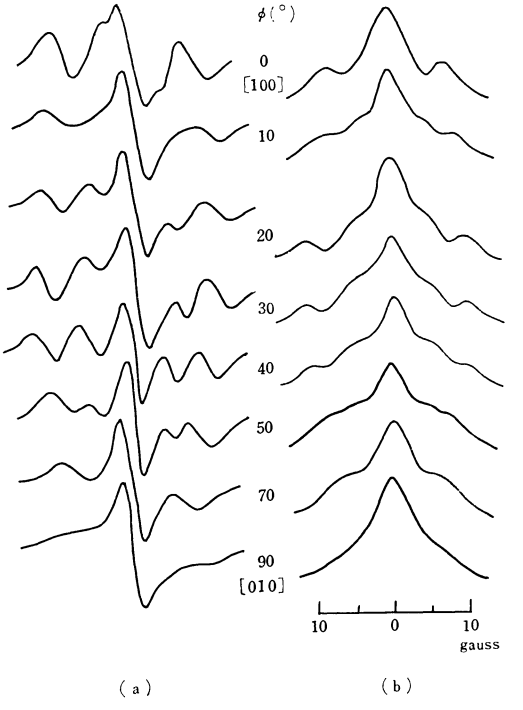


Fig. 3. Resonance patterns for various directions of H_0 in the *ab*-plane at 110°K, (a) derivatives, (b) integrals.

However, some additional evidence concerning the orientation of proton pairs may be drawn from this experiment as follows: (i) the maximum peak-to-peak separation, $2\Delta H$, for proton pair I occurs at $\phi=\pm25°$ from the *a*-axis, and both p-p vectors lie very nearly in the *ab*-plane. The maximum separation is 21.6 gauss, corresponding to a p-p distance, *r*, of 1.58 Å. The ratio of the area under these outer peaks to that under the rest of the curve is close to the expected 1 : 4; (ii) each resonance spectrum seems always to have some component lines with an ΔH of 2~5 gauss, so that the other proton pair II may be about 60° out of the *ab*-plane; (iii) near $\phi=90°$, the absorption curves were unduly broad. This broadening obviously means that some of the protons of adjacent water molecules might be close together in the *b*-axis direction.

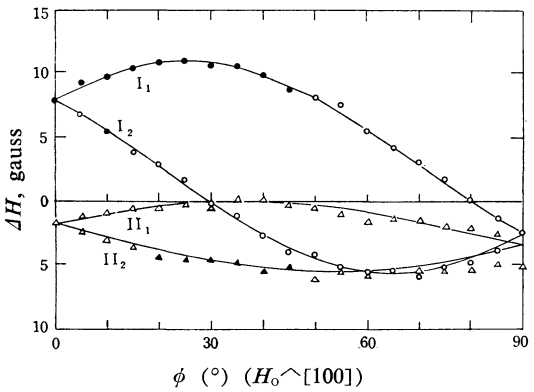


Fig. 4. Angular variation of the peak displacement ΔH in the *ab*-plane at 110°K. Calculated curves: I_1 and I_2, $\phi_0=\pm25.2°$, $\delta=2.5°$, $\alpha=5.4$ g.; II_1 and II_2, $\phi_0=\pm36°$, $\delta=54.5°$, $\alpha=5.4$ g.

The result of the measurement at 110°K with H_0 in the *bc*-plane did not contradict that obtained in the case of the *b*-axis rotation. By taking the values of ϕ_0 and δ and by using spherical trigonometry, one can compute the direction angles of the p-p lines with respect to the crystallographic axes. They were $\alpha_0=25°$, $\beta_0=65°$ and $\gamma_0=97°$ for proton pair I, while they were $\alpha_0=118°$, $\beta_0=70°$ and $\gamma_0=27°$ for proton pair II. These angles are measured away from the positive sides of the crystallographic axes, *a*, *b* and *c* respectively.

The Position of Protons below the Transition Temperature.—Although the positions of hydrogen atoms can not be determined directly from the results of the present study, it is possible to locate the most likely sites for them within the framework of the heavy atoms. As has been described above, the atomic arrangement in the low temperature form is almost the same as that of the room temperature form and the change in interatomic distances in the transition is negligible. Therefore, there is no trouble in locating the p-p vector based on the structure of the room temperature form. As the water molucule H_2O-I is coordinated to the cupric ion directly, it should orient itself by placing two protons opposite the "positive" copper ion. Thus, the direction of the p-p vector in H_2O-I will be nearly parallel to the *ab*-plane. Furthermore, the protons of H_2O-I will not deviate much from the two O-O lines where the hydrogen bonds were predicted by X-rays. It has therefore been concluded that the proton pair I should be assigned to that of H_2O-I and, consequently, the other pair II, to that of H_2O-II.

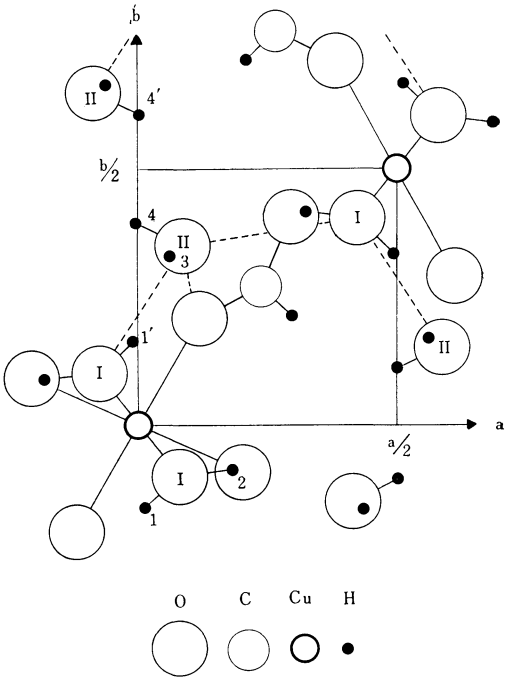


Fig. 5. Projection of the structure of $Cu\cdot(HCO_2)_2\cdot4H_2O$ on the (001) plane. Broken lines represent possible hydrogen bonds.

By using the p-p separations and the orientations of the p-p vectors, and assuming the O–H distance in the water molecule to be 0.96 Å[8], the location of the hydrogen atoms can be obtained. The deduced parameters of water hydrogen atoms are given in Table I. The projections on (001) and (010) are shown in Figs. 5 and 6 respectively. It appears that two protons (H_1 and H_2) of H_2O-I form two non-linear hydrogen bonds with two adjacent

8) G. Herzberg, "Infrared and Raman Spectra of Polyatomic Molecules", Von Nostrand, New York (1945), p. 489.

oxygens of H_2O-II in the same water layer; meanwhile one proton (H_3) of H_2O-II serves to bind the water oxygen to one oxygen of formate ion, and the other proton (H_4) is free from any hydrogen bond. With respect to packing in the *b* direction, hydrogen atoms neighbor each other as expected from the breath of the absorption spectrum. Consequently, some of the hydrogen atoms along the *b*-axis are separated by 1.9~2.3 Å, a little less than twice the van der Waals radius of 1.2 Å for the hydrogen atom.

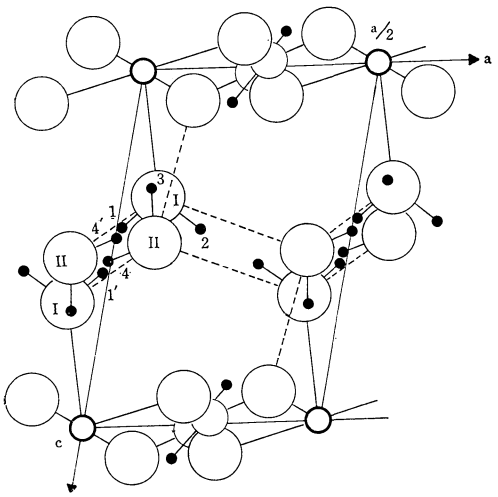


Fig. 6. Projection of the crystal structure on (010).

TABLE I. SET OF POSSIBLE COORDINATES FOR PROTONS IN WATER MOLECULES

		x	*y*	*z*
H_1	(H_2O-I)	0.01_2	-0.16_2	0.43_9
H_2	(H_2O-I)	0.18_0	-0.09_2	0.44_7
H_3	(H_2O-II)	0.06_1	0.33_1	0.33_1
H_4	(H_2O-II)	-0.00_6	0.39_3	-0.46_5

The present study is based upon Pake's method, which is applicable to the model of a "two-proton system", but the structure of this substance is much more complex than such an ideal case in two important respects: first, the water molecules lie close to each other, forming a sheet structure, and then the broadening of the fundamental line shape is so great that details are somewhat obscured; second, one must consider the effect of the cupric ions, which prevents one from using the second moment method for the purpose of structure determination. In spite of these difficulties, the positional determination of the proton pair has been fairly successful, since the resonance line shape fortunately retained the characteristic feature of the two-proton system. However, for further refinement of the proton position, a direct method of determination, such as neutron diffraction analysis at low temperatures, would be desirable.

Proton Resonance above the Phase Transition Temperature and Motion of the Water Molecules

The resonance pattern observed at the lowest temperature measured did not significantly change up to 233°K, a few degrees below the phase transition temperature, T_{tr}, 237°K. It is, therefore, certain that the hydrated water molecules are effectively stationary within the crystal lattice of the low temperature phase. When the temperature reached T_{tr}, absorption lines began to narrow with the increasing temperature at all settings of the single crystal. Two typical series of resonance line integrals for various temperatures are shown in Fig. 7, where ϕ is the angle between the applied field H_0 and the *a*-axis in the *ac*-plane. The outer peaks on the absorption curves at $\phi=0°$ and 120° have been assigned just above to the proton pairs of H_2O-I and H_2O-II respectively. In the direction of $\phi=0°$, the peak-to-peak separation, $2\Delta H$, gradually decreased from 16 to 12.5 gauss over a range of about 40° above T_{tr}, and these peaks retained prominent features well until 287°K. Then the outer

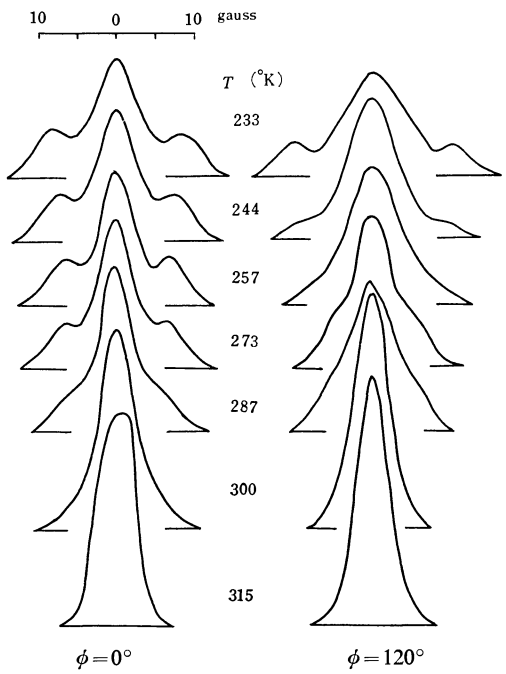


Fig. 7. Resonance absorption lines at various temperatures above T_{tr} for two special ϕ's of the single crystal. ϕ is the angle between the *a*-axis and H_0.

peaks started to collapse towards the center of the spectrum, a process which continued until the temperature was 300°K. At 300°K the absorption curve consisted of a single peaks 3.0 gauss wide, the line width being defined as the distance between the points of maximum slope. As the temperature was raised further, this single line then split up, so that at 315°K the spectrum seemed to consist of three peaks. On the other hand, the separation between the well-resolved peaks on the absorption line at $\phi=120°$ decreased much more rapidly than those at $\phi=0°$ in the temperature range 237~287°K so that prominent features of the outer peaks were barely observable even at 257°K. Then the spectrum showed further narrowing to a single peak 3.3 gauss wide between 300 and 315°K. In this temperature range the proton magnetic resonance curves at particular settings of the crystal are completely resolved into three peaks, as we shall see later.

It is known that the second moment of a resonance spectrum should be theoretically independent of the thermal motion of the nuclei[9]. However, side-spectra on absorption curves developed by thermal motions are usually too weak to be observed. If these side-spectra are neglected, the second moment of the central line would be affected by the motion. The experimental second moments for both single crystal and powdered samples are plotted against temperature in Fig. 8. The contribution of the dipole-interaction between the protons to the total second moment in the rigid state was calculated by Van Vleck's formula[10]. This value amounted to about 28.6 gauss^2 for the powder, while the experimental value was 29.0 gauss^2. The apparent change in the second moment extends over a wide temperature range from 235° to 310°K, and its total reduction for the powdered sample was 24 gauss^2. This large change indicates that the reorientation of the water molecules occurs around one axis or even more than one axis.

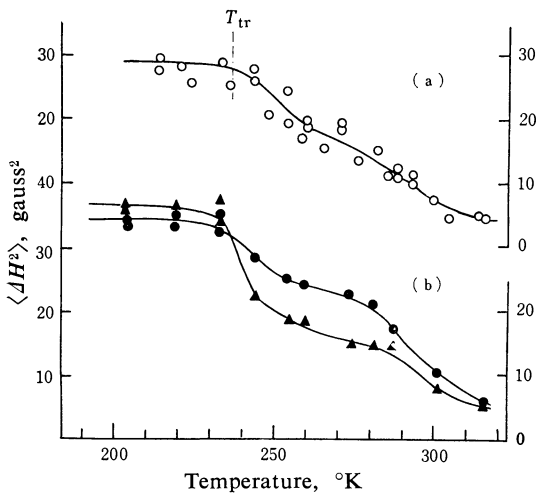


Fig. 8. Second moment as a function of temperature: for the powdered sample, (a); for the single crystal, (b).
○ Powder, ● $\phi=0°$, ▲ $\phi=120°$

In the middle of the line-width transition region, the second moment decreased with the temperature much less rapidly than at the ends of the transition region. The rather discontinuous change in the separation between the peaks or the line width, particularly near $\phi=0°$, was responsible for this stepwise decrease of the second moment. Because of the r^{-6} dependence of the second moment, a 0.2% increase in the c lattice dimension occurring at T_{tr} should produce only a 1% decrease in the second moment; hence it seems unlikely that the change in the second moment near 240°K is only a result of the lattice expansion. A study of the changes in the derivative curves indicates that both kinds of water molecule are set in motion just above the phase transition temperature and that the reorientation becomes sufficiently rapid to collapse the characteristic rigid hydrate spectra at different temperatures for the water molecules at two non-equivalent lattice sites. As is to be expected from the crystal structure, H_2O-I is subjected to a higher energy barrier to rotation than that to which H_2O-II is subjected, this being a main cause of the observed stepwise reduction in the second moment.

If the motion of the water molecule at higher temperatures is rapid rotation or reorientation about an arbitrary axis, as in Fig. 9,

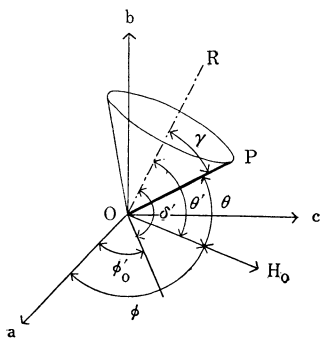


Fig. 9. Diagram showing definition of the angles for the rotating proton pair system.

9) E. R. Andrew and R. A. Newing, *Proc. Physic. Soc.*, **72**, 959 (1958).

10) J. H. Van Vleck, *Phys Rev.*, **74**, 1168 (1948).

then the absorption line should have two component lines, as given by the formula[11].

$$\Delta H = \pm(\alpha/2)(3\cos^2\gamma - 1)(3\cos^2\theta' - 1)$$

Then

$$\Delta H = \pm(\alpha/2)(3\cos^2\gamma - 1) \times [3\cos^2\delta' \cos^2(\phi - \phi_0') - 1] \qquad (3)$$

where γ, θ', δ', ϕ and ϕ_0' are as shown in the figure; OP is the vector r joining the two protons of the water molecule, and OR is the rotation axis making angle θ' with H_0 and angle γ with r.

In the temperature range of 300° to 315°K, the absorption curves with the magnetic field in the *ac*-plane consisted of a central peak and only one double line, whose separation strongly depended on the orientation of the crystal. The central peak was assigned to the proton of the formate ion, and the doublet to the water molecule. Some of the measured derivatives and the angular variation of the line-pair separation, $2\Delta H$, at 310°K are shown in Fig. 10. The extreme separations were 4.5 and 5.3 gauss respectively. Assuming that the peak-to-peak separation of 5.3 gauss corresponds to $\phi - \phi_0 = 90°$ in Eq. 3, and using $r = 1.58$ Å, as given in the previous section, the value of angle γ is computed to be 90° or 35°. Since the water molecule has a symmetry axis perpendicular to the p-p line, the former figure seems to be more acceptable. If, however, γ equals 90° for all p-p vectors, this form of motion of H_2O would not affect the dielectric properties. The large dielectric absorption and the corresponding dispersion found above T_{tr} lead us to postulate that one isolated hydroxyl group, O–H_4, of H_2O-II does reorient about the remaining O–H_3 bond in the same water molecule (see Figs. 5 and 6). On the basis of the nature of the chemical bonds between each water molecule in two different sites and its surroundings as well as of the character of the dielectric anisotropy, it is suggested that the value of γ for H_2O-II should be 35° rather than 90°, whereas the angle γ for H_2O-I has the expected value of 90°.

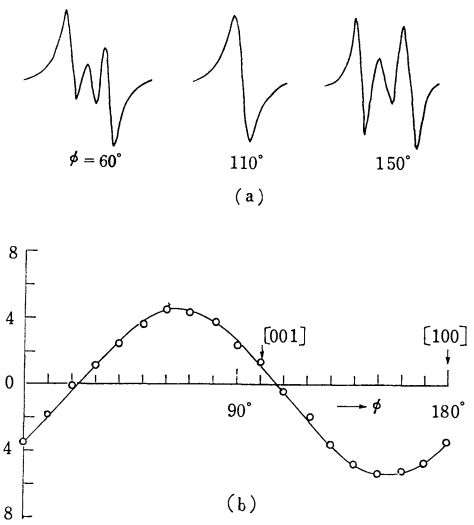


Fig. 10. Resonance patterns as the single crystal is turned about the *b*-axis at 310°K, (a) derivatives in three directions of H_0, (b) angular variation of the peak-to-peak separation.

If the data in Fig. 10 conforms to Eq. 3, the remaining parameters, ϕ_0' and δ', may be estimated from the field splittings at various orientations. The maximum line-pair separation occurs in the region of 60~70°; this yields a value for ϕ_0' of 65°. The ratio of the extreme separations is 4.5/5.3, and, also, ΔH appears to pass through zero at $\phi = 15°$ and 105°. These results lead to an estimate for projection angle δ of 38°. Thus, a set of plausible values for the parameters in Eq. 3 are $\phi_0' = 65°$, $\delta = 38°$, and $(\alpha/2)(3\cos^2\gamma - 1) = 2.7$ gauss; the continuous line in Fig. 10 indicates the corresponding line-pair separations. It is to be noted that there is no difference between the rotational states of two non-equivalent water molecules over the last few degrees before reaching the dehydration point at 319°K.

Now one can estimate the proton contribution to the second moment for the powdered sample in the rotational state. It may be considered that the component line shown in Fig. 10 owes its width to the inter-molecular broadening. The smallest values of the line width are found from the single crystal data, to be 1.2 gauss for the doublet and 0.8 gauss for the central line, the inter-molecular broadening being estimated to be about 0.4 gauss[2]. The rigid lattice second moment of an isolated water molecule is 23 gauss[2] for an H–H distance of 1.58 Å. When the water molecules rotate about an axis making an angle γ of 90° or 35° with the interproton line, the second moment may be reduced to $23/4 = 5.7$ gauss[2]. Since the water molecules include 4/5 of the protons in the chemical formula, the total second moment is expected to be 5.0 gauss[2], which is in good agreement with the observed value at 315°K.

Summary

The proton magnetic resonance spectra of $Cu(HCO_2)_2 \cdot 4H_2O$ have been investigated over the range 110° to 315°K, using both single crystal and powdered samples. The water molecules are effectively rigid below the phase transition temperature, 237°K, and the most

11) H. S. Gutowsky and G. E. Pake, *J. Chem. Phys.*, **18**, 162 (1950).

probable positions of the protons of the two non-equivalent water molecules are postulated on the basis of Pake's method.

The narrowing of the absorption line occurs above 237°K; this implies the gradual onset of a certain motion of both kinds of water molecules. The absorption spectra in the higher temperature range of 300~315°K indicate that the reorientation of the water molecules takes place almost exclusively about one axis.

The author wishes to express her sincere thanks to Professor Isamu Nitta, Professor Junkichi Itoh and Professor Ryôiti Kiriyama for their valuable discussions and continued interest, and to Mr. Teruo Yukitoshi for his collaboration in some of the experiments.

The Institute of Scientific and Industrial Research
Osaka University
Sakai, Osaka

Factors which Determine Solubility

By Kōzō SHINODA

(Received January 24, 1962)

The factors which determine solubility in regular solutions have been analyzed by Hildebrand[1]. After being trained by Hildebrand, I have directed my efforts toward applying the regular solution concept to various non-regular solutions. I have been able to extend it to many non-regular systems[2]. However, there are also many systems where the aspects of dissolution are quite different from those in regular solutions. Particularly, the solutions of a surface active agent, a polymer (including polyelectrolyte) and a poly-soap are markedly different from regular solutions. Yet these solutions are very important for practical purposes and are interesting to tackle. The present paper was undertaken to analyse the dominant factors which determine the solubility of these substances.

Factors which Determine Solubility in Regular Mixtures.—The entropy of mixing, the heat of mixing and the free energy of the solute in equilibrium with the solute molecule in solution are the most important factors controling solubility in regular solutions. The basic solubility equation of the regular solution theory is[1]:

$$\ln a_2 = \ln x_2 + \frac{V_2\phi_1^2(\delta_1-\delta_2)^2}{RT} \qquad (1)$$

where a_2 is the relative activity of the solute in equilibrium with the solute molecule in solution, x_2, the solubility expressed as mole fraction, V_2, the molal volume of solute, ϕ_1, the volume fraction of the solvent, and δ_1 and δ_2, the solubility parameters of the solvent and the solute.

Accordingly, devices to increase the solubility of certain substances at a constant temperature are 1) to decrease the heat of the solution by selecting a suitable solvent, 2) to increase the activity of the solute, for example, to increase the solute pressure in the case of gas solubility, and 3) to use a solvent of a small molecular size so that when the solubility expressed as the mole fraction, x_2, remains the same, the amount which dissolves in the same volume of solvent is large. If the use of solutes of a small molecular volume and of similar chemical properties is permitted, the solubility increases very much, because the heat of solution can be reduced by a factor of V_2'/V_2. (V_2' is the molal volume of a solute of chemical properties similar to those of solute 2.)

If the super-cooled liquid state is easily attainable and relatively stable, the solubility can be increased metastably by cooling (at the temperature at which the crystal is a preferred state for the solute). In this case a solubility increase results from the enhanced free energy. In polymer, poly-soap, and surface active agent solutions this process is a rather important one as a means of increasing the solubility.

If the temperature can be changed, one way to increase the solubility of ordinary substances is to raise the temperature, because 1) the heat of mixing usually decreases with the temperature and the heat term (second term

1) J. H. Hildebrand and R. L. Scott, "The Solubility of Nonelectrolytes", Reinhold Publishing Corp., New York (1950), p. 131. "Regular Solutions", Prentice-Hall Inc., New Jersey (1962).

2) a) K. Shinoda and E. Hutchinson, *J. Phys. Chem.*, **66**, 577 (1962); b) K. Shinoda, T. Nakagawa, B. Tamamushi and T. Isemura, "Colloidal Surfactants", Academic Press Inc., New York (1962).

in Eq. 1), which is divided by the temperature, decreases more rapidly, and because 2) the relative activity of the solid increases so very rapidly that the solubility of the solid also increases very rapidly. The relative activity does not change in a liquid solute, and the solubility does not increase so much as in the case of a solid at a temperature well below critical mixing. In the case of gases, the solubility, which is usually measured under constant pressure, decreases somewhat, usually because the relative activity decreases as compared with the liquid state.

If there is a strong dipole-dipole interaction or a dipole-induced dipole interaction, the molecules orientate so as to decrease the heat of mixing. Any intermolecular force, such as hydrogen bonding or differences in the positive and negative character of the components, causes a deviation from regular behavior and increases solubility. We should now add a charge transfer force[3] as a new type of intermolecular force. These, the ordinary procedures to increase the solubility, are widely applicable in many non-regular systems.

Pseudo-phase Dispersion of Surface Active Agent.—The substances studied in the solution theory are usually nearly symmetrical in their physical nature. However, molecules which have completely different properties at either end show quite non-regular behavior. Yet this type of molecule, the surface active molecule, is becoming more and more important in almost all fields of industry. In the case of surface active substances, the mechanism of dissolution is quite different. If we immerse a dry surface active agent in water, the water molecule penetrates into the hydrophilic layer so that the distance between bimolecular leaflets becomes large. If the temperature is high enough for the interior of bimolecular leaflet, i. e. the hydrocarbon chain, to be in the liquid state, the hydrocarbon chains orient end to end and the hydrophilic groups are directed to the aqueous environment. This particle, consisting of scores of surface active agent molecules (ions), is called a micelle. Since the micelle is slightly more stable than the solid hydrated surface active agent, as has been discussed elsewhere[2], a large amount of surface active agent disperses into the solution. The micelle is a small particle compared with the wave length of light and gives a clear transparent solution. Micelles are in equilibrium with singly-dispersed surface active molecules (ions), and this saturation concentration stays almost constant above the concentration at which micelle formation begins. Hence, the solubility of a surface active agent proceeds at first, up to the critical concentration for the formation of the micelle, just like an ordinary solution, but above the CMC the solubility increases very much, without any appreciable difference in the partial molal heat, entropy or free energy. The solubility of sodium dodecyl sulfate just below the Kraff point (above this temperature, the liquid state becomes preferable) is about 0.2%, but above the Kraff point it is about 10~20%. The longer the chain of surface active salts, the larger the ratio of the solubility. It becomes several hundred times more soluble as a result of micellar dispersion. The temperature rise is the most important process in increasing the solubility. Another device may be to change the structure of the molecule or to add a third component, such as alcohol, thus depressing the Krafft point. We may assume complete random mixing, as in the regular solution for singly dispersed molecules, but micelle formation is treated on the basis of a complete orientation and a complete non-mixing of water and surface active ions in the micelle.

Dissolution by the Addition of a Third Component.—We well know that the addition of a third component, such as acetic acid, to the benzene+water system increases the mutual solubility of water and benzene, finally leading to a single homogeneous phase. This is more or less a result of the orientation of the acetic acid. The methyl group will be directed more strongly toward the benzene molecule, and the carboxylic group may be bonded to the water molecules, on a statistical average.

The extreme case would be micelle formation by the third component and the solubilization of the second component by the micelle. In this case, the acetic acid is replaced by a paraffin chain salt. Alcohols, hydrocarbons, etc. dissolve in the aqueous phase and in the micelle. The process is something like dissolution into a heterogeneous mixture of water+hydrocarbon, the hydrocarbon chain aggregate of the surface active agent comprising the hydrocarbon medium[4]. In addition, it is known that the addition of surface active agent as a third component increases the solubility of some substances, such as dimethyl phthalate[5] and some kinds of dyes, which are rather difficult to dissolve in either water or hydrocarbon. We may classify this process as partition dissolution in aqueous solution containing a pseudo-phase.

3) H. A. Benesi and J. H. Hildebrand, *J. Am. Chem. Soc.*, **71**, 2703 (1949).

4) M. E. L. McBain and E. Hutchinson, "Solubilization and Related Phenomena", Academic Press Inc., New York (1955).

5) J. W. McBain, "Colloid Science", Heath, Boston (1950).

Solubility of the Macromolecule.—Flory and Huggins[6] proposed to use the excess entropy of mixing due to an excess configuration based on the lattice model of a liquid. However, as was revealed by a recent study[7], the Flory-Huggins excess entropy is certainly an overestimate for a molecule which is not completely flexible.

If a polymer (macromolecule) in an equilibrium with solution is in the crystalline form, it is rather difficult to dissolve. Even a very small heat of mixing per unit volume results in a large heat of mixing per mole of polymer. However, if the polymer is in the liquid state, the solvent molecule, which is usually much smaller than the polymer, can easily dissolve because of the small heat of mixing. Even the more concentrated phase of the two phases which are in equilibrium contains much more solvent than polymer[8]. Hence, it is very important that a macromolecule be in the liquid state in order for it to dissolve in a solvent.

This can be seen from the basic solubility equation of a liquid-liquid mixture[1]:

$$\ln x'_2+\frac{V_2\phi'^2_1(\delta_1-\delta_2)^2}{RT}=\ln a_2$$

polymer rich phase

$$=\ln x_2+\frac{V_2\phi_1^2(\delta_1-\delta_2)^2}{RT} \qquad (2)$$

solvent rich phase

or

$$\ln \phi'_2+\phi'_1\left(1-\frac{V_2}{V_1}\right)+\frac{V_2\phi'^2_1(\delta_1-\delta_2)^2}{RT}=\ln a_2$$

$$=\ln \phi_2+\phi_1\left(1-\frac{V_2}{V_1}\right)+\frac{V_2\phi_1^2(\delta_1-\delta_2)^2}{RT} \qquad (2')$$

Flory-Huggins entropy of mixing is used in Eq. 2'.

In the ordinary liquid-liquid solubility of sparingly soluble compounds, $\phi_1'^2$, the volume fraction of the solvent in the solute phase, is very small, so that $\ln x'_2 \cong \ln a_2 \cong 1$.

Hence,

$$-\ln x_2 \cong \frac{V_2\phi_1^2(\delta_1-\delta_2)^2}{RT} \cong \frac{V_2(\delta_1-\delta_2)^2}{RT}$$

If the heat of mixing is large, this is compensated for by a very small value of x_2. However, in the case of polymer solutions, the volume fraction of solvent in the polymer phase is large. This is because the heat of solution of the solvent molecule in the polymer is much smaller than in the inverse process. This means that the heat term on the left-hand side of Eqs. 2 or 2' largely cancels the heat term on the right-hand side of the equation or, in other words, that the heat of the transfer of the polymer molecule from the concentrated phase to the dilute phase is small because the volume fraction of the solvent in both phases is large. Hence, we can conclude that the dissolution of a polymer (macromolecule) essentially means the dissolution of solvent in the polymer. Polymers which do not swell in a solvent do not dissolve well.

Effect of Dissociation.—If a compound contains an ionic bond and it the solvent has a large dielectric constant, the compound dissociates in solution. Dissociation proceeds as a result of the increase of entropy, and the electrical energy for dissociation acts so as to supress dissociation. If either anion or cation is readily soluble in the solution and the opposite ion is not, the soluble ion dissolves first and the solid phase in equilibrium with the solution becomes charged and becoms more soluble because of the electrical repulsion. If the anion and cation have the same tendency to dissolve, the separate solute phase may not be charged. However, the solubility is very large because the heat of solution per ion is much smaller, approximately one half, as compared with that of an ionic pair. The solubility expressed in the unit of mole fraction increases to roughly the square root as compared with a hypothetical non-dissociated species. In fact, the saturation concentrations of a single dispersion of ionic agents are roughly the square root of those of non-ionic agents which have the same oleophilic group and a similar hydrophilic group except with regard to dissociation[2b].

Solubility of Poly-soap.—In the case of the dissolution of a poly-soap polymer, to the long chain of which soap-like side chains are attached[9], many factors come into play. The poly-soap is a polymer; hence, the molecule has to have a shape and properties which make it difficult to crystallize in order for the solvent to dissolve into poly-soap. Poly-soaps have oleophilic groups as well as hydrophilic groups in the molecule. At least a fairly large part of the molecule must be strongly solvated with solvent in order to decrease the heat of mixing. However, the most important factor in the dissolution of poly-soap seems to be 1) a large amount of dissolution of the solvent into the poly-soap and 2) something similar to an inversion of the phase in the poly-soap rich phase. This means that in the first

6) M. L. Huggins, *J. Chem. Phys.*, **9**, 440 (1941); P. J. Flory, ibid., **9**, 660 (1941).

7) K. Shinoda and J. H. Hildebrand, *J. Phys. Chem.*, **61**, 789 (1957); **62**, 481 (1958); J. H. Hildebrand, *Z. physik. Chem. [N. F.]*, **16**, 3 (1958).

8) P. J. Flory, "Principles of Polymer Chemistry", Cornell University Press, New York (1953), p. 546.

9) U. P. Strauss and B. L. Williams, *J. Phys. Chem.*, **65**, 1390 (1961).

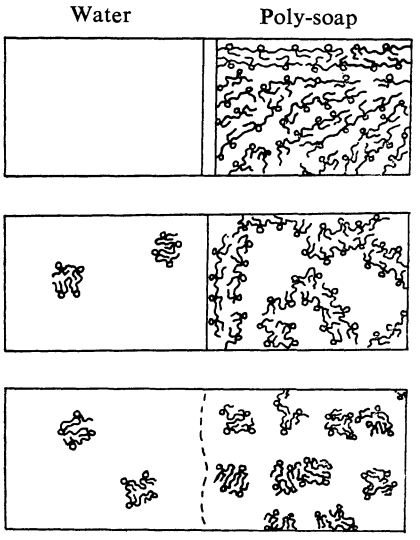


Fig. 1. Schematic diagram to illustrate probable mode of mutual dissolution of water—poly-soap.

instance the poly-soap is the solvent medium and that water (a common solvent for poly-soap) is the dispersed solute in the poly-soap phase, but in the next step the poly-soap molecules orient themselves so as to decrease the heat of mixing, hydrophilic groups being oriented outside and less hydrophilic groups inside, and finally water becomes the solvent medium and the poly-soap molecules the solute particles. Once this pseudo-phase inversion occurs in the poly-soap phase, the dispersion can be easily diluted by the very dilute poly-soap solution, formerly a separate liquid phase in an equilibrium with the poly-soap phase. The micro-Brownian motion, convection current, etc. may be sufficient for mixing. The solution is transparent because both phases are transparent. The solution may show a relatively intense light-scattering owing to the fluctuations of the concentration and the large size of the poly-soap molecule.

The addition of a certain amount of surface active agent as a third component seems to promote the solubility of the surface active polymers[10], including protein[11] in some systems.

Summary

The factors which determine solubility in various systems have been analyzed and discussed. The orientation of the molecule, the pseudo-phase dispersion, the liquid state of the solute, solvation and the pseudo-phase inversion are important factors in increasing solubility in various non-regular solutions.

The author wishes to thank Professor E. Hutchinson for his interest in and discussions about this work while he spent summer at the Stanford University in 1961.

Department of Chemistry
Faculty of Engineering
Yokohama National University
Minami-ku, Yokohama

10) T. Isemura and Y. Kimura, *J. Polymer Sci.*, **16**, 90 (1955).
11) K. Aoki, *J. Am. Chem. Soc.*, **80**, 2904 (1958).

New Addition Reactions. II. Addition of Aliphatic Epoxides to Schiff Bases

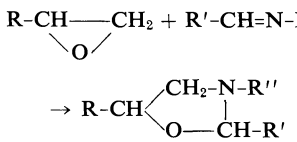
By Ryohei ODA, Masaya OKANO, Shohei TOKIURA and Akira MIYASU

(Received January 24, 1962)

Some studies of the formation of five-membered heterocycles by the addition of epoxides to aldehydes, ketones, esters and isocyanates have already been reported. We described in a previous paper[1] the results of a new reaction of epoxides with ketene. By analogy, the addition of epoxides to Schiff bases may be expected to produce oxazolidines. In 1950, Doughty et al.[2] observed the formation of these compounds by a similar addition of ethylenimine to aldehydes or ketones. It has now been found that in the presence of catalytic amounts (5~10 mol.%) of stannic chloride, the expected cyclization of aliphatic epoxides with Schiff bases proceeds smoothly, according to the following equation:

1) R. Oda, S. Munemiya and M. Okano, *J. Org. Chem.*, **26**, 1341 (1961).

2) J. B. Doughty, C. L. Lazzell and A. H. Collett, *J. Am. Chem. Soc.*, **72**, 2866 (1950).



All reactions were carried out in carbon tetrachloride at 10~20°C for three hours. The results of several experiments are shown in Table I. Unfortunately, in a similar reaction with styrene oxide, the attempt to isolate the desired adduct was unsuccessful, probably because of contamination with a hydroxyl compound (see Experimental).

The yields in this addition were generally not very high, and they were not improved by varying the reaction temperature or time. The use of boron trifluoride as a catalyst resulted in a lower yield of the desired product. It is of interest to note that *N-tert*-butylazomethine is capable of reaction with epoxides, even in the absence of a catalyst. This may be due to its high nucleophilicity. In the case of the reaction with benzalaniline, a considerable amount (ca. 70~90%) of the unreacted Schiff base could be recovered, but complete recovery was impossible because of the thermal instability of the product. On the other hand, when *N-tert*-butylazomethine was used as a Schiff base, a great loss (ca. 50%) of this compound was observed in a blank experiment, presumably due to simultaneous evaporation on distillation of the solvent and hydrolysis during the after-treatment. Therefore, no effort was made to recover it from the reaction mixture.

To ascertain the direction of the ring-opening of the substituted ethylene oxides, the adduct from propylene oxide and *N-tert*-butylazomethine was compared with two authentic specimens, i. e., 3-*tert*-butyl-4-methyl- and 3-*tert*-butyl-5-methyloxazolidines, prepared by the usual condensation method[3]. The results of mixed melting point determinations as their picrates showed that the product was the 3, 5-isomer. Moreover, vapor phase chromatographic analysis indicated that the liquid adduct did not contain any 3, 4-isomer. The structure of the solid propyleneoxide-benzalaniline adduct was also confirmed by independent synthesis from 1-anilino-2-propanol and benzaldehyde. In the case of epichlorohydrin, it has been shown that ring-opening always occurs at the primary position[4]; hence, the exclusive formation of the 3, 5-isomer would be expected.

Based on the observed orientation, an S_N2-like mechanism[5], which involves a nucleophilic attack by the Schiff base on the epoxide, may be postulated, but some additional evidence would seem to be desirable before a detailed mechanism can be proposed.

Experimental[6]

Some illustrative examples are given below.

3-*tert*-Butyl-5-methyloxazolidine.—A solution of 6.6 g. (0.025 mol.) of stannic chloride in 60 ml. of carbon tetrachloride was dropped over a period of 1 hr. into a stirred solution of 21.2 g. (0.25 mol.) of *N-tert*-butylazomethine (prepared by the procedure of Hurwitz[7]) and 15.9 g. (0.275 mol.) of propylene oxide in 100 ml. of carbon tetrachloride. The addition was carried out at 10~15°C. After additional stirring for 2 hr. at 20°C, the solution was poured into 100 ml. of water, and filtered to remove stannic hydroxide. The aqueous layer was separated from the organic layer and extracted with 50 ml. of carbon tetrachloride. The combined carbon tetrachloride layers were washed with water, dried, and evaporated. Distillation in vacuo gave 8.6 g. (24%) of the base, b. p. 56~57°C (20 mmHg). The picrate (monohydrate), after recrystallization from 98% ethanol, melted at 180°C. No mixed melting point depression was observed with the picrate of authentic 3-*tert*-butyl-5-methyloxazolidine, but there was a lower mixed melting point with the picrate of authentic 3-*tert*-butyl-4-methyloxazolidine.

Vapor phase chromatographic analysis of the crude distillate was carried out, using a 1-meter column containing polyethylene glycol 1500-Celite 545 (3 : 7 by weight), with nitrogen as a carrier gas, at 70°C. The chromatogram indicated that the product consisted mainly of the 3,5-isomer. No trace of the 3,4-isomer was detected.

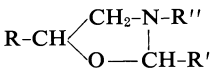
In this case, the authentic 3,5-isomer was synthesized by condensation between 1-bromo-2-propanol and *tert*-butylamine, followed by cyclization with formaldehyde. The pure base boiled at 53~54°C (15 mmHg), and its picrate (monohydrate) melted at 180~181°C (Analytical data are included in Table I). The authentic 3,4-isomer was similarly prepared from ethyl α-bromopropionate, via ethyl α-(*N-tert*-butyl)aminopropionate and 2-(*N-tert*-butyl)aminopropanol. The pure base boiled at 52~53°C (19 mmHg), and its picrate melted at 185~186°C.

The free base. Found: C, 67.01; H, 12.18; N, 9.56. Calcd. for $C_8H_{17}NO$: C, 67.09; H, 11.96; N, 9.78%. The picrate. Found: C, 45.20; H, 5.57; N, 15.03. Calcd. for $C_{14}H_{20}N_4O_8$: C, 45.16; H, 5.41; N, 15.05%.

5-Methyl-2, 3-diphenyloxazolidine.—A solution of 3.3 g. (0.0125 mol.) of stannic chloride in 30 ml. of carbon tetrachloride was added, drop by drop, over a period of 1 hr., to a solution of 45.3 g. (0.25 mol.) of benzalaniline and 15.9 g. (0.275 mol.) of propylene oxide in 100 ml. of carbon tetrachloride maintained at 10°C. Stirring was continued at

3) Cf. R. C. Elderfield, "Heterocyclic Compounds", Vol. 5, John Wiley, New York, N. Y. (1957), p. 391.
4) "Epichlorohydrin", Shell Chem. Corp., New York, N. Y. (1949).
5) Cf. R. E. Parker and N. S. Isaacs, *Chem. Revs.*, **59**, 742 (1959).
6) All temperatures are uncorrected.
7) M. D. Hurwitz, U. S. Pat., 2582128 (1952); *Chem. Abstr.*, **46**, 8146 (1952).

TABLE I. FORMATION OF OXAZOLIDINES FROM ALIPHATIC EPOXIDES AND SCHIFF BASES



R in epoxide[a]	R′ and R″ in Schiff base	Catalyst (Mol.%)[b]	Yield[c] %	B. p., °C (mmHg)	M. p. of picrate, °C
R=H[d]	R′=H, R″=$(CH_3)_3C$	$SnCl_4$ (10)	18	63～64(32)[e]	155[f]
R=H[d]	R′=H, R″=$(CH_3)_3C$	None	6	60～61(27)	155
R=CH_3	R′=H, R″=$(CH_3)_3C$	$SnCl_4$ (10)	24	56～57(20)[g]	180[h]
R=CH_3	R′=H, R″=$(CH_3)_3C$	BF_3 (100)	8	56～57(20)	180
R=CH_3	R′=H, R″=$(CH_3)_3C$	None	4	51～52(15)	180
R=CH_2Cl	R′=H, R″=$(CH_3)_3C$	$SnCl_4$ (10)	59	93～94(19)[i]	156[j]
R=H[d]	R′=R″=C_6H_5	$SnCl_4$ (5)	14(37)	84[k,l]	
R=CH_3	R′=R″=C_6H_5	$SnCl_4$ (5)	30(79)	88[k,m]	
R=CH_3	R′=R″=C_6H_5	None	Unreacted		
R=CH_2Cl	R′=R″=C_6H_5	$SnCl_4$ (5)	70	114～115[k,n]	
R=CH_2Cl	R′=R″=C_6H_5	BF_3 (10)	25(63)	114～115[k]	

a Ten mol.% excess of epoxides were used, unless otherwise indicated.
b Based on Schiff bases.
c Conversions based on consumed benzalaniline are shown in parentheses.
d Two equivalents of epoxide were used, because of its low boiling point.
e Found: C, 65.03; H, 11.73; N, 10.92. Calcd. for $C_7H_{15}NO$: C, 65.07; H, 11.70; N, 10.84%.
f Monohydrate. Found: C, 41.73; H, 5.33; N, 15.01. Calcd. for $C_{13}H_{20}N_4O_9$: C, 41.49; H, 5.36; N, 14.89%.
g Found: C, 66.84; H, 11.70; N, 9.93. Calcd. for $C_8H_{17}NO$: C, 67.09; H, 11.96; N, 9.78%.
h Monohydrate. Found: C, 43.17; H, 5.77; N, 14.62. Calcd. for $C_{14}H_{22}N_4O_9$: C, 43.07; H, 5.68; N, 14.35%.
i Found: C, 53.79; H, 9.30; N, 7.66; Cl, 20.05. Calcd. for $C_8H_{16}NOCl$: C, 54.07; H, 9.08; N, 7.88; Cl, 19.91%.
j Monohydrate. Found: C, 39.79; H, 5.11; N, 13.89; Cl, 8.70. Calcd. for $C_{14}H_{21}N_4O_9Cl$: C, 39.59; H, 4.99; N, 13.16; Cl, 8.35%.
k M. p.
l Reported m. p. 84～85°C [G. A. R. Kon and J. J. Roberts, *J. Chem. Soc.*, **1950**, 980].
m Reported m. p. 88.5～89.5°C (Ref. 8).
n Found: C, 70.00; H, 6.04; N, 5.22; Cl, 13.23. Calcd. for $C_{16}H_{16}NOCl$: C, 70.19; H, 5.89; N, 5.12; Cl, 12.95%.

20°C for an additional 2 hr. The reaction mixture was then poured into 100 ml. of water, made slightly basic with aqueous potassium hydroxide, and filtered. The organic layer was washed, dried, evaporated and distilled in vacuo to remove unreacted benzalaniline (28 g.). Recrystallization of the residue from ethanol afforded 18.0 g. (30%) of the product, m. p. 88°C. A mixed melting point with the authentic material prepared by condensation between 1-anilino-2-propanol and benzaldehyde[8] showed no depression.

5-Chloromethyl-2,3-diphenyloxazolidine.—The procedure employed was similar to that used for the preparation of 5-methyl-2,3-diphenyloxazolidine, except that 25.4 g. (0.275 mol.) of epichlorohydrin was employed. The product which separated from the carbon tetrachloride solution at the end of reaction was filtered, washed with water, and dried. Some additional product was also obtained from the solvent layer. Recrystallization from an ethanol-dimethylformamide mixture gave 47.8 g. (70%) of pale yellow crystals, m. p. 114～115°C.

An Attempt to Prepare the Adduct from Styrene Oxide and *N-tert*-Butylazomethine.—In a similar way, 33 g. of styrene oxide was treated with 21.2 g. of *N-tert*-butylazomethine in the presence of a stannic chloride catalyst. The isolated basic fraction, b. p. 111～113°C (4 mmHg), weighed 8.5 g. Even after duplicate vacuum distillations, its elemental analysis disagreed with that of the expected adduct. However, the infrared spectrum was similar to those of other 3-*tert*-butyloxazolidines except for the appearance of a strong hydroxyl absorption in the 3400 cm^{-1} region. The picrate obtained from this product melted at 152～154°C and showed analytical data corresponding to the picrate of the desired adduct.

Found: C, 52.69; H, 5.35; N, 12.61. Calcd. for $C_{19}H_{22}N_4O_8$: C, 52.53; H, 5.10; N, 12.90%.

No further study of the structure of the product was undertaken.

The authors are indebted to the Ube Industries, Ltd., for financial support of this work. They also wish to thank Dr. Toshihiko Oiwa for his vapor phase chromatographic analysis.

Institute for Chemical Research
Kyoto University
Takatsuki, Osaka

8) K. D. Petrov, *Sbornik Statei Obshchei Khim., Akad. Nauk. S. S. S. R.*, **1**, 374 (1953); *Chem. Abstr.*, **49**, 997 (1955).

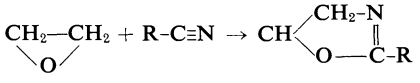
New Addition Reactions. III. Addition of Aliphatic Epoxides to Nitriles

By Ryohei ODA, Masaya OKANO, Shohei TOKIURA and Fujio MISUMI

(Received January 24, 1962)

In a previous paper[1], the formation of oxazolidines by the cyclic addition of Schiff bases to epoxides in the presence of Lewis acid catalysts was described. In this connection, the early study of a similar addition of sodium cyanamide to ethylene oxide to yield 2-amino-2-oxazoline by Fromm et al.[2] is of interest.

We have now extended this addition to study the reactions of aliphatic or aromatic nitriles with aliphatic epoxides in concentrated sulfuric acid. The formation of the cyclic adduct is illustrated by the following equation. When a Lewis acid catalyst was employed, however, no product, except for a polymeric product of the epoxide, was obtained:



R=CH_3, C_6H_5, etc.

In this concentrated sulfuric acid medium, some competitive reactions — e. g., addition of water and sulfuric acid to the epoxide, and hydrolysis of the nitrile—may be expected. In fact, the reaction of ethylene oxide with phenylacetonitrile afforded a 37% yield of phenylacetamide, in addition to the desired adduct (5%) and the unchanged nitrile (51%). However, isolation of the by-products derived from the epoxide was difficult because of their water-soluble nature, but the observation that, in a blank experiment with epichlorohydrin, the loss amounted to roughly 80% and no water-insoluble product except for the unchanged epoxide was isolated, seems to support the possibility of the occurrence of the above-mentioned side-reactions.

In view of the appreciable loss of epoxide, all reactions were carried out in a molar ratio of 2 epoxide to 1 nitrile. The reaction temperature was maintained at 5~10°C. The results of several experiments are shown in Table I. At somewhat higher temperatures, a decrease in the yield of the desired product was observed. Moreover, an attempted reaction with styrene oxide was unsuccessful owing to its rapid hydration.

In the addition of propylene oxide to acetonitrile, two isomers of the product, i. e., 2, 4- and 2, 5-dimethyl-2-oxazolines, are possible. In fact, although only one basic fraction was obtained by distillation, vapor phase chromatographic analysis indicated that it was composed of 70% of the 2, 4-isomer and 30% of the 2, 5-isomer. A similar orientation was observed on the addition of the same epoxide to benzonitrile. Here, the authentic materials used for the assignments of structure were prepared by a condensation reaction[3]. The predominant ring-opening at secondary carbon suggests an S_N1-like mechanism[4] which involves a nucleophilic attack by nitrile on the carbonium ion resulting from the ring-opening of the protonated epoxide. On the other hand, the reaction of epichlorohydrin with acetonitrile afforded only one isomer which was chromatographically homogeneous; no characterization of it was made because of the failure of an attempted independent synthesis. If the orientation is much influenced by the electron-withdrawing chlorine atom, as is seen in other acidic additions to epichlorohydrin[5], the 2, 5-isomeric structure rather than the 2, 4-isomeric structure for the adduct would be more likely.

Experimental[6]

Illustrative examples are given below.

2-Phenyl-2-oxazoline.—Benzonitrile (51.5 g., 0.50 mol.) was gradually dissolved in 55 ml. of concentrated sulfuric acid at ca. 0°C. Into this solution 44.5 g. (1.00 mol.) of ethylene oxide was dropped over a period of 3 hrs. with stirring. The temperature was maintained at 5~10°C. After completion of this addition, stirring at 10°C was continued for 2 hr. The reaction mixture was then allowed to stand overnight below 10°C and poured slowly into ca. 200 ml. of ice and water. The solution was made slightly acidic below 20°C with aqueous sodium hydroxide, and the precipitated mixture of sodium sulfate and benzamide was filtered off. The filtrate was extracted with benzene to remove the unchanged nitrile and then made strongly basic by the addition of a concentrated sodium hydroxide solution. It was then extracted with three 100 ml. portions of ether. The combined ether extracts were washed with a saturated sodium chloride solution and

1) R. Oda, M. Okano, S. Tokiura and A. Miyasu, This Bulletin, **35**, 1216 (1962).
2) E. Fromm et al., *Ann.*, **442**, 130 (1925).
3) H. Wenker, *J. Am. Chem. Soc.*, **57**, 1079 (1935).
4) Cf. R. E. Parker and N. S. Isaacs, *Chem. Revs.*, **59**, 742 (1959).
5) "Epichlorohydrin", Shell Chem. Corp., New York., N. Y. (1949).
6) All boiling and melting points are uncorrected.

TABLE I. FORMATION OF 2-OXAZOLINES FROM ALIPHATIC EPOXIDES AND NITRILES

Epoxide	Nitrile	Product	B. p., °C (mmHg)	Yield[a] %	M. p. of picrate, °C
Ethylene oxide	Acetonitrile	2-Methyl-2-oxazoline	110[b]	7	162[c]
Ethylene oxide	Isobutyronitrile	2-Isopropyl-2-oxazoline	137～138[d]	21(29)	134[e]
Ethylene oxide	Phenylacetonitrile	2-Benzyl-2-oxazoline	136～137 (20)[f]	5(10)	141[g]
Ethylene oxide	Benzonitrile	2-Phenyl-2-oxazoline	121(13)[h]	19(42)	177[i]
Propylene oxide	Acetonitrile	Mixt. of 2,4- and 2,5-dimethyl-2-oxazolines (70 : 30)[j]	116～118[k]	8	
Propylene oxide	Benzonitrile	Mixt. of 4- and 5-methyl-2-phenyl-2-oxazolines (70 : 30)[j]	127～129 (22)[l]	5(12)	
Epichlorohydrin	Acetonitrile	4- or 5-Chloromethyl-2-methyl-2-oxazoline	73～75 (9)[m]	12	127[n]
Epichlorohydrin	Acrylonitrile	4- or 5-Chloromethyl-2-vinyl-2-oxazoline	92～93 (22)	2	

a The figures in parentheses represent conversions based on consumed nitriles.
b Ref. 3 gives b. p. 111°C.
c Ref. 3 gives m. p. 163°C.
d Found: C, 63.49; H, 9.80; N, 12.60. Calcd. for $C_6H_{11}NO$: C, 63.68; H, 9.80; N, 12.39%.
e Found: C, 41.84; H, 3.79; N, 16.44. Calcd. for $C_{12}H_{14}N_4O_8$: C, 42.11; H, 4.12; N, 16.37%.
f Found: C, 74.81; H, 6.66; N, 8.81. Calcd. for $C_{10}H_{11}NO$: C, 74.51; H, 6.88; N, 8.69%.
g Monohydrate. Found: C, 47.81; H, 4.24; N, 13.75. Calcd. for $C_{16}H_{16}N_4O_9$: C, 47.06; H, 3.95; N, 13.72%.
h Ref. 3 gives b. p. 247°C.
i Ref. 3 gives m. p. 177°C.
j Determined by v. p. c. analysis.
k Found: C, 60.69; H, 9.19; N, 14.01. Calcd. for C_5H_9NO: C, 60.58; H, 9.15; N, 14.13%.
l Found: C, 74.53; H, 6.80; N, 8.42. Calcd. for $C_{10}H_{11}NO$: C, 74.51; H, 6.88; N, 8.69%.
m Found: C, 44.96; H, 6.13; N, 10.19; Cl, 26.62. Calcd. for C_5H_8NOCl: C, 44.95; H, 6.04; N, 10.49; Cl, 26.54%.
n Found: C, 36.77; H, 3.20; N, 15.63. Calcd. for $C_{11}H_{11}N_4O_8Cl$: C, 36.43; H, 3.06; N, 15.45%.

dried. The solvent was removed by evaporation, and the resulting oil was distilled to yield 13.9 g. (19%) of 2-phenyl-2-oxazoline, b. p. 121°C/13 mmHg. The recovered benzonitrile from the benzene extact weighed 28.4 g. (54%).

A Mixture of 2, 4- and 2, 5-Dimethyl-2-oxazolines.—Into a solution of 20.5 g. (0.50 mol.) of acetonitrile in 55 ml. of concentrated sulfuric acid, 58 g. (1.00 mol.) of propylene oxide was dropped over a period of 3 hr. at 5～10°C. Stirring was continued at 10°C for an additional 2 hr. After the solution had stood overnight below 10°C, the reaction mixture was gradually poured into 200 ml. of ice and water. The solution was then neutralized with aqueous sodium hydroxide, and the resulting precipitate was filtered off. The filtrate was made strongly basic with concentrated sodium hydroxide and extracted three times with 100 ml. of ether. After the removal of the ether, the residue was distilled and 4.1 g. (8%) of the product, b. p. 116～118°C, was obtained. Recovery of unchanged acetonitrile was difficult due to its water-solubility. A redistilled sample prepared for elemental analysis was chromatographed on a 2-meter column containing polyethylene glycol 4000-Celite 545 (3 : 7 by weight), with hydrogen as a carrier gas, at 70°C. Data showed that it was composed of 70% of 2,4-dimethyl-2-oxazoline (low retention) and 30% of the 2,5-isomer (high retention). Authentic 2,4- and 2,5-dimethyl-2-oxazolines used as references were prepared by the method of Wenker[3] from 2-amino-1-propanol and 1-amino-2-propanol with acetic acid respectively. The 2-amino-1-propanol used here was synthesized by esterification of *dl*-alanine[7], followed by reduction with lithium aluminum hydride[8]. 1-Amino-2-propanol was commercially available. The pure 2,4-isomer boiled at 116～117°C [lit.[9] 30°C/35 mmHg], and its picrate melted at 130～131°C (lit.[9] 130～135°C). The 2,5-isomer boiled at 117～118°C (lit.[10] 117～119°C), and its picrate at 114～115°C (lit.[10] 114～115°C).

***x*-Chloromethyl-2-vinyl-2-oxazoline and its Polymer.**—The procedure employed was similar to that used for the preparation of the above oxazoline except that a small amount of hydroquinone was added as a polymerization inhibitor. The product, b. p. 92～93°C/22 mmHg, easily polymerized on

7) S. D. Brewer and R. M. Herbst, *J. Org. Chem.*, **6**, 870 (1941).
8) D. Karrer, P. Portmann and M. Suter, *Helv. Chim. Acta*, **31**, 1617 (1948).
9) N. V. Organon, Dutch Pat. 81868; *Chem. Zentr.*, **1959**, 3971.
10) A. Uekinck, *Ber.*, **32**, 975 (1899).

standing. No effort was made to characterize the structure of the adduct. In the bulk polymerization using benzoyl peroxide as an initiator, a hard, clear, colorless polymer was obtained. This polymer is soluble in water and *m*-cresol, but insoluble in ethanol and benzene.

Found: C, 48.75; H, 5.43; N, 9.73; Cl, 24.15. Calcd. for $(C_6H_8NOCl)_n$: C, 49.50; H, 5.54; N, 9.62; Cl, 24.35%.

The authors wish to express their gratitude to the Ube Industries, Ltd., for financial support of this study. They also wish to express their deep appreciation to Dr. Toshihiko Oiwa for his vapor phase chromatographic anaysis.

Institute for Chemical Research
Kyoto University
Takatsuki, Osaka

High-Kinetic Energy Fragment Ions from Aliphatic Hydrocarbons under Electron Impact. I. Measurement and High-Kinetic Energy Methyl Ions from 1,3-Butadiene

By Toshikazu TSUCHIYA

(Received November 20, 1961)

It has long been known that fragment ions from diatomic and polyatomic molecules by electron impact often have appreciable kinetic energies. The distribution of kinetic energies among the fragment ions formed from the diatomic molecules of a given species can now be explained satisfactorily on the basis of potential energy diagrams of the normal state and of the various ionized states using the Franck-Condon principle[1].

Fragment ions from polyatomic molecules have not been so thoroughly studied as those from diatomic molecules. Hustrulid et al.[2], in a study of the mass spectrum of benzene, showed that the satellite peak on the high mass side of each of the peaks of the masses *m/e* 15, 26, 27, 14, 13 and 12, is caused by ions to which the dissociation process has imparted a large kinetic energy lying within a narrow range. It was suggested that the high energy ion came from the dissociation of doubly charged molecules into two singly charged fragments. The appearance potential of the satellite peaks was found to be much higher than the main peaks, a finding consistent with this explanation.

Hipple et al.[3] gave the collector of their mass spectrometer a positive potential, relative to the analyzer, sufficient to stop all ions of a zero initial velocity, and so was able to record the satellite peak alone. This experimental result shows that the satellite peak came from ions with a high initial velocity, too. Mohler et al.[4] measured the kinetic energies and intensities of satellites which accompany the *m/e* 15 spectra of 15 hydrocarbons; they also discussed the reaction mechanism by which the high kinetic energy ions are produced. Their mass spectrometer was provided with a metastable ion suppressor slit between the exit slit of the analyzer and the ion collector. The slit could be set at an adjustable positive potential to stop any ions which have lost kinetic energy while traversing the analyzer tube. The slit had a focusing action for ions and increased the resolving power of the instrument. They observed satellites on *m/e* 15 by applying the appropriatepoten tial to the suppressor slit and by using very low ion-accelerating voltages ranging from 500 to 145 V.

Berry[5], in a study of discrimination effect, has measured the velocity distribution of methyl ions from *n*-butane, and of various other ions, by deflecting the ion beam parallel to the magnetic field by an electric field. He confirmed that there are two groups of ions, one with a thermal distribution and the other with a high kinetic energy.

In this paper a method for measuring high energy ions with a conventional analytical mass spectrometer without any such equipment as an additional deflecting electrode or a metastable ion suppressor slit, and some results are described.

1) H. D. Hagstrum, *Rev. Modern Phys.*, 23, 185 (1951).
2) A. Hustrulid, P. Kusch and J. T. Tate, *Phys. Rev.*, 54, 1037 (1938).
3) J. A. Hipple, R. E. Fox and E. U. Condon, ibid., 69, 347 (1946).
4) F. L. Mohler, V. H. Dibeler and R. M. Reese, *J. Chem. Phys.*, 22, 394 (1954).
5) C. E. Berry, *Phys. Rev.*, 78, 597 (1950).

Experimental

A Consolidated Model 21-103C analytical mass spectrometer with a dual collector slit was used in this research. This instrument has a mass-resolving power of about 600 when a 7 mil (ca. 0.2 mm.) slit is used. With the slit, if the magnetic field is reduced and the m/e 15 ion of propane is focused at about 500 V. or less, the satellite peak described by Mohler et al. appears. Figure 1 illustrates the mass spectrum of propane, m/e 15 and 14 under these conditions. The m/e 15 satellite originates from ions having excess kinetic energies* as has been well established[4]. However, if a satellite peak is observed in the mass spectrum of a new substance, the satellite may be a KE peak, or a peak which originates from metastable ions or from ordinary TE ions having an m/e value slightly different from the m/e value of the "mother" peak. We must, therefore, distinguish KE peaks from those peaks mentioned above. In the experiments made by Mohler et al. metastable ions, if desired, could be eliminated by the use of a metastable ion-suppressor slit.

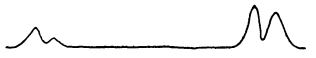


Fig. 1. Doublets at m/e 14 and m/e 15 in the spectra of propane.
Electron current; 19.5 μA, $V_i \fallingdotseq 500$ V., $V_r = 0$ V.

In order to study KE ions by means of a conventional mass spectrometer, we shall consider, for a moment, how to distinguish KE peaks from the other peaks in the spectrum. For this purpose, we shall now study the properties of the following doublets and peaks by varying the ion-accelerating and ion-repeler voltages: (1) m/e 15 doublets in the spectrum of n-butane and propane, (2) the m/e 31.9 peak of n-butane, and (3) the m/e 44 peaks of propane and carbon dioxide. The higher mass side peak of the m/e 15 doublet is the KE peak; the m/e 31.9 peak is a metastable peak, and the m/e 44 peaks are TE peaks.

Distinction between KE and Other Peaks.—*Influence of* V_i.—Figure 2 shows the effect of varying the ion-accelerating voltage, V_i, on various peaks. The spectra were taken by voltage scanning in appropriate magnetic fields. Curve 1 in this figure represents the m/e 15 peak ratio, I_k/I_t, for propane. The ion-repeler voltage, V_r, was about 5 V. Curve 2 is the peak ratio $(m/e\ 31.9)/(m/e\ 30)$ for n-butane. V_r's were set at optimum positions for m/e 31.9 peak focusing. Curve 3 is the m/e 44 peak ratio of propane to the carbon dioxide in a mixture of these compounds. V_r's were about 0.5 V.

Curve 1 in Fig. 2, which gives the m/e 15 intensity ratio, I_k/I_t, for propane, has a large positive

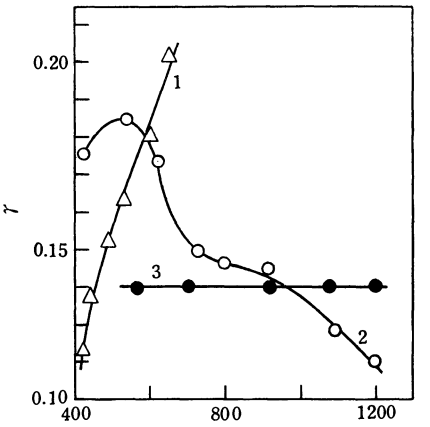


Fig. 2. Peak ratios γ versus ion accelerating voltage, V_i.
Curve 1: m/e 15 peak height ratio of propane, (Higher mass side peak)/(Lower mass side peak).
Curve 2: Peak height ratio of n-butane, $(m/e\ 31.9)/(m/e\ 30)$.
Curve 3: m/e 44 peak height ratio, $(C_3H_8)/10\times(CO_2)$.

gradient, and can easily be distinguished from curves 2 and 3 in the same figure. According to Berry[5], the larger the initial kinetic energies of the ions, the larger the absolute value of the tangent of the ion intensity versus V_i curve. The behavior of curve 1 can be well explained by assuming that the ions on the higher mass side peak have greater kinetic energies.

Metastable peaks result from the spontaneous dissociation of an ion after the ion has been accelerated but before it has passed very far into the analyzing magnetic field. The peaks do not follow the equation

$$m/e \propto H^2/V_i$$

where H is the magnetic field. The point where the dissociation takes place depends on the speed of the mother ion and is a function of V_i. Curve 2 in Fig. 2, which gives the peak intensity ratio $(m/e\ 31.9)/(m/e\ 30)$ of n-butane, shows that the metastable peak intensity, I_m, tends to decrease relative to the normal ion intensity, I_t, as V_i is reduced in the range of V_i larger than about 500 V. This may be explained as follows. The smaller the V_i value is, the nearer to the point of formation of ordinary ions is the point of dissociation of the mother ion, and consequently, the more efficiently focused is the beam of the dissociated product ions. The details of curve 2 may be explained by the potential distribution in the various parts of the ion source. This explanation is a tentative one, and, moreover, the experiment concerns only the m/e 31.9 ion of n-butane. Therefore, to establish that the behavior of the metastable ion is proper to all metastable ions, further investigations on various ions are, of course, necessary. However, if a doublet is observed and if the ratio of the peak intensities

* For convenience, ions having excess kinetic energies will hereafter be called KE ions, and the peaks due to KE ions will be called KE peaks. Similarly, ions having thermal energies corresponding to the temperature of the ion-source will be called TE ions, and the peaks due to TE ions will be called TE peaks. The intensities of the KE and TE peaks will be indicated by I_k and I_t respectively.

for the components behaves in the way shown by curve 2 in Fig. 2, the peaks invariably do not come from KE ions. The distinction between curves 1 and 2 is outstanding, as may be seen from a comparison of curves in Fig. 2.

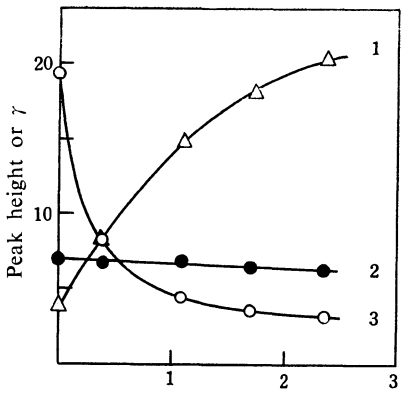


Fig. 3. KE peak height, I_k, TE peak height, I_t, and the ratio I_k/I_t versus ion repeller voltage, V_r.
n-Butane. $V_i \fallingdotseq 500$ V., electron current: 19.5 μA. Peak height is represented by an arbitrary scale.
Curve 1: I_t, *m/e* 15 lower mass side peak height.
Curve 2: I_k, *m/e* 15 higher mass side peak height.
Curve 3: $10\times(I_k/I_t)$.

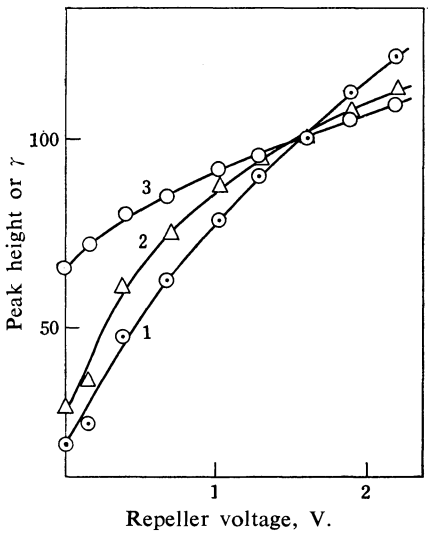


Fig. 4. Metastable ion peak height, I_m, TE peak height, I_t, and the ratio, I_m/I_t versus ion repeller voltage, V_r.
n-Butane. $V_i \fallingdotseq 500$ V., electron current: 19.5 μA. Peak height is represented by an arbitrary scale.
Curve 1: I_m, $(m/e\ 31.9)\times 10$
Curve 2: I_t, $(m/e\ 30)$
Curve 3: γ, $(I_m/I_t)\times 10^3$

Curve 3 in Fig. 2, which gives the *m/e* 44 peak ratio of propane to carbon dioxide, concerns two spepcies of ions which are produced at a normal position in the ionization chamber and which have close *m/e* values. These ions have only a kinetic energy corresponding to the temperature of the ionization chamber. The curve shows that the influences of V_i on these ions are nearly the same.

Influences of V_r.—Figures 3 and 4 show the influences of the ion-repeller voltage, V_r, on various peaks. The data in Fig. 3 were obtained by measurements of the doublet at *m/e* 15 of *n*-butane, with the V_i being fixed at about 500 V. In Fig. 3, curve 1 shows the I_t, i.e., the lower mass side peak height of the doublet, while curve 2 shows the I_k, the higher mass side peak height of the doublet, and curve 3 shows the ratio I_k/I_t. In Fig. 4, the height, I_m, of the *m/e* 31.9 metastable peak (curve 1), the height, I_t, of the *m/e* 30 peak (curve 2), and the ratio, I_m/I_t, (curve 3) are given as functions of V_r.

The *m/e* 44 peak versus the V_r curves for both propane and carbon dioxide showed much the same tendency as curve 1 in Fig. 3, and the ratio of the two peaks was almost constant over the range of V_r used.

The influence of the ion-repeller voltage, V_r, on metastable ion peaks was investigated by Hipple et al.[3] They showed that an increase in V_r increases both normal TE ion peaks and metastable ion peaks, and that the effect is more pronounced in the case of metastable peaks. They also pointed out that KE ions are less affected by V_r than TE ions. Curve 3 in Fig. 4, which represents the ratio of the metastable peak to the TE peak, has a positive tangent, as they demonstrated. Curve 3 in Fig. 3, which represents the ratio of the KE peak to the TE peak, has a negative tangent.

The ions produced in the ionization chamber are pushed out through the ionization chamber slit into the ion accelerating system by the action of the repeller voltage, V_r. When a small voltage V_r is applied to the repeler, I_t is increased by this action, as may be seen from curve 1 in Fig. 3. If ions with an initial kinetic energy are produced in the ionization chamber and have a velocity component perpendicular to the plane of the exit slit of the chamber, the ions are expected to pass through the slit irrespective of V_r values above zero. This expectation is shown to be true by curve 2 in Fig. 3, which, as Hipple et al. pointed out qualitatively, shows that the V_r values have only a slight effect on these ions, which are considered to have appreciable kinetic energies.

The finding that the ratio of the *m/e* 44 peaks of propane to carbon dioxide was practically independent of V_r shows that the influences of V_r on TE peaks are the same.

Measurement. — The KE peak, TE peak, metastable peak, and their ratios have been investigated as functions of V_r and V_i, by taking the peaks of *n*-butane and propane as examples. As is clear from a consideration of the results, the properties shown in Figs. 2, 3 and 4, except for the $I_m \sim V_i$ relation, are not specific to the substances taken as examples, but are specific to each species of ions.

To distinguish between the TE, KE, and metastable peaks, we may vary V_i or V_r and examine the resulting influences on the intensity, I, of the peak under consideration or on the intensity ratio of I to a peak which is known to be a TE peak.

All the KE ions observed so far have accompanied TE ions and have appeared as doublets. When a doublet spectra appeared in the mass spectrum of a compound, the high mass side peak was examined by the procedure mentioned above to determine whether or not it was KE peak. After a peak was identified as a KE peak, the kinetic energy, E, the ion-accelerating voltage difference of the doublet[4], was measured by one or both of the following procedures: (a) The ion accelerating voltages of the doublet are measured by setting the voltage manually on each peak, with the potentiometer supplied with the instrument to calibrate the mass scale. E is obtained as the difference of the voltages. (b) The ion-accelerating voltages of the two peaks just before and after a doublet are measured. From these values and the distances, recorded on the chart, between the two peaks and between the peaks of the doublet, the ion-accelerating voltage difference corresponding to the doublet is calculated by interpolation.

When the resolution and intensity are favorable, the reproducibility of the measurements was within ± 0.2 eV.

The influences of the ion-accelerating voltage, V_i, and the ion-repeller voltage, V_r, on the measured kinetic energy values were checked by varying V_i and V_r values in the ranges 400~600 and 0~10 V. respectively. The results showed that the variation in these voltages has no influence on the measured kinetic energies.

Because of the overlapping of the tails of the major and minor peaks of a doublet, an error in locating the maximum point of the minor peak may result from a marked unbalance of the peak heights of a doublet. To minimize the effect of the overlapping of peak tails on the measured E value, all E values were measured with a repeller voltage of $V_r=0$.

Results and Discussion

Table I summarizes the results of the measurements of the kinetic energy peaks for methyl ion in ethane, propane, *n*-butane, isobutane, propylene, and 1, 3-butadiene. Since the first four substances were investigated by Mohler et al.[4], their results are also listed in the table as a check.

The second column gives the kinetic energy value found in the present work, and the fifth column, the value reported by Mohler et al. Taking the accuracies of measurements into account, the coincidence of data is reasonable.

The third column gives the intensity, found by the present measurements, of the satellite peak relative to the thermal energy peak, and the sixth column, the intensity found by Mohler et al. A comparison of the data shows that the values of the present work are about 10 times larger than those of Mohler et al. As can be seen from curve 1 in Fig. 2 and curve 3 in Fig. 3, these ratios depend markedly on the ion-accelerating voltage, V_i, and the ion-repeler voltage, V_r. The values of V_i and V_r used in this work were, respectively, about 500 and 0 V. On the other hand, the value of V_i used by Mohler et al. was 140 V.; their V_r value was not indicated. The discrepancies in the intensity ratios may be due to the differences in these experimental conditions.

In the present experiment, the m/e 15 KE ion of an appreciable intensity was found in the spectrum of 1, 3-butadiene. KE ions of m/e 14 were detected by Hipple et al.[3] in the spectrum of this compound. The m/e 15 peaks of 1, 3-butadiene are rearrangement peaks, and are unique in that the intensity of the KE peak is about four times higher than that of the TE peak. This phenomenon may be explained as follows: The first and fourth carbon atoms of the compound are more reactive than the second and third atoms. In an excited state, proposed by Eyring et al.[6], of the compound under electron impact, the more reactive first or fourth carbon atom takes the hydrogen atom from the adjacent second or third carbon atom and forms a methyl group. During this transfer, the equilibrium C=C distance is assumed to remain approximately the same. Since the equilibrium distance of CH_3–C is longer than that of CH_2=C, the Franck-Condon region corresponding to the CH_2=C bond of the mother compound crosses the CH_3–C potential energy curve for an upper state at a region higher than the dissociation asymptote of the curve; thus, the methyl ion, formed by rearrangement, dissociates with a high kinetic energy.

Hustrulid et al.[2] suggested that these ions of a high kinetic energy result from the dissociation of doubly-charged ions formed by electron impact. Mohler et al.[4] computed the repulsive energies of various compounds on this assumption. The "Coulomb energy" calculated by them, i. e., the calculated repulsive energy, is cited in the last column of Table I. When a molecular ion dissociates into two fragments, these fragments have equal momenta. By assuming that doubly-charged ions dissociate into two fragments, one of the two being methyl ion, and that the law of conservation of momenta holds, the total kinetic energy of both fragments has been computed from the value in column 2; this is listed in the fourth column of Table I. In the seventh column the total energy calculated by Mohler et al. is

6) H. M. Rosenstock, M. B. Wallenstein, A. L. Wahrhaftig and H. Eyring, *Proc. Natl. Acad. Sci. U. S.*, 38, 667 (1952).

TABLE I. CH_3^+ IONS OF HIGH KINETIC ENERGY IN MASS SPECTRA OF HYDROCARBONS

Compound	Present experiment			Result of Mohler et al.*			
	KE of satellite	Relative intensity	Total KE	KE of satellite	Relative intensity	Total KE	Coulomb energy
Ethane	2.5	0.54	5.0	2.3	0.03	4.6	5.6
Propane	2.4	0.89	3.6	2.2	0.076	3.3	3.7
Propylene	2.6	0.52	4.0	—	—	—	—
n-Butane	2.3	1.41	3.1	2.2	0.137	3.0	2.9
Isobutane	2.5	1.16	3.4	2.6	0.11	3.5	3.7
1,3-Butadiene	2.5	4.15	3.3	—	—	—	—

Energy unit is eV.

* F. L. Mohler, V. H. Dibeler and R. M. Reese, *J. Chem. Phys.*, **22**, 394 (1954).

given for purposes of comparison. In the cases of ethane and propane, the total energies found in this work are nearer to the "Coulomb energy" than those found by Mohler et al. The total energies of other substances are nearly the same in both cases.

If the mechanism proposed by Hustrulid-Mohler* is valid, the total energy is approximately inversely proportional to the distance between the carbon atoms at both ends of the molecular chain[4]. In the cases of two series of substances, ethane, propane, and *n*-butane, and propylene and propane, this expectation is realized qualitatively, as may be seen from the fourth column, Table I; the assumption of H-M appears to be true from this consideration. However, if a doubly-charged ion actually dissociates into two fragment ions, two species of ions with the same momentum must be observed. To clarify the origin of high kinetic energy ions from this point of view, it is desirable to study the kinetic energies of all the fragment ions of a compound.

Taking ethylene as an example, all peaks were examined, and kinetic energy satellites were found at *m/e* 13 and 14. Table II summarizes the results of these measurements. The first column gives the *m/e* values at which kinetic energy satellites were found; the second and third columns give, respectively, the kinetic energy value and the intensity of the satellite peak. The conditions of measurements were much the same as those for the measurements in Table I.

The following reactions were studied for the fragmentation of ethylene, according to the H-M mechanism:

$$C_2H_4 \rightarrow C_2H_4^{2+} \rightarrow \begin{cases} 2CH_2^+ & (1) \\ CH_2^+ + CH^+ + H & (2) \end{cases}$$

From Table II, the measured total energy for reaction 1 is 4.4 eV., if it is assumed that the fragments have only translational kinetic

* Abbreviated as H-M.

TABLE II. IONS OF HIGH KINETIC ENERGY IN MASS SPECTRA OF C_2H_4

m/e	KE of satellite	Intensity (arbitrary unit)
13	2.1 eV.	2.4
14	2.2 eV.	6.6

energies. If the H-M assumption were valid, the total energy for the fragmentation of KE ions of ethane would be smaller than that for reaction 1. However, since the value for ethane is 5.6 eV. according to the computation by Mohler et al.[4], is 5.0 eV. according to the computation made in the present work (Table I), the H-M mechanism of fragmentation does not hold for reaction 1.

If it is assumed that the H-M mechanism holds and that the hydrogen atom produced carries away a large amount of kinetic energy, the reaction represented by Eq. 2 can take place. However, according to the relation between the ion intensities of methylene ion and methylidyne ion in Table II, it is considered that all the methylene ions are not formed by the reaction. It follows that, from the standpoint of the H-M mechanism, a fraction of methylene KE ions is produced, together with neutral fragments.

Summary

With a conventional analytical mass spectrometer and without any additional electrodes, fragment ions produced with excess kinetic energies by electron impact can be detected and studied quantitatively. Mainly methyl KE ions in the spectra of seven hydrocarbons have been measured. A comparison of the results on methyl ions in four hydrocarbons with reported values showed a satisfactory consistency.

An appreciable part of the *m/e* 15 rearrangement ions of 1,3-butadiene had excess kinetic energies. The mechanism of the formation of the ions has been proposed which assumes a transfer of the hydrogen atom from a second

carbon atom of the molecule to the first carbon atom followed by the recoil of the resulting two groups of atoms. The study of the KE ions in the spectra of the ethylene molecule from the standpoint of the H-M assumption shows that the mechanism of the formation of various KE ions is complicated and deserves more detailed study.

Government Chemical Industrial Research Institute, Tokyo
Shibuya-ku, Tokyo

Infrared Spectra of Acyclic Imides. V. Infrared Spectra and Structure of Acyclic Imides in Solutions

By Toyozo UNO and Katsunosuke MACHIDA

(Received January 11, 1962)

In earlier papers of this series[1-4], it has been shown that the infrared spectra of saturated acyclic imides in the crystalline state are closely related to the configuration of the -CONHCO- group. Some higher homologs of diacetamide (R-CONHCO-R', R=CH_3, C_2H_5 and *n*-C_3H_7; R'=C_2H_5 and *n*-C_3H_7) have been proved to be crystallized in a stable form taking the trans-trans configuration[2,3]. The characteristic frequencies of the trans-trans -CONHCO- group have been assigned, and their similarity to the characteristic frequencies of the trans -CONH- group has been pointed out[2]. No example of the trans-cis -CONHCO- group, however, has been found to exist in the crystalline state except for the stable form (form A) of diacetamide[1], the first member of the homologous series. In connection with these results, the present paper deals with the infrared spectra (4000 to 900 cm^{-1}) of these acyclic imides dissolved in various non-polar solvents. It will be shown that the higher homologs, as well as diacetamide itself, take the trans-cis configuration when dissolved in a non-polar solvent, such as carbon tetrachloride, tetrachloroethylene or carbon disulfide. The characteristic frequencies of the trans-cis -CONHCO- and -CONDCO- groups in the rock salt region will also be discussed in detail.

Results and Discussion

Diacetamide in Non-polar Solvents.—In the infrared measurements of the solutions of diacetamide, the three non-polar solvents, carbon tetrachloride, tetrachloroethylene and carbon disulfide, lead to nearly identical spectra except for covering the regions where their own absorptions arise. By using these solvents in turn, an almost complete range of the spectra of diacetamide dissolved in a non-polar solvent at a concentration between 0.25 and 0.01 mol./l. can be recorded from 4000 to 900 cm^{-1}. The infrared spectra thus obtained for several solutions of diacetamide and diacetamide-*d* are shown in Fig. 1[5].

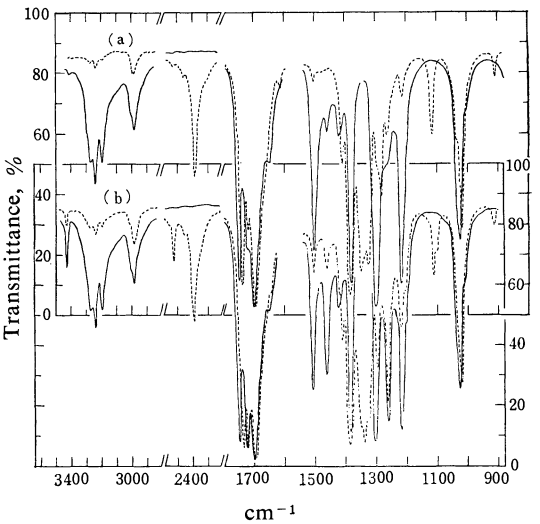


Fig. 1. Infrared spectra of diacetamide (solid line) and diacetamide-d (broken line); (a) 0.34 mol./l., (b) 0.012 mol./l.

1) T. Uno and K. Machida, This Bulletin, **34**, 545 (1961).
2) T. Uno and K. Machida, ibid., **34**, 551 (1961).
3) T. Uno and K. Machida, ibid., **34**, 821 (1961).
4) T. Uno, K. Machida and I. Hamanaka, ibid., **34**, 1448 (1961).

5) The infrared spectra shown in Figs. 1, 2, 4 and 5 were recorded with the use of the following cell length and solvents: (a) 0.1 mm.; CCl_4: (b) 2.85 mm.; 3500~1600 and 1480~1300 cm^{-1}, CCl_4: 1550~1480 cm^{-1}, C_2Cl_4; 1300~900 cm^{-1}, CS_2.

TABLE I. THE INFRARED FREQUENCIES (cm^{-1}) DUE TO ASSOCIATED MOLECULES

	Diacetamide	*N*-Acetylpropionamide	Dipropionamide	*N*-Propionyl-*n*-butyramide	Di-*n*-Butyramide
R	CH_3	CH_3	C_2H_5	C_2H_5	$n\text{-}C_3H_7$
R′	CH_3	C_2H_5	C_2H_5	$n\text{-}C_3H_7$	$n\text{-}C_3H_7$
R-CONHCO-R′					
Imide Ia+Imide II	3277 sh[b]	3275 sh	3273 sh	3273 sh	3269 sh
ν_{N-H}[a]	3222 m	3220 m	3220 m	3219 m	3218 m
Imide Ib+Imide II	3170 m	3168 m	3160 m	3157 m	3152 m
ν_{C-H}	2998 w	2988 m	2985 m	2980 m	2969 s
	—	2948 sh	2942 w	2942 sh	2937 sh
	—	2889 w	2886 sh	2883 w	2879 w
Imide Ia ($\nu_{C=O}$ free)	1747 s	1747 s	1747 s	1746 s	1743 s
Imide Ib ($\nu_{C=O}$ bonded)	1698 vs	1698 vs	1694 vs	1694 vs	1690 vs
Imide II (δ_{N-H}, ν_{C-N-C} antisym.)	1503 s	1502 s	1498 s	1496 s	1495 s
CH_3 asym. deform., CH_2 bend.	—	1462 w	1461 m	1461 m	1461 m
	1423 w	1423 w	1421 w	1420 w	1420 sh
CH_3 sym. deform.	1383 s	1382 s	1383 s	1382 s	1394 s, 1377 sh
CH_2 twist., CH_2 wag.	—	—	1301 w	1337 sh, 1300 w	1321 w, 1295 w
Imide III					
(ν_{C-N-C} sym.)	1301 s	1302 s, 1220 s	1214 s	1215 s	1205 s
(δ_{N-H}, ν_{C-N-C} antisym.)	1216 s	1159 m	1160 m	1160 m	1160 m
$\nu_{skeletal}$, CH_3 rock., CH_2 rock.	—	—	—	—	1100 m
	—	1075 w	1083 m	1081 m	1054 w
	1028 s	1030 w	1060 sh	1063 sh	1041 w
	—	—	—	—	990 w
	—	924 w	931 w	933 w	973 w
R-CONDCO-R′[c]					
ν_{N-D}	2390 m	2390 m	2385 m	2380 m	2380 m
Imide Ia ($\nu_{C=O}$ free)	1737 s	1737 s	1736 s	1735 s	1733 s
Imide Ib ($\nu_{C=O}$ bonded)	1695 vs	1694 vs	1689 vs	1688 vs	1687 vs
CH_3 asym. deform., CH_2 bend.	—	1463 w	1462 m	1462 m	1462 m
	1418 w	1420 sh	1435 w	1434 w	1435 w
CH_3 sym. deform.	1385 s	1384 s, 1357 sh	1385 vs, 1359 sh	1397 sh, 1386 s	1397 s, 1380 sh
Imide II′					
(ν_{C-N-C} antisym.)	1350, 1326 db, s	1328 sh, 1314 s	1300 s	1304 s	1335 s, 1312 m
(ν_{C-N-C} sym.)	1286 m	1211 m	1208 m	1208 m	1200 m
δ_{N-D}, $\nu_{skeletal}$, CH_3 rock., CH_2 rock.	1112 m	1109 w	—	—	1103, 1086 db, m
	—	1078 m	1079 s[d]	1078 s[d]	
	—	—	1059 sh	1060 w	1058 w
	1024 s	1034 s[d]	1025 w	1026 w	1043 w
	—	980 w	984 w	981 w	1007 m[d]
	913 w	959 w	959 w	961 w	994 w

a) ν, stretching; δ, in-plane deformation.

b) vs, very strong; s, strong; m, medium; w, weak; sh, shoulder; db, doublet.

c) The ν_{C-H} frequencies are the same as the corresponding undeuterated compounds.

d) Probably the imide III′ frequencies.

Most of the bands observed for the concentrated solution show, in intensities as well as in frequencies, marked correspondences with the bands of the crystal of diacetamide in form A[1] (see Table I). The N–H stretching band appears near 3220 cm^{-1}, indicating the presence of hydrogen bonds. The complicated feature of this band is quite analogous to that of the triplet observed in the same region for the crystal in form A. The 0.34 mol./l. solution shows two C=O stretching (imide I) bands, at 1747 and 1698 cm^{-1}, of which the band with the lower frequency is stronger than the other, as in the case of form A. The analogy in infrared spectra between the concentrated solution and the crystal in form A is preserved

TABLE II. THE CHARACTERISTIC FREQUENCIES (cm^{-1}) DUE TO THE MONOMERS[a]

	Diacetamide	*N*-Acetylpropionamide	Dipropionamide	*N*-Propionyl-*n*-butyramide	Di-*n*-butyramide
R-CONHCO-R′					
ν_{N-H}	3416	3416	3416	3416	3416
Imide I	1720	1718	1718	1718	1715
Imide II	1465	1462[b]	1461[b]	1461[b]	1461[b]
Imide III	1263	1265 1187	1187	1186	1180
R-CONDCO-R′					
ν_{N-D}	2523	2523	2523	2523	2523
Imide I	1717	1717	1715	1715	1712
Imide II′	1339 1260	1183	1183	1180	1177

a) Only the frequencies were listed which differ appreciably from those of the associated molecules.
b) Overlapped by the CH_3 asymmetric deformation bands.

on deuteration. For instance, the bands at 1503, 1301 and 1216 cm^{-1} observed for diacetamide in the solution disappear on deuteration. Instead, diacetamid-*d* shows a strong doublet near 1340 cm^{-1} and a weak band at 1286 cm^{-1}. These features of spectral change have also been observed for form A in a quite similar way[1].

It has been pointed out previously[1] that the difference in the configurations of the N–H and the C=O bonds in the –CONHCO– group results in the marked difference in the characteristic bands of this group. In this connection, the present results strongly suggest that the configuration of the –CONHCC– group of diacetamide in the concentrated solution in the non-polar solvents is similar to that involved in the crystal in form A, that is, it is similar to the trans-cis configuration. The dimeric association of diacetamide dissolved in nitrobenzene has been suggested on the basis of the cryoscopic study[6]. Although the difference in the nature of the solvents must be taken into account, it seems quite probable that the association of diacetamide dissolved in the non-polar solvents is also dimeric, the two molecules involved being in the trans-cis configuration. If this is valid, the characteristic bands of the –CONHCO– group observed for the concentrated solution must be given reasonable assignments on the basis of the trans-cis configuration. Taking into account the spectral change on deuteration, we can pick up several characteristic bands of the –CONHCO– group besides the C=O stretching (imide I) bands, which may be assigned without question. Thus, the imide II, III and II′ frequencies shown in Table I were determined by analogy with the corresponding characteristic frequencies of the trans-trans configuration[2]. In the following sections, the nature of these characteristic bands will be discussed in relation to the configuration of the –CONHCO– group.

The frequency shifts on the change from the crystal in form A to the concentrated solution in the non-polar solvents are rather small for these characteristic bands. This is analogous to the case of *N*-methylacetamide, the characteristic bands of which have been reported to show small frequency shifts on the change from the crystal in the stable form above the transition point to the concentrated solution in carbon tetrachloride[7]. The characteristic bands of diacetamide dissolved in the non-polar solvents undergo marked changes on the change in concentration. The N–H stretching and the imide II bands (3222 and 1503 cm^{-1}) of the associated molecules are replaced gradually by the monomer bands at 3416 and 1465 cm^{-1} respectively on successive dilution. The directions of these frequency shifts are in agreement with those of the corresponding characteristic bands of monosubstiuted amides[7]. On the other hand, the imide I and III bands of the monomers are observed at 1720 and 1263 cm^{-1} respectively for the solutions at a concentration below 0.1 mol./l. Thus, it is seen that a monomer band appears between the two dimer bands for each of these characteristic vibrations (see Tables I and II). In this respect, the situation for diacetamide, involving two C=O, and two C–N bonds, seems to be different from the case of monosubstituted amides.

6) L. Hunter and N. Raynolds, *J. Chem. Soc.*, **1950**, 2857.

7) T. Miyazawa, *J. Chem. Soc. Japan, Pure Chem. Sec.* (*Nippon Kagaku Zassi*), **77**, 171, 321 (1956); T. Miyazawa, T. Shimanouchi and S. Mizushima, *J. Chem. Phys.*, **24**, 408 (1956).

Besides the characteristic bands described above, all the bands due to the CH_3 deformation vibrations are easily assigned, except for those due to the CH_3 rocking modes. The bands at 1424 and 1383 cm^{-1} are assigned to the CH_3 asymmetric and symmetric deformation vibrations respectively. Appreciable frequency shifts for these bands do not occur on either deuteration or dilution.

Higher Homologs in Non-polar Solvents.— The infrared spectra of the higher homologs of diacetamide dissolved in the three non-polar solvents are shown in Figs 2—5[5]. In some cases, the concentrations of the saturated solutions at room temperature are so small that the observed band intensities are not sufficient for the 0.1 mm. cell. Thus, infrared spectra in which the monomer bands are absent could not be recorded for some of these higher homologs. It is seen, however, that these higher homologs show, at a variety of concentrations, infrared spectra resembling that of diacetamide at the corresponding concentration. This fact is in marked contrast with the case of the crystalline state, in which the stable form (form A) of diacetamide shows a quite different spectrum from those of the higher homologs[2]. The spectral difference between diacetamide and the higher homologs in the crystalline state was explained as resulting from the difference in the configuration of the

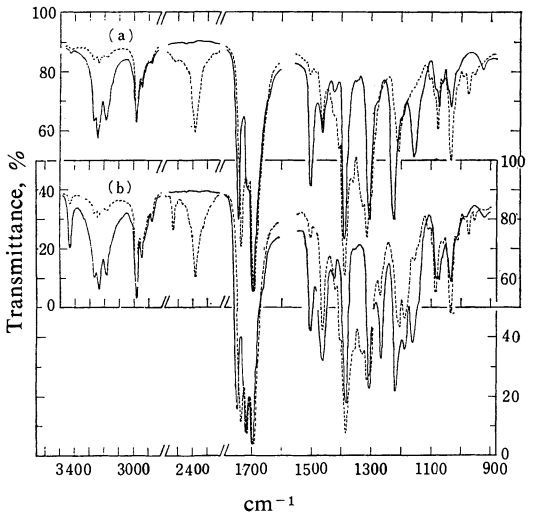


Fig. 2. Infrared spectra of *N*-acetylpropionamide (solid line) and *N*-acetylpropionamide-d (broken line); (a) 0.20 mol./l. (b) 0.01 mol./l.

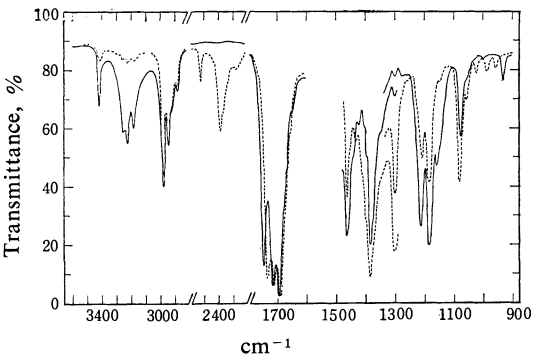


Fig. 3. Infrared spectra of dipropionamide (solid line) and dipropionamide-d (broken line); 2.85 mm. cell; 3500~1300 cm^{-1}, 0.01 mol./l. in CCl_4; 1300~900 cm^{-1}, 0.007 mol./l. in CS_2.

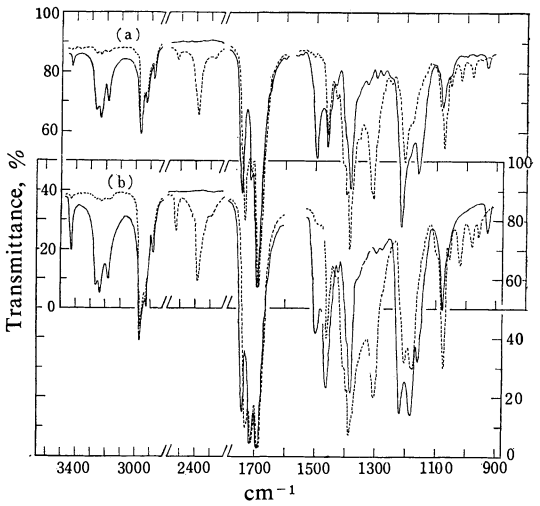


Fig. 4. Infrared spectra of *N*-propionyl-*n*-butyramide (solid line) and *N*-propionyl-*n*-butyramide-d (broken line); (a) 0.14 mol./l. (b) 0.01 mol./l.

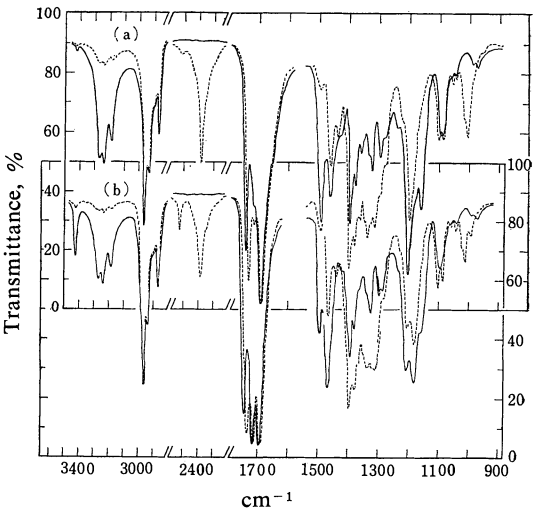
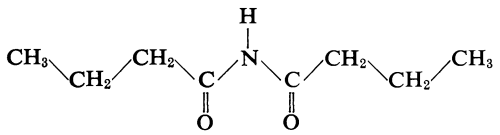


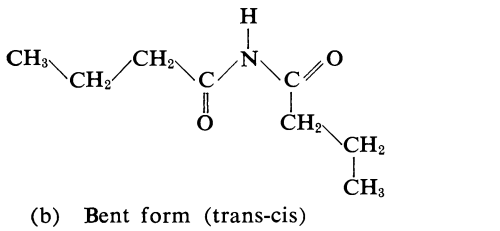
Fig. 5. Infrared spectra of di-*n*-butyramide (solid line) and di-*n*-butyramide-d (broken line); (a) 0.30 mol./l. (b) 0.01 mol./l.

–CONHCO– group[1,2]. That is to say, diacetamide in form A takes the trans-cis configuration, while the higher homologs are in the trans-trans configuration. The present results suggest, however, that the higher homologs take the same configuration as diacetamide takes when dissolved in the non-polar solvents. In other words, the higher homologs undergo an inversion of the –CONHCO– group from the trans-trans to the trans-cis configuration in going from the crystals to the solutions in the non-polar solvents. Previously[4] we found that the addition of some alkali halides to diacetamide in form A gives rise to the inversion from the trans-cis to the trans-trans configuration and pointed out that this inversion is due to the electrostatic and steric effects of the cations and of the anions of the alkali halide added. Similarly, the above inversion of the higher homologs suggested as taking place on the change of state can be interpreted in terms of the analogous effects of the functional group and of the alkyl residues of these molecules.

With respect to an isolated molecule, the trans-trans configuration is expected to be less stable than the trans-cis configuration since the strong electrostatic dipole-dipole interaction between the two C=O groups may be involved in the former. On the other hand, if the alkyl chains of the higher homologs are assumed to be in the trans zigzag arrangement, the molecules involving the trans-trans and the trans-cis –CONHCO– group may be considered to take the linear and the bent form respectively. Di-*n*-butyramide in these two forms is illustrated in Fig. 6. With respect to the packing of the molecules in a unit cell, the linear form is expected to have greater advantages than the bent form. Thus, in the case of the higher homologs in the crystalline state, the advantage for the molecular packing overcomes the electrostatic interaction. In the case of diacetamide, however, difference between the linear and the bent form is not so distinct as in the higher homologs. Thus, the electrostatic interaction determines the configuration of diacetamide in the crystalline state; the trans-cis –CONHCO– group is therefore involved in the stable form (form A). On the other hand, diacetamide as well as the higher homologs takes the trans-cis configuration when dissolved in the non-polar solvents; in this case the advantage for the packing is not required, so only the electrostatic interaction may determine the configuration. The trans-cis acyclic imides dissolved in the non-polar solvents may be associated to construct the cyclic dimers involving the two equivalent hydrogen bonds of the N–H···O type. From the above considerations, it may be seen that both the electrostatic and the steric effects play important roles in determining the configuration of the –CONHCO– group.



(a) Linear form (trans-trans)



(b) Bent form (trans-cis)

Fig. 6. The configurations of di-*n*-butyramide with the trans zigzag alkyl groups.

The Characteristic Bands of the trans-cis Imides.—The characteristic bands of the associated trans-cis –CONHCO– group in the rock salt region are listed in Table I. The assignment of these bands will now be discussed in comparison with the results for the trans-trans[2] and the cis-cis[8] –CONHCO– groups.

Imide I Bands.—Since the –CONHCO– group contains two C=O and two C–N bonds, we may expect two bands for each of the C=O and the C–N stretching vibrations. It has been pointed out, however, that the symmetric arrangement of atoms in the trans-trans configuration results in a decrease in intensity or even in the vanishing of the C=O out-of-phase and the C–N–C symmetric stretching bands[2]. On the other hand, the reduced symmetry of the trans-cis configuration may result in agreement between the number of possible stretching modes and the number of observed bands. In fact, as shown in Fig. 1, two C=O stretching bands are observed for the 0.34 mol./l. solution of diacetamide. For convenience, the weaker band at 1747 cm^{-1} and the stronger band at 1698 cm^{-1} will be called the imide Ia and Ib band respectively. The higher homologs show these bands in a quite similar way. As the first approximation, the Ia and Ib bands are attributable to the free and the bonded C=O stretching vibration respectively, although the coupling between the two C=O stretching vibrations is more or less expected[9]. With respect to the features of the C=O stretching bands, the trans-cis –CONHCO– group of these

8) T. Uno and K. Machida, This Bulletin, **35**, 276 (1962).
9) R. A. Abramovitch, *J. Chem. Soc.*, **1957**, 1413; H. K. Hall, Jr. and R. Zwinden, *J. Am. Chem. Soc.*, **80**, 6428 (1958).

acyclic imides is rather similar to the cis-cis –CONHCO– group of succinimide and maleimide[8], except that the ring strain raises the free C=O stretching frequency of these cyclic imides by about 30 cm^{-1} in comparison with acyclic imides. This may be related to the similarity in the hydrogen bonds resulting from these two configurations. By X-ray diffraction study[10], the crystal of succinimide has been proved to consist of ring dimers involving both the bonded and the free C=O bonds.

Imide II Band.—In contrast with the case of the imide I bands, the presence of the imide II band near 1500 cm^{-1} differentiates the infrared spectra of the trans-cis –CONHCO– group from those of the cis-cis group. This band results from the coupling between the N–H in-plane deformation and the C–N stretching vibrations of the –CONHCO– group containing the trans –CONH– group. Thus, the imide II band is characteristic of the trans-cis and the trans-trans –CONHCO– group, although the vibrational modes involved may be different for these two configurations. Table I shows that the difference in the alkyl frameworks hardly affects the imide II frequency, suggesting that the vibration is almost localized in the –CONHCO– group.

Imide III Bands.—As has been seen for the imide I bands previously, the features of the imide III bands are also affected by the difference in symmetry between the trans-trans and the trans-cis –CONHCO– group. The two strong bands at 1301 and 1216 cm^{-1} observed for diacetamide dissolved in the non-polar solvents disappear on deuteration. This fact may be well elucidated since the trans-cis –CONHCO– group, for which all the in-plane vibrations belong to the same symmetry species, A′, involves two C–N stretching modes being allowed to couple with the N–H in-plane deformation vibration. The imide III frequencies of the trans-cis –CONHCO– group, as in the case of the trans-trans group, vary with the change in alkyl framework. This means that the coupling between the vibrations of the functional group and the alkyl frameworks is appreciable with respect to the imide III bands. The higher homologs other than *N*-acetylpropionamide show the two imide III bands, consistent with the above consideration for diacetamide. On the other hand, the three imide III bands of *N*-acetylpropionamide (Fig. 2) seem to indicate the presence of the rotational isomers. The trans-cis –CONHCO– group of *N*-acetylpropionamide differentiates the two configurations in which the C=O bond in the acetyl group takes the trans and the cis position with respect to the N–H bond. In the infrared spectra of fatty acid esters, the acetyl group is distinguished from other acyl groups with respect to the C–O–C antisymmetric stretching frequency[11]. A similar peculiarity of the acetyl group was observed for the imide III frequencies of acyclic imides in the trans-trans configuration[2]. Thus, the imide III frequencies may be different for the two trans-cis configurations of *N*-acetylpropionamide, so that in carbon tetrachloride solutions this compound shows more than two bands related to the C–N stretching vibrations in the region 1350 to 1100 cm^{-1}.

Imide II′ and III′ Bands.—The difference in the alkyl framework affects the imide II′ and III′ frequencies of the *N*-deuterated compounds. Each of the acyclic imides investigated has turned out to show the two imide II′ bands in the region 1360 to 1150 cm^{-1} on deuteration. These bands are due to the two C–N stretching vibrations released from the coupling with the N–H in-plane deformation vibration. The contribution of the framework vibrations seems to remain on deuteration, since in some cases the band with the higher frequency shows a complicated feature with several peaks. This band is always stronger than the other band with the lower frequency. The frequency of the weaker band for each compound is 10 to 20 cm^{-1} lower than the higher imide III frequency of the corresponding undeuterated compound (see Table I). On the basis of these results, it is suggested that the antisymmetric and the symmetric C–N–C stretching vibrations are related to the stronger and the weaker band respectively. For the former band, however, the amplitude of the stretching coordinate of the shorter C–N bond may be greater than that of the longer bond, and vice versa for the latter band. As with the related compounds[7,12], the N–D in-plane deformation vibration seems to couple appreciably with the framework vibrations. The two bands at 1112 and 913 cm^{-1} of diacetamide-d are considered to result from such a coupling, in which an in-plane vibration contributing to the band at 1028 cm^{-1} of diacetamide is expected to be involved on deuteration. In fact, the features of the band at 1028 cm^{-1} are also changed on deuteration. This interpretation is consistent with the product rule applied to diacetamide in the trans-cis configuration. For the in-plane (A′) frequencies below 2000 cm^{-1}, the observed and the theoretical ratios,

10) R. Mason, *Acta Cryst.*, **9**, 405 (1956).

11) H. W. Thompson and P. Torkington, *J. Chem. Soc.*, **1945**, 640; the recent investigation by K. Toriyama and T. Shimanouchi (unpublished) must also be referred to.

12) T. Miyazawa, *J. Mol. Spectroscopy*, **4**, 155 (1960).

$\Pi(\nu_H/\nu_D)$, are 1.41[13] and 1.44 respectively. Here, the theoretical ratio has been calculated from the same molecular constants as those used in the calculation of the A'' ratio[1]. The high-frequency separation has been made in analogy with that applied to succinimide[8]. For the solution of the higher homologs of diacetamide, the bands in the 1100 to 900 cm^{-1} region are much obscured by the destruction of the trans-zigzag arrangement of the alkyl chains. As with the imide III' band, however, each *N*-deuterated compound shows a fairly strong band in this region which is not observed for the corresponding undeuterated compound. Although this band results mainly from the N-D in-plane deformation vibration, the varying of the frequency with the alkyl groups seems to indicate some contribution of the framework vibrations.

N-H and N-D Stretching Bands.—As has been seen for the trans-trans[3] and the cis-cis[8] configurations, the features of the N-H and N-D stretching bands of the trans-cis configuration may well be elucidated in terms of Fermi resonance. All the in-plane vibrations of the trans-cis configuration belong to a single symmetry species, A', of the point group C_s. Thus, the imide Ia and Ib vibrations of this configuration can combine with the imide II vibration to give rise to two combination tones, which take part in the Fermi resonance with the N-H stretching vibration. The three peaks in the 3280 to 3150 cm^{-1} region observed for each undeuterated compound are attributed to this Fermi resonance (see Table I). It is seen from Figs. 1—5 that the vanishing of the resonance on deuteration leads to a single peak near 2390 cm^{-1} for the N-D stretching band of the trans-cis -CONDCO- group. It may be noted here that the intermolecular interaction is improbable as the cause of the splitting of the N-H stretching band in this case, since the symmetry of the associated ring dimer in the solution leads to only one infrared active N-H stretching vibration.

13) Calculated from the following frequencies: diacetamide, 1747, 1698, 1503, 1301, 1216, 1028; diacetamide-d, 1737, 1695, 1338 (the mean value of 1350 and 1326), 1286, 1112, 913.

Conclusion

The infrared spectra of the aliphatic acyclic imides dissolved in the non-polar solvents indicate that the -CONHCO- group of these compounds takes the trans-cis configuration in the associated molecules. This means that the higher homologs of diacetamide (trans-trans in the crystalline state) undergo an inversion of the configuration of the -CONHCO- group upon the change of state. One of the anomalous features observed for the infrared spectra of the higher homologs of diacetamide is the marked decrease (30～40 cm^{-1}) in the frequencies of the strongest C=O stretching band on going from the crystals to the solutions in the non-polar solvents. This may result not only from the change in the vibrational modes due to the change in the configuration, but also from the change in the force constants due to the change in the type of hydrogen bond.

Experimental

The samples used in the present study are the same as those reported previously[1,2]. Commercially available, guaranteed-pure grade carbon tetrachloride, tetrachloroethylene and carbon disulfide were dried with silica gel and redistilled before use. The infrared measurements were made with a Perkin Elmer Model 221 spectrophotometer equipped with a lithium fluoride prism (4000～2600 cm^{-1}) and a Koken DS-301 spectrophotometer equipped with two rock salt prisms (2600～900 cm^{-1}). The water vapor and the polystyrene bands were used for the wave number calibration.

The authors wish to express their thanks to Dr. Tatsuo Miyazawa of Osaka University and to Dr. Kiyoshi Nakamura of the Research Laboratory, Dainippon & Co., Ltd., for their helpful advice throughout this work. Thanks are also due to Dr. Kunio Fukushima of Osaka University for his measurement in the 4000 to 2600 cm^{-1} region.

Faculty of Pharmacy
Kyoto University
Sakyo-ku, Kyoto

Kolbe's Reaction of Higher Fatty Acids. III. Anode Potential in the Electrolysis of Lauric Acid with Platinum Anode

By Ryoichi MATSUDA, Takeo HISANO, Toshio TERAZAWA and Norio SHINOHARA

(Received April 26, 1961)

Several investigators who have dealt with the anodic potentials of Kolbe's reaction and of those closely related to it in the electrolysis of acetic acid[1-5] have found that there are two stages of the anodic potential with a smooth platinum anode. They are 1.8~2.0 and 2.2~2.8 V. vs. hydrogen electrode, which are regarded as the potentials of oxygen evolution and the discharge of acetate ion respectively. In the electrolysis of the aqueous solution of acetic acid, Kolbe's reaction normally occurs. In other words, the discharge of acetate ions, which have a higher discharge potential than hydroxyl ions, predominates over that of the latter under ordinary conditions. This fact will be, according to Hickling[1], a formidable problem for any theory of anodic reactions. Adam and others[6] have stated that the formation of a surface film of acetate ions would disturb the discharge of hydroxyl ions and give rise to a higher potential. However, Hickling emphasized that the anode showed the higher potential from the very beginning of the electrolysis; therefore, it was not a question of the replacement of a lower potential process by one of a higher potential after the electrolysis had been run for some time. Aoyagi and Sugino[4] have mentioned that the realization of the higher potential stage was caused by the adsorption by the anode of such ions as were not oxidized or discharged at the potential of oxygen evolution.

The present authors have not come across any work on the characteristic nature of the anodic potential in the Kolbe reaction of higher fatty acids, which might behave somewhat unlike the lower members, and so have undertaken the study of the anodic potential with a smooth platinum anode in the electrolysis of lauric acid.

Experimental

Electrolyte Solution.—Either ethanol or methanol is often employed, together with water, to increase the poor solubility of lauric acid in water. In order to avoid the effect of such an alcohol as that mentioned above on the anodic potential, however, electrolyte solutions were made by adding an aqueous solution of potassium hydroxide of a proper concentration to a solution of lauric acid and potassium carbonate which had been prepared by treating a mixture of these two solutes with warm water. The composition of the electrolyte solutions employed is shown in Table I, in which [La], [K_1] and [K_2] denote the concentrations in mol./l. of lauric acid, potassium hydroxide and potassium carbonate respectively. The lauric acid was obtained by recrystallizing two times a raw lauric acid which was 99.9% pure with a mixture of ethanol and water. The other chemicals were of the special grade for analysis.

Apparatus and Electrodes.—The electrolytic cell employed in the current-potential and time-potential measurements was a glass cylinder, and 100 ml. of the electrolyte solution were used for each run. The anode was a smooth platinum plate with a total surface area of 0.5 cm^2. To keep the current distribution as uniform as possible, the anode was surrounded by a platinum plate cathode which had an area of about 5 cm^2 on each side, almost large enough to avoid the effect of cathodic polarization. Before electrolysis, both electrodes were thoroughly cleaned with ethanol, with concentrated nitric acid and finally with pure water. The reproducibility of the equilibrium potential of the anode in the electrolyte solution was about ± 0.02 V. The Luggin capillary, which was 1 mm. in outside diamete at its tip, was filled with the electrolyte solution and then connected to a saturated calomel electrode through a potassium chloride solution. At the middle of the capillary tube a glass stop cock was fitted; this was kept closed during the experiment to prevent the contamination of the electrolyte solution with potassium chloride. The potential was measured by an electronic valve potentiometer, the imput impedance of which was 10 MΩ.

Since Kolbe's reaction of lauric acid produces docosane[7], which is solid and oily at room

1) A. Hickling, *Discussions Faraday Soc.*, **1**, 227 (1947).
2) B. G. Preuner and E. B. Ludlam, *Z. physik. Chem.*, **59**, 682 (1907).
3) S. N. Shukla and O. J. Walker, *Trans. Faraday Soc.*, **27**, 722 (1931).
4) S. Aoyagi and K. Sugino, *J. Chem. Soc. Japan, Pure Chem. Sec.* (*Nippon Kagaku Zasshi*), **79**, 1202 (1958).
5) S. Aoyagi and K. Sugino, *J. Electrochem. Soc.*, **103**, 166 (1956).
6) N. K. Adam et al., *Discussions Faraday Soc.*, **1**, 248 (1947).
7) T. Mizuta, T. Hisano and R. Matsuda, This Bulletin, **33**, 700 (1960).

TABLE I. COMPOSITION OF ELECTROLYTE SOLUTIONS

Solute	Soln. 1	2	3	4	5	6	7	8
[La]	0.012	0.012	0.100	0.057	0.114	0.171	0.229	0.057
[K_1]	1.776	0.306	0.100	0.857	0.714	0.571	0.429	0
[K_2]	0.017	0.017	0.145	0.031	1.062	0.093	0.124	0.031
[K_1]/[La]	150	25	1.0	15	6.3	3.3	1.9	0
[K_2]/[La]	1.4	1.4	1.4	0.54	0.54	0.54	0.54	0.54

temperature and 40°C respectively, the electrolysis was conducted at 40±0.5°C without any mechanical agitating device.

Determination of the Current Efficiency of Oxygen Evolution.—Both the anode and cathode employed in this case had a larger surface area (7 and 100 cm^2 respectively) than those mentioned above. The electrolytic cell was fitted with a side tube in order to adjust the level of the electrolyte solution, and the cell was completely filled with the solution before electrolysis. During electrolysis the constant anodic potential was maintained by manual adjustment of the current. The evolved gas, which was collected into a syringe of a 20 ml. capacity, was treated with potassium hydroxide and alkaline pyrogallol solutions succesively. Special attention was paid to prevent the entrance of air into the gas samples. The efficiency of the oxygen evolution at the anode was calculated, assuming that the efficiency of hydrogen evolution was 100% at the cathode and that the residual gas after absorption contained hydrogen only. According to these assumptions, the current efficiency of oxygen evolution will be lower than it should be if the electrolytic gas contained any unabsorbable gas other than hydrogen.

Results and Discussion

From Fig. 1, showing the relation between the current and anodic potential in the

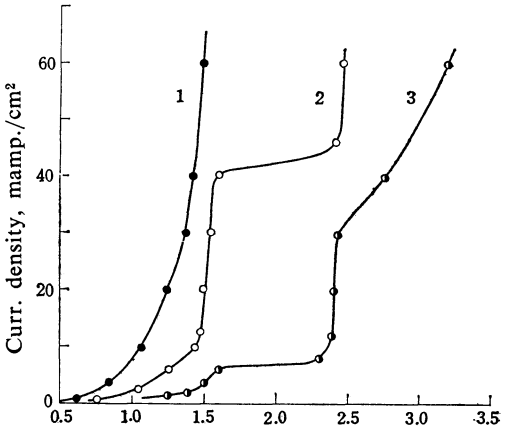


Fig. 1. Relation between anodic current and potential. Curves 1, 2 and 3 are related to solutions 1, 2 and 3 respectively.

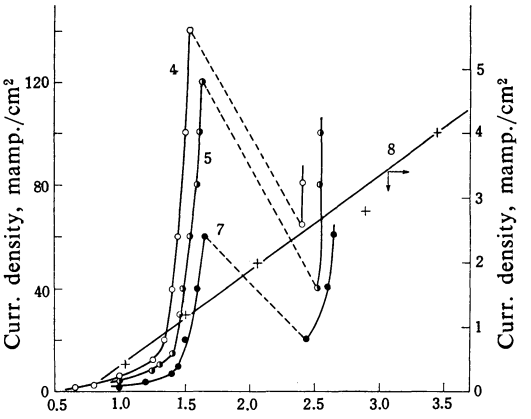


Fig. 2. Relation between anodic current and potential. Curves 4, 5, 7 and 8 are related to solutions 4, 5, 7 and 8 respectively.

electrolysis of solutions 1, 2 and 3, in which the value of [K_2]/[La] was always equal to 1.4, the following two facts may be observed. First, when [K_1] is not very high compared with [La], as in the cases of curves 2 and 3, two stages of anodic potential are clearly marked. The first stage lies at 1.5~1.6 V., and the second at a potential a little higher than about 2.3 V. Secondy, when [K_1] is very large compared with [La], the current increases so much that it reaches beyond the estimation range, and the second stage of potential disappears. In the potential range between 1.5 and 2.4 V., both curves 2 and 3 have a plateau which looks as if it were a saturation or limiting current. However, strictly speaking, this is not the case, since it is impossible to maintain a constant current at a constant potential, particularly in a part of the potential range below 2.4 V. The current decreases if the potential is kept constant. Moreover, as the current approaches a certain high value, the potential increases more rapidly than with the former. For these reasons curves 2 and 3 were obtained by reading the potential immediately after adjusting the current to as constant a level as possible. The values of the height of the plateau in curves 2 and 3 are, consequently, not very precise. Yet it is clear that the height

of the plateau has a close connection with the value of $[K_1]$.

The relation between the current and potential was also observed for solutions 4, 5, 6, 7 and 8. In this case the current was left without adjustment during the rapid potential transition. Some of the results are represented in Fig. 2. According to these curves, there occurs a phenomenon something like the passivity of a soluble anode. The first and second potential stages are situated like that case, at 1.5~1.6 V. and 2.4~2.6 V. vs. S. C. E. respectively. Curve 8 represents the case of a solution which contains lauric acid and potassium carbonate but no potassium hydroxide. This curve is nearly linear and shows that a higher anodicpot ential is attained by a lower current density than with the other curves. It can well be considered that this is due to the resistance overpotential caused by some filmy substance on, in the vicinity of, the anode. As a matter of fact, a transparent viscous substance was observed on the anode during electrolysis, although it disappeared after opening the circuit. This is probably potassium laurate liberated.

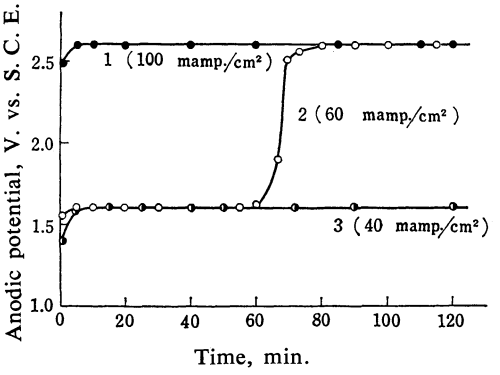


Fig. 3. Variation of anodic potential during electrolysis of solution 7 at constant current.

Figure 3 shows typical curves observed as to the variation in anodic potential during the electrolysis of solution 7 under a constant current. Whereas curves 1 and 3 reach 2.6 and 1.6 V. respectively soon after the commencement of electrolysis, and both remain constant as time goes on, curve 2 proceeds along with curve 3 for the first period and then ascends quickly to 2.6 V. and remains constant thereafter. With an ordinary electronic valve potentiometer, the potential under high current densities is observed to be 2.4~2.6 V. from the beginning of electrolysis, as illustrated by curve 1. A cathode ray oscillograph, however, shows distinctly that, under the same conditions as mentioned above, the rapid displacement of the potential stage from the first to the second still occurs at the moment of closing the circuit. At any rate, it is evident from these observations that the displacement of the potential stage takes place at a certain time after the beginning of the electrolysis of alkali laurate.

The relation between current density and the time of potential displacement will be reported on later.

From the result mentioned above, the transition of the potential and the realization of the higher potential stage in preference to the lower one may by supposed to be caused by the formation of some sort of film on the anode surface. Three possible types of film which can bring about an abnormally high overpotential are as follows;

(1) a highly resistant film of the oxide of the anode material;

(2) a film of a resistant substance formed of discharged anion, and

(3) a film of adsorbed anion[4].

In the present study, (2) or (3) is likely to occur, but (1) is unlikely since it is already known[8] that the steady evolution of oxygen on a platinum anode occurs on its oxide layer, which has an unusual capacity for electron conduction.

Table II. Electrolyses at two constant potentials

Anode area, 7.0 cm²; Solution, 6.

Anode potential, V.	1.5~1.6	2.5~2.6
Mean curr. density, mamp/cm²	11	57
Quantity of electricity, coulombs	ca. 300	120~345
Curr. efficiency of O_2 evolution, %	99.2±0.1	25.0±2.4
Docosane formation	None	Confirmed

Table II represents the current efficiency of oxygen evolution at two constant anode potentials. The value at the lower potential stage amounts to 99% and differs decidedly from that at the higher stage. That is, the anode reaction occuring at the lower potential was almost entirely the evolution of oxygen. In the electrolysis at the higher stage of anode potential, the solution became utterly opaque soon after the commencement of electrolysis, and a floating substance, which was identified by its melting point as docosane, rose to the surface of the solution. During electrolysis at the lower potential, the solution was clear or only slightly opaque. If docosane be formed at the lower potential stage, its appearance on the surface of the solution would be perceptible

8) H. A. Laitinen and C. G. Enke, *J. Electrochem. Soc.*, 107, 773 (1960).

after the electrolysis had been conducted with a sufficiently large quantity of electricity, since it is sparingly soluble in the solution employed. However, no floating substance was found after electrolysing 250 ml. of solution 6 with 8000 coulombs of electricity at the constant potential of 1.5~1.6 V. Although the above-mentioned method is not complete for the detection of docosane, it seems not to be right, by reason of the following observation, to suppose that the displacement of the anode potential is due to the formation of a resistant film of docosane which is produced out of the discharged laurate ions. The displacement of the lower potential by the higher one was observed not immediately but some time after the start of a second run of electrolysis at the lower potential of a certain solution which, for the first time, had been electrolyzed for a long time at the higher potential and, therefore, should have been saturated with docosane and other products.

In conclusion, it seems, to the authors, as far as the present study is concerned, that the most probable mechanism of the displacement of the anode potential stages in the electrolysis of the alkali laurate solution is related to the formation of an adsorbed film of laurate ions, and that at the lower potential stage of 1.5~1.6 V. vs. S. C. E. the main reaction is the evolution of oxygen. As laurate ions are adsorbed on the anode surface, the effective surface area of the latter for the discharge of hydroxyl ions decreases; therefore, the potential rises to 2.4~2.6 V., at which point laurate ions begin to discharge.

As has previously been reported[9] docosane is formed on a graphite anode with a pulsating direct current, whereas with ordinary direct current there occurs a rapid diminution of current; thus it will be interesting to investigate the behavior of graphite and platinized platinum anodes in the light of the anodic potential, since these have atomically irregular surfaces, on which large laurate ions may be expected to be adsorbed in a manner somewhat dissimilar to that which is the case with a smooth platinum surface.

9) R. Matsuda, T. Hisano and D. Kubota, This Bulletin, 34, 649 (1961).

Summary

An aqueous solution of lauric acid, containing potassium hydroxide and potassium carbonate, was electrolysed at 40±0.5°C with smooth platinum electrodes. Not only were two constant anodic potential stages, 1.5~1.6 and 2.4~2.6 V. vs. S. C. E., clearly found, but also an abrupt shift from the lower stage to the higher one was distinctly observed. The main reaction at the lower stage is the evolution of oxygen. In addition, at the higher stage the discharge of laurate ions is accompanied by an oxygen evolution that is markedly retarded compared with that at the lower stage. It may therefore, be inferred that the transition of potential from the lower stage to the higher is caused by the formation of a film of adsorbed laurate ions.

The authors wish to express their thanks to Nippon Oils and Fats Co., Ltd., which kindly provided them with lauric acid.

Department of Applied Chemistry
Faculty of Engineering
Tokushima University
Tokushima

NOTES

Relation between Vapor Pressure and Internal Pressure in Solutions and Pure Liquids

By C. V. SURYANARAYANA and
K. K. JANARDHANAN PILLAI

(Received October 13, 1961)

Recently Suryanarayana[1] proposed internal pressure as the basis of a unified theory of solutions. If it should be tenable, several fundamental properties of solutions as well as pure liquids should be explicable on the basis of internal pressure. A search has been made by us if vapor pressure over a liquid, be it pure or a solution, has any relation with the internal pressure. For computing internal pressure, recently Suryanarayana and Govindaswamy[2] formulated an equation,

$$\Pi = K \cdot \rho^{4\frac{1}{3}} / M^{1/3} \qquad (1)$$

based on a relationship pointed out by Young[3] and Leplace[4]. In Eq. 1 K is an incomputable constant independent of temperature, whereas Π, ρ and M are internal pressure, density and molecular weight of the medium respectively. Equation 1 is applicable to solutions in the form,

$$\Pi = K \cdot \rho^{4\frac{1}{3}} / (M_1 x_1 + M_2 x_2)^{1/3} \qquad (2)$$

where x_1 and x_2 are the mole fractions of the two components, for example in a binary solution, and M_1 and M_2 are respectively the molecular weights. Suryanarayana and Govindaswamy (loc. cit) showed that Eq. 2 is applicable to solutions of nonelectrolytes and fully dissociated electrolytes. The computable part on the right hand sides of Eqs. 1 and 2 has been called the Π-factor. For purposes of comparison of internal pressures a study of the Π-factor must be sufficient and reliable.

Vapor pressure data for electrolyte solutions of sodium carbonate, lithium bromide, nitric acid, hydrochloric acid, sodium sulfate, sulfuric acid, ammonium chloride, sodium chloride, sodium nitrate, sodium hydroxide, potassium sulfate, sodium iodide, ammonium sulfate and sodium bromide, at least at six temperatures in each case were obtained from the International Critical Tables, Vol. III, 1928. Graphical studies showed that in almost all cases vapor pressure varies linearly with the internal pressure of a solution,

$$P = A - B\Pi' \qquad (3)$$

where P is the vapor pressure, Π' the Π-factor and A and B cnstants. Substituting the Π-factor for pure water in Eq. 3, computed from its density and molecular weight, we can get the vapor pressure P at a given temperature. Values thus obtained from Eq. 3 agreed excellently with those given in standard tables at all the temperatures tested. The following table gives at 40°C a comparison of vapor pressure values between the standard ones and those obtained from 3 of different salts by substituting Π' of water in the respective equations.

TABLE I. DATA AT 40°C*

Electrolyte	Vapor pressure of water from the equation mmHg	% deviation from the accepted value
Sodium carbonate	55.25	−0.1266
Lithium bromide	55.14	−0.3254
Nitric acid	55.03	−0.5242
Hydrochloric acid	57.98	+4.808
Sodium sulfate	55.08	−0.4338
Sulfuric acid	57.56	+4.049
Ammonium chloride	54.55	−1.392
Sodium chloride	55.46	+0.253

* The accepted vapor pressure of water at 40°C is 55.32 mmHg.

Sodium nitrate, bromide, iodide, hydroxide, potassium sulfate and ammonium nitrate solutions give for a plot of vapor pressure versus Π-factor in each case two straight lines intersecting at a point. These can be explained on the basis of 1-1, 1-2 and 2-2 interactions.

The internal pressure of a liquid increases as the temperature decreases. At each temperature probably a quantitative relationship exists between the vapor pressure and internal pressure of a liquid. In expectation of a fundamental relationship between the two, thirty liquids namely, methyl sulfide, diethyl amine, ethyl propyl ether, methyl ethyl ether, cyclohexane, isopropyl isobutyrate, chlorobenzene, methyl acetate, *n*-propyl acetate, benzene, methyl formate, ethyl formate, ethyl acetate, methyl isobutyrate, ethyl sulfide, methyl propionate, ethyl

1) C. V. Suryanarayana. *J. Sci. Ind. Research (India)*, **A20**, 141 (1961).
2) C. V. Suryanarayana and S. Govindaswamy, *Acta Chim. Hung.*, **25**, 341 (1960).
3) T. Young, *Phil. Trans.*, **1**, 65 (1805).
4) P. S. Laplace, "Oeuvres", Vol. IV, 389.

propionate, acetic acid, methyl alcohol, *n*-propyl alcohol, diethyl ether, *n*-pentane, bromobenzene, ethyl alcohol, methyl *n*-butyrate, *n*-propyl formate, acetone, isopropyl alcohol, carbon tetrachloride, and water have been studied. Data of vapor pressure and density for the first six are from International Critical Tables (McGraw-Hill), Vol. III, 1928 and for the rest from Timmermans Physico-chemical Constants of Pure Organic Compounds, Amsterdam, 1950. In almost all cases we found the simple relationship,

$$\log P = A - B\Pi \qquad (4)$$

applicable in almost all cases excepting *n*-propyl formate and water, which requir to be explained.

Thus in solutions we observe from Eq. 3 that the vapor pressure varies linearly with internal pressure, whereas in the case of pure liquids the logarithm of the vapor pressure is found to vary as in Eq. 4 linearly with the internal pressure. In the case of solutions, the causative factor that changes internal pressure is the solute concentration whereas in the the case of pure liquids it is the temperature. Normally speaking, provided the vapor pressure and the internal pressure are quantitatively related, whatever may be the causative factor that changes the internal pressure, the fundamental relation between the two should remain universal and undisturbed. Invalidation of this expectation and the existence of two types of relations as in Eqs. 3 and 4 signifies a difference in the mechanism of change of internal pressure in the two cases. A detailed study of these and other aspects will be published elsewhere in due course.

Department of Chemisty
Mysore University
Mysore, India

Microhardness of Coal Immersed in Various Solvents

By Yuzō SANADA and Hidemasa HONDA

(Received November 29, 1961)

The intrinsic mechanical strength of coal, shown by the microhardness number, may be related to inter and/or intramolecular forces[1-3]. When coal is immersed in a solvent, the solvent penetrates into coal, causing swelling. The resultant loosening of inter and/or intramolecular forces leads to changes in the mechanical strength of the coal. Recently, the microhardness of coals immersed in pyridine has been measured[4]. The hardness ratio, $H_k/H_{k,o}$, where H_k is the equilibrium Knoop hardness number of the coal immersed in in pyridine and $H_{k,o}$ is the Knoop hardness number of the original coal, when plotted against the rank of coal, shows a characteristic curve with a minimum at about an 80% carbon content[4].

In the present paper, the microhardness of coals immersed in various solvents has been measured further. The solvents used are benzene, ethanol, *p*-dioxan and dimethyl formamide (DMF). The details of measurement and the degree of error in the determination of the Knoop hardness number have been described elsewhere[1,4].

The Knoop hardness number of coal decreases with the increase in immersion time and reaches an equilibrium value after a few hours for all solvents as well as for pyridine[4]. The relation between the $H_k/H_{k,o}$, when coal is immersed in DMF and benzene respectively, and the rank of coal is shown in Fig. 1. In the case of immersion in DMF, the variation of $H_k/H_{k,o}$ in relation to the rank of coal is similar to that of pyridine, but the action of DMF is smaller than that of pyridine. In the case of benzene, the minimum in the curve of $H_k/H_{k,o}$ plotted against the rank shifts to a higher carbon content. As the constitution of coal is complex, it is difficult to explain these phenomena precisely, but the marked variation

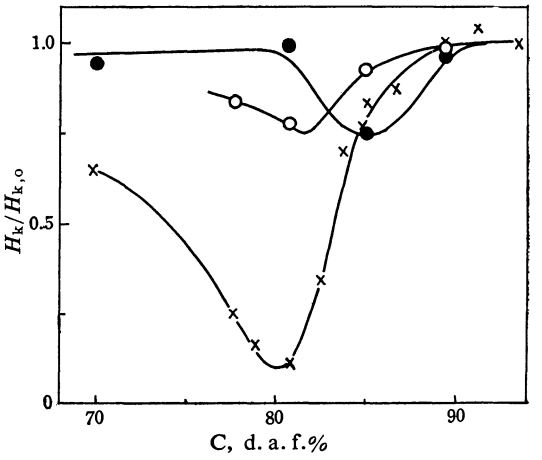


Fig. 1. Relation between hardness ratio and rank of coal.
○ DMF, ● Benzene, × Pyridine[4]

1) H. Honda and Y. Sanada, *Fuel*, **36**, 403 (1957).
2) Y. Sanada, N. Mochida and H. Honda, This Bulletin, **33**, 1479 (1960).
3) D. W. van Krevelen and J. Schuyer, "Coal Science, Aspects of Coal Constitution", Elsevier, Amsterdam (1957), p. 264.
4) Y. Sanada and H. Honda, *Fuel*, **40**, 327 (1961).

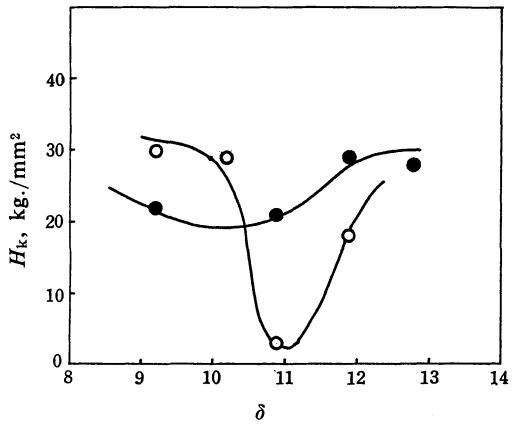


Fig. 2. Relation between equilibrium hardness number and solubility parameter of solvent, for Yūbari and Bibai vitrain immersed in solvent.
○ Bibai vitrain, ● Yūbari vitrain

in the value of $H_k/H_{k,o}$ with the rank would be expected to depend on the physical or chemical properties of the solvent and of the coal.

Figure 2 shows the relation between the H_k of Yūbari (d. a. f. 85%C) or Bibai (d. a. f. 81%C) coal immersed in solvents, and the solubility parameter*, δ, of solvents. It shows that H_k has a minimum at around 10 and 11 in the values of δ for Yūbari and Bibai coal respectively. It is known that the swelling of the polymer by various organic liquids correlates to a large extent with the cohesive energy density (CED) of the solvent and the polymer[5,6]. Such a relationship between the CED of solvents, including very highly polar ones, and the yield of extract of coals has been found[7]. Consequently, it seems that the CED is an important factor determining the solvent action on the mechanical behavior of coal.

Resources Research Institute
Kawaguchi, Saitama

* The square of δ means CED; the values of δ in solvent are available in "Chemical Handbook (Kagaku Binran)", ed. by the Chem. Soc. Japan, Maruzen, Tokyo (1958), p. 1247.

5) G. Gee, *Quart. Rev.*, **1**, 288 (1947).
6) E. E. Walker, *J. App. Chem.*, **2**, 470 (1952).
7) Y. Sanada and H. Honda, This Bulletin, to be published.

Mechanism of the Carbonization of Chromium(III) Oxide

By Hiroaki TAGAWA and Hitoshi NAKAJIMA

(Received on November 8, 1961)

Many kinds of carbides are formed by the solid state reaction of metal oxides with carbon at high temperatures. As most solid-solid reactions occur by counter diffusion of the cations of the reactants through the product layer, the kinetics of compound formation are considered to depend on the nature of the reactant and of the product. In the present study, the carbonization of chromium oxide was thermogravimetrically examined, and the mechanism was compared with that of the previously reported reaction of calcium oxide with carbon[1].

Experimental.—Extra pure chromium(III) oxide was obtained from Wako Chemicals Co. The particles were about 1 μ in diameter. Artificial graphite ($d_{002}=3.389$ Å, pulverized below 250 mesh sieve) for an atomic pile was used as carbon. A mixture of 1.00 g. of carbon and 2.92 g. of chromium oxide was compressed at about 1 ton/cm^2 into a cylindrical pellet, 15 mm. in diameter and 8 mm. in height. It was found by X-ray and chemical analysis that only chromium carbide, Cr_3C_2, was formed on the reaction of chromium oxide with carbon in the temperature range between 1060 and 1200°C and at 2×10^{-2} mmHg. The mixing ratio of carbon to chromium oxide was chosen according to the following equation: $3Cr_2O_3+13C=2Cr_3C_2+9CO$.

The apparatus for the kinetic experiments consisted of a spring balance in a vacuum electric furnace[1]. In the hot zone of the furnace a graphite bucket was suspended with fine molybdenum wire from the spring. The shrinkage of the spring upon a loss in weight was observed with a microscope with an eyepiece scale. The elongation of the spring against weight was 1.036 cm./g. The reaction temperature was measured with a platinum-platinum·13% rhodium thermocouple and was maintained at a desired value within ±3°C with the aid of an automatic temperature controller. The electric furnace was evacuated to 2×10^{-2} mmHg during the course of the experiments.

Results and Discussion.—All the curves of the weight decrease against time were parabolic in the temperature range 1060 to 1200°C. Figure 1 shows the course of the reaction at four temperatures.

Generally, the rate of solid state reaction determined by a diffusion process is expressed by the following equation:

$$(1-\sqrt[3]{1-x})^2=2kt \qquad (1)$$

1) H. Tagawa, H. Sugawara and H. Nakajima, *J. Chem. Soc. Japan, Ind. Chem. Sec.* (*Kogyo Kagaku Zasshi*), **64**, 1751 (1961).

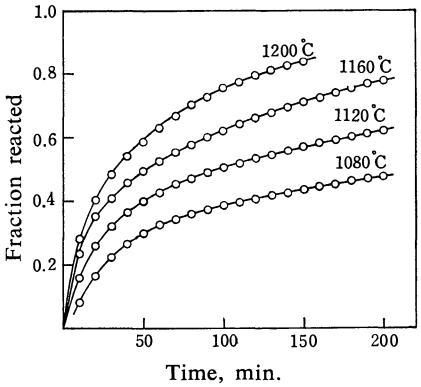


Fig. 1. Relation between fraction reacted and time.

where x is the fraction reacted, t the time, and k the reaction rate constant. To determine whether the reaction followed the parabolic kinetics shown in Eq. 1, the data in Fig. 1 were plotted as the values of $(1-\sqrt[3]{1-x})^2$ vs. time in Fig. 2. The linearity of the curve suggests that the diffusion process is rate-controlling. The constant k in Eq. 1 was found from the slope of each curve. The logarithm of the slope was plotted against the reciprocal of the absolute temperature in Fig. 3. The activation energy was calculated as 89.4±3.4 kcal./mol. from the least-squares slope of this plot.

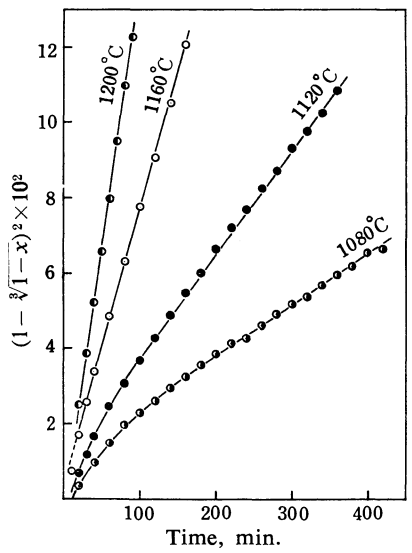


Fig. 2. Relation between $(1-\sqrt[3]{1-x})^2$ and time.

Boericke[2] has concluded that the reduction of chromium oxide with carbon involves four distinct, consecutive and reversible reaction steps:

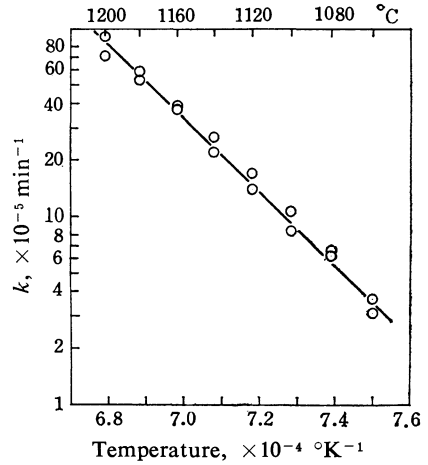


Fig. 3. Relation between the reaction velocity and reciprocal absolute temperature in the reaction of chromium oxide with carbon.

$$3Cr_2O_3 + 13C = 2Cr_3C_2 + 9CO \quad (2)$$

$$5Cr_2O_3 + 27Cr_3C_2 = 13Cr_7C_3 + 15CO \quad (3)$$

$$5Cr_2O_3 + 14Cr_7C_3 = 27Cr_4C + 15CO \quad (4)$$

$$Cr_2O_3 + 3Cr_4C = 14Cr + 3CO \quad (5)$$

It has been shown in this experiment that Cr_3C_2 is formed as an intermediate compound between chromium oxide and metallic chromium. The predominant formation of Cr_3C_2 is to be expected, as the equilibrium carbon monoxide pressure in Eq. 2 is the largest one in the reaction system of chromium oxide with carbon.

It is recognized that calcium vapor and carbon monoxide are formed in the reaction of calcium oxide with carbon below 1400°C in vacuo according to the following equation: $CaO+C=Ca+CO$[3]. As has previously been reported[1], when the plot of the weight decrease vs. time became linear, the reaction rate constant was obtained from the slopes of these curves. The activation energies from the Arrhenius plots were 92±5, 136±10 and 147±6 kcal./mol. for calcium oxides burned at 900, 1100 and 1300°C respectively for 3 hr. The difference in activation energy may be due to the sintering of calcium oxide during the course of the experiments and to the decrease in the reactivity with carbon.

When chromium carbide and calcium carbide are formed by the diffusion of cations through the oxide and the product layer, the reaction rate may depend on the mobility of the cations and on the reactivity of carbon as a reducing agent at the interface. Oxygen ions may not be considered to play an important role in

2) F. S. Boericke, *U. S. Bur. Mines, Tech. Paper*, R. I. 3747 (March, 1944).

3) N. Kameyama, "Electrochemistry: Theory and Practice", Vol. III-2, Maruzen, Tokyo (1956), p. 131.

carbonization, as their mobility is small in comparison with that of the cations.

The solid state reaction of carbon with chromium oxide and calcium oxide is considered from the standpoint of diffusion phenomenon. The self-diffusion coefficient of chromium ions in the oxide was determined by Lindner[4], the activation energy being 100 kcal./mol. The activation energy of the self-diffusion of calcium ions in the oxide was 80 kcal./mol.[5], while that of ^{14}C in graphite was 163 kcal./mol.[6] In the reaction of carbon with chromium oxide and with calcium oxide, the activation energy was 89 and 147 kcal./mol. respectively, the former value being similar to the activation energy for the self-diffusion of chromium ions in the oxide and the latter being similar to that of the self-diffusion of carbon and the lattice energy of graphite (170.9 kcal./.g.atom)[7]. Consequently, it may be considered that the rate determing factor is closely related to the diffusion of chromium ions in the oxide in the chromium carbide formation and to the structure of the carbons for the reduction of the oxide in the reaction with calcium oxide.

Research Laboratory
Nippon Carbide Industries Co., Inc.
Uozu, Toyama

4) R. Lindner and Å. Åkstrom, *Z. physik. Chem.* (*N. F.*), 6, 162 (1956).
5) J. A. Hedvall, "Einführung in die Festkörperchemie", Friedr. Vieweg & Sohn, Braunschweig (1952), p. 85.
6) M. A. Kanter, *Phys. Rev.*, **107**, 655 (1957).
7) D. Smith, A. S. Dworkin and E. R. van Artsdanlen, *J. Am. Chem. Soc.*, **77**, 1654 (1955).

Structure of the So-called Tricoordinated Copper Complexes

By Michihiko KISHITA and Masaji KUBO

(Received February 10, 1962)

We have determined the magnetic moments of a number of tricoordinated copper(II) complexes such as acetylacetone-mono-(*o*-hydroxyanil) copper(II)[1]. From the observed subnormal magnetic moments 0.87~1.37 B.M. per copper atom, it was concluded that binuclear complex molecules are formed in crystals, in which pairs of copper atoms exist: the Cu-Cu distance being so small as to permit exchange interaction between two copper atoms in a pair. Attention was called to the fact that all tricoordinated copper(II) complexes showing a subnormal magnetic moment so far investigated have a planar monomeric structure, because the copper atom is involved in two rings, both of which are either a five-membered ring or a six-membered one having conjugated double bonds[2]. These conclusions have been confirmed by the recent X-ray analysis of a single crystal of acetylacetone-mono-(*o*-hydroxyanil) copper(II) carried out by Barclay et al.[3] It was found that two copper atoms are 3.00 Å distant from each other in a dimer molecule having a planar configuration shown in Fig. 1. In this binuclear complex, each copper atom has one nitrogen and three oxygen atoms as coordinating atoms at the corners of a slightly distorted square.

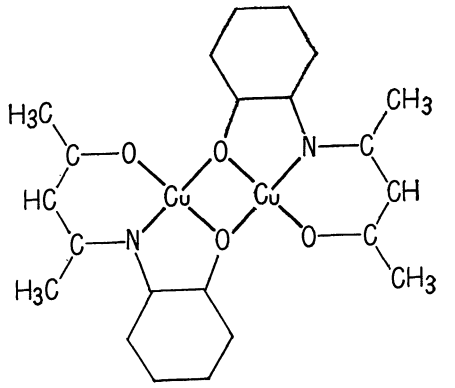


Fig. 1. Binuclear structure of acetylacetone-mono-(*o*-hydroxyanil) copper(II).

We have found[2] that some tricoordinated copper(II) complexes show a normal moment slightly greater than the spin moment for one unpaired electron 1.73 B.M. 5-Nitrosalicylalanthranilic acid copper(II) is an example. It was pointed out that these copper complexes showing a normal magnetic moment have a carbonyl group, the oxygen atom of which is capable of being coordinated on a copper atom and that they contain a six-membered chelate ring possibly having a three-dimensional structure, because only one double bond is involved in the ring[4].

In order to explain the observed moments, we propose a new binuclear structure for the so-called tricoordinated copper(II) complexes having a normal magnetic moment. The structure is shown in Fig. 2 with 5-nitrosalicylalanthranilic acid copper(II) as an example. It is analogous to that shown in Fig. 1 in that the two copper atoms in the binuclear complex have

1) M. Kishita, Y. Muto and M. Kubo, *Naturwissenschaften*, **44**, 372 (1957); *Australian J. Chem.*, **10**, 386 (1957).

2) M. Kishita, Y. Muto and M. Kubo, *Naturwissenschaften*, **44**, 612 (1957); *Australian J. Chem.*, **11**, 309 (1958).

3) G. A. Barclay, C. M. Harris, B. F. Hoskins and E. Kokot, *Proc. Chem. Soc.*, **1961**, 264.

4) K. Sakashita, *J. Chem. Soc. Japan, Pure Chem. Sec.* (*Nippon Kagaku Zassi*), **74**, 315 (1953).

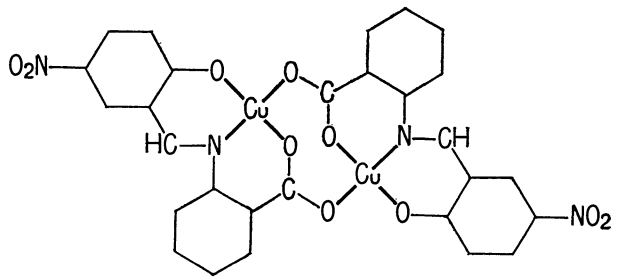


Fig. 2. Binuclear structure of 5-nitrosalicylalanthranilic acid copper(II).

a square coordination of nitrogen and oxygen atoms. It differs from the latter structure in that the copper atoms are involved in an eight-membered ring instead of forming a square with two oxygen atoms and are farther apart from each other than in the structure shown in Fig. 1. Consequently, the direct spin interaction between the two copper atoms is negligible, i.e., the low diamagnetic singlet energy level of the pair of spins practically coincides with the higher paramagnetic triplet level, leading to a situation equivalent to the independent orientation of each spin in the external magnetic field. The eight-membered ring and two six-membered rings adjacent to it are presumably nonplanar for reasons described above. As a result, the distance between two oxygen atoms closest to the center of symmetry of the dimer molecule is of reasonable magnitude as a non-bonded distance between oxygen atoms (ca. 3.0 Å). In fact, the configuration of Cu–O–C–O–Cu links in the eight-membered ring is quite analogous to the anti-syn bridging arrangement determined by X-ray diffraction experiments carried out by Barclay and Kennard[5] for the royal-blue modification of anhydrous copper(II) formate. The stereochemical requirements such as the normal values for bond lengths and valency angles, the coplanar structure of conjugated systems, the absence of appreciable steric hindrance, etc. are well satisfied and one can construct a plausible molecular model for this structure.

The proposed structure implies that the so-called tricoordinated copper(II) complexes are really binuclear complexes having copper atoms of ligancy 4, regardless of whether they show a subnormal or normal magnetic moment and that "tricoordinated" copper(II) complexes in the literal sense of the word do not exist. It must be recalled that the unusual coordination number 3 for a copper atom has been conceived from the method of synthesis and the chemical analysis of the complexes along with the tridentate nature of the single ligand molecules under a tacit assumption that the complex molecules have only one copper atom. It is evident that the normal magnetic moment of a copper(II) complex does not necessarily lead to the conclusion for the existence of separate monomeric molecules in crystals. Mention should be made here of the cryoscopic determination of the molecular weights of *N*-salicylidene-*N'*-*n*-caprinylhydrazino copper(II) and *N*-salicylidene-*N'*-*n*-palmitylhydrazino copper(II) by Ohta[6], who found that these tricoordinated copper(II) complexes form dimer molecules. However, Grün and Freiesleben[7] found monomeric molecular weights for some nickel complexes of formazyls in benzene and are of opinion that the nickel atom has the coordination number 3.

In the monopyridine derivatives of the so-called tricoordinated copper(II) complexes, all of which show a normal magnetic moment, a nitrogen atom of pyridine is presumed to be coordinated on a copper atom to complete the square coordination. As a result, the molecule of these monopyridine derivatives must have a single copper atom.

In short, the coordination number 3 for a copper atom does not afford the only possible interpretation nor the most probable one. On the contrary, with the concept of binuclear complexes, one can dispense with the unusual coordination number 3 in favor of the ligancy 4, irrespective of whether or not the so-called tricoordinated copper(II) complexes show a normal moment.

Chemistry Department
Nagoya University
Chikusa, Nagoya

5) G. A. Barclay and C. H. L. Kennard, *J. Chem. Soc.*, **1961**, 3289.

6) H. Ohta, This Bulletin, **33**, 202 (1960).

7) W. Freiesleben and F. Grün, *Chimia*, **9**, 276 (1957); F. Grün and W. Freiesleben, *Helv. Chim. Acta*, **41**, 574 (1958).

SHORT COMMUNICATIONS

The Reductive Aminations of α-Keto Acids with Cobalt Complex Ions in Homogeneous Solution

By Masuo MURAKAMI and Jung-Wong KANG

(Received March 24, 1962)

It has been known[1] that the reductive amination of α-keto acid with aqueous ammonia can be carried out with an active metal such as platinum, palladium and Raney-nickel. However, the same reaction using metal complex ion under homogeneous conditions is still unknown. It has been shown recently[2] that various unsaturated compounds using cyano cobalt complex which prepared from cobaltous chloride and five moles of potassium cyanide were hydrogenated in aqueous solution.

In this communication, we wish to report that reductive amination of α-keto acids with aqueous ammonia can be made either with cyano cobalt complex as a catalyst or chloropentamminecobalt(III) chloride as a reagent of the reductive amination in alkaline solution.

Most of the experiments using cyano cobalt complex were carried out at 30~70°C under a hydrogen pressure of 50 kg./cm^2 using 6% aqueous ammonia. The results of the reductive amination of α-keto acids are summarized in Table I.

When the reaction was carried out at room temperature under an atmospheric pressure,

TABLE I

Compound	Run	Keto acid/ $CoCl_2 \cdot 6H_2O$	Temp. °C	Time hr.	Corresponding amino acid, %	Co Deposited
$C_6H_5CH_2CCOOH$ (O)	1	1	30	8	—[a]	None
	2	3	40	8	85.6	None
	3	1	70	5	95.0	None
	4	10	70	5	76.5	None
	5	1	70	5	36.3[b]	None
CH_3COOH (O)	6	1	40	8	73.2	None
$HOOC(CH_2)_2CCOOH$ (O)	7	1	40	8	36.4	None

a) The reaction was carried out at a hydrogen pressure of one atmosphere.
b) Potassium cyanide was not added in the reaction system.

TABLE II

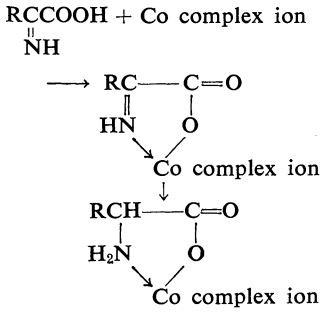
Compound	Run	*n*KCN	Keto acid/ Complex	Corresponding amino acid, %	Co Deposited
$C_6H_5CH_2CCOOH$ (O)	1	5	1	29.6	Small
	2	5	5	53.0	None
	3	5	2	96.4	None
	4	5	1	94.0	None
CH_3CCOOH (O)	5	5	2	85.0	None

1) F. Knoop and H. Oesterlin, *Z. Physiol. Chem.*, **148**, 294 (1925); **170**, 185 (1927).
2) M. Iguchi, M. Takahashi et al., Presented in part at the 9-11th Annual Meetings of the Chemical Society of Japan, Tokyo and Kyoto, April, 1956-1958; B. Devries, *Koninkle. Ned. Akad. Wetenshap, Proc.*, **B63**, 443 (1960); N. Kelso King and M. E. Winfield, *J. Am. Chem. Soc.*, **83**, 3366 (1961); J. Kwiatek, I. L. Mador and J. K. Seyler, *J. Am. Chem. Soc.*, **84**, 304 (1962); M. Murakami and J. W. Kang, Presented in part at the 15th Annual Meeting of the Chemical Society of Japan, Kyoto, April, 1962.

phenylalanine was not detected among the products even by the paper chromatographic analysis of the products.

At run 5, the reductive amination of phenylpyruvic acid was carried out with cobaltous chloride under the similar conditions. Comparison of runs 3 and 5 indicated that the yield of phenylalanine increases appreciably by the addition of potassium cyanide to the reaction mixture.

The above results also indicated that cyano cobalt complex acts as a catalyst for the reductive amination of α-keto acids with aqueous ammonia. The mechnism of this reaction seems to be as follows: the unstable intermediate, α-imino acid, coordinates with cobalt complex ion and then the complex is reduced.



When α-keto acids were treated with chloropentamminecobalt(III) chloride[3] alone or together with potassium cyanide at 70°C under hydrogen pressure of 50 kg./cm^2 for five hours in alkaline solution, α-amino acids were obtained. The results of the reductive aminations with $[Co(NH_3)_5Cl]Cl_2$ are summarized in Table II.

While the reductive amination of phenylpyruvic acid with $[Co(NH_3)_5Cl]Cl_2$ gave phenylalanine in 29.6% yield, the yield was greatly increased by the addition of five moles of potassium cyanide. The yield of the amino acid decreased with the decrease of the molar ratio of $[Co(NH_3)_5Cl]Cl_2$ to α-keto acid.

The mechanism of this reaction seems to be similar to that of the reductive amination of α-keto acid with aqueous ammonia using cyano cobalt complex. A more detailed description of this work will be published shortly

The Institute of Scientific and Industrial Research
Osaka University
Sakai, Osaka

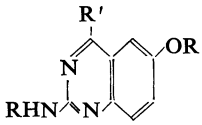
3) T. Inoue, "Mukikagaku Seizo Jikken", Shokabo Ltd., Tokyo (1949), p. 358.

Structure of the C_8-Base, an Acid Degradation Product of Tetrodotoxin

By Toshio Goto, Yoshito Kishi and Yoshimasa Hirata

(Received May 1, 1962)

Alkaline degradation of tetrodotoxin[1] (swellfish poison) afforded a yellow compound (C_9-base), whose structure was reported in the previous communication[2]. Tetrodotoxin also gave another yellow compound (C_8-base) when treated with sulfuric acid. That the C_8-base is 2-amino-6-hydroxyquinazoline (I) is deduced from the following evidences.



(II) R=R′=H
(II) R=CH_3CO, R′=H
(III) R=H, R′=CH_3

Tetrodotoxin was dissolved in concentrated sulfuric acid and the solution allowed to stand at room temperature for three days. Then the reaction mixture was neutralized with aqueous barium hydroxide and filtered. The filtrate was acidified with hydrochloric acid, evaporated to dryness under vacuum, and the residue was sublimed to give the C_8-base hydrochloride, m. p. over 250°C (in a sealed tube). Treatment of the hydrochloride with acetic andydride and pyridine afforded the diacetate (II), m. p. 198°C (in a sealed tube), $C_8H_5ON_3(COCH_3)_2$ (Found: C, 58.64; H, 4.55; N, 17.31. Calcd.: C, 58.77; H, 4.52; N, 17.14%); λ_{max}^{EtOH} mμ (log ε): 248 (4.3), $\lambda_{max}^{NaOH-EtOH}$ 258 (4.1); ν_{KBr} 1745 (phenol ester), 1675 cm^{-1} (amide).

2-Amino-4-methyl-6-hydroxyquinazoline (III) was synthesized for comparison of its ultraviolet spectrum with that of the C_8-base. 2-Nitro-5-hydroxyacetophenone[3], m. p. 146~147°C, was reduced catalytically (H_2/PtO_2) to give 2-amino-5-hydroxyacetophenone, m.p. 183~187°C (decomp.), which was then condensed with cyanamide. The quinazoline III thus obtained was converted to its hydrochloride, m. p. over 250°C (in a sealed tube). The ultraviolet spectrum of the C_8-base hydrochloride [$\lambda_{max}^{H_2O}$ mμ (log ε): 233 (4.3), λ_{max}^{NaOH} 245 (4.4)] was almost superimposable with that of the quinazoline III hydrochloride [$\lambda_{max}^{H_2O}$ mμ (log ε): 233 (4.3), λ_{max}^{NaOH}

1) H. Kakisawa, Y. Okumura and Y. Hirata, *J. Chem. Soc. Japan, Pure Chem. Sec.* (*Nippon Kagaku Zasshi*), **80**, 1483 (1959).
2) T. Goto, Y. Kishi and Y. Hirata, This Bulletin, **35**, 1045 (1962); K. Tsuda et al. also reported the same conclusion, *Chem. Pharm. Bull.*, **10**, 247 (1962).
3) A. R. Osborn and K. Schofield, *J. Chem. Soc.*, **1955**, 2100.

245 (4.4)]. For a methyl substituent at C_4-position would not contribute much to the ultraviolet spectrum of the quinazoline III, the C_8-base must have the structure I. The NMR spectrum of C_8-base in deuterium oxide shows only three signals (all singlets) at -2, -23 and -73 c. p. s.[4] (area ratio 1 : 2 : 1), which were assigned to one proton at C_4, two at C_7 and C_8, and one at C_5, respectively.

The author wish to thank Fujisawa Pharmaceutical Co. Ltd., for collecting ovaries of swellfish and to express appreciation to the Public Health Service, National Institutes of Health, for support of this work under Research Grant RG-7969.

Chemical Institute
Faculty of Science
Nagoya University
Chikusa, Nagoya

4) Spectrum was taken on a Nihondenshi JM (40 Mc.) spectrometer using D_2O containing NaOD as solvent, and external benzene as a reference (0 c. p. s.).

Isomerization of Flavan-3, 4-diols during the Formation of Isopropylidene Derivatives

By Shin-ichiro FUJISE, Shinzaburo HISHIDA, Toshio ONUMA, Koichiro ADACHI, Yutaka FUJISE and Takashi MUNEKATA

(Received May 10, 1962)

The stereochemistry of flavan-3, 4-diols is being studied in recent years. Corey et al.[1] reported that *cis*- and *trans*-flavan-3, 4-diols could respectively be converted to cyclic carbonates and that one of these carbonates was a trans derivative. Bokadia et al.[2] have shown that *trans*-flavan-3, 4-diol, *trans*-5-methylflavan-3, 4-diol, and *trans*-5-methyl-4′-methoxyflavan-3, 4-diol afforded the isopropylidene derivatives of the corresponding *cis*-diols. These results show that the formation of a cyclic derivative could no longer be regarded as diagnostic for a *cis*-configuration.

TABLE I

Flavan-3, 4-diols			Isopropylidene derivatives	
		M. p. °C	M. p. °C	Yield[h] %
Non-substituted	I[a]	161.5～162.5	110～111	60
	II[a]	142.5～143.5	None	
	III[b]	152～153	135～136	70
4′-Methoxy-	IV[a]	158.5～159.9	114～115	55
	V[a]	173～174	None	
	VI[b]	134～136		
7-Methoxy-	VII[a]	135～136	None[c]	(50)
	VIII[a]	117～118	113～114	60
	IX[b]	107～108		
7, 3′, 4′-Trimethoxy-	X[a]	172～173	135[d]	35 (55)
	XI[a]	149.5～150.5		3 (45)
	XII[b]	151～152	108～109[e]	(70)
5, 7, 3′, 4′-Tetramethoxy-	XIII[a]	206.5～207.5	141～142[f]	70
	XIV[a]	165.5～166.5		75
	XV[b]	153～154	141～142	45
5, 7, 3′, 4′, 5′-Pentamethoxy-	XVI[a]	195～196	172～173[g]	50
	XVII[a]	184～185		60
	XVIII[b]	186～187	164～165	30 (60)

a Synthesized from 3-hydroxyflavanones.
b Synthesized from flavonols.
c The same isopropylidene derivative which was obtained from VIII, was obtained by the reaction with acetone in the presence of concentrated hydrochloric acid. Yield, 50%.
d Obtained from both X and XI.
e Obtained in the presence of concentrated hydrochloric acid.
f Obtained from both XIII and XIV.
g Obtained from both XVI and XVII.
h The yield in parentheses show that obtained in the presence of concentrated hydrochloric acid.

1) E. J. Corey, E. M. Philbin and T. S. Wheeler, *Tetrahedron Letters*, No. 13, 429 (1961).

2) M. M. Bokadia et al., *J. Chem. Soc.*, **1961**, 4663.

Authors report analogous results shown below (Table I). The two stereoisomers of flavan-3, 4-diols (at C-4) were synthesized by the reduction (with $NaBH_4$, $LiAlH_4$, or catalytic hydrogenation) of the corresponding 3-hydroxyflavanones and the third isomers were synthesized by catalytic hydrogenation of the corresponding flavonols in the presence of copper chromium oxide, Raney nickel, or platinium oxide. The isopropylidene derivatives were obtained from flavan-3, 4-diols by the reaction with acetone in the presence of anhydrous cupric sulfate at room temperature.

Some pairs of flavan-3, 4-diols, X and XI, XIII and XIV, XVI and XVII, gave the same isopropylidene derivatives. The stereochemical change in the course of the formation of isopropylidene derivatives may be caused by the ionization of the benzylic 4-carbon atom.

Department of Chemistry,
Faculty of Science
Tohoku University
Katahira-cho Sendai

The Color of Liquid Caustic Soda Produced by the Ammonia-Soda Process

By Hiroshi AWAYA

(Received January 7, 1961)

Inasmuch as the chromium in an electrolyte has an influence on chlorine-caustic electrolysis in the electrolytic-soda process, small amounts of chromium in the electrolyte and in the products have been measured, but in the ammonia-soda process, the amount of chromium in the products has not yet been measured.

Caustic liquor produced by the ammonia-soda process has a characteristic yellow color. For the present article, the cause of such coloring was studied by polarographic and spectrophotometric methods, and it was found that the coloring was due to a chromate contained as an impurity in the caustic liquor.

Then the chromate content in many steps of the manufacturing process was determined. As a result of this experiment, it was found that the chromate in the caustic liquor comes from the milk of lime used for causticization.

Preliminary Experiments

Polarographic Method.—Caustic liquor samples from both ammonia and electrolytic processes were used. The sample of the ammonia process had a marked tinge of yellow. This sample was diluted with water and tartaric acid was added to make 0.2 M of an acid tartrate solution (pH 4.5). A small quantity of gelatin was also added. The polarograms of these solutions are shown in Fig. 1.

The polarogram of the sample from the ammonia process shows an abnormal wave. This wave seems to be due to a hydrolysis current[1].

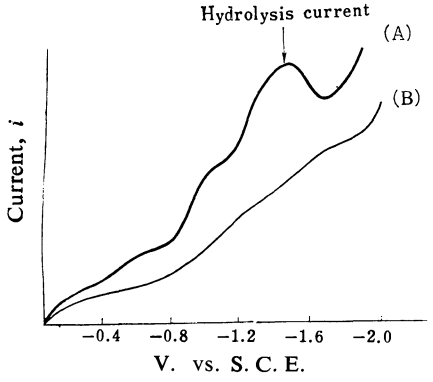


Fig. 1. Polarograms of caustic liquor as 0.2 M acid tartrate (pH=4.5).
(A) Ammonia-soda process
(B) Electrolytic process

Although the polarographic study of chromate ions by Lingane and Kolthoff[2] did not describe this hydrolysis current, and the half-wave potential did not coincide exactly with the values obtained by Lingane for chromate ions[3]; it seems to the author that the existence of chromate in the sample caused this hydrolysis current. This method did not give however, reproducible results. It might be that the coloring was due to the chromate, but this could not be confirmed by the polarographic method.

Absorption Spectra. — If the coloring of the caustic liquor was caused by the chromate contained as an impurity, the absorption spectra of the sample would show an absorption maximum at the wavelength of 370 mμ[4]. Therefore, the absorption spectra of many sorts of caustic soda were determined.

The samples were diluted to a 25% solution, and their absorbancy was determined photometrically over the wavelength range from 340 to 700 mμ. The data obtained are shown in Fig. 2.

The caustic liquor produced by the ammonia

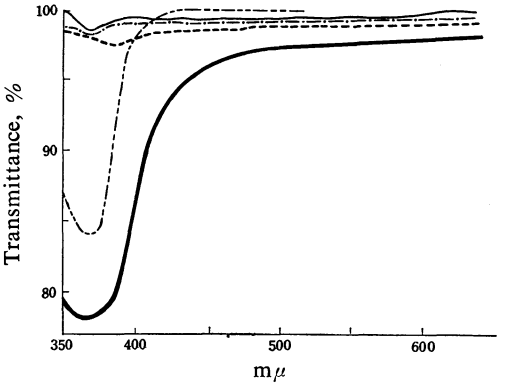


Fig. 2. Absorption spectra of caustic soda. 25% NaOH solution, 1 cm.-glass cell
—— Chemical pure reagent
-·-· Caustic liquor (electrolytic)
---- Caustic solid (ammonia)
▬▬ Caustic liquor (ammonia)
·---- Chromate solution (Cr : 2.5 p. p. m.)

1) M. Shinagawa, "Polarographic Determination", Kyoritsu Shuppan Co., Tokyo (1950), p. 126.
2) J. J. Lingane and I. M. Kolthoff, *J. Am. Chem. Soc.*, **62**, 852 (1940).
3) J. J. Lingane and R. L. Pecsock, ibid., **71**, 425 (1949).
4) E. B. Sandel, "Colorimetric Determination of Traces of Metals", Interscience Publishers, Inc., New York (1959), p. 390.

process had an absorption maximum at 370 mμ, agreeing with the characteristic absorption band of chromate. When the caustic liquor was concentrated to an anhydrous solid, even if it was produced by the ammonia process, it showed no absorption maximum at 370 mμ. This was due to the addition of sulfur, used as a refining reagent for solid caustic soda.

Experimental and Results

The Determination of Chromium. — As it was established that the coloring of the caustic liquor produced by the ammonia process was caused by chromate, the chromium content at many steps of the caustic manufacturing process was determined[5].

The chromium content in the electrolytic caustic soda was also determined.

Preparation.—Liquid caustic soda (50%): Dilute 50 ml. of the sample with water to about 200 ml.

Sodium carbonate solution: Dilute 100 ml. of the sample with water to about 200 ml.

Salt: Heat 100 g. of the sample with 100 ml. of 1 : 9 hydrochloric acid, add water until dissolution, and filter the solution in order to remove insoluble substance.

Limestone and burned lime: Take 20 g. of limestone and 5 g. of burned lime respectively. Moisten the sample powder with water, add 6 N hydrochloric acid until the bubbles of the carbon dioxide gas disappear, and dilute the mixture with water. Then heat the solution and, after cooling, filter it for removal of the insoluble substance.

Milk of lime: Dilute 10 ml. of the sample with water, and 6 N hydrochloric acid until the bubbles of the carbon dioxide gas disappear, and dilute the mixture with water. Then heat the solution.

Operation of Analysis.—If the sample solution is neutral of alkaline, add hydrochloric acid to the solution until it is acidic (pH 1~2). If the sample solution is highly acidic, add aqueous ammonia. Heat the solution carefully, add 5 ml. of a ferrous solution (1 mg. Fe^{2+} per mol.) for the reduction of the chromate and, after a while, add 0.5 ml. of concentrated nitric acid in order to oxidize the ferrous ion. Add aqueous ammonia (12 N) excessively to the solution at 30 to 40°C. The precipitates of ferric and chromium hydroxides are filtered and dissolved with 20 ml. of hot mixed acid (10% concentrated sulfuric acid, 10% concentrated phosphoric acid, and 80% water by volume). Dilute to about 40 ml. with water, heat the solution and, keeping it warm, add the potassium permanganate solution (0.5%), drop by drop, until the solution comes to have a tinge of the purple color of the permanganate for 10 min. After cooling, add 10 ml. of a urea solution (10%) and then sodium nitrite solution (10%), drop by drop, until the pink color disappears. Stir the solution vigorously until the bubbles are broken, transfer the solution to a 100 ml. volumetric flask. Add 3 ml. of diphenylcarbazide solution (0.2% alcoholic solution) and then shake it and allow it to settle for a minute. Add 5 ml. of hydrofluoric acid (4%) in order to mask the ferric ion, dilute to 100 ml., determine the absorbancy photometrically at 540 mμ using a blank solution (containing ferric ion and all reagents) as a reference and compare it with the calibration curve.

5) Japanese Industrial Standards, JIS G-1217 (1958).

Table I. Determination of chromium on the soda industry

Materials			Cr, %
Salt	Egypt-salt		<0.000004
	Aden-salt		<0.000004
	Formosa-salt		<0.000004
	Taku-salt		<0.000004
Brine (electrolytic soda process)			
	Purified brine		0.0000030
	Depleted brine		0.0000045
Limestone			0.00027
Burned lime			0.0025
Milk of lime		No. 1	0.00038
		No. 2	0.00026
Na_2CO_3-solution (before the causticization)			0.00000
Liquid caustic soda (45%)			
	Ammonia process		
		No. 1	0.00019
		No. 2	0.000084
		Maker A	0.000115
		Maker B	0.000133
		Maker C	0.000135
	Electrolytic process		
		No. 1	0.000005
		Maker A	0.000048
Solid caustic soda		No. 1	0.000007
		No. 2	0.000062

The results of the determination of chromium content are shown in Table I.

The chromate was also found in the caustic liquor produced by several ammonia process makers in Japan.

As shown in Table I, the salts used as raw material and the sodium carbonate solution used for causticization contained little chromium. A considerable amount of chromium was found in limestone, burned lime and milk of lime. It was thus confirmed that the chromate in the caustic liquid came from the limestone.

Discoloring of the Yellow Colored Caustic Liquor.—Discoloring of the caustic liquor produced by the ammonia process was attempted.

The caustic liquor samples used were 10% solutions.

Treatment 1.—Add the powder of ferrous sulfate or strontium sulfate up to 1% of the solution, then stir and filter the solution. The chromate in the solution was reduced by this method, precipitated as chromium hydroxide and removed from the solution.

Treatment 2. — Let the sample solution pass through a column of anion exchange resin (Amberlite IRA-410, OH-form). The chromate in the solution was adsorbed in the resin, and the solution was purified. After each treatment, the

TABLE II. DISCOLORING OF CAUSTIC LIQUOR

Treatment	Cr, %
Before treatment	0.000034
Addition of excess of $FeSO_4$	0.000012
Addition of excess of $SrSO_4$	0.000014
Treatment with anion exchange resin*	0.000008

* Amberlite IRA-410, OH-form

chromium content of these solutions was determined. These results are shown in Table II.

Yellow colored caustic liquor was discolored by the addition of ferrous sulfate or strontium sulfate.

The application of anion exchange resins was also effective.

Summary

It is found that the coloring of caustic liquor produced by the ammonia-soda process is due to chromate in the milk of lime given to the sodium carbonate solution for causticization. But the solid caustic soda, even produced by the ammonia-soda process, contains a little chromate. The coloring of caustic liquor by chromate is found in products of all ammonia process makers in Japan.

The existence of chromate not only gives the yellow color to the product, but also has an undesirable effect on viscose production in the rayon industry.

Yellow-colored caustic liquor can be discolored by the addition of the reducing reagent. Refining by anion exchange resin is also effective, but there is a risk of the corrosion of the resin by the caustic liquor. As the chromate was identified in the caustic liquor, it was concluded that the abnormal wave of the polarogram caustic liquor was probably due to the hydrolysis current.

By measuring the absorbancy of caustic liquor at the wavelength of 370 mμ, the chromate content can be nearly exactly determined.

As much limestone contains a considerable impurities, it is not desirable to use the milk of lime for the purification of the brine in the electrolytic-soda process also.

Thanks are due to Professor Mutsuaki Shinagawa of Osaka University for his helpful advice.

Tokuyama Soda Co., Ltd.
Research Division
Tokuyama

On Glumamycin, a New Antibiotic. II[*1]. *Isolation and Identification of Amino Acids Constituting Glumamycin*

By Michitaka INOUE[*2]

(Received March 31, 1961)

Glumamycin[1-3], an antibiotic isolated from the culture broth of a soil streptomyces *Streptomyces zaomyceticus* No. 7548, shows a strong activity against Gram positive bacteria, particularly penicillin- and tetracycline-resistant bacteria such as *M. aureus* and *B. subtilis*. It is interesting to note that glumamycin is more active in vivo than in vitro[4]. The author has long been engaged in the investigation of glumamycin, and as described in previous communications[2,3] the antibiotic was found to consist of the following amino acids; L-aspartic acid, α(L), β-methylaspartic acid, L-proline, L-valine, glycine, D-pipecolic acid, and α, β-diaminobutyric acid. This paper deals with the identification of these amino acids.

As already reported[1,2] glumamycin was extracted from a filtered broth with isoamylalcohol or *n*-butanol at pH 2.0, transferred to water at pH 7.0~8.0, and separated from brown pigments by column chromatography on active carbon. Further purification was effected by Craig's countercurrent distribution (300 transfers).

Pure glumamycin, a white crystalline powder, is soluble in water and methanol, and when dissolves in a sodium hydrogen carbonate solution, produces carbon dioxide. But it is insoluble in chloroform, benzene and ethyl acetate. Analysis of glumamycin gives a value consistent with the molecular formula of $C_{59}H_{91}O_{20}N_{13}$. The antibiotic is an optically

*1 This constitutes Part XXXI of a series entitled "Studies on Antibiotics" by S. Tatsuoka.

*2 Present address: Osaka Factory, Takeda Chemical Industries, Ltd., Juso, Higashiyodogawa, Osaka.

1) M. Inoue, K. Nakazawa, A. Miyake et al., *J. Antibiotics*, A15, 1 (1962).
2) M. Inoue et al., This Bulletin, 33, 1014 (1960).
3) M. Inoue, ibid., 34, 885 (1960).
4) Y. Oka, M. Matsui and T. Araki, *Ann. Rept. Takeda Research Lab.*, 20, 207 (1961).

active substance and gives biuret reaction but no ninhydrin reaction. Infrared spectrum of glumamycin shows the presence of the linkage characteristic of peptide, but its ultraviolet spectrum exhibits no specifuity. From these results glumamycin was presumed to be an acidic peptide, so its amino acids were investigated by hydrolytic degradation. Hydrolysis of glumamycin with 6 N hydrochloric acid separated an oily substance, which was removed by extraction with ether. In the water layer seven amino acids were detected by paper chromatography and paper electrophoresis, of which two were acidic, one was basic, and the remaining four were neutral. In general, peptide-type antibiotics so far known belonged to D-series or specific amino acids, so the seven amino acids were isolated by a combination of ion-exchange chromatography and partition chromatography, and their properties were investigated.

One of the two acidic amino acids was L-aspartic acid and three of the four neutral amino acids were L-proline, L-valine and glycine, and they were identified by their infrared spectrum, optical activity and behavior in paper chromatography.

One of the remaining three amino acids was obtained as fine needles, $C_5H_9NO_4$, and though acidic, it was not identical with glutamic acid on paper chromatography. The compound was presumed to be methylaspartic acid from detection of one C–CH_3 group by the Kuhn-Roth method, and identified as α(L), β-methylaspartic acid[5] from its optical rotation, melting point and infrared spectrum*3.

Another compound of the three unidentified amino acids was isolated as a neutral amino acid, fine needles, $C_6H_{11}NO_2 \cdot HCl$, and containing no *N*-methyl group and no amino-nitrogen, and giving a specific color with ninhydrin, it was presumed to be a piperidine carboxylic acid. The compound was compared with synthetic DL-pipecolic acid (piperidine-α-carboxylic acid) and its isomers by paper chromatography, and it was assumed to be pipecolic acid. Further, as the optical rotation of the compound was in reverse relation with that of L-pipecolic acid monohydrochloride obtained from a plant[6], it was presumed to be D-pipecolic acid. Therefore, its (+)tartrate[7] was compared with D-pipecolic acid (+)tartrate obtained by optical resolution of synthetic DL-pipecolic acid, and they were observed to be in good agreement in the melting point, optical rotation and infrared spectrum. These findings establish conclusively that the neutral amino acid is D-pipecolic acid.

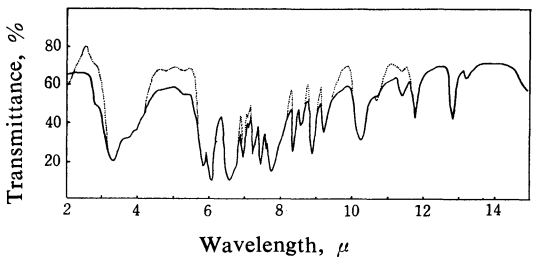


Fig. 1. Infrared absorption spectrum of α(L), β-methylaspartic acid.
—— α(L), β-Methylaspartic acid (from glumamycin), KBr
····· α(L), β-Methylaspartic acid (H. A. Barker[5]), KCl

Table I. R_f Values of three isomers of piperidine carboxylic acid on P. P. C. by various solvent systems

	Solvent systems		
	A	B	C
DL-Pipecolic acid	0.45 (0.44)	0.48 (0.45)	0.92 (0.92)
D-Pipecolic acid (from glumamycin)	0.45	0.48	0.92
L-Proline	0.34 (0.34)	0.36 (0.34)	0.90 (0.90)
Nipecotic acid	(0.34)	(0.33)	(0.95)
Isonipecotic acid	(0.34)	(0.28)	(0.95)

R_f Values in bracket are from "Chromatographic Technique" ed. by I. Smith, William Heinemann Medical Books, Ltd. London (1958).

The remaining one of the three unidentified amino acids, which was basic on paper electrophoresis, was isolated as hydrochloride, $C_4H_{10}N_2O_2 \cdot HCl$. Although the molecular formula of this amino acid was in accord with that of α, γ-diaminobutyric acid obtained from

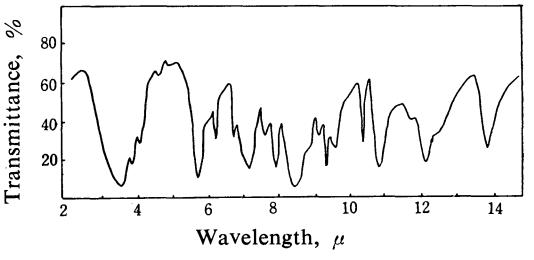


Fig. 2. Infrared absorption spectrum of D-pipecolic acid, KBr.

5) H. A. Barker et al., *Arch. Biochem. Biophys.*, **78**, 468 (1958).

*3 The author thanks Dr. N. Bohonos and Dr. J. Martin, Lederle Laboratories Division of American Cyanamid Co., for their kind information on IR spectrum of α(l), β-methylaspartic acid.

6) R. M. Zacharins, J. F. Tompson and F. C. Steward, *J. Am. Chem. Soc.*, **76**, 2908 (1954).

7) R. L. Morrison, *Biochem. J.*, **50**, 474 (1953).

Table II. Comparison with α, β-diaminobutyric acid and α, γ-diaminobutyric acid

	M. p., °C		R_f Value Solvent systems	
	Monohydrochloride	Monopicrate	A	B
α, β-Diaminobutyric acid (from glumamycin)	202	209	0.15	0.32
α, γ-Diaminobutyric acid (synthetic)	228~230	184~185	0.13	0.20

such antibiotics as Polymixin B[8], it seems different from α, γ-diaminobutyric acid because it gave a values of nearly one mole of C-CH_3 by the Kuhn-Roth method, and the melting points of its hydrochloride and picrate and its R_f-value were all different from those of α, γ-diaminobutyric acid. So this basic amino acid was presumed to be α, β-diamino-*n*-butyric acid or α, β-diaminoisobutyric acid. To clarify its identity the amino acid was deaminated with one mole of sodium nitrate carefully and resulting ninhydrin positive product $C_4H_9O_3N \cdot H_2O$, which gave acetaldehyde on oxidation with periodic acid, was assumed to be α-hydroxy-β-aminobutyric acid, and thus the above-mentioned basic amino acid was established to be α, β-diamino-*n*-butyric acid.

To confirm the result more positively, attempt was made on the synthesis of α, β-diaminobutyric acid. As to the synthesis there is found no other report than that of Neuberg[9], who effected it with α, β-dibromobutyric acid and aqueous ammonia under pressure, but as the product was a syrupy substance, it was isolated as phenylisocyanate or picrate. However, since the α-bromine seems readily to be split off in this method as pointed out by Neuberg[9], the present author employed the method used by Horner[10] for the synthesis of β-alanine. Namely, ethyl α, β-dibromobutyrate (I) was allowed to react with sodium azide, the resulting ethyl α, β-diazidobutyrate (II) was further reacted with triphenylphosphine, and the phosphinimide thus produced was hydrolyzed with hydrobromic acid to give α, β-diaminobutyric acid (IIIa). The diamino acid was also obtained by reducing the diazide compound under high pressure and hydrolyzing the reaction mixture directly, but in this case, besides IIIa, its isomer IIIb crystallizable as hydrochloride was obtained.

Benzoylation of IIIa and IIIb by Schotten-Baumann's method afforded IVa, m. p. 216°C and IVb, m. p. 106~108°C, respectively. Dehydration of IVa with benzoyl chloride in pyridine yielded a substance assumable as the corresponding azlactone, which was converted to ethyl α, β-dibenzoylaminobutyrate (Va) by boiling with ethanol. The infrared spectrum of the product was in accord with that of α, β-dibenzoylaminobutyrate prepared by the same method from the dibenzoyl compound derived from glumamycin.

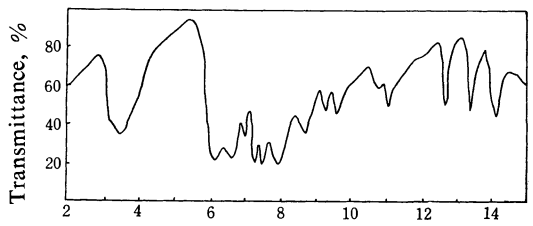


Fig. 3. Infrared spectrum of α, β-diaminobutyric acid monopicrate, KBr.

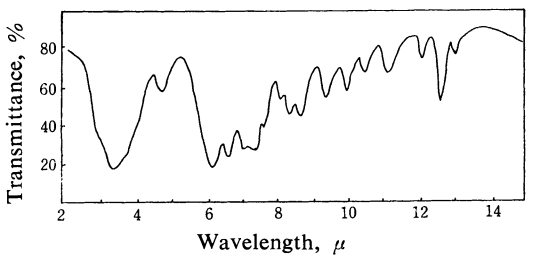


Fig. 4. Infrared absorption spectrum of α, β-diaminobutyric acid monohydrochloride, KBr.

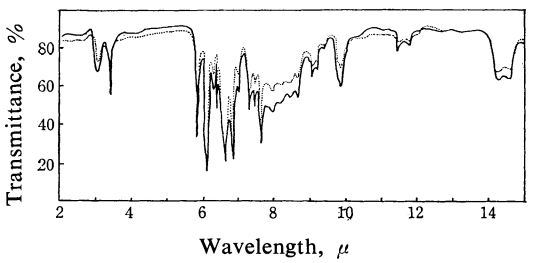


Fig. 5. Infrared absorption spectrum of ethyl dibenzoylaminobutyrate, KBr.
—— From glumamycin
····· Synthetic

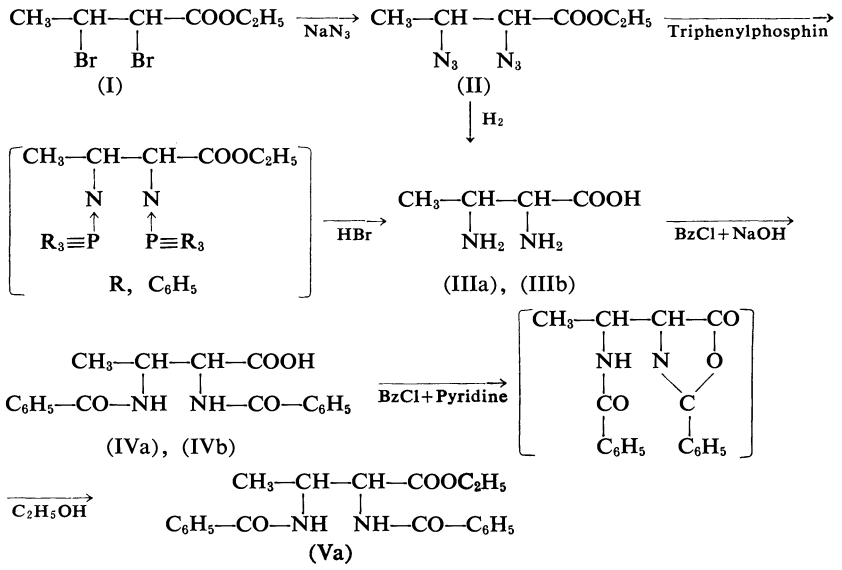
From the results mentioned above the plane structure of the basic amino acid of glumamycin was established to be α, β-diamino-*n*-butyric acid.

Of the seven amino acids constituting glumamycin, α(L), β-methylaspartic acid, D-pipecolic acid and α, β-diaminobutyric acid are the first to be isolated as components of peptide-type compounds. It was found that glumamycin

8) W. Hausmann, *J. Am. Chem. Soc.*, **78**, 3668 (1956).

9) C. Neuberg, *Biochem. Z.*, **1**, 282 (1960).

10) L. Horner and A. Gross, *Ann.*, **591**, 117 (1955).



also follows the rule that peptide-type antibiotics contain always D-series amino acids.

Experimental

Paper Chromatography.—Whatman No. 1 paper and Toyo Roshi No. 50 paper were employed with the following solvent systems: A, *n*-butanol-acetic acid water (4 : 1 : 5); B, *n*-butanol-pyridine-water (1 : 1 : 1); C, phenol-water (4 : 1).

Paper Electrophoresis. — Whatman No. 1 paper employed with the following conditions: Buffer; 2 N acetic acid. Voltage; 300 V. Time; 3 hr.

Glumamycin. — The crude antibiotic which was obtained as described in a previous paper[1] was purified by countercurrent distribution (300 transfer: 20 ml.) in the system chloroform-methanol-0.02 hydrochloric acid (2 : 2 : 1). The materials in the tubes (158~168), whose distribution corresponded closely to the theoretical $k=1.17$, were combined and recrystallized to yield the material for all degradative studies. Glumamycin was obtained as a white crystalline powder by recrystallization from a methanol-ethyl acetate mixture, m. p. 230°C (decomp.), $[\alpha]_D^{20}$ +8.5±0.5 (*c* 1, in ethanol).

Found: C, 54.58; H, 7.25; N, 13.60. Calcd. for $C_{59}H_{91}O_{20}N_{13}$: C, 54.25; H, 6.99; N, 13.99%.

Acid Hydrolysis.—Hydrolysis of glumamycin at 110°C for 12 hr. with 6 N hydrochloric acid and, after removing the ether soluble material and working up in the usual way, gave a mixture of amino acids which, when examined by paper chromatography (solvent system A, Toyo Roshi No. 50) and paper electrophoresis, was found to contain seven amino acids. Prolonged heating with hydrochloric acid did not change the composition of this mixture.

Separation and Identification of Hydrolyzate.—The acid hydrolyzate of the antibiotic (5 g.) was treated with ether and concentrated in vacuo in the usual way.

Aspartic Acid.—The above residue was dissolved in 200 ml. of water. The solution was put on a column (3 cm.×20 cm.) of Amberlite IR-4B (OH-form). The column was eluted with 1 N hydrochloric acid, the ninhydrin positive fraction was collected and concentrated under reduced pressure, and the residue was recrystallized from ethanol to give colorless granular crystals, m. p. 160°C $[\alpha]_D^{23}$ +23° (*c* 8, in 6 N hydrochloric acid).

Found: C, 36.10; H, 5.41; N, 10.30%.

α(L), β-Methylaspartic Acid.—The mother liquor from the aspartic acid was evaporated to dryness and the residue was subjected to partition chromatography, using a column (3 cm.×35 cm.) of cellulose powder and developing with *n*-butanol-acetic acid-water (120 : 30 : 50). Amino acids were detected in the eluate fractions (5 ml.) by subjecting them to paper chromatography (solvent system A). The fractions showing a single spot at about R_f 0.35, which colored purplish red with ninhydrin, were combined and evaporated to dryness. The residue was dissolved in water, the solution was passed through a column of Amberlite IR-120 (H-form), and the column, after washing with water and 0.2 N acetic acid, was eluted with 0.2 N aqueous ammonia. The eluate was concentrated under reduced pressure, the residue was dissolved in aqueous butanol, the acetone was added to the solution, giving colorless needles, which were purified by recrystallization from aqueous ethanol, m. p. 254~256°C (decomp.), $[\alpha]_D^{21}$ +13.0° (*c* 1, in 5 N hydrochloric acid).

Found: C, 40.52; H, 6.18; N, 9.27; C-CH_3, 10.33. Calcd. for $C_5H_9NO_4$: C, 40.80; H, 6.12; N, 9.52; C-CH_3, 10.20%.

Separation of Neutral Amino Acids.—The above effluent from Amberlite IR-4B was combined with the washing and evaporated to dryness in vacuo. The residue was dissolved in 20 ml. of ammonium acetate buffer (pH 5.0), the solution was passed through a column (8 cm.×40 cm.) of Dowex 50-X8 (100~200 mesh) treated beforehand with the same buffer, and the column was eluted with the same buffer. The effluent was collected in fractions of 200 ml. each and investigated by paper ionophoresis, finding that all neutral amino acids were eluted out in 200~800 ml. of the effluent.

This portion of the effluent was evaporated to dryness under reduced pressure and the residue was extracted several times with 30 ml. portions of methanol to divide it into methanol soluble and methanol insoluble parts.

D-Pipecolic Acid.—The solution of the methanol soluble part was evaporated to dryness and developed on a column (3 cm.×35 cm.) of cellulose powder with *n*-butanol-acetic acid-water (4 : 1 : 5). Of the effluent the part which flowed out first and gave a single spot coloring bluish purple with ninhydrin was evaporated under reduced pressure, and the residue was recrystallized from a mixture of methanol and ether, m. p. 240°C (decomp.), $[\alpha]_D^{21}$ +10.0° (*c* 1, in water).

Found: C, 43.82; H, 7.47; N, 8.76; Cl, 22.61. Calcd. for $C_6H_{11}NO_2 \cdot HCl$: C, 43.50; H, 7.30; N, 8.76; Cl, 21.40%.

D-Pipecolic Acid (+)Tartrate. — According to the method of Morrison[7], an aqueous solution of 250 mg. of the above pipecolic acid monohydrochloride was passed through a column (0.9 cm.× 6.0 cm.) of Amberlite IR-4B (OH-form) to remove the hydrochloric acid and evaporated to dryness. The residue and 232 mg. of (+)tartaric acid were dissolved in 2.5 ml. of hot methanol and the solution was allowed to cool, precipitating the desired product, which melted at 187°C after recrystallization from ethanol.

Found: C, 43.54; H, 6.06; N, 4.80. Calcd. for $C_{10}H_{17}O_8N$: C, 43.00; H, 6.14; N, 5.02%. $[\alpha]_{25}^{D}$ +20° (*c* 10, in water). D-Pipecolic acid (+)tartrate[7], m. p. 187°C, $[\alpha]_D^{25}$ +18° (*c* 10, in water).

Proline.—In the treatment of the methanol soluble part mentioned before, an effluent giving a yellow ninhydrin reaction flowed out after the eluate of D-pipecolic acid. This portion was evaporated and the residue was recrystallized from *n*-butanol to yield prisms, m. p. 218°C (decomp.) $[\alpha]_D^{21}$ −82° (*c* 1, in water).

Found: C, 52.13; H, 8.04; N, 11.87%.

Valine.—The methanol insoluble part mentioned above was developed on a column of cellulose powder with *n*-butanol-acetic acid-water (4 : 1 : 5). The effluent which flowed out first and gave a single ninhydrin positive spot was evaporated and the residue was recrystallized from water, furnishing colorless prisms, m. p. 312°C, $[\alpha]_D^{23}$ +25° (*c* 3.4, in 6 N hydrochloric acid).

Found: C, 51.10; H, 9.46; N, 11.98%.

Glycine.—The eluate which flowed out after valine and which exhibited a single ninhydrin positive spot corresponding to glycine was evaporated and the residue was recrystallized from aqueous methanol yielding prisms, m. p. 233°C.

Found: C, 32.34; H, 7.20; N, 18.69%.

Synthesis of DL-Pipecolic Acid. — A mixture of 10 g. of α-bromo-ε-benzoylaminocapric acid, 100 ml. of water, 100 g. of acetic acid, 100 g. of concentrated hydrochloric acid was boiled under reflux for 6 hr. The reaction mixture was evaporated under reduced pressure to remove the hydrochloric acid and acetic acid, and an aqueous solution of the residue was passed through a column of Amberlite IR-120 (H-form), the effluent being discarded. The column was washed with water and eluted with 0.5 N aqueous ammonia, and the eluate was evaporated to dryness under reduced pressure. The residue was extracted with ethanol, the extract, after addition of a small amount of hydrochloric acid, was evaporated again to dryness, and the residue was recrystallized from a mixture of ethanol and acetone to yield colorless needles, m. p. 240°C (decomp.), $[\alpha]_D^{21}$ 0 (*c* 1, in water).

Found: C, 43.62; H, 7.42; N, 8.80; Cl, 22.34%.

Optical Resolution of DL-Pipecolic Acid. — D-Pipecolic acid (+)tartrate was prepared from DL-pipecolic acid monohydrochloride by the method of Morrison[7] as in the case of D-pipecolic acid described before. The melting point and optical rotation were 187∼188°C and $[\alpha]_D^{25}$ +20° (*c* 1, in water), respectively.

Found: C, 43.80; H, 6.06; N, 4.08. Calcd. for $C_{10}H_{17}O_8N$: C, 43.00; H, 6.14; N, 5.02%.

α,β-Diaminobutyric Acid Monohydrochloride.— The column Dowex 50-X8, which was eluted with 1000 ml. of ammonium acetate buffer (pH 5.0) as mentioned before, was further eluted with 0.25 N aqueous ammonia, and it was found by paper ionophoresis that 400∼800 ml. of the effluent contained a basic amino acid. This fraction was evaporated under reduced pressure, the residue was dissolved in a small amount of hydrochloric acid, and the solution, after addition of mathanol and ether, was allowed to stand in a cool place, whereupon colorless needles melting at 202°C (decomp.) after recrystallization from aqueous ethanol precipitated.

Found: C, 31.39; H, 7.30; N, 17.64; Cl, 21.99. Calcd. for $C_4H_{10}O_2N_2 \cdot HCl$: C, 31.06; H, 6.48; N, 18.11; Cl, 22.95%. $[\alpha]_D^{22}$ +19° (*c* 1, in 6 N hydrochloric acid), $[\alpha]_D^{22}$ +16° (*c* 1, in water), $pk_a' < 2$, 6.6, 9.6. Treated with picric acid it gave α,β-diaminobutyric acid monopicrate, m. p. 209°C (decomp.).

Found: C, 34.72; H, 3.84; N, 19.95. Calcd. for $C_4H_{10}N_2O_2 \cdot C_6H_3O_7N_3$: C, 34.59; H, 3.74; N, 20.10%.

Benzoylated by the Schotten-Bauman's method it gave α,β-dibenzoylaminobutyric acid, m. p. 210°C.

Found: C, 66.14; H, 5.59; N, 8.42. Calcd. for $C_{18}H_{18}O_4N_2$: C, 66.24; H, 5.56; N, 8.58%.

α-Hydroxy-β-aminobutyric Acid.—To a solution in 30% acetic acid of 1 g. of α,β-diaminobutyric acid from glumamycin was added dropwise a solution of 4.5 g. of sodium nitrite in 10 ml. of water over a period of about 1 hr. with stirring and cooling with ice water. The reaction mixture was left standing for 10 hr. The product, diluted with water, was absorbed on a column of Amberlite IR-120 (H-form) and the column was eluted with 1 N aqueous ammonia. The eluate was evaporated in vacuo, and the residue was recrystallized from water, m. p. 123°C (decomp.).

Found: C, 35.08; H, 7.98; N, 9.81; H_2O, 13.98. Calcd. for $C_4H_9O_3N \cdot H_2O$: C, 35.03; H, 8.03; N, 10.21; H_2O, 13.00%.

Periodic Acid Oxidation of α-Hydroxy-β-aminobutyric Acid. — To a solution of 113 mg. of α-hydroxy-β-aminobutyric acid in 10 ml. water was added dropwise a solution of 230 mg. periodic acid in 5 ml. of water with stirring and cooling with ice water. The reaction mixture was left standing

for 2 hr. at room temperature and the product was distilled with 20 ml. of water. To the distillate was added a solution of 180 mg. of dimedon in aqueous alcohol and the resulting colorless substance was recrystallized from aqueous alcohol, m. p. 140°C. Yield, 220 mg. A mixed melting point with authentic acetaldodimedon (m. p. 140°C) showed no depression and infrared spectrum of the two were quite identical.

Ethyl α, β-Diazidobutyrate (II).—To a solution of 27.4 g. of ethyl α, β-dibromobutyrate (I) in 137 ml. of ethanol was added dropwise a solution of 19.5 g. of sodium azide in 78 ml. of water over a period of about 3 hr. with stirring and heating on a water-bath. After the reaction was completed by heating about one hour more, the ethanol was distilled off under reduced presssure, and the aqueous solution was extracted with benzene. The benzene solution, after washing with water, diluted hydrochloric acid and sodium hydrogen carbonate solution successively and drying over anhydrous sodium sulfate, was evaporated under reduced pressure, leaving 16.8 g. of a residue. The residue was distilled in vacuo and the portion b. p. 70~85°C/2 mmHg. (11.2 g. or 56.6%) was redistilled to give the diazide compound, b. p. 80~83°C/2 mmHg.

DL-α, β-Dibenzoylaminobutyric Acid (IVa), (IVb).—i) To a solution of 5 g. of the diazide compound II in 100 ml. of benzene was added dropwise a benzene solution of 13 g. of triphenylphosphin with stirring, when a reaction set in with evolution of heat and nitrogen gas. The reaction temperature was kept at 30°C. After addition of triphenylphosphin the reaction mixture was heated on the water-bath for 2 hr. and then the benzene was distilled off. The crude phosphinimine compound thus obtained was heated with 50 ml. of 40% hydrobromic acid, the reaction mixture was concentrated under reduced pressure and after dilution with water, the precipitate was filtered off. The filtrate was passed through a column of Amberlite IR-120 (H-form), the column was eluted with 4 N aqueous ammonia, and the eluate was evaporated to dryness under reduced pressure, leaving a residue, which gave crystals by addition of ethanol, m. p. 178°C (decomp.).

This compound IIIa was benzoylated by the method of Schotten-Baumann and the resulting crude product was recrystallized from ethanol after treating it with ligroin, m. p. 216~218°C.

Found: C, 66.14; H, 5.41; N, 8.73. Calcd. for $C_{18}H_{18}O_4N_2$: C, 66.24; H, 5.56; N, 8.58%.

ii) A solution of 20 g. of the azide compound in 80 ml. of ethanol was reduced on Adams platinum oxide at room temperature under 100 atmospheric pressure. The catalyst was filtered and the filtrate was evaporated under reduced pressure to give a light yellow syrupy substance. The substance was boiled with 175 ml. of 20% hydrochloric acid for 3 hr., the hydrolyzate was evaporated in vacuo, and the residue was allowed to stand with ethanol-ether, separating 5.5 g. (37.6%) of white prisms (IIIb), m. p. 199~201°C (decomp.). The mother liquor was concentrated in vacuo, the residue was dissolved in water, and the solution was treated by the same method in IIIa, giving 3 g. of IIIa, m. p. 178°C.

Compound IIIb was benzoylated by the same method and the resulting product was recrystallized from aqueus ethanol, yielding white needles, m. p. 106~108°C.

Found: C, 62.82; H, 5.81; N, 8.20. Calcd. for $C_{18}H_{18}O_4N_2 \cdot H_2O$: C, 62.78; H, 5.85; N, 8.14%.

DL-Ethyl α, β-Dibenzoylaminobutyrate (Va). To a solution of 700 mg. of the dibenzoyl compound (IVa) in 7 ml. of pyridine was added 0.2 ml. of benzoyl chloride under cooling with ice water. After one hour, the reaction mixture was poured onto chipped ice, neutralized with hydrochloric acid, and extracted with ethyl acetate. The extract, after washing with water, sodium hydrogen carbonate solution and water successively and drying over anhydrous sodium sulfate, was evaporated under reduced pressure and the residue was treated with ether, leaving a substance, m. p. 187°C, which was assumed to be an azlactone. The substance, was dissolved in ethanol, the solution, after being boiled for one hour, evaporated and the residue was recrystallized from aqueous ethanol to given colorless needles, m. p. 187°C.

Found: C, 67.00; H, 6.20; N, 7.68. Calcd. for $C_{20}H_{24}O_4N_2$: C, 67.78; H, 6.26; N, 7.91%.

Summary

Isolation of the amino acids constituting glumamycin, a new antibiotic, was effected. As a result, α(L), β-methylaspartic acid, besides L-aspartic acid was obtained as an acidic amino acid. In addition to L-valine, glycine, and L-proline, D-pipecolic acid was yielded as a neutral amino acid. Further, α, β-diaminobutyric acid was obtained as a basic amino acid and its structure was established to be α, β-diamino-*n*-butyric acid. For positive confirmation of the structure the acid was synthesized, and it was found that the *N*, *N*-dibenzoyl ethyl ester of the synthetic product and that of the basic amino acid derived from glumamycin were in complete agreement.

The author wishes to express his sincere thank to Dr. Satoru Kuwada, the Director of Research Laboratories, Dr. Sueo Tatsuoka, Vice Director of Research Laboratories, Dr. Kuniyoshi Tanaka, the Head of the 2nd Division of Research Laboratories, for their guidance and encouragement, and to Drs. Kôichi Nakazawa, Akira Miyake, Jisaburo Ueyanagi and Mr. Masahiko Fujino for their kind advices. The author is indebted to Messrs. Masami Kan, Hironobu Kashiwagi and Miss Fusa Suzuki and Mrs. Yoshiko Tsukamoto for performing microanalysis and to Messrs. Hideo Kamio and Hideo Nakamachi for determination of spectra.

Research Laboratories
Takeda Chemical Industries, Ltd.
Juso, Higashiyodogawa-ku, Osaka

On Glumamycin, a New Antibiotic. III[*1]. *Fatty Acid, a Constituent of the Antibiotic*

By Michitaka INOUE[*2]

(Received March 31, 1961)

Investigations reported in previous papers of this series[1] have found that the constituents of the peptide portion of glumamycin are seven kinds of amino acids, i. e. L-aspartic acid, α(L), β-methylaspartic acid, D-pipecolic acid, L-proline, L-valine, glycine and α, β-diaminobutyric acid. An acid hydrolysis of glumamycin, however, gave an oily substance which was insoluble in water, soluble in ether, and, when dissolved in sodium hydrogen carbonate solution, produced carbon dioxide. In the present work, investigation is made of the oily substance.

This substance boiled at 139°C/1 mmHg and corresponded to an unsaturated fatty acid having an empirical formura of $C_{13}H_{24}O_2$, and its hydrogenation product and *S*-benzylthiuronium salt consisted of $C_{13}H_{26}O_2$ and $C_{13}H_{24}O_2 \cdot C_8H_{10}N_2S$ respectively. Since the substance was optically active and its C-CH_3 value, as measured by the Kuhn-Roth method, was 1.2 mol., it was presumed to be an unsaturated fatty acid possessing more than one side-chain.

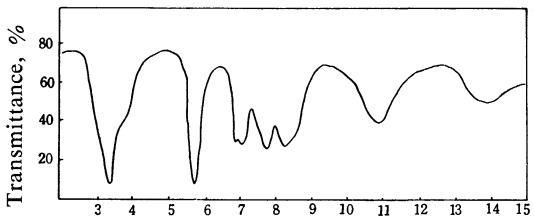


Fig. 1. Infrared absorption spectrum of $C_{13}H_{24}O_2$ from glumamycin.

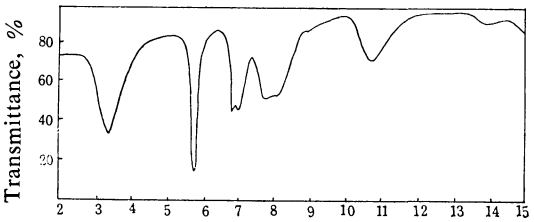


Fig. 2. Infrared absorption spectrum of $C_{13}H_{26}O_2$.

The 2-tridecenoic acid ($C_{13}H_{24}O_2$) obtained by Ogawa et al.[2] from the decomposition product of esperin, an antibiotic produced by *B. mesentercius*, was a straight chain compound and differed from the present substance in its infrared spectum. Therefore, the substance was oxidized with ozone, and then the product was further oxidized with silver oxide, giving a saturated fatty acid corresponding to $C_{10}H_{20}O_2$ and a dibasic acid of $C_3H_4O_4$.

$$C_{13}H_{24}O_2 \xrightarrow{O_3} C_{10}H_{20}O_2 + C_3H_4O_4$$
$$\downarrow H_2$$
$$C_{13}H_{26}O_2$$

The former was like capric acid in constitution but was optically active, and the mixed melting point of its amide with that of capric

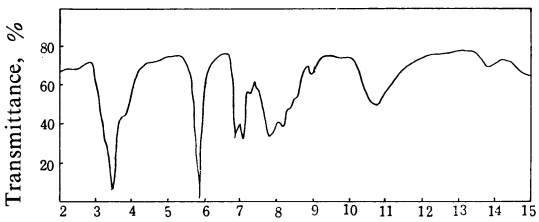


Fig. 3. Infrared absorption spectrum of $C_{10}H_{20}O_2$ from C_{13}-monounsaturated fatty acid.

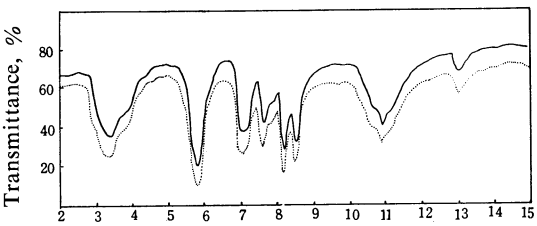


Fig. 4. Infrared absorption spectrum of malonic acid.
—— Malonic acid from C_{13} monounsaturated fatty acid
..... Authentic sample

*1 This constitutes Part XXXII of a series entitled "Studies on Antibiotics" by S. Tatsuoka.

*2 Present address: Osaka Factory, Takeda Chemical Industries, Ltd., Juso, Higashiyodogawa-ku, Osaka.

1) M. Inoue, This Bulletin, 35, 1249 (1962).

2) H. Ogawa, *J. Agr. Chem. Soc. Japan* (*Nippon Nogei-Kagaku Kaishi*), 26, 432 (1952).

acid showed a clear depression; hence, it was assumed to be isocapric acid.

From the above results, the fatty acid ($C_{13}H_{24}O_2$) contained in glumamycin seems to have a double bond at position 3 and side chains at the $C_9H_{19}CH=$ part, and it may be represented by a partial constitution (C_9H_{19}·CH=CHCH$_2$COOH) of 3-isotridecenoic acid.

There has been found no report on the fatty acid parts of amphomycin[3,4] and zaomycin[5] which resemble glumamycin. Crystallomycin[6] contains a straight chain fatty acid with 17 carbon atoms, and aspartocin is also different from glumamycin at the fatty acid portion, according to a private letter from Dr. N. Bohonos of Lederle Laboratory.

Experimental

***S*-Benzylthiuronium Salt of 3-Isotridecenoic Acid.**—A mixture of 10 g. of pure glumamycin and 200 ml. of 6 N hydrochloric acid was heated at 110°C for 24 hr., and the reaction mixture, after being diluted with 200 ml. of water, was extracted with two 100 ml. portions of ether. The ether solution was washed with water, dried and evaporated to give 1.4 g. of a light brown oil. The oil was suspended in 100 ml. of water, and sodium hydrogen carbonate was added portionwise until the pH of the mixture became 7.5, when the oil dissolved completely. A solution of 1.5 g. of *S*-benzylthiuronium chloride in 100 ml. of ethanol was added to the solution, and the resulting *S*-benzylthiuronium salt was recrystallized from 50% ethanol to give 1.4 g. of colorless plates, m. p. 141°C.

Found: C, 66.57; H, 9.11; N, 7.01; S, 8.40. Calcd. for $C_{21}H_{34}N_2SO_2$: C, 66.63; H, 9.05; N, 7.40; S, 8.46%.

3-Isotridecenoic Acid.—A solution of 1.1 g. of the *S*-benzylthiuronium salt in 150 ml. of 50% ethanol was passed through a column of ion exchange resin Amberlite IR-120 (H-form) previously treated with the same solvent, the column was washed well with 50% ethanol, and the combined washings were evaporated, giving a colorless oil. The oil was taken in ether, and the ether solution was dried over anhydrous sodium sulfate and evaporated to afford 400 mg. of a colorless oil, b.p. 139°C/1 mmHg, $[\alpha]_D^{22}$ +4.0° (*c* 1, in ethanol), $[\alpha]_D^{22}$ +4.2° (*c* 10, ethanol).

Found: C, 73.40; H, 11.33. Calcd. for $C_{13}H_{24}O_2$: C, 73.53; H, 11.39%. Mol. wt., Found: 225±25 (Barger's method), 210 (titration method), Calcd: 212.

The brown oil obtained by the hydrolysis of glumamycin was purified directly by distillation in vacuo to give a colorless oil, b. p. 139°C/1 mmHg.

Found: C, 73.45; H, 11.55. Calcd. for $C_{13}H_{24}O_2$: C, 73.53; H, 11.39%. The *S*-benzylthiuronium salt of the oil, m. p. 131°C.

Found: C, 66.53; H, 9.30; N, 7.42%. Calcd. for $C_{21}H_{34}N_2O_2S$: C, 66.63; H, 9.05; N, 7.40%.

Isotridecanoic Acid.—A portion of 50 mg. of 3-isotridecenoic acid was subjected to catalytic reduction on palladium carbon as usual, and the product was distilled in vacuo, giving a colorless oil, b. p. 150°C/2 mmHg.

Found: C, 72.74: H, 12.19. Calcd. for $C_{13}H_{26}O_2$: C, 72.84; H, 12.23%. The *S*-benzylthiuronium salt, m. p. 149°C.

Found: C, 66.36; H, 9.65; N, 7.05. Calcd. for $C_{21}H_{36}O_2N_2S$: C, 66.28; H, 9.54; N, 7.36%.

Ozone Oxidation of 3-Isotridecenoic Acid.—A solution of 10 g. of the unsaturated fatty acid ($C_{13}H_{24}O_2$) in 100 ml. of pure chloroform was oxidized with ozone for one hour's cooling with ice (flux: 1 l./min., voltage: 8000 V., content of O_3: 6%), and the reaction mixture was evaporated under reduced pressure, leaving a colorless syrup. The ozonide thus obtained was decomposed by heating with 100 ml. of water for 30 min. on the waterbath, and the resulting hot solution was stirred, drop by drop, into a suspension of 30 g. of silver oxide in 100 ml. of a 2% sodium hydroxide solution at 60°C.

After about one hour, when a test for aldehyde became negative, the silver oxide was filtered and washed well with water. The combined filtrate and washing were acidified with hydrochloric acid and extracted two times with 100 ml. of ether, and the extract was washed with water.

Isocapric Acid.—The above ether solution was evaporated and the residue was distilled under reduced pressure, giving a colorless oil, b. p. 145°C/2 mmHg.

Found: C, 70.03; H, 11.62. Calcd. for $C_{10}H_{20}O_2$: C, 69.72; H, 11.70%. $[\alpha]_D^{21}$ +3° (*c* 1, in ethanol).

Isocapric Acid Amide.—A mixture of 200 mg. of the above oil and 1 g. of thionylchloride was heated on the water-bath for one hour, the excess thionylchloride was distilled off, and 20 ml. of cool concentrated aqueous ammonia was added to the residue to separate a white precipitate, which was purified by recrystallization from 50% ethanol, m. p. 93°C.

Found: C, 69.81; H, 12.37; N, 8.25; Calcd. for $C_{10}H_{21}ON$: C, 70.12; H, 12.34; N, 8.13%. $[\alpha]_D^{21}$ +8° (*c* 1, in ethanol). Mixed melting point determination of the product with capric acid amide prepared in the same manner from capric acid showed a depression.

Malonic Acid.—The filtrate from the silver oxide was combined with the washing of the above ether extract and concentrated to 100 ml. The concentrate was extracted with ether, the extract was evaporated and the residue was recrystallized from a mixture of ether and petroleum ether to give colorless prisms, m. p. 134°C (decomp.). Mixed melting point with authentic malonic acid showed no depression.

Summary

Investigation was made of the ether soluble part of glumamycin hydrolysate. After this oily substance was purified by distillation, the distillate corresponded to unsaturated fatty

3) B. Heineman, M. A. Kaplan et al., *Antibiotics & Chemotherapy*, 3, 1239 (1953).
4) G. Giolitii, G. Corti et al., *Giorn., Microbiol.*, 3, 70 (1957).
5) Y. Hinuma, *J. Antibiotics*, A7, 134 (1954).
6) N. N. Lomakina and M. G. Branzhikova, *Biokhimya*, 24, 425 (1959).

acid, having an epimerical formula $C_{13}H_{24}O_2$.

This unsaturated fatty acid was optically active and by oxidation with ozone gave an optically active saturated fatty acid $C_{10}H_{20}O_2$ and malonic acid $C_3H_4O_4$. Therefore, the fatty acid constituted glumamycin corresponding to 3-isotridecenoic acid.

The author wishes to express his sincere thanks to Dr. Satoru Kuwada, the Director of the Takeda Research Laboratories, Dr. Sueo Tatsuoka, Vice Director of the Research Laboratories, and Dr. Kuniyoshi Tanaka, the Head of the 2nd Division of the Research Laboratories, for their guidance and encouragement, and to Drs. Kôichi Nakazawa, Akira Miyake, and Jisaburo Ueyanagi and Mr. Masahiko Fujino for their kind advice. The author is also indebted to Messrs. Masami Kan and Hironobu Kashiwagi and to Miss Fusa Suzuki and Mrs. Yoshiko Tsukamoto for performing microanalysis, and to Messrs. Hideo Kamio and Hideo Nakamachi for the determination of spectra.

Research Laboratories
Takeda Chemical Industries, Ltd.
Higashiyodogawa-ku, Osaka

The Secondary-emission Electron Multiplier Tube Used on a Mass Spectrometer and its Amplification of Ion Currents

By Toshio SUGIURA

(Received June 13, 1961)

The requirement for a detector both reliable and very sensitive for the measurement of ion beam currents in mass spectrometry has greatly increased in the past few years. This requirement can be attributed largely to the following:

1. Studies of the measurement of ionization potentials, especially by means of the ionization produced by vacuum-ultraviolet light.
2. The measurement of very small amounts of inert gases occluded in minerals or meteorites in order to determine their age.
3. The mass spectrometric measurement of ions produced by the alpha-ray in the study of ion-molecular reactions.

Various types of electrometers and electrometer tube amplifiers have been used to measure the ion currents collected by the Faraday cage of the mass spectrometer. By such means, ion currents as low as 10^{-14} amp. have been detected. Probably the best commercially available device for the reliable measurement of very small ion currents is the vibrating-reed electrometer, but this instrument has two important limitations which cause trouble at low input currents. First, the time constant of the input reed circuit increases to about 1 sec. when a 10^{11} ohms resistor is used, and, second, the alpha particle activity of about 1 alpha particle per 2 min., which results from the radioactive elements present in the vibrating-reed head in trace amounts, gives rise to bursts of charge. It is generally accepted that the measurement of very small ion currents of less than 10^{-16} amp. are extremely difficult to measure by ordinary methods.

In order to carry out this type of measurement, the secondary-electron emission multiplier is useful. Several types of electron multipliers have been used in mass spectrometry, namely, the electro-static focused multiplier[1-3], the magnetic focused multiplier[4,5], and the scintillator type multiplier[6,7]. The construction of the electrode system in the magnetic-focused electron multiplier is simple, but the preparation of the emitter of the secondary electrons is difficult. On the scintillator type multiplier, a scintillator fit to use in high vacuum conditions is difficult to obain. The electro-static focused type electron multiplier is considered to be the most convenient for use as an amplifier of very small amounts of ions in mass spectrometric studies. The author has already investigated the characteristics of the secondary electron emission by positive ions from the surface of copper-beryllium for the purpose of making use of the dynode

1) R. E. Halsted and A. O. Nier, *Rev, Sci. Instr.*, **21**, 1019 (1950); M. J. Higatsberger, H. L. Demorest and A. O. Nier, *J. Appl. Phys.*, **25**, 883 (1954).
2) J. S. Allen, *Phys. Rev.*, **55**, 966 (1939); *Rev. Sci. Instr.*, **18**, 739 (1947).
3) F. A. White and T. L. Collins, *Appl. Spectroscopy*, **8**, 17, 169 (1954).
4) L. G. Smith, *Rev. Sci. Instr.*, **22**, 3, 166 (1951).
5) L. Heroux and H. E. Hintereger, ibid., **31**, 280 (1960).
6) P. I. Richards and E. E. Hays, ibid., **21**, 99 (1950).
7) N. R. Day, ibid., **31**, 264 (1960).

material for the electro-static focused type secondary electron multiplier[8-10].

There are, in the literature, a large number of papers reporting investigations of the characteristics of the electron multiplier, but many of these papers are contradictory because of the large number of variables involved in this phenomenon[11]. Thus, with respect to the reported results concerning the mass dependency of the amplification factor of the electron multiplier for various ions, Nier et al.[1] have reported that its multiplicity for inert gas ions is inversely proportional to the square root of the ion mass, while, on the other hand, White and Collins[3] have reported that the multiplicity of the electron multiplier is independent of ion mass, and Barnett et al.[12] have produced evidence which purports to show that the mass dependency of the multiplicity of the electron multiplier depends on the conditions for treating the dynodes.

In this study, the author has designed and constructed a 12-stage secondary electron multiplier tube using copper-beryllium dynodes treated with electro-polish and with activation by oxidation, and the electron multiplier so constructed has been installed to with the mass spectrometer. The amplification factor of the secondary electron multiplier for inert gas ions has been measured as a function of the supplied voltage to the conversion dynode of the electron multiplier, and the results have been compared with those obtained with the multiplier using electro-polished and activated dynodes. The best amplification was obtained 2×10^5 by the electron multiplier constructed with activated dynodes for helium ions.

Experimental

The Mass Spectrometer its Reconstruction.—In this study, the instrument used was a modified Hitachi RMC-1 type mass spectrometer, which is of the 90° sector type, its radius of the curvature of the ion path and its maximum resolution in mass units being 135 mm. and 150 respectively.

In order to install the secondary electron multiplier and to determine the amplification factor of the ion current by the secondary electron multiplier, the collector block of the mass spectrometer was reconstructed of stainless steel, as is shown in Fig. 1. As may be seen in Fig. 1, the 96 mm. square collector block was welded to the analyzer tube in order to have the center of the collector block deviate by 10 mm. from the center of the analyzer tube. In Fig. 1, S_E and S_S are the earth slit and the suppresser plate for the Faraday cage F respectively. The width of the earth slit is variable over a range from 0 to 5 mm. by means of the driving screw, shown as D.S. in the diagram. The Faraday cage, F, may be moved a distance of 30 mm. without breaking the vacuum condition, for the purpose of measuring the amplification factor of the electron multiplier in the same ion path. After removing the Faraday cage, the electron multiplier tube can approach the earth slit, S_E, shown in Fig. 1. The maximum range of displacement of the electron multiplier tube is 30 mm. The electron multiplier was assembled on the E. M. flange by the method described below.

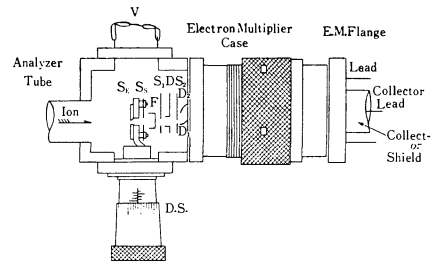


Fig. 1. Schematic diagrams of the collector block of the mass spectrometer and the electron multiplier. D.S. is the driving screw for variation of the width of the earth slit S_E, V is the pumping line, S_S is suppressor plates for secondary electrons from Faraday cage F, S_1, D, S_2, D_1 and D_2 are entrance slit of the ion beam, ion deflecting plate, second entrance slit, conversion dynode and second dynode of the electron multiplier, respectively.

Electron Multiplier Tube Design.—The electron multiplier tube was designed by reference to the electron multiplier used by Nier et al.[1] * The assembly and the details of the actual electrode system of the electron multiplier are shown in Fig. 2. In Fig. 2, B, S_E, S_S and F are the baffle slit, the earth slit, the suppressor plate for secondary electrons from the Faraday cage and the Faraday cage respectively. To the right of S_1 in Fig. 2, the assembly of the electrodes of the electron multiplier is shown. In Fig. 2, S_1 and S_2 are disks, 40 mm. in diameter and 1 mm. in thickness, made from stainless steel; each disk has an entrance slit of 10×3 mm^2 for the ions; D indicates the ion deflector plates, that were constructed from two plates, 4×10 mm^2 in area, installed parallel to each other at a distance of 7 mm. D_1 is the conversion dynode which gives off secondary electrons which are accelerated and focused onto a second dynode, D_2. The electrodes from D_2 to D_{12} are a succession of dynodes which give off multiplied secondary electrons which are accelerated and focused onto the following dynode. These dynodes are pressed from a copper-beryllium plate, 0.2 mm. in thickness,

8) T. Sugiura and T. Hayakawa, This Bulletin, **34**, 58 (1961).
9) T. Sugiura, ibid., **34**, 1475 (1961).
10) T. Sugiura, ibid., **35**, 218 (1962).
11) M. G. Inghram, "A Handbook on Mass Spectroscopy", National Academy of Sciences (1954), p. 41.
12) C. F. Barnett, G. C. Evods and P. M. Stier, *Rev. Sci. Instr.*, **25**, 1112 (1954).

* The details of the specifications of the multiplier tube are from a private communication from Professor A. O. Nier to Professor K. Ogata of Osaka University.

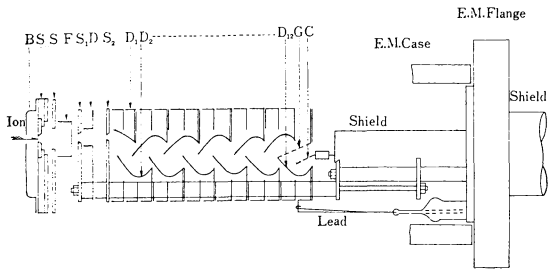


Fig. 2. Schematic diagram of the secondary-emission electron multiplier tube. B, S_E, S_S and F are the buffle slit, earth slit, suppressor slit and movable Faraday cage, respectively. S_1, D, S_2 are the entrance slit for the ion beam, ion deflecting plates, and second entrance slit of the electron multiplier tube, respectively. D_1 is the conversion dynode, the electrodes indicated from D_2 to D_{12} are succeeding dynodes, C and G are the electron collector and its shielding grid.

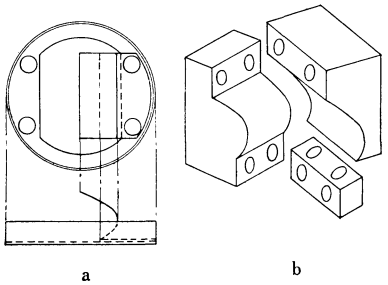


Fig. 3. Schematic diagram of a dynode of the electron multiplier and its shielding plate (a), and schematic view of the mold for shaping the dynodes of the electron multiplier (b).

in the mold shown in Fig. 3b. C and G in Fig. 2 are the electron collector and the shielding grid of the electron collector respectively. Both C and G are in the form of a grid made from tungsten wire 0.07 mm. in diameter, and the rim is made from stainless steel 0.1 mm. in thickness. The electron collector, C, is supported by a molybdenum rod fixed in the center of the E. M. flange by means of a glass-kovar seal. Each dynode was treated after shaping by the method described below, after which each dynode was put into the shielding plate, with a shielding rim 5 mm. in height and 0.3 mm. in thickness, as is shown in Fig. 3a; the shielding plates and the dynodes successively installed pass through four supporting rods, one on top of another, electrically insulated from each other by the quartz spacers. The supporting rods were made from stainless steel 3 mm. in diameter and covered by slender quartz tubes 4.8 mm. in outer diameter and 3.2 mm. in inner diameter. The quartz spacers, 6 mm. in length, were carved from a quartz tube 8 mm. in outer diameter and 5 mm. in inner diameter, and these quartz spacers were burnished up 1/100 mm. precision in length. The electrical connection for each dynode and electrode was provided from the fifteen lead connections

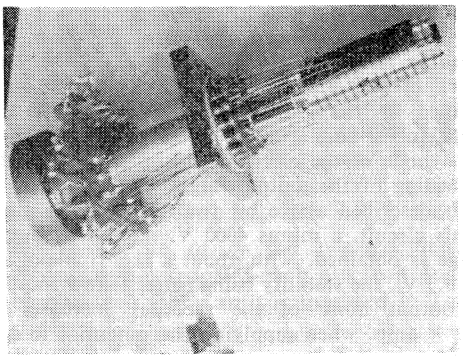


Fig. 4. The electrode structure of a electron multiplier tube used on a mass spectrometer, and the quartz insulators and dynode (lower part of the figure).

sealed by the glass-kovar seal surrounding the collector lead on the E.M. flange. In Fig. 4, a picture of the electron multiplier tube is shown, together with the quartz insulators and the dynodes.

Electronic Circuit for Supplying the High Voltage.—The electronic circuit for supplying a high voltage to each dynode of the secondary electron multiplier, as shown in Fig. 5, was constructed by the author himself. To obtain a high voltage, a commercially offered flyback-transformer was employed, as were a 6CM5 tube as a high frequency input supply for the flyback-transformer, and a 12AU7 tube as a symmetrical multi-vibrator for the rectangular input of the 6CM5 oscillator. The high voltage obtained by the flyback-transformer was rectified by a 1B3-GT tube and a simple RC filter. The oscillator, flyback-transformer, rectifier and RC filter were constructed

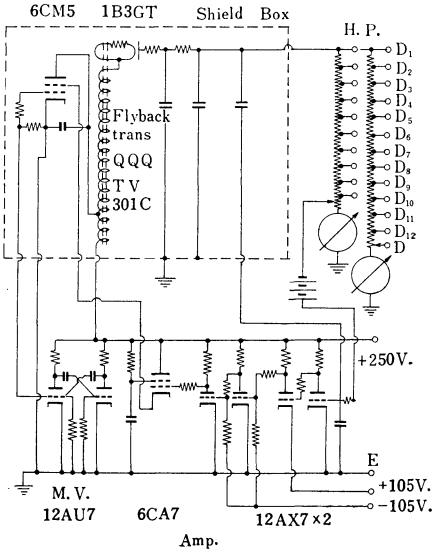


Fig. 5. Electrical circuit of the high potential supply for the electron multiplier tube. H.P. is the output of the high potential, M. V. is the symmetrical multivibrator using 12AU7 tube, Amp. is the d. c. amplifier.

in the shieled box, which was made from copper net. The output voltage was stabilized by means of feeding back to the screen grid of the oscillator a part of the output current after it had been amplified by the amplifier, which employed two 12AX7 tubes and a 6CA7 tube. The voltage to each dynode of the electron multiplier was supplied by dividing of the output high voltage from the circuit described above by twelve 3 MΩ resistors. By this circuit, a minus 4000 V. maximum output voltage is obtained, with about a 8kc. ripple of less than 0.1 V., the stability being better than 2.5×10^{-5}. The output noise of the recorder increases by 2×10^{-14} amp. when supplying the potential to each dynode.

Activation of Dynodes.—The apparatus for the activation of the dynodes of the electron multiplier has been described in previous papers[8,9]. The dynodes of the electron multiplier were activated in the following manner: The shaped and electro-polished dynodes were placed in a quartz tube and evacuated to higher than 5×10^{-6} mmHg at about 800°C for about three hours. Then the temperature of the quartz tube was lowered to 420°C, and oxygen was introduced at an initial pressure of 1 mmHg. After 20 min. the oxygen was pumped out, and the temperature was lowered to room temperature.

Experimental Procedure.—For the measurement of the ion and the amplified electron currents, a conventional type D.C. amplifier was used; this amplifier employed a HT-1005 tube, a modified 6C6 tube as a priamplifier tube, and a 6SN7 tube as a second-stage differential amplifier. For the recorder a four-element oscillo-galvanometer was used. In order to determine the total gain of the secondary electron multiplier, high resistances of 1×10^{10} ohms for direct measurement of the ion current and 1×10^{8} ohms for measurement of the electron current amplified by the electron multiplier were used in the circuit of the D.C. amplifier.

Results

The amplification factors of the 12-stage secondary electron multipliers, which are constructed from electro-polished copper-beryllium dynodes and from activated copper-beryllium dynodes, were obtained for inert gas ions, using different voltage supplies to the conversion dynodes. In Figs. 6 and 7, the amplification factors for the electron multiplier using inert gas ions are plotted as functions of the supplied voltage to the conversion dynode in the range from −1800 to −3000 V. In these

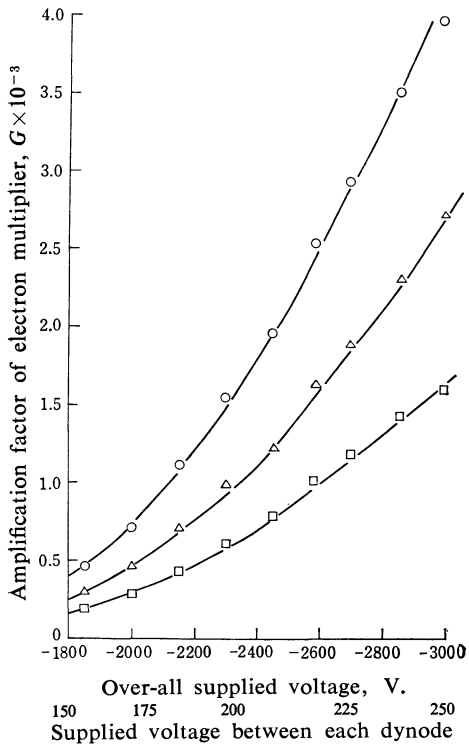


Fig. 6. Amplification factor of the electron multiplier tube using the electro-polished dynodes, as functions of supplied voltage to conversion dynode for inert gas ions. Circular, triangular and square points indicate results for $^{4}He^{+}$, $^{20}Ne^{+}$ and $^{40}A^{+}$ ions, respectively.

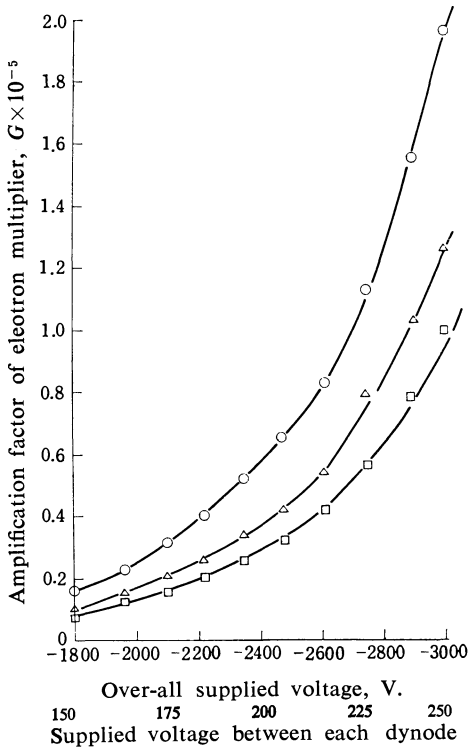


Fig. 7. Amplification factor of the electron multiplier tube constructed by the activated dynodes, as functions of supplied voltage to conversion dynode for inert gas ions. Circular, triangular and square points indicate the results for $^{4}He^{+}$, $^{20}Ne^{+}$ and $^{40}A^{+}$ ions, respectively.

figures, circles, triangles and squares indicate the results for helium 4, neon 20 and argon 40 ions respectively. The ions were accelerated by 1200 V. to earth potential during these measurements.

Discussion

The Influence of Ion Species on the Amplification Factor of the Secondary Electron Multiplier.—As may be seen from Figs. 6 and 7, the amplification factors of the electron multiplier are different for different ion species under the same conditions. In these results, the amplification factors of the ion currents were in the sequence, helium, neon and argon ions. In the results from the electro-polished dynodes, the ratios of the amplification factors are $He^+ : Ne^+ : A^+ = 2.45 : 1.79 : 1.00$ with each voltage. These ratios indicate that the amplification factors are roughly inversely proportional to the square root of the ion mass. This correlation obtained from the electro-polished dynodes agrees with the results obtained by Nier et al.[1] On the other hand, the ratios of the amplification factors obtained from the electron multiplier constructed with the activated dynodes are approximately $He^+ : Ne^+ : A^+ = 2.00 : 1.28 : 1.00$ for each voltage. These ratios indicate that the amplification factors have not the same correlation as the results from the electro-polished dynodes. These results indicate that the amplification factors vary according to the conditions of the treatment of the dynodes, a finding which is in agreement with the results obtained by Barnett et al.[12]

Average Yield of Secondary Electrons by Electron Bombardment. — The amplification factor of the electron multiplier, G, is given by the following relation:

$$G=\gamma_i\times\bar{\delta}^{n-1}$$

when γ_i is the ratio of the number of secondary electrons to positive ions at the conversion dynode, $\bar{\delta}$ is the average ratio of primary to secondary electrons on the succeeding dynodes, and n is the number of stages of the secondary-electron multiplier. γ_i is governed by the following factors: the chemical and physical natures of the dynode, the incident angle of the ions, the kinetic and potential energies of ions and ionic charge, etc., $\bar{\delta}$ is governed by the chemical and physical natures of the dynode, and the kinetic energy of the incident electrons. With regard to the results of this study, the kinetic energy of the ions bombarding the conversion dynode is the difference between the ion acceleration potential and the supplied voltage to the conversion dynode. Assuming that the ion energy dependency of the value γ_i is not varied in the ion energy above 1200 V. the value of γ_i can be obtained by the extrapolation of the data measured in a previous study[8]. The values of γ_i for ion energy obtained in the manner described above are shown in Tables I and II for the electro-polished and activated copper-beryllium dynodes. By using these γ_i values, the value of $\bar{\delta}$, the average yield of the secondary electrons at each electron energy, can be obtained; they are summarized in Tables I and II.

Influence of the Activation of Dynodes on the Amplification Factor of the Secondary Electron Multiplier.—For comparison of the electro-polished dynodes with the activated dynodes, the logarithms of the amplification factors are plotted as functions of the supplied voltage to the conversion dynode; they are shown in Fig. 8. In Fig. 8, the upper three curves are the results obtained from activated dynodes, while the lower three curves are the results obtained from electro-polished dynodes; the circles, triangles and squares indicate the helium, neon and argon ions respectively. As

Table I. Variation of $\bar{\delta}$ with electron energy and γ_i ($^{40}A^+$) with ion energy from electro-polished Cu-Be

Ion energy V.	γ_i Electrons / Ion	Electron energy V.	$\bar{\delta}$ Electrons / Electron
3050	2.65	154	1.47
3200	2.80	167	1.54
3350	2.95	179	1.58
3500	3.13	192	1.59
3650	3.28	204	1.65
3780	3.38	215	1.68
3910	3.53	226	1.69
4060	3.68	238	1.72
4200	3.80	250	1.74

Table II. Variation of $\bar{\delta}$ with electron energy and γ_i ($^{40}A^+$) with ion energy from activated Cu-Be

Ion energy V.	γ_i Electrons / Ion	Electron energy V.	$\bar{\delta}$ Electrons / Electron
3000	8.30	150	1.87
3160	8.75	163	1.92
3300	9.15	175	1.95
3440	9.50	186	1.99
3550	9.80	196	2.04
3680	10.1	207	2.07
3820	10.5	218	2.12
3940	10.8	228	2.18
4000	11.2	240	2.24
4200	11.5	250	2.29

is seen in Fig. 8, the amplification factors of the electron multiplier were radically increased by the activation of the dynodes, and the results show that the amplification factor increased almost exponentialy with the increasingly supplied voltage for all ions, while this was not so in the case of the electro-polished dynodes. When Tables I and II are compared, the values of γ_i and $\bar{\delta}$ show an increase as a result of the dynode activation. The voltage dependency of the amplification factor is mainly governed by the value of $\bar{\delta}$. From the value of $\bar{\delta}$ shown in Tables I and II, the difference in the energy dependency of the value $\bar{\delta}$ due to dynode activation is not clear, but from a comparison of the results in Fig. 8, the energy dependency of $\bar{\delta}$ is considered to be larger for the activated dynodes than for the electro-polished dynodes. In the previons studies[8-10], the increase in the secondary electron yield by activation of the copper-beryllium was explained by the contribution of the beryllium oxide formed near the surface, while for the ions having an energy higher than 1200 V. it was explained by the fact that the stopping power of the beryllium oxide is larger than that of the copper oxide. The increased values of $\bar{\delta}$ by dynode activation for electrons having an energy between 150 and 250 V. can be understood in the same way.

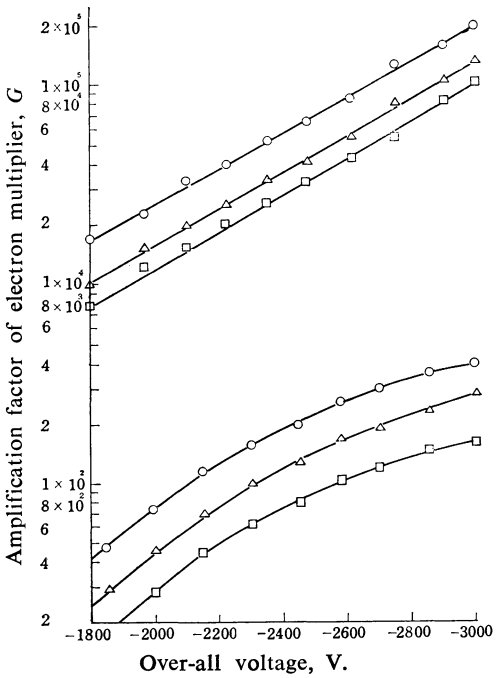


Fig. 8 Semilog plots of the amplification factor of the electron multiplier tube as a function of supplied voltage to conversion dynode for inert gas ions. Upper three curves are the results for activated dynodes, and lower three curves are the results for electro-polished dynodes, the signs of the curves are same as Figs. 6 and 7.

Summary

For the purpose of measuring very small ion currents by the mass spectrometer, a secondary electron multiplier, using the dynodes of copper-beryllium, has been constructed and installed. The amplification by the electron multiplier of various supplied voltages to the conversion dynode was measured for inert gas ions, and the amplification factor and its variation with the supplied voltage to the conversion dynode was compared with both the activated and the electro-polished dynode. For the electron multiplier using the electro-polished dynodes, the amplification was roughly inversely proportional to the square root of the ion mass, while for the activated dynode this was not the case. The average yield of the secondary electrons impacted by electrons on the copper-beryllium dynodes was determined, using the values of γ_i which had been estimated by extrapolation of the data obtained in a previous study. The increase of the amplification factors of the electron multiplier due to the dynode activation was explained on the basis of an increase in γ_i and $\bar{\delta}$ due to dynode activation, an increase to be attributed to the formation of beryllium oxide layers. In this study, an amplification factor of a 10^5 order for inert gas ions has been obtained with the electron multiplier constructed with dynodes made from activated copper-beryllium. By using this electron multiplier, ion currents of 10^{-19} amperes are easily detectable with a mass spectrometer using a conventional D. C. amplifier.

The author wishes to acknowledge his indebtedness to Professor Shyoji Shida of the Tokyo Institute of Technology, Professor Teruo Hayakawa and Professor Osamu Toyama of the University of Osaka Prefecture, and to Professor Koreichi Ogata of Osaka University, under whose direction and guidance this work was carried out.

The expense has been defrayed in part by a grant given by the Ministry of Education, to which the author's thanks are due.

Departmet of Applied Chemistry
College of Engineering
University of Osaka Prefecture
Sakai, Osaka

The Behavior of Fission Products Captured in Graphite Powder by Nuclear Recoil. V. Effect of Fission Fragment Damage on the Diffusion of the Fission Product Xenon

By Seishi YAJIMA, Sumio ICHIBA, Kazumi IWAMOTO and Koreyuki SHIBA

(Received November 18, 1961)

The radiation damage to graphite caused by neutron irradiation is of great importance in reactor technology, and many studies have been made in this field[1-4]. However, in the case of the dispersed type of fuel, when the fissionable material is dispersed throughout a matrix of graphite powder, the damage from fission fragments is more severe than the neutron damage[5-8].

The present authors have been studying[9-12] the behavior of fission products captured in several kinds of graphite powder by fission recoil.

For the present work, diffusion experiments on Xe-133 and Xe-135 captured in graphite powder were carried out over an extensive range of fission product concentrations. It has become clear through this work that with natural graphite the diffusion behavior of xenon in graphite is far more strongly affected by fission fragment damage than by neutron damage to the graphite crystal, and that the behavior changed markedly with an increase in the fission product concentration. However, in the case of artificial graphite, the effects of both fission fragment damage and neutron damage were insignificant over the range of fission product concentrations covered in this experiment.

Experimental

Preparation and Irradiation of Samples.—The graphite samples examined in this experiment were of two kinds, natural graphite (NG-1) and artificial graphite (AG), as described in our previous report[12]. Mixed with this graphite was natural uranium in the form of dioxide powder with a particle size of less than 1 μ, which ensured that most of the fission products would recoil out of the uranium dioxide particles into the surrounding graphite. The relation of the fission product capturing factor of the graphite to the uranium dioxide ratio of the mixture were discussed in detail in a previous report[5].

The mixing ratios adopted for the samples in the present experiments were 33 : 1 and 1 : 1 by weight, at which ratios the capturing factors were 0.95 and 0.70 respectively.

The prepared mixtures were sealed in quartz ampules in a vacuum and were irradiated in the JRR-1*1, the JRR-2*2 and the research reactor of the Brookhaven National Laboratory. Data concerning the preparation and irradiation of the samples are given in Table I. In this table the fission product concentration was calculated according to the equation given in the footnote below*3.

Since the radioactivity of samples numbered 13, 14, 15 and 16 was too strong for them to be handled immediately upon initial irradiation, these samples were cooled for four months. After this time, they were reirradiated with thermal neutrons to a ϕt ratio of 8 to produce the fission-recoiled Xe-133 in the samples.

Samples No. 17 and No. 18, after four months' cooling, were treated with nitric acid*4 to remove the uranium dioxide; then the remaining graphite powder was washed with water and acetone, and dried. The powder was then heated for 2 hr. in an argon flow at 1000 and 1440°C respectively. After the heat treatment, the graphite powder was again mixed with uranium dioxide powder to a

1) W. K. Woods, L. P. Bupp and J. F. Flecher, Proceedings of the First International Conferences on Peaceful Uses of Atomic Energy, Geneva (United Nations, New York, 1956), Vol. 7, p. 455.
2) G. H. Kinchin, ibid., Vol. 7, p. 472.
3) G. R. Henning and J. E. Hove, ibid., Vol. 7, p. 666.
4) W. Bollman, *J. Appl. Phys.*, 32, 869 (1961).
5) E. Nishibori, R. Ueda, S. Yajima, S. Ichiba, Y. Kamemoto and K. Shiba, *Plansee Berichite*, to be published.
6) L. D. Loch and J. A. Slyh, CF-53-3-276(Del.), Radiation damage Conference, Part I, p. 93, Dec. 20, 1954.
7) R. H. Kernoban, ibid., p. 98.
8) R. J. Harrison, ibid., p. 113.
9) T. Nakai, S. Yajima, K. Shiba, J. Osugi and D. Shinoda, This Bulletin, 33, 494 (1960).
10) T. Nakai, S. Yajima, K. Shiba, J. Osugi and D. Shinoda, ibid., 33, 497 (1960).
11) S. Yajima, S. Ichiba, Y. Kamemoto and K. Shiba, ibid., 34, 493 (1961).
12) S. Yajima, S. Ichiba, Y. Kamemoto and K. Shiba, ibid., 34, 697 (1961).

*1 Japan Research Reactor-1, water boiler type, operated at 50 kW thermal out-put.
*2 Japan Research Reactor-2, CP-5 type, operated at 1000 kW thermal out-put.
*3 The number of fission product atoms captured in a unit volume of graphite was calculated according to the following equation:

$$\text{Number of f. p. atoms/cm}^3 \text{ of graphite} = 2 \cdot {}^{235}\mathrm{U} \cdot \sigma \cdot \phi \cdot t \cdot \alpha \cdot d$$

where,
^{235}U : Number of U-235 atoms
σ : Fission cross-section of U-235
ϕ : Neutron flux
t : Irradiation time
α : Capturing factor of fission products in graphite
d : Density of graphite

*4 The fission products captured in graphite did not leach out of the graphite to any significant extent by this nitric acid treatment[9].

weight ratio of 33 : 1 and reirradiated with thermal neutrons to a ϕt ratio of 8, to produce the fission-recoiled Xe-133 in the samples.

Samples No. 19 and No. 20 were irradiated at 500°C and, after four months' cooling, were reirradiated with thermal neutrons to a ϕt ratio of 2, to produce the fission-recoiled Xe-133 in the samples.

The difference between the effects on the diffusion of xenon in the graphite of neutron damage and of fission fragment damage was examined with sample No. 21. In this sample natural graphite powder alone was first irradiated with neutron to a ϕt ratio of 58 in JRR-2; then, after this irradiation, the powder was mixed with uranium dioxide powder to a weight ratio 33 : 1, and reirradiated with neutrons to a ϕt ratio of 1 to produce the fission-recoiled Xe-133 in the sample.

Obtaining the Heating Curve.—To obtain the heating curves, Xe-133 was used as the tracer for most experiments, but in some cases of low fission product concentration, Xe-135 was used as the tracer. The optimum cooling times for the experiments, after irradiation or reirradiation, were 1 day for Xe-135 and 7 days for Xe-133. After cooling, the samples were dissolved in nitric acid to remove the uranium dioxide, and the remaining graphite powder was washed with water and acetone and then dried.

The apparatus used for the diffusion experiment was the same as that described in a previous report. A prepared graphite sample was placed in an alundum boat and inserted into an alundum tube, forming the core of an electric furnace with a platinum heater. The temperature was raised at the rate of 5°C/min. The radioactive xenon released from the graphite crystal was carried off with purified argon*5 and trapped in an activated charcoal trap cooled with dry ice. To remove the undesirable radioactive iodine released from the graphite with the radioactive xenon, a trap of glass wool with a silver nitrate deposit was inserted in front of the charcoal trap. The charcoal trap was changed every five minutes until the temperature reached 1500°C. Then the graphite sample was fired with oxygen mixed with argon (volume ratio 1 : 1) at 1200°C, and the residual xenon which had not diffused out of the graphite during heating was caught in the charcoal trap. The excess oxygen and carbon dioxide were removed with a mixture of pyrogallol and potassium hydroxide solutions, and then the water vapor was trapped with a phosphorus pentoxide drying tube.

The Xe-133 and Xe-135 collected in the charcoal traps were placed in a sodium iodide well (2 inches in diameter by 1.75 inches high) attached to a Baird Atomic γ-ray spectrometer to obtain their spectra.

When Xe-133 was used as the tracer, the spectra obtained were radioactively pure, but with Xe-135, traces of the Xe-133 spectrum were discernible along with the Xe-135 spectrum. The portion of

*5 The argon used was 99.99% pure and was further passed through a copper gauze bed heated to 400°C, a phosphorus pentoxide trap, and a sponge titanium bed heated to 800°C to remove the small amounts of oxygen, water vapor and other impurities.

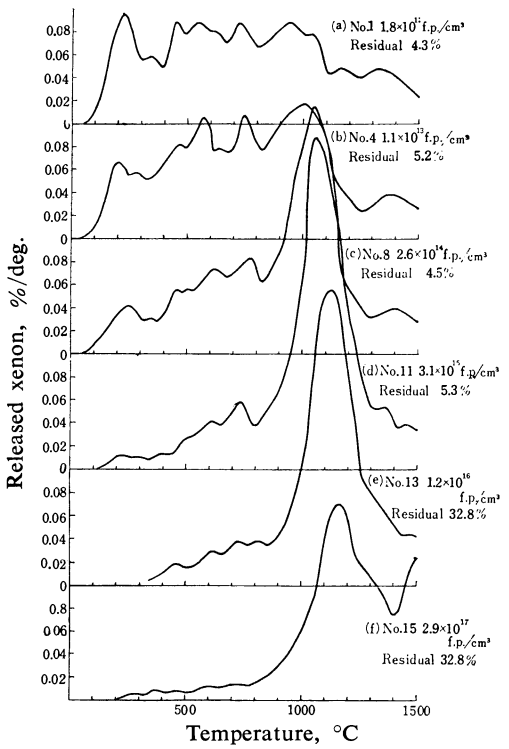


Fig. 1. Heating curves (5°C/min.) of natural graphite (NG-1).

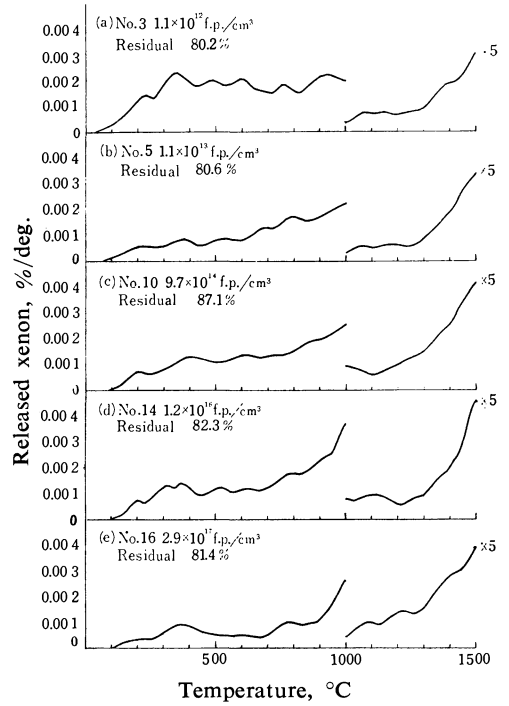


Fig. 2. Heating curves (5°C/min.) of artificial graphite (AG).

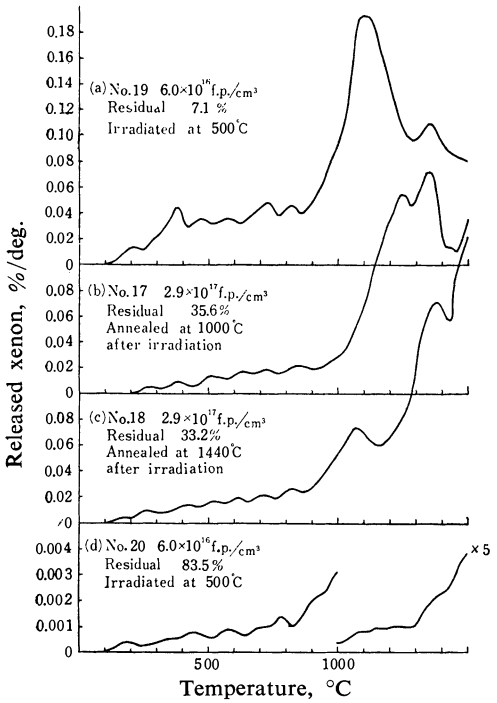


Fig. 3. Heating curves (5°C/min.) of heat-treated graphite sample.

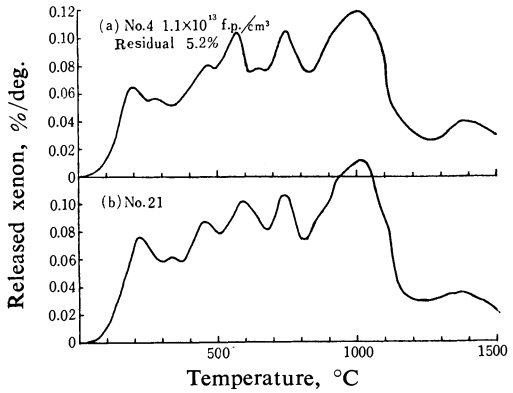


Fig. 4. Heating curve (5°C/min.) of preliminarily neutron-irradiated graphite sample.

Xe-133 was, therefore, subtracted from the obtained total spectrum area. The portion of Xe-135 was, furthermore, calibrated by means of its decay curve, because the Xe-135 nuclide is short-lived.

The fraction of the total activity formed by the activity of each charcoal trap was divided by the temperature rise in the 5 min. interval during which the trap was in use. The plots of this value against the temperature (heating curve) are shown in Figs. 1, 2, 3 and 4.

Determination of Activation Energy.—As is shown in Fig. 1, the heating curves of natural graphite change markedly with the fission product concentration. The activation energy for the

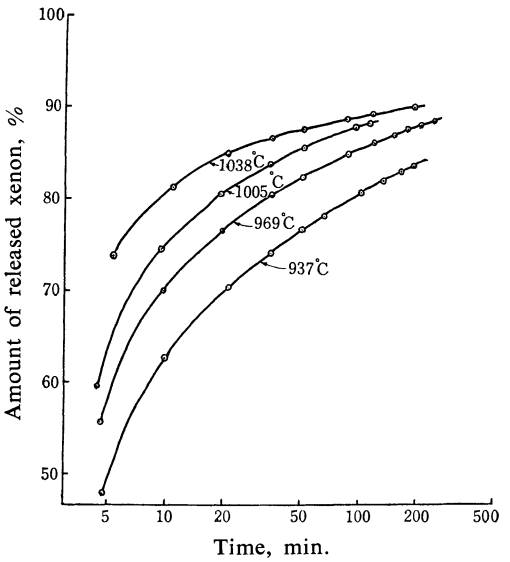


Fig. 5. Isothermal curves in the range 937~1038°C.

diffusion of xenon in natural graphite at a temperature corresponding to the peak seen in Fig. 1 (about 1000°C) was measured by Dienes' method[13]. The furnace was maintained at a fixed temperature, and the graphite sample inserted into the heating tube as rapidly as possible. The released xenon was trapped in a charcoal trap, which was replaced by a new one at the optimum time interval of about 3 hr. The radioactivity of the charcoal traps was plotted against the time (isothermal curve) (Fig. 5). The samples were prepared by the same irradiation treatment as No. 4 in Table I. These samples were preheated to 700°C for 30 min. to eliminate the spectra from xenon released in the range below 700°C and thereby to bring out the isothermal curves of diffusion at about 1000°C. Thus, the ordinate in Fig. 5 does not represent the fraction of released xenon referred to the total activity but the fraction referred to the residual after the preheat treatment. The isothermal curves were obtained for 937, 969, 1005 and 1038°C respectively. The relation between the annealing time (plotted logarithmically) and the temperature (reciprocal of the absolute temperature) is given in Fig. 6. The activation energy can be obtained from the slopes of the $1/T$ plot according to the following equation, derived by Dienes et al.:

$$t \times e^{-E/RT} = C$$

where,

t = diffusion time required to obtain a certain diffusion fraction of the isothermal curve
E = activation energy, cal./mol.
R = gas const., 1.978 cal./deg.
T = temperature, °K
C = constant

13) G. J. Dienes and W. E. Parkins, "An Improved Method for Determining Activation Energies of Relaxation Processes", NAA-SR-60.

TABLE I. DESCRIPTION OF SAMPLES

Sample No.	Kind of*1 graphite	UO_2 mixed with 1 g. graphite mg.	Thermal neutron*2 dose, n/cm²	ϕt ratio*3 Initial irrad.	ϕt ratio*3 Reirrad.	Irrad. temp., °C	Fission product concn.
1	NG-1	30	1.5×10^{14}	1/60		40	1.8×10^{11}
2	NG-1	30	9.0×10^{14}	1/10		40	1.1×10^{12}
3	AG	30	9.0×10^{14}	1/10		40	1.1×10^{12}
4	NG-1	30	9.0×10^{15}	1		40	1.4×10^{13}
5	AG	30	9.0×10^{15}	1		40	1.4×10^{13}
6	NG-1	30	5.4×10^{16}	6		125	6.4×10^{13}
7	AG	30	5.4×10^{16}	6		125	6.4×10^{13}
8	NG-1	30	2.2×10^{17}	24		125	2.6×10^{14}
9	NG-1	30	8.2×10^{17}	91		125	9.7×10^{14}
10	AG	30	8.2×10^{17}	91		125	9.7×10^{14}
11	NG-1	30	2.6×10^{18}	288		125	3.1×10^{15}
12	AG	30	2.6×10^{18}	288		125	3.1×10^{15}
13	NG-1	30	9.9×10^{18}	1092	8	125	1.2×10^{16}
14	AG	30	9.9×10^{18}	1092	8	125	1.2×10^{16}
15	NG-1	1000	9.9×10^{18}	1092	8	125	2.9×10^{17}
16	AG	1000	9.9×10^{18}	1092	8	125	2.9×10^{17}
17	NG-1	1000	9.9×10^{18}	1092	8	125	2.9×10^{17}
18	NG-1	1000	9.9×10^{18}	1092	8	125	2.9×10^{17}
19	NG-1	1000	2.4×10^{18}	482	4	500	6.0×10^{16}
20	AG	1000	2.4×10^{18}	482	4	500	6.0×10^{16}
21	NG-1	30	5.0×10^{17}	58	1	40	1.1×10^{13}

*1 NG-1 and AG respectively represent natural and artificial graphite powders of certain specifications.

*2 In every case the doses of fast neutrons were 1/10 of those of thermal neutrons. The thermal neutron dose was measured with cobalt monitoring wire and fast neutron dose with nickel monitoring wire.

*3 The flux time was compared with that of sample No. 4, taken as standard.

4 The Xe nuclide used as a tracer on diffusion experiment was Xe-135 for samples of Nos. 1—3 and Xe-133 for samples of Nos. 4—21, respectively.

5 The samples of Nos. 1—4 were irradiated in JRR-1, the samples of Nos. 5—20 were irradiated in Graphite Research Reactor of the Brookhaven National Laboratory and the sample of No. 21 was irradiated in JRR-2.

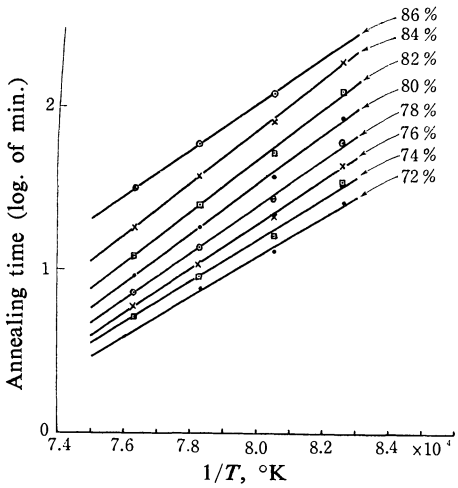


Fig. 6. Annealing time versus $1/T$ in the range 937~1038°C.

The activation energies thus obtained are shown in Table II.

TABLE II. ACTIVATION ENERGIES IN THE RANGE 937~1038°C

Fraction	Slope $\times10^3$ deg.	Activation energy kcal./mol.
0.72	1.24	56.6
0.74	1.26	57.8
0.76	1.40	63.9
0.78	1.43	65.3
0.80	1.53	70.1
0.82	1.59	72.7
0.84	1.60	73.2
0.86	1.40	64.7
	Mean value	65.5

Results

The heating curves of natural graphite sample (Nos. 1, 4, 8, 11, 13 and 15) are shown in Fig. 1, and those of artificial graphite samples (Nos. 3, 5, 10, 14 and 16), in Fig. 2. The curves of natural and artificial graphite samples irradiated under heat (Nos. 17 and 18) and

natural and artificial graphite samples annealed after irradiation (Nos. 19 and 20) are shown in Fig. 3. Figure 4 represents the neutron-irradiated natural graphite sample (No. 21).

The following remarks may be made on the basis of the above figures.

1) Sample No. 15 was irradiated with the same doses as No. 13, but the fission product concentration of No. 15 was 24 times larger than that of No. 13, and their heating curves (e) and (f) in Fig. 1 were found to differ considerably from each other.

The graphite portion of sample No. 21 was preliminarily irradiated with a dosage 58 times larger than that of No. 4, but the fission product concentrations in both samples stayed almost identical in shape (Fig. 4). From this, it can be said that the effect of neutron irradiation on the heating curve spectra is very much smaller than the irradiation of fission fragments, at least in the range of the dosage in question.

2) The heating curves of natural graphite represent a continuous spectrum, possessing several peaks.

3) The positions of these peaks do not change appreciably with the fission product concentration.

4) To determine the influence of the fission products concentration on the temperatures at which radiation damage is mainly brought about, three temperature ranges, A (0～850°C), B (850～1350°C) and C (above 1350°C), were arbitrarily established. The fraction of the total xenon released in each temperature range was plotted against the fission product concentration (Fig. 7). In this figure, the fraction. of xenon released in range A is seen to begin

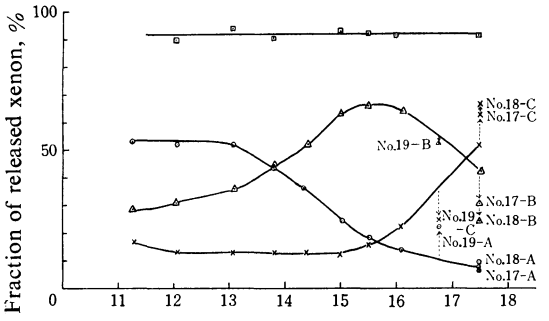


Fig. 7. Change of xenon fraction released from three temperature ranges A, B and C with fission product concentration in unit volume of graphite.

⊙ Natural graphite, range A (0～850°C)
△ Natural graphite, range B (850～1350°C)
× Natural graphite, range C (>1350°C)
⊡ Artificial graphite, range C (>1350°C)

decreasing at about 10^{13} f. p./cm³ graphite, but the fraction of range B goes on increasing with the fission product concentration to reach its maximum at about 10^{15}～10^{16} f. p./cm³ graphite. The fraction of C stays unchanged up to 10^{15} f. p./cm³ graphite; from there on, it increases rapidly. This would appear to indicate that with the increasing fission product concentration, the imperfections of graphite crystal corresponding to range A are taken over by imperfections corresponding to range B and, further, to range C.

5) Returning to Fig. 1, the position of the peak near 1000°C (in range B) shifts toward higher temperatures with the increase in fission product concentration; that is, the position of the peak is 1010°C in curve (b) and shifts with the increasing fission product concentration to reach 1170°C in curve (f). This temperature shift might be explained as a lag of the release rate of xenon against the rising temperature, taking account of the fact that the chance of xenon being captured before diffusing out of the graphite increases with the number of imperfections, which influences the position of the peak, which in turn would depend on the fission product concentration. Another explanation is that the trapping power of the imperfections corresponding to this peak increases gradually with the fission product concentration; that is, the depth of imperfection becomes deeper with the increasing fission product concentration. This temperature shift is not observed in other peaks found in the lower temperature range.

6) As in the case of natural graphite, the heating curves of artificial graphite (Fig. 2) were translated into a curve relating the portion of the released xenon to the fission product concentration (uppermost curve in Fig. 7). This curve represents the fraction of xenon released in range C and indicates that the fraction of C retains a constant value of over 90% and is thus predominant over those of both A and B, which are so small as to be within the range of experimental error. In conclusion, it is obvious that, in the range of fission product concentration examined in this experiment, xenon trapped in natural graphite can more easily diffuse out than that trapped in artificial graphite.

7) The curves of heat-treated samples, Nos. 17, 18 and 19 (Fig. 3), were also analyzed; they are plotted in Fig. 7. It is seen that the fraction of xenon release in temperature range C is greater for samples 17 and 18 than that of the corresponding non-treated sample, No. 15. From this it may be said that heat treatment at 1000 or 1440°C after irradiation will heal radiation damage corresponding to ranges

A and B, but not to that of range C. It may also be seen that the fission fragment damage due to reirradiation is very small compared with the residual from range C caused by initial irradiation.

In the same figure, the plot for sample No. 19 lies above the curve for non heat-treated samples in the case of the fraction for range A. This means that heat treatment of the sample at 500°C during irradiation will impede damage in range C. It may be concluded that heat treatment after irradiation is not effective in removing damage corresponding to higher temperatures, but, on the other hand, that heat treatment during irradiation will considerably reduce this damage. This phenomenon is in accord with the release curve of stored energy in artificial graphite irradiated with fast neutrons of the order of 10^{20} nvt. (see remark 8 below). The heating curve of sample No. 20 in Fig. 3 does not differ from that of the samples unheated during irradiation in Fig. 2.

8) The release of stored energy in artificial graphite irradiated with fast neutrons of the order of 10^{20} nvt. has already been extensively studied[1,4]. The release curve of stored energy (an example was given in Fig. 8) has peaks at points apparently in good correspondence with the xenon release curve of natural graphite. This correspondence might be explained by considering that they both represent the progress of annealing or recovery from strain caused in the graphite crystal by neutrons or by fission fragments, manifesting itself on the one hand in a release of stored energy and, on the other hand, in a release of xenon from the crystal. It should be noted that, while the stored energy release curve represents by the temperature scale, the absolute quantity as well as the depth of damage, the xenon heating curve represents only the depth of damage by the same scale.

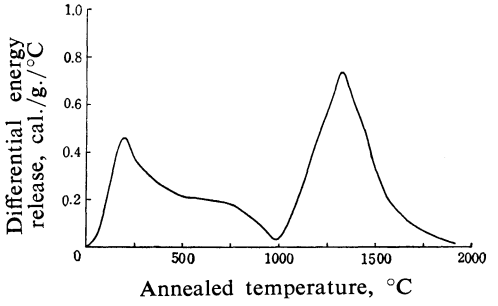


Fig. 8. Differential stored energy release (after Woods et al.[1]).

Xenon atoms trapped in imperfections of graphite crystal are released from the imperfections by heating at a given temperature, when some of them will diffuse out from the graphite particles*6 and others will be trapped again in other imperfections of a higher trapping power. The probability of either happening will be determined by the chemical and physical state of the diffusing atom, the depth of the trapping power of the imperfection, and the number of imperfections per unit volume.

The release curve of stored energy in artificial graphite irradiated with neutrons indicates that the imperfections corresponding to temperature range C are insignificantly few in number (Fig. 8), but the heating curves of artificial graphite (Fig. 2) indicate the fraction of the range C to far surpass those of ranges A and B. This brings out the significance of the studies that should be undertaken on the capturing process of xenon in artificial graphite.

9) The activation energy of xenon diffusion in natural graphite at the peak of about 1000°C in the heating curves is 65.5 kcal./mol. According to Suzuki's study[15], the imperfections existing in ranges A and B may be presumed to be interstitial cluster and mono-vacancy respectively.

The diffusion experiments of highly irradiated samples (Nos. 6—20) were carried out at the Brookhaven National Laboratory. S. Yajima and K. Iwamoto, those of the present authors who went to the Laboratory to undertake the experiment, are particularly indebted to Dr. F. T. Miles, Dr. D. H. Gurinsky Dr. E. Fujita and Mr. H. Munkelwitz for invaluable help and suggestions during their work at Brookhaven.

Japan Atomic Energy Research Institute
Tokai, Ibaraki-ken

*6 Suzuki et al.[14] reported that the xenon atoms which exist between the layers of graphite crystal diffuse very easily and that the calculated activation energy of this diffusion is about 0.03 eV.

14) T. Iwata, E. Fujita and H. Suzuki, *J. Phys. Soc. Japan*, **16**, 197 (1961).
15) H. Suzuki, private communication.

Molecular Rotations of Glucides in Relation to their Structures. VIII[1]. *On the Product of the ζ-Coefficients of the Hydroxyl and the Methyl Groups*

By Shukichi YAMANA

(Received December 12, 1961)

Recently, the author introduced an adjustable parameter, the ζ-coefficient, in order to make up Kirkwood's polarizability theory of optical rotatory power; he named this manner of the calculation of optical rotation the "PM-method"[2]. By using the PM-method, it is possible to explain logically the relation between the $[M]_D^{20}$(W) of some optically active substances (i.e. glucocides, polyhydroxycyclohexanes[4] and menthol-like substances[5]) and their molecular structure. Moreover, the product of the ζ-coefficient of the hydroxyl group and that of the methyl group, $\zeta_{OH}\zeta_{CH_3}$, was calculated as about $1.6\{3/((n^2+2)\}$ in molecules which have a cyclohexane-ring (i.e. (−)-trans-2-methylcyclohexanol and menthol-like substances[5]). Nevertheless, in the case of carbohydrates which have an aldopyranose-ring in their molecules, the value of $\zeta_{OH}\zeta_{CH_3}$ had been calculated as either $0.3096\{3/((n^2+2)\}$[6] (when using the $[M]_D^{20}$(W) of β-L-arabinose written in Bates' book[8]) or $0.6671\{3/(n^2+2)\}$[9] (when using the $[M]_D^{20}$(W) of β-L-arabinose observed by Hudson[10]), which values are fairly different from that in the case of molecules which have a cyclohexane-ring, as has been mentioned above. For these reasons, the recalculation of the value of $\zeta_{OH}\zeta_{CH_3}$ in carbohydrates (methyl pentose) becomes necessary.

New Treatment Applied

Into the "Method Proposed" of the previous paper[7], the following two alterations were introduced:

(i) Molecular Model. — In the previous paper[7], the molecular model which had been determined by McDonald and Beevers[11] from the results of the X-ray analysis of crystalline α-D-glucose (hexose) was used. Strictly speaking, however, the shape of its aldopyranose-ring is not perfectly the same as that in methyl pentose. Therefore, as with the molecular model in this article, the one proposed by Geachin and Beevers[12] in the case of crystalline α-rhamnose monohydrate is used. However, this change in the molecular model will not cause much difference[13].

(ii) The $[M]_D^{20}$(W) of α-D-Isorhamnose. — In this series of studies, the data for $[M]_D^{20}$(W) which are listed in Bates' book[8] have been used preferentially. However, after its publication (1942), new data on the $[M]_D^{20}$(W) of carbohydrates have been reported year after year, and those new data should be taken into account. Particularly, in 1951 Hudson reported 163.7 as the $[M]_D^{20}$(W) of α-D-isorhamnose[15], a value which is far different from that listed in Bates' book, 120.3. Therefore, it should be discussed here which of these two values should be chosen. Generally, the $[M]_D^{20}$(W) of an aldopyranose changes widely as time elapses (this phenomenon is called "mutarotation"), and the determination of the initial $[M]_D^{20}$(W) at the time of resolution is difficult. However, the $[M]_D^{20}$(W) of its methyl glycoside is almost constant and can be easily observed. Therefore, it is desirable that an experimental datum of the $[M]_D^{20}$(W) of an aldopyranose should be examined by using the $[M]_D^{20}$(W) of its methyl glycoside.

On the other hand, concerning $[M]_D^{20}$(W)-Diff<methyl glycoside−cor. al. pyranose[16]>[17], Hudson's empirical rule is well known. This

1) Part VII: S. Yamana, This Bulletin, **32**, 597 (1959).
2) Footnote* 17 in Ref. 3.
3) S. Yamana, This Bulletin, **31**, 558 (1958).
4) S. Yamana, ibid., **33**, 1741 (1960); **34**, 1212 (1961).
5) S. Yamana, ibid., **34**, 1414 (1961).
6) Eq. 4 in Ref. 7.
7) S. Yamana, This Bulletin, **31**, 564 (1958).
8) F. J. Bates et al., "Polarimetry, Saccharimetry and the Sugars", United States Government Printing Office, Washington (1942).
9) Eq. 4, in footnote* 17 of Ref. 7.
10) E. Montgomery and C. S. Hudson, *J. Am. Chem. Soc.*, **56**, 2074 (1934).
11) T. R. R. McDonald and C. A. Beevers, *Acta Cryst.*, **5**, 654 (1952).
12) H. Mc. D. McGeachin and C. A. Beevers, *Acta Cryst.*, **10**, 227 (1957).
13) Cf. footnote* in Ref. 14.
14) S. Yamana, This Bulletin, **30**, 203 (1957).
15) E. Zissis, N. K. Richtmyer and C. S. Hudson, *J. Am. Chem. Soc.*, **73**, 4714 (1951).
16) "cor." and "al." mean "corresponding" and "aldo-" respectively.
17) In order to represent the difference between A and B simply, the abbreviated symbol, Diff <A−B>, will be used hereafter. For example, $[M]_D^{20}$(W)-Diff<methyl α-D-isorhamnoside−α-D-isorhamnose> means the difference in $[M]_D^{20}$(W) between methyl α-D-isorhamnoside and α-D-isorhamnose, and so on.

TABLE I. $[M]_D^{20}$(W)-DIFF.<METHYL GLYCOSIDE −COR. AL. PYRANOSE[16]>[17]

Name	$[M]_D^{20}$(W) of methyl glycoside	$[M]_D^{20}$(W) of cor. al. pyranose	$[M]_D^{20}$(W)-Diff.
β-L-Arabinose	403.0[8]	303.3[10]	99.7
α-L-Arabinose	28.4[8]	133.6[10]	−105.2
α-D-Xylose	252.6[8]	140.5[8]	112.1
α-D-Fucose	351.2[21]	251.0[8]	100.2
β-D-Fucose	−25.3[21]		
α-D-Isorhamnose	272.1[22]	163.7[15]	108.4
β-D-Isorhamnose	−97.3[22]		
α-D-Rhamnose	111.4[8]	15.7[8]	95.7
β-D-Rhamnose	−170.0[8]	−63.0[8]	−107.0
α-D-Galactose	380.5[8]	271.5[8]	109.0
β-D-Galactose	0.0[8]	95.1[8]	−95.1
α-D-Glucose	308.6[8]	202.1[8]	106.5
β-D-Glucose	−66.4[8]	33.7[8]	−100.1
α-D-Mannose	153.8[8]	52.8[8]	101.0
β-D-Mannose	−135.5[8]	−30.6[8]	−104.9
		Mean of the absolute value	103.5

rule says that the absolute value of this $[M]_D^{20}$(W)-Diff. is not far from 100[18-20].

By using this rule, the approximate value of the $[M]_D^{20}$(W) of α-D-isorhamnose can be obtained by the following equation:

$$272.1^{23,18)} - 100 = 172.1$$

Accordingly, Hudson's datum of the $[M]_D^{20}$(W) of α-D-isorhamnose, 163.7, seems to be more reliable than that in Bates' book, 120.3.

Data Used

Therefore, Table I of the previous paper[7] is rewritten as Table II of this article.

The optical data of the unit groups used in the previous paper[7] are adopted again without any correction[24]. An optical center of the unit group is located at the center of the mass of the bond with which it is combined.

Re-calculation

$\zeta_{OH}\zeta_{CH_3}$.—By using Table II in this article, Eqs. 1, 2 and 3 of the previous paper[7] can be

TABLE II

Name	Unit groups	$[M]_D^{20}$(W)	Lit.
α-D-Xylose	[$(OH)^{1\alpha}$, $(OH)^{2\alpha}$, $(OH)^{3\beta}$, $(OH)^{4\alpha}$, Ring]	140.5°	8)
β-L-Arabinose	[$(OH)^{1\alpha}$, $(OH)^{2\alpha}$, $(OH)^{3\beta}$, $(OH)^{4\beta}$, Ring]	303.3°	10)
α-D-Isorhamnose	[$(OH)^{1\alpha}$, $(OH)^{2\alpha}$, $(OH)^{3\beta}$, $(OH)^{4\alpha}$, $(CH_3)^{5\beta}$, Ring]	163.7°	15)
β-D-Isorhamnose	[$(OH)^{1\beta}$, $(OH)^{2\alpha}$, $(OH)^{3\beta}$, $(OH)^{4\alpha}$, $(CH_3)^{5\beta}$, Ring]		
α-D-Fucose	[$(OH)^{1\alpha}$, $(OH)^{2\alpha}$, $(OH)^{3\beta}$, $(OH)^{4\beta}$, $(CH_3)^{5\beta}$, Ring]	251.0°	8)

TABLE III. $[\mu]_{D\,calcd}^{20}\{3/(n^2+2)\}$, CAUSED BY THE DYNAMICAL COUPLING EFFECT BETWEEN ANY TWO MEMBERS OF UNIT GROUPS (EXCEPT RING) IN MCGEACHIN AND BEEVERS' MOLECULAR MODEL

	$(CH_3)^{5\beta}$	4β	4α	3β	3α	2β	2α
1α	−5.57 (−4.32)	0.05 (0.15)	0.02 (0.01)	2.54 (2.20)	−1.93 (−1.83)	1.51 (0.76)	12.17 (6.64)
1β	1.26 (0.65)	−0.26 (−0.18)	0.02 (0.01)	−0.82 (−0.44)	−1.47 (−1.33)	12.60 (7.00)	−12.22 (−6.42)
2α	−0.61 (−0.31)	1.96 (1.65)	−0.15 (−0.08)	11.05 (6.28)	−11.12 (−6.28)		
2β	1.28 (0.82)	−0.66 (−0.64)	−1.80 (−1.53)	−11.28 (−6.37)	0.31 (0.17)		
3α	3.62 (3.00)	0.17 (0.08)	12.46 (6.93)				
3β	0.25 (0.12)	11.52 (6.18)	−12.01 (−6.52)				
4α	24.52 (12.37)						
4β	−24.38 (−12.50)						

Note: The values, calculated by supposing that the optical center of (OH) group is located at its O atom, and that of $(CH_3)^{5\beta}$ group is at its C atom, are given in parentheses.

18) Cf. Table I.
19) C. S. Hudson, *J. Am. Chem. Soc.*, **47**, 268 (1925).
20) The author proposes to name this empirical rule "Hudson's methyl glycoside rule".
21) R. C. Hockett, F. P. Phelps and C. S. Hudson, *J. Am. Chem. Soc.*, **61**, 1658 (1939).
22) W. D. Maclay, R. M. Hann and C. S. Hudson, ibid., **61**, 1660 (1939).
23) This is the $[M]_D^{20}$(W) of methyl α-D-isorhamnoside.
24) The mean polarizability, α, of OH is 1.04×10^{-24} cc.; the α of CH_3 is 2.27×10^{-24} cc.; the anisotropy ratio, β, of OH is 0.35 and the β of CH_3 is 0.35. The refractive index, *n*, is 1.34.

rewritten as the following Eqs., 1', 2' and 3', respectively.

$$\text{Yo. Diff.}\langle\alpha\text{-D-isorhamnose}-\alpha\text{-D-fucose}\rangle^{17)} = 163.7-251.0^{25)} = -87.3 \equiv (F-E)$$
$$= \{(4\alpha)\,\text{Å}\,(1\alpha) + (4\alpha)\,\text{Å}\,(2\alpha) + (4\alpha)\,\text{Å}\,(3\beta) + (4\alpha)\,\text{Å}\,(\text{CH}_3)^{5\beta} + (4\alpha)\,\text{Å R}\} - \{(4\beta)\,\text{Å}\,(1\alpha) + (4\beta)\,\text{Å}\,(2\alpha) + (4\beta)\,\text{Å}\,(3\beta) + (4\beta)\,\text{Å}\,(\text{CH}_3)^{5\beta} + (4\beta)\,\text{Å R}\} \quad (1')$$

$$\text{Yo. Diff.}\langle\alpha\text{-D-xylose}-\beta\text{-L-arabinose}\rangle = 140.5-303.3^{25)} = -162.8 \equiv \{(4\alpha)-(4\beta)\}\,\text{Å}\{(1\alpha)+(2\alpha)+(3\beta)+\text{R}\} = \{(4\alpha)\,\text{Å}\,(1\alpha) + (4\alpha)\,\text{Å}\,(2\alpha) + (4\alpha)\,\text{Å}\,(3\beta) + (4\alpha)\,\text{Å R}\} - \{(4\beta)\,\text{Å}\,(1\alpha) + (4\beta)\,\text{Å}\,(2\alpha) + (4\beta)\,\text{Å}\,(3\beta) + (4\beta)\,\text{Å R}\} \quad (2')$$

$$\{(4\alpha)\times(\text{CH}_3)^{5\beta} - (4\beta)\times(\text{CH}_3)^{5\beta}\}\zeta_{\text{OH}}\zeta_{\text{CH}_3} \times\{(n^2+2)/3\} = 75.5 \quad (3')$$

On the other hand, all $[\mu]^{20}_{\text{D calcd}}\{3/(n^2+2)\}$, values caused by the dynamical coupling effect between any two members of the unit groups (except the ring) in the molecular model are calculated by using the theoretical formulae of Kirkwood and are shown in Table III.

It is apparent in Table III that $(4\alpha)\times(\text{CH}_3)^{5\beta}$ and $(4\beta)\times(\text{CH}_3)^{5\beta}$ are 24.52 and −24.38 respectively[26]. By using these values in Eq. 3',

$$\{24.52-(-24.38)\}\zeta_{\text{OH}}\zeta_{\text{CH}_3}\{(n^2+2)/3\} = 75.5$$

or
$$\zeta_{\text{OH}}\zeta_{\text{CH}_3} = 1.5440\{3/(n^2+2)\} \quad (4')$$

The value of $\zeta_{\text{OH}}\zeta_{\text{CH}_3}$ in Eq. 4' is nearly equal to $1.6\{3/(n^2+2)\}$ which was obtained as the values of $\zeta_{\text{OH}}\zeta_{\text{CH}_3}$ in the case of those substances which have a cyclohexane-ring.

$[M]^{20}_{\text{D}}$(W) of β-D-Isorhamnose.—In the footnote *29 of a previous paper[7], the author proposed an equation to presume an approximate value of the $[M]^{20}_{\text{D}}$(W) of β-D-isorhamnose, now unknown, without using any ζ-coefficient. That is the {$[M]^{20}_{\text{D}}$(W) of the An. Diff.[27] of D-mannose} minus the {$[M]^{20}_{\text{D}}$(W) of the An. Diff. of D-rhamnose}=the {$[M]^{20}_{\text{D}}$(W) of the An. Diff. of D-glucose} minus the {$[M]^{20}_{\text{D}}$(W) of the An. Diff. of D-isorhamnose} (*29)

On the other hand, some $[M]^{20}_{\text{D}}$(W) values had already been observed, as below[18]:

52.8 (α-D-mannose), −30.6 (β-D-mannose),
15.7 (α-D-rhamnose), −63.0 (β-D-rhamnose),
202.1 (α-D-glucose), 33.7 (β-D-glucose)
and 163.7 (α-D-isorhamnose).

Therefore, if the $[M]^{20}_{\text{D}}$(W) of β-D-isorhamnose is y,

$$\{52.8-(-30.6)\}-\{15.7-(-63.0)\} = \{202.1-33.7\}-\{163.7-y\}$$
$$\therefore\quad y = 0.0$$

As the $[M]^{20}_{\text{D}}$(W) of methyl β-D-isorhamnoside is −97.3[18], $[M]^{20}_{\text{D}}$(W)-Diff.⟨methyl β-D-isorhamnoside−β-D-isorhamnose⟩ = −97.3 −0.0 = −97.3.

As the absolute value of this $[M]^{20}_{\text{D}}$(W)-Diff. is about equal to 100, it can be said that the $[M]^{20}_{\text{D}}$(W) of β-D-isorhamnose, presumed above, 0.0, satisfies Hudson's methyl glycoside rule[20] and may be trusted.

Discussion

In the previous paper[7], the value of $\zeta_{\text{OH}}\zeta_{\text{CH}_3}$ then obtained was first applied in the calculation of the $[\mu]^{20}_{\text{D obs}}$ of the An. Diff.[27] of D-rhamnose, and the calculated $[\mu]^{20}_{\text{D obs}}$ coincided with its corresponding observed value, $[M]^{20}_{\text{D}}$(W). But in that paper, the $[M]^{20}_{\text{D}}$(W) of β-D-isorhamnose was calculated as −46.6[28]. In that case,

$$[M]^{20}_{\text{D}}\text{(W)-Diff.}\langle\text{methyl }\beta\text{-D-isorhamnoside}-\beta\text{-D-isorhamnose}\rangle = -97.3 - (-46.6) = -50.7$$

The absolute value of this $[M]^{20}_{\text{D}}$(W)-Diff., 50.7, deviates greatly from 100. (In other words, −46.6 of the $[M]^{20}_{\text{D}}$(W) of β-D-isorhamnose does not satisfy Hudson's methyl glycoside rule.) Therefore, −46.6 seems to be unreliable as a presumed value of the $[M]^{20}_{\text{D}}$(W) of β-D-isorhamnose. The principal reason for that mis-presumption in the previous paper[7] may be the inadequacy of using 120.3 as the $[M]^{20}_{\text{D}}$(W) of α-D-isorhamnose; accordingly, the value of $\zeta_{\text{OH}}\zeta_{\text{CH}_3}$ then obtained, 0.3096 $\{3/(n^2+2)\}$ (or $0.6671\{3/(n^2+2)\}$), may be untrustworthy. Concerning the accidental coincidence of $[\mu]^{20}_{\text{D obs}}$ with its corresponding $[M]^{20}_{\text{D}}$(W) for the case of the An. Diff. of D-rhamnose in the previous paper[7], further examination will be necessary in the future.

Summary

By using a new molecular model and the new datum concerning the $[M]^{20}_{\text{D}}$(W) of α-D-isorhamnose, the $\zeta_{\text{OH}}\zeta_{\text{CH}_3}$ in the case of methyl pentose and the $[M]^{20}_{\text{D}}$(W) of β-D-isorhamnose, now unknown, were re-calculated. The obtained value of $\zeta_{\text{OH}}\zeta_{\text{CH}_3}$ was nearly equal to that in the case of substances which have a

25) Cf. Table II.
26) Cf. footnote* 32 in Ref. 3.
27) This is the difference in optical rotation between the α and β D-aldoses (or the β and L-aldoses).
28) Without using $\zeta_{\text{OH}}\zeta_{\text{CH}_3}$, 'the $[M]^{20}_{\text{D}}$(W) of β-D-isorhamnose was calculated as −43.4 in footnote* 29 of Ref. 7.

cyclohexane-ring. The new value of the $[M]_D^{20}$(W) of β-D-isorhamnose satisfies Hudson's methyl glycoside rule.

Department of Chemistry
Kyoto Gakugei University
Fushimi-ku, Kyoto

Chlorination by Sulfuryl Chloride. II[1]. *Action of Sulfuryl Chloride on the Methylenedioxy-ring*

By Mannosuke ARAI

(Received December 25, 1961)

In the first part of this series[1], the author reported on the action of sulfuryl chloride on aromatic aldehyde (including anisaldehyde) in the presence of benzoyl peroxide. The reaction resulted in the formation of the corresponding acid chlorides by the attack of chlorine on aldehydic hydrogen. At the same time, the author noticed that the reaction with phenolic aldehyde usually leads to nuclear chlorination, the aldehydic hydrogen being intact. The investigation of this type of reaction has now been extended to an aromatic aldehyde, such as piperonal, with etheric linkage.

The reaction of sulfuryl chloride on piperonal has already been reported on in a patent[2]. On heating at 130°C, the reaction proceeded to give dichloropiperonal, which afforded protocatechualdehyde on being hydrolyzed. Later investigation by Weisse[3] indicated that no reaction took place by heating, but that, after the substance had been allowed to stand for two days at room temperature, only nuclear chlorination occurred, the methylenedioxy bridge being intact.

A survey has now also been made using methyl piperonylate and 1, 2-methylenedioxy-4-nitrobenzene in the presence of benzoyl peroxide in order to see which of the reactions, nuclear chlorination or cleavage of the ethereal ring, would occur preferentially.

Results and Discussion

To confirm Weisse's findings, piperonal and sulfuryl chloride were heated without a solvent. After hydrolysis with water, 6-chloropiperonal (89%) and protocatechualdehyde (8%) were obtained, showing that mainly nuclear chlorination had occurred. When carbon tetrachloride was used as a solvent, complete recovery of the starting material resulted.

Following the procedure of the previous paper[1], piperonal was heated in benzene with two moles of sulfuryl chloride in the presence of benzoyl peroxide. On treatment of the reaction products with aniline, protocatechuic anilide, not piperonyl anilide, was obtained. An attempt was made to isolate the chlorinated product by distillation under reduced pressure. However, polymerization occurred as a result of the heat, and the attempt failed to obtain any pure substance.

Moreover, piperonal was submitted to the reaction with one or two moles of sulfuryl chloride, followed by hydrolysis with water. The results, shown in Table I, indicate that protocatechualdehyde and protocatechuic acid are the reaction products and that no 6-chloropiperonal, a nuclear substitution product, is detectable. The quantitative formation of protocatechuic acid with two moles of sulfuryl chloride indicates that one mole of the reagent attacks the methylenedioxy bridge and the other the aldehyde group. It is also clear that the chlorination occurred first at the methylenedioxy bridge and then at the aldehyde group, since no piperonylic acid is formed in a benzene solution.

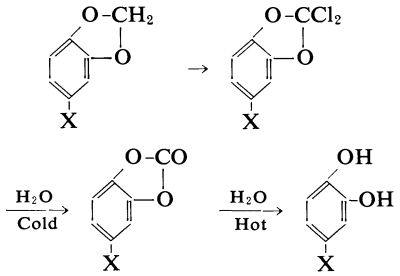
The chlorination of the methylenedioxy-ring and its cleavage has been studied. The dichloro-compound is considered to be produced by chlorination with phosphorous chloride[4,5], thionyl chloride[5], sulfur chloride[2,3,6] or gaseous chlorine[7], and its hydrolysis is assumed to proceed through the cyclic carbonate, as is shown in the following scheme:

1) M. Arai, *J. Chem. Soc. Japan, Pure Chem. Sec.* (*Nippon Kagaku Zasshi*), **81**, 1450 (1960).
2) German Pat. 165727 (1906).
3) K. Weisse, *Ber.*, **43**, 2605 (1910).
4) R. Fittig and I. Remsen, *Ann.*, **159**, 128 (1871); H. Pauly, *Ber.*, **40**, 3096 (1907); P. Hoering and F. Baum, ibid., **41**, 1914 (1908).
5) G. Barger, *J. Chem. Soc.*, **93**, 563 (1908).
6) H. Pauly, *Ber.*, **42**, 417 (1907).
7) L. Schmidt, *Chem. Zentr.*, **1914**, II, 1080; **1921**, II, 358.

TABLE I. CHLORINATION OF PIPERONAL BY SULFURYL CHLORIDE[a)]

Exp. No.	Reactants: Piperonal mol.	Reactants: SO_2Cl_2 mol.	Reactants: Solvent ml.	React. time. hr.	Products, %[b)]: Protocatechuic acid	Products, %[b)]: Protocatechualdehyde	Products, %[b)]: Piperonylic acid
1	0.01	0.01	C_6H_6, 15	6	30 (60)	36	
2	0.01	0.02	C_6H_6, 15	8	90	8 (4)	
3	0.01	0.01	CCl_4, 15	48	54 (108)	8	4
4	0.01	0.02	CCl_4, 15	48	98		

a) In the presence of benzoyl peroxide at 85°C.
b) Based upon the amount of piperonal used, and the numerical values in parentheses are based upon the amount of SO_2Cl_2.



As had been reported by the author[1)], chlorination by sulfuryl chloride is a radical chain reaction. Therefore, the intermediate is assumed to be a monochloro-compound. In Experiment 3), piperonylic acid was formed, and the yield of protocatechuic acid was greater than that expected from the amount of sulfuryl chloride. This result suggests a further radical reaction of piperonal and carbon tetrachloride during the reaction.

In order to confirm this cleavage reaction, methyl piperonylate was heated in benzene with sulfuryl chloride in the presence of benzoyl peroxide. After distillation of the solvent, the chlorinated product was hydrolyzed with water to give methyl protocatechuate quantitatively. The titration curve (Fig. 1)

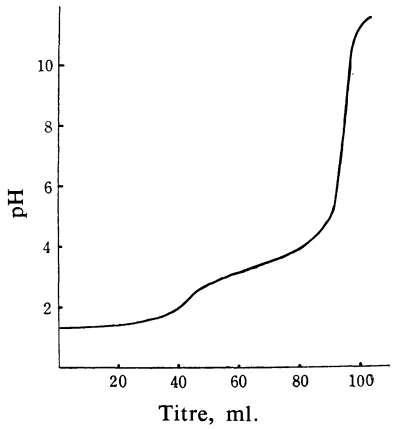
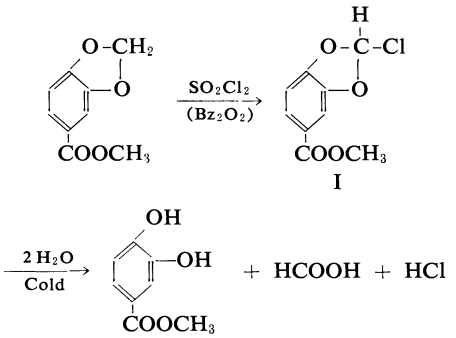


Fig. 1. Titration curve of the mother liquor for the hydrolysis of chlorinated products of methyl piperonylate by 0.1 N NaOH (f=0.985).

of the mother liquor for hydrolysis indicates that the liquor contains two kinds of acids, the one being stronger in acidity than the other. The latter was identified as formic acid by the formation of *p*-bromophenacyl ester (Kubota and Matsuura's method[8)]), and the former must be hydrochloric acid formed by the decomposition of the monochloro compound I. Consequently, the entire course of the reaction should be depicted as follows:



This reaction sequence was also supported by the quantitative isolation of viscous fuming oil, b.p. 101~101.5°C/0.15 mmHg, which yielded methyl protocatechuate on the addition of water, and an equivalent number of chloride ions (Mohr's method). The infrared absorption spectrum of the oil (Fig. 2) lacks the peaks to be expected at 2780, 925, 720 cm^{-1} judging from the methylenedioxy group in the starting substance, while it exhibits a newly developed broad peak at 705 cm^{-1} attributable to the C–Cl bond.

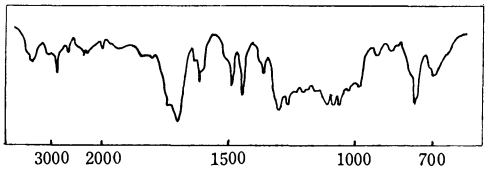


Fig. 2. Infrared absorption spectrum of chlorinated methyl piperonylate (I).

8) T. Kubota and T. Matsuura, *J. Chem. Soc. Japan, Pure Chem. Sec. (Nippon Kagaku Zassi)*, **72**, 482 (1951).

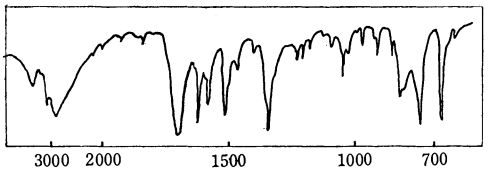
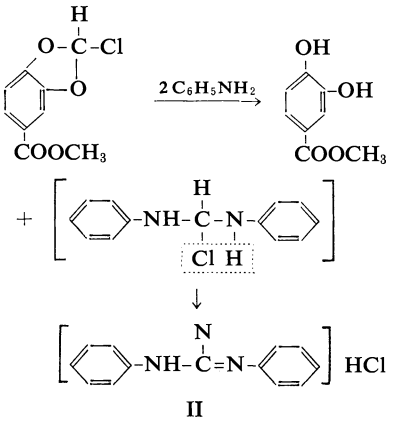


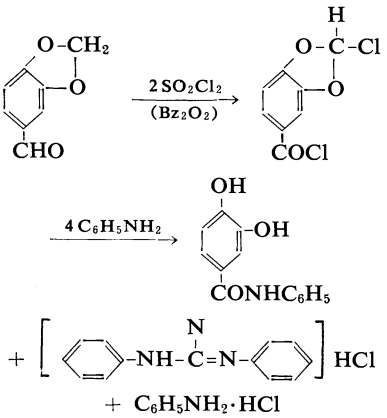
Fig. 3. Infrared absorption spectrum of *N*, *N'*-diphenylformamidine (II) hydrochloride.

Treatment of the oil with aniline gave a colorless featherly crystalline substance, $C_{13}H_{18}N_2Cl \cdot H_2O$, m. p. 253°C, besides methyl protocatechuate. The infrared absorption spectrum of this substance shows a strong absorption at 1700 cm^{-1} ($\nu_{C=N}$), suggesting the hydrochloride of compound II.



II

The free base II, m. p. 139°C, has an absorption maximum at 274 mμ. The value[9] for *N*, *N'*-diphenylformamidine supports the figure of II. The imide II was also obtained, together with protocatechuic anilide, by the reaction of two moles of sulfuryl chloride on piperonal, followed by treatment with aniline.

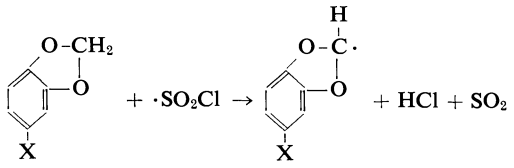


9) L. Claisen, *Ann.*, **287**, 366 (1895); Brit. Pat. 353138 (1930); French Pat. 717145 (1932); W. Bradley and I. Wright, *J. Chem. Soc.*, **1956**, 640; R. N. Roberts and R. H. De. Walfe, *J. Am. Chem. Soc.*, **76**, 2411 (1954).

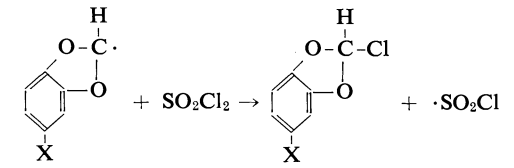
Further chlorination of the oil I was attempted under the same conditions, but the inertness of the tertiary hydrogen of I for chlorination by stlfuryl chloride was recognized upon obtaining *N*, *N'*-diphenylformamidine hydrochloride by treatment with aniline.

In another experiment, a similar chlorination of 4-nitromethylenedioxy-benzene was carried ont. The quantitative formation, 4-nitrocatechol, was recognized after treatment with water, though the reaction rate was rather small.

From the results mentioned above, the mechanism of this chlorination is shown to be as follows;



III



IV

The chlorosulfonyl radical (·SO_2Cl), formed by the reaction of sulfuryl chloride and benzoyl peroxide, attacks the methylenedioxy group and abstracts a hydrogen atom to produce the radical III, hydrogen chloride and sulfur dioxide. The radical III stabilizes by abstracting a chlorine atom from sulfuryl chloride to form the compound IV and the chlorosulfonyl radical, completing a radical chain. The preference for the chlorosulfonyl radical over the chlorine atom for the first step of the chain reaction is based on the fact that the dichloro-compound, which should have resulted from the reaction of the molecular chlorine[7], was not produced in this reaction. It is quite natural to assume that the chlorosulfonyl radical is not capable of attacking compound IV, but is capable of attacking only the methylenedioxy group of the starting substance in preference to decomposing to sulfur dioxide and a chlorine atom.

Experimental

Reaction of Piperonal and Sulfuryl Chloride.—1) In the Absence of Benzoyl Peroxide. — *a) Without a Solvent.*—A mixture of 1.50 g. of piperonal and 2.70 g. of sulfuryl chloride was heated under reflux in an oil bath at 105~110°C for 2 hr., with moisture excluded. After the mixture had been cooled, water (20 ml.) was added to the reaction mixture, which was then made alkaline and extracted with ether. The evaporation of ether gives 1.65 g.

of colorless needles, which were recrystallized from ethanol to 6-chloropiperonal, m. p. 115°C (Found: C, 52.39; H, 2.68%). An alkali-soluble part gives, by separation with toluene, 0.11 g. of plates which give a dark green coloration with ferric chloride. The 2,4-dinitrophenylhydrazone of this compound, m. p. 273°C, (Found: N, 17.54%), coincides with that of protocatechualdehyde.

b) *In Carbon Tetrachloride.*—The same reaction was carried out in carbon tetrachloride (10 ml.). After refluxing for 10 hr., the starting material was completely recovered and identified as 2, 4-dinitrophenylhydrazone.

2) **In the Presence of Benzoyl Peroxide.**—In an atmosphere of dry nitrogen, piperonal and sulfuryl chloride (1 or 2 equiv.) were heated at 85°C in benzene or carbon tetrachloride in the presence of benzoyl peroxide (1% of the amount of sulfuryl chloride) until the evolution of hydrogen chloride ceased. After evaporation of the solvent, the product was decomposed by the addition of a small amount of water, and the resultant mixture was fractionated with benzene. Protocatechuic acid was obtained from the insoluble part and protocatechualdehyde from the benzene-layer, as is shown in Table I.

3) **Treatment with Aniline.**—The same reaction was carried out using more than 2 mol. of sulfuryl chloride. After the solvent was removed, a solution of 4 mol. of aniline in ether was added to the resultant viscous oil. A vigorous reaction took place, and an yellow solid was separated out. The solid was washed with 5% hydrochloric acid and recrystallized from dilute methanol to give colorless prisms, m. p. 166~167°C. The solid was identified with protocatechuanilide by the melting point test, and gave a dark green color with ferric chloride (Found: N, 6.01%).

The yellow solid described above was treated with 5% of an aqueous solution of sodium hydroxide, filtered, and washed with a small amount of ether. The crystals remaining were recrystallized from benzene-peteroleum ether to give colorless needles, m. p. 139°C. The compound obtained was identified as *N,N'*-diphenylformamidine, obtained from methyl piperonylate, by the mixed-melting point test (vid. Fig. 3).

Reaction with Methyl Piperonylate. — In an atmosphere of nitrogen, 0.90 g. (0.005 mol.) of methyl piperonylate, an equivalent of sulfuryl chloride and 10 mg. of benzoyl peroxide were heated in 10 ml. of benzene at 85°C for 6 hr. in an oil bath. After the complete evaporation of the solvent in vacuo at 80°C, the addition of cold water (ca. 1.5 ml.), the filtration of the separated crystal and, washing with cold water, 0.82 g. of colorless crystals were obtained. Recrystallization from water gave methyl protocatechuate, m. p. 134°C, in a 97.6% yield. Dark green on conbination with ferric chloride (Found: C, 57.08; H, 4.76%). The filtrate and washing were combined and titrated with 0.1 N of an aqueous solution of sodium hydroxide (titration curve: Fig. 1). After adjusting the pH value to 7, the titrated solution was evaporated to dryness, and the residue was triturated with absolute ethanol (50 ml.) and absolute methanol (5ml.). The alcoholic solution was treated with *p*-bromophenacyl bromide, giving *p*-bromophenacyl formate as colorless plates, m. p. 100°C.

The same reaction was carried out using 4.50 g. of methyl piperonylate at 85°C for 15 hr. The reaction mixture was distilled in vacuo to give a viscous liquid, b. p. 101~101.5°C/0.15 mmHg, in a quantitative yield (The infrared absorption spectrum is shown in Fig. 2). On standing in the air, the liquid decomposed to give methyl protocatechuate.

Found: Cl, 16.22 (Mohr's method). Calcd. for $C_9H_7O_4Cl$; Cl, 16.53%.

After evaporation of the solvent, a solution of 2 mol. of aniline in ether was added, drop by drop, to the reaction mixture under cooling. The precipitate formed was filtered. Methyl protocatechuate was obtained quantitatively from the ether-layer, and feathery crystals, m. p. 253°C, were obtained after recrystallization of the precipitate from water. The infrared absorption spectrum of the latter indicates that the product is *N, N'*-diphenylformamidine hydrochloride, as is shown in Fig. 3.

Found: C, 62.39; H, 6.13; N, 11.34. Calcd. for $C_{13}H_{13}N_2Cl \cdot H_2O$; C, 62.24; H, 6.25; N, 11.17%.

After treatment of the hydrochloride with 5% of an aqueous solution of sodium hydroxide, the free base was obtained as colorless needles, m. p. 139°C.

Found: N, 14.57. Calcd. for $C_{13}H_{12}N_2$; N, 14.28%.

Reaction with 4-Nitromethylenedioxybenzene.—4-Nitromethylenedioxybenzene (0.64 g.) was submitted to the reaction described above with an equivalent amount of sulfuryl chloride. After the decomposition with water, the reaction mixture gave yellow needles, m. p. 176°C (4-nitrocatechol melts at 175°C[10]). The needles gave a dark green color when treated with ferric chloride solution.

Found: N, 9.17. Calcd. for $C_6H_5O_4N$; N, 9.03%.

The author wishes to express his gratitude to Professor Mamoru Yamaguchi of Tohoku University for his constant guidance in the course of this work. He also wishes to thank the members of Professor Fujise's laboratory of the Faculty of Science for their microanalyses.

Kawauchi College
Tohoku University
Kawauchi, Sendai

10) E. Bamberger and M. Czerkis, *J. prakt. Chem.*, (2), **68**, 480 (1903).

The Kinetics of the Formation of Calcium Carbide in a Solid-Solid Reaction

By Hiroaki TAGAWA and Hideo SUGAWARA

(Received January 22, 1962)

Calcium carbide is generally made from calcium oxide and carbon according to the following equation:

$$CaO + 3C = CaC_2 + CO \quad (1)$$

Our fundamental information on the kinetics of this reaction, however, is limited.

The most extensive thermodynamic investigations into calcium carbide formation from calcium oxide and carbon have been made by the Kameyama's group[1]. They have found that the reaction of calcium oxide with carbon involves the following two main steps:

$$CaO + C = Ca + CO \quad (2)$$

$$Ca + 2C \rightleftharpoons CaC_2 \quad (3)$$

They concluded that the carbon monoxide pressures of Eqs. 1 and 2 were equal at 1460°C, and that the reaction of Eq. 1 was predominant in comparison with that of Eq. 2 above 1460°C.

Calcium carbide is commercially produced in the molten phase and in a complex reaction system. In order to clarify the kinetics of the reaction of calcium oxide with carbon, the corbonization of calcium oxide was, in the present study, thermogravimetrically examined in a solid-solid reaction at temperatures between 1600 and 1800°C and at various carbon monoxide pressures.

Experimental

Materials. — Calcium oxide was produced by burning precipitated calcium carbonate in an electric furnace at 1200°C for 2 hr. The carbon specimen used was charcoal which had been preheated at 1000°C for 2 hr. in order to remove volatile matters. Calcium oxide and carbon were pulverized to pass through a 200 mesh sieve and mixed at a ratio of 1 : 3 by mole. Nine grams of the mixture were compressed at about 1 ton/cm^2 into a cylindrical pellet, 20 mm. in diameter and 30 mm. in height.

Apparatus.—The apparatus used for the kinetic experiments consisted of a spring balance in a vacuum electric furnace of which the internal volume was about 150 l.[2] The pumping speed of a connected rotary pump was 1600 l./min. A graphite bucket, 45 mm. in diameter and 35 mm. in height, was suspended from the spring in the hot zone of the furnace by a fine molibdenum wire. The shrinkage of the spring by the weight loss of the sample was observed with a microscope with an eyepiece scale. The sensitivity of the spring was 0.278 g./mm. The reaction temperature was measured with a radiation pyrometer and was maintained at a desired value within ±3°C with the aid of an automatic temperature controller. The error in temperature measurement caused by the calcium vapor and the carbon monoxide atmosphere was corrected with a W/50%W-Mo thermocouple[3], which had been calibrated by an optical pyrometer in vacuo. The electric furnace was kept at the desired carbon monoxide pressure during the course of the experiments. The pressures were 50, 100 and 200 mmHg.

Procedure. — The velocity of the formation of calcium carbide was determined as follows. The reaction was stopped at a defined time, and the residual specimen was chemically analyzed for calcium carbide and for residual calcium oxide and carbon. If the formation expressed in Eq. 1 and the decomposition of the calcium carbide formed occur as main reactions in these experimental conditions, there are the following relationships among the analyzed quantities:

Weight loss = CO (evolved)
+ Ca (from decomposed CaC_2)

Residual CaC_2 = CaC_2 (formed)
− CaC_2 (decomposed)

Residual CaO = CaO (unreacted)

Residual C = C (unreacted)
+ C (from decomposed CaC_2)

Each quantity was obtained from the material balance calculations in the above equations.

The notations used in Figs. 2 to 6 and in the kinetic equation are as follows:

Reaction ratio = Formed CaC_2/Theoretically formed CaC_2

Decomposition ratio = Decomposed CaC_2/Theoretically formed CaC_2

Residual ratio (yield) = Reaction ratio
− Decomposition ratio

1) N. Kameyama, "Electrochemistry: Theory and Application", Vol. III-2, Maruzen, Tokyo (1956), p. 134.
2) H. Tagawa and H. Nakajima, This Bulletin. 35, 1239 (1962).
3) T. Tomonari, M. Takahashi, S. Togawa and H. Arakawa, *J. Electrochem. Soc. Japan (Denki Kagaku)*, **26**, 479 (1958); F. H. Morgan and W. E. Danforth, *J. Appl. Phys.*, **21**, 112 (1950).

Results

All curves of the weight decrease against the time were parabolic in the temperature range 1600 to 1800°C and at 50, 100 and 200 mmHg of carbon monoxide pressure. Figure 1 shows the course of the reaction at five temperatures and at 100 mmHg of carbon monoxide. The weight loss is presumed to be due to the evolution both of carbon monoxide produced in the formation of calcium carbide and of calcium vapor produced by the decomposition of the freshly formed calcium carbide. The curves of the reaction ratio vs. time, the residual ratio vs. time, and the decomposition ratio vs. time at 100 mmHg of carbon monoxide are shown in Figs. 2, 3 and 4 respectively. The reaction ratio curves are parabolic, whereas the decomposition curves are approximately linear with time. The curves of the residual ratio vs. time and of the decomposition ratio vs. time at 1760°C are shown in Figs. 5 and 6 respectively. The decomposition ratio decreases with the increasing carbon monoxide pressure at any temperature.

The reaction ratio curves were parabolic in all experiments. The rate of solid state reaction when the diffusion process is rate-determining is expressed by the following equation[4]:

$$(1-\sqrt[3]{1-x})^2=kt \qquad (4)$$

where x is the reaction ratio, t the time, and k the reaction rate constant. This is derived from the reaction of a sphere of component A completely surrounded by spheres of component B. To determine whether the reaction followed the parabolic kinetics given in Eq. 4, the data in Fig. 2 were plotted as the value of $(1-\sqrt[3]{1-x})^2$ vs. time in Fig. 7. The linearity of the $(1-\sqrt[3]{1-x})^2$ vs. time curve means that the reaction is apparently diffusion-controlled. The apparent rate constant, k, in Eq. 4 was found from the slope of each line.

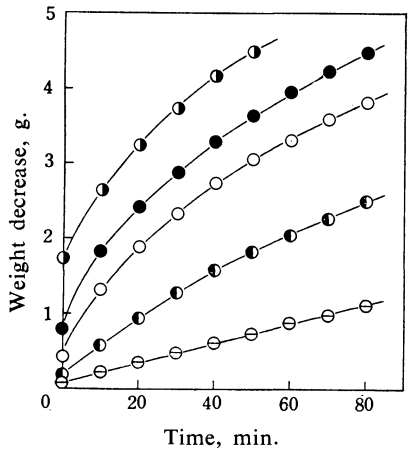


Fig. 1. Relation between weight decrease and time at 100 mmHg of CO.
◑, 1800 ●, 1760 ○, 1720 ◐, 1680 ⊖, 1640°C

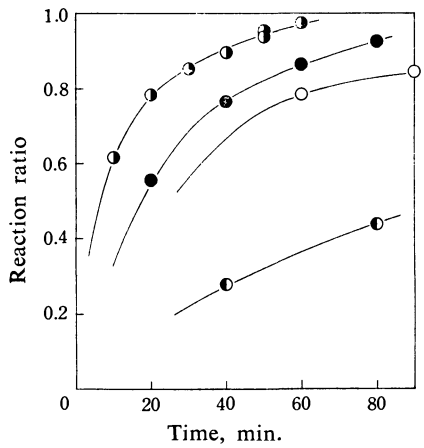


Fig. 2. Relation between reaction ratio and time at 100 mmHg of CO.

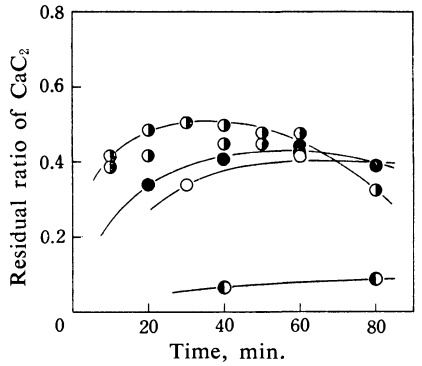


Fig. 3. Relation between residual ratio of CaC_2 and time at 100 mmHg of CO.

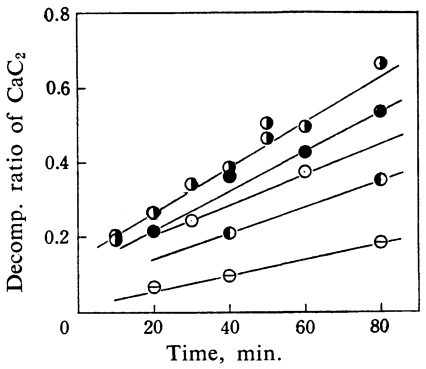


Fig. 4. Relation between decomposition ratio of CaC_2 and time at 100 mmHg of CO.

4) W. Jander, *Z. anorg. u. allgem., Chem.*, **111**, 78 (1927).

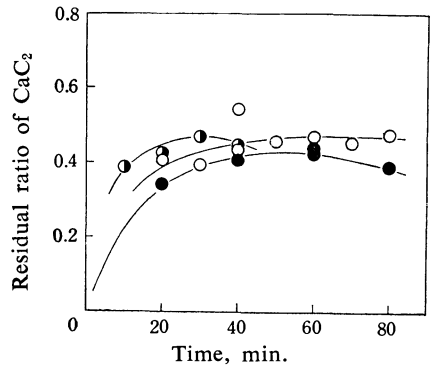


Fig. 5. Relation between residual ratio of CaC_2 and time at 1760°C.
◑, 50 ●, 100 ○, 200 mmHg

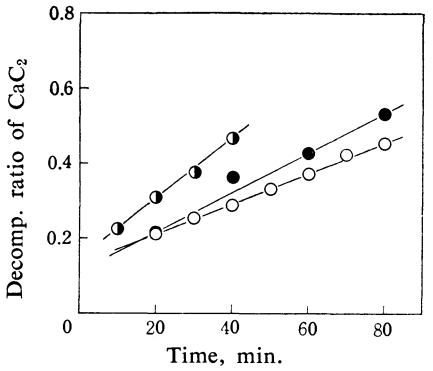


Fig. 6. Relation between decomposition ratio of CaC_2 and time at 1760°C.

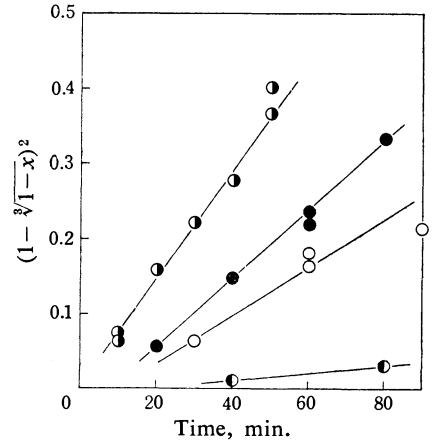


Fig. 7. Relation between $(1-\sqrt[3]{1-x})^2$ and time at 100 mmHg of CO.
◑, 1800 ●, 1760 ○, 1720 ◐ 1680°C

The logarithm of the slope was plotted against the reciprocal of the absolute temperature at 50, 100 and 200 mmHg of carbon monoxide in Fig. 8. The rate constant decreases as the pressure of carbon monoxide increases.

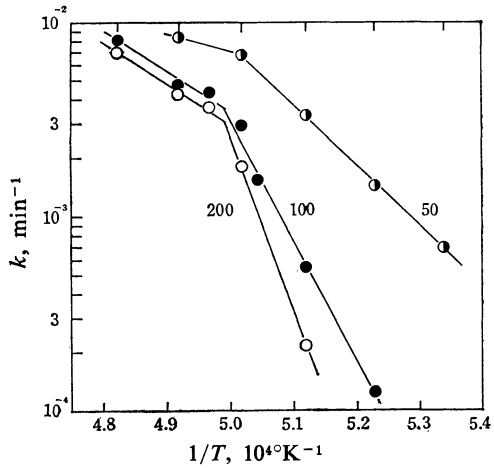


Fig. 8. Relation between logarithm of reaction velocity and the reciprocal absolute temperature at 50, 100 and 200 mmHg of CO.

Discussion

The formation of calcium carbide in a solid state reaction has been studied by Kameyama et al.[1] and by Mukaibo and Yamanaka[5]. Kameyama has found that calcium carbide is formed by the following successive reactions.

$$CaO + C = CaO\cdot C \text{ (Interdiffusion state)} \quad (5)$$

$$CaO\cdot C \text{ (Interdiffusion state)} = Ca + CO \quad (6)$$

$$Ca + 2C = CaC_2 \quad (7)$$

It has been found that the interdiffusion between calcium oxide and carbon occurs at temperatures above 1000°C. Although the reactions of 5 and 6 are determined by diffusion, the kinetics of $CaO+C=Ca+CO$ is described as a zero-order reaction because the products of the reaction of calcium oxide with carbon vaporized from the surface of the reactants[2,5]. The activation energy of the reaction was 147 kcal./mol.[2]

The formation of calcium carbide is apparently expressed by the following equation: $(1-\sqrt[3]{1-x})^2=kt$. In this kinetics, the following steps are considered to be rate-determining:

1) Diffusion of carbon into calcium oxide, and vice versa.
2) Diffusion of carbon monoxide through the product layer.

The apparent activation energy at 50 mmHg of carbon monoxide obtained from Fig. 8 was 143 kcal./mol., while that above 100 mmHg was more than 200 kcal./mol. The effect of the varied carbon monoxide pressure on the

5) T. Mukaibo and Y. Yamanaka, *J. Chem. Soc. Japan, Ind. Chem. Sec.* (*Kōgyō Kagaku Zassi*), **58**, 643 (1955).

activation energy may be involved in the pressure term of the kinetics equation, but the general formula of this kinetics has not yet been determined. From the fact that the velocity, k, depends on the pressure of carbon monoxide and that the activation energy is close to that of the first step of the carbide formation at about 1400°C, the rate-determining step may be the diffusion of gas through the product layer as well as that of solids into the solid and product layer. As the calcium carbide formed simultaneously enters upon consecutive decomposition, the reaction velocity, k, is considered to be not an absolute measure, but a relative one.

The apparent reaction rate vs. the reciprocal absolute temperature curves have a break point at about 1700°C. It is considered that reactions expressed in Eqs. 8 and 9, besides the reaction of $CaO+3C=CaC_2+CO$, occur at higher temperature, above 1700°C:

$$mCaC_2 + nCaO = mCaC_2 \cdot nCaO \quad (8)$$

$$mCaC_2 \cdot nCaO = (m-1)CaC_2 \cdot (n-2)CaO + 3Ca + 2CO \quad (9)$$

Summary

The kinetics of the formation of calcium carbide in the solid state reaction of calcium oxide with carbon has been examined by using a thermobalance in the temperature range 1600 to 1800°C and at 50, 100 and 200 mmHg of carbon monoxide. The reaction ratio vs. time curves were parabolic in all experimental runs, and the reaction followed parabolic kinetics: $(1-\sqrt[3]{1-x})^2=kt$. On the other hand, the decomposition of calcium carbide as a successive reaction occurred from the specimen surface and was described as a zero-order reaction. As the reaction velocity depended strongly on the pressure of carbon monoxide, it is considered that the reaction rate is governed by the diffusion process of gas through the product layer, as well as that of solids into the solid and product layer.

Research Laboratory
Nippon Carbide Industries Company
Uozu, Toyama

Infrared Spectra and Normal Vibrations of Acetamide and its Deuterated Analogues

By Isao SUZUKI

(Received January 25, 1962)

It has been shown in previous papers[1,2] that normal coordinate analyses of formamide and *N*-methylformamide molecules can be made satisfactorily by employing the Urey-Bradley force field and that the force constants determined for formamide can be used without any significant alternations in value in the normal coordinate treatment of *N*-methylformamide. As a continuation of this research, the acetamide molecule is treated in the present paper.

Only a limited number of spectroscopic investigations of acetamide have been reported[3-5], and the main interests of these authors have been focused rather on the protonated systems of the molecule than on acetamide itself. The vibrational assignments for this molecule are very uncertain. Therefore, infrared measurements have been made not only of CH_3CONH_2, but also of three deuterated species of acetamides, CH_3COND_2, CD_3CONH_2 and $CD_3CO\cdot ND_2$. From the combined results of these measurements and of the calculation of normal vibrations, the nature of the observed frequencies is discussed in detail in the present paper. The Urey-Bradley force constants obtained in the present work are compared with those in formamide and in *N*-methylformamide, and the values of some constants are discussed.

1) I. Suzuki, This Bulletin, 33, 1359 (1960).
2) I. Suzuki, ibid., 35, 540 (1962).
3) M. Davies and H. E. Hallam, *Trans. Faraday Soc.*, 47, 1170 (1951).
4) N. Albert and R. M. Badger, *J. Chem. Phys.*, 29, 1193 (1958).
5) E. Spinner, *Spectrochim. Acta*, 15, 95 (1959).

Experimental

Materials.—*Acetamide* CH_3CONH_2. — Acetamide was obtained from a commercial source and was purified by the method of ether precipitation from

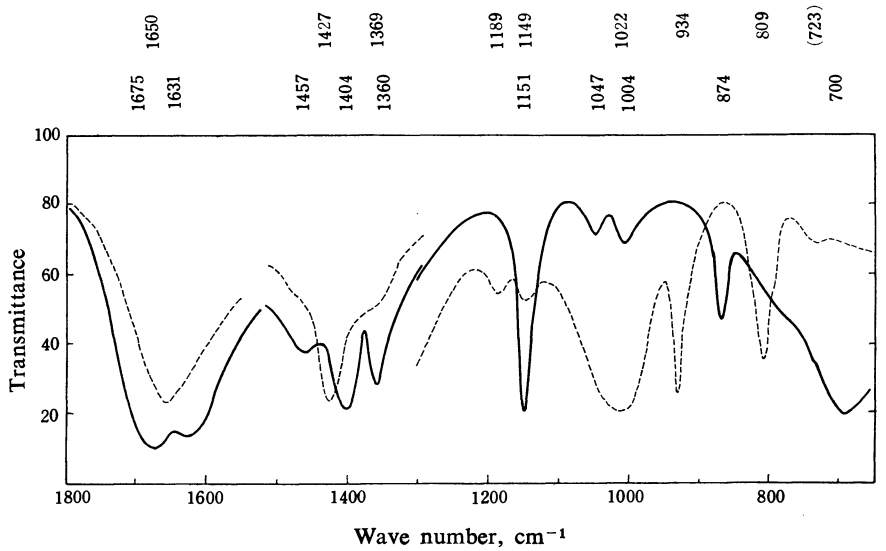


Fig. 1. Infrared spectra of CH_3CONH_2 (solid line) and CH_3COND_2 (broken line) in the solid state in the region from 1800 to 650 cm^{-1}.

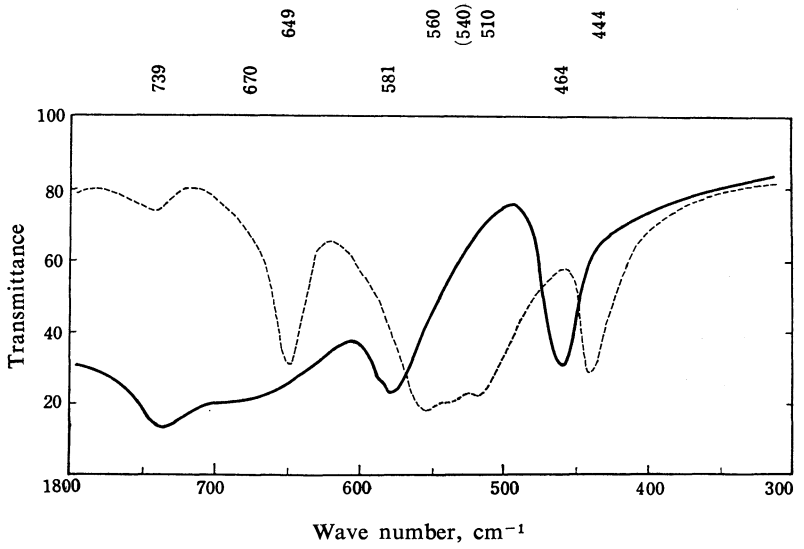


Fig. 2. Infrared spectra of CH_3CONH_2 (solid line) and CH_3COND_2 (broken line) in the solid state in the region from 800 to 300 cm^{-1}.

an alcohol solution[6]. The acetamide precipitated was collected, dried in vacuum, and used in the measurements; m. p., 80°C.

C-Deuterated Acetamide CD_3CONH_2.—First, CD_3COOD was prepared by the thermal decomposition of $CD_2(COOD)_2$, which was obtained from the exchange reaction of $CH_2(COOH)_2$ with D_2O[7]. Then, CD_3COOD was reacted with liquid ammonia. The ammonium acetate obtained was heated at about 200°C for four hours in a sealed tube, and the CD_3COND_2 (containing CD_3CONHD) thus formed was distilled out in vacuum. It was purified by the method described above.

The exchange reaction with D_2O was employed to replace the amide hydrogen atoms by deuterium.

Infrared Spectra.—The measurements of the infrared spectra were made in the region from 4000 to 650 cm^{-1} with a Hitachi EPI spectrophotometer equipped with sodium chloride optics, and in the region from 800 to 300 cm^{-1} with a Nippon Bunko grating spectrophotometer equipped with a cesium bromide foreprism. The infrared spectra of CH_3CONH_2 and CH_3COND_2 were measured in the solid and liquid states and in solutions. The solid state

6) E. C. Wagner, *J. Chem. Educ.*, **7**, 1135 (1930).
7) J. O. Halford and L. C. Anderson, *J. Am. Chem. Soc.*, **58**, 736 (1936).

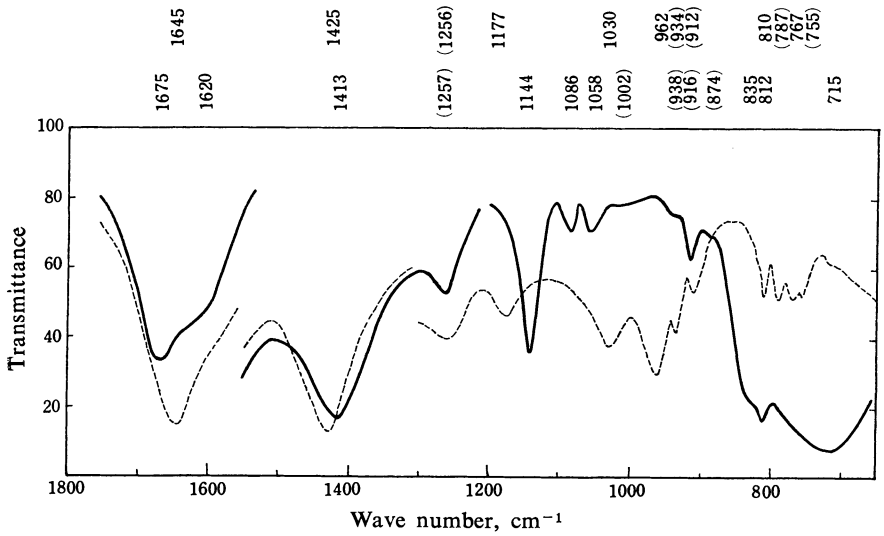


Fig. 3. Infrared spectra of CD_3CONH_2 (solid line) and CD_3COND_2 (broken line) in the solid state in the region from 1800 to 650 cm^{-1}.

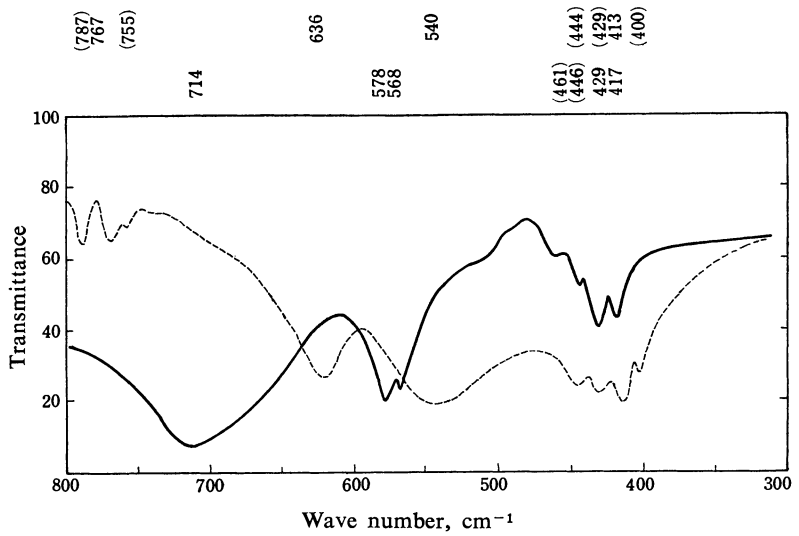


Fig. 4. Infrared spectra of CD_3CONH_2 (solid line) and CD_3COND_2 (broken line) in the solid state in the region from 800 to 300 cm^{-1}.

spectra were taken in Nujol or hexachlorobutadiene mulls and are shown in Figs. 1 and 2. A small heating cell was used to obtain the spectra in the liquid state. The observed frequencies are summarized in Table I. The spectra of CD_3CONH_2 and CD_3COND_2 in the solid state are shown in Figs. 3 and 4. As may be seen from these figures, the spectra of both CD_3CONH_2 and CD_3COND_2 are complicated, particularly in the region below 1000 cm^{-1}. This is due to the presence of bands arising from the CHD_2-species which are contained in the samples. Therefore, the assignments of those vibration bands which are mainly associated with the CD_3 rocking and CC' in-plane deformation vibrations are uncertain. When the values of the force constants were refined, they were not used as frequency data.

Normal Coordinate Treatment

The calculation of normal vibrations was made as a nine-body problem by Wilson's method[8]. The planar model (C_s), except for two hydrogen atoms attached to the methyl carbon atom (C')*[1], was adopted (see Fig. 5).

8) E. B. Wilson, *J. Chem. Phys.*, **7**, 1047 (1930); **9**, 96 (1941).

*1 C and C' denote the carbonyl and methyl carbon atoms respectively.

TAELE I. OBSERVED FREQUENCIES (IN cm^{-1}) OF ACETAMIDE

(a) CH_3CONH_2			(b) CH_3COND_2		
Solid	Liquid	$CHCl_3$ soln.	Solid	Liquid	$CHCl_3$ soln.
3340	3355	3520(3360)	2920	2937	(2980)
3163	3165	3403(3161)	2505	2555	2537
2820	2815		2395	2405	(2460)
			2315		2372
1675	1660?	1680	1650	1634?	1668
1632	1600	1594		(1468)	
1457	1458	1440?	1427	1405	1390
1404	1388	1378	1369	1360	1355
1360	1345	1336	1189	1174	
1152	1138	1118	1150		
1047	1048	1041	1022	1035	(1035)
1005	998	981	934	921	
874	865	872	809	801	
(739)			649		613*
667		527*	560		538*
581		557*	560		518*
464		443*	516		400*
			444		433*

* CH_3CN solution

TABLE II. SYMMETRY COORDINATES

S_i	$S=UR$	Vibrational mode	Abbr.
S_1	Δr_{14}	CN stretching	ν(CN)
S_2	Δr_{45}	CC′ stretching	ν(CC′)
S_3	Δr_{46}	CO stretching	ν(CO)
S_4	$(2\Delta\alpha_{23}-\Delta\alpha_{42}-\Delta\alpha_{34})/\sqrt{6}$	NH_2 bending	$b(NH_2)$
S_5	$(\Delta\alpha_{42}-\Delta\alpha_{34})/\sqrt{2}$	NH_2 rocking	$r(NH_2)$
S_6	$(2\Delta\alpha_{61}-\Delta\alpha_{15}-\Delta\alpha_{56})/\sqrt{6}$	NCO deformation	δ(NCO)
S_7	$(\Delta\alpha_{15}-\Delta\alpha_{56})/\sqrt{2}$	CC′ deformation	δ(CC′)
S_8	$(2\Delta\alpha_{89}-\Delta\alpha_{78}-\Delta\alpha_{79})/\sqrt{6}$	CH_3 asym. deformation	$\delta_a(CH_3)$
S_9	$(\Delta\alpha_{47}+\Delta\alpha_{48}+\Delta\alpha_{49}-\Delta\alpha_{78}-\Delta_{79}-\Delta\alpha_{89})/\sqrt{6}$	CH_3 sym. deformation	$\delta_s(CH_3)$
S_{10}	$(2\Delta\alpha_{47}-\Delta\alpha_{48}-\Delta\alpha_{49})/\sqrt{6}$	CH_3 rocking	$r(CH_3)$

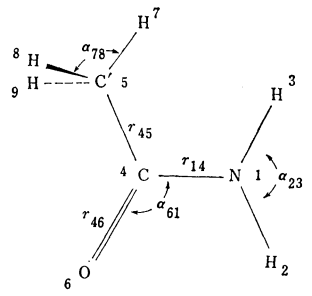


Fig. 5. Molecular structure and internal coordinates of acetamide.

The normal vibrations are classified into 14 in-plane (A′) and 7 out-of-plane (A″) vibrations, of which the in-plane vibrations are treated. The structural parameters used in the present work are as follows: the bond lengths of r(C=O) = 1.28 Å, r(C–N) = 1.38 Å, r(C–C′) = 1.51 Å, r(N–H) = 1.02 Å and r(C′–H) = 1.09 Å[9] and the bond angles of 120° for those around the N and C atoms and of 109°47′ for those around the C′ atom. To simplify the calculation, lower frequencies are separated from four higher frequencies which are mainly associated with the CH and NH(D) stretching vibrations[8]. The symmetry coordinates used are given in Table II (see also Fig. 5 for definitions of the internal coordinates).

Force Constants.—As has already been mentioned, the potential function used in the calculation is of the Urey-Bradley type[10]:

$$2V=\sum_i K_i(\Delta r_i)^2+\sum_{i\neq j} H_{ij}r_i^0r_j^0(\Delta\alpha_{ij})$$
$$+\sum_{i\neq j} F_{ij}(\Delta q_{ij})^2+\text{Linear terms}$$

The same notations as in the preceding papers[1,2] are used. In addition, the intramolecular tension, κ, is introduced in the elements of the F-matrix when the linear terms are eliminated by a redundancy condition[10].

9) F. Senti and D. Harker, *J. Am. Chem. Soc.*, **62**, 2008 (1940).

10) T. Shimanouchi, *J. Chem. Phys.*, **17**, 245, 734, 848 (1949).

TABLE III. FORCE CONSTANTS IN md./A*

	K_{CN}	5.75 (6.15)	H_{HNH}	0.40 (0.40)	$F_{H(N)H}$	**0** (0)
A	K_{CO}	8.50 (8.80)	H_{HNC}	0.32 (0.32)	$F_{H\cdots C}$	0.46 (0.46)
			H_{NCO}	0.34 (0.34)	$F_{N\cdots O}$	1.50 (1.50)
B	K_{CC}	2.40	H_{CCN}	0.30	$F_{C\cdots N}$	0.70
			H_{CCO}	0.32	$F_{C\cdots O}$	0.72
C	κ	**−0.05** (md·A)	H_{HCH}	**0.43**	$F_{H(C)H}$	**0.03**
			H_{HCC}	0.25	$F_{H(C)C}$	0.47

* Initial set of values for the force constants in group A are given in parenthesis.

Therefore, eighteen force constants are necessary to calculate normal vibrations of the acetamide molecule. As may be seen from Table III, these force constants are classified into three groups, A, B and C, and their values were first determined by the following method: The constants in group A were directly transferred from the formamide molecule[1]. The constants in group B are associated with the "joint" of the CH_3 and amide groups, and $K_{CC}=3.00$ md./A, $H_{CCN}=0.23$ md./A, $H_{CCO}=0.31$ md./A, and $F_{C\cdots N}=F_{C\cdots O}=0.50$ md./A were first assumed*2. Those belonging to group C are associated with the methyl group. In our laboratory, a number of compounds containing methyl groups have been studied, and it has been found that one set of constants, $H_{HCH}=0.43$ md./A, $F_{H\cdots H}=0.03$ md./A and $\kappa=-0.05$ md·A, always gives a good frequency fit with the observed data. These values have also been adopted in the present work; they are not varied in the course of refinements. As for other constants, $H_{HCC}=0.25$ md./A and $F_{H\cdots C}=0.45$ md./A were used.

The normal vibrations were calculated from these force constants, and they give fairly good agreement with the observed frequencies. Then the values of the constants were refined as indicated by the Jacobian matrix[12] to obtain a better frequency fit. At the first step of the refinements, only the frequencies of CH_3CONH_2 and CH_3COND_2 were used. Then at the final step those of CD_3CONH_2 and CD_3COND_2 above 1000 cm^{-1} were also taken into account. However, the frequencies of the latter two molecules found below 1000 cm^{-1} *3 were not used for the reason indicated in the preceding section. At first the force constants in group B were subjected to refinements, since their values were less certain than those in groups A and C.

Although only five constnats were refined, the frequency fit between the observed and the calculated was improved remarkably. In fact, the agreements were so good that refinement was practically unnecessary for the constants in groups A and C, except for two stretching constants, K_{CN} and K_{CO}. The final set of force constants is listed in Table III.

Results and Discussion

Assignments of Vibration Bands. — The frequencies calculated from the force constants given in Table III are compared with the observed frequencies in Tables IV(a)—(d) for each isotopic species of acetamide. In Tables IV(a)—(d), the potential energy distribution among the symmetry coordinates is also given for each normal mode. This represents the quantitative assignment.

In CH_3CONH_2, each normal vibration takes place along one or two symmetry coordinates and is easily identified. As expected, the band at 1676 cm^{-1} of acetamide is associated with the ν(CO) mode. However, the ν(CN) and $b(NH_2)$ vibrations also contribute to this band. The bands at 1632 and 1152 cm^{-1} are mainly associated with the $b(NH_2)$ and $r(NH_2)$ vibrations respectively, and the fact that they move to lower frequencies in a $CHCl_3$ solution is consistent with the above assignments. The bands at 1457, 1360 and 1005 cm^{-1} are associated with the methyl deformation vibrations and are assigned, respectively, to the $\delta_a(CH_3)$, $\delta_s(CH_3)$ and $r(CH_3)$ vibrations. The nature of the 1404 cm^{-1} band is a little complicated. This band can be called the ν(CN) band, although there are considerable contributions from the $\nu(CC')$, $r(NH_2)$, δ(NCO) and $\delta_s(CH_3)$ vibrations. The band at 864 cm^{-1} is associated with the $\nu(CC')$ vibrations, while the bands at 581 cm^{-1} and 464 cm^{-1} are associated with δ(NCO) and $\delta(CC')$ vibrations respectively.

Instead of the 1632 cm^{-1} band, a band appears at 1189 cm^{-1} in CH_3COND_2; this is assigned to an almost pure $b(ND_2)$ vibration. The ν(CO) band is lowered, probably by the decoupling of the $b(NH_2)$ vibrations, while the ν(CN) band moves to a higher frequency and appears at 1427 cm^{-1}. The $b(ND_2)$ vibration

*2 Miyazawa et al., obtained a good frequency agreement for the skeletal deformation vibrations of *N*-methylacetamide[11] from the values of $H_{CH_3\text{-}C\text{-}N}=H_{CH_3\text{-}C=O}=0.30$ md./A and $F_{CH_3\cdots N}=F_{CH_3\cdots O}=0.50$ md./A, although they treated the methyl group as a dynamic unit.

*3 Those frequencies are given in parentheses in the first column of Tables IV (c) and (d).

TABLE IV. OBSERVED AND CALCULATED FREQUENCIES, AND POTENTIAL ENERGY DISTRIBUTIONS AMONG SYMMETRY COORDINATES; $(F_{ii}L_{is}^2/\lambda_s)\times 100$

(a) CH_3CONH_2

					P. E. D.									
Q_i	ν_{obs}	ν_{calcd}	$\Delta\nu$	Δ	S_1	S_2	S_3	S_4	S_5	S_6	S_7	S_8	S_9	S_{10}
Q_1	1676	1678	− 2	0.1	**28**	1	**59**	**16**	4	1	7	1	0	4
Q_2	1632	1630	+ 2	0.1	1	1	**17**	**80**	2	1	1	0	0	1
Q_3	1457	1462	− 5	0.4	1	1	3	0	1	1	0	**82**	0	9
Q_4	1404	1396	− 8	0.6	**48**	**13**	2	4	**10**	**14**	2	5	**12**	0
Q_5	1360	1366	− 6	0.5	6	**20**	1	0	2	2	0	0	**92**	0
Q_6	1152	1133	+19	1.7	7	1	**16**	6	**70**	1	1	0	0	0
Q_7	1005	1002	+ 3	0.3	5	0	2	0	1	0	3	**11**	0	**81**
Q_8	874	892	−18	2.1	**10**	**61**	4	1	7	8	0	0	0	0
Q_9	581	580	+ 1	0.2	0	10	0	0	3	**74**	5	0	0	0
Q_{10}	464	465	+ 1	0.2	1	0	1	0	2	5	**82**	2	0	5

(b) CH_3COND_2

					P. E. D.									
Q_i	ν_{obs}	ν_{calcd}	$\Delta\nu$	Δ	S_1	S_2	S_3	S_4	S_5	S_6	S_7	S_8	S_9	S_{10}
Q_1	1650	1666	−16	1.0	**24**	2	**75**	1	3	1	9	1	0	6
Q_2	(1455)	1461	—	—	1	1	4	0	0	1	0	**81**	0	8
Q_3	1427	1419	+ 8	0.5	**56**	**13**	7	**13**	3	**12**	1	5	7	0
Q_4	1369	1367	+ 2	0.1	4	**16**	1	1	0	1	0	0	**98**	0
Q_5	1189	1191	− 2	0.2	1	**14**	0	**72**	3	8	2	1	0	2
Q_6	1022	1006	+16	1.6	1	3	9	0	5	2	3	**10**	0	**70**
Q_7	934	936	− 2	0.2	**13**	5	7	**10**	**36**	6	0	1	0	**10**
Q_8	809	818	− 9	1.1	6	**50**	0	3	**35**	0	0	0	0	0
Q_9	560	556	+ 4	0.8	0	6	1	0	7	**64**	**15**	0	0	1
Q_{10}	444	442	+ 2	0.5	1	0	0	0	8	**12**	**70**	0	0	4

(c) CD_3CONH_2

					P. E. D.									
Q_i	ν_{obs}	ν_{calcd}	$\Delta\nu$	Δ	S_1	S_2	S_3	S_4	S_5	S_6	S_7	S_8	S_9	S_{10}
Q_1	1675	1672	+ 3	0.2	**29**	1	**57**	**21**	4	1	7	0	0	2
Q_2	1620	1629	− 9	0.6	**0**	2	**22**	**75**	2	1	2	0	0	1
Q_3	1413	1394	+19	1.4	**56**	**27**	3	4	**12**	**17**	2	0	0	1
Q_4	1144	1133	+11	0.9	7	0	**16**	0	**70**	1	1	0	0	0
Q_5	1086	1092	− 6	0.6	1	**30**	0	0	2	0	0	0	**86**	0
Q_6	1058	1048	+10	0.9	0	0	0	0	0	0	1	**91**	0	5
Q_7	(835)	842	− 7	0.9	**11**	**14**	0	0	2	8	6	3	6	**45**
Q_8	(812)	839	−27	3.3	1	**23**	5	0	5	9	3	3	9	**35**
Q_9	(578)	553	−25	4.3	0	**13**	0	0	2	**68**	3	0	4	1
Q_{10}	(429)	429	0	0	1	0	0	0	1	3	**78**	4	0	**12**

(d) CD_3COND_2

					P. E. D.									
Q_i	ν_{obs}	ν_{calcd}	$\Delta\nu$	Δ	S_1	S_2	S_3	S_4	S_5	S_6	S_7	S_8	S_9	S_{10}
Q_1	1645	1658	−13	0.8	**25**	2	**78**	1	3	1	9	0	0	3
Q_2	1425	1416	+ 9	0.6	**61**	**22**	**10**	**15**	3	**14**	1	0	0	0
Q_3	1177	1192	−15	1.3	1	**22**	0	**67**	3	8	1	0	6	1
Q_4	—	1089	—	—	3	**16**	1	9	0	1	0	0	**82**	0
Q_5	1030	1049	−19	1.8	0	0	0	0	0	0	1	**91**	0	5
Q_6	(962)	940	−22	2.3	5	1	**13**	5	**48**	9	3	0	3	4
Q_7	(810)	823	−13	1.7	7	0	1	2	2	1	6	5	0	**77**
Q_8	(767)	764	+ 3	0.4	5	**38**	1	2	**29**	3	0	0	**11**	1
Q_9	(540)	530	+10	1.9	0	9	1	0	7	**64**	8	1	3	2
Q_{10}	(413)	404	+ 9	2.2	1	0	0	0	5	7	**74**	3	0	8

$\Delta\nu=\nu_{obs}-\Delta\nu_{calcd}$, $\Delta=|\Delta\nu|/\nu_{obs}$

also contributes to the latter band. The $r(ND_2)$ vibration takes part in both the 934 and 809 cm^{-1} bands. The $\nu(CN)$, $b(ND_2)$ and $r(CH_3)$ vibrations also contribute to the former band, and the $\nu(CC')$ vibration to the latter.

The nature of the 1676, 1632, 1404 and 1152 cm^{-1} bands of CH_3CONH_2 is not much affected by the *C*-deuteration; they are found at 1672, 1620, 1413 and 1144 cm^{-1} in CD_3CONH_2, The 1414 cm^{-1} band is assigned to a composite mode in which the $\nu(CN)$, $\nu(CC')$ $r(NH_2)$ and $\delta(NCO)$ vibrations take place. In $CD_3 \cdot COND_2$, it is found at 1425 cm^{-1}, and the $b(ND_2)$ vibration contributes to this band instead of $r(NH_2)$ vibration. The $\delta_a(CD_3)$ vibration occurs at 1058 cm^{-1}, which is lower by 28 cm^{-1} than the $\delta_s(CD_3)$ vibration. The reversal of these two methyl deformation vibrations is often observed in the spectra of compounds containing CD_3 groups[13]. For the CD_3-species of acetamide, the vibrational assignments of the observed bands below 1000 cm^{-1} are very difficult, because of the presence of the bands arising from the CHD_2-species contained in the sample. (The 1257 cm^{-1} band is assigned to the CH bending vibration of the CHD_2-species.) Aside from the bands of the CD_3-species, CD_2 wagging, bending, rocking and twisting vibrations are expected to appear in this region. Therefore, the assignments given in Table IV are tentative. The features of the $\delta(CC')$ vibration region are very interesting; four small peaks are observed around 420 cm^{-1} in the spectra of both CD_3CONH_2 and CD_3COND_2. The present calculations indicate that an interaction takes place between the $\delta(CC')$ and $r(CD_3)$ vibrations. It is also probable the vibrational interaction occurs between the $r(CD_2)$ and $\delta(CC')$ modes. However, the degrees of the interaction depend on the mutual positions of the CHD_2 group to the plane determined by the amide group. Several stable but non-equivalent configurations can be considered as for the positions of the CHD_2 group, and this may be the cause of the complexity of the $\delta(CC')$ bands.

Several bands can be assigned to the out-of-plane vibrations. In the NH_2-species, a broad band is found around 700 cm^{-1} and is assigned to the NH_2 wagging vibration. The NH_2 twisting band may overlap with this band. The corresponding bands are found around 500 cm^{-1} in the ND_2-species. A strong band found at about 640 cm^{-1} in the ND_2-species may be associated with the CC' out-of-plane vibration*4. but the ND_2 twisting and wagging vibrations may also contribute to this band.

Force Constants. — The force constants in group A are associated with the $O\!\!\nearrow\!\!C\text{-}N\!\!\swarrow^{H}_{H}$ part of the molecule and are transferred form formamide[1]. As may be seen from the process of determining their values, they can be used without significant alternations in value. This is the second example of showing a fine transferability of the constants determined in the formamide molecule[2]. A stretching force constant, *K*, has often been used as a measure of the bond order or character of the corresponding bond. In the series of amides, the K_{CO} and K_{CN} values are always found, respectively, around 8.50 and 6.00 md./A and are considered to indicate the partial single and double bond characters of the respective C=O and C–N bonds. In urea, however, the K_{CO} value falls to 6.47 md./A[14]. The lowering of the K_{CO} value may partly be accounted for by the presence in urea of two C–N bonds adjacent to the C=O bond*5. In the Urey-Bradley force field, the value of a given stretching constant is closely correlated with those of the repulsive constants around the bond. It is often odserved for a molecule which contains conjugated systems that some repulsion constants become very large[17]. In such a molecule, the resonance term $k_{ab}(\Delta r_a)(\Delta r_b)$*6, which is neglected in the Urey-Bradley field, is of considerable magnitude and affects the corresponding force constant $F_{a\ldots b}$. In the present case, the $F_{N\ldots O}$ value is found to be as large as 1.50 md./A. The lowering of the K_{CO} value in urea as compared with that in acetamide can be explained by the superposed effect of $F_{N\ldots O}$ from two adjacent C–N bonds. It should be noted that the direct comparison of stretching constants sometimes leads to an incorrect conclusion, especially when some repulsive force constants are considerably large.

The force constants in group B are primarily

11) T. Miyazawa, T. Shimanouchi and S. Mizushima, ibid., **29**, 611 (1958).
12) T. Miyazawa, *J. Chem. Soc. Japan, Pure Chem. Sec. (Nippon Kagaku Zassi)*, **76**, 1132 (1955).
13) For example, H. C. McMurry and V. Thornton, *J. Chem. Phys.*, **19**, 1014 (1951).
14) A. Yamaguchi, *J. Chem. Soc. Japan, Pure Chem. Sec. (Nippon Kagaku Zassi)*, **78**, 1319, 1467 (1957).

*4 In the NH_2-species, the corresponding band can not be found; it is probable that the band is overlapped with that of the $\delta(NCO)$ vibration at about 560 cm^{-1}.
*5 However, the reported value of 1.26 Å for the C=O bond in urea[15] is not much different from that of 1.255 Å in formamide[16] and only a little shorter than that of 1.28 Å in acetamide[9].
15) A. Yamaguchi, T. Miyazawa, T. Shimanouchi and S. Mizushima, *Spectrochim. Acta*, **17**, 719 (1961).
16) J. Landall and B. Post, *Acta Cryst.*, **7**, 559 (1954).
17) T. Miyazawa, *J. Chem. Soc. Japan, Pure Chem. Sec. (Nippon Kagaku Zassi)*, **77**, 381 (1956).
*6 r_a and r_b denote the bonds resonated with each other, and k_{ab} is a force constant. In fact, Scherer and Overend include the analogous term in the normal vibration calculation of the benzene molecule[18].
18) J. R. Scherer and J. Overend, *Spectrochim. Acta*, **17**, 719 (1961).

concerned with the C–C bond of the molecule. The present results, if combined with those of *N*-methylformamide, give the reliable set of force constants necessary to describe the peptide skeletals: $\overset{C}{\underset{O}{\rangle}}C-N\langle^{H}_{C'}$. The force constants in group C are concerned with the CH_3 group, and it is shown that the values of the force constants recommended in our laboratory can also be used in this molecule.

The present author wishes to express his deep gratitude to Professor Takehiko Shimanouchi for his kind guidance and encouragement in the present work. His thanks are also due to Professor Hidetoshi Takahashi for the use of a PC-1 computer.

Department of Chemistry
Faculty of Science
The University of Tokyo
Hongo, Tokyo

Infrared Spectra and Normal Vibrations of Thioamides. I. Thioformamide

By Isao SUZUKI

(Received February 2, 1962)

As has been reported in previous papers[1-3], the values of the Urey-Bradley type force constants for the simple primary and secondary amides, $HCONH_2$, CH_3CONH_2 and $HCONH \cdot CH_3$ were determined from their vibrational frequencies, and it was shown that these constants are transferable throughout the series of the molecules and that they give a good account of the nature of the normal vibrations of these molecules. About the vibrational spectra of the thioamides, on the other hand, few systematic investigations have yet been reported, and there are ambiguities in the assignments of many observed bands. As has been shown in the previous papers[1-3], all the values of the force constants necessary to calculate the normal vibrations of simple thioamides are now known except those concerning the sulfur atom. Therefore, the work has been extended to the thioamide group for the purpose of clarifying the nature of the normal vibrations of these molecules as well as to make a further check on the transferability of force constants of the Urey-Bradley type. The nature of the C=S and C–N bonds in thioamides is also discussed in connection with the force constants obtained. In the present paper, the results of infrared measurements and normal vibration calculations of thioformamide $HCSNH_2$, the first member of the series, are reported. The results for CH_3CSNH_2, $HCSNHCH_3$ and $CH_3CSNHCH_3$ will be given in subsequent papers.

1) I. Suzuki, This Bulletin, 33, 1359 (1960).
2) I. Suzuki, ibid., 35, 540 (1962).
3) I. Suzuki, ibid., 35, 1279 (1962).

Thioformamide and *N*-deuterated thioformamide were prepared, and their infrared spectra were measured in both liquid and solid states. The spectrum of $HCSNH_2$ in the liquid state corresponds well with that given earlier by Davies and Jones[4], except the band found at 439 cm^{-1} with medium intensity which was not reported. The assignments of the observed bands, however, differ considerably from theirs. The normal vibrations for thioformamide were first calculated with the force constants which were directly transferred from formamide[1] and thiourea[5]. Since the computed frequencies show a good agreement with the observed, the assignments of the infrared absorption bands can be made without difficulty. Then the values of the force constants were refined to obtain a better frequency fit. Based on the results of this calculation, the nature of the observed bands is explained in terms of the potential energy distributions and the vibrational amplitudes.

Experimental

Samples. — Thioformamide was prepared from formamide and P_2S_5 suspended in tetrahydrofuran[6] and was purified by the method shown in Ref. 7.

Exchange reaction with D_2O was employed to displace the amide hydrogen atoms by deuterium. Since thioformamide slowly decomposes at room temperature, the sample was mixed with a large

4) M. Davies and W. J. Jones, *J. Chem. Soc.*, 1958, 955.
5) A. Yamaguchi, R. B. Penland, S. Mizushima, T. J. Lane, C. Curran and J. V. Quagliano, *J. Am. Chem. Soc.*, 80, 527 (1958).
6) S. Gabriel, *Ber. deut. chem. Ges.*, 49, 1110 (1916).
7) R. Willstäter and T. Werth, ibid., 42, 1908 (1909).

excess of D_2O and shaken vigourously for a minute, and then the excess D_2O was quickly pumped out with a method analogous to freeze drying and measured immediately. Although thioformamide was reported to form monohydrate[7], no deuterium oxide seems to remain with the sample by this procedure; we did not detect the 1200 cm^{-1} band which is characteristic of D_2O.

Infrared Spectra.—The infrared spectra of these compounds were measured with a Hitachi EPI spectrophotometer equipped with sodium chloride optics, in the region from 4000 to 650 cm^{-1}, and with a Nippon Bunko grating spectrophotometer equipped with a cesium bromide foreprism in the region from 800 to 300 cm^{-1}. The solid state spectra were obtained with a low temperature cell[8] cooled with mixture of dry ice and methanol.

Infrared Spectra

The infrared spectra of $HCSNH_2$ in the liquid and solid states are shown in Figs. 1 (a)—(c), and those of $HCSND_2$, in Figs. 2 (a)—(c). As may be seen from Fig. 2, the spectra of the deuterated species are a little complicated by the presence of the bands arising from monodeuterated thioamides (HCSNHD,

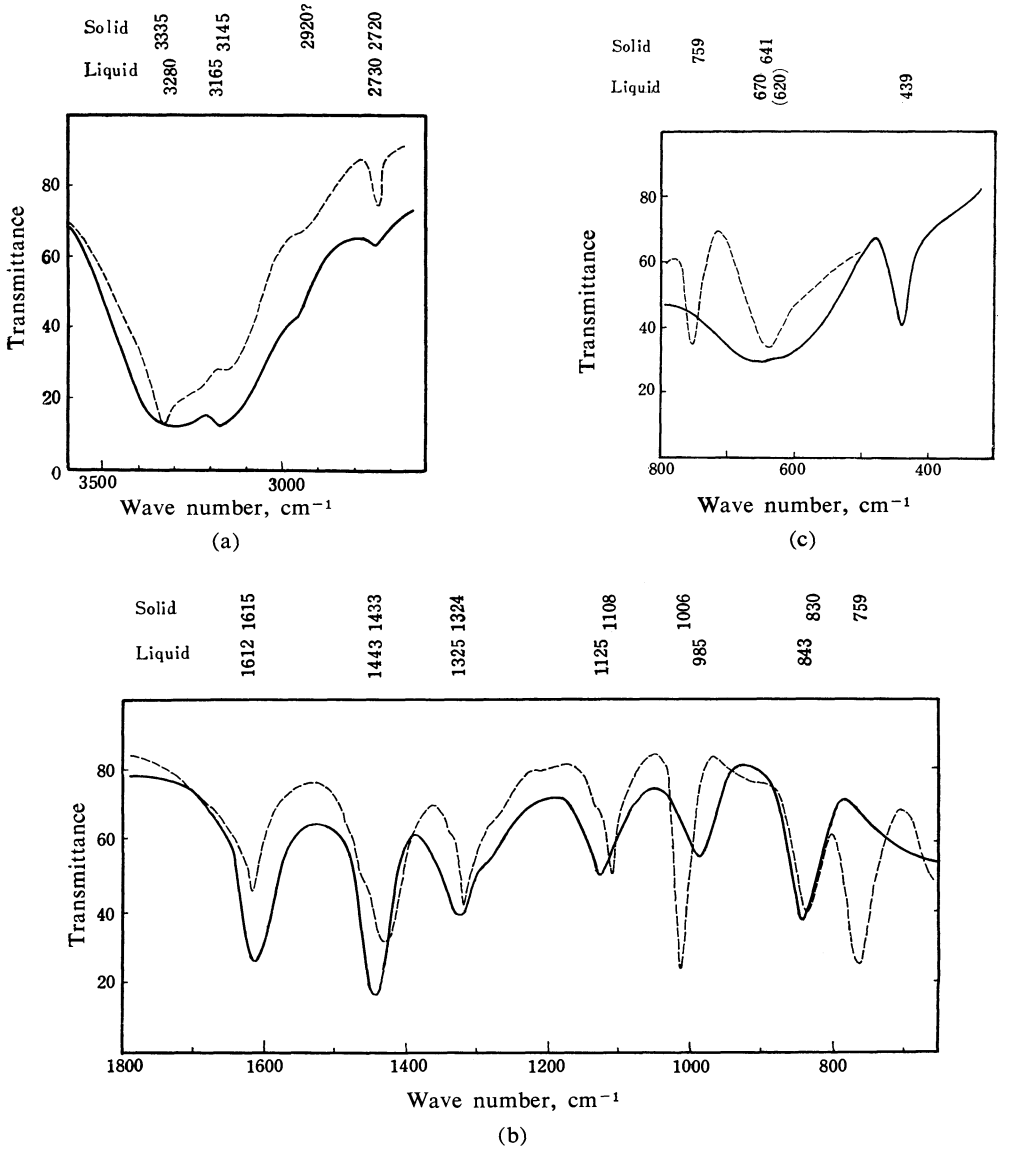


Fig. 1. Infrared spectra of $HCSNH_2$ in the liquid (solid line) and solid states (broken line). (a) 3600~2600 cm^{-1}, (b) 1800~650 cm^{-1}, (c) 800~300 cm^{-1}

8) T. Miyazawa, *J. Chem. Soc. Japan, Pure Chem. Sec.* (*Nippon Kagaku Zassi*), **76**, 821 (1955).

cis and trans) as well as of those from dideuterated species. When the sample was exposed to the atmosphere for a while, the former bands became strong in intensity as a result of the partial hydrogenation caused by the atmospheric vapor, while the latter became weak. In this way, the bands due to the NHD species could be identified. In Fig. 2, the bands whose wave numbers are given in parentheses are those arising from the NHD species.

Spectral changes due to the state of aggregation are sometimes very helpful in assigning the observed bands. In the case of $HCSNH_2$, changes in the spectra by solidification are not so significant as are those of formamide, and little change is observed in a number of vibration bands, including those chiefly associated with the NH_2 stretching, NH_2 bending, CN stretching and CH bending vibrations. However, the 985, 670 and 620 cm^{-1} bands in the liquid state change their positions considerably, and are found respectively at 1002, 759 and 641 cm^{-1} in the solid state. It will be shown in subsequent sections that these bands can reasonably be assigned to three out-of-plane (A'') vibrations: namely, the CH out-of-plane, NH_2 wagging and NH_2 twisting (CN torsional) vibrations; π(CH), $w(NH_2)$ and $t(NH_2)$.

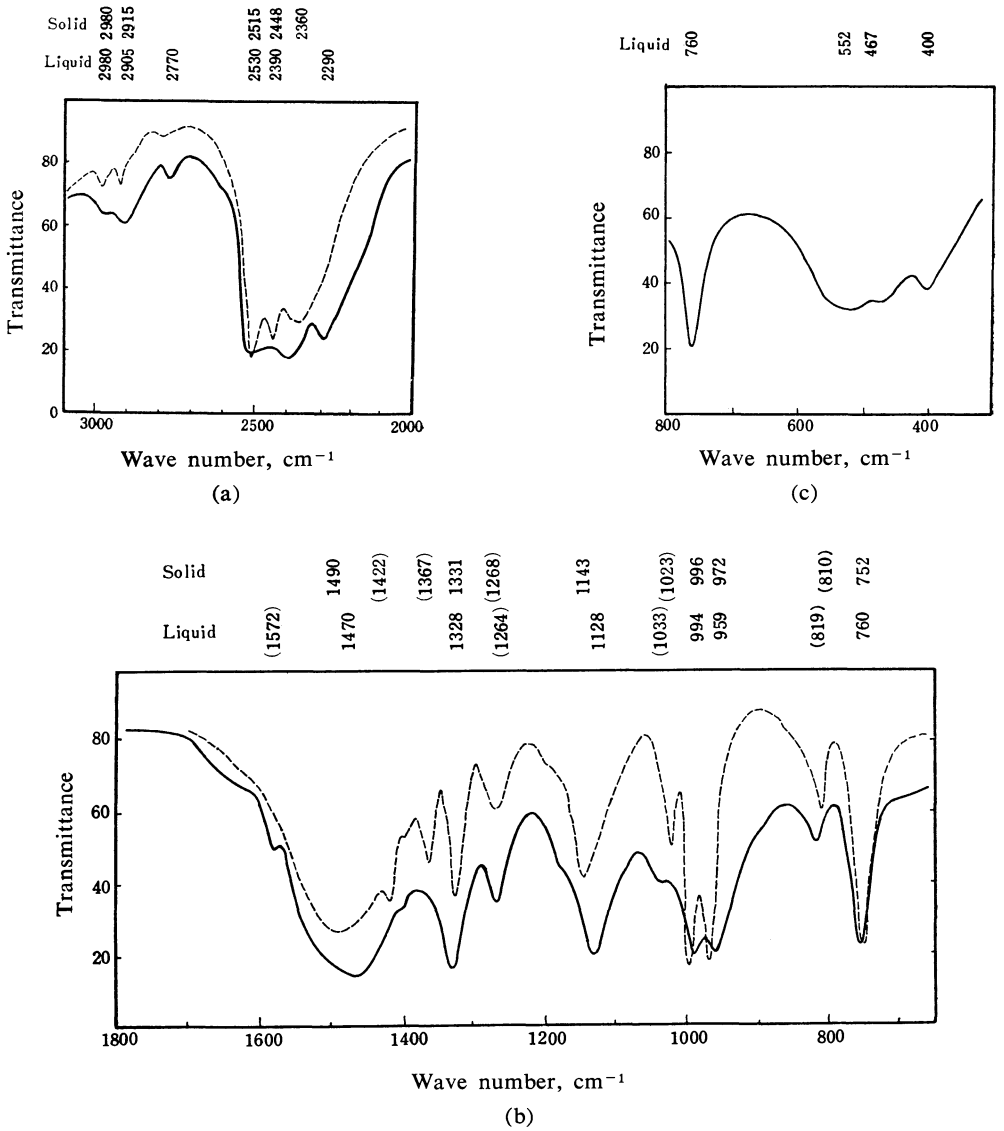


Fig. 2. Infrared spectra of $HCSND_2$ in the liquid (solid line) and solid states (broken line). (a) 3100~2000 cm^{-1}, (b) 1800~650 cm^{-1}, (c) 800~300 cm^{-1}

The difference in the strength of the NH···S hydrogen bonding between the solid and liquid states seems to be small, but the force field perpendicular to the molecular plane may be affected by solidification.

The assignment of the observed bands is chiefly based on the calculation of the normal vibration for $HCSNH_2$ and $HCSND_2$ molecules, so it will be discussed together with the results of that calculation.

Normal Coordinate Treatment

The calculation of the normal vibrations was made according to Wilson's method[9]. It was assumed that the molecule is planar, so the normal vibrations can be classified into 9 inplane (A′) and 3 out-of-plane (A″) vibrations. In the present paper the inplane vibrations are mainly treated*1. The structural parameters used in the present calculations are as follows, the bond lengths of $r(NH)=1.04$Å, $r(CH)=1.07$Å, $r(CN)=1.324$Å and $r(CS)=1.713$Å. All the bond angles are assumed to be 120°*2.

The symmetry coordinates used in the calculation are given in Table I.

Force Constants. — The potential function employed in the calculation is of the Urey-Bradley type[13]:

$$2V=\sum_i K_i(\Delta r_i)^2+\sum_{i\neq j} H_{ij}r_i^0 r_j^0(\Delta\alpha_{ij})^2 + \sum_{i\neq j} F_{ij}(\Delta q_{ij})^2+\text{Linear terms}$$

where r_i and r_j are bond lengths with the equilibrium values r_i^0 and r_j^0; α_{ij}'s are bond angles, and q_{ij}'s, distances between nonbonded atoms. K, H, and F are stretching, bending and repulsive force constants respectively.

As has already been mentioned, the values of these force constants were first transferred from formamide[1] and thiourea[5]*3 they are given in the first column of Table II. The

Table I. Symmetry coordinates

S_i	$S=UR$	Vibrational mode	Abbr.
S_1	$(\Delta r_{NH_a}-\Delta r_{NH_b})/\sqrt{2}$	NH_2 antisym. stretching	$\nu_a(NH_2)$
S_2	$(\Delta r_{NH_a}+\Delta r_{NH_b})/\sqrt{2}$	NH_2 sym. stretching	$\nu_s(NH_2)$
S_3	Δr_{CH}	CH stretching	ν(CH)
S_4	Δr_{CN}	CN stretching	ν(CN)
S_5	Δr_{CS}	CS stretching	ν(CS)
S_6	$(2\Delta\alpha_{HNH}-\Delta\alpha_{CNH_a}-\Delta\alpha_{CNH_b})/\sqrt{6}$	NH_2 bending	$b(NH_2)$
S_7	$(\Delta\alpha_{CNH_a}-\Delta\alpha_{CNH_b})/\sqrt{2}$	NH_2 rocking	$r(NH_2)$
S_8	$(2\Delta\alpha_{NCS}-\Delta\alpha_{HCN}-\Delta\alpha_{HCS})/\sqrt{6}$	NCS bending	b(NCS)
S_9	$(\Delta\alpha_{HCN}-\Delta\alpha_{HCS})/\sqrt{2}$	CH bending	b(CH)
$S_{R'}$	$(\Delta\alpha_{HNH}+\Delta\alpha_{CNH_a}+\Delta\alpha_{CNH_b})/\sqrt{3}$	Redundant	—
$S_{R''}$	$(\Delta\alpha_{NCS}+\Delta\alpha_{HCN}+\Delta\alpha_{HCS})/\sqrt{3}$	Redundant	—

Table II. The values of the force constants (in md./A)

	I	II		I	II		I	II
K_{NH}	5.57[a]	5.52	H_{HNH}	0.40[a]	0.43	$F_{H\cdots H}$	0[a]	0
K_{CH}	3.74[a]	3.88	H_{NHC}	0.32[a]	0.27	$F_{N\cdots C}$	**0.46**[a]	**0.46**
K_{CN}	6.15[a]	6.35	H_{NCH}	0.18[a]	0.17	$F_{N\cdots H}$	0.70[a]	0.74
K_{CS}	3.50[b]	3.95	H_{HCS}	0.18[c]	0.13	$F_{H\cdots S}$	0.70[c]	**0.60**
			H_{NCS}	0.19[b]	0.15	$F_{N\cdots S}$	0.98[b]	**1.02**

I: Initial set of the values
a: transferred from $HCONH_2$
b: transferred from $(NH_2)_2CS$
c: assumed
II: Final set of the values

9) E. B. Wilson, *J. Chem. Phys.*, **7**, 1047 (1939); **9**, 96 (1941).

*1 Since the force field for the out-of-plane vibrations is quite different in nature from that for the in-plane vibrations, it is treated separately and will be reported on elsewhere, together with the results for other amides, such as $HCONH_2$, CH_3CONH_2, CH_3CSNH_2 and $HCSNHCH_3$ (see also Ref. 3).

*2 No structural analysis has yet been reported for $HCSNH_2$, so the values of the C-N and C=S bonds are taken from those of CH_3CSNH_2[10], and the others from $HCONH_2$[11,12].

10) M. R. Truter, *J. Chem. Soc.*, **1960**, 997.

11) C. P. Post and J. Ladell, *Acta Cryst.*, **7**, 559 (1954).

12) R. A. Krombrout and G. B. Moulton, *J. Chem. Phys.*, **25**, 35 (1955).

13) T. Shimanouchi, ibid., **17**, 245, 734, 848 (1949).

*3 The values adopted here are slightly different from those in Ref. 5. The present values are based on an unpublished work by Yamaguchi in which, starting with the values in Ref. 5, she obtained the values of the force constants to give the frequency fit with in 4% for all the bands of thiourea and deuterated thiourea.

TABLE III. THE OBSERVED AND CALCULATED FREQUENCIES, POTENTIAL ENERGY DISTRIBUTIONS; $(F_{ii}L_{is}^2/\lambda_s)\times 100$, AND PERCENT DEVIATIONS; $\Delta=(\nu_{obs}-\nu_{calcd})\times 100/\nu_{obs}$

(a) $HCSNH_2$

	Frequency					P. E. D.								
	ν_{obs}	ν^{I}_{calcd}	Δ^{I}	ν^{II}_{calcd}	Δ^{II}	S_1	S_2	S_3	S_4	S_5	S_6	S_7	S_8	S_9
ν_1	3287	3300	−0.2	3287	0.0	**101**	0*	0	0	0	0	0	0	0*
ν_2	3165	3204	−1.3	3191	−0.8	0*	**99**	0*	0*	0*	0*	0*	0*	0*
ν_3	(2905)	2872		2908		0	0	**102**	0*	0*	0	0	0	0
ν_4	1612	1620	−0.5	1623	−0.8	0*	1	0*	**20**	1*	**88**	0	0*	1*
ν_5	1443	1498	−4.0	1450	−0.5	0*	0	0*	44	11	8	2*	0*	**57**
ν_6	1325	1315	0.7	1308	0.5	0	0*	0*	**39**	0*	5*	4*	2*	**40**
ν_7	1125	1189	−5.6	1130	−0.5	0	0	0	0*	13*	0	**74**	8	6
ν_8	843	829	1.6	850	0.8	0	0*	1*	2	**81**	0*	17	5*	0
ν_9	439	451	−2.7	441	−0.5	0*	0	0	0	1	0*	4*	**90**	0

(b) $HCSND_2$

	ν_{obs}	ν^{I}_{calcd}	Δ^{I}	ν^{II}_{calcd}	Δ^{II}	S_1	S_2	S_3	S_4	S_5	S_6	S_7	S_8	S_9
ν_1		2446		2434		**101**	0*	0	0	0*	0	1	0	0*
ν_2	2290	2317	−1.2	2307	−0.8	0	**98**	0	2*	0	1*	0	0	0*
ν_3	2905	2873	1.1	2908	−0.1	0*	0*	**102**	0*	0*	0	0	0	0
ν_4	1470	1507	−2.6	1477	−0.5	0*	1	0*	**74**	10*	8	0	0*	35*
ν_5	1328	1372	−3.4	1345	−1.3	0	1	0*	**16**	0	13	1*	1*	64
ν_6	1128	1110	1.6	1111	1.5	0*	1	0	9*	8	**74**	0*	0	3*
ν_7	994	1025	−3.1	1001	−0.7	0*	0*	0*	3	43	3*	**39***	19*	1*
ν_8	760	750	1.3	750	1.3	0	0	0*	2	**46**	1*	**48**	0	1
ν_9	400	414	−3.5	399	0.5	0*	0	1	0	0	0*	11*	**85**	0

* The asterisk means that the corresponding L-matrix element is negative.

frequencies calculated from these values are given in the second column of Table III. As the force constants, H_{HCS} and $F_{H\cdots S}$, for which few data were available, the values of 0.18 and 0.70 md./A respectively were assumed. Then the values of the force constants were refined to obtain a better frequency agreement. The final set of their values are given in the second column of Table II.

Results of Calculations.—With the values of the force constants given in the second column of Table II (Set II), the normal vibrations have been calculated. In Tables III (a) and (b), the observed and calculated frequencies, the percent deviations, and the potential energy distributions (P. E. D.) among the symmetry coordinates for each normal mode, as well as the signs of the corresponding L-matrix elements, are given. In Tables III (a) and (b), the calculated frequencies based on Set I of the force constants are also given for comparison.

In order to visualize the features of the normal mode, it is preferable to compute the elements of the L^x matrix, which is defined, in matrix expression, as:

$$X=L^xQ$$

where X is the column vector of the Cartesian coordinates of the atoms involved and Q is the normal coordinate vector. From the calculated values of the corresponding elements

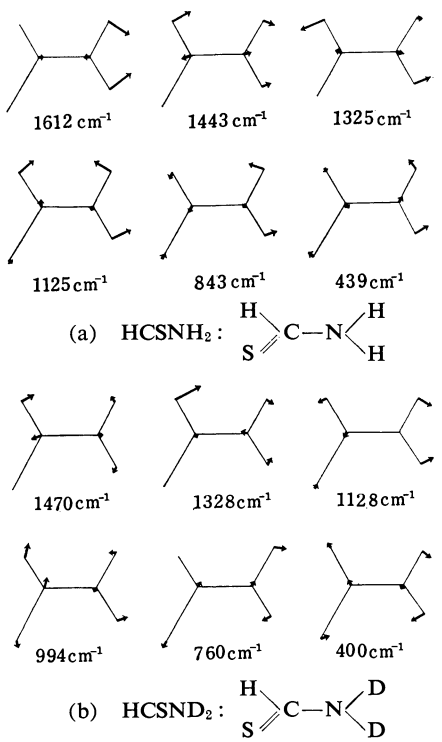


Fig. 3. The in-plane normal modes of thioformamides in Cartesian displacement vectors (A/unit change in normal coordinate).

of the L^x matrices, the vibrational feature of each normal mode is schematically shown in Figs. 3 (a) and (b) for both $HCSNH_2$ and $HCSND_2$. The features corresponding to the three higher frequencies are hydrogen (or deuterium) stretching vibrations and are obvious, so they are omitted from the figures.

The numerical computations were carried out with a PC-1 computer; the routines and the methods employed in the calculations have been described in detail in Refs. 14 and 15 and so are not discussed here.

Discussion

Force Constants.—As has been shown in the previous paper[1], the nature of the normal vibrations of the formamide molecule has been well elucidated from the simple Urey-Bradley force field without the terms $C_{ij}(\Delta q_{ij})^2$, which were used to refer to the repulsion between two nonbonded atoms situated at the cis position[16]. It has also been shown that the force constants obtained for $HCONH_2$ can be used without significant alteration in their values for $HCONHCH_3$ and CH_3CONH_2 molecules[2,3]. These facts suggest that the force field of this type can safely be applied in the study of thioamide groups, and that the force constants concerning the HC-NH_2 part of the molecule, at least as a starting set of values, may be assumed to be the same as those of formamide. A few additional data concerning the force constants involving the sulfur atom are transferred from thiourea.

The values of the force constants, Set I, of Table II, were determined in this way. As can be seen from Table II, the agreements between the observed and calculated frequencies, ν^{I}_{calcd}, are far better than one might expect, the maximum deviation being 5.5% and the average, 2.2%. This shows that the assumption that was made was not far from the truth. The agreements are good enough to make the assignment of each observed band without ambiguities, except in the case of $HCSND_2$, which will be discussed later.

Once the assignment is settled, it is not difficult to refine the values of the force constants due to the indication given by the elements of the Jacobian matrix $(\delta\lambda_i/\delta K_j)$[17,18]. Such refinements were repeated, and the force constants given in the second column of Table II (Set II) were obtained. They give most of the calculated frequencies within 1% of the observed values; the maximum deviation is only 1.5%.

The values of some force constants are worth mentioning. The present calculation gives the value of K_{CN} to be 6.35 md./A, which is only 0.20 larger than that of $HCONH_2$. The value of K_{CN} is correlated closely with some repulsion force constants, such as $F_{H\cdots H}$, $F_{H\cdots C}$ and $F_{N\cdots S}$ ($F_{N\cdots O}$), and it is somewhat indefinite. However, it is sure that there is little difference between formamide and thioformamide in the nature of the C-N bond, and it has a considerable double bond character. Therefore, the value of K_{CS} obtained (3.95 md./A) should be considered to be much lower than that corresponding to the pure C=S bond*4.

It is of interest to compare the values of $F_{H\cdots S}$ and $F_{N\cdots S}$ with those of $F_{H\cdots O}$ and $F_{N\cdots O}$ in $HCONH_2$. Although the sulfur atom has a larger van der Waals radius and is bulkier than the oxygen atom, the former values are about two-thirds of the latter. This is probably due to the much longer N···S or S···H distances. In this case, the distance between two non-bonded atoms becomes a dominant factor in determining the magnitudes of the repulsion constants.

Assignments of the Observed Bands.—For each in-plane normal vibration, the potential energy distributions among symmetry coordinates and Cartesian displacement vectors have been calculated; they are given, respectively, in Table III and Fig. 3. Based on these values, the qualitative assignments of the observed bands will be described.

The Bands above 2000 cm^{-1}.—The bands at 3280 and 3165 cm^{-1} of $HCSNH_2$ undoubtedly correspond to the $\nu_a(NH_2)$ and $\nu_s(NH_2)$ vibrations respectively. The band associated with the ν(CH) motion is found around 2900 cm^{-1}, but it is too weak for its precise position to be determined. The spectrum of $HCSND_2$ is rather complicated. The bands at 2530 and 2290 cm^{-1} might be associated with the $\nu_a(ND_2)$ and $\nu_s(ND_2)$, vibrations respectively, while the 2448 cm^{-1} is associated with the ν(ND) of the HCSNHD molecule. However, if these assignments were correct, the separation of the $\nu_a(ND_2)$ and $\nu_s(ND_2)$ frequencies is much larger than that of the $\nu_a(NH_2)$ and $\nu_s(NH_2)$

14) T. Shimanouchi and I. Suzuki, *J. Mol. Spectroscopy*, **6**, 277 (1961).
15) T. Shimanouchi and I. Suzuki, ibid., **8**, 222 (1962).
16) D. E. Mann, T. Shimanouchi, J. H. Meal and L. Fano, *J. Chem. Phys.*, **27**, 43 (1957).
17) W. T. King, I. M. Mills and B. C. Crawford, ibid., **27**, 455 (1957).
18) T. Miyazawa, *J. Chem. Soc. Japan, Pure Chem. Sec. (Nippon Kagaku Zassi)*, **76**, 1132 (1955).

*4 Truter suggests, from her recent X-ray investigation of thioacetamide, that the obtained values of 1.32 Å for the C-N bond length and 1.713 Å for the C-S bond length probably represent the lengths of the pure single C-N and double C-S bonds respectively[10]. However, the value of K_{CN} corresponding to the pure C-N bond is around 3.15~3.20 md./A[3,19]. The high values found in various amides and thioamides exclusively indicate the partial double bond character of the C-N bond.
19) A. Yamaguchi, ibid., **80**, 1105 (1959).

frequencies. This is highly improbable. In addition, the central peak is too strong in intensity and behaves somewhat differently from other peaks arising from the NHD species when the sample is exposed to atmospheric air. In the spectrum of $HCSNH_2$, a weak but well-defined band is found at 2454 cm^{-1}; this is probably due to the combination tone of the 1325 and 1125 cm^{-1} frequencies. In the N-dideuterated species, two bands are found at 1328 and 1128 cm^{-1}. Fermi resonance probably occurs between the $\nu_a(ND_2)$ vibration and the combination tone of the above two frequencies. This, as well as the coexistence of the ν(ND) band of HCSNHD, is the cause of the complexity of the spectrum. The unperturbed $\nu_a(ND_2)$ frequency is estimated as about 2450~2460 cm^{-1}.

The Band at 1612 cm^{-1}. — The band at 1612 cm^{-1} of $HCSNH_2$ can be assigned to an almost pure $b(NH_2)$ vibration; this is in agreement with the assignment by Davies and Jones[4]. In addition, there is small contribution of the ν(CN) mode. As seen in Fig. 3 (a), the C–N bond stretches when the HNH angle increases in this mode. In the deuterated species, the band corresponding to an almost pure $b(ND_2)$ vibration occurs at 1128 cm^{-1}. Contributions of the other vibrational modes to this band are found to be very small.

The Bands at 1443 and 1325 cm^{-1}.—Davies and Jones assigned the 1443 cm^{-1} band of $HCSNH_2$ to the ν(CN) vibration, and the 1325 cm^{-1} band to the δ(CH) vibration. The present calculations establish that these two vibrational modes couple with each other almost completely, and that each of the bands can not be assigned to a particular vibrational mode. The δ(CH) and ν(CN) vibrations also couple with each other in $HCONH_2$[1], but they are not so strong as in the case of $HCSNH_2$. The force constants H_{HCS} and $F_{H...S}$ are smaller in value than H_{HCO} and $F_{H...O}$ and lower the intrinsic frequency of the δ(CH) vibration, while that of the ν(CN) vibration increases as a result of the absence of the ν(CO) mode. This may be the cause of such a strong coupling. On deuteration, the band at 1443 cm^{-1} shifts towards higher frequencies by 27 cm^{-1}, while the 1325 cm^{-1} band scarcely moves.

The Bands at 1125 and 843 cm^{-1}.—The band at 1125 cm^{-1} $HCSNH_2$ is chiefly associated with the $r(NH_2)$ vibration, although there is a small contribution from the ν(CS) vibration. It is of general interest in the infrared investigation of thioamides to determine in what region the frequency characteristic of the ν(CS) mode appears. Various authors indicate various ranges for the ν(CS) vibration*5; e. g., 1500~1470 cm^{-1}, around 1300 cm^{-1}, around 1100 cm^{-1}, etc. In thiolactams, Mecke and Mecke assigned the bands around 1100 cm^{-1} to this mode[21]. In the case of $HCSNH_2$, Davies and Jones indicated that the interaction probably occurs between the ν(CS) and ν(CN) modes and gives rise to the two frequencies at 1443 and 1288 cm^{-1}. However, as may be seen from Fig. 1 (b), the 1288 cm^{-1} band is a weak shoulder of the strong 1325 cm^{-1} band, and, it can hardly be assigned to one of the fundamental frequencies. The present calculations show that the 843 cm^{-1} band of $HCSNH_2$ corresponds to an almost pure ν(CS) mode, while there is a small contribution from the $r(NH_2)$ vibration to this band. It is true that there are some difficulties in specifying tne characteristic C=S frequency as suggested by Davies and Jones. As will be shown in the subsequent papers, the ν(CS) vibration interacts with several vibrational modes in CH_3CSNH_2, $HCSNHCH_3$ and $CH_3CSNHCH_3$, and it is rather hard to tell which band is to be called the C=S stretching band. However, in the case of $HCSNH_2$, the band at 843 cm^{-1} corresponds to an almost pure ν(CS) vibration.

In *N*-dideuterated species, the vibrational interaction occurs between the $r(ND_2)$ and the ν(CS) modes; this gives rise to two observed frequencies at 994 and 760 cm^{-1}. Energetically, both the ν(CS) and $r(ND_2)$ vibrations contribute to these modes in approximately the same degree. The above facts suggest that the intrinsic frequency of the ν(CS) vibration lies in the region from 900 to 850 cm^{-1}.

Close to the 994 cm^{-1} band, another strong band is found in $HCSND_2$ at 959 cm^{-1}. This band is assigned to the π(CH) vibration. It may be possible to reverse the assignment for these two bands. However, the present assignment is supported by the following evidence: (1) A band is found at 985 cm^{-1} in $HCSNH_2$ which is assigned to the π(CH) mode without doubt. If we adopt the reverse assignment, the π(CH) band would seem to shift towards a higher frequency on *N*-deuteration. This is quite improbable. (2) The 985 cm^{-1} band of $HCSNH_2$ shifts to a higher frequency by 21 cm^{-1} on solidification. The 959 cm^{-1} band of $HCSND_2$ also moves to a higher frequency by 13 cm^{-1}, while the 994 cm^{-1} band shifts very little*6. (3) The computed frequency always favors the present assignment.

*5 As a summary of the ν(CS) frequency, see Ref. 20, p. 350.

20) L. J. Bellamy, "The Infrared Spectra of Complex Molecules", Methuen & Co., Ltd., London (1958), p. 350.

21) R. Mecke and R. Mecke Jr., *Ber. deut. chem. Ges.*, **89**, 343 (1959).

*6 In $HCONH_2$[8], and in $HCONHCH_3$[3], the bands associated with the π(CH) mode shift towards higher frequencies on solidification.

The Band at 439 cm^{-1}.—Present calculation shows this band arises from the δ(NCS) vibration and corresponds well with the 412 cm^{-1} band of thiourea[5]. On *N*-deuteration, the $r(ND_2)$ vibration interacts with the $\delta(NCS_2)$ mode and lowers the band by 39 cm^{-1}. This is in good agreement with the calculated shift.

The Out-of-plane (A'') Vibrations.—Once the assignments for the in-plane normal vibrations are settled, it is not difficult to pick up the bands associated with the out-of-plane vibrations. In $HCSNH_2$, they are found at 985, ca. 670 and ca. 620 cm^{-1}. The absorption around 650 cm^{-1} in the liquid spectrum is very broad, and it is difficult to judge whether it is due to a single, very broad band or to two broad bands overlapping each other. The inspection of the spectrum taken in the solid phase shows that the latter is the case. It gives two distinct bands at 641 and 759 cm^{-1}. The 985 cm^{-1} band is assigned to the π(CH) vibration without ambiguity, while the bands at 670 (759) and 620 (641) cm^{-1} are assigned to the $w(NH_2)$ and $t(NH_2)$ vibrations respectively. The $t(NH_2)$ vibration is closely associated with the nature of the C–N bond, since it should accompany the torsional movement around the C–N bond. The bands at 1443 and 1325 cm^{-1}, which are associated with the ν(CN) vibration, are insensitive to solidification; therefore, the band less sensitive to solidification is chosen as due to the $t(NH_2)$ vibration. In $HCSND_2$, the band found at 959 cm^{-1} is assigned to the π(CH) vibration, as has been described above. The bands corresponding to the $w(ND_2)$ and $t(ND_2)$ vibrations are found at 552 cm^{-1} and 467 cm^{-1} respectively.

Thus complete assignments for the observed bands of both the $HCSNH_2$ and $HCSND_2$ molecules have been made. The present assignment for the $HCSNH_2$ molecule considerably differs from that made by Davies and Jones. However, this assignment is supported firmly by the calculations of the normal vibrations and by the change in the spectrum due either to *N*-deuteration or to solidification.

The author wishes to express his deep gratitude to Professor Takehiko Shimanouchi for his guidance and encouragement throughout this work, and to Professor Hidetoshi Takahashi for the use of a PC-1 computer. His thanks are also due to Dr. Akiko Hirakawa, who made her unpublished data on thiourea available to him.

Department of Chemistry
Faculty of Science
University of Tokyo
Hongo, Tokyo

Temperature Dependences of the Nuclear Quadrupole Resonance Frequencies in 1,4-Dihalogenocyclohexanes

By Tadashi TOKUHIRO

(Received January 24, 1962)

By our studies of the halogen nuclear quadrupole resonance in *cis*-1, 4-dibromo- and diiodo-cyclohexanes, it has been found that the chemical inequivalence of the two halogen nuclei, which are, respectively, in the 1e and 4a positions[1] of the cyclohexane ring, leads to doublet lines. As for *trans*-1, 4-dibromo- and diiodo-cyclohexanes, it is no surprise that only one line was observed in the iodo-derivative and that two lines, separated by only 0.11 Mc./sec., were observed in the bromo-derivative, since both the halogen atoms in these compounds occupy the e-positions of the ring in the solid. From only a comparison of the frequencies of the doublet lines in the cis-compound with those in the trans-compound, the assignment of the doublet lines could not be made, however, be cause two frequencies of the doublet lines are not close to those in the trans-compound. However, as it has been found that the doublet separation varies considerably with the rising temperature, it seemed probable that this phenomenon is due to the different contribution from molecular torsional motions to the temperature dependence of the resonance frequency of each line and that a consideration of this would shed light on the assignments. In an attempt to clarify this

1) D. H. R. Barton, O. Hassel, K. S. Pitzer and V. Prelog, *Nature*, **172**, 1096 (1953); *Science*, **119**, 49 (1953).

point, the following studies have been carried out.

Experimental

Preparations of 1,4-Dibromocyclohexanes. — A mixture of quinit and a hydrobromic-sulfuric acid solution was allowed to stand overnight[2] and was then heated for 3 hr. on a steam bath. By standing at room temperature, an oily layer was separated from the solution. The product was washed with water and dried over calcium chloride. A fractional distillation of the product under reduced pressure gave two parts of the distillates, namely, *trans*-1,4-dibromocyclohexane, and a mixture of *trans*- and *cis*-1,4-dibromocyclohexanes. The trans-isomer was recrystallized from ethyl alcohol. By fractional crystallizations, in which ethyl alcohol and petroleum ether were alternately used as solvents, the cis-isomer was isolated from the mixture. The trans-isomer had a m. p. of 112°C, the cis-isomer, a m. p. of 49°C. These values agreed with those reported previously[3]. The purity for both isomers was ascertained by infrared spectra.

Preparations of 1,4-Diiodocyclohexanes. — By using a method similar to that of Kwestroo et al.[4], *trans*- and *cis*-1,4-diiodocyclohexanes were prepared from quinit and a 52% hydroiodic acid solution. The melting point values for the isomers (trans-, 142°C; cis-, 67°C) agreed with those reported by Kwestroo. By infrared evidence it was shown that no impurity was contained in either of the isomers.

Apparatus.—The spectrometer used in this work was a frequency-modulated (50 c./sec.) super-regenerative oscillator with 955 acon tubes[5]. A push-pull oscillator with a transmission line-tuned circuit was quenched by an oscillator of a few kilocycles. By displacing the movable reflecting disk and the 955 acon tubes at points $\lambda/2$ and $\lambda/4$ of the transmission line in the plate circuit respectively, the oscillator has a workable range of from 160 to 360 Mc./sec. In this frequency range, the quenching frequencies were from 100 to 300 Kc./sec. In order to obtain the maximum sensitivity of the detector, the quenching frequency, the quenching voltage, and shorted point of the transmission line in the cathode circuit were suitably chosen. The signal was picked up through the anode resistance, amplified by four stage audio-amplifiers (12AX7×2), and displayed on a cathode-ray oscilloscope screen. For the line-width measurement, the derivative of the signal was recorded by the help of a narrow-band lock-in system, followed by a chart-recorder. The resonance frequencies were measured with a heterodyne frequency-meter calibrated within the order of 10^{-5}.

The sample tube was directly immersed in liquid nitrogen and in petroleum ether cooled with dry ice for the measurements at −196 and −76°C respectively. For measurements at temperatures between −76 and 0°C, temperature regulation was achieved by using a gear pump and a wide-mouthed, 1.5 liter Dewar vessel with a cover of styrofoam as a thermal insulator. The vessel was filled with a high-boiling petroleum ether, in which the sample tube was immersed. The intermediate temperatures of petroleum ether in the vessel were reached by passing ethyl alcohol cooled with dry ice through a helicoid-type tube which was immersed in the petroleum ether of the vessel. The sample coil and the transmission line were connected through condensers to prevent heat conduction. The temperature was measured by means of a copper-constantan thermocouple placed at the surface of the sample tube. In order to avoid the temperature inhomogeneity of the sample, the measurements of the resonance frequencies were carried out after the sample tube had been placed in petroleum ether for one hour. By using the above procedure for temperature regulation, petroleum ether gave a temperature stability of about ±0.1°C.

Results and Discussion

The temperature dependences of the ^{79}Br and ^{127}I nuclear quadrupole resonance frequencies measured in 1,4-dibromo- and diiodo-cyclohexanes are shown in Fig. 1.

At the temperature of liquid nitrogen the resonance lines of the cis-dibromo- and diiodo-derivatives showed a similar pattern of strong doublet lines, except that the latter gave rather a larger doublet separation than the former. The doublets are undoubtedly due to the fact that the two halogen atoms in

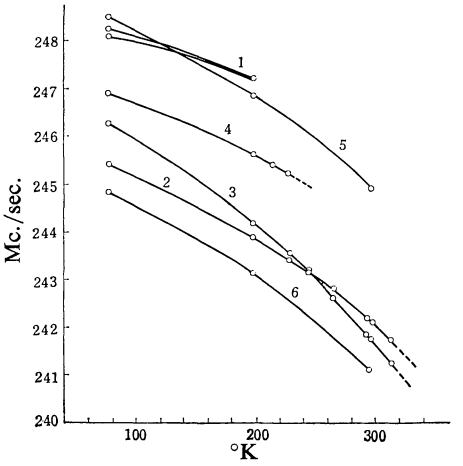


Fig. 1. Temperature dependences of ^{79}Br and ^{127}I nuclear quadrupole resonance frequencies measured in 1,4-dihalogenocyclohexanes.
1 *trans*-1,4-Dibromocyclohexane
2 (ν_1) and 3 (ν_2), *cis*-1,4-Dibromocyclohexane
4 *trans*-1,4-Diiodocyclohexane
5 (ν_1) and 6 (ν_2), *cis*-1,4-Diiodocyclohexane

2) "Organic Syntheses", Coll. Vol. 1, p. 25 (1948).
3) M. B. Rothstein, *Ann. Chim.*, **14**, 461 (1930).
4) W. Kwestroo, F. A. Meijer and E. Havinga, *Rec. trav. chim. Pay-Bas*, **73**, 717 (1954).
5) S. Kojima, K. Tsukada, A. Shimauchi and Y. Hinaga, *J. Phys. Soc. Japan*, **9**, 795 (1954).

these molecules are in two chemically inequivalent positions, namely the 1e and 4a positions, although the crystal structures of these compounds are not known.

According to the results of X-ray analysis[6], both crystals of the trans-isomers of dibromo- and diiodo-derivatives contain two equivalent molecules in a unit cell. Therefore, it would be very natural for the resonance to give a singlet line since the two halogen atoms in the isomer are in chemically equivalent positions (1e and 4e) in the free molecule. In the case of the iodo-derivative, this is actually the case. However, the pattern of the trans-dibromo-derivative gave doublet lines near one another. The doublet separation in frequency, about 110 Kc./sec. at 77°K, may reflect the effect of the intermolecular forces which render the two bromine positions in the unit cell somewhat inequivalent.

In the case of cis-compounds, the bromine and the iodine resonance lines were observable in the solid up to their melting points. However, the bromine and the iodine resonance lines in the solid trans-compounds faded out at temperatures considerably below their melting points. In the trans-dibromo-compound, the line at −77°C was so broad that the signal could hardly be detected, and the iodine resonance of the diiodo-derivative was found to fade out at about −43°C, although it does not melt until 142°C.

As shown in Fig. 1, it is easily seen that the resonance frequencies of the trans- and the cis-isomers of 1, 4-dihalogenocyclohexanes continuously decrease with the rising temperature, but the temperature dependences of the frequencies differ slightly. From this fact, it follows that no phase transitions in these solids occur within the temperature range described above and that the temperature dependence of the frequency may be ascribed to molecular torsional motions in the solids.

The theory and the extensive experimental results of the effect of temperature and pressure on nuclear quadrupole resonance frequencies have been discussed in detail by Kushida, Benedek and Bloembergen[7]. In molecular crystals, they found that the temperature dependence of the resonance frequency was due primarily to the explicit temperature dependence of the amplitudes of lattice vibrations, namely Bayer's effect[8], because of a much smaller contribution of the volume dependence of the resonance frequency. In the present article also we shall confine our attention only to Bayer's effect.

It is assumed that the direction of the maximum principal axis of the field gradient tensor at the halogen nucleus coincides with the direction of the C–X bond (X denotes halogen), and that the gradient has axial symmetry about the C–X bond (asymmetry parameter $\eta=0$). When a molecule containing the C–X bond executes torsional motions about an axis perpendicular to the C–X bond, the inclination, θ, of the C–X bond relative to its equilibrium direction in the solid gives rise to the shift of the resonance frequency $\nu(T)$ given by Eq. 1:

$$\nu(T)=\nu_0(1-3\theta^2/2) \tag{1}$$

where ν_0 is the resonance frequency when $\theta=0$. Since the frequencies of molecular vibrations and of lattice vibrations are much higher than the nuclear quadrupole resonance frequencies, the square of angular displacement, θ^2, must be averaged over all vibrational states. Therefore, we should replace θ^2 of Eq. 1 by the mean square of the angular displacement $\langle\theta^2\rangle$ of the C–X axis relative to its equilibrium direction.

When a torsional vibration can be approximated by a harmonic oscillator, $\langle\theta^2\rangle$ is expressed as follows:

$$\langle\theta^2\rangle=\frac{\boldsymbol{h}}{4\pi^2 I_t\nu_t}\left[\frac{1}{2}+\frac{1}{\exp(\boldsymbol{h}\nu_t/\boldsymbol{k}T)-1}\right] \tag{2}$$

where ν_t is the torsional frequency, I_t the corresponding moment of inertia, T the absolute temperature, $\boldsymbol{h}$ Planck's constant, and $\boldsymbol{k}$ Boltzmann's constant. From Eqs. 1 and 2 the temperature coefficient of the resonance frequency can be expressed as follows:

$$\frac{\Delta\nu}{\Delta T}=-\frac{3\boldsymbol{h}^2\nu_0}{8\pi^2\boldsymbol{k}T^2}\frac{1}{I_t}\frac{\exp(\boldsymbol{h}\nu_t/\boldsymbol{k}T)}{[\exp(\boldsymbol{h}\nu_t/\boldsymbol{k}T)-1]^2} \tag{3}$$

From Eq. 3 it can be seen that the contribution to the temperature coefficient of the resonance frequency from any other normal (intramolecular) vibrations is negligible, as compared with that of the torsional vibrations around the principal molecular axes, because the torsional frequencies, in general, are considerably lower than the frequencies of molecular vibrations.

When the torsional vibration does not take place about an axis perpendicular to the C–X bond, Eq. 3 should be modified. For this purpose a parameter, α, given by the following relation is introduced:

$$\theta=\alpha\phi$$

where θ and ϕ are the angular displacements of the C–X bond from its equilibrium direction caused by the torsional motions about an axis

6) E. Halmony and O. Hassel, *Z. physik. Chem.*, **B16**, 234 (1930).
7) T. Kushida, G. B. Benedek and N. Bloembergen, *Phys. Rev.*, **104**, 1356 (1956).
8) H. Bayer, *Z. Physik*, **130**, 227 (1951).

TABLE I. THE VALUES OF THE SQUARE OF PARAMETER α_i FOR THE EQUATORIAL AND THE AXIAL HALOGEN ATOMS IN 1,4-DIHALOGENOCYCLOHEXANES

	cis-1,4-Dibromocyclohexane		*cis*-1,4-Diiodocyclohexane		*trans*-1,4-Diiodocyclohexane
Positions	e	a	e	a	e
$\alpha_a^2\times10^2$	7.1	99.5	8.8	99.8	3.1
$\alpha_b^2\times10^2$	92.9	0.5	91.2	0.2	96.9
$\alpha_c^2\times10^2$	100.0	100.0	100.0	100.0	100.0

TABLE II. OBSERVED FREQUENCIES ν_1 AND ν_2 OF ^{79}Br NUCLEAR QUADRUPOLE RESONANCE IN THE *cis*-1,4-DIBROMOCYCLOHEXANE AT 77, 196 AND 295°K, AND VALUES OF TORSIONAL FREQUENCIES $\langle\nu_t\rangle$ AND ν_a CALCULATED FROM Eq. 8

Temp. °K	Resonance frequencies		Case I[1]		Case II[2]			
	ν_1 Mc./sec.	ν_2 Mc./sec.	$\langle\nu_t\rangle$ cm^{-1}	ν_a cm^{-1}	$\langle\nu_t\rangle$ cm^{-1}	g_t $\times10^3$	ν_a cm^{-1}	g_a $\times10^3$
77	245.425±0.020	246.296±0.020	44.7	39.1	35.7		77.9	
196	243.873±0.050	244.128±0.050	34.0	30.6	27.5	1.91	58.6	2.06
295	242.118±0.040	241.729±0.040	29.1	26.5	23.8	1.53	49.2	1.68

1) ν_1 and ν_2 are assigned to the equatorial and the axial bromine nucleus respectively.
2) The assignment of ν_1 and ν_2 is the reverse of case I.

perpendicular to the C–X bond and about an axis of the principal molecular axes respectively. By considering the relation between the geometrical configurations of molecules and the three principal molecular axes, the value of α can be evaluated. The method is similar to that used by Tatsuzaki and Yokozawa[9]; the values of the square of α_i for the equatorial and the axial halogen atom in 1,4-dihalogenocyclohexanes are listed in Table I. Since molecules in the solid undergo torsional motions about the three principal molecular axes, $\langle\theta^2\rangle$ can be written by Eq. 4 as:

$$\langle\theta_i^2\rangle=\alpha_i^2\langle\phi_i^2\rangle, \qquad \langle\theta^2\rangle=\sum_i\langle\theta_i^2\rangle \tag{5}$$

where i denotes one of the principal molecular axes. Upon consideration of the first relation of Eq. 5, the following modification of Eq. 2 is obtained:

$$\langle\theta_i^2\rangle=\frac{\alpha_i^2\hbar}{4\pi^2I_i\nu_i}\left[\frac{1}{2}+\frac{1}{\exp(\hbar\nu_i/kT)-1}\right] \tag{6}$$

where I_i is the moment of inertia around the i axis, and ν_i the corresponding torsional frequency. From the second relation of Eq. 5 and Eq. 6, Eq. 3 should be modified as follows:

$$\frac{\Delta\nu}{\Delta T}=-\frac{3\hbar^2\nu_0}{8\pi^2kT^2}\sum_i\frac{\alpha_i^2}{I_i}\left[\frac{\exp(\hbar\nu_i/kT)}{\{\exp(\hbar\nu_i/kT)-1\}^2}\right] \tag{7}$$

where the summation runs over the three principal axes (the a, b and c axes).

As for *cis*-1,4-dihalogenocyclohexanes, there is a considerable difference between the values of α_a^2 and α_b^2 for the equatorial and the axial halogen atom. Therefore, there may be expected to be some difference between the temperature coefficients of the resonance frequencies of the equatorial and the axial halogen atom. This is actually the case (Fig. 1). The theoretical value of the temperature coefficient cannot be obtained by the use of Eq. 7, since the vibrational spectra of isomers in the solid state over low frequency regions have not yet been measured. So far as the cis-isomer is concerned, it may approximately be assumed that the torsional frequencies ν_b and ν_c are nearly the same because the moments of inertia around the b and the c axis of the molecule are almost identical in magnitude. When ν_b or ν_c, and I_b or I_c, of Eq. 7 are replaced by the average value of $\langle\nu_t\rangle$ and $\langle I_t\rangle$ respectively, Eq. 7 becomes:

$$\frac{\Delta\nu_j}{\Delta T}=-\frac{3\hbar^2\nu_0}{8\pi^2kT^2}\left[\frac{\alpha_b^2+\alpha_c^2}{\langle I_t\rangle}\frac{\exp(\hbar\langle\nu_t\rangle/kT)}{\{\exp(\hbar\langle\nu_t\rangle/kT)-1\}^2}+\frac{\alpha_a^2}{I_a}\frac{\exp(\hbar\nu_a/kT)}{\{\exp(\hbar\nu_a/kT)-1\}^2}\right] \tag{8}$$

where ν_j denotes one of the doublet lines. By using Eq. 8, the calculated moments of inertia, $\langle I_t\rangle$ and I_a, and the experimental values of $\Delta\nu_j/\Delta T$ at various temperatures, the torsional frequencies $\langle\nu_t\rangle$ and ν_a are calculated. The results thus obtained for the bromo-derivative are tabulated in Table II. In a similar way, $\langle\nu_t\rangle$ and ν_a for the iodo-derivative are calculated. The results thus obtained are given in Table III. Two cases are shown in Tables II and III, since a complete blank in our knowledge of the X-ray analysis of the crystal structure and of the Zeeman pattern for the nuclear quadrupole resonance of the cis-isomer

9) I. Tatsuzaki and Y. Yokozawa, *J. Phys. Soc. Japan*, 12, 802 (1957).

TABLE III. OBSERVED FREQUENCIES ν_1 AND ν_2 OF ^{127}I NUCLEAR QUADRUPOLE RESONANCE IN THE *cis*-1,4-DIIODOCYCLOHEXANE AT 77, 196 AND 293.5°K, AND VALUES OF TORSIONAL FREQUENCIES $\langle\nu_t\rangle$ AND ν_a CALCULATED FROM Eq. 8

Temp. °K	Resonance frequencies		Case I[1]		Case II[2]			
	ν_1 Mc./sec.	ν_2 Mc./sec.	$\langle\nu_t\rangle$ cm^{-1}	ν_a cm^{-1}	$\langle\nu_t\rangle$ cm^{-1}	g_t $\times10^3$	ν_a cm^{-1}	g_a $\times10^3$
77	248.458±0.045	244.848±0.030	31.7	37.0	30.1		42.2	
196	246.837±0.035	243.133±0.035	24.5	29.3	23.5	1.83	32.4	1.95
293.5	244.874±0.02	241.082±0.040	21.2	25.6	20.4	1.49	27.9	1.56

1) ν_1 and ν_2 are assigned to the equatorial and the axial bromine nucleus respectively.
2) The assignment of ν_1 and ν_2 is the reverse of case I.

TABLE IV. OBSERVED FREQUENCIES OF ^{127}I NUCLEAR QUADRUPOLE RESONANCE IN THE *trans*-1,4-DIIODOCYCLOHEXANE AT 77, 196 AND 213.5°K, VALUES OF TORSIONAL FREQUENCIES $\langle\nu_t\rangle$ CALCULATED FROM Eq. 7 AND LINE-WIDTHS

Temp. °K	Resonance frequencies Mc./sec.	$\langle\nu_t\rangle$ cm^{-1}	g_t $\times10^3$	$\Delta\nu_{msl}$[1] kc./sec.
77	246.890±0.020	31.0		24.3±3
196	245.594±0.030	21.5	2.56	23.6±4
213.5	245.343±0.020	20.8	2.40	

1) The frequency difference between the points of maximum slope in the absorption curve.

does not permit us to determine the assignment of the doublet.

As may be seen in Table II, in case I, where the two resonance lines, ν_1 and ν_2, are assigned to the equatorial and the axial bromine nucleus respectively, it is found that the difference between the two torsional frequencies, $\langle\nu_t\rangle$ and ν_a, is small and that ν_a is rather smaller than $\langle\nu_t\rangle$ at any temperature. On the other hand, in case II, where the assignment of ν_1 and ν_2 is the reverse of case I, the value of ν_a is about twice as large as that of $\langle\nu_t\rangle$.

The simple sinusoidal potential was assumed, because the form of the potential barrier for the torsional vibration in the crystal is hard to assess theoretically. Therefore, the frequency ν_i is given by:

$$\nu_i=\frac{n}{2\pi}\sqrt{\frac{V_0}{2I_i}} \quad (i=t \text{ or } a)$$

where V_0 is the height of the potential barrier with an n-fold symmetry, and I_i, the moment of inertia. If the heights of the potential barriers for different torsional axes have the same order of magnitude, the frequency, ν_i, is exclusively determined by the magnitude of the moment. From the study of the temperature dependence of the resonance frequency, of the asymmetry parameter and of the Raman spectra for the *p*-diiodobenzene, Shimauchi[10] have recently pointed out that the heights of the potential barriers for the three torsional vibrations are nearly the same.

10) A. Shimauchi, *Science of Light (Japan)*, **10**, 59 (1961).

As for 1,4-dihalogenocyclohexanes, it seems probable that the molecules execute torsional vibrations under the influence of the same heights of the potential barriers, since the molecular structures of 1,4-dihalogenocyclohexanes are not so different from those of *p*-dihalogenobenzenes. Therefore, ν_a in the cis-dibromo-compound becomes about 1.3~1.4 times as large as $\langle\nu_t\rangle$, because the moment of inertia, I_a, is about a half of $\langle I_t\rangle$ in magnitude. As is shown in Table II, case II, where ν_a is nearly twice as large as $\langle\nu_t\rangle$, seems to be more reasonable than case I. It therefore follows that the line of higher frequency at 77°K may be assigned to the equatorial bromine nucleus.

As for the cis-diiodo-derivative, the results obtained are analogous to those of the bromine-compound, but the assignment of the doublets is even more difficult, because the experimental temperature coefficients for each line do not appreciably differ when compared with those of the cis-dibromo-compound.

In the trans-compound, it may be assumed that the contribution to the temperature coefficient from the torsional motion around the a-axis is negligible, because the square of parameter α_a is very small as compared with the square of the other parameters. However, the fact that the resonance in the trans-diiodo-derivative gives a singlet line makes it impossible to determine the two torsional frequencies around the b- and the c-axes by the use of Eq. 7. Therefore, the values of the average torsional frequency, $\langle\nu_t\rangle$, at 77, 196

and 213.5°K were calculated. The average moment of inertia, $\langle I_t \rangle$, is $(I_b+I_c)/2$, and $\langle \nu_t \rangle$ denotes the corresponding frequency. The results thus obtained are listed in Table IV.

As is seen in Tables II, III and IV, all the torsional frequencies, $\langle \nu_t \rangle$ and ν_a, decrease with the increasing temperature. Such a variation of $\langle \nu_t \rangle$ and ν_a with temperature seems to imply the variations of the intermolecular potentials in the crystal caused by the thermal expansion. On the other hand, it was found, from Raman studies on various molecules, that the frequencies of lattice vibrations or torsional vibrations in molecular crystals vary with the temperature and that the experimental formula can be expressed as

$$\nu_i = \nu_i^0(1-g_i t)$$

where g_i is a constant and has a value of the range $(5\sim1.5)\times10^{-3}$ deg^{-1}, ν_i is the torsional frequency at an arbitrary temperature, ν_i^0 is the torsional frequency at some definite temperature t^0, and t is the temperature measured from t^0. By using the value of $\langle \nu_t \rangle$ or ν_a given in Tables II, III and IV, the constant, g_i, is calculated as shown in the seventh or the ninth column in Tables II and III, and in the fourth column in Table IV. As is seen in Tables II, III and IV, the agreement between the constant, g_i, obtained and those obtained by Ichishima[11] may be regarded as satisfactory.

A final point to be noticed concerns the fade-out of the resonance of the trans-compound. In the solids CCl_3CCl_3[9,12], and $CH_3 \cdot CCl_3$[12,13], it has been established that the fade-out of the resonance at a temperature far below the melting point arises from the re-orientational motion around the C–C axis. This motion leads to an exponential broadening of the line-width with the increasing temperature. In order to investigate whether or not the fade-out of the resonance of the trans-compound can be attributed to the similar motion, the line-width for the *trans*-1, 4-diiodocyclohexane was measured[14]; the results obtained are given in the fifth column of Table IV. From a comparison of the experimental value of the line-width at 77°K with those at 196°K, it is likely that the re-orientational motion responsible for the fade-out does not occur at 196°K.

In order to establish this point, the investigation of the proton magnetic resonance was carried out at room temperature and at the temperature of liquid nitrogen. Whereas it was expected that such motions would produce drastic changes in the line-width and in the line-shape of the proton magnetic resonance in solids[16], and that, for *trans*- and *cis*-1, 4-dihalogenocyclohexanes, the motion would give rise to a narrowing of the line-width of the resonance, no marked changes in the line-width or in the line-shape with the increasing temperature could be observed for either isomer. It follows that the motion cannot be responsible for the fade-out of the nuclear quadrupole resonance of the trans-isomer. To understand what causes may produce the fade-out of the nuclear quadrupole resonance of the trans-isomer, it would be necessary to measure the relaxation times at various temperatures.

Summary

The temperature dependences of the ^{79}Br and ^{127}I nuclear quadrupole resonance frequencies in 1, 4-dihalogenocyclohexanes were investigated. According to Bayer's theory (Eq. 8), the torsional frequencies were calculated by the use of the calculated moments of inertia and the experimental values of the temperature coefficients of the resonance frequencies at various temperatures. From a comparison of the torsional frequencies, the line of higher frequency at 77°K in *cis*-1, 4-dibromocyclohexane may be assigned to the equatorial bromine nucleus. All the calculated torsional frequencies decrease with the increasing temperature. Such variation in the frequencies agrees with the variation obtained by Raman studies of various molecules in crystals. The resonance lines in the trans-compounds fade out at temperatures considerably below their melting points.

The author wishes to express his deep thanks to Professor Kunio Kozima for his kind guidance and encouragement throughout this work. The author wishes also to thank Dr. Akira Shimauchi of the Institute for Optical Research, Tokyo University of Education, for his helpful advice in the development of the instrumentation. He is grateful to Professor Yoshinobu Kakiuchi and Dr. Takehiko Chiba of the Institute for Solid

11) I. Ichishima, *J. Chem. Soc. Japan. Pure Chem. Sec.* (*Nippon Kagaku Zassi*), **71**, 607 (1950).
12) M. Bule-Bodin, *Ann. de Physique*, **10**, 533 (1955).
13) H. S. Gutowsky and D. W. McCall, *J. Chem. Phys.*, **32**, 548 (1960).
14) The super-regenerative quench method is not reliable for the measurement of the true line-shape. As has been suggested by Tatsuzaki et al.[9] and Tsukada[15], however, the line-width obtained by this method provides rather useful information concerning the dynamic structure in the solid when a strong and sharp signal is detected at the temperature of liquid nitrogen or hydrogen, whereas no resonance line is observed at much higher temperatures.
15) Tsukada, *J. Phys. Soc. Japan*, **11**, 956 (1956).
16) For example, H. S. Gutowsky and G. E. Pake, *J. Chem. Phys.*, **18**, 162 (1950).

State Physics, the University of Tokyo, for their interest and kind advice throughout the measurement of the proton magnetic resonance.

Research Laboratory of Spectroscopy
Tokyo Institute of Technology
Meguro-ku, Tokyo

Studies on Fluorene Derivatives. XIX[1]*. The Clemmensen Reduction of 2-Bromofluorenone*

By Kazuo SUZUKI, Tsutomu MAEDA, Nagateru NAWA and Yoshitomo SŌDA

(Received January 27, 1962)

Some interesting findings noted during the Clemmensen reduction of fluorenone were reported in a preceding paper[2] of this series. Thus, fluorene was obtained in a poor yield, but a great part of the fluorenone was converted abnormally into the related dimeric products, dibiphenylene-ethylene, -ethane, 10, 10-diphenylene-9-phenanthrone, 9, 10-diphenylenephenanthrene and other intermediates through 9, 9-dihydroxy-9, 9'-bifluorenyl (fluorenopinacol).

The present study deals with the effect on this reduction of an electron-attracting group such as bromine at the 2-position of fluorenone. This is of interest because the substituent influences may be transmitted to the carbonyl at the 9-position, both directly through the substituted ring and indirectly through the unsubstituted ring.

There is only one reference in the literature to the Clemmensen-Martin reduction of 2-bromofluorenone (I), that by Miller and Bachman[3], who reported a nearly quantitative yield of 2-bromofluorene (II).

In this study, I was submitted to the same procedure as was fluorenone[2]. I was refluxed vigorously for twenty-four hours with amalgamated zinc, water, concentrated hydrochloric acid and toluene or xylene, more acid being added at intervals of about six hours. From this reduction, II, 2-bromofluorenol (III) and

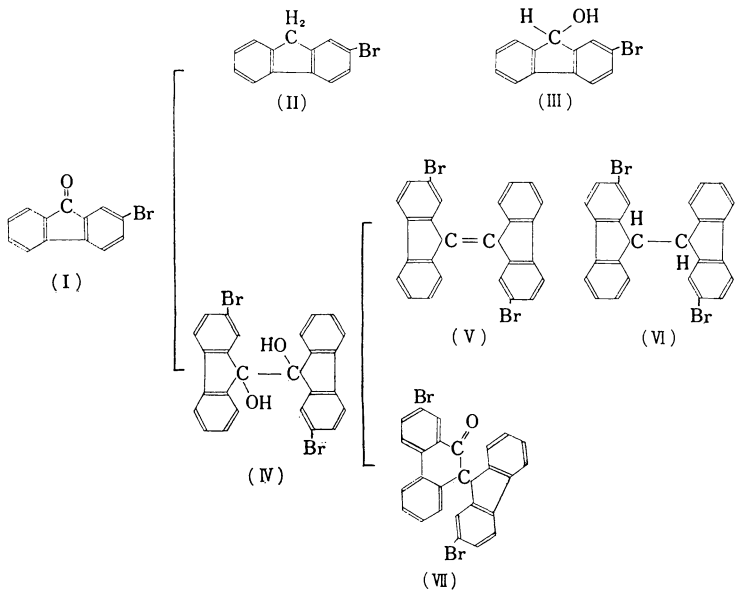


Chart 1.

1) XVIII of this series: K. Suzuki, *J. Org. Chem.*, 27 No. 6 (1962).

2) XV of this series: K. Suzuki, This Bulletin, 35, 735 (1962).

3) H. F. Miller and G. B. Bachman, *J. Am Chem. Soc.*, 57, 2447 (1935).

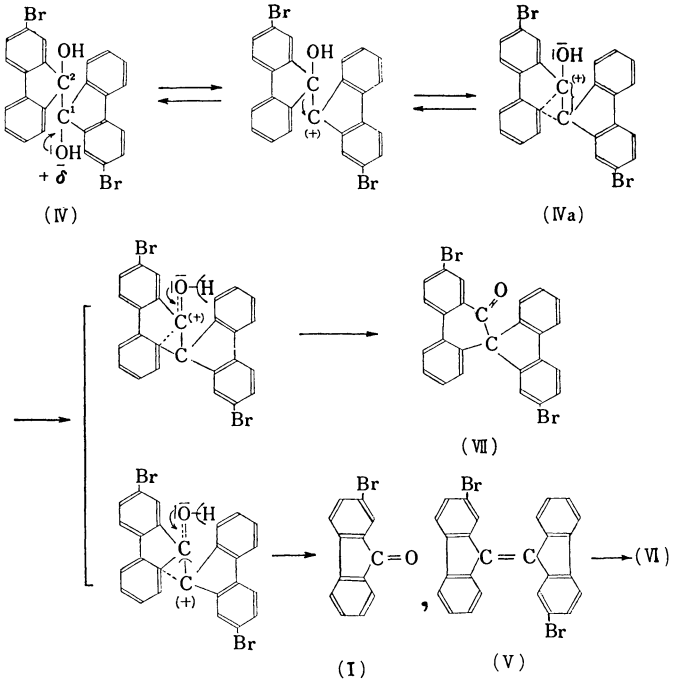


Chart 2.

several dimeric reaction products, namely 2, 2'-dibromo-9, 9-dihydroxy-9, 9'-bifluorenyl (2, 2'-dibromofluorenopinacol) (IV), 2, 2'-dibromodibiphenylene-ethylene (V)[4], -ethane (VI)[4] and a trace of spiro-[2-bromofluorene-9, 9'(10')-2'-bromophenanthrone] (VII), were isolated by means of a combination of recrystallization and column chromatography.

These reaction products are shown in Chart 1.

The reduction of I is very slow; only 11% of it was recovered after 72 hr. On the other hand, III was isolated after just a 24 hr.-period, while fluorenol has the short reduction period of 2 hr. of fluorenone. The yield of IV is increased by the use of a more concentrated hydrochloric acid, as is shown in Table I (No. 4).

IX was, however, not isolated from this series, in contrast to the comparable reduction of fluorenone. The formation of IX is controlled by the formation of VII from IV. Actually, VII was obtained only in trace amounts by this reduction, as is described in the experimental section.

First, the results can mean that the oxygen atom of the hydroxyl group attached to the carbon, C^1, is positively charged by the electron-attracting bromine in IV. For this reason, the hydroxyl group is relatively more hindered for the elimination than it is in fluorenopinacol[2] owing to the electron-repelling effect on the protonation. Under these conditions, carbonium ion formation is unlikely.

A second possible explanation is that, due to being stabilized by the formation of the transition carbonium ion, IVa, by resonance, the hydroxyl group is dehydrated from the carbon, C^1. However, state IVa must cross a high energy barrier to reach stable state VII.

These sequences can be visualized, as in Chart 2.

It seems that the formation of I and V from IVa occurs preferentially to that of VII. This is indicated in view of the following experimental evidence.

Traces of VII, V and VI were also obtained by the Clemmensen reduction of I (Table I, No. 2). I, V and VI were isolated from IV by the same reduction procedure.

Therefore, IV was treated with hydrochloric acid in toluene under the same conditions but without amalgamated zinc; a small amount of I and V was isolated.

Subsequently the quantity of the reduced form of V and VI was gradually increased after 72 hr. (Table I, No. 3).

On the other hand, the fairly large amount of VII accompanying I and V was obtained from IV by pinacol rearrangement.

The following new compounds: VII, spiro-[2-bromofluorene-9, 9'-(10')-2'-bromophenanethrol] (VIII), 2, 2'-dibromophenanthreno-9',10':

4) K. Suzuki, *J. Chem. Soc. Japan, Pure Chem. Sec.* (*Nippon Kagaku Zassi*), 75, 714 (1954); J. Schmidt and H. Wagner, *Ann.*, 387, 155 (1912).

TABLE I. REDUCTION OF I UNDER VARIOUS CONDITIONS

Exp. No.	I g.	Solvent ml.	React. time hr.	II g.	III g.	IV g.	V g.	VI g.	Recvd. I g.	Other
1	20	Toluene 40	24	1.41	0.1	4.7	0.04	0.47	4.0	
2	20	Xylene 40	24	2.7	0.26	4.7	0.01	0.8	2.2	VII, 0.005 g.
3	20	Xylene 40	72	1.3			0.01	6.6	2.2	
4*	20	Toluene 40	24	1.21	1.7	10.0	0.01	1.35	1.4	m. p. >300°C Orange-red needles, trace

* In this case, 15 ml. of water and 85 ml. of concentrated hydrochloric acid were used.

9, 10-phenanthrene (IX) and 2, 11-dibromotetrabenzocyclodecane-9, 18-dione (X), were synthesized separately by the same procedure as that with which the corresponding compounds were obtained in the case of fluorenone[2].

VII was reduced to VIII by zinc and ammonium hydroxide in an alcoholic solution and then converted into IX by retropinacol rearrangement with hydrochloric acid in acetic acid. IX was also obtained directly by the Clemmensen reduction of VII in toluene, or by hydrogen iodide and red phosphorus in acetic acid.

IX was converted into X by sodium bichromate in acetic acid, and X was also reduced to IX by hydrogen iodide in acetic acid.

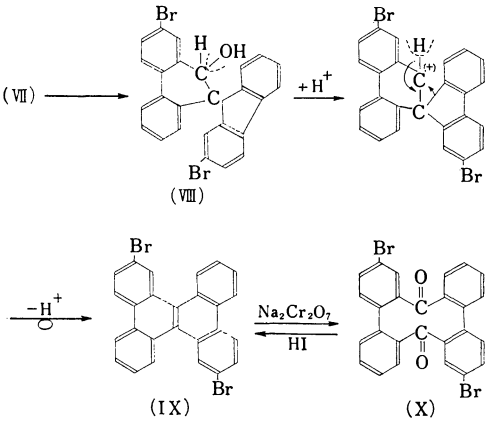


Chart 3.

Experimental*

General Procedure for the Clemmensen Reduction of 2-Bromofluorenone (I). — *Materials.* — Amalgamated zinc filings were prepared according to Martin's method[5].

2-Bromofluorene was obtained by the bromination of fluorene in chloroform; it was then oxidized to I[6] in over 80% yields.

About 0.077 mol. (20 g.) of the ketone I was refluxed vigorously for 24 hr. with 40 g. of amalgamated zinc, 30 ml. of water, 70 ml. of concentrated hydrochloric acid and 40 ml. of xylene in a 1000 ml. flask.

Concentrated hydrochloric acid (20 ml.) was added every six hours, according to Martin's method. The xylene layer turned an orange-red color after 24 hr.

When the mixture had been left standing, the crystals in the xylene layer were recrystallized from benzene, m. p. 195~196°C (4.7 g.), identical with 2,2'-dibromofluorenopinacol (IV).

Found: C, 59.99; H, 3.13. Calcd. for $C_{26}H_{16}O_2Br_2$: C, 60.02; H, 3.10%. IR 3450 (OH) cm^{-1} (KBr-disk).

The products which coated the surface of the zinc were filtered, dried and dissolved in benzene by heating; upon cooling, VI (m. p. 274°C, 0.36 g.) was obtained and I (m. p. 140°C, 0.5 g.) was recovered from the benzene mother solution. The identity of both compounds was confirmed by mixed melting point determination.

The original xylene mother liquor was evaporated, and VI (m. p. 275°C, 0.05 g.), VII (m. p. 253~254°C, 0.005 g.), and recovered I (m. p. 140°C, 0.35 g.) were isolated by fractional recrystallization. VII was identical with the material which had been prepared by the pinacol rearrangement of IV with sulfuric acid in acetic acid.

Found: C, 61.95; H, 2.70. Calcd. for $C_{26}H_{14}OBr_2$: C, 62.18; H, 2.81%.

The xylene mother solution was steam-distilled to remove the solvent, and II (m. p. 112°C, 2.7 g.) was obtained; this was confirmed by mixed melting point determination.

The orange residue was filtered and dried, and VI (m. p. 275°C, 0.38 g.), V (m. p. 264°C, 0.01 g.), I (m. p. 140°C, 1.3 g.) and III (m. p. 130°C, 0.26 g.) were separated by a combination of fractional recrystallization and chromatography in benzene on an alumina column. Mixed melting points established the nature of the products.

Clemmensen Reduction of IV. — A mixture of amalgamated zinc (11 g.), concentrated hydrochloric acid (18.2 ml.), water (6.5 ml.), toluene (13.4 ml.) and IV (4.2 g.) were refluxed for 24 hr. A 5 ml. portion of concentrated hydrochloric acid was added every six hours.

The toluene layer turned yellow after five minutes, and orange-yellow after 12 hr.

After the mixture had been left standing 24 hr., the deposited products were filtered and then recrystallized from benzene, whereupon (m. p. 195°C,

* All the melting points are uncorrected.

5) E. L. Martin, "Organic Reactins", Vol. 1, Chapman and Hall, London (1942), p. 155.

6) J. Schmidt and K. Bauer, *Ber.*, **38**, 3753 (1905).

1.2 g.) was recovered. Then V (m. p. 263°C, 0.2 g.) was isolated by evaporation and recrystallization from the mother liquor.

The last toluene mother liquor was subjected to steam distillation, and the yellow residue was filtered and recrystallized from benzene to yield VI (m. p. 273°C, 0.005 g.), then IV (m. p. 195°C, 0.8 g.) and I (m. p. 140°C, 0.51 g.) from the benzene mother solution. These compounds were confirmed by mixed melting point determinations.

Reaction of IV with Hydrochloric Acid. — IV (0.5 g.), toluene (2 ml.), water (0.8 ml.) and concentrated hydrochloric acid (1.8 ml.) were refluxed for 24 hr. A 0.5 ml. portion of hydrochloric acid was added every six hours.

The toluene layer turned an orange-yellow color after 20 hr. When the mixture had been left standing, the precipitate was filtered and recrystallized from benzene, m. p. 193°C (0.21 g.), identical with the recovered IV. The toluene mother liquor was steam-distilled to remove the solvent, yielding I (m. p. 140°C, 0.05 g.), which was recrystallized from alcohol.

The residual products were filtered; I (m. p. 142°C, 0.06 g.) and V (m. p. 263°C, 0.002 g.), obtained by means of chromatography in benzene on alumina, were confirmed by mixed melting point determinations.

Pinacol Rearrangement of IV to VII.—IV (5 g.) was dissolved in acetic acid (50 ml.), and concentrated sulfuric acid (0.5 ml.) was added; the mixture was then refluxed for 30 min. When the mixture had cooled, the deposited products were filtered and recrystallized from acetic acid to yield VII (m. p. 252°C, 3.0 g.) as colorless crystals. The mother liquor was poured into water, the precipitate was filtered, and additional VII (m. p. 252°C, 0.42 g.), recovered pinacol (IV) (m. p. 194°C, 0.06 g.) and I (m. p. 141°C, 0.11 g.) were separated by a combination of recrystallization and column chromatography in benzene on alumina. Moreover, a small amount of V (m. p. 264°C) was isolated from the mother liquor by recrystallization.

Reduction of VII to VIII.—Finely powdered VII (1 g.) was suspended in 600 ml. of ethyl alcohol, zinc dust (3 g.) and concentrated ammonium hydroxide (30 ml.) were added, and the mixture was refluxed for 10 hr. Concentrated ammonium hydroxide (30 ml.) was added every 3 hr. The reaction mixture was filtered, and the filtrate was evaporated to half volume. The white product deposited was filtered, then recrystallized from benzene to give unreacted VII (m. p. 253°C, 0.31 g.). The first mother liquor was evaporated to a small volume, and the precipitate was recrystallized from benzene to give crystals, m. p. 153~154°C (0.05 g); these were identical with VIII.

Found: C, 62.21; H, 3.32. Calcd. for $C_{26}H_{16}OBr_2$: C, 61.93; H, 3.20%. IR 3484 (OH) cm^{-1} (KBr-disk).

Rearrangement of VIII to IX.—To a solution of VIII (0.2 g.) in acetic acid (10 ml.) there was added 1.5 ml. of concentrated hydrochloric acid, and the mixture was refluxed for 2 hr. When the mixture had cooled, the precipitate was filtered and recrystallized from benzene, m. p. 305°C, (0.05 g.); this was identical with IX.

Found: C, 64.11; H, 3.07. Calcd. for $C_{26}H_{14}Br_2$: C, 64.22; H, 2.90%.

Rearrangement of VII to IX by Reduction.—A mixture of VII (1 g.), acetic acid (190 ml.), hydrogen iodide (10 ml.) and red phosphorus (1 g.) was refluxed for 9.5 hr. Upon cooling, the reaction mixture was filtered, and the filtrate was poured into water. The precipitate was then filtered and washed well with water. It was recrystallized from benzene to give IX (m. p. 305~307°C, 0.2 g.) as small colorless needles; unreacted ketone VII (m. p. 253°C, 0.4 g.) was also recovered.

Clemmensen Reduction of VII to IX.—A mixture of amalgamated zinc (6.0 g.), water (1.5 ml.), toluene (10 ml.), concentrated hydrochloric acid (5 ml.) and VII (1 g.) was refluxed vigorously for 24 hr. in a 100 ml., round-bottomed flask. A 1 ml. portion of concentrated hydrochloric acid was added every 6 hr. After reaction, the deposited material was filtered and recrystallized from benzene to yield IX (m. p. 305°C, 0.5 g.). Then VIII (m. p 150~152°C, 0.005 g.) and unreacted VII (m. p. 253°C, 0.66 g.) were also isolated from the mother liquor by fractional recrystallization.

Oxidation of IX to X.—IX (0.4 g.) in a mixture of acetic acid (700 ml.) and sodium bichromate (6 g.) was refluxed for 13 hr. Upon cooling, the reaction mixture was poured into water. The white amorphous product was recrystallized from benzene, m. p. 224~225°C (0.25 g.); this was identical with X.

Found: C, 60.53; H, 2.91. Calcd. for $C_{26}H_{14}O_2Br_2$: C, 60.26; H, 2.72%. IR 1672 (C=O) cm^{-1} (KBr-disk).

Reduction of X to IX.—A mixture of X (0.1 g.), acetic acid (15 ml.), hydrogen iodide (1 ml.), and red phosphorus 0.1 g. was refluxed for 9 hr. Then the reaction mixture was filtered, and the filtrate was poured into water; the white precipitate was recrystallized from benzene, m. p. 305°C, (0.05 g.). This compound was identical with IX, as was shown by mixed melting point determination.

It is a pleasure to acknowledge our helpful discussions of problems related to this paper with Drs. John and Elizabeth Weisburger of National Institutes of Health and with Dr. Yoshiro Ogata of Nagoya University, and to thank Dr. Shoji Kajigaeshi for his assistance.

We are also indebted to Idemitsu Industries Co., Ltd., for the infrared spectra measurement.

Department of Chemistry
Faculty of Technology
Yamaguchi University
Tokiwadai, Ube

Raman Spectrum of γ-Glycine

By K. BALASUBRAMANIAN, R. S. KRISHNAN and Yoichi IITAKA*

(Received January 30, 1962)

A study of Raman spectra of crystalline glycine and its addition compounds is of great interest because of the existence of strong hydrogen bonding in these substances. A systematic study of Raman effect in single crystals of these substances was therefore undertaken in the Department of Physics of the Indian Institute of Science a few years ago. The Raman spectra of α-glycine[1], triglycine sulfate[2], diglycine nitrate[3], diglycine hydrochloride[3] and diglycine hydrobromide[3] have already been reported. It is well known that besides the α-form, two other polymorphic forms of glycine exist. These are (1) an unstable β-form first described by Fischer[4] and (2) γ-form the existence of which was reported by one of us[5]. The crystal structure of the γ-form has been determined very accurately[6]. This γ-variety can be obtained in single crystal form and is quite stable. It is therefore considered desirable to have its Raman spectrum photographed and compared with that of α-glycine.

Experimental Details

Single crystals of γ-glycine were grown in the following way[5,6]. A saturated aqueous solution of α-glycine was prepared at 60 to 80°C. This was made acidic with 15% acetic acid and was cooled slowly in an ice-box with seeding γ-glycine crystals. They usually grow in massive aggregates; but, with some difficulty single crystals of small size could be obtained. Two specimen of roughly 5 mm. in size were used for taking the Raman spectrum using λ 2536.5 excitation. Exposure for about one day was found to be necessary for recording a satisfactory spectrogram with a Hilger medium quartz spectrograph. The crystals did not get spoiled due to irradiation with ultraviolet light.

Results

An enlarged photograph of the Raman spectrum of γ-glycine obtained with λ 2536.5 excitation is reproduced in Fig. 1 (b) and the corresponding microphotometer record is shown in Fig. 1(c). Fig. 1(a) represents the Raman spectrum of α-glycine taken under identical conditions. The frequency shifs in cm^{-1} of the observed Raman lines are marked in the microphotometer record. They are also tabulated in Table I, column 2. The figures given in brackets are the intensities of the lines for the unspecified orientation that was used. These intensities are estimated spectrophotometrically. The Raman frequency shifts of α-glycine[1] are also entered in column 1 of Table I. On the whole 39 Raman lines are

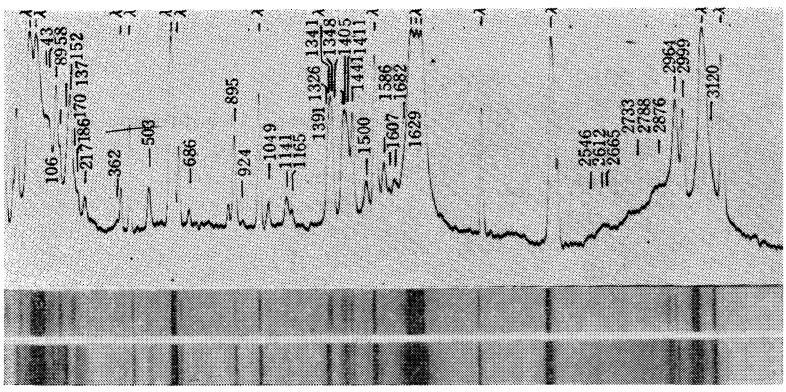


Fig. 1. (a) Raman spectrum of α-glycine with λ 2536 excitation.
(b) Raman spectrum of γ-glycine with λ 2536 excitation.
(c) Microphotometer record of Raman spectrum of γ-glycine.

* Faculty of Pharmaceutical Science, the University of Tokyo, Hongo, Tokyo.

1) R. S. Krishnan and K. Balasubramanian, *Proc. Ind. Acad. Sci.*, **48A**, 55 (1958).
2) R. S. Krishnan and K. Balasubramanian, ibid., **48A**, 138 (1958).
3) K. Balasubramanian, ibid., **53A**, 105 (1961).
4) E. Fischer, *Ber. dtsch. chem. Ges.*, **38**, 2917 (1905).
5) Y. Iitaka, *Proc. Japan Acad.*, **30**, 109 (1954).
6) Y. Iitaka, *Acta Cryst.*, **14**, 1 (1961).

TABLE I. RAMAN FREQUENCIES OF CRYSTALLINE γ-GLYCINE

α-Glycine	γ-Glycine Raman effect	γ-Glycine Infrared	Assignment
	43(10)		Lattice
53(30)	58(15)		
74(23)	89(48)	90.3(i)	
90(?)		101(w)	
109(61)	106(20)	105(i)	
588		116(w)	
		127(w)	
	137(15)	138(i)	
164(33)	152(40)		
	170(6)	173(i)	
183(25)	186(8)		NH·····O
199(15)	217(9)	243	NH·····O
358(11)	362(2)	357	NCC
499(18)	503(14)	503	COO^- nocking
588		557, 560	NH_3^+ torsion
		602, 607	$-COO^-$ wagging
697(7)	686(4)	684, 689	$-COO^-$ sym. bend.
896(42)	895(27)	888, 893	CCN sym. stretch.
925	924(?)	924, 929	CH_2 rocking
1038(12)	1045(?)	1044	CCN antisym. stretch.
	1049(8)	1050	
		1126	
1112(9)	1141(10)	1135	NH_3^+ rocking
1140(10)	1165(6)	1154	〃
1320(60)	1326(25)	1317	CH_2 wagging
1330(60)	1341(35)	1324	〃
		1340	
	1348(35)		〃
1395	1391(30)	1389	$-COO^-$ sym. stretch.
	1405(30)	1397	〃
1414(41)	1411(25)		〃
1441(27)	1441(31)	1435	CH_2 sym. bend.
1459(20)			
1506(14)	1500(7)	1492	NH_3^+ sym. defmn.
1563(25)	1586(10)	1575	NH_3^+ deg. defmn.
		1585	
	1607(5)	1620	
1640(12)	1629(5)		$-COO^-$ antisym. stretch.
1668(8)	1682(?)	1660	NH_3^+ deg. defmn.
2530(5)	2546(3)		N-H bonded oscillations
2630(11)	2612(5)		〃
	2663(5)		〃
2750(10)	2733(8)		〃
	2788(8)		〃
2830(14)	2876(11)		〃
2895(17)			〃
2974(47)	2964(41)		C-H stretch.
3008(36)	2999(35)		C-H stretch.
3145(15)	3120(5)		NH_3^+ stretch.

i, Intense; w, Weak

recorded in γ-glycine of which the first nine lines (43～270 cm^{-1}) belong to low frequency spectrum and the remaining 30 lines belonging to internal oscillations. The Raman spectrum of α-glycine reproduced in Fig. 1 (a) is more intense than that of γ-glycine. This is due to the fact that the specimen of γ-glycine used was less perfect than that of α-glycine.

Discussion

γ-Glycine crystallizes in hexagonal class with space group $P3_1$ or $P3_2$ and shows piezoelectric properties along the c-axis. The cell dimensions are $a=7.037$ Å and $c=5.483$ Å. There are 3 molecules in the unit cell. Here also the glycine units exist in the zwitter ion form as in α-glycine. According to the detailed structure analysis carried out by one of us (Iitaka[6]) the N atom is 0.309 Å (12.8°) out of the best plane through C_I, C_{II}, O_I, O_{II} as against 0.436 Å (18.6°) in α-glycine. The N atoms are surrounded by 5 oxygen atoms at short distances out of which 3 short distances are attributed to be making hydrogen bonds (N–H···O); these hydrogen bond (N–H···O) distances are as follows; 2.801 Å, 2.817 Å and 2.970 Å. In α-glycine two hydrogen atoms are participating in strong hydrogen bonds which hold the molecule in a sheet and the third hydrogen atom forms a weak bifurcated bond with glycines in the next sheet. Whereas, in γ-glycine there is no such bifurcated bond and all these bonds are nearly of equal strength. The directional properties of the hydrogen bonds are more fully satisfied in γ-glycine than that in the other form. The hydrogen bonding between amino N and carboxyl O atoms links the molecules in helical chains about the 3-fold screw axis. These chains are linked together by lateral hydrogen bonds forming the 3-dimensional network of hydrogen bonds.

Internal Oscillations.—The frequencies corresponding to the absorption maxima of γ-glycine in infrared reported by Tsuboi and others[7] are given in column 3 of Table I. The data on the far-infrared absorption spectrum of γ-glycine (85～200 cm^{-1}) was supplied by Tsuboi[8]. There is a very close correspondence between the frequency shifts observed in the Raman spectrum of γ-glycine and its infrared absorption frequencies. This is not surprising because the crystal belongs to the hexagonal class $P3_1$ or $P3_2$ for which the selection rules are such that the Raman effect and infrared absorption are not mutually exclusive. Some additional maxima are observed in the

7) M. Tsuboi, T. Onishi, I. Nakagawa, T. Shimanouchi and S. Mizushima, *Spectrochim. Acta.*, 12, 253 (1958).
8) M. Tsuboi, unpublished work.

infrared. The Raman line corresponding to the absorption 602~607 cm^{-1} in infrared can not be identified in the spectrum taken with λ 2536.5 excitation as it falls very close to the mercury line λ 2576.3Å. In the infrared absorption, above 1700 cm^{-1} no data are available for comparison with the observed Raman frequencies.

As is to be expected there is a close agreement between the Raman frequencies of γ-glycine and α-glycine. From a comparative study of the two spectra the assignments have been given for most of the internal oscillations. Many of the internal oscillations are influenced by the hydrogen bonds and especially those which contain N–H group. A very careful comparison of the spectra of α-glycine and γ-glycine reveals the fact that the influence of hydrogen bonds on some of the internal frequencies is different in the two crystals. This is not surprising if one remembers the fact that in γ-glycine there are 3 equally strong hydrogen bonds, whereas in α-glycine there are only two strong hydrogen bonds and one comparatively weaker bond. As in the case of α-glycine and other glycine addition compounds, a large number of Raman frequency shifts are observed in the spectrum of γ-glycine in the region 2500~2900 cm^{-1}, the intensity increasing with increasing frequency shift. They are all assigned to N–H ··· O oscillations. The presence of the Raman line at 3120 cm^{-1} adjacent to intense mercury line λ 2752.8 clearly indicates the existense of NH_3^+ group. This supports the X-ray evidence that the glycine molecules in γ-glycine exist in the zwitter ion configuration. The planarity of the glycine molecule is different in the α and γ forms. This appears to have some influence on the C–H stretching frequency. The C–H frequencies in γ-glycine, in which the glycine molecule is more planar, are lower than the corresponding frequencies of α-glycine, whereas the difference in the frequency shifts between the symmetric and antisymmetric (C–H) oscillations remains the same. Similar observations have also been made with addition compounds of glycine (Balasubramanian[3]).

Low Frequency Spectrum.—In the Raman spectrum, one observes 9 distinct lines in this region, some of them being very intense. Of these the lines at 186 and 217 which are also observed in the spectrum of α-glycine should be attributed to the vibrations of hydrogen bond i. e., NH···O (Gross[9]). The remaining seven low frequency Raman lines belong to the lattice oscillation of rotatory and translatory types of glycine units. There is practically no similarity between the lattice spectra of α- and γ-glycine. This is not surprising because they belong to two different crystal systems. In infrared absorption, Tsuboi[8] has also observed seven maxima. However, only four of them with frequencies 90.3, 105, 138 and 173, which are the intense ones, agree closely with those observed in Raman effect.

From a group theoretical analysis, taking each glycine molecule as an individual unit, it can be shown that there are, on the whole (for the unit cell of γ-glycine) only 10 external oscillations, which are active both in infrared and Raman effect. These are as follows: 2 translatory and 3 rotatory oscillations coming under the symmetric class, and 2 translatory and 3 rotatory coming under the doubly degenerate class. Taking all the observed frequencies in infrared as well as in Raman effect, one observes that they are actually twelve in number. Therefore, at least two of them should be assigned to combination or overtones. The oscillations with frequencies 101, 116 and 127 appear very weakly in infrared absorption and do not appear in Raman effect. It is possible that with a better and more clear specimen of γ-glycine and a longer exposure these faint lines may also be recorded in Raman effect. The appearance of two lowest frequency lines 43 and 58 in infrared absorption is yet to be confirmed. Tsuboi's observations in infrared extends only up to 85 cm^{-1}. The Raman line at 152 cm^{-1} is extremely intense and sharp while the corresponding frequency is absent in infrared absorption. This might be due to the fact that for this particular oscillation though there might be a great change in polarizability, the change in dipole moment may not be appreciable.

Summary

Using λ 2536.5 excitation the Raman spectrum of single crystal of γ-glycine has been recorded for the first time. Thirty-nine Raman frequencies have been reported. Comparing the spectrum of γ-glycine with its infrared absorption spectrum and also with the Raman spectrum of α-glycine, proper assignments have been given to the internal frequencies. The lattice lines observed in Raman effect and infrared absorption have been satisfactorily accounted for.

The authors wish to express their grateful thanks to Professor San-ichiro Mizushima and Professor Masamichi Tsuboi for their kind interest in the work and also for supplying the far-infrared absorption data of γ-glycine.

Department of Physics
Indian Institute of Science
Bangalore, India

9) E. F. Gross, "Hydrogen Bonding" by D. Hadži, Pergamon Press (1959), p. 203.

Adsorption of Cesium by Japanese Acid Clay

By Noboru Oi and Eijiro Ohashi

(Received February 3, 1962)

We have already reported[1] the separation of uranium from fission products by the adsorption of the latter to Japanese acid clay in an organic solution. We pointed out the strong preference for adsorbing cesium to other fission product nuclides. This phenomenon was found also in aqueous solutions, so we extended the survey to aqueous systems, especially in regard to the effect of the heat treatment of the clay on adsorption.

Experimental

Sample Description.—Japanese acid clay, from Ōmi, Niigata prefecture, was obtained from the Koso Chemicals Co. The clay was used without pretreatment or was used after heating it at different temperatures up to 1200°C for 1.5~2 hr., followed by gradual cooling.

The ion exchange capacities were determined by using the barium-saturation-acid titration technique described by Suto[2].

The Measuring of the K_d Values of Cesium.—About 10 ml. of an aqueous solution, containing 1~2μC. of carrier free cesium-137, was placed in a graduated glass cylinder with a stopper, and 30~50 mg. of the clay were added. After equilibrium was reached with intermittent shaking, the solution was centrifuged. One milliliter of aliquot was counted in a well-type scintillation counter with a NaI (Tl) crystal, after the mixture had been left standing for 20 min. to ensure radioactive equilibrium with ^{137m}Ba. The K_d values were then calculated by the following equation:

$$K_d = \frac{[\text{Cs concn. of the sample soln. before adding the clay (c. p. m./ml.)} - \text{Cs concn. after equilibration (c.p.m./ml.)}] \times [\text{Vol. of the soln. (ml.)}]}{[\text{Weight of the clay (g.)}] \times [\text{Cs concn. after equilibration(c. p. m./ml.)}]}$$

The time of equilibration was almost the same in various solutions, either carrier free, with carrier, or containing a salt such as sodium nitrate: this time was found to be 0.5~1.0 hr.

Compared with the data of montmorillonite[3] and kaolinite[4], where the times of equilibration for the cesium adsorption in aqueous systems were 16~696 hr. and 40 days, the adsorption by Japanese acid clay is rapid. Presumably this is due to the ease of defloculation of this clay; a larger proportion of sites is soon made available for exchange. It was also noticed that the adsorption of cesium was better at a lower temperature; for example the K_d values of cesium from aqueous solution were 6430, 6450, 5570, 5470, 4270 and 3980 at 0, 10, 20, 30, 40 and 50°C respectively.

Results and Discussion

The Meaning of the K_d Values.—Many surveys have been made of the ion-exchange properties of clay minerals. Almost all of them, however, treated the results of the experiments by hold-up volume or by the percentage of adsorption at various concentrations and various pH values. This seems due to a lack of information as to whether the phase equilibrium really exists, even in the case of clay minerals. We confirmed this point by the following two methods and discussed all the data using K_d values.

(1) In some K_d value measurements, the volume of the solution and the amounts of the clay to be added were changed, only to find that the calculated K_d values were changed only a little with varying these two factors.

(2) Cesium was adsorbed to the clay from a 0.2 M nitric acid aqueous solution, and the supernatant solution was rejected. This clay was next brought in contact with 0.2 M nitric acid, the K_d value of the desorption being measured. The same experiments were repeated, and the changes in the K_d values of desorption were observed. The results are shown in Table I. The gradual increase in K_d

Table I. Desorption of cesium-137 which was adsorbed on Japanese acid clay

No.	Total activity (c.p.m.)	Desorbed activity (c.p.m.)	K_d
1	1246000	109140	2080
2	1137640	91400	2280
3	1046240	77660	2500
4	968580	65270	2760
5	903310	238150*	3160

Desorption: 0.2 M. nitric acid, 10 ml. (*50 ml.) Japanese acid clay, 50 mg. Time of equilibration, 1.5 hr.

1) N. Oi and T. Kamada, Presented at the 14th Annual Meeting of the Chemical Society of Japan, Tokyo, April, 1961.
2) T. Suto, "Clay minerals", Iwanami, Tokyo (1958), p. 146.
3) T. Tamura and D. G. Jacobs, *Health Physics*, **2**, 391 (1960).
4) M. A. Tamers and H. C. Thomas, *J. Phys. Chem.*, **64**, 29 (1960).

values seems to show the existence of some irreversible adsorption, but on the whole we can probably assume a phase equilibrium.

The Influence of the Concentration of Acid, Alkali and Salt.—The K_d values of cesium-137 at various concentrations of nitric acid, hydrochloric acid, ammonia, sodium chloride, sodium nitrate, aluminum nitrate and cesium nitrate in an aqueous solution were measured; they are shown in Figs. 1 and 2. Here it must be pointed out that the adsorption of cesium by this clay is much more highly specific than that of these ions: H^+, Na^+, NH_4^+ and Al^{3+}. It was also shown that the cesium adsorption was at its maximum in water (pH=7), the K_d value then being 7000. When the concentration of the solute in the solution increased except in the case of ammonia, which is one of the weak electrolytes, the K_d values decreased rapidly, and to almost the same value; the K_d value was below 1000 above 0.2 M. This indicates, on the contrary, the possibility of cesium desorption by a solution of a higher concentration.

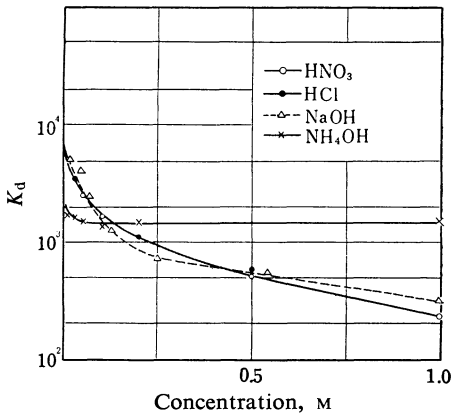


Fig. 1. Influence of acids and alkalis on the K_d values of cesium.

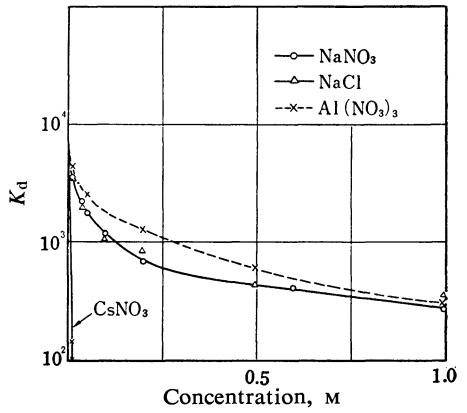


Fig. 2. Influence of salts on the K_d values of cesium.

Above all, it seems to indicate that the adsorption is a cationic exchange in nature and that the decrease in K_d values is due to the competition between cesium and other ionic species at the higher concentrations.

Influences of the Heat Treatment of Japanese Acid Clay.—It is known that the adsorbability for cesium of clay minerals, especially montmorillionite, is enhanced by heat treatment. In this case, the basal diffraction of the X-ray diffraction pattern changes from 15~17 Å to about 10 Å. Tamura et al.[3-5] suggested the importance of this 10 Å c-axis spacing for the adsorption of cesium; they also pointed out the affinity for cesium of illite and synthetic micas, which have a 10 Å c-axis spacing.

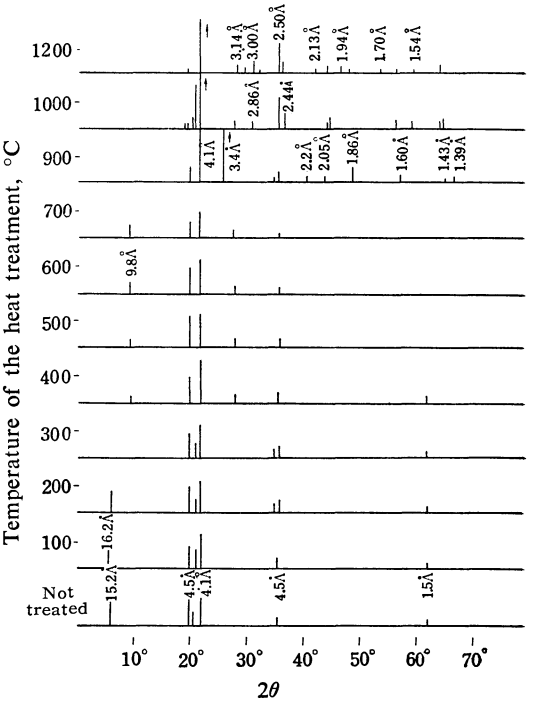


Fig. 3. X-Ray diffraction patterns of the heat treated Japanese acid clay.

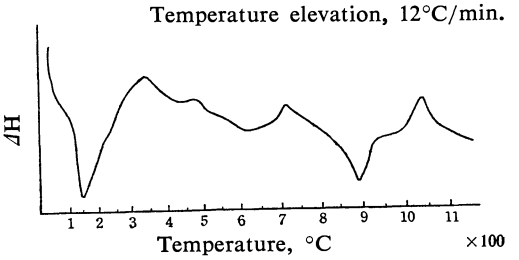


Fig. 4. Curve obtained by the differential thermal analysis of the Japanese acid clay.

5) T. Tamura and D. G. Jacobs, *Health Physics*, 5, 149 (1961).

We carried out the experiment with heat-treated clay and considered our results using X-ray diffraction patterns (Fig. 3) and differential thermal analysis (Fig. 4). The changes in the K_d values of some systems are shown in Fig. 5. It is shown that the selectivity for cesium was most improved by heating it to a temperature in the 400~500°C range. By comparing these results, the following conclusions[6] were reached:

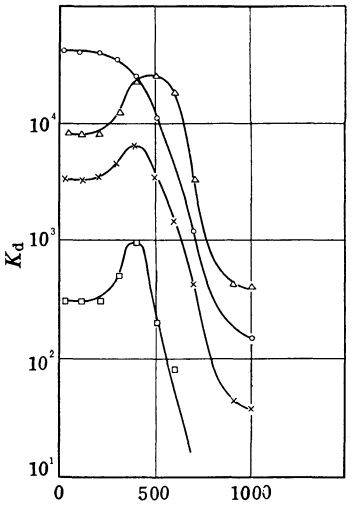


Fig. 5. Changes of the K_d values of cesium by using heat treated Japanese acid clay.
—○— *n*-Butylacetate, uranyl nitrate 0.1 M
—×— 0.1 M uranyl nitrate aqueous solution
—△— Water
—□— 1 M Nitric acid

(1) Japanese acid clay loses about 10%. of its weight at 100~150°C by the removal of its absorbed water. This process, however, does not work positively but rather somewhat negatively in cesium adsorption.

(2) Up to 700°C, the patterns of X-ray diffraction show little change except in their basal reflection. This changes from 15~16 Å at 100~200°C to about 10 Å at 400~700°C, while its intensity also increased. The process of the formation of the 10 Å axis corresponds to the maximum point of the adsorption.

(3) The endothermic peak of 350~650°C is due to the removal of the structural water (or -OH), and in this process the c-axis changes to 10 Å. After the complete dispersion of the structural water, the K_d values drop. The pattern of differential thermal analysis indicates two stage changes within this temperature range, one rather moderate in the range of 350~450°C and the other slightly steep up to 500°C. The clay of the first stage showed the maximum K_d values.

(4) The endothermic-exothermic peak of the 850~1100°C range corresponds to the change in colloidal silica, which is one of the components of this clay, to α-crystobalite via α-quartz. This is clear from the X-ray patterns. Here the K_d values decreased to a minimum.

Thus, the K_d maximum corresponds to the process of 10 Å c-axis formation and also to the removal of the structural water. These results qualitatively agree with Tamura et al's data[3].

Fripiat et al.[7] studied the relation of the dehydration of montmorillonite to its infrared spectroscopy. They pointed out the increase in the stretching vibration frequency of the hydroxyls as the dehydration progressed. We also took infrared spectra of the untreated and heat treated clays, but we could not clearly determine the relation between the increase in OH stretching and the maximum K_d value. This is presumably because the K_d maximum is due to the structural factor and not to the ion exchange character.

In Fig. 5. a curve showing the K_d changes in *n*-butylacetate is also included. This shows no maximum value. This seems to indicate that the mechanism of the adsorption in an organic solution is mainly molecular and is different from that in an aqueous solution, ion exchange adsorption.

On the other hand, when cesium was adsorbed by this clay and was heated for half an hour at about 1000°C, it was fixed to the clay and was not eluted even when boiled with large amounts of water.

The Cesium Concentration and the Change in K_d Values.—The experiment above was carried out using carrier-free (about 10^{-7} mol./l.) cesium-137. However, as much as 10^{-4} mol./l. of cesium is handled in high-level waste. Besides, the behavior of cesium at a higher concentration also seems interesting with regard to the adsorption mechanism: therefore, we carried out experiments up to 0.1 mol./l., using both untreated and heat-treated clays at 400°C. The results are shown in Fig. 6. In the cesium concentration range of below 10^{-6} mol./l. heat-treated clay showed higher K_d values, but at a higher cesium concentration untreated clay showed better adsorption. The adsorption isotherms of both clays at a higher cesium concentration indicated a maximum adsorption, the amounts of adsorption being almost the same as their ion exchange capacities, 0.45 and

6) Cf. G. W. Brindley, "X-Ray Identification and Crystal Structures of Clay Minerals", The Mineralogical Society, London, (1951), p. 118.

7) J. J. Fripiat, J. Chaussidon and R. Touillaux, *J. Phys. Chem.*, **64**, 1234 (1960).

0.14 meq./g. and 59 and 17 mg. of cesium adsorption per gram of the clay for untreated and for treated clays respectively. These results show that ion exchange plays a major role in the adsorption of cesium, but that at a lower cesium concentration a somewhat specific, perhaps structural adsorption takes place and causes an increase in the K_d values.

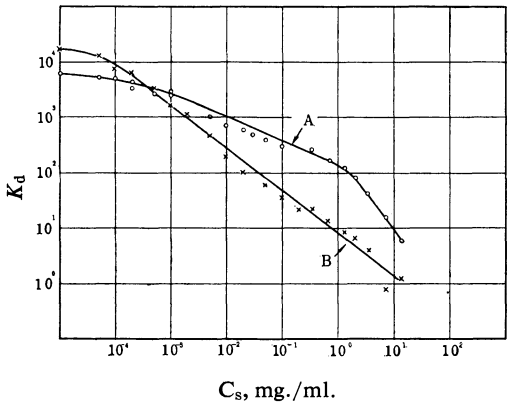


Fig. 6. Changes of the K_d values of cesium by increasing cesium nitrate concentration in water.
A, Untreated clay
B, Heat treated clay at 400°C

Adsorption of Cesium-137 from Fission Products Mixture.—A simple survey of cesium adsorption from the fission products of this clay showed that cerium, zirconium and niobium were adsorbed at about 1% of the K_d value of cesium. Ruthenium was eliminated more efficiently. The behavior of nuclides was altered by the heat treatment of the clay; for example, in the case of 200 day-cooled fission products, the gross K_d values of total γ-activities in water were 460 and 16, by the untreated clay and the clay treated at 500°C respectively.

Summary

Japanese acid clay, a montmorillonite-type one, exhibited a special affinity for cesium-137 from an aqueous solution. The phase epuilibrium of the adsorption was confirmed, and the K_d values were used to analyze the data.

The K_d value of cesium was highest in pure water, but it was decreased by increasing the aqueous acid, alkali and salt concentration.

When clay which had been treated at 400~500°C was used, the K_d value increased two- or three-fold. This phenomenon corresponds to the formation of 10 Å c-axis spacing and the dispersion of the structural water of the clay. This peculiarity, however, appears only at a low cesium concenration, below 10^{-6} mol./l. At a higher cesium concentration, the adsorption of cesium depends simply on the cation exchange capacity of the clay; heat-treated clay showed a poorer adsorption.

The adsorption of cesium from a fission products mixture was also simply examined.

The authors wish to express their deep thanks to Dr. Kakuzo Tada and Dr. Tsutomu Takamura of Toshiba Central Research Laboratory for their encouragement and valuable advice.

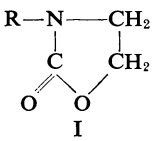
Central Research Laboratory
Tokyo Shibaura Electric Co., Ltd.
Kawasaki

Studies of 2-Oxazolidinones. I. A Convenient Synthesis of 3-Substituted 2-Oxazolidinones

By Ryohei ODA, Masahiko MIYANOKI and Masaya OKANO

(Received February 2, 1962)

Although several methods for the formation of 3-substituted 2-oxazolidinones (I) are known, these preparative routes may be classified into three general groups: (i) the condensation of β-hydroxyethylamines with carbonic acid derivatives such as dialkyl carbonates[1], urea[2], or phosgene[3]; (ii) the addition of isocyanates to



I

1) A. H. Homeyer, U. S. Pat. 2399118; *Chem. Abstr.*, **40**, 4084 (1946).
2) J. M. Stratton and F. J. Wilson, *J. Chem. Soc.*, **1932**, 1133.
3) P. Otto, *J. prakt. Chem.*, [2], **44**, 17 (1891).

TABLE I. β-CHLOROETHYL CARBAMATES

N-Sub. β-chloroethyl carbamates	Method	Total yield[a]	M. p.	Solvent of crystn.[b]	C, %		H, %		N, %	
					Calcd.	Found	Calcd.	Found	Calcd.	Found
n-Butyl	B	66	113(4.3)[c,d]							
t-Butyl	A	58	90(7)[c]		46.80	46.69	7.86	7.80	7.96	7.96
Phenyl	B	80	160(5)[c]; 49[e]							
p-Tolyl	B	75	61[f]	B						
o-Tolyl	A	91	45[g]	L						
p-Nitrophenyl	B	88	116	B	44.19	44.47	3.71	3.97	11.45	11.57
o-Nitrophenyl	A	91	70.5	B-L	44.19	44.80	3.71	4.09	11.45	11.65
p-Carbethoxyphenyl	A	86	145	B-E	53.05	53.09	5.19	5.05	5.16	5.38
p-Chlorophenyl	A	69	69[h]	B						
1-Anthraquinonyl	A	84	184[i]	E-Dm						
Ethylene-bis	A	39	136[j]	E						
Tetramethylene-bis	B	50[k]	118[l]	B						
m-Phenylene-bis	B	79	115.5	Dm-W	44.88	45.13	4.39	4.63	8.37	8.36
p-Phenylene-bis	B	78	202	Dm-W	44.88	45.15	4.39	4.48	8.37	8.25

a. In method A the yield was calculated as 93% for β-chloroethyl chloroformate synthesis (see Experimental). b. B=Benzene, Dm=Dimethylformamide, E=Ethanol, L=Ligroin, W=Water. c. B. p. (mmHg). d. Reported b. p. 98°C (1 mmHg), Ref. 11. e. Reported b. p. 134°C (2 mmHg), Ref. 11; m. p. 51°C, Ref. 6. f. Reported m. p. 63°C, Ref. 8. g. Reported m. p. 46°C, Ref. 8. h. Reported m. p. 63°C, Ref. 7; 69°C, Ref.8. i. Reported m. p. 186°C, A. Noguchi, *J. Soc. Org. Synth. Chem. Japan (Yūki Gōsei Kagaku Kyokai Shi)*, **13**, 78 (1955). j. Reported m. p. 136.5°C, R. Delaky et al., *Bull. soc. chim. France*, 396 (1951). k. This low value is due to a poor yield of the diisocyanate prepared from the corresponding acid. l. Reported m. p. 118.5°C, Ref. 10.

epoxides[4,5]; (iii) the dehydrochlorination of β-chloroethyl carbamates[6-9]. Among instances of route iii, β-chloroethyl carbamates have recently been obtained by the condensation of amines with ethylene carbonate, followed by the chlorination of the resulting β-hydroxyethyl carbamates[9,10]. However, the authors have considered that Nemirowsky's well-known method A[6-8,11] may have an abvantage over the above method from the synthetic standpoint.

Method A:

$$COCl_2 + HOCH_2CH_2Cl \rightarrow ClCOOCH_2CH_2Cl$$

$$RNH_2 + ClCOOCH_2CH_2Cl \rightarrow RNHCOOCH_2CH_2Cl$$

Making another combination of the three reactants, the following method B may be considered, although it has not previously been reported.

Method B:

$$RNH_2 + COCl_2 \rightarrow RNCO$$

$$RNCO + HOCH_2CH_2Cl \rightarrow RNHCOOCH_2CH_2Cl$$

Method B is a modification of the method ii mentioned above.

This paper deals with the preparation of β-chloroethyl carbamates by method A or B and with the ring-closure of these compounds to form 3-substituted 2-oxazolidinones. The results of the carbamate syntheses are summarized in Table I. These results seem to prove that our method B is comparable to method A in yields and is applicable as a convenient method of 2-oxazolidinone synthesis.

In the dehydrochlorinative ring-closure of β-chloroethyl carbamates, many workers have used more than one molar equivalent of alkali. However, it is known that the oxazolidinones are less stable in alkaline media and are easily hydrolyzed by aqueous alkali to yield β-hydroxyethylamines[3,7]. In this research, optimum yields were obtained by the use of approximately one molar equivalent of sodium ethoxide in dioxane or ethanol. For example, although Naiki[12] failed in the synthesis of 3-(1-anthraquinonyl)-2-oxazolidinone using aqueous alkali as a ring-closure agent, we have succeeded in this synthesis using an equivalent amount of

4) G. D. Speranza and W. J. Peppel, *J. Org. Chem.*, **23**, 1922 (1958).
5) K. Gulbins and K. Hamann, *Angew. Chem.*, **70**, 705 (1958).
6) J. Nemirowsky, *J. prakt. Chem.*, [2], **31**, 173 (1885).
7) R. Adams and J. B. Segur, *J. Am. Chem. Soc.*, **45**, 785 (1923).
8) A. F. Mckay and R. O. Braun, *J. Org. Chem.*, **16**, 1829 (1951).
9) R. Delaby, P. Chabrier and H. Najer, *Bull. soc. chim. France*, 1616 (1955).
10) R. Delaby, P. Chabrier and H. Najer, *Compt. rend.* **235**, 376 (1952).
11) D. B. Sprinson, *J. Am. Chem. Soc.*, **63**, 2249 (1941).
12) K. Naiki, *J. Soc. Org. Synth. Chem. Japan (Yūki Gōsei Kagaku Kyokai Shi)*, **14**, 84 (1956).

TABLE II. 3-SUBSTITUTED 2-OXAZOLIDINONES

3-Sub. 2-Oxazolidinone	Solvent of reaction[a]	Yield %	M. p.	Solvent of crystn.[a]	C, % Calcd.	C, % Found	H, % Calcd.	H, % Found	N, % Calcd.	N, % Found
n-Butyl	D	80	122(4)[b,c]							
t-Butyl	E	62	94(2)[b]		58.72	58.88	9.51	9.44	9.78	9.90
Phenyl	E	94	118[d]	B						
p-Tolyl	D	70	91[e]	B-L						
o-Tolyl	E	81	170(4)[b,f]							
p-Nitrophenyl	E	95	154.5	B-E	51.92	52.14	3.87	4.06	13.46	13.31
o-Nitrophenyl	E	94	165	B	51.92	52.21	3.87	4.10	13.46	13.61
p-Carbethoxyphenyl	E	97	110[g]	B						
p-Chlorophenyl	E	85	121[h]	B						
1-Anthraquinonyl	D	85	226.5	Dm	69.62	69.36	3.78	4.00	4.78	4.76
Ethylene-bis	E	80	107[i]	E						
Tetramethylene-bis	D	85	118	E	52.62	52.68	7.07	7.32	12.27	12.00
m-Phenylene-bis	D	62	175	B	58.06	57.78	4.87	5.05	11.29	11.40
p-Phenylene-bis	D-Dm	68	253	Dm	58.06	58.31	4.87	5.02	11.29	11.49

a. D=Dioxane, E=Ethanol, B=Benzene, L=Ligroin, Dm=Dimethylformamide. b. B. p. (mmHg). c. Reported b. p. 94°C (1 mmHg), Ref. 1. d. Reported m. p. 118°C, J. R. Caldwell, U. S. Pat. 2656328 [*Chem. Abstr.*, **48**, 2415 (1954)]; 122°C, Ref. 3; 124°C, Ref. 6. e. Reported m. p. 91°C, Ref. 7. f. Reported b. p. 180~185°C (3 mmHg), Ref. 7. g. Reported m. p. 110°C, Ref. 4. h. Reported m. p. 121°C, Ref. 8. i. Reported m. p. 108°C, Ref. 10.

alcoholate. In preparing 3-*p*-nitrophenyl-2-oxazolidinone, the use of alcoholate gave a satisfactory result, but the use of aqueous alkali resulted in the formation of *N*-*p*-nitrophenylethanolamine. Data on the dehydrochlorination of β-chloroethyl carbamates are given in Table II.

Experimental

All melting and boiling points are uncorrected.

β-Chloroethyl Chloroformate.—The preparation of the ester was carried out by a modification of the procedure of Nekrassow et al.[13] Phosgene was passed rapidly into 161 g. of ethylene chlorohydrin for 3 hr. at 0°C. The reaction mixture was then allowed to stand at room temperature (approximately 15°C) until the evolution of hydrogen chloride had subsided; it was then weighed. If the weight increase did not approach the theoretical expectation, this procedure was repeated. The resulting liquid was then refluxed for 2 hr. Upon distillation, 263 g. (93%) of the ester, b. p. 149~153°C (lit.[13] b. p. 152~153°C), was obtained.

Isocyanates.—Except for tetramethylenediisocyanate, all isocyanates were prepared from the corresponding amine hydrochlorides according to the well-known phosgene method[14]. The boiling points (or melting points) and yields of the isocyanates obtained were as follows: *n*-butyl-, b. p. 114°C (lit.[14] 115°C), 80%; phenyl-, b. p. 50~51°C/10 mmHg lit.[14] 56°C/16 mmHg, 82%; *p*-tolyl-, b. p. 110°C/72 mmHg lit.[14] 67.7°C/10 mmHg, 75%; *p*-nitrophenyl-, m. p. 57°C (lit.[14] 56~57°C), 88%; *m*-phenylenedi-, m. p. 51°C (lit.[14] 51°C), 79%; *p*-phenylenedi-, m. p. 94°C (lit.[14] 95°C), 85%. Tetramethylenediisocyanate was synthesized by a Curtius rearrangement of adipodiazide prepared from adipic acid[15]. The over-all yield was 50%. The product boiled at 80.5°C/5 mmHg, lit.[15] 93°C/7 mmHg.

***N*-Substituted β-Chloroethyl Carbamates.**—Typical examples are given below.

By Method A.—(*a*) *N-tert-Butyl-β-chloroethyl Carbamate.*—β-Chloroethyl chloroformate (59 g., 0.41 mol.) was stirred, drop by drop, into a mixture of 25 g. (0.34 mol.) of *tert*-butyl amine and 41 g. (0.41 mol.) of triethylamine. The reaction mixture was heated to 70°C for 30 min. and then poured into 200 ml. of water. The mixture was extracted with two 100 ml. portions of ether. The extract was dried over anhydrous sodium sulfate, and the ether was distilled off. When the residue was fractionated under reduced pressure, 38 g. (63%) of the carbamate, b. p. 90°C/7 mmHg, was obtained.

(*c*) *N-o-Nitrophenyl-β-chloroethyl Carbamate.*—A mixture of 43 g. (0.30 mol.) of β-chloroethyl chloroformate and 34.5 g. (0.25 mol.) of *o*-nitroaniline was heated to 120°C. Heating and stirring were continued for ca. 1 hr., until the evolution of hydrogen chloride ceased. Owing to the intermediate formation of the amine hydrochloride, the reaction mixture became heterogeneous, but subsequently it became clear again. This clear mixture was then cooled, and the precipitate of the carbamate was filtered, washed with ethanol, and dried. It weighed 61 g. (98%). Recrystallization from a benzene-ligroin mixture gave the pure product, m. p. 70.5°C.

By Method B. (*a*) *N-n-Butyl-β-chloroethyl Carbamate.*—A mixture of 25 g. (0.25 mol.) of *n*-butyl-isocyanate and 21 g. (0.26 mol.) of ethylene

13) W. Nekrassow and J. F. Komissarow, *J. prakt. Chem.*, [2], **123**, 163 (1929).

14) W. Siefken, *Ann.*, **562**, 75 (1949); R. L. Shriner et al., "Organic Syntheses", Coll. Vol. II., (1943), p. 453.

15) Y. Iwakura et al., "Experiments in Polymer Chemistry (Kōbunshi Zikken Kagaku Kōza)", Vol. II, Kyōritsu, Tokyo (1958), p. 141.

chlorohydrin in 50 ml. of dry benzene was refluxed for 5 hr. After evaporation of the benzene, distillation of the residue yielded 39 g. (83%) of the carbamate, b. p. 113°C/4.3 mmHg.

(b) N-p-Tolyl-β-chloroethyl Carbamate.—A mixture of 33.3 g. (0.25 mol.) of *p*-tolylisocyanate and 21 g. (0.26 mol.) of ethylene chlorohydrin in 50 ml. of dry toluene was refluxed for 2 hr. Removal of the solvent gave 54 g. of the crude product, and the yield was nearly quantitative. Recrystallization from benzene afforded the pure compound, m. p. 61°C.

3-Substituted 2-Oxazolidinones.—In all experiments, sodium ethoxide was used as a ring-closure agent and the reaction was carried out in dioxane or ethanol. A few examples follow.

(a) 3, 3'-Tetramethylene-bis-(2-oxazolidinone).—A solution of sodium ethoxide, prepared from 7.5 g. (0.33 g. atom) of sodium and 50 ml. of absolute ethanol, was stirred, drop by drop, into a solution of 48.5 g. (0.16 mol.) of *N, N'*-tetramethylene-bis-(β-chloroethyl carbamate) in 50 ml. of dioxane at 70~80°C. After completion of the addition, stirring and heating were continued for another hour. The precipitate of sodium chloride was filtered from the warm mixture. After evaporation of the solvent form the filtrate, 31 g. (95%) of the bis-(2-oxazolidinone) was obtained. The pure compound had a m.p. of 118°C after recrystallization from ethanol.

(b) 3-Phenyl-2-oxazolidinone.—A solution of 5.0 g. (0.22 g. atom) of sodium in 50 ml. of ethanol was gradually stirred into 39.5 g. (0.20 mol.) of *N*-phenyl-β-chloroethyl carbamate in 50 ml. of ethanol at 65~70°C. After the addition was complete, this temperature was maintained for 1 hr.; 100 ml. of water was then stirred into the reaction mixture to dissolve the sodium chloride. The crude 3-phenyl-2-oxazolidinone which separated on cooling was collected by filtration, washed with ethanol, and dried. The yield was 30 g. (94%). The pure product melted at 118°C after recrystallization from benzene.

(c) 3-p-Nitrophenyl-2-oxazolidinone.—A ca. 10% sodium ethoxide solution was stirred, drop by drop, into 46.5 g. (0.19 mol.) of *N-p*-nitrophenyl-β-chloroethyl carbamate in 150 ml. of ethanol at 75°C, until the reaction mixture became slightly brown. The consumption of the sodium ethoxide was nearly the theoretical expectation. Upon the stirring in of 300 ml. of water to the above mixture, 37.5 g. (95%) of 3-*p*-nitrophenyl-2-oxazolidinone crystallized out as yellow needles. Recrystallization from a benzene-ethanol mixture gave the pure compound, m. p. 154°C.

When an alcoholic solution of *N-p*-nitrophenyl-β-chloroethyl carbamate was treated with two molar equivalents of 30% aqueous potassium hydroxide at 60°C, crude *N-p*-nitrophenylethanolamine separated out in a nearly quantitative yield. This was recrystallized from benzene, and the pure product melted at 109°C. Its structure was confirmed by elemental analysis and by infrared measurement.

Found: C, 52.72; H, 5.79; N, 15.77. Calcd. for $C_8H_{10}N_2O_3$: C, 52.74; H, 5.53; N, 15.38%.

Summary

A convenient synthesis of 3-substituted 2-oxazolidinones starting from three components —aliphatic or aromatic amines, phosgene and ethylene chlorohydrin—has been developed.

The author wish to express their gratitude to Hodogaya Kagaku Co., Ltd., for the gift of phosgene and to Mr. A. Miyasu for the preparation of some isocyanates.

Department of Synthetic Chemistry
Faculty of Engineering
Kyoto University
Sakyo-ku, Kyoto (*R. O. & M. M.*)
Institute for Chemical Research
Kyoto University
Takatsuki, Osaka (*M. O.*)

The Behavior of Silver in Glass. I. The Diffusion of Silver into Glass from a Melt of Silver Nitrate[*1]

By Taro Ito

(Received February 10, 1962)

Previously the present author, together with his co-worker, studied[1] the diffusion of silver into a glass material in a temperature range somewhat below the softening temperature, namely, from 500 to 600°C. It was ascertained that a colorless glass gradually turned yellow or, further, brown as a result of the immigration of silver therein. According to previous authors, the following three consecutive stages of change are involved: first, the immigration of silver ions due to exchanges between silver

*1 The major part of this report was presented at the 8th Annual Meeting of the Chemical Society of Japan, Tokyo, April, 1955.

1) S. Kinumaki and T. Ito, *Sci. Repts. Research Inst., Tohoku Univ.*, **A8**, 60 (1956).

and sodium ions[2], second, the reduction of the ions[3], and, last, the formation of silver colloid in the glass medium[4]. The first quantitative investigations of the immigration were done by Schulze[2], who observed that silver diffuses from a silver nitrate melt into Thuringian glass and stains it intensively and that ions of silver and of sodium are exchanged. However, as to how each of these stages contributes respectively to the coloring, we do not have sufficient knowledge, especially in the former two cases; the problem must be studied in the future. However, in any cases, the degree of coloring may be taken as a measure corresponding to the immigration of silver into the glass material.

Consequently, the amount of silver immigrated in the glass material can be estimated by measuring the absorption of light at a characteristic wavelength, if it exists. The present investigation attempted to study the problem of the penetration of silver into a glass medium in particular connection with the light absorption.

Experimental

Material and Measurement of Absorbance. — The specimens were made from a glass plate, 1.93 $\pm$0.03 mm. thick, the composition of which was the same*2 as that glass used in the previous work. This glass plate was cut into rectangles 12×50 mm^2 as the optimum size of the specimens; in addition, as a point of reference, a piece was cut out of the same glass plate next to every piece, in order to eliminate the discrepancies in the following observations due to fluctuation in the composition or in the thickness of the glass material.

The specimens were immersed for definite periods in melts of silver nitrate, which were kept at the constant temperatures of 250, 280, 310, 340, 370 and 400$\pm$1°C. Then they were taken out of the melts, cooled and washed with distilled water to remove the salt clinging to the surface of the glass.

Absorption spectra were measured on these glass plates with a Shimadzu QB-50 type spectrophotometer.

After the optical measurements, the border parts of the glass plates were cut off in order to avoid the boundary effects in the diffusion processes; then the residual parts were cut into rectanglar pieces 6×12 mm^2 for the sake of simple calculation. These pieces were used as specimens for measuring the changes in density due to the silver immigration. As points of reference, pieces cut out of the original pile, as mentioned above, were used, having been heat-treated to have the same thermal histories as salt-immersed pieces.

Measurement of the Shifting of Glass Densities. —We know that we can coveniently determine the density of a tiny piece of a solid material when we have a liquid the density of which can vary over a range including that of the specimen. Thus, if the density of the liquid be adjusted so that the specimen can stay at any depth in the liquid, neither rising nor sinking, then the density of liquid, determinable with a pycnometer or by other means, can be taken to be that of the solid. For this purpose, in the present work, solutions were prepared as follows: a suitable quantity of red mercuric iodide was suspended in water; then potassium iodide was added thereto, enough for the bulk to become a clean solution, probably due to the formation of some complex ions. By such processes we can obtain solutions of desired densities, in the range from unity to 3.5, corresponding to the concentrations; moreover, we can, in the above-mentioned range, increase or decrease the densities of given solutions by the evaporation or addition of water. Thus, the solution consisting of 113 g. of mercuric iodide, 91 g. of potassium iodide and 46 g. of water, the total weight amounting to 250 g. and the volume to 100 ml., has a density of 2.5, which is nearly equal to those of the glasses. This was, therefore, suitable as the starting solution.

As, in the present work, the change in the density of the glass due to the immigration, rather than its absolute values, was essential, the following procedures were preferred: a piece of salt-treated glass, together with a piece of the original glass, was put into a solution denser than both of them, and thereinto was poured, little by little, pure water from a micro buret, the volume being read frequently. First, the denser one of the two pieces reached the state of suspension; then, after the addition of a definite quantity of water, the other reached suspension. Thus, from the quantity of added water between the two suspensions, the required value can be calculated.

Then, because of the small density differences, the density differences between the specimens were evaluated by interpolation from the rising or sinking velocity measures instead of adjusting the densities of the liquids exactly to the perfect suspension of the specimens.

On the original glass, it was confirmed by the same procedure that the density remains unchanged on the thermal exposure in the temperature range from 250 to 400°C; this fact about glass of a similar kind has already been indicated by previous authors[5].

Thermostat.—All through the measurements of the densities, the temperature was kept at 25$\pm$0.001°C by means of a thermostat regulated by a combination of an infrared radiator and a water cooler. The room temperature was 25$\pm$3°C.

2) For instance, A. G. Schulze, *Ann. Phys.*, **40**, 335 (1913).
3) J. Halberstadt, *Z. anorg. allgem. Chem.*, **211**, 185 (1933).
4) W. Jander, ibid., **143**, 277 (1925); W. A. Weyl, "Coloured Glasses", Soc. Glass Tech., Sheffield, England (1951), p. 407; H. Tober, *Glastech. Ber.*, **34**, 456 (1961).
*2 Composition of sample glass: SiO_2, 70.89; Na_2O, 14.11; CaO, 8.22; MgO, 4.43; Al_2O_3, 1.31; Fe_2O_3, 0.13; TiO_2, 0.03; total, 99.12 wt.%.
5) H. Salmang und K. von Soesser, *Glastech. Ber.*, **8**, 463 (1930).

Results and Calculation

Absorbance.—The absorption spectrum of non-treated sodium-glass was obtained with the usual profile, as is shown in Fig. 1; it was ascertained that this spectrum does not suffer any annealing effect. The absorption of silver-glass was obtained with reference to this non-treated glass. Accordingly, the measure of absorbance is the difference between the absorptions of silver- and sodium-glasses and may be regarded as corresponding to the change in composition due to the immigration of silver. Typical curves of the absorbance spectra of silver-glass obtained as mentioned above are shown in Fig. 2. These curves all have one resemblance. The depth of penetration layer was estimated by the diminution of the thickness of the specimen ground until the yellow layer had disappeared. Now it was obtained as about 0.4 mm. under these conditions of treatment. As is seen in Fig. 2, the maxima of the absorbance curves lie at a wavelength of 314±1 mμ. Thus, the wavelengths of maximum absorption can be taken to have a constant value, the small deviation in the above-mentioned results being attributable to the fluctuation in the properties of the particular glass pieces. The heights of peaks are dependent on the time and the temperature of treatment. The relations, at various temperatures, between the heights of the maxima and the times of treatment are shown in Fig. 3.

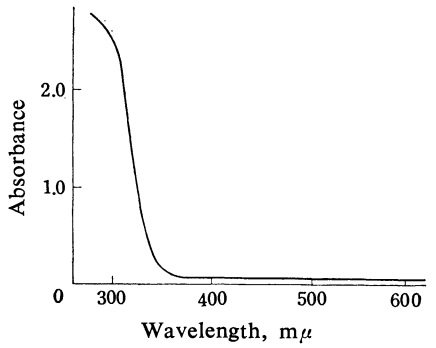


Fig. 1. Absorbance spectrum of sample glass refered to air. Since the conversion into the value per unit thickness is not important in this case, this is a figure obtained from non-converted values.

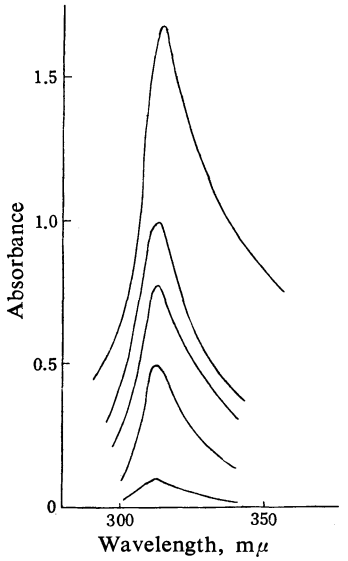


Fig. 2. Absorbance spectra of silver-containing glasses refered to the glass of Fig. 1.

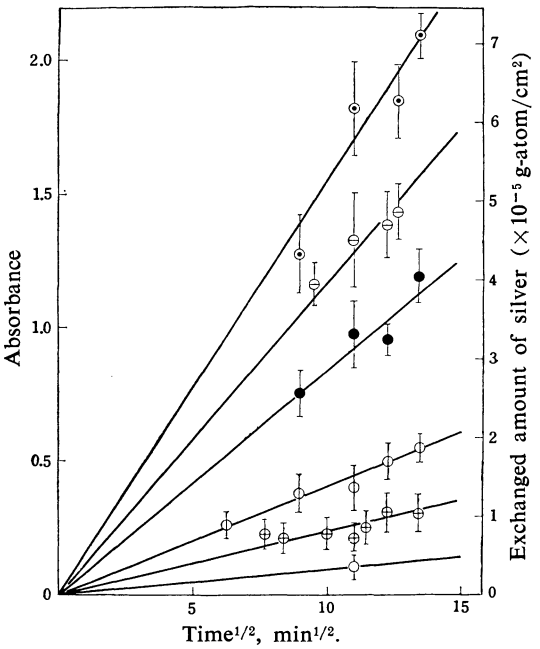


Fig. 3. Values of absorbance maxima as function of time at five temperatures:
○ 250, ⊕ 280, ◐ 310,
● 340, ⊖ 370, ⊙ 400C
Errors are indicated by the lengths of the vertical lines.

Calculation of Density.—The pieces used in the measurement of density differences were selected particularly from those specimens which had reasonable values of absorbance as ascertained by the above-mentioned methods. We will denote the volume of water added to the reference solution from the beginning to the first suspension state by a in ml., and the volume, the weight and the density of the solution in this state by V, W and ρ respectively. Further, the volume of water added from the first to the second suspension states is v, the volume, the weight and the density of the solution thus arrived at being V_0, W_0

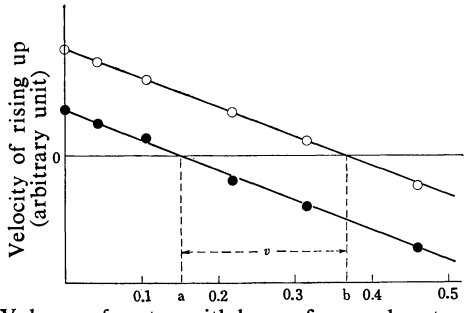


Fig. 4. The relation of the velocity of rising up against the volume of water withdrawn.
-○- Sodium-glass -●- Silver-glass

and ρ_0 respectively. One of the relations of the rising or sinking velocity against the volume of withdrawn water was plotted as shown in Fig. 4. The difference in density between the two glass pieces is given by:

$$\Delta\rho=\rho-\rho_0=\frac{W}{V}-\rho_0$$

Then $$W=W_0-w=V_0\rho_0-vd$$

where v, w and d are the volume, the weight and the density*3 of the water withdrawn from the buret.

So $$\Delta\rho=\frac{V_0\rho_0-vd-V\rho_0}{V}$$

$$=\frac{(V_0-V)\rho_0-vd}{V}$$

In the present work, it was confirmed that the volume contraction due to the dilution of the solution does not exceed the limit of acceptable approximation, namely $V_0-V=v$.

Consequently, $$\Delta\rho=\frac{v(\rho_0-d)}{V}$$

The value thus obtained is the change in the weight of the glass per ml. caused by the immigration of silver. The area of the precise rectangle through which silver ions had penetrated into the glass was measured with a screw micrometer. The penetrated amounts per unit area thus calculated are plotted against absorbance in Fig. 5.

Diffusion Constant.—It has been described how both the absorbance and the change in density resulting from an immersion treatment occur as a result of a diffusion of silver ions and depend on the total amount of exchanged silver. With the inclination of the straight line given in Fig. 5, the absorbance can be converted into the amount of silver. The ratio of the exchanged amount of silver per unit

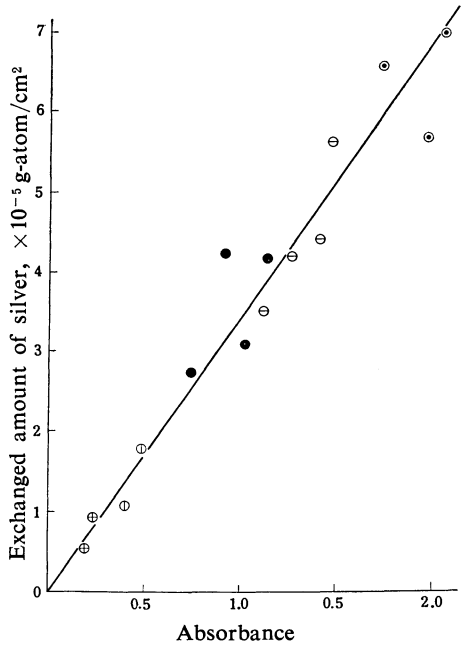


Fig. 5. The relation of the exchanged amount of silver against absorbance (cf. Fig. 3 for notes).

area vs. the absorbance was obtained as follows:

$$r=\frac{\text{amount per area}}{\text{absorbance}}=3.408\times10^{-5}\ \text{g-atom/cm}^2$$

The results of the conversion are placed vertically on the right of Fig. 3. On the other hand, according to Fick's law[6], the amount of silver can be represented with

$$M=2N\sqrt{\frac{Dt}{\pi}} \qquad (1)$$

Accordingly, $$D=\left(\frac{M}{\sqrt{t}}\right)^2\frac{\pi}{4N^2} \qquad (2)$$

where M is the immigrated amount of silver, N the saturation concentration, and t the reaction time. The $M/\sqrt{t}$ was obtained from the inclination of the straight lines in Fig. 3 at the respective temperatures. N can be taken as the concentration of sodium ions in the glass. It was calculated with the following equation:

$$N=\rho_0\times C\times\frac{1}{1/2(Na_2O)}$$

Inserting $\rho_0=2.511$, $C=14.11/100$ (the wt.% of Na_2O) and $Na_2O=61.98$ (molecular weight),

$$N=1.31\times10^{-2}\ \text{g-atom/ml.}$$

Putting these values into Eq. 2, the diffusion constant, D, was obtained. The logarithms of

*3 $d=0.9971\pm0.0007$ (at 25 ± 3°C), according to Landolt-Bernstein, "Physikalisch-Chemische Tabellen".

6) J. Crank, "The Mathematics of Diffusion", Clarendon Press, Oxford (1956), p. 31.

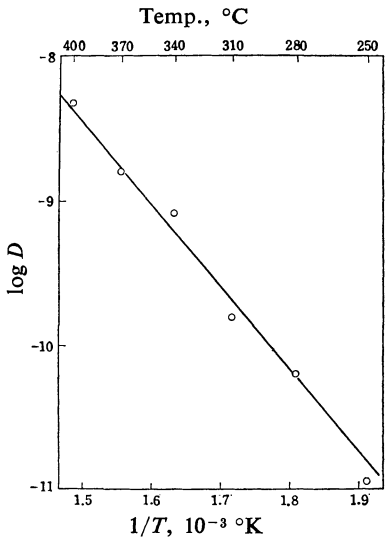


Fig. 6. The relation between $\log D$ and $1/T$.

D thus obtained are plotted against the reciprocal absolute temperature in Fig. 6. The relation of $\log D$ to $1/T$ is linear, as is seen in this figure. From the inclination of the line, the energy of activation, E, can be calculated to be

$$E=26.3 \text{ kcal./mol.}$$

also $$D_0=9.85\times10^{-1} \text{ cm}^2/\text{sec.}$$

Discussion

By measuring the electrical resistance, the diffusion of sodium in glass was studied[7]. In this work the means of absorbance has been successfully applied to the calculation of the diffusion, accompanied with the measurement of density difference.

The value of $E=26.3$ kcal./mol. is of the same order as that obtained in the previous work[1]. The value of $D_0=9.85\times10^{-1}$ cm^2/sec., on the other hand, is slightly larger than that obtained previously. However, they are both reasonable values. In this work, treatment at temperatures above 400°C could not be carried out because of the instability of the nitrate and because of the anomaly of glass-density in its thermal history.

7) R. W. Douglas and J. O. Isard, *J. S. Glass Thechnol.*, 33, 289 (1949).

The figures in many reports of the absorption spectra of silver-containing glass have not agreed with each other. According to Wells[8], the coloration of silver salts depends on the length of the Ag—O bonds. Helmholz[9], on the contrary, has suggested that the color is related to the nature of the Ag—O bonds.

Most silver salts are colorless, although some of them are yellow or a similar color. Their absorption spectra have relatively low bands at wave lengths near 300 mμ[10]. Glass is not crystalline but amorphous. Therefore, the coloration, as well as the diffusion, involves more complicated problems than the salts, the space conditions in the glass media being in chaos. The absorption spectrum of silver-containing glass annealed at higher temperatures had a different band[1]. The coloration of glass has been, hitherto, dealt with in terms of the formation of the colloid of some metals in glass. The color of various kinds of silver glass would depend on the chemical state of silver, that is, on whether it is ionic, atomic or colloidal. The color obtained in the present experiment was yellow and not fluorescent, so it should be regarded as due to the state of the ions[11]. A detailed study of this problem will be carried out in the future.

The author wishes to express his deep gratitude to Professor Susumu Kinumaki of the Chemical Research Institute of Non-Aqueous Solutions, Tohoku University, for his helpful counsel and for supplying the author with material help of various kinds in the course of this study.

Faculty of Liberal Arts and Science
Yamagata University
Yamagata City

8) A. F. Wells, "Structural Inorganic Chemistry", 2nd ed., Clarendon Press, Oxford (1950), p. 215.
9) L. Helmholz and R. Levine, *J. Am. Chem. Soc.*, **64**, 354 (1942).
10) Y. Shibata et al., *J. Tokyo Chem. Soc.*, **40**, 411 (1919); J. W. Mellor, "A Comprehensive Treatise on Inorganic and Theoretical Chemistry", Vol. III, Longmans Green and Co., London (1923), p. 463; H. Fesefeldt, *Z. Physik*, **64**, 741 (1930); A. R. Ubbelohde et al., *Proc. Roy. Soc.*, **A251**, 156 (1959).
11) W. A. Weyl, "Coloured Glasses", loc. cit., p. 459; W. A. Weyl, *J. Phys. Chem.*, **57**, 756 (1953).

Proton Magnetic Resonance of Ammonia-Borane Derivatives

By Osamu OHASHI, Yukio KURITA, Tetsushi TOTANI, Haruyuki WATANABE, Toshio NAKAGAWA and Masaji KUBO

(Received February 19, 1962)

The present authors have already studied the proton magnetic resonance of borazole and some of its derivatives[1,2]. There is another group of compounds having a bond between boron and nitrogen known as ammonia-boranes (or borazanes), i.e., the derivatives of ammonia-borane H_3NBH_3[3]. For instance, both boron trichloride (or trichloroborane) BCl_3 and triethylborane $B(C_2H_5)_3$ are known to form addition compounds with amines through a donor-acceptor bond. Whereas borazole is isoelectronic with benzene, ammonia-borane is isoelectronic with ethane. Accordingly, one has in ammonia-boranes a typical example of donor-acceptor bonds as contrasted with the case of borazoles, in which covalent σ bonds are involved in addition to donor-acceptor bonds between boron and nitrogen. This paper presents the results of investigation on the proton magnetic resonance of ammonia-boranes.

Experimental

Triethylborane was prepared by adding the calculated amount of the addition compound between boron trifluoride and *n*-butyl ether, $BF_3 \cdot O(C_4H_9)_2$, drop by drop to the solution of ethylmagnesium bromide in *n*-butyl ether at room temperature. The resulting triethylborane was purified by distillation in the stream of nitrogen at ordinary pressure, b.p. 95~96°C (lit.[4] 94~97°C).

Trimethylamine-triethylborane $(CH_3)_3NB(C_2H_5)_3$ was synthesized by a method due to Brown[4]. Triethylborane was treated with an excess of trimethylamine. After the excess was removed by distillation from the reaction mixture, the liquid was subjected to distillation at low temperature under reduced pressure, m.p. −47 to −46°C (lit.[4] −46 to −45°C).

Triethylamine-triethylborane $(C_2H_5)_3NB(C_2H_5)_3$ was synthesized from triethylborane and excess triethylamine and purified in the same manner as above. This compound decomposes in the gas phase at room temperature, decomposition products being presumed to exist in the liquid state also. No data are available in the literature for comparison.

Trimethylamine-trichloroborane $(CH_3)_3NBCl_3$ was prepared by allowing boron trichloride to react with the equivalent amount of trimethylamine in carbon tetrachloride at −70°C. The addition compound was soluble with difficulty in this solvent. After filtration, the precipitates were recrystallized from ethanol, m.p. 243~244°C (lit.[5] 243~244°C). Anal. Calcd. for $(CH_3)_3NBCl_3$: N, 7.96%. Found: N, 7.89%.

Triethylamine-trichloroborane $(C_2H_5)_3NBCl_3$ was synthesized from boron trichloride and triethylamine in a similar manner to above and was recrystallized from methanol. It decomposed on melting at 81~83°C (lit.[6] 75°C). Anal. Calcd. for $(C_2H_5)_3NBCl_3$: N, 6.42%. Found: N, 6.16%.

The proton magnetic resonance spectra were recorded at room temperature by means of a JNM-3 high-resolution NMR spectrometer of Japan Electron Optics Laboratory Company operating at 40 Mc. Chemical shifts were evaluated using appropriate internal standards so as to avoid the overlap of signals of samples under investigation with that of the standard used. In case when samples were unstable, they were sealed in a cell with an external standard. No correction was made for the bulk magnetic susceptibility of the samples.

Assignments

The NMR spectra of triethylborane were recorded in pure liquid state as well as in carbon tetrachloride solution with cyclohexane as an internal standard. These spectra were essentially identical with each other. The spectra showed a fairly sharp composite signal attributable to ethyl groups bonded to boron as illustrated in Fig. 1a.

Trimethylamine-triethylborane was examined in pure liquid state with water as an external standard. A very sharp intense line appearing at −0.77 p.p.m. as calculated with cyclohexane as the standard* was ascribed to protons in methyl groups bonded to nitrogen. In addition,

1) K. Ito, H. Watanabe and M. Kubo, *J. Chem. Phys.*, **32**, 947 (1960); This Bulletin, **33**, 1588 (1960).
2) K. Ito, H. Watanabe and M. Kubo, *J. Chem. Phys.*, **34**, 1043 (1961).
3) S. G. Shore and R. W. Parry, *J. Am. Chem. Soc.*, **77**, 6084 (1955); **80**, 8 (1958).
4) H. C. Brown, ibid., **67**, 374 (1945).
5) E. Wiberg and W. Sütterlin, *Z. anorg. u. allgem. Chem.*, **202**, 31 (1931); J. Goubeau, M. Rahtz and H. J. Becher, ibid., **275**, 161 (1954).
6) F. Gallais and J. P. Laurend, *Compt. rend.*, **244**, 1636 (1957); H. C. Brown, P. F. Stehle and P. A. Tierney, *J. Am. Chem. Soc.*, **79**, 2020 (1957).

* Numerical values for chemical shifts given below refer to cyclohexane as the standard. Conversion was made with the proton chemical shifts −3.4 and +1.6 p.p.m. of water and tetramethylsilane referred to cyclohexane. J. A. Pople, W. G. Schneider and H. J. Bernstein, "High-resolution Nuclear Magnetic Resonance", McGraw-Hill, New York (1959), pp. 89, 236.

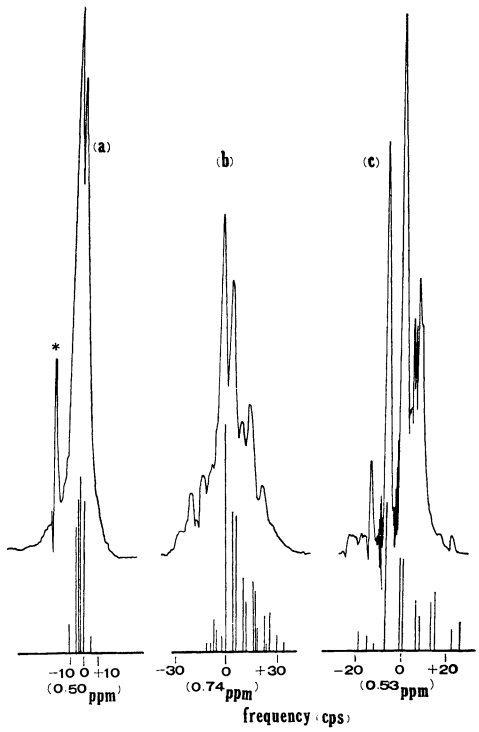


Fig. 1. $B\text{-}C_2H_5$ proton signals of (a) triethylborane, (b) trimethylamine-triethylborane and (c) triethylamine-triethylborane. The theoretical patterns are shown below. For the sake of clarity, some sets of closely spaced theoretical lines are shown by single bars. The peak marked with an asterisk is the reference line of cyclohexane. In order to increase resolution, a different sweep rate was employed for (c).

a group of weak peaks appeared on the lower field side of this peak. Presumably, some decomposition products were responsible for it. Ethyl groups in this compound yielded a complicated group of lines shown in Fig. 1b, suggesting that intermediate coupling exists rather than weak coupling, in which case one would have a simple three-four pattern for the signal of ethyl groups[7].

Triethylamine-triethylborane was studied in pure liquid state with water as an external reference. The spectrum showed a quartet at −2.13 p.p.m. attributable to methylene protons in ethyl groups bonded to nitrogen. The separation between multiplet components yielded the spin coupling constant J_{HH} equal to 6.7 c.p.s. The corresponding signal of methyl protons appeared at about 0.16 p.p.m., although the triplet structure was not very clear because of masking by BC_2H_5 signals described below. As in the spectra of the foregoing two compounds, ethyl groups bonded directly to boron gave rise to a complicated signal shown in Fig. 1c. This compound readily decomposes in the gaseous state. In fact, signals presumed to be due to some decomposition products from intensity considerations appeared between the triplet and the quartet of ethyl groups bonded to nitrogen, rendering unequivocal assignment very difficult.

Trimethylamine-trichloroborane was dissolved in chloroform and the NMR spectrum was recorded with tetramethylsilane as an internal reference. The spectrum showed a group of closely spaced lines centered at −1.57 p.p.m. in addition to a very strong peak attributable to chloroform, which was accompanied by spinning side bands and weak satellites due to $^{13}CHCl_3$. Unlike the signals of NCH_3 protons in *N*-trimethylborazoles, which were found to be rather sharp, that of this compound consisted of four almost equally spaced quartet lines separated by 2.6 c.p.s., a line at the highest field being weaker than three others. The small separation of this magnitude[2] suggests spin coupling between protons and a nitrogen nucleus separated by two chemical bonds, although the reason for the appearance of a quartet rather than a triplet is not clear.

Triethylamine-trichloroborane was dissolved in chloroform and the spectrum was taken with tetramethylsilane as an internal standard. The spectrum was comprised of a typical 1 : 2 : 1 triplet centered at 0.04 p.p.m. attributable to methyl protons in ethyl groups and a quartet centered at −2.37 p.p.m. originating from methylene protons. The spin coupling constant J_{HH} was evaluated at 7.6 c.p.s. In addition, a very strong peak due to $^{12}CHCl_3$, weak satellites arising from $^{13}CHCl_3$ and spinning side bands were recorded.

Discussion

The numerical values of chemical shifts and spin coupling constants are summarized in Table I. Those of trimethylamine[8], triethylamine[8] and borazoles[1,2] also are listed for comparison. The observed chemical shifts and spin coupling constants are of the correct order of magnitude compared with those of borazole[1,2] already studied, indicating the adequacy of the present assignments.

The observed NCH_2 and $NCCH_3$ proton chemical shifts of triethylamine, triethylamine-triethylborane and triethylamine-trichloroborane decreases in this order in agreement with increasing extent of charge transfer from nitrogen to boron due to the formation of an

7) P. L. Corio, *Chem. Revs.*, **60**, 363 (1960).

8) B. P. Dailey and J. N. Shoolery, *J. Am. Chem. Soc.*, **77**, 3977 (1955).

TABLE I. PROTON CHEMICAL SHIFTS (p.p.m.) AND SPIN COUPLING CONSTANTS J (c.p.s.) OF TRIETHYLBORANE AND SOME AMMONIA-BORANES. REFERENCE: CYCLOHEXANE.

Compounds	NCH_2	NCH_3	$NCCH_3$	BC_2H_5	J
$B(C_2H_5)_3$				0.00−0.74	
$(CH_3)_3NB(C_2H_5)_3$		−0.77		0.14−1.54	
$(C_2H_5)_3NB(C_2H_5)_3$	−2.13		0.16	0.16−0.84	$J_{HH}=6.7$*
$(CH_3)_3NBCl_3$		−1.57			$J_{NCH}=2.6$
$(C_2H_5)_3NBCl_3$	−2.37		0.04		$J_{HH}=7.6$
$N(CH_3)_3$		−0.77			
$N(C_2H_5)_3$	−1.33		0.50		
Borazoles**	−2.20 −1.98 −2.17	−1.75 −1.60 −1.58 −1.50	0.38 0.40 0.40	0.45 0.52 1.05	$J_{HH}=8.0, 7.2, 8.1$ $J_{NCH}=3.0$

* In ethyl groups attached to nitrogen. ** For detailed description of borazole derivatives, see Ref. 2.

N→B bond and the effect of electronegative chlorine atoms. The same trend is observed for the NCH_3 proton chemical shifts of trimethylamine, trimethylamine-triethylborane and trimethylamine-trichloroborane.

A striking difference between ammonia-boranes and borazoles is that whereas ethyl groups attached to boron in the latter compounds give rise to a single sharp signal of proton resonance, those in the former yield a group of lines showing a complicated pattern of line spacings and relative intensities. The observed ethyl signals of triethylborane, trimethylamine-triethylborane and triethylamine-triethylborane were compared with theoretical calculations by Corio[7] for an A_3B_2 spin system. In other words, further splitting of ethyl proton signals due to magnetic boron nuclei was disregarded for the following reasons. In the first place, the spin coupling constants between a boron nucleus having a small atomic number and ethyl protons across two or more chemical bonds are presumed to be small[9]. Secondly, because boron nuclei have an electric quadrupole moment, spin decoupling is presumed to take place between boron nuclei and protons. In fact, Onak et al.[10] have observed the ^{11}B nuclear magnetic resonance spectra of a number of boron compounds including triethylborane and evaluated spin coupling constants between directly bonded boron and hydrogen but not those between boron nuclei and protons separated by two or more chemical bonds. Considering possible overlap of closely spaced theoretical lines, the relative internal shifts δ (unmodified by spin interactions) between methyl and methylene proton signals and spin-spin coupling constants were evaluated as shown in Table II. Theoretical spectra calculated with these values yield a fairly good fit with experiments as shown in Fig. 1.

TABLE II. THE INTERNAL CHEMICAL SHIFTS (p.p.m.) AND THE SPIN-SPIN COUPLING CONSTANTS (c.p.s.) OF BC_2H_5 PROTONS IN TRIETHYLBORANE AND RELATED COMPOUNDS.

Compound	$\Delta CH_3-\Delta CH_2$	J	Electro-negativity of boron
$B(C_2H_5)_3$	+0.19	7.2	1.8, 2.2*
$(CH_3)_3NB(C_2H_5)_3$	−0.47	7.1	1.4, 1.8*
$(C_2H_5)_3NB(C_2H_5)_3$	−0.43	7.3	1.4, 1.8*

* The modified Dailey-Shoolery equation was employed in the calculation.

Dailey and Shoolery[8] have shown that the methyl signal and the methylene signal of an ethyl group showing the characteristic three-four pattern ($J \ll \delta$)* draw together as the electronegativity of an atom bonded to the ethyl group decreases: a linear relation holds between the electronegativity and the difference, $\delta=\Delta CH_3-\Delta CH_2$, between the chemical shifts of methyl protons and methylene protons in an ethyl group.

$$\text{E.N.}=0.695(\Delta CH_3-\Delta CH_2)+1.71$$

When the difference between the chemical shifts (in frequency units) of these two groups becomes small and comparable with the spin-spin coupling constant, one has the case of intermediate coupling ($J \approx \delta$) as in triethylborane. In the extreme case in which the spin-spin coupling predominates over the effect of chemical shifts ($J \gg \delta$), a single sharp line results as in *B*-triethylborazoles[11]. When δ

9) P. T. Narasimhan and M. T. Rogers, *J. Chem., Phys.*, **34**, 1049 (1961).
10) T. P. Onak, H. Landesman, R. E. Williams and I. Shapiro, *J. Phys. Chem.*, **63**, 1533 (1959).

* The sign of J is trivial in interpreting the present spectra. J refers to absolute values and hence is positive.
11) J. A. Pople, W. G. Schneider and H. J. Bernstein, "High-resolution Nuclear Magnetic Resonance", McGraw-Hill, New York (1959), p. 116.

decreases further to assume a negative value with its absolute value comparable with the spin-spin coupling constant, we have again the case of intermediate coupling as in trimethylamine-triethylborane and triethylamine-triethylborane. The negative internal chemical shifts between methyl and methylene protons have already been reported for aluminum triethyl, diethylaluminum chloride[12], some mercury dialkyls[13], mercury diethyl[14] and tin tetraethyl[9].

The aforementioned empirical equation first proposed by Dailey and Shoolery for electronegativity values ranging over 2.6~3.9 was found by Baker[12] to be valid approximately even for electronegativity values less than 1.71, i.e., for negative internal shifts of ethyl groups. The electronegativity of boron calculated for triethylborane and related compounds are shown in Table II along with values calculated by the modified Dailey-Shoolery equation[15], in which the constant in the original equation is changed from 1.71 to 2.10 for atoms of low electronegativity.

The present results lead to the conclusions that the formation of an N→B bond interchanges the positions of the methyl and methylene signals of triethylborane and that boron in ammonia-boranes is less electronegative than that in borazoles. This supports the view that the extent of electron transfer from nitrogen to boron in ammonia-boranes is almost the same as but slightly greater than that in borazoles.

Mention should be made in this connection that Becher[16] has determined the dipole moments of some ammonia-boranes (ammonia-trimethylborane $H_3NB(CH_3)_3$ and trimethylamine-trimethylborane $(CH_3)_3NB(CH_3)_3$) and aminoboranes (aminodimethylborane $H_2NB(CH_3)_2$ and dimethylaminodimethylborane $(CH_3)_2NB(CH_3)_2$) in benzene solutions and evaluated from them the NB bond moment in ammonia-boranes and aminoboranes (or borazenes). The former was found to amount to about 30% of the value calculated for the N→B bond. This implies that ammonia-boranes resonate between the no-bond structure $R_3N.BR_3$ and the donor-acceptor bond structure $R_3N{\rightarrow}BR_3$ (R=alkyl group), the contribution of the latter being about 30%. On the other hand, from the measurement of the diamagnetic susceptibilities of borazole and some of its derivatives, the present authors[17] have estimated the diamagnetic anisotropy of a borazole ring and concluded that the contribution of the donor-acceptor double bond structure to the normal state of borazole is 24%.

From the greater extent of the donor-acceptor bond character in ammonia-boranes than that in borazoles, one might expect that nitrogen in the former compounds is more electronegative and hence the chemical shift difference $\Delta CH_3-\Delta CH_2$ of ethyl groups attached to nitrogen is greater than the corresponding values of the latter compounds. However, as shown in Table III, the chemical shift differences of triethylamine-triethylborane and triethylamine-trichloroborane are smaller than those of hexaethylborazole and *B*-trichoro-*N*-triethylborazole, respectively. The reason for this is presumed to be twofold. In the first place, the diamagnetic ring current induced by the external magnetic field in a borazole ring makes a negative contribution[18] to the chemical shifts of protons in the same molecule. Owing to the greater distance from the ring, the effect is smaller for methyl protons than for methylene protons. As a result, the diamagnetic ring current increases the internal chemical shift of ethyl groups in borazoles, regardless of whether the ethyl groups are attached to nitrogen or boron. Secondly, although charge migration from nitrogen to boron is slightly greater in ammonia-boranes than in borazoles, electron withdrawal by nitrogen from three ethyl groups in ammonia-boranes rather than one as in borazoles, more than compensates the decrease in the electronic population of the nitrogen atom due to the formation of an N→B bond. Accordingly, the nitrogen in ammonia-boranes becomes less electronegative than that in borazole derivatives

TABLE III. THE INTERNAL CHEMICAL SHIFTS (p.p.m.) OF NC_2H_5 PROTONS IN TRIETYLAMINE, TRIETHYLAMINE-BORANES AND *N*-TRIETHYLBORAZOLES.

Compound	$\Delta CH-\Delta CH_2$	Electronegativity of nitrogen
$N(C_2H_5)_3$	1.83*	2.98
$(C_2H_5)_3NB(C_2H_5)_3$	2.29	3.30
$(C_2H_5)_3NBCl_3$	2.41	3.38
$[(C_2H_5)NB(CH_3)]_3$	2.38	3.36
$[(C_2H_5)NB(C_2H_5)]_3$	2.57	3.50
$[(C_2H_5)NBCl]_3$	2.58	3.50

* Coyle and Stone give 1.50 p.p.m. See Ref. 19.

12) E. B. Baker, *J. Chem. Phys.*, **26**, 960 (1957).
13) R. E. Dessy, T. J. Flautt, H. H. Jaffé and G. F. Reynolds, ibid., **30**, 1422 (1959).
14) P. T. Narasimhan and M. T. Rogers, ibid., **31**, 1430 (1959); *J. Am. Chem. Soc.*, **82**, 34 (1960).
15) J. N. Shoolery, Lecture Notes, Varian Associates Conference (Nov. 1957). See also Ref. 14.
16) H. J. Becher, *Z. anorg. u. allgem. Chem.*, **270**, 273 (1952).
17) H. Watanabe, K. Ito and M. Kubo, *J. Am. Chem. Soc.*, **82**, 3294 (1960).
18) H. J. Bernstein, W. G. Schneider and J. A. Pople, *Proc. Roy. Soc.*, **A236**, 515 (1956).

as was actually found by the present investigation. This complication does not arise in discussing the BC_2H_5 proton resonance, because electron transfer between boron and ethyl groups is inappreciable as suggested by the electronegativity of boron in triethylborane, which is close to that of a free boron atom equal to 2.0. For this reason, BC_2H_5 proton signals are more suitable than NC_2H_5 signals in discussing the nature of NB bonds in ammonia-boranes and borazoles.

Coyle and Stone[19] have reported the results of measurements on the proton chemical shifts in some boron-containing addition compounds of Lewis bases and showed that the chemical shift criterion is not uniformly successful in predicting the stabilities of addition compounds. However, direct comparison between their results and the present conclusion is not feasible, because no compounds were examined both by them and by the present authors.

19) T. D. Coyle and F. G. A. Stone, *J. Am. Chem. Soc.*, **83**, 4138 (1961).

Summary

The proton magnetic resonance spectra of triethylborane, trimethylamine-triethylborane, triethylamine-triethylborane, trimethylamine-trichloroborane and triethylamine-trichloroborane were recorded at room temperature using an NMR spectrometer operating at 40 Mc. The assignments of observed signals were made and the chemical shifts and spin coupling constants were evaluated. The extent of electron transfer from nitrogen to boron in ammonia-boranes is slightly greater than that in borazoles.

Chemistry Department
Nagoya University
Chikusa-ku, Nagoya
(O.O., Y.K. & M.K.)
Shionogi Pharmaceutical Company
Fukushima-ku, Osaka
(T.T., H.W. & T.N.)

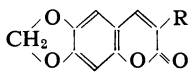
Synthetic Studies of Sesamol Derivatives. I. A New Synthesis of Ayapin

By Kenji FUKUI and Mitsuru NAKAYAMA

(Received February 23, 1962)

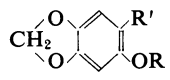
Ayapin, a coumarin isolated from the leaves of *Eupatorium ayapana Vent.*[1,2] is an interesting compound because of its biological activity[3]. Its chemical structure has been established by Späth, Bose and Schläger[2] as Ia, and it is the only known natural methylenedioxycoumarin. It was synthesized by the action of methylene iodide on aesculetin (6,7-dihydroxycoumarin)[2].

This paper describes an improved synthesis of Ia by two routes, that is, by the Knoevenagel and by the Perkin reaction from 2-hydroxy-4,5-methylenedioxybenzaldehyde (IIb).



I

a) R=H
b) R=$COOC_2H_5$
c) R=$COCH_3$
d) R=COOH



II

a) R=R'=H
b) R=H, R'=CHO
c) R=CH_3CO, R'=CHO

2-Hydroxy-4,5-methylenedioxybenzaldehyde (IIb), which was used as the starting material, was readily prepared from seamol (IIa)[4,5], either by formylation by the Gattermann reaction[5] or by the dimethylformamide method. The aldehyde IIb was acetylated to the 2-acetoxy-4,5-methylenedioxybenzaldehyde (IIc), m.p. 125~126°C, with acetic anhydride in the presence of pyridine or anhydrous sodium acetate.

The condensation of hydroxyaldehyde (IIb) with ethyl malonate by the Knoevenagel reaction gave ethyl 6,7-methylenedioxycoumarin-3-carboxylate (Ib), m.p. 190~191°C. On the other hand, when IIb was treated with ethyl acetoacetate in absolute ethanol, it gave 3-acetyl-6,7-methylenedioxycoumarin (Ic), m.p.

1) P. K. Bose and A. Ch. Roy, *J. Indian Chem. Soc.*, **13**, 586 (1936) (*Chem. Abstr.*, **31**, 1787 (1937)).
2) E. Späth, P. K. Bose and J. Schläger, *Ber.*, **70**, 702 (1937).
3) P. K. Bose and P. B. Sen, *Ann. Biochem. and Exptl. Med.*, **1**, 311 (1941); **5**, 1 (1945) (*Chem. Abstr.*, **37**, 3835 (1943); **40**, 2224 (1946)); D. P. Chakraborty, A. D. Gupta and P. K. Bose, ibid., **17**, 59 (1957) (*Chem. Abstr.*, **52**, 1352 (1959)).
4) J. Boeseken, W. D. Cohen and C. J. Kip, *Rec. Trav. Chem.*, **55**, 815 (1936) (*Chem. Abstr.*, **31**, 1017 (1937)); M. Beroza, *J. Agr. Food Chem.*, **4**, 49 (1956) (*Chem. Abstr.*, **50**, 6737 (1956)).
5) H. Suginome, *Tetrahedron Letters*, **1960**, No. 19, 16.

237～238°C. Compound Ib was easily converted by alkaline hydrolysis to acid (Id), m. p. 263～265°C. This acid Id was also obtained by the reaction of IIb with malonic acid, cyanoacetic acid and ethyl cyanoacetate. It was then decarboxylated in quinoline with copper powder to ayapin (6,7-methylenedioxycoumarin) (Ia), m.p. 227～228°C.

In an alternate route, Ia was prepared by the Perkin reaction. This substance exhibited no melting point depression when mixed with the above sample.

Experimental *

2 - Hydroxy - 4, 5 - methylenedioxybenzaldehyde (IIb).—*a) Dimethylformamide Method.*—To a solution of sesamol (IIa) (2.0 g.) in dimethylformamide (3.0 ml.), phosphorous oxychloride (2.0 ml.) was added drop by drop with ice cooling. The reaction mixture was heated on a steam bath for 1 hr. and frequently shaken. After being cooled in an ice bath, the solution was diluted with a saturated sodium acetate solution (ca. 50 ml.) and was heated for 0.5 hr. on a steam bath. Upon cooling of the mixture, the solid which had deposited was collected and recrystallized from ethanol to give IIb in the form of colorless needles, m. p. 125～126°C (reported m. p. 125～126°C)[6], with a blue violet ferric reaction in ethanol; yield, 1.9 g. (79%).

Found: C, 57.84; H, 3.70. Calcd. for $C_8H_6O_4$: C, 57.83; H, 3.64%.

b) Gattermann Reaction.—This aldehyde IIb was prepared from sesamol (IIa) (2.0 g.) and zinc cyanide (4.0 g.) by the Gattermann reaction[4]; m. p., 124～125°C; yield, 2.0 g. (83%). This substance showed no depression of the melting point on admixture with the specimen derived by the above-mentioned method a).

2 - Acetoxy - 4, 5 - methylenedioxybenzaldehyde (IIc).—a) A mixture of IIb (500 mg.), acetic anhydride (3 ml.) and pyridine (5 ml.) was kept at room temperature for 24 hr. and then poured into dilute hydrochloric acid. The precipitates were collected and recrystallized from ethanol to give IIc in the from of colorless needles, m. p., 125～126°C (reported m. p. 126～7°C)[7], with a negative ferric reaction; yield, 620 mg. (99%).

Found: C, 57.64; H, 3.88. Calcd. for $C_{10}H_8O_5$: C, 57.69; H, 3.87%.

b) A mixture of IIb (1.0 g.) and anhydrous sodium acetate (1.2 g.) in acetic anhydride (10 ml.) was refluxed for 4 hr. The cooled mixture was poured into water, and the precipitates were collected. This was recrystallized from ethanol to give IIc in the form of colorless needles; m. p. 125～126°C; yield, 1.0 g. (78%). This substance showed no depression of the melting point on admixture with the specimen derived by the above-mentioned method a).

Ethyl 6,7-methylenedioxycoumarin-3-carboxylate (Ib).—To a solution of IIb (2.0 g.) in pyridine (20 ml.), ethyl malonate (3.0 g.) and piperidine (5 drops) were added. The mixture was refluxed for 0.5 hr., kept at 100°C for 2 hr., and then poured into dilute hydrochloric acid (150 ml.). The precipitates were collected and recrystallized from ethanol to give Ib in the from of pale yellow needles, m. p. 190～191°C, with a strong fluorescence in concentrated sulfuric acid (green) and in ethanol (blue) and with a negative ferric reaction; yield, 2.6 g. (81%); IR; 1739 (C=O); 1029, 938 cm^{-1} (O—CH_2—O) (Nujol)[8].

Found: C, 59.97; H, 4.14. Calcd. for $C_{13}H_{10}O_6$: C, 59.54; H, 3.84%.

3-Acetyl-6,7-methylenedioxycoumarin (Ic).—To a solution of IIb (1.5 g.) in warm absolute ethanol (20 ml.), ethyl acetoacetate (1.5 g.)and piperidine (3 drops) were added. The mixture was refluxed for 5 min. After the mixture had been cooled, the crystalline products were filtered and recrystallized from ethanol to give Ic in the torm of pale yellow needles, m. p. 237～238°C (decomp.), with a fluorescence in ethanol (pale blue) and a negative frric reaction; yield, 2.0 g. (95%); IR; 1725, 1682 (C=O); 1030, 926 cm^{-1} (O—CH_2—O) (Nujol).

Found: C, 61.84; H, 3.43. Calcd. for $C_{12}H_8O_5$: C, 62.07; H, 3.47%.

6, 7 - Methylenedioxycoumarin-3-carboxylic Acid (Id).—*a) From Ib.*—A suspension of ester Ib (1.0 g.) in a 4% sodium hydroxide solution (50 ml.) was stirred for 10 hr. The resulting mixture was filtered, the filtrate was acidified with dilute hydrochloric acid, and the precipitates were collected and recrystallized from ethanol to give Id in the form of pale yellow needles, m. p. 263～265°C, with a strong fluorescence in concentrated sulfuric acid (green) and in ethanol (blue); yield, 0.7 g. (89 %); IR: 1736, 1674 (C=O); 1026, 918 cm^{-1} (O—CH_2—O) (Nujol).

Found: C, 56.43; H, 2.58. Calcd. for $C_{11}H_6O_6$: C, 56.42; H, 2.58%.

b) From IIb.—To a solution of IIb (1.0 g.) and malonic acid (1.3 g.) in pyridine (10 ml.), aniline (5 drops) was added. The mixture was heated on an oil-bath at 55°C for 4 hr. and then poured into dilute hydrochloric acid (150 ml.). The precipitates were collected and recrystallized from ethanol to give Id, m. p. 263～265°C, with a negative ferric reaction; yield, 1.0 g. (71%). This was found to be identical with the specimen obtained by method a).

c) From IIb.—A mixture of IIb (1.0 g), a 20% sodium hydroxide solution (30 ml.) and cyanoacetic acid (1.0 g.) was stirred at room temperature for 24 hr. The resulting mixture was acidified with dilute hydrochloric acid, and the precipitates were collected and recrystallized from ethanol to give Id, m. p. 260～262°C, with a negative ferric reaction; yield, 1.1 g. (78%). This was found to be identical with the specimen obtained by method a).

d) From IIb.—By a method similar to that described for Ic, the products were obtained from IIb (1.0 g.), ethyl cyanoacetate (1.0 g.), piperidine

* All melting points are uncorrected.

6) K. N. Campbell, P. F. Hopper and B. K. Campbell, *J. Org. Chem.*, **16**, 1736 (1951).

7) R. T. Arnold and F. Bordwell, *J. Am. Chem. Soc.*, **64**, 2983 (1942).

8) L. H. Briggs, L. D. Colebrook, H. M. Fales and W. C. Wieldmann, *Anal. Chem.*, **29**, 904 (1957).

(3 drops) and absolute ethanol (20 ml.). Then, a mixture of the products and a 5% sodium hydroxide solution was heated on a steam bath for 8 hr. and kept at room temperature for 12 hr. The resulting mixture was filtered, and the filtrate was acidified with dilute hydrochloric acid. The precipitates were collected and recrystallized from ethanol to give Id, m. p. 263~264°C, with a negative ferric reaction; yield, 400 mg. (38%). This was found to be identical with the specimen obtained by method a).

Ayapin (6,7-Methylenedioxycoumarin) (Ia)—*a) From Id.* —A mixture of the acid (Id) (500 mg.), copper powder (500 mg.) and quinoline (20ml.) was heated while being stirred in an atmosphere of nitrogen for 20 min. at 200~220°C until the evolution of carbon dioxide ceased. The cooled mixture was diluted with ether (100 ml.), filtered and extracted with 8% hydrochloric acid. After being washed with aqueous sodium bicarbonate and then with water, the ethereal solution was dried and evaporated. The residue was recrystallized from ethanol to give Ia in the form of colorless crystals; m. p. 227~228°C (reported 231~232°C in sealed tube)[2]; yield, 350 mg. (86%); IR: 1712 (C=O); 1036, 938 cm^{-1} (O—CH_2—O)[9] (Nujol).

Found: C, 63.36; H, 3.39. Calcd. for $C_{10}H_6O_4$: C, 63.16; H, 3.18%,

9) IR spectrum of ayapin: H. Bickel and H. Schmid, *Helv. Chem. Acta*, **36**, 670 (1953).

b) From IIb.—A mixture of IIb (1.0 g.), anhydrous sodium acetate (1.5 g.) and acetic anhydride (15 ml.) was vigorously refluxed for 10 hr. The cooled mixture was poured into water, and the precipitates were collected. These recrystallized from ethanol to give Ia in the from of colorless crystals, m. p., 226~227°C, with a negative ferric reaction; yield, 700 mg. (61%). This substance showed no depression of its melting point on admixture with the specimen derived by the above-mentioned method a).

The authors are grateful to Professor M. Nakajima of Kyoto University and Professor T. Matsuura of Hiroshima University for their IR spectroscopy and to Professor T. Mitsui and his associates, Kyoto University, for their annalyses. This work was partially supported by a grant-in-aid for Scientific Research from the Ministry of Education, which is acknowledged with gratitude.

Department of Chemistry
Faculty of Science
Hiroshima University
Higashi Sendamachi, Hiroshima

Infrared and Ultraviolet Spectra of α- and γ-Pyrones

By Kiyoyuki YAMADA

(Received February 26, 1962)

There have been known a number of pyrone derivatives; both synthetic ones and naturally occurring ones. The characteristic features of infrared and ultraviolet spectra of the pyrone nucleus itself cannot be obtained from those of benzopyrones, i. e. coumarines and chromones, owing to the presence of the fused benzene ring. It is, therefore, necessary to examine the pyrone derivatives without any fused aromatic rings, in order to obtain the spectral properties of pyrones. In connection with the investigation of aureothin[1], the studies of various pyrones without aromatic rings were carried out, and in the present paper, the spectroscopic aspects of pyrones are reported.

Infrared Spectra. — Since α- and γ-pyrones show some aromatic nature, the bands associated with the double bonds of the ring as well as carbonyl band are characteristic for the identification of pyrone rings. The effects of the substituents on these bands were examined.

α-Pyrone.—Since the position and the shape of the carbonyl band are, in many cases, sensitive to the condition of measurement[2], the band positions were compared in the same

1) Y. Hirata, H. Nakata, K. Yamada, K. Okuhara and T. Naito, *Tetrahedron*, **14**, 252 (1961).

2) As to α-pyrone and 5-methyl-α-pyrone, Jones and his coworkers[3] observed anomalous absorption in the carbonyl stretching region; the single absorption band expected for these compounds is replaced by two bands, the relative intensities of which are dependent on the solvent polarity and temperature. Various interpretations including Fermi resonance were presented but they could not reach any conclusion regarding this phenomenon.

3) R. N. Jones, C. L. Angell, T. Ito and R. J. D. Smith, *Can. J. Chem.*, **37**, 2007 (1959).

No.	R_1	R_2	R_3	R_4
1*1	H	H	H	H
2	H	CH_3	H	CH_3
3	Br	CH_3	H	CH_3
4	H	OCH_3	H	CH_3
5	Br	OCH_3	H	CH_3
6*2	H	OH	H	CH_3
7*3	Br	OH	H	CH_3
8	CH_3	OCH_3	CH_3	
9*4	H	H	$COOCH_3$	H
10	H	H	$COOCH_3$	CH_3
11	H	CH_3	COOH	CH_3
12	$COCH_3$	OH	H	CH_3
13	$COCH_3$	OCH_3	H	CH_3
14	NO_2	OH	H	CH_3

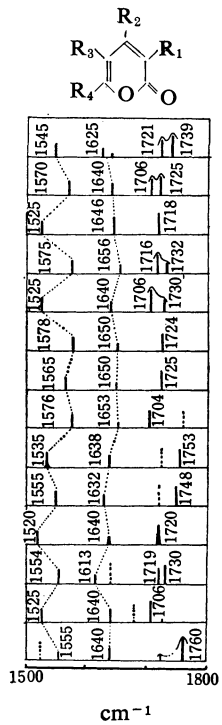
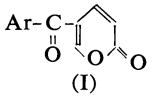


Fig. 1. Infrared spectra of α-pyrone derivatives ($CHCl_3$ solution).

*1 Data from R. N. Jones et al. (Ref. 3)
*2 Dioxane solution.
*3 $\nu_{C=O}$ appears at 1735 cm^{-1} in dioxane solution.
*4 A band written by dotted line is due to a group in side chain.

solvent. The carbonyl frequency was reported[4,5] to be in the range of 1720~1750 cm^{-1}, and the variance in the band position is mainly due to the substituents, as illustrated later. As characteristic bands of α-pyrones, there appear two bands arising from the double bonds of the ring; one lies usually within the range 1650~1630 cm^{-1}, and the other within 1570~1520 cm^{-1}. In general, the lower band shows stronger intensity than the higher one, but the reverse is sometimes observed (4, 6-dimethyl-3-bromo-α-pyrone, methyl coumalate). The infrared spectra of substituted α-pyrones are shown in Fig. 1. In comparison with the conjugated systems of ketones and lactones, the effect of the substituent on the position of a carbonyl band is unique in some respects, which may be ascribed to the aromatic character of the pyrone ring. While an electron-donating substituent conjugated with a $>C=O$ group has a small influence on the carbonyl band (i.e., variance of $\nu_{C=O}$ in No. 2→No. 4 and No. 3→No. 5 in Fig. 1), an electron-attracting group shifts the carbonyl band to a higher frequency[6]. (Changes of $\nu_{C=O}$ in No. 1→No. 9 and No. 1→No. 10. $\nu_{C=O}$ of the type I was reported[8] to fall within 1760~1750 cm^{-1}). When the

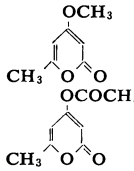


(I)

4) a) R. H. Wiley and C. H. Jarboe, *J. Am. Chem. Soc.*, **78**, 624 (1956); b) R. H. Wiley and C. H. Jarboe, ibid., **78**, 2398 (1956); c) R. H. Wiley, C. H. Jarboe and F. N. Hayes, ibid., **79**, 2602 (1957); d) K. Meyer, *Helv. Chim. Acta*, **38**, 1631 (1955); e) R. H. Wiley and C. L. de Silva, *J. Org. Chem.*, **21**, 841 (1956); f) I. Chimielewska, J. Cieslak and T. Kraczkiewicy, *Roczniki Chem.*, **30**, 1009 (1956); g) I. Chimielewska, J. Cieslak, K. Gorczynska, B. Kontnik and Pitakowska, *Tetrahedron*, **4**, 36 (1958); h) D. Herbest, W. B. Mors, O. R. Gottlieb and C. Djerassi, *J. Am. Chem. Soc.*, **81**, 2427 (1959); i) R. H. Wiley and J. G. Esterle, *J. Org. Chem.*, **22**, 1257 (1957).

5) Y. Hirata, "Infrared Absorption Spectrum", Vol. 12, Nankodo, Tokyo (1961), pp. 93—105.

6) A good example reported[7] is the difference of pyrone carbonyl bands of A and B. A compound A has stronger electron-donating group (OCH_3), than a compound B.



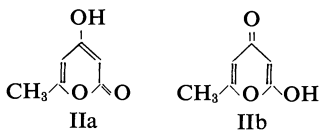
1712 (sh.)
1701 cm^{-1} (A)

1739 cm^{-1} (B)

7) E. A. Chandross and P. Yates, *Chem. & Ind.*, **1960**, 149.

8) R. H. Wiley and S. C. Slaymaker, *J. Am. Chem. Soc.*, **78**, 2393 (1956).

substituent R_3 in Fig. 1 is an ester group (No. 9, No. 10), there appear two carbonyl bands, one of which at higher frequency is considered to be a band due to a pyrone carbonyl group. It has been known that halogen substitution in the alpha position of a carbonyl group results in a high-frequency shift of the carbonyl absorption as illustrated in α-haloketones[9], α-halo-esters[9] and $\Delta^{\alpha,\beta}$-α-halo-γ-lactone[10]. This general finding is expected for 3-bromo-α-pyrone derivative, but in fact this phenomenon was not an actual case and there was an indication that α-bromination rather resulted in a lowering of a carbonyl frequency[11] (see $\nu_{C=O}$ change in No. 2→No. 3 and No. 4→No. 5 in Fig. 1). This fact would be explicable if a factor leading to a low-frequency shift of $\nu_{C=O}$ (plausible one is +M effect of bromine[12]) is operative in addition to the dipole-dipole interaction which causes a high-frequency shift of carbonyl band. This apparent anomaly is not observed, when the more electronegative substituent is introduced into an α-position of carbonyl group (3-nitro-α-pyrone derivatives), and in this case $\nu_{C=O}$ appears at fairly high frequency region. The effects of substituents on the bands related to the double bonds of pyrone ring seem to be complicated, but the clear points worthy of mention are that two bands appear in every case examined and that the band at a higher frequency is insensitive to the introduction of the substituent whereas the other is deeply influenced. As mentioned before, the carbonyl band differs in shape and position according to the condition of measurement—that is, solution or solid state. A remarkable example is triacetic lactone (II) (No. 6 in Fig. 1), the infrared spectrum of which taken in a solid state is complex in comparison with that in dioxane[13]. Two tautomeric forms IIa, IIb are possible for this compound and it is evident



IIa IIb

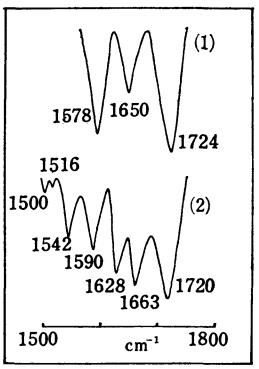


Fig. 2. Infrared spectra of triacetic lactone. (1) Dioxane (2) KBr

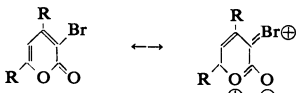
that IIa is an overwhelmingly predominant form in solution on the infrared and ultraviolet evidence (see Fig. 1 and Table I). In the solid state, II exhibits a complicated pattern of bands in 1800～1500 cm^{-1} region as shown in Fig. 2, and the bands due to strong hydrogen bonds are observed. It should be noted that a spectrum of II is similar to that of methyl-ether of IIa (No. 4 in Fig. 1) in 1000～700 cm^{-1} region.

γ-Pyrone.—As in α-pyrone series, the most characteristic frequencies available for detection of a γ-pyrone ring arise from carbonyl and C=C double bond vibrations. Usually a band near 1660 cm^{-1} (first band) is believed to originate from the carbonyl group[4h,14] and the bands (second and third bands) observed in 1650～1560 cm^{-1} would correspond to the double bonds of γ-pyrone (see Fig. 3). However, intense couplings among $\nu_{C=C}$ and $\nu_{C=O}$ might occur in the compound of this series and the definite assignments of the bands are therefore difficult[15]. According to the data available from literatures[4h,14] and in Fig. 3, the introduction of a substituent makes but a small influence on the position of the first band near 1660 cm^{-1} and no significant change on this band was observed under various conditions of measurement. Though the carbonyl absorption of γ-pyrone itself shows the doublet peaks, no such phenomenon was found on the substituted γ-pyrones examined. In general, there appear two bands (the second band, the third band) associated with the double bonds. In comparison with those of α-pyrone series, the two bands are separated to a smaller

9) L. J. Bellamy, "The Infrared Spectra of Complex Molecules", Methuen & Co. Ltd., London (1958), p. 400.

10) Y. Hata, *J. Chem. Soc. Japan, Pure Chem. Sec.* (*Nippon Kagaku Zassi*), **79**, 1531 (1958).

11) Similar result was obtained under the different conditions; i. e., in carbon tetrachloride solution and in solid state.

12) 

13) Similar phenomenon was observed on 4-hydroxy-coumarin. No definite conclusion as to the structure in the solid state was obtained: R. A. Abramovitch and J. R. Gear, *Can. J. Chem.*, **36**, 1501 (1958).

14) a) L. L. Woods, *J. Am. Chem. Soc.*, **77**, 3161 (1955); b) C. D. Hurd and S. Trofimenko, *J. Org. Chem.*, **23**, 1276 (1958); c) R. J. Light and C. R. Hauser, ibid., **25**, 538 (1960).

15) Cook assigned a band of the highest-frequency in 1600 cm^{-1} region to a ring stretching mode on the basis of the magnitude of the band shift observed on the various salts prepared from 2, 6-dimethyl-γ-pyrone and Lewis acids: D. Cook, *Can. J. Chem.*, **39**, 1184 (1961).

No.	R_1	R_2	R_3	R_4
1	H	H	H	H
2	CH_3	H	H	CH_3
3	OCH_3	CH_3	CH_3	
4	OCH_3	H	H	CH_3
5*	H	OH	H	H
6*	CH_3	OH	H	H
7	CH_3	OCH_3	H	H
8*	CH_2OH	H	OCH_3	H
9*	CH_2OH	H	OH	H

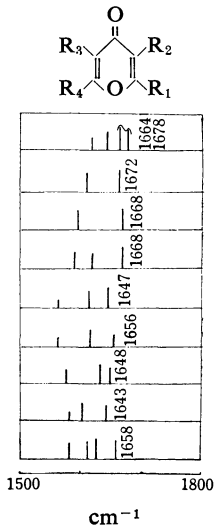


Fig. 3. Infrared spectra of γ-pyrone derivatives ($CHCl_3$ solution).
* KBr

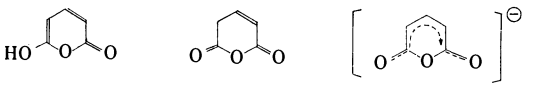
extent and their relative intensities to that of the carbonyl band are fairly strong.

Ultraviolet Spectra. — *α-Pyrone.* — Ultraviolet spectra of a few α-pyrones were already reported[4h,7,16], especially 6-methyl-4-hydroxy-α-pyrone[17]. In order to avoid the factors of conjugation and/or strain, α-pyrone derivatives examined in the present study are those without fused rings—aromatic or alicyclic. In Table I are listed the ultraviolet spectra of various α-pyrones. Almost all the compounds recorded in Table I have their maxima near 300 mμ, and in some type of the substituted pyrones, the second absorption maximum with the higher intensity appears in the short wavelength region (250 mμ). In general, the introduction of substituents such as alkyl, carbonyl, bromine, etc. causes a bathochromic shift of the absorption band near 300 mμ.

γ-Pyrone. — The absorption maxima of γ-pyrones appear in the shorter wavelength region (near 250 mμ) in comparison with those of α-pyrones. In Table II are shown absorption maxima of some γ-pyrone derivatives. The properties of the substituents are not so widely varied in the present study as well as in the compounds already reported[16c,18], as to permit to infer the substituent effect on the ultraviolet absorption.

On the Structural Problems of Some Pyrone Derivatives.—With these spectral characteristics at hand, the structural problems of pyrones are easily solved in some cases.

1) Tautomerism of Glutaconic Anhydride. — Glutaconic anhydride (III) and its derivatives have been assigned 6-hydroxy-α-pyrone structure (IIIa) on evidence from their chemical behaviors[19].



IIIa IIIb IIIc

In the infrared spectra of III, bands appeared at 1805, 1740, 1650 cm^{-1} in the solid state (KBr) and at 1800, 1760, 1650(w) cm^{-1} in chloroform solution and no hydroxyl bands were observed. Thus, it becomes evident that glutaconic anhydride exists as normal anhydride form IIIb in the solid state and chloroform solution. This conclusion is supported from the fact that no strong absorptions ascribable to α-pyrone structure IIIa were detected in the ultraviolet region (chloroform solution). In contrast to the transparency of III in chloroform solution, the ultraviolet absorptions with high intensities (λ_{max} 350 mμ, log ε, 4.21 ; 233 mμ, log ε, 3.91) were observed in ethanol, which are expected and accounted for by assuming the presence of the anion IIIc, since III is strongly acidic and hence is likely to dissociate in polar solvent such as

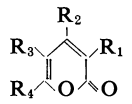
16) a) R. B. Woodward and G. Small, *J. Am. Chem. Soc.*, **72**, 1297 (1950); b) J. A. Berson, ibid., **74**, 5172 (1952); c) J. A. Berson, W. M. Jones and S. L. F. O'Callaghan, ibid., **78**, 622 (1956); d) S. Pataki and K. Meyer, *Helv. Chim. Acta*, **38**, 1631 (1955).

17) It was established that α-form absorbs at longer wavelength than γ-form when there are two isomeric α- and γ-pyrones such as 6-methyl-2,4-pyronone[4f,4h].

18) a) J. A. Berson, *J. Am. Chem. Soc.*, **75**, 3521 (1953); b) W. M. McLamore, E. Gelblum and A. Bavley, ibid., **78**, 2816 (1956).

19) a) N. Bland and J. F. Thorpe, *J. Chem. Soc.*, **101**, 856 (1912); b) R. H. Wiley and C. H. Jarboe Jr., *J. Am. Chem. Soc.*, **77**, 403 (1955).

TABLE I. ULTRAVIOLET SPECTRA* OF α-PYRONE

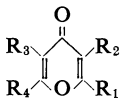


No.	Compound				λ_{max} (mμ)	log ε
	R_1	R_2	R_3	R_4		
1	H	H	CH_3	H	298	3.7**
2	H	CH_3	H	CH_3	290	3.78
3	Br	CH_3	H	CH_3	305	3.89
4	H	CH_3	COOH	CH_3	304	3.79
5	H	CH_3	$COOC_2H_5$	CH_3	292 (246	3.7 3.8)
6	H	H	$COOCH_3$	CH_3	293 (246	3.71 4.03)
7	H	H	$COOCH_3$	H	290 (245	3.61 3.96)
8	H	H	H	COOH	304 (225	3.87 —)
9	H	OH	H	CH_3	284	3.80
10	H	OCH_3	H	CH_3	280	3.86
11	NO_2	OH	H	CH_3	327 (306 (235	3.74 3.70) 3.95)
12	Br	OH	H	CH_3	296	3.94
13	$COCH_3$	OH	H	CH_3	310 (225	4.00 3.95)
14	$COCH_3$	OCH_3	H	CH_3	312	3.75
15	CH_3	OCH_3	CH_3		295	

* Measurements were made in ethanol. Absorption maxima in shorter wavelength region are put in parentheses.

** J. Fried and R. C. Elderfield, *J. Org. Chem.*, **6**, 566 (1941).

TABLE II. ULTRAVIOLET SPECTRA OF γ-PYRONE



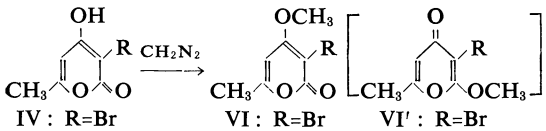
No.	Compound				λ_{max} (mμ)	log ε
	R_1	R_2	R_3	R_4		
1	H	H	H	H	248 (253) (260)	
2	CH_3	H	H	CH_3	247	4.02
3	H	OH	H	H	272	3.82
4	CH_3	OH	H	H	276	3.88
5	CH_3	H	H	OCH_3	240	4.05
6	CH_2OH	H	OH	H	266	3.85
7	CH_2OH	H	OCH_3	H	265	3.86
8		CH_3	CH_3	OCH_3	263 (248	3.90 3.84)

* Measurements were made in ethanol. A figure in parenthesis shows a position of the shoulder of the absorption.

ethanol. Upon addition of a drop of hydrochloric acid, the absorption maximum at 350 mμ disappeared and instead the new absorption appeared at 328 mμ (log ε, 3.04). Considering the α-pyrone structure IIIa, the new absoption, though quite reasonable as to its position, is unusually weak in intensity, implying that the equilibrium between two undissociated forms IIIa, IIIb is in favor of keto-form IIIb even in the polar solvent and

a fraction of an enol form IIIa is small[20].

2) Structures of Triacetic Lactone Derivatives.—Both α- and γ-pyrone forms are possible for the 2, 4-pyronone system and it is a matter of importance, which of the two predominates in various substituted 2, 4-pyronones. As shown before, triacetic lactone (No. 6 in Fig. 1) exists as an α-form and the same result was obtained on 4-hydroxycoumarin[21], while the preferential existence of γ-form under the subtle influences of substituents and fused rings was reported[4h,22] in some derivatives of 2, 4-pyronone. There was some confusion as to the structures of triacetic lactone methylether, but two isomers were unambiguously isolated and assignments of the isomers to α- and γ-forms were carried out[23]. As one of the problems regarding the isomeric α- and γ-pyrones, Arndt and Avan reported the methylethers of 3-bromotriacetic lactone and 3-nitrotriacetic lactone[24]. It is evident from the spectral viewpoints (Fig. 1 and Table I) that α-pyrone structures are assigned to 3-bromotriacetic lactone (IV) and 3-nitrotriacetic lactone (V)[25], to which no structural reference was made by Arndt et al. Methylation of IV and V under conditions employed by Arndt et al., gave corresponding methylethers VI, VII.



IV : R=Br VI : R=Br VI′ : R=Br
V : R=NO_2 VII : R=NO_2 VII′ : R=NO_2

Arndt and Avan assigned γ-pyrone structures VI′, VII′ to these methylethers on the basis of their solubilities to concentrated hydrochloric acid. However, this conclusion is unacceptable. The infrared spectrum of bromo-derivative VI in solution is, as shown in Fig. 1, typical of α-pyrone structure and also in solid state the same is true (bands at 1703, 1640 and 1522 cm^{-1}). The ultraviolet spectral result also favors the α-pyrone structure for VI (λ_{max} 305 mμ, log ε, 3.95). Similarly, α-pyrone structure is established for nitro derivative (VII) from the infrared (bands at 1735, 1644, 1543 and 1525 cm^{-1} in chloroform) and ultraviolet (λ_{max} 310 mμ, log ε, 3.68 : 300 mμ, log ε, 3.75) spectral data. Accordingly, the methylethers obtained by Arndt et al., in fact, have α-pyrone structures.

Experimental

Infrared spectra were measured with a Hilger H 800 Model. The ultraviolet spectra were measured with a Beckman DK-2 spectrophotometer.

Synthesis and Characterization of Compounds.—*Dehydroacetic Acid (No. 12 in Fig. 1).*—Commercial sample recrystallized from ethanol, m. p. 107～108°C.

Dehydroacetic Acid Methylether (No. 13 in Fig. 1).—Prepared as described by Perkin[26], m. p. 89～90°C.

Triacetic Lactone (No. 6 in Fig. 1).—Obtained by the procedure of Collie[27], m. p. 185～186°C.

6-Methyl-4-methoxy-α-pyrone (No. 4 in Fig. 1) and 6-Methyl-2-methoxy-γ-pyrone (No. 4 in Fig. 3).—Treatment of triacetic lactone with ethereal diazomethane gave a mixture of two isomers, the separation of which was carried out by the salt formation of γ-pyrone isomer[23b]; α-isomer, m. p. 85～86°C; γ-isomer, m. p. 93～94°C.

3-Bromotriacetic Lactone (No. 7 in Fig. 1) and 3-Nitrotriacetic Lactone (No. 14 in Fig. 1).—Prepared as described by Arndt and Avan[24]. Bromo compound decomposed above 210°C. Found : C, 35.51; H, 2.53. Calcd. for $C_6H_5O_3Br$: C, 35.14; H, 2.46%. Nitro compound had m. p. 162～164°C. Found : C, 41.83; H, 3.16; N, 8.23. Calcd. for $C_6H_5O_5N$: C, 42.11; H, 2.95; N, 8.19%.

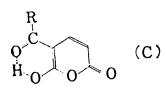
6-Methyl-4-methoxy-3-bromo-α-pyrone (No. 5 in Fig. 1) and 6-Methyl-4-methoxy-3-nitro-α-pyrone.—Prepared as described by Arndt and Avan[24]. 3-Bromo compound, m. p. 151～152°C. Found : C, 38.59; H, 3.31. Calcd. for $C_7H_7O_3Br$: C, 38.38; H, 3.23%. Nitro compound, m. p. 165～167°C. Found : C, 45.34; H, 3.93; N, 7.69. Calcd. for $C_7H_7O_5N$: C, 45.41; H, 3.81; N, 7.57%.

Isodehydroacetic Acid (No. 11 in Fig. 1).—Prepared from ethyl acetoacetate and concentrated sulfuric acid[28]. M. p. 152～154°C.

4, 6-Dimethyl-α-pyrone (No. 2 in Fig. 1).—Isodehydroacetic acid (or ethyl isodehydroacetate) was heated with concentrated sulfuric acid at 160°C, and a mixture was diluted with water and extracted with ether[28], m. p. 49～50°C.

4, 6-Dimethyl-3-bromo-α-pyrone (No. 3 in Fig. 1).—Prepared from 4, 6-dimethyl-α-pyrone[29], m. p. 102～104°C.

20) In some cases where there are structural factors that would stabilize the hydroxy-anhydride form as encountered in C, it has been known that α-pyrone structure predominates:



(C)

H. Schmid and W. Bencze, *Helv. Chim. Acta*, **36**, 1468 (1953); F. Gautschi, O. Jeger, V. Prelog and R. B. Woodward, ibid., **37**, 2280 (1954).

21) a) V. C. Farmer, *Spectrochim. Acta*, **1959**, 870; b) E. Knobloch and Z. Prochazka, *Chem. listy*, **47**, 1285 (1953).

22) a) C. H. Stammer, E. Walton, A. N. Wilson, R. W. Walker, N. R. Trenner, F. W. Holly and K. Folkers, *J. Am. Chem. Soc.*, **80**, 137 (1958); b) C. F. Spencer, J. O. Rodin, E. Walton, F. W. Holly and K. Folkers, ibid., **80**, 140 (1958); c) Y. Kawase, This Bulletin, **32**, 11 (1959); d) I. Chimielewska and J. Cieslak, *Tetrahedron*, **4**, 135 (1958).

23) a) I. Chimielewska and J. Cieslak, *Przemysl Chem.*, **8**, 196 (1952); b) S. Janiszewska-Drabarek, *Roczniki Chem.*, **27**, 456 (1953).

24) F. Arndt and S. Avan, *Chem. Ber.*, **84**, 343 (1951).

25) α-Form for V was already suggested by Dallacker et al.: F. Dallacker, P. Kratzer and M. Lipp, *Ann.*, **643**, 97 (1961).

26) W. H. Perkin, *J. Chem. Soc.*,. **51**, 496 (1887).

27) J. N. Collie, ibid., **59**, 607 (1891).

28) R. H. Wiley and N. R. Smith, *J. Am. Chem. Soc.* **73**, 3533 (1951).

29) R. H. Wiley and N. R. Smith, ibid., **74**, 3893 (1952).

Methyl Coumalate (No. 9 in Fig. 1). — Coumalic acid was treated with 1.5 equivalent amount of ethereal diazomethane, m. p. 71~72°C.

Methyl 6-Methylcoumalate (No. 10 in Fig. 1). — Coumalic acid was treated with a large excess amount of diazomethane (3~4 mol. equiv.) at room temperature. In this case, *C*-methylation took place at 6-position of coumalic acid, in addition to *O*-methylation (ester formation). Recrystallization from ether gave rectangular plates, m. p. 83~85°C (reported 86~87°C[30]).

2,6-Dimethyl-γ-pyrone (No. 2 in Fig. 3). — Decarboxylation of dehydroacetic acid, m. p. 128~130°C.

Pyromeconic Acid (No. 5 in Fig. 3). — M. p. 114~115°C.

Maltol (No. 6 in Fig. 3).—M. p. 158~160°C.

Maltol Methylether (No. 7 in Fig. 3). — Prepared from maltol and diazomethane, colorless liquid, b. p. 122~125°C/20 mmHg.

Kojic acid (No. 9 in Fig. 3).—M. p. 150~151°C.

Kojic Acid Monomethylether (No. 8 in Fig. 3).—Action of ethereal diazomethane on kojic acid gave needles, m. p. 161~163°C.

Glutaconic Anhydride (III). — Prepared by dehydration of glutaconic acid with acetic anhydride and purified by distillation under reduced pressure, m. p. 84~86°C, recrystallization from benzene.

30) J. Fried and R. C. Elderfield, *J. Org. Chem.*, **6**, 577 (1941).

Summary

Effects of substituents on the characteristic bands of pyrones were examined in the infrared spectra. Ultraviolet spectra of various α- and γ-pyrones were recorded and the application of the spectroscopic results obtained, disclosed the problems of tautomerism and isomerism concering some of the pyrone derivatives.

The author is greatly indebted to Professor Yoshimasa Hirata of this University of his guidance and encouragement in this work and is also grateful for the fellowship from Parke Davis & Co., Michigan, U. S. A. This work was supported by a research grant from the Ministry of Education, to which the author's thanks are due.

Chemical Institute
Faculty of Science
Nagoya University
Chikusa-ku, Nagoya

Reduction of Pyrones with Complex Metal Hydrides[1]

By Kiyoyuki YAMADA

(Received February 26, 1962)

It has been known that α- and γ-pyrones have an aromatic character which is reflected on their physical properties—for example, their infrared spectra. The aromatic nature of γ-pyrone is also reflected on its chemical properties; in comparison with a normal ketone, carbonyl group of γ-pyrone is generally unreactive, which is illustrated by the fact that γ-pyrone does not form 2, 4-dinitrophenylhydrazone[2]. However, condensation of γ-pyrone with an active methylene compound was reported[3] and in this case γ-pyrone reacted as a normal ketone. α-Pyrone behaves as α, β-γ, δ-unsaturated lactone[2] in various reactions including ozonization, hydrolysis, catalytic hydrogenation[4] and Diels-Alder reaction. So far, little is known about the reduction of α- and γ-pyrones with various complex metal hydrides except for limited examples of benzo-α-[5,6], benzo-γ-pyrones[7] and xanthone[8]. In case of benzo-α-pyrones, the formation of diol expected for the usual reduction of a lactone was reported. An α-pyrone derivative was known to be unreactive towards sodium borohydride under mild condition[9]. As to benzo-

1) Preliminary communication. K. Yamada, M. Ishizaka and Y. Hirata, This Bulletin, **34**, 1873 (1961).

2) R. C. Elderfield, "Heterocyclic Compounds", Vol. I, John Wiley, (1950), pp. 343—396.

3) a) L. L. Woods, *J. Am. Chem. Soc.*, **80**, 1440 (1958); b) M. Ohta and H. Kato, This Bulletin, **32**, 707 (1959).

4) In catalytic hydrogenation of α-pyrone derivative, it was reported that in addition to the formation of saturated δ-lactone, the hydrogenolytic cleavage of 1, 6-linkage of an α-pyrone ring took place to yield a saturated carboxylic acid[2]. The analogous result of the bond cleavage is found in the catalytic hydrogenation of β-alkoxy-α, β-unsaturated ketone.

5) a) F. A. Hochstein, *J. Am. Chem. Soc.*, **71**, 305 (1949); b) P. Karrer and P. Banerjea, *Helv, Chim. Acta*, **32**, 1692 (1949).

6) J. P. Freeman and M. F. Hawthorne, *J. Am. Chem. Soc.*, **78**, 3366 (1956).

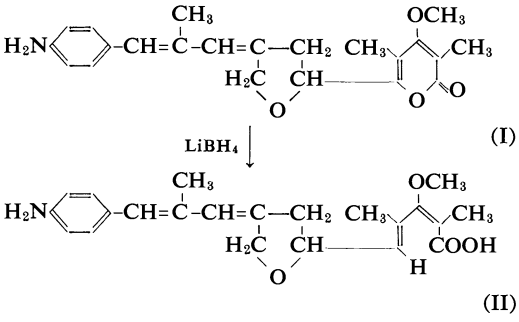
7) a) R. Robinson and R. Mirza, *Nature*, **166**, 929 (1950); b) R. Mirza and R. Robinson, ibid., **166**, 997 (1950).

8) A. Mustafa and M. K. Hilmy, *J. Chem. Soc.*, **1952**, 1343.

9) M. Bharucha, H. Jäger, K. Meyer, T. Reichstein and O. Schindler, *Helv. Chim. Acta*, **42**, 1395 (1959).

γ-pyrone derivatives[7], it was reported that the expected reduction of a ketone group to γ-pyranol took place.

In isoaureothamine (I) which is one of the derivatives of natural nitro compound aureothin[10], the presence of an α-pyrone ring was inferred from infrared and ultraviolet spectral data. Treatment of I with sodium borohydride or lithium borohydride led to a product aminol H, which was acidic and still showed a carbonyl band in the infrared spectrum[11]. Later, structure II was assigned to aminol H[12]. This would be regarded as unusual reduction product if α-pyrone moiety of I is expected to behave like a lactone. Admitting the correctness of the structure II, there remained a problem whether or not this unexpected reduction occurred under the influence of other part of the molecule.

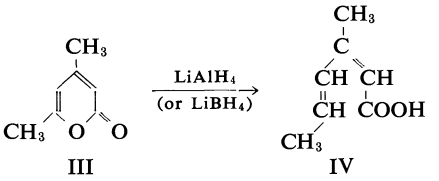


(I)

(II)

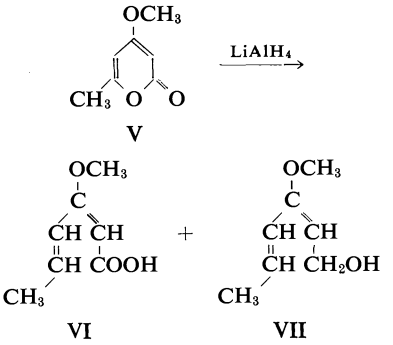
The result obtained in the reduction of isoaureothamine (I) is, thus quite different from those in benzo-α-pyrones, suggesting that the presence of the fused benzene ring in benzo-α-pyrone would account for this difference. From this viewpoint, monocyclic α-pyrones were prepared and their reductions with various complex metal hydrides were examined.

Reduction of α-Pyrones.—Firstly, reduction of 4, 6-dimethyl-α-pyrone (III) was carried out as a simple and standard α-pyrone. On treatment with sodium borohydride under various conditions (temperature, 20, 50, 70°C: solvent, ethanol or tetrahydrofuran) no reaction took place, though the reaction conditions employed in the present study were more drastic than that of Bharucha et al.[9] Lithium borohydride treatment of III in tetrahydrofuran, though a considerable amount of III was recovered, gave a reduction product identified as β-methylsorbic acid (IV) from the melting point and elemental analysis. When the more powerful reducing reagent, lithium aluminum hydride was used, the acid IV was obtained from III in fairly good yield (about 60%) and hence the recovery of III was decreased in amount (ca. 20%) as compared with lithium borohydride treatment.



III IV

Secondly, 6-methyl-4-methoxy-α-pyrone (V) was employed in the reduction reaction. The enhanced reactivity of V towards reducing reagents is evident from the following results. Even on treatment with sodium borohydride in ethanol, β-methoxysorbic acid (VI) was obtained from V, besides a large amount of starting material. Considerable amount of VI was produced from V in the reduction using lithium borohydride together with a small amount of starting material. Lithium aluminum hydride reduction of V afforded the acid VI in rather poor yield and the neutral product VII, which turned out to be a diene-alcohol derived from VI by further reduction of carboxyl group to hydroxymethyl group[13].



V VI VII

A large excess amount of lithium aluminum hydride (molar ratio, V/$LiAlH_4$=1/2) was used in the reduction of V, and the formation of VII becomes predominant with a raise of temperature (Table I).

Since the product ratio VII/VI is sensitive to the reaction conditions, it was necessary to carry out the experiments shown in Table I under the same concentrations and the same mode of addition, i.e., "inverse" addition method[14]. In order to get an information on the product ratio VII/VI from the other point of view, the influence of the relative amount of lithium aluminum hydride to V was examined (Table II). As indicated in Table II, large excess amount of lithium aluminum hydride

10) Y. Hirata, H. Nakata, K. Yamada, K. Okuhara and T. Naito, *Tetrahedron*, 14, 252 (1961).

11) K. Yamada, Y. Hirata, K. Okuhara, H. Nakata, T. Naito and K. Iwadare, *J. Chem. Soc. Japan, Pure Chem. Sec.* (*Nippon Kagaku Zassi*), 79, 384 (1958).

12) K. Yamada, T. Naito, K. Okuhara, H. Nakata and Y. Hirata, This Bulletin, 33, 1303 (1960).

13) The neutral product (VII) was independently prepared by reduction of VI with lithium aluminum hydride.

Table I. Reduction of 6-methyl-4-methoxy-α-pyrone (V). Temperature dependence of products

Temp. °C	Reactant V g.	Reactant $LiAlH_4$ g.	Product VI g.	Product VII g.	VII/VI[a]
0~3[b]	1.00	0.62	0.14	0.2	1.6
25~27	3.00	1.81	0.24	1.11	5.1
48~50	3.00	1.82	0.01	2.15	238

a) Molar ratio
b) Starting material V was partly recovered.

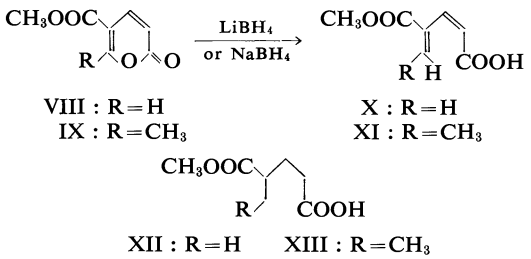
Table II. Reduction of 6-methyl-4-methoxy-α-pyrone. Dependence of product proportions on the amount of lithium aluminum hydride

Temp. °C	Reactant V mg.	Reactant $LiAlH_4$[a] mg.	Product VI mg.	Product VII mg.
10~12	280	45	90	—[b]
58~60	280	48	85	—[c]
10~12	280	110	84	(50)[d]
58~60	280	115	50	(60)[d]
10~12	280	220	65	140
58~60	280	220	Trace	205

a) The purity of $LiAlH_4$ was determined before use (Ref. 13, p. 8).
b) The formation of VII was very small in amount. As a neutral fraction, starting material (80 mg.) was recovered.
c) VII was detected by infrared spectrum, but the main part of the neutral fraction (110 mg.) was V.
d) In these cases, the neutral fraction was a mixture of VII and V and, on account of incomplete separation of two compounds, these figures would overestimate the amount of VII.

is markedly effective for the production of the alcohol VII even at rather low temperature. When the different mode of addition, normal addition[14] was applied in the reduction of V with lithium aluminum hydride, the acid VI and a neutral fraction were obtained. From the infrared analysis, this neutral fraction was shown to be a mixture of a ketonic compound[15] and the alcohol VII.

Further, methylesters of coumalic acid and 6-methylcoumalic acid, VIII, IX were treated with lithium borohydride and sodium borohydride. These α-pyrones showed enhanced reactivities and especially methyl coumalate VIII was so reactive as to form immediately a deeply colored complex near 0°C with lithium borohydride. The product was ester-carboxylic acid in each case. From the infrared and ultraviolet spectral evidence, structure X and XI were assigned to the products. These were further supported by the fact that the reduced products X, XI could by catalytic hydrogenation be led to XII and XIII, obtained[16] directly by catalytic hydrogenation of VIII and IX respectively (identification by comparison of infrared spectra).



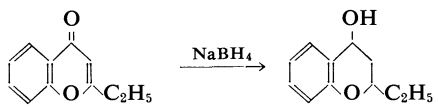
VIII : R=H
IX : R=CH3

X : R=H
XI : R=CH3

XII : R=H XIII : R=CH3

In order to avoid reduction of the ester group of the side chain, an experiment using lithium aluminum hydride was not undertaken.

Reduction of Benzo-γ-pyrone.—From the infrared evidence, a carbonyl group of monocyclic γ-pyrone in aureothin was reported[11] to be reduced with lithlum borohydride, but the structure of product is still uncertain. In connection with the reduction of aureothin, 2, 6-dimethyl-γ-pyrone (XIV) was treated with complex metal hydrides ($LiAlH_4$, $LiBH_4$) to give a liquid mixture from which no definite compounds could be isolated[17]. While the monocyclic γ-pyrone (XIV) was inert to sodium borohydride, benzo-γ-pyrone showed an enhanced reactivity and was reduced with this reagent, as follows. Treatment of 2-ethylchromone (XV) with sodium borohydride under the same condition as employed in XIV, gave 2-ethyl-4-hydroxychroman (XVI).



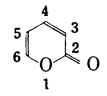
XV XVI

When treated with lithium borohydride, XV afforded, in addition to XVI, an oily product, the formation of which increased further with lithium aluminum hydride reduction.

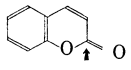
14) N. G. Gaylord, "Reduction with Complex Metal Hydrides", Interscience Publishers Inc., New York (1956), p. 1008.
15) In spite of the repeated experiments under various conditions, this compound was produced in poor yield. Though the structure is still ambiguous on account of difficulties in separation and purification, this would arise from the reduction of 1, 2-linkage of V, which means the normal lactonic behavior of α-pyrone.
16) J. Fried and R. C. Elderfield, *J. Org. Chem.*, 6, 566 (1941).
17) Main fraction of the products showed a strong band at 1710 cm^{-1}.

Discussion

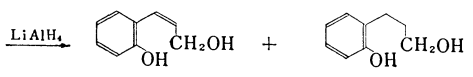
Reduction with complex metal hydride is considered as nucleophilic reaction involving hydride ions, though the active entity during the reduction process is still uncertain. Nucleophilic attack of hydride ion at 2-position of α-pyrone led to the same result as encountered in a usual lactone and, in fact, this mode of

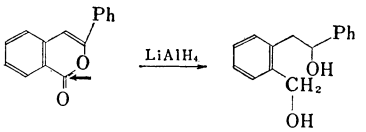


reaction is found in lithium aluminum hydride reductions (hydride ion as a nucleophile) and Grignard reactions (carbanion as a nucleophile) of benzo-α-pyrones XVII[5,6], XVIII[18].



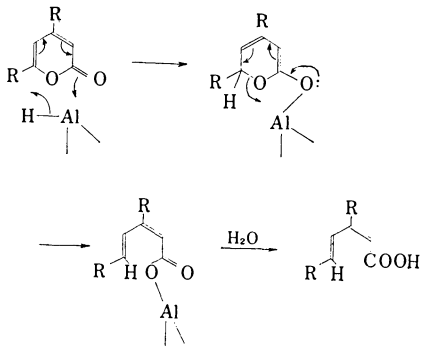
XVII





XVIII

A reaction of monocyclic α-pyrone with Grignard reagent involving an attack at 2-position of an α-pyrone was reported[19] recently, while, as described in this paper, the results of reduction of monocyclic α-pyrones with complex metal hydrides are unique, i.e., a general type of reduction of monocyclic α-pyrone with complex metal hydride reagent is a hydrogenolytic cleavage of 1, 6-linkage to afford an α, β-γ, δ-unsaturated carboxylic acid. This result is, at first sight, unexpected for the lactonic property of α-pyrone but can be explained as follows. According to the concept of vinylogy in reaction, possible points of attack by a nucleophile are 2-, 4- and 6-positions of an α-pyrone. In a complex metal hydride reduction, an attack of hydride to 6-position (1, 6-conjugate addition) occurs selectively and then the redistribution of electrons under the participation of metal ion takes place to afford a carboxylic acid, as shown in the scheme.



The difference of the reaction centers of monocyclic α-pyrone between hydride reduction and Grignard reaction[19] would be accounted for by considering the bulkiness of the reagent and/or a role of metallic ion involved in each reaction. Though a role of metallic ion in the hydride reduction is important, a precise mechanism of its participation during the reaction is not clear and hence aluminum is tentatively shown in the scheme as an electron acceptor. A high reactivity at 6-position of an α-pyrone is expected to be furthermore increased by introducing an electron-attracting substituent at 5-position[20], and this is encountered in the coumalic acid derivatives which were reduced under mild conditions.

In benzo-α-pyrone, carbon-carbon double bond of α-pyrone constitutes a part of benzene skeleton and the electronic displacement illustrated in the scheme would be accomplished with reluctance or prohibited[21], thus leading to a preferential attack of a nucleophile at a lactone-carbonyl carbon.

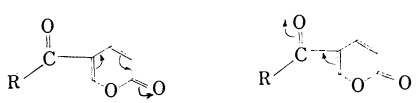
In the reduction of V, there were obtained an acid VI and an alcohol VII, and the amount of VII increased with a raise of temperature, when a large excess of hydride reagent was used—this is an expected result. The relative amount of the reducing reagent to V was found to have a more remarkable effect on the product proportions VI, VII, than temperature change. In the present case, reduction of COOH→ CH_2OH is sensitive to the amount of the reagent (Table II).

Reduction of 2-ethylchromone (XV) takes place under milder conditions, than in case of

18) S. Siegel and S. Coburn, *J. Am. Chem. Soc.*, **73**, 5494 (1951).

19) R. Gompper and O. Christmann, *Chem. Ber.*, **94**, 1784 (1961).

20) Electropositive property of 6-position is increased by an addional effect of electronic displacement in B besides A.



(A) (B)

21) In other words, an electropositive character at 6 position of monocyclic α-pyrone is weakened in benzo-α-pyrone system by supply of electrons from a benzene ring.

monocyclic γ-pyrone (XIV), indicating that a carbonyl group of XV loses an inert character of γ-pyrone carbonyl and instead has a property of a usual conjugated ketone. In case of XV, the first stage of the reaction is, of course a conjugate addition (1, 4-addition) of hydride ion, followed by further reduction of the ketone group.

Experimental

The infrared spectra were measured with a Hilger H 800 Model and Nihonbunko model IR-S. The ultraviolet spectra were measured with a Beckmann DK-2 spectrophotometer.

4, 6-Dimethyl-α-pyrone. — Prepared from ethyl acetoacetate[22]. M. p. 48~49°C.

Reduction of 4, 6-Dimethyl-α-pyrone.—*a) Sodium Borohydride.*—To an ethanolic solution (10 ml.) of 500 mg. of sample was added 300 mg. of sodium borohydride. The mixture was kept at 70°C for 2.5 hr. After cooling, a small amount of hydrochloric acid was added, and on removal of the solvent at reduced pressure, the residue was extracted with ether. The ethereal solution was dried with anhydrous sodium sulfate and after filtration, ether was removed to afford colorless crystals (460 mg.), m. p. 45~48°C which were identified as starting material. To the residue was added hydrochloric acid until the solution became strongly acidic and the aqueous solution was extracted with ether. From this ethereal solution, the expected carboxylic acid IV could not be obtained. The same procedure was repeated at 50 and 20°C only to recover a starting material. When tetrahydrofuran was employed as solvent, sodium borohydride was suspended in it.

b) Lithium Borohydride.—A suspension of lithium borohydride in tetrahydrofuran (240 mg./10 ml.) was added to a solution of a sample in tetrahydrofuran (720 mg./10 ml.) and the mixture was kept under reflux for 3 hr. The solution became yellow and turbid. After removal of the solvent under reduced pressure, 5 ml. of water was added to decompose the formed complexes and excess reagent. The aqueous solution was extracted with ether (50 ml.). From this ethereal layer, starting material was recovered. On acidification of the aqueous layer with hydrochloric acid, a white precipitate appeared, was collected and recrystallized from benzene, 120 mg. M. p. 97~98°C (reported 98~99°C)[23]: this acid proved to be β-methylsorbic acid.

Found: C, 67.00; H, 8.10. Calcd. for $C_7H_{10}O_2$: C, 66.64; H, 7.99%.

UV: λ_{max}^{EtOH}, 260 mμ (log ε, 4.22).

c) Lithium Aluminum Hydride.—To a solution of 5.0 g. of a sample in tetrahydrofuran (15 ml.) was gradually added a suspension of 1.0 g. of lithium aluminum hydride in tetrahydrofuran (30 ml.). The mixture was stirred at 40°C for 4 hr. After cooling, the solvent was removed under reduced pressure and water was added to decompose complexes and excess reagent. The aqueous solution was extracted with ether and starting material (1 g.) was recovered from this ethereal layer. After filtration, the aqueous layer was acidified with hydrochloric acid to afford white crystals which was identical with an acid obtained with lithium borohydride treatment, yield 3 g.

6-Methyl-4-methoxy-α-pyrone.—Triacetic lactone was prepared from dehydroacetic acid with concentrated sulfuric acid at 130°C. Treatment of triacetic lactone with ethereal diazomethane gave 6-methyl-4-methoxy-α-pyrone contaminated with a small amount of isomeric γ-pyrone.

After separation[24] of γ-isomer, 6-methyl-4-methoxy-α-pyrone melted at 83~85°C.

Reduction of 6-Methyl-4-methoxy-α-pyrone.—*a) Sodium Borohydride.*—To a solution of 500 mg. of sample in ethanol (10 ml.) was added a solution of 300 mg. of sodium borohydride. The mixture was worked up in a manner identical with that used for 4, 6-dimethyl-α-pyrone. From the ethereal layer, starting material was recovered (350 mg.). To the residue was added 5 ml. of water and after filtration, aqueous solution was acidified with hydrochloric acid to give a white solid. Recrystallization from benzene gave colorless prisms (β-methoxysorbic acid), 25 mg., m. p. 146~148°C (reported 152°C (decomp.)[25]).

Found: C, 59.17; H, 7.13. Calcd. for $C_7H_{10}O_3$; C, 59.14; H, 7.09%.

UV: λ_{max}^{EtOH}, 264 mμ (log ε, 4.1).

b) Lithium Borohydride.—To a solution of 500 mg. of sample in tetrahydrofuran (10 ml.) was added 300 mg. of lithium borohydride in tetrahydrofuran (10 ml.) and the mixture was kept under reflux for 1 hr.

After removal of the solvent, 5 ml. of water was added to decompose yellow complexes. The aqueous solution was extracted with ether (40 ml.). From the ethereal layer was obtained an oily product, which gradually solidified and was identified as starting material (80 mg.). The aqueous solution was acidified to give a white precipitate which was collected, dried and recrystallized from benzene, m. p. 147~149°C (β-methoxysorbic acid), 305 mg.

c) Lithium Aluminum Hydride. — To a solution of 4.5 g. of sample in anhydrous tetrahydrofuran (60 ml.) was added with stirring a solution of lithium aluminum hydride (2.6 g.) in tetrahydrofuran (50 ml.) gradually. The mixture was kept at 30°C for 2 hr. Greenish precipitates appeared and the solution became yellow. Water was added carefully and the precipitates were removed by filtration.

The filtrate was concentrated to give an aqueous solution (an alcohol VII separated from the aqueous layer).

The aqueous solution was extracted with 150 ml. of ether. From the aqueous layer, β-methoxysorbic acid was obtained, 820 mg. The ethereal solution was dried with anhydrous sodium sulfate and the

22) R. H. Wiley and N. R. Smith, *J. Am. Chem. Soc.*, **73**, 3531 (1951).

23) R. Kuhn and M. Hoffer, *Ber.*, **65**, 651 (1932).

24) S. Janiszewska-Drabarek, *Roczniki Chem.*, **27**, 456 (1953).

25) a) E. R. H. Jones and M. C. Whiting, *J. Chem. Soc.*, **1949**, 1423; b) H. B. Henbest and E. R. H. Jones, ibid., **1950**, 3628.

solvent was removed to give a yellow liquid, of 3.1 g. This was fractionally distilled under reduced pressure in a small apparatus. Almost the whole part of the liquid was distilled between 100~104°C 16 mmHg. This was again distilled, yielding a colorless liquid, b. p. 102~104°C/16 mmHg.

IR, 3600, 3470(br.), 1665, 1605 cm^{-1} ($CHCl_3$) : UV, λ_{max}^{EtOH}, 239 mμ (log ε, 3.9).

Found : C, 65.92; H, 9.60. Calcd. for $C_7H_{12}O_2$: C, 65.59; H, 9.44%. Methoxyl analysis (Zeisel) : 0.93 group.

This liquid was obtained also from β-methoxysorbic acid (500 mg.) and lithium aluminum hydride (200 mg.) in tetrahydrofuran (20 ml.) at 40°C for 30 min. This substance is 3-methoxy-2, 4-hexadienol and is rather unstable when exposed to air and light and becomes colored and viscous.

d) Experiment on Table II.—When reduction of V was carried out using various amounts of lithium aluminum hydride, it was sometimes necessary to separate V from VII in a mixture of neutral fraction. Though complete separation was difficult, a small difference of solubility of carbon tetrachloride was used for the separation. The extent of separation was checked by infrared spectrum.

e) Reduction using a Normal Addition. — To a solution of 800 mg. of lithium aluminum hydride in 20 ml. of tetrahydrofuran was added 2.0 g. of a sample of tetrahydrofuran (40 ml.). The mixture was kept at 30°C with stirring for 2 hr. The reaction mixture was worked up in the same manner as described in the inverse addition method and β-methoxysorbic acid (280 mg.) was obtained.

The neutral fraction (1.1 g.) showed a carbonyl band at 1710 cm^{-1} in addition to the bands at 1665 and 1605 cm^{-1} of VII and is positive for iodoform test.

Methyl Coumalate.—Coumalic acid was treated with 1.5 equivalent amount of ethereal diazomethane, m. p. 71~72°C.

Methyl 6-Methylcoumalate.—Coumalic acid was treated with a large excess amount of diazomethane (3~4 mol. equiv.) at room temperature. M. p. 83~85°C.

Reduction of Methyl Coumalate.—To a solution of 460 mg. of sample in 10 ml. tetrahydrofuran was added 100 mg. of lithium borohydride in 10 ml. tetrahydrofuran under cooling. The solution immediately turned yellow and then became brown. After 20 min., the mixture became dark-red and brown complexes appeared. After removal of the solvent, water (20 ml.) was added and the brown solution was extracted with ether. From the colorless ethereal layer nothing could be obtained. Yellow aqueous solution was acidified with 4 N sulfuric acid. The solution was tubid and extracted with ether (40 ml.). From the ethereal solution, a slightly yellow liquid was obtained (420 mg.). Infrared spectrum, 1725(sh), 1705, 1650(w), 1610 (w) cm^{-1} (film). UV, λ_{max}^{EtOH}, 263 mμ.

Neutralization of the liquid with sodium bicarbonate (or triethylamine) gave a solid, which showed bands at 1720, 1590(s) cm^{-1}. Catalytic hydrogenation (PtO_2 as catalyst) of this liquid in methanol, gave, after uptake of about two equivalent moles of hydrogen, a liquid which was chromatographed on silicic acid. The main fraction thus obtained was identical with liquid obtained[16] by direct hydrogenation of methyl coumalate by infrared comparison. The same result was obtained, when the sample (500 mg.) was treated with sodium borohydride (200 mg.) in ethanol (20 ml.) at room temperature.

Reduction of Methyl 6-Methylcoumalate.—To a solution of 670 mg. of sample in 10 ml. of tetrahydrofuran was added 110 mg. of lithium borohydride in 10 ml. of tetrahydrofuran at room temperature (10~15°C). The solution became yellow and then orange red. The same procedure as described in methyl coumalate was employed.

Reduction of 2-Ethylchromone.—To an ethanolic solution (200 ml.) of 1.04 g. of sodium borohhydride was added 2.06 g. of 2-ethylchromone[26] in ethanol (50 ml.) and the mixture was kept under reflux for 3 hr. The solvent was removed under reduced pressure, and the extraction with ether was repeated. Concentration of ethereal solution gave an oil which gradually solidified. The solid was recrystallized from petroleum ether to give white feathery needles, 1.3 g., m.p. 77~78°C (reported for 2-ethyl-4-hydroxychroman, 78~79°C[27]).

Found : C, 74.19; H, 7.83. Calcd. for $C_{11}H_{14}O_2$: C, 74.13; H, 7.92%.

Summary

Reduction using complex metal hydrides was carried out on monocyclic α-pyrones and benzo-γ-pyrone. It was established that generally the hydrogenolysis of the 1, 6-linkage of an α-pyrone ring occurred. In benzo-γ-pyrone, carbon-carbon double bond and ketone were reduced. The effects of the substituents on the reactivity of α-pyrone were discussed.

The author is greatly indebted to Professor Yoshimasa Hirata of this University for his guidance and encouragement throughout this work and also expresses his gratitude to Mr. M. Ishizaka and Mr. Y. Kato for their technical assistance. The author is grateful for the fellowship from Parke Davis and Co., Michigan, U. S. A. This work was supported by a research grant from the Ministry of Education, to which the author's tkanks are due.

Chemical Institute
Faculty of Science
Nagoya University
Chikusa-ku, Nagoya

26) "Organic Syntheses", Coll. Vol. III, p. 387.
27) R. Mozingo and H. Adkins, *J. Am. Chem. Soc.*, **60**, 669 (1938).

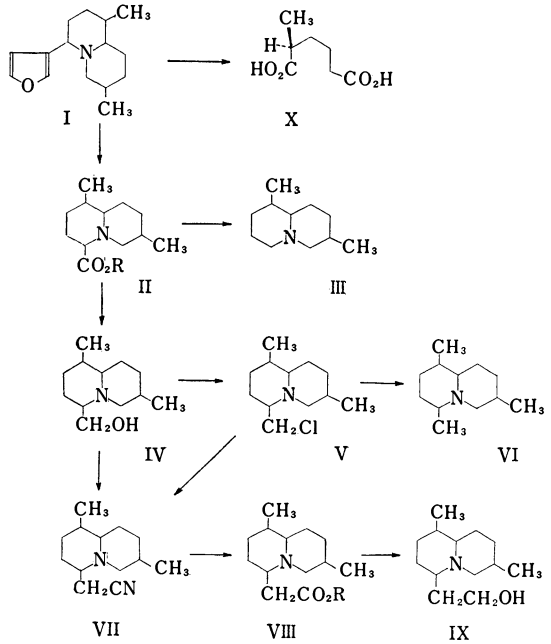
The Stereochemistry of Deoxynupharidine: The Absolute Configuration of Deoxynupharidine[1]

By Munio KOTAKE, Ichiro KAWASAKI, Tadashi OKAMOTO, Shigeru MATSUTANI, Shiro KUSUMOTO and Takeo KANEKO

(Received February 27, 1962)

In 1956, Kotake, Kusumoto and Ohara[2] assigned structure I to deoxynupharidine, an alkaloid isolated from the roots of the water lily *Nuphar japonicum*, DC., and a compound that seemed to have the same structure was synthesized[3]. Though the infrared spectrum of synthetic deoxynupharidine could almost be superimposed on that of the natural product, a slight difference was found in the fingerprint region. Since the 2-[5-methyl-pyridyl-(2)]-5-[furyl-(3)]-pentane obtained by the dehydrogenation of the synthetic sample had an infrared spectrum identical with that obtained from natural deoxynupharidine by the same procedure, the synthetic deoxynupharidine was probably a mixture of diastereomers. In this paper the determination of the absolute configuration of deoxynupharidine by means of a conformational analysis using the NMR spectrum is reported on.

1,7-Dimethylquinolizidine (III) (defuryldeoxynupharidine) was obtained by the sodalime distillation of nupharidinic acid hydrochloride, which was obtained by the oxidation of deoxynupharidine. On the other hand, the methyl ester of II was reduced with lithium aluminum hydride to alcohol IV, which was converted with thionyl chloride to chloro compound V, and V was then reduced with palladium on charcoal to 1, 4, 7-trimethylquinolizidine (VI), which has a 4-methyl group in place of the β-furyl group of deoxynupharidine. Nitrile VII, obtained from chloro compound V by treatment with sodium cyanide, was hydrolized and esterified to VIII. Methyl ester VIII was reduced with lithium aluminum hydride to 1, 7-dimethyl-4-hydroxyethylquinolizidine (IX). In this compound IX, an equatorial hydroxyethyl group would make intramolecular hydrogen bonding between the hydroxyl and nitrogen possible. Actually, the absorption band of the hydroxyl group of IX in the infrared region appeared at 3260 cm^{-1} (in carbon tetrachloride), and a dipole moment of 2.63 D was found[4]. These results suggested that compound IX had an equatorial hydroxyethyl group.



Recently, the determination of the conformation of methylquinolizidine by means of the NMR spectrum has been reported on briefly[5]. Independently, we have prepared 1-, 3- and 4-methylquinolizidines with a definite conformation, and their NMR spectra have been compared in order to determine the configuration of deoxynupharidine with those of di- and trimethylquinolizidines, III and IV.

The preparation of the diastereomer of 1-methylquinolizidine was as follows: diethyl 2-[pyridyl-(2)]-allylmalonate[6] (XI) gave diethyl

1) A part of this work was presented to the 5th Meeting on Natural Organic Compounds of the Chemical Society of Japan at Sendai on October 12, 1961.

2) M. Kotake, S. Kusumoto and T. Ohara, *Ann.*, **606**, 148 (1957).

3) M. Kotake, I. Kawasaki, T. Okamoto, S. Kusumoto and T. Kaneko, ibid., **636**, 158 (1960).

4) J. Ratusky, A. Reiser and F. Sorm, *Collection Czechoslov. Chem. Communs.*, **20**, 798 (1955).

5) T. M. Moynehan, K. Schofield, R. A. Y. Jones and A. R. Katritzky, *Proc. Chem. Soc.*, **1961**, 218. In the course of the preparation of the manuscript of this contribution, we discovered Moynehan's communication.

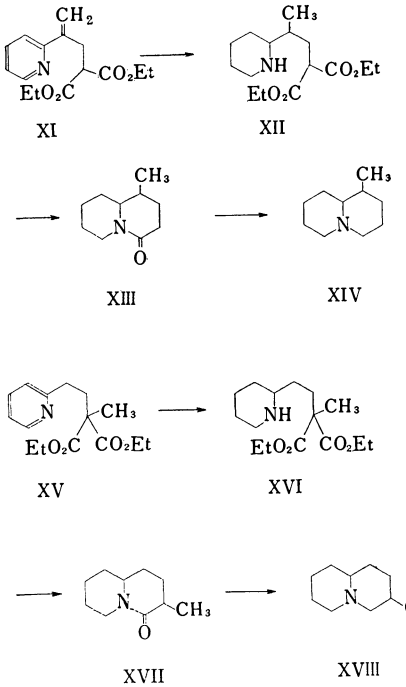
6) F. Bohlmann. N. Ottawa and R. Keller, *Ann.*, **587**, 162 (1954); E. E. Tamelen and F. S. Baran, *J. Am. Chem. Soc.*, **80**, 4659 (1958).

2-[piperidyl-(2)]-propylmalonate (XII) by hydrogenation at an ordinary pressure and temperature over a platinum catalyst. This diester, XII, afforded 1-methyl-4-ketoquinolizidine (XIII) through successive hydrolysis, esterification and cyclization. The hydride reduction of XIII gave an epimeric mixture of 1-methylquinolizidine (XIV), which was separated into two racemates by chromatography on alumina; the picrates were formed, m. p. 185~188 and 162~164°C. On the other hand, synthetic 1-lupinine has been separated, by chromatography on alumina[7], to *dl*- and *epi*-isomers, which were converted into 1-methylquinolizidine by Karrer's method[8]. The isomer from *dl*-lupinine formed a picrate which melted at 180~181°C, while the isomer obtained from the *epi*-isomer melted at 160~161°C. From these results, it is suggested that the higher melting picrate has the axial methyl group, while the other has the equatorial methyl group.

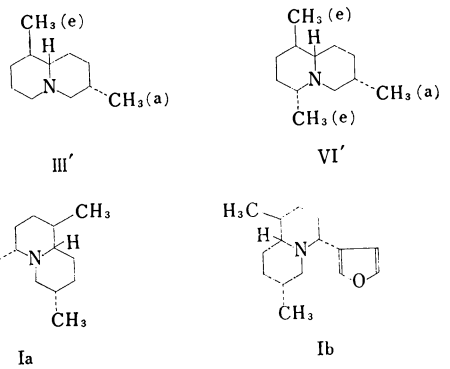
3-Methylquinolizidine (XVIII) was prepared from diethyl 2-[pyridyl-(2)]-ethyl methylmalonate (XV)[9] through XVI and XVII by the same manner as that used in the preparation of 1-methylquinolizidine, which was separated on an alumina chromatogram into two isomers. The corresponding picrates melted at 151~152 and at 183~185°C. Moreover, synthetic 3-lupinine was separated into *dl*- and *epi*-forms by the same manner as that used for 1-lupinine. The reduction of 3-*dl*-lupinine afforded an isomer, its picrate melted at 151~152°C, and 3-*epi*-lupinine gave a higher melting picrate, m. p. 177~178°C. Thus, we have suggested that the isomer of the lower melting picrate has the axial methyl group and the other has the equatorial methyl group.

The diastereomers of 4-methylquinolizidine have been obtained previously[10,11], and Boekelheide[12] has suggested that the methyl group of the higher melting picrate can be assigned to the equatorial group. We obtained 4-methylquinolizidine by the catalytic hydrogenation of 1-[pyridyl-(2)]-4-pentanone with simultaneous cyclization, and the two racemates which were separated by chromatography on alumina formed picrates; m. p. 193~196 and 187~190°C.

The NMR spectra of methylquinolizidines in a benzene solution (Figs. 1—6) showed that in the 1- and 3-methyl compounds the peak for an axial methyl group is at a lower field than that for the corresponding equatorial methyl group, but that for the 4-methylquinolizidine, in which the methyl group seemed to be equatorial, the peak is at a lower field than that of the axial isomer[5].



A doublet of 350~354 c. p. s. and another doublet of 327~333 c. p. s., present in the spectrum of 1, 7-dimethylquinolizidine (III), were assigned to 1-equatorial and 3-axial methyl groups respectively. A doublet of 337~344 c. p. s. in the spectrum of 1, 4, 7-trimethylquinolizidine (VI) was assigned to a 4-equatorial methyl group, since the intensity of the peak at 337 c. p. s. was twice that of the peak at 354.



The relative configurations of these compounds can thus be shown as III′ and VI′,

7) J. Ratusky and F. Sorm, *Collection Czechoslov. Chem. Communs.*, **19**, 340 (1954).
8) P. Karrer and A. Vogt, *Helv. Chim. Acta*, **13**, 1073 (1930).
9) V. Boekelheide and S. Rothchild, *J. Am. Chem. Soc.*, **71**, 879 (1949).
10) N. J. Leonard, A. S. Hay, R. W. Fulmer and V. W. Gash, ibid., **77**, 439 (1955).
11) R. Lukes and F. Sorm, *Colleation Czechoslov. Chem. Communs.*, **12**, 356 (1947).
12) V. Boekelheide and J. M. Ross, *J. Am. Chem. Soc.*, **77**, 5691 (1955).

and the absolute configuration of deoxynupharidine, as either Ia or Ib. Since the configuration of (−)-α-methyladipic acid (X), obtained from the Hofmann degradation of deoxynupharidine, was found to have an s(−)-configuration[13], we came to the conclusion that the formula Ib shows the absolute configuration of deoxynupharidine.

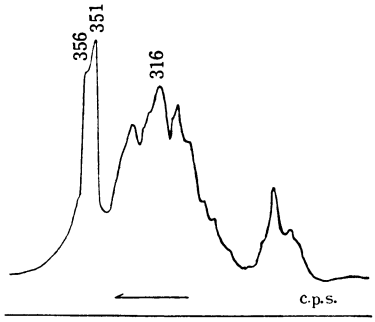


Fig. 1. NMR spectrum of 1(e)-Methylquinolizidine [picrate; m. p. 162~164°C].

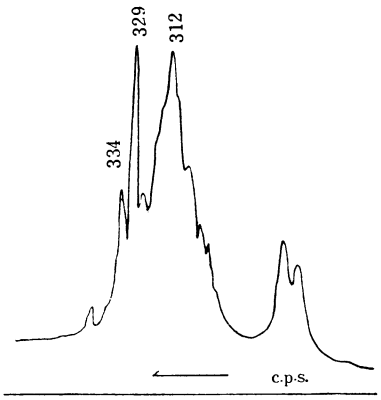


Fig. 2. NMR spectrum of 1(a)-Methylquinolizidine [picrate; m. p. 185~188°C].

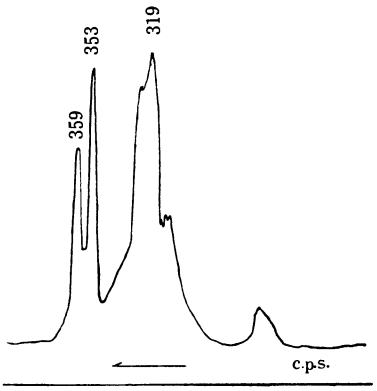


Fig. 3. NMR spectrum of 3(e)-Methylquinolizidine [picrate; m. p. 183~185°C].

13) T. Kaneko, K. Wakabayashi and H. Katsura, This Bulletin, 35, 1149 (1962).

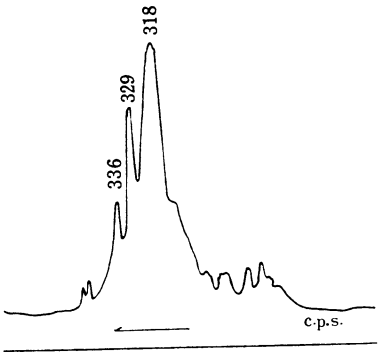


Fig. 4. NMR spectrum 3(a)-Methylquinolizidine [picrate; m. p. 151~153°C].

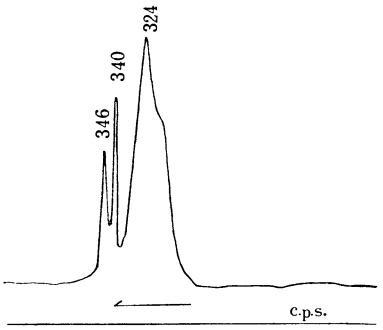


Fig. 5. NMR spectrum of 4(e)-Methylquinolizidine [picrate; m. p. 193~196°C].

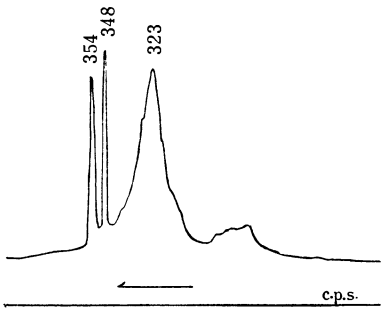


Fig. 6. NMR spectrum of 4(a)-Methylquinolizidine [picrate; m. p. 181~190°C].

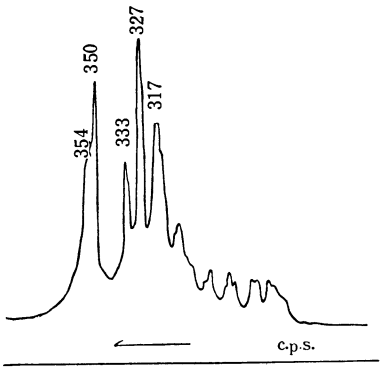


Fig. 7. NMR spectrum of 1,7-dimethylquinolizidine (III).

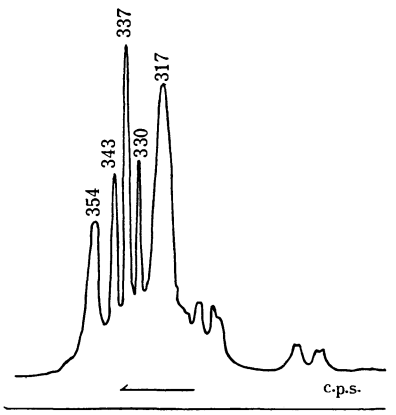


Fig. 8. NMR spectrum of 1, 4, 7-trimethylquinolizidine (VI).

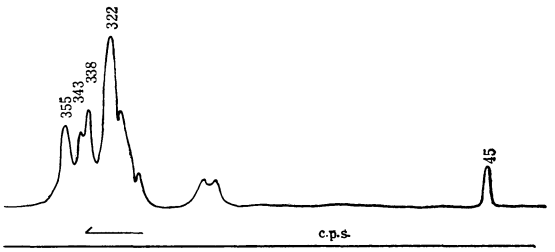


Fig. 9. NMR spectrum of deoxynupharidine (I).

Experimental

The NMR spectra were measured in a benzene solution at 56.4 Mc/sec. using a Varian Associates 4300 C instrument and the c.p.s. value was calculated from benzene.

Dehydrogenation of Synthetic Deoxynupharidine.—A mixture of 500 mg. of synthetic deoxynupharidine and 100 mg. of palladium black was heated at 280~290°C for 1 hr. After filtration of the catalyst, 250 mg. of pale yellow oil, b.p. 87~90°C/0.02 mmHg, was obtained.

The infrared spectrum of this oil was identical with that of 2-[5-methyl-pyridyl-(2)]-5-[furyl-(3)]-pentane derived from natural deoxynupharidine.

Nupharidinic Acid (II).—Hydrochloride: $[\alpha]_D$ −40.3° (*c* 1.18, ethanol), $[\alpha]_D$ −68.05° (*c* 1.44, water), $[\alpha]_D$ −75.16° (*c* 3.02, 6 N hydrochloric acid). (Found: C, 58.31; H, 9.02; N, 5.66. Calcd. for $C_{12}H_{21}O_2N \cdot HCl$: C, 58.16; H, 8.95; N, 5.65%).

Methyl ester; b. p. 87~90°C/1 mmHg, $[\alpha]_D$ −76.15° (*c* 2.78, ethanol).

1, 7-Dimethylquinolizidine (III).—A mixture of 3.7 g. of II-HCl salt and 10 g. of soda lime was distilled. The distillate was dissolved in dilute hydrochloric acid and extracted with ether, and the aqueous layer was made basic with potassium carbonate and extracted with ether. The basic ether extracts were washed with water and dried over sodium sulfate, and the solvent was distilled off. The residue was distilled at 65°C/15 mmHg; yield 1.0 g. (40%) (Found: C, 79.16; H, 12.36. Calcd. for $C_{11}H_{21}N$: C, 78.97; H, 12.65%), $[\alpha]_D$ −34.28° (*c* 2.45, ethanol). The picrate crystallized from ethanol as orange yellow prisms, m. p. 124~125°C (Found: C, 51.66; H, 6.05; N, 14.09. Calcd. for $C_{17}H_{24}O_7N_4$: C, 51.51; H, 6.10; N, 14.14%). The picrolonate from ethanol was in the form of yellow needles, m. p. 200~204°C (Found: C, 58.71; H, 6.92; N, 16.03. Calcd. for $C_{22}H_{29}O_5N_5$: C, 58.95; H, 6.77; N, 16.23%).

Alcohol (IV).—A solution of 12.3 g. of methyl ester of II in 30 ml. of absolute ether was added, drop by drop, to a solution of 2 g. of lithium aluminum hydride in 100 ml. of ether, After being heated under reflux for 3 hr. the reaction mixture was decomposed with the required amount of water and the precipitated hydroxide was extracted with boiling ether, the extracts evaporated and the residue distilled. The product was a colorless oil, b. p. 119~122°C/3.5 mmHg; yield 9.6 g. (90%) (Found: C, 72.76; H, 11.69; N, 6.93. Calcd. for $C_{12}H_{23}ON$: C, 73.04; H, 11.75; N, 7.10%). $[\alpha]_D$ −37.10° (*c* 2.57, ethanol). The infrared absorption band in carbon tetrachloride was at 3460 cm^{-1} (OH). The hydrochloride, prepared in an ethereal solution with dry hydrogen chloride and recrystallized from acetone-ethanol, was colorless and cubic; m. p. 195~196°C (Found: C, 61.41; H, 10.27; N, 5.88. Calcd. for $C_{12}H_{23}ON \cdot HCl$: C, 61.65; H, 10.35; N, 5.99%). The methiodide recrystallized from acetone-ethanol as colorless prisms; m. p. 173~174°C (Found: C, 46.17; H, 7.65; N, 4.39. Calcd. for $C_{12}H_{23}ON \cdot CH_3I$: C, 46.02; H, 7.72; N, 4.13%).

Chloride (V).—To a solution of 7.6 g. of IV in 200 ml. of ether was added 30 ml. of thionyl chloride, and the mixture was refluxed for 2 hr. The reaction mixture was evaporated in vacuo and added to a small amount of ice. The solution was carefully made basic with potassium carbonate and extracted with ether, and the solvent was removed and residue distilled at 93~95°C/1 mmHg; yield 7.1 g. (86%). $[\alpha]_D$ −69.4° (*c* 4.27, ethanol) (Found: C, 67.18; H, 10.40; N, 6.26. Calcd. for $C_{12}H_{22}NCl$: C, 66.80; H, 10.28; N, 6.49%).

1, 4, 7-Trimethylquinolizidine (VI).—A solution of 1.1 g. of V in 20 ml. of ethanol was shaken with hydrogen at atmospheric pressure in the presence of 500 mg. of 5% palladium charcoal. After 7 hr., the catalyst was filtered off and the solvent evaporated. Distillation of the residue in vacuo gave trimethylquinolizidine; b. p. 74~78°C/15 mmHg, yield 0.7 g. (76%). $[\alpha]_D$ −47.8° (*c* 2.56, ethanol) (Found: C, 78.96; H, 12.76. Calcd. for $C_{12}H_{23}N$: C, 79.49; H, 12.79%). It was volatile. The picrolonate recrystallized from ethanol as yellow needles, m. p. 180~184°C (Found: C, 59.17; H, 7.13; N, 15.57. Calcd. for $C_{22}H_{31}O_5N_5$: C, 59.31; H, 7.01; N, 15.72%). The methiodide recrystallized from acetone as colorless needles, m. p. 189~191°C (Found: C, 48.21; H, 8.13; N, 4.17. Calcd. for $C_{12}H_{23}N \cdot CH_3I$: C, 48.30; H, 8.11; N, 4.33%).

Nitrile (VII).—A solution of 3.4 g. of chloride V in 40 ml. of ethanol was added, drop by drop, to a boiling solution of 2.4 g. of sodium cyanide in 36 ml. of ethanol and 12 ml. of water. After being heated under reflux for 8 hr., the reaction mixture was evaporated in vacuo. The residue was

extracted several times with boiling chloroform, and the combined extracts were evaporated to an oil, which was distilled, b. p. 96~99°C/1 mmHg, yield 2.5 g. (76%). The infrared absorption spectrum was at 2280 cm^{-1} (CN). $[\alpha]_D$ −78.1° (*c* 3.52, ethanol) (Found: C, 75.75; H, 10.81. Calcd. for $C_{13}H_{22}N_2$: C, 75.67; H, 10.75%).

Methyl Ester (VIII R=CH_3).—A solution of 10.0 g. of nitrile VII in 100 ml. of concentrated hydrochloric acid was heated for 2 hr. and evaporated to dryness. The residue was dissolved in 100 ml. of methanol and saturated with hydrogen chloride. After standing overnight at room temperature, the solvent was removed in vacuo. Water was added to the residue, and the solution was made basic with potassium carbonate; it was then extracted with ether and the extract dried. On distillation there was obtained 10.3 g. (89%), b. p. 105~108°C/1.5 mmHg, $[\alpha]_D$ −30.2° (*c* 4.97, ethanol) (Found: C, 70.59; H, 10.76; N, 6.21. Calcd. for $C_{14}H_{15}O_2N$: C, 70.25; H, 10.53; N, 5.85%).

1,7-Dimethyl-4-hydroxyethylquinolizidine (IX).—A solution of 4.0 g. of methyl ester VIII in 10 ml. of absolute ether was added to a solution of 1 g. of lithium aluminum hydride in 60 ml. of ether. The reaction mixture was refluxed for 2 hr., decomposed with the required amount of water, and the precipitate extracted several times with boiling ether. The extracts were evaporated, and the residue distilled. The product was obtained as an oil (b.p. 122~124°C/1.5 mmHg, yield 3.1 g. (88.5%)), which solidified and which was recrystallized from acetone as colorless needles, m. p. 84~85°C. The infrared absorption band of the hydroxyl group was at 3140 cm^{-1} (Nujol) and 3260 cm^{-1} (carbon tetrachloride). $[\alpha]_D$ −18.8° (*c* 1.06, ethanol) (Found: C, 73.67; H, 11.83; N, 6.39. Calcd. for $C_{13}H_{25}ON$: C, 73.88; H, 11.92; N, 6.63%).

The dipole moment was determined in a benzene solution. The dielectric constants were measured at 25°C with a measuring condenser of 300 p*F* and a liquid condenser of 30 p*F*. The density was determined at 25°C in a Lipkin's Pyknometer. The refraction of compound IX was calculated from the atomic refraction. The results were evaluated according to the procedure of Halverstadt and Kumler[14] and are summarized below:

ω	ε^{25}	d^{25}
0.0000	2.2724	0.8729
0.0048	2.2938	0.8736
0.0088	2.3035	0.8738
0.0115	2.3165	0.8742
0.0165	2.3343	0.8747
0.0205	2.3476	0.8751
0.0288	2.3787	0.8759
0.0311	2.3852	0.8760

R_D=63.30, P=207.1, μ=2.63

α-Methyladipic Acid (X).—$[\alpha]_D$ −12.0° (*c* 3.00, ethanol).

1-Methyl-4-ketoquinolizidine (XIII).—A solution of diethyl 2-[pyridyl-(2)]-allylmalonate (XI) in a glacial acetic acid was hydrogenated over platinum oxide at room temperature and atmosphere. After filtration of the catalyst, the solvent was removed in vacuo and concentrated hydrochloric acid was added and then refluxed for 6 hr. The solution was evaporated to dryness. Absolute ethanol was then added to the residue, and the solution was saturated with hydrogen chloride and left to stand overnight. The solution was concentrated and neutralized with potassium carbonate. After extraction with ether, the ethereal solution dried over sodium sulfate. The solvent was then distilled off, and the residue, on heating to 180~200°C, began to distill at 102~105°C/1 mmHg with an overall yield of 60%.

1-Methylquinolizidine (XIV) and its Chromatogram.—A solution of XIII (15.2 g.) in 100 ml. of absolute ether was added, drop by drop, to a solution of lithium aluminum hydride (3.5 g.) in ether (200 ml.), and the mixture was refluxed for 3 hr., and then decomposed with the required amount of water. The precipitated hydroxides were extracted several times with boiling ether, and the solvent was then distilled off. The residue, on distillation under reduced pressure, yielded 10 g. (72%) of a colorless oil, b. p. 76~78°C/11 mmHg. This product (5.6 g.) was dissolved in petroleum ether and chromatographed on alumina (75 g.).

Fraction	Eluent	Volume ml.	Weight g.
1	Petroleum ether	200	2.5
2,3	Petroleum ether	400	1.1
4	Petroleum ether : benzene (1 : 1)	200	0.6

The picrate from fraction-1 was in the form of yellow plates, m. p. 185~188°C (Found: C, 50.46; H, 5.73; N, 14.62. Calcd. for $C_{16}H_{22}O_7N_4$: C, 50.26; H, 5.80; N, 14.65%). The picrate from fraction-2, 3 melted at 167~175°C. The picrate from fraction-4 was in the form of yellow needles, m. p. 162~164°C (Found: C, 50.46; H, 5.86; N, 14.56%). The picrate from mother liquids of fraction-1 melted at 163~165°C; that of fraction-2, 3 at 164~166°C, and that of fraction-4 at 175~177°C.

1-Methylquinolizidine from 1-Lupinine.—Synthetic 1-lupinine (18.6 g.) was dissolved in petroleum ether and chromatographed on alumina (100 g.).

Fraction	Eluent	Volume ml.	Weight g.	Residue
1	Petroleum ether	300	6.80	B.p. 100~103°C/2.2 mmHg
2	Petroleum ether	120	3.00	M.p. 73~80°C
3	Ether	200	5.50	M.p. 81°C
4	Ether	250	1.80	M.p. 81°C
5	Ether	280	7.50	M.p. 76~80°C
6	Methanol	190	1.20	

To 1-*dl*-lupinine (fraction-1; 5.5 g.) was added, drop by drop, thionyl chloride (8 g.) under ice cooling. The mixture was kept at 50°C for 10 min. and evaporated in vacuo. Ice was added to the residue, and the mixture was made basic with sodium carbonate and then extracted with ether.

14) I. F. Halverstadt and W. D. Kumler, *J. Am. Chem. Soc.*, **64**, 2988 (1942).

The ether extract was dried, and the solvent was removed. On distillation, there was obtained a colorless oil, b. p. 105~107°C/9 mmHg, yield 4.3 g.

A solution of 4.3 g. of the above chloride in 50 ml. of absolute alcohol at the reflux temperature was treated with 4 g. of sodium, added in small pieces. After completion of the addition, the reaction mixture was heated under gentle reflux for 4 hr. The excess sodium was then decomposed by the addition of ethanol and water. The mixture was acidified with 6 N hydrochloric acid and was concentrated to remove the ethanol in vacuo. The residue was then made basic with sodium carbonate and extracted with ether. The ether extract was dried, and the ether was removed. The residual oil was distilled at 81°C/15 mmHg, yield 2.2 g. The picrate was prepared in and recrystallized from ethanol, m. p. 180~181°C (Found: C, 50.07; H, 5.82; N, 14.40%).

Following the procedure given above for 1-*dl*-lupinine, 1-*epi*-lupinine (fraction-3,4; m. p. 81°C, 3.8 g.) was reduced to 1-*epi*-lupinane (b. p. 72~75°C/12 mmHg, 1.3 g.). The picrate melted at 160~161°C (Found: C, 50.26; H, 6.04; N, 14.26%).

Diethyl 2-[Pyridyl-(2)]-ethyl Methylmalonate (XV).—B. p. 132~135°C/1 mmHg.

3-Methylquinolizidine (XVIII) from XV.—Following the procedure given above for the preparation of 1-methylquinolizidine, the product (9.2 g.) was dissolved in petroleum ether and chromatographed on alumina (100 g.).

Fraction	Eluent	Volume ml.	Weight g.
1-3	Petroleum ether	600	7.5
4-9	Petroleum ether	1200	0.5
10	Ether	200	0.7

The picrate from fraction 1-3 was in the form of yellow plates, m. p. 150~153°C, (Found: C, 50.13; H, 5.90; N, 15.08%). The picrate from fraction 4-9 appeared as yellow needles, m. p. 183~185°C. The picrate from fraction 10 was also in the form of yellow needles, m. p. 183~185°C (Found: C, 50.09; H, 5.80; N, 14.79%).

3-Methylquinolizidine from 3-Lupinine.—Synthetic 3-lupinine (38 g.) was dissolved in petroleum ether and chromatographed on alumina (400 g.).

Fraction	Eluent	Volume ml.	Weight g.	Residue
1—5	Petroleum ether	1300	0.9	M.p. 49~52°C
6	Petroleum ether	300	3.2	M.p. 56~58°C
7	Ether	300	2.1	M.p. 55~57°C
8	Ether	300	1.5	M.p. 51~53°C
9	Ether	400	1.7	M.p. 50~52°C
10	Ether	300	0.8	M.p. 48~51°C
11—16	Ether	2500	3.3	Oil
17	Methanol	500	24.3	Oil

Following the procedure given above for the preparation of 1-lupinane from 1-lupinine, 3-*dl*- and 3-*epi*-lupinine were converted to 3-*dl*- and 3-*epi*-lupinane. 3-Methylquinolizidine (1.6 g., b. p. 71~72°C/15 mmHg) was obtained from 1.5 g. of 3-*dl*-lupinine (m. p. 57~58°C, fraction-6, 7). The picrate was prepared in and recrystallized from ethanol, m. p. 151~152°C, in the form of yellow plates (Found: C, 49.83; H, 5.86; N, 14.74%).

On distillation of the oil (fraction-17), there were obtained 3 fractions: b. p. ~118°C/5 mmHg, 1.0 g; b. p. 118~123°C/5 mmHg, 17.9 g.; b. p. 123~125°C/5 mmHg, 4.9 g.

The product (10 g., b. p. 118~123°C/5 mmHg) was chromatographed on alumina (100 g.).

Fraction	Eluent	Volume ml.	Weight g.	Residue
18	Petroleum ether : Ether	200	1.5	Oil
19	Ether	200	1.4	Oil
20	Ether	160	0.6	Oil
21	Ether	200	1.0	Oil
22	Ether	230	0.9	Oil
23	Ether	200	0.8	Oil
24	Ether	40	0.5	Oil
25	Ethanol	270	3.4	Oil

Two and half grams of fractions 19, 20 and 21 was converted into 3-lupinane b. p. 77~79°C/15 mmHg, 1.1 g.; the picrate melted at 144~151°C and at 163~165°C (trace). The product (4.9 g., b. p. 123~125°C/5 mmHg) was chromatographed on alumina (100 g.).

Fraction	Eluent	Volume ml.	Weight g.	Residue
26	Petroleum ether : Ether	300	0.3	Oil
27	Ether	450	0.3	Oil
28	Ether	380	0.4	Oil
29	Ether	300	0.2	Oil
30	Ethanol	250	3.8	Oil

Nine tenths grams of fractions 27, 28 and 29 was converted into 3-lupinane, b. p. 79~81°C/17 mmHg, 0.6 g. The picrate was in the form of yellow needles, m. p. 177~178°C (Found: C, 50.32; H, 5.74; N, 14.99%).

4-Methylquinolizidine.—The hydrogenation of 1-[pyridyl-(2)]-pentan-4-one was carried out at an ordinary temperature and pressure over a platinium catalyst. 4-Methylquinolizidine was taken up in the usual manner and distilled at 17 mmHg, 81~86°C; yield 74%. The product (9.1 g.) was dissolved in petroleum ether and chromatographed on alumina (100 g.).

Fraction	Eluent	Volume ml.	Weight g.	M. p. of picrate
1—2	Petroleum ether	200	8.2	190~196°C
3	Petroleum ether	100	1.2	193~196°C
4—6	Petroleum ether	300	0.8	193~196°C
7	Ether	100	0.6	189~193°C
8	Ether	100	0.5	187~192°C

The picrate from fraction-3 was recrystallized three times from ethanol; it appeared as yellow prisms,

m. p. 193～196°C (Found: C, 50.07; H, 5.88; N, 14.56%). The picrate from fraction 8 was recrystallized three times from ethanol, appearing as small yellow plates, m. p. 187～190°C (Found: C, 50.51; H, 5.82; N, 14.50%).

The author wishes to thank Professor Yasuhide Yukawa for his helpful discussions, and Mr. Naohiro Hayakawa, of the Japan Atomic Energy Research Institute, and Mr. Shiro Sato, of the Institute of Scientific and Industrial Research, Osaka University, for their measurement of the NMR spectra.

Department of Chemistry
Faculty of Science
Osaka University
Nakanoshima, Osaka

Studies of the Cross-linking and Glass Transition of Fatty Acid-Modified Alkyd Resins

By Jū Kumanotani, L. W. Chen and Tsutomu Kuwata

(Received February 27, 1962)

The air drying of oil paints and varnishes has been considered to proceed by the autoxidative polymerization of the unsaturated part of the acyl groups. Reactions in the process of air-drying have been studied, resulting in some information, but how the unsaturated part of the acyl groups takes part in the cross-linking has scarcely been studied. It is well known that alkyd resin, a thermosetting amorphous polymer, is used as one of the main consituents of synthetic resin varnishes. In this paper, using fatty acid-modified alkyd resins, several factors which might have an influence on the degree of cross-linking and on the glass transition temperature of the films made from the resin have been investigated in order to get further information about the cross-linking reactions of acyl groups and some suggestions for the improvement of synthetic varnishes. The factors studied were:

a) The constitution of alkyd resins, i. e., the ratio of reactants (fatty acid, phthalic anhydride and glycerol).

b) The reaction time (the molecular weight changes with the reaction time).

c) The method of film formation (with or without the addition of a drier, air-drying or baking).

d) The aging of the films.

Experimental

Reagents.—The reagents used, phthalic anhydride, glycerol, lineseed oil fatty acids and soybean oil fatty acids, were chemically pure. The iodine values of the linseed oil fatty acids and soybean oil fatty acids were 183 and 128 respectively (as measured by Wijs' method). Xylene, the thinning solvent, was also chemically pure. Naphthenates of cobalt, lead and manganes were employed as the driers.

Synthesis of Alkyd Resins. — A 300 ml. four-necked flask with a glass stirrer was used, into one neck introducing carbon dioxide gas, into one neck inserting a thermometer, and into another one inserting a 25 ml. Stark & Dean trap for dehydration. The flask was immersed in a silicon oil bath and heated by a gas burner. The reagents were all introduced at once, and the temperature was raised to 230°C within $1^1/_2$ hr. and kept at that temperature for 5 hr.

The Process of Making Films. — The varnishes were prepared in 50% xylene solutions. The varnishes, with or without driers, were brushed on tin plates and dried in air or by baking. The quantity of the drier added to the resin was Mn 0.05%, Co 0.1% and Pb 0.2%. Since film more than 0.1 mm. thick is desirable, the varnishes were brushed 8 times every other day in the case of air drying, and the films were heated 8 times in an electric drier at 105°C for 8 hr. each time in the case of baking.

The Glass Transition Temperature (T_g) and the Degree of Cross-linking.—*The Physical Meaning of T_g and the Degree of Cross-linking.*—The term "glass transition" refers to the characteristic change in polymer properties from those of a relatively hard, brittle, glassy state to those of a softer, more flexible rubbery state as the temperature is raised through the glass transition temperature (T_g). Below the T_g, thermal energy is not available to allow the segments of the chain to move as a whole. The motions of the individual atoms are restricted to small excursions around their equilibrium positions. As the temperature approaches the T_g, the increased thermal energy becomes sufficient to allow larger molecular motions involving the coordinated movement of several atoms. Of course, the rigidity modulus G of a polymer decreases sharply with temperatures near the T_g,

until it reaches a definite value enough above the T_g; on further raising of the temperature, the value keeps constant or rises a little. Since the chain segments can move freely at higher temperatures, the rigidity is sustained by the entropy elasticity of the network chains. As predicted by the kinetic theory of rubber elasticity, the rigidity modulus at high temperatures (G_h) is in proportion to the degree of cross-linking.

The Torsional Pendulum Method. — The torsional pendulum method[1] developed by Inoue was employed for observing the T_g and G of the dried films. The period and the amplitudes of the damping oscillation of the film were measured; then the rigidity modulus G and logarithmic decrement λ were calculated. The temperature dependences of G and λ were measured in the range of $-70\sim90$°C. When these were plotted on a graph, a kind of characteristic spectrum of the polymer similar to a relaxation spectrum was obtained. As λ is defined as the ratio of the energy consumed by internal friction to the supplied energy, λ is considered to reach its maximum at T_g; reversely, T_g is found from λ_{max} on the garph. The rigidity modulus at high temperatures (G_h) is a direct measure of the degree of cross-linking.

Apparatus.—The inner structure of the films was considered to be at mechanical and thermal equilibrium when the films were left at room temperature for a time. The procedure of the measurement was separated into two parts, one part heating up from room temperature and another part cooling drown from room temperature. For the former, as is shown in Fig. 1, an electric drier was devised for hanging down the films and oscillating the pendulum from the outside. The temperature of the cabinet was controlled by a slide regulator and was raised at the rate of 0.5°C/min. For the latter, as is shown in Fig. 2, a core was installed in an ethanol-dry ice bath. The device for oscillating the pendulum, the same as in the electric drier, was set on the upper part of the core. The crushed dry-ice was thrown in the bath for cooling at the rate of 0.5°C/min. The core was equipped with a small fan for keeping the distribution of the temperature homogeneous, and nitrogen gas was suplied to the core continuously to prevent the freezing of moisture on the films.

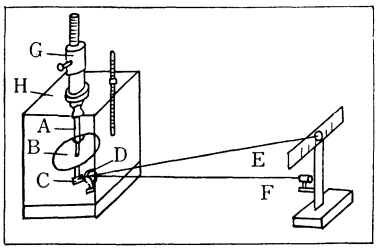


Fig. 1. Heating apparatus for torsional pendulum method.

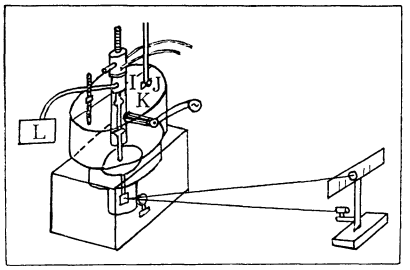


Fig. 2. Cooling apparatus for torsional pendulum method.
A Sample, B Inertia disk, C Mirror, D Lens, E Scale, F Lamp, G Device for twisting, H Electric drier, I Core J Dryice-ethanol bath, K Fan, L Thermocouple

1) Y. Inoue, *J. Chem. Soc., Japan. Ind. Chem. Sec.* (*Kogyo Kagaku Zassi*), 55, 262 (1952).

Results and Discussion

The Influence of Oil Length*. — Linseed oil fatty acid-modified alkyd resins of oil lengths 50%, 60% and 70% were prepared. Their acid values were 10.1, 7.5 and 5.1; their molecular weights were 1000, 740 and 690 respectively (as measured by Rast's method). The results are shown in Figs. 3 and 4, and in Table I**.

G_h increased with the oil length; i.e., 2×10^8 dyn./cm^2 for 50%, 2.7×10^8 dyn./cm^2 for 60% and 1.5×10^9 dyn./cm^2 for 70% in the case of baked film without the addition of a drier

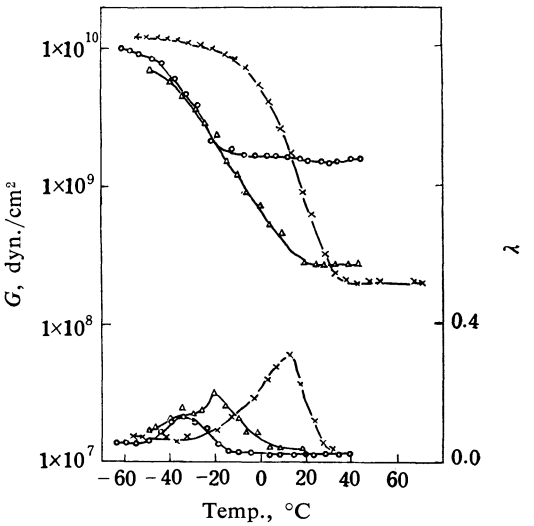


Fig. 3. Influence of oil length. Baking film of linseed oil fatty acid modified alkyd resin without addition of drier, measured at 6 months after preparation.
○ Oil length 70% △ Oil length 60%
× Oil length 50%

* $\text{Oil length} = \dfrac{\text{oil}}{\left(\begin{array}{c}\text{oil+glycerol+phthalic}\\ \text{anhydride−water(calcd.)}\end{array}\right)} \times 100$

** Sample films were exposed to the air for 6 months.

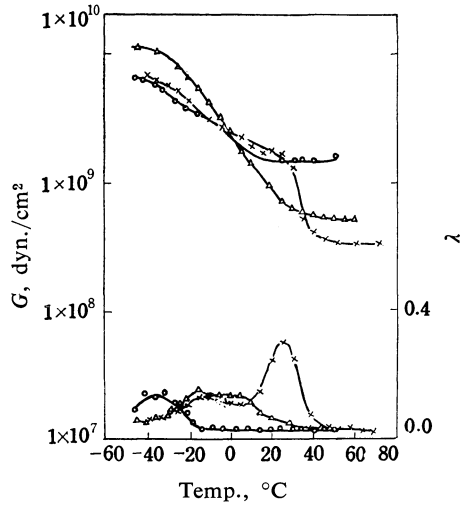


Fig. 4. Influence of oil length. Baking film of linseed oil fatty acid modified alkyd resin with addition of drier, measured at 6 months after preparation.
○ Oil length 70% △ Oil length 60%
× Oil length 50%

and 3.2×10^8 dyn./cm² for 50%, 5.0×10^8 dyn./cm² for 60% and 1.5×10^9 dyn./cm² for 70% in the case of baked film with the addition of a drier. Therefore, the degree of cross-linking increased with the oil length. Since the double bond is considered to be the source of cross-linking and the number of double bonds to increase with the increase in oil length, it is reasonable to assume that the degree of cross-linking increased with the increase in oil length. On the contrary, the T_g decreased with the increase in oil length; i.e., 12°C for 50%, −20°C for 60% and −33°C for 70% in the case of baked film without the addition of a drier, and 25°C for 50%, 0°C for 60%, and −35°C for 70% in the case of baked film with the addition of a drier. The benzene ring plays an important role in preventing molecular movements, resulting in the elevation of the T_g. It is reasonable to assume that the T_g decreased with the increase in oil length, as the concentration of the benzene ring increased with the decrease in oil length. It is also known that the T_g rises as the degree of cross-linking increases. The authors conclude that, in raising the T_g, the steric hindrance of the benzene ring plays a more important role than the degree of cross-linking. The λ_{max} increased with the decrease in oil length as a result of the internal friction of the benzene ring, the cohesive energy of which is relatively large.

The Effect of the Molecular Weight. — Fifty per cent oil length linseed oil fatty acid-modified resin was prepared under the conditions mentioned above. In the course of preparation, the samples of prepolymers of different molecular weights, 430, 570, 1000 and 1400, were taken, and air dried as well as baked film (heated for 16 hr. each time) was prepared from each prepolymer. The results are shown in Figs. 5 and 6 and in Table II. In the case of baked films without

Table I. Influence of oil length*

Oil length %	T_g °C	G_h dyn./cm²	λ_{max}	Prepolymer A. V.	Prepolymer Mol. wt.	Remarks
50	12	2.0×10^8	0.32	10.0	1000	Baking without addition of drier
60	−20	2.7×10^8	0.20	7.5	740	
70	−33	15×10^8	0.14	5.1	690	
50	25	3.2×10^8	0.30	10.0	1000	Baking with addition of drier
60	0	5.0×10^8	0.13	7.5	740	
70	−35	15×10^8	0.14	5.1	690	

* Measured at 6 months after preparation of the films

Table II. Effect of molecular weight

Oil length %	T_g °C	G_h dyn./cm²	λ_{max}	Mol. wt. of prepolymer	Remarks
50[a]	− 1	—	0.58	430	Baking without addition of drier
50[a]	18	0.6×10^8	0.75	1000	
50[a]	28	0.75×10^8	0.98	1400	
50[b]	5	—	0.67	570	Air drying with addition of drier
50[b]	20	0.28×10^8	1.24	1000	
50[b]	20	0.40×10^8	1.4	1400	

a Measured at 2 weeks after preparation of the films
b Measured at 2 months after preparation of the films

the addition of a drier, the T_g and G_h values were: 28°C, 0.75×10^8 dyn./cm^2 for mol. wt. 1400, 18°C; 0.6×10^8 dyn./cm^2 for mol. wt. 1000, and −1°C for mol. wt. 430*, and in the case of air-dried films with the addition of a drier, those values were: 20°C, 0.4×10^8 dyn./cm^2 for mol. wt. 1400, 20°C, 0.28×10^8 dyn./cm^2 for mol. wt. 1000, and −5°C for mol. wt. 570*. The results show that both the T_g and the G_h increase with the increase in the molecular weight of the prepolymer. The results may be considered as follows:

a) The configuration of the prepolymers of a high molecular weight may favor cross-linking.

b) The prepolymers of a low molecular weight contain more unreactant, which act as plasticizers for the polymer.

In the glass transition state, both the *G-T* and λ-*T* curves were sharp compared with the curves found in the samples of the same oil length used above, because the cross-linking was not fully completed, and the λ_{max} increased with the increase in the molecular weight of the prepolymer. This suggests that the λ-*T* curve's tendency to be flat is not a mere result of the progress of the cross-linking.

The Effect of Excess Glycerol. — In connection with reducing the acid value of resins less than 10, which is important practically, two 50% soybean oil fatty acid-modified resins were prepared: (A) with an equivalent weight of glycerol and (B) with a 20% excess (by weight) of glycerol. The acid values were

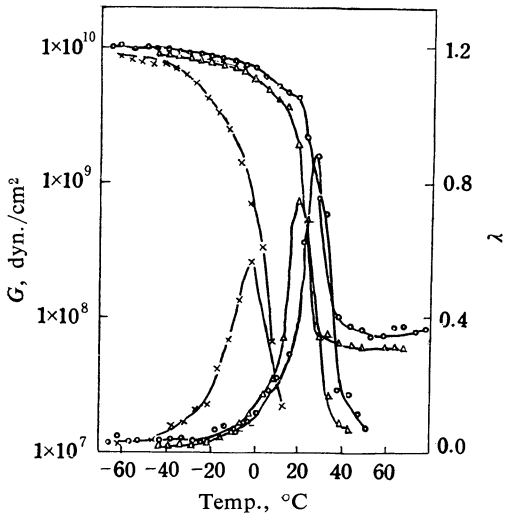


Fig. 5. Effect of molecular weight. Baking film of 50% oil length linseed oil fatty acid modified alkyd resin without addition of drier, measured at 2 weeks after preparation.
○ Mol. wt. 1400 △ Mol. wt. 1000
× Mol. wt. 430

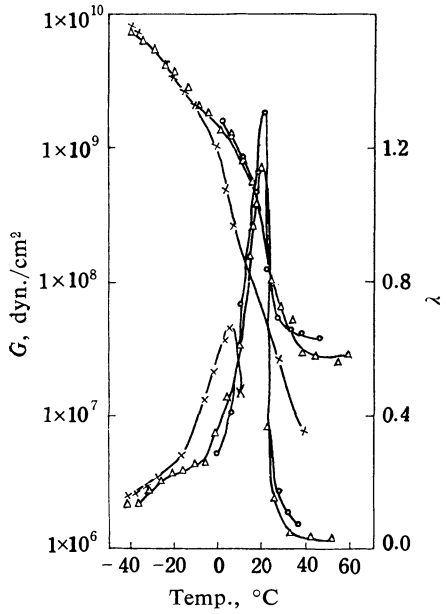


Fig. 6. Effect of molecular weight. Air drying film of 50% oil length linseed oil fatty acid modified alkyd resin, measured at 2 months after preparation.
○ Mol. wt. 1400 without drier
△ Mol. wt. 1000 with drier
× Mol. wt. 570 with drier

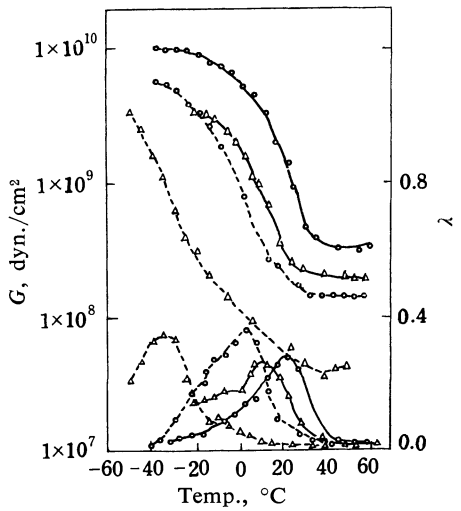


Fig. 7. Effect of excess glycerol. 50% oil length soybean oil fatty acid modified alkyd resin, measured at 6 months after preparation.
○ 20% excess glycerol
△ Equilibrium weight of glycerol
—— Baking film, with drier
---- Air drying film, with drier

* No G_h values of the sample were observed, since the films elongated and broke off at high temperatures.

TABLE III. EFFECT OF EXCESS GLYCEROL*

	T_g °C	G_h dyn./cm²	λ_{max}	A. V. of prepolymer	Remarks
A	10	2.0×10^8	0.27	32.7	Baking
B	21	3.2×10^8	0.28	9.6	
A	−11	0.4×10^8	0.34	32.7	Air drying
B	2	1.5×10^8	0.36	9.6	

* Measured at 6 months after preparation of the films

TABLE IV. EFFECT OF DRIER AND METHOD OF DRYING

	T_g °C	G_h dyn./cm²	λ_{max}	A. V. of prepolymer	Remarks
A_1	13	1.8×10^8	0.38	26.1	Measured at 6 months after preparation of the films
A_2	13	3.2×10^8	0.30	26.1	
B_1	23	5.4×10^8	0.26	26.1	
B_2	28	11×10^8	0.16	26.1	
A_1	22	2.5×10^8	0.50	26.1	Measured at 10 months after preparation of the films
A_2	26	4.0×10^8	0.36	26.1	
B_1	41	7.8×10^8	0.26	26.1	
B_2	52	11×10^8	0.18	26.1	

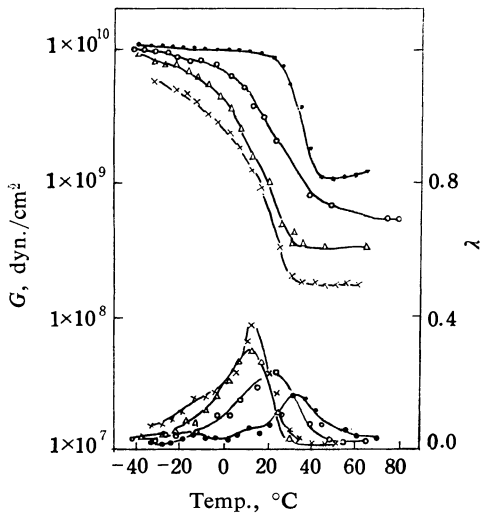


Fig. 8. Effect of drier and method of drying. 40% oil length linseed oil fatty acid modified alkyd resin, measured at 6 months after preparation.
● Baking with drier
○ Baking without drier
△ Air drying with drier
× Air drying without drier

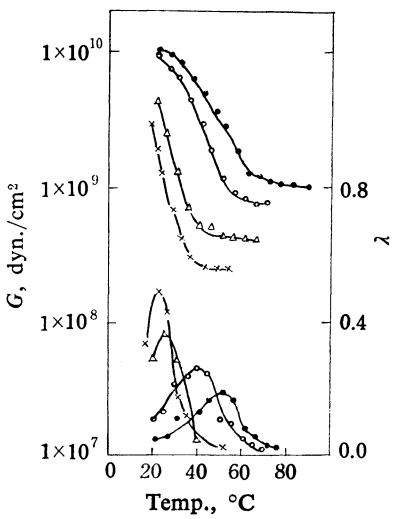


Fig. 9. Effect of drier and method of drying. 40% oil length linseed oil fatty acid modified alkyd resin, measured at 10 months after preparation.
● Baked with drier
○ Baked without drier
△ Air dried with drier
× Air dried without drier

32.7 for A and 9.6 for B. The results are shown in Fig. 7 and Table III. The G_h and T_g values were 3.2×10^8 dyn./cm², 21°C for B, 2.0×10^8 dyn./cm², 10°C for A in the case of baked films and 1.5×10^8 dyn./cm², 20°C for B, 0.4×10^8 dyn./cm², −11°C for A in the case of air-dried films. The results show that both the T_g and the G_h of B were larger than those of A. This may be considered to be result of the effects of the molecular weight and of the plasticizing action of the unreactant for the polymer.

The Effect of the Drier and the Method of Drying.—A 40% oil length, linseed oil fatty acid-modified resin was prepared under the same reaction conditions mentioned above, except

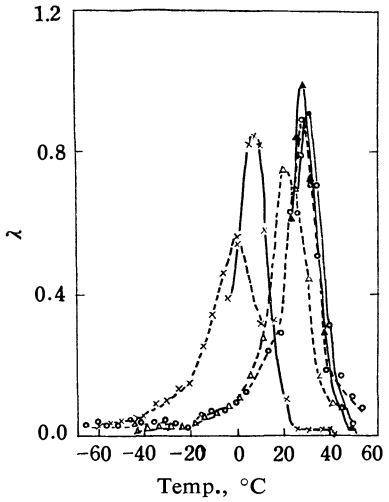


Fig. 10. λ-T relation of 50% oil length linseed oil fatty acid modified alkyd resin at early period of drying.
●, ○ Mol. wt. 1400 ▲, △ Mol. wt. 1000
× Mol. wt. 430
—— Baked film without drier measured at 2 months after preparation
---- Baked film without drier measured at 2 weeks after preparation

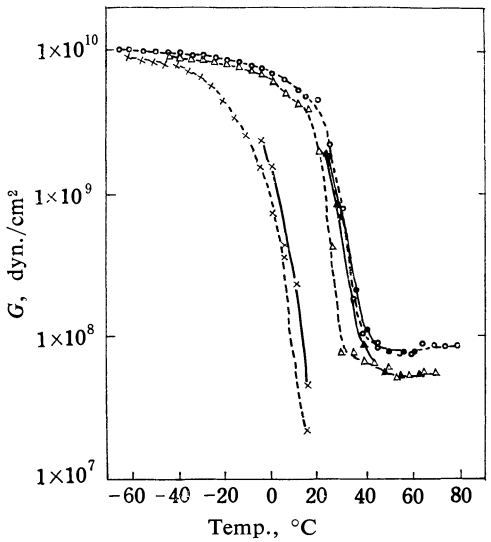


Fig. 11. G-T relation of 50% oil length linseed oil fatty acid modified alkyd resin at early period of drying.
●, ○ Mol. wt. 1400 ▲, △ Mol. wt. 1000
× Mol. wt. 430
—— Baked film without drier measured at 2 months after preparation
---- Baked film without drier measured at 2 weeks after preparation

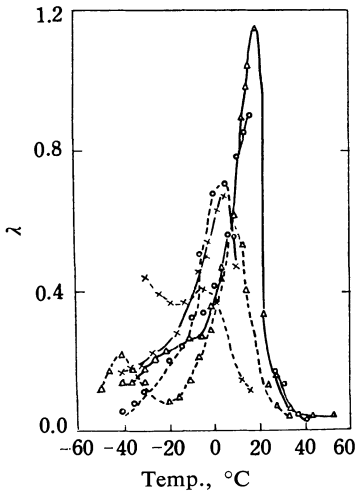


Fig. 12. λ-T relation of 50% oil length linseed oil fatty acid modified alkyd resin at early period of drying.
○ Mol. wt. 1400 without drier
△ Mol. wt. 1000 with drier
× Mol. wt. 570 with drier
—— Air dried film measured at 2 months after preparation
---- Air dried film measured at 2 weeks after preparation

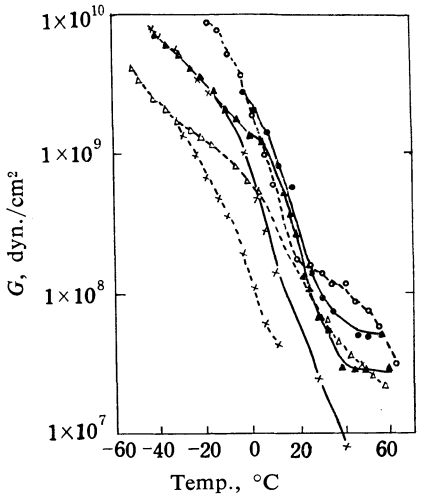


Fig. 13. G-T relation of 50% oil length linseed oil fatty acid modified alkyd resin at early period of drying.
●, ○ Mol. wt. 1400 ▲, △ Mol. wt. 1000
× Mol. wt. 570
—— Air dried film measured at 2 months after preparation
---- Air dried film measured at 2 weeks after preparation

that the reaction time was limited to 2 hr. in order to avoid gelation. Because the functionality per mole is larger in this case, it gels at a higher acid value[2]. The acid value of the resin in this case was relatively large, i. e., 26.1. Air-dried (A) and baked film (B) with a drier (A_2, B_2) and without a drier (A_1, B_1) were

2) W. H. Carothers, *Trans. Faraday Soc.*, 32, 39 (1936).

Table V. Early period of drying

Mol. wt. of prepolymer	Exposed time	T_g °C	G_h dyn./cm²	λ_{max}	Remarks
430	2 weeks	0	—	0.57	Baking
430	2 months	6	—	0.9	
1000	2 weeks	20	0.54×10^8	0.75	
1000	2 months	27	0.54×10^8	1.2	
1400	2 weeks	28	0.8×10^8	0.98	
1400	2 months	30	0.8×10^8	1.02	
570	2 weeks	− 5	—	0.41	Air drying
570	2 months	5	—	0.67	
1000	2 weeks	9	—	0.59	
1000	2 months	19	0.18×10^8	1.25	
1400	2 weeks	5	—	1.0	
1400	2 months	20	0.4×10^8	1.0	

prepared. The results are shown in Figs. 8 and 9 and in Table IV. The degree of cross-linking was in the order of $A_1<A_2<B_1<B_2$; the T_g was in the same order, and the λ_{max} decreased in this order. The G at a sufficiently low temperature was 10^{10} dyn./cm², and the same G values were observed in other films.

Aging of Films.—*Early Period of Drying.*—A 50% oil length linseed oil fatty acid-modified resin was prepared, from which air-dried and baked films were made. Their properties were measured 2 weeks and 2 months after the preparation. The results are shown in Figs. 10, 11, 12 and 13 and in Table V. For baked films, no distinguishable difference in the T_g and the G_h was observed between the films prepared from the prepolymer of a larger molecular weight. For air-dried films, the elevation of the G-T curve and the T_g (about 10°C) were observed, and the cross links were developed to the extent of sustaining the applied load.

Aging at a Later Period.—A 40% oil length linseed oil fatty acid-modified resin was prepared, from which air-dried and baked films were made. The results of the measurement 6 months and 10 months after the preparation are shown in Fig. 14. In the course of 4 months, the elevation of the G-T curve and the raising of the T_g (10~20°C) were observed. The λ_{max} was larger, and the λ-T curve tended to be sharp. It is notable that, in the case of baked film with the addition of a drier, no change in the G_h was observed, although the T_g was raised more than 10°C. This may be explained by the fact that, in the course of time, the film was gradually air-oxidized with the formation of polar groups, with the result that their cohesive energy became larger and led to a rise in the T_g. Owing to the increase in the energy consumed by the internal friction caused by the increase in the concentration of

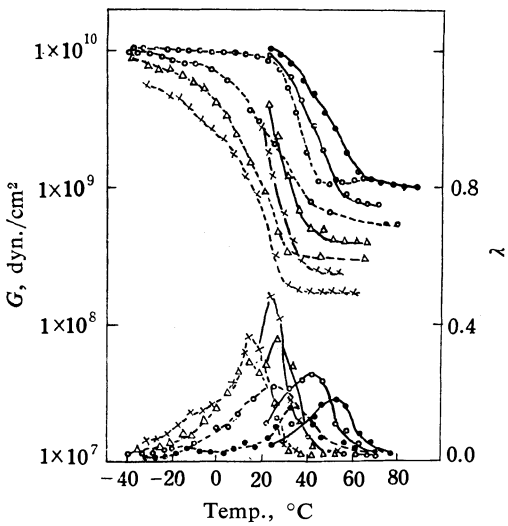


Fig. 14. The aging of the films of 40% oil length linseed oil fatty acid modified alkyd resin.
- ● Baked with drier
- ○ Baked without drier
- △ Air dried with drier
- × Air dried without drier
- —— Measured at 10 months after preparation
- ---- Measured at 6 months after preparation

the polar group, the λ_{max} became larger. Generally the driers accelerate the drying of film in the early period, resulting in the G_h values of the films with a drier being higher than those of the films without a drier (measured 6 months after the preparation of the films); this effect of acceleration still held even 10 months after the preparation of the films. Both the T_g and the G_h were larger in the case of baked films. Comparing the baked to the air-dried films, the authors found that the effect of heating held even 10 months after the preparation of the films. Concerning

TABLE VI. AGING AT LATER PERIOD

Exposed time	T_g** °C	λ_{max}**	T_g* °C	λ_{max}*	G_h dyn./cm²	Remarks
6 months	5	0.14	−33	0.32	—	Baking
10 months	3	0.17	−32	0.24	0.75×10^8	Baking
6 months	—	—	−35	0.36	0.4×10^8	Air drying
10 months	11	0.32	−33	0.28	0.84×10^8	Air drying

* Values at sub-glass transition
** Values at main glass transition

the acceleration of the cross-linking, heating was found to be more effective than driers. It may be suggested that the mechanism of cross-linking is not the same in the case of baking and of air-drying.

Sub-glass Transition. — In some experiments, two glass transition points were observed; the authors have named the higher one, the main glass transition point, and the lower one, the sub-glass transition point. The sub-glass transition was observed between −30 to −40°C. In the case of air-dried film prepared from the prepolymer of a low molecular weight, the sub-glass transition was found in the early period of drying (Fig. 15). Comparing the films two weeks and two months after preparation, the λ_{max} of the sub-glass transition tended to be small and the λ-T curve at the sub-glass transition state became flat; on the other hand, the λ_{max} of the main glass transition tended to be larger and the λ-T curve at the main glass transition state became sharp. The same glass transition phenomenon was observed in the case of a 50% oil length soybean oil fatty acid-modified resin using an equivalent weight of glycerol even 10 months after the preparation of the films (Fig. 16 and Table VI). Though the reasons are not fully understood, this finding suggests that such a kind of sub-glass transition is due to the unrestrained chain of the acryl groups.

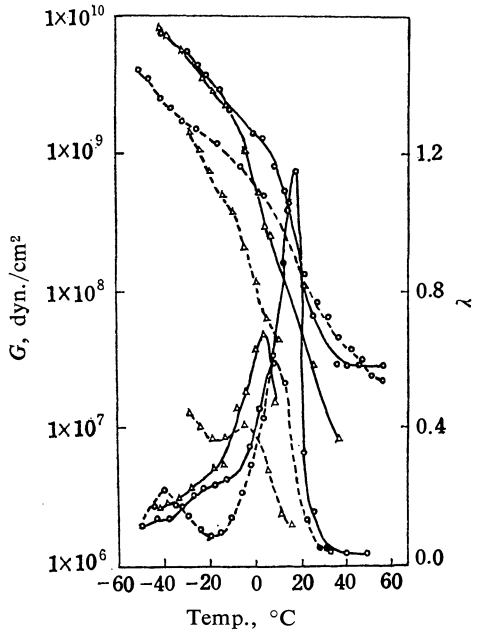


Fig. 15. Sub-glass transition. 50% oil length linseed oil fatty acid modified alkyd resin at early period of drying with addition of drier.
○ Mol. wt. 1000 △ Mol. wt. 570
—— Measured at 2 months after preparation
---- Measured at 2 weeks after preparation

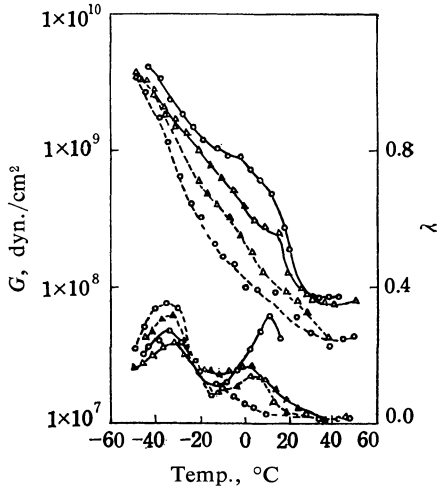


Fig. 16. Sub-glass transition. Air dring films of 50% oil length soybean oil fatty acid modified alkyd resin with equivalent weight of glycerol.
○ With drier △ Without drier
—— Measured at 10 months after preparation
---- Measured at 6 months after preparation

Summary

a) The degree of cross-linking observed in films of fatty acid modified alkyd resins increases with the content of unsaturated acids. Moreover, cross-linking is not so effective in raising the T_g as the benzene ring, which has a larger cohesive energy.

b) Both the T_g and the degree of cross-linking increase with the increase in the molecular weight of the prepolymer.

c) The excess of glycerol employed in fatty acid-modified alkyd resin is effective in raising the T_g and encouraging the progress of the cross-linking.

d) Generally, the cross-linking is not soon completed; as time elapses, the T_g rises, and the cross-linking progresses. No change in the G_h with the elevation of the T_g (baked film with the addition of a drier) is considered to be caused by the formation of polar groups by air-oxidation.

e) In the early period of drying, a sub-glass transition caused by the unrestrained chain of the acyl groups is observed.

Department of Applied Chemistry
Faculty of Engineering
The University of Tokyo
Hongo, Tokyo

*Studies of the Structure and Properties of Aromatic Polyamide. I. Physical Properties of Poly(m-xylyleneadipamide)**

By Naoya YODA

(Received March 13, 1962)

It has been reported that *m*-xylylenediamine reacts with various aliphatic dibasic acids to form high molecular weight polyamides[1].

The polymer of *m*-xylylenediamine and adipic acid shows the effects caused by a reversal of the position of the carbonyl groups relative to the amide nitrogen, compared to that of the polymer of isophthalic acid and hexamethylenediamine[2,3]. *m*-Xylylenediamine has the characteristic high reactivity of aliphatic diamines mainly due to the side-chain methylene group, which is considerably more reactive than aromatic diamines[4,5]. The present investigation was undertaken to study the physical properties of a melt-spun filament of aromatic polyamide obtained from *m*-xylylenediamine and adipic acid; as described herein, studies of the dynamic mechanical properties as well as of the chemical behavior of the polymer reveal that it possesses properties intermediate between poly-ε-capramide and polyethylene terephthalate.

Experimental

Polymerization of *m*-Xylylenediamine and Adipic Acid.—Commercially available *m*-xylylenediamine was distilled under reduced pressure, and the fraction boiling at 114°C/1 mmHg was used for the polymerization. The purified adipic acid (m. p. 133°C) was obtained by crystallization of commercially available dibasic acid from aqueous ethanol. The *m*-xylylenediamine adipic acid salts were prepared according to the following procedure[6]: 14.6 g. (0.1 mol.) of adipic acid was added into a solution of 13.6 g. (0.1 mol.) of *m*-xylylenediamine in 28.2 ml. of water in order to obtain a concentrated warm solution of the salt. When the solution had been cooled, a white crystalline solid precipitated out slowly. In order to complete the precipitation of the salt, 113 ml. of isopropanol was added. The white solid was filtered, washed with isopropanol, and dried under vacuum at 60°C. The yield of salt was 93%, m. p. 193~194°C. The nylon salt thus obtained was polymerized at an elevated temperature with the following procedure: Excess adipic acid (0.075 mol. %) was added as a stabilizer, and the salt was heated at 180 to 190°C in a Claisen flask under a nitrogen atmosphere. Then the polymerization temperature was gradually raised to 260°C over a 1~1.5 hr. period. The polymer was held at 260°C for 2 hr. at atmospheric pressure before applying a vacuum (1 to 5 mmHg) for 0.5 to 1 hr. to complete the polymerization. The resulting polymer had a melting point of 243°C, $d_4^{25}=1.2059$, and the intrinsic viscosity measured in *m*-cresol at 25°C was 0.96. It showed the typical infrared spectrum of polyamide, indicating a NH band (hydrogen bonding) at 3297 cm^{-1}, an amide I band at 1639 cm^{-1} and an amide II band at 1545 cm^{-1}. Experimental details will be discussed in a forthcoming paper**.

Melt-spinning of Poly(*m*-xylyleneadipamide).—A small scale melt-spinning instrument, composed of a heating cylinder, plunger, spinneret (0.5029 mm. diameter, 0.402 mm. length) and with a

* This paper was presented in part before the 12th Annual Meeting of the Chemical Society of Japan, Kyoto, April, 1959.

1) E. F. Carlston and F. G. Lum, *Ind. Eng. Chem.*, **49**, 1239 (1957).

2) F. G. Lum and E. F. Carlston, ibid., **44**, 1595 (1952).

3) A. J. Yu and R. D. Evans, Abstracts of papers, 135th Am. Chem. Soc. Meeting, Boston, Mass. (April 5-10, 1959), p. 23s.

4) P. J. Flory, U. S. Pat. 2244192 (June 3, 1941).

5) W. W. Triggs, Brit. Pat 525516 (Aug. 29, 1940).

** N. Yoda and I. Matsubara, *J. Polymer Sci.* (1962), in press.

6) W. H. Carothers, U. S. Pat. 2130947 (Sept. 20, 1938).

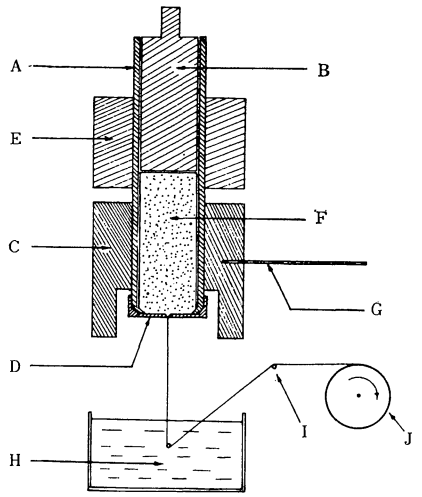


Fig. 1. Melt-spinning apparatus of polymer.

A Heating cylinder	F Polymer block (candle)
B Plunger	G Thermometer
C Heating jacket	H Cooling bath
D Spinneret	I Guide
E Cooling jacket	J Take-up roller

heating and cooling jacket, a cooling bath and a take-up roller, as shown in Fig. 1, was used as the apparatus.

The spinning block of the polymer was prepared by melting the polymer flakes in a sillicone-varnished (DC 20) glass cylinder under dry nitrogen atmosphere under vacuum at an elevated temperature. After pressing the melt with the steel plunger to complete the deairation at 245~250°C, it was cooled gradually to form the polymer block, which was ready to use for spinning.

The following spinning conditions were employed for the melt-spinning of poly(*m*-xylyleneadipamide) shown in Table I.

TABLE I. MELT-SPINNING CONDITIONS OF POLY-(*m*-XYLYLENEADIPAMIDE)

Item	Condition
Spinning temperature	265°C
Diameter of polymer block	27 mm.
Pressing speed	0.260 cm./min. (press, 282 r. p. m.)
Diameter of spinneret	0.5029 mm. (length : 0.402 mm.)
Rate of take up	30 m./min.
Length of air cooling	1.5 m. (at 25°C)
Cooling bath temperature	5°C

Drawing and Heat-setting of the Undrawn Filament. — The undrawn filament thus obtained was heat-stretched in a water bath at 79°C, the draw ratio of 3.4—4.5 was found to be the optimum. (Low speed, 5 m./min., high speed 25 m./min.) The stretched filament was treated either at 180°C for 5 min. or at 187°C for 10 min. in a thermostat drier for the heat setting.

Measurement of Density. — A mixed solvent composed of carbon tetrachloride and toluene was used, and the density was measured by the flotation method[7].

Measurement of the Stress-strain Curves of the Filaments.—Stress (g./D) and strain (%) curves were obtained by the use of an Instron tensile-testing instrument.

Measurement of Light Resistance.—The drawn filaments were exposed to light by means of a Atlas Fade-O-meter for a certain period of time and the tensile strength of the irradiated specimens was then measured.

Results and Discussion

Stress-strain Diagram of Poly(*m*-xylylene-adipamide) Mono-filament.—The stress-strain curves of melt-spun mono-filaments are shown in Fig. 2. The stress-strain characteristics change as expected with an increase in the strain rate. The tenacity of the drawn filament is 5.93 g./D., whereas the heat-set filament shows a tenacity of up to 6.79 g./D.

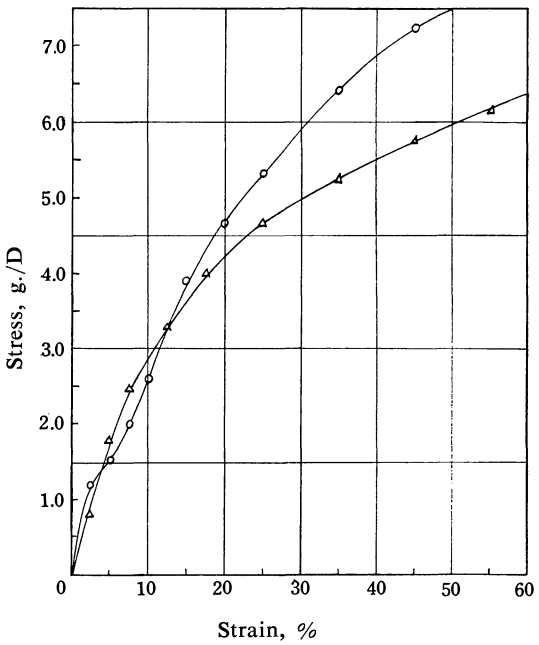


Fig. 2. Stress-strain curve of poly (*m*-xylylene-adipamide) mono-filament.
○ Heat-set filament △ Drawn filament

Wet and Dry Knot, and Loop Tenacity.—The wet and dry knot, and the loop tenacity are compared with those of polycapramide and polyethylene terephthalate in Table II and Fig. 3.

7) C. E. Black and M. Dole, *J. Polymer Sci.*, 3, 358 (1948).

Table II. Dry and wet knot, and loop tenacity

Polymer	Dry, knot, and loop tenacity g./D	Wet, knot, and loop tenacity g./D
MXDA-6	5.36	4.18
Polyester	4.5—7.0	4.5—7.0
Polycapramide	4.5—7.0	4.0—6.5

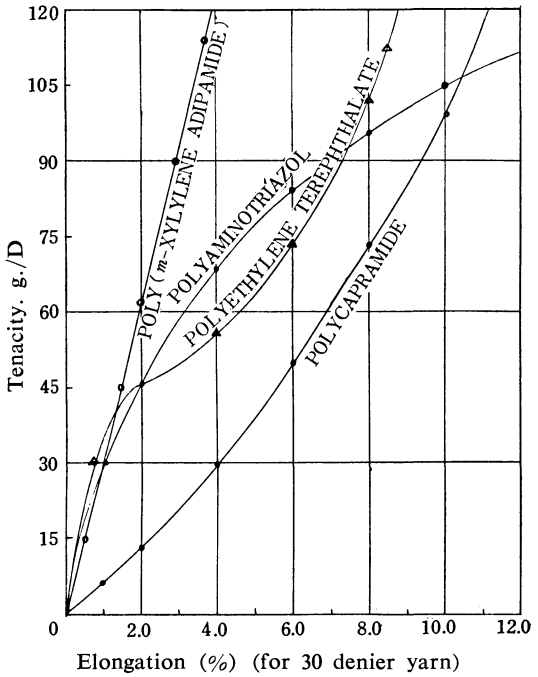


Fig. 3. Relation between elongation and tenacity of poly(*m*-xylyleneadipamide) mono-filament[8].

Measurement of Shrinkage.—The shrinkage of the heat-set filament in boiling water was measured at 4.0%.

Measurement of Light-resistance.—The light-resistance of the heat-set filament was measured by means of an Atlas Weather-o-Meter over the periods of 10, 20, 40 and 80 hr.

The ratio of the tenacity of irradiated to that of unirradiated filament is plotted against the irradiation time in Fig. 4. It can be seen in Fig. 4 that a 25% decrease in the tenacity was observed for 40 hr. irradiation, and 30% for 80 hr. exposure.

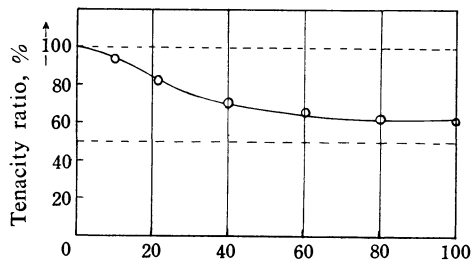


Fig. 4. Relation between irradiation time and tenacity ratio.

Elastic Recovery of the Heat-set Filament.—The elastic recovery was measured by the Instron instrument at a 5% elongation and a 10% elongation, the results are summarized in Tables III and IV respectively.

Table III. Elastic recovery of poly-(*m*-xylyleneadipamide) filament

No.	Immediate recovery	Delayed recovery	Deformation
1	57/81=0.705	24—20/81=0.0495	20/81=0.247
2	67/80=0.815	15—12/80=0.0376	12/80=0.150
3	54/77=0.700	23—20/77=0.0390	20/77=0.261
$\overline{X}$	0.740	0.042	0.219

Table IV. Elastic recovery of poly-(*m*-xylyleneadipamide) filament

No.	Immediate recovery	Delayed recovery	Deformation
1	110/197=0.560	87—54/197=0.167	54/197=0.273
2	110/196=0.561	86—55/196=0.158	55/196=0.280
3	110/196=0.561	86—53/196=0.168	54/196=0.270
$\overline{X}$	0.561	0.164	0.274

It was found that the elastic recovery of the filament is 78.2% or better at the 5% elongation and that at the 10% elongation the elastic contribution (immediate plus delayed) drops

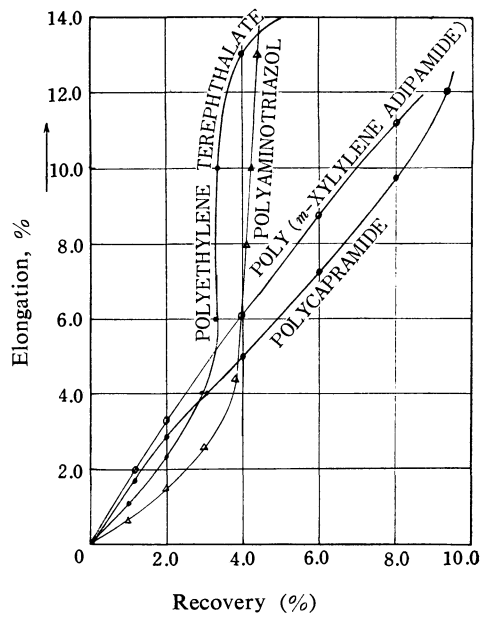


Fig. 5. Elastic recovery and elongation of poly (*m*-xylyleneadipamide) yarn, as compared with other fibers.

to 72.5%. Similar results were obtained from the repeated stress data. The elastic recovery of the poly(*m*-xylyleneadipamide) filament is compared with that of polyester, polycapramide and polyaminotriazole in Fig. 5.

Measurement of the Dynamic Modulus of Elasticity and of the Loss Factor (tan δ).—The dynamic modulus of elasticity, E_2, is expressed in terms of the product of the frequency, ω, and the dynamic coefficient of the viscosity, η, as follows;

$$E_2 = \omega\eta \quad (1)$$

The loss factor, tan δ is expressed in Eq. 2, where E_1 is the modulus of the elasticity.

$$\tan\delta = E_2/E_1 \quad (2)$$

The observed data in Eqs. 1 and 2 are shown in Table V.

TABLE V

Filament	Dynamic modulus of elasticity, $E_2\times10^{10}$ dyn./cm^2,	Loss factor tan δ $\times10^{-2}$
Stretched and nonheat-set filament	5.08	2.2
Stretched and heat-set filament	5.34	1.9

The values thus obtained are compared with those of polycapramide and polyethyleneterephthalate in Table VI.

TABLE VI

Polymer	Dynamic modulus of elasticity, $E_2\times10^{10}$ dyn./cm^2	Loss factor tan δ $\times10^{-2}$
Nylon 6	4.2	10
Nylon 6.10	4.5	4.4
Polyester ($\times5$ drawn)	4.5	1.5
Polyester ($\times7$ drawn)	1.3	1.5

It can be seen from Table VI that the poly(*m*-xylyleneadipamide) filament possesses physical properties intermediate between nylon 6 and polyester.

Measurement of Density.—The density was measured by the floating method, using a toluene/carbon tetrachloride solvent mixture. A modified pycnometer was employed at 25.0°C for the measurement.

The observed values are summarized in Table VII.

TABLE VII. DENSITY OF POLY-(*m*-XYLYLENEADIPAMIDE)

Density	Un-stretched	Stretched	Annealed
d_4^{25}	1.2059	1.2219	1.2248

It was again concluded that the density of poly(*m*-xylyleneadipamide) shows a value intermediate between polycapramide and polyethylene terephthalate, as is shown in Table VIII.

TABLE VIII

Density	Polycapramide	Poly (MXD-6)	Polyethylene terephthalate
d_4^{25}	1.14	1.23	1.38

Viscosity Measurement.—The intrinsic viscosity was measured in *m*-cresol at 25.0°C.

$$[\eta]_{m\text{-cresol}}^{25°C} = 0.96$$

In a diluted concentration range of the *m*-cresol solution, an abnormal increase in specific viscosity was observed, as is shown in Fig. 6.

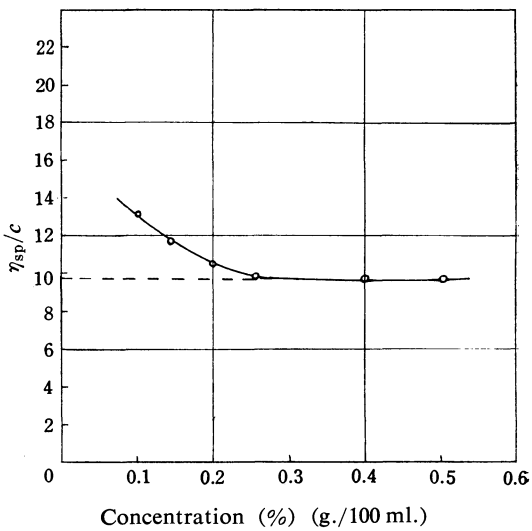


Fig. 6. Relation between reduced viscosity and concentration of poly(*m*-xylyleneadipamide) measured in *m*-cresol at 25°C.

Summary

Poly(*m*-xylyleneadipamide) was synthesized by the polycondensation of *m*-xylylenediamine and adipic acid, and the resulting polymer was melt-spun to afford a mono-filament. The physical properties of the undrawn filament, the stretched filament, and the stretched and annealed filament were investigated. It was found that the dynamic mechanical behavior and the chemical property of the aromatic polyamide are intermediate between poly-ε-capramide and polyethylene terephthalate.

The author takes pleasure in acknowledging the support and interest of Dr. Haruo Kobayashi, the Director of the Research Department of

8) J. W. Fisher, *J. Applied Chem.*, **4**, 212 (1954).

Toyo Rayon Company, and in thanking him for his permission to publish these findings. Thanks are also due to Dr. Masamoto Watanabe, Dr. Akihisa Miyake and Dr. Tatsuo Kawaguchi for their valuable discussions.

Central Research Laboratories
Research Department
Toyo Rayon Co., Ltd
Otsu, Shiga

The Kinetics of the Transition of Titanium Dioxide

By Akira SUZUKI and Yoshihide KOTERA

(Received February 24, 1962)

The kinetics of the transition of anatase to rutile have previously been investigated[1,2]. In these studies samples, after being heated, were analyzed by means of the X-ray diffraction method. The rate of the transition of compounds such as titanium dioxide, germanium dioxide and silica is complicated by the variation in the size of the particles, the temperature, the surrounding atmosphere and the presence of small amounts of impurity.

Attention should be paid to the values of the activation energy of the transition. It has been reported that the value of the activation energy of the transition was equal to that of the sublimation energy in some organic compounds[3,4] and in sulfur[5], while the value of a compound such as mercuric iodide was not equal to that of the sublimation energy[6]. It is, therefore, important to determine the value of the activation energy in the transition of titanium dioxide as correctly as possible and to compare it with other thermodynamic values.

Meanwhile, it has been proved that there is a large difference between the dielectric constants of anatase and rutile; from this fact it was possible to analyze both elements in the mixture. We have measured the transition rate of anatase to rutile, analyzing their mixture by the dielectric constant method, and have obtained some interesting results to explain the transition process.

Experimental

In this study the raw materials of titanium dioxide (anatase) was prepared by the following procedure. Titanium tetrachloride was distilled after the impurities in it had been precipitated by letting hydrogen sulfide pass through it. The distillate was added, drop by drop, to a 50% sulfuric acid solution, and the mixture was heated to drive off hydrochloric acid until no Cl^- was detected. The solution thus obtained was diluted with distilled water and then hydrolyzed at 90~100°C. The precipitated gel was washed with distilled water, and then the product obtained was heated for five hours at 700°C in an electric furnace. Two kinds of samples, "a" and "b" were used in this study, both being prepared in the same manner. It was later proved that they have different rates of transition.

Zn, Mg, Pb, Fe, Al, V, Ca, Cu, Ga, Cr and Sn were not detected spectroscopically, while the lines of Si were faintly observed. According to the electron-microscopic observation, the crystal size of the raw materials was 0.09~1 μ, while the crystal size of sample "a" was a little larger than that of sample "b". The pattern of rutile was not detected by the X-ray diffraction.

The dielectric constant of the mixture of anatase and rutile was measured by the method reported by Oehme[7]. The measuring equipment used was a DK Scope, type 59 (Yanagimoto Co., Ltd.). In the measurement of the dielectric constant of powder by the immersion method, it is necessary to eliminate completely the foams of air occluded in the powder. By using the coaxial cylindrical cells shown in Fig. 1, it is possible to measure the difference in capacity between liquid and powder suspension. 0.700 g. of the sample was accurately weighed and put into A in the figure. After pouring aceton into A and B until half the height of a bakelite cylinder was reached, the powder suspension in A cell was agitated carefully by a stainless steel wire until no bubble rose. By switching C on the respective side, the capacities of the A and B cells were compared with one other. From the difference in the readings on the scale, ΔS, it is possible to determine the proportion of rutile or anatase in powder. Figure 2 shows the calibration curve obtained in this work.

1) A. W. Czanderna, C. N. R. Rao and J. M. Honig, *Trans. Faraday Soc.*, **54**, 1069 (1958).
2) C. N. R. Rao, *Can. J. Chem.*, **39**, 498 (1961).
3) N. H. Hartshorne, G. S. Walter and W. O. William, *J. Chem, Soc.*, **1935**, 1860.
4) A. Hodkin and D. Taylor, ibid., **1955**, 489.
5) N. H. Hartshorne and M. H. Roberts, ibid., **1951**, 1097.
6) D. G. Fade and N. H. Hartshorne, ibid., **1938**, 1636.
7) F. Oehme, *Z. Naturforsch.*, **14b**, 779 (1959).

The X-ray diffraction patterns of the samples were obtained by the Geiger Counter X-ray Diffractometer, and the results were compared with those of the dielectric constant method.

The sample in the sintered alumina boat was placed in a quartz tube, which was then set in a platinum electric furnace equipped with a voltage transformer and a chromel-alumel thermocouple. The position where the sample was placed in the furnance was selected so as not to be affected by the temperature variation in the furnace. In any given run, the temperature fluctuation did not exceed ±2°C. The temperatures of the experiments were established within 3 min. after the boat had been put in the furnace.

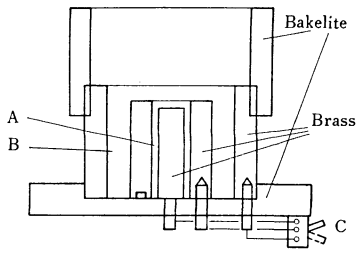


Fig. 1. Coaxial cylindrical cell for the analysis of the anatase-rutile mixture by means of the dielectric constant measurements.

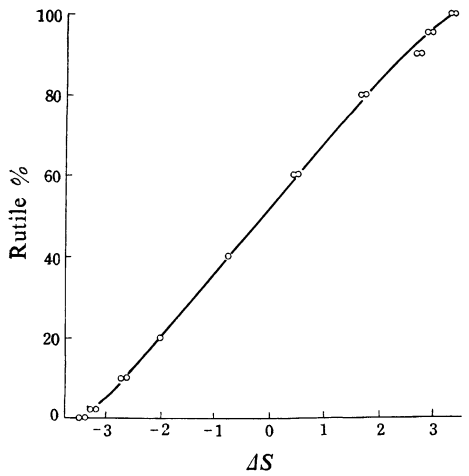


Fig. 2. Calibration curve for the analysis of the anatase-rutile mixture by means of the dielectric constant measurements.

The oxygen atmosphere was obtained from a bomb containing oxygen prepared electrolytically from distillated water. The oxygen was dried by letting it pass through sulfuric acid and calcium chloride. By using a u-type flow meter, the flow velocity of the oxygen was controlled.

Potassium chloride or lithium chloride was added to the samples in the form of solutions, and the mixtures were dried at 150°C before heating.

Experimental Results

The results of experiments on many samples, which were subjected to different heat treatments or surrounding atmospheres and which contained different additives, are sammarized in Figs. 3—6. Within the range of experimental uncertainty, no variation in the lattice parameter was encountered for any sample, and the diffraction patterns of anatase and rutile agreed fairly well, with respect to both the *d* values and the relative intensities, with those previously reported[8] by means of the

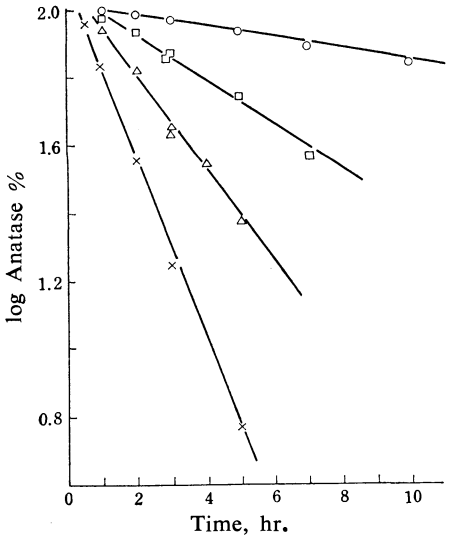


Fig. 3. First-order plots of the data in the sample "a" in air.

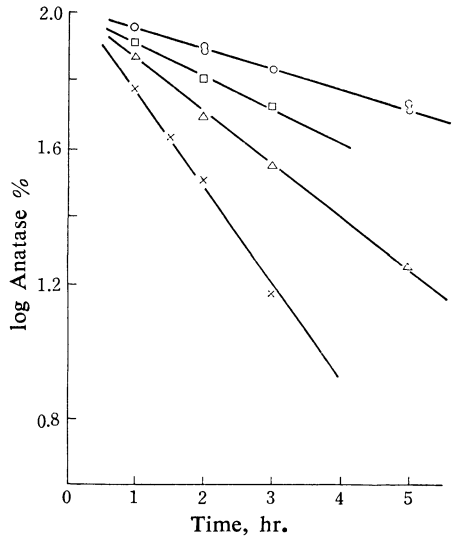


Fig. 4. First-order plots of the data in the sample "b" in air.

8) A. S. T. M. X-ray powder diffraction card.

X-ray diffraction method. No line broadening was encountered throughout the whole stage, nor was there any evidence for the existence of solid solutions, i. e., of disordered structures.

The color of most samples turned from white to yellowish as the transition proceeded, but the color of the sample with potassium chloride turned greyish.

Transition of Pure Titanium Dioxide in Air. —The transition from anatase to rutile modification was found to occur between 750 and 800°C in pure titanium dioxide in air. The rate of transition depends on the heating time and the temperature. Figures 3 and 4 show the transition of pure titanium dioxide in air, log(Anatase %) against time being illustrated. Fig. 3 shows the transition of "a", and Fig. 4, that of "b". These data were treated as previously reported by Czanderna, Rao and Honig[1] and by Rao[2]. In this study the data were plotted for the first-order equation; the data follow the first-order law fairly well for two kinds of samples, "a" and "b". However, there was a large difference between the rates of the transition of "a" and "b" as shown in Table I. In Table I the values of the rate constants, k, are shown for the transitions without and also with flux.

The activation energy was computed from the standard Arrenenius plot of $\log k$ against $1/T$ shown in Fig. 7. The deviation of each plot from the straight line is within the range of experimental error. The values of the activation energy thus obtained were 110 and 116 kcal./mol. for "a" and "b" respectively.

Attention should be paid to the fact that the values of activation energy do not differ significantly between "a", and "b" even

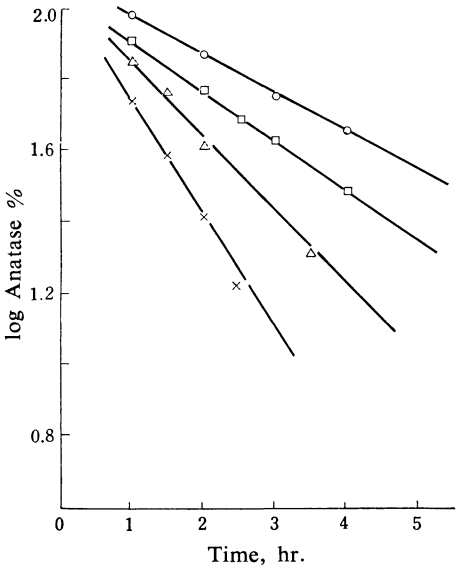


Fig. 5. First-order plots of the data in the sample "b" in O_2.

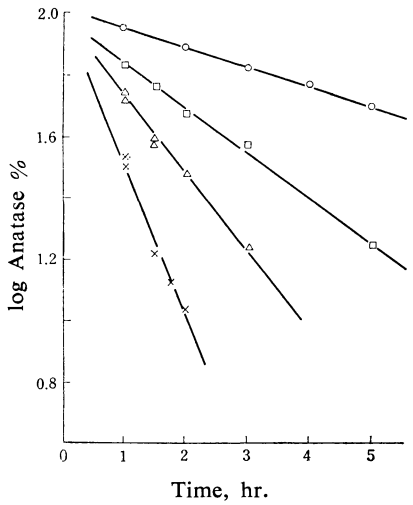


Fig. 6. First-order plots of the data in the sample "b" with LiCl in air.

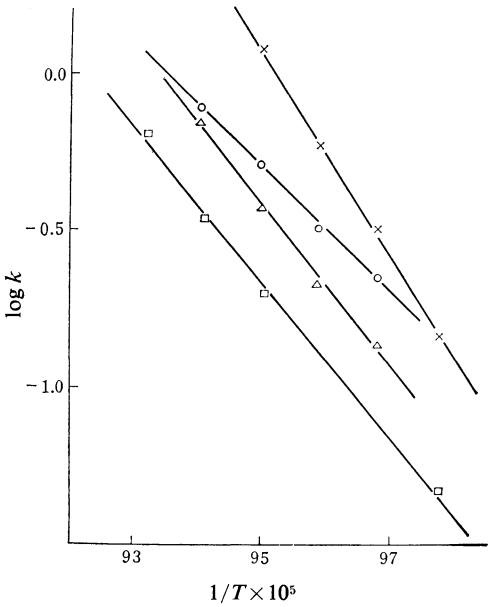


Fig. 7. Arrhenius plots of $\log k$ against $1/T$.

-□- a, air; -×- a, air, LiCl
-△- b, air; -○- b, O_2

TABLE I

Sample	Heating condition	Rate constant, $k\times10^2$, hr^{-1}	
		780°C	790°C
a	Air	19.6	34.5
a	Air, LiCl	100.0	—
b	Air	36.5	69.2
b	O_2	51.8	78.1

though the difference in rates is large.

Transition of Pure Titanium Dioxide in an Oxygen Atmosphere. — Czanderna, Rao and Honig[1] reported that the transition was not significantly affected by the atmosphere. In this study, the "b" samples were heated in an oxygen atmosphere; the results obtained are shown in Fig. 5. The rate of transition was greater in an oxygen atmosphere than in air, as is shown in Table I. The deviations from the first-order rate law and the standard Arrhenius plot are very small. The value of activation energy estimated from Fig. 7 was 92 kcal./mol.

Transition of Titanium Dioxide with Flux.— The rate of transition with lithium chloride was determined with sample "a" in the same way as has been described above. Figure 6 illustrates the transition in air with 1% lithium chloride. The rate of transition in the presence of lithium chloride was greater than that without lithium chloride, as is shown in Table I, and the deviations from the first-order rate law and from the standard Arrhenius plot are small. The value of the activation energy estimated from Fig. 7 was 150 kcal./mol.

The transition with potassium chloride was very different from that with lithium chloride. We could not estimate rate constants because of the fluctuation of the data. The percentages of rutile in the samples after heating them till 800°C did not exceed 15%.

Discussion

A large number of polymorphic transitions of chemical compounds have been studied in recent years, and it has been pointed out that in those cases difficulties remain in obtaining reproducible data. These difficulties are perhaps, partly caused by the fluctuation in the behavior of the starting materials. In the present study attention was directed to the following items in order to obtain the starting material of titanium dioxide; (a) it was made as chemically pure as possible, (b) the crystal growth of anatase ended in it, and (c) it contained no rutile-type compound. Thus, it was possible in this study to obtain reproducible data for one sample. Nevertheless, different transition rates were found for two samples prepared by the same procedure, as was seen in the transition of pure titanium dioxide in air. This may be caused by the facts that the preparing conditions were not yet completely controlled and that the physicochemical behavior of the samples, for example, in the particle size and in the number of lattice defects differed; therefore, the frequency factors in the equation of transition rates were different.

The kinetics of the transition of anatase to rutile have been studied by Rao et al.[1,2], by means of the X-ray diffraction method. In the present study the transition rate was measured from the change in the dielectric constant of the samples. It might be suggested that the analysis of a mixture of anatase and rutile by the X-ray diffraction method, in which the heights of the diffraction peaks of the two components are compared, is accompanied by error when the crystal growth of anatase is incomplete. The analysis of the anatase-rutile mixture by the measurement of the dielectric constant, which has recently been described by Oehme[7], was tried in this study; it was proved that the analysis could also be successfully carried out in a sample which contains anatase below 10% or above 90%. The analysis of such a sample is known to be difficult to perform by the X-ray diffraction method.

The activation energy for the anatase-rutile transition in air was measured by Czanderna, Rao and Honig[1] as 110 ± 10 or 90 ± 10 kcal./mol., and later by Rao alone[2] as 80 ± 10 kcal./mol. They empolyed as a starting material anatase obtained by precipitation from an ammoniacal solution of titanium after elimination of the impurities. However, in our study the value of this energy is calculated as 110 kcal./mol. or 116 kcal./mol. It is thought that this discrepancy is caused by the fact that Rao et al. dried their samples at a relatively low temperature (160°C). It is difficult to dehydrate completely the titania gel prepared by hydrolysis in an aqueous solution of titanium salt; furthermore, the crystal growth of anatase is incomplete in this case.

It was assumed by Czanderna et al. that atmosphere had no effect upon the anatase-rutile transition, but it was recognized in our experiment that the value of the activation energy of this transition is somewhat larger in air than in oxygen.

As for the effect of the flux, it is probable that the lithium or potassium atom may enter into the lattice of titanium dioxide, and/or that flux may react with titanium dioxide to form a titanate of lithium or potassium. It was proved by flame photometric analysis that the lithium or potassium ion was not found in the washing liquid obtained by the cold or hot washing of the samples which had been heated with flux. However, it was found that the lithium or potassium ion was present in that solution which had been obtained by dissolving the samples in sulfuric acid. On the other hand, it was impossible to recognize the change in the lattice constant by means of X-ray diffraction analysis. Also, there was

no abnormal change in the dielectric constant of the samples. It might be necessary to carry out accurate measurements in order to clarify the atomic behavior of the flux.

The rate of tranision has been theoretically treated by Avrami[9], and his equation has been applied to explain the phenomena in the transition of several materials. However, in the transition of titanium dioxide, it has been proposed that treatment by Avrami's equation may provide only a formal account of the conversion process. The results obtained in our experiments fit fairly to the first-order rate law, the deviations from the straight line being found not to exceed the range of experimental error. The induction period might exist in the case of the transition of sample "a" in air, but it was impossible to clarify this phenomena because of the fluctuation of the analytical process. The data fluctuate when the conversion takes place only in a small amount of anatase or rutile, especially below 2%.

It might be worth comparing the values of the activation energy in the transition with those of the thermodynamical properties. It has been reported that the activation energy is equal to the energy of sublimation, e. g., in the transition of sulfur[5], *o*-nitroaniline[3] and azoxybenzene, but not in mercuric iodide[6]. Meanwhile, de Boer[10] has proposed that the transition of the tridymite form of silicon dioxide into the cristobalite form would resemble that of wurtzite into zinc-blende. He has assumed that it might be neccessary to break the links between the Si- and O-atoms before SiO_4 tetrahedra can be shifted and that after such shifts the Si-O links might be re-established; consequently, such a transition might not proceed easily.

It might be assumed that the transition would be accompanied by the rupture of the bond in such compounds as AB_2, e. g., in silica, germanium dioxide, or titanium dioxide, and that the bond energy would be nearly equal to the activation energy. In the quartz-tridymite transition of silica, it has been reported that the activation energy is 96 kcal./mol., while the bond energy of Si-O is calculated to be 89.3 kcal./mol. by Pauling[11] and 101 kcal./mol. by Huggins[12]. Furthermore, it will be reported that the activation energy is about 100 kcal./mol. in the hexagonal-tetragonal transition of germanium dioxide[13], while the bond energy of Ge-O was reported to be 104 kcal./mol. as calculated from Huggins' data[12], It was impossible to find the bond energy of Ti-O, but, with the assumption that the bond energy would be obtained by dividing the heat of formation[14] by the number of bonds per stoichiometric molecule of such compounds as titanium dioxide, it is possible to establish the bond energy of Ti-O as 109 kcal./mol., which value is nearly equal to the activation energy of the anatase-rutile transition. Such an assumption might also explain the transition in mercuric iodide. It might be necessary, however, to carry out an investigation into the transition in compounds similar to titanium dioxide in order to prove the above idea.

Summary

The kinetics of the transition of anatase to rutile have been studied in the temperature range 750~800°C by means of dielectric constant measurements. The kinetic data can be fitted reasonably well by the first order equation. The transition rate is significantly affected by the heating atmosphere and the flux, and the values of the activation energy show a significantly large difference in these cases. In an air or oxygen atmosphere the value of the activation energy in the transition of pure titanium dioxide is 110 or 116 kcal./mol. and 90 kcal./mol. respectively. When 1% of lithium chloride is added to the titanium dioxide, the value of the activation energy of the transition is 150 kcal./mol.

The authors wish to thank Dr. R. Ishida for his spectroscopic analysis of samples, Dr. Y. Kamura for his discussion of the measurement of the dielectric constant, and Mr. E. Asada for his discussion of analysis by the X-ray diffraction method.

Government Chemical Industrial Research Institute, Tokyo
Shibuya-ku, Tokyo

9) M. Avrami, *J. Chem. Phys.*, **7**, 1103 (1939); **8**, 212 (1940); **9**, 177 (1941).
10) J. H. de Boer, *Discussions Faraday Soc.*, **23**, 176 (1957).
11) L. Pauling, "The Nature of the Chemical Bond", Cornell University Press, Ithaca (1940), Chap. 2.
12) M. L. Huggins, *J. Am. Chem. Soc.*, **75**, 4123 (1953).
13) Y. Kotera and M. Yonemura, unpublished work.
14) "Selected Value of Chemical Thermodynamic Properties", Nat. Bur. Standards (1952). U. S. Government Printing office, Washington, D. C.

*Solvent Extraction of Coal—Relation between the Yield of Extract and the Solubility Parameter of the Solvent**

By Yuzō SANADA and Hidemasa HONDA

(Received November 29, 1961)

In spite of the obvious variations in the yield of extract found with different solvents, only a few workers have attempted to study systematically the solvent effect of extraction for coal. The most extensive work on the extraction of coal has been done by Dryden[1-3]. Dryden developed an interesting classification of suitable coal solvents from his results, and observed that the yield of extract obtained from a given coal varies largely with the type of solvent employed and that the better solvents for coals, such as ethylene diamine, have structures containing a nitrogen or oxygen atom possessing an available unshared pair of electrons. Recently Halleux and Tschamler have, from a study of coal extraction with a series of closely related pyridine bases[4], expanded the hypothesis put forward by Dryden. These investigators indicate that the acid-base interaction is important in explaining the relative solvation power of pyridine bases for coal.

The most important studies made of the relation between the physical or chemical nature of solvents and the yield of extract are those by Kiebler[5,6]. A statistical analysis was done from the values of the yield of extract and from the various physical properties of the solvent. The physical properties considered were internal pressure, surface tension, dipole moment, dielectric constant, refractive index, and so on. Of these properties, the internal pressure had the most significant relationship to the yield of extract as shown by correlation coefficients. Kiebler showed that the relation between the yield of extract and the internal pressure of solvent at a given temperature is approximately linear, and that deviations from the resulting regression line could not be related to any physical properties[5,6]. There are, however, several reasons why Kiebler's conclusions are not wholly acceptable[2]: (i) Kiebler rejected a number of solvents on the suspicion of chemical effects; therefore, his experiments were based on a selected range of liquids; (ii) he excluded water and glycol, because their dissolving power against coal is poor in spite of their high internal pressures; (iii) his extraction method was not based on the Soxhlet principle; therefore, it is doubtful whether the completeness of extraction by all solvents is of the same order.

According to the regular solution theory, on the other hand, cohesive energy density (CED)** is an important factor in determining the action of a solvent on a solute[7]. It is also well known that the solvation of a polymer by various organic liquids correlates to a large extent with the CED of the solvent and the polymer[8,9]. Consequently, one may expect some relationship between the CED of the solvent and the yield of extract obtained from coal.

Experimental

The coal specimen was pulverized enough to pass through a 30-, and to stand on a 60-, Tyler mesh sieve. The lighter fraction, with a specific gravity of less than 1.30, was isolated by the float-or-sink method, using a mixture of benzene and carbon

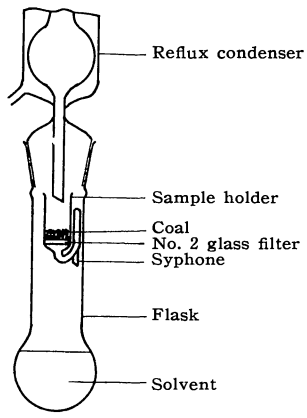


Fig. 1. Modified soxhlet extractor.

* Presented at the 13th Annual Meeting of the Chemical Society of Japan, Tokyo, April, 1960.

1) I. G. C. Dryden, *Nature*, **162**, 959 (1948); **163**, 141 (1949); **166**, 561, 606 (1950).
2) I. G. C. Dryden, *Fuel*. **29**, 197, 221 (1950).
3) I. G. C. Dryden, ibid., **30**, 39, 145, 217 (1951); **31**, 176 (1952).
4) A. Halleux and H. Tschamler, ibid., **38**, 291 (1959).
5) M. W. Kiebler, *Ind. Eng. Chem.*, **32**, 1389 (1940).
6) H. H. Lowry, ed., "Chemistry of Coal Utilization", Vol. I, John Wiley & Sons, Inc., New York (1947), p. 736.

** CED and internal pressure are of the same meaning.

7) J. H. Hildebrand and R. L. Scott, "Solubility of Nonelectrolytes", Reinhold Publishing Corp., New York (1950).
8) G. Gee, *Quart. Revs. (London)*., **1**, 288 (1947).
9) E. E. Walker, *J. Appl. Chem.*, **2**, 470 (1952).

TABLE I. CHARACTERISTICS OF SAMPLES USED

Source	Proximate analysis, %				Ultimate analysis d. a. f., %		
	Moisture	Ash	Volatile matter	Fixed carbon	C	H	O+N+S
Yūbari	1.7	2.4	42.0	53.9	85.2	6.3	8.5
Ashibetsu	3.0	4.1	42.9	50.0	81.1	5.5	13.4

tetrachloride. These fractions have ash contents of less than 3% and are estimated to be almost vitrain. The characteristics of the various vitrains are listed in Table I. All solvents were commercial reagents (grade: guaranteed reagent or extra pure) and were used without further purification.

Instead of the customary method of Sexhlet extraction, a modified Soxhlet method at the boiling temperature of the solvent was used. The apparatus is shown in Fig. 1. The extraction was done exactly at the boiling temperature of the solvent. Vitrain samples (dried in vacuo at 110°C) were extracted under the standard conditions, namely, a coal to solvent ratio of 150 mg. to 30 ml. and under dry air for 48 hr. The extraction residue was dried in vacuo at 110~180°C for 7 hr. The extraction residues by the higher boiling solvents were washed with acetone before drying. The extraction yield was determined by direct weighing of the residue. The absorption effect of the solvent on the residue was not considered, because examination of ethyene diamine, one of the more powerful solvents, showed only a small difference (about 2% or so between the yield obtained by the direct weighing method and that obtained by calibrating the nitrogen in increase in the residue.

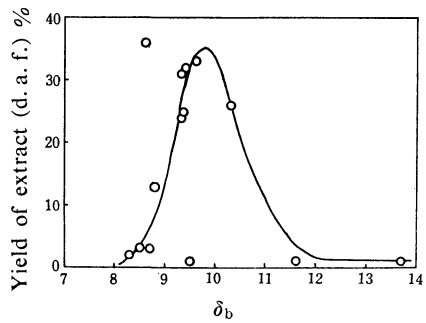


Fig. 2. Relation between yield of extract and solubility parameter of solvent at b. p. (Yūbari vitrain).

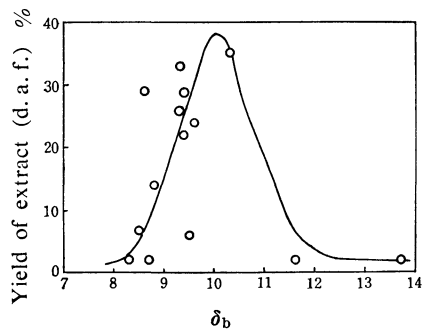


Fig. 3. Relation between yield of extract and solubility parameter of solvent at b. p. (Ashibetsu vitrain).

Experimental Results

The CED of the solvent, e_{ss} (cal./cc.), was calculated from the following relationship:

$$e_{ss}=(L_b-\mu RT)/V_b \quad (1)$$

where L_b is the latent heat of vaporization at the boiling point in cal./mol., V_b is the molecular volume at a normal boiling point in cc./mol., R is the gas constant, T is the boiling temperature in °K, and μ is the correction term in $\mu=PV/RT$. (For substances boiling above 50°C, and, therefore, for all solvents used, the μ correction can be neglected.) The V_b value was calculated by the additive method using LeBas's volume increments[10]. The average error for the compound tested was 4.7%. The value of L_b was available in the references[11-13].

TABLE II. YIELD OF EXTRACT AT BOILING TEMPERATURE TOGETHER WITH CERTAIN PHYSICAL DATA FOR THE SOLVENTS USED

Solvent	t_b, °C	δ_b	Yield of extract d. a. f., %	
			Yūbari	Ashibetsu
Chloroform	61	8.7	2.6	2.3
Methanol	64	13.7	0.9	1.5
Ethanol	78	11.6	0.6	1.8
Ethyl methyl ketone	80	8.5	3.4	7.0
Benzene	80	8.3	1.8	1.6
Pyridine	116	9.6	33.2	23.8
Ethylene diamine	117	10.3	26.2	34.9
Butanol	118	9.5	0.8	5.0
Dimethyl formamide	153	9.3	24.0	25.6
Cyclohexanone	156	9.4	25.0	29.1
Cyclohexanol	161	8.8	13.0	13.5
Phenol	182	9.4	32.0	21.9
Cresol	185~193	9.3	30.7	32.6
Acetophenone	202	8.6	35.6	29.1

10) R. C. Rein and T. K. Sherwood, "The Properties of Gases and Liquids", McGraw-Hill, New York (1958), p. 51.
11) T. Kuwata "Yōzai", Maruzen, Tokyo (1940).
12) A. Weissberger, ed., "Organic Solvents", Interscience Pub., New York (1955).
13) The Chem. Soc. of Japan, "Chemical Handbook" ("Kagaku Binran"), Maruzen, Tokyo (1958).

If L_b was unknown, the estimation was made by the Watson-Negishi method according to the following equation[14]:

$$L_b = 2.48\ (t_b+273)^2/(A+0.11t_b) \qquad (2)$$

where A is the constant within a given homologus series, and t_b is the boiling point in °C. Therefore, the solubility parameter, δ_b, at the boiling point is deduced from the CED as follows:

$$\delta_b = \sqrt{e_{ss}} \qquad (3)$$

The yields of extract for Yūbari coal and for Ashibetsu coal by various solvents are presented in Table II, together with the t_b and δ_b values of various solvents. Figures 2 and 3 show the relation between the yield of extract and the value of δ_b for Yūbari coal and for Ashibetsu coal respectively. The yield of extract increases with the increase of δ_b, reaches a maximum at about 10 of δ_b, and then decreases with the increase of δ_b.

Discussion

Several attempts to find a correlation between the yield of extract and some physical properties of the solvents have been proposed[5,6,15-17]. These methods can, however, be successful in only a limited number of case, for example, in a series of chemically related solvents[4].

In spite of the fact that the solvents we used included various chemically different types, including alcohols (though they were excluded by Kiebler), and have a wide range of boiling temperatures from 61 to 202°C, a good relationship between the yield of extract and the δ_b value of the solvents has been found, as is shown in Figs. 2 and 3, with the exception of acetophenone and butanol.

The poor dissolving power of alcohol and water against coal, in spite of their high CED values, may be explained by the following reasons. Alcohol and water are strongly hydrogen-bonded substances and have high CED values, owing to their hydroxyl associations. These liquids are all substances which form 'solvent-solvent' contacts (hydrogen bonds) with the evolution of a large amount of energy. It seems that they form 'solvent-coal' contacts less readily and that the energy gained in forming these contacts does not balance the energy lost in breaking the 'solvent-solvent' and 'coal-coal' contacts.

From these results, it appears that the CED value is one of the most important factors determining the solvent action of liquids on coal. Moreover, our conclusions, based on the Soxhlet principle and resulting from the employment of solvents having CED values over a wide range, should be borne in mind.

It is possible to propose the following explanations for the deviations from the resulting correlation curves. The solvents include various chemically different types and have a wide range of boiling temperatures. The various polar groups in solvents, therefore, may have some specific influences on coal. Coal is a mixture of complex compounds, and the CED value of coal varies with the temperature. Moreover, the estimation error of the CED value at the boilng temperature may contribute to the deviation.

Further strict experiments on the action of solvents on coal have been made; these results will be reported later[18].

Resources Research Institute
Kawaguchi, Saitama-ken

14) K. Satō, "Bussei Zyōsū Suisanho", Maruzen, Tokyo (1957), p. 240.
15) W. Ostwald and H. Ortlov, *Kolloid Z*, **59**, 25 (1932).
16) D. J. W. Kreulen, *Brennstoff-Chem.*, **16**, 165 (1935); *Fuel (London)*, **25**, 99, 104 (1946).
17) G. Agde and R. Hubertus, *Brennstoff-Chem.*, **17**, 149 (1936); *Braunkohlenarchiv*, **No. 46**, 3 (1936).
18) Y. Sanada and H. Honda, in preparation.

On the Association of Condensed Polycyclic Aromatic Compounds in Concentrated Sulfuric Acid

By Takashi HANDA

(Received February 25, 1961)

Several investigations have been made of the aggregation of dye molecules or ions in aqueous solutions, and it seems clear that some dyes form dimers and polymers under suitable conditions. Qualitative discussions of the factors determining the associations and also of the spectral shifts caused by them have also been made[1-9].

The polycyclic aromatic hydrocarbons and their related quinons in concentrated sulfuric acid possess strong absorptions in the visible region which are ascribed to monomeric proton-complexes. Some of these spectral responses show a blue shift with an increasing concentration of the solute. These phenomena are interpreted as being caused by association of molecules.

These associates are considered, from experimental spectral facts, to be in equilibrium with the monomeric proton-complexes. For instance, dibenzopyrene forms successively, an octamer and the higher polymers in 96 per cent sulfuric acid with an increase in the concentration of the solute. However, it forms a dimer in 86 per cent sulfuric acid and shows no eminent blue spectral shift. Also the case of some of the related quinones such as anthraquinone, which forms a tetramer, *p*-naphthoquinone, and anthanthrone, which forms dimers, no blue shift is observed either. Moreover, tetracene and benzoanthrone form no polymers up to 10^{-2} mol. per liter of the concentration of the solutes.

The object of the present paper is to report these points, with some discussion of the mechanism or of the association of these compounds with reference to the considerations of the above-described investigations[1-9].

1) E. Rabinowitch and L. F. Epstein, *J. Am. Chem. Soc.*, **63**, 69 (1941).
2) S. E. Sheppard, *Rev. Mod. Phys.*, **14**, 303 (1942).
3) S. E. Sheppard and A. L. Geddes, *J. Am. Chem. Soc.*, **66**, 1955, 2003 (1944).
4) V. L. L. Leoshin, *Acta Physicochim.* U. S. S. R., **1**, 685 (1935).
5) M. Koizumi and N. Mataga, This Bulletin, **27**, 194 (1954).
6) V. Zanker, *Z. physik. Chem.*, **199**, 225 (1955); **200**, 250 (1952).
7) N. Mataga, This Bulletin, **30**, 375 (1957).
8) Y. Mori, Symposium of π-Electronic State, Chem. Soc. Japan, 1955.
9) Th. Förster, "Fluoreszenz Organischer Verbindungen", Vandenhoech und Ruprecht, Göttingen (1951).

Experimental

The measurement of the absorption spectra was carried out with a Beckman DU-type spectrophotometer with quartz-cells, 1.0, 0.1 and 0.05 cm. thick, and with, in the visible region, a thin, transparent glass plate 0.01 cm. thick. The read-off value of the spectral measurement was the mean value of three readings in the concentrated region of solute molecules.

The specimen used in this experiment was prepared and recrystallized from appropriate solvents and was further purified by the repeated sublimation in vacuo of 10^{-3} to 10^{-4} mmHg. The concentrated sulfuric acid used in this experiment was an extra pure grade reagent of the Kanto Chemical Co., Ltd., which was considered to be chemically pure and to be transparent in the visible region of the spectrum. The concentration of the acid was to be ca. 98 per cent.

The solutions of different concentrations used in this experiment were prepared by dilution of the concentrated stock solution, the concentration of which was about 10^{-2} to 10^{-3} mol. per liter and which was freshly prepared before each measurement.

Results and Discussion

Dibenzopyrene (I). — Two strong absorption bands appear in succession in the spectra of the sulfuric acid solution, 10^{-6} mol. per liter,

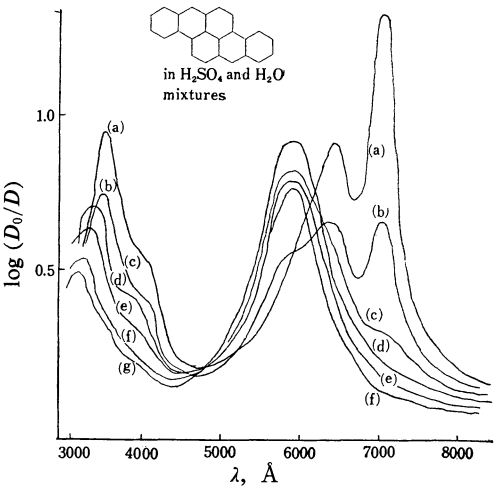


Fig. 1. The absorption spectra of dibenzopyrene in H_2SO_4 of 96% (a), 90% (b), 85% (c), 80% (d), 75% (e) and 70% (f).

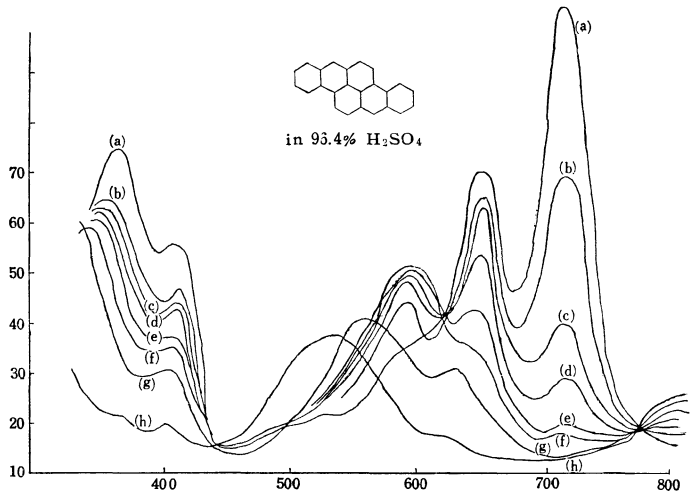
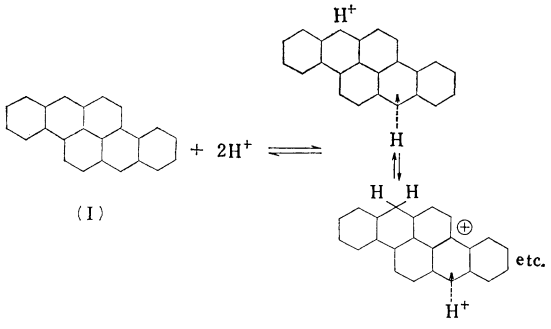


Fig. 2. The absorption spectra of dibenzopyrene with its concentration of $2.7\times10^{-6}\sim 5.4\times10^{-5}$ (a), 6.75×10^{-5} (b), 9×10^{-5} (c), 1.35×10^{-4} (d), 2.7×10^{-4} (e), 9×10^{-4} (f), 2.7×10^{-3} (g) and 1.4×10^{-2} mol./l. (h) in 96.4% sulfuric acid.

with the increase in acidity, as is shown in Fig. 1. When this hydrocarbon is dissolved in 86 per cent sulfuric acid, the peak of the absorption band is found in the region of 580 mμ. When 98 per cent sulfuric acid is used, the band shifts to the longer wavelength region, 725 mμ. Both are considered to be in equilibrium with each other and with the protons in the acid. Therefore, the dibenzopyrene molecule is considered to be doubly protonated*. The protons which form a complex with the molecule are believed to be attached to the position of the largest charge-density as follows:



However, a discrepancy from Beer's law occurs with the increase of the concentration of solute up to 10^{-3} mol. per liter in 98 per cent sulfuric acid. New absorption bands appear near 595, 555 and 535 mμ with solute concentrations of 10^{-5}, 10^{-4} and 10^{-3} mol. per liter respectively. They may be interpreted as corresponding to the blue shift of the absorption band at 712 mμ by the influence of association and as being in equilibrium with each other; they have isobestic points near 770, 620, 570, 500, 465, 440 and 350 mμ, as is illustrated in Fig. 2.

Anthrone and Anthraquinone. — No new absorption peaks are found in the wavelength range from 350 to 1000 mμ, and only a decrease in the extinction coefficient at the absorption peak of monomer is observed with an increase in the concentration of the solute.

In the case of anthraquinone, however, a slight increase in the extinction coefficient is found beyond the region of the isobestic point near 460 mμ, in the skirt of the strong absorption peak of the monomer, with an increase in the concentration. This increase may be interpreted as being due to the slight change in the electronic state of monomer as a result of a weak intermolecular hydrogen bond formation between two molecules. As the configuration of the associate, a proton and a $(H_3SO_4)^+$ ion may be supposed to be resonating among a pair of two oxygen atoms of the molecules, which are assumed to take a parallel plane configuration. The structure is centrally symmetrical and possesses many resonating structures in the ground and excited states, unlike the model of the acridine-orange double ion by Zanker[6], which is anti-symmetric for one axis.

On the other hand, the absorption peak of anthrone in sulfuric acid, where polymerization of the 16th-degree occurs, shows a red-shift,

* As was reported in a preceding paper (T. Handa, This Bulletin, **28**, 483 (1953)), we were able to obtain the two pK_B values of −5.0 and −7.4.

as is illustrated in Fig. 3, and also a slight increase in the extinction coefficient in the skirt of the main absorption band beyond the isobestic point near 415 mμ with an increase in the solute concentration. The configuration of the associate is supposed not to be coplanar and to be anti-symmetric like the acridine-orange double cation.

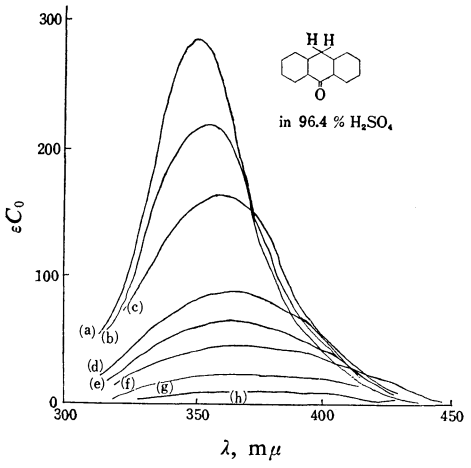


Fig. 3. The spectral response of the absorption spectra of anthrone with its concentration of 5.5×10^{-5} (a), 9.6×10^{-5} (b), 1.45×10^{-4} (c), 2.9×10^{-4} (d), 3.4×10^{-4} (e), 5.6×10^{-4} (f), 1.05×10^{-3} (g), and 5.78×10^{-3} (h) in 96.4% sulfuric acid.

Several quinones, such as *p*-naphthoquinone, anthanthrone and isoviolanthrone in sulfuric acid, whose degrees of polymerization are 2, 4 and 2 respectively, exhibit similar behavior.

Benzanthrone and Benzonaphthenone.—These compounds form no polymers. It is considered that, because of the larger weight of the existence of π-complexes in the ground state which gives the resonating carbonium ion, the potential barrier in the Morse curve in Fig. 5 may be higher than those in other cases because of the electrostatic repulsion of carbonium ions and the fact that they can not ride over this potential barrier to form stable polymers.

From the foregoing experimental facts, the association constant, k, and the degree of polymerization have been estimated.

When the equilibrium between monomer and polymer, an associate of n-th degree, exists, the association constant, k, is expressed as

$$k=\frac{X}{nC_0{}^{n-1}(1-X)^n} \qquad (1)$$

where X is the fraction of polymer and C_0 is the concentration of the solute molecule.

The apparent extinction coefficient, ε, at a definite wavelength is expressed as:

$$\varepsilon=\frac{X}{n}\varepsilon_n+(1-X)\varepsilon_m \qquad (2)$$

where ε_n and ε_m are the extinction coefficients of the polymer and the monomer respectively.

From Eqs. 1 and 2, we can obtain the following relation:

$$\log C_0(1-\varepsilon/\varepsilon_m) =\log(Ck)+n\log C_0\left(\frac{\varepsilon}{\varepsilon_m}-\frac{\varepsilon_n}{n\varepsilon_m}\right) \qquad (3)$$

where

$$C=n^n\left(n-\frac{\varepsilon_n}{\varepsilon_m}\right)^{1-n}$$

As a rough approximation, we can neglect $\varepsilon_n/\varepsilon_m$ as compared with $\varepsilon/\varepsilon_m$; therefore

$$\log C_0\left(1-\frac{\varepsilon}{\varepsilon_m}\right) =\log(Ck)+n\log C_0\left(\frac{\varepsilon}{\varepsilon_m}\right) \qquad (4)$$

When we apply Eq. 4 to determine the n for the dibenzopyrene molecule in 96 per cent concentrated sulfuric acid this degree is 8, as is shown in Fig. 4. Further, the new absorption band at the wavelength of 985 mμ may correspond to that of the octamer of the dibenzopyrene diprotonium cation, while the equilibrium constant, k, at 20°C is estimated to be approximately 3×10^{28}. We may expect the qualitative dimerization of the octamer of the dibenzopyrene diprotonium cation from the new absorption band near 555 mμ. The high degree polymerization proceeds in successive steps with the increase in the concentration of the dibenzopyrene molecule in such a manner as 8, 16, 32, and so on.

With the elevation of the temperature of the solution from 20 to 70°C, the intensity of the

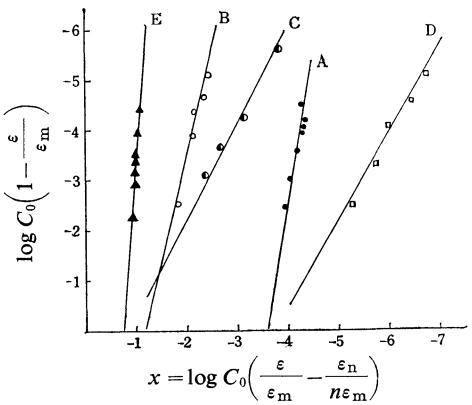


Fig. 4. The equilibrium relation (Eq. 3) between the monomer and the polymer of dibenzopyrene (A), anthraquinone (B), isoviolanthrone (C), anthanthrone (D) and anthrone (E) in sulfuric acid.

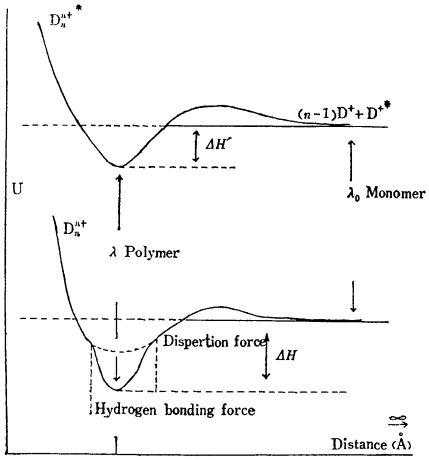


Fig. 5. The assumed Morse-curve of the polymers of the mono-protonium cations of a condensed aromatic compound in concentrated sulfuric acid.

absorption band at 580 mμ, which corresponds to the optical absorption of the octamer, decreases, while that at 710 mμ, corresponding to the monomer, increases. This may be understood as being due to the thermal decomposition of the polymers. The values of $\log k$ at temperature of 20, 45 and 70°C are 28.5, 25.4 and 22.3 respectively. From the above temperature dependency of the equilibrium constant, the heat of the association of the octamer of dibenzopyrene in concentrated sulfuric acid is estimated to be 54 kcal./mol. from the following equation (Eq. 3):

$$\Delta H = \frac{RT_1T_2 \ln k_2/k_1}{T_2 - T_1} \qquad (5)$$

where k_1 and k_2 are association constants at temperatures of T_1 and T_2 respectively. The value of the entropy may be estimated, for the association of the dibenzopyrene octamer, as 47 cal./mol. deg.

From these experimental results, the equilibrium constants of isoviolanthrone at temperatures 20, 45 and 70°C are determined to be 3.4, 3.0 and 2.7 respectively. Therefore, the heat of association for this molecule is roughly estimated as 6.4 kcal./mol.

Discussion

The foregoing results suggest that the formation of the associates of complexes among sulfuric acid and the condensed polycyclic aromatic hydrocarbons and their related quinones are divided into three types. The first type exhibits a blue-shift of the absorption-peaks of the spectra of the associates and forms the higher associates in successive steps with the increase in the concentration of the solute. A typical example is the case of doubly protonated dibenzopyrene in 96 per cent sulfuric acid.

The second type does not exhibit any blue-shift of the absorption-peaks of the spectra of the associates but forms one kind of associate with a definite degree of association and does not form the higher associate with the increase of the concentration of the solute. Examples are singly protonated dibenzopyrene in 86 per cent sulfuric acid and singly protonated anthraquinone in 96 per cent sulfuric acid. The third type forms no associate. An example of this is benzoanthrone in 96 per cent sulfuric acid.

Concerning the cause of association, we may imagine, firstly, the London-type dispersion force and, secondly, a hydrogen bonding-like force among proton and oxygen atoms. It is very uncertain whether or not such forces are exerted on monomers in a strongly polarized solvent. Rabinowitch and Epstein have ascribed the cause of the dimerisation of thionine molecules in water and ethanol to the London-type dispersion force and have estimated the stable intermolecular distance, r_0, by assuming that the minimum potential energy, U_0, in the Morse curve is approximately equal to the heat of association.

When we ascribe the cause of the association in the case of doubly protonated dibenzopyrene with the association degree of 8, to the London-type dispersion force, we can estimate the mean intermolecular distance, r_0, as do Rabinowitch et al.*, on the assumption that the heat of association per pair of the octamer or $\Delta H/7$ is equal to the minimum potential energy, U_0, in this case. The estimated value of r_0 is approximately 3.2 Å when we put the experimental oscillation-strength, f, as equal to 0.53 and λ as equal to 6825 Å, which figures are estimated from the absorption spectrum, and the refractive index of the solvent, n as 1.44.

This is a reasonable value compared with the one estimated in the case of the dimerization of thionic molecules studied by Rabinowitch et al. and compared with the van der Waals radii of the aromatic molecule in the solid state.

When we assume the experimental heat of association to consist of only the dispersion energy in the case of the singly protonated dibenzopyrene (where no blue-shift is observed dimerization), the intermolecular distance, r_0, is estimated to be ca. 2.6 Å, which is considered to be unreasonably small. This is also the

* $$\partial U/\partial r = 0 \qquad (1)$$

$$U_0 = -1.74\times10^{-7} f^2 \lambda_0^3/r^6 \quad -3.287\times10^{-10} f^3 \lambda_0^4/r^8 - 5.825\times10^{-13} f^4 \lambda_0^5/r^{10} + 330/D_T + x/r^{12} \qquad (2)$$

$$f \fallingdotseq 4.32\times10^{-9} \times n \int \varepsilon \, d(1/\lambda) \qquad (3)$$

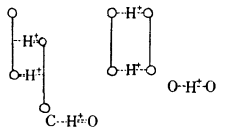
TABLE I

Name of substance	pK	Degree of polymerization	log K*1	f*2	λ_0 Å	H*3 kcals./mol.
p-Naphthoquinone	−7.5	1.7	1.9	0.21	4100	
Anthraquiaone	−7.5	4.1	12.3	0.39	4100	ca. 23
Anthanthrone	−7.4	1.9	2.5	0.24	6360	
Isoviolanthrone	−6.8	1.85	3.2	0.27	7170	6.4
Anthron	−6.5	16	60	0.59	3500	ca. 114
Dibenzopyrene (I)	−5.0	2.0	3.3	0.34	5800	
Dibenzopyrene (II)	−7.4	7.8	28.5	0.30	7100	54.5

*1 log K: The equilibrium-constant at 20°C.
*2 f: The empirical oscillator-strength obtained from the graphs.
*3 H: The experimental heat of the association.

case for isoviolanthrone in 96 per cent sulfuric acid. In this case, the r_0 is estimated to be ca. 2Å, as it is in the cases of anthraquinone, anthanthrone, *p*-naphthoquinone and anthrones.

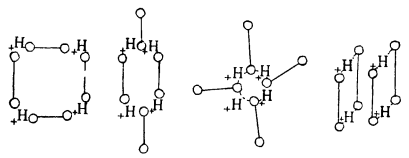
These intermolecular distances are considered to be unreasonably small. In these compounds, we can not observe the blue-shift of the absorption-peak of the monomers.



(I) (II)

(a)

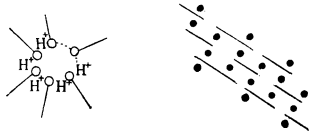
Isoviolanthrone (I)
Anthanthrone (II)
Mono-protonium cation dimer



Plane-parallel Semi-plane-parallel Non-plane-parallel Dimer-dimer

(b)

Various configuration of tetramer of anthraquinone-mono-protonium cation.



Non-coplanar

(c) (d)

Fig. 6. The assumed configuration of several polymers of polycyclic aromatics: Mono-protonium cation dimer of isoviolanthrone and anthanthrone (a), tetramer of anthraquinone-mono-protonium cation (b), 16th-mer of anthrone mono-protonium cation (c) and octamer of dibenzopyrene diprotonium cation (d).

○ Oxygen atom ● $H_3^+SO_4$ ion
—— Dibenzopyrene (d)

Therefore, it may be necessary to assume some force like the intermolecular hydrogen-bonding which such combinations as O···H^+···O, C···H^+···O and C···H^+···C exert within a certain range of the intermolecular distance in the Morse curve, in addition to the dispersion force as illustrated in Fig. 5, in the strongly polarized environment with both positive and negative charges. The experimental heat of association may be put approximately as the sum of the potential energy, U', of the dispersion force and the heat of the formation of the weak intermolecular hydrogen-bonding, U''.

In the case of the related quinones, the effect of the intermolecular hydrogen-bonding, O···H^+···O and O^+···H···O, may be considered to play an important role in the association compared with the effect of the dispersion force. The amount of the hydrogen-bonding may be estimated as 2∼4 kcal./mol., assuming the state of the existence of polymer to be as is illustrated in Fig. 6.

In the case of benzoanthrone, the term from the electrostatic repulsive energy among those positive charges in the carbon skelton which are caused by the larger basicity of the molecule might play an important role in the above considerations.

Summary

The effect of the concentration on the absorption spectra of condensed polycyclic aromatic hydrocarbons and their related carbonyl derivatives in concentrated surfuric acid was studied in the concentration range from 10^{-6} to 10^{-3} mol. per liter. The free energies and heats of formation of these associates were also measured.

In the case of the dibenzopyrene molecule in 96 per cent sulfuric acid, it is observed that various kinds of association, such as 8, 16 etc., were obtained in successive steps with the

increase in the concentration of the solute, while in the case of carbonyl derivatives, only one kind of associate was observed, the number of degree of association of which was observed to be 2, 4 and 16.

In the case of dibenzopyrene in 96 per cent sulfuric acid, where it is believed to be doubly protonated, the cause of association might be explained by the dispersion effect, while the blue-shift of the absorption peak of the monomer is clearly observed in successive steps succession with the increase in the concentration of the solute.

However in the case of carbonyl derivatives and dibenzopyrene in 86 per cent sulfuric acid, where they are singly protonated, it is observed that they do not show any blue-shift of their absorption peaks but a lowering of the extinction coefficient.

As is illustrated in Table I, their experimental heat of association may possibly not be explained by the dispersion effect alone. It may be necessary to take into consideration some kind of hydrogen-bonding between the carbonyl oxygen atoms and the proton.

Department of Chemistry
Faculty of Science
The University of Tokyo
Hongo, Tokyo

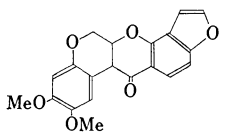
Synthetic Studies on the Benzofuran Derivatives. VIII. Synthesis of Furo[2,3-f]chromeno[3,4-b]chromone[*1]

By Yoshiyuki KAWASE and Chûji NUMATA

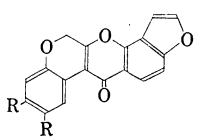
(Received October 20, 1961)

Miyano and Matsui[1] have succeeded in the reduction of chromenochromones to give chromanochromanones, and recently the total syntheses of rotenone[2], deguelin[3] and munduserone[4] have been accomplished by this method.

Therefore, it seems desirable for the synthesis of elliptone[5] (I), a kind of rotenoids, to prepare dehydroelliptone (II) because I may be obtained from II by the method mentioned above.



I



II) R=OMe
III) R=H

Now the synthesis of furo[2,3-f]chromeno-[3,4-b]chromone (III), the parent nucleus of II, has been carried out by two routes. Both routes started from 7-hydroxy-2'-methoxy-2-ethoxymethylisoflavone (IV), but differed from each other in the order of furan-ring construction and chromen-ring closure.

For the preparation of chromenochromones, two methods are available; those are by chromenochromone-ring formation of phenoxyacetic acid-2-(2-hydroxy)-acetophenone[6] (the Robertson's method) and by chromen-ring formation of 2-methyl[7] or 2-ethoxymethyl[8] derivatives of 2'-methoxyisoflavone (the Seshadri's method). In the latter method, Mehta and Seshadri reported that 7-hydroxy-2'-methoxy-2-ethoxymethylisoflavone (IV) was converted directly by the action of hydrogen bromide in acetic acid into 2', 7-dihydroxy-8-bromomethylisoflavone (VI) which was converted into 9-hydroxychromeno[3,4-b]chromone (VII), and Seshadri and Varadarajan reported that VII was also obtained by the action of potassium carbonate in acetone on 2', 7-dihydroxy-2-hydroxymethylisoflavone (V) which

*1 Brief report: Y. Kawase and C. Numata, *Chem. & Ind.*, **1961**, 1361.

1) M. Miyano and M. Matsui, *Bull. Agr. Chem. Soc. Japan*, **22**, 128 (1958); *Chem. Ber.*, **91**, 2044 (1958).

2) M. Miyano, A. Kobayashi and M. Matsui, *Bull. Agr. Chem. Soc. Japan*, **24**, 540 (1960); *Agr. Biol. Chem.*, **25**, 673 (1961).

3) H. Fukami, J. Toda, G. Sakata and M. Nakajima, *Bull. Agr. Chem. Soc. Japan*, **24**, 123 (1960); *Agr. Biol. Chem.*, **25**, 252 (1961).

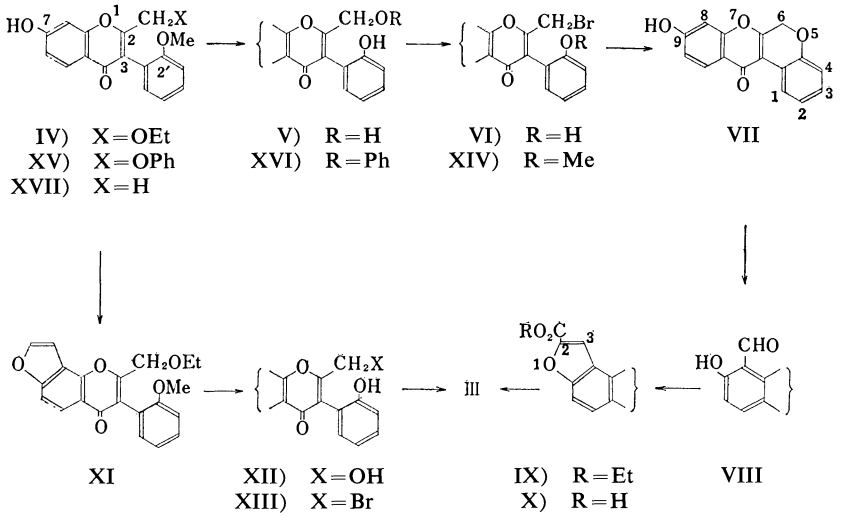
4) J. R. Herbert, W. D. Ollis and R. C. Russell, *Proc. Chem. Soc.*, **1960**, 177.

5) S. H. Harper, *J. Chem. Soc.*, **1939**, 1099, 1424; ibid., **1942**, 587.

6) A. Robertson, ibid., **1933**, 489, 1163.

7) T. R. Seshadri and S. Varadarajan, *Proc. Indian Acad. Sci.*, **37A**, 784 (1953).

8) A. C. Mehta and T. R. Seshadri, ibid., **42A**, 192 (1955).



was prepared from 7-hydroxy-2'-methoxy-2-methylisoflavone (XVII) through four steps.

But in the author's experiments, the hydroxybromomethyl compound VI was not obtained directly from IV but only the 2'-methyl ether (XIV) of VI was obtained by the procedure reported by Mehta and Seshadri, and also some attempts to obtain the 2-halomethyl analog of VI from IV by the action of other reagents (e. g. hydrochloric, hydrobromic or hydroiodic acid in acetic acid or pyridine hydrochloride) resulted in a failure. Further, the 2-phenoxy analog (XV) of IV was not affected by hydrogen bromide in acetic acid, and was converted into only the 2'-demethylated compound XVI by the action of anhydrous aluminum chloride.

On the other hand, IV was readily converted by the action of anhydrous aluminum chloride into the trihydroxy compound V which had been, with difficulty, prepared from XVII. But it proved to be impossible to convert this compound V directly into the chromenochromone VII by the procedure reported by Seshadri and Varadarajan, and also by other dehydrating reagents (e.g. *p*-toluenesulfonic acid in benzene, concentrated sulfuric acid, polyphosphoric acid, acetic anhydride, and tosyl or thionyl chloride in pyridine). Therefore, the trihydroxy compound V was made to react with hydrogen bromide in acetic acid to give the hydroxybromomethyl compound VI smoothly, which was readily converted into the chromenochromone VII*2 by the action of potassium carbonate in acetone.

Then, constructing the chromenochromone-ring by the above-mentioned modification of the Seshadri's method and building up the furan-ring by a method analogous to that reported previously for isoflavones[9], the authors synthesized the furochromenochromone III from IV as follows:

In one route, the chromenochromone VII was formylated by the hexamine method to give the 8-formyl compound VIII, which was converted into furochromenochromone-2-carboxylic acid (X) by the action of ethyl bromomalonate and potassium carbonate followed by alkaline hydrolysis. Decarboxylation of this acid X furnished the furochromenochromone III, slightly red colored microcrystals, m. p. 239.5~240°C.

In the other route, the furochromenochromone III was obtained more smoothly by the chromen-ring closure of 2'-methoxy-2-ethoxymethylfuro-[2,3-f] isoflavone (XI), its preparation from the isoflavone IV was reported in the previous paper[9]: Furoisoflavone XI was treated with aluminum chloride in nitrobenzene not in benzene to give the dihydroxy compound XII, which was converted into the bromo compound XIII and then finally into III, slightly orange colored microneedles, m. p. 241.5~242.5°C, identical with the other sample. The structure of III and of the other intermediates was confirmed by ultraviolet and infrared spectroscopy and by microanalysis.

Experimental*3

7-Hydroxy-2'-methoxy-2-bromomethylisoflavone (XIV).—A mixture of IV (1 g.), acetic acid (10 ml.) and hydrogen bromide-acetic acid (50%, 10 ml.) was allowed to stand over night, then the mixture

*2 This VII was also prepared by the Robertson's method.

9) T. Matsumoto et al., This Bulletin, 31, 688 (1958); Y. Kawase and K. Fukui, ibid., 31, 693 (1958); Y. Kawase et al., ibid., 33, 1240 (1960).

*3 Melting points are uncorrected and infrared spectra were measured in Nujol unless otherwise noted.

was heated for 45 min. on a steam-bath with the addition of more hydrogen bromide-acetic acid (50%, 10 ml.). Ice water was added to the cooled solution, and the solid products obtained were recrystallized from ethanol to give XIV in colorless microcrystals, m. p. 192~193°C, which gave a positive Beilstein test.

Found: C, 57.22; H, 3.79. Calcd. for $C_{17}H_{13}O_4Br$: C, 56.53; H, 3.63%.

7-Hydroxy-2'-methoxy-2-phenoxymethylisoflavone (XV).—To a solution of 2,4-dihydroxyphenyl 2-methoxybenzyl ketone (2.6 g.) in pyridine (50 ml.) was added phenoxyacetyl chloride (5 g.) drop by drop with ice cooling and stirring. By the usual treatment of the mixture, XV was obtained in colorless microcrystals, m. p. 232~233°C (from ethanol); yield 1.25 g. (33.5%).

Found: C, 73.34; H, 4.86. Calcd. for $C_{23}H_{18}O_5$: C, 73.79; H, 4.85%.

2',7-Dihydroxy-2-phenoxymethylisoflavone (XVI).—Anhydrous aluminum chloride (1.5 g.) was added to a solution of XV (0.5 g.) in benzene (or nitrobenzene), and the mixture was refluxed for 2.5 hr. on a steam-bath. The solvent was removed (by steam-distillation in the case of nitrobenzene), and the cooled residue was treated with ice water and hydrochloric acid. Next day, the precipitates were collected, washed with water, dissolved in aqueous sodium carbonate, and the alkaline solution was filtered and acidified. The crystaline products obtained were recrystallized from ethyl acetate or from dilute ethanol to give XVI in colorless microcrystals, m. p. 218~220°C; yield 0.2 g. (40%). IR: 3600, 3000 (broad) (OH), 1630 cm^{-1} (γ-pyrone).

Found: C, 73.03; H, 4.75. Calcd. for $C_{22}H_{16}O_5$: C, 73.33; H, 4.44%.

2',7-Dihydroxy-2-hydroxymethylisoflavone (V).—Powdered anhydrous aluminum chloride (12 g.) was added to a solution of IV (4 g.) in benzene (200 ml.) or in nitrobenzene (100 ml.), and the mixture was treated similarly as described for XVI. The product obtained from the sodium carbonate soluble part was crystallized from dilute ethanol to give V in colorless microcrystals, m. p. 225~226°C (decomp.)*4, identical with the sample kindly sent from Seshadri; yield 3 g. (86%). IR: 3200 (OH), 1630 cm^{-1} (γ-pyrone) (KBr).

Found: C, 67.56; H, 4.35. Calcd. for $C_{16}H_{12}O_5$: C, 67.60; H, 4.22%.

2',7-Dihydroxy-2-bromomethylisoflavone (VI).—A mixture of V (2.2 g.), acetic acid (22 ml.) and hydrogen bromide-acetic acid (50%, 33 ml.) was heated gradually to 100°C (20 min.) and kept for 45 min. at the temperature. Ice water was added to the cooled solution, and the crystalline product obtained was washed with water and with ethyl acetate, then was recrystallized from ethanol to give VI in colorless microcrystals, m. p. 221~224°C (decomp.)*5, which gave a positive Beilstein test and was identical with the sample from Seshadri; yield 2.1 g. (82%).

9-Hydroxychromeno[3,4-b]chromone (VII).—Anhydrous potassium carbonate (9 g.) was added to a solution of VI (0.9 g.) in anhydrous acetone (300 ml.), and the mixture was refluxed for 4 hr. and then for further 6 hr. with the addition of more potassium carbonate (9 g.). The solvent was distilled off, and the residue was dissolved in water, filtered and acidified. The crystalline product obtained was recrystallized from ethanol to give VII in colorless needles, m. p. 245~250°C (decomp.), identical with the sample prepared by the Robertson's method; yield 0.7 g. (quantitative).

UV λ_{max}^{EtOH} mμ (log ε): 270 (5.02), 297 (4.55).

9-Hydroxy-8-formylchromeno[3,4-b]chromone (VIII).—A mixture of VII (1.5 g.), hexamine (8 g.) and acetic acid (60 ml.) was heated on a steam-bath for 6 hr. and then for further 10 min. with the addition of hot hydrochloric acid (20%, 27 ml.). The crystalline product obtained from the cooled solution was recrystallized from ethyl acetate to give VIII in slightly yellow colored needles, m. p. 261~262°C, which gave a red ferric chloride reaction; yield 0.7 g. (40%). IR: 1730 (CHO), 1630 cm^{-1} (γ-pyrone).

Found: C, 69.18; H, 3.69. Calcd. for $C_{17}H_{10}O_5$: C, 69.39; H, 3.43%.

Furo[2,3-f]chromeno[3,4-b]chromone-2-carboxylic Acid (X).—Anhydrous potassium carbonate (4 g.) was added to a solution of VIII (0.9 g.) and ethyl bromomalonate (1.2 g.) in anhydrous acetone (130 ml.), and the mixture was refluxed for 8.5 hr. Acetone was distilled off, and the residual product was crystallized from ethanol to give ethyl furo[2,3-f]chromeno[3,4-b]chromone-2-carboxylate (IX) in slightly brown colored microcrystals, m. p. 225~226°C; yield 0.4 g. (36%).

A mixture of this ester IX (0.4 g.), acetone (115 ml.) and 5% aqueous sodium hydroxide (30 ml.) was refluxed for 3 hr. The resulting mixture was acidified by hydrochloric acid, acetone was distilled off, and the crystaline product was collected and recrystallized from ethanol to give X in orange colored plates, m. p. 300°C (decomp.); yield 0.25 g. (68%). IR: 3500, 3320, 1700 (CO_2H), 1630 cm^{-1} (γ-pyrone).

Found: C, 66.33; H, 3.68. Calcd. for $C_{19}H_{10}O_6 \cdot 1/2\,H_2O$: C, 66.47; H, 3.23%.

2'-Hydroxy-2-hydroxymethylfuro[2,3-f]isoflavone (XII).—Powdered aluminum chloride (1.2 g.) was added to a solution of 2'-methoxy-2-ethoxymethylfuro[2,3-f]isoflavone[9] (XI)*6 (0.4 g.) in nitrobenzene (30 ml.), and the mixture was heated for one hour on a steam-bath. The resulted solution was treated with a little dilute hydrochloric acid, nitrobenzene was removed by steam-distillation, and the residue was extracted with ethyl acetate. The ethyl acetate solution was washed with dilute hydrochloric acid and then extracted with 5% aqueous sodium hydroxide. The precipitates obtained by acidifying the alkaline solution were recrystallized from ethanol to give XII in colorless microcrystals, m. p. 224~225°C; yield 0.2 g. (50%). IR: 3280 (OH), 1630 cm^{-1} (γ-pyrone).

Found: C, 70.32; H, 4.25. Calcd. for $C_{18}H_{12}O_5$: C, 70.12; H, 3.93%.

*4 Melting point was 212~214°C (decomp.) when the temperature was raised slowly.

*5 Melting point was 212~214°C (decomp.) when the temperature was raised slowly.

*6 M. p. 119~120°C; UV λ_{max}^{EtOH} mμ (log ε): 240 (4.98), 307 (4.14); IR: 1640 cm^{-1} (γ-pyrone) (KBr).

2'-Hydroxy-2-bromomethylfuro[2,3-f]isoflavone (XIII).—A mixture of XII (0.15 g.), acetic acid (2 ml.) and hydrogen bromide-acetic acid (50%, 3 ml.) was treated similarly as described for VI. The product was recrystallized from ethyl acetate to give XIII in colorless microcrystals, m. p. 210°C (decomp.), which gave a positive Beilstein test; yield 0.1 g. (60%). IR: 3380, 3190 (OH), 1630 cm^{-1} (γ-pyrone).

Found: C, 58.46; H, 3.06. Calcd. for $C_{18}H_{11}O_4Br$: C, 58.24; H, 2.98%.

Furo[2,3-f]chromeno[3,4-b]chromone (III).—*a) From the Acid X.*—A mixture of X (0.2 g.), copper powder (0.1 g.) and quinoline (10 ml.) was heated on an oil-bath (190~210°C) for 20 min. under nitrogen gas stream with stirring until the evolution of carbon dioxide ceased. The resulting mixture was filtered from copper, quinoline was removed by steam-distillation, and the crystalline product obtained was dissolved in ethyl acetate. The ethyl acetate solution was washed successively with dilute sulfuric acid, aqueous sodium hydroxide and water. The solvent was removed and the residual product was crystallized from ethanol then from ethyl acetate to give III in slightly red colored microcrystals, m. p. 239.5~240°C, identical with the other sample; yield 0.1 g. (70%).

b) From the Furoisoflavone XIII.—Anhydrous potassium carbonate (1.2 g.) was added to a solution of XIII (0.12 g.) in acetone (40 ml.), and the mixture was refluxed for 4 hr. and then for further 4 hr. with the addition of potassium carbonate (1.2 g.). Acetone was removed from the filtered solution, and the residual product was treated with dilute hydrochloric acid. Recrystallization from ethanol then from ethyl acetate furnished III in slightly orange colored microneedles, m. p. 241~242.5°C. UV λ_{max}^{EtOH} mμ (log ε): 264 (4.93), 304 (4.48); IR: 1630 cm^{-1} (γ-pyrone).

Found: C, 74.26; H, 3.67; Mol. wt. (Rast), 300. Calcd. for $C_{18}H_{10}O_4$: C, 74.48; H, 3.47%; Mol. wt., 290.

The authors are grateful to Dr. Mitsuru Nakayama for assistance, to the members of the Faculty of Pharmacology of this University for microanalysis and to the members of the Institute of Agricultural Chemistry of Kyoto University for microanalysis and infrared spectroscopy.

Faculty of Literature and Science
Toyama University
Gofuku, Toyama

Chloromethylation of 7-Methoxyisoflavone

By Yoshiyuki KAWASE, Mitsuru NAKAYAMA* and Shigeru MATSUTANI

(Received March 31, 1962)

Chloromethylation of flavones has already been carried out by Nakazawa and Matsuura[1] and by Da Re and Verlicchi[2] to give 6- and 8-chloromethyl derivatives from acacetin 7-methyl ether and 8-chloromethyl derivative from 7-methoxy-3-methylflavone respectively, and of flavanones by Matsuoka[3], but that of isoflavone has not yet been reported. Now the chloromethylation of 7-methoxyisoflavone (II) has been carried out.

For the reaction are available two methods, those are by the action of formaline or paraformaldehyde[2] and hydrochloric acid and by that of chloromethyl methyl ether and acetic acid[1,3].

In this experiment, II was chloromethylated by the paraformaldehyde-hydrochloric acid method to give 7-methoxy-8-chloromethylisoflavone (III), colorless needles, m. p. 143~144°C, in 59% yield. The structure of III was confirmed by converting it into 8-acetoxymethyl derivative IV by the action of sodium acetate and acetic anhydride, and further by an alkaline hydrolysis of IV into 8-hydroxymethyl derivative V, which was identical with the authentic sample prepared from 7-hydroxy-8-formylisoflavone[4] (VI) by another route: Reduction of VI by the Meerwein-Ponndorf method or by sodium borohydride*2 furnished 8-hydroxymethyl derivative VII, which was methylated by diazomethane to give V as shown in the Chart.

The chlorine atom of III is fairly reactive: The methoxy- or ethoxy-methyl derivative (VIII or IX) was obtained by the action of sodium

*1 Present address: Faculty of Science, Hiroshima University, Hiroshima.

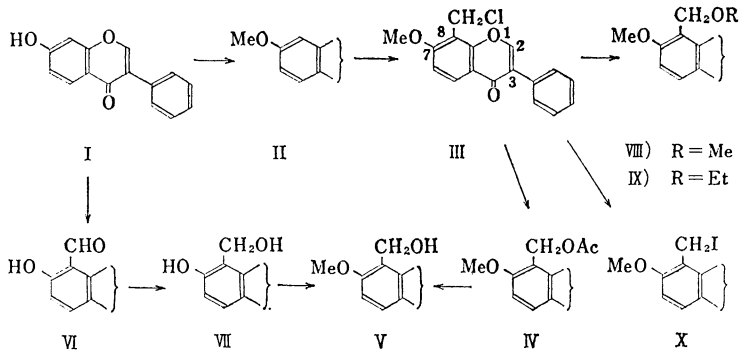
1) K. Nakazawa and S. Matsuura, *J. Pharm. Soc. Japan*, **73**, 481, 484 (1953).

2) P. Da Re and L. Verlicchi, *Ann. Chim. (Rome)*, **46**, 904 (1956).

3) K. Matsuoka, *J. Chem. Soc. Japan, Pure Chem. Sec., (Nippon Kagaku Zasshi)*, **80**, 64 (1959).

4) K. Fukui and Y. Kawase, This Bulletin, **31**, 693 (1958).

*2 It was confirmed that this reagent does not affect the isoflavone nucleus.



methoxide or ethoxide and the iodomethyl derivative X by the action of potassium iodide in acetone, and only the acetoxymethyl derivative IV instead of the reduced compound was obtained by the action of zinc and acetic acid. An attempted chloromethylation of 7-hydroxyisoflavone (I) by the similar method was unsuccessful.

Experimental*3

7-Methoxyisoflavone (II).—*a) By Methyl Iodide.* To a stirred mixture of 7-hydroxyisoflavone (I) (30 g.), anhydrous potassium carbonate (30 g.) and anhydrous acetone (350 ml.) was added dropwise a solution of methyl iodide (18 g.) in acetone (50 ml.), and the mixture was refluxed for 6 hr. and then treated as usual to give II, m. p. 156~157°C (from benzene), identical with the other sample; yield 21.5 g. (67%).

b) By Diazomethane.—To a suspension of I (20 g.) in benzene (500 ml.) was added an ethereal solution of diazomethane (prepared from 7.8 g. of nitrosomethylurea), and the mixture was allowed to stand for 2 days. By the usual treatment, 9.8 g. (46.5%) of II was obtained through recrystallization from benzene; m. p. 156~157°C.

Found: C, 76.06; H, 4.66. Calcd. for $C_{16}H_{12}O_3$: C, 76.18; H, 4.80%.

7-Methoxy-8-chloromethylisoflavone (III).—A mixture of II (9.8 g.), paraformaldehyde (4 g.), acetic acid (98 ml.) and concentrated hydrochloric acid (49 ml.) was saturated with hydrogen chloride under stirring and heating at 60~70°C, and then was allowed to stand at room temperature over night. The solid product obtained was washed with water and recrystallized from acetone to give III in colorless needles, m. p. 143~144°C, giving a positive Beilstein test; yield 7.1 g. (59%). IR: 1645 cm^{-1} (γ-pyrone).

Found: C, 67.29; H, 4.43. Calcd. for $C_{17}H_{13}O_3Cl$: C, 67.89; H, 4.36%.

7-Methoxy-8-acetoxymethylisoflavone (IV).—*a) From III by Sodium Acetate and Acetic Anhydride.*—A mixture of III (2 g.), anhydrous sodium acetate (1.4 g.) and acetic anhydride (20 ml.) was heated for 3 hr. on an oil-bath (170~180°C). By the usual treatment, 1.7 g. of IV was obtained in colorless needles, m. p. 197~198°C (from ethanol). IR: 1720 (acetate), 1650 cm^{-1} (γ-pyrone).

Found: C, 70.21; H, 4.92. Calcd. for $C_{19}H_{16}O_5$: C, 70.36; H, 4.98%.

b) From III by Zinc and Acetic Acid.—A mixture of III (0.3 g.), zinc powder (1 g.) and acetic acid (80%, 5 ml.) was heated at 80°C for 2 hr., and the resulting mixture was poured into water. The crystalline product obtained was recrystallized from ethanol to give IV, m. p. 196~198°C.

c) From V.—A mixture of V (0.2 g.), sodium acetate (0.15 g.) and acetic anhydride (2 ml.) was treated similarly as described for a) to give IV, m. p. 196~198°C.

7-Hydroxy-8-hydroxymethylisoflavone (VII).—*a) By the Meerwein-Ponndorf Method.*—To a solution of 7-hydroxy-8-formylisoflavone[4] (VI) (0.5 g.) in absolute isopropyl alcohol (15 ml.) was added aluminum isopropoxide (prepared from 2.75 g. of aluminum ribbon and 30 ml. of isopropyl alcohol), and the mixture was heated on an oil-bath for 4 hr., most of the solvent was distilled off in the meantime. Dilute sulfuric acid was added to the residue, and the crystalline product obtained was recrystallized from ethanol then from ethyl acetate to give VII in colorless microcrystals, m. p. 172°C (decomp.); yield 0.2 g. IR: 3300~2400 (OH), 1620 cm^{-1} (γ-pyrone).

Found: C, 71.56; H, 4.54. Calcd. for $C_{16}H_{12}O_4$: C, 71.63; H, 4.51%.

b) By Sodium Borohydride.—A solution of sodium borohydride (0.2 g.) in water (100 ml.) was added to a solution of VI (1 g.) in 1% aqueous sodium hydroxide (50 ml.), and the solution was heated at 60~70°C for 2 hr. on a steam-bath. The cooled solution was acidified with dilute hydrochloric acid, and the crystalline product obtained was recrystallized from ethanol then from ethyl acetate; m. p. 172°C (decomp.), identical with the other sample.

7-Methoxy-8-hydroxymethylisoflavone (V).—*a) From VII.*—To a suspensin of VII (0.1 g.) in benzene (150 ml.) was added an ethereal solution of diazomethane (prepared from 1.5 g. of nitrosomethylurea), and the mixture was allowed to stand over night. The solvent was removed, and the residual product was washed with 5% aqueous sodium hydroxide then was recrystallized from benzene to give V in colorless microcrystals, m. p. 185~186°C. IR: 3300 (OH), 1625 cm^{-1} (γ-pyrone).

Found: C, 72.23; H, 5.03. Calcd. for $C_{17}H_{14}O_4$: C, 72.33; H, 5.00%.

*3 Melting points are uncorrected and infrared spectra were measured in Nujol.

b) From IV.—A mixture of IV (0.5 g.), ethanol (5 ml.) and 0.5 N ethanolic potassium hydroxide (2 ml.) was refluxed for 1.5 hr. The cooled solution was diluted with water and the crystalline product obtained was recrystallized from benzene to give V in colorless microcystals, m. p. 186~187°C, identical with the other sample; yield 0.2 g.

Found: C, 72.51; H, 5.02. Calcd. for $C_{17}H_{14}O_4$: C, 72.33; H, 5.00%.

7-Methoxy-8-methoxymethylisoflavone (VIII).—To a solution of III (1.5 g.) in benzene (100 ml.) was added methanolic sodium methoxide (prepared from 0.1 g. of sodium and 5 ml. of methanol), and the mixture was refluxed for 4 hr. The resulting mixture was filtered, the solvent was distilled off, and the residual product was crystallized from ethanol to give VIII in colorless needles, m. p. 142~143°C; yield 1 g.

Found: C, 72.58; H, 5.47. Calcd. for $C_{18}H_{16}O_4$: C, 72.96; H, 5.44%.

7-Methoxy-8-ethoxymethylisoflavone (IX).—A similar treatment of III with sodium ethoxide furnished IX in colorless needles, m. p. 115~117°C (from acetone).

Found: C, 72.80; H, 5.68. Calcd. for $C_{19}H_{18}O_4$: C, 73.53; H, 5.85%.

7-Methoxy-8-iodomethylisoflavone (X).—A mixture of III (1 g.), potassium iodide (1 g.) and acetone (20 ml.) was refluxed for 1.5 hr. The acetone was distilled off, and the residual product was washed with water and then was crystallized from acetone to give X in colorless needles, m. p. 166~167°C, giving a positive Beilstein test; yield 1 g.

Found: C, 51.98; H, 3.39. Calcd. for $C_{17}H_{13}O_3I$: C, 52.06; H, 3.34%.

The authors are grateful to Mr. Shinichi Nakamoto for assistance and to the members of the Faculty of Pharmacology of this University for microanalysis and also to the members of the Institute of Agricultural Chemistry of Kyoto University for microanalysis and infrared spectroscopy.

Faculty of Literature and Science
Toyama University
Gofuku, Toyama

The Molecular Structure of trans-4-Halogenocyclohexanol

By Yoshiko TAKEOKA

(Received December 12, 1961)

It has been well established that the cyclohexane ring has a chair form and that some cyclohexane derivatives have mutually convertible isomers, viz., inverted isomers. Since *trans*-4-halogenocyclohexanol should also have such isomers, it seemed very interesting to study the stability of the isomers in these compounds.

Experimental

Preparation of *trans*-4-Halogenocyclohexanol.—*trans*-4-Chlorocyclohexanol was prepared by adding hydrochloric acid to 1,4-epoxycyclohexane which had been obtained from 1,4-cyclohexanediol by dehydration with activated alumina. The product was recrystallized from ligroin, m. p. 82.0～83.0°C[1,2].

The preparation of *trans*-4-bromo- and of *trans*-4-iodocyclohexanol was similar to that of the chloro-derivative. The melting point of the bromo-derivative is 81.0～81.5°C, while that of the iodo-derivative is 59.2～60.3°C.

The Bromo-derivative. — Found: C, 39.95; H, 6.28. Calcd. for $C_6H_{11}OBr$: C, 40.24; H, 6.19%.

1) E. A. Fehnel, *J. Am. Chem. Soc.*, 73, 4978 (1951).
2) E. L. Bennett and C. Niemann, ibid., 74, 5076 (1952).

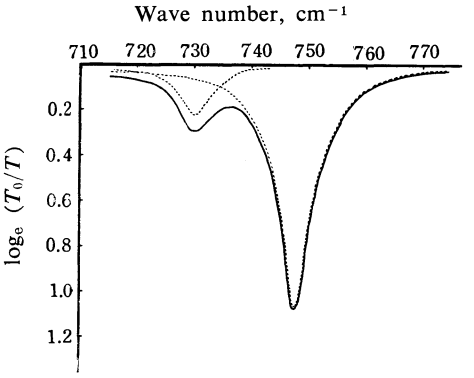


Fig. 1. Bands of C-Cl stretching vibration in the carbon disulfide solution (0.030 mol./l.).

The Iodo-derivative.—Found: C, 32.28; H, 5.41. Calcd. for $C_6H_{11}OI$: C, 31.88; H, 4.91%.

Dipole Moment. — The dipole moment of the chloro-derivative was obtained, by Debye's solution method, in the dilute carbon tetrachloride solution at 20.0°C. The dielectric constants were measured by the usual heterodyne beat method. The results are listed in Table I.

Infrared Spectra. — The measurements of the spectra were made with a Perkin-Elmer spectrometer

TABLE I. DIPOLE MOMENT OF *trans*-4-CHLOROCYCLOHEXANOL

Solvent; Carbon tetrachloride
Temperature; 20.0°C

	Molar fraction	Density	Dielectric constant	P_2
	0.0000	1.5952	2.2396	
Soln. I	0.00309	1.5938	2.2540	107
Soln. II	0.00425	1.5930	2.2594	108
Soln. III	0.00496	1.5929	2.2613	104
Soln. IV	0.00909	1.5910	2.2797	103
	$P_{2\infty}=107$		$\mu=1.87$ D	

TABLE II. INFRARED SPECTRA OF *trans*-4-HALOGENOCYCLOHEXANOL (cm^{-1})

Chloro-derivative		Bromo-derivative		Iodo-derivative	
Liquid	Solid	Liquid	Solid	Liquid	Solid
400~800 (bm)	480~830 (bs)	400~800 (bm)	450~830 (bs)	400~750 (bm)	430~800 (bs)
459 (w)	460 (w)	453 (bw)	453 (m)	448 (bw)	453 (vw)
	479 (w)	472 (w)	474 (m)	469 (bw)	470 (w)
		491 (m)	487 (w)		
552 (vs)	556 (vs)	534 (vs)	538 (vs)	521 (vs)	522 (vs)
628 (m)	629 (w)	609 (w)	609 (w)	596 (w)	597 (w)
				680 (m)	681 (m)
		708 (s)	706 (s)		
730 (m)	—				
745 (s)	744 (s)				
805 (m)	—	799 (w)	—	790 (vw)	—
817 (s)	818 (s)	808 (s)	809 (s)	803 (s)	805 (s)
860 (vw)	862 (vw)	860 (w)	862 (vw)	859 (w)	861 (vw)
883 (m)	885 (s)	879 (s)	881 (s)	877 (s)	877 (s)
899 (m)	900 (s)	899 (s)	899 (s)	897 (s)	896 (m)
947 (s)	950 (s)	944 (vs)	946 (s)	942 (vs)	942 (s)
965 (m)	965, 969 (m)	963 (m)	967 (s)	966 (m)	967 (m)
1007 (m)	1012 (m)	1003 (s)	1007 (s)	997 (s)	1002 (s)
1034 (vw)	1035 (vw)	1031 (vw)	1032 (vw)	1031 (vw)	1033 (vw)
1062 (vs)	1067 (vs)	1060 (vs)	1064 (vs)	1059 (vs)	1061 (vs)
1110 (vw)	1113 (w)	1099 (m)	1101 (m)	1084 (s)	1086 (s)
1135 (vw)	1135 (w)	1132 (w)	1135 (m)	1130 (w)	1139 (w)
1196, 1207 (m)	1200, 1210 (s)	1180 (s)	1183 (s)	1162 (s), 1199 (w)	1165 (s), 1199 (w)
1256 (m)	1254 (w)	1233 (m)	1232 (m)	1222 (m)	1223 (m)
1279 (w)	1288 (m)	1279 (m)	1289 (m)	1279 (m)	1286 (w)
1308 (vw)	1311 (w)				1301 (m)
1327 (vw)	1333 (w)	1330 (m)	1335 (m)	1324 (m)	1322 (w)
1344 (vw)	1345 (w)				
1366 (m)	1365 (s)	1364 (s)	1365 (s)	1363 (s)	1362 (s)
1405 (bw)	1415 (bw)	1405 (bw)	1417 (bw)	1406 (bw)	1420 (bw)
1452 (s)	1450 (s)	1450 (s)	1447 (s)	1450 (s)	1450 (s)
2687 (vw)	2699 (vw)	2685 (vw)	2684 (vw)	2672 (vw)	2675 (vw)
2870 (s)	2875 (s)	2874 (s)	2864 (s)	2834 (s)	2862 (s)
2939 (vs)	2948 (vs)	2936 (vs)	2932 (vs)	2925 (vs)	2937 (vs)
3420 (vs)	3325 (vs)	3373 (vs)	3289 (vs)	3358 (vs)	3317 (vs)

w=weak, m=medium, s=strong, v=very and b=broad

model 112 equipped with potassium bromide or sodium chloride prism. Although the solid spectra were observed both for the Nujol mull and for the solid obtained by cooling the molten sample, no significant difference in intensity could be found between them. The liquid spectra were observed for the molten compounds. The results are shown in Table II.

Measurement of the Integrated Intensities.—The intensities of the two bands at 730 and 748 cm^{-1} of

TABLE III. TEMPERATURE DEPENDENCE OF THE RELATIVE INTENSITIES

Carbon disulfide solution (0.030 mol./l.)

Temp. °C	Wave number	Form	$\log_e\left(\frac{T_0}{T}\right)_{max}$	$\Delta\nu^a_{1/2}$	$c_a A_a / c_e A_e$
27	730	(1a, 4a)	0.225	6.4	0.20
	748	(1e, 4e)	1.08	6.1	
−27	730	(1a, 4a)	0.237	6.6	0.15
	748	(1e, 4e)	1.35	6.7	

the chloro-derivative were observed by the use of a potassium bromide prism. The slit width used was 0.248 mm., and the spectral widths were 3.8 cm^{-1} at 730 cm^{-1} and 4.0 ml^{-1} at 748 cm^{-1}. Measurements were made at 27 and −27°C. The cell thickness was 3 mm. Since these bands partly overlap each other, these were separated by assuming that the band shapes are given by Lorentz's equation, as is shown in Fig. 1. The integrated intensities A of the bands were obtained by Ramsay's method[3] of direct integration corrected for finite slit widths. The intensities are given by the following equation:

$$A = (K/cl) \log_e (T_0/T)_{max} \times \Delta\nu^a_{1/2}$$

where c is the concentration of the solute in moles per liter, l is the cell length in cm., T_0 and T are the apparent intensities of the incident and transmitted radiation when the spectrometer is set at frequency ν_{max}, and $\Delta\nu^a_{1/2}$ is the apparent half-intensity width.

The values of K were obtained from Ramsey's table[3]. The results are listed in Table III.

Discussion

It has been concluded on the basis of chemical evidence that the compound obtained by adding hydrochloric acid to the epoxy-compound is the trans-isomer. In order to confirm this conclusion, the dipole moment of this molecule was determined. The results obtained are shown in Table I. As may be seen in the table, the molecular polarization, P_2, depends upon the concentration of the solution. However, at concentrations lower than 0.00425 in molar fraction, it takes a constant value, 107. It was shown, by infrared absorption measurement, that in Soln. I there is practically no intermolecular hydrogen bond. Therefore, the P_2 value of 107 was taken as that for the extreme dilution ($P_{2\infty}$). From this value of $P_{2\infty}$, the dipole moment was calculated as 1.87 D.

Since it is very probable that the cyclohexane ring of this compound has the chair form, stable forms may be expected for both the trans- and the cis-isomer of this compound. These structures may be schematically represented as in Fig. 2. The positions of the atoms attached to the cyclohexane ring are represented by the usual symbols, e and a[4].

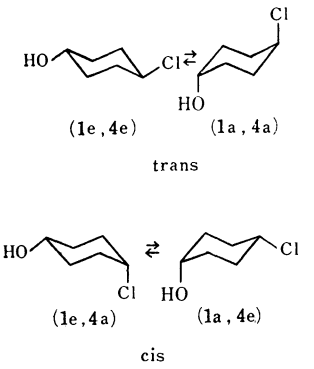


Fig. 2. Inverted isomers of 4-chlorocyclohexanol.

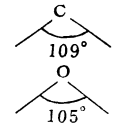
TABLE IV. BOND MOMENTS AND VALENCY ANGLES

$\mu_{C-O} = 0.8$ D

$\mu_{H-O} = 1.5$ D

$\mu_{C-Cl} = 1.6$ D

$\mu_{H-C} = 0.3$ D



Beginning from the law of the vector addition of bond moments, and by assuming that an almost free rotation of the OH group around the C–O axis is possible, it can be easily seen that the values of the dipole moments of both the cis- and the trans-isomer are not changed by converting the cyclohexane ring; viz., the value of the (1e, 4e)-form is equal to that of the (1a, 4a)-form, and the value of the (1e, 4a)-form is equal to that of the (1a, 4e)-form. Upon the basis of simple vector addition and by using the values shown in Table IV, the values of 2.3 and 1.9 D were obtained for the cis- and the trans-isomer respectively. Since the observed value, 1.87 D, agrees well with the calculated value of 1.9 D for the trans-isomer, it is very probable that the compound is the trans-isomer.

The wave numbers of the infrared bands of these compounds in the liquid and in the solid states are listed in Table II. Because similar methods were used for the preparation of these compounds and because the spectra of the bromo- and the iodo-derivative are similar to that of the chloro-derivative, it may be concluded that the bromo- and the iodo-derivative

3) D. A. Ramsay, ibid., **74**, 72 (1952).
4) D. H. R. Barton, O. Hassel, K. S. Pitzer and V. Prelog, *Nature*, **172**, 1096 (1953); *Science*, **119**, 49 (1953).

are the same geometrical isomers as that of the chloro-derivative, viz., the trans-isomer.

As for the trans-isomers of these compounds, the existence of two mutually convertible or "inverted" isomers is probable. As can be seen from Table II, the bands at 730 and 805 cm^{-1} for the chloro-derivative disappear when the state is changed from liquid to solid. From this fact, it follows that the equilibrium of the two isomers, which exists in the liquid, breaks down in the course of crystallization and that only one isomer persists in the solid. Therefore, it seemed interesting to determine the form of the isomer.

It has been known that chlorocyclohexane[5] has two mutually convertible isomers, viz., the (e)- and the (a)-form, in the vapor and in the dilute carbon disulfide solution, and that the energy difference between them is about 0.3 kcal./mol. in these states, the (e)-form being stable. Cyclohexanol[6] also has the (e)- and the (a)-form in solutions and in the liquid, and the energy difference between them seems to be larger than that for chlorocyclohexane.

Considering the energy difference for chlorocyclohexane and that for cyclohexanol, it seems very probable that the stable form of *trans*-4-chlorocyclohexanol is the (1e, 4e)-form and that only this form exists in the solid state. However, since it has been known[5] that the energy difference between the two isomers of *trans*-1, 4-dichlorocyclohexane, viz., the (1e, 4e)- and the (1a, 4a)-form, is not twice that between the two isomers of chlorocyclohexane, further, evidence for this is needed.

The bands at 730 and 745 cm^{-1} in the liquid spectrum may be assigned to the C–Cl stretching vibrations. As for the bands assigned to the C–Cl stretching vibrations of the chloro-derivatives of cyclohexane, it is known[7] that the frequencies of the bands which are due to the chlorine atoms attached to the (e)-position of cyclohexane ring are higher than those of the bands due to the chlorine atoms of the (a)-position. Therefore, the band at 730 cm^{-1}, which disappears in the solid state, can be assigned to the (1a, 4a)-form. Then the same conclusion as described above can be drawn from this information.

According to the other experimental rule[8] that the frequency of the breathing vibration of the molecule of cyclohexane derivatives having substituents in the (a)-position does not markedly shift from that of cyclohexane, viz., 802 cm^{-1}, the band at 805 cm^{-1} may be assigned to the (1a, 4a)-form. The fact that this band disappears in the solid spectrum favors the above conclusion.

In order to determine the energy difference between the two isomers of the chloro-derivative, the ratios of the integrated intensity of the band at 730 cm^{-1} of the (1a, 4a)-form to that at 748 cm^{-1} of the (1e, 4e)-form were measured in a carbon disulfide solution at 27 and $-27°C$. As for the solution of 0.4 mol./l., the very broad band assigned to the out-of-plane deformation vibration of the intermolecular bonded OH group appears in the region from about 400 to 800 cm^{-1}. Therefore, the measurements were made in the more dilute solution, in which no bands assigned to the hydrogen bond could be detected. From the data of Table III, we can calculate as usual the difference, ΔE, between the energy, E_a of the (1a, 4a)-form and the energy, E_e, of the (1e, 4e)-form ($\Delta E = E_a - E_e$) by the equation;

$$c_a A_a / c_e A_e = (\alpha_a f_a / \alpha_e f_e) \exp(-\Delta E / RT)$$

where A_a and A_e are the true integrated absorption intensities of the bands at 730 and 748 cm^{-1}, c_a and c_e the concentrations (mol./l.), α_a and α_e, the molar absorption coefficients, and f_a and f_e, the partition functions of the forms shown by the suffixes. As the measurements were made at two temperatures, the unknown quantity ($\alpha_a f_a / \alpha_e f_e$) can be eliminated. The ratio of the partition functions, f_a/f_e, is taken to be constant, because of the narrow temperature range. The value obtained for ΔE is 0.76 kcal./mol., the (1e, 4e)-form being more stable.

By using this value of the energy difference and by assuming as usual that f_a is nearly equal to f_e, a rough estimate of the abundance ratio, n_a/n_e, can be made by the equation:

$$n_a/n_e = f_a/f_e \, e^{-\Delta E/RT}$$

The value of the ratio obtained is 1/3.6 at room temperature. From this it can be surmised that a small number of the bands disappear when the state is changed from liquid to solid.

It is expected that the bromo- and the iodo-derivative also have the (1a, 4a)- and the (1e, 4e)-forms, since their structures are similar to that of the chloro-derivative. From the fact that the energy difference between the (a)- and the (e)-form of halogenocyclohexanes, where the halogen is chlorine, bromine or iodine, becomes larger with the increasing atomic number of the halogens[5,9], it is very probable that in the case of *trans*-4-halogenocyclohexanol also the energy differences for the bromo- and the iodo-derivative are larger than that of the

5) K. Kozima and K. Sakashita, This Bulletin, **31**, 796 (1958).
6) Y. Takeoka, unpublished.
7) K. Kozima, *Bull. T. I. T.*, 1952, 1.
8) K. Sakashita, *J. Chem. Soc. Japan, Pure Chem. Sec.*, (*Nippon Kagaku Zasshi*), **80**, 13 (1959).
9) K. Kozima and Y. Takeoka, unpublished.

chloro-derivative. From this it may be surmised that, for the spectra of the bromo- and the iodo-derivative, only the one weak band disappears when the state is changed from liquid to solid, as is shown in Table II.

The author wishes to express her sincere thanks to Professor Kunio Kozima for his kind guidance. Her thanks are also due to Dr. Asaji Kondo for his elementary analyses.

Laboratory of Chemical Spectroscopy
Tokyo Institute of Technology
Meguro-ku, Tokyo

Studies on Mixture Dyeing. I. The Kinetics of the Mixture of Benzopurpurine 4B and Sky Blue 6B

By Minoru SEKIDO and Zenzo MORITA

(Received December 22, 1961)

In practical dyeing, dye mixtures are usually used to produce a desirable shade. Moreover, some commercial dyes are deliberate mixtures in order to provide certain specific properties and shades. This implies that to study dyeing is practically the same as to study mixture dyeing. However, little has been done in the quantitative study of such mixture dyeing. Neale and Stringfellow[1] and recently Horiki et al.[2,3] have investigated the equiliburium adsorption of binary direct dye mixtures, but the diffusion of dye mixtures has been little studied. Recently, however, many studies of diffusion in multi-component systems have been made from the view point of the thermodynamics of irreversible processes[4]. Uedaira[5] and Tsuda[6] applied this theory to the mixture dyeing process.

For this paper, the kinetics of the single dyeing of Benzopurpurine 4B (C. I. 23500) and of Sky Blue 6B (C. I. 24410) has been investigated in detail in order to study quantitatively their behavior in mixture dyeing. Then the kinetics of mixture dyeing has been studied theoretically on the basis of the information about the single dyeing.

Experimental

Purified dyes were used throughout. They were prepared from commercial dyes (Diacotton Benzopurpurine 4B (MCI) and Diacotton Sky Blue 6B (MCI)) by the method of Robinson and Mills[7]. The high purity of these samples was checked by titanometry and also by the ashing method. The absence of colored impurities was confirmed by paper chromatography.

A cellophane sheet, made by Tokyo Cellophane Co., Ltd., was used as the dyeing substrate. It was cut into pieces 6 cm. wide and 55 cm. long, which pieces were then scoured by distilled water and layered round on a glass tube. This cylindrical cellophane-film roll[8] was dyed under certain conditions. After dyeing, the film roll was rinsed in a dilute sodium chloride solution for a short time. Then the dyed cellophane was unrolled and dried. The dried sample was cut, layer by layer, for colorimetry by a Hitachi EPB-V type spectrophotometer, or the dyes adsorbed by each layer were stripped with 25% aqueous pyridine and the dye content of the solution was measured by the spectrophotometer. The mean thickness of each swollen cellophane sheet was 4.66×10^{-3} cm.

In single dyeing, the concentration of dye in the dye bath was 1.0, 2.5, 5.0, or 10.0×10^{-5} mol./l., while that of sodium chloride was 0.01, 0.02, 0.03, or 0.04 mol./l. In mixture dyeing, the experimental conditions were as shown in Tables IV and V. The dyeing time was 3000 min. (90°C); 4500 min. (85°C); 6000 min. (80°C) or 7500 min. (75°C).

Theoretical

The cylindrical cellophane roll[8] may well be considered a semi-infinite media in the direction of the center of the roll. The surface dye concentration of rolled cellophane is maintained constant throughout the whole period of dyeing by means of the infinite dye bath condition.

1) S. M. Neale and W. A. Stringfellow, *J. Soc. Dyers Colourists*, **59**, 243 (1943).
2) Y. Horiki, Y. Tanizaki and N. Ando, This Bulletin, **33**, 163 (1960).
3) Y. Horiki, ibid., **33**, 974 (1960).
4) D. G. Miller, *Chem. Revs.*, **60**, 15 (1960).
5) H. Uedaira, *J. Soc. Textile Cellulose Ind. Japan (Sen-i Gakkaishi)*, **14**, 967 (1958).
6) K. Tsuda, the 13th Annual Meeting of the Chemical Society of Japan, 1959.
7) C. Robinson and H. A. T. Mills, *Proc. Roy. Soc.*, **A131**, 576 (1931).
8) M. Sekido, *Annual Report of the 120th Committee of Science Promoting Society of Japan*, **5**, 113 (1953); **6**, 75 (1954); **7**, 56 (1955); **8**, 39 (1956).

Single Dyeing.—Assuming that the diffusion coefficient of dye through the dyeing substrate, D (cm^2/min.), is constant at a given temperature and concentration of dye and electrolyte in the dye bath, the diffusion equation is

$$\frac{\partial C}{\partial t}=D\frac{\partial^2 C}{\partial x^2} \tag{1}$$

where C (mol./cm^3 s. c.*) denotes the concentration of dye in the substrate, t (min.), the time, and x (cm.), the distance measured from the surface to the center. The solution of Eq. 1 for this system is

$$\frac{C}{C_0}=\mathrm{erfc}\frac{x}{2\sqrt{Dt}} \tag{2}$$

where

$$\mathrm{erfc}\,x=\frac{2}{\sqrt{\pi}}\int_x^\infty e^{-\eta^2}d\eta \tag{3}$$

and C_0 is the surface concentration of dye.

The calculation of the diffusion coefficient and of the surface dye concentration can be made by the method of Sekido and Matsui[9].

Mixture Dyeing.—The diffusion of a mixture of dyes has recently been studied by Uedaira[5] and by Tsuda[6]. Assuming for the diffusion coefficient the same conditions as those in the case of single dyeing, the diffusion equations of binary mixture dyeing[5,10] are

$$\frac{\partial C_1}{\partial t}=D_{11}\frac{\partial^2 C_1}{\partial x}+D_{12}\frac{\partial^2 C_2}{\partial x^2} \tag{4}$$

$$\frac{\partial C_2}{\partial t}=D_{21}\frac{\partial^2 C_1}{\partial x^2}+D_{22}\frac{\partial^2 C_2}{\partial x^2} \tag{5}$$

where C_1 and C_2 are the concentrations of dyes 1 and 2 respectively, D_{11} and D_{22} are the main diffusion coefficients, and D_{12} and D_{21} are the cross-term diffusion coefficients.

These equations may be solved by the method of Fujita and Gosting[11], as was done by Uedaira[5]. The initial and boundary conditions are

$$C_1=C_2=0, \qquad x>0, \qquad t=0 \tag{6}$$

$$C_1=C_1^\circ, \qquad C_2=C_2^\circ, \qquad x=0, \qquad t>0 \tag{7}$$

where C_1° and C_2° are the surface concentrations of dyes 1 and 2 respectively.

Therefore, the solutions of these equations are

$$\frac{C_1}{C_1^\circ}=K_1^+\,\mathrm{erfc}\frac{\sqrt{\sigma_+}}{2\sqrt{t}}x+K_1^-\,\mathrm{erfc}\frac{\sqrt{\sigma_-}}{2\sqrt{t}}x \tag{8}$$

$$\frac{C_2}{C_2^\circ}=K_2^+\,\mathrm{erfc}\frac{\sqrt{\sigma_+}}{2\sqrt{t}}x+K_2^-\,\mathrm{erfc}\frac{\sqrt{\sigma_-}}{2\sqrt{t}}x \tag{9}$$

where

$$K_1^+=\frac{(D_{22}-D_{11})+\sqrt{(D_{22}-D_{11})^2+4D_{12}D_{21}}-2D_{12}C_2^\circ/C_1^\circ}{2\sqrt{(D_{22}-D_{11})^2+4D_{12}D_{21}}} \tag{10}$$

$$-K_1^-=\frac{(D_{22}-D_{11})-\sqrt{(D_{22}-D_{11})^2+4D_{12}D_{21}}-2D_{12}C_2^\circ/C_1^\circ}{2\sqrt{(D_{22}-D_{11})^2+4D_{12}D_{21}}} \tag{11}$$

$$K_2^+=\frac{(D_{11}-D_{22})+\sqrt{(D_{22}-D_{11})^2+4D_{12}D_{21}}-2D_{21}C_1^\circ/C_2^\circ}{2\sqrt{(D_{22}-D_{11})^2+4D_{12}D_{21}}} \tag{12}$$

$$-K_2^-=\frac{(D_{11}-D_{22})-\sqrt{(D_{22}-D_{11})^2+4D_{12}D_{21}}-2D_{21}C_1^\circ/C_2^\circ}{2\sqrt{(D_{22}-D_{11})^2+4D_{12}D_{21}}} \tag{13}$$

$$\sigma_+=\frac{(D_{22}+D_{11})+\sqrt{(D_{22}-D_{11})^2+4D_{12}D_{21}}}{2(D_{11}D_{22}-D_{12}D_{21})} \tag{14}$$

$$\sigma_-=\frac{(D_{22}+D_{11})-\sqrt{(D_{22}-D_{11})^2+4D_{12}D_{21}}}{2(D_{11}D_{22}-D_{12}D_{21})} \tag{15}$$

The surface concentrations C_1° and C_2° are determined by extrapolation of the dye distribution curves in the cellophane roll. The four diffusion coefficients should be determined simultaneously. However, the calculation of these coefficients from the dye distribution curve is not possible. It is assumed that the main diffusion coefficients, D_{11} and D_{22}, are the diffusion coefficients of each single dyeing whose surface concentration is equal to that in the mixture dyeing. Therefore, the cross-term diffusion coefficients, D_{12} and D_{21}, are determined by the trial and error from Eqs. 8—15, using the values of C_1°, C_2°, D_{11} and D_{22} obtained above.

Results

Single Dyeing.—The results for single dyeings are shown in Tables I (Benzopurpurine 4B) and II (Sky Blue 6B), which show the surface dye concentrations and the diffusion coefficients of single dyeing. According to the theory of activated diffusion, the observed diffusion coefficient at a given temperature is given by the equation

$$\log D=\log D_0-E/2.303RT \tag{16}$$

where E is the apparent activation energy of the diffusion.

From the experiments at various dye concentrations, the apparent activation energy of

* s. c.=Swollen cellophane.

9) M. Sekido and K. Matsui, Meeting of the Society of Textile and Cellulose Industries, Japan (1959).

10) R. L. Baldwin, P. J. Dunlop and L. J. Gosting, *J. Am. Chem. Soc.*, **77**, 5235 (1955).

11) H. Fujita and L. J. Gosting, ibid., **78**, 1099 (1956).

TABLE I. THE DIFFUSION COEFFICIENTS AND THE SURFACE CONCENTRATIONS OF BENZOPURPURINE 4B

(5.0×10^{-5} mol. dye/l. dyeing liquor)

Temp. °C	NaCl concn. mol./l.	$C_0\times10^5$ mol./cm³ s.c.	$D\times10^8$ cm²/min.
90	0.01	0.89	3.5
	0.02	1.1	4.0
	0.03	1.7	4.4
	0.04	1.8	5.0
85	0.03	1.8	2.1
80	0.03	2.0	1.7
75	0.03	2.2	1.3

TABLE II. THE DIFFUSION COEFFICIENTS AND THE SURFACE CONCENTRATIONS OF SKY BLUE 6B

(5.0×10^{-5} mol. dye/l. dyeing liquor)

Temp. °C	NaCl concn. mol./l.	$C_0\times10^6$ mol./cm³ s.c.	$D\times10^8$ cm²/min.
90	0.01	1.3	3.9
	0.02	2.5	5.6
	0.03	2.7	5.8
	0.04	5.6	5.8
85	0.03	4.3	5.1
80	0.03	5.2	3.1
75	0.03	6.8	2.5

the diffusion at a certain surface concentration can be obtained. Figures 1 and 2 show the relation between the logarithm of the diffusion coefficient and the reciprocal of the absolute temperature ($1/T$ °K^{-1}) at a constant surface concentration, and some numerical results obtained from these figures are given in Table III.

Mixture Dyeing*.—The dye distributions at

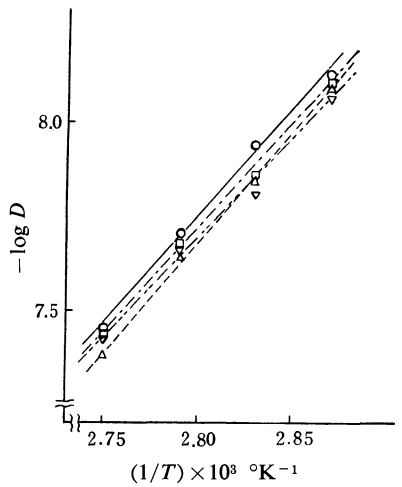


Fig. 1. Effect of temperature on diffusion coefficient of Benzopurpurine 4B.
—○— 0.01 ; --△-- 0.02 ; -·-□-·- 0.03 ; -···▽-··· 0.04 mol. NaCl/l.

* Dye 1 denotes Benzopurpurine 4B and dye 2 denotes Sky Blue 6B.

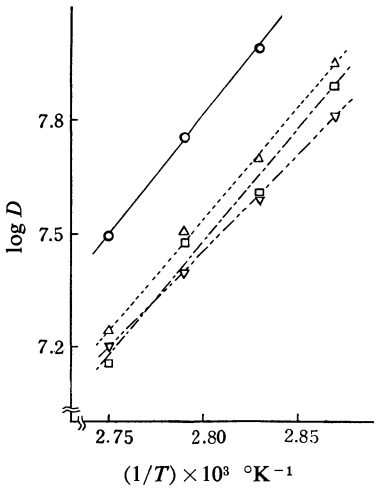


Fig. 2. Effect of temperature on diffusion coefficient of Sky Blue 6B.
—○— 0.01 ; --△-- 0.02 ; -·-□-·- 0.03 ; -···▽-··· 0.04 mol. NaCl/l.

TABLE III. APPARENT ACTIVATION ENERGY OF DIFFUSION

	E kcal./mol.	$C_0\times10^6$ mol./cm³ s.c.	NaCl concn. mol./l.
Benzopurpurine 4B	25.6	8.	0.01
	26.8	11.	0.02
	25.2	14.	0.03
	24.2	16.	0.04
Sky Blue 6B	28.5	1.3	0.01
	27.2	2.7	0.02
	26.4	3.6	0.03
	23.8	4.6	0.03

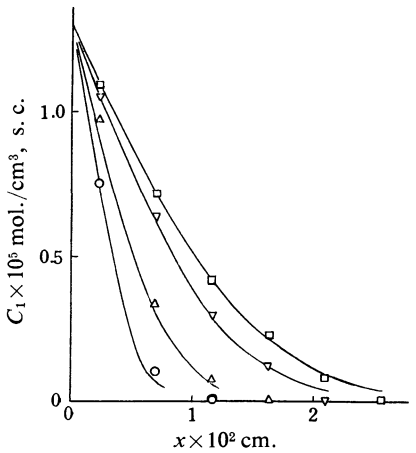


Fig. 3. The distributions of Benzopurpurine 4B at various times of mixture dyeing.
○ 187 ; △ 540 ; ▽ 1448 ; □ 2130 min.
—— theoretical curve.
each dye concn. = 5.0×10^{-5} mol./l., 90°C ; 0.03 mol. NaCl/l.

TABLE IV. FOUR DIFFUSION COEFFICIENTS AND SURFACE CONCENTRATIONS IN MIXTURE DYEING* (at 90°C)

NaCl concn. mol./l.	D_{11}	D_{22}	D_{12}	D_{21}	$C_1^\circ \times 10^5$	$C_2^\circ \times 10^6$
	($\times 10^8$ cm²/min.)				(mol./cm³ s. c.)	
0.01	2.9	2.0	−0.01	0.10	0.49	0.38
0.02	3.1	2.3	−0.01	0.40	0.97	0.96
0.03	3.3	3.0	−0.01	0.80	1.3	1.6
0.04	3.3	4.0	−0.09	1.1	1.5	2.2

TABLE V. FOUR DIFFUSION COEFFICIENTS AND SURFACE CONCENTRATIONS IN MIXTURE DYEING* (0.03 mol. NaCl/l.)

Temp. °C	D_{11}	D_{22}	D_{12}	D_{21}	$C_1^\circ \times 10^5$	$C_2^\circ \times 10^6$
	($\times 10^8$ cm²/min.)				(mol./cm³ s. c.)	
85	2.5	1.8	-0.01_6	0.74	1.4_5	1.8
80	1.6	1.3	-0.04_4	0.57	1.6	2.2
75	1.2	0.80	-0.01_4	0.22	1.6	2.0

* Concentration of each dye $= 5.0 \times 10^{-5}$ mol./l.

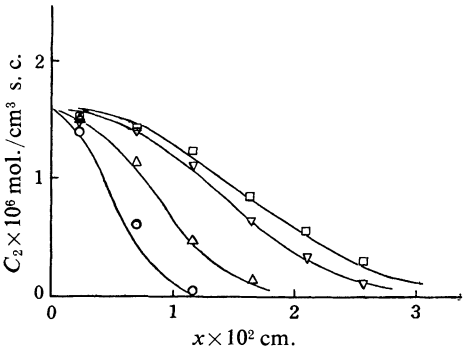


Fig. 4. The distributions of Sky Blue 6B at various times of mixture dyeing.
○ 187; △ 540; ▽ 1448; □ 2130 min.
—— theoretical curve
each dye concn. $= 5.0 \times 10^{-5}$ mol./l.; 90°C; 0.03 mol. NaCl/l.

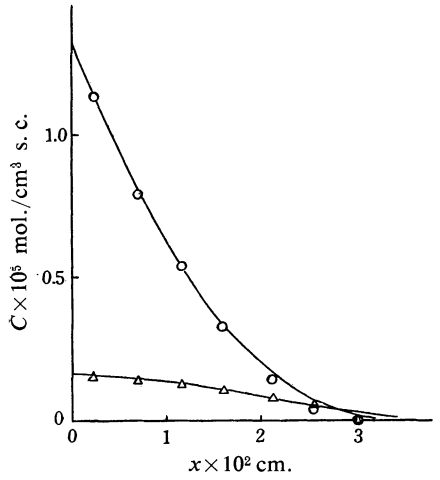


Fig. 5. Dye distributions in mixture dyeing.
○ Benzopurpurine 4B; △ Sky Blue 6B;
—— theoretical curve;
each dye concn. $= 5.0 \times 10^{-5}$ mol./l.; 90°C; 3000 min.; 0.03 mol. NaCl/l.

various times in the dyeing process are shown in Figs. 3 (Benzopurpurine 4B) and 4 (Sky Blue 6B).

The salt effects on mixture dyeing were also examined at 90°C, the results are shown in Table IV. The dye distributions in one of these experiments are shown in Fig. 5, where the solid curves are theoretical curves derived from Eqs. 8 and 9.

The temperature effects on mixture dyeing at a certain sodium chloride concentration (3.0×10^{-2} mol./l.) are shown in Table V.

Discussion

Activation Energy of Diffusion.—The apparent activation energy of the diffusion of Sky Blue 6B, as determined by Boulton and Morton[12], is in the range of 15~19 kcal./mol. for viscose rayon. These values are for a constant dye bath concentration. However, as the diffusion coefficient of a dye is a function of the dye content in a substrate, and since under the conditions of a constant dye bath concentration the surface dye concentration decreases with the increasing temperature, the activation energy of the diffusion should be estimated for a constant dye content, i. e., at a constant surface concentration.

The values we found for Sky Blue 6B, as shown in Table IV, are greater than those of Boulton and Morton[12]. These differences may be attributed to the concentration dependence of the diffusion coefficients. If the values of the activation energy of the diffusion for a constant dye bath concentration (5.0×10^{-5} mol./l.) are calculated, they are 22~25 kcal./mol. for Benzopurpurine 4B and 13~19 kcal./mol. for Sky Blue 6B. The values for Sky

12) J. Boulton and T. H. Morton, quoted by T. Vickerstaff, "The Physical Chemistry of Dyeing", 2nd Ed., Oliver & Boyd, London (1954), p. 268.

Blue 6B are similar to those of Boulton and Morton[12].

Mixture Dyeing.—As is shown in Figs. 3 (Benzopurpurine 4B) and 4 (Sky Blue 6B), the dye distributions in the mixture dyeing are considerably different from that in the single dyeing, and the surface concentration of each dye is maintained constant throughout the whole period of mixture dyeing.

Let us consider the case of Fig. 5. The surface concentration of each dye is smaller in the mixture dyeing than that in the single dyeing, irrespective of the constant dye concentrations in the dye bath. Clearly the diffusion of Sky Blue 6B cannot be described by means of Fick's law, as given in Eq. 1. Owing to the concentration dependence, the (main) diffusion coefficient of each dye should decrease with the decrease in surface concentration. If the main diffusion coefficients are obtained from the experiments of single dyeing and if the cross-term diffusion coefficients are estimated properly, as is mentioned in the theoretical section, the theoretical curves derived from Fqs. 8 and 9 agree well with the dye distributions of the mixture dyeing. The diffusion of Sky Blue 6B was greatly accelerated by the presence of Benzopurpurine 4B, as the value of the cross-term diffusion coefficient of blue dye is plus. In the case of Figs. 3 and 4, too, there are good agreements between the experimental results and the theoretical curves.

The effect of salt and temperature on mixture dyeing is very difficult to study, for the main diffusion coefficients and the surface concentrations vary with the salt concentration and temperature. According to the findings on the salt effect on mixture dyeing at 90°C, in which only the concentration of sodium chloride is varied from 0.01 to 0.04 mol./l., the interaction between two dyes will increase with an increase in the concentration of sodium chloride, for the absolute values of the cross-term diffusion coefficients change more than those of the main diffusion coefficients do. It is considered that the effect of a decrease in temperature is similar to that of an increase in salt concentration.

In mixture dyeing there may be two different interactions between two dyes, one in the dye bath and the other in the substrate. The interaction in the dye bath reduces the surface dye concentration below its normal value, as was studied earlier by Neale and Stringfellow[1] and by Horiki et al.[2,3] The cause of the interaction in the substrate may be that Sky Blue 6B is easy to diffuse, as a large amount of Benzopurpurine 4B adsorbed in the substrate reduces the available surface for the blue dye.

Summary

1. The single and mixture dyeing of Benzopurpurine 4B (C. I. 23500) and Sky Blue 6B (C. I. 24410) were examined kinetically.

2. The diffusion coefficient of each dye decreased with a decrease in the surface concentration. The apparent activation energy of diffusion at a constant surface concentration was evaluated.

3. In mixture dyeing, the dye distributions in the substrate were considerably different from that in the single dyeing, but there was good agreement between the dye distributions experimentally determined and those theoretically calculated in terms of the thermodynamics of irreversible processes.

4. The interaction between two dyes in the substrate increased with an increase in the sodium chloride concentration in the dye bath and with a decrease in the temperature.

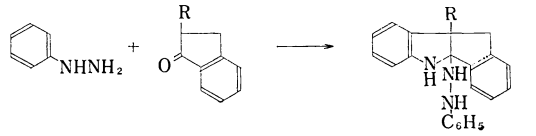
Laboratory of Dyeing Chemistry
Tokyo Institute of Technology
Meguro-ku, Tokyo

*Medium Ring-size Effect in 2′, 3-Polymethylen-3-alkyl-2-phenylindolenines**

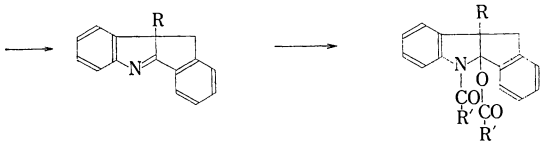
By Masao NAKAZAKI and Minoru MAEDA

(Received September 15, 1961)

The pronounced reactivity of the C=N group of indolenine[1] to add various reagents was first observed when Leuchs and his co-workers[2] heated 2-benzyl-1-indanone (Ia) with excess phenylhydrazine at 130°C to yield a substance, $C_{28}H_{25}N_3$, m. p. 192°C, which, on treatment with hydrochloric acid, lost the phenylhydrazine and formed the hydrochloride (decomp. p. 206~208°C) of the expected indolenine IIIa ($C_{22}H_{17}N$, m. p. 123~124°C). It was soon

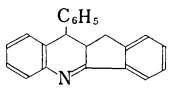


Ia R=$CH_2C_6H_5$ IIa R=$CH_2C_6H_5$
b R=CH_2CH_3 b R=CH_2CH_3

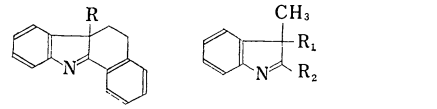


IIIa R=$CH_2C_6H_5$ IV
b R=CH_2CH_3

found that the indolenine IIIa was formed directly without a catalyst and that IIIa then immediately added phenylhydrazine to form the addition compound IIa. The C=N group adds not only amines, ammonia and phenylhydrazine, but also acid anhydrides (acetic, benzoic and phthalic anhydride) to give the indoline derivatives which have the general formula of IV.



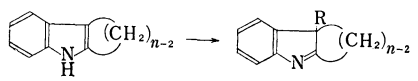
V



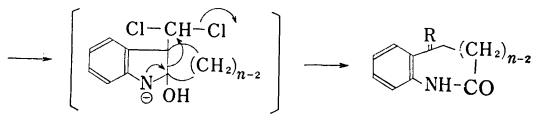
VIa R=$CH_2C_6H_5$ VIIa R_1=CH_3, R_2=C_6H_5
b R=CH_2CH_3 b R_1=$CH_2C_6H_5$, R_2=CH_3

A possibility that the active methylene of the benzyl group might be involved in the ring closure reaction giving the dihydroquinoline V, and that it is V instead of the indolenine IIIa which is responsible for the facile addition reactions, was ruled out by their subsequent findings. It was found that 2-ethyl-1-indanone (Ib) also gave a compound ($C_{17}H_{15}N$, m. p. 79~80°C) which, because of the lack of the active methylene of the benzyl group, should have the indolenine structure of IIIb, but which behaved like an aldehyde[3], e. g., by the addition of amines, ammonia and acid anhydrides as well as of sodium bisulfite.

Their further observation[4] that VIIa and the six-membered analogues of IIIa, b (VIa, b) were incapable of adding phenylhydrazine and sodium bisulfite led them to the conclusion that ring system III, with a five-membered ring fused to the indolenine nucleus, is essential to



VIIIa n=5 IXa n=5, R=$CHCl_2$
b n=6 b n=6, R=$CHCl_2$
c n=5, R=OOH
d n=6, R=OOH



Xa n=5, R=CHCl
b n=6, R=CHCl
c n=5, R=O
d n=6, R=O

* A preliminary communication has appeared in *Chem. & Ind.*, **1960**, 719.

1) For a general discussion of the reactions of indolenines, see P. L. Julian, E. W. Meyer and H. C. Pring, "The Chemistry of Indoles", in R. Elderfield, "Heterocyclic Compounds", Vol. 3, John Wiley and Sons, Inc., New York (1952), p. 108.
Unfortunately, the formula which appear on pp. 108—110 of their article are incorrect as a result of mistaking β-benzyl-α-hydrindone as 1-benzyl-2-indanone.

2) a) H. Leuchs, J. Wutke and E. Giesler, *Ber.*, **46**, 2200 (1913); b) H. Leuchs and K. Winzer, ibid., **58**, 1520 (1925); c) H. Leuchs, C. D. Philpot, P. Sauder, A. Heller and K. Köhler, *Ann*, **461**, 27 (1928).

3) Facile addition reactions to the C=N bond in the indolenines without a fused ring have been noticed. G. Plancher, *Ber.*, **31**, 1488 (1898); G. Plancher and D. Bettinelli, *Gazz. chim. ital.*, **29**, I, 106 (1899).

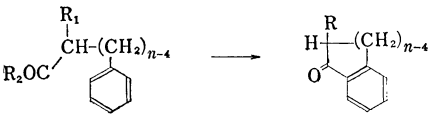
4) H. Leuchs, A. Heller and A. Hoffmann, *Ber.*, **62**, 871 (1932).

smooth addition reactions. The same sort of ring-size effect on the reactions of indolenines was encountered in our study[5] of "Plancher's base"[6] (Xa) and of the mechanism of its formation from pentindole (VIIIa) with alkali and chloroform.

Whereas tetrahydrocarbazole (VIIIb) affords stable 11-dichloromethyltetrahydrocarbazolenine (IXb), which can be converted into the lactam Xb only by prolonged reflux in the presence of alkali[7], the lactam Xa ("Plancher's base) is a sole product isolated from the reaction mixture of pentindole (VIIIa) with alkali and chloroform, presumably because of the enhanced reactivity of the C=N group in the intermediate IXa, which has a five-membered ring fused to the indolenine nucleus. It is not surprising, therefore, to find that the hydroperoxide, IXd, is stable enough to be isolated as such, but that the hydroperoxide IXc, from pentindole, is directly rearranged to the lactam Xc[8], suggesting a close relationship between the reactivity of indolenine and the size of the ring fused with it.

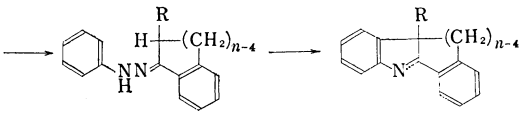
This paper will report on the preparation of 2′,3-polymethylen-3-alkyl-2-phenylindolenines (XIV) and on the observations of the changes of their properties as the ring members are varied from 5 to 6, 7 and 8, compared with those of 3,3-dimethyl-2-phenylindolenine (VIIa)[9] and 2,3-dimethyl-3-benzylindolenine (VIIb)[10].

The indolenines (XIV)[11,12] were prepared by Fischer-Brunner's method from 4-alkyl-1,2-benzocycl-1-en-3-one (XII); of these the seven-membered ketone (XIIa) (b. p. 153~160°C/28 mmHg; semicarbazone, m. p. 197~198°C) and



XIa $n=7$, $R_1=CH_3$
b $n=8$, $R_1=CH_3$

XIIa $n=7$, $R=CH_3$
b $n=8$, $R=CH_3$
c $n=6$, $R=CH_3$
d $n=5$, $R=CH_2CH_3$



XIII

XIVa $n=5$, $R=C_2H_5$
b $n=6$, $R=CH_3$
c $n=7$, $R=CH_3$
d $n=8$, $R=CH_3$

the eight-membered ketone (XIIb) (b. p. 109~111°C/1 mmHg; 2,4-dinitrophenylhydrazone, m. p. 170~171°C) were prepared from the corresponding acids (XIa, b) by polyphosphoric acid cyclization[13] (61%) and high dilution

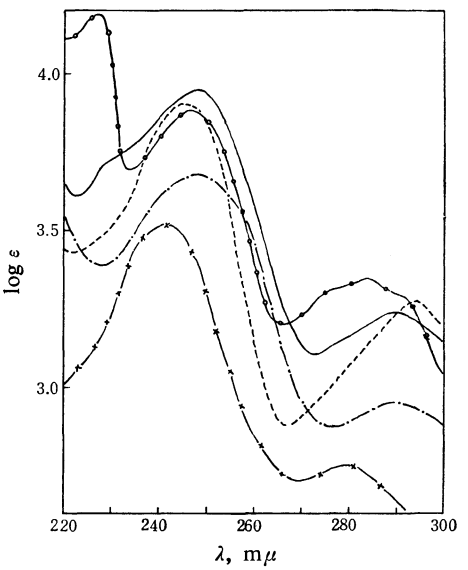
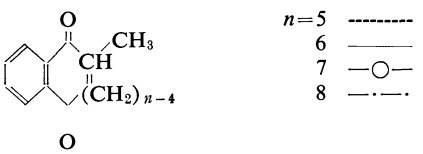


Fig. 1



5) M. Nakazaki, *J. Chem. Soc. Japan, Pure Chem. Sec.* (*Nippon Kagaku Zassi*), **76**, 1169 (1955).

6) G. Plancher, B. Cecchetti and E. Ghigi, *Gazz. chim. ital.*, **59**, 340 (1929).

7) M. F. Bartlett, D. F. Dickel and W. I. Taylor, *J. Am. Chem. Soc.*, **80**, 126 (1958).

8) B. Witkop, J. B. Patrick and M. Rosenblum, ibid., **73**, 2641 (1951).

9) H. M. Kissman, D. W. Farnsworth and B. Witkop, ibid., **74**, 3948 (1952); M. Nakazaki, K. Yamamoto and K. Yamagami, This Bulletin, **33**, 471 (1960). According to a recent publication (F. J. Evans and R. E. Lyle, *Chem. & Ind.*, **1960**, 597.), 3,3-dimethyl-2-phenylindolenine prepared by the polyphosphoric acid method is contaminated by isomeric 2,3-dimethyl-3-phenylindolenine.
The indolenine VIIa used here was regenerated from the purified picrate, m. p. 170~171°C, recrystallized from ethanol.

10) T. Hoshino, *Ann.*, **500**, 35 (1932); M. Nakazaki, S. Isoe and K. Tanno, *J. Chem. Soc. Japan, Pure Chem. Sec.* (*Nippon Kagaku Zassi*), **76**, 1263 (1955).

11) See footnote 2 c). Several attempts to prepare XIV, $n=5$, $R=CH_3$ failed.

12) M. Nakazaki, K. Yamamoto and K. Yamagami, (This Bulletin, **33**, 471 (1960)) reported 6a-methyl-5,6-dihydro-6a-benzo(a)carbazole (XIVb) as an oil, b. p. 160~164°C/2 mmHg; picrate, m. p. 169~170°C, but XIVb crystallized on prolonged standing in a refrigerator. The specimen used in the present work was recrystallized from diluted ethanol and melted at 98~98.5°C.

13) R. Gilman, Jr., and W. J. Horton, *J. Am. Chem. Soc.*, **73**, 1411 (1951).

TABLE I

Indolenine	M. p. or b. p., °C	M. p. of picrate, °C	UV spectra λ_{max}, mμ (log ε)		pK_a'	$-E_{1/2}$(S.C.E.) pH 2.20	$-E_{1/2}$(S.C.E.) pH 4.95	IR spectra μ
XIVa	150~155/1 mmHg	165~167	240(3.96)	304(3.67)	—	—	0.88	6.35
XVIIa	156~159/1 mmHg	154~155	227(4.11)	308(4.18)	2.2	0.88	1.17	
XIVb	98~98.5	167~168	235(4.16)	309(4.18)	2.6	0.92	1.13	6.44
XIVc	105~106	183~184	226(4.22)	290(4.16)	2.1	1.01	1.11	6.48
XIVd	145~147	119~120		266(3.97)	1.8	>1.1	1.28	6.48
VIIb	48~49	141~142		260(3.72)	—	>1.1	>1.3	6.37

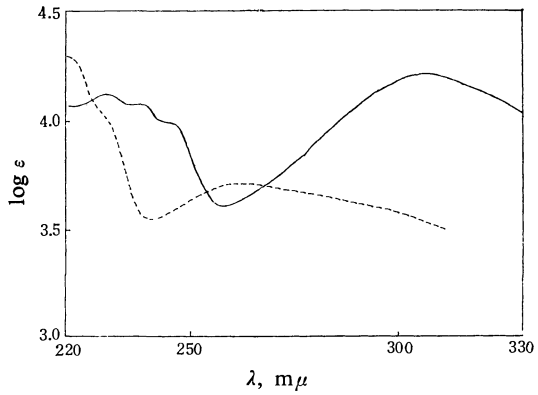
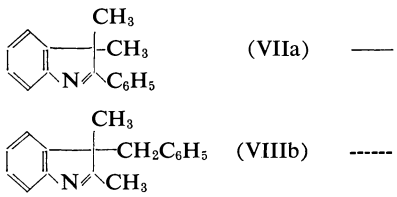


Fig. 2



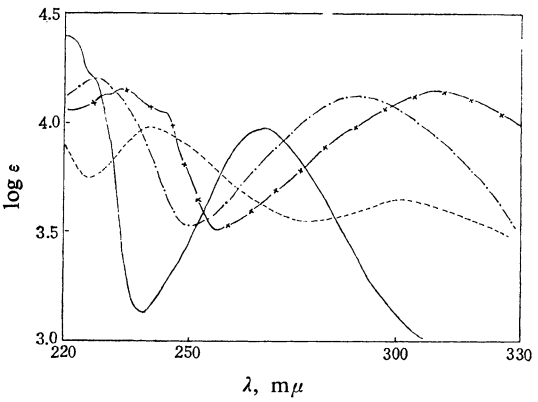
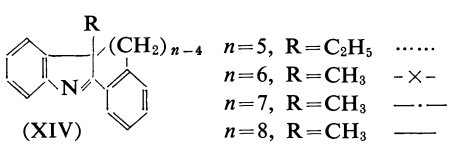


Fig. 3



Friedel-Crafts cyclization (62%) respectively[14].

The ultraviolet absorption spectra of the ketone XIIa, b, c, d[15] and isobutyrophenone are shown in Fig. 1.

In Table I the properties of these indolenines are summarised, together with those of VIIa and VIIb.

Ultraviolet Absorption Spectra[16] (See Table I, Figs. 2 and 3).—The six-membered indolenine XIVb exhibits almost the same ultraviolet spectrum as the indolenine VIIa, which has a phenyl group capable of conjugating with the indolenine system by free rotation. Moreover, the coincidence of the fine structures of their absorption pattern at a shorter wavelength is remarkable. However, a different situation arises in the seven- and eight-membered indolenines (XIVa, b), in which the polymethylene bridge pushs the ortho position of the phenyl group aside so as to force the benzene ring to pivot around out of the plane of the indolenine conjugate system, thus decreasing the effective conjugation between the indolenine system and the benzene ring. An inspection of the molecular model of the eight-membered indolenine (Fig. 4) reveals



Fig. 4

14) R. Huisgen, W. Rapp, I. Ugi and H. Walz, *Ann.*, **586**, 52 (1952). Their yield for the eight-membered ketone (XIIb, without a methyl group) was 70% by the high dilution Friedel-Crafts cyclization technique. For a general discussion of the synthetic methods of large ring compounds, see K. Ziegler's excellent article in Houben-Weyl, "Methoden der organischen Chemie", Ed. by E. Muller, Band IV, Teil 2, George-Thiem Verlag, Stuttgart (1955), p. 930.

15) The ultraviolet spectra of 1,2-benzocycl-1-en-3-one (XII) without methyl substitution have been thoroughly discussed. R. Huisgen, W. Rapp, I. Ugi, H. Walz and E. Mergenthaler, *Ann.*, **586**, 1 (1954).

16) Their infrared absorption spectra (C=N streching band) are summarized in Table I, but no conspicuous regular change in absorption maximum with the ring size can be found.

17) Free from Baeyer strain. The conformational relationships among the four methylene groups, 1—2 is semieclipsed, while 2—3 and 3—4 are skew.

that, to achieve the most favorable conformation[17], the benzene ring must be brought almost perpendicular to the indolenine ring, which explains the fact that eight-membered indolenine XIVd shows marked hypsochromic shifts of the absorption bands associated with its diminished extinction coefficients. Although its ultraviolet absorption maximum and ultraviolet absorption minimum become quite close to those of VIIb, which has no phenyl group at the C_2 position, the higher extinction coefficient of XIVd seems to show that complete steric inhibition of the mesomerism is not attainable, even in the eight-membered indolenine. The parallel observation of the medium ring-size effect on ultraviolet spectra in the indole series XV was reported by Huisgen and Ugi[18].

It is of interest also to note the extraordinarily low extinction coefficient of the absorption (in both the 240 mμ and 300 mμ regions) of the five-membered indolenines XIVa, whose positions of absorption bands are not shifted much from that of the six-membered indolenine XIVb. Although its detailed theoretical interpretation presents considerable difficulties[19,20], there is no doubt that the Baeyer strain imposed upon the five-membered ring (normal bond angle: 108°) with three sp^2 carbon atoms (normal bond angle: 120°) deforms the conjugated system of the indolenine to a great extent, thus causing the pattern of the absorption band to deviate considerably from that of the indolenines, which do not suffer Baeyer strain[21].

Dissociation Constant[22].—As can be seen from Table I, the p*Ka*′ values of the indolenines XIV are also effected by the size of the ring fused to the indolenine nucleus.

Table I summarizes the values of p*Ka*′ of the conjugated acids of the indolenines determined spectrophotometrically[23], while Fig. 5 reproduces typical spectra of the seven-membered indolenine at different pH values which show clearly marked isosbestic points. If the

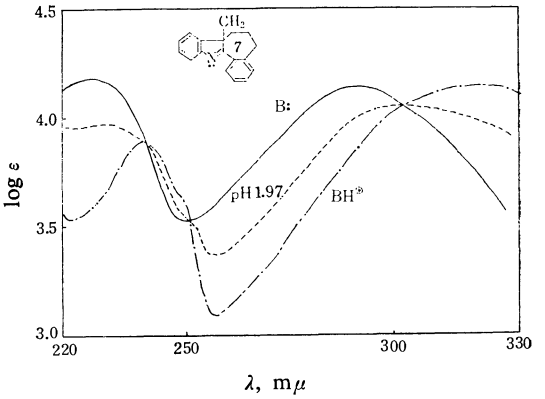


Fig. 5

phenyl group is allowed to be coplanar with the indolenine conjugation system, the +M effect of the phenyl group will be such as to increase the electron density at the nitrogen atom (XVI), i. e., to increase the basic strength of the indolenine. From the evidence previously adduced from the spectroscopic data (vide supra), there can be expected a considerable steric inhibition of the mesomerism and, hence, a decrease in the basic strength of the eight-membered indolenine XIVd; Table I shows this to be the case.

Polarographic Half-wave Potential.—If the polarographic electrode process[24] of indolenine

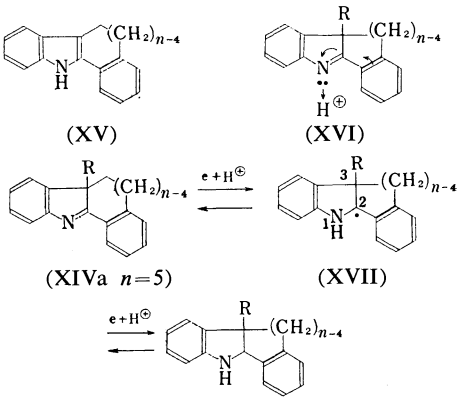


Fig. 6

18) R. Huisgen and I. Ugi, *Ann.*, **610**, 57 (1957).

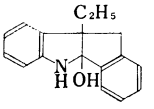
19) For the medium ring-size effect in 1,2-benzocycl-1-en-3-one and related compounds, see Huisgen's excellent review. R. Huisgen, *Angew. Chem.*, **69**, 341 (1957).

20) Ultraviolet absorption in relation to steric conformation about a single bond in a conjugated system is fully discussed in W. Klyne, "Progress in Stereochemistry", Vol. 1, Butterworths Pub. Ltd., London (1954), p. 136 and Vol. 2, (1958), p. 99. Numerous papers presented in G. W. Gray, "Steric Effects in Conjugated Systems", Butterworths Pub. Ltd., London (1958) are also worth consulting.

21) This Baeyer strain is reflected much more clearly in the polarographic study and will be discussed more thoroughly there.

22) H. C. Brown, D. H. McDaniel and O. Häfliger, "Dissociation Constants", in E. A. Braude and F. C. Nachod, "Determination of Organic Structures by Physical Methods", Academic Press, Inc., New York (1955), p. 567, and the literature cited in footnotes 19) and 20).

23) Attempts to measure the dissociation constant of XIVa were fruitless because its ultraviolet absorption spectra at various pH values did not show any clear isosbestic points, probably owing to the irreversible formation of (i) by the addition of water.



(i)

24) J. M. Kolthoff and J. K. Kingane, "Polarography", Vol. 1, Interscience Pub. Inc., New York (1952), p. 685; P. Pasternak, *Helv. Chim. Acta*, **31**, 753 (1948).

can be expressed as in Fig. 6, the stability of the intermediate free radical XVII may be expected to influence the half-wave potential.

When the π-orbital of the sp^2 center of XVII at C_2 can overlap effectively with the π-orbital of the phenyl group at C_2, the intermediate XVII will be stabilized and the half-wave potential will shift to positive. The high value of $-E_{1/2}$ of the eight-membered indolenine is clearly to be ascribed to the non-co-planarity of the iodolenine system and the phenyl group at the C_2 carbon atom.

The remarkable susceptibility of five-membered indolenine XIVa to polarographic reduction[25] is remarkable, conceivably because of the Baeyer strain being relieved in a five-membered ring with three sp^2 carbon atoms fused to a five-membered indolenine ring.

Experimental[26]

Diethyl Benzylethylmalonate.—To a stirred suspension of 4.6 g. of sodium powder (pulverized under boiling xylene and decanted from it) in 30 cc. of benzene was added slowly 23 cc. of absolute ethanol. After the sodium had been completely converted into sodium ethoxide, 35.4 g. of diethyl benzylmalonate was added over a 10 min. period. This mixture was refluxed while being stirred for 10 min.; then 46.5 g. of ethyl iodide was added over a period of 25 min. The temperature of the mixture was kept at 60~70°C for 5.5 hr. and then at 70~80°C for 7.5 hr. The solvent was then removed on a water bath, and water was added to dissolve the precipitated salt. The reaction mixture was extracted with ether. After the ether extract had been washed with water and dried over anhydrous sodium sulfate, the solvent was removed to yield an oil, b. p. 143~147°C/3 mmHg, 33.4 g. (85% yield) (literature[27]; b. p. 184°C/18 mmHg).

1-Benzyl-*n*-butyric Acid (XI) ($n=5$, $R_1=C_2H_5$, $R_2=OH$).—A mixture of 32.6 g. of diethyl benzylethylmalonate and 100 cc. of 45% aqueous potassium hydroxide was refluxed for 2 hr. (the mixture became homogenous after 20 min.) The aqueous solution was made acidic with dilute hydrochloric acid and extracted continuously with ether for 6 hr. Removal of the solvent gave a residue which was decarboxylated by heating at 180°C for 1 hr.; the residual oil was distilled to give 20.0 g. of a viscous oil (96% yield), b. p. 127~140°C/3 mmHg (literature[28]; b. p. 172~174°C/13 mmHg).

1-Benzyl-*n*-butyroyl Chloride (XI) ($n=5$, $R_1=C_2H_5$, $R_2=Cl$).—After a mixture of 19 g. of 1-benzyl-*n*-butyric acid and 17.8 g. of thionyl chloride had been heated on a water bath, the excess thionyl chloride was removed in a vacuum. Distillation of the residue afforded an oil, b. p. 124~131°C/15 mmHg, 20 g. (96% yield) (literature[27]; b. p. 128~131°C/15 mmHg). The anilide prepared from it was recrystallized from diluted ethanol, m. p. 86~87°C (literature[28]; m. p. 88~89°C).

2-Ethyl-1-indanone (XIId).—To a stirred mixture of 18.8 g. of powdered aluminum chloride and 50 cc. of carbon disulfide was added a solution of 1-benzyl-*n*-butyroyl chloride in 50 cc. of carbon disulfide over a period of 15 min. After being refluxed for 50 min., the reaction mixture was decomposed with ice and water. The usual working up gave an liquid with a pleasant smell, b. p. 130~136°C/13 mmHg, 14.8 g. (91% yield) (literature[29]; b. p. 143~144°C/22 mmHg). The semicarbazone was recrystallized from ethanol, m.p. 201.5~202.5°C (literature[29]; m.p. 202°C).

8b-Ethyl-2, 3-benzo-1, 2, 3, 4-tetrahydrocyclopent-(b)*pseudo*indole (XIVa)[30].—After a mixture of 2.0 g. of the indanone XIId, 1.4 g. of phenylhydrazine and 0.5 g. of sodium acetate was heated on a water bath for 2 hr., a solution of 12.5 g. of zinc chloride in 10 cc. of ethanol was added; this reaction mixture was kept at 150~155°C for 4 hr. Then 1 N hydrochloric acid was added to precipitate a complex salt which was collected and washed with 1 N hydrochloric acid and then with ether. Aqueous ammonia was added to the suspension of the complex salt on ether to liberate the indolenine XIVa, which was extracted with ether. After being washed with water and dried over anhydrous sodium sulfate, the solvent was evaporated to give a residual oil which distilled at 156°C/1 mmHg and which weighed 1.9 g. The crude indolenine was directly converted into the picrate and was recrystallized from ethanol to give yellow crystals, m. p. 164~165°C which were suspended on ether and decomposed with 0.5 N sodium hydroxide to regenerate the indolenine XIVa, b. p. 150~155°C/1 mmHg[31].

Found: C, 87.35; H, 6.61; N, 6.01. Calcd. for $C_{17}H_{15}N$: C, 87.51; H, 6.48; N, 6.00%.

The picrate was recrystallized from ethanol, m.p. 166~167°C.

Found: C, 59.49; H, 3.84; N, 12.33. Calcd. for $C_{23}H_{18}O_7N_4$: C, 59.74; H, 3.92; N, 12.12%.

Diethyl 3-Phenylpropylmalonate.—After 6 g. of sodium had been pulverized by vigorous stirring under 60 cc. of boiling toluene, the toluene was removed by decantation and was replaced by 50 cc. of benzene. Then 27 cc. of absolute ethanol was carefully added in order to convert the sodium powder into sodium ethoxide, and 63 cc. of freshly distilled diethyl malonate was added over a 45 min. period. To the refluxing reaction mixture was added a solution of 35 g. of 3-phenylpropyl bromide[32] in

25) On the medium ring-size effect of 1, 2-benzocyclo-1-en-3-one and related compounds on its half-wave potential, see the literature cited in footnote 15) and also H. Adkins, R. M. Elofson, A. G. Rossow and C. C. Robinson, *J. Am. Chem. Soc.*, **71**, 2622 (1949).

26) All ultraviolet spectra were measured in ethanol with an EP-2 Hitachi pen-recording spectrophotometer. The analyses were performed in the Microanalytical Laboratory of the Department of Chemistry, Osaka City University.

27) E. Mohr, *J. prakt. Chem.*, (2), **71**, 330 (1905).

28) B. Anschütz and W. Berns, *Ann.*, **261**, 307 (1891).

29) E. A. Speight, A. Stevenson and J. F. Thorpe, *J. Chem. Soc.*, **125**, 2191 (1924).

30) According to the nomenclature of A. M. Patterson and L. T. Capell, "The Ring Index", Reinhold Pub. Corp., New York (1940).

31) Leuchs and his coworkers (cf. footnote 2 c)) reported this indolenine as a crystal, m.p. 79~80°C, b.p. 202~204°C/14 mmHg, but our attempts to crystallize failed.

32) Prepared from 3-phenylpropanol according to the procedure of O. Kamm and C. S. Marvel, "Organic Syntheses", Coll. Vol. I, 25 (1948). B. p. 128~134°C/30 mmHg (86% yield).

50 cc. of benzene; the refluxing was then continued for 7 hr. on a water bath. After water was added, the reaction mixture was made acidic with dilute hydrochloric acid, and the benzene layer was separated. The aqueous solution was extracted with ether, and the ether extract was combined with benzene extract. After the mixture had been washed with water and dried over anhydrous sodium sulfate, the solvent was removed to give an oil which distilled at 143~149°C/1 mmHg and which weighed 44.7 g. (91.4% yield) (literature[33]; b. p. 189~194°C/13 mmHg).

Diethyl Methyl-3-phenylpropylmalonate.—To a sodium ethoxide solution prepared from 5.3 g. of sodium and 80 cc. of ethanol was added 44.4 g. of diethyl 3-phenylpropylmalonate. Into the stirred, refluxing solution, 39.2 g. of methyl iodide was add and then, after 2 hr. 10 g. of methyl iodide was added to make the solution neutral to wet litmus paper.

After the solvent had been removed, water was added and the mixture was extracted with ether. After the ether extract had been washed with water and dried over anhydrous magnesium sulfate, the ether was removed and the residual oil was distilled. The malonate distilled at 140~145°C/1 mmHg, and weighed 40.6 g. (87% yield) (literature[34]; b. p. 194°C/13 mmHg).

1-(3-Phenylpropyl)propionic Acid (XIa) (R_2=OH).—A mixture of 39.9 g. of diethyl methyl-3-phenylpropylmalonate, 90 g. of potassium hydroxide and 110 cc. of water was refluxed for 2~3 hr. The reaction mixture was then chilled in an ice bath and was made acidic with concentrated hydrochloric acid to precipitate crystals (methyl-3-phenylpropylmalonic acid), which were collected and washed with water. The malonic acid was decomposed by heating at 180°C and was distilled to give the acid XIa, b. p. 141~143°C/1 mmHg, 23.1 g. (88% yield) (literature[35]; b. p. 190°C/12 mmHg).

Found: C, 74.77; H, 8.89. Calcd. for $C_{12}H_{16}O$: C, 74.87; H, 8.39%.

The anilide was recrystallized from aqueous ethanol, m. p. 78.5~79.5°C.

Found: C, 80.85; H, 8.03; N, 5.45. Calcd. for $C_{18}H_{21}ON$: C, 80.86; H, 7.92; N, 5.24%.

4-Methyl-1,2-benzocyclohept-1-en-3-one (XIIa).—To stirred polyphosphoric acid prepared from 60.5 g. of phosphorus pentoxide and 38.7 g. of concentrated phosphoric acid was added 10 g. of the acid XIa; the reaction mixture was then heated at 100°C for 2 hr. The temperature of the mixture was raised to 160°C over a 1-hour period, and the reaction mixture was decomposed with water and extracted with ether. The ether extract was washed with 2 N sodium hydroxide and water, then dried over anhydrous sodium sulfate. Removal of the solvent gave a residual oil which distilled at 153~160°C/28 mmHg and which weighed 5.5 g. (61% yield). From alkaline washing, 1 g. of the acid XIa was recovered.

Found: C, 84.36; H, 8.14. Calcd. for $C_{12}H_{14}O$: C, 82.72; H, 8.10%.

The semicarbazone was recrystallized from aqueous ethanol, m. p. 197~198°C.

Found: C, 69.19; H, 7.51. Calcd. for $C_{13}H_{17}ON_3$: C, 67.50; H, 7.41%.

10a-Methyl-6,7-benzo-5,6,7,8,9,10-hexahydrocyclohept(b)*pseudo*indole (XIVc)[30]. — A mixture of 2 g. of the ketone XIIa and 1.3 g. of phenylhydrazine was heated on a water bath for 1.5 hr., the generated water was then removed by azeotropic distillation with benzene. After removal of the benzene, the residue was dissolved in 20 cc. of absolute ethanol and the solution was saturated with dry hydrogen chloride gas while being chilled in an ice-salt cooling bath. After being allowed to stand at room temperature for 5 hr., the solution was diluted with water and washed with ether to remove any neutral substance. The ether washing was extracted with dilute hydrochloric acid, and the acidic aqueous extracts were combined. The combined aqueous solution was then made basic with 2 N sodium hydroxide to precipitate the indolenine XIVc, which was extracted with ether. Removal of the solvent afforded a viscous oil which was purified via picrate. The picrate (2.1 g.) melted at 182~183°C after being recrystallized from ethanol and was decomposed with 0.5 N sodium hydroxide, then extracted with ether. The pale yellow ether extract was washed three times with 0.5 N sodium hydroxide until the ether layer became colorless; it was then washed with water and dried over anhydrous sodium sulfate. The solvent was removed to give a residue which was recrystallized from aqueous ethanol, m. p. 105~106°C.

Found: C, 87.56; H, 6.92; N, 5.91. Calcd. for $C_{18}H_{17}N$: C, 87.41; H, 6.93; N, 5.66%.

The picrate was recrystallized from ethanol to give yellow needles, m. p. 182~183°C.

Found: C, 60.61; H, 4.29; N, 11.58. Calcd. for $C_{24}H_{20}O_7N_4$: C, 60.50; H, 4.23; N, 11.76%.

4-Phenyl-*n*-butanol.—A mixture of 56 g. of ethyl 3-phenyl butyrate[36] and 7 g. of copper chromite catalyst was hydrogenated in a 500 cc. steel bomb at 98 atm. of hydrogen and at 256°C for 2 hr. After being separated from the catalyst, the alcohol was distilled to give a viscous oil, b. p. 145~151°C/26 mmHg, 33.5 g. (76.6% yield) (literature[37]; b. p. 137°C/14 mmHg).

4-Phenylbutyl Bromide.—This bromide was prepared from 4-phenyl-*n*-butanol following Kamm and Marvel's procedure[32], b. p. 142~148°C/24 mmHg (literature[38]; b. p. 132°C/12 mmHg).

Diethyl 4-Phenylbutylmalonate.—This was prepared from 4-phenylbutyl bromide following the procedure described in the preparation of diethyl 3-phenylpropylmalonate, b. p. 148~155°C/1 mmHg (91% yield) (literature[33]; b. p. 215~218°C/11 mmHg)

Diethyl Methyl-4-phenylbutylmalonate.—This was prepared from diethyl 4-phenylbutylmalonate by alkylation with methyl iodide following the procedure described in the preparation of diethyl

33) J. v. Braun and O. Kruber, *Ber.*, **45**, 386 (1912).
34) J. v. Braun and G. Kirschbaum, ibid., **45**, 1257 (1912).
35) J. v. Braun, H. Deutsch and A. Schmatloch, ibid., **45**, 1257 (1912).
36) B. p. 144~149°C/18 mmHg. Prepared from 3-phenylpropyl bromide by malonic ester synthesis.
37) H. Adkins, B. Wojcik and L. W. Covert, *J. Am. Chem. Soc.*, **55**, 1669 (1933).
38) P. W. Clutterbuck and J. B. Cohen, *J. Chem. Soc.*, **123**, 2510 (1923).

methyl-3-phenylpropylmalonate. The yield was 87.3%, and the malonate distilled at 155~160°C/1 mmHg.

Methyl-4-phenylbutylmalonic Acid.—Diethyl methyl-4-phenylbutylmalonate was hydrolyzed with 45% potassium hydroxide to give the malonic acid, which melted at 109~110°C after recrystallization from aqueous ethanol.

Found: C, 67.69; H, 7.50. Calcd. for $C_{14}H_{18}O_4$: C, 67.18; H, 7.25%.

1-(4-Phenylbutyl)propionic Acid. (XIb) (R_2=OH).—Methyl-4-phenylbutylmalonic acid was decomposed by heating at 180°C, and the propionic acid XIb was distilled, b. p. 138~149°C/1 mmHg (75.6% yield).

Found: C, 75.86; H, 9.15. Calcd. for $C_{13}H_{18}O_2$: C, 75.69; H, 8.80%.

The anilide was recrystallized from aqueous ethanol, m. p. 118~119°C.

Found: C, 80.89; H, 8.73; N, 5.09. Calcd. for $C_{19}H_{23}ON$: C, 81.10; H, 8.24; N, 4.98%.

1-(4-Phenylbutyl)propionyl Chloride (XIb) (R_2=Cl).—A mixture of 21.3 g. of the acid XIb and 17.8 g. of thionyl chloride was heated on a water bath for 1 hr., and the excess thionyl chloride was distilled off. The residual oil distilled at 161~167°C/15 mmHg, and weighed 23.2 g.

4-Methyl-1,2-benzocyclooct-1-en-3-one (XIIb).—The simplified Ziegler's high dilution apparatus[39] consists of a 3-l. three-necked round-bottomed flask equipped with a Vibro-Mischer and an efficient Dimroth condenser. The acid chloride solution is introduced at the middle point of the arm which connects the flask and the condenser, so the solution is immediately diluted and is carried down into the reaction flask by the solvent running down from the condenser. In the flask was placed 900 cc. of carbon disulfide; a small amount of the solvent was distilled off through the condenser in order to dry the apparatus while the cooling water was temporarily cut off. Then 37 g. of powdered aluminum chloride was introduced, and the mixture was refluxed on a water bath while being vigorously stirred. To the mixture was added a solution of 23.2 g. of the acid chloride XIb (R_2=Cl) in 750 cc. of carbon disulfide over a period of 76.5 hr., during which time 11 g. of powdered aluminum chloride was added at the 24th, 34th, 49th, 64th and 74th hr. from the starting point of the reaction. After 1.2 l. of the solvent had been removed, the reaction complex was decomposed with ice, water and concentrated hydrochloric acid. After being saturated with sodium chloride, the mixture was extracted with ether. A dark colored solid which appeared between the aqueous layer and ether layer was collected and treated separately.

After the ether extract had been washed and dried over anhydrous sodium sulfate, the solvent was removed to give a residual oil which distilled at 105~110°C/1 mmHg and which weighed 6.0 g. The collected dark colored solid was continuously extracted with benzene for 6 hr., and the benzene extract was washed with water and dried over anhydrous sodium sulfate. After removal of the solvent, the extract gave 6.1 g. of an oil which distilled at 109~111°C/1 mmHg and which raised the total yield to 62.3%. On one more distillation, 9.8 g. of the crude ketone gave 8.6 g. of purified ketone, which boiled at 104~112°C/1 mmHg.

Found: C, 82.91; H, 8.74. Calcd. for $C_{13}H_{16}O$: C, 82.93; H, 8.57%.

The 2,4-dinitrophenylhydrazone was recrystallized from ethanol, m. p. 170~171°C.

Found: C, 61.68; H, 5.27; N, 14.95. Calcd. for $C_{19}H_{20}O_4N_4$: C, 61.94; H, 5.47; N, 15.21%.

11a-Methyl-6,7-benzo-5,6,7,8,9,10-hexahydrocyclooct(b)*pseudo*indole (XIVd)[30].—A mixture of 2.0 g. of the ketone XIIb and 1.2 g. of phenylhydrazine was heated on a water bath, and the generated water was removed by azeotropic distillation with benzene. After removal of the benzene, the residue was dissolved in 19 cc. of absolute ethanol, and the chilled solution was saturated with dry hydrogen chloride gas. After the solvent had been evaporated in a vacuum, the reaction mixture was diluted with water and washed with ether. The aqueous layer was made basic with a concentrated ammonia solution, and the basic fraction liberated was extracted with ether. Removal of the solvent afforded a solid which crystallized upon cooling and trituration. Recrystallization from aqueous ethanol yielded crystals, m. p. 145.5~146.5°C.

Found: C, 87.15; H, 7.40; N, 5.41. Calcd. for $C_{19}H_{19}N$: C, 87.31; H, 7.33; N, 5.36%.

The picrate was recrystallized from ethanol to give yellow crystals which deteriorated on heating at 100°C and were found to have 1 mol. of ethanol of crystallization.

Found: C, 60.19; H, 5.38; N, 10.46. Calcd. for $C_{25}H_{22}O_7N_4 \cdot C_2H_5OH$: C, 60.44; H, 5.26; N, 10.44%.

After being heated at 65°C and 3 mmHg for 12 hr., the picrate melted at 119~120°C.

Found: N, 11.56. Calcd. for $C_{25}H_{22}O_7N_4$: N, 11.42%.

Polarographic Measurement.—The apparatus used for the measurement of the polarographic half-wave potential was a Yanagimoto pen-recording polarograph model P-B 4, while the pH values were measured on a Beckman pH meter model G.

The supporting electrolyte and buffer solution were that used by Huisgen and his co-workers[15]: 50% isopropanol containing potassium chloride (0.1 M), phosphoric acid (0.05 M) and acetic acid (0.05 M), the pH value was adjusted by the addition of 6 N ammonia in 50% isopropanol. The indolenine solution (ca. 10^{-4} M) was mixed with a gelatin solution, incuvated in a thermostat (26°C), and swept by a stream of nitrogen to replace the oxygen, which process took 30~90 min.

The authors are very grateful to Dr. Ken-ichi Takeda and Dr. Masakazu Inaba, The Shionogi Research Laboratory, Shionogi & Co., Ltd., for making it possible for them to use their polarograph. They are also indebted to Mr. Eiichi Togashi, Shiono Koryo Kaisha,

39) K. Ziegler, H. Eberle and H. Ohlinger, *Ann.*, **504**, 123 (1933). See also the literature cited in footnote 14) for a more simplified apparatus.

40) Laboratoriums-Vibro-Mischer, Model El, AG. für Chemie-Apparatebau, Zürich.

for his generous gift of phenethyl alcohol and cinnamic acid, and to the Nitto Kasei Co. for its financial support. This work was partially supported by a grant-in-aid for Fundamental Scientific Research from the Ministry of Education, to which the author's thanks are due.

Department of Chemistry
Osaka City University
Kita-ku, Osaka

Absolute Configuration of (+)-Occidol

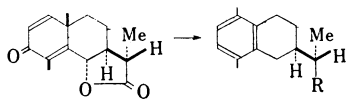
By Masao NAKAZAKI

(Received March 30, 1962)

(+)-Occidol (I), a new sesquiterpene alcohol, m. p. 69~70°C, $[\alpha]_D$ +163.7° (in chlorofom) isolated as a minor constituent from the neutral fraction of the essential oil of *Thuja occidentalis* L. was shown to have the structure I by degradative works[1] and by the comparison of its infrared spectrum with a synthetic racemic compound[2].

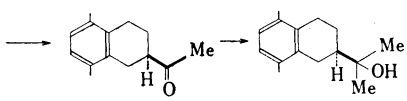
Because this compound has an unusual structure feature, which is apparently derived from eudesmane sesquiterpene precursor by the dienol-benzene rearrangement or similar mechanism[3], determination of the absolute configuration of this alcohol is interesting from a biogenetic point of view.

This paper is concerned with the correlation of C_7 absolute configuration with (−)-santonin (II)[4].



II

III R=CO_2H
IV R=COCl
V R=COMe
VI R=OAc
VII R=OH



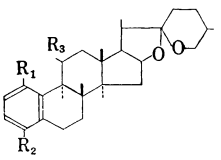
VIII I

Hyposantonous acid (III), prepared from (−)-santonin (II) via the oxime and hyposantonin, was converted by thionyl chloride into acid chloride IV, which afforded the ketone V with dimethycadmium. Baeyer-Villiger oxidation of V with perbenzoic acid in chloroform gave the acetate VI, which was separated from the unchanged ketone V using Girard P reagent. The crude acetate VI was hydrolyzed directly with methanolic potassium hydroxide to alcohol VII. Chromatography on Florisil gave a viscous oil, b. p. 140~180°C/0.5 mmHg. The alcohol VII was oxidized with chromic anhydride-pyridine complex to ketone VIII. Grignard reaction of ketone VIII with methylmagnesium iodide afforded a tertiary alcohol which was purified by chromatography on Florisil. Recrystallization from petroleum ether gave crystals, m. p. 69~70°C, $[\alpha]_D$ +76.7° (in chloroform), the identity of which with (+)-occidol[5] was established by the mixed melting point determination and comparison of infrared spectra in chloroform.

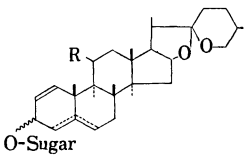
These findings show that (+)-occidol has the *R* configuration at C_7, typical of the natural eudesmane type sesquiterpenes and this fact suggests the close relationship of (+)-occidol with eudesmane type compounds[4]. In the steroid field, compounds which have an aromatic A ring are common, especially among female hormones, where the biological passway involving the splitting of the angular methyl group at C_{10}, has been worked out thoroughly.

However, there had not been reported a steroid with an aromatic ring containing the methyl group originally attached to C_{10}. Recently the sapogenins, meteogenine and luvigenin, isolated from *Metanarthecium luteo-virid* Maxim. were shown to have the structures IX and X, respectively[6], and as possible

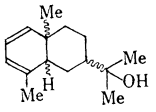
1) Y. Hirose and T. Nakatsuka, *Bull. Agri. Chem. Soc. Japan*, **23**, 143 (1959).
2) Y. Hirose and T. Nakatsuka, ibid., **23**, 253 (1959).
3) M. J. Gentles, J. B. Moss, H. L. Herzog and E. B. Hershberg, *J. Am. Chem. Soc.*, **80**, 3702 (1958); H. Dannenberg and Ch. H. Doering, *Z. physiol. Chem.*, **311**, 84 (1958); H. Dannenberg, Ch. H. Doering and D. Dannenberg-von Dresler, ibid., **317**, 174 (1959); H. Dannenberg and Hans-Günter Neumann, *Ann.*, **646**, 148 (1961).
4) W. Cocker and T. B. H. McMurry, *Tetrahedron*, **8**, 181 (1960).
5) Generously supplied by Dr. Hirose, Department of Agriculture, Tokyo University.
6) K. Takeda, T. Okanishi, K. Igarashi and A. Shimaoka, *Tetrahedron*, in the press; K. Igarashi, *Chem. Pharm. Bull.*, **9**, 722, 729 (1961).



IX R_1=Me, R_2=H, R_3=OH
X R_1=H, R_2=Me, R_3=H



XI



XII

precursors the dienol-glycosides (XI) were suggested.

Although its absolute configuration is still to be elucidated, (+)-occidentalol (XII)[7], isolated as the major constituent of the essential oil of *Thuja occidentalis* L., might be a precursor of (+)-occidol (I). It is suggested that a careful examination of the mother liquor of the extract of the sapogenins IX and X might reveal the existence of the $\Delta^{1,3}$-sapogenins.

Experimental*

Hyposantonin[8].—To a solution of 26 g. of (−)-santonin oxime in 1 l. of 90% ethanol, 50 cc. of concentrated sulfuric acid was added, and was chilled to 20°C. After a solution of 1 g. of copper sulfate in 5 cc. of water was added, 150 g. of zinc powder was added slowly and the reaction temperature was kept below 40°C with vigorous stirring (with Vibro-Mischer) and cooling. After the initial exothermic reaction had subsided (50 g. of zinc powder), the remainder of zinc powder could be added rapidly. The stirring was continued for 10 hr. and during this time the temperature was kept at 31~35°C.

The zinc powder was filtered and washed repeatedly with warm ethanol (40°C), and the filtrate and washings were combined. After evaporation of the solvent at 40°C, the viscous residue was extracted twice with 350 cc. of warm water (40°C). The combined extracts were freed from polymeric viscous mass by filtration through a layer of Hyflo super cell, and was boiled to precipitate hyposantonin, which weighed 14 g., m. p. 142~149°C. Recrystallization from aqueous ethanol gave cystals, m. p. 151~152°C, $[\alpha]_D^{23}$ +36.1° (*c* 1.05, in benzene) (literature[9]; m. p. 152~153°C, $[\alpha]_D$ +32.75° (*c* 2.4), in benzene).

Hyposantonous Acid (III)[8].—Three hundred grams of zinc powder was adedd in two portions to a boiling solution of 24.3 g. of hyposantonin in 1.5 l. of acetic acid with vigorous stirring (Vibro-Mischer). After heating under reflux with stirring for 16 hr., the zinc powder was removed by filtration, and washed with hot acetic acid. The combined acetic acid solutions were concentrated under reduced pressure, and the viscous residue was diluted with water to precipitate crystals, which were recrystallized from aqueous acetic acid to give colorless prisms, 16 g., m. p. 92~94°C. The mother liquor was evaporated and the residue was distilled to afford a viscous oil, b. p. 155°C/0.01 mmHg (bath temp. 200~210°C), which solidified by scratching, 5.6 g., m. p. 91°C, and made total yield 93%. $[\alpha]_D^{12}$ +85.0° (*c* 0.31, in 95% ethanol) (literature[10]; m. p. 95.5°C, $[\alpha]_D^{28}$ +75.95° in ethanol).

Hyposantonous Acid Chloride (IV).—A mixture of 11.6 g. of hyposantonous acid, 13 g. of thionyl chloride and 15 cc. of benzene was refluxed for 1 hr. After the solvent and excess thionyl chloride were removed at reduced pressure, the residue was distilled to afford 11.6 g. (93% yield) of an oil, b. p. 133~137°C/0.5 mmHg, n_D^{18} 1.5480. After standing at room temperature it solidified to give srystals, m. p. 45~46°C. IR spectrum: 1765 cm^{-1} (in chloroform).

Anilide: recrystallized from aqueous ethanol, m. p. 138~141°C.

Found: C, 82.09; H, 8.25; N, 4.77. Calcd. for $C_{21}H_{25}ON$: C, 82.04; H, 8.25; N, 4.56%.

3-(5, 8-Dimethyl-1, 2, 3, 4-tetrahydro-2-naphthyl)-butanone-2 (V).—To a suspension of 1 g. of magnesium in 60 cc. of absolute ether, a stream of methyl bromide was passsed with stirring for 1 hr. until the magnesium disappeared. Then, at room temperature and in an atmosphere of nitrogen, 2.3 g. of cadmium chloride (dried at 130°C) was added during 5 min., and the reaction mixture was refluxed for 45 min. After 28 cc. of ether was removed by distillation, 30 cc. of benzene was added and then 28 cc. of benzene-ether mixture was evaporated under vigorous stirring to disperse the solid mass which formed. After 25 cc. of benzene was added, the viscous material adhering to the wall of the reaction flask was dislodeged by scratching with a spatula. A solution of 6 g. of the acid chloride IV in 10 cc. of benzene was slowly added, and stirring under refluxing was continued for 1.5 hr. The reaction mixture was decomposed by adding a mixture of 20 cc. of water and 20 cc. of 4 N sulfuric acid, and extracted twice with benzene. After washing with water, 5% sodium carbonate solution and saturated aqueous sodium chloride, the benzene solution was dried over anhydrous magnesium sulfate. Evaporation of the solvent gave an oil, which distilled at 154~155°C/0.5 mmHg (bath temp. 180~200°C) and weighed 3.8 g. (yield, 69%), n_D^{18} 1.5342, $[\alpha]_D^{22}$ +69.5° (*c* 2.74, in 95% ethanol). IR spectrum: 1700 cm^{-1} (in chloroform).

Found: C, 82.31; H, 9.61. Calcd. for $C_{12}H_{22}O$: C, 83.43; H, 9.63%.

7) T. Nakatsuka and Y. Hirose, *Bull. Agr. Chem. Soc. Japan*, **20**, 215 (1956); ibid., **23**, 140 (1959).

* All melting points are uncorrected. The analyses were performed in the Microanalytical Laboratory of the Institute of Polytechnics, Osaka City University.

8) Elsevier's "Encyclopedia of Organic Chemistry", Series III, Vol. 12B, Elsevier Pub. Co. Inc., New York-Amsterdam (1948), pp. 3326, 3456.

9) D. Gucci, *Gazz. chim. ital.*, **19**, 367 (1889) (*Chem. Zentr.*, **1889**, II, 595); G. Grassi-Gristaldi, ibid., **19**, 382 (1889) (*Chem. Zentr.*, **1889**, II, 597).

10) G. Grassi-Cristaldi, ibid., **26**, 459 (1896) (*Chem. Zentr.*, **1897**, I, 170).

Semicarbazone: recrystallized from ethanol, decomp. p. 216~225°C.

Found: C, 71.07; H, 9.05; N, 14.80. Calcd. for $C_{17}H_{25}ON_3$: C, 71.04; H, 8.77; N, 14.62%.

1-(5, 8-Dimethyl-1,2,3,4-tetrahydro-2-naphthyl)-ethanol (VII).—A mixture of 3.12 g. of the ketone V and 32 cc. of chloroform which contained 2.53 g. of perbenzoic acid was kept in a dark place at room temperature for one week. After 50 cc. of ether was added, the solution was washed with 1N sodium hydrogen carbonate and saturated sodium chloride solution. After drying with anhydrous magnesium sulfate, the solvent was removed to give a viscous oil, which was dissolved in a solution of 1.7 g. of the Girard P reagent in 40 cc. of 99% ethanol. Then 2.31 g. of acetic acid was added, and the solution was refluxed on a water bath for 1 hr. The pale yellow solution was cooled in an ice bath, and brought to pH 7 by adding a solution of 1.85 g. of sodium carbonate in 200 cc. of water. The turbid aqueous solution was extracted with six portions of 50 cc. of benzene.

The Acetate Fraction.—The benzene extract was washed with saturated sodium chloride solution and dried over anhydrous magnesium sulfate. Removal of the solvent gave a viscous oil, which was directly hydrolyzed by boiling with a mixture of 0.8 g. of potassium hydroxide in 15 cc. of methanol for 2 hr. After the solvent was removed on a water bath, the residue was diluted with 20 cc. of water and extracted with ether. The ether extract was washed with water and saturated sodium chloride solution and dried over anhydrous magnesium sulfate. The solvent was removed and the residue was distilled to give 0.8 g. of an oil, b. p. 140~180°C (bath temp.)/0.1 mmHg. Since the infrared spectrum showed the contamination with a small amount of the unchanged ketone V, the alcohol VII was purified by chromatography on Florisil (10 g.). Elution with petroleum ether (b. p. 60~80°C) gave unchanged ketone, followed by alcohol VII which was eluted with benzene-petroleum ether. IR spectrum: 3340 cm^{-1} (in chloroform). $[\alpha]_D^{20}$ +63.2° (c 2.12, in pyridine).

The Ketone Fraction.—From the aqueous solution separated from the ester, 0.84 g. of ketone V was recovered.

(5, 8-Dimethyl-1,2,3,4-tetrahydro-2-naphthyl)-methylketone (VIII).—Pyridine-chromic anhydride complex was prepared by careful addition of 0.9 g. of chromic anhydride in 16 cc. of pyridine cooled at 15~20°C. A solution of 0.618 g. of alcohol VII in 16 cc. of pyridine was added to the suspension of the complex, and the solution was allowed to stand at room temperature overnight. After being diluted with 400 cc. of water, the reaction mixture was extracted six times with total amount, of 500 cc. of ether. The ether extract was washed with saturated sodium sulfate solution four times, and dried over anhydrous magnesium sulfate.

After evaporation of the solvent, the residue distilled at 120~140°C (bath temp.)/0.1 mmHg and weighed 0.589 g. IR spectrum: 1700 cm^{-1} (in chloroform). $[\alpha]_D^{21}$ +51.6° (c 1.95, in ethanol), 2,4-Dinitrophenylhydrazone: bright yellow needles from ethanol-ethyl acetate, m. p. 206~207°C. Found: C, 62.93; H, 6.08; N, 14.48. Calcd. for $C_{20}H_{22}O_4N_4$: C, 62.81: H, 5.80 N, 14.65%.

(+)-Occidol (I).—To the Grignard solution prepared from 0.3 g. of magnesium and 0.54 g. of methyl iodide in 20 cc. of anhydrous ether, a solution of 0.5 g. of ketone VIII in 10 cc. of ether was added, and the reaction mixture was refluxed for 1 hr. The Grignard complex was decomposed by adding 1.5 cc. of saturated ammonium chloride solution, and the clear ether supernatant was decanted. The residue was washed three times with ether, and the combined extracts and washings were dried over anhydrous magnesium sulfate. Removal of the solvent gave a viscous oil (0.574 g.) which was purified by chromatography on 13 g. of Florisil. The fractions which were eluted with petroleum ether-benzene (17 : 3), after evaporation of the solvent, crystallized upon rubbing and weighed 0.388 g. Recrystallization from petroleum ether (b. p. 50~60°C) gave crystals which melted at 69~70°C.

The mixed melting point determination and the comparison of infrared spectra (in chloroform) with an authentic sample established their identity. $[\alpha]_D^{17}$ +76.7° (c 0.90, in chloroform). Found: C, 82.35; H, 10.22. Calcd. for $C_{15}H_{22}O$: C, 82.51; H, 10.16%.

The author is very grateful to Dr. H. Watanabe, Fujisawa Pharm. Co., for his generous supply of (−)-santonin. This work was partially supported by the grant-in-aid for Fundamental Scientific Research from the Ministry of Education to which the author's thanks are due.

Department of Chemistry
Osaka City University
Kita-ku, Osaka

Catalytic Activities of Copper-nickel Alloys for Hydrogenating Reactions

By Toyosaburo TAKEUCHI, Masakazu SAKAGUCHI, Ikkei MIYOSHI and Takeo TAKABATAKE

(Received October 23, 1961)

The catalytic activities of copper-nickel alloys for hydrogenating reactions have been interpreted by Dowden and Reynolds[1] in the light of the modern electronic theory of metals. In their studies, massive copper-nickel alloys (foils) were employed as the catalysts. Since an early study by Schwab and Brennecke[2], many investigations[3-7] of hydrogenating reactions have been carried out employing granular copper-nickel alloys prepared chemically. However, no such obvious relation to the number of holes per atom in the 3d-band of these alloy has been found as Dowden and Reynolds found for the massive alloys. Moreover, the results are not in accordance with one another. The cause of this discrepancy in the results has not yet been explored. It was sometimes proposed that the granular catalyst might be joined with a homogeneous alloy as in the case of the massive alloys. As a result of previous studies[8,9] with an electron diffraction of the reactions between hydrogen chloride and the catalysts, the writers proposed that the concentration of nickel at the surface of the granular copper-nickel alloy differs from that of the interior of the composing particles. The present work is concerned with the catalytic activities of hydrogenations of ethylene and benzene over two copper-nickel series, i. e., granular and massive alloys, in order to make sure whether the discrepancy in catalytic activities between granular alloys and massive alloys can be explained by the nonuniform distribution of nickel in the granular alloys. In addition, the heat of the adsorption of hydrogen and the amounts of hydrogen adsorbed on granular alloys were measured in order to confirm the previous data reported by the writers[10] and to discuss the relation between the heat of adsorption and the catalytic activity of the copper-nickel alloy.

Experimental

The tests of the activity of two series of catalysts (granular and massive alloys) were made by a static method, using ethylene. The test of benzene was made only for granular alloys by a flow method.

Granular alloys were prepared from solutions of copper and nickel nitrates and their mixtures, by evaporating them to dryness and by igniting them to metal oxides in a furnace at 500°C, in a way which was described elsewhere[8,9,11]. Prior to use, the oxides were then reduced at 200°C for about three weeks in an atmosphere of hydrogen, which was replaced about five times. At the end of the reduction period, the catalysts were evacuated for several hours at 200°C to a pressure of 10^{-5} mmHg. Several samples of each catalyst were analyzed for total nickel and total copper to provide data for a study of the composition variable.

Massive alloys were prepared from mixtures of electrolytic copper and nickel by completely melting them in a furnace. The ingots containing less than 40% nickel were rolled in the form of a sheet 0.1 mm. thick, while those of 65% and 80% nickel were cut down in the form of a plate 1 mm. thick. These sheets and plates were polished with emery paper and washed by pure alcohol and distilled water; then they were reduced in an atmosphere of hydrogen.

The ethylene used was prepared by the dehydration of ethyl alcohol with sulfuric acid and was purified by vacuum distillation using a liquid oxygen bath. The benzene used was commercially available material which was purified by stirring it with sulfuric acid, with sodium hydroxide solution and then with water, and which was dried by contact with calcium chloride and then distilled.

The hydrogen used for the adsorption measurement or for the hydrogenation reaction of ethylene was prepared by the electrolysis of water and was purified by diffusion through a palladium thimble, preceded and followed by liquid oxygen traps. The commercial electrolytic hydrogen was used for the test of the activity of benzene. It was purified by

1) P. W. Reynolds, *J. Chem. Soc.*, **1950**, 265; D. A. Dowden and Reynolds. *Discussions Faraday Soc.*, **8**, 184(1950).
2) G. -M. Schwab and W. Brennecke, *Z. physik. Chem.*, **B24**, 393 (1933).
3) J. H. Long, J. C. W. Frazer and E. Ott, *J. Am. Chem. Soc.*, **56**, 1101 (1934).
4) V. N. Ipatieff, B. B. Corson and I. D. Kurvatov, *J. Phys. Chem.*, **43**, 598 (1939).
5) P. H. Emmett and N. Skau, *J. Am. Chem. Soc.*, **65**, 1029 (1943).
6) R. J. Best and W. W. Russell, ibid., **76**, 838 (1954).
7) W. K. Hall, Thesis, Univ. of Pittsburgh (1956); W. K. Hall and P. H. Emmett, *J. Phys. Chem.*, **62**, 816 (1958).
8) T. Takeuchi and M. Sakaguchi, This Bulletin, **29**, 117 (1957).
9) T. Takeuchi, F. Shibata and M. Sakaguchi, *Z. physik. Chem., N. F.*, **14**, 339 (1958).
10) T. Takeuchi and T. Okano, Abstract of the 10th Annual Meeting of the Chemical Society of Japan, (1957); T. Takeuchi, *Yukagaku*, **8**, 231 (1959).
11) T. Takeuchi and M. Sakaguchi, This Bulletin, **29**, 182 (1957).

copper wire at 350°C, followed by anhydrous calcium chloride.

The apparatus used for the hydrogenation of benzene was a modification of that of Ipatieff[4]. The diameter of the reaction tube was 20 mm., and the length of tube was 30 cm. In every experiment, 20 g. of oxide was mounted on a glass boat 25 cm. in length. After the end of the reduction of the oxide at 200°C with the stream of hydrogen, the mixture of hydrogen and benzene at atmospheric pressure was passed in a volume ratio of 8 : 1 at a flow rate 100 ml./min. over the catalyst at 190°C; then about 2 l. of hydrogen were used to sweep the catalysate which remained in the catalyst into the receiver. Three grams of benzene was used for each run. The composition of the liquid catalysate, a mixture of benzene and cyclohexane, was determined by means of the refractive index.

The apparatus used for the hydrogenation of ethylene and for the adsorption of hydrogen was the same as that described in a previous paper[11]. In the case of the hydrogenation of ethylene, the apparatus was connected with a U-tube manometer of apiezon oil to facilitate the measurement of the pressure change in the reactions. The volume of the reaction vessel which included the U-tube manometer was 155 cc. For the test of activity, about 0.5 or 2 g. of granular oxide or about 0.2 m^2 (apparent area) of massive alloy were loaded in the vessel. Care was taken by using a liquid oxygen trap or a dry-ice trap, to prevent the contamination of the catalyst. A mixture of ethylene and hydrogen in a volume ratio of 1 : 1 and a total pressure of 20 mmHg was admitted into the reaction vessel; then the decrease in pressure was followed by the manometer, controlling the temperature of the reaction vessel at a constant value. The temperatures of the reaction were 100, 120, 140 and 160°C. In every interval of the test, catalysts were reduced afresh with hydrogen for two or three days at 200°C. The isotherms of the hydrogen adsorption on granular samples, i.e., 2.0 g. of 40% nickel and 0.5 g. of 86% nickel and pure nickel, were obtained at three temperatures, 100, 120 and 140°C, in the same way as has been described elsewhere[11]. The samples used for the adsorption of hydrogen were of 40% nickel, 86% nickel and pure nickel. After the catalyst testing had been completed, each sample was evacuated at 200°C for about three hours until a pressure of better than 10^{-5} mmHg had been attained. The B. E. T. area measurements were then made on each catalyst by ethylene, its cross-sectional area being taken to be 17.2 $Å^2$.

Results

In the hydrogenation of ethylene, both on the granular and the massive alloys, the relation of the logarithms of the rates to the time was represented by linear lines, except for a few minutes of the initial stage of the reaction. Figure 1 shows examples of the massive 80% nickel alloy. As can be recognized in the figure, the inclination of the linear part of the curve is not practically affected by the reaction temperature. In order to know the cause of the discontinuity in these curves, the adsorptions of hydrogen and ethylene were observed under the same initial pressures as in the hydrogenation, and a comparison between the two pressure changes was made. It was concluded after the comparison that the steep decrease in every initial stage of the hydrogenating reaction is probably due to the adsorption of ethylene on the catalyst. Figure 2 shows the relation of the activities in the hydrogenation of ethylene to the nickel percentage in the massive catalysts. The rates in the figure, at 120°C, were obtained from the inclination of each linear part of the curve. The figure shows that the pure copper was practically

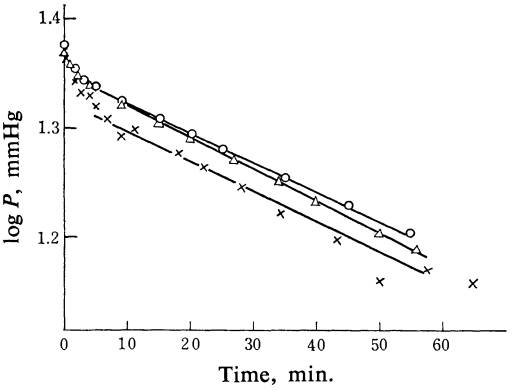


Fig. 1. Rates of hydrogenation of ethylene on massive 80% Ni alloy.
—×— 100°C, —○— 120°C, —△— 160°C

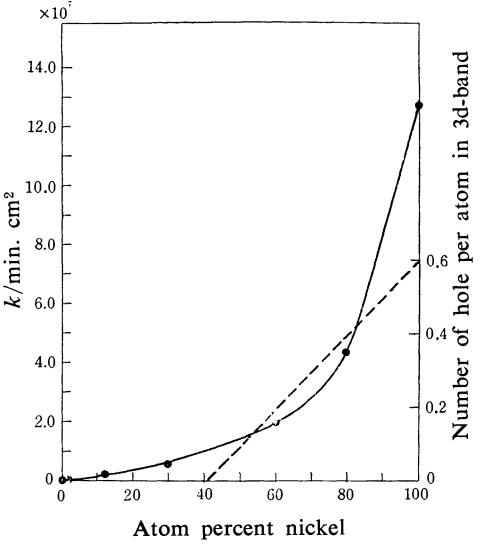


Fig. 2. Catalytic activities of massive Cu, Ni and Cu-Ni for the hydrogenation of ethylene at 120°C.
---- Number of hole per atom in 3d-band

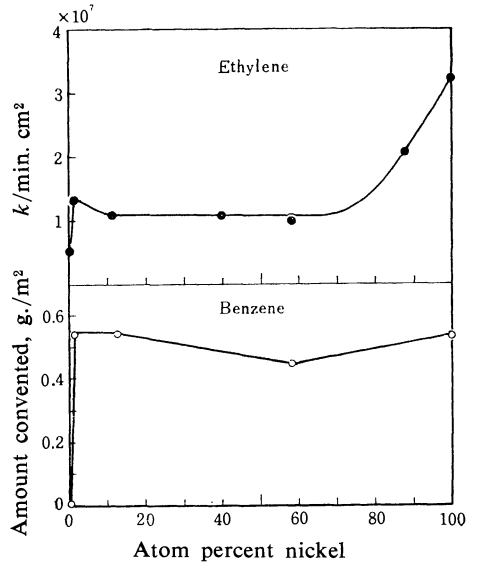


Fig. 3. Catalytic activities of granular Cu, Ni and Cu-Ni for the hydrogenations of ethylene and benzene.
—●— Ethylene, at 120°C by static method
—○— Benzene, at 190°C by flow method

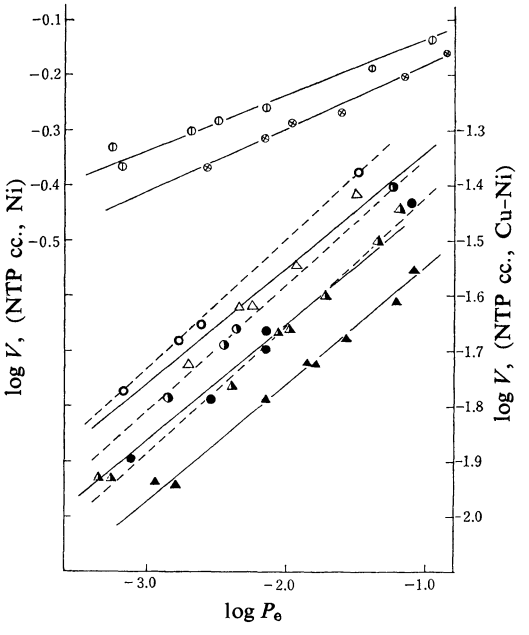


Fig. 4. Adsorption isotherms of granular Ni and Cu-Ni.

—◐—	Pure Ni (0.5 g.)	100°C
—⊗—		120°C
--○--	40% Ni (2.0 g.)	100°C
--◑--		120°C
--●--		140°C
—△—	86% Ni (0.5 g.)	100°C
—◭—		120°C
—▲—		140°C

inactive for the reaction, and that alloying 60% or less of nickel with copper causes a gradual rise in the activity, while increasing the nickel content to over 70% causes a conspicuous rise in the activity, showing a maximum in pure nickel. Figure 3 shows the results of the hydrogenation of ethylene at 120°C and that of benzene at 190°C over the granular alloys. In the case of ethylene, the activity of pure copper is quite small, while it increases markedly on a slight addition of nickel (1%). The activity does not increase, but declines slightly on a further increasing of the nickel content; it is

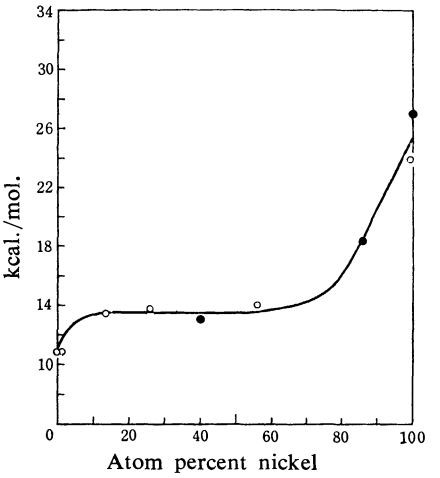


Fig. 5. Heats of adsorption of hydrogen on granular Cu, Ni and Cu-Ni.

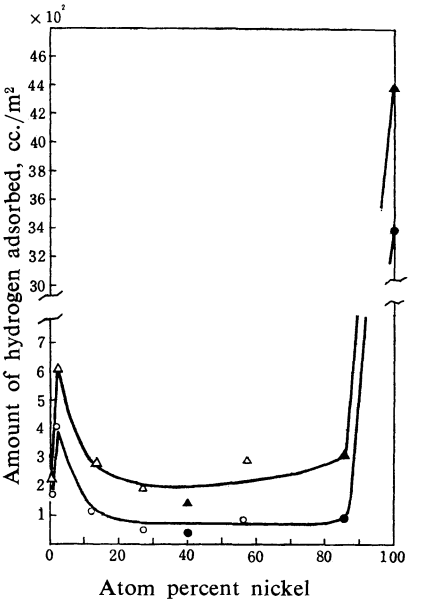


Fig. 6. Amount of hydrogen adsorbed on granular Cu, Ni and Cu-Ni.
-○- $P_e=10^{-3}$ mmHg, -△- $P_e=10^{-1}$ mmHg

kept constant for the wide range of nickel content from about 10% to 60% and then increases again, showing a maximum in pure nickel. In the case of benzene, the activity is taken as the amount (in the unit, g.) of benzene converted to cyclohexane per unit area of the catalysts while 3.0 g. of benzene was being passed at a constant velocity over the catalysts. The figure shows that the activity of the alloyed catalysts is not substantially affected by the nickel content. Figure 4 shows the isotherms of the adsorption of hydrogen on 40, 86 and 100% nickel alloys of a granular form. Figures 5 and 6 show the relation of the heat of the adsorption of hydrogen at sparse coverage and of the amount of hydrogen adsorbed to the component of granular alloys findings which were given by the isotherms. The heats were calculated by adapting the Clausius-Clapeyron equation to the isotherms. The open circles and triangles in the figure show findings previously determined[10]. Linear relations can be found within the range of experimental accuracy over a wide range of alloy composition, except in the high-content range of both copper and nickel, as in the case of the hydrogenations of the same alloys. Table I shows the B. E. T. areas of the alloys used.

TABLE I. THE B. E. T. AREAS OF Cu, Ni AND Cu-Ni ALLOYS

Massive alloys reduced at 200°C (Total area)		Granular alloys reduced at 200°C	
Ni, %	m^2	Ni, %	$m^2/g.$
0	0.31	0	0.69
1	0.29	1	0.80
12	0.27	12	3.3
30	0.25	26	4.0
60	0.52	40	4.6
80	0.22	57	4.7
100	0.20	86	6.1
		100	3.0

Discussion

The results reveal that the activities of the massive copper-nickel alloys in the hydrogenation of ethylene may be interpreted by the Dowden theory. However, the activities of the granular alloys can not be interpreted simply by his theory.

The surface of the granular copper-nickel alloy has been discussed over a long period by many researchers[3,12-15]. Among them, Best and Russell[6] and Hall and Alexander[15] have proposed that the surface is composed of an equilibrium alloy. Their opinion were based on the coincidence of the lattice parameters given by X-ray diffraction with those of the equilibrium alloys. Problems will remain, however, in accepting their opinion inasmuch as the rather strong penetrating power of X-rays is not suitable for the investigation of the surface.

Our previous studies[16] of the granular copper-nickel alloys by an electron diffraction had led to the conclusion that the surface of copper-nickel powder is composed of microcrystals of various compositions. A more detailed conclusion could be derived from studies[8,9] of the reaction of the granular alloys (1 and 12% nickel) with hydrogen chloride gas. These results show that the amount of nickel was greater in the upper layer of the composing particle than in the interior and that the amount per unit area of the catalyst was smaller in the 12% nickel alloy than in the 1% nickel alloy. From these facts, it can be surmised that the great increase in activity caused by a slight addition of nickel (1% nickel) in a granular alloy depends upon the preferential aggregation of nickel on the surface and that the activity is determined mainly by the amount of nickel on the surface. The decline in activity caused by the increase in the concentration of nickel from 1 to 12% would be due to the decrease in the amount of nickel on the surface, and the extensive and essentially linear portion of the catalytic activity would reveal an invariablity in the concentration of nickel on the surface. Interpretations can be made in the same way for the heat of adsorption and for the amount of hydrogen adsorbed on the granular alloys. A discrepancy can be recognized, however, between the heat of adsorption and the amount adsorbed in the 1% nickel alloy. The heat seems to be quite small in the light of the great amount of hydrogen adsorbed. This would be due to the following troublesome fact which has been established by the present writers[11] concerning the adsorption of hydrogen on pure copper and on the 1% nickel alloy: the rates of the adsorption of hydrogen on these catalysts were too slow for it to be possible to find readily a distinct equilibrium pressure, because of the irreversibility of adsorption.

It has been recognized by many researchers[17]

12) G. Wagner, G. -M. Schwab and R. Staeger, *Z. physik. Chem.*, **27**, 493 (1935).
13) N. Kadota and S. Ikeda, *J. Am. Chem. Soc.*, **73**, 4475 (1951).
14) J. A. Sabatka and P. W. Selwood, *J. Phys. Chem.*, **61**, 1564 (1957).
15) W. K. Hall and L. Alexander, ibid., **61**, 242 (1957).
16) S. Yamaguchi and T. Takeuchi, *Kolloid Z.*, **150**, 69 (1957); *J. Colloid Sci.*, **12**, 263 (1957); *Z. anorg. u. allgem. Chem.*, **294**, 254 (1958); *J. Phys. Chem.*, **61**, 1023 (1957).
17) For a discussion with references, see D. D. Eley in "Advances in Catalysis", I, Academic press, New York (1948), p. 157.

that the reaction is of the first order with respect to hydrogen and of zero order with respect to hydrocarbons. This would indicate that the amount of hydrogen adsorbed on a catalyst is far less than that of hydrocarbon. We can now understand the fact, established in our study, that the adsorbing ability of hydrogen is related to the catalytic activity.

Shallcross and Russell[18] have recently studied the ortho-parahydrogen interconversion over granular copper-nickel alloys prepared by a solution of ammonium bicarbonate. They found a constant activity in the alloy region from about 10 to 95% nickel. The shape of the curve for the activity of the reaction is substantially the same as those for the hydrogenation reactions of the granular alloys used in our study. In their report, they claimed that the catalysts were homogeneous both in bulk and on the surface. Very recently, Shield and Russell[19] have studied the heats of the adsorption of hydrogen on the same catalysts. In their paper, they ignored our results, which we had shown to them. Their scanty results are, however, quite similar to those measured by the writers. The agreement in both heats would indicate that the surfaces of the two granular alloys do not differ from one another.

In our study, the activity of granular pure nickel was the greatest for the hydrogenation of ethylene, but not for that of benzene. These results do not agree with those reported in other papers. Schwab[2] and Hall[7] found the maximum activity for the hydrogenation of cinnamic acid and benzene in a nickel-rich region, but Best and Russell[6] found the greatest for that of ethylene in a copper-rich region. The situation is very complicated. However, it can be noted that the results which gave the maximum activity in an alloy were obtained by the flow method. In the case of the flow method, the hydrogen used for the reduction of the catalyst occasionally remains in the catalyst because of the difficulty in evacuating sufficiently due to the characteristics of the apparatus. Attention should be called to the recent work of Hall[7]. He has found that the hydrogen added in the temperature range 100 to 300°C acts as a promoter for copper-nickel catalysts but as an inhibitor for pure nickel. Although a theoretical interpretation of his results has not yet been established, it seems certain that the decrease in the activity found in the studies of the pure nickel and nickel-rich regions might be related to the hydrogen preadsorbed on (or dissolved in) alloys or pure nickel.

Many other factors might cause the decrease in the catalytic activity in the nickel-rich region and the disagreement in the relation of the activity to the composition of the alloy between studies. It should be emphasized, however, that the activity of the granular copper-nickel alloy may best be discussed by taking account of the non-uniform distribution of nickel on the surface.

18) P. B. Schallcross, Thesis, Brown University, (1958); P. B. Schallcross and W. W. Russell, *J. Am. Chem. Soc.*, **81**, 4132 (1959).

19) L. S. Shield and W. W. Russell, *J. Phys. Chem.*, **64**, 1952 (1960).

Summary

The hydrogenation of ethylene and benzene on two series of copper-nickel alloys, i. e., massive alloys prepared physically and granular alloys prepared chemically, was carried out in order to determine the cause of the disagreement of the catalytic activities which have been found in these alloys. The adsorption of hydrogen on granular alloys was also examined to learn the heat of adsorption and the amount adsorbed; the results were compared with the activities of the alloys.

The activities of massive alloys may be interpreted by the Dowden theory, but those of granular alloys could not. The activities of granular alloys were interpreted in connection with the concentration of nickel at the surface, which can be considered to be different from that in the interior. It was concluded that the amount of hydrogen adsorbed, the heat of adsorption, and the catalytic activity of granular alloy are related to the concentration of nickel at the surface.

Faculty of Literature and Science
Toyama University, Toyama

*Syntheses of Chelating Agents. I. Stability of the Metal Chelate of Benzylamine-N, N-diacetic Acid and its Nitro Derivatives**

By Takeshi ANDO

(Received November 30, 1961)

Although many papers[1-7] have been published concerning the stabilities of the metal chelates of iminodiacetic acid and its derivatives, no investigation has been undertaken of the stability of its benzyl derivatives.

During the course of our search for new chelating agents of the aminopolycarboxylic acid type, benzylamine-*N*, *N*-diacetic acid and two of its nitro derivatives have been synthesized.

This paper is to report on the syntheses of new ligands as well as on the stabilities of their metal chelates, with an attempt to correlate the structure of the ligand with the stability of the metal chelates.

The synthesis of benzylamine-*N*, *N*-diacetic acid (BADA) has been reported on in the literature[8]. The syntheses of the new ligands, *o*- and *p*-nitrobenzylamine-*N*, *N*-diacetic acid (*o*-NBADA and *p*-NBADA), has been carried out by the standard procedure[9] from the corresponding nitrobenzylamine and monochloroacetic acid.

The chelate stability measurements were carried out by the pH titration method on these ligands only for a 1 : 1 ratio of the ligand to the metal ion, and the first stability constants have been obtained.

For BADA, the chelate stability constants with copper(II), nickel(II), cobalt(II), lead(II), zinc(II), calcium(II) and magnesium(II) were obtained. The results indicate that the behavior of BADA in relation to metal ions is similar to that of iminodiacetic acid. The copper chelate is so stable that it exists even in a strongly acid solution where the undissociated form of the ligand predominates. It forms relatively stable chelates with nickel, zinc, lead and cobalt, and forms very unstable chelates with magnesium and calcium. It was also noted that the pH titration curves indicated the formation of hydrogen complexes with some metal ions in the low pH region.

For *o*- and *p*-nitrobenzylamine-*N*, *N*-diacetic acid, the stability constants of magnesium(II) and calcium(III) have been obtained, the results indicated that the nitro substitution on the benzene ring had an appreciable effect on the dissociation constant of the ligand as well as on the stability constant of the chelates.

Experimental

Syntheses of Ligands.—BADA, which had been prepared according to the method of Chase and Downer[8], was purified by repeated recrystallization from water. The pure product decomposed at 204°C.

Found: N, 6.17. Calcd. for $C_{11}H_{13}NO_4$: N, 6.28%.

Syntheses of *o*-NBADA and *p*-NBADA.—These were synthesized from *o*- and *p*-nitrobenzylchloride respectively, according to the following reaction scheme, in which both compounds were processed in the way otherwise mentioned:

$$C_6H_4(NO_2)CH_2Cl \xrightarrow[\text{in dimethylformamide}]{C_6H_4(CO)_2NK} C_6H_4(NO_2)CH_2N(CO)_2C_6H_4 \xrightarrow[\text{dil.HCl}]{H_2NNH_2}$$

(I)

$$C_6H_4(NO_2)CH_2NH_2\cdot HCl \xrightarrow{ClCH_2CO_2H}$$

(II)

$$C_6H_4(NO_2)CH_2N(CH_2CO_2H)_2$$

(III)

o- and p-Nitrobenzylphthalimide (I). — The corresponding nitrobenzylchloride (18 g.) and potassium phthalimide (18 g.) were suspended in dimethylformamide**, and the mixture was heated while being stirred in an oil bath at 100~110°C. The temperature was kept below 120°C to prevent any side reaction. After two hours, the mixture was cooled; then it was poured into 500 ml. of water and stirred well. After the mixture had been left

* Contribution No. 23 from the Department of Organic Synthesis, Faculty of Engineering, Kyushu University.

1) S. Chaberek, Jr. and A. E. Martell, *J. Am. Chem. Soc.*, **74**, 5052 (1952).
2) S. Chaberek, Jr., R. C. Courtney and A. E. Martell, ibid., **74**, 5057 (1952).
3) G. Schwarzenbach, E. Kamplitsh and R. Steiner, *Helv. Chim. Acta*, **29**, 364 (1946).
4) G. Schwarzenbach, A. Wili and R. O. Bach, ibid., **30**, 1303 (1947).
5) G. Schwarzenbach and W. Biedermann, ibid., **38**, 1492 (1951).
6) G. Anderegg and G. Schwarzenbach, ibid., **38**, 1940 (1951).
7) G. Schwarzenbach, G. Anderegg, W. Schneider and H. Senn, ibid., **38**, 1147 (1955).
8) B. H. Chase and A. M. Downer, *J. Chem. Soc.*, **1953**, 3874.
9) G. Schwarzenbach and H. Ackermann, *Helv. Chim. Acta*, **31**, 1029 (148).

** The use of dimethylformamide, which was recently suggested by Sheehan and Bolhofer, has an advantage of a lower reaction temperature with an increased yield, while avoiding tar formation (*J. Am. Chem. Soc.*, **72**, 2786 (1950)).

standing for a while, the separated precipitate was filtered off and washed repeatedly. The crude product was purified by recrystallization from acetic acid. The melting point was 218°C for *o*-nitrobenzylphthalimide and 174°C for *p*-nitrobenzylphthalimide.

Found: *o*-isomer N, 9.91. *p*-isomer N, 9.92. Calcd. for $C_{15}H_{10}N_2O_6$: N, 9.91%.

o- and p-Nitrobenzylamine (II).—The corresponding phthalyl compounds I were decomposed with hydrazine hydrate and dilute hydrochloric acid in an ordinary manner[10]. The hydrochlorides thus obtained were recrystallized several times from 95% ethanol and were then used for the next step. *o*- and *p*-Nitrobenzylamine hydrochloride decomposed at 248 and 249°C respectively.

o- and p-NBADA. — The same general procedure was also followed in this step. To 70 ml. of a 2 M aqueous solution of monochloroacetic acid which had been carefully neutralized with sodium hydroxide, 10 g. of the corresponding nitrobenzylamine hydrochloride was added. The pH value of the mixture was adjusted to 10 by dropping in a 2 N sodium hydroxide solution. After the mixture had been stirred for three hours at 50°C, the temperature was raised to 70~80°C to complete the reaction, while the pH value of the reaction mixture was maintained between 7 and 10 by the intermittent addition of a sodium hydroxide solution. After it had cooled, the reaction mixture was filtered to remove some precipitates. The crude acid was precipitated as barium salt from the filtrate, and free acid was regenerated by treating barium salt with the theoretical amount of sulfuric acid.

The free acid was further purified by repeated recrystallization from 70% ethanol or methanol. Colorless crystls of *o*-NBADA, which decomposed at 189°C, were obtained in a 50% yield. Pale yellow crystals of *p*-NBADA, which decomposed at 201~202°C, were obtained in a 40% yield.

Found for *o*-NBADA: C, 49.31; H, 4.47; N, 10.65. Found for *p*-NBADA: C, 49.46; H, 4.41; N, 10.45. Calcd. for $C_{11}H_{12}N_2O_6$: C, 49.26; H, 4.51; N, 10.45%.

Both compounds were slightly soluble in water (about 1.8×10^{-2} mol./1000 ml. water) and were appreciably soluble in ethanol.

Measurement of Dissociation and Chelate Stability Constants.—The experimental method consisted of the potentiometric titration of the ligand in both the absence and the presence of the metal ion being investigated. The ionic strength was kept constant ($\mu=0.1$) by using potassium nitrate as a supporting electrolyte and by employing relatively low concentrations (about 2×10^{-3} mol.) of the metal ion and the ligand. The titrations were carried out on a solution of only a 1:1 ratio of the ligand to the metal ion concentration. All measurements were carried out at 25±0.1°C.

The titration assembly consisted of a Hitachi-Horiba model P pH meter with glass and calomel electrodes and of a jacketed glass titration cell 130 ml. in capacity. Instead of using the standard buffer, the calibration of the pH meter was carried out under a constant ionic strength ($\mu=0.1$) by referring to the hydrogen ion concentration calculated from the hydrochloric acid-sodium hydroxide titration system for the regions below pH 3 and above pH 7, and from the acetic acid-sodium hydroxide system for the region between pH 3~7.

The titrations were carried out by the usual procedure in an atmosphere of carbon-dioxide free nitrogen. The pH reading were taken until the pH value reached 10.5~11.0 for each titration. The concentrations of the ligand and the metal ion were about 2×10^{-3} mol. for BADA, and about 8×10^{-4} mol. for *o*- and *p*-NBADA because of their low solubilities. The concentrations of the metal ion stock solutions were determined by the EDTA titration.

All reagents used in this investigation were of the analytical grade.

Calculation

Calculation of Acid Dissociation Constants.—The acid dissociation constants were calculated from the titration curves of ligands in the absence of metal ions (Figs. 1, 2 and 3). The equilibria involved and the dissociation constants to be determined are:

$$H_2A \rightleftarrows HA^- + H^+ ; \quad k_1=(H^+)(HA^-)/(H_2A) \tag{1}$$

$$HA^- \rightleftarrows A^{2-} + H^+ ; \quad k_2=(H^+)(A^{2-})/(HA^-) \tag{2}$$

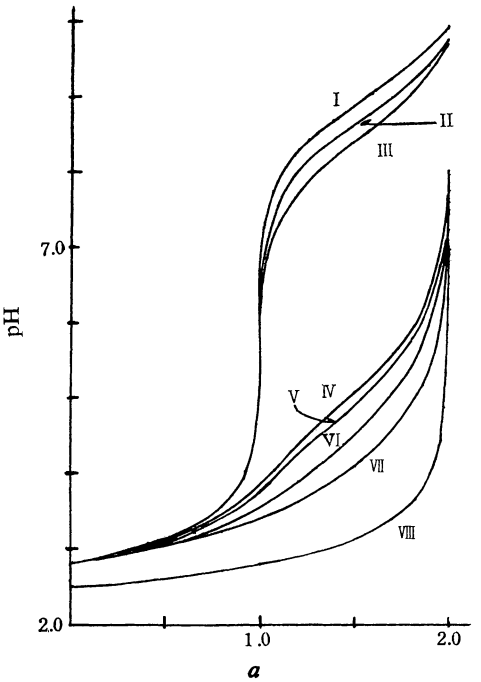


Fig. 1. Titration of BADA in the presence of equimolar concentrations of metal ions.
I, 2×10^{-3} M BADA with 0.1 N NaOH; II, Mg(II); III, Ca(II); IV, Co(II); V, Zn(II); VI, Pb(II); VII, Ni(II); VIII, Cu(II).
a, denotes moles of base added per mole of acid.

10) H. R. Ing and R. H. F. Manske, *J. Chem. Soc.*, 1926, 2348.

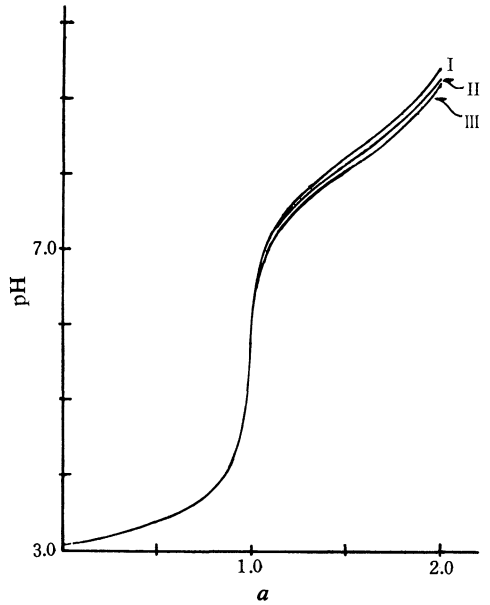


Fig. 2. Titration of *o*-NBADA in the presence of equimolar concentrations of Mg(II) and Ca(II) ions.
I, 8×10^{-4} M *o*-NBADA with 0.1 N NaOH; II, Mg(II); III, Ca(II).
a, denotes moles of base added per mole of acid.

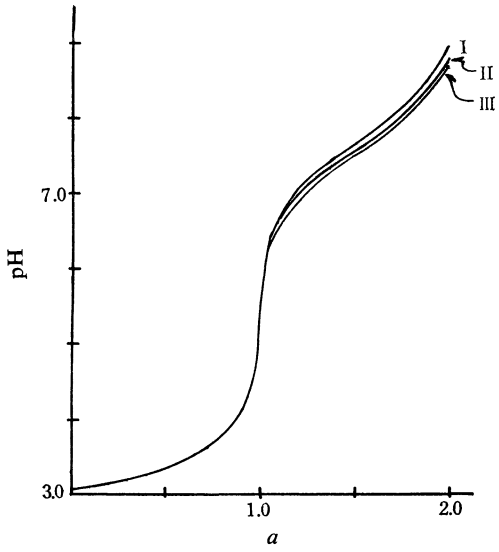


Fig. 3. Titration of *p*-NBADA in the presence of equimolar concentrations of Mg(II) and Ca(II) ions.
I, 8×10^{-4} M *p*-NBADA with 0.1 N NaOH; II, Mg(II); III, Ca(II).
a, denotes moles of base added per mole of acid.

where H_2A represents the undissociated ligand. As is shown in Figs. 1, 2 and 3, the two buffer regions are so clearly separated that each dissociation stage can be treated independently. If C_A represents the total concentraions of the ligand species and a represents the number of moles of the base added per mole of the ligands present, it follows that in the low pH buffer region

$$C_A=(H_2A)+(HA^-) \tag{3}$$

$$aC_A+(H^+)=(HA^-) \tag{4}$$

Also, the first dissociation constant may be calculated from the following equation:

$$k_1=\frac{(H^+)\,[aC_A+(H^+)]}{C_A-[aC_A+(H^+)]} \tag{5}$$

In the high pH buffer region, the concentration of the acid form (H_2A) of the ligand may be neglected, and Eqs. 3 and 4 can be rewritten as

$$C_A=(HA^-)+(A^{2-}) \tag{6}$$

$$(a-1)C_A-(H^+)/K_W=(A^{2-}) \tag{7}$$

Under these conditions, k_2 may be expressed as

$$k_2=\frac{(H^+)\,[(a-1)C_A-(H^+)/K_W]}{C_A-[(a-1)C_A-(H^+)/K_W]} \tag{8}$$

where $K_W=(H^+)(OH^-)$. Alternatively, the second dissociation constant could be obtained directly from the titration curve, if one preserved a relationship in which the value of pk_2 is equal to the pH value at $a=1.5$ on the titration curve of the ligand. In this investigation, the k_2 value of BADA was determined by both methods, while the k_2 value of *o*-NBADA and *p*-NBADA were obtained only by the graphical method.

Calculation of the Chelate Stability Constants.—It has been reported[1] that, in the case of iminodiacetic acid and iminodipropionic acid, the formation of 1:2 chelate (MA_2) could be neglected in the region around $a=1.5$ in the titration curve of a 1:1 metal ligand mixture. Accordingly, it may be safe to assume for BADA chelates that in the pH range corresponding to *a* values of about 1.0~1.8, the equilibria involved in the chelate formation may be expressed as follows:

$$M^{2+}+A^{2-} \rightleftarrows MA;$$

$$K_{MA}=(MA)/(M^{2+})(A^{2-}) \tag{9}$$

where M represents the divalent metal ion used. Therefore, K_{MA} can be calculated by the following equation, which was derived by Chaberek and Martell[1]:

$$K_{MA}=\frac{C_A-\alpha(A^{2-})}{(A^{2-})\,[C_M+\alpha(A^{2-})-C_A]}=\frac{C_A-\alpha(A^{2-})}{\alpha(A^{2-})^2} \tag{10}$$

The last formula in Eq. 10 may be obtained because $C_A=C_M$ in this case. In this equation, (A^{2-}) and α are expressed as

$$(A^{2-}) = \frac{(2-a)C_A - (H^+) + (OH^-)}{2(H^+)^2/k_1k_2 + (H^+)k_2} \quad (11)$$

$$\alpha = (H^+)^2/k_1k_2 + (H^+)/k_2 + 1 \quad (11')$$

where C_M represents the total concentration of the metal ion species.

In general, Eqs. 10, 11 and 11' can be used for the calculation of the stability constants of divalent metal chelates. However, in the case of calcium and magnesium chelates, they can be simplified, as will be discussed below. It can be seen from the titration curves (Figs. 1, 2 and 3) of these chelates that the chelate formations occur in approximately the region of $a=1.0\sim2.0$, where the first dissociation step of the ligand can be neglected. Therefore, the following stoichiometric relationships can be written for ligand ion species, metal ion species and the titrable hydrogen ion respectively:

$$C_A = (HA^-) + (A^{2-}) + (MA) \quad (12)$$

$$C_M = (M^{2+}) + (MA) \quad (13)$$

$$(2-a)C_A = (H^+) - (OH^-) + (HA^-) \quad (14)$$

Since $C_A = C_M$, as defined in the experimental conditions, Eqs. 2, 12 and 13 may be combined to give

$$K'_{MA} = \frac{C_A - \alpha'(A^{2-})}{(A^{2-})^2} \quad (15)$$

Here K'_{MA} represents the stability constants for magnesium and calcium chelates, while α' and (A^{2-}) can be given in the more simplified form:

$$(A^{2-}) = \frac{(2-a)C_A + (OH^-) - (H^+)}{(H^+)/k_2} \quad (16)$$

$$\alpha' = (H^+)/k_2 + 1 \quad (16')$$

with the aid of Eqs. 15, 16 and 16', the stability constants of magnesium and calcium chelates of BADA, *o*-NBADA and *p*-NBADA were calculated.

Finally, as there is an indication of the formation of a hydrogen complex in the relatively low pH region in certain ions, the stability constants of the hydrogen complex were calculated. If one assume that, in a low pH region, only the formation of the hydrogen complex is predominant, the other reactions being negligible, the equilibria involved in this pH range can be given as follows:

$$H_2A \rightleftarrows H^+ + HA^-;$$

$$k_1 = (H^+)(HA^-)/(H_2A) \quad (17)$$

$$M^{2+} + HA^- \rightleftarrows MHA^+;$$

$$K_{MHA} = (MAH^+)/(M^{2+})(HA^-) \quad (18)$$

Also the total concentration of the ligands, metal ions and titrable hydrogen ions are given respectively by;

$$C_A = (H_2A) + (HA^-) + (MHA^+) \quad (19)$$

$$C_M = (M^{2+}) + (MHA^+) \quad (20)$$

$$(2-a)C_A = (H^+) - (OH^-) + (MHA^+) + (HA^-) + 2(H_2A) \quad (21)$$

On the basis of these equations, K_{MHA} is expressed as

$$K_{MHA} = \frac{aC_A + (H^+) - \beta k_1/(H^+)}{\beta^2 k_1/(H^+)\,[1 + k_1/(H^+)]} \quad (22)$$

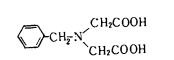
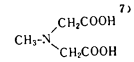
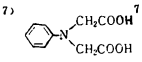
where $\beta = (H_2A) = C_A(1-a) - (H^+)$. Calculations were carried out with the aid of the above equations, employing the data taken from the $a=0.5\sim0.8$ region of the titration curves (Fig. 1)

Results and Discussion

The acid dissociation constants of BADA and its chelate stability constants are listed in Table I. If one consider the basicity of the donor nitrogen, the value of the second dissociation constant and the chelate stability constants of BADA may be expected in between those of aniline-*N*, *N*-diacetic acid[7] and of methylamine-*N*, *N*-diacetic acid[7]. The data obtained are in good accordance with our estimates, as is shown in Table I.

The other of the decreasing stability of the metal chelate is Cu(II)>Ni(II)>Pb(II)>Zn(II)>Co(II)>Ca(II)>Mg(II), as is listed in Table I. These values were calculated using Eqs. 15 and 16 for calcium and magnesium, and 10 and 11 for the rest of the metal ions, employing the data obtained from nine points on the titration curve in the $a=1.1\sim1.8$ range for each metal ion. The calculated values on each metal ion are found to be in good agreement within the range of experimental error, thus indicating the reasonableness of the assumption. The order of chelate stability for

TABLE I. THE STABILITY CONSTANTS OF CHELATES OF BADA AND RELATED LIGANDS
$\mu=0.1$ (KNO_3)

Ligand		 [7]	 [7]
	25°C	20°C	20°C
pk_1	2.24	2.12	2.40
pk_2	8.90	9.65	4.96
log K_{MA} for			
Cu(II)	10.51	10.09	6.57
Ni(II)	7.98	8.73	3.53
Pb(II)	7.39	—	3.49
Zn(II)	6.97	7.66	3.22
Co(II)	6.88	7.62	2.90
Ca(II)	3.13	3.75	1.50
Mg(II)	2.63	3.44	1.15

these ions is quite similar to that of methylamine-*N*, *N*-diacetic acid, as is shown in Table I. Moreover, the decreased values for the BADA chelates may be due to the electronegative effect of the phenyl group through $-CH_2-$ linkage.

Although we tried to apply this calculation to the range below $a=1.0$ for copper, nickel, zinc, lead and cobalt, it was only successful in the case of copper and nickel, failing for the rest of metal ions. For copper and nickel, the consistent values were obtained even in this earlier part of the titration curve, and their mean values were identical with those obtained from the later part of the curve.

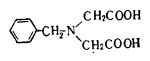
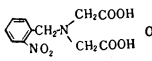
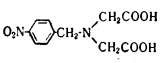
If one carefully examines the titration curves for zinc, lead and cobalt, a slight inflection will be noticed at a point near $a=1.0$. This inflection may indicates that the chelate formation reaction proceeds in two steps. The first step involves the formation of a hydrogen complex which predominates at the first buffer region of $a=0.8$, while the second step involves the formation of a neutral complex which predominates at the second buffer region of $a=1.3$. In the $a=0.8\sim1.3$ region, both reactions proceed simultaneously. Proceeding from this assumption, the stability constants of the hydrogen complex (K_{MHA}) with three metal ions were calculated in the first buffer region of $a=0.5\sim0.8$, the points used for the calculation being only five. The calculated values were found to be fairly consistent for the hydrogen complexes of cobalt and zinc, but not for lead. The values for cobalt and zinc thus determined are found to be $\log K_{CoHA}=2.7$ and $\log K_{ZnHA}=3.0$.

As the data used for the calculation were obtained from a relatively narrow range, these values may not be accurate enough. However, the formation of a hydrogen complex will be quite probable for zinc and cobalt. Although the calculation of the stability constant of a hydrogen complex for lead did not give satisfactory results, the formation of the hydrogen complex may also occur to some extent in this case.

The acid dissociation constants of *o*- and *p*-NBADA, as well as their chelate stability constants for calcium and magnesium, are listed in Table I. The first and second dissociation constants of both compounds indicate that these are more acidic than BADA. The higher acidity can be attributed to the electron inductive effect of the nitro group, which decreases the basicity of the donor nitrogen through $-CH_2-$ linkage. In the case of the *o*-isomer, the coplanarity of the nitro group is so hindered by the neighboring bis-(carboxymethyl)-iminomethylene group that the resonance of nitro group is decreased, which in turn reduces the inductive effect of the nitro group. Thus, the *o*-isomer is less acidic than the *p*-isomer, whose nitro group does not suffer from steric hindrance.

Table II. Alkaline earth chelating tendencies of BADA and its nitro derivatives

$t=25°C$, $\mu=0.1$ (KNO_3)

Ligand			
pk_1	2.24	1.99	1.80
pk_2	8.90	8.29	7.65
$\log K_{MA}$ for			
Ca(II)	3.13	2.93	2.53
Mg(II)	2.63	2.65	1.6

The stability constants of these two ligands with calcium and magnesium are found to be reasonable in comparison with those of BADA, and their stabilities decrease with the decreasing pk_2 values. The accuracy of the stability constant of magnesium chelate of *p*-NBADA is attained only to one decimal place on account of its low stability.

Summary

1. The acid dissociation constants of benzylamine-*N*, *N*-diacetic acid, and the stability constants of its chelates with Cu(II), Ni(II), Pb(II), Zn(II), Co(II), Ca(II) and Mg(II) at 25°C and 0.1 ionic strength, have been determined by the pH titration method.

2. *o*- and *p*-Nitrobenzylamine-*N*, *N*-diacetic acid have been newly synthesized from the corresponding benzylamine.

3. The acid dissociation constants of the above two ligands, and the stability constants of its chelates with Ca(II) and Mg(II), have been determined at 25°C and 0.1 ionic strength.

The author wishes to express his gratitude to Professor Keihei Ueno for his guidance and to Assistant Professor Yukito Murakami for his kind advice during the course of this investigation. He also wishes to thank Mr. Michio Shido, Miss Sachiko Indo and Miss Takeko Tahara for their microanalysis.

Finally, the expenses have been defrayed in part by a grant given by the Ministry of Education, to which the author's thanks are due.

Department of Organic Synthesis
Faculty of Engineering
Kyushu University
Hakozaki, Fukuoka

Concentration and Temperature Profiles in a Tubular Reactor for Methanol Synthesis with an Outer-wall of Uniform Temperature. I. Profiles in a Reactor without a Heat Exchanger in a Catalyst Bed

By Hiroshi UCHIDA, Yoshisada OGINO, Masaaki OBA and Kinya SHIMOMURA

(Received January 6, 1962)

The heat transfer problem concerning methanol synthesis reactor placed in a bath of boiling heat transfer medium has been discussed in a paper by Wirth[1], but his paper deals with neither the concentration profile nor the temperature profile in the catalyst bed. The present paper provides sets of concentration and temperature profiles obtained by the use of a tubular reactor for the methanol synthesis. The reactor was placed in a bath of flowing hot oil, and the determination of the profiles was conducted in essentially the same way as that used with the Fischer-Tropsch synthesis reactors in this laboratory[2,3]. Starting with the experimental concentration profile, calculation of the axial temperature profile by means of the conventional procedure was attempted in order to find out the reasonable values of heat transfer coefficients by comparison of the resultant profile with the experimental profile. In view of the most favorable temperature profile for methanol production, the experimental profile, in conjunction with the heat transfer efficiencies thus obtained, may be helpful in predicting a suitable means for improving the reactor performance.

Experimental

The synthesis gas, consisting of three parts hydrogen and one part carbon monoxide plus a small amount of inert gas (5~7% nitrogen), was furnished in a gas holder (400 m^3) by adding an amount of electrolytic hydrogen to water-gas produced in a water-gas generator. Before this addition, the water-gas was passed through a gas purification train in a method described elsewhere[1], and the sulfur content was reduced to about 1 p.p.m. Figure 1 shows a schematic diagram of the methanol synthesis. The synthesis gas was compressed by a gas compressor (A) to 250 kg./cm^2 and was then introduced into a high pressure gas storage (B), from which the compressed gas was injected as a make-up gas into a synthesis loop through a reducing valve (V_1). The synthesis loop consisted of a gas purifier (D) filled with active charcoal, a preheater (E) for

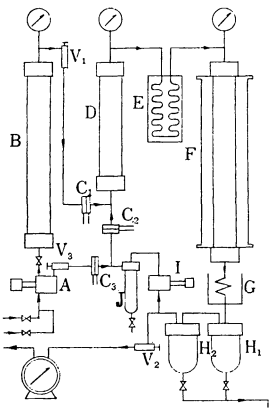


Fig. 1. Schematic diagram of methanol synthesis.

the synthesis gas, a reactor (F), a cooler (G), two methanol separators (H_1 and H_2), a gas circulating pump (I), and an oil separator (J) for removal of oil from the pump. Injection of the make-up gas was made immediately before the purifier in the synthesis loop in order that the gas might be removed from the last traces of sulfur prior to its entering the reactor. Part of the circulating gas was always being purged from the loop through a reducting valve (V_2) to keep the inert gas content below a certain limit, and the flow rate of purged gas was determined by means of a gas meter at atmospheric pressure. Moreover, the compressor was connected in order to allow compression of hydrogen into the synthesis loop through a reducing valve (V_3). The flow rates of the make-up gas and the circulating gas were determined by means of high pressure flow meters, C_1 and C_2 respectively.

A detailed sketch of the reactor is given in Fig. 2. The reactor had a total length of 2 m., an outer diameter of 100 mm., and an inner diameter of 50 mm., and was made of chromium steel (13% Cr). It was placed coaxially in a cylinder 300 mm. in diameter. Into the bottom of the cylinder, a heat tranfer medium (Kanechlol) was fed at a flow rate of 1.2 m^3/hr.; it passed upwards through an annular space between the reactor and the cylinder wall to the top, where the medium was allowed to flow down into a reservoir maintained at a fixed high temperature. The catalyst charge was 1.74 l. with a layer of 1 l. copper granules placed above the catalyst bed. The catalyst bed was 950 mm. high, occupying the intermediate range of the

1) G. Wirth, *Chem. Tech.*, 5, 253 (1953).
2) M. Kuraishi, H. Ichinokawa, K. Ogawa, K. Kurita, T. Hosoya and H. Uchida, *J. Chem. Soc. Japan, Ind. Chem. Sec.* (*Kogyo Kagaku Zasshi*), 63, 1588 (1960).
3) M. Kuraishi, M. Kurita, T. Hosoya, H. Ichinokawa, K. Ogawa and H. Uchida, This Bulletin, 34, 780, 1101 (1961).

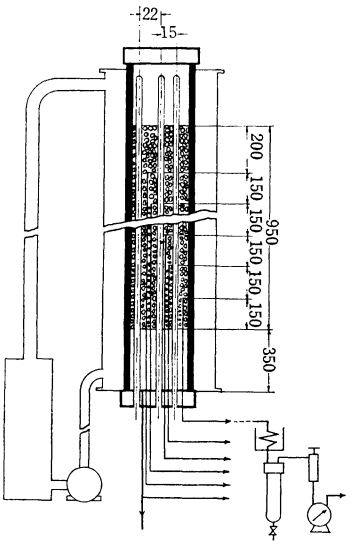


Fig. 2. Methanol synthesis reactor.

reactor between 350 and 1300 mm. from the bottom. Three thermocouple protection tubes of stainless steel went through the whole length of the catalyst bed. One of the tubes was a center thermocouple tube 8 mm. in outer diameter and with a thickness of 2 mm., while the others were off-center thermocouple tubes 5 mm. in outer diameter with a thickness of 1 mm. and were arranged in such a manner that they went through the bed 13 mm. and 22 mm. apart from the center axis respectively. The thermocouples could be moved upwards and downwards to permit scanning of the axial temperature profiles along the protection tubes.

Five small copper tubes, 2 mm. in outer diameter and 0.5 mm. thick, of different lengths were placed parallel in the catalyst bed, and from five successive ports, at 150, 300, 450, 600 and 750 mm. above the bottom of the bed, small portions of the fluid in the catalyst bed were withdrawn at a flow rate of 30 l./hr. out of the reactor; they then passed separately through small coolers and separators (50 cc. in volume) in order to produce the liquid product. Moreover, a small portion was led in the same way from the outlet tube by way of a tee placed immediately after the reactor. The gaseous product was reduced to atmospheric pressure, metered and analyzed, while the liquid product obtained in the small separators was weighed and analyzed. The analyses were made by means of gas chromatography as well as by conventional chemical methods. From the results of the analyses and the amounts of methanol obtained in the separators, the composition of the fluids at the five ports in the catalyst bed, as well as that of the exit gas, could be calculated.

For satisfactory performance of the reactor, caution had to be exercised, particularly at the beginning of the synthesis, to avoid a sudden temperature rise in the catalyst bed, which would cause an ignition of the catalyst granules. The entire system, accordingly, was first charged with hydrogen, which was circulated at about 100 kg./cm^2, while the heat transfer medium was heated up to 295°C. The make-up gas was then gradually introduced until the total pressure reached 200 kg./cm^2. The carbon monoxide content was subsequently increased by discharging continuously part of the circulating gas and by charging, in turn, the make-up gas until the synthesis could allow the collection of reliable performance data.

A three-component catalyst consisting of oxides of zinc, chromium and copper was used in this synthesis. Prepared in the way described previously[4], it contained zinc, chromium and copper in the atom ratios of Cr/Zn=0.49 and Cu/Zn=0.16. Before use in the synthesis, the catalyst was reduced in a separate oven at about 240°C in a current of the synthesis gas at atmospheric pressure. The catalyst granules were 3 mm. in diameter by 4 mm. high, and 1.74 l. of the reduced granules weighed 2.43 kg.

Results

Methanol Yield.—The methanol yields are illustrated in Table I, together with the corresponding operation variables. The yield, expressed by the space-time yield of the reactor, is rather lower than is usual with commercial reactors. It becomes higher as either the flow rate of the inlet gas is increased or as the

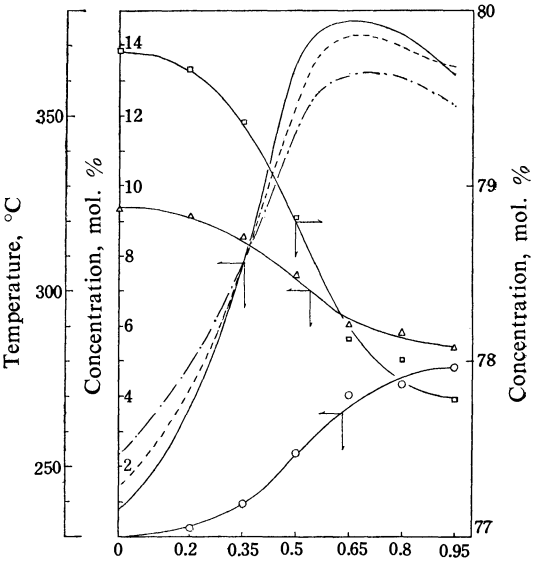


Fig. 3. Axial concentration and temperature profiles. Exp. 1.
Temperature profiles
—— Center profile
------ Off-center profile at r=15 mm.
—·— Off-center profile at r=22 mm.
Concentration profiles
—○— Methanol
—△— Carbon monoxide
—□— Hydrogen

4) Y. Ogino, M. Oba and H. Uchida, ibid., 33, 358 (1960).

TABLE I. OPERATION VARIABLES AND METHANOL YIELD

Exp.	Flow rate of inlet gas	Composition of inlet gas[a]	Oil bath temperature	Bed temperature		Methanol yield	Space-time-yield
				top	bottom		
	l./hr.	H_2/CO	°C	°C	°C	kg./day	kg./l. hr.
1	33570	8.5(10.9)	295±1	246	359	50.6	1.21
2	30000	8.6(10.8)	295±1	245	362	50.4	1.21
3	34600	9.1(10.1)	295±1	235	359	48.9	1.17
4	38740	8.0(9.2)	295±1	243	364	60.3	1.44
5	31070	9.1(9.8)	295±1	256	356	47.2	1.13
6	24680	9.7(10.0)	295±1	243	359	41.2	0.99
7	19430	10.7(9.5)	295±1	256	328	35.1	0.84
8	19980	10.5(10.4)	295±1	255	332	33.1	0.79
9	41130	4.8(6.9)	295±1	232	385	56.0	1.34
10	34470	3.0(7.7)	295±1	239	374	42.2	1.01

[a] Numerals in bracket indicate the inert gas content (vol. %).

ratio of hydrogen to carbon monoxide is decreased. The synthesis product contains only 1~3% water and 0~0.3% methyl formate as its impurities. Very little carbon dioxide or methane was detected in the exit gas from the reactor.

Temperature and Concentration Profiles in Catalyst Bed.—As is shown by the examples in Figs. 3 and 4, the axial profiles differ in minor details, even though the flow rate of the inlet gas and the composition of the synthesis gas vary within a certain range. The bed temperature remains below the oil bath temperature in the top zone of the catalyst bed, it rises rapidly in the intermediate zone, and, after having its maximum value, it decreases slowly in the bottom zone. In contrast to this, the methanol concentration is extremely low in the top zone, begins to rise in the intermediate zone, and continues to rise more slowly until the equilibrium concentration is attained at the bottom of the bed.

As is shown in Fig. 5, the radial temperature profile is concave upwards at the top of the bed, becomes flat in the intermediate zone, and finally turns convex upwards at the lower zone. The temperature rise over a cross section of the catalyst bed reaches as high as about 40°C in the bottom zone. Within the present

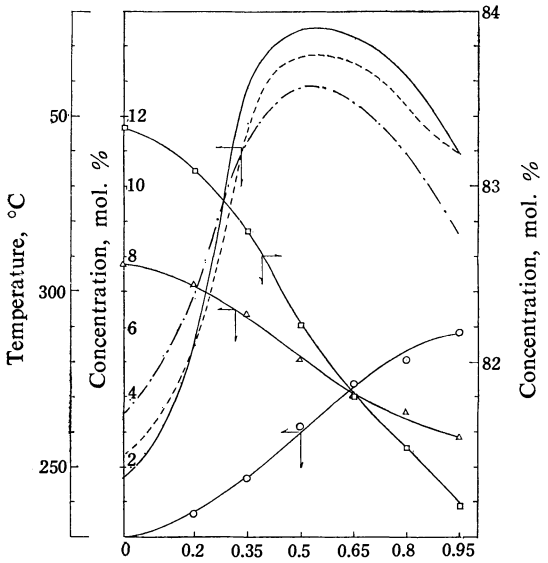


Fig. 4. Axial concentration and temperature profiles. Exp. 7.
Temperature profiles
—— Center profile
------ Off-center profile at r=15 mm.
—·— Off-center profile at r=22 mm.
Concentration profiles
—○— Methanol
—△— Carbon monoxide
—□— Hydrogen

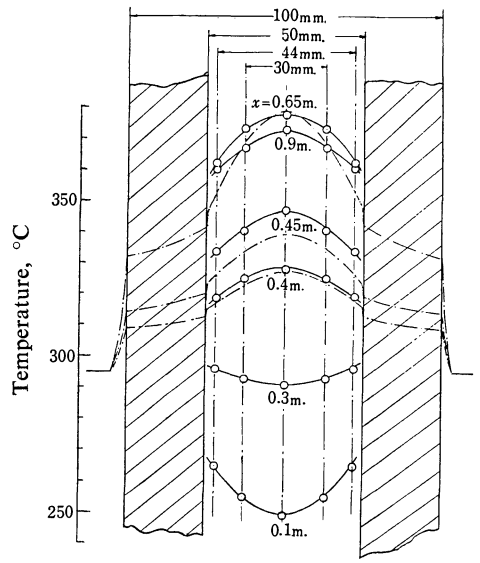


Fig. 5. Radial temperature profiles. Exp. 1.
—○— Experimental profiles
—·— Calculated profiles

range of operation conditions, the magnitude of the temperature rise increases with a decreasing ratio of hydrogen to carbon monoxide.

Axial Distribution of Reaction Heat.—The combination of the concentration data along the bed with the methanol yield of the reactor, as well as with the flow rate of the inlet gas, leads to the methanol flow rate as a function of the bed length (cf. the solid-line curve in Fig. 6). When the whole bed length is divided into six steps according to the heights of the ports at which a small portion of the fluid is withdrawn, the methanol yield within each step can be readily obtained from the flow rate curve (cf. the step-by-step dotted-line plot). Multiplication of the methanol yield by Thomas'[5] thermochemical data on the reaction heat of the methanol synthesis results in a step-by-step plot of the reaction heat (cf. the dotted and dashed-line plot). In the multiplication, the reaction heat is assumed to take a value corresponding to the temperature averaged throughout each step on the basis of the average temperature over a cross section.

Catalyst Activity.—The activities for the methanol synthesis of the catalyst samples before and after the present synthesis have been determined by the use of a small separate reactor (catalyst bed, 10 cc.), as has been reported previously[6]. The operating variables

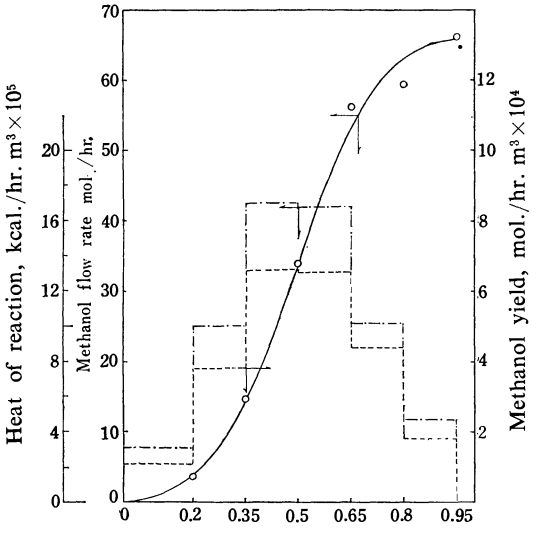


Fig. 6. Methanol flow rate, methanol yield and reaction heat of methanol synthesis as function of bed length. Exp. 1.
—○— Methanol flow rate
--------- Methanol yield
—·—· Heat of reaction

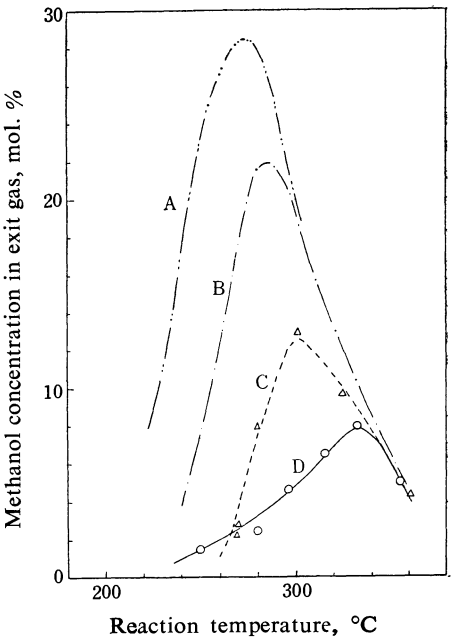


Fig. 7. Catalyst activity for methanol synthesis.
—·—· Activity after reduction at 250°C
—·—· Activity after heating at 360°C
---△--- Activity after heating at 450°C
—○— Activity after runs 1—10

were as follows: the pressure was 150 kg./cm², the space velocity was 1×10^4 hr^{-1}, and the H_2/CO ratio was 2. The results are shown in Fig. 7. Although the activity is high immediately after the reduction of the raw catalyst at 250°C (plot A), it becomes lower as the catalyst undergoes heating at higher temperatures, as is shown by plots B and C, obtained with the catalyst samples after heating them at 360 and 450°C for two hours respectively. The activity of the catalyst sample after the synthesis runs (plot D) 1—10 lies even lower than plot C. This low activity is probably due to the poisoning effect of sulfur, a minute amount of which is perhaps contained in the inlet gas.

Discussion

Calculation of Temperature Profiles.—The heat balance equation for a tubular reactor packed with catalyst granules is given generally as

$$C_pG\frac{\partial t}{\partial x}=\frac{1}{r}\left\{\frac{\partial}{\partial r}\left(\lambda_r\cdot r\frac{\partial t}{\partial r}\right)+\frac{\partial}{\partial x}\left(\lambda_x\cdot r\frac{\partial t}{\partial x}\right)\right\}+Q \qquad (1)$$

where C_p is the heat capacity of the fluid, G is the mass velocity based on an empty tube,

5) W. J. Thomas, *Ind. Eng. Chem.*, **50**, 967 (1958).
6) H. Uchida and Y. Ogino, This Bulletin, **31**, 45 (1958).

t is the over-temperature in the catalyst bed (which is defined by $t_b - t_w$, where t_b is the bed temperature and t_w is the temperature of heat transfer medium), x is the distance from the catalyst inlet, λ_x and λ_r are the respective thermal conductivities of the bed in the axial and lateral directions, and Q is the heat of the reaction. Strictly speaking, Q in Eq. 1 is to be given as a function of the reaction rate, and hence as a function of the temperature and concentration. For the sake of simplicity, the reaction heat was sometimes approximated to a function of x alone, and Eq. 1 was solved after this substitution. This approach was made by Kodama and Fukui, by Shindo, by Maeda, by Kjaer, and by Kuraishi et al., who have proposed the following formulae: $Q = q_0 e^{-cx}$ with $\lambda_x = \lambda_r$[7], or with $\lambda_x \neq \lambda_r$[8], $Q = Ae^{-cx} + B$[9], and $Q = c_1 e^{-Mx} + c_2 e^{-Nx}$[2], where q_0 is the reaction heat at the catalyst inlet and c, A, B, c_1, c_2, M, and N are constants conveniently chosen to fit the profile of the reaction heat. None of the above formulae, however, could express the present axial distribution data of the reaction heat. The solution of Eq. 1 along this line has, therefore, been given up, and a more simplified method, a step by step calculation of the temperature profile, has been adopted. In this method, the total bed length is divided into steps, and throughout each of the steps the heat of the reaction is assumed to be constant.

Under the further assumptions that the catalyst bed is cylindrical[10] and that λ_x and λ_r are identical and equal to λ_e, the solutions of the heat balance equations for the individual steps with the following boundary conditions,

$$(t_i)_{x=0} = t_{0i} - t_w, \quad (\lambda_e \partial t_i/\partial r + U t_i)_{r=R} = 0$$

are summarized by Eq. 2:

$$t_i = (t_i)_{x_i=0} \sum_{n=1}^{\infty} \frac{2J_0(a_n r/R) e^{-\alpha^2 y}}{a_n (1 + a_n^2/b^2) J_1(a_n)} + (Q_i/\lambda_e) \sum_{n=1}^{\infty} \frac{(R/a_n)^2 2J_0(a_n r/R)(1 - e^{-\alpha^2 n y})}{a_n (1 + a_n^2/b^2) J_1(a_n)} \tag{2}$$

in which the following abbreviations are introduced:

$$b = UR/\lambda_e, \quad A = (\lambda_e/C_p G)^2, \quad \text{and} \quad y = \lambda_e x_i / C_p G$$

In the above equations, t_i is the bed over-temperature, t_{0i} is the bed temperature at the top of the ith step ($x_i = 0$), R is the inner radius of the reactor tube, and U is the overall heat transfer coefficient, which is based upon the temperature difference between the catalyst bed at $r = R$ and the heat transfer medium and which is referred to the inner diameter of the reactor. Further, a_n's and α_n's are the positive roots of the following auxiliary equations, $a_n J_1(a_n) = b J_0(a_n)$ and $A\alpha_n^4 + \alpha_n^2 - a_n^2/R^2 = 0$, respectively. J_0 and J_1 are Bessel functions of the first kind, zero and first order respectively.

In the calculation of t by Eq. 2, the constants, such as C_p, k (the thermal conductivity of fluid) and μ (the viscosity of fluid), are evaluated in the sampe way as has been described elsewhere[1]; from k and μ thus obtained, λ_e is determined by the aid of the formula proposed by Hatta and Maeda[11]. U is usually defined by the equation:

$$1/U = 1/h + (1/h_L)(R/R_O) + (R/\lambda_s) \ln R_O/R \tag{3}$$

where h and h_L are the heat transfer coefficients referred to the inner and outer tube surfaces respectively, λ_s is the thermal conductivity of the reactor tube material, and R_O is the outer radius of the reactor tube. However, the evaluation of U is impossible, because the characteristic constants of the heat transfer medium, and consequently of h_L, are not available. As it is, a trial and error method has been adopted for the determination of U, as is described in the next paragraph.

The step lengths used in the calculation of the temperature profiles are 0.2 m. for the first step and 0.15 m. for the other steps; the Q_i corresponding to each step is found in Fig. 6. Furthermore, it should be noted that the application of Eq. 2 to the step by step calculation is permissible only if the radial temperature profile is uniform at the top of each step (cf. footnote 13). This, however, is not the case with the present experimental profiles. A more conventional procedure is, therefore, adopted to calculated the axial profile based on the average temperature over a cross section. Under the assumption that the catalyst inlet

7) S. Kodama and K. Fukui, *Chem. Eng.* (*Kagaku Kikai*), **14**, 259 (1950); S. Shindo, *Memoir Muroran Univ. Eng.*, **1**, 51 (1950).

8) S. Maeda, *Chem. Eng.* (*Kagaku Kogaku*), **19**, 212, 263 (1955).

9) L. Kjaer, "Measurement and Calculation of Temperature and Conversion in Fixed-bed Catalytic Reactors", Jul. Gjellerups Vorlag, Copenhagen (1958), p. 85.

10) The assumption is rather conventional. A similar solution of Eq. 1 for an annular-shaped cylindrical bed, through which passes a thermocouple tube, and a calculation of t by the aid of the solution were also made. The results have proved to be almost identical with those obtained by the use of Eq. 2. The cooling effects due to the other thin tubes placed in the bed are conventionally ignored in the present calculations.

11) $\lambda_e/k = 0.209(R_{ep})^{0.87}$, $R_{ep} = d_p G/\mu$, where R_{ep} is the modified Reynolds number, d_p is the diameter of catalyst granules (cf. footnote 12).

12) S. Hatta and S. Maeda, *Chem. Eng.* (*Kagaku Kikai*), **12**, 56 (1948).

13) M. Shindo and H. Kubota, ibid., **19**, 487 (1955).

TABLE II. THERMODYNAMICAL DATA, OVERALL HEAT TRANSFER COEFFICIENT AND OTHER MATTERS

Exp.	C_p kcal./kg.°C	μ kg./m.hr.	k kcal./m.hr.°C	λ_e kcal./m.hr.°C	G kg./m²hr.	R_{ep}	U kcal./m²hr.°C
1	0.9987	0.0793	0.2548	6.528	5.698×10^3	2.515×10^2	2.912×10^2
7	1.0934	0.0768	0.2605	3.814	2.901×10^3	1.322×10^2	2.912×10^2
9	0.8703	0.0824	0.2479	7.930	7.642×10^3	3.246×10^2	2.912×10^2

temperature is radially uniform with an arithmetically average temperature of the three experimental temperatures, the calculation of t at the end of the first step by the aid of Eq. 2 leads to a radial profile which is reduced to an average temperature over the cross section[14]. The average temperature is, then, assumed to be equal to that at the top of the second step; the same calculation is repeated as regards the second step, and so forth. In the calculation, a value of U was chosen in order that the calculated average temperature might fit the experimental temperature based on the arithmetically average one of Exp. 1 as closely as possible. The value of U thus obtained is given in Table II, together with the other constants. The procedure was then applied to the data of Exps. 7 and 9 as well as of Exp. 1; the resultant average temperatures are plotted as a function of the bed length in Fig. 8. For the sake of comparison, the figure includes the experimental profiles based on the arithmetically average temperature. The comparison shows that the profiles are almost, though not entirely, consistent with each other.

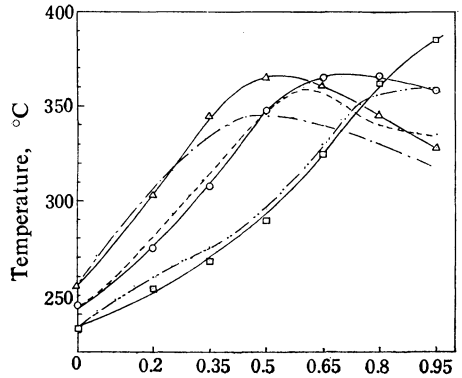


Fig. 8. Comparison between experimental and calculated profiles based on average temperature over cross section.
—○— Experimental Exp. 1
—△— Experimental Exp. 7
—□— Experimental Exp. 9
--------- Calculated Exp. 1
—·—· Calculated Exp. 7
—··— Calculated Exp. 9

14) The average temperature t_{av}, is calculated by means of the equation: $t_{av}=\int_0^R 2\pi rtdr/\pi R^2$.

This, however, may be the order of accuracy to be expected in the present performance data.

On the basis of the experimental facts in Exp. 1 that the radial temperature profile happens to be flat at a cross section 0.35 m. from the catalyst inlet and that the Q_i's are nearly equal between the third and the fourth steps (cf. Fig. 6), Eq. 2 may be applied to the calculation of the radial temperature profiles over cross sections within these steps. The calculated profiles are shown in Fig. 5. The discrepancy between the experimental and calculated profiles is small at the cross section very near the top of the third step, but it tends to increase to some extent with the increasing bed length.

Once U has been obtained for the present synthesis, h_L, in turn, is obtained from Eq. 3, since h in the equation can be calculated from the formula of Hatta and Maeda[15]. The values of h_L thus obtained are listed in Table III, together with those of U, h, and λ_s. By the use of these values, radial temperature profiles in the range from the bed at $r=R$ to the heat transfer medium can be drawn in the same way as has been reported previously[2]. Sample profiles are given in Fig. 5 for Exp. 1. The figure, like the table, clearly indicates that the heat transfer resistance is largest at the outer tube surface.

TABLE III. HEAT TRANSFER CONSTANTS

Exp.	h kcal./m²hr.°C	h_L kcal./m²hr.°C	λ_s kcal./m.hr.°C
1	2.797×10^3	2.091×10^2	2.530×10
7	2.859×10^3	2.084×10^2	2.530×10
9	2.722×10^3	2.099×10^2	2.530×10

Optimum Reaction Temperatures.—The determination of the optimum reaction temperature, at which the maximum rate of methanol synthesis is attained, is of interest in estimating the optimum operation conditions for a reactor. The determination can be conducted by the aid of a chart in which lines of constant conversion, with reaction rates as ordinates and temperatures as abscissas, are drawn.

As has been stated previously[4], the rate of

15) $hD/\lambda_e=254(R_{ep}d_p/D)^{-0.87}$, where D is the equivalent diameter of the catalyst bed (cf. footnote 12).

methanol synthesis is represented by the following equation:

$$r=k_d(a_{CO}a^2_{H_2})^{0.7}\ (1-a_{CH_3OH}/Ka_{CO}a^2_{H_2}) \qquad (4)$$

Upon substitution of the following relation for the reaction rate in a fixed-bed reactor, $r=(273\,\boldsymbol{R}c_mA)^{-1}\cdot dF/dx$, and subsequent rearrangement, Eq. 4 is rewritten as:

$$k=273\,\boldsymbol{R}c_mk_d=(dF/Adx)/(a_{CO}a^2_{H_2})^{0.7} \times(1-a_{CH_3OH}/Ka_{CO}a^2_{H_2}) \qquad (5)$$

In the equation, k_d is the rate constant, $\boldsymbol{R}$ is the gas constant, a is the activity, c_m is the mean compressibility coefficient of gas at a normal state, K is the equilibrium constant of methanol synthesis, F (m^3 (N. T. P.)/hr.) is the flow rate of methanol, and A is the cross sectional area of the bed. By the aid of Eq. 5, k at any x is calculated from experimental data, for instance, from the data of Fig. 6. Furthermore, one can draw an Arrhenius' plot of k, because the average temperature over a cross section at the x is determined from the experimental radial temperature profile. The plot is shown in Fig. 9, where an approximate activation energy of the methanol synthesis is found to be 15 kcal./mol. From combining the rate constants with the activation energy thus obtained, the rates at various methanol concentrations and temperatures in Exp. 1 are calculated by Eq. 4, and the resultant data are plotted in Fig. 10 as the lines mentioned above. This chart is restricted to a pressure of 200 kg./cm^2 of the synthesis gas, with a fixed composition and flow rate corresponding to those of Exp. 1. In the figure, the maximum rate curve, which indicates the most favorable temperature profile in the catalyst bed, is given by a thick broken-line curve, whereas the experimental rate curve is given by a thick solid-line curve. Comparison of the two curves discloses that. for attaining the efficient performance of the reactor, the temperature in the zone of low methanol concentration, or in the top zone of the catalyst bed, is too low, whereas the temperature in the zone of high methanol concentration, or in the bottom zone, is too high.

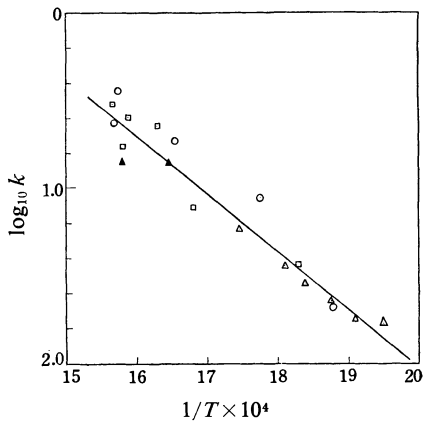


Fig. 9. Arrhenius' plot of rate constant.
○ Exp. 1 □ Exp. 7 ▲ Exp. 9
△ After use in runs 1—10 (refer to Fig. 7)

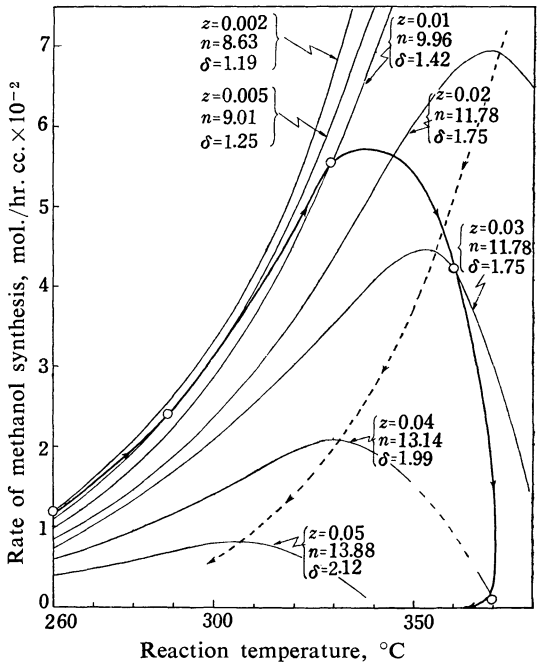


Fig. 10. Effect of temperature and conversion on rate of methanol synthesis.
------ Maximum rate curve
—— Rate curve for Exp. 1
z, methanol concentration $n=H_2/CO$,
δ=inert gas/CO

If the heat transfer referred to the outer tube surface is improved, the axial temperature profile could be more uniform, becoming higher in the top zone and lower in the bottom zone, and, as a consequence, the experimental rate curve would approach the maximum rate curve. Nevertheless, this improvement alone would not necessarily diminish the large magnitude of the temperature rise in the catalyst bed. With the increasing methanol output, the magnitude is liable to increase more considerably in the bottom zone. An alternate means of providing a suitable control of the bed temperature is the use of a heat exchanger in the catalyst bed, by which the temperature could be controlled by radial heat transfer through the bed. The effect of a heat exchanger on the bed temperature profile, and consequently on the reactor performance, will be described in our next paper.

Summary

On the basis of the experimental concentration and temperature profiles for one of the synthesis runs, the experimental rate curve has been drawn on a chart in which lines of constant conversion with reaction rates are given as ordinates and temperatures as abscissa. In a step by step calculation of the temperature profiles from the experimental profiles by the use of a set of analytical solutions of the heat balance equation, which includes the respective constant reaction heat terms given by the step by step distribution plot, the heat transfer coefficients are conveniently chosen to match the calculated profiles with the experimental ones. Taking the heat transfer efficiencies thus obtained into consideration, a comparison of the experimental rate curve with the maximum rate curve on the afore-mentioned chart discloses that, for attaining an efficient performance of the reactor, not only should the heat transfer referred to the outer tube surface be improved, but also the temperature rise in the catalyst bed should be controlled by a suitable means.

Government Chemical Industrial Research Institute, Tokyo
Shibuya-ku, Tokyo

Investigation of Chemisorption by Desorption Rate Measurement; CO_2 on ZnO and NiO; CO on NiO

By Yutaka KUBOKAWA and Osamu TOYAMA

(Received January 31, 1962)

The importance of desorption rate measurements in the investigation of chemisorption has been emphasized in recent work[1] by one of the present authors. It would seem that the most general method would be to determine the heats of adsorption from adsorption isotherms at various temperatures, but in this case the measurements are often limited to a narrow range of coverage because of a slow attainment of equilibrium, particularly at low temperatures. On the other hand, measurements of the desorption rate have no such limitations, permitting an investigation over a wide range of coverage; they also make it possible to obtain information concerning the energy relation for a given chemisorption. In addition, it has been shown that desorption measurements can lead to definite conclusions concerning the relation between the electronic state of an oxide and its chemisorption, the nature of surface heterogeneity, and also the problem of whether or not two types of chemisorption are operative. The present work describes an extension of such desorption experiments to a number of chemisorption systems.

The chemisorption of carbon dioxide on zinc oxide has been investigated by Kwan et al.[2], who have shown that the heat of adsorption as determined from adsorption isotherms ranges from 35 to 48 kcal./mol. On the other hand, the calorimetric measurements carried out by Garner and Veal[3] have shown that the heat of adsorption is only 13 kcal./mol. As for the chemisorption of carbon monoxide on nickel oxide, there seems to have been no studies made of the heat of adsorption apart from the calorimetric measurements of Dell and Stone[4]. Further work is necessary to obtain a complete knowledge of all of the above systems. According to the electron barrier theory suggested by Hauffe and others[5], both systems mentioned above belong to a class characterized by anionic chemisorption on an *n*-type conductor or by cationic chemisorption on a *p*-type conductor, in which a depletion of charge carriers occurs in the boundary layer. If the formation of such a depletive layer played a large part in determining the behavior of the chemisorption, the amount adsorbed and other properties would be seriously affected by oxygen treatment at a high temperature, which would be expected to change the concentration of carriers markedly. Thus, in the present work, the energy relations of, as well as the effects of oxygen treatment

1) Y. Kubokawa, This Bulletin, **33**, 546, 550, 555, 739, 747, 936 (1960).

2) T. Kwan, T. Kinuyama and Y. Fujita, *J. Res. Inst. Catalysis, Hokkaido Univ.*, **3**, 31 (1953).

3) W. E. Garner and E. J. Veal, *J. Chem. Soc.*, **1935**, 1487.

4) R. M. Dell and F. S. Stone, *Trans. Faraday Soc.*, **50**, 501 (1954).

5) K. Hauffe and H. J. Engell, *Z. Elektrochem.*, **56**, 366 (1952); **57**, 763, 773 (1953); P. B. Weisz, *J. Chem. Phys.*, **21**, 1531 (1953).

on, both of these systems have been investigated by making use of desorption measurements.

Experimental

Materials. — Nickel oxide was prepared by the thermal decomposition of nickel nitrate at 400°C and then by sintering it at 700°C for 5 hr. Zinc oxide was prepared from zinc oxalate in a method described in a previous paper[1]. The reagents were of an extra pure grade. Carbon dioxide and oxygen were obtained from the thermal decomposition of magnesium carbonate and potassium permanganate respectively. Carbon monoxide was prepared by the reaction of air-free formic acid and concentrated sulfuric acid. All the gases used were purified as usual with liquid nitrogen.

Apparatus and Procedure.—The amount adsorbed was determined by using a conventional constant volume apparatus. The method for measuring the rate of desorption has been described previously and will be repeated here only in outline. The chemisorbed gas was desorbed by means of a mercury diffusion pump, and the desorbed gas was collected in a McLeod gauge and its pressure followed at definite intervals. The activation energy of desorption was determined as follows: The temperature of desorption was lowered abruptly during the desorption experiment, and the rates before the temperature drop were extrapolated to those for the smaller amounts adsorbed when the measurements were carried out after the temperature drop. Thus, the rates at the two temperatures corresponded to the same amount adsorbed, and, hence, the activation energy of desorption could be obtained. It was found that the process of readsorption had no effect on the rates of desorption, or at least on the activation energy of the desorption or on the value of $d \ln v_{des}/dq$ (v_{des}, rate of desorption; q, adsorbed amount).

Prior to the chemisorption experiments, all the adsorbents were evacuated for five hours at 450°C. The weight of the adsorbent and the surface area determined by the B. E. T. method using nitrogen adsorption are shown in Table I.

TABLE I

Adsorbent	Weight g.	Surface area $m^2/g.$
ZnO	16.72	6.1
NiO I	5.49	3.1
NiO II	28.61	3.4

NiO I was used for CO_2 chemisorption and NiO II for CO chemisorption.

Results and Discussion

Activation Energies of Desorption at Various Coverages.—*Carbon Dioxide Chemisorption on Zinc Oxide and Nickel Oxide.* — After carbon dioxide had been allowed to chemisorb at about 300°C for 2 hr., the temperature of the specimen was raised from −30 to 400°C in stages, at each of which the activation energy of the desorption was determined in the manner given above. The results are shown in Fig. 1. It is seen that in the range below room temperature the activation energy of the desorption is about 16 kcal./mol., while above room temperature it increases with the temperature of the desorption, up to 40 kcal./mol. After carbon dioxide had been adsorbed at about 400°C, the adsorption isotherms were determined by successive withdrawals of the gas by a method described in the previous paper[1]. The isotherms thus determined were reproducible on increasing or decreasing the pressure. The results are represented in Fig. 2. The heats of adsorption determined from these isotherms are represented in Fig. 1,

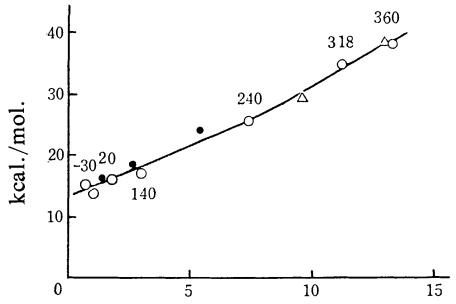


Fig. 1. Activation energies of desorption of carbon dioxide chemisorbed on zinc oxide. The amount adsorbed at room temperature before desorption was 14.33 cc. before oxygen treatment and 13.31 cc. after oxygen treatment. Figures indicate the temperature of desorption. -○-, before treatment; -●-, after treatment. The symbol △ refers to the heat of adsorption.

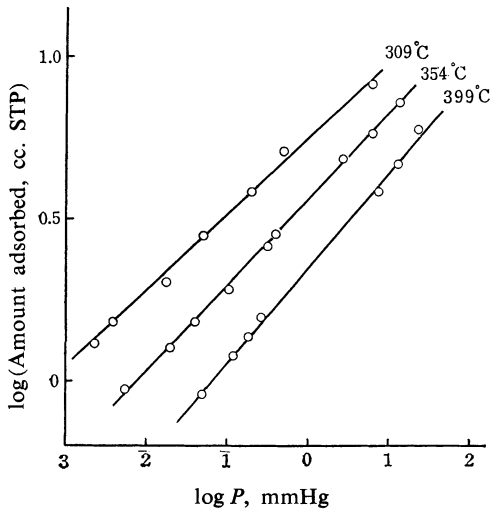
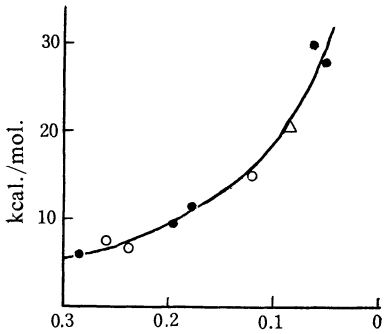


Fig. 2. Adsorption isotherms of carbon dioxide on zinc oxide.



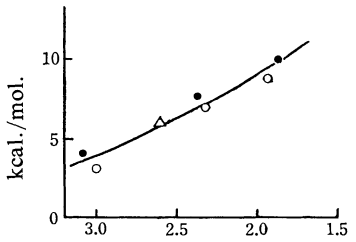
q or cq
(q, Amount adsorbed, cc. STP; $c=1.45$)

Fig. 3. Activation energies of desorption of carbon dioxide chemisorbed on nickel oxide. The amount adsorbed at room temperature before desorption was 0.357 cc. before oxygen treatment and 0.263 cc. after oxygen treatment. -○-, befor treatment; -●-, after treatment. The symbol -△- refers to the heat of adsorption.

together with the activation energy of the desorption. It follows from this figure that, for the range with an activation energy of desorption of 40 kcal./mol., which is close to the maximum value for this system, the chemisorption involves no activation energy. Consequently, for the range with a lower activation energy of desorption, the same conclusion may also be applicable.

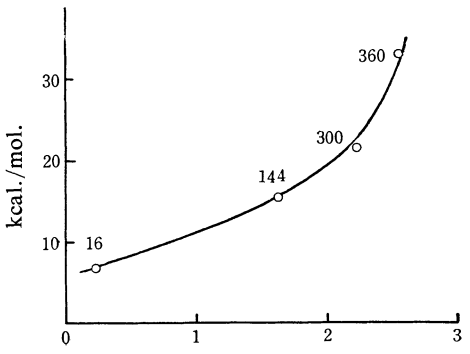
For carbon dioxide chemisorption on nickel oxide, the activation energies of desorption at various coverages were determined in a similar manner. The results are represented in Fig. 3. A comparison with the heats of adsorption determined from the adsorption isotherms shows that the chemisorption is also of a non-activated type. It is evident from Figs. 1 and 3 that the activation energy of desorption, as well as the adsorbed amount per unit area, is much less on nickel oxide than on zinc oxide.

Carbon Monoxide Chemisorption on Nickel Oxide. — After carbon monoxide had been chemisorbed at room temperature, the activation energies of desorption were determined in a similar manner in the range below room temperature. The results are represented in Fig. 4. Figure 5 shows similar results obtained with a specimen on which carbon monoxide chemisorption had been carried out at about 260°C. The carbon dioxide content of the desorbed gas was examined by immersing the trap attached to the McLeod gauge in liquid nitrogen. As is seen in Fig. 6, the content is negligibly small below room temperature, but it increases steadily with the increasing temperature of the desorption. At 250°C, most of the desorbed gas consists of carbon dioxide.



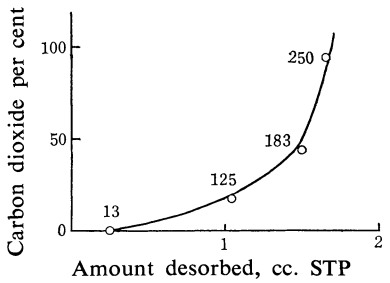
Amount left adsorbed, cc. STP

Fig. 4. Activation energies of desorption of carbon monoxide chemisorbed on nickel oxide. The amount adsorbed at room temperature before desorption was 2.82 cc. before oxygen treatment and 2.64 cc. after oxygen treatment. -○-, before treatment; -●-, after treatment. The symbol -△- refers to the heat of adsorption.



Amount desorbed, cc. STP

Fig. 5. Activation energies of desorption of carbon monoxide chemisorbed on nickel oxide. Carbon monoxide was chemisorbed at about 260°C. Figures indicate the temperature of desorption. The amount adsorbed at room temperature before desorption was 2.69 cc.



Amount desorbed, cc. STP

Fig. 6. Carbon dioxide content of the desorbed gas. Figures indicate the temperature of desorption.

Such behavior indicates the existence of two types of chemisorption, one being reversible, the other, irreversible. As is seen in Fig. 6, most of the carbon monoxide reversibly adsorbed can be desorbed below 200°C, suggesting that the upper limit of the activation energy of the desorption for the reversible type is about 16~20 kcal./mol. (Fig. 5).

The adsorption isotherms were determined to be between 0°C and −22°C in a manner similar to that described above. The heat of adsorption determined from these isotherms is represented in Fig. 4. It follows from this figure that the reversible chemisorption is of a non-activated type. On the other hand, it was found that the adsorption isobar obtained on increasing the temperature of the specimen, which had chemisorbed carbon monoxide at room temperature, showed a maximum at about 250°C, suggesting that some part of the irreversible chemisorption involves an activation energy.

Two Types of Chemisorption and their Behavior in Desorption.—According to previous work by one of the present authors[1], there seems little doubt that, at least in the case of the chemisorption on oxides, the heat of the adsorption or the activation energy of the desorption increases with the adsorbed amount mainly as a result of an a priori heterogeneity of the surface rather than an induced heterogeneity[6] or interaction between the adsorbed species. For such a heterogeneous surface the rate of desorption can be derived by introducing the following method, first given in a previous work[7]. The surface may be divided into a number of sets of identical sites, each of which has a particular activation energy of desorption. At any moment during the desorption experiments, there exists a certain set of sites, S_m, for which the rate of desorption passes through a maximum. Such a maximum rate may be assumed to be approximately proportional to the rate for the whole surface. The rate expression thus derived is given as

$$\mathrm{d} \ln v_{\mathrm{des}}/\mathrm{d}q = -(\mathrm{e}^{\beta}/RTN\theta)$$

where θ and N are the coverage at equilibrium and the distribution function of the sites respectively, both referring to the set of sites, S_m, mentioned above, and β is a constant associated with the distribution of sites. As was described in a previous work, the term of e^{β} is of secondary importance in determining the value of $\mathrm{d} \ln v_{\mathrm{des}}/\mathrm{d}q$. It may therefore be expected that the value of $\mathrm{d}q/\mathrm{d} \ln v_{\mathrm{des}}$ will increase with the increasing value of $N\theta$ and vice versa.

In the desorption rate measurements, if the temperature of the specimen is raised in stages, as has been described above, the set of sites, S_m, will be shifted in the direction of a higher activation energy of desorption, that is, of a higher value of θ, with the increasing temperature of the desorption. The variation of N, accompanied by such a shift of S_m, depends upon the distribution of sites; without any information about this, however, a quantitative discussion of it does not seem feasible. However, at least for the case in which only one type of adsorption is operative, it would not be expected that the value of N, and hence the product $N\theta$, would pass through a minimum with the progress of the desorption, since θ is increased with the increasing temperature of the desorption. Thus, the occurrence of such a minimum in $N\theta$, i.e., $\mathrm{d}q/\mathrm{d} \ln v_{\mathrm{des}}$, suggests that the adsorption sites are divided into two groups, which is to be expected for two types of chemisorption. As an illustration, we can mention the results of the chemisorption of carbon monoxide on nickel oxide, for which the existence of two types of chemisorption has been confirmed. From the plots of $\log v_{\mathrm{des}} - q$ at various temperatures for this system, the values of $\mathrm{d}q/\mathrm{d} \log v_{\mathrm{des}}$ at different amounts adsorbed were determined to be as shown in Fig. 7. It is seen that this value shows a minimum at 150~170°C, below which temperature most of the carbon monoxide reversibly chemisorbed can be desorbed (Fig. 6), thus confirming the above conclusion.

Similar treatments were carried out using

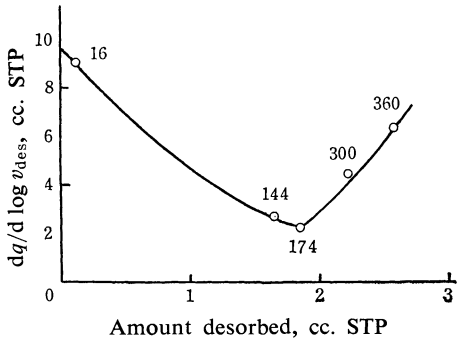


Fig. 7. Values of $\mathrm{d}q/\mathrm{d} \log v_{\mathrm{des}}$ for carbon monoxide chemisorption on nickel oxide. Figures indicate the temperature of desorption.

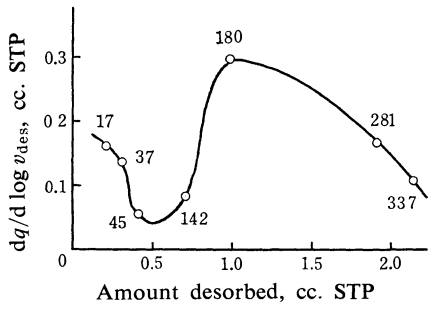


Fig. 8. Values of $\mathrm{d}q/\mathrm{d} \log v_{\mathrm{des}}$ for carbon dioxide chemisorption on zinc oxide. The weight of adsorbent used in these runs was 3.51 g. Figures indicate the temperature of desorption.

6) M. Boudart, *J. Am. Chem. Soc.*, **74**, 3556 (1952).
7) Y. Kubokawa, This Bulletin, **33**, 734, 1226, 1227 (1960).

the results of desorption experiments on other systems. For carbon dioxide chemisorption on zinc oxide, a similar minimum is observed, as may be seen in Fig. 8. This suggests the existence of two types of chemisorption, the existence of which has been recently supported by the work of Matsushita[8] on the infrared spectrum of carbon dioxide chemisorbed on zinc oxide. On the other hand, for the carbon dioxide-nickel oxide system, somewhat different results were obtained, the value of $dq/d \log v_{des}$ decreasing steadily with the increasing temperature of the desorption. Such behavior is inconsistent with that expected for the two types of chemisorption. Further study, therefore, seems necessary before we can understand the difference between the nickel oxide and zinc oxide systems and clarify the true nature of the two types of chemisorption on zinc oxide.

Effect of Oxygen Treatment on the Chemisorption.—This problem was investigated in the following way. All the adsorbents were treated with oxygen at about 450°C, followed by evacuation at 260°C for carbon dioxide and at 100°C for carbon monoxide chemisorption. The activation energies of the desorption at various coverages were then determined in a similar manner. As may be seen in Figs. 1 and 4, for carbon monoxide on nickel oxide and for carbon dioxide on zinc oxide such an oxygen treatment has little or no effect on either the adsorbed amount or on the activation energy of the desorption. This indicates that both chemisorptions are essentially independent of the electronic state of the adsorbents. It may, therefore, be concluded that the formation of an electrical double layer at the interface, which has been emphasized by Hauffe and others, probably plays no significant role in determining the features of the chemisorption already mentioned, although some contribution by ionic binding to the adsorption bond is undeniable. It seems likely that the above-mentioned marked change in the activation energy of the desorption with the change in coverage is mainly to be attributed to a heterogeneity of the surface, as was concluded in a previous work. Such a conclusion is supported by a marked variation in the value of $dq/d \log v_{des}$ with a slight change in the coverage, examples being given in Figs. 7 and 8. As has been described previously, such a phenomenon seems very difficult to explain in terms of the concept of induced heterogeneity.

For carbon dioxide on nickel oxide, somewhat different results were obtained, the amount adsorbed being appreciably reduced after the oxygen treatment. However, if q is replaced by cq (c, constant) in the plots of the activation energy of the desorption against q, then the resulting plots before and after the oxygen treatment lie on the same curve, as may be seen in Fig. 3. This slight effect on the activation energy of the desorption and the results obtained with zinc oxide suggest that the decrease of the adsorbed amount is not closely associated with a change in the electronic state.

Carbon dioxide chemisorption on doped zinc oxide has been investigated by Hart and Sebba[9]. According to their work, the doping with aluminum oxide, which increases the electrical conductivity of zinc oxide, increased the heat of the adsorption, while the doping with lithium oxide had a reverse effect; they have discussed such effects in terms of the change in the Fermi level of zinc oxide. As has been suggested by various workers, however, it should be taken into consideration that such doping will change the surface heterogeneity as well as the electronic state of zinc oxide, both changes affecting the features of the chemisorption. It seems questionable, therefore, to attribute the effect of doping to only the change in the electronic state, as these workers have done. In fact, rather unusual behavior is observed in their work, since they show that the adsorbed amount per unit area is the largest on lithium-doped zinc oxide, which shows the lowest heat of adsorption.

Summary

As an extension of previous work, the study of chemisorption by desorption rate measurement was carried out for carbon dioxide adsorbed on zinc oxide and nickel oxide, and also for carbon monoxide adsorbed on nickel oxide. For the chemisorption of carbon dioxide, the activation energy of the desorption was increased with the decreasing amount adsorbed from 16 to 40 kcal./mol. on zinc oxide and from 7 to 30 kcal./mol. on nickel oxide. In the case of the chemisorption of carbon monoxide, where the two types of chemisorption are seemingly operating, the activation energy of the desorption for the reversible type ranged from 5 to 18 kcal./mol. A method of distinguishing these two types of chemisorption from the behavior on desorption has been proposed, for it has been found that there are two types of chemisorption for the carbon dioxide-zinc oxide system. From the effect of oxygen treatment at high temperatures on the chemisorption, it was concluded that the effect

8) S. Matsushita and T. Nakata, *J. Chem. Phys.*, **36**, 665 (1962).

9) P. M. G. Hart and F. Sebba, *Trans. Faraday Soc.*, **56**, 551 (1961).

of the surface barrier, emphasized by Hauffe and others, seems to be only of secondary importance in the above system.

We wish to express our sincere thanks to Mr. Seishi Takeuchi and Mr. Hironori Kushiro for their collaboration in this work.

Department of Applied Chemistry
College of Engineering
University of Osaka Prefecture
Sakai-shi, Osaka

Polymerization of Isoprene with a Tin Tetraalkyl-Titanium Tetrachloride Catalyst

By Nobuyuki ASHIKARI, Hirotaka HIRATA and Kazuo YANAGISAWA

(Received January 31, 1962)

Many studies[1,2] of the polymerization of isoprene have been undertaken in an attempt to prepare a natural rubber-like polymer using such a typical Ziegler catalyst as aluminum trialkyl-titanium tetrachloride. Moreover, Saltman et al.[3] studied the mechanism of isoprene polymerization with aluminum triisobutyl-titanium tetrachloride.

There is a patent[4] concerning isoprene polymerization using tin tetraalkyl as a component of the catalyst system of SnR_4-$TiCl_4$-$AlCl_3$. However, the catalyst system is so complicated that any analysis of the reaction scheme is comparatively difficult. The authors, therefore, studied the polymerization by a comparatively simple catalyst system consisting of two components, tin tetraalkyl and titanium tetrachloride, in order to obtain fundamental data prior to treating a more complicated system.

Experimental

Materials. — Isoprene was synthesized by the thermal decomposition of limonene according to Staudinger's method[5] and was purified by redistillation. Commercial solvents such as *n*-hexane, benzene and toluene were purified by distillation after drying them with sodium. Titanium tetrachloride was treated with copper dust and distilled. Tin tetraalkyl was synthesized by the usual method[6], i. e., by the reaction between a Grignard reagent and tin tetrachloride in ether, and was employed after a by-product, R_3SnCl, had been removed.

Polymerization. — In every case, the catalyst complex was prepared by mixing the two components at room temperature in a polymerization tube filled with gaseous nitrogen. Then the complex was aged at that temperature for about 30 min., except for the case of finding the effect of the aging time on the polymerization rate. The complex thus produced was usually a large block. After a solvent, benzene or hexane, had been poured into the tube, the block was divided as finely as possible by high speed shaking. Then the tube was cooled in dry ice-methanol and sealed after a desired amount of monomer had been introduced into it. The reaction was started by transferring the tube into a constant temperature bath. The polymer produced was dipped in methanol containing hydrochloric acid to decompose the catalyst residue, filtered, washed thoroughly with methanol, and dried.

Investigation of Microstructure. — The microstructure of the polymer was investigated by infrared-measurement of the absorption bands in the 750～900 cm^{-1} region. The sample was placed between two rock salt plates to protect it from oxidation during the measurement. This protective procedure was found to be necessary, particularly in the case of measurements at elevated temperatures.

Measurement of Viscosity. — The Viscosity of the soluble part of the polymer was measured in toluene as a solvent at 30°C. Thus, the intrinsic viscosity was obtained.

Results

Effect of the Aging Time on the Polymerization Rate.—The relation between the aging time and conversion is shown in Fig. 1. In this case, the polymerization was carried out with a tin tetraethyl-titanium tetrachloride catalyst at 25°C for one hour. The Sn/Ti ratios shown by the A, B and C lines were 1.40, 2.25 and 0.28 respectively. The polymerization rate dropped suddenly in the initial stage and became almost constant after

1) E. g., H. E. Adams, R. Stearns, W. A. Smith and J. L. Binder, *Ind. Eng. Chem.*, **50**, 1507 (1958).
2) N. G. Gaylord and H. F. Mark, "Linear and Stereoregular Addition Polymers", Interscience Publishers, Inc., New York (1959), p. 372.
3) W. M. Saltman, W. E. Gibbs and J. Lal, *J. Am. Chem. Soc.*, **80**, 5615 (1958).
4) Solvay and Cie., Belg. Pat. 547618 (1956).
5) H. Staudinger and H. W. Klever, *Ber.*, **44**, 2212 (1911).
6) P. Pfeiffer and K. Schnurmann, ibid., **37**, 319 (1904).

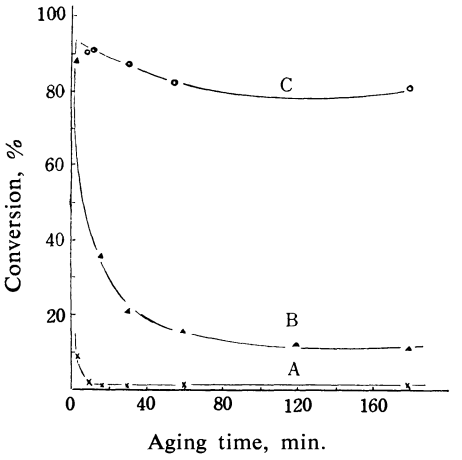


Fig. 1. Effect of aging time on the polymerization rate. Catalyst composition (Sn/Ti) ;
A: 1.40, B: 2.25, C: 0.28
$TiCl_4$, 5.46×10^{-3} mol.; monomer, 5 cc.; hexane, 5 cc.

a certain aging time although the time required for this constancy to be attained was different according to the variation in the molar ratio of the catalyst components.

Effect of Catalyst Composition on the Properties of the Polymer.—Here, properties of polymer' indicates the solubility, the intrinsic viscosity and the microstructure. The experiments for investigating these properties were performed on the polymers produced by the $Sn(i\text{-}C_3H_7)_4$-$TiCl_4$ catalyst at 40°C. In this case, the amount of monomer used was 10 cc. in each polymerization. The polymer was extracted by boiling toluene after being purified. Solubility and intrinsic viscosity are summarized in Table I.

Table I. Polyisoprene produced by $Sn(i\text{-}C_3H_7)_4$-$TiCl_4$

No.	SnR_4 $\times10^2$ mol.	Sn/Ti	Soluble part %	$[\eta]\times10^2$
1	0.203	0.22	71.0	5.64
2	0.406	0.44	90.8	5.68
3	0.812	0.88	75.4	4.88
4	1.218	1.31	73.3	4.57
5	1.624	1.75	81.3	5.30

$TiCl_4$, 9.26×10^{-3} mol.; monomer, 10 cc.; benzene, 10 cc.; temp., 40°C, time, 4 hr.

From the table it can be concluded that the yield of a soluble part and the intrinsic viscosity have no direct connection with the catalyst composition. Generally, the molecular weight (deduced from the intrinsic viscosity) of polyisoprene produced by the SnR_4-$TiCl_4$ catalyst seems to be low.

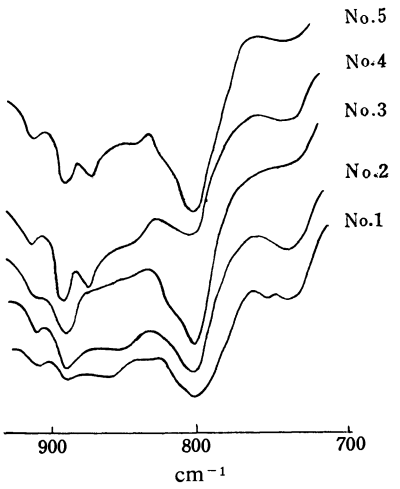


Fig. 2. Infrared spectra of the samples produced by $Sn(i\text{-}C_3H_7)_4$-$TiCl_4$.

Microstructure.—The infrared spectra of the samples shown in Table I are represented in Fig. 2. The spectra indicate that the microstructure of the polymers is similar to that of gattapercha, shown in Fig. 3. Therefore, it is clear that the polymers consist for the most part of *trans*-1, 4 structure.

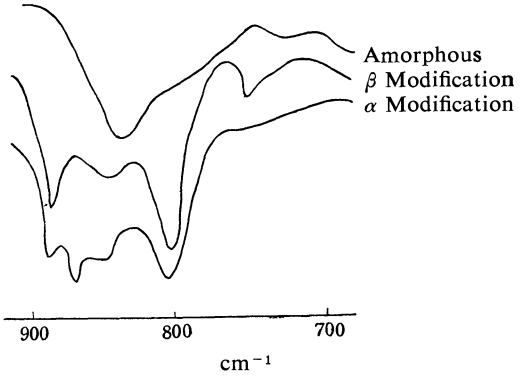


Fig. 3. Infrared spectra of guttapercha, cited from Richardson's paper[7].

Later some of the absorption bands which appeared in 750~900 cm^{-1} region will be discussed. Here, let it only be noticed that the microstructure is greatly affected by the catalyst composition. When the tin tetraalkyl increased to some extent, the microstructure had a close resemblance to that of the α type of guttapercha.

Crystalline Band.—The infrared spectra of the sample of No. 5 were observed in a molten and annealed state (Fig. 4). The specimen was treated carefully to prevent it from oxidation. Figure 4 shows the results obtained

7) W. S. Richardson and A. Sacher, *J. Polymer Sci.*, **14**, 353 (1953).

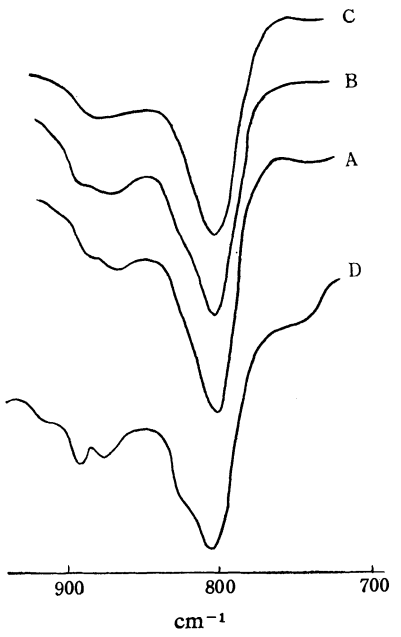


Fig. 4. Infrared spectra of No. 5 at various temperatures.
A: 85°C, B: 105°C, C: 150°C, D: annealed.

at 85, 105 and 150°C and in the annealed state. Since the intensity of the bands at 870 and 890 cm^{-1} decreased with an increase in the temperature and since they reappeared in the re-cooled state, it may be said that they resulted from the crystalline structure.

Here, it must be noted that the crystalline band does not reappear, even if the polymer is crystallizable, when the observation is made as soon as the specimen is re-cooled. The facts was confirmed by a preliminary experiment using a crystalline guttapercha.

Simple Kinetics.—The effects of monomer and catalyst concentration on the polymerization rate were investigated using the $SnEt_4$-$TiCl_4$ catalyst, in which the Sn/Ti ratio is constant (1.09). Tables II and III show the results obtained from the polymerization with a constant concentration of monomers and a constant concentration of catalysts respectively. The tables show that the over-all reaction rate is of the first order with respect to the

TABLE II. POLYMERIZATION UNDER CONSTANT CONCENTRATION OF MONOMER

[C] (mol./l.) $\times 10$	R_p (mol./l./sec.) $\times 10^5$
0.618	1.88
1.853	3.20
3.705	5.35
6.176	8.38

Monomer, 5 cc.; hexane, 10 cc.; Sn/Ti, 1.09

TABLE III. POLYMERIZATIONS UNDER CONSTANT CONCENTRATION OF CATALYST

Monomer cc.	*n*-Hexane cc.	R_p (mol./l./sec.) $\times 10^5$
5	25	4.81
15	15	13.1
20	10	18.1

$SnEt_4$, 10.12×10^{-3} mol.; $TiCl_4$, 9.26×10^{-3} mol.; temp., 21°C

concentration of the catalysts and monomers, [C] and [M].

$$R_p = k\,[C]\,[M]$$

Here, [C] means the concentration of titanium tetrachloride.

Over-all Energy of Activation. — In all experiments at various temperatures, 0.1 mol. of monomer was polymerized in 5 cc. of an *n*-hexane solution containing 10.12×10^{-3} mol. of tin tetraethyl and 9.26×10^{-3} mol. of titanium tetrachloride. The results are represented in Fig. 5. By plotting the R_p calculated from Fig. 5 against $1/T$, Fig. 6 was obtained. Therefore, the value of the apparent activation energy was obtained as 13.6 kcal./mol.

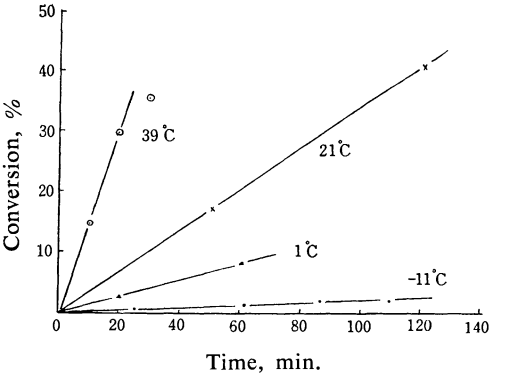


Fig. 5. Polymerization rates at various temperatures.

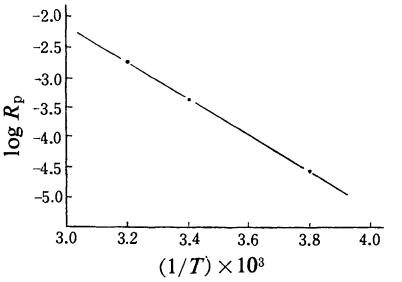


Fig. 6. Relation between log R_p and $1/T$.

Discussion

From the reaction of SnR_4 and $TiCl_4$, such reaction products as R_3SnCl, R_2SnCl_2, etc., and

$RTiCl_3$, R_2TiCl_2, etc., can be expected. However, any one product may have little or no catalytic activity, so that the true catalyst causing the polymerization to start might be a complex the form of which is not clear.

As we[8] discussed previously in connection with the polymerization of propylene with the same catalyst, the catalyst system has a cationic or an anionic character according to the existence of either $TiCl_4$ or SnR_4 in excess.

Since the polymerization rate is of the first order with respect to the concentration of the catalysts, the reaction mechanism can be considered to be a typical ionic type-probably a coordinated anionic type. It was also considered that termination will occur as a result of the abstraction of the hydrogen from the solvent or from other materials.

The comparatively small value of the activation energy is also in good agreement with a concept of an ionic mechanism. The value is slightly smaller than that (14.4 kcal./mol.) obtained by Saltmann, who used an aluminum triisobutyl titanium tetrachloride catalyst.

It must be noted that when SnR_4 is used as a catalyst component, the charactor of the complex depends not only on the catalyst composition but also on the aging time, because the reaction between SnR_4 and $TiCl_4$ is rather slower than the reaction between AlR_3 and $TiCl_4$. As is well known, the reaction of the latter combination is so violent that the complex is produced as soon as the two components are mixed. In the case of the former combination, so long as the reaction of the components is incomplete, free titanium tetrachloride remains in the catalyst system. which gives rise to a comparatively rapid polymerization. Figure 1 clearly shows the relationships. The abrupt drop in the polymerization rate which appeared at the initial stage of reaction (hence, a shorter aging time), means a decrease in the free titanium tetrachloride and an increase in the catalyst complex.

The reason why the catalytic activity of C is the highest will be due to the somewhat cationic character of the catalyst system because of excess titanium tetrachloride. The other lines, A and B, represent anionic polymerization except for the initial stage, because tin tetraalkyl was used in excess. The fact that the B line is higher than the A line may be attributed to the existence of more effective complexes in the former than in the latter.

We will now discuss the results shown in Fig. 2. The following descriptions concerning the assignment of various absorption bands are based on Richardson's paper[7]. Absorption bands are present at 750, 800 and 909 cm^{-1} in every polymer (Nos. 1—5); the bands represent β modification, a crystalline type of *trans*-1,4 structure, or a *cis*-1,4, *trans*-1,4 and 1,2 structure respectively.

Other specific bands in the polymers of Nos. 4 and 5 (the first group) exist at 870 and 890 cm^{-1}; the former band is attributed to α modification and the latter to both α- and β modification. Comparing the two bands, the latter is relatively more intense than the former, and hence the polymer in the first group can be considered to be a mixture of the two modifications. The variation in crystalline type between α and β is affected by the temperature, so that both types may exist as a mixture at a suitable temperature.

A specific band in the other polymers (Nos. 1—3, the second group), at 887 cm^{-1}, is attributed to the 3,4 structure. If the polymer were an example of β modification, a specific band for the type would be present at 890 cm^{-1}. Therefore, the band at 750 cm^{-1} mentioned above may be due to the *cis*-1,4 structure. After all, it is not clear from the infrared study whether or not the crystallinity is present in the polymers of the second group.

Further investigation concerning the spectra is being undertaken from the viewpoint of catalyst composition. The polymers in the first group are produced by the complex where the Sn/Ti ratio is larger than unity, while those in the second group are produced under the reverse conditions. Accordingly, it may be said that a complex having an anionic character produces a crystalline polymer, exemplifying α- and β-modification of *trans*- 1,4-polyisoprene, and that that having a cationic character produces a polymer consisting of various structures.

In addition to the infrared study, we examined the X-ray diffraction pattern of the sample, which had been considered a crystalline polymer as a result of the infrared study, but we could not obtain the crystalline pattern. This may be because the crystallite contained in the polymer is too small to represent the crystalline X-ray pattern, while it is large enough to represent the crystallinity in infrared measurement.

The Electrical Communication Laboratory
Nippon Telegraph and Telephone
Public Corporation
Musashino-shi, Tokyo

8) N. Ashikari and M. Honda, This Bulletin, **34**, 767 (1961).

NOTES

Thermodynamics of Ionization of Substituted Benzoic Acids: 3, 4, 5-Trimethoxybenzoic Acid

By R. K. CHATURVEDI and Sarvagya S. KATIYAR

(Received December 18, 1961)

The studies on the dissociation of carboxylic acids at different temperatures were undertaken by us originally in connection with our studies on the interaction of these acids with the metal ions[1]. The knowledge of dissociation constant of these acids which we found essential to have, led to some interesting conclusions regarding the influence of the substituents on the dissociation of the acids. It was, therefore, considered of value to examine this latter aspect by studying a number of substituted benzoic acids. The present paper reports the pH metric determination of dissociation constant of 3, 4, 5-trimethoxybenzoic acid in the temperature range 20~60°C and the thermodynamic functions associated with the dissociation of this acid.

Experimental

3, 4, 5-Trimethoxybenzoic acid was synthesized by the method described in the literature[2]. Recrystallization from water gave a product of satisfactory purity with m. p. 169°C (reported 168°C[3]). Solutions of the acid prepared in double distilled water were titrated pH metrically against standard sodium hydroxide solution prepared from a Merck "Guaranteed" reagent. All the pH metric measurements were made with a Beckmann pH meter model G employing the extension electrode assembly. The arrangement for the temperature control was the same as described earlier[4].

Results and Discussion

Figure 1 gives the typical set of results on the pH metric titration of the acid against standard sodium hydroxide solution. The curves refering to different temperatures (indicated in the body of the Fig. 1) show a marked inflexion characteristic of the carboxylic acids. The values of the classical dissociation constant of the acid at different temperatures were calculated from the data in Fig. 1 by the method discussed by Britton[5]; these values at various temperatures are returned in Table I,

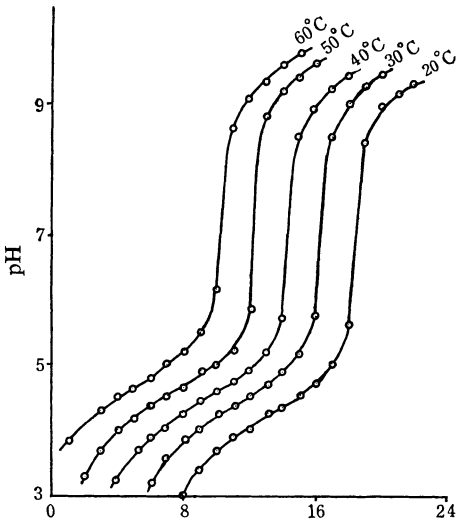


Fig. 1

TABLE I. DISSOCIATION CONSTANT OF 3, 4, 5-TRIMETHOXYBENZOIC ACID

Temperature °K	pk*	pK*
293	4.17	4.19
303	4.27	4.30
313	4.36	4.38
323	4.49	4.53
333	4.62	4.65

* Mean deviation of the order of ±0.05

column 2. The values of the thermodynamic dissociation constants of the acid were obtained by using the modified Debye-Hückel equation[6] and with the values of the Debye-Hückel constant A due to Bates and coworkers[7]; these values are presented in column 3 of

1) N. A. Ramaiah and R. K. Chaturvedi, *Proc. Ind. Acad. Sci.*, **51**, 177 (1960).
2) M. T. Bogart and B. B. Coyne, *J. Am. Chem. Soc.*, **51**, 571 (1929).
3) C. D. Hodgman, R. C. Weast and S. M. Selby, "Hand Book of Chemistry & Physics", Chemical Rubber Publishing Co., Ohio (1955), p. 789.
4) N. A. Ramaiah and R. K. Chaturvedi, *Z. physik. Chem.*, **216**, 184 (1960).
5) H. T. S. Britton, "Hydrogen Ions", Macmillan & Co., London (1942), p. 217; See also Ref. 1.
6) E. A. Guggenheim and F. Schindler, *J. Phys. Chem.*, **38**, 539 (1934).
7) G. G. Manov, R. G. Bates, W. H. Hamer and S. E. Acree, *J. Am. Chem. Soc.*, **65**, 1765 (1943).

Table I. It may be seen from these data that increase in the temperature causes an increase in the pK of the acid; the values, for example, are 4.30±0.07 and 4.65±0.05 at 30 and 60°C respectively.

By applying the method of least squares the following equation,

$$-\ln K = \frac{7430.55}{T} - 44.24 - 9.725 \times 10^{-2} T \quad (1)$$

was derived[8] which governed satisfactorily the variation of pK with T. From the values of the constant of Eq. 1 the thermodynamic functions such as change in free energy, entropy, enthalpy and heat capacity were computed from the well known thermodynamic relationships[8]; the values of these quantities at different temperatures are given in Table II.

Table II. Thermodynamic functions of dissociation of 3, 4, 5-trimethoxybenzoic acid

Temperature °K	ΔF kcal./mol.	ΔH kcal./mol.	ΔS cal./mol. deg.	ΔC_p cal./mol. deg.
293	5.59	−1.83	−25.33	−113.24
303	5.87	−2.98	−29.19	−117.10
313	6.18	−4.17	−33.06	−120.96
323	6.53	−5.39	−36.93	−124.83
333	6.92	−6.66	−40.79	−128.69

For a number of substituted benzoic acids it was shown by Shorter and Stubbs[9] that the total effect of the substituents in different positions on ionization of the parent acid is roughly the sum of the individual contributions of the substituents; this is especially true in case the substituent occupies meta or para positions. These observations indicating the additivity of pK have been theoretically well discussed by a number of workers[10]. It is of interest to examine the applicability of the additivity principle to the data on pK of the 3, 4, 5-trimethoxybenzoic acid. From the data in column 3 of Table III, it may be seen that the substitution of a methoxy group in meta position lowers the pK of benzoic acid by 0.12 unit while that in the para position enhances the same by 0.26 unit. These consideration suggest, by the application of the above principle, a value of 4.23 at 25°C for pK of the acid under investigation is good agreement with our values in this temperature range.

Table III. Observed and calculated values of pK and ΔF

Acid	pK	Contribution to pK	ΔF kcal./mol.	Contribution to ΔF
Benzoic	4.21	—	5.74	—
m-Methoxybenzoic	4.09	−0.12	5.58	−0.16
p-Methoxybenzoic	4.47	+0.26	6.09	+0.35
3, 4, 5-Trimethoxybenzoic	4.23	+0.02	5.77	+0.03

Further, the change in free energy of ionization obeys additivity principle in cases in which steric effects are not significant. Even in certain cases when steric effects are considerable the additivity of ΔF is maintained presumably because of the compensation of the steric effects on ΔH and $T\Delta S$[11]. Besides steric effects, the solvent effects are also known to influence the additivity of ΔF. But the large size of −COO group and the fact that the charge is carried by both the oxygen atoms because of resonance, minimizes the possibility of a significant solvent effect in case of benzoic acids[12,13]. The data in column 4 of Table III gives the ΔF values for benzoic and methoxybenzoic acids. From the contribution to ΔF of methoxy group in *p*- and *m*-positions we get a value of 5.77 kcal./mol. at 25°C in good agreement with our value in the same temperature range. The application of the additivity principle to ΔF values might lead to the view that purely polar effects arising out of inductive influences are operative. But the consideration of the ΔS value clearly shows that this is not the case. It is known that purely polar effects hardly cause any change in ΔS. Thus for example ΔS for *m*-methoxybenzoic acid (−18.5) and *p*-methoxybenzoic acid (−18.5) are hardly different from the value of −18.9 for benzoic acid whereas the value of ΔS for 3, 4, 5-trimethoxybenzoic acid is significantly different from that of benzoic acid.

Author's grateful thanks are due to Dr. Hrishikesh Trivedi, Principal, for facilities and kind encouragement and to Dr. Jagraj Behari Lai for his kind interest in the work.

Chemistry Department
Indian Institute of Technology
Kanpur, India (*S. S. K.*)

Harcourt Butler Technology Institute
Kanpur, India (*R. K. C.*)

8) H. S. Harned and R. A. Robinson, *Trans. Faraday Soc.*, **36**, 973 (1940).
9) J. Shorter and F. J. Stubbs, *J. Chem. Soc.*, **1949**, 1180.
10) See for example, E. Remick, "Electronic Interpretation of Organic Chemistry", John Wiley & Sons, New York (1949); C. K. Ingold, "Structure and Mechanism in Organic Chemistry", G. Bell & Co., Ltd., London (1953), p. 738.
11) K. J. Laidler, *Trans. Faraday Soc.*, **55**, 1725 (1959).
12) T. W. Zawidzki, H. M. Papee and K. J. Laidler, ibid., **55**, 1743 (1959).
13) H. C. Brown, D. H. McDaniel and O. Hafliger, "Determination of Organic Structures by Physical Methods", Chap. 14.

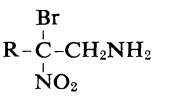
Preparation of 2-Bromo-2-nitro-pentylamine

By Mitsuo MASAKI and Masaki OHTA

(Received March 8, 1962)

Only a few β-halogeno-β-nitro amines are known to be the products of the addition of ammonia or amines to α-halogeno-α-nitro-olefines. The reaction of β-bromo-β-nitrostyrene with ammonia gives 2-bromo-2-nitro-1-phenylethylamine[1], and the reaction of 1-bromo-1-nitrobutene with ammonia or amines gives unstable adducts[2], but in most cases the products have not been characterized.

We wish to report the preparation of 2-bromo-2-nitro-pentylamine (I, $R=C_3H_7$) required for other work by a new method, which involves the reaction of 1, 2-dibromo-2-nitropentane with potassium phthalimide.



2-Nitropentene-1[3] (b. p. 73~74°C/45 mmHg), which was prepared in a good yield by the direct dehydration of 2-nitropentanol using the technique of Buckley and Scaife[4], was converted, by the addition of bromine in chloroform, into 1, 2-dibromo-2-nitropentane (II), a colorless oil with a b. p. of 99~100.5°C/7.5 mmHg. (Found: N, 4.93; C, 21.87; H, 3.48. Calcd. for $C_5H_9O_2 \cdot NBr_2$: N, 5.09; C, 21.82; H, 3.27%).

The dibromide II was heated under reflux with potassium phthalimide in acetone for 30 hr., cooled to room temperature, and filtered to remove the potassium bromide. After the bulk of acetone had been removed by distillation, the resultant syrup was crystallized by the addition of ethanol and then recrystallized from ethanol, giving colorless prisms of 1-phthalimide-2-bromo-2-nitropentane (III). M. p. 90~92°C (yield 70%). (Found: N, 8.35; C, 45.68; H, 3.99. Calcd. for $C_{13}H_{13}O_4N_2Br$: N, 8.22; C, 45.75; H, 3.81%).

The reaction of III with hydrazine hydrate in ethanol gave I ($R=C_3H_7$), which was isolated as its stable hydrochloride IV; the latter was then recrystallized from ethylacetate or ethanol-ether to give colorless needles with a m. p. of 126~127°C (yield 63%). (Found: N, 11.35; C, 23.84; H, 5.31. Calcd. for $C_5H_{11}O_2N_2Br \cdot HCl$: N, 11.31; C, 24.24; H, 4.85%). The infrared absorption band in IV at 1440 cm^{-1}, which has disappeared in I ($R=C_3H_7$), is ascribed to $-\overset{+}{C}H_2\overset{+}{N}H_3$; therefore, I ($R=C_3H_7$) is not the alternative nitro-amine, 1-bromo-2-amino-2-nitropentane.

This nitro-amine (I, $R=C_3H_7$) was also characterized by its conversion into the picrate (m. p. 156~157°C. Found: N, 15.64. Calcd. for $C_{11}H_{14}O_9N_5Br$: N, 15.86%), its reduction on Raney nickel to the corresponding diamine[5] (picrate m. p., 224~227°C. Found: N, 19.79; C, 36.79; H, 3.80. Calcd. for $C_{17}H_{20}N_8O_{14}$: N, 20.00; C, 36.43; H, 3.57%), its benzoylation to give the *N*-benzoyl compound of I ($R=C_3H_7$) (m. p. 90~91°C. Found: N, 8.63. Calcd. for $C_{12}H_{15}O_3N_2Br$: N, 8.89%), and its reaction with phenyl isocyanate to give the corresponding derivative of urea (m. p. 103~104°C. Found: N, 12.36. Calcd. for $C_{12}H_{16}O_3N_3Br$: N, 12.73%).

The applicability of this method in the preparation of other β-bromo-β-nitro-alkylamines (I) is now under study in this laboratory.

We are indebted to Mr. Keiji Naruse for performing the microanalyses.

Laboratory of Organic Chemistry
Tokyo Institute of Technology
Meguro-ku, Tokyo

1) J. Loevenich and H. Gerber, *Ber.*, **63**, 1707 (1930).
2) J. Loevenich, J. Koch and U. Pucknet, ibid., **63**, 636 (1930).
3) H. B. Hass, A. G. Susie and R. L. Heider, *J. Org. Chem.*, **15**, 8 (1950).
4) G. D. Buckley and C. W. Scaife, *J. Chem. Soc.*, **1947**, 1471.
5) R. C. Elderfield and C. Ressler, *J. Am. Chem. Soc.*, **72**, 4059 (1950).

On the Nitration of 2-Thenyl Acetate

By Tyo SONE, Kensuke TAKAHASHI and Yasuo MATSUKI

(Received March 14, 1962)

A recent paper[1] has reported that the nitration of 2-thenyl acetate with acetic anhydride-nitric acid at 10°C gives a 65% yield of 5-nitro-2-thenyl acetate (I), b. p. 132°C/0.3 mmHg, m. p. 35°C, but also that in spite of some attempts, the formation of 3-nitro-2-thenyl acetate (II), which can be expected from the presence of the *o*-, *p*-directing acetoxymethyl group in the 2-position of the thiophene ring, is not observed.

During the identification and the structural investigation of thenyl derivatives by means of the NMR technique, we early examined the same reaction and observed, unlike the paper mentioned above, the formation of II as a by-product in a relatively high proportion. To a solution of 2-thenyl acetate (15.6 g.) in acetic anhydride (30 ml.), a mixture of nitric acid (d=1.50, 6 ml.) and acetic anhydride (12 ml.) was added at −10°C, and the reaction mixture was stirred at −5∼0°C for 2.5 hr. Nitro-2-thenyl acetate was obtained as a pale yellow oil (13.6 g., 67.6%), b. p. 120∼125°C/2∼2.5 mmHg (Found: C, 42.02; H, 3.27; N, 6.47%), which, on being left standing, partially solidified to colorless needles, m. p. 38∼39°C[2] (from low boiling petroleum ether). The NMR spectrum (Fig. 1a[3], 40 Mc., cyclohexane as an internal reference) of the oil shows several lines with a medium intensity in the aromatic region, in addition to the four lines (227.8, 231.9, 252.7 and 256.6 c. p. s., J=4.0 c. p. s.) on the basis of which the major part of the oil can be identified as I, 2,5-disubstituted thiophene[4]. Besides these, two lines (155 and 168 c. p. s.) due to the methylene group and a line (31 c. p. s.) due to the methyl group are observed at the high field side. This indicates the presence of an isomer other than I. Upon treating the acetate (b. p. 120∼125°C/2∼2.5 mmHg) with 10% sulfuric acid, the corresponding nitro-2-thenyl alcohol (b. p. 115∼118°C/2 mmHg) was obtained in a 72% yield (Found: C, 38.03; H, 2.87; N, 8.61; Calcd. for $C_5H_5 \cdot NO_3S$: C, 37.73; H, 3.17; N, 8.80%). Benzoate, m. p. 97.5∼99°C (from alcohol) (Found: N, 5.25; Calcd. for $C_{12}H_9NO_4S$: N, 5.32%). In the NMR spectrum (Fig. 1b) of the alcohol, the shifts and the coupling constants (J=4.1 and 5.4 c. p. s.) obviously show the alcohol to be a mixture of 5-nitro- and 3-nitro-2-thenyl alcohol. Thus, it is evident that the original nitro-2-thenyl acetate is also a mixture of I and II. From the relative peak area of the NMR spectra, the ratio of II to I in the nitration products of 2-thenyl acetate under the conditions studied is of the order of 1 to 8 or higher. There has been hitherto little systematic or quantitative investigation of the ratio of isomer formed in the electrophilic substitution of thiophene derivatives with an *o*-, *p*-directing group in the 2-position; it has been assumed that the substitution occurs almost exclusively at the 5-position and at the 3-position, if at all, to a minor extent. However, from the results of the nitration of 2-methoxy thiophene[5] and 2-thenyl chloride[6] and of the present study, it seems that 3-substitution occurs in a relatively higher proportion than had been expected.

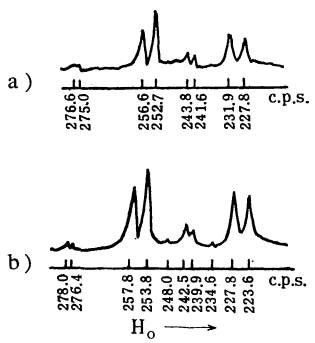


Fig. 1. NMR spectra in the aromatic region of:
a) A mixture of 3-nitro-, and 5-nitro-2-thenyl acetate
b) A mixture of 3-nitro-, and 5-nitro-2-thenyl alcohol

Chemical Research Institute of Non-Aqueous Solutions
Tohoku University
Katahira-cho, Sendai

1) M. Berçot-Vatteroni, R. C. Moreau and P. Reynaud, *Compt. rend.*, **252**, 2419 (1961).
2) The lines due to II are not observed in the NMR spectrum.
3) The two extra peaks at the low field side are probably due to the presence of the dinitro isomer.
4) S. Gronowitz and R. A. Hoffman, *Arkiv. Kemi.*, **13**, 279 (1958); ibid., **16**, 563 (1960); K. Takahashi, Y. Matsuki, T. Mashiko and G. Hazato, This Bulletin, **32**, 156 (1959); K. Takahashi, Y. Matsuki, Y. Miyake and G. Hazato, ibid., **34**, 1599 (1961).
5) J. Sicé, *J. Am. Chem. Soc.*, **75**, 3697 (1953).
6) T. Sone and Y. Matsuki, *J. Chem. Soc. Japan, Pure Chem. Sec.* (*Nippon Kagaku Zasshi*), **83**, 496 (1962).

Molecular Rotations of Glucides in Relation to their Structures. IX[1]. *The Value of the ζ-Coefficient of the Hydroxyl Group in Hydro-D-xylal*

By Shukichi YAMANA

(Received March 19, 1962)

The value of the ζ-coefficient of the hydroxyl group, ζ_{OH}, in hydro-D-xylal has been calculated. The unit groups in the molecule and its $[M]_D^{20}(W)$ are shown in Table I (Fig. 1).

TABLE I

Name	Unit groups	$[M]_D^{20}(W)$
Hydro-D-xylal	$[(OH)^{3\beta}, (OH)^{4\alpha}, Ring^{0}$ [2]$]$	−53.0[3]

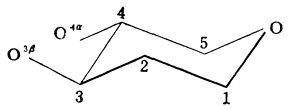


Fig. 1. Perspective drawing of the molecular model of hydro-D-xylal.

In the aldopyranose-ring, R^0 [2], of hydro-D-xylal, the O atom is combined with two methylene radicals, (i. e. $-C^1H_2-$ and $-C^5H_2-$). Therefore, the shape of R^0 is considered to be almost symmetrical. Therefore, in order to simplify the calculations, an ideal model of glucide[4] is used here. By using the PM-method[6],

$$[M]_D^{20}(W) \text{ of hydro-D-xylal,}$$

$$-53.0 \equiv \sum [\mu]_{D\,obs}^{20} \text{ of hydro-D-xylal}$$

$$= (3\beta)\,\Lambda\,(4\alpha) + (3\beta)\,\Lambda R^0 + (4\alpha)\,\Lambda R^0 \qquad (1)$$

As R^0 is symmetrical,

$$(3\beta)\,\Lambda R^0 = 0 \qquad (2)$$

On the other hand, as the orientation of 4α is almost parallel with the average plane of R^0 (equatorial bond), it is expected that the absolute value of $(4\alpha)\,\Lambda R^0$ will be very small[7]. Therefore, for the sake of simplicity of calculation, the next equation is available;

$$(4\alpha)\,\Lambda R^0 \simeq 0 \qquad (3)$$

Combining Eqs. 1, 2 and 3,

$$-53.0 \simeq (3\beta)\,\Lambda\,(4\alpha) \qquad (4)$$

However,

$$(3\beta)\,\Lambda\,(4\alpha) = \{(3\beta) \times (4\alpha)\}\zeta^2_{OH}\{(n^2+2)/3\}^{9)}$$

$$= \{[\mu]_{D\,calcd}^{20} \text{ between } (OH)^{3\beta} \text{ and } (OH)^{4\alpha}\}$$

$$\times \{3/(n^2+2)\}\zeta^2_{OH}\{(n^2+2)/3\}^{11)}$$

$$= -A\zeta^2_{OH}\{(n^2+2)/3\}^{12)}$$

$$= -11.73\zeta^2_{OH}\{(n^2+2)/3\} \qquad (5)$$

From Eqs. 4 and 5,

$$-53.0 \simeq -11.73\zeta^2_{OH}\{(n^2+2)/3\}$$

or

$$\zeta^2_{OH} \simeq 4.5183\{3/(n^2+2)\}$$

This value is almost equal to the value of ζ^2_{OH} in (−)1/2 cyclohexanediol, which has only two hydroxyl groups in its molecule, $4.1091\{3/(n^2+2)\}$[13]. This fact may mean that the value of the ζ-coefficient of a unit group is nearly constant, regardless of the kind of ring in the molecule with which it is concerned.

Department of Chemistry
Kyoto Gakugei University
Fushimi-ku, Kyoto

1) Part VIII, S. Yamana, This Bulletin, **35**, 1269 (1962).
2) Ring^0 (or R^0) means an aldopyranose-ring which has not any hydrogen bond producing group at its 1- or 5-position.
3) H. G. Fletcher, Jr. and C. S. Hudson, **71**, 3682 (1949).
4) This model can be made from the ideal model of polyhydroxycyclohexane by replacing the C^6-atom of its cyclohexane-ring by the ring-O-atom. (Cf. previous papers[5,6]). For this model, $[\mu]_{D\,calcd}^{20}\{3/(n^2+2)\}$ is given by Table I of a previous paper[5] and, more precisely, by Table II of a previous paper[6].
5) S. Yamana, This Bulletin, **30**, 207 (1957).
6) S. Yamana, ibid., **33**, 1741 (1960).
7) Concerning the reason for this deduction from the relative geometry of the unit groups, cf. Eq. 1 of a previous paper[8].
8) S. Yamana, This Bulletin, **30**, 203 (1957).
9) Equation 32 of a previous paper[10] is used.
10) S. Yamana, This Bulletin, **31**, 558 (1958).
11) Cf. footnote *10 of the previous paper[5].
12) Table II of the previous paper[6] is used.
13) Cf. footnote 4, S. Yamana, This Bulletin, **34**, 1414 (1961).

SHORT COMMUNICATIONS

A Synthetic Resin Catalyzing Racemization of Amino Acids. I

By Koji Toi, Yoshiharu Izumi and Shiro Akabori

(Received March 19, 1962)

It has been demonstrated that salicylaldehyde, a benzene analogue of pyridoxal, catalyzes the racemization of amino acids in the presence of metal ion[1]. In the present work a resin which contain the salicylaldehyde group was prepared from *o*-cresol-formaldehyde resin by converting the methyl substituent of *o*-cresol to aldehyde. Crushed resin was oxidized with chromium trioxide in a mixture of acetic acid and acetic anhydride, and the acetal produced was hydrolyzed with 4 N hydrochloric acid. The formyl content of the resin was found to be 0.16 mmol./g. of dry resin. This synthetic resin was used as a catalyst for the racemization of amino acids in the presence of cupric ion.

The racemization experiment was conducted with L-alanine, L-glutamic acid, and L-aspartic acid. An aqueous solution of each amino acid, which was adjusted to pH 10 with sodium hydroxide and which contained 0.2 mol. of amino acid and 0.9 g. of cupric chloride in a total volume of 100 ml., was prepared. Fifteen milliliters of the above solution, 15 ml. of 0.2 M borate buffer of pH 10, and 5 g. of the resin were stirred at 100°C. The reaction mixture was removed at varing intervals of time and diluted with 12 N hydrochloric acid, and its optical rotation was measured. The amino acid content of the reaction mixture was checked by the ninhydrin colorimetric method during

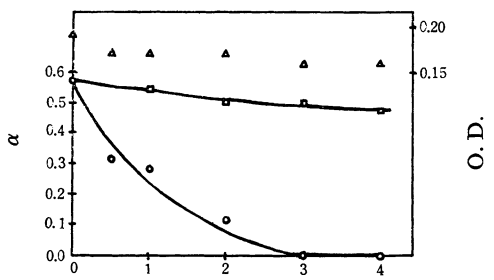


Fig. 1. Racemization of L-alanine.

○ Optical rotation shown in the reaction catalyzed by resin
□ Optical rotation shown in the reaction without resin
△ Optical density by ninhydrin method

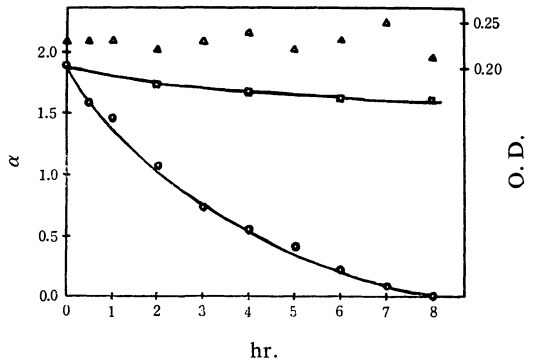


Fig. 2. Racemization of L-aspartic acid.

○ Optical rotation shown in the reaction catalyzed by resin
□ Optical rotation shown in the reaction without resin
△ Optical density by ninhydrin method

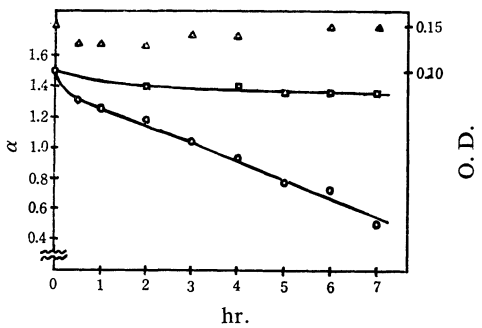


Fig. 3. Racemization of L-glutamic acid.

○ Optical rotation shown in the reaction catalyzed by resin
□ Optical rotation shown in the reaction without resin
△ Optical density by ninhydrin method

1) K. Ohno, I. Sasaji and M. Hara, Abstract of the 12th Annual Meeting of the Chemical Society of Japan (Apr., 1959), p. 27.

the course of the racemization. The results are shown in Figs. 1—3.

Division of Organic Chemistry
Institute for Protein Research
Osaka University
Kita-ku, Osaka

Abnormal Reaction of Ferrocene with Unsaturated Dibasic Acid Chloride and NMR Spectra of Ferrocene Derivatives

By Noboru SUGIYAMA and Tsutomu TEITEI

(Received April 2, 1962)

Treatment of ferrocene (10.0 g., 0.054 mol.) with fumaryl chloride (4.1 g., 0.027 mol.) in presence of aluminum chloride (7.2 g., 0.054 mol.) in methylene chloride (150 ml.) gave a mixture from which were isolated a saturated compoud, 1, 2-diferrocenoylethane (I, 2.3 g.), orange needles, m. p. 185~186°C, not depressed on admixture with an authentic specimen[1], and β-ferrocenoylpropionic acid (4.5 g.). The expected *trans*-diferrocenoylethylene was not obtained as in the case of benzene[2]. Found: C, 63.58: H, 4.83. Calcd. for $C_{24}H_{22}O_2Fe_2$: C, 63.44; H, 4.85%.

Dihydropyridazine derivative of I; brown needles, m. p. 266°C (decomp.). Found: N, 6.27. Calcd. for $C_{24}H_{22}N_2Fe_2$: N, 6.22%. Infrared, ultraviolet and NMR spectra of I are identical with those of 1, 2-diferrocenoylethane[1]; IR, 1660 cm^{-1} (>CO) (KBr), UV (95% ethanol), 460 mμ (ε, 910). The NMR spectrum of I contains one singlet at $\tau=6.86$ (methylene protons), and another singlet at $\tau=5.76$ (unsubstituted ring protons) and two widely separated triplets at $\tau=5.51$ and 5.18; $J=1.64$ c.p.s. (substituted ring protons).

Under the same conditions as above 1, 2-diferrocenoylpropane (II, 1.8 g.) and 1-methyl-2-ferrocenoylpropionic acid (III, 5.2 g.) were obtained by reaction of ferrocene (10 g.) with citraconyl chloride (4.5 g.).

2, 4-Dinitrophenylhydrazone of II; purple crystals, m. p. 234°C. Found: C, 56.84; H, 4.15; N, 8.53. Calcd. for $C_{31}H_{28}O_5N_4Fe_2$: C, 57.41; H, 4.32; N, 8.64%. IR, 1665 (>CO), 1615 (>C=N-), 1518, 1500, 1320 cm^{-1} ($-NO_2$) (KBr). *p*-Bromophenacyl ester of III (IV); light orange needles, m. p. 149~150°C. Found: C, 55.71; H, 4.24. Calcd. for $C_{23}H_{21}O_4BrFe$: C, 55.53; H, 4.23%. IR; 1740 (ester CO), 1715 (PhCO-), 1665 cm^{-1} (FcCO-) (KBr). UV (95% ethanol), 464 mμ (ε, 435). The NMR spectrum of IV contains three singlets at $\tau=5.76$, 5.51 and 5.20 (ferrocene ring protons), with an expected doublet at $\tau=8.66$; $J=6.22$ c.p.s. (methyl protons) and multiplet at $\tau=6.60\sim7.16$ (methylene protons and a proton at a tertiary carbon). Besides these it contains two quartets at $\tau=4.70$; $J=8.2$ c.p.s. and 2.32; 8.53 (benzene ring and methylene protons respectively) due to the phenacyl group.

It is a very interesting fact that the monosubstituted ferrocene derivatives (I and IV) have three peaks in the NMR specta. Rinehart[3] reported that the spectrum of 1, 1'-(tetramethylethylene)-ferrocene contains the expected methyl proton singlet at $\tau=8.74$, but the ring protons are found in two widely separated triplets at $\tau=6.11$ and 5.37; $J=1.6$ c.p.s.; and the considerable chemical shift is best explained as arising from the ring proton's unequal distance from the iron nucleus in a molecule where the rings are tilted. However, the chemical shift in our case is best explained as arising from the unequal inductive effect of carbonyl group on the ring protons. Thus α protons are assigned to the lower peak and β protons to the higher one in the substituted ring. This interpretation is in accord with the reactivity of acetylferrocene[4].

The authors wish to express their thanks to Professor Koji Nakanishi and his co-workers for their kind advices.

Department of Chemistry
Faculty of Science
Tokyo Kyoiku University

1) N. Sugiyama et al., This Bulletin, in press.
2) "Organic Syntheses", Coll. Vol. III, p. 248.
3) K. L. Rinehart, *J. Am. Chem. Soc.*, **82**, 2082 (1960); **82**, 4111 (1960).
4) A. N. Nesmeyanov et al., *Doklady Akad. Nauk S. S. S. R.*, **111**, 605 (1956).

Infrared Absorption Spectrum of Boron Carbide

By Hiroaki TAGAWA and Shin'ichi MATSUDA

(Received May 7, 1962)

Boron is dissolved in boron carbide at high temperature[1] and the ratio of boron and carbon in boron carbide prepared by reaction of boron oxide with carbon always becomes greater than four[2-4]. Although lattice dimension of boron carbide increases with dissolving boron, a detail of the structural change has not yet been explained. In this communication, the infrared absorption spectra of boron carbide having various B/C ratios are presented with the result of X-ray examination of the change of lattice dimension.

Samples of boron carbide employed were fabricated by the reaction of boron oxide with carbon black at about 2800°C by means of 40 kW closed electric furnace. Crystalline boron (purity, more than 99 percent; tetragonal) was provided from Borax Consolidated Ltd. (England). The infrared absorption spectra were observed by using potassium bromide pellet techniques.

The infrared absorption spectra of boron carbide and boron in the range between 1600 and 700 cm^{-1} are shown in Fig. 1 and they agree with the results reported by Brame[5]. The absorption bands at 1158, 1084, 798 and 781 cm^{-1} remain unaffected by the difference of composition, and are the same as that of elemental boron. On the other hand, the band at 1578 cm^{-1} moves gradually toward to small wave number region with the increase of the B/C ratio. It is evident from Fig. 2 that the variation of the wave number with carbon content has some regularity, and the knee point is found at 17.5 percent of carbon. The result of the examination of these carbides by X-rays is shown in Fig. 3, values of 2θ of the (603) reflections are plotted against atom percent of carbon. The carbon content of the reflection point shown in Fig. 3, which agrees with the result found in Fig. 2, may show the limitation of solubility of carbon into boron carbide. The structural unit of boron carbide is linear chain of three carbon atoms and a group of twelve boron atoms arranged at the vertices of a regular icosahedron, and these are distributed approximately in an NaCl type of structure[6]. The shift of the absorption band at 1578 cm^{-1} by dissolving boron may be closely related to the change of the structure; the central carbon of the linear chain of three carbons connecting between boron icosahedron is replaced by a boron atom, which is 14 percent larger than carbon in atomic radius.

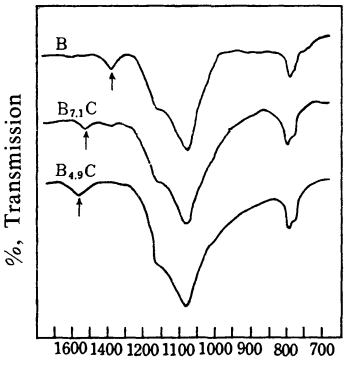


Fig. 1. Infrared absorption spectra of boron and boron carbide.

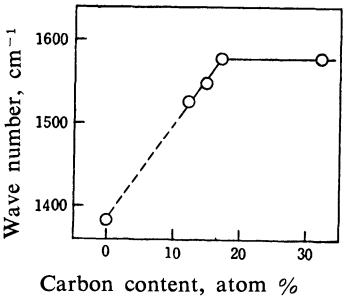


Fig. 2. Characteristic absorption band of boron-carbon system.

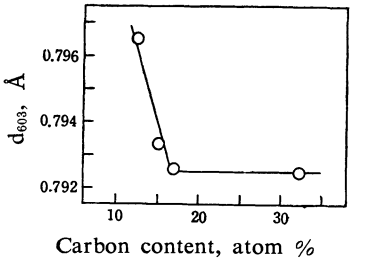


Fig. 3. Interplaner distance of (603) reflection of boron-carbon system.

Research Laboratory
Nippon Carbide Industries Co., Inc.
Uozu, Toyama

1) G. B. Samsonov, *J. Phys. Chem.* (*U. S. S. R.*), **32**, 2424 (1958).
2) R. D. Allen, *J. Am. Chem. Soc.*, **75**, 3582 (1953).
3) F. W. Glaser and D. Moskowitz, *J. Appl. Phys.*, **24**, 731 (1953).
4) G. S. Zhdanov et al., *J. Phys. Chem.* (*U. S. S. R.*), **28**, 1076 (1954).
5) E. G. Brame, *J. Inorg. Nucl. Chem.*, **5**, 48 (1957).
6) H. K. Clark and J. L. Hoard, *J. Am. Chem. Soc.*, **65**, 2115 (1943).

Crystallinity of Boron Nitride Fabricated in Various Ways

By Hiroaki TAGAWA and Kikuo ISHII

(Received May 7, 1962)

Crystallinity of boron nitride fabricated in variety of ways has been investigated by means of X-ray diffraction. The structure of boron nitride is very similar to that of graphite[1]. As is shown in graphitizing nature of carbon, the physical and chemical properties of boron nitride may vary considerably according to the nature of starting materials and the conditions of preparation. This communication describes the difference between the crystallinity of boron nitride fabricated by the gas phase reaction and that of the one prepared by the solid state reaction.

The methods of preparation of boron nitride used were as follows; (1) gas phase reaction of boron trichloride with ammonia on a SiC resistor heated at 900 or 1050°C[2], (2) decomposition at 800 or 1000°C of the complex formed by the reaction of boron trichloride with ammonia in gas phase at room temperature[3], (3) solid-gas reaction of boron oxide coated on tri-calcium phosphate with ammonia at 800 or 1000°C for four hours[4], (4) solid-gas reaction of sodium tetraborate with ammonia at 800 or 1000°C for two hours, and (5) solid-solid reaction of boron oxide with sodium amide (mixing ratio by mole, 1 : 3) at 800°C in nitrogen[5,6].

Interlayer spacings of (002), and La- and Lc-dimensions of crystallite of boron nitride fabricated by the methods mentioned above were measured using an automatic recording X-ray spectrometer. As the observed diffraction maximum is not corrected for polarization and absorption, the true value may slightly become less than the measured one. La-dimension, the width of the graphite-like layer, was obtained from (10) band or (100) line, and Lc-dimension, the thickness of the parallel packet of layers, was obtained from (002) line.

The result of X-ray measurement is summarized in Table I. The crystallinity of boron nitride fabricated at 1000°C is more developed than that at 800°C. Interlayer spacing of the

TABLE I. BORON NITRIDE FABRICATED IN A VARIETY OF WAYS

Starting material	Reaction temp. °C	d_{002} Å	La Å	Lc Å
1) BCl_3+NH_3	900	3.619	45	12
	1050	3.591	49	13
2) Decomposition of the complex ($BCl_3 \cdot 4NH_3$)	800	3.624	56	14
	1000	3.594	68	14
3) $B_2O_3+NH_3$	800	3.389	71	45
	1000	3.339	290	66
4) $Na_2B_4O_7+NH_3$	800	3.349	265	88
	1000	3.339	1160	282
5) $B_2O_3+NaNH_2$	800	3.389	243	115

nitride fabricated in gas phase is larger than that of the nitride prepared in solid-gas and solid-solid reaction, while La- and Lc-dimensions of the former being smaller than those of the latter. Boron nitrides fabricated at 800°C in the reaction of boron trichloride with ammonia and in the reaction of boron oxide on tri-calcium phosphate with ammonia were heated at 1400, 1600, 1800 and 2000°C in nitrogen atmosphere of 200 mmHg. The relation between La- and Lc-dimensions of these nitride is shown with the values of starting materials in Fig. 1.

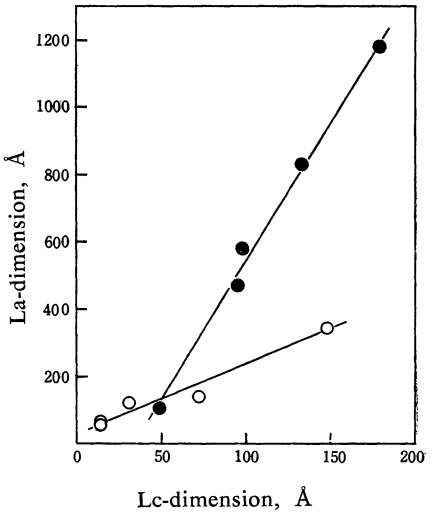


Fig. 1. Crystallite growth of boron nitride by heat treatment.

○ Boron nitride fabricated by the reaction of BCl_3 with NH_3

● Boron nitride fabricated by the reaction of B_2O_3 with NH_3

It is shown from Fig. 1 that crystallization of boron nitride formed in solid phase is preferable to that of the nitride in gas phase. It seems that boron nitride formed by gas phase

1) R. S. Pease, *Acta Cryst.*, 5, 356 (1952).
2) Th. Renner, *Z. anorg. u. allgem. Chem.*, **298**, 22 (1959).
3) F. Meyer and R. Zappner, *Ber.*, **54B**, 560 (1921).
4) K. M. Tayler, U. S. Navy, Bureau of Ordnance Research Contract NOrd 10982 (1949).
5) J. Kamlet, U. S. Pat. 2865715 (1958).
6) H. Tagawa and O. Itouji, This Bulletine, in press (1962).

reaction and that prepared by solid phase one correspond to non-graphitizing and graphitizing carbons respectively.

Research Laboratory
Nippon Carbide Industries Co., Inc.
Uozu, Toyama

Intramolecular-Intermolecular Polymerization of Glutaraldehyde[1]

By Chuji Aso and Yuzo Aito

(Received May 7, 1962)

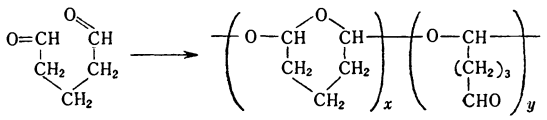
Recently, many studies were reported on the intramolecular-intermolecular polymerization of nonconjugated diolefins[2]. This reaction process was extended to the addition polymerization of glutaraldehyde (I). It was reported that certain dialdehydes yielded glassy materials without catalyst, but their structures were not described[3].

I was polymerized to the white, powdery polymer with an organometallic catalyst such as triethylaluminum or partially hydrolyzed one. Boron trifluoride-ether complex and other cationic catalysts were also effective. These polymers cantained a few residual aldehyde groups by infrared analysis. This suggests that the ring formation was occurred during the propagation process.

Some results of the polymerization with triethylaluminum-water catalyst are shown in Table I. The soluble fraction (II) of considerably high viscosity and low residual aldehyde content, melted at about 75~85°C, and was depolymerized quantitatively to I by pyrolysis in vacuo. II has the strong infrared absorption bands at 1150~950 cm^{-1}, which are assigned to ether bond. The sharp absorption bands are also observed at 805 and 855 cm^{-1}. A sample of 2-ethoxycyclooxahexane prepared for comparison shows the corresponding bands at 811 and 872 cm^{-1}.

Therefore, it would seem reasonable to believe that II posessed the six-membered cyclic ether units and the linear nature evidenced by solubility and fusibility.

It was presumed from these results that the polymerization proceeded mainly by intramolecular-intermolecular mechanism and the polymer thus obtained had the ring structure as shown below:



where the ratio of x to y was nearly equal to ten.

The soluble tetramer or pentamer obtained from I after being kept at room temperature without catalyst, contained about one aldehyde group per one molecule, and showed the similar infrared spectrum to that of II. The polymers obtained with the cationic catalysts, on the other hand, were less soluble and showed the different infrared spectrum from II.

The authors are grateful to the Asahi Glass Technical Aide Association for the fund to this investigation.

Department of Organic Synthesis
Faculty of Engineering
Kyushu University
Fukuoka

TABLE I. EXAMPLES OF POLYMERIZATION OF GLUTARALDEHYDE WITH $Al(C_2H_5)_3$-H_2O (1 : 1) IN TOLUENE AT −76°C (CATALYST CONCENTRATION 5.0 mol.% TO MONOMER)

Monomer g./ml.	Time hr.	Conversion %	Soluble[a] fraction %	Soluble fraction $[\eta]$[b] dl./g.	Soluble fraction Residual[c] aldehyde, %
0.050	1.5	27.4	17.9	0.26	6.4
0.058	2.7	51.4	27.6[d]	0.24	8.7

a) Soluble fraction of polyglutaraldehyde in cold benzene.
b) Intrinsic viscosity of benzene solution at 30°C.
c) Determined by infrared absorption at 1730 cm^{-1}.
d) Analysis: Found: C, 59.20; H, 8.16. Calcd. for $(C_5H_8O_2)_n$: C, 59.98; H, 8.05%.

1) Presented at the 15th Annual Meeting of the Chemical Society of Japan, Kyoto, April, 1962.
2) G. B. Butler and R. J. Angelo, *J. Am. Chem. Soc.*, **79**, 3128 (1957); C. S. Marvel and R. D. Vest, ibid., **79**, 5771 (1957); C. Aso, *J. Chem. Soc. Japan, Ind. Chem. Sec.* (*Kogyo Kagaku Zasshi*), **63**, 363 (1960); and etc.
3) C. Harries and L. Tank, *Ber.*, **41**, 1701 (1908); and etc.

The Color and the Structure of Tetramineplatinum(II) Tetrahalogenoplatinate(II)

By Shoichiro YAMADA

(Received June 4, 1962)

Magnus's green salts having an empirical formula of $[Pt(NH_3)_4][PtCl_4]$ and a related compound, $[Pt(NH_3)_4][PtBr_4]$ are peculiar in that the salts in the crystalline state are green, whereas the component complex ions are colorless and red in solution. In order to elucidate this peculiarity of the color, the present author formerly determined the dichroism of the compounds in the visible and near-ultraviolet region, and concluded that the unusually deep color of the compounds was due most probably to a weak bond between platinum ions along the needle axis[1]. It was also found that compounds represented by a general formula of $[Pt(amine)_4][PtCl_4]$ are colored either red or green, depending upon the amine[2]. The compounds of the pink series show a dichroism similar to that of $K_2[PtCl_4]$, in which no specific bond is involved between platinum ions, while the green compounds show a dichroism which differs remarkably from that of the potassium salt. The main difference between the two series lies in the following point. The green series shows an absorption band in the longer wavelength region than the red series, and the band is polarized along the c-axis of the crystal, along which the Pt-Pt bond is assumed to occur. The difference in the dichroism as well as in the color between the two series of compounds is so marked that it is possible to tell, by using the dichroism or the color as a criterion, whether a compound with an empirical formula of $[Pt(amine)_4][PtCl_4]$ involves the Pt-Pt bond or not. The results of the examinations are given in Table I, together with the previous data.

A similar examination has been extended to the corresponding bromo-complexes, $[Pt(amine)_4][PtBr_4]$, the results being included in Table I. Thus dichroism of $[Pt(NH_2CH_3)_4][PtBr_4]$, which has been determined by the present author using the microscopic method[3], shows the main features similar to that of Magnus's green salt.

Inspection of Table I shows that a drastic change occurs between methylamine and ethylamine in the case of $[Pt(amine)_4][PtCl_4]$. This may be ascribed to the steric factor[2]. Comparison of $[Pt(amine)_4][PtCl_4]$ with $[Pt(amine)_4][PtBr_4]$ also indicates that the bromo-complexes are more favorable for the formation of the Pt-Pt bond than the corresponding chloro-complexes. Since the bromide ion is larger than the chloride ion, this difference is not to be ascribed to the steric factor, but must be due to the difference in the inductive effect of the halide ions on the electronic state of the platinum ion. Similar results were obtained when a binuclear complex, $[Pt_2Br_6]^{2-}$, was used instead of $[PtBr_4]^{2-}$.

The same thing is again observed for the iodo-complexes. Thus $[PtI_4]^{2-}$ is colored dark-red, in the form of the potassium salt, but its combination with $[Pt(amine)_4]^{2+}$ ions yields complexes with color of greenish yellow, where amine represents ammonia, methylamine, *n*- and isopropylamine, *n*-butylamine, *n*-amylamine, ethylenediamine and propylenediamine.

The consideration, in the light of the criterion used in the cases of the chloro- and the bromo-complexes, indicates that these iodo-complexes all involve the Pt-Pt bond. It is most probable

TABLE I. Pt-Pt BOND IN THE CRYSTALS OF $[Pt(amine)_4][PtX_4]$

Amine	X=Cl		X=Br		X=I	
	Color	Pt-Pt bond	Color	Pt-Pt bond	Color	Pt-Pt bond
NH_3	Green	Present	Green	Present	Green-yellow	Present
CH_3NH_2	Green	Present	Green	Present	Green-yellow	Present
$C_2H_5NH_2$	Pink	Absent	Green	Present	Green-yellow	Present
n-$C_3H_7NH_2$	Pink	Absent	Green	Present	Green-yellow	Present
iso-$C_3H_7NH_2$	Pink	Absent	Green	Present	Green-yellow	Present
n-$C_4H_9NH_2$	Pink	Absent	Green	Present	Green-yellow	Present
n-$C_5H_{11}NH_2$	Pink	Absent	Green	Present	Green-yellow	Present
$H_2NCH_2CH_2NH_2$	Pink	Absent	Green	Present	Green-yellow	Present
$CH_3CH(NH_2)CH_2NH_2$	Pink	Absent	Green	Present	Green-yellow	Present

1) S. Yamada, *J. Am. Chem. Soc.*, **73**, 1579 (1951); S. Yamada and R. Tsuchida, *J. Chem. Soc. Japan, Pure Chem. Sec.* (*Nippon Kagaku Zassi*), **70** 142 (1949).

2) S. Yamada and R. Tsuchida, This Bulletin, **31**, 813 (1958).

3) R. Tsuchida and M. Kobayashi, "The Color and the Structure of Metallic Compounds" (Kinzokukagōbutsu no Iro to Kōzō), Zoshindo, Osaka (1944), p. 180.

that in the iodo-complexes the inductive effect, together with the π-bonding, is more important for the Pt-Pt bond formation than the steric factor, since the iodide ion is much larger than the bromide ion as well as the chloride ion.

It is interesting to note the difference between $[Pd(amine)_4][PtCl_4]$ and $[Pd(amine)_4] \cdot [PtBr_4]$, where amine represents those used in the other series of the complexes. It is found that the former show normal color of pink and the latter abnormal color of green. This fact seems to show that the Pd-Pt bond is absent in the former, while the bond exists in the latter. This result is in agreement with the conclusion derived in the foregoing part of the present communication.

The author wishes to thank the late Professor Ryutaro Tsuchida for his encouragement during the course of this work.

Department of Chemistry
Faculty of Science
Osaka University
Nakanoshima, Osaka

NMR Spectra of Methylene Protons in Benzyl Sulfites and Benzenesulfinate

By Michinori Ōki and Hiizu Iwamura

(Received June 7, 1962)

Abnormal splitting of the methylene proton signal in diethyl sulfite found by Finegold[1] could be due either to i) the non-equivalence of the two methylene groups, because of a) a different bond character of S–O linkages contributed differently with $\pi_{p,d}$- bonding orbital[1], b) geometrical asymmetry, or c) internal C–H ···O–S hydrogen bonding of one side of the ethyl groups with the other left intact, or to ii) the long-range spin-spin coupling effect. Waugh and Cotton[2] rejected all the above possibilities by finding the same phenomenon also in ethyl benzenesulfinate, and attributed it to the magnetic non-equivalence of two protons on a methylene group caused by neighbors of asymmetric center (S atom)[3]. Lately Kaplan and Roberts[4] have shown that the analysis of the spectra of diethyl sulfite as ABC_3 spin system leads to a good agreement with those observed. Thus, it seems to be a timely contribution to offer a conclusive experimental support for the computation results.

The syntheses and the physical properties of the samples will be reported later. Spectral measurement was carried out with a Varian model DP 60 NMR spectrometer at 60 Mc./sec. The samples were dissolved in carbon tetrachloride to give 10% solution, except the nitro-derivative for which the saturated solution in chloroform was employed. Cyclohexane (1%) added to the solvent served as an internal standard, the side band technique[5] being employed throughout the reading of the signals.

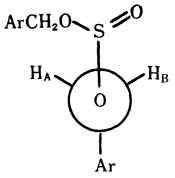
The methylene protons in these benzyl esters give a typical quartet signal of AB spin system[6] which can rigorously be solved to afford the $\nu_A-\nu_B$ and J_{AB} values in Table I. The skewness of the spectra of alkyl sulfites may be interpreted similarly.

Since $\nu_A-\nu_B$ is independent of the ring substituents in spite of the dependence of $(\delta_A+\delta_B)/2$ on them, it must be the S=O bond anisotropy that shifts a hydrogen signal to the lower applied magnetic field by the amount observed. Moreover, as $\nu_A-\nu_B$ is about 7 c.p.s. and is comparable with that in rather rigid ethylene sulfite[7], the most populating conformation of benzyl sulfites can be regarded as I and its residence time should be relatively long as suggested by the scarce temperature dependence of the signal. In benzyl benzenesulfinate, $\nu_A-\nu_B$ rises up to 31.38 c.p.s. In this case (II), H_B is suffering from the S=O bond anisotropy, while H_A is situated in the diamagnetic second field produced by the ring current of the benzene ring in the magnetic field[8], resulting in a large $\nu_A-\nu_B$ value.

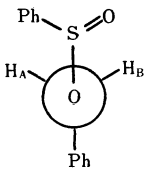
Table I. Methylene proton resonance of benzyl sulfites and benzenesulfinate measured at 60 Mc./sec.

$(X\cdot C_6H_4CH_2O)_2SO$ X	$(\delta_A+\delta_B)/2$ τ Value	$\nu_A-\nu_B$ c.p.s.	J_{AB} c.p.s.
p-NO_2	4.85	7.77	12.81
p-Cl	5.17	6.43	12.03
H	5.19	7.44	11.87
p-Me	5.22	7.23	11.78
p-MeO	5.24	6.90	11.57
$PhS(=O)OCH_2Ph$	5.34	31.38	11.37

1) H. Finegold, *Proc. Chem. Soc.*, **1960**, 283.
2) J. S. Waugh and F. A. Cotton, *J. Phys. Chem.*, **65**, 562 (1961).
3) P. M. Nair and J. D. Roberts, *J. Am. Chem. Soc.*, **79**, 4565 (1957).
4) F. Kaplan and J. D. Roberts, ibid., **83**, 4668 (1961).
5) J. T. Arnold and M. E. Packard, *J. Chem. Phys.*, **19**, 1608 (1951).
6) J. A. Pople, W. G. Schneider and H. Bernstein, "High-resolution Nuclear Magnetic Resonance Spectra", McGraw-Hill Book Co., Inc., New York, (1959), p. 119.
7) J. G .Pritchard and P. C. Lauterbur, *J. Am. Chem. Soc.*, **82**, 2105 (1961).
8) J. A. Pople, *J. Chem. Phys.*, **24**, 1111 (1956).



I



II

Department of Chemistry
Faculty of Science
The University of Tokyo
Hongo, Tokyo

Far Infrared Spectra and Torsional Vibrations of Polyoxymethylene

By Hiroyuki TADOKORO, Masamichi KOBAYASHI, Shunsuke MURAHASHI, Akiyoshi MITSUISHI and Hiroshi YOSHINAGA

(Received June 13, 1962)

In the previous paper[1], it was reported that the results of the calculation of the normal vibrations of polyoxymethylene (POM) were in fairly good agreement with the observed infrared and Raman frequencies. In that case, the measurements were limited to the region higher than 300 cm^{-1}, and the torsional coordinates were neglected in the calculation. Although the infrared spectra of POM and POM-d_2 have been already measured in the region of 5000~300 cm^{-1} by Novak and Whalley[2], the spectra in the far infrared region have not yet been reported. In this communication, we will report the results of the far infrared measurements of POM and POM-d_2, and of the consideration about the torsional vibrations of the skeletal chain.

The spectra were measured by using a single beam far infrared spectrophotometer constructed in the Faculty of Engineering of this University. The detail of the spectrophotometer was described in the previous report[3]. A film sample of POM (3 cm.×7 cm.×0.03 mm.) was prepared from pellets of Delrin-acetal resin (du Pont Corporation) by rolling between a couple of heated rolls. The polarization spectra of POM were also measured by using a transmission polarizer made of polyethylene sheets[4]. The spectrum of POM-d_2 (paraformaldehyde-d_2 manufactured by Merck & Co., Inc.) was measured as Nujol paste.

The results are shown in Fig. 1. A parallel band (belonging to the A_2 species) was found at 235 cm^{-1} in the spectra of POM[5] and a band was found at a slightly lower frequency (212 cm^{-1}) in the spectrum of POM-d_2.

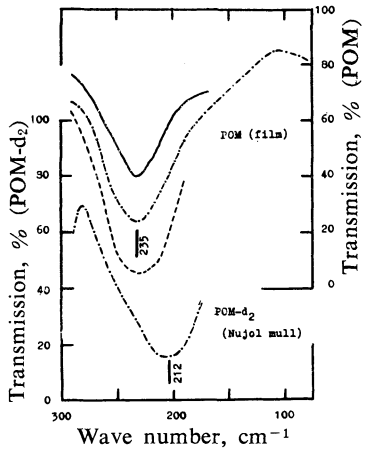


Fig. 1. Far infrared spectra of POM and POM-d_2.

-·-· Unpolarized
—— Electric vector perpendicular to the orientation direction
---- Electric vector parallel to the orientation direction.

The calculation of the normal vibrations was carried out by using the Urey-Bradley potential field according to the method described in the previous papers[6]. In this calculation the torsional displacement coordinates of the skeleton were taken into account. The numerical computation was made by using a NEAC 2203 electronic digital computer installed in the Computation Center of this University. The results show fairly good agreement between the observed and calculated frequencies. The maximum and average deviations are 6.15 and 2.19% for POM, and 9.90 and 2.51% for POM-d_2, respectively. The detailed results of the vibrational calculations will be reported in elsewhere.

As to the bands at near 200 cm^{-1}, the calculated frequencies [POM: 237 cm^{-1} (A_2), POM-d_2: 212 cm^{-1} (A_2)], are in good agreement with the observed results. The potential energy distributions calculated for the A_2 235

1) H. Tadokoro et al., *J. Chem. Phys.*, **35**, 369 (1961).
2) A. Novak and E. Whalley, *Trans. Faraday Soc.*, **55**, 1484 (1959).
3) H. Yoshinaga et al., *J. Opt. Soc. Am.*, **48**, 315 (1958).
4) A. Mitsuishi et al., ibid., **50**, 433 (1960).
5) This frequency (235 cm^{-1}) agrees with the calculated values, 253 cm^{-1}, for the skeletal model of POM by Miyazawa (*J. Chem. Phys.*, 35, 693 (1961)).
6) H. Tadokoro. *J. Chem. Phys.*, **33**, 1558 (1960); **35**, 1050 (1961).

and 212 cm^{-1} bands are $\tau_a(96\%)+r(CH_2)(3\%)$ and $\tau_a(93\%)+r(CD_2)(5\%)$, respectively[7]. The E_1 fundamental of the lowest frequency (calculated as 22 cm^{-1} for POM and 21 cm^{-1} for POM-d_2) corresponds to the approximately pure torsional vibration of the skeleton with the potential energy distribution $\tau_s(56\%)-\tau_a(40\%)$ for both POM and POM-d_2[7]. These bands could not be observed definitely because of the difficulties in the experimental technique in this region.

The torsional force constant F_τ was defined so that the diagonal elements of the $\boldsymbol{F}$-matrix associated with the torsional coordinates are expressed as $R_0^2 \sin^2\Theta_0 F_\tau$, where R_0=equilibrium C–O distance and Θ_0=equilibrium COC or OCO angles. The value of F_τ was calculated to be 0.061 md/Å, from which the height of the potential barrier for the internal rotation about the C–O bond, V_0, can be estimated by using a sinusoidal potential function

$$V=(V_0/2)(1-\cos 3\phi)$$

where $\phi=\tau-\tau_0$. V_0 was found to be 3.6 kcal./mol.

The authors express their gratitude to Professor Kenzo Joh and Dr. Saburo Makinouchi for the use of the computer and the helpful suggestions for programming.

Department of Polymer Science
Faculty of Science
Osaka University
Nakanoshima, Osaka
(H. T., M. K. & S. M.)

Department of Applied Physics
Faculty of Engineering
Osaka University
Higashinoda, Osaka
(A. M. & H. Y.)

7) τ_a and τ_s denote the antisymmetric and symmetric combinations of two torsional coordinates for adjacent skeletal bonds, respectively.

Cobalt(II) Complexes with Schiff's Bases Derived from Salicylaldehyde and ortho-Substituted Aromatic Amines

By Hiroaki NISHIKAWA and Shoichiro YAMADA

(Received June 18, 1962)

It has been generally believed that quadri-co-ordinate cobalt(II) complexes are not formed with Schiff's bases having substituents on the carbon atom in the 2-position (I)[1]. In fact, bis(salicylidene-2-anisilato)cobalt(II) was reported, but the formation of the compound was ascribed to extra stabilization due to the additional linkage of the oxygen atom of the methoxygroup with the cobalt(II) ion to complete sexa-co-ordination[1]. The present authors have recently succeeded in preparing several cobalt(II) compounds with Schiff's bases having substituents in the 2-position, which are listed in Table I.

The main procedure of the preparations was to add the mixture of $Co(salal)_2 \cdot 2H_2O$*1 (0.015 mol.) and one of the amines (about 0.045 mol.) into a flask which contained ethanol and was filled with its vapor above the liquid phase, keep the reaction mixture closed tightly, allow it to stand overnight and cool it eventually. Red or orange-red crystals are then obtained. In the case of the *o*-chloroaniline, dark-brown crystals are obtained by this procedure. These crystals were recrystallized from pyridine, and the resulting crystals of $Co(2\text{-}Cl \cdot C_6H_4 \cdot N : CH \cdot C_6H_4 \cdot O)_2 \cdot (py)_2$*2 were heated at 70°C in vacuo to yield orange-yellow crystals of $Co(2\text{-}Cl \cdot C_6H_4 \cdot N : CH \cdot C_6H_4 \cdot O)_2$.

Absorption spectra of these compounds in non-co-ordinating organic solvents have been determined in the present study. Since all these compounds display similar absorption spectra, only some of the typical spectra are shown in Fig. 1, together with the absorption spectra of bis(salicylidene-methyliminato)- and bis(salicylidene - isopropyliminato) - cobalt(II). Most bis(salicylidene-alkyliminato)cobalt(II) complexes, absorption spectra of which were recently reported by the present authors[2], are stable in the air at least during the measurements, except for the methyliminato compound of cobalt(II), which is unstable in the air. Since the measurements in the previous

1) B. O. West *Nature*, **173**, 1187 (1954).

*1 The notation, salal, denotes an anion derived when a molecule of salicylaldehyde loses a hydrogen ion of the phenolic hydroxylgroup.

*2 The notation, py, denotes a molecule of pyridine.

2) H. Nishikawa, S. Yamada and R. Tsuchida, *Z. anorg. u. allgem. Chem.* (1962), in press.

TABLE I. BIS(SALICYLIDENE-ARYLIMINATO)COBALT(II), $Co(O\cdot C_6H_4\cdot CH:N\cdot R)_2$

R	Solvents used in preparation	C, %		H, %		N, %	
		Calcd.	Found	Calcd.	Found	Calcd.	Found
2-Methylphenyl	Ethanol	70.2	69.9	5.05	5.08	5.84	5.92
2-Chlorophenyl	Ethanol	60.0	60.3	3.49	3.61	5.38	5.22
2,6-Dimethylphenyl	Methanol	71.0	71.1	5.56	5.52	5.52	5.22
2,4-Dimethylphenyl	Ethanol	71.0	70.8	5.56	5.65	5.52	5.34
2,3-Dimethylphenyl	Methanol	71.0	70.7	5.56	5.53	5.52	5.86
α-Naphthyl	Methanol	74.0	73.6	4.39	4.36	5.08	4.96

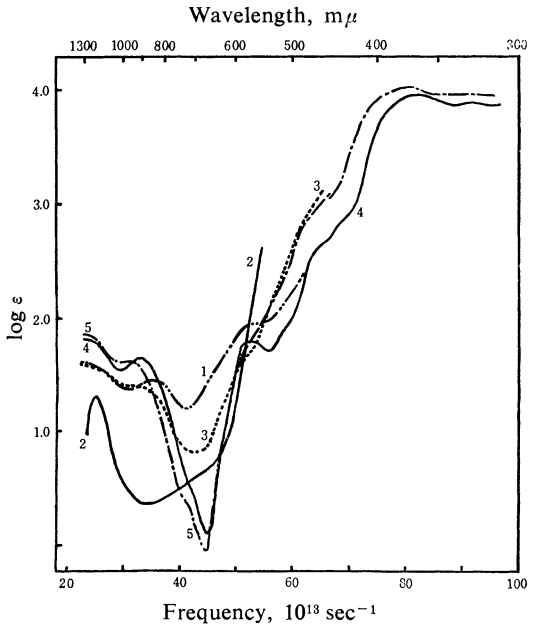


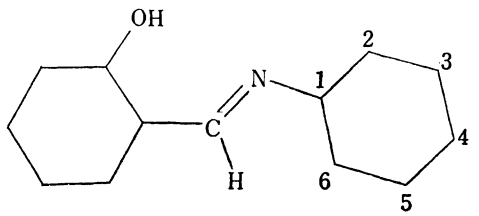
Fig. 1. Ultraviolet-absorption spectra of 1. $Co(O\cdot C_6H_4\cdot CH:N\cdot CH_3)_2$ in chloroform, 2. "salcomine" in chloroform, 3. $Co(O\cdot C_6H_4\cdot CH:N\cdot 2\text{-}Cl\cdot C_6H_4)_2$ in benzene, 4. $Co(O\cdot C_6H_4\cdot CH:N\cdot 2\text{-}CH_3\cdot C_6H_4)_2$ in benzene, and 5. $Co(O\cdot C_6H_4\cdot CH:N\cdot 2,6\text{-}(CH_3)_2C_6H_3)_2$ in benzene.

work[2] were done in the presence of air, it seems likely that the oxidation of the methyliminato compound may have taken place during the measurements. The measurements in the present work with bis(salicylaldehyde)ethylenediimine-cobalt(II), ("salcomine"), bis(salicylaldehyde)propylenediimine-cobalt(II) and bis(salicylidene-methyliminato)cobalt(II), which are most readily oxidized in the air, have been carried out in the atmosphere of nitrogen to avoid the undesirable oxidation.

It was formerly found that the absorption spectra, especially the ligand field bands, of the compounds of this sort are diagnostic in determining the configuration of these compounds[2]. Actually the present measurements indicate that "salcomine" and the corresponding propylenediimine complex, which have square-planar configuration, show absorption spectra quite different from the spectra of the methyliminato- and other alkyliminato-derivatives, which were concluded to have a configuration distorted from the square-plane[2,3]. The main difference between the two types lies in that the complexes of the series having a configuration distorted from the square-plane show ligand field bands with characteristic shape in the near-infrared region, while "salcomine" with square-planar configuration does not show a similar pattern, but a rather sharp band in that wavelength region.

Bis(salicylidene-2,6-xylidinato)cobalt(II), which suffers steric hindrance against forming the square-planar co-ordination around a cobalt(II) ion, shows absorption spectrum, similar to those of bis(salicylidene-alkyliminato)-cobalt(II) complexes. Moreover, all the compounds with a substituent on the carbon atom in the 2-position show absorption spectra which are similar to each other, having the main features observed for bis(salicylidene-alkyliminato)-cobalt(II) complexes. The spectra of these compounds, however, are different from the spectrum of "salcomine". It is concluded, therefore, that all these compounds synthesized in the present study, as well as bis(salicylidene-methyliminato)cobalt(II), have a configuration distorted from the square-plane.

It is concluded in a similar way that bis(salicylidene-anilinato)cobalt(II) is also distorted from the square-planar co-ordination, since the compound shows ligand field bands with features similar to those of bis(salicyl-



(I)

3) H. Nishikawa, S. Yamada and R. Tsuchida, *Z. Naturforsch.*, **17b**, 78 (1962).

idene-2, 6-xylidinato)cobalt(II). In the former there is only slight steric hindrance between the hydrogen atom in the 2-position and the oxygen atom of the neighboring ligand. The favorable condition in energy, together with this slight steric hindrance, may be one of the main factors which give rise to the distortion from the square-planar co-ordination in this type of compounds.

The present authors wish to thank the late Professor Ryutaro Tsuchida for his encouragement during the course of this work.

Department of Chemistry
Faculty of Science
Osaka University
Nakanoshima, Osaka

The Determinations of Some Metal Ions by Using Hexamminecobalt(III) Chloride and Sodium Thiosulfate as Precipitants

By Jun YOSHIMURA, Yoshimasa TAKASHIMA, Yoshio MURAKAMI and Toyoaki KUSABA

(Received January 16, 1962)

Many studies for the determinations of various metals using hexamminecobalt(III) chloride as the reagent have been reported. For example, indium has been determined gravimetrically[1,2], colorimetrically[3,4], volumetrically[3], and radiometrically[3] in the form of $[Co(NH_3)_6]InCl_6$ in a hydrochloric acid system. Moreover, thallium has been determined as $[Co(NH_3)_6]TlCl_6$[5-9], aluminum as $[Co(NH_3)_6]AlF_6$[10], gallium as $[Co(NH_3)_6]GaF_6$[11], scandium as $[Co(NH_3)_6]ScF_4$[12,13], iron as $[Co(NH_3)_6]FeF_6$[14], phosphate as $[Co(NH_3)_6]PO_4 \cdot 4H_2O$[15-18], vanadate as $[Co(NH_3)_6](VO_3)_3$[19], and beryllium as $[Co(NH_3)_6][(H_2O)_2Be_2(CO_3)_2(OH)_3] \cdot 3H_2O$[20,21].

Recently Yatsimirskii and Roslyakova have studied the precipitation reactions of copper and lead, using hexamminecobalt(III) chloride and sodium thiosulfate as precipitants[22]; that is, when these reagents were added to the solutions of the metal ions mentioned above, these metals were precipitated, forming insoluble complexes such as $[Co(NH_3)_6]_5[Cu(S_2O_3)_3]_3 \cdot 12H_2O$ and $[Co(NH_3)_6]_2[Pb_2(S_2O_3)_5]$; they have also developed iodometric determination methods. As one of a series of these studies, and in order to develop Yatsimirskii's method, this work was performed.

It was found in this study that silver, cadmium, mercury and bismuth were precipitated forming insoluble complex salts immediately, when hexamminecobalt(III) chloride and sodium thiosulfate solutions were added to the solutions of the metal ions mentioned above; the compositions of these complex salts, except bismuth salt were confirmed to be $[Co(NH_3)_6][Ag(S_2O_3)_2]$, $[Co(NH_3)_6]_4[Cd(S_2O_3)_3]_3 \cdot 6H_2O$ and $[Co(NH_3)_6]_4[Hg(S_2O_3)_3]_3 \cdot 10H_2O$ respectively. The composition of the slightly soluble complex salt which is formed by adding a hexamminecobalt(III) chloride solution to a sodium thiosulfate solution was found to be $[Co(NH_3)_6](S_2O_3)Cl \cdot H_2O$, while Rãy prepared the complex salt $[Co(NH_3)_6]S_2O_3Cl$ by the addition of ammonia to a mixed solution of cobalt(II) chloride, ammonium chloride and sodium thiosulfate in a current of air[23].

We have studied various methods of the determination of metal ions based on the formation of metal complexes; that is, we studied silver by measuring volumetrically the excess of sodium thiosulfate with a standard iodine solution, copper and mercury by weighing gravimetrically their complex salts, and mercury and lead by EDTA titration after their salts had been decomposed.

Experimental

Preparation of Hexamminecobalt(III) Chloride Thiosulfate.—To 10 ml. of a 0.1 M hexamminecobalt(III) chloride solution, an equimolar solution of sodium thiosulfate was added and stirred; after a while a precipitate was obtained. The precipitate was then filtered through a glass filter (1G No. 4), washed 2~3 times successively with 5 ml. of distilled water, and dried on calcium chloride in a dessicator for a month.

Preparation of Silver, Cadmium and Mercury Complexes.—To the mixture of 1.0 ml. of 0.1 M metal chloride and 15 ml. of 1 M ammonium acetate solutions, 10 ml. each of 0.1 M hexamminecobalt(III) chloride and 0.1 M sodium thiosulfate solutions were added. A precipitate of the metal

1) F. Ensslin, *Metall. u. Erz.*, **28**, 305 (1941).
2) F. Ensslin and H. Dreyer, *Z. anorg. u. allgem. Chem.*, **249**, 119 (1942).
3) T. Ishimori et at., *Japan Analyst*, **5**, 329 (1956).
4) T. Nozaki, *J. Chem. Soc. Japan, Pure Chem. Sec.* (*Nippon Kagaku Zassi*), **77**, 1751 (1956).
5) G. Spacu and A. Pope, *Z. anal. Chem.*, **120**, 322 (1940).
6) Y. Murakami, This Bulletin, **22**, 206 (1949).
7) T. Ishimori, ibid., **26**, 336 (1953).
8) T. Ishimori and Y. Takashima, *J. Chem. Soc. Japan, Pure Chem. Sec.* (*Nippon Kagaku Zassi*), **76**, 858 (1955).
9) T. Nozaki, ibid., **77**, 493 (1956).
10) Y. Takashima, ibid., **80**, 619 (1959).
11) Y. Takashima, ibid., **80**, 622 (1959).
12) Y. Takashima, ibid., **79**, 243 (1958).
13) Y. Takashima, ibid., **79**, 246 (1958).
14) Y. Takashima, ibid., **79**, 248 (1958).
15) H. A. Laitinen and L. W. Burdétt, *Anal. Chem.*, **23**, 1265 (1951).
16) H. W. McCune and G. T. Arquette, ibid., **27**, 401 (1955).
17) T. Matsuo, *Japan Analyst*, **4**, 108 (1955).
18) Y. Takashima, *Memoirs. Kyushu Univ.*, **C2** 161 (1957).
19) C. Duval and A. Morette, *Compt. rend.*, **230**, 545 (1950).
20) T. I. Pirtea and G. Mihail, *Z. anal. Chem.*, **159**, 205 (1958).
21) S. Misumi and T. Taketatsu, This Bulletin, **32**, 593 (1959).
22) K. B. Yatsimirskii and E. N. Roslyakova, *Report on Symposium*; "*Sovrem Metody Anal. Metall., M., Metallurgizdat*", **1955**, 124; Ref. *Anal. Abstr.*, **4**, 1126 (1957).
23) P. R. Rãy, *Quart. J. Indian Chem. Soc.*, **4**, 64 (1927).

complex salt was formed immediately. The precipitate was filtered through a glass filter, washed repeatedly with 5 ml. of water and dried on calcium chloride for a month.

Analytical Methods of Complex Salts.—*Determination of the Hexamminecobalt(III) Ion.*—A known quantity of the dried precipitate was dissolved in a 10% sodium hydroxide solution and boiled untill the black brown precipitate of cobalt(III) hydroxide was obtained. The solution containing the precipitate was acidified by adding hydrochloric acid and boiled to dissolve the cobalt(III) hydroxide. After the solution had been allowed to cool the concentration of cobalt(III) ion in the solution was determined by the nitroso-R and EDTA methods. The quantity of hexamminecobalt(III) ion was calculated by making use of their factors.

Determination of the Thiosulfate Ion.—In the case of hexamminecobalt(III) chloride thiosulfate, a known quantity of the sample was dissolved in distilled water and the thiosulfate ion was determined by iodometric titration. As for the metal complexes, after the metal complex formed had been filtered off through a glass filter, the concentration of thiosulfate ion in the filtrate was determined by iodometric titration, and then the content of this ion in the complex was calculated from the difference between the total concentration of this ion and that in the filtrate.

Determination of the Chloride Ion.—After the sample had been treated with a 10% hot sodium hydroxide solution, the cobalt(III) hydroxide formed was filtered off. Then a few milliliters of 3% hydrogen peroxide were added to the filtrate, and this mixture was warmed in boiling water, to oxidize the thiosulfate to the sulfate ion or to sulfur[24]; this treatment was followed by the addition of copper(II) nitrate for the decomposition of the excess of hydrogen peroxide[25]. After the solution had been allowed to cool, the concentration of the chloride ion was determined by Mohr's method.

Determination of the Water of Crystallization.—The sample was dried again up to a constant weight on the phosphorus pentoxide under reduced pressure (below 20 mmHg), and the water content was calculated from the weight difference.

Determination of the Silver Ion.—After the sample had been decomposed by the same treatment as in the determination of the hexamminecobalt(III) ion in the complex salt, the silver hydroxide formed was filtered and dissolved again in dilute aqueous ammonia; then silver chloride was precipitated by acidifying the solution with nitric acid, and the concentration of silver ion was determined gravimetrically.

Determination of the Cadmium and Mercury Ions.—After alkali and acid treatments, these metals were determined by EDTA titration.

Procedures.—*General Procedure for the Determination of Silver by Iodometric Titration.*—To about 10 ml. of a solution containing 5~50 mg. of silver and 15 ml. of a buffer solution, 10 ml. each of 0.1 M hexamminecobalt(III) chloride and equimolar thiosulfate solutions were added and stirred, so a precipitate of silver complex was formed immediately. After the solution had been left standing for 5 min., the precipitate was filtered through a glass filter (1G, No. 4), washed 3 times with 10 ml. of distilled water, and the filtrate and the washings were collected into a 100 ml. dry flask. The filtrate was titrated with a standard iodine solution to determine the excess of sodium thiosulfate, and the number of thiosulfate ions in the precipitate was calculated from the difference between the total thiosulfate concentration added and that in the filtrate. The concentation of silver was determined indirectly by making use of their factors.

Procedure for Determination of Copper, Mercury and Lead by the Gravimetric Method.—To a sample solution containing about 2 ml. of a 0.03~0.1 M metal chloride solution, 15 ml. of a buffer solution and 10 ml. each of the two reagents were added; a precipitate of the metal complex was then formed. After the solution had been left standing for about 15 min., the precipitate was filtered through a weighed glass filter (1G No. 4) and washed with distilled water and then with alcohol and ether. It was dried in an air bath at 50°C for 3 hr. and weighed after cooling.

Procedure for the Determination of Mercury and Lead by EDTA Titration.—A precipitate formed by the same procedure as in the gravimetric method was filtered through filter paper (Toyo-roshi 5C) and washed with distilled water, transferred to the beaker, and decomposed with the alkali and acid treatments previously mentioned; then the concentration of metal ions was determined by EDTA titration.

Results and Discussion

Stability of Sodium Thiosulfate in Solutions of Various pH Values from 1 to 10.5.—In this study, the most important finding was that the hexamminecobalt(III) chloride and sodium thiosulfate used as precipitants were stable under the experimental conditions. It is well known that hexamminecobalt(III) chloride is very stable in solutions over this pH range. Sodium thiosulfate, on the other hand, was unstable in solutions with pH values below 4 and decomposed, separating out sulfur, but it was stable in solutions with pH values above 5; therefore, the experiment could not be done below this pH value.

Effect of the Ammonium Acetate Solution Added.—When a 0.1 M sodium thiosulfate solution was mixed with a 0.1 M hexamminecobalt(III) chloride solution and stirred, an orange, needle-shaped precipitate [hexamminecobalt(III) chloride thiosulfate] was formed; the coprecipitation of this salt with a metal complex salt caused a large error in the determination of the metal ions, but the formation of this complex salt was repressed by adding a certain amount of acetate salt. When 10 ml. of each

24) S. Utsumi, *J. Chem. Soc. Japan, Pure Chem. Sec.* (*Nippon Kagaku Zassi*), **74**, 608 (1953).
25) S. Utsumi, ibid., **74**, 609 (1953).

precipitant was added to 15 ml. of a 1 M ammonium acetate solution, this complex salt was not formed at least for 20 min. It was evident from this fact that the ammonium acetate solution acted not only as a buffer but as a masking agent. It was then decided to use 10 ml. of each 0.1 M precipitant and 15 ml. of the 1 M ammonium acetate solutions in the following study.

Possibility of the Formation of Various Metal Complexes.—By adding 1 ml. of a 0.1 M solution of various metal ions to the mixed solution of the three reagents mentioned above, the possibility of the formation of various metal complex salts was examined. The elements used in this examination were lithium, sodium, potassium, silver, beryllium, magnesium, calcium, strontium, barium, zinc, cadmium, mercury, boron, aluminum, gallium, indium, thallium, scandium, germanium, tin, arsenic, antimony, bismuth, vanadium, chromium, molybdenum, tungsten, uranium, manganese, iron, cobalt and nickel. It was also found that, in addition to copper and lead, silver, mercury and cadmium were precipitated, forming an insoluble complex salt in solutions with 5.0~10.5 pH values and that bismuth precipitated as its hydroxide in the neutral solution, but formed an insoluble complex in the solution with a pH value of 3.

Determination of the Compositions of Various Complexes.—

1) Hexamminecobalt(III) chloride thiosulfate.

Found: $[Co(NH_3)_6]^{3+}$, 49.4; $S_2O_3^{2-}$, 34.3; Cl^-, 11.6; H_2O, 5.0. Calcd. for $[Co(NH_3)_6](S_2O_3)Cl\cdot H_2O$: $[Co(NH_3)_6]^{3+}$, 49.3; $S_2O_3^{2-}$, 34.3; Cl^-, 10.9; H_2O, 5.5%.

2) Silver complex.

Found: $[Co(NH_3)_6]^{3+}$, 31.3; Ag^+, 21.9; $S_2O_3^{2-}$, 45.1. Calcd. for $[Co(NH_3)_6][Ag(S_2O_3)_2]$: $[Co(NH_3)_6]^{3+}$, 32.6; Ag^+, 21.8; $S_2O_3^{2-}$, 45.4%.

3) Mercury complex.

Found: $[Co(NH_3)_6]^{3+}$, 26.9; Hg^{2+}, 24.0; $S_2O_3^{2-}$, 42.0; H_2O, 7.4. Calcd. for $[Co(NH_3)_6]_4[Hg(S_2O_3)_3]_3\cdot 10H_2O$: $[Co(NH_3)_6]^{3+}$, 26.5; Hg^{2+}, 24.7; $S_2O_3^{2-}$, 41.4; H_2O, 7.4%.

4) Cadmium complex.

Found: $[Co(NH_3)_6]^{3+}$, 31.2; Cd^{2+}, 15.8; $S_2O_3^{2-}$, 48.8; H_2O, 5.2. Calcd. for $[Co(NH_3)_6]_4[Cd(S_2O_3)_3]_3\cdot 6H_2O$: $[Co(NH_3)_6]^{3+}$, 30.7; Cd^{2+}, 16.1; $S_2O_3^{2-}$, 48.1; H_2O, 5.2%.

5) Bismuth complex.

As has been previously mentioned, this complex was formed in the solution with a pH value of 3, but the composition of this complex was not determined, for this complex could not be separated from the sulfur formed as a result of the decomposition of the sodium thiosulfate reagent.

Relation between the Amount of the Precipitate and the pH Value of the Solution.—As the compositions of the silver, cadmium and mercury complexes were determined in addition to those of copper and lead, we studied on the determination methods for these metal ions based on the formation of a complex salt. At first, the relation between the amount of the precipitate and the pH value of the solution was studied under the same conditions as for the preparation of a metal complex. The results are shown in Figs. 1a and 1b. From these results, the cadmium complex was shown not to precipitate quantitatively; when the pH value of the solution became larger than 8, lead did not precipitate as its complex salt, but as its hydroxide, and the gravimetric determination of lead by making use of its complex became useless.

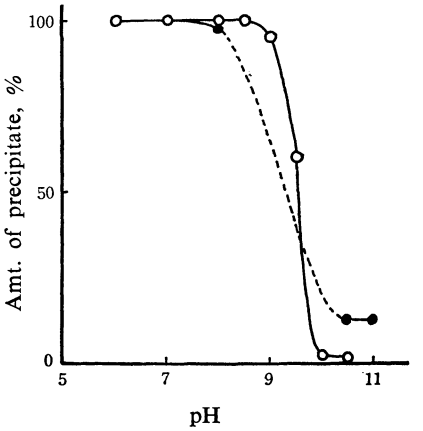


Fig. 1a

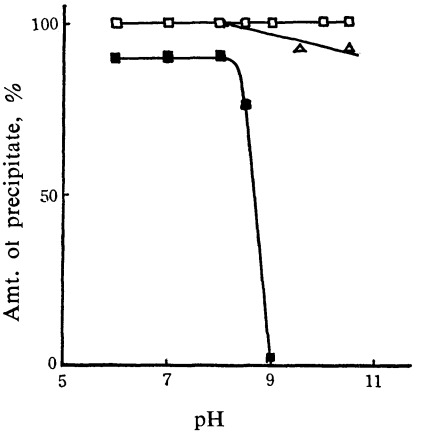


Fig. 1b

Figs. 1a and 1b. Relation between the amount of the precipitate and the pH value of the solution.

—○— Copper —△— Silver
—●— Lead —■— Cadmium
—□— Mercury

The Effect of Ammonium Acetate on the Precipitation of the Metal Complex. — We studied the effect of ammonium acetate on the precipitation of a silver complex by measuring the concentration of excess sodium thiosulfate by iodometry, for we were afraid that the acetate repressed not only the formation of hexamminecobalt(III) chloride thiosulfate but also that of the metal complex. The results are shown in Table I. It is evident from this table that the addition of 2~30 ml. of a 1 M ammonium acetate solution does not repress the formation of the silver complex.

TABLE I. EFFECT OF AMMONIUM ACETATE IN THE PRECIPITATION OF SILVER COMPLEX

Ag taken mg.	1 M ammonium acetate added ml.	Ag found mg.
10.8	0	10.8
10.8	3	10.7
10.8	5	10.7
10.8	10	10.8
10.8	15	10.8
10.8	30	10.7

Relation between the Amount of the Precipitate and the Time Allowed for the Precipitate to Form.—The effect of the time on the amount of the precipitate was studied under general conditions. The results are shown in Fig. 2. From these results, the time which the solution should be allowed to stand after the precipitants had been added to the sample solution was concluded to be 5 min. for the volumetric method for silver and 20 min. for the other metals.

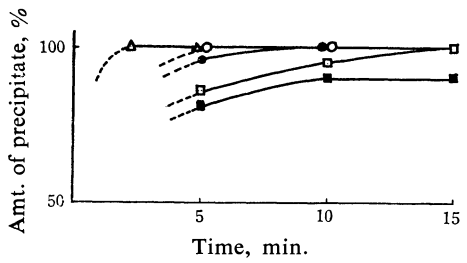


Fig. 2. Relation between the amount of the precipitate and the time allowed for the precipitate to form.
—○— Copper —△— Silver
—●— Lead —■— Cadmium
—□— Mercury

Washing and Drying of Metal Complexes.—Metal complexes were almost insoluble in water, acid, alcohol, ether, acetone, etc., while hexamminecobalt(III) chloride thiosulfate was fairly soluble in water. These salts were decomposed by heating above 60°C but were stable below 50°C, so in the gravimetric determination the precipitate was washed with water, alcohol and ether and then dried in an air bath at 50°C.

Volumetric Determination of Silver.—Silver was precipitated, forming the insoluble complex salt in the neutral solution by adding hexamminecobalt(III) chloride and sodium thiosulfate solutions to a silver nitrate solution. We studied the determination method of silver by measuring volumetrically the excess of sodium thiosulfate, and various concentrations of silver were determined by the general procedure; the results are shown in Table II. It was also concluded that the indirect titration of silver was satisfactorily carried out. As has been previously mentioned, copper, cadmium, mercury and lead were precipitated together with

TABLE II. DETERMINATION OF VARIOUS CONCENTRATIONS OF SILVER BY GENERAL PROCEDURE

Ag taken mg.	Ag found mg.	Ag found/ Ag taken %
5.4	5.4	99.8
10.8	10.7	100.5
21.6	21.7	99.0
53.9	53.8	99.4

TABLE III. DETERMINATION OF SILVER IN THE PRESENCE OF FOREIGN IONS

0.1 M sodium thiosulfate added, ml.	2.5	5.0	10.0
Foreign ion	Ag found, mg.		
Mg(II)	4.6	5.4	—
Ca(II)	5.4	5.5	—
Al(III)	4.6	5.5	—
Cr(III)	4.8	5.4	—
Mn(II)	4.4	4.7	5.3
Fe(III)	4.4	4.6	5.4
Co(III)	5.5	5.4	—
Ni(III)	4.9	5.4	—

Silver added: 5.4 mg.
Each foreign ion added: 2.5 mg.

TABLE IV. GRAVIMETRIC DETERMINATIONS OF VARIOUS CONCENTRATIONS OF COPPER, MERCURY AND LEAD

Metal	Metal taken mg.	pH of solution	Metal found mg.	Error mg.
Cu	3.4	7.4	3.5	+0.1
	6.9	7.4	7.2	+0.3
	14.5	7.4	14.8	+0.3
Hg	5.4	7.4	5.4	0.0
	10.8	7.4	10.8	0.0
	21.6	7.4	21.9	+0.4
	10.8	11.0	11.0	+0.2
Pb	3.0	7.4	3.0	0.0
	6.0	7.4	6.2	+0.2
	12.1	7.4	12.5	+0.4

TABLE V. DETERMINATIONS OF MERCURY AND LEAD BY EDTA TITRATION

Metal	Metal taken mg.	pH of solution	Foreign ion taken mg.	Metal found mg.	Error mg.
Hg	5.4	7.4		5.5	+0.1
	10.8	7.4		10.8	0.0
	21.6	7.4		21.5	−0.1
	10.8	11.0		10.7	−0.1
	10.8	11.0	Cu: 2.9	10.6	−0.2
	10.8	11.0	Cd: 11.5	10.8	0.0
	10.8	11.0	Cu: 6.9 Cd: 11.5	10.7	−0.1
Pb	3.0	7.4		3.1	+0.1
	6.0	7.4		5.8	−0.2
	12.1	7.4		12.1	0.0

silver, forming insoluble complex salts, and this causes serious interference on the determination of the silver. When the sample solution contained calcium, magnesium, aluminum, chromium, manganese, iron, cobalt and nickel together with silver, the precipitate of the silver complex was not formed quantitatively, for the foreign ions existing in the solution formed thiosulfate complexes and, consequently, the free thiosulfate ion in the solution decreased and was not enough to produce the insoluble silver complex perfectly. In this case, good results in the determination were obtained by adding a large excess of sodium thiosulfate. The results are shown in Table III.

Gravimetric Method.—We studied the gravimetric determination of copper, mercury and lead, for these metals are precipitated quantitatively, producing insoluble complex salts. The results obtained by the general procedure are shown in Table IV. The positive error of the observed value in every run seems to be caused by the water adhering to the precipitate.

Determination by EDTA Titration. — As mercury and lead existing in the solution together with cobalt can be determined by EDTA titration without being separated from cobalt[26,27], these metal ions were determined by this method after their complexes had been decomposed by alkali and acid treatments. The results obtained by the general procedure are shown in Table V.

Studies of the Isolation of these Complex-forming Metals.—In order to mask the formation of bismuth hydroxide in the neutral solution and of lead hydroxide in a solution with a pH value above 8, the masking actions of ammonium oxalate, ammonium citrate, ammonium succinate and ammonium tartrate solutions were examined; among them only the ammonium citrate solution was effective in preventing the hydroxides from forming, but at the same time this reagent repressed the formation of the metal complex to be measured and so was found to be useless. It is evident from the results described above that silver and mercury could be separated from copper and cadmium, but that the ultimate isolation of each element could not be effected.

Summary

1) When hexamminecobalt(III) chloride and sodium thiosulfate solutions were mixed, a precipitate was formed; the composition of this salt was found to be

$$[Co(NH_3)_6](S_2O_3)Cl\cdot H_2O$$

2) In addition to copper and lead, silver, cadmium, mercury and bismuth were precipitated, forming insoluble metal complexes, by adding hexamminecobalt(III) chloride and sodium thiosulfate solutions as precipitants to the solutions of these metal ions. The compositions of these salts, except for bismuth salt, were found to be

$$[Co(NH_3)_6][Ag(S_2O_3)_2],$$
$$[Co(NH_3)_6]_4[Cd(S_2O_3)_3]_3\cdot 6H_2O \text{ and}$$
$$[Co(NH_3)_6]_4[Hg(S_2O_3)_3]_3\cdot 10H_2O$$

3) Various determination methods based on the formation of metal complexes were studied; that is, silver was studied by volumetrically measuring the excess of sodium thiosulfate with an iodine solution, copper and mercury, by gravimetrically weighing their complex salts, and mercury and lead, by EDTA titration after their complex salts had been decomposed.

Department of Chemistry
Faculty of Science
Kyushu University
Hakozaki, Fukuoka

26) G. Schwarzenbach, "Die Komplexometrische Titration", Ferdinand Enke Verlag, Stuttgart (1957), p. 82.
27) H. Flaschka, *Z. anal. Chem.*, **138**, 332 (1953).

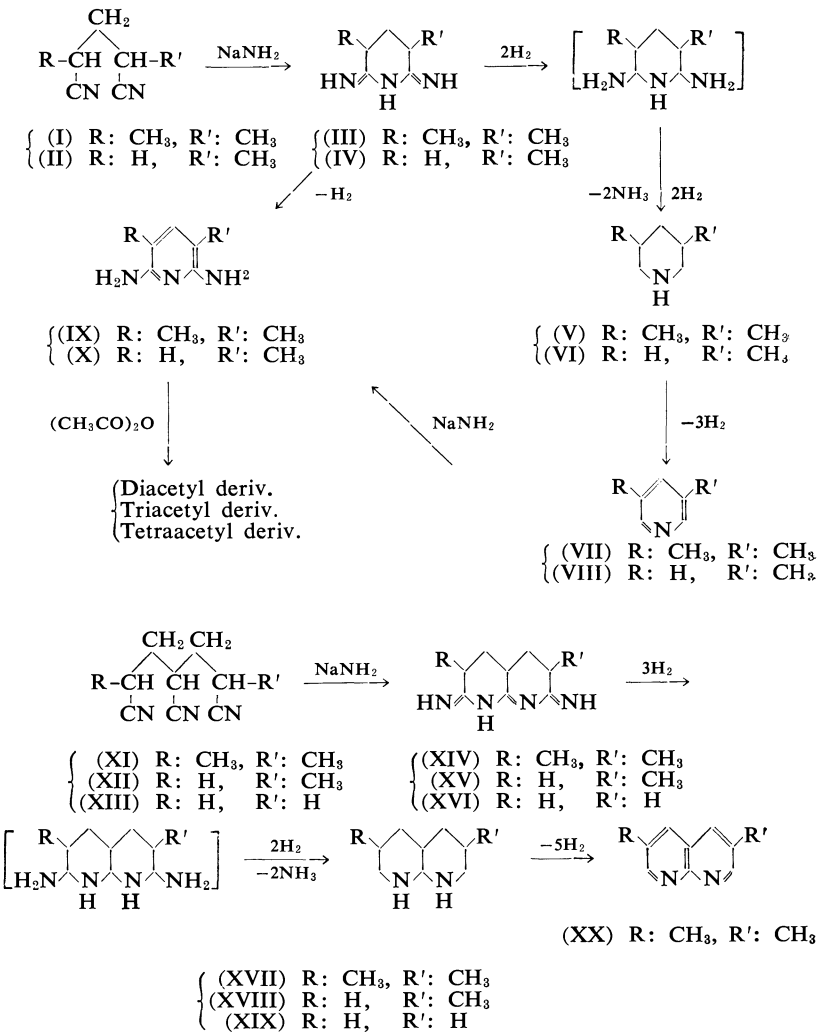
Synthesis of Methylpyridine and 1, 8-Naphthylidine Derivatives

By Toshihiro TAKATA

(Received January 18, 1962)

Usually, pyridine and 1, 8-naphthylidine derivatives are prepared from carbonyl compounds and from α-aminopyridines respectively[1,2]. The present paper describes a synthesis of those derivatives from aliphatic dinitriles[3] or from trinitriles accomplished through the scheme shown below:

The ring-closure reactions of dinitriles (I and II) and trinitriles (XI, XII and XIII) were carried out according to the techniques of Elvidge[4] for succinonitrile, using sodium amide to give glutaroimidine derivatives (III and IV) or diimino-1, 8-naphthylidine derivatives (XIV, XV and XVI).

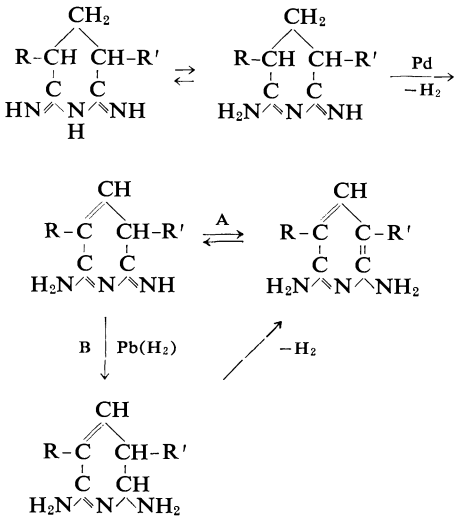


1) T. Matsukawa et al., "Dai Yūki Kagaku", Vol. 16, Asakura Shoten, Tokyo (1959), pp. 390—391.
2) C. F. Allen, *Chem. Revs.*, **47**, 275 (1950).
3) T. Takata and M. Taniyama, *Kōbunshi Kagaku*, **16**, 693 (1959).
4) J. A. Elvidge and R. P. Linstead, *J. Chem. Soc.*, **1954**, 442.

Those cyclic imidine-type compounds (III, IV, XIV, XV and XVI) were hydrogenated in an alcoholic solution with sodium to give piperidine derivatives (V and VI) or decahydro-1,8-naphthylidine derivatives (XVII, XVIII and XIX), the imino groups were eliminated almost quantitatively as ammonia, as in the case of α-aminopyridine[5].

Dehydrogenations of the cyclic compounds (III, IV, V, VI and XVII) were carried out by treating them with a palladium catalyst to yield α, α'-diaminopyridines (IX and X), methylpyridines (VII and VIII), or dimethyl-1,8-naphthylidine (XX). Monomethyl-α, α'-diaminopyrine (X) was also obtained from VIII by treating it with sodium amide[6]; between the infrared spectra of the X derived from VIII and that derived from IV, no difference could be detected, as is shown in Fig. 1.

Therefore, the formation of α, α'-diaminopyridines from glutaroimidines suggests the possibility of the mechanism shown below, in which reaction B may be more probable than A.



As another route for the synthesis of 1,8-naphthylidines, we followed the procedure of Reissert[7,8] except for the preparation of the δ-carboxyheptamethylene diamines, which had been prepared from γ-bromopropylphthalimide and diethyl malonate by Reissert, but which we derived from diethyl malonate and acrylonitrile or methacrylonitrile. This scheme is shown below.

5) A. E. Tschitschibabin and M. P. Gertschuk, *Ber.*, **63**, 1153 (1930).
6) A. E. Tschitschibabin and Seide, *Chem. Zentr.*, **1915**, I. 1065.
7) A. Reissert, *Ber.*, **26**, 2137 (1893).
8) A. Reissert, ibid., **27**, 980 (1894).

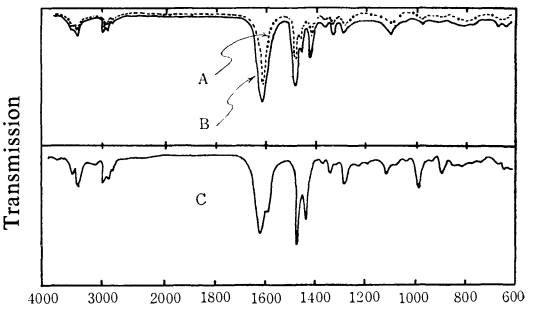
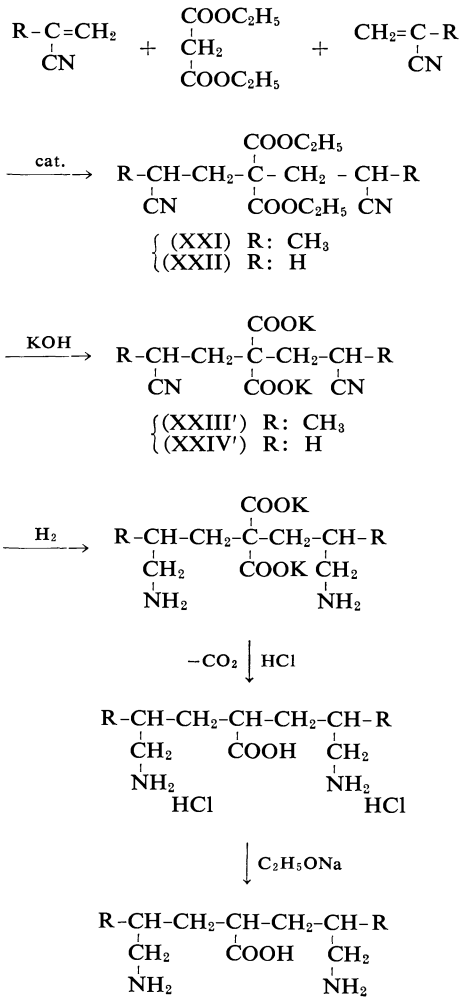
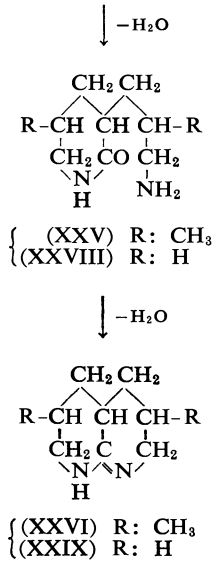


Fig. 1. Infrared spectra of 2,6-diamino-pyridine derivatives in chloroform.
A: 2,6-Diamino-3-methylpyridine (X), derived from 3-methylpyridine (VIII)
B: 2,6-Diamino-3-methylpyridine (X), derived from 2-methylglutaroimidine (IV)
C: 2,6-Diamino-3,5-dimethylpyridine (IX), derived from α, α'-Dimethylglutaroimidine (III)





In this route γ,γ-diethoxycarbonylpimeronitriles (XXI and XXII) were prepared from diethyl malonate and acrylonitrile (by the use of potassium hydroxide[9] as a catalyst, although Koelsh[10] used sodium ethoxide for this purpose) or from methacrylonitrile (by using sodium ethoxide).

The compounds XXI and XXII were then saponified with potassium hydroxide to potassium salts (XXIII' and XXIV'), which were hydrogenated in the presence of a Raney-nickel catalyst to diaminodicarboxylic acid derivatives. When these diaminodicarboxylic acids were treated with concentrated hydrochloric acid, decarboxylation occurred and the hydrochlorides of diaminomonocarboxylic acids were formed; these hydrochlorides were not isolated but were treated with sodium ethoxide in ethanol to liberate diaminomonocarboxylic acids. These diaminomonocarboxylic acids were pyrolyzed to lactam derivatives (XXV and XXVIII), which also were not isolated but which were identified by infrared spectra and by the formation of picrates.

By the pyrolysis of XXV and XXVIII, the octahydro-1, 8-naphthylidines (XXVI and XXIX) reported by Reissert[7,8] were not obtained, but dimethyltetrahydro-1, 8-naphthylidine (XXVII) and hexahydro-1, 8-naphthylidine (XXX) were obtained. This fact suggests that the dehydrogenation[11] with air was accompanied with dehydration in order to give XXVI and XXIX in the thermal treatments of XXV and XXVIII.

In Fig. 2 below, the infrared spectra of dimethyldecahydro-, dimethyltetrahydro- and dimethyl-1, 8-naphthylidine are compared with one other.

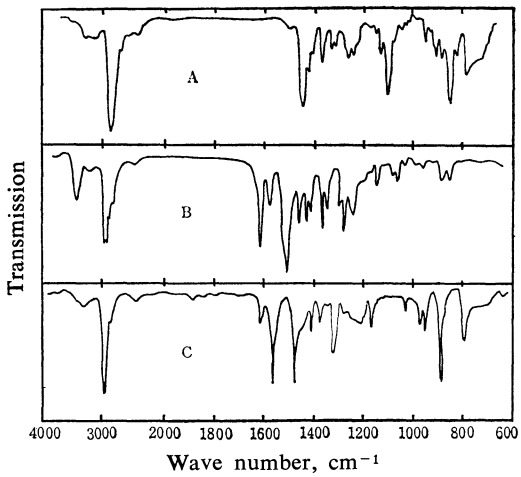


Fig. 2. Infrared spectra of 3, 6-dimethyl-1, 8-naphthylidine derivatives in chloroform.
A: 3, 6-Dimethyldecahydro-1, 8-naphthylidine (XVII)
B: 3, 6-Dimethyltetrahydro-1, 8-naphthylidine (XXVII)
C: 3, 6-Dimethyl-1, 8-naphthylidine (XX)

Experimental

α,α'-Dimethylglutaroimidine (III). — α,α'-Dimethylglutaronitrile (I)[3] (43 g.) was added to a cooled solution of sodium amide (30 g.) in formamide (258 ml.); after standing for 2 days at room temperature, this solution gave a crystalline product, which was collected by filtration, washed with *n*-propanol, ethyl acetate, and ether, and recrystallized from absolute ethanol, affording III (41.0 g., 83.7%) as colorless prismatic needles, m. p., 209~210°C (decomp.).

Found: C, 59.81; H, 9.39; N, 30.04. Calcd. for $C_7H_{13}N_3$: C, 60.40; 9.41; N, 30.19%.

α-Methylglutaroimidine (IV). — By a method similar to that described above, IV was obtained from α-methylglutaronitrile (II)[3] (37 g.) and sodium amide (26 g., in 222 ml. of formamide) in the form of colorless prismatic needles, m. p., 154~155°C (decomp.) (from absolute ethanol); yield. 30.0 g. (70.1%).

Found: C, 57.71; H, 8.88; N, 30.31. Calcd. for $C_6H_{11}N_3$: C, 57.57; H, 8.86; N, 35.57%.

3, 5-Dimethylpiperidine (V).—Into a solution of III (7 g.) in absolute ethanol (100 ml.) on an oil bath at 130~140°C were alternately stirred sodium (98 g.) and absolute ethanol in small portions. Then the reaction mixture was submitted to steam distillation. The distillate was acidified with hydrochloric acid, concentrated, and treated with excess sodium hydroxide to liberate the free base, from which 4.6 g. (80.7%) of V was obtained by distillation; b. p., 144°C, d_4^{20} 0.8532, n_D^{20} 1.4560.

During this reaction the evolved gas was bubbled

9) H. Zahn and P. Schäfer, ibid., **92**, 736 (1959).
10) C. F. Koelsch, *J. Am. Chem. Soc.*, **65**, 2458 (1943).
11) A. V. Topchiyev et al., *Chem. & Ind.*, **1960**, 184.

through aqueous sulfuric acid; by titration of this sulfuric acid solution, 1.45 g. of ammonia was detected. (The calculated amount of ammonia from 7 g. of III is 1.71 g.).

The Picrate of V.—M. p., 184°C (from water). Found: C, 45.60; H, 5.35; N, 16.22. Calcd. for $C_{13}H_{18}N_4O_7$: C, 45.61; H, 5.30; N, 16.37%.

3-Methylpiperidine (VI).—By a method similar to that described above, VI was obtained from IV (7 g. in 100 ml. of absolute ethanol), sodium (98 g.) and absolute ethanol (600 ml.). B. p., 125~126°C, d_4^{20} 0.8570, n_D^{20} 1.4506; yield, 3.2 g. (58.2%).

In this reaction 1.68 g. of eliminated ammonia was detected. (The calculated amount of ammonia for 7 g. of IV is 1.90 g.).

The Picrate of VI.—M. p., 105°C (from water). Found: C, 44.08; H, 4.92; N, 17.14. Calcd. for $C_{12}H_{16}N_4O_7$: C, 43.90; H, 4.91; N, 17.07%.

3, 5-Dimethylpyridine (VII).—In an atmosphere of nitrogen, compound V (0.5 g.) was heated at 230°C for 5 hr. in the presence of a palladium catalyst (0.2 g.). Then 0.35 g. (74.5%) of VII was obtained by distillation; b. p., 168~171°C, d_4^{20} 0.9096, n_D^{20} 1.4501.

The Picrate of VII.—M. p., 242~243°C (decomp.) (from water). Found: C, 46.26; H, 3.61; N, 16.44. Calcd. for $C_{13}H_{12}N_4O_7$: C, 46.43; H, 3.60; N, 16.66%.

3-Methylpyridine (VIII).—By a method similar to that described above, 0.35 g. (74.5%) of VIII was obtained from VI (0.5 g.). B. p., 142°C, d_4^{20} 0.9556, n_D^{20} 1.5053.

The Picrate of VIII.—M. p., 149~150°C (from ethyl acetate). Found: C, 44.73; H, 3.23; N, 17.35. Calcd. for $C_{12}H_{10}N_4O_7$: C, 44.73; H, 3.13; N, 17.39%.

2, 6-Diamino-3, 5-dimethylpyridine (IX).—In an atmosphere of nitrogen, compound III (1 g., in 4 ml. of diphenyl ether) was heated at 300°C for 11 hr. in the presence of a palladium catalyst (0.6 g.). The reaction mixture was then dissolved in ether and shaken with dilute hydrochloric acid. The aqueous layer was treated with sodium hydroxide to liberate the basic product, which was extracted with ether. The crystals obtained after evaporation of the ether were recrystallized from benzene to give IX, in the from of colorless needles; m. p., 186~187°C, yield, 0.3 g. (30.6%).

Found: C, 61.62; H, 8.18; N, 31.00. Calcd. for $C_7H_{11}N_3$: C, 61.28; H, 8.08; N, 30.63%.

Tetraacetyl-2,6-diamino-3,5-dimethylpyridine.—Compound IX (21 mg.) was treated with acetic anhydride (1 ml.) at 170°C for 1 hr. in a sealed glass tube. After removal of the acetic acid and unreacted acetic anhydride by distillation, the residue was recrystallized from benzene to give the tetraacetyl derivative of IX as colorless crystals; m. p., 149°C; yield, 20.7 mg. (44.2%).

Found: N, 13.77. Calcd. for $C_{15}H_{19}N_3O_4$: N, 13.76%.

Diacetyl-2, 6-diamino-3, 5-dimethylpyridine. — Compound IX (17 mg.) was treated with acetic anhydride (1 ml.) at 95°C for 1 hr. to give the diacetyl derivative of IX in the form of colorless crystals; m. p., 197°C; yield, 5 mg. (18.2%).

Found: N, 18.43. Calcd. for $C_{11}H_{15}N_3O_2$: N, 18.99%.

2, 6-Diamino-3-methylpyridine (X). — *a) By the Tschitschibabin-Seide Method*[6]. — Compound VIII (12.2 g.) was treated with sodium amide (16 g.) in tetraline (16 g.) at 150~153°C for 4 hr. and thereafter at 198~200°C for 17 hr. The reaction mixture was then poured into water and extracted with benzene. From the benzene extract X was obtained in the form of colorless plates; m. p., 156~157°C (from benzene); yield, 2.5 g. (15.5%).

Found: C, 58.48; H, 7.31; N, 34.54. Calcd. for $C_6H_9N_3$: C, 58.51; H, 7.37; N, 34.12%.

b) By the Dehydrogenation of IV.—By a method similar to that described for IX, X was obtained from IV (0.5 g.) as colorless plates; m. p., 156~157°C (from benzene), undepressed on admixture with the specimen derived from VIII; yield, 0.15 g. (30.6%).

Triacetyl-2, 6-diamino-3-methylpyridine.—By a method similar to that described for tetraacetyl-2, 6-diamino-3, 5-dimethylpyridine, compound X (99.8 mg.) was treated with acetic anhydride (3 ml.) at 170~180°C for 3 hr., giving the triacetyl derivative of X in the from of colorless crystals; m. p., 142~144°C (from benzene); yield, 53.4 mg. (26.4%).

Found: N, 16.72. Calcd. for $C_{12}H_{15}N_3O_3$: N, 16.86%.

Diacetyl-2, 6-diamino-3-methylpyridine. — Compound X (100.3 mg.) was treated with acetic anhydride (2 ml.) at 90~100°C for 1 hr. to give the diacetyl derivative of X as colorless crystals; m. p., 220~221°C (from petroleum ether); yield, 78.1 mg. (46.4%).

Found: N, 20.39. Calcd. for $C_{10}H_{13}N_3O_2$: N, 20.28%.

3, 6-Dimethyl-2, 7-diaminooctahydro-1,8-naphthylidine (XIV).—By a method similar to that described for III, XIV was obtained from 2, 4, 6-tricyano-*n*-heptane (XI)[3] (75 g.) and sodium amide (50 g., in 300 ml. of formamide) in the form of pale greenish-yellow crystals; m. p., 222~224°C (decomp.); yield, 71.6 g. (87%).

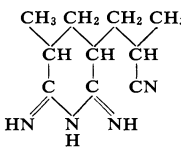
Found: C, 62.50; H, 8.46; N, 29.23. Calcd. for $C_{10}H_{16}N_4$*: C, 62.47; H, 8.39; N, 29.14%.

3-Methyl-2, 7-diiminooctahydro-1, 8-naphthylidine (XV).—By a method similar to that described for III, XV was obtained from 1, 3, 5-tricyano-*n*-hexane (XII)[3] (77 g.) and sodium amide (52 g., in 310 ml. of formamide) in the form of pale greenish yellow crystals; m. p., 204~206°C (decomp.); yield, 55.3 g. (65.0%).

Found: C, 60.26; H, 7.74; N, 31.09. Calcd. for $C_9H_{14}N_4$: C, 60.65; H, 7.92; N, 31.44%.

---

* The calculaled value for $C_{10}H_{16}N_4$ also satisfies the structure:



but this possibility can be omitted because of the lack in the infrared spectrum of the absorption band (near 2250 cm^{-1}) due to CN.

2, 7-Diiminooctahydro-1, 8-naphthylidine (XVI).—By a method similar to that described for III, XVI was obtained from 1, 3. 5-tricyano-*n*-pentane (XIII)[9] (33 g.) and sodium amide (22 g., in 123 ml. of formamide) in the form of pale greenish-yellow crystals; m. p., 205~206°C (decomp.); yield, 31.3 g. (82.3%).

Found: C, 58.25; H, 7.27; N, 34.04. Calcd. for $C_8H_{12}N_4$: C, 58.51; H, 7.37; N, 34.12%.

3,6-Dimethyldecahydro-1,8-naphthylidine (XVII). To a solution of XIV (1.5 g.) in amyl alcohol (240 ml.) was added sodium (21 g.) at 130~140°C. The reaction mixture was then submitted to steam distillation. The distillate was acidified with hydrochloric acid, concentrated, and treated with excess sodium hydroxide to liberate the free base, from which by extraction with ether, was obtained XVII in the form of colorless needles; m. p., 162~163°C (from benzene); yield, 1.0 g. (75.3%).

Found: C, 72.14; H, 11.27; N, 16.88. Calcd. for $C_{10}H_{20}N_2$: C, 72.24; H, 10.91; N, 16.85%.

In this reaction, 0.254 g. of eliminated ammonia was detected. (The calculated amount of ammonia for 1.5 g. of XIV is 0.266 g.).

The Dipicrate of XVII.—M. p., 213°C (decomp.) (prepared in ethyl acetate).

Found: C, 42.28; H, 4.23; N, 17.85. Calcd. for $C_{22}H_{26}N_8O_{14}$: C, 42.18; H, 4.18; N, 17.89%.

3-Methyldecahydro-1,8-naphthylidine (XVIII).—By a method similar to that described for XVII, XVIII was obtained from XV (7 g., in 800 ml. of amyl alcohol) and sodium (98 g.) in the form of colorless needles; m. p., 113~114°C (from benzene); yield, 4 g. (66.7%).

Found: C, 69.79; H, 11.79; N, 17.69. Calcd. for $C_9H_{18}N_2$: C, 70.07; H, 11.76; N, 18.17%.

The Dipicrate of XVIII.—M. p., 205°C (decomp.) (prepared in ethyl acetate).

Found: C, 41.47; H, 4.16; N, 17.93. Calcd. for $C_{21}H_{24}N_8O_{14}$: C, 41.18; H, 3.95; N, 18.30%.

Decahydro-1, 8-naphthylidine (XIX).—By a method similar to that described for XVII, XIX was obtained from XVI (1.2 g., in 200 ml. of amyl alcohol) and sodium (17 g.) in the form of colorless needles; m. p., 116~117°C (from benzene); yield, 0.9 g. (90.0%).

Found: C, 68.42; H, 11.50; N, 19.78. Calcd. for $C_8H_{16}N_2$: C, 68.52; H, 11.50; N, 19.98%.

The Dipicrate of XIX.—M. p., 195°C (decomp.) (prepared in ethyl acetate).

Found: C, 40.26; H, 3.93; N, 18.54. Calcd. for $C_{20}H_{22}N_8O_{14}$: C, 40.14; H, 3.71; N, 18.74%.

3, 6-Dimethyl-1, 8-naphthylidine (XX).—In an atmosphere of nitrogen, compound XVII (0.15 g., in 2 ml. of diphenyl ether) was heated at 200~270°C for 20 hr. in the presence of a palladium catalyst (0.2 g.). Thereafter, treatment by a method similar to that described for IX gave XX as light yellowish-orange, prismatic needles; m. p., 191~192°C (from benzene); yield, 0.1 g. (71.0%).

Found: C, 75.66; H, 6.36; N, 17.70. Calcd. for $C_{10}H_{10}N_2$: C, 75.92; H, 6.37; 17.71%.

The Monopicrate of XX.—M. p., 210~211°C (decomp.) (prepared in benzene).

Found: C, 49.57; H, 3.45; N, 17.90. Calcd. for $C_{16}H_{13}N_5O_7$: C, 49.62; H, 3.38; N, 18.08%.

α, α'-Dimethyl-γ, γ-dicarbethoxy-pimeronitrile (XXI).—Into a mixture of diethyl malonate (320 g., 2 mol.) and methacrylonitrile (280 g., 4.2 mol.) sodium ethoxide (11 g., in 80 g. of absolute ethanol) was stirred at 32~50°C for 8 hr. and thereafter at 80~90°C for 2 hr. After neutralization with hydrochloric acid, this mixture was poured into water to separate an oily substance, which was submitted to distillation to give XXI; b. p., 175°C/2 mmHg; m. p., 61~63°C; yield, 338 g. (57.5%).

Found: C, 61.25; H, 7.52; N, 9.47. Calcd. for $C_{15}H_{22}N_2O_4$: C, 61.20; H, 7.54; N, 9.52%.

γ, γ-Dicarbethoxy-pimeronitrile (XXII).—To a cooled and stirred mixture of diethyl malonate (187 g., 1.1 mol.), acrylonitrile (123 g., 2.3 mol.) and dioxane (233 g.) a methanolic 30% potassium hydroxide solution (10.6 ml.) was slowly added below 20°C and thereafter stirred for 2 hr. at room temperature. After neutralization with hydrochloric acid, the mixture was poured into water to separate an oily substance, which crystallized slowly and which was recrystallized from ethanol to give XXII; m. p., 60~62°C; yield, 224 g. (76.4%).

Found: C, 58.75; H, 6.90; N, 10.18. Calcd. for $C_{13}H_{18}N_2O_4$: C, 58.63; H, 6.81; N, 10.52%.

α, α'-Dimethyl-γ, γ-dicarboxy-pimeronitrile (XXIII).—A mixture of XXI (115 g.) and potassium hydroxide (55 g.) in absolute ethanol (500 ml.) was left for a few days at room temperature to precipitate the potassium salt of XXIII, which was then collected by filtration; yield, 106 g. (86.2%).

The potassium salt was dissolved in water, acidified with hydrochloric acid, and extracted with ethyl acetate to give XXIII; m. p., 134~136°C (decomp.) (from water).

Found: C, 55.27; H, 6.30; N, 11.76. Calcd. for $C_{11}H_{14}N_2O_4$: C, 55.45; H, 5.88; N, 11.76%.

γ, γ-Dicarboxypimeronitrile (XXIV).—By a method similar to that described above, from XXII (133 g.) and potassium hydroxide (65 g., in 650 ml. of absolute ethanol) was obtained the potassium salt of XXIV (135 g., 94.4%), from which XXIV was obtained after acidification with hydrochloric acid and extraction with ethyl acetate; m. p., 158°C (decomp.) (from water).

Found: C, 51.87; H, 4.90; N, 12.87. Calcd. for $C_9H_{10}N_2O_4$: C, 51.43; H, 4.80; N, 13.33%.

3-(β-Methyl-ω-amino-*n*-propyl)-5-methylpiperidone-2 (XXV).—In a 220 ml. autoclave, the potassium salt of XXIII (47.1 g., in 50% aqueous ethanol) was hydrogenated under ca. 100 atm. of hydrogen pressure below 60°C in the presence of a Raney-nickel catalyst (from 38 g. of Ni-Al alloy 50 : 50). The reaction mixture was concentrated and acidified with 300 ml. of concentrated hydrochloric acid and heated on a water bath to complete the decarboxylation. After concentration, this mixture was heated at 200°C for another 3 hr. to remove thoroughly the volatile component; the residue was then extracted with absolute ethanol. This ethanolic solution was treated with sodium ethoxide to liberate the free aminolactam (XXV) from the hydrochloride. After elimination of the sodium chloride and evaporation of the ethanol crude XXV (20 g.) was obtained, a hygroscopic sticky substance which was not purified, but in the infrared spectrum of

which there was detected the characteristic absorption band at 1670 cm^{-1} which was assigned to the lactam groups of the six-membered ring[12].

The Picrate of XXV.—M. p., 184~186°C (prepared in ethanol).

Found: N, 17.65. Calcd. for $C_{16}H_{23}N_5O_8$: N, 16.94%.

3,6-Dimethyltetrahydro-1,8-naphthylidine (XXVII).—By pyrolysis of crude XXV (0.71 g.) at 330°C a crystalline substance (carbonate of XXVII ?) was deposited on the neck of the reaction flask. This crystalline product was acidified with hydrochloric acid and treated with excess sodium hydroxide to liberate the free base, which was then extracted with benzene to give XXVII in the form of colorless plates; m. p., 110~111°C (from benzene-petroleum ether); yield, 0.02 g.

Found: C, 74.33; H, 8.65; N, 17.41. Calcd. for $C_{10}H_{14}N_2$: C, 74.03; H, 8.63; N, 17.26%.

The Monopicrate of XXVII.—M. p., 256°C (decomp.) (prepared in benzene). Found: C, 49.42; H, 4.49; N, 17.93. Calcd. for $C_{16}H_{17}N_5O_7$: C, 49.16; H, 4.38; N, 17.90%.

Dehydrogenation of XXVII.—In an atmosphere of nitrogen, compound XXVII (0.11 g., in 2 ml. of diphenyl ether) was heated at 250~280°C for 20 hr. in the presence of a palladium catalyst (0.2 g.). The reaction mixture was treated by a method similar to that described for XX in order to obtain the dehydrogenated product (0.05 g.); m. p., 191~192°C (from benzene), undepressed on admixture with the specimen of XX.

Hydrogenation of XXVII.—By a method similar to that described for XVII, compound XXVII (0.2 g., in 130 ml. of amyl alcohol) was treated with sodium (7 g.). A hydrogenated product (0.2 g.) was obtained; m. p., 162~163°C (from benzene), undepressed on admixture with the specimen of XVII.

3-(ω-Amino-*n*-propyl)-piperidone-2 (XXVIII).—By a method similar to that described for XXV, potassium salt of XXIV (28 g.) was hydrogenated in the presence of a Raney-nickel catalyst (prepared from 25 g. of Ni-Al alloy 50 : 50), giving crude XXVIII (13 g.).

The Picrate of XXVIII.—M. p., 207°C* (prepared in ethanol). Found: N, 18.11. Calcd. for $C_{14}H_{19}N_5O_8$: N, 18.18%.

Hexahydro-1,8-naphthylidine (XXX).—By a method similar to that described for XXVII, crude XXX was obtained from XXVIII in the form of a basic sticky substance which gave the picrate.

The Monopicrate of XXX.—M. p., 228~230°C (decomp.) (prepared in benzene). Found: C, 46.59; H, 4.00; N, 18.94. Calcd. for $C_{14}H_{15}N_5O_7$: C, 46.03; H, 4.14; N, 17.91%.

The author is grateful to Mr. Masatomo Kusunose (manager of Research Institute, Toho Rayon Co., Ltd.), Mr. Masahiko Takikawa (chief of the Laboratory to which the author belongs), Dr. Masakazu Taniyama (Toho Beslon Co., Ltd.), Dr. Torakichi Yoshioka (Profossor of Tokushima Univ.), Dr. Hisaya Tani (Professor of Osaka Univ.), Dr. Minoru Imoto (Professor of Osaka City Univ.) and Dr. Eizi Ochiai (ITSUU Lab., Tokyo) for their valuable advice on his experiments; to Mr. Takumi Okauchi, Mr. Yukihide Furutsu and Mr. Hiroshi Saijo for their help; to Mr. Toshikazu Inoue, Miss Keiko Yano and Miss Akiko Hiroshe, who helped him with the elementary analysis, and to Mr. Yoshiyuki Nishiyama and Mr. Kiyosumi Kubo, who helped him with the infrared spectra work.

Research Institute, Toho Rayon Co., Ltd.
Kitajima Chō, Itano-Gun, Tokushima

12) K. Nakanishi, "Sekigai Kyūshū Supekutoru" (Infrared Absorption Spectra), Nankōdō, Tokyo (1960), p. 51.

* This melting point agrees with that reported by Reissert[8].

Determination of Aluminum, Cerium(III) and Lead with Fluoride by an Amperometric Indicator Method

By Asha VARMA

(Received November 25, 1961)

In a recent study in these laboratories, it has been shown that the amperometric indicator method with polarized electrodes can be applied with success for the determination of barium, lanthanum and thorium with fluoride involving precipitation reactions[1]. The field of application of this method is wide and the method is more general than conventional voltammetry. However, formation of complexes and neutralization, in general, had scarcely been made use of as titration reactions.

This paper reports the results of determination of aluminum, cerium and lead with fluoride involving both complex forming and precipitation reactions, using two identical polarized platinum electrodes at constant applied voltage in the presence of small amounts of ferric chloride as an indicator and the appropriate supporting electrolytes.

Various methods for the determination of aluminum[2-4], cerium[2,5] and lead[2,6-9] have been developed. Ringbom and Wilkman[3] titrated aluminum with fluoride amperometrically at the dropping mercury electrode versus saturated calomel electrode using trivalent iron as indicator whose reduction at the cathode produces diffusion current. So long as the ferric iron remains uncomplexed, it can be reduced at the dropping mercury cathode and the current passes through the cell; and excess fluoride complexes the ferric ions and stops the current. This method is much simpler in technique and has several advantages over conventional potentiometric or amperometric method.

Experimental and Results

Standard potassium fluoride solutions were prepared by accurate dilution of a more concentrated solution which has been standardized potentiometrically[10]. Stock solution of aluminum chloride was prepared by dissolving a weighed quantity of pure aluminum wire in dilute hydrochloric acid, which was transferred to 500 ml. standard volumetric flask. The amount of aluminum was determined potentiometrically by the Scott's method[4]. Cerium chloride solution was prepared by dissolving the weighed quantity of Merck's extrapure cerium carbonate in dilute hydrochloric acid in 250 ml. standard flask. Hydrogen peroxide was added to aliquot, a weakly ammoniacal solution of cerous chloride to oxidize it completely to ceric form, and the resulting solution was titrated by potentiometric method[11] and also amperometrically with two polarized electrodes[12] against standard ferrous ammonium sulfate solution. The stock solution of Merck's extrapure lead nitrate was standardized amperometrically with standard potassium dichromate solution[13]. Conductivity water was used for the preparation of all solutions, and test solutions were obtained after appropriate dilution of the stock solution with air-free water. All other chemicals used were of reagent grade.

Experimental arrangements for the amperometric titrations were essentially the same as described earlier[12,14]. Two platinum electrodes were immersed in the titration cell and a constant voltage of 0.04 V. was applied to these electrodes. Current through the cell was measured using a sensitive galvanometer, 0.5 μA with lamp and scale arrangements. The solution was stirred uniformly during the titration using a magnetic stirrer. Twenty milliliters of titration mixture in an appropriate buffer containing the suitable supporting electrolyte and a small amount of indicator was placed into the titration cell. Titrant (10^{-1} to 10^{-3}M)

1) D. Singh and A. Varma, *J. Sci. Res. BHU.*, in press.
2) W. Wagner et al., "Advanced Analytical Chemistry", Reinhold Publishing Co., New York (1956), pp. 146—148, 152—153 and 172—174.
3) A. Ringbom and W. Wilkman, *Acta. Chem. Scand.*, **3**, 22 (1949).
4) A. H. Bushey, *Anal. Chem.*, **20**, 169 (1948).
5) C. W. Leonard, H. J. Kelly and D. H. Hume, *Anal. Chim. Acta.*, **16**, 185 (1957).
6) L. Farkas and N. Uri, *Anal. Chem.*, **20**, 236 (1948).
7) J. Cihalik and E. Kuornovska-Pavlikova, *Chem. Listy.*, **49**, 1640 (1955); *Collection Czechoslov Chem. Communs.*, **21**, 718 (1956).
8) F. R. Cropper, *Analyst*, **76**, 370 (1951).
9) Yu I. Usatenko and M. A. Vitikina, *Zavodskya Lab.*, **23**, 427 (1957).
10) S. T. Talipov and J. Z. Teodorovich, ibid., **15**, 529 (1949).
11) N. H. Willard and P. Young, *J. Am. Chem. Soc.*, **50**, 1379 (1928).
12) D. Singh, A. Varma and V. S. Agarwala, *Z. anal. Chem.*, in press.
13) I. M. Kolthoff and Y. D. Pan, *J. Am. Chem. Soc.*, **61**, 3402 (1939).
14) D. Singh and A. Varma, *J. Sci. Res. BHU*, **11**, 125 (1960).

TABLE I. TITRATION OF ALUMINUM BY FLUORIDE WITH TWO POLARIZED ELECTRODES AT 40 mV. USING 0.5 ml. OF 0.05 M FERRIC CHLORIDE AS AN AMPEROMETRIC INDICATOR

Volume of the titration mixture: 20 ml. Medium: 0.05 M NH_4Cl+Acetate buffer, pH 6.2.

Determinations made	Amount of aluminium, mg.		Experimental error, %	
	Taken	Found	Average	Maximum
3	4.568	4.568	0.00	0.00
4	2.284	2.291	+0.42	+0.64
4	0.3219	0.3233	+0.44	+0.86
5	0.1407	0.1396	−0.82	−0.96
3	0.0704	0.0698	−1.14	−1.56
5	0.0226	0.0221	−2.38	−2.60
6	0.0113	0.0116	+3.54	+5.32

TABLE II. TITRATION OF CERIUM(III) BY FLUORIDE WITH TWO POLARIZED ELECTRODES AT 40 mV. USING 1.0 ml. OF 0.05 M FERRIC CHLORIDE AS AN AMPEROMETRIC INDICATOR

Volume of titration mixture containing equal volume of 96% ethyl alcohol, 20 ml. Medium: 0.05 M NH_4Cl+Acetate buffer, pH 6.0 to 6.5; Temperature, 40±1.0°C

Determinations made	Amount of cerium(III), mg.		Experimental error, %	
	Taken	Found	Average	Maximum
4	16.114	16.103	−0.08	−0.16
5	3.223	3.223	+0.04	+0.12
5	1.612	1.608	−0.30	−0.55
3	0.8060	0.8093	+0.56	+0.72
4	0.3223	0.3233	+0.44	+0.68
6	0.0806	0.0810	+0.86	+1.12
5	0.0322	0.0314	−2.79	−5.09

TABLE III. TITRATION OF LEAD BY FLUORIDE WITH TWO POLARIZED ELECTRODES AT 40 mV. USING 1.0 ml. OF 0.05 M FERRIC CHLORIDE AS AN AMPEROMETRIC INDICATOR

Volume of titration mixture containing equal volume of 96% ethyl alcohol, 20 ml. Medium: 0.1 M KCl or KBr+Acetate buffer, pH 5.5 to 6.2

Determination made	Amount of lead, mg.		Experimental error, %	
	Taken	Found	Average	Maximum
5	20.655	20.655	+0.32	+0.64
3	10.355	10.361	+0.04	+0.08
4	2.788	2.785	−0.16	−0.25
5	2.066	2.059	−0.54	−0.96
6	1.033	1.030	−0.59	−0.84
5	0.8276	0.8289	+0.18	+0.25
4	0.2066	0.2072	+0.44	+0.68
4	0.1033	0.1029	−0.77	−1.00
6	0.0517	0.0528	+2.70	+3.10

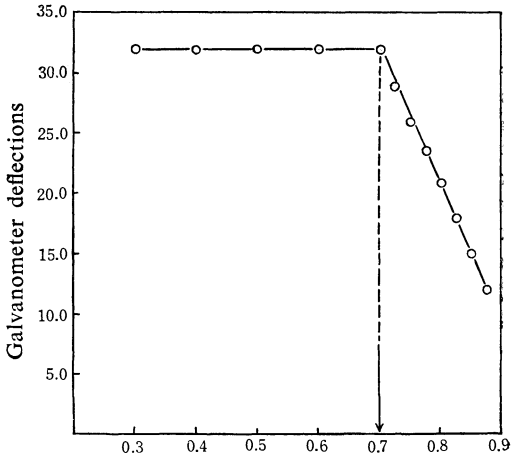


Fig. 1 Titration of 2.788 mg. lead with fluoride in 20 ml. acetate buffer, pH 5.5~6.5, containing 0.1 M KBr in equal volume of 96% ethyl alcohol, at 40 mV. with two polarized electrodes, indicator; $FeCl_3$.

was administered from 2 ml. semimicroburette with 0.01 ml. divisions. Readings were taken at uniform regular intervals, usually one minute, after each addition of the titrant. Equivalence points were found graphically by the usual plot of galvanometer deflections against the volume of titrant added. A typical titration curve is shown in Fig. 1. The end points were quite reproducible. A large number of experiments were carried and each determination was repeated several times for good and satisfactory results. Summarized results for the determination of aluminum, cerium(III) and lead are recorded in Tables I—III respectively. In column three is given the best experimental value observed for these estimations at the particular concentration.

Discussion

It has been observed that fluoride is an excellent titrant in precipitation and complex forming reactions. The fluoride ion is the smallest and the least deformable of the halide ions, and it should form the fewest complexes in accordance with the covalency rule, yet it forms far more complexes by electrostatic forces similar to those which hold "ion pairs" together[15,16]. This view is supported from the paramagnetism of such double salts as K_3FeF_6; the bonding is covalent and the electrons are paired and the molecules diamagnetic. Fluorine, having small size of the fluoride ion, brings

15) N. Bjerrum, *Kgl. Danske. Videnskb. Selskabs.*, **7**, 9 (1926).
16) R. M. Fuoss, *Chem. Revs.*, **17**, 27 (1935).

out the highest coordination number of the atom with which it combines.

Fluoride ions have greater tendency to complex aluminum ions than trivalent iron ions and in neutral solution aluminum reacts with fluoride to form stable, AlF_6^{3-} ion; therefore on addition of potassium fluoride to the titration mixture, reaction shifts towards the formation of potassium cryolite:

$$AlCl_3 + 6\,KF \rightarrow AlF_3,\ 3\,KF \downarrow + 3\,KCl$$

Aluminum first precipitates out as aluminum trifluoride, and this reacts with excess potassium fluoride forming the said stable complex.

Fluoride precipitates cerium trifluoride at pH 6.0 to 6.5, $CeCl_3 + 3\,KF \rightarrow CeF_3 \downarrow + 3\,KCl$; and the precipitate is insoluble in excess potassium fluoride. Lead is partially precipitated as lead chloride in presence of potassium chloride or as lead bromide in presence of potassium bromide in the titration mixture. On addition of potassium fluoride, the reaction proceeds towards completion yielding leadchlorofluoride or leadbromofluoride. These precipitation reactions are stoichiometric and quantitative especially in presence of equal volume of 96% ethyl alcohol, at pH 5.5 to 6.5.

In all these determinations, upto the equivalence point, corresponding to the stoichiometric completion of the reaction, current remains constant. After it, the excess fluoride ions complex the indicator ferric ions whose reduction constitutes the end point, and the current falls (cf., curve Fig. 1). The end point is sharp and quite reproducible.

Data recorded in Tables I–III show that the results are good and satisfactory with excellent accuracy upto 10^{-4} M. At lower concentrations, the maximum error is about $\pm 5.0\%$.

Summary

Determinations of aluminum, cerium(III) and lead by fluoride involving complex formation, $KAlF_6$ and precipitations, CeF_3 and PbClF or PbBrF have been carried out successfully using amperometric indicator method at 0.04V. with two identical polarized platinum electrodes. A small amount of ferric chloride is used as an indicator, the reduction of which beyond end point constitutes the indicating system. Upto the equivalence point, current remains constant, and then it falls due to the reduction of the trivalent iron complex which is formed on addition of excess fluoride. The method is simpler in technique, sensitive and rapid, and the results obtained are good and satisfactory with accuracy of the right order of magnitude even at lower concentrations, as low as 10^{-4} M. At still higher dilutions the maximum error rises to about $\pm 5.0\%$.

My sincere thanks are due to Dr. D. Singh, Department of Chemistry, BHU, for suggesting the problem, his continuous guidance, valuable criticism and advice.

Department of Chemistry
Banaras, Hindu University
India

Reaction of Styrene Glycol with Aqueous Acids

By Tsutomu MATSUDA and Masahiko SUGISHITA

(Received January 18, 1962)

Although Zincke[1] reported in 1882 that, when treated with aqueous acid, styrene glycol yielded phenylacetaldehyde (I), together with higher boiling materials, there have been few investigations to examine the utility of the procedure for the synthesis of I, except that Emerson[2] has reported a vapor phase isomerization of styrene glycol to I in a yield of 74%. This reaction is a well-known pinacolic rearrangement and it may be a possible synthetic route for I. As styrene glycol[2] is easily prepared from styrene, we undertook to explore the procedure to clarify the course of reaction and to find the most suitable conditions for the preparation of I.

1) Th. Zincke, *Ann.*, **216**, 295 (1882).
2) W. S. Emerson, *J. Am. Chem. Soc.*, **67**, 516 (1945).

Results and Discussion

Effect of Reaction Conditions.—As Zincke's paper was concerned chiefly with the structure of the higher boiling material and did not disclose any optimum conditions for obtaining I, we first examined the effect of reaction conditions upon the yield of I, varying the kind of acids, the acid concentrations and the

TABLE I. EFFECTS OF KIND AND CONCENTRATION OF ACIDS

Reaction time: 2 hr.

Acid			Product		
Kind	Concn.	H_0*	Phenylacetaldehyde	Higher fraction**	
	mol./l.		%	%	n_D^{25}
H_2SO_4	1.00	−0.25	2.3	36.8[a]	1.5691
HCl	1.09		3.5	44.9	1.5670
H_3PO_4	3.06		2.9	34.9[a]	1.5698
H_2SO_4	2.33	−1.00	18.7	69.0	1.5740
HCl	2.89		12.9	67.6	1.5798
H_3PO_4	5.99		17.3	71.9[b]	1.5728
H_2SO_4	3.79	−1.75	12.9	73.4	1.5820
HCl	4.57		5.8	53.2[c]	1.6150
H_3PO_4	7.85		14.4	76.3	1.5818

* H_0 values were quoted from M. Z. Paul and F. A. Long, *Chem. Revs.*, **57**, 12 (1957).

** Products a and b were combined and redistilled and analyzed for elemental composition.

TABLE II. EFFECT OF REACTION TIME*

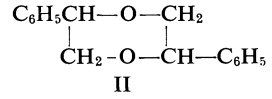
Aqueous acid: 2.24 mol./l. sulfuric acid

Time	Product		
	Phenylacetaldehyde	Higher fraction	
hr.	%	%	n_D^{25}
1.0	11.5	73.4	1.5682
1.5	15.8	70.5	1.5689
2.0	18.7	69.0	1.5740
2.5	17.3	63.3	1.5776
3.0	17.3	66.2	1.5782
5.0	14.4	50.4	1.5925

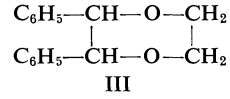
* Mixtures of styrene glycol (10 g.) and the aqueous acid (15 ml.) were refluxed for the specified periods.

reaction times. The results are summarized in Tables I and II.

These results reveal that the yield of I in the simple treatment was relatively low but that a higher boiling material was formed in an appreciable quantity; however, severe conditions, prolonged reaction periods, or treatment with more concentrated acid solutions lowered the yields of the higher boiling material. It was also noticed that, under the more severe conditions, the refractive indices of the higher boiling materials were higher and that the intensity of their infrared absorptions at 1730 and 1698 cm^{-1} were stronger. Especially, the product c (indicated in Table I) was found at 1130 cm^{-1} to lack the C–O–C absorption which appeared in the others. These observations seemed to indicate that another type of by-product was formed under the more severe conditions, especially on treatment with an aqueous hydrochloric acid. The higher boiling fractions, with a lower refractive index (product a and b in Table I), were combined and redistilled. The results of the elemental analysis of the redistilled product (Found: C, 80.43; H, 6.80%: hereafter named "dimer A") coincided well with the composition of phenylacetaldehyde dimer ($C_{16}H_{16}O_2$), to which Zincke assigned either structure II or III and which he considered as an intermediate to I.



II



III

As Zincke pointed out that dimer A also afforded I on treatment with aqueous acid, dimer A was treated with aqueous sulfuric acid repeatedly in order to confirm the formation of I. The results are shown in Table III.

TABLE III. PRODUCT RATIOS WITH REPEATED TREATMENT

Reaction time: 2 hr.

Aqueous acid: 3.0 mol./l. sulfuric acid

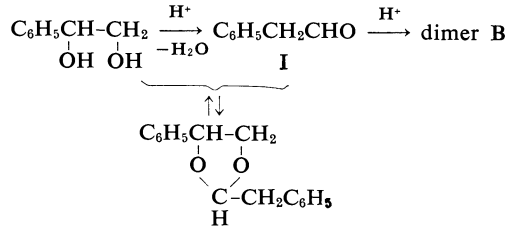
No.	Phenylacetaldehyde	Higher fraction recovered	
	%	%	n_D^{25}
1	13.6	80.3	1.5772
2*	14.0	70.0	1.5900
3	13.3	76.7	1.5960

* The recovered dimer A in No. 1 (n_D^{25} 1.5772) was used as the reactant in experiment No. 2, and so on.

The results show that, in each run, the ratios of I to the higher boiling fraction were kept nearly constant, but that the refractive indices of the recovered dimer A increased gradually in this case, too. These results seemed strongly to support the hypotheses that dimer A was not a simple intermediate but was in equilibrium with I and that any device to remove I from the reaction mixture would increase the yield. A preliminary experiment was made, in which styrene glycol was treated with acid in methanol and in ethanol instead of in water in order to remove I in the form of the acetals, but the products isolated were neither the expected acetals nor dimer A respectively. In another attempt, the reaction mixture obtained from styrene glycol with aqueous acid was steam-distilled; this procedure seemed to be promising because I was isolated in a 31% yield.

Structure of Dimer A.—If such an equilibrium between dimer A and I existed, we could expect that I would give a similar equilibrium mixture in the treatment of I with an acid solution. After being refluxed for two hours

with aqueous acid, I gave a product which was found to consist of recovered I (18%) and of a higher boiling material. The higher boiling material showed a boiling range similar to that of dimer A but a somewhat higher refractive index. The infrared spectrum of the latter (hereafter named "dimer B") revealed that the product thus obtained was different from dimer A but was identical with the product c in Table I. In the reaction with aqueous acid, dimer A did not give I and was recovered unchanged in a 90% yield. These results lead us to the presumption that another structure of dimer A, one which can account for its molecular formula ($C_{16}H_{16}O_2$) and for its infrared absorption behavior, should be sought. Among others[3], the structure of 2-benzyl-4-phenyl-1, 3-dioxorane (IV) could well interpret the observed results, especially that dimer A was hydrolyzed easily in acidic conditions and that both styrene glycol and I were necessary for the formation of dimer A. The acetal IV was prepared in a yield of 94% by the reaction of I and styrene glycol in benzene in the presence of monochloroacetic acid as a catalyst. The product was proved to be identical with dimer A by its infrared spectrum and yielded 18% of I and 70% of the starting material when treated with aqueous sulfuric acid, but the latter was proved to be contaminated with a small amount of dimer B by the presence of a weak absorption in its carbonyl range and by its higher refractive index. Thus we have concluded that dimer A was 2-benzyl-4-phenyl-1, 3-dioxorane and that the equilibrium mixture of I, styrene glycol and IV is rapidly formed in the reaction of the glycol with an aqueous acid under suitable conditions, while I gradually changed to dimer B. The course of the reaction may be represented by the following scheme;



IV (dimer A)

Preparation of Phenylacetaldehyde. — Based upon the above-mentioned results, the following procedure was used for the preparation of I. A mixture of styrene glycol and of an aqueous acid was refluxed for one hour; steam was then introduced immediately into the reaction mixture to distill out the I, avoiding the dimerization resulting from prolonged contact with the acid. The volume of the reaction mixture was kept almost constant during the course of the steam distillation by applying a controlled external heating. By this technique we realized a significantly higher yield (as much as 70%) of I, as is summarized in Table IV.

TABLE IV. PREPARATION OF PHENYLACETALDEHYDE

No.	Materials	Acid		Yield of phenylacetaldehyde %
		Kind	Concn. mol./l.	
1	Styrene glycol	H_2SO_4	2.24	31.3*
2	Styrene glycol	H_2SO_4	1.01	62.2
3	Styrene glycol	H_2SO_4	1.78	70.2
4	Styrene glycol	H_2SO_4	2.29	63.3
5	Styrene glycol	H_2SO_4	3.49	56.4
6	Dimer A	H_2SO_4	2.23	66.7
7	Styrene glycol	H_3PO_4	5.03	70.2
8	Styrene glycol	H_3PO_4	5.96	57.5

* Steam distillation was performed without external heating.

Experimental

Styrene Glycol. — Styrene glycol was prepared from styrene by the method of Emerson[2] through styrene chlorohydrin; it appeared as white needles; m. p., 67.0~67.5°C.

Reaction of Styrene Glycol with Aqueous Acid. —A mixture of styrene glycol (10 g.) and aqueous acid (150 ml.) was refluxed for two hours. The reaction mixture was then cooled and extracted with ether (50 ml.×3), and the combined extract was washed with a 5% sodium carbonate solution and water and dried over anhydrous sodium sulfate. The ether was distilled off, and the residue was vacuum-distilled to yield: 1. phenylacetaldehyde (b. p. 56.0~58.0°C/5 mmHg); 2. a higher boiling fraction (b. p. 150~157°C/5 mmHg). The yields of these fractions under a variety of conditions are shown in Tables I and II. Redistillation of the combined fraction 1 gave pure phenylacetaldehyde, b. p. 57.0~57.5°C/5 mmHg, n_D^{25} 1.5319, semicarbazone, m. p. 150~151°C. The higher boiling fractions a and b indicated in Table I were combined and redistilled; b. p., 157~158°C/5 mmHg, n_D^{25} 1.5697.

Found: C, 80.42; H, 6.80. Calcd. for $C_{16}H_{16}O_2$: C, 80.00; H, 6.70%.

Reaction of Phenylacetaldehyde with Aqueous Acid.—A mixture of phenylacetaldehyde (5 g.) and 2.42 mol./l. aqueous sulfuric acid (100 ml.) was refluxed for two hours, and the reaction mixture was treated as above to give: 1. phenylacetaldehyde, 0.9 g. (18%) (b. p. 55.5~58.0°C/5 mmHg); 2. a higher boiling fraction, 3.5 g. (70%) (b. p. 158~161°C/5 mmHg, n_D^{25} 1.5970). The latter showed strong absorptions at 1730 and 1698 cm^{-1} but lacked

3) L. A. Bryan, W. M. Smedley and R. K. Summerbell (ibid., 72, 2206 (1950)) have reported that 2, 5-diphenyl-1, 4-dioxane (II) was a solid with a m. p. of 121~122 and of 173°C (cis and trans forms respectively).

them in the 1150~1100 cm^{-1} region, and treatment with an aqueous sulfuric acid gave only the recovered material in a yield of 90%.

2-Benzyl-4-phenyl-1, 3-dioxorane (IV). — A mixture of styrene glycol (5 g.), phenylacetaldehyde dimethylacetal (6 g.), and monochloroacetic acid (4 g.) in 50 ml. of benzene was refluxed for two hours. Thirty milliliters of benzene was distilled off from the reaction mixture, and the residue was neutralized with a 5% sodium carbonate solution, washed with water, and dried over anhydrous sodium sulfate. Distillation under vacuum gave 8.3 g. (94%) of 2-benzyl-4-phenyl-1,3-dioxorane; b. p., 187~188°C/14 mmHg, n_D^{25} 1.5669. Treatment of the compound with 2.42 mol./l. aqueous sulfuric acid gave an 18% yield of phenylacetaldehyde and a 70% yield of dimer A; b. p., 177~182°C/12mmHg, n_D^{25} 1.5675.

Preparation of Phenylacetaldehyde.—A mixture of styrene glycol (10 g.) and 1.78 mol./l. aqueous sulfuric acid (150 ml.) was refluxed for one hour. The reaction mixture was then immediately steam-distilled under external heating of the flask so that the volume of the content was kept constant. The distillate was saturated with sodium chloride and extracted with ether (50 ml.×3). The combined extract was washed with a 10% sodium bicarbonate solution and water and dried over anhydrous sodium sulfate. The ether was distilled off, and the residue was vacuum-distilled to give 6.1 g. (70.2%) of phenylacetaldehyde. The results under other conditions are given in Table IV.

Department of Organic Synthesis
Faculty of Engineering
Kyushu University
Hakozaki, Fukuoka

Infrared Spectra and Normal Vibrations of Thioamides. II. Thioacetamide

By Isao SUZUKI

(Received February 2, 1962)

In a preceding paper (hereafter refered to as (I))[1], the results of a normal coordinate analysis of thioformamide, the first member of the thioamide group, as well as its *N*-deuterated analogue, were reported on. It was shown in (I) that the Urey-Bradley force field[2] can be applied to the $HCSNH_2$ molecule successfully, and that it gives a very good account of the nature of the normal vibrations of the molecule. As a continuation of that research, an analysis of the vibrational spectra of thioacetamide and *N*-dideuterated thioacetamide has now been made; the results will be given in the present paper.

The Raman and infrared spectra of thioacetamide have been studied by several investigators[2-7] and the assignments of some vibration bands have been reported. Recently Kutzelnigg and Mecke studied the infrared spectra of thioacetamide and its complexes and presented assignments for the observed frequencies[7]. In order to make a detailed analysis of the nature of normal vibrations and to determine the values of the force constants more precisely, it is vitally important to investigate the spectrum of CH_3CSND_2 as well as that of CH_3CSNH_2. Therefore, *N*-dideuterated thioacetamide was prepared, and the infrared spectra of both CH_3CSNH_2 and CH_3CSND_2 were measured in the solid and liquid states and in solutions. A normal coordinate treatment for the in-plane vibrations of these molecules was undertaken, the Urey-Bradley force field being employed in the calculations.

Experimental

Sample.—Thioacetamide (CH_3CSNH_2) was obtained from a commercial source and was purified by recrystallization from chloroform; m. p., 110.5°C (uncorr.).

Exchange reaction with deuterium oxide was employed to prepare *N*-dideuterated thioacetamide (CH_3CSND_2); thioacetamide was mixed with excess D_2O and was heated until it was completely dissolved in D_2O. Then the solution was cooled and the excess D_2O was pumped out in vacuum; this procedure was repeated until the NH stretching bands around 3200 cm^{-1} became almost undetectable.

1) I. Suzuki, This Bulletin, **35**, 1286 (1962).
2) T. Shimanouchi, *J. Chem. Phys.*, **17**, 245, 734, 848 (1949).
3) K. W. F. Kohlrahsch and J. Wagner, *Z. physik. Chem.*, **B45**, 229 (1940).
4) R. Mecke and H. Speisecke, *Chem. Ber.*, **89**, 1110 (1956).
5) E. Spinner, *Spectrochim. Acta*, **15**, 95 (1959).
6) L. J. Bellamy and P. Z. Rogasch, *J. Chem. Soc.*, **1960**, 2218.
7) W. Kutzelnigg and R. Mecke, *Spectrochim. Acta*, **17**, 530 (1961).

TABLE I. OBSERVED FREQUENCIES (IN cm^{-1}) OF THIOACETAMIDES

(a) CH_3CSNH_2

Solid	Liquid	Solution			Assignment
		CS_2	$CHCl_3$	CH_3CN	
3290	3305	3515	3496	3440	$\nu_a(NH_2)$
3165	3160	3391	3381	3230	$\nu_s(NH_2)$
2945	2948		2962		$\nu_a(CH_3)$
2860					
2670					
2620	2613				
1648	1627		1606	1632	$b(NH_2)$
1478	1472				$\delta_a(CH_3)$
1393	1400 br.	1425 (CCl_4)			$\nu(CN)$
1364	1364	1357	1367		$\delta_s(CH_3)$
1306	1302	1315	1316	1309	Skeletal$+r(NH_2)$
1030	1020				$r(NH_2)+r(CH_3)$
975	970	967	966	975	$\nu(CC)+r(CH_3)+\nu(CS)$
718	715			719	$\nu(CS)+\nu(CC)$
709	625 br.			650 br.	$w(NH_2)$ and $t(NH_2)$
517	512			511	$\pi(CC)$
471, 460	448			445	$\delta(NCS)$
375	373				$\delta(CC)$

(b) CH_3CSND_2

Solid	Liquid	Solution			Assignment
		CS_2	$CHCl_3$	CH_3CN	
	(2960)				$\nu_a(CH_3)$?
	2925				$\nu_s(CH_3)$
2470	2540	2622	2612	2580	$\nu_a(ND_2)$
2340	2390	2465	2461	2425	$\nu_s(ND_2)$
1500, 1495			1488		$\delta_a(CH_3)+\nu(CN)$
1423	1400 br.				$\nu(CN)+\delta_a(CH_3)$
1365	1369	1346	1365		$\delta_s(CH_3)$
1238	1238	1249	1250	1244	Skeletal$+r(ND_2)$
1160	1158			1166	$b(ND_2)$
1075					
	1050				$r(CH_3)$ (A''?)
1025					
981	981		982	984	$r(CH_3)$
	865			867	
838	826			828	$\nu(CC)+r(ND_2)$
699, 694	695			703	$\nu(CS)$
580					
556	552			553	$w(ND_2)$
521					$t(ND_2)$
478	479 br.			476	$\pi(CC)$
	452 br.			454	
427	415			405	$\delta(NCS)$
374	374			(368)	$\delta(CC')$

Infrared Spectra. — The infrared spectrophotometers used in the present work were the same as described in (I), and the measurements were made in the region from 3500 to 300 cm^{-1}. The spectra in the solid state were measured as Nujol or hexachlorobutadiene mulls; they are given in Figs. 1 (a)—(c). Those in the liquid state were obtained by heating samples between KCl or KRS-5 plates

to slightly above the melting point with a heater embedded between two thin mica plates*1. Acetonitrile, chloroform and carbon disulfide were used as solvents for the measurements in solutions. Owing to the low solubility of the sample in nonpolar solvents, the measurements were made with a variable thickness cell with a thickness up to 5 mm. The results of these measurements are summarized in Tables I (a) and (b).

Normal Coordinate Treatment

The normal vibrations were calculated as a nine-body problem, assuming a planar structure for the molecule similar to that of acetamide. The procedures of the calculation are quite analogous to those for the acetamide molecule[8], so they are not described here. The

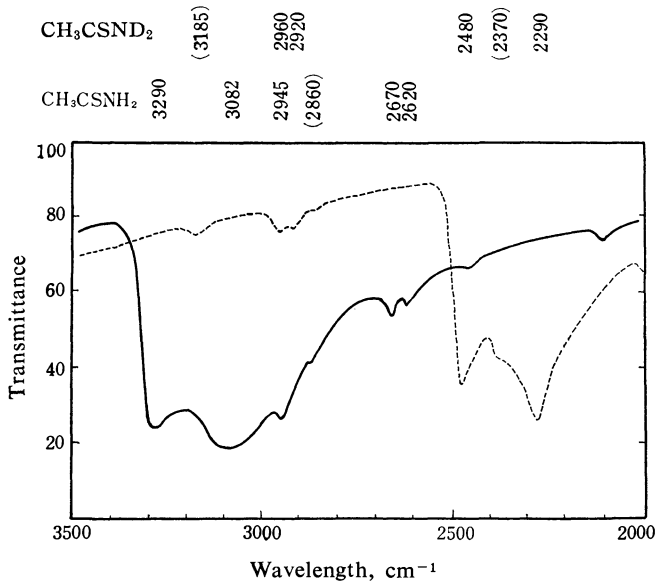


Fig. 1 (a)

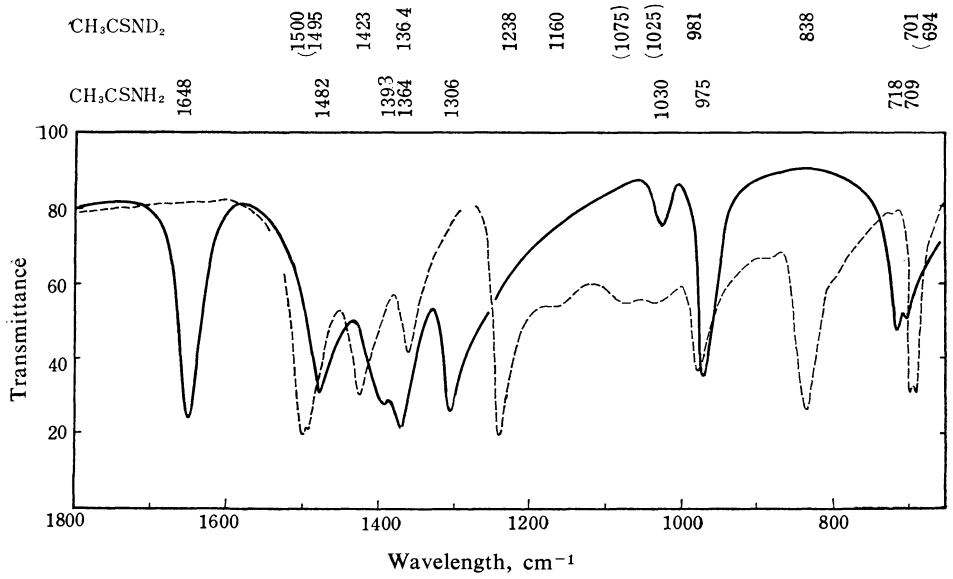


Fig. 1 (b)

*1 Since thioacetamide is less stable under these conditions, the positions of the observed bands were determined by repeating the measurements several times.

8) I. Suzuki, This Bulletin, 35, 1279 (1962).

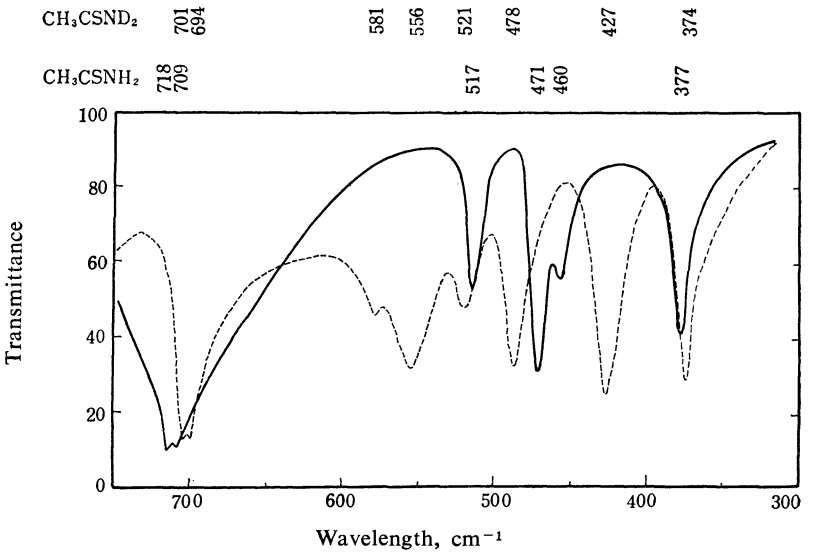


Fig. 1 (c)

Fig. 1. Infrared spectra of CH_3CSNH_2 (solid line) and CH_3CSND_2 (broken line) in the solid state.
(a) 3500~2000 cm^{-1}, (b) 1800~650 cm^{-1}, (c) 800~300 cm^{-1}

structural parameters used are the bond lengths of r(C=S) = 1.713 Å, r(C–N) = 1.324 Å, r(C'C)*2 = 1.494 Å, r(N–H) = 1.02 Å and r(C–H) = 1.09 Å, and the bond angles of 120° for those around the C and N atoms and of 109°47' for those around the C' atom[9],*3. The symmetry coordinates used are listed in Table II.

TABLE II. SYMMETRY COORDINATES*

S_i	Vibrational Modes	Abbr.
S_1	CN stretching	ν(CN)
S_2	CC' stretching	ν(CC)
S_3	CS stretching	ν(CS)
S_4	NH_2 bending	$b(NH_2)$
S_5	NH_2 rocking	$r(NH_2)$
S_6	NCS deformation	δ(NCS)
S_7	CC' deformation	δ(CC')
S_8	CH_3 asym. deformation	$\delta_a(CH_3)$
S_9	CH_3 sym. deformation	$\delta_s(CH_3)$
S_{10}	CH_3 rocking	$r(CH_3)$

* Higher frequencies are separated from lower frequencies[10,11]. Combinations of the internal coordinates in each symmetry coordinate are shown in Ref. 8.

All the numerical computations were carried out with a parametron computer, PC-1. The methods and the routines used in the present study are the same as those described in Refs. 12 and 13.

Results and Discussion

Force Constants.—A considerable amount of data has now been accumulated on the values of the Urey-Bradley force constants for simple amides and thioamides; this is summarized in Table III. It is not difficult to select an appropriate set of force constants for this molecule. The normal vibrations were first calculated from the constants mainly transferred from $HCSNH_2$[1] and CH_3CONH_2[8]; then the values of the constants were refined so as to obtain a better frequency fit. The final set of these values are given in the last column of Table III.

The force constants listed in Table III can be roughly classified into two groups: (A) the constants involving the sulfur or oxygen atoms, and (B) those concerned with other atoms. As was pointed out in (I), the repulsive force constants involving the sulfur atom are found to be always smaller than the corresponding constants involving the oxygen atom. This is also the case for the stretching,

*2 C and C' denote the thiocarbonyl and methyl carbon atoms respectively.

9) M. Truter, *J. Chem. Soc.*, **1960**, 997.

*3 The bond lengths are based on recent X-ray investigation of thioacetamide[9]. The bond angles are assumed, for the sake of simplicity, to be tetrahedral and 120°; these values are not, however, far from the reported values.

10) E. B. Wilson, *J. Chem. Phys.*, **7**, 1047 (1939); **9**, 76 (1941).

11) E. B. Wilson, J. C. Decius and P. C. Cross, "Molecular Vibrations", McGraw-Hill Co., New York (1955), p. 74.

12) T. Shimanouchi and I. Suzuki, *J. Mol. Spectroscopy*, **6**, 277 (1961).

13) T. Shimanouchi and I. Suzuki, ibid., **8**, 222 (1962).

TABLE III. FORCE CONSTANTS OF AMIDES AND THIOAMIDES, (md./A)*,**

	$HCONH_2$	$HCSNH_2$	$HCONHCH_3$		CH_3CONH_2	CH_3CSNH_2	
K_{NH}	5.80	5.52					
K_{CH}	3.74	3.88					
K_{CX}	8.80	**3.95**	8.80		8.50	**3.40**	
K_{CN}	6.15	6.35	6.15		5.75	5.70	
H_{HNH}	0.40	0.43			0.40	0.41	
$F_{H\cdots H}$	0	0			0	0	
H_{HNC}	0.32	0.27	0.30		0.32	0.32	
$F_{H\cdots C}$	0.46	0.46	0.46		0.46	0.44	
H_{HCN}	0.18	0.17	0.18	H_{CCN}	0.30	0.27	
$F_{H\cdots N}$	0.70	0.74	0.72	$F_{C\cdots N}$	0.70	0.68	
H_{HCX}	0.20	**0.13**	0.20	H_{CCX}	0.32	**0.27**	
$F_{H\cdots X}$	0.92	**0.60**	0.92	$F_{C\cdots X}$	0.72	**0.44**	
H_{NCX}	0.34	**0.15**	0.37		0.34	**0.24**	
$F_{N\cdots X}$	1.50	**1.02**	1.50		1.50	**1.17**	
$K_{C'N}$			3.15	K_{CC}	2.40	2.70	
H_{HCH}			0.43		0.43	0.43	N-CH_3 or C-CH_3 part
$F_{H\cdots H}$			0.03		0.05	0.05	
$H_{HC'N}$			0.28	H_{HCC}	0.25	0.25	
$F_{H\cdots N}$			0.52	$F_{H\cdots C}$	0.47	0.50	
κ (md.·A)			−0.04		−0.05	−0.05	
$F'=-F/10$							

* The definitions of K, H and F are the same as in (I), κ is an intramolecular tension defined by Shimanouchi[2].

** X denotes oxygen or sulfur atom. In this table, values of the force constants associated with the sulfur atom are given in bold-faced letters.

and bending force constants*4. The force constants belonging to (B) show excellent transferability throughout the series of thioamides as well as that of amides. The nature of the NH_2, CN and CH_3 groups seems to be scarcely affected by the substitution for the oxygen of the sulfur atom.

The repulsive force constants $F_{N\cdots S}$ are found to be comparatively large, as in the case of $F_{N\cdots O}$. The Urey-Bradley type force field does not contain resonance terms such as $k_{NS}(\Delta r_{CS})\cdot(\Delta r_{CN})$ explicitly, where K_{NS} is a force constant. Therefore, the value of $F_{N\cdots S}$ is partly affected by the resonance force constant k_{NS} and is somewhat effective.

Assignments of the Observed Bands. — The computed frequencies given in Tables IV (a) and (b) are obtained from the force constants listed in the final column of Table III, and correspond to the observed frequencies very closely. Therefore, the potential energy distributions among the symmetry coordinates given in Tables IV (a) and (b) can be considered to represent the quantitative assignments of the observed frequencies. In order to visualize the normal vibration modes corresponding to these vibration bands, the Cartesian displacement vectors have also been calculated*5; they are illustrated in Figs. 2 (a) and (b). Based on the results of calculation, the nature of some vibration bands characteristic of the thioamide group is discussed in this section.

As has been pointed out by Kutzelnigg and Mecke, one of the difficulties in interpreting the spectrum of thioacetamide is the complexity of the spectrum in the region from 1500 to 1300 cm^{-1}. However, the present calculation gives a good account of the nature of these bands. Among the four bands observed in this region, the 1364 cm^{-1} band can reasonably

*4 It is interesting to note that the ratio of K_{CO}/K_{CS} obtained from carbon dioxide and carbon disulfide ($K_{CO}=15.5$, $K_{CS}=7.5$) is close to the value obtained here[14].

14) Ref. 11, p. 311.

*5 In the present calculation, the CH and NH stretching frequencies are separated from the lower frequencies. Therefore, care should be taken in calculating the L^X matrix, which is usually obtained by equation 1.

$$L^X=M^{-1}B'G^{-1}L \qquad (1)$$

Miyazawa and the author have found that the process for higher frequency separation is equivalent to transforming G into $G^*=TGT'$, where G, G^* and T have the following expressions, if we adopt Wilson's notation[14]:

$$G=\begin{Vmatrix} G_{11} & G_{12} \\ G_{21} & G_{22} \end{Vmatrix}, \quad G^*=\begin{Vmatrix} G_{11} & 0 \\ 0 & G_{22}-G_{21}G_{11}^{-1}G_{12} \end{Vmatrix}$$

$$\text{and } T=\begin{Vmatrix} E_{11} & 0 \\ -G_{21}G_{11}^{-1} & E_{22} \end{Vmatrix}.$$

Instead of Eq. 1, one should employ the following equation for obtaining the L^X matrix:

$$L^X=M^{-1}B'T'G^{*-1}L \qquad (2)$$

TABLE IV. THE OBSERVED AND CALCULATED FREQUENCIES, PERCENT DEVIATIONS, AND POTENTIAL ENERGY DISTRIBUTIONS AMONG THE SYMMETRY COORDINATES, $(F_{ii}L_{is}^2/\lambda_s)\times 100$

(a) CH_3CSNH_2

Q_i	ν_{obs}	ν_{calcd}	$\Delta\nu$*	Δ*	P. E. D. S_1	S_2	S_3	S_4	S_5	S_6	S_7	S_8	S_9	S_{10}
Q_1	1648	1634	+14	0.8	13	0	0	**93**	0	0	0	0	0	0
Q_2	1482	1478	+ 4	0.3	9	0	2	2	0	0	1	**68**	0	**16**
Q_3	1393	1396	− 3	0.2	**62**	5	4	**5**	0	3	7	16	6	1
Q_4	1364	1374	−10	0.7	4	10	1	0	0	0	1	1	**99**	0
Q_5	1306	1310	− 4	0.3	0	**26**	**17**	0	**50**	**15**	6	2	0	2
Q_6	1030	1028	+ 2	0.2	4	12	4	0	**29**	1	2	8	0	**46**
Q_7	975	964	+11	1.1	9	**34**	**14**	0	**16**	2	0	4	0	**28**
Q_8	718	718	0	0	5	**16**	**57**	0	1	0	6	1	0	3
Q_9	471	468	+ 3	0.7	0	3	2	0	4	**76**	8	0	0	0
Q_{10}	377	388	+11	2.9	1	2	8	0	0	11	**73**	1	0	3

(b) CH_3CSND_2

Q_i	ν_{obs}	ν_{calcd}	$\Delta\nu$*	Δ*	P. E. D. S_1	S_2	S_3	S_4	S_5	S_6	S_7	S_8	S_9	S_{10}
Q_1	1495	1487	+ 8	0.6	**28**	1	3	3	0	0	2	**50**	0	16
Q_2	1423	1431	− 8	0.6	**54**	5	2	10	0	2	5	**35**	1	0
Q_3	1364	1374	−10	0.7	1	9	0	0	0	0	0	0	**104**	0
Q_4	1238	1231	+ 7	0.6	0	**43**	**28**	0	**21**	**19**	6	3	0	6
Q_5	(1160)	1179	—	—	1	5	2	77	0	1	4	2	0	8
Q_6	981	978	+ 3	0.3	12	1	4	6	4	1	0	9	0	**65**
Q_7	838	836	+ 2	0.2	3	31	3	1	57	1	1	0	0	0
Q_8	696	702	− 6	0.9	6	9	**58**	3	6	0	6	0	0	3
Q_9	427	433	− 6	1.4	0	1	1	0	**12**	**66**	**14**	0	0	1
Q_{10}	374	362	+12	3.2	1	4	7	0	0	**18**	**62**	1	0	2

* $\Delta\nu=\nu_{obs}-\nu_{calcd}$, $\Delta=|\Delta\nu|/\nu_{obs}$

be assigned to an almost pure $\delta_s(CH_3)$ vibration. Of the remaining three, the 1482 cm^{-1} band is found to be chiefly associated with the $\delta_a(CH_3)$ vibration, while the band at 1392 cm^{-1}, with the ν(CN) vibration, although a coupling between these two vibrational modes takes place. In the *N*-dideuterated species, the coupling occurs more strongly than in the normal species; this gives rise to two observed bands at 1495 and 1423 cm^{-1}.

The present calculations show that the nature of the 1306 cm^{-1} band of CH_3CSNH_2 is very complicated and that it cannot be attributed to one or two vibration modes. This may be the cause of the difficulty in interpreting the nature of this band. The $r(NH_2)$, ν(CC), ν(CS) and δ(NCS) vibrations contribute to this band. As may be seen from Fig. 2 (a), this normal vibration involves the rocking motion of the NH_2 group as well as the movements of the two carbon atoms perpendicular to the C–N bond and antiparallel to each other. In the *N*-dideuterated species, the band found at 1238 cm^{-1} corresponds to this normal mode, although the contribution of the $r(NH_2)$ motion to this mode decreases considerably, while that of the ν(CC) vibration increases.

The band at 1030 cm^{-1} is assigned to the hybridized vibration containing the $r(NH_2)$ and $r(CH_3)$ vibrations, and these two vibrations also contribute to the 975 cm^{-1} band. It is of interest to seek in which region the band chiefly associated with the ν(CS) vibration appears. In the case of $HCSNH_2$, it was found that the band at 843 cm^{-1} corresponds to an almost pure ν(CS) vibration. In thioacetamide, the situation is rather complicated by the existence of the C–C bond adjacent to the C=S bond. The ν(CC) and ν(CS) vibrations are coupled with each other. In fact, the normal vibrations at 1306, 975 and 718 cm^{-1} of CH_3CSNH_2 involve considerable contributions from the ν(CC) and ν(CS) vibrations. Above all, the contribution of the ν(CS) vibration to the 718 cm^{-1} band is comparatively large; the energy associated with this motion is about 60% of the total. This is consistent with the fact reported by Kutzelnigg and Mecke that this band is shifted by 29 cm^{-1} toward a lower frequency on the

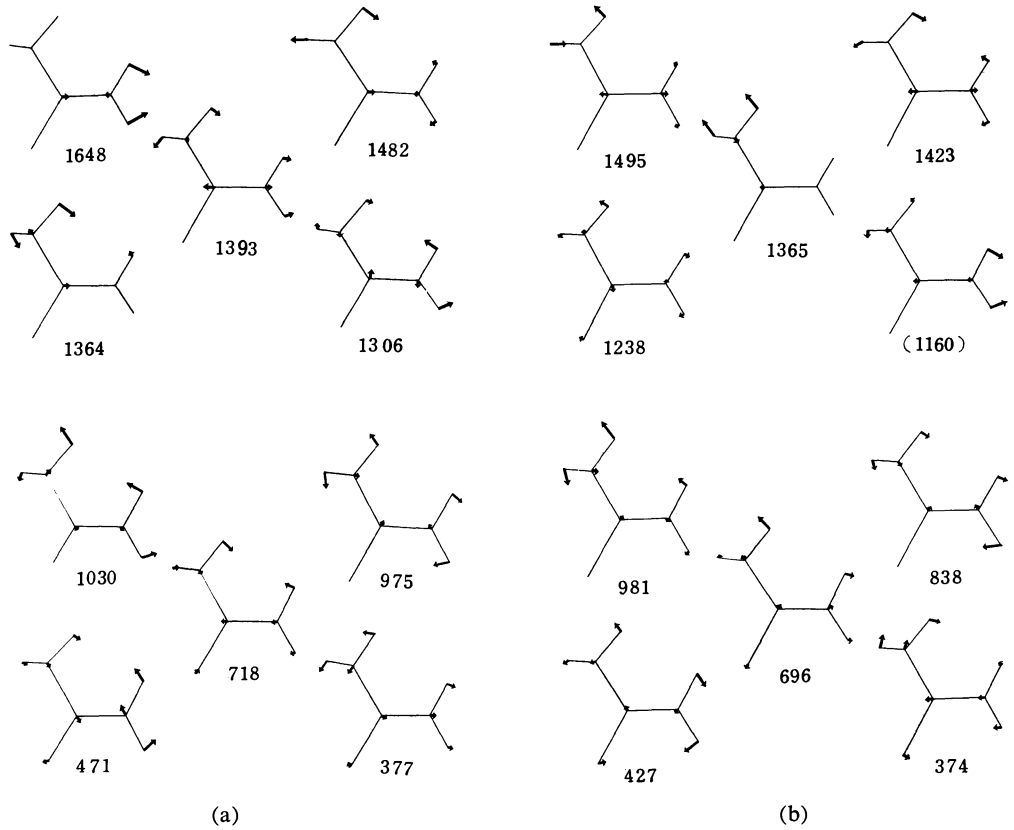
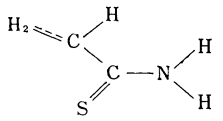
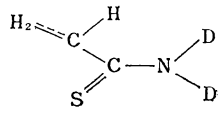


Fig. 2. The normal modes of CH_3CSNH_2 and CH_3CSND_2 in Cartesian displacement vectors projected to the molecular plane. (A/unit change in normal coordinate)

(a) CH_3CSNH_2:



(b) CH_3CSND_2:



formation of a complex with cupper chloride[7].

In the region below 800 cm^{-1}, the bands of CH_3CSNH_2 found at 471 and 377 cm^{-1} are assigned to two skeletal deformation vibrations. The spectrum of CH_3CSND_2 is complicated, since some out-of-plane vibrations also occur in this region, but the bands found at 427 and 374 cm^{-1} can safely be assigned to these deformation vibrations. The approximate assignment of each observed band is given in the last column of Tables I (a) and (b).

Three out-of-plane (A'') vibrations are expected to appear in the region below 800 cm^{-1}. They are the NH_2 wagging, NH_2 twisting and CC out-of-plane bending vibrations, $w(NH_2)$, $t(NH_2)$ and τ(CC); the assignments for these modes are also included in Tables I (a) and (b). The present assignments are based on the fact that the out-of-plane vibrations are sensitive to change in the states in which the substance is measured. In order to check the assignments of the out-of-plane vibrations, the product rule is applied[15]. The ratio of the three observed frequencies is $(700\times700\times517)/(556\times476\times454)=1.83$ for the solid state spectra*6, and $(650\times650\times512)/(553\times476\times454)=1.81$ for the solution spectra. This is in good agreement with the theoretical value of 1.83[2].

A more detailed analysis of the out-of-plane vibrations is now in progress for various

*6 The $w(NH_2)$ and $t(NH_2)$ frequencies appear around 700 cm^{-1}. In $HCSNH_2$, they occur at 670 and 620 cm^{-1} in the liquid state and at 754 and 645 cm^{-1} in the solid state (I). Although we cannot resolve the absorption around 700 cm^{-1}, it seems reasonable to assume that these vibrations happen to be at approximately the same frequency. It should be emphasized that three distinct bands are found at 769, 735 and 690 cm^{-1} in the spectrum of the CH_3CSNH_2-CuCl complex[7].

amides and thioamides; the results will be published elsewhere.

The present author wishes to express his deep gratitude to Professor Takehiko Shimanouchi for his guidance and encouragement throughout this work. His thanks are also due to Professor Hidetoshi Takahashi for the use of a PC-1 computer.

Department of Chemistry
Faculty of Science
The University of Tokyo
Hongo, Tokyo

Infrared Spectra and Normal Vibrations of Thioamides. III. N-Methylthioformamide and N-Methylthioacetamide

By Isao SUZUKI

(Received February 2, 1962)

It has been shown in preceding papers[1,2],*1 that a normal coordinate analysis of the $HCSNH_2$ and CH_2CSNH_2 molecules can be made quite successfully by applying the Urey-Bradley force field[3]. The nature of normal vibrations have been clarified, and the values of the force constants have now been settled for these primary thioamides. The work has also been extended to secondary thioamides, RCSNHR', and in this paper the results obtained for *N*-methylthioformamide and *N*-methylthioacetamide will be presented.

N-Methylthioformamide and *N*-methylthioacetamide, as well as their *N*-deuterated analogues, were prepared, and their infrared spectra were measured in the solid and liquid states and in solution. It is now well accepted that the simple secondary amides, RCONHR', predominantly take the planar configurations in which R and R' are in the trans-position with regard to each other[4]. It will be shown in the present investigation that the vibrational spectra of secondary thioamides are also interpreted satisfactorily in terms of the trans planar models. The in-plane normal vibrations of $HCSNHCH_3$ and $HCSNDCH_3$ have been calculated from the force constants directly transferred from $HCSNH_2$ (I) and $HCONHCH_3$[5]; the calculated frequencies for the trans configuration agree well with the observed frequencies.

In the present paper, the results of these measurements and calculations are reported. Based on these results, the nature of the normal vibrations and the problem of a stable configuration for the secondary thioamides are discussed.

Experimental

Materials.—*N-Methylthioacetamide* $CH_3CSNHCH_3$. —This compound was prepared by heating *N*-methylacetamide, with phosphorus pentasulfide suspended in benzene at about 50°C for 3 hr.[6] The sample was purified by recrystallization from ether containing petroleum ether; m. p., 59°C (uncorr.).

N-Methylthioformamide $HCSNHCH_3$. — This was prepared from *N*-methylformamide by a method analogous to that used for *N*-methylthioacetamide. This compound is not as stable as *N*-methylthioacetamide, and it was usually kept in a refrigerator as an ethereal solution. When it was distilled, it showed obvious signs of decomposition, even at a reduced pressure. Therefore, it was purified by recrystallization from ether containing petroleum ether at about −50°C.

The exchange reaction with deuterium oxide was used to replaced the amide hydrogen atom with deuterium.

Infrared Spectra. — The infrared measurements of $HCSNHCH_3$ were made in the liquid and solid states and in solutions; the results are given in Figs. 1 and 3, and the observed frequencies, in Table I(a). Those of $HCSNDCH_3$ are given in Figs. 2 and 3. A low temperature cell[7] cooled with a mixture of dry ice and methanol was used to obtain the spectra in the solid state. The infrared measurements of $CH_3CSNHCH_3$ were also made in the solid and liquid states and in solutions; the results are given in Figs. 4 and 5, and the observed frequencies, in Table I(b). Those of the deuterated species are given in Figs. 4 and 5. The spectra in

1) I. Suzuki, This Bulletin, **35**, 1286 (1962).
2) I. Suzuki, ibid., **35**, 1449 (1962).
*1 Hereafter referred to as (I) and (II).
3) T. Shimanouchi, *J. Chem. Phys.*, **17**, 245, 734, 848 (1945).
4) For example, T. Miyazawa, T. Shimanouchi and S. Mizushima, ibid., **24**, 408 (1956); **29**, 611 (1958).
5) I. Suzuki, This Bulletin, **35**, 540 (1962).
6) I. L. Knunyants and L. V. Razadovskaya, *J. Gen. Chem.* (*U. S. S. R.*), **9**, 557 (1939) (*Chem. Abstr.*, **34**, 391 (1940)).
7) T. Miyazawa, *J. Chem. Soc. Japan, Pure Chem. Sec.* (*Nippon Kagaku Zassi*), **76**, 821 (1955).

TABLE I(a). THE OBSERVED FREQUENCIES (IN cm^{-1}) OF $HCSNHCH_3$

Solid (−50°)	Liquid	Solution			Assignment
		CCl_4 concn.	or CS_2 dil.	$CHCl_3$	
3160	3230	3233 −70	3434	3415	ν(NH)
3047	3047				
2960	2985		2963	2965	$\nu_a(CH_3)$
			2933		$\nu_s(CH_3)$
2850					
1550	1537			1525	$\nu(CN)+\delta(NH)$
1492	1479		1482	1480	$\delta_a(CH_3)+\delta(CH)+\delta(NH)$
1470	1463		1460	1461	$\delta_a(CH_3)$ (A″)
1440	1443			(1437)	$\delta(CH)+\nu(CN)$
1392	1393		1399	1394	$\delta_s(CH_3)$
1370			1348		
1308	1297	1300	1277	1288	$\delta(CH)+\delta(NH)+\nu(CN)$
1138	1136		1135	1137	$r(CH_3)+\nu(C'N)$
	(1010)		1025	1020	π(CH) (A″)
992	987		992	992	$r(CH_3)+\nu(C'N)+\nu(CS)$
985 / 946					
912	920	927	915	923	
874 / 865	868	873	878	873	$\nu(CS)+\nu(C'N)$
739	680		667 (CH_3CN)		π(NH) (A″)
	600		606 (CH_3CN)		$\delta(NCS)-\delta(CNC')$
	467		467 (CH_3CN)		
	363		357 (CH_3CN)		τ(CN) (A″)
	$(200)_{calcd}$				$\delta(NCS)+\delta(CNC')$

TABLE I(b). THE OBSERVED FREQUENCIES (IN cm^{-1}) OF $CH_3CSNHCH_3$

Solid	Liquid	Solution			Assignment
		CCl_4 / CS_2	$CHCl_3$	CH_3CN	
3207	3283	3428 / 3240	3425 / 3250		ν(NH)
3077	3063	(3045)	(3050)		
3019					
2977	2985				$\delta_a(CH_3)_{N \text{ and } C}$
2935	2928	2930			$\delta_s(CH_3)_{N \text{ and } C}$
1565	1547		1534		$\delta(NH)+\nu(CN)$
1473	1460		(1469)		$\delta_a(CH_3)_C$
1425	1438		1438		$\delta_a(CH_3)_N$
1370			1375 sh		$\delta_s(CH_3)_N$
	1360				
1357		1348	1360		$\delta_s(CH_3)_C$ and $\nu(CN)+\delta(NH)$
1243	1242	(1246)			
1211	1210	1212			
1099	1100	1100	1099		$\nu(CC)+\nu(CS)+r(CH_3)_N$
1074	(1060)	(1055 ?)			
1023	1020	1038	1022		$r(CH_3)_N$ and $r(CH_3)_C$
955	950	945	952		$\nu(C'N)+\nu(CS)$
746	690			690 br.	π(NH)
684	690	699		703	$\nu(CS)+\nu(CC)$
559	555			552	$\delta(NCS)-\delta(CNC')$
538	533			532	$\pi(CC')$
503	(503)				
374	370				$\delta(CC')$
387	(287)				$\delta(NCS)+\delta(CNC')$

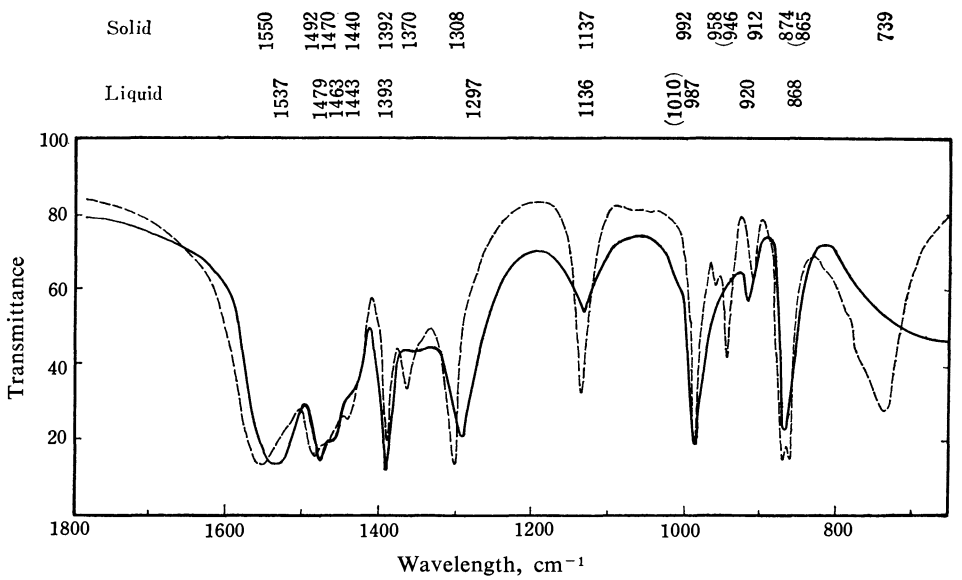


Fig. 1. Infrared spectra of $HCSNHCH_3$ in the liquid state (solid line) and in the solid state (broken line) in the region from 1800 to 650 cm^{-1}.

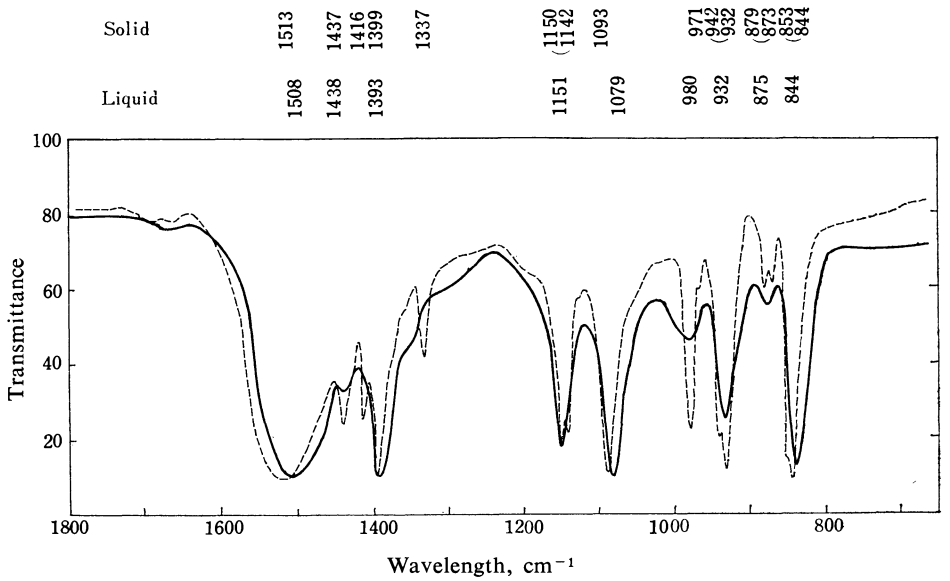


Fig. 2. Infrared spectra of $HCSNDCH_3$ in the liquid state (solid line) and in the solid state (broken line) in the region from 1800 to 650 cm^{-1}.

the solid state were obtained as Nujol or hexachlorobutadiene mulls. A small heating cell was used to measure the spectrum in the liquid state. Carbon tetrachloride, carbon disulfide or chloroform were used as solvents in the region from 3500 to 800 cm^{-1} and acetonitrile in the region from 800 to 400 cm^{-1}.

The spectrophotometers used in the present work are the same as those described in (I). In addition, a high-resolution Perkin-Elmer 112G grating spectrophotometer equipped with a KBr fore-prism was employed for the measurement of the NH stretching bands in carbon tetrachloride in the 3μ region. The results are given in Fig. 6.

Normal Coordinate Treatment

The normal coordinate treatments were undertaken for the in-plane vibrations of $HCSNHCH_3$ and $HCSNDCH_3$ as a nine-body problem, assuming a trans planar structure for the molecule which was analogous to $HCONHCH_3$[5]. The calculation procedures

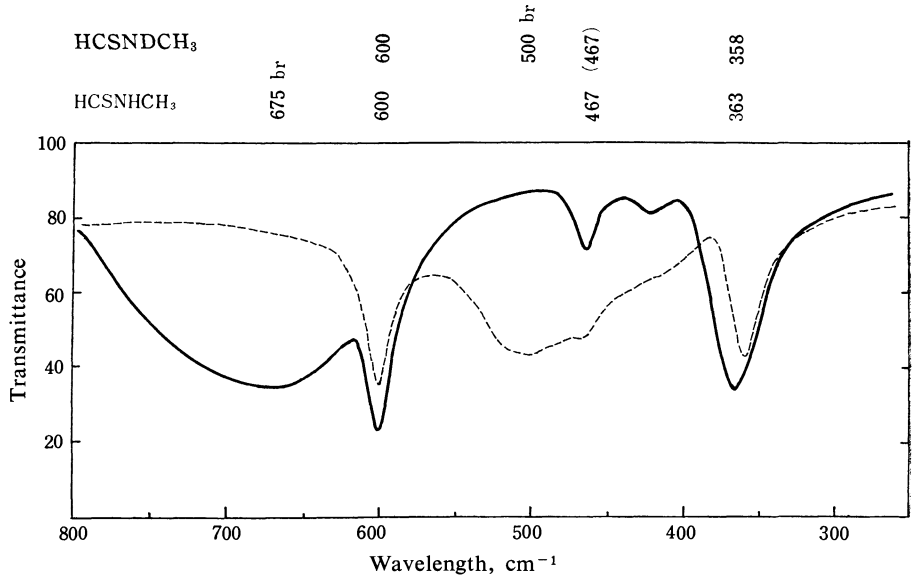


Fig. 3. Infrared spectra of $HCSNHCH_3$ (solid line) and $HCSNDCH_3$ (broken line) in the liquid state in the region from 800 to 260 cm^{-1}.

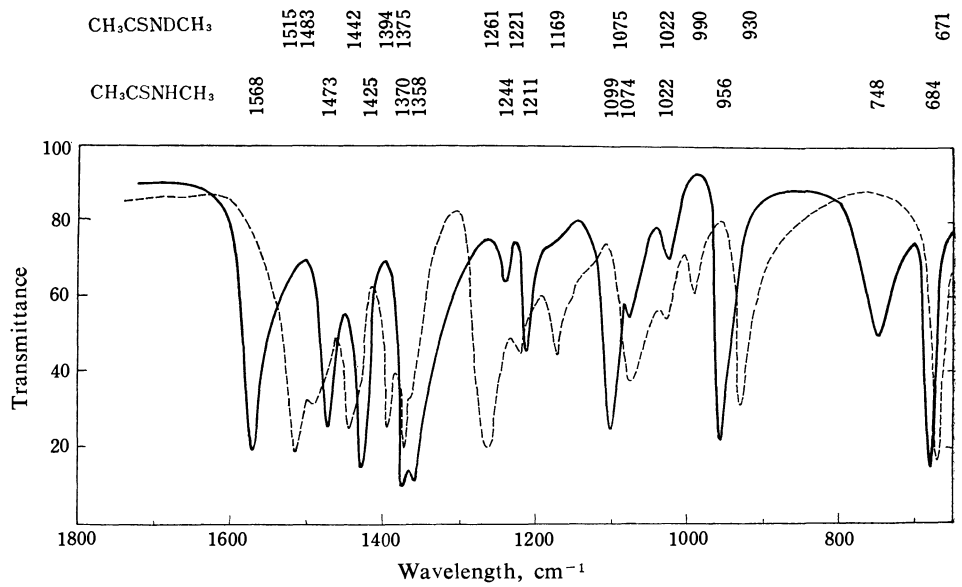


Fig. 4. Infrared spectra of $CH_3CSNHCH_3$ (solid line) and $CH_3CSNDCH_3$ (broken line) in the solid state in the region from 1800 to 650 cm^{-1}.

are similar to those for the $HCONHCH_3$ molecule and do not be described here. The structural parameters used in the calculation are the bond lengths of $r(C{=}S) = 1.713$ Å, $r(C{-}N) = 1.324$ Å, $r(C'{-}N)$*2 $= 1.47$ Å, $r(C'{-}H) = r(C{-}H) = 1.07$ Å, and the bond angles of 120° for those around the C and N atoms and of 109°47′ for those around the C′ atom. The symmetry coordinates used in the calculation are listed in Table II; the combinations of

*2 C and C′ denote the thiocarbonyl and methyl carbon atoms respectively.

Table II. Symmetry coordinates

S_i	Vibrational mode	Abbr.
S_1	CS stretching	ν(CS)
S_2	CN stretching	ν(CN)
S_3	C′N stretching	ν(C′N)
S_4	NH deformation	δ(NH)
S_5	CH deformation	δ(CH)
S_6	CNC′ deformation	δ(CNC′)
S_7	NCS deformation	δ(NCS)
S_8	CH_3 sym. deformation	$\delta_s(CH_3)$
S_9	CH_3 rocking	$r(CH_3)$
S_{10}	CH_3 asym. deformation	$\delta_a(CH_3)$

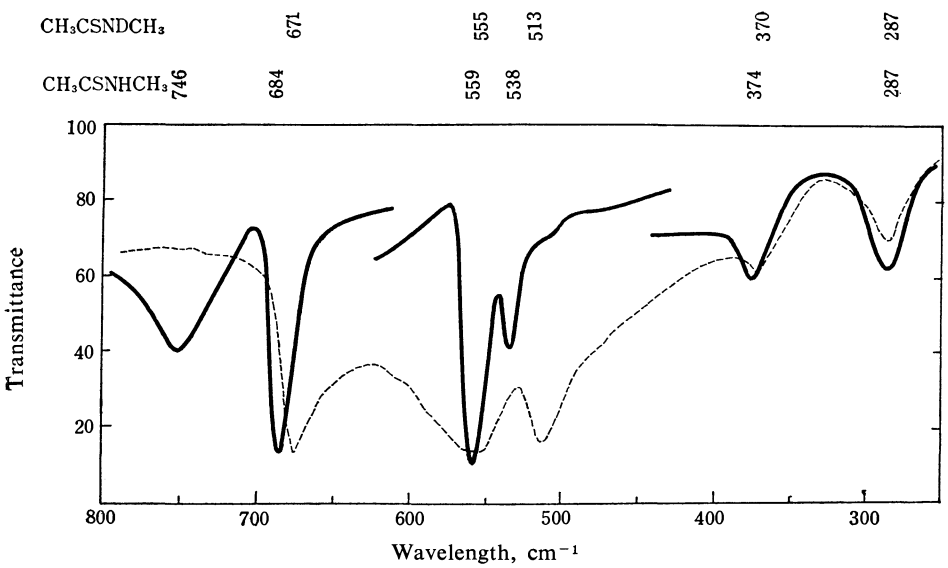


Fig. 5. Infrared spectra of $CH_3CSNHCH_3$ (solid line) and $CH_3CSNDCH_3$ (broken line) in the solid state in the region from 800 to 260 cm^{-1}.

TABLE III. FORCE CONSTANTS (md./A)

	K_{CN}	6.15	$H_{CNC'}$	0.35	$F_{C\cdots C'}$	0.30
I	$K_{C'N}$	3.15	H_{CNH}	0.30	$F_{C\cdots H}$	0.46
			$H_{C'NH}$	0.25	$F_{C'\cdots H}$	0.36
	K_{CS}	3.95	H_{NCS}	0.15	$F_{N\cdots S}$	1.02
II			H_{NCH}	0.17	$F_{N\cdots H}$	0.74
			H_{HCS}	0.13	$F_{H\cdots S}$	0.60
	κ	−0.05	$H_{NC'H}$	0.28	$F_{N\cdots H}$	0.52
III		(md.·A)	$H_{HC'H}$	0.43	$F_{H\cdots H}$	0.05

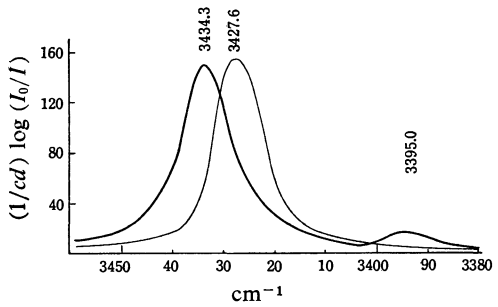


Fig. 6. Infrared absorptions of $HCONHCH_3$ (——) and $CH_3CSNHCH_3$ (▬▬) in carbon tetrachloride solutions in the region from 3460 to 3380 cm^{-1} (The effective slit width is about 1.8 cm^{-1}).

the interal coordinates in each symmetry coordinate are given in Ref. 5 and so are not reproduced here. Four higher frequencies corresponding to the CH and NH(D) steretching vibrations are separated from the lower frequencies[8].

8) E. B. Wilson, *J. Chem. Phys.*, **7**, 1047 (1939); **9**, 96 (1941).

Force Constants. — As in (I) and (II), the Urey-Bradley force field was employed in the calculation. In Table III, the values of the force constants used are listed. They were determined by the following methods: the values of the force constants in group I were directly transferred from the $HCONHCH_3$[5] molecule, while those in group II are from the $HCSNH_2$ molecule (I). The force constants belonging to group III are related to the N–CH_3 part of the molecule. They are also transferred from $HCSNHCH_3$, but slightly modified values were used*3.

Results of Calculation.—The computed frequencies from the force constants given in Table III are shown in Tables IV (a) and (b). They show a surprisingly good agreement with the observed frequencies, with a maximum deviation of 3.6%. The agreement is so good that the refinement of the force constants is unnecessary

*3 The Urey-Bradley force constants have been obtained in our laboratory for a number of compounds containing methyl groups. The set of H_{HCH}=0.43 md./A, $F_{H\cdots H}$=0.03 md./A and κ=−0.05 md.·A has been found to be the best choice for explaining the frequency data.

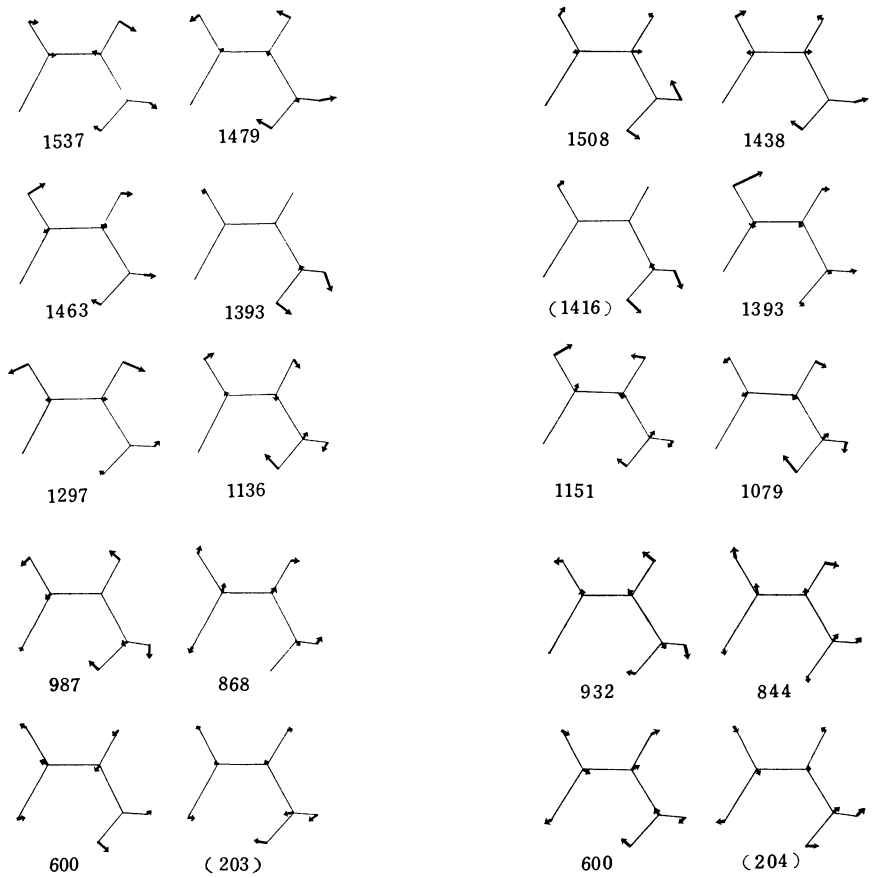
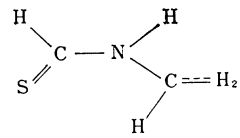
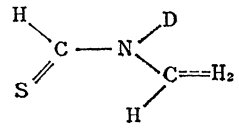


Fig. 7. The in-plane normal modes of *N*-methylthioformamides in Cartesian diplacement vectors projected to the molecular plane (A/unit change in normal coordinate).

(a) $HCSNHCH_2$:



(b) $HCSNDCH_3$:



for the present purposes. Tables IV (a) and (b) list the potential energy distributions among the symmetry coordinates, as well as the signs of the corresponding elements of the L matrix. The Cartesian displacement vectors*4 obtained from the L^x matrix have also been calculated; they are given in Figs. 7 (a) and (b).

The numerical computations were carried out with a PC-1 computer; the routines and methods of calculations are described in Refs. 9 and 10 and so are not described here.

*4 Special treatment is necessary to calculate the L^x matrix when higher frequencies are separated from lower ones. The details were given in (II).

9) T. Shimanouchi and I. Suzuki, *J. Mol. Spectroscopy*, **6**, 277 (1961).

10) T. Shimanouchi and I. Suzuki, ibid., **8**, 222 (1962).

Discussion

Possible Rotational Isomers. — As shown in (I) and (II), the C–N bonds of the thioamide molecules possess a considerable double-bond character, and the molecules take approximately planar configurations. Therefore, the secondary thioamides have two possible configurations, cis and trans, in which the amide hydrogen and thiocarbonyl sulfur atoms take, respectively, the cis and trans positions with regard to each other. Russell and Thompson[11] have proposed that the two closely situated NH stretching bands of the secondary amides in dilute carbon tetrachloride solutions arise from these two isomers;

11) R. A. Russell and H. W. Thompson, *Spectrochim. Acta*, **8**, 138 (1956).

Table IV. The observed and calculated frequencies, percent deviations, and potential energy distributions among the symmetry coordinates, $(F_{ii}L_{is}^2/\lambda_s \times 100)$

(a) $HCSNHCH_3$

Q_i	ν_{obs}	ν_{calcd}	$\Delta\nu$	Δ	S_1	S_2	S_3	S_4	S_5	S_6	S_7	S_8	S_9	S_{10}
Q_1	1537	1539	− 2	0.1	1*	**44**	7*	**50**	0*	0*	1*	1*	6	3
Q_2	1479	1476	+ 3	0.2	2*	1	1	15*	10*	0*	0	0	11	**59**
Q_3	1443	1442	+ 1	0.1	10	**25***	0*	5	**55**	2	0*	0*	1	**19**
Q_4	1393	1405	− 8	0.5	0	0	9*	0	0	0	0*	**100**	0	0*
Q_5	1297	1285	+12	0.8	2*	**21**	3*	**26***	**35**	0*	0*	0*	0	1*
Q_6	1136	1097	+39	3.6	1*	0*	**27**	0	2	11*	5	0	**45**	10*
Q_7	987	987	0	0	**22**	3*	**29***	3*	1*	2	4*	0*	**32**	7*
Q_8	868	883	−15	1.8	**57**	10	**24**	1*	0	1	9*	0	1*	0
Q_9	600	589	+11	1.8	12*	0	6	0*	0*	**35**	**35***	0	4	1*
Q_{10}	—	204	—	—	0*	1	0	0*	0*	**52**	**49**	0	1	0*

(b) $HCSNDCH_3$

Q_i	ν_{obs}	ν_{calcd}	$\Delta\nu$	Δ	S_1	S_2	S_3	S_4	S_5	S_6	S_7	S_8	S_9	S_{10}
Q_1	1508	1503	+ 5	0.3	4*	**50**	4*	4	8*	1*	0*	0*	13	**27**
Q_2	1438	1452	−14	1.0	4	**31***	2	3*	11	1	0	1	4	**54**
Q_3	(1416)	1406	—	—	0*	0	5*	0*	3*	0*	0	**101**	0*	0*
Q_4	1393	1395	− 2	0.2	3	3	13*	11	**70**	1	2*	3	0	1*
Q_5	1151	1114	+37	3.3	18	4*	20	24	11*	9	6*	0	8*	2
Q_6	1079	1068	+11	1.0	8	5*	3	15	0*	2*	0	0	**57**	12*
Q_7	932	922	+10	1.1	0	4	**50**	**23**	0	1*	0	0	14	3*
Q_8	844	863	−19	2.3	**57**	8	5	**21***	0	3	11*	0*	0	0*
Q_9	600	584	+16	2.7	13*	0	5	0*	0*	**35**	**34***	0	4	1*
Q_{10}	—	204	—	—	0*	1	0	0*	0*	**50**	**52**	0	1	0*

$\Delta\nu = \nu_{obs} - \nu_{calcd}$, $\Delta = |\Delta\nu|/\nu_{obs}$

* The asterisk means that the corresponding $\boldsymbol{L}$ matrix element is negative.

the band with a higher frequency corresponds to the NH stretching vibration of the trans form, and the band with a lower frequency, to that of the cis form. This proposal was supported by our dielectric and infrared measurements of some anilides over a wide range of concentrations[12,13], although there is a certain limitation in applying the rule, especially to aromatic amides[14]. It was also shown that the rule is applicable not only to secondary amides but also to thioamides[13].

The infrared absorption curves of $HCSNHCH_3$ and $CH_3CSNHCH_3$ in dilute carbon tetrachloride solutions are shown in Fig. 6. Only a single absorption peak is observed at 3427.6 cm^{-1} for $CH_3CSNHCH_3$. In addition to the main peak at 3434.3 cm^{-1}, $HCSNHCH_3$ shows a satellite peak at a lower frequency. The positions and the relative intensities*5 of these two bands correspond well to those of $HCONHCH_3$. Therefore, it can be concluded that $CH_3CSNHCH_3$ takes the trans configuration, even in a dilute non-polar solvent, and that $HCSNHCH_3$ takes both trans and cis forms, of which the former is predominant. In analogy with the secondary amides, these facts indicate that thioamides are also in the trans form in the condensed phases. The calculations of the normal vibrations of $HCSNHCH_3$ and $HCSNDCH_3$ described below also indicate that the vibrational spectra of these molecules are satisfactorily explained by assuming that the molecules are predominantly in the trans form.

Assignments of the Observed Frequencies.— As has already been stated, the computed frequencies of $HCSNHCH_3$ and $HCSNDCH_3$ given in Tables IV (a) and (b) are in good agreement with the results of observation. Not only does it indicate the excellent transferability of the Urey-Bradley force constants, but it also shows that the assumption of the trans planar model for the molecule is generally correct. Therefore, the potential energy distributions among the symmetry coordinates given in Tables IV (a) and (b), as well as the Cartesian

12) I. Suzuki, *J. Chem. Soc. Japan, Pure Chem. Sec.* (*Nippon Kagaku Zasshi*), **80**, 353, 697 (1959).
13) I. Suzuki, M. Tsuboi, T. Shimanouchi and S. Mizushima, *Spectrochim. Acta*, **16**, 471 (1960).
14) I. Suzuki, M. Tsuboi and T. Shimanouchi, ibid., **16**, 467 (1960).
*5 The relative intensity of the satellite band to the main band is a little stronger than that of $HCONHCH_3$; this is consistent with the results obtained from anilides and thioanilides[12,13].

displacement vectors given schematically in Figs. 7 (a) and (b), can be considered to represent the quantitative assignments of the observed frequencies.

Next, the out-of-plane vibrations should be treated in order to complete the vibrational assignments of *N*-methylthioformamide. Of seven out-of-plane vibrations, four are chiefly associated with the CH_3 group vibrations. The methyl asymmetric stretching, asymmetric deformation and rocking vibrations are expected to occur around the corresponding in-plane vibrations. The methyl torsional vibration is expected to appear at a much lower frequency and to lie beyond the limits of the present investigation. The remaining three are the NH and CH out-of-plane and CN torsional vibrations, π(NH), π(CH) and τ(CN). The 680 and 363 cm^{-1} bands of $HCSNHCH_3$ correspond well with those at 720 and 353 cm^{-1} of $HCONHCH_3$ in their positions, intensities, and spectral changes due to *N*-deuteration and to the alternation of the states of aggregation as well. They are assigned, respectively, to the π(NH) and τ(CN) vibrations*6. The assignment of the π(CH) vibration is slightly ambiguous. In $HCSNH_2$ it was found at 985 cm^{-1}, and a band found at 980 cm^{-1} of $HCSNDCH_3$ is probably to be assigned to this vibration. In $HCSNHCH_3$, there is a strong band at 987 cm^{-1} belonging to one of the in-plane vibrations. Therefore, it is not clear whether a weak shoulder band at 1010 cm^{-1} is to be ascribed to the π(CH) mode or it overlaps the strong band mentioned above. In the last column of Table I (a), the approximate assignments of the observed frequencies are given.

If we combine the results of the normal coordinate analysis of $HCSNHCH_3$ with those of CH_3CSNH_2 and $CH_3CONHCH_3$[4], it is not difficult to assign the observed bands of $CH_3CSNHCH_3$. The results of these vibrational assignments are given in the last column of Table I (b). In the next section vibrational assignments of some bands in $CH_3CSNHCH_3$ and $CH_3CSNDCH_3$ are discussed in connection with the characteristic frequencies of secondary thioamides.

The Characteristic Frequencies of Secondary Thioamides. — The nature of some vibration bands characteristic of the secondary thioamides will now be discussed in detail on the basis of the assignments described in the previous section.

The Band around 1550 cm^{-1}.—As can be seen from Table IV (a) and Fig. 7 (a), the band at 1537 cm^{-1} of $HCSNHCH_3$ is assigned to the mixed vibration of the ν(CN) and δ(NH). The nature and the frequency of the band, as well as its change due to the states of aggregation, correspond to those of the amide II band in secondary amides[4]. In $CH_3CSNHCH_3$ this band is found at 1564 cm^{-1} in the solid state and at 1547 cm^{-1} in the liquid state. On *N*-deuteration, this band moves to a frequency lower by about 30 cm^{-1}. Instead of the δ(NH) vibration, the $\delta_a(CH_3)$ vibration couples with the ν(CN) motion in *N*-deuterated species; this gives rise to two frequencies at 1508 and 1438 cm^{-1} in $HCSNDCH_3$. In the case of $CH_3CSNDCH_3$, the $\delta_a(CH_3)_C$*7 vibration also couples with the ν(CN) vibration, as in the case of CH_3CSND_2 (II), the three frequencies are observed at 1515, 1483 and 1442 cm^{-1}.

The Band around 1300 cm^{-1}. — The band at 1297 cm^{-1} of $HCSNHCH_3$ is also assigned to the mixed δ(NH) and ν(CN) vibrations and corresponds to the amide III band of monosubstituted amides. However, the δ(CH) vibration also contributes to this band considerably. Although the spectra of *N*-methylthioacetamides are complicated, it is quite probable that a strong band at 1261 cm^{-1} of the *N*-deuterated species corresponds to the band at 1238 cm^{-1} of CH_3CSND_2 (II) in its nature, which is assigned to the composite vibration of skeletal stretching and deformation. In $CH_3CSNHCH_3$ a vibrational interaction certainly takes place between this skeletal and the δ(NH) modes, and the features of the vibration would resemble those of the amide III band. The amide III band occurs at 1299 cm^{-1} in $CH_3CONHCH_3$, which is about 50 cm^{-1} higher than that of $HCONHCH_3$. If we take the above facts into account, the position of the amide III-like band of $CH_3CSNHCH_3$ is estimated at around 1350 cm^{-1} and probably overlaps the $\delta_s(CH_3)_C$ band. This explains the lowering of the band in the carbon tetrchloride solution*8.

The Skeletal Stretching Vibrations.—As has been pointed out in (II), the values of the force constants, K_{CS}, K_{CC} and $K_{C'N}$, are close to each other, and interactions occur between the ν(C'N), ν(CS) and ν(CC) vibrations. Therefore, the nature of the observed frequencies in the region from 1100 to 800 cm^{-1} becomes complicated. In addition, the $r(CH_3)_N$ and $r(CH_3)_C$ vibrations are also in this region.

Both (C'N) and ν(CS) vibrations take place in the normal modes of 987 and 868 cm^{-1} of

*6 In $HCSNDCH_3$, the bands at ca. 500 and 358 cm^{-1} are assigned, respectively, to the π(ND) and τ(CN) vibrations.

*7 In $CH_3CSNHCH_3$, $(CH_3)_C$ and $(CH_3)_N$ are used to refer to the methyl groups attached, respectively, to the carbon and nitrogen atoms.

*8 The intensity of the band becomes very strong.

$HCSNHCH_3$. The $r(CH_3)$ vibration also contributes to the former vibration. As for the 868 cm^{-1} band, the energy associated with the ν(CS) vibration is about 55% of the total, and so this band may be called the ν(CS) band. In *N*-deuterated species, the δ(ND) vibration should also be taken into account; the bands at 932 and 844 cm^{-1} are assigned to the mixed vibrations of the ν(C'N) and δ(ND), and of the ν(CS) and δ(ND), respectively.

In $CH_3CSNHCH_3$, three strong bands at 1099, 955 and 684 cm^{-1} are assigned to the skeletal stretching vibration. The $r(CH_3)_N$ vibration may also contribute considerably*9 to the 1099 cm^{-1} band. The band at 684 cm^{-1} corresponds to the 718 cm^{-1} band of CH_3CSNH_2 and is certainly associated with the mixed mode of the ν(CS) and ν(CC) vibrations, of which the former is predominant. In *N*-deuterated species, the 956 cm^{-1} band is split into two bands at 990 and 930 cm^{-1}; the δ(ND) vibration probably takes place in both of these vibrations.

The NH Out-of-plane Vibrations. — The π(NH) band is termed the amide V band in secondary amides, and can easily be identified by its broadness and sensitivity to a change in states. In secondary thioamides it also occurs at about 680 cm^{-1} in the liquid state and on solidification moves to a frequency higher by about 60 cm^{-1}. The π(ND) band is found at about 500 cm^{-1}.

The Skeletal Deformation Vibrations.—The band at 600 cm^{-1} of $HCSNHCH_3$ (and of $HCSNDCH_3$) is assigned to one of the skeletal deformation vibrations. The rather high frequency*10 of the deformation vibration is explained by the vibrational coupling of the δ(NCS) and δ(CNC') modes. In this vibration the N–C=S angle increases while the C–N–C' angle decreases, or vice virsa. In other words, it corresponds to a kind of asymmetrical deformation vibration. Therefore, the band corresponding to the "symmetrical" deformation vibration falls at too low a frequency to be detected.

In $CH_3CSNHCH_3$ the bands at 559, 374 and 287 cm^{-1} are assigned to the skeletal deformation vibrations. The 374 cm^{-1} band corresponds to the band at 378 cm^{-1} of CH_3CSNH_2 and is assigned to the δ(CC') vibration, while the other two are assigned to the "asymmetric" δ(NCS) and δ(CNC') and "symmetric" δ(NCS) and δ(CNC') vibrations respectively.

Thus, the complete assignments of two secondary thioamides, $HCSNHCH_3$*11 and $CH_3CSNHCH_3$, have been made from the calculation of the normal vibrations and from the correspondence of the bands between the related molecules. It has been shown that the assignments of the vibration bands can be made by the trans planar model for the molecules. It has also been shown that the Urey-Bradley force constants so far obtained[1,2,5] have an excellent transferability and can be used without any modification of their values.

The author wishes te express his deep gratitudes to Professor Takehiko Shimanouchi for his guidance and encouragement throughout this work. His thanks are also due to Professor Hidetoshi Takahashi for the use of a PC-1 computer.

Department of Chemistry
Faculty of Science
The University of Tokyo
Hongo, Tokyo

*9 The band at 1099 cm^{-1} of $CH_3CSNHCH_3$ probably corresponds to those around 1100 cm^{-1} of thiolactams which are assigned to the ν(CS) vibration[15].

*10 The δ(NCS) vibration usually occurs at about 450 cm^{-1} (I), and the δ(CNC'), at 350 cm^{-1} [5].

15) R. Mecke and R. Mecke Jr., *Ber. deut. chem. Ges.*, 89, 343 (1959).

*11 In the spectrum of $HCSNHCH_3$, there remain two bands unassigned, e. g. the bands at 467 and 920 cm^{-1}. As has been pointed out previously, the vibration associated with the δ(NCS) mode usually occurs about 450 cm^{-1}. Like the band around 600 cm^{-1} found in $HCONHCH_3$[5], this band may be assigned to the δ(NCS) vibration of the cis isomer, in which the interaction between the δ(NCS) and δ(CNC') vibrations is considerably weaker than in the trans form.

*An Attempt to Prepare Linear Chelate Polymers**

By Shunsuke MURAHASHI and Hiroaki KUBOTA

(Received February 16, 1962)

Three new tetraoximes, in which two pairs of glyoxime groups are linked together by hexamethylene, decamethylene or a *p*-phenylene group, have been synthesized. The possible formation of coordinated high polymers by the coordination reaction between these tetraoximes and some metal ions has been studied. In the case of aliphatic tetraoximes, instead of the expected coordinated linear polymers, cyclization was found to have occurred, giving multimembered ring compounds of a low molecular weight. The aromatic tetraoxime also gave coordination compounds, but the product was infusible and insoluble in all solvents tested. Although there was a possibility of obtaining high polymers and the possibility may be considered reasonable from the study of molecular models, the high polymeric nature of the product could not be fully established experimentally.

The main chain of synthetic high polymers is usually linked by covalent bonds. Recently there have appeared in the literature descriptions of some polymeric materials having coordinated bonds with metal ions in the main chain. Such polymeric materials would be of interest from the standpoint of practical importance as well as of academic interest, since they lie on a borderline between organic and inorganic polymers and could be expected to introduce an inorganic character into conventional organic polymers.

Owing to their insolubility in general, there had been no reliable proof of the formation of high polymers before the present authors started their work. The reaction between dimethylglyoxime and the nickel ion has been well studied in chelate chemistry, and the structure of the complex of nickel(II) dimethylglyoximate has been established as having stable coordination bonds in it.

Attempts were made, therefore, on the basis of the above considerations, to prepare linear coordination polymers which would have stable coordination bonds in the main chain and would be easily soluble in organic solvents.

Three new tetraoximes with two symmetrically situated glyoxime groups were synthesized. One has two glyoxime groups connected by a *p*-phenylene group, which will give little flexibility to the main chain of the resulting polymer owing to the rigidity of the *p*-phenylene group. The other two have their oxime groups connected with polymethylene groups of a different number, which will dilute the mutual polar effect of the glyoxime groups and give more or less flexibility. The reaction between these oximes and metal ions, especially the nickel ion, was carried out.

Results

Bis-α-dioximes were synthesized in the following scheme:

$$2CH_3COCH_2COOC_2H_5 + Br(CH_2)_nBr \xrightarrow{C_2H_5ONa} CH_3COCH(CH_2)_nCHCOCH_3$$
$$\qquad\qquad\qquad

The intermediate I, II and III hydroxyiminoketones as well as the IV, V and VI tetraoximes are all new compounds; their infrared spectra are presented in Figs. 1 and 2. The I, II and III compounds have absorption bands for the carbonyl and hydroxy groups at 1640~1680 and at 3200~3400 cm^{-1} respectively. In IV, V and VI, the strong absorption band of the carbonyl group disappeared, and instead a strong and broad band for hydroxyl group was seen at around 3250 cm^{-1}. Many geometrical isomers of each one of the tetraoximes may exist; attempts were made to determine whether the product was a mixture of isomers or not, but only one species, presumably the most stable one, was isolated.

Coordination compounds of tetraoximes with metal ions have been prepared by the reaction of tetraoximes with metal salt in dry dimethylformamide or in an aqueous dimethylformamide solution in the presence of or absence of ammonia. The properties of the coordination compounds are shown in Table I. The oximes were allowed to react with Cu^{2+}, Co^{2+} and Fe^{2+} to yield precipitates of black, dark brown, and brown color respectively, but the reaction medium did not show any appreciable increase in viscosity during the reaction. The coordination compounds with nickel ion were all microscopically amorphous, but the VII and IX complexes showed crystalline X-ray patterns (Figs. 3 and 4).

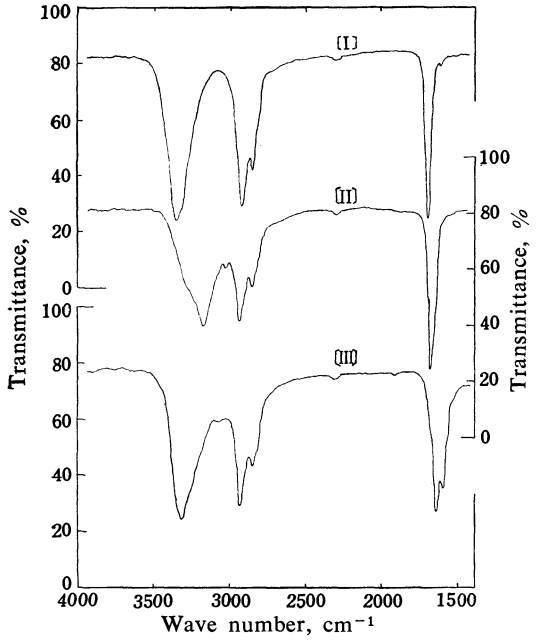


Fig. 1. Infrared spectra of hydroxyiminoketones [I], [II] and [III].

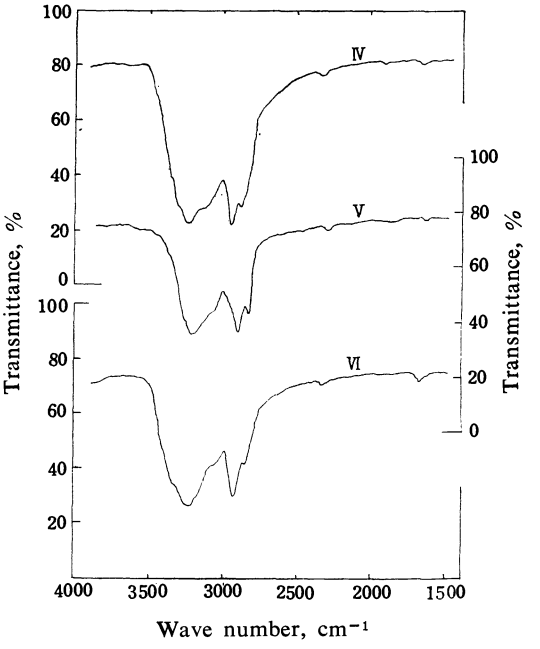


Fig. 2. Infrared spectra of tetraoximes [IV], [V] and [VI].

TABLE I. Ni-CHELATE COMPOUNDS OF THE TETRAOXIMES

Tetraoxime	R in oxime*	Ni-Chelate compound	Appearance	Mol. wt. found.	Solvent	Towards aq. alkali hydroxide
IV	$-(CH_2)_6-$	VII	Orange-red powder	400~600	Sparingly sol. in hot pyridine	Stable
V	$-(CH_2)_{10}-$	VIII	Orange-yellow powder	560~620	Pyridine, hot nitrobenzene. Sparingly sol. in chloroform and hot benzene	Stable
VI	$-C_6H_4-$	IX	Orange-red powder	—	None	Became dark red

* General formula $CH_3-\underset{\underset{NOH}{\|}}{C}-\underset{\underset{NOH}{\|}}{C}-R-\underset{\underset{NOH}{\|}}{C}-\underset{\underset{NOH}{\|}}{C}-CH_3$

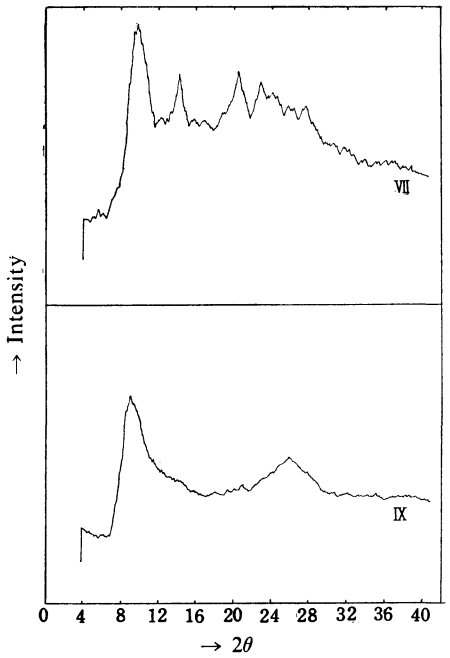


Fig. 3. X-Ray powder spectra (Cu K_α) of [VII] and [IX].

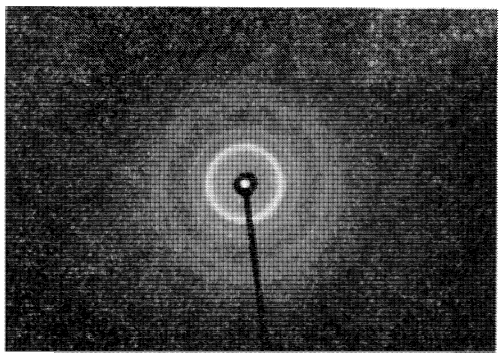


Fig. 4. X-Ray diffraction pattern of (VII). (CuK_α).

The infrared spectra of these coordination compounds are shown in Fig. 5. The broad absorption band of tetraoximes at 3250 cm^{-1} disappeared completely, and new bands appeared at 1560 cm^{-1} in VII and VIII and at 1545 cm^{-1} in IX. There are no indications of the presence of the oxime end-group, and the spectra showed a great resemblance to that of nickel-(II) dimethylglyoximate. Therefore, it may be concluded that the complete coordination of the glyoxime group to the nickel ion took place. A broad and weak band at about 1775 cm^{-1} in the spectra of VII and VIII, and a very weak one in that of IX, may be considered due to hydrogen bonding in the planar coordination structure around the central nickel ion[1]. It may also be deduced that the

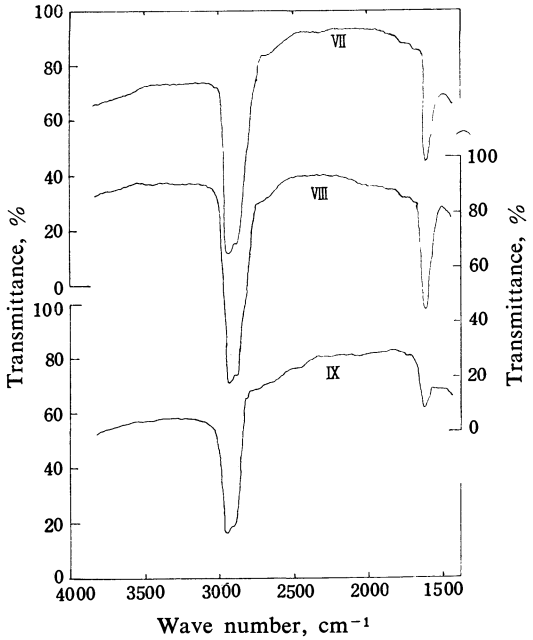


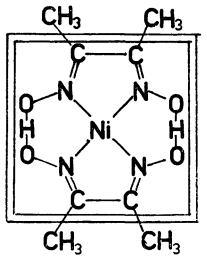
Fig. 5 Infrared spectra of Ni-complexes [VII], [VIII] and [IX].

glyoxime groups coordinated to the nickel ion have the same structure as that of nickel(II) dimethylglyoximate.

Molecular weight measurement by the Rast method, using *p*-phenylphenol or *p*-nitrophenol as the solvent, showed that VII has a molecular weight of about 400 to 610 (empirical formula weight 343) and VIII, of about 560 to 620 (empirical formula weight 399). The molecular weight of IX was not measured because of its insolubility in the solvents.

Discussion

The coordination structure of nickel(II) dimethylglyoximate is known to be planer with the central nickel ion and with the two hydrogen bonds between the two dimethylglyoxime molecules, as is shown below[2].



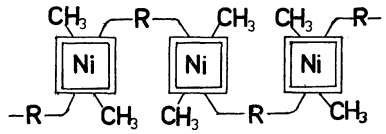
The planer chelate structure of nickel(II) dimethylglyoximate

1) R. E. Rundle and M. Parasol, *J. Chem. Phys.*, **20**, 1487 (1952).
2) L. E. Godycki and R. E. Rundle, *Acta Cryst.*, **6**, 487 (1953).

The planer units are piled up on one another in the crystal. On the basis of the above-mentioned facts, the coordination complexes of the tetraoximes with the nickel ion are considered to have the same chelated structure as that of nickel(II) dimethylglyoximate. Leaving aside the problem of steric effect and the tendency of ring formation, and the possible structures of complexes can be represented as either one or as a mixture of the A, B, C and D forms.

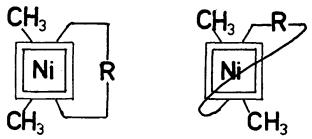
According to the inspection of the Stuart model, the A structure is possible for all the tetraoxime complexes. The B structure is possible only for V, since VII can not take the B structure because of the rigidity of the *p*-phenylene group, nor can IV owing to the shortness of the polymethylene chain. The C structure is probable for IV and V, but is unprobable for VI because of the rigidity of the *p*-phenylene group.

A



Linear polymer

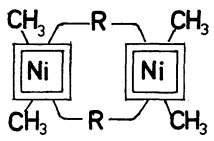
B



cis trans

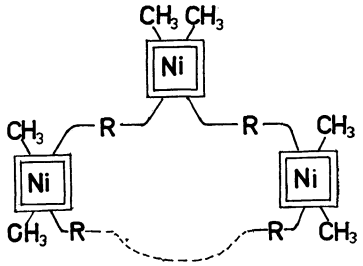
Monomer

C



Dimer

D



Cyclic polymer

Ni = The planer chelate structure with a central nickel atom

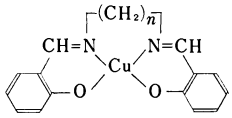
R = $-(CH_2)_6-$ IV

R = $-(CH_2)_{10}-$ V

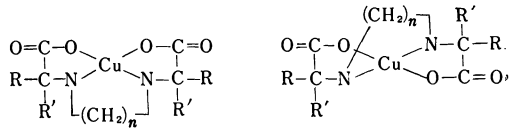
R =  VI

Except for the A structure with end groups, the forms B, C and D have the same composition and can not be distingished from each other by mere chemical analysis. In order to draw a conclusion about the structural assignment, further information must be acquired from a detailed examination of the product or from measurements of molecular weight.

The formation of cyclic low-molecular-weight compounds by condensation polymerization is known to occur in the case of polyamides and polyesters: it depends on the length of the chain unit and is modified by the existence of aromatic rings. Since Carothers and his co-workers explored this problem, a large amount of evidence has been accumulated indicating that, unless the formation of stable 5- or 6-member rings were expected in the reaction, the linear polymerization could occur exclusively. In chelate chemistry, although it is known that the formation of the 5- or 6-membered chelate ring is most feasible, the formation of larger membered rings are, surprisingly, just as feasible. For instance, Pfeiffer and his co-workers were able without difficulty to prepare 7-, 8- and 13-membered compounds X (n=4, 5 and 10 respectively) by the reaction

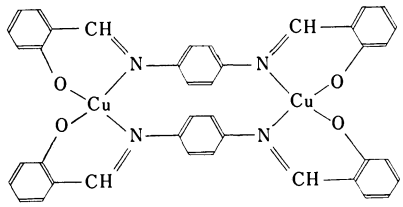


[X] (Pfeiffer)



cis trans

[XI] (Schlesinger)



[XII] (Pfeiffer)

of the cupric ion with bis-salicylaldehyde-polymethylene diimine[3]. The formation of the XI and XII complexs are other examples described by Schlesinger[4] and Pfeiffer[5] respectively. From these facts, it is apparent that

3) P. Pfeiffer et al., *Ann.*, **503**, 804 (1933).
4) N. Schlesinger, *Ber.*, **58**, 1877 (1925).
5) P. Pfeiffer and H. Pitzer, *J. prakt. Chem.*, **145**, 243 (1936).

the relation between the ring formation and the structural unit in the usual linear condensation polymerisation does not hold in the formation of the co-ordination polymer. Therefore, in assigning the reaction product it seems necessary to study carefully what kinds of unit structure have been or will be favorable to form the linear polymer in each type of coordination compound.

The results of molecular weight measurement indicate that the coordination product VII may be either B or C. The infrared spectrum of VII did not show the absorption band for the oxime end-group, pointing to either a B or C structure, or a mixture thereof. From the study of molecular models, however, the VII compound is considered unable to take the monomeric form B because of the short polymethylene chain. Thus, the VII product may be assigned to the dimer C.

The VIII product also did not show the infrared absorption band for the oxime end-group, and so it may have the structure of either the monomeric B or of the C or D. From the determination of the molecular weight, it may considered to be a mixture of types B and C.

The product IX did not show the oxime end-group in the infrared spectrum and showed a little amorphous character in an X-ray diffraction pattern. From the consideration of molecular models, it may be plausible to consider either the IX product has the A (high molecular weight) or D polymeric structure. However, the polymeric nature of the IX product could not be established definitely owing to its insolubility and infusibility.

Experimental

Dodecane-2, 3, 10, 11-tetraone-3, 10-dioxime (I).—Into a solution of 4.6 g. (0.2 atom) of sodium in 60 ml. absolute alcohol was stirred 30 g. (0.23 mol.) of ethyl acetoacetate. Hexamethylene bromide (27 g., 0.11 mol.) was then added slowly for about one hour at about 100°C (bath temperature). The reaction temperature was maintained at about 100°C until the solution became neutral, about 12 to 15 hr. of continuous stirring being required. Ethanol was distilled off from the reaction mixture by heating it up to 140°C, and there was obtained a viscous brown oil containing a white precipitate. To the oil was added just enough water to dissolve the precipitates and the mixture was extracted with ether. The ether layer was washed with water and dried over anhydrous sodium sulfate. Then the ethereal solution was evaporated and the residue was stripped under 5 mmHg until no distillate was obtained by heating it up to 170°C; about 34 g. of brown viscous syrup was obtained.

To the syrup was added a solution of 12 g. (0.3 mol.) sodium hydroxide in 120 ml. water; hydrolysis was effected at room temperature with constant stirring. The heterogeneous mixture was made into a solution in about twenty hours; a clear orange solution was obtained. To this solution was added 16 g. (0.23 mol.) of sodium nitrite, and it was kept below 5°C. An aqueous solution of 10% sulfuric acid was stirred in order to retain the color of potassium iodide-starch paper at least for fifteen minutes.

Aqueous sodium hydroxide was stirred in until all the solid that had separated by the acidification had dissolved. The alkaline solution was extracted with ether to remove any unreacted materials. The alkaline layer was cooled in an ice-salt bath and acidified by stirring in 2 N sulfuric acid. The solid separated by acidification was extracted with ether, producing an orange-red extract. The ether extract was washed with an aqueous 2 N sodium carbonate solution until the aqueous layer became almost colorless. The ether layer was washed with water and dried over anhydrous sodium sulfate. Evaporation of the solvent gave a solid product, which was recrystallized from a mixture of 10 ml. of ether and 120 ml. of benzene to give 9.6 g. of crude, faintly yellow crystals. The crude product was further recrystallized, using active charcoal, to yield 7.8 g. of colorless crystals; m. p., 129.5~131°C (corr.). The overall yield was 22.6%.

Found: C, 56.24; H, 7.73; N, 10.88. Calcd. for $C_{12}H_{20}O_4N_2$: C, 56.23; H, 7.85, N, 10.93%.

The compound I was easily soluble in ether, alcohol, dimethylformamide and pyridine, was soluble in hot benzene, was sparingly soluble in cold benzene and was inslouble in petroleum benzine and petroleum ether. It was soluble in alkali hydroxide solutions, giving a yellow solution, and also a little soluble in concentrated aqueous ammonia, again yielding a yellow solution.

After being heated in a water bath at about 80°C with a nickel salt in an alcohol solution, compound I showed no reaction, but gave, in the presence of ammonia, red precipitates. It gave carbonyl derivatives of hydroxylamine, *p*-nitrophenylhydrazine and semicarbazide. *p*-Nitrophenylhydrazone was soluble in dimethylformamide, pyridine and hot nitrobenzene and was recrystallized from nitrobenzene to give yellow crystals; m. p., 232~233°C (decomp.) (corr.).

Found: N, 21.08. Calcd. for $C_{24}H_{30}O_6N_8$: N, 21.28%.

Dodecane-2, 3, 10, 11-tetraonetetraoxime (IV).—To a mixture of 2.5 g. of I (0.01 mol.), 2 g. of hydroxylamine hydrochloride (0.03 mol.), 1.5 g. of sodium carbonate (0.015 mol.) and 30 ml. of alcohol water was added bit by bit so as to make the mixture clear. The solution was refluxed for more than ten hours and was kept standing overnight. The white precipitates thus formed were filtered and washed with water till no chloride ion were detected. The precipitates were dissolved in 10 ml. of dimethylformamide, and the solution was filtered. Methanol (40 ml.) was then added to the solution and the mixture was kept at room temperature overnight to yield 2 g. of colorless crystals, which decomposed at 250~253°C (corr.). Yield, 70%.

Found: C, 50.39; H, 7.50; N, 19.21. Calcd. for $C_{12}H_{22}O_4N_4$: C, 50.33; H, 7.74; N, 19.57%.

Compound IV was soluble in almost all organic solvents. It was also soluble in an alkali hydroxide solution.

The reaction of IV with Ni^{2+}, Co^{2+} and Cu^{2+} salts in aqueous dimethylformamide solutions immediately gave orange, dark brown and almost black precipitates respectively in the presence of ammonia or alkali hydroxide. In the absence of an alkali catalyst, the reaction took a long time by standing at room temperature and several hours by heating.

Nickel Complex of Dodecane-2, 3, 10, 11-tetra-one-tetraoxime (VII).—Nickel was purified through its hexammine complex. Hexaamminenickel bromide (0.231 g. 0.5 mmol.) was decomposed by boiling it with water until no more evolution of ammonia was detected. A few drops of concentrated hydrochloric acid were added, and the solution was evaporated on a water bath. This procedure was repeated several times, a yellowish-brown residue being obtained. To this residue was added just enough water to dissolve the residue, 2 ml. of dimethylformamide and a few drops of concentrated aqueous ammonia, resulting in a homogeneous solution. A solution of 143 mg. (0.0005 mol.) of IV in 6 ml. of dimethylformamide was added to the solution, an orange precipitates being formed immediately. The mixture was heated on a steam bath for 20 hr. and kept standing overnight. The precipitates were filtered out, washed with hot dimethylformamide to remove the unreacted tetraoxime, with water until no more Ni^{2+} and Cl^- were detected, and finally with methanol, and then dried in vacuo at 100°C to yield 150 mg. (92.6%) of the VII complex of an orange color.

Found: C, 41.90; H, 5.81; N, 16.66; Ni, 17.23. Calcd. for $C_{12}H_{20}O_4Ni$: C, 42.05; H, 5.88; N, 16.34; Ni, 17.11%.

The compound showed neither a definite melting point nor a decomposition point. Upon being heated over 300°C in a capillary tube, it changed to a black powder. It was slightly soluble in hot pyridine to give an orange-red solution, was sparingly soluble in nitrobenzene and was insoluble in a wide variety of organic solvents. It was insoluble in 4 N sodium hydroxide and was decomposed with 6 N sulfuric acid and formic acid, but it was not attacked by boiling acetic acid.

Hexadecane-2, 3, 14, 15-tetraone-3, 14-dioxime (II).—The preparation was carried out in the same way as that of compound I. From 4.6 g. of sodium (0.2 atom.), 100 ml. absolute alcohol, 30 g. of ethyl acetoacetate and 33 g. of decamethylene bromide (0.11 mol.), 40 g. of the condensation product was obtained. Hydrolysis of the condensation product and the following formation of oxime gave a crude product, II, which was recrystallized from a benzene-ether mixture to give colorless crystals; m. p., 138~139°C (corr.). The overall yield was 5.4 g. (17.2%).

Found: C, 61.63; H, 8.85; N, 8.87. Calcd. for $C_{16}H_{28}O_4N_2$: C, 61.51; H, 9.03; N, 8.97%.

The compound was soluble in alcohol, ether and hot benzene and sparingly soluble in cold benzene, but it was insoluble in petroleum benzine or in petroleum ether. The behavior of this compound was similar to that of I.

Hexadecane-2, 3, 14, 15-tetraone-tetraoxime (V).—Preparation of this compound was carried out in the same way as that of IV. The yield of oximation was 88%; m. p., 240~242°C (corr.).

Found: C, 56.40; H, 8.70; N, 16.07. Calcd. for $C_{16}H_{30}O_4N_4$: C, 56.12; H, 8.83; N, 16.36%.

Compound V was soluble in dimethylformamide, in pyridine, and in hot nitrobenzene, but insoluble in a wide variety of other organic solvents.

Reactions of V with Ni^{2+}, Co^{2+} and Cu^{2+} salt in an aqueous dimethylformamide solution gave orange, dark brown and black precipitates respectively when heated for several hours, or immediately in the presence of ammonia.

Nickel Complex of Hexadecane-2, 3, 13, 14-tetra-one-tetraoxime (VIII).—The preparation was carried out in the same way as that of VII, except that the mixture was kept for a week at room temperature (93.3% yield).

Complex VIII was an orange yellow powder, showing no melting point. When heated, it sintered at about 165°C and changed to a black solid at from 220 to 360°C.

Found: C, 48.60; H, 6.93; N, 14.07; Ni, 14.77. Calcd. for $C_{16}H_{28}O_4N_4Ni$: C, 48.15; H, 7.07; N, 14.04; Ni, 14.71%.

Complex VIII was hydrophobic and soluble in pyridine, yielding an orange-red solution. In hot nitrobenzene it became paste-like at first and, after a long time of heating, dissolved to give an orange-red solution. In chloroform, it became paste-like but was sparingly soluble, forming a faintly yellow solution. It was insoluble in a wide variety of other organic solvents.

It was decomposed with formic acid at room temperature, but it was stable with acetic acid.

Terephthaloyl Chloride.—This compound, obtained by heating the mixture of powdered phosphorus pentachloride and terephthalic acid, recrystallized from ligroin in the form of colorless needles; m. p., 81~82°C (93% yield).

***N, N, N', N'*-Tetraethyl Terephthalic Diamide.**—The compound was synthesized from terephthalyl chloride and diethylamine by Schotten-Baumann reaction in benzene. It was recrystallized from benzene in the form of colorless crystals; m. p., 128~129°C (127°C in the literature[6]) (88.5% yield).

***p*-Dipropionylbenzene.**—The compound was obtained by the method of Maxim from *N, N, N', N'*-tetraethylterephthalodiamide and ethylmagnesium bromide in ether, with the by-product of 4-propionylbenzodiethylamide. The yield was 56.5% in the form of colorless crystals; m. p., 102.5~103.5°C (corr.) (100°C in the literature[7]).

Found: C, 75.83; H, 7.42. Calcd. for $C_{12}H_{14}O_2$: C, 75.76; H, 7.27%.

Dioxime was prepared in the usual manner and was recrystallized from alcohol in the form of colorless crystals; m. p., 226~228°C (corr.).

Found: C, 65.45; H, 7.28; N, 12.10. Calcd. for $C_{12}H_{16}N_2O_2$: C, 65.43: H, 7.32; N, 12.72%.

***p*-Bis(1, 2-dioxopropyl)benzene-2, 2'-dioxime (III).**—*p*-Dipropionylbenzene (5.7 g., 0.03 mol.) was

6) N. Maxim, *Ann. Chim.*, [10] **9**, 66.
7) N. Maxim, *Compt. rend.*, **184**, 690 (1927).

dissolved in 60 ml. of dry benzene, and then dry hydrogen chloride and dry methyl nitrite were introduced to the solution, the temperature being kept below 50°C by constant stirring. The reaction mixture was left standing overnight. The mixture was shaken vigorously after the addition of 60 ml. of water. The precipitates formed were filtered, washed thoroughly with water, dried, and then boiled with 20 ml. of benzene and filtered again. The crude product was recrystallized from aqueous alcohol to give 4.8 g. of colorless needles (64.6% yield).

Found: C, 58.11; H, 4.44; N, 11.06. Calcd. for $C_{12}H_{12}O_4N_2$: C, 58.06; H, 4.87; N, 11.29%.

Compound III was soluble in dimethylformamide, tetrahydrofuran, boiling alcohol and boiling ether. It was also soluble in aqueous alkali hydroxide and slightly soluble in aqueous concentrated ammonia, yielding an yellow solution. It did not show any reaction with Ni^{2+} salt in a hot alcohol solution after 8 hr., but, in the presence of ammonia, it formed dark brown precipitates.

p-Bis(1, 2-dioxopropyl)benzene-tetraoxime (VI).—The tetraoxime was prepared by refluxing a mixture of 2.1 g. (0.03 mol.) of hydroxylamine hydrochloride, 1.5 g. (0.015 mol.) of sodium carbonate, and 1.2 g. (0.015 mol.) of *p*-bis(1,2-dioxopropyl)-benzene-2,2'-dioxime in aqueous alcohol for 30 hr. The crude tetraoxime was dissolved in hot dimethylformamide and precipitated by adding methanol, yielding 0.46 g. of colorless crystals, which did not show any melting point (40% yield).

Found: C, 51.77; H, 4.83; N, 19.61. Calcd. for $C_{12}H_{14}O_4N_4$: C, 51.79; H, 5.07; N, 20.14%.

The compound was soluble in hot dimethylformamide and in hot pyridine.

Nickel Complex Compound of *p*-Bis(1, 2-dioxopropyl)benzene-tetraoxime (IX).—The chelate compound of VI with nickel ion was prepared in the same way as that of VII, an orange-red powder being obtained. The unreacted tetraoxime was removed from the product by extraction with hot dimethylformamide. The yield was 83%. Compound IX did not show any melting point or definite decomposition point up to 360°C; it darkened at about 260°C and changed to a black powder at about 300°C.

Found: C, 42.61; H, 3.85; N, 15.96; Ni, 17.72. Calcd. for $C_{12}H_{12}O_4N_4Ni$: C, 43.03; H, 3.61; N, 16.73; Ni, 17.52%.

The compound was insoluble in a wide variety of organic solvents and even in hot phenol, hot nitrophenol and *p*-phenylphenol. It was decomposed by 6 N sulfuric acid and by formic acid at room temperature, but it was not decomposed by boiling acetic acid. It is a marked difference of this complex from the other two that it was slowly attacked by 4 N sodium hydroxide to give a dark red solution.

The authors wish to thank Dr. M. Huggins for his interest in their work during his stay at their University in 1956.

Department of Polymer Science
Faculty of Science
Osaka University
Kita-ku, Osaka

Relations between the Degree of Orientation and the Conditions of the Deposition of Pyrolytic Graphite

By Tokichi NODA, Michio INAGAKI and Hajime KATO

(Received February 23, 1962)

Pyrolytic graphite is produced by the thermal decomposition of a carbonaceous gas. Recently, this graphite has attracted considerable attention and has been widely studied because it possesses many interesting physico-chemical properties. In a number of investigations concerning pyrolytic graphite, it has been found that its electrical, thermal, and mechanical properties are extremely different from those of ordinary graphitized products. Its tensile strength along a deposition surface is about ten times higher than that of ordinary graphitized products[1], and its strength-to-weight ratio is the highest of all high-temperature materials[2]. This graphite has a high density and a high impermeability to gases. In addition, it is more resistant to oxidation. Its thermal and electrical conductivities are strongly anisotropic, higher in a plane parallel to the deposition surface than in a plane perpendicular to it, because the crystallites in pyrolytic graphite are highly oriented in placing their layer-planes parallel to the deposition surface. It can be said that many interesting physico-chemical properties of pyrolytic graphite are largely dependent upon the orientation of the crystallites. However, the direct

1) H. E. Martens and J. D. Jaffe, *J. Appl. Phys.*, **31**, 1122 (1960).

2) Anon., *Industrial Heating*, **27**, 593 (1960).

measurement of the orientation for pyrolytic graphite had not yet been carried out. Therefore, the present work was carried out to discover the relations between the degree of orientation and the conditions of the deposition, such as the rate of flow of hydrocarbon gas and the temperature of the deposition. The degree of orientation was directly measured by means of the X-ray diffraction method. The graphitizability of pyrolytic graphite is also discussed on the basis of X-ray diffraction profiles.

Experimental

Preparation of Pyrolytic Graphite. — Pyrolytic graphite was prepared by passing gaseous hydrocarbons on the heated surface of an electrographitized carbon rod. The rod was 9 mm. in diameter and had a reduced central part 9 mm. wide, 1 mm. thick and 60 mm. long; it was placed in a bell-jar type metallic chamber. The rod was heated by the passage of electric current directly through it, and the temperature of the surface of the reduced part was measured with the aid of an optical pyrometer. The pressure of gas in the chamber was measured with a mercury manometer, and the rate of gas flow, with a flowmeter. The gas used was a commercial propane gas which was a mixture of light hydrocarbons, such as propane, propyrene, butane, and butene. After the chamber had been evacuated, the propane gas was admitted at a constant rate of gas flow—45, 115, 330, 665 or 1110 cc./min., and then the rod was heated to the desired temperature of deposition—1600, 1800, 2000, 2200 or 2400°C. The heating of the rod was performed in a moment. Deposition was carried out at a constant temperature of the deposition surface and at a constant rate of gas flow until the deposited graphite had thickness enough.

The Anisotropy Factor and the X-Ray Diffraction Profile.—The orientation function, $I(\phi)$, of graphite crystallites in a specimen was obtained from a (002) diffraction ring[3] taken by using unfiltered CuK radiation. In order to make a specimen, the deposited graphite was sliced in the direction perpendicular to the deposition surface.

The orientation anisotropy factor (σ_{oz}/σ_{ox}) proposed by Bacon[3] can be calculated as

$$\sigma_{oz}/\sigma_{ox}=2\cdot\frac{\int_0^{\pi/2}I(\phi)\cdot\cos^2\phi\cdot\sin\phi\cdot d\phi}{\int_0^{\pi/2}I(\phi)\cdot\sin^3\phi\cdot d\phi} \quad (1)$$

The orientation functions of all slices could well be approximated to curves of $\cos^n\phi$, that is to say, $I(\phi)=\cos^n\phi$. Therefore, Eq. 1 can be reduced to

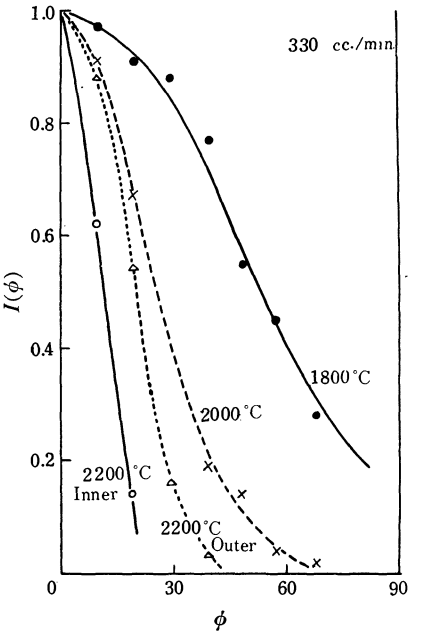
$$\sigma_{oz}/\sigma_{ox}=n+1 \quad (2)$$

The profiles of the (002) or (004) diffraction of the deposited graphites were obtained by using a recording diffractometer.

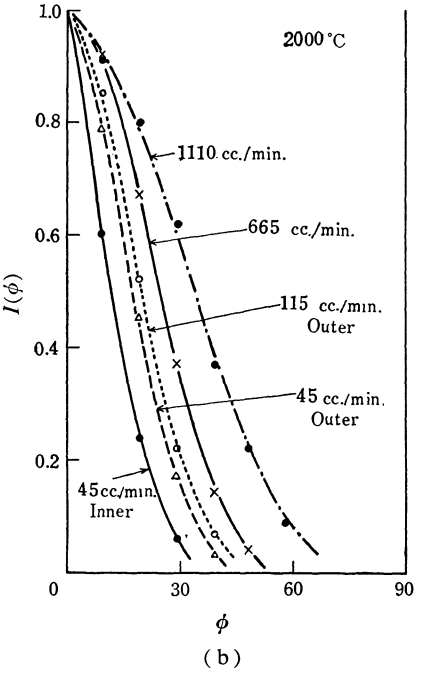
3) G. E. Bacon, *J. Appl. Chem.* (*London*)., **6**, 477 (1956).

Results and Discussion

Relations between the Anisotropy Factor and the Conditions of Deposition.—The orientation functions of the deposited graphites, which were produced at a constant rate of gas flow, i. e., 330 cc./min., and at various temperatures of deposition, are shown in Fig. 1a. The

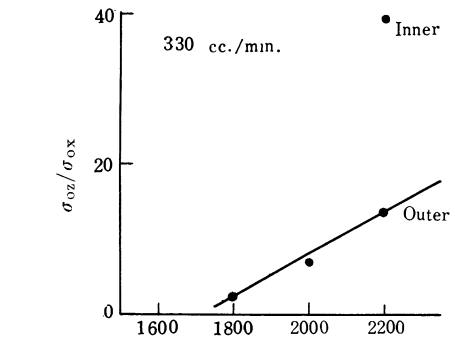


(a)

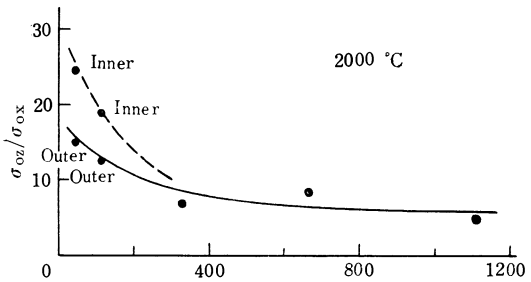


(b)

Fig. 1. Orientation functions of pyrolytic graphites.



(a)



(b)

Fig. 2. Anisotropy factors (σ_{oz}/σ_{ox}) of pyrolytic graphites.

anisotropy factor, which was calculated from the orientation function, is shown in Fig. 2a as a function of the temperature of deposition. From the two figures, it can be seen that the degree of crystallite orientation in the pyrolytic graphite increases with the increase in the temperature of deposition and that the anisotropy factor is directly proportional to the deposition temperature between 1800 and 2400°C, when the anisotropy factor is taken as a measure of the crystallite orientation. Brown and Watt[4] reported that the electrical resistivity of pyrolytic graphite decreases in the direction parallel to the deposition surface and increases in the direction perpendicular to it as the temperature of deposition rises. This strong dependence of the electrical resistivity on the temperature of deposition has been explained on the assumption that the graphite crystallites are more highly oriented as the temperature of deposition increases. In the present work, this assumption is experimentally verified by the direct measurement of the orientation.

The orientation functions of deposited graphites which were produced at a constant temperature, i. e., 2000°C, and at various rates of gas flow are shown in Fig. 1b. The variation of the anisotropy factor with the rate of gas flow is shown in Fig. 2b. On the basis of the two figures, it can be said that the degree of crystallite orientation increases and that, accordingly, the anisotropy factor becomes larger as the rate of gas flow decreases.

A cross-section of the deposited graphite, which was produced at a temperature above 2000°C, consisted of two or three layers. These layers were easily distinguishable from one another on the basis of their lusters. An inner layer, which was closer to the graphite substrate, had more metallic luster than an outer one.

The anisotropy factor of an inner layer was found to be larger than that of an outer one. These large anisotropy factor values of the inner layer have never been found in ordinary graphitized products[3,5]. It has been previously reported, however, that graphite crystallites in carbon which had been obtained by vacuum evaporation were highly oriented with their layer-planes parallel to the evaporated surface and that the degree of orientation increased with the increase in the temperature of the heat-treatment[6].

X-Ray Diffraction Profiles.—As is shown in Fig. 3, almost all the (002) or (004) diffraction profiles of the deposited graphites have been found to be asymmetrical and to be apparently composed of two kinds of profiles, whose values of c_0 are 6.72 and 6.86Å. Similar phenomena have been observed with charcoals heat-treated at various temperatures[7,8]. The similarity of the asymmetrical diffraction profile of pyrolytic graphite to that of charcoal is of great interest in regard to their graphitization.

Diefendorf reported that soot particles, produced in a gas phase by the thermal decomposition of methane, were incorporated in pyrolytic graphite when the pressure of the gas was above 5 mmHg[9]. The observed asymmetry of the diffraction profile of the pyrolytic graphite may be caused by the incorporation of these soot particles.

The profile of an inner layer of the deposited graphite was sharply defined, and its c_0 value was 6.71~6.72Å; i. e., the inner layer of the deposited graphite was highly graphitized. Because the crystallites were strongly oriented, the thermal conductivity in a direction perpendicular to the deposition surface was very

4) A. R. G. Brown and W. Watt, "Industrial Carbon and Graphite", Society of Chemical Industry, London (1958), p. 85.

5) T. Noda and M. Inagaki, *J. Chem. Soc. Japan, Ind. Chem. Sec.* (*Kogyo Kagaku Zasshi*), **62**, 1300 (1959).

6) T. Noda and H. Matsuoka, ibid., **64**, 2083 (1961).

7) T. Noda, M. Inagaki and N. Fusisawa, ibid., **64**, 1370 (1961).

8) R. E. Franklin, *Proc. Roy. Soc.*, **A209**, 196 (1951).

9) R. J. Diefendorf, *J. Chim. Phys.*, **4**, 815 (1960).

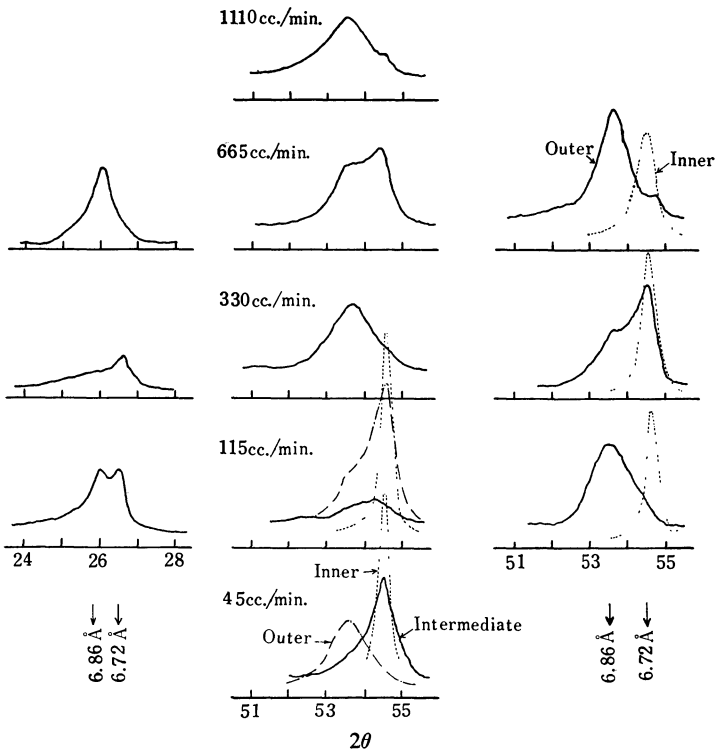


Fig. 3. X-Ray diffraction profiles of pyrolytic graphites.

low[2] and a large temperature gradient seemed to be produced in the deposited graphite. Therefore, it is thought that the temperature of an inner layer is higher than that of the deposition surface.

Petroleum coke is the most easily graphitizable carbon of all raw carbon materials, but the c_0 value of one sample of petroleum coke (Greate Lake Co.) was not less than 6.718Å, even when it was heat-treated at 3400°C[7]. It has also been reported that vacuum-evaporated graphite had a c_0 value of 6.710Å when it was heat-treated at 2800°C under atmospheric pressure[6]. The inner layer of pyrolytic graphite had a c_0 value of 6.71~6.72Å. It can be said that a carbon in which graphite crystallites are strongly oriented, such as pyrolytic graphite and evaporated graphite, is much more graphitizable than ordinary raw carbon materials, for instance, coke and carbon black.

Summary

Pyrolytic graphites were deposited on carbon rods by the thermal decomposition of a commercial propane gas at various temperatures and at various rates of gas flow. The orientation functions of the graphite crystallites in the deposited graphites were measured by means of the X-ray diffraction method. It was shown that the degree of orientation in the deposited graphites increased with the increase in the temperature of deposition and decreased with the increase in the rate of gas flow. The graphites deposited at temperatures above 2000°C were composed of two layers; the inner layers had a larger degree of orientation and a higher graphitizability than the outer layers. Almost all the (0 0 l) diffraction profiles of the deposited graphites were found to be asymmetrical and to the apparently composed of two kinds of profiles, whose c_0 values were 6.72 and 6.86Å.

Department of Applied Chemistry
Faculty of Engineering
Nagoya University
Chikusa-ku, Nagoya

An NBMO Method for Saturated Compounds

By Kenichi Fukui, Hiroshi Kato and Teijiro Yonezawa

(Received March 12, 1962)

By the use of the extremely simple character of the nonbonding molecular orbital (NBMO) method, explanations have been offered of some physico-chemical properties of conjugated systems, for instance, the chemical reactivity, radical stability, and the basicity[1,2].

In the present paper, we will apply this method to σ electron systems. Consider, for example, a fission of a C–C or a C–H bond in a saturated hydrocarbon molecule (or vice versa, a recombination of the two corresponding radicals). It may be reasonable to assume in the first place that an "unpaired" sp^3 hybridized orbital of carbon* might appear just after the fission (or just before the recombination). Our previous papers[3,4] treated the saturated compounds by the simple LCAO MO method. This can also be applied to those compounds with an unpaired sp^3 hybridized orbital. In these compounds with an odd electron, the highest half-occupied orbital has an energy nearly equal to that of the Coulomb integral of an sp^3 hybridized orbital of a carbon atom (α). We will attempt to discuss the bond strength and the reactivity of the saturated compounds by using the characteristic regularity of the electron distribution in this half-occupied orbital. For the sake of simplicity, the compounds with an unpaired "σ" hybridized orbital are hereafter represented by the notation** R–, while the highest half-occupied molecular orbital is referred to as the "σ NBMO". The R– compounds treated in the present paper are CH_3–, C_2H_6–, n-C_3H_7–, n-C_4H_9–, i-C_3H_7–, t-C_4H_9– and so on. At the same time, the compounds which have an unpaired sp^2 hybridized orbital such as C_2H_3(vinyl)– and C_6H_5(phenyl)–, are also treated, together with those having an sp^3 unpaired orbital, since the procedure of calculation is common to both classes of compounds.

* The unpaired hybridized orbital stands for the AO of the carbon atom, which does not participate into the C-C or C-H bonding.

1) H. C. Longuet-Higgins, *J. Chem. Phys.*, **18**, 283 (1950).

2) M. J. S. Dewar, *J. Am. Chem. Soc.*, **74**, 3357 (1952).

3) K. Fukui, H. Kato and T. Yonezawa, This Bulletin, **34**, 442 (1961).

4) K. Fukui, H. Kato and T. Yonezawa, ibid., **34**, 1111 (1961).

** R– should be discriminated from the species usually represented by R·, in which the reorganization of the odd electron may in general have already taken place.

The Electronic Energy Levels and the Electron Distribution in R– Compounds

The calculations are carried out by the simple LCAO MO method, including all bonding atomic orbitals in the saturated compounds[3,4]. Hence, the calculated molecular orbital energies of the occupied orbitals of R– compounds are obtained in terms of $\lambda_i = \varepsilon_i - \alpha/\beta$, in which α is the Coulomb integral of sp^3 (or sp^2 in, e. g., the C_6H_5–) hybridized orbital of a carbon atom and β is the resonance integral between the sp^3 (or sp^2) orbitals of the adjacent carbon atoms. These values are listed in Fig. 1, together with those of the corresponding parent RH compounds. The calculated energies of σ NBMO (λ_N) and the electron distributions of the σ NBMO in these R– compounds are shown in Fig. 2.

The following conclusions can be derived from these results:

1) The energy value of σ NBMO in R– compounds is nearly equal to α. It may be observed in Fig. 1 that one σ-MO localized at the C–H bond in the parent RH compound disappears and that an NBMO appears in the R– compound. The energy difference between the corresponding occupied orbitals of the R– and RH compounds is very small.

2) The odd electron of the σ NBMO is largely located in the unpaired hybridized orbital, the odd electron density at this orbital being nearly equal to unity, while those of the other hybridized orbitals are alternately equal to zero and the value of the non-zero density rapidly decreases with the distance from the unpaired hybridized orbital. This implies that the R– compounds are very unstable and that the most reactive position is that of the unpaired hybridized orbital.

3) The odd electron density of the unpaired hybridized orbital in various R– compounds decreases in the order CH_3– > C_2H_5– > n-C_3H_7– > n-C_4H_9– > i-C_3H_7– > i-C_4H_9– > t-C_4H_9–. The density values are listed in Table I, along with the energy values of the σ NBMO.

According to the conclusions stated above, one can say that the energy of the σ NBMO is nearly equal to α, as it was in the π NBMO, whereas the mode of the odd electron distribution in the σ NBMO shows a remarkable

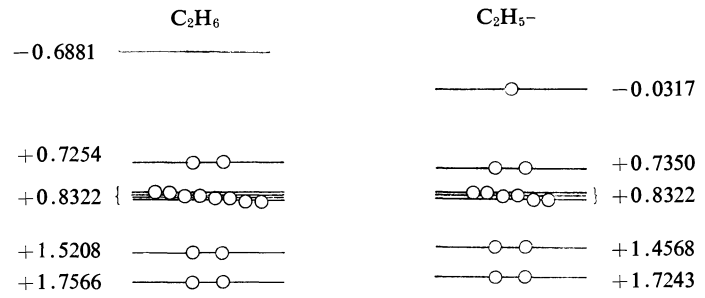


Fig. 1. The relation of energy levels of occupied orbitals between C_2H_6 and C_2H_5-.

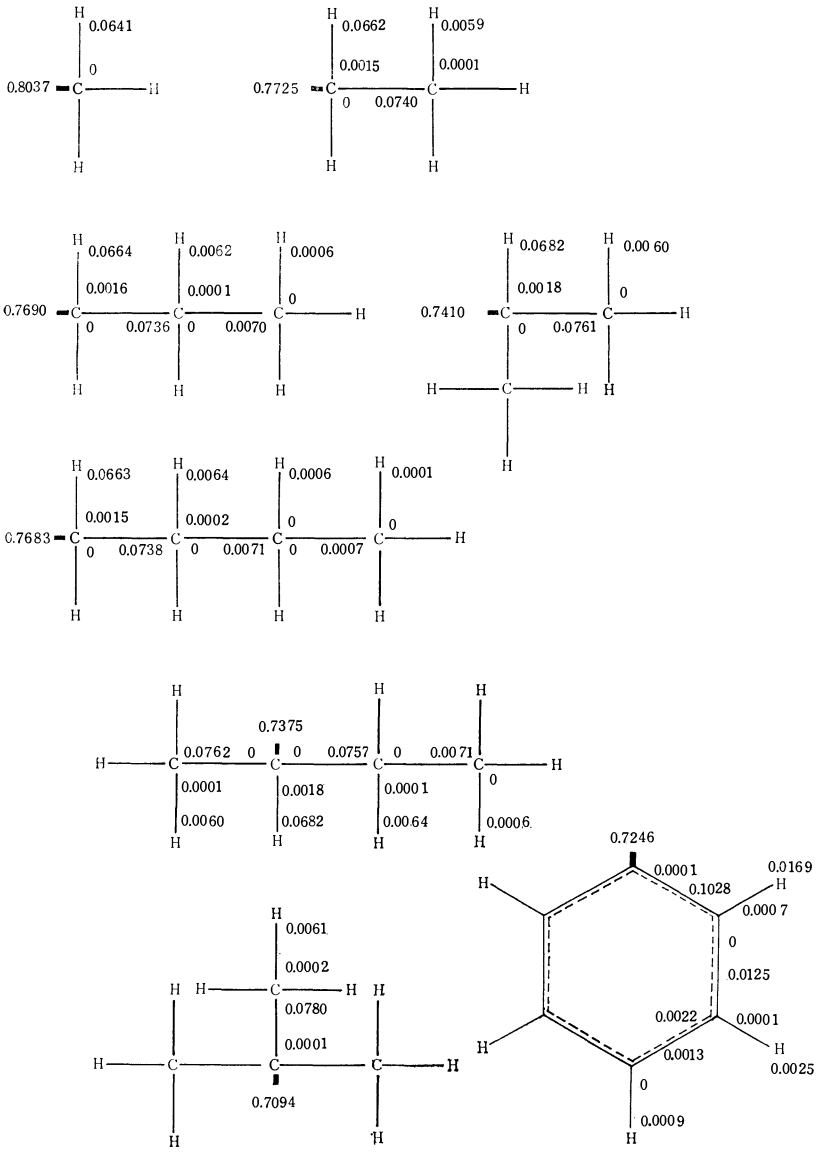


Fig. 2. The odd electron distributions in the σ NBMO of some R- compounds.

difference from that of the π NBMO; i.e., the former localizes and the latter does not (see appendix). In the following sections, it will be shown that the reactivity of alkyl compounds and the bond strength of C–C bonds in saturated compounds can be discussed by means of the extremely simple calculations based upon the properties of the σ NBMO.

The Reactivity Indecis Derived from the σ NBMO Method

In this section, some indecis for the chemical reactivity of saturated compounds are derived by means of the σ NBMO method. It may be worthwhile to recollect here that the activation energy of the reaction in the frontier electron theory has been discussed in terms of the stabilization energy at the transition state. Once the stabilization energy, ΔE, can be obtained, the activation energy, E, is written in the form:

$$E=C-\Delta E \tag{1}$$

in which C is a constant denoting the repulsive term due to the interaction between the reactant and the reagent[2,5]. For a definite type of reaction, it may be assumed that C is a constant and that E is determined only by the difference in the magnitude of ΔE.

In some types of reactions of saturated compounds, the stabilization of the σ-electronic energy, ΔE_σ, may easily be obtained by the σ NBMO method in the following way:

Abstraction Reaction.—The abstraction reaction in saturated compounds is represented by the following formula:

$$RX+Y\cdot \rightarrow [R\text{—}X\cdots Y] \rightarrow R\cdot+XY$$

where RX is a saturated compound and Y· is an odd electron system. In this case, ΔE_σ is given by

$$\Delta E_\sigma=2\left(\sum_j^{occ}\sum_i^{unocc}-\sum_i^{occ\text{-}N}\sum_j^{unocc}\right)\times\frac{(C_r^j)^2(C_s^i)^2}{\lambda_j(RX)-\lambda_i(Y)}+\left(\sum_j^{occ}-\sum_j^{unocc}\right)\times\frac{(C_r^j)^2(C_s^N)^2}{\lambda_j(RX)-\lambda_N(Y)} \tag{2}$$

(in units of $\gamma(-\beta)$)

in which C_r^j and C_s^j are the coefficients of the r-th atomic orbital in the j-th molecular orbital of the RX molecule and of the s-th atomic orbital in the i-th molecular orbital of the reagent Y·; N denotes the half-occupied molecular orbital of Y; $\lambda_j(RX)$ is the energy of the j-th molecular orbital of the RX compound, and $\lambda_i(Y)$ is that of the i-th molecular orbital of Y: compound respectively. The unit is $\gamma(-\beta)$, which represents the absolute value of the resonance integral between the two NBMO's, X and Y. Since it may reasonably be considered that the radical Y· is converted to the Y– form in the transition state, λ_N is nearly equal to zero and the values of $(C_s^N)^2$ are larger than those of $(C_s^i)^2(N\neq i)$. Thus, the first term in Eq. 2 can be ignored, since this should be much smaller than the second term. In this way, we obtain a simplified formula of ΔE_σ as

$$\Delta E_\sigma\cong D_r^{(R)}(C_s^N)^2 \tag{3}$$

in which $D_r^{(R)}$ is nothing but what we called "delocalizability", derived for the radical reaction of saturated compounds in our previous paper[4],*. That is, ΔE_σ is the reactivity index obtained by considering the interaction explicitly between the σ orbitals of the reactant molecule and the attacking radical.

Radical or Ionic Recombination Reaction.—A similar procedure is applicable when discussing the easiness of the reactions which are covered by the following general equation:

$$R+X \rightarrow [R\cdots X] \rightarrow RX$$

In this equation, the type of reaction may be classified as follows according to the number of electrons occupying the σ NBMO of R and X:

1. One electron each exists in both the NBMO's, R and X (R·+X· → RX: radical recombination).
2. Two electrons in the NBMO of R, and none in the NBMO of X, or vice versa ($R^-+X^+\rightarrow RX$ or $R^++X^-\rightarrow RX$: ionic recombination).

It may be considered that both R and X have one σ NBMO each in the transition state. If we can ignore the energy difference between the two σ NBMO's**, ΔE_σ can be obtained by the first order perturbation theory. Hence, ΔE_σ for all the cases stated above may be simply given as follows:

$$\Delta E_\sigma=2|C_r^N C_s^N| \text{ (in unit of } \gamma(-\beta)) \tag{4}$$

In the series of reactions in which X does not change, the coefficient C_s^N is a constant, so ΔE_σ is proportional only to $|C_r^N|$.

Radical or Ionic Dissociation Reaction.—Consider a dissociation reaction proceeding:

5) T. Yonezawa, K. Hayashi, C. Nagata, S. Okamura and K. Fukui, *J. Polymer. Sci.*, **14**, 312 (1954).

* Delocalizability, $D_r^{(R)}$, for the radical reaction was defined by the following formula[4]:

$$D_r^{(R)}=\sum_j^{occ}\frac{(C_r^j)^2}{\lambda_j}+\sum_j^{unocc}\frac{(C_r^j)^2}{-\lambda_j}$$

** In general, the energies of the two -NBMO's of R and X are not exactly the same. Both of these levels, however, lie very close to α, so that it might be possible to ignore the difference.

$$RX \rightarrow [R\cdots X] \rightarrow R+X$$

In this case we also assume that both the R and X compounds have a σ NBMO each in the transition state. The magnitude of ΔE_σ is shown to be a measure of the activation energy. Namely, the activation energy, E, of the reaction is given by

$$E=\varepsilon(R\cdots X)-\varepsilon(RX) \qquad (5)$$

where $\varepsilon(R\cdots X)$ and $\varepsilon(RX)$ denote the total energy of R···X and RX respectively. Equation 5 may be written in another form as:

$$E=\{E(R\cdots X)-E(R+X)\} -\{E(RX)-E(R+X)\} \qquad (6)$$

As was pointed out in the last section, the first term is put equal to $(C-\Delta E_\sigma)$. The term in the second parenthesis may become $(C-\Delta E'_\sigma)$ so long as one considers that the energy $E(RX)$ may be deemed an extreme of $E(R\cdots X)$ and that the stabilization due to the covalent interaction between R and X may be proportional to ΔE_σ, resulting from an incipient bond*. Therefore, the prime of ΔE_σ indicates that the resonance integral $(\gamma\beta)$ between R and X has a very large value. Let it be $\gamma'\beta$.

Based on these considerations, we can conclude that the activation energy of the dissociation reaction may be proportional to the difference between $\Delta E'_\sigma$ and ΔE_σ as

$$E=F_{rs}\simeq\Delta E'_\sigma-\Delta E_\sigma\simeq 2|C_r^N C_s^N| \quad \text{(in units of } |(\gamma'-\gamma)(-\beta)|) \qquad (7)$$

in which F_{rs} is σ new index representing the relative strength of the bond (rs).

In the present simplified treatment, the activation energy of the dissociation reaction does not vary according to whether it takes place in the radical or in the ionic mechanism. From this equation it is found that the larger the stabilization in the formation of the incipient bond between R and X, the less easily does the dissociation of the compound RX into R and X proceed.

Results and Discussion

Hydrogen Abstraction Reaction.—The reaction, $RH+R'\cdot \rightarrow R\cdot+R'H$, has also been discussed in our previous paper in terms of the reactivity indecis $f_r^{(R)}$ and $D_r^{(R)}$[3,4]. On that occasion we discussed the comparison of the reactivity of various RH's against a common R'· radical, so the energetical contribution of the attacking radicals was not taken into account. The new reactivity index, ΔE_σ, in Eq. 2, which has been derived by considering both the reactant molecule and the reagent with a σ NBMO in the transition state, enables us also to compare, e. g., the reactivity of RH against various alkyl-radicals. In Table II, the calculated values of ΔE_σ and $D_r^{(R)}$ for the hydrogen abstraction of saturated hydrocarbons are listed, together with values of the observed activation energy, E (kcal./mol.)[6]. In Fig. 3, the values of ΔE_σ are plotted against those of E. The linearity between the calculated and the observed values is seen; therefore, the value of $|C_r^N|$ in ΔE_σ for radical reactions may be said to reflect the reactivity of the alkyl radical.

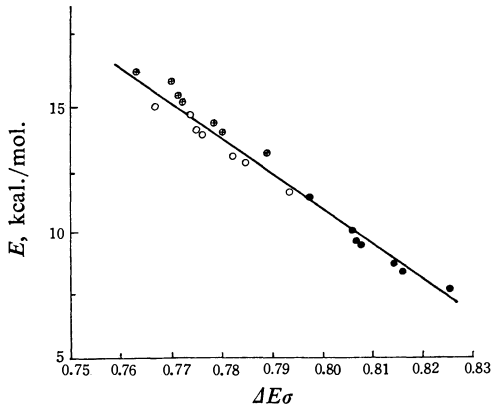


Fig. 3. The activation energy, E, of the reaction $RH+R'\cdot\rightarrow R\cdot+R'H$ vs. $\Delta E_\sigma=D_r^{(R)}(C_s^N)^2$.

Ionic Reaction.—The ionic dissociation reaction of saturated compounds is represented by the general formula $RX\rightarrow R^+ + X^-$, where X is, e. g., a halogen atom or a OH group. The quantity, F_{rs}, in Eq. 7 is adopted as the reactivity index of this type of reaction, assuming that the energy of the half-occupied orbital appearing in the X group in the transition state is nearly equal to α. Referring to the absolute value of the coefficient of the σ NBMO of various R– compounds, $|C_r^N|$, the order of easiness of dissociation of alkyl groups is predicted as follows:

$$CH_3 < C_2H_5 < n\text{-}C_3H_7 < n\text{-}C_4H_8 < i\text{-}C_3H_7 < i\text{-}C_5H_{12} < t\text{-}C_4H_9$$

In Fig. 4, the values of the heat of the gas-phase ionic dissociation of alkyl derivatives[7] are plotted against the $|C_r^N|$ values of the alkyl groups. Here, the upper oblique line corresponds to the dissociation reaction of ROH, the lower one, to that of RCl. In Fig. 5, the values of the heat of the reaction of the $RH\rightarrow R^+ + H^-$ type are plotted against

* It may be allowed to consider that repulsion term in RX does not differ so much from that in R···X.

6) N. N. Tikhomirova and V. V. Voevodski, *Chem. Abstr.*, **45**, 9940 (1951).

7) A. Streitwiesser, *Chem. Revs.*, **56**, 571 (1956).

TABLE I. THE CALCULATED VALUES OF ODD ELECTRON DENSITY OF UNPAIRED HYBRIDIZED ORBITAL AND THOSE OF NBMO ENERGY OF SOME R- COMPOUNDS

Compound		$(C_r^N)^2$	λ_N
CH_3-	—	0.8037	−0.0415
C_2H_5-	Primary	0.7725	−0.0317
n-C_3H_7-	Primary	0.7690	−0.0308
n-C_4H_9-	Primary	0.7683	−0.0308
$(CH_3)CCH_2$-	Primary	0.7604	−0.0288
i-C_3H_7-	Secondary	0.7410	−0.0219
i-C_4H_9-	Secondary	0.7375	−0.0211
i-C_5H_{11}-	Secondary	0.7340	−0.0202
t-C_4H_9	Tertiary	0.7094	−0.0129
$(C_2H_5)(CH_3)_2C$-	Tertiary	0.7051	−0.0114

TABLE II. THE CALCULATED VALUES OF $D_r^{(R)}$ (H) AND $\Delta E_\sigma = D_r^{(R)}(H)\cdot(C_s^N)^2$ AND THE EXTRACTION REACTION OBSERVED VALUES OF ACTIVATION ENERGY, E (kcal./mol.), FOR HYDROGEN EXTRACTION REACTION OF SEVERAL SATURATED HYDROCARBONS

Compound		Attacking radical					
		$CH_3\cdot$		$C_2H_5\cdot$		*n*-$C_3H_7\cdot$	
	$D_r^{(R)}$	ΔE_σ	E	ΔE_σ	E	ΔE_σ	E
CH_3-H	0.9926	0.7978	11.5	0.7668	15.0	0.7633	16.6
C_2H_5-H	1.0029	0.8060	10.0	0.7747	14.8	0.7712	16.2
n-C_3H_7-H	1.0037	0.8067	9.5	0.7754	14.2	0.7718	15.5
n-C_4H_9-H	1.0040	0.8072	9.3	0.7758	13.9	0.7723	15.3
$(CH_3)_2CHCH_2$-H	1.0049	0.8076	—	0.7763	—	0.7728	—
$(CH_3)_2CH$-H	1.0135	0.8146	8.7	0.7829	13.3	0.7794	14.5
$CH_3CH_2(CH_3)CH$-H	1.0152	0.8167	8.2	0.7849	12.7	0.7813	14.1
$(CH_3)_3C$-H	1.0268	0.8254	7.7	0.7933	11.6	0.7898	13.4

TABLE III. THE CALCULATED VALUES OF C-C BOND STRENGTH AND *G*-VALUES OF RADIOLYSIS IN HEXANE ISOMERS

Hexane isomer	Bond	Calculated bond energy kcal./mol.	F_{rs}	Observed *G*-values
C(1)–C(2)–C(3)–C–C–C	1	82.4	1.572	0.2
	2	80.2	1.540	0.55
	3	80.2	1.538	0.45
C(1)–C(2)(C)–C(3)–C(4)–C	1	80.2	1.524	0.6
	2	78.1	1.510	1.6
	3	80.2	1.532	—
	4	82.4	1.560	—
C(1)–C(2)–C(3)(C)–C–C	1	82.4	1.546	—
	2	78.1	1.496	1.2
	3	80.2	1.526	0.5
C(1)–C(2)(C)–C(C)–C	1	80.2	1.534	0.2
	2	76.0	1.482	1.2
C(C)–C(1)–C(2)–C(3)	1	78.1	1.514	0.8
	2	76.0	1.480	3.9
	3	82.4	1.566	—

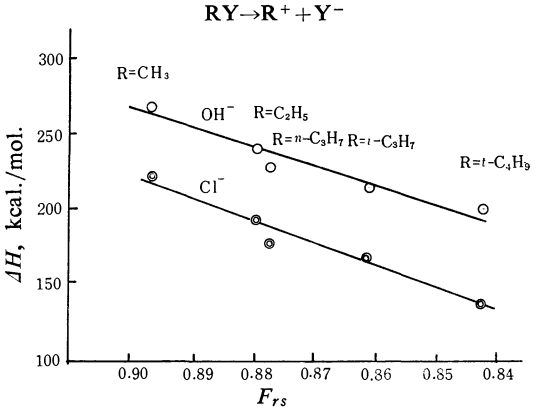


Fig. 4. The heat of reaction, ΔH, of gaseous ionic dissociation of alkyl compounds vs. $F_{rs}=\text{const}\times|C_r^N|$.

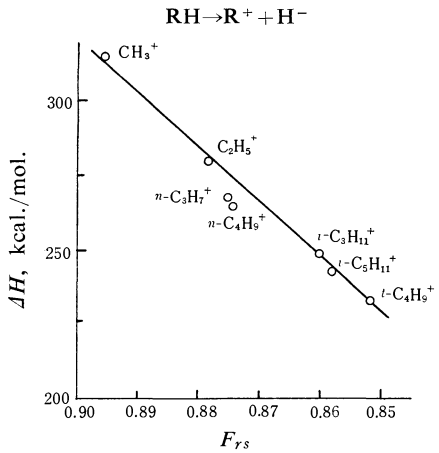


Fig. 5. The heat of reaction, ΔH, in the ionic dissociation of paraffins vs. $F_{rs}=\text{const}\times|C_r^N|$.

those of the $|C_r^N|$ values of various alkyl groups. The parallelism between the observed and the calculated values is obvious.

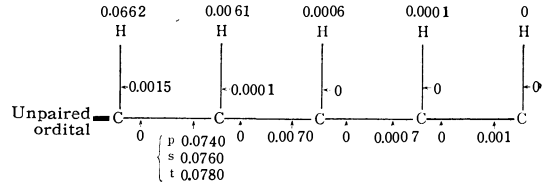
C–C Bond Fission.—How to obtain easily the strength of the C–C bond of a hydrocarbon molecule is a problem of interest not only from a theoretical but also from a practical point of view. The fission of a C–C bond is in general represented by

$$R\text{–}S \rightarrow R + S$$

in which R and S are alkyl groups. Using the σ NBMO method, we can easily obtain from Eq. 7 the activation energy of a C–C fission which we can adopt as a measure of the relative strength of the C–C bond. Namely,

$$F_{rs}=2|C_r^N C_s^N|$$

in which F_{rs} is the relative strength of the bond (rs) of the parent molecule. The calculated values of F_{rs} to each C–C bond in the isomeric hexanes are listed in Table III, together



(The notations p, s, and t stand for the cases where the carbon atom having the unpaired hybridized orbital is a primary, a secondary, and a tertiary carbon, respectively.)

Fig. 6. Diagram of approximate distribution of odd electron density of saturated hydrocarbons.

with the calculated bond energies[8] and the observed G-values obtained by radiolysis[9]. The parallelism between the calculated and the observed results is good. The calculated values of $|C_r^N|$ are obtained by means of the approximate values of odd electron distribution, as shown in Fig. 6, which is estimated by the regularity, as shown in Fig. 1. In Fig. 7, two calculated values[10] for the squalane molecule ($C_{30}H_{62}$) are given. The agreement between the calculated and the observed results[10] is almost entirely on satisfactory. From the two examples stated above, one can see that the F_{rs} index is a good and extremely simple index for the relative strength of a C–C bond.

The next problem is the catalytic cracking of hydrocarbons. Consider the decomposition of a carbonium ion represented by

$$R_1^+ \rightarrow R_2^+ + \text{olefin}$$

Several examples of this type of reaction are as follows:

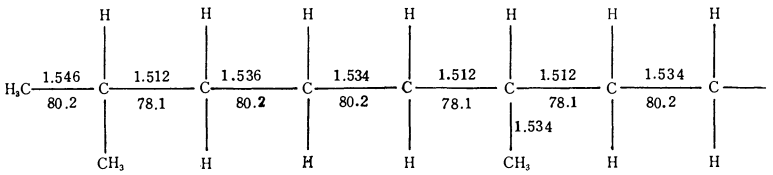
1 $R\text{–}CH_2\text{–}CH_2^+ \rightarrow R^+ + C_2H_4$

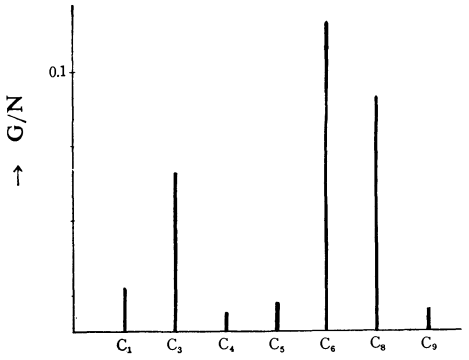
2 $R\text{–}CH_2\text{–}CH^+\text{–}CH_3 \rightarrow R^+ + C_3H_6$

3 $R\text{–}CH(CH_3)\text{–}C^+(CH_3)\text{–}CH_3 \rightarrow R^+ + i\text{-}C_4H_9$

In this case, the observed energy of the bond fission, ΔH (kcal./mol.)[11], is expected to be parallel to the value of F_{rs}, provided that one can assume the appearance of two σ NBMO's at the R_r–C_s bond in the transition state. In each series, 1, 2 and 3, of the reactions indicated above, the olefin molecule produced is the same, so the value of F_{rs} is proportional to the $|C_r^N|$ value of R only. In Fig. 8, the calculated $|C_r^N|$ values of R and the observed values of ΔH are given for the sake of comparison.

8) K. Fueki and K. Hirota, *J. Chem. Soc. Japan, Pure Chem. Sec.* (*Nippon Kagaku Zassi*), **77**, 985 (1956).
9) H. A. Dewhurst, *J. Am. Chem. Soc.*, **80**, 5607 (1958).
10) H. Yamazaki and S. Shida, *J. Chem. Phys.*, **33**, 950 (1960).
11) T. Amamiya, "Sekiyu Kagaku", Sangyo Tosho, Tokyo (1959), p. 131.





Number of carbon
(N is the number of equivalent bonds)

Fig. 7. The calculated values of F_{rs} and bond energy (kcal./mol.)[10], the observed G-values for irradiated squalane molecule.

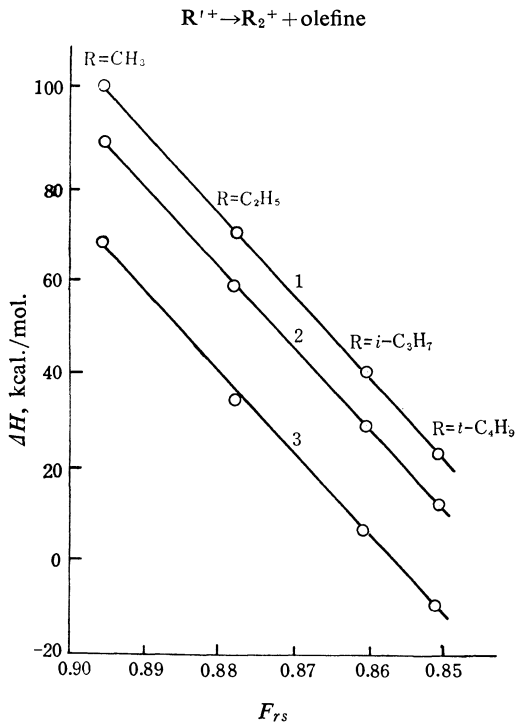


Fig. 8. The heat of reaction, ΔH, of C-C bond fission in alkyl cations vs. $F_{rs}=\text{const}\times|C_r^N|$ at the bond rs in R'^+ to be cloven.
1 $R\text{-}CH_2\text{-}CH_2^+ \rightarrow R^+ + C_2H_4$
2 $R\text{-}CH_2\text{-}CH^+\text{-}CH_3 \rightarrow R^+ + C_3H_6$
3 $R\text{-}CH_2\text{-}C^+(CH_3)\text{-}CH_3 \rightarrow R^+ + C_4H_8$

β-Fission Rule.—The C–C bond, β, to the charged carbon atom in an alkyl cation is often selectively cloven. This phenomenon is well known as the β-fission rule. This rule is satisfactorily explained by the relative bond strength of F_{rs}. That is, in the actual species of an alkyl ion or an alkyl radical, the hybridization of the carbon atom in question may be changed from sp^3 to sp^2. The odd electron distribution of some alkyl, i. e., $\overset{*}{C}H_2$–, $\overset{*}{C}H_2CH_2$– and $\overset{*}{C}H_2CH_2CH_2$–, are calculated by using the parameters of the sp^3 and sp^2 hybridized orbitals for the carbon atom designated by *[12]. The calculated results are shown in Fig. 9. For a long straight chain hydrocarbon, the $|C_s^N|$ coefficient of the unpaired hybridized orbital in the σ NBMO of the radical R′ appearing as the result of the fission of the rs bond $|C_s^N|$ (see the figure below) is almost independent of the position s. Hence, the relative C–C bond strength of these * compounds is measured by the $|C_r^N|$ values with respect to the C–C bond in question.

$$\underbrace{\overset{*}{C}H_2\text{–}CH_2\cdots CH_2}_{R}\overset{r\ \ s}{\text{——}}\underbrace{CH_2\cdots\cdots CH_3}_{R'}$$

These results are summarized in Fig. 10, where it is observed that the value of $|C_r^N|$ is the smallest at the β bond to the carbon atom

12) K. Fukui, H. Kato, T. Yonezawa, K. Morokuma, I. Imamura and C. Nagata, This Bulletin, 35, 38 (1962).

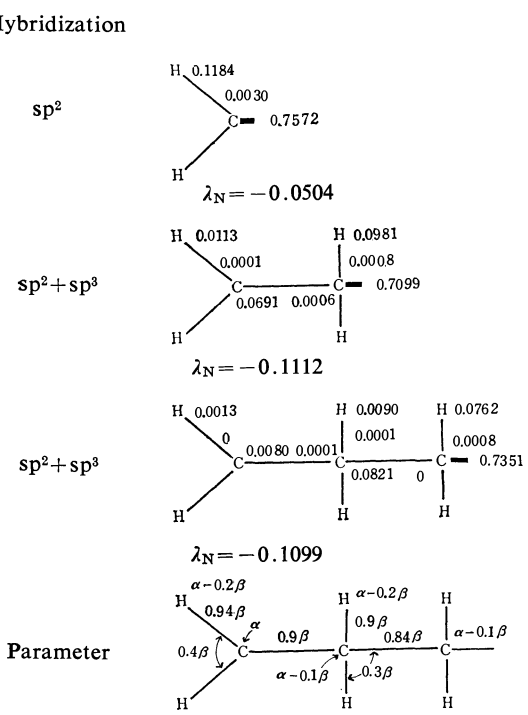


Fig. 9. The odd electron distribution of the σ NBMO in sp^2 or (sp^2+sp^3) systems and the values of parameter used.

designated by *. It is thus found that the β C–C bond becomes the weakest owing to the change in the hybridization of the * carbon atom.

This procedure will also be applied to treating the β fission problem of alkyl aromatics.

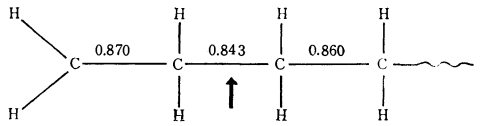


Fig. 10. The mode of β-C–C bond fission. The calculated values of $F_{rs}=\text{const}\times|C_s^N|$ in (sp^2+sp^3) systems.

A part of the calculation has been carried out on a KDC-I digital computer at Kyoto University.

Faculty of Engineering
Kyoto University
Sakyo-ku, Kyoto

Appendix

The tendency toward the degradation of the odd electron density becomes more apparent when R-compounds are treated by the C–C skeleton method[13,14]. That is to say, in this more simplified procedure the energy value of the σ NBMO is just equal to α[14], as it is in the NBMO of π electron systems, while in the case of straight chain R-compounds, the coefficients of the hybridized orbitals in the σ NBMO are alternately equal to zero, those of non-zero orbitals being given by $-ma$, $+m^2a$, $-m^3a$, $+m^4a$ and so forth, as is seen in Fig. 11. (m is the coefficient of the resonance integral between sp^3 hybridized orbitals of the same carbon atom.) The odd electron distribution in the more complex R- compounds can be obtained by means of this simplified procedure. The results are given in Fig. 12. The odd electron densities at the unpaired hybridized orbital of primary, secondary and tertiary carbon atoms decrease in the order

$$(C_r^N)^2_{prim} > (C_r^N)^2_{sec} > (C_r^N)^2_{tert}$$

which is in accordance with the results obtained in Section I.

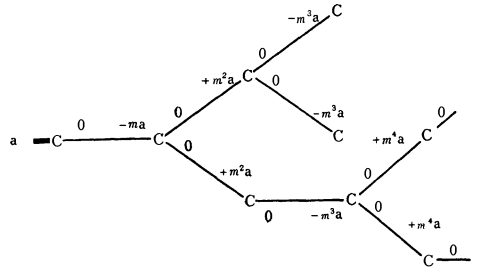


Fig. 11. The coefficients of sp^3 hybridized orbitals in the σ NBMO of an R- compound obtained by the C-C skeleton method.

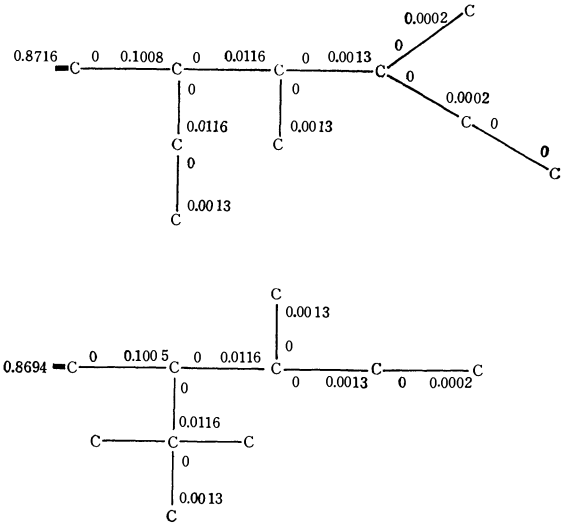


Fig. 12. The odd electron distribution of the σ NBMO calculated by the C-C skeleton method.

13) K. Fukui, H. Kato and T. Yonezawa, This Bulletin, 33, 1198 (1960).
14) H. Yoshizumi, *Trans. Faraday Soc.*, 53, 125 (1957).

A Molecular Orbital Treatment of cis- and trans-Dichloroethylenes

By Shinhachiro SAITO*

(Received March 15, 1962)

It is well known that, for the 1,3-butadienes, the trans isomer is more stable than the cis isomer. Parr and Mulliken[1] have carried out SCF MO[2] calculations for the π electrons of these molecules, confirming this view theoretically.

Dichloroethylenes are a special case in that the cis isomer has the lower energy. This fact has been investigated by many authors[3] on the basis of thermodynamic or vibrational data. Pitzer and Hollenberg[3] suggested that the anomalous stability of the cis isomer of dichloroethylene is associated with the unlike charges between those on the Cl atom for the cis isomer and for the trans isomer. For *cis*- or *trans*-dichloroethylene, no LCAO SCF treatment such as Parr and Mulliken's has ever been made. In the present paper, LCAO SCF MO calculations of the π electrons in their ground state are undertaken. The double bond characters, the ionization potentials and the energy difference between cis and trans isomers are discussed in comparing the results with experimental data.

Ground State Orbitals and Energy

The internuclear distances and the bond angles of *cis*- and *trans*-dichloroethylenes, based on microwave or electron diffraction data, are given in the literature[4,5]. They are listed in Table I. In these calculations, it has been assumed that the cis and the trans isomer have the same internuclear distances and the same bond angles. The properly-averaged numerical values based upon Table I are as follows: the skeletones Cl–C–C′–Cl′ are planar; Cl–C–C′ and C–C′–Cl′ angles, 122°; C–C′ distances, 1.38 Å; C–Cl and C′–Cl′ distances, 1.69 Å, as is shown on the last line of Table I and in Fig. 1. These values are consistent with the experimental data in Table I; also permit us to appropriate the integrals given in the literature[6] to these calculations. Bray and Barnes[7] have shown, in their nulear quadrupole resonance study of multichlorobenzenes, that, in *o*-dichlorobenzene, the out-of-plane bending of the C–Cl bonds causes an increase in the double-bond character. If the same is true for *cis*-dichloroethylene, the ground state orbitals and energy may also be affected by the out-of-plane bending of the C–Cl bond. Therefore, a trial calculation are carried out for a staggered form* (see Fig. 2) of cis isomer at the same time with the planar cis and the trans isomer. The penetration, exchange and hybrid integrals, which are not seen in the literature, have been evaluated by the use of a uniformly-charged sphere model[6,8] and of

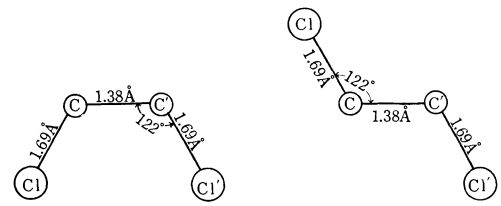
TABLE I. BOND DISTANCES AND BOND ANGLES FOR *cis*- AND *tras*-DICHLOROETHYLENE[a]

Form	Method	d_{C-C} Å	d_{C-Cl} Å	∠C=C-Cl
Cis	(E. D.)*	1.38	1.67	123.5°
	(M. S.)**	1.32	1.70	121°.33′
Trans	(E. D.)	1.38	1.69	122.5°
The adopted values for both forms in this work		1.38	1.69	122.0°

* (E. D.) is abbreviation of the method of electron diffraction.

** (M. S.) is abbreviation of the method of microwave spectra.

a) See Refs. 4 and 5.



Cis form (planar) Trans form (planar)

Fig. 1

* Present address: The Research Institute for Iron, Steel and Other Metals, Tohoku University, Katahira-cho, Sendai.

1) R. G. Parr and R. S. Mulliken, *J. Chem. Phys.*, **18**, 1338 (1950).

2) J. C. C. Roothan, *Rev. Mod. Phys.*, **23**, 69 (1951).

3) R. E. Wood and D. P. Stevenson, *J. Am. Chem. Soc.*, **63**, 1650 (1941); K. S. Pitzer and J. L. Hollenberg, ibid., **76**, 1493 (1954); Bernstein and Ramsay, *J. Chem. Phys.*, **17**, 556 (1949); Bernstein and Pullin, *Can. J. Chem.*, **30**, 963 (1952).

4) R. Wirel, *Ann. Physik*, **13**, 453 (1932); J. Y. Brockway et al., *J. Am. Chem. Soc.*, **57**, 2693 (1935).

5) T. Shimizu and H. Takuma, *J. Phys. Soc. Japan*, **15**, 646 (1960).

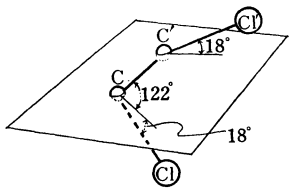
6) M. Simonetta, G. Favini and S. Carra, *Mol. Phys.*, **1**, 181 (1958).

7) P. J. Bray, R. G. Barnes and R. Bersohn, *J. Chem. Phys.*, **25**, 813 (1956).

* In this case, the overlap in the C-Cl bond is evaluated by the following equation (see Ref 7):

$$<\pi_C/\pi_{Cl}>\cos^2 18° + <\pi_C/\pi_{Cl}>\sin^2 18°$$

8) R. Pariser and R. G. Parr, ibid., **21**, 466 (1953).



Cis form (staggered)

Fig. 2

TABLE II

Overlap integrals (dimensionless)

	Cis	Trans	Cis 18°
$S_{CC'}$	0.266	0.266	0.266
S_{CCl}	0.166	0.166	0.182
$S_{CCl'}$	0.022	0.022	—*
$S_{ClCl'}$	0.006	0.000	—*

Penetration integrals (in eV.)

	Cis	Trans
Cl' : CCl = Cl : C'Cl'	0.024	0.043
Cl : CCl' = Cl' : C'Cl	0.015	0.018
C : ClCl' = C' : ClCl	0.001	0.000
Cl' : ClCl' = Cl : ClCl'	0.090	0.005

The symbolism for the integrals adopted here is the same as in the Refs. 1 and 6.

* These values were assumed to be the same as that of cis planer form.

Mulliken's approximation[9]. The overlap integrals are calculated by the equation given by Mulliken et al.[10] Except for the integrals referred to in the literature[1,6], the estimated values of integrals are listed in Table II. Prior to SCF calculations, the starting orbitals were calculated by the simple LCAO MO method. In these calculations, the Coulomb integrals of the chlorine atoms (denoted by α_{Cl}) were evaluated by Coulson's prescription[11], and the resonance integrals between the C and the Cl atom, β_{C-Cl}, were evaluted by Wheland's expression[12]:

$$\alpha_{Cl}-\alpha_C=(X_{Cl}-X_C)\beta_{cc}$$
$$\beta_{C-Cl}=(S_{C-Cl}/S_{cc})\beta_{cc}$$

where X_{Cl} and X_C are the electronegativities of the Cl and the C atoms, and S_{C-Cl} and S_{cc}, the overlap integrals of the C–Cl and C–C' bonds respectively. The molecular orbitals were obtained as follows:

$$\left.\begin{aligned}
\phi_1&=0.4024(\chi_{Cl}+\chi_{Cl'})+0.5815(\chi_C+\chi_{C'})\\
\phi_2&=0.6612(\chi_{Cl}-\chi_{Cl'})+0.2506(\chi_C-\chi_{C'})\\
\phi_3&=0.5815(\chi_{Cl}+\chi_{Cl'})-0.4024(\chi_C+\chi_{C'})\\
\phi_4&=0.2506(\chi_{Cl}-\chi_{Cl'})-0.6612(\chi_C-\chi_{C'})
\end{aligned}\right\} \quad (1)$$

After eight trials using these orbitals, the four orthonormal SCF orbitals, ϕ_i, and the corresponding energy levels, ε_i, were found as follows:

$$\left.\begin{aligned}
\phi_1&=\begin{Bmatrix}0.2117\\0.2357\\0.2436\end{Bmatrix}(\chi_{Cl}+\chi_{Cl'})+\begin{Bmatrix}0.5688\\0.5585\\0.5518\end{Bmatrix}(\chi_C+\chi_{C'})\\
\phi_2&=\begin{Bmatrix}0.6636\\0.6614\\0.6575\end{Bmatrix}(\chi_{Cl}-\chi_{Cl'})+\begin{Bmatrix}0.1893\\0.1900\\0.1975\end{Bmatrix}(\chi_C-\chi_{C'})\\
\phi_3&=\begin{Bmatrix}0.6828\\0.6772\\0.6750\end{Bmatrix}(\chi_{Cl}+\chi_{Cl'})-\begin{Bmatrix}0.2876\\0.3072\\0.3224\end{Bmatrix}(\chi_C+\chi_{C'})\\
\phi_4&=\begin{Bmatrix}0.2786\\0.2781\\0.2984\end{Bmatrix}(\chi_{Cl}-\chi_{Cl'})-\begin{Bmatrix}0.8157\\0.8154\\0.8168\end{Bmatrix}(\chi_C-\chi_{C'})
\end{aligned}\right\} \quad (2)$$

where the upper value of the coefficients are for the trans-, the middle for planar cis-, and the lower for the staggered cis- form respectively. The orbital energies for the six π-electrons in the field of the core are (in eV.):

ε_1	cis	−18.2491
	trans	−18.5648
	cis(staggered)	−18.5445
ε_2	cis	−12.2857
	trans	−12.0196
	cis(staggered)	−12.3744
ε_3	cis	−10.1897
	trans	− 9.0793
	cis(staggered)	− 9.4966
ε_4	cis	− 6.6847
	trans	− 6.6423
	cis(staggered)	− 7.1360

while the π-electron densities on the chlorine atoms, denoted by q_{Cl}, and the bond order of C–Cl bond, P_{C-Cl}, are:

q_{Cl}	cis	1.9113
	trans	1.9109
	cis(staggered)	1.9032
P_{C-Cl}	cis	0.2854
	trans	0.2860
	cis(staggered)	0.2995

Discussion

In comparing Eqs. 1 and 2, we can see that the results obtained by the simple LCAO MO method agree qualitatively with those resulting from the LCAO SCF calculations.

Although many assumptions are included in the SCF calculations, agreement between the calculated (ε_3) and the experimental (cis: 9.61[13] or 9.66[14]; trans: 9.91[13] or 9.96[14]) values of the ionization potential is fairly good.

As has been shown in the introductory part, the energy of the cis isomer is lower than that

9) R. S. Mulliken, *J. Chim. Phys.*, **46**, 675 (1946).
10) R. S. Mulliken, C. A. Rieke, D. Orloff and H. Orloff, *J. Chem. Phys.*, **17**, 1248 (1949).
11) C. A. Coulson, "Valence", Oxford University Press, London (1952), p. 242.
12) G. W. Wheland, *J. Am. Chem. Soc.*, **64**, 900 (1942).
13) T. M. Sugden, A. D. Walsh and W. C. Price, *Nature*, **148**, 372 (1941).
14) A. D. Walsh, *Trans. Faraday Soc.*, **41**, 35, 76 (1945).

of the trans isomer. It is generally known that one cannot expect the energy difference between the cis and the trans isomer quantitatively with the results of the ground state energy obtained from the MO treatment mentioned above. However, for a comparison with the experimental data, the energy difference between the cis and the trans isomers is thus estimated from the ground state total π-electron energy, E_n, by the method used by Parr and Mulliken for *cis*- and *trans*-butadienes:

$$E_n \text{ (trans)} - \left\{ \begin{matrix} E_n\text{(cis) or} \\ E_n\text{(cis, staggered)} \end{matrix} \right\} \approx 11 \text{ eV}.$$

This is surprising when compared with experimental data[3], but the calculated sign agrees with the experimetal data in that the cis isomer is more stable than the trans isomer.

The numerical values of the bond order P_{C-Cl} show that the double-bond character in the cis isomer is nearly equal to that of the trans isomer, and that the P_{C-Cl} for the staggered cis form is larger than those of the planar isomers. On the other hand, the nuclear quadrupole coupling constants[15] of the ^{35}Cl atom in the solid cis isomer are smaller than those in the solid trans isomer.

If the ionic character and the *s* character[16] in the chlorine atoms are the same for both molecules, and if the C−Cl bond of the cis isomer is to be staggered from the molecular plane in the solid state, such as in Fig. 2, the difference in the nuclear quadrupole coupling constants of the cis and trans isomers (cis: 70.00 (average), trans: 71.16) may be explained in terms of the difference in the double-bond character of the two molecules.

The author wishes to express his thanks to Dr. Siro Maéda of the Defense Academy, with whom he has been able to discuss this work.

Department of Chemistry
Defense Academy
Yokosuka

15) R. Livingston, *J. Phys. Chem.*, **57**, 496 (1952).
16) C. H. Towns and B. P. Dailey, *J. Chem. Phys.*, **17**, 782 (1949).

The Formation of Acetylenic Bond by the Elimination Reaction of Some Enol-esters. I. Syntheses of Enol-esters

By Masazumi NAKAGAWA, Gen NAKAMINAMI, Fumio OGURA and Hiroshi ONO

(Received March 20, 1962)

In recent years the wide distribution of various kinds of polyacetylenic compounds in the plant kingdom was well recognized[1], and considerable attention has been directed towards the mode of the formation of such a labile molecule containing a large amount of energy in a living cell. The most plausible one among the proposed several hypotheses[2] seems to be the dehydration mechanism of an enol of a β-dicarbonyl compound by way of a suitable

$$RCOCH_2COR' \rightarrow RC(OX)=CHCOR' \rightarrow RC\equiv CCOR'$$

enol derivative. This hypothesis has been supported indirectly by recent biochemical evidence which was obtained by the ^{14}C tracer technique[3].

Quite recently, Jones has suggested that the decarboxylative elimination of pyrophosphate anion from the pyrophosphate of acetylmalonyl coenzyme A is a possible route in the formation of an acetylenic bond in vivo[4], and the mechanism has been supported experimentally by the formation of phenylpropiolic acid from enol-brosylate of diethyl benzoylmalonate in an alkaline medium[5]. But the full explanation of the Jones' hypothesis and the detail of the experimental support are not ready for our hands.

Independently we have carried out the experimental confirmation of the formation of triple bond by simple elimination reaction of several enol-esters. The present paper deals with the synthesis of some enol-esters and the formation of acetylenic compounds from them will be reported in the following papers.

1) For review on this field, see, F. Bohlmann, *Angew. Chem.*, **67**, 389 (1955); E. R. H. Jones, *Proc. Chem. Soc.*, **1960**, 199; N. A. Sörensen, ibid., **1961** 98.

2) J. D. Bu'Lock, *Quart. Revs.*, **10**, 371 (1956).

3) J. D. Bu'Lock and H. Gregory, *Biochem. J.*, **72**, 322 (1959); J. D. Bu'Lock, D. C. Allport and W. B. Turner, *J. Chem. Soc.*, **1961**, 1654.

4) *Chem. & Ind. News*, **39**, No. 12, 46 (1961).

5) I. Fleming and J. Harey-Mason, *Proc. Chem. Soc.*, **1961**, 245.

$$RC(OX)=CHCOR'$$

I : R, R' = C_6H_5
a : X = $PO(OC_6H_5)_2$
b : X = COC_6H_5

II : R = C_6H_5, R' = OCH_3
a : X = $PO(OC_6H_5)_2$
b : X = $SO_2C_6H_4$-*p*-CH_3

III : R = CH_3, R' = OC_2H_5
a : X = $PO(OC_6H_5)_2$
b : X = $SO_2C_6H_4$-*p*-CH_3

IV : R, R' = CH_3, X = $PO(OC_6H_5)_2$

$$[RCOCHCOR']Na + ClPO(OC_6H_5)_2 \ (V) \rightarrow RC(OPO(OC_6H_5)_2)=CHCOR'$$

The following seven enol-esters were synthesized in the present work. These hitherto unknown enol-phosphates were obtained in good yield by the reaction of the sodium derivatives of the corresponding β-dicarbonyl compounds with diphenyl phosphorochloridate (V). Diphenyl 1, 3-diphenyl-2-propen-1-on-3-yl phosphate (Ia) and diphenyl β-methoxycarbonyl-α-styryl phosphate (IIa) were obtained in crystalline form, while diphenyl 1-ethoxycarbonyl-1-propen-2-yl phosphate (IIIa) and diphenyl 3-penten-2-on-4-yl phosphate (IV) were obtained in liquid form. The last one could not be purified owing to the decomposition in the attempted distillation even under a high vacuum. The structures of these compounds were confirmed by analyses except in the case of the phosphate IV, and also by the fact that all of these were insoluble in a dilute aqueous alkali solution and gave no coloration with ferric chloride. As will be reported later, elimination reaction was successfully realized in the cases of Ia and IIa affording the correspoding acetylenic compounds.

It has long been known that *C*-acylated products are mainly obtained, when sodium derivatives of various β-dicarbonyl compounds are treated with acyl halides. However, exclusive *O*-acylation was observed in the abovementioned phosphorylation, and no *C*-acylated product was detected. The usual method of *O*-acylation with acyl halides in pyridine gave no satisfactory result for the synthesis of phosphate Ia. No reaction appeared to occur, when the copper complex of methyl benzoylacetate was treated with phosphorochloridate (V).

Although many investigations were carried out until now about the reaction of the sodium derivatives of β-dicarbonyl compounds with various sulfonyl chlorides[6], the corresponding enol-sulfonates could not be obtained except at one instance. Kohler and MacDonald[6a], and Findeisen[6b] obtained sodium *p*-toluenesulfinate, ethyl chloroacetoacetate and ethyl diacetosuccinate, when the sodium derivative of ethyl acetoacetate was treated with *p*-toluenesulfonyl chloride in dry ether. The present authors carried out the reaction in acetone and obtained 4, 4'-dimethyldiphenyldisulfone[7] together with an oil. The oily material could be distilled under a high vacuum, but a small amount of chlorine containing impurity could not be removed. The distillate was insoluble in a dilute alkali solution and gave a negative test against ferric chloride and it is likely to consist mainly of enol-tosylate of ethyl acetoacetate (IIIb). The formation of the disulfone, in the present case, is attributable to the reaction of sulfonyl chloride with the sulfinate which is produced at the first stage[7].

The sodium derivative of methyl benzoylacetate was treated with *p*-toluenesulfonyl chloride in ether, yielding crude methyl *p*-toluenesulfonyloxycinnamate (IIb) in crystals. The pure material was obtained in only a few per cent yield owing to the difficulty in the removal of a considerable amount of contaminant. The assigned structure of the tosylate IIb was supported by analysis and the fact that the substance is insoluble in aqueous alkali and gives a negative test against ferric chloride*.

Treatment of dibenzoylmethane and methyl benzoylacetate with *p*-toluenesulfonyl chloride in pyridine did not afford the desired tosylates. Also the reaction of the copper complex of the above ketoester with the sulfonyl chloride gave unsatisfactory result.

β-Benzoyloxychalcone (Ib) was prepared according to the literature[8].

Experimental**

Diphenyl 1, 3-Diphenyl-2-propen-1-on-3-yl Phosphate (Ia). — A solution of dibenzoylmethane[9] (17.3 g., 0.077 mol.) in absolute ethanol (340 ml.) was added dropwise at room temperature to a stirred solution of sodium ethoxide (from 1.8 g., 0.078 g. atom, of sodium and 175 ml. of absolute ethanol).

Ethanol was evaporated (below 40°C) under reduced pressure, and the residual yellow solid was collected on a funnel, and washed with ether. A further crop was obtained from the filtrate and washings. The well dried solid was pulverized, suspended in dry ether (150 ml.), and a solution

6) a) E. P. Kohler and M. B. MacDonald, *Am. Chem. J.*, **22**, 227 (1899); b) T. v. Findeisen, *J. prakt. Chem.*, [2] **65**, 529 (1902); c) H. Böhme and H. Fischer, *Ber.*, **76**, 92, 99 (1943); d) E. M. Philbin, E. R. Stuart, R. F. Timoney and T. S. Wheeler, *J. Chem. Soc.*, **1957**, 2338.

7) E. P. Kohler and M. B. MacDonald, *Am. Chem. J.*, **22**, 219 (1899).

* In a preliminary experiment, the tosylate (IIb) afforded phenylpropiolic acid by the action of sodium *tert*-butoxide. This also supports the assignment.

8) L. Claisen and E. Haase, *Ber.*, **36**, 3674 (1903).

** All melting points and boiling points are uncorrected.

9) C. F. H. Allen, R. D. Abell and J. B. Normington, "Organic Syntheses", Coll. Vol. I (1948), p. 205.

of diphenyl phosphorochloridate[10] (V) (19.7 g., 0.074 mol.) in dry ether (150 ml.) was added dropwise with stirring at room temperature to this suspension during 30 min. The mixture was stirred for 3 1/4 hr., refluxed with stirring for 13 hr., and was then left at room temperature for 79 hr. After addition of water (90 ml.), the insoluble solid was filtered, washed with water and ether and recrystallized from ethanol to give the fairly pure phosphate Ia (20.7 g., 59% based on dibenzoylmethane), m. p. 112.5~115°C, which was further recrystallized twice from the same solvent to yield the analytical sample, light yellow cubes, m. p. 113.5~115°C.

Found: C, 70.64; H, 4.53. Calcd. for $C_{27}H_{21}O_5P$: C, 71.05; H, 4.64%.

Dibenzoylmethane (4.2 g.) was recovered from the ethereal layer of the above-mentioned filtrate and washings.

Diphenyl β-Methoxycarbonyl-α-styryl Phosphate (IIa).—The sodium compound prepared from methyl benzoylacetate[11] (10.0 g., 0.056 mol.) was mixed with diphenyl phosphorochloridate (V) (15.0 g., 0.056 mol.) according to the same manner as described above. The reaction mixture was stirred at room temperature for 6.5 hr., allowed to stand overnight and then refluxed with stirring for 4 hr. Water (90 ml.) was added to the ice-cooled reaction mixture, and the solid phosphate was filtered and washed successively with water and ether. A further crop was obtained from the ethereal solution. Recrystallization of the combined crops from light petroleum (b. p. 60~80°C) afforded almost pure material (14.2 g., 62%), m. p. 74~76°C, which was further recrystallized from the same solvent as colorless needles, m. p. 75~76°C.

Found: C, 64.75; H, 4.69; P, 7.27. Calcd. for $C_{22}H_{19}O_6P$: C, 64.39; H, 4.67; P, 7.55%.

Diphenyl 1-Ethoxycarbonyl-1-propen-2-yl Phosphate (IIIa).—The sodium derivative (10.7 g., 0.07 mol.) of ethyl acetoacetate was mixed with diphenyl phosphorochloridate (V) (18.9 g., 0.07 mol.) as described above. The mixture was stirred for 13 hr., and kept at room temperature for several hr. Water was added and the ethereal layer was washed successively with a 5% sodium hydroxide solution and a sodium chloride solution, and dried (Na_2SO_4). After evaporation of the solvent, the residue was distilled under reduced pressure to give the phosphate IIIa (16.1 g., 63.5%) as a colorless liquid, b. p.167~172°C/2×10^{-3} mmHg, n_D^{20} 1.5336.

Found: C, 59.79; H, 5.32; P, 8.48. Calcd. for $C_{18}H_{19}O_6P$: C, 59.67; H, 5.29; P, 8.56%.

Diphenyl 3-Penten-2-on-4-yl Phosphate (IV).—The sodium compound, prepared from acetylacetone (23.6 g., 0.24 mol.), and diphenyl phosphorochloridate (V) (63.2 g., 0.24 mol.) were mixed as above. The reaction mixture was stirred at room temperature for 9 hr., left overnight, and was then treated as in the case of the phosphate IIIa affording an orange oil (54.0 g., 69%). An attempt to distill the oil was unsuccessful even under a high vacuum (3×10^{-4} mmHg) because of its slow decomposition at a bath-temperature above 150°C.

Methyl β-p-Toluenesulfonyloxycinnamate (IIb).—A mixture of methyl sodiobenzoylacetate (prepared from 3.6 g., 0.02 mol. of the ester) and *p*-toluenesulfonyl chloride (3.8 g., 0.02 mol.) obtained in the manner as used for the phosphate, was stirred at room temperature for 9 hr., refluxed for 23 hr., and left at room temperature about 100 hr. After addition of water, the ethereal solution separated was washed successively with dilute aqueous sodium hydroxide and water, and dried (Na_2SO_4). Removal of the ether afforded a solid, which was separated from a concomitant oil by filtration, washed with ether, and recrystallized from methanol to give the tosylate IIb as colorless plates (0.5 g., 7.5%), m. p. 103~104°C.

Found: C, 61.26; H, 4.83; S, 9.71. Calcd. for $C_{17}H_{16}O_5S$: C, 61.43; H, 4.85; S, 9.65%.

Ethyl β-p-Toluenesulfonyloxycrotonate (IIIb).—*p*-Toluenesulfonyl chloride (38.0 g., 0.2 mol.) in anhydrous acetone was added to a suspension of sodium compound prepared from ethyl acetoacetate (26.0 g., 0.2 mol.) in the same solvent. The reaction mixture was stirred at room temperature for 6 hr., refluxed for 5.5 hr., and then allowed to stand at room temperature for 2 days. After a large amount of water was added to the reaction mixture, a white crystalline material and an oil separated which were extracted repeatedly with benzene. The combined benzene extracts were washed with a 5% sodium hydroxide solution and with a sodium chloride solution, and dried. Evaporation of benzene gave a crystalline material together with an oil. The oil was distilled under a high vacuum affording the tosylate IIIb as light yellow viscous oil (21.9 g., 38.5%), b. p. 126~128°C/4×10^{-4} mmHg, $n_D^{20.5}$ 1.5270.

Found: C, 54.12; H, 5.55. Calcd. for $C_{13}H_{16}O_5S$: C, 54.57; H, 5.97%.

The crystals were recrystallized twice from benzene yielding 4, 4'-dimethyldiphenyldisulfone as colorless needles (2.1 g.), m. p. 208.5~209.5°C (decomp.), [lit.[7], m. p. 212°C (decomp.)].

Found: C, 54.31; H, 4.54; S, 20.36. Calcd. for $C_{14}H_{14}O_4S_2$: C, 54.17; H, 4.55; S, 20.66%.

The present authors wish to thank the Ministry of Education for a grant-in-aid. They are also grateful to Dr. Tetsuo Shiba, Dr. Saichi Misumi, Mr. Masakazu Okumiya, Miss. Kiku Koike and Mr. Kenji Yoshimura for the microanalyses.

Department of Chemistry
Faculty of Science
Osaka University
Nakanoshima, Osaka

10) E. Baer, "Biochemical Preparations", Vol. 2, John Wiley and Sons, Inc., New York (1952), p. 97.
11) A. Wahl, *Compt. rend.*, **147**, 72 (1908).

The Formation of Acetylenic Bond by the Elimination Reaction of Some Enol-esters. II. Fission of C–C Bond in α, β-Acetylenic Carbonyl Compounds by the Action of Amide Anion

By Masazumi NAKAGAWA, Gen NAKAMINAMI, Fumio OGURA and Hiroshi ONO

(Received March 20, 1962)

The nucleophilic addition of various bases to the triple bond of α, β-acetylenic carbonyl compounds has been well known. Benzoylphenylacetylene (I), for example, readily adds amines[1] or alcohols[2] in the presence of the corresponding alcoholates giving β-amino- or β-alkoxy-chalcones, respectively. Therefore the reagents and the reaction conditions, which do not cause such addition reaction, had to be found out for the study of the elimination reaction of enol-esters to yield acetylenic compounds.

Sodium amide was first examined, because its action on the ketone I had never been known. The ketone I was treated with sodium amide in liquid ammonia resulting in the formation of phenylacetylene (II), benzoic acid (III) and benzamide (IV), while any substance arising from the addition reaction

$$\underset{\text{(I)}}{2\,C_6H_5C{\equiv}CCOC_6H_5} \rightarrow 2\,\underset{\text{(II)}}{C_6H_5C{\equiv}CH} + \underset{\text{(III)}}{HO_2CC_6H_5} + \underset{\text{(IV)}}{H_2NCOC_6H_5}$$

could not be detected at all. This fact suggests the breaking of the bond between the acetylenic carbon and the carbonyl carbon atoms. Only an example of such a bond fission has been reported in which acetylphenylacetylene is decomposed to phenylacetylene and acetic acid by the action of aqueous potassium hydroxide[3]. Under similar condition, the ketone I decomposed to yield acetophenone and benzoic acid possibly via dibenzoylmethane which was produced by the hydration of the triple bond[3].

Benzoylphenylacetylene (I) was recovered unchanged in an 80% yield when it was treated with liquid ammonia in the absence of sodium amide, indicating the essential role of amide anion for the bond fission of the acetylenic ketone. If the reaction proceeds in one step by the attack of amide anion to the carbonyl carbon displacing phenylethynyl anion, only phenylacetylene (II) and benzamide (IV) ought to be produced and the corresponding free acid should not be obtained at all. The possibility of the hydrolysis of the amide IV in the course of the isolation of the reaction products was excluded by the fact that the amide IV was recovered unchanged in about 75% yield and the acid III was obtained only in a minor quantity, when IV was treated in the same manner as in the isolation procedure. Therefore, the formation of the free acid III seems to be involved in the main reaction path, but detailed studies were not undertaken.

Diphenyl 1, 3-diphenyl-2-propen-1-on-3-yl phosphate (V)[4] was treated with four equivalents of sodium amide in liquid ammonia. Expectedly, phenylacetylene (II) and benzamide (IV) were obtained. Also diphenyl β-methoxycarbonyl-α-styryl phosphate (VI)[4] was treated with sodium amide affording phenylacetylene (II). Phenylpropiolic acid (VII, R=H) or its derivative (VII, R=CH_3 or NH_2) could not

$$\underset{\text{(V)}}{C_6H_5C(OPO(OC_6H_5)_2){=}CHCOC_6H_5} \rightarrow \underset{\text{(II)}}{C_6H_5C{\equiv}CH} + \underset{\text{(IV)}}{H_2NCOC_6H_5}$$

$$\underset{\text{(VI)}}{C_6H_5C(OPO(OC_6H_5)_2){=}CHCO_2CH_3} \rightarrow \underset{\text{(VII)}}{(C_6H_5C{\equiv}CCO_2R)} \rightarrow \underset{\text{(II)}}{C_6H_5C{\equiv}CH}$$

be detected at all. Also no basic material was obtained indicating, that no nucleophilic addition occured in this reaction.

It was confirmed from the above-mentioned results, that an acetylenic linkage can be formed by the elimination reaction of enol-ester, but it was found to be difficult to isolate the corresponding α, β-acetylenic carbonyl compound without decomposition under the above stated reaction condition.

Further studies on the elimination reaction will be reported in the following paper.

1) E. André, *Compt. rend.*, **152**, 525 (1911); E. André, *Ann. chim.*, [8] **29**, 569 (1913); E. R. Watson, *J. Chem. Soc.*, **85**, 1319 (1904).

2) M. C. Dufraisse and P. Gérald, *Bull. soc. chim. France*, [4] **31**, 1285 (1922); M. C. Dufraisse and A. Gillet, *Ann. chim.*, [10] **6**, 295 (1926).

3) C, Moureu and R. Delange, *Compt. rend.*, **130**, 1259 (1900).

4) M. Nakagawa, G. Nakaminami, F. Ogura and H. Ono, This Bulletin, **35**, 1485 (1962).

Experimental*

Reaction of Benzoylphenylacetylene (I) with Sodium Amide in Liquid Ammonia. — A solution of the ketone I[5] (4.1 g., 0.02 mol.) in dry tetrahydrofuran (50 ml.) was added dropwise to a stirred suspension of sodium amide (0.022 mol.) in liquid ammonia (50 ml.) during 45 min. After stirring for a further 3 hr., ammonium chloride (1.5 g.) was added with stirring, and the ammonia was removed. Ether (50 ml.) and then saturated aqueous sodium chloride solution (50 ml.) were added to the stirred mixture under cooling by ice. A small amount of insoluble material was filtered off and washed with ether. The ethereal solution was separated from the aqueous solution, (solution A), washed successively with sodium chloride solution (solution B), dilute sulfuric acid (solution C), and sodium chloride solution, and dried ($MgSO_4$). The oily residue, obtained by removal of the solvent through a Widmer column, separated crystals on standing. A small amount of light petroleum was added to complete the crystallization. Recrystallization of the solid (0.25 g., 10%) from aqueous methanol and then from benzene afforded benzamide as colorless plates, m. p. 126.5~128°C, which was undepressed on admixture with the authentic specimen.

Distillation (at 75.5~77.5 mmHg) of the unsolidified fraction gave phenylacetylene as colorless liquid (0.7 g.) which was converted to the mercury compound according to the usual way[6]. It was recrystallized 3 times from ethanol as colorless plates, m. p. 123~124.5°C, which showed no depression in the melting point on admixture with the authentic specimen[6]. The yield of the mercury compound was 1.0 g. (25% based on the ketone I) in a fairly pure state.

A solid was separated, on acidification with sulfuric acid (Congo red) from the combined solutions of A and B. The solid was separated by filtration, and the filtrate was extracted with ether. The ethereal solution was concentrated to give a further crop of the solid (combined yield, 1.2 g., 49%). Sublimation of the solid under reduced pressure afforded benzoic acid as colorless plates, m. p. 121~122°C, undepressed on admixture with the authentic specimen.

The solution C was made alkaline with dilute sodium hydroxide and extracted with ether to give orange crystals which could not be identified owing to its minor quantity.

Treatment of Benzoylphenylacetylene (I) with Liquid Ammonia. — A solution of the ketone I (2.0 g., 0.01 mol.) in dry tetrahydrofuran (30 ml.) was added dropwise while stirring to liquid ammonia (50 ml.). After stirring for 5 min., ammonium chloride (0.6 g., 0.011 mol.) was added in a portion, and the mixture was stirred for a further 4 1/4 hr. The ammonia was evaporated, water (50 ml.) and ether (50 ml.) were added to the residue under stirring. The ethereal solution was washed successively with dilute sodium hydroxide solution, water, dilute sulfuric acid and water, and dried (Na_2SO_4). The solvent was evaporated and the residue was distilled giving a yellow liquid (1.6 g., 80%), b. p. 153.5~160°C/2 mmHg. The infrared spectrum of the liquid was identical with that of an authentic specimen of I. The entire liquid crystallized when seeded with a piece of crystal of ketone I.

Reaction of Diphenyl 1, 3-Diphenyl-2-propen-1-on-3-yl Phosphate (V) with Sodium Amide. — A solution of the phosphate V[4] (4.6 g., 0.01 mol.) in dry tetrahydrofuran was added dropwise to a stirred suspension of sodium amide (0.04 mol.) in liquid ammonia (45 ml.) during a period of 15 min. The reaction mixture was stirred for 3 1/2 hr., and the ammonia was evaporated. A saturated solution of sodium chloride was added to the residue under stirring and cooling (ice-bath). A small amount of insoluble material was removed by filtration, and the aqueous layer was extracted with ether. The combined organic solutions were washed with sodium chloride solution, and dried (Na_2SO_4). The solvent was evaporated, and the residue deposited a solid on standing. Light petroleum was added to complete the deposition. The solid (0.8 g., 66%) was separated and then recrystallized 3 times from benzene to give benzamide as white plates, m. p. 126~127°C, which was undepressed on admixture with the authentic specimen.

Found: C, 69.43; H, 5.95; N, 11.37. Calcd. for C_7H_7ON: C, 69.40; H, 5.83; N, 11.56%.

Distillation of the unsolidified part gave phenylacetylene as a colorless liquid, b. p. 60~100°C (bath)/75~77.5 mmHg, which was converted to the mercury derivative according to the usual method[6]. Recrystallization of the mercury compound gave colorless needles or plates, m. p. 123.5~124.5°C, undepressed on admixture with authentic specimen.

The Reaction of Diphenyl β-Methoxycarbonyl-α-styryl Phosphate (VI) with Sodium Amide. —A solution of the phosphate VI[4] (15.0 g., 0.037 mol.) in dry ether (500 ml.) was added dropwise to a stirred suspension of sodium amide (0.2 mol.) in liquid ammonia (250 ml.) during 1 3/4 hr. The mixture was stirred for 1 1/4 hr. The ammonia was evaporated, and a solution of ammonium chloride (12.0 g.) in water (38 ml.) was added to the residue under stirring and cooling (ice-bath). A small amount of insoluble material was filtered and washed with ether. The organic layer separated from the lower (solution A) was washed successively with dilute sodium hydroxide solution (solution B) and water, and dried. The ethereal solution was worked up yielding phenylacetylene (1.05 g., 28%) as a colorless liquid, b. p. 72~73°C/73~73.5 mmHg, whose infrared spectrum and mercury derivative (colorless needles or plates, m. p. 123~124°C) were identical with those of the authentic specimen.

Phenylpropiolic acid or its derivatives were not detected at all whether in the solution A nor in the residue in the distilling flask.

Phenol was obtained from the ether-extract of

* All melting points and boiling points are not corrected.

5) E. André, *Ann. chim.*, [8] **29**, 564 (1913). Cf., K. Bowden, I. M. Heilbron, E. R. H. Jones and B. C. L. Weedon, *J. Chem. Soc.*, **1946**, 39.

6) J. R. Johnson and W. L. McEwen, *J. Am. Chem. Soc.*, **48**, 471 (1926).

the acidified solution **B**. Benzoylation by Schotten-Baumann's method afforded phenyl benzoate (4.1 g., 28% based on VI), which was crystallized from ethanol yielding light yellow needles, m. p. 67.5~69.5°C, undepressed on admixture with authentic specimen.

The authors are indebted to Mr. Masakazu Okumiya for the microanalyses. A part of the expenses of this research was defrayed from the grant-in-aid of the Ministry of Education to which the authors' thanks are also due.

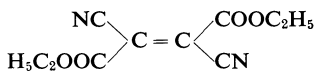
Department of Chemistry
Faculty of Science
Osaka University
Nakanoshima, Osaka

*Studies on trans-Dicyanodiethoxycarbonyl Ethylene. I. The Determination of the Structure**

By Ken-ichi KUDO

(Received March 28, 1962)

Cairns and coworkers[1] synthesized tetracyanoethylene containing four cyano groups and investigated its derivatives. However, there were only a few reports for the compounds of this class. Accordingly, studies on the properties and the behaviors of *trans*-dicyanodiethoxycarbonyl ethylene (I) containing two cyano and two ethoxycarbonyl groups were attempted in comparison with tetracyanoethylene in the present paper.



(I)

In 1955, Felton[2] reported that I was prepared in about 10% yield from ethyl cyanoacetate by the oxidation with selenium dioxide. Furthermore, it was also found that dicyanodiethoxycarbonyl ethane reported by Naik[3] in 1921 was identical to the ethylene compound I prepared by the Felton method. The precise structure of I, however, was not yet determined completely.

Consequently, the physical and the chemical properties of I were investigated to determine its structure. When I was dissolved in aromatic bases (e. g., benzene, toluene, xylenes, etc.), the solutions gave intense yellow colors. These colored solutions were attributed to the formation of π-comlexes between the aromatic bases and I. The π-complex spectra of I with the aromatic bases were shown in Fig. 1.

Furthermore, the concentration dependence

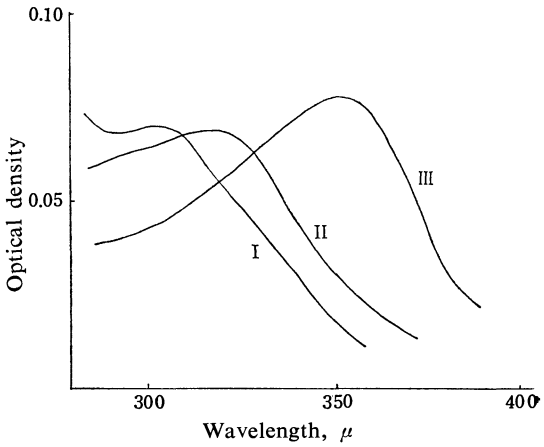


Fig. 1. The π-complex spectra of I with aromatic bases.
I (I) 0.514×10^{-4} mol./l., benzene
II (I) 0.522×10^{-4} mol./l., toluene
III (I) 0.522×10^{-4} mol./l., *o*-xylene

of these spectra was analyzed by the mothod of Keefer and Andrews[4], and Merrifield and Phillips[5]. The relation, then, is given as

$$[\mathrm{I}]\,l/\log(I_0/I) = 1/K\varepsilon\,[\mathrm{B}] + 1/\varepsilon$$

where [I] and [B] are the molar concentration of I and the mole fractions of aromatic bases, respectively, K is the association constants, log I_0/I is the optical density, and l is the cell length.

If the complex is 1 : 1 as in the case of

* This work was presented at the 14th Annual Meeting of the Chemical Society of Japan, April, 1961.

1) T. L. Cairns et al., *J. Am. Chem. Soc.*, **80**, 2775 (1958).
2) D. G. I. Felton, *J. Chem. Soc.*, **1955**, 515.
3) K. G. Naik, ibid., **119**, 1239 (1921).
4) R. M. Keefer and L. J. Andrews, *J. Am. Chem. Soc.*, **72**, 4677 (1950); L. J. Andrews and R. M. Keefer, ibid., **73**, 462 (1951).
5) R. E. Merrifield and W. D. Phillips, ibid., **80**, 2778 (1958).

TABLE I. π-COMPLEXES FORMED BETWEEN I AND AROMATIC BASES
(Solvent, CH_2Cl_2; Temperature, 20°C)

π-Base	K	λ_{max} mμ	ε $l \cdot cm^{-1}\ mol^{-1}$	K	λ_{max} mμ	ε $l \cdot cm^{-1}\ mol^{-1}$
Benzene	4.1	308	1300	—	—	—
Toluene	3.3	320	1250	—	—	—
o-Xylene	1.3	355	2632	—	—	—
m-Xylene	1.1	354	2900	—	—	—
p-Xylene	2.6	340	2000	—	—	—
Naphthalene	14.5	324	454	1.6	405	1333
Chlorobenzene	9.8	315	633	—	—	—
Anisole	10.7	310	649	1.9	390	909
Pyridine	1.2	315	826	—	—	—

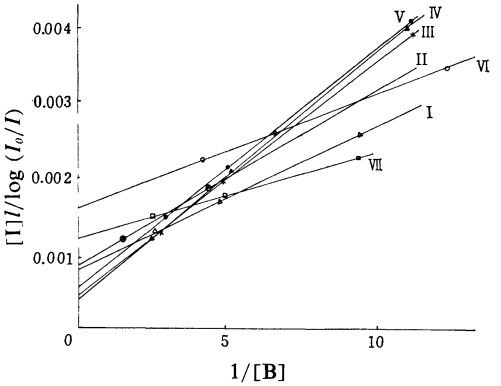


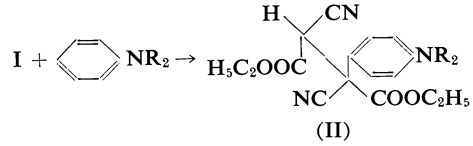
Fig. 2. Determination of K and ε for some I-aromatic complexes in CH_2Cl_2.
I Benzene II Toluene
III *o*-Xylene IV *m*-Xylene
V *p*-Xylene VI Chlorobenzene
VIII Pyridine

tetracyanoethylene, a plot of $[I]l/\log(I_0/I)$ vs. $1/[B]$ should be linear and yield ε as the reciprocal of the intercept, and the product $K\varepsilon$ as the reciprocal of the slope. These plots of I-aromatic complexes were shown in Fig. 2. Association constants, K, wavelength of maximum absorption, λ_{max}, and extinction coefficients for maximum absorption, ε, for nine I-aromatic complexes were listed in Table I.

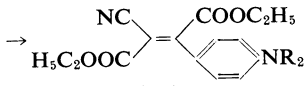
From these data it appears that I is a π-acid like tetracyanoethylene[5]. However, I does not appear to be nearly as strong a π-acid; the complexes of I have an absorption maxima at shorter wavelengths than do the corresponding complexes of tetracyanoethylene. Furthermore, whereas the π-complexes of tetracyanoethylene show a progressive increase of K and λ_{max} with increasing methylation of benzene, the complexes of I do not show a similar increase.

The ultraviolet absorption spectrum of I showed a band at λ_{max} 242 mμ (log ε; 4.0313). The infrared absorption spectrum showed two bands at 1740 cm^{-1} and 1260 cm^{-1} which were attributed to the stretching vibration of C=O and C–O of ester groups, respectively, but the conjugated alkyl C≡N band at 2225±10 cm^{-1} could not be detected (Fig. 3). These results, however, are not unexpected from the fact[6] that the introduction of an oxygenated group into the molecule results in a "quenching" of the C≡N absorption intensity to a remarkable extent. The Raman spectrum showed an intense band at 1650 cm^{-1} which was attributed to the symmetrical ethylenic double bond. As a chemical evidence, the ethanolysis of I gave ethyl ethylenetetracarboxylate.

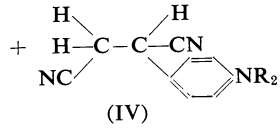
Finally, the geometrical structure of I was determined by the following manner. The reaction of I with tertiary aromatic amines



(II)



(III)



(IV)

resulted in addition of a benzene nucleus to the ethylenic double bond with the formation of 4-α, β-dicyano-α, β-diethoxycarbonyl-*N*, *N*-dialkylanilines (II). When the products II were heated with 10% aqueous sodium carbonate solution, 4-*trans*-α,β-diethoxycarbonyl-β-cyanovinyl-*N*, *N*-dialkylaniline (III) and 4-α, β-dicyanoethyl-*N*, *N*-dialkylanilines (IV) were obtained.

These addition reactions were accompanied by the production of a transient color, which would be attributed to formation of the π-complexes between I and *N*,*N*-dialkylaniline,

6) R. E. Kitson and N. E. Griffith, *Anal. Chem.*, **24**, 334 (1952).

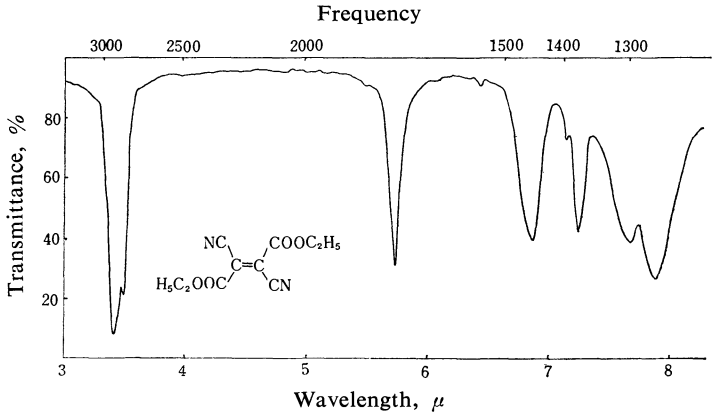
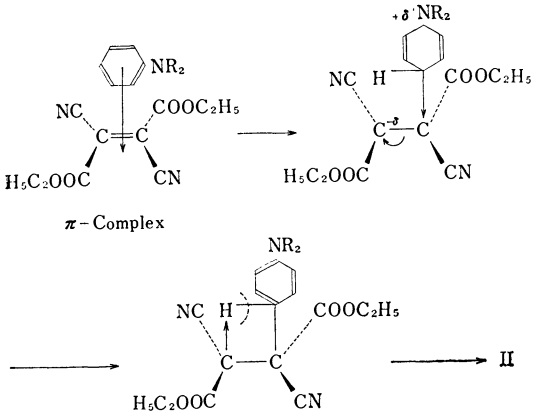


Fig. 3. Infrared absorption spectrum of I in Nujol mull.

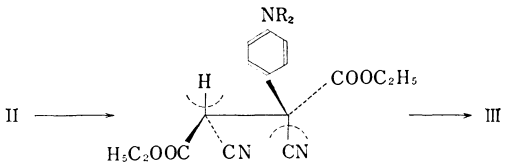
since the intense electronic absorption bands of the reaction mixture at λ_{max} 323 mμ and λ_{max} 560 mμ are attributable to neither I nor *N,N*-dimethylaniline, but to the π-complex itself as a new molecular species.

Furthermore, the course of the addition reactions was sterically specific.

From these data it appears that the addition reactions of I with *N,N*-dialkylanilines are initiated by an ionic reaction involving electron transfer from the benzene nucleus to I. This step is probably rapid and results in th π-complex formation. The second, probably rate controlling, step in the addition reactions is a rearrangement of the π-complex to yield the adducts II. Accordingly, the course of the addition reactions would be a purely cis addition as follows:



It is generally recognized that most of the base-catalized elimination reactions, e.g., elimination of hydrogen halide or cyanide, to form a new carbon-carbon double bond proceed in a trans steric course. Accordingly, the elimination of hydrogen cyanide of II should occur in a H and a CN trans orientation (staggered form) driven by a rotation about the central carbon-carbon bond.



Thus, the evidence that the elimination product III had only a ethoxycarbonyl-ethoxycarbonyl trans geometry would drive to the conclusion that I had a trans geometry for the cyano and cyano groups.

The structures of II and IV were estimated on the basis of the infrared absorption spectra (Fig. 4). The structure of III was established definitely by the following manner. The infrared absorption spectrum of III (R ; CH_3), showed C=O bands at 1720 cm^{-1} and 1736 cm^{-1} and a C≡N band at 2220 cm^{-1} (Fig. 4). As a chemical evidence, the hydrolysis of III (R ; CH_3) with sulfuric acid gave an intramolecular acid anhydride. In addition, the structure was confirmed by the use of mixture melting points of the material with 4-*trans*-α,β-diethoxycarbonyl-β-cyanovinyl-*N,N*-dialkylaniline synthesized by an another method. Finally, the geometrical structure of III was determined on the basis of the infrared absorption spectrum. As described above, the ester C=O bands at 1736 cm^{-1} and 1720 cm^{-1} were attributed to the ester groups of α- and β-position for the benzene nucleus, respectively. Since the ester group of α-position is sterically more hindered than the other ester group, the frequency of the ester group on the α-position should shift toward a shorter wavelength from the normal position. In addition, the infrared absorption spectrum of 4-α-ethoxycarbonyl-β,β-dicyanovinyl-*N,N*-dimethylaniline[7] (V) showed an ester band at 1736 cm^{-1} (Fig. 4). The fact that the infrared absorption band of the ester on the α-position

7) B. C. McKusick et al., *J. Am. Chem. Soc.*, **80**, 2806 (1958).

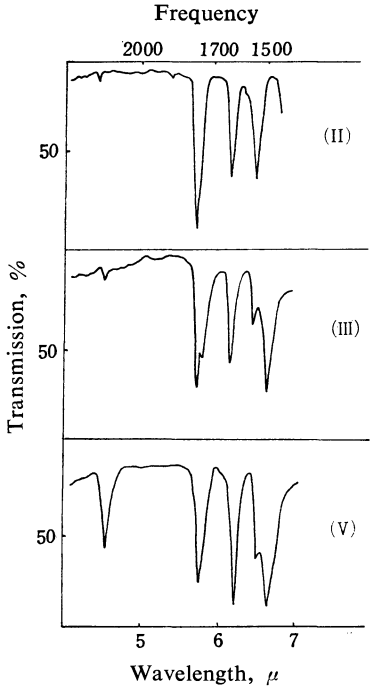
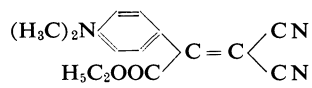


Fig. 4. Infrared absorption spectra of II, III and V.

of V coincided completely with that of the ester on the α-position of III (R ; CH_3) suggests that the α-ester group of III (R ; CH_3) is also hindered by a benzene and a cyano group, but not by an another ester group. Incidentally, Felton[8] reported that the ester C=O frequency



(V)

shifts of compounds, in which more than one ester or cyano group is attached to an ethylenic double bond, depended upon mainly the steric repulsion between these substituents. Consequently, it seems to be plausible that the configuration of III is concluded to be a trans type.

Experimental

Hydrolysis of I to Ethyl Ethylenetetracarboxylate. — A mixture of 4.4 g. of (I), 8 g. of 95% ethanol, and 8 g. of 98% sulfuric acid was heated under reflux for 7 hr. After cooling, the mixture was extracted with ether. The extract was washed with 5% sodium carbonate solution, dried with sodium sulfate, and distilled to expel ether and the residue crystallized to a colorless crystal, m. p. 54.5~55.5°C.

II(R ; CH_3).—A mixture of 22 g. (0.1 mol.) of I and 17 g. (0.14 mol.) of *N*, *N*-dimethylaniline in 50 ml. of dimethylformamide was heated at 50~60°C with stirring for 20 min. After cooling, the solvent was evaporated under reduced pressure, the residue was triturated with 50% methanol, and stood in an ice-box for several days. The solidified product was collected by filtration, washed with 50% methanol, and recrystallized from methanol-water to give 33 g. (97%) of II (R ; CH_3), m. p. 81~88°C, as colorless crystals.

Found : C, 63.07 ; H, 6.24 ; N, 12.31 ; mol. wt., 337(Rast). Calcd. for $C_{18}H_{21}O_4N_3$: C, 62.96 ; H, 6.16 ; N, 12.24% ; mol. wt., 343

Its infrared absorption spectrum had a C≡N band at 2250 cm^{-1} and a C=O band at 1760 cm^{-1}.

II(R ; C_2H_5).—In a similar procedure, II(R ; C_2H_5), m. p. 86~87.5°C, was obtained in 80% yield.

Found : C, 64.36 ; H, 6.54 ; N, 11.49 ; mol. wt., 366(Rast). Calcd. for $C_{20}H_{25}O_4N_3$: C, 64.67 ; H, 6.78 ; N, 11.31% ; mol. wt., 371.

Its infrared absorption spectrum had a C≡N band at 2250 cm^{-1} and a C=O band at 1740 cm^{-1}.

Decarbethoxylation or Elimination of Hydrogen Cyanide of II(R ; CH_3).—A mixture of 5 g. II (R ; CH_3) and 5 g. of sodium carbonate in 45 ml. of water was heated under reflux for about 20 min. to give a red oily layer. The oily layer was separated from the aqueous layer, recrystallized from benzene-petroleum benzine, and gave III (R ; CH_3), m. p. 121~122°C, as the red crystals.

Found : C, 64.45 ; H, 6.51 ; N, 8.77. Calcd. for $C_{17}H_{20}O_4N_2$: C, 64.54 ; H, 6.37 ; N, 8.86%

The crystals from the aqueous layer were collected by filtration, washed with water, and recrystallized from ethanol-water. There was obtained IV (R ; CH_3), m. p. 98~100.5°C. as yellow crystals.

Found : C, 72.25 ; H, 6.64 ; N, 21.28 ; mol. wt., 196(Rast). Calcd. for $C_{12}H_{13}N_3$: C, 72.33 ; H, 6.57 ; N, 21.09% ; mol. wt., 199.

The ultraviolet absorption spectrum of III (R ; CH_3) showed a band at λ_{max} 252 mμ (log ε ; 3.978). The infrared absorption spectrum of IV (R ; CH_3) had a C≡N band at 2250 cm^{-1} and benzene bands at 1620 cm^{-1} and 1530 cm^{-1}.

Synthesis of III (R ; CH_3) from Ethyl 4-Dimethylaminophenyl Glyoxylate.—A solution of 4 g. (0.02 mol.) of ethyl 4-dimethylaminophenyl glyoxylate, 9 g. (0.08 mol.) of ethyl cyanoacetate, and 0.5 ml. of piperidine in 7 ml. of absolute ethanol was refluxed for 30 hr. The mixture was concentrated under reduced pressure to dryness. The residue was recrystallized from benzene-petroleum benzine to give 2.8 g. (48%) of III (R ; CH_3) as red crystals, m. p. 121~122°C.

Cyclization of III (R ; CH_3) to 4-Dimethylaminophenylmaleic Anhydride.—A solution of 5 g. of III (R ; CH_3) in 40 ml. of 75% sulfuric acid was heated on boiling water for 6 hr. After cooling, the solution was poured into 100 ml. of ice-water under stirring and the aqueous mixture was neutrallized with sodium carbonate. The precipitated crystals were collected by filtration and recrystallized from acetone. There was obtained 0.8 g. (21%) of intramolecular acid anhydride in the form of dark red crystals, m. p. 179~179.5°C.

Found : C, 66.58 ; H, 5.18 ; N, 6.28 ; mol. wt., 219(Rast). Calcd. for $C_{12}H_{11}O_3N$: C, 66.35 ; H, 5.10 ; N, 6.45% ; mol. wt., 217.

8) D. G. I. Felton et al., *J. Chem. Soc.*, 1955, 2170.

Its infrared absorption spectrum showed C=O bands at 1820 cm^{-1} and 1775 cm^{-1}.

The author wishes to express his heartfelt thanks to Professor Risaburo Nakai of the Institute for Chemical Research of Kyoto University for his cordial encouragement and suggestion throughout the work. He also desires to state his sincere gratitude to Professor Ryozo Goto of Kyoto University for his invaluable advice in the course of this work. Thanks are due to Mr. Tohru Takenaka of the Institute for Chemical Research of Kyoto University for infrared spectral measurement.

Institute for Chemical Research
Kyoto University
Takatsuki, Osaka

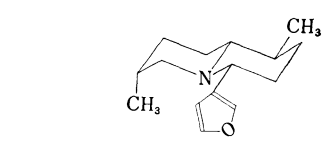
*Resolution of dl-Deoxynupharidine; The Total Synthesis of Nupharidine**

By Munio KOTAKE, Ichiro KAWASAKI, Shigeru MATSUTANI, Shiro KUSUMOTO and Takeo KANEKO

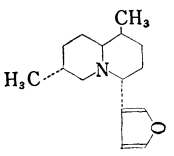
(Received April 2, 1962)

Recently we have suggested that the absolute configuration of deoxynupharidine should be represented as formula I[1]. In the course of the synthetic route of deoxynupharidine, it seems that the 7-axial methyl group has mainly been produced by catalytic reduction of the pyridine nucleus of ethyl 4-[5-methyl-pyridyl-(2)]-valerate and the 4-equatorial furyl group has been produced by catalytic reduction of 1, 7-dimethyl-4-[furyl-(3)]-dehydroquinolizidine-3. From the results that 3-methylquinolizidine obtained from 2, 5-lutidine through catalytic reduction of pyridine nucleus afforded mainly 3(a)-methyl form[2] and 4-methylquinolizidine obtained by Murakoshi's method[3] afforded only one diastereomer of 4-methylquinolizidine the synthetic mixture of deoxynupharidine[4] may be contained isomer Ia and Ib predominantly. A chromatography of the diastereoisomeric mixtures of synthetic sample on alumina[5] resulted in the separation of the following fractions. The first fraction eluted by petroleum ether gave an isomer, which was crystallized as hydrochloride. This isomer could not be lead to *N*-oxide and to iodomethylate by the same condition as used with

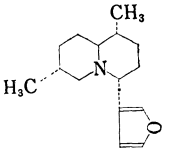
Chart I



I



Ia



Ib

success in case of a natural product. From the suggestion, that the 1(a)-methyl group of this isomer will hinder sterically the above reactions and from the evidence of NMR spectra, this isomer should be presented as 1-epimer (Ib). The fraction eluted by petroleum ether-ether, which has the infrared and NMR spectrum similar to that of natural deoxynupharidine, was oxidized with hydrogen peroxide to *N*-oxide and recrystallized as its hydrochloride (infrared spectrum in Nujol was found to be identical with that of nupharidine hydrochloride), and then reduced smoothly with palladium charcoal to give *dl*-deoxynupharidine. The treatment of *dl*-form with *l*-tartaric acid afforded *l*-deoxynupharidine *l*-tartrate as less soluble salt and the regenerated *l*-base from the tartrate oxidized to *d*-nupharidine, which was identical with a natural product in all aspects. The *d*-base also has been isolated with the aid of *d*-tartaric acid.

* Short communication, This Bulletin, 35, 698 (1962).

1) M. Kotake et al., ibid., 35, 697 (1962).

2) T. Kaneko et al., *J. Chem. Soc. Japan, Pure Chem. Sec.* (*Nippon Kagaku Zasshi*), 83, 949 (1962).

3) I. Murakoshi, *J. Pharm. Soc. Japan* (*Yakugaku Zasshi*) 78, 594 (1958).

4) M. Kotake, I. Kawasaki, T. Okamoto, S. Kusumoto and T. Kaneko, *Ann.*, 636, 158 (1960).

5) In the course of this resolution, we found the contribution of F. Bohlmann, E. Winterfeld, P. Studt, H. Laurent, G. Boroschewoki and K-M. Kleine, *Chem. Ber.*, 94. 3151 (1961).

6) Y. Arata and T. Asai, *J. Pharm. Soc. Japan* (*Yakugaku Zasshi*), 79, 1442 (1959).

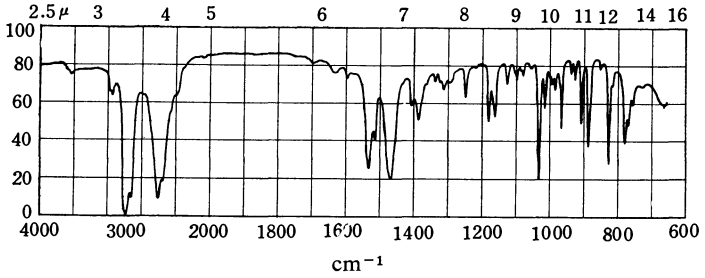


Fig. 1. *dl*-Nupharidine hydrochloride (Nujol).

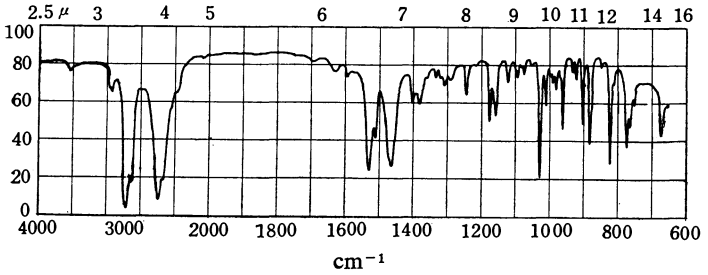


Fig. 2. Nupharidine hydrochloride (natural) (Nujol).

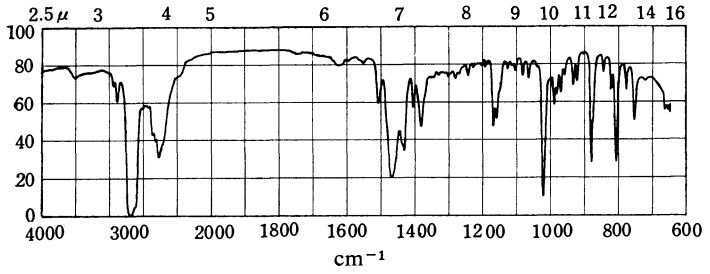


Fig. 3. 1(epi)-Deoxynupharidine hydrochloride (Nujol).

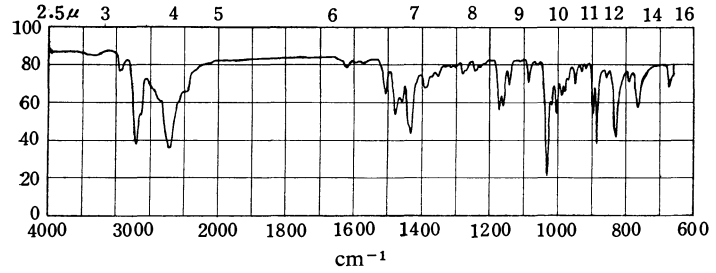


Fig. 4. *dl*-Deoxynupharidine hydrochloride (Nujol).

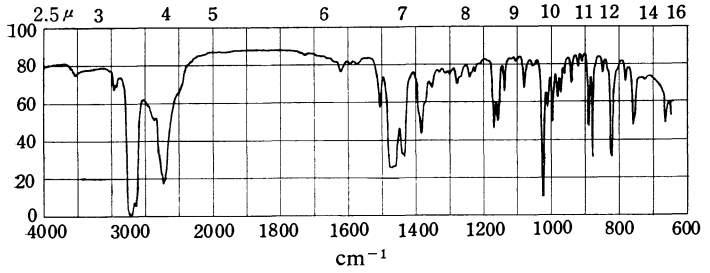


Fig. 5. Deoxynupharidine hydrochloride (natural) (Nujol).

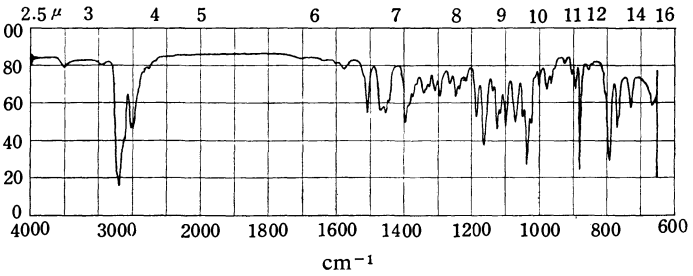


Fig. 6. *l*-Deoxynupharidine (synthetic) (liquid).

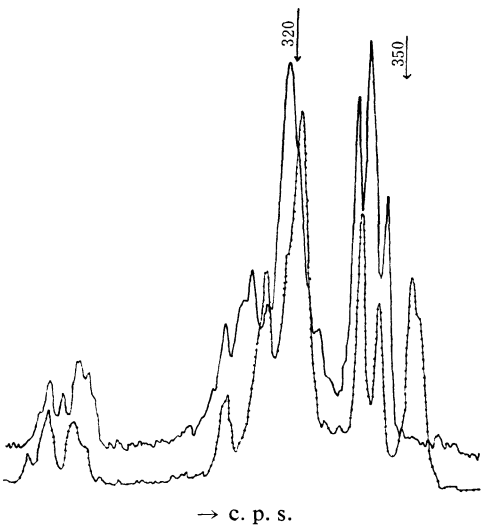


Fig. 7. The NMR spectra were measured in benzene solution at 56.4 Mc. using a Varian spectrometer and c. p. s. values calculated from benzene.
—— 1(epi)-Deoxynupharidine
------ *dl*-Deoxynupharidine

Experimental

To purify the reaction product, diethyl 2-[5-methylpyridyl-(2)]-allylmalonate was reduced partially with Pd-C in ethanol to diethyl 2-[5-methyl-(2)]-propylmalonate (picrate from ether, m. p. 84～85.5C, Found: C, 50.54; H, 5.01; N, 10.76. Calcd. for $C_{22}H_{26}O_{11}N_4$; C, 50.57; H, 5.02; N, 10.72%)[6] and then hydrolyzed to 4-[5-methylpyridyl-(2)]-valeric acid (m. p. 77～77.5°C, Found: C, 68.45; H, 7.88; N, 7.06. Calcd. for $C_{11}H_{15}O_2N$: C, 68.35; H, 7.82; N, 7.25%, the hydrochloride, m. p. 145～146°C, Found: C, 57.42; H, 7.06; N, 5.88. Calcd. for $C_{11}H_{15}O_2N$-HCl: C, 57.51; H, 7.02; N, 6.09%). Ethyl 4-[5-methyl-pyridyl-(2)]-valerate (b. p. 102～104°C/2 mmHg) was reduced with platinum oxide in acetic acid and then acylated with furoyl chloride immediately to give furoyl derivatives.

Natural Deoxynupharidine.—$[\alpha]_D$ −109.86° (*c* 1.16, in ethanol), the hydrochloride, m. p. 261～263°C, $[\alpha]_D$ −21.4° (*c* 0.98, in 1 N HCl).

Natural Nupharidine.—$[\alpha]_D$ +17.2° (*c* 1.10, in ethanol).

***l*-Deoxynupharidine-*l*-tartrate.** —*l*-Deoxynupharidine (0.76 g.) and *l*-tartaric acid (0.5 g.) were mixed in acetone (8 ml.) and deposited the tartrate (1.3 g.), which recrystallized from acetone-ethanol and ethyl methyl ketone, m. p. 151～152°C, $[\alpha]_D$ −14.65° (*c* 1.11, in ethanol).

Found: C, 59.26; H, 7.73; N, 3.59. Calcd. for $C_{19}H_{29}O_7N$: C, 59.51; H, 7.62; N, 3.65%.

***d*-Nupharidine-*d*-camphorsulfonate.** — *d*-Nupharidine (0.3 g.) and *d*-camphorsulfonic acid (0.3 g.) were mixed in chloroform (10 ml.) and the deposited salt (0.5 g.) recrystallized from ether-ethanol in needles, m. p. 182～183°C (decomp.), $[\alpha]_D$ +39.0° (*c* 0.9, in ethanol).

Found: C, 61.86; H, 8.25; N, 2.85. Calcd. for $C_{25}H_{40}O_6NS$: C, 62.21; H, 8.35; N, 2.90%.

Chromatography of Synthetic Deoxynupharidine. —The synthetic deoxynupharidine (42.15 g., b. p. 93～98°C/2 mmHg was chromatographed on alumina and resulted in the separation of following fractions (the fraction was checked by the infrared NMR spectroscopy);

Chromatography No. 1—1

Synthetic sample (13.3 g.) was dissolved in petroleum ether (50 ml.) and chromatographed on alumina (80 g.).

Fraction	Eluent	Volume ml.	Weight g.
1—1	Pet. ether	200	3.4
2—1	Pet. ether	200	1.7
3—1	Pet. ether	200	0.25
4—1	Pet. ether : Ether	100	0.8
5—1	Ether	100	0.65
6—1	Ether	310	0.2
7—1	Ethanol	120	4.4

Chromatography No. 1—2

Synthetic sample (15.5 g.) was dissolved in peteroleum ether (100 ml.) and chromatographed on alumina (100 g.).

Fraction	Eluent	Volume ml.	Weight g.
1—2	Pet. ether	200	2.3
2—2	Pet. ether	100	4.5
3—2	Pet. ether : Ether	100	0.8
3—2	Ether	100	1.9
5—2	Ether	200	0.3
6—2	Ether	400	0.2
7—2	Ethanol	150	4.5

Chromatography No. 1—3

Synthetic sample (13.35 g.) was dissolved in petroleum ether (100 ml.) and chromatographed on alumina (100 g.).

Fraction	Eluent	Volume ml.	Weight g.
1—3	Pet. ether	200	3.4
2—3	Pet. ether	100	4.5
4—3	Pet. ether	100	0.3
4—3	Pet. ether : Ether	100	0.5
5—3	Ether	100	2.9
6—3	Ether	200	0.3
7—3	Ethanol	150	1.9

Chromatography No. 2

Fractions except 7 of chromatography No. 1—1, 2, 3 were dissolved in peteroleum ether (50 ml.) and chromatographed on alumina (125 g.).

Fraction	Eluent	Volume ml.	Weight g.
8	Pet. ether	200	21.7
9	Pet. ether	100	2.1
10	Pet. ether : Ether	100	0.6
11	Pet. ether : Ether	100	2.8
12	Ether	225	1.5
13	Ether	200	0.5
14	Ethanol	100	0.3

Chromatography No. 3

The fractions 8 and 9 (23.8 g.) were dissolved in petroleum ether (100 ml.) and chromatographed on alumina (130 g.).

Fraction	Eluent	Volume ml.	Weight g.
15	Pet. ether	200	14.4
16	Pet. ether	100	5.2
17	Pet. ether : Ether (7 : 3)	100	0.8
18	Pet. ether : Ether (7 : 3)	100	3.7
19	Ether	100	0.3
20	Ether	300	0.05
21	Ether	120	Trace

Chromatography No. 4

The fractions 15 and 16 (19.6 g.) were dissolved in petroleum ether (80 ml.) and chromatographed on alumina (115 g.).

Fraction	Eluent	Volume ml.	Weight g.
22	Pet. ether	100	11.1
23	Pet. ether	100	4.7
24	Pet. ether : Ether (7 : 3)	100	0.7
25	Pet. ether : Ether (7 : 3)	100	2.5
26	Ether	100	0.05
27	Ether	300	0.05
28	Ethanol	125	Trace

Chromatography No. 5

The fractions 22 and 23 (15.8 g.) were dissolved in petroleum ether (60 ml.) and chromatograph on alumina (125 g.).

Fraction	Eluent	Volume ml.	Weight g.
29	Pet. ether	200	10.6
30	Pet. ether	100	2.2
31	Pet. ether : Ether (7 : 3)	100	2.2
32	Pet. ether : Ether (7 : 3)	100	1.6
33	Ether	100	Trace
34	Ether	300	Trace
35	Ethanol	120	Trace

Infrared spectra of the fractions 11, 18, 25 and 32 were similar to that of natural deoxynupharidine.

***dl*-Nupharidine Hydrochloride.**—A part (2.2 g.) of the above fractions 11, 18, 25 and 32 was dissolved in acetone and added 15% of hydrogen peroxide (2.3 g.) The reaction mixture was heated on a steam bath at 50°C for 3 hr. and then evaporated in vacuo. The residue was dissolved in ethanol (4.5 g.) and added concentrated hydrochloric acid (0.7 ml.) and ether (38 ml.) and then kept in a refrigerator to give a precipitate (m. p. 193 ~196°C), which was recrystallized from ethanol-ether in needles, m. p. 222~223°C (decomp.).

Found: C, 62.85; H, 8.29; N, 4.98. Calcd. for $C_{15}H_{23}O_2N \cdot HCl$: C, 63.03; H, 8.46; N, 4.90%.

***dl*-Deoxynupharidine Hydrochloride.**—*dl*-Nupharidine hydrochloride (1 g.) was dissolved in ethanol (30 ml.), added 10% palladium charcoal (0.4 g.) and hydrogenated at ordinary pressure and temperature. Eighty-seven milliliters of hydrogen (theoretical amount, 79 ml.) were absorbed in 2 hr. The catalyst was filtered off and the filtrate was evaporated in vacuo. The residue recrystallized from ether and ethanol gave *dl*-deoxynupharidine hydrochloride (0.85 g.), m. p. 218~220°C, yield 93%. Analytical sample obtained by further recrystallization melted at 224~225°C.

Found: C, 66.69; H, 8.84. Calcd. for $C_{15}H_{23}ON \cdot HCl$: C, 66.77; H, 8.97%.

Resolution of *dl*-Deoxynupharidine.—The *dl*-base (1.5 g.) which was obtained by several runs as above mentioned and *l*-tartaric acid (0.6 g.) were dissolved in acetone (9 ml.) and ether (ca. 0.5 ml.) and left overnight in the refrigerator. The precipitated crude tartrate (0.5 g., m. p. 141~144°C) was recrystallized several times from ethyl methyl ketone. The final product (0.2 g.) melted at 151.5 ~152°C (mixed melting point with authentic *l*-deoxynupharidine *l*-tartrate, 152~154°C) and showed $[\alpha]_D$ −11.54° (*c* 1.00, in ethanol).

Found: C, 59.30; H, 7.64; N, 3.58%.

The base recovered from the above tartrate showed $[\alpha]_D$ −68.82° (*c* 1.01, in ethanol), the hydrochloride, $[\alpha]_D$ −17.03° (*c* 1.02, in 1 N HCl), m. p. 258~261°C.

Found: C, 66.82; H, 8.96; N, 5.03%.

***d*-Nupharidine.**—The synthetic *l*-deoxynupharidine (64 mg.) was dissolved in acetone (2 ml.) and added 15% hydrogen peroxide (0.6 ml.). The mixture was kept at 50°C for 2 hr. and the solvent was evaporated under reduced pressure. The residue was dissolved in chloroform and washed with water. The residue (68 mg.) obtained from the

chloroform solution by evaporation was recrystallized from acetone in plates (8 mg.), 222°C (decomp.), $[\alpha]_D$ +13.00° (*c* 0.38, in ethanol). Found: C, 71.81; H, 9.57%. The hydrochloride, m. p. 245~246°C (decomp.).

Found: C, 63.25; H, 8.48%.

***d*-Deoxynupharidine-*d*-tartrate.** — The mother-liquor from the first crop of *l*-deoxynupharidine *l*-tartrate was evaporated, the residue dissolved in water, basified, and extrated with ether, giving the crude *d*-base (1.0 g.). This was combined with *d*-tartaric acid (0.64 g.) in ethyl methyl ketone (10 ml.) and the *d*-tartrate (0.9 g. m. p. 138~140°C) repeatedly crystallized from ethyl methyl ketone, the last fraction (0.35 g.) having m. p. 152~154°C, $[\alpha]_D$ +13.5° (*c* 1.66, in ethanol).

Found: C, 59.48; H, 7.62; N, 3.76%.

***d*-Deoxynupharidine.** — *d*-Deoxynupharidine recovered from the above showed $[\alpha]_D$ +108.58° (*c* 0.99, in ethanol), the hydrochloride, m. p. 259~261°C. Found: C, 66.50; H, 8.85; N, 5.18%.

1-(epi)-Deoxynupharidine.—Fraction 29 (10.6 g.) was dissoved in ethanol (50 ml.) and concentrated hydrochloric acid (5 ml.) and then added ether (50 ml.). The precipitated hydrochloride (7.7 g. m. p. 220~222°C) was recrystallized from acetone-methanol in prisms, m. p. 224~225°C.

Found: C, 66.65; H, 8.87; N, 5.36%.

The free base (400 mg.) was dissolved in acetone (6 ml.) and added 15% hydrogen peroxide (1 ml.). After the mixture was kept at 50°C for 2 hr., the solvent was removed in vacuo and the residue dissolved in chloroform. The chloroform solution was washed with water and then evaporated. The residual oil (400 mg.) was identical with starting material in infrared spectra.

The free base (350 mg.) was mixed with methyl iodide (5 ml.) and then left overnight. To the reaction mixture ether was added and the ethereal solution washed with bisulfite solution. By removing of solvent, starting material was recovered (350 mg.).

The author wishes to thank Mr. Naohiro Hayakawa of Japan Atomic Energy Research Institute for measurement of the NMR spectra.

Deartment of Chemistry
Faculty of Science
Osaka University
Nakanoshima, Osaka

On Olefin Synthesis with Phosphonate Carbanions

By Hidetaka TAKAHASHI, Kazuyoshi FUJIWARA and Masaki OHTA

(Received May 7, 1962)

A number of methods to the synthesis of olefins by using organo-phosphorus compounds have been reported.

Wittig[1] has described the conversion of a carbonyl compound into an olefin in which the oxygen atom of the carbonyl group was replaced with an alkylidene group by the reaction of an alkylidene triphenylphosphorane.

Horner and Hoffmann[2] have reported the preparation of olefins from phosphine oxides and aldehydes by refluxing the mixture in toluene for about ten hours in the presence of potassium *tert*-butoxide.

Also, Wadsworth[3] has recently reported the preparation of olefins by the reaction of phosphonate carbanions which had been prepared by the addition of the phosphonate to a slurry of sodium hydride in 1, 2-dimethoxyethane at room temperature with carbonyl compounds.

In this paper, a method of preparing phosphonate carbanions by the action of sodium amide with phosphonates and the reaction of aldehydes and ketones with the carbanions derived from diethyl carbethoxymethylphosphonate, diethyl cyanomethylphosphonate, diethyl formylmethylphosphonate diethylacetal and diethyl acetonylphosphonate are described.

Diethyl carbethoxymethylphosphonate carbanion was prepared by the reaction of diethyl carbethoxymethylphosphonate with sodium amide as a proton-accepter in tetrahydrofuran or in ether as an aprotic solvent at room temperature; it was treated with such aldehydes as *n*-butylaldehyde, crotonaldehyde, benzaldehyde and cinnamaldehyde, or with such ketones as acetone, acetophenone, benzophenone and cyclohexanone.

The reaction proceeded smoothly under mild conditions with a variety of aldehydes and ketones, resulting in α, β-unsaturated esters in fairly good yields.

The reaction can be formulated by the following scheme; the results are summarized in the Table.

1) U. Schöllkopf, *Angew. Chem.*, **71**, 260 (1959).
2) L. Horner and H. Hoffmann, *Chem. Ber.*, **92**, 2499 (1959).
3) W. S. Wadsworth, *J. Am. Chem. Soc.*, **83**, 1733 (1961).

TABLE

R_1	R_2	Yield %	III Formula	B. p. °C/mmHg
H	$CH_3CH_2CH_2$	67	$C_8H_{14}O_2$	65/12
H	$CH_3CH=CH$	47	$C_8H_{12}O_2$	79~79.5/13
H	C_6H_5	82	$C_{11}H_{12}O_2$	135~136/13
H	$C_6H_5CH=CH$	72	$C_{13}H_{14}O_2$	135~136/3
CH_3	CH_3	61	$C_7H_{12}O_2$	72~73/49
CH_3	C_6H_5	77	$C_{12}H_{14}O_2$	132~134/11
C_6H_5	C_6H_5	87	$C_{17}H_{16}O_2$	180~181/760
$CH_2(CH_2)_4CO$		76	$C_{10}H_{16}O_2$	98~99/11

$$(C_2H_5O)_2\overset{O}{\overset{\uparrow}{P}}-CH_2COOC_2H_5$$
(I)

$$\xrightarrow{NaNH_2} (C_2H_5O)_2\overset{O}{\overset{\uparrow}{P}}-\overset{\ominus}{C}HCOOC_2H_5$$
(II)

$$II + \begin{matrix}R_1\\R_2\end{matrix}\!\!>\!C=O$$

$$\rightarrow \begin{matrix}R_1\\R_2\end{matrix}\!\!>\!C=CHCOOC_2H_5 + (C_2H_5O)_2\overset{O}{\overset{\uparrow}{P}}O^{\ominus}$$
(III)

Diethyl cyanomethylphosphonate (IV), prepared from bromoacetonitrile and triethylphosphite, gave an anion when treated with sodium amide at a low temperature; this anion reacted with benzaldehyde and benzophenone to produce cinnamonitrile (Vb) and β-phenylcinnamonitrile (Va).

$$\begin{matrix}R_1\\R_2\end{matrix}\!\!>\!C=O + (C_2H_5O)_2P(O)CH_2CN$$
(IV)

$$\xrightarrow{NaNH_2} \begin{matrix}R_1\\R_2\end{matrix}\!\!>\!C=CHCN$$
(V)

R_1: C_6H_5 R_2: C_6H_5, H
(Va) (Vb)

Diethyl formylmethylphosphonate diethylacetal (VI), prepared by the heating of ethyl bromoacetal with triethylphosphite, was added to a suspension of sodium amide in tetrahydrofuran at room temperature, and the resulting diethyl formylmethylphosphonate diethylacetal carbanion was treated with benzaldehyde at about 20°C to give cinnamaldehyde diethylacetal (VII), which was hydrolyzed and identified with 2, 4-dinitrophenylhydrazone.

$$C_6H_5CHO + (C_2H_5O)_2P(O)CH_2CH(OC_2H_5)_2$$
(VI)

$$\xrightarrow{NaNH_2} C_6H_5CH=CHCH(OC_2H_5)_2$$
(VII)

In the same way, diethyl acetonylphosphonate carbanion, prepared from diethyl acetonylphosphonate (VIII), was treated with benzaldehyde to give the expected benzalacetone (IX) in a poor yield.

$$C_6H_5CHO + (C_2H_5O)_2P(O)CH_2COCH_3$$
(VIII)

$$\xrightarrow{NaNH_2} C_6H_5CH=CHCOCH_3$$
(IX)

Experimental

The phosphonates were prepared by means of the Michaelis-Arbuzov reaction[4]. The sodium amide was a commercial product.

Ethyl Cinnamilideneacetate.—Diethyl carbethoxymethyl phosphonate (11.20 g., 0.05 mol.), prepared from ethyl bromoacetate and triethylphosphite, in dry tetrahydrofuran (20 ml.) was added dropwise with stirring to a suspension of sodium amide (1.95 g., 0.05 mol.) in dry tetrahydrofuran (30 ml.) at about 20°C. The solution was then stirred at room temperature under a slow stream of nitrogen to sweep out the evolved ammonia.

Into the resulting yellow solution, cinnamaldehyde (6.60 g., 0.05 mol.) in the same solvent (20 ml.) was added dropwise over a one-hour period at 20~25°C. During this addition, a gummy precipitate appeared.

The solvent was removed, and then the residue was taken up in water. The aqueous solution was extracted with ether. The ether extract was dried over sodium sulfate and evaporated, and the residue was distilled under reduced pressure, giving 7.3 g. (72.5%) of liquid; b. p., 135~136°C/2 mmHg. This product crystallized; m. p., 26~27°C.

Found: C, 77.10; H, 6.92. Calcd. for $C_{13}H_{14}O_2$: C, 77.20; H, 6.98%.

β-Phenylcinnamonitrile (Va).—Sodium amide (1.95 g., 0.05 ml.) was placed in dry tetrahydrofuran (30 ml.). Diethyl cyanomethylphosphonate (8.86 g., 0.05 mol.), prepared from bromoacetonitrile and triethylphosphite, in dry tetrahydrofuran (20 ml.) was added dropwise with stirring to the suspension at 0~5°C, and then the resulting red solution was stirred at 15°C for about three hours under a slow stream of nitrogen. After removal of

4) G. M. Kosolapoff, "Organophosphorus Compounds", 1st. ed., J. Wiley & Sons, Inc., New York, N. Y. (1950), Chap. 7.

the ammonia, (benzophenone 9.1 g., 0.05 mol.) in the same solvent (20 ml.) was added dropwise with stirring at room temperature, and the solution was allowed to stand overnight. The solvent was removed after cooling, water was added to the residue, and the product was extracted with ether. The ether, after being dried over sodium sulfate, was removed, and the residue was distilled under reduced pressure giving 4.5 g. of liquid (b. p., 170~171°C/5.5 mmHg), which solidified, giving crystals (m. p. 43~44°C).

Found: C, 87.50; H, 5.39; N, 6.77. Calcd. for $C_{15}H_{11}N$: C, 87.77; H, 5.40; N, 6.82%.

Cinnamonitrile (Vb). — Diethyl cyanomethylphosphonate carbanion was prepared from diethyl cyanomethylphosphonate (8.86 g., 0.05 mol.) and sodium amide (1.95 g., 0.05 mol.) in the same way. Benzaldehyde (5.3 g., 0.05 mol.) in dry tetrahydrofuran (20 ml.) was added with stirring at −15~−10°C to the carbanion. After this addition, the solution was stirred for 30 min. at 15°C and allowed to stand overnight. The ether extract was dried over sodium sulfate. After removal of the ether, the residue was distilled, giving 5.5 g. of liquid (b. p., 121~123°C/9 mmHg). The liquid was hydrolyzed to give crystals of cinnamic acid (m. p., 131~133°C).

Cinnamaldehyde Diethylacetal (VII). — Diethyl formylmethylphosphonate diethylacetal (12.7 g., 0.05 mol.), prepared from bromoacetoaldehyde diethylacetal and triethylphosphite, in dry tetrahydrofuran (20 ml.) was added dropwise with stirring at 18~20°C into sodium amide (1.95 g., 0.05 mol.) in dry tetrahydrofran (30 ml.); then nitrogen was passed into the solution for several hours. After removal of the ammonia, benzaldehyde (5.3 g., 0.05 mol.) in the same solvent (20 ml.) was added dropwise with stirring at 17~18°C. The solution was stirred for an additional three hours and allowed to stand overnight. The solvent was evaporated, and the oily residue was taken up in water. The aqueous solution was extracted with ether, and the ether extract was dried over sodium sulfate and evaporated and the residue was distilled, giving 6.3 g. of liquid (b. p., 126~127°C/10 mmHg). The product was hydrolyzed and identified with the 2,4-dinitrophenylhydrazone (m. p., 149~151°C).

Benzalacetone (IX). — Diethyl acetonylphosphonate was prepared from bromoacetone and triethylphosphite. The phosphonate (9.2 g., 0.05 mol.) in dry tetrahydrofuran (20 ml.) was added dropwise with stirring at 3~5°C into a suspension of sodium amide(1.95 g., 0.05 mol.) in dry tetrahydrofran (30 ml.), and then nitrogen was passed into the solution to sweep out the ammonia. Into the solution, benzaldehyde (5.3 g., 0.05 mol.) in the same solvent was added dropwise with stirring at 5~8°C. The solution was stirred for an hour and allowed to stand overnight. The solvent was then evaporated. Steam-distillation gave IX; m. p., 39~40°C.

Found: C, 81.86; H, 7.24. Calcd. for $C_{10}H_{10}O$: C, 82.16; H, 6.90%.

We are indebted to Mr. Keiji Naruse for performing the microanalyses.

Laboratory of Organic Chemistry
Tokyo Institute of Technology
Meguro-ku, Tokyo

Studies on the Effects of the Substituents for 1-Arylaminoanthraquinones

By Takayuki HAYASHI and Masaki MATSUO*1

(Received May 8, 1962)

In recent years, much effort has been expended in devising a series of anthraquinone acid dyes that are resistant to decomposition by light and to severe washing. The method which has been adopted most widely is to introduce large non-sulfonated groups into established simpler dyes, thereby increasing the molecular size and the affinity for fiber and decreasing the solubility in water[1]. Prior to a discussion of the anthraquinone acid dyes, 1-arylaminoanthraquinones, the parent compounds, will be considered in this paper. Substituent groups (X) include nitro, chloro, methyl, methoxy and amino groups. Their visible and infrared absorption spectra have been measured in solution and in solid respectively. On the basis of these results, the effects of the substituent groups (X) will be discussed in view of various properties, such as wavelengths of absorption maxima and C=O and NH frequencies, similar to the previous discussion of the properties of acylaminoanthraquinones[2].

*1 Present Address: Institute of Industrial Science, The University of Tokyo, Minato-ku, Tokyo.

1) W. Bradley, "Recent Progress in the Chemistry of Dyes and Pigments", Royal Institute of Chemistry, London (1958), p. 61.

2) T. Hayashi and R. Shibata, This Bulletin, **34**, 1116 (1961).

Results and Discussion

Visible Absorption Spectra.—The visible absorption spectra of some 1-arylaminoanthraquinones were observed by Hida[3] in a trichlorobenzene solution. For this paper, their spectra have been measured in an *o*-dichlorobenzene solution, and the effects of the substituents on the wavelength of the absorption maximum have been considered.

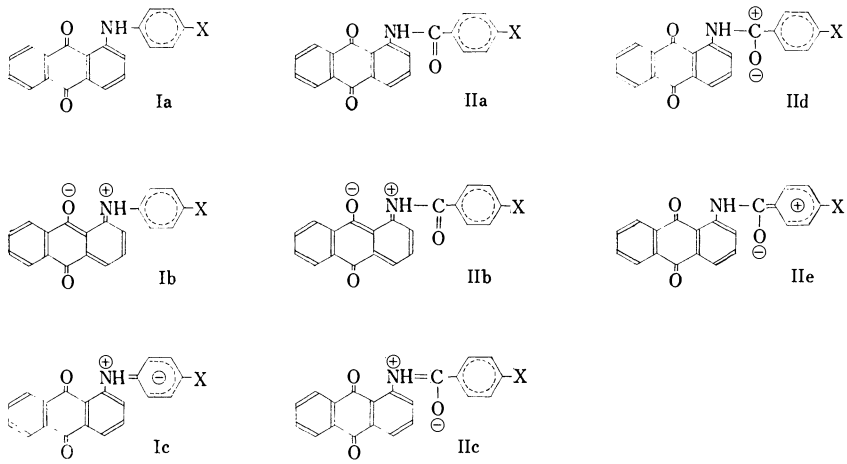
For 1-phenylaminoanthraquinone (I), the contribution of structure Ib to the resonance would be larger and, owing to the $-T$ effect of the phenyl group, the wavelength of the absorption maximum would become longer than that of 1-aminoanthraquinone*2. For 1-benzoylaminoanthraquinone (II), the contribution of structure IIb to the resonance would be the largest, but, since this is repressed by the contribution of structure IIc, the wavelength of the absorption maximum becomes shorter than that of 1-aminoanthraquinone. From the results indicated in Table I, one can see that the general pattern of effects on the absorption maxima agrees with the well-known effects[2,4-5] of substituents on the amino group.

TABLE I. VISIBLE ABSORPTION PEAKS OF 1-ARYLAMINOANTHRAQUINONES

X	Peak
H[a]	508 (5920)*3
p-NO_2[b]	487 (10700)
m-NO_2	489 (6460)
o-NO_2	483 (9370)
p-Cl	505 (7130)
m-Cl	501 (7220)
o-Cl	499 (6610)
p-NHCOMe	513 (6200)
o-NHCOMe	482 (6220)
p-Me	514 (6190)
o-Me	506 (6390)
p-OMe	516 (6000)
o-OMe	517 (5970)
p-NH_2[c]	525 (5990)
m-NH_2	515 (6910)
o-NH_2	492 (5980)

The peaks of a), b) and c) appeared at 511 (7590), 488±3 (10000) and 520 mμ (6920)*3 respectively in trichlorobenzene[3].

In the previous case of 1-acylaminoanthraquinones[2] (II), a plot of the wave numbers of the absorption maximum against the corresponding Hammett σ values[6] concaved upwards, but against the corresponding Brown σ^+ values[7,8] gave a linear relationship. For 1-arylaminoanthraquinones, on the contrary while, the plot of the wave numbers against the former does give a linear relationship, against the latter it does not do so, as is indicated in Figs. 1 and 2. In general, the electron-releasing para substituent, such as amino, methoxy and methyl groups, show the electron-release described by Hammett σ values in a nucleophilic reaction, but they show a greater electron-release than that described by them in an electrophilic reaction. In the latter, the deviations of the plots for these groups may reasonably be attributed to the differing capacities of the substituents for the resonance stabilization of a positively-charged transition state;



3) Presented at the Meeting of the Society of Organic Synthetic Chemistry of Japan, Tokyo, October, 1960.

*2 A peak of 1-aminoanthraquinone appeared at 464 mμ (5980)*3 in *o*-dichlorobenzene.

*3 Wavelength, mμ, (molar extinction coefficient).

4) R. H. Peters and H. H. Sumner, *J. Chem. Soc.*, **1953**, 2101.

5) W. Bradley and H. Kaiwar, ibid., **1960**, 2859.

6) H. H. Jaffé, *Chem. Revs.*, **53**, 191 (1953).

7) H. C. Brown and Y. Okamoto, *J. Am. Chem. Soc.*, **80**, 4979 (1958).

8) H. C. Brown, "Steric Effects in Conjugated Systems", Ed. by G. W. Gray, Butterworths Scientific Publications, London (1958), p. 100.

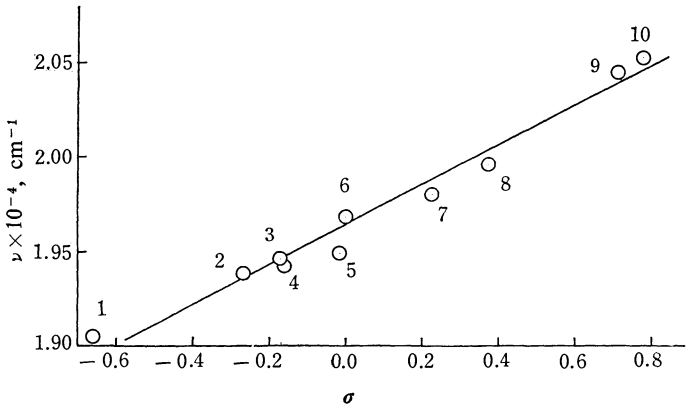


Fig. 1. Plot of wave numbers of the visible absorption maximum against Hammett σ values for 1-arylaminoanthraquinones.

1. *p*-NH_2, 2. *p*-OMe, 3. *p*-Me, 4. *m*-NH_2, 5. *p*-NHCOMe, 6. H, 7. *p*-Cl, 8. *m*-Cl, 9. *m*-NO_2, 10. *p*-NO_2

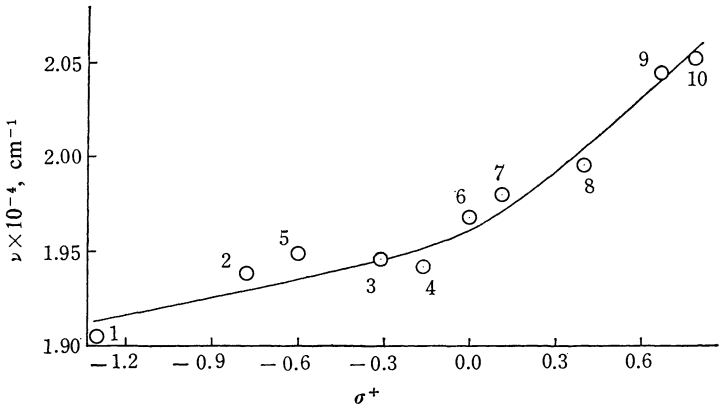


Fig. 2. Plot of wave numbers of the visible absorption maximum against Brown σ^+ values for 1-arylaminoanthraquinones.

the positive charge must be delocalized through resonance interaction, while it is the negative charge which must so be delocalized on the former. Therefore, although some attempts to correlate electrophilic reactions with an alternative set of substituent constants have been proposed by various authors, Brown's set[7,8] is apparently the one with the most general applicability. Here, too, the same considerations as noted above are employed in the case of the shifts of absorption maxima. For 1-acylaminoanthraquinones (II), the positive charge indicated in structure IId would be delocalized through resonance with electron-releasing groups, as indicated in structure IIe, but for 1-arylaminoanthraquinones(I), unshared electrons of nitrogen in structure Ia would be delocalized through the resonance with electron-attracting groups, as indicated in structure Ic. The former is consistent with the previous data for 1-acylaminoanthraquinones[2], and the latter, with the present data for 1-arylaminoanthraquinones.

For the visible absorption spectra of 7-substituted derivatives of 3,4- and of *N*-methyl-3,4-phthaloylacridones reported by Bradley[5], a plot of the wave numbers of the absorption maximum against the corresponding Hammett σ values gives a linear relationship, as is indicated in Fig. 3. This fact shows that the type of electron displacement for 3,4-phthaloylacridone is similar to that of 1-phenylaminoanthraquinone, as was deduced from the similarity in their chemical structures. It has been suggest by Bradley[5] that 3,4-phthaloylacridone's similarity to 1-phenylaminoanthraquinone in its red-violet color, indicates that it is a true acridone, not a hydroxyacridone. The establishment of this linear relationship may also support Bradley's suggestion.

Here, too, as in the previous case of 1-acylaminoanthraquinones[2], the wavelength of the

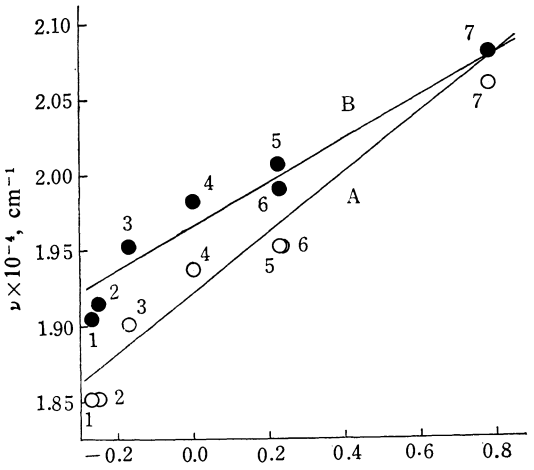


Fig. 3. Plot of wave numbers of the visible absorption maximum against Hammett σ values for 7-substituted derivatives of 3,4- and of *N*-methyl-3,4-phthaloylacridones.
A: 3,4-Derivatives
B: *N*-Methyl-3,4-derivatives
1. OMe, 2. OEt, 3. Me, 4. H, 5. Cl, 6. Br, 7. NO_2

absorption maximum is shorter for the *o*-nitro-derivative than for the *m*- and *p*-isomers; such a relation is also seen in the other *o*-derivatives, except for the *o*-methoxy derivative, as Table I indicates. The wavelength and intensity of the absorption maximum for the *o*-methyl derivative differ little from those of 1-methylaminoanthraquinone*4. The effect of the *o*-tolyl group for the former should, therefore, be much the same as that of the methyl group for the latter; this fact shows that the aryl ring is twisted around the C–N linkage between the aryl ring and the imino group in the arylamino group. The twisting may be attributed to the steric hindrance or to the repulsion between the *o*-methyl and CH groups in the 2 position of the anthraquinone nucleus. For the *o*-nitro derivative, too, the hypsochromic shift is probably due to such a twisting of the aryl ring. If it were due to the twisting of the nitro group around the C–N linkage between the benzene ring and the nitro group, the wavelengths of the absorption maxima of the *o*- and *m*-isomers would be much the same, but the wavelengths increase in the order of the *o*-, *p*- and *m*-isomers. For the *o*-amino derivative, since the wavelengths increase in the order of the *o*-, *m*- and *p*-isomers and since, moreover, the wavelength is for the first shorter than for 1-phenylaminoanthraquinone, the twisting may also arise. For the *o*-methoxy derivative, the wavelength of the absorption maximum differs little from that of the *p*-isomer; this fact shows that such twisting may not arise because of the reduced extent of the steric hindrance or because of the repulsion due to the free rotation of the methyl group in the methoxy group.

*4 A peak of 1-methylaminoanthraquinone appeared at 504 mμ (6480)*3 in *o*-dichlorobenzene.

Infrared Absorption Spectra. — Three micron infrared absorption spectra bands for a few 1,4-diarylaminoanthraquinones have been observed as Nujol mull[9], but the spectra of 1-arylaminoanthraquinones have not yet been observed. In this work, the latter were observed as Nujol mull on account of their limited solubility; then information was gained about their structure in the solid.

Table II. 3 and 6 μ-Bands of Solid 1-Arylaminoanthraquinones

X	3 μ-Bands, cm^{-1} (NH frequencies)	6 μ-Bands, cm^{-1} (C=O frequencies) (a)	(b)
H[a]	3236	1672	1634
p-NO_2	3311	1672	1639
m-NO_2	3268	1675	1637
o-NO_2	3257	1675	1650
p-Cl	3236	1678	1637
m-Cl	3257	1681	1637
o-Cl	3279	1672	1645
p-Me	3247	1684	1629
o-Me	3247	1678	1637
p-OMe	3215	1678	1626
o-OMe	3289	1672	1634
p-NH_2	3236, 3378, 3460[b]	1664	1623
m-NH_2	3236, 3390, 3484[b]	1681	1631
o-NH_2	3236, 3390, 3472[b]	1681	1629

a) NH, C=O (a) and (b) frequencies were observed at 3247, 1678 and 1639 cm^{-1} respectively by the potassium bromide disk technique.
b) The two higher frequencies are assigned to the respective NH vibration of the amino group.

Table II lists the observed NH and C=O frequencies of 1-arylaminoanthraquinones, while those of 1-phenylaminoanthrquinone are indicated in Figs. 4 and 5. For every item in this table, as in the previous case of 1-acylaminoanthraquinones[2,10], the first carbonyl bands at a higher frequency are assigned to the respective C=O (a) vibrations, since these frequencies (1660~1680 cm^{-1}) are closer than the others to the C=O frequency (1676 cm^{-1})[11] of anthraquinone; the second carbonyl bands at a lower

9) D. N. Shigorin, "Hydrogen Bonding", Ed. by D. Hadzi, Pergamon Press, London (1959), p. 191.
10) T. Hayashi, *J. Chem. Soc. Japan, Ind. Chem. Sec.* (*Kogyo Kagaku Zasshi*), **63**, 1985 (1960).
11) M. S. C. Flett, *J. Chem. Soc.*, **1948**, 1441.

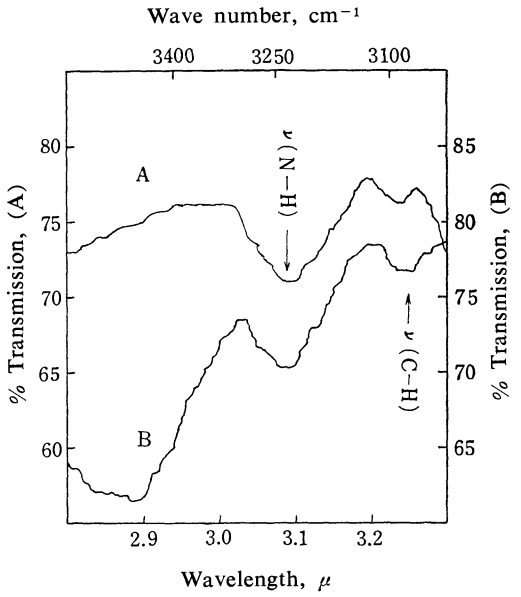


Fig. 4. 3 μ-Bands of 1-phenylaminoanthraquinone.

A : Nujol mull technique
B : KBr disk technique

frequency are assigned to the respective C=O (b) vibrations in the peri-position of the arylamino group.

For visible absorption spectra in solution, the wavelengths of the absorption maximum for 1-methylamino- and 1-dimethylaminoanthraquinones were longer than for 1-aminoanthraquinone; the wavelengths of the first and the second were alike, but their intensity decreased in the order of the first, last, and second[4]. The fact that 1-methylaminoanthraquinone had a longer wavelength than would be expected was attributed to the resonance possibility developed by the formation of the chelate structure, while the considerably reduced intensity of 1-dimethylaminoanthraquinone was thought to be due to the steric hindrance between the methyl and the C=O (b) group[4,12]. Similar phenomena have been seen in some other cases[4-5,13-14]. On the other hand, as is indicated in Table III, the fact that a C=O (b) frequency was higher for 1-methylamino- than for 1-aminoanthraquinones was attributed to the reduction of resonance by the methyl group within the former chromophoric system, and the unusually high frequency of 1-dimethylaminoanthraquinone was partly attributed to the similar reduction by methyl groups and partly to the steric hindrance between the methyl and the C=O (b) groups[11]. Similar results have been reported in some other cases[13-14]. Here, too, for visible absorption spectra in solution, the wavelength of the absorption maximum was longer for 1-phenylamino- than for 1-amino- and 1-methylamino-anthraquinones, although the C=O (b) frequency for the first was higher than for the second and was the same as that of the last. This fact may not be attributable to steric hindrance, but to the reduction by the phenyl group of resonance within the chromophoric system of the first, this being similar to the above-mentioned reduction by the methyl group for the last.

TABLE III. NH AND C=O (b) FREQUENCIES OF SOLID 1-SUBSTITUTED ANTHRAQUINONES

	NH frequency cm^{-1}	C=O (b) frequency cm^{-1}
1-Aminoanthraquinone[11]	3420, 3300	1612
1-Methylaminoanthraquinone[11]	3300	1635
1-Phenylaminoanthraquinone	3236	1634
1-Benzoylaminoanthraquinone[2]	3175	1669
1-Dimethylaminoanthraquinone[11]		1645

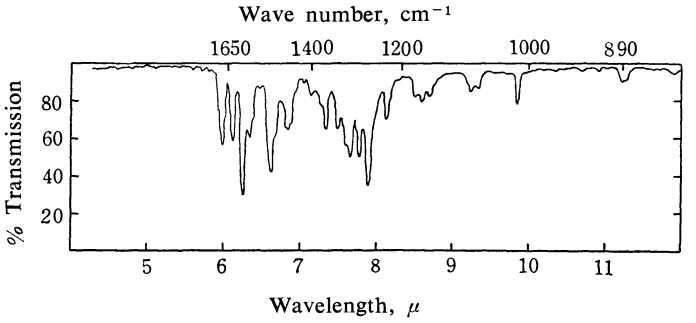


Fig. 5. The infrared spectrum of 1-phenylaminoanthraquinone by Nujol mull technique.

12) W. R. Brode, "The Roger Adams Symposium", John Wiley & Sons, Inc., New York (1955), p. 16.
13) J. Weinstein and C. Merritt, Jr., *J. Am. Chem. Soc.*, **81**, 3759 (1959).
14) R. A. Durie and J. S. Shannon, *Australian J. Chem.*, **11**, 189 (1958).

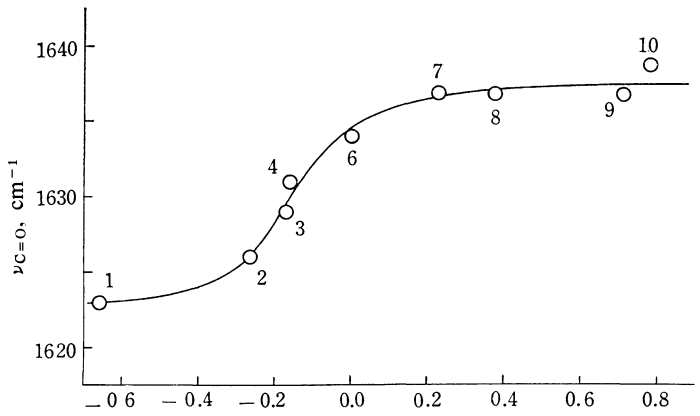
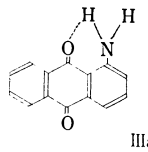
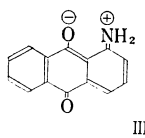


Fig. 6. Plot of C=O frequencies against Hammett σ values for 1-arylaminoanthraquinones.

As is indicated in Table III, the NH frequency lowers in the order of 1-amino-, 1-methylamino-, 1-phenylamino- and 1-benzoylamino-anthraquinones, and the reverse is found to be true for a C=O (b) frequency. For 1-aminoanthraquinone III, it seems that it is impossible to form a powerful hydrogen bonding, as in IIIa, between the amino and C=O (b) groups, and that, therefore, a contribution



IIIa



IIIb

of the ionic structure IIIb to the resonance, rather than the weak hydrogen bonding, was responsible for the considerable lowering of the C=O (b) frequency, the hydrogen bonding serving only to stabilize the ionic structure[11,15]. On the other hand, for 1-methylamino- and 1-phenylamino-anthraquinones, such resonance within chromophoric systems was reduced by the methyl and phenyl groups respectively. The above-mentioned order of the lowering of NH frequencies, therefore, suggests that the smaller the contribution of the ionic structure to the resonance becomes, the greater the contribution of the hydrogen bonding.

As is indicated in Table II, for *m*- and *p*-substituted 1-arylaminoanthraquinones, the C=O (b) frequency lowers for the ones with electron-releasing substituents, while the reverse is found to be true for the derivatives with electron-attracting groups, as in the case of those for 1-acylaminoanthraquinones[10]. These results are similar to the general pattern of substituent effects on the shift of the visible absorption maximum in solution. The effects of these substituents on the shift of the C=O (a) frequency were small, similar to those for 1-acylaminoanthraquinones[10].

A plot of the C=O (b) frequencies obtained from solids of 1-acylamino-anthraquinones against the corresponding Hammett σ values gave an S-shaped relationship; this result served to explain the shades of dyed cotton[10]. Here, too, a similar plot for 1-arylaminoanthraquinones gives the same result, as is indicated in Fig. 6. The C=O (b) bond was, therefore, strengthened to much the same degree for the derivatives with any of the electron-attracting substituents. This fact may also serve to elucidate the shades of anthraquinone acid dyes on fiber.

Here, as indicated in Table II, the C=O (b) frequency of the *o*-nitro derivative is considerably higher than those of the *m*-, *p*-isomers and 1-methylaminoanthraquinone; it is a little higher than that of 1-dimethylaminoanthraquinone, in which the unusually high C=O (b) frequency was partly attributed to steric hindrance, as has been noted above. These facts show that the aryl ring of the *o*-nitro derivative is twisted around the C–N linkage between the aryl ring and the imino group, and that the twisting may be attributed to the above-mentioned steric hindrance or to repulsion, as in the case of the molecule in solution. On the contrary, the C=O (b) frequencies of the other *o*-derivatives are 6~8 cm^{-1} higher than those of the corresponding *p*-isomers. It seems probable, therefore, that the above-mentioned twisting of the aryl rings for *o*-chloro and *o*-methyl derivatives does not arise in a solid, as in the cases of *o*-methoxy and *o*-amino derivatives, this being different from the molecule in solution. For former

15) H. Bloom, L. H. Briggs and B. Cleverley, *J. Chem. Soc.*, **1959**, 178.

o-derivatives, such twisting may be suppressed in a solid where the molecules are packed closely.

Experimental

Materials and Apparatus. — 1-Arylaminoanthraquinones with methyl or methoxy group as a substituent were prepared by condensing 1-chloroanthraquinone with substituted aniline in nitrobenzene, but nitro derivatives were prepared by condensing 1-aminoanthraquinone with the appropriate chloronitrobenzene in nitrobenzene, as has been described by Ullmann[16] and Takegawa[17]. They were obtained in good yields. Chloro derivatives were prepared in only a poor yield by either above-mentioned method. Acetylamino derivatives were prepared by acetylation of the corresponding amino derivatives with acetic anhydride, these having been prepared by reduction of the corresponding nitro derivatives with sodium dithionite at 65°C, as has been described by Ullmann[16]. All materials were purified by recrystallization and then by chromatography or hot chromatography on alumina in benzene, monochloro- or dichloro-benzene. The results are given in Table V.

TABLE V. 1-ARYLAMINOANTHRAQUINONES

X	M. p.[a] °C	N, % Found	N, % Calc.
H	146[b]	4.64	4.68
p-NO_2	314[c]	8.09	8.14
m-NO_2	246	8.11	8.14
o-NO_2	295[d]	8.13	8.14
p-Cl	212	4.15	4.20
m-Cl	202[e]	4.12	4.20
o-Cl	227	4.17	4.20
p-NHCOMe	176[f]	7.81	7.86
o-NHCOMe	266[g]	7.80	7.86
p-Me	163[h]	4.46	4.47
o-Me	192[i]	4.44	4.47
p-OMe	155[j]	4.24	4.25
o-OMe	177[k]	4.21	4.25
p-NH_2	204[l]	8.85	8.91
m-NH_2	212	8.88	8.91
o-NH_2	204[m]	8.86	8.91

a) All melting points are uncorrected.
b), d), f), g) and m) Ullmann[16] gives m. p. 147.5, 293, 176, 257 and 204°C (corr.) respectively.
c) and l) Takegawa[17] gives m. p. 311 and 206~206.5°C (corr.) respectively.
e) and i) D. R. Pat. 251103; Frdl., 11, 251 (1912), gives m. p. about 190°C.
h) Zahn[18] gives m. p. 156~157°C.
j) and k) Cook[19] gives m. p. 153~154 and 177°C respectively.

The visible absorption spectra were obtained by a Shimadzu spectrophotometer, type QB-50. The infrared absorption spectra were obtained using the Nujol mull technique; a Perkin-Elmer Model 21 double beam spectrophotometer fitted with a rock-salt prism was also used. Purification of *o*-dichlorobenzene was done by the method recommended for monochlorobenzene[20].

The authors wish to express their deep thanks to Professor Yoshio Nagai and Professor Shimpachiro Kato of the University of Tokyo for their helpful suggestions and encouragement in the course of this work, and also to Mr. Akira Hara of the Tokuyama Research Laboratory of the Idemitsu Kōsan Co. for their infrared measurements.

Department of Chemistry
Faculty of Literature and Science
Yamaguchi University
Ushirogawara, Yamaguchi-shi

16) F. Ullmann and O. Fodor, *Ann.*, **380**, 317 (1911).
17) Y. Takegawa et al., *J. Chem. Soc. Japan, Ind. Chem. Sec.* (*Kogyo Kagaku Zasshi*), **60**, 595 (1957).
18) K. Zahn and H. Koch, *Ber.*, **71**, 172 (1938).
19) A. H. Cook and W. Waddington, *J. Chem. Soc.*, **1945**, 402.
20) A. Weissberger and E. S. Proskauer, "Organic Solvents", Interscience Publishers, New York (1955), p. 407.

The Mutual Interaction between Solutes in Gas Chromatography

By Kazuo AMAYA and Kazuko SASAKI

(Received March 29, 1962)

In principle, it is expected that the solutes will interact with each other in the liquid phase and that the retention volume of one component will be affected by the presence of the other components. In gas chromatography (gas-liquid partition gas chromatography), howevr, it is generally accepted that solutes do not, in fact, interact with each other in the liquid phase and that the retention volume of one solute is independent of the presence of the other components, because the concentration of each component is infinitely small. In order to elucidate the above problem, a theoretical consideration of the problem will be made from the standpoint of strictly regular solutions, and also a little experimental evidence will be given.

Theoretical Considerations

In considering the effect of the presence of other components on the retention volume of one particular component, the partial vapor pressure of the one component, which relates to its partition coefficient, in the presence of the other component must first be considered. We consider two kinds of components 1 and 2 in samples as solutes and the liquid of the stationary phase as the solvent, and we regard the portion of the stationary phase liquid in which solutes 1 and 2 are dissolved as a uniform ternary system. The system is composed of N_1 molecules of solute 1, N_2 molecules of solute 2, and N_s molecules of the solvent; for the sake of simplicity, it is also assumed that solutes 1 and 2 and the solvent have the same molecular sizes and that these molecules are arranged in $(N_1+N_2+N_s)$ sites of a quasi-crystalline lattice with z nearest neighbors. For zeroth approximation, the configurational free energy F_c of the system is given by

$$F_c=\frac{1}{2}z(N_1+N_2+N_s)\left\{\frac{N_s^2}{(N_1+N_2+N_s)^2}u_{ss}+2\frac{N_sN_1}{(N_1+N_2+N_s)^2}u_{s1}+2\frac{N_sN_2}{(N_1+N_2+N_s)^2}u_{s2}+\frac{N_1^2}{(N_1+N_2+N_s)^2}u_{11}+\frac{N_2^2}{(N_1+N_2+N_s)^2}u_{22}+2\frac{N_1N_2}{(N_1+N_2+N_s)^2}u_{12}\right\}+\boldsymbol{k}T\left(N_s\ln\frac{N_s}{N_1+N_2+N_s}+N_1\ln\frac{N_1}{N_1+N_2+N_s}+N_2\ln\frac{N_2}{N_1+N_2+N_s}\right) \quad (1)$$

where u_{ij} denotes the mutual interaction energy of the ij pair, $\boldsymbol{k}$ is the Boltzmann constant, and T is the absolute temperature. The chemical potential of solute 1 in the liquid phase, μ_1^l can be obtained by differentiating Eq. 1 with respect to N_1. μ_1^l is then expressed as

$$\left(\frac{\partial F_c}{\partial N_1}\right)=\mu_1^l=-x_s^2u_{ss}+2x_s(1-x_1)u_{s1}-2x_sx_2u_{s2}+x_1(2-x_1)u_{11}-x_2^2u_{22}+2x_2(1-x_1)u_{12}+\boldsymbol{k}T\ln x \quad (2)$$

where x, x_1 and x_2 denote $N_s/(N_1+N_2+N_s)$, $N_1/(N_1+N_2+N_s)$ and $N_2/(N_1+N_2+N_s)$ respectively. If we define the quantities w_{s1}, w_{s2} and w_{12} as

$$\left.\begin{aligned}w_{s1}&=2u_{s1}-u_{ss}-u_{11}\\w_{s2}&=2u_{s2}-u_{ss}-u_{22}\\w_{12}&=2u_{12}-u_{11}-u_{22}\end{aligned}\right\} \quad (3)$$

and use the relation that $x_1+x_2+x_s=1$, Eq. 2 can be rewritten as

$$\mu_1^l=x_{s2}w_{s1}+x_2^2w_{12}+x_2x_s(w_{12}+w_{s1}-w_{s2})+u_{11}+\boldsymbol{k}T\ln x_1 \quad (4)$$

Similarly, the chemical potential of Solute 2, μ_2^l, is given by

$$\mu_2^l=x_s^2w_{s2}+x_1^2w_{12}+x_1x_s(w_{12}-w_{s1}+w_{s2})+u_{22}+\boldsymbol{k}T\ln x_2 \quad (5)$$

For the gas phase, the solute molecules are assumed to be perfect and to have no interaction with other molecules. Therefore, if we neglect the contribution of the internal degrees of freedom to the chemical potential, the chemical potentials of solutes 1 and 2, μ_1^g and μ_2^g respectively, are given by:

$$\mu_1^g=\boldsymbol{k}T\ln N_1^g/V \quad (6)$$

$$\mu_2^g=\boldsymbol{k}T\ln N_2^g/V \quad (7)$$

where N_1^g and N_2^g denote the number of molecules of solutes 1 and 2 respectively in the gas phase of volume V. In equilibrium, the chemical potential of each species is equal in both the liquid and gas phases; therefore, by equating 4 with 6 and 5 with 7, the following relations are obtained;

$$kT \ln N_1^g/V = x_s^2 w_{s1} + x_2^2 w_{12} + x_2 x_s (w_{12} + w_{s1} - w_{s2}) + u_{11} + kT \ln x_1 \quad (8)$$

$$kT \ln N_2^g/V = x_s^2 w_{s2} + x_1^2 w_{12} + x_1 x_s (w_{12} - w_{s1} + w_{s2}) + u_{22} + kT \ln x_2 \quad (9)$$

Since the partition coefficient is the ratio of the mumber of solute molecules in the unit volume of the stationary liquid phase to that in the gas phase, the partition coefficient of solute 1, k_1^m, and that of solute 2, k_2^m, for their mixture are given by:

$$\ln k_1^m = \ln N_1 x_1 - \ln N_1^g/V = -(1/kT)\cdot\{x_s^2 w_{s1} + x_2^2 w_{12} + x_2 x_s (w_{12} + w_{s1} - w_{s2}) + u_{11}\} \quad (10)$$

$$\ln k_2^m = \ln N_1 x_2 - \ln N_2^2/V = -(1/kT)\cdot\{x_s^2 w_{s2} + x_1^2 w_{12} + x_1 x_s (w_{12} - w_{s1} + w_{s2}) + u_{22}\} \quad (11)$$

where N_1 is the number of molecules in the unit volume of the stationary liquid phase. The partition coefficients k_1^o and k_2^o for the pure solutes 1 and 2 respectively are obtained by equating x_2 or x_1 in Eqs. 10 and 11 with zero and are given by:

$$\ln k_1^0 = \ln N_1 x_{10} - \ln N_1^g/V = -(1/kT)\cdot(x_{s1}^2 w_{s1} + u_{11}) \quad (12)$$

$$\ln k_2^0 = \ln N_1 x_{20} - \ln N_2^g/V = -(1/kT)\cdot(x_{s2}^2 w_{s2} + u_{22}) \quad (13)$$

where x_{10} and x_{20} denote the mole fraction of solutes 1 and 2 respectively, and x_{s1} and x_{s2} denote the corresponding mole fraction of the solvent when only a single solute is present. From Eqs. 10, 11, 12 and 13 the ratio of partition coefficients for the mixture to that for the pure component, when there is an equal concentration in the stationary liquid phase, that is, $x_{10}=x_1$ and $x_{20}=x_2$, k_1^m/k_1^o and k_2^m/k_2^o, are given by using the relation $x_{s1}=x_s+x_2$ or $x_{s2}=x_s+x_1$:

$$\ln k_1^m/k_1^o = -(1/kT)\cdot\{x_2^2(w_{12}-w_{s1}) + x_2 x_s (w_{12} - w_{s1} - w_{s2})\} \quad (14)$$

$$\ln k_2^m/k_2^o = -(1/kT)\cdot\{x_1^2(w_{12}-w_{s2}) + x_1 x_s (w_{12} - w_{s1} - w_{s2})\} \quad (15)$$

Generally, the right sides of Eqs. 14 and 15 are not equal to zero, and k_1^m and k_2^m differ from k_1^o and k_2^o respectively; consequently, the retention volume for the mixture differs from that for the pure component.

Experimental

The experiments were performed for the equivolume mixture of chloroform-ethyl methyl ketone with a column of apiezon J and those of the chloroform-carbon tetrachloride and chloroform-toluene mixture with a column of P. E.; also, the position of each peak was compared with that obtained for the pure substances. In this case the quantity of each component was kept equal. The results obtained are shown in Table I.

Discussions

If $x_2 \ll 1$, and $x_1 \ll 1$, x_s is approximated to be equal to 1, and the term containing x_1^2 or x_2^2 is neglected as too small, and if, in expanding the exponential function, the terms higher than the second are also neglected, Eqs. 14 and 15 can be approximated as

$$k_1^m = k_1^o\{1 - (1/kT)\cdot x_2(w_{12} - w_{s1} - w_{s2})\} \quad (16)$$

Table I. Comparison of the retention time for mixtures (T_r^m) with that for pure components (T_r^o). (The quantity of each component is 25μl.)

Sample	T_r^o, min.	T_r^m, min.	ΔT_r, min.	$\Delta T_r/T_r^o$
Ethyl methyl ketone	7.60	7.83	0.23	0.030
Chloroform	10.95	11.63	0.68	0.062

Experimental Conditions —— Temp.: 52°C; Press.: 34.75 mmHg; Column: Cu pipe; Stationary phase: Apiezon J 420 g.; Support: C-22; Firebrick: 1200 g. 42~60 mesh; Carrier gas: H_2; Flow rate: 94 cc./min.

Sample	T_r^o, min.	T_r^m, min.	ΔT_r, min.	$\Delta T_r/T_r^o$
Carbon tetrachloride	4.55	4.64	0.10	0.022
Chloroform	10.16	10.35	0.19	0.019

Experimental conditions —— Temp.: 70.2°C; Press.: 26.2 mmHg; Column: Cu pipe 4 m; Stationary phase: P. E. G. 3; Support: Celite 10; Carrier gas; H_2; Flow rate: 77 cc./min.

Sample	T_r^o, min.	T_r^m, min.	ΔT_r, min.	$\Delta T_r/T_r^o$
Toluene	13.74	14.02	0.26	0.019
Chloroform	8.97	9.05	0.08	0.009

Experimental conditions —— Temp.: 70.2°C; Press.: 31.0 mmHg; Flow rate: 83 cc./min; Other conditions were the same as above.

$$k_2^m = k_2^o\{1-(1/\boldsymbol{kT})\cdot x_1(w_{12}-w_{s1}-w_{s2})\} \quad (17)$$

These equations show that the effect of interaction with a foreign substance is proportional to its concentration.

It may also be inferred that the partition coefficient in the mixture increases or decreases as the sign of $(w_{12}-w_{s1}-w_{s2})$ is positive or negative. This indicates that the position of the peak for a particular component is shifted to either the shorter or longer side according to the kind of other component in the mixture.

In the above discussions, it is tacitly assumed that the two solutes coexist and that the concentration of each solute does not change with time. However, in actuality, the concentration of each solute changes with time and the two solutes are gradually separated as they proceed through a column and are finally completely separated where the effect of interaction with the other solute does not occur. This means that the k_1^m/k_1^o or k_2^m/k_2^o ratio changes with time, even if the two solutes are always both present, if not, its value approaches 1 when the two solutes are completely separated. The time required for the value of k_1^m/k_1^o or k_2^m/k_2^o to reach 1 is dependent on the kind of solute. If the retention times of solutes 1 and 2 are denoted by T_1 and T_2 respectively, the effect of the interaction becomes larger as T_1/T_2 approaches 1.

The assumption that the solute and the solvent have the same molecular size is far from the actual case, for the molecular size of the stationary liquid phase is of an order ten times greater than that of most samples. However, the effect of the difference in molecular size is not significant if the mole fractions in the expressions are replaced by the volume fractions.

As for the experimental results, in the mixture of chloroform (1) and ethyl methyl ketone (2) it was found that the component peaks shifted to a positive direction compared with those for single component samples when an apiezon J column is used. This is interpreted as follows: the heat of the mixing of chloroform with ethyl methyl ketone may be negative, since the two components may form a hydrogen-bonded complex as chloroform and acetone do; hence, the value of w_{12} may be negative.

Further, since both component molecules, 1 and 2, have dipoles and since the stationary phase liquid apiezon J(s) is a homologue of aliphatic hydrocarbons, the heats of the mixing of s with 1 and with 2 may both be positive and the values of w_{s1} and w_{2} may be positive. Accordingly, the value $(w_{12}-w_{1}-w_{2})$ in Eqs. 16 and 17 may be negative; it therefore follows that $k_1^m > k_1^o$ and $k_2^m > k_2^o$ and the position of each component peak in the mixture may be shifted in the positive direction. This prediction coincides with the experimental results. An example of the reverse case, in which the relation $k_1^m < k_1^o$ and $k_2^m < k_2^o$ holds, has not yet been found.

For a quantitative discussion of this problem we must further derive those expressions which relate the concentration of the single component sample in the column with the time which has transpired after the sample injection under the assumption that the partition coefficient of each component varies with its concentration in the column; then we must integrate the contribution due to mutual interaction at each concentration. Further, the same procedure must be repeated for the mixture samples and the latter results compared with the former. We do not intend to deal with this problem here.

Theory predicts that the shift of each component peak due to mutual interaction will occur in the same direction. The experimental results coincide with this prediction.

It should be noted that an apparent shift in the two peaks occurs when they approach, but that the directions of the shifts are such that the two peaks come close together and are opposite each other, which effect can easily be discriminated from what originates from the mutual intearction.

Although in the present experiment a considerable quautity of samples (25μl.) was used, the relative shift of the peaks was 6% at most, which wonld be a much smaller value if much smaller quantity of samples were used. In actuality, the quantity of samples is usually of an order of a few μl. and the effect of mutual interaction can be neglected. However, when the minor component is analysed by using large amount of the sample, the effect may become important.

Summary

The influence of the mutual interaction between the molecules of different components in the sample on the retention volume of each component has been discussed from the standpoint of a strictly regular solution. The retention volume of each component in the mixture either increases or decreases, compared with that in the single component samples, according to the kinds of sample and of stationary phase liquid.

The authors wish to express their thanks to Mr. Ichiro Takeda for his helpfulness in the experimentation and also for his valuable discussions throughout this work. The authors

also wish to express their thanks to Dr. Yōichiro Mashiko for his constant encouragement throughout this work.

Government Chemical Industrial Research Institute, Tokyo
Shibuya-ku, Tokyo

Studies on Tritium-labeled Compounds. VI[1]. *The Platinum-catalyzed Exposure Technique*

By Teruhiko MESHI and Tadao TAKAHASHI

(Received March 22, 1962)

The gas exposure technique developed by Wilzbach[2] has greatly simplified the labeling of many organic compounds, including such biologically active materials as insulin[3]. Its use is somewhat restricted, however, by the fact that multicuric quantities of tritium are required to obtain levels of activity, satisfactorily high for tracer experiments.

Up to the present, workers have tried to increase the labeling by adding to the system such external activation energy as is obtained from electric discharge[4-7], microwave discharge[7], ultraviolet irradiation[7], and γ-radiation[5]. These methods increase the specific activities remarkably, but they also produce a large amount of decomposition products. The aim of our experiments is also to obtain higher labeled products by the Wilzbach method but not by adding external activation energy. We have also tried to increase the efficiency of labeling by a larger exploitation of the β-ray energy of tritium.

Since the β-particle from tritium has a range of only 0.7 mg./cm^2, complete absorption of energy occurs within the layers of 7 μ if the organic material has a specific weight of 1 g./cm^3. Therefore, it is quite clear that labeling will occur at or near the surface of the organic compound.

The possibility of increasing the labeling efficiency by reducing the size of the particle of the organic compound is very limited, as Rosenblum et al.[8] have already shown.

Recently Wenzel et al[9] reported that higher specific activities in the range of 2~130 fold were obtained by adsorbing the compound on charcoal. When hydrogenation catalysts were applied to a salicylic acid-T_2 system, a large increase in specific activity was observed. This paper presents the results of this new modification for labeling organic compounds by the Wilzbach procedure.

Experimental

Chemicals.—All chemicals used were of analytical reagent grade and were not subjected to any further purification.

Platinum black was prepared by hydrogenation of Adams platinum oxide[10] made from chloroplatinic acid.

Palladium black was prepared by hydrogenation of palladium oxide[11] made from palladium chloride. Raney nickel was developed from a Ni-Al alloy consisting of 50% nickel by the W-2 method. The tritium gas was purchased from the Radiochemical Center, Amersham, and was 98% T_2, the rest being H_2.

Exposure. — Glass ampoules with a volume of about 5 ml. and with a breakoff seal were used for exposure.

All the samples were thoroughly mixed with 100 mg. of the catalysts and then brought into a reaction vessel. The reaction vessel was connected with the apparatus described in the previous paper[1] and was throughly degassed by pumping.

After some hours of evacuation, about 100 mc. of tritium was transferred to the reaction vessel by means of the Toepler pump, and then the capillary was sealed off. After the exposure, the reaction vessel was remounted on the apparatus, the breakoff

1) Part V: Y. Sato, T. Takahashi and T. Meshi, *Radioisotopes*, **10**, 488 (1961).
2) K. E. Wilzbach, *J. Am. Chem. Soc.*, **79**, 1013 (1957).
3) C. Holt and L. Holt, *Naturwiss.*, **12**, 289 (1958).
4) K. E. Wilzbach and L. M. Dorfman, *J. Phys. Chem.*, **63**, 799 (1959).
5) F. L. Jackson, G. W. Kittinger and F. P. Krause, *Nucleonics*, **18**, 102 (1960).
6) Y. Sato, T. Meshi, T. Takahashi and N. Sugimoto, *Japanese J. Pharm. and Chem.*, **32**, 317 (1960).
7) T. Westermark, H. Lindroth and B. Enander, *Intern. J. Appl. Rad. Isotopes*, **7**, 331 (1960).
8) C. Rosenblum and H. T. Meriwether, Proceedings of the Symposium on Advances in the Tracer Applications of Tritium (1958), p. 3.
9) M. Wenzel and H. Wollenberg, Symposium on the Detection and Use of Tritium in the Physical and Biological Sciences, Vienna (1961).
10) R. Adams, V. Voohees and R. L. Shriner, "Organic Syntheses", Col. vol. I, (1948), p. 463.
11) R. L. Shriner and R. Adams, *J. Am. Chem. Soc.*, **46**, 1683 (1924).

seal was opened, and the tritium was transferred to a storage vessel.

Purifications. — The exposed products were dissolved in a hydroxylic solvent, and the catalyst was filtered off.

The solvent was removed from the filtrate by distillation in vacuo. This operation was repeated three times to remove the exchangeable tritium completely. The residue was recrystallized from a suitable solvent and radiochemically purified through paper-chromatography, using Toyo Roshi No. 526. L-Valine and thiamine were purified with *n*-butanol-acetic acid-water (4 : 1 : 1), inositol with *n*-butanol-ethanol-water (4 : 1.1 : 1.9), and predonisolone with toluene-methanol (3 : 1). Sublimation was chosen for purification of salicylic acid, and solvent extraction for that of benzoic acid. The radiochemical purity was established by cutting the chromatograms of the labeled compounds in 10 mm. segments, extracting each segment with distilled water or alcohol, and counting the tritium activity of each extract in a windowless gas-flow counter.

Measurement of Radioactivity. — The specific activities of the tritiated products were determined by liquid scintillation counting. An aliquot of a suitable concentration of a compound in a mixture of alcohol and water was added to toluene dissolving phenylbiphenyloxadiazole (4 g./l.) and 1,4-di(2,5-phenyloxazole)-benzene (100 mg./l.) and was counted with a Pachard Tri-Carb liquid scintillation spectrometer cooled to −10°C. This system had an efficiency of approximately 13% if the sample was nonquenching.

An internal standard was used to correct for quenching and to estimate the efficiency of counting.

Results

Listed in Table I are the results of the new method of labeling with tritium catalyzed by three different typical hydrogenation catalysts.

As is shown in Table I, the platinum catalyst is the most effective in promoting tritium labeling. With platinum oxide, there is also an increase in the specific activity, but the increase is much lower because most of the tritium is used to form the tritium oxide. The addition of a small amount of platinum oxide plus platinum, however, gave a greater

Table I. Increase of the specific activity by the catalyzed exposure technique*

Compound	Catalyst mg.	Tritium gas mc.	Exposure time days	Specific activity μc./mg.	Increase of specific activity	Recovery %
Salicylic acid	Control	150	2	0.05	1	78
Salicylic acid	Charcoal (100)	150	5	0.06	1.2	53
Salicylic acid	Raney nickel (100)	150	2	0.06	1.2	59
Salicylic acid	Nickel oxide (100)	150	2	0.007		62
Salicylic acid	Pd black (100)	150	3	13.8	276	48
Salicylic acid	Pd-PdO (50 : 50)	150	3	20.0	400	49
Salicylic acid	Pt black (100)	150	5	108	2018	33
Salicylic acid	$Pt\text{-}PtO_2 \cdot H_2O$ (65 : 35)	150	5	146	2920	30
Salicylic acid	$PtO_2 \cdot H_2O$ (100)	150	5	1.0	20	54
Salicylic acid	Control	100	3	0.068	1	76
Salicylic acid	Charcoal (100)	100	3	0.090	1.3	49
Salicylic acid	Charcoal (200)	100	3	0.060		45
Salicylic acid	Pd black (100)	100	3	11.8	173	48
Salicylic acid	Pt black (100)	100	3	88	1290	37
Salicylic acid	Pt black (200)	100	3	128	1880	31
L-Valine	Control	100	20	0.30	1	80
L-Valine	Charcoal (100)	100	20	0.30	1	66
L-Valine	Charcoal (200)	100	20	0.26		63
L-Valine	Pd black (100)	100	7	0.57	1.9	72
L-Valine	Pt black (100)	100	20	8.6	29	62
L-Valine	Pt black (200)	100	20	6.2	21	59
Predonisolone	Control	100	22	0.40	1	67
Predonisolone	Charcoal (100)	100	22	0.28		63
Predonisolone	Pt black (100)	100	22	2.32	5.8	60
Benzoic acid	Control	100	5	0.10	1	74
Benzoic acid	Pt black (100)	100	5	21.0	210	53
Inositol	Control	100	4	0.24	1	68
Inositol	Pt black (100)	100	4	4.55	19	41
Thiamine	Control	100	7	0.95	1	68
Thiamine	Pt black (100)	100	7	3.05	3.2	56

* One hundred mg. of each sample was exposed to tritium gas.

TABLE II. SPECIFIC ACTIVITY OF TRITIUM IN LABILE AND NONLABILE POSITIONS IN SALICYLIC ACID AS A FUNCTION OF TIME OF EXPOSURE TO TRITIUM GAS*

Condition	Exposure time hr.	Total tritium incorporated A, μc./mg.	Increase of A	Nonlabile tritium B, μc./mg.	Increase of B	Survival B/A
Salicylic acid	1	5.4	1	0.041	1	0.76
+Pt black	1	660	122	100	2440	15.2
Salicylic acid	3	5.7	1	0.036	1	0.63
+Pt black	3	555	97	91	2530	16.4
Salicylic acid	10	5.9	1	0.024	1	0.42
+Pt black	10	426	72	84	3500	19.7
Salicylic acid	30	6.0	1	0.020	1	0.33
+Pt black	30	372	63	78	3900	21.0

* One hundred mg. of salicylic acid was exposed to about 100 mc. of tritium either in the presence or in the absence of the platinum catalyst.

TABLE III. EFFECT OF TEMPERATURE ON LABELING OF L-VALINE*

Platinum catalyst mg.	Exposure time days	Temperature °C	Specific activity μc./mg.	Increase of specific activity	Recovery %
	7	Room temp.	0.45	1	80
100	7	Room temp.	106	235	62
	4	80	0.58	1.3	68
100	4	80	2.25	5	58

* One hundred mg. of L-valine was exposed to about 100 mc. of tritium.

increase in specific activity than that of platinum alone. This is probably due to the fact that tritium gas is more readily adsorbed on platinum oxide than on platinum. The conditions employed and the results obtained in the labeling of six compounds by the catalyzed exposure technique are listed in Table I. The increase in labeling varies considerably with different compounds, but it is present in all of the compounds studied.

The aromatic compounds are more readily labeled than the aliphatic compounds. Table II shows the rates of the labeling of salicylic acid in the presence of or in the absence of the platinum catalyst.

In the absence of the catalyst, the total amount of tritium incorporated increases with the exposure time, while the amount of nonlabile tritium attached to the carbon atoms decreases with the time. In the presence of the catalyst, both the total amount of tritium (A) and the amount of nonlabile tritium (B) decrease with the exposure time beyond one hour.

These results indicate that the exposure for a longer time greatly increases the radiation damage in salicylic acid and so that the highest specific activity is obtainable when exposure is less than one hour. This is in contradiction to the report of Rydberg et al.[12] that the specific activity generally increased with the exposure time when p-aminosalicylic acid was exposed to tritium gas.

The data in Table III show the effect of temperature on labeling.

The amount of labeling increases with the exposure temperature without the catalyst, but in the presence of platinum the increase in the specific activity at 80°C is much lower than that at room temperature. Probably the amount of the adsorption of tritium gas on the platinum catalyst is substantially dependent on the temperature.

Discussion

The favorable effect of the platinum catalyst in the system is obviously related to the properties of platinum, as is shown in Table I. One probable effect of the platinum addition is to increase the absorption of β-ray energy from tritium in the system by making the contact closer between tritium and organic molecules on the catalyst surface by chemisorption.

The exchange reaction between tritium and hydrogen atoms of organic molecules is undoubtedly induced by the radioactive decay of the tritium and by the beta radiation associated therewith, as is shown below[13]:

12) J. Rydberg and A. Hanngren, *Acta Chem. Scand.*, **12**, 332 (1958).

13) T. H. Pratt and R. Wolfgang, *J. Am. Chem. Soc.*, **83**, 10 (1961).

$$T_2 \xrightarrow{-\beta^-} HeT^+ \quad (1)$$

$$RH \rightsquigarrow \text{Ions and excited species} \quad (2)$$

$$T_2 \rightsquigarrow \text{Ions and excited species} \quad (3)$$

where RH is the organic compound being irradiated.

If the tritium is to be used efficiently without adding external activation energy to the system, it is necessary to promote such ionization and excitation reactions as 2 and 3 by completely absorbing the decay energy in the system and also to increase the probability of reactions between HeT^+ and the organic compound.

When tritium and an organic compound are sealed in an ampoule without a catalyst, the beta energy is dissipated by the formation of ions and of excited molecules of both constituents and by the loss due to the absorption to the wall.

When the catalyst is present in the system, the wall loss should be small; the decay energy would be spent efficiently in the formation of the ions and of the excited molecules by the chemisorption of tritium on the catalyst.

The chemisorption of molecular tritium and organic molecules on the surface of the catalyst also increases the probability of reactions between HeT^+ and organic molecules.

Another effect of platinum addition may be seen in the catalytic exchange of hydrogen atoms, an exchange which has been employed for the preparation of tritium-labeled compounds using tritium oxide[14]. Farkas et al.[15] have already demonstrated the catalytic exchange of hydrogen atoms between molecular tritium and the nonpolar solvent, cyclohexane.

In the absence of a catalyst, the ratio of the total tritium to the nonlabile tritium attached to carbon atoms was less than one per cent, while in the presence of the catalyst, the B/A ratio increased to more than 15%, as is shown in Table II.

If the labeling is promoted only by increased absorption of the decay energy in the system, the B/A ratio must be independent of the presence of the catalyst.

Therefore, the great increase in the B/A ratio by platinum addition should be attributed to the catalytic exchange of hydrogen atoms, which presumably occurs through CH bond rupture. The relative amount of exchange for aliphatics is lower than for aromatics, as is shown in Table I. The observed tendency in the relative amount of exchange may be attributed to different strengths of chemisorption and to the fact that chemisorption of unsaturated hydrocarbons on a platinum catalyst occurs through π-complex formation.

It may be considered that chemisorption involving aliphatic compounds is relatively weak, or, alternatively, that strong chemisorption may occur only at very active, and hence less abundant, catalyst sites. In the case of salicylic acid, doubling the amount of platinum in the system increases the specific activity, but in that of valine, an increase in the amount of catalyst causes no increase in tritiation.

Furthermore, there is apparently an optimum concentration of platinum beyond which an increase in the amount of catalyst reduces the specific activity of the compound. The decrease in specific activity with the increase in platinum concentration beyond an optimum can be explained on the basis of an increasing probability of the ion neutralization and of the disappearance of the excited molecules before an effective collision (one leading to labeled-product formation) can occur.

On the other hand, charcoal also adsorbs the organic compounds, and so an increase in labeling is expected. However, a drop in the specific activity was observed when the amount of charcoal was doubled.

It could be that a part of the β-ray energy is used in vain to ionize and excite the charcoal, because the tritium gas is not adsorbed on charcoal at room temperature[9], and that consequently the efficiency of the labeling decreases.

The data in Table III indicate that the chemisorption of tritium gas on the catalyst is a very important factor in promoting the labeling. The addition of the platinum catalyst appears to promote the radiolysis of organics, but the amount of radiolysis by-products is not very large, as is shown in the recovery column of Table I.

Salicylic acid became somewhat brownish in color after 3 days of irradiation, and only 31 mg. of a radiochemically pure product could be obtained. This recovery of 31% is presumably due to the increased radiation decomposition caused by the more intense irradiation.

The low recovery in the presence of charcoal can be ascribed to the incomplete elution of the charcoal-adsorbed compound, because only about 70% of the compound used was recovered when the test blank of elution was carried out with 20 ml. of alcohol. The platinum-addition method has some advantages over the original exposure technique in that the amount of tritium required is reduced and in that the time required for labeling becomes substantially

14) J. L. Garnett, L. J. Henderson and W. A. Sollich, Symposium on the Detection and Use of Tritium in the Physical and Biological Sciences, Vienna (1961).

15) A. Farkas and L. Farkas, *Trans. Faraday Soc.*, 35, 917 (1937).

shorter—a few day by this new technique as compared to a few weeks by the Wilzbach procedure for obtaining the same amount of activity.

Summary

To increase the efficiency of labeling according to the Wilzbach procedure by absorbing the β-ray energy of tritium in the system, three typical hydrogenation catalysts were applied to the salicylic acid-T_2 system.

The platinum catalyst was found to be most effective in promoting the labeling. The results obtained in labeling six compounds by the platinum-catalyzed-exposure technique showed that by this procedure higher specific activities in the range of 3~1880 fold were obtained.

The increase in labeling changed considerably with different compounds, and the relative amount of labeling for aromatics was higher than for aliphatics.

The authors wish to express their deep gratitude to Dr. Norio Sugimoto and Dr. Yoshio Kowa for their helpful advice and encouragement throughout this work. They are also indebted to Mr. Kiyoteru Yamada for the exposure apparatus.

Osaka Research Laboratory
Tanabe Seiyaku Co., Ltd.
Higashiyodogawa-ku, Osaka

Electronic States of p-Benzoquinone. VII. Intensity of the Symmetry-forbidden Electronic Absorption Bands of p-Benzoquinone

By Akira SADÔ

(Received July 26, 1961)

In Parts I[1] and II[2] of this series, we calculated the energy levels of the *p*-benzoquinone molecule and showed that the absorption bands of this molecule, appearing around 2900Å, are a superposition of three transitions, the $^1B_{1g}\leftarrow{}^1A_g$ transition, which corresponds to the π-π transition, and ^1A_u and $^1B_{2g}\leftarrow{}^1A_g$ transitions, which correspond to the n-π transitions. These transitions are all forbidden by the molecular symmetry, but are allowed through the vibronic interaction with the allowed $^1B_{2u}\leftarrow{}^1Ag$ transition. If this assignment is correct, the spectrum will appear with its transition moment along the long axis of the molecule (connecting two oxygen atoms). This is in agreement with the results of the spectroscopic studies of crystalline *p*-benzoquinone by Fixl and Schauenstein[3], Brand and Goodwin[4], and Sidman[5]. The absorption intensity around

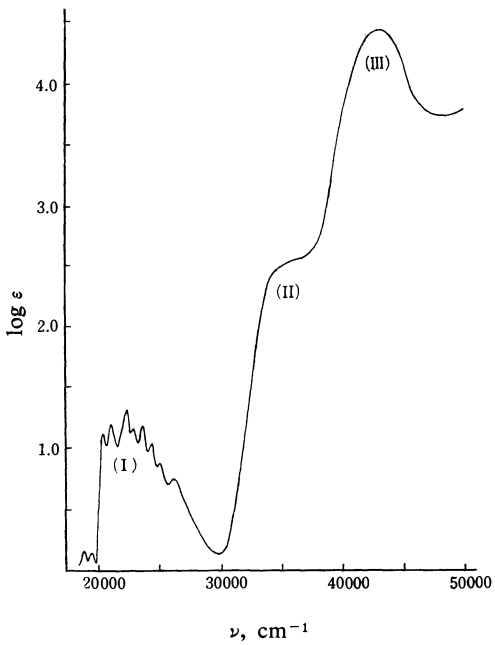


Fig. 1. The absorption spectrum of *p*-benzoquinone in *n*-hexane.

1) T. Anno, I. Matubara and A. Sadô, This Bulletin, **30**, 168 (1957).
2) T. Anno, A. Sadô and I. Matubara, *J. Chem. Phys.*, **26**, 967 (1957).
3) J. O. Fixl and E. Schauenstein, *Monatsh.*, **81**, 598 (1950); *Chem. Abstr.*, **45**, 4136f (1951).
4) J. C. D. Brand and T. H. Goodwin, *Trans. Faraday Soc.*, **53**, 295 (1951).
5) J. W. Sidman, *J. Am. Chem. Soc.*, **78**, 2363 (1956); *J. Chem. Phys.*, **27**, 820 (1957).

2900Å in a *n*-hexane solution is greater than the absorption intensity around 4500Å,

$$f_{\mathrm{I}}/f_{\mathrm{II}} \fallingdotseq 1/10 \tag{1}$$

where

$$f=\int \varepsilon_{\nu} \mathrm{d}\nu \tag{2}$$

and where subscripts I and II refer to the absorption systems around the 4500Å and 2900Å regions respectively. Therefore, we may calculate the absorption intensity as a means of determining the nature of the absorption. In the description of vibronic interaction, spatially-fixed electronic wave functions are assumed.

Theoretical Considerations

The symmetry-forbidden electronic transitions are allowed by vibronic interaction with the allowed transition. This vibronic interaction has been treated by several authors[6-8]. According to the first-order perturbation method, the oscillator strength, f, for the forbidden electronic transition is described by the following formula:

$$f_{0\to k}=\sum_{s}(E_{0\to k}/E_{0\to s})C_{sk}(\boldsymbol{s})^2 f_{0\to s} \tag{3}$$

and

$$C_{sk}(\boldsymbol{s})=(W_{sk})/(E_{0\to s}-E_{0\to k}) \tag{4}$$

where $\boldsymbol{s}$ is the displacement from the equilibrium configuration in the ground electronic state, where subscript $0\to k$ indicates that the transition is from the ground state to the k state, where $0\to k$ and $0\to s$ transitions correspond to the forbidden and the allowed transitions respectively, and where $E_{0\to k}$ is the energy of the $0\to k$ transition. If we write

$$(W_{sk})_Q=\int \Theta_s^*(\boldsymbol{r})\sum_i\sum_a\{Z_a e^2 \boldsymbol{r}_a(i)\boldsymbol{s}_{Qa}/|\boldsymbol{r}_a(i)|^3\} \times\Theta_k(\boldsymbol{r})\mathrm{d}\boldsymbol{r} \tag{5}$$

then,

$$(W_{sk})^2=\sum_Q (W_{sk})_Q \tag{6}$$

where $\boldsymbol{s}_{Qa}$ is the displacement of the atom a in the normal mode Q, $\Theta_s(\boldsymbol{r})$ is the molecular electronic wave function of the quantum state, s, for the equilibrium configuration in the ground electronic state, $\boldsymbol{r}$, the symbol for the electronic coordinate, Z_a, the effective nuclear charge, and $|\boldsymbol{r}_a(i)|$, the distance from atom a to electron i. The introduction of the molecular orbital theory to give an approximate form for the electronic wave functions $\Theta_s(\boldsymbol{r})$ and $\Theta_k(\boldsymbol{r})$ leads to a considerable simplification of Eq. 5:

$$(W_{sk})_Q=\pm e^2\int \psi_1(\boldsymbol{r})\sum_a(Z_a \boldsymbol{r}_a \boldsymbol{s}_{Qa}/|\boldsymbol{r}_a|^3) \times\psi_2(\boldsymbol{r})\mathrm{d}\boldsymbol{r} \tag{7}$$

where ψ_1 and ψ_2 are the ummatched molecular orbitals in $\Theta_k(\boldsymbol{r})$ and $\Theta_s(\boldsymbol{r})$, respectively. This expression is now a one-electron integral and represents the electrostatic energy of the interaction between a set of dipoles, μ_a, and the electronic distribution, $e\psi_1\psi_2$.

If MO is constructed by the LCAO approximation, we can write

$$\psi_1=\sum_b c_{1b}\chi_b(\boldsymbol{r}) \tag{8}$$

where χ_b is the atomic orbital for atom b and c_{1b} is the coefficient of χ_b in ψ_1. From Eqs. 7 and 8,

$$(W_{sk})_Q=\pm e^2\int \sum_a\sum_b c_{1b}\chi_b(\boldsymbol{r})(\boldsymbol{r}_a \boldsymbol{s}_{Qa}/|\boldsymbol{r}_a|^3) \times\sum_c c_{2c}\chi_c(\boldsymbol{r})\mathrm{d}\boldsymbol{r} \tag{9}$$

since,

$$\boldsymbol{r}_a=\boldsymbol{r}_b+\boldsymbol{r}_{ab} \tag{10}$$

where $|\boldsymbol{r}_{ab}|$ is the distance from atom a to atom b and where it is constant, and if we neglect the differential overlap formally, we obtain,

$$(W_{sk})_Q=\pm e^2\int \sum_a\sum_b c_{1b}\chi_b(\boldsymbol{r}) \times\{(\boldsymbol{r}_b+\boldsymbol{r}_{ab})\boldsymbol{s}_{Qa}/|\boldsymbol{r}_a|^3\}c_{2b}\chi_b(\boldsymbol{r})\mathrm{d}\boldsymbol{r} \tag{11}$$

but

$$\int \chi_b(\boldsymbol{r})(\boldsymbol{r}_b \boldsymbol{s}_{Qa}/|\boldsymbol{r}_a|^3)\chi_b(\boldsymbol{r})\mathrm{d}\boldsymbol{r}=0 \tag{12}$$

and if we assume

$$\boldsymbol{r}_{ab}=\boldsymbol{r}_a \tag{13}$$

Eq. 11 becomes

$$(W_{sk})_Q=\pm e^2\int \sum_a\sum_b Z_a c_{1b}c_{2b}\chi_b(\boldsymbol{r})\boldsymbol{r}_{ab}\boldsymbol{s}_{Qa} \times\chi_b(\boldsymbol{r})\mathrm{d}\boldsymbol{r}/|\boldsymbol{r}_{ab}|^3 \tag{14}$$

Using Eq. 14, we can calculate Eq. 7 numerically.

The quantities μ_a can be evaluated by the standard method[9]:

$$\mu_a=\boldsymbol{s}_a Z_a e \tag{15}$$

Thus,

$$\boldsymbol{s}=\boldsymbol{M}^{-1}\boldsymbol{B}'(\boldsymbol{L}^{-1})'\boldsymbol{Q} \tag{16}$$

6) J. N. Murrell and J. A. Pople, *Proc. Phys. Soc.*, A61, 245 (1956).
7) J. A. Pople and J. W. Sidman, *J. Chem. Phys.*, 27, 1270 (1957).
8) A. D. Liehr, *Can. J. Phys.*, 35, 1123 (1957).
9) E. B. Wilson, Jr., J. C. Decius and P. C. Cross, "Molecular Vibrations", McGraw-Hill Book Co., Inc., New York (1955), Chap. 4.

where M^{-1} is a diagonal matrix whose elements are the reciprocal masses of the appropriate atoms. B' is the transpose of the matrix B, which transforms the Cartesian displacement coordinates s into the symmetry coordinates S. $(L^{-1})'$ is the transpose of the matrix (L^{-1}), which transforms the symmetry coordinates, S, into the normal coordinates, Q. The B matrix can be evaluated from the geometry and atomic mass of *p*-benzoquinone.

Normal Coordinates

Assuming the V_h structure of the *p*-benzoquinone molecule, the transitions from the ground A_g state to the B_{2u} and B_{3u} states can appear with the transition moments along the y and x axes (both lying in the molecular plane; see Fig. 1) respectively, while the transitions to the B_{1u} state appear with moment along the z axis (perpendicular to the molecular plane)[1,2]. As is shown by Eqs. 3 and 4, the contribution of a perturbing state to the absorption intensity is inversely proportional to the energy difference between the perturbing state and the perturbed state. The absorption spectrum[3-5] of the *p*-benzoquinone crystal, using a low temperature of 20°K, appears around 2900Å with its transition moment along the y axis. Therefore, the perturbing state belongs to species B_{2u}, and we can consider vibrations belonging to b_{3u} ($B_{1g}\times b_{3u}=B_{2u}$), b_{2g}($A_u\times b_{2g}=B_{2u}$) and a_u($B_{2g}\times a_u=B_{2u}$). Since vibrations belonging to species b_{2g} and a_u have been calculated[10], we can calculate the vibration belonging to species b_{3u}.

The normal coordinate was calculated by using the method of Wilson[9]. Thereby, a matrix equation

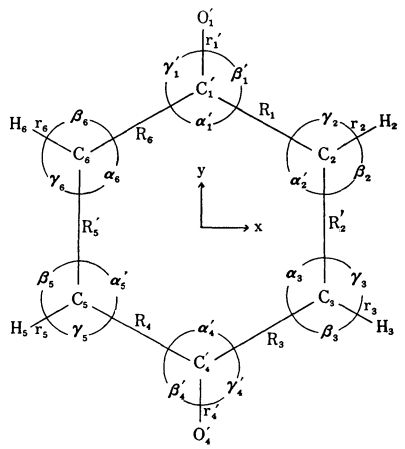


Fig. 2. Notations expressing bond angles and bond lengths and the numbering of atoms for the *p*-benzoquinone molecule.

$$(GF-\lambda I)S=0 \qquad (17)$$

was obtained. The G and F matrices are the inverse kinetic energy matrix and the force constant matrix respectively, and I is the unit matrix.

The symbols used to describe various atoms, bond lengths and bond angles in the *p*-benzoquinone molecule are shown in Fig. 2. Denoting the increase in bond lengths and angles by placing Δ in front of the symbols for these quantities, the internal symmetry coordinates, whose symbols are chosen to be as consistent as possible with those of benzene[11], are

$$\left.\begin{aligned}
S_{14} &= (1/\sqrt{6})(-\Delta R_1+\Delta R_2'-\Delta R_3+\Delta R_4 \\
&\quad -\Delta R_5'+\Delta R_6) \\
S_{15} &= (1/\sqrt{6})(-\Delta\phi_1'+\Delta\phi_2-\Delta\phi_3+\Delta\phi_4' \\
&\quad -\Delta\phi_5+\Delta\phi_6) \\
S_{18b} &= (1/\sqrt{12})(2\Delta\phi_1'+\Delta\phi_2-\Delta\phi_3 \\
&\quad -2\Delta\phi_4'-\Delta\phi_5+\Delta\phi_6) \\
S_{19b} &= (1/\sqrt{12})(\Delta R_1+2\Delta R_2'+\Delta R_3 \\
&\quad -\Delta R_4-2\Delta R_5'-\Delta R_6) \\
S_{20b} &= (1/2)(\Delta r_2+\Delta r_3-\Delta r_5-\Delta r_6) \\
S_D &= (1/2)(\Delta\alpha_2+\Delta\alpha_3-\Delta\alpha_5-\Delta\alpha_6)
\end{aligned}\right\} \qquad (18)$$

where $\Delta\phi_i=(1/2)(\Delta\gamma_i-\Delta\beta_i)$ ($i=1$, 2, 3, 4, 5 and 6).

In calculating the numerical values of G and B matrix elements, the following values of

Table I. Values of force constants of *p*-benzoquinone

$D=5.548\times10^5$ dyn./cm.
$D''=9.313\times10^5$ dyn./cm.
$F=5.065\times10^5$ dyn./cm.
$I=1.0142\times10^{-11}$ erg./rad²
($I''=1.7086\times10^{-11}$ erg./rad²)[a]
$H=(1/3)(H+2H'')$
$=1.3418\times10^{-11}$ erg./rad²

a) Evaluated value, see text.

Table II. Calculated and observed frequencies of b_{3u} vibrations of *p*-benzoquinone (cm^{-1})

	Normal coordinate	Calcd.	Obs.[a]
C-H stretching	Q_1	3068	3049
C-C stretching	Q_4	1142	944
C-C breathing	Q_3	1402	1064
C=O bending	Q_5	(370)[b]	370
C-H bending	Q_2	1836	1356

a) T. Anno and A. Sadô, This Bulletin, **31**, 734 (1958).
b) The value in parentheses is used to calculate the C=O bending force constant.

10) T. Anno and A. Sadô, This Bulletin, **31**, 728 (1958).

11) B. L. Crawford, Jr., and F. A. Miller, *J. Chem. Phys.*, **17**, 249 (1949).

TABLE III

N matrix[a)]

b_{3u}	X_1	X_2	X_3	X_4	X_5	X_6
S_{14}	$2A/\sqrt{6}$	$-A/\sqrt{6}$	0	0	$(1-B)/\sqrt{6}$	0
S_{15}	$1/\sqrt{6}r'$	$D/\sqrt{6}r$	$-1/\sqrt{6}r'$	$-D/\sqrt{6}r$	$A/\sqrt{6}r$	$-(2C/r+A/R)/\sqrt{6}$
S_{18b}	$3B/\sqrt{12}R$ $-1/\sqrt{3}r'$	$-\sqrt{3}B/4R$ $+D/\sqrt{12}r$	$1/\sqrt{3}r'$	$-D/\sqrt{12}r$	$\sqrt{3}C/4R$ $+C/\sqrt{12}r$	$-(2C/r+A/R)/\sqrt{12}$
S_{19b}	$-A/\sqrt{3}$	$A/\sqrt{12}$	0	0	$B/\sqrt{12}+1/\sqrt{3}$	0
S_{20b}	0	$-C/2$	0	$C/2$	$D/2$	$-D/2$
S_D	B/R	$B/2R$	0	0	$-A/R$	0

a) $A=\sin\alpha$, $B=\cos\alpha$, $C=\sin\beta$, $D=\cos\beta$

TABLE IV

L^{-1} matrix

b_{3u}	S_{14}	S_{15}	S_{18b}	S_{19b}	S_{20b}	S_D
Q_1	−0.005174	0.000178	−0.002246	−0.016444	0.122330	0.001894
Q_2	0.110382	0.026871	0.020412	0.124886	0.014495	−0.008061
Q_3	−0.123996	−0.003126	0.079654	0.196126	0.021796	−0.029465
Q_4	−0.079997	0.122540	0.046664	0.190321	−0.013264	0.021185
Q_5	0.524840	−0.977320	1.348043	−1.519523	−0.054969	0.212170

the interatomic distances and the bond angles for the ground electronic state are used:

$$r_i'=1.23\text{Å} \qquad r_i=1.08\text{Å}$$
$$R_i=1.461\text{Å} \qquad R_i'=1.349\text{Å}$$
$$\alpha_i'=116^\circ \qquad \alpha_i=\beta_i'=\gamma_i'=122^\circ$$
$$\text{and} \quad \beta_i=\gamma_i=119^\circ$$

The source of these data may be found in a previous paper[10].

The potential function assumed was a simple valence-force field type,

$$\begin{aligned}2V=&D\{(\Delta R_1)^2+(\Delta R_3)^2+(\Delta R_4)^2+(\Delta R_6)^2\}\\&+D''\{(\Delta R_2')^2+(\Delta R_5')^2\}\\&+F\{(\Delta r_2)^2+(\Delta r_3)^2+(\Delta r_5)^2+(\Delta r_6)^2\}\\&+H\{(\Delta\alpha_2)^2+(\Delta\alpha_3)^2+(\Delta\alpha_5)^2+(\alpha\Delta_6)^2\}\\&+I\{(\Delta\phi_2)^2+(\Delta\phi_3)^2+(\Delta\phi_5)^2+(\Delta\phi_6)^2\}\\&+I''\{(\Delta\phi_1')^2+(\Delta\phi_4')^2\}\end{aligned} \tag{19}$$

The numerical values of the force constant, the same as those used in a previous paper[12] except for I'', are given in Table I. I'' is determined in such a way that a calculated value of the frequency agrees with the experimental frequency assigned to the b_{3u} C=O bending vibration ($\nu=370\,\text{cm}^{-1}$ in the ground state). The calculated and the observed frequencies are shown in Table II. The Cartesian coordinate system at each atom is defined in such a way that the positive direction of the y axis runs parallel to a line running from atom O_4 to atom O_1 and the xy plane coincides with the molecular plane. In Table III, the N' matrix is shown; it is defined by the following relation:

$$S=NX \tag{20}$$

and N' is the transpose of the matrix N. The matrix X represents the external symmetry coordinates, which are defined by using the Cartesian displacement coordinates:

$$\left.\begin{aligned}X_1&=x_{C_1'}+x_{C_4'}\\X_2&=x_{C_2}+x_{C_3}+x_{C_5}+x_{C_6}\\X_3&=x_{O_1'}+x_{O_4'}\\X_4&=x_{H_2}+x_{H_3}+x_{H_5}+x_{H_6}\\X_5&=y_{C_2}-y_{C_3}+y_{C_5}-y_{C_6}\\X_6&=y_{H_2}-y_{H_3}+y_{H_5}-y_{H_6}\end{aligned}\right\} \tag{21}$$

The L^{-1} matrix is given in Table IV.

Intensity Calculation

A dipole moment is calculated from the following formulae:

$$\mu_a=Z_a e(\overline{s_a^2})^{1/2} \tag{22}$$

and

$$\overline{s_a^2}=(\overline{x_a^2}+\overline{y_a^2}+\overline{z_a^2})\frac{h}{8\pi^2\nu_Q} \tag{23}$$

where Z_a is the "effective charge" at atom a and we use three kinds of value: (i) Z_a is the one which has been used by Murrell and Pople[11] and by Sidman[7]; (ii) each atomic displacement acts towards the π-electrons and the non-bonding electrons on its non-neighbors as a small dipole, but it is completely screened by the combined σ-electron, π-electron and non-bonding electron density from the

12) T. Anno and A. Sadô, ibid., 32, 1611 (1960).

π-electrons and non-bonding electron on its neighbors[13]. Therefore, Z_a is given the value of zero for its neighbor electron, but it is given Slater's effective nuclear charge for the 3p orbital in a negative ion of atom a (Z_C= 0.6 and Z_O=0.9) for its non-neighbors. (iii) Since the *p*-benzoquinone molecule has an unbalanced electron density, screening constants are calculated by considering the electron density. The electron densities used are given in Table V; they have been determined by the method of Moffitt[14]. The molecular orbital used for the calculation was determined in a previous paper[1]. The electronic wave functions for the equilibrium configuration were determined by a semi-empirical MO method, taking CI into account, but for the B_{2g} state only one configuration was used.

TABLE V. FORMAL CHARGE OF *p*-BENZOQUINONE (AS A RESULT OF EXCITATION)

	O_1'	C_1'	C_2
A_u(I)[a] B_{2g}(I)	+0.0121	—[b]	—[b]
A_u(II)[a] B_{2g}(II)	+0.0209	—[b]	—[b]
B_{1g}	−0.7456	+0.2314	+0.2576

a) (I) and (II) show the lowest and the second lower states.
b) In the present calculation, these values are unnecessary.

Results and Discussion

For observing the absorption spectrum, a model EPS-2 Hitachi recording spectrophotometer was used, the oscillator strength was obtained graphically with a planimeter. The *p*-benzoquinone sample was prepared in the same manner as in Part V of this series[15] from hydroquinone. *n*-Hexane was used for the solvent, which was purified in the usual manner[16]. The experimental results are shown in Fig. 1.

The Cartesian displacement coordinates are given in Table VI. The calculated values of intensities are shown in Tables VII and VIII for the 4500Å and 2900Å regions respectively. From these results, we may conclude that the band around 2900Å corresponds to the transition belonging to $^1B_{1g}\leftarrow{}^1A_g$, and that the perturbing vibration is almost the b_{3u} C=O bending vibration (370 cm^{-1} in the ground state).

For the absorption band around 4500Å, the calculated intensity is very small. This is due to the facts that the interaction between the non-bonding electron of oxygen and the electronic dipole corresponds to the interaction

TABLE VI. CARTESIAN DISPLACEMENT OF b_{3u} VIBRATION (in 10^{-2}Å)

	Q_1	Q_2	Q_3	Q_4	Q_5
$x_{C_1'}$[a]	0.00194	0.03111	−0.12066	−0.06844	−0.15682
x_{C_2}	−0.01564	−0.02150	0.04219	0.02755	−0.28131
$x_{O_1'}$	−0.00023	0.00021	0.01358	−0.00704	0.57370
x_{H_2}	0.18758	0.06967	0.10904	0.13631	−0.27291
y_{C_2}	−0.01154	0.08433	0.02199	0.04554	−0.02752
y_{H_2}	0.10612	−0.05081	−0.06958	0.32805	−0.05135

a) Other displacements are evaluated from symmetrical character.

TABLE VII. OBSERVED AND CALCULATED VALUES OF THE INTENSITY OF ABSORPTION BAND APPEARING AROUND 4500Å AND THE CONTRIBUTION OF NORMAL VIBRATIONS

	Z_a=1	Z_a by method (ii)	Z_a by method (iii)
$f_{Au(I)}/f_{B_{2u}}$[a]	1.44×10^{-10}	0.52×10^{-10}	0.53×10^{-10}
$f_{B_{2g}(I)}/f_{B_{2u}}$	6.96×10^{-10}	2.50×10^{-10}	2.59×10^{-10}
Q_1[b]	0.50×10^{-10}	0.18×10^{-10}	0.19×10^{-10}
Q_2	6.46×10^{-10}	2.32×10^{-10}	2.40×10^{-10}
f_I/f_{III}[c]		8.77×10^{-4}	

a) $f_{Au(I)}$ shows the oscillator strength of ^1A_u(I)$\leftarrow{}^1A_g$ transition, (I) showing the lowest excited state belonging to the species.
b) Contribution of Q_1 vibration belonging to a_u species, and so on.
c) f_I and f_{III} show observed oscillator strengths of the first and the third longest wavelength absorptions, respectively.

13) D. P. Craig, *J. Chem. Soc.*, **1950**, 59.
14) W. Moffitt, *J. Chem. Phys.*, **22**, 1820 (1954).
15) T. Anno and A. Sadô, ibid., **32**, 1602 (1960).
16) A. E. Gillam and E. S. Stern, "An Introduction to Electronic Absorption Spectroscopy in Organic Chemistry", Edward Arnold (Publishers), Ltd. London (1954), p. 262.

TABLE VIII. OBSERVED AND CALCULATED VALUES OF THE INTENSITY OF ABSORPTION BAND APPEARING AROUND 2900 Å AND THE CONTRIBUTION OF NORMAL VIBRATIONS

	$Z_a=1$	Z_a by method (ii)	Z_a by method (iii)
$f_{Au(II)}/f_{B_{2u}}$[a]	8.58×10^{-11}	3.09×10^{-11}	3.27×10^{-11}
$f_{B_{2g}(II)}/f_{B_{2u}}$	4.16×10^{-10}	1.49×10^{-10}	1.59×10^{-10}
Q_1[b]	0.30×10^{-10}	0.11×10^{-10}	0.11×10^{-10}
Q_2	3.86×10^{-10}	1.39×10^{-10}	1.46×10^{-10}
$f_{B_{1g}}/f_{B_{2u}}$	3.39×10^{-3}	3.39×10^{-5}	1.07×10^{-3}
Q_1	0.00×10^{-3}	0.22×10^{-5}	$0.00_4\times10^{-4}$
Q_2	0.03×10^{-3}	0.13×10^{-5}	$0.00_3\times10^{-3}$
Q_3	0.71×10^{-3}	0.20×10^{-5}	$0.00_1\times10^{-3}$
Q_4	0.24×10^{-3}	0.00×10^{-5}	$0.00_0\times10^{-3}$
Q_5	2.40×10^{-3}	2.84×10^{-5}	1.06×10^{-3}
f_{II}/f_{III}[c]		1.77×10^{-2}	

a) $f_{Au(II)}$ shows oscillator strength of $^1A_u(II)\leftarrow{}^1A_g$ transition, (II) showing the second lowest excited state belonging to the species.
b) Contribution of Q_1 vibration belonging to a_u species, and so on.
c) f_{II} and f_{III} show observed oscillator strengths of the second and the third longest wavelength absorptions, respectively.

between an electric quadrupole and a dipole and that in the present calculation only this interaction contributes to the "n-π transition". Therefore, we considered the s-character of the non-bonding electron, but this effect was excluded from a consideration of the molecular symmetry. Assuming a V_h structure of p-benzoquinone[17,18], the non-bonding orbital of oxygene cannot be a hybridized s- and p_x-orbital, because the "s-p_x hybrid orbital" is symmetric to the yz plane. If the non-bonding orbital in oxygen is the s-orbital or the s-p_y hybrid orbital, according to the notations in Part I of this series[1], the non-bonding orbitals of p-benzoquinone ϕ_{n1} and ϕ_{n2} belong to the A_g and B_{2u} species respectively, and the $(n_1\rightarrow5)$ and $(n_2\rightarrow5)$ states belong to species B_{3g} and B_{1u}. Therefore, one of the "n-π transitions" should be an allowed transition. This fact is inconsistent with the vibrational analysis of the absorption of p-benzoquinone vapor around 4500 Å[15]. We must consider other effects or other higher-order interactions.

17) J. M. Robertson, *Proc. Roy. Soc.*, **A150**, 106 (1955).
18) S. M. Swingle, *J. Am. Chem. Soc.*, **76**, 1409 (1954).

Summary

The intensity of the symmetry-forbidden electronic absorption band of p-benzoquinone, whose excited states belong to $^1B_{2g}$, ^1A_u and $^1B_{1g}$, has been calculated by the perturbation method. It has been concluded that the absorption band around 2900 Å corresponds to the $^1B_{1g}\leftarrow{}^1A_g$ transition, which is allowed through vibronic interaction with the allowed $^1B_{2u}\leftarrow{}^1A_g$ transition. The interaction is contributed to almost entirely by b_{3u} C=O bending vibration, whose frequency is 370 cm^{-1} in the ground state.

The author wishes to express his deep thanks to Professor Sunao Imanishi and Dr. Yoshiya Kanda of Kyushu University for their encouragement throughout this research, and to Dr. Tosinobu Anno for his helpful guidance and discussions.

Department of Chemistry
Faculty of Science
Kanazawa University
Kanazawa

Electronic States of p-Benzoquinone. VIII. Vibrational Analysis of the Vapor Absorption Spectrum around 2900 Å

By Akira SADÔ

(Received July 26, 1961)

In Part VII[1] of series, the present author showed that the absorption spectrum around 2900Å of the *p*-benzoquinone molecule due to the $^1B_{1g}\leftarrow{}^1A_g$ (π-π) transition. This transition is forbidden by molecular symmetry but allowed through vibronic interaction with the allowed $^1B_{2u}\leftarrow{}^1A_g$ transition. For this interaction, the perturbing vibration is almost b_{3u} C=O bending vibration only. Solvent effect study[2] revealed that this absorption spectrum is due to a π-π ($^1B_{1g}\leftarrow{}^1A_g$) transition. In Parts I and II[3,4], the author has calculated the energy levels of this molecule and shown that there are three transitions, ^1A_u, $^1B_{2g}$ and $^1B_{1g}\leftarrow{}^1A_g$, which are superposed in this region.

The vapor spectrum in this region has been studied by Light[5] and by Seshan[6]. Light observed 21 bands. Seshan observed 32 bands between 3145~2530Å and represented them by the following formula:

$$\nu = 31780 + 450n - 230p \qquad (1)$$

where n and p are integers, n, running 0~17, and $p=0$ or 1. However, nothing was mentioned in his paper as to the nature of the electronic transition concerned.

In order to clarify the nature of the absorption band of *p*-benzoquinone around 2900Å, the vibrational analysis of vapor spectrum of this molecule has now been investigated.

Experimental

The sample of *p*-benzoquinone from hydroquinone was prepared in the same manner as in Part V[7]. The spectrum was taken on a "Fuji process" plate. The spectrograph used was a quartz spectrograph whose dispersion was 7Å/mm. at 3000Å. The absorption cell with quartz windows was 40 cm. long; to it a small side tube was attached. The sample was immediately placed in the side tube, and the absorption cell was evacuated, while its side arm was being cooled by using a freezing mixture of ice and sodium chloride to prevent the *p*-benzoquinone sample from sublimation, and sealed off. The temperature of the absorption cell was controlled between 40 and 120°C in a manner described elsewhere[8].

Results

The absorption spectrum of *p*-benzoquinone in the region between 2580~3290Å appears at a lower temperature than that in the 4500Å region. The microphotometer tracing curves of the spectrograms of this molecule is shown in Fig. 1, while Table I contains the measured frequencies and relative intensities of the main absorption bands, together with their interpretations. We have obtained about eightly bands. From a comparison of this table with Table I in Seshan's paper[6], it can be seen that the present observation corresponds with region II of his work and that

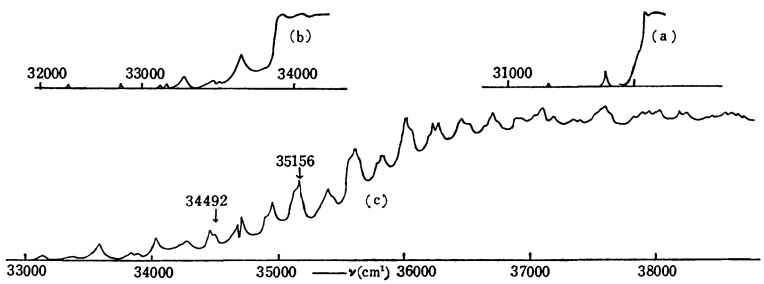


Fig. 1. Microphotometer tracing curves of the absorption spectrum of *p*-benzoquinone vapor; (a) 120°C, (b) 100°C, (c) 90°C.

1) A. Sadô, This Bulletin, **35**, 1514 (1962).
2) S. Nagakura and A. Kuboyama, *J. Chem. Soc. Japan, Pure Chem. Sec.* (*Nippon Kagaku Zassi*), **74**, 499 (1953); *J. Am. Chem. Soc.*, **76**, 1003 (1954).
3) T. Anno, I. Matubara and A. Sadô, This Bulletin, **30**, 168 (1957).
4) T. Anno, A, Sadô and I. Matubara, *J. Chem. Phys.*, **26**, 967 (1957).
5) L. Light, *Z. physik. Chem.*, **122**, 414 (1926).
6) P. K. Seshan, *Proc. Ind. Acad. Sci.*, **3A**, 172 (1936).
7) T. Anno and A. Sadô, *J. Chem. Phys.*, **32**, 1602 (1960).
8) T. Anno and I. Matubara, ibid., **23**, 796 (1955).

TABLE I. ABSORPTION BANDS OF *p*-BENZOQUINONE VAPOR

Wave number cm^{-1}	Intensity[a]	Assignment
		$t=120°C$
31 329	w	ν_I
778	m	ν_I+450
32 042	w	$0+\nu'-7\times444-45$
091	w	$0+\nu'-7\times444$
218	s	$\nu_I+2\times450$
		$t=90°C$
32 218	w	$\nu_I+2\times450$
676	w	$\nu_I+3\times450$
937	vw	$0+\nu'-5\times444-45$
976	vw	$0+\nu'-5\times444$
33 128	m	$\nu_I+4\times450$
367	w	$0+\nu'-4\times444-45$
414	w	$0+\nu'-4\times444$
587	s	$\nu_I+5\times450$
804	w	$0+\nu'-3\times444-45$
833	w	$0+\nu'-3\times444$
34 032	s	$\nu_I+6\times450$
		$t=60°C$
33 128	vw	$\nu_I+4\times450$
587	vw	$\nu_I+5\times450$
804	vw	$0+\nu'-3\times444-45$
833	vw	$0+\nu'-3\times444$
34 032	w	$\nu_I+6\times450$
228	vw	$0+\nu'-2\times444-45$
272	vw	$0+\nu'-2\times444$
406	vw	
472	w	$0-\nu''-45$
492	w	$0-\nu''$
674	w	$0+\nu'-444-45$
712	w	$0+\nu'-444$
840	vw	
899	w	$0-\nu''+435-45$
939	m	$0-\nu''+435$
35 099	vw	
111	w	$0+\nu'-45$
156	m	$0+\nu'$
340	w	$0-\nu''+2\times435-45$
390	w	$0-\nu''+2\times435$
444	vw	
558	m	$0+\nu'+435-45$
591	m	$0+\nu'+435$ $0-\nu''+692+435-45$
630	m	$0-\nu''+692+435$
804	w	$0+\nu'+692-45$
35 841	w	$0+\nu'+692$
		$t=60°C$ (Continued)
36 024	m	$0+\nu'+2\times435$ $0-\nu''+1560-45$
067	w	$0-\nu''+1560$
238	w	$0+\nu'+1560-444-45$
281	w	$0+\nu'+1560-444$ $0-\nu''+2\times692+435-45$
320	w	$0-\nu''+2\times692+435$
424	vw	
466	m	$0-\nu''+1560+435-45$
511	w	$0-\nu''+1560+435$
629	vw	
678	m	$0+\nu'+1560-45$
708	m	$0+\nu'+1560$ $0-\nu''+1560+692-45$
754	w	$0-\nu''+1560+692$
880	w	$0-\nu''+1560+2\times435-45$
910	vw	
922	w	$0-\nu''+1560+2\times435$
970	w	$0+\nu'+1125$
37 034	vw	
065	m	$0+\nu'+1560+435-45$
118	s	$0+\nu'+1560+435$
139	s	$0-\nu''+1560+692+435-45$
199	m	$0-\nu''+1560+692+435$
362	m	$0+\nu'+1560+692-45$
411	m	$0+\nu'+1560+692$
508	m	$0+\nu'+1560+2\times435-45$
550	s	$0+\nu'+1560+2\times435$
583	s	$0-\nu''+2\times1560-45$
632	m	$0-\nu''+2\times1560$
810	m	$0+\nu'+1560+692+435$
836	w	$0-\nu''+1560+2\times692+435-45$
891	w	$0-\nu''+1560+2\times692+435$
938	w	$0+\nu'+1560+3\times435-45$
38 026	m	$0+\nu'+1560+3\times435$
196	w	$0+\nu'+2\times1560-45$
244	w	$0+\nu'+2\times1560$
391	w	
441	vw	
469	vw	
562	vw	
613	w	$0+\nu'+2\times1560+435-45$
658	w	$0+\nu'+2\times1560+435$
717	w	$0-\nu''+2\times1560+692+435-45$
763	vw	$0-\nu''+2\times1560+692+435$

a) v=very, w=weak, m=medium, s=strong

the main bands agree with those reported by him, although his one band is resolved into several components. Moreover, we can classify the bands into two groups by their characters. One of the two groups (group 1) consists of sharp and single bands and corresponds to Sidman's (d) band[9] observed for a crystalline sample. The other band group (group 2)

9) J. W. Sidman, *J. Am. Chem. Soc.*, **78**, 2363 (1956); *J. Chem. Phys.*, **27**, 820 (1957).

consists of broad bands, each of which has two components, the frequency separation being 45 cm^{-1}

Analysis and Discussion

We have shown[3,4] that, if the *p*-benzoquinone molecule belongs to the V_h point group[10,11], three transitions (^1A_u, $^1B_{2g}$ and $^1B_{1g}\leftarrow{}^1A_g$) are superimposed in this region, and that these transitions are all forbidden by molecular symmetry but allowed through vibronic interaction with allowed $^1B_{2u}\leftarrow{}^1A_g$ transition[3,4]. If this assignment is correct, the spectrum should appear with the transition moment along the molecular axis (connecting two oxygen atoms). This is in agreement with the spectroscopic studies of crystalline *p*-benzoquinone by Fixl and Schauenstein[12], by Brand and Goodwin[13] and by Sidman[9]. The perturbing state and perturbing vibration in this case, are shown in Table II.

TABLE II. COMBINATIONS OF PERTURBED AND PERTURBING STATES OF *p*-BENZOQUINONE

Perturbing state	Perturbing vibration	Perturbed state
	b_{2g}	A_u
B_{2u}	a_u	B_{2g}
	b_{3u}	B_{1g}

In the first place, we will consider group 2. The band at 35156 cm^{-1} is taken as the origin of the analysis, which corresponds to the transition from the vibrationless ground state to the electronic excited state upon which a perturbing vibration is suberimposed by one quantum ($0+\nu''$). This band is the origin of two pregressions: one has a frequency separation of 444 cm^{-1} for a long wavelength, and the other has a frequency separation of 435 cm^{-1} for a short wavelength. They may be totally symmetric vibration frequencies in the ground and excited electronic states, as will be discussed later. Similarly, the band at 34492 cm^{-1} is the transition from the ground state upon which a perturbing vibration is superimposed by one quantum to the vibrationless electronic excited state ($0-\nu'$). The difference between the two bands is 665 cm^{-1}, and the frequencies of the perturbing vibration may be 250~400 cm^{-1}. From Table IV in Part IV of this series[14] and Table II here, the C=O bending vibration belonging to the b_{3u} species whose frequency is 370 cm^{-1} may be considered to be the perturbing vibration. This result is consistent with the absorption intensity calculation[1]. Therefore, the absorption bands of group 2 can be assigned to the $^1B_{1g}\leftarrow{}^1A_g$ transition.

The observed frequencies forming the main progressions are shown in Table III and are compared with the data of the Raman spectrum and the data from the 4500Å region absorption. The obtained frequencies, 444 in the ground state and 435, 692 and 1560 cm^{-1} in the excited state, are assigned to the a_g vibration. The 435, 692 and 1560 cm^{-1} frequencies in the excited state may correspond to the ground state frequencies of 444, 770 and 1667 cm^{-1}.

We have not been able to observe that band corresponding to the transition from the ground state in which both the perturbing vibration and the (totally symmetric) 444 cm^{-1} vibration are excited by one quantum each to the vibrationless excited state ($0-\nu''-444$), probably because this band is hidden by a band of group 1 ($\nu_I+6\times450$). The band at 36970 cm^{-1} is assigned to $0+\nu'+1125+692$, but other bands can be assigned using 1560($=1125+435$ cm^{-1}). The frequency of 1125 cm^{-1} is uncertain.

Group 1 has seven components at equal intervals of about 450 cm^{-1} between 31336 cm^{-1}

TABLE III. FUNDAMENTAL FREQUENCIES OF TOTALLY SYMMETRIC VIBRATION OF *p*-BENZOQUINONE

Raman effect[a]	3500Å region[b]		Present work		
	Ground state	Excited state	Ground state	Excited state	
444	440	436	444	435	Ring bending
770	770	796		692	C-C breathing
1149	1144	1109			C-H bending
1667	1667	1220		1560	C=O stretching
1688					C-C stretching
3058					C-H stretching

a) H. Stammreich and R. Formeris, *Z. Naturforsch.*, **7a**, 756 (1952).
b) T. Anno and A. Sadô, *J. Chem. Phys.*, **32**, 1602 (1960).

10) J. M. Robertson, *Proc. Roy. Soc.*, **A150**, 106 (1935).
11) S. M. Swingle, *J. Am. Chem. Soc.*, **76**, 1409 (1954).
12) J. O. Fixl and E. Schauenstein, *Monatsh.*, **81**, 598 (1950); *Chem. Abstr.*, **45**, 4136f (1951).
13) J. C. D. Brand and T. H. Goodwin, *Trans. Faraday Soc.*, **53**, 295 (1957).
14) T. Anno and A. Sadô, This Bulletin, **31**, 734 (1958).

(ν_I) and 34032 cm^{-1} ($\nu_I+6\times450$). The shapes of these bands are sharp and they are distinguished from the shape of the bands in group 2. It is probable, though not certain, these absorption bands are due to the n-π (^1A_u or $^1B_{2g}\leftarrow{}^1A_g$) transition. The bands belonging to group 1 are shown by the form $\nu_I+n\times450$ in Table I.

Summary

The absorption spectrum of *p*-benzoquinone vapor was observed at 2900Å region and the vibrational analysis was carried out. Two absorption groups were found. The bands in group 1 are sharp and single, but the nature of the transition is uncertain. Group 2 is composed of a doublet whose frequency separation is 45 cm^{-1}. It corresponds to the $^1B_{1g}\leftarrow{}^1A_g$ transition and is allowed by vibronic interaction with the allowed $^1B_{2u}\leftarrow{}^1A_g$ transition. The perturbing vibration is a C=O bending vibration belonging to the b_{3u} species whose frequency is 370 cm^{-1} in the ground state. The vibration frequencies of the main progression are 444 cm^{-1} and 435, 692 and 1560 cm^{-1} in the ground and excited electronic states respectively.

The author wishes to express his sincere thanks to Professor Sunao Imanishi and Dr. Yoshiya Kanda of Kyushu University for their encouragement throughout this research, and to Dr. Tosinobu Anno for his helpful guidance and discussions. Thanks are also due to Dr. Ryoichi Shimada and Dr. Ikuo Matubara for guidance and assistance in the experiments.

Department of Chemistry
Faculty of Science
Kanazawa University
Kanazawa

Studies on Long Chain Alkyl Amides of Water-soluble Poly-α-amino Acids. II. Infrared Spectra of Poly-DL-alanine Dodecylamide

By Shoichi IKEDA and Toshizo ISEMURA

(Received March 30, 1962)

Infrared spectral studies of synthetic polypeptides have been an important method for elucidation of the molecular conformation. Experimental investigations have been made by Elliott[1-4], Bamford[1,5] and Blout[6-8] to correlate the conformation of various polypeptide specimens with the frequency of characteristic band in infrared spectra, and recently a semiempirical interpretation of the spectra has been developed by Miyazawa[9,10].

Blout and Asadourian[6] found that an L-polypeptide, poly-γ-benzyl-L-glutamate, consists of different amounts of the α- and β-forms, depending on the mode of preparation and the degree of polymerization. The α-form was characterized by an absorption around 1655 cm^{-1} in the amide I band, and the β-form by an absorption around 1630 cm^{-1}. Bamford, Happey and Hanby[5] reported the dependence of the infrared spectra and the conformation of copoly-1 : 1-(DL-phenylalanine, DL-leucine) on the degree of polymerization, and Robinson and Bott[11] correlated the conformation of copoly-1 : 1(γ-methyl-L-glutamate, DL-phenylalanine) with the degree of polymerization.

On the other hand, the mechanism of the polymerization reaction of *N*-carboxy-α-amino acid anhydride with primary amine initiation[12] leads us to expect that the polypeptide produced by this reaction should link with the amine residue on its terminal carboxyl group by a peptide bond. No direct evidence for such a linkage has yet been found, however. Infrared spectral study of this kind of polypeptides would also provide information to demonstrate such a terminal structure, if the

1) C. H. Bamford, A. Elliott and W. E. Hanby, "Synthetic Polypeptides", Academic Press, New York (1956).
2) E. J. Ambrose and A. Elliott, *Proc. Roy. Soc.*, **A205**, 47 (1950).
3) E. J. Ambrose and A. Elliott, ibid., **A208**, 75 (1951).
4) A. Elliott, ibid., **A221**, 104 (1953).
5) C. H. Bamford, W. E. Hanby and F. Happey, ibid., **A206**, 407 (1951).
6) E. R. Blout and A. Asadourian, *J. Am. Chem. Soc.*, **78**, 955 (1956).
7) E. R. Blout and M. Idelson, ibid., **80**, 4909 (1958).
8) E. R. Blout, C. deLozé, S. M. Bloom and G. D. Fasman, ibid., **82**, 3787 (1960).
9) T. Miyazawa, *J. Chem. Phys.*, **32**, 1647 (1960).
10) T. Miyazawa and E. R. Blout, *J. Am. Chem. Soc.*, **83**, 712 (1961).
11) C. Robinson and M. J. Bott. *Nature*, **168**, 325 (1951).
12) S. G. Waley and J. Watson, *Proc. Roy. Soc.*, **A199**, 499 (1949).

primary amine for initiation was properly chosen.

We have studied a long-chain alkyl amide of water-soluble poly-α-amino acid, which we call poly-DL-alanine dodecylamide[13]. In this paper we will report the results of the infrared spectral study on poly-DL-alanine dodecylamide (PADA) with reference to poly-DL-alanine. Our original interests have been directed towards the confirmation of the presence of a dodecyl group in the molecule and the dependence of the molecular conformation on the mode of preparation or on the degree of polymerization. For these purposes, the polymers were investigated in the solid state. However, the spectra of the polymers in Nujol mull or in potassium bromide disk were found to exhibit some complications[13]. Thus the polymers were exclusively examined in the state of film which had been cast from solutions in various solvents.

The observed infrared spectra themselves reflected the difference in structure as well as in conformation, depending on the mode of preparation. Furthermore, they were found to be also strongly dependent on the state of solution from which the film had been cast. These were interpreted as a result of conformational change of the polymer in the dissolved state.

Experimental

Materials.—Poly-DL-alanine dodecylamide was prepared as previously described, and all the specimens except one were the same as in the previous investigation[13]. PADA obtained from the anhydride/initiator molar ratio, [A]/[I], of 5 to 30 was found to have a number average degree of polymerization approximately equal to [A]/[I]. Poly-DL-alanine was prepared by triethylamine initiation or by sodium methoxide initiation.

The number average degree of polymerization of the polymers was determined by the anhydrous titration of a terminal amino group.

PADA and poly-DL-alanine were soluble in formic acid, dichloroacetic acid, trifluoroacetic acid and *m*-cresol. When PADA of [A]/[I] higher than 5 and poly-DL-alanine were dissolved in formic acid to a concentration of about 10%, the solutions gelled after a few hours to a few days. The gelation occurred faster, as the [A]/[I] value was lower. The polymer solutions in the other solvents did not show any such tendency to gel.

PADA of [A]/[I] higher than 15 and poly-DL-alanine were soluble in distilled water*. All the polymers were soluble in aqueous hydrochloric acid solution, the pH value of which was lower than 5.5. When PADA of [A]/[I] higher than 5 or poly-DL-alanine was dissolved in aqueous hydrochloric acid or in distilled water to a concentration of about 10%, the solution gelled at room temperature after several hours to several days, and the gelation occurred faster as the pH of the solution was lower. The solution gelled also by heat.

Some properties of these polymers are listed in Table I.

Infrared Measurements.—Films for infrared measurements were cast on silver chloride plates from about 10% polymer solutions in various solvents, whether they were fluid or gelled. Films cast from formic acid solution or from aqueous solution were dried at room temperature for 4 hr. or more. Dichloroacetic acid or trifluoroacetic acid could be removed from cast films with great difficulty, merely by drying them by heat (ca. 50°C) in vacuo (4 mmHg) for several hr.; the remaining solvent greatly affected the spectra and the conformation of the polymer. It was more difficult to remove the solvent, as the [A]/[I] value of the polymer was higher.

All infrared spectral measurements were performed on a Perkin-Elmer 221 spectrophotometer using a sodium chloride prism. The temperature was about 20°C, and the relative humidity was about 40%.

Results

Poly-DL-alanine. — Poly-DL-alanine obtained from [A]/[I] of 50 or more with either sodium methoxide or triethylamine initiation showed identical spectra when measured in

TABLE I. PROPERTIES OF PADA AND POLY-DL-ALANINE

Sample No.	[A]/[I]	Degree of polymerization	Amount of HCl added to bring aqueous solution to pH 5.5 (mmol./g.)	Approximate % of each conformation	
				Random coil	β-Form
A431 (PADA)	5	5.4	1.13	5	95
A432 (PADA)	10	10.2	0.50	15	85
A433 (PADA)	15	14.6	0.24	45	55
A434 (PADA)	20	18.5	0.12	85	15
A605 (PADA)	30		—	98	2
A203 (Et_3N)	50		—	100	0
A808 (NaOMe)	150	49	—	100	0

13) T. Isemura, S. Ikeda, F. Tokiwa and J. Noguchi, This Bulletin, 34, 1236 (1961).

* Poly-DL-alanine contained a small amount of insoluble material, which was stated to have a cyclic structure at the terminal residue (Ref. 1, p. 298).

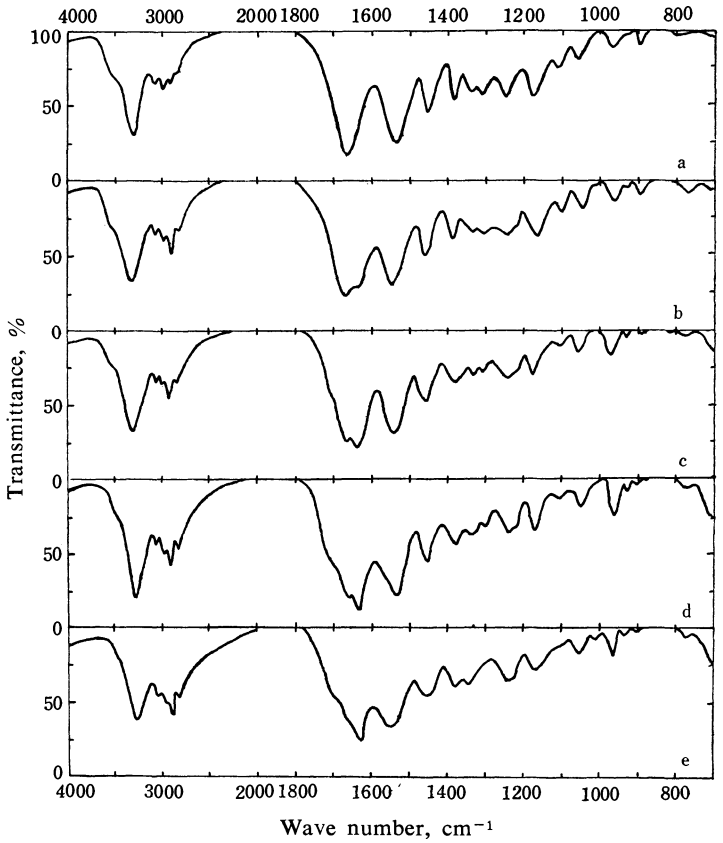


Fig. 1. Infrared spectra of poly-DL-alanine and poly-DL-alanine dodecylamides. Films cast from formic acid solutions. a. Poly-DL-alanine, A808; b. [A]/[I]=20; c. [A]/[I]=15; d. [A]/[I]=10; e. [A]/[I]=5

films cast from formic acid solution or from aqueous solution. A typical spectrum is shown in Fig. 1, curve a. This spectrum is identical with that reported by Elliott[1,4]. The characteristic absorptions at the amide I and II bands were relatively broad and were located at 1661 cm^{-1} and 1536 cm^{-1} respectively. Elliott[4,14] attributed the amide I band at 1661 cm^{-1} to the α-form. However, from the results referred to below, it is more likely that this absorption is due to the random coil form of poly-DL-alanine. Furthermore, it is now established that the amide I band of the random coil form lies at almost the same frequency as that of the α-helix[10,15]. Deuterium-hydrogen exchange experiments provide additional evidence for the random coil form of poly-DL-alanine, although it is in an aqueous solution[16].

The correlation of the amide II frequency with the polypeptide conformation is not clear. An absorption in the amide III band appeared at 1248 cm^{-1}, whatever the polypeptide conformation was, as will be described below. The N–H stretching mode was observed at a relatively high frequency, 3311 cm^{-1}. The relatively weak absorptions at 2985 and 2933 cm^{-1} may be assigned to the antisymmetric and the symmetric C–H stretching modes of the side chain methyl group respectively. The data concerning the main absorption bands are summarized in Table II.

Film cast from gel obtained by aging the solution either in formic acid or in distilled water gave an absorption spectrum as shown in Fig. 2, curve b. In comparison with curve a, obtained from a fresh, fluid solution, the amide I band had a weak shoulder at 1630 cm^{-1} in addition to the original peak at 1661 cm^{-1}. The shoulder may be assigned to the amide I band of the β-form, following Elliott[14] and after Miyazawa and Blout[10]. Thus, the gelation of the poly-DL-alanine solutions accompanies the partial conversion of the random coil form to the β-form.

Structure and Conformation of PADA.—The infrared spectra of PADA in films cast from a

14) A. Elliott, *Nature*, **170**, 1066 (1952).
15) G. D. Fasman and E. R. Blout, *J. Am. Chem. Soc.*, **82**, 2262 (1960).
16) W. P. Bryan and S. O. Nielsen, *Biochim. Biophys. Acta*, **42**, 552 (1960).

TABLE II. CHARACTERISTIC ABSORPTIONS OF PADA AND POLY-DL-ALANINE films cast from formic acid solutions

Characteristic band[a]	Wave number (cm^{-1}) and intensity[b]		
	PADA	[A]/[I]=5 → 30	Poly-DL-alanine
NH str.		3279(s) → 3300(s)	3311(s)
Antisym. CH_3 str.		2967(m) → 2985(m)	2985(m)
Sym. CH_3 str.		— —	2933(m)
Antisym. CH_2 str.		2907(s) → 2924(w)	
Amide I ↑↓ β	ca 1690	w → 0	
Amide I r	1661	w → s	1661(s)
Amide I β	1630	s → w	
Amide II	1530~1550	s s	1536(s)
Amide III	1244	m m	1248(m)
Amide III β	1222	m → 0	

a) r=random coil conformation, β=β-conformation, ↑↓ β=antiparallel β-conformation[9]
b) s=strong, m=medium, w=weak

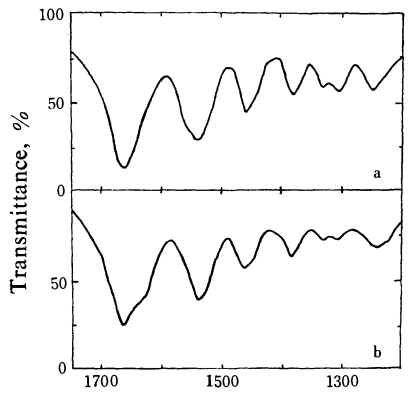


Fig. 2. Infrared spectrum of poly-DL-alanine. a. Film cast from formic acid solution; b. Film cast from gelled solution in formic acid

formic acid solution in a fluid state (immediately after dissolution) are shown in Fig. 1, curves b, c, d and e. It should be first noted that the intensity of the antisymmetric C–H stretching mode at 2920 cm^{-1} is varied from weak to strong with decreasing the [A]/[I] ratio or the degree of polymerization. No doubt this dependence of the spectra on the [A]/[I] ratio reflects the difference in the structure of the polymer dependent on the degree of polymerization. The band may be associated with the methylene groups of the terminal dodecyl group in the PADA molecule. Since the number of mole of dodecyl group per, say, peptide group increases with decreasing the [A]/[I] ratio, the change in intensity of the band at 2920 cm^{-1} indicates the formation of a linkage between the dodecylamino group and the poly-DL-alanine part.

While poly-DL-alanine of different modes of preparation was in the random coil conformation, as has been mentioned before, PADA obtained from [A]/[I] ratios of less than 30 exhibited a different situation. The amide I absorption of the [A]/[I] 20 preparation lay at 1661 cm^{-1} with a weak shoulder at 1630 cm^{-1}, suggesting that the polymer consisted mostly of the random coil form but partly of the β-form. With decreasing [A]/[I] ratio, the absorption at 1661 cm^{-1} became weaker and that at 1630 cm^{-1} stronger. For the [A]/[I] 5 preparation, the latter band was predominant and the former appeared as a weak shoulder. The dependence of the spectra on the [A]/[I] value manifests a conformational change of PADA with the degree of polymerization. That is, a greater amount of the β-form and a smaller amount of the random coil were included in PADA, as the [A]/[I] value or the degree of polymerization was lower. The lowest [A]/[I] preparation was mostly composed of the β-form. The relative amounts of the two conformations were estimated from the ratio of the intensities of the two amide I absorptions, assuming equal molar extinction coefficients. The results are given in Table I. In addition, a shoulder at 1690 cm^{-1} became apparent as the peak at 1630 cm^{-1} became higher. This indicates that the β-form consists of antiparallel chains, provided that Miyazawa's theory[9] can be extended to such low molecular weight polypeptides.

The amide II band showed no such striking correlation of spectra with the [A]/[I] value as the amide I band, but it appeared to be slightly broader as the [A]/[I] value was decreased.

A characteristic change of spectra was also observed in the amide III band. While this band was located at 1244 cm^{-1} for the [A]/[I] 20 and 30 preparations, corresponding to 1248 cm^{-1} for poly-DL-alanine, the lower [A]/[I] preparations absorbed two frequencies, 1244 and 1222 cm^{-1}, the latter becoming stronger

with decreasing [A]/[I] value. Accordingly, the absorption at 1222 cm^{-1} should be associated with the β-form, while the one at 1244 cm^{-1} is independent of the conformation.

The N–H stretching mode at about 3300 cm^{-1} changed not in intensity but in frequency as the [A]/[I] value was varied. While poly-DL-alanine gave an absorption at 3311 cm^{-1}, the observed frequency of PADA of [A]/[I] 5 was 3279 cm^{-1} and the higher [A]/[I] preparations absorbed an intermediate frequency, 3289 to 3300 cm^{-1}. This variation also seems to accompany the conformational change with the degree of polymerization. PADA absorbed a higher frequency of the N–H stretching vibration in the random coil form, and, with an increasing amount of the β-form, it absorbed a lower frequency. This kind of behavior has already been observed for other polypeptides by Ambrose and Elliott[2].

All the above correlations of the infrared spectra with the mode of preparation are tabulated in Table II. The conformation of PADA and poly-DL-alanine can be most distinctly identified by observing the amide I absorptions at 1661 and 1630 cm^{-1}.

Film cast from dichloroacetic acid or trifluoroacetic acid solution in which the solvent was still retained always showed a stronger absorption at 1661 cm^{-1} than that from a formic acid solution. This observation suggests that PADA is strongly solvated by dichloroacetic acid or trifluoroacetic acid, which is known to be a "random coil solvent", and that PADA is more favorably stabilized in the random coil form in the presence of the solvent. The band at 1661 cm^{-1} may, therefore, be associated with the random coil form rather than with the α-helix.

Ionization of the Terminal Amino Group of PADA.—The pH value of an aqueous solution of PADA was dependent on the [A]/[I] value when dissolved or suspended in aqueous hydrochloric acid of the same concentration, since PADA combined with different numbers of hydrogen ions[13]. The pH value of the solution should be lower as the [A]/[I] value is higher. Thus the [A]/[I] 5 preparation was insoluble in 0.1 N hydrochloric acid solution, while the others were soluble. However, we may use the concentration of hydrochloric acid instead of the pH value as a measure of the ionization of the terminal group of dissolved polymer.

The infrared spectra of film cast from aqueous hydrochloric acid solution or suspension, the acidity of which was varied from 0.1 N to 0.4 N, were compared with that from formic acid solution. It was found that the spectra of PADA of [A]/[I] higher than 15 were not distinguished from those cast from the formic acid solution and were scarcely influenced by the acid strength. However, the lower [A]/[I] preparations revealed the effect of the ionization on the spectra. For the preparations of [A]/[I] 5 and 10, these changes are illustrated in Fig. 3, in which are shown the spectra of films cast from formic acid solution and from 0.1 N and 0.2 N hydrochloric

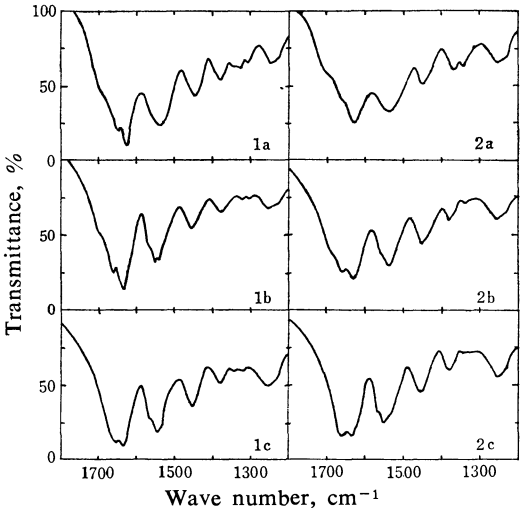


Fig. 3. Infrared spectra of poly-DL-alanine dodecylamide. Films cast from solutions in different solvents. 1. [A]/[I]=10; 2. [A]/[I]=5; a. Formic acid; b. 0.1 N Hydrochloric acid; c. 0.2 N Hydrochloric acid

acid solutions. The effect of the ionization was more enhanced as the [A]/[I] value was higher, and the absorption at 1661 cm^{-1} was stronger and the one at 1630 cm^{-1} was weaker as the degree of ionization was higher. Thus the random coil form is more stable in the ionized state than the β-form.

Gelation of PADA Solution in Formic Acid or in Aqueous Hydrochloric Acid.—When PADA was dissolved in formic acid, the lower [A]/[I] (10 and 15) preparations gelled within several hours, while the higher [A]/[I] preparations gelled after a day or two. Film cast from the gel gave a spectrum different from that obtained from the original fluid solution. With the higher [A]/[I] preparations, the absorption at 1661 cm^{-1} became weaker and that at 1630 cm^{-1} stronger, as in the case of poly-DL-alanine. Correspondingly, the bands at 1690 and 1222 cm^{-1} appeared or became slightly stronger. These are shown in Fig. 4, curves 1. Thus, the gelation of the higher [A]/[I] preparations in formic acid accompanies a conformational change characterized by the transformation of a part of the random coil to the β-form.

With the lower [A]/[I] preparations the

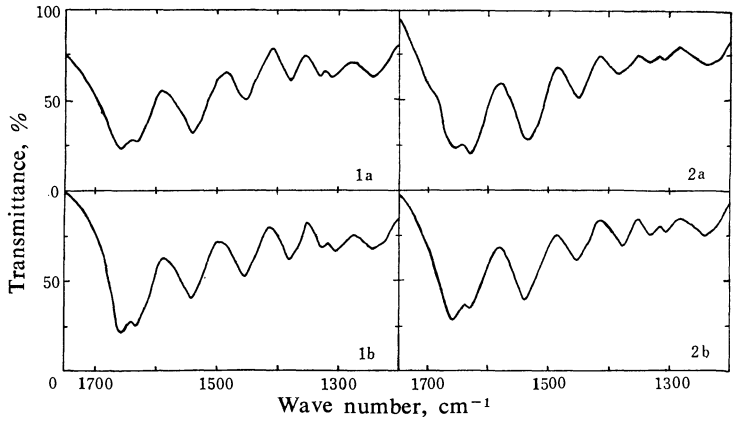


Fig. 4. Infrared spectra of poly-DL-alanine dodecylamide. 1. [A]/[I]=20; 2. [A]/[I]=15; a. Film cast from formic acid solution; b. Film cast from gelled solution in formic acid

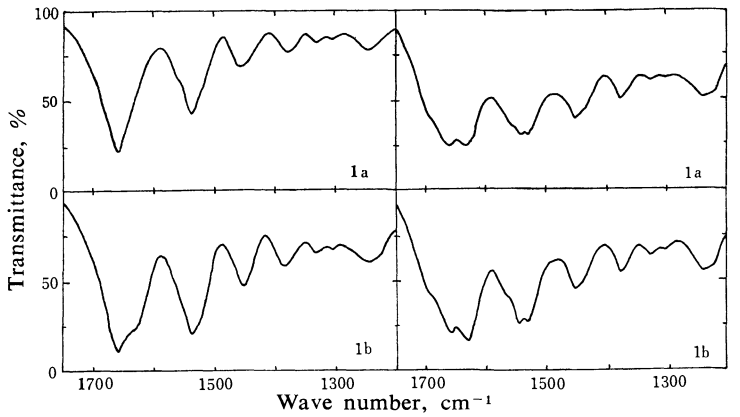


Fig. 5. Infrared spectra of poly-DL-alanine, A 808 (1) and poly-DL-alanine dodecylamide, [A]/[I] 15 (2). a. Film cast from 0.2 N hydrochloric acid solution; b. Film cast from gelled solution in 0.2 N hydrochloric acid

TABLE III. CONFORMATIONAL CHANGE DURING GELATION[a)]

PADA	Formic acid solution			0.2 N HCl Solution		
	Sol	Gel		Sol	Gel	
[A]/[I] 5	r, % 5 β, % 95	not gelled		r, % 45 β, % 55	not gelled	
[A]/[I] 10	r, % 15 β, % 85	30 70	β→r	r, % 40 β, % 60	15 85	r→β
[A]/[I] 15	r, % 45 β, % 55	75 25		r, % 45 β, % 55	40 60	
[A]/[I] 20	r, % 85 β, % 15	75 25	r→β	—	—	
[A]/[I] 30	r, % 98 β, % 2	—		—	—	
Poly-DL-ala (A808)	r, % 100 β, % 0	90 10		r, % 100 β, % 0	90 10	

a) r=random coil conformation, β=β-conformation

reverse situation was encountered during the gelation. The change of the spectra by gelation is illustrated in Fig. 4, curves 2. The absorption at 1661 cm^{-1} became stronger and that at 1630 cm^{-1} weaker. Simultaneously, the bands at 1690 and 1222 cm^{-1} vanished or weakened. In the case of the lower [A]/[I] preparations in formic acid, therefore, the β-form is partly transformed into the random coil during the gelation.

When PADA was dissolved in aqueous hydrochloric acid and kept at room temperature for several days or heated on boiling water for several minutes, the solution of PADA (except for the lowest [A]/[I] preparation) became gel. Film cast from the gel was always characterized by the increased intensity of the absorption at 1630 cm^{-1} and by the decreased intensity of 1661 cm^{-1}, as compared with that from the original fluid solution. Thus the gelation of PADA in aqueous hydrochloric acid is always associated with the change of a part of the random coil form to the β-form.

All these conformational changes followed by the gelation are summarized in Table III, in which the relative amounts of the random coil and the β-form estimated as before are given.

Discussion

According to Blout and Asadourian[6], low molecular weight poly-γ-benzyl-L-glutamate produced from the *N*-carboxyanhydride by *n*-hexylamine initiation could be separated into two components, the α- and the β-forms, by the difference in solubility in formic acid. The α-polypeptide had a higher molecular weight and absorbed a frequency at 1655 cm^{-1} in the amide I band when cast in film, but the β-polypeptide was of a lower molecular weight and showed an absorption at 1630 cm^{-1}. The portion of each form in poly-γ-benzyl-L-glutamate was independent of the solvent species from which film had been cast.

According to Bamford et al.[5,17], on the other hand, low molecular weight copoly-1 : 1-(DL-phenylalanine, DL-leucine) was less soluble in benzene as the degree of polymerization was lower. The copolymer was composed of the α- and β-forms, and the decreased solubility was attributed to the increased amount of the β-form. The α-form absorbed 1655 cm^{-1}* and the β-form absorbed 1636 cm^{-1} when the copolymer was examined in a film state. Unlike as in poly-γ-benzyl-L-glutamate, however, the portions of the two forms were dependent on the solvent species and the method for the regeneration into film. Formic acid was more favorable in producing the β-form, and dichloroacetic acid preferred the formation of the α-form. Similar results were obtained for poly-DL-phenylalanine[17].

Poly-DL-alanine obtained from dodecylamine initiation, PADA, was found to consist of the random coil form and the antiparallel β-form. The former form gave an absorption at 1661 cm^{-1} in the amide I band, while the latter absorbed at 1630 cm^{-1}. The portion of the β-form was greater, and the solubility in distilled water was lower, as the degree of polymerization was lower. However, the solubility of this polymer in water might not be attributable to the conformational difference alone but also to the hydrophobicity of the dodecyl group. As compared with that from formic acid solution, film cast from dichloroacetic acid solution contained a greater amount of the random coil form, but the difference would be caused by the presence of remaining solvent and will disappears after the complete removal of the solvent. Thus, the conformation of PADA in the solid state is defined mainly by the degree of polymerization.

There are two factors to stabilize a given conformation of a polymer chain, i. e., energy and entropy contributions. The former is determined by the potential of internal rotation around backbone linkages, the hydrogen bonding between peptide bonds, etc. The latter arises mainly from the Brownian motion of the constituent residues. In high molecular weight PADA and poly-DL-alanine, the entropy contribution is greater than the energy contribution; then the random coil form is made more stable. With lowering of the degree of polymerization, the conformational entropy decreases and the energy contribution becomes predominant. The energetically stable form would be the interchain hydrogen-bonded β-form, and then the β-form becomes abundant in low molecular weight PADA. In PADA, the van der Waals cohesion between dodecyl groups should play an additional role in stabilizing the β-form, the long chain alkyl groups tending to be held together. Further, the antiparallel-chain β-form would be more stable than the parallel one, as far as the potential of the internal rotation was concerned[18].

The effect of the dissolved state on the regenerated conformation of PADA may be interpreted as follows. In dichloroacetic acid or trifluoroacetic acid solution, the polymer is probably in a solvated random coil form,

17) C. H. Bamford, W. E. Happy and F. Happey, *Proc. Roy. Soc.*, **A205**, 30 (1950).

* Elliott[4] recorded this frequency as 1661 cm^{-1}.

18) T. Miyazawa, *J. Polymer Sci.*, **55**, 215 (1961).

irrespective of the degree of polymerization, owing to the strong ability of the solvent to break hydrogen bonds, and no further conformational change occurs in the course of time. The conformation of PADA in the dissolved state is considered to be reversible to the original one in the solid state when the polymer is made free from the solvent.

In formic acid solution, however, PADA will be in a randomly coiled form immediately after dissolution. This form may be less solvated and less randomly coiled than in dichloroacetic acid solution, since formic acid is a weaker hydrogen bond-breaking agent. However, this state of dissolution is considered to be reversible to the initial solid state of the polymer. The conformation of PADA in formic acid solution is no doubt much more abundant in the random coil form than in the initial solid state. However, this solution undergoes aging, probably owing to the weak polymer-solvent interaction and the high polymer concentrations such as 10%. In the course of aging, the dissolved random coils are in contact with one another and are then linked by interchain hydrogen bonds. As a result, the random coil is partly converted into the β-form, and the formation of cross-linkages makes the fluid solution into gel. PADA in the gelled state can no longer return to the initial solid state, even if the solvent is completely removed. When the regenerated solid state is compared with the original solid state, the aging or the gelation apparently accompanies the partial conversion of the β-form to the random coil for the [A]/[I] 10 and 15 preparations, but it produces the reverse conversion for the higher [A]/[I] preparations. The chain length of PADA of [A]/[I] 5 is too short to bring about gelation.

In aqueous hydrochloric acid solution, the terminal amino groups of PADA are, at least, partially ionized, as the pH titration data indicate. The electrostatic repulsion is then operative between polymers and the polymer chain takes a random coil. From the pH titration and the surface tension data, it is evident that most of the hydrochloric acid required to make the pH value of the solution lower than 5.5 is not bound to the polymer, but merely suppresses the electrostatic repulsion as neutral electrolyte does. When the solvent is removed, however, the free hydrochloric acid or the ionic atmosphere is reduced and the interchain distance is decreased. Thus, the electrostatic repulsion is very strong in the regenerated PADA, which is partially ionized. As compared with the unionized PADA regenerated from formic acid solution, the ionized PADA regenerated from aqueous hydrochloric acid solution has a higher portion of the random coil form, since the interchain hydrogen bonds maintaining the β-form are ruptured by the electric repulsion. The effect of the repulsive force is greater, as the degree of polymerization is lower and the degree of ionization is higher.

The aqueous solution of PADA or poly-DL-alanine forms a gel by aging. The random coil form of PADA in solution will be partly converted into the β-form during this process. The cross-linkages formed by the aging will be retained even after the removal of the solvent, and the increased amount of the β-form results in the ionized PADA regenerated from the gel. In solution, the contact or the aggregation of ionized PADA is disturbed by the interchain repulsion between ionized terminal groups. In concentrated hydrochloric acid solution, however, most of ions produced from the acid are free from PADA and only serve to reduce the electrostatic repulsion, Thus, the contact of ionized PADA with one another is made easier and the gelation can occur faster, as hydrochloric acid is more concentrated.

Summary

The infrared spectra of poly-DL-alanine and poly-DL-alanine dodecylamide were measured on film cast from various solutions, and the conformation of the polymers were elucidated on the basis of the location and intensity of absorptions, mainly in the amide I and III bands.

The polymer showed an absorption at 1661 cm^{-1} in the amide I band if it was in the random coil form, but it showed two absorptions at 1630 and 1690 cm^{-1}, if it was in the antiparallel β-form. While the amide III band was located at 1244 cm^{-1} irrespective of the polymer conformation, the band had an additional absorption at 1222 cm^{-1} for the β-conformation.

From the above correlation of the spectra with the polymer conformation, it was found that poly-DL-alanine and PADA prepared with high [A]/[I] ratios are in the random coil form but that PADA of [A]/[I] ratios lower than 30 is composed of both the random coil and the antiparallel β-forms when it is regenerated from formic acid solution. PADA contained a greater amount of the β-form as the [A]/[I] value or the degree of polymerization was lower. The [A]/[I] 5 preparation was mostly in the β-form.

In the ionized PADA obtained from aqueous hydrochloric acid solution, the portion of the random coil form increased relative to that in the unionized PADA derived from formic

acid solution, and the effect of the ionization was enhanced for the lower [A]/[I] preparations.

Poly-DL-alanine and PADA in formic acid or aqueous hydrochloric acid solution underwent a partial transformation from the random coil to the β-form during the aging of concentrated solution, which process accompanied gelation. The solution of the lowest [A]/[I] preparation did not gel. In the state regenerated from gel, poly-DL-alanine and PADA, except for the unionized lower [A]/[I] preparations, had an increased amount of the β-form as compared with that from an initial fluid solution. In the lower [A]/[I] preparations obtained from formic acid solution, the reverse transformation apparently occured, when the films cast before and after the gelation were compared.

The authors wish to thank Dr. Kunio Fukushima for helpful discussion on the infrared data. The expense of this work was partly defrayed by a grant from the Ajinomoto Co.

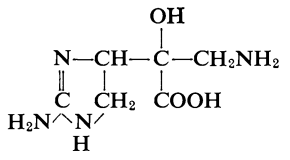
Faculty of Science (*S. I. & T. I.*)
and
Institute for Protein Research (*T. I.*)
Osaka University
Kita-ku, Osaka

*An Attempt at the Synthesis of Roseonine**

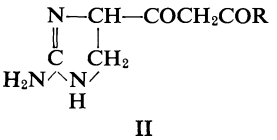
By Tadashi SATO

(Received December 11, 1961)

In 1954, Nakanishi et al. isolated a new amino acid, roseonine, as one of the hydrolysis products of a peptide antibiotics roseothricin; they proposed that the structure was 2-amino-4-(1-carboxy-1-hydroxy-2-amino)-ethyl-2-imidazoline (I)[1]. Since the compounds firmly



I



II

identified as the degradation products of roseonine were very few in number, information about its structure was obtained mainly from a comparison of its physicochemical properties with those of many model compounds. Later, some similar amino acids were isolated from other sources and were named differently (e. g., geamine isolated from geomycin[2]), but they were proved to be identical with roseonine.

In order to confirm the structure of this amino acid, the synthesis of roseonine was attempted. As the most facile path to roseonine appeared to be through a ketonic compound II, the studies were directed to the preparation of this ketonic compound. When 2,3-diaminopropionic acid monohydrobromide (III) was treated with bromocyan in the presence of two moles of sodium hydroxide, 2-amino-2-imidazoline-4-carboxylic acid (IV) was obtained. The acetylation of IV with a mixture of acetic acid, acetic anhydride and concentrated sulfuric acid afforded a monoacetyl derivative. The acetyl derivative was formulated as V in view of the following reaction sequence. Ethanolic hydrogen chloride converted V into its ester, VI. Numerous attempts to effect the condensation of VI with ethyl acetate or acetone in order to afford II were unsuccessful. However, ethyl acetoacetate condensed with it in the presence of sodium ethylate, and the product was isolated as its hydrochloride. Based on the following physicochemical properties and reactions of this condensation product, the bicyclic structure VIIa was assigned to it. IV and V may have a dipolar structure, judging from their pK_a values (Table II). The infrared spectra of IV, V, VI and VIIa in the 1800~

* After the manuscript of this article was submitted for publication, a revised structure was proposed for roseonine: H. E. Carter et al., *J. Am. Chem. Soc.*, 83, 4297 (1961).

1) K. Nakanishi, T. Ito, M. Ohashi, I. Morimoto and Y. Hirata, This Bulletin, **27**, 539 (1954); K. Nakanishi and M. Ohashi, ibid., **30**, 725 (1957).

2) H. Brockmann and H. Musso, *Chem. Ber.*, **88**, 648 (1955).

Chart 1

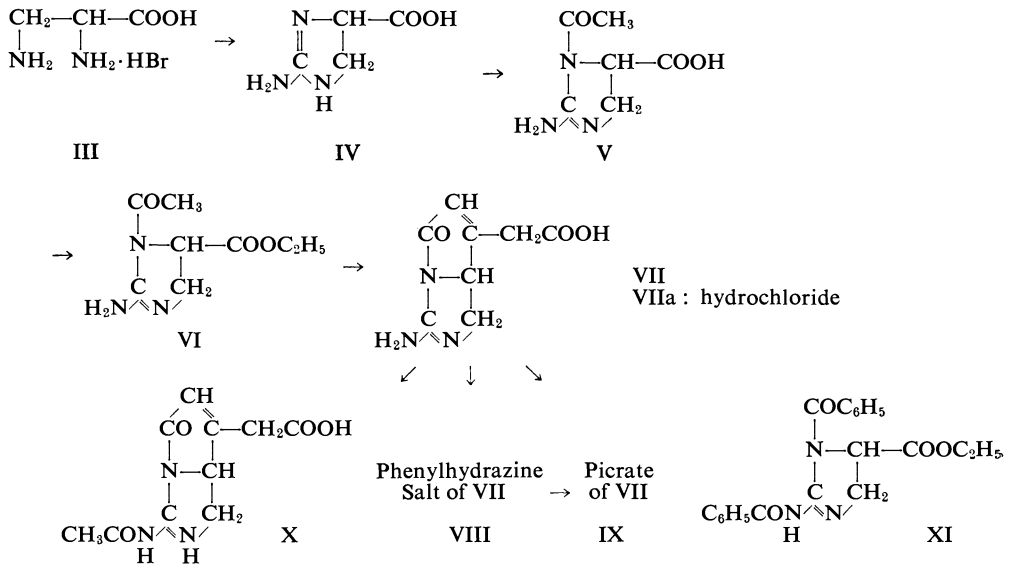
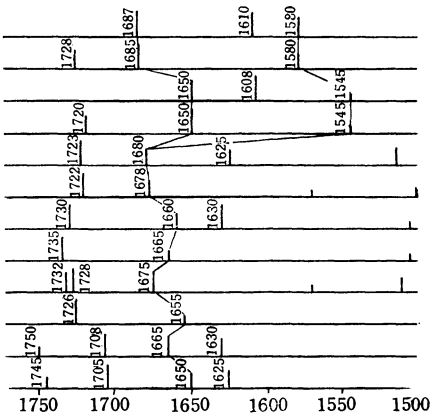


TABLE I. INFRARED SPECTRA

A	IV (KBr)
B[a]	IV hydrochloride (KBr)
C[b]	IV (D_2O solution)
D[b]	IV (D_2O-HCl solution)
E	V (KBr)
F[a]	V hydrochloride (KBr)
G[b]	V (D_2O solution)
H[b]	V (D_2O-HCl solution)
I[a]	VI hydrochloride (KBr)
J[b]	VI (D_2O-HCl solution)
K	VIIa (KBr)
L[b]	VIIa (D_2O solution)



a. Determined for the sample obtained by dissolving IV, V or VI in a slight excess of 5% hydrochloric acid and keeping the solution over solid sodium hydroxide and then over phosphorus pentoxide at room temperature (1 mmHg.).
b. Determined in a KRS cell.

1500 cm^{-1} region were measured in different states and were compared with each other (Table I). The carboxylate band (1630~1608 cm^{-1} in A, C, E, G) of IV and V shifted to the carboxyl band (1735~1720 cm^{-1} in B, D, F, H) in the acidic state. Goto et al.[3] reported that the disubstituted guanidium group generally showed in the 1700~1580 cm^{-1} region, two bands separated from each other by 90 cm^{-1}; they were named guanidium I and II. The bands at 1687 and 1580 cm^{-1} of IV were, therefore, thought to be guanidium I and II; in accordance with this expectation, they shifted to a lower wave number in the deuteriated state (C, D). However, V and VI have only one band that shifted when deuteriated. It was assumed from this result that the two guanidium bands of IV were reduced to one band by acetylation. The bands at 1735~1720 cm^{-1} of V and VI, which were unaffected by the change in state, were assigned to amide carbonyl[4] overlapped by carboxyl in

3) T. Goto, K. Nakanishi and M. Ohashi, This Bulletin, 30, 723 (1957).

4) It has been reported that the amide carbonyl band shifts toward a higher wave number when the amide nitrogen atom constitutes a five-membered ring system (*N*-acetylimidazole, *N*-acetylindol, etc.): W. Otting, *Chem. Ber.*, 89, 1940 (1956); H. A. Staab, ibid., 90, 1320 (1957).

Table II. Values of pK_a's

Compound	pK_{a1}	pK_{a2}
IV	2.5	12.1
V	1.6	8.7
VI	—	7.7
VIIa	2.0	3.8
X	3.1	—

the case of F and H in Table I or by ester in the case of I and J.

Bearing these facts in mind, the band assignments of VIIa were made as follows: 1750 cm^{-1} to amide carbonyl (shifted to a higher wave number by five-membered cyclization), 1708 cm^{-1} to carboxyl, 1665 cm^{-1} to guanidium (shifted to a lower wave number by deuterium substitution in the case of L), and 1630 cm^{-1} to a C=C double bond.

Further evidence supporting this structure (VIIa) was also obtained. Phenylhydrazine reacted with VIIa, but the product was not the phenylhydrazone, but the phenylhydrazine salt of VII (VIII), because phenylhydrazine was easily removed from VIII by the action of picric acid to afford the picrate of VII (IX). The hydrochloride VIIa was not susceptible to the acid or to alkali hydrolysis, and the titration with alkali revealed the presence of two titratable groups, which were attributable to the guanidine and carboxyl groups (see below). The acetylation of VIIa afforded the acetyl derivative X, which had only one titratable group. Although the observations described above were consistent with the bicyclic structure VIIa, the hydrochloride exhibited unexpectedly low pK_a values, 2.0 and 3.8. Even when the higher observed value of pK_a was attributed to the ionization of the guanidine group, it appeared to be too low to be regarded as the pK_a value of normal guanidine derivatives. A specific steric environment caused by the fusion of two rings is probably responsible for this unusually low pK_a value.

In order to prevent the cyclization of the acetyl derivative VI to VIIa, the benzoylation of IV was carried out. However, the dibenzoyl ester (XI or its isomer, according to the position of the benzoyl groups), which was directly obtained from IV, resisted condensation with ethyl acetate or acetone to prepare II.

As α,β-diamino compounds were found to be a convenient starting material for the synthesis of 2-amino-2-imidazoline derivatives, an artifice of synthesizing from the side chain was next adopted. As the immediate synthetic objective, an olefinic compound XII was chosen in order to prepare for the desired diamino compound XIII.

Chart 2

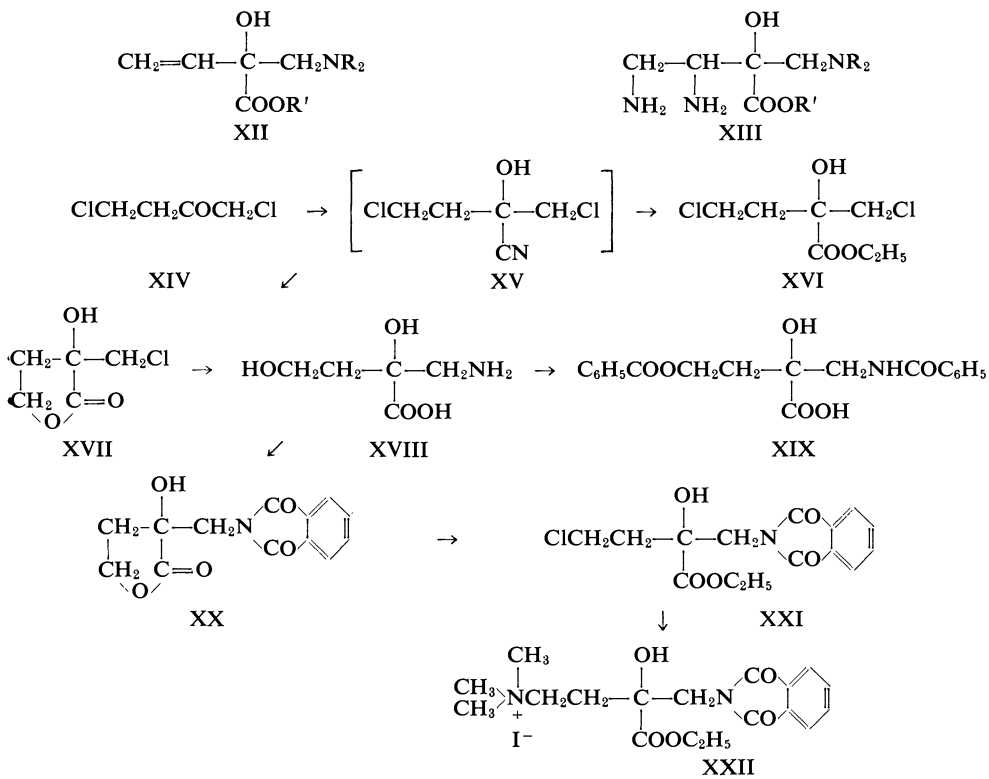
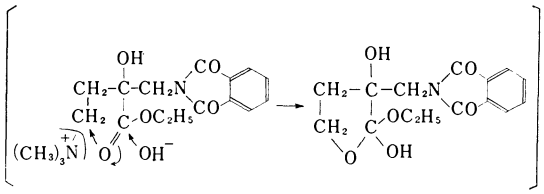


Chart 3



XXIII XXIV

When 1,4-dichloro-2-butanone (XIV) was treated with sodium bisulfite and then with potassium cyanide, an oil was obtained. This oil, despite its fairly constant boiling point, contained the starting ketone, which was detected by infrared analysis. The oil exhibited bands of hydroxyl and nitrile in its infrared spectrum and afforded a considerable amount of the starting ketone on being left standing. It may be inferred from these results that the oil is an equilibrium mixture of the cyanhydrin XV and the starting ketone XIV. Further support for the cyanhydrin structure was obtained by converting it into its chloroester XVI by ethanol and concentrated sulfuric acid, and into a chlorolactone XVII by hydrochloric acid in acetic acid. The amino acid XVIII was obtained from the lactone XVII by aqueous ammonia at 100°C. Chemical evidence for the β-amino-γ-hydroxy acid structure of XVIII was obtained by Schotten-Baumann benzoylation, which afforded the dibenzoylcarboxylic acid XIX, and by reaction with phthalic anhydride in pyridine, which afforded the phthaliminolactone XX. The amino acid XVIII has a side chain of roseonine, and its behavior in reaction against ninhydrin was similar to that of roseonine dihydrochloride. Ethanolic hydrogen chloride converted the phthaliminolactone XX into the ester XXI. As the direct dehydrochlorination of XXI was unsuccessful, it was converted into tertiary amine methiodide XXII. The Hofmann degradation of XXII afforded a glassy substance. The structure of this substance may be assumed to be the hemiacetal XXIV derived from the hydroxide XXIII by the scheme shown in Chart 3, since it afforded the starting lactone XX on treatment with dilute hydrochloric acid.

Experimental

The infrared spectra were determined on a Koken infrared recording spectrophotometer, model DS 301.

The acid constants refer to apparent values derived with a glass electrode system in water.

2-Amino-2-imidazoline-4-carboxylic Acid (IV).—Eleven grams of 2,3-diaminopropionic acid monohydrobromide were dissolved in 48 ml. of 10% sodium hydroxide and 50 ml. of an aqueous solution containing 6.3 g. of bromocyan were added. After being left standing overnight, it was evaporated to dryness in vacuo, and the residue was recrystallized from water. Yield, 3.5 g.; m. p., 303°C (decomp.).

Found: C, 36.90; H, 5.41; N, 32.80. Calcd. for $C_4H_7N_3O_2$: C, 37.21; H, 5.43; N, 32.55%.

The picrate was prepared and recrystallized from water, m. p., 208°C.

Found: N, 23.73. Calcd. for $C_{10}H_{10}N_6O_9$: N, 23.46%.

1-Acetyl-2-amino-2-imidazoline-5-carboxylic Acid (V).—Seventy milliliters of acetic anhydride and one drop of concentrated sulfuric acid were added to a solution of 8 g. of IV in 70 ml. of glacial acetic acid, and the solution was kept at 40~45°C for 45 min. After concentration in vacuo on a water bath, 200 ml. of methanol were added. The resulting crude product (m. p. 225°C (decomp.)) was recrystallized from glacial acetic acid-methanol; m. p., 232°C (decomp.).

Found: N, 24.73. Calcd. for $C_6H_9N_3O_3$: N, 24.55%.

Ethyl 1-Acetyl-2-amino-2-imidazoline-5-carboxylate (VI).—A suspension of 5 g. of the acid V in 100 ml. of ethanol was saturated with dry hydrogen chloride without cooling and then left to stand for 2 hr. After concentration in vacuo, the residue was neutralized with aqueous sodium carbonate and taken up in chloroform. The extract was dried over sodium sulfate, and the solvent was distilled. The residual ester was recrystallized from chloroform-petroleum ether; m. p., 152~154°C.

Found: C, 48.14; H, 6.72; N, 21.42. Calcd. for $C_8H_{13}N_3O_3$: C, 48.23; H, 6.58; N, 21.10%.

The picrate was prepared in water and recrystallized from ethanol; m. p., 163~165°C.

Found: N, 19.74. Calcd. for $C_{14}H_{16}N_6O_{10}$: N, 19.62%.

Bicyclic Compound VII.—A mixture of 0.3 g. of the ester VI, 0.3 g. of ethyl acetoacetate, and 1.1 ml. of a sodium ethylate solution (prepared by dissolving 1 g. of sodium in 20 ml. of ethanol) was heated at reflux for 1.5 hr. The solid was then filtered out and dissolved in a small amount of water. The solution was acidified with hydrochloric acid (1 : 1) and concentrated in vacuo. The resulting solid was recrystallized from ethanol; m. p., 242°C.

Found: C, 41.37; H, 4.56; N, 18.00. Calcd. for $C_8H_{10}ClN_3O_3$: C, 41.54; H, 4.31; N, 18.11%.

The phenylhydrazine salt VIII was obtained by heating a mixture of the hydrochloride and phenylhydrazine in ethanol for 10 min. Recrystallization from ethanol afforded white needles; m. p., 162~163°C.

Found: C, 55.65; H, 5.72; N, 23.07. Calcd. for $C_{14}H_{17}N_5O_3$: C, 55.53; H, 5.62; N, 23.11%.

The picrate IX was prepared from the hydrochloride VIIa or the phenylhydrazine salt VIII by treatment with picric acid in water; m. p., 125°C.

Found: N, 19.27. Calcd. for $C_{14}H_{12}N_6O_{10}$: N, 19.85%.

The acetyl derivative X was prepared by heating a solution of the hydrochloride in a mixture of glacial acetic acid and acetic anhydride (1 : 1) in the presence of a small amount of pyridine and then recrystallizing it from ethanol; m. p., 224°C (decomp.).

Found: C, 50.90; H, 4.70; N, 17.59. Calcd. for $C_{10}H_{11}N_3O_4$: C, 50.75; H, 4.64; N, 17.72%.

Ethyl 1-Benzoyl-2-benzoylamino-2-imidazoline-4-carboxylate (XI).—A suspension of 1 g. of IV in 20 ml. of ethanol was saturated with dry hydrogen chloride without cooling. After 2 hr., the ethanol was removed in vacuo. The resulting oil was dissolved in a small amount of ethanol, and the ethanol was again removed in vacuo. The same procedure was once repeated with ethanol and then twice with pyridine, and 3.6 g. of benzoic anhydride was added. The solution was heated at reflux for 4 hr., and the pyridine was removed in vacuo. The resulting oil, when triturated with a small amount of ethanol, crystallized; this was then recrystallized from ethanol in the form of white needles; m. p., 189~190°C.

Found: C, 65.85; H, 5.60; N, 11.80. Calcd. for $C_{20}H_{19}N_3O_4$: C, 65.74; H, 5.24; N, 11.50%.

2-Chloromethyl-2-hydroxy-4-chlorobutyronitrile (XV).—A solution of 89 g. of sodium bisulfite in 222 ml. of water was added to 62 g. of 1,4-dichloro-2-butanone (XIV), and the mixture was shaken vigorously for 20 min. To the resulting homogeneous solution, some crushed ice, 150 ml. of ether, and then a solution of 56 g. of potassium cyanide in 168 ml. of water were added. The ether layer was separated, and the aqueous layer was shaken with ether several times. The combined ether solution was dried over sodium sulfate and distilled; b. p., 102~103°C/1 mmHg.

The infrared spectrum showed bands of hydroxyl (3340 cm^{-1}) and nitrile (2219 cm^{-1}). The carbonyl band (1724 cm^{-1}) of the starting ketone was also observed.

Ethyl 2-Chloromethyl-2-hydroxy-4-chlorobutyrate (XVI).—A mixture of 5 g. of the cyanhydrin XV, 25 ml. of ethanol and 7.5 ml. of concentrated sulfuric acid was heated at reflux for 5 hr. and then poured onto crushed ice. This was shaken with ether, and the ether extract was dried over sodium sulfate. After the solvent had been removed, the residue was distilled; b. p. 111~115°C/4 mmHg.

Found: C, 38.43; H, 5.32. Calcd. for $C_7H_{12}Cl_2O_3$: C, 39.23; H, 5.58%.

The infrared spectrum showed an ester band at 1733 cm^{-1}.

α-Chloromethyl-α-hydroxy-γ-butyrolactone (XVII).—A mixture of 61 g. of the cyanhydrin (XV), 92 ml. of glacial acetic acid and 183 ml. of concentrated hydrochloric acid was heated on a water bath for 6 hr. After the ammonium chloride had been filtered off, the filtrate was concentrated in vacuo and extracted with ether. The ether extract was dried over sodium sulfate, and the solvent was removed. Vacuum distillation afforded a white viscous oil. Yield, 39 g.; b. p., 128~136°C/5 mmHg.

Found: C, 38.46; H, 4.69. Calcd. for $C_5H_7ClO_3$: C, 39.84; H, 4.65%.

The infrared spectrum showed a lactone band at 1760 cm^{-1}.

2-Aminomethyl-2,4-dihydroxybutyric Acid (XVIII).—A mixture of 6 g. of the lactone (XVII) and 120 ml. of concentrated aqueous ammonia was heated at 100°C in an autoclave for 5 hr. The solution was evaporated to dryness in vacuo, and the resulting solid was recrystallized from water. Yield, 3.5 g.; m, p. 237°C (decomp.).

Found: C, 40.39; H, 7.55; N, 9.31. Calcd. for $C_5H_{11}NO_4$: C, 40.26; H, 7.43; N, 9.39%.

The amino acid showed no color development on treatment with ninhydrin at 100°C. However, a purple-brown precipitate was obtained when the reaction was carried out at 150°C in a sealed tube.

2-Benzaminomethyl-2-hydroxy-4-benzoxybutyric Acid (XIX).—A small amount of the amino acid XVIII was dissolved in 10% aqueous sodium hydroxide and shaken with benzoyl chloride, with the solution being kept alkaline. Acidification with hydrochloric acid afforded white crystals, which were washed with ether to remove any benzoic acid. The ether-insoluble product was recrystallized from 50% ethanol; m. p., 173°C.

Found: N, 3.86. Calcd. for $C_{19}H_{19}NO_6$: N, 3.93%.

α-Hydroxy-α-phthaliminomethyl-γ-butyrolactone (XX).—A mixture of 3.5 g. of the amino acid XVIII, 5.5 g. of phthalic anhydride, 50 ml. of pyridine was heated at reflux for 6 hr. The solution was concentrated in vacuo, and water was added. The resulting solid (5.5 g., m. p. 147~149°C) was recrystallized from ethanol; m. p., 155°C.

Found: N, 5.26. Calcd. for $C_{13}H_{11}NO_5$: N, 5.37%.

Ethyl 2-Hydroxy-2-phthaliminomethyl-4-chlorobutyrate (XXI).—A suspension of 15 g. of the lactone XX in 350 ml. of ethanol was saturated with dry hydrogen chloride without cooling. After standing for 2hr. at room temperature, the solution was concentrated in vacuo. The addition of water afforded an oil which soon solidified. Recrystallization from 50% ethanol afforded white needles of XXI; m. p., 99~100°C.

Found: C, 55.47; H, 5.16; N, 4.32. Calcd. for $C_{15}H_{16}ClNO_5$: C, 55.22; H, 4.90; N, 4.28%

Ethyl 2-Hydroxy-2-phthaliminomethyl-4-dimethylaminobutyrate Methiodide (XXII).—Four grams of the chloroester XXI were dissolved in 20 ml. of ethanol containing 2.8 g. of dimethyl amine and then heated at 100°C for 4 hr. in a sealed tube. The ethanol was removed in vacuo, and the residue was extracted with ether (Soxhlet). Evaporation of the ether afforded a pale yellow viscous oil. The oil was dissolved in 50 ml. of dry acetone, and 15 g. of methyl iodide was added. A yellow solid was recrystallized from water; m. p., 219°C.

Found : C, 44.44 ; H, 5.56 ; N, 5.91. Calcd. for $C_{18}H_{25}IN_2O_5$: C, 45.31 ; H, 5.25 ; N, 5.87%.

Thermal Decomposition of the Hydroxide Obtained from XXII.—Wet silver oxide which had freshly been prepared from 1.5 g. of silver nitrate was added to a solution of 1.5 g. of the methiodide XXII in 30 ml. of water, stirred for 30 min., and filtered. The filtrate was evaporated to dryness under reduced pressure and kept at 150°C for 2 hr. (2 mmHg.). The residue was taken up in chloroform and treated with charcoal. Evaporation of the chloroform afforded a white glassy substance. Treatment of this substance with dilute hydrochloric acid afforded the lactone XX ; m. p. and mixed m. p., 155°C.

The author wishes to express his deep thanks to Professor Masaki Ohta, Tokyo Institute of Technology, for his guidance throughout this work. The author is also indebted to Professor Koji Nakanishi, Tokyo University of Education, for his helpful discussions and to Dr. Asaji Kondo for his microanalyses. Moreover, he is grateful to the Kawakami Memorial Foundation for financial support.

Department of Applied Chemistry
School of Science and Engineering
Waseda University
Shinjuku-ku, Tokyo

The Formation and Crystalline Nature of Boron Nitride in the Reaction of Boron Oxide with Sodium Amide

By Hiroaki TAGAWA and Otokichi ITOUJI

(Received March 20, 1962)

Boron nitride has extremely interesting chemical properties and physical characteristics. As the structure is very similar to that of graphite, it is sometimes called white graphite. Boron nitride is an excellent refractory material and is used as a thermal insulator in high frequency induction vacuum furnaces, as a material for the manufacture of refractory crucibles, and as an anti-sticking agent in contact with molten glass or metals. It is also an excellent lubricant and is used as a heat-resistant lubricant.

Boron nitride has been known for the more than one hundred years since it was first prepared by Balmain in 1842[1]. Since then it has been investigated by many researchers, and many methods of fabrication have been described in the literature and by patents.

Boron nitride is prepared by the reactions of a compound containing boron with a compound containing nitrogen; it the many processes by which it is produced may be summarized by the following equations:

$$4NH_3 + BCl_3 = BN + 3NH_4Cl$$[2-4]

$$2B + N_2 = 2BN$$[5]

$$B_2O_3 + 2NH_3 = 2BN + 3H_2O$$[6-8]

$$B_2O_3 + 3NaNH_2 = 2BN + NH_3 + 3NaOH$$[9]

$$B_2O_3 + 2NH_4Cl = 2BN + 2HCl + 3H_2O$$[10]

As with carbon, the physical and chemical properties of this material may vary considerably according to the nature of the starting materials and of the fabricating condition, but they may be thought of as depending mainly on such structural factors as the crystallinity and the state of the condensed system of the triboron-triazin ring.

In this article, boron oxide and sodium amide were selected as the starting materials in the preparation of boron nitride. Sodium amide is a chemically strong reducing agent; its great reactivity is coupled with the relatively low melting point of 210°C. The boron nitride which was formed in the reaction of boron oxide with sodium amide was investigated for the effect of the producing conditions on its structure and properties. The behavior of the reaction was examined by differential thermal analysis and thermogravimetry, and the crystalline nature of the boron nitride thus formed

1) W. H. Balmain, *J. prakt. Chem.*, **27**, 422 (1842); **32**, 494 (1844); *Phil. Mag.*, **21**, 170 (1842).
2) F. Meyer and R. Zappner, *Ber.*, **54B**, 560 (1921).
3) I. E. Compbell et al., *J. Electrochem. Soc.*, **96**, 318 (1948).
4) Th. Renner, *Z. anorg. u. allgem. Chem.*, **298**, 22 (1959).
5) R. Lorenz and J. Wooleock, ibid., **211**, 41 (1928).
6) E. Podzus, *Z. angew. Chem.*, **30**, 156 (1917); German Pat. 282701, 282748 (1913).
7) The British Thomson Houston Co., Ltd., Brit. Pat. 483201 (1938).
8) K. M. Tayler, U. S. Navy, Bureau of Ordnance Research Contract NOrd 10982 (1945).
9) J. Kamlet, U. S. Pat. 2865715 (1958).
10) R. Heyder, *J. Soc. Chem. Ind.*, **32**, 600 (1913).

was investigated by X-ray analysis and infrared absorption measurement.

The Nature of the Reaction of Boron Oxide with Sodium Amide

Experimental.—*Material.*—Boron oxide (Junsei Chemicals Co.) was dehydrated at 1000°C for 1hr., and then pulverized and screened with a 16 to 32 mesh sieve in a dry box. The sodium amide used in this experiment was obtained from the Kongo Chemicals Co.; it was pulverized below a 100 mesh sieve. The purity of this material was 93%; the rest was sodium hyroxide.

Differential Thermal Analysis.—A specimen, mixed to a 1 : 3 (by mol.) ratio of boron oxide to sodium amide was examined by differential thermal analysis with a three-hole nickel holder within an atmosphere of nitrogen. The difference in temperature between the sample and the reference (aluminium oxide) was measured by a thermocouple of chromel-alumel with two pairs in series. The differential thermoelectric motive force was recorded on the chart of electric recorder.

The temperature of the electric furnace was elevated continuously at a constant heating rate of 5°C/min.

Thermogravimetry.—The behavior of the reaction of boron oxide with sodium amide was also examined by using a thermogravimetric apparatus, which allowed a continuous measurement of the weight loss against the time. The apparatus consisted of a torsion type thermobalance (Shimadzu Manufacturing Co.) using a fine tungsten wire and of an electric furnace. The weight changes were measured by the rotation of the wheel, which applied sufficient torsion to the fiber to restore the arm to the null position. Its capacity and sensitivity were 1 g. and 5 mg. respectively. The thermobalance system could be evacuated.

The specimen used in this experiment was a mixture of boron oxide and sodium amide (mixing ratio, 1 : 3 by mol.). The powdered sample was placed in a nickel crucible and was suspended from the arm by a molybdenum wire. The weight changes by dehydration and nitridation were observed during the elevation of the sample temperature at a constant rate of heating of 5°C/min, within an atmosphere in nitrogen.

Results and Discussion.—*Differential Thermal Analysis.* — Differential thermograms of the reaction of boron oxide with sodium amide and of that of only sodium amide are shown in Fig. 1. The reaction of boron oxide with sodium amide in Fig. 1 (a) shows two peaks at 163 and 205°C, while in the reaction of boron oxide with sodium amide, involving 65% of sodium hydroxide, only one peak appears, at 163°C. Although the melting point of sodium amide is 210°C, it may be found in Fig. 1 (c) that the melting point is lowered in the presence of sodium hydroxide to about 165°C. The endothermic peaks at 155 and 201°C correspond with the melting of the sodium amide containing large amounts of

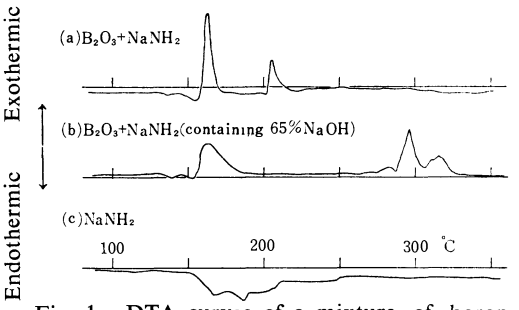


Fig. 1. DTA curves of a mixture of boron oxide and sodium amide (mixing ratio by mol. = 1 : 3).

sodium hydroxide and pure sodium amide respectively. The reaction peak at 205°C shows that the reaction of boron oxide with sodium amide occurs as soon as the sodium amide melts, which agrees with finding of Kamlet[9]. It may therefore be concluded that this reaction needs the melting of sodium amide and that the reaction temperature is lowered in the presence of sodium hydroxide, as sodium amide appears to make a solid solution with sodium hydroxide. The several peaks at about 300°C in the reaction of boron oxide with sodium amide involving large amounts of sodium hydroxide in Fig. 1 (b), seem to be due to the formation of sodium borates by the reaction of sodium hydroxide with the unreacted boron oxide.

Thermogravimetry. — The thermogravimetric curve of a mixture of 1.5 g. of boron oxide (16~32 mesh) and 2.5 g. of sodium amide is shown in Fig. 2. In this curve the weight loss observed is plotted against the temperature

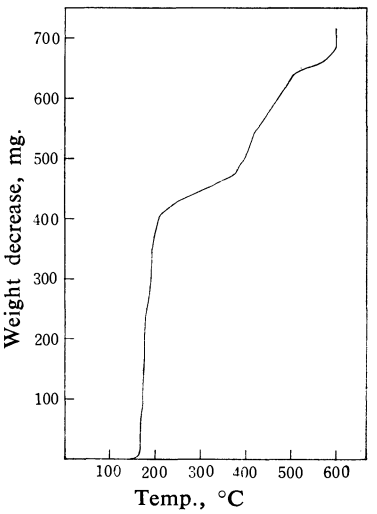


Fig. 2. Thermogravimetric curve of a mixture of boron oxide and sodium amide in hydrogen. B_2O_3; 1.5 g., $NaNH_2$; 2.5 g., heating rate; 5°C/min., retention time at 600°C; 30 min.

up to 600°C. A steep weight loss occurs in the temperature range from 170 to 200°C. The finding of this decrease in weight above 170°C is correspondent with that of the differential thermal analysis. The weight of the sample decreases gradually with the raising of the temperature, even above 200°C. At temperatures above 400°C, some sodium amide was condensed at the cold part of the quartz tube.

The mixing ratio of boron oxide was chosen as 1 : 3 by mole according to the following equation :

$$B_2O_3 + 3NaNH_2 = 2BN + NH_3 + 3NaOH$$

Theoretically, 1.5 g. of boron oxide reacts with 2.5 g. of sodium amide to form 1.1 g. of boron nitride and 0.36 g. of ammonia. The actual weight decrease is two times larger than the calculated quantity of evolved ammonia. Chemical analysis indicates that only 29.9% of the boron oxide changes into boron nitride. Consequently, this large weight loss may be due to the reaction of the sodium hydroxide formed with the amide and to the sublimation of the amide.

Crystalline Nature of the Boron Nitride Formed

Experimental.—*Preparation of Boron Nitride.*—Boron nitride for X-ray analysis and for infrared absorption measurement was produced by heating a mixture of boron oxide and sodium amide (mixing ratio, 1 : 3 by mole) at a desired temperature between 200 and 800°C in an ammonia atmosphere. The apparatus consisted of a quartz tube 50 mm. in inner diameter, a suspended crucible 30 mm. in diameter and 40 mm. in height, and an electric furnace. The tube containing the mixture could be evacuated for the exchange of atmosphere. The sample was suspended in a nickel bucket in the hot zone of the tube with fine tungsten wire from the top of the tube.

Five grams of boron oxide and 13.3 g. of sodium amide were ground together, charged into the nickel crucible, and heated in the electric furnace at temperatures from 200 to 800°C. In order to examine the behavior of the reaction during heating, a thermocouple was put in the mixture. The reaction commenced at about 170°C and proceeded vigorously at about 210°C with the evolution of ammonia. When the furnace temperature stood at 210°C, it was shown that the temperature of the mixture was temporarily brought up to 350°C. The reaction mixture was kept at the desired terminal temperature between 200 and 800°C for more than 30 minutes. The product in the crucible was obtained as a gray porous material. The substance was broken up and vigorously stirred into ice water. The insoluble boron nitride was filtered off, washed free of soluble matter with water, and then dried. The yields of boron nitride based on boron oxide were always about 30 percent in the top temperature range from 200 to 800°C. This boron nitride was analyzed for boron and nitrogen using the method mentioned by Finlay et al.[11]

X-Ray Measurement.—Changes in the interlayer spacing and crystallite growth were observed as a function of the terminal temperature. The diffraction patterns were recorded by an automatic recording X-ray spectrometer (Rigaku Denki Co.) and were calibrated by referring to a standard quartz specimen. The diffraction maximum did not directly give the true interlayer spacing for the polarization and absorption, as in the case of carbon[12], but the measured values were used.

The crystallite size was obtained from the broadening of the X-ray diffraction lines according to the procedure described by Klug and Alexander[13]. The crystallite dimension was calculated according to the following equation :

$$L = K\lambda/\beta\cos\theta$$

where L is the average effective dimension of the crystallite in a direction perpendicular to the reflecting plane at the glancing angle θ, λ is the wave length of the X-ray, K is a shape factor, and β is defined as the half-maximum line breadth. The L_c-dimension, the thickness of the parallel packets of layers, was obtained from the (002) line by using $K=0.9$. The L_a-dimension could not be obtained because of the obscure shape of the (10) band.

The diffraction conditions employed were as follows; the target was copper filtered by nickel, the filament voltage and current were 30 kV. and 15 mamp. respectively, the divergent slit was 1°, the receiving slit, 1° and 0.1 mm., the time constant, 4 sec., and the scanning speed, 2°/min.

Infrared Absorption Spectra.—The infrared spectra in the 4000 to 650 cm^{-1} region of boron nitride were obtained by using a Nippon Bunko model DS-301 spectrophotometer (with a potassium bromide prism) and by using potassium bromide pellet techniques.

Results and Discussion.—*X-Ray Analysis.*—The X-ray diffraction patterns of boron nitride formed at several temperatures between 200 and 800°C are shown in Fig. 3. Geometrically, the structure is very similar to that of graphite[14]. The peak at about 26° of the Bragg angle corresponds with the interlayer spacing. A terminal temperature of 800°C for the reaction mixture scarcely affects the yield of boron nitride, but the crystallinity increases with an increase in the top temperature. The X-ray diagrams of the boron nitride formed at 200 to 600°C show diffuse bands corresponding to the positions of the (002) and (100) lines, indicating a two-dimensional structure. In the case of boron nitride produced at 800°C, the deformation of the (10) band is already visible, and the

11) G. R. Finlay and G. H. Fetterley, *Ceram. Bull.*, **31**, 141 (1952).
12) W. R. Ruston, *Fuel*, **31**, 52 (1953).
13) H. P. Klug and L. E. Alexander, "X-Ray Diffraction Procedures", John Wiley, New York (1954), p. 491.
14) R. S. Pease, *Acta Cryst.*, **5**, 356 (1952).

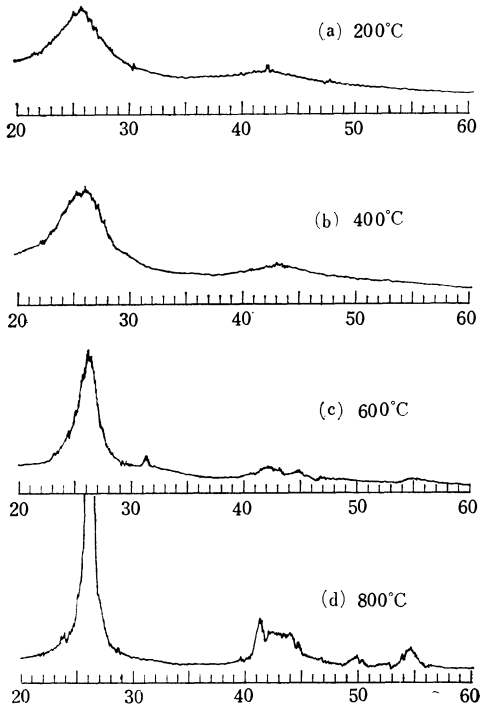


Fig. 3. X-ray patterns of boron nitride of various terminal temperatures.

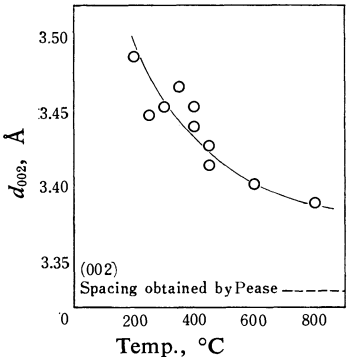


Fig. 4. Relationship between the apparent interlayer spacing and the terminal temperatures.

separation of the (100) and (101) reflexions may be clearly recognized.

By increasing the terminal temperature of the reaction mixture, the diameter of the boron nitride layers and the number of layers per parallel packet is increased, and the (002) spacing decreases. The results of these measurements are shown in Figs. 4 and 5. In the case of carbon, a decrease in the interlayer spacing, which accompanies an increase in the degree of graphitization, has already been

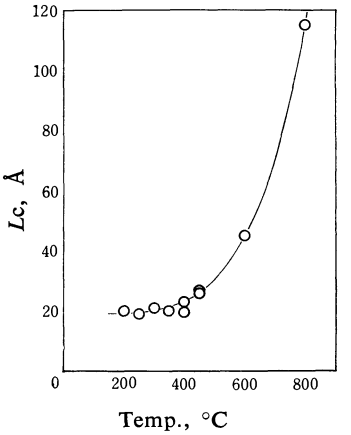


Fig. 5. Relationship between the *Lc*-dimensions of the parallel layer groups and the terminal temperature.

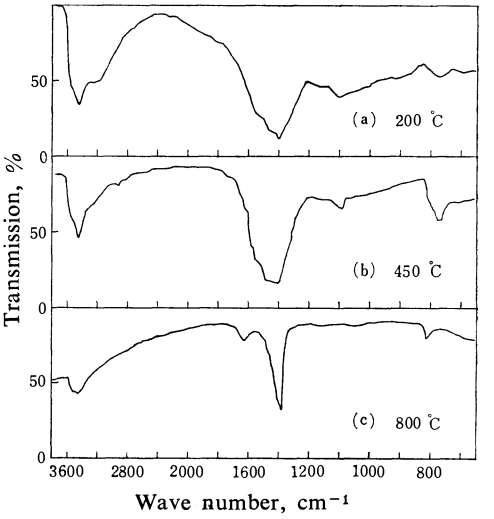


Fig. 6. Infrared absorption spectra of boron nitride of various terminal temperatures.

shown by Rooksby[15], Bacon[16] and Franklin[17]. The different graphitizing behavior of carbon may be a result of the nature of the original carbonaceous material and of the conditions under which they have been carbonized. On the other hand, the crystallization of boron nitride, like that of carbon, seems to be due to the processes and conditions of various methods of production. The increase of crystallite above 400°C, as shown in Fig. 5, is thought to be accelerated in the presence of molten salts, such as boric anhydride and sodium hydroxide.

Infrared Absorption Spectra. — The infrared absorption spectra of boron nitride formed at

15) H. P. Rooksby, *Elect. Times*, **102**, 19 (1942).
16) G. E. Bacon, *Acta Cryst.*, **3**, 137, (1950).
17) R. E. Franklin, ibid., **4**, 153 (1951).

200, 450 and 800°C are shown in Fig. 6. The absorption band at about 1400 cm^{-1} for boron nitride may be assigned as an in-plane B–N ring deformation. The spectrum of boron nitride obtained at 200°C, especially the B–O streching vibration at 1450 cm^{-1}, is different from the infrared absorption spectrum of boron oxide[18]. The absorption spectrum of boron nitride formed at 800°C agrees with the finding of Miller[19] and Brame[20]. The broadness of the absorption band at 1400 cm^{-1} and the O–H stretching band due to boron nitride hydrolyzed become somewhat smaller with an increase in the terminal temperature. The fundamental infrared absorption spectrum of boron nitride is scarcely influenced by the fabrication temperature. Although the melting point of boron nitride is above 3000°C, the skeletal structure of B–N hexagonal layers is complete even in the formation at 200°C, which finding agrees with the results of X-ray diffraction.

18) J. L. Parsons and M. E. Milberg, *J. Am. Cer. Soc.*, **43**, 326 (1960).
19) F. A. Miller, *Anal. Chem.*, **24**, 1253 (1952).
20) E. G. Brame, *J. Inorg. Nucl. Chem.*, **5**, 48 (1957).

Summary

The reaction of boron oxide with sodium amide has been investigated using differential thermal analysis and thermogravimetry. The reaction occurs at 210°C, the melting point of sodium amide, while in the presence of a large amount of sodium hydroxide, the reaction temperature is lowered to 165°C. It has been shown from the results of the differential thermal analysis that the reaction of boron oxide with sodium amide commences as soon as the sodium amide melts.

The boron nitride formed completes the skeletal structure of B–N hexagonal layers even at 200°C. The fundamental infrared absorption spectra of boron nitride is very little influenced by the fabrication temperature. The crystallinity of boron nitride as shown by the interlayer spacing and the crystallite size increases with the reaction temperature.

Research Laboratory
Nippon Carbide Industries Co., Inc.
Uozu, Toyama

Radiation Induced Reaction of Silicon Hydride

By Wataru ANDO and Shigeru OAE

(Received May 10, 1962)

Several publications have disclosed the addition of silicon hydrides to a number of alkenes with activated peroxide or under ultraviolet light. White and Rochow[1] obtained ethyl-, diethyl-, and triethylsilane by exposing a mixture of silane and ethylene to mercury vapor discharge. They indicated that the initial reaction is the decomposition of silane from the major amounts of products obtained by the irradiation of the mixture of silane and ethylene with mercury discharge in a flow system, and then concluded that the initial step involved must be the formation of hydrogen atom and silyl(SiH_3-) radical from silane. Fritz[2] also gave the mechanism in which the addition of the silicon hydrides to alkenes is free radical chain reaction. However, the exact course of the addition could not be determined, since further reactions of the initial products were extensive under these conditions.

The present investigation differs primarily from the above work in that the reaction was carried out at room temperature using gamma rays from 3.8 kilocurie ^{60}Co source.

No direct studies of the radiation chemistry of pure silane have been reported. The results of irradiation of pure silane and that with water, carbon dioxide and acetylene will be investigated.

Experimental

Reagents.—The reaction of silicon tetrachloride with lithium tri-*tert*-butoxaluminohydride was used for the preparation of silane[3]. In this case the reaction was carried out in a 500 ml. flask with flow of dry nitrogen. Commercially available carbon dioxide was purified by fractional distillation at low

1) D. G. White and E. G. Rochow, *J. Am. Chem. Soc.*, **76**, 3897 (1954).
2) G. Fritz, *Z. Naturforsch.*, **7b** 507 (1952).
3) S. Sujishi and J. Kieth, *J. Am. Chem. Soc.*, **80**, 4138 (1958).

temperature. Acetylene was made from the reaction of carbide and water, and was purified by repeated distillations.

Reaction Vessel.—The vessel in which the gaseous irradiations were carried out was consisted of pyrex tube of 16 mm. outside diameter and 22 mm. length, and equipped with a breakoff seal.

Analysis of Products.—Separation of products was achieved by a serial fractional distillations and condensations following the known procedure[4]. The yield of each fraction was measured by observing the pressure exerted when the entire fraction was vaporized into a calibration column. Vapor pressure at below room temperature was measured by the conventional method. The molecular weight of each product was calculated from its vapor density. Gamma field intensity was determined by the ferrous sulfate dosimeter.

Results and Discussion

Radiation Induced Reaction of Pure Silane.—The results of the irradiation of pure silane at different pressures and radiation doses are shown in Tables I and II. In these experiments, the separation of the products was achieved by taking the advantage of the different volatilities of the products; unreacted silane was distilled at −160°C, and di- and higher silanes at −111.8 and −45°C. The noncondensable gas at 196°C was introduced into a calibrated column with a Toepler pump. Higher silicon hydrides data are not shown in the following tables because of the low concentrations and the poor precision in their analyses.

In all of the reactions, the rate of hydrogen formation did decrease with the total radiation dose and the original silane pressure increased. In each experiment, a thin layer of light brown amorphous solid deposited on the wall of the reaction vessel. It was a polymeric compound having an empirical formula $(SiH_2)_x$, which was identified by measuirng the amounts of hydrogen and silicon after decomposing the solid by heating in an incinerator.

Under the described conditions, it is assumed that SiH_3, SiH_2, Si_2H_5 and H radicals or ions are formed in the irradiation of silane. These results when plotted as a function of initial silane pressure (Fig. 1) show that the rate of hydrogen formation in irradiation decreases with increasing silane pressure. At high pressure of gas the dependence of the energy absorption upon the pressure is not linear with density. This will acount for at least a part of the effect of pressure upon $G(H_2)$: i.e. Table I.

However, this relation will depend upon the composition and the geometry of the reaction vessel and the pressure of the gas in a

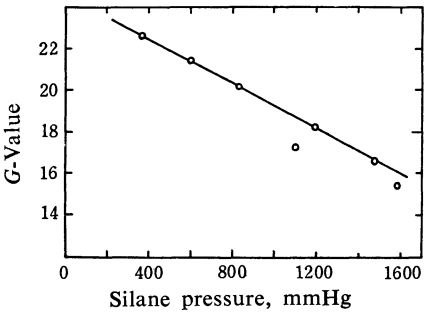


Fig. 1. Pressure dependence of hydrogen formation on the radiolysis of silane.

Table I. Pressure effect on the radiolysis of silane*

SiH_4 Pressure	Products, mmol.×10³			
mmHg	H_2	$G(H_2)$	Si_2H_6	Higher silanes
380	3.19	22.8	1.27	Trace
600	4.66	21.7	1.57	Trace
820	6.13	20.5	1.56	Trace
1100	6.88	17.2	1.33	Trace
1200	7.92	18.3	0.93	Trace
1480	8.98	16.8	1.47	None
1580	9.02	15.8	1.95	None

* Total dose was 5.81×10^{20}eV./g. for each experiment.

Table II. Radiation dose effect on the radiolysis of silane at 380 mmHg pressure*

	Irradiation time, hr.							
Product	2	4	6.5	7.8	10	12.8	16	20.3
H_2, mmol.×10³	1.27	1.34	1.32	1.75	1.88	2.15	2.51	3.14
$G(H_2)$	42.3	38.2	31.1	32.6	27.6	24.3	23.1	22.8

* Radiation dose rate was 2.87×10^{19}eV./g./hr.

4) R. T. Sanderson, "Vacuum Manipulation of Volatile Compound", John Wiley and Sons. Inc., New York, N. Y. (1948).

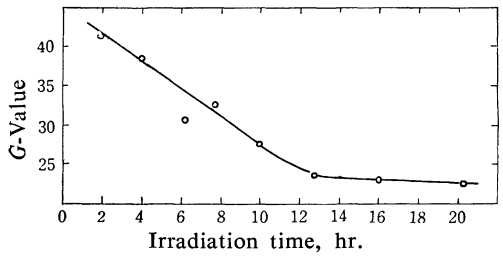


Fig. 2. Hydrogen formation as function of energy absorbed on radiolysis of silane.

complicated manner. Figure 2 shows that the rate of hydrogen formation at the low pressure (in these experimental range) decreases with irradiation time. These trend seems to favor the radical-radical reaction rather than ion-molecule reaction.

These facts suggest that unimolecular decomposition of silane might be considerd as taking place initially in two ways.

$$SiH_4 \sim\sim\sim\rightarrow SiH_2 + H_2 \quad (1)$$

$$SiH_4 \sim\sim\sim\rightarrow \cdot SiH_3 + H \quad (2)$$

There is no definite evidence as to which is primary reaction. But the energy of dissociation of reaction 1 very probably is not greater than the activation energy. On the other hand, the energy of dissociation for reaction 2 should be considerably greater than that of the activation. Hogness, Wilson and Johnson[5] have concluded that silylene radical is the primary product in the decomposition of silane. If this is the case, silyl radical becomes the secondary product arising from reaction such as

$$SiH_2 + SiH_4 \rightarrow 2 \cdot SiH_3 \quad (3)$$

In this case some of SiH_2 radical loses its energy and forms polymeric solid: $(SiH_2)_x$. The formation of hydrogen produced by radical process is probably due to the reaction; the primary process may be proposed as the reaction 1 and then 3, which is followed by the following chain propagating processes;

$$\cdot SiH_3 + SiH_4 \rightarrow Si_2H_6 + \cdot H \quad (4)$$

$$\cdot SiH_3 + Si_2H_6 \rightarrow Si_3H_8 + \cdot H \quad (5)$$

and chain ending processes

$$2H \cdot \rightarrow H_2 \quad (6)$$

$$2 \cdot SiH_3 \rightarrow Si_2H_6 \quad (7)$$

Radiation Induced Reaction of Silane with Carbon Dioxide, Water and Acetylene.—Mixtures of silane and carbon dioxide were sealed into the reaction vessels in various ratios. The results of four experiments were given in Table III, only for the hydrogen formation. Analysis of the material volatile at room temperature showed the presence of silane, disilane and higher silanes in addition to the bulk of non-condensable hydrogen at −196°C. Here again a thin layer of light brown solid deposited on the wall of the reaction vessel.

TABLE III. RADIOLYSIS OF SILANE-CARBON DIOXIDE MIXTURES*

SiH_4 mmol.	CO_2 mmol.	Ratio CO_2/SiH_4	Product, H_2 mmol. $\times 10^3$	$G(H_2)$
0.455	0.		3.19	22.8
0.450	0.129	0.29	3.57	25.7
0.480	0.478	1.0	9.24	65.3
0.136	0.443	3.2	3.57	84.8

* Total dose for these experiments was 5.81×10^{20} eV./g.

The result from the radiolysis of silane with water are shown in Table IV. In case of radiolysis of a mixture of silane and acetylene, the observed G-value for the formation of hydrogen was 52.7.

TABLE IV. RADIOLYSIS ON THE MIXTURE OF SILANE AND WATER*

SiH_4 mmol.	H_2O mmol.	Product, H_2 mmol. $\times 10^3$	$G(H_2)$
0.482	3.2	17.7	119
0.487	0.005	11.1	77
0.482	0.003	7.72	52
0.422	trace	4.78	37

* Total dose was 5.81×10^{20} eV./g. in each experiment.

Striking difference was observed in the amounts of hydrogen in the radiolysis of mixiures of silane and carbon dioxide from that of pure silane even when the silane pressure and radiation dose were similar in those experiments. The increase in the G-value with carbon dioxide concentration seems to suggest that original energy absorbed by carbon dioxide somehow transfers to the silane, be it the transfer of charge or of excitation. Such transfer manifests itself as an increase in the rate of silane conversion. This effect has been noted previously in the radiolysis of acetylene[6-8], butadiene, and several inorganic gases[6].

In case of water-silane mixtures, in view of the very little reactivity of silicon hydrides toward pure water[9], the observed G-value of

5) T. R. Hogness, T. L. Wilson and W. C. Johnson, *J. Am. Chem. Soc.*, **58**, 108 (1936).

6) S. C. Lind and D. C. Bardwell, ibid., **48**, 1575 (1926).

7) R. C. Palmer and D. C. Badwell, Presented at the 134th National Meeting of the American Chemical Society, Chicago, Illinois, September, 1958.

8) L. M. Dorfman and A. C. Wahl, *Radiation Research*, **10**, 680 (1956).

9) H. J. Emeleus and J. S. Anderson, "Modern Aspect of Inorganic Chemistry", 2nd Ed., Van Norstand (1952), p. 283.

hydrogen formation was extremely high as compared to that of pure silane radiolysis. The observed results is very interesting. Energy transfer from water to silane cannot be attributed as the amounts of water used was less than one per cent. One possibility would be that the excited water molecule will abstract hydrogen atom from silane by short chain reaction, but little is known about what happens to the resulting radical in the gaseous medium. The exact nature of the chain reactions is not clear.

By comparion with a simple charge transfer reaction in the radiolysis of silane-carbon dioxide system, charge transfer reaction is not possible in the radiolysis of silane-acetylene mixtures because acetylene have a lower ionization potential than that of silane. In this system, charge transfer producing chemical changes has been known to be supressed[10]. Perhaps, the compound containing vinyl group attached to the silicon might be formed by the following reactions[1].

10) P. S. Rudolph and C. E. Melton, *J. Chem. Phys.*, **32**, 586 (1960).

$$\cdot SiH_3 + C_2H_2 \rightarrow \dot{C}H{=}CHSiH_3 \quad (8)$$

$$\dot{C}H{=}CHSiH_3 + SiH_4 \rightarrow CH_2{=}CHSiH_3 + \cdot SiH_3 \quad (9)$$

Summary

Silane, at various pressures, has been irradiated with 3.8 kilocuries gamma rays. In all experiments, gaseous products of the reaction were hydrogen, disilane and higher silanes, while *G*-value for the formation of hydrogen depends on initial silane pressure and total dose. Some polymeric material with the approximate empirical formula of $(SiH_2)_x$ is also formed.

Mixtures of silane with carbon dioxide, water and acetylene were also irradiated with gamma rays, and the rate of hydrogen formation was found to increase with increasing carbon dioxide and water. This was explained by a charge transfer mechanism.

Radiation Center of Osaka Prefecture
Sakai, Osaka

*Equilibria in the $PdS-H_2-Pd_4S-H_2S$ and $Pd_4S-H_2-Pd-H_2S$ Systems**

By Kichizo NIWA, Toshio YOKOKAWA and Toshiro ISOYA

(Received January 31, 1962)

It is known that in the palladium-sulfur system there are three stable compounds, namely PdS_2, PdS and Pd_4S. The sulfur pressure associated with the dissociation of PdS_2 to PdS has been measured by Biltz and Laar[1], while the thermodynamic properties of the other two compounds are not yet known. The present studies have been undertaken to measure the dissociation pressures of PdS and Pd_4S on the basis of measurements of the equilibrium between a hydrogen-hydrogen sulfide gaseous mixture and a PdS–Pd_4S or Pd_4S–Pd solid mixture. From the experimental results, the free energies of the formation of the three sulfides were calculated.

Experimental

Materials. — PdS was prepared from palladium chloride of a guaranteed reagent. From a 5% hydrogen chloride aqueous solution of palladium chloride, PdS was precipitated by the introduction of gaseous hydrogen sulfide. Pd_4S was not prepared as a pure substance, but was produced in the solid phase in the intermediate state of a reduction of PdS to Pd (or in the sulfidization of Pd to PdS). This compound was identified by X-ray analysis.

Apparatus and Procedures.—A streaming method was employed. The reaction tube is shown in Fig. 1. In the figure, A is a pyrex tube 30 cm. in length and 1 cm. in inner diameter. The right hand portion of the tube is expanded downwards to be charged with the sulfide mixture. B is a pyrex outlet tube 9 mm. in outer diameter and 5 mm. in inner diameter. The heating element is a nichrome resistance furnace. The temperature of the furnace was controlled manually within ±1°C. The temperature was measured by a platinum vs platinum—rhodium thermocouple at

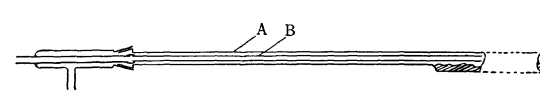


Fig. 1. Schematic diagram of the reaction tube.

* Presented at the 14th Annual Meeting of the Chemical Society of Japan, April, 1961.

1) W. Biltz and J. Laar. *Z. anorg. u. allgem, Chem.*, **228**, 257 (1936).

the outside of the reaction tube. The temperature of the inner space of the reaction tube was proved to be equal to that of the outside by a preliminary test. Hydrogen gas was generated by electrolysis of a potassium hydroxide solution. Oxygen was eliminated by introducing the gas into a heated copper net. The hydrogen thus prepared was found by gas-chromatographic analysis to contain a trace of oxygen and about 2% nitrogen. These impurities were disregarded, since any error due to these minor quantities falls within the normal scattering of experimental results. For the sake of uniform mixing, the gas mixture of hydrogen and hydrogen sulfide was stored before use above vacuum pump oil in a glass vessel. After the reaction, the gas mixture was led into a potassium hydroxide aqueous solution and then gathered in a glass vessel, where the volume of the hydrogen was measured. The amount of hydrogen sulfide in the alkaline solution was determined by iodometric titration. The rate of gas flow appropriate for attaining equilibrium was examined at 625°K. No change in apparent equilibrium composition was detected when the flow rate was changed from 7 to 60 cc./min. Another confirmation of the attainment of equilibrium is given by the fact that the apparent equilibrium compositions of the gaseous mixture were consistent with each other, irrespective of the direction of reaction, as will be seen below.

Results

PdS–Pd_4S System. — The equilibrium was measured over the temperature range of 613 to 795°K. The ratios of the equilibrium partial pressure of hydrogen sulfide to that of hydrogen are summarized in Table I. The reaction is represented by the following equation:

TABLE I. EQUILIBRIUM CONSTANTS OF THE REACTION, $4/3\ PdS+H_2=1/3\ Pd_4S+H_2S$

Temp., °K	P_{H_2S}/P_{H_2}
612	3.68×10^{-2}
613	3.74×10^{-2}
622	3.50×10^{-2}
622	4.40×10^{-2}
622	4.29×10^{-2}
622	4.00×10^{-2}
663	8.94×10^{-2}
678	1.09×10^{-1}
*713	1.53×10^{-1}
731	1.84×10^{-1}
747	2.40×10^{-1}
773	3.28×10^{-1}
788	3.22×10^{-1}
791	3.75×10^{-1}
791	3.13×10^{-1}
*791	3.64×10^{-1}
795	3.08×10^{-1}

* From sulfidization side

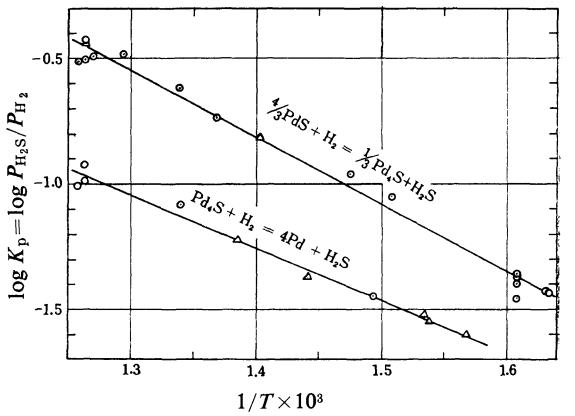


Fig. 2. Logarithm of the equilibrium constants plotted against reciprocal temperature.

$$\frac{4}{3}PdS+H_2=\frac{1}{3}Pd_4S+H_2S,\ K_p=P_{H_2S}/P_{H_2} \quad (1)$$

The logarithms of equilibrium constants are plotted against the reciprocal temperature in Fig. 2. By the least-aquare method, the following equation was derived for the standard free energy change of this reaction:

$$\Delta G^0=(12200\pm300)-(13.4\pm0.5)T$$
$$(\pm130\ \text{cal./mol. at } 613\sim798°K) \quad (1')$$

Pd_4S–Pd System.—The temperatures of the measurements ranged from 638 to 795°K. The equilibrium constants, defined below, are shown in Table II and in the lower portion of Fig. 2.

TABLE II. EQUILIBRIUM CONSTANTS OF REACTION, $Pd_4S+H_2=4Pd+H_2S$

Temp., °K	P_{H_2S}/P_{H_2}
*638	2.50×10^{-2}
*650	2.83×10^{-2}
*652	3.01×10^{-2}
670	3.57×10^{-2}
*694	4.27×10^{-2}
*722	6.00×10^{-2}
746	8.29×10^{-2}
791	1.03×10^{-1}
791	1.20×10^{-1}
795	9.87×10^{-2}

* From sulfidization side

From these values, the free energy equation can be derived as follows:

$$Pd_4S+H_2=4Pd+H_2S,\ K_p=P_{H_2S}/P_{H_2} \quad (2)$$
$$\Delta G^0=(9600\pm400)-(7.7\pm0.6)T$$
$$(\pm90\ \text{cal./mol. at } 638\sim795°K) \quad (2')$$

In Eqs. 1′ and 2′, the figures after the ± sign denote the standard deviations.

Discussion

Combining Eqs. 1 and 2 with that of the thermal dissociation of hydrogen sulfide, one can calculate the dissociation pressures of these two sulfides. Within the temperature range of this experiment, the free energy change associated with the dissociation of hydrogen sulfide is given by[2]:

$$H_2S = H_2 + \frac{1}{2}S_2 \quad (3)$$

$$\Delta G^0 = 21200 - 11.3T \quad (3')$$

Therefore,

$$\frac{3}{8}PdS = \frac{2}{3}Pd_4S + S_2 \quad (4)$$

$$\log P(\text{atm.}) = -14600/T + 10.8 \quad (4')$$

$$2Pd_4S = 8Pd + S_2 \quad (5)$$

$$\log P(\text{atm.}) = -13500/T + 8.3 \quad (5')$$

and

$$2PdS_2 = 2PdS + S_2 \quad (6)$$

$$\log P(\text{atm.}) = -7330/T + 8.45 \quad (6')$$

Here, the temperature equation for PdS_2 was calculated from the data of Biltz and Laer's measurement at three temperatures.

Next, on the basis of Eqs. 4, 5 and 6, the free energies of the formation of Pd_4S, PdS and PdS_2 are:

$$4Pd + \frac{1}{2}S_2(g.) = Pd_4S \quad (7)$$

$$\Delta G^0 = -30800 + 19.0T \quad (7')$$

$$Pd + \frac{1}{2}S_2(g.) = PdS \quad (8)$$

$$\Delta G^0 = -32800 + 23.3T \quad (8')$$

$$Pd + S_2 = PdS_2 \quad (9)$$

$$\Delta G^0 = -49700 + 41.7T \quad (9')$$

The standard free energies of the formation of these sulfides at 298°K cannot be obtained because of a lack of knowledge about their heat contents.

2) K. K. Kelley, *Bur. Mines Bulletin*, No. 406 (1937).

Summary

Equilibrium measurements were carried out by a streaming method on the systems of palladium sulfides and of hydrogen-hydrogen sulfide gaseous mixtures. From the results, the dissociation pressures of PdS and Pd_4S were calculated, and the free energies of the formation of PdS_2, PdS and Pd_4S from palladium metal and sulfur diatomic gas were obtained.

Department of Chemistry
Faculty of Science
Hokkaido University
Sapporo

Spectroscopic Studies of Methylamine Adsorption on Gamma-alumina

By Kozo HIROTA, Kenji FUEKI and Tokuji SAKAI

(Received April 14, 1962)

In our previous reports[1], the state of formic acid adsorbed on dehydrated silica and on alumina was investigated by means of nuclear magnetic resonance and infrared absorption methods. We thereby concluded that the acid adsorbed on silica was in an undissociated state, but that the free motion of the proton bonded to oxygen was hindered markedly, while a part of the acid dissociated into formate ions on alumina similarly to the way it did on several metal catalysts[2].

As the next substance to be studied along these lines and to be reported on in this paper, methylamine, which has a basic character contrary to that of formic acid, was adopted, while gamma-alumina was adopted as the adsorbent. The present research will also be interesting because of the fact that several amines are used so as to estimate the acidities of such oxide-catalysts.

Experimental

Materials. — *Methylamine.* — Methylamine of a chemically pure grade was used after dehydration.

Deuteromethylamine CH_3ND_2. — Methylamine was deuterated by the following exchange reaction.

$$CH_3NH_2 + D_2O \rightarrow CH_3ND_2 + H_2O$$

1) K. Hirota, K. Fueki, K. Shindo and Y. Nakai, This Bulletin, **31**, 783 (1958); **32**, 1261 (1959).

2) K. Hirota, K. Kuwata and Y. Nakai, This Bulletin, **31**, 861 (1958); J. Fahrenfort and H. F. Hazebrock, *Z. physik. Chem., N. F.*, **20**, 105 (1959).

Alumina.—Aluminum hydroxide, which was prepared from aluminum nitrate, was dried at 130°C for 10 hr. Then, after drying at 450°C for 8 hr., it was further degased at the same temperature for 100 hr. in vacuo (10^{-4} mmHg). The sample thus produced was a porous powder, its apparent density being 0.49 g./cm^3. According to X-ray measurement, it was almost amorphous, and it could be concluded to be gamma-alumina.

Measurement.—The essential measurement procedures were the same as has been reported already[1]. The infrared spectrum of methylamines adsorbed on the alumina powders was obtained on the sample pressed on a NaCl plate placed in a cell with NaCl windows. The infrared apparatus was a Perkin-Elmer Model 221, installed at the Institute of Protein Research, Osaka University. The nuclear magnetic resonance (NMR) spectrum was obtained at a fixed measuring frequency of 60 Mc./sec. with a Varian-V3600 C, installed at the Japan Atomic Energy Research Institute. The chemical shift of the proton resonance spectrum was determined by employing benzene as an external reference substance in a spinning, coaxial-sample tube arrangement (the double-tube method). Other experimental details will be described when necessary.

Results

The Infrared Spectra.—The infrared spectra of the adsorbed state are shown in Fig. 1, where the contribution of gaseous amine to the spectra, if it existed, was eliminated with a compensation cell. The spectra were obtained when the surface coverage, θ, of amines was ca. 0.2. Though the s/n ratio was large, three bands due to adsorption may be clearly identified in Fig. 1. In Table I they are assigned to gaseous amines of strong intensities. A detailed assignment of the bands will be undertaken below. It must be noted that the intensity of the degenerate stretching vibration ($\nu(CH_3)$) of CH_3 is markedly decreased by adsorption as compared with those of the other two bands, $\delta(CH_3)$ and $\delta(NH_2)$.

The NMR Spectra.—Figure 2 shows the NMR spectra of the normal and deuterated amines in liquid and adsorbed states measured at room temperature. It was found that only one signal could be identified over the range up to $\theta=1.2$; i. e., the other signal became too broad. By comparing the spectra of both amines, it is evident that the observed signal corresponds to that of the proton attached to the carbon atom rather than to that attached to the nitrogen atom. As ought to be expected, the half-width of this signal decreased and became sharp with the surface coverage, θ, as is shown in Fig. 3, where θ was determined

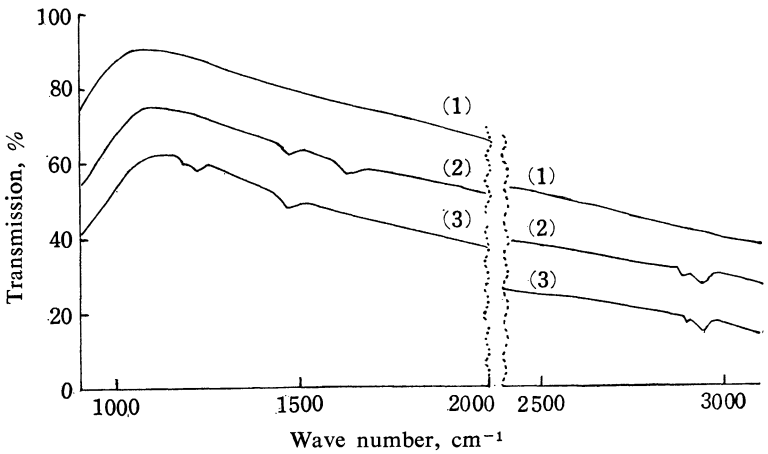


Fig. 1. Infrared spectra of the adsorbed methylamines.
(1) Gamma-alumina, (2) CH_3NH_2 on alumina, (3) CH_3ND_2 on alumina

Table I. The IR adsorption bands of methylamines

Modes of vibration	Gaseous state*		Adsorbed state	
	CH_3NH_2 cm^{-1}	CH_3ND_2 cm^{-1}	CH_3NH_2 cm^{-1}	CH_3ND_2 cm^{-1}
(a) ν (CH_3), Degenerated stretching vibration of CH_3	2961	2961	2927	2927
(b) δ (CH_3), Degenerated deformation vibration of CH_3	1473	1468	1470	1465
(c) δ (NH_2), Scissoring vibration of NH_2	1623	1234	1603	1214

* The bands determined were practically the same as those of the literature (A. P. Gray and R. C. Lard, *J. Chem. Phys.*, **26**, 690 (1957)).

under the assumption that the molecular cross section of methylamine was 18 Å^2. Another interesting point is the chemical shift to the adsorbed state from the liquid state. Since the so-called "bulk effect" is superposed on this effect, a quantitative discussion, besides the relation shown in Fig. 3, will be postponed to later paragraphs.

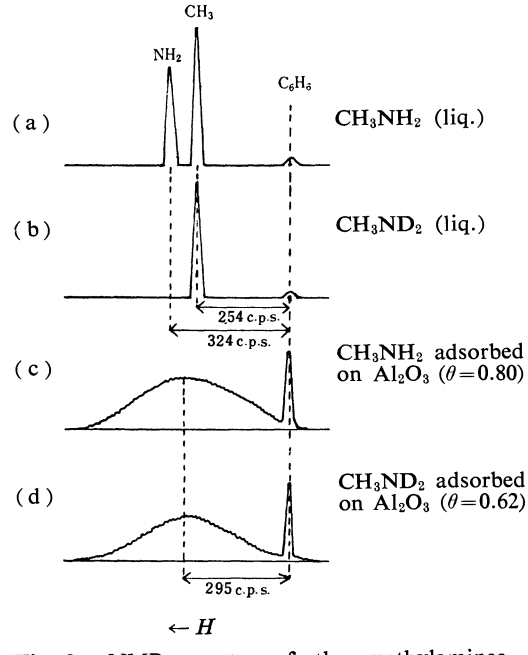


Fig. 2. NMR spectra of the methylamines adsorbed on alumina (schematic).

Discussion

Adsorbed States of Amines.—In the region between 1100~3300 cm^{-1}, three strong bands are observed on gaseous methylamine, e. g., 2961, 1473 and 1623 cm^{-1}; these are assigned to be $\nu(CH_3)$, $\delta(CH_3)$ and $\delta(NH_2)$ respectively, while the corresponding ones are observed on deuterated methylamine, CH_3ND_2, at 2961 cm^{-1} ($\nu(CH_3)$), 1468 cm^{-1} ($\delta(CH_3)$) and 1234 cm^{-1} ($\delta(ND_2)$) respectively. It is natural, therefore, to correlate them, as has been done in Table I, to the three bands observed when both amines were adsorbed. However, there were some shifts to a lower frequency in $\nu(CH_3)$, $\delta(NH_2)$ and $\delta(ND_2)$. These shifts seem to suggest the occurrence of some structural change of methylamines due to adsorption. The same conclusion will be derived from the data of the NMR spectra below.

As has already been mentioned, two marked changes were observed in the NMR spectra when either of the two methylamines was adsorbed on alumina: a disappearance of the signal of the aminyl-proton and a broadening of that of the methyl-proton.

Judging from these results, methylamine seems to be adsorbed in such a state that the hydrogen of the aminyl group is more resticted than that of the methyl group; i. e., amine is bonded to alumina via the nitrogen atom. Such a model is convenient to explain the change of the δ (NH_2) absorption band, because the bond angle between the N–H groups would be deformed due to adsorption, even though the three bonds of nitrogen atom orient one another so as to take a pyramidal structure, according to microwave-spectroscopic research[3].

The Nature of the Bond between Amines and Alumina.—It is, therefore, highly probable that both methylamines are adsorbed on alumina, making the nitrogen atom nearer to the surface than the carbon atom. Let us investigate the nature of the interaction of both atoms from the viewpoint of the adsorbent.

According to recent research[4], extremely dehydrated alumina acts as a Lewis acid; e. g., the aluminum atom of such alumina can accept a pair of electrons in its vacant *p*-orbitals, making a kind of bond with the adsorbate molecule. On the present drastically dehydrated alumina, it is natural to assume, therefore, that part of the unpaired electrons of the nitrogen atom will move to the aluminum atom. However, considering the fact that the adsorption heat is not very high, the degree of electron transfer may not be very high*.

Such an electron transfer due to adsorption may also be shown to be possible by the NMR spectra, which give the direction of the transfer by the chemical shift. As is shown by Fig. 2, the signal of the methyl proton shifts to a higher field, apparently suggesting the increase of electrons at the carbon atom, though the reverse result would be expected. The above discrepancy will disappear if the bulk-susceptibility correction is taken into consideration.

When the double-tube method was adopted, the net shift, δ, may be given from the observed shift, δ_{obs}, by the following formula[6]:

$$\delta = \delta_{obs} + \frac{2\pi}{3}(\chi_{ref} - \chi) \qquad (1)$$

where χ_{ref} and χ denote the volume magnetic

3) K. Shimoda, T. Nishikawa and T. Itoh, *J. Phys. Soc. Japan*, **9**, 974 (1954); T. Itoh, ibid., **11**, 264 (1956); T. Nishikawa, ibid., **12**, 668 (1957).

4) Cf., Actes du II Congrès International de Catalyse, Technip, Paris (1960).

* According to the results of Sakai[5], the heat of the adsorption of methylamine on alumina is 7.9 kcal./mol. at room temperature.

5) T. Sakai, K. Fueki and K. Hirota, 14th Annual Meeting of the Chemical Society of Japan, Tokyo, April, 1961, No. 3360.

6) Cf., J. A. Pople, W. G. Schneider and H. J. Bernstein, "High-resolution Nuclear Magnetic Resonance", McGraw-Hill Book Co., New York (1959), p. 81.

susceptibilities of the reference substance and of the adsorbate respectively. The chemical shift observed, Δ, corresponds to the difference in δ's between the liquid and the adsorbed state of methylamine, irrespective of the reference substance, benzene. Thus, Δ is given from Eq. 1 by

$$\Delta = (\delta_{liq} - \delta_{ads})_{obs} + \frac{2\pi}{3}(\chi_{ads} - \chi_{liq}) \qquad (2)$$

where the volume susceptibility of methylamine χ_{liq} is calculated to be -0.67×10^{-6} from the specific susceptibility[7] and its density, (0.767 g./cc.). Thus, Δ may be calculated to be 0.35 p. p. m., if the specific susceptibility of alumina is assumed to be that of a dehydrated alumina, i. e., -0.350×10^{-6} [8]. Therefore, it can be said that the net shift was to the lower field, suggesting an electron transfer from the carbon atom. Such a result will be noteworthy if compared with formic acid/silica system[1], where such a chemical shift due to adsorption may be practically neglected (+0.01 p. p. m.).

On the other hand the conclusion already mentioned is supported by the fact that electron density decreased at the carbon atom as a result of adsorption; the decrease of ν (CH_3) in wavelength can be explained by this model. However, it is difficult at the present stage of study to estimate quantitatively either the increase in electron density at the aluminum atom or the exact nature of the bond between the amine and alumina.

If the amine molecule is chemisorbed on alumina via the nitrogen atom, as has been suggested above, it is not strange that the motion of the aminyl group will be hindered so much more than that of the methyl group that the proton signal of the former may become very broad. For the same reason, it is possible that the signal of the latter may become sharp as the amount of adsorption increases. Thus, the results shown in Fig. 3 may be explained qualitatively.

Finally, it may be added that, according to our recent spectroscopic research, an aromatic amine, aniline, seems to be adsorbed also via its nitrogen atom on alumina[9], though it takes not a pyramidal but a planar structure. On the other hand, such an adsorbed model will provide other evidence on the role of the Lewis acid sites of alumina, recently proposed by Peri[10], on the isomerization catalyst.

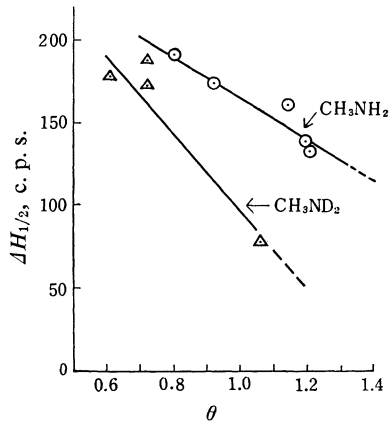


Fig. 3. Change of the half-width of NMR signal of the adsorbed methylamines.

Summary

It can be confirmed directly by means of NMR and infrared spectra that methylamine is chemisorbed on dehydrated gamma-alumina at room temperature, making a bond probably with the aluminum atom via the nitrogen atom; this conclusion is supported by the fact that the proton signal of the aminyl group cannot be observed at such a surface coverage when that of the methyl group is observed, and the fact that the deformation band of the NH_2 group and the stretching band of CH_3 group change as a result of adsorption.

The authors wish to express their deep thanks to Dr. Naohiro Hayakawa of the Japan Atomic Energy Research Institute for his NMR measurement.

Department of Chemistry
Faculty of Science
Osaka University
Nakanoshima, Osaka

7) "Kagaku-Benran", Maruzen, Tokyo (1958), p. 642.
8) P. Pascal, *Compt. rend.*, 178, 481 (1924).
9) K. Fueki, K. Hirota and H. Otouma, 15th Annual Meeting of the Chemical Society of Japan, Kyoto, April, 1962, No. 21 303.
10) J. B. Peri, Actes du II Congrès International de Catalyse, Technip, Paris (1960), p. 1333.

Polarography of Pyridine N-Oxide and its Alkyl Derivatives[*1]

By Tanekazu KUBOTA and Hiroshi MIYAZAKI

(Received April 23, 1962)

Several authors have reported on the polarographic behavior of such aliphatic and aromatic *N*-oxides as pyridine, nitrogen mustard and narcotin *N*-oxides, showing that these *N*-oxides give one or more reduction waves involving two electrons and are reduced to the corresponding amines[1-4]. Especially, Foffani and Fornasari have found that pyridine *N*-oxide in various buffer solutions gives one reduction wave whose height decreases rapidly at above pH≈6 and disappears in alkali[4]. The mechanism of such polarographic behavior, however, has not yet been studied in detail. In order to obtain further information about this mechanism, the present authors have attempted detailed polarographic investigations.

Experimental

A Yanagimoto pen-recording polarograph, model PB-4, a Beckman pH meter, model G, and a Hitachi recording spectrophotometer, model EPS-2, were used for the measurement of polarograms, pH values, and ultraviolet absorption spectra respectively. The characteristics of the dropping mercury electrode used were: $m=1.23$ mg./sec., $h=65$ cm. and $t=4.35$ sec. (open circuit). The ionic strength of the buffer solutions used, had been adjusted to 0.45 by adding sodium chloride; these buffer solutions were as follows: NaAc+HCl (pH=1.09~3.79), NaAc+HAc (pH=3.80~5.60), KH_2PO_4+NaOH (pH=6.20~7.40), and glycocol+NaCl+NaOH (pH=8.53~11.01). Polarograms were taken in the above buffer solutions after bubbling nitrogen gas for 10 min. to remove the dissolved oxygen in the solutions, saturated calomel electrode being used as the external reference electrode. In this case, the temperature was controlled within ±0.1°C by a thermostat, and the measurements were usually made at 25±0.1°C. Experiments were carried out three times on the same electrolytic solution. The values thus obtained were averaged.

Pyridine, 4-methylpyridine and 4-ethylpyridine *N*-oxides were prepared and purified by the standard method[5], and their melting points were determined to be 66, 184~185 and 108~109°C respectively. Infrared spectra and microanalytical data show good agreement with the data in the literature[6] and with the calculated values.

Results and Discussion

Polarograms of pyridine *N*-oxide at various pH values are illustrated in Fig. 1. The pH-dependence of the limiting current in pyridine and 4-methylpyridine *N*-oxides is also shown in Figs. 2 and 3. From Figs. 1, 2 and 3, it can be clearly seen that the reduction wave decreases rapidly with the increasing pH value in pH values above 5. Since the ultraviolet absorption spectra of each of the above *N*-oxides in a region of pH≈7 to 1 N sodium hydroxide coincide almost completely in both the maximum wavelength and the intensity, no change in the structure is expected in alkali. On the other hand, the acid dissociation constants (pK_a's) of pyridine and 4-methylpyridine *N*-oxides have previously been determined by the spectrophotometric method as 0.79 and 1.29 respectively[7,8]. Moreover, the experimental results of the temperature dependence and the mercury pressure dependence on the reduction wave in the acidic pH region and in the pH region in which the limiting current decreases rapidly are shown in Table I.

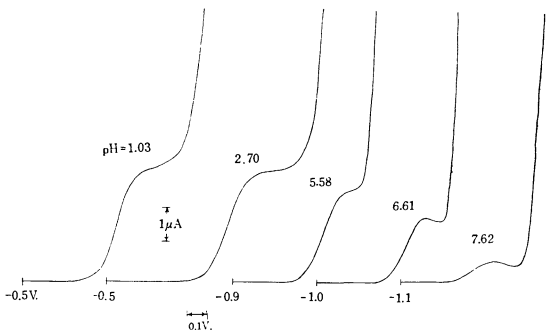


Fig. 1. Polarograms of pyridine *N*-oxide at various pH's.
Concn.: 5.28×10^{-4} mol./l., temp.: 25°C, ionic strength: 0.45

*1 Polarographic Study of Aromatic *N*-Oxides I.

1) E. Ochiai, *J. Pharm. Soc. Japan* (*Nippon Yakugaku Zasshi*), **69**, 1 (1949).
2) I. Aiko, *Pharm. Bull.*, **1**, 335 (1953).
3) Y. Asahi, This Bulletin, **34**, 1185 (1961).
4) A. Foffani, and F. Fornasari, *Gazz. Chim. Ital.*, **83**, 1051, 1059 (1953).
5) E. Ochiai, *J. Org. Chem.*, **18**, 534 (1953).
6) H. Shindo, *Chem. & Pharm. Bull.*, **7**, 791 (1959); **6**, 117 (1958); **4**, 460 (1956).
7) a) T. Kubota, *J. Pharm. Soc. Japan* (*Nippon Yakugaku Zasshi*), **75**, 1546 (1955); b) T. Kubota, *J. Spectroscopical Soc. Japan*, **10**, 83 (1962).
8) H. H. Jaffé and G. O. Doak, *J. Am. Chem. Soc.*, **77**, 4441 (1955).

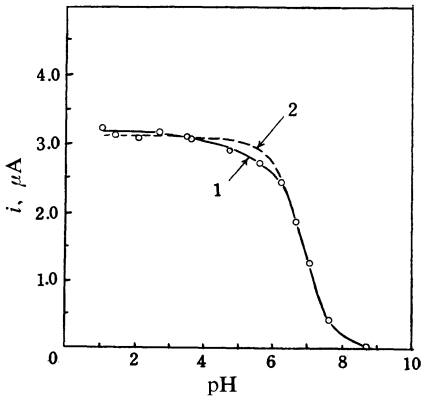


Fig. 2. The pH dependence of the limiting current of pyridine *N*-oxide.
Concn.: 5.28×10^{-4} mol./l., temp.: 25°C, ionic strength: 0.45. The relationship between pH and $E_{1/2}$ (in volt) fulfills the equation $-0.865[pH]-0.849$ in a region of pH=1.5~6.7.
1: Experimental curve
2: Calculated curve

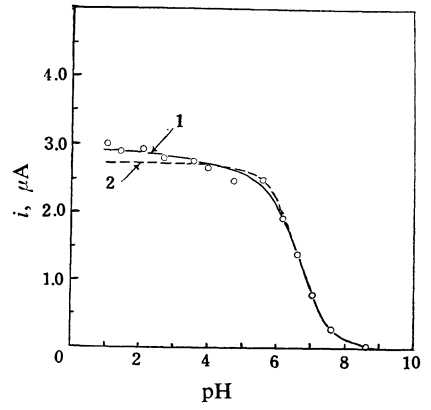
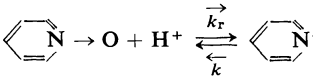


Fig. 3. The pH dependence of the limiting current of 4-methylpyridine *N*-oxide.
Concn.: 5.07×10^{-4} mol./l., temp.: 25°C, ionic strength: 0.45. The relationship between pH and $E_{1/2}$ fulfills the equation $E_{1/2}=-0.0948[pH]-0.883$ in a region of pH=1.5~6.7.
1: Experimental curve
2: Calculated curve

In the case of pH 7.0, the temperature coefficient of the reduction wave is much greater than that at pH 2.91. Moreover, the mercury pressure dependence at pH 7.0 did not show a good relationship between i and $\sqrt{h}$, where i and h denote the limiting current (μA) and the height of a mercury electrode in cm. (corrected with the reverse pressure of mercury height) respectively. In the case of pH 2.91, however, a linear relationship of i to $\sqrt{h}$ was obtained. In addition, the limiting current independent of $\sqrt{h}$ is zero or vevy small at pH 2.91 on the pyridine and 4-methylpyridine *N*-oxides, as may be seen in Table I.

From the viewpoint of the recent kinetic current theory[9], therefore, it may be reasonably considered on the basis of the above experimental results that the pH dependence of the limiting current is due to the kinetic current, which can be represented as Eqs. 1 and 2, which were derived by Matsuda and by Koutecky[10,11].



$$\longrightarrow \text{N}^{+}\text{-H} + \text{H}_2\text{O} \qquad (1)$$

$$i = i_d \cdot [1/[1+1.128(\vec{k}_r \cdot t \cdot [H^+]^2/K_a)^{-1/2}]] \qquad (2)$$

Hence, i_d is the diffusion current corresponding to the total concentration of *N*-oxides. In our case, the i appearing in the region of high proton concentrations becomes equivalent to i_d, which may show the normal temperature and mercury pressure dependences, as was observed at pH 2.91 on the above *N*-oxides, because in this condition the term in the brackets on the right hand side of Eq. 2 is reduced to 1.

Using Eq. 2 and the K_a value above stated, we have determined the rate constant, $\vec{k}_r$, of the recombination process in Eq. 1, whereas for the drop time, t, the values measured under the same condition as the determination of limiting current were used, so as to satisfy the pH dependence of the limiting current; $\vec{k}_r = 3.0\times10^{12}$ and $\vec{k}_r = 3.7\times10^{11}$ (mol./l.)$^{-1}$(sec.)$^{-1}$ were obtained for pyridine *N*-oxides and 4-methylpyridine *N*-oxide respectively*2.

The rate constants thus obtained are of the same order as the theoretical value obtained by Onsager[12] and as the experimental values of the other compounds determined by other workers[11]. The current-pH relationships calculated by using these k_r values are also shown in Figs. 2 and 3. A good agreement with the experiments is obtained on the whole. Some discrepancy, however, can be found in the acidic pH region. No quantitative explanation could be made for this, but it seems that the other miscellaneous effects on the *N*-oxide

9) See the following reviews; M. Takagi, *Review of Polarography*, **9**, 53 (1961); M. Senda, ibid., **6**, 95 (1958); H. W. Nürnberg, *Angew. Chem.*, **72**, 433 (1960).
10) a) J. Koutecky, *Coll. Czecho. Chem. Communs.*, **18**, 183, 597 (1953); **19**, 857 (1954); b) H. Matsuda and Y. Ayabe, This Bulletin, **28**, 422 (1955).
11) R. Bridicka, *Z. Elektrochem.*, **64**, 16 (1960).
*2 Applying Ilkovic's equation, $i_d = 607 n.c. D^{1/2} m^{2/3} t^{1/6}$, with i_d, m and t at pH=2.5~4.7 and $D=7.7$ or 8.68×10^{-6} cm^2/sec., which figures are estimated from the molecular weight or from the equivalent conductance at an infinite dilution of such analogous organic ions as benzoic acid, $n=2.1$~2.4 is obtained.
12) L. Onsager, *J. Chem. Phys.*, **2**, 599 (1934).

TABLE I. THE TEMPERATURE AND THE PRESSURE DEPENDENCES FOR THE REDUCTION WAVE AT VARIOUS pH'S

Compound	Temperature coefficient (deg^{-1})[a]		Pressure dependence[b]	
Pyridine *N*-oxide	pH=2.91	pH=7.0	pH=2.91	pH=7.0
	1.05%	2.42%	$i=0.476\cdot\sqrt{h}$	c)
4-Methylpyridine *N*-oxide	pH=3.30	pH=6.61	pH=3.30	pH=6.61
	1.31%	2.06%	$i=0.304\sqrt{h}+0.375$	d)

a) Calculated at compound interest method.
b) h and i denote the height of a mercury electrode in cm. (corrected against the reverse pressure) and the limiting current (μA), respectively.
c) No good relationship between i and $\sqrt{h}$ exists.
d) No rigid relationship between i and $\sqrt{h}$ is obtained, but can be roughly expressed as $i=0.71+0.092\sqrt{h}$.

group, such as the hydration and the acid catalytic reactions, may contribute somewhat in the acidic pH region*3.

The current pH relationship of 4-ethylpyridine *N*-oxide also showed the same tendency as in Figs. 2 and 3. In this case, $\vec{k_r}=5.5\times10^{11}$ $(mol./l.)^{-1}(sec.)^{-1}$ was obtained by using Eq. 2, and $pK_a\fallingdotseq1.21$, which is estimated from the relationship between pK_a and Hammett's σ values[8].

Under the conditions used here, the reduction wave corresponding to the free *N*-oxide group could not be found; this point differs from that in such aliphatic compounds as narcotin *N*-oxide. As a result of the resonance effect between $\geqslant N\rightarrow O$ group and pyridine ring, as is well known, the aromatic *N*-oxide group shows a great resistance to the reductive reaction[5,7b].

*3 In addition the error owing to the drawing figure for the determination of the limiting current may also not be neglected.

Summary

The polarographic behavior of pyridine, 4-methylpyridine and 4-ethylpyridine *N*-oxides has been investigated. The reduction wave of these *N*-oxides decreases rapidly with the increasing pH value in pH values above 5 and disappears in alkali. It was clearly shown by the polarographic and spectroscopic investigations that the main reason for this phenomenon is the kinetic current. Quantitative treatment of the pH-dependence of the limiting current was also carried out.

The authors are grateful to Professor Shinzi Koide of Mukogawa Women's University, in Nishinomiya, and to Dr. Masanosuke Takagi of University of Osaka Prefecture for various discussions.

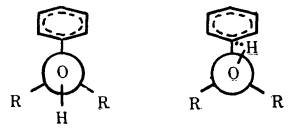
Shionogi Research Laboratory
Shionogi & Co., Ltd.
Fukushima-ku, Osaka

Intramolecular Interaction between Hydroxyl Group and π-Electrons. XVI.[1] ν_{O-H} *Absorption Spectra of Aryldimethylcarbinols and Related Compounds*

By Michinori Ōki and Hiizu Iwamura

(Received March 20, 1962)

It has been shown in a previous paper[2] that the benzyl alcohols show doublet O–H stretching vibration spectra (ν_{O-H}) in the 3 μ region owing to the rotational isomerism about the C_α–O bond. The hydroxyl group in one (II) of the isomers takes part in the intramolecular interaction with π-electrons of the benzene nucleus and shows the lowered ν_{O-H} when compared with the normal one. Ring



I II

substitution at *p*- or *m*-position to the hydroxymethyl group has been found to alter considerably the apparent ν_{O-H} curve, that is, the relative amount of the two rotational isomers. Furthermore, the phenomenon has been ascribed solely to the change in the proton accepting power of the π-electrons on the benzene ring. In reference to the Hammett's sigma constants of the substituents, the π-electron density at the carbon atom to which the hydroxymethyl group is attached, has been found to have the greatest influence, and a "cis" structure is proposed for the isomer as expressed by model II.

Evans[3] has observed that in benzyl alcohol an unusual vibrational coupling takes place between the aromatic C–H in-plane deformation mode and a stretching mode of $-CH_2-O-$ group at 1020 cm^{-1}. According to the literature, this coupling should be permitted only when C_α–O bond lies in the plane perpendicular to that of the benzene ring. This configuration is in accordance with that of the "cis" structure proposed by the present authors.

There seems to be, however, another factor in the apparent substituent effects, that is, the proton donating character of the α-hydroxyl group might also be influenced by the ring substituent and the apparent substituent effects would be the result of a counteraction between the two effects just as is the case in 2-hydroxybiphenyls[4].

To clarify the ambiguity in the electronic effect, and to obtain further support on the configuration of the interacting form, aryldimethylcarbinols and the related tertiary carbinols in which the hyperconjugative electronic interaction between the hydroxyl group and the aromatic residue may be minimal, have been submitted to the ν_{O-H} spectral measurement.

Experimental

Spectral Measurement.—A Perkin Elmer 112 G grating infrared spectrometer was operated to measure ν_{O-H} absorption as described previously[5].

Materials.—They were prepared by action of an excess of methyl- or ethyl-magnesium halide on the corresponding ketones or carboxylic esters, unless otherwise stated. Decomposition of the reaction mixtures was always effected by an aqueous solution of ammonium chloride to avoid dehydration catalyzed by a trace of acid in the later process. Despite all the tests no *p*-dimethylamino derivative could be obtained, *p*-dimethylamino-α-methylstyrene, m. p., 75°C[6], being the sole product.

The two nitro derivatives were obtained by oxidation of the corresponding nitrocumenes as described for the *p*-isomer[7].

p-Methoxycarbonyl derivative was prepared by refluxing the silver salt of 2-(*p*-carboxyphenyl)-2-propanol[8] with methyl iodide in methanol.

Physical constants and analytical data, if necessary, of the samples are listed in Tables I and II.

Results and Discussion

In Fig. 1 are presented the apparent ν_{O-H} absorption curves of dimethylphenylcarbinol and the two extreme derivatives with respect to the Hammett's sigma constants of the substituents. All the numerical band properties are listed in Table III.

1) Part XV. M. Ōki and H. Iwamura, This Bulletin, **35**, 283 (1962).
2) M. Ōki and H. Iwamura, ibid., **32**, 955 (1959).
3) J. C. Evans, *Spectrochim. Acta*, **17**, 129 (1961).
4) M. Ōki and H. Iwamura, This Bulletin, **34**, 1395 (1961).
5) M. Ōki and H. Iwamura, ibid., **32**, 567 (1959).
6) Y. Okamoto and H. C. Brown, *J. Am. Chem. Soc.*, **80**, 4978 (1958).
7) H. Kwart and P. S. Francis, ibid., **77**, 4907 (1955).
8) Y. Okamoto, T. Inukai and H. C. Brown, ibid., **80**, 4971 (1958).

TABLE I. PHYSICAL CONSTANTS AND ANALYTICAL DATA OF THE ARYLDIMETHYLCARBINOLS, X-C_6H_4·CMe_2·OH

X	M. p. or b. p. observed (lit.)	Ref. index	Anal. Found C	Found H	Found N	Calcd. C	Calcd. H	Calcd. N
H	35°C (91°C/8 mmHg)[7]							
p-MeO	103°C/1 mmHg	n_D^{26} 1.5251	72.10	8.67		72.26	8.49	
m-MeO	34°C(34~35°C)[9]							
p-Me	78°C/1.5 mmHg (101°C/10 mmHg)[10]							
m-Me	100°C/7 mmHg (73°/3 mmHg)[10]							
m-Me_2N	73°C (73°C)[6]							
p-*tert*-Bu	79°C (79°C)[11]							
p-Cl	44°C (43.3°C)[12]							
m-Cl	87°C/3.5 mmHg, (88°C/2 mmHg)	n_D^{22} 1.5355 n_D^{20} 1.5370)[12]						
p-CO_2Me	122°C/3.5 mmHg		68.07	7.46		68.02	7.27	
p-NO_2	134°C/3.5 mmHg, (120.5~121°C/2 mmHg)	n_D^{24} 1.5520 n_D^{20} 1.5552)[7]						
m-NO_2	63~64°C		59.60	6.13	7.79	59.66	6.12	7.73

TABLE II. PHYSICAL CONSTANTS OF TERTIARY ALCOHOLS RELATED TO DIMETHYLPHENYLCARBINOL

	M. p. or b. p. (lit.)
Diethylphenylcarbinol	73°C/3.5 mmHg, n_D^{16} 1.5172 (79~82°C/3 mmHg, n_D^{20} 1.5178)[13]
1-Methyl-1, 2, 3, 4-tetrahydro-1-naphthol	88°C (88.5~88.7°C)[14]
1-Phenylcyclohexanol	62°C (60°C)[15]

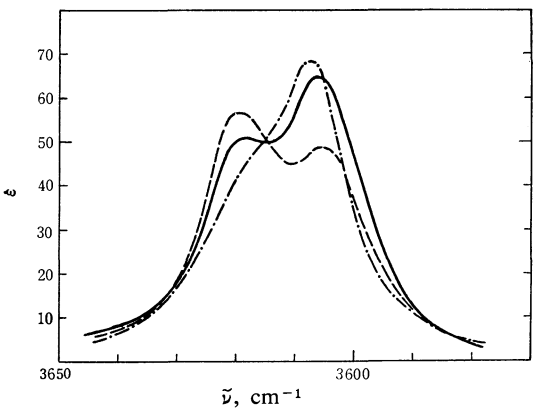


Fig. 1. ν_{O-H} Absorption of aryldimethylcarbinols.
Ph·CMe_2·OH ———
p-MeO·C_6H_4·CMe_2·OH —·—·—
p-NO_2·C_6H_4·CMe_2·OH — — —

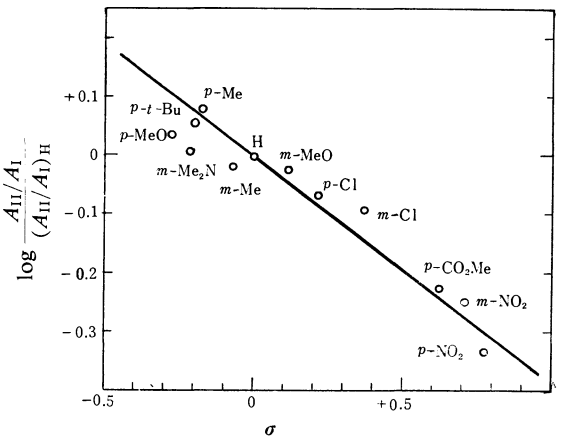


Fig. 2. Relation between $\log\frac{A_{II}/A_I}{(A_{II}/A_I)_H}$ and the Hammett's sigma constant.

In contrast with the benzyl alcohols[2] which have the ν_{O-H}'s at 3636 and 3617 cm^{-1}, all the present carbinols have doublet ν_{O-H}'s at 3620 and 3606 cm^{-1}. This is the due consequence of the tertiary nature of the hydroxyl group[16].

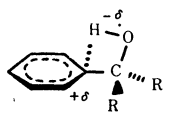
The relative intensity, A_{II}/A_I, which may be put approximately equal to the equilibrium constant, K, between I and II, varies considerably as the electron-releasing substituents in the benzene ring enhance the lower lying band, while the electron-withdrawing ones reduce it, relative to the higher absorption. In Fig. 2, it is illustrated quantitatively as the relation between $\log(A_{II}/A_I)$ and the Hammett's sigma constants. The inclination expressed as $\rho = -0.357$ is as large as that of the benzyl alcohols, $\rho = -0.475$[2], and suggests a similar mechanism

9) Y. Okamoto and H. C. Brown, ibid., **79**, 1912 (1957).
10) H. C. Brown, J. D. Brady, M. Grayson and W. H. Bonner, ibid., **79**, 1897 (1957).
11) H. Walther, *J. pharm. chim.*, **27**, 476 (1938).
12) H. C. Brown, Y. Okamoto and G. Ham, *J. Am. Chem. Soc.*, **79**, 1907 (1957).
13) A. Dierichs and E. Preu, *Chem. Ber.*, **90**, 1208 (1957).
14) T. Kusama and D. Koike, *J. Chem. Soc. Japan, Pure Chem. Sec. (Nippon Kagaku Zassi)*, **72**, 685 (1951).
15) C. D. Nenitzescu and I. Necsoni, *J. Am. Chem. Soc.*, **72**, 3483 (1950).
16) M. Ōki and H. Iwamura, This Bulletin, **32**, 950 (1959).

Table III. ν_{O-H} Absorptions of aryldimethylcarbinols, X-C_6H_4·CMe_2·OH

X	ν_{O-H}	ν_{max} cm^{-1}	$\Delta\nu^a_{1/2}$ cm^{-1}	A 10^3 mol^{-1} l. cm^{-2}	$\Delta\nu_{max}$ cm^{-1}	$\log(A_{II}/A_I)$
p-MeO	I	3620.1	16.4	1.50	13.4	0.310
	II	3606.7	15.0	3.06		
m-Me_2N	I	3619.8	19.4	1.66	13.6	0.280
	II	3606.2	14.0	3.16		
p-*tert*-Bu	I	3620.7	19.0	1.55	13.7	0.336
	II	3607.0	16.0	3.36		
p-Me	I	3620.3	16.2	1.53	12.7	0.353
	II	3607.6	15.6	3.45		
m-Me	I	3620.2	18.8	1.74	13.0	0.255
	II	3607.2	15.0	3.13		
H	I	3620.4	15.2	1.72	13.5	0.276
	II	3606.9	14.4	3.25		
m-MeO	I	3620.7	17.2	1.85	14.0	0.251
	II	3606.7	15.0	3.30		
p-Cl	I	3620.2	15.0	2.01	14.2	0.203
	II	3606.0	15.8	3.21		
m-Cl	I	3620.7	15.0	2.13	15.2	0.184
	II	3605.5	15.8	3.25		
p-CO_2Me	I	3621.2	13.4	2.64	14.6	0.050
	II	3606.6	17.0	2.96		
m-NO_2	I	3620.2	15.0	2.69	15.3	0.024
	II	3604.9	16.0	2.84		
p-NO_2	I	3619.5	14.6	3.17	14.6	−0.067
	II	3604.9	15.8	2.72		

of interaction. If the interaction bore a fairly polarized mechanism with considerable contribution of the intramolecularly charge-transferred structure, III, the electronic interaction between the substituent and the site of the interaction would be pronounced and the σ^+



III

proposed by Brown and Okamoto[9], rather than the original σ constants would have given the better linearity. Since this is not the case, the interaction may be considered to include but little contribution by such a structure. A slight diminution in the absolute value may be due to the weakened ability of the tertiary carbinols as proton donors rather than the primary ones.

There is no doubt about assigning the isomer II, having the intramolecular interaction with the π-electrons, to the band at lower frequency, 3606 cm^{-1}. Then the apparent variation in A_{II}/A_I may be, as a first approximation, attributed to the change in the proton attracting power of the π-electron on the benzene ring. Since the doublet ν_{O-H} maxima vary only within the experimental error, the ring substituents might be regarded to be indifferent to the force constant of the hydroxyl group. ν_f which appears at 3620 cm^{-1} can validly be said to be indifferent to the ring substituent in contrast to the substituted phenols[17] in which ν_f's are in linear relation with the sigma constants of the ring substituents. It is, however, rather dangerous to conclude from the apparent constancy in the wave number that the hydroxyl groups having the intramolecular interaction with the π-electrons are also independent of the substituents.

With the intention of making it clear that the ring substituents might not be concerned with the donor ability of the hydroxyl group,

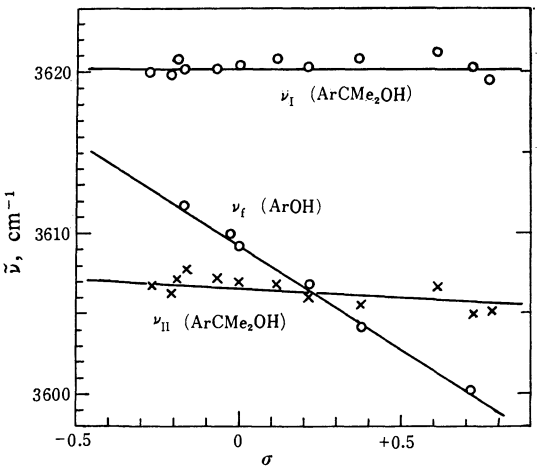


Fig. 3. The effect of the nuclear substitution on the ν_{O-H} maxima of aryldimethylcarbinols and phenols.

17) P. J. Stone and H. W. Thompson, *Spectrochim. Acta*, **10**, 17 (1957).

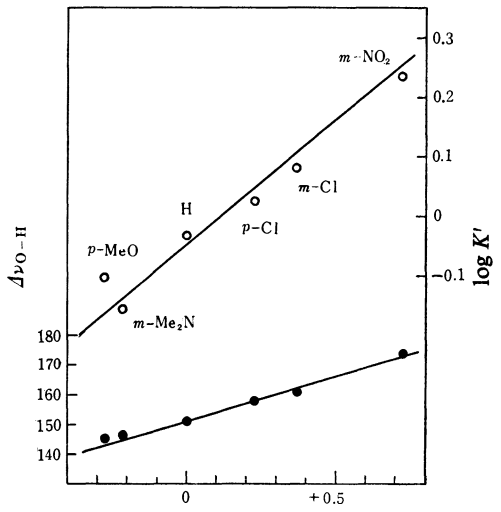


Fig. 4. The association between aryldimethylcarbinols and diethyl ether in carbon tetrachloride.
● Shift of ν_{O-H} maxima.
○ Equilibrium constant defined by
$$K' = \frac{[Ar \cdot CMe_2 \cdot OH \cdots OEt_2]}{[Ar \cdot CMe_2 \cdot OH]}$$
the denominator being estimated from the intensity of the remaining free ν_{O-H}.

but solely with the π-electron system as the proton acceptors, the intermolecular association of these carbinols with diethyl ether as a common proton acceptor in carbon tetrachloride was investigated. Unexpectedly, the association IV was found to be dependent on the substituents as is seen from the ν_{O-H} of the hydroxyl group taking part in the association, and from the association constants (K'), in Fig. 4. The electron-withdrawing group such as nitro

$$Ar \cdot CMe_2 \cdot \overset{-\delta}{O}\text{-}H \cdots \overset{+\delta}{O}Et_2$$
IV

tends to strengthen, while the electron-releasing one weakens, the association between the aryldimethylcarbinols and diethyl ether. Compared with the free ν_{O-H}'s which are quite independent of the ring substitution, it has become reasonable to conclude here that the effect of the ring substituents on the hydroxyl group becomes the more conspicuous, when the hydroxyl group is more polarized by the formation of hydrogen bonding or the like interactions. The electronic structure of the hydroxyl group should be expressed as a resonance hybrid between V, VI and VII. The increased contribution of the structures VI and VII by any mechanism will lower the force constant of O–H which in turn makes sharper response to the electronic changes in the rest of the

R-O-H	$R\text{-}\bar{O}\text{-}\overset{+}{H}$	$R\text{-}\overset{+}{\bar{O}}\text{-}H$
V	VI	VII

molecule, R. This finding bears a resemblance to the substituent effects on the reaction kinetics and the ultraviolet spectra, in which the excited state rather than the ground state suffers from more distinguished electronic effect of the substituents.

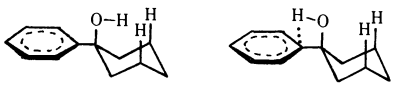
Since the strength of, and the polarization in the hydroxyl group by, the O–H$\cdots\pi$ interaction, as realized in aryldimethylcarbinols, may be regarded to lie between the two extremes, the effect of the substituent on the proton donor character of the hydroxyl group will be medium and can not be evaluated quantitatively. The effect of the substituent in this sense will make ν_i's lower by way of strengthening the proton donor character, as the electron-withdrawing power of the substituent increases, and may be opposite to the direct substituent effect on the proton accepting ability of the π-electrons. Thus, it is rather practical to assume that the apparent constancy of ν_i's over a wide range of aryldimethylcarbinols would be the result of the counterbalance between a favorable effect on the proton donor and an unfavorable influence on the proton acceptor in the case of the electron attracting substituent. The same interpretation will also be operative of the electron releasing groups.

In Table IV are listed ν_{O-H} data of diethylphenylcarbinol, 1-phenylcyclohexanol and 1-methyl-1, 2, 3, 4-tetrahydro-1-naphthol. Though the hydroxyl groups in these compounds are in the same structural position as those of the aryldimethylcarbinols with respect to the benzene ring, and the π-electron density as a proton acceptor is common, they have the

Table IV. ν_{O-H} Absorptions of tertiary alcohols

	ν_{O-H}	ν_{max} cm^{-1}	$\Delta\nu^a_{1/2}$ cm^{-1}	A 10^3 mol^{-1} l. cm^{-2}	$\Delta\nu_{max}$ cm^{-1}	log (A_{II}/A_I)
Diethylphenylcarbinol	I	3618.2	17.8	2.71	10.0	−0.10
	II	3608.2	19.0	2.16		
1-Phenylcyclohexanol	I	3620.5	17.7	1.10	15.3	0.57
	II	3605.2	12.8	4.10		
1-Methyl-1, 2, 3, 4-tetrahydro-1-naphthol	I	3616.0	10.2	1.85	12.2	0.16
	II	3603.8	13.6	2.65		

varied value of log (A_{II}/A_I). The phenomenon can not be attributed to the electronic effect, but rather to the steric effect. Taking 1-phenylcyclohexanol as an example, the hydroxyl



Ia IIa

hydrogen in Ia has a steric interference with the axial hydrogens at 3- and 5-positions of the cyclohexane ring. Thus the stability of isomer Ia relative to IIa will be diminished considerably, and the value of log (A_{II}/A_I) is the largest ever examined for a compound of this type.

The authors are indebted to Professor Yoshiyuki Urushibara for his encouragement and discussion throughout this work. The authors' thanks are also due to the Ministry of Education for the grant-in-aid for fundamental scientific research.

Department of Chemistry
Faculty of Science
The University of Tokyo
Hongo, Tokyo

On Glumamycin, a New Antibiotic. IV. The Amino Acid Moiety*

By Michitaka INOUE**

(Received April 19, 1962)

As we have reported previously[1-4], glumamycin[5], a new acidic peptide-type antibiotic, is composed of seven kinds of amino acids and one mono-unsaturated fatty acid. They are aspartic acid, α(L), β-methylaspartic acid, proline, valine, glycine, pipecolic acid, α,β-diaminobutyric acid, and 3-isotridecenoic acid.

In the present work, the nature of the amino acids was determined and an investigation was made of the free amino group of glumamycin.

Experimental

Preparation of the Sample for Determination of the Amino Acids.—Ten milligrams of glumamycin purified by counter current distribution[5] were hydrolyzed with 3 ml. of 6 N hydrochloric acid in a sealed tube at 110°C for 24 hr., and the hydrolysate was then treated in the usual way to remove the excess hydrochloric acid.

Determination of the Amino Acids by the Moore-Stein Method[6]. — First the determination was carried out by Moore-Stein's method. The results are shown in Table I.

Determination of the Amino Acids by the Paper-DNP Method.—Next, determination of the amino acids was conducted by the paper-DNP method.

A definite volume of the above hydrolysate was dinitrophenylated by the method of Levy[7]. The mixture of DNP-amino acids thus obtained was subjected to two-dimensional paper chromatography (Solvent system: first, *n*-butanol saturated with 2 N aqueous ammonia, and then a 1.5 M phosphate buffer[8]). The yellow spots on the paper chromatogram (Fig. 1) were cut out and extracted with 5 ml. of 1% sodium hydrogen carbonate solution[7]. Colorimetry of the extract was effected at 360 mμ for the usual amino acids, at 385 mμ for proline, and at 395 mμ for pipecolic acid. This determination was conducted on three sheets of paper chromatogram, and the amino acid contents were calculated from the mean values of the experimental millimole extinction coefficients obtained in the next experiment. The results are shown in Table III.

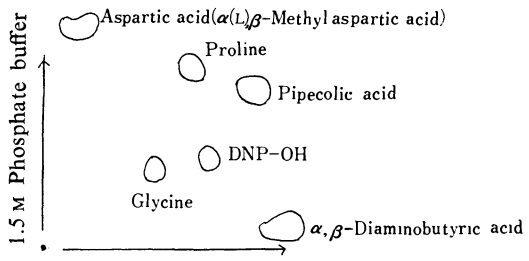


Fig. 1. Two dimensional paper chromatogram of DNP-derivatives of amino acids in 24 hr.-hydrolysate of glumamycin.

* Sueo Tatsuoka, Studies on Antibiotics, Part XXXIII.

** Present address: Osaka Factory, Takeda Chemical Industries, Ltd., Juso, Higashiyodogawa, Osaka.

1) M. Inoue et al., This Bulletin, **33**, 1014 (1960).
2) M. Inoue, ibid., **34**, 885 (1961).
3) M. Inoue, ibid., **35**, 1249 (1962).
4) M. Inoue, ibid., **35**, 1255 (1962).
5) M. Shibata et al., *J. Antib. (Japan)*, **A15**, 1 (1962).
6) S. Moore and W. H. Stein, *J. Biol. Chem.*, **176**, 367 (1948); ibid., **192**, 663 (1951).
7) A. L. Levy, ibid., **213**, 187 (1955); ibid., **213**, 487 (1955); *Nature*, **174**, 126 (1954).
8) K. Satake et al., *Kagaku no Ryoiki, Supplementum*, **34**, 77 (1959).

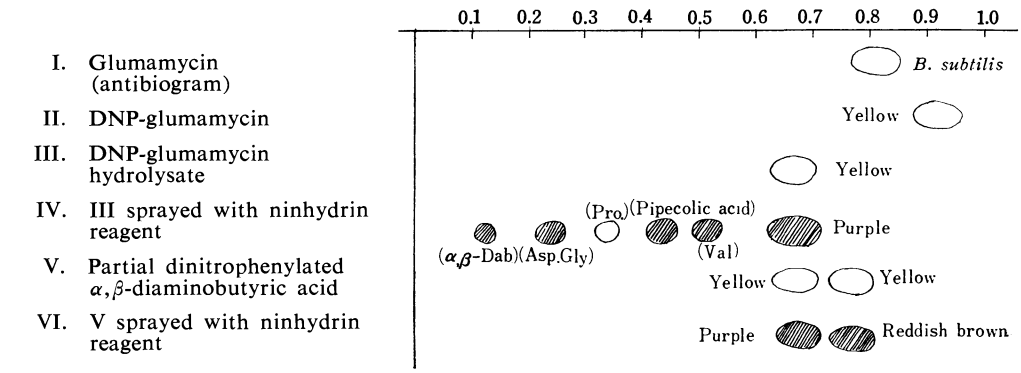


Fig. 2. Paper chromatograms of glumamycin and related compounds (Solvent system; *n*-butanol, acetic acid, water (4 : 1 : 5)).

Measurement of the Experimental Millimole Extinction Coefficients of Various Amino Acids.—Aspartic acid, glycine, proline, valine, pipecolic acid, and α, β-diaminobutyric acid were dissolved in three consecutive concentrations. The solutions, after being dinitrophenylated by Levy's method[7], were subjected to two-dimensional paper chromatography (Solvent system: the same as has been mentioned above). The yellow sports were cut out and extracted in the same way as above. The experimental millimole extinction coefficients of the amino acids were calculated from the absorptions at their respective wavelengths, and finally the mean values of the solutions in three concentrations were obtained (Table II).

Hydrolysis of DNP-Glumamycin.—Ten milligrams of DNP-glumamycin obtained by Sanger's method[9] were hydrolyzed with 3 ml. of 6 N hydrochloric acid in a sealed tube at 110°C for 24 hr. The hydrolysate was diluted and treated with ether in the usual way. No ether-soluble DNP-amino acid was obtained. The yellow aqueous layer was evaporated in a dark place, to remove the excess hydrochloric acid. The residue thus obtained was submitted to paper chromatography (Fig. 2).

Paper Chromatography.—The paper chromatograms (I—VI) in Fig. 2 were obtained by developing them with the solvent system *n*-butanol, acetic acid and water (4 : 1 : 5). All the processes were conducted by the descending method.

Partial Dinitrophenylation of α, β-Diaminobutyric Acid.—α, β-Diaminobutyric acid[8] isolated from the hydrolysate of glumamycin was dinitrophenylated by Sanger's method[9], but the reaction time was limited to 30 min. The reaction mixture was immediately shaken with ether to remove the unreacted dinitrofluorobenzene and di-DNP-α, β-diaminobutyric acid. The yellow aqueous layer thus obtained was submitted to paper chromatography.

Results and Discussion

The amino acids contents of glumamycin was estimated by the Moore-Stein method; as a result, 4 mol. of aspartic acid, 1 mol. of valine, and 2 mol. of glycine were detected, as is shown in Table I. The other amino acids were not detected, probably because α(L), β-methylaspartic acid was eluted in the same fraction as that of aspartic acid, because pipecolic acid was not colored favorably with ninhydrin, and because α, β-diaminobutyric acid was not eluted by this method. That ammonia was not detected means that asparagine does not exist therein despite the presence of 4 mol. of aspartic acid.

TABLE I. AMINO ACIDS COMPOSITION OF GLUMAMYCIN DETERMINED BY MOORE-STEIN'S METHOD

Amino acid	Calcd. ratio in 48 hr. hydrolysate	Assumed ratio of amino acid residue
Aspartic acid	4.23	4
Glycine	2.12	2
Valine	1.00	1
Proline	1.05	1
Amino N	0	0

Next, the determination was carried out by the paper-DNP method. The DNP-derivatives of the amino acids in glumamycin hydrolysate were obtained by Levy's method, and their two-dimensional paper chromatograms are shown in Fig. 2. The DNP-derivatives of the two acidic amino acids, i.e. α(L), β-methylaspartic acid and aspartic acid were not separated clearly, so their ratio could not be determined. However, the ratio of the two compounds was estimated to be about one to three or more, judging from the sizes of their spots colored with ninhydrin in the paper chromatography of the acidic amino acid fraction of glumamycin hydrolysate. The spots of the DNP-derivatives of valine and pipecolic acid also overlapped, but the ratio of their contents could be calculated since their absorption maxima were different. This method of determining amino acids was carried out

9) F. Sanger, *Biochem. J.*, **39**, 507 (1945); ibid., **45**, 563 (1949).

TABLE II. EXPERIMENTAL mM EXTINCTION COEFFICIENT

Amino acid	Experimental	Extinction coefficient $k\times10^{-3}$ at λ_{max}	Recovery %
Aspartic acid	15.74	18.1	87
Glycine	15.39	17.0	90
Valine	15.75	18.0	87
Proline	16.80	18.5	91
α,β-Diaminobutyric acid	20.85	29.2	71
Pipecolic acid	15.51	15.8	98

TABLE III. AMINO ACID COMPOSITION OF GLUMAMYCIN DETERMINED BY PAPER-DNP METHOD

Amino acid	Calcd. ratio	Assumed ratio of amino acid residue
Aspartic Acid	4.12	4
Glycine	1.94	2
Proline	1.00	1
Valine	0.89	1
Pipecolic acid	0.97	1
α,β-Diaminobutyric acid	1.93	2

after confirming the fact that the dinitrophenylation of each amino acid and the elution of the product were reproducible with an error of ±4%, and that, therefore, this method was usable. The results are shown in Table II. From the experimental data, the nitrogen content of the amino acids was calculated; from the recovery rate of nitrogen (108%), the molecular ratio shown in Table III seems reasonable and is in accord with the results obtained by the Moore-Stein method.

On the basis of the above results, glumamycin is considered to contain 4 mol. of aspartic acid (including α(L), β-methylaspartic acid), one mol. each of proline, valine and pipecolic acid, and 2 mol. each of glycine and α,β-diaminobutyric acid; judging from the analytical results[3], 1 mol. of an unsaturated fatty acid[4] also seems to be present.

Further, investigation was made into the free amino group of glumamycin. As is shown in Fig. 2, the water-soluble DNP-amino acid in the hydrolysate of DNP-glumamycin was identified as mono-substituted DNP-α,β-diaminobutyric acid. The results of the paper chromatography are as follows;

1) Paper chromatogram I is the antibiogram of glumamycin (microorganism; *B. subtilis*), 2) Paper chromatogram II shows the yellow spot of DNP-glumamycin, 3) Paper chromatogram III shows the yellow spot at R_f 0.68 of the DNP-amino acid in the DNP-glumamycin hydrolysate; when the chromatogram is sprayed with the ninhydrin reagent, all the amino acids contained in glumamycin are colored and the yellow spot at R_f 0.68 turns purple (paper chromatogram IV), 4) Paper chromatogram V indicates two yellow spots of partially dinitrophenylated α,β-diaminobutyric acid at R_f 0.68 and 0.75; when the paper chromatogram is sprayed with the ninhydrin reagent, the yellow spot at R_f 0.68 turns purple and the spot at R_f 0.75, reddish brown.

Judging from the color reaction paper chromatogram VI, it is assumed that the substance with R_f 0.68 is mono-DNP-α,β-diaminobutyric acid in which the α-amino group is free and that the β-amino group is dinitrophenylated, while the substance with R_f 0.75 is also the same acid, but its α-amino group is dinitrophenylated and β-amino group is free. On the basis of this assumption, the free amino group of glumamycin is assumed to be the β-amino group of α,β-diaminobutyric acid, and the α-amino group is assumed to participate in peptide linkage. In addition, as another spot of α,β-diaminobutyric acid is found at R_f 0.1 on paper chromatogram V, 1 mol. α,β-diaminobutyric acid of each two in glumamycin takes part in the peptide-linkage through both the α- and the β-amino groups.

Summary

Separatory determination was conducted on the seven amino acids contained in glumamycin. By the Moore-Stein method and by paper chromatography of the DNP-derivatives of the amino acids, 4 mol. of aspartic acid (including α(L), β-methylaspartic acid), 2 mol. each of glycine and α,β-diaminobutyric acid, and 1 mol. each of valine, pipecolic acid and proline were detected. Also, investigation was made into the free amino group of this antibiotic.

The hydrolysate of DNP-glumamycin showed one yellow spot at R_f 0.68, which spot turned purple with ninhydrin.

Compared these results with paper chromatogram of partially dinitrophenylated α,β-diaminobutyric acid, it was assumed that the β-amino group of one of the acids, is free, that the α-amino group participates in the peptide linkage in glumamycin, and that both amino groups of another α,β-diaminobutyric acid take part in the peptide linkage.

The author wishes to express his thanks to Dr. Satoru Kuwada, the Director of the Research Laboratories, Dr. Sueo Tatsuoka, Vice-Director of the Research Laboratories, and Dr. Kuniyoshi Tanaka, the Head of the Second Division of the Research Laboratories for their guidance and encouragement, and to Drs.

Kôichi Nakazawa, Akira Miyake, Jisaburo Ueyanagi and Mr. Masahiko Fujino for their kind advice.

Research Laboratories
Takeda Chemical Industries, Ltd.
Juso, Higashiyodogawa, Osaka

Electric Properties of the Single-crystal and Thin Film of α,α'-Diphenyl-β-picrylhydrazyl

By Hiroo INOKUCHI, Yoshiya HARADA and Yusei MARUYAMA

(Received May 19, 1962)

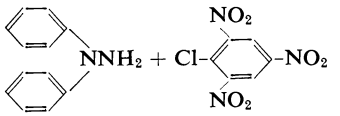
It is known that α,α'-diphenyl-β-picrylhydrazyl (DPPH) has one unpaired electron. The magnetic properties of the stable free radical have been studied by a number of investigators[1-4]. The unpaired electron localized on the nitrogen atoms of the molecule converts para-hydrogen into ortho-hydrogen at low temperature[5]. The conversion mechanism is a paramagnetic (physical) one, as absence of the hydrogen-deuterium exchange reaction rules out a dissociative chemisorption of hydrogen molecules by the free valencies of surface.

The works on the role of the unpaired electron in the interaction between free radicals and adsorbed oxygen or complexed organic solvents have been reported[6,7]. These results expressed that no change of the concentration of unpaired electrons is found with this interaction.

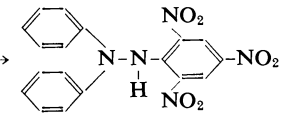
However, few articles concerning the electronic properties for solid free radicals have been published[5,8]. In this paper, we are presenting the electronic conduction and its related phenomena of the single crystal and the thin film of α,α'-diphenyl-β-picrylhydrazyl. Further, the relation between the orientation of molecules in the crystal and the electronic conduction will be discussed.

Experimental Procedures

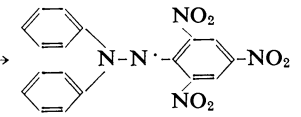
α,α'-Diphenyl-β-picrylhydrazyl was prepared by reaction of α,α'-diphenylhydrazine (I) with picryl-chloride (II) in chloroform. The strong heating of this solution yielded precipitates of white crystallites, diphenylhydrazine hydrochloride. After separation of these precipitates from the solution, the addition of ether caused beautiful scarlet-red crystal, α,α'-diphenyl-β-picrylhydrazine (III), to precipitate. After the method of Goldschmidt and Renn[9], the oxidation of hydrazine with lead dioxide and anhydrous sodium sulphate, produced the violet crystal, α,α'-diphenyl-β-picrylhydrazyl (IV).



(I) (II)



(III)



(IV)

The solvent-free single crystal (dimension: 0.3×0.3×1.3 mm., weight: about 1 mg.) of the free radical was grown from the carbon disulphide solution. Two types of thin film cells of DPPH were prepared by a vacuum evaporation as described in the previous report[10]. This evaporation had to be operated rapidly at a vacuum of the order of 10^{-5} ~10^{-6} mmHg to avoid the decomposition of the free radical in specimen vessel under heating (80~130°C). The decomposition of the prepared thin free radical film was also accelerated by a contact with air and/or by an illumination of ultraviolet light. Therefore, the observation of its physicochemical properties was carried out in short period (one or two days) after preparation.

The semi- and photo-conductivities of the DPPH

1) E. Müller, I. Müller-Rodloff and W. Bunge, *Ann.*, **520**, 235 (1935).
2) H. J. Gerritsen, R. Okkes, H. M. Gijsman and J. van den Handel, *Physica*, **20**, 13 (1954).
3) J. V. Zanchetta, Thesis, The University of Bordeaux 1961.
4) H. Inokuchi and M. Kinoshita, This Bulletin, **33**, 1627 (1960).
5) D. D. Eley and H. Inokuchi, *Z. Elektrochem.*, **63**, 29 (1959).
6) J. E. Bennett and E. J. H. Morgan, *Nature*, **182**, 199 (1958).
7) J. A. Lyons and W. F. Watson, *J. Polymer Sci.*, **18**, 141 (1955).
8) D. D. Eley and G. D. Parfitt, *Trans. Faraday Soc.*, **51**, 1529 (1955).
9) S. Goldschmidt and K. Renn, *Ber.*, **55**, 628 (1922).
10) H. Inokuchi, H. Kuroda and H. Akamatu, This Bulletin, **34**, 746 (1961).

specimen were measured with an aid of vibration-reed electrometer. During the measurement, the specimen was kept in a vacuum vessel. The absorption spectra of the free radical were observed with a Cary recording spectrophotometer, model-14.

Results and Discussion

The electrical resistivity*, ρ, and its activation energy of the DPPH single crystal were fairly high in comparison with the previous results[5,8]. It was found that a great anisotropy of these values occurs in the direction of the crystal: The conductivity along the long axis (c-axis) of needle crystal is higher than that perpendicular to the axis by a factor of 10^5 as listed in Table I.

From a preliminary results, the crystal structure of DPPH is orthorhombic one, with four molecules in a unit cell of dimensions a=17.6Å, b=18.9Å and c=7.59Å and molecules in the crystal seem to be arranged perpendicular to the c-axis and the molecular planes are parallel with each other. The unpaired electron in the molecule is localized on the nitrogen atoms and the direction of its orbitals extends perpendicularly from the molecular plane as shown in Fig. 1. Therefore, the overlapping of the orbitals is expected to be large in the direction perpendicular to the molecular plane, but not in the parallel one to the plane. Since charge carriers in the free radical transfer through the overlapping, the anisotropy of conductivity might be a consequence of substantial anisotropy of the overlapping in the crystal.

As is illustrated in Table I, no direction dependency was found in the values of energy

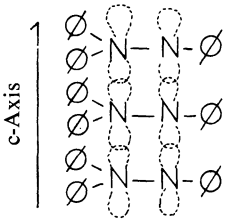


Fig. 1. The arrangement of DPPH molecules in crystal.

TABLE I. THE ELECTRONIC CONDUCTION IN DPPH

Sample	Single crystal		Thin film	
Direction	c-Axis ∥	c-Axis ⊥	Sandwich type	Surface type
ρ_{15}	$1\times10^{10}\,\Omega$ cm.	$1\times10^{15}\,\Omega$ cm.	$\sim10^{13}\,\Omega$ cm.	$\sim10^{10}\,\Omega$ cm.
$\Delta\varepsilon$	1.5 eV.	1.6 eV.	2.7 eV.	1.7 eV.
ρ_0	$10^{-3}\,\Omega$ cm.	$10^{2}\,\Omega$ cm.	$10^{-4}\,\Omega$ cm.	$10^{-2}\,\Omega$ cm.

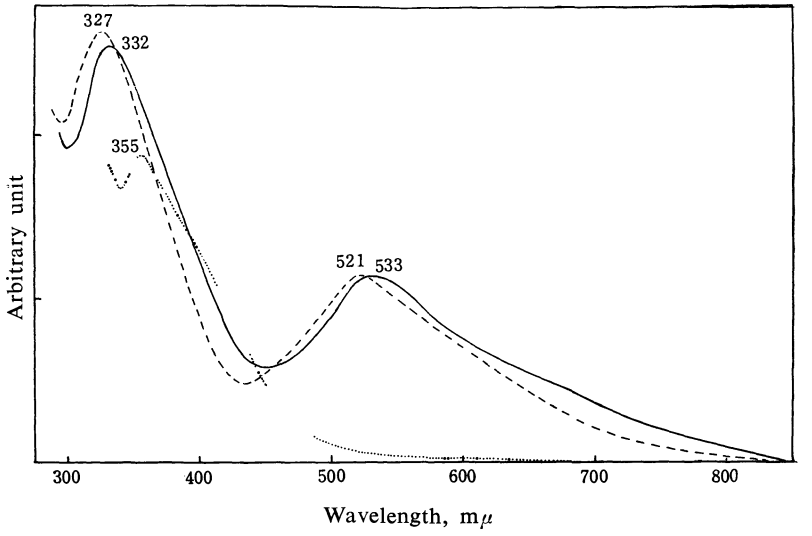
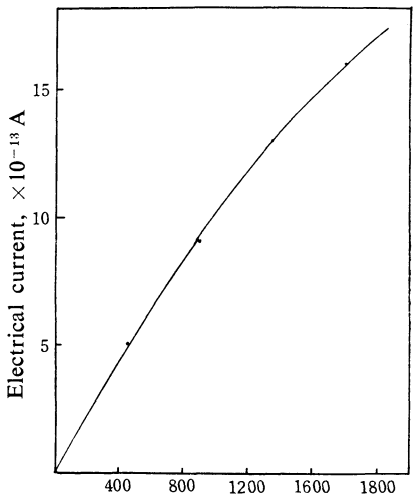


Fig. 2. The spectral responses of optical absorption and photoconduction for α,α'-diphenyl-β-picrylhydrazyl.
—— Absorption spectrum of solid (film)
---- Absorption spectrum of benzene solution
····· Photoconduction for sandwich-type cell

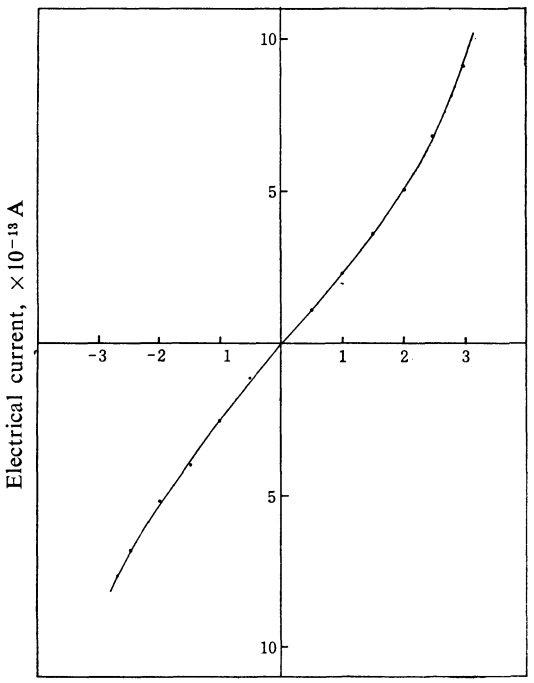
* The electrical resistivity, ρ, is expressed as $\rho=\rho_0\exp(\varepsilon/2kT)$.

gap, $\Delta\varepsilon$. Hence, there should be a large difference in the mobility of charge carriers depending on the direction of the crystal.

Polycyclic aromatic molecules of thin film are in alignment with their ab plane with the film surface as reported in the previous paper[10]. The DPPH thin film is expected to be a similar behaviour. The anisotropic values of the resistivity of its two directions—the direction perpendicular to the film (sandwich-type cell) and that along to the surface (surface-type cell)—are also explained by the orientation of unpaired electron orbitals.



(a)



(b)

Fig. 3. The current-voltage relation of DPPH thin film cells.
(a) I-V curve of the surface type DPPH cell.
(b) I-V curve of the sandwich type DPPH cell.

A great difference was found on the characteristics of photoconduction and current-voltage relation in these two types of cells. The photoconduction for sandwich-type cell, Al||DPPH||Al[11], was found under an illumination of visible light but little for surface type one. The spectral response for photoconduction is illustrated in Fig. 2 as a dotted line.

In comparison with the absorption spectra of the DPPH crystal, which possess two absorption peaks, 332 and 533 mμ, the spectral response for photoconduction is in a good agreement with that for optical absorption for the shorter wavelength peak of 332 mμ, but not for the longer wavelength peak of 533 mμ, which is completely missed in the response for photoconduction.

The variation of the current with the applied potential obeyed Ohm's law for the lower fields used. At the higher fields (over 10^3 V./cm.), however, its voltage dependence was strongly curved for sandwich-type cell and became more linear for surface-type one as illustrated in Fig. 3.

Summary

The electronic conductivity of two forms of α,α'-diphenyl-β-picrylhydrazyl, the single crystal and the thin film, was observed. The resistivity (ρ_{15}) at room temperature along c-axis (1×10^{10} Ω cm.) is 10^5 times lower than that perpendicular to the axis (1×10^{15} Ω cm.), but its activation energy ($\Delta\varepsilon$) against temperature is in good agreement (1.5 and 1.6 eV.). These large anisotropy may be introduced from that of the arrangement of molecules in the crystal. In the case of thin film, the values of ρ_{15} and of $\Delta\varepsilon$ are $\sim10^{10}$ Ω cm., 1.7 eV. for surface type cell and $\sim10^{13}$ Ω cm., 2.7 eV. for sandwich-type cell respectively. A great difference on the characteristics of photoconduction and on the current-voltage relation in these two types of cell was found.

The Institute for Solid State Physics
The University of Tokyo
Azabu, Tokyo

11) H. Inokuchi, Y. Maruyama and H. Akamatu, This Bulletin, 34, 1093 (1961).

*Dye-sensitized Photopolymerization of Vinyl Compounds. Polymerization of Acrylonitrile by Stannous Chloride and Acriflavine. II**

By Ai WATANABE**

(Received February 8, 1962)

In the previous paper[1], the present author and Koizumi studied the polymerization of acrylonitrile (AN), which takes place when a solution of AN, acriflavine (D) and stannous chloride in the mixed solvent of water and dimethylformamide (DMF) is illuminated by visible light. They found that neither oxygen nor water is of primary importance for the initiation of polymerization, as a mechanism they proposed that a transient tin ion of odd valency is produced and that this, by interacting with the monomer, initiates the polymerization.

The aim of the present work is to make the proposed scheme more definite by ascertaining whether it also fits the photosensitized polymerization of AN in DMF (with no addition of water and in vacuo) in the presence of stannous chloride and acriflavine.

Experimental

Materials.—AN from the Union Carbide Corporation was distilled at atmospheric pressure and was further distilled twice in an atmosphere of nitrogen under reduced pressure. Commercial acriflavine was recrystallized twice from water and dried in vacuo. Stannous chloride dihydrate (G. R) was dehydrated in vacuo at room temperature. DMF from Du Pont was purified as has been described previously[1].

Procedure.—As the light source, a tungsten projection lamp 100 V.-500 W was operated at 80 V., as has been described in Part I. The distance between the light source and the reaction cell in a thermostat was 10 cm. A Matsuda color filter V-Y3C and a heat-cutoff filter were put between the reaction cell and the light source. The reaction cells and dilatometers were the same as have been described in Part I except for the one shown in Fig. 1, which was used to study the influence of oxygen upon the rate of polymerization. The solution to be studied was poured into cell A and then degassed after being frozen in a dry-ice bath. When the degassing was complete, a definite quantity of air was introduced through B and the dilatometer was sealed off at constricted Part B. When the contents thawed, the air was dissolved by shaking the cell, and the solution was poured through capillary C into the reaction cell D by tilting the unit. The drop of meniscus in the capillary, E, was followed by the use of a travelling microscope. All the experiments were done at 30°C, and the solutions were degassed by repeating the vacuum distillation except when otherwise described.

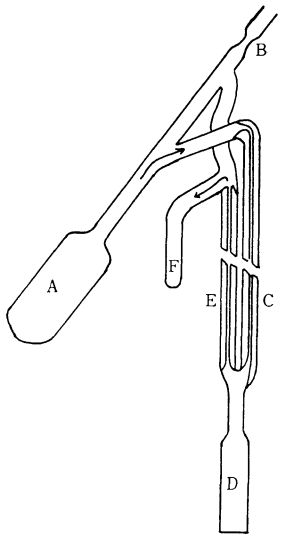


Fig. 1. Dilatometer.

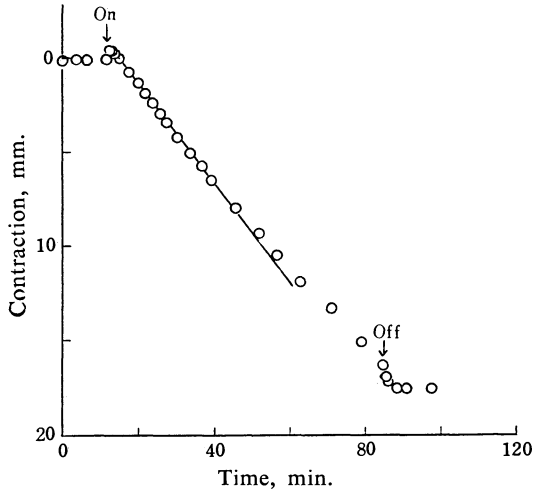


Fig. 2. The polymerization~time curve. $[D]=1.0\times10^{-4}$ M ; $[SnCl_2]=1.25\times10^{-2}$ M ; $[AN]=5.0$ M

* Presented at the 14th Annual Meeting of the Chemical Society of Japan, Tokyo, April, 1961.

** Present address: Nichiban Co., Nerima-ku, Tokyo.

1) A. Watanabe and M. Koizumi, This Bulletin, **34**, 1086 (1961).

The apparatus employed for making a sample of a bleaching reaction was almost the same as that used for the polymerization. The solutions were thoroughly degassed and were poured into two reaction cells in vacuo. They were sealed off, separately; one was used for the dark-reaction, and the other for the photo-reaction. At various time intervals during the reaction, reaction cells were taken out and the dye concentration of solutions was measured by a spectrophotometer.

Results

The Polymerization.—Induction periods were observed in almost none of the experiments, and after a short period of constant rate the rate fell off gradually. Figure 2 shows a typical curve for the polymerization. During the course of polymerization, the polymer did not deposit. In all cases, the rate was evaluated from the initial linear portion of the curve. The reproducibility of experiments was not excellent enough to correlate the data of a different series of experiments.

The Effect of Dye Concentration.—In Fig. 3 is shown the variation of the rate with the concentration of acriflavine. It is apparent from the figure that, at a concentration of dye of less than 1×10^{-5} M, the rate increases linearly with the square root of the dye concentration and that the log(rate)~log[D] curve gives the slope of 0.4. The rate decreases when the concentration of dye exceeds 1×10^{-4} M.

The Effect of the Concentration of Stannous Chloride.—The effect of the concentration of stannous chloride on the rate is shown in Fig.

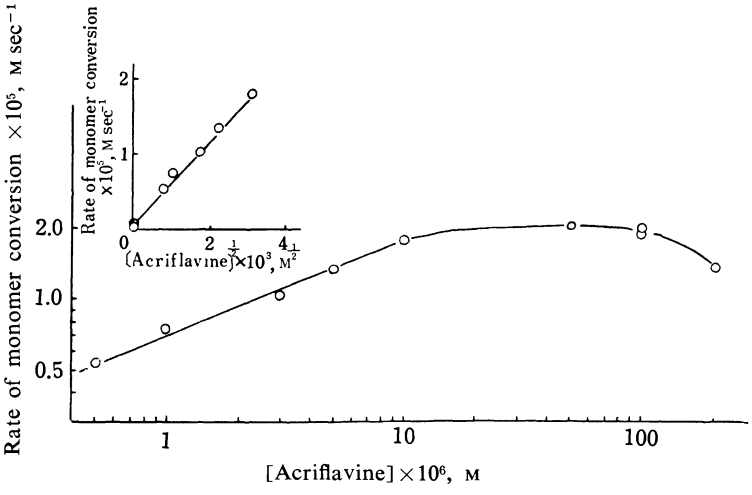


Fig. 3. The dependence of the initial polymerization rate on acriflavine concentration.
$[SnCl_2]=1.25\times10^{-2}$ M; [AN]=5.0 M

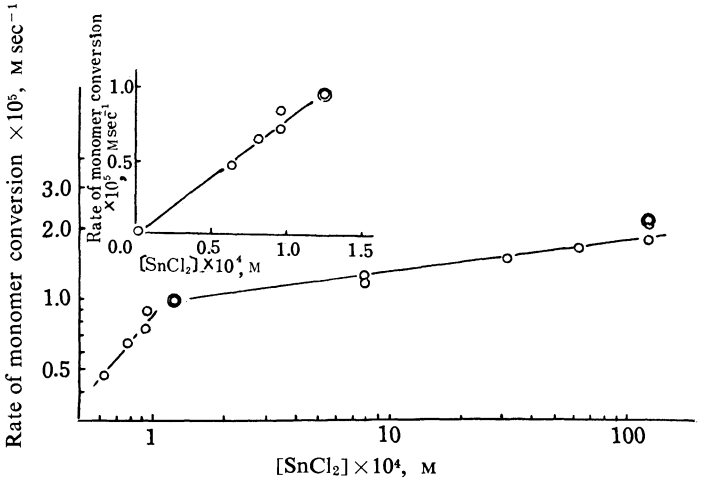


Fig. 4. The dependence of the initial polymerization rate on $SnCl_2$ concentration.
$[D]=1.0\times10^{-4}$ M; [AN]=5.0 M

4. When the concentration of stannous chloride is less than 1×10^{-4} M, the linearity holds between the rate and the concentration of stannous chloride, this being also confirmed by the slope of 0.95 for the log(rate)~log[$SnCl_2$] plot, although there exists some scattering of the experimental points. In the region where the concentration of stannous chlorde is more than ca. 1×10^{-4} M, the rate increases at a lower rate.

The Effect of the Monomer Concentration.—As is shown in Fig. 5, the rate depends on the second power of the monomer concentration. The log(rate)~log[AN] plot gives a straight line of the slope of 2.2.

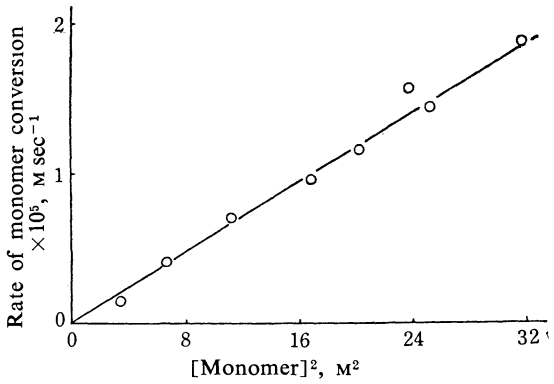


Fig. 5. The dependence of initial polymerization rate on acrylonitrile concentration.
[D]=2.0×10^{-4} M; [$SnCl_2$]=1.25×10^{-2} M

The Effect of the Pressure of Oxygen.—In Fig. 6, the rate is plotted against the pressure of oxygen. It is evident that the polymerization in the degassed solution has a rate somewhat smaller than that in the non-degassed solution, the ratio of the rate in the two cases being about 0.5. Thus, the presence of oxygen is not of primary importance for the occurrence of the reaction.

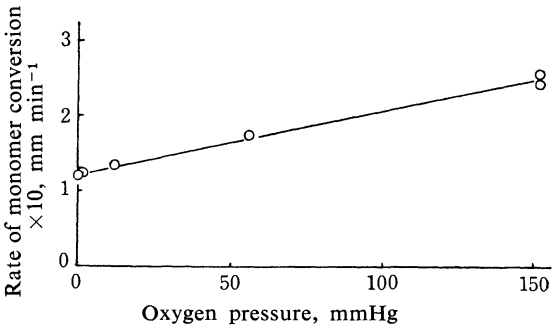


Fig. 6. The dependence of the initial polymerization rate on oxygen pressure.
[D]=1.0×10^{-4} M; [$SnCl_2$]=1.25×10^{-2} M; [AN]=5.0 M

The Effect of the Light Intensity. — The intensity of the exciting light was changed to 50, 25 and 12% of the standard light by the use of neutral filters. The samples used in these experiments contained a quantity of dye large enough to absorb almost all the effective light. As is shown in Fig. 7, the intensity exponent is about 0.35.

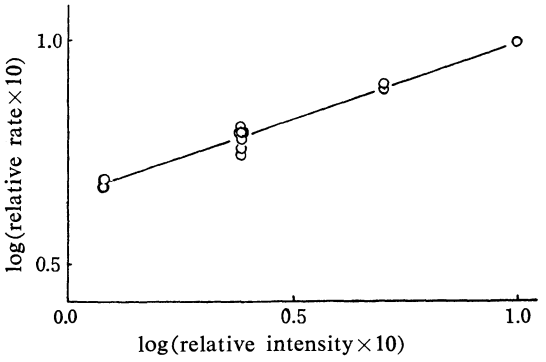


Fig. 7. The intensity exponent.
[D]=1.0×10^{-4} M; [$SnCl_2$]=1.25×10^{-2} M; [AN]=5.0 M

The Bleaching.—*The Bleaching of Dye in the DMF Solution.*—When the degassed solution of dye in DMF was illuminated, the bleaching occurred, whereas not a slight bleaching was observed in the dark. In Fig. 8 the absorption spectrum of the sample after illumination is (2), and that of the original sample is (1). A slow restoration of the absorption curve was realized even in vacuo when the illuminated sample was kept in the dark (3). On the

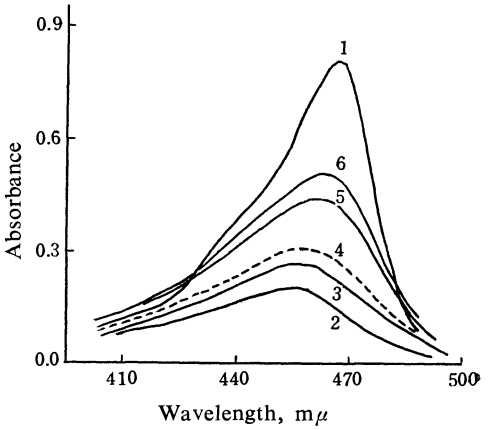


Fig. 8. Spectrum changes of acriflavine in DMF solution degassed.
1 Initial ([D]=1.4×10^{-5} M)
2 1.2 hr.-illumination at 30°C
3 15 hr.-standing of (2) in the dark
4 Aeration of (3)
5 5.4 hr.-standing of (4) in the dark
6 47.5 hr.-standing of (4) in the dark

introduction of air into the illuminated sample, the absorption curve was further restored to some extent.

The rate of photobleaching was reduced by the addition of stannous chloride, and it was found that the bleached solution in this case never completely regains its color upon the introduction of air. The bleaching did not occur in the dark. The reversible photobleaching was scarcely observed at about 6.25×10^{-3}M stannous chloride and the absorption spectrum showed a slight shift of λ_{max} toward a longer wavelength.

In Fig. 9, the absorbance at the wavelength corresponding to the maximum of the original sample is plotted against the reaction time. This figure does not allow a rigorous comparison of the rates of photobleaching because of the superposition of the reversible and irreversible bleaching, the latter especially giving an absorption curve due to the remaining dye and the product. However, the rates can be compared semiquantitatively from this figure, and it is clear that the rate decreases as the concentration of stannous chloride is increased.

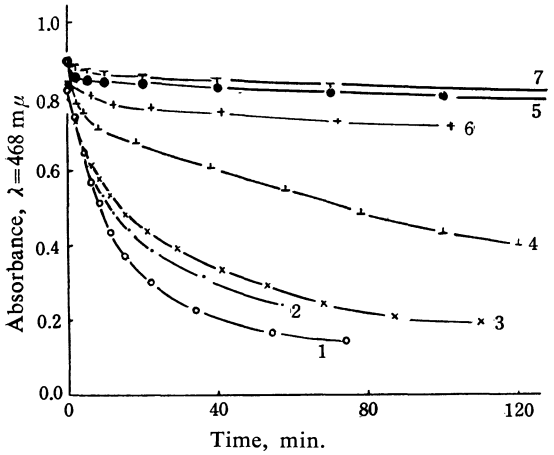


Fig. 9. The photobleaching~time curves of acriflavine in DMF solution degassed.
$[D]\approx1.4\times10^{-5}$ M

	$[SnCl_2]$, M
1	0
2	6.25×10^{-6}
3	1.25×10^{-5}
4	2.50×10^{-5}
5	1.25×10^{-4}
6	1.25×10^{-3}
7	1.25×10^{-2}

The Bleaching of Dye in the DMF-AN Solution. —When AN is added to the DMF solution, the spectrum of dye showed little change, but the rate of photobleaching was reduced. Furthermore, the photobleaching of dye in the degassed DMF-AN solution was irreversible, and the absorption spectra of the illuminated solution showed a shift of λ_{max} to longer wavelengths. When stannous chloride is added, the rate of photobleaching is appreciably

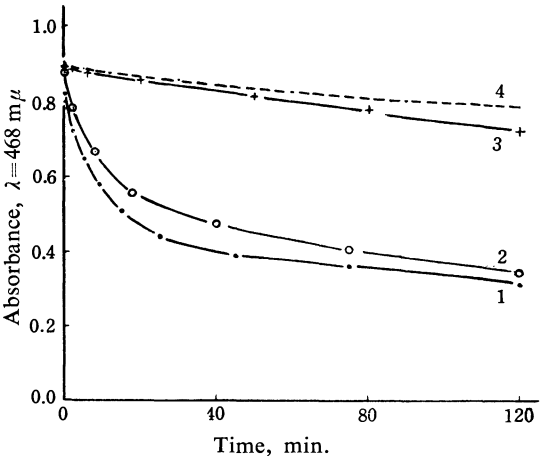


Fig. 10. The photobleaching~time curves of acriflavine in DMF-AN solution degassed in the presence of $SnCl_2$.
Volume ratio, DMF/AN=9;
$[D]\approx1.4\times10^{-5}$ M

	$[SnCl_2]$, M
1	0
2	1.25×10^{-5}
3	1.25×10^{-4}
4	1.25×10^{-2}

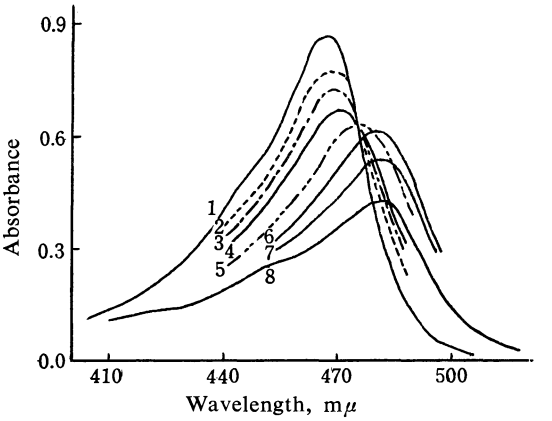


Fig. 11. Spectrum changes of acriflavine in DMF-AN solution degassed in the presence of $SnCl_2$.
Volume ratio, DMF/AN=9; $[SnCl_2]=1.25\times10^{-5}$ M; $[D]=1.4\times10^{-5}$ M
1 Initial
2 2 min.-illumination
3 4 min.-illumination
4 8 min.-illumination
5 18 min.-illumination
6 40 min.-illumination
7 75 min.-illumination
8 120 min.-illumination

reduced, as is shown in Fig. 10; the bleaching is irreversible. The bleaching does not occur in the dark. An example of the spectral change caused by illumination is shown in Fig. 11.

Though the feature of photobleaching is complicated and it is desirable to study it more quantitatively, some qualitative discussion may be given about the relation between photobleaching and photopolymerization on the basis of the above results. In broad outline, the photobleaching of dye occurs in the absence of stannous chloride though the photopolymerization does not occur. The rate of photobleaching is reduced by the addition of stannous chloride which, on the other hand, causes the photopolymerization to occur. Consequently, it may be concluded that the photobleaching of dye does not occur parallel with the photopolymerization.

Discussion

As expected, the polymerization of AN was initiated by visible light in the presence of stannous chloride and acriflavine in vacuo. It will be discussed below whether the experimental results can be interpreted on the basis of the schemes proposed in the previous paper. One of the schemes proposed for the initiation process involves the assumption that a complex is formed between the Sn^{2+} ion and the dye. However, this seems rather implausible in view of the finding that the shift of the absorption spectrum of dye in the visible region was not observed by the addition of stannous chloride in a DMF-AN or a DMF-AN-H_2O solution. Moreover, the essential steps are common in the two schemes. Hence, to avoid confusion, the discussion is limited to the other scheme, which is described below:

$$\begin{array}{ccccccccc} D & \xrightarrow[(1)]{h\nu} & D^* & \xrightarrow[(3)]{D} & D^t & \xrightarrow[(5)]{Sn^{2+}} & (D^- \text{ — } Sn^{3+}) & \xrightarrow[(7)]{Sn^{2+}} & \\ & & \downarrow (2) & & \downarrow (4) & & \downarrow (6') & \downarrow (6) & \\ & & D & & D & & D+Sn^{2+} & Leuco+Sn^{4+} & \end{array}$$

$$D + Sn^+ + Sn^{3+} \xrightarrow[(8)]{} D + 2Sn^{2+}$$

$$(\text{or } D^- + Sn^{3+}) \qquad (\text{or } D + Sn^{2+})$$

$$Sn^{3+} + M \xrightarrow{k_i} R$$

$$(\text{or } Sn^+ + M \rightarrow R)$$

The essential points in this scheme are that the two kinds of ionic species of a radical nature produced by process (7) react almost exclusively in such a way as to produce stable ions, and that only a small fraction of them react with the monomer to initiate the polymerization. It is assumed, in addition, that the reaction attains the steady state and that the termination of the growing polymer is spontaneous.

The experimental overall rate formula in the present case may be expressed as follows,

$$v \propto [D]^{1/2}[SnCl_2][M]^2 \qquad (I)$$

provided that [D] and $[SnCl_2]$ are small. Thus, the rate is 1/2-order with respect to the dye concentration, whereas it is first order in the previous system, containing water and oxyen, which was treated in Part I. This difference in the order of reaction with respect to the dye concentration can be explained on the assumption that the transition from a singlet (D^*) to a triplet (D^t) excited state occurs in this case as is described below, whereas this is induced by the ground state dye molecule[2] in the previous system, as was discussed in Part I:

$$\begin{array}{ccccccc} D & \xrightarrow[(1)]{h\nu} & D^* & \rightarrow & D^t & \rightarrow & \text{same as the above scheme} \\ & & \downarrow (2)(3) & & \downarrow (4) & & \\ & & D & & D & & \end{array}$$

From this scheme, the initiation rate (v_i) and v can be derived as follows:

$$v_i = \left[\left(\frac{I_0 k_1 k_3}{k_2 + k_3}\right)\left(\frac{k_5[Sn^{2+}]}{k_4 + k_5[Sn^{2+}]}\right) \times \left(\frac{k_7[Sn^{2+}]}{k_6 + k_6' + k_7[Sn^{2+}]}\right)\right]^{1/2} \frac{k_i}{k_8^{1/2}}[M] \qquad (II)$$

and

$$v = \frac{k_1 k_p}{k_t k_8^{1/2}}[M]^2\left[\left(\frac{I_0 k_1 k_3}{k_2 + k_3}\right)\left(\frac{k_5[Sn^{2+}]}{k_4 + k_5[Sn^{2+}]}\right) \times \left(\frac{k_7[Sn^{2+}]}{k_6 + k_6' + k_7[Sn^{2+}]}\right)\right]^{1/2} \qquad (III)$$

From Eq. III, the following relations are obtained, satisfying the experimental results:

i) When [D] is small, $I_0 k_1$ may be put as approximately proportional to [D]. Hence, $v \propto [D]$.
ii) When $[Sn^{2+}]$ is small, $v \propto [Sn^{2+}]$.
iii) In all cases, $v \propto [M]^2$.
iv) $v \propto I_0^{1/2}$

It is regrettable that the value of the intensity exponent experimentally obtained, i.e., 0.35 (which is much less than 0.5), can not be explained satisfactorily.

To sum up, all the features of the present reaction, except a single point mentioned above, can well be interpreted on the basis of a scheme quite similar to that proposed in the previous paper. In addition, the rate of the photobleaching of dye decreases with the increasing stannous chloride concentration, whereas the rate of the photopolymerization increases appreciably with it. This result also supports the view that the photopolymerization

2) F. Millich and G. Oster, *J. Am. Chem. Soc.*, **81**, 1357 (1959).

does not accompany the transient photobleaching of dye, which finding is naturally expected according to the proposed scheme.

Summary

The photosensitized polymerization of AN in DMF by acriflavine and stannous chloride in vacuo was investigated. The reaction rate was shown as: $v \propto [D]^{1/2}[SnCl_2][M]^2$, where [D] and $[SnCl_2]$ were small. The experiments performed examining the photobleaching of dyestuff in various conditions led to the finding that the photopolymerization does not occur by virtue of the transiently-reduced dye. The scheme proposed in Part I, in which the transient tin ion of odd valency (Sn^{3+} and/or Sn^{+}) initiates the polymerization by interacting with the monomer, was further substantiated.

The author wishes to expess her hearty thanks to Professor Masao Koizumi and Dr. Shunji Kato of Tohoku University for their helpful discussion, and to Professor Ryoichi Fujishiro for his encouragement.

Department of Chemistry
Faculty of Science
Osaka City University
Kita-ku, Osaka

Adsorption Characteristics of ^{60}Co-ions towards Polystyrene Treated with Sulfuric Acid Relative to Radioactive Decontamination

By Tsutomu SEIMIYA and Tsunetaka SASAKI

(Received April 6, 1962)

The surface treatment of plastics has drawn the attention of many investigators since it has much to do with such practical problems as anti-electrification, adhesion, radioactive decontamination, etc. It is also a problem of theoretical interest from the viewpoint of the relation of the adsorption to the nature of the surface concerned[1]. Concerning these problems, it is of basic importance to know the amount of solute adsorbed on a solid surface, about which much literature is available[2]. In such studies, however, the total uptakes of a solute have often been roughly treated as the adsorption and no due distinction has been drawn between the adsorption and adhesion[3], especially concerning practical problems, in spite of the fact that such a distinction is rather important in the practice, for instance, of decontamination. Further, as for the adsorption which is measured as a surface excess, several types have been distinguished according to their natures[4], but in practice they have also often been treated without distinction. In order to contribute to the study of such problems we have studied the details of the adsorption of cobalt ions on a polystyrene surface, and also the effect of sulfuric acid treatment on the adsorption.

1) M. Muramatsu and T. Sasaki, *Radioisotopes*, **7**, 36, 42 (1958) (in Japanese); T. Sasaki, M. Muramatsu, H. Hotta and Y. Wadachi, ibid., **7**, 47 (1958) (in Japanese); P. C. Tompkins et at., *Ind. Eng. Chem.*, **42**, 1475 (1950).
2) J. H. Schulman et al., *Kolloid-Z.*, **146**, 77 (1956).
3) C. V. King and B. Levy, *J. Phys. Chem.*, **59**, 910 (1955).
4) C. H. Giles et al., *J. Chem. Soc.*, **1960**, 3973.

Experimental

The samples of plastics used in these experiments were polystyrene ("Styron-666-General Purpose" of Asahi-Dow Ltd.) cut in $0.2\times2\times2$ cm. plates. The sulfuric acid used was of a commercial pure grade. An aqueous solution of cobaltous chloride (8×10^{-7} mol./l.) tagged with ^{60}Co-ions was used for the adsorption experiment. The specific activity under the experimental geometry was 6.7×10^{-14} g./cm^2 c.p.m. The sample plates cleaned with a soap solution were immersed under various conditions of dipping time and temperature into sulfuric acid, withdrawn, rinsed with distilled water, and dried in a desiccator. The samples thus treated were weighed and floated on the surface of 4 cc. of an aqueous solution of radioactive cobaltous chloride. After 30 minutes' contact, which was considered to be sufficient for equilibration, they were then taken out of the radioactive solution, weighed to measure the amounts of liquids which adhered to the samples, and dried using an infrared lamp. The radioactivities of the samples were then mesured with a GM-Counter (Ten Model SA-10, 100 Scaler), equipped with a GM-tube with a 2.95 mg./cm^2 mica window (Ten GM 131). The amount of adsorption was determined as the difference between the total radioactivity taken up by the plastics samples and that radioactivity due to the solution adhering to the polystyrene sample, under

the assumption that the concentration of ^{60}Co-ions is the same for both the adhering solution and the bulk of the solution. The specific activity of cobalt ions necessary for this calculation was measured at the same time under the same geometry as for the standard sample, which was prepared by evaporating a known amount of a radioactive sample solution put in 20 spots on a polystyrene sample. For the measurement of the radioactivity, only β-ray counting was used, the difference between the counting rates taken with and without a γ-ray filter. The samples of plastics were further dipped into 50 cc. of various rinsing liquids and were taken out of them after a desired immersion time. The remaining radioactivities on the plastics surface were then measured, and from the values obtained, the amount of the desorption of ^{60}Co-ions from the samples was determined. For each successive dipping, the rinsing liquid was renewed.

Results

Figure 1 shows the changes in the uptake of ^{60}Co-ions with the immersion time of polystyrene in sulfuric acid at 40°C. The desorption of cobalt ions using various rinsing liquids was measured; these results are shown in Figs. 2 and 3. The polystyrene samples appearing in Fig. 3 had been immersed in a sulfuric acid solution for 30 sec. at 85 to 88°C; those in Fig. 2 had not been so treated. The amounts of ^{60}Co-ions remaining on the plate taken as a vertical axis, were expressed as percentages of the original amount of ^{60}Co-ions adsorbed, as was stated in the preceding section. The values above 100 per cent came from the adhering portion of the liquid which was used for the cobalt ion adsorption. Here we can notice that, although the cobalt ions adsorbed initially on an untreated surface (Fig. 2) are much fewer than those on a treated surface (Fig. 3), the former as a whole is rather harder to remove by rinsing than the latter, regardless of the nature of the rinsing liquid; i. e., the steady portion of the curves of Fig. 2 attained after prolonged rinsing is higher (2.95×10^{-11} g./cm^2) than would be presumed from the small initial amount of cobalt ion uptake. This may come from the irreversible portion of the adsorption of cobalt ions due to the impurities in the original sample; the impurities may possibly be removed or altered to the center of reversible adsorption during the sulfuric acid treatment.

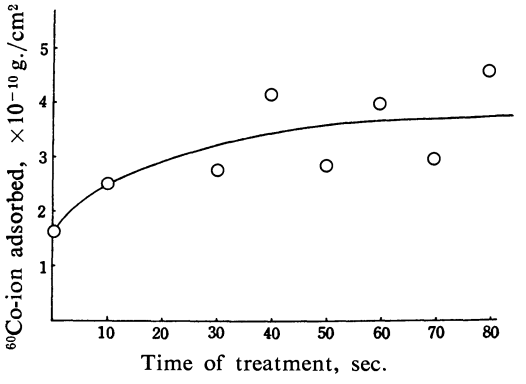


Fig. 1. Change of adsorption of ^{60}Co-ion on polystyrene with time of immersion into sulfuric acid.

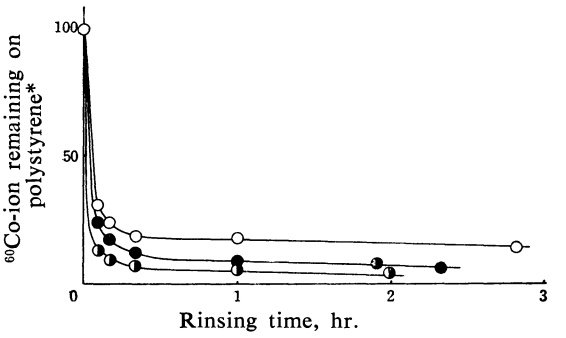


Fig. 2. Desorption of ^{60}Co-ion from polystyrene not treated with sulfuric acid.
Initial activity being 2500 c.p.m.; rinsing liquid used being 0.1 mol. aqueous cobalt chloride (○), distilled water (●) and aqueous 1 % EDTA solution all at pH 7.8 (◑).
* Relative counting rate of ^{60}Co-ion

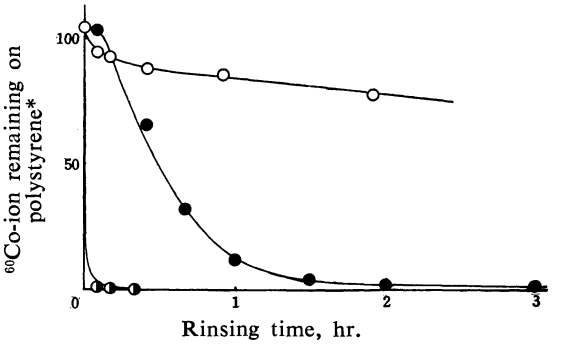


Fig. 3. Removal of ^{60}Co-ion-contamination from polystyrene treated with sulfuric acid.
Initial radioactivity; 15000~5000 c.p.m. (^{60}Co; $4.1\sim1.4\times10^{-9}$ g.) rinsing liquids; absolute ethanol (○); distilled water (●); 0.1 mol. aqueous cobaltous chloride solution (◑).
* Relative counting rate of ^{60}Co-ion

It can be seen in Fig. 3 that, in the case of treated polystyrene, the initial amount of adsorption is much larger than that of an untreated surface and that the desorption curves change markedly with the nature of the rinsing liquids. Thus, the rinsing with distilled water gradually decreases the adsorbed cobalt ions, while almost all of the cobalt ions are removed instantly by rinsing with a non-radioactive 0.1 mol. aqueous cobaltous chloride solution; this reduces the residual amount of

cobalt ion adsorption to less than 3.08×10^{-12} g./cm^2. On the basis of this desorption behavior, shown in Figs. 2 and 3, it may be concluded that the major part of the adsorption of cobalt ions by the treated (sulfonated) polystyrene is the ion-exchange adsorption. This conclusion is further confirmed by the fact that the rate of desorption by the anhydrous ethyl alcohol is smaller than that by distilled water. Here we employed ethyl alcohol because it is a nonionizing solvent, thus offering no ions for ion-exchange with the adsorbed ion, and yet it shows a larger solubility for cobaltous chloride than does distilled water. The desorption curves are also shown in Fig. 3.

In this situation, we should like to draw further attention to the problem of radioactive contamination and decontamination. Concerning these problems, Jackson and Garard made a similar experiment[5] for plastics surfaces using nuclear fission products as contaminants. The amount of adsorbed fission products they obtained, as well as the final amount of activity after rinsing the contaminated sample with 5 per cent ammonium citrate, is higher than those of our results for the sulfonated (ion-exchanging) polystyrene surface. In our case, the sulfonation of polystyrene was mainly restricted to its surface, and it was shown that, in such a case, adsorbed cobalt ions are rather readily desorbed; even a simple water (a weakly ionizing liquid) rinsing is fairly effective, as is shown in Fig. 3.

In the case of radioactive decontamination, it is the easy and widespread practice to use water, a detergent solution or an acid solution as the rinsing liquid or decontaminant. Quite often, howeve, these treatments leave some persistent contamination behind, though a large portion of contamination is readily removed. This residual contamination, though small in amount, may often be quite undesirable. Our present findings on the adsorption and desorption of ^{60}Co-ion by polystyrene have some bearing on this problem. It may be said that, if the sample of polystyrene is properly treated with sulfuric acid, such residual contamination will be reduced practically to zero even by a simple rinsing with water, though the surface is rendered rather susceptible to contamination. However, the problem still remains to find the optimum conditions, giving minimum susceptibility, for such a surface treatment.

In conclusion, we should like to emphasize that, judging from the results of the present experiment on the adsorption characteristics of cobalt ions on a polystyrene sample, the information concerning the properties of solid surfaces and the nature of the adsorption of a solute on them can properly be obtained from such experiments as sulfuric acid treatment and from the measurement of desorption curves for treated and untreated surfaces using various rinsing liquids.

5) E. W. Jackson and L. Garard, *Nature*, **171**, 442 (1953).

Summary

The adsorption of cobalt ions by polystyrene treated with sulfuric acid was measured using the radiotracer technique. We also studied the type of adsorption of the cobalt ions by polystyrene, with or without sulfuric acid treatment, by observing the rate of desorption by the use of several rinsing liquids. It was confirmed that, although cobalt ion adsorption on an untreated surface is much less than that on a treated surface, the former is rather harder to remove by rinsing than the latter, regardless of the nature of the rinsing liquid.

The authors wish to express their thanks to the Ministry of Education for the Scientific Research Expenditure Grant given to T. Sasaki. They also wish to thank the Asahi-Dow, Ltd., and the Mitsui Chemical Ind. Co. for the samples given to them.

Department of Chemistry
Faculty of Science
Tokyo Metropolitan University
Setagaya-ku, Tokyo

Effect of Sulfuric Acid and Chromic Acid Mixture Treatments of Plastics on their Wettability towards Water

By Teruo TSUNODA, Tsutomu SEIMIYA and Tsunetaka SASAKI

(Received April 6, 1962)

The wettability of polymer surfaces has been studied by several workers with reference to the theoretical problems of surface chemistry as well as the practical processes of printing, adhesion, friction, anti-electrification, surface electrical conductivity, etc., and many problems of the surface chemical and physical treatment of a polymer substance and plastics have been studied along these lines[1].

In most of these experiments with surface treatment, however, no full attempt has been made to establish a definite relation between the amount of surface attack and the magnitude of the surface properties affected thereby. In the present experiment, the effect of the sulfuric acid treatment of polystyrene and of the chromic acid mixture treatment of polyethylene on their wettability towards water was studied.

Experimental

Materials.—The plastics used in this experiment were polystyrene ("Styron-666-General Purpose" made by the Asahi-Dow, Ltd.) and polyethylene ("Hi-Zex" made by the Mitsui Chemical Ind. Co.), both 0.2 cm. in thickness and cut into 2×1 cm. plates. Sulfuric acid of a pure grade and a chromic acid mixture prepared from commercial potassium dichromate, sulfuric acid and water in the ratio of 5 : 100 : 8 by weight were used for the surface treatment of polystyrene and polyethylene respectively.

Procedure.—Sample plates cleaned with a soap solution were immersed, under varying conditions of dipping time and temperature, into a sulfuric acid solution in the case of polystyrene and into a chromic acid mixture in the case of polyethylene; they were then withdrawn, rinsed with distilled water, dried in a desiccator, and used for the contact angle measurement by a Wilhelmy-type torsion balance, in a manner similar to that reported previously[2]. The cobalt adsorption on the treated polystyrene surface was measured by the radiotracer method, using a cobaltous chloride solution tagged with ^{60}Co. The details of this, as well as the results of the measurement, have already been reported in a preceding paper[3].

Contact Angles.—Figure 1 shows the change in the contact angles of water on polyethylene with the time of immersion in a chromic acid

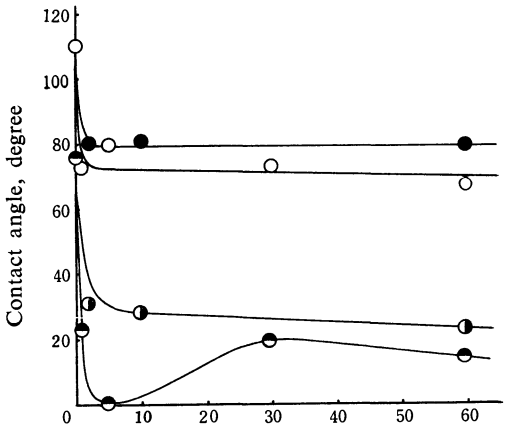


Fig. 1. Change of wettability of polyethylene towards water with time of immersion into chromic acid mixture.
- ● Advancing contact angle; immersion temperature 13°C
- ○ Advancing contact angle; immersion temperature 23°C
- ◑ Receding contact angle; immersion temperature 13°C
- ◓ Receding contact angle; immersion temperature 23°C

mixture at 23 and 13°C. In both cases, the polyethylene surfaces are rendered wettable soon after immersion into the chromic acid mixture. This can reasonably be explained by the oxidation of the polyethylene surfaces by the chromic acid mixture, as may be seen from a similar oxidation reaction which constitutes the basic reaction of the quantitative determination of the number of side chains in a polyethylene molecule[4]. A similar oxidation is observed in a surface treatment by an aqueous solution of chromic acid and

1) E. G. Shafrin and W. A. Zisman, *J. Phys. Chem.*, **64**, 519 (1960); R. G. Craig, G. C. Berry and F. A. Peyton, ibid., **64**, 514 (1960); F. E. Bartell and B. Roger Ray, *J. Am. Chem. Soc.*, **74**, 778 (1952); K. Kawasaki, *J. Colloid Sci.*, **15**, 402 (1960); B. Roger Ray, J. R. Anderson and J. J. Scholz, *J. Phys. Chem.*, **62**, 1220, 1227 (1958).

2) T. Sasaki, H. Kumanomido and T. Tsunoda, Second. International Congress of Surface Activity, III, Butterworths, London (1957), p. 153.

3) T. Seimiya and T. Sasaki, This Bulletin, **35**, 1567 (1962).

4) K. Tani, *Kobunshikagaku*, (in Japanese) **28**, 104 (1948).

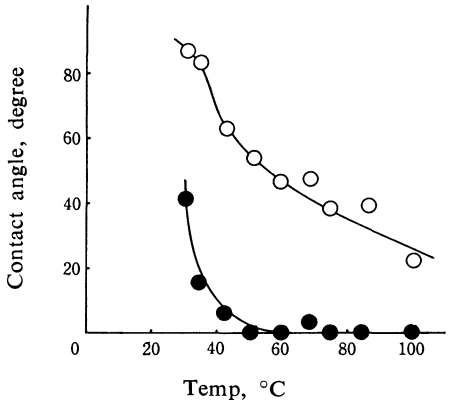


Fig. 2. Change of wettability of polystyrene towards water with temperature of immersion into sulfuric acid.
Time of immersion 10 sec.
○ Advancing contact angle
● Receding contact angle

potassium permangante, while no increase in the wettability can be seen in a treatment by sulfuric acid or phosphoric acid. The relation between the contact angle of the water and the temperature of the sulfuric acid treatment for polystyrene is given in Fig. 2, which shows a zero receding contact angle for temperatures above 50°C. The higher the temperature of treatment is raised, the more wettable becomes the polystyrene surface towards water. The sulfonation of the polystyrene surface by the sulfuric acid may reasonably be considered responsible for this wettability[5]. The change in the contact angle of water on polystyrene

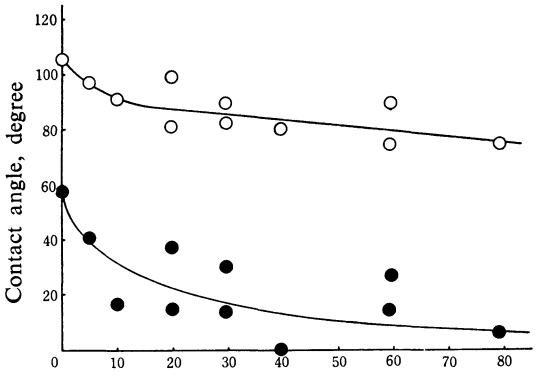


Fig. 3. Change of wettability of polystyrene towards water with time of immersion into sulfuric acid.
○ Advancing contact angle
● Receding contact angle
} immersion temp. 30°C

5) For example, H. Shimizu, "Ion-Exchange Resin", Kyoritsu Pub. Co., Tokyo (1958) (in Japanese).

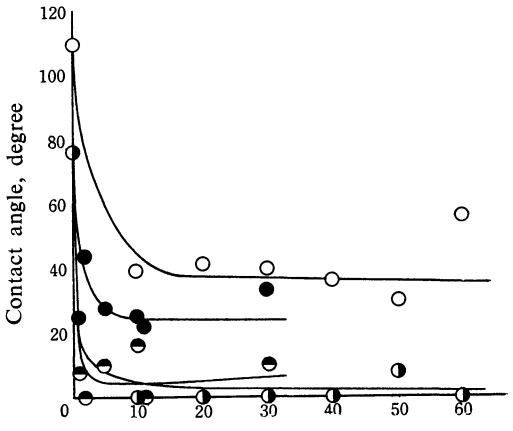


Fig. 4. Change of wettability of polystyrene towards water with time of immersion into sulfuric acid.
○ Advancing contact angle; immersion temperature 85~88°C
● Advancing contact angle; immersion temperature 100°C
◑ Receding contact angle; immersion temperature 85~88°C
◓ Receding contact angle; immersion temperature 100°C

with the time of immersion into sulfuric acid was also measured at the immersion temperatures of 30°C, from 85 to 88°C and at 100°C (Figs. 3 and 4). For the cases of both 85 to 88°C and of 100°C, a rapid increase in wettability is observed within 10 sec. of immersion, while a rather gradual increase in wettability is exhibited at 30°C.

The Relation between Wettability and the Degree of Surface Attack.—Various equations for the relation between the wettability of a solid surface and the adsorption of the liquid or solute upon it have been proposed[6].

We ourselves have presented the following equation[2]:

$$\cos\theta = \frac{\sigma_1 + \sigma_w}{\sigma_1}(a\Gamma + b) - 1 \qquad (1)$$

where θ is the contact angle of the wetting liquid (aqueous solution) with a surface tension of σ_1 on the surface of a solid where the solute adsorption of the amount Γ takes place, σ_w, the surface tension of the solvent (water), an a and p, constants. The value a is positive or negative according to whether the adsorption renders the surface hydrophobic or hydrophilic. This equation can be reduced

6) P. A. Rhebinder et al., *Kolloid-Z.*, **65**, 268 (1933); M. A. Cook et al., *J. Phys. Colloid Chem.*, **55**, 1219 (1951); K. S. Doss et al., *Proc. Ind. Acad. Sci.*, **7A**, 117 (1938); M. Wada, *Nippon Kogyo Kaishi*, **59**, 681 (1943) (in Japanese); L. S. Bartell et al., *J. Phys. Chem.*, **64**, 514 (1960).

to Doss' Eq. 5 for wetting by a pure liquid (water) where $\sigma_1=\sigma_w$ and $\Gamma=0$.

We have already confirmed that Eq. 1 is valid both in the case of the wetting of a paraffin surface by an aqueous ethyl alcohol solution and in the case of the dewetting of a galena surface by an aqueous xanthate solution[2]. Now let us apply this equation in the present case to explain the wetting of a polystyrene surface by water. Here σ_1 is equal to σ_w and the equation is simplified to:

$$\cos\theta=2(a\Gamma+b)-1 \qquad (2)$$

In the original Eq. 1, Γ represents the amount of adsorption, which can be interpreted to be the extent of the portion of the surface suffering from the change in wetting properties. It is quite legitimate here to equate Γ with the extent of the surface rendered wettable by the sulfuric acid, or with the degree of surface sulfonation if such an expression may be used for the sake of brevity. Then we can interpret Eq. 2 as the wetting isotherm for the sulfonation of a polystyrene surface. Now if we assume that the amount of cobalt adsorption, x, for the sulfonated surface is proportional to Γ, we have

$$\cos\theta=2(apx+b)-1 \qquad (3)$$

where p is the proportionality constant. We should, however, notice that the untreated surface also gives a cobalt adsorption of the amount x_w. This, together with x, gives the total cobalt adsorption, X, namely

$$X=x+x_w \qquad (4)$$

From Eqs. 3 and 4, we obtain

$$\cos\theta=\cos\theta_w+2ap(X-x_w) \qquad (5)$$

Here $X-x_w$ expresses the net amount of surface sulfonation. From Eq. 5 we should expect a linear relation between $\cos\theta$ and $X-x_w$. Figure 5 shows the experimental results. Here the values of θ were those measured one minute after the samples were dipped in water, and the corresponding X values were measured by the radiotracer method[3]. Now, we can observe a linear relation as a whole, in the cases of both an advancing and a receding contact angle, thus confirming a linear change of wettability with the degree of sulfonation as far as the present experiment is concerned. We can, of course, expect in this diagram that the region of saturation may appear on further attack, where the incerase of $X-x_w$ will no longer result in an increase in $\cos\theta$. This may be explained chiefly by the fact that, under such a condition, the attack may proceed deep under the surface, thus contributing little to the wetting properties of the surface.

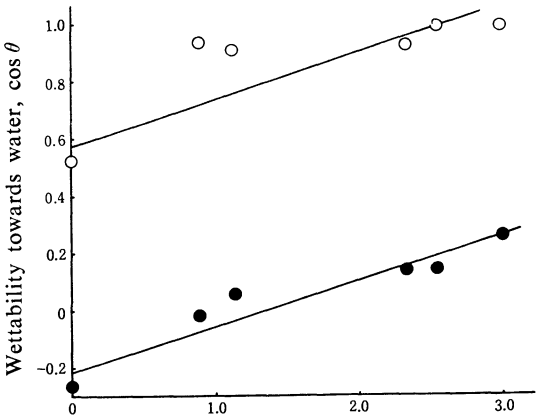


Fig. 5. Change of wettability with degree of surface attack of polystyrene.
○ Receding contact angle
● Advancing contact angle

The authors wish to express their thanks to the Ministry of Education for the Scientific Research Expenditure given to T. Sasaki. They also wish to thank the Asahi-Dow, Ltd., and the Mitsui Chemical Ind. Co. for the samples given to them.

Department of Chemistry
Faculty of Science
Tokyo Metropolitan University
Setagaya-ku, Tokyo

Dissolution and Anion Exchange Behavior of the Rare Earth Elements in Potassium and Ammonium Carbonate Solutions

By Tomitsugu TAKETATSU

(Received May 21, 1962)

It has been reported by several investigators[1-4] that tracer amounts of thorium and yttrium, as well as macro amounts of uranium(VI), thorium, cerium(IV) and beryllium, are firmly adsorbed on an anion exchange resin in a carbonate solution. No systematic studies of the dissolution of rare earth carbonates and of the anion exchange behavior of macro amounts of rare earth ions dissolved in a carbonate solution have yet been reported. In the present paper, however, the relation between the amounts of rare earth elements dissolved and the concentration of potassium or ammonium carbonate will be studied. Moreover, the minimum concentration of potassium or ammonium carbonate necessary to dissolve the precipitate of the rare earth carbonate completely will be determined, and the distribution coefficients (K_d) of rare earth ions between an anion exchange resin and a potassium or ammonium carbonate solution more concentrated than the minimum will be measured. The state of the dissolution and the anion exchange behavior of the rare earth elements will be discussed using these results.

Experimental

Standard solutions of rare earth elements were prepared by dissolving the oxides of the elements in dilute hydrochloric acid, while the concentrations of the rare earth ions were determined volumetrically with ethylenediaminetetraacetic acid (EDTA) by using Xylenol Orange as the indicator.

As the anion exchange resin, Dowex 1, X-8 in carbonate form, of a 50~100 mesh, was used.

All the other chemicals used were of analytical reagent grade.

The measurements of the amounts of rare earth elements dissolved and of the distribution coefficients K_d, of rare earth ions between an anion exchange resin and a potassium or ammonium carbonate solution were carried out as follows:

A known amount of the rare earth solution was put into a glass-stoppered conical flask, and the solution was dried on a water bath to remove any excess hydrochloric acid. One hundred milliliters of a series of potassium carbonate solutions of various concentrations was added to the residue in the flask. The precipitate of basic rare earth carbonate was thereby formed. The flask was vigorously shaken by a mechanical shaker for an hour and left to stand overnight to dissolve the precipitate.

(A) When the precipitate was not dissolved completely, it was filtered with No. 5C Toyo filter paper. The precipitate on the filter paper was dissolved in dilute hydrochloric acid, and the solution was poured into a beaker. The rare earth ion in the solution was titrated with EDTA.

(B) When the precipitate was dissolved completely, one gram of the resin was added to the carbonate solution. After the solution had been shaken by a shaker for 3 to 4 hr., the resin was rapidly separated by suction from the solution with a glass filter and transferred into a column. The rare earth element adsorbed on the resin was eluted by dilute hydrochloric acid. Although at the beginning of the elution the resin bed was disturbed by the release of carbon dioxide, it gradually settled down and was packed in the column. This disturbance did not affect the elution, since only the rare earth ion was adsorbed on the resin. The amount of rare earth ion was determined by a method similar to that described above.

All the procedures in the case of ammonium carbonate solution were similar to those used for the potassium carbonate solution, except that, because of the instability of ammonium carbonate, a magnetic stirrer was used instead of a shaker to stir the solution.

All the experiments were carried out at room temperature, which was about 20°C.

Results and Discussion

The quantities of rare earth ions used in this experiment, as well as the quantities of thorium and uranyl ions used for comparison are shown in Table I.

Relation between the Concentration of Potassium or Ammonium Carbonate Added and the Amount of Rare Earth Carbonate Dissolved. —When an excessive amount of a potassium or ammonium carbonate solution was added to the rare earth chloride, the basic rare earth carbonate was precipitated; the precipitate was then dissolved partially or completely by shaking or stirring. The plots of the amounts of the rare earth ions dissolved against various concentrations of potassium and ammonium carbonate are shown in Figs. 1 and 2. The

1) T. Ishimori and H. Okuno, This Bulletin, **29**, 78 (1956).
2) N. Saito and T. Sekine, ibid., **30**, 561 (1957).
3) S. Misumi and T. Taketatsu, ibid., **32**, 877 (1959).
4) N. Saito and T. Sekine, *Nature*, **180**, 753 (1957).

TABLE I. QUANTITIES OF RARE EARTH, THORIUM AND URANYL IONS USED

Ions	Taken mg.	Concn. 10^{-4} mol./1.
La^{3+}	7.452	5.363
Ce^{3+}	7.546	5.385
Pr^{3+}	7.169	5.087
Nd^{3+}	7.056	4.891
Sm^{3+}	7.214	4.798
Gd^{3+}	7.772	4.942
Er^{3+}	10.424	6.232
Y^{3+}	4.208	4.732
Sc^{3+}	1.595	3.537
Th^{4+}	14.802	6.377
UO_2^{2+}	18.145	6.703

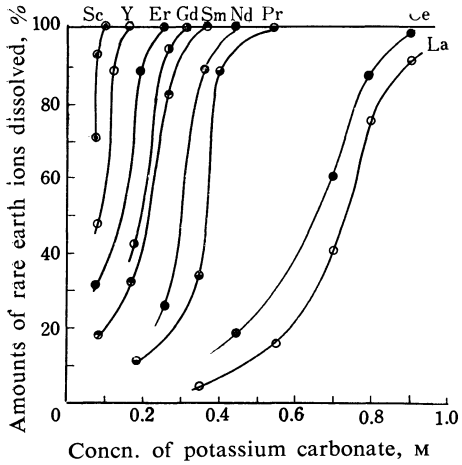


Fig. 1. Relation between the concentration of potassium carbonate and the amounts of rare earth ions dissolved.

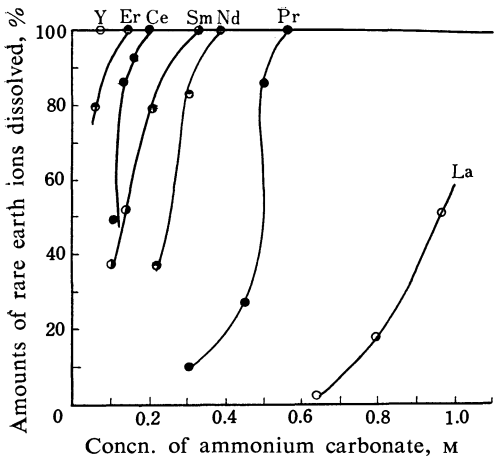


Fig. 2. Relation between the concentration of ammonium carbonate and the amounts of rare earth ions dissolved.

molar concentration of ammonium carbonate is represented by the molecular formula of $NH_4CO_2NH_2 \cdot NH_4HCO_3$, but the concentration is not accurate owing to the instability of ammonium carbonate.

From these results, it can be seen that the amounts of rare earth elements dissolved increase with the increase in the concentration of carbonate, and also with the increase in atomic number, except for cerium, yttrium and scandium. For example, the precipitates of praseodymium, neodymium, samarium, gadolinium, erbium, yttrium and scandium carbonates are dissolved completely in potassium carbonate solutions more concentrated than about 0.55, 0.45, 0.35, 0.30, 0.25, 0.15 and 0.10 M respectively. The precipitate of lanthanum carbonate could not be dissolved completely even in 1.0 M. As cerium is oxidized to the tetrapositive state in a potassium or ammonium carbonate solution, its behavior differs from that of other rare earth elements. In an ammonium carbonate solution more cnocentrated than 0.2 M, cerium is able to exist as stable orange-yellowish solution; on the other hand, in a potassium carbonate solution more concentrated than 0.4 M, it is dissolved completely

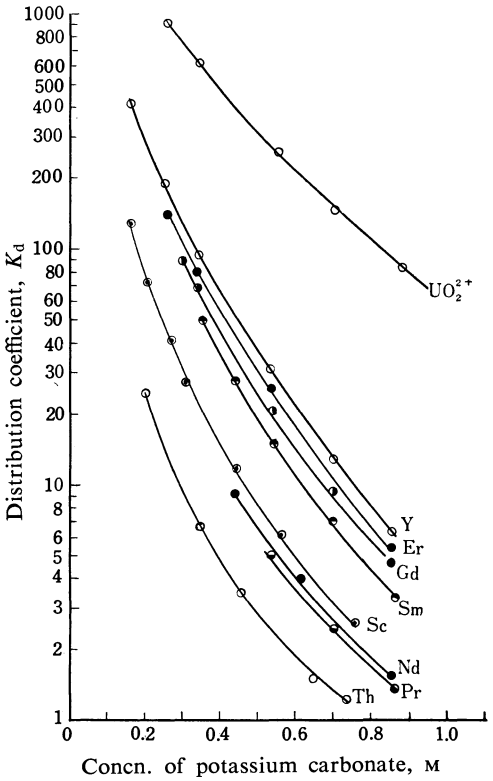


Fig.3. Distribution coefficient of rare earth and uranyl and thorium ions between Dowex 1 and potassium carbonate solution.

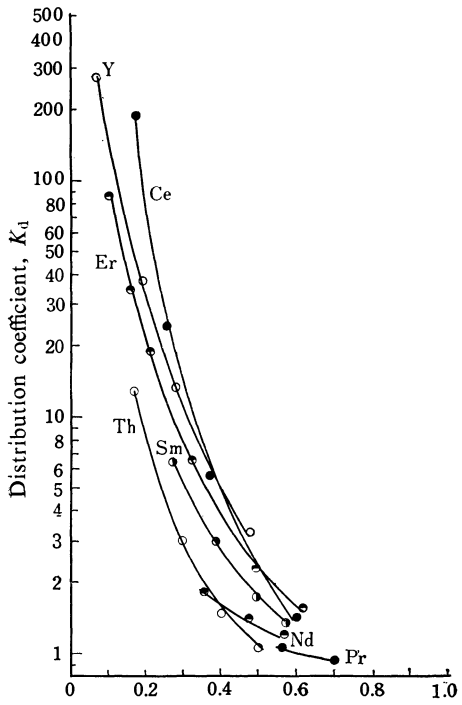


Fig. 4. Distribution coefficient of rare earth ions between Dowex 1 and ammonium carbonate solution.

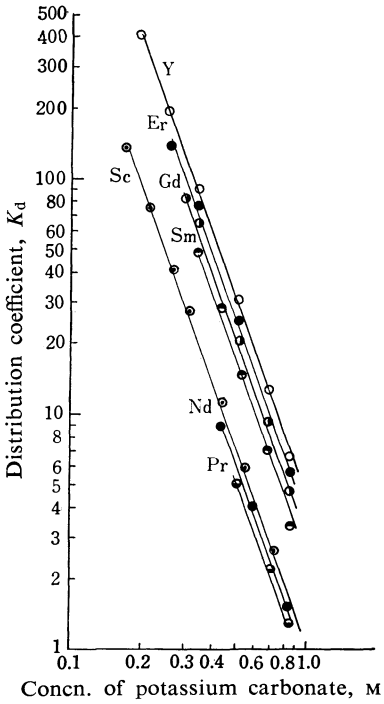


Fig. 5. Distribution coefficient of rare earth ions between Dowex 1 and potassium carbonate solution.

at first, although the precipitate of the carbonate is formed again when the solution is left over night.

Relation between the Adsorbabilities of the Rare Earth Elements and the Concentrations of Potassium and Ammonium Carbonate. — When the precipitates of rare earth carbonates were dissolved completely by the procedure described above, the anion exchange behavior of these elements was studied. The distribution coefficient, K_d, is given by:

$$K_d = [M_r]/[M_s] \quad \text{(ml./g.)}$$

where M_r and M_s represent the amount of rare earth ion in 1 g. of the resin and in 1 ml. of the solution respectively.

The plots of the distribution coefficients, K_d, of rare earth ions against various concentrations of potassium and ammonium carbonates are shown in Figs. 3 and 4. It can be seen that the adsorbability of rare earth elements decreases as the concentration of potassium or ammonium carbonate increases and that the order of the K_d values is Y> Er> Gd > Sm> Sc> Nd> Pr in a potassium carbonate solution. In an ammonium carbonate solution, the K_d value of tetrapositive cerium is larger than that of samarium and the slope of tetrapositive cerium is more similar to that of thorium than to the slopes of other rare earth elements. For purposes of comparison, the K_d values for uranyl and thorium ions in a potassium carbonate solution obtained by the same procedure as that for rare earth ion are shown in Fig. 3. From the distinct difference in the values of K_d, it is expected that the rare earth elements can be effectively separated from uranium(VI) and thorium(IV) by an anion exchange resin, with the potassium carbonate solution as the eluting agent.

A logarithmic diagram of the K_d values of rare earth ions against the concentrations of potassium carbonate is given in Fig. 5. Since the slope of the curve $\log K_d$ vs. $\log (CO_3^{2-})$ shows linearity and since the lines are parallel to one another with a negative slope, it has been concluded, according to a method developed by Kraus et al.[5] for determining the composition of metal complex species using an anion exchange resin, that the rare earth ions dissolved in a carbonate solution have an identical negative charge.

Summary

The amounts of rare earth elements dissolved in potassium and ammonium carbonate solutions of various concentrations have been

5) K. A. Kraus and F. Nelson, "Anion Exchange Studies of the Fission Products" in "Peaceful Uses of Atomic Energy", Proceedings of the International Conference in Geneva (United Nations) Vol. VII, (1955), p. 113.

determined. These amounts increase with the increase in the concentration of the carbonate and also with the increase in atomic number, except for cerium, yttrium and scandium. When the precipitates of the rare earth elements were completely dissolved in carbonate solutions more concentrated than a certain known concentration, the distribution coefficients, K_d, of the rare earth carbonate ions between an anion exchange resin of a carbonate form and potassium or ammonium carbonate solutions of various concentrations were determined. The values of K_d increased both with the decrease in the concentration of carbonate ions and with the increasing atomic number of the rare earth elements. Since the slopes of the curve $\log K_d$ vs. $\log(CO_3^{2-})$ in a potassium carbonate solution are found to be almost the same value for all the rare earth elements investigated, it has been concluded that the soluble complex of rare earth elements possesses an identical negative charge.

The author wishes to express his gratitude to Professor S. Misumi for his valuable discussions and encouragement.

General Education Department
Kyushu University
Otsubo-machi, Fukuoka

Influence of Substituent Groups on Nuclear Reactivity in the Formation of Substituted Biphenyls by Reaction of Aromatic Diazo and Related Compounds with Aromatic Liquids. V. Phenylation of Nitrobenzene and Anisole

By Takashi INUKAI, Katsumi KOBAYASHI and Osamu SIMAMURA

(Received May 22, 1962)

A semi-quantitative determination of the partial rate factors for nitrobenzene in the homolytic phenylation by phenyl radicals produced by decomposition of *N*-nitrosoacetanilide and of diazobenzene hydroxide was reported in Part I[1] of this series. Subsequent quantitative experiments[2] on various substiuted benzenes using column chromatography, spectrophotometry, etc., showed that the reactivity towards the phenylation differs rather slightly from compound to compound. Consequently for the comparison of the values of partial rate factors obtained from competitive phenylation to be significant it became necessary to improve the precision of the product analysis. We accordingly have adopted the radioisotope dilution analysis as reliable means accurate enough for the desired determination, and we now report the partial rate factors for phenylation of nitrobenzene and of anisole obtained by this method.

N-Nitrosoacet(anilide-^{14}C) was allowed to decompose in a large excess of a mixture of known amounts of benzene and nitrobenzene at 20°C. The reaction mixture was analyzed for biphenyl and the three isomeric nitrobiphenyls by the isotope dilution method. The results are presented in Table I. The results of a similar experiment in a mixture of benzene and anisole at 20°C are shown in Table II. The partial rate factors, the relative rates compared with the rate for benzene and the isomer distributions derived from the data shown in these tables are listed in Table III.

The high precision of the present analytical method is evident from the agreement of two independent determinations of the yield of biphenyl in any of the three experiments, as will be seen from the last columns of Tables I and II. Such an excellent agreement, however, was not observed in the partial rate factors for nitrobenzene calculated from the data of Exps. 1 and 2. This is deemed not due to defects in the analytical method, but apparently due to incontrollable minor fluctuations in experimental conditions, which we do not intend to study further for the present.

Recently Hey, Orman and Williams[3] redetermined the relative rate of the homolytic

1) O. Simamura, T. Inukai and M. Kanazashi, This Bulletin, **23**, 205 (1950).

2) O. Simamura, T. Inukai and M. Kurata, ibid., **25**, 76 (1952); O. Simamura and T. Migita, ibid., **27**, 228 (1954); and unpublished results.

3) D. H. Hey, S. Orman and G. H. Williams, *J. Chem. Soc.*, **1961**, 565.

TABLE I. ISOTOPE DILUTION ANALYSIS OF THE PRODUCTS FROM DECOMPOSITION OF *N*-NITROSOACET(ANILIDE-^{14}C) IN A MIXTURE OF BENZENE AND NITROBENZENE AT 20.0°C

Experiment 1: *N*-Nitrosoacetanilide (14.45±0.08 mc./mol.), 5.607 mmol.; Benzene, 666.7 mmol.; Nitrobenzene, 666.7 mmol.

Portion of the reaction mixture (133.697 g.)	Carrier added: Compound	Carrier added: mmol.	Specific activity of recovered material mc./mol.	Yield[a] mmol.
A (42.578 g.)	Biphenyl	6.472	0.286±0.002	0.410
	o-Nitrobiphenyl	8.540	0.629±0.006	1.230
	p-Nitrobiphenyl	5.484	0.492±0.005	0.606
B (45.335 g.)	Biphenyl	3.221	0.607±0.006	0.415
	m-Nitrobiphenyl	2.496	0.300±0.003	0.156

Experiment 2: *N*-Nitrosoacetanilide (14.18±0.07 mc./mol.), 1.844 mmol.; Benzene, 248.8 mmol.; Nitrobenzene, 275.7 mmol.

Portion of the reaction mixture (53.384 g.)	Carrier added: Compound	Carrier added: mmol.	Specific activity of recovered material mc./mol.	Yield[a] mmol.
A (27.062 g.)	Biphenyl	3.242	0.228±0.002	0.105
	o-Nitrobiphenyl	6.803	0.390±0.004	0.380
	p-Nitrobiphenyl	4.285	0.293±0.002	0.180
B (26.280 g.)	Biphenyl	3.197	0.226±0.002	0.105
	m-Nitrobiphenyl	2.535	0.124±0.002	0.0452

a) The amount of each compound in the total reaction mixture.

TABLE II. ISOTOPE DILUTION ANALYSIS OF THE PRODUCTS FROM DECOMPOSITION OF *N*-NITROSOACET(ANILIDE-^{14}C) IN A MIXTURE OF BENZENE AND ANISOLE AT 20.0°C

N-Nitrosoacetanilide (14.18±0.07 mc./mol.), 3.883 mmol.; Benzene, 231.4 mmol.; Anisole, 741.8 mmol.

Portion of the reaction mixture (98.296 g.)	Carrier added: Compound	Carrier added: mmol.	Specific activity of recovered material mc./mol.	Yield[a] mmol.
A (49.030 g.)	Biphenyl	3.204	0.514±0.004	0.249
	o-Methoxybiphenyl	7.089	0.892±0.008	0.954
	p-Methoxybiphenyl	4.013	0.299±0.003	0.173
B (48.904 g.)	Biphenyl	3.879	0.445±0.004	0.253
	m-Methoxybiphenyl	6.123	0.281±0.002[b]	0.249

a) The amount of each compound in the total reaction mixture.
b) The radiochemical assay was made on *m*-hydroxybiphenyl.

phenylation of nitrobenzene by phenyl radicals produced by decomposition of benzoyl peroxide and revised the former value[4], which was considered as a maximum value since it was based on results which may be subject to an error due to loss of rather volatile biphenyl during the course of the analysis. Obviously the isotope dilution analysis adopted in the present work is not liable to such errors due to fractionation of components to be determined. The revised value of 2.94 for the relative rate leads to new values for the partial rate factor of 5.5, 0.86 and 4.9 for the *o*-, *m*- and *p*-position, respectively, of nitrobenzene, whereas the present authors' corresponding values are 9.38, 1.16 and 9.05, respectively, for the phenylation by phenyl radicals produced by the decomposition of *N*-nitrosoacetanilide. The discrepancy between these two sets of values could be accounted for partly on the ground that, although both reactions are of the homolytic nature, the detailed mechanism may not necessarily be the same. But a more important cause is probably the difference in reaction temperature; the decomposition of *N*-nitrosoacetanilide was carried out at 20°C, whereas that of benzoyl peroxide at 80°C, and elevation of the reaction temperature would tend to change the partial rate factors towards unity, it being assumed that both reactions proceed

4) D. R. Augood, D. H. Hey and G. H. Williams, ibid., 1952, 2094.

TABLE III. PARTIAL RATE FACTORS, RELATIVE RATES AND ISOMER DISTRIBUTION IN PHENYLATION OF NITROBENZENE AND ANISOLE

Compound PhX		Partial rate factors			Relative rates	Isomer distribution of $C_6H_5C_6H_4X$, %		
		o	*m*	*p*		*o*	*m*	*p*
$PhNO_2$	Exp. 1	8.95	1.14	8.82	4.83	61.8	7.8	30.4
	Exp. 2	9.80	1.17	9.28	5.20	62.8	7.4	29.8
	Mean	9.38	1.16	9.05	5.02	62.3	7.6	30.1
PhOMe		3.56	0.93	1.29	1.71	69.3	18.1	12.6

by the same mechanism and that the frequency factor in the Arrhenius equation remains constant. Thus it is readily shown that partial rate factors $f(T_1)$ and $f(T_2)$, at two temperatures, T_1 and T_2, are related with each other by the following equation:

$$T_1 \log f(T_1) = T_2 \log f(T_2)$$

Substitution of the value for the partial rate factor of the *o*-position obtained by the *N*-nitrosoacetanilide reaction and of the corresponding value by the benzoyl peroxide reaction for $f(T_1)$ and $f(T_2)$ in this equation, respectively, gives 1.31 as the value for T_2/T_1, which should actually be $353/293=1.20$. A similar substitution of the values for the *p*-position gives 1.39. The approximate agreement of these values with the actual value seems to indicate the validity of this explanation for the observed difference in the partial rate factors, although the values for the meta position give no reasonable value for T_2/T_1. Huisgen and Grashey[5] quoted a value of 2.0 for the relative rate of phenylation of anisole by means of *N*-nitrosoacetanilide at 25°C. This value is fairly close to our value of 1.71. As there are no previous data for the partial rate factors for anisole available for comparison, we have calculated, similarly to Williams's calculation[6], the partial rate factors by using the free valence values, 0.422, 0.395 and 0.406 for the *o*-, *m*- and *p*-position of phenol, respectively, derived from Sandorfy's bond order values[7]. In adopting these values as the free valence values of anisole we have neglected the polar effect of the methyl group, which tends to lower the electronegativity of the oxygen atom. The predicted values for the partial rate factors at 20°C are 4.06, 0.84 and 1.60 for the *o*-, *m*- and *p*-position, which compare favourably with the present experimental values of 3.56, 0.93 and 1.29.

Although separate experiments[8] show that the abstraction of a hydrogen atom by aryl radicals produced from *N*-nitrosoacetanilides occurs only to a very limited extent in an aromatic compound which contains no reactive methyl group, in the decomposition of *N*-nitrosoacetanilide in a mixture of anisole and benzene the phenyl radicals generated should readily abstract a hydrogen atom from the methyl group of anisole resulting in the formation of benzene-^{14}C. To examine this probability the benzene recovered from the reaction mixture was nitrated with a mixture of fuming nitric acid and concentrated sulphuric acid, and the resulting *m*-dinitrobenzene was recrystallized from ethanol to give a specimen of a constant activity of 0.018 ± 0.001 mc./mol. This value corresponds to the production of 0.30 ± 0.02 mmol. of benzene-^{14}C, and shows that 15.4% of the phenyl radicals generated and accounted for as biphenyls and benzene gave benzene by abstracting a hydrogen atom.

Experimental

All melting points are corrected.

Materials.—Thiophene-free benzene was purified by repeated fractional freezing, m. p. 5.7°C. Nitrobenzene, prepared from the above benzene by nitration, was fractionally distilled and further purified by repeated fractional freezing, m. p. 5.7°C. Anisole was prepared by methylation of purified phenol and purified by distillation and fractional freezing, m. p. −37.5°C.

Commercial biphenyl was repeatedly recrystallized from 90% ethanol and sublimed under reduced pressure, m. p. 70°C.

Nitrobiphenyls and 4-methoxybiphenyl were prepared from the corresponding nitroanilines and anisidine by the Gomberg-Bachmann reaction[9] and purified by recrystallization from methanol; the melting points were: 2-NO_2, 37; 3-NO_2, 61; 4-NO_2, 113.5; and 4-MeO, 91°C.

2-Methoxybiphenyl was similarly prepared from *o*-anisidine, recrystallized twice from petroleum ether, and converted into 2-hydroxybiphenyl, m. p. 58.5°C (from petroleum ether), by heating (210~220°C, 16 hr.) with pyridine hydrochloride[10], and

5) R. Huisgen and R. Grashey, *Ann.*, **607**, 46 (1957).
6) G. H. Williams, "Homolytic Aromatic Substitution", Pergamon Press, Oxford (1960), p. 15.
7) C. Sandorfy, *Bull. soc. chim. France*, **1949**, 615.
8) T. Inukai, K. Kimura, O. Simamura and T. Suehiro, This Bulletin, **35**, 129 (1962); R. Itô, T. Migita and O. Simamura, to be published.
9) W. E. Bachmann and R. A. Hoffman, "Organic Reactions", Vol. II, John Wiley and Sons, Inc., New York, (1944), p. 247.
10) V. Prey, *Ber.*, **74**, 1219 (1941) **75**, 350 (1942).

this compound was methylated with dimethyl sulphate again to afford pure 2-methoxybiphenyl, m. p. 32°C (from methanol).

3-Methoxybiphenyl was prepared from 3-nitrobiphenyl by reduction to 3-aminobiphenyl (b. p. 187~188°C/18 mmHg), diazotization and hydrolysis in diluted sulphuric acid at 65°C to give 3-hydroxybiphenyl, m. p. 76.8°C (from petroleum ether), which was then methylated with dimethyl sulphate to afford pure 3-methoxybiphenyl, b. p. 159°C (12 mmHg), a colourless oil.

N-Nitrosoacet(anilide-^{14}C) was prepared from benzene-1-^{14}C (The Radiochemical Centre, Amersham) by nitration and catalytic reduction to aniline followed by acetylation and finally by nitrosation of the resulting acetanilide. The experimental procedure is described elsewhere[11].

Decomposition of *N*-Nitrosoacet(anilide-^{14}C) in a Mixture of Benzene and Nitrobenzene.—The results are tabulated in Table I. *N*-Nitrosoacet-(anilide-^{14}C) with a specific activity of 14.45 mc./mol., (920.42 mg., 5.607 mmol.) was dissolved in a mixture of 52.0 g. of benzene (666.7 mmol.) and 82.0 g. of nitrobenzene (666.7 mmol.) maintained at 20.0°C in a thermostat and allowed to decompose until at last the nitrogen evolved reached a final value of 68% of the theoretical. A portion (A, 42.578 g.) was weighed out from the reaction mixture (133.697 g.), and to this portion were added 0.9975 g. (6.472 mmol.) of biphenyl, 1.7011 g. (8.540 mmol.) of *o*-nitrobiphenyl, and 1.0924 g. (5.484 mmol.) of *p*-nitrobiphenyl. From the resulting solution benzene and nitrobenzene were removed under reduced pressure. The residue was distilled through a Vigreux column 15 cm. in height giving a biphenyl fraction, b. p. 117~120°C (6.5 mmHg), an *o*-nitrobiphenyl fraction, b. p. 140~150°C (5 mmHg), and a *p*-nitrobiphenyl fraction, b. p. 155~160°C (5 mmHg). Biphenyl and *o*-nitrobiphenyl were purified by chromatography on activated alumina in petroleum ether, and *p*-nitrobiphenyl was purified by chromatography on acetivated alumina in 1 : 1 mixture of petroleum ether and benzene. Another portion (B, 45.335 g.) was taken from the original reaction mixture, and to this portion were added 0.4962 g. (3.221 mmol.) of biphenyl and 0.4972 g. (2.496 mmol.) of *m*-nitrobiphenyl. The mixture was worked up as above, that is, by distillation to give a biphenyl and a *m*-nitrobiphenyl fraction and by chromatography of these fractions on activated alumina in petroleum ether. The two specimens of biphenyl from portion A and portion B were finally purified by repeated recrystallizations from 90% ethanol and sublimation under vacuum (1~2 mmHg). Nitrobiphenyls were further purified by recrystallization from methanol. The purification was deemed complete when the specific activity of a specimen remained constant on further recrystallization. A second experiment was carried out in a similar way.

Decomposition of *N*-Nitrosoacet(anilide-^{14}C) in a Mixture of Benzene and Anisole.—The results are summarized in Table II. *N*-Nitrosoacet(anilide-^{14}C) with a specific activity of 14.18 mc./mol., (637.43 mg., 3.883 mmol.), was dissolved in a mixture of 18.08 g. of benzene (231.4 mmol.) and 80.22 g. of anisole (741.8 mmol.) and allowed to decompose at 20.0°C; nitrogen evolved amounted to 82.5% of the theoretical value. Two portions (A, 49.030 g., and B, 48.904 g.) were weighed out from the reaction mixture (98.296 g.). To portion A were added 0.4942 g. (3.204 mmol.) of biphenyl, 1.3061 g. (7.089 mmol.) of 2-methoxybiphenyl, and 0.7393 g. (4.018 mmol.) of 4-methoxybiphenyl, and from the resulting solution benzene and anisole were removed under reduced pressure. The residue was dissolved in a mixture of petroleum ether and benzene (4 : 1), and subjected to chromatography on activated alumina in petroleum ether to afford biphenyl, 2-methoxybiphenyl and 4-methoxybiphenyl by elution with petroleum ether (b. p. 40~60°C). To portion B above were added 0.5982 g. (3.879 mmol.) of biphenyl and 1.1281 g. (6.123 mmol.) of 3-methoxybiphenyl, and from the resulting solution benzene and anisole were removed under reduced pressure. The residue was chromatographed on activated alumina in petroleum ether to give biphenyl and 3-methoxybiphenyl. The specimens of biphenyl from portions A and B were purified by recrystallization and sublimation as in the experiments in a mixture of nitrobenzene and benzene. 2- and 4-Methoxybiphenyl were purified by repeated recrystallizations from methanol. The oily 3-isomeride was converted into 3-hydroxybiphenyl by heating with pyridine hydrochloride, and this was purified by repeated recrystallizations from petroleum ether to a constant activity of 0.281±0.002 mc./mmol.

Radioactivity Determination.—Radiocarbon assays were carried out by oxidizing samples according to the method of Van Slyke and Folch[12] and by converting the resulting carbon dioxide into barium carbonate, the activity of which was then counted with an end-window Geiger-Müller counter on an "infinitely thick" layer.

Summary

N-Nitrosoacet(anilide-^{14}C) has been decomposed at 20°C in a mixture of benzene with nitrobenzene or with anisole, and the reaction products have been analyzed for biphenyl and isomeric nitrobiphenyls or isomeric methoxybiphenyls by isotope dilution method. From these results the partial rate factors for the phenylation have been calculated to be for nitrobenzene: *o*, 9.38; *m*, 1.16; and *p*, 9.05; and for anisole: *o*, 3.56; m, 0.93; and *p*, 1.29.

Department of Chemistry
Faculty of Science
The University of Tokyo
Hongo, Tokyo

11) H. Koyama, N. Morikawa, T. Migita, R. Itô and G. Tsuchihashi, *Radioisotopes (Tokyo)*, **9**, 112 (1960).

12) D. D. Van Slyke and J. Folch, *J. Biol. Chem.*, **136**, 509 (1940).

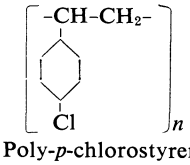
The Solution Behavior of Polystyrene Derivatives: Poly-p-chlorostyrene

By Takahide SAITO

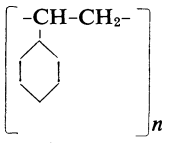
(Received May 23, 1962)

It has been revealed by the studies of the viscosity and light-scattering characteristics of polymers that the solution behavior of polymers is, in general, affected by the polarity of the solvent, the branching of the polymer, the structure and the configuration of the monomer unit, etc. Therefore, it has been interesting for the present author to study the solution properties of polystyrene derivatives, especially the effects of the variation in monomer structure on their solution behavior.

In this paper the viscosity and light-scattering characteristics of poly-*p*-chlorostyrene in butanone and in toluene have been compared with those of polystyrene.



Poly-*p*-chlorostyrene



Polystyrene

Experimental

Materials. — *p*-Chlorostyrene[1],* was redistilled under reduced pressure (b. p., 69.0°C/20 mmHg) before use. The monomer (ca. 70 g.) was sealed in a glass tube and polymerized without an initiator for 48 hr. at 100°C. Then the polymerization product was dissolved in butanone, and the polymer was precipitated with methanol. Reprecipitation was carried out twice, and, after being washed with methanol, the polymer was dried under reduced pressure. The conversion rate was about 87%.

Butanone was refluxed with potassium permanganate for one day in order to oxidize some organic impurities. The butanone distilled from this mixture was dried with potassium carbonate for a week and then redistilled. The fraction (b. p., 79.5~80.0°C) was used. Toluene was washed successively with sulfuric acid, water, a dilute solution of sodium hydroxide, and finally again with water until it was neutralized. It was then dried with metallic sodium and distilled. The fraction which distilled at 110.0~110.5°C was used.

The sample of poly-*p*-chlorostyrene was divided into two parts; each part was independently fractionated as follows: About 20 g. of polymer was dissolved in one liter of butanone. Ten fractions were fractionally precipitated with methanol by the successive precipitation method at 35°C. Each fraction was redissolved in butanone and was precipitated to eliminate the part with a lower molecular weight. Seven fractions were used for the measurements in butanone, and six in toluene.

Measurements.—The solutions for the light-scattering and viscosity studies were rendered free from dust by centrifuging for one hour at 20000 g., using a "Spinco Ultra Centrifuge, Type E" and were filtered into the light-scattering cell or into the reservoir of the viscometer, through a sintered glass filter No. 5, just before the measurements. The viscosity measurements were carried out on the butanone solutions at 25°C and on the toluene solutions at 30°C. A conventional Ubbelohde viscometer was modified so that successive dilution could be performed. The intrinsic viscosity, $[\eta]$, and the Huggins constant, k', were obtained according to the equation:

$$\eta_{sp}/C=[\eta]+k'[\eta]^2C$$

where η_{sp} is the specific viscosity and C is the concentration of polymer in g./100 ml.

An Aminco photometer[2] was used for the measurements of the light scattering. Measurements covering the angular range of 30~140° were performed at room temperature; the wavelengths used for the measurements were 436 mμ and 546 mμ. The weight-average molecular weight, M_w, the second virial coefficient, A_2, and the z-average-root-mean-square-end-to-end distance, $<D^2>_z^{1/2}$, were calculated, using the Zimm plot, according to the equations:

$$KC/R_\theta=1/M_wP(\theta)+2A_2CP(\theta)$$

$$K=2\pi^2n_0^2(dn/dc)^2/N_A\lambda^4$$

where

$P(\theta)$: the factor expressing the reduction in scattered intensity at angle θ
λ : the wavelength of light in vacuum
N_A : Avogadro's number
R_θ : Rayleigh ratio at angle θ

R_θ is calculated according to the equation[3]:

$$R_\theta=(n_0^2/\pi h)\,Y(G_\theta/G_0^p)S_dXV$$

where

G_θ: the galvanometer reading at angle θ
G_0^p: the galvanometer reading at angle 0° when the incident beam falls to photo tube through the opal-glass standard diffuser located at the center of the cell holder
S_d: the transmittance of the opal-glass standard diffuser,
T : the total transmittance of the neutral filters used in measuring G_0^p

* The monomer used was synthetized by the author of Ref. 1.

1) A. Kotera, *Chem. High Polymer*, **1**, 1 (1944).

2) G. Oster, *Anal. Chem.*, **25**, 1165 (1953).

3) D. K. Carpenter and W. R. Krigbaum, *J. Chem. Phys.*, **24**, 1041 (1956).

h : the width of the slit of the receiver
n_0 : the refractive index of pure solvent
X : a calculation constant determined by the Rayleigh ratio of benzene, 48.5×10^{-6}
V : the volume correction approximated by $1/\sin\theta$

The values of dn/dc, the increments of the refractive index of the solution with concentration, were determined by a Zeiss interferometer to be 0.212 ml./g. in butanone and 0.106 ml./g. in toluene at room temperature.

Results and Discussion

Results.—The plots of the reduced viscosity, η_{sp}/C, vs. the concentration, C, in butanone and in toluene are shown in Figs. 1 and 2 respectively, and the intrinsic viscosity, $[\eta]$, and the Huggins constant, k', are determined from these plots. The Zimm plots for A–6 in butanone and B 2–2 in toluene are shown in Figs. 3 and 4 as examples of the light-scattering measurements. The weight-average molecular weight, M_w, the second virial coefficient, A_2, and the z-average-root-mean-square-end-to-end distance, $\langle D^2\rangle_z^{1/2}$, for each fraction are determined from these figures.

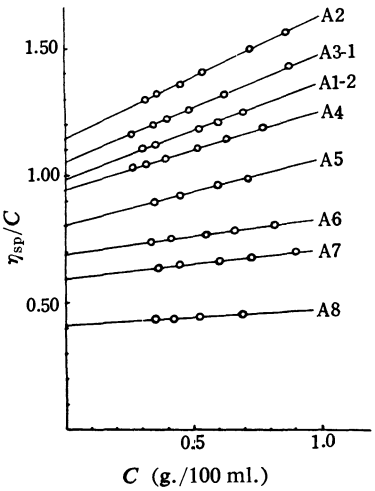


Fig. 1. Relation between reduced viscosity and concentration of poly-*p*-chlorostyrene in butanone at 25°C.

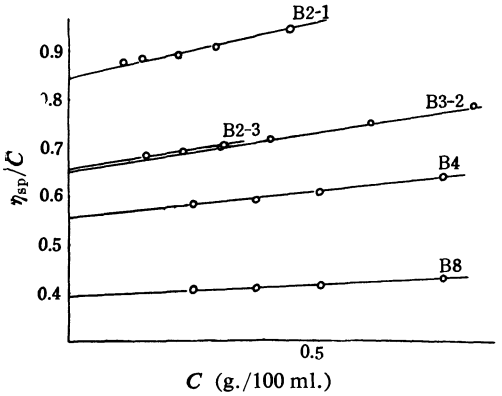


Fig. 2. Relation between reduced viscosity and concentration of poly-*p*-chlorostyrene in toluene at 30°C.

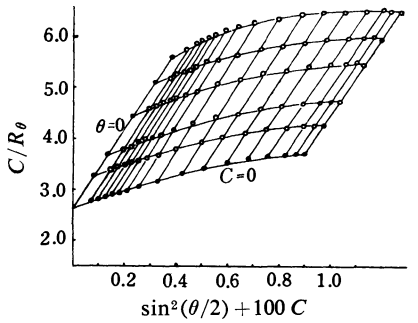


Fig. 3. Zimm plot of poly-*p*-chlorostyrene fraction A 6 in butanone for $\lambda=436$ mμ.

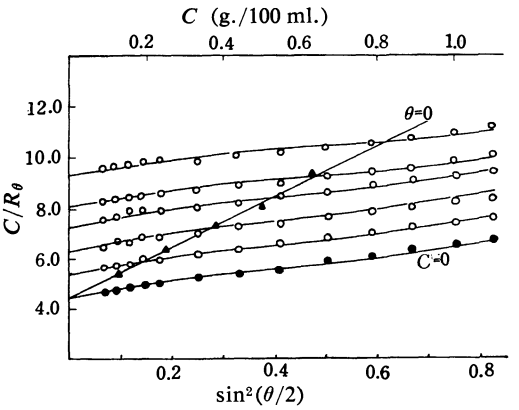


Fig. 4. Incomplete Zimm plot of poly-*p*-chlorostyrene fraction B 2-2 in toluene for $\lambda=436$ mμ. Upper abscissa shows concentration and lower abscissa shows $\sin^2(\theta/2)$. Plots of C/R_θ vs. concentration for each angle except a line for $\theta=0°$ are not shown in this figure.

The results of the viscosity and light-scattering measurements in butanone and in toluene are summarized in Tables I and II respectively.

The molecular weight (degree of polymerization) dependences of the intrinsic viscosity, $[\eta]$, the z-average-root-mean-square-end-to-end distance, $\langle D^2\rangle_z^{1/2}$, and the second virial coefficient, A_2, are usually represented by the equations:

$$[\eta]=KM_w^{\alpha} \tag{1}$$

$$\langle D^2\rangle_z^{1/2}\sim M_w^{\beta} \tag{2}$$

$$A_2\sim M_w^{\gamma} \tag{3}$$

where the constants, K, α, β and γ, are experimentally determined from a plot of $\log X$ against $\log M_w$ (or $\log P$), where X is $[\eta]$, A_2,

TABLE I. THE EXPERIMENTAL RESULTS OF POLY-*p*-CHLOROSTYRENE IN BUTANONE. THE VALUES OF M_w, A_2 AND $<D^2>_z^{1/2}$ ARE DETERMINED BY THE LIGHT SCATTERING MEASUREMENTS AND ARE AVERAGE ON THE RESULTS AT TWO WAVELENGTHS, 436 AND 546 mμ

Fraction	$[\eta]$	k'	$M_w\times10^{-4}$	$A_2\times10^4$	$<D^2>_z^{1/2}$ mμ	$\Phi\times10^{-21}$
A 1-2	0.986	0.38	110	1.5_0	130	1.6
A 2	1.114	0.40	115	1.3_0	127	1.6
A 3-1	1.051	0.39	101	1.4_0	114	1.5
A 4	0.940	0.36	76	1.7_0	101	1.4
A 6	0.688	0.33	49	2.5_7	78	1.4
A 7	0.592	0.32	36	1.7_7	68	1.5
A 8	0.410	0.36	31	2.1_8	63	2.0

Notation; M_w : Weight average molecular weight
A_2 : Second virial coefficient
$<D^2>_z^{1/2}$: Root-mean-square-end-to-end distance
k' : Huggins constant
Φ : Flory parameter
$[\eta]$: Intrinsic viscosity

TABLE II. THE EXPERIMENTAL RESULTS OF POLY-*p*-CHLOROSTYRENE IN TOLUENE. THE VALUES OF M_w, A_2 AND $<D^2>_z^{1/2}$ ARE DETERMINED BY THE LIGHT SCATTERING MEASUREMENTS FOR 436 mμ

Fraction	$[\eta]$	k'	$M_w\times10^{-4}$	$A_2\times10^4$	$<D^2>_z^{1/2}$ mμ	$\Phi\times10^{-21}$
B 2-1	0.847	0.31	102	0.7_0	95	1.0
B 2-2	0.850		99	0.7_0	93	
B 2-3	0.658	0.37	75	0.8_0	78	1.0
B 3-2	0.652	0.38	66	0.9_0	75	1.0
B 3-4	0.556	0.34	47	1.1_0	57	1.4
B 8	0.395	0.29	33		49	1.1

The notations used in this table are the same as those used in Table I.

or $<D^2>_z^{1/2}$ *. The log-log plots of the intrinsic viscosity, the second virial coefficient and the end-to-end distance against the molecular weight are shown in Figs. 5, 6 and 7 respectively.

Equations 1, 2 and 3 for poly-*p*-chlorostyrene are

$[\eta]=2.9_4\times10^{-4}M_w^{0.59}$ in butanone at 25°C
$[\eta]=1.2_8\times10^{-4}M_w^{0.64}$ in toluene at 30°C
$<D^2>_z^{1/2}\sim M_w^{0.55}$ in butanone
$<D^2>_z^{1/2}\sim M_w^{0.60}$ in toluene
$A_2\sim M_w^{-0.17}$ in butanone
$A_2\sim M_w^{-0.40}$ in toluene

Discussion.—A solvent, the polymer solution of which shows a higher value of A_2, $<D^2>_z^{1/2}$ or $[\eta]$, is called a "*good*" solvent. In the case of poly-*p*-chlorostyrene, butanone is considered to be a better solvent than toluene according to this definition, because poly-*p*-chlorostyrene in the former solvent shows higher values of A_2 and of $<D^2>_z^{1/2}$ than in the latter.

To discuss the influence of the substituent in the para position of the benzene ring on the solution behavior, the constants, K, α, β and γ, for poly-*p*-chlorostyrene and polystyrene

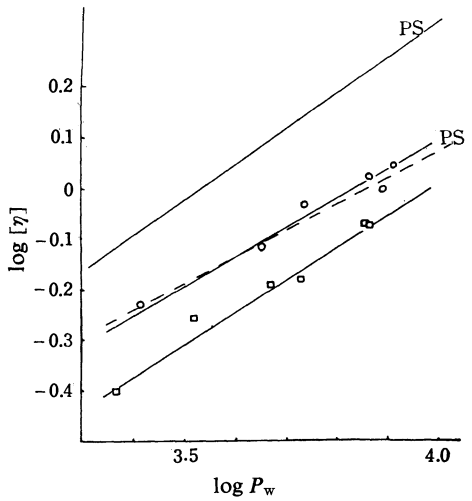


Fig. 5. Plot between intrinsic viscosity and degree of polymerization.
—PS : Polystyrene-toluene
- - -PS : Polystyrene-butanone
-□- : Poly-*p*-chlorostyrene-toluene
-○- : Poly-*p*-chlorostyrene-butanone

* The value shown as $<D^2>_z^{1/2}$ gives the length $\sqrt{6}$ times as long as the root-mean-square radius of gyration, and it gives the end-to-end distance only in the case of the Gaussian chain. For convenience, however, the value is used as a relative measure of chain extension in the case of the non-Gaussian chain also.

TABLE III. COMPARISON OF THE DEPENDENCES OF SOLUTION BEHAVIORS ON MOLECULAR WEIGHT FOR POLYSTYRENE AND POLY-*p*-CHLOROSTYRENE IN BUTANONE AND TOLUENE

Solvent	Polymer	$K\times10^4$	α	β	γ
Butanone 25°C	Poly-*p*-chlorostyrene	2.9	0.59	0.55	−0.17
	Polystyrene	3.9	0.58	0.58	−0.23
Toluene 30°C	Poly-*p*-chlorostyrene	1.2	0.64	0.60	−0.40
	Polystyrene	1.3	0.70	0.68	−0.33

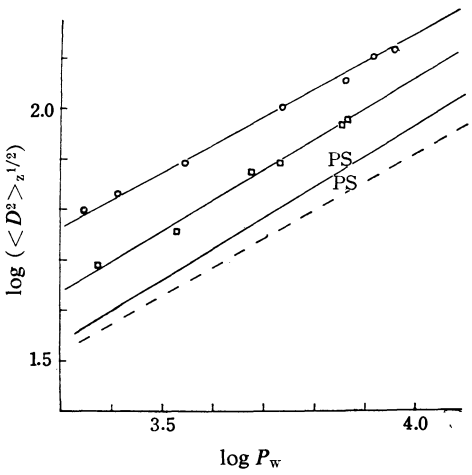


Fig. 6. Comparison of extensions of chain for poly-*p*-chlorostyrene in toluene and butanone with those of polystyrene at the same degree of polymerization.

-□-: Poly-*p*-chlorostyrene-toluene
-○-: Poly-*p*-chlorostyrene-butanone
—PS: Polystyrene-toluene
- - -PS: Polystyrene-butanone

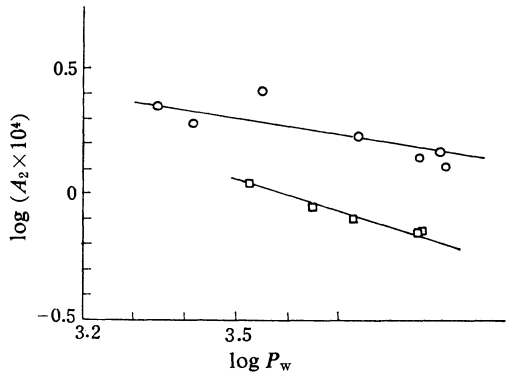


Fig. 7. Relation between second virial coefficient and degree of polymerization of poly-*p*-chloro-styrene.

-□-: Poly-*p*-chlorostyrene-toluene
-○-: Poly-*p*-chlorostyrene-butanone

are summarized and compared in Table III **.

The values of the K, α, β and γ of poly-*p*-chlorostyrene are nearly the same as those of polystyrene.

Moreover, some interesting results in their solution behavior may be deduced from a detailed comparison. (1) The value of the $[\eta]$ of poly-*p*-chlorostyrene in toluene is smaller than that of polystyrene. (2) The $[\eta]$ of polystyrene in butanone is nearly the same as that of poly-*p*-chlorostyrene. (3) The values of the $\langle D^2\rangle_z^{1/2}$ of polystyrene in butanone and toluene are all smaller than those of poly-*p*-chlorostyrene. (4) The values of $[\eta]$ and $\langle D^2\rangle_z^{1/2}$ for poly-*p*-chlorostyrene in toluene are smaller than those in butanone.

Generally speaking, it is not exact to define a solvent as a "*good*" or "*bad*" solvent only on the basis of a comparison of the chain extensions of various polymers in a solvent regardless of differences in their structures. However, when the basic structures of the chain molecules are similar to one another, a comparison of the chain extensions in a solvent may be used as a relative measure of the effects of solvent on polymer configurations.

On the basis of the third result described above, it may be said that both butanone and toluene act as better solvents for poly-*p*-chlorostyrene than polystyrene.

To show this result more clearly, the ratio for polystyrene and poly-*p*-chlorostyrene of $\langle D^2\rangle_z^{1/2}$ to D_f, where D_f is the end-to-end distance, assuming a free rotation model for the chain configuration, are compared in Table IV at the weight-average degree of polymerization of $p_w=10^4$. To obtain quantitative information on the effect of the solvent on chain extension, it is necessary to take, as a parameter to be used for comparison, a ratio of $\langle D^2\rangle_z^{1/2}/\langle D_0^2\rangle_z^{1/2}$ instead of $\langle D^2\rangle_z^{1/2}/D_f$,

** The formulas which have been reported for the dependence of the intrinsic viscosity of polystyrene are;

$[\eta]=1.7\times10^{-4}M_w^{0.69}$ in toluene at 25°C[4]
$[\eta]=1.2\times10^{-4}M_w^{0.71}$ in toluene at 30°C[5]
$[\eta]=0.92\times10^{-4}M_w^{0.74}$ in toluene at 30°C[6]
$[\eta]=3.9\times10^{-4}M_w^{0.58}$ in butanone at 25°C[4]
$[\eta]=2.3\times10^{-4}M_w^{0.62}$ in butanone at 30°C[7]

The equation quoted in Table III seems to be appropriate with regard to the temperature and to the measured range of the molecular weight.

4) P. Outer, C. I. Carr and B. H. Zimm, *J. Chem. Phys.*, **18**, 830 (1950).
5) T. Oyama and K. Kawahara, *J. Chem. Soc. Japan, Pure Chem. Sec. (Nippon Kagaku Zassi)*, **78**, 484 (1957).
6) S. N. Chinai et al., *J. Polymer Sci.*, **22**, 527 (1956).
7) T. Oyama and K. Kawahara, *J. Chem. Soc. Japan, Pure Chem. Sec. (Nippon Kagaku Zassi)*, **79**, 727 (1958).

TABLE IV. VALUES OF $<D^2>_z^{1/2}/D_f$ FOR POLYSTYRENE AND POLY-*p*-CHLOROSTYRENE IN BUTANONE AND TOLUENE AT $P_w=10^4$. VALUES OF POLYSTYRENE ARE CALCULATED FROM THE DATA IN REFS. 4 AND 5.

Polymer	$<D^2>_z^{1/2}/D_f$ Solvent	
	Butanone	Toluene
Poly-*p*-chlorostyrene	3.23	2.65
Polystyrene	1.86	2.14

where $<D_0^2>_z^{1/2}$ is a z-average-root-mean-square-end-to-end distance of an unperturbed chain, because the unperturbed extension of polymer molecules with different structures varies according to differences in the dipole-dipole interaction and in the steric effects of the substituents. However, even though the values of $<D^2>_z^{1/2}/D_f$ are directly related to the effects of solvents on the polymer configuration in solution, it should be noted that the dimensions of poly-*p*-chlorostyrene in butanone are particularly extensive compared with the dimensions of poly-*p*-chlorostyrene in toluene and/or of polystyrene in toluene and butanone.

According to Flory and Fox, the relation between the intrinsic viscosity and the end-to-end distance for a linear polymer may be expressed as follows:

$$[\eta]=\Phi\frac{<D^2>_z^{3/2}}{M_w} \qquad (4)$$

where Φ is defined as an universal constant independent of the temperature, solvent and basic structure of the polymer[8]. Therefore, when Φ is a constant regardless of the solvent, the same tendencies must exist in the relations between $[\eta]$ and solvents as in the case of $<D^2>_z^{1/2}/D_f$. However, the experimental results with reference to the intrinsic viscosity which are summarized above as results 1 and 2 are not in accord with result 3. These conflicting results are substantially derived from the differences of the Φ of poly-*p*-chlorostyrene in the two solvents, as is shown in Tables I and II. The author can not explain at present why the values of Φ in the two solvents differ.

8) P. J. Flory and T. Fox, *J. Phys. Chem.*, 53, 197 (1957).

Summary

The polar group in the para position of the benzene ring of poly-*p*-chlorostyrene has a remarkable influence on the solution behavior and that, especially, the chain in the polar solvent is particularly extensive because of the interaction between the C–Cl group in the para position and the polar solvent.

The author is deeply grateful to Professor Akira Kotera and Professor Keizo Suzuki for their helpful suggestions and discussion. He also wants to thank Dr. Hideomi Matsuda and Dr. Yuji Miyazawa, who made some of the measurements of viscosity and light scattering, and Miss Michiko Takahashi, who made the centrifuging of the solutions, for their kindness. This research was supported in part by a Scientific Research Encouragement Grant from the Ministry of Education, to which the author's thanks are due.

Department of Chemistry
Faculty of Science
Tokyo University of Education
Otsuka, Tokyo

Electronic Interactions between Molecules and Atoms (Radicals) Involving Excited States

By Yuji MORI

(Received February 21, 1961)

A number of reactions can be discussed from the standpoint of the potential-energy surface[1]. The chemical reactivity of conjugated molecules for a radical attack can sometimes be interpreted in terms of the enegy change of the ground state of the system arising from the radical attack[2]. The quenching of excited (^{2}P) sodium by a molecule is interpreted on the basis of the potential-energy surfaces[3] of the system, involving the excited state of the sodium

1) S. Glasstone, K. J. Laidler and H. Eyring, "The Theory of Rate Processes", McGraw-Hill Book Co., Inc., New York (1941).

2) R. D. Brown, *J. chim. phys.*, **50**, 109 (1953).

3) K. J. Laidler, "Chemical Kinetics of Excited States", Oxford University Press, London (1955).

atom. In the present paper the chemical reactivity of conjugated molecules and the quenching of excited sodium will be discussed on the basis of the electronic structures of the molecules by giving the energy change for a radical attack or the potential-energy surfaces of the system. The importance of the lowest triplet states of molecules in their chemical reactivity to a radical attack, in addition to the role of the electron-transfer states in the quenching of excited sodium, will be discussed.

In previous papers[4,5], the present author has given a theoretical interpretation of the electronic spectrum of the benzyl radical under the assumption that the benzyl radical is composed of a benzene ring and a methylene radical. Since the electronic system, composed of an atom (or a radical) and a molecule, is similar to that of the benzyl radical, a theoretical treatment similar to those of the previous papers will be undertaken in the present work.

Wave Functions

The configurational wave functions of the whole system can be written as follows:

a) Doublet states ($M_S=+1/2$)

$$\Psi_0=\phi_0\cdot\chi_0^\alpha$$

$$\Psi_S(i-l)=\phi_s(i-l)\cdot\chi_0^\alpha$$

$$\Psi_T^1(i-l)=1/\sqrt{3}\{\phi_i^0(i-l)\cdot\chi_0^\alpha-\sqrt{2}\phi_i^1(i-l)\cdot\chi_0^\beta\}$$

$$\Psi_X=\phi_0\cdot\chi_1^\alpha$$

$$\Psi_C(i-\chi_0)=(1^\alpha1^\beta\cdots\cdots i^\alpha\cdots\cdots n^\alpha n^\beta\chi_0^\alpha\chi_0^\beta)$$

$$\Psi_C(\chi_0-l)=(1^\alpha1^\beta\cdots\cdots n^\alpha n^\beta l^\alpha)$$

b) Quartet states ($M_S=+3/2$)

$$\Psi_T^2(i-l)=\phi_i^1(i-l)\cdot\chi_0^\alpha$$

where $\phi_s(i-l)$, $\phi_i^0(i-l)$ and $\phi_i^1(i-l)$ are the wave functions of the excited states of the molecule, in which one electron has been excited from an occupied MO (i) to a vacant MO (l).

$$\phi_0=(1^\alpha1^\beta\cdots\cdots i^\alpha i^\alpha\cdots\cdots n^\alpha n^\beta)$$

$$\phi_s(i-l)=1/\sqrt{2}\{(1^\alpha1^\beta\cdots\cdots i^\alpha l^\beta\cdots\cdots n^\alpha n^\beta)-(1^\alpha1^\beta\cdots\cdots i^\beta l^\alpha\cdots\cdots n^\alpha n^\beta)\}$$

$$\phi_i^0(i-l)=1/\sqrt{2}\{(1^\alpha1^\beta\cdots\cdots i^\alpha l^\beta\cdots\cdots n^\alpha n^\beta)+(1^\alpha1^\beta\cdots\cdots i^\beta l^\alpha\cdots\cdots n^\alpha n^\beta)\}$$

$$\phi_i^1(i-l)=(1^\alpha1^\beta\cdots\cdots i^\alpha l^\alpha\cdots\cdots n^\alpha n^\beta)$$

The abbreviations are as follows:

i: an occupied MO of the molecule
l: a vacant MO of the molecule
χ_0: the singly occupied orbital in the ground state of the atom (or the radical)
χ_1: an excited orbital of the atom

In the above wave functions, Ψ_0, $\Psi_S(i-l)$, $\Psi_T^1(i-l)$ and Ψ_X correspond to the ground state, the excited singlet state $\phi_s(i-l)$, the triplet state $\phi_t(i-l)$ and the excited state of the atom respectively. $\Psi_T^2(i-l)$ corresponds to the triplet state. $\Psi_C(i-\chi_0)$ and $\Psi_C(\chi_0-l)$ show the electron-transfer configurations from i to χ_0 and from χ_0 to l respectively.

The energies and wave functions of the resulting states of the whole system can be given by solving the secular determinant. However, in order to avoid complications, a simplification of the treatment will be undertaken.

Reactivity of Conjugated Molecules

The object in this section is to find the energy change of the ground state of the whole system arising from interaction, relative to that in a large intermolecular distance where there is no interaction between the molecule and the radical.

In some theories of the chemical reactivity of conjugated molecules which have dealt with the energy of the reacting system by explicitly taking into account the interaction between the molecule and the radical[2,6], only the effect of the electron transfer has been discussed; no discussion has been given of the effect of the exchange of electrons. It is supposed that interaction by exchange of electrons between the molecule and the radical is as important as that by electron transfer, because the bond between the molecule and the radical may have the character of a σ-bond rather than of a π-bond in the activated complex.

From this viewpoint, the problem will be treated by taking into account the following configurational wave functions of the whole system:

$$\Psi_0,\ \Psi_S(i-l),\ \Psi_T^1(i-l),\ \Psi_C(i-\chi_0),\ \Psi_C(\chi_0-l)$$

By applying a perturbation theory for the small interactions, the energy of the ground state, W_0, is obtained as follows:

$$W_0=(\Psi_0\mathrm{H}\Psi_0)+\sum_i^{\mathrm{occ}}\sum_l^{\mathrm{vac}}\left\{\frac{(\Psi_0\mathrm{H}\Psi_S(i-l))^2}{(\Psi_0\mathrm{H}\Psi_0)-(\Psi_S(i-l)\mathrm{H}\Psi_S(i-l))}+\frac{(\Psi_0\mathrm{H}\Psi_T^1(i-l))^2}{(\Psi_0\mathrm{H}\Psi_0)-(\Psi_T^1((i-l)\mathrm{H}\Psi_T^1(i-l))}\right\}+\sum_i^{\mathrm{occ}}\frac{(\Psi_0\mathrm{H}\Psi_C(i-\chi_0))^2}{(\Psi_0\mathrm{H}\Psi_0)-(\Psi_C(i-\chi_0)\mathrm{H}\Psi_C(i-\chi_0))}+\sum_l^{\mathrm{vac}}\frac{(\Psi_0\mathrm{H}\Psi_C(\chi_0-l))^2}{(\Psi_0\mathrm{H}\Psi_0)(\Psi_C(\chi_0-l)\mathrm{H}\Psi_C(\chi_0-l))}$$

4) Y. Mori, This Bulletin, **34**, 1031 (1961).
5) Y. Mori, ibid., **34**, 1035 (1961).
6) K. Fukui, T. Yonezawa and C. Nagata, *J. Chem. Phys.*, **27**, 1274 (1957).

Neglecting overlap integrals, the matrix elements can be written as follows:

$$(\Psi_0 H \Psi_0) = E_0 - \sum_i^{occ} k^0_{i\chi}$$

$$= E$$

$$(\Psi_S(i-l) H \Psi_S(i-l))$$

$$= E + \Delta E_s(i-l) + 1/2(k^0_{i\chi} - k^0_{l\chi})$$

$$(\Psi^1_T(i-l) H \Psi^1_T(i-l))$$

$$= E + \Delta E_t(i-l) + 3/2\, k^0_{i\chi} + 1/2\, k^0_{l\chi}$$

$$(\Psi_C(i-\chi_0) H \Psi_C(i-\chi_0))$$

$$= E - \varepsilon_i + a^0_\chi + (\chi_0 H^+_i \chi_0)$$

$$(\Psi_C(\chi_0-l) H \Psi_C(\chi_0-l))$$

$$= E - \varepsilon^0_\chi + a_l + (l H^+_X l)$$

$$(\Psi_0 H \Psi_S(i-l)) = -1/\sqrt{2}\ (i\chi_0 H \chi_0 l)$$

$$(\Psi_0 H \Psi^1_T(i-l)) = \sqrt{3/2}(i\chi_0 H \chi_0 l)$$

$$(\Psi_0 H \Psi_C(i-\chi_0)) = -(i H \chi_0)$$

$$(\Psi_0 H \Psi_C(\chi_0-l)) = (l H \chi_0)$$

where E_0 is the energy of the ground state of the system without interaction, and $\Delta E_s(i-l)$ and $\Delta E_t(i-l)$ are the excitation energies of the molecule to the singlet and triplet states respectively. The integrals in these expressions are:

$$k^0_{i\chi} = (i\chi_0 H \chi_0 i)$$

$$\varepsilon_i = (i H_0 i)$$

$$a_l = (l H_0 l) + \sum^{occ} \{2(ll : ii) - (li : li)\}$$

$$\varepsilon^0_\chi = (\chi_0 H_0 \chi_0)$$

$$a^0_\chi = (\chi_0 H_0 \chi_0) + (\chi_0\chi_0 : \chi_0\chi_0)$$

$$(\chi_0 H^+_i \chi_0) = (\chi_0 H \chi_0) - (\chi_0 H_0 \chi_0) - (ii : \chi_0\chi_0)$$

$$(l H^+_X l) = (l H l) - (l H_0 l) - (ll : \chi_0\chi_0)$$

where H and H_0 respectively the Hamiltonian of the whole system with and without interaction between the molecule and the radical.

The integrals are reduced by disregarding non-neighbors and the difference between H and H_0 as follows:

$$(\chi_0 H^+_i \chi_0) = -(ii : \chi_0\chi_0)$$

$$(l H^+_X l) = -(ll : \chi_0\chi_0)$$

$$(i H \chi_0) = C_{ir} \cdot \beta^0_{r\chi}$$

$$(l H \chi_0) = C_{lr} \cdot \beta^0_{r\chi}$$

$$(i\chi_0 H \chi_0 l) = C_{ir} \cdot C_{lr} \cdot \alpha^0_{r\chi}$$

$$k^0_{i\chi} = (C_{ir})^2 \cdot \alpha^0_{r\chi}$$

where C_{ir} and C_{lr} are the coefficients of the r-th AO in the molecular orbitals i and l respectively; $\beta^0_{r\chi}$ is the resonance integral and $\alpha^0_{r\chi}$ is the exchange energy between the redical and the r-th atom in the molecule.

Therefore, the energy change of the ground state ΔW_0 is

$$\Delta W_0 = -1/2 \cdot q_r \cdot \alpha^0_{r\chi} - \sum_i^{occ} \sum_l^{vac} \left\{ \frac{(C_{ir} \cdot C_{lr})^2}{\Delta E_s(i-l) + 1/2(k^0_{i\chi} - k^0_{l\chi})} + \frac{(C_{ir} \cdot C_{lr})^2}{\Delta E_t(i-l) + 3/2\, k^0_{i\chi} + 1/2\, k^0_{l\chi}} \right\} (\alpha^0_{r\chi})^2 - \left\{ \sum_i^{occ} \frac{(C_{ir})^2}{-\varepsilon_i + a^0_\chi - (ii : \chi_0\chi_0)} + \sum_l^{vac} \frac{(C_{lr})^2}{-\varepsilon^0_\chi + a_l - (ll : \chi_0\chi_0)} \right\} (\beta^0_{r\chi})^2 \qquad (2)$$

wher q_r is the electron density at the position of the r-th atom in the molecule.

The first term, $-1/2 \cdot q_r \cdot \alpha^0_{r\chi}$, in Eq. 2 represents the exchange repulsion between the molecule and the radical, since $\alpha^0_{r\chi}$ has a negative value. In the first bracket of Eq. 2, the first term arises from the excited singlet states, and the second term shows the effect of the triplet states of the molecule. The exchange energy gives rise to these stabilization energies. These two terms are represented by $-1/8\,\pi^S_{rr}$ and $-3/8\,\pi^T_{rr}$ respectively, which are similar to the figures for atom-atom polarizability[7]. By disregarding interelectronic interaction and exchange energy, these terms can be reduced to $-1/8\,\pi_{rr}$ and $-3/8\,\pi_{rr}$, because

$$\Delta E_s(i-l) + 1/2(k^0_{i\chi} - k^0_{l\chi}) = \varepsilon_l - \varepsilon_i$$

$$\Delta E_t(i-l) + 3/2\, k^0_{i\chi} + 1/2\, k^0_{l\chi} = \varepsilon_l - \varepsilon_i$$

The two terms in the second bracket of Eq. 2, arising from electron-transfer interaction, are similar to the figures for superdelocalizability[6,8] for a radical attack and may be abbreviated as follows:

$$\gamma^+_r = -\sum_i^{occ} \frac{(C_{ir})^2}{-\varepsilon_i + a^0_\chi - (ii : \chi_0\chi_0)}$$

$$\gamma^-_r = -\sum_l^{vac} \frac{(C_{lr})^2}{-\varepsilon^0_\chi + a_l - (ll : \chi_0\chi_0)}$$

$$\gamma_r = \gamma^+_r + \gamma^-_r$$

Using the above abbreviations, Eq. 2 can be written as follows.

$$\Delta W_0 = -1/2 \cdot q_r \cdot \alpha^0_{r\chi} + (1/8\,\pi^S_{rr} + 3/8\,\pi^T_{rr})(\alpha^0_{r\chi})^2 + \gamma_r(\beta^0_{r\chi})^2 \qquad (3)$$

The uniform charge distribution for alternant

7) C. A. Coulson and H. C. Longuet-Higgins, *Proc. Roy. Soc.*, A191, 39 (1947).

8) K. Fukui, K. Morokuma, T. Yonezawa and C. Nagata, *J. Chem. Phys.*, 32, 1743 (1960).
If interelectronic repulsion is disregarded, we obtain:

$$-\gamma_r = Z_0/(\beta^0_{r\chi})^2$$

where Z_0 is the superdelocalizability for the radical attack.

hydrocarbons has been given by Pople[9]. Therefore, in a simple approximation, the chemical reactivity of conjugated molecules for a radical attack can be determined approximately by π_{rr} and Z_0, as has been concluded by other authors[2,7,8].

Equation 2 or 3 has an interesting feature in that the chemical reactivity of molecules is affected directly by the excited states; moreover, the triplet states are more important than the excited singlet states. The importance of the triplet states is also due to the fact that a triplet state has a lower energy than that singlet state with the same electron configuration.

Quenching of Excited (^{2}P) Sodium

The experimental work by Norrish and MacF. Smith[10] on the quenching of excited sodium by hydrocarbons shows that the hydrocarbons fall into two classes according to their cross-sections for the excited sodium, as is shown in Table I. The saturated hydrocarbons have

Table I. Quenching cross-sections*

	Cross-section, Å^2
Hydrogen	7.4
Nitrogen	14.5
Methane	0.11
Ethane	0.17
Propane	0.2
Butane	0.3
Cyclohexane	0.4
Ethylene	44.0
Propylene	52.0
1-Butene	58.0
2-Butene	58.0
Cyclohexene	59.0
Benzene	75.0

* R. G. W. Norrish and W. MacF. Smith, *Proc. Roy. Soc.*, **A176**, 295 (1940).

very small quenching cross-sections. On the other hand, the unsaturated hydrocarbons have large cross-sections. Hydrogen and nitrogen have the intermediate quenching cross-sections of 7.4 Å^2 and of 14.5 Å^2 respectively. These differences can be explained by the potential energy surfaces, as will be shown below.

The potential-energy surfaces may well be represented by taking into account the ground configuration as well as the electron-transfer configurations from the sodium atom to the molecule, because of the low ionization potential of sodium. (The excitation energy to ^{2}P of sodium is 2.12 eV., and the ionization potential is 5.14 eV.). Since the excited states of the molecules under consideration have much higher energies than the ^{2}P of sodium, the energy transfer from the sodium atom to the molecule will be disregarded. Therefore, the discussion is carried out by taking into account Ψ_0 (the ground state of the system), Ψ_X (the excited state of the sodium atom), and Ψ_C (the electron-transfer state).

Diatomic Molecules.—The quenching cross-section of hydrogen for excited sodium has been discussed theoretically by Laidler[3] and by Magee and Ri[11], who have shown the potential-energy surfaces for the sodium-hydrogen system with the aid of the VB theory. In the present work, the problem is discussed from the point of view of the transfer of the electron from the sodium atom to the molecule.

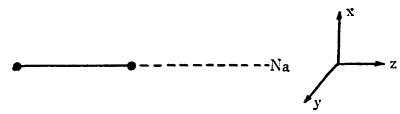


Fig. 1. The coordinate system for linear configuration in the case of diatomic molecule.

Linear Configuration. — The wave functions used are as follows[12]:

$$^2\Sigma^+ \quad \Psi_0 = \phi_0 \cdot \chi_0^{\alpha}(3s)$$

$$^2\Pi \begin{cases} \Psi_X^x = \phi_0 \cdot \chi_1^{\alpha}(3p_x) \\ \Psi_X^y = \phi_0 \cdot \chi_1^{\alpha}(3p_y) \end{cases}$$

$$^2\Sigma^+ \quad \Psi_X^z = \phi_0 \cdot \chi_1^{\alpha}(3p_z)$$

$$\Psi_C = \phi(\chi_0 - v)$$

The symmetry of the electron-transfer configuration, Ψ_C, is $^2\Sigma^+$ in the case of hydrogen and $^2\Pi$ in the case of nitrogen[13].

The diagonal matrix elements are as follows:

$$(\Psi_0 H \Psi_0) = E_0 - \sum_i^{occ} k_{i\chi}^0$$

$$(\Psi_X^x H \Psi_X^x) = E_0 + \Delta E(\chi_0 - \chi_1) - \sum_i^{occ} k_{i\chi}^x$$

$$(\Psi_X^y H \Psi_X^y) = E_0 + \Delta E(\chi_0 - \chi_1) - \sum_i^{occ} k_{i\chi}^y$$

$$(\Psi_X^z H \Psi_X^z) = E_0 + \Delta E(\chi_0 - \chi_1) - \sum_i^{occ} k_{i\chi}^z$$

$$(\Psi_C H \Psi_C) = E_0 - \varepsilon_\chi^0 + a_v + (v H_X^+ v)$$

and the non-vanishing off-diagonal elements are, for hydrogen:

$$(\Psi_0 H \Psi_X^z) = -\sum_i^{occ} (i\chi_0 H \chi_1(3p_z) \cdot i)$$

9) J. A. Pople, *Trans. Faraday Soc.*, **49**, 1375 (1953).
10) R. G. Norrish and W. MacF. Smith, *Proc. Roy. Soc.*, **A176**, 295 (1940).
11) J. L. Magee and T. Ri, *J. Chem. Phys.*, **9**, 638 (1941).
12) The lowest vacant MO of a diatomic molecule is represented by v.
13) The lowest vacant MO of hydrogen is σ_u^+, and that of nitrogen is π_g.

$$(\Psi_0 H \Psi_C) = (v(\sigma_u^+) H \chi_0)$$
$$(\Psi_X^z H \Psi_C) = (v(\sigma_u^+) H \chi_1(3p_z) \cdot i)$$

and for nitrogen:

$$(\Psi_0 H \Psi_X^z) = -\sum_i^{occ} (i\chi_0 H \chi_1(3p_z) \cdot i)$$
$$(\Psi_X^x H \Psi_C^x) = (v(\pi_g^x) H \chi_1(3p_x))$$
$$(\Psi_X^y H \Psi_C^y) = (v(\pi_g^y) H \chi_1(3p_y))$$

The potential energy surfaces of the configurational states Ψ_0, Ψ_X^x, Ψ_X^y and Ψ_X^z are repulsive toward the approach of the sodium atom to the molecule owing to the exchange repulsion[14], and that of Ψ_C(electron-transfer state) is attractive owing to the Coulomb interaction between the negatively-charged molecule and the sodium ion. The schematic potential-energy surfaces of these configurational states may be shown by the dotted lines in Fig. 2 (for hydrogen) and in Fig. 3 (for nitrogen).

The resulting potential-energy surfaces may be shown by the full lines in the figures by the consideration of the off-diagonal matrix elements.

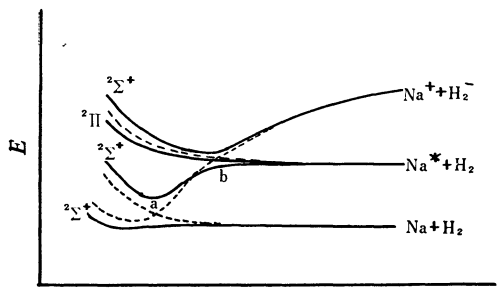


Fig. 2. The potential-energy surfaces for hydrogen (linear configuration).

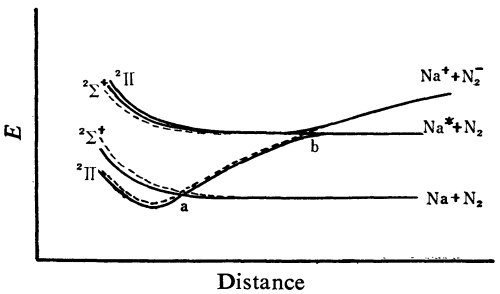


Fig. 3. The potential-energy surfaces for nitrogen (linear configuration).

14) Some of the exchange energies have positive values. In the case of hydrogen, for instance, the exchange energy $k_{1\chi}$, has a positive value, since

$$k_{1\chi}^x = (1\chi_1^x H \chi_1^x 1) = (1\chi_1^x : \chi_1^x 1)$$

Therefore, the surface of Ψ_X^x for the linear configuration of the sodium-hydrogen system may be slightly attractive, but this attractive nature of the surface is unimportant in the present discussion.

The resonance splitting at a in Fig. 2 is not small, since $(v(\sigma_u^+)H\chi_0)$, which is the off-diagonal element between Ψ_0 and Ψ_C, is given by the resonance integral between σ_u^+ and χ_0,

$$(v(\sigma_u^+) H \chi_0) = \beta(\sigma_u^+ - \chi_0)$$

In these circumstances, the reaction system on a upper surface has a small probability of passing to a lower one via crossing[3]. The resulting lower and upper surfaces do not cross, as is shown by the full lines in Fig. 2; the quenching reaction is brought about by a radiationless transition from the upper state to the lower one, which transition gives rise to a sudden acceleration of the motion of the nuclei. This radiationless transition, however, is forbidden by the Franck-Condon principle[15] and has a small probability of occurring if the energy difference between the lower and upper states is not small.

The potential-energy surfaces for the nitrogen-sodium system shows that the quenching reaction will be brought about by a transition at crossing a. The radiationless transition at a is highly probable due to the small interaction between the lower state and the upper state (electron-transfer state); this interaction may arise from the small bending distortion of the linear configuration of the nuclei.

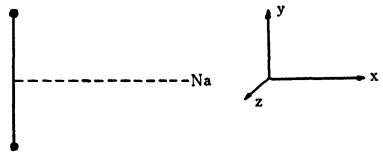


Fig. 4. The coordinate system for triangular configuration in the case of diatomic molecule.

Triangular Configuration.—In this case, the configurational wave functions and their symmetries are, for the hydrogen-sodium system, as follows:

$^2A_1$ $\quad \Psi_0 = \phi_0 \cdot \chi_0^a(3s)$
$^2A_1$ $\quad \Psi_X^x = \phi_0 \cdot \chi_1^a(3p_x)$
$^2B_1$ $\quad \Psi_X^y = \phi_0 \cdot \chi_1^a(3p_y)$
$^2B_2$ $\quad \Psi_X^z = \phi_0 \cdot \chi_1^a(3p_z)$
$^2B_1$ $\quad \Psi_C = \phi(\chi_0 - v)$

The non-vanishing interconfigurational interactions are as follows:

$$(\Psi_0 H \Psi_X^x) = -\sum_i^{occ} (i\chi_0 H \chi_1(3p_x) \cdot i)$$
$$(\Psi_X H \Psi_C) = (\sigma_u^+ H \chi_1(3p_y))$$

For considerations similar to those in the

15) G. Herzberg, "Spectra of Diatomic Molecules", 2nd Ed., D. Van Nostrand Co., New York (1950).

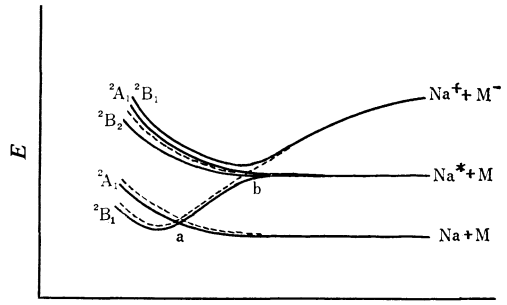


Fig. 5. The potential-energy surfaces for triangular configuration.

case of the linear configuration, the schematic potential-energy surfaces may be given as in Fig. 5. The potential-energy surface for $^2B_1$ (electron-transfer state) is cut by the surface of the lowest state. Since the interconfigurational interaction will be small, the quenching reaction may be brought about by the process:

$$H_2 + Na^*(^2P) \rightarrow H_2 \cdots Na^*(^2B_1) \rightarrow H_2^- - Na^+(^2B_1)$$
$$\rightarrow H_2 \cdots Na(^2A_1) \rightarrow N_2 + Na(^2S)$$

In the case of nitrogen, the wave functions, excepting those of the electron-transfer states, are similar to those of the hydrogen-sodium system. The wave functions of the electron-transfer states are as follows:

$$^2B_1 \quad \Psi_C^x = \phi(\chi_0 - v(\pi_g^x))$$
$$^2B_2 \quad \Psi_C^y = \phi(\chi_0 - v(\pi_g^y))$$

The features of these potential-energy surfaces are quite similar to those of the electron-transfer state of the hydrogen-sodium system. Both of these surfaces are cut by that of the lowest state, ($^2A_1$). Therefore, the reaction system on any surface of the electron-transfer states has a large probability of passing to the lowest state via the crossing, and then the quenching reaction can proceed.

Methane. — The lowest vacant orbital of methane may belong to the irreducible representation of a_1 (totally symmetrical). In the two cases shown in Fig. 6, the wave functions of the reacting system and their symmetries are as follows:

$$^2A_1 \quad \Psi_0 = \phi_0 \cdot \chi_0^\alpha(3s)$$
$$^2E \begin{cases} \Psi_X^x = \phi_0 \cdot \chi_1^\alpha(3p_x) \\ \Psi_X^y = \phi_0 \cdot \chi_1^\alpha(3p_y) \end{cases}$$
$$^2A_1 \begin{cases} \Psi_X^z = \phi_0 \cdot \chi_1^\alpha(3p_z) \\ \Psi_C = \phi(\chi_0 - v) \end{cases}$$

Since both Ψ_0 (the lowest configuration) and Ψ_C (the electron-transfer configuration) belong to the same symmetry class, ($^2A_1$), and since the interconfigurational interaction between Ψ_0 and Ψ_C is not small, it can not be expected that the resulting potential-energy surface of the upper state (the electron-transfer configuration) will be cut by that of the lowest state[16]. These circumstances are similar to those in the case of the linear configuration of the hydrogen-sodium system. The low efficiency of the quenching reaction with excited sodium will, therefore, be interpreted as due to the "non-crossing" of potential-energy surfaces.

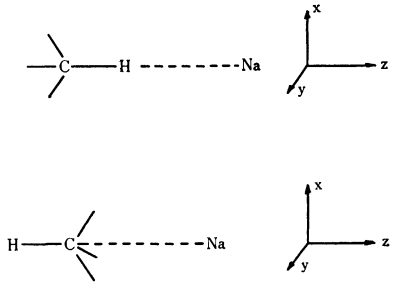


Fig. 6. The configurations for methane.

Discussion

Reactivity of Conjugated Molecules.—It has been shown that the triplet state has an effect on the chemical reactivity of conjugated molecules for a radical attack. If the energy of the lowest triplet state of a molecule is low, the role of the triplet state is clear.

The approach of a radical to a molecule causes a decrease in the exchange energy, $\alpha_{r\chi}^0$, between the radical and the r-th atom in the molecule. Since the energy difference between Ψ_0 (the lowest configuration) and $\Psi_T^1(n-n+1)$ (which corresponds to the lowest triplet state) is expressed by the relation:

$$\Delta E_T^1(n-n+1)$$
$$= (\Psi_T^1(n-n+1)\,H\Psi_T^1(n-n+1)) - (\Psi_0 H \Psi_0)$$
$$= \Delta E_t(n-n+1) + 3/2\, k_{n\chi}^0 + 1/2\, k_{n+1,\chi}^0$$
$$= E_t(n-n+1) + (3/2\,|C_{nr}|^2 + 1/2\,|C_{n+1,r}|^2)$$

the energy difference, $\Delta E_T^1(n-n+1)$, decreases with the approach of the radical to the molecule. When the radical approaches very close to the molecule, the energy of $\Psi_T^1(n-n+1)$ will be lower than that of Ψ_0 owing to the decrease in the exchange energy. In theses cases, the most important interconfigurational interaction is that between Ψ_0 and $\Psi_T^1(n-n+1)$, which is expressed by the nearest neighbor approximation as:

$$(\Psi_0 H \Psi_T^1(n-n+1)) = (C_{nr} \cdot C_{n+1,r}) \cdot \alpha_{r\chi}^0$$

16) Non-crossing may be due to the low electron affinity of methane.

where C_{nr} and $C_{n+1,r}$ are the coefficients at the r-th atom in the molecular orbitals n and $n+1$. If the activated complex or the transition state of the reaction is defined by the condition

$$\Delta E_T^1(n-n+1)=0$$

the activation energy for the reaction may be approximated as follows:

$$\begin{aligned}\Delta W_0 \fallingdotseq & -1/2\{\Delta E_t(n-n+1)/(3/2\,k_{n\chi}^0 \\ & +1/2\,k_{n+1,\chi}^0)\}\alpha_{r\chi}^0+|C_{nr}\cdot C_{n+1,r}|\alpha_{r\chi}^0 \\ = & -1/2\{\Delta E_t(n-n+1)/(3/2\,|C_{nr}|^2 \\ & +1/2|C_{n+1,r}|^2)\}+|C_{nr}\cdot C_{n+1,r}|\alpha_{r\chi}^0 \end{aligned} \quad (4)$$

The experimental work by Szwarc[17] on the radical affinity of conjugated molecules has shown that the radical affinity of a conjugated molecule depends on the energy of the lowest triplet state. This result can be interpreted by Eq. 4. Equation 4 shows that the activation energy decreases with a decrease in the energy difference, $\Delta E_t(n-n+1)$, between the ground state and the lowest triplet state.

In regard to the theoretical approximations of the present paper, the effect of the σ-bonds in the molecule was ignored completely. The use of the wave functions of the whole electron system, including the σ-electrons, would have complicated the theory and may not have affected the results greatly.

Quenching of Excited Sodium.—If the radiationless transition at a is fast, the activated state of the quenching reaction will correspond to b, which is the crossing between Ψ_C (the electron-transfer state) and Ψ_X (the excited state of sodium). The maximum value of the quenching cross section is determined by the distance between the center of the molecule and the sodium atom at b. In the case of hydrogen, the distance is found to be about 4 Å, taking the electron affinity of hydrogen as -0.28 eV.[18] This value may be compared with an experimental value of 2.7 Å $=7.4^{1/2}$ calculated from the quenching cross section (7.4 Å^2) in Table I.

The distance at b, σ, is determined mainly by the electron affinity of the molecule. Table II shows the relation between the electron affinity and the value of σ. In the calculation of the table, the small energy change of Ψ_X due to the interaction was ignored, and the integral $(v\mathrm{H}_X^* v)$ was approximated by $-e^2/R$, where R is the distance between the center of the molecule and the sodium atom. From this relation and by assuming that the activated state corresponds to b, the quenching cross sections of the molecules can be explained except in the case of the saturated hydrocarbons.

The lowest vacant orbital of ethylene will be the anti-bonding π orbital with the nodal plane between the two carbon atoms. The potential-energy surfaces and the quenching reaction process may be similar to those in the case of a triangular configuration for hydrogen, because the lowest state, Ψ_0, and the electron-transfer state, Ψ_C, have symmetry characters different from one other if the sodium atom lies in that nodal plane. Therefore, the quenching process will be as follows[19]:

$$\begin{aligned}\mathrm{C_2H_4+Na^*(^2P)} & \rightarrow \mathrm{C_2H_4\cdots Na^*(^2B_1)} \\ & \rightarrow \mathrm{C_2H_4^- - Na^*(^2B_1)} \rightarrow \mathrm{C_2H_4\cdots Na(^2A_1)} \\ & \rightarrow \mathrm{C_2H_4+Na(^2S)}\end{aligned}$$

The molecular plane of ethylene is the nodal plane of its π-orbital, but this will be unimportant since the hydrogen atoms prevent the approach of the sodium atom to the molecule.

Although the electron affinity of ethylene is unknown, the value of σ (6.6 Å) which is found from the value of the quenching cross-section in Table I can be fit into the relation shown in Table II by assuming the value of electron affinity of ethylene to be 0.9 eV.

TABLE II. THE RELATION BETWEEN σ AND ELECTRON AFFINITY

Electron affinity eV.	σ Å
−2.0	2.86
−1.0	3.57
0	4.75
1.0	7.09
2.0	13.98

The quenching cross-sections of unsaturated hydrocarbons can be explained by a consideration similar to that as in the case of ethylene. The lowest vacant orbital of the π-electrons of the unsaturated group will have the largest electron affinity in the molecule; it also has the nodal plane on which the sodium atom can approach. If the sodium atom lies in that nodal plane, the matrix element, the interconfigurational interaction between Ψ_0 and Ψ_C, is very small. The resonance splitting at crossing a will not be large, and hence, the radiationless transition can take place. The value of the quenching cross-section can, therefore, be determined by the electron affinity and by the size of the molecule.

The lowest vacant orbital of saturated hydrocarbons will have no nodal plane on which

17) M. Szwarc, *J. Chem. Phys.*, 23, 204 (1955).
18) I. Fisher-Hjalmars, *Arkiv Fysik*, 16, 33 (1959).
19) The sodium atom lies on the symmetry axis perpendicular to the molecular plane.

the sodium atom can approach. This is similar to the case of methane. The quenching cross-section of a saturated hydrocarbon may be small due to the large resonance splitting at crossing a.

It may be concluded that the efficiency of the quenching reaction with sodium (^{2}P) depends on the symmetry of the lowest vacant MO and on the electron affinity of the molecule.

Summary

In the first section, the chemical reactivity of conjugated molecules toward a radical attack has been explained. The index of chemical reactivity for a radical attack can be represented in terms of polarizability (π^S_{rr}, π^T_{rr}) and of γ_r, which is similar to the superdelocalizability for a radical attack. The role of the lowest triplet states of molecules in a radical reaction has been discussed.

Secondly, the quenching of excited (^{2}P) sodium was discussed. It has been concluded that the quenching cross-section is determined by the symmetry character of the lowest electron-transfer state and by the electron affinity of the molecule.

The author wishes to express his thanks to Professor Ikuzo Tanaka of this loboratory for his encouragement and discussion throughout this work.

Laboratory of Physical Chemistry
Tokyo Institute of Technology
Meguro-ku, Tokyo

Electronic Structures of Benzyl Cation and Related Compounds

By Yuji MORI

(Received February 21, 1961)

In previous papers[1,2], the author has shown a theoretical interpretation of the electronic structure of the benzyl radical, with relation to the electronic structure of a separate fragment (benzene). The calculations suggested that the lowest excited state of the benzyl radical, $^2B_2$, can be related to the lowest triplet state of benzene, $^3B_{1u}$.

Longuet-Higgins and Pople[3] have interpreted the spectra of odd alternant hydrocarbon radicals and corresponding cations on the basis of the molecular orbital theory. They have shown that odd alternant hydrocarbon radicals may have absorption bands with a weak intensity in the vicinity of the absorption bands of corresponding cations. For the benzyl radical and cation, a similar result has been reported by Bingel[4].

It will, therefore, be interesting to investigate the electronic structure of the benzyl cation from the viewpoint of the electronic structures of the separate fragments, as was done in the case of the benzyl radical.

The first problem of the present paper will be to show an interpretation of the electronic structure of the benzyl cation based on those of the composite system. This will be followed by an interpretation of the electronic spectra of diphenyl-methyl and triphenyl-methyl cations from the same standpoint, utilizing a simple treatment.

The Benzyl Cation

In the calculations, it is assumed that the system is composed of the benzene ring and the positively-charged methylene group ($-CH_2^+$). The calculations are based on the method of composite systems[5] and are carried out by taking into account the locally excited configurations in the benzene ring and the electron-transfer configurations in which an electron has been transferred from the benzene ring to $-CH_2^+$.

The LCAO MO's of benzene ring are

$$\varphi_0 = 1/\sqrt{6}\,(\chi_1+\chi_2+\chi_3+\chi_4+\chi_5+\chi_6)$$

$$\varphi_1 = 1/\sqrt{12}\,(2\chi_1+\chi_2-\chi_3-2\chi_4-\chi_5+\chi_6)$$

1) Y. Mori, This Bulletin, **34**, 1031 (1961).
2) Y. Mori, ibid., **34**, 1035 (1961).
3) H. C. Longuet-Higgins and J. A. Pople, *Proc. Phys. Soc.*, **A68**, 591 (1955).
4) W. Bingle, *Z. Naturforschg.*, **A10**, 462 (1955).
5) A. London, *J. Chem. Phys.*, **13**, 396 (1945); H. C. Longuet-Higgins and J. A. Pople, *Proc. Phys. Soc.*, **A68**, 601 (1955); Y. Mori, This Bulletin, **28**, 291 (1955). A similar treatment is described by Nagakura and Tanaka; S. Nagakura and J. Tanaka, *J. Chem. Phys.*, **22**, 236 (1954); S. Nagakura, ibid., **23**, 1441 (1955); J. Tanaka and S. Nagakura, ibid., **24**, 1274 (1956).

$$\varphi_2=1/2(\chi_2+\chi_3-\chi_5-\chi_6)$$
$$\varphi_3=1/\sqrt{12}(2\chi_1-\chi_2-\chi_3+2\chi_4-\chi_5-\chi_6)$$
$$\varphi_4=1/2(\chi_2-\chi_3+\chi_5-\chi_6)$$
$$\varphi_5=1/\sqrt{6}(\chi_1-\chi_2+\chi_3-\chi_4+\chi_5-\chi_6)$$

where χ_r is the $2p\pi$ AO of the r-th carbon atom in the benzene ring.

The bond is formed between the methylene group ($-CH_2^+$) and the carbon atom 1 of the benzene ring. The $2p\pi$ AO of $-CH_2^+$ is expressed by χ_7.

The electronic configurations are shown in Fig. 1, while the wave functions corresponding to these configurations are given in Table I.

TABLE I. THE WAVE FUNCTIONS OF THE BENZYL CATION

$^1A_1$ $\left\{\begin{array}{l}\Psi_1=(001122)=\phi_1\\ \Psi_2=\phi_2(1\to\chi_7)\\ \Psi_3=\phi_3(0\to\chi_7)\end{array}\right.$

$^1B_1$ $\Psi_4=\phi_4(2\to\chi_7)$

$^1A_1$ $\left\{\begin{array}{l}\Psi_5=1/\sqrt{2}\{\phi_5(1\to3)+\phi_6(2\to4)\}\\ \Psi_6=1/\sqrt{2}\{\phi_5(1\to3)-\phi_6(2\to4)\}\end{array}\right.$

$^1B_1$ $\left\{\begin{array}{l}\Psi_7=1/\sqrt{2}\{\phi_7(1\to4)+\phi_8(2\to3)\}\\ \Psi_8=1/\sqrt{2}\{\phi_7(1\to4)-\phi_8(2\to3)\}\end{array}\right.$

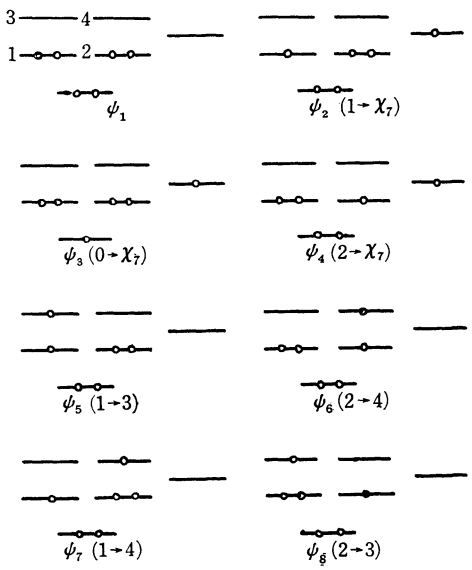


Fig. 1. The electron configurations of the benzyl cation.

In the table, Ψ_5, Ψ_6, Ψ_7 and Ψ_8, which represent the locally excited states of the benzene ring, are introduced for the purpose of considering the effect of the polarization in the benzene ring induced by $-CH_2^+$. The wave functions, Ψ_2, Ψ_3 and Ψ_4, correspond to the electron-transfer configurations, in which one electron has been transferred from the benzene ring to the $2p\pi$ AO of $-CH_2^+$.

A standard bond length, 1.39 Å, is assumed for all C–C bonds throughout the present work. The values for the molecular integrals are taken from the work of Pariser[6], and the penetration integrals from neutral carban atoms are disregarded.

The matrix elements are given in Table II, and the calculared energy levels of the benzyl cation are shown in Table III. The energy of the ground state is -61 kcal., relative to the energy of Ψ_1.

TABLE II. THE MATRIX ELEMENTS OF THE BENZYL CATION (eV.)

	1	2	3	5	6
1	0				
2	−1.9359	−0.0865			
3	−1.3689	0	+3.0295		
5	−1.9290	−0.9680	0	+6.7595	
6	+0.0350	−0.9680	0	0	+5.9595

	4	7	8
4	−0.0865		
7	−0.9680	+4.7095	
8	+0.9680	+0.3303	+6.7595

TABLE III. THE ENERGY LEVELS OF THE BENZYL CATION

Symmetry	Energy, eV.	Polarization*
$^1A_1$	0	
$^1B_1$	2.23	⊥
$^1A_1$	3.91	∥
$^1A_1$	6.24	∥
$^1B_1$	7.54	⊥

* ⊥ and ∥ mean perpendicular and parallel polarization with respect to the long axis in the benzyl cation.

The wave functions of the ground state and of the two excited states are as follows:

($^1A_1$; 0)

$$\Phi_1=0.7118\cdot\Psi_1+0.6435\cdot\Psi_2+0.1715\cdot\Psi_3+0.2121\cdot\Psi_5+0.0694\cdot\Psi_6$$

($^1A_1$; 3.91 eV.)

$$\Phi_2=0.5396\cdot\Psi_1-0.7124\cdot\Psi_2+0.4178\cdot\Psi_3+0.0639\cdot\Psi_5-0.1508\cdot\Psi_6$$

($^1B_1$; 2.23 eV.)

$$\Phi_4=0.9735\cdot\Psi_4+0.1928\cdot\Psi_7-0.1232\cdot\Psi_8$$

The calculated charge distributions of the ground state are shown in Fig. 2. In the calculation of the electron densities, it is necessary to take into account the interconfigurational electron densities. The interconfigurational electron density can be defined by the following expression for a small change in the Coulomb

6) R. Pariser, *J. Chem. Phys.*, **24**, 250 (1956).

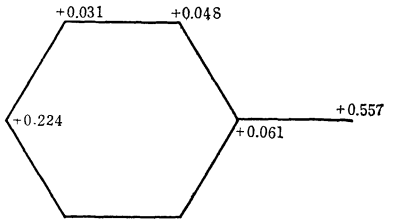


Fig. 2. The charge distribution of the benzyl cation.

integral $\Delta\alpha_r$ at the r-th atom:

$$q_r(ij)=\frac{\partial}{\partial(\Delta\alpha_r)}\Delta W_r(ij)$$

where

$$\Delta W_r(ij)=\int\Psi_i\Delta\alpha_r\Psi_j d\tau$$

Also, $q_r(ii)$ can be defined by the expression:

$$q_r(ii)=\frac{\partial}{\partial(\Delta\alpha_r)}\cdot\Delta W_r(ii)$$

Then the electron density at the carbon atom r may be written as follows:

$$q_r=\frac{\partial}{\partial(\Delta\alpha_r)}\cdot\int\Phi_1\Delta\alpha_r\Phi_1 d\tau$$
$$=\sum_i\sum_j C_iC_j\cdot q_r(ij)$$

where $\Phi_1=\sum_i C_i\cdot\Psi_i$

From the wave functions and wave numbers obtained in this section, the oscillator strengths[7] may be given as follows:

$$f_{12}=0.34$$
$$f_{14}=0.11$$

It seems that there has been no reliable experimental observation of the electronic absorption spectrum of the benzyl cation. The calculations, however, may be compared with the absorption spectrum of the carbonium ion in a sulfuric acid solution of benzyl alcohol. Grace and Symons[8] have observed that the solution shows an absorption band at 4700 Å (2.6 eV.) and so have assigned it to the benzyl cation.

The calculations show a qualitative agreement with those by Bingel[4] and by Longuet-Higgins and Pople[3]. The energy and charge distribution of the ground state are similar to the results of the calculations by Brickstock and Pople[9].

7) R. S. Mulliken and C. A. Rieke, *Repts. Progr. Phys.*, **8**, 231 (1941).
8) J. A. Grace and M. C. R. Symons, *J. Chem. Soc.*, **1959**, 958.
9) A. Brickstock and J. A. Pople, *Trans. Faraday Soc.*, **50**, 901 (1954).

The transition moment of the $\Phi_1-\Phi_4$ transition arises from the local transition in the benzene ring, and the direction of this is orthogonal to the long axis of the system, i. e., the direction of the electron transfer. The transition moment from Φ_1 to Φ_2 is due to the electron transfer and is parallel to the direction of the electron transfer.

The charge density on $-CH_2^+$ is +0.05 in the lowest excited state, $^1B_1$, according to the wave function obtained in the present paper. Therefore, the lowest excited state, $^1B_1$, can be represented approximately by the single configuration, Ψ_4, the electron-transfer configuration from φ_2 to χ_7. In a similar way, the approximate wave function of the ground state of the benzyl cation can be represented by the linear combination of Ψ_1 and Ψ_2, Ψ_2 being the electron-transfer configuration from φ_1 to χ_7. According to the above simple approximation, the longest absorption band of the benzyl cation may be interpreted as the band arising from the transition from the ground state to the excited state which is represented by Ψ_4. This relation is shown in Fig. 3. This simple treatment will be applied in the calculations of diphenyl-methyl and triphenyl-methyl cations in the next section.

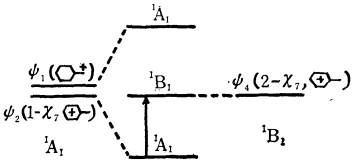


Fig. 3. Effect of electron transfer interaction in the benzyl cation.

Diphenyl-methyl and Triphenyl-methyl Cations. —In the preceding section, it was shown that the role of the electron-transfer configurations is important for the ground and the lowest excited states of the benzyl cation, and that the role of the locally excited configurations is minor. In this section, therefore, calculations will be carried out taking into account only the interactions arising from electron-transfer configurations of low energies.

The LCAOMO's of the benzene rings in the diphenyl-methyl cation are similar to those in the case of the benzyl cation. The MO which belongs to a benzene ring A or B is denoted by a subscript a or b, and the $2p\pi$ AO of $-CH^+-$ in the diphenyl-methyl cation is represented by χ_7.

The electronic wave functions of the diphenyl-methyl cation are shown in Table IV. In the table, Ψ_1 represents the state in which the positive charge is localized on $-CH^+-$, while Ψ_2, Ψ_3, Ψ_4 and Ψ_5 are the electron transfer states.

TABLE IV. THE WAVE FUNCTIONS OF THE DIPHENYL-METHYL RADICAL CATION

$$^1A_1 \begin{cases} \Psi_1 = (0_a0_a1_a1_a2_a2_a)\,(0_b0_b1_b1_b2_b2_b) \\ \Psi_2 = 1/\sqrt{2}\,\{\phi(1_a\rightarrow\chi_7)+\phi(1_b\rightarrow\chi_7)\} \end{cases}$$

$$^1B_1 \begin{cases} \Psi_3 = 1/\sqrt{2}\,\{\phi(1_a\rightarrow\chi_7)-\phi(1_b\rightarrow\chi_7)\} \\ \Psi_4 = 1/\sqrt{2}\,\{\phi(2_a\rightarrow\chi_7)+\phi(2_b\rightarrow\chi_7)\} \end{cases}$$

$$^1A_1 \quad \Psi_5 = 1/\sqrt{2}\,\{\phi(1_a\rightarrow\chi_7)-\phi(2_b\rightarrow\chi_7)\}$$

A planar configuration of the diphenyl-methyl cation is assumed in the calculation, although the system may not be planar. The possible effect of nonplanarity on the energy levels will be discussed in a later section. The matrix elements are shown in Table V. The calculated energy levels are given in Table VI.

TABLE V. THE MATRIX ELEMENTS OF THE DIPHENYL-METHYL RADICAL CATION

Values are given in eV.

	1	2	5
1	0		
2	−2.738	−0.086	
5	0	0	−0.086

	3	4
3	−0.086	
4	0	−0.086

TABLE VI. THE ENERGY LEVELS OF DIPHENYL-METHYL RADICAL CATION

Symmetry	Energy, eV.
$^1A_1$	0
$^1A_1$	2.69
$^1B_1$	2.69
$^1B_1$	2.69
$^1A_1$	5.48

The calculations may be compared with the absorption spectrum of the solution of diphenyl-methanol in the mixture of trichloroacetic acid and benzene, which has been observed by Grace and Symons[8]. They assign the absorption band at 4420 Å (2.81 eV.) to the diphenyl-methyl cation. In spite of their very simple calculations, the results seems satisfactory as an explanation of the characteristic features of the absorption band of the diphenyl-methyl cation. Also, the calculations will serve for the qualitative interpretation of the absorption band of the protonated compound of anthracene at 4100 Å[10], since this compound may have a structure similar to that of the diphenyl-methyl cation.

In the case of the triphenyl-methyl cation, a similar calculation has been carried out for the energy levels. The wave functions are shown in Table VII. The subscripts a, b and c denote the benzene rings A, B and C respectively, while χ_7 represents the $2p\pi$ AO of the carbon atom at the center of the system. The matrix elements are shown in Table VIII.

TABLE VII. THE WAVE FUNCTIONS OF THE TRIPHENYL-METHYL RADICAL CATION

$$^1A'_1 \begin{cases} \Psi_1 = (0_a0_a1_a1_a2_a2_a)\,(0_b0_b1_b1_b2_b2_b)\,(0_c0_c1_c1_c2_c2_c) \\ \Psi_2 = 1/\sqrt{3}\,\{\phi(1_a\rightarrow\chi_7)+\phi(1_b\rightarrow\chi_7)+\phi(1_c\rightarrow\chi_7)\} \end{cases}$$

$$^1A'_2 \quad \Psi_3 = 1/\sqrt{3}\,\{\phi(2_a\rightarrow\chi_7)+\phi(2_b\rightarrow\chi_7)+\phi(2_c\rightarrow\chi_7)\}$$

$$^1E' \begin{cases} \Psi_4 = 1/\sqrt{3}\,\{\phi(1_a\rightarrow\chi_7)+\exp(\pm 2\pi i/3)\phi(1_b\rightarrow\chi_7) \\ \qquad +\exp(\pm 4\pi i/3)\phi(1_c\rightarrow\chi_7)\} \\ \Psi_5 = 1/\sqrt{3}\,\{\phi(2_a\rightarrow\chi_7)+\exp(\pm 2\pi i/3)\phi(2_b\rightarrow\chi_7) \\ \qquad +\exp(\pm 4\pi i/3)\phi(2_c\rightarrow\chi_7)\} \end{cases}$$

TABLE VIII. THE MATRIX ELEMENTS OF THE TRIPHENYL-METHYL RADICAL CATION

Values are given in eV.

	1	2
1	0	
2	−3.353	−0.086

$H_{33} = -0.086$

	4	5
4	−0.086	
5	0	−0.086

TABLE IX. THE ENERGY LEVELS OF THE TRIPHENYL-METHYL RADICAL CATION

Symmetry	Energy, eV.
$^1A'_1$	0
$^1A'_2$	3.27
$^1E'$	3.27
$^1E'$	3.27
$^1A'_1$	6.71

The energy levels given in Table IX are relative to the energy of the ground state. The system may not be planar, but the calculations may be compared with the absorption spectrum of the triphenyl-methyl cation, which has its first absorption band at about 4300 Å[11] (2.88 eV.). The calculated value is too high compared with the observed value. However, in view of the simple calculation and the assumed planar structure, it would be reasonable to say that this absorption band arises from the electron-transfer configuration.

Discussion

The charge distribution of the benzyl cation calculated in the present paper is similar to that calculated by Brickstock and Pople[9]. According to the prediction by the simple

10) G. Dallinga, E. L. Makor and A. A. V. Stuart, *Mol. Phys.*, **1**, 123 (1958).

11) T. L. Chu and S. I. Weissman, *J. Chem. Phys.*, **22**, 21 (1954).

MO theory, the positive charge densities are identical at the para- and ortho-positions, and there is no apparent charge at the meta-position. This charge distribution differs from that of the present calculations shown in Fig. 2. This difference may be due to the effect of polarization.

The stabilization energy, 61 kcal., of the ground state, that is, the resonance energy of the benzyl cation relative to that of benzene, is large compared to that of the benzyl radical[9,12]. Brickstock and Pople[9] have obtained a value of 21.9 kcal. for the benzyl radical. This is due to the facts that the electron affinity of $-CH_2^+$ (benzyl cation) is much larger than that of $-CH_2$ (benzyl radical), and that the largest contribution to this energy comes from the electron-transfer interaction.

The transition moment from Φ_1 to Φ_4, which is orthogonal to the direction of the electron transfer, is due to the (interconfigurational) dipole matrix elements between Ψ_3 and Ψ_4 and between Ψ_1 and Ψ_8. The dipole matrix element

$$q_{34}=e\int \Psi_3 \sum_{\nu} q(\nu)\Psi_4 \mathrm{d}V$$

corresponds to that of the one-electron transition between φ_0 and φ_2 in the positively-charged benzene ring, while q_{18} corresponds to that of the transition ($^1A_{1g}$–$^1E_{1u}$) of benzene.

A simple treatment, which deals with only the three electron-configurations, Ψ_1, Ψ_2 and Ψ_4, can interpret the characteristic features of the absorption band of the benzyl cation. However, there are some difficulties in explaining the charge distribution of the ground state and the intensity of the absorption band. The charge distribution which will be given by this simple treatment will show the same positive charge densities on the carbon atoms 1 and 4, and also on the carbon atoms 2 and 3. The transition moment from the ground state to the lowest excited state, $^1B_1$, will be zero, since no contributions from the non-vanishing dipole matrix elements, q_{34} and q_{18}, can be expected.

For the diphenyl-methyl and triphenyl-methyl cations, the planar configuration has been assumed, although the benzene rings in these systems may not be coplanar. The matrix element H_{12} (Tables V and VIII), the inter-configurational interaction between Ψ_1 and Ψ_2 (Tables IV and VII), can be expressed by the resonance integral between the benzene ring and the carbon atom at the center of the system. If the bond is twisted by an angle θ, the resonance integral $\beta(\theta)$ is given by the relation

$$\beta(\theta)=\beta(0)\cos\theta$$

Therefore, the excitation energies from the ground states to the lowest excited states of these systems will decrease with the increase in the angle of twist. However, it is difficult to determine the angle of twist for these cations from the results of the present calculations, because the calculations are so very simple that there must be some errors in them which would affect the results.

Any transition from the ground state to the excited state ($^1A_2$) of the triphenyl-methyl cation is forbidden in the planar configuration. This transition is allowed in the twisted configuration, which has a transition moment perpendicular to the σ-bonds of the central atom of the system. (This transition corresponds to that from Φ_1 to Φ_4 in the case of the benzyl cation.)

The three excited levels of the diphenyl-methyl cation have the same energy, and for the triphenyl-methyl cation a similar degeneracy of the energy levels has been found. This may be due to disregarding the configurations in which more than one electron has been transferred and the locally excited configurations in the benzene rings.

Summary

The electronic structure of the benzyl cation has been calculated on the basis of an approximation of the composite systems in order to explain the electronic spectrum of the benzyl cation from the point of view of electron-transfer interaction between the fragments. The calculations show a satisfactory agreement with the experimental observations.

For the electronic spectra of some other cations, simple calculations have been carried out as an application of the treatment for the benzyl cation. The results for the diphenyl- and triphenyl-methyl cations show qualitative agreement with the experimental results.

The author is greatly indebted to Professor Ikuzo Tanaka for his continuous encouragement.

Laboratory of Physical Chemistry
Tokyo Institute of Technology
Meguro-ku, Tokyo

12) A value of 17 kcal. has been elsewhere calculated by the present author (cf. footnote 2).

The Kinetics of Substitution Reactions Involving Metal Complexes. V. Reaction between Copper(II) and Ethylenediaminetetraacetatocadmate(II) Complexes in Aqueous Solutions

By Nobuyuki TANAKA and Minoru KAMADA

(Received April 13, 1962)

The substitution reaction of copper(II) ion and ethylenediaminetetraacetatocadmate(II) complex (Cd(II)-EDTA) was first studied by Ackermann and Schwarzenbach[1]. From the polarographic measurement of the reaction rate at 0°C and ionic strength 1.0 at 5×10^{-6} to 1.4×10^{-4} M of hydrogen ion, they concluded that the reaction proceeds simultaneously through four different reaction paths. Although their measurements were carried out in acetate buffer solutions and the decrease of the reaction rate was observed with increasing concentrations of acetate ion, Ackermann and Schwarzenbach did not take consideration of this fact in the treatment of the reaction kinetics.

This observation and a series of kinetic studies on the substitution reactions involving metal complexes[2-5] carried out in this laboratory suggested us to reinvestigate the substitution reaction of copper(II) ion and Cd(II)-EDTA and to compare the mechanisms and the rate constants of those substitution reactions obtained under the same experimental conditions.

In this study, therefore, the reaction rates were measured by the polarographic method at 5 and 15°C at lower concentrations of hydrogen ion than those reported by Ackermann and Schwarzenbach. The effect of acetate ion on the reaction rate was taken into consideration. A new reaction path was found in which the rate was inversely proportional to the hydrogen ion concentration of the solution. The contribution of this reaction path was more important at lower hydrogen ion concentrations.

Experimental

Reagents.—Preparations and standardizations of the solutions of copper(II) nitrate, cadmium(II) nitrate, disodium ethylenediaminetetraacetate (EDTA) and sodium acetate-acetic acid buffers were described in the previous paper[6]. The cadmium nitrate solution was found to contain 0.08% of lead(II) ion as impurity, being determined by the a. c. polarographic method. The preliminary experiments indicated that this concentration of lead(II) ion gave no appreciable effect on the reaction rate under investigation and therefore no further purification was carried out. Other reagents used for supporting electrolytes were of guaranteed reagent grade and used without further purification.

Apparatus and Procedure.—The rate of the reaction between copper(II) ion and Cd(II)-EDTA complex was followed by measuring the change of polarographic limiting current of copper(II) ion at −0.12 V. vs. SCE with time. A Shimadzu RP-2 pen-recording polarograph was employed for the measurement of current-time curves. The dropping mercury electrode used had an m value of 2.57 mg./sec. and a drop time t_d of 3.52 sec. in an air-free acetate buffer of pH 4.7 containing 0.1 M acetate, 0.1 M potassium nitrate and 0.01% gelatin at 25°C with open circuit. A saturated calomel electrode (SCE) was used as reference electrode which was connected to the electrolytic solution with the aid of a Hume and Harris type agar bridge[7]. Dissolved oxygen in the solution was removed by bubbling nitrogen gas through the solution. Gelatin was added as maximum suppressor by 0.01% in concentration. The pH of solution was measured by means of Hitachi EHP-1 pH meter, within the accuracy of 0.02 pH unit, immediately after the measurement of current-time curve.

The reactions were initiated by injecting the known amount of the deaerated copper(II) nitrate solution at the rate of 1 ml. per second with a calibrated syringe into acetate buffer solution which contained cadmium(II) ion and Cd(II)-EDTA complex in excess. The ionic strength of the solution was adjusted to be 0.2 with potassium nitrate. The solution was thoroughly stirred by bubbling nitrogen gas for ten seconds. With this technique, a reproducible current-time curve was obtained from 20 sec. after the initiation of reaction.

Results and Discussion

Copper(II) forms mono- and diacetato complexes, whereas cadmium(II) does only monoacetato complex in the solution which contains less than 0.2 M of acetate ions. The overall substitution reaction between copper(II) ion

1) H. Ackermann and G. Schwarzenbach, *Helv. Chim. Acta*, 35, 485 (1952).
2) N. Tanaka, K. Kato and R. Tamamushi. This Bulletin, 31, 283 (1958).
3) N. Tanaka and K. Kato, ibid., 32, 1376 (1959).
4) K. Kato, ibid., 33, 600 (1960).
5) N. Tanaka and K. Kato, ibid., 33, 1236 (1960).
6) N. Tanaka, M. Kamada, H. Osawa and G. Satô, ibid., 33, 1412 (1960).
7) D. N. Hume and W. E. Harris, *Ind. Eng. Chem., Anal. Ed.*, 15, 465 (1943).

and Cd(II)-EDTA complex in acetate buffer solution is represented with the following equations.

$$Cu^{2+} + 2OAc^- \rightleftarrows CuOAc^+ + OAc^- \rightleftarrows Cu(OAc)_2 \quad (1)$$

$$Cu^{2+} + CdY^{2-} \rightleftarrows CuY^{2-} + Cd^{2+} \quad (2)$$

$$Cd^{2+} + OAc^- \rightleftarrows CdOAc^+ \quad (3)$$

In Eq. 2, Y^{4-} denotes tetravalent EDTA anion. In the case when both Cd^{2+} and CdY^{2-} are present in a large excess over the copper(II) ion, Eq. 2 can be simplified to

$$Cu^{2+} \underset{k^-}{\overset{k^+}{\rightleftarrows}} CuY^{2-} \quad (4)$$

The rate equation for Eq. 4 is written as

$$-\frac{d[Cu^{2+}]_{app}}{dt} = k^+[Cu^{2+}]_{app} - k^-[CuY^{2-}] \quad (5)$$

where $[Cu^{2+}]_{app}$ is the apparent concentration of copper(II) ion that can be determined polarographically, or the sum of hydrated copper(II) ion and mono- and diacetato copper-(II) complexes.

Integrating Eq. 5

$$\ln\{[Cu^{2+}]_{app} - [Cu^{2+}]_{e,app}\} = -(k^+ + k^-)t + \ln\{[Cu^{2+}]_{0,app} - [Cu^{2+}]_{e,app}\} \quad (6)$$

is obtained, where suffixes 0 and e denote the initial and the equilibrium state respectively. At the equilibrium the following relation may be satisfied.

$$k^+/k^- = \frac{[CuY^{2-}]_e}{[Cu^{2+}]_{e,app}} \fallingdotseq K^{Cu}_{Cd,app}\frac{[CdY^{2-}]_0}{[Cd^{2+}]_{0,app}} \quad (7)$$

$K^{Cu}_{Cd,app}$ means the apparent equilibrium constant of Eq. 2 at a certain acetate concentration, and is given as

$$K^{Cu}_{Cd,app} = \frac{[CuY^{2-}]_e[Cd^{2+}]_{e,app}}{[Cu^{2+}]_{e,app}[CdY^{2-}]_e} \quad (8)$$

The values of $K^{Cu}_{Cd,app}$ were determined polarographically to be 102 at 15°C and 113 at 5°C in the presence of 0.091 M of acetate. These values were introduced in Eq. 7, and k^+ was determined from Eqs. 6 and 7.

The apparent overall rate constants of forward reaction of Eq. 4 ($k^+/[CdY^{2-}]_0$) were measured at varied initial concentrations of copper(II) ion and those of Cd(II)-EDTA complex under other conditions kept constant, and found to be independent of the variables as shown in Table I. This observation led to the conclusion that the overall substitution reaction proceeds according to the pseudo first order rate law.

Table I. $k^+/[CdY^{2-}]_0$ values at various initial concentrations of copper(II) ion or Cd(II)-EDTA complex
(15°C, μ=0.2, $[OAc^-]$=0.091 M, pH=5.50, $[Cd^{2+}]_{0,app}=1.028\times10^{-2}$ M)

$[Cu^{2+}]_{0,app}$ M×10⁴	$[CdY^{2-}]_0$ M×10³	$k^+/[CdY^{2-}]_0$ l.mol⁻¹ sec⁻¹
0.99	5.00	0.72_4
1.98	5.00	0.73_2
2.97	5.00	0.73_2
1.98	9.98	0.72_0

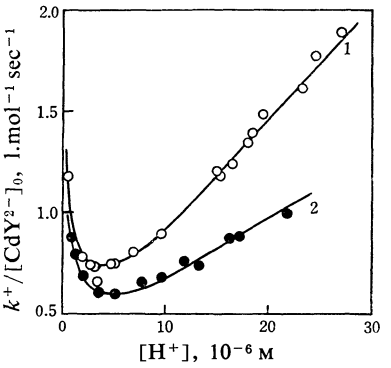


Fig. 1. $k^+/[CdY^{2-}]_0$ as a function of the hydrogen ion concentration in acetate buffer-potassium nitrate solutions of ionic strength 0.2 at 15°C. Initial concentrations are: $[Cu^{2+}]_{0,app}=1.98\times10^{-4}$ M; $[CdY^{2-}]_0=5.00\times10^{-3}$ M; $[Cd^{2+}]_{0,app}=1.028\times10^{-2}$ M (curve 1) and 2.056×10^{-2} M (curve 2). Concentration of free acetate is 0.091 M.

Two sets of $k^+/[CdY^{2-}]_0$, in each of which the values of $k^+/[CdY^{2-}]_0$ were measured at various hydrogen ion concentrations under other conditions kept constant, were obtained at two different concentrations of cadimium-(II) ion. The values obtained are plotted against the hydrogen ion concentration as shown in Fig. 1, where it should be noticed that, in the region of low hydrogen ion concentration, $k^+/[CdY^{2-}]_0$ increases with decreasing concentration of hydrogen ion.

These experimental results suggest that the substitution reaction between copper(II) ion and Cd(II)-EDTA complex proceeds simultaneously through the following four reaction paths:

i) $Cu^{2+} + CdY^{2-} \underset{k_1^+}{\rightleftarrows} CuY^{2-} + Cd^{2+}$ (9)

ii) $CdY^{2-} + H^+ \rightleftarrows CdHY^-$ (10a)

$CuHY^- + Cu^{2+} \underset{k_{II}^+}{\rightleftarrows} CuHY^- + Cd^{2+}$ (10b)

$CuHY^- \rightleftarrows CuY^{2-} + H^+$ (10c)

iii) $CdY^{2-} + H^+ \rightleftarrows Cd^{2+} + HY^{3-}$ (11a)

$Cu^{2+} + HY^{3-} \underset{k_{III}^+}{\rightleftarrows} CuY^{2-} + H^+$ (11b)

iv) $CdY^{2-} + H_2O \rightleftarrows CdOHY^{3-} + H^+$ (12a)

$$Cu^{2+} + CdOHY^{3-} \overset{k_{IV}^+}{\rightleftarrows} CuOHY^{3-} + Cd^{2+} \quad (12b)$$

$CuOHY^{3-} + H^+ \rightleftarrows CuY^{2-} + H_2O$ (12c)

If the substitution reaction is assumed to proceed only through the hydrated ions which are in equilibrium with the acetato complexes, the apparent rate of the forward reaction ($v^+ = k^+ [Cu^{2+}]_{app}$) is represented by Eq. 13.

$$v^+ = k^+ [Cu^{2+}]_{app} = \left\{ \frac{k_1^+ + k_2^+ [H^+] + k_3^+ [H^+] \frac{1 + K_{CdOAc}[OAc^-]}{[Cd^{2+}]_{app}} + k_4^+ \frac{1}{[H^+]}}{1 + \sum_{n=1}^{2} K_{Cu(OAc)_n} [OAc^-]^n} \right\} \times [Cu^{2+}]_{app} [CdY^{2-}] \quad (13)$$

$$\left. \begin{aligned} k_2^+ &= k_{II}^+ K_{CdHY}^H \qquad k_3^+ = k_{III}^+ / K_{CdY} K_{HY} \\ k_4^+ &= k_{IV}^+ K_{CdOHY} \end{aligned} \right\} \quad (14)$$

In Eqs. 13 and 14, K_{CdHY}^H means the equilibrium constant of reaction 10a, K_{CdY}, the formation constant of CdY^{2-}, K_{HY}, the fourth dissociation constant of ethylenediaminetetraacetic acid, K_{CdOHY}, the equilibrium constant for reaction 12a, and K_{CdOAc} and $K_{Cu(OAc)_n}$ represent the overall formation constants of acetatocadmium(II) and acetatocopper(II) complexes, respectively. Some of these constants were determined in our laboratory[6,8] and others were cited from literatures, if necessary, after correction for the ionic strength and/or temperature with the same procedures as described previously[2-4]. These constants are given in Table II.

TABLE II. EQUILIBRIUM CONSTANTS AT IONIC STRENGTH 0.2 AT VARIOUS TEMPERATURES

Temp., °C	5	15	20
$\log K_{CdY}$	16.53	16.34	—
pK_{HY}	10.34	10.16	—
$\log K_{CdHY}^H$	—	—	2.8
K_{CuOAc}	—	41	—
$K_{Cu(OAc)_2}$	—	190	—
K_{CdOAc}	—	27	—

From Eq. 13 is obtained,

$$K^+ / [CdY^{2-}]_0 = A[H^+] + B + C\frac{1}{[H^+]} \quad (15)$$

$$\left. \begin{aligned} A &= \frac{k_2^+ + k_3^+ \frac{1 + K_{CdOAc}[OAc^-]}{[Cd^{2+}]_{0,app}}}{1 + \sum_{n=1}^{2} K_{Cu(OAc)_n} [OAc^-]^n} \\ B &= k_1^+ / (1 + \sum_{n=1}^{2} K_{Cu(OAc)_n} [OAc^-]^n) \\ C &= k_4^+ / (1 + \sum_{n=1}^{2} K_{Cu(OAc)_n} [OAc^-]^n) \end{aligned} \right\} \quad (16)$$

8) N. Tanaka and K. Kato, This Bulletin, 33, 417 (1960).

where the initial concentrations, $[Cd^{2+}]_0$ and $[CdY^{2-}]_0$, are substituted for $[Cd^{2+}]$ and $[CdY^{2-}]$, respectively.

Rearranging Eq. 15,

$$k^+ [H^+] / [CdY^{2-}]_0 = A[H^+]^2 + B[H^+] + C \quad (17)$$

$$\left(\frac{k^+ [H^+]}{[CdY^{2-}]_0} - C \right) \Big/ [H^+] = A[H^+] + B \quad (18)$$

are obtained. Since both Cd^{2+} and CdY^{2-} are present in the reaction mixture in a large excess over the concentration of copper(II) ion, the change of their concentrations during the reaction can be neglected.

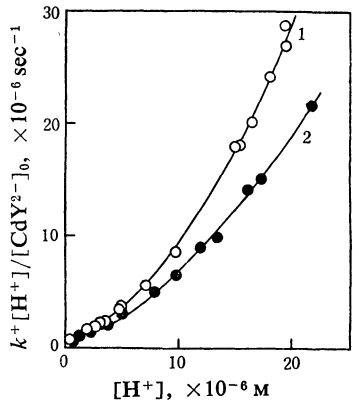


Fig. 2. $k^+[H^+]/[CdY^{2-}]_0$ as a function of the hydrogen ion concentration in acetate buffer-potassium nitrate solutions of ionic strength 0.2 at 15°C. Initial concentrations are: $[Cu^{2+}]_{0,app} = 1.98 \times 10^{-4}$ M; $[CdY^{2-}]_0 = 5.00 \times 10^{-3}$ M; $[Cd^{2+}]_{0,app} = 1.028 \times 10^{-2}$ M (curve 1) and 2.056×10^{-2} M (curve 2). Concentration of free acetate is 0.091 M.

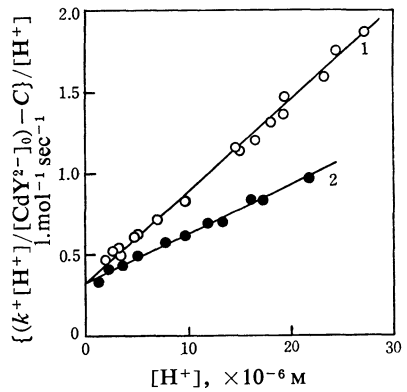


Fig. 3. $\{(k^+[H^+]/[CdY^{2-}]_0) - C\}/[H^+]$ as a function of the hydrogen ion concentration in acetate buffer-potassium nitrate solutions of ionic strength 0.2 at 15°C. Initial concentrations are: $[Cu^{2+}]_{0,app} = 1.98 \times 10^{-4}$ M; $[CdY^{2-}]_0 = 5.00 \times 10^{-3}$ M; $[Cd^{2+}]_{0,app} = 1.028 \times 10^{-2}$ M (curve 1) and 2.056×10^{-2} M (curve 2). Concentration of free acetate is 0.091 M.

TABLE III. RATE CONSTANTS IN EQ. 13 OBTAINED EXPERIMENTALLY, AND THOSE FOR REACTIONS 10b, 11b AND 12b AT IONIC STRENGTH 0.2 AT VARIOUS TEMPERATURES

Temp. °C	Rate constant					
	k_1^+ l.mol^{-1} sec^{-1}	k_2^+ l^2 mol^{-2} sec^{-1}	k_{II}^+ l.mol^{-1} sec^{-1}	k_3^+ l.mol^{-1} sec^{-1}	k_{III}^+ l.mol^{-1} sec^{-1}	k_4^+ sec^{-1}
5	0.95	$1.7_0\times10^4$	26.9	$3.7_6\times10^2$	$5.7_0\times10^8$	$9.4_5\times10^{-7}$
15	2.2	$2.9_0\times10^4$	45.9	$9.0_7\times10^2$	$1.3_2\times10^9$	$3.7_8\times10^{-6}$

In Figs. 2 an 3, $k^+[H^+]/[CdY^{2-}]_0$ and $\{(k^+[H^+]/[CdY^{2-}]_0)-C\}/[H^+]$ are plotted against $[H^+]$, respectively, using the values of k^+ obtained at various hydrogen ion concentrations. The values for *A*, *B* and *C* were determined from these plots; *A* from the slope of the plot in Fig. 3, *B* from the intercept of the plot in Fig. 3 and *C* from the intercept of the plot in Fig. 2. With these values and equilibrium constants given in Table II, the rate constants were calculated using Eqs. 14 and 16, and they are summarized in Table III.

The rate constant k_{III}^+ had been determined in the kinetic studies of the substitution reaction between copper(II) ion and lead(II)-EDTA complex[2,3], and that between copper(II) ion and zinc(II)-EDTA complex[4]. It is in reasonable agreement with the value of k_{III}^+ obtained in this study, as shown in Table IV.

TABLE IV. THE RATE CONSTANTS OF ELEMENTARY REACTIONS OF THE SUBSTITUTION REACTION, $M^{m+}+M'Y^{(m'-4)+} \rightleftarrows MY^{(m-4)+}+M'^{m'+}$, AT 15°C $\mu=0.2$ AND $[OAc^-]=0.09$ M

M	M'	k_1^+ l.mol^{-1} sec^{-1}	k_{II}^+ l.mol^{-1} sec^{-1}	k_{III}^+ l.mol^{-1} sec^{-1}
Cu^{2+}	Pb^{2+}	1.7	10	1.7×10^9
Cu^{2+}	Zn^{2+}	19	60	2.0×10^9
Cu^{2+}	Cd^{2+}	2.2	45.9	$1.3_2\times10^9$
Pb^{2+}	Zn^{2+}	4.6	800	1.0×10^{10}

Ackermann and Schwarzenbach[1] investigated the kinetics of the substitution reaction between copper(II) ion and Cd(II)-EDTA complex at 0°C in the solutions of ionic strength 1.0 containing 0.09 M of acetate ion and $5\times10^{-6}\sim1.4\times10^{-4}$ M of hydrogen ion, when they concluded that the reaction proceeds simultaneously through four different paths as follows:

$$Cu^{2+}+\left\{\begin{array}{l} CdY^{2-} \\ \downarrow\uparrow \\ CdHY^- \\ \downarrow\uparrow \\ Cd^{2+}+HY^{3-} \\ \downarrow\uparrow \\ Cd^{2+}+H_2Y^{2-} \end{array}\right\} \rightarrow Cd^{2+}+CuY^{2-}+\left\{\begin{array}{l} H^+ \\ H^+ \\ 2H^+ \end{array}\right\}$$

Their experimental conditions, however, were apparently unfavorable to find out the reaction path given by Eqs. 12a, 12b and 12c.

Equation 13 predicts that the reaction rate decreases with the increasing concentration of acetate ion. This was previously recognized experimentally by Ackerman and Schwarzenbach, who stated that the decrease in reaction rate was due to the formation of acetato copper(II) complex. Using Eqs. 15 and 16, the values of $k^+/[CdY^{2-}]_0$ were calculated at various concentrations of acetate ion with the rate constants given in Table III. These values are plotted against acetate ion concentration in Fig. 4, where the experimental values for $k^+/[CdY^{2-}]_0$ obtained at various concentrations of acetate ion are also given. Figure 4 indicates that the calculated values of $k^+/[CdY^{2-}]_0$ considerably deviate from the experimental ones. This tendency has been noticed in the studies on other substitution reactions[3-5]. The discrepancy seemed to come from the assumption that the reaction proceeds through only hydrated ions.

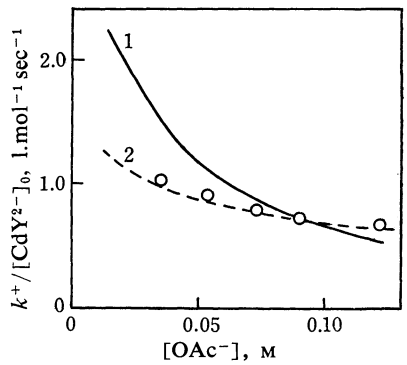


Fig. 4. $k^+/[CdY^{2-}]_0$ as a function of the acetate ion concentration in acetate buffer-potassium nitrate solutions of pH 5.50 and ionic strength 0.2 at 15°C. Initial concentrations are: $[Cu^{2+}]_{0,app}=1.98\times10^{-4}$ M; $[CdY^{2-}]_0=5.00\times10^{-3}$ M; $[Cd^{2+}]_{0,app}=1.028\times10^{-2}$ M. ○ indicates the experimental value. Curve 1 is calculated with Eq. 13 and curve 2, with Eq. 19.

Then, the reaction was assumed as to proceed through both hydrated ion and monoacetato complex. The rate-determining steps in the simultaneous substitution reaction are as follows.

$$\text{i)}\quad Cu^{2+}+CdY^{2-} \overset{k_{1h}^+}{\rightleftarrows} CuY^{2-}+Cd^{2+} \qquad (9')$$

$$CuOAc^+ + CdY^{2-} \overset{k_{1c}^+}{\rightleftarrows} CuY^{2-}+CdOAc^+ \qquad (9'')$$

ii) $Cu^{2+} + CdHY^- \overset{k_{IIh}^+}{\rightleftarrows} CuHY^- + Cd^{2+}$ (10b')

$CuOAc^+ + CdHY^- \overset{k_{IIc}^+}{\rightleftarrows} CuHY^- + CdOAc^+$ (10b'')

iii) $Cu^{2+} + HY^{3-} \overset{k_{IIIh}^+}{\rightleftarrows} CuY^{2-} + H^+$ (11b')

$CuOAc^+ + HY^{3-} \overset{k_{IIIc}^+}{\rightleftarrows} CuY^{2-} + H^+ + OAc^-$

iv) $Cu^{2+} + CdOHY^{3-} \overset{k_{IVh}^+}{\rightleftarrows} CuOHY^{3-} + Cd^{2+}$ (12b')

$CuOAc^+ + CdOHY^{3-} \overset{k_{IVc}^+}{\rightleftarrows} CuOHY^{3-} + CdOAc^+$ (12b'')

where k_{ih}^+ and k_{ic}^+ mean the rate constants of the reactions which proceed through the hydrated ion and monoacetato complex, respectively. Since it seemed extremely difficult, however, to determine all of these rate constants separately because of insufficient accuracy in the measurement, the following procedure was taken up as the first approximation. In all reactions from (9') to (12b'') the ratios of k_{ic}^+ to k_{ih}^+ (i.e. k_{ic}^+/k_{ih}^+) are assumed to be the same and denoted with x. The rate equation is written as Eq. 19.

$$v^+ = \frac{k_{1h}^+ + k_{2h}^+[H^+] + k_{3h}^+ \dfrac{1+K_{CdOAc}[OAc^-]}{[Cd^{2+}]_{app}} + k_{4h}^+ \dfrac{1}{[H^+]}}{1+\sum_{n=1}^{2} K_{Cu(OAc)_n}[OAc^-]^n} \times (1+xK_{CuOAc}[OAc^-])[Cu^{2+}]_{app}[CdY^{2-}] \quad (19)$$

Comparing Eq. 19 with Eq. 13,

$$k_i^+ = k_{ih}^+(1+xK_{CuOAc}[OAc^-]) \quad (20)$$

is derived. With the values of k_i^+ obtained experimentally at various concentrations of acetate ion k_{ih}^+ and x were determined by the graphical method. For the latter, 0.26 at 5°C and 0.37 at 15°C were obtained. The apparent rate constants $k^+/[CdY^{2-}]_0$ at various concentrations of acetate ion were evaluated with the values of k_{ih}^+ and x using Eq. 20. The results are in satisfactory agreement with the experimental values as shown in Fig. 4 (curve 2). Although this treatment is not strictly rigorous, it proves that the substitution reaction proceeds through both hydrated ions and monoacetato complexes.

Summary

The kinetic study of the substitution reaction of copper(II) and ethylenediaminetetraacetatocadmate(II) complexes in acetate buffer solutions has been carried out by the same method as reported previously[2-5]. The reaction was found, under the experimental conditions, to proceed simultaneously through four different reaction paths, and the rate constants for the elementary reactions of those reaction paths were determined at ionic strength 0.2 at 5 and 15°C. It was confirmed also that this substitution reaction proceed through both hydrated ion and monoacetato complex.

The authors thank the Ministry of Education for the financial support granted for this research.

Department of Chemistry
Faculty of Science
Tohoku University
Katahira-cho, Sendai

*The Crystal Structure of m-Aminobenzenearsonic Acid**

By Akira SHIMADA

(Received May 23, 1962)

The crystal and molecular structure of benzenearsonic acid and its *p*-amino derivative have been recently investigated by the present author[1,2]. These two structures are closely related in both having endless chains formed by the hydrogen bonds between arsonic acid groups, although the molecule in the latter is to be regarded as a zwitterion and although the $-NH_3^+$ group in this ion forms additional hydrogen bonds to link the chains. In connection with the above work, the crystal structure of *m*-aminobenzenearsonic acid, $H_2N \cdot C_6H_4AsO(OH)_2$, was examined as part of a program to contribute to the structural chemistry of organoarsenic compounds.

* The major part of this papar was read at the 14th Annual Meeting of the Chemical Society of Japan, Tokyo, April, 1961.

1) A. Shimada, This Bulletin, **32**, 309 (1959); A. Shimada, ibid., **33**, 301 (1960).

2) A. Shimada, ibid., **34**, 639 (1961).

Experimental

Crystals suitable for X-ray work were selected from specimens kindly prepared and supplied by Prof. H. Nakata of Konan University. They were colorless, transparent, and lath-like needles with a long dimension in the c direction. The crystals used in this experiment had square cross sections 0.16×0.15 mm. for $(h\,k\,0)$, 0.22×0.24 mm. for $(0\,k\,l)$, and 0.26×0.29 mm. for $(h\,0\,l)$. Oscillation and Weissenberg photographs around three principal axes were taken with CuK_α radiation; it was found from an examination of them that the unit cell is monoclinic with the following dimensions:

$a=13.35$, $b=15.60$, $c=7.46$ Å and $\beta=92.7°$

This choice of axes, which makes the unit cell base-centered, is unconventional in the case of the monoclinic system, but the crystal was referred to these axes for the sake of experimental convenience, since the c axis lies along a needle direction and since the a axis is almost perpendicular to the needle direction by this choice of axes. The cell size of this crystal gave a calculated density of 1.857 g. cm^{-3} on the assumption that there are eight formula units in a unit cell. This calculated density is close to the value found for the *p*-amino derivative.

The extinctions observed, $h\,k\,l$ when $h+l$ is odd, $h\,0\,l$ when h and l is odd, and $0\,k\,0$ when k is odd, indicate that the space group is $C_{2h}^5-B2_1/a$. By comparing these results with a calibrated scale, visual intensity measurements were made with the aid of both multiple exposure and multiple-film techniques. They were corrected for the appropriate Lorentz and polarization factors, and the correction for absorption ($\mu=58.6\,cm^{-1}$) was evaluated on the assumption that the specimens were cylindrical rods.

Structure Determination

The structure was determined by making use of the heavy atom technique. Thus, the Patterson projection $P(UV)$ along the c axis was first synthesized because of the short c axis. In this projection were found trains of peaks along the b axis at approximately $U=0$ and $U=a/4$ due to vectors from the heavy arsenic atom to the lighter atoms; peaks due to vectors between arsenic atoms were also found. This striking appearance suggests that the planes of benzene rings are perhaps almost parallel to the (100) plane and pack one above the other, with a separation of one quarter of a period along the a axis. This fact was confirmed by the minimum function based on the rotation peak between arsenic atoms and also by the preliminary electron-density map, the Fourier terms of which were observed structure amplitudes with signs determined only by the approximate coordinates of arsenic atoms derivable from the Patterson function. Hence, it was not so difficult to locate plausible positions of the lighter atoms in this projection with this feature of the packing mode of benzene rings, although there was a heavy overlapping of the carbon atoms of benzene rings.

Referring to this feature of the structure, the Patterson and electron-density maps along the a axis were synthesized by the same procedure. These two maps along the a axis, together with the aid of the projection along the c axis, were sufficient to give all of the atomic positions except those of the hydrogen atoms; the projection along the b axis was also tried in order to confirm the atomic positions derived by the other projections.

Refinement of the coordinates of atoms was carried out by successive Fourier syntheses and also by difference syntheses at later stages. In the calculation of the structure factors, McWeeny's scattering curves[3] for the nitrogen atom, of "valence states" for carbon and of $1/3(f^{\parallel}+2f^{\perp})$ for the oxygen atom, were used,

Table I. Atomic coordinates

Atom	x/a	y/b	z/c
As	0.087_4	0.162_5	0.135_1
O_1	0.172	0.238	0.215
O_2	−0.040	0.196	0.136
O_3	0.112	0.138	−0.092
C_1	0.111	0.059	0.268
C_2	0.109	−0.022	0.184
C_3	0.130	−0.092	0.300
C_4	0.137	−0.089	0.488
C_5	0.141	−0.008	0.563
C_6	0.124	0.061	0.457
N	0.143	−0.179	0.221

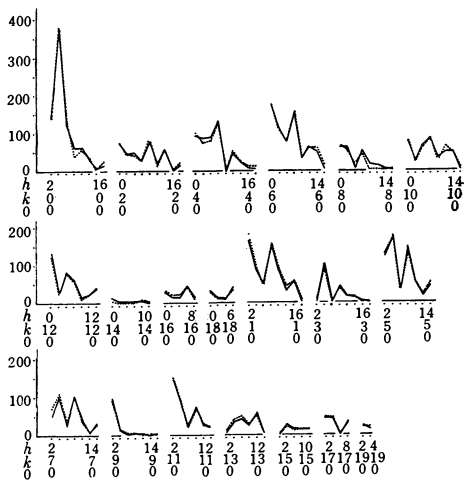


Fig. 1a. Comparison of observed and calculated structure factors, $F(h\,k\,0)$.
—— F_{obs} ····· F_{calcd}

3) R. McWeeny, *Acta Cryst.*, **4**, 513 (1951).

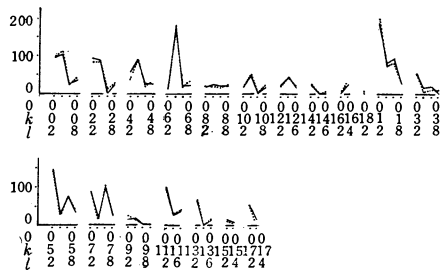


Fig. 1b. Comparison of observed and calculated structure factors, $F(0kl)$.
—— F_{obs} ····· F_{calcd}

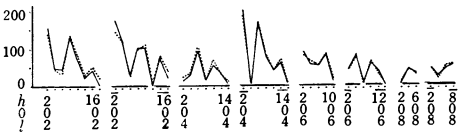


Fig. 1c. Comparison of observed and calculated structure factors, $F(h0l)$.
—— F_{obs} ····· F_{calcd}

while that given by Berghuis et al.[4] was used for the arsenic atom. The isotropic temperature factors were estimated to be 2.7 Å^2 for all atoms. The R indices for the final coordinates listed in Table I were 10.0, 11.8 and 11.6% for $(hk0)$, $(0kl)$ and $(h0l)$ respectively, excluding terms too weak to be observed. The observed structure factors are compared with those calculated in Fig. 1.

Description of the Structure

The configuration of a molecule and the molecular arrangement in the crystal may be seen in Figs. 2a, 2b and 2c, which represent the c, a and b axes projections for this crystal. The arsenic atom is surrounded by a group of three oxygen atoms, O_1, O_2 and O_3 of the arsonic acid, and one carbon atom C_1 of the benzene ring. The average As–O distance is 1.76 Å, and the As–C distance is 1.91 Å. The disposition of bonds from the arsenic atom appears to be nearly tetrahedral, the angles between the bonds being about 110°. The benzene ring is planar, and the average distance between adjacent carbon atoms is 1.39 Å, individual values ranging from 1.35 Å to 1.41 Å. The N–C distance is 1.49 Å, and the nitrogen atom is found to lie on the plane of a benzene ring within the limit of experimental error. This molecular configuration is considered to be in accordance with those of benzenearsonic acid and its *p*-amino derivative.

The molecules are held together by a beautiful network of hydrogen bonds. There are four hydrogen atoms available for hydrogen bonding in an asymmetric unit. Two of them come from the *m*-amino group, and two come from the arsonic acid group. There is one hydrogen bond between oxygen atoms, and there are three hydrogen bonds between oxygen and nitrogen atoms in the crystal. The hydrogen bond, with a length of 2.56 Å from the O_3

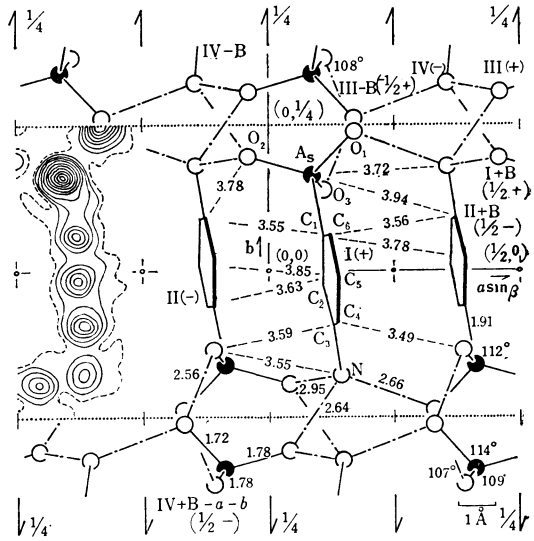


Fig. 2a. The structure and the electron-density projection along the c axis, with bond angles, intra- and intermolecular distances (Å). Contours at arbitrary scale. Dot-dash lines indicate hydrogen bonds.

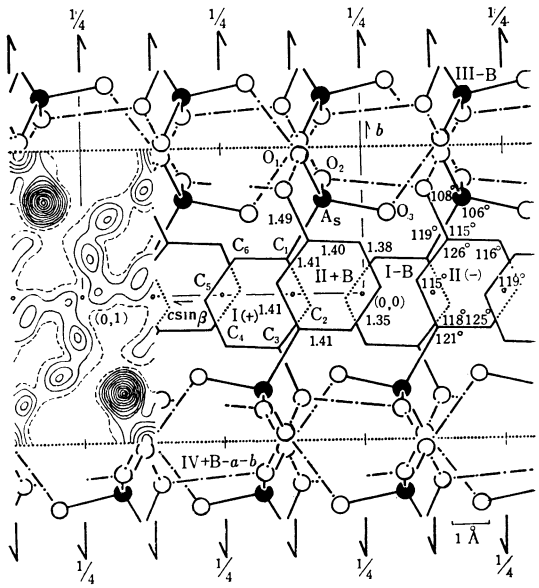


Fig. 2b. The structure and the electron-density projection along the a axis, with bond angles and intramolecular distances (Å). Contours at arbitrary scale. Dot-dash lines indicate hydrogen bonds.

4) J. Berghuis, I. M. Haanappel, M. Potters, B. O. Loopstra, C. H. MacGillavry and A. L. Veenedaal, ibid., 8, 478 (1955).

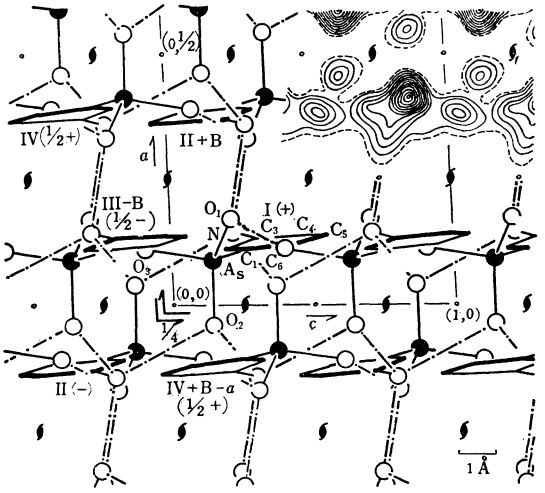


Fig. 2c. The structure and the electron-density projection along the b axis. Contours at arbitrary scale. Dot-dash lines indicate hydrogen bonds.

atom of I molecule to the O_1 atom of the III–B molecule, links the molecules with each other to form endless chains along the c axis. The nitrogen atom in the *m*-amino group of molecule I forms three hydrogen bonds, the first with a length of 2.95Å to the O_2 atom of II molecule, the second with a length of 2.64Å to the O_2 atom of IV+B−a−b molecule, and the third with a length of 2.66Å to the O_1 atom of the II+B molecule. This triple hydrogen-bond formation of a nitrogen atom suggests that one of the hydrogen atoms is transferred from an arsonic acid group to the *m*-amino group. On this basis, the formula of the molecule should be written as $NH_3^+ \cdot C_6H_4 \cdot AsO_2(OH)^-$, which indicates that the molecule is in the zwitterion form in the crystal.

Three hydrogen bonds around a nitrogen atom connect the chains mentioned above to form a sheet which is perpendicular to the b axis and is located around a glide plane. These sheets of hydrogen bonds are interlocked through the benzene rings, which are found to stack with each other along the a axis. This mode of packing of the molecule is similar to that of *p*-aminobenzenearsonic acid, while only hydrogen-bonded chains are packed together by van der Waals forces in benzenearsonic acid. All the intermloecular distances correspond to normal van der Waals interactions; the shorter contacts are illustrated in Fig. 2.

The author is much indebted to Professor Isamu Nitta of Kwansei Gakuin University and to Professor Tokunosuke Watanabé of Osaka University for their interest and encouragement, to Professor Hisakazu Nakata of Konan University for providing the specimens, and to Dr. Kenji Osaki of Osaka University for his sharing of his computation programs and for his instructions about structure-factor calculations using the NEAC electronic computer, which was generously made available by Dr. Shigeki Sakurai of the Electrical Communication Laboratory. Part of the computations for this study were also carried out with a KDC-I electronic computer; deep appreciation is expressed to Professor Tetsuro Tanaka, Professor Takeshi Kiyono and Mr. Koichi Toyoda of Kyoto University for their kind assistance with these calculations. The present study was supported partly by a scientific research grant from the Ministry of Education.

Department of Chemistry
Faculty of Science
Osaka City University
Kita-ku, Osaka

Semiconductivities and Charge Transfer Spectra of Solid Molecular Complexes of 1, 3, 5-Trinitrobenzene

By Haruo KURODA, Keitaro YOSHIHARA and Hideo AKAMATU

(Received April 30, 1962)

The solid molecular complexes formed by the interaction of polycyclic aromatic hydrocarbons with halogens are semiconductors of a high electrical conductivity[1]. In such molecular complexes, a charge transfer interaction between the molecules contributes to the solid formation, where halogen molecules behave as electron acceptors, while hydrocarbon molecules behave as electron donors. These solid molecular complexes exhibit a strong electron spin resonance absorption[2,3], which indicates a strong electron transfer from the donor to the acceptor molecules. There are, however, a number of charge transfer complexes which do not show any appreciable electron spin resonance absorption. In such molecular complexes, the intermolecular charge transfer between donor and acceptor molecules is relatively weak in the ground state. In these cases, Mulliken's theory of charge transfer interaction can be successfully applied to a discussion of the electronic state[4]. We shall temporarily call such complexes by the name of "loose molecular complexes". The complexes formed from polycyclic aromatic hydrocarbons, as the donor, and tetracyanoethylene or 1, 3, 5-trinitrobenzene (TNB), as the acceptor, are of this kind.

In a previous paper[5], we have shown, with a series of tetracyanoethylene-complexes, that the energy gap, twice the activation energy for the electrical conduction, determined from the temperature dependence of the electrical resistivity is approximately equal to the energy corresponding to the peak of the charge transfer band in the absorption spectrum of the crystal. In order to explain such a result, we presumed that a charge carrier is produced through a charge transfer from a donor to an acceptor molecule. If this is actually the case, a similar relation will be found with other loose molecular complexes. It seems, therefore, of interest to compare the activation energy for the electrical conduction with the frequency of the charge transfer band observed with such other loose molecular complexes as TNB-complexes.

1) H. Akamatu, H. Inokuchi and Y. Matsunaga, This Bulletin, **29**, 219 (1956).
2) Y. Matsunaga, *J. Chem. Phys.*, **30**, 855 (1959).
3) L. S. Singer and J. Kommandeur, ibid., **34**, 133 (1961).
4) R. S. Mulliken, *J. Am. Chem. Soc.*, **74**, 811 (1952).
5) H. Kuroda, M. Kobayashi, M. Kinoshita and S. Takemoto, *J. Chem. Phys.*, **36**, 457 (1962).

Experimental

The TNB-complexes, in which the mole ratios of the donors to TNB were 1 : 1, were prepared by cooling hot solutions containing equivalent amounts of the donors and of TNB. The crystals of the complexes usually precipitate as fine needles.

The electrical resistivity of each complex was measured by the D. C. method. A crystalline powder of the complex was packed in a quartz cell, and the resistivity was measured under a compression of 116 kg./cm^2. The field applied externally for the resistivity measurement was below 2000 V./cm., where the resistivity obeyed Ohm's law. The temperature dependence of the resistivity was studied in a range from room temperature to a little below the melting point.

The visible and ultraviolet absorption spectra of the crystalline powders were measured by means of the KBr-pellet method with a Cary spectrophotometer.

Results

Absorption Spectra. — The absorption spectrum of the solid complex formed between *N, N, N', N'*-tetramethylbenzidine and TNB is shown in Fig. 1. The absorptions at wavelengths shorter than 500 mμ can be assigned to the excitation of either the donor or the TNB molecules, while the band extending from 500 to 800 mμ is the characteristic absorption band for the complex formation. Almost every

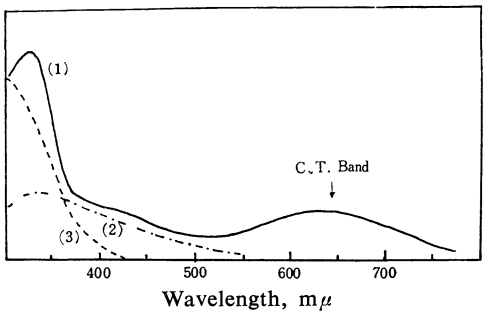


Fig. 1. Absorption spectrum of tetramethylbenzidine-TNB complex in the crystalline state: (1) solid complex, (2) tetramethylbenzidine (solid), (3) TNB (solid).

TABLE I. CHARGE TRANSFER SPECTRA OF TNB-COMPLEXES

Donor	Ionization potential of donor eV.	Solution (in CCl_4) $\tilde{\nu}_{max}$ $10^3\,cm^{-1}$	Crystal $\tilde{\nu}_{max}$ $10^3\,cm^{-1}$	$\Delta\tilde{\nu}$ $(=\tilde{\nu}(soln.)-\tilde{\nu}(solid))$ $10^3\,cm^{-1}$
Anthracene	7.55[a]	22.5	20.4	2.1
			21.5	1.0
			22.6	−0.1
Phenanthrene	8.03[a]	26.8	24.3	2.5
Pyrene	7.55[b]	22.5	21.5	1.0
Chrysene	7.8[b]	23.3	22.5	0.8
Perylene	7.15[b]	19.6	18.0	1.6
Anthanthrene	(7.1)[c]	18.5	17.9	0.6
Aniline	7.70[d]	25.0	22.7	2.3
Dimethylaniline	7.3[b]	20.9	19.6	1.3
Benzidine		20.0	17.6	3.4
Tetramethylbenzidine		17.1	16.0	1.1
p-Phenylenediamine	7.15[b]	20.0	17.3	2.7
α-Naphthylamine		21.7	20.9	0.8

a) M. E. Wacks and V. H. Dibeler, *J. Chem. Phys.*, **31**, 1958 (1959).
b) D. Brieglebs and J. Czekalla, *Z. Elektrochem.*, **63**, 6 (1959).
c) F. A. Matsen, *J. Chem. Phys.*, **24**, 602 (1956).
d) K. Watanabe and J. R. Mottl, ibid., **26**, 1773 (1957).

solid complex studied here has such a characteristic band, which is always very broad and without any fine structure, the width at half of the intensity maximum being more than 8000 cm^{-1} in wave number. The solid complex of anthracene was found to be an exception in this respect; it showed an absorption band with a fine structure which we shall mention later.

The wavelength at the peak of the characteristic band is given in Table I, together with the wavelength of the charge transfer band observed with the carbon tetrachloride solution of the complex. McGlynn and Boggus[6] have shown that the frequency of the charge transfer band of TNB-complexes of polycyclic aromatic hydrocarbons in solutions is linearly dependent on the ionization potential of the donor. The frequency of the charge transfer band in carbon tetrachloride, $\nu_{C.T.}(soln.)$, given in Table I, can be described as:

$$h\nu_{C.T.}(soln.) = 0.85I_p - 3.65 \quad [eV.] \qquad (1)$$

where I_p is the ionization potential of the donor. The relation between the frequency of the characteristic band of the solid complexes, $\nu_{C.T.}(solid)$, and the ionization potential of the donor can also be described by a similar equation:

$$h\nu_{C.T.}(solid) = 0.85I_p - 3.82 \quad [eV.] \qquad (2)$$

The regularity mentioned above implies, in the first place, that the characteristic absorption bands observed with the solid complexes are also due to the excitation associated with a charge transfer from the donor to the TNB molecules, and that, in the second place, the energy of the charge transfer excitation is, in the crystalline state, lower by an average of 0.17 eV. than that of the isolated complex in carbon tetrachloride. In other words, we can consider that the charge transfer band shows a red-shift as a result of the crystallization. The magnitude of the red-shift in each complex is given in the last column of Table I.

The absorption spectrum of the solid complex of anthracene-TNB is shown in Fig. 2. The absorption in the wavelength region of 400~500 mμ is the charge transfer band. In this band we can observe three peaks separated from each other by 1070 cm^{-1}. Lower, Hochstrasser, and Reid[7] have observed the absorption spectrum of a single crystal of

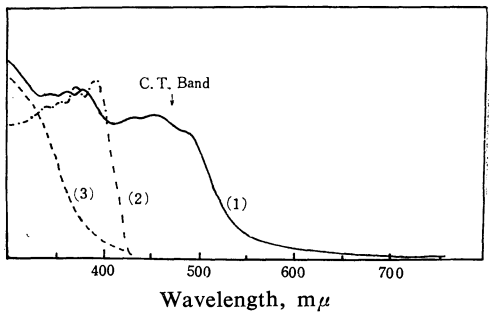


Fig. 2. Absorption spectrum of anthracene-TNB complex in the crystalline state: (1) solid complex, (2) anthracene (solid), (3) TNB (solid).

6) S. P. McGlynn and J. D. Boggus, *J. Am. Chem. Soc.*, **80**, 5096 (1958).

7) S. K. Lower, R. M. Hochstrasser and C. Reid, *Mol. Phys.*, **4**, 162 (1961).

anthracene-TNB at the temperature of liquid nitrogen and have found a similar fine structure in the change transfer band. They assigned the fine structure to the TNB-ring stretching vibration, 1070 cm^{-1}, an intermolecular vibration, 250 cm^{-1}, and their combinations. This fine structure can be observed in the crystalline state only; the charge transfer band in the absorption spectrum of the complex in solution shows no structure.

Electrical Resistivity. — All the TNB-complexes studied here are poor semiconductors, exhibiting an electrical resistivity of $10^{13}\sim10^{20}$ Ω·cm. at room temperature. As is known to be the case for many organic semiconductors, the resistivity is exponentially dependent on the reciprocal of the temperature. A typical example of the temperature dependence is given in Fig. 3. The resistivity can be described, therefore, with the following equation:

$$\rho = \rho_0 \exp(E/kT) \qquad (3)$$

where E is the activation energy for the electrical conduction, and ρ_0 is a constant. The experimental results are summarized in Table II. It is to be noted that the activation energy required for the electrical conduction

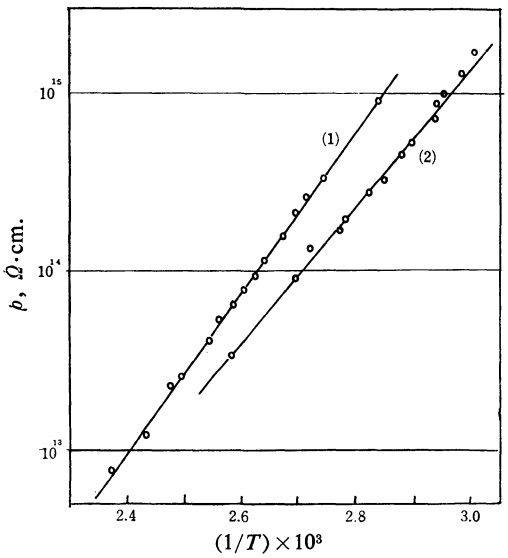


Fig. 3. Temperature dependence of the electrical resistivity: (1) anthracene-TNB, (2) tetramethylbenzidine-TNB.

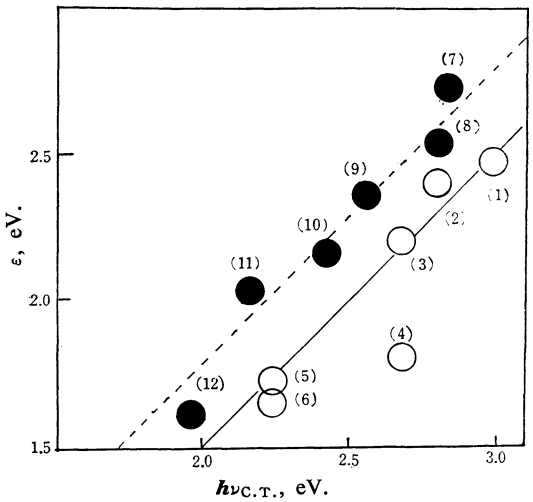


Fig. 4. Energy gap and energy of charge transfer excitation: (1) TNB complexes of phenanthrene, (2) chrysene, (3) pyrene, (4) anthracene, (5) anthanthrene, (6) perylene, (7) *p*-chloroaniline, (8) aniline, (9) α-naphthylamine, (10) *N,N'*-dimethylaniline, (11) *p*-phenylenediamine, (12) *N,N,N',N'*-tetramethylbenzidine.

—— $\varepsilon = h\nu - 0.5$ [eV.]
---- $\varepsilon = h\nu - 0.2$ [eV.]

TABLE II. ELECTRICAL RESISTIVITIES OF TNB-COMPLEXES

Donor	$\rho_{(15°C)}$	ρ_0	Activation energy E	Energy gap ε	Energy of C.T. excitation $h\nu_{C.T.}$
	Ω·cm.	Ω·cm.	eV.	eV.	eV.
Anthracene	9×10^{17}	3×10^{1}	0.9	1.8	2.53
Phenanthrene	7×10^{18}	1×10^{-4}	1.24	2.48	3.01
Pyrene	1×10^{20}	2	1.10	2.20	2.66
Chrysene	7×10^{18}	2×10^{-3}	1.20	2.40	2.78
Perylene	1×10^{19}	5×10^{3}	0.83	1.66	2.23
Anthanthrene	1×10^{18}	2×10^{2}	0.86	1.72	2.22
Violanthrene	5×10^{13}	2×10^{3}	0.57	1.14	—
N,N,N',N'-Tetramethylbenzidine	1×10^{17}	2×10^{2}	0.81	1.62	1.98
Aniline	1×10^{17}	4×10^{-7}	1.27	2.54	2.82
p-Phenylenediamine	8×10^{16}	2×10^{2}	1.02	2.04	2.14
p-Chloroaniline	5×10^{13}	5×10^{-12}	1.36	2.72	2.82
N,N-Dimethylaniline	1×10^{16}	7×10^{-4}	1.04	2.08	2.42
α-Naphthylamine	3×10^{7}	1×10^{-4}	1.18	2.36	2.58

is very high in TNB-complexes, being comparable with or even higher than that of the donor hydrocarbons.

In Fig. 4, the energy gap, twice the activation energy for the electrical conduction, is plotted against the energy of the charge transfer excitation as determined from the frequency at the peak of the charge transfer band in the solid state. It can easily be seen in Fig. 4 that there is a very close correlation between these two values. They agree well with each other in the complexes formed with aromatic amines. In hydrocarbon-TNB complexes, the energy gap is a little lower than the energy of the charge transfer excitation, although there is a linear relation between them; it coincides, rather, with the absorption edge.

Discussion

In a previous paper[5] we have pointed out that, in several solid complexes formed between TCNE and polycyclic aromatic hydrocarbons, the energy gap, ε, determined from the temperature dependence of the electrical resistivity agrees well with the energy of the charge transfer excitation measured from the wavelength at the peak of the charge transfer band. We have confirmed in the present study that these two values are also closely related with each other in many TNB-complexes. We can not say, however, that they exactly equal one other. The relation between them may be expressed in general by the following equation:

$$\varepsilon = h\nu_{C.T.}(\text{solid}) - \Delta \qquad (4)$$

where Δ is nearly constant in a group of molecular complexes with a fixed acceptor if the donors are molecules of a same type. The average value of Δ is -0.1 eV. in polycyclic aromatic hydrocarbon-TCNE complexes, and 0.2 and 0.5 eV. in TNB-complexes of aromatic amines and in those of polycyclic aromatic hydrocarbons respectively.

Although we have compared here the energy gap with the energy corresponding to the absorption maximum, there is no theoretical reason to take that energy figure instead of the energy of the absorption edge, which is lower than the other by about 0.5 eV. in these solid complexes. We can say that, in the molecular complex mentioned above, the energy gap is equal to or a little higher than the energy of the absorption edge.

If we presume that the band model can be applied to the electronic state of the crystal of the molecular complex, and that the absorption spectrum is associated with an excitation of an electron from the highest filled energy band to the conduction band, the experimental results mentioned above can be explained rather simply. In such a case, the highest filled band may be supposed as one formed from the overlapping between the highest filled molecular orbitals of the donor molecules, and the lowest conduction band, from that of the lowest empty molecular orbitals of the acceptors. Therefore, the excitation of an electron from the filled band to the conduction band corresponds to the transfer of an electron from the donor to the acceptor; hence it is a charge transfer. According to this model, the thermal excitation needed to produce the charge carriers will be identical in its nature with the charge transfer excitation in the optical process.

It is questionable, however, whether or not the observed spectrum is actually associated with such a "band-to-band" excitation as has been postulated above. The energy of the charge transfer excitation in a (1 : 1)-complex formed in solution can be expressed by the following equation, providing the charge transfer interaction is very weak:

$$h\nu_{C.T.} = I_p - A - (e^2/\overline{R}_{D^+\cdot A^-}) - \Delta W \qquad (5)$$

where I_p is the ionization potential of the donor, A, the electron affinity of the acceptor, $\overline{R}_{D^+\cdot A^-}$, the average distance between the positive and the negative charges in the excited state, and ΔW, the energy difference which is not given by the first three terms of this equation. It can be seen that the Coulomb interaction makes quite a large contribution to determining the magnitude of $h\nu_{C.T.}$. In the crystal, on the other hand, if the electron excited from a donor molecule is not localized on the neighboring acceptor molecule, but occupies an orbital that is a little more extended over the crystal lattice, a marked decrease in the Coulomb term will result, which decrease will contribute to a blue-shift of the charge transfer band of the crystal from that of the solution. On the other hand, if the excited electron remains localized on the neighboring acceptor molecule, forming an ion pair, and if the surrounding molecules affect it as a dielectric medium, a red-shift is to be expected, since the charge transfer band of the solution is known to make a red-shift, as the refractive index of the medium is higher[8].

The wavelength of the charge transfer band in the solid complex can be determined by balancing these two opposing effects. The observation that the energy of the charge transfer excitation in the crystalline state is a

8) J. Czekalla and K.-O. Meyer, *Z. physik. Chem. N. F.*, 27, 185 (1961).

little lower in TNB-complexes than the corresponding energy of a (1 : 1)-complex in carbon tetrachloride, suggest that it is not a delocalized electron, but an neighboring ion pair, that is produced in the crystal by the charge transfer absorption. It has also been suggested by Lower, Hochstrasser and Reid[7], on the basis of their studies of the vibrational structure and of the Davydov splitting of the charge transfer band of a single crystal of anthracene-TNB complex, that the exciton in this crystal is an ion pair localized at a lattice position for a relatively long time.

if the charge transfer state in the crystal is such a one as has been discussed above, the charge carriers may not be produced directly through such an excitation process; consequently, the energy of the charge transfer need not coincide with the energy gap as determined from the electrical conduction. We can imagine a number of electronic states which can contribute to the electrical conduction in a crystal of a loose molecular complex. Let us consider a widely separated ion pair. If the distance between a positively-charged donor molecule and a negatively-charged acceptor molecule is so large that the electrostatic interaction between them is completely negligible, the positive charge can change its position from one donor molecule to another donor molecule without requiring additional energy, or at least, with a small activation energy. The same can be said about the movement of the negative charge on acceptor molecules. Thus, the widely separated ion pair can contribute to the electrical conduction. This will be the lowest conduction state; hence, the energy necessary to produce a widely separated ion pair will be equal to the energy gap. This energy can be estimated by the following energy cycle: a donor molecule is taken out from the crystal to the vacuum, then ionized and returned into the original lattice position, and a similar procedure is true for an acceptor molecule at a lattice position sufficiently separated from the positive ion of the donor. The total work necessary to complete such a process, or the energy gap, can be described as:

$$\varepsilon = I_p - A - (W_p^+ + W_p^-) \qquad (6)$$

where W_p^+ and W_p^- represent the polarization energy arising from the positive and negative ions respectively. On the other hand, the energy required to form a neighboring ion pair in the crystal can be expressed by Eq. 5. Therefore, the relation between the energy gap and the energy of the charge transfer can be expressed as:

$$\varepsilon = h\nu_{C.T.} - \delta \qquad (7)$$

$$\delta = (W_p^+ + W_p^-) - (e^2/\bar{R}_{D^+\cdot A^-} + \Delta W)$$

If the donors are molecules of a same type in a series of the complex of an acceptor, $(W_p^+ + W_p^-)$ will not change very much. δ will be nearly constant in this case. The value of δ seems to be less than 1 eV. in TNB-complexes. According to this model, ε is not necessarily equal to $h\nu_{C.T.}$, although it is linearly dependent on the other. The model given above seems to give a probable explanation for the experimental results.

Summary

A series of solid complexes of aromatic hydrocarbons and amines, with 1, 3, 5-trinitrobenzene as the common electron acceptor, were prepared. These complexes were of the loose molecular complex type, and the charge transfer bands were observed with the solid complexes, which showed only small red-shifts from the corresponding bands of the solutions. These solid complexes are poor semiconductors, and the energy gap for the excitation to the conduction state is relatively large, and is nearly coincident with the energy for the charge transfer excitation. From these results, it has been suggested that the charge transfer state in the crystal may not be very different from the corresponding state in the isolated (1 : 1)-complex in the solution. The relation between the charge transfer state and the conduction state has been discussed, and a probable model for the formation of a charge carrier has been suggested.

The cost of research has been defrayed by a Scientific Research Encouragement Grant from the Ministry of Education, to which the authors' thanks are due.

Department of Chemistry
Faculty of Science
The University of Tokyo
Hongo, Tokyo

The Absorption Spectra of the Molecular Complexes of Aromatic Compounds with p-Bromanil

By Minoru KINOSHITA

(Received May 17, 1962)

The characteristic absorption spectra of molecular complexes have already been interpreted by the charge transfer theory of Mulliken[1,2]. By the approximation of the theory, the parabolic or linear relation between the energy of the charge transfer transition ($h\nu$) and the ionization potential of the donor (I_p) has been derived and experimentally confirmed[3-6].

$$h\nu = I_p - c_1 + \frac{c_2}{I_p - c_1} \quad (1)$$

$$h\nu = aI_p + b \quad (2)$$

Here, a, b, c_1 and c_2 are assumed to be characteristic constants for the complexes of any one acceptor. Equation 1 is based on Mulliken's theory more strictly than is Eq. 2. However, for weak complexes where the third term in Eq. 1 is rather small, the simple form of Eq. 2 can be a sufficient approximation.

If the coefficients in these equations are known for complexes of various acceptors, the positions of the charge transfer bands in the absorption spectra of the complexes can be predicted from the ionization potentials of donors, or vice versa; also, a comparison of the so-called "apparent electron affinities"[6] of the acceptors can be made. Therefore, it is desirable to obtain these relations in many series of complexes. In this short note, the coefficients of Eq. 2 are determined for the complexes of aromatic hydrocarbons and amines with *p*-bromanil, and the ionization potentials of several donors are estimated.

The charge transfer spectra of the complexes were measured in a carbon tetrachloride solution by the use of a Cary model-11 spectrophotometer at room temperature. The observed results are summarized in Tables I and II, along with the ionization potentials of the donors, which have been given by Watanabe[7] and by Briegleb and Czekalla[4]. Using these ionization potentials, we obtained the following relations:

$$h\nu = 0.928I_p - 4.95 \text{ eV}. \quad (3)$$

for the complexes of the polycyclic aromatic hydrocarbons in Table I, and

$$h\nu = 0.973I_p - 5.27 \text{ eV}. \quad (4)$$

for the complexes of the substituted aromatic compounds. On the other hand, Foster[6] has examined the absorption spectra for many molecular complexes with several acceptors and has shown that coefficient "a" in Eq. 2

TABLE I. MAXIMA OF CHARGE TRANSFER BANDS FOR COMPLEXES OF POLYCYCLIC AROMATIC HYDROCARBONS WITH *p*-BROMANIL IN CARBON TETRACHLORIDE

No.	Donor	Maximum of charge transfer band		Ionization potential[a], eV.
		λ, mμ	$h\nu$, eV.	
1	Naphthalene	486	2.55	8.12[b]
2	Anthracene	630	1.97	7.4
3	Phenanthrene	465	2.67	8.1
4	Pyrene	608	2.04	7.55
5	Chrysene	562	2.21	7.8
6	Triphenylene	487	2.55	8.1
7	1,2-Benzanthracene	587	2.11	7.6
8	Perylene	738	1.68	7.15
9	Anthanthrene	756	1.64	—

a) from Ref. 4 b) from Ref. 7

1) R. S. Mulliken, *J. Am. Chem. Soc.*, **74**, 811 (1952).
2) R. S. Mulliken, *J. Phys. Chem.*, **56**, 801 (1952).
3) S. H. Hasting, J. L. Franklin, J. C. Schiller and F. A. Matsen, *J. Am. Chem. Soc.*, **75**, 2900 (1953).
4) G. Briegleb and J. Czekalla, *Z. Elektrochem.*, **63**, 6 (1959).
5) H. McConnell, J. S. Ham and J. R. Platt, *J. Chem. Phys.*, **21**, 66 (1953).
6) R. Foster, *Tetrahedron*, **10**, 96 (1960).
7) K. Watanabe, *J. Chem. Phys.*, **26**, 542 (1957).

TABLE II. MAXIMA OF CHARGE TRANSFER BANDS FOR COMPLEXES OF SUBSTITUTED AROMATIC COMPOUNDS WITH *p*-BROMANIL IN CARBON TETRACHLORIDE

No.	Donor	Maximum of charge transfer band		Ionization potential[a], eV.
		λ, mμ	$h\nu$, eV.	
10	1-Methylnaphthalene	418	2.97	7.96[b]
		503	2.46_5	
11	Acenaphthene	566	2.19	—
12	Diphenyl	410	3.02	8.45
13	*p*-Xylene	424	2.92	8.445[b]
14	Mesitylene	421	2.94_5	8.39[b]
15	Aniline	560	2.21	7.70[b]
16	Dimethylaniline	657	1.89	7.3
17	*p*-Chloroaniline	500	2.48	—
18	*o*-Phenylenediamine	638	1.94	7.45
19	Diphenylamine	655	1.89	7.4
20	Phenyl-α-naphthylamine	718	1.73	—
21	Phenyl-β-naphthylamine	706	1.75_6	—
22	α-Naphthylamine	632	1.96	7.4
23	*p*-Toluidine	586	2.12	7.65
24	*o*-Toluidine	558	2.22	7.75
25	Phenothiazine	665	1.86_5	—
		> 800	—	
26	Acridine	493	2.51_6	—

a) from Ref. 4 b) from Ref. 7

is usually 0.85. If we use this value as "*a*", coefficient "*b*", or the apparent electron affinity for the present acceptor, can be calculated as −4.32 eV. by the method of the least squares.

$$h\nu = 0.85 I_p - 4.32 \text{ eV.} \quad (5)$$

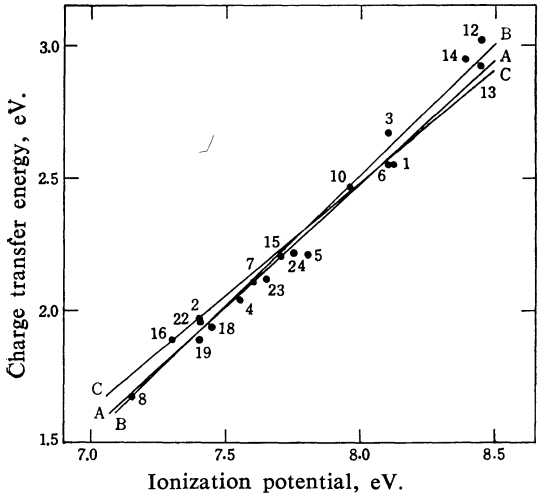


Fig. 1. Plot of energy of charge transfer absorption versus ionization potential. Donors are represented by the corresponding number in Tables I and II.
A : $h\nu = 0.927 I_p - 4.95$
B : $h\nu = 0.973 I_p - 5.27$
C : $h\nu = 0.85 I_p - 4.32$

TABLE III. IONIZATION POTENTIALS OF DONORS ESTIMATED FROM EQ. 5

Donor	Ionization potential calculated from Eq. 5, eV.
Naphthalene	8.08
Anthracene	7.40
Phenanthrene	8.22
Pyrene	7.48
Chrysene	7.68
Triphenylene	8.08
1,2-Benzanthracene	7.56
Perylene	7.06
Anthanthrene	7.01
1-Methylnaphthalene	7.98
Acenaphthene	7.66
Diphenyl	8.64
p-Xylene	8.52
Mesitylene	8.55
Aniline	7.68
Dimethylaniline	7.31
p-Chloroaniline	8.00
o-Phenylenediamine	7.36
Diphenylamine	7.31
Phenyl-α-naphthylamine	7.12
Phenyl-β-naphthylamine	7.15
α-Naphthylamine	7.39
p-Toluidine	7.58
o-Toluidine	7.69
Phenothiazine	7.28
Acridine	8.04

As is shown in Fig. 1, no serious difference is found between these equations in the I_p range from 7.0 to 8.5 eV. In consequence, a comparison of the apparent electron affinity of the acceptor can be conveniently made by using the last equation. The apparent electron affinity of *p*-bromanil is slightly larger than that of *p*-chloranil, 4.16 eV.; this seems to be quite reasonable. The ionization potentials of the donors, which were determined from the observed charge transfer energy in association with Eq. 5, are given in Table III.

Among the complexes of polycyclic aromatic hydrocarbons, perylene and pyrene gave crystalline complexes with *p*-bromanil. Their charge transfer bands were found at 755 and 650 mμ respectively, by employing the KBr-disk method. The solid complexes of some aromatic amines, such as tetramethyl-*p*-phenylenediamine, dimethylaniline, etc., with *p*-bromanil have been found to give electron spin resonance absorptions[8-10]. However, the complexes of perylene and pyrene with *p*-bromanil were found to give no electron spin resonance in their crystalline state. Considering that perylene and pyrene possess nearly the same ionization potential values as the amines, the difference in the magnetic property of the molecular complexes can not be explained simply by the difference in the ionization potential of the donors.

The author wishes to express his hearty thanks to Professor Hideo Akamatu for his kind direction and advice, and also to Dr. Haruo Kuroda for his continuous advice in the course of this work.

Department of Chemistry
Faculty of Science
The University of Tokyo
Hongo, Tokyo

8) D. Bijl, H. Kainer and A. C. Rose-Innes, ibid., **30**, 765 (1959).
9) Y. Matsunaga and C. A. McDowell, *Nature*, **185**, 916 (1960).
10) H. Inokuchi, K. Ikeda and H. Akamatu, This Bulletin, **33**, 1622 (1960).

The Precipitation Reaction of Various Metallic Ions with Phenylarsonic Acid and its Derivatives

By Hisakazu NAKATA, Yuzuru KUSAKA and Shigeaki KIKKAWA

(Received May 11, 1962)

Phenylarsonic acid and its derivatives have been used extensively as precipitation reagents to separate and determine zirconium, titanium, thorium, bismuth, iron, tin and so on[1-4]. In these separation procedures it is very important to keep a sample solution at an appropriate acidity in order to complete the separation. For ortho, meta and para derivatives of aminophenylarsonic acid and nitrophenylarsonic acid, the pH values at which precipitation begins to occur have been reported for forty elements[3,4]. In these reports, however, the experimental conditions, such as the concentration of reagents and metallic ions and the precipitation procedure, were not described. Moreover, the exact acidities less than a pH value of 1 in which zirconium, titanium, tin and so on are precipitated were not reported.

We have studied the precipitation reactions of about twenty-five metallic elements with phenylarsonic acid and its derivatives. Under definite experimental conditions, the acidities in which the precipitation began and was then completed were measured and compared with each other. The acidities to be measured were over a broad region, such as from 12 N in hydrochloric acid to almost neutral. Phenylarsonic acid, *p*-hydroxy, *p*-amino, *o*-nitro, *m*-nitro, *p*-nitro and *p*-hydroxy-*m*-nitrophenylarsonic acid were used as the reagents. The results obtained are reported here.

Experimental

Materials.—*Phenylarsonic Acid and its Derivatives.* —These were synthesized in our laboratory, phenylarsonic acid by the Palmer-Adams method[5],

1) J. F. Flagg, "Organic Reagents Used in Gravimetric and Volumetric Analysis", Interscience Publisher, New York (1948), p.107.
2) F. J. Welcher, "Organic Analytical Reagents", Vol. IV, D. Van Nostrand Co., Princeton (1948), p. 49.
3) R. Pietsch, *Mikrochim. Acta*, 1955, 954.
4) R. Pietsch, ibid., 1955, 1019.
5) C. S. Palmer and R. Adams, *J. Am. Chem. Soc.*, **44**, 1356 (1922).

p-hydroxy phenylarsonic acid by the Jacobs-Heiderberger method[6], *p*-aminophenylarsonic acid by the Jacobs-Heiderberger-Rolf method[7], and *o*-, m- and *p*-nitrophenylarsonic acid by the Bart method[8]. Only *p*-hydroxy-*m*-nitrophenylarsonic acid was obtained already intact from Prof. Risaburo Nakai of Kyoto University. All were purified by the conventional recrystallization method.

Metallic Salts. — The usual analytical-grade reagents were used. Most of them were chlorides, except for the silver, lead, uranium and thorium as nitrates.

Measurement Instruments.—A photometric Titrator PT-1 of the Yanagimoto Co. and a pH meter M-3 of the Horiba Inst. Co. were used for the measurements. In the former, a red filter was used when the sample solution was colorless. When the solution had some color, as in the case of copper, a filter whose color was the same as that of the solution was used in the experiment. The pH meter was calibrated by Sörensen buffer solutions, solutions mixed with various ratios of 0.1 N hydrochloric acid and 0.1 M sodium citrate.

Precipitation Procedures. — For the elements which were precipitated by an arsonate reagent in pH 1.0~9.0, 8 ml. of 0.05 M metallic ion solution in 0.1 N hydrochloric acid was mixed with 24 ml. of a 0.05 M solution of the arsonate reagent in 0.1 N hydrochloric acid*. Then, by adding a 2.7 N ammonium hydroxide solution drop by drop until the pH value of the solution became 3, the precipitation phenomenon was observed. For the neutralization in more than pH 3, 0.54 N ammonium hydroxide solution was used. As the volume of these ammonia to be added did not exceed 4 ml. in all the experiments, the concentration of metallic ions in the precipitation system was in the range of 0.011~0.013 M.

The formation and the completion of precipitation were investigated with a photometric titrator which measured the transparency or the turbidity of the solution. The pH value of the solution was measured with the pH meter.

For the elements which were precipitated in a more acidic medium than with a pH value of 1, the acidities in which the precipitation occured were determined by a two-step method. First, an approximate region of the acidity was determined. Each 1 ml. of a 0.05 M metallic ion solution whose acidities were adjusted to 6, 5, 4, 3, 2 and 1 N for hydrochloric acid was put in a separate test tube, and then 3 ml. of a 0.05 M arsonate reagent solution of the same acidity as that of the metallic ion solution was added. By this technique, an approximate acidity in which the precipitation is occured was determined; for example, zirconium *p*-hydroxy phenylarsonate is precipitated in a 5~4 N hydrochloric acid solution. In the next step, the more accurate acidity was determined by a similar method. For example, 8 ml. of a 0.05 M zirconium chloride solution in 5 N hydrochloric acid was mixed with 24 ml. of a 0.05 M *p*-hydroxy phenylarsonic acid solution in 5 N hydrochloric acid. Then, 13.5 N ammonium hydroxide was added drop by drop. The arsonate precipitation phenomenon was investigated by the photometric titrator, and the acidity in the precipitation was calculated from the amount of ammonia added to the solution.

For the elements which were precipitated in a stronger acidic medium than 6 N in hydrochloric acid, the experiment was performed by almost the same method as has been described above. In this case, however, only an approximate region of the acidity was determined by a method similar to the first step in the above experiment, and the next step of determining a more accurate acidity in the precipitation was ommited, because ammonium chloride was precipitated by adding ammonia in such a strong hydrochloric acid solution.

In all cases, the experiments were performed at room temperature (about 15°C); this temperature did not exceed 20°C even in the evolution of neutralization heat.

Results and Discussion

Typical examples of the results in the experiments of lead and cadmium phenylarsonates in a weak acidic medium and of thorium and uranium *p*-nitrophenylarsonates in a strong acidic medium are shown in Figs. 1 and 2.

As these figures show, the acidities at which the precipitation began and then was completed could be elucidated by measuring the acidity and the transparency depression in the solution. The turbidity was measured only as a subsidiary means to the transparency measurement. For example, when some color change of ions, based on an acidity change in solution, occured, as in the case of chromic ion, the turbidity measurement played an important role.

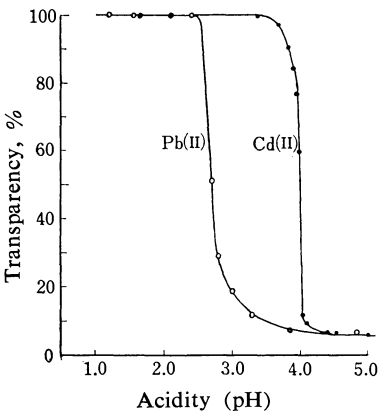


Fig. 1. Lead and cadmium phenylarsonate precipitations in weak acidic medium.

6) W. A. Jacobs and M. Heiderberger, ibid., **41**, 1440 (1919).
7) W. A. Jacobs, M. Heiderberger and I. P. Rolf, ibid., **40**, 1580 (1918).
8) H. Bart, *Ann.*, **429**, 106 (1922).
* In the cases of silver and lead, nitric acid was used instead of hydrochloric acid because of their chloride precipitations.

TABLE I. ARSONATE PRECIPITATION IN A STRONG ACIDIC MEDIUM
(Normality of acid)

	Phenyl.	*p*-OH phenyl.	*p*-NH_2 phenyl.	*o*-NO_2 phenyl.	*m*-NO_2 phenyl.	*p*-NO_2 phenyl.	*p*-OH-*m*-NO_2 phenyl.
Nb(V)	10	9	9	10	11	12	10
	9	8	8	9	9	11	8
Ta(V)	12	7	10	7	7	10	8
	8	6	9	6	6	8	7
Ti(IV)	9	6	0.4	1.8	9	11	8
	8	6	0.3	1.1	8	9	7
Zr(IV)	6	4.9	1.3	0.6	6	6	6
	6	3.7	0.5	0.1	6	6	6
Sb(V)	2.2	2.5	0.5	—	3.5	2.6	2.1
	1.9	2.2	0.3	—	3.4	2.3	1.7
Sn(II)	1.4	0.7	0.5	1.7	3.0	3.0	2.0
	0.5	0.6	0.4	0.7	0.8	0.8	0.02*
Sb(III)	0.6	0.6	0.4	2.0	1.0	1.8	1.1
	0.3	0.3	0.2	1.6	0.8	0.4	0.7
U(VI)	0.2	0.4	0.6	0.2	1.0	1.0	1.0
	0.03	0.3	0.5	0.2	0.5	0.5	0.7
Th(IV)	0.3	0.2	0.2	0.07	1.9	2.3	0.5
	0.01	0.1	0.1	0.07	0.9	0.9	0.06
Bi(III)	0.03	0.4	0.4	0.1	0.03	0.5	0.01
	0.003	0.3	0.3	0.1	0.01	0.5	0.004
Fe(III)	0.1	0.003	0.02	0.005	2.0	2.0	0.2
	0.07	0.002	0.004	0.003	1.0	0.9	0.07
Sn(IV)	2.0	0.5	0.5	1.8	—	—	1.8
	1.4	0.05	0.4*	0.7	—	—	1.1

* Beyond these acidities, these precipitates were dissolved in a more basic region.

TABLE II. ARSONATE PRECIPITATION IN A WEAK ACIDIC MEDIUM
(pH)

	Phenyl.	*p*-OH phenyl.	*p*-NH_2 phenyl.	*o*-NO_2 phenyl.	*m*-NO_2 phenyl.	*p*-NO_2 phenyl.	*p*-OH-*m*-NO_2 phenyl.
Pb(II)	2.5	1.5	2.5	2.5	2.2	2.1	1.8
	3.3	3.1	2.8	2.9	2.5	3.4	2.5
Zn(II)	3.5	4.4	2.4**	4.3	2.4	2.2	2.9
	4.5	4.7	4.9	4.9	2.6	3.8	3.2
Ag(I)	4.4	4.1	1.6	5.1	3.2	1.0	3.2
	5.1	5.5	2.5	5.4	4.3	1.0	4.5
Ce(III)	3.4	3.3	3.4	2.5	4.5	2.7	3.2
	3.5	3.5	3.9	3.4	6.2	3.3	3.7
La(III)	3.3	3.2	4.1	5.9	2.5	2.6	3.0
	3.5	3.3	4.3	6.5	3.5	3.5	3.4
Cd(II)	3.5	4.4	2.3	7.2	2.5	2.3	1.8
	4.5	5.4	3.0	7.6	2.6	3.2	2.3
Cu(II)	—	3.0	2.5	5.3	2.7	1.7	2.9
	—	3.4	3.5	5.6	3.0	3.1	3.4
Cr(III)	—	4.5	4.0	4.0	2.3	1.5	3.5
	—	5.7	5.2	7.1	3.8	2.5	7.5
Mn(II)	2.1**	5.0	2.4**	—	1.0**	1.0	1.5
	5.0	6.2	5.5	—	4.5	4.4	4.6
Co(II)	6.2	6.5	5.8	8.2	4.4	1.6**	7.0
	6.7	7.4	6.9	9.2	5.0	6.0	7.6
Ni(II)	—	7.0	—	—	—	—	—
	—	7.7	—	—	—	—	—

** Beyond these acidities, a part of the precipitates were dissolved.

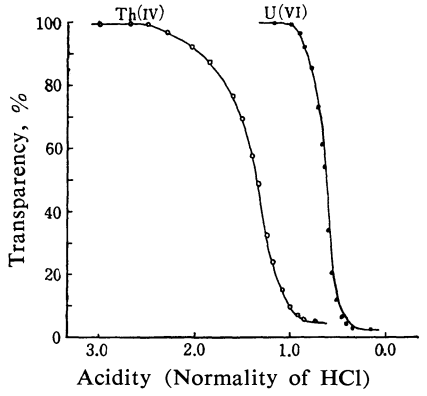


Fig. 2. Thorium and uranium *p*-nitrophenylarsonate precipitations in strong acidic medium.

The experimental results which were obtained for various metallic ions are shown in Tables I and II, in which the former is the precipitation in a strong acidic medium and the latter that in a weak acidic medium. In the tables, the numbers of the first line for each element indicate the acidity at which the precipitation began, and those of the second line indicate that point at which the precipitation is completed.

As the tables show, it seems possible to formurate some general rules on the precipitation of various elements by phenylarsonic acid and its derivatives. Although a few exceptions are found in each reagent, the general order of the elements precipitated from a strong acidic to a weak acidic medium is the order of elements shown in the tables, that is, up to down in the tables.

In each arsonate, especially when they are compared with the phenylarsonates, the nitro derivatives seem to be precipitated in a more acidic medium. In the nitro derivatives, the order is generally from the para and the meta and to the ortho form. The para hydroxy and the para amino derivatives seem to be precipitated in a more basic medium.

The authors wish to express their thanks to Messrs. Hideo Kitai, Mitsuro Tsubosaka, and Mrs. Akiko Ueshima, who contributed to this study by their synthesis of arsonic acid reagents and by their primary study of the precipitations of various metallic ions. Thanks are also due to Mr. Haruo Tsuji for his frequent assistance and to Dr. Risaburo Nakai for his gift of *p*-hydroxy *m*-nitro phenylarsonic acid.

Department of Chemistry
Faculty of Science
Konan University
Higashinada, Kobe

Rotatory Dispersion and Stereochemistry of Organic Compounds. IV. On the Optical Rotatory Contribution of Hydroxyl Groups in Glucose. (Preliminary Report)*

By Yojiro TSUZUKI, Katsumi TANAKA and Koko TANABE

(Received May 25, 1962)

The rotatory dispersion of hydroxy compounds usually shows plain curves, so that the configurational environments around the asymmetric center can not be revealed by the curves. Therefore, it would be desirable to convert the hydroxyl group to one which exhibits a Cotton effect in a convenient spectral region.

The chromophore C=S, one of the most suitable for this purpose, was introduced by Tschugaeff[1] in the form of xanthates and dithiourethans; it has already been experimentally demonstrated by Lowry[2] to produce anomalous rotatory dispersion, and later Fredga[3] and Djerassi et al.[4] successfully applied it to a number of hydroxy acids.

In the present investigation, the authors have prepared various derivatives of D-glucose containing such a chromophore, namely 1,2-5,6-*O*-diisopropylidene-D-glucofuranose-3-(*S*-methyl)-xanthate (II), μ-thioglucoxazoline (III),

* I. This Bulletin, **11**, 586 (1936); II. *Sci. Pap. Inst. Phys. Chem. Res. (Tokyo)*, No. 890, Vol. 35, 425 (1939); III. ibid., No. 901, Vol. 36, 31 (1939).

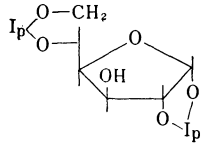
1) L. Tschugaeff, *Ber.*, **42**, 2244 (1909); L. Tschugaeff and A. Ogorodnikoff, *Z. physik. Chem.*, **74**, 503 (1910) and later papers.

2) T. M. Lowry and H. Hudson, *Phil. Trans. Roy. Soc. London*, **A232**, 117 (1933).

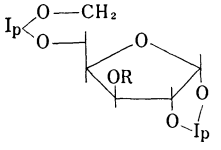
3) A. Fredga, *Svensk. Kem. Tidskr.*, **53**, 221 (1941); **54**, 26 (1942).

4) C. Djerassi, "Optical Rotatory Dispersion", McGraw-Hill Book Co., New York, N. Y. (1960), p. 203.

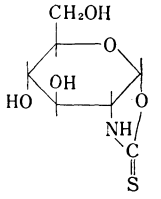
tetraacetyl-μ-thioglucoxazoline (IV), and methyl-2, 3, 4-*O*-triacetyl-α-D-glucopyranosyl-6-(*S*-benzyl)-xanthate (V); the rotatory dispersion was measured with a Rudolph spectropolarimeter at room temperature over the wavelength region of from 300 to 700 mμ, with a view of getting information on the rotatory contribution of the hydroxyl groups in sugars.



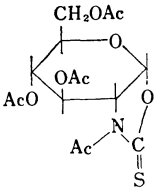
(I) Ip=$-CH(CH_3)_2$



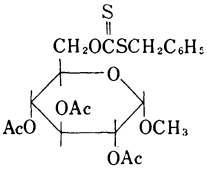
(II) R=$-C(=S)-SCH_3$



(III)



(IV) Ac=$-COCH_3$



(V)

TABLE I. MEASUREMENT OF RD

Compound	Solvent	Concn. gr./100 cc.	Light source
I	Methanol	1.0304	Zr
II	Methanol	0.1244	Xe
III	Water	1.0132	Xe
IV	Chloroform	0.1240	Xe
V	Chloroform	0.1002	Xe

Results and Discussion

Compound I exhibits a negative, plain, rotatory dispersion curve, since in the measured wavelength region the compounds has no optically-active absorption band (Fig. 1).

C_3-OH, which is the only free hydroxyl group in this compound, has an L-configuration according to the Fischer-Tollens projection formula. The rotatory dispersion curve II of compound II, which was obtained by treating I with metallic sodium, carbon disulfide and methyl iodide in absolute ether, first exhibits a broad extreme (trough) near 500 mμ and then a sharp extreme (peak) near 375 mμ, thus producing an anomalous dispersion curve. The former trough (ca. 550 mμ) is of no special significance, but the latter sharp peak is related

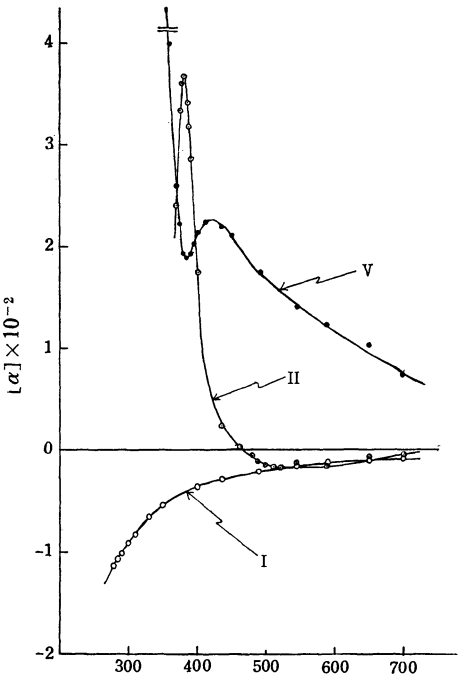


Fig. 1. RD of derivatives of glucose.
○ I, ⊙ II, ● V

to the configuration, judging from its ultraviolet absorption spectrum, which does not exhibit a peak between 400 and 700 mμ.

The ultraviolet absorption maxima appear at 280 mμ (ε=13000) and at 358 mμ (ε=49.21); the peak at 280 mμ is attributed to the C=S moiety, and the maximum at 358 mμ, to the $-\overset{S}{\overset{\|}{C}}-S-$ group.

The anomalous rotatory dispersion curve is caused by the ultraviolet, optically-active absorption band near 375 mμ due to the $-\overset{S}{\overset{\|}{C}}-S-$ group.

Although no data are available below 370 mμ, because of the difficulty of measurement, the extrapolated curve intersects the abscissa at about 360 mμ, a point which is substantially identical with the wavelength of maximum ultraviolet absorption, 358 mμ.

The positive Cotton effect seen in curve II is considered to be due to the C_3- group of the L-configuration; this would, however, be expected to give a negative partial rotation[5].

5) One of the authors has inferred from an analysis of the rotatory dispersion and various experimental facts that the OH group of L-hydroxy acids should contribute to the negative rotation, and has therefore given a rational interpretation to the anomalous behavior of the optical rotation of some hydroxy carboxylic acids. Y. Tsuzuki, *Sci. Pap. Inst. Phys. Chem. Res. (Tokyo)*, No. 890, Vol. 35, 425 (1939); No. 901, Vol. 36, 31 (1939); *J. Chem. Soc. Japan, (Nippon Kwagaku Kwaisi)*, **64**, 282, 290 (1943); Y. Tsuzuki et al., *J. Chem. Soc. Japan, Pure Chem. Sec. (Nippon Kagaku Zasshi)*, **78**, 764 (1957).

On the contrary, the xanthate group on the hydroxyl of L-types of lactic, malic and mandelic acids is clearly responsible for the positive rotation which has been demonstrated by Tschugaeff[1], by Fredga[3], and particularly by Djerassi's rotatory dispersion studies[4].

The reason for this is not clear; however, the authors think that inversion of the sign of rotation may occur when the order of the magnitude of the substituents attached to the asymmetric center is inverted, such as:

$$COOH > OH \text{ (negative)}$$

$$COOH < O\text{–}CSSR \text{ (positive)}$$

Thus, the observed rotatory contribution of the C_3 of glucose becomes comprehensible, quite in harmony with the former views and observations.

The rotatory dispersion of III, both in a neutral and in an acidic solution, exhibits obviously single Cotton effect curves (Fig. 2).

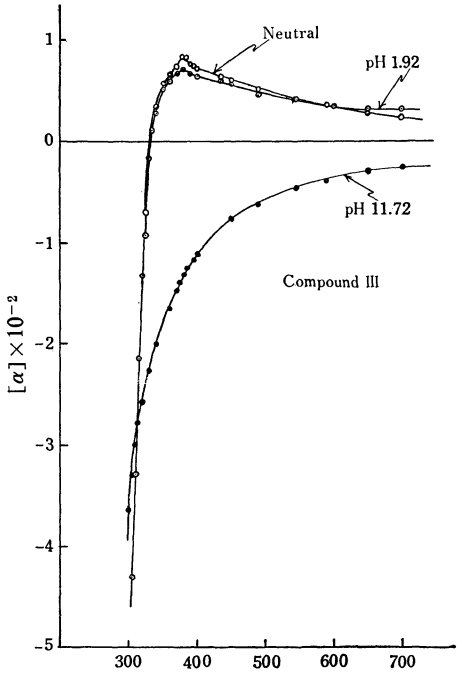
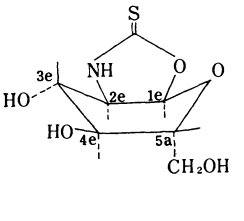
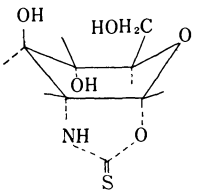


Fig. 2. RD of III.
○ Neutral, ⊙ pH=1.92, ● pH=11.72

However, compound III and its acetyl derivative IV present a complicated and difficult problem for the interpretation of the rotational behavior. Undoubtedly this anomalous dispersion originates in the partial contribution of C_1 and C_2, the possible form of which may be shown as follows (IIIa):



(IIIa)



(IIIb)

The hydrogen atoms directly attached to the ring carbon atoms are ommited for the sake of simplicity. The pyranose must be at the same time of both the α- and the boat forms; otherwise, a five-membered ring including 1- and 2-carbon atoms cannot be formed. All the hydrogen atoms except C_5–H are axial. The alternate boat form, IIIb, in which the oxazoline five-membered ring and the two OH groups are axial is clearly more unstable than IIIa and is therefore to be left out of consideration.

Acetyl derivative IV of compound III also exhibits a single positive Cotton effect, however, with a larger amplitude, as may be seen by a comparison of the RD-curves of III and IV. In compound IV the thion moiety is well preserved even by acetylation, giving a maximum absorption at 345 mμ (ε=35.6) and also a nearly corresponding Cotton effect (zero rotation point at about 385 mμ) (Fig. 3). Compound III shows no ultraviolet maxima, being transparent in this spectral region. This

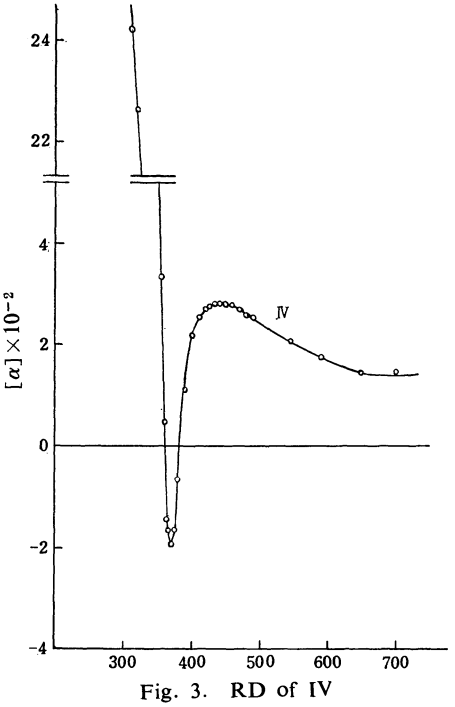


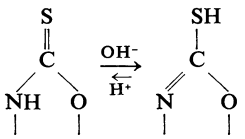
Fig. 3. RD of IV

TABLE II. DISPERSION CONSTANTS FOR GLUCOSE DERIVATIVES

$$[M]=\frac{A}{\lambda^2-\lambda_0^2}+\frac{B}{\lambda^2}$$

Compound	A	B	λ_0 mμ	Peak		Trough		UV absorption 10^{-2} mol./l.	
				mμ	[M]	mμ	[M]	mμ	ε
II	4.54	−37.82	380	380	321.54	—	—	358	49.21
III neutral	−0.11	27.73	367	385	191.49	—	—	no absorption	
III pH 1.92			308	380	154.76	—	—	no absorption	
III pH 11.72	−25.62	0.893	243	—	—	—	—	240~245	
IV	−9.99	280.24	407	445	1104.3	370	−759.17	345	35.65
V	2.53	193.09	399	410	1078.9	385	918.4	358	77.73

compound is considered to be in the non-chromatic μ-thiol form of the following tautomerism:



thion-form thiol-form

In the hydrogen chloride solution (pH=1.92) the rotatory dispersion curve was almost identical with that observed in the neutral solution except that the rotation at the peak is lower. In the sodium hydroxide solution (pH =11.72), the RD curve is shown by a negative plain curve. Thus, it is revealed by these curves that the >C=S moiety of compound III has no influence on the thion-thiol equilibrium when acidic, but in an alkaline solution the equilibrium is displaced so completely towards the enol form that the optically-active absorption band disappears and only a negative plain dispersion curve is obtained. This somewhat unexpected feature may be due to the basic rotation of the boat form.

Compound V, in which C_6 is benzylated, exhibits a rotatory dispersion curve with an obvious single positive Cotton effect near 400 mμ; however, the amplitude is small. This Cotton effect is responsible for the partial contribution of the C_5- carbon. The small amplitude implies that the effect of benzyl xanthate is lessened considerably by the intervention of the C_6-methylene group. The positive sign of this small Cotton effect is in harmony with the L-type of the C_5-$CH_2OCSCH_2C_6H_5$ group, namely, the inversion of the sign of rotation. The ultraviolet absorption maximum of compound V was found to be 358 mμ (ε=77.7), in chloroform, which absorption is responsible for the –C–S– group, perhaps being optically active. The basically strong positive rotation, the peak of which is presumably below 250 mμ, is no doubt related to the D-type of C_1-configuration (α-D-glucoside).

On the Two-term Drude Equation

It is to be expected that the dispersion data can be expressed by the two-term Drude equation:

$$[M]=\frac{A_1}{\lambda^2-\lambda_1^2}+\frac{A_2}{\lambda^2-\lambda_2^2}$$

and that the physical meaning of the values of λ_1 and λ_2 can be interpreted with relation to the chromophores of the molecules; however, for the sake of simplicity the authors have attempted for the present to see whether the experimental data conform to the following abbreviated two-term expression:

$$[M]=\frac{A}{\lambda^2-\lambda_0^2}+\frac{B}{\lambda^2}$$

The first term depends on a particular chromophore, while the second term is concerned with the sum of all the other chromophores or with the remainder of the molecule. The calculations were carrried out by means of the least square method with an electronic computer. The results are shown in Table II.

It may be seen in Table II that the optically-active absorption band in all cases shifted more or less towards wavelengths longer than the corresponding ultraviolet absorption maximum. The values of A, namely, the partial rotatory contribution of the particular chromophores, is negative in sign, in compounds III and IV, and positive in the others.

Experimental

The derivatives of glucose were prepared according to the methods of the literature.

1,2,5,6-*O*-Diisopropylidene-D-glucofuranose (compound I)[6]; m. p., 108~110°C.

1,2,5,6-*O*-Diisopropylidene-D-glucofuranose-3-(*S*-methyl)-xanthate (compound II)[7]; m. p., 59.8~60.5°C.

6) E. Fischer and C. Rund, *Ber.*, **49**, 93 (1916).
7) K. Freudenberg and A. Wolf, ibid., **60**, 232 (1927).

μ-Thioglucoxazoline (compound III)[8]; m. p., 172°C.

Tetraacetyl-μ-thioglucoxazoline (compound IV)[8]; m. p., 119~120°C.

Methyl-2,3,4-*O*-triacetyl-α-D-glucopyranosyl-6-(*S*-benzyl)-xanthate (compound V)[9]; m. p., 106°C.

Department of Chemistry
Tokyo College of Science
Shinjuku-ku, Tokyo

8) G. Zemlén, A. Grecs and M. Rados, ibid., **69**, 748 (1936).

9) J. J. Willard and E. Pascu, *J. Am. Chem. Soc.*, **82**, 4347 (1960).

Studies on Antibiotics and Related Substances. XV. Syntheses of Acetobromo Derivatives of 3-Amino-3-deoxyglucose and 6-Amino-6-deoxyglucose[1]

By Yukio Itō, Shinkiti Kōtō and Sumio Umezawa

(Received June 9, 1962)

Acetohalogeno derivatives of sugars are important intermediates used for the synthesis of glycosides, however, the corresponding derivatives of aminosugars represent a relatively unexplored territory. In the course of our studies on the synthesis of glycosides relating to carbohydrate-antibiotics, such as kanamycin and paromomycin, a program was instituted toward the synthesis of acetobromo derivatives of aminosugars. The synthesis of 2, 4, 6-tri-*O*-acetyl-3-amino-α-1-bromo-1, 3-dideoxy-D-glucopyranose (III), 2, 3, 4-tri-*O*-acetyl-6-amino-α-1-bromo-1, 6-dideoxy-D-glucopyranose (VII) and their derivatives is the subject of this paper.

The synthesis of III and their derivatives is outlined in the following Chart A:

Methyl 3-acetamido-2,4,6-tri-*O*-acetyl-3-deoxy-α-D-glucopyranoside (I) was synthesized by a modification of the route described by Peat and Wiggins[2]. When this route was followed, the yield of α-anomer of methyl 2, 4, 6-tri-*O*-acetyl-3-*O*-(p-toluene-sulfonyl)-D-glucoside was found to be too low to make progress in further synthesis. The difficulty has been overcome by the transformation of β-anomer to α-anomer by a modification of the method described by Ohle and Wilcke[3]. It has been found that treatment with titanium tetrachloride in chloroform transformed the β- to α-anomer in 91% yield. It has also been found that isopropanol is an appropriate solvent for the crystallization of α-anomer resulting in a

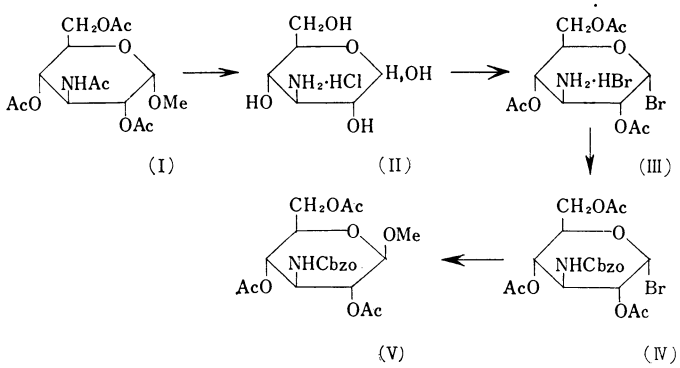


Chart A

1) Presented at the Division of Organic Chemistry of the 15th Annual Meeting of the Chemical Society of Japan, Kyoto, April, 1962.

2) S. Peat and L. F. Wiggins, *J. Chem. Soc.*, 1938, 1092, 1810.

3) H. Ohle and H. Wilcke, *Ber.*, 71, 2327 (1938).

relatively good yield (28.9%)[4]. Thus the total yield of α-anomer has been raised to 62.5%. The α-anomer has been subjected to ammonolysis by methanolic ammonia in an autoclave at 150°C, followed by acetylation, to give methyl 3-amino-3-deoxy-α-D-glucoside tetraacetate (I) by the method of Peat and Wiggins. Attempts have been made to effect ammonolysis of β-anomer by analogous procedure, followed by acetylation, but these have not been successful.

3-Amino-3-deoxy-D-glucose has been obtained by hydrolysis of the above tetraacetate. Acid hydrolysis studies revealed optimum conditions, namely, refluxing in 6 N hydrochloric acid for three hours, whereby 79.2% of the tetraacetate has been converted to 3-amino-3-deoxy-D-glucopyranose hydrochloride (II).

When treated with acetyl bromide at room temperature for three hours, 3-amino-3-deoxy-D-glucopyranose hydrochloride gave 2, 4, 6-tri-*O*-acetyl-3-amino-α-1-bromo-1, 3-dideoxy-D-glucopyranose hydrobromide (III) in a 96.2% yield.

Masking of the amino group of III with the carbobenzoxy group by treatment with carbobenzoxy chloride in potassium bicarbonate solution gave 2,4,6-tri-*O*-acetyl-α-1-bromo-3-carbobenzoxyamino-1, 3-dideoxy-D-glucopyranose (IV) in a 53.2% yield.

An attempt to prepare a glycoside from IV proved to be practical. When shaken with methanol in the presence of mercuric cyanide by Koenigs-Knorr reaction, methyl 2, 4, 6-tri-*O*-acetyl-3-carbobenzoxyamino-3-deoxy-β-D-glucopyranoside (V) has been obtained in a 77.4% yield.

Synthesis of 2, 3, 4-tri-*O*-acetyl-6-amino-α-1-bromo-1, 6-dideoxy-D-glucopyranose (VII) and their derivatives is outlined in the following Chart B:

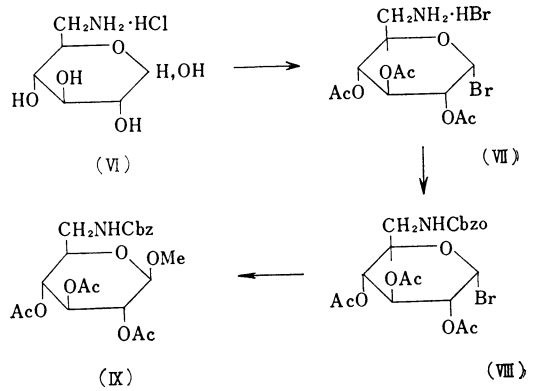


Chart B

6-Amino-6-deoxy-D-glucopyranose hydrochloride (VI) was synthesized from tetra-*O*-acetyl-α-D-glucopyranosyl bromide via benzylglucoside-derivatives by the route described by Cramer et al.[5] Reaction of VI with acetyl bromide at room temperature for seventy-four hours yielded 2,3,4-tri-*O*-acetyl-α-1-bromo-1,6-dideoxy-D-glucopyranose hydrobromide (VII), m. p. 162~164°C (decomp.), in a 96.3% yield. It should be noted that VII is almost insoluble in chloroform and other common organic solvents, while the corresponding derivative III is soluble in chloroform.

When a suspension of VII in chloroform was shaken with carbobenzoxy chloride in the presence of a saturated solution of potassium bicarbonate at 0°C for twenty minutes, the reaction product dissolved in chloroform-layer, from which 2, 3, 4-tri-*O*-acetyl-α-1-bromo-6-carbobenzoxyamino-1, 6-dideoxy-D-glucopyranose (VIII) was obtained in a 76% yield. When subjected to Koenigs-Knorr reaction, using

Table I

Compound	Specific rotation	IR absorption, cm^{-1}
III	$[\alpha]_D^{15}$ +127.5° (*c* 1.77, $CHCl_3$)	undetectable
VII	—	843 (weak)
IV	$[\alpha]_D^{15}$ +131.6° (*c* 1.77, $CHCl_3$)	847
VIII	$[\alpha]_D^{17}$ +156° (*c* 1.62, $CHCl_3$)	833
V	$[\alpha]_D^{12}$ −19.6° (*c* 1.77, $CHCl_3$)	885
IX	$[\alpha]_D^{15}$ +4.5° (*c* 2.00, $CHCl_3$)	900
2ABG*	$[\alpha]_D^{19}$ +148° (*c* 0.84, CH_3COCH_3)[6]	—
2ABCG**	$[\alpha]_D$ +146.5° (*c* 1.6, $CHCl_3$)[7]	845
2MACG***	$[\alpha]_D$ +17° (*c* 3.4, $CHCl_3$)[7]	—

* 3,4,6-Tri-*O*-acetyl-2-amino-α-1-bromo-2-deoxy-D-glucopyranose hydrobromide
** 3,4,6-Tri-*O*-acetyl-α-1-bromo-2-carbobenzoxyamino-1,2-dideoxy-D-glucopyranose
*** Methyl 3,4,6-tri-*O*-acetyl-2-carbobenzoxyamino-2-deoxy-β-D-glucoside

4) Yield reported by Peat and Wiggins, loc. cit., was 19.4%.
5) F. Cramer, O. Otterbach and H. Springman, *Chem. Ber.*, **92**, 384 (1959).
6) W. O. Cutler, W. N. Haworth and S. Peat, *J. Chem. Soc.*, **1937**, 1979.
7) L. Zervas and S. Konstas, *Chem. Ber.*, **93**, 435 (1960).

mercuric cyanide as a catalyst, VIII gave methyl 2,3,4-tri-*O*-acetyl-6-carbobenzoxyamino-6-deoxy-α-D-glucopyranoside (IX) in a 61.2% yield. The same reaction using silver carbonate-calcium sulfate as a catalyst gave the same product IX in a 57% yield.

Infrared spectra of the acetobromo derivatives (IV, VII, VIII) showed absorptions near 840 cm^{-1} which is characteristic of α-configuration, while the methylglucosides (V, IX) prepared from IV and VIII showed absorptions near 890 cm^{-1}, indicating that the methylglycosides have a β-configuration, as anticipated from the usual results of the Koenigs-Knorr reaction. Moreover, values of specific rotation of the above-mentioned derivatives are consistent with the spectroscopic results, as shown in Table I, where these data are shown together with those of the corresponding derivatives of 2-amino-2-deoxy-D-glucose.

Experimental

Methyl 2,4,6-Tri-*O*-acetyl-3-*O*-(*p*-toluenesulfonyl)-α-D-glucoside. — A solution of 84 g. of 1,2:5,6-di-*O*-isopropylidene-3-*O*-(*p*-toluenesulfonyl)-α-D-glucofuranose[8] in 650 g. of 2% methanolic hydrogen chloride was refluxed for 15 hr. on a steam bath. After being cooled, the reaction mixture was neutralized with basic lead carbonate, filtered and the filtrate was evaporated under reduced pressure to give a yellowish syrup. A mixture of the syrup, 67 g. of anhydrous sodium acetate and 335 ml. of acetic anhydride was heated at 110°C for 3 hr. The reaction mixture was cooled and then poured into 500 g. of ice-water, followed by stirring for 30 min. The resulting mixture was extracted with six 100 ml. portions of chloroform. The chloroform extracts were combined, washed with a saturated solution of sodium carbonate, and then with water thoroughly to give a neutral chloroform-solution, which was dried over sodium sulfate and filtered. Evaporation of the filtrate at 55°C under reduced pressure gave a reddish-brown syrup, which was crystallized from 100 ml. of ether to give 32.2 g. of methyl 2,4,6-tri-*O*-acetyl-3-*O*-(*p*-toluenesulfonyl)-β-D-glucopyranoside, m. p. 126.9~130°C., yield 33.6%.

The mother liquor separated from the above-mentioned β-anomer was evaporated to dryness to give a syrup. When dissolved in 35 ml. of hot isopropanol and allowed to stand, the syrup gave the corresponding α-anomer, the title compound, m. p. 94~95°C, yield 27.8 g. (28.9%). The crude product was used for amination. Peat and Wiggins[2] reported m. p. 97°C, $[\alpha]_D^{16}+87.1°$ ($CHCl_3$) and 19.4% yield.

Transformation of Methyl 2,4,6-Tri-*O*-acetyl-3-*O*-(*p*-toluenesulfonyl)-β-D-glucoside to its α-Anomer. —The transformation was effected by a modified method of Ohle and Wilcke[3] as follows: To a solution of 10 g. of methyl 2,4,6-tri-*O*-acetyl-3-*O*-(*p*-toluenesulfonyl)-β-D-glucoside in 120 g. of dry chloroform was added a solution of 5 g. of titanium tetrachloride in 80 g. of dry chloroform and the mixture was refluxed on a water bath for 75 min. After being cooled, the reaction mixture was poured into 200 g. of ice-water and shaken vigorously. The chloroform-layer was separated and the aqueous layer was extracted with three 10 ml. portions of chloroform. The chloroform extracts were combined, washed with water and dried over sodium sulfate. After being filtered, the chloroform solution was evaporated to dryness under reduced pressure. The resulting brown syrup was dissolved in 5 ml. of hot isopropanol and allowed to stand in the refrigerator to give a crystalline solid of methyl 2,4,6-tri-*O*-acetyl-3-*O*-(*p*-toluenesulfonyl)-α-D-glucopyranoside, m. p. 96.8~97.4°C, $[\alpha]_D^{20.7}+89°$ (*c* 2.0, $CHCl_3$), yield 9.1 g. (91%). Mixed melting point of the product with the above-described α-anomer showed no depression. The product was also used for amination.

3-Amino-3-deoxy-D-glucopyranose Hydrochloride (II).—A solution of 4.0 g. of methyl 3-acetamido-2,4,6-tri-*O*-acetyl-3-deoxy-α-D-glucoside[9] in 80 ml. of 6 N hydrochloric acid was heated on a steam bath for 3.5 hr. The reaction mixture was evaporated to dryness at 50°C in vacuo. The residue was dissolved in 2 ml. of methanol and evaporated again to dryness. The evaporation to remove water was repeated seven times to give a pale-yellow spongy residue. The residue was dissolved in 60 ml. of warm methanol, neutralized with silver carbonate and shaken with 1 g. of decolorizing charcoal for 30 min., followed by filtration. The filtrate was evaporated to dryness in vacuo at about 50°C to give 2.4 g. of a spongy residue. The residue was dissolved in 15 ml. of warm methanol, added dropwise with isopropanol until the solution became somewhat turbid and the mixture was allowed to stand in a refrigerator to give a hygroscopic powder of 3-amino-3-deoxy-D-glucopyranose hydrochloride, yield 1.2 g. (79.2%).

Found: C, 33.37; H, 6.96; N, 6.76. Calcd. for $C_6H_{13}NO_5 \cdot HCl$ (215.6): C, 33.42; H, 6.54; N, 6.50%.

Paperchromatography of the product showed a single spot by ninhydrin coloration and gave the same R_f value with that of a natural specimen which was obtained from the hydrolyzate of kanamycin.

2,4,6-Tri-*O*-acetyl-3-amino-α-1-bromo-1,3-dideoxy-D-glucopyranose Hydrobromide (III).—A mixture of 2.27 g. of 3-amino-3-deoxy-D-glucopyranose hydrochloride (II) and 10 g. of freshly distilled acetyl bromide was allowed to stand for 3 hr. at room temperature with frequent shaking. The resulting solution was subjected to distillation in vacuo to remove unchanged acetyl bromide and the residue was dried in a brown vacuum-desiccator over sodium hydroxide overnight. The residue was dissolved in 25 ml. of hot chloroform, added with 1 g. of decolorizing charcoal and refluxed for 15 min. After the mixture was filtered, 100 ml. of absolute ether was added to the solution and the mixture was allowed to stand in a refrigerator overnight to

8) K. Freundenberg and O. Ivers, *Ber.*, 55, 929 (1922).

9) S. Peat and L. F. Wiggins, *J. Chem. Soc.*, 1938, 1810

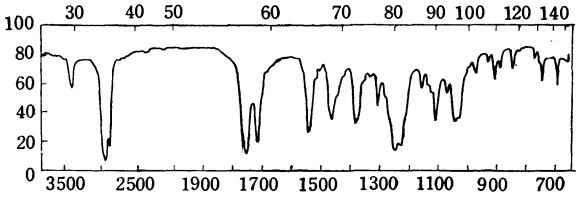


Fig. 1. Infrared spectrum of 2,4,6-tri-*O*-acetyl-α-1-bromo-3-carbobenzoxyamino-1,3-dideoxy-D-glucopyranose (IV) in Nujol.

to precipitate colorless powdery 2,4,6-tri-*O*-acetyl-3-amino-α-1-bromo-1,3-dideoxy-D-glucopyranose hydrobromide (III). The mother liquor was concentrated and added with absolute ether to obtain a second crop. The total yield was 4.56 g. (96.2%). The first crop showed m. p. 131~135°C, $[\alpha]_D^{15}$ +127.5° (*c* 1.77, $CHCl_3$).

Found: C, 31.30; H, 4.19; N, 3.38. Calcd. for $C_{12}H_{19}O_7NBr_2$ (449.1): C, 32.09; H, 4.26; N, 3.12%.

The infrared spectrum of the product in potassium bromide shows absorption bands at 3225 (νNH), 1759, (νC=O in OAc), 1593 (δNH_3^+), and 1219 (νC-O in OAc).

2, 4, 6-Tri-*O*-acetyl-α-1-bromo-3-carbobenzoxyamino-1, 3-dideoxy-D-glucopyranose (IV).—A mixture of the first and second crops of 2,4,6-tri-*O*-acetyl-3-amino-α-1-bromo-1,3-dideoxy-D-glucopyranose (III) was used for the following preparation: A mixture of 4.36 g. of III, 3 ml. of carbobenzoxy chloride (purity 58.5%), 77 ml. of chloroform and 41 ml. of saturated solution of potassium bicarbonate was stirred vigorously at −5°C for 20 min. The chloroform layer was separated and the aqueous layer was extracted with three 5 ml. portions of chloroform. The chloroform extracts were combined, washed three tmies with each 5 ml. of water and dried over 10 g. of sodium sulfate for 3 hr. The filtrate was concentrated under reduced pressure to yield a residue of colorless crystals of 2,4,6-tri-*O*-acetyl-α-1-bromo-3-carbobenzoxyamino-1,3-dideoxy-D-glucopyranose. To the residue was added 30 ml. of ether, allowed to stand overnight and then filtered; m. p. 146~148°C (decomp.), $[\alpha]_D^{10}$ +131.6° (*c* 1.77, $CHCl_3$), yield 2.59 g. (53.2%).

Found: C, 47.90; H, 4.64; N, 3.03; Br, 15.67. Calcd. for $C_{20}H_{24}O_9NBr$ (502.3): C, 47.82; H, 4.81; N, 2.79; Br, 15.91%.

The infrared spectrum of the product in Nujol shows absorption bands at 3383, (νNH), 1753 (ν C=O in OAc), 1714 (νC=O in Cbzo), 1540 (δNH), 1244, 1225 (νC-O in OAc), 848 (type 2a of pyranose ring) and 776, 748, 698 (phenyl) (Fig. 1).

Methyl 2,4,6-Tri-*O*-acetyl-3-carbobenzoxyamino-3-deoxy-β-D-glucopyranoside (V).—A mixture of 0.2 g. of 2,4,6-tri-*O*-acetyl-α-1-bromo-3-carbobenzoxyamino-1,3-dioxy-D-glucopyranose (IV) and 0.05 g. of mercuric cyanide in 1.0 ml. of absolute methanol was shaken at 27°C for 1.0 hr. to obtain a yellowish solution. The solution was cooled in ice-water and added with water dropwise, whereupon the solution became turbid and then there were colorless crystals of methyl 2,4,6-tri-*O*-acetyl-3-carbobenzoxyamino-3-deoxy-β-D-glucopyranoside deposited, which were collected and washed with water until the washings became neutral; yield 0.14 g. (77.4%), m. p. 139°C, $[\alpha]_D^{12}$ −19.6° (*c* 1.77, $CHCl_3$).

Found: C, 55.50; H, 5.99; N, 3.12; OCH_3, 6.58. Calcd. for $C_{21}H_{27}O_{10}N$ (453.5): C, 55.62; H, 6.00; N, 3.09; OCH_3, 6.84%.

The infrared spectrum of the product in chloroform shows absorption bands at 3415 (νNH), 1753 (νC=O in OAc), 1735 (νC=O in Cbzo) 1520 (δNH), 1227, 1210 (νC-O in OAc) and 895 (type 2b of pyranose ring).

2, 3, 4-Tri-*O*-acetyl-6-amino-α-1-bromo-6-deoxy-D-gulcopyranose Hydrobromide (VII).—A mixture of 0.2 g. of 6-amino-6-deoxy-D-glucose hydrochloride[5] and 0.72 g. of freshly distilled acetyl bromide was placed in a brown flask and allowed to stand for 74 hr. with frequent shakings. The resulting mixture was subjected to vacuum-distillation to remove unchanged acetyl bromide and the residue was dried thoroughly in a vacuum-desiccator over sodium hydroxide overnight. The residue was triturated with 8 ml. of chloroform to give colorless crystals of 2,3,4-tri-*O*-acetyl-6-amino-α-1-bromo-6-deoxy-D-glucopyranose hydrobromide, which were washed three times with a portion of 2.0 ml. of chloroform each, yield 0.4 g. (96.3%), m. p. 142°C (decomp.). A specific rotation pattern of the product could not be ascertained because it is not soluble enough for the determination in ordinary organic solvents. A small quantity of the product was recrystallized from a large quantity of dioxane-tetrahydrofuran for the elementary analysis; m. p. was raised to 162~164°C (decomp.).

Found: C, 31.81; H, 4.61; N, 3.04. Calcd. for $C_{12}H_{19}O_7NBr_2$ (449.1): C, 32.09; H, 4.26; N, 3.12%.

The infrared spectrum of the product in potassium bromide shows 3218 (νNH) 1765 (νC=O in OAc), 1594 (δNH_3^+), 1249, 1224 (νC-O in OAc) 843 (type 2a of pyranose ring).

2, 3, 4-Tri-*O*-acetyl-α-1-bromo-6-carbobenzoxyamino-1, 6-dideoxy-D-glucopyranose (VIII).—A mixture of 0.2 g. of 2,3,4-tri-*O*-acetyl-6-amino-α-1-bromo-6-deoxy-D-glucopyranose hydrobromide (VII), 0.12 g. of carbobenzoxy chloride, 3.5 ml. of chloroform and 1.5 ml. of a saturated solution of sodium bicarbonate was shaken at about 0°C for 20 min. Thereby the suspension of VII which is almost insoluble in both chloroform and water disappeared, resulting in two layers of clear chloroform and aqueous solutions. The chloroform layer was separated, washed with water and dried over sodium sulfate. The filtrate was evaporated under reduced

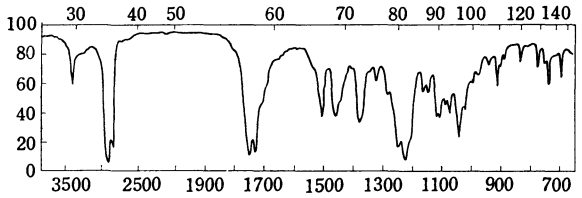


Fig. 2. Infrared spectrum of 2,3,4-tri-*O*-acetyl-α-1-bromo-6-carbobenzoxyamino-1,6-dideoxy-D-glucopyranose (VIII) in Nujol.

pressure and the resulting residue was recrystallized twice from ether-petroleum ether to give colorless tiny crystals of 2,3,4-tri-*O*-acetyl-α-1-bromo-6-carbobenzoxyamino-1,6-dideoxy-D-glucopyranose; yield 0.17 g. (76%), m. p. 89°C, $[\alpha]_D^{17}$ +156° (*c* 1.67, $CHCl_3$).

Found: C, 48.29; H, 4.72; N, 2.91; Br, 15.43. Calcd. for $C_{20}H_{24}O_9NBr$ (502.3): C, 48.72; H, 4.81; N, 2.79; Br, 15.92%.

The infrared spectrum of the product in Nujol shows absorption bands at 3390 (νNH), 1751 (νC=O in OAc), 1731 (νC=O in Cbzo), 1507 (δNH), 1249, 1222 (νC-O in OAc), 833 (type 2a of pyranose ring) and 776, 732, 739, 697 cm^{-1} (phenyl) (Fig. 2).

Methyl 2, 3, 4-Tri-*O*-acetyl-6-carbobenzoxyamino-6-deoxy-β-D-glucopyranoside (IX). — *By Mercuric Cyanide as a Condensing Reagent.*—A mixture of 0.2 g. of 2, 3, 4-tri-*O*-acetyl-α-1-bromo-6-carbobenzoxyamino-1,6-dideoxy-α-D-glucopyranose (VIII), 0.05 g. of mercuric cyanide in 1.0 ml. of absolute methanol was placed in a brown flask and shaken at 29°C for 1 hr. and then poured into 8 ml. of ice-water. The resulting viscous precipitate was taken in chloroform and washed with water. After drying over sodium sulfate, the chloroform solution was evaporated to dryness and the residue was triturated with isopropanol to start crystallization, yield 0.11 g. (61.2%), m. p. 95~100°C. Recrystallization from isopropanol raised the m. p. to 103~104°C; $[\alpha]_D^{15}$ +4.5° (*c* 2.00, $CHCl_3$).

Found: C, 55.77; H, 5.76; N, 3.11; OCH_3, 6.44. Calcd. for $C_{21}H_{27}O_{10}N$ (453.5): C, 55.62; H, 6.00; N, 3.09, OCH_3, 6.84%.

The infrared spectrum of the product in chloroform shows absorption bands at 3465 (νNH), 1764 (νC=O in OAc), 1734 (νC=O in Cbzo), 1519 (δNH), 1245, 1215 (νC-O in OAc), 903 (type 2b of pyranose ring).

By Silver Carbonate as a Condensing Reagent.—A mixture of 0.2 g. of 2,3,4-tri-*O*-acetyl-α-1-bromo-6-carbobenzoxyamino-1, 6-dideoxy-D-glucopyranose, 9.1 ml. of methanol, 1.2 g. of silver carbonate, 0.61 g. of calcium sulfate and 9.1 ml. of chloroform was sealed in a test tube to keep completely free from moisture and shaken at 29°C for 4.5 hr. The reaction mixture was filtered through active charcoal placed on a filter paper and the active charcoal was washed ten times with a portion of 2 ml of methanol. The filtrate and washings were combined and evaporated to dryness under reduced pressure. The residue was recrystallized from isopropanol to give colorless crystals of m. p. 99~101°C, yield 0.1 g. (57%). Mixed melting point of the product and the sample obtained by the above method showed no depression and the respective infrared spectra were completely superimposable.

The authors are indebted to Mr. Saburo Nakada for microanalysis and are grateful to Mr. Sadaaki Hashimoto for helping their experiments.

Department of Applied Chemistry
Faculty of Engineering
Keio University
Koganei-shi, Tokyo

NOTES

Oxidaton of Tetralin with tert-Butyl Chromate

By Tamon MATSUURA, Takayuki SUGA and Takashi SAKAO

(Received April 23, 1962)

Previous works on the oxidation of cyclohexene[1a,b] and of terpenoids[2a-e] with *tert*-butyl chromate have revealed that an active methylene group adjacent to a double bond was preferentially oxidized to an α,β-unsaturated ketonic group. Also, some aromatic compounds[3] have been oxidized with the same oxidant; e. g., dihydrosafrole was mainly oxidized to piperonylic acid. The present work deals with the oxidation of tetralin with this oxidant.

Experimental

Tetralin, distilled repeatedly, was used as the sample; b. p. 90°C/18 mmHg, n_D^{25} 1.5388, d_4^{25} 0.9669. Gas chromatography using a column of P. E. G. −6000 on celite at 150°C and helium (60 cc./min.) as a carrier gas showed that the sample tetralin was contaminated by 2.9% of naphthalene.

Experiment I.—A *tert*-butyl chromate solution was prepared from 197 g. of chromic anhydride, 394.5 g. of *tert*-butyl alcohol, 1100 g. of benzene, 50 g. of glacial acetic acid and 100 g. of acetic anhydride in the same manner as in the previous report[2c] except that the oxidant solution was concentrated to 66% in volume before use. This oxidant solution was added drop by drop, to a solution of 50 g. of tetralin in 75 g. of benzene, and the oxidation was carried out under the conditions shown in Table I. Then, the whole reaction mixture was treated as usual (cf. Ref. 1b or 2c). In this manner, 44.5 g. of a neutral product and 1.8 g. of an acidic one were obtained. The latter (1.8 g.) was chromatographed on silica gel using ethyl alcohol-chloroform mixture, The first fraction gave 0.5 g. of *o*-carboxyhydrocinnamic acid (m. p. 166~167°C[4]; Found: C, 61.62; H, 5.54%) and the other fraction gave *o*-phthalic acid (m. p. and mixed m. p., 191~191.5°C).

A gas chromatogram of the neutral product showed three peaks, which corresponded to those of tetralin (retention time at 160°C: 5 min.), naphthalene (10 min.) and α-tetralone (32 min.) respectively. The chromatogram indicated the presence of 3.1% of naphthalene in the neutral product, corresponding to 2.8% for the tetralin used.

A portion (10 g.) of the neutral product was chromatographed on silica gel using mixture of ethyl acetate and *n*-hexane. The first fraction gave 5.5 g. of tetralin unchanged (b. p., n_D^{25}, d_4^{25}; the IR spectrum accorded with that of tetralin), while the second one gave 3.5 g. of α-tetralone (b. p. 124~125°C/10 mmHg, n_D^{25} 1.5655, d_4^{25} 1.0914, λ_{max}^{EtOH} 247 mμ[5]: ε 11790), which in turn gave 2, 4-dinitrophenylhydrazone (m. p. 255°C (decomp.)) (Found: N, 17.01%), semicarbazone (m. p. 219~221°C) (Found: N, 20.80%), and oxime (m. p. 102~103°C) (Found: N, 8.46%). As for the determination of the α-tetralone in the neutral product, Fujita's procedure[6] was used. The reliability of this procedure was confirmed by using a known mixture containing pure α-tetralone in tetralin.

Experiment II.—A *tert*-butyl chromate solution was prepared in the same manner as above, except that the benzene solution was concentrated to 55% in volume. To this oxidant, 50 g. of tetralin in 50 g. of benzene was added drop by drop. After the oxidation had been carried out under the conditions shown in Table I, the reaction mixture was treated as in Experiment I.

Results

The results are summarized in Table I. It was found that a methylene group adjacent to a benzene nucleus of tetralin was preferentially oxidized to a ketonic group, with *tert*-butyl chromate giving α-tetralone. However, no formation of 1,4-naphthoquinone was observed, unlike the *tert*-butyl chromate oxidation of cyclohexene, which afforded *p*-benzoquinone, and also unlike the chromic acid oxidation of α-tetralone[7], in acetic acid which gave 1, 4-naphthoquinone. A slight degradative oxidation

1) a) R. V. Oppenauer and H. Oberrauch, *Anales Asoc. Quim. Argentina*, **37**, 246 (1949); b) T. Suga, *J. Chem. Soc. Japan, Pure Chem. Sec.* (*Nippon Kagaku Zasshi*), **80**, 906 (1959).

2) a) G. Dupont, R. Dulou and O. Mondou, *Bull. soc. chim. France*, **1953**, 60; b) K. Fujita, *J. Chem. Soc. Japan, Pure Chem. Sce.* (*Nippon Kagaku Zassi*), **78**, 1112 (1957); c) T. Suga, This Bulletin, **31**, 569 (1958); d) K. Fujita, ibid., **34**, 968 (1961); e) T. Matsuura, K. Saito and Y. Shimakawa, ibid., **23**, 1151 (1960).

3) I. Iwai and Y. Okajima, *J. Pharm. Soc. Japan* (*Yakugaku Zasshi*), **78**, 1252 (1958); T. Suga, *J. Chem. Soc. Japan, Pure Chem. Sec.* (*Nippon Kagaku Zasshi*), **80**, 948 (1959); T. Kuraoka, ibid., **82**, 50 (1961); Y. Fujita and T. Ueda, ibid., **78**, 655 (1957); **82**, 397 (1961).

4) W. Hückel and E. Vevera, *Chem. Ber.*, **89**, 2109 (1956).

5) R. Huisgen and W. Rapp, ibid., **85**, 831 (1952).

6) Y. Fujita and K. Nakahara, *J. Chem. Soc. Japan* (*Nippon Kwagaku Kwaishi*), **61**, 77 (1940).

7) T. Shoji, *J. Pharm. Soc. Japan* (*Yakugaku Zasshi*), **79**, 1034 (1959).

TABLE I. CONDITIONS AND RESULTS IN THE OXIDATION OF TETRALIN

Experiment	Reaction condition: Sample/Chromic acid	Reaction condition: Temp. °C	Reaction condition: Time day	Reaction product (wt % to the sample): α-Tetralone	o-Carboxyhydrocinnamic acid	o-Phthalic acid	Tetralin unchanged
I	1 : 5.2	18~25	16	35	1	0.6	48
II	1 : 5.2	18 then, 46~48	1 15	45	2	12	17

of α-tetralone occurred to give *o*-carboxyhydrocinnamic acid and *o*-phthalic acid. Undoubtedly, *o*-carboxyhydrocinnamic acid is the degradative product of α-tetralone through 1, 2-diketone, i. e., 3, 4-dihydro-1, 2-naphthoquinone, while *o*-phthalic acid is produced by the further oxidation of *o*-carboxyhydrocinnamic acid.

Summary

The oxidation of tetralin with *tert*-butyl chromate gave a relatively good yield of α-tetralone as the major product. Thus, it was seen that this oxidant oxidizes a methylene group of an alicyclic ring, adjacent to a benzene nucleus, to a ketonic group, forming α-ketone.

Department of Chemistry
Faculty of Science
Hiroshima University
Hiroshima

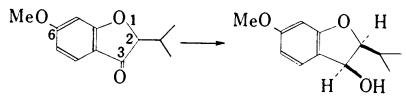
A New Method of Preparing 2-Alkylbenzofuran from 2-Alkyl-3(2H)-benzofuranone

By Yoshiyuki KAWASE and Shinnichi NAKAMOTO

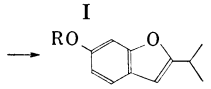
(Received May 29, 1962)

For the preparation of 2-alkylbenzofurans, two methods seem to be generally applicable, by the reduction of 2-alkyl-3(2*H*)-benzofuranone oxims followed by deamination[1], and by the dehydrogenation of 2, 3-dihydro-2-alkylbenzofurans[2]. However, neither method is entirely satisfactory because of their low yields and too many steps. In the case of the 2-isopropyl derivatives, they have been prepared from 2-acetyl derivatives by the Grignard reaction[3].

Now a new, easier method for the synthesis of general 2-alkylbenzofuran from 2-alkyl-3-(2*H*)-benzofuranone has been explored; the ketone was reduced with lithium aluminum hydride or with sodium borohydride to give 2, 3-dihydro-2-alkyl-3-benzofuranol, which was then readily converted into 2-alkylbenzofuran by dehydration.



I II



III R=Me
IV R=H

Reduction of 2-isopropyl-6-methoxy-3(2*H*)-benzofuranone (I), followed by subsequent treatment with acetic acid, furnished *cis*-2, 3-dihydro-2-isopropyl-6-methoxy-3-benzofuranol (II) in the form of colorless crystals with a sharp odor. The hydroxyl group of II seems to be cis to the isopropyl group, considering its formation procedure, the difficulty with which it forms nitrobenzoate, and the easiness with which it can be dehydrated. The distillation of II or the use of hydrochloric acid in the above-mentioned reduction of I readily furnished 2-isopropyl-6-methoxybenzofuran (III). The reflux of II with anhydrous pyridine hydrochloride furnished 6-hydroxy-2-isopropylbenzofuran (IV).

Experimental*

***cis*-2, 3-Dihydro-2-isopropyl-6-methoxy-3-benzofuranol (II).**—(*a*) *By Lithium Aluminum Hydride.*—A solution of 2-isopropyl-6-methoxy-3(2*H*)-benzofuranone[4] (I, m. p. 74~75°C, IR: ν_{CO} 1675 cm^{-1} (KBr), 2 g.) in anhydrous ether (20 ml.) was stirred into a suspension of lithium aluminum hydride

1) R. Stoermer and W. König, *Ber.*, **39**, 492 (1906); P. Friedländer, ibid., **47**, 1919 (1914); B. Kamthong and A. Robertson, *J. Chem. Soc.*, **1939**, 933; K. Horváth, *Monatsh.*, **82**, 901 (1951).

2) B. Klarmann, *J. Am. Chem. Soc.*, **73**, 4476 (1951); H. Bickel and H. Schmid, *Helv. Chim. Acta*, **36**, 664 (1953).

3) A. Robertson, *J. Chem. Soc.*, **1949**, 2057; M. Miyano and M. Matsui, *Chem. Ber.*, **92**, 2487 (1959).

* Melting and boiling points are uncorrected.

4) J. Arima and T. Okamoto, *J. Chem. Soc. Japan* (*Nippon Kwagaku Kwaishi*), **50**, 344 (1929); W. Bridge, A. J. Crocker, T. Cubin and A. Robertson, *J. Chem. Soc.*, **1937**, 1530.

(0.4 g.) in ether (80 ml.), and the mixture was then refluxed for one hour. The cooled mixture was acidified with dilute aqueous acetic acid, and the ether layer was separated and washed with dilute aqueous sodium hydroxide. The crystalline product obtained from the ethereal solution was recrystallized from petroleum benzine to give II in the form of colorless crystals; m. p., 108~109°C; yield, 1 g. (50%). IR: ν_{OH} 3220 cm^{-1} (KBr) or 3480 cm^{-1} ($CHCl_3$). Found: C, 69.24; H, 7.74. Calcd. for $C_{12}H_{16}O_3$: C, 69.21; H, 7.74%.

(*b*) *By Sodium Borohydride.*—A solution of sodium borohydride (0.5 g.) in ethanol (20 ml.) was slowly added to a solution of the ketone I (1 g.) in ethanol (30 ml.), and the mixture was heated at 65~70°C for 2 hr. In this reduction, the reaction temperature was important, for the starting material was recovered only when the temperature was lower. Most of the ethanol was removed in vacuo; the residue was acidified with dilute aqueous acetic acid and extracted with ether. The ethereal solution was washed with dilute aqueous sodium hydroxide, and the product was recrystallized from petroleum benzine; m. p., 107~109°C. Yield, 0.5 g. (50%).

2-Isopropyl-6-methoxybenzofuran (III).—Distillation of II in vacuo or treatment with dilute hydrochloric acid instead of acetic acid in the above-mentioned reduction of I gave III as a colorless oil; b. p., 130~135°C/3 mmHg. Picrate: red crystals; m. p., 60~61°C (from ethanol). Found: N, 10.75. Calcd. for $C_{18}H_{17}O_9N_3$: N, 10.02%.

6-Hydroxy-2-isopropylbenzofuran (IV).—A mixture of II (0.3 g.) and anhydrous pyridine hydrochloride (1.5 g.) was refluxed for 20 min. on an oil-bath (220°C). The cooled product was treated with dilute hydrochloric acid and extracted with ether. The ethereal solution was extracted with dilute aqueous sodium hydroxide, and the product obtained by acidifying the alkaline solution was distilled in vacuo (b. p., 130°C/0.001 mmHg) and then crystallized from petroleum benzin to give IV in the form of colorless microcrystals; m. p., 75~76°C; yield, 0.1 g. The reported m. p. is 75~76°C[1]. Found: C, 74.72; H, 7.03. Calcd. for $C_{11}H_{12}O_2$: C, 74.97; H, 6.86%.

The authors are grateful to Dr. Matao Kanaoka of the Faculty of Pharmacology of this University and to Dr. Sōichi Misumi of the Faculty of Science of Osaka University for their microanalyses and infrared spectroscopy.

Faculty of Literature and Science
Toyama University
Gofuku, Toyama

SHORT COMMUNICATION

High Pressure Hydrogenation with Rhodium-Platinum Oxide

By Shigeo NISHIMURA and Hisaaki TAGUCHI

(Received July 23, 1962)

In previous papers[1], it was shown that the rhodium-platinum oxide of Adams' type is an excellent catalyst in activity and in selectivity in the hydrogenation of various organic compounds at ordinary temperature and pressure. The effects of platinum in the rhodium-platinum oxide were also reported[2].

Subsequently the use of the rhodium-platinum oxide under high pressure of hydrogen has been found extremely effective in many hydrogenations. Under the pressures of 70 to 100 kg./cm^2, most hydrogenations proceed rapidly at room temperature with (7 : 3) rhodium-platinum oxide (see Table I). Usually in acetic acid rapid absorptions of hydrogen begin with the reduction of the oxide almost instantly at 50°C and in 10 to 30 min. at room temperature at the pressure of 100 kg./cm^2. The rate in hydrogenation of benzene increased greatly with the increase of hydrogen pressure in the range of 75 to 132 kg./cm^2. The activity of (7 : 3) rhodium-platinum oxide under high pressures is not only much greater, but also more stable than that of platinum oxide[3]. Accordingly, with rhodium-platinum oxide only a small amount of the catalyst is required for rapid and complete hydrogenation of most unsaturated organic compounds. With

1) S. Nishimura, This Bulletin, **33**, 566 (1960); **34**, 32 (1961).
2) S. Nishimura, ibid., **34**, 1544 (1961).
3) High pressure hydrogenations with platinum oxide were reported to be effective [R. H. Baker and R. D. Schuetz, *J. Am. Chem. Soc.*, **69**, 1250 (1947)]. But in most cases, for the completion of hydrogenations within a short time, fairly a good amount of the catalyst must be used because of the decrease of the activity during hydrogenation.

TABLE I. HIGH PRESSURE HYDROGENATION WITH (7 : 3) RHODIUM-PLATINUM OXIDE[a]

Compound	Amount g.	Catalyst g.	Temp. °C	H_2 press. kg./cm^2	Time min.	Product (Yield, %)
Benzene	7.81	0.05*	24	75～49	11	Cyclohexane (Not isolated)
Benzene	7.81	0.05*	24	99～70	8	Cyclohexane (Not isolated)
Benzene	7.81	0.05*	24	132～99	5	Cyclohexane (Not isolated)
Benzene	7.81	0.025	50	99～70	6	Cyclohexane (Not isolated)
Toluene	9.21	0.05	25	99～66	12	Methylcyclohexane (85)
Ethyl benzoate	15.0	0.05	24	98～68	45	Ethyl hexahydrobenzoate (91)
Aniline	9.31	0.10*	23	75～24	76	Cyclohexylamine (68) Dicyclohexylamine (20)
Aniline	9.31	0.05	50	80～51	35	Cyclohexylamine (56) Dicyclohexylamine (29)
Phenol	9.41	0.05	32	99～65	12	Cyclohexanol (85)
Acetophenone	12.0	0.05	27	100～70	55	Cyclohexylmethylcarbinol (82) Ethylcyclohexane (6)
Pyridine	7.91	0.05	50	100～71	20	Piperidine (Not isolated)

a) 50 ml. of acetic acid was used as solvent.
* The oxide was pre-reduced in the absence of the substrate.

the catalyst aniline gives a better yield of cyclohexylamine than with platinum oxide[4]. Phenol and acetophenone gave with good yields the corresponding saturated alcohols. Pyridine hydrogenates rather slowly at room temperature, but rapidly at 50°C. Thus, the high pressure hydrogenation with rhodium-platinum oxide is a very useful synthetic method. Its high acitivity at low temperatures may be advantageous in many selective hydrogenations. Further studies on the catalytic activity and selectivity of the rhodium-platinum oxide under high pressures are in progress.

The authors are indebted to Mitsubishi Chemical Industries Co. for the support of this work.

The Institute of Physical and Chemical Research
Bunkyo-ku, Tokyo

4) With platinum oxide under similar conditions, cyclohexylamine and dicyclohexylamine were obtained in yields of 17 and 23% respectively (Ref. 3); cf. G. S. Hier and R. Adams, *Ber.*, **59**, 162 (1926).

The Question of a Diversity of Mechanisms in Friedel-Crafts Acylation Reactions

By P. H. GORE

(Received March 13, 1962)

In a recent paper Yamase[1] adopted the view proposed earlier[2-4] that the literature data pertaining to Friedel-Crafts acylation reactions are consistent with a concept of a duality of mechanisms. According to the type and reactivity of reagent and substrate, the mechanism of acylation is considered to involve either an attack on the aromatic substrate by the acyl cation $RCO^{\oplus}$, or by the bulkier acyl halide complex RCOX, AlX_3. Evidence had been adduced earlier[3] in favour of the view that the latter mechanism operated in most "normal" acylation reactions, whilst attack by $RCO^{\oplus}$ would be likely only when steric circumstances become dominant.

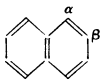
If, for instance, the acyl halide RCOX is sterically hindered, then formation of the addition complex RCOX, AlX_3 becomes energetically unfavourable*, and ionization giving the reactive acyl cation would be promoted, viz.

$$RCOX + AlX_3 \rightleftarrows RCO^{\oplus} + AlX_4^{\ominus}$$

Alternatively, when the reactive nuclear position of the substrate is sterically inaccessible, the small reagent $RCO^{\oplus}$ may be able to approach closely to the site of substitution, whilst the bulky addition complex may not. The theory of a duality of mechanisms has found a measure of general acceptance[1,6-9], whilst Brown and Jensen[6] contributed a further mechanism (i.e. involving attack by the ion-pair $(RCO^{\oplus})(AlX_4^{\ominus})$), which is not considered further here.

The data which Yamase and Goto[10,11] have recently put forward appear relevant to the concept of a duality of mechanisms. Their study of the relative reactivities of a series of acyl halides RCOX, in the presence of AlX_3, with a series of substrates, employed measurement of the "temperature of incipient reaction" (i.e. "the temperature at which the velocity of reaction becomes sufficient to cause visible bubbles (of hydrogen halide) to be evolved"), which was valuable enough in Calloway's[12] study of 1937, but which no longer can be regarded as a more than very approximate kinetic criterion.

It is of interest to consider whether the present theoretical framework of the concept of a diversity of mechanisms in the Friedel-Crafts acylation reaction would accomodate, for example, the "abnormal" substitution of naphthalene. Acylations of naphthalene[cf.4] exhibit wide variations of α- and β-isomer formation, depending on the solvent used, ranging from about 95% α- (with ethylene dichloride) to about 25% α- (with nitrobenzene). This has usually been attributed (in vague terms) to complex formation between the addition complex and solvent (S) molecules. The bulky complex RCOX, AlX_3, S would be more easily accomodated in the β-position of naphthalene[13-18]. One must admit that there is little doubt that such solvated complexes are capable of being formed under the usual reaction conditions.

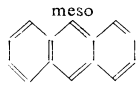


The effect of such solvation would indeed be a reduction in the electron-demand (and hence of the reactivity) of the reagent, as found experimentally. However, this clear-cut and simple role of the solvent cannot, in the present view, be supported in the light of the

* This is akin to the formation of aroyl cations from aromatic carboxylic acids (ArCOOH) on dissolution in concentrated sulphuric acid, when two ortho substituents are present. (In their absence $ArCOOH_2^{\oplus}$ is formed) (Ref. 5).

1) Y. Yamase, This Bulletin, **34**, 484 (1961).
2) J. M. Tedder, *Chem. & Ind.*, **1954**, 630.
3) P. H. Gore, ibid., **1954**, 1385.
4) P. H. Gore, *Chem. Revs.*, **55**, 229 (1955).
5) M. S. Newman, *J. Am. Chem. Soc.*, **63**, 2431 (1941).
6) H. C. Brown and F. R. Jensen, ibid., **80**, 2291 (1958).
7) C. D. Gutsche and A. J. Lauck, *Chem. & Ind.*, **1955**, 116.
8) J. Hine, "Physical Organic Chemistry", McGraw-Hill Book Company, Inc., New York (1956), p. 338.
9) F. R. Jensen, G. Marino and H. C. Brown, *J. Am. Chem. Soc.*, **81**, 3303 (1959).
10) Y. Yamase, This Bulletin, **34**, 480 (1961).
11) Y. Yamase and R. Goto, *J. Chem. Soc. Japan, Pure Chem. Sec.* (*Nippon Kagaku Zasshi*), **81**, 1906 (1960).
12) N. O. Calloway, *J. Am. Chem. Soc.*, **59**, 1474 (1937).
13) G. Baddeley, *J. Chem. Soc.*, **1949**, S. 99.
14) E. Berliner, "Organic Reactions", Vol. 5, John Wiley & Sons, Inc., New York (1949), p. 229.
15) G. Chiurdoglu and P. J. C. Fierens, *Bull. soc. chim. France*, [5] **17**, D27 (1950).
16) L. Chopin, ibid., [4] **35**, 610 (1924).
17) L. F. Fieser and M. Fieser, "Natural Products related to Phenanthrene", A. C. S. Monograph No. 70, Reinhold Publishing Corporation, New York (1949) p. 87.
18) S. M. Rivkin, *Zhur. Obshchei Khim.*, **5**, 277 (1935).

following: 1) If in nitrobenzene a bulky acylating complex is formed, why does concurrent α-substitution proceed in naphthalene, sometimes to the extent of 40%? Why can anthracene be acylated in this same solvent in its sterically hindered *meso*-position, as with benzoyl chloride in 79% yield[19], or with cinnamoyl chloride in 52% yield[4]? 2) Why

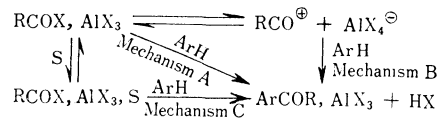


are such wide variations in isomer ratio observed with changing acyl halide? An α-/β-isomer ratio of 2.1 is obtained in the benzoylation of naphthalene in nitrobenzene, whilst under identical experimental conditions acetylation gives an isomer ratio of 0.5[13]. 3) How can appreciable β-substitution be explained in solvents such as carbon disulphide (e. g. 65% in acetylation[20]), which cannot readily solvate the aluminium chloride complexes. 4) An increase in temperature should result in increased substitution at the more sterically hindered position, whatever the solvent*. Data exist[4] for benzoylation of naphthalene, which show an increase in actual yield of β-naphthyl phenyl ketone from 24% (at 35°C) to 33% (at 150°C)[13].

The closely analogous pattern to the reversible sulphonation of naphthalene prompted the suggestion[3,4] that certain acylations may be reversible in polycyclic systems. In this theory "normal" substitution in these systems would depend on rapid precipitation of the ketone-catalyst addition complex from solution (as occurs, for example, in ethylene dichloride), whilst "abnormal" substitution would result from deacylation and resynthesis, occurring in the solution phase. Reversibility of acylation in substituted naphthalenes and higher polycyclics has now been established[4,21,22], but it appears to be of little importance[21,23] in the case of naphthalene itself, or one must surmise, with simple benzene derivatives.

The abnormal results, and the role of the solvent, in the acylations of naphthalene have not, therefore, been adequately accounted for. For this reason, and to explain recent data obtained by Jensen[23], an explanation has been sought[24] in terms of the alternative mechanisms, which may operate generally in an acylation system, viz. ArH/RCOX/S (where S = solvent).

Let it be assumed that the following reactions are possible, i. e. that the ketone ArCOR may be formed by any of three mechanistic pathways, (A) by means of the unsolvated acyl halide/catalyst complex (high reactivity, and of medium steric requirements), (B) by the free acyl carbonium ion (of high reactivity, and of low steric requirements), and (C) by a solvated acyl halide/catalyst complex (low reactivity, and of large steric requirements). It is further held that these mechanisms are not merely alternative possibilities, but that they may proceed simultaneously, their relative importance being a function of the reactivities of the reactants, and the solvating power of the solvent.



According to this view, then, α-substitution in naphthalene will proceed via mechanisms A and B, with the former predominating[3,4]. If the acyl halide is itself sterically hindered[3], mechanism B alone will operate. β-Substitution will take place by mechanisms A and C, with a trace only of B. Of these mechanisms C will become increasingly important in solvents of the type nitrobenzene, or with excess acyl halide. In solvents which tend to give "normal" (i. e. predominant α-) substitution, solvation is minimal, viz. mechanism A will operate mainly, and the product will be mostly α-, with some β- ketone. That portion of the reaction operating by mechanism B will tend to increase the percentage of α-ketone formed.

The use of excess benzoyl chloride in the benzoylation of naphthalene has recently been shown[23] to produce an increase in the proportion of β-isomer, and a marked decrease in overall yield. In the present view the effect of increasing the concentration of benzoyl chloride would here be to increase the contribution by mechanism C (at the expence of mechanism A), i. e. the proportion of β-isomer will increase. Also, since the solvated acyl complex is of low reactivity, the overall rate will decrease, and thus, presumably, will the overall yield in an equivalent experiment.

Toluene may be acetylated in ethylene dichloride solution[25] to give a p/o ratio = 83.4, whilst benzoylation[26] under similar experimental conditions involves a ratio = 9.6. It

* This assumes rate differences to be mainly due to changes in activation energy.

19) F. Krollpfeifer and F. Schütz, *Ber.*, **56**, 2360 (1923).

20) H. F. Bassilios, S. M. Makar and A. Y Salem, *Bull. soc. chim. France*, [5] **21**, 72 (1954).

21) P. H. Gore and R. B. Girdler, unpublished.

22) P. H. Gore, *J. Org. Chem.*, **22**, 135 (1957).

23) F. R. Jensen, *J. Am. Chem. Soc.*, **79**, 1226 (1957).

24) P. H. Gore, in "Friedel-Crafts and Allied Reactions". Ed. by G. A. Olah, Interscience Publishers, Inc., New York, in the press.

25) H. C. Brown, G. Marino and L. M. Stock, *J. Am. Chem. Soc.*, **81**, 3310 (1959).

26) H. C. Brown and G. Marino, ibid., **81**, 3308 (1959).

was concluded[25] that the steric requirements for acetylation under these conditions (with a non-coplanar configuration of the methyl group in the acetylating species) are larger than those for benzoylation.

In the present theory, it is suggested that whilst mechanism C will not operate in the solvent used[25], viz. ethylene dichloride, the ortho and para positions may both be substituted by mechanisms A and B (the former always predominating). Ionization to $RCO^{\oplus}$ will be favoured in the case of benzoyl chloride, due to resonance stabilisation, and thus the contribution of mechanism B will increase in this case, resulting here in a higher percentage ortho substitution.

Increasing concentrations of excess benzoyl chloride have been reported[23] not to affect the rate of, and the percentage ortho isomer in, the benzoylation of toluene. Since mechanism C will not operate here, this result is here to be predicted.

The data obtained by Jensen[23] led him to conclude that the acylating species for his benzoylations of toluene and naphthalene are different. We would here add the conclusion, that the differences are due in these systems to different combinations of competing substitution processes.

Brunel College
Woodlands Avenue
London, W. 3, England

The Formation of Acetylenic Bond by the Elimination Reaction of Some Enol-esters. III. Formation of α, β-Acetylenic Carbonyl Compounds

By Gen NAKAMINAMI

(Received March 20, 1962)

As described in the preceding paper[1], an α, β-acetylenic ketone is readily decomposed by the action of amide anion to yield the corresponding ethynyl compound and acid amide. Therefore, in order to obtain an α, β-acetylenic carbonyl compound by the elimination reaction of enol-esters, it was hoped to employ a suitable base to avoid the cleavage reaction. The nucleophilic addition of the base to a triple bond must also be avoided. The present paper deals with the studies along this line.

According to the studies of Dufraisse and his coworkers[2], primary and secondary alcohols add readily to the triple bond in acetylenic ketone II, but *tert*-alcohols were left untouched up to now. Therefore, the action of sodium *tert*-butoxide on ketone II was examined.

When ketone II was treated with sodium *tert*-butoxide in *tert*-butanol, there was obtained β-*tert*-butoxychalcone (III), as the main product, together with minor amounts of phenylacetylene (IV) and benzoic acid (V). The formation of IV and V clearly indicated that the bond-splitting reaction[1] occured subsidiarily in II.

$$C_6H_5C(OR)=CHCOC_6H_5 \rightarrow C_6H_5C\equiv CCOC_6H_5$$
(Ia, b) (II)

$$\rightarrow C_6H_5C(O\text{-}tert\text{-}C_4H_9)=CHCOC_6H_5$$
(III)

$$+ C_6H_5C\equiv CH + HO_2CC_6H_5$$
(IV) (V)

a : R = $PO(OC_6H_5)_2$ b : R = COC_6H_5

$$C_6H_5C(OPO(OC_6H_5)_2)=CHCO_2CH_3 \rightarrow C_6H_5C\equiv CCO_2R$$
(VI) (VIIa, b, c)

$$+ C_6H_5COCH_2CO_2CH_3 + (C_6H_5O)_3PO$$
(VIII) (IX)

a : R = *tert*-C_4H_9 b : R = CH_3 c : R = H

The structure of III was confirmed by its analytical data and infrared spectrum, and supported also by the formation of dibenzoylmethane on heating the enol-ether under reduced pressure. These results indicate that neither the addition nor the bond-fission reaction can be suppressed by the use of sodium *tert*-butoxide in *tert*-butanol.

It was found after several experimentations

1) M. Nakagawa, G. Nakaminami, F. Ogura and H. Ono, This Bulletin, 35, 1488 (1962).
2) M. C. Dufraisse and P Gérald, *Bull. soc. chim. France*, [4] 31, 1285 (1922); M. C. Dufraisse and A. Gillet, *Ann. chim.*, [10] 6, 295 (1926).

that ketone II was recovered unchanged in a fair yield, when treated with sodium *tert*-butoxide in benzene, therefore all elimination reactions in the present work were carried out in benzene as the solvent. A solution of enol-phosphate was added dropwise to a stirred suspension of sodium *tert*-butoxide in benzene, and the reaction mixture was stirred further in adequate periods. Benzoylphenylacetylene (II) was obtained from the phosphate Ia[3] and the benzoate Ib[3] in 76 and 58% respectively. Not any appreciable amount of by-product could be isolated in these cases. Similarly *tert*-butyl phenylpropiolate (VIIa) was obtained in a 24% yield from the phosphate VI[3]. The structure of VIIa was inferred from its infrared spectrum in which the characteristic absorptions ascribed to a disubstituted acetylene, an ester-carbonyl group and a *tert*-butyl group were clearly indicated. The ester VIIa was converted into methyl ester by refluxing in methanol in the presence of a small amount of sulfuric acid. The ester VIIb thus obtained was hydrolyzed to give free acid VIIc, which was readily purified by sublimation followed by recrystallization. In another experiment, the acid VIIc was isolated from the reaction mixture in a 28% yield. In the reaction of phosphate VI with sodium *tert*-butoxide, triphenylphosphate IX and methyl benzoylacetate VIII were also obtained.

The formation of keto-ester VIII and phosphate IX is probably due to ester-exchange reaction. The reaction of this type was found to be the main reaction in the case of phosphate Xa[3] by the isolation of triphenylphosphate IX and phenol from the reaction products, and no elimination reaction was observed. The elimination reaction of tosylate Xc[3] under similar conditions resulted in the formation

$CH_3C(OR)=CHCO_2C_2H_5$ (Xa, c) $\quad CH_3C(OP(OC_6H_5)_2)=CHCOCH_3$ (XI)

a : $R=PO(OC_6H_5)_2$

c : $R=SO_2C_6H_4$-*p*-CH_3

of a small amount of a liquid, the main constituent of which was assigned to be ethyl tetrolate on the basis of the infrared spectrum. Alkaline hydrolysis of this material afforded a small amount of crystals, whose identification could not be performed owing to its minor quantity. The phosphate XI[3] gave no well-defined product on treatment with sodium *tert*-butoxide.

The above-mentioned results appear to provide a support for the elimination mechanism of triple bond biosynthesis through enol derivative*.

3) M. Nakagawa, G. Nakaminami, F. Ogura and H. Ono, This Bulletin, **35**, 1485 (1962).

Experimental**

Action of Sodium *tert*-Butoxide on Benzoylphenylacetylene (II).—A solution of *tert*-butoxide (0.013 mol.) in dry *tert*-butanol (50 ml.) was warmed at 25~30°C. A solution of ketone II[4] (2.0 g., 0.01 mol.) in dry ether (30 ml.) was added dropwise while stirring into the above solution during 40 min. The reaction mixture was stirred for a further 2 hr. at the same temperature, and set aside at room temperature for 16 hr. A solution of glacial acetic acid (0.8 g., 0.013 mol.) in dry ether (25 ml.) was added dropwise while stirring and cooling (ice-bath), and then water (50 ml.) was added. The aqueous solution was extracted twice with ether, and combined ethereal solutions were washed successively with sodium hydrogen carbonate solution, 5% potassium hydroxide solution and water, dried (sodium sulfate) and concentrated. The residue was dissolved in ethanol (6 ml.), and treated with mercuric chloride-potassium iodide solution in the Johnson-McEwen's procedure[5]. An oil and an amorphous solid were separated. The solid was filtered, washed with 50% aqueous ethanol, pressed on a porous plate, left overnight to remove an oily material as well as possible, and recrystallized twice from ethanol to give a mercury compound of phenylacetylene as colorless needles, m. p. 122~123.5°C, undepressed on admixture with an authentic specimen.

On acidification (Congo Red) of the sodium hydrogen carbonate washings, an oil was separated and extracted with ether. The combined ether-extracts were washed with sodium chloride solution, dried (sodium sulfate), and evaporated. To the residue dissolved in acetic acid, water was added precipitating a solid (0.7 g., 57%), which was sublimed under reduced pressure and recrystallized twice from water to give benzoic acid as colorless plates, m. p. 121.5~122°C. It showed no depression in the melting point on admixture with an authentic specimen.

In another experiment using 0.04 mol. of acetic acid only 0.1 g. of the crude benzoic acid was obtained, and from the neutral part crystals (0.5 g.) of *β-tert*-butoxychalcone (III) were yielded, which were treated with charcoal in methanol and recrystallized twice from the same solvent to afford light yellow plates, m. p. 97~98°C.

Found: C, 81.54; H, 7.25. Calcd. for $C_{19}H_{20}O_2$: C, 81.39; H, 7.19%.

* As mentioned previously[3], quite recently, Jones [*Chem. & Ind. News*, **39**, No. 12, 46 (1961)] has suggested that the decarboxylative elimination of pyrophosphate anion from the pyrophosphate of acetylmalonyl coenzyme A is a possible route in the formation of an acetylenic bond in vivo, and the mechanism has been supported experimentally by the formation of phenylpropiolic acid from enol brosylate of diethyl benzoylmalonate in an alkaline medium (I. Fleming and J. Harey-Mason, *Proc. Chem. Soc.*, **1961**, 245.).

** All melting points and boiling points are uncorrected.

4) E. André, *Ann. chim.*, [8], **29**, 564 (1913). Cf. K. Bowden, I. M. Heilbron, E. R. H. Jones and B. C. L. Weedon, *J. Chem. Soc.*, **1946**, 39.

5) J. R. Johnson and W. L. McEwen, *J. Am. Chem. Soc.*, **48**, 471 (1926).

IR (Nujol): >C=O, 1662 cm^{-1}.

The enol-ether III gave the same deep red color as dibenzoylmethane, when it was treated with ferric chloride in ethanol, but the development of the color required several minutes. A similar behavior against ferric chloride was observed also in the case of β-methoxychalcone[2].

Thermal Decomposition of β-*tert*-Butoxychalcone (III).—The enol-ether III (0.1 g.) was heated at 180~200°C (bath) under reduced pressure (aspirator) in a sublimation apparatus. Light yellow crystals adhered gradually on the cold finger, and finally only a small amount of oil was left at the bottom of the vessel. The crystals furnished dibenzoylmethane on recrystallization from methanol as light yellow needles, m. p. 77.5~78.5°C, which showed no melting point depression on admixture with an authentic specimen[6].

Found: C, 80.62; H, 5.44. Calcd. for $C_{15}H_{12}O_2$: C, 80.33; H, 5.39%.

Elimination Reaction of Diphenyl 1, 3-Diphenyl-2-propen-1-on-3-yl Phosphate (Ia) by Sodium *tert*-Butoxide.—Sodium (0.95 g., 0.041 gram atom) was dissolved in hot dry *tert*-butanol (150 ml.), and the solvent was driven off at 50~55°C (bath) under reduced pressure as well as possible, affording almost colorless needles of sodium *tert*-butoxide. Dry benzene (150 ml.) was added to the crystals, and then the phosphate Ia (18.3 g., 0.04 mol.) in dry benzene (200 ml.) was added dropwise with stirring at room temperature to the resulting suspension during 1 hr. The mixture was stirred for a further 13.5 hr. at room temperature, and set aside for 28 hr. Water was added, and the benzene layer was washed successively with 5% potassium hydroxide solution and water and dried (sodium sulfate). All of the aqueous solutions were combined and extracted with ether. The combined ether-extracts were washed with water and dried (sodium sulfate). Evaporation of the solvent followed by distillation of the residue gave benzoylphenylacetylene (II) as a yellow oil (6.3 g., 76%), b. p. 142~144°C/0.5 mmHg, without affording any appreciable amount of low-boiling or high-boiling material. The oil was solidified completely, when seeded with a piece of crystal of authentic II, to give crystals melted at 42~47°C which was recrystallized twice from light petroleum (b. p. 40~60°C) to yield slightly yellow needles, m. p. 48~48.5°C, undepressed on admixture with an authentic specimen. Its infrared spectrum also showed the identity with that of the authentic specimen.

Found: C, 87.54; H, 5.04. Calcd. for $C_{15}H_{10}O$: C, 87.35; H, 4.89%.

A crystalline material which seemed to be diphenyl phosphate was obtained from the aqueous solution left after the extraction of ketone II.

Elimination Reaction of β-Benzoyloxychalcone (Ib) with Sodium *tert*-Butoxide.—A suspension of sodium *tert*-butoxide (0.022 mol.) in dry benzene (50 ml.) was prepared as above. A solution of the benzoate Ib[3] (6.6 g., 0.02 mol.) in dry benzene (50 ml.) was added dropwise with cooling (cold water) to the stirred suspension during 40 min. The mixture was stirred for 6 hr. with cooling by cold water, for a further 10 hr. at room temperature, and allowed to stand for about 30 hr. Water (150 ml.) was added with cooling by cold water, and the aqueous layer was extracted twice with benzene and twice with ether. The combined organic extracts were washed with sodium chloride solution and dried (sodium sulfate). Evaporation followed by distillation of the residue afforded ketone II as an oil (3.0 g.), b. p. 162~169°C/2.5 mmHg, which was solidified completely when seeded as described before. The solid so far obtained was dissolved in ether and washed successively with 5% potassium hydroxide solution and water. The ether was altered with benzene and the benzene solution was chromatographed on alumina (4.0 g.). Removal of the solvent from the eluate gave II (2.6 g., 58%) which was recrystallized from light petroleum (b. p. 40~60°C) as yellow plates, m. p. 46.5~49.5°C, and identified by infrared spectrum.

Elimination Reaction of Diphenyl β-Methoxycarbonyl-α-styryl Phosphate (VI) with Sodium *tert*-Butoxide.—A suspension of sodium *tert*-butoxide (0.044 mol.) in dry benzene (120 ml.) was prepared as above. A solution of the phosphate VI[3] (17.8 g., 0.043 mol.) in dry benzene (120 ml.) was added dropwise at room temperature to this stirred suspension during 1 hr. The mixture was stirred for a further 7 hr. at room temperature, left standing overnight, and then treated with water (120 ml.). The aqueous solution (solution A) was extracted twice with ether, and the combined organic solutions were washed successively with a 4% potassium carbonate solution (100 ml.×2), ice-cooled 0.5 N sodium hydroxide solution (100 ml.×2) and water, and dried (sodium sulfate). Evaporation followed by distillation gave a colorless liquid (product A) (2.1 g.), b. p. 93.5~96°C/1 mmHg, and an orange oily residue (product B).

The sodium hydroxide washings were acidified at 0°C, and then extracted 3 times with ether. The combined extracts were washed with sodium chloride solutionand dried (sodium sulfate). Evaporation followed by distillation afforded an oil (1.6 g., 30%), b. p. 100~101°C/1 mmHg, which was identified with methyl benzoylacetate[7] by infrared spectrum. The copper complex provided by the above oil exhibited m. p. 200~202°C and showed no melting point depression on admixture with an authentic specimen[7].

Found: C, 57.81; H, 4.42. Calcd. for $C_{20}H_{18}O_6Cu$: C, 57.48; H, 4.34%.

The above-mentioned potassium carbonate washings and the solution A afforded an oil on acidification (Congo Red) and ether-extraction. The oil appeared from its infrared spectrum as a mixture of diphenyl phosphate and a small amount of phenylpropiolic acid (VIIc), but no detailed study was taken.

Product A.—Its infrared spectrum [(liquid film): 2215, 2250 (-C≡C-); 1710 (>C=O ester); 1397, 1373 (C-H *tert*-C_4H_9); 1300, 1150 cm^{-1} (O=C-O-)] was found to be consistent with the structure of *tert*-butyl phenylpropiolate (VIIa), although the analytical

6) C. F. H. Allen, R. D. Abell and J. B. Normington, "Organic Syntheses", Coll. Vol. 1 (1948), p. 205.

7) A. Wahl, *Compt. rend.*, **147**, 72 (1908).

data indicated the presence of an impurity. A mixture of the product A (1.0 g.), absolute methanol (20 ml.) and concentrated sulfuric acid (4 drops) was refluxed for 12.5 hr., left to stand at room temperature for about 30 hr., and poured into ice-water. An oil was separated and extracted 3 times with ether. The combined extracts were washed successively with water, sodium hydrogen carbonate solution and water, and dried (sodium sulfate). After evaporation of the solvent, the residue was distilled giving a light yellow liquid (0.8 g., 100%), b. p. 78.5~81°C/2 mmHg, (lit.,[8] b. p. 132~133°C/16 mmHg), which was proved to consist mainly of methyl ester VIIb on the basis of the infrared spectrum [(liquid film): 2220 (-C≡C-); 1715 (>C=O ester); 2820 cm^{-1} (C-H CH_3O)].

A mixture of methyl ester VIIb (0.5 g.), potassium hydroxide (0.3 g., 1.5 equiv.), ethanol (8 ml.) and water (4 ml.) was refluxed for 30 min., and cooled immediately. On addition of water (10 ml.) a small amount of oil was separated. After removal of the oil by ether-extraction, the remaining aqueous solution was acidified (Congo red) with dilute sulfuric acid at 0°C. An oil was separated, and soon began to crystallize. The product was taken up in ether, washed with sodium chloride solution and dried. Evaporation of the ether afforded phenylpropiolic acid VIIc, (0.3 g., 65%) which was sublimed under reduced pressure, and recrystallized twice from carbon tetrachloride and once from water as colorless needles, m. p. 135~137°C, (lit.[9], m. p. 137°C).

Found: C, 73.89; H, 4.22. Calcd. for $C_9H_6O_2$: C, 73.96; H, 4.14%.

IR (Nujol): 2205, 2240 (-C≡C-); 1675 (>C=O carboxyl); 3200~2400 cm^{-1} (O-H carboxyl).

Product B.—On storage in an ice-box, product B deposited some amounts of the recovered phosphate VI, which was removed by filtration. The filtrate was distilled and the fraction, boiling at 140~173°C/3×10^{-4} mmHg, was collected, then it was seeded with a piece of crystal of triphenyl phosphate[10] IX and stored in an ice-box. A solid was separated (1.4 g., 16%) and recrystallized from light petroleum (b. p. 40~60°C) to give phosphate IX as colorless needles, m. p. 48.5~50°C, which showed no melting point depresssion on admixture with an authentic specimen. Its infrared spectrum also agreed with that of the authentic specimen.

Reaction of Diphenyl 1-Ethoxycarbonyl-1-propen-2-yl Phosphate (Xa) with Sodium *tert*-Butoxide.—The phosphate[3] Xa (160.8 g., 0.44 mol.) was added dropwise at room temperature to a stirred suspension of sodium *tert*-butoxide (0.45 mol.) in dry benzene. The mixture was stirred for 20 hr., set aside for 1 day, and treated with water. The benzene layer was washed successively with 5% sodium hydroxide solution and sodium chloride solution, and dried. Benzene was removed, the residue was distilled and a fraction boiling over 130°C/3×10^{-3} mmHg, was collected. The fraction solidified, and it was recrystallized twice from light petroleum to give triphenyl phosphate (IX) as colorless needles, m. p. 49~49.5°C, identified by infrared spectrum.

A low boiling liquid obtained above was redistilled to give a liquid, b. p. 95~105°C/1×10^{-3} mmHg, n_D^{20} 1.4838, which was clearly different from the starting phosphate Xa, but its infrared spectrum resembled Xa. Although the product was supposed to be produced by ester-exchange reaction, the analytical value did not agree with the calculated ones for any possible compounds. Perhaps it is a mixture of various products at different stages in ester-exchange reaction.

From the sodium hydroxide extract stated above, some amount of phenol was obtained by acidification and ether-extraction.

Reaction of Ethyl β-*p*-Toluenesulfonyloxy-crotonate (Xc) with Sodium *tert*-Butoxide.—The tosylate Xc[3] (13.4 g., 0.047 mol.) was added dropwise at room temperature to a stirred suspension of sodium *tert*-butoxide (0.048 mol.) in dry benzene. The mixture was stirred at room temperature for 38 hr., left standing for 75 hr., and treated with water. The aqueous layer was extracted with ether, and the combined organic layers were washed successively with 5% sodium hydroxide solution and salt solution. Evaporation followed by distillation gave ethyl tetrolate as colorless, sweet smelling liquid (0.5 g.), b. p. 63~64°C/10 mmHg, (lit.[11], b. p. 164.5~165.0°C/760 mmHg).

IR (liquid film): 2240 (-C≡C-); 1712 cm^{-1} (>C=O ester).

A mixture of the liquid (0.3 g.) and 0.5 N potassium hydroxide (15 ml.) was refluxed for 40 min., cooled, and extracted with ether to remove a small amount of insoluble material. Acidification and ether-extraction afforded a very small amount of crystals, which could not however be identified.

The author wishes to express his sincere thanks to Professor Masazumi Nakagawa of Osaka University for his guidance and encouragement throughout this work. The author's thanks are also due to the Ministry of Education for the grant-in-aid.

Note added in proof (August 31, 1962).

Since this paper was submitted a short communication by J. Cymerman Craig and M. Moyle (*Proc. Chem. Soc*, **1962**, 149) has appeared in which they realized the formation of some acetylenic compounds treating the enol diethyl phosphates of the corresponding carbonyl compounds with sodium amide in liquid ammonia.

Department of Chemistry
Faculty of Science
Osaka University
Nakanoshima, Osaka

8) C. Moureu, *Ann. chim.*, [8] **7**, 536 (1906).
9) F. Barisch, *J. prakt. Chem.*, [2] **20**, 173 (1879).
10) G. Jacobson, *Ber.*, **8**, 1523 (1875); P Brigl and H. Müller, ibid., **72**, 2121 (1939).
11) E. A. Halonen, *Acta Chem. Scand.*, **9**, 1492 (1955).

Studies of the Solvent Extraction of Niobium-95 in the Tribenzyl Amine-Hydrochloric Acid System

By Takashi OMORI and Nobuo SUZUKI

(Received February 22, 1962)

There are many reports on the solvent extraction of metals, but these extraction methods are only applicable to the particular cases described in these papers. The present authors have undertaken a quantitative investigation of solvent extraction and have made an effort to elucidate the chemical behavior of metals in the case of solvent extraction. One of the authors has already reported the quantitative treatment of the solvent extraction of ^{144}Ce with acetylacetone[1]. Recently, we both reported the mutual separation of ^{95}Zr and ^{95}Nb with acetylacetone[2].

Since about 1958 there has been a rapid developement in amine extraction, particularly for uranium extraction[3]. It has been reported that the mechanism of amine extraction is similar to that of anion exchange[3-5]. However, phenomena which can not be completely explained as anion exchange mechanism have been found in a few reports[6-8].

In the present paper, the distribution coefficients of ^{95}Nb between hydrochloric acid and amine are investigated. Based on the results, the mechanism of amine extraction and the species of niobium in hydrochloric acid are discussed.

Experimental

Reagents.—Carrier-free ^{95}Nb was separated from $^{95}Zr(^{95}Nb)$ by the anion exchange method and was stored in 18 N sulfuric acid, as has been described in a previous paper[2]. Before being used for experiments, ^{95}Nb was extracted with acetylacetone and was converted into the chloride form by back-extraction with hydrochloric acid.

Tribenzylamine (TBA) obtained from the Tokyo Kasei Co., Ltd. was of a high purity as indicated by melting point measurement and was used without further purification. A standard solution of TBA was prepared by dissolving TBA in chloroform. TBA was converted into the hydrochloride form (TBA-Cl) before being used for experiments by shaking the TBA solution in chloroform with 6 M hydrochloric acid for 30 min.

E. P. grade chloroform was treated with concentrated sulfuric acid and then purified by distillation.

All other chemicals were of guaranteed reagent grade.

Distribution Measurement. — All equilibrations were carried out in glass-stoppered tubes. These tubes were shaken with a mechanical shaking device in a constant temperature bath. The experiments were carried out at 25±0.5°C unless otherwise stated. The distribution coefficients, D, were determined as follows: ^{95}Nb was previously extracted from concentrated hydrochloric acid with TBA-Cl in chloroform. An aliquot of this organic solution, containing ^{95}Nb, was shaken for one hour with aqueous solutions of various conditions. After the phases had disengaged, the phases were transferred into two test tubes and the γ-activities of both tubes were measured with a scintillation counter. Studies of the equilibration rate have shown that complete equilibration was attained in less than 30 min.; however, the shaking time of one hour was chosen for this work.

The determination of the acidity of both phases was necessary. The aqueous phase was titrated with a standard solution of sodium hydroxide, using methyl orange as the indicator. The acid in the organic phase was titrated with a stadard sodium hydroxide solution in ethanol by the aid of a pH meter.

Results and Discussion

Extraction Mechanism and Some Related Equations. — The authors consider that the anionic species of niobium in the aqueous phase is transferred to the organic phase as follows:

$$Nb(OH)_pCl_q^{+5-p-q} + (p+q-5)RCl \rightleftharpoons R_{p+q-5}Nb(OH)_pCl_q + (p+q-5)Cl^- \quad (1)$$

followed by the reaction of the above species with TBA-Cl in the organic phase, containing large amounts of TBA-Cl:

$$R_{p+q-5}Nb(OH)_pCl_q + iRCl \rightleftharpoons R_{p+q-5}Nb(OH)_pCl_q \cdot iRCl \quad (2)$$

1) N. Suzuki and S. Oki, This Bulletin, **35**, 233, 237 (1962).
2) N. Suzuki and T. Omori, ibid., **35**, 595 (1962).
3) C. F. Coleman, K. B. Brown, J. G. Moore and K. A. Allen, A/Conf. 15/P/510 (1958); C. F. Coleman, K. B. Brown, J. G. Moore and D. J. Crouse, *Ind. Eng. Chem.*, **50**, 1756 (1958), W E. Keder, J. C. Sheppard and A. S. Wilson, *J. Inorg. Nucl. Chem.*, **12**, 327 (1960).
4) J. Y Ellenburg, G. W. Ledicotte and F. L. Moore, *Anal. Chem.*, **26**, 1045 (1954).
5) G. E. Boyd and Q. V. Larson, *J. Phys. Chem.*, **64**, 988 (1960).
6) K. A. Allen, *J. Am. Chem. Soc.*, **80**, 4133 (1958).
7) W. J. McDowell and C. F. Baes. Jr., *J. Phys. Chem.*, **62**, 777 (1958).
8) S. Matsuo, *J. Chem. Soc. Japan, Pure Chem. Sec.* (*Nippon Kagaku Zasshi*), **82**, 458 (1961).

where RCl indicates TBA-Cl and $6 \leq (p+q) \leq 8$.

The extraction constant for Eq. 1 and the formation constant for Eq. 2 are:

$$K_{p,q} = \frac{(R_{p+q-5}Nb(OH)_pCl_q)_o(Cl^-)_a{}^{p+q-5}}{(Nb(OH)_pCl_q{}^{+5-p-q})_a(RCl)_o{}^{p+q-5}} \quad (3)$$

$$K_i = \frac{(R_{p+q-5}Nb(OH)_pCl_q \cdot iRCl)_o}{(R_{p+q-5}Nb(OH)_pCl_q)_o(RCl)_o{}^i} \quad (4)$$

where the subscripts a and o detote the aqueous and organic phases respectively.

On the other hand, the next reaction can be considered with respect to the formation of an anionic complex of niobium in the aqueous solution. For the sake of simplicity, it is reasonable to consider the typical form of $Nb(OH)_2Cl_4^-$ as the predominant species based on the following experimental results:

$$Nb(OH)_mCl_n{}^{+5-m-n}* + (m-2)H^+ + (4-n)Cl^- \rightleftarrows Nb(OH)_2Cl_4^- + (m-2)H_2O \quad (5)$$

The equilibrium constant for Eq. 5 is defined as

$$\beta_{m,n} = \frac{(Nb(OH)_mCl_n{}^{+5-m-n})_a}{(Nb(OH)_2Cl_4^-)_a \times (H^+)_a{}^{m-2}(Cl^-)_a{}^{4-n}} \quad (6)$$

The solubility of TBA-Cl in the aqueous solution can be ignored. The distribution coefficient for niobium, D, therefore, is derived in terms of activities from Eqs. 3, 4 and 6:

$$D = \frac{\sum_p\sum_q\sum_i (R_{p+q-5}Nb(OH)_pCl_q \cdot iRCl)_o}{\sum_m\sum_n (Nb(OH)_mCl_n{}^{+5-m-n})_a} = \frac{(Cl^-)_a{}^5}{\sum\sum(\beta_{m,n} \cdot (H^+)_a{}^{-m}(Cl^-)_a{}^n)} \times [\sum\sum\sum\sum(K_{p,q} \cdot K_i \cdot \beta_{p,q} \cdot (H^+)_a{}^{-p} \times (Cl^-)_a{}^{-p}(RCl)_o{}^{p+q+i-5}] \quad (7)$$

On the basis of the above equations, it is possible to indicate the factors which influence the extractability of niobium. The dependence of the hydrogen ion activity on D is given by the differentiation of Eq. 7 with respect to the hydrogen ion activity at a constant chloride level. Thus,

$$\frac{\partial \ln D}{\partial \ln (H^+)_a} = \bar{m} - \bar{p} \quad (8)$$

Proceeding as above, we obtain

$$\frac{\partial \ln D}{\partial \ln (Cl^-)_a} = 5 - \bar{p} - \bar{n} \quad (9)$$

where $\bar{m}$ and $\bar{n}$ denote, respectively, the average number of hydroxide and chloride groups per Nb in the aqueous phase, and $\bar{p}$, the average number of hydroxide groups per Nb in the organic phase.

In this experiment it is difficult to maintain the ionic strength constant; the analysis of the results obtained at such higher ionic strengths is possible only by the use of "activity" instead of "molar concentration". Therefore, the results are shown in terms of the activity. The activities for the hydrogen ion and the chloride ion are assumed to be:

$$(H^+)_a = [H^+]_a\gamma_{\pm HCl}$$
$$(Cl^-)_a = [Cl^-]_a\gamma_{\pm LiCl} \quad (10)$$

where brackets are used to indicate the molar concentrations. The mean activity coefficients for hydrochloric acid, $\gamma_{\pm HCl}$, and lithium chloride, $\gamma_{\pm LiCl}$, are calculated from the data listed in Harned and Owen[9]. For the sake of simplicity, is assumed that the species in the organic phase are monomeric and that their activity coefficients are equal to 1.

Distribution of Hydrochloric Acid.—Hydrochloric acid of various acidities ranging from 1 M to 11.4 M were shaken with a 0.1 M TBA solution in chloroform. As is shown in Fig. 1, the acid concentration in the organic phase

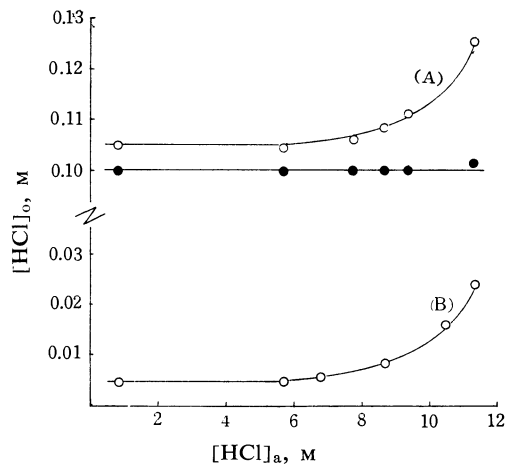


Fig. 1. Distribution of hydrochloric acid at 25°C.

○, (A) 0.100 M TBA in $CHCl_3$; (B) pure $CHCl_3$

●, Difference between curve (A) and curve (B)

abruptly increases with the increasing acidity of hydrochloric acid, but the difference in the acid concentration between the cases of TBA and pure chloroform is just 0.1 M, equivalent to the TBA concentration.

* $Nb(OH)_mCl_n{}^{+5-m-n}$ shows the general form of the niobium chloro-complex in the aqueous solution.

9) H.S. Harned and B.B. Owen, "The Physical Chemistry of Electrolytic Solutions", 2nd. Ed., Reinhold Pub. Co., New York (1950).

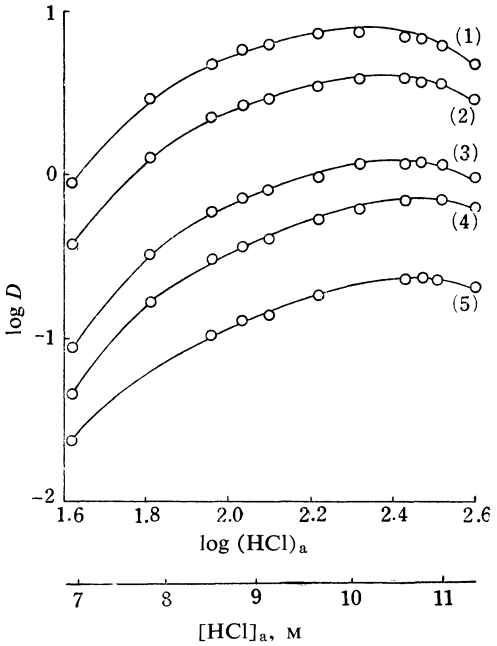


Fig. 2. Distribution of niobium between hydrochloric acid and TBA-chloroform at 25°C.

(1) (2) (3) (4) (5)
$[RCl]_o$: 0.200, 0.150, 0.100, 0.075, 0.050 M

Dependence of the Extractability of ^{95}Nb on Hydrochloric Acid.—The distribution of ^{95}Nb between hydrochloric acid and a TBA-Cl chloroform solution was determined. As is shown in Fig. 2, the distribution of ^{95}Nb increases with an increase in the concentration of TBA-Cl, and there is a maximum at about 10.5 M of hydrochloric acid. In this experiment, of course, the results are influenced by the concentration of hydrogen and chloride ions.

Dependence on Chloride Ion Activity. — To examine the effect of the chloride ion activity, a series of experiments were carried out. By using hydrochloric acid-lithium chloride mixtures, the concentration of hydrochloric acid was held at 7.62 M, while the chloride ion activity was varied by the addition of lithium chloride. As is shown in Fig. 4, the slope of the curve varies from 0.5 to 2.5. According to Eq. 9:

$$\frac{\partial \log D}{\partial \log (Cl^-)_a} = 5 - \bar{p} - \bar{n} \simeq 0.5 \sim 2.5 \qquad (9')$$

Dependence on Hydrogen Ion Activity.—The details of these experiments were similar to those of the above experiment, but in this case the chloride levels were held at 8.85 M and 11.4 M while the hydrogen ion activity was varied. At constant chloride levels, D is not so much affected by the hydrogen ion activity,

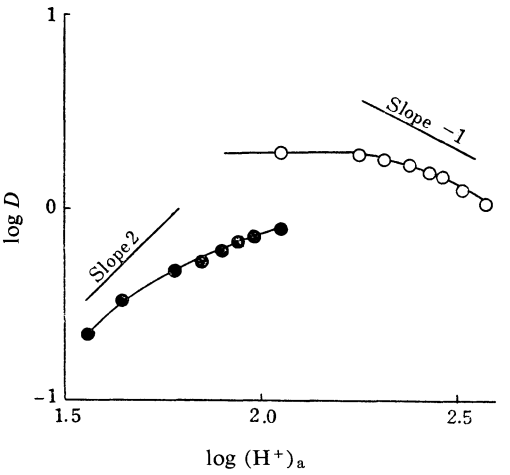


Fig. 3. Acid dependence of D values for niobium at 25°C.

○, $[Cl^-]_{a,\,total}$=11.4 M
●, $[Cl^-]_{a,\,total}$=8.85 M

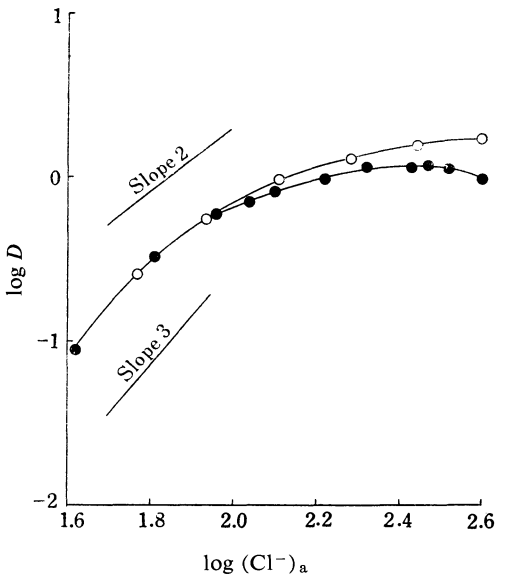


Fig. 4. Chloride dependence of D values for niobium at 25°C.

○, HCl-LiCl mixture. $[H^+]_a$=7.62 M
●, Pure HCl

as may be seen in Fig. 3. Although D remains constant at high chloride levels, 11.4 M, D decreases with a slope of −1 as the hydrogen ion activity increases. According to Eq. 8:

$$\frac{\partial \log D}{\partial \log (H^+)_a} = \bar{m} - \bar{p} \simeq 0 \sim -1.2 \qquad (8')$$

At low chloride levels, the decrease in D is suspected as being due mainly to the hydrolysis of niobium, i.e., $\bar{m} > \bar{p}$.

From Eqs. 8' and 9', we find:

$$1.2 \leq \bar{p} \leq 2.5$$

It seems reasonable, however, to consider that p $(=\bar{p})$ is constant in these conditions, probably equal to two, because the values of D are constant in the $\bar{m}=\bar{p}$ region and decrease gradually for $\bar{m} \lesssim \bar{p}$. Thus, the decrease of the D values with a slope of -1 may be explained by the following reaction (cf. the following paragraph):

$$Nb(OH)_2Cl_4^- + H^+ \rightleftharpoons Nb(OH)Cl_4 + H_2O \quad (11)$$

Species and Reaction in the Organic Phase.— In order to estimate the niobium species in the organic phase, ^{95}Nb was extracted from 10 M hydrochloric acid with various concentrations of TBA-Cl solutions in chloroform. There was no difference between the two cases of D values; viz., in one case D values were obtained by direct extraction of ^{95}Nb in hydrochloric acid with TBA-Cl, and in another case D values were obtained by the backward equilibration of the organic phase containing ^{95}Nb with hydrochloric acid. The resulting plot shown in Fig. 5 has a slope of 3.0 above 0.1 M TBA-Cl and of 2.1 below 0.1 M, indicating that one molecule of the niobium complex associates with up to three molecules of amine.

When the aqueous phase conditions are held constant, Eq. 7 can be replaced by:

$$D=A(RCl)_o+B(RCl)_o^2+C(RCl)_o^3 \quad (12)$$

where A, B and C are the constants. Therefore, if a plot of $D/(RCl)_o$ against $(RCl)_o$ fits the quadratic curve and if the intercept is not equal to zero, i. e., $K_{p,q(p+q=6)} \neq 0$, it can be considered that one molecule of amine exchages with the niobium chloro-complex.

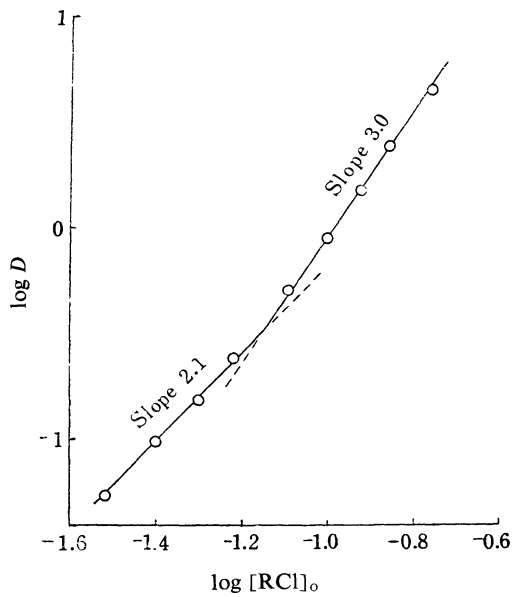


Fig. 5. TBA dependence of D values for niobium at 25°C.

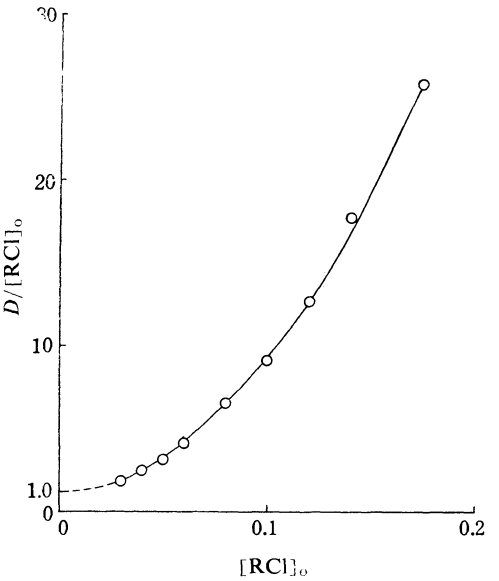


Fig. 6. Plot of $D/[RCl]_o$ vs. $[RCl]_o$.

The resulting curve is shown in Fig. 6, which indicates that the charge number of the niobium chloro-complex extracted is probably -1. It was found that the p value in the formula of $Nb(OH)_pCl_q^-$ was equal to two; therefore, this would mean that the complex in the organic phase is $RNb(OH)_2Cl_4 \cdot iRCl$ $(i=1$ and $2)$.

These considerations lead to the conclusion that the typical extractable species of niobium is $Nb(OH)_2Cl_4^-$. Other extractable species [i. e., $Nb(OH)_3Cl_3^-$, $Nb(OH)_2Cl_5^{-2}$, $Nb(OH)Cl_5^-$, etc.] will be present in very small amounts if such species exist at all. The species of niobium in hydrochloric acid have been investigated by the anion exchange method[10] and by the spectrophotometric method, indicating the presence of $Nb(OH)_2Cl_4^-$ in a 10.5 M hydrochloric acid solution[11].

From a plot of $D/(RCl)_o$ vs. $(RCl)_o$, $K_{i=1}$ and $K_{i=2}$ can be obtained as 4.4 and 786 respectively. If it is assumed that only $Nb(OH)_2Cl_4^-$ is the extractable species, $K_{p=2,\ q=4}$ can be calculated as about 940.

Temperature Effect.—There are few papers which have investigated the effect of temperature in a solvent extraction, but the authors consider that temperature is one of the most important factors. Equilibration experiments were carried out at 10 and 40°C. These results are shown in Fig. 7. At a low temperature,

10) E. H. Huffman, *J. Am, Chem. Soc.*, **74**, 4714 (1952); K. A. Kraus, ibid., **71**, 3885 (1949).
11) J. H. Kanzelmeyer, J. Ryan and H. Freund, ibid., **78**. 3020 (1956).

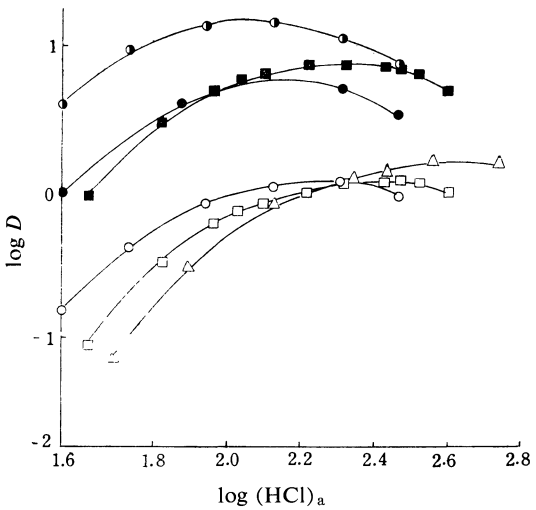


Fig. 7. Temperature dependence of D values for niobium.
○, 40±0.5°C; □, 25±0.5°C; △, 10±0.5°C
◑, $[RCl]_0$=0.30 M; ●, 0.20 M; ■, 0.10 M

the extraction curve is similar to that shown in Fig. 4 (chloride dependence). The solubility of TBA-Cl in chloroform* is relatively small, so it is better to raise the temperature in order to use a high concentration of the TBA-Cl solution. The shapes of extraction curves are not equal to each other at different temperatures. At lower temperatures D shows a maximum in the region of higher acidity. The acidity at which it shows a maximum of D shifts to a lower acidity with an increase in the temperature. These results suggest that the reaction expressed in Eq. 11 and the formation of the niobium chloro-complex are promoted with an increase in the temperature.

Conclusion

The extraction processes of ^{95}Nb from hydrochloric acid with tribenzyl amine are shown by the following reactions:

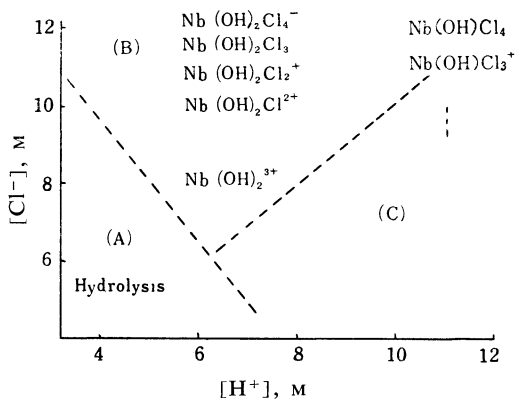
$$Nb(OH)_2Cl_4^- + RCl \rightleftarrows RNb(OH)_2Cl_4 + Cl^- \quad K_{p=2,\,q=4}=940$$

$$RNb(OH)_2Cl_4 + RCl \rightleftarrows RNb(OH)_2Cl_4\cdot RCl \quad K_{t=1}=4.4$$

$$RNb(OH)_2Cl_4\cdot RCl + RCl \rightleftarrows RNb(OH)_2Cl_4\cdot 2RCl \quad K_{t=2}=786$$

The $K_{p=2,\,q=4}$ value is comparatively small, but it is interesting that the apparent D values are large. This fact suggests that the secondary reaction, as shown in Eq. 2, occurs in the organic phase; therefore, the overall extraction ratio increases. The formation constants for niobium chloro-complexes cannot be obtained owing to their complexity, but the authors present in Table I a scheme concerning the niobium species in the chloride system. In region A, the hydrolysis (and/or polymerization) of niobium may occur; $Nb(OH)_2Cl_n^{+3-n}$ species exist in region B and C, and $Nb(OH)Cl_n^{+4-n}$ may exist in region C only. As the temperature rises, the formation of niobium chloro-complexes will be promoted, but dehydroxylation may occur simultaneously; therefore, the situation is not simple.

Table I. Niobium species in hydrochloric acid-lithium chloride solutions at 25°C



The authors wish to express their hearty thanks to Professor Kunio Seto for his kind suggestions made in the course of this work.

Department of Chemistry
Faculty of Science
Tohoku University
Katahira-cho, Sendai

* The maximum concentration is about 0.2M TBA-Cl at 25°C.

Concentration and Temperature Profiles in a Tubular Reactor for Methanol Synthesis with the Outer-wall of a Uniform Temperature. II. Profiles in Reactors with a Heat Exchanger Tube in the Catalyst Bed

By Yoshisada OGINO*, Masaaki OBA, Kinya SHIMOMURA and Hiroshi UCHIDA

(Received April 12, 1962)

For better performance in methanol synthesis of the previously described tubular reactor, which was placed in a heat transfer medium of flownig oil and which was packed with a catalyst bed with no heat exchanger tube, it was pointed out that any large magnitude of temperature rise along the catalyst bed should be reduced[1]. The use of a heat exchanger tube in the catalyst bed was naturally expected to be a means of providing suitable control of the bed temperature. In this connection, several workers, such as Kodama et al.[2,3], Shindo et al.[4] and Matsuyama et al.[5], have discussed the temperature profiles in catalytic reactors equipped with various types of heat exchanger tubes, but their papers have provided no detailed experimental data on this subject. On the other hand, Kjaer[6] provided the data on the basis of which he had calculated the temperature profiles in both the catalyst bed and the heat exchanger tube, with an industrial reactor for the ammonia synthesis, but his treatment did not deal with the comparative merits of the different types of heat exchanger tubes.

In this paper, the experimental data on the profiles of methanol concentration and on the temperature measured with reactors which were individually equipped with three different types of heat exchanger tubes are presented, and their effects upon the profiles, as well as on the methanol yield, are discussed.

Experimental

The same methanol synthesis reactor as was described in the preceding paper[1] was equipped successively with three different types of heat exchanger tubes, all three types of heat exchanger tubes were copper; the first and second ones were countercurrent types (types A and B), while the last one was a concurrent type (type C). Detailed sketches of them are shown in Figs. 1A and 1B. The A-type heat exchanger tube was a single tube of 10 mm. O. D. and 8 mm. I. D.; it was placed at the center-axis of the reactor. A thermocouple protection tube of stainless steel, 5 mm. O. D. with a thickness of 1 mm., went coaxially through the heat exchanger tube and permitted scanning of the temperature along the whole length by moving the thermocouple. The heat exchangers of types B and C were double tubes of the same dimensions. They consisted of an outer tube, sealed at one end, of 10 mm. O. D. and an inner tube of 6 mm. O. D., each of them having a thickness of 1 mm. For both the B and C types of heat exchangers, the thermocouple protection

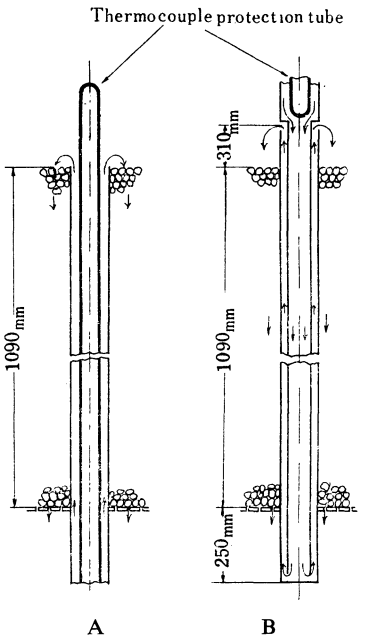


Fig. 1A. Heat exchanger tube (Type A and Type B).

* Present address, Faculty of Engineering, Tohoku University, Sendai

1) H. Uchida, Y. Ogino, M. Oba and K. Shimomura, This Bulletin, 35, 1400 (1962).

2) S. Kodama, K. Fukui and K. Takagi, *J. Chem. Soc. Japan, Ind. Chem. Sec.* (*Kōgyō Kagaku Zasshi*), 52, 123, 221 (1949).

3) S. Kodama, K. Fukui, K. Tame and K. Takagi, ibid., 53, 148 (1950).

4) M. Shindo and S. Araki, *Bull. Faculty Eng., Hokkaido Univ.*, 5, 143 (1951).

5) T. Matsuyama, Y. Sugawara and K. Matsuo, *Chem. Eng.* (*Kagaku Kikai*). 14, 229 (1950).

6) J. Kjaer, Measurement and Calculation of Temperature and Conversion in Fixed-bed Catalytic Reactors," Jul. Gjellerups Forlag, Copenhagen (1958).

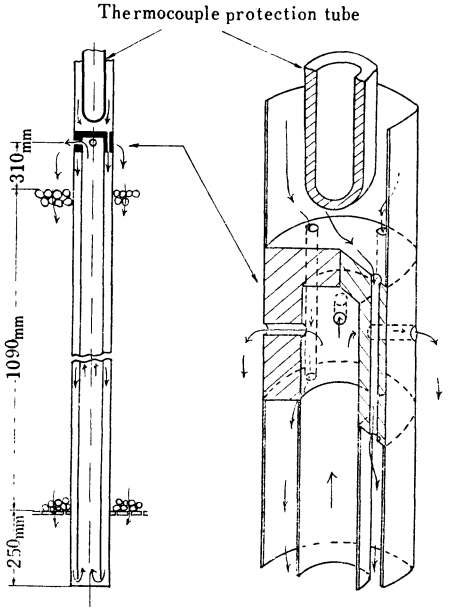


Fig. 1B. Heat exchanger tube (Type C).

tube was too thick to be inserted in the inner tube. The path of the gas stream in the reactor is indicated by arrows in the figures. It should be noted that, in the B-type heat exchanger, the synthesis gas introduced into the reactor at the top first flows downwards through the inner tube, whereas in the C-type exchanger it first flows downwards through the annular space between the outer and the inner tubes. For the sake of simplicity, the previous reactor with no heat exchanger will be hereafter denoted as the O reactor, while the individual reactors equipped with the heat exchangers of type A, type B, and type C will be termed the A, B, and C reactors respectively.

The catalyst used in the present study was a three-component catalyst (ZnO-Cr_2O_3-CuO) of the same composition and prepared by the same procedure as those of the catalyst in the preceding study[1]. Two liters of the reduced catalyst granules (3 mm. in diameter by 4 mm. high), weighing 3.012 kg., were charged into the reactor, and the catalyst bed attained as high as 1090 mm., occupying the intermediate range of the reactor between 1440 and 350 mm. from the bottom.

The operating procedure of the methanol synthesis was quite the same as has been described previously[1]. In this study, however, the bed temperature profile along the center-axis could not be measured, because the heat exchanger tube occupied the center-axis. As it was, only the off-center profiles at radial distances of 15 and 22 mm. from the center-axis were measured by means of two thermocouples in the protection tubes (5 mm. O. D. with a 1 mm. thickness) placed parallel in the bed.

The axial concentration profile was determined in the same way as in the preceding study[1], but the catalyst bed heights at which small portions of the fluid were withdrawn for the composition determinations varied somewhat according to the kinds of reactors[7].

Results

Methanol Production.—The methanol yields are listed in Table I, together with the operation variables. For the sake of comparison, the table also includes the previous data on the synthesis runs (Exps. I and I') using the O reactor. The A reactor produced a much larger amount of methanol than the O reactor, and the space-time-yield attained as much as twice the yield of the O reactor (compare Exp. I with Exp. 3), provided the synthesis gas was preheated at a higher temperature (cf. the data of Exps. 2 and 3). The B reactor could also produce a larger amount of methanol than the O reactor, but the production increase was rather low compared with that of the A reactor (compare Exp. 1 with Exp. 6). Contrary to the above findings, reliable performance data could not be collected with the C reactor until the introducing gas had been preheated to a much higher temperature (cf. Exp. 7). In this reactor, the heat exchanger tube cooled the catalyst bed so much that the bed temperature would decrease too low to allow the progress of the synthesis.

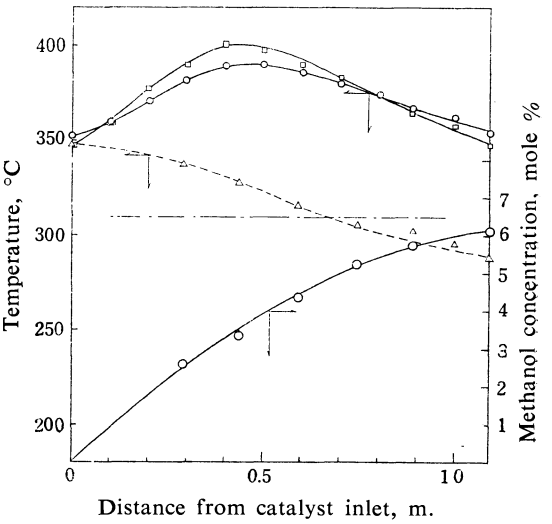


Fig. 2. Axial temperature and concentration profiles. Exp. 4.
—□— Off-center temperature profile at $r=15$ mm.
—○— Off-center temperature profile at $r=22$ mm.
···△··· Temperature profile in heat exchanger tube.
—·—· Oil bath temperature.
—○— Methanol concentration profile.

7) The bed heights will be seen by the lengths of the abscissa corresponding to the marks along the experimental concentration profiles.

TABLE I. METHANOL YIELD AND OPERATION VARIABLES

Exp.	Heat exchanger	Flow rate of inlet gas l./hr.	Composition of inlet gas H_2/CO	Oil bath temp. °C	Preheated temp.[b] °C	Methanol yield kg./day	Space-time-yield of reactor kg./l. hr.
1	Type A	32170	2.92 (11.0)[a]	310	210	89	1.86
2	Type A	27810	2.92 (9.4)	315	208	90	1.87
3	Type A	56650	2.71 (13.3)	310	275	104.5	2.27
4	Type A	54570	4.59 (10.2)	310	275	101	2.11
5	Type B	32080	4.40 (3.3)	310	240	69	1.44
6	Type B	32170	3.15 (7.2)	302	222	67.5	1.41
7	Type C	44050	2.50 (9.2)	310	310	80.5	1.68
I	none	34470	3.0 (7.7)	295	295	42.2[c]	1.01
I'	none	33570	8.5 (10.5)	295	219	50.6[c]	1.21

Every run was made at 200 kg./cm² of the synthesis gas.
a) Numerals in the parentheses give the inert gas content (vol. %).
b) The temperature was measured immediately after the preheater.
c) In Exps. I and I', 1.74 l. of the reduced catalyst was used.

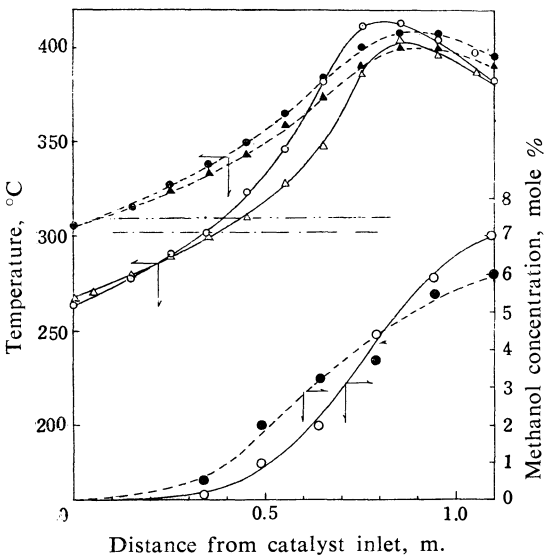


Fig. 3. Axial temperature and concentration profiles. Exps. 6 and 7.

Off-center temperature profile at $r=15$ mm. —○— Exp. 6. ···●··· Exp. 7.
Off-center temperature profile at $r=22$ mm. —△— Exp. 6. ···▲··· Exp. 7.
Oil bath temperature. — · — Exp. 6. —·· — Exp. 7.

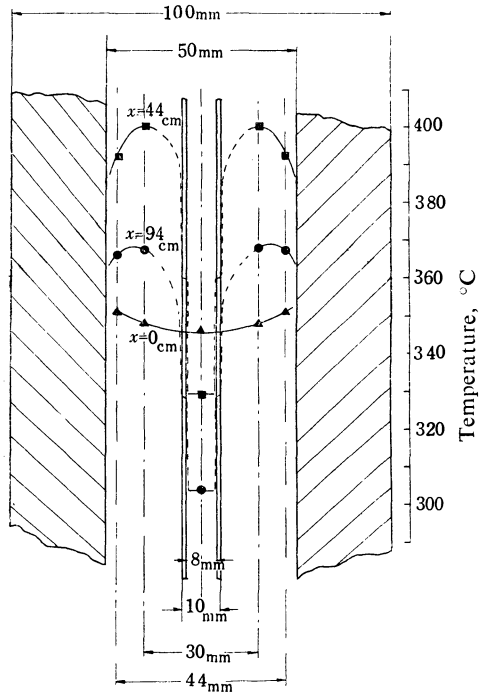


Fig. 4. Radial temperature profile.

Concentration and Temperature Profiles.— Figure 2 shows the concentration and temperature profiles for the synthesis run with the A reactor (Exp. 4), while Fig. 3 shows the profiles for the runs with the B reactor (Exp. 6) and the C reactor (Exp. 7.). The major difference observed among the temperature profiles of the three reactors is that the maximum of the temperature profile appears in the upper half of the catalyst bed of A reactor whereas it appears near the bottom of the bed of B and C reactors. Moreover, the temperature at the catalyst inlet of the B and C reactors is kept considerably lower than that of the A reactor even when the gas is preheated at higher temperatures. In the bed of the A reactor, methanol has already been produced at the top zone of the bed and increases in amount rather monotonously with the bed length, whereas in the beds of reactors B and C only a small amount of methanol begins to appear after the gas has passed through more than a quarter of the bed length. The concentration and temperature profiles observed with the B and C reactors are essentially the same in tendency as those observed with the O reactor[1].

The off-center temperatures, as well as the temperature in the heat exchanger tube measured at the different bed lengths of 0, 0.44, and 0.94 m., are given as full marks in Fig. 4 for Exp. 4. A rough estimation of the radial profile from the available data leads us to expect a steep temperature rise in the middle across the annular-shaped cylindrical bed.

Discussion

Heat Transfer between Gases in the Catalyst Bed and the Heat Exchanger Tube.—Since the synthesis runs using the A reactor provide the experimental axial temperature profiles in the heat exchanger tube as well as in the catalyst bed, a quantitative treatment of the heat transfer phenomena between the gas in the catalyst bed and the gas in the heat exchanger tube will be made with this reactor. The heat balance equation for the bulk catalyst has the form:

$$S_1C_{p1}G_1dt_1/dx = S_1v\Delta H - F_{12}U_{12}(t_1-t_2) - F_{1b}U_{1b}(t_1-t_b) \quad (1)$$

while the equation for the gas in the heat exchanger tube is given by;

$$S_2C_{p2}G_2dt_2/dx = F_{12}U_{12}(t_1-t_2) \quad (2)$$

In the equations, S is the cross sectional area, C_p is the heat capacity of the gas, G is the mass velocity of the gas, v is the reaction rate based on the unit volume of the catalyst bed, ΔH is the reaction heat, F is the cooling area per unit length, and U is the overall heat transfer coefficient. Subscripts 1, 2, and b indicate the catalyst bed, the heat exchanger tube, and the oil bath respectively.

Because of the complicated nature of the first term on the right hand-side of Eq. 1, it is necessary to use a step by step integration of the differential equations. Under the assumptions that $S_1C_{p1}G_1$ and $S_2C_{p2}G_2$ are identical and that v is constant within the step length Δx, the differential equations can be directly transformed to the following difference equations:

$$A(t_{1no}-t_{1n1})/\Delta x = \Delta Q_n - F_{12}U_{12}\{(t_{1no}+t_{1n1}) - (t_{2no}+t_{2n1})\}/2 - F_{1b}U_{1b}\{(t_{1no}+t_{1n1})/2 - t_b\} \quad (3)$$

$$-A(t_{2no}-t_{2n1})/\Delta x = F_{12}U_{12}\{(t_{1no}+t_{1n1}) - (t_{2no}+t_{2n1})\}/2 \quad (4)$$

In Eqs. 3 and 4, A stands for $S_1C_{p1}G_1 = S_2C_{p2}G_2$, ΔQ_n for $S_1v_n\Delta H$ where v_n is the v in the n-th step, and the subscripts ni and no indicate the inlet and outlet of the n-th step respectively. The difference equations are solved to result in the following respective expressions of $U_{12}F_{12}/A$, t_{1no}, and t_{2no}:

$$U_{12}F_{12}/A = (t_{2n1}-t_{2no})/\Delta x\{(t_{1n1}-t_{2n1}) + \Delta t/2\} \quad (5)$$

$$t_{1no} = b/a + t_{2no}c/a \quad (6)$$

$$t_{2no} = (ap-lb)/(lc+aq) \quad (7)$$

in which the following abbreviations are introduced:

$$\Delta t = (t_{1no}-t_{1n1}) - (t_{2no}-t_{2n1}),\ a = A + F_{1b}\cdot U_{1b}\Delta\chi/2,\ b = \Delta Q + A(t_{1n1}-t_{2n1}) + F_{1b}U_{1b}\cdot \Delta x(t_b-t_{1n1}/2),\ l = B\Delta x/2,\ p = t_{2n1}\ (1\text{-}B\Delta x/2) - B\Delta x(t_{1n1}/2-t_{2n1}),\ q = (1-B\Delta x/2),\ \Delta Q = \Delta Q_n\Delta x$$

The left-hand side term of Eq. 5 corresponds to the cooling coefficient of the heat exchanger tube and will be denoted by B hereafter.

Let us calculate B by the aid of Eq. 5 on the basis of the experimental profiles of Exps. 1, 2, 3, and 4. In the calculation, t_1 is conventionally chosen to fit the arithmetic mean temperature between the two measured off-center temperatures. The step lengths used in the calculation are 0.29 m. for the first step and 0.15 m. for the other steps, corresponding to the bed heights at which small portions of the fluid in the bed were drawn for the composition determination. The B thus obtained is denoted by B_{exp} and is shown in Fig. 6 as a function of x. The figure shows that B_{exp} is different according to the bed lengths and that a maximum appears at about $x=0.4$ m.

The B_{exp}'s are then averaged over the whole bed length (denoted by $\bar{B}_{exp}$ hereafter), and the $\bar{B}_{exp}$ is compared with the value of B_{calc}, which can be calculated by usual means. In the comparison, B_{calc} averaged over the whole bed length, for the sake of convenience, is taken into account[8]; it is usually given by the following formulae:

$$B_{calcd} = U_{12}F_{12}/A \quad (8)$$

where U_{12} is defined either by

$$1/U_{12} = 1/h + (1/h_a)(r_2/r_1) + r_2/\lambda_s\ln(r_2/r_1) \quad (9)$$

or by

$$1/U_{12} = 1/h' + (1/h_a)(r_2/r_1) + r_2/\lambda_s\ln(r_2/r_1) + r_2/\lambda_e\ln(r_3/r_2) \quad (10)$$

In the above formulae, h is the heat transfer coefficient based upon the difference between the average catalyst temperature and the temperature of the outer-wall of the heat exchanger tube, whereas h' is the coefficient across

8) The calculation of individual B's at different bed lengths is very time-consuming, since the thermodynamic data must be evaluated at different bed lengths.

TABLE II. FORMULAE FOR EVALUATION OF h AND h'

Symbol	Formula	Ref.
A	$hD/k=21.3(R_{ep})^{0.6}\exp(-5.72d/D)d^{0.15}$	9)
B	$hD/k=4.9(R_{ep})^{0.6}\exp(-2.2d/D)$	10)
C	$hD/k=3.5(R_{ep})^{0.7}\exp(-4.6d/D)$	11)
D	$hD/k=0.813(R_{ep})^{0.9}\exp(-6d/D)$	12)
E	$h=60+0.083R_{ep}$	13)
F	$h'D/\lambda_e=254(R_{ep}d/D)^{-0.87}$ $\lambda_e/k=0.209(R_{ep})^{0.87}$	14)

TABLE III. THERMODYNAMIC DATA AND OTHER MATTERS

Exp.	C_p kcal./kg. °C	μ kg./m. hr.	k kcal./m. hr. °C	λ_e kcal./m. hr. °C	G kg./m². hr.	R_{ep} in catalyst bed	R_{ep} in heat exchanger tube
1	0.654	0.0972	0.204	6.15	8.41×10^3	3.03×10^2	3.62×10^3
2	0.701	0.0948	0.210	5.15	6.47×10^3	2.39×10^2	2.85×10^3
3	0.607	0.1001	0.205	10.47	15.90×10^3	5.56×10^2	6.64×10^3
4	0.800	0.0936	0.222	9.21	11.68×10^3	4.37×10^2	5.22×10^3

TABLE IV. HEAT TRANSFER COEFFICIENTS

Heat transfer coefficient kcal./m² hr. °C		Formula for evaluation	Exp. 1	Exp. 2	Exp. 3	Exp. 4
h_a	$\times10^{-2}$		6.36	6.07	16.54	15.57
h	$\times10^{-2}$	A	7.76	6.33	11.22	10.53
	$\times10^{-3}$	B	1.43	1.27	2.06	1.94
	$\times10^{-2}$	C	7.79	6.79	11.96	10.96
	$\times10^{-2}$	D	3.40	2.90	6.03	5.26
	$\times10$	E	8.51	7.98	10.62	9.63
h'	$\times10^{-3}$	F	2.70	2.78	2.71	2.94
U_{12}	$\times10^{-2}$	A	3.07	2.85	6.06	5.69
	$\times10^{-2}$	B	3.74	3.51	8.04	7.56
	$\times10^{-2}$	C	3.07	2.83	6.27	5.82
	$\times10^{-2}$	D	2.04	1.82	4.14	3.69
	$\times10$	E	7.29	6.85	9.82	9.22
	$\times10^{-2}$	F	2.97	2.74	5.76	5.45

the gas film on the outer surface of the tube, h_a is the coefficient from the cooling gas to the inner-wall of the heat exchanger tube material (315 kcal./m. hr. °C), λ_e is the effective thermal conductivity of the catalyst bed, r_1 and r_2 are the inner and the outer radii of the heat exchanger tube, and r_3 is the radius to give the area which is equivalent to a half of the cross sectional area of the catalyst bed. The last term on the right-hand side of Eq. 10 has no strict meaning in theory, but it is introduced conventionally because the $1/U_{12}$ should include any term of the heat transfer resistance through the catalyst bed. The term may stand for the mean value of the transfer resistance.

The evaluation of h can be made by the aid of several kinds of formulae (A[9], B[10], C[11], D[12], and E[13]), while h' can be evaluated by the aid of formula F[14], as listed in Table II. The symbols not explained earlier are as follows: R_{ep} is the modified Reynolds number, D is the equivalent diameter of the annular shaped bed, and μ is the viscosity of the gas. Moreover, either one of the following formulae can give h_a according as whether the gas flow is laminar or turbulent[15]:

9) S. Maeda and K. Kawazoe, *Chem. Eng.* (*Kagaku Kikai*), **15**, 5, 9, 312 (1951).
10) S. Hatta and S. Maeda, ibid., **12**, 56 (1948).
11) M. Leva, M. Weintaub, M. Gummer and E. L. Clark, *Ind. Eng. Chem.*, **40**, 747 (1948).
12) M. Leva, ibid., **39**, 857 (1947).
13) S. Sugawara and S. Sato, *Coll. Papers Chem. Eng.* (*Kagaku Kikai Ronbunshu*), **13**, No. 45, 164 (1947).
14) S. Hatta and S. Maeda, *Chem. Eng.* (*Kagaku Kikai*), **12**, 56 (1948), **13**, 79 (1949).
15) In view of the magnitude of R_{ep} in Table III, the gas flow is laminar for the cases with Exps. 1 and 2, whereas it is turbulent for the cases with Exps. 3 and 4.

Table V. Comparison of B_{calcd} with $\bar{B}_{exp}$

Exp.	$\bar{B}_{exp}$ m^{-1}	B_{calc} from formula A	B	C	D	E	F
1	1.005	0.954	1.163	0.955	0.630	0.227	0.922
2	0.880	1.077	1.325	1.068	0.685	0.259	1.033
3	0.837	1.073	1.423	1.110	0.732	0.174	1.020
4	0.942	1.046	1.388	1.068	0.678	0.169	0.999

Table VI. Heat transfer resistances

Exp.	$1/U_{12}$	$1/h'$	$(1/h_a)(r_2/r_1)$	$(r_2/\lambda_s)\ln(r_2/r_1)$	$(r_2/\lambda_e)\ln(r_3/r_2)$
1	3.370×10^{-3}	3.701×10^{-4}	1.967×10^{-3}	3.537×10^{-6}	1.026×10^{-3}
4	1.837×10^{-3}	3.401×10^{-4}	8.029×10^{-4}	3.537×10^{-6}	6.867×10^{-4}

$$h_a = 1.75(k/D_e)(C_pG/SkL)^{1/3}$$
for a laminar flow (11)

$$h_a = 0.023(k/D_e)(D_eG/\mu)^{0.8}(C_p\mu/k)^{0.4}$$
for a turbulent flow[16] (12)

where k is the thermal conductivity of the gas, D_e is the equivalent diameter of the heat exchanger tube, and L is the catalyst bed length. Table III summarizes the thermodynamic and other data with respect to Exps. 1, 2, 3 and 4. In Table V, $\bar{B}_{exp}$ is compared with the B_{calcd} obtained by putting into Eq. 8 the values of the heat transfer coefficients as listed in Table IV. A comparison shows that the B_{calcd}'s obtained by the use of h's from the A, C, and E formulae, and also the B_{calcd} obtained by the use of h' from formula F, are consistent with the $\bar{B}_{exp}$.

In addition, the calculation of $1/U_{12}$ by means of Eq. 10 provides the content of the overall heat transfer resistance between the gas in the catalyst bed and the gas in the heat exchanger tube; this is shown in Table VI. The table shows that the heat transfer resistance across the catalyst bed is so high as to account for about one-third of the overall heat transfer resistance.

Calculation of Axial Temperature Profiles in the A Reactor.—Under the assumption that the catalyst inlet temperature is identical with the temperature at the end of the heat exchanger tube, a step by step calculation of the axial temperature profiles in both the catalyst bed and the heat exchanger tube is possible with the aid of Eqs. 6 and 7, if ΔQ_n, U_{1b}, and B, besides the thermodynamic data, are available. In this connection, ΔQ_n is given as a function

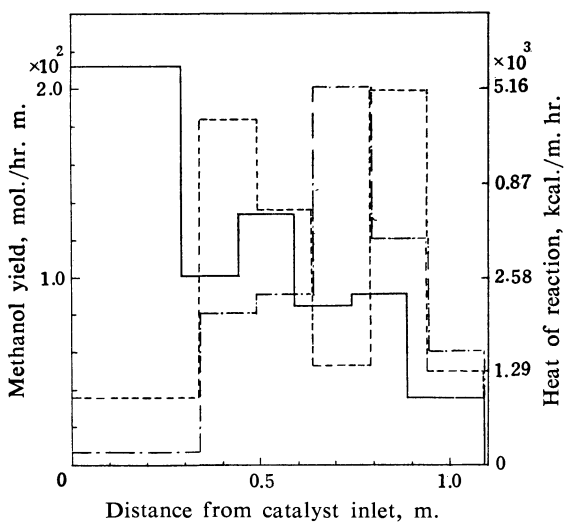


Fig. 5. Methanol yield and reaction heat of methanol synthesis as function of bed length.
—— Exp. 4. —·— Exp. 6. ····· Exp. 7.

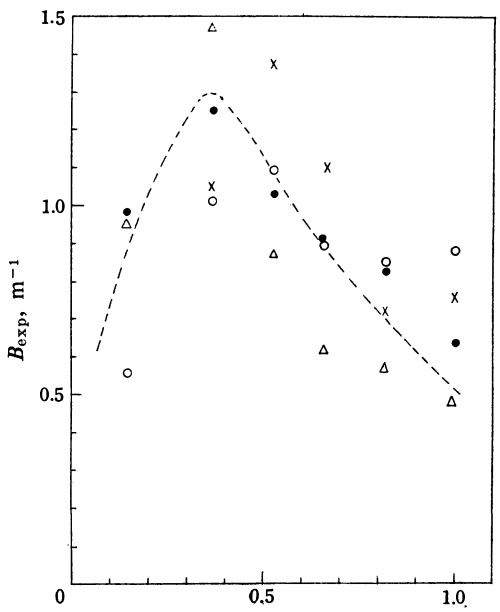


Fig. 6. Cooling coefficient as function of bed length.
× Exp. 1. ○ Exp. 2. △ Exp. 3. ● Exp. 4.

16) McAdams, "Heat Transmission", McGraw-Hill Book Co. Inc., New York (1954), pp. 219, 232.

of x in Fig. 5, while B_{exp} is given in Fig. 6 also as such. U_{1b} can be evaluated as a function of x by the following equation:

$$U_{1b}F_{1b}\{(t_{1ni}+t_{1no})/2-t_b\}\Delta x=\Delta Q-A\Delta t \quad (13)$$

For the sake of simplicity, however, B_{calcd} evaluated from the formula of Leva et al.[11] and U_{1b} averaged over the whole bed length are used in the present calculations. The choice of B_{calcd} is due to the afore-mentioned finding that the evaluated B_{calcd} was very approximate to the $\bar{B}_{exp}$.. The calculations are now made on the basis of the data of Exp. 4[17], and the resultant profiles are shown in Fig. 7 in comparison with the experimental ones. The accordance between the two sets of profiles is good. This indicates that an adequate value of B_{calcd} evaluated from any of the formulae thus far proposed can be used for the profile calculation without causing any serious errors.

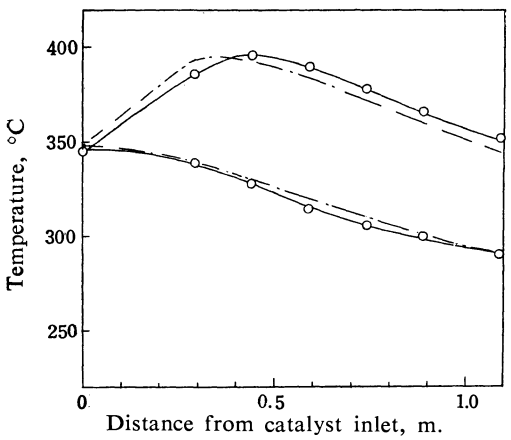


Fig. 7. Comparison between experimental and calculated temperature profiles. Exp. 4.
—○— Experimental profile.
—·—· Calculated profile.

Radial Temperature Profile across the Reactor.—Because only four measurements of the temperatures, namely, the temperatures at the center axis of the heat exchanger tube, the off-center temperatures at $r=15$ and 22 mm. in the catalyst bed, and the oil bath temperature, were made at several different bed lengths, the experimental radial profile across the reactor has not yet been obtained. In view of the estimated value of h', as well as of those of the respective heat transfer coefficients across the films on the outer and the inner surfaces of the reactor (h_L and h'')[18], steep temperature rises are expected at the outer surface of the heat exchanger tube and at the inner and the outer surface of the reactor. However, nothing decisive can be said in this respect.

Axial Temperature Profiles in B-Type and C-Type Heat Exchanger Tubes.—An attempt has been made to calculate the temperature profiles in the heat exchanger tubes of the B and C types. The calculations have been made by starting with a set of the following heat balance equations (14, 15, and 16):

$$Adt_1/dx=\Delta Q-F_{1b}U_{1b}(t_1-t_b)-F_{12}U_{12}(t_1-t_2) \quad (14)$$

$$\mp Adt_2/dx=F_{12}U_{12}(t_1-t_2)-F_{23}U_{23}(t_2-t_3) \quad (15)$$

$$\pm Adt_3/dx=F_{23}U_{23}(t_2-t_3) \quad (16)$$

The respective minus and plus signs on the left hand-side of Eqs. 15 and 16 are used as with the B-type heat exchanger tube, while the corresponding plus and minus signs are as with the C type one. The subscript 1 indicates the catalyst bed, as has been mentioned, and the subscripts 2 and 3 indicate the annular-shaped space and the inner tube of a double tube heat exchanger respectively. Since the thermodynamic as well as the mechanical data, such as C_p, U, G ΔQ, S and F, have already been

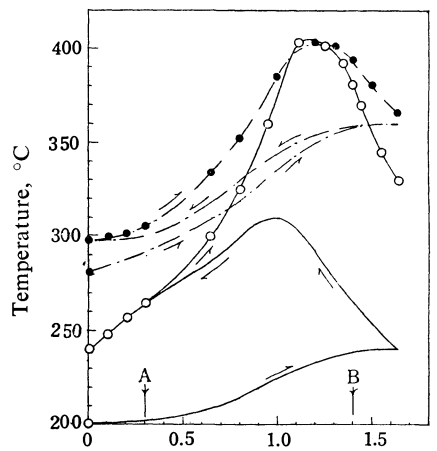


Fig. 8. Calculated temperature profiles in heat exchanger tube. Exps. 6 and 7.
Exp. 6. ——— Calculated profile in heat heat exchanger tube.
—○— Experimental profile in catalyst bed.
Exp. 7. —·—· Calculated profile in heat exchanger tube.
—·●—· Experimental profile in catalyst bed.
A; catalyst inlet, B; catalyst outlet.

17) In Exp. 4, the catalyst inlet temperature was 348°C. Evaluation of U_{1b} and B_{calcd} resulted in 1.524×10^2 kcal./m²hr.°C and 1.0684 m^{-1} respectively.

18) The value of h_L was estimated to be 2.091×10^2 kcal./m² hr. °C (cf. 1)), while that of h'' is evaluated, for instance, to be 2.465×10^3 kcal./m² hr. °C for the case of Exp. 4.

TABLE VII. HEAT TRANSFER COEFFICIENTS WITH B AND C TYPES HEAT EXCHANGER TUBES

Exp.	Passage I			Passage II		
	R_{ep}	h kcal./m². hr. °C	Formula for evaluation	R_{ep}	h_a kcal./m². hr. °C	Formula for evaluation
6	2.97×10^2	7.698×10^2	A in Table II	3.55×10^3	6.361×10^2	(11) in this paper
7	4.05×10^2	9.072×10^2	A in Table II	4.84×10^3	1.302×10^3	(11) in this paper

Exp.	Passage III			Overall heat transfer coefficient		
	R_{ep}	h_a kcal./m² hr. °C	Formula for evaluation	U_{12}	U_{23} kcal./m² hr. °C	U_{1b}
6	1.24×10^4	1.399×10^3	(12) in this paper	3.060×10^2	3.771×10^2	8×10^2
7	8.46×10^3	2.038×10^3	(12) in this paper	4.841×10^2	6.615×10^2	1.27×10^2

available and since dt_1/dx can readily be obtained from the experimental temperature profiles, t_2 can be calculated by the aid of Eq. 14. Once t_2 is obtained as a function of x, t_3 can be calculated by the substitution of the value of dt_2/dx into Eq. 15.

The calculations have been conducted on the basis of the experimental data of Exps. 6 and 7; the results are shown in Fig. 8. The values of the heat transfer coefficient necessary for the calculations are listed in Table VII, in which the symbols I, II, and III stand for the passages as indicated in Fig. 9. The figure and the table disclose that, owing to the efficient heat transfer between the gases in the II and III passages, the temperature profiles in the second passage always slope down markedly in the upper zone, and that, as a consequence, the catalyst inlet temperature is kept comparatively low. These facts may have led to the axial temperature profile in the catalyst bed being almost identical in tendency with that for the reactor with no heat exchanger tube. Taking the most favorable temperature profile for the methanol synthesis (cf. 1)) into consideration, any remarkable effect in increasing the methanol yield is scarcely to be expected from the use of heat exchanger tubes of the B and C types, unless special treatment lowers the U_{23} in the upper part of the tubes. This may have resulted in the lower methanol yields of the B and C reactors as compared with the yield of the A reactor.

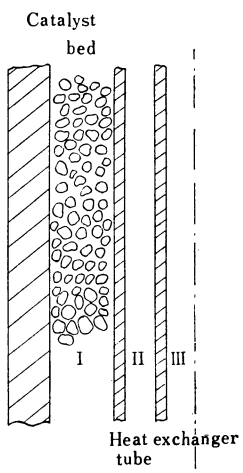


Fig. 9. Schematic diagram of flow passages.

Summary

Among the three types of heat exchanger tubes, a single tube countercurrent type, a double tube countercurrent type, and a double tube concurrent type, only the first one serves to increase the methanol production considerably compared with the effect of the previously tested reactor with no heat exchanger tube. On the basis of the experimental temperature profiles in both the catalyst bed and the single tube-heat exchanger tube, the cooling coefficient with the tube has been calculated to give the value as a function of the bed length. The value, when averaged over the whole bed length, agrees with the calculated value from the heat transfer coefficients, h or h' and h_a, available from certain formulae. By the use of this value, the average temperature profiles in the bed have been calculated on the basis of the experimental concentration profile; the resultant profile agrees well with the experimental one.

As regards the double tube-heat exchanger tubes, the temperature profiles for both the annular-shaped space and the inner tube have been calculated from the experimental bed temperature profiles. The results show that the profiles in the second passage of the tubes always slope down markedly in the upper zone and that, as a consequence, the bed temperature profiles are apt to remain almost identical with that for the previously tested reactor with no heat exchanger tube.

Government Chemical Industrial Research Institute, Tokyo
Shibuya-ku, Tokyo

A Simple Molecular Orbital Method for Discussing the Electronic Structures of Stereoisomers—The Theoretical Method and ESR Hyperfine Splittings of the Terephthalaldehyde Anion

By Keiji MOROKUMA, Teijiro YONEZAWA and Kenichi FUKUI

(Received May 8, 1962)

The various different properties of the stereoisomers of organic compounds have long excited the interest of chemists in their chemical reactivities, physical properties, spectroscopic data, and so forth.

From the point of view of molecular orbital (MO) treatment, stereoisomers may be divided into two classes, one consisting of geometrical (cis- and trans-) and rotational (gauche- and trans-) isomers, and the other containing optical isomers. The following discussion will be limited to the isomers of the first class.

The electronic structures of these isomers are calculated to be identical when the simple LCAO MO method, in which electronic interactions are formally neglected, is used, for in this method the secular equation of one of the isomers is equal to that of the other. In the discussion of the differences in energy of the first class steroisomers, classical electrostatic calculation has been found useful, as has the ASMO (antisymmetrized MO) calculation, including electronic interactions. In a discussion of their electron distribution the ASMO SCF (self-consistent field) calculation is both necessary and adequate; a typical example would be the strict calculation of the π-electron distribution of trans- and cis-butadiene by Parr and Mulliken[1]. In such non-polar compounds as butadiene, indeed, such a strict but very troublesome calculation is indispensable in order to show any difference of distribution. However, in a compound containing polar groups, some differences of electron distribution between the isomers, which may be sufficient for a qualitative comparison, may be obtained by a simple LCAO MO method, with the parameters modified by considering the electronic interaction between polar groups.

In this paper, such a modified simple molecular orbital method is to be determined for conjugated molecules; it is then to be applied to the interesting differences between terephthalaldehyde anion isomers in the proton hyperfine couplings in ESR (electron spin resonance) spectroscopy recently investigated by Maki[2].

As to the structural isomers, the electronic structures are, of course, different even in the simple LCAO MO calculation. In this simple method, however, it is difficult sufficiently to take into account the effects of near-by polar groups, while actually the electronic interactions cause a considerable change in the electron distribution. The simple MO method with modified parameters which is utilized for geometrical isomers is also of use for this class of isomers. Applications to actual problems of structural isomers—nuclear coupling constants and asymmetric parameters in PQR (pure nuclear quadrupole resonance) spectra, dipole moments, etc.—will be given in the next paper[3].

Theoretical Method

In the Hückel MO theory, by solving the secular equation

$$\sum_{s=1}^{n}(a_{rs}^{0}-\lambda_i\delta_{rs})C_{ir}^{\pi}=0 \quad (r=1,2,\cdots,n) \quad (1)$$

molecular orbitals are obtained as a linear combination of atomic orbitals (AO's) as follows:

$$\phi_i^{\pi}=\sum_{r=1}^{n}C_{ir}^{\pi}\chi_r^{\pi} \quad (i=1,2,\cdots,n) \quad (2)$$

where n is the number of π AO's, χ_r^{π} is the rth π AO, C_{ir} is the coefficient of the rth AO in the ith MO, λ_i is the ith eigenvalue of Eq. 1, and a_{rr}^{0} and a_{rs}^{0} are the parameters standing for the Coulomb integral of the rth AO and the resonance integral between the rth and the sth AO's, respectively.

The molecular orbitals of σ electrons are similarly calculated as a linear combination of σ atomic orbitals (sp^2 or sp^3 hybridized orbitals on carbon atoms, hydrogen 1s orbitals

1) R. G. Parr and R. S. Mulliken, *J. Chem. Phys.*, **18**, 1182 (1950).

2) A. H. Maki, ibid., **35**, 761 (1961).

3) K. Morokuma, T. Masuda and K. Fukui, to be published in this Bulletin.

and σ atomic orbitals on substituents)[4-6]*:

$$\psi_j^{\sigma}=\sum_{t=1}^{N}C_{jt}^{\sigma}\chi_t^{\sigma} \qquad (j=1,2,\cdots,N) \quad (3)$$

with parameters b_{tt}^0 and b_{tu}^0 defined as

$$\left.\begin{array}{ll}\text{Coulomb integral} & \alpha_t^{\sigma}=\alpha_{\sigma}+b_{tt}^0\beta_{\sigma}\\ \text{resonance integral} & \beta_{tu}^{\sigma}=b_{tu}^0\beta_{\sigma}\end{array}\right\} \quad (4)$$

where N is the number of σ AO's and β_{σ} is the resonance integral of the standard C–C σ bond of benzene. From these MO's, the π and the σ electron densities, q_r^{π} and q_t^{σ} respectively, are calculated:

$$\left.\begin{array}{l}q_r^{\pi}=\sum_{i}^{\text{occ}}\nu_i^{\pi}(C_{ir}^{\pi})^2\\ q_t^{\sigma}=\sum_{j}^{\text{occ}}\nu_j^{\sigma}(C_{jt}^{\sigma})^2\end{array}\right\} \quad (5)$$

where ν_i represents the number of electrons in the ith MO.

Suppose that q_r^{π} and q_t^{σ} have already been calculated by the use of assumed parameters. We call them the densities and the parameters, respectively, of the zero order. Of course, the results are identical with respect to the cis- and the trans-isomers. If the compound has an even number of electrons (closed shell), Fock's operater of the pth atomic orbital on the Ath atom with electron-electron interaction, which corresponds to the Coulomb integral in the simple MO treatment, may be given as follows[7]:

$$F_{pp}=W_p(q_p)+\frac{1}{2}q_p\gamma_{pp}+(Z_A-1)\xi_{pA}+\sum_{r\ (\text{on }A)}^{\text{all AO's}}q_r\gamma_{pr}+\sum_{r\ (\text{not on }A)}^{\text{all AO's}}q_r\gamma_{pr}+\sum_{B\ (\neq A)}^{\text{all cores}}Z_B\xi_{pB} \quad (6)$$

The first four terms are concerned with the electrons and the core of atom A, and the last two represent the interactions with electrons and cores on the other atoms; γ_{pr} and ξ_{pB} are the electron repulsion integral and the electron core atraction integral, respectively, which are represented by

$$\left.\begin{array}{l}\gamma_{pr}=\int\chi_p^*(1)\chi_p(1)\dfrac{e^2}{r_{12}}\chi_r^*(2)\chi_r(2)\,d\tau_1 d\tau_2\\ \xi_{pB}=-\int\chi_p^*(1)\dfrac{e^2}{r_{1B}}\chi_p(1)\,d\tau_1\end{array}\right\} \quad (7)$$

γ_{pp} and ξ_{pA} are the corresponding one-center integrals, and Z_B is the charge of the core B. $W_p(q_p)$ is the energy of an electron on the pth AO in its valence state, which is a function of the electron density, q_p.

If one assumes that, when the rth and the qth AO's belong to the same atom, B, γ_{pr} is equal to γ_{pq} wherever each of them may be directed, and that, further, ξ_{pB} is equal to them (hereafter they are designated by γ_{AB}), then the latter two terms may be written as follows:

$$-\sum_{B\ (\neq A)}Q_B\gamma_{AB} \quad (8)$$

where Q_B is the net charge on atom B

$$Q_B=Z_B-\sum_{r\ (\text{on }B)}^{\text{all AO's}}q_r \quad (9)$$

The assumption is acceptable in this simple qualitative discussion. Because W_p becomes more positive and $-(1/2)q_{pp}$ more negative when q_{pp} is set larger, the sum W_p^0

$$W_p^0=W_p-\frac{1}{2}q_p\gamma_{pp}-\xi_{pA} \quad (10)$$

might be independent of the density*. Thus, the remainder of the former terms are reduced to

$$-Q_A\gamma_{AA} \quad (11)$$

Moreover, a simple expression,

$$F_{pp}=W_p^0-\sum_{B}^{\text{all atoms}}Q_B\gamma_{AB} \quad (12)$$

is obtained, W_p^0 being a constant, depending only on the kind and the hybridization of the atom (sp^2 carbon, sp^3 carbon, hydrogen, and so forth). We choose a certain atom as the standard, putting 0 on the shoulder as follows:

$$F_{qq}^0=W_q^0-\sum_{B}^{\text{all atoms}}Q_B\gamma_{DB} \quad (13)$$

At this stage, we return to the simple LCAO MO treatment, regarding the F_{pp} as the new Coulomb integral, α_p, modified with electronic interactions, and F_{qq}^0 as the standard integral, α_q^0, assumed to be equal to that of the zero order (Eqs. 1 and 4). Therefore, the new Coulomb integrals for the π electrons are:

4) K. Fukui, H. Kato and T.Yonezawa, This Bulletin, **34**, 442, 1111 (1961).
5) K. Fukui, H. Kato, T. Yonezawa, K. Morokuma, A. Imamura and C. Nagata, ibid., **35**, 38 (1962).
6) K. Morokuma, H. Kato and K. Fukui, to be published in this Bulletin.
* If the compound in question is a conjugated system, sp^2 hybridized orbitals should be used. When the compound is a saturated one, π MO's (Eq. 2) do not appear and the σ MO's are composed of sp^3 hybridized orbitals.
7) J. A. Pople, *Trans. Faraday Soc.*, **49**, 1375 (1953).

* In stereoisomers, the assumption expressed by Eq. 10 is unnecessary. The assumption is needed only in structural isomers.

$$\left.\begin{aligned} \alpha_q^0 &= \alpha_\pi + a_{qq}^0 \beta_\pi \\ \alpha_p &= \alpha_p^0 + (F_{pp} - F_{qq}^0) \end{aligned}\right\} \quad (14)$$

or the new parameters a_{pp}^1 and a_{qq}^1 are:

$$\left.\begin{aligned} a_{qq}^1 &= a_{qq}^0 \\ a_{pp}^1 &= a_{pp}^0 + (F_{pp} - F_{qq}^0)/\beta_\pi \end{aligned}\right\} \quad (15)$$

Also, for σ electrons,

$$\left.\begin{aligned} b_{qq}^1 &= b_{qq}^0 \\ b_{pp}^1 &= b_{pp}^0 + (F_{pp} - F_{qq}^0)/\beta_\sigma \end{aligned}\right\} \quad (16)$$

With these new parameters of the first order, which do, of course, differ between the two geometrical isomers, are calculated the π and σ electron distributions of the first order, showing the difference between the isomers.

Instead of Eqs. 15 and16, Eq. 17

$$\left.\begin{aligned} a_{pp}^1 &= a_{pp}^0 + k(F_{pp} - F_{qq}^0)/\beta_\pi \\ b_{pp}^1 &= b_{pp}^0 + k(F_{pp} - F_{qq}^0)/\beta_\sigma \end{aligned}\right\} \quad (17)$$

might better be used. The value of k is unity in Eqs. 15 and 16, but this value might lead to an over-estimation of the effects; therefore, so as to get nearer to self-consistency, k might be better settled as $0 < k < 1$.

ESR Hyperfine Splittings of the Terephthalaldehyde Anion

Recently an ESR spectrum of a terephthalaldehyde mononegative ion radical produced by the electrolytic reduction of the aldehyde has been observed by Maki[2]; it has been found that the hyperfine splittings of the spectrum cannot be interpreted without taking them as rising from two radical species, each of which has three pairs of protons with these coupling constants; species A: 2.08, 0.70 and 3.89 gauss, and species B: 1.54, 1.16 and 3.81 gauss (absolute value). Maki regarded them as cis- and trans-isomers of the anion radical, distinguished in the ESR spectrum because of the restricted rotation of the aldehyde groups; he suggested that species A was the cis isomer, whereas B was the trans isomer.

It would be interesting to apply the method developed in the preceding paragraph and to see which species may be assigned to which isomer and, furthermore, which coupling constant may be assigned to which proton.

As the terephthalaldehyde anion is a radical, Fock's operator in the radical is a little different from that in Eq. 6[8]. For this qualitative discussion, however, the simplified expression, Eq. 12, may rationally be adopted even for a radical; thus, no special notice to its being open shell is paid in this paragraph.

Evaluation of Atomic Integrals.—The electron repulsion integrals necessary to the evaluation of Fock's operator are estimated, in the form used by Mataga et al.[9], as follows:

$$\gamma_{AB} = \frac{14.39}{a_{AB} + r_{AB}} \text{eV.} \quad (17')$$

where a_{AB} is the distance in Å from atom A to atom B and is constant settled so as to fit experimental values at $r_{AB}=0$ (ionization potential minus electron affinity) if A and B are atoms of the same kind. When A and B are of different kinds, an arithmetical mean may roughly be adopted. The values of a_{AB} are tabulated in Table I.

The values of β_π and β_σ, standard resonance integrals, are taken as follows:

Table I. Values of a_{AB} for various pairs of atoms

B \ A	C	H	O
C	1.29	1.20	1.14
H	1.20	1.12	1.05
O	1.14	1.05	0.99

Table II. Values of parameters a_{rr}^0, a_{rs}^0, b_{tt}^0 and b_{ru}^0 of the zero order*

a_{rr}^0: Coulomb integral of π AO's

O	+2
C_{II}	+0.2
C (others)	0

a_{rs}^0: Resonance integral between π AO's

C_{II}-O	+1.4
C-C	+1

b_{tt}^0: Coulomb integral of σ AO's

O	+0.3
C	0
H	−0.2

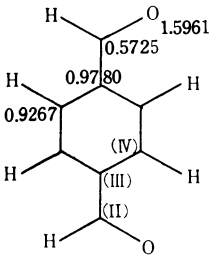
b_{tu}^0: Resonance integral between σ AO's

C-O	+1.1
C-H	+0.94
C-C (bonding)	+1
C-C (on the same atom)	+0.38

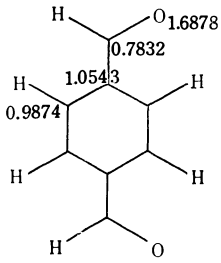
* As to numbering of AO's, see Fig. 1.

8) C. C. J. Roothaan, *Rev. Modern Phys.*, 32, 179 (1960); J. A. Pople and R. K. Nesbet, *J. Chem. Phys.*, 22, 571 (1954).

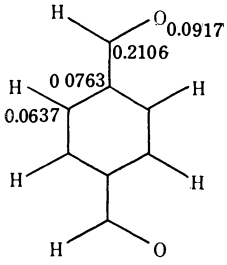
9) N. Mataga and K. Nishimoto, *Z. physik. Chem.*, 13, 140 (1957).



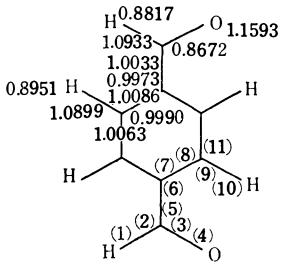
π Elctron density of the neutral aldehyde (numbering of π AO's)



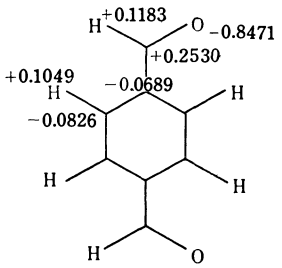
π Electron density of the aldehyde anion



π Spin density of the anion



σ Electron density (numbering of σ AO's)



Net charge of the anion

Fig. 1. Electron distribution of the zero order (numbering of AO's in parentheses).

$$\left.\begin{aligned}\beta_\pi &= -2.5 \text{ eV.}\\ \beta_\sigma &= -8.0 \text{ eV.}\end{aligned}\right\} \qquad (18)$$

and k is set as unity.

The geometry of the aldehyde and its anion is considered to be planar, with bond lengths of 1.40Å for C–C (aromatic), 1.52Å for C–C (substituent), 1.08Å for C–H, and 1.22Å for C=O and with all bond angles of 120°.

Parameters of the Zero Orders.—The parameters of the zero order for the π and σ electron systems are collected in Table II. The values of a_{rr}^0 and a_{rs}^0 for π electron systems are similar to those popularly used. As to the σ system, the values in the table, except for O and C=O, are taken from a paper by the present authors[6]. The values of a_{OO}^0 and a_{CO}^0 have been settled anew by referring to the ionization potentials and electron affinities of oxygen, and to the bond energy of the C–O single bond of alcohols or ethers and the ratio of the overlap integrals for C=O and C–O bonds respectively.

Electron Distributions of the Zero Order.—In Fig. 1 are given electron distributions calculated on the basis of the parameters of the zero order. Since, of course, the results are identical for both isomers, the patterns for only the cis isomer are represented in the figure.

Parameters of the First Orders. — By using the net charge of the anion given in the Fig. 1 and the integrals of γ_{AB}, β_π and β_σ given in the foregoing section, new parameters of the first order have been derived.

As for the π electron system, as the circumstances affecting π AO's C_{II} and C_{III} are not affected by the isomerism, the a_{rr}^1's have been taken to be equal to a_{rr}^0's*. For carbons IV and V, which are indistinguishable in the zero order, new parameters have been estimated by looking tentatively on the $C_V\pi$AO in the trans isomer as a standard; for oxygens, the $O_I\pi$AO in the trans isomer has been taken as a standard.

A similar standardization and calculation of the parameters have also been carried out for σ AO's. The values of the parameters a_{rr}^1 and b_{tt}^1 of the first order thus calculated for both isomers are tabulated in Table III.

Results and Discussion. — The π and σ electron densities and the π spin density of the isomers of the terephthalaldehyde anion have been calculated with the parameters of the first order; the results are given in Fig. 2.

As would be expected from a simple electrostatic consideration, in both isomers the π electron density on C_V is larger than that on C_{IV}, since to the latter the electron-rich and, accordingly, repulsive center of oxygen is located nearer. A similar tendency is found also in σ electron densities on ring hydrogens and ring carbons. The π spin density is

* For the numbering of π AO's, see Figs. 1 and 2.

TABLE III. VALUES OF PARAMETERS a_{rr}^1 AND b_{tt}^1 OF THE FIRST ORDER*

Cis		Trans	
a_{rr}^1: Coulomb integral of π AO's		a_{rr}^1: Coulomb integral of π AO's	
O_I	+1.976	O_I	+2.0 (standard)
C_{II}	+0.2 (invariant)	C_{II}	+0.2 (invariant)
C_{III}	0 (invariant)	C_{III}	0 (invariant)
C_{IV}	−0.230	C_{IV}	−0.146
C_V	+0.084	C_V	0 (standard)
b_{tt}^1: Coulomb integral of σ AO's		b_{tt}^1: Coulomb integral of σ AO's	
H_1	−0.193	H_1	−0.2 (standard)
C_2, C_3, C_5	0 (invariant)	C_2, C_3, C_5	0 (invariant)
O_4	+0.292	O_4	+0.3 (standard)
C_6, C_7, C_{12}	0 (invariant)	C_6, C_7, C_{12}	0 (invariant)
C_8, C_9, C_{11}	−0.072	C_8, C_9, C_{11}	−0.046
H_{10}	−0.336	H_{10}	−0.299
C_{13}, C_{14}, C_{16}	+0.026	C_{13}, C_{14}, C_{16}	0 (standard)
H_{15}	−0.164	H_{15}	−0.2 (standard)

* As to numbering of AO's, see Fig. 2.

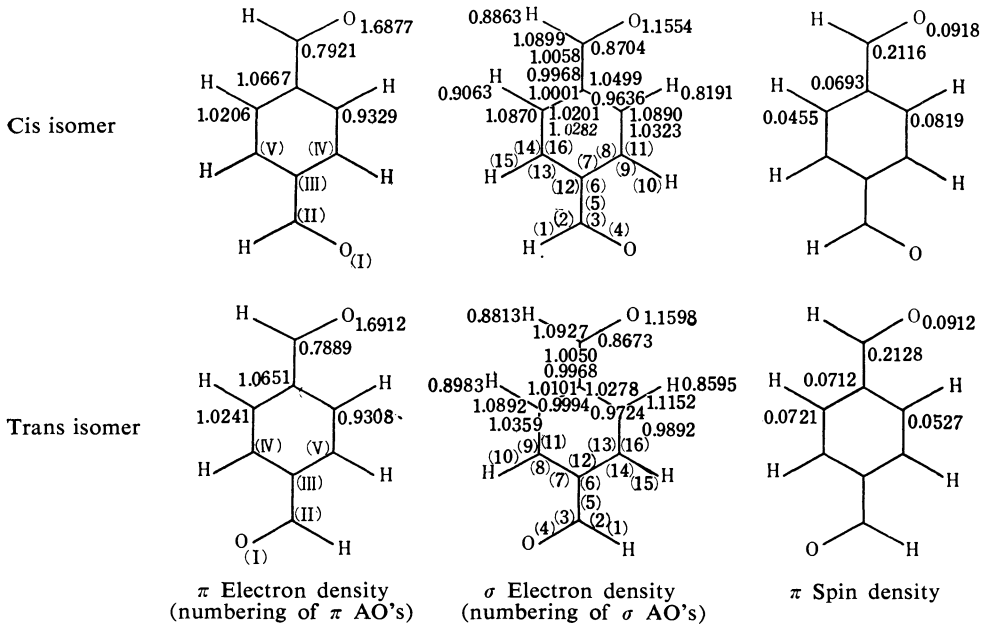


Fig. 2. Electron densities of the first order of the aldehyde anion isomers (numbering of AO's in parentheses).

calculated as the density of the half-occupied level of the anion.

In order to compare these findings in the calculations, the experimental proton hyperfine coupling constants, a_H, have been converted into spin densities on the adjacent carbons, ρ_C, by the equation

$$a_H = Q\rho_C \qquad (19)$$

where the constant, Q, is equal to −23 gauss[10]. Strictly speaking, the constancy of Q would not hold in this case, for the different polarity of each C–H bond, as may be seen in Fig. 2, would yield a different value of Q; in a qualitative discussion like this, however, such a slight difference is of little significance.

On collating the calculated spin densities with the experimental findings indicated in Table IV, we find a good mutual agreement, thus obtaining the following assignments:

(1) The A species is the cis isomer and the B species is the trans isomer, in agreement with Maki's proposition.

10) H. M. McConnell, *J. Chem. Phys.*, **24**, 632, 764 (1956).

TABLE IV. CALCULATED AND EXPERIMENTAL SPIN DENSITIES AND ASSIGNMENT OF COUPLING CONSTANTS OF TEREPHTHALALDEHYDE ANION

Calculated (cis isomer)		Experimental (species A)
Position	Spin density	Spin density
C_{II}	0.212	0.169
C_{IV}	0.082	0.090
C_V	0.046	0.030

Calculated (trans isomer)		Experimental (species B)
Position	Spin density	Spin dencity
C_{II}	0.213	0.166
C_{IV}	0.053	0.050
C_V	0.072	0.067

(2) In each isomer, the largest (in absolute value) and nearly invariant coupling constant originates from the aldehyde proton.

(3) In the trans isomer, the order of the spin density on ring carbons is $C_V > C_{IV}$. On the other hand, in the cis isomer, the spin density on C_{IV} is much larger than that on C_V. This result is of great interest because the order of the spin density is inverse to that of the total π electron density and is contradictory to a simple electrostatic presumption. On inspecting the calculated electron distribution of each molecular orbital (Table V), such a presumption seems to be attributable to the total density and to the distribution of molecular orbitals of a lower energy, but not necessarily to a distribution molecular orbitals of a higher energy or of a less bonding or antibonding nature, as the half-occupied orbital of the anion discussed here.

TABLE V. ELECTRON DENSITY OF EACH OCCUPIED π MO

1. Cis isomer

Orbital energy λ_i	Symmetry**	Electron density	
		C_{IV}	C_V
−0.1498*	A′	0.0819	0.0455
+0.9204	A′	0.2662	0.2253
+1.1815	A″	0.0493	0.0652
+1.9686	A′	0.1001	0.1838
+2.8555	A″	0.0015	0.0017
+2.8876	A′	0.0085	0.0117

* Half occupied level
** Symmetry in C_{1h} group

2. Trans isomer

Orbital energy λ_i	Symmetry**	Electron density	
		C_{IV}	C_V
−0.1383*	A	0.0527	0.0721
+0.9240	B	0.2661	0.2255
+1.1872	B	0.0291	0.0922
+1.9597	A	0.1334	0.1469
+2.8716	B	0.0014	0.0016
+2.9021	A	0.0090	0.0097

* Half occupied level
** Symmetry in C_2 group

Summary

A new simple molecular orbital method with parameters modified by electronic interactions was developed so as to discuss simply the difference in electron distributions between stereoisomers. An application was made to the proton hyperfine coupling constants of the cis- and trans-isomers of the terephthalaldehyde anion radical, and the assignment of the constants was proposed on the basis of molecular orbital calculations.

Most of the numerical calculations were carried out on the KDC-I digital computor of Kyoto University.

Faculty of Engineering
Kyoto University
Sakyo-ku, Kyoto

Changes of the Lattice Constants and Crystallite Sizes of Various Types of Carbons with Heat Treatment

By Michio INAGAKI and Tokiti NODA

(Received June 7, 1962)

Measurements of the lattice constants and crystallite sizes of a number of raw carbon materials, heat-treated at various temperatures, have been carried out by many investigators. However, in most of the investigations, the heat treatments were made in a vacuum or in an inert atmosphere, such as of nitrogen or argon, using laboratory-type furnaces. On the other hand, the present authors thought it necessary to study the effect of the atmosphere of heat treatment on the graphitization of carbon, because it had previously been reported that carbon was only with difficulty graphitized in a vacuum[1,2]. For the present work, several kinds of raw carbon materials were heat-treated at temperatures between 1500 and 3400°C in a resistance furnace under atmospheric pressure. The lattice constants and crystallite sizes of these carbons were measured by means of the X-ray diffraction method in order to investigate their changes with heat treatment. The heterogeneity of the interlayer spacing in a parallel layer group and the relation between the crystallite size and the particle size of carbon black will also be discussed.

Experimental

Heat Treatment of Raw Carbon Materials.—The raw carbon materials used in the present work are shown in Table I, together with technical analysis data of these materials. Each of the raw carbon materials was placed in a graphite crucible and heat-treated in a carbon granular-resistance furnace of a type similar to the industrial graphitizing furnace. The temperature of the crucible was measured with an optical pyrometer focusing through a graphite tube. Because it was difficult to keep the heating temperature constant during the heat treatment, the arithmetical mean of the temperature, t_{20}, at which the crucible was kept for 20 min. and the highest temperature, t_h, in the run was taken as the temperature of the heat treatment, t_m, as is illustrated in Fig. 1. The calibration of the scale of the optical pyrometer and the correction for the absorption by the window glass of the sighting pipe were made by using a standard lamp for the optical pyrometery.

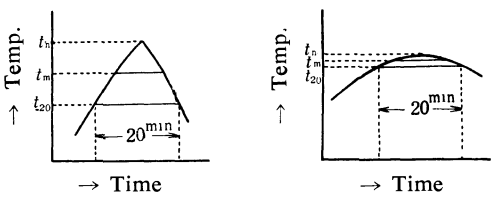


Fig. 1. Scheme of determination of heat treatment temperature.

X-Ray Diffraction Analysis.—Each sample was pulverized to pass through a 150-mesh sieve and mixed with an extra-pure silicon powder as an inner standard to the amount of 10%. The particle sizes of the standard silicon powder used were from about 20 to 40 μ, and its lattice constant, a_0, was measured as 5.4310±0.0004 Å. For X-ray diffraction analysis, a recording diffractometer and CuK_α

TABLE I. TECHNICAL ANALYSIS DATA OF RAW CARBON MATERIALS

Sample	Moisture %	Volatile matter %	Vanadium p. p. m.	Free carbon %	Ash %	Sulfur %	Apparent density g./cm³	Powder resistance Ω·cm.
Petroleum coke	0.13	0.52	278	99.03	0.32	1.54	2.043	0.128
Pitch coke	0.13	0.19	20	99.43	0.25	0.45	2.009	0.218
Thermal black	0.15	1.72	12	97.26	0.87	0.186	1.895	0.911
Lamp black								
Furnace black A	0.87	1.88	13	97.07	0.18	0.686	1.822	0.452
Furnace black B	0.30	2.13	13	97.45	0.12	0.766	1.854	0.311
Channel black	2.38	4.65	11	97.96	0.14	0.339	1.790	0.325
Acetylene black	0.47	1.43	11	92.85	0.12	0.783	1.740	3.137
Charcoal	2.33	13.77	10	82.94	0.96	0.186	1.414	—

1) T. Ichiki, *The Hitachi-Hyoron*, **30**, 247 (1949).

2) T. Noda and H. Matsuoka, *J. Chem. Soc. Japan, Ind. Chem. Sec.* (*Kogyo Kagaku Zasshi*), **64**, 2083 (1961).

radiation were used. All the profiles of the (422) and (331) diffractions, and some profiles of the (311) diffraction, of standard silicon, were graphically separated into the α_1 and α_2 profiles by means of the Rachinger method[3], the α_1 profiles were used for the present measurements. The lattice constant, c_0, and the thickness of the graphite crystallite along the c-axis, L_c, were obtained from the (002) and (004) diffractions of carbon, the lattice constant, a_0, and the width of the crystallite along the a-axis, L_a, from the (110) diffraction, and the spacing, d_{112}, and size of three-dimensional crystallite, L_{112}, from the (112) diffraction. The crystallite sizes were calculated from half-maximum breadths of the diffraction profiles[4]. The profile of the (002) diffraction was corrected for various intensity factors, such as the Lorentz-polarization factor, the absorption factor and the square of the atomic scattering factor, by using a method similar to Ruston's[5].

Results and Discussion

Changes of Lattice Constants and Crystallite Sizes with Heat Treatment.—The lattice constant, c_0, and the crystallite sizes, L_c, L_a and L_{112}, of the samples are shown as a function of the temperature of heat treatment in Fig. 2. The c_0 and L_c values of all raw carbon materials changed very slightly at temperatures above 2500°C, apparently approaching a finite value. The c_0 values of a petroleum coke and a pitch coke, i. e., the so-called graphitizing carbons, were not less than 6.718Å, even when they were heat-treated up to 3400°C. According to Walker and Imperial, the c_0 values of four carbons heat-treated at about 3600°C under a pressure of 10 atm. of argon were not less than 6.714Å[6]. The same c_0 value as of natural graphite, 6.708Å, was obtained only when carbon was melted[7]. From the results of our experiment and of the reported experiments, it can be concluded that the graphitizability of carbon is affected by the original texture of the carbon—crystallite arrangement, pore distribution, criss-cross linkage between crystallites, etc.—even at such a high temperature as 3600°C, in the same way as at 3000°C or below.

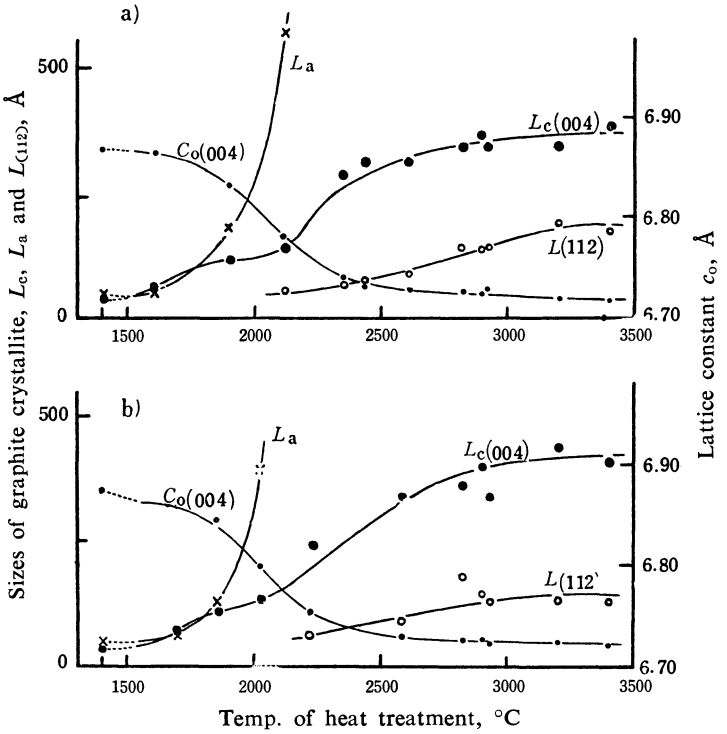
In carbon blacks heat-treated at 3400°C, i. e., a thermal black, a lamp black, two furnace blacks, a channel black and an acetylene black, the c_0 values were 6.77, 6.76, 6.81, 6.83, 6.85 and 6.82Å, and the L_c values obtained from the (002) diffractions, were 220, 190, 110, 89, 64 and 91Å respectively. The particle sizes of these carbon blacks were about 3000, 5000, 500, 350, 300 and 300Å respectively. These experimental results revealed that the c_0 value became smaller and the L_c value larger with the increase in the particle size of carbon black. Therefore, it can be said that the degree of graphitization of carbon black depends on its particle size. This is very interesting in regard to the mechanism of crystal growth in a particle of carbon black. This subject will be discussed below in more detail.

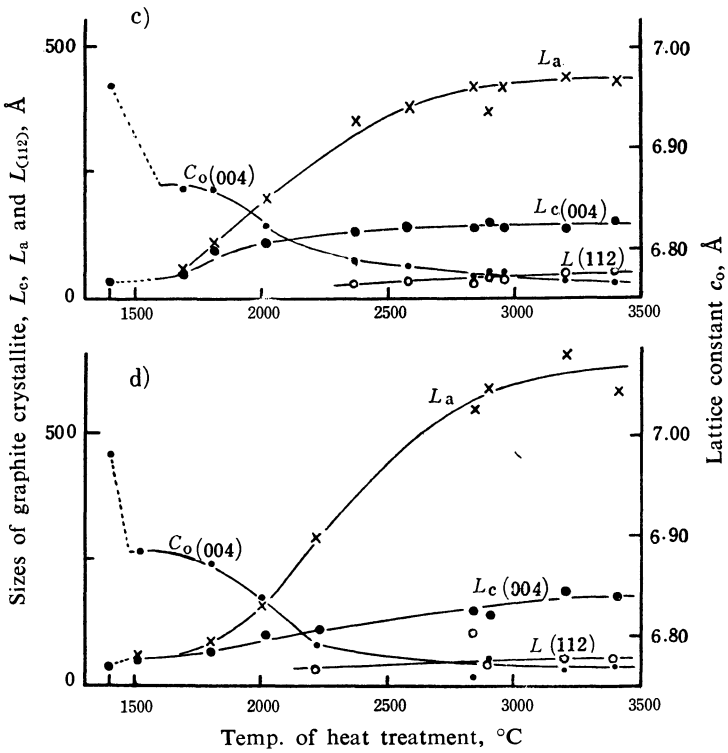
The a_0 value increased with the increase in the temperature of heat treatment, approaching the a_0 value of natural graphite, 2.461Å. The a_0 values of the cokes heat-treated at temperatures above 2400°C and the values of the thermal black and the lamp black heat-treated above 3000°C were 2.461Å, but the values of other carbon blacks did not increase over 2.456Å even when they were heat-treated up to 3400°C.

The value of spacing, d_{112}, was always 1.156Å, independent of the temperature of heat treatment. The modulation of the (11) diffraction profile, which reveals the appearance of a three-dimensional (112) diffraction, was observed in the cokes heat-treated at temperatures above 1800°C, the L_a values of the cokes being larger than 100Å. This experimental finding coincides with Warren's observation[8]. In the thermal black and the lamp black, the (112) diffraction was observed when the L_a value was more than 150~200Å. In all the other carbon blacks, however, no (112) diffraction could be observed.

Heterogeneity of Interlayer Spacing in Crystallite.—Usually, the L_c value obtained from the (002) diffraction of a carbon, $L_{c(002)}$, is larger than that from the (004) diffraction of the same carbon, $L_{c(004)}$. The broadening of the (002) or (004) diffraction profile may be caused not only by the smallness of the crystallite but also by the heterogeneity of the interlayer spacing. The interlayer spacing of the turbostratic structure is said to be 3.44Å and that of graphite structure, 3.354Å, so the broadening for the (004) diffraction due to the heterogeneity of the spacing is twice as large as that for the (002) diffraction. The broadening due to the smallness of the crystallite should be the same for both the (002) and (004) diffractions, provided that the diffraction angle is taken into consideration. As the crystallite size is calculated from the observed broadening, the above discrepancy between $L_{c(002)}$ and $L_{c(004)}$ must be caused mainly by the heterogeneity of the spacing. If we put $\{L_{c(002)}-L_{c(004)}\}/L_{c(002)}$ as $\Delta L/L$, the

3) W. A. Rachinger, *J. Sci. Instruments*, **25**, 254 (1948).
4) H. P. Klug and L. E. Alexander, "X-ray Diffraction Procedures", John Wiley (1954), p 491.
5) W. R. Ruston, *Fuel*, **32**, 53 (1953).
6) P. L. Walker and G. Imperial, *Nature*, **180**, 1184 (1957).
7) T. Noda and H. Matsuoka, *J. Chem. Soc. Japan, Ind. Chem. Sec.* (*Kogyo Kagaku Zasshi*), **63**, 465 (1960).
8) B. E. Warren, "Proc. Conf. on Carbon" Univ. of Buffalo (1956), p. 49.


a)
b)
L_a
$L_c(004)$
$C_o(004)$
$L(112)$
500
0
1500
2000
2500
3000
3500
6.90
6.80
6.70
Sizes of graphite crystallite, L_c, L_a and $L_{(112)}$, Å
Lattice constant c_o, Å
Temp. of heat treatment, °C


c)
d)
L_a
$L_c(004)$
$C_o(004)$
$L(112)$
500
0
1500
2000
2500
3000
3500
7.00
6.90
6.80
Sizes of graphite crystallite, L_c, L_a and $L_{(112)}$, Å
Lattice constant c_o, Å
Temp. of heat treatment, °C

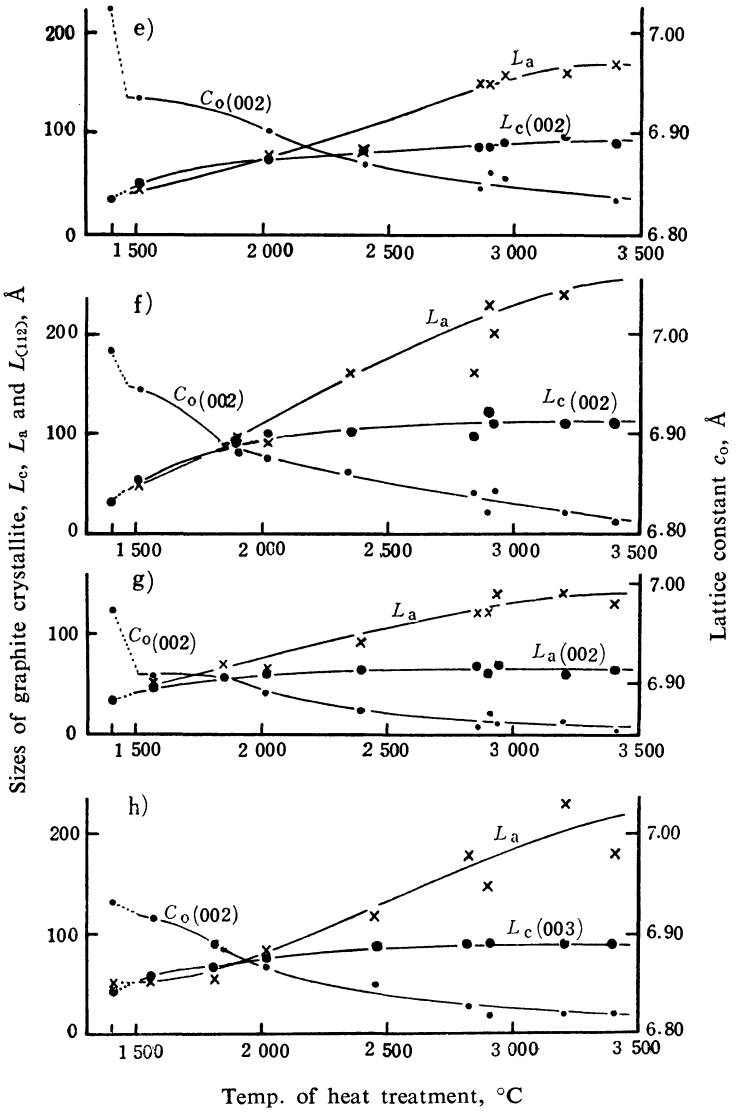


Fig. 2. Changes of lattice constant and crystallite sizes of carbon with heat treatment.
a) Petroleum coke, b) Pitch coke, c) Thermal black, d) Lamp black, e) Furnace black A, f) Furnace black B, g) Channel black, h) Acetylene black

value of $\Delta L/L$ may be taken as a measure of the heterogeneity of the spacing of the graphite-like layers in a parallel layer group.

The relation between $\Delta L/L$ and the temperature of heat treatment is shown in Fig. 3. The curves of $\Delta L/L$ for the petroleum coke, the pitch coke, and the thermal black were similar. These curves might be interpreted as follows. Up to 2000°C treatment, the turbostratic structure of graphite-like layers predominates in the samples, but a part of the graphite-like layers begin to take on a three-dimensional ordering, i. e., the graphite orientation, from 1800°C treatment (this was proved by the modulation of the (11) diffraction as mentioned above). Therefore, the heterogeneity of the interlayer spacing in crystallite increases, and the value of $\Delta L/L$ increases rapidly from 1800°C upward. At temperatures above 2000°C, the graphite orientation predominates in the samples, while the turbostratic structure decreases; i. e., the heterogeneity in crystallite decreases with the increase in the temperature of heat treatment. Therefore, the value of $\Delta L/L$ becomes maximum at about 2000°C and then decreases as the temperature

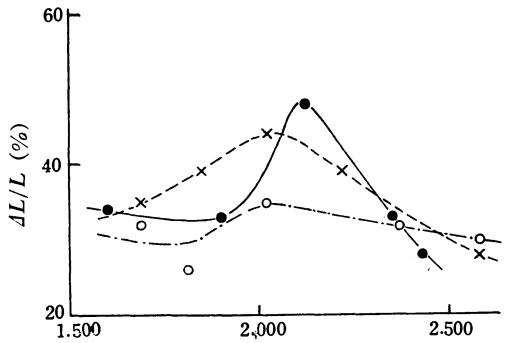


Fig. 3. Relations between $\Delta L/L$ and temperature of heat treatment of carbon.
—●— Petroleum coke
--×-- Pitch coke
-·○·- Thermal black

of the heat treatment increases. With samples heat-treated at temperatures above 2600°C and having crystallite sizes larger than 300Å, the error in $\Delta L/L$ was very large, so a discussion of the signification of $\Delta L/L$ may become meaningless. Tagawa and Nakashima[9] obtained a similar curve by investigating the relation between the temperature of heat treatment and the activation energy of the wet oxidation reaction of heat-treated petroleum coke.

Relation between the Particle Size and the Crystallite Size of Carbon Black.—It is said that particle size is the main limiting factor for the growth of graphite crystallite in carbon black[10]. In Fig. 4, the crystallite size, L_c or L_a, of the thermal black, the two furnace blacks, and the channel black is represented as a function of the average particle size, $2R$. Because the lamp black had a peculiar distribution of particle size and because the acetylene black seemed to behave differently in its crystal growth from other carbon blacks, they were omitted from this discussion. From the two figures, it can be seen that the particle size has some effect on the crystal growth along the a-axis and also along the c-axis. This is consistent with the assumption that the minute crystallite whose layer plane is aligned parallel to the surface of the carbon black particle coalesces with its adjacencies into a larger crystallite[11] and that, in consequence, the angle between the c-axes of adjacent parallel layer group is the main limiting factor for crystal growth in carbon black. If it is the only limiting factor, the value of $L_a/2R$, which corresponds to the average angle between the c-axes of adjacent parallel layer groups, should

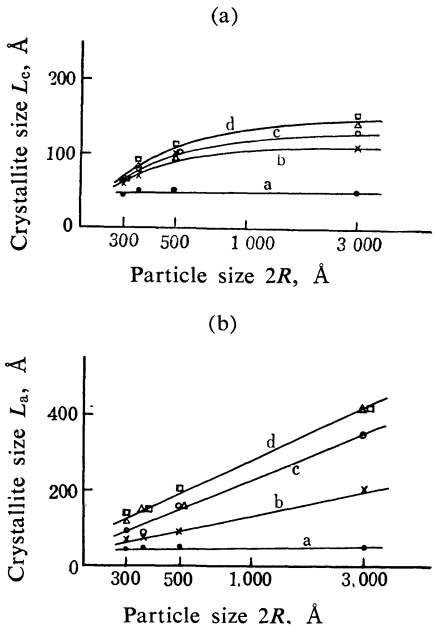


Fig. 4. Relations between particle size and crystallite sizes of carbon black.
a: 1550 b: 2020
c: 2400 d: 2800~3400°C

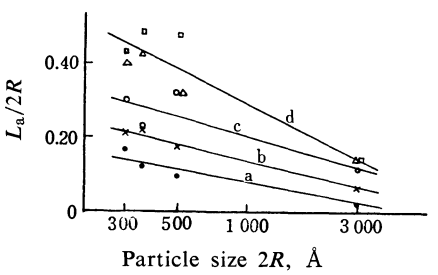


Fig. 5. Relation between particle size and $L_a/2R$ of carbon black.
a: 1550 b: 2020
b: 2400 d: 2800~3400°C

be the same in all carbon blacks. However, it can be seen in Fig. 5 that the value of $L_a/2R$ is larger as the particle size is smaller. Therefore, there must be another limiting factor besides the angle between the c-axes of adjacent crystallites. It might be the micropores between the crystallites.

Graphitization of Charcoal.—All diffraction profiles of charcoals heat-treated at various temperatures are asymmetrical and seem to be composite profiles[12], as is shown in Fig. 6. The profiles can be separated into three different ones by appearance, i. e., two peaks at about 3.43 and 3.36Å and a broad band.

9) H. Tagawa and H. Nakashima, *J. Chem. Soc. Japan, Ind. Chem. Sec.* (*Kogyo Kagaku Zasshi*), **63**, 1690 (1960).
10) H. T. Pinnick, *J. Chem. Phys.*, **20**, 756 (1952).
11) H. Akamatu et al., This Bulletin, **29**, 574 (1956).
12) T. Noda and M. Inagaki, "Proc. 4th Conf. on Carbon", (in press).

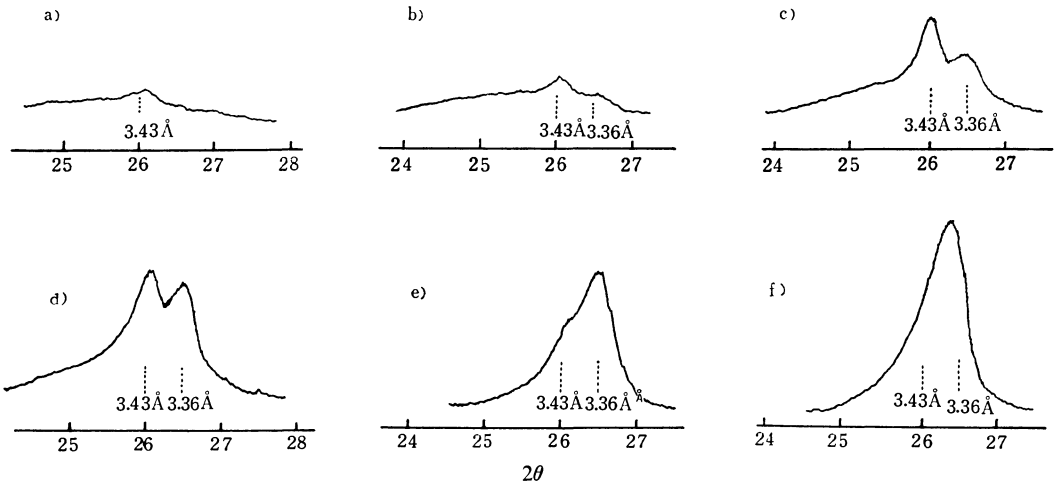


Fig. 6. Profiles of heat-treated charcoals.
a) 1820 b) 2120 c) 2370 d) 2450 e) 2820 f) 3200°C

The peak at 3.43Å increases its intensity up to 2500°C. The peak at 3.36Å, which is feeble as a temperature lower than 2000°C, increases its intensity with the increase in temperature of heat treatment and surpasses the peak of 3.43Å above 2500°C. Franklin[13] first noticed this phenomenon, calling it three-phase graphitization.

Summary

Two kinds of cokes, six kinds of carbon black and a charcoal were heat-treated at temperatures between 1500 and 3400°C in a resistance furnace under atmospheric pressure. The lattice constants and crystallite sizes of these carbons were measured by means of the X-ray diffraction method, using extra-pure silicon as an inner standard.

The c_0 values of the graphitizing carbons, such as the petroleum coke and the pitch coke, were not less than 6.718Å, even when these carbons were heat-treated at 3400°C. It was concluded that the graphitizability of carbon was affected by its original texture even at such a high temperature as 3400°C.

The c_0 value of carbon black became smaller and the value of L_c, larger with the increase in the particle size of carbon black. It has been said that the particle size is the main limiting factor for the growth of graphite crystallite in carbon black, but the experimental results suggest that such other properties as micropores may also be limiting factors.

The discrepancy between the L_c values calculated from the (002) and (004) diffractions was accounted for by the heterogeneity of the interlayer spacing in crystallite.

With the charcoal, so-called three-phase graphitization was observed.

Department of Applied Chemistry
Faculty of Engineering
Nagoya University
Chikusa-ku, Nagoya

13) R. E. Franklin, *Proc. Roy. Soc.*, **A209**, 196 (1951).

*Nuclear Magnetic Resonance Spectra of Amino Acids and their Derivatives. I. DNP Amino Acids**

By Shizuo FUJIWARA, Yoji ARATA, Naohiro HAYAKAWA and Hironao MOMOI

(Received June 8, 1962)

The molecular structure of amino acids has already been investigated by a variety of physical and chemical techniques. High-resolution NMR spectroscopy has also been used for this purpose. Using it, Takeda and Jardetzky[1], Jardetzky and Jardetzky[2], and Bovey and Tiers[3] have measured the proton chemical shift of NH and CH groups in amino acids.

Our aim is to study the NMR spectra of amino acids in more detail in order to compile fundamental data for the investigation of the structure of polypeptides and proteins by the NMR method.

The signal due to the NH proton of an amino acid cannot usually be observed in a water solution, since the NH proton of the amino group is subject to rapid exchange between neighboring molecules. However, in an *N*-(2, 4-dinitrophenyl) amino acid (DNP amino acid), when the sample is dissolved in dehydrated dioxane, the exchange of the NH proton is slow enough to permit the observation of the signal.

The patterns of the spectra arising from the protons on the NH and DNP groups are found to be useful for the identification of DNP amino acids.

Experimental

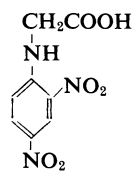
Materials. — All of the samples were purchased from Wako Chemicals & Co. Solutions (10%, w/v) of each DNP amino acid were prepared in dehydrated dioxane, and 2,4-dinitroaniline was dissolved in dehydrated acetone. The solutions were sealed in 5 mm. o. d. sample tubes. Sixteen kinds of DNP amino acids were used in this experiment: *N*-(2,4-dinitrophenyl) derivatives of glycine (Gly), L-alanine (Ala), L-serine (Ser), L-methionine (Met), L-threonine (Thr), L-allothreonine (Althr), L-leucine (Leu), L-isoleucine (Ileu), L-valine (Val), L-lysine (Lys), L-aspartic acid (Asp), L-glutamic acid (Glu), L-phenylalanine (Phe), L-tryptophan (Try), L-proline (Pro) and L-hydroxyproline (Hyp).

Spectrometer.—A Varian Associates model V4300C NMR spectrometer, operating at 56.44 Mc./sec., was employed for all measurements.

Calibration of the Spectra. — The frequency separations of the spectra with reference to the dioxane signal were determined by the usual side-band technique. The chemical shift data, expressed in p. p. m., are summarized in Fig. 3.

Results

The signals of the three protons of the 2, 4-dinitrophenyl group are easily identified, as is shown in the spectrum of DNP-glycine (Fig. 2). The assignment is found to be unambiguous if the spectrum is compared with that of



2, 4-dinitroaniline (Fig. 2d). In these spectra the signals due to $H_{(3)}$ and $H_{(6)}$ are both doublet; the spin-spin coupling constant between these protons (J_{36}) is estimated to be smaller than 1 c. p. s. J_{35} and J_{56} are found to be 2.8 and 9.2 c. p. s. respectively.

The signal due to the NH proton of DNP-glycine is observed as a slightly broad triplet at the high field side of the $H_{(3)}$ signal (Fig. 2a). The splitting can be attributed to the spin-spin coupling with CH_2 protons. The spin-spin coupling constant is 5.6 c. p. s. When a small amount of water is added, the signal is further broadened. This can be interpreted in terms of an increasing exchange rate of the NH proton (Fig. 2b, 2c). A detailed analysis of the broadening of the signal will be the subject of a forthcoming paper.

In all the other DNP amino acids except DNP-lysine, the NH proton signals are doublet, and in some cases they are overlapped by the $H_{(3)}$ signals. DNP-lysine gives rise to two signals of the NH protons; one is due to the α-NH proton, and the other is due to the ε-NH proton. These signals are split into doublet and triplet, respectively, by interaction with $C_{(2)}$-H and $C_{(6)}$-H protons.

* Presented at the lst symposium on High Resolution NMR, held by the Chemical Society of Japan, Tokyo, November, 1961.

1) M. Takeda and O. Jardetzky, *J. Chem. Phys.*, **26**, 1346 (1957).

2) O. Jardetzky and C. D. Jardetzky, *J. Biol. Chem.*, **233**, 383 (1958).

3) F. A. Bovey and G. V. D. Tiers, *J. Am. Chem. Soc.*, **81**, 2870 (1959).

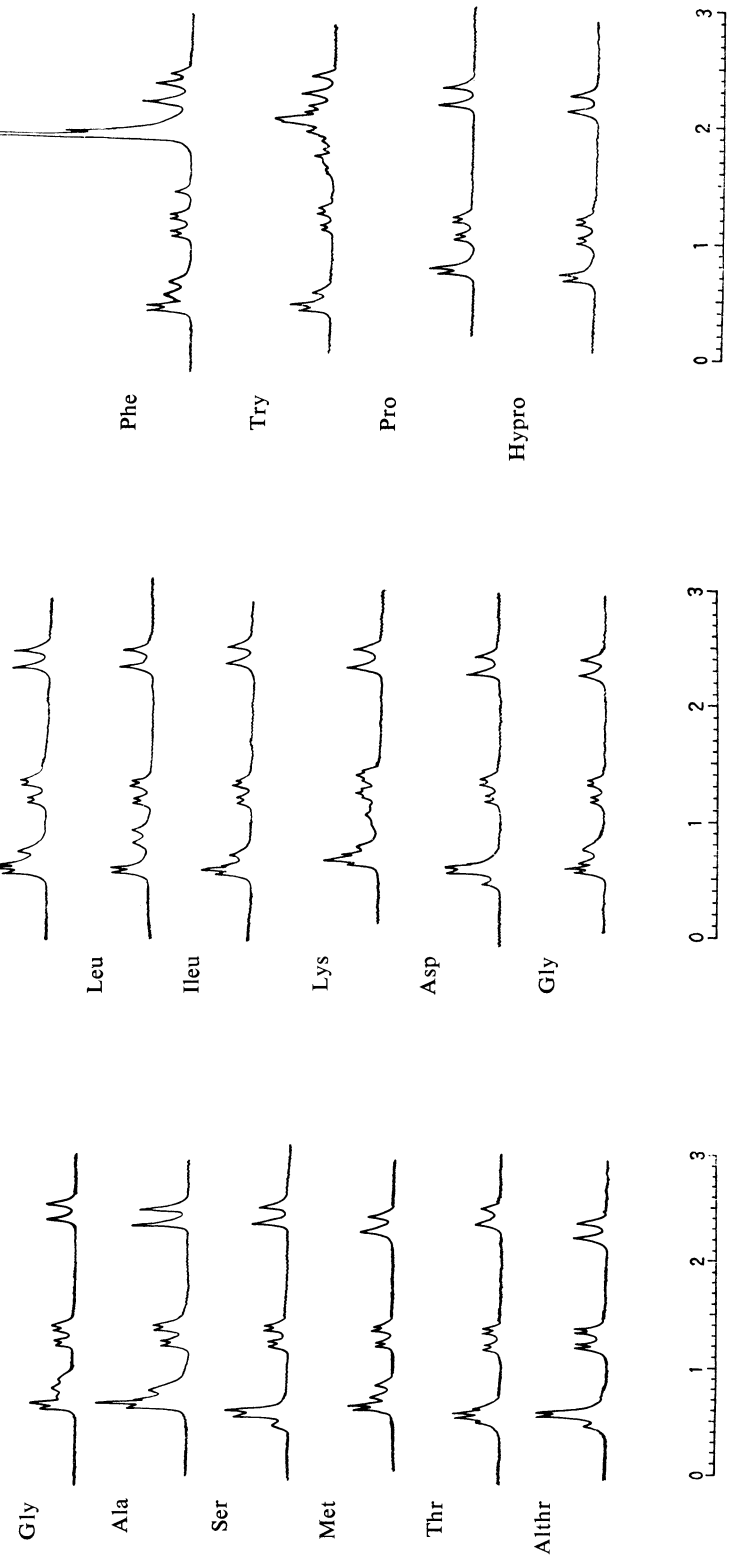


Fig. 1. The proton resonance spectra of the NH and 2,4-dinitrophenyl groups in DNP amino acids. Magnetic field increases from left to right.

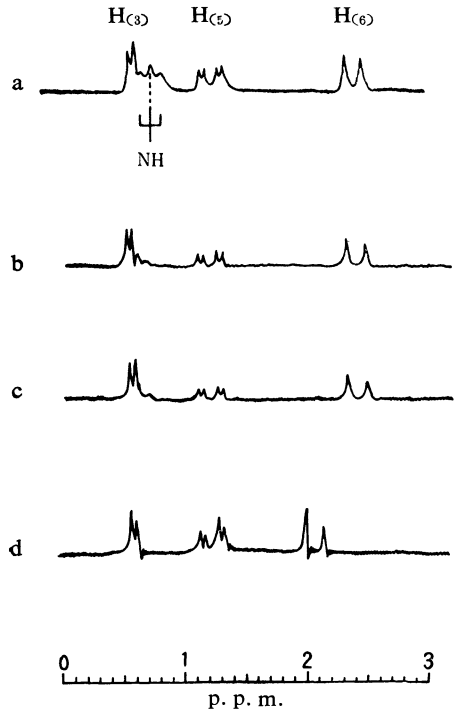


Fig. 2. The proton resonance spectra of DNP-glycine (a), (b) and (c) and of 2,4-dinitroaniline (d).
(a) Assignment of the signals. (b) Distortion of the NH proton signal caused by addition of a small amount of water. (c) The distortion by further addition of water.

In the spectra of DNP-proline and DNP-hydroxyproline, which have no NH proton, signals corresponding to those mentioned above are not observed. This also confirms the assignment of the NH proton signal.

The patterns of the spectra arising from the protons of the NH and DNP groups are sensitive to a slight change in the molecular structure. Thus, DNP-threonine and DNP-allothreonine can easily be discriminated. The same is true for DNP-leucine, DNP-isoleucine, and DNP-valine, and also for DNP-aspartic acid and DNP-glutamic acid.

In DNP-proline and DNP-hydroxyproline, the chemical shift between $H_{(3)}$ and $H_{(5)}$ is small compared with that in the other DNP

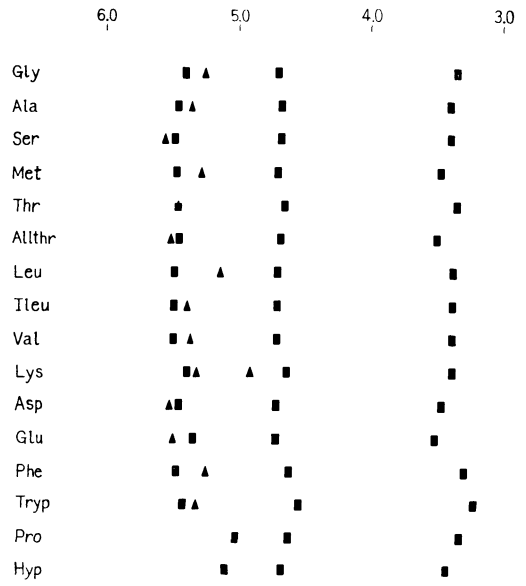


Fig. 3. Proton chemical shifts in p. p. m. of the NH and 2,4-dinitrophenyl groups referred to dioxane. Magnetic field increases from left to right. In the figure ▲ and ■ represent the center of the NH and CH proton signals, respectively.

amino acids. This may be interpreted in terms of a twisting of the NO_2 group at carbon 2 of the DNP group caused by the presence of the bulky 2-carboxy-1-pyrrolidyl group.

Signals due to alkyl chain protons cannot be identified in a dioxane solution. Therefore, an investigation of the signals of free amino acids in a D_2O solution is now in progress. The results will be discussed in the next paper.

Department of Chemistry
Faculty of Science
The University of Tokyo
Hongo, Tokyo (S. F.)

University of Electro-communications
Chofu, Tokyo (Y. A.)

Japan Atomic Energy Research Institute
Tokai-mura, Ibaragi (N. H.)

School of Medicine
The University of Tokyo
Hongo, Tokyo (H. M.)

*Accurate Determination of Interatomic Distances of Carbon Disulfide**

By Yonezo MORINO and Takao IIJIMA

(Received June 16, 1962)

In some recent studies[1,2] of molecular structure by gas electron diffraction, attentions have been paid to the physical meanings of various distance-parameters for comparing the results obtained by different techniques. In almost all cases, however, it has been impossible to show the consistency of the results of electron diffraction with those of spectroscopy because of the limited knowledge on the anharmonicity of molecular vibration.

The interatomic distances in a molecule are not constant but vary periodically because of the molecular vibrations. The distance averaged over the vibration is denoted by r_g in the sense that r_g is the center of gravity of the distribution function. In the studies of electron diffraction by gas molecules, we obtain r_g from the experimental data by a simple analytical procedure. In the spectroscopy, however, it is r_0 that is usually obtained from the rotational constant of the ground vibrational state. The r_g can be calculated if the equilibrium distance r_e and the anharmonic potential constants, especially the cubic constants, are known. Carbon disulfide is one of the simple molecules of which detailed spectroscopic data are available. The purpose of the present work is to examine if the results of the electron diffraction experiment are consistent with those of the spectroscopy by taking carbon disulfide as an example.

Among a number of spectroscopic studies for carbon disulfide, a high resolution Raman spectrum by Stoicheff[3], and an analysis of infrared rotation-vibration spectra by Guenther, Wiggins, and Rank[4], combined with another infrared study by Allen, Plyler and Blaine[5], provide us with information necessary for this work.

Calculation of r_g from Spectroscopic Data

An instantaneous distance of the C–S atom pair is expressed by

$$r = r_e + \Delta z + \frac{\Delta\rho^2}{2r_e} \tag{1}$$

in terms of internal coordinates, Δz and $\Delta\rho$, where Δz denotes the relative displacement of the atoms C and S along the molecular axis and $\Delta\rho$ is the relative displacement perpendicular to the axis. $\Delta\rho^2$ is sometimes written as $\Delta x^2+\Delta y^2$. By taking an average of Eq. 1 with respect to the distribution function, the average C–S distance r_q(C–S) is expressed by

$$r_g = r_e + \langle\Delta z\rangle + \frac{\langle\Delta\rho^2\rangle}{2r_e} \tag{2}$$

The internal coordinates Δz and $\Delta\rho$ are related to the normal coordinates by the following relations,

$$\Delta z_1 = b_1 q_1 + b_3 q_3 \tag{3a}$$

$$\Delta z_2 = b_1 q_1 - b_3 q_3 \tag{3b}$$

and

$$\Delta\rho^2 = b_{22}(q_{2a}^2 + q_{2b}^2) \tag{3c}$$

where Δz_1 and Δz_2 denote the displacements of the two C–S atompairs, respectively, and q's are the dimensionless normal coordinates which are related to the normal coordinate Q's as $q_i = 2\pi(c\omega_i/h)^{1/2}Q_i$. The coefficients b's are given by the standard treatment of normal vibrations, as

$$b_1 = \left(\frac{h\mu_s}{8\pi^2 c\omega_1}\right)^{1/2} \tag{4a}$$

$$b_3 = \left[\frac{h}{8\pi^2 c\omega_3}(\mu_s + 2\mu_c)\right]^{1/2} \tag{4b}$$

$$b_{22} = \frac{h}{8\pi^2 c\omega_2}(\mu_s + 2\mu_c) \tag{4c}$$

μ_s and μ_c are the inverse masses of S-atom and C-atom, respectively.

The $\langle\Delta z\rangle$ is thus calculated as,

$$\langle\Delta z\rangle = b_1\langle q_1\rangle \tag{5}$$

in terms of the average of the totally symmetric normal coordinate q_1, because the averages of all the linear terms of normal coordinates vanish except for the term of q_1. The general expression of $\langle q_1\rangle$ has been derived by Morino, Toyama and Oka[6], and it is reduced to the following equation for the case of a linear symmetric triatomic molecule,

* A part of this work was reported at the International Conference on Magnetism and Crystallography, Kyoto, September, 1961.

1) L. S. Bartell and R. A. Bonham, *J. Chem. Phys.*, **31**, 400 (1959).

2) L. S. Bartell and R. C. Hirst, ibid., **31**, 449 (1959).

3) B. P. Stoicheff, *Can. J. Phys.*, **36**, 218 (1958).

4) A. H. Guenther, T. A. Wiggins and D. H. Rank, *J. Chem. Phys.*, **28**, 682 (1958).

5) H. C. Allen, E. K. Plyler and L. R. Blaine, *J. Am. Chem. Soc.*, **78**, 4843 (1956).

6) Y. Morino, M. Toyama and T. Oka, to be published.

TABLE I. MOLECULAR CONSTANTS OF CS_2

ω_1^e	671.36 cm^{-1}	α_1	0.000156 cm^{-1}	k_{111}	−14.90 cm^{-1}	B_0	0.10910 cm^{-1}
ω_2^e	398.62 cm^{-1}	α_2	−0.000256 cm^{-1}	k_{122}	50.10 cm^{-1}	B_e	0.10928 cm^{-1}
ω_3^e	1551.92 cm^{-1}	α_3	0.000711 cm^{-1}	k_{133}	−129.56 cm^{-1}	r_e	1.5532 Å

$$\langle q_1\rangle = -\frac{1}{2\omega_1}\left[3k_{111}\coth\frac{hc\omega_1}{2kT} + 2k_{122}\coth\frac{hc\omega_2}{2kT} + k_{133}\coth\frac{hc\omega_3}{2kT}\right] + \left(\frac{8\pi^2 c\omega_1}{h\mu_s}\right)^{1/2}\frac{kT}{f_{11}r_e} \quad (6)$$

when the potential energy expression for a CS_2 type molecule is given by,

$$V = \frac{hc}{2}[\omega_1 q_1^2 + \omega_2(q_{2a}^2 + q_{2b}^2) + \omega_3 q_3^2] + hc[k_{111}q_1^2 + k_{122}q_1(q_{2a}^2 + q_{2b}^2) + k_{133}q_1 q_3^2] \quad (7)$$

The quartic and higher-order terms are neglected in this work, because the average interatomic distances are strongly affected by the asymmetric deformation of the distribution function which is mainly dependent on the cubic terms of the potential function. The first term of Eq. 6 is due to the anharmonicity of vibrations and the second term to the centrifugal stretching for which the mean rotational energy is approximated by kT. The f_{11} is the force constant of the totally symmetric stretching vibration. The $\langle\Delta\rho^2\rangle$ is simply calculated by inserting the relation $\langle q_i^2\rangle = (1/2)\coth(hc\omega_i/2kT)$, into Eq. 3c.

The cubic potential constants k_{ijk}'s are calculated from α_i's, the variation of the rotational constants which have been obtained through the relations[7],

$$\alpha_1 = -\frac{6B_e^2}{\omega_1} - 6\sqrt{2}\left(\frac{B_e}{\omega_1}\right)^{3/2}k_{111} \quad (8a)$$

$$\alpha_2 = -\frac{B_e^2}{\omega_2}\cdot\frac{3\omega_2^2+\omega_3^2}{\omega_2^2-\omega_3^2} - 2\sqrt{2}\left(\frac{B_e}{\omega_1}\right)^{3/2}k_{122} \quad (8b)$$

and $$\alpha_3 = -\frac{2B_e^2}{\omega_3}\cdot\frac{3\omega_3^2+\omega_2^2}{\omega_3^2-\omega_2^2} - 2\sqrt{2}\left(\frac{B_e}{\omega_1}\right)^{3/2}k_{133} \quad (8c)$$

The values of α_i's used and those of k_{ijk}'s obtained from them are listed in Table I.

As the result of numerical computation, $\langle\Delta z\rangle$ was found to be 0.0013 Å, which included the contribution of the centrifugal stretching 0.0003 Å, and $\langle\Delta\rho^2\rangle/2r_e = 0.0035$ Å was obtained for $T = 288°K$. Accordingly, r_g(C–S) is calculated to be

$$r_g(\text{C–S}) = r_e + \langle\Delta z\rangle + \frac{\langle\Delta\rho^2\rangle}{2r_e} = 1.5532 + 0.0013 + 0.0035 = 1.5580\text{ Å}$$

Similarly for the S–S distance,

$$r_g(\text{S–S}) = r_e + \langle\Delta z_1 + \Delta z_2\rangle = r_e + 2\langle\Delta z\rangle = 3.1064 + 0.0026 = 3.1090\text{ Å}$$

where it is noted that $\Delta\rho$ is zero for the S–S distance.

The apparent non-linearity or the shrinkage[8] $\delta_g = 2r_g(\text{C–S}) - r_g(\text{S–S})$ is equal to $\langle\Delta\rho^2\rangle/r_e$, and it was found to be 0.0070 Å by the calculation.

According to Stoicheff[3], $\alpha_1 = 0.00018\ cm^{-1}$ may be preferable when the effect of Fermi resonance is considered. This alternative value of α_1 leads to $k_{111} = -16.27\ cm^{-1}$ and $\langle\Delta z\rangle = 0.0011$ Å. The equilibrium distance r_e is also affected by this change: it becomes 1.5530 Å. However, the average distance r_g is little altered: it was found to be 1.5579 Å. Therefore, the uncertainty in the value of α_1 due to Fermi resonance gives no serious error in the present study.

Measurement of r_g by Electron Diffraction

Experimental.—The diffraction photographs were taken by the apparatus[9,10] equipped with an r^3-sector, with the camera length of 12 cm. and the accelerating voltage of about 45 kv which was calibrated by the transmission pattern of a gold-foil. The beam current was about 0.025 μamp., and the exposure time was about 3 min. Fuji Process Plates were used to record the diffraction patterns and developed by the FD-131 developer at 20°C.

Three photographic plates were mounted in the camera at one time, fixed on a disk which was held nearly perpendicular to the main beam. Each plate was set at the exposure position one by one, by rotating the disk from outside. Photographic plates in the unit are, therefore, not exactly but only nearly perpendicular to the beam, so that the value of $L\lambda$ obtained by measuring the diameter of the gold-foil pattern recorded along the edge of the plate may differ from that of the diffraction pattern recorded on the center of the plate. The correction factor for $L\lambda$ was obtained by taking the photographs of gold-foil patterns both on the edge and on the center of the plate. The measurement was repeated

7) H. H. Nielsen, *Revs. Modern Phys.*, **23**, 90 (1951).

8) Y. Morino, J. Nakamura and P. W. Moore, *J. Chem. Phys.*, **36**, 1050 (1962).

9) T. Ino, *J. Phys. Soc. Japan*, **8**, 92 (1953).

10) Y. Morino et al., "Jikken Kagaku Koza", Vol. 3, Maruzen Co. Ltd., Tokyo (1957), p. 253.

four times, that is, for twelve (4×3) plates and two gold-foil patterns on each, the corrections of $L\lambda$ were found to be,

A $-0.3\pm0.03\%$
B $0.0\pm0.05\%$
C $0.0\pm0.03\%$

for the three positions, A, B and C, of the plate on the disk, with the standard deviations among the four measurements.

In order to get the exact value of the camera length for the photograph of the gas electron diffraction, the reference gold-foil should be put at the same place as the center of the gas distribution at the nozzle. It was confirmed by an examination with a microscope that there was no considerable deficiency in the geometrical design and in the screwing mechanism of the nozzle. There is, however, an anxiety pointed out by Murata[11], that the center of the gas distribution might deviate slightly backwards, because the nozzle aperture has an asymmetric form along the beam axis, i. e., it is widened at the front side by a cone-shape cut to avoid the shielding of the scattered beam by the edge. The effect was examined by taking diffraction photographs with the nozzle turned around by 180°. The result showed no significant deviation as compared with the results of the ordinary nozzle orientation. This is in contrast to the case of $SiCl_4$[11] for which a slight deviation was really observed. The difference might be caused by the different rates of flow of gas samples.

The photographs were traced with a Rigaku-Denki MP-3 microphotometer. The full scale of the transmittancy axis on the recording chart is 24 cm. As it is not wide enough to record minute feature of diffraction patterns, an expanding device was attached to the unit to facilitate expanded recordings along the transmittancy axis, in the scale five times as large as the ordinary one.

During the tracing, the plate was rotated around the center of the pattern to average out irregularities. The recorded photometer curve became narrower as the plate was rotated more rapidly. It was observed, however, that when the pen of the recorder showed no high-frequency vibration due to the irregularities as the result of a rapid rotation, a remarkable retardation of the recording took place, presumably because of the inertia of the recording system. Accordingly, the speed of rotation was kept rather slow, about 150~500 r. p. m., and varied during the scanning so as to maintain a high-frequency vibration of the pen in an appreciable amplitude. (The width is 0.5~1 mm.)

To avoid ambiguity caused by the calibration of density into intensity of scattered electrons, the exposure was kept in the range where the linearity held between density and intensity. The linearity was shown to be valid in the range of density less than 0.6, by an application of the pair method[12] to the diffraction patterns of a gold-foil. It was confirmed for FD-131 (diluted twice in volume and developed for 5 min. at 20°C) and for D72 (diluted twice in volume, developed for 3 min. at 20°C), but the linearity was found rather poor for D76.

The nozzle was covered with a liquid-air trap though not in contact with it. The temperature decrease of the nozzle was tested with a thermocouple inserted in place of the nozzle-head. Even after the trap was charged with liquid-air, no temperature decrease was observed unless the gas was led into the apparatus. By the same rate of gas flow as in the experiment, a decrease of 5°C was observed. The temperature decrease due to adiabatic expansion of the gas was estimated to be negligibly small. Therefore it seems reasonable to assume that the temperature of gas molecules is nearly equal to the room temperature.

The lattice constant of the gold-foil used in the present study was examined by two methods. By an X-ray diffractometer, Geigerflex, the lattice constant was determined to be $a_0=4.072\pm0.003$ Å, from four diffraction peaks, (400), (331), (420) and (422), obtained by Cu-$K\alpha$. On the other hand, the lattice constant was also confirmed by the comparison of electron diffraction rings of the foil with those of thallium chloride which was proved by H. Reather* to be suitable for the use as a standard substance of wavelength measurement. An evaporated film of TlCl was deposited on a thinned gold-foil and diffraction rings of gold and TlCl were recorded simultaneously on a photographic plate by 45 kv electron beam. By taking the value of the lattice constant of TlCl, 3.8424 Å, (or 3.8347 kX[13]), the lattice constant of the gold foil was determined to be $a_0=4.067\pm0.003$ Å.

A mean of this value and that obtained by the X-ray diffraction leads to the value $a_0=4.070\pm0.002$ Å. This is 0.2% smaller than the value for pure gold, 4.078 Å**, probably became copper was contained by an amount of ca. 0.55% by weight. Chemical analysis revealed that the amount of copper in the gold-foil used in the present study was 0.47% by weight.

Analysis.—The analysis of the intensity curves to obtain molecular intensity and radial distribution curve was carried out by the same procedure as that usually applied. Elastic scattering factors given by several authors are compared in Fig. 1, and the values on the full line, those by McWeeny[16] and Berghuis et al.[15] for C-atom, and those by Tomiie and Stam[17] for S-atom, were used in the present analysis. The phase factors due to the failure of the Born approximation were obtained from the table calculated by Ibers and Hoerni[19].

11) Y. Morino and Y. Murata, to be published.
12) J. Karle and I. L. Karle, *J. Chem. Phys.*, **18**, 957 (1950).

* Private Communication.
13) M. Straumanis, A. Ievinš and K. Karlsons, *Z. physik. Chem.*, **B42**, 143 (1939).
14) E. R. Jette and F. Foote, *J. Chem. Phys.*, **3**, 605 (1935).
** The X-ray value of the lattice constant of gold usually adopted is 4.070[14], but it is to be noted that this is expressed in kX unit, not in Å. (1 kX=1.0020 Å)
15) J. Berghuis and C. H. MacGillavry et al., *Acta Cryst.*, **8**, 478 (1955).
16) R. McWeeny, ibid., **4**, 513 (1951).
17) Y. Tomiie and C. H. Stam, ibid., **11**, 126 (1958).
18) H. Viervoll and O. Ogrim, ibid., **2**, 277 (1949).
19) J. A. Ibers and J. A. Hoerni, ibid., **7**, 405 (1954).

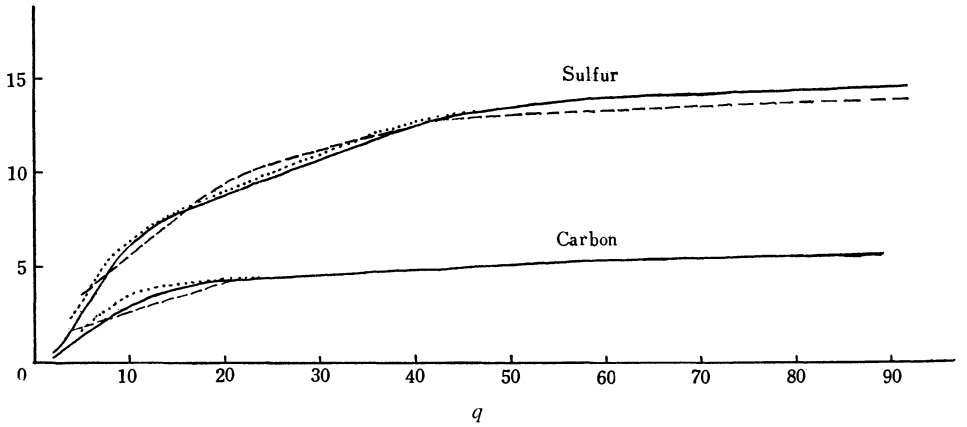


Fig. 1. The atomic scattering factors of carbon and sulfur.
—— Refs. 15 and 16 for carbon, and Ref. 17 for sulfur
..... Ref. 18
--- Ref. 19

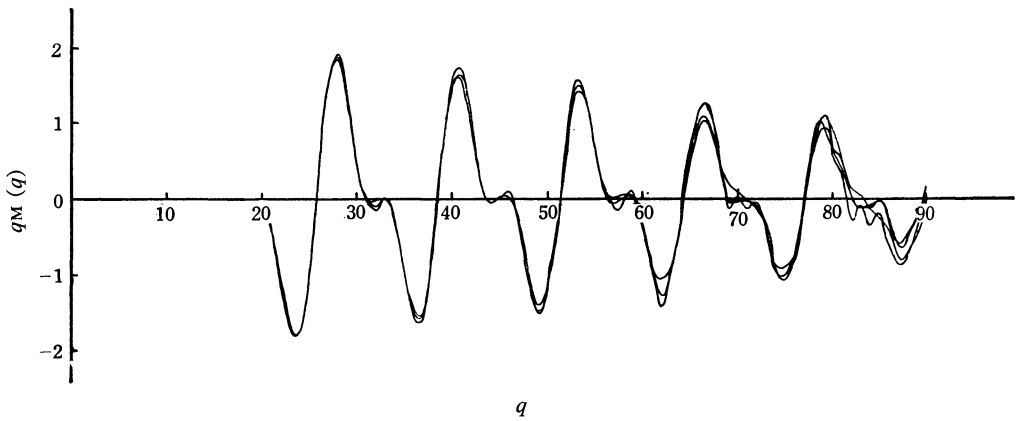


Fig. 2. The four observed molecular intensity curves of CS_2.

Inelastic scattering factors were calculated by the function given by Bewilogua[20].

Least-Squares Analysis[21,22].—Four molecular intensity curves were separately analyzed by the least-squares method described in the previous paper[21]. Each molecular intensity curve was fitted to the following equation,

$$F=i\{C_1(1/r_a'_1)\exp(-a_1s^2)\sin r_a'_1s + C_2(1/r_a'_2)\exp(-a_2s^2)\sin r_a'_2s\} \quad (9)$$

where the subscript 1 denotes the atom pair of C–S, and 2 the atom pair of S–S, and r_a' stands for $r_a-\kappa s^2$. Rigorously speaking, the r_a' in the denominators should be r_e, but it can be approximated by r_a', as adopted in the present treatment. The coefficients C's are,

$$C_1=\frac{4|F_c^e(s)||F_s^e(s)|\cos\Delta\eta}{\sum_i|F_i^e(s)|^2+\sum_i s_i(s)} \quad (10a)$$

$$C_2=\frac{2|F_i^e(s)|^2}{\sum_i|F_i^e(s)|^2+\sum_i S_i(s)} \quad (10b)$$

F_i^e and S_i denote the elastic and the inelastic scattering factors of atom i, respectively.

The distance-parameter r_a' to be determined by this method should be interpreted as the weighted mean of $r_a-\kappa s^2$, averaged over the observed range of s. It is not successful to attempt to determine κ as one of the parameters of the least-squares treatment, except for the case when κ is sufficiently large. The magnitude of κ theoretically expected is of the order of 10^{-6} A^3, and it was shown in the study of $GeCl_4$ that the magnitude of the standard deviation of κ was equal to or ten times as large as κ itself[21]. Therefore no significant value of κ can be expected to be determined.

20) L. Bewilogua, *Physik. Z.*, 32, 740 (1931).
21) Y. Morino, Y. Nakamura and T. Iijima, *J. Chem. Phys.*, 32, 643 (1960).
22) O. Bastiansen, K. Hedberg and L. Hedberg, ibid., 27, 1311 (1957).

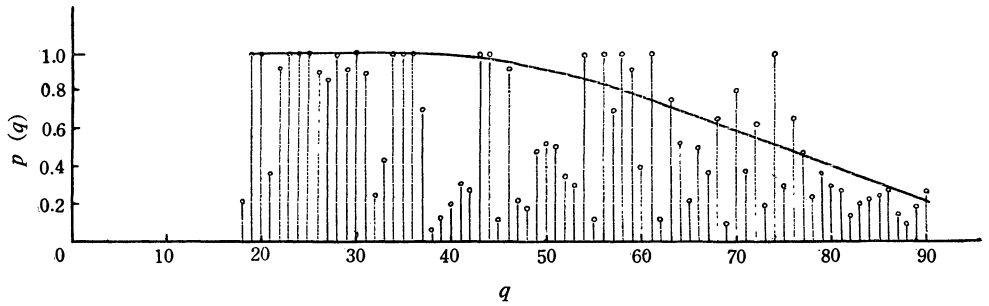


Fig. 3. The weight function: The weight determined as inversely proportional to σ^2 at each q. The smooth curve shows the general tendency.

Moreover the value of r_a may be strongly affected by the correlation between r_a and κ. Accordingly, it is more reasonable to determine the value of r_a from r_a' by the use of κ calculated from the cubic term of the distribution function.

In order to estimate the weight of the observed values of the molecular intensity at each q, $(q=(10/\pi)s)$, the standard errors of the molecular intensity were evaluated by the fluctuation among the four molecular intensity curves. The weight function was assumed to be inversely proportional to the square of the standard error at each q. It is graphically shown in Fig. 3. The results of the least squares calculation obtained by the discontinuous weight function coincided with those obtained by taking the smooth function which expresses the general tendency of the observed $1/\sigma^2$. By the second refinement of the least-squares, the convergence of the parameters was found to be sufficiently good. The results are tabulated in Table II. As the standard deviations σ are nearly the same for every intensity curve, the greatest ones are tabulated.

The standard deviations σ_{av} attached to the averaged values were evaluated from the fluctuation among the results of four intensity curves. It is expected that σ_{av} is nearly equal to $1/\sqrt{4}$ of the σ of the parameters determined for an individual curve, if sufficiently large number of plates are analyzed, or it may be somewhat greater because of the possible systematic errors independently included in each plate. The expectation that σ_{av} is almost equal to $(1/\sqrt{4})\sigma$, is nearly realized, and it may accordingly be stated that the systematic error specific to each plate is not a predominant factor.

Table II. The results of the least squares treatment

Plate	Index	r_a'(C-S)	r_a'(S-S)	l(C-S)	l(S-S)
I	0.97	1.5564	3.1085	0.0347	0.0481
II	1.00	1.5590	3.1136	0.0368	0.0484
III	1.01	1.5572	3.1121	0.0419	0.0515
IV	1.02	1.5587	3.1133	0.0368	0.0509
σ	0.02	0.0011	0.0016	0.0020	0.0022
Average	1.00	1.5578	3.1119	0.0376	0.0497
σ_{av}	0.01	0.0006	0.0012	0.0015	0.0008

Corrections.—As was stated in the preceding section, the distance r_a' is related to the r_a as,

$$r_a' \cong \langle r_a - \kappa s^2 \rangle_s = r_a - \kappa \langle s^2 \rangle_s \qquad (11)$$

where κ is related to the cubic coefficient β_3 of the distribution function as[21],

$$\kappa = l^6 \cdot \beta_3 \qquad (12)$$

and

$$\langle s^2 \rangle_s = \sum_s p(s)s^2 / \sum_s p(s) \qquad (13)$$

Thus κ for C–S was estimated to be 1.0×10^{-6} Å^3, and similarly 0.6×10^{-6} Å^3 for S–S. The weighted mean of s^2 was roughly estimated to be 250 Å^{-2}, and therefore $\kappa\langle s^2\rangle$ is 0.3×10^{-3} Å for C–S and 0.2×10^{-3} Å for S–S, respectively*. Accordingly, we have,

r_a(C–S): 1.5581 Å

and r_a(S–S): 3.1121 Å

The average interatomic distances r_g are easily obtained from r_a by the relation[21],

$$r_g = r_a + \frac{l^2}{r_e} \qquad (14)$$

With values of l^2/r_e, 0.0011 Å for C–S, and 0.0005 Å for S–S, the final results were obtained as follows,

r_g(C–S): 1.5592 Å

and r_g(S–S): 3.1126 Å

The root mean square amplitudes were corrected for the finite sample size around the

* Rigorously speaking,

$$\frac{\sum_s p(s)s^4\exp(-2as^2)\cos^2 r_a s}{\sum_s p(s)s^2\exp(-2as^2)\cos^2 r_a s}$$

should be taken in place of $\langle s^2\rangle_s$, if the correlation is assumed to be considerable only between r_a and κ. This expression was estimated to be nearly 300 Å^{-2}. Therefore the approximation by $\langle s^2\rangle_s$ is practically acceptable.

nozzle, by −0.0012Å for C–S and −0.0049Å for S–S, respectively. These corrections were calculated from the distribution of the gas molecule, which was estimated by the discrepancy of the observed background intensity from the theoretical one in the region of q larger than 70[23]. Thus the corrected values of l's are,

l(C–S) : 0.0364Å

and l(S–S) : 0.0448Å

Estimation of Reliabilities.—The reliabilities of the results of the present work are indicated by *the 99 per cent confidence intervals*, where both random and systematic errors were taken into consideration. The greater of the σ_{av} and $(1/\sqrt{4})\sigma$ of each parameter was regarded as the standard deviation originating from the random error, and 2.5 times that amount was considered to specify the 99 per cent confidence interval in the sense that the probability of finding the result of any observation outside this interval would be less than 1%[24].

The sources and the amounts of several systematic errors for both interatomic distances and root mean square amplitudes were thoroughly examined by Kuchitsu[23]. Although most of his estimates remain valid in the present work, there are required slight modifications due to some differences in experimental and analytical procedures. The systematic errors not negligible were estimated as follows corresponding to the 99 per cent confidence intervals, although there was no statistical evidence available to show that they were really so.

i) For atomic distances.

The drift of the wavelength of the primary electron beam ; 0.05%. (The accelerating voltage was regulated constant within 0.1%.)

Uncertainty of the lattice constant of the gold-foil ; 0.05%.

Errors associated with the corrections for the inclination of plates ; 0.075%. (From the standard deviations σ_A, σ_B and σ_C of the correction factors for the three plate-positions A, B and C, the standard deviation σ_P due to this correction was estimated for the average value obtained from four plates by

$$\sigma_P=\frac{1}{4}[\sigma_A{}^2+(2\sigma_B)^2+\sigma_C{}^2]^{1/2}$$

because these four consisted of one photographed at A, two at B and one at C. The 2.5 times σ_P was found to be 0.075%.)

Thus the total amounts to 0.10%, because these systematic errors are independent of each other.

ii) For root mean square amplitudes.

Errors associated with the correction for the distribution of gas molecules ; 1% for C–S, 4% for S–S. (They were tentatively taken as 50% of the correction.)

Uncertainty of the values of η in the correction for the Born approximation ; 2% for C–S.

Errors due to the arbitrary choice of the weight function[11] ; 2%.

Thus the total amounts 3% for C–S and 5% for S–S, respectively.

The confidence intervals were estimated from the square root of the sum of $(2.5\sigma)^2$ and (systematic error)^2, as summarized in Table III, and the final results of the present work are listed in Table IV, in comparison with the values calculated from the spectroscopic data.

TABLE III. ESTIMATION OF THE 99 PER CENT CONFIDENCE INTERVALS

	σ (random)	System. error	2.5σ (random)	Confidence interval
i	0.01		0.025	0.029
r_g(C–S)	0.0006	0.0016	0.0015	0.0022
r_g(S–S)	0.0012	0.0031	0.0030	0.0044
l(C–S)	0.0015	0.0012	0.0038	0.0040
l(S–S)	0.0011	0.0025	0.0028	0.0038

TABLE IV. INTERATOMIC DISTANCES, ROOT-MEAN-SQUARE AMPLITUDES AND SHRINKAGE OF CS_2 AT 15°C, WITH THE 99 PER CENT CONFIDENCE INTERVALS

	E. D.	Spectr.
Index i	1.00 ±0.03	
r_g(C–S)	1.5592±0.0022 Å	1.5580±0.0005 Å
r_g(S–S)	3.1126±0.0044 Å	3.1090±0.0010 Å
l(C–S)	0.0364±0.0040 Å	0.0391 Å
l(S–S)	0.0448±0.0038 Å	0.0412 Å
δ_g	0.0058±0.0042 Å	0.0070 Å

Conclusion

As shown in Table IV, the results obtained by electron diffraction are in good agreement with those obtained from spectroscopic data. Thus the consistency between electron diffraction and spectroscopy has been well confirmed : it gives a support to the present interpretation of the distance-parameters and the effect of molecular vibrations upon them. Moreover, it should be noted that the r_0 of the C–S distance obtained by spectroscopy is 1.5545± 0.0003Å, and r_e is 1.5532±0.0005Å[3], and they are significantly shorter than the r_g obtained by electron diffraction. This fact clearly shows that it is important to take accurately the physical meanings of various distance-parameters

23) K. Kuchitsu, This Bulletin, 32, 748 (1959).
24) W. A. Wallis and H. V. Roberts, "Statistics", The Free Press, Glencoe, Illinois (1956), p. 456.

into consideration, in comparing them with each other. The shrinkage effect has been confirmed as well.

The authors wish to express their gratitude to Professor Hidetoshi Takahashi and his co-workers, in the Department of Physics, for the use of PC-1 computer. They are indebted to the Central Research Institute of Mitsubishi Metal Industry Co. Ltd., for the chemical analysis of the gold-foil. They are also indebted to the Ministry of Education of Japan for the research grant.

Department of Chemistry
Faculty of Science
The University of Tokyo
Hongo, Japan

Assignments of the ^{35}Cl Nuclear Quadrupole Resonance Spectra in Multichlorobenzenes by the Measurement of the Zeeman Effect

By Yonezo MORINO, Masaharu TOYAMA, Koichi ITOH* and Saburo KYONO

(Received June 26, 1962)

The ^{35}Cl nuclear quadrupole resonance lines in multichlorobenzenes were first assigned by Bray, Barnes, and Bersohn to the chlorine atoms in the molecules[1]. The assignment was, however, based on the assumption that the atoms having more numbers of ortho chlorine neighbors give rise to the resonances at the higher frequencies. This assumption is supported by the fact that the resonance frequencies in *ortho*-dichlorobenzene are higher than those in meta- and para-derivatives. The frequency shifts were interpreted in terms of the induction effect due to the substituted chlorine atoms, in particular, at the ortho neighbors. For the confirmation of this effect, it is necessary to make assignments without any assumption for the derivatives with more than two chlorine atoms. The Zeeman effect of a single crystal is suitable for this purpose, as was shown in the study of benzene hexachlorides[2].

A quadrupole resonance line splits into several Zeeman components in the presence of a static magnetic field. The splittings depend on the orientation of the applied field with respect to the principal axes of the electric field gradient at the nucleus. It has been realized that in the case of the chlorine atom in a C–Cl bond, the bond direction coincides to a high degree of approximation with that of the principal z axis, the direction giving the largest component of the electric field gradient ($|q_{xx}| \leqq |q_{yy}| \leqq |q_{zz}|$). The bond direction can, therefore, be determined by observing the angular depedence of the Zeeman effect in a single crystal. If the crystal structure is known, each resonance frequency can be assigned to one of chlorine atoms in a unit cell, by comparing the directions of the z axes with those of the C–Cl bonds, or the observed Zeeman patterns with those expected from the structure. Even when the crystal structure is unknown, the assignment is made to some extent, if the molecular structure can be inferred from other information: for instance, the resonance lines due to two chlorine atoms disposed mutually at the para positions of a benzene ring are expected to display the same Zeeman patterns at any orientation of the applied field.

The present study was originally made for the purpose to investigate the steric repulsion between the ortho chlorine neighbors in multichlorobenzenes. It was reported by Bastiansen and Hassel that the interatomic distances in hexachlorobenzene observed in electron diffraction were accounted for with assuming the distortion of the C–Cl bonds by 12° successively above and below the plane of the benzene ring[3]. The samples studied in the present work are 1, 3, 5-trichlorobenzene, 1, 2, 3, 4-tetrachlorobenzene and pentachlorobenzene. In 1, 3, 5-trichlorobenzene, the principal z axis of a chlorine atom was found to be inclined at $1.6 \pm 1.0°$ with respect to the plane determined by those of the other two[4]. Since the chlorine atoms in this

* Present address: The Institute for Solid State Physics, The University of Tokyo, Minato-ku, Tokyo.

1) P. J. Bray, R. G. Barnes and R. Bersohn, *J. Chem. Phys.*, **25**, 813 (1956).

2) Y. Morino, T. Chiba, T. Shimozawa, M. Toyama and K. Itoh, *Rev. Univ. des Mines*, 9e Sér. T. XV, 591 (1959).

3) O. Bastiansen and O. Hassel, *Acta Chem. Scand.*, **1**, 489 (1947).

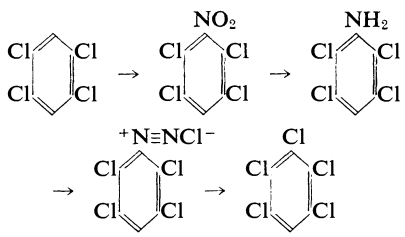
4) Y. Morino and M. Toyama, *J. Phys. Soc. Japan*, **15**, 288 (1960).

molecule are substituted at the meta positions with respect to one another, the observed distortion was attributed to the effect of crystal field. In the other compounds, it was difficult to prepare single crystals large enough for the Zeeman study. The crystals obtained were imperfect so that it was unsuccessful to perform a precise determination of the principal axes[5]. This article will present the assignments of the spectral lines for these multichlorobenzenes made in the course of the investigations.

Experimental

A self-quenched super-regenerative oscillator-detector of Dean's type[6] was used for detecting the absorption spectra. The signals detected were suitably amplified by a narrow-band amplifier, and then recorded through a phase-sensitive detector followed by a pen-recorder, for obtaining a high signal-to-noise ratio. The modulation frequency was 230 c/sec. and the quench frequency was nearly 50kc./sec. The magnet used for the Zeeman study was an air-cooled Helmholtz coil described previously[7], which supplied up to 150 gauss of magnetic field in the continuous operation. All the Zeeman experiments were carried out at room temperature.

The sample of pentachlorobenzene was synthesized from 1, 2, 4, 5-tetrachlorobenzene by Sandmeyer's method:



The product recrystallized from alcoholic solution was colorless needle-like crystals with m. p. 84~85°C. The infrared spectrum indicated little contamination in the reactants and the intermediate products. Further purification was performed by the repetition of zone-melting to remove impurities at the tracer level. The existence of such a small amount of impurities as those detected neither by the melting point nor by the infrared spectrum made the intensity of the nuclear quadrupole resonance spectrum considerably weak. For other samples, use was made of the commercial products after the purification by the similar procedures.

Single crystals were prepared by Bridgeman's method[7]. The apparatus for this purpose was an electric furnace, whose lower end was followed by a cooler place to give a large temperature gradient between the two regions. About 10 g. of each sample, put in an evacuated glass ampule with a capillary sealed at the bottom, was heated in the furnace and then slowly lowered down into the cooler place (at a rate of 2~4 mm./hr.). A single crystal gradually grew up from the bottom of the capillary, when it came to this cooler region.

Results

1, 3, 5-Trichlorobenzene

Zeeman study was made for three ^{35}Cl resonance lines designated ν_a, ν_b and ν_c in the order of increasing frequency, as was reported previously[4]. In Table I are listed the quadrupole coupling constants, the asymmetry parameters of the electric field gradients, and the direction cosines of the principal z axes with respect to the symmetry axes of the crystal, X, Y and Z. The relative orientation of the principal axes led to the unit-cell structure with the orthorhombic symmetry. The analysis of the crystal structure by X-ray diffraction was reported by Milledge and Pant[8]. As was expected from the Zeeman study, the crystal was found to be orthorhombic with the space group $P2_12_12_1$ and the unit-cell dimensions:

TABLE I. QUADRUPOLE COUPLING CONSTANTS, ASYMMETRY PARAMETERS, AND DIRECTION COSINES OF THE PRINCIPAL AXES AND OF THE CORRESPONDING C-Cl BONDS WITH RESPECT TO THE CRYSTAL AXES IN 1,3,5-TRICHLOROBENZENE

Lines (^{35}Cl)		eQq_{zz}[a] Mc./sec.	η	Direction cosines			$\Delta\alpha$[b]
				a(X)	b(Y)	c(Z)	
ν_a	z axis	71.1_2	0.09_3	-0.423_1	0.864_7	0.270_8	1.1°
	C-Cl_3			-0.436_4	0.854_9	0.280_6	
ν_b	z axis	71.8_6	0.11_1	-0.474_4	-0.865_9	0.158_9	1.1°
	C-Cl_1			-0.486_1	-0.861_9	0.144_2	
ν_c	z axis	72.2_8	0.12_9	0.913_6	-0.000_0	-0.406_7	0.8°
	C-Cl_5			0.908_1	-0.006_2	-0.418_7	

a) The value extraporated to 0°K.
b) The angle between the principal z axis and the corresponding C-Cl bond.

5) Recently, Dean, Richardson and Sakurai also made a Zeeman study of 1, 2, 3, 4-tetrachlorobenzene [*Molecular Physics*, **4**, 95 (1961)]. Their results showed that the molecule was planar within ±3/4°. Bastiansen reinvestigated hexachlorobenzene by the electron diffraction method and concluded a planar structure, in contrast with the previous results (private communication).

6) C. Dean and M. Pollak, *Rev. Sci. Instr.*, **29**, 630 (1958).

7) Y. Morino, T. Chiba, T. Shimozawa and M. Toyama, *J. Phys. Soc. Japan*, **13**, 869 (1958).

8) H. J. Milledge and L. M. Pant, *Acta Cryst.*, **13**, 285 (1960).

$a=13.93$ Å, $b=13.19$ Å, $c=3.91$ Å
and $Z=4$ at 20°C

Fractional coordinates in the unit-cell were also given for each constitutive atom.

The assignment of spectral lines is made by comparing the directions of the principal z axes with those of the C–Cl bonds calculated from the fractional coordinates. The results are best explained by assigning the lines ν_a, ν_b and ν_c to the atoms Cl_3, Cl_1 and Cl_5, respectively, with the symmetry axes X, Y and Z corresponding to the crystal axes *b*, *a* and *c*, respectively. Here the suffixes 1, 3 and 5 represent the ring positions designated by Milledge and Pant. Agreement of the directions of the principal z axes with those of the C–Cl bonds is satisfactory as seen in Table I. Table II shows the mutual angles of the principal z axes of the three chlorine atoms in a molecule and those of the corresponding C–Cl bonds. It is to be noted that each principal z axis is appreciably inclined with respect to the plane determined by the remaining two, while the three C–Cl bonds are coplanar within the experimental uncertainty. In this respect the further improvement of the X-ray analysis would be desirable.

Table II. Angles between the principal z axes of the field gradients and those between the corresponding C–Cl bonds in 1, 3, 5-trichlorobenzene

	Cl_1Cl_3	Cl_3Cl_5	Cl_5Cl_1	$\Delta\theta$[a]
z Axes	120.3°	119.8°	119.9°	1.6°
C–Cl bonds	119.0°	121.3°	119.8°	0.0°

a) The angle which each z axis or each C–Cl bond makes with respect to the plane determined by the remaining two. The experimental uncertainty is estimated to be ±1.0° for the Zeeman study and ±2.5° for the X-ray study.

1, 2, 3, 4-Tetrachlorobenzene

Four resonance lines were observed by Bray et al.[1]: $\nu_a=36.297$, $\nu_b=36.333$, $\nu_c=36.635$ and $\nu_d=36.763$ Mc./sec. at 301°K; the two lower frequency lines ν_a and ν_b coalesce to one line at the liquid-nitrogen temperature. The crystal structure has not been reported. The present Zeeman study of a single crystal revealed that the lines ν_a and ν_b gave similar Zeeman patterns at any orientation of the applied magnetic field, while ν_c and ν_d gave the patterns different from any of others. The lines ν_a and ν_b are, therefore, assigned to the pair of chlorine atoms Cl_1 and Cl_4, which are substituted at the para positions with respect to each other, and the lines ν_c and ν_d to Cl_2 and Cl_3. The assignments completely agree with those expected by Bray et al.

Pentachlorobenzene

Five resonance lines were observed by Bray et al.[1] (Table III). with the single hydrogen atom bonded to the ring carbon 1, they also made a tentative assignment on the basis of Hammett sigma values and the frequency grouping: two lowest frequencies ν_a and ν_b to the chlorines 2, 6; a middle frequency ν_c to the chlorines 3, 5; two highest frequencies ν_d and ν_e to the chlorine 4. The assignment, however, seems to be very unusual. If it were true, the relative intensity of the five resonance lines should be 1 : 1 : 2 : 1/2 : 1/2 in the order of increasing frequency. In the actual spectrum, all the lines have nearly the same absorption intensities, and do not split further by the change in temperature.

The study with a single crystal indicates that the resonace lines are classified into three groups: (ν_a, ν_c), (ν_b, ν_e) and ν_d. The lines in each group show the Zeeman pratterns similar to each other but entirely different from those in other groups. The single line ν_d is then assigned to the chlorine 4 whose bond direction is different from those of other chlorines. The other line pair, (ν_a, ν_c) or (ν_b, ν_e), is assigned to either of the atom pairs, (Cl_2, Cl_5) or (Cl_3, Cl_6), the atoms in each pair being substituted at the para positions with respect to each other. Here eight possible choices of the assignments remain unexcluded, as shown in Table III. For

Table III. Assignments of the ^{35}Cl resonance frequencies in pentachlorobenzene with the single hydrogen atom bonded to carbon 1

Resonance frequency at 306°K, Mc./sec.	Assignment[a]								
	I	I′	II	II′	III	III′	IV	IV′	0
ν_a 36.782	2	6	2	6	5	3	5	3	2,6
ν_b 36.961	6	2	3	5	6	2	3	5	6,2
ν_c 37.112	5	3	5	3	2	6	2	6	3,5
ν_d 37.413	4	4	4	4	4	4	4	4	4
ν_e 37.512	3	5	6	2	3	5	6	2	4

a) The assignments I–IV′ are the possible ones revealed by the present Zeeman study, of which I and I′ are the most probable. The last column 0 presents the assignment by Bray et al.

discussing the effect of the ortho chlorine neighbors, it is necessary to assign each line to each atom in the molecule. It is, however, impossible by the present study alone. An assumption, which is not so serious as that made by Bray et al., will be employed here: the line of the highest frequency ν_e comes from one of the atoms Cl_3, Cl_4 and Cl_5, and that of the lowest one ν_a from the atom Cl_2 or Cl_6. The possible assignments are then reduced to the two cases denoted by I and I′ in Table III. These two cases are completely equivalent to each other, so long as the effect of the crystal field is ignored. The result is more reasonable than that by Bray et al., since one absorption line corresponds to one chlorine atom in a molecule. It is to be noted that the line ν_d is assigned without any assumption to the Cl_4, and the line of the highest frequency ν_e to the other one.

The angular dependence of the Zeeman patterns suggests that the orientation of the molecules in a unit-cell is symmetric with respect to three planes perpendicular to one another. It is then likely that the crystal system is orthorhombic with $Z=4$, the molecules in a unit-cell being all equivalent to one another.

Discussion

First of all it should be noted that the four resonance lines in 1, 2, 3, 4-tetrachlorobenzene have been grouped into two groups: two lower frequencies due to Cl_1 and Cl_4 and two higher ones due to Cl_2 and Cl_3; similarly the five resonance lines in pentachlorobenzene into two groups: two lower frequencies due to Cl_2 and Cl_6 and three higher ones due to Cl_3, Cl_4 and Cl_5. This fact indicates that the intramolecular effect is of predominant importance for the shifts of resonance frequencies. As for the origin of these shifts, considerations will be first made on the contribution from the charges at the neighboring atoms within the molecule. The direct field produced by the charges, which is, in general, very weak, distorts the electronic cloud around the nucleus in resonance to make a considerable contribution to the field gradient. Sternheimer has theoretically shown that the total increment of the field gradient may be approximated by the direct one Δq times a constant factor[9]:

$$\Delta q^{\text{total}} = \Delta q(1-R)$$

R is usually called Sternheimer factor which has been estimated for a Cl^- ion to be -57.7[10]. Actually, the differences in the six resonance frequencies of α-isomer of benzene hexachloride and those of γ-isomer have been satisfactorily interpreted in terms of this effect by assuming the multiplying factor $(1-R)\cong 50$[2]. Similar interpretation may be applied to the frequency differences in multichlorobenzenes.

Figure 1 presents a diagram of the observed frequencies in multichlorobenzenes plotted against the zz component of the direct field gradient calculated with disregarding the intermolecular effect. In the calculation, a formal charge placed at the center of each atom has been assumed from the information of the bond moment and of the coupling constant of the chlorine nucleus in monochlorobenzene: $-0.20e$ at the chlorine atom, $0.20e$ at the carbon atom bonded to the chlorine atom, $-0.05e$ at the carbon atom bonded to a hydrogen atom, and $0.05e$ at the hydrogen atom. The interatomic distances have been assumed to be $r(C-C)=1.39$ Å, $r(C-Cl)=1.71$ Å and $r(C-H)=1.08$ Å, and the bond angles to be all hexagonal. The plot has been made on the basis of the above assignments for 1, 2, 3, 4-tetrachlorobenzene and for pentachlorobenzene, and also of those by Bray et al.[1] for other derivatives. Roughly speaking, the frequencies are linearly correlated with Δq_{zz}, and the frequency shifts are accounted for by assuming the same multiplying factor as that in benzene hexachlorides. It will be recognized by a closer examination, however, that the frequencies are aligned on three nearly parallel lines, depending on the number of ortho chlorine neighbors. It is apparent from the trends of the three lines that the contributions from the ortho neighbors are relatively over-estimated by this direct interaction alone. Similar tendencies have been found by Bray et al. in the diagram of frequency versus Hammett sigma values[1].

Two origins should be mentioned in relation to such complicated feature of the resonance frequencies. One is the displacement of the center of the electronic charges from that of the nucleus. A simple estimate will then be attempted here for the position of the formal charge on each atom. If sp^2 hybrid orbitals are assumed for the carbon atoms, the average position of the positive charge in the C^+Cl^- bond or of the negative charge in the C^-H^+ bond is calculated by the following formula:

$$\langle z_C \rangle = (2\sqrt{2}/3)\int z_C \chi_{2s}\chi_{2pz}\mathrm{d}\tau$$

where z_C denotes the displacement of the charge measured from the center of the carbon nucleus towards that of either the chlorine or the hydrogen nucleus, and χ_{2s} and χ_{2pz} the 2s and $2p_z$ atomic orbitals of the carbon atom, respectively. The displacement of the charge

9) R. M. Sternheimer, *Phys. Rev.*, **95**, 736 (1954).
10) R. M. Sternheimer and H. M. Foley, ibid., **102**, 731 (1956).

centers also takes place in the chlorine atom of the covalent C–Cl bond: a negative charge at the center of the chlorine nucleus and a positive charge at the distance

$$\langle z_{Cl}\rangle = 2\sqrt{s(1-s)}\int z_{Cl}\chi_{3s}\chi_{3pz}d\tau$$

from the chlorine nucleus to the carbon one[11], s denoting the s character of the bonding orbital of the chlorine atom. By making use of Slater functions[12] for the atomic orbitals χ's, the equation gives $\langle z_C\rangle = 0.453$ Å and $\langle z_{Cl}\rangle = 0.376$ Å, where the s character is assumed to be 0.15 for the chlorine atom according to the estimate by Townes and Dailey[13]. This amount of displacement of the charges in the covalent C–Cl bond produces a bond moment of 1.80 D, slightly larger than the observed one[14]. The change in the field gradients thus estimated, however, rather enhances the trends of the three lines found in Fig. 1, contrary to the expectation.

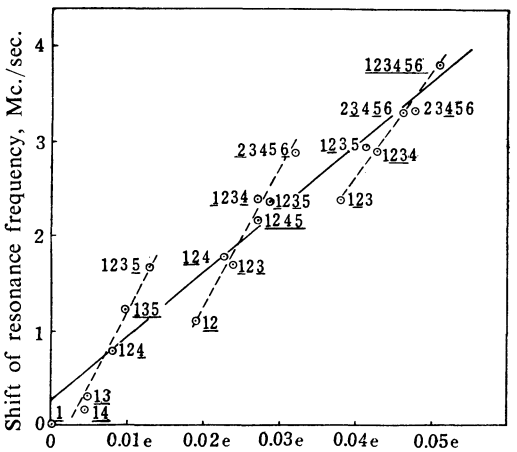


Fig. 1. Plot of the ^{35}Cl resonance frequency in multichlorobenzenes versus the direct field gradient arising from the distribution of the effective charges within the molecule. The diagram is drawn with reference to monochlorobenzene. The names of the compounds are represented by the ring positions of the substituted chlorine atoms and the assignment of each spectral line is indicated with underlines.

Another origin to be mentioned is the indirect induction effect propagated through the chemical bonds. Since chlorine is more electronegative than carbon, the bonding electrons in the C–Cl bond are, in general, attracted towards the chlorine atom. In multichloro-derivatives, however, the attractive forces of other chlorine atoms counteract that of the one in question through the bonds to produce a decrease in the ionic character of the C–Cl bond. The resonance frequency thus tends to increase with increasing number of chlorine atoms substituted in the molecule. The observed trend of the frequencies suggests that such indirect induction effect is considerably propagated to the meta and the para positions, too. An evidence for such effect was also observed in the nuclear magnetic resonance spectra[15]: the protons in monochlorobenzene, for example, give rise to a single resonance with a chemical shift $\tau = 2.756$, independent of the ring positions relative to the chlorine atom.

The contribution of the intermolecular effect has been estimated for the three resonance lines in 1, 3, 5-trichlorobenzene, on the basis of the crystal structure. Table IV shows the direct field gradients calculated by assuming an effective charge at the center of each atom in the crystal as mentioned above. The convergence has been substantially reached by the summation up to the first neighboring lattices along the a and b axes and to the third neighbors along the c axis. The sequence of the field gradients Δq_{zz} thus calculated does not agree with that of the observed coupling constants, except for Cl_3. The agreement does not seem to be attained by making any plausible

Table IV. Calculated field gradients at the chlorine nuclei directly arising from the charge distribution in crystalline 1, 3, 5-trichlorobenzene

Chlorine site	Δq_{zz}-$\Delta q_{zz}(Cl_3)$ in 10^{24} c. g. s. e. s. u.	Δq_{xx}-Δq_{yy} in 10^{24} c. g. s. e. s. u.
Cl_1	0.0130e	−0.0125e
Cl_3	0.0000e	−0.0124e
Cl_5	0.0086e	0.0015e

11) With regard to the charge distribution in the covalent C–Cl bond, one may be tempted to presume a model with the positive charge at the position of the chlorine nucleus and the negative charge at the distance $\langle z_{Cl}\rangle$ from the nucleus in the direction of the anti-bonding orbital. Such a model, however, has neglected the quadrupolar field due to the lone-pair electrons in the $3p_x$ and the $3p_y$ orbitals which is expected to have a significant influence, especially, on the ortho neighbors. In this respect, the model employed above seems more reasonable, because the positive charge has been treated as a defect of an electronic charge from the spherically symmetric configuration Cl^-.

12) J. C. Slater, *Phys. Rev.*, **36**, 57 (1930).

13) C. H. Townes and B. P. Dailey, *J. Chem. Phys.*, **17**, 782 (1949); C. H. Townes and A. L. Schawlow, "Microwave Spectroscopy", McGraw-Hill Inc., New York (1955), p. 237*ff*.

14) Even if the s character is taken to be 0.10, the moment is only reduced to 1.52 D. The consideration suggests that the distribution of the effective charges in the C–Cl bond should be approximated by that in a purely covalent bond with an appropriate amount of s character.

15) P. L. Corio and B. P. Dailey, *J. Am. Chem. Soc.*, **78**, 3043 (1956); A. A. Bothner-By and R. E. Glick, *J. Chem. Phys.*, **26**, 1651 (1957).

TABLE V. DISTANCES BETWEEN THE CHLORINE ATOMS IN THE MOLECULE 1 AND THE ATOMS IN THE NEIGHBORING MOLECULES IN THE CRYSTAL OF 1, 3, 5-TRICHLOROBENZENE

Atoms in molecule 1[a]	Atoms in the neighboring molecules			
	Cl		H	
Cl_1	(5—6)[a)]	3.63 Å	(4—7)	2.96 Å
	(3—5)	3.75 Å		
	(1—8 and 8′)	3.91 Å		
	(5—7)	4.04 Å		
	(3—5′)	4.15 Å		
Cl_3	(1—5′)	3.75 Å	(2—5)	2.97 Å
	(3—8 and 8′)	3.91 Å	(6—3)	2.98 Å
	(5—3)	4.13 Å	(2—5′)	3.21 Å
	(1—5)	4.15 Å		
Cl_5	(1—2)	3.63 Å		
	(5—4)	3.65 Å		
	(5—4′)	3.65 Å		
	(5—8 and 8′)	3.91 Å		
	(1—3)	4.04 Å		
	(3—7)	4.13 Å		

a) The first figure in each parenthesis denotes the ring position of the neighboring atom and the second one the molecule in which the atom locates. The position of each molecule must be interpreted as follows: 1, (x,y,z); 2, $(1/2+x,1/2-y,1-z)$; 3, $(1-x,1/2+y,1/2-z)$; 4, $(3/2-x,1-y,1/2+z)$; 4′, $(3/2-x,1-y,-1/2+z)$; 5, $(1/2-x,1-y,-1/2+z)$; 5′, $(1/2-x,1-y,1/2+z)$; 6, $(-1/2+x,1/2-y,1-z)$; 7, $(1-x,-1/2+y,1/2-z)$; 8, $(x,y,z+1)$; 8′, $(x,y,z-1)$, where the fractional coordinates (x,y,z) correspond to those given by Milledge and Pant (see Table 1 in Ref. 8).

correction to the amounts nor to the position of the effective charges. The situation is quite the same for the asymmetry parameters. Since the three chlorine atoms are substituted symmetrically with respect to one another in the molecule, the intramolecular effect is not expected to produce any difference in the field gradients. The shifts of the resonance frequencies in this derivative should, therefore, be produced only through the intermolecular interactions. The disagreement may suggest either a limitation to the application of the Sternheimer theory to molecular crystals, or the existence of an extra process to propagate the effects between the neighboring molecules.

A process to be considered is the one through the distortions of the bonds. In 1, 3, 5-trichlorobenzene, however, there are no significant differences in the lengths of the C–Cl bonds, in particular, between C_1–Cl_1 and C_5–Cl_5; $r(C_1\text{–}Cl_1)=1.710$ Å, $r(C_3\text{–}Cl_3)=1.714$ Å and $r(C_5\text{–}Cl_5)=1709$ Å[8]. Considerable differences have been observed rather in the interatomic distances between the neighboring molecules. As easily seen from Table V, the number of the neighboring atoms increases in the order of positions 3, 1 and 5 for the chlorine neighbors, and in the inverse order for the hydrogen ones. Since the hydrogen atom, in general, has an electric property opposite to the chlorine atom, the observed order of the coupling constants is reasonably interpreted by considering an intermolecular induction effect independent of the directions, such as those analogous to the intramolecular one propagated through the chemical bonds. An evidence for such an extra process may also be seen in the fact that the resonance lines due to the chlorine atoms, which should be equivalent in the free molecule, are distributed over a wide range of frequency, compared with those in other chloro-derivatives of benzene.

Summary

Assignments of the ^{35}Cl nuclear quadrupole resonance spectra have been made for some multichlorobenzenes by the Zeeman studies of single crystals. Three resonance lines in 1, 3, 5-trichlorobenzene, have been assigned, in the order of increasing frequency, to Cl_3, Cl_1 and Cl_5 designated by Milledge and Pant in their X-ray study; two lower frequencies in 1, 2, 3, 4-tetrachlorobenzene to Cl_1 and Cl_4 and two higher ones to Cl_2 and Cl_3; and in pentachlorobenzene, the second highest frequency to the chlorine atom at the para position with respect to the single hydrogen atom. The shifts of the resonance frequencies have been accounted for in terms of the induction effect. It is likely that the ortho

effect is produced by the direct field arising from the charges on the neighboring atoms rather than the indirect one propagated through the chemical bonds. The interpretation of the three frequencies in 1, 3, 5-trichlorobenzene has also been attempted from the viewpoint of the intermolecular effect. It has been suggested that an induction effect independent of the directions takes place in this crystal among the neighboring molecules.

The authors would like to express their thanks to Professor Hidetoshi Takahashi, Department of Physics, the University of Tokyo, for the use of a parametron computer (PC-1) in the calculation of the crystal field in 1, 3, 5-trichlorobenzene. They are also indebted to the Ministry of Education for the expense in this experiment.

Department of Chemistry
Faculty of Science
The University of Tokyo
Hongo, Tokyo

Decomposition of Peroxybenzoic Acid in Solution. I. Decomposition in Alcohols

By Katsumi TOKUMARU, Osamu SIMAMURA and Masaru FUKUYAMA

(Received June 25, 1962)

In the course of an investigation of epoxidation of olefins with peroxybenzoic acid in this Laboratory, peroxybenzoic acid was found to decompose appreciably in ethyl alcohol at room temperature[1]. Search of the literature revealed that, concerning the decomposition of organic peroxyacids in alcohols, only Swern and coworkers' report[2] was available, which stated that long chain aliphatic peroxyacids such as peroxylauric acid decomposed appreciably in methyl alcohol at 25°C. We then undertook investigation on the decomposition of peroxybenzoic acid in alcohols and some other solvents. During our research, Swern and coworkers[3] again reported the decomposition of peroxylauric acid in solvents and offered a non-radical, concerted mechanism.

After our work had been completed, Lefort, Paquot, and Sorba[4] proposed a radical mechanism for the decomposition of peroxylauric acid in petroleum ether. More recently Lefort, Sorba, and Rouillard[5] published a study on the decomposition of the same acid mainly in cyclohexane, and Heywood, Phillips, and Stansbury[6] presented a radical mechanism for the decomposition of peroxyacetic acid in hydrocarbon solutions. Further, Cohen and Edwards[7] made a kinetic study of decomposition of peroxybenzoic acid in benzene and 1-butanol in the presence of 2, 2-diphenyl-1-picrylhydrazyl and concluded a free radical cleavage of peroxybenzoic acid. We now report our results and propose a radical chain mechanism for the decomposition of peroxybenzoic acid in alcohols.

Experimental

Materials. — Peroxybenzoic acid was prepared from benzoyl peroxide according to Braun's procedure[8] as modified by Kolthoff et al.[9] Methylene chloride was used for extraction of peroxybenzoic acid. The extract was dried with sodium sulphate, the solvent removed by suction with a water-jet aspirator, and the remaining peroxybenzoic acid sublimed[10] several times under reduced pressure of a rotary vacuum pump to give samples of 96~99% purity (determined by iodometric titration[11]).

Methyl alcohol was refluxed with silver nitrate and potassium hydroxide and distilled. The distillate was refluxed with magnesium methoxide and distilled before use. Ethyl alcohol was similarly purified. Isopropyl alcohol was refluxed with 2,4-dinitrophenylhydrazine and distilled. The distillate

1) M. Fukuyama, Thesis (Tokyo University), 1958.
2) W. E. Parker, C. Riccuiti, C. L. Ogg and D. Swern, *J. Am. Chem. Soc.*, 77, 4037 (1955).
3) W. E. Parker, L. P. Witnauer and D. Swern, ibid., **80**, 323 (1958).
4) D. Lefort, C. Paquot and J. Sorba, *Bull. soc. chim. France*, **1959**, 1385.
5) D. Lefort, J. Sorba and D. Rouillard, ibid., **1961**, 2219.
6) D. L. Heywood, B. Phillips and H. A. Stansbury, Jr., *J. Org. Chem.*, **26**, 281 (1961).
7) S. R. Cohen and J. O. Edwards, *J. Phys. Chem.*, **64**, 1086 (1960).
8) G. Braun, "Organic Syntheses", Coll. Vol. I (1946), p. 431.
9) I. M. Kolthoff, T. S. Lee and M. A. Mairs, *J. Polymer Sci.*, **2**, 199 (1947).
10) C. G. Overberger and R. W. Cummins, *J. Am. Chem. Soc.*, **75**, 4250 (1953).
11) D. Swern, "Organic Reactions", Vol. VII, John Wiley and Sons, Inc., New York (1953), p. 378.

was refluxed with aluminium isopropoxide and distilled. *tert*-Butyl alcohol was purified by repeated partial freezing and finally distilled.

Nitrogen was freed from oxygen according to Fieser's directions[12]. Oxygen was passed through aqueous potassium permanganate acidified with sulphuric acid and dried with sulphuric acid.

Product Study.—A typical experiment for each alcohol is described.

Decomposition in Ethyl Alcohol. — Peroxybenzoic acid (9.7 g., 70 mmol.) was dissolved in 100 ml. of ethyl alcohol and left to stand in the dark for two months at room temperature until peroxybenzoic acid had been decomposed completely. The solvent was distilled, and fresh alcohol added to the residue and distilled to remove low boiling volatile matter. The combined distillates, on treatment with 2,4-dinitrophenylhydrazine, gave 2,4-dinitrophenylhydrazone of acetaldehyde (11 mmol.), m. p. (from ethyl alcohol) and mixed m. p. with an authentic sample, 168°C. Subsequent distillation of the residue under reduced pressure gave acetic acid, which was characterized as the *p*-toluidide (16 mmol.), m. p. and mixed m. p. with an authentic sample, 147°C. The residue from the distillation consisted of almost pure benzoic acid, (8.2 g., 67 mmol.), m. p. 121°C.

Decomposition in Isopropyl Alcohol.—Peroxybenzoic acid (10.3 g., 75 mmol.) was dissolved in 80 ml. of isopropyl alcohol and allowed to stand in the dark until peroxybenzoic acid had completely disappeared. The reaction mixture was distilled, and the distillate, treated with 2,4-dinitrophenylhydrazine, yielded 2,4-dinitrophenylhydrazone of acetone (42 mmol.), m. p. 126°C. The solid residue was benzoic acid (9.1 g., 75 mmol.), m. p. 121°C. When peroxybenzoic acid (0.5 g., 3.6 mmol.) was allowed to decompose in isopropyl alcohol (50 ml.) at 60°C for 4 hr., the reaction mixture, worked up as above, gave acetone, identified as 2,4-dinirophenylhydrazone (2.2 mmol.), m. p. 126°C, and benzoic acid (0.4 g., 3.3 mmol.).

Decomposition in Methyl Alcohol. — Peroxybenzoic acid (0.5 g., 3.6 mmol.) was decomposed in boiling methyl alcohol (50 ml.) for 10 hr., under a stream of nitrogen. Distillation of the reaction mixture gave formaldehyde, identified as 2,4-dinitrophenylhydrazone (1.5 mmol.), m. p. 165°C and benzoic acid (0.4 g., 3.3 mmol.).

Analysis of Gaseous Products.—A solution of peroxybenzoic acid was placed in a reaction flask. The flask was cooled with dry ice-ethyl alcohol, evacuated to remove oxygen, and let stand to warm up, and after introduction of nitrogen and chilling with the cooling mixture the system was evacuated again. After the cycle of these operations was repeated three times, the reaction was started by immersing the flask in a thermostat and gas was collected, as it evolved from the reaction mixture, on mercury in a gas burette connected to the reaction flask. When the reaction was complete, the gas was analyzed for carbon dioxide and oxygen by absorption in potassium hydroxide solution and in alkaline pyrogallol solution, respectively.

In one run, decomposition of 3.2 g. (23 mmol.) of peroxybenzoic acid in 40 ml. of isopropyl alcohol at 58°C gave 0.5 mmol. of carbon dioxide and 0.3 mmol. of oxygen.

Kinetic Measurements. — In a 200 ml. round bottomed flask equipped with a gas inlet tube and a spiral condenser carrying a calcium chloride tube at the top was placed a measured amount of an alcohol and the flask was immersed in a thermostat kept at a specified temperature. Nitrogen was passed through the alcohol to exclude oxygen, a weighed amount of peroxybenzoic acid was added, and after dissolution the concentration of the acid was determined iodometrically (normally about 0.1 mol./l.) The time of the sampling was taken as time zero for the kinetic run. Aliquots (2.00 ml.) were withdrawn at intervals and titrated in the usual manner.

At first kinetic results were not reproducible. We then found that the following treatment of reaction vessels gave tolerably reproducible results. A reaction vessel was first washed with concentrated methyl alcoholic solution of potassium hydroxide followed by water, and with concentrated nitric acid followed by water; then dilute solution of peroxybenzoic acid in the organic solvent in which the reaction was to be run was placed in the vessel and kept at 60°C for 3 hr.; and finally the vessel was thoroughly washed with this solvent and dried.

When the effect of light was investigated, a quartz flask or a glass flask coated with black enamel was used. In usual runs no special precaution was taken to exclude diffuse room light; control experiments established that this had no detectable effect upon the reaction rate.

Normally, at 30°C, an induction period ranging from ten to sixty minutes was observed, and sometimes it continued as long as three hours, but it

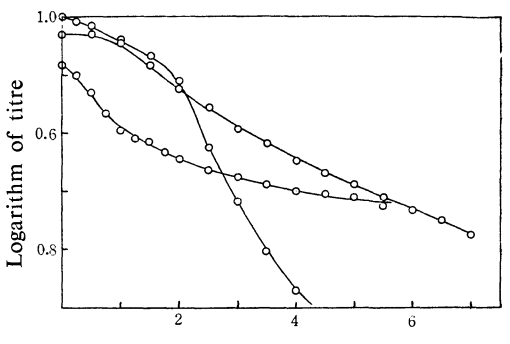


Fig. 1. Rate of decomposition of peroxybenzoic acid in isopropyl alcohol at 30°C (initial concentration of peroxybenzoic acid, ca. 0.1 mol./l.). A plot against time of logarithm of the concentration of peroxybenzoic acid expressed in titre (in ml.) of standard thiosulphate solution (0.04 N) consumed for an aliquot (2 ml.) of peroxybenzoic acid solution.

12) L. F. Fieser, "Experiments in Organic Chemistry", D. C. Heath and Co., Boston, 3rd Ed. (1955), p. 299.

seldom was observed above 50°C. The induction period was followed by a rapid and steady decomposition, but after a few hours the rate began to decrease gradually; some typical runs are shown in Fig. 1. The first-order rate constant for the decomposition was obtained from the slope of the straight part of the curve drawn through plots against time of logarithm of the concentration of peroxybenzoic acid. The mean values of the rate constants from several determinations with standard deviations are shown in Table II.

Results and Discussion

The results of the product study are shown in Table I.

The results of kinetic runs are summarized in Table II, which shows that the apparent decomposition rate in alcohols decreases in the order: isopropyl > ethyl > methyl alcohol. The rate in *tert*-butyl alcohol was nil at 30°C.

The rate of decomposition was larger in an atmosphere of nitrogen than in an atmosphere of oxygen or air for the respective alcohols. In the presence of *p*-benzoquinone in isopropyl alcohol in an atmospherere of nitrogen the decomposition took place much slower, as shown in Fig. 2. When solution of peroxybenzoic acid in isopropyl alcohol was irradiated with ultraviolet light in a quartz flask, a very rapid decomposition occurred. Acceleration by ultraviolet light was also observed in benzene solution, although it took place to a much smaller extent than in isopropyl alcohol.

These findings suggest that radicals are involved in the decomposition of peroxybenzoic acid in alcohols. It is quite natural and reasonable to assume homolytic rupture of the oxygen-oxygen bond of peroxybenzoic acid as a radical initiation process, giving a benzoyloxy and a hydroxyl radical:

$$C_6H_5C(=O)OOH \rightarrow C_6H_5C(=O)O\cdot + HO\cdot$$

The radicals thus formed attack a molecule of

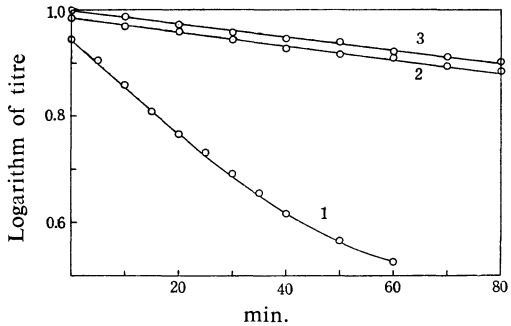


Fig. 2. Rate of decomposition of peroxybenzoic acid in isopropyl alcohol at 55°C (initial concentration of peroxybenzoic acid, ca. 0.1 mol./l.). A plot against time of logarithm of the concentration of peroxybenzoic acid expressed in titre (in ml.) of standard sodium thiosulphate solution (0.04 N) consumed for an aliquot (2 ml.) of peroxybenzoic acid solution.
1, Reaction in a stream of nitrogen
2, In the presence of *p*-benzoquinone (7×10^{-3} mol./l.) in a stream of nitrogen
3, Reaction in an atmosphere of oxygen

Table I. Products formed in decomposition of peroxybenzoic acid in alcohols

Alcohol	Temp.	Products from alcohol		Products (yield, %) Benzoic acid	Carbon dioxide	Oxygen
Methyl	Under reflux	Formaldehyde	42	92		
Ethyl	Room temp.	Acetaldehyde	15	96		
		Acetic acid	22			
Isopropyl	Room temp.	Acetone	56	100		
Isopropyl	60°C	Acetone	61	92		
Isopropyl	58°C				1.2	2

Table II. Apparent pseudo-first order rate constants for decomposition of peroxybenzoic acid in several alcohols at 30°C

Alcohol	in Air $k_1\times10^5$ sec^{-1}	in Nitrogen $k_1\times10^5$ sec^{-1}	Relative rate	Relative rate per α-hydrogen
Methyl	0.23±0.04	0.32±0.10	0.3	0.2
Ethyl	0.34±0.07	1.1 ±0.3	1	1
Isopropyl	0.52±0.05 (0.42±0.04)*	2.7 ±0.8	2.5	5
tert-Butyl	0	0	0	

* This value is for the decomposition in an atmosphere of oxygen.

TABLE III. RELATIVE RATE CONSTANTS FOR SOME PROCESSES IN THE REACTIONS OF BENZOYL PEROXIDE AND FENTON'S REAGENT WITH ALCOHOLS

Alcohol	Benzoyl peroxide[13]		Fenton's reagent[14]	
	Apparent first-order constant at 60°C (relative value)	k_2 for reaction 2 at 60°C	k_{3B}/k_4 at 60°C	$k_{2'}$ for reaction 2' at room temp.
Methyl	0.20			0.42
Ethyl	1.00	1.00	1.00	1.00
Isopropyl	3.58	3.08	11.36	1.58
tert-Butyl	0.004			

solvent alcohol, abstracting a hydrogen atom α to the hydroxyl group and giving a 1-hydroxyalkyl radical, which will hereafter in this report be briefly called "solvent radical".

Since the apparent decomposition rates were different in various alcohols and the effects of oxygen and *p*-benzoquinone were observed, it is concluded that the induced decomposition of peroxybenzoic acid by solvent radicals must have occurred. If the induced decomposition had not occurred, the apparent decomposition rate of peroxybenzoic acid would have been larger in ethyl alcohol than in isopropyl alcohol, since acetaldehyde primarily formed in the former is more easily oxidized by peroxybenzoic acid than acetone formed in the latter as shown by a separate experiments.

These results suggest a mechanism comprising the following series of reactions.

$$PhCO_3H \rightarrow PhCO_2\cdot + HO\cdot \quad (1)$$

$$PhCO_2\cdot \rightarrow Ph\cdot + CO_2 \quad (1')$$

$$PhCO_2\cdot + RR'CHOH \rightarrow PhCO_2H + RR'\dot{C}OH \quad (2)$$

$$HO\cdot + RR'CHOH \rightarrow H_2O + RR'\dot{C}OH \quad (2')$$

$$PhCO_3H + RR'\dot{C}OH \rightarrow PhCO_2\cdot + RR'C(OH)_2 \quad (3)$$

$$PhCO_3H + RR'\dot{C}OH \rightarrow HO\cdot + PhCO_2CRR'OH \quad (3')$$

$$PhCO_2\cdot + RR'\dot{C}OH \rightarrow PhCO_2CRR'OH \quad (4)$$

$$HO\cdot + RR'\dot{C}OH \rightarrow RR'C(OH)_2 \quad (4')$$

$$PhCO_2CRR'OH \rightarrow PhCO_2H + RR'CO$$

$$RR'C(OH)_2 \rightarrow H_2O + RR'CO$$

Reaction 1' represents the well known decomposition of the benzoyloxy radical. It turned out, however, that this reaction did not take place to an appreciable extent in alcohols, since, the yield of benzoic acid was invariably nearly quantitative.

Reactions 2 and 2' are abstraction by radicals of a hydrogen atom from a molecule of alcohol; the former has already been proposed by Mashio and Kato[13] for the decomposition of benzoyl peroxide in alcohols, and the latter by Merz and Waters[14] for the reaction of the Fenton reagent with alcohols. They estimated the relative rate constants for reactions 2 and 2', which are shown in Table III. The relative rates decrease in the order: isopropyl > ethyl > methyl alcohol. This order can be interpreted as indicating that a larger rate constant corresponds to a larger resonance stabilization of the solvent radical formed.

Reactions 3 and 3' represent the induced decomposition of peroxybenzoic acid by solvent radicals. Although which of reactions 3 or 3' is the more important could not be determined, the results with hydrocarbons to be subsequently reported suggest that it probably is reaction 3 that took place predominantly. Similar reactions have been also proposed for the induced decomposition of benzoyl peroxide[13,15,16], acetyl peroxide[17], and persulphate[18] by 1-hydroxyalkyl radicals. It has been reported that the induced decomposition of benzoyl peroxide is readily caused by 1-hydroxyalkyl radicals or 1-alkoxyalkyl radicals among various radicals[15,16].

Mashio and Kato[13] has estimated the rate constant k_{3B} for the following reaction relative to the rate constant for reaction 4.

$$PhCO_2OCOPh + RR'\dot{C}OH \rightarrow PhCO_2CRR'OH + PhCO_2\cdot \quad (3B)$$

Since k_4's can be assumed to be nearly equal for various alcohols, the magnitude of k_{3B}/k_4 is regarded as a measure for k_{3B}. As seen from Table III, k_{3B}/k_4 is larger for isopropyl alcohol than for ethyl alcohol. It therefore

13) S. Kato and F. Mashio, *J. Chem. Soc. Japan, Ind. Chem. Sec.* (*Kogyo Kagaku Zassi*), **59**, 380 (1956); F. Mashio and S. Kato, *Science and Technology* (*Kyoto Techn. Univ.*), **5**, 51 (1956).
14) J. H. Merz and W. A. Waters, *Discussions Faraday Soc.*, **2**, 179 (1947).
15) W. E. Cass, *J. Am. Chem. Soc.*, **68**, 1976 (1946).
16) K. Nozaki and P. D. Bartlett, ibid., **69**, 2299 (1947).
17) M. S. Kharasch, J. L. Rowe and W. H. Urry, *J. Org. Chem.*, **16**, 905 (1951).
18) K. B. Wiberg, *J. Am. Chem. Soc.*, **81**, 252 (1959).

seems that k_{3B} is larger for the more electron-donating 1-hydroxyalkyl radical, since the electron-donating property decreases in the order: 1-hydroxy-1-methylethyl > 1-hydroxyethyl > hydroxymethyl radical.

Reactions 4 and 4' are written as termination reactions; the former has also been suggested for the decomposition of benzoyl peroxide[13].

Evidently, rapid decomposition of peroxybenzoic acid requires the presence of a hydrogen at the α-carbon atom in alcohol; indeed the decomposition was not noticeable in *tert*-butyl alcohol at room temperature. Table II indicates that the rate constant depends upon the nature of the α-hydrogen atom. Moreover, it is interesting to note that there seems to be a parallelism in the apparent decomposition rate between peroxybenzoic acid and benzoyl peroxide as shown by comparison of the values in Table II with those in Table III.

In the present mechanism, the induced decomposition of peroxybenzoic acid by solvent radicals is the major process which distinguishes solvents in the decomposition rate. This process is controlled, in the first place, by the stationary concentration of solvent radicals and, secondly, by their reactivity towards peroxybenzoic acid. The stationary concentration of solvent radicals would tend to increase, other things being equal, according as an α-hydrogen atom of the alcohol is abstracted more readily. The resulting 1-hydroxyalkyl radicals are resonance-stabilized in the order: 1-hydroxy-1-methylethyl > 1-hydroxyethyl > hydroxymethyl. The order of the efficiency with which they are formed from the corresponding alcohols therefore falls in the order: isopropyl > ethyl > methyl alcohol. The reactivity of solvent radicals towards peroxybenzoic acid can be assumed to be parallel to that towards benzoyl peroxide, that is, to be governed by their electron-donating property. Then for this property again the same order as above is valid, as mentioned earlier. Thus alcohols will favour the induced decomposition in the order: isopropyl > ethyl > methyl alcohol, in agreement with the findings in the rate study.

The evolution of oxygen observed in the case of the decomposition in isopropyl alcohol at 58°C might suggest participation of peroxybenzoate anions, since dissociation of peroxybenzoic acid as an acid would be favoured in a polar solvent like alcohols, and the peroxybenzoate anion has been shown to react with peroxybenzoic acid giving oxygen[19]. Oxygen is also formed from α-cumyl hydroperoxide both in aqeous alkaline solution and in cumyl alcohol[20].

Summary

Decomposition of peroxybenzoic acid was studied in methyl, ethyl, isopropyl and *tert*-butyl alcohol. The primary and the secondary alcohols were oxidized to the corresponding carbonyl compounds, which were sometimes further oxidized. The apparent decomposition rate of peroxybenzoic acid in alcohols decreased in the order: isopropyl alcohol > ethyl alcohol > methyl alcohol ≫ *tert*-butyl alcohol. For these decompositions a radical mechanism, which involves the homolytic rupture of peroxybenzoic acid and its induced decomposition by 1-hydroxyalkyl radicals derived from the respective alcohols, was proposed. A possible participation of peroxybenzoate anions in these decompositions was suggested.

Department of Chemistry
Faculty of Science
The University of Tokyo
Hongo, Tokyo

19) W. Kirmse and L. Horner, *Chem. Ber.*, **89**, 836 (1956).
20) M. S. Kharasch, A. Fono and W. Nudenberg, *J. Org. Chem.*, **16**, 113 (1951); M. S. Kharasch, A. Fono, W. Nudenberg and B. Bischof, ibid., **17**, 207 (1952).

Decomposition of Peroxybenzoic Acid in Solution. II. Decomposion in Hydrocarbons

By Katsumi TOKUMARU and Osamu SIMAMURA

(Received June 25, 1962)

In the preceding paper[1] we have proposed a radical chain mechanism for the decomposition of peroxybenzoic acid in alcohols. In alcohols, peroxybenzoic acid decomposes not only through the initial homolytic rupture, but also through the induced decomposition due to attack by 1-hydroxyalkyl radicals formed from alcohol molecules. In the decomposition of benzoyl peroxide, it is well known that the induced decomposition of the oxygen-oxygen bond by radicals derived from solvent molecules does not occur as readily in hydrocarbons as in alcohols or ethers[2]. Therefore, by analogy with benzoyl peroxide, we first imagined that peroxybenzoic acid might decompose in hydrocarbons with a lesser extent of the induced decomposition by solvent radicals and the apparent decomposition rate might approximate the initial decomposition rate of peroxybenzoic acid. The present report deals with the decomposition of peroxybenzoic acid in several hydrocarbons; it has turned out that peroxybenzoic acid also is extensively attacked by solvent radicals in hydrocarbons.

Experimental

Materials. — Peroxybenzoic acid was prepared according to the procedure previously described[1]. *n*-Heptane was shaken with sulphuric acid, followed by aqueous sodium hydroxide solution, dried with calcium chloride and then with sodium metal, and distilled. Cyclohexane was treated with nitric acid-sulphuric acid mixture, washed with aqueous sodium hydroxide, dried with calcium chloride and then with sodium metal, and distilled. Cyclohexanol was washed with aqueous sodium hydroxide, dried with anhydrous sodium sulphate, purified with repeated freezing, and distilled. Cumene was shaken with sulphuric acid, washed with aqueous sodium hydroxide solution, dried with calcium chloride and then with sodium metal, and distilled under an atmosphere of nitrogen. Benzene and toluene were shaken with sulphuric acid, washed with sodium hydroxide solution, dried with calcium chloride and then with sodium metal and distilled; benzene was further purified with repeated freezing and finally distilled over sodium. Carbon tetrachloride was refluxed with a mixture of aqueous potassium hydroxide solution and ethyl alcohol, washed with sulphuric acid and then with aqueous sodium hydroxide, dried with calcium chloride, and distilled.

Kinetic Measurements.—In some kinetic runs the procedure was essentially the same as described in Part I[1]. In most runs aliquots (2 ml.) of a solution of peroxybenzoic acid (0.1 mol./l.) were placed in glass tubes, the tubes were evacuated thoroughly with alternate chilling and warming to remove oxygen, sealed, and immersed in a thermostat kept at 79°C, and the contents were analyzed iodometrically for peroxybenzoic acid at intervals. Typical runs are shown in Fig. 1. Under the present experimental conditions no induction period

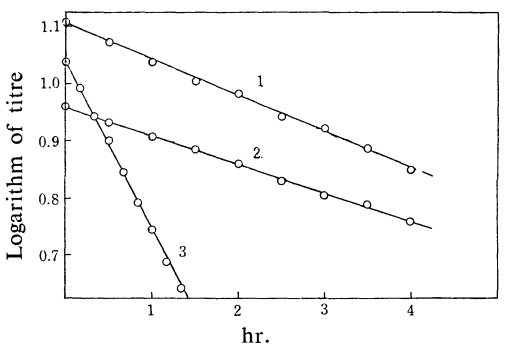


Fig. 1. Rate of decomposition of peroxybenzoic acid in hydrocarbons at 79°C (initial concentration of peroxybenzoic acid, ca. 0.1 mol./l.). A plot against time of logarithm of the concentration of peroxybenzoic acid expressed in titre (in ml.) of standard thiosulphate solution (0.04 N) consumed for an aliquot (2 ml.) of peroxybenzoic acid.
1, 2 in cyclohexane, 3 in cumene

TABLE I. APPARENT PSEUDO-FIRST ORDER RATE CONSTANTS FOR DECOMPOSITION OF PEROXYBENZOIC ACID IN SOME SOLVENTS
at 79°C; initial concentration, ca. 0.1 mol./l.

Solvent	$k_1 \times 10^4$ sec^{-1}
Carbon Tetrachloride	0.02
Benzene	0.26±0.02
n-Heptane	0.33±0.02
Cyclohexane	0.37±0.02
Toluene	1.6 ±0.1
Cumene	1.9 ±0.1
Cyclohexanol	~40

1) K. Tokumaru, O. Simamura and M. Fukuyama, This Bulletin, 35, 1673 (1962).
2) P. D. Bartlett and K. Nozaki, *J. Am. Chem. Soc.*, 68, 1686 (1946); K. Nozaki and P. D. Bartlett, ibid., 69, 2299 (1947).

was observed. The first-order rate constant for the decomposition was obtained from the slope of the straight part of the curve drawn through plots against time of logarithm of the concentration of peroxybenzoic acid. The mean values of the rate constants from several determinations together with deviation are shown in Table I.

Product Study.—The decomposition was carried out in a three-necked round bottomed flask equipped with an inlet tube for nitrogen and a spiral condenser, to the top of which were connected, in order of mention, a trap cooled with dry-ice ethyl alcohol, a calcium chloride tube and a potash bulb. A weighed amount of peroxybenzoic acid dissolved in a solvent was placed in the flask which was immersed in a thermostat and allowed to decompose in a slow stream of nitrogen. The decomposition was carried out until no more absorption of carbon dioxide in the potash bulb was observed. Then the reaction mixture was worked up.

For analysis of gaseous products, a solution of small amount of peroxybenzoic acid was decomposed in a closed system, and the gas evolved was analysed for carbon dioxide and oxygen by absorption method as described in Part I[1].

Decomposition in n-Heptane. — Peroxybenzoic acid (9.3 g., 67 mmol.) dissolved in 250 ml. of *n*-heptane (the initial concentration of peroxybenzoic acid, 0.27 mol./l.) was heated at 90°C for 19 hr. in a stream of nitrogen. After the decomposition was over, benzoic acid, deposited in the reaction flask, was filtered off; a little water was observed to have been formed. The filtrate was extracted repeatedly with 5% aqueous sodium hydrogen carbonate. The organic layer was dried with anhydrous sodium sulphate and distilled giving heptane and two fractions, b. p. 45~50°C at 22 mmHg (0.75 g.) and b. p. ca. 68°C at 22 mmHg (0.8 g.), respectively. The former was shown to be a mixture of heptanols and heptanones and the latter a mixture of C_7 esters, such as amyl acetate, by comparison of the infrared spectra with those of authentic specimens. The aqueous extract, on acidification with hydrochloric acid and extraction with ether, afforded benzoic acid, m. p. 121°C. The total amount of this acid formed in this reaction was 5.7 g. (46.8 mmol.).

The amount of the carbon dioxide formed as estimated from the increment of the weight of the potash bulb was 0.70 g. (15.8 mmol.). No formation of oxygen was observed in the reaction in heptane.

Decomposition in Cyclohexane. — Solution of peroxybenzoic acid (10.5 g., 76 mmol.) in 250 ml. of cyclohexane (the initial concentration, 0.3 mol./l.), was heated at 79°C for 27 hr. in a stream of nitrogen. The reaction mixture was cooled and the deposited benzoic acid filtered off; a small amount of water was noticeable in the reaction mixture. The filtrate was shaken with water; the aqueous layer, on treatment with 2,4-dinitrophenylhydrazine, gave 2,4-dinitrophenylhydrazone of cyclohexanone (trace), m. p. 158°C. It was then extracted with aqueous sodium hydrogen carbonate to isolate benzoic acid. Most of the solvent was removed from the organic layer on a water bath, and in the recovered cyclohexane benzene was detected by its characteristic ultraviolet absorption at 220~270 mμ. The residue was subjected to fractionation giving cyclohexanol (0.4 g., 4 mmol.), b. p. 68°C at 20 mmHg, which was identified by infrared spectrum measurement, and characterized as 3,5-dinitrobenzoate, m. p. 112°C, and a small amount of a colourless viscous liquid, b. p. 110°C at 2 mmHg, which was identified with ε-caprolactone by converting it into ε-hydroxycaproic acid hydrazide (Found: C, 49.31; H, 9.79. Calcd. for $C_6H_{14}N_2O_2$: C, 49.30; H, 9.63%.), m. p. 114~115°C[3,4] The residue in the distilling flask was shown to be a mixture of ε-caprolactone and its polymers by treatment with hydrazine hydrate on a boiling water-bath, ε-hydroxycaproic acid hydrazide being obtained. The total amount of ε-caprolactone in the monomeric and the polymeric form was about 2 g. (18 mmol.). In this experiment benzoic acid recovered amounted to 6.1 g. (50 mmol.) and carbon dioxide, 0.83 g. (19 mmol.). A separate small scale experiment in a closed system showed that no oxygen was formed in cyclohexane.

Decomposition in Cyclohexanol. — Peroxybenzoic acid, (1.4 g., 10 mmol.) was decomposed in cyclohexanol (40 ml.) (the initial concentration, 0.26 mol./l.) at 79°C for 1 hr. under an atmosphere of nitrogen. The reaction mixture was diluted with benzene, and extracted with water. The aqueos extract, on treatment with 2,4-dinitrophenylhydrazine, gave 2,4-dinitrophenylhydrazone of cyclohexanone (0.2 mmol.), m. p. 158°C. The organic layer was worked up as described for the experiment with cyclohexane to give benzoic acid (1.15 g., 9.5 mmol.) and ε-caprolactone (0.07 g., 0.6 mmol.), identified as ε-hydroxycaproic acid hydrazide, m. p. 114~115°C.

Decomposition in Cumene. — Peroxybenzoic acid (12.5 g., 90 mmol.) was decomposed in cumene (200 ml., the initial concentration of the acid, 0.35 mol./l.) at 79°C for 8 hr. in a stream of nitrogen. A small amount of water was detected. The reaction mixture was extracted with aqueous sodium hydrogen carbonate, and the aqueous extract gave benzoic acid (9.9 g., 81 mmol.) on acidification. The organic layer was extracted with aqueous sodium hydroxide; the aqueous extract was reddish brown, but gave no identifiable substance. Distillation of the organic layer afforded cumene and cumyl alcohol (2.1 g., 15 mmol.), b. p. 63~66°C at 2 mmHg, a considerable amount of tarry matter (ca. 0.5 g.) remaining. Cumyl alcohol was purified by repeated sublimations under reduced pressure, m. p. 33°C, (Found: C, 79.33; H, 9.05. Calcd. for $C_9H_{12}O$: C, 79.37; H, 8.88%). The infrared spectrum of the crude cumyl alcohol showed the presence of acetophenone in trace amount.

In separate experiments, oxygen was not detected by the absorption method.

Decomposition in Toluene. — Peroxybenzoic acid (3.5 g., 25 mmol.) was decomposed in toluene (70 ml., the initial concentration of the acid, 0.36 mol./l.) at 79°C for 5 hr. in a stream of nitrogen.

3) F. J. Van Natta, J. W. Hill and W. H. Carothers, *J. Am. Chem. Soc.*, **56**, 455 (1934).
4) S. L. Friess, ibid., **71**, 2571 (1949).

Extraction of the reaction mixture with aqueous sodium hydrogen carbonate gave benzoic acid (3.5 g., 28 mmol.). Distillation of the organic layer gave toluene, benzyl alcohol, (0.2 g., 2 mmol.), b. p. 105°C at 20 mmHg, and a tarry residue (ca. 0.2 g.). The benzyl alcohol was characterized by formation of 3,5-dinitrobenzoate, m. p. 112°C, and by the infrared spectrum.

Decomposition in Carbon Tetrachloride in the Presence of Iodine.—Peroxybenzoic acid (5.1 g., 37 mmol.) and iodine (10.0 g., 39.5 mmol.) were dissolved in carbon tetrachloride (130 ml.) and the solution was heated under reflux for 90 hr.

The precipitate formed was filtered off and washed with carbon tetrachloride and ethyl alcohol until the colour due to iodine was no longer observed in washings. After being dried, it was identified as diiodine pentoxide (0.4 g., ca. 1 mmol.), by determining both neutralization and oxidation equivalent (Found: neutralization equivalent, 165.9; oxidation equivalent, 27.4. Calcd. for I_2O_5: neutralization equivalent, 166.9; oxidation equivalent, 27.82.). The filtrate was shaken with aqueous sodium thiosulphate solution to remove iodine, and extracted with aqueous sodium hydrogen carbonate. The aqueous extract gave benzoic acid (4.0 g., 33 mmol.). Carbon tetrachloride was distilled, and the residue from the distillation was subjected to steam distillation. From the distillate hexachloroethane (0.1 g.). was obtained and identified by infrared spectrum measurement, m. p. (from ethyl alcohol) and mixed m. p. with an authentic sample measured in a sealed tube, 185°C.

Results and Discussion

The results of kinetic runs are shown in Table I. The apparent decomposition rates varied from solvent to solvent, and the tendency of variation was not always similar to that in the case of benzoyl peroxide[2].

When a small amount of *p*-benzoquinone was added in *n*-heptane solution of peroxybenzoic acid, apparent decomposition was retarded: at 90°C, with an initial concentration of 0.1 mol./l. of peroxybenzoic acid, k_1 was 1.5×10^{-4} sec^{-1} in the absence of *p*-benzoquinone, and 1.4×10^{-5} sec^{-1} in its presence ($0.6\sim1.2\times10^{-2}$ mol./l.).

The results of the product study are summarized in Table II. The sum of the amounts in which benzoic acid and carbon dioxide were formed is a measure of the amount of the CO_3H group decomposed, and it amounted nearly to 100% of the peroxybenzoic acid used, as seen from this table. However, in the reaction in toluene, the yield of benzoic acid exceeds the amount of the peroxybenzoic acid decomposed. This suggests that part of the benzoic acid probably was formed by the oxidation of toluene by way of benzyl alcohol and benzaldehyde.

As in the case of the reaction in alcohols, the radical nature of the decomposition of peroxybenzoic acid in hydrocarbons is indisputable. On the basis of the results of the kinetic and the product analysis, the following series of reactions are postulated which include the induced decomposition (reaction 3) of peroxybenzoic acid by solvent radicals (S·) generated from molecules of a hydrocarbon (SH) by abstraction of a hydrogen atom (reactions 2, 2′ and 2″).

$$PHCO_3H \rightarrow PhCO_2\cdot + HO\cdot \quad (1)$$

$$PhCO_2\cdot \rightarrow Ph\cdot + CO_2 \quad (1')$$

$$PhCO_2\cdot + SH \rightarrow PhCO_2H + S\cdot \quad (2)$$

$$HO\cdot + SH \rightarrow H_2O + S\cdot \quad (2')$$

$$Ph\cdot + SH \rightarrow PhH + S\cdot \quad (2'')$$

$$PhCO_3H + S\cdot \rightarrow SOH + PhCO_2\cdot \quad (3)$$

$$S\cdot + HO\cdot \rightarrow SOH \quad (4)$$

$$S\cdot + PhCO_2\cdot \rightarrow PhCO_2S \quad (4')$$

$$S\cdot + S\cdot \rightarrow S_2 \quad (4'')$$

$$SOH \rightarrow \text{Oxidation products} \quad (5)$$

TABLE II. YIELDS (IN %) OF PRODUCTS FORMED IN DECOMPOSITION OF PEROXYBENZOIC ACID IN SOME SOLVENTS

Solvent	Temp. °C	Products from solvents	Benzoic acid	Carbon dioxide	Remark
n-Heptane	90	Heptanols Heptanones C_7-Ester	69	23	Water detected
Cyclohexane	79	Cyclohexanol 5 Cyclohexanone trace ε-Caprolactone 24	66	25	Water and benzene detected
Cyclohexanol	79	Cyclohexanone 2 ε-Caprolactone 6	95		
Cumene	79	α,α-Dimethyl-benzyl alcohol 17 Distillation residue	89	8	Water detected
Toluene	79	Benzyl alcohol 8 Benzoic acid Distillation residue	112		

Reaction 1′ is the well known decomposition of the benzoyloxy radical. This reaction takes place to an appreciable extent in hydrocarbons, competing with the abstraction of a hydrogen atom from a solvent molecule (reaction 2). Reaction 1′ is less important in cumene and toluene, which possess a hydrogen atom at the α position available for ready abstraction by the benzoyloxy radical; in fact in these hydrocarbons the yield of benzoic acid was nearly quantitative. In contrast to this, the yield of benzoic acid was lower and that of carbon dioxide higher in cyclohexane and heptane; in these hydrocarbons hydrogen atoms are not as liable to attack as the α-hydrogen atom in cumene and toluene. However, in cumene and toluene, such possibility could not be excluded that the oxidation of the aromatic nucleus by peroxybenzoic acid through an ionic or molecular mechanism may occur in which peroxybenzoic acid transfers an atom of oxygen to the aromatic nucleus, being itself converted into benzoic acid.

Radicals generated in the reacting solution abstract a hydrogen atom from a molecule of hydrocarbon (SH) giving rise to a hydrocarbon radical (S·), which appears to react mainly by decomposing peroxybenzoic acid. The products from this induced decomposition are the corresponding alcohol (SOH) and the benzoyloxy radical. The alcohol may further be oxidized (reaction 5) to the corresponding carbonyl compound, carboxylic acid and ester according to the scheme set forth in Part I[1]. In fact, the successive oxidation of cyclohexanol, the primary product from cyclohexane, to cyclohexanone and ε-caprolactone was borne out as described in the experimental part.

The retarding action of *p*-benzoquinone indicates that the induced decomposition is important. In the absence of the induced decomposition water ought to have been formed in much larger amount than actually found, and the benzoate ester ($PhCO_2S$) derived from the hydrocarbon would have been formed at least in an amount comparable to that of the alcohol (SOH, reactions 4 and 4′), because hydroxyl radicals would abstract a hydrogen atom from a molecule of hydrocarbon more efficiently than benzoyloxy radicals do, the stationary concentration of the latter radical thus becoming larger than that of the former. In fact no such benzoate ester was detected at all.

A similar mechanism has recently been postulated by other workers for the induced decomposition of other organic peroxyacids. Thus, Lefort, Paquot and Sorba[5] have found that decomposition of peroxylauric acid in petroleum ether gave *n*-undecanol in a good yield and postulated attack of a *n*-undecyl radical generated by decomposition of a lauroyloxy radical on a molecule of peroxylauric acid giving a molecule of *n*-undecanol and a lauroyloxy radical.

$$C_{11}H_{23}\cdot + C_{11}H_{23}CO_3H \rightarrow C_{11}H_{23}OH + C_{11}H_{23}CO_2\cdot$$

More recently Heywood, Phillips and Stansbury[6] have studied decomposition of peroxyacetic acid in several solvents and proposed a radical chain mechanism very similar to ours. There, the induced decomposition of peroxyacetic acid by solvent radicals (S·) has also been postulated, giving rise to a molecule of the corresponding alcohol and a acetyloxy radical, which decomposes to a methyl radical and carbon dioxide.

$$S\cdot + CH_3CO_3H \rightarrow SOH + CH_3CO_2\cdot$$

Further, Lefort, Sorba and Rouillard[7] have presented a similar mechanism for the formation of cyclohexanol in the decomposition of peroxylauric acid in cyclohexane.

It is noteworthy that peroxybenzoic acid is, as shown in the present work, readily attacked at the peroxidic oxygen atom even by the radical derived from hydrocarbon, which is usually regarded as rather inefficient in causing the induced decomposition of benzoyl peroxide[2] compared with radicals from ethers and alcohols. In this respect, peroxybenzoic acid is rather similar to hydroperoxides than to benzoyl peroxide. Thus, Fordham and Williams[8] have postulated the attack of α,α-dimethylbenzyl radicals on α,α-dimethylbenzyl hydroperoxide to produce a molecule of α,α-dimethylbenzyl alcohol and an α,α-dimethylbenzyloxy radical in decomposition of α,α-dimethylbenzyl hydroperoxide in cumene. Further, Bateman and Hughes[9] have assumed induced decomposition of cyclohexenyl hydroperoxide by cyclohexenyl radicals giving cyclohexenol and a cyclohexenoxy radical, whereas in the decomposition of benzoyl peroxide in cyclohexane[10,11], such a mode of decomposition does not seem to be significant.

As regards the initiation process in alcohols and hydrocarbons, we have proposed a unimolecular homolysis of the oxygen to oxygen

5) D. Lefort, C. Paquot and J. Sorba, *Bull. soc. chim. France*, **1959**, 1385.

6) D. L. Heywood, B. Phillips and H. A. Stansbury, Jr., *J. Org. Chem.*, **26**, 281 (1961).

7) D. Lefort, J. Sorba and D. Rouillard, *Bull. soc. chim. France*, **1961**, 2219.

8) J. W. R. Fordham and H. L. Williams, *Can. J. Research*, **B27**, 943 (1949).

9) L. Bateman and H. Hughes, *J. Chem. Soc.*, **1952**, 4594.

10) P. H. Hermans and J. Van Eyk, *J. Polymer Sci.*, **1**, 407 (1946).

11) C. Walling and E. S. Savas, *J. Am. Chem. Soc.*, **82**, 1738 (1960).

bond of peroxybenzoic acid producing a benzoyloxy radical and a hydroxyl radical (reaction 1). Since peroxybenzoic acid was found to be consumed very slowly in carbon tetrachloride, it was at first thought that the rate of the homolysis of the oxygen to oxygen bond had been measured, the induced decomposition by the solvent radical, the trichloromethyl radical, having hardly occurred. If peroxybenzoic acid decompose by a similar reaction scheme in carbon tetrachloride to that in alcohols and hydrocarbons, the benzoyloxy radical initially formed will predominatly decompose to carbon dioxide and a phenyl radical, which abstracts a chlorine atom from carbon tetrachloride and yields chlorobenzene and a trichloromethyl radical; the latter will then give hexachloroethane by dimerization or phosgene and hydrogen chloride through its attack on peroxybenzoic acid or its combination with a hydroxyl radical. In fact the decomposition products in carbon tetrachloride contained only negligible traces of chlorobenzene, hexachloroethane and phosgene[12]. These findings therefore lead us to conclude that the decomposition rate of peroxybenzoic acid observed in carbon tetrachloride cannot be regarded as representing the unimolecular homolysis of peroxybenzoic acid.

If peroxybenzoic acid decomposed in benzene predominantly by the radical path, biphenyl and phenol ought to have been obtained. Actually, among the decomposition products in benzene neither biphenyl nor phenol was detected and only a trace of carbon dioxide was formed[12], indicating that the benzoyloxy radical was produced only to a limited extent. It is true that any phenol produced might have been further oxidized by peroxybenzoic acid[13], but the above findings strongly suggest that most part of peroxybenzoic acid reacted by oxidizing the benzene nucleus through a mechanism other than homolytic.

In order to get a deeper insight into the initiation process, decomposition of peroxybenzoic acid in carbon tetrachloride in the presence of iodine was carried out with the intention of catching benzoyloxy radicals according to Hammond's[14] procedure used in his study on benzoyl peroxide. However, in the present experiment, unexpectedly, diiodine pentoxide was obtained, showing that peroxybenzoic acid oxidized iodine to diiodine pentoxide, and that this method was not suitable for the study of the unimolecular homolytic decomposition of peroxybenzoic acid.

12) K. Tokumaru and O. Simamura, unpublished.
13) K. Akiba and O. Simamura, unpublished.
14) G. S. Hammond and L. M. Soffer, *J. Am. Chem. Soc.*, **72**, 4711 (1950).

Meanwhile in this laboratory peroxybenzoic acid has been shown to initiate a radical polymerization of methyl methacrylate[15] and kinetic measurements of this polymerization have yielded the following expression for the rate constant of the initiation, the initiation efficiency of unity being assumed:

$$2.11\times10^{4}\exp(-15400/\boldsymbol{RT})\,\mathrm{sec}^{-1}$$

This rate constant may well be taken to be that for the initial homolytic rupture of the oxygen to oxygen bond in peroxybenzoic acid. Indeed it is extremely striking that both activation energy and frequency factor are so small as compared with the corresponding values for other organic peroxides. Thus, for example, with benzoyl peroxide, the following value[16] is reported.

$$3.0\times10^{13}\exp(-29600/\boldsymbol{RT})\,\mathrm{sec}^{-1}$$

Recently Cohen and Edwards[17] have carried out kinetic study of decomposition of peroxybenzoic acid in the presence of 2, 2-diphenyl-1-picrylhydrazyl in benzene or in *n*-butyl alcohol at 60 and 65°C, estimated the rate constant of the free-radical cleavage of peroxybenzoic acid and calculated the activation energy to be about 30 kcal./mol. in benzene. Since there is no cogent reason for assuming that there exists no interaction at all between peroxybenzoic acid and 2, 2-diphenyl-1-picrylhydrazyl other than the latter is consumed by being attacked by radicals generated from the former, the values obtained by the American workers must be accepted with some reservation. However, if this value of 30 kcal./mol. is correct for the activation energy for the unimolecular homolysis of the oxygen to oxygen bond in peroxybenzoic acid, the abnormal value obtained by us suggests that the initiation might occur rather through some interaction between peroxybenzoic acid and the vinyl monomer. Moreover, the alternative possibility can not be overlooked that peroxybenzoic acid may decompose by interaction with a molecule of solvent (H–S), producing radicals, as represented in reaction (1a).

$$PhCO_3H + H\text{–}S \rightarrow PhCO_2\cdot + H_2O + S\cdot \qquad (1a)$$

A similar mode of decomposition has been

15) O. Simamura, T. Suehiro and H. Terada, presented at the 13th Annual Meeting of the Chemical Society of Japan, Tokyo, April, 1960; H. Terada, *J. Soc. Organic Synthetic Chem. Japan* (*Yuki-gosei Kagaku Kyokaishi*), **19**, 721 (1961); **20**, 74, 158 (1962).
16) C. E. H. Bawn and S. F. Mellish, *Trans. Faraday Soc.*, **47**, 1216 (1951). Similar data are tabulated in A. V. Tobolsky and R. B. Mesrobian, "Organic Peroxides", Interscience Publishers, New York (1954), p. 78.
17) S. R. Cohen and J. O. Edwards, *J. Phys. Chem.*, **64**, 1086 (1960).

suggested by Semenov[18] and Thomas and Harle[19] for the decomposition of hydroperoxides.

Summary

Decomposition of peroxybenzoic acid was studied in *n*-heptane, cyclohexane, cumene, and toluene. The hydrocarbons were oxidized to the corresponding alcohols, which were often oxidized further. For these decompositions, a radical chain mechanism was proposed, which involves the homolytic rupture of the oxygen-oxygen bond of peroxybenzoic acid as the initiation process and an induced decomposition of this bond by solvent radicals derived from hydrocarbon molecules.

Department of Chemistry
Faculty of Science
The University of Tokyo
Hongo, Tokyo

18) N. N. Semenov, "Some Problems of Chemical Kinetics and Reactivity" (translated by J. E. S. Bradley), Vol. II, Pergamon Press, London (1959), p. 128.
19) J. R. Thomas and O. L. Harle, *J. Phys. Chem.*, **63**, 1027 (1959).

Spectrophotometric Determination of Cerium(III) and Some Rare Earths with Xylenol Orange[1]

By Kôichi TONOSAKI and Makoto OTOMO

(Received July 9, 1962)

Since xylenol orange was first prepared by Körbl and others[2,3] as a metallochromic indicator of the "complexone type", this reagent has widely been used by a number of investigators in complexometric titrations. However, only a few workers have applied this reagent to the spectrophotometric determination of metals; zirconium, hafnium, iron and bismuth have been thus determined by Cheng[4-8], and recently bitsmuth, by Onishi and Ishiwatari[9].

The present investigation was undertaken to evaluate the applicability of xylenol orange as a spectrophotometric reagent for various metal cations. From the results, a new spectrophotometric method for the determination of cerium(III) and of some rare earth elements is proposed. As in the other cases[4-9], the molar ratio of the complex between rare earth and this reagent is also 1 : 1.

Experimental

Reagents. — Stock solutions of rare earths were prepared separately by dissolving the purified oxide of rare earths (cerium, lanthanum, neodymium and yttrium) and were standardized by EDTA titration, using xylenol orange as an indicator[10].

About 10^{-3} M of a xylenol orange solution was prepared by dissolving Dotite XO reagent Dôjindô) & Co., Kumamoto) in distilled water. According to Ueno[11], this solution is stable for several months.

Apparatus. — All the absorption measurements were made with a Hitachi model EPU-2A spectrophotometer, using 1 cm. cells.

Procedure. — From 0 to 100 μg. of one of the rare earths was transferred to a 25 ml. volumetric flask. (When cerium was to be determined, 1 ml. of a 0.5% solution of ascorbic acid was added to prevent oxidation of the cerium(III) to the ceric state). Three to four milliliters of a xylenol orange solution and 15 ml. of an acetate buffer solution (pH 6.1±0.1, 0.17 M as acetate ions) were then added. After the mixture had been diluted to the mark with water and mixed, the absorbance of the solution was measured at the wavelengths mentioned below.

Results and Discussion

Absorption Spectra. — Figure 1 shows the absorption spectra of xylenol orange and its cerium complex at a pH of 6.1. Both the reagent and the complex have an absorption maximum at about 580 mμ. When a correction for the reagent blank is applied, an absorption peak of the complex is found at 575 mμ. A wavelength of 575 mμ, therefore, has been

1) Presented at the 14th Annual Meeting of the Chemical Society of Japan, Tokyo, April, 1961.
2) J. Körbl, R. Pribil and A. Emr, *Collection Czech. Chem. Communs.*, **22**, 961 (1957).
3) J. Körbl and R. Pribil, *Chemist Analyst*, **46**, 102 (1956).
4) K. L. Cheng, *Talanta*, **2**, 61 (1959).
5) K. L. Cheng, ibid., **2**, 266 (1959).
6) K. L. Cheng, ibid., **3**, 81 (1959).
7) K. L. Cheng, ibid., **3**, 147 (1959).
8) K. L. Cheng, ibid., **5**, 254 (1960).
9) H. Ônishi and N. Ishiwatari, This Bulletin, **33**, 1581 (1960).
10) K. Ueno, "Chelate Titration", Nankôdô, Tokyo (1960), p. 328.
11) Ibid., p. 125.

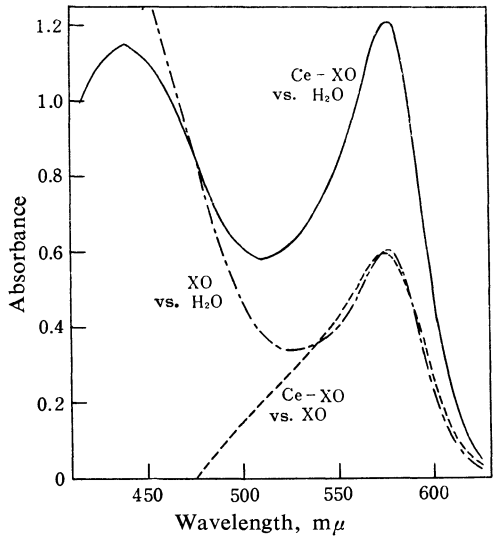


Fig. 1. Absorption spectra of xylenol orange and its cerium complex.
Ce: 1.9×10^{-5} M XO: 1.2×10^{-4} M

adopted in the determination of cerium. (At this wavelength the absorbance of the complex is about six times that of the reagent itself.) The complexes of lanthanum, neodymium and yttrium exhibit similar tendencies with the cerium complex. Their absorption peaks are found at 576 mμ for lanthanum and 578 mμ for neodymium and yttrium.

Effect of pH.—The effect of pH on the color development of the cerium complex was studied with solutions varying in pH value from 4 to

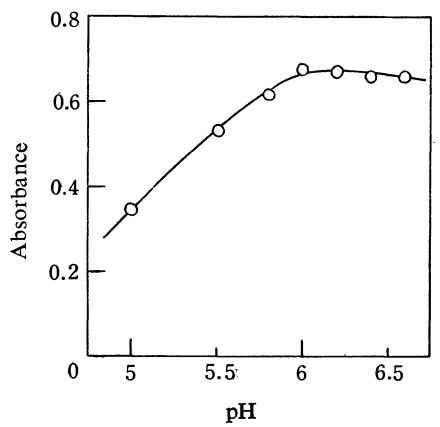


Fig. 2. Effect of pH on color development.
Ce: 65 μg.

7. Figure 2 shows that the maximum color development is obtained over the pH range of 6.0 to 6.5. Similar results are also obtained for the other rare earths.

Effect of Xylenol Orange. — A practically constant absorbance is obtained by adding 3

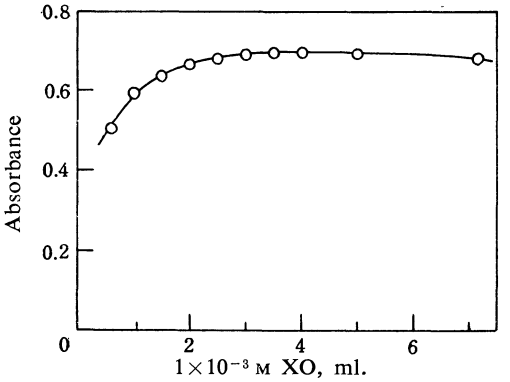


Fig. 3. Effect of addition of xylenol orange.
Ce: 65 μg.

to 5 ml. of a 1×10^{-3} M xylenol orange solution (Fig. 3). Too large amounts of the dye tend to decrease the absorbance. It seems, therefore, that in the presence of a large excess of the dye, these rare earths may form a complex other than a 1 : 1 complex.

Stability of Complex.—Figure 4 shows the stability of the colored complex of cerium. Since the color is stable at room temperature for at least 2 hr., no particular attention need be paid to the time of standing.

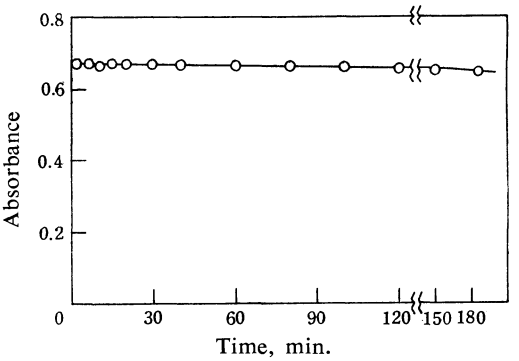


Fig. 4. Stability of Ce-XO complex.
Ce: 65 μg.

Calibration Curve. — As is shown in Fig. 5, a linear relationship exists between the absorbance and the rare earth concentration over the range investigated. The optimum concentration range was then determined by Ringbom's procedure[12] and was found to lie between 20 to 100 μg. cerium. At the measured wavelength, the molar extinction coefficients of the xylenol orange complexes of lanthanum, cerium, neodymium and yttrium are 32000, 31000, 38000 and 48000 respectively. From these high sensitivities, xylenol orange is found to be the

12) A. Ringdom, *Z. anal. Chem.*, **115**, 332 (1938/9).

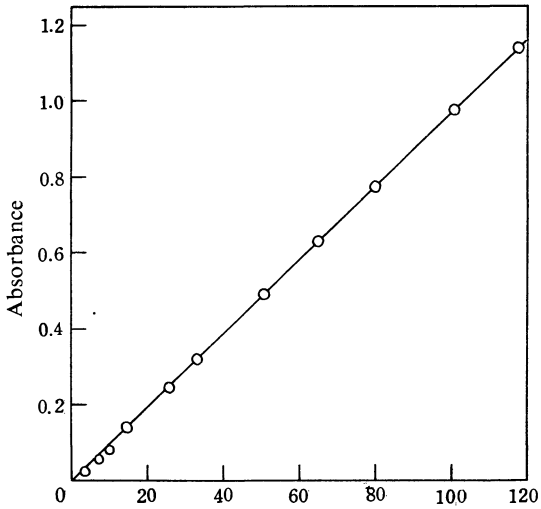


Fig. 5. Calibration curve.

most convenient reagent for spectrophotometric determination of trace amounts of rare earths.

Formation Constant.—The mole ratio method and the continuous variation method (Job's method) were applied to establish the mole ratio of the complex in solution. From Figs. 6 and 7, it is evident that cerium forms a 1 : 1 complex with xylenol orange. The formation constant was calculated from the curves shown in Fig. 7, based on the method described by Cheng[5] and et al. It was found to be 3×10^5 at 25°C. Because of its low formation constant, it is easily understood why xylenol orange has been successfully used as an indicator in the EDTA titration of rare earths. Lanthanum, neodymium and yttrium also form a 1 : 1 complex with xylenol orange; their formation constants are calculated to be 7×10^5, 1×10^6 and 3×10^5 respectively. These values are slightly lower than those of zirconium-[5], hafnium-[6] and bismuth-xylenol orange[8,9] complexes.

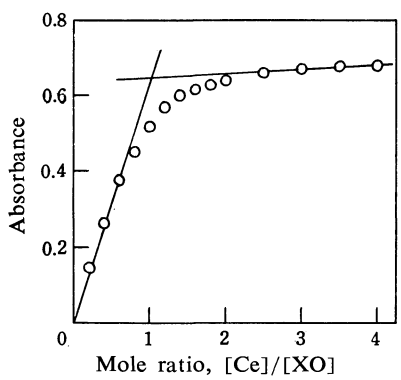


Fig. 6. Mole ratio method.
XO: 2×10^{-5} M

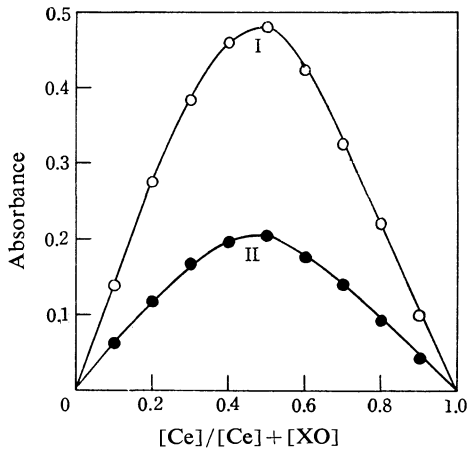


Fig. 7. Continuous variation method.
I: $[Ce]+[XO]=4\times10^{-5}$ M
II: $[Ce]+[XO]=2\times10^{-5}$ M

TABLE I. EFFECT OF ANIONS ON CERIUM DETERMINATION

Anion		Cerium	
Present	Added μ mol.	Taken μg.	Found μg.
Chloride	250	98.1	98.1
	500		97.0
Fluoride	1	92.5	88.4
	5		74.1
	10		46.5
Nitrate	250	98.1	96.6
	500		99.5
Sulfate	250		100.3
	500		99.7
Thiosulfate	8	97.4	96.3
	20		93.3
Oxalate	2.5		88.3
	5		82.2
Phosphate	1	98.1	43.5
	2.5		15.5
	5		5.2
Tartrate	5	97.4	91.9
Citrate	0.2		91.7
	1		88.0
NTA	0.5	92.5	92.3
	1.5		81.9
EDTA	0.01		73.0
	0.05		2.0
	0.2		1.0

Effect of Anions.—Table I indicates the effect of anions on the determination of cerium. Chloride, nitrate, sulfate and thiosulfate do not interfere. Large amounts of fluoride, oxalate, tartrate and citrate decrease the absorbance considerably. NTA (nitrilotriacetic

acid) and EDTA, which may form a stable complex with the rare earths, seriously inhibit the color development of the complex.

Summary

A method has been described for the spectrophotometric determination of 20 to 100 μg. of a rare earth element using xylenol orange. The complexes of cerium(III), lanthanum(III), neodymium(III) and yttrium(III) with xylenol orange have an absorption maximum at 575 to 578 mμ vs. the reagent blank. Each of them is a 1 : 1 complex and has a formation constant of approximately 10^5 under the conditions studied. Anions such as NTA and EDTA inhibit the color development of the complexes.

The authors wish to express their thanks to Miss Iku Mizuki for her assistance in the measurements.

Department of Chemistry
Faculty of Literature and Science
Hirosaki University
Hirosaki, Aomori

*The Stereoregularity of Poly-p-bromostyrene Polymerized by the Ziegler Catalyst**

By Koichi HATADA, Takao NIKI, Shun-ichi NOZAKURA and Shunsuke MURAHASHI

(Received January 10, 1962)

Since stereospecific polymerization was discovered by Natta[1] in 1955, many crystalline structures have been investigated and determined on a number of stereoregular polymers. Crystallizability is not always dependent on the stereoregularity of the polymer, and some of the polymers polymerized by the so-called stereospecific catalysts appear to be amorphous, it not being certain whether they are stereoregular or not[2]. For instance, poly-*p*-methylstyrene and poly-*m*-methylstyrene polymerized by the Ziegler catalyst were originally considered to be amorphous. Later it was found, from the infrared spectroscopic study of these polymers, that the polymers might have stereoregularity[3]. This led to the preparation of effectively oriented samples of the polymers and to the determination of their crystalline structures[4].

Natta and his coworkers found that poly-*p*-chlorostyrene polymerized by the stereospecific catalyst was amorphous, but the polymer was proved to be stereoregular by its giving of crystalline polyvinylcyclohexane as the result of catalytic hydrogenation. They ascribed the noncrystallinity of the original poly-*p*-chlorostyrene to the steric effect of the chlorine atom in crystalline orientation[5]. Poly-*p*-chlorostyrene polymerized by the Ziegler catalyst was found by Nagai to contain a small fraction of the polymer insoluble in cold xylene; this fraction gave an infrared spectrum different from that of the amorphous fraction soluble in cold xylene[6].

For the present work, the authors investigated the stereoregularity of poly-*p*-bromostyrene polymerized by the Ziegler catalyst and were led to the conclusion that the polymer was, in this particular case, not stereoregular, this conclusion being different from Natta's for poly-*p*-chlorostyrene.

Experimental

Materials. — *p-Bromostyrene.* — *p*-Bromoacetophenone was prepared from bromobenzene and acetic anhydride using aluminum chloride as the catalyst[7] and was purified by recrystallization from methanol-water to make it free from the ortho isomer. The pure *p*-bromoacetophenone (m. p., 49.5~50.0°C) was reduced to the corresponding carbinol by the Meerwein-Pondorf method[8]. The carbinol was

* Paper X in a series on "Stereoregular Polymers". Presented at the 13th Annual Meeting of the Chemical Society of Japan, Tokyo, April, 1960. For paper IX, see This Bulletin, **34**, 1673 (1961).

1) G. Natta, *J. Polymer Sci.*, **16**, 143 (1955).

2) G. Natta, F. Danusso and D. Sianesi, *Makromol. Chem.*, **28**, 253 (1958).

3) H. Tadokoro, S. Murahashi, T. Kitazawa, Y. Yasuhara and S. Nozakura, This Bulletin, **32**, 313 (1959).

4) S. Murahashi, S. Nozakura and H. Tadokoro, ibid., **32**, 534 (1959).

5) G. Natta, P. Corradini and I. W. Bassi, *Makromol. Chem.*, **33**, 247 (1959); G. Natta, ibid., **35**, 94 (1960).

6) K. Nagai, M. Kobayashi and E. Nagai, This Bulletin, **32**, 771 (1959).

7) R. Adams and C. R. Noller, "Organic Synthesis", Coll. Vol. I (1956), p, 109.

8) A. L. Wilds, "Organic Reactions", Vol. II, John Wiley & Sons, Inc., New York (1944), p. 178.

dehydrated to *p*-bromostyrene by potassium bisulfate[9]. The product was dried over calcium chloride and distilled under reduced pressure. A fraction boiling at 69~92°C/13 mmHg was collected and fractionally crystallized several times, about one-sixth of the product being discarded each time as an unfrozen liquid. Pure *p*-bromostyrene was obtained by redistillation of the residue of the final crystallization; b. p., 90.5~91.0°C/13 mmHg, n_D^{20} 1.588.

n-Heptane.—Commercial *n*-heptane was purified in the usual manner[10], dried, and stored over metallic sodium.

Aluminum Triethyl.—Aluminum triethyl was supplied by the Mitsui Chem. Ind. Co. and was used without further purification.

Titanium Tetrachloride.—The titanium tetrachloride was a product of the Osaka Titanium Co.

Titanium Trichloride.—A commercial product (Stauffer Chem. Co.) was washed three times with *n*-heptane before use.

n-Butyllithium.—A benzene solution was prepared according to Ziegler's method[11] from *n*-butylchloride and lithium.

Lithium Aluminum Hydride.—The lithium aluminum hydride was a commercial product of Metal Hydride Inc.

Tetrahydrofuran.—Tetrahydrofuran was refluxed and distilled over sodium before use.

Polymerization.—The polymerization was carried out in a method similar to that described in a previous paper[12]. After the vessel had been flushed by dry nitrogen, 20 ml. of *n*-heptane and 0.38 g. of titanium tetrachloride were introduced into the vessel. While the solution was boiled gently, 0.225 g. of triethylaluminum was added slowly; the heating was continued for a further 5 min. and then the solution was cooled. After the precipitation of a solid complex, the supernatant liquid was removed by a syringe under dry nitrogen. The solid was washed three times with 20 ml. of *n*-heptane, and 20 ml of *n*-heptane and 0.225 g. of triethylaluminum were added. The monomer was then added to the catalyst suspension and polymerized.

When the catalyst was prepared from titanium trichloride and aluminum triethyl, 0.20 g. of triethylaluminum was added to 1.5 g. of titanium trichloride suspended in 20 ml. of *n*-heptane at room temperature.

The polymer produced was precipitated by pouring the reaction mixture into methanol containing hydrochloric acid, washed thoroughly with methanol, and dried in vacuo at 130~150°C.

Reaction of Poly-*p*-bromostyrene with *n*-Butyllithium.—A three-necked flask was fitted with a reflux condenser, a separatory funnel and a glass tube equipped with a rubber cap. After the flask had been flushed by dry nitrogen, 20 ml. of benzene and a benzene solution of *n*-butyllithium (600 mg.) were introduced with a hypodermic syringe through the rubber cap. While the solution was stirred with a magnetic stirrer and maintained at the reaction temperature, a solution of about 200 mg. of poly-*p*-bromostyrene in 20 ml. of benzene was slowly added, drop by drop, over a period of from 2 to 4 hr. After the addition was complete, stirring was continued for 2 hr.; then the mixture was poured into a large amount of methanol to hydrolyze the lithiated polymer. After the mixture had stood overnight, the polymer was collected, washed with methanol, and dried in vacuo at 70~100°C.

Reduction of Poly-*p*-bromostyrene by Lithium Aluminum Hydride.—A mixture of about 300 mg. of poly-*p*-bromostyrene and 0.5 g. of finely powdered lithium aluminum hydride in 300 ml. of tetrahydrofuran was brought to solution by warming; the solution was then refluxed under dry nitrogen for about 6 days. In the course of the reaction, two portions of 5 ml. of benzene each were added to the reaction mixture in order to solubilize the partially debrominated polymer and to complete the reaction. The reaction mixture was poured into 300 ml. of methanol containing a small amount of hydrochloric acid to decompose the excess lithium aluminum hydride and to precipitate the polymer. The product was then purified by reprecipitation from toluene and methanol.

Measurements of Softening Points and Viscosities.—Softening points were measured using a hot-stage microscope. Intrinsic viscosities are measured in benzene at 20°C using a Ubelhode-type dilution viscometer.

Results and Discussion

It was reported in a previous paper that bromobenzene does not impair the isotactic polymerization of styrene with the Ziegler catalyst[12]. This fact prompted us to prepare the isotactic polymer of *p*-bromostyrene with the catalyst.

p-Bromostyrene was easily polymerized with the catalyst to give a high polymer in good yields. The results of the polymerization are summarized in Table I. Polymerization with the addition of thiophene to the catalyst system gave almost the same results. The addition of thiophene was tried since a good stereospecificity was observed with it in the case of the polymerization of styrene[12]. The polymer showed an amorphous X-ray pattern and the same infrared spectrum as that of the polymer obtained by radical polymerization.

In order to determine the stereoregularity of poly-*p*-bromostyrene, the polymer was reduced to polystyrene and the properties of the resulting polystyrene were compared with those of isotactic and amorphous polystyrenes. Debromination was attempted by two methods, i. e., halogen-metal conversion with butyllithium, followed by hydrolysis (Braun's method)[13] and reduction with lithium aluminum hydride.

9) C. Walling, *J. Am. Chem. Soc.*, **70**, 1537 (1948).
10) A. Weissberger et al., "Organic Solvents", 2nd. Ed., Interscience Publishers, Inc., New York (1955), p. 311.
11) K. Ziegler and H. G. Gellert, *Ann.*, **567**, 179 (1950).
12) S. Murahashi, S. Nozakura and K. Hatada, This Bulletin, **34**, 939 (1961).
13) D. Braun, *Makromol. Chem.*, **30**, 85 (1959).

TABLE I. POLYMERIZATION OF *p*-BROMOSTYRENE WITH ZIEGLER TYPE CATALYSTS
Solvent: *n*-Heptane, 20 ml.

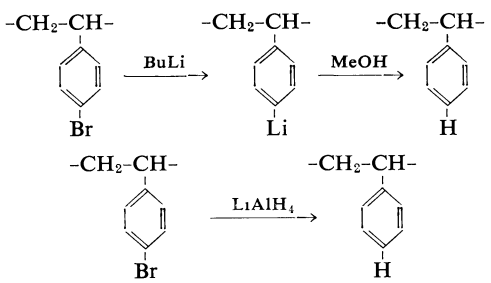
Catalyst g.	Monomer g.	Polymerization Temp. °C	Polymerization Time hr.	Polymer Conv. %	Polymer M. p.[b] °C	Polymer Elemental anal.[c], % C	H	Br	Ash	Polymer [η] dl./g.
$AlEt_3$-$TiCl_4$	7.0	70	6	92.2	218~224	52.73	3.77	43.41	0.63	0.259
$AlEt_3$-$TiCl_4$[a]	6.3	60	6	87.2	214~219	52.29	3.91	43.49	0.53	0.244
$AlEt_3$-$TiCl_3$	4.2	10	75	72.0	192	53.11	3.98	43.34	0	0.167
$AlEt_3$-$TiCl_4$	3.5	−35	36	0	—	—	—	—	—	—

a) Thiophene (0.46 g.) was added.
b) The softening point of poly-*p*-bromostyrene prepared by thermal polymerization was 215°C. $[\eta]=0.280$ dl./g.
c) Calcd. for $(C_8H_7Br)_n$: C, 52.49; H, 3.86; Br, 43.65%.

TABLE II. REDUCTION OF POLY-*p*-BROMOSTYRENE WITH *n*-BUTYLLITHIUM
n-BuLi, 600 mg.; Solvent, Benzene 40 ml.

Exp. No.	Polymer g.	Reaction Temp. °C	Reaction Time hr.	Reduced polymer Yield g.	Elemental anal., % C	H	Br	Ash
H-2[a]	0.203	20	3.3	0.133	75.25	6.21	17.62	0.59
H-1	0.206	20	2.2	0.137	69.17	5.46	24.27	0.35
H-4[b]	0.112	20	5.8	0.087	85.43	7.11	6.34	0.89
H-7[c]	0.070	20	6.0	0.063	88.06	7.29	3.49	1.32
H-3[d]	0.200	80	5.3	0.110	91.81	7.68	0.73	0
H-8	0.156	43	5.0	0.065	82.08	7.08	9.09	0.51

a) The polymer was polymerized thermally.
b), c) Specimens H-4 and H-7 were obtained by successive reductions of H-1.
d) Elemental analysis was given for the soluble part of the reduction product.



Braun demonstrated the recovery of an isotactic polystyrene from an amorphous iodinated product which had been derived by the iodination of isotactic polystyrene[14]. He attempted to apply the method to the determination of the stereoregularity of poly-*p*-chlorostyrene and poly-*p*-bromostyrene, resulting in incomplete dehalogenation.

In the present work it was also ascertained that the lithiation of poly-*p*-bromostyrene with butyllithium could not be accomplished satisfactorily. The results of the reduction of poly-*p*-bromostyrene by butyllithium are shown in Table II. When the reaction temperature of 20°C was employed, only a half of the bromine of the polymer was removed. The three successive reactions at the same temperature gave a product still 3.49% bromine. When the reaction was carried out at the boiling point of benzene, the debromination was almost complete, but 90% of the product was insoluble and infusible. This must be a cross-linked polymer produced by the Wurtz-Fittig coupling between the lithiated phenyl group and the bromophenyl group in the polymer chains.

Prolonged reduction of poly-*p*-bromostyrene using lithium aluminum hydride as a reducing agent gave a polystyrene containing a negligible amount of bromine, although in this reaction a large excess of lithium aluminum hydride was required[15]. The results of the reduction are shown in Table III. Elemental analysis of the product showed a good agreement with that of polystyrene except that a trace of ash could not be removed from the samples.

14) D. Braun, *J. Polymer Sci.*, **40**, 578 (1959).

15) The necessity of a large excess of lithium aluminum hydride may be explained, according to Bailey[15], as follows: as the reduction proceeds, the produced aluminum tribromide reacts with lithium aluminum hydride and gives aluminum hydride. Both aluminum hydride and lithium aluminum hydride may cause a ring cleavage of the solvent tetrahydrofuran and may thus be consumed. (W. J. Bailey and F. Marktscheffel, *J. Org. Chem.*, **25**, 1797 (1960).)

TABLE III. REDUCTION OF POLY-*p*-BROMOSTYRENE WITH $LiAlH_4$

$LiAlH_4$: 0.5 g.
Solvent: Tetrahydrofuran, 30 ml.
Reaction temp: 66°C (b. p. of tetrahydrofuran)

Exp. No.	Polymer g.	React. time hr.	Reduced polymer				
			Yield	Elemental analysis[b], %			
			g.	C	H	Br	ash
H-11	0.316	6	0.247	60.70	4.54	35.07	0.63
H-12	0.300	145	0.130	91.62	7.69	0	0.67
H-13[a]	0.300	145	0.126	91.11	7.55	0.36	0.80

a) Poly-*p*-bromostyrene obtained by thermal polymerization
b) Calcd. for polystyrene $(C_8H_8)_n$: C, 92.26; H, 7.74%

TABLE IV. A COMPARISON OF THE REDUCED POLYMER WITH ISOTACTIC AND ATACTIC POLYSTYRENES

Polystyrene	Reducing agent	M. p. °C	Solubility[d]		X-Ray diffraction
			EMK[e]	Toluene	
Amorph. P. S.[a]	—	110~3	+	+	Amorph.
Isot. P. S.[b]	—	230~3	−	+	Cryst.
From PPBS[c],[f]	*n*-BuLi	120	+	+	Amorph.
From PPBS	$LiAlH_4$	150~5	+	+	Amorph.
From PPBS[g]	$LiAlH_4$	146~9	+	+	Amorph.

a) Amorphous part of the polymer obtained by the polymerization of styrene with the Ziegler catalyst
b) Isotactic part of the polymer obtained by the polymerization of styrene with the Ziegler catalyst
c) PPBS: Poly-*p*-bromostyrene
d) +: Soluble, −: Insoluble
e) EMK: Ethyl methyl ketone
f) The soluble fraction of the polymer reduced at 80°C
g) A specimen obtained by the reduction of a thermally polymerized poly-*p*-bromostyrene

The polystyrene obtained by the reduction was not separated into fractions having different properties with usual organic solvents. The polymer was heat-treated at 100°C for eight hours, but no crystallization by the treatment was detected. It was soluble in ethyl methyl ketone, gave only amorphous X-ray patterns, and showed a softening point of 150~155°C and the same infrared spectrum as that of atactic polystyrene. In the infrared spectrum, no absorption band was observed at 1364 and 1297 cm^{-1}, which bands had been proved to be characteristic of isotactic polystyrene[16]. A comparison of the reduced polymers with isotactic and atactic polystyrenes is shown in Table IV.

It may well be assumed that no change in the steric configuration of the main chain occurred through the reduction process. On the basis of these results, we may draw the conclusion that poly-*p*-bromostyrene polymerized with the Ziegler catalyst is substantially atactic in the steric configuration of the main chain. A major factor in the lack of stereoregularity may be the disturbance of stereoregulation at the site of polymerization by the bulky bromine atom attached to the para position of the benzene ring.

It is also to be noted that the polystyrene obtained by the reduction of poly-*p*-bromostyrene has a softening temperature of about 150°C. This is about 40°C higher than that of the conventional atactic polystyrene (ca. 110°C). Similarly, a polystyrene which was obtained by the lithium aluminum hydride reduction of thermally polymerized poly-*p*-bromostyrene showed the unusual softening point of 146~149°C. Therefore, there may be a possibility that the elevation of the softening point is due to a minor change in the chemical structure during the reduction, to, that is, for instance, a small extent of cross-linking.

Department of Polymer Science
Faculty of Science
Osaka University
Nakanoshima, Osaka

16) H. Tadokoro, T. Kitazawa, S. Nozakura and S. Murahashi, This Bulletin, **34**, 1209 (1959).

Spectroscopic Studies of 1, 2- and 3, 4-Phthaloylacridones

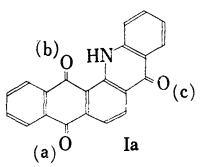
By Takayuki HAYASHI and Jun-ichirō MAEHARA*

(Received May 19, 1962)

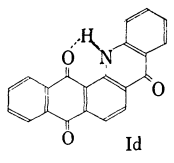
Phthaloylacridones are compounds of a high melting point and a low solubility in organic solvents. 1, 2-Phthaloylacridone, quite similar to acridone in its orange color, is a relatively strong acid which dissolves in alcoholic potassium hydroxide with a violet color[1]. The *N*-methyl derivative is non-acidic, more soluble in organic solvents, and lower-melting than 1, 2-phthaloylacridone, the properties of which are probably the result of intermolecular hydrogen bonding[2]. 3, 4-Phthaloylacridone is similar to 1-phenylaminoanthraquinone in its red-violet color, which indicates that its molecule exists in a true acridone, not a hydroxyacridone, structure, and it is lower-melting and more soluble in organic solvents than isomeric 1, 2-phthaloylacridone, suggesting the occurrence of intramolecular hydrogen bonding[2]. As the infrared, visible and ultraviolet regions of the spectra might yield more interesting information, it seemed desirable to investigate the spectra of these phthaloylacridones and their related compounds.

Results and Discussion

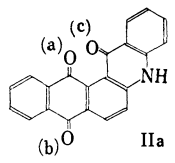
Visible Absorption Spectra.—For 1-benzoylaminoanthraquinone, a IIIb structure has been largely discredited[3]; also, its molecule could not exist in structure IIIc, since amide-type resonance is not possible for IIIc[4]. 1-Benzoylaminoanthraquinone is the resonance hybrid of the forms IIIa, IIId and IIIe[4]. The phthaloylacridones are chemically closely similar to the acylaminoanthraquinones[5], and 3, 4-phthaloylacridone is a vinylog of 1-benzoylaminoanthraquinone. It seems probable, therefore, that the molecule of the former can not exist in either the structure Ib or Ic, that the former is the resonance hybrid of the forms



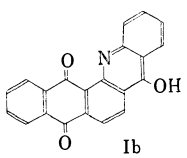
Ia



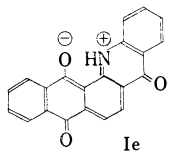
Id



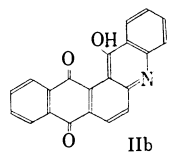
IIa



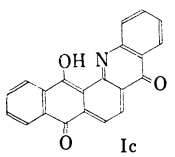
Ib



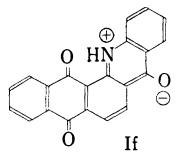
Ie



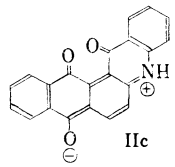
IIb



Ic



If



IIc

* Present address: The Research Laboratory of Idemitsu Kōsan Co., Tokuyama-shi.

1) F. Ullmann and P. Ochsner, *Ann.*, **381**, 1 (1911); F. Ullmann and M. Sone, ibid., **380**, 336 (1911); T. Maki and K. Eguchi, *J. Chem. Soc. Japan, Ind. Chem. Sec.* (*Kōgyō Kagaku Zassi*), **44**, 788 (1941).

2) W. Bradley and H. Kiwar, *J. Chem. Soc.*, **1960**, 2859.

3) L. Valentine, *J. Soc. Dyers & Colorists*, **72**, 286 (1956).

4) T. Hayashi and R. Shibata, This Bulletin, **34**, 1116 (1961).

5) W. Bradley, "Recent Progress in the Chemistry of Dyes and Pigments", The Royal Institute of Chemistry, London (1958), p. 4.

TABLE I. VISIBLE ABSORPTION PEAKS OF SUBSTITUTED AMINOANTHRAQUINONES AND PHTALOYLACRIDONES

	In *o*-dichlorobenzene	In pyridine	In conc. sulfuric acid
Anthraquinone			410 (7400)[8]
1-Aminoanthraquinone	466 (5980)*		380 (6000)[9]
2-Aminoanthraquinone	413 (3800)		375 (7100)[9]
1-Phenylaminoanthraquinone	508 (5920)		
1-Aminoanthraquinone-2-carboxylic acid	495 (7900)		355 (3300)
1-(*o*-Carboxyphenyl)-aminoanthraquinone	500 (6600)		370 (4100)
1-Benzoylaminoanthraquinone	421 (5900)[4]	415 (6350)[7]	
1,2-Phthaloylacridone		400 (11300)[2]	385 (7900)
			505 (11800)
3,4-Phthaloylacridone	516 (8000)[2]	516 (8000)[2]	365 (7200)**
			465 (3890)
5,6-Phthaloyl-1,2-benzacridone	515 (9000)[2]		

* Wavelength, mμ (molar extinction coefficient)
** The peak in 94% sulfuric acid appeared at 365~370 mμ[10].

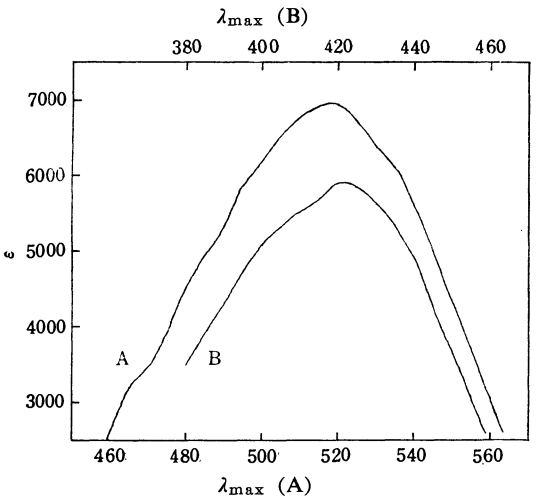


Fig. 1. Visible absorption spectra.
A: 3,4-Phthaloylacridone
B: 1-Benzoylaminoanthraquinone

Ia, Ie and If and that the carbonyl group in the nitrogen-bearing ring for the former shows an insulating effect similar to that in the benzoylamino group for the latter[4]. Their spectra in the visible region are shown in Fig. 1. As in the case of 5,6-phthaloyl-1,2-benzacridone[6], 3,4-phthaloylacridone gives a absorption curve broadly similar to that of 1-benzoylaminoanthraquinone, illustrating the insulating effect of the carbonyl group in the nitrogen-bearing ring. Such a fact is consistent with the above-mentioned deduction that both visible absorption bands are due to the same chromophore.

As is indicated in Table I, a comparison of the peaks of 3,4-phthaloylacridone and 1-benzoylaminoanthraquinone indicates a bathochromic shift of 95 mμ; the peak of the former shifts towards a longer wavelength than those of 1-aminoanthraquinone-2-carboxylic acid and 1-(*o*-carboxyphenyl)- and 1-phenyl-aminoanthraquinones. This fact can probably be attributed to the increased coplanarity of the molecule owing to the existence of the nitrogen-bearing ring for 3,4-phthaloylacridone. This interpretation is supported by the following thesis: the coplanarity on the molecule of 5,6-phthaloyl-1,2-benzacridone should be the same degree as for 3,4-phthaloylacridone, and therefore the effective area of the π-electron system[11] seems to be larger for the former than for the latter. As is clear from the results in Table I, the peak of the former appears at the same wavelength as for the latter, and the intensity is greater for the former than for the latter.

This fact is also deduced from the following results: though a comparison of the peaks of 3,4-phthaloylacridone and 1-aminoanthraquinone indicates a bathochromic shift of 53 mμ, that of 1,2-phthaloylacridone and 2-aminoanthraquinone makes only a slight hypsochromic shift of 13 mμ. For 1-amino-, 1-benzoylaminoanthraquinones[4,12] and 1,1'-dianthrimide[8], mesomeric shifts in their chromophoric systems contributed mainly to the shifts of their absorption peaks. Therefore, as will be clear from the results of the study of the infrared

6) J. J. Moran and H. I. Stonehill, *J. Chem. Soc.*, **1957**, 765.
7) R. H. Peters and H. H. Sumner, ibid., **1953**, 2101.
8) R. A. Durie and J. S. Shannon, *Australian J. Chem.*, **11**, 189 (1958).
9) K. A. Durie and J. S. Shannon, ibid., **11**, 168 (1958).
10) A. M. Lukin, P. M. Aronovich and G. P. Brin, *Zhur. Obshchei Khim.*, **20**, 2219 (1950); *Chem. Abstr.*, **45**, 7124 (1951).
11) E. A. Braude, *J. Chem. Soc.*, **1950**, 379; R. H. Peters and H. H. Sumner, *J. Soc. Dyers & Colorists*, **71**, 130 (1955).
12) G. S. Egerton and A. Roach, ibid., **74**, 401 (1958).

spectra of 3,4-phthaloylacridone, the carbonyl group is hydrogen-bonded with the imino group, though probably hydrogen bonding is not the main cause of such a large difference between the shifts of 3,4- and 1,2-phthaloylacridones. Such a hypsochromic shift of the peak for 1,2-phthaloylacridone is, therefore, to be attributed to the reduced mesomeric shift, leading to the IIc structure, owing to the decreased coplanarity of the molecule, which is due to the repulsion between two vicinal carbonyl-type oxygen atoms.

In aminoanthraquinones and phthaloylacridones, the protonation of their carbonyl oxygen atoms can occur, but it is not possible to say positively whether one, two or three carbonyl oxygen atoms are protonated[9,13]. As is indicated in Table I, the peaks of 1- and 2-aminoanthraquinones in concentrated sulfuric acid are shifted to shorter wavelengths and lower intensities compared with anthraquinone, and appear at shorter wavelengths than those in organic solvents. These hypsochromic shifts are most probably caused by the protonation of the amino group. On the contrary, as is indicated in Table I, 1,2-phthaloylacridone absorbs at a greatly longer wavelength in concentrated sulfuric acid than in pyridine. Similar phenomena were also seen in indanthrone. The absorption peaks of indanthrone appeared at 371, 422, 482, 554, 598 and 635 mμ in ethanol[6], at about 620, 675 and 740 mμ in 1,2,4-trichlorobenzene[14], and at 390, 462 and 818 mμ in concentrated sulfuric acid[8]. Its absorption peak at the longest wavelength indicates a marked bathochromic shift at the last. Furthermore, in concentrated sulfuric acid indanthrone absorbed at longer wavelengths than did 1,2-diaminoanthraquinone. This fact was attributed to the strong amide-type resonance in the former persisting in concentrated sulfuric acid and to the inhibited protonation of the imino groups, though the amino groups of the latter were protonated[8]. On the contrary, since the phthaloylacridones are chemically closely similar to the acylaminoanthraquinones[5], the amide-type resonance for the former is not so strong as for indanthrone; therefore, the protonation of the imino nitrogen atoms of the former can occur. Consequently, the absorption peak at the longest wavelength in concentrated sulfuric acid for 1,2- and 3,4-phthaloylacridones should be attributed to the production of new chromophoric systems by protonation. In concentrated sulfuric acid, two absorption peaks of 1,2-phthaloylacridone appear at respectively longer wavelengths than do corresponding ones of 3,4-phthaloylacridone, but in pyridine the reverse is found to be true.

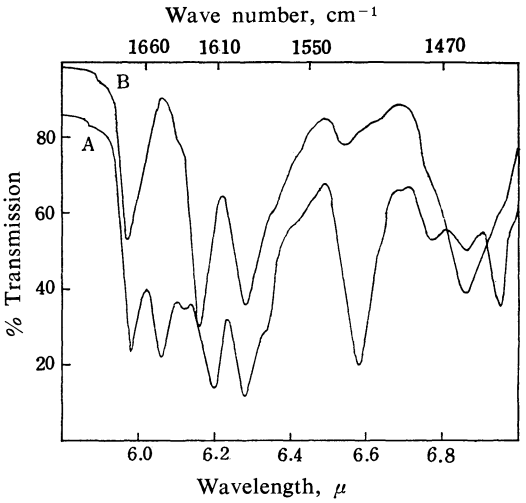


Fig. 2. 6 μ-Region of infrared absorption spectra.
A: 3,4-Phthaloylacridone
B: 1,2-Phthaloylacridone

TABLE II. 3 AND 6 μ-BANDS OF SOLID SUBSTITUTED ANTHRAQUINONES AND PHTHALOYLACRIDONES

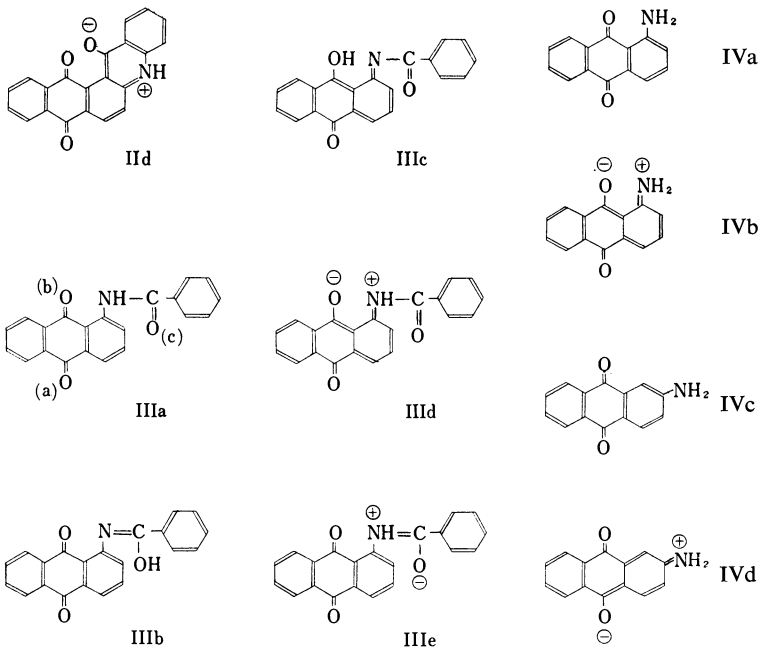
	3 μ-Bands, cm^{-1} (NH frequencies)	6 μ-Bands, cm^{-1} (C=O frequencies)		
		(a)	(b)	(c)
Anthraquinone[15]		1676		
1-Aminoanthraquinone[15]	3420, 3330	1665	1612	
2-Aminoanthraquinone[15]	3470, 3330, 3220	1676	1625	
1-Benzoylaminoanthraquinone[4]	3175	1681	1669	1637
1,2-Phthaloylacridone*	3300, 3215	1675	1675	1623
3,4-Phthaloylacridone*	3226, 3195	1672	1650	1613
5,6-Phthaloyl-1,2-benzacridone	3236	1678	1656	1608

* The C=O(a), (b) and (c) frequencies for 1,2- and 3,4-phthaloylacridones were observed at 1675, 1675 and 1623, and at 1672, 1653 and 1618 cm^{-1}, respectively, by the potassium bromide disk technique.

13) R. A. Hebert, M. B. Goren and A. A. Vernon, *J. Am. Chem. Soc.*, **74**, 5779 (1952); A. Geake, *Trans. Faraday Soc.*, **37**, 68 (1941).

14) J. Weinstein and C. Merritt, *J. Am. Chem. Soc.*, **81**, 3759 (1959).

15) M. S. C. Flett, *J. Chem. Soc.*, **1948**, 1441.



This bathochromic shift is probably due to the fact that, since the molecule of the former has a decreased coplanarity compared with the latter, the reduced effect of the strongly electron-attracting $-NH_2^+-$ group contributes to the resonance hybrid.

Infrared Absorption Spectra.—Three and six μ bands of aminoanthraquinones and phthaloylacridones suspended in Nujol are shown in Table II, and the spectra in the 6 μ region of the latter are shown in Fig. 2. As 3, 4-phthaloylacridone is a vinylog of 1-benzoylaminoanthraquinone, the 1672, 1650 and 1613 cm^{-1} bands for the former are assigned, respectively, to vibrations of the C=O(a), C=O (b) and C=O(c) groups indicated in Ia, similar to those of the latter[4,16]. In the same manner, the 1675 cm^{-1} band for 1, 2-phthaloylacridone is assigned to vibrations of both the C=O(a) and C=O(b) groups indicated in IIa, and the 1623 cm^{-1} band, to the vibration of the C=O(c) group. In such unsymmetrically substituted anthraquinones as amino- and hydroxy-derivatives, two bands appear, since the strengths of the two C=O bonds are unequal, but unsymmetrically substituted anthraquinones such as nitro-, chloro-, methoxy- and methyl-derivatives, on which the absorption peaks hardly appear in the visible region, give a single C=O frequency, since the dissymmetry is insufficient for two separate bands to be observed[15]. Therefore, two carbonyl groups of the anthraquinone nucleus for 1, 2-phthaloylacridone, the visible absorption peak of which appears at 400 mμ, seem to give only one band in the infrared region. On the contrary, those of 3, 4-phthaloylacridone, the visible absorption peak of which appears at 516 mμ, give two bands. Its C=O(c) frequency agrees with the C=O(b) frequency of 1-aminoanthraquinone IVa, and a relation between If and IVb for them corresponds to that between the IId of 1, 2-phthaloylacridone and the IVd of 2-aminoanthraquinone. It is probable, therefore, that the frequency at 1623 cm^{-1} for 1, 2-phthaloylacridone, being equal to the C=O(b) frequency for 2-aminoanthraquinone, may be assigned to the vibration of the C=O(c) group. Such facts about the C=O frequencies of 1, 2-phthaloylacridone are to be attributed to the reduced mesomeric shift leading to the IIc structure owing to the above-mentioned decreased coplanarity of the molecule. This interpretation is supported by the fact that the C=O(c) frequency of 1, 2-phthaloylacridone is about the same as for *N*-methyl-γ-quinolone[17], the C=O frequency of which appeared at 1625 cm^{-1}.

The absorption of both the 1, 2- and 3, 4-phthaloylacridones obtained using the potassium bromide disk technique occurred at 1580 cm^{-1}. Frequencies for the C=N groups[18] are most probably found in the frequency range 1690 to 1640 cm^{-1}, and the influence of conjugation is usually small. The observed frequencies in

16) T. Hayashi. *J. Chem. Soc. Japan, Ind. Chem. Sec.* (*Kogyo Kagaku Zasshi*), **63**, 1985 (1960).

17) P. I. Ittyerah and F. G. Mann, *J. Chem. Soc.*, **1958**, 467.

18) L. J. Bellamy, "The Infrared Spectra of Complex Molecules", John Wiley & Sons, Inc., New York (1958), p. 267.

phthaloylacridones at 1580 cm^{-1} appear, therefore, at too low a frequency to be normally attributed to the C=N vibration. Furthermore, when C=N and C=C groups are in conjugation, particularly in cyclic systems, it is doubtful whether either group can be regarded as retaining its individual character; therefore, the assignment of C=N frequencies under such circumstances is not reliable[18]. The 1575 cm^{-1} band for 1, 1'-dianthrimide was not attributed to the C=N vibration, but to the ring vibration[8]. The 1582 cm^{-1} band for 1-benzoylaminoanthraquinone was also attributed to the ring vibration[16]. Furthermore, since not only amino-substituted anthraquinones, indanthrones, and anthraquinoneazines, but also anthraquinone, had medium to strong bands in the vicinity of 1587 cm^{-1}, the 1580 cm^{-1} band of indanthrone could not be reasonably assigned to the C=N vibration; these bands were, rather, attributed to ring vibrations[14]. Thus, there is no precedent for assigning the 1580 cm^{-1} band of phthaloylacridones to the C=N vibration; it also is probably to be assigned to the ring vibration. Consequently, this band can not be used to support the structures containing the C=N bond (Ib, Ic, IIb). This interpretation of the molecular structure in a solid is the same as the deduction on that in solution on the basis of the results of the visible absorption; moreover, chemical evidence does not favor the Ib, Ic and IIb structures.

The spectra in the 3 μ region of 1, 2- and 3, 4-phthaloylacridones mulled in Nujol are shown in Fig. 3. The frequencies for the O–H groups are usually found in the frequency range of 3450~3650 cm^{-1}, and the influence of conjugation is quite large[19]. Many of the frequencies for O–H groups of oxanthrone, anthraquinol and their substituted derivatives in a solid[15] were found in the 3300~3500 cm^{-1} frequency range. Moreover, neither the 3175 cm^{-1} band of 1-benzoylaminoanthraquinone nor the 3165 cm^{-1} band of indanthrone was assigned to the O–H vibration; rather, both were assigned to the N–H vibration[4,14]. For indigo and 5, 5', 7, 7'-tetrabromoindigo, in which an amide-type resonance contributes greatly to their resonance hybrids, the 3268 cm^{-1} band for the former and the 3367 cm^{-1} band for the latter were both assigned to the N–H vibration[20]. Broad and distinct bands at 3226 and 3195 cm^{-1} for 3, 4-phthaloylacridone may appear, therefore, at too low a frequency to be normally assigned to the O–H vibration; therefore, this band can not be used to support

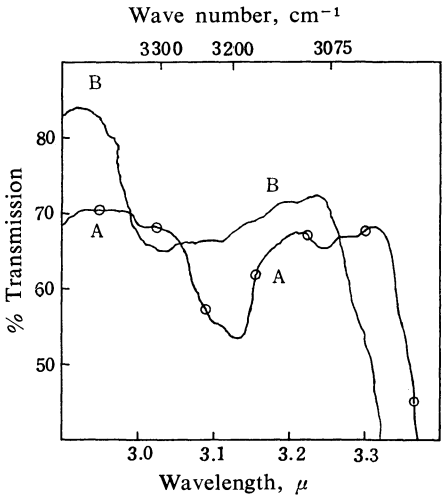


Fig. 3. 3 μ-Region of infrared absorption spectra.
A: 3, 4-Phthaloylacridone
B: 1, 2-Phthaloylacridone

the structures Ib and Ic. Consequently, the 3195 cm^{-1} band should be assigned to the N–H vibration of the true acridone structure. This interpretation of the molecular structure in a solid is the same as the deduction on that in solution on the basis of the results of the visible absorption; moreover, chemical evidence favors the true acridone structure. According to this view, the molecules of 1, 2-phthaloylacridone should also exist in a true acridone structure, in a way similar to that of the 3, 4-phthaloylacridone molecules.

It may be clearly seen in Fig. 3 that 1, 2-phthaloylacridone has two bands at 3300 and 3215 cm^{-1}. 2-Naphthylamine and 2-aminoanthraquinone in a solid gave a triple N–H band; therefore, these phenomena might not be attributable to the C=O group, but to intermolecular interactions between NH_2 groups[15]. 1-Benzoylaminoanthraquinone as a potassium bromide disk[16] also gave a double N–H band at 3226 and at 3115 cm^{-1}. Both of two bands for 1, 2-phthaloylacridone, therefore, may be attributed to the N–H vibration; therefore, the 3215 cm^{-1} band is assigned to the intermolecularly hydrogen-bonded N–H vibration. It is not possible, however, to state whether or not the occurrence of the 3300 cm^{-1} band is caused by intermolecular interaction between NH groups. The frequencies and broad shapes of the two N–H bands of 3, 4-phthaloylacridone at 3226 and 3195 cm^{-1}, similar to those of 1-benzoylaminoanthraquinone as Nujol mull[16], indicate some degree of hydrogen bonding. This view is supported by the fact that acridone in a carbon tetrachloride solution[21] gives a

19) L. J. Bellamy, ibid., p. 96.
20) G. M. Wyman, *J. Am. Chem. Soc.*, **78**, 4599 (1956); W. R. Brode, E. G. Pearson and G. M. Wyman, ibid., **76**, 1034 (1954).
21) A. V. Karyakin and A. V. Shablya, *Doklady Akad. Nauk S. S. S. R.*, **116**, 969 (1957); *Chem. Abstr.*, **52**, 4324 (1958).

N–H band at 3440 cm^{-1}. The proximity of the C=O and NH groups and the possibility for the formation of a six-membered ring suggest that one bonding is intramolecular, as is indicated in Id. Furthermore, 1-benzoylaminoanthraquinone as Nujol mull[16] gave a intramolecular N–H band at 3175 cm^{-1}, and the frequency of 3, 4-phthaloylacridone at 3226 cm^{-1} is in the vicinity of the intermolecular hydrogen-bonded N–H frequency of 1,2-phthaloylacridone at 3215 cm^{-1}. Therefore, the 3226 and 3195 cm^{-1} bands are most probably to be assigned to intermolecularly and to intramolecularly hydrogen-bonded N–H vibration respectively. This view is supported by the general tendency that, for β-amino-α, β-unsaturated ketones, the intramolecular hydrgen-bonded N–H bands occur at lower frequencies than the intermolecular hydrogen-bonded N–H bands[22]. The extent of conjugation between the imino and the C=O group in the nitrogen-bearing ring should be higher for *N*-phenylacridone than for 3, 4-phthaloylacridone, but the C=O frequency of the latter is lower than that of the former[23], this being 1632 cm^{-1}. This lowering seems also to be caused by intermolecular interaction between the NH and the C=O group for the latter.

22) J. Weinstein and G. M. Wyman, *J. Org. Chem.*, **23**, 1618 (1958).
23) E. R. H. Jones and F. G. Mann, *J. Chem. Soc.*, **1958**, 294.

Experimental

Materials and Apparatus.—The compounds used in this investigation were purified by repeated crystallization and then by chromatography or hot chromatography on alumina in suitable solvents.

The visible absorption spectra were obtained by a Shimadzu spectrophotometer type QB-50. The infrared absorption spectra were obtained using the Nujol mull technique; a Perkin-Elmer Model 21 double beam spectrophotometer fitted with a rock-salt prism was also used. *o*-Dichlorobenzene was purified by the method recommended for monochlorobenzence[24].

The authors wish to express their deep gratitude to Mr. Akira Hara of the Tokuyama Research Laboratory of Idemitsu Kōsan Co. for his infrared measurements.

Department of Chemistry
Faculty of Literature and Science
Yamaguchi University
Ushirogawara, Yamaguchi-shi

24) A. Weissberger and E. S. Proskauer, "Organic Solvents", Interscience Publishers, New York (1955), p. 407.

*Ultraviolet Spectra of β-Furyl Ketone and its Derivatives**

By Teruo MATSUURA, Keizo NAYA, Nobutaka ICHIKAWA and Takashi KUBOTA

(Received May 28, 1962)

Koltzin and Bulfson[1] have reported that β-furyl ketones of the A and B types have an ultraviolet absorption maximum at 240~270 mμ and 442~460 mμ respectively. Since these types of compounds possess another chromophoric group which is unconjugated or conjugated to the β-furoyl group, the present authors hoped to examine the ultraviolet spectrum of simple β-furyl ketones. For the present paper, the ultraviolet spectra of fifteen β-furyl ketones and their derivatives, which have been isolated from natural sources or have been synthesized in this laboratory, have been examined; the results are listed in the Table I.

Simple β-furyl ketones (I–V) have a broad absorption maximum at 205~208 mμ which is regarded as due to the furan nucleus[2], and also a considerably sharp maximum at 251~255 mμ (ε 3000~8000). The latter maximum, in the longer wave length region, is considered to be usable for analytical purposes as the maximum characteristic of a β-furyl ketone. The β-furyl ketone band of the VI acid appears as a shoulder under the influence of the strong band of the *a*, β-unsaturated acid group at 218 mμ.

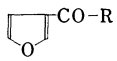
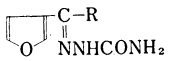
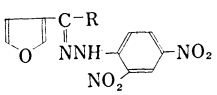
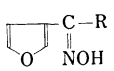
The longest wavelength bands of the semicarbazones (VII–IX) at 265 mμ and of the 2, 4-dinitrophenylhydrazones (X–XII) at about 380 mμ are located at almost the same position as those of the semicarbazone and the

* Natural Furan Derivatives, Part XII. Part XI: T. Tokoroyama and T. Matsuura, *J. Chem. Soc. Japan, Pure Chem. Sec.* (*Nippon Kagaku Zasshi*), **83**, 630 (1962).

1) V. E. Koltzin and N. S. Bulfsone, *J. Gen. Chem., U. S. S. R.*, **30**, 3091 (1960).

2) T. Kamikawa and T. Kubota, *Tetrahedron*, **12**, 262 (1961) and cited references.

TABLE I

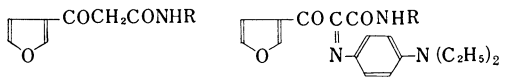
Type of compound	No.	R	λ_{max}^{EtOH}, mμ	ε_{max}
	I[8]	$-CH_2CH_2CH(CH_3)_2$	207 253	14100 5800
	II[9]	$-CH_2CH_2COCH_3$	208 251	16600 7700
	III[10]	$-CH_2CH_2\underset{\displaystyle CH_3}{\underset{\vert}{C}}HCH_2COCH_2CH(CH_3)_2$	207 251	14100 6200
	IV[11]	$-CH_2CH_2\underset{\displaystyle CH_3}{\underset{\vert}{C}}HCOOH$	ca. 205 252	7400 3100
	V[12]	$-CH_2CH_2N(CH_3)_2\cdot HCl$	ca. 205 255	8000 3600
	VI[13]	$-CH_2CH_2\underset{\displaystyle CH_3}{\underset{\vert}{C}}=CHCOOH$	218 255(infl.)	19400 4100
	VII[12]	$-CH_3$	218 264	7900 17700
	VIII[12]	$-CH_2CH_2\underset{\displaystyle CH_3}{\underset{\vert}{C}}HCOOH$	218 265	8400 20000
	IX	$-CH_2CH_2\underset{\displaystyle CH_3}{\underset{\vert}{C}}=CHCOOH$	216 265	22400 19600
	X	$-CH_3$	251[a] 380[a]	14900 26600
	XI[11]	$-CH_2CH_2\underset{\displaystyle CH_3}{\underset{\vert}{C}}HCOOH$	251[a] 380[a]	13400 25600
	XII[8]	$-CH_2CH_2CH(CH_3)_2$	ca. 253[a] 382	11200 21300
	XIII[9]	$-CH_2CH_2C(=NNH-C_6H_3(NO_2)_2)CH_3$	241[a] 369[a]	30500 39000
	XIV[10]	$-CH_2CH_2\underset{\displaystyle CH_3}{\underset{\vert}{C}}HCH_2C(=NNH-C_6H_3(NO_2)_2)CH_2CH(CH_3)_2$	ca. 260[a] 373[a]	24200 47800
	XV[8]	$-CH_2CH_2CH(CH_3)_2$	209 229	6300 5000

a) Determined in chloroform

3) A. E. Gillam and E. S. Stern, "An Introduction to Electronic Absorption Spectroscopy in Organic Chemistry", 2nd Ed., Edward Arnold Ltd., London (1957), p. 114 ff.
4) K. Hirayama, in "Jikken Kagaku Koza", Ed. by the Chemical Society of Japan, Maruzen Co., Tokyo (1957)., Vol. 1, p. 85 ff.
5) Ibid., p. 57.
6) A. E. Gilliam and E. S. Stern, "An Introduction to Electronic Absorption Spectroscopy in Organic Chemistry", 2nd Ed., Edward Arnold Ltd., London (1957), p. 57.
7) T. Ueda and Y. Fujita, 15th Annual Meeting of the Chemical Society of Japan, Kyoto, April, 1961.
8) T. Matsuura, This Bulletin, **30**, 430 (1957).
9) T. Kubota and N. Ichikawa, *J. Chem. Soc. Japan, Pure Chem. Sec.* (*Nippon Kagaku Zasshi*), **75**, 450 (1954).
10) T. Kubota and T. Matsuura, This Bulletin, **31**, 492 (1958).
11) T. Kubota and K. Naya, *J. Chem. Soc. Japan, Pure Chem. Sec.* (*Nippon Kagaku Zasshi*), **77**, 86 (1956).
12) K. Naya, ibid., **77**, 759 (1956).
13) T. Matsuura, ibid., **78**, 389 (1957).

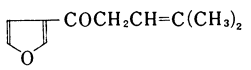
2, 4-dinitrophenylhydrazone of α, β-unsaturated ketones[3,4]. On the other hand, the bis-2, 4-dinitrophenylhydrazones, XIII and XIV, which have the additional 2, 4-dinitrophenylhydrazone group of a saturated ketone in the molecule, show a maximum at about 370 mμ with twice the absorption intensity. This hypsochromic shift is apparently due to the overlapping of the band of the unsaturated ketone derivative with the band of the saturated ketone derivative[5,6].

The ultraviolet absorption maxima[7] of egomaketone (β-dehydroperillaketone) (XVI) and of its ketonic derivatives show a good agreement with those discussed above.



A (R=Aryl)

B (R=Aryl)



XVI

Experimental

The ultraviolet spectra were determined with a Hitachi recording spectrophotometer, model EPS 2.

Semicarbazone IX of 2-Methyl-4-(β-furoyl)-1-butene-1-carboxylic Acid.—The acid[13] (0.1 g.) was treated with semicarbazide hydrochloride (0.1 g.) and potassium acetate (0.1 g.) in dilute ethanol for two days. The crystals which separated were collected (0.12 g.) and recrystallized from dioxane to give colorless plates; m. p., 200~201°C (decomp.).

Found: C, 54.40; H, 6.11; N, 14.49. Calcd. for $C_{12}H_{15}O_4N_3 \cdot 1/4\ (C_4H_8O_2)$: C, 54.35; H, 5.97; N, 14.63%.

2,4-Dinitrophenylhydrazone (X) of 3-Acetylfuran.—3-Acetylfuran[12] was treated with 2, 4-dinitrophenylhydrazine-sulfuric acid in ethanol. Recrystallization from ethyl acetate gave orange needles; m. p., 227~228°C.

Found: C, 49.97; H, 3.57; N, 19.45. Calcd. for $C_{12}H_{10}O_5N_4$: C, 49.66; H, 3.47; N, 19.31%.

The authors are indebted to Miss Ayako Yoshihara for her technical assistance.

Faculty of Science
Osaka City University
Sumiyoshi-ku, Osaka

Analysis of Complex Species Produced by the Szillard-Chalmers Process from Hexaquo-chromium Chloride $Cr(H_2O)_6Cl_3$ and Tetraquo-chromium Chloride $[Cr(H_2O)_4Cl_2]\cdot Cl\cdot 2H_2O$

By Niro MATSUURA, Yoshimi KURIMURA and Yoshikazu TSUNODA

(Received May 17, 1960)

Radioactive ^{51}Cr compound of a high specific activity can easily be obtained in a reactor by the Szillard-Chalmers process, using as a target an inner complex salt of chromium[1]. For example, Harbottle et al.[2] obtained hexavalent chromate or bichromate salt with a retention value of more or less 90%, depending on the nature of the counter-cation. They also obtained similar retention values for several trivalent chromium compound. In our present work, the retention of the chromium aquo-complex was investigated with a view to finding the way the energy of radioactive recoil is dissipated under the influence of a complex ligand field. Two different kinds of chromium chloride isomers were used as targets in this work, and neutron irradiation was effected in the JRR-1 reactor of the Japan Atomic Energy Research Institute. The activated products were separated into several portions of complex species by ion-exchange chromatography, and two samples of the separated portions were put into radiometric analysis for determining the ^{51}Cr yields and into colorimetric analysis for determining the total chromium content.

Experimental

Preparation of Chromium Complex.—Hexaquo- (purple) and tetraquo- (green) chloride complex salts were prepared by the method described in "Inorganic Synthesis"[4]; confirmation of the

1) N. Shibata and K. Yoshihara, This Bulletin, **32**, 422 (1959)

2) G. Harbottle, *J. Chem. Phys.*, **22**, 1083 (1954); A. G. Maddock et al., *Nature*, **164**, 788 (1949).

3) J. W. Cobble and G. E. Boyd, *J. Am. Chem. Soc.*, **74**, 248 (1952).

4) Ed. by T. Inoue, Y. Tsunoda and T. Takeuchi, "Inorganic Preparation", Conference of Complex Chemistry in Japan, No. 202 (November 23, 1959).

purity was made with a Beckman D. U.-type spectrophotometer using the salts absorption spectra. Two pure stable salts of chromium chloride isomers were obtained; however, they could not be stored, even in a sulfuric acid desiccator, without partial degradation. It was found that the one isomer changed into the other by the degradation, even at room temperature. For obtaining the net yield of the radiolytic decomposition of the Szillard-Chalmers reaction, we must know the yield of natural degradation, probably caused by thermal and photochemical reactions, as a function of the time elasped before irradiation.

Irradiation.—The irradiation was effected in a closed silica or polyethylene tube containing several grams of silica gel, which was used as a desiccating agent. For neutron irradiation the target sample was placed in the No. 12 hole of JRR-1, which provided a thermal neutron flux of 2×10^{11} n/cm^2/sec. together with a γ flux of 4.5×10^5 r/hr. For γ irradiation, the sample was placed 20 cm. apart from the ^{60}Co source of 1000 curie in the Radiochemical Laboratory, the Institute of Physical and Chemical Research; this provided a dose rate of 4.5×10^4 r/hr.

Separation of Complex Species. — About 0.1 mequiv. weight of the target chromium complex was dissolved in thrice-distilled water, and the 0.1 M solution thus prepared was passed through a cation-exchange resin column 1.5 cm. in diameter and 15 cm. in length, with 12 g. of air-dried Amberlite IR-120. Then, the resin column was washed successively with water, 0.05 N perchloric acid, a 0.05 N sodium hydroxide solution, and 2 N hydrochloric acid. These eluants, proposed by Gustavson and Kawamura[6], permitted us to separate the complex species in the order given below:

Chromate, tetraquo-dichloro chromim(III), pentaquo-monochloro chromium(III) and hexaquo chromium(III) complex.

Colorimetry of the Total Chromium.—The solutions of each effluent from the cation-exchange resin column were made alkaline with 0.2 N sodium hydroxide, and the resulting alkaline solutions were treated with hydrogen peroxide in order to convert chromium(III) into chromium(VI). The developed yellow color was measured with a Beckman D.U.-type spectrophotometer[7].

Radioactivity Measurement.—After cooling for two weeks, the neutron-irradiated sample was dissolved in a small quantity of water. Then, the species of the chromium complex tagged with radioactive ^{51}Cr were separated by ione-xchange chromatography. For measuring the radioactivity due to ^{51}Cr in the separated fractions, a given amount of inactive chromium(III) salt was added as a carrier: this provided uniform precipitates of a given thickness for radioactive assay. Chromium-(III) was converted into hexavalent chromate by oxidation with hydrogen peroxide in an alkaline medium, and lead chromate was precipitated. The yellow precipitates of lead chromate, containing ^{51}Cr, were filtered off, dried and mounted for radioactivity measurement. A bell-type G. M. counter was generally used for the activity measurement, but a dipping-type counter with a wall thickness of 37 mg./cm^2 was also used when simultaneous determinations of the total and of the radioactive chromium were needed. The main radioactive impurity was ^{35}S, produced by (n, p) reaction from ^{35}Cl in chromic chloride. This interference could be avoided by absorbing the soft β rays with an aluminum absorber 8.9 mg./cm^2 thick. The radioactive ^{32}P, even if produced by a fast neutron by a (n, α) reaction with an cross section of 0.13 barn, did not interfere with our measurement of ^{51}Cr, because anionic phosphate could be eliminated during the chemical separations by cation-exchange resin and by precipitation. Actually, ^{32}P was not detected in such an amount as to affect the determination of ^{51}Cr.

Results

Separation and Recovery by Ion-exchange Chromatography.—A synthetic mixture of pure tetraquo- and hexaquo-complex salts was dissolved in water to produce a 0.2 M solution with regard to each component, and the complex species were adsorped on a hydrogen-form cation-exchange resin column. The separation was effected by the eluants as described above (Experimental). The elution chromatogram in Fig. 1 shows the quantitative recovery of two isomers.

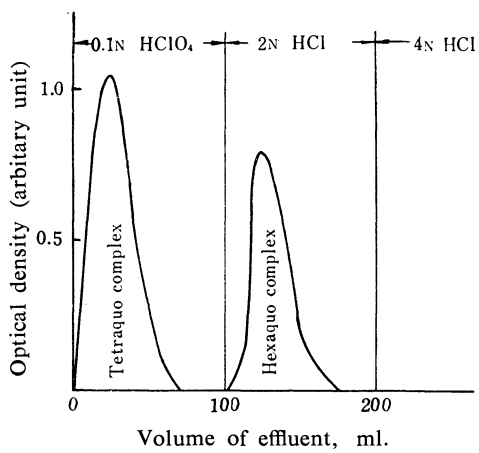


Fig. 1. Elution curve of a mixture of tetraquo- and hexaquo-complex.

Radioactive Species.—The yields of radioactive chromium complex species produced by neutron activation were determined radiochemically after separaion by ion-exchange chromatography. Each 5 ml. portion of the effluents was taken for counting the radioactivity in the course of the elution. The results of the measured radioactivity and the calculated enrichment factors are presented in Fig. 2.

5) M. Kondo, The First Conference of Utilisation of Radioisotopes in Japan (1957).

6) K. H. Gustavson, *Sv. Kem. Tid*, **56**, 14 (1944); R. Kawamura, *Jap. Analyst*, **4**, 277 (1955).

7) E. B. Sandell, "Colorimetric Determination of Traces of Metals", New York (1950), p. 388.

TABLE I. γ-RAY DECOMPOSITION AND NATURAL DEGRADATION YIELD OF TETRAQUO-DICHLORO COMPLEX SALT (A) AND HEXAQUO-COMPLEX SALT (B)

Decomp. products opt. dens./100 ml.	i) Neutron and γ in a pile	ii) γ from ^{60}Co	iii) Natural degradation
A)			
Sample taken	0.204 (100%)	0.222 (100%)	0.283 (100%)
H_2O fraction (neutral and anionic)	0.000 (0%)	0.000 (0%)	0.000 (0%)
0.1 N $HClO_4$ fraction (tetraquo)	0.265 (94.5%)	0.202 (91%)	0.186 (91%)
HCl fraction (hexaquo)	0.028 (10%)	0.028 (7%)	0.018 (9%)
Summation deviation	0.010 (−4%)	0.004 (2%)	0.000 (0%)
B)			
Sample taken	0.360 (100%)	0.247 (100%)	0.286 (100%)
H_2O fraction (neutral and anionic)	0.012 (3%)	0.000 (0%)	0.005 (2%)
0.1 N $HClO_4$ (tetraquo)	0.042 (12%)	0.070 (28%)	0.051 (18%)
HCl fraction (hexaquo)	0.275 (77%)	0.172 (70%)	0.211 (74%)
Summation deviation	0.028 (8%)	0.005 (2%)	0.009 (7%)

The first effluent of the ion-exchange chromatograms contains unknown neutral and anionic species. The second activity peak in Fig. 2 indicates the presence of tetraquo-dichloro chromium-51, corresponding to the Szillard-Chalmers retention value. Similarly, the third peak shows the eluted pentaquo-monochloro chromium-51. The last effluent, obtained by a hydrocholoric acid stronger than 2 N, is ascribed to the hexaquo chromium-51 fraction according to the results of the preliminary test on the ion-exchange chromatography. The observed specific activities or enrichment factors of the first and third peaks were nearly the same, but each was a hundred times as large as that of the second. This is because of the partial degradation of the tetraquo-complex into the hexaquo-complex during the times of irradiation and storage. Besides, the treatment with a 0.05 N sodium hydroxide solution for eluting pentaquo-complex species causes a sort of degradation of the hexaquo-complex in the resin phase, forming a species which can not easily be eluted with 2 N hydrochloric acid. The effect of the natural degradation of the

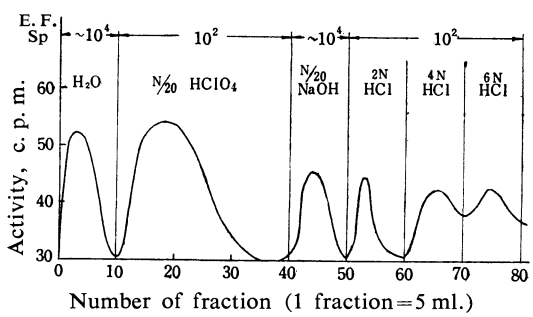


Fig. 2. Distribution of decomposition products by neutron-irradiated tetraquo-complex.
Sp; Specific activity (activity/optical density)
E. F.; Enrichment factor

TABLE II. PERCENT YIELD OF ^{51}Cr BY THE ELUTION WITH HCl MORE THAN 2 N. COMPARISON WAS MADE BETWEEN THE YIELDS WITH AND WITHOUT PRETREATMENT USING 1/20 N NaOH

Treatment	Eluant: 4 N HCl	Eluant: 6 N HCl
Yield with treatment	17%	12%
Yield without treatment	less than 3%	less than 3%

tetraquo-complex target on the yield of radioactive complex species can be clearly seen in Table I; and the similar effect of pretreatment with 0.05 N sodium hydroxide is shown in Table II.

It is supposed that an unstable chlomium complex in a valency state higher than three might be produced by neutron activation and that the absorption of this species on the resin is too strong to be eluted with 2 N hydrochloric acid. If chromium(IV) or chromium(V) were formed in the irradiated sample, then the chloride of chromium trichloride would act as a reducing agent against chromium-(IV) or chromium(V) which is probably a powerful oxidizing agent. For this reason, an elution was carried out with 2 N hydrochloric acid in the presence of excess sulfurous acid, but no appreciable change was observed in the elution characteristics; the conclusion was drawn that there was no chromium(IV) or chromium(V).

Radioactive Complex Species Produced from the Hexaquo- and Tetraquo-complex Target.— The yield of radioactive chromium complex species produced by neutron activation from two different targets, the hexaquo- and tetraquo-complex isomers, is presented in Figs. 3 and 4. Beside these, the amount of chromium found in each fraction of chromatograms, as

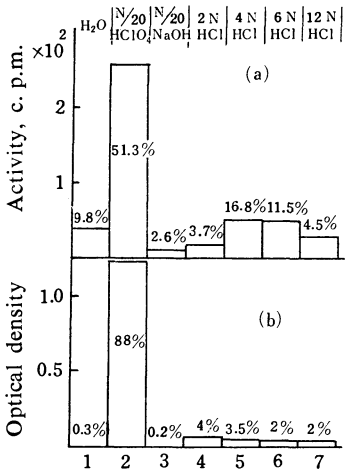


Fig. 3. Irradiated tetraquo-complex.
(a) Comparison of the amount of ^{51}Cr (expressed in radioactivity), (b) the amount of the total chromium (expressed in optical density) in the sample.

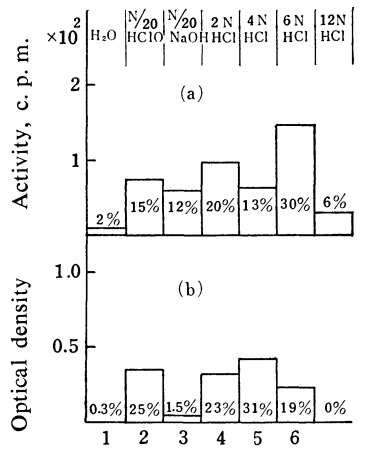


Fig. 4. Irradiated hexaquo-complex.
(a) Comparison of the amount of ^{51}Cr (expressed in radioactivity), (b) the amount of the total Cr (expressed in optical density) in the sample.

determined by colorimetric analysis, is shown in Figs. 3 and 4.

As the hexaquo-complex is much more labile than the tetraquo-complex, not only to radiation decomposition but also to natural degradation in air, the contribution of the latter effect must be considered in order to obtain the correct yield of the radiation decomposition of the hexaquo-complex. However, this effect is so small for the tetraquo-complex that the correction is not necessary. The corrected yields for the radioactive chromium species are shown in Fig. 5 for the hexaquo-chromium target and in Fig. 3 for the tetraquo-chromium target.

Anionic Species of the Activated Chromium Complex.—The first effluent produced by exchange chromatography was passed through a column filled with anion-exchange resin, Dowex 1-X8. Less than 8% of the radioactive chromium was adsorbed on the anion-exchange resin. Therefore, the remaining 92% is considered to be present in a non-ionic form, but the chemical species of the latter was not identified. As to the anionic species, the extraction of chromium as perchromic acid by ethyl acetate was undertaken from acetic acid and a sodium acetate buffer solution at pH 1.6 in order to prove the presence of the chromate anion. The extracted radioactivity was less than 5% of the total present in the first effluent produced by cation-exchange chromatography.

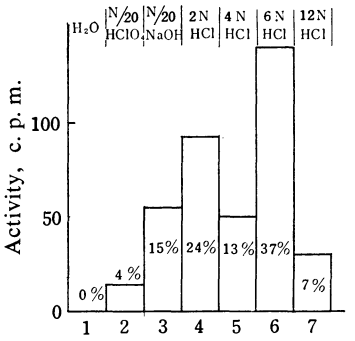


Fig. 5. Corrected distribution of ionic species for neutron irradiated hexaquo-complex.

Discussion

The yields of complex species of radioactive chromium(III) are summarized in Table III. As the retention values for two different isomers differ greatly from one another, we

TABLE III. SUMMARY OF YIELD

Decomp. product	Yield, % $[Cr(H_2O)_4Cl_2]\cdot Cl\cdot 2H_2O$ target %		$[Cr(H_2O)_6]Cl_3$ target %	
Anionic ^{51}Cr salt	2			
Neutral ^{51}Cr salt	8			
Tetraquo ^{51}Cr salt	50			
Pentaquo ^{51}Cr salt	3		15	
Hexaquo ^{51}Cr salt	4			
Eluant by 2 N HCl	4		24	
4 N HCl	17	37	13	80
6 N HCl	12		37	
12 N HCl	4		7	
Retention	50		80	

hoped from stereochemistry of the complex to get some information about the energy dissipation of the recoil chromium atom under the influence of the ligand field. The energy liberation by the process $^{50}Cr(n, \gamma)^{51}Cr$ was evaluated to be 9.2 MeV. from the atomic mass difference between ^{50}Cr and ^{51}Cr. From this, the recoil energy imparted to the ^{51}Cr atom by the emission of γ rays is estimated to be 839 eV. This energy must be imparted to the surrounding ligand atoms in different ways depending on the geometrical arrangement of the ligand in the chromium chloride complex. The actually observed Szillard-Chalmers effect is not the same with respect to the yield of the radioactive chromium complex for the two different isomers, hexaquo- and tetraquo-chromium chloride.

As the positively charged (+3e) recoil chromium atom is so heavy compared to the surrounding ligand atoms, the former can not escape from the interior of the crystal without any interaction. First, we suppose the recoil energy is imparted equally to three ligand atoms on the same plane of the octahedral surface; therefore these atoms will be expelled out of the complex crystal and caught by some interstitial site of the crystal. The radioactive recoil chromium atom will then recombine by statistical chance with an atom or a water molecule at the nearest neighbor's forming a certain species of the complex. As six water molecules and three chloride ions are the nearest neigbors in the present case, the yield of the radioactive complex species can be ruled out by simple statistics. With this assumption, the radioactive chromium complex yields must be 2/10 for the formation of the hexaquo-complex species, 3/10 for that of the pentaquo-complex, and 2/10 for that of the tetraquo-complex, regardless of the target complex. However, this hypothesis can not account for the experimental results shown in Table IV.

Secondly, the whole energy is transferred to one special ligand atom by head-on collision, and the kinetic energy of the recoil atom is effectively absorbed by this ligand atom. If the recoil energy is not greater than the binding energy between the central metal ion and the ligand atom, the retention value can be estimated as follows. The binding energy of one ligand water molecule to the central chromium atom is estimated to be $48/6=8$ eV. from the hydration energy of the chromium ion. However, this value must be multiplied by the factor of M°/M, for the available energy for bond-breaking is smaller than the recoil energy by this factor since momentum partition between the water molecule and the recoil chromium atom takes place. Therefore, the minimum energy is $8\times(159/18)=70.6$ eV. for breaking one ligand bond. The energy, required to remove successively one more ligand water amounts to $70.6\times(141/18)=555$eV. From this consideration, the recoil atom having less energy than this threshold energy of 70.6 eV. must retain its initial ionic form of the complex. Similarly, in the recoil chromium atom having between 70.6 and 555 eV. of energy the yields of radioactive chromium complex are different in ligand number by one from the initial form of the target complex. In the case of the tetraquo-complex as the terget the energy necessary to remove one chlorine atom from the complex crystal field can be estimated from the absorption spectroscopic data to be one-half of the energy needed for the water molecule. However, the reduction factor of the available energy for bond-breaking, M/M°, is twice as large as that of the water molecule. Therefore, the threshold energy for breaking the ligand chlorine bond is nearly one-fourth that of the evaluated energy for ligand water.

Table IV. Comparison of the Szillard-Chalmers yield of chromium chloride complex with the theoretical yield based on complete dissociation and statistical rearrangement of ligand atoms

Target complex	Tetra isomer	Hexa isomer	Theoretical
Product		yield, %	
Tetra form	50 (Retention)	4	28.5
Penta form	3	15	43
Hexa form	37	80 (Retention)	28.5

The Effect of the Multicascade of γ Emission. —The calculation of the recoil energy is not so simple as has been discussed above, since γ emission in the neutron gamma process generally takes place through several steps in cascade. In this discussion, we treat the problem as if γ emission occurred in two steps, since the final result does not differ essentially from that of multicascade emission. Assuming that successive γ photons of the same energy are emitted in two directions with an angle α, we can expect the relation between the recoil energy with no cascade, E°, and with a two-steps cascade, E', given by the Eq. 1:

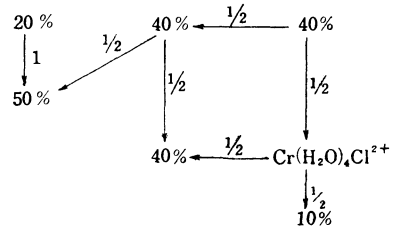
$$E'=E^\circ\cos^2(\alpha/2) \quad (1)$$

As successive γ emission takes place in a random direction, the angle α divided by π gives a probability of the event where a successive γ emission occurs between 0 and α. In Fig. 6 the α/π value is plotted against the

Table V. The effect of multicascade γ emission on the Szillard-Chalmers reaction yields. The tentative calculation of the yields for recoil intermediates and final products was based on the spatial recoil energy distribution by two successive γ emission

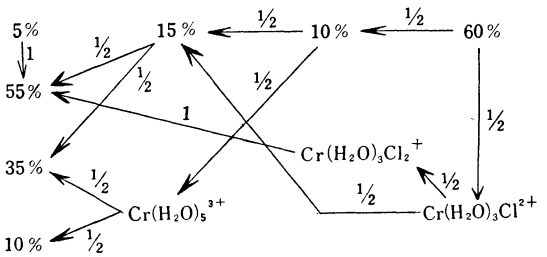
a) Hexaquo-dichloro complex target

Recoil process	Zero ligand dissociation	One ligand dissociation	Two ligand dissociation
Threshold energy	less than 70.5 eV.	70.5 eV.	555 eV.
Assumed species and its initial yield	$Cr(H_2O)_6^{3+}$	$Cr(H_2O)_5^{3+}$	$Cr(H_2O)_4^{3+}$
Products and its observed yield			
$Cr(H_2O)_6^{3+}$ (80%)			
$Cr(H_2O)_5Cl^{2+}$ (15%)			
$Cr(H_2O)_4Cl_2^{+}$ (4%)			



b) Tetraquo-dichloro complex target

Recoil process	Zero ligand dissociation	One ligand dissociation	Two ligand dissociation	Three ligand dissociation
Threshold energy	less than 17.6 eV.	17.6 eV.	70 eV.	more than 280 eV.
Assumed species and its initial yield	$Cr(H_2O)_4Cl_2^{+}$	$Cr(H_2O)_4Cl^{2+}$	$Cr(H_2O)_4^{3+}$	$Cr(H_2O)_3^{3+}$
Products and its observed yield				
$Cr(H_2O)_4Cl_2^{+}$ (50%)				
$Cr(H_2O)_5Cl^{2+}$ (3%)				
$Cr(H_2O)_6^{3+}$ (37%)				



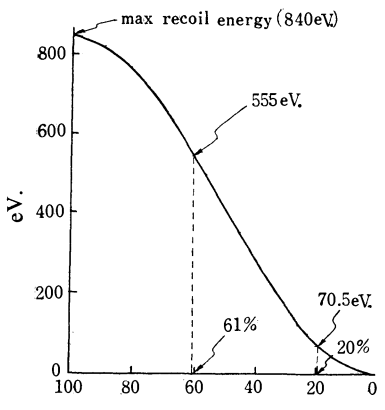


Fig. 6. Recoil energy of ^{51}Cr calculated from Eq. 1 vs. $(1-\alpha/\pi)\times 100$ which represents percentage of ^{51}Cr having recoil energy E'.

recoil energy, E', for a two-cascades emission of γ rays by the aid of Eq. 1. Taking the threshold energy value, E', for bond-breaking, we can determine the probability, α/π, from the curve shown in Fig. 6, which gives the yield of the complex species of radioactive chromium produced by neutron-gamma reaction. The α/π fraction for the given threshold, E', insufficient to break one bond, gives the retention yield of radioactive chromium. Similarly, the α/π value for the threshold corresponding to the breaking of two or more bonds, gives the yield of the complex species of radioactive chromium differing by one or more ligand atom. An intermediate complex, lacking one or more ligand atom, reproduces a normal six-ligand complex species by picking up either a water molecule or a chlorine atom depending on the relative abundance of the surrounding ligand species. For example, an intermediate $Cr(H_2O)_5^{3+}$ will reproduce either one of two stable complex six-ligand species, $Cr(H_2O)_5^{3+}$ or $Cr(H_2O)_6Cl^{2+}$, with equal probability. Therefore, on the basis of the above assumption, the final products of the radioactive chromium complex can be

estimated; the schemata are presented in Table Va for a hexaquo target and in Table Vb for a tetraquo target.

The tables show that double γ emission schema plausibly improve the agreement between the calculated and observed results more than the simple cascade scheme does.

College of General Education
The University of Tokyo
Meguro-ku, Tokyo

Studies on Modified Hydrogenation Catalyst. I. Selective Hydrogenation Activity of Modified Raney Nickel Catalyst for Carbonyl Group and C=C Double Bond

By Hideaki FUKAWA, Yoshiharu IZUMI, Shinichiro KOMATSU and Shiro AKABORI

(Received February 1, 1962)

Recently, Izumi et al.[1-3] developed an entirely new series of hydrogenation catalysts, which are unique in that silk fibroin serves as carrier for metals. These catalysts have highly selective hydrogenation activity, having high activity for unsaturated compounds and aromatic nitro compounds but no activity for aliphatic carbonyl compounds. It was suggested that the specificity of these catalysts resides in the special structure of the carrier, silk fibroin.

It therefore seemed possible that if Raney nickel (R-Ni) catalyst is treated with amino acid, peptide or protein, these modified R-Ni catalysts may possess selective hydrogenation activity similar to that of the silk-metal catalyst. Isoda and Ichikawa[4] have, in fact reported the occurrence of asymmetric hydrogenation with the use of R-Ni catalyst on which optically active amino acids had been adsorbed.

As is well known, enzymatic reactions are highly specific, but their velocities can be modified by means of various reagents. Accordingly, methods of competitive inhibition or antagonism in enzymology should also be applicable to the study of non-enzymatic catalytic reactions. On the basis of these conceptions, the hydrogenation activity of the R-Ni catalyst modified with amino acids and other chelating agents has been systematically studied.

R-Ni catalyst treated with these reagents had diminished hydrogenation activity only for the carbonyl group. In particular, R-Ni catalyst modified by various amino acids, possessed this property to a greater extent than that modified by other reagents. The present paper describes the hydrogenation activity and some characteristics of the modified R-Ni catalyst.

Results and Discussion

Allyl alcohol and ethyl methyl ketone were used as substrates for most of this investigation. As modifying agent, L-glutamic acid or its monosodium salt was generally used because of its selectivity.

As summarized in Table I, the hydrogenation activity of R-Ni catalyst for ethyl methyl

TABLE I. CONCENTRATION OF MODIFYING SOLUTION

Modifying reagent	Concn. %	Hydrogenation activity EMK 10°C	EMK 60°C	AA 10°C
Untreated	—	2	20	34
Untreated*	—	3	20	—
L-Glu	0.02	0.5	17	34
	0.5	0	3	34
	1.0	0	1.5	34
L-MSG	1.0	0	2	30
	2.0	0	2	30
	4.0	0	0.5	16
Gly-Gly	1.0	0	2	45
	2.0	0	0	21

* Allowed to stand for 5 hr. at room temperature

1) Y. Izumi, This Bulletin, **32**, 932, 936, 942 (1959).
2) A. Akamatsu, Y. Izumi and S. Akabori, ibid., **34**, 1067, 1302 (1961).
3) Y. Izumi, A. Akamatsu and S. Akabori, in preparation.
4) T. Isoda, A. Ichikawa and T. Shimamoto, *J. Sci. Res. Inst.* (*Riken hokoku*), **34**, 143 (1958).

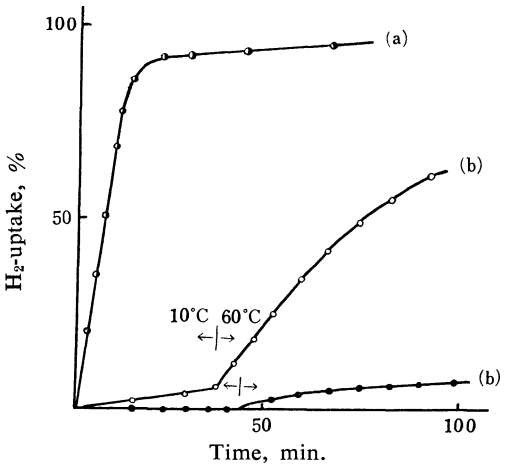


Fig. 1. Hydrogenation of allyl alcohol (a) at 10°C and ethyl methyl ketone (b) at 10°C and 60°C.
○ With unsaturated catalyst
● With modified catalyst (0.5% Glu)

ketone was almost lost at 10°C when the catalyst was treated with a solution of L-glutamic acid or sodium L-glutamate of greater concentration than 0.5%, and was greatly diminished at 60°C. On the other hand, no appreciable change in its hydrogenation activity for allyl alcohol occurred upon treatment with sodium L-glutamate solutions in concentration up to 4%. When the catalyst was treated with sodium L-glutamate at concentrations greater than 4%, the hydrogenation activity for ethyl methyl ketone was almost lost even at higher temperatures. Figure 1 shows a typical hydrogenation curve of ethyl methyl ketone (a) and allyl alcohol (b) carried out with untreated and modified R–Ni catalyst.

The effect of modifying the time of immersion of R–Ni catalyst in L-glutamic acid solution on hydrogenation activity is shown in Table II. Immersion for 15 min. was sufficient to cause a pronounced decrease in hydrogenation activity for ethyl methyl ketone. Further treatment resulted in a more gradual decrease in activity. It thus appears that most of the modifying effect of L-glutamic acid took place in the first 15 min. On the other hand, immersion of R–Ni catalyst in water as long as 5 hr. did not change its hydrogenation activity.

TABLE II. TIME OF MODIFYING

Modifying reagent	Time of immersion	Hydrogenation activity EMK 10°C	EMK 60°C	AA 10°C
0.5% L-Glu	15 min.	0	4	34
	2 hr.	0	3	—
	16 hr.	0	2	30
4% L-MSG	2 hr.	0	1	16
	16 hr.	0	0	14

Treatment with various other amino acids and some other types of compounds has been carried out, and the results are summarized in Table III. All of the amino acids tested gave selective hydrogenation activity to R–Ni catalyst. Dibasic amino acids and phenylalanine had the greatest effect among the α-amino acids tested to date. Other types of chelating agents had a lesser effect than amino acids.

An interesting finding was, that the hydrogenation activity of R–Ni catalyst for allyl alcohol was promoted by the treatment with dimethylglyoxime. As will be described below, it was observed, that the hydrogenation activity of the modified R–Ni catalyst increased to three times that of the untreated catalyst in the hydrogenation of nitrobenzene. The surface of the catalyst modified with dimethylglyoxime turned pink in color. This change suggests the formation of a chelated complex between nickel and dimethylglyoxime.

Table IV summarizes the results of the hydrogenation of various ketones and unsaturated compounds with the modified R–Ni catalyst. The catalyst in these experiments was prepared by immersion in 2% sodium L-glutamate solution for 2 hr. at 10°C. The hydrogenation activity at low temperature for ketones was lost by this treatment, and even at 60°C the activity decreased from one tenth

TABLE III. VARIOUS MODIFYING REAGENTS

Modifying reagent	Concn. %	pH	Hydrogenation activity EMK 10°C	EMK 60°C	AA 10°C
L-Glu	1.0	4	0	1.5	36
L-MSG	1.2	7	0	2	30
L-ASP	1.0	4	0	2	35
L-Leu	1.0	7	0	3.5	34
Gly	1.0	7	0	3	35
DL-Thr	1.0	7	0	3	35
L-Hypro	1.0	7	0	3	38
L-Phe	1.0	7	0	1–0.5	36
L-Arg	1.0	11	0	3.5	22
Gly-Gly	1.0	5	0	2	45
Gelatin*	0.5	6	0.5	1.5	38
EDTA·2Na	1.85	4	0.5	4	37
Succinic acid	1.3	3	0	3–3.5	25
Sodium acetate	0.5	5	2	6	—
Dimethyl-glyoxime**	0.8	—	0.5	5.5	(50)
Ethylenediamine hydrochloride	1.0	7	0	3	(52)

* Reaction was stopped at the hydrogen uptake of nearly half of the theoretical.
** In methanol

Table IV. Hydrogenation of various substrate

Substrate	Hydrogenation activity[a] 10°C Control	10°C Modified	60°C Control	60°C Modified
Ketone				
Acetone	5.7	0	55	8
Ethyl methyl ketone	2	0	20	2
Acetophenone	8	0	120	22
Cyclohexanone	1.8	0	24.3[b]	7
C=C Double bond				
Allyl alcohol	34	34		
Cinnamic acid	16	16		
Maleic acid	41	63		
Ethyl acrylate	5 min.[c]	3 min.		
Diethyl maleate	5 min.[c]	4 min.		
Mesityl oxide[d]	28	14	6	1
Cinnamic aldehyde	12.5	0.5	14	—

a) Hydrogenation activity is expressed by % hydrogen uptake in initial 30 min. in the case of ketone and in initial 5 min. in the case of C=C double bond.
b) This compound was reduced at 80°C.
c) Time of reaction finished.
d) Losses of carbonyl group in the products were 11% and 3%, respectively.

to one sixth of that of the untreated catalyst. Hydrogenation activity of R-Ni catalyst for unsaturated compounds was almost unchanged by this treatment, and the activity increased in the case of hydrogenation of maleic acid. Similarly, the rates of hydrogenation of ethyl maleate and of ethyl acrylate were increased by this treatment.

When mesityl oxide was the substrate of hydrogenation, hydrogen uptake ceased, when the uptake of hydrogen was one mol. per mol. of substrate, and isobutyl methyl ketone was obtained in high yield. This result shows that the C=C double bond was predominantly hydrogenated while the carbonyl group was almost unaffected when mesityl oxide was hydrogenated with this modified catalyst.

This conclusion was confirmed by examining the infrared spectrum and determining the carbonyl content of the hydrogenated products. The only negative result occurred with cinnamaldehyde. Neither its C=C double bond nor its carbonyl group was hydrogenation activity of R-Ni catalyst for nitrobenzene was depressed by treatment with amino acid as shown in Table V, but was increased two-fold by treatment with dimethylglyoxime.

The results thus for obtained suggest the possibility that the surface of activated R-Ni catalyst is inhomogeneous and that C=C and

Table V. Hydrogenation activity for nitrobenzene

Modifying reagent	Hydrogenation activity* 10°C	40°C
Untreated	9	16
2% L-MSG	2	8
0.8% Dimethylglyoxime	32	45

* % Hydrogen uptake (%) in initial 10 min.

C=O bonds are reduced at different hydrogenating centers on the surface. When the catalyst was modified with an amino acid capable of chelating with nickel ion, the hydrogenated centers for carbonyl compounds were inhibited, whereas the centers for C=C double bond remained unaffected.

In this investigation, carbonyl-containing substrates used were limited to some ketones, and the conditions of hydrogenation were also limited. In order to obtain further information concerning the mechanism of this modification and to provide a basis for its practical application, further studies are required. It is expected that such studies will shed some light on the mechanism of catalytic hydrogenation reactions.

Experimental

Preparation of Catalyst. — The catalyst used in this work, was prepared by the following method. One and a half grams of Raney nickel alloys (aluminum content 45%, manufactured by Kawakami Lab. Co. Ltd.,) was added to 20 ml. of 20% sodium hydroxide solution in small portions during a period of 5 min., and was allowed to stand for 45 min. at 80°C. The activated catalyst was washed several times with water. All of hydrogenation reaction in this work was carried out with this quantity of R-Ni catalyst.

Modification of Catalyst. — Fifty milliliters of an amino acid solution was added to the activated catalyst, and the mixture was allowed to stand with occasional shaking at room temperature (10~15°C) for 2 hr. After the modifying solution was removed by decantation, the catalyst was washed once with water and two times with methanol, and centrifuged. Dry weight of the catalyst was about 0.7 g. Glycylglycine hydrochloride and acetic acid were used after their solution were adjusted to pH 5 by dilute alkali. Dimethylglyoxime was used in methanol solution.

Reaction Vessel.—A shaking autoclave of 100 ml. capacity was used as the vessel for hydrogenation reaction.

Activity of Catalyst. — Hydrogenation activity was measured by the rate of hydrogen uptake at the initial period of reaction and was represented as percent of theoretical hydrogen absorption per specified period of time.

Hydrogenation Reaction. — *1) Hydrogenation of C=C Double Bonds. — a) Hydrogenation of Allyl Alcohol.*—Seventeen grams (0.3 ml.) of allyl alcohol

were hydrogenated with hydrogen 95 kg./cm² at 10°C with R-Ni prepared from 1.5 g. alloy. Reaction velocity was represented by percent hydrogen uptake in the initial 5 min.

b) Hydrogenation of Cinnamic Acid, Maleic Acid, Ethyl Acrylate and Diethyl Maleate.—7.5 g. cinnamic acid in 50 ml. methanol, 17.5 g. maleic acid in 50 ml. methanol, 15 g. ethyl acrylate in 40 ml. methanol and 17.2 g. diethyl maleate in 50 ml. methanol were hydrogenated by the same procedure as allyl alcohol.

2) Hydrogenation of Ketones.—a) Hydrogenation of Ethyl Methyl Ketone.—Twenty grams (0.3 mol.) of ethyl methyl ketone were hydrogenated with hydrogen (70 kg./cm²) at 10°C. Reaction velocity represented hydrogen uptake in the initial 30 min. Temperature of the reaction was initially maintained at 10°C for 3 hr. and then was raised to 60°C.

b) Hydrogenation of Acetone.—Acetone (11.6 g., 0.2 mol.) was hydrogenated by the same procedure as ethyl methyl ketone.

c) Hydrogenation of Acetophenone.—Twelve grams (0.1 mol.) of acetophenone dissolved in 50 ml. methanol were hydrogenated by the same procedure as ethyl methyl ketone.

d) Hydrogenation of Cyclohexanone.—Cyclohexanone (19.6 g., 0.2 mol.) was hydrogenated by the same procedure as ethyl methyl ketone, except that the hydrogenation at higher temperature was carried out at 80°C instead of 60°C.

3) Hydrogenation of Mesityl Oxide. — Mesityl oxide was purified by fractional distillation (128~130°C, b. p.) after being washed with dilute alkali to remove contaminating iodine. Purified mesityl oxide (19.6 g., 0.2 mol.) was hydrogenated with hydrogen 90 kg./cm² initially at 10°C. After the hydrogen uptake was 0.2 mol., temperature was raised to 60°C and reaction was continued still further for 2 hr. Reaction velocity was represented by hydrogen uptake in the initial 5 min. at 10°C and during the first 30 min. at 60°C and was expressed as percentage of the theoretical amount for each radical.

4) Hydrogenation of Nitrobenzene. — Four grams (0.03 mol.) of nitrobenzene dissolved in 50 ml. methanol were hydrogenated with hydrogen (80 kg./cm²). The temperature, which initially was 10°C, rose to 40°C during the reaction. Reaction velocity was presented by percent hydrogen uptake in the first 10 min.

Determination of the Carbonyl Group. — The carbonyl group was assayed by the hydroxylamine method after Fritz and Yamamura[5].

Summary

Hydrogenation activity of the Raney nickel catalyst for carbonyl compounds was greatly diminished, when the catalyst was treated with a solution of amino acid. On the other hand, no appreciable change in its hydrogenation activity for C=C double bonds occurred upon this treatment. When mesityl oxide was used as a substrate, selective hydrogenation was most clearly demonstrated.

The effect of conditions of modification, such as concentration of the modifying solution, immersion time and kind of modifying reagent on the activity of the modified catalyst, were investigated.

Division of Organic Chemistry
Institute for Protein Research
Osaka University
Kita-ku, Osaka

5) J. S. Fritz and S. S. Yamamura, *Anal. Chem.*, 31, 260 (1959).

Studies on the Silk-Rhodium Catalyst

By Akira AKAMATSU*, Yoshiharu IZUMI and Shiro AKABORI

(Received May 16, 1962)

A series of the hydrogenation catalysts, composed of highly dispersed metal on fibers of silk fibroin, has recently been studied. The silk-palladium[1] and silk-platinum[2] catalysts, have shown a number of interesting properties that probably depend upon the nature of the carrier silk-fibroin fibers. In particular, catalysts of this type are highly selective with respect to the reactions that they catalyze. The metal used in the present study was rhodium which was recently found to be an excellent catalyst for the reduction of aromatic or heterocyclic double bond. The silk-rhodium catalyst was prepared by boiling silk-fibroin fibers with an aqueous solution of rhodium chloride and then hydrogenating the resulting silk-$RhCl_3$-complex.

The silk-palladium catalyst selectively hydrogenated the C=C double bond without reducing

* Present address: Central Research Laboratory of Ajinomoto Co., Inc., Suzukicho, Kawasaki.

1) For example, S. Akabori, S. Sakurai, Y. Izumi and Y. Fujii, *Nature*, **178**, 323 (1956); Y. Izumi, This Bulletin, **32**, 932, 936, 942 (1959).

2) A. Akamatsu, Y. Izumi and S. Akabori, ibid., **34**, 1067 (1961); ibid., **34**, 1302 (1961).

the carbonyl group in an aliphatic molecule, which contains both groups. In the case of silk-rhodium catalyst, it appears that the selectivity was much increased. In the present work, it was found that this catalyst easily catalyzes the hydrogenation of C=CHCH$_2$OH and C=CHCOOH type of the C=C double bonds, while carbonyl groups, including those of aromatic compounds, could not be hydrogenated at all. This catalyst was relatively less active for the hydrogenation of the other type of the C=C double bonds, such as C=CHCO–R, and of nitro groups.

Results and Discussion

Conditions for Preparation of the Catalysts. — In order to obtain a catalyst with high activity and to minimize expensive loss of rhodium, optimal conditions were sought for the preparation of the silk-rhodium chelate and for the activation of the resulting chelate to the catalyst.

In Fig. 1a the rhodium contents in the chelate prepared in the different preparations are shown: when 400 mg. of silk-fibroin fibers were boiled with an aqueous solution containing 100 mg. of rhodium chloride ($RhCl_3$) for 25 min. The concentration was varied by changing the volume of water, and maximum chelation occurred in a mixture containing 100 mg. of silk-fibroin fibers in 0.5% aqueous $RhCl_3 \cdot H_2O$.

The optimal volume of the 0.5% $RhCl_3$ solution and boiling time was then determined. The results are summarized in Figs. 1b and 1c. Two hundred milligrams of each of the resulting chelate was activated by reduction in an autoclave, with ca. 90 kg./cm^2 of hydrogen in 50 ml. of water at 160°C for 1.5 hr., and the activities of the obtained catalysts were measured. The activity yield ($y \cdot v$), the product of the reaction velocity (v) and gravity yield (y)[2] is a measure of activity of the catalyst for a given amount of the metal in the catalyst. Reaction velocity (v) was measured during hydrogenation of allyl alcohol to propyl alcohol with the same amount of catalyst, and was calculated by the equation; $v=100/t$, where t is the time in minutes required for 70% uptake of hydrogen.

As can be seen from data described here, the most favorable result was obtained, when 400 mg. of silk-fibroin fibers were boiled with 30 ml. of a 0.5% aqueous solution of rhodium chloride for ca. 30 min. The obtained silk-rhodium chelate consisted of golden-colored fibers which contained approximately 3.6% of the metal. This preparation was used for the work described in the following section of this paper.

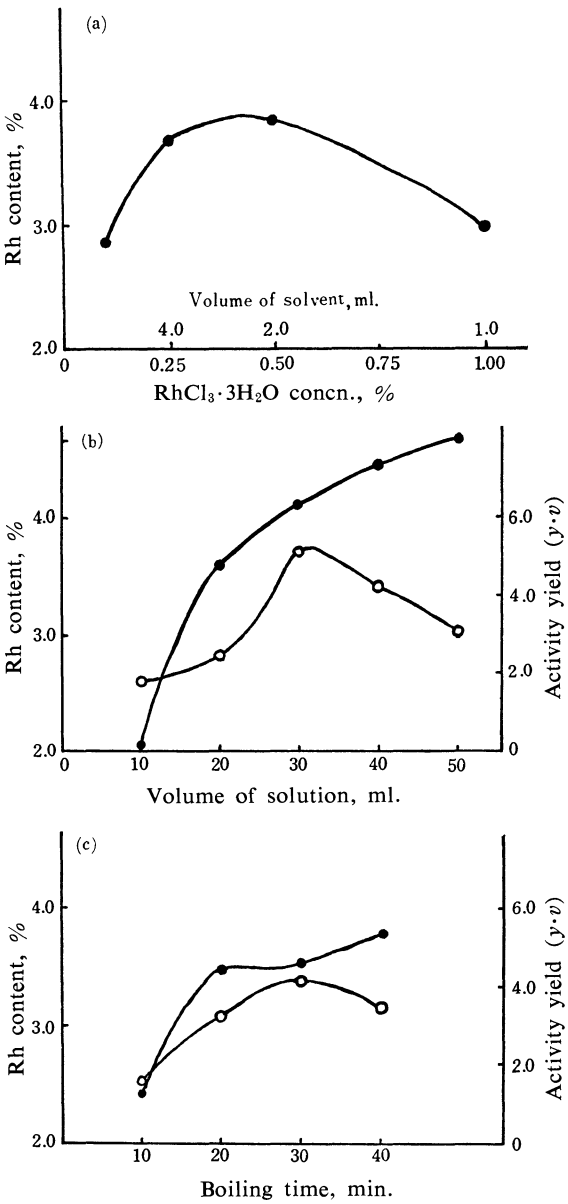


Fig. 1. Rhodium content of chelate under various conditions and activity yield of activated catalyst.
● Rhodium content
○ Activity yield
Silk-fibroin 400 mg. was boiled (a) in an aq. solution containing 100 mg. of $RhCl_3 \cdot 3H_2O$ for 25 min., (b) in a 0.5% $RhCl_3 \cdot 3H_2O$ aq. solution for 25 min., and (c) in 30 ml. of the solution.

Table I is a summary of experiments in which chelate was activated by reduction in an autoclave with ca. 90 kg./cm^2 of hydrogen in 50 ml. of water at various temperatures for different periods. The activity of the obtained catalyst, represented by the reaction

Table I. Activity of the catalyst prepared under various conditions

No.*	Precursor chelate, mg.	Temp. °C	Time hr.	Grav. yield y, %	React. vel. at 32°C, v	Act. yield $y \cdot v$
a-1			2	82	5.3	4.3
a-2			3	89	6.6	5.9
a-3		100	4	82	8.0	6.6
a-4			5	86	6.8	5.8
a-5			2	78	5.2	4.1
a-6			3	81	5.7	4.6
a-7		120	4	77	5.8	4.5
a-8	200		5	70	3.1	2.2
a-9			1	73	6.6	4.8
a-10			2	68	5.8	3.9
a-11		140	3	63	5.6	3.5
a-12			4	65	6.9	4.5
a-13			1	56	12.7	7.1
a-14		160	2	57	11.3	6.4
a-15			4	51	11.2	5.7
b-1	200	140	3	63	7.6	4.8
b-2	1000	140	3	57	8.3	4.7
b-3	200	160	2	31	15.0	4.7
b-4	1000	160	2	31	15.5	4.8

* a differs from b in lot of the chelate prepared.

velocity (v) and the activity yield ($y \cdot v$) during the hydrogenation of allyl alcohol to propyl alcohol, was as dependent upon the temperature and time of activation as that of the silk-platinum catalyst. Increasing the amount of the precursor chelate used with respect to the amount of the solvent (water) did not influence the activity.

Stability of the Catalyst.—The reaction velocities measured by the method described above are shown in Table II. The catalyst was used both immediately after its activation and after it was dried and stored for several days in a stopped bottle. Storage of the catalyst for a long period resulted in considerable increase of activity.

Table II. Stability of catalyst

Storage time days	React. vel. at 32°C, v
1	8.8
3	8.5
8	15.2
15	14.2
47	9.0

The activity of the silk-rhodium catalyst was strongly inhibited by some substances. The inhibitory effects of certain poisons on the hydrogenation of 0.1 mol. of allyl alcohol in methanol in the presence of 20 mg. (containing ca. 10^{-5} mol. of Rh) of the catalyst was investigated. The results are shown in Table III. The behavior of this catalyst towards metal ions was similar to that of the silk-platinum catalyst. It was found that silk-rhodium catalyst poisoned with both ferric and cupric ions could be reactivated by treatment with ethylenediaminetetraacetic acid (EDTA).

Table III. Poisoning of catalyst

	Addition $\times 10^{-6}$ mol.	React. vel. at 32°C, v
$PhCH_2SH$	None	9.0
	1	4.4
	2	3.4
	3	0.1
$Fe(NO_3)_3 \cdot 12H_2O$	10	1.9
	(treated with EDTA)*	4.4
	50	1
$Cu(NO_3)_3 \cdot 3H_2O$	50	5.0
	200	5.0
	410	2.7
	440	1.8
	460	0.5
	(treated with EDTA)**	2.7

* 75% of the catalyst was recovered and treated with EDTA.

** 56% of the catalyst was recovered to be treated.

Acetylation of this catalyst scarcely affected the activity. The reaction velocity (v), as defined above, with an acetylated catalyst was 10.4 at 32°C.

TABLE IV. CATALYTIC REDUCTIONS OF VARIOUS COMPOUNDS

Substrate g.	Solvent ml.	Cat. mg.	Temp. °C	H_2-Uptake %	Time min.	Product	Yield %
Acetaldehyde (11)		50	40	3	390	—	—
Benzaldehyde (25)		50	10	9	390	—	—
Benzaldehyde (25)		50	80	6	215	—	—
Ethyl methyl ketone (36)		200	80	2	390	—	—
Allyl alcohol (5.8)		20	16	100	37	Propanol	100*
Maleic acid (11.6)	MeOH(50)	20	55	100	74	Succinic acid	62
Diethyl maleate (34.5)		40	11	8	300	—	—
Diethyl maleate (34.5)		40	45	9	330	—	—
Cinnamic acid (7.4)	MeOH(50)	10	10	100	160	2-Phenylpropionic acid	87
Cinnamic acid (3.7)	aq. NaOH(50)	10	9	100	320	2-Phenylpropionic acid	72
Acrolein (5.6)	EtOH(50)	20	17	100	250	Propionaldehyde	93*
Crotonaldehyde (14)	MeOH(50)	40	15	18	350	—	—
Cinnamaldehyde (13)	MeOH(50)	20	15	9	210	—	—
Mesityl oxide (24.5)		50	55	20	270	Isobutyl methyl ketone	20*
2-Butyne-1,4-diol (4.3)	MeOH(50)	20	19	100	245	1,4-Butanediol	100
Nitrobenzene (4)	MeOH(50)	40	10	10	330	—	—
Nitrobenzene (4)	MeOH(50)	40	90	88	300	Aniline	60**
p-Nitrotoluene (4.6)	MeOH(50)	40	90	100	30	*p*-Toluidine	70**
Nitromethane (6.1)	Ac_2O(50)	60	50	2	250	—	—
Diethyl nitromalonate (4.2)	Ac_2O(50)	20	40	8	128	—	—
m-Nitrocinnnamic acid (4.8)	aq. NaOH(50)	10	70	80	100	*m*-Aminocinnamic acid *m*-Amino-2-phenylpropionic acid	29 29

* Estimated directly by gas-chromatography of the reaction mixture.
** Estimated by isolating the products as *N*-acetyl derivatives.

Selectivity of the Catalyst.—The catalytic efficiency of the silk-rhodium catalyst on various substrates was examined. For each mole of hydrogen required for complete reduction, 200 mg. of the catalyst were used under ca. 90kg./cm^2 of hydrogen in a 100 ml. autoclave. The results are summarized in Table IV.

In an earlier study it was observed that hydrogenation of both acetaldehyde and benzaldehyde did not take place in the presence of a silk-platinum catalyst, when hydrogen was introduced into the reaction vessel before the reactant had been heated to a reaction temperature; however, when catalyst and aldehyde were pre-heated and then hydrogen was introduced, the reaction occurred. All the compounds tested in the present work, were heated before introduction of hydrogen.

Hydrogenation of the Carbonyl Group.—In the presence of this catalyst the carbonyl group was not hydrogenated in any of the aldehydes and ketones listed in the Table IV.

Hydrogenation of the C=C Double Bonds.—This catalyst is extremely active in hydrogenating C=C double bonds in compounds of the types C=CHCOOH and C=CHCH$_2$OH, such as allyl alcohol, maleic acid, and cinnamic acid. On the other hand, the hydrogenation of the C=C double bonds attached to an ester group or conjugated with a carbonyl group seems to be difficult with this catalyst, and hydrogen uptake by diethyl maleate, cinnamaldehyde and crotonaldehyde was very low. Mesityl oxide absorbed a small amount of hydrogen, yielding only isobutyl methyl ketone, and preserving its carbonyl group intact. The C=C double bond in acrolein, which is conjugated with carbonyl group, behaved typically in that it could be easily hydrogenated at low temperature. The carbonyl group was not attacked, and propionaldehyde was produced in a nearly quantitative yield.

Thus it appears that the silk-rhodium catalyst is capable of easily catalyzing the hydrogenation of the aliphatic C=C double bonds in some molecules leaving unaltered their coexisting carbonyl groups. The double bonds in benzene rings were not hydrogenated in the presence of this catalyst.

Reduction of Nitro Groups.—The hydrogenating activity of silk-platinum catalyst was reported to be extremely high for nitro groups attached to aromatic rings and low for aliphatic nitro groups and C=C double bonds. In the present work, however, the catalyst showed comparatively little activity in the hydrogenation of aromatic nitro groups, and the aliphatic nitro groups of nitromethane and diethyl

nitromalonate were not reduced at all in the presence of acetic anhydride.

Nitrobenzene was not reduced except at high temperature, but the substituted nitrobenzenes, *p*-nitrotoluene and *m*-nitrocinnamic acid, were easily reduced.

2-Butyne-1, 4-diol.—It was easily hydrogenated to give 1, 4-butanediol quantatively.

Experimental

Determination of Rhodium.—Rhodium was determined by the stannous iodide method[3], after the chelated sample had been treated as follows; about 25 ml. of the chelated sample was accurately weighed in a test tube and heated with 0.5 ml. of concentrated nitric acid on a steam bath for 1 hr. The mixture was diluted with 4 N hydrochloric acid to 50.0 ml. Exactly 5.00 ml. of the solution was used for each ascertainment.

The standard curve was made with a solution containing accurately weighed rhodium chloride trihydrate to which was added a certain amount of silk-fibroin decomposed by the method described above for the chelated sample.

Measurement of the Reaction Velocity.—Twenty milligrams of the catalyst to be tested and 5.8 g. (0.1 mol.) of allyl alcohol dissolved in 50 ml. of methanol were placed in a 100 ml. autoclave. Hydrogen was then introduced to a pressure of 90 kg./cm^2, and the time required for 70% of the theoretical hydrogen uptake measured.

Preparation of Catalyst. — Five grams of the silk-rhodium chelate prepared as described previously were reduced in a 300 ml. autoclave with 90 kg./cm^2 of hydrogen in 150 ml. of water, at 140°C for 3 hr. The catalyst obtained was washed with water, methanol, and ether in succession, and then dried in vacuo; yield: 3.2 g. (65%), rhodium content: ca. 5.4% (calculated from rhodium content in the precursor chelate and the yield).

Treatment of the Inhibited Catalysts by Ethylenediaminetetraacetic Acid (EDTA). — The inhibited catalyst was boiled with 100 ml. of 0.5% aqueous solution of EDTA for 5 min., filtered, washed with water, methanol and ether, and finally dried in vacuo.

Acetylation of the Catalyst.—One hundred milligrams of the catalyst were boiled with 50 ml. of acetic anhydride for 2 hr., filtered, washed with ether, and dried in vacuo. The activity of this catalyst was measured by the same procedure used in testing nonacetylated catalyst.

Isolation of the Product.—*Hydrogenation of Allyl Alcohol, Acrolein and Mesityl Oxide.*—The reaction mixture was filtered and the filtrate was treated by gas chromatography; the products were identified as propyl alcohol, propionaldehyde, and isobutyl methyl ketone, respectively, and the yield estimated.

Hydrogenation of Maleic Acid.—The reaction mixture was filtered, the filtrate evaporated to 20 ml., and to this was added 20 ml. of water. After standing overnight, 3.7 g. of succinic acid (m. p. 179~181°C) was obtained. It was confirmed by infrared spectroscopy that the product had no unsaturated bond.

Found: C, 41.25; H, 5.17. Calcd. for $C_4H_6O_4$: C, 40.68; H, 5.12%.

Hydrogenation of Cinnamic Acid.—(i) The reaction mixture was filtered, the filtrate evaporated to 10 ml., and to this was added 20 ml. of 1 N hydrochloric acid. After standing in a refrigerator overnight, 6.4 g. of 2-phenylpropionic acid (m. p. 47.5°C) was obtained.

Found: C, 72.36; H, 6.74. Calcd. for $C_9H_{10}O_2$: C, 72.98; H, 6.71%.

(ii) An aqueous solution of cinnamic acid adjusted to pH 7.0 with sodium hydroxide, was subjected to hydrogenation. The reaction mixture was evaporated to 20 ml., and then acidified with 15 ml. of 2 N hydrochloric acid. After standing in a refrigerator overnight, 2.7 g. of 2-phenylpropionic acid (m. p. 49°C) was obtained.

Found: C, 72.15; H, 6.62. Calcd. for $C_9H_{10}O_2$: C, 71.98; H, 6.71%.

These products were proved to have no unsaturated bond, by infrared spectroscopy.

Reduction of Nitrobenzene and p-Nitrotoluene.—After filtration of the reaction mixture 10 g. of acetic anhydride was added to the filtrate. It was evaporated to dryness and the residue treated with a small amount of water. After standing 2.7 g. of acetanilide (m. p. 113~115°C) and 3.5 g. of *p*-acetotoluidide (m. p. 149°C) was obtained from aniline and *p*-toluidine, respectively.

Acetanilide. Found: N, 10.30. Calcd. for C_8H_9NO: 10.37%.

p-Acetotoluidide. Found: N, 9.28. Calcd. for $C_9H_{11}NO$: 9.39%.

Reduction of m-Nitrocinnamic Acid.—The reaction mixture was evaporated, and to this was added 25 ml. of 2 N hydrochloric acid. Obtained precipitate was filtered off, washed with water and dried in vacuo. (Dried weight, 800 mg.). The fiiltrate was concentrated to 50 ml., to the residue was added 2.5 g. of acetic anhydride and 2 g. of sodium acetate, and the mixture was stirred for 3 hr. Then, a mixture of *m*-acetaminocinnamic acid and 2-*m*-acetaminophenylpropionic acid was precipitated. *m*-Acetaminocinnamic acid content was estimated to be 49.5% by measuring hydrogen uptake on further hydrogenation of this mixture in methanol with Pd-C catalyst.

The mixture. Found: C, 63.15; H, 6.21; N, 6.83. Calcd. for $C_{11}H_{13}O_3N+C_{11}H_{11}O_3N$ (1 : 1): C, 64.07; H, 5.68; N, 6.80%.

Hydrogenation of 2-Butyne-1, 4-diol.—After filtration of the reaction mixture, the solvent was removed from the filtrate by evaporation, and the residue was dried in vacuo. The product was identified as 1, 4-butanediol by infrared spectroscopy.

Summary

1) The most active catalyst was obtained when 400 mg. of silk-fibroin was boiled with 30 ml. of 0.5% aqueous solution of rhodium chloride for ca. 30 min., and the resulting chelate was then reduced.

3) E. B. Sandell, "Colorimetric Determination of Traces of Metals", Interscience Publishers, New York (1959), p. 774.

2) The activity of this catalyst was not influenced significantly by the conditions for its preparation and was maintained or even increased greatly on storage for a long period. Benzyl mercaptan, ferric and cupric ions poisoned the catalyst, but the inhibition by the metal ions could be restored by ethylenediaminetetraacetic acid.

3) This catalyst was extremely active for the hydrogenation of the types C=C double bonds $C{=}CHCH_2OH$ and $C{=}CHCOOH$ but inactive for carbonyl groups. For the hydrogenation of other types of C=C double bonds and of nitro groups, the catalyst seems to be less active.

The authors are indebted to Dr. Heavey A. Itano of the National Institutes of Health, U. S. A., for his advice on preparing this manuscript. The authors wish to express their sincere thanks to Mr. Masami Imaida for his technical assistance throughout this investigation and to Miss Kiku Koike and Miss Masako Kawakita of this Institute for the elemental analysis.

Division of Organic Chemistry
Institute for Protein Research
Osaka University
Kita-ku, Osaka

The Anodic Behavior of Tin in an Alkaline Solution

By Masayoshi KATOH

(Received February 1, 1962)

In this paper, the anodic behavior of tin in an alkaline solution will be described.

Lowenheim[1] demonstrated that tin is anodically polarized through two potential stages in an alkaline solution. In the first stage, the anodic film of tin dissolves into the alkaline solution to form stannite ions at a relatively less noble potential. In the second stage, the anode becomes passive and shows quite a noble potential. Wakked[2] observed the same two stages, and he also showed that the film in the first stage consists of stannous hydroxide.

In contrast with the results of these previous investigators, in the present experiment the author has found three clearly distinguishable potential stages in the anodic polarization curves. This paper presents not only the polarization curves but also the nature of the film in each stage. The rate-determining step in the anodic dissolution process is also discussed.

Experimental

The study of the anodic polarization curves was carried out in a 100 ml. beaker containing a sodium hydroxide solution. The anode was polarized against a platinum cathode, and the anodic potentials were measured against a Hg-HgO reference electrode. The cell was sealed from the atmosphere and was so constructed as to bubble nitrogen or oxygen gas into the electrolytic solution through finely sintered glass.

A circular tin plate was used as the anode. Before being used, this specimen was polished with different grades of emery paper, and then its surface was rubbed with degreased cotton which had been wet by hot water. Finally it was rinsed with ethyl alcohol. Immediately after this treatment, the specimen was placed between two methacrylic resin plates. One of the plates had a circular hole, 0.3 cm^2 in area; this sized area was, therefore, exposed to the electrolytic solution as an anodically polarized electrode.

Results and Discussion

The Anodic Polarization Curves.—The anodic polarization curves of tin in a 0.1 N sodium hydroxide solution are shown in Fig. 1. It may be seen that these curves show three stages of dissolution potentials.

In order to examine the current efficiency and potential variation with time, experiments on the anodic dissolution of tin were carried out for several hours, under constant current densities at the potentials selected within the potential ranges of each stage in Fig. 1. These results are shown in Figs. 2 and 3.

In addition to these experiments, reversible

Part of this paper was reported in *J. Chem. Soc. Japan, Ind. Chem. Sec.* (*Kogyo Kagaku Zasshi*), **62**, 1488 (1959); **64**, 851 (1961).

1) F. A. Lowenheim, *Metal Finishing*, **49**, 60 (1951).

2) S. E. S. E. L. Wakked, *J. Chem. Soc.*, **1954**, 3103.

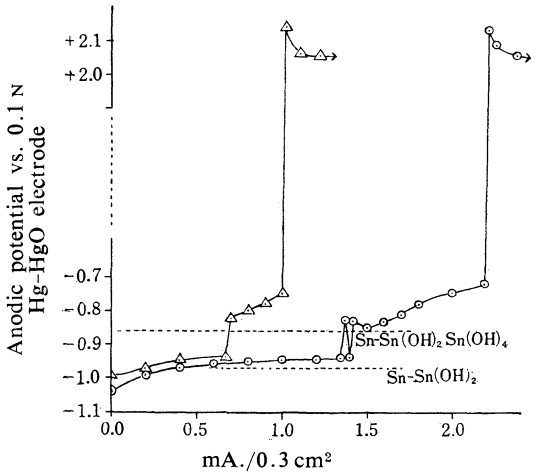


Fig. 1. Anodic polarization curves in 0.1 N sodium hydroxide solution at 25°C.
⊙ N_2 atmosphere △ O_2 atmosphere

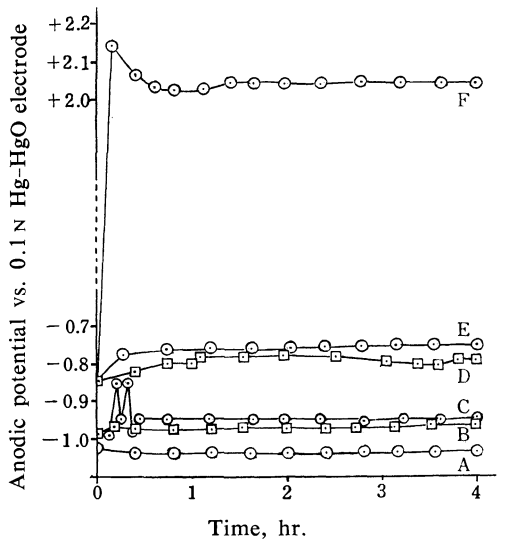


Fig. 2. Potential-time curves at constant current densities in nitrogen atmosphere.
A: 0 mA (simple immersion)
B: 0.6 mA, Curr. eff.=106.0%
C: 0.9 mA, Curr. eff.=103.2%
D: 1.5 mA, Curr. eff.=79.0%
E: 2.0 mA, Curr. eff.=77.6%
F: 2.2 mA, Curr. eff.=7.6%

potentials calculated from thermodynamic data[3] were taken into consideration. These values are given in Table I.

It will be seen from Fig. 1 that potentials in the former two stages nearly correspond to those listed in the first and the second lines, respectively, of Table I although the experimental values are slightly more noble than the table values. In the third stage, however, the anode indicates its passive state; here the potential becomes considerably more noble compared with any value listed in Table I. Since the first line of Table I shows the reversible potential value of the tin-stannous hydroxide system, the anodic film in the first stage seems to be stannous hydroxide. This was supported by the fact, shown in Fig. 2, that the current efficiencies in the first stage were nearly equal to 100%, if the current efficiencies were determined from the actual weight loss of anode and from the theoretical weight loss calculated by Faraday's law, assuming that tin was dissolved as a divalent species, i. e., stannous ion. In another experiment, the concentration of stannite ion and the total of tin in the electrolytic solution were determined after the electrolysis; the ratio between the two was found to be 0.9. This provides another evidence as to the nature of the anodic film mentioned above.

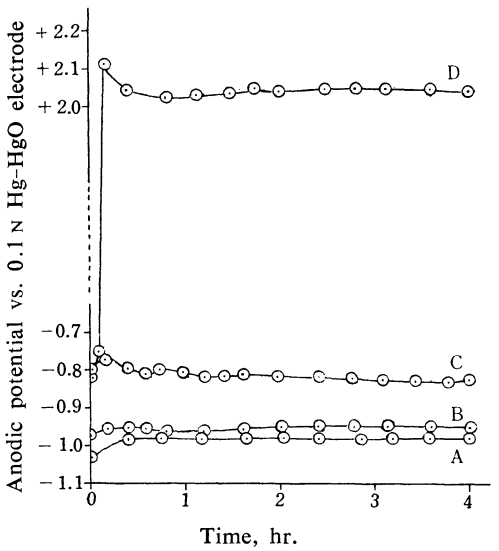


Fig. 3. Potential-time curves at constant current densities in oxygen atmosphere.
A: 0 mA (simple immersion)
B: 0.3 mA, Curr. eff.=162.3%
C: 0.9 mA, Curr. eff.=96.5%
D: 1.0 mA, Curr. eff.=10.0%

TABLE I. REVERSIBLE POTENTIALS OF HALF CELLS CALCULATED EROM FREE ENERGY

Half cell	Potential vs. Hg-HgO-0.1 N NaOH V.
$Sn-Sn(OH)_2$-0.1 N NaOH	−0.973
$Sn(OH)_2-Sn(OH)_4$-0.1 N NaOH	−0.873
$Sn-Sn(OH)_4$-0.1 N NaOH	−0.923
Sn-SnO-0.1 N NaOH	−1.036
$SnO-SnO_2$-0.1 N NaOH	−1.193

3) W. M. Latimer, "The Oxidation States of the Elements and their Potentials in Aqueous Solutions", Prentice-Hall Inc., New York (1952), p. 148.

In the second stage, the potential nearly corresponds to that of the stannous hydroxide-stannic hydroxide system, as can be seen from Table I. This result may allow us to suppose that the film consists of stannic hydroxide under which stannous hydroxide is present. However, it was found from the experiment represented by Fig. 2 that the film dissolved into both stannite and stannate ions, since the current efficiencies in that stage were about 70 to 80% and the ratio, defined as before, was about 0.64 in a nitrogen atmosphere. Moreover, the film did not have the characteristic white appearance of stannic hydroxide, but, rather, was black. The film in the second stage, therefore, can not be stannic hydroxide; it is more appropriate to consider that the film consists of some sorts of reaction products from stannic and stannous hydroxides. In order to ascertain this, another experiment was performed in which four kinds of half cells were constructed from freshly prepared components. The potentials of these cells are tabulated in Table II. The results indicate that the potential at the second stage in Fig. 1 approximately coincides with that of the third line in the table, although the former potential is slightly more noble than the latter, probably owing to ohmic polarization. This confirms the reasonableness of the consideration described above.

Table II. Potentials of half cells which were freshly prepared

Half cell	Potential vs. Hg-HgO-0.1 N NaOH V.
$Sn-Sn(OH)_2$-0.1 N NaOH	−0.980
$Sn-Sn(OH)_4$-0.1 N NaOH	−0.73～−0.75
$Sn-Sn(OH)_2$ and $Sn(OH)_4$ mix. −0.1 N NaOH	−0.86～−0.89

Some other knowledge of the nature of the film can be derived from Figs. 2 and 3. As can be seen from Fig. 2, the open circuit potential of tin in a nitrogen atmosphere is the same as that of the fourth line in Table I, so that a protective layer of stannous oxide, which is sparingly soluble, may be presumed to exist on the tin surface. In an oxygen atmosphere, however, the open circuit potential corresponds well to that of the first lines in both Tables I and II. This indicates that stannous hydroxide is present on the tin surface even as a result of simple immersion; thus, it can easily be supposed that stannous hydroxide is formed not only by electrochemical reaction but also by chemical reaction. The abnormally high current efficiency, over 100% in the oxygen atmosphere, as shown in Fig. 3,

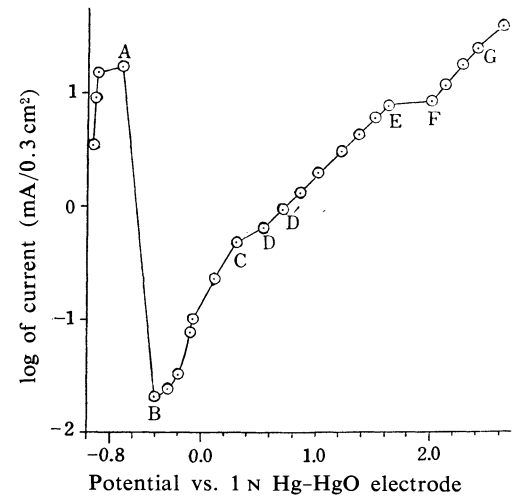


Fig. 4. Anodic polarization curve in 1.0 N sodium hydroxide solution.
A : Point just before passivation
B : Frade potential
C : Point adopted for investigation of decay curve
D : Reversible potential for oxygen evolution
D′: Oxygen evolution was actually observed.

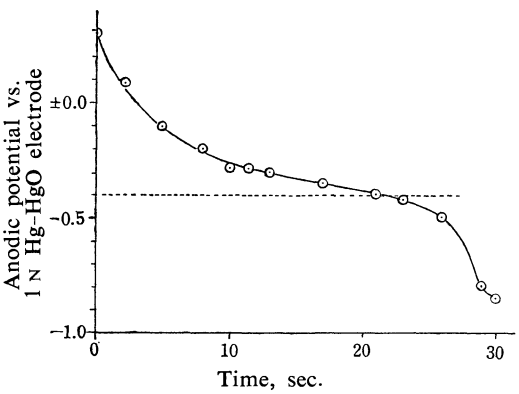


Fig. 5. Decay curve after cutting off the current at C in Fig. 4.

can be attributed to such a chemical process. It may also be found from Figs. 2 and 3 that a long duration of electrolysis at the first or the second stage does not give any passivity to the anode which might be caused by the growth of the film.

When the current density was increased beyond the second stage to reach the third stage, passivation occurred in which oxygen evolved at the anode. The process of this passivation can be more clearly observed in Fig. 4, in which the logarithm of current density is plotted against the anodic potential. The potential bordered on activation and passivation, which is generally known as the Frade potential, can be seen to be −0.400 V.

vs. the 1 N Hg–HgO reference electrode, which is indicated at B in Fig. 4. A decay curve of the potential after the current at C in Fig. 4 had been cut off was also drawn from the measured values, where a stagnation was observed at about −0.40 V., as is shown in Fig. 5. This potential coincides well with the potential at B in Fig. 4. As the anode was polarized beyond the Frade potential, three different stages were observed, the first of which was in BC before the oxygen evolution. If the anodic potential reached D', oxygen was evolved and a bright yellow surface was observed until the potential was raised to E. Further polarization, however, altered the surface state considerably; the color of the film changed to dark black from bright yellow and a different Tafel line appeared. The yellow film in the D'E region was found to be relatively more soluble compared with the dark film in FG and dissolved to give a stannate ion with about a 10% current effiiciency. In the electroplating process of tin, the anode is generally controlled to maintain the yellow color in order to obtain the stannate ion, and so it can be seen that this state corresponds to that of the D'E region.

Relation between the Alkaline Concentration and the Limitting Current Density.—The same type of polarization curves as shown in various alkaline concentrations, so that the limiting current densities reaching the second or the third stage from the first or the second stage could be measured for various concentrations. The experiment was carried out under atmospheric conditions, and the electrolytic solution was not stirred. These results are shown in Fig. 6.

It has been seen from the previous experiments that the limiting current density is governed by the transference of the hydroxide ion from the bulk of the solution to an active site where the anode takes part in the reaction. In this case, it is not necessary to make consider the diffusion of the stannate or stannite ions from the active site to the bulk of the solution, because changes in the concentration of either ion did not appreciably alter the limiting current density. According to Fick's law, the current density I, which responds to the transference of the hydroxyl ions from the bulk of the solution to the surface of the film, is given by[4]:

$$I=\frac{D\cdot nF}{(1-t_{OH^-})\delta}(a-a_c) \tag{1}$$

where t_{OH^-} and D represent the transference number and the diffusion coefficient of the hydroxide ion respectively, δ is the thickness of the diffusion layer in the solution, a and a_c are the activities of the ion in the bulk of the solution and at the surface of the film respectively, and n is the valency of the ion.

In order for the anodic reaction to take place, the hydroxide ion must reach the active site by passing through the film. Although the mechanism concerning such an ionic transference is little known, Fick's law may also be adopted in this case; it so, the current density I in the film may be expressed by the following equation:

$$I=\frac{D'\cdot nF}{(1-t'_{OH^-})\delta'}(a_c-a_d) \tag{2}$$

where t'_{OH^-} and D' are the transference number and the diffusion coefficient of the hydroxide ion in the film respectively, δ' is the thickness of the film, and a_d is the activity of the hydroxide ion at the active site. Since the current densities I in both Eqs. 1 and 2 should be equal, Eq. 1 can be combined with Eq. 2, in which case the current density I may be rewritten as:

$$I=\frac{a-a_d}{(1-t_{OH^-})\delta/D\cdot nF+(1-t'_{OH^-})\delta'/D'\cdot nF} \tag{3}$$

When the current density is increased to the maximum value, which is represented by I_L, a_d should be almost epual to zero, and hence I_L is given by:

$$I_L=\frac{a}{(1-t_{OH^-})\delta/D\cdot nF+(1-t'_{OH^-})\delta'/D'\cdot nF} \tag{4}$$

It follows from this equation that the relation of the limiting current density to the concentration of the hydroxide ions would be a linear function provided that the denominator of Eq. 4 is constant. As can be seen from Fig. 6, this relation is actually satisfied in the region

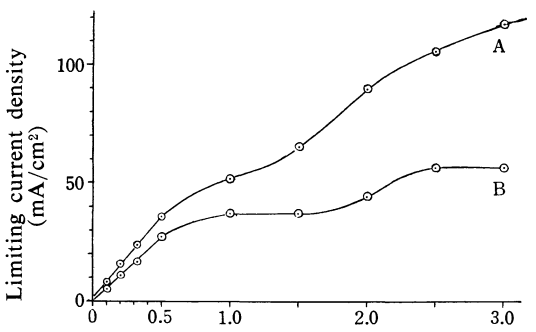


Fig. 6. Relation between alkaline concentration and limiting current density, I_L.
A I_L, from the second stage to the passive stage
B I_L, from the first stage to the second stage

of 0~0.5 N sodium hydroxide. In the denominator of Eq. 4, it is considered that the first and the second terms correspond to resistances for the transference of hydroxide ions throughout the diffusion layers in solution and in film respectively. Therefore, if each term is known, it can be determined in which layer the rate-determining step exists. In the case of the limiting current density reaching the third stage from the second stage, the first term was calculated to be 0.44×10^{-2} up to a 0.5 N concentration at 30°C by introducing the following values:

$t_{OH^-}=0.817$, $F=96500$ coulombs,

$\delta=0.05$ cm.[4], $D=2.14\times10^{-5}$ cm$^2\cdot$sec^{-1}

The sum of the first and the second terms in the denominator of Eq. 4 (i. e., a/I_L), could be obtained from the slope of the straight line in Fig. 6; it was 1.0×10^{-2} up to a 0.5 N concentration. Thus, the second term could be evaluated by subtracting the first term from a/I_L; it was found to be 0.56×10^{-2}. From these values, it may be stated that the diffusion layers in solution and in film both equally resist the transference of hydroxide ions up to a 0.5 N concentration.

As the concentration is increased beyond 0.5 N, however, the slope in Fig. 6 tends to become less steep, although still not proportional to the concentration, and the linear function no longer obtains. This indicates that the denominator of Eq. 4 begins to increase and shows no constant value. According to one table[5], any value in the first term is almost independent of the alkaline concentration. This means, therefore, that the second term tends to increase and is not constant. Since the increase of the second term means an increase of δ' and a decrease of D', it follows that thickening of the film should occur. Therefore, it can be concluded that the rate-determining step is the process in which hydroxide ions reach the active site by passing through the film.

The limiting current density reaching the second stage from the first stage can be treated in the same manner as above. Equation 4 may still be employed, because the electrode process still proceeds by replenishment of the hydroxide ions.

Since a linear function was obtained in the region of 0~0.5 N sodium hydroxide solutions, the first and the second terms of the denominator in Eq. 4 were calculated to be 0.44 and 1.19 respectively. This indicates that the rate of the transference of the hydroxide ion is practically determined by the rate of its passage through the film of stannous hydroxide; that is, the film of the first stage resists the transference of the hydroxide ion more intensely than the film of the second stage.

Department of Applied Chemistry
Faculty of Science
Tokyo College of Science
Shinjuku-ku, Tokyo

4) G. Kortum and J. O'M. Bockris, "Textbook of Electrochemistry", Elsevier Publishing Co., New York (1951), p. 402.

5) National Research Council, "International Critical Table", Vol. VI, McGraw-Hill Book Co., New York (1929).

Relations between the Electronic Absorption Spectra and the Spatial Configurations of Conjugated Systems. XII. The Intensity and the Shape of the Conjugation Band

By Hiroshi SUZUKI

(Received June 22, 1962)

The preceding parts[1] of this series dealt mainly with a rather restricted aspect of the theme. That is, they dealt mainly with the relation between the wavelength position of the absorption maximum of the conjugation band and the most probable configuration of the molecule in some conjugated hydrocarbon systems, such as biphenyl, styrene and stilbene. In the present paper, other aspects of the subject, especially the relations between the intensity, as well as the shape of the conjugation band, and the spatial configuration of the molecule, are discussed for the foregoing systems as representatives of alternant hydrocarbon systems.

1) H. Suzuki, This Bulletin, (I) **32**, 1340; (II) 1350; (III) 1357 (1959); (IV) **33**, 109; (V) 379; (VI) 389; (VII) 396; (VIII) 406; (IX) 410; (X) 613; (XI) 619 (1960).

Calculation of the Transition Moment as a Function of the Angle of Twist

It is well known that in such conjugated hydrocarbon system as the foregoing, steric hindrance to the planarity of the system exerts a hypochromic as well as a hypsochromic effect on the conjugation band.

The steric hindrance may be considered to be relieved, to a first approximation, only by a twist of the formally single bond or bonds, e.g., the co-annular bond in the biphenyl system, the bond linking the phenyl group to the ethylenic carbon atom in the styrene system, and the similar bonds in the stilbene system. (These "single" bonds are referred to as the pivot bonds.) On the basis of this assumption, in the preceding parts of this series, the energy of a one-electron transition from the highest occupied π-orbital, ψ_{+1}, to the lowest vacant one, ψ_{-1}, was calculated, by the simple LCAO MO method, as a function of the angle of the twist of the pivot bond for each of these systems and was correlated with the wavelength of the maximum of the conjugation band for a number of the compounds of the system. In spite of the simplicity of the method used, the correlation was almost completely satisfactory. Thus, it may be said that an almost satisfactory explanation of the steric hypsochromic effect in these conjugated systems was obtained. Therefore, it may be of some interest to see whether the steric hypochromic effect, i.e., the reduction of the intensity of the band due to steric hindrance to the planarity of the conjugated system, can be explained by extending the simple MO treatment.

The resonance integral of the atomic orbitals χ_i and χ_j is denoted by $\rho_{ij}\beta$, β representing the π-π resonance integral for adjacent carbon atoms in the benzene ring. The parameter, ρ_{ij}, is determined by the distance, R_{ij}, between atoms i and j as well as by the angle of twist, θ_{ij}, of the bond, i.e., the angle by which the axes of χ_i and χ_j are twisted with respect to each other. If it is assumed that the bond length, R_{ij}, is constant, ρ_{ij} can be taken to be proportional to $\cos\theta_{ij}$.

On the basis of the orbital energies calculated as functions of ρ_{piv} in the preceding parts of this series, the coefficients of the atomic orbitals in the molecular orbitals ψ_{-1} and ψ_{+1} and then the transition moment, $M_{-1,+1}$, have been calculated as functions of ρ_{piv}. The transition moment is, needless to say, expressed as:

$$M_{-1,+1}=\sqrt{2}\int\psi_{-1}\,q\psi_{+1}\mathrm{d}\tau$$

where q and $\mathrm{d}\tau$ are the position coordinate of the electron and the volume element of the space of the coordinate respectively. By the way, the subscript $-1,+1$ refers to quantities concerning the transition from ψ_{+1} to ψ_{-1}, while the subscript piv refers to quantities concerning the pivot bond. These subscripts are subsequently often omitted for the sake of brevity if no confusion is possible. In the calculations, the relation between ρ and θ as well as R assumed in the preceding parts has been used for each system, and all the bond angles at the carbon atoms in the conjugated skeleton have been assumed to be 120°. The results are shown in Fig. 1, in which the values of the square of the transition moment, namely, the dipole strength of the transition (in units of Å^2), are plotted against θ_{piv}.

The oscillator strength, f, is related to the transition moment by the usual equation;

$$f=1.085\times10^{-5}\nu M^2$$

where ν is the wave number (in cm^{-1}) at which the absorption due to the transition occurs. In the previous papers, the wave number to be observed was correlated with the transition energy, ΔE, calculated as a function of θ for each of the systems. Accordingly, by the use of the relation, the f-value can be calculated as a function of θ for each system. The calculated f-value, which is designated as f_{theor}, for the stilbene system is also graphed in Fig. 1.

It can be clearly seen in this figure that the dipole strength of the transition, as well as the oscillator strength, of each system becomes

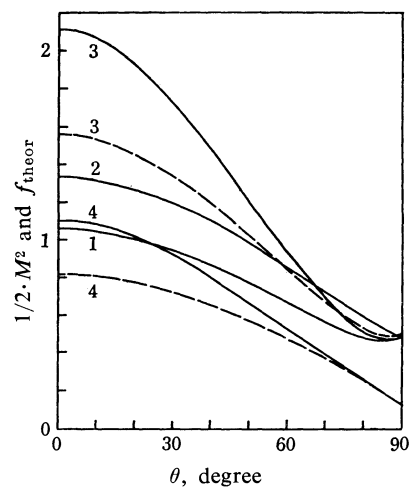


Fig. 1. Relations between the transition moment, M, as well as the calculated oscillator strength, f_{theor}, of the conjugation band and the angle of twist of the "single" bond, θ. Solid lines are for $1/2\cdot M^2$ (in Å^2); broken lines, for f_{theor} 1, styrene 2, biphenyl 3, *trans*-stilbene 4, *cis*-stilbene.

smaller as the value of θ becomes larger. This means that the intensity of the conjugation band will become lower as the deviation from the planarity of the conjugated system increases, a trend which is in agreement with observation. It may be noted here that the variation in the dipole strength of the transition associated with the variation of ρ_{piv} is roughly linear in each of the systems.

A Comparison of the Theoretical Values with the Experimental Values of Oscillator Strength

The oscillator strength can be estimated from the absorption curve by means of the usual equation:

$$f=4.317\times10^{-9}\int\varepsilon_{\nu}\mathrm{d}\nu$$

where ε_{ν} is the molar extinction coefficient at wave number ν and the integral is the integrated intensity of the absorption band concerned. The value of the oscillator strength estimated from the observed spectrum is designated as f_{exp}.

In Table I, for some compounds of the conjugated systems under consideration and, in addition, for butadiene, the values of f_{theor} and f_{exp} are listed, together with some relevant data.

The f_{theor}-Values.—The values of θ are those evaluated from the wavelengths of the absorption maxima in the previous parts of this series, and the transition moments have been calculated on the basis of these θ values. That is, the transition moment of each compound has been calculated for the most probable configuration of the conjugated system, and no electronic (probably small hyperchromic) effects which the substituents may exert on the absorption intensity have been taken into account.

For tetraphenylethylene, the model in which all of the phenyl groups are rotated out of the plane of the central ethylenic bond to the same extent was used as the basis for the calculation of the transition moment, according to the conclusion made in Part VI of this series.

For butadiene, the calculation has been carried out on the basis of the planar s-trans model in which the lengths of the "double" bonds and of the "single" bond are 1.34Å and 1.48Å respectively.

The f_{exp}-Values.—The f_{exp}-values for most compounds were estimated from the absorption spectra reported in Parts I, II, V and VII of this series. The spectra of biphenyl, tetraphenylethylene and tolan reported in Parts I and VI were found to be somewhat inaccurate with respect to the absorption intensity. Accordingly, the f_{exp}-values for these compounds (the entry numbers 4, 13 and 14) were estimated on the basis of the newly redetermined spectra. The experimental data for the entry

Table I

No.	Compound	λ mμ	ε $\times10^{-2}$	θ degree	M^2 Å^2	f_{theor}	f_{exp}	$\frac{f_{\mathrm{theor}}}{f_{\mathrm{exp}}}$	$\frac{f_{\mathrm{exp}}}{\varepsilon}\times10^{7}$	$\Delta\nu$ $\times10^{-1}$ cm^{-1}
1	Butadiene (in *n*-hexane)	217	209	0	2.334	1.167	0.53	2.20	254	—
2	Styrene	248	148	0	2.120	0.927	0.327	2.84	222	—
3	Biphenyl (KCl disk)	253	—	0	2.677	1.148	—	—	—	—
4	Biphenyl	247	167	23	2.503	1.100	0.411	2.68	246	254
5	Biphenyl (vapor, 170°C)	238	121	42	2.159	0.984	0.316	3.11	262	—
6	*o*-Methylbiphenyl	235	100	58	1.772	0.818	0.261	3.13	261	260
7	*trans*-Stilbene	294	280	0	4.221	1.557	0.739	2.11	264	307
8	*trans*-α, α'-Dimethylstilbene	243	123	58	1.951	0.870	0.350	2.49	285	323
9	*trans*-α, α'-Diethylstilbene	237	111	63	1.696	0.778	0.330	2.36	298	335
10	*cis*-Stilbene (in ethanol)	280	105	28	1.882	0.729	0.323	2.26	309	311
11	*cis*-α, α'-Dimethylstilbene	252	89	52	1.276	0.549	0.329	1.67	371	450
12	*cis*-α, α'-Diethylstilbene (in ethanol)	244	77	58	1.110	0.494	0.270	1.83	349	372
13	Tetraphenylethylene	309	142	35	2.566	0.902	0.393	2.30	278	266
14	Tolan	280	316	0	4.804	1.862	0.700	2.66	222	233

The notation is as follows: λ and ε, the wavelength and the molar extinction coefficient of the maximum of the conjugation band respectively; θ, the angle of twist of the "single" bond in the most probable configuration; M, the calculated transition moment; f_{theor} and f_{exp}, the theoretical and the experimental oscillator strength respectively; $\Delta\nu$, the wave number interval between the absorption maximum and the point of half the maximum intensity at a longer wavelength than the maximum.

numbers 1[2,3], 2[4], 3[5] and 5[6] have been taken from papers of other authors. All the spectral data are for the solution in *n*-heptane at room temperature except where otherwise indicated.

It is difficult to determine unambiguously the intrinsic band envelope and, hence, the integrated intensity of the conjugation band as differentiated from neighboring bands. For each of the compounds of entry numbers 4, 7, 10, 13 and 14, the area under the absorption curve at wave numbers lower than the absorption minimum between the conjugation band and the neighboring band lying at higher wave numbers was taken as an approximation of the integrated intensity of the conjugation band, since with these compounds the conjugation band is comparatively well resolved from its neighbor.

With the compounds of entry numbers 6, 8, 9, 11 and 12, the conjugation band itself is situated at quite a high wave number and has quite a low intensity; hence, the resolution of the band from the neighboring band is very unsatisfactory. Therefore, for these compounds, twice the area under the absorption curve at wave numbers lower than the absorption maximum was taken as a rough appoximation of the integrated intensity of the conjugation band.

Comparison of f_{theor}- and f_{exp}-Values.—It is well known that the value of f calculated by the simple MO method is in general too high by a factor of about 2~3. This general tendency is considered to be due to the essential character of the method, which does not take account of interactions among electrons and hence tends to over-estimate the delocalization of the molecular orbitals[7]. This appears to be inevitable when any one single electronic configuration is used. In this respect, the present calculation is not an exception. Thus, the ratios of f_{theor} to f_{exp} are about 2~3.

Apart from the discrepancy in the absolute values, quite a good correspondence is found between the f_{theor} values and the f_{exp} values. This can be seen more clearly in Fig. 2, in which the f_{theor} values are plotted against the corresponding f_{exp} values. Considering the uncertainty involved in the estimation of the f_{exp} values, as well as the simplification made in the calculation of the f_{theor} values, it may be said that the correspondence is rather

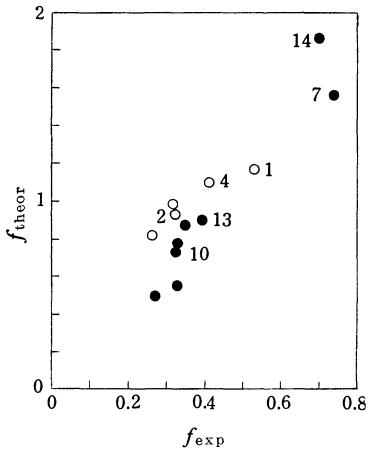


Fig. 2. Relations between the theoretical values, f_{theor}, and the experimental values, f_{exp}, of the oscillator strength of the conjugation band. ○, for the compounds of the entry numbers 1—6 in Table I; ●, for the compounds of the entry numbers 7—14 (the compounds of the stilbene system, including tolan).

unexpectedly good. Especially, it may be noted that the points for the compounds belonging to the stilbene system (entry numbers 7, 8, 9, 10 and 13), with the exception of two *cis*-dialkylstilbenes and tolan, fall nearly on a smooth line passing through the origin.

This almost satisfactory correspondence of the f_{theor} values to the f_{exp} values may be considered to validate the present treatment. Thus, it may be concluded that the reduction of the intensity, as well as the shift toward shorter wavelengths, of the conjugation band caused by steric hindrance to the planarity of the conjugated system has been almost satisfactorily explained solely by the change in the π-electronic states of the molecule associated with the change of the most probable configuration.

Basic Assumptions in the Present Treatment

One of the basic assumptions underlying the treatment developed throughout the present series of papers is that the steric hindrance to the planarity of the conjugated system is relieved to a first approximation only by a twist of the formally single bond or bonds. Any twist of such a bond should not affect the σ-bond energy, and, since such a bond has a relatively low π-bond order in the electronic ground state, the loss of the delocalization energy of the π-electrons associated with the twist should be relatively small. Furthermore, it is expected that such a twist will, in most cases, rapidly reduce the steric repulsion

2) K. B. Alberman, R. N. Haszeldine and F. B. Kipping, *J. Chem. Soc.*, **1952**, 3284.
3) C. A. Coulson and J. Jacobs, *Proc. Roy. Soc.*, **A206**, 287 (1951).
4) D. F. Evans, *J. Chem. Phys.*, **23**, 1429 (1955).
5) J. Dale, *Acta Chem. Scand.*, **11**, 650 (1957).
6) F. Almasy and H. Laemmel, *Helv. Chim. Acta*, **33**, 2092 (1950).
7) See, for example, Ref. 3, and also R. S. Mulliken and C. A. Rieke, *Rep. Progr. Phys.*, **8**, 231 (1941).

between non-bonding atoms. The above assumption is quite admissible.

Two other important underlying assumptions are that the molecules with the most probable configuration in the electronic ground state make the most important contribution to the absorption band and that the absorption maximum corresponds to the vertical transition in such molecules. These assumptions might appear to be self-evident. However, since the explanations of the steric hypochromic effect proposed by some other authors seem to be based on an idea quite opposed to this assumption, and, further, in order to provide a basis for a later discussion of the shape of the band, they will be discussed here in some detail.

The potential energy curve of any electronic state for the twist of a "single" bond can be considered to be determined primarily by the sum of the π-electronic energy of the state and of the steric repulsion energy as functions of the angle of twist. Such a potential energy curve may be relatively shallow; hence, the separations of the vibrational levels may be relatively small, compared, for example, with those for the stretching vibrational mode of a "double" bond.

According to the classical theory, the molecules in each vibrational level can be considered to stay predominantly at the turning points of the vibrational motion. Therefore, according to the Franck-Condon principle, the most probable of the electronic transitions which a molecule in a vibrational state associated with the electronic ground state can give rise to should be the transition vertically upward in the potential energy diagram from each of the turning points of the vibrational level to the point on the potential energy curve of the electronic upper state. The energy of such a vertical transition is the difference between the potential energies of the two points and, hence, should be equal to the difference between the π-electronic energies in the configuration characterized by the angle of twist, the contributions of other factors such as steric repulsion energy and σ-electronic energy to the potential energies of the two points being considered to be identical because the transition does not involve any change in the spatial configuration of the molecule. This consideration justifies that treatment in the present series by which the energy difference between the two π-orbitals, ψ_{-1} and ψ_{+1}, calculated as a function of θ, namely, $\Delta E_{-1,+1}(\theta)$, has been correlated directly with the wave number of the observed absorption band.

The wave number corresponding to $\Delta E(\theta)$ is denoted by $\nu(\theta)$, and the transtion moment and the oscillator strength of this transition are denoted by $M(\theta)$ and $f(\theta)$ respectively. The population ratio of the configuration characterized by θ in the electronic ground state is denoted by $P^G(\theta)$. The value of θ at which the value of $P^G(\theta)$ is at its maximum is denoted by θ^G_{max}, which may be considered to agree approximately with the value of θ at the minimum of the potential energy curve, namely, θ^G_{eq}, in which the subscript eq is an abbreviation for "equilibrium".

The contribution of any configuration to the absorption is proportional to the product of the population ratio of the configuration and the transition probability in the configuration. Accordingly, the absorption intensity, $\varepsilon(\theta)$, at the wave number, $\nu(\theta)$, can be taken to be approximately proportional to $f(\theta)\cdot P^G(\theta)$.

The value of f, as well as that of M^2, decreases comparatively slowly as the value of θ becomes larger, as is seen in Fig. 1. Roughly speaking, the larger the value of θ, the larger the increase of f as well as of M^2 associated with a decrease of θ. Thus, in the conjugated hydrocarbon systems treated in the present paper, the variation of f as well as of M^2 is approximately linear to cos θ.

On the other hand, the distribution curve of $P^G(\theta)$ versus θ may be relatively steep. Thus, the value of $P^G(\theta)$ may decrease comparatively rapidly as the value of θ is separated in both directions from that of θ^G_{max}. In cases where steric hindrance is involved, the larger the steric hindrance, the larger the value of θ^G_{max} and, probably, the larger the decrease of $P^G(\theta)$ associated with a decrease of θ from θ^G_{max}.

Therefore, it is quite reasonable to expect that the angle of twist, θ, at which the value of $f(\theta)\cdot P^G(\theta)$ is at its maximum agrees almost completely with θ^G_{max}, i. e., the angle of twist in the most probable configuration. Thus, the maximum of the absorption band may be considered to originate in molecules with the most probable configuration.

The oscillator strength of the band should be expressed as:

$$f=\int f(\theta)\cdot P^G(\theta)\cdot d\theta$$

Judging from the above-mentioned feature or the dependence of $f(\theta)$ as well as of $P^G(\theta)$ on θ, it is evident that f can be well approximated by $f(\theta^G_{max})$.

On Some Other Explanations of the Steric Hypochromic Effect

The Explanation of Jaffé and Orchin.—Jaffé and Orchin[8] recently proposed a "Franck-Condon effect" as an important cause of the

8) H. H. Jaffé and M. Orchin, *J. Chem. Soc.*, 1960, 1078.

steric hypochromic effect observed with the conjugation band of such sterically hindered compounds as sterically hindered stilbenes. Their basic theory is that only the vertical transitions to the lowest vibrational level of the electronic upper state should be allowed. Thus, according to them, if the values of θ at the turning points of the lowest vibrational level of the twisting mode of the "single" bond in the electronic excited state are denoted by $\theta^{E}_{<}$ and $\theta^{E}_{>}$, only the molecules with the value of θ in the range between $\theta^{E}_{<}$ and $\theta^{E}_{>}$ in the electronic ground state can give rise to a transition to the electronic excited state, and any transition in the molecules with θ outside the range is forbidden. Accordingly, the observed intensity of the band should be reduced below the value predicted from the theoretical oscillator strength by the ratio of the number of the molecules with θ in the range to the whole number of the molecules in the electronic ground state. The greater the steric hindrance, the smaller this ratio will be. This is the gist of Jaffé and Orchin's explanation of the "Franck-Condon effect".

This explanation is in conflict with the basic assumptions of the present treatment. From the considerations given above, it is evident that the explanation by Jaffé and Orchin is invalid. In addition, they seem to confuse the probability density distribution in the lowest vibrational state in the electronic ground state with the distribution of population among various vibrational states in the electronic state; furthermore, it seems not to be clear whether they discuss the intensity of the absorption maximum or the integrated intensity of the entire band.

The Explanation of Braude.—The argument of Jaffé and Orchin is similar to the explanation by Braude of the so-called type 1 steric effect, i. e., the decrease in the intensity of the conjugation band without any appreciable accompanying wavelength displacement of the band observed with sterically hindered compounds, e. g., *o*-substituted acetophenones, as compared with the sterically unhindered parent compound. Braude and his co-workers[9,10] ascribed this decrease in the intensity to the decrease in the population ratio of the planar or near-planar configuration in the electronic ground state. This theory means that, with sterically hindered compounds, the maximum absorption does not originate in the most probable non-planar configuration but in the less probable, energetically unfavorable, planar or near-planar configuration; this is contrary to the basic assumptions of the present treatment. The theory of Braude is evidently based on the concept that the absorptions at nearly identical wavelengths should be due to the transitions in the nearly identical configurations; it also tacitly involves the assumption that the transition in non-planar configurations is impossible or nearly so.

In general, the direction and the magnitude of the change of the transition energy caused by a twist of a bond depend on the sign and the magnitude of the change in the π-bond order of the bond associated with the transition[11,12] and, hence, essentially on the nature of the orbitals between which the transition occurs[13]. In some cases, it is possible that a quite large change of the molecular configuration results in substantially no change or a very small change in the transition energy. Therefore, absorptions at the identical wavelength do not necessarily mean that they originate in the identical configuration.

As is shown above, the transition moment varies continuously with θ in the cases of the conjugated hydrocarbon systems. As will be discussed later in this series, the situation is not so very different in the case of the phenylcarbonyl system, i. e., the acetophenone or benzaldehyde system, which was cited by Braude as representative of the systems exhibiting the so-called type 1 steric effect. The assumption that the transition in non-planar configurations is substantially impossible is untenable. Furthermore, it has been demonstrated experimentally by Waight and Erskine[14] that the maximum absorption should be considered to originate in the transition in the most probable non-planar configuration, even in the case of sterically hindered acetophenones.

The Shape of the Conjugation Band

Potential Energy Curves for the Twisting Mode.—It is a notable fact that the conjugation band of *trans*-stilbene exhibits a well-resolved vibrational fine structure, even at room temperature, whereas the bands of sterically-hindered related compounds are structureless. A similar situation can be found in many other conjugated systems.

We shall now attempt, on the basis of the considerations so far described, to relate the shape of the conjugation band to the steric hindrance to the planarity of the conjugation system. With this end in view, the potential

9) E. A. Braude and F. Sondheimer, ibid., **1955**, 3754.
10) W. F. Forbes, "Steric Effects in Conjugated Systems", Ed. by G. W. Gray, Butterworths Scientific Publications, London (1958), p. 62 ff.
11) E. Heilbronner and R. Gerdil, *Helv. Chim. Acta*, **39**, 1996 (1956).
12) R. I. T. Cromartie and J. N. Murrell, *J. Chem. Soc.*, **1961**, 2063.
13) J. N. Murrell, ibid., **1956**, 3779.
14) E. S. Waight and R. L. Erskine, Ref. 10, p. 73 ff.

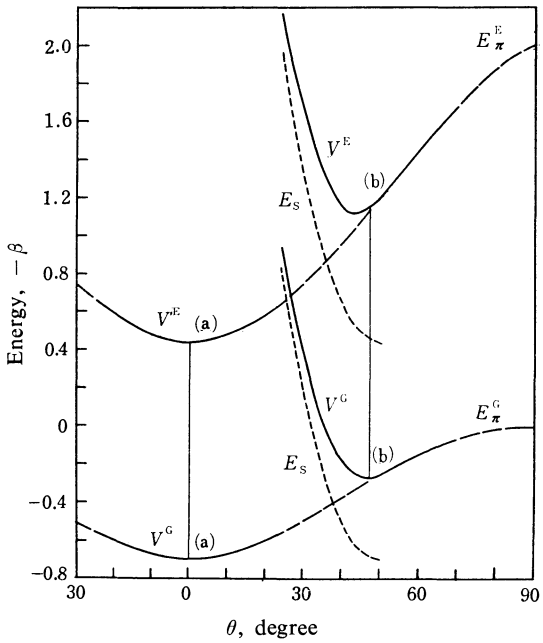


Fig. 3. Potential energy diagram for the stilbene system. V, potential energies (solid lines) as functions of the angle of twist of the "single" bonds, θ: (a) for the sterically unhindered compound; (b) for a sterically hindered compound. E_π, π-electronic energies (broken lines). E_S, steric repulsion energy (dotted lines).

energy curves for the twisting of the pivot bonds are first examined.

In Fig. 3, the calculated π-electronic energy ($E^G{}_\pi$) of the ground state of the stilbene system and that ($E^E{}_\pi$) of the excited state which arises from the transition of an electron from ψ_{+1} to ψ_{-1} are plotted against θ, these curves being shown as broken lines. In this figure, the energy of the ground state when θ is 90° is taken as the reference zero energy, while the unit of energy is $-\beta$. By the way, the superscripts G and E refer to the electronic ground state and the electronic excited state respectively throughout the present paper. The quantity $-E^G{}_\pi$ is the so-called extra-resonance energy and is approximately proportional to $\rho^2{}_{piv}$ and, hence, to $\cos^2\theta_{piv}$. The difference between $E^E{}_\pi$ and $E^G{}_\pi$ is the transition energy and increases, roughly speaking, linearly with the decreasing value of ρ_{piv} and, hence, of $\cos\theta_{piv}$. The $E^E{}_\pi$-curve is, of course, steeper than the $E^G{}_\pi$-curve.

Also in Fig. 3, the curves for the steric repulsion energy (E_S) as a function of θ for a hindered case are arbitrarily depicted as dotted lines. The curves for the resultant potential energy (V) as the sum of E_π and E_S for the unhindered case and for the hindered case are shown as solid lines.

In the unhindered case, the V-curves coincide with the E_π-curves; therefore, $\theta^G{}_{eq}=\theta^E{}_{eq}=0°$, where θ_{eq} represents the equilibrium angle of the twist, i.e., θ at the minimum of the V-curve.

In the hindered case, the V of each electronic state is regarded as the sum of E_π of the state and E_S, which is considered to be identical in both the states. Since $E^E{}_\pi$ increases more rapidly than $E^G{}_\pi$ does as θ becomes larger, there must be this relation: $\theta^G{}_{eq}>\theta^E{}_{eq}>0°$.

The E_S-curve may be quite steep. The E_π-curves are steeper at a larger value of θ, except when θ is extremely large. Therefore, if the steric hindrance is not so slight, the V-curves in the sterically hindered case may be steeper than the corresponding ones in the unhindered case. At least, there seems to be no reason to believe that the latter should be distinctly steeper than the former.

Distribution of Configurations in the Ground State.—As has been mentioned above, the V^G-curve in the sterically hindered case may be steeper than that in the unhindered case. Accordingly, the distribution curve of the population of configurations characterized by θ in the electronic ground state, namely, the $P^G(\theta)\sim\theta$ curve, which can be considered to have its maximum at $\theta^G{}_{eq}$, may be broader in the unhindered case than in the hindered case.

However, if $P^G(\theta)$ is plotted against $\Delta E(\theta)$ or $\nu(\theta)$ instead of θ, a distribution curve with quite different features will result. As has been mentioned already, the configuration characterized by θ can be considered to be characterized also by $\Delta E(\theta)$ or $\nu(\theta)$. $\Delta E(\theta)$ and $\nu(\theta)$ vary roughly linearly with ρ and, hence, with $\cos\theta$. Therefore, if $\theta^G{}_{eq}$ is small, even though the distribution curve with respect to θ is comparatively broad, the distribution curve with respect to $\Delta E(\theta)$ or $\nu(\theta)$ will be quite steep. This means that, in this case, even quite a wide variation of θ will give rise to the transition in quite a narrow range of wave numbers. On the other hand, if $\theta^G{}_{eq}$ is fairly large, even if θ varies within a comparatively limited range around $\theta^G{}_{eq}$, the variation of θ will give rise to the transition in a comparatively wide range of wave numbers. Thus, from the consideration of the distribution of configurations in the electronic ground state, it may be expected that the conjugation bands of the sterically hindered compounds are broader than that of the unhindered parent compound.

By the way, since $-E^G{}_\pi$, i.e., the extra-resonance energy, can be considered to be approximately proportional to $\cos^2\theta$, it can be roughly related with $\Delta E(\theta)$ and $\nu(\theta)$ as follows:

$$-E^{G}{}_{\pi}(\theta) \propto [\Delta E(90°) - \Delta E(\theta)]^2$$
$$\propto [\nu(90°) - \nu(\theta)]^2$$

Intensity Distribution among Transitions of Vibrational Progression.—The total probability of the transition from a vibrational state associated with the electronic ground state to the electronic excited state is distributed among transitions to vibrational states associated with the electronic excited state in proportion to the square of the overlap integral of the eigenfunctions of the two vibrational states involved.

The vibrational quantum number is represented by v and, as has been mentioned already, the electronic states are denoted by the superscripts G and E respectively. The lowest vibrational state associated with the electronic ground state, i. e., the state for which v^G is 0, is admittedly most densely populated, and the transition from this state should make the most important contribution to the absorption band, as has been discussed above.

In general, for $v=0$, there is a broad maximum of the probability density distribution approximately above the minimum of the potential energy curve. On the other hand, for $v \neq 0$, there is a broad maximum of the probability density distribution in the neighborhood of each of the classical turning points of the vibrational motion, but lying somewhat more toward the center. In a series of transitions from the state for which $v^G=0$, the overlap integral has a maximum value for the transition to the v^E state which has the broad maximum of its probability distribution vertically above the minimum of the potential energy curve of the electronic ground state. Therefore, the further the minima of the potential energy curves of the two electronic states are separated from each other, and the steeper the upper potential energy curve, the higher the v^E-value of the most probable transition from the $v^G=0$ state will be and the greater the variety of v^E states will be, among transitions to which the total transition probability is distributed[15].

As has been mentioned above, in the unhindered case, $\theta^G{}_{eq}=\theta^E{}_{eq}=0°$. Therefore, in this case, the transition probability from the $v^G=0$ state will be concentrated mostly in the 0−0 band. On the other hand, in the hindered case, $\theta^G{}_{eq} > \theta^E{}_{eq} > 0°$, and the upper potential energy curve may be steeper than that in the unhindered case. Therefore, in this case, the transition probability from the $v^G=0$ state will be broadly distributed among transitions to a comparatively large number of v^E states.

The Shape of the Band.—From the considerations of both the distribution of the population of configurations in the electronic ground state and of the intensity distribution among transitions from the most probable vibrational state associated with the electronic ground state to various vibrational states associated with the electronic excited state, it is expected that, in the unhindered case, the absorption will occur over a comparatively narrow range of wavelengths and that the greater the steric hindrance, the wider the range of wavelengths over which the absorption will occur. Thus, as far as the twisting mode about the single bonds is concerned, it is expected that the absorption band will be broadened by the steric hindrance.

This expected effect of steric hindrance in broadening the absorption band may be of two kinds: (a) a broadening of the whole band system or (b) a broadening of individual absorption lines originating in the other kind of vibrational mode and, consequently, a blurring of the fine structure of the band.

The half-band-width, as well as the ratio of the integrated intensity or the oscillator strength to the intensity of the absorption maximum, may be taken as a measure of the broadness of the band as a whole. In Table I, instead of the half-band-width, the wave number interval between the absorption maximum and the point of half the intensity of the maximum at a longer wavelength than the maximum, which is referred to as $\Delta\nu$, is presented, together with the $f_{exp}/\varepsilon_{max}$ ratio for each compound.

It seems that there is, in gross, a trend in conformity with the above expectations, although it is doubtful, because of uncertainty involved in the estimation of these data, whether much significance can be attached to this apparent trend. Thus, the effect of steric hindrance of broadening the band as a whole is not clear, although its possibility can not be excluded.

On the other hand, the effect of blurring the fine structure of the band and, eventually, of making the band structureless seems to be more convincing.

As was shown in Fig. 1 of Part V of this series, the conjugation band of *trans*-stilbene exhibits quite a well-resolved fine structure. The separations of the fine structure are about 1340 cm^{-1} at 20°C; these become 1480 cm^{-1} at −130°C[16]. The conjugation bands of *p*-phenylstilbene, *p*,*p'*-diphenylstilbene[I-IX] and styrene[4] exhibit a similar, though somewhat more blurred, fine structure. In contrast with the conjugation bands of these probably

15) See, for example: G. Herzberg, "Molecular Spectra and Molecular Structure, I. Spectra of Diatomic Molecules", 2nd ed., D. Van Nostrand Company, Inc., New York (1950), p. 193 ff.

16) R. N. Beale and E. M. F. Roe, *J. Chem. Soc.*, 1953, 2755.

unhindered compounds, the bands of probably nonplanar related compounds are almost perfectly structureless. (By the way, the conjugation band of biphenyl is structureless.)

According to Beale and Roe[16], the fine structure of the conjugation band of *trans*-stilbene is considered to originate in an ethylenic C=C stretching frequency. This bond undergoes the largest change in π-bond order on the excitation of the molecule; hence, the minima of the potential energy curves of the electronic ground state and of the electronic excited state for the stretching vibration of this bond are probably at values of the bond length considerably different from each other. (Since the π-bond order decreases on the excitation, the equilibrium bond length in the upper state is probably longer than that in the lower state.) Therefore, it must be possible for transitions from the lowest vibrational level of the electronic ground state to several vibrational levels of the electronic excited state to occur and, since the energy separations of the vibrational levels must be comparatively large, they will probably be revealed as the progression of the fine structure.

As has been mentioned above, the transition probability is considered to be concentrated in a considerably restricted wavelength range in the unhindered case, in so far as the twisting mode about the single bonds is concerned. Consequently, in this case, the progression originating in the C=C stretching mode is not so blurred and will reveal itself as a comparatively well-resolved fine structure.

On the other hand, in the case of hindered molecules, the transition probability is considered to be distributed among a greater variety of transitions covering a wider range of wavelengths; the fine structure will thereby be blurred. The same explanation will be applicable to the other systems.

Summary

The moment of the transition from the highest occupied orbital to the lowest vacant orbital has been calculated, by the simple LCAO MO method, as a function of the angle of the twist of the " single " bond for biphenyl, styrene and stilbene, each as a representative of alternant hydrocarbon systems. Thereby, it has been shown that the decrease in the intensity of the conjugation band observed with sterically hindered compounds, as compared with the band of the sterically unhindered parent compound, can be explained almost entirely satisfactorily by the decrease in the transition moment associated with the deviation of the most probable configuration of the molecule from the planarity. In this connection, Jaffé and Orchin's explanation, as well as Braude's explanation, of the steric hypochromic effect has been criticized.

From a consideration of the potential energy curves of the electronic ground state and of the electronic excited state for the twist of the "single" bond, an explanation has been suggested of the notable fact that the conjugation bands of sterically hindered stilbenes are almost structureless in contrast with the band of *trans*-stilbene, which has quite a well-resolved fine structure.

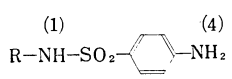
Department of Chemistry
College of General Education
The University of Tokyo
Meguro-ku, Tokyo

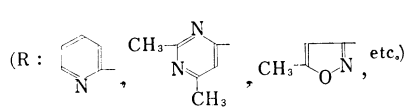
*Relationship between Acid Dissociaiton Constants of N_1-Arylsulfanilamides and the Hammett Equation**

By Mitsuru YOSHIOKA, Kaname HAMAMOTO and Tanekazu KUBOTA

(Received June 25, 1962)

It has been known that there are close and important relationships between acid dissociation constants of sulfa drugs and such chemotherapeutic properties as bacteriostatic activity[1], absorption[2], excretion[2], and so on. The general formula of the drugs is as follows:





* Presented in part at the Symposium on the Electronic States of the Molecule, Sapporo, August, 1960, and in part at the Symposium on the Mechanism of Organic Reactions, Sendai, October, 1961.

1) P. H. Bell and R. O. Roblin, Jr., *J. Am. Chem. Soc.*, **64**, 295 (1942).

2) L. S. Schanker, "Annual Review of Pharmacology", Vol. I, Annual Reviews. Inc. California (1961), p. 29.

where R are usually heterocyclic substituents.

Therefore, it seems very important to investigate in detail a effect of the substituent R on the acid dissociation constant. In the case of heterocyclic compounds, a quantitative investigation of the effect would involve various, complicated problems. On the other hand, in the case of N_1-arylsulfanilamides (R: Ar; $ArNHSO_2C_6H_4NH_2$), such an investigation could be carried out by applying the Hammett equation (Eq. 1).

$$\log (k/k_0) = \rho\sigma \qquad (1)$$

In this equation k and k_0 are equilibrium (or rate) constants for a meta or para-substituted and for the unsubstituted aromatic compounds respectively. σ is the substituent constant, which depends solely on the substituent, and ρ is the reaction constant, which depends on the specific reaction. A different substituent constant, σ^-, for a para electron-attracting group has been used on dissociations (or reactions) of anilines and phenols. Little examination of dissociation of anilides, however, has been made so it is not clear whether or not σ^- [3] should be used with the dissociation of sulfanilamides which belong to the anilides[4]. The purpose of this paper is to clear up this point and to make a quantitative examination of a relationship between the acid dissociation constants of N_1-arylsulfanilamides and the Hammett equation.

Experimental

Materials.—N_1-Arylsulfanilamides were prepared by known procedures[5] and were purified by repeated recrystallizations from aqueous alcohol.

Dissociation Constant Determination.—Bell and Roblin[1] have reported that all the sulfanilamides used in their study, except for the very acidic ones, are in the "non-zwitter ion" form. Accordingly, acid dissociation of the sulfanilamides used here can be expressed by Eq. 2:

$$\underset{BH^+}{Ar\cdot NH\cdot SO_2C_6H_4NH_2} + H_2O \rightleftharpoons \underset{B}{Ar\cdot N^-\cdot SO_2C_6H_4NH_2} + H_3O^+ \qquad (2)$$

The acid dissociation constant, K_{NH}[6], can be given by Eq. 3:

$$K_{NH} = [Ar\cdot N^-\cdot SO_2C_6H_4NH_2][H_3O^+]/Ar\cdot NH\cdot SO_2C_6H_4NH_2] = [B][H_3O^+]/[BH^+] \qquad (3)$$

Equation 4 can be obtained easily by applying Lanbert and Beer's law to Eq. 3:

$$pK_{NH} = pH - \log \frac{E_{BH^+} - E_{obs}}{E_{obs} - E_B} \qquad (4)$$

where E_{BH^+}, E_B and E_{obs} are optical densities of BH^+, B, and a mixture at a given pH, in the same concentration at a wavelength. Therefore, we can accurately determine pK_{NH} ($-\log K_{NH}$) values by the spectrophotometric method. The ultraviolet spectra of N_1-phenylsulfanilamide and determination of its pK_{NH} value by applying Eq. 4 are shown in Figs. 1 and 2 as typical examples.

A stock solution (2 cc.) of sulfanilamides in an aqueous 0.001 N sodium hydroxide solution or in

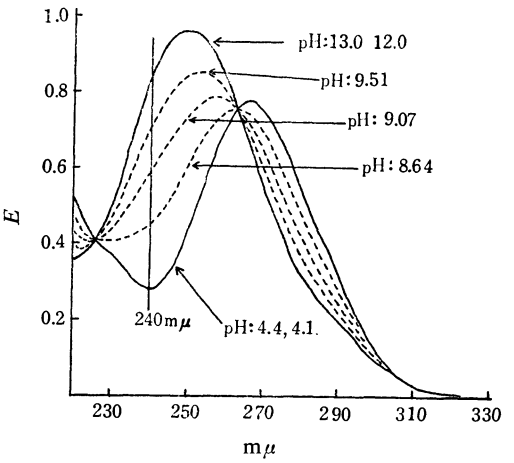


Fig. 1. Ultraviolet spectra of N_1-phenylsulfanilamide at various pH in 4.74×10^{-5} M solution.

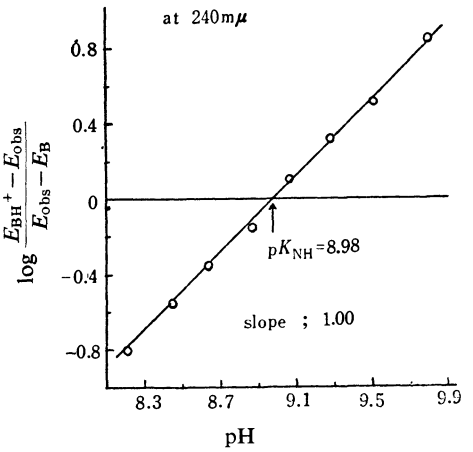


Fig. 2. Determination of the pK_{NH} value of N_1-phenylsulfanilamide at 240 mμ: The mean value of pK_{NH} values at 240, 243, 246 and 249 mμ, is given to be 8.97.

3) This constant, σ^-, is the same as Jaffé's σ^*[4].

4) H. H. Jaffé, *Chem. Revs.*, **53**, 191 (1953).

5) A. E. Senear et al., *J. Org. Chem.*, **11**, 378 (1946); H. Kaplan and G. W. Leubner, *J. Am. Chem. Soc.*, **67**, 1076 (1945); J. H. Gorrin, *J. Chem. Soc.*, **1945**, 734.

6) There is another dissociation constant of the sulfanilamides, $K_{NH_3^+}$, as is shown in the following equations:

$$ArNHSO_2\cdot C_6H_4\cdot NH_3^+ + H_2O \rightleftharpoons ArNHSO_2\cdot C_6H_4\cdot NH_2 + H_3O^+$$

$$K_{NH_3^+} = [ArNHSO_2\cdot C_6H_4\cdot NH_2][H_3O^+]/[ArNHSO_2\cdot C_6H_4\cdot NH_3^+]$$

Examination of this dissociation will appear elsewhere.

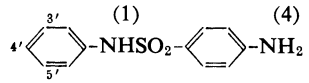
an aqueous 0.033 N ethanolamine solution[7] was diluted to 25 cc. with Britton-Robinson's universal buffer solutions[8], the ionic strength of which had been adjusted to 0.2 by adding sodium chloride. The pH values of sample solutions were measured with a Beckman model G pH meter at 25±2°C, and the spectra were recorded with a Hitachi model EPS-2 recording spectrophotometer at 27±2°C, using a 1 cm. cell. An improved spectrophotometric method[9] was applied for the pK_{NH} determination of the sulfanilamides with a SO_2NH_2 group, because they have overlapping dissociation constants (pK_{NH} and $pK_{SO_2NH_2}$).

Results and Discussion

Acid Dissociation Constants and Melting Points of Sulfanilamides. — The dissociation constants, pK_{NH}, and the melting points are listed in Table I. The elementary analysis of each compound listed here agrees well with the corresponding formula unless otherwise stated.

TABLE I. pK_{NH} AND MELTING POINTS OF N_1-ARYLSULFANILAMIDES

Substituent[a]	pK_{NH}	M. p. °C
3',5'-$(NO_2)_2$	6.19	206.0~209.0
3'-NO_2, 5'-Cl	6.92	201.0~202.0
4'-NO_2	6.97	167.0~169.0
3'-NO_2, 4'-Cl	7.16	159.0~161.0
4'-CN	7.36	176.7~177.5
4'-SO_2NH_2	7.45	119.0~121.0[b]
3',5'-Cl_2	7.54	147.0~148.5
3'-NO_2	7.67	172.5~174.0
4'-$COCH_3$	7.61	193.5~194.5
3'-SO_2NH_2	7.81	122.5~124.5[c]
3'-CN	7.83	188.0~191.5
3'-Cl	8.28	133.0~134.0
3'-$COCH_3$	8.34	187.5~189.0
4'-Cl	8.56	199.0~199.5
3'-OCH_3	8.72	162.0~164.0
H	8.97	195.0~196.5
3'-CH_3	9.05	132.0~133.0
4'-CH_3	9.25	188.5~191.0
4'-OCH_3	9.34	195.0~197.0
3'-$N(CH_3)_2$	9.01	152.0~154.0
4'-$N(CH_3)_2$	9.46	227.0~228.5 (decomp.)

a) 

b) The analysis fits the formula $C_{12}H_{13}O_4 \cdot N_3S_2 \cdot {}^1/_2H_2O$

c) The formula $C_{12}H_{13}O_4N_3S_2 \cdot {}^1/_2C_2H_5OH$ was indicated by analysis.

Substituent Constants (σ and σ^-). — Since Jaffé's[4] evaluation of normal substituent constants (σ values), they have been re-evaluated by McDaniel, and Brown[11] and by Bekkum et al.[12] We have examined their papers and have selected McDaniel's σ values[11] except for the *m*- and *p*-substituents of SO_2NH_2 and NMe_2, because McDaniel's values have been evaluated from dissociation constants of substituted benzoic acids and so seem to be most reliable and reasonable. It seems to us that McDaniel made a mistake in evaluating the σ values of *m*- and *p*-SO_2NH_2, so Zollinger's original values[13] are adopted for them. At present, the σ values for *m*- and *p*-NMe_2 are quite complicated. McDaniel has given −0.83 for *p*-NMe_2, whereas Jaffé and Bekkum respectively, have given −0.60 and −0.266[14] for it. McDaniel's values for NMe_2 were evaluated from dissociation constants of dimethylaminobenzoic acids, which exist to some extent as the zwitterions. Jaffé's value for *p*-NMe_2 is an average of seventeen values ranging from −1.049 to −0.206. Bekkum calculated the σ value of *p*-NMe_2 from equilibria involving anilines. Therefore, Bekkum's value for *p*-NMe_2 is most reliable and his values for *p*- and *m*-NMe_2 are selected here.

As for σ^- values, Jaffé's estimates are adopted for *p*-NO_2, *p*-CN and *p*-$COCH_3$ and

TABLE II. SELECTED SUBSTITUENT CONSTANTS

Subst.	σ	σ^-
p-NO_2	0.778	1.270
m-NO_2	0.710	
p-CN	0.660	1.000
m-CN	0.56	
p-SO_2NH_2	0.62	0.94
m-SO_2NH_2	0.60	
p-$COCH_3$	0.502	0.874
m-$COCH_3$	0.376	
p-Cl	0.227	
m-Cl	0.373	
p-OCH_3	−0.268	
m-OCH_3	0.115	
p-CH_3	−0.170	
m-CH_3	−0.069	
p-NMe_2	−0.266	
m-NMe_2	−0.049	

7) The ethanolamine solution was used for preparation of a stock solution of the compounds having a CN group, because this group is hydrolzyed easily in an alkaline solution.

8) H. T. S. Britton and R. A. Robinson, *J. Chem. Soc.*, **1931**, 1457.

9) M. Yoshioka, K. Hamamoto and T. Kubota, *J. Chem. Soc. Japan, Pure Chem. Sec.* (*Nippon Kagaku Zasshi*), **83**, 229 (1962).

10) Melting points were measured on a micro hotstage and were not corrected.

11) D. H. McDaniel and H. C. Brown, *J. Org. Chem.*, **23**, 420 (1958).

12) H. V. Bekkum, P. E. Verkade and B. M. Wepster, *Rec. trav Chim.*, **78**, 815 (1959).

13) H. Zollinger and C. Wittmer, *Helv. Chim. Acta*, **39**, 351 (1956).

14) A σ value from equilibria involving anilines.

Zollinger's estimate is adopted for p-SO_2NH_2, because there is no other value for these groups.

Table II lists the substituent constants (σ and σ^-) we have selected.

Plot of log K_{NH} ($-pK_{NH}$) against σ (or σ^-). —Figure 3 represents a relation of the dissociation constants of sulfanilamides with the substituent constants. A good, linear relationship between log K_{NH} and σ is obtained except for p-NO_2, p-CN, p-$COCH_3$ and p-SO_2NH_2. For these electron-attracting groups, neither σ values nor σ^- values give a good fit. This result clearly indicates that neither σ nor σ^- for these groups may be applicable to the dissociation of sulfanilamides.

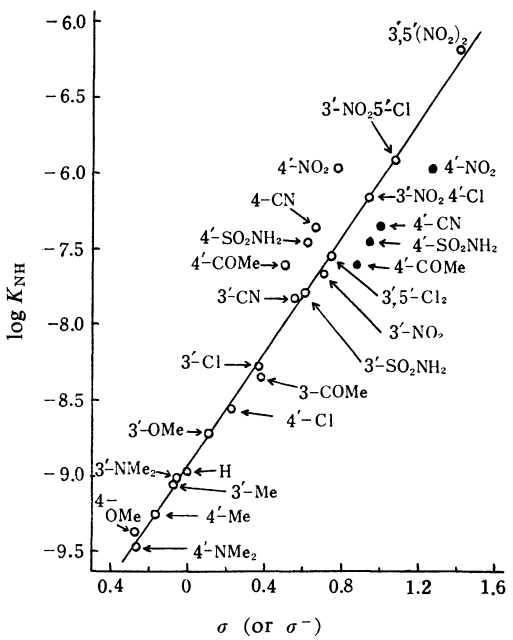


Fig. 3. Plot of log K_{NH} against substituent constants. Open circles, σ ; Closed circles, σ^-

A Modified Hammett Equation. — The only other known irregular relationship of this kind for electron-attracting groups in nucleophilic reactions ($\rho > 0$) is in the case of thiophenols[4]. In electrophilic reactions ($\rho < 0$), however, a similar irregular relationship for such electron-releasing groups as p-NH_2, p-OCH_3 and p-CH_3 has been observed in many reactions and equilibria. Yukawa and Tsuno have proposed the following modified Hammett relationship (Eq. 5) ; this relationship has been applied successfully to many electrophilic reactions[15] ($\rho < 0$).

$$\log (k/k_0) = \rho(\sigma + r\Delta\sigma_R^+)$$
$$\Delta\sigma_R^+ \equiv \sigma^+_{\text{Brown and Okamoto}} - \sigma \qquad (5)$$

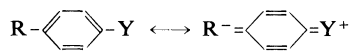
where r is a reaction constant describing the degree of the transition state resonance and $\Delta\sigma_R^+$ is a substituent constant suggesting the resonating capacity of an electron-releasing substituent at the para-position

A similar modification could be made in nucleophilic reactions[16], and a modified Hammett equation can be expressed by Eq. 6 for nucleophilic reactions and equilibria ($\rho > 0$) :

$$\log (k/k_0) = \rho(\sigma + r'\Delta\sigma_R^-)$$
$$\Delta\sigma_R^- \equiv \sigma^- - \sigma \qquad (6)$$

Here r' (a resonance reaction constant), $\Delta\sigma_R^-$ (a resonance substituent constant of an electron-attracting p-substituent), and σ^- for nucleophilic reactions correspond to r, $\Delta\sigma_R^+$, and σ^+ Brown and Okamoto respectively for electrophilic reactions.

This modified equation (Eq. 6) may be connected with mesomeric para interactions in nucleophilic reactions (or equilibria), as is shown in the following limiting structures:



R : NO_2, CN, etc. Y : NH_2, SH, etc.

Consequently, Eq. 6. can be applied to the acid dissociation of sulfanilamides. In this case, the ρ value should be calculated only from the data of the m-substituted sulfanilamides. However, the data for such p-substituents as CH_3O, CH_3 and Cl may be used also, for in these groups the mesomeric para interactions are very weak for the sulfanilamides discussed here. On the other hand, the data for such substituents as m-SO_2NH_2, m-NMe_2 and p-NMe_2 should be excluded from the calculation of the ρ value, because σ values for these groups[17] have not been determined definitely and are less reliable than for other groups. Thus, the ρ value was calculated by means of the least square method, using the data for m-substituents of NO_2, CN, and CH_3CO, m- and p-substituents of Cl, CH_3, and CH_3O and H. The calculated values of ρ, log $K_{0,NH}$, S[18], and the correlation

TABLE III. $\Delta\sigma_R^-$ VALUES

Subst.	$\Delta\sigma_R^- \equiv \sigma^- - \sigma$
p-NO_2	0.492
p-CN	0.340
p-SO_2NH_2	0.32
p-$COCH_3$	0.372

15) Y. Yukawa and Y. Tsuno, This Bulletin, 32, 971 (1959).

16) Y. Yukawa and Y. Tsuno, "Progress in Organic Reaction Mechanisms", Vol. I, Maki-shoten, Tokyo (1958), p. I (in Japanese).

17) It is worth noting that the selected values for these groups in Table II give a good fit, as is shown clearly in Fig. 3.

18) The standard deviation of experimental results from the regression line.

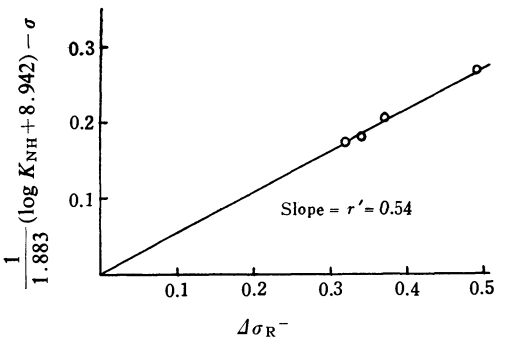


Fig. 4. Determination of r' for the dissociation of N_1-arylsulfanilamides.

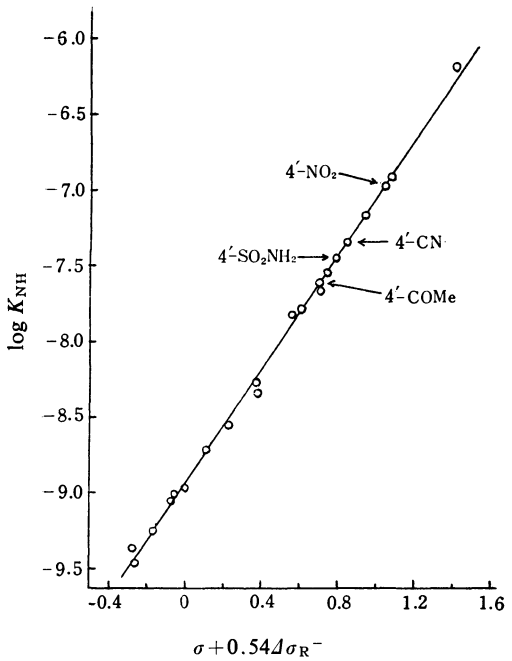


Fig. 5. Correlation of the dissociation of N_1-arylsulfanilamides with the modified Hammett equation.

coefficient are 1.883, −8.942, 0.07 and 0.998 respectively. In Table III are given the $\Delta\sigma_R^-$ values calculated from the substituents constants listed in Table II. From the plot of $[(1/\rho)\log(K_{NH}/K_{0,NH})-\sigma]$ against $\Delta\sigma_R^-$, as shown in Fig. 4, r' is given as 0.54. As is seen in Fig. 5, the acid dissociation of N_1-arylsulfanilamides is expressed well by Eq. 7:

$$\log K_{NH}=1.883(\sigma+0.54\ \Delta\sigma_R^-)-8.942 \quad (7)$$

Dissociation of *N*-Arylbenzenesulfonamides ($ArNHSO_2C_6H_5$). — Willi[19] has reported a relationship between dissociation constants of *N*-arylbenzenesulfonamides and the Hammett equation. He has concluded that σ^- should be applied for the electron-attracting groups at the para-position in the case of these sulfonamides. These compounds have a –NH– group of the same type as that of the N_1-arylsulfanilamides discussed above, so the modified Hammett equation (Eq. 6) may be applied also to the dissociation of *N*-arylbenzenesulfonamides. Willi's data were treated as in the case of sulfanilamides. The σ values[12] selected for p-COO^-, and p-NH_2 are 0.120 and −0.423, and the σ^- value for p-COO^- is 0.367[20]. The ρ value, $\log K_0$, S[18], and the correlation coefficient are calculated to be 1.833, −8.285, 0.059 and 0.998 respectively, using the data for m-NO_2, p-Cl, H, p-CH_3, p-OCH_3 and p-NH_2. From Fig. 6, r' is given as 0.68.

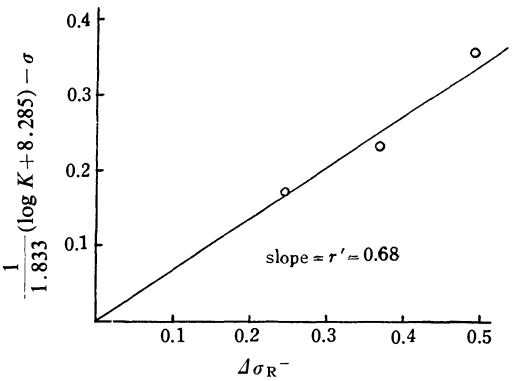


Fig. 6. Determination of r' for the dissociation of *N*-arylbenzenesulfonamide.

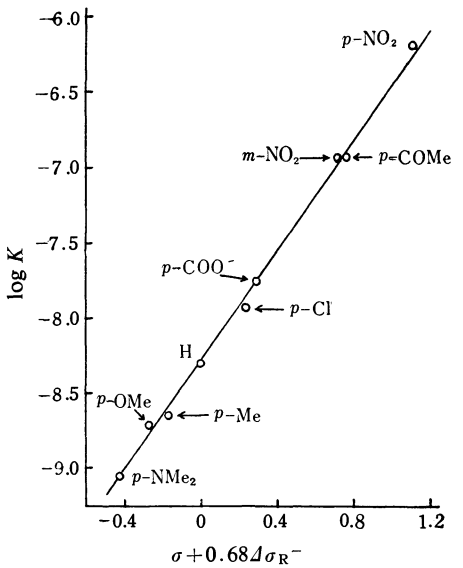


Fig. 7. Correlation of the dissociation of *N*-arylbenzenesulfonamide.

19) A. V. Willi, *Helv. Chim. Acta*, **39**, 46 (1959).

20) A. V. Willi and T. F. Stocker, ibid., **38**, 1279 (1955). In this paper the σ^- value of p-COO^- has been given as 0.335; this is an average of the 0.367 obtained from dissociation of phenols and the 0.335 obtained from that of $ArNHSO_2C_6H_5$. Only the former value should be adopted.

Therefore, the dissociation of *N*-arylbenzenesulfonamides can be expressed well by Eq. 8, as is shown in Fig. 7:

$$\log K = 1.833(\sigma + 0.68\ \Delta\sigma_R^-) - 8.285 \qquad (8)$$

Since the number of the substituents is only eight and some of them are not reliable enough, the values of ρ and r' will be somewhat uncertain. Nevertheless, clearly the modified Hammett equation (Eq. 6) can be applied also to the dissociation of these sulfonamides.

The results obtained from the sulfanilamides ($ArNHSO_2C_6H_4NH_2$) and the benzenesulfonamides ($ArNHSO_2C_6H_5$) show that the modified Hammett relationship for nucleophilic reactions should be applied to the dissociation of Ar–NH–SO_2– type anilides.

Summary

1. Acid dissociation constants of twenty-one N_1-arylsulfanilamides ($ArNHSO_2C_6H_4NH_2$) were exactly determined by the spectrophotometric method at 27±2°C and in an ionic strength of 0.2.

2. A modified Hammett relationship for nucleophilic reactions (Eq. 6) can be applied to acid dissociation of N_1-arylsulfanilamides and also of *N*-arylbenzenesulfonamides ($Ar\cdot NHSO_2C_6H_5$).

3. These results show that the modified Hammett relationship should be applied to the dissociation of Ar–NH–SO_2– type anilides.

The authors wish to thank Professor Yasuhide Yukawa of Osaka University for his valuable advice, Mr. Tsunetoshi Honma for his assistance in the preparation of the samples, and Mr. Hiroshi Miyazaki and Mr. Itaru Tanaka for their ultraviolet spectral measurements.

Shionogi Research Laboratory
Shionogi & Co., Ltd.
Fukushima-ku, Osaka

Studies of the Photochemical Reactions. IV. The Synthesis of Dimethyl-α-tetralylcarbinol by the Photochemical Reaction of Acetone in Tetralin[1]

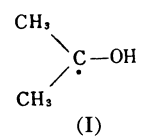
By Kensuke SHIMA, Yasuo SHIGEMITSU and Shigeru TSUTSUMI

(Received June 2, 1962)

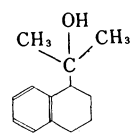
In a previous paper[2], the reactions of photoactivated acetone in cyclohexane or methylcylclohexane was reported on. In these reactions, it was ascertained that photoactivated acetone abstracted hydrogen from the hydrogen donor solvent to form an intermediate radical, the dimethylhydroxymethyl radical (I).

In order to use this radical (I) for synthetic purposes, tetralin, having the reactive α-hydrogen for autoxidation[3] or other radical reactions[4], was chosen as the hydrogen donor solvent. The present paper reports on the synthesis of dimethyl-α-tetralylcarbinol (II), which can only with considerable difficulty be prepared by other methods[5].

In this experiment, an ultraviolet light from a 400 W high pressure mercury lamp was used. A mixture of acetone and tetralin (mole ratio: 1 : 4 and 1 : 2 respectively) was irradiated in a nitrogen atmosphere at 10～15°C for 100, 25 and 10 hr., and then the reaction products were fractionated and analyzed chromatographically.



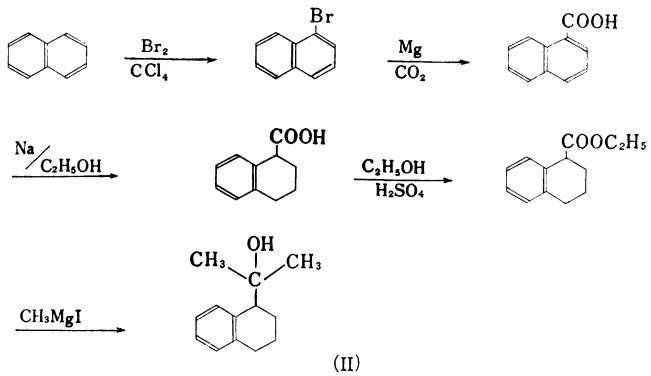
(I)



(II)

From the lower boiling fraction, isopropyl alcohol was obtained, and the fraction (b. p. 124～126°C/4 mmHg) was identified as dimethyl-α-tetralylcarbinol (II), the adduct of the (I) radical and the α-tetralyl radical. The infrared spectrum, shown in Fig. 2, was identical with that of an authentic sample, and the mixed melting point of its phenyl urethane was not depressed. The authentic sample was prepared by the following procedure[5]:

1) Reported at the 15th Annual Meeting of the Chemical Society of Japan, Kyoto, April, 1962.
2) K. Shima and S. Tsutsumi, *J. Chem. Soc. Japan, Ind. Chem. Sec.* (*Kogyo Kagaku Zasshi*), **64**, 460 (1961).
3) M. Hartmann and M. Seiberth, *Helv. Chim. Acta*, **15**, 1390 (1932); H. Hock and W. Suemihl, *Ber.*, **66**, 61 (1933).
4) G. Sosnovsky and N. C. Yang, *J. Org. Chem.*, **25**, 899 (1960)
5) F. W. Kay and A. Morton, *J. Chem. Soc.*, **105**, 1571 (1914).



(II)

Table I. The reaction conditions and the yields of products

Reaction number	1	2	3
Reaction time, hr.	100	25	10
Acetone used, g.	43.5	45.0	26.4
Tetralin used, g.	194.5	201.3	240.0
Tetralin/Acetone (mol. ratio)	2	2	4
Unreacted acetone, g.	6.7	30.2	15.6
Unreacted tetralin, g.	116.9	156.4	214.0
Acetone consumed, g.	36.8	14.8	10.8
Tetralin consumed, g.	77.6	44.9	26.0
Isopropyl alcohol, g.	12.6	4.0	1.6
II, g.	35.4	17.9	11.7
High boiling residue, g.	58.3	31.3	16.2
Wt. % of II in the products*	33.3	33.7	39.7
Ultimated yield of II, based on acetone consumed, mol. %	30.2	37.0	33.1
Ultimated yield of II, based on tetralin consumed, mol. %	31.7	27.7	31.4

* Isopropyl alcohol, II, and high boiling residue.

The reaction conditions and the yields of the products are summarized in Table I. The amounts of unreacted acetone and isopropyl-alcohol were estimated by gaschromatographic analysis.

It is of interest to note that dimethyl-α-tetralylcarbinol (II) is easily produced in a fairly high yield by the photochemical reaction of acetone in tetralin.

Experimental[6]

Materials.—Tetralin was purified by fractional distillation over sodium ; b.p., 81.5~83°C/14 mmHg, n_D^{20} 1.5380. Acetone was purified by the ordinary method[7] ; b. p. 56.5~57°C, n_D^{20} 1.3588.

The Photochemical Reaction of Acetone in Tetralin.—A mixture of acetone (45 g., 0.77 mol.) and tetralin (201.3 g., 1.53 mol.) was placed in a 300 ml. reaction vessel and irradiated at 10~15°C in a nitrogen atmosphere for 25 hr. The reaction apparatus is shown in Fig. 1. After this irradiation, the reaction product was fractionally distilled under atmospheric and reduced pressure to give the following fractions :

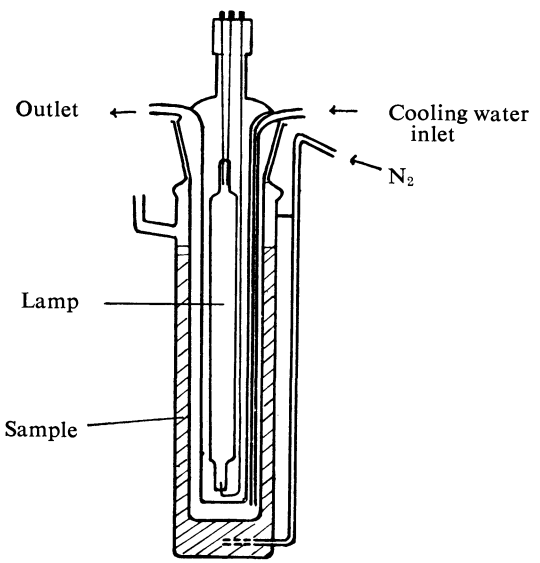


Fig. 1. Reaction apparatus.

	B. p.	Weight g.	n_D^{20}
(1)	57.5~59°C	20.5	1.3588
(2)	59.5~83°C	7.7	1.3645
(3)	~30°C/14 mmHg	6.0	1.3838
(4)	76 ~96.5°C/14 mmHg	156.4	1.5364
(5)	118~129°C/4 mmHg	17.9	1.5452
(6)	Residue	31.3	

By gaschromatographic analysis, it was assumed that 1, 2 and 3 fractions were unreacted acetone, a mixture of acetone and isopropyl alcohol, and isopropyl alcohol respectively. The 3, 5-dinitrobenzoate of fraction 3 (m. p. 120~121°C, recrystallized from ethanol) was confirmed to be the 3, 5-dinitrobenzoate of isopropyl alcohol by the mixed melting point test.

6) The boiling and melting points are uncorrected.
7) A. Bramley, *J. Chem. Soc.*, **59**, 10 (1916).

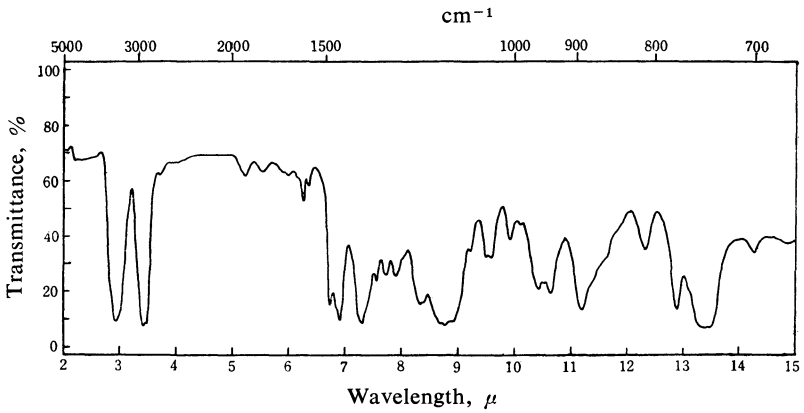


Fig. 2. Infrared spectrum of dimethyl-α-tetralylcarbinol (II).

The amounts of unreacted acetone and isopropyl alcohol were estimated by gaschromatographic analysis: column, D. N. P. 3 m.; carrier gas, H_2, 0.3 kg./cm^2; bridge current 160 mA; column temp., 50°C; retention time, acetone: 5 min., isopropyl alcohol: 7 min.

Fraction 4 identified as unreacted tetralin by the gaschromatographic analysis.

Fraction 5 gave positive results to the Denigés test[8] and so was identified as dimethyl-α-tetralylcarbinol.

Found: C, 82.24; H, 9.60. Calcd. for $C_{13}H_{18}O$: C, 82.06; H, 9.54%.

Phenyl urethane was synthesized and recrystallized from ligroin; m. p., 84~85°C, and its mixed melting point with an authentic sample showed no depression.

Found: C, 77.63; H, 7.49. Calcd. for $C_{20}H_{23}O_2N$: C, 77.64; H, 7.49%.

Synthesis of Dimethyl-α-tetralylcarbinol.—α-Bromonapthalene was prepared by the reaction of naphthalene with bromine in carbon tetrachloride according to the procedure of Clarke and Brethen[9]; b. p. 130~133°C/11 mmHg.

α-Naphthoic acid[10] was prepared by the carbonation of α-naphthylmagnesium bromide, formed by the action of magnesium on α-bromonaphthalene in ether; m. p. 161~162°C.

Ethyl tetrahydro-α-naphthoate[5] was prepared by the reaction of tetrahydro-α-naphthoic acid with ethanol in the presence of concentrated sulfuric acid under reflux conditions; b. p. 123~125°C/12 mmHg, n_D^{20} 1.5241.

Dimethyl-α-tetralylcarbinol (II)[5] was prepared by the reaction of methylmagnesium iodide with ethyl tetrahydro-α-naphtoate; b. p. 121~123°C/3 mmHg, n_D^{20} 1.5460, phenyl urethane, m. p. 84~85°C.

Department of Chemical Technology
Faculty of Engineering
Osaka University
Miyakojima-ku, Osaka

8) G. Denigés, *Compt. rend.*, **126**, 1048, 1277 (1898).

9) H. T. Clarke and M. R. Brethen, "Organic Syntheses", Coll. Vol. I (1948), p. 121.

10) H. Gilman, N. B. St. John and F. Schulze, ibid., Coll. Vol. II (1948), p. 425.

*Studies of trans-Dicyanodiethoxycarbonylethylene. II. Reactions with Ammonia and Primary Aromatic Amines**

By Ken-ichi KUDO

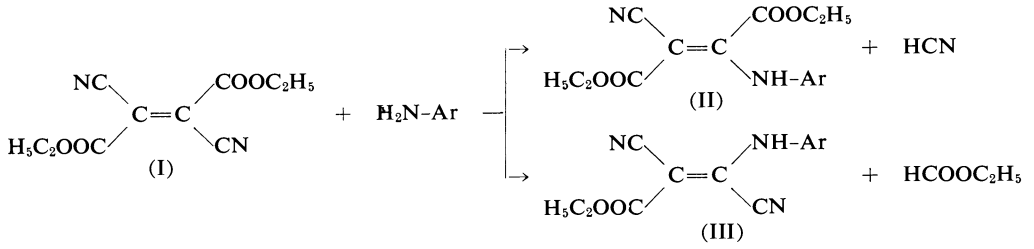
(Received May 22, 1962)

As has been described in a previous paper[1], the reactions of *trans*-dicyanodiethoxycarbonylethylene (I) with tertiary aromatic amines resulted in the addition of a benzene nucleus to the ethylenic double bond with the formation of 4-α, β-dicyano-α, β-diethoxycarbonyl-*N*, *N*-dialkylanilines. In the present paper, the reactions of I with ammonia or primary aromatic amines are investigated.

Reactions with Primary Aromatic Amines. — When a mixture of primary aromatic amine

* This work was presented at the 14th Annual Meeting of the Chemical Society of Japan, Tokyo, April, 1961.

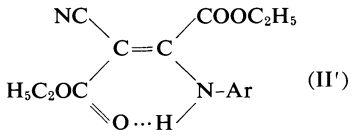
1) Part I, K. Kudo, This Bulletin, 35, 1490 (1962).



II Ar; *p*-CH_3O-C_6H_4, *p*-CH_3-C_6H_4, or *p*-Cl-C_6H_4
III Ar; *p*-CH_3O-C_6H_4, *p*-CH_3-C_6H_4, *p*-Cl-C_6H_4, *m*-NO_2-C_6H_4, or β-$C_{10}H_7$

and I in an organic medium was heated, *N-trans*-α, β-diethoxycarbonyl-β-cyanovinylamines (II) and *N-trans*-α, β-dicyano-β-ethoxycarbonylvinylamines (III) were obtained. In these reactions, when the molar ratio of I to primary amine was 1 : 2, II products, resulting from the substitution of a cyano group with an amine group, predominated. On the other hand, III products, resulting from the substitution of an ethoxycarbonyl group, predominated when the molar ratio of I to primary amine was 2 : 1. Neither II nor III products were obtained by the reaction of I with α-naphthylamine or *p*-nitroaniline, while with *m*-nitroaniline or β-naphthylamine only III products were obtained. These results are shown in Table I.

The structures of III and II were determined in the following manner. By the hydrolysis of II or III with a 10% aqueous sodium hydroxide solution, the parent amine was recovered in a good yield. This result suggests that the vinyl group is attached to the nitrogen atom rather than to the carbon atom. The infrared absorption spectrum of III (Ar; *p*-CH_3-C_6H_4) showed an NH band at 3115 cm^{-1}, C≡N bands at 2227 and 2247 cm^{-1}, and a C=O band at 1680 cm^{-1} (Fig. 1). The infrared absorption spectrum of II (Ar; *p*-CH_3-C_6H_4) showed an NH band at 3185 cm^{-1}, a C≡N band at 2227 cm^{-1}, and C=O bands at 1672 and 1754 cm^{-1} (Fig. 1). The facts that the ester groups of II showed two bands at 1672 and 1754 cm^{-1} and that of III only a band at 1680 cm^{-1} suggest that the bands at 1754 and 1672 cm^{-1} are to be attributed to the ester groups attached to the α- and β-carbon atoms in the aromatic amine group respectively. Similarly, it is expected that the C≡N bands at 2247 and 2227 cm^{-1} are to be attributed to the C≡N groups attached to the α- and β-carbon atoms respectively. (Incidentally, it is generally known that the carbonyl and nitrile frequencies are shifted from their normal positions toward longer wavelengths by conjugation with the vinyl group and also by strongly electronegative substituents on the α-carbon atom, while the α,β-unsaturated carbonyl and nitrile frequencies shift from their normal position toward shorter wavelength in the case of sterically hindered compounds[2].) The geometrical structures of II and III were established on the basis of the considerations of the C=O frequencies of the β-esters of II and III. It was already known that a C=O frequency of β-amino-α, β-unsaturated ester is shifted toward a low frequency by the formation of a chelate hydrogen-bond structure[3]. Thus, the evidence that the β-ester of II had a lower C=O frequency than that of



(II')

III would indicate that II had an intramolecular chelate structure II'. Accordingly, it should be concluded that II and III have ester-ester and nitrile-nitrile trans geometries respectively.

Further chemical evidence for II was obtained

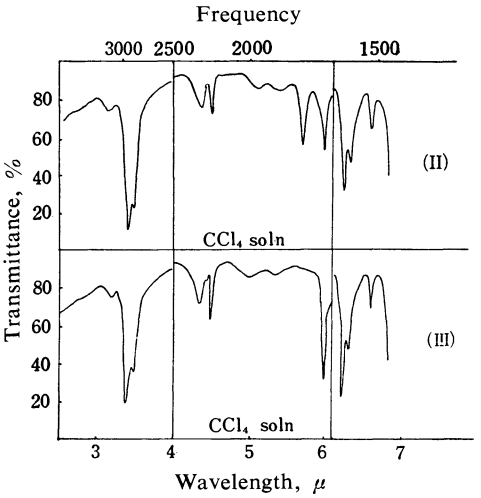
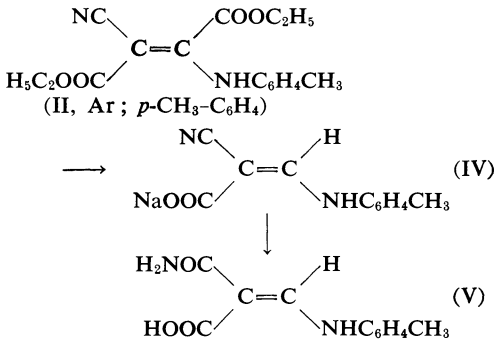


Fig. 1. The infrared absorption spectra of (II, Ar; *p*-CH_3-C_6H_4) and (III, Ar; *p*-CH_3-C_6H_4). A lithium fluoride prism was used for the measurement of C=O and C≡N bands in carbon tetrachloride and one of rock salt for the other bands in Nujol mull.

2) D. G. I. Felton and S. F. D. Orr, *J. Chem. Soc.*, **1955**, 2170.
3) B. Witkop, *J. Am. Chem. Soc.*, **78**, 2873 (1956).

by step by step hydrolysis and decarboxylation of II (Ar; p-CH_3-C_6H_4) to β-p-toluidino-α-carbamoylacrylic acid (V) via sodium β-p-toluidino-α-cyanoacrylate (IV). While the

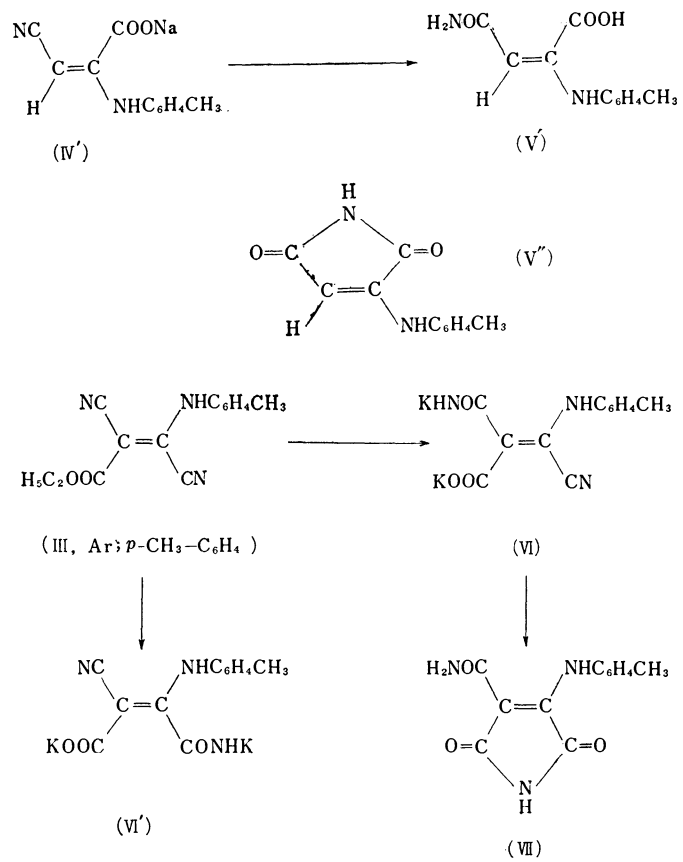


(II, Ar; p-CH_3-C_6H_4)

infrared absorption spectra of IV and V did not exclude the possibility that these compounds may possess the corresponding isomeric forms, IV' and V', this possibility was rejected when cyclic imide V'', the expected product from IV', was not obtained by the hydrolysis of IV' with dilute hydrochloric acid.

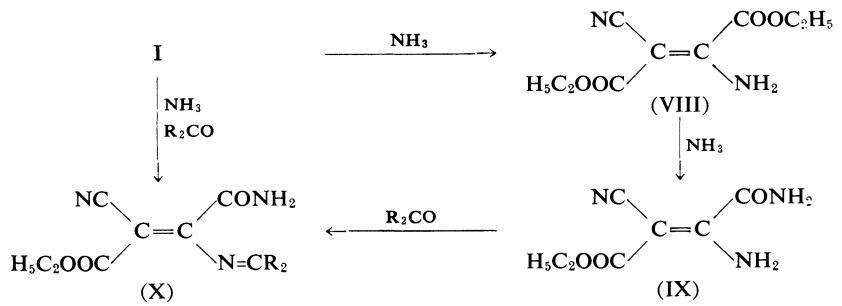
III (Ar; p-CH_3-C_6H_4) was also hydrolyzed with a 10% methanolic potassium hydroxide solution to give potassium β-p-toluidino-β-cyano-α-potashcarbamoylacrylate (VI). When the solution of VI was acidified, α-p-toluidino-α'-carbamyl maleimide (VII) was formed readily by the intramolecular cyclization of the CN and COOH groups. If the VI' structure were correct, the C=O frequency would be shifted toward a shorter wavelength by deviation from the planar configuration which was attributed to the steric repulsion between the aryl and the amide C=O groups. Consequently, the VI' structure should be excluded on the evidence that the spectrum showed its low frequency at 1650 cm^{-1}.

Kissinger and Ungnade[4] discovered that α, α-dinitro-ester, $RC(NO_2)_2COOC_2H_5$, undergoes the substitution of an ethoxycarbonyl group with alcoholic hydrazine hydrate. Thesing[5] and Dornow[6] described how the displacement of a nitrile group of acylcyanides occurs readily in reaction with nucleophilic reagents in a neutral and especially in a weak alkaline



(IV') (V') (V'') (III, Ar; p-CH_3-C_6H_4) (VI) (VI') (VII)

4) L. W. Kissinger and H. E. Ungnade, *J. Org. Chem.*, **23**, 1340 (1958).
5) J. Thesing and D. Witzel, *Angew. Chem.*, **68**, 425 (1956).
6) A. Dornow and H. Grabhöfer, *Ber.*, **91**, 1824 (1958); A. Dornow, *Angew. Chem.*, **70**, 400 (1958).



solution. Thus, as indicated by Middleton[7], if the $\rangle C{=}C\langle^{CN}_{COOC_2H_5}$ group may be analogous to the $\rangle C{=}O$ group in its electron-drawing effects, the formation of II or III respectively by the substitution of C≡N or $COOC_2H_5$ with aromatic amine derivatives seems to be reasonable.

The mechanism of these substitution reactions would be similar to the reaction mechanism of the formation of 4-*trans*-α, β-diethoxycarbonyl-β-cyanovinyl-*N*, *N*-dialkylaniline from I described in the previous paper[1]. Namely, these reactions would be initiated by the formation of the π-complexes between I and primary aromatic amines, since the intense electronic absorption bands of the reaction mixture at λ_{max} 315~365 mμ and λ_{max} 440~510 mμ are attributable to neither the I products nor to the primary aromatic amines, but to the π-complex itself as a new molecular species. The second step in the reaction appears to be an addition of primary aromatic amine to give an adduct, although the adduct as an intermediate was not isolated. The final step is an elimination of hydrogen cyanide or ethyl formate to yield II or III respectively.

Reaction with Ammonia.—The reaction of I and ammonia with a molar ratio of 1 : 1 gave only one product, *trans*-α, β-diethoxycarbonyl-β-cyanovinylamine (VIII), in a good yield. By a similar procedure, α-carbamoyl-β-cyano-β-ethoxycarbonylvinylamine (IX) was obtained from I via VIII by ammonolysis of an ester group with the excess of ammonia in a good yield, but diamide derivatives of VIII were not obtained. The infrared absorption spectrum of VIII showed NH bands at 3401 and 3279 cm^{-1}, a C≡N band at 2212 cm^{-1}, and C=O bands at 1761 cm^{-1} (α-ester) and 1687 cm^{-1} (β-ester) (Fig. 2). The infrared absorption spectrum of IX had NH bands at 3448, 3356, 3257 and 3185 cm^{-1}, a C≡N band at 2222 cm^{-1}, and C=O bands at 1695 (β-ester) and 1667 cm^{-1} (α-amide) (Fig. 2). In these spectral data, the evidence that the β-esters of VIII and IX had low C=O frequencies is to be attributed to the formation of an intramolecular hydrogen-bond[3] between the C=O and amino groups. Further chemical evidence for VIII and IX was supplied by the synthesis of the acetyl derivatives and by the formation of Schiff bases X respectively. X products were also obtained directly from I. The X structures were established on the bases of the synthesis of the acetyl derivatives and supported by the fact that X products were hydrolyzed with an aqueous sodium hydroxide solution to give the parent ketone, which would indicate that the ketone was attached to the nitrogen atom rather than to the carbon atom.

The mechanism of the formation of VIII products would be similar to the reaction mechanism of the formation of II products described above.

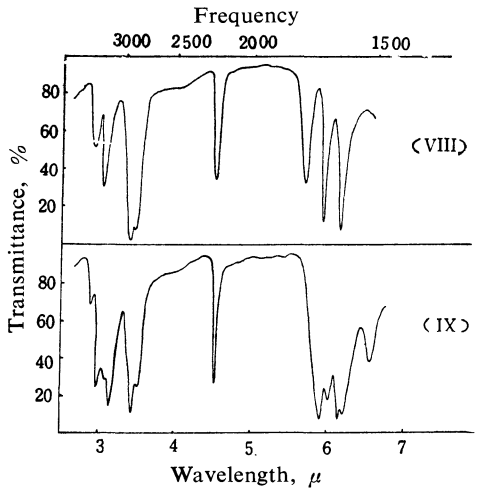


Fig. 2. The infrared absorption spectra of VII and IX.

Experimental

***N*-*trans*-α, β-Dicyano-β-ethoxycarbonylvinylamines (III).**—III products were generally prepared by the reaction of primary aromatic amines with the excess of I in dimethylformamide at 50~60°C. Other solvents, such as pyridine, acetonitrile and ethyl formate, were also used. In a typical experiment, a mixture of 4.3 g. (0.04 mol.) of *p*-toluidine

7) W. J. Middleton and V. A. Engelhart, *J. Am. Chem. Soc.*, **80**, 2788 (1958).

TABLE I. PROPERTIES OF II, $H_5C_2OOC(NC)C:C(COOC_2H_5)NHAr$ AND III, $H_5C_2OOC(NC)C:C(CN)NHAr$

Compound Ar		Yield* %	M. p. °C	λ_{max} mμ	log ε	Formula	Found (Calcd.) Mol. wt.	C, %	H, %	N, %
p-CH_3-C_6H_4	II	28	103 ~104	310	4.184	$C_{16}H_{18}O_4N_2$	315 (302)	63.36 (63.56)	5.98 (6.00)	9.13 (9.27)
	III	92	116.5~116.7	225 355	3.915 4.059	$C_{14}H_{13}O_2N_3$	246 (255)	65.82 (65.87)	5.18 (5.13)	16.54 (16.46)
p-CH_3O-C_6H_4	II	30	92.5~ 93.5	225 305	4.029 4.175	$C_{16}H_{18}O_5N_2$	314 (318)	60.11 (60.36)	5.75 (5.72)	8.90 (8.79)
	III	43	141 ~143.5	230 360	4.087 4.080	$C_{14}H_{13}O_3N_3$	274 (271)	61.88 (61.96)	4.77 (4.83)	15.77 (15.48)
p-Cl-C_6H_4	II	11	99.5~100.5	225 310	3.859 4.154	$C_{15}H_{15}O_4N_2Cl$	322 (323)	55.88 (55.79)	4.63 (4.67)	8.89 (8.73)
	III	36	165 ~165.5	230 360	4.280 4.314	$C_{13}H_{10}O_2N_3Cl$	261 (275)	56.62 (56.63)	3.70 (3.66)	15.27 (15.22)
m-NO_2-C_6H_4	III	trace	120.5~121.5	230 345	4.145 4.224	$C_{13}H_{10}O_4N_4$	275 (286)	54.37 (54.55)	3.68 (3.52)	—
β-$C_{10}H_7$	III	trace	148 ~150	358	4.239	$C_{23}H_{17}O_2N_3$	289 (291)	70.02 (70.09)	4.47 (4.50)	—

* In the media of dimethylformamide

and 18 g. (0.08 mol.) of I in 30 ml. of dimethylformamide was heated at 50~60°C while being stirred for 30 min. The solvent was distilled off in vacuo, and the red residue was kept in an ice-box for several days. The solidified residue was recrystallized from ethanol-water to give 9 g. (92%) of III (Ar; p-CH_3-C_6H_4) (m. p. 116.5~117°C) in the form of yellow crystals (Table I).

***N*-*trans*-α, β-Diethoxycarbonyl-β-cyanovinylamines (II).**—II products were prepared from I with an excess of primary aromatic amines by a similar procedure. For example, from 12 g. (0.06 mol.) of I and 12 g. (0.12 mol.) of p-toluidine, II (Ar; p-CH_3-C_6H_4) (m. p. 103~104°C) was obtained in a 5 g. (28%) yield (Table I).

Hydrolysis of III (Ar; p-Cl-C_6H_4) to p-Chloroaniline.—A mixture of 1 g. of III (Ar; p-Cl-C_6H_4) and 50 ml. of a 10% sodium hydroxide solution was refluxed for 3.5 hr. and then steam distilled. The distillate was cooled to give 0.3 g. (77%) of p-chloroaniline; m. p., 68~69°C. The p-chloroaniline was dissolved in a solution of 4 ml. of pyridine and a small quantity of ether. The addition of 0.3 ml. of acetyl chloride to the solution gave p-chloroacetanilide (m. p. 177~179°C, alone or mixed with an authentic sample). Similarly, the other II and III products also gave the corresponding parent amines.

Hydrolysis of II (Ar; p-CH_3-C_6H_4) to Sodium β-p-Toluidino-α-cyanoacrylate (IV).—A mixture of 3 g. of II (Ar; p-CH_3-C_6H_4) and 5 g. of sodium carbonate in 45 ml. of water was heated under reflux for 2.5 hr. and then cooled to 0°C. The precipitated IV was filtered off and recrystallized from ethanol-water to give colorless crystals (m. p. 232~233.5°C (decomp.)).

Found: C, 58.82; H, 4.23. Calcd. for $C_{11}H_{19}O_2N_2Na$: C, 58.93; H, 4.05%.

Its infrared absorption spectrum had bands at 3230 cm^{-1} (NH), 2200 cm^{-1} (C≡N) and 1640 cm^{-1} (C=O).

Hydrolysis of Sodium β-p-Toluidino-α-cyanoacrylate (IV) to β-p-Toluidino-α-carbamoylacrylic Acid (V).—A clear solution of 2 g. of IV in 100 ml. of water was acidified with hydrochloric acid to pH 3. The precipitated crystals were recrystallized from ethanol. There was obtained 1 g. of V (m. p. 166.5~168.5°C) as yellow crystals.

Found: C, 60.08; H, 5.48. Calcd. for $C_{11}H_{12}O_3N_2$: C, 59.99; H, 5.49%.

Its infrared absorption spectrum showed bands at 3330 cm^{-1} and 3170 cm^{-1} (NH), and 1655 and 1645 cm^{-1} (C=O).

Hydrolysis of III (Ar; p-CH_3-C_6H_4) to Potassium β-p-Toluidino-β-cyano-α-potashcarbamoylacrylate (VI).—A mixture of 2.6 g. of III (Ar; p-CH_3-C_6H_4), 5 g. of potassium hydroxide, 25 ml. of methanol, and 25 ml. of water was heated on a boiling water bath for 2 hr. After cooling, the precipitated crystals were recrystallized several times from ethanol-water to give 1.3 g. of VI (m. p. 274~275°C) as colorless crystals.

Found: C, 42.20; H, 3.43; N, 12.40. Calcd. for $C_{12}H_{11}O_4N_3K_2$: C, 42.45; H, 3.27; N, 12.38%.

Its infrared absorption spectrum showed peaks at 3480, 3340, 3200, 2160 and 1650 cm^{-1}.

Cyclization of Potassium β-p-Toluidino-β-cyano-α-potashcarbamoylacrylate (VI) to α-p-Toluidino-α'-carbamoylmaleimide (VII).—A solution of 3 g. of VI in 100 ml. of water was acidified with hydrochloric acid. The precipitated crystals were collected, washed with water, and recrystallized from dimethylformamide-ethanol to give VII (m. p. 276~277°C) as yellow crystals.

Found: C, 58.77; H, 4.60; N, 17.25. Calcd. for $C_{12}H_{13}O_3N_3$: C, 58.77; H, 4.52; N, 17.14%.

Its infrared absorption spectrum showed bands at 3420 and 3200 cm^{-1} (NH), 1760 and 1730 cm^{-1} (succinimide type C=O), and 1665 cm^{-1} (amide C=O).

***N*-*trans*-α, β-Diethoxycarbonyl-β-cyanovinylamine (VIII).**—*With Ammonium Hydroxide.*—Three grams (0.05 mol.) of 28% ammonium hydroxide were slowly stirred into a mixture of 11 g. (0.05 mol.) of I and 60 ml. of acetonitrile at 5~8°C. The solvent was evaporated at room temperature, and the residue was crystallized to give 10 g. (94%) of VIII (m. p. 78~79°C).

Found: C, 50.82; H, 5.65; N, 13.33. Calcd. for $C_9H_{12}O_4N_2$: C, 50.94; H, 5.70; N, 13.20%.

With Ammonia Gas.—A mixture of 2.8 g. (0.013 mol.) of I and 15 ml. of acetonitrile was placed in a 50 ml. three-necked flask equipped with a mechanical stirrer and a gas inlet tube. After the flask had been cooled in an ice-salt bath at −10~15°C and the mechanical stirring had been started, ammonia gas was slowly passed into the mixture for 2~3 min. until an orange color appeared; the reaction was then allowed to proceed for 20 min. When the acetonitrile was removed by vacuum distillation, the residue solidified to give 2.1 g. (75%) of VIII (m. p. 78~79°C) as colorless crystals.

α-Carbamoyl-β-cyano-β-ethoxycarbonylvinylamine (IX).—A mixture of 11 g. (0.05 mol.) of I and 60 ml. of acetonitrile was placed in a three-necked flask equipped with a sealed mechanical stirrer, a gas inlet tube, and a gas outlet tube protected with a calcium chloride tube. Ammonia gas was vigorously passed for 2 hr. into the mixture, which had been cooled throughly in an ice-salt bath. The solvent was removed by distillation, and the residue was crystallized. After recrystallization from alcohol, the yield of IX (m. p. 145~146°C (decomp.)) as colorless crystal was 7.5 g. (82%).

Found: C, 46.09; H, 5.03; N, 22.66. Calcd. for $C_7H_9O_3N_3$: C, 45.90; H, 4.95; N, 22.94%.

Preparation of Schiff Bases (X).—*From I.*—A mixture of 11 g. (0.05 mol.) of I and 100 ml. of acetone was treated with ammonia gas by a procedure similar to that used in the preparation of IX. The yield of X (R; CH_3) (m. p. 235~236°C) as colorless crystals was 3.2 g. (30%).

Found: C, 53.82; H, 6.02; N, 18.77. Calcd. for $C_{10}H_{13}O_3N_3$: C, 53.80; H, 5.87; N, 18.83%.

The infrared absorption spectrum of X (R; CH_3) had bands at 3322, 3226, 2220, 1733 and 1692 cm^{-1}.

In a similar procedure, X (R; C_2H_5) was obtained in a 84% yield.

Found: C, 57.06; H, 6.90; N, 16.75. Calcd. for $C_{12}H_{17}O_3N_3$: C, 57.38; H, 6.82; N, 16.72%.

From N-trans-α, β-Diethoxycarbonyl-β-cyanovinylamine (VIII) and α-Carbamoyl-β-cyano-β-ethoxycarbonylvinylamine (IX).—In a similar procedure, the yields of X from VIII and from IX were 86 and 79% respectively.

Hydrolysis of Schiff Bases (X).—A mixture of 1 g. of X and 100 ml. of a 5% aqueous sodium hydroxide solution was placed in a two-necked flask equipped with a gas inlet tube and a condenser with a gas outlet tube leading to a trap containing a 2,4-dinitrophenylhydrazine solution. The mixture was refluxed, and nitrogen gas was slowly passed into the mixture. Acetone 2,4-dinitrophenylhydrazone (m. p. 126°C) was precipitated as red needle crystals.

Acetylation of *N*-*trans*-α, β-Diethoxycarbonyl-β-cyanovinylamine (VIII).—*With Acetic Anhydride.*—A mixture of 4.2 g. (0.02 mol.) of VIII, 10 ml. of acetic anhydride, and three drops of concentrated sulfuric acid was heated under reflux for 8 hr. After cooling, the dark brown residue was crystallized to give 1.8 g. (33%) of α-ethoxycarbonyl-α'-diacetylaminomaleimide (m. p. 173~174°C) as colorless crystals.

Found: C, 49.45; H, 4.95; N, 10.52. Calcd. for $C_{11}H_{12}O_6N_2$: C, 49.25; H, 4.51; N, 10.45%.

Its infrared absorption spectrum had bands at 3344, 1812, 1779, 1745, 1704 and 1681 cm^{-1}.

With Acetyl Chloride.—A two-necked flask, equipped with a dropping funnel and a reflux condenser protected with a calcium chloride tube, was charged with 17 g. (0.08 mol.) of VIII and 200 ml. of acetone. The mixture was heated under reflux, and 150 ml. of acetyl chloride was added over a period of a few minutes. After the mixture had been refluxed for an additional 2 hr., the solvent was removed by vacuum distillation at room temperature and a dark red residue was crystallized. By recrystallization several times from acetone, α, β-diethoxycarbonyl-β-cyanovinylacetylamine (m. p. 215~216°C) was obtained in a 2.2 g. (11%) yield.

Found: C, 51.90; H, 5.42. Calcd. for $C_{11}H_{14}O_5N_2$: C, 51.96; H, 5.55%.

Its infrared absorption spectrum had bands at 3226, 2222, 1802, 1709 and 1654 cm^{-1}.

Acetylation of Schiff Bases X with Acetyl Chloride.—A mixture of 1 g. (0.004 mol.) of X, 10 ml. of acetic anhydride, and a few drops of concentrated sulfuric acid was refluxed for 10 min. After cooling, the mixture was crystallized to give α-*N*-acetylcarbamoyl-β-ethoxycarbonyl-β-cyanovinylisopropylidenamine (m. p. 200~201°C) in a 10% yield.

Found: C, 54.38; H, 6.05; N, 15.80. Calcd. for $C_{12}H_{15}O_4N_3$: C, 54.33; H, 5.70; N, 15.84%.

The author wishes to express his gratitude to professor Risaburo Nakai of the Institute for Chemical Research, Kyoto University, for his cordial encouragement and suggestions throughout this work. He also desires to state his gratitude to Professor Ryozo Goto of Kyoto University for his invaluable advice in the course of this work. Thanks are also due to Mr. Tatsuo Azuma of the Institute for Chemical Research, Kyoto University for his earnest assistance.

Institute for Chemical Research
Kyoto University
Takatsuki, Osaka

NOTES

Synthesis of N-Vinylsuccinamides

By Kiyoshi KATO

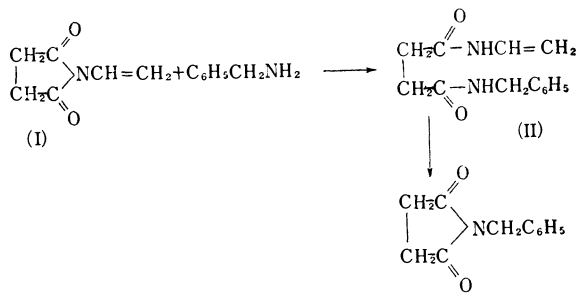
(Received February 19, 1962)

In 1959 Yanagi[1] reported a reaction of *N*-vinylsuccinimide with amines at room temperature. Under his experimental conditions, a white precipitate was given as an addition product, and he presumed the addition of amines to occur on the vinyl double bond. However, the reaction of *N*-vinylsuccinimide with amines may take place in two ways, to yield either an addition product to the double bond or *N*-vinylamide by the opening reaction of the imide ring.

Therefore, the present author has tried to prepare *N*-vinylamide derivatives through the latter reaction. When *N*-vinylsuccinimide (I) was treated with benzylamine at room temperature, a reaction occurred immediately and gave a solid flake (II), m. p. 172~173°C (decomp.). II was converted into *N*-benzylsuccinimide by the thermal decomposition. The infrared spectrum of II (Fig. 1) showed the absorption bands[2] at 3.02, 6.10 and 6.50 μ which suggested the existence of an amide radical. The existence of a double bond in the product was recognized by the Baeyer test and by bromination. Thus, II was concluded to be *N*-vinyl-*N'*-benzylsuccinamide.

Similarly, *N*-vinylsuccinimide reacted with various primary and secondary aliphatic, aromatic and heterocyclic amines and gave the respective vinyl compounds (see Table I).

N-Vinylsuccinamide copolymerized readily with such a monomer as methyl methacrylate or acrylonitrile.



Experimental

Only a few typical procedure are described in detail.

The physical properties and analyses of products are collected in Table I.

Preparation of *N*-Vinyl-*N'*-benzylsuccinamide.—A mixture of 1.1 g. of *N*-vinylsuccinimide and 1.25 g. of benzylamide was kept at room temperature for thirty minutes. The purified sample melted at 172~173°C (decomp.) and weighed 2.21 g. (95.2%).

TABLE I

N-Vinylsuccinamides $ROCCH_2CH_2CONHCH{=}CH_2$

R	M. p. (decomp.) °C	Yield %	Crystn.[a] solvent	Formula	Analyses C, % Calcd.	C, % Found	H, % Calcd.	H, % Found	N, % Calcd.	N, % Found
CH_3NH	153.5~154.5	94.8	E	$C_7H_{12}O_2N_2$	53.83	53.88	7.75	7.91	17.94	18.12
C_2H_5NH	180 ~181	87.0	E	$C_8H_{14}O_2N_2$	56.45	56.30	8.30	8.34	16.46	16.46
C_3H_5NH	158.5~159.5	93.0	M	$C_9H_{14}O_2N_2$	59.32	59.51	7.75	7.68	15.37	15.33
n-C_3H_7NH	168 ~168.5	94.2	E	$C_9H_{16}O_2N_2$	58.67	58.94	8.75	9.12	15.21	15.20
i-C_3H_7NH	164.5~165.5	90.2	E	$C_9H_{16}O_2N_2$	58.67	58.91	8.75	8.85	15.21	15.02
C_7H_7NH	172 ~173	95.2	E	$C_{13}H_{16}O_2N_2$	67.18	67.23	6.94	7.21	12.06	12.20
C_2H_5ONH	134.5~135.5	94.8	BE	$C_8H_{14}O_3N_2$	51.60	51.62	7.59	7.64	15.05	14.87
C_2H_6N	132.5~133	62.9	E	$C_8H_{14}O_2N_2$	56.45	56.58	8.30	8.42	16.46	16.45
$C_5H_{10}N$	86 ~ 87	91.9	AE	$C_{11}H_{18}O_2N_2$	62.82	63.01	8.64	8.72	13.32	13.33

a) AE, Ethyl acetate; BE, Benzene-ethanol; E, Ethanol; M, Methanol

1) K. Yanagi, *J. Org. Chem.*, **24**, 1121 (1959).
2) L. J. Bellamy, "The Infrared Spectra of Complex Molecules", John Wiley and Sons, Inc., New York (1954), p. 176.

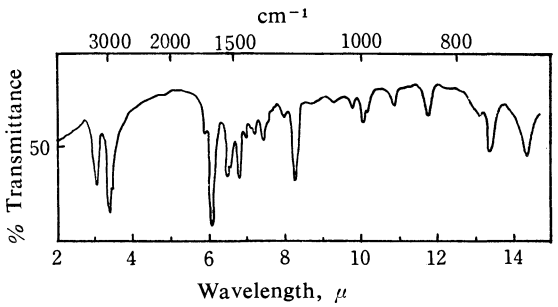


Fig. 1. Infrared spectrum of II (Nujol).

Thermal Decomposition of *N*-Vinyl-*N'*-benzylsuccinamide.—When II was heated at about 180°C for a few minutes, a red liquid was obtained. After recrystallization of the product from methanol, crystals were obtained; m. p. 98~99°C, undepressed by admixture with an authentic compound (Found: N, 7.28%).

Synthesis of *N*-Vinyl-*N'*-2-hydroxyethylsuccinamide.—A mixture of 1.25 g. of *N*-vinylsuccinimide and 0.6 g. of monoethanolamine in 2 ml. of benzene was kept at room temperature for few minutes. The precipitate was then filtered and dried. The product was recrystallized from benzene-ethanol. The purified sample melted at 134.5~135.5°C (decomp.); the yield was 1.75 g. (94.8%).

Reaction of *N*-Vinylsuccinimide with Morphorine.—*N*-Vinylamide was expected to be produced in this run, too, but it was not obtained in an analytically pure state. In the infrared spectrum of the crude material, absorption bands were observed at 3.02, 6.58 and 10.06 μ; these were assigned to the NH stretching vibration of a secondary amide and to CH out-of-plane deformation.

Copolymerization of *N*-Vinyl-*N'*-*n*-propylsuccinamide with Methyl Methacrylate.—A solution of 0.2 g. of *N*-vinyl-*N'*-*n*-propylsuccinamide, 1.8 g. of methyl methacrylate and 0.02 g. of benzoyl peroxide in 7 ml. of dioxane was heated at 65~66°C in a water bath for 6 hr. The polymer solution was poured into 70 ml. of methanol. After filtration and drying, the polymer weighed 0.41 g. (N, 1.69%). It was soluble in acetone, tetrahydrofurane, dioxane, benzene, toluene, chloroform, tetrachloroethane and ethyl acetate.

The author is indebted to Professor Niro Murata of the University of Osaka Prefecture for his invaluable advice and encouragement. Thanks are also due to Dr. Seibei Yoshikawa for his encouragement.

Government Industrial Research Institute, Osaka
Oyodo-ku, Osaka

Ultracentrifugal Determination of Micellar Molecular Weights of Polyoxyethylene Dodecyl Ether

By Fumikatsu TOKIWA* and Toshizo ISEMURA

(Received May 15, 1962)

Several investigations[1-5] of non-ionic detergents in aqueous solutions have shown that the micellar molecular weights are highly dependent on the structures of the detergents. The chain-lengths of the polyoxyethylene of non-ionic detergents are also considered to be one of the factors that affect the micellar molecular weights.

An analytical ultracentrifuge provides a convenient method for the determination of the micellar molecular weights of non-ionic detergents. The transient-state method of determining micellar molecular weights in the analytical ultracentrifuge may be useful in avoiding independent determinations of the diffusion coefficients[6], and the synthetic boundary method may be used to determine relative optical concentrations without independent determinations of specific refractive increments[7]. The treatment of the data obtained from the Schlieren optics of analytical ultracentrifuge has already been given in detail[5,8] and will not be repeated here. The equation required for weight-average micellar molecular weight determination by the transient-state method is:

$$M=\frac{RT}{(1-\bar{V}\rho)\omega^2}\left(\frac{dc/dx}{xc}\right)_{m \text{ or } b}$$

Here M is the molecular weight, R the gas constant, T the absolute temperature, $\bar{V}$ the partial specific volume of the solute, ρ the density of the solution, ω the angular velocity, c the solute concentration, and x the distance from the axis of rotation to some point in the

* Present address: Research Laboratory, Kao Soap Co., Ltd., Sumida-ku, Tokyo.

1) A. M. Mankowich, *J. Phys. Chem.*, **58**, 1027 (1954).
2) J. Stauff and J. Rasper, *Kolloid-Z.*, **151**, 148 (1957).
3) L. M. Kushner, W. D. Hubbard and A. S. Doan, *J. Phys. Chem.*, **61**, 371 (1957).
4) T. Nakagawa, H. Inoue and K. Kuriyama, *J. Chem. Soc. Japan, Pure Chem. Sec.* (*Nippon Kagaku Zassi*), **79**, 345 (1958).
5) C. W. Dwiggins, Jr., R. J. Bolen and H. N. Dunning, *J. Phys. Chem.*, **64**, 1175 (1960).
6) H. K. Schachman, "Ultracentrifugation in Biochemistry", Academic Press, New York, N. Y. (1959), pp. 181—199.
7) S. M. Klainer and G. Kegeles, *J. Phys. Chem.*, **59**, 952 (1955).
8) S. M. Klainer and G. Kegeles, *Arch. Biochem. Biophys.*, **63**, 247 (1956).

TABLE I. PROPERTIES OF PODE SOLUTIONS AND MICELLES AS A FUNCTION OF POLYOXYETHYLENE CHAIN-LENGTH

Sample[a]	Concn. %	Temp. °C	Partial specific volume ml./g.	Micellar molec. wt. $\times 10^{-4}$	Molecules[c] per micelle
PODE- 7.6	1.08	18	0.931	3.76	72
PODE-10.6	1.09	21	0.910	3.17	49
PODE-20.4	1.06	18	0.890	3.75	35
PODE-38.6	1.10	21	0.866	3.50	19
PODE-67.3	1.03	18	0.825	2.06	6.5
PEG[b]	1.05	18	0.808	0.41	1

a) Number written after PODE represents the average number of oxyethylene groups per molecule.
b) Approximate molecular weight is 4000 (which is taken from the manufacture's literature).
c) See the text.

solution; the values of c and dc/dx must, on the other hand, be determined. The symbols m and b denote the meniscus and the bottom of the liquid column respectively.

Experimental

The detergents studied were polyoxyethylene dodecyl ether (abbreviated to PODE), $C_{12}H_{25}O\cdot(CH_2CH_2O)_nH$, which were prepared from dodecyl alcohol of high purity. The average degrees of the polymerization of ethylene oxide in these samples used are listed in Table I. The purification of the detergents was carrried out by an extraction method[9] using water-saturated *n*-butanol and *n*-butanol-saturated water. It was confirmed, by testing through paper chromatography[10], that the purified samples contained no detectable free polyethyleneglycol (abbreviated to PEG). The molecular weights of the samples (m) were determined by the freezing point depression of their benzene solutions. PEG (Carbowax 4000) was purchased from the Carbide and Carbon Chemicals Co. The detergent solutions were prepared by weight in freshly distilled water and stored for a few days.

The ultracentrifugal experiments were performed in a Hitachi model UGA-1 type ultracentrifuge. Centrifugations were done at 18 ± 0.2°C or 21 ± 0.2°C. In the present work, micellar molecular weights were determined only from the meniscus of the column, because it was found that the detergent solutions gave insufficient refractive-index gradients to permit measurement of the micellar molecular weight at the bottom of the column.

Partial specific volumes were determined from pycnometric measurements of solution densities at the same temperature as centrifugation was performed. The values of partial specific volumes are given in Table I.

Results and Discussion

The results for the micellar molecular weight (M) determination of PODE having various chain-lengths of polyoxyethylene are summarized in Table I. As expected, the micellar molecular weight or the aggregation number (the number of molecules per micelle, M/m) is highly dependent on the chain-length of polyoxyethylene. The aggregation number represented by M/m is used here as a measure of the degree of the aggregation, since the molecular weights of PODE should always have some distribution and the molecular weights obtained from different methods differ from one another. The aggregation number decreased with an increase in the chain-length, and PEG, a high molecular weight condensate composed of hydrophilic ethylene oxide, was found to be dissolved as a single molecule. Concerning the effect of polyoxyethylene chain-lengths on the aggregation numbers, Nakagawa et al.[4] have obtained similar results from light-scattering and diffusion-viscosity experiments over a relatively limited range of chain-lengths, using methoxy polyoxyethylene decyl and dodecyl ether. It would be desirable to have data for lower concentrations, but even a small error in reading the concentration gradient curves for concentrations lower than about 0.8~1.0 g./100 ml. would introduce much error.

The finding that the aggregation number decreases with the increase in the chain-length of polyoxyethylene indicates that the micelle formation of non-ionic detergents has some relation with the steric effect of the polyoxyethylene chain as well as with the hydrophility of the polyoxyethylene chain. It is a doubtful postulate that ordinary micelles are formed in a solution of such a non-ionic detergent as is encountered in ionic detergent solutions if the polyoxyethylene chain becomes sufficiently long. In the case of PODE of $n=67.3$ the aggregation number is only 6.5, and it is doubtful that a micelle, in the generally accepted meaning of the term, could be formed with

9) K. Nagase and K. Sakaguchi, *J. Chem. Soc. Japan, Ind. Chem. Sec.* (*Kogyo Kagaku Zasshi*), **64**, 635 (1961).
10) T. Nakagawa and I. Nakata, ibid., **59**, 710, 1154 (1956).

such an insufficient number of molecules. PEG shows no micelle formation, assuming that the molecular weight reported for the PEG studied is correct. Such behavior is not unexpected since light-scattering[1] and ultracentrifugal[5] experiments have shown that similar compounds, Pluronics, which are high molecular weight condensates of ethylene and propylene oxides, do not form micelles.

The authors express their hearty thanks to Mr. K. Kakiuchi for his measurements of ultracentrifugal sedimentation.

Institute for Protein Research
Osaka University
Kita-ku, Osaka

Recoil Reactions in Irradiated Tris-(nitrosonaphtholato)- and Tris-(dimethylglyoximato)-cobalt(III) Complexes

By Nobufusa SAITO, Takeshi TOMINAGA and Hirotoshi SANO

(Received May 28, 1962)

Hot-atom chemistry of radiocobalt has been studied by several authors on the irradiated octahedral cobalt(III) complexes of the formula, CoA_3, containing organic bidentate ligands, A (A=glycinate, acetylacetonate, oxinate, etc.)[1-4]. With a view to clarifying the relationship between distribution of induced ^{60}Co activity in various chemical forms and any chemical or physical property of the ligand, the present authors have selected, in addition to those mentioned above, three complex compounds of the similar type, tris-(α-nitroso-β-naphtholato)-,

TABLE I. PERCENTAGE OF ^{60}Co ACTIVITY SEPARABLE AS Co(II)

Target	Time of irradiation hr.	Time of storage*	^{60}Co activity separable as Co(II) %	Method of separation**
Tris-(α-nitroso-β-naphtholato)-cobalt(III)	1	1 day	39.1	a
		5 days	21.0	a
		2 months	17.2	a
	5	2 days	27.4	a
		5 days	27.0	a
		2 months	14.3	a
Tris-(β-nitroso-α-naphtholato)-cobalt(III)	1	1 day	28.9	a
		5 days	16.0	a
		2 months	10.9	a
	5	1 day	17.4	a
		5 days	16.9	a
		2 months	9.1	a
Tris-(dimethylglyoximato)-cobalt(III)	1	1 day	82.2	a
		4 days	77.4	a
		4 days	74.6	b
		2 months	75.4	a
	5	5 days	83.9	a
		5 days	83.3	b
		5 days	73.7	c
		5 days	85.0	d
		2 months	57.6	a
		2 months	57.1	b
		2 months	42.6	c
		2 months	57.6	d

* Storage at room temperature

** a: solvent extraction, b: precipitation, c: ion exchange, d: paper electrophoresis

1) A. Zuber, USAEC Document NYO-6142 BNL.
2) A. Nath, J. Shankar and S. B. Srivastava, Proc. 2nd Intern. Conf., Peaceful Uses of Atomic Energy, Geneva, **20**, 58 (1958).
3) A. Nath, J. Shankar et al., Papers presented at the IAEA Symposium on the Chemical Effects of Nuclear Transformations, Prague, 1960.
4) L. L. Williams, N. Sutin and J. M. Miller, *J. Inorg. Nuclear Chem.*, **19**, 175 (1961).

tris-(β-nitroso-α-naphtholato)- and tris-(dimethylglyoximato)-cobalt(III) complexes, and investigated the recoil reactions of radiocobalt in such compounds.

These crystalline complex compounds were irradiated in an experimental hole in JRR-1 reactor for one or five hours at ambient temperature. Thermal neutron flux was approximately 3×10^{11} n/cm^2·sec. All bombardments were made in the presence of air.

After the bombardments tris-(nitrosonaphtholato)-cobalt(III) complexes were dissolved in chloroform, and shaken four times with (1 : 1) nitric acid. The ^{60}Co activity as cobalt(II) was extracted into aqueous phase with enrichment factors more than 150, while ^{60}Co as complexes remained in organic phase.

The irradiated tris-(dimethylglyoximato)-cobalt(III) complex was dissolved in water and ^{60}Co-labeled species were separated by means of procedures involving paper electrophoresis (in acetate buffer or in 1% sodium chloride solution), solvent extraction (cobalt(II) extracted into benzene as β-nitroso-α-naphtholato-complex), precipitation, or ion exchange. By the solvent extraction method, ^{60}Co was extracted into benzene with enrichment factors more than 100. For the dimethylglyoximato-complex, the ^{60}Co activity separable as cobalt(II) was considerably decreased unless the irradiated complex was dissolved in water containing cobalt(II) carrier beforehand. Since no isotopic exchange was observed in practice between ^{60}Co(II) and tris-(dimethylglyoximato)-cobalt(III) complex within 6 hr. (at 24.5°C), the decrease might be mainly attributed to consumption of ^{60}Co(II) (in micro quantities) due to probable comlpex formation with free dimethylglyoximate ions present in the solution. Therefore adequate amounts of cobalt(II) carrier was added beforehand to minimize the loss of activity.

The percentages of ^{60}Co activity separable as cobalt(II) for samples irradiated and stored for varied times were summarized in Table I.

As seen in Table I, nitrosonaphtholato-cobalt(III) complexes showed considerably low percentages for cobalt(II) fraction. Since it was reported that more than 70% of the induced ^{60}Co activity could be separated as cobalt(II) from most of the CoA_3 type complexes freshly irradiated*, such a low extractability seemed to be rather unusual.

It is worthy of mentioning that α-nitroso-β-naphtholato-complex represented higher extractability of radiocobalt as cobalt(II) than β-nitroso-α-naphtholato-complex. This fact might possibly be related to some differences in configuration of their ligands or chemical properties of these complexes.

Department of Chemistry
Faculty of Science
The University of Tokyo
Hongo, Tokyo

* Based on the values reported in the papers cited above (1—4) as well as those for tris-(dimethylglyoximato)-cobalt(III) reported in the present paper. Though the irradiation condition employed by different authors were not identical the integrated neutron flux and gamma flux in the present experiment were estimated rather lower than those employed by other authors. Most irradiations by the other authors were also made at pile temperature.

Self-diffusion of the Sulfate Ion in Gelatin Gels

By Hirondo KURIHARA*1, Hiroshige HIGUCHI*2, Takeshi HIRAKAWA*3 and Ryohei MATUURA

(Received May 28, 1962)

The self-diffusion of ions in gels has not been studied so extensively as in aqueous solutions. In general, the diffusion process in gels is made more complicated than in liquid systems by such factors as the geometry of the diffusion path and the adsorption of the ion by the gel substance. Clearly these factors are closely related to the structure of gels. It is expected that the study of the self-diffusion of ions will give us useful information about the structure of gels as well as the nature of the transport phenomena in gels. In this paper the self-diffusion of the sulfate ion in gelatin gels will be investigated.

Experimental

The gelatin used in the present experiment was Merck's reagent for chemical use. In order to minimize its salt content, the aqueous solution (sol) of the gelatin was passed through an ion-exchange column. After that the salt content was found to be 0.3%. ^{35}S labeled sodium sulfate was obtained from the Radiochemical Center, England, as a carrier-free material. It was isotopically diluted to a proper concentration and purified by recrystallization.

For the measurement of diffusion, the layer analysis method was used. The diffusion cell was almost identical with that of Nachtrieb and Petit[1],

*1 Present address: Faculty of Engineering, Ehime University, Niihama, Ehime.
*2 Present address: Fukuoka Senior High School, Fukuoka.
*3 Present address: Shin Nippon Chisso Hiryo K. K., Central Research Laboratory, Yokohama.

1) N. H. Nachtrieb and J. Petit, *J. Chem. Phys.*, **24**, 746 (1956).

although some details were modified. The cell was made up of six disks (denoted from the top as disk No. 1 to disk No. 6) of poly(methyl methacrylate) Each disk, 40 mm. in diameter and 5 mm. in thickness, could be rotated around a common vertical axis. Disks No. 2 to No. 5 bore holes 5 mm. in diameter at a point 1 cm. from the center. They were aligned by means of a locating pin so that they formed a straight diffusion column. The two ends of the diffusion column were covered by disks No. 1 and No. 6, which bore no holes.

The gelatin sol, which contained inactive sodium sulfate of a known concentration, was poured into the holes of disks No. 3 to No. 5, which had been aligned. The same sol also containing radioactive sodium sulfate of the same concentration as above was poured into the hole of disk No. 2. They were then left to stand in a constant temperature bath. After complete gelation, the two gel blocks were placed in contact with each other by rotating the disks and by aligning the holes by the locating pin, as has been stated above. This time of contact was taken as time zero for diffusion. After an appropriate time (usually, 4 to 5 hr.), the cell was taken out of the bath and each disk was rotated with respect to its neighbor in order to shear the column of gel into four sections. The radioactivity of the sodium sulfate in each section (C) was measured after it had been mounted on a porcelain dish as a uniform film. The self-absorption correction was not made, since each disk contained exactly the same amount of gelatin and we needed only the relative intensity of radioactivity with respect to the initial one in disk No. 2 (C_0). The self-diffusion coefficient of the sulfate ion was thus calculated from the observed value of C/C_0 with the aid of the Stefan-Kawalki Tables[2].

The temperature of most of the diffusion, experiment was 25°C. For the measurement of the activation energy for self-diffusion, the temperature ranged from 10 to 28°C with 11% gelatin gel containing sodium sulfate of 0.001 mol./l.

Results and Discussion

In Fig. 1 the self-diffusion coefficient of the sulfate ion in gelatin gels, D_g, at 25°C is plotted against the square root of the concentration of sodium sulfate in the gel. Each value of the diffusion coefficient is a mean of three separate runs. The standard deviation was less than 3%. For the sake of comparison, the self-diffusion coefficient of the sulfate ion in aqueous solutions at 25°C, D_w, as measured by Nielsen et al.[3], is also shown in Fig. 1.

It may be seen from Fig. 1 that the D_g value in 11% gel is about half as large as D_w when the concentration of sodium sulfate is very low, but at higher concentrations of sodium sulfate the two values approach each other. As the gel concentration increases, the D_g value decreases; also, the dependence of the D_g value on the

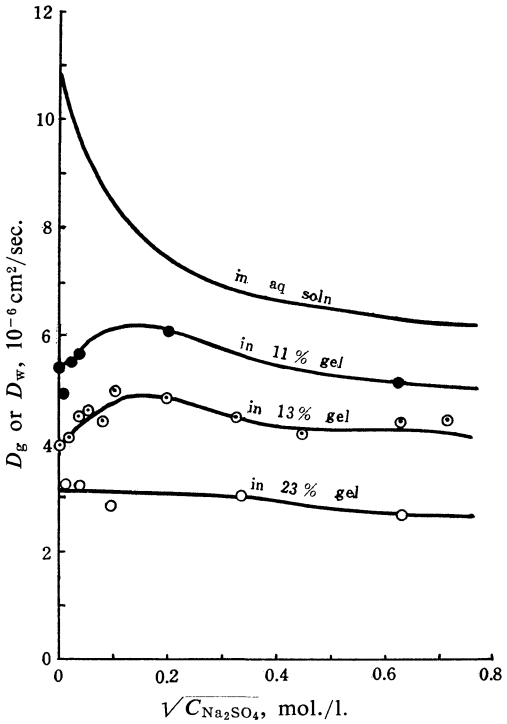


Fig. 1. Self-diffusion coefficient of sulfate ion vs. square root of concentration of Na_2SO_4 in gelatin gels (D_g) and in aqueous solutions (D_w) at 25°C.

concentration of sodium sulfate becomes smaller. The initial linear decrease of the D_w value with respect to the square root of the concentration of sodium sulfate in aqueous solutions may be explained in terms of the Onsager theory of ionic diffusion[4,5]. This behavior is quite different in gels, where the D_g initially increases a little but decreases slightly as the concentration of sodium sulfate increases further. In 23% gel, no initial increase in the D_g is observed.

It has reasonably been assumed that the sulfate ion is adsorbed strongly by the gelatin molecule to form intra- or intermolecular cross-linking. Indeed, we found that the "melting point" of gelatin gel[6] increases as the addition of sodium sulfate increases. The activation energy for the self-diffusion of the sulfate ion in 11% gel at the sulfate concentration of 0.001 mol./l. was found to be 5.9 kcal./mol. This value is of the same order of magnitude as that for the self-diffusion of ions in ion-exchange resins[7]. It is to be concluded, therefore, that the self-diffusion of the sulfate

2) W. Kawalki, *Ann. Physik*, **52**(2), 166 (1894).
3) J. M. Nielsen, A. W. Adamson and J. W. Cobble, *J. Am. Chem. Soc.*, **74**, 446 (1952).
4) L. Onsager, *Ann. N. Y. Acad. Sci.*, **46**, 241 (1945).
5) L. J. Gosting and H. S. Harned, *J. Am. Chem. Soc.*, **73**, 159 (1951).
6) J. Bello, H. C. A. Riese and J. R. Vinograd, *J. Phys. Chem.*, **60**, 1299 (1956).

ion in gelatin gels proceeds via the exchange of the adsorbed ion. Of course, the geometry of the diffusion path plays an important role in the diffusion of the adsorbed ion, since the self-diffusion coefficient decreases appreciably as the concentration of gel increases.

Bloksma[8] measured the self-diffusion of sodium and iodide ions and of urea in clay pastes. He separated two labyrinth factors, geometry and adsorption, and proposed to determine them. It is, however, not easy to determine each factor separately unless some assumptions are made. Probably the combined effects are responsible for the curious dependence of the D_g value on the concentration of sodium sulfate.

Department of Chemistry
Faculty of Science
Kyushu University
Fukuoka

7) G. E. Boyd and B. A Soldano, *J. Am. Chem. Soc.*, **75**, 6091 (1953); B. A. Soldano and G. E. Boyd, ibid., **75**, 6099 (1953).
8) A. H. Bloksma, *J. Colloid Sci.*, **12**, 40 (1957).

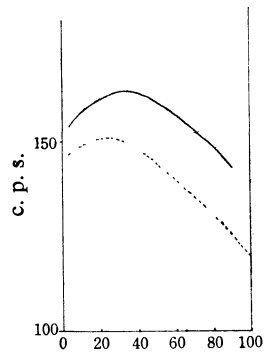


Fig. 1
Cyclopentane-1,2-diol
Solvent : Pyridine
cis ---- trans ——

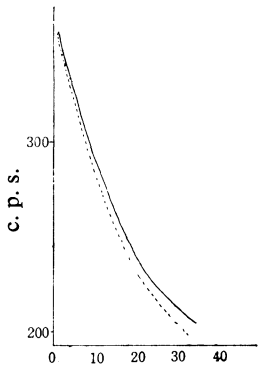


Fig. 2
Cyclohexane-1,2-diol
Solvent : CH_3COOH
cis ---- trans ——

*NMR Spectra of α-Glycols**

By Shin-ichiro FUJISE, Genjiro HAZATO, Tsuneo IKENOUE, Shin-ichi SASAKI and Yasuhisa SENDA

(Received June 7, 1962)

We wish to report that the NMR spectra of α-glycols show a deviation caused by the differences in the steric configurations of the hydroxyl groups.

In the spectra of α-glycols, a characteristic difference between two isomers appeared in the chemical shift of the hydroxyl protons. The experimental results are shown in Table I. These findings are very interesting in comparison with those reported by Kuhn[1].

1) In α-glycol, which is in a liquid state at ordinary temperatures, the signal of the hydroxyl proton of the erythro-isomer was generally observed at a lower magnetic field than that of the threo-isomer, and in the trans rather than in the cis state.

2) When α-glycols are dissolved in a basic solvent, these hydroxyl protons are exchanged with the base; therefore, their signals show a single peak and the chemical shifts show a curve with a shape like that of Fig. 1, without exception between two isomers.

3) In organic acid, the protons of the carboxyl group and the hydroxyl group are exchanged, and their signals appear as a concentration shift. The shape of the curve in the two-phase system is different from that in a basic solvent (Fig. 2), but its behavior between two isomers is the same as in those cases without a solvent or in a base.

The following are the exceptions to our experimental rule which were observed.

4) In the spectrum of five-membered ring compounds such as cyclopentane-1,2-diol or α,β-dihydroxyvalerolactone, which take the planar conformation, the signal of the hydroxyl proton of the cis-isomer in acidic solvents was less shielded than that of the corresponding

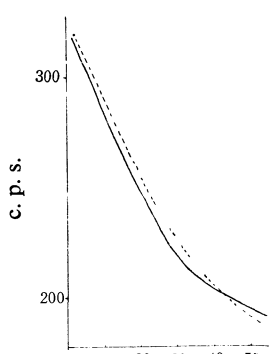


Fig. 3
Cyclopentane-1,2-diol
Solvent : CF_3COOH
cis ---- trans ——

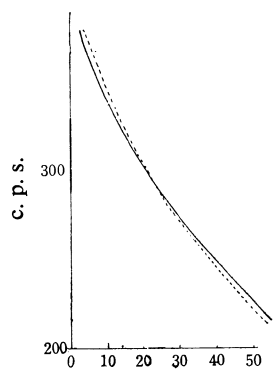


Fig. 4
Cyclopentane-1,2-diol
Solvent : CH_3COOH
cis ---- trans ——

* Read at the 11th Annual Meeting of the Chemical Society of Japan, Tokyo, April, 1958.

1) L. P. Kuhn, *J. Am. Chem. Soc.*, **76**, 4223 (1954).

TABLE I

1) Solvent: Pyridine

Sample	Isomer	Concn. mol. %	Shifts c. p. s.	Diff. c. p. s.
α, β-Dihydroxybutyric acid	erythro threo	14.1	315.3 304.3	11.0
Methyl α, β-dihydroxybutyrate	erythro threo	32.5	221.3 195.3	26.0
Tartaric acid	meso DL	33.4	322.6 271.2	51.4
Dimethyl tartrate	meso DL	31.3	151.3 144.7	6.6
Cyclopentane-1,2-diol	cis trans	43.9	150.0 167.7	17.7
Cyclohexane-1,2-diol	cis trans	32.3	163.2 185.7	22.5
α, β-Dihydroxyvalerolactone	cis trans	34.0	240.5 257.8	17.3
9,10-Dihydroxystearic acid	erythro thero	11.1	293.4 290.8	2.6
Octadecane-1,9,10-triol	erythro threo	5.9	192.1 179.1	13.0

2) Solvent: Acetic acid

Sample	Isomer	Concn. mol. %	Shifts c. p. s.	Diff. c. p. s.
Methyl α, β-dihydroxybutyrate	erythro threo	31.3	276.1 254.6	21.5
Dimethyl tartrate	meso DL	25.0	360.5 315.4	45.1
Cyclopentane-1,2-diol	cis trans	35.3	256.8 259.7	2.9
Cyclohexane-1,2-diol	cis trans	31.7	252.4 259.9	7.5
α, β-Dihydroxyvalerolactone Solvent: CF_3COOH	cis trans	18.0	319.1 312.4	−6.7

trans-isomer in areas of a higher acid content (Figs. 3 and 4). This fact was recognized when trifluoroacetic acid instead of acetic acid was used as a solvent, a smaller amount of trifluoroacetic acid being sufficient to show this experimental fact, it is also well known that triflouroacetic acid is weaker than acetic acid in acidity.

The NMR spectra were obtained with a Varian V-4300 high resolution spectrometer at a fixed frequency of 40 Mc./sec., and the chemical shifts of the hydroxyl proton were relative to the signal of the proton of the group which was seen at the highest field in the spectra.

Chemical Research Institute of
Non-Aqueous Solution
Tohoku University
Katahira-cho, Sendai
(G. H. & T. I.)

Department of Chemistry
Faculty of Science
Tohoku University
Katahira-cho, Sendai
(S. F., S. S. & Y. S.)

4-Chloro-3-methylcrotonic Acid Derivatives and Phosphonates

By Kazuyoshi FUJIWARA, Hidetaka TAKAHASHI and Masaki OHTA

(Received June 15, 1962)

3-Methylcrotonic acid derivatives are important intermediates for the synthesis of Vitamin A or of carotenoid. The present authors have found a very convenient procedure for the preparation of 4-chloro-3-methylcrotonic acid derivatives by the use of phosphonates. Recently, Wadsworth and Emmons[1] described how carbonyl compounds reacted with phosphonates by the action of sodium hydride to give olefinic compounds. In this study, ethyl

1) W. S. Wadsworth and W. D. Emmons, *J. Am. Chem. Soc.*, **83**, 1733 (1962).

4-chloro-3-methylcrotonate and 4-chloro-3-methylcrotononitrile were obtained from chloroacetone and appropriate phosphonate by the aid of sodium amide or of hydride in dry ether or tetrahydrofuran.

$$ClCH_2\overset{CH_3}{\overset{|}{C}}O + (EtO)_2\overset{O}{\overset{\|}{P}}CH_2R \rightarrow ClCH_2\overset{CH_3}{\overset{|}{C}}=CHR \quad (I)$$

(R, CO_2Et or CN)

Phosphonate in dry ether or tetrahydrofuran was stirred into a slurry of sodium amide or hydride in the same solvent at about 20°C. After this addition, the solution was stirred at room temperature while the evolved gas was removed under a slow stream of nitrogen. To the yellow solution, maintained below 25°C, chloroacetone in the same solvent was added drop by drop, a gummy precipitate appearing. After the reaction mixture had been stirred at room temperature for 1 hr., much excess water was added and then the product was extracted with ether. The ether, after being dried over sodium sulfate, was removed and the residue distilled under reduced pressure. I, R=CO_2Et; yield, 58%; b. p., 83~84°C/15 mmHg. Found: C, 51.38; H, 6.47; Cl, 21.41. Calcd. for $C_7H_{11}ClO_2$: C, 51.70; H, 6.82; Cl, 21.81%. I, R=CN; yield, 72%; b. p., 89~90°C/22 mmHg. Found: C, 51.92; H, 5.31; N, 12.09. Calcd. for C_5H_6ClN: C, 51.96; H, 5.23; N, 12.12%.

The 4-chloro-3-methylcrotonic acid derivatives condensed with triethyl phosphite at 180~200°C to give phosphonates. II, R=CO_2Et; yield, 81%; b. p., 157~158°C/8 mmHg. Found: C, 49.68; H, 8.11. Calcd. for $C_{11}H_{21}O_5P$: C, 49.99; H, 8.01%. II, R=CN; yield, 89%; b. p., 135~136°C/4 mmHg. Found: C, 49.58; H, 7.44; N, 6.44. Calcd. for $C_9H_{16}NO_3P$: C, 49.76; H, 7.43; N, 6.45%.

$$ClCH_2\overset{CH_3}{\overset{|}{C}}=CHR + (EtO)_3P \rightarrow (EtO)_2\overset{O}{\overset{\|}{P}}CH_2\overset{CH_3}{\overset{|}{C}}=CHR \quad (II)$$

Further investigation into the reaction between haloketones and phosphonates is now in progress; details will be presented elsewhere.

Laboratory of Organic Chemistry
Tokyo Institute of Technology
Meguro-ku, Tokyo

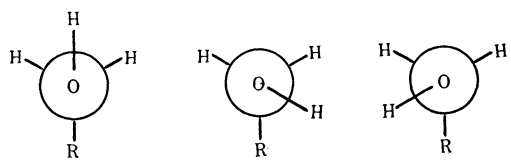
ν_{O-H} *Absorption and Rotational Isomerism of Fluoro-alcohols*[1]

By Michinori Ōki and Hiizu Iwamura

(Received June 15, 1962)

In a previous paper[2] it was presented that the ordinary saturated alcohols possess doublet character of O–H fundamental stretching vibration (ν_{O-H}). Considering the lack of this character in methanol and *tert*-butyl alcohol, and classifying the ν_{O-H} frequencies in reference to the types of the alcohols, the authors have succeeded in a tentative explanation that the occurrence of the doublet bands should be due to the rotational isomerism about the C–O bond as an axis.

In the meantime, Piccolini and Winstein[3] have been led to the same conclusion based on the measurement with some seventy saturated alcohols. Partly because of the fact that they took advantage of the spectra in the first overtone 1.4 μ region, their data are not always in quantitative agreement with the present authors'. In this respect, it seems desirable to add another example to confirm the existence of the rotational isomers about the C–O bond in alcohols.



I II II'

Of the three rotational isomers, I, II and II', in primary alcohols, relative stabilities will be determined by the interaction between the hydroxyl group and group R. As far as R is an alkyl group, only the van der Waals repulsive force is to be considered, hence I is expected to be predominant over II and II'. In this connection it was shown[2] that the intensity of the band corresponding to I is about twice as stronger as that of (II+II'), in spite of just the reverse statistical factor, and that the ratio of the integrated intensities, A_I/A_{II}, amounts to 6.0 when R is *tert*-butyl. Since it is unlikely that the molar absorption intensity

1) Part XVII of the "Intramolecular Interaction between Hydroxyl Group and π-Electrons", Part XVI: M. Ōki and H. Iwamura, This Bulletin, **35**, 1552 (1962).
2) M. Ōki and H. Iwamura, ibid., **32**, 950 (1959).
3) R. Piccolini and S. Winstein, *Tetrahedron Letters*, No. 13, 4 (1959).

TABLE I. ν_{O-H} ABSORPTIONS OF FLUORO-ALCOHOLS

	Band	ν_{max} cm^{-1}	$\Delta\nu^a_{1/2}$ cm^{-1}	$A\times10^{-3}$ mol^{-1} l. cm^{-2}	A_I/A_{II}
FCH_2CH_2OH	I	3634.6	25.6	1.17	0.43
	II	3620.9	20.0	2.74	
CF_3CH_2OH	I	3636.2	12.4	0.30	0.042
	II	3619.8	22.2	6.87	
$CF_3CF_2CH_2OH$	I	3635.5	19.4	2.46	0.29
	II	3619.8	23.6	8.60	

of ν_{O-H} differs appreciably in I and II, A_I/A_{II} may be a good estimate of the population ratio between I and II. Then it comes out that I is about 400 cal./mol. more stable than II. The ratio, B_1/B_2, of ca. 8 by Piccolini and Winstein[3] will produce unreasonably great energy difference between the two rotational isomers.

When a hetero-atom is introduced in group R, another situation will arise in addition to the mere repulsive force. The apparent absorption curves and ν_{O-H} data of the fluorinated primary alcohols measured in dilute carbon tetrachloride solution (ca. 0.003 mol./l.) are shown in Fig. 1 and in Table I, respectively. They were determined with a Perkin-Elmer 112G grating IR spectrometer with the spectral slit width of 1 cm^{-1} [4,5].

All three show doublet ν_{O-H} at 3635 and 3620 cm^{-1}, respectively. The former is as high as that of methanol and can validly be assigned to the conformation I of the ordinary primary alcohols. According to the generalization put forward in the previous paper[2], conformational isomer II should have its ν_{O-H} at 3626~3629 cm^{-1}. There is a slight shift to the lower frequency in the present examples. The intensities of the doublet bands have suffered from more conspicuous effect. Contrary to the corresponding ethanol and 1-propanol, the lower-lying bands have acquired superiority over the higher ones, as shown in the A_I/A_{II} column in Table I. These data are in accord with the idea of the rotational isomerism around the C–O bond and may be explained as follows.

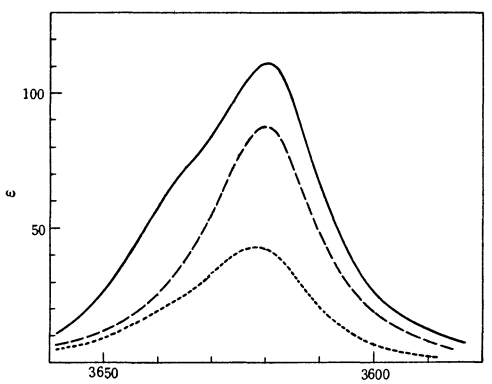


Fig. 1

····· FCH_2CH_2OH
– – – $CF_3CH_{20}OH$
—— $CF_3CF_2CH_2OH$

In isomers II and II′, it is possible for the hydroxyl group to take part in some kinds of O–H···F interaction which stabilizes the molecule. In ethylene fluorohydrin there seems to be no apparent energy difference between I and II, because A_I/A_{II} is nearly equal to the frequency factor of 1/2. However, the statement is not strictly true, since (II+II′) contains further isomerism with respect to the $C_\alpha-C_\beta$ axis. Band II, therefore, consists of the sum of these isomers and it is the mean energy of them that is comparable with that of I. When the number of the fluorine atoms at β-carbon atom is raised to three, rotational degree of freedom about the $C_\alpha-C_\beta$ bond produces no isomerism and all conformations belonging to (II+II′) have O–H···F interaction with the consequence of almost exclusive population in these isomers. In pentafluoropropanol, the existence of one or two of the rotational isomers in respect of the $C_\alpha-C_\beta$ axis in type (II+II′) become impossible, because of overcrowding of the CF_3 and OH groups. This effect disfavors the residence of the molecule in conformation (II+II′) relative to I, and has already been observed in a pair of ethanol and 1-propanol which have their A_I/A_{II} of 1.8 and 2.6, respectively[2]. The rates of the increase in the relative intensity are 1.44 in ethanol—1-propanol, and 6.9 in trifluoroethanol —pentafluoropropanol. Exaltation in the latter is the due consequence of the longer C–F bond length and the larger van der Waals radius of fluorine atom.

It may be concluded that, by introducing fluorine atom in R of primary alcohols,

4) M. Ōki and H. Iwamura, This Bulletin, 32, 567 (1959).
5) Samples of trifluoroethanol and pentafluoropropanol were given by Dr. Robert West of the University of Wisconsin, U. S. A., to whom the authors' thanks are due. Ethylene fluorohydrin was prepared according to the literature: B. C. Saunders, G. J. Stacey and I. G. E. Wilding, *J. Chem. Soc.*, **1949**, 773. Their physical constants agreed well with those in the literatures.

RCH_2OH, the relative population between the isomers around C–O axis has been reversed, and thus another example has been complied favorably for the existence of the rotational isomerides about the C–O bond as an axis.

Department of Chemistry
Faculty of Science
The University of Tokyo
Hongo, Tokyo

*Metal Ketyls of Benzophenone Derivatives. I**

By Ryozo GOTO, Kazuhiro MARUYAMA, Rikuhei TANIKAGA and Yasuo DEGUCHI

(Received June 28, 1962)

The metal ketyls of benzophenone (I), *p*-methylbenzophenone (II), *p,p'*-dimethylbenzophenone (III), *p-tert*-butylbenzophenone (IV), *p,p'*-di-*tert*-butylbenzophenone (V), and dimesityl ketone (VI) were studied by electron spin resonance spectroscopy**. Metalic potassium was used as the alkali metal, and tetrahydrofuran as the solvent. A hyperfine structure was obtained for each spectrum of these ketyls (Fig. 1 (I)—Fig. 6 (VI)).

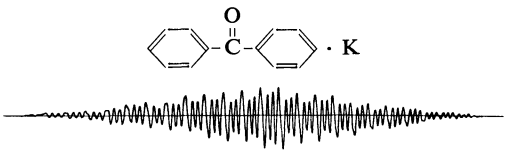


Fig. 1

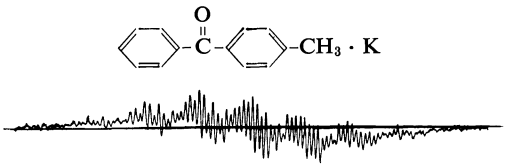


Fig. 2

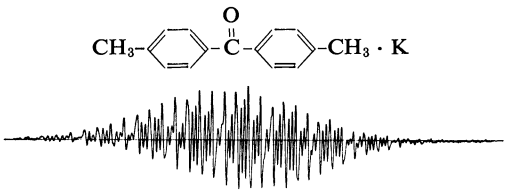


Fig. 3

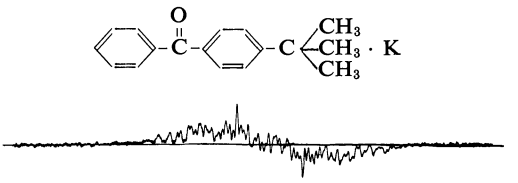


Fig. 4

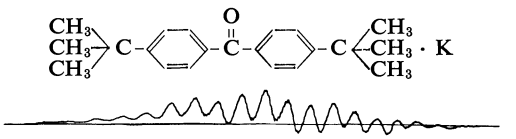


Fig. 5

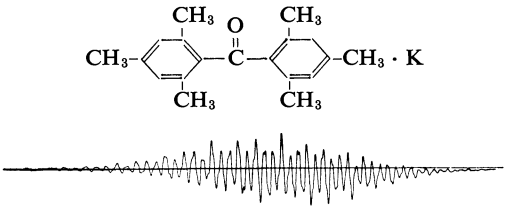
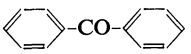
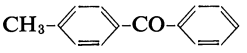
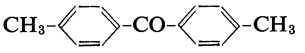
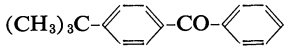
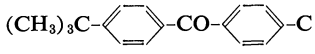
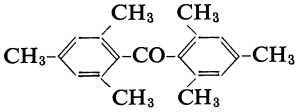


Fig. 6

TABLE I. OVERALL PROTON HYPERFINE SPLITTING OF SPECTRA

Benzophenone derivatives		Number of hydrogen atoms				Factor F	Overall splitting S, gauss	S/F
		o	*m*	*p*	*α*			
	(I)	4	4	2	0	16	24.5	1.54
	(II)	4	4	1	3	17	26.8	1.58
	(III)	4	4	0	6	18	29.1	1.60
	(IV)	4	4	1	0	14	22.2	1.58
	(V)	4	4	0	0	12	19.2	1.58
	(VI)	0	4	0	18	22	33.7	1.54

* The present work was presented at the 15th Annual Meeting of the Chemical Society of Japan, Kyoto, April, 1962.

** A spectrometer, 3B-type. Japan Electron Optics Laboratory Co., Ltd. (Tokyo, Japan) was used.

The present authors found that the molecular symmetry of ketyls has a considerable influence on the total shape of the spectra. Although there has as yet been no explanation for these experimental facts, the present writers are rather inclined to consider that the cause of the poor resolution of the spectra of the ketyls (II, IV) which have different phenyl groups seems to be due to the different contributions of the two phenyl groups to the free electron.

We have not yet been able to assign their hyperfine structures, but there seems to be a relation between the number of hydrogen atoms and the overall proton hyperfine splitting of the spectra, as can be seen from Table I.

Factor F was calculated assuming that the weight of the ortho- and para-hydrogen atoms was 2, and that of meta- and α-hydrogen atoms, 1. For example, in the case of compound I, $F=4\times2+4\times1+2\times2=16$.

The authors wish to thank the Ministry of Education for its grant.

Department of Chemistry
Faculty of Science
Kyoto University
Sakyo-ku, Kyoto

SHORT COMMUNICATIONS

Complex of Boron Fluoride with Olefin on the Low-temperature

By Ryohei NAKANE, Tsunao WATANABE and Osamu KURIHARA

(Received July 2, 1962)

In our recent paper[1] we showed by the measurements of isotopes effect that boron trifluoride can form the complexes with chloro- and chlorodifluoromethane only at the low-temperature. In the present work the possibility of the presence of complexes of boron trifluoride with olefins was examined by the same method and the relation of them with the mechanism of the boron trifluoride catalyzed polymerization reaction is discussed. Propylene was chosen as an olefin, being suitable for our purpose, because it was found against Booth's claim[2] that a well-purified boron trifluoride - propylene mixture is condensed together at $-112°C$ (m. p. of carbon disulfide) without polymerization, but only the passage of moist air through its mixture can initiate polymerization.

We measured the equilibrium constants for isotopic exchange between boron trifluoride gas and boron trifluoride in propylene solution at $-112°C$ and $-96.5°C$ (m. p. of cumen) in a shaking type gas-liquid contactor, used in a previous work[1]. The two phases of boron trifluoride gas and propylene solution of boron trifluoride were kept in a glass flask, which was vigorously shaken in the low-temperature bath

TABLE I. EQUILIBRIUM CONSTANT FOR BORON ISOTOPE EXCHANGE BY BORON TRIFLUORIDE-PROPYLENE SYSTEM

Temp. °C	Mole ratio of propyrene to BF_3 in the liquid phase	Vapor press. mmHg	Equilibrium constant $\left[\frac{^{10}B}{^{11}B}\right]_{liq}/\left[\frac{^{10}B}{^{11}B}\right]_{gas}$
−112	0	300	1.011±0.002
−112	0.05, 1, 3	—	—*
−112	4	95	1.021±0.003
− 96.5	0	(1000)	(1.007)**
− 96.5	0.05, 1, 2.3	—	—*
− 96.5	3.4	400	1.016±0.003
− 96.5	5.3	310	1.016±0.003

* Solid

** Obtained by extrapolation from values at other temperatures

1) R. Nakane and O. Kurihara, *Sci. Papers Inst. Phys. Chem. Research (Tokyo)*, **56**, 161 (1962).

2) H. Booth and D. Martin, "Boron Trifluoride and its Derivatives", John Wiley & Sons, Inc., New York (1949), p 42.

for several hours. The equilibrium constant could be determined by measuring the $^{10}B/^{11}B$ ratio in the gas phase before and after equilibrations on a mass spectrometer, since a large excess of boron trifluoride was used in the liquid phase and hence the isotopic composition in the liquid phase remained practically unchanged throughout the experiments. On warming to room temperature after the experiments, the mixture, when evaporated, leaving only a trace amount of polymer on the vessel wall.

Results are shown in Table I. The equilibrium constant at $-112°C$ on no propylene in the liquid phase was also secured. In this case, isotopic exchange occurs between gaseous boron trifluoride and liquid boron trifluoride as follows;

$$^{10}BF_3(gas) + {}^{11}BF_3(liq) \overset{K}{\rightleftharpoons} {}^{11}BF_3(gas) + {}^{10}BF_3(liq)$$

$$K=\frac{[^{10}BF_3(liq)]}{[^{11}BF_3(liq)]} \Big/ \frac{[^{10}BF_3(gas)]}{[^{11}BF_3(gas)]}$$

$$=1.011\pm0.002 \quad (-112°C)$$

Thus, this constant is identical with the vapor pressure ratio of isotopic molecules, $^{11}BF_3$ and $^{10}BF_3$.

We found that the values of the equilibrium constants were much larger when there was propylene in the liquid, than the value when there was no liquid propylene, as in the case of boron trifluoride-chloromethane and boron trifluoride-chlorodifluoromethane systems. These results show that isotopic exchange occurs between gaseous boron trifluoride and a new liquid compound, being quite different from liquid boron trifluoride, because the equilibrium constant for isotopic exchange is well correlated with the translational, rotational and vibrational energy states of molecules. Boron trifluoride is known to coordinate with many compounds and the equilibrium constants for isotopic exchange between these liquid complexes and gaseous boron trifluoride are always larger than the vapor pressure ratio of isotopic molecules. Therefore, we consider that its new liquid compound is the complex of boron trifluoride with propylene, and isotopic exchange is shown by following equation;

$$^{10}BF_3(gas) + {}^{11}BF_3\cdot CH_2CHCH_3(liq) \overset{K}{\rightleftharpoons} {}^{11}BF_3(gas) + {}^{10}BF_3\cdot CH_2CHCH_3(liq)$$

$$K=\frac{[^{10}BF_3\cdot CH_2CHCH_3(liq)]}{[^{11}BF_3\cdot CH_2CHCH_3(liq)]} \Big/ \frac{[^{10}BF_3(gas)]}{[^{11}BF_3(gas)]}$$

$$=1.021\pm0.003 \quad (-112°C)$$

Although Evans et al.[3] claimed in their investigation on the mechanism of the polymerization that boron trifluoride did not form a stable complex with isobutylene, our result suggests that Evans' conclusion is wrong and the complex, $BF_3\cdot CH_2C(CH_3)_2$, can also exist at low-temperature.

However, these liquid complexes are stable only at low-temperature, because it was found that the solubility of boron trifluoride in propylene solution decreased markedly with the increase in temperature and, for example, boron trifluoride could scarcely be dissolved into liquid propylene even at $-78°C$.

For comparison, the system of boron trifluoride and paraffin such as propane was also investigated and it was found that the two liquids are practically immiscible at $-96.5°C$ or $-112°C$. Therefore the formation of any complex can not be considered.

Thus, we could detect the formation of the stable liquid complexes of boron trifluoride with an unsaturated hydrocarbon such as propylene at the low-temperature, and would like to conclude that these stable complexes have no concern with the mechanism of the polymerization and are not the intermediate products for polymerization, because the polymerization of both propylene and isobutylene can not proceed as long as there is no co-catalyst such as water, albeit the complexes can exist always at the low-temperature.

The Institute of Physical and Chemical Research
Bunkyo-ku, Tokyo

3) A. Evans and M. Polanyi, *J. Chem. Soc.*, 1947, 253.

High Resolution NMR Spectra of Stereoregulated Polyvinyl Alcohol

By Akibumi DANNO and
Naohiro HAYAKAWA

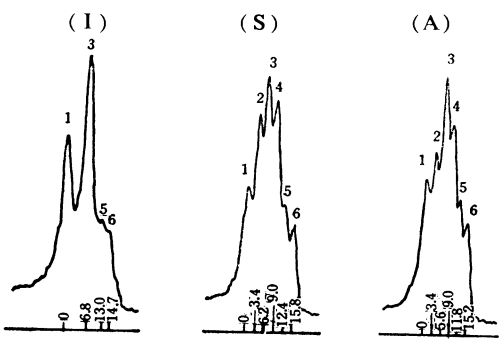
(Received July 19, 1962)

In order to study the stereoregulated structure of polyvinyl alcohol (PVA), the high resolution NMR spectra of PVA dissolved in heavy water (about 3% PVA in weight) were examined. The samples used in the present work were isotactic rich (I), syndiotactic rich (S) and atactic PVA (A). The sample I obtained from poly-*tert*-butyl ether, and S from polyvinyl formate which was polymerized from vinyl formate at $-78°C$. The sample A was prepared from thermally polymerized polyvinyl

acetate. NMR measurements were made with a Varian V-4300-C spectrometer operating at 56.4 Mc.

The spectra of PVA consist of three signals corresponding to the three nonequivallent proton groups, namely, methylene, methine and hydroxyl groups. Among them, the hydroxyl proton signal appears in the lowest magnetic field at room temperature, shifts remarkably to higher magnetic field with increasing sample temperature (about 0.6 p. p. m. over the temperature range from 24 to 110°C). This shift is believed to be assigned to breaking of hydrogen bond[1]. The methine signal is seen in the magnetic field higher than that for hydroxyl signal at room temperature. However, its structure can not be resolved separately from hydroxyl signal in higher temperature, as the shift of hydroxyl signal results an overlapping on the methine signal. Finally, methylene signal appears in the highest magnetic field. Raising the temperature of sample makes the methylene signal narrower, and gives a hyperfine structure above 70°C. It is clear that the above narrowing is due to the more free segmental motion of PVA molecule at higher temperature.

The methylene signals obtained at 110°C show different patterns depending on the structures of the stereoregulated PVA molecules as shwon in Fig. 1. In this figure, the spectrum I, S and A stand for isotactic rich, syndiotactic rich and atactic PVA, respectively. In the isotactic rich PVA the peaks 1 and 3 are predominant, while in the syndiotactic rich PVA other peaks 2, 4 and 6 are also observed. The syndiotactic rich PVA used in the present work was so abundant in isotactic structure that the difference between the spectrum S and A was not so markedly.



Relative line positions measured from the lowest peak, c./sec.

Fig. 1. Spectra of methylene group of stereoregulated PVA at 110°C. The spectrum I, S and A stand for isotactic rich, syndiotactic rich and atactic PVA, respectively.

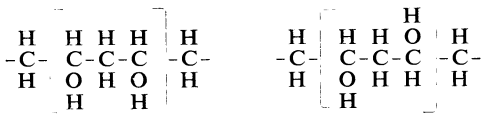


Fig. 2. Structure of the ideal isotactic and syndiotactic PVA.

As shown in Fig. 2, cis- and trans-configurations of a proton and a hydroxyl group around –C–C– chain are most remarkable difference between the isotactic and the syndiotactic PVA molecule as far as ideal structures concern. In a PVA molecule, two protons of a given methylene group are affected both by the spin-spin interaction with the proton of the methine and by the magnetic anisotropic effect of the hydroxyl group[2]. Therefore, it is explained that the differences in both effects mentioned above bring about the difference in hyperfine structures observed. Details of the work will be published in the near future in this journal.

The authours wish to express their heartly thanks to Dr. Hiroyuki Tadokoro and Dr. Masakazu Matsumoto for kind preparation of the stereoregulated PVA samples and also for their helpful discussions.

Division of Radiation Applications
Japan Atomic Energy Research Institute
Tokai, Ibaraki-ken

1) J. A. Pople, W. G. Schneider and H. J. Bernstein, "High-Resolution Nuclear Magnetic Resonance", McGraw-Hill Book Co., New York, (1959), p. 400.

2) M. Karplus, *J. Phys. Chem.*, **64**, 1793 (1961).

Structure of Isojervine[1]

By Tadashi MASAMUNE, Mitsuo TAKASUGI, Hiroshi SUZUKI, Shozo KAWAHARA, Masatoshi GOHDA and Toshi IRIE

(Received July 18, 1962)

Isojervine[2], $C_{27}H_{39}O_3N$, an unexpected product obtained on acid treatment of pseudojervine or jervine[3] (I), has received no generally accepted structural assignment. We

1) When we have completed this work, Dr. O. Wintersteiner, the Squibb Inst., and Prof. W. G. Dauben, California Univ., kindly informed us that they have arrived at the same structure as ours.

2) W. A. Jacobs and L. C. Craig, *J. Biol. Chem.*, 155, 565 (1944).

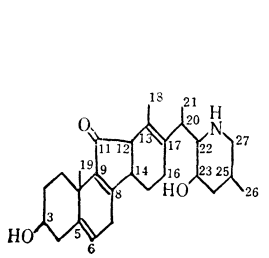
3) J. Fried, O. Wintersteiner, M. Moore, B. M. Iselin

wish to report that the structure II is consonant with all chemical and spectral data for isojervine[4], which is a secondary base with two acylable hydroxyl groups and one $\alpha\beta$-unsaturated keto group. IR[5], 1684, 1630 and 1063 cm^{-1}, UV[4], 330 mμ (ε, 250), 252 mμ (inflexion, ε, 2900) and end absorption (ε, 9000 at 211 mμ).

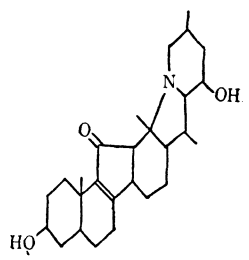
Reduction of II with lithium and methanol in liquid ammonia at $-70°C$ has now afforded α-dihydrojervinol[4], thus establishing the skeleton and the position of all oxygen-containing functional groups of II.

The location of a double bond at C_5–C_6 was confirmed by the Oppenauer oxidation of II with cyclohexanone and aluminum isopropoxide to isojervone[6], m. p. 112~114°C, $[\alpha]_D$ +140° (ethanol), IR, 1682, 1642 and 1620 cm^{-1}, UV, 234 mμ (ε, 22000). Hydrogenation of II over platinum in acetic acid resulted in preferential reduction of the C_5–C_6 double bond to yield dihydroisojervine (III), m. p. 153~155°C (as hydrate) and 171.5~172.5°C (after drying), IR, 1679, 1625 and 1040 cm^{-1}, UV, 238 mμ (ε, 9400); that is, the Oppenauer oxidation of III produced dihydroisojervone, m. p. 108~110°C, IR, 1712, 1687 and 1629 cm^{-1}, UV, 238 mμ (ε, 9900), only in a low yield. Hydride reduction of II yielded isojervinol (IV), m. p. 210~211°C, which exhibited only a weak end absorption (ε, 6400 at 212 mμ). The spectroscopic behavior of II, III and IV completely paralleled that of 1-acetyl-1, 4-cyclohexadiene[7], suggesting that another double bond would exist at C_8–C_9. The NMR spectral data (deuterochloroform, 60 Mc.) supported this view; the C_{19}-methyl signal of triacetate (IIa) of II appeared at the lower field (8.68 τ) as compared with that (8.97 τ) of diacetate (Ia) of I. The observed shift would be explained by assuming the field due to magnetic anisotropy not only of the C_8–C_9 double bond itself[8,9] but also associated with interaction[7] between the C_5–C_6 and C_8–C_9 double bonds. The C_{19}-methyl signals of triacetate, m. p. 203~205°C, of III and of diacetyl-Δ^{13}-jervine[5] appeared at the normal positions (8.98 and 8.87 τ) and the ultraviolet absorptions of these compounds were devoid of anomalies as observed with II.

The NMR spectrum of IIa showed a broad multiplet centered at 4.53 τ due to *one* olefinic proton (C_6-hydrogen) and a sharp singlet of methyl group attached to olefinic carbon at 8.06 τ instead of that at 7.77 τ due to C_{18}-methyl of Ia. The Birch reduction of III led to reduction of the C_8–C_9 double bond to yield two crystalline substances, α-tetrahydroisojervine (V), m. p. 147~149°C, IR, 1731 cm^{-1}, and β-isomer (VI), m. p. 138~142°C (chloroform addition compound), IR, 1741 cm^{-1}. However, neither triacetate, m. p. 179~182°C, of V, nor the corresponding β-isomer, m. p. 168~168.5°C, was found to be identical with 22, 27-imino-Δ^{17-20}-jervene-3, 23-diol-11-one triacetate prepared by Wintersteiner et al.[10] Treatment of III with 1 N potassium *t*-butoxide in refluxing *t*-butanol[11] under nitrogen for an hour yielded a crystalline compound (VII), m. p. 142~144°C, IR, 1670, 1621 and 1036 cm^{-1}, chloroform, 1678 and 1630 cm^{-1}, UV 239 mμ (ε, 8600). It was a *weak* tertiary base; (1) the pK_a value of VII, II and III were 6.12, 6.92 and 7.08 in 50% ethanol. (2) Acetylation of VII with acetic anhydride and pyridine on steam bath for 3 hr. gave exclusively an amorphous *O,O*-diacetate, IR, chloroform, 1725, 1685 and 1632 cm^{-1}, pK_a, 4.47. In view of the analogous examples[12], the formula VII was assigned to the m. p. 144°C compound. Similar reactions were observed with V and VI. Apparently these reactions involve migration of C_{13}-C_{17} double bond to $\alpha\beta$-position of the carbonyl group followed by cyclization. Thus, the formula II is the most favorable structure of isojervine.



(II)



(VII)

We express our sincere thanks to Dr. T. Ikegami, Tohoku University, and Dr. K. S. Brown, University of Wisconsin, for the NMR spectra.

Department of Chemistry
Faculty of Science
Hokkaido University, Sapporo

and A. Klingsberg, *J. Am. Chem. Soc.*, **73**, 2970 (1951).

4) W. A. Jacobs and C. F. Heubner, *J. Biol. Chem.*, **170**, 635 (1947); W. A. Jabobs and Y. Sato, ibid., **181**, 55 (1949).

5) B. M. Iselin and O. Wintersteiner, *J. Am. Chem. Soc.*, **77**, 5318 (1955). Unless otherwise stated, IR spectra were taken in Nujol and UV spectra in ethanol.

6) All new compounds reported in this paper had acceptable carbon, hydrogen and nitrogen analyses.

7) E. A. Braude, E. R. H. Jones, F. Sondheimer and J. B. Toogood, *J. Chem. Soc.*, **1949**, 607.

8) R. F. Zürcher, *Helv. Chim. Acta*, **44**, 1380 (1961).

9) J. S. G. Cox, E. O. Bishop and R. E. Richards, *J. Chem. Soc.*, **1960**, 5118.

10) O. Wintersteiner, M. Moore and B. M. Iselin, *J. Am. Chem. Soc.*, **76**, 5609 (1954).

11) R. Hirschmann, C. S. Snoddy, Jr., C. F. Hiskey and N. L. Wendler, ibid., **76**, 4013 (1954).

12) O. Wintersteiner and M. Moore, ibid., **78**, 6193 (1956).

Electrolytically Regenerated Ceric Sulfate for the Oxidation of Organic Compounds. I. Oxidation of p-Xylene to p-Tolualdehyde

By R. RAMASWAMY, M. S. VENKATACHALAPATHY and H. V. K. UDUPA

(Received April 15, 1961)

The use of ceric sulfate as "oxygen carrier" is described in many electro-organic oxidation processes[1-3]. These carriers act as depolarizers and ceric sulfate belongs to the group of ionic oxidizing agents which act only as electron-abstracting agents[21]. The reaction of the oxidized reagent with the organic compound to give the desired product is also expected to take place. If the latter is true, it would be a most convenient and economical procedure[4] to carry out the oxidation reaction in two stages, the first stage of electrolytically oxidizing cerous sulfate into ceric sulfate and the second stage of reacting the ceric sulfate with the organic compound to obtain the desired product. The oxidation of trivalent to tetravalent ceric sulfate[5-7] at a lead dioxide anode for the use of oxidation of xylenes and the electrolytic regeneration of ceric sulfate for further use have therefore been studied. Such a two-stage process has recently been developed in this laboratory, using manganous sulfate for the oxidation of aromatic hydrocarbons[11,12].

Kinetic studies of the oxidation of organic compounds by ceric sulfate have been described in literature[8-10,20]. A kinetic study of the oxidation of *p*-xylene by manganic sulfate was reported[11], but no kinetic study of the reaction between *p*-xylene and ceric sulfate appears to have been carried out. Ceric sulfate brings about controlled oxidation of *p*-xylene to *p*-tolualdehyde and a kinetic study of this oxidation using Ce^{4+} cation in sulfuric acid is described in the present article.

Experimental

Electrolytic Cell.—A glass trough of diameter of 12 cm. and height of 6.5 cm. with a suitable perspex lid carrying four holes for the electrodes, diaphragms, and thermometer respectively was used as electrolytic cell. Cylindrical lead anode with an effective area of 40 cm^2 was used as rotating anode. In the case of divided cells, two ceramic diaphragms of outer diameter of 2.5 cm. and height of 10 cm. and two narrow lead strips of 2 cm. wide and 14 cm. long were used as cathodes. In the case of investigating the use of stationary electrode with the same cylindrical lead anode, a glass stirrer was used for effective agitation in the cell. The anode potential was measured by Crompton potentiometer against a saturated calomel electrode. The other experimental conditions employed are given in the tables.

Analysis.—When electrolysis was over, 5 cc. of the oxidized solution was added to a known volume (20 cc.) of N/10 ferrous sulfate solution and then the excess of ferrous sulfate was titrated with a standard permanganate solution. In the case of electrolysis in the state of suspension, a known weight of the paste was added to excess ferrous sulfate solution and titrated in the same way and the current efficiency was calculated from the titre values knowing the total weight of the paste.

Kinetic Study of the Oxidation of *p*-Xylene with Ceric Sulfate

Materials.—Distilled *p*-xylene (b. p. 138°C) was used in the study. Cerous sulfate and all other chemicals were of A. R. quality. The ceric sulfate was prepared by the anodic oxidation of cerous sulfate in sulfuric acid as described before.

Measurement of Reaction Kinetics.—Ceric sulfate solution (350 cc.) in 5% sulfuric acid was taken in a three-necked flask and maintained at a desired temperature in a thermostat. Forty cc. of *p*-xylene was added to the flask containing ceric sulfate. A blade-type stirrer with a constant r.p.m. of 200 was employed to ensure identical agitation conditions. No attempt has been made to study the reaction in the absence of air. After five minutes of starting the reaction, stirring was stopped and the emulsion allowed to clear (30 sec.)

1) S. Glasstone, "Introduction to Electrochemistry", D. Van Nostrand Co. Inc., New York (1947), p, 512.
2) C. L. Mantell, "Industrial Electrochemistry", 3rd Ed., McGraw-Hill Co., New York (1950), p. 104.
3) C. J. Brockmann, "Electro-Organic Chemistry", John Wiley & Sons, New York (1926), p. 14.
4) M. S. Venkatachalapathy, R. Ramaswamy and H.V. K. Udupa, Indian Pat. 62379, 62426.
5) Hengstenberger, "Electrolytic Oxidation of Cerous Salts and Chlorination Experiments in Contact with Cerous Chloride", Munisch, Germany, J. Feller (1947).
6) G. Smith, G. Frank and A. E. Kott, *Ind. Eng. Chem., Anal. Ed.*, **12**, 268 (1940).
7) J. L. Culbertson and C. Rutkowski, *Trans. Electrochem. Soc.*, **81**, 185 (1942).
8) J. Shorter and C. Hinshelwood, *J. Chem. Soc.*, **1950**, 3425, 3276.
9) S. V. Gorbarchev and Ya. I. Vabel, *Chem. Abstr.*, **49**, 3630 (1955).
10) Shas Min. Chzlcov and S. V. Garbarchev, ibid., **52**, 15213 (1958).
11) M. S. Venkatachalapathy, R. Ramaswamy and H. V. K. Udupa, *Bull. acad. Polon. Sci.*, **7**, No. 9, 629 (1959).
12) M. S. Venkatachalapathy, R. Ramaswamy and H. V. K. Udupa, Proc. Symposium on "Electrolytic Cells", Central Electrochemical Research Institute, Karaikudi (India) (1961), p. 147.

and an aliquot part (2 cc.) was pipetted out almost from the bottom of the flask and added to excess ferrous sulfate and then back titrated against standard potassium permanganate. Determinations were carried out at 90, 85, 80 and 75°C in the manner just described and with the experimental data curves were drawn for log C vs. time where C indicates the concentration of ceric sulfate. The slopes of all these straight lines in Fig. 1 are within experimental error. A blank was run at 90°C to make suitable corrections, but it was found that there was no appreciable decomposition of ceric sulfate during 25 min.

Reaction of *p*-Xylene with Ceric Sulfate.—Ceric sulfate solution or paste was taken in a three necked flask fitted with a mercury seal and stirrer, reflux condenser and thermometer. Required volume of *p*-xylene was added and the flask kept in the thermostat so that the oxidation could be carried out at 80°C. The contents of the flask were well agitated until the reaction was over.

Isolation of Aldehyde. — After cooling, the *p*-xylene layer was separated from the paste or solution and washed well with water to remove any sulfuric acid. Then the layer was treated with a saturated solution of sodium bisulfite to get *p*-tolualdehyde addition compound which on decomposition with soda ash and steam distillation, gave *p*-tolualdehyde.

Purification of used Electrolyte.—The used electrolyte was well extracted with xylene to remove all organic materials and after separation of xylene-layer the electrolyte was distilled under reduced pressure. The distillation was continued until a few cc. of water (5~15 cc.) was collected and the electrolyte after being made up to the original strength was recycled to the cell for regeneration of ceric sulfate, thereby making the process continuous and cyclic.

Results

The relationship between current efficiency and current density using stationary anode is shown in Fig. 2. Figure 3. shows the variation of anode potential with current density. The current efficiency obtained varying the concentration of sulfuric acid is given in Table I. Table II gives the current efficiency obtained using a divided or undivided cell. Table III gives the current efficiency obtained using a suspension of cerous sulfate in the electrolyte. The influence of anode material on current efficiency and yield is given in Table IV.

Values of the rate constants obtained in the kinetic study of the oxidation of *p*-xylene are given in Table V. Similarly the results of chemical oxidation of *p*-xylene by ceric sulfate are given in Table VI. Table VII includes the

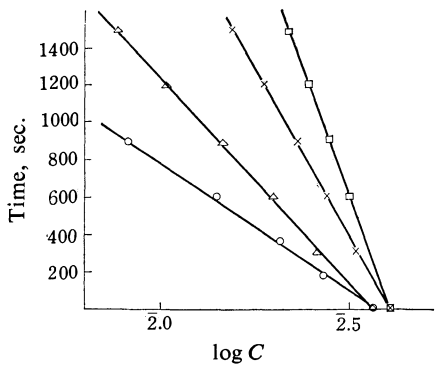


Fig. 1. Plot of log C against time (in sec.). ○, 90°C; △, 85°C; ×, 80°C; □, 75°C

TABLE I. INFLUENCE OF THE CONCENTRATION OF SULFURIC ACID ON THE CURRENT EFFICIENCY

Temp., 30°C; anode, PbO_2 on Pb; anolyte, 20 g. cerous sulfate in 400 cc. of sulfuric acid; catholyte, 5% sulfuric acid; cathode, lead strip; current density, 1 amp./dm²; r. p. m. of the electrode, 3000.

Concn. of sulfuric acid %	Cell voltage V.	Current efficiency %
3	3.6	83.5
10	3.0	79.8
20	2.9	73.8
30	2.8	43.0

TABLE II. CURRENT EFFICIENCY WITH DIVIDED AND UNDIVIDED CELL

Concentration of sulfuric acid in anolyte, 10%; interelectrode distance, 3 cm.; cell voltage, 3~3.2 V.; current density, 1 amp./dm²; cathode current density in undivided cell, 30 amp./dm². All other conditions same as it Table I.

Type of cell	Motion of anode	Current efficiency, %
Undivided	Stationary	60.5
Divided	Stationary	69.9
Undivided	Rotated	69.1
Divided	Rotated	75.4

TABLE III. INFLUENCE OF SUSPENSION OF CEROUS SULFATE IN SULFURIC ACID ON THE CURRENT EFFICIENCY

Concentration of sulfuric acid, 5%; temp. 35°C; stationary anode; undivided cell; anode current density, 2 amp./dm²; cathodic current density, 30 amp./dm²; current strength, 3.4 amp.

Nature of electrolyte	Cell voltage V.	Current efficiency %	Duration of electrolysis hr.
100 g. cerous sulfate suspended in 250 cc. of sulfuric acid	4.0	66.1	1.03
150 g. cerous sulfate suspended in 250 cc. of sulfuric acid	4.1	59.7	1.51
200 g. cerous sulfate suspended in 250 cc. of sulfuric acid	4.2	57.3	2.06

TABLE IV. EFFECT OF ANODE MATERIAL ON THE CURRENT EFFICIENCY AND YIELD

Stationary anode; concentration of sulfuric acid, 5%; undivided cell; cell voltage, 2.9~3.0 V.; current density, 1 amp./dm^2.
All other conditions same as in Table I.

Anode material	Current efficiency %	Duration hr.	Yield %
Lead	67.8	1	67.8
	49.0	2	98.0
Antimonial lead	50.5	1	50.0
PbO_2 on graphite	71.6	1	71.6
	54.0	1.83	98.0
Lead	65.1*	1	65.0
Lead	62.8*	1	63.0
Lead	62.0*	1	62.0

* Results obtained in the first, second and third regeneration experiments respectively.

TABLE V. RATE CONSTANTS EOR THE OXIDATION OF *p*-XYLENE WITH CERIC SULFATE

Temp. °C	$1/T$ °K$\times 10^3$	$k\times 10^4$	$\log k$
90	2.755	16.89	$\bar{3}.2276$
85	2.793	10.47	$\bar{3}.0199$
80	2.833	6.33	$\bar{4}.8016$
75	2.874	4.03	$\bar{4}.6053$

results of the effect of cathodic reduction of ceric sulfate.

Discussion

The results indicate that the anodic oxidation of cerous sulfate in sulfuric acid is dependent upon a number of factors. Figure 2 shows that high current efficiencies are obtained at low current density values. The anode potential rapidly increases with current density as seen from Fig. 3. The decrease of current efficiency with increase of current density is therefore to be attributed to simultaneous oxygen evolution taking place at higher anode potentials. Results in Table I indicate that the concentration of sulfuric acid exerts a marked influence on the current efficiency because of the above reason. The difference in current efficiency obtained with divided and undivided cells is shown in Table II. The application of the rotating anode technique gave improved current efficiency due to the decrease of polarization. In subsequent experiments only stationary anodes were employed as the results obtained were satisfactory for the present purpose. The difference in current efficiency between divided and undivided cell is not large and the use of diaphragm can therefore be avoided by employing high cathodic current density.

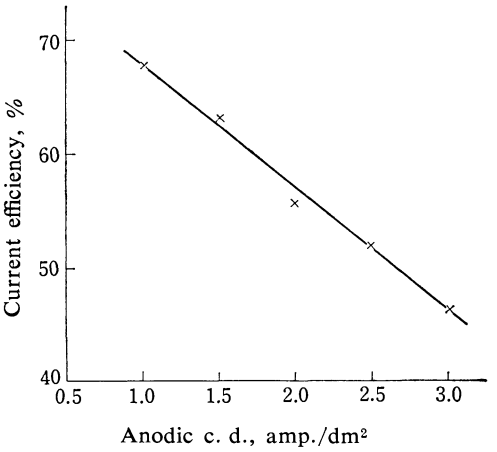


Fig. 2. Current efficiency against current density.

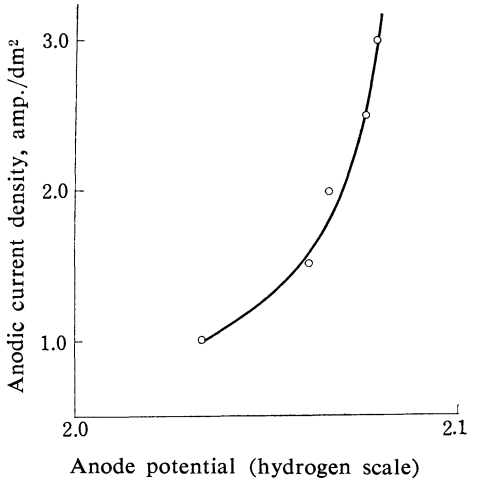


Fig. 3. Current density against anode potential (hydrogen scale).

Technique of avoiding the use of diaphragms in electrolytic cells is an important aspect to be considered on a practical scale and should lead to energy economics in addition to making cell design simple. Although this fact is known in developing practical scale production techniques, it is necessary to examine various aspects of the reaction itself. In the oxidation of manganous to manganic sulfate, evidence has been found for the existence of trivalent manganese in the complex form $H_2[Mn_2(So_4)_4]$. The reduction of the trivalent manganese in the anion $[Mn_2(So_4)_4]^{2-}$ at the cathode may be prevented especially at high current densities so that an undivided[12,13] cell can be advantageously employed. The direct reduction of the Mn^{+3} to Mn^{+2} at the cathode has thus been found to be negligible, especially when

13) M. S. Venkatachalapathy, R. Ramaswamy and H. V. K. Udupa, *Curr. Sci. (India)*, **28**, 63 (1959).

TABLE VI. RESULTS OF OXIDATION OF *p*-XYLENE BY CERIC SULFATE.PASTE
Temp., 80°C; 40 cc. of *p*-xylene was added in each case

Strength of sulfuric acid	Current passed	Quantity of ceric sulfate	Current efficiency for Ce^{3+} to Ce^{4+}	*p*-Tolualdehyde formed	Oxidation efficiency based on ceric sulfate used	Overall current efficiency for aldehyde formation
%	amp.-hr.	g.	%	g.	%	%
20	5.3	32.00	47.1	1.4	54.2	23.3
5	7.0	51.3	59	2.1	50.7	26.7
5	10.5	78.00	60	3.15	50.0	30.0

TABLE VII. EFFECT OF CATHODIC REDUCTION ON CERIC SULFATE
Catholyte, 4.3 g. of ceric sulfate in 300 cc. of 5% sulfuric acid; divided cell; lead electrodes, temp., 30°C

Current density amp./dm²	Current efficiency %
50	4.9
30	5.3
15	12.3
5	31.3

the ratio of anode area to cathode area is sufficiently high. In a similar manner, ceric sulfate is also known to exist as the complex[6,14] sulfato-ceric acid, $H_4[Ce(So_4)_4]$ so that the reduction of Ce^{4+} in this anion should be prevented. The effect of cathodic reduction of ceric sulfate can be seen from Table VII and it is clear that the efficiency of reduction is very much affected, especially when the cathodic current density is above 15 amp./dm².

The results given in Table III are quite interesting and reveal the fact that the current efficiency remains more or less the same even when a cerous sulfate suspension in sulfuric acid is used for the oxidation. The portion of cerous sulfate in solution gets oxidized to ceric sulfate and a corresponding amount of the former dissolves in the electrolyte from the suspended state. However, when the solution becomes saturated with ceric sulfate, further formation of the same leads to a separation of the salt giving finally a suspension of ceric sulfate in the electrolyte. The effect of anode material on the current efficiency is shown in Table IV and it indicates that either lead dioxide electrodeposited on graphite[15] or lead dioxide on lead electrode can be used. By passing excess current, the yields obtained are almost theoretical even though the current efficiency bared on the ceric sulfate is somewhat lowered.

The electrochemical oxidation of *p*-xylene[16-19] in a single stage process using ceric sulfate as oxygen carrier has been reported to give very poor current efficiency. The oxidation carried out in two stages gives overall current efficiency of 23 to 30% as seen from Table VI, even though the efficiency of the oxidation of *p*-xylene with reference to ceric sulfate is more than 50%.

Energy of Activation for the Oxidation of *p*-Xylene by Ceric Sulfate

The reaction appears to be essentially homogenous, the dissolved *p*-xylene mainly taking part in the reaction. The efficient agitation was helpful in maintaining the solution saturated with *p*-xylene.

Figure 4 shows plot of log k against $1/T$ (°K). From the slope, the calculated apparent energy of activation is 23840 cal./mol., which would be inclusive of the effect of change of solubility of *p*-xylene in the medium with temperature.

Oxidation of hydrocarbons generally requires severe conditions and is usually retarded by bases, but is catalyzed by acids. The mechanism appears to be a single electron transfer reaction

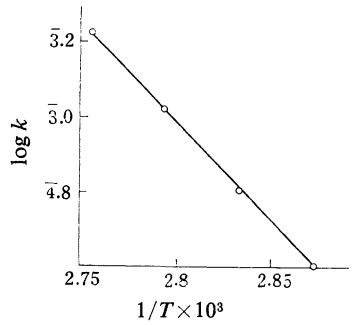
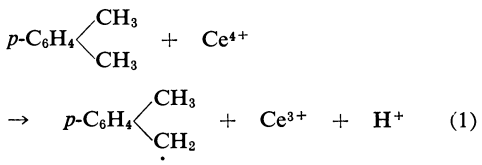


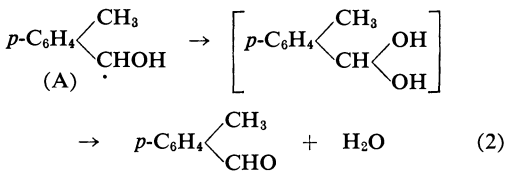
Fig. 4. Plot of log k against $1/T\times10^3$.

14) E. G. Jones and F. G. Soper, *J. Chem. Soc.*, **1935**, 802.
15) K. C. Narasimham and H. V. K. Udupa, Proc. Symposium on "Electrolytic Cells", Central Electrochmical Research Institute, Karaikudi (India) (1961), p. 22.
16) H. D. Law and F. M. Perkin, *Trans. Faraday Soc.*, **1**, 32 (1905).
17) F. Fichter and R. Stocker, *Ber.*, **47**, 2003 (1914).
18) M. S. Venkatachalapathy and H. V. K. Udupa, Proc. Symposium on "Electrolytic Cells", Central Electrochemical Research Institute, Karaikudi (India) (1961), p. 204.
19) H. V. K. Udupa and M. S. Venkatachalapathy, Indian Pat. 66175.
20) J. S. Littler and W. A. Watters, *J. Chem. Soc.*, **1960**, 2767.
21) W. A. Waters, "Oxidation Processes", Vol. IV, Chap. 12, Organic Chemistry by Gilman, John Wiley & Sons, New York (1953).

and by the action of tetravalent ceric ion, exclusive oxidation of one of the methyl groups takes place and the initial attack may occur by hydrogen abstraction according to the reaction 1 given below:



The reaction of the substituted benzyl radical then takes place to yield tolylcarbinol which again reacts with Ce^{4+} to give the radical A which immediately reacts to give *p*-tolualdehyde as in Eq. 2.



Summary

1. The current efficiency for the oxidation of cerous sulfate in sulfuric acid at a lead dioxide in an undivided cell was generally found to be 70%.

2. By using a paste of cerous sulfate in sulfuric acid, ceric sulfate reagent is obtained in a concentrated form.

3. A kinetic study of the oxidation of *p*-xylene by ceric sulfate is described and apparent energy of activation is calculated.

4. The process of oxidation of *p*-xylene to *p*-tolualdehyde is made cyclic and continuous by regeneration of ceric sulfate at a lead dioxide anode.

The authors thank Professor K. S. G. Doss, Director of the Institute for his keen interest in this investigation. They also thank Shri K. C. Narasimham of this Institute for preparing graphite substrate lead dioxide anode.

Central Electrochemical Research Institute
Karaikudi-3, India

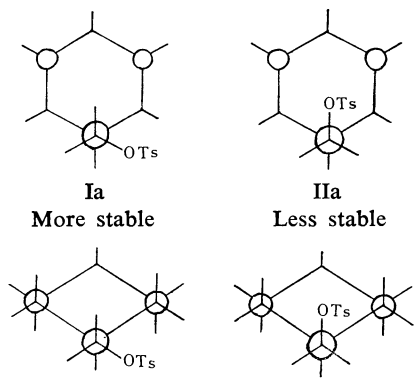
Conformational Analysis of Isomeric 4-Substituted Cyclohexylcarbinyl p-Tosylates

By Nobuo Mori

(Received May 22, 1961)

In a previous work[1] which was carried out to investigate the difference in reactivity between the axial and the equatorial *p*-toluenesulfoxymethyl group in a cyclohexane system, it was found that *cis*-4-methylcyclohexylcarbinyl *p*-tosylate was solvolyzed more rapidly in acetic acid and more slowly in ethanol than the trans-isomer. From the observed rates and the consideration for their possible conformations, it was suggested that conformation Ia rather than IIa should be favorable for the axial *p*-toluenesulfoxymethyl group and conformation Ie rather than IIe for the equatorial one.

However, the above tosylates are unsuitable to provide a precise solution for the above problem, since each of them may exist in two interconvertible chair-conformations, the conformations and their relative rates of reaction must be taken into account estimating reactivity. Consequently, it is desirable to study a pair of diastereoisomeric compounds whose chair conformations are entirely pure.



Ia More stable — IIa Less stable

Ie More stable — IIe Less stable

Fig. 1

1) N. Mori, This Bulletin, **34**, 1299 (1961).

A detailed study has now been made of solvolysis of *cis*- and *trans*-4-*t*-butylcyclohexylcarbinyl *p*-tosylate under the assumption that the *t*-butyl group is more bulky than the *p*-toluenesulfoxymethyl group so that it is entirely restricted in the equatorial orientation and exerts no direct polar or steric effect across the cyclohexane ring, as in the case of *t*-butylcyclohexyl *p*-tosylates[2,3].

The results obtained show that the *cis*-*t*-butylcyclohexyl compound with an axial toluenesulfoxymethyl group is solvolyzed more rapidly by a factor of 4 in acetic acid and more slowly by a factor of 0.5 in ethanol than the trans-form with an equatorial toluenesulfoxymethyl group and the free energy difference ($e-a$) is $-1.7\sim-1.8$ kcal./mol., which is surprisingly almost equal to $-1.6\sim-1.8$ kcal./mol.[4] for the methyl group and which supports the assumption that the *t*-butyl group is entirely restricted in the equatorial orientation.

Experimental

Samples. — *cis*- and *trans*-4-*t*-Butylcyclohexylcarbinyl *p*-tosylate were prepared from the corresponding *cis*- and *trans*-4-*t*-butylcyclohexylcarbinols according to the method[5] previously reported by the author. The former melted at 95~95.5°C and the latter at 84°C.

Acetolysis of Cyclohexylcarbinyl *p*-Tosylate.— Cyclohexylcarbinyl *p*-tosylate[1] (6 g.) and an approximately equivalent amount of anhydrous sodium acetate in acetic acid (50 cc.) in a sealed ampoule were heated at 110°C for 60 hr. The reaction mixture was neutralized with sodium carbonate and extracted with ether. After drying, the ether solution was concentrated and the residue was heated with a methanolic sodium hydroxide solution for a short period. The mixture was evaporated and extracted with ether, and the ether extract was washed with water, dried and distilled. The distillation gave only one fraction (2 g., 80% yield) boiling at 89~90°C/19 mmHg and having $n_D^{21}=1.4638$, which was identical with cyclohexylcarbinol having b. p. 91°C/18 mmHg and $n_D^{20}=1.4649$. The above methanol distilled out, on addition of a salt solution, deposited an oily product (ca. 40 mg., 1.5% yield), which absorbed bromine and was therefore probably methylenecyclohexane boiling at 103°C.

Procedure for Rate Measurements. — Solvolysis was followed in ethanol (98.5% by weight) and in acetic acid containing a slight excess of acetic anhydride to 20~50% completion at 99.8±0.1°C or to 40~60% completion at 110±0.1°C by the usual ampoule technique[6] and first order rate constants calculated were steady to ±3% in the acetolysis and to ±5% in the ethanolysis. Table I lists the data for a typical run with *cis*-4-*t*-butylcyclohexylcarbinyl *p*-tosylate at 99.8°C in acetic acid.

Table I. Acetolysis of *cis*-4-*t*-butylcyclohexylcarbinyl *p*-tosylate at 99.8°C

Time sec.	Tosylate 10^2 mol./l.	$k_1\times10^5$/sec.
0	1.550	
5400	1.450	1.23
9000	1.385	1.28
12600	1.326	1.23
16200	1.279	1.24
19800	1.219	1.21
22200	1.180	1.23
25200	1.144	1.20
28800	1.100	1.20
	Mean	1.23

Unsubstituted and 4-methyl substituted cyclohexylcarbinyl tosylates[1] previously used were also solvolyzed at 110°C. Heats and entropies of activation were calculated by means of the equation given by Eyring[7].

The rate constants obtained are summarized in Table II, along with those of some other primary alkyl *p*-tosylates for comparison.

Discussion

Behavior in Solvolysis.—Since unsubstituted and substituted cyclohexylcarbinyl *p*-tosylates are regarded as members of a β-branched primary alkyl series, a similarity of behavior in solvolysis would be expected between these *p*-tosylates and, for example, isobutyl *p*-tosylate. In fact, Table II shows that the rates and $\Delta H^{\neq}$ and $\Delta S^{\neq}$ values of acetolysis of all cyclohexylcarbinyl *p*-tosylates used in the present work agree substantially with those of primary alkyl *p*-tosylates such as ethyl and isobutyl *p*-tosylate[8]. Further, an upward trend in rate as going from acetic acid to ethanol is not only observed for the former tosylates except *cis*-*t*-butylcyclohexycarbinyl tosylate, but also similarly for the latter tosylates, as shown in Table III. Such an upward trend in the rate attending the solvent change has not been found for secondary alkyl *p*-tosylates in general as well as cyclohexyl *p*-tosylates, while for these tosylates a downward trend in rate is observed which probably arises from the electron repelling inductive effect of α-alkyl substituents. Additionally, the absence of such α-substituents would be expected to result in lower acetolysis rates (10^{-5}/sec. at 100°C) of the primary alkyl and the cyclohexylcarbinyl *p*-tosylates, as compared

2) S. Winstein and H. J. Holness, *J. Am. Chem. Soc.*, **77**, 5562 (1955).
3) E. L. Eliel and C. A. Lukach, ibid., **79**, 5986 (1957).
4) M. Newman, "Steric Effects in Organic Chemistry", John Wiley and Sons, Inc., New York, N. Y. (1956), p. 18.
5) N. Mori, This Bulletin, **34**, 1567 (1961).
6) N. Mori, ibid., **33**, 1144 (1960).
7) S. Glasstone, K. J. Laider and H. Eyring, "The Theory of Rate Processes", McGraw-Hill Book Co., Inc., New York, N. Y. (1941), p. 196.
8) S. Winstein and H. Marshall, *J. Am. Chem. Soc.*, **74**, 1120 (1952).

TABLE II. SUMMARY OF SOLVOLYSIS RATES

4-Substituent	Solvent	Tosylate 10^2 mol./l.	Temp. °C	$k_1 \times 10^5$/sec.	$\Delta H^{\neq}$ kcal./mol.	$\Delta S^{\neq}$ e. u.
cis-t-Bu	EtOH	1.55	99.8	0.935	27.9	−7.1
	EtOH	1.30	110	2.48		
	AcOH	1.55	99.8	1.23		
	AcOH	1.55	110	3.35		
trans-t-Bu	EtOH	1.55	99.8	1.85	27.1	−12
	EtOH	1.30	110	4.45		
	AcOH	1.55	99.8	0.290		
	AcOH	1.40	110	0.768		
cis-Me	EtOH	1.79	99.8	1.28[1]	26.1	−13
	AcOH	1.78	99.8	0.723[1]		
	AcOH	1.40	110	1.85		
trans-Me	EtOH	1.79	99.8	1.83[1]	26.8	−12
	AcOH	1.81	99.8	0.298[1]		
	AcOH	1.40	110	0.782		
H	EtOH	1.60	99.8	1.40[1]	27.3	−11
	EtOH	1.64	110	2.97		
	AcOH	1.58	99.8	0.378[1]		
	AcOH	1.64	110	1.00		
EtOTs[8]	AcOH	3.8~4.3	99.6	0.847	24.4*	−16.7
iso-BuOTs[8]	AcOH	2.5~2.8	99.7	0.379	28.2*	−8.0

* Value at 75°C

TABLE III. RELATIVE RATES

4-Substituent	EtOH/AcOH		AcOH	EtOH	AcOH	EtOH
	99.8°C	110°C	99.8°C		110°C	
cis-t-Bu	0.76	0.74	4.23	1.00	4.36	1.00
cis-Me	1.77	—	2.49	1.37	2.41	—
H	3.7	3.0	1.30	1.50	1.30	1.20
trans-Me	6.1	—	1.03	1.95	1.02	—
trans-t-Bu	6.4	5.8	1.00	1.97	1.00	1.78
EtOTs	39*					
iso-BuOTs	6.2*					
neo-PentOTs	0.28*					

* Values at 75°C (lit. 8)

to those (10^{-3}/sec. at 100°C) of the secondary alkyl and the cyclohexyl *p*-tosylates.

In view of the result to be published in a subsequent paper that rates of acetolysis of isomeric 1, 2-bis-*p*-toluenesulfoxymethylcyclohexanes are not influenced by the presence of sodium acetate, the acetolysis of the cyclohexylcarbinyl *p*-tosylates is essentially of the unimolecular type involving a carbonium ion. Further, the acetolysis of cyclohexylcarbinyl *p*-tosylate gave predominantly one substituted product with a very small amount of olefin (see Experimental). This fact means that the acetolysis of the isomeric cyclohexylcarbinyl tosylates probably consists substantially of a substitution reaction while an elimination reaction is practically of unimportance. The ethanolysis of these compounds also may mainly consist of a substitution reaction. This expection is also supported by the fact[9] that bimolecular reaction of dimethanesulfonates of *cis*- and *trans*-1, 3-dihydroxymethylcyclohexanes with sodium iodide in acetone gives the corresponding *cis*- and *trans*-diiodide in 41 and 94% yield, respectively, and hydrolysis of the above two dimethanesulfonates in aqueous potassium hydroxide solution gives the corresponding *cis*- and *trans*-dicarbinol in a major yield (70% or more) and 4-methylenecyclohexylcarbinol in a minor yield (ca. 7%).

9) G. A. Haggis and L. N. Owen, *J. Chem. Soc.*, **1953**, 404.

Table IV. Relative rates of cis/trans

4-Substituent	99.8°C		110°C	
	EtOH	AcOH	EtOH	AcOH
t-Bu	0.51	4.2	0.55	4.3
Me	0.69	2.4	—	2.4

From Tables III and IV in which relative rates are shown, it will be seen that behavior in solvolysis of *cis-t*-butylcyclohexylcarbinyl tosylate in different solvents is essentially different from that of the trans-isomer. That is to say, the cis-form is acetolyzed more rapidly than the trans-form and on the contrary the former is ethanolyzed more slowly than the latter. The rate ratios of cis/trans in the acetolysis and in the ethanolysis are respectively 4.2 and 0.51 at 99.8°C which are almost the same as the values at 110°C, and these values agree essentially with 2.4 and 0.69 for 4-methylcyclohexylcarbinyl tosylates.

Further, the tables show that *trans*-4-*t*-butylcyclohexylcarbinyl tosylate is solvolyzed more rapidly in ethanol than in acetic acid and the ratio of EtOH/AcOH is 6.4. This value agrees substantially with 6.1 for *trans*-4-methylcyclohexylcarbinyl tosylate and also with similar values for primary alkyl tosylates, especially with a value of 6.2 for isobutyl tosylate at 75°C. This increase in rate attending the solvent change suggests that participation of the solvent, as shown in Fig. 2, which is a part of a driving force for ionization is more important in the ethanolysis of these compounds than in the acetolysis, since ethanol is of more nucleophilic nature than acetic acid.

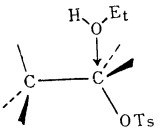
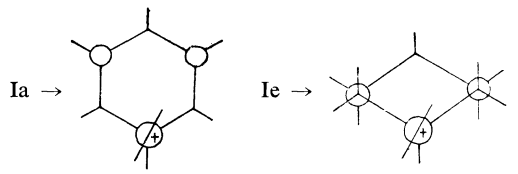


Fig. 2

On the contrary, *cis*-4-*t*-butylcyclohexylcarbinyl tosylate was solvolyzed more slowly in ethanol than in acetic acid and the rate ratio of EtOH/AcOH averages 0.75. The corresponding ratio for unsubstituted and *cis*-4-methyl substituted cyclohexylcarbinyl tosylates, however, are respectively 3.7 and 1.8 which are lower than 6.1 for *trans*-4-methylcyclohexylcarbinyl tosylate. The lowest value of 0.75 for the *cis*-4-*t*-butyl-compound would be due to the cause that the ethanolysis of this compound does not substantially involve participation of the solvent such as shown in Fig. 2 for the case of the corresponding trans-form, as will be detailed later. The relatively high ratios of EtOH/AcOH for the unsubstituted and *cis*-4-methyl substituted compounds arise from their interconvertible chair conformations.

Conformational Analysis.—In Fig. 1, the possible conformations for the axial and the equatorial toluenesulfoxymethyl group which were proposed in the previous paper[1] are projected along the C_7–C_1 axis. Conformation Ie is more stable than IIe, since the former is free from the two 1, 3-diaxial interactions which are present in the latter. On the other hand, conformation Ia is more stable than IIa, since the bulky toluenesulfoxy group in the former is separated far from the two axial hydrogens on C_3 and C_5.

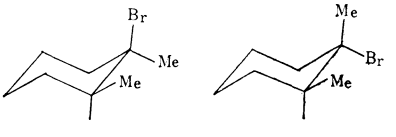
According to the consideration in the previous paper[1], in the conformation Ia there is very high crowding between the two axial hydrogens on C_3 and C_5 and the inside hydrogen on C_7. In the course of formation of the carbonium ion IIIa from the ground state Ia in Fig. 3, a large strain originally exerted on the inside hydrogen on C_7 decreases to a considerable extent. If the decrease in strain is much



IIIa IIIe

Fig. 3

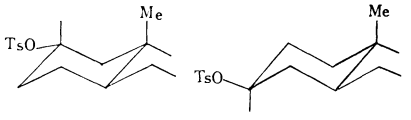
larger than that in the case of formation of the carbonium ion IIIe from the ground state Ie, that is to say, the difference in energy between Ia and IIIa is lower than that between Ie and IIIe, this would provide a convenient explanation for the high rate ratio (higher than 1) of cis/trans observed in the acetolysis of isomeric 4-*t*-butylcyclohexylcarbinyl tosylates. Such a consideration may be supported by the experimental fact[10] that *trans*- and *cis*-1, 2-dimethylcyclohexyl bromides I and II are solvolyzed at an equal rate, and therefore steric interaction affecting the axial methyl group on C_1 in the cis-form II accelerates ionization of the equatorial bromine atom, to an almost equal extent with that of the so called 1, 3-diaxial interaction-accelerate-ionization of the axial bromine atom in the trans-form.



I II

10) T. D. Nevitt and G. S. Hammond, *J. Am. Chem. Soc.*, 76, 4124 (1954).

Further, it is supported also by the fact[11] that cholestan-2α-yl tosylate (III) is solvolyzed more rapidly by a fact of 3 than cholestan-3β-yl tosylate (IV), owing to relatively high interaction between the axial hydrogen on C_2 and the methyl group in the former tosylate.



III IV

On the other hand, as described above, the ethanolysis of the 4-*t*-butylcyclohexylcarbinyl tosylate would involve a solvent participation, but in the case of the cis-isomer such a participation would not be involved. Examination of the molecular models shows that in the conformation Ia a back-side entry of nucleophilic molecules, as shown in Fig. 2, is hindered by the axial hydrogen on C_3 or C_5, but in the conformation Ie such a steric hindrance is absent. This examination can give a convenient reason for the observed lower rate ratio of of EtOH/AcOH for the cis-form containing an axial toluenesulfoxymethyl group, as compared to that for the trans-form containing an equatorial one.

Summarizing the above consideration, in the acetolysis of the compound containing a toluenesulfoxymethyl group in an axial or an equatorial position, the decrease in steric strain controls the rate. On the other hand, in the ethanolysis of the compound containing an equatorial toluenesulfoxymethyl group, a driving force for ionization consists of the decrease in strain and the high solvent participation effecting to push the toluenesulfoxy radical, where the former being less important than the latter, while in the case of the compound containing an axial toluenesulfoxymethyl group the steric hindrance results in less importance of the solvent participation and only the decrease in strain effects a substantial driving force for ionization.

Although the conformations Ia and Ie may be respectively more stable than the corresponding IIa and IIe, this does not mean that these tosylates must react only in these stable conformations, since the energy barriers for their interconversion are probably less than the activation energies involved in the solvolysis.

Further, from the above conformations, it is easily understood that steric strain for the toluenesulfoxy group and for the inside hydrogen in the respective *trans*- and *cis*-4-*t*-butylcyclohexylcarbinyl tosylates is much higher by considerable factors than in cyclohexyl tosylates in general, and such high strain would result in a high rate of solvolysis. However, α-alkyl substituents or their electron-donating inductive effect can give much higher rate-increasing effects than steric strain does, and this has been borne out by the lower acetolysis rates of the former tosylates than that of the latter tosylates.

Free Energy Difference between Axial and Equatorial Toluenesulfoxymethyl Group. — Winstein and Holness[2] proposed a very useful relationship between the specific reaction rate k for any reaction of a molecule which exists in the two interconvertible chair conformations and has a departing group directly bound to the ring, the mole fractions N_a and N_e of the two conformations at equilibrium and the respective individual rate constants k_a and k_e, as follows:

$$k = N_a \cdot k_a + N_e \cdot k_e \quad (1)$$

On the other hand, Eliel and Lukach[3] gave an equivalent relationship, as follows:

$$k = (k_e \cdot K + k_a)/(K+1) \quad (2)$$

where K is the equilibrium constant N_e/N_a between the two conformations. From this equation Eq. 3 may be derived.

$$K = (k_a - k)/(k - k_e) \quad (3)$$

If the proportions of Ia and IIa and of Ie and IIe are affected by any substituent present in the tosylates, the above equations are applicable to solvolysis of the tosylates. In Table V are listed the conformational equilibrium constants derived from the rate constants in Table II by Eq. 3 in which k is the rate constant for the compound indicated, k_a is the rate constant for the purely axial isomer *cis*-4-*t*-butylcyclohexylcarbinyl tosylate and k_e is the rate constant for the purely equatorial isomer *trans*-4-*t*-butylcyclohexylcarbinyl tosylate. $\Delta F°$ in the table is the free energy difference between the chair-conformational isomers derived from the K value by Eq. 4.

$$\Delta F° = -2.3RT \log K \quad (4)$$

The $\Delta F°$ values require comment. It must be realized that these values no more than indicate orders of magnitude, since K in Eq. 3 is obtained as a quotient of two differences, one of which is usually small and therefore affected by a large relative error. Therefore, the values for the ethanolysis, in which measurement errors have been relatively high, are unsatisfactory (not shown in the table).

The conformational equilibrium constant for cyclohexylcarbinyl tosylate in acetolysis listed in Table V indicates that about 90% of the molecules exists with the toluenesulfoxymethyl

11) S. Nishida, ibid., 82, 4290 (1960).

Table V. Summary of K and ΔF° values in acetic acid

4-Substituent	99.8°C			110°C		
	K	ΔF° kcal./mol.	N_a %	K	ΔF° kcal./mol.	N_a %
cis-t-Bu	0	—	100	0	—	100
cis-Me	1.17	−0.12	46	1.3	−0.20	44
H	9.6	−1.7	10	8.7	−1.8	9.0
trans-Me	116	−3.5	0.8	183	−5.1	0.54
trans-t-Bu	∞*	—	0.0	∞*	—	0.0

* Assumed

group equatorial in equilibrium with 10% whose toluenesulfoxymethyl group is axial. The ΔF° value of −1.7∼1.8 kcal./mol. for the cyclohexylcarbinyl tosylate seems to be reasonable for the difference ΔF°_{TsOMe} in free energy between the equatorial and axial toluenesulfoxymethyl group.

The conformational free energy differences ΔF°_{cis} and ΔF°_{trans} for *cis*- and *trans*-4-methylcyclohexylcarbinyl tosylates should be related to that of cyclohexylcarbinyl tosylate by the equations:

$$\Delta F^\circ_{cis} = -\Delta F^\circ_{Me} + \Delta F^\circ_{TsOMe}$$

and

$$\Delta F^\circ_{trans} = \Delta F^\circ_{Me} + \Delta F^\circ_{TsOMe}$$

The ΔF°_{Me} is the difference in free energy between an equatorial and an axial methyl group or the energy required for moving a methyl group from an equatorial to an axial position and may be taken as −1.6 kcal./mol.[4] Since the corresponding value ΔF°_{TsOMe} for toluenesulfoxymethyl group is −1.7 kcal./mol. at 99.8°C, the calculated free energy difference ΔF°_{cis} for *cis*-4-methylcyclohexylcarbinyl tosylate with an equatorial toluenesulfoxymethyl group and its conformational isomer with an axial one is 1.6−1.7 or −0.1 kcal./mol.

Similarly, from the values of −1.8 kcal./mol. at 110°C for the toluenesulfoxymethyl group, the corresponding value is −0.2 kcal./mol. The calculated values of −0.1 and −0.2 kcal./mol. are in good agreement with the observed −0.12 and −0.2 kcal./mol.

For *trans*-4-methylcyclohexylcarbinyl tosylate, the value for moving a methyl and a toluenesulfoxymethyl group from axial to equatorial positions is −1.6 −1.7 or −3.3 kcal./mol. at both temperatures, which is in good agreement with the experimental values of −5.1 and −3.5 kcal./mol.

The value of 1.7∼1.8 kcal./mol. for the difference in free energy between the conformations with a toluenesulfoxymethyl group in an equatorial and an axial position respectively is almost equal to 1.6∼1.8 kcal./mol. for the methyl group[4] and 0.7∼1.7 kcal./mol. for the toluenesulfoxy group[2,3] but lower than 2.1 kcal./mol. for the ethyl and the *n*-propyl group[2]. The relatively low value of 1.7∼1.8 kcal./mol. appears quite reasonable, however, since in view of varying experimental conditions such as difference in solvents and temperatures, complete agreement of the ΔF° values should perhaps not be expected and the value of 1.7∼1.8 kcal./mol. would not be expected to be very different, as compared to that for the other groups.

The author wishes to express his sincere thanks to Professor Yojiro Tsuzuki for his advice.

Tokyo College of Science
Shinjuku-ku, Tokyo

Rates of Solvolysis of Bis-p-toluenesulfoxymethylcyclohexanes

By Nobuo Mori

(Received June 17, 1961)

According to the previous work[1] dealing with solvolytic reactivity of a departing group such as a toluenesulfoxy group bound through a methylene linkage to a cyclohexane ring, the compound with a toluenesulfoxy group in an axial position is solvolyzed at a rate 4.2 times as fast and one half as fast as the corresponding isomer with that group in an equatorial position in acetic acid and in ethanol, respectively.

In the present work, the investigation has been extended to similar solvolysis of *cis*- and *trans*-1, 2- and 1, 4-bis-*p*-toluenesulfoxymethylcyclohexanes (described as ditosylates herein).

Experimental and Results

Samples. — All samples were prepared according to the methods by Haggis and Owen[2,3] with some modifications. The four ditosylates so obtained had the following melting points, respectively:

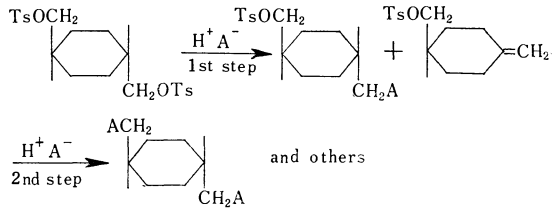
Position of $TsOCH_2$	M. p., °C	M. p. (reported)
cis-1,2	88	84 ~85[2]
cis-1,4	94.5~ 95	95[3]
trans-1,2	107.5~108	108[2]
trans-1,4	163 ~163.5	162~163[3]

Procedure for Rate Measurements. — Rate measurements were carried out in a similar manner to the previously employed method[4]. Rate constants were calculated from the formula

$$k=2.3/t\cdot\log 2a/(2a-x) \qquad (1)$$

in which a was the initial molar concentration of a ditosylate and x was the molar concentration of sulfonic acid liberated at time t.

Solvolysis was followed to 30~50% completion at 99.8±0.1°C in neutral ethanol (98.5% by weight) and in dry acetic acid containing a slight excess of sodium acetate. Concentrations were 0.01~0.015 mol./l. for the 1, 2-ditosylates and 0.002 mol./l. for the 1, 4-ditosylates, since especially the latter were difficulty soluble in these solvents. The solvolysis proceeds substantially in two steps with different rates where in the first step monotosylates are predominantly produced which in the second step are converted into final products, for example, as illustrated in the case of the *trans*-1, 4-ditosylate by the following formula:



where H^+A^- is the solvent and TsO is the toluenesulfoxy group. In all cases, however, the rate constants derived by Eq. 1 were nearly of the first order with a maximum error of 6%. Table I shows the data of a typical run with the *cis*-1, 2-ditosylate in ethanol at 99.8°C.

The acetolysis rates of the isomeric 1, 2-ditosylates were not substantially influenced by

Table I. Ethanolysis of *cis*-1,2-bistoluenesulfoxymethylcyclohexane at 99.8°C

Time sec.	Tosylate mol./l.×10²	$k_1\times10^5$/sec.
0	1.06	
6000	0.955	(1.73)
10800	0.890	1.61
14400	0.835	1.65
20400	0.763	1.61
27000	0.684	1.62
		Mean 1.6

Table II. Summary of solvolysis rates at 99.8°C

Position of $TsOCH_2$	Solvent	Tosylate mol./l.×10²	$k_1\times10^5$/sec.
cis-1,2	EtOH	1.06	1.6
	AcOH*	1.00	0.31
	AcOH	1.33	0.31
trans-1,2	EtOH	0.884	3.4
	AcOH*	1.00	0.26
	AcOH	1.33	0.27
cis-1,4	EtOH	0.349	1.0
	AcOH**	0.530	0.49
trans-1,4	EtOH	0.200	1.5
	AcOH**	0.530	0.21

*, ** Contained AcONa in 0.0300 and 0.0150 mol./l., respectively.

1) N. Mori, This Bulletin, **35**, 1755 (1962).
2) G. A. Haggis and L. N. Owen, *J. Chem. Soc.*, **1953**, 389.
3) G. A. Haggis and L. N. Owen, ibid., **1953**, 404.
4) N. Mori, This Bulletin, **33**, 1144 (1960).

TABLE III. RELATIVE RATES

Position of $TsOCH_2$		k_{EtOH}/k_{AcOH}	k_{cis}/k_{trans} EtOH	k_{cis}/k_{trans} AcOH
cis-1,2		5.1	0.47	1.2
trans-1,2		13		
cis-1,4		2.6	0.68	2.3
trans-1,4		7.1		
4-*t*-Butylcyclohexylmethyl tosylate[1],	*cis*	0.76	0.51	4.2
	trans	6.4		

the absence of sodium acetate. The rate constants and the relative rates are summarized in Tables II and III.

Discussion

In the isomeric 1, 4-ditosylates, the trans-form may substantially exist in a diequatorial conformation while a diaxial conformation is negligible, since the energy required for moving the toluenesulfoxymethyl group from an equatorial to an axial position is 1.7 kcal./mol.[1] and therefore the free energy difference between the two conformations may be 3.4 kcal./mol. which indicates the proportion of the former conformation in the ground state to be more than 99%. On the other hand, especially in the *trans*-1, 2-ditosylate there are probably some interactions such as the steric and the electrostatic repulsion between the two bulky and polar toluenesulfoxymethyl groups, and therefore for this ditosylate a diaxial conformation may be preferable, as shown in various *trans*-1,2-disubstituted cyclohexanes[5] containing dipolar groupings such as halogen and others, which are mainly in a diaxial conformation. Accordingly, from the considerations based on the conformational preference at the ground state and the previous results described above, it is expected that the *cis*-1, 4-ditosylate is acetolyzed more rapidly than the trans-isomer with a relatively low ratio of k_{cis}/k_{trans}, as compared with the value of 4.2 for 4-*t*-butylcyclohexylmethyl tosylate, because in the cis-form one of the two toluenesulfoxymethyl groups is always axial. On the other hand, in the 1, 2-ditosylates it may be difficult to expect their solvolysis behavior.

According to the experiments, the rate ratio in acetolysis is 2.3 for the 1, 4-ditosylate and also 1.2 for the 1, 2-ditosylate.

Further, the *cis*-1, 4-ditosylate and also the *cis*-1, 2-ditosylate are ethanolyzed more slowly than the corresponding trans-isomers with a similar trend in rate ratio to that (0.51) for the 4-*t*-butyl compound, as seen in Table III.

Further, a ratio of k_{EtOH}/k_{AcOH} is 0.76 for the *cis*-4-*t*-butyl compound and 6.4 for the trans-isomer. The high ratios of 5.1 and 2.6 for the *cis*-1, 2 and 1, 4-ditosylates should be due to one equatorial toluenesulfoxymethyl group present in them.

Tokyo College of Science
Shinjuku-ku, Tokyo

5) H. A. Smith and F. P. Byrne, *J. Am. Chem. Soc.*, 72, 4406 (1950); K. Kozima and T. Yoshino, ibid., 75, 166 (1953); M. Kilpatrick and J. G. Morse, ibid., 75, 1846 (1953); A. Tulinskie, A. D. Giacomo and C. P. Smyth, ibid., 75, 3552 (1953).

The Radiation-Induced Exchange Reaction of Oxygen Atoms in Carbon Dioxide

By Kozo Hirota, Hideo Terasaki and Motoyoshi Hatada

(Received July 12, 1962)

There have been several reports on the radiation-induced reactions of carbon dioxide since the classical paper of Lind[1]. Recently Harteck and Dondes[2] obtained a small G value on the decomposition of carbon dioxide in relation to the study on the production of carbon suboxide and its polymers. However, they concluded[3] that this is due to the presence of the backward reaction, because the G-value became higher by the inhibition of the backward reaction with nitrogen dioxide. In relation to the above conclusion on the decomposition of carbon dioxide by Harteck

1) S. C. Lind and D. C. Barwell, *J. Am. Chem. Soc.*, **47**, 2675 (1925).

2) P. Harteck and S. Dondes, *J. Chem. Phys.*, **23**, 902 (1955); **26**, 1727 (1957).

3) P. Harteck and S. Dondes, *Z. Elektrochem.*, **64**, 983 (1960).

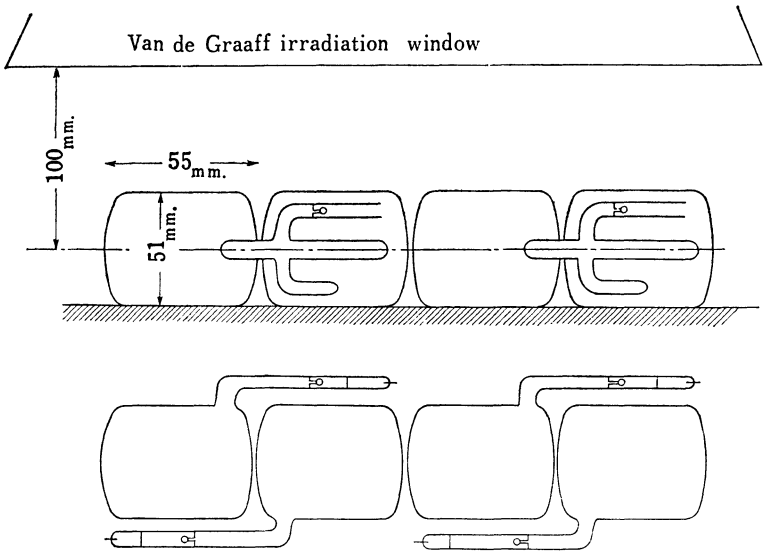


Fig. 1. Arrangement of the irradiation ampoules.

et al., it will be interesting to study the radiation-induced oxygen exchange between normal and labeled carbon dioxide: $C^{18}O_2 + C^{16}O_2 \rightarrow 2C^{16}O^{18}O$. Our purpose in the present paper is to report the investigation actually carried out on this line.

Experimental

Labeled Carbon Dioxide $C^{18}O_2$. — The enriched carbon dioxide $C^{18}O_2$ used in this experiment was prepared by the thermal diffusion method at the Faculty of Science, Osaka University[4]. The ^{18}O content was ca. 29 atom % and the ratio $C^{16}O_2$: $C^{16}O^{18}O$: $C^{18}O_2$ was 51.1 : 39.9 : 8.5*.

Normal Carbon Dioxide. — Commercial carbon dioxide was used after vacuum distillation.

Irradiation. — Definite amounts of the normal and the labeled carbon dioxide were taken and introduced into a cylindrical glass ampoule (80 cc.) with a break-off-tip by using liquid nitrogen cold trap. A set of such ampoules were arranged as shown in Fig. 1 and was irradiated simultaneously with 1.5 MeV. electron beam from the Van de Graaff accelerator (High Voltage Eng. Co., Model AKS).

Analysis. — After the irradiation, the samples were taken out from the ampoules and were analyzed by use of a mass-spectrometer (Hitachi, RMU-5 type).

Results and Discussion

The results in addition to the conditions of the irradiation are described in Table I. In the case of No. 4, glass wool was inserted into the ampoule.

Effect of the Irradiation Time. — The logarithm of the excess amount of heavy carbon dioxide in mole from the equilibrium value is plotted against the irradiation time t. The rate constant k was estimated to be $1.5_2\ hr^{-1}$, assuming that this exchange reaction proceeds according to 1st order, i. e.,

$$\ln\frac{[CO_2^*] - [CO_2^*]_\infty}{[CO_2^*]_0 - [CO_2^*]_\infty} = -kt$$

and reaches the equilibrium, the thermal equilibrium constant of which is as follows.

$$[COO^*]^2/[CO_2^*]\,[CO_2] = 4.0$$

where $[COO^*]$, $[CO_2^*]$ and $[CO_2]$ are the amounts of COO^*, CO_2^* and CO_2 in mol./unit volume, respectively.

Determination of the Apparent G Value. — The G^{exc}-value of the exchange reaction is given by the decrease of CO_2^* as follows:

$$G(-CO_2^*) = \frac{\text{Number of the } CO_2^* \text{ exchanged} \times 100}{\text{Energy absorbed in eV.}} \quad (1)$$

This value will be called an apparent one of G^{exc}, because only the value of the labeled CO_2 is determined.

In order to evaluate the energy absorbed by carbon dioxide in Eq. 1, effective thickness of the ampoules was calculated to be 2.1 mm. in No. 1—3, while it was estimated to be 2.2 mm. in No. 4 by considering the thickness corresponding to a half amount of the glass wool besides. The dose rate I thus calculated in

4) K. Hirota, Y. Kobayashi, M. Takahashi and Y. Yoshikawa, *Isotopes and Radiation (Tokyo)*, **2**, 235 (1959).

* Hereafter O^{18} will be denoted by O* while ^{16}O by O.

* In the equation N_A is the Avogadro number.

Table I. Experimental results

		Blank	No. 1	No. 2	No. 3	No. 4
Dose rate $\times 10^5$ rad/sec.		0	0.88	0.88	0.88	0.55[b]
Irradiation time, min.		0	60	120	180	180
Before the irradiation	Labeled carbon[a] dioxide, $\times 10^{-5}$ mol.	5.23	5.41	5.50	5.48	4.02
	Normal carbon dioxide, $\times 10^{-5}$ mol.	16.24	16.11	16.08	16.16	12.38
	Total CO_2, $\times 10^{-5}$ mol.	21.48	21.52	21.58	21.64	16.41
	Normal CO_2 : Labeled CO_2	3.10	2.98	2.93	2.95	3.08
After the irradiation	CO_2 (%)	(88.6)[c]	86.6	86.3	86.6	86.7
	COO* (%)	(9.5)	12.7	12.4	13.0	12.4
	CO_2* (%)	(1.90)	0.11	0.84	0.45	0.94

N. B. a) Isotopic composition of the carbon dioxide used (CO_2 : COO* : CO_2* = 51.1 : 39.9 : 8.5)
b) The value corrected for the energy absorption by glass wool in the reaction vessels.
c) Percentages in parentheses are those of the blank.

both cases was 0.88×10^5 rad/sec. and 0.55×10^5 rad/sec., respectively.

First, mean $G(-CO_2^*)$ value was estimated to be 0.3_7 from No. 1, 2 and 3. In the case where glass wool was contained in the ampoule, the $G(-CO_2^*)$ value was calculated to be 0.3_5 using the dose rate corrected for the energy absorbed by the glass wool. Since $G(-CO_2^*)$ was not altered by the addition of the glass wool, it may be reasonable to regard the effect of the wall of the vessel negligible to the reaction.

However, the result observed after 3 hr. irradiation (No. 3) should be eliminated from the data for discussion, because the isotopic equilibrium may have been completed at that time and the isotopic composition of this system was not changed by further irradiation. Therefore, it is more reasonable to calculate the G-value of the exchange reaction of oxygen atoms between carbon dioxide molecules by the following equation,

$$G_{corr}(-CO_2^*)=\frac{([CO_2^*]_0-[CO_2^*]_\infty)k\times N_A}{I\cdot W\cdot 6.25\times10^{11}}$$

where I is the dose rate in rads/hr., and W is the amount of carbon dioxide in grams. The G value calculated by this equation was 1.7_2. In the discussion $G_{corr}(-CO_2^*)$ will be used hereafter.

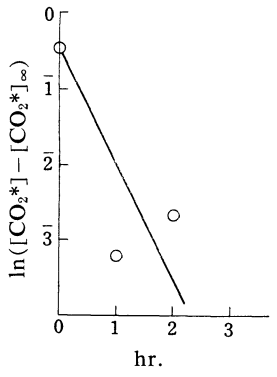


Fig. 2. Irradiation time vs. $\ln([CO_2^*]-[CO_2^*]_\infty)$. $k=1.5\ hr^{-1}$

Total G Value of the Exchange Reaction. — The apparent G values calculated above correspond to the exchange reaction a between CO_2* and CO_2. However, there are several similar reactions b—f in this system, which are not observed because of the situation that the species of the reactant and the product are the same.

$$CO_2^*+CO_2 \rightarrow COO^*+COO^* \quad (a)$$
$$CO_2^*+COO^* \rightarrow COO^*+CO_2^* \quad (b)$$
$$CO_2^*+CO_2^* \rightarrow CO_2^*+CO_2^* \quad (c)$$
$$COO^*+CO_2 \rightarrow COO^*+CO_2 \quad (d)$$
$$COO^*+COO^* \rightarrow COO^*+COO^* \quad (e)$$
$$CO_2+CO_2 \rightarrow CO_2+CO_2 \quad (f)$$

Fraction of the reaction a to all the reactions is calculated by

$$\frac{l\cdot n}{l\cdot n+l\cdot m+m\cdot n+\frac{l^2}{2}+\frac{m^2}{2}+\frac{n^2}{2}}=\frac{l\cdot n}{\frac{1}{2}(l+m+n)^2}$$

where l, m and n are the initial molar fractions of CO_2*, COO* and CO_2, respectively. Thus, the total G value of carbon dioxide G_{total}^{exc} in such a kind of exchange reaction is given by

$$G_{total}^{exc}=G_{corr}(-CO_2^*)\cdot\frac{1}{2\cdot l\cdot n} \quad (2)$$

Since $2\cdot l\cdot n$ equals to 0.033_7, G_{total}^{exc} was calculated to be 51 using the $G_{corr}(-CO_2^*)$ value of 1.7_2.

Comparison of the G Value of the Radiation-Induced Exchange Reaction with That of Radiolysis.—Harteck et al.[3] reported a rather small G^{dec} value (0.005) for the radiolysis of carbon dioxide at 1 atm. and concluded that

this small value was resulted from the simultaneous backward reaction induced by radiation. This conclusion was based on the fact that the G^{dec} value increased to 8.5 ± 1 when nitrogen dioxide (NO_2) was added as inhibitor to the backward reaction[3]. In our experiment, the forward and backward reactions under irradiation may give rise to exchange reaction of oxygen atoms between carbon dioxide molecules as actually shown by the present experiment. Therefore the G^{exc}_{total} must correspond to Harteck's G^{dec} in which the contribution of the backward reaction was eliminated. However, since the G^{exc}_{total} is determined to be 51, it is larger to some extent than G^{dec} of Harteck (8.5). This discrepancy may be attributed to the fact that the nitrogen dioxide added in Harteck's experiment may have some roles other than as an inhibitor of the backward reaction, whereas the samples in our experiment did not contain any impurities.

Summary

Oxygen exchange of carbon dioxide induced by β-ray irradiation has been investigated by use of oxygen isotope O*. From the decrease of O* amount, the apparent and total values of the exchange reaction, $G_{corr}(-CO_2^*)$ and G^{exc}_{total}, have been calculated to be 1.7_2 and 51, respectively. The latter value 51 would be equivalent to the forward reaction, but has been shown to be larger than the corresponding value (8.5) in Harteck's experiment.

Appreciation is expressed to Mr. Yohta Nakai for his collaborations in operation of the Van de Graaff accelerator and also to Dr. Yasushi Kobayashi and Mr. Masashi Takahashi for their preparation of heavy carbon dioxide.

Department of Chemistry
Faculty of Science
Osaka University
Nakanoshima, Kita-ku, Osaka (*K. H.*)

Osaka Laboratory
Japanese Association for
Radiation Research on Polymers
Neyagawa City, Osaka (*K. H., H. T. & M. H.*)

Action des Ions du Fer Trivalent sur la Chalcopyrite

Par Masami ICHIKUNI

(Reçu le 15 Novembre 1961)

Comme la désagrégation qui a lieu dans la nature est composée de plusieurs processus: mécaniques, chimiques et microbiologiques, l'interprétation des descriptions faites aux mines offre une difficulté considérable. On trouve dans la littérature de nombreux travaux, soit géologiques, soit minéralogiques. Cependant on ne rencontre que très rarement des études géochimiques, qui présentent un grand intérêt aux géologues et géochimistes. Dans un travail antérieur[1], le présent auteur signalait la décomposition de la chalcopyrite en solution par de l'oxygène libre. Les décompositions oxydatives des minéraux sulfurés peuvent être provoquées principalement par l'oxygène et les ions du fer trivalent. Avec les expériences effectuées au laboratoire, on est capable de poursuivre uniquement l'action des ions du fer trivalent sans intervention de l'oxygène, ainsi on peut estimer avec facilité l'importance des facteurs géochimiques participant à ce phénomène. Le but de ce rapport est d'examiner par voie expérimentale la décomposition de la chalcopyrite en solution acide contenant des ions du fer trivalent.

1) M. Ichikuni, Ce Bulletin, 33, 1052 (1960).

Expérience

Les échantillons utilisés dans ce rapport sont un grand monocristal de pyrite, produit à la mine de Kanaborizawa, département d'Aomori et une masse de cristaux de chalcopyrite, produite à la mine d'Ani, département d'Akita, dont la description détaillée a été donnée ailleurs[1]. L'examen à l'aide des rayons X a montré que cettre chalcopyrite ne présente pas de phase cristalline étrangère. Ces minéraux ont été broyés, et passés au tamis de 200 mesh. Des sulfures mixtes de composition connue ont été préparés par mélange soigneux des deux minéraux pesés.

Comme la chalcopyrite est facilement attaquée par l'oxygène en milieu fortement acide, la réaction entre ce minéral et les ions du fer trivalent doit être effectuée à l'abri de l'oxygène atmosphérique. Dans une solution acide chlorhydrique, contenant

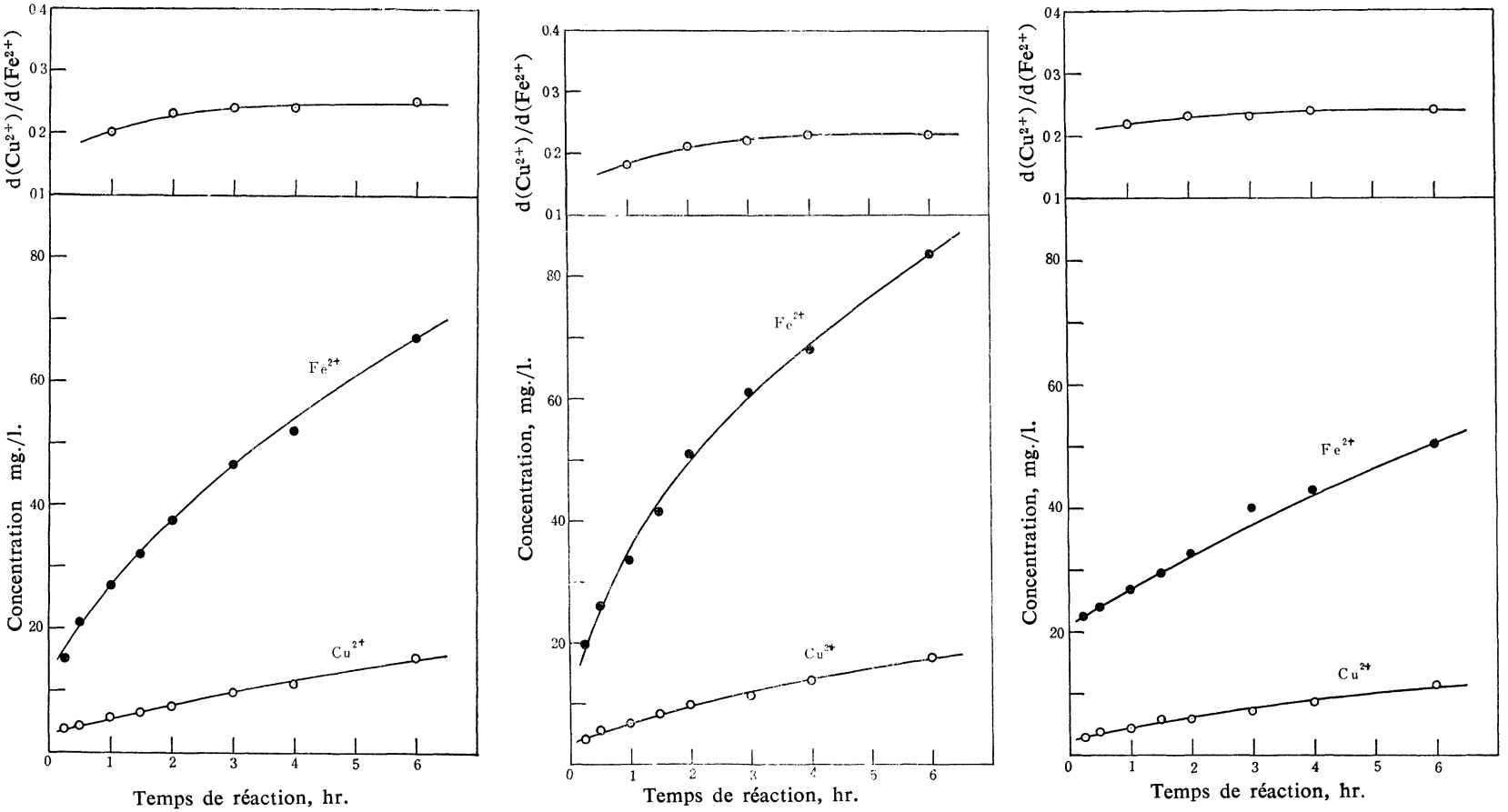


Fig. 1. Variation des concentrations de Cu^{2+} et de Fe^{2+} ainsi que du rapport $d(Cu^{2+})/d(Fe^{2+})$ en fonction du temps.

des ions du fer trivalent en concentration de 100 mg./l., préalablement chauffée à 50°C, on introduit un courant de dioxyde de carbone pour entraîner l'oxygène dissous. On ajoute ensuite 500 mg. de chalcopyrite ou de sulfures mixtes. De la solution agitée vigoureusement à l'aide d'un agitateur magnétique, on effectue plusieurs prélèvements de 5 ml. de liqueur avec des intervals appropriés. Ces liqueurs, immédiatement filtrées, sont diluées à 50 ml., d'où on prend 5 ou 10 ml. pour doser le cuivre, le fer divalent, le sulfate et le soufre libre. L'analyse du premier s'effectue par la colorimétrie avec le cupférazone[2], et celle du dernier, avec l'*o*-phénanthroline.

Résultats et Discussion

La décomposition de la chalcopyrite, causée par l'action des ions du fer trivalent, donne des ions du cuivre et du fer divalent, et du soufre libre, mais pas d'ions sulfate, d'où on déduit l'équation suivante:

$$CuFeS_2 + 4Fe^{3+} \rightarrow Cu^{2+} + 5Fe^{2+} + 2S \qquad (1)$$

L'analyse des résultats d'expériences révèle que le rapport de la vitesse de formation d'ions du cuivre sur celle d'ions du fer divalent $d(Cu^{2+})/d(Fe^{2+})$ varie avec le temps de réaction. Si la réaction avait lieu exactement comme indiquée par l'équation 1, le rapport serait de Cu/5Fe, soit de 0.23, indépendamment du temps de réaction. On voit sur la Fig. 1 que le rapport est légèrement inférieur à 0.23 au départ de la réaction, augmente lentement et s'approche de 0.23 environs.

Le présent auteur propose un mécanisme de réaction pour expliquer ces résultats: les atomes du fer contenus dans la chalcopyrite sont plus facilement libérés par l'attaque des ions du fer trivalent que ceux du cuivre, ce qui aboutit à un enrichissement en cuivre à la surface du minéral. Cette fois, les ions du fer trivalent peuvent réagir plus aisément sur les atomes du cuivre et le rapport $d(Cu^{2+})/d(Fe^{2+})$ augmente. L'enrichissement en cuivre ne peut donc être très imporant, et le minéral se décomposera entièrement en présence d'un excès d'ions du fer trivalent.

Il semble que la réaction ralentisse avec l'augmentation de l'acidité de solution et que la variation du rapport $d(Cu^{2+})/d(Fe^{2+})$ en fonction du temps soit influencée par le pH, mais il peut y avoir d'autres facteurs qui jouent un rôle important dans ce processus.

Une autre série d'expériences a été effectuée sur des sulfures mixtes, dont la proportion pondérale, chalcopyrite/pyrite+chalcopyrite, a varié de 5 à 100%. L'acidité de solution a été constamment de 0.01 N en acide chlorhydrique. Au terme de la réaction, où les ions du fer se trouvent tous à l'état divalent, on a fait le dosage des ions du cuivre et du fer. On peut trouver facilement les quantités augmentées de cuivre et de fer en solution, en sachant la concentration initiale en ions du fer.

Tableau I. Quantités de cuivre et de fer dissous a partir de 500 mg. de sulfures mixtes sous l'action de 20 mg. d'ions du fer trivalent

Composition de sulfures mixtes		Cu dissous mg.	Fe dissous mg.	Fe provenant de la pyrite mg.
Chalcopyrite %	Pyrite %			
5	95	0.38	2.2	1.9
10	90	0.66	2.4	1.8
20	80	1.2	2.6	1.5
40	60	2.1	2.8	1.0
100	0	5.4	4.8	0

Le Tableau I montre les quantités de cuivre et de fer dissous par la décomposition de sulfures mixtes. En admettant que la chalcopyrite donne 1 mol. de fer pour 1 mol. de cuivre en se décomposant sous les conditions d'expériences, on a calculé la quantité de fer libéré à partir de la pyrite. La Fig. 2 indique que la quantité de cuivre est proportionnelle à la teneur en chalcopyrite des sulfures mixtes, et que celle de fer provenant de la pyrite l'est à la teneur en pyrite.

Ces résultats mènent à une conclusion importante que les ions du fer trivalent réagissent sur des sulfures mixtes d'une façon peu sélective par rapport à l'oxygène. Notons que l'oxygène favorise une forte dissolution de la chalcopyrite associée à une quantité considérable de pyrite[3]. On a souvent remarqué que les minéraux sulfurés associés se

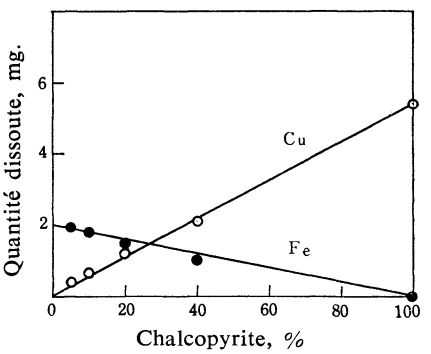


Fig. 2 Quantités de cuivre dissous de la chalcopyrite et de fer dissous de la pyrite en fonction de la teneur en chalcopyrite des sulfures mixtes.

2) C. R. Elliott et al., *Analyst*, **84**, 237 (1959).

3) M. Ichikuni, Ce Bulletin, **33**, 1156 (1960).

dissolvent chacun avec une vitesse différente lors de la désagrégation. Ce phénomène peut être expliqué par la différence du potentiel de contact existant entre de différents minéraux. Cette explication ne semble pas toujours s'appliquer à la désagrégation simultanée de minéraux associés, provoquée par les ions du fer trivalent. Toutefois des expériences répétées sur d'autres minéraux associés seront encore exigées pour faire la preuve de cette conclusion hardie.

Résumé

Sous l'action des ions du fer trivalent, la chalcopyrite libère tout d'abord plus de fer que du cuivre, ce qui aboutit à un enrichissement en cuivre à la couche superficielle du minéral. Cette couche est attaquée à son tour par les ions du fer trivalent, ainsi la décomposition avance en tout comme l'équation 1 l'indique. Pour la chalcopyrite associée à la pyrite, l'action des mêmes ions ne favorise pas de dissolution sélective d'un des deux minéraux. Répétons que l'action de l'oxygène accélère la dissolution de la chalcopyrite en milieu acide, si elle est associée à la pyrite. On trouve ici les caractéristiques des actions de l'oxygène et des ions du fer trivalent sur les minéraux sulfurés associés.

L'auteur se permet d'adresser ses remerciements sincères à Monsieur le professeue Kimio Noguchi et à Monsieur le professeur Takahisa Hanya qui lui ont donné des conseils utiles au cours de l'exécution de ce travail, et à Monsieur le professeur Takeo Watanabé, à l'Université de Tokyo, qui a bien voulu lire le manuscrit de ce rapport.

Faculté des Sciences
Université Métropolitaine de Tokyo
Sétagaya-ku, Tokyo

Physico-chemical Studies on the Composition of Thiosulfates of Metals. I. Thermometric Studies of Bismuth Thiosulfate Complexes

By Mahendra Singh BHADRAVER

(Received April 11, 1962)

The composition of bismuth thiosulfate has been studied by the method of thermometric titrations between bismuth nitrate and sodium thiosulfate in aqueous and alcoholic medium. The direct titrations curve suggest the formation of $Na_3Bi(S_2O_3)_3$ in which the ratio of $Bi : S_2O_3$ is 1 : 3. In the reverse titrations also the formation of $Na_3Bi(S_2O_3)_3$ is indicated.

There is a meager amount of literature on the study of the composition of bismuth thiosulfate. Carnot and Hauser[1] suggested the formula $R_3Bi(S_2O_3)_3 \cdot nH_2O$ and he pointed out that the solutions of these salts contain $Bi(S_2O_3)^{3-}$ which breaks up readily. There is however hardly any reference in literature on the study of bismuth thionsulfate by physicochemical methods. Hence the present investigation by applying thermometric method was considered worthwhile.

In view of the difficulties associated with analytical work and to throw further light on the composition of bismuth thiosulfate, attempts have been made in this paper to study the composition of these complexes by thermometric method. With the results of potentiometric, conductometric and amperometric measurements in progress, the results of thermometric method have been incorporated and discussed in this paper.

Experimental

The Reagents used were of E. Merck quality. Standard solutions were prepared by weighing. In case of sodium thiosulfate few drops of chloroform were added during the preparation of the solution so that the solution may be serviceable for a longer time. The strength of the sodium thiosulfate solution was further checked by standard KIO_3 solution[2]. Bismuth nitrate $Bi(NO_3)_3 \cdot 5H_2O$ was prepared by direct weighing and the solution was estimated as bismuth oxy-iodide[3].

The arrangement for thermometric titrations was the same as has been described by Naldar[4]. Using different concentrations of the two salts in solution,

1) O. Hauser, *Bull. soc. chim. France*, **35**, 1 (1903).

2) A. I. Vogel, "A Text Book of Quantitative Inorganic Analysis", p. 335.

3) A. I. Vogel, ibid., pp. 425 and 426.

4) B. C. Halder, *J. Ind. Chem. Soc.*, **23**, 147 (1946).

TABLE I. SUMMARY OF THERMOMETRIC OBSERVATIONS

Table No.	Fig. No.	Curve No.	$Bi(NO_3)_3$ concn.	$Na_2S_2O_3$ concn.	Points Med.	Showing Calcd.	Breaks Obs.	Formula Supported	Ratio
Direct titration									
1	1	1	M/5	M/20 20 cc.	Aq.	1.66	1.6	$Na_3Bi(S_2O_3)_3$	1 : 3
2	1	2	M/5	18	Alc. 10%	1.50	1.5	$Na_3Bi(S_2O_3)_3$	1 : 3
3	1	3	M/5	16	20%	1.33	1.4	$Na_3Bi(S_2O_3)_3$	1 : 3
4	1	4	M/5	M/25 20	Aq.	1.33	1.4	$Na_3Bi(S_2O_3)_3$	1 : 3
5	1	5	M/5	18	Alc. 10%	1.20	1.2	$Na_3Bi(S_2O_3)_3$	1 : 3
6	1	6	M/5	16	20%	1.06	1.1	$Na_3Bi(S_2O_3)_3$	1 : 3
Reverse titration									
7	2	1	M/80 20 cc.	M/5	Aq.	3.75	3.7	$Na_3Bi(S_2O_3)_3$	3 : 1
8	2	2	18	M/5	Alc. 10%	3.375	3.4	$Na_3Bi(S_2O_3)_3$	3 : 1
9	2	3	16	M/5	20%	3.00	2.9	$Na_3Bi(S_2O_3)_3$	3 : 1
10	2	4	M/125 20 cc.	M/10	Aq.	4.80	4.8	$Na_3Bi(S_2O_3)_3$	3 : 1
11	2	5	18	M/10	Alc. 10%	4.32	4.30	$Na_3Bi(S_2O_3)_3$	3 : 1
12	2	6	16	M/10	20%	3.84	3.80	$Na_3Bi(S_2O_3)_3$	3 : 1

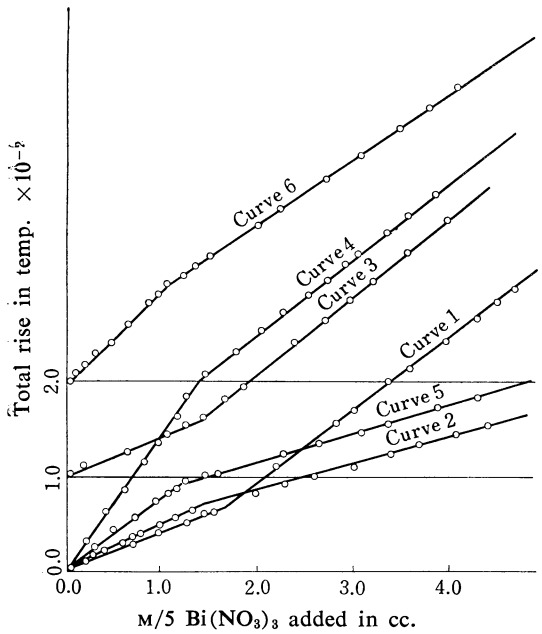


Fig. 1. Direct-titrations.
Curves 1, 2, 3 M/5 $Bi(NO_3)_3$ and M/20 sodium thiosulfate
Curves 4, 5, 6 M/5 $Bi(NO_3)_3$ and M/25 sodium thiosulfate

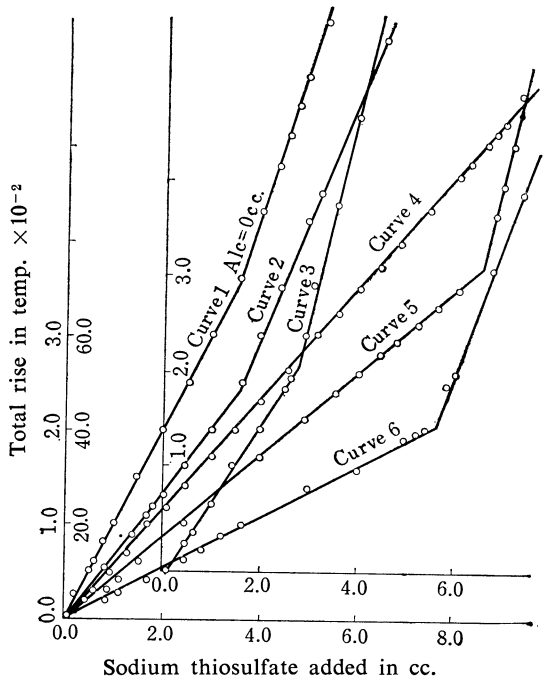


Fig. 2. Reverse-titrations.
Curve 1, 2, 3 M/5 sodium thiosulfate and M/80 $Bi(NO_3)_3$
Curve 4, 5, 6 M/10 sodium thiosulfate and M/125 $Bi(NO_3)_3$

the titrations were followed by the direct and reverse methods (i. e. when $Bi(NO_3)_3$) was added from burette to sodium thiosulfate solution in thermos flask and vice versa).

Titrations were also carried out in presence of alcohol up to 20% by volume. The total rise in temperature was then plotted against the titre in cc.

Discussion

It is evident from the summary of the observations of thermometric titrations that in the direct titrations the theoretical titre values required for the formation of $[Na_3Bi(S_2O_3)_3]$ would be (Table Nos. 1 to 6) 5.0, 4.5, 4.0, 2.0, 1.8 and 1.6 respectively in the ratio of 1 : 3. In the direct titrations one break occurs at the point of equivalence in the ratio 1 : 3. The theoretical values calculated for the reverse titrations accordingly for the ratio 1 : 1 are (Table Nos. 7 to 12) 1.25, 1.125, 1.00, 1.6, 1.44 and 1.28 respectively and therefore the theoretical titre values required for the ratio 3 : 1 would be 3.75, 3.375, 3.00, 4.80, 4.32 and 3.84 respectively. The observed values in the reverse titrations are in agreement with the values for the ratio 3 : 1. Thus the formation of the same compound $Na_3Bi(S_2O_3)_3$ is supported.

With a view to show the discrepancy between the observed and calculated titre values, a summary of observations in aqueous and alcoholic solutions is given above for comparison.

The results of our thermometric method are accurate and fairly support the views of Hauser[5].

Grateful thanks are due to Dr. J. N. Gaur, Maharaja College, Jaipur for his kind guidance in this piece of investigation.

Chemical Laboratories
Lohia College
Churu
Rajasthan, India

5) J. W. Mellor, "Treatise on Inorganic Chemistry", Vol. 10, p. 552.

Physico-chemical Studies on the Composition of Complex Arsenites of Metals. I. Conductometric and Thermometric Studies on the Composition of Copper Arsenite (Scheele's Green) Complexes

By Mahendra Singh BHADRAVER

(Received April 11, 1962)

The formation and composition of copper arsenite (Scheele's Green) has been investigated by conductometric and thermometric titrations between copper sulfate and sodium arsenite at several dilutions of the reactants by direct and reverse methods. The composition arrived at both by conductometric and thermometric titrations is $Cu(AsO_2)_2$.

There are variable formulae suggested in literature for the composition of copper arsenite: $CuHAsO_3$ or $Cu_3(AsO_3)_2 \cdot 2H_2O$ (Bornemann 1922; Inorganic Chemistry Partington p. 628). There is hardly any reference in literature on the composition of copper arsenite by applying physico-chemical methods. In order to arrive at decisive conclusions and to throw light on the composition of copper arsenite it was considered worthy of interest to study its composition by conductometry and thermometry.

A. R. (B. D. H.) reagents were used. Standard sodium arsenite solution was prepared and estimated as described (Vogel; Text Book of Quantitative Inorganic Analysis, p. 342). Copper sulfate solution was standardized against standard sodium thiosulfate solution.

Using different concentrations of the solutions of copper sulfate and sodium arsenite, conductometric and thermometric titrations were carried out by direct and reverse methods, i. e., when copper sulfate solution was added from micro-burette to sodium arsenite solution taken in conductivity cell or thermos flask and vice versa. The titrations were performed both in aqueous and aqueous alcoholic medium, the maximum alcoholic concentration in the latter case being 20% by volume. The results are shown in Figs. 1, 2 and 3.

Considering the strength of solutions of copper sulfate (M/10, M/20) and sodium arsenite (M/40, M/80), the observed titre values in conductometric titrations are 2.6, 2.2, 2.1, 2.6, 2.3

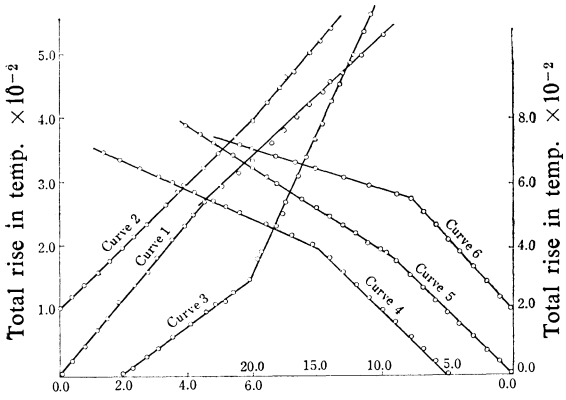


Fig. 1. Direct-titrations.
Curves 1, 2, 3 M/5 $CuSO_4$ and M/20 $NaAsO_2$
Curves 4, 5, 6 M/5 $CuSO_4$ and M/10 $NaAsO_2$

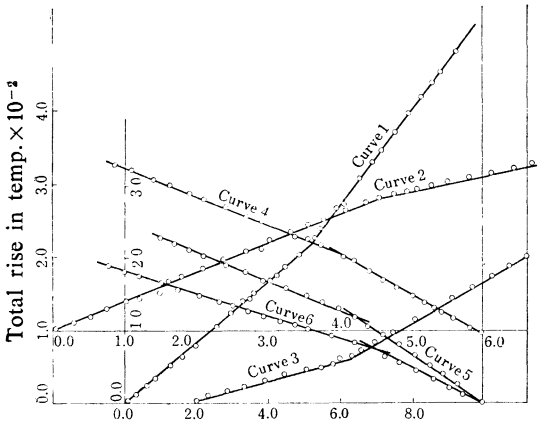


Fig. 2. Direct-titrations.
Curves 1, 2, 3 M/5 $NaAsO_2$ and M/20 $CuSO_4$
Curves 4, 5, 6 M/5 $NaAsO_2$ and M/10 $CuSO_4$

and 2.1 which are in agreement with the theoretical values 2.5, 2.25, 2.0, 2.5, 2.25, and 2.0 for 20.18 cc. and 16 cc. of sodium arsenite in case of direct titrations. The observed values in reverse titrations show a fair agreement

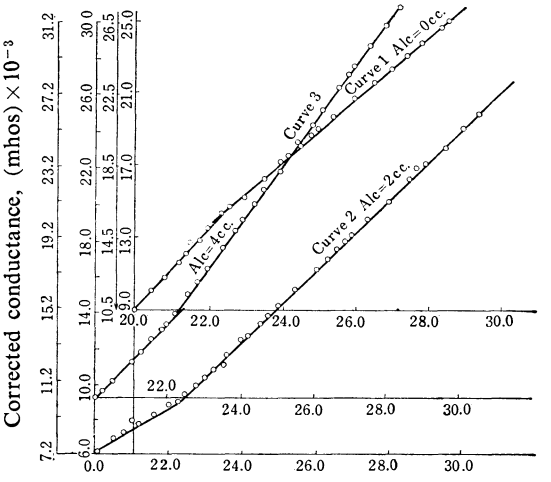


Fig. 3. Reverse-titrations.
Curves 1, 2, 3 M/5 $NaAsO_2$ and M/40 $CuSO_4$
Curves 1, 2, 3 M/10 $NaAsO_2$ and M/80 $CuSO_4$

with the theoretical values. Similarly in thermometric titrations the theoretical titre values calculated for 20.18 cc. and 16 cc. of solution in thermos flask show a notable agreement with the observed values, both in direct and reverse titrations. The details have not been given for the sake of brevity.

Thermometric and conductometric titration curves, both in direct and reverse methods, show one break corresponding to the point of equivalence in the ratio of 1 : 2 ($CuSO_4$: $NaAsO_2$) suggesting the formation of $Cu(AsO_2)_2$ which can be explained on the basis of the following equation:

$$CuSO_4 + 2NaAsO_2 = Cu(AsO_2)_2 + Na_2SO_4 \quad (1)$$

Studies on the complex by potentiometric titrations and Job's method of continued variation are in progress and the results will be communicated shortly.

Chemical Laboratories
Lohia College
Churu
Rajasthan, India

Further Studies on Kinetics of Reaction of Malachite Green with Acids. Influence of Temperature

By Sarvagya S. KATIYAR

(Received April 16, 1962)

Lapin and Gein[1] suggested the use of malachite green (MG) as an analytical reagent especially for the colorimetric estimation of Sb^{3+}, Au^{3+} and Tl^{+}. For these estimation the interaction between metal ions and malachite green has been found sensitive to acidity. In acid medium, however, malachite green reacts with acid[2-4], resulting in the loss of characteristic color which sets a limitation to its usefulness in acid medium. This instability of malachite green in acid medium was hitherto uninvestigated in detail and therefore, warranted investigations for the elucidation of the mechanism involved therein. The variation of velocity constant with temperature could be utilized for the computation of energy, heat and entropy of activation, which are of immense value for the elucidation of reaction mechanism. In the present paper are reported the investigations on the reaction of MG with hydrochloric acid at different temperatures in aqueous medium as well as in media containing varying percentages of organic solvents.

Experimental

Malachite green of B. D. H. quality was purified in the manner described by Lewis and coworkers[5]. The purified product used for kinetic study was obtained as sulfate. The hydrochloric acid used was Merck GR sample.

Acetone of B. D. H. Analar Grade was purified by refluxing over calcium oxide and distilling[6].

Dioxane, the extra pure product of E. Merck was purified by refluxing with acid and then over sodium and finally distilling according to procedure of Hess and Frahm[7].

The organic solvent water mixtures containing varying amounts of dioxane and acetone were made by volume percent. The reaction mixtures were so prepared that the final volume was the same containing fixed quantities of MG and acid but varying amounts of dioxane or acetone.

The progress of the reaction of MG with hydrochloric acid was investigated with the help of Beckman DU spectrophotometer by making optical density measurements at the wavelength of maximum absorption at different intervals of time. Corex cells of 10 mm. width were employed. The temperature in the cell compartment was maintained at the desired value by circulating water in the dual thermospacer set fixed in the spectrophotometer, from an external thermostat controlled by an electronic micro relay. By this arrangement temperature could be controlled with a precision of ± 0.05°C.

Results and Discussion

Malachite green is known[4,5] to exhibit absorption maximum at $\lambda = 617.5$ mμ in aqueous medium. This absorption maximum is, however, affected by the presence of organic solvents such as dioxane or acetone which shift it to 620.0 and 622.5 mμ respectively. The kinetic studies at different temperatures were therefore carried out at $\lambda = 617.5$ mμ in water, 620 mμ in acetone and at 622.5 mμ in dioxane water mixtures. At these wavelengths MG obeys Beer's law and the reaction products do not show any absorption.

Time Variant Nature of the Reaction: First Order Nature.—In presence of acids the characteristic green color of MG decreases continuously and progressively with time. The data given in Fig. 1 illustrate the variation with time of optical density in presence of 60 mM hydrochloric acid. Here curves 1 to 6 refer to different initial concentration of MG employed, in the range 0.006~0.014 mM. Thus the concentration of hydrochloric acid is in very great excess over that of MG. Under this experimental condition the reaction obeyed first order law, when analyzed by differential method. The average value of n, the order of reaction corresponded to 1.11. The first order nature of the reaction is further substantiated by what follows.

For establishing the order of a reaction and to calculate velocity constant k from the values

1) L. N. Lapin and V. O. Gein, *Trudy Komisii Anal. Khim., Akad. Nauk, S. S. S. R. Inst. Geokhim. i Anal. Khim.*, **7**, 217 (1956).
2) S. S. Katiyar, *Naturwissenschaften*, **49**, 325 (1962).
3) S. S. Katiyar, *Z. physik. Chem. N. F.*, in press.
4) N. V. Sidgwick and T. S. Moore, *J. Chem. Soc.*, **95**, 889 (1909), cf. *Chem. Abstr.*, **3**, 2799 (1909).
5) G. N. Lewis, T. T. Magel and D. Lipkin, *J. Am. Chem. Soc.*, **64**, 1774 (1942).
6) A. I. Vogel, "Practical Organic Chemistry", Longmans Green and Co., Ltd., London (1959), p. 171.
7) L. F. Fieser, "Experiments in Organic Chemistry", 2nd Ed., D. C. Heath and Co., New York, N. Y. (1941), p. 368.

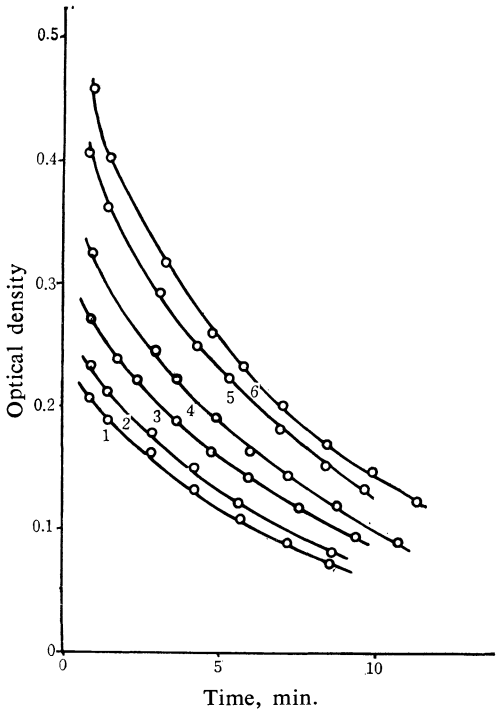


Fig. 1. Kinetic runs for the reaction of MG and HCl at varying MG concentrations.

1, 0.006 2, 0.007 3, 0.008
4, 0.01 5, 0.12 6, 0.14 mM

of C at time t, a number of methods[8] have been proposed from time to time. The following is the familiar equation for obtaining the first order rate constants

$$\ln C = \ln C_0 - kt$$

where C_0 is the initial concentration and C the concentration at time t. According to this equation the plot of log C vs. t would yield a straight line for a first order reaction. It is of interest to note from Fig. 2 that the plots of log C vs. t are sensibly linear confirming thereby the first order nature of the reaction. As mentioned above that $C_{MG} \ll C_{H^+}$ therefore the real velocity constant k' was obtained as follows:

$$k' = \frac{(\Delta \log C_{MG})}{\Delta t\ (C_{H^+})}\ \text{l. mol}^{-1}\,\text{sec}^{-1} \qquad (2)$$

Dependence of k' on Temperature in Aqueous Medium.—The data given in Fig. 2 show the variation of log (OD) with time of malachite green solutions at different temperatures in the range 298~313°K. For these experiments the

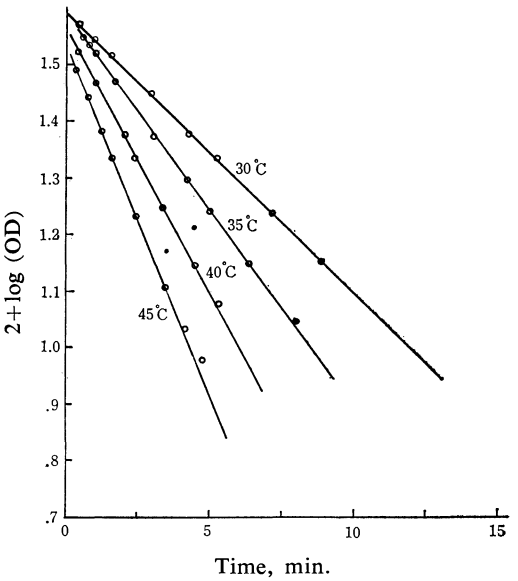


Fig. 2. Variation of log (OD) with time at different temperatures in aqueous medium.

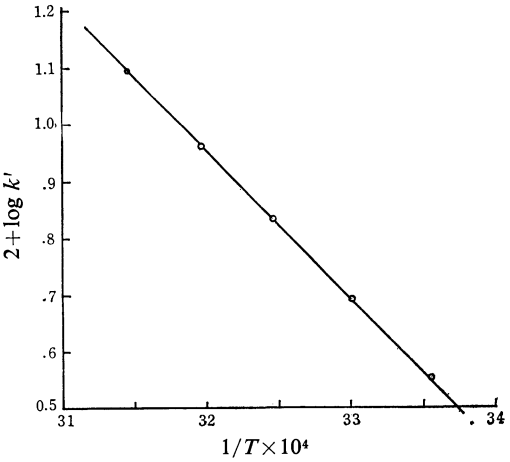


Fig. 3. Linear variation of log k' with $1/T$ in aqueous medium.

initial concentrations of MG and hydrochloric acid were 0.008 and 40 mM respectively. From the slope of these plots and the known initial concentration of hydrochloric acid k' was computed and the values obtained are reported in Table I; k' were 3.56×10^{-2} and 6.77×10^{-2} l. mol^{-1} sec^{-1} at 298 and 308°K respectively. The data of Table I were analyzed by the Arrhenius equation

$$\ln k' = \ln A - \frac{RT}{E^*} \qquad (3)$$

and the results are given in Fig. 3. It is interesting to note that sensibly linear plot of log k' vs. $1/T$ was obtained in accord with the

8) See for example, E. A. Guggenheim, *Philos. Mag.*, **2**, 538 (1926); A. A. Frost and R. G. Pearson, "Kinetics and Mechanism", John Wiley & Sons, Inc., New York (1953), p. 40.

TABLE I. VELOCITY CONSTANT FOR THE REACTION OF MG AND HCl AT DIFFERENT TEMPERATURES IN AQUEOUS MEDIUM

Temp. °K	$k' \times 10^2$ l./mol. sec.
298	3.56
303	4.91
308	6.77
313	9.12
318	12.40

TABLE II. THERMODYNAMIC QUANTITIES OF ACTIVATION IN AQUEOUS MEDIUM AT 25°C

E^*	11.91	kcal.
A	1.92×10^7	l./mol.sec.
ΔF^*	19.42	kcal./deg.mol.
ΔS^*	−27.20	cal./deg.mol.
ΔH^*	11.32	kcal.

above equation. The slope of this plot yielded a value of 11.91 kcal. for E^*, the energy of activation. This value of E^* together with k' (given in Table I) gave a value of 1.92×10^7 l. mol^{-1} sec^{-1} for A, the frequency factor. Further, these data were also utilized for the computation of other thermodynamic quantities of activation such as free energy (ΔF^*), entropy (ΔS^*) and heat (ΔH^*) of activation with the aid of following equations[9]

$$\Delta F^* = 2.303\, RT\left(\log \frac{RT}{Nh} - \log k'\right) \qquad (4)$$

$$\Delta S^* = 2.303\, R\left(\log A - \log e\frac{RT}{Nh}\right) \qquad (5)$$

The values of themodynamic quantities are summarized in Table II. It is seen from this table that ΔS^* corresponded to −27.2 cal./deg. mol. This negative value of ΔS^* indicates that the reaction is occurring between ionic species[10,11].

Dependence of Velocity Constant on Temperature in Dioxane and Acetone - Water Medium.— A typical set ot kinetic data obtained in 10% dioxane - water and 10% acetone-water is shown in Figs. 4 and 5 respectively. Similar type of data were obtained in 5 and 15% composition of these solvents. For these experiments the initial concentration of MG and hydrochloric acid were 0.008 and 80 mM respectively. The values of rate constants k' obtained from these data are listed in Table III. It may be noted from this table that k' decreased with

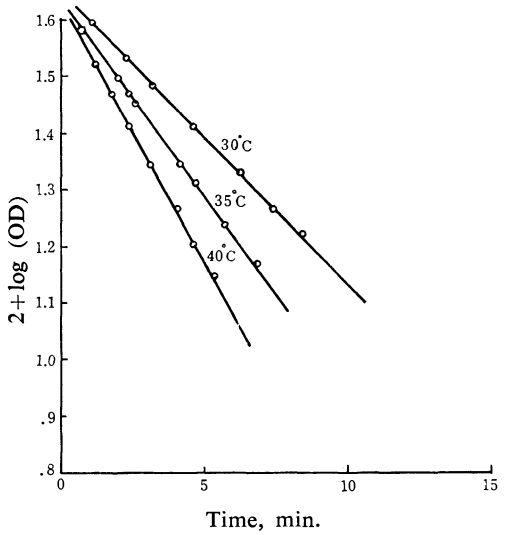


Fig. 4. Typical kinetic data for the reaction of MG and HCl in 10% dioxane.

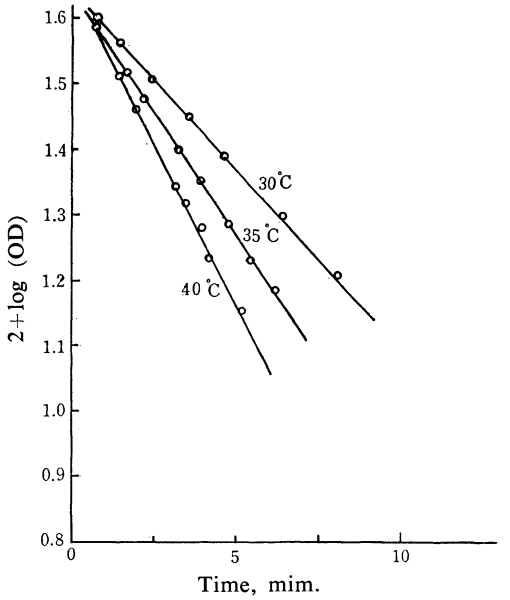


Fig. 5. Typical kinetic data for the reaction of MG and HCl in 10% acetone.

the increase in percentage of organic solvent at a particular temperature. This lowering of k' with decrease of dielectric constant of the medium when examined from Bronsted, Christiansen and Scatchard[12] equation points out towards the like charged nature of reactants involved in the reaction. This aspect has already been discussed in detail in a separate communication[2,3]. Further, at a fixed composition of solvent, however, rate constant

9) S. Glasstone, K. J. Laidler and H. Eyring, "The Theory of Rate Processes", McGraw Hill Book Co., Inc., New York, N. Y. (1941), pp. 195—199.
10) D. P. Ames and J. E. Willard, *J. Am. Chem. Soc.*, **73**, 164 (1951).
11) Cf. Ref. 9., p. 433.
12) G. Scatchard, *Chem. Revs.*, **10**, 229 (1932).

Table III. Velocity constants for the reaction of MG and HCl at varying temperatures in organic solvent water mixtures

Temp. °K	$k' \times 10^2$ l./mol.sec. 5%	10%	15%
	Dioxane		
298	2.32	1.85	1.44
303	3.27	2.48	1.90
308	4.47	3.33	2.58
313	6.00	4.42	3.43
	Acetone		
298	2.28	1.85	1.44
303	3.31	2.64	2.04
308	4.67	3.60	2.71
313	6.61	4.71	3.65

Table IV. Thermodynamic quantities of activation in organic solvent water mixtures

Thermodynamic quantities		Percentage of organic solvent 5%	10%	15%
		Dioxane		
E^*,	kcal.	11.68	11.27	10.68
A,	l./mol.sec.	0.84×10^7	0.34×10^7	0.78×10^6
ΔF^*,	kcal./deg.mol.	19.68	19.82	19.95
ΔS^*,	cal./deg.mol.	−28.84	−30.67	−33.13
ΔH^*,	kcal.	11.09	10.68	10.09
		Acetone		
E^*,	kcal.	12.75	11.70	11.16
A,	l./mol.sec.	3.11×10^7	0.70×10^7	0.22×10^7
ΔF^*,	kcal./deg.mol.	19.68	19.81	19.95
ΔS^*,	cal./deg.mol.	−26.24	−29.20	−31.52
ΔH^*,	kcal.	12.16	11.11	10.57

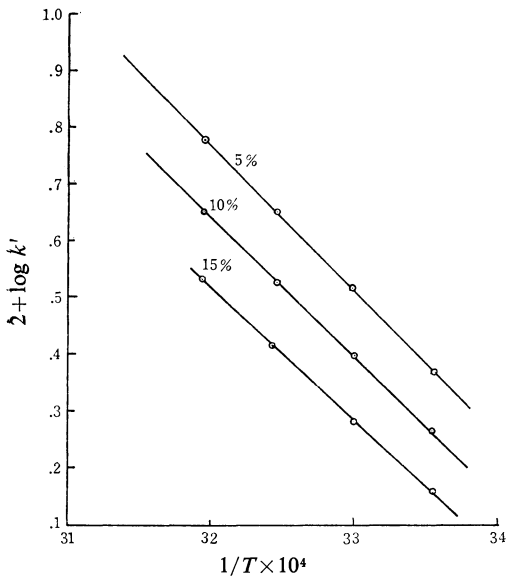


Fig. 6. Variation of log k' with $1/T$ in dioxane-water.

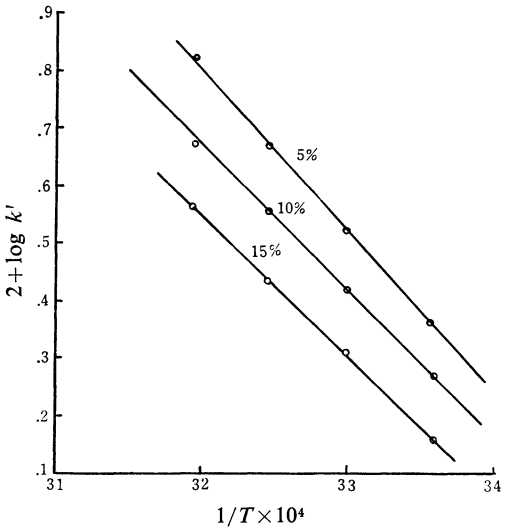


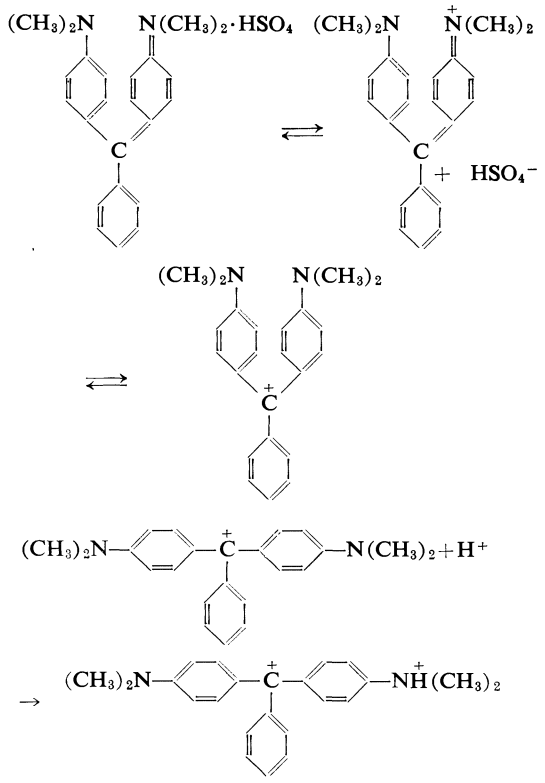
Fig. 7. Variation of log k' with $1/T$ in acetone-water.

k' was found to increase with increasing temperature. Thus, e. g. in 5% dioxane k' was 2.32×10^{-2} and 4.47×10^{-2} l. mol^{-1} sec^{-1} at temperatures 298 and 308°K respectively. This gave a value of 1.92 for temperature coefficient which is of the same order as observed in case of a numder of other reactions[13].

The data of Table III were also employed for the calculation of E^* in different composition of organic solvent. The plots of log k' vs. $1/T$ are shown in Figs. 6 and 7, for dioxane and acetone water mixtures. These plots as required by Eq. 3 are straight lines and the values of E^* obtained from the slopes are returned in Table IV. It is instructive to note that E^* decreases slightly with increasing percentage of organic solvent. Further the data of Table IV were also employed for the computation of thermodynamic quantities of activation such as ΔS^*, ΔH^* and ΔF^*. The values of these in different solvent compositions are summarized in Table IV. It is instructive to observe that ΔS^* becomes more negative with increasing percentage of organic solvents. This is probably due to solvated nature of intermediate complex. This observation also suggests that the species involved in the reaction responsible for the fading of color of MG in acid media are similarly charged[14] and this is in accord with the earlier findings.

Reaction Mechanism.—The results obtained by the kinetic studies on the reaction of malachite green and hydrogen ions led the author to suggest the following mechanism

13) S. Glasstone, "A Text Book of Physical Chemistry", MacMillan and Co., Ltd., London (1956), p. 1087.
14) Cf. Ref. 9, p. 122.



It is suggested that the first step represented by an equilibrium between the HSO_4^- and MG^+ ion does not contribute to the kinetic studies as the ionic recombination processes are known to be very fast[15,16]. Therefore, the second step involving the formation of acid salt is the rate determining step. It is instructive to note here that the second step points out towards reaction between positively charged ions, which is in complete agreement with the kinetic data obtained and presented in this paper and other communications[2,3]. It will be of interest to refer in this connection the observation of Branch and Tolbert[17] and Newman and Deno[18] who have also suggested the formation of acid salt for the reaction of malachite green with acids at pH 1.

Author's thanks are due to Professor P. K. Kelkar, Director of Indian Institute of Technology, Kanpur, for encouragement and kind interest in the work and to Director of N. S. I. Kanpur for the facilities of a spectrophotometer.

Department of Chemistry
Indian Institute of Technology
Kanpur, India

15) M-Eigen, *Discussions Faraday Soc.*, **17**, 194 (1954).
16) P. Delahay and T. J. Adams, *J. Am. Chem. Soc.*, **74**, 1437 (1952).
17) G. E. K. Branch and B. M. Tolbert, ibid., **71**, 781 (1949).
18) M. S. Newman and N. C. Deno, ibid., **73**, 3644 (1951).

*Thortveitite from Kobe, Omiya, Kyoto, Japan**

By Kin-ichi SAKURAI**, Kozo NAGASHIMA and Akira KATO***

(Received May 12, 1962)

In 1960, T. Hisano, an amateur mineral collector in Kyoto, presented several mineral specimens gathered from Shiroishi pegmatite at Kobe, Omiya, Naka-gun, Kyoto, to the first author for identification. Of these, a small greenish gray crystal, after being subjected to X-ray diffraction, X-ray fluorescent and emission spectrochemical studies, turned out to be the first thortveitite fonnd in Japan.

Thortveitite, a soro-silicate of the scandium and yttrium group rare earths, was first described by Schetelig[1] in 1911 as gathered from a pegmatite at Iveland, Saetersdalen, Norway. Since then, only one locality, Befanamo, Madagascar, has been added, by Lacroix[2]. The material from this locality, containing more zirconium and less yttrium than that from Iveland material, was called by the variety name of befanamite.

In 1924, Goldschmidt and Thomassen showed the selective assemblage of rare earth elements in this mineral, the surprisingly high content of ytterbium, and the higher contents of scandium and yttrium[3]. Also, Goldschmidt alone has demonstrated an average of as much

* This paper was read at the 15th Annual Meeting of the Chemical Society of Japan, Kyoto, April, 1962.

** Present address: The National Science Museum, Taito-ku, Tokyo.

*** Present address: Faculty of Science, The University of Tokyo, Hongo, Tokyo.

1) J. Schetelig, *Vidensk. Skrift*, No. 151 (1922).

2) A. Lacroix, *Compt. rend.*, **171**, 421 (1922).

3) V. M. Goldschmidt and L. Thomassen, *Videndsk. Skrift. I. Mat. -naturv. Klasse*, No. 5 (1924).

as 20 p. p. m. scandium in the gabbro-amphibolite of Iveland and has suggested that the scandium in the thortveitite did not originate from granitic residual material but from the surrounding gabbro-amphibolite penetrated by the pegmatite dikes[4].

The peculiarity of this rare silicate is also found in its unusually high HfO_2/ZrO_2 ratio[5,6], which reaches 0.5 in the Norwegian thortveitite associated with zircons, with $HfO_2/ZrO_2=0.02$ as an average. Furthermore, as is frequently mentioned in textbooks of crystal chemistry, this mineral is one of the most representative species among soro-silicates[7,8].

Occurrence

The Shiroishi pegmatite is enclosed by a late Cretaceous biotite granite overlain by Miocene volcanic sediments about 10 km. north of the pegmatite[10]. The granite body contains many pegmatites, as at Oro, Mie, Morimoto, Ushio Mine, and also this Shiroishi pegmatite.

The pegmatite from which this mineral was derived is called Shiroishi pegmatite and is composed chiefly of perthite, quartz, biotite, muscovite and many such rare accessory minerals as kobeite[10,11], perrierite[12,13], euxenite, monazite, radioactive zircon, allanite, tourmaline, magnetite and ilmenite.

There are only two specimens that have been identified as thortveitite. One is a prismatic crystal $10\times4\times3.5$ mm. in size, while the other is much smaller, $9\times2\times2$ mm. Minute crystals of zircon are attached to the surface of the latter. Because both of them were found in the waste of the quarry, the minerals in the paragenetic relation are uncertain except for the zircon. The fresh surface is greenish gray in color with a glassy luster, but when altered it turns somewhat brownish. The streak color is white.

Emission Spectrochemical Analysis

As the amount of the sample available was so small, the emission spectrochemical technique was applied for the estimation of the scandium, yttrium, ytterbium, zirconium and hafnium. Sodium chloride contaminated by 0.01% palladium as the internal standard was used as the spectrochemical buffer to depress the intensities of the cyanogen bands, which may interefere with many sensitive lines of rare earth elements.

A graduated standard series covering the 0.002~2.0% range as the oxide of each element was prepared by diluting a mixture of scandium oxide, yttrium oxide, ytterbium oxide, zirconium oxide and hafnium oxide with a buffer. Samples were mixed according to one of the following ratios: (a) one part of sample to 9 parts of buffer, or (b) one part of sample to 99 parts of buffer. The wall of the cavity of the graphite electrode was cut as thin as possible so as to aid the quick burning of the sample, and higher amperage was applied to reduce the volatility differences between the elements.

Working conditions were as follows:

Instrument: Shimadzu Littrow type spectrograph.
Spectral region: 4400~2700 Å.
Electrode: National Carbon's special-grade 1/8 inch graphite electrode.
Loaded sample: About 10 mg.
Analytical gap: 3 mm.
Voltage: 230 V. D. C.
Current: 9 amp. anode excitation.
Exposure: 0~50 sec.
Photographic plate: Fuji Spectroscopic Process.

In the sample with 1:9 dilution, such elements as aluminum, calcium, dysprosium, erbium, iron, hafnium, lutetium, magnesium, manganese, scandium, silicon, yttrium, ytterbium and zirconium were detected. Of these, except for silicon, scandium, yttrium and ytterbium the main components of this mineral, the lines of only iron and manganese were strong enough to be estimated as much as the order of 1%. Beryllium, often reported in this mineral, was not found.

Adopting the line pairs of Sc 3365/Pd 3481, Y 3242/Pd 3481, Yb 3298/Pd 3481, and Zr 3391/Pd 3481, smooth calibration curves were drawn for each element except hafnium at lower concentrations. Taking account of the previous lack of study of error for actual analysis, the range of values for each oxide is shown in Table I.

Table I. Spectrochemical analysis

Sc_2O_3	10 %
Y_2O_3	3~10 %
Yb_2O_3	3~10 %
ZrO_2	0.1~0.3 %
HfO_2	0.01~0.03%

4) V. M. Goldschmidt, *Geol. Foren. Forh.*, **56**, 385 (1934).
5) G. von Hevesy and V. Thal Jantzen, *Z. anorg. Chem.*, **136**, 387 (1924).
6) M. Fleischer, *U. S. Geol. Survey Bull.*, No. 1021 (1955).
7) W. H. Zachariasen, *Z. Krist.*, **73**, 1 (1930).
8) F. Liebau, *Acta Cryst.*, **14**, 1103 (1961).
9) O. Hirokawa and K. Kuroda, Geological Map of Miyazu (1/50000) and Explanatory Text, Geol. Survey of Japan (1960) (in Japanese).
10) J. Takubo, Y. Ukai and T. Minato, *J. Geol. Soc. Japan*, **56**, 509 (1950) (in Japanese).
11) K. Masutomi, K. Nagashima and A. Kato, *Mineral. J.*, **3**, 139 (1961).
12) J. Takubo and S. Nishimura, *J. Min. Soc. Japan*, **1**, 51 (1953) (in Japanese).
13) S. Bonatti, *Am. Mineral.*, **44**, 115 (1959).

Such other minerals as kobeite, monazite, zircon, ilmenite, and feldpars were analyzed in the same way; only in kobeite 0.1~0.3 % scandium oxide was determined.

X-Ray Powder Studies

A very small fraction of the thortveitite was examined by X-ray powder study using a Norelco X-ray diffractometer. These powder data were compared with those of the thortveitite from Befanamo, Madagascar,[14] as given in Table II.

As may easily be seen, there are consistent discrepancies in the respective corresponding diffractions; that is, their *d*-values are always smaller in the Befanamo material. The discrepancies are to be ascribed to the increase of lattice constants due to the substitution for the smaller ion (Zr^{4+}=0.86Å) of the larger ion (Y^{3+}=1.00Å), both of which replace scandium.

TABLE II. X-RAY POWDER DATA FOR THORTVEITITES FROM BEFANAMO, MADAGASCAR AND KOBE, KYOTO, JAPAN

1		2	
d, Å	*I*	*d*, Å	*I*
5.13	100	5.18	30
4.57	5	4.57	20
4.48	5		
4.29	5		
3.45	5	3.45	20
3.36	10	3.35	10
3.14	90	3.16	50
3.12	100	3.13	100
2.93	80	2.96	80
2.60	30	2.62	40
2.55	80	2.59	50
		2.44	10
2.17	30	2.19	30
2.13	5	2.15	5
2.09	10b	2.11	20
2.05	30	2.08	20b
1.932	10		
1.975	10	1.883	10
		1.768	10
1.700	40	1.738	10vb
1.694	30	—1.708	
1.646	30	1.660	20b
1.594	20	1.590	10b
1.572	10		
1.552	10	1.537	30
1.509	20	1.510	10
1.422	20	1.434	10
1.358	40	1.346	10b

b=broad, vb=very broad

1 Thortveitite (Befanamite), Befanamo, Madagascar. Cu/Ni radiation[14].

2 Thortveitite, Kobe, Kyoto, Japan. Cu/Ni radiation.

14) Geological Survey of Japan, X-ray Powder Data for Radioactive Minerals, (1958), p. 112, (unpublished data).

Distribution of Lanthanum Series Elements

The distribution of lanthanum series elements was determined by the X-ray fluorescent method. The results are graphically configured in Fig. 1 and compared with those of Goldschmidt and Thomassen. The figure indicates the prevailing dominance of ytterbium among the lanthanide elements and how the elements belonging to the cerium-, gadolinium- and terbium-groups are quite deficient (detection limit: 0.01 % as R_2O_3). Although there are slight discrepancies between the present results and those of Goldschmidt and Thomassen in point of the distribution of the lighter lanthanides, a good coincidence was attained for those of the heavier lanthanides according to Oddo-Harkin's law.

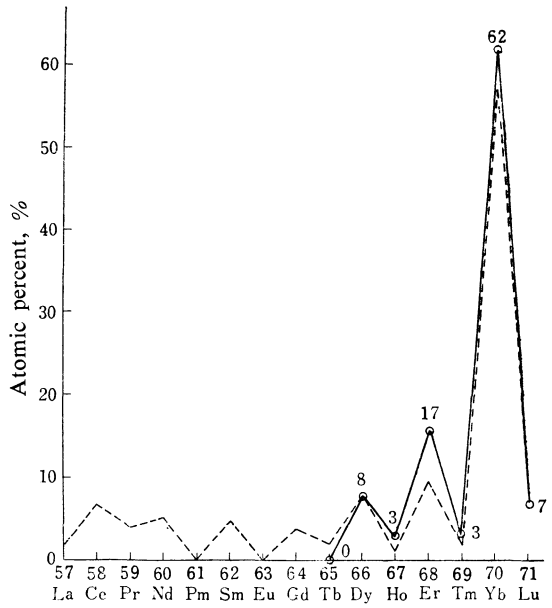


Fig. 1. Distribution of the Lanthanum series elements.
—— Present mineral
--- Goldschmidt's thortveitite type (recalculated)

Discussion

From the results of X-ray powder study, X-ray fluorescent and emission spectrochemical analyses, it is quite certain that the mineral in question is thortveitite.

As for the contents of the yttrium group of rare earths, that is, a summation of yttrium oxide and the oxides of the yttrium group

lanthanide elements, values by older analyses fall in the range between 8.89~17.7 % which range includes the present value.

The zirconium contents in thortveitites vary considerably. For example, Schetelig found 5 % zirconium oxide from the Iveland material[15], but a newer analysis[16] shows the absence of zirconium in other thortveitite from the same locality, suggesting a fluctuation in zirconium content even in samples from the same locality. Therefore, the rather low zirconium content of the present material is not particularly unusual; moreover, as may easily be seen from Table I, the extraordinary concentration of hafnium with respect to zirconium is in good harmony with the results of Hevesy and Jantzen[5].

Our discovery of thortveitite and detection of scandium in kobeite from the Shiroishi pegmatite indicates a notable accumulation of scandium in the magmatic residue of the granitic rock in this area in which no vestige of basic rock is found. In this respect, Goldschmidt's opinion is not applicable to the genesis of the thortveitite from the Shiroishi pegmatite.

Very recently, Neumann[17] has suggested the origin of scandium in several kinds of minerals in pegmatites of the Iveland district, where some thortveitite-bearing pegmatite dikes are developed.

The writers wish to express their hearty thanks to Mr. Takeshi Hisano for his kind presentation of the material used in this study. Our study was aided by a grant from the Scientific Research Fund of the Ministry of Education.

College of General Education
The University of Tokyo
Meguro-ku, Tokyo

15) C. Doelter, "Handbuch der Mineralchemie," III-2, 554 (1917).
16) J. P. Marble and J. J. Class, *Am. Mineral.*, **27**, 696 (1924).
17) H. Neumann. *Norsk. Geol. Tidssk.*, **41**, 197 (1961).

*Isomerization of Cyclohexyl Phenyl Ketoxime in Liquid Sulfur Dioxide**

By Niichiro TOKURA and Katsuo SHIINA

(Received May 16, 1962)

It has been shown by Waterman et al.[1] that the cis-trans isomerization of olefins is carried out by sulfur dioxide at 100~140°C. As to the elaidination of oleic acid by sulfur dioxide, many papers have been published[2] since the first paper on this subject appeared in 1894 by Saytzeff[3]. The carbon-carbon double bonds of steroids are also rearranged by liquid sulfur dioxide or by sulfur dioxide vapor[4]. Recent works by Cunneen et al.[5] are concerned with the cis-trans isomerization of polybutadiene and polyisoprene by sulfur dioxide at high temperatures.

The isomerization of a ketoxime in liquid sulfur dioxide was first found by Tada, Masubuchi and Tokura[6], the isomerization taking place even at low temperatures. According to their view[6], the rate of the Beckmann rearrangement of a ketoxime in liquid sulfur dioxide is so fast that the isomerization of the ketoxime is not competitive with the Beckmann rearrangement in liquid sulfur dioxide, the product of the reaction being a pure and single acidamide.

On the other hand, Brown et al.[7a] have reported on an ordinary case of Beckmann rearrangement in which the isomerization was predominant over the rearrangement, the product being a mixtue of the acidamides.

* The Beckmann Rearrangement in Liquid Sulfur Dioxide. Part X.

1) H. I. Waterman and C. Boelhower, "Advances in Catalyst", **9**, Ed. by A. Farkas, Academic Press, New York (1957), p. 294.

2) a) H. I. Waterman et al., *Chem. Abstr.*, **42**, 2787 (1948).
b) H. I. Waterman et al., ibid., **44**, 3884, (1950).
c) H. I. Waterman et al., *Chemie et Industrie*, **64**, 557 (1950).
d) H. I. Waterman et al., *Chem. Abstr.* **45**, 5946 (1951).
e) A. Kenzenkamp et al. *J. Am. Oil Chem. Assoc.*, **26**, 479 (1949).

3) A. Saytzeff, *J. Prakt. Chem.*, **50**, 73, 81 (1894).

4) a) C. D. Laubach, *J. Am. Chem. Soc.*, **78**, 4744 (1956).
b) A. W. D. Hudgell, J. H. Turnbull and W. Wilson, *J. Chem. Soc.*, **1954**, 814.

5) a) J. I. Cunneen and F. W. Sirley, *J. Polymer Sci.*, **34**, 260 (1959); **36** 77 (1959).
b) J. I. Cunneen and H. F. Watson, ibid., **38**, 521, 533 (1959); **40**, 1 (1959).

6) R. Tada, Y. Masubuchi and N. Tokura, This Bulletin, **34**, 209 (1961).

7) a) R. F. Brown, M. van Gulic and C. H. Schmid, *J. Am. Chem. Soc.*, **77**, 1094 (1955).
b) Y. Yukawa, "Jikken Kagaku Koza", Vol. **18**, Ed. by the Chemical Society of Japan, Maruzen, Tokyo (1957), p. 426.

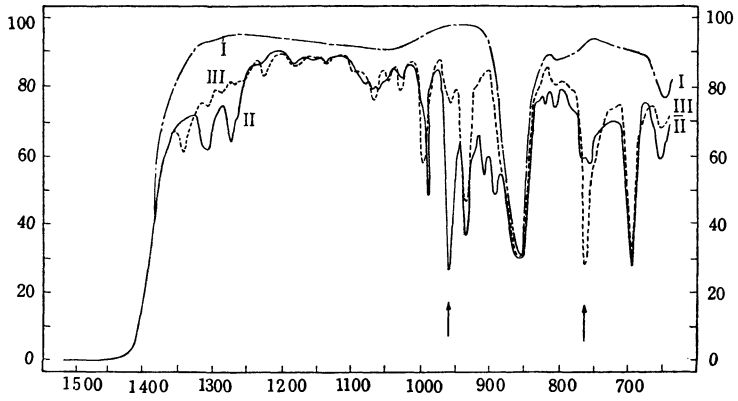
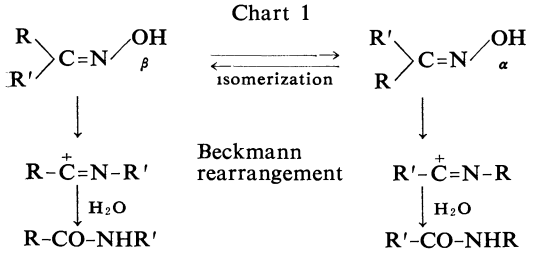


Fig. 1. Infrared spectra of the oximes in carbon disulfide.
I —·— CS_2 II —— α-Oxime III --- β-Oxime

derived from both the initial and the isomerized oximes. Yukawa et al. have tried the Beckmann rearrangement of cyclohexyl phenyl ketoxime in order to obtain various mixtures of the two acidamides, the proportions of which were dependent upon the reagents used for the rearrangement[7b].

Chart 1



In the present paper, the present authors should like to submit their findings on the kinetics of the liquid sulfur dioxide-catalyzed isomerization of β-cyclohexyl phenyl ketoxime ($R=C_6H_{11}$, $R'=C_6H_5$) to the α-isomer.

Experimental

Liquid Sulfur Dioxide.—Sulfur dioxide was dehydrated by phosphoric acid anhydride[6].

Preparation and Separation of Cyclohexyl Phenyl Ketoxime.—The method used in the preparation and separation of the α and β-oximes was that described in a preceding paper[6].

Experimental Procedure.—In a 200 ml. glass pressure vessel about 250 mg. of the β-oxime(m. p., 114.5°C) was dissolved into liquid sulfur dioxide to make up a 40 ml. solution of the reaction mixture, the temperature of which was kept constant throughout the preparation[8] and the runs by means of a thermostat. At definite time intervals 8 ml. portions of the solution were withdrawn from the mixture. The aliquot was mixed with ice water and neutralyzed with an ammonia solution, and the precipitate was filtered, dried and analyzed for the oxime content. The run in dark was also carried out to compare the photochemical effect on the isomerization.

Analysis of the Isomeric Oximes.—The infrared spectrophotometric method was employed for this analysis. A Perkin-Elmer double-beam model 21 type spectrometer was used. As may be seen in Fig. 1, the characteristic absorption curves of α and β-oximes in carbon disulfide (curves II and III respectively) offer absorption maxima at 762 and 957 cm^{-1} for use as key bands for the analysis of the oximes. The simultaneous Eqs. 1 and 2 were used to calculate the content of the oximes.

$$E_m^{762}=C_\alpha\cdot E_\alpha^{762}+C_\beta\cdot E_\beta^{762} \quad (1)$$

$$E_m^{957}=C_\alpha\cdot E_\alpha^{957}+C_\beta\cdot E_\beta^{957} \quad (2)$$

where, E_α^{762}, E_β^{762}, E_α^{957}, and E_β^{957} are the molecular extinction coefficients of α-oxime and of β-oxime at 762 and 957 cm^{-1} respectively, the upper suffixes corresponding to the wave numbers and the lower suffixes to the α- and β-oximes, E_m^{762} and E_m^{957} are the extinction coefficients of the sample at the respective wave numbers, and C_α and C_β are the contents of the oximes in the sample. Beer's law was obeyed throughout the experimental conditions, and the experimental error of this analytical method was within three percent.

Results and Discussion

The isomerization of the β-oxime to the α-oxime is a slow reaction, as was expected. The conversions, in percentages, were 27 at 48 hr. and 20 at 12 hr., the initial concentrations of the oxime being, 2.46×10^{-2} mol./l. and 4.31×10^{-2} mol./l. at 0°C in diffused-room daylight. The reaction was accelerated by light and retarded by the addition of hydroquinone (H.Q.) (Fig. 2). In Fig. 3 the effects of the degree of dehydration of the liquid sulfur dioxide and of the addition of

8) N. Tokura, M. Matsuda and F. Yazaki, *Makromol. Chem.*, **42**, 108 (1960).

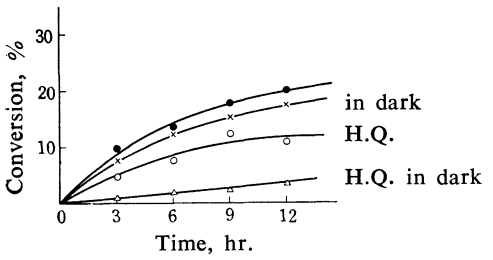


Fig. 2. Isomerization at 0°C in liquid sulfur Dioxide
[β-oxime] 4.31×10^{-2} mol./l.
[H. Q.] 1.0×10^{-2} mol./l.

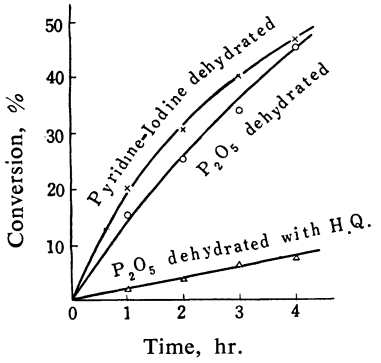


Fig. 3. Effect of degree of dehydration of liquid sulfur dioxide.
[β-oxime] 4.31×10^{-2} mol./l., Temp. 30°C

hydroquinone at 30°C in diffused daylight are visualized together. Liquid sulfur dioxide dried with phosphorus pentoxide (assuming the water content to be 100~50 p. p. m.)[9] or liquid sulfur dioxide dried with pyridine and iodine (estimating the water content as 30 p. p. m.)[10] has produced little difference in the rate of isomerization, whereas the addition of hydroquinone produced a marked depression of the rate at this temperature also.

These results are consistent with the radical nature of the isomerization reaction, as was shown in the cases of the cis-trans isomerization of olefins at higher temperatures[1-5]. However, acid catalysis by sulfur dioxide in part may not completely be ruled out since Tokura et al.[11] have found that a cationic polymerization by sulfur dioxide itself can be carried out in preference to a radical reaction in liquid sulfur dioxide.

To avoid the effect of light, all of the following kinetic runs were performed in the dark. The extent of the isomerization for the kinetical analysis was confined to a low conversion as much as possible. The reactions were carried out at 0, 10 and 20°C, the initial concentration of the β-oxime being 4.31×10^{-2} mol./l. The $\ln\{a/(a-x)\}$ vs. time plots are shown in Fig. 4. The results fit well with a first-order rate expression with respect to the concentration of the β-oxime. The rate constants, k, for the respective temperatures are listed in Table I.

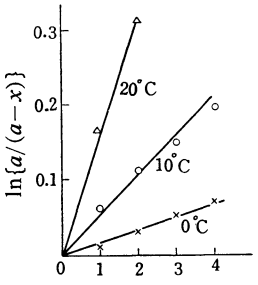


Fig. 4

Table I. The rate constants of the isomerization
Rate=k·[oxime]

Temp., °C	Rate constant, k $\times10^5$ sec^{-1}
0 (dark)	0.41
10 (dark)	1.58
20 (dark)	4.66
0 (diffused daylight)	0.65

Table II. The Arrhenius parameters

Activation energy:	E_a	19.1 kcal./mol.
Frequency factor:	A	6.3×10^{11} sec^{-1}
Rate constant:	k	$=6.3\times10^{11}\times\exp[-19.1/RT]$ sec^{-1}

Table III. Attempted isomerization in various solvents
(In the dark at 0°C and over a 12-hr. period)

Solvent	Isomerization
Ethanol	None
Acetone	None
Benzene*	None
CCl_4	None
Acetic acid*	None
Dimethyl sulfoxide*	None
Dimethylformamide	None

* At room temperature

The Arrhenius parameters are obtained from the linear plot, $\log k$ vs. $1/T$, and are listed in Table II.

To compare these results with the catalytic action of the ordinary solvents with the syn-anti isomerization of the oxime, the β-oxime

9) D. Murakami and N. Tokura, This Bulletin, 31, 431 (1958).
10) T. Hata and T. Asano, *Bull. of Res. Inst. of Non-Aqueous. Solns.* (*Hisuiken Hokoku*), 9, 79 (1960).
11) N. Tokura, M. Matsuda, I. Shirai, K. Shiina, Y. Ogawa and Y. Kondo, This Bulletin, 35, 1043 (1962).

was dissolved in a number of solvents and the mixtures were allowed to stand for 12 hr. at 0°C in the dark. As is shown in Table III, no isomerization was observed.

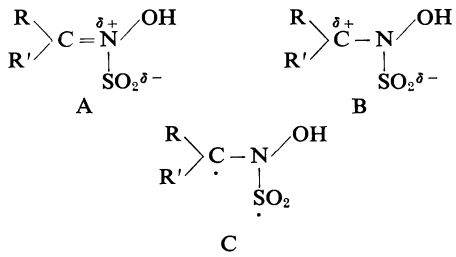
Tada, Shoji and Tokura[12] have shown that oxime is liable to form a 1 : 1 complex with sulfur dioxide:

$$\text{Oxime} + SO_2 \rightleftharpoons \text{Oxime}\cdot SO_2 \text{ (complex)} \quad (3)$$

The postulated dual (radical and ionic) nature of sulfur dioxide catalysis upon isomerization may well be elucidated by such a complex formation as an intermediate, as such is often the case in sulfur dioxide catalyses[1-5].

In the absence of light, the isomerization may be subject to acid catalysis via form B in Chart 2 through a rotating of the C–N axis conducted by a carbonium ion mechanism.

Chart 2



On the other hand, in the presence of light complex A may be excited to make easy the formation of the carbon radical, as is seen in form C in Chart 2, the rotation of the C–N axis being carried out through this radical form. That sulfur dioxide is an excellent radical acceptor by using the expanded orbital (3d orbital) of the sulfur atom has already been recognized in many instances.

For the early stage of the oxime conversion and in the case of a large excess of liquid sulfur dioxide, the rate of the isomerization, R, may be expressed as Eq. 4, the rate-determining step being assumed as the isomerization of the complex.

$$R = k_o[\text{complex}] = k_o K[\beta\text{-oxime}][SO_2] = k[\beta\text{-oxime}] \quad (4)$$

where K is an equilibrium constant for Eq. 3, k_o and k are the rate constants of the isomerization for the second order and the pseudo-first order reactions respectively, and the brackets indicate the concentrations of the respective components.

As has been described above, the isomerization of the oxime in liquid sulfur dioxide is a very slow reaction in comparison with the fast Beckmann rearrangement, the latter reaction being much too fast to be measured accurately and the rearrangement being completed within 5 min. at 0°C[6].

However, the conclusion that liquid sulfur dioxide is an excellent solvent for such a Beckmann rearrangement should be taken with many reservations, since there remains another possibility of the isomerization during the Beckmann rearrangement, viz., an acid-catalyzed isomerization accompanied by this rearrangement. The acid may be either the acid (Lewis acid) itself used as the reagent for the Beckmann rearrangement or a Brønsted acid derived from Lewis acid. Experiments on an acid-catalyzed isomerization in liquid sulfur dioxide are now in progress; and the results will be published in a following article.

Summary

1. The syn-anti isomerization of β-cyclohexyl phenyl ketoxime is carried out in liquid sulfur dioxide.

2. The isomerization is accerelated by light and retarded by hydroquinone. The degree of the dehydration of liquid sulfur dioxide has little effect on the rate of isomerization.

3. The kinetic result has shown that the reaction is of the first order with respect to the concentration of the oxime and that the rate constant, k for $R = k[\beta\text{-oxime}]$, may be expressed as:

$$k = 6.3 \times 10^{11} \exp\ [-19.1/RT]$$

4. A complex between the oxime and sulfur dioxide is assumed as the intermediate step, the isomerization of the complex being the rate-determining step. The dual (radical and ionic) nature of the isomerization in liquid sulfur dioxide may well be elucidated by such an assumption.

The Chemical Research Institute of Non-Aqueous Solutions
Tohoku University
Katahira-cho, Sendai

12) R. Tada, K. Shoji and N. Tokura, unpublished.

Synthesis of Mononitro-, Monoamino- and Monohalo-p-terphenyls, and their Solubility and Specific Gravity

By Tadashi NOZAKI and Yûhei HARADA

(Received May 21, 1962)

Many physical properties of monosubstituted *p*-terphenyls should vary greatly according to the variety in the nature and the position of the substituent. This is because, since *p*-terphenyl (in general, a para-polyphenyl) is a long planar molecule having many π-electrons, the change in its energy levels caused by a substituent should usually be large, with the mode and degree of the change depending more strongly on the nature and the position of the substituent than in the case of an aliphatic or a condensed aromatic compound. Therefore, various kinds of isomeric monosubstituted *p*-terphenyls seem to be an interesting example regarding the influence of a substituent on physical properties of organic compounds. Studies on their synthesis and physical properties would also be useful for further development in the basic study of organic scintillator and organic semiconductor.

Various synthetic methods for mononitro-, monoamino-, monochloro-, monobromo- and monoiodo-*p*-terphenyls were examined and compared with one another, and suitable methods of preparation are presented in this paper. All isomers of these compounds, including several new compounds, were synthesized and purified. Their solubility and specific gravity were measured, and other physical properties including absorption spectra are now under measurement.

Synthesis.—Ames reviewed the synthesis of substituted terphenyls in 1958[1]. We reported a suitable condition for the mononitration of *p*-terphenyl[2]. In general, the following processes seem to be available for the synthesis of the compounds in question: (1) direct nitration or halogenation of *p*-terphenyl, (2) reaction of 4-(*N*-nitrosoacetamido)-biphenyl (abbreviated as NAB) or *p*-phenylbenzenediazonium oxide (abbreviated as PBDO) with nitrobenzene or halobenzene, (3) reaction of monosubstituted NAB or monosubstituted PBDO with benzene, (4) conversion of another monosubstituted *p*-terphenyl into the desired compound, (5) dehydrogenation of monosubstituted 4-cyclohexylbiphenyl, (6) reaction of monosubstituted *N*-nitrosoacetanilide with biphenyl. The process 1, 2 and in some cases 4 offer a mixture of isomeric monosubstituted *p*-terphenyls. For the separation, column chromatography followed by recrystallization is usually suitable.

The mono-nitration of *p*-terphenyl[2] gave a mixture of 2-nitro-*p*-terphenyl (15~25%), 4-nitro-*p*-terphenyl (ca. 60%) and 2'-nitro-*p*-terphenyl (15~20%). This reaction is suitable for preparing 4-nitro-*p*-terphenyl, since it is easily separated from the mixture owing to its low solubility. But, separation of other two isomers required very tedious processes because of their marked similarity in many physical properties. Earlier workers obtained[3] 2-nitro-*p*-terphenyl and 4-nitro-*p*-terphenyl by treating NAB with nitrobenzene and separating the product by fractional recrystallization. According to our experimental result, PBDO could be used in place of NAB to give almost the same yield of the product, and PBDO was prepared much more easily than NAB. Further, 3-nitro-*p*-terphenyl, a new compound, was obtained by column-chromatographic separation of the reaction products, though the yield was poor. 3-nitro-*p*-terphenyl was more conveniently prepared by deacetamidating a nitration product of 4-acetamido-*p*-terphenyl (overall yield, 40% based on 4-amino-*p*-terphenyl). 2'-Nitro-*p*-terphenyl had been obtained by dehydrogenating 3-nitro-4-cyclohexylbiphenyl[4]. This compound was synthesized more conveniently, contrary to the description in a literature[3], by the reaction of nitrosated 3-nitro-4-acetamidobiphenyl with benzene. Although pure 3-nitro-NAB was not obtained, the yield of purified 2'-nitro-*p*-terphenyl was satisfactory (30~40% based on 3-nitro-4-acetamidobiphenyl).

Nitro-*p*-terphenyl was reduced to amine hydrochloride with tin(II) chloride almost quantitatively, and iodo-*p*-terphenyl was obtained by the Sandmeyer reaction of the diazotized amine with a good yield (50~60%). The

1) R. G. Ames, *Chem. Revs.*, **58**, 895 (1958).
2) T. Nozaki et al., This Bulletin, **33**, 1331 (1960).
3) H. France et al., *J. Chem. Soc.*, **1938**, 1368.
4) F. R. Basford, ibid., **1937**, 1442.

yield of chloro- and bromo-*p*-terphenyls except 4-chloro- and 4-bromo-*p*-terphenyls by this method, however, was poor. Several new compounds, i. e. 2'-chloro-, 2'-bromo-, 2-, 3- and 2'-iodo-*p*-terphenyls, were thus obtained.

The earlier workers[3] also prepared 2-, 3-, 4-chloro-, 2-, 3- and 4-bromo-*p*-terphenyls by similar processes as they used for preparing 2- and 4-nitro-*p*-terphenyls. In these cases, too, PBDO was found to be used preferably to NAB. Separation of isomeric halo-*p*-terphenyls was more tedious than in the case of the nitro-compounds, requiring repeated chromatographic separation and recrystallization. Hence, for preparing a definite quantity of 2- and 3-chloro (or 2- and 3-bromo), it is preferable to separate a part of 2- and 3-chloro (or 2- and 3-bromo) in pure state from a larger quantity of the mixture. Some of the compounds have considerably higher melting points than the values in the literature[5]. The reaction of PBDO or NAB with iodobenzene, however, gave only traces of iodo-*p*-terphenyls with a much larger quantity of 4-iodobiphenyl.

3-Chloro-4-acetamidobiphenyl had been prepared[6] by chlorinating 4-acetamidobiphenyl with sodium hypochlorite and treating the product with hot acetic acid. Crude 3-bromo-4-acetamidobiphenyl had also been prepared[7] by treating 4-acetamido-biphenyl with bromine in acetic acid and removing less soluble by-products. The two halo-acetamidobiphenyls were nitrosated and converted into 2'- (30~40% yield based on 4-acetamidobiphenyl) and crude 2'-bromo compounds, the latter being purified chromatographically. These processes compare favorably with the syntheses from 2'-nitro-*p*-terphenyl.

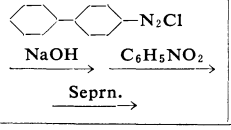
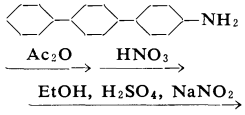
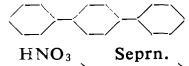
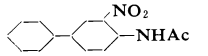
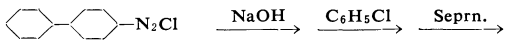
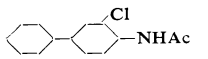
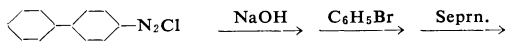
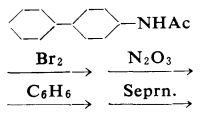
Direct bromination and iodination of *p*-terphenyl under a suitable condition offer 4- and 4-iodo respectively, but the products are contaminated by 4, 4''-dihalo-*p*-terphenyl, which is removed with great difficulty on recrystallization and vacuum sublimation. Column-chromatographic separation with the aid of the absorption technique of a soft γ-ray, however, was very useful for obtaining a small quantity (less than a few grams) of 4-bromo or 4-iodo in pure state, as reported previously[8].

Efforts were made to obtain some kinds of monosubstituted *p*-terphenyl by the reaction of substituted *N*-nitrosoacetanilide with biphenyl in a suitable solvent. The yield of the desired compound, however, was always poor, and by-products were removed with great difficulty.

Suitable processes for preparing the monosubstituted *p*-terphenyls are listed in Table I, and melting points summarized in Table II.

Solubility and Specific Gravity.—Tables III and IV show the solubility, and Fig. 1 shows the relationship between the melting point and the solubility in *n*-hexane at 25°C. Both values are more strongly influenced by the position of the substituent than by its nature. Among 2-halo-*p*-terphenyls, the melting point becomes lower in the order of chloro- iodo-

Table I. Suitable preparation methods for mononitro-, monoamino- and monohalo-*p*-terphenyls

Substituent	Position			
	2	3	4	2'
NO_2				
NH_2	the reduction of the nitro-compound			
Cl			the Sandmeyer reaction	
Br			the Sandmeyer reaction	
I	the Sandmeyer reaction			

5) H. France et al., ibid., **1938**, 1368.
6) F. Bell et al., ibid., **1926**, 1246.
7) J. Kenyon et al., ibid., **1926**, 3051.
8) T. Nozaki, This Bulletin, **35**, 1035 (1962).

TABLE II. MELTING POINT OF SUBSTITUTED *p*-TERPHENYLS (°C)

Substituent	Position			
	2	3	4	2'
NO_2	129	176~177	213	131
NH_2	162~163	179	201	177
Cl	112~113	142	222	100~101
Br	87~ 88	151~152	234	98
I	101	155~156	247	99~100

p-Terphenyl 213°C

TABLE III. SOLUBILITY OF SUBSTITUTED *p*-TERPHENYLS IN *n*-HEXANE AT 25°C (g. in 100 ml. solution)

Substituent	Position			
	2	3	4	2'
NO_2	0.118	0.036	0.015	0.136
NH_2	0.121	0.028	0.019	0.076
Cl	1.59	0.35	0.096	2.19
Br	3.3	0.293	0.073	2.66
I	1.50	0.288	0.038	1.36

TABLE IV. SOLUBILITY OF SUBSTITUTED *p*-TERPHENYLS IN VARIOUS SOLVENTS AT 25°C (g. in 100 ml. solution)

Solute	Solvent		
	n-Hexane	Benzene	Ethanol
p-Terphenyl	0.084	1.20	0.056
2-Cl	1.59	27	1.16
3-Cl	0.36	6.5	0.199
4-Cl	0.096	1.74	0.084
2'-Cl	2.19	28	1.18
4-NO_2	0.015	0.75	0.035
4-NH_2	0.018	1.00	0.31
4-Br	0.073	1.34	0.047
4-I	0.038	0.67	0.028

In ethyl acetate: *p*-Terphenyl, 0.500, 4-Cl, 0.719

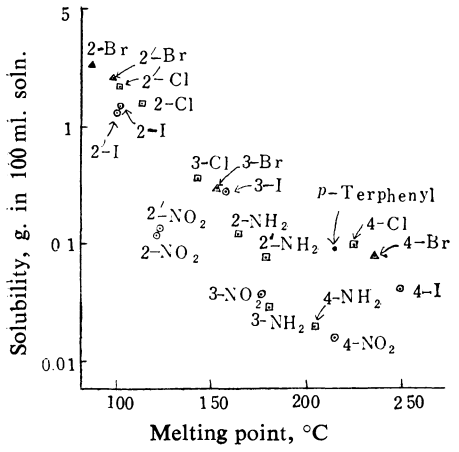


Fig. 1. Relationship between the melting point and the solubility in *n*-hexane at 25°C.

and bromo-*p*-terphenyl. The same order is seen for 2'-halo-*p*-terphenyls, though the differences are small. For 3- or 4-halo-*p*-terphenyls, on the other hand, the order is iodo-, bromo- and chloro-*p*-terphenyl. The 2- and 2'-halo-*p*-terphenyls are apt to form supersaturate solutions. Table V indicates the specific gravity at 25°C. It is, of course, quite sensitive to the nature of the substituent. The influence of the position of the substituent, on the other hand, is less clear and less systematic on the specific gravity than on the melting point and the solubility.

TABLE V. SPECIFIC GRAVITY AT 25°C

Substituent	Position			
	2	3	4	2'
NO_2	1.293	1.296	1.321	1.283
NH_2	1.205	1.225	1.236	1.215
Cl	1.226	1.264	1.271	1.234
Br	1.437	1.439	1.466	1.425
I	1.634	1.596	1.635	1.582

p-Terphenyl 1.236

Figure 2 shows the dependence of the solubility on the temperature. The heat of solution is calculated by the use of the Clapeyron's equation (Eq. 1) with the assumption (Eq. 2):

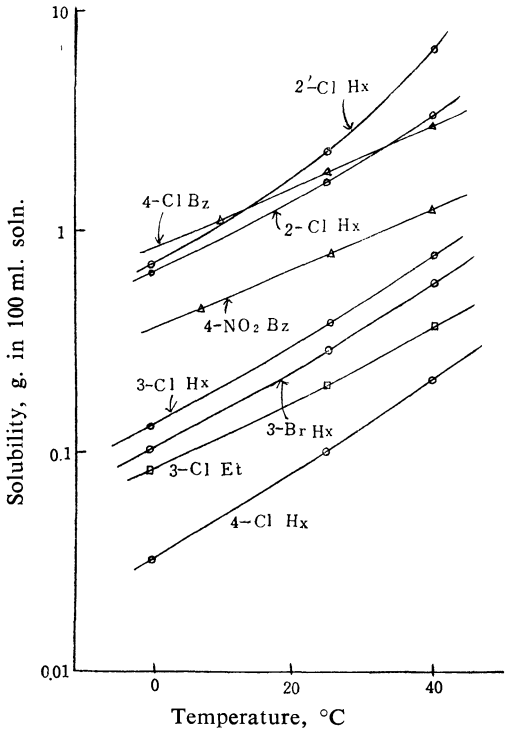


Fig. 2. Temperature dependence of the solubility.

$$\frac{dP}{dT}=\frac{\Delta H}{T(V_L-V_S)} \quad (1)$$

$$P=kC,\ V_L \gg V_S,\ kCV=RT \quad (2)$$

where ΔH is the molar heat of the solution, V_L the molar dilution, V_S the molar volume of solid solute, C the concentration and k a coefficient independent of temperature.

Since

$$\Delta H=\frac{RT^2}{C}\cdot\frac{dC}{dT} \quad (3)$$

and dC/dT is known from Fig. 2, ΔH can be calculated. The result is shown in Table VI.

Table VI. Partial molar heat and entropy of solution at 25°C for the saturation concentration (kcal./mol.)

Solute	Solvent	ΔH	TS_m	$\Delta H-TS_m$
2-Cl	Hx	4.0	2.9	1.1
3-Cl	Hx	4.1	3.8	0.4
4-Cl	Hx	4.1	4.5	−0.4
2'-Cl	Hx	5.1	2.7	2.4
3-Cl	Et	3.5	4.6	−1.1
4-Cl	Bz	3.3	3.0	0.3
3-Br	Hx	3.9	4.0	−0.1
4-NO_2	Bz	3.0	3.6	−0.5

Hx: *n*-Hexane; Et: Ethanol; Bz: Benzene
ΔH: Partial molar heat of solution
S_m: Entropy of mixing for perfect gases (cratic quantity)
T: Absolute temperature

Since this ΔH is the partial molar heat of solution at the saturation concentration, the value with the opposite sign is the product of partial molar entropy of solution and the temperature. The partial molar entropy of solution for a dilute solution consists of two terms[9]: (1) a term depending only on the concentration (cratic term or entropy of mixing of perfect gases), (2) terms independent of concentration (unitary quantity). The term 1, S_m, is expressed by

$$S_m=-R\ln\{x/(1-x)\} \quad (4)$$

where x is the molar fraction of the solute to the solution. Table VI also shows the value of TS_m and that of $H-TS_m$. The term 2, on the other hand, is dependendent on the various quantities: the degree of symmetry and flexibility of the solute molecule, the shape and size of the solute and of the solvent molecule, the translation and rotation of the solute molecule in solution, the lattice vibration of the solute substance in a solid state and the intramolecular motion of the solute substance both in solution and in solid state. A higher degree of symmetry of 4-substituted compounds is one reason for low solubility. Since the translational and the rotational entropy should not differ largely from compound to compound in question, the difference in the term $H-TS_m$ in Table VI should be due mainly to the degree of flexibility and to a different mode of intramolecular motions. These two are intercorelated.

Studies on absorption spectra, specific heat, X-ray crystallography etc. are necessary for quantitative treatment of such phenomena.

9) e.g. R. W. Gurney, "Ionic Processes in Solution", Chapter 5, McGraw-Hill, New York (1953)

Experimental

Preparation of Nitro-, Chloro- and Bromo-*p*-terphenyls by the Reaction of PBDO with Nitrobenzene, Chlorobenzene and Bromobenzene.—The procedure for the synthesis of 4-bromobiphenyl described in the "Organic Syntheses"[10] was successfully applied to the synthesis of the present compounds with a slight modification: 4-aminobiphenyl was diazotized in a mortar under grinding with a pestle at 8~10°C with occasional addition of ice. When the reaction of PBDO with nitrobenzene, chlorobenzene or bromobenzene was completed, the remaining monosubstituted benzene was removed by distillation. The residue was distilled under reduced pressure, and the distillate subjected to column-chromatographic separation, the solvent and eluant being benzene for nitrocompounds or a mixture of petroleum benzine (b. p., 70~90°C) and benzene for halo-compounds (the molar fraction of benzene being increased with progress of elution). Complete separation was not attained, but the following three fractions were obtained: (1) pure 2-nitro (or 2-chloro or 2-bromo), (2) 3-nitro (or 3-chloro or 3-bromo) containing 2-nitro (or 2-chloro or 2-bromo), (3) 4-nitro (or 4-chloro or 4-bromo) containing the other two isomers. From fractions 2 and 3, 3-nitro (3-chloro or 3-bromo) and 4-nitro (4-chloro or 4-bromo)-*p*-terphenyls were obtained respectively by recrystallization from a mixture of ethanol and ethyl acetate. The compounds in the mother-liquor of the recrystallization were separated by repeating column chromatography and recrystallization. From each 21 g. portion of 4-aminobiphenyl the following products were obtained: 2-nitro, 3.7 g.; 3-nitro, 1.3 g. and 4-nitro, 5.2 g.; 2-chloro, 5 g.; 3-chloro, 2.5 g. and 4-chloro, 4.5 g; 2-bromo, 4 g.; 3-bromo, 2.5 g. and 4-bromo, 5 g.

3-Nitro-*p*-terphenyl was identified as follows: (1) analysis (Found: C, 78.70; H, 4.72; N, 5.00. Calcd. for $C_{18}H_{13}NO_2$: C, 78.53; H, 4.76; N, 5.09%); (2) it gave an amine on reduction, which was converted into 3-chloro by the Sandmeyer reaction.

Synthesis of 3-Nitro from 4-Nitro-*p*-terphenyl.—4-Nitro was reduced to 4-amino (see below). To a warm solution of 4-amino (5 g.) in acetic acid (250 ml.) was added acetic anhydride (30 ml.) to give a fine suspension. This was treated with nitric acid (d=1.38, 20 ml.), gradually warmed to

10) R. Adams, "Organic Syntheses", Vol. 8 (1928), p. 42.

60°C and poured into water. The precipitate was filtered off, boiled in a mixture of ethanol (300 ml.) and sulfuric acid (200 ml.) for 1 hr. Sodium nitrite (20 g.) was added in small portions to the hot mixture, which was then diluted with water. The precipitate was filtered off, distilled in vacuo and purified by column-chromatography. Pure 3-nitro compound (2.3 g.) was obtained in pale yellow plates (from a mixture of ethanol and ethyl acetate).

Synthesis of 2'-Nitro-*p*-terphenyl from 3-Nitro-4-acetamidophenyl. — 3-Nitro-4-acetamidobiphenyl (30 g.) in a mixture of acetic acid (700 ml.) and acetic anhydride (300 ml.) was nitrosated at 10~15°C by passing nitrous fumes for 4 hr. and adding simultaneously solid sodium nitrite (10 g.). When the green solution was poured into water with stirring, an orange oil separated, which gradually solidified into a hard yellow mass. This material contained slightly less nitrogen than the theoretical value for 3-nitro-NAB. The solid was dried, dissolved in dry benzene (1.5 l.), warmed with care and eventually refluxed for 5 hr. until the evolution of nitrogen ceased. After benzene was removed from the solution, the residue was under reduced pressure, and the distillate subjected to column-chromatography. 2'-Nitro-*p*-terphenyl (12 g.) was obtained as almost colorless plates (from ethanol). A considerable quantity of 3-nitro-4-acetamidobiphenyl was recovered.

Reduction of Nitro-*p*-terphenyls.—Hot solution of 2-nitro, 3-nitro or 2'-nitro compound (3 g.) in ethanol (30 ml.) or in a mixture of ethanol and ethyl acetate was added to a warm solution of tin(II) chloride ($SnCl_2 \cdot 2H_2O$ 15 g.) in hydrochloric acid (11 N, 20 ml.), and boiled for 20 min. On cooling, the amino-*p*-terphenyl hydrochloride precipitated as colorless small crystals in a nearly quantitiative yield. In some cases, the precipitate contained some tin salt, which, however, was easily removed by treatment with dilute hydrochloric acid. Free amine (2-, 3- or 2'-amino compound) was obtained by treating the amine hydrochloride with an aqueous solution of sodium hydroxide. For the reduction of 4-nitro-*p*-terphenyl other solvents were preferably used[2] owing to its low solubility in ethanol, and 4-amino-*p*-terphenyl was obtained by treating the hydrochloride with hot solution of sodium ethylate in a mixture of ethanol and toluene.

The Sandmeyer Reaction.—The amine hydrochloride (2 g.) was dissolved in a mixture of acetic (70 ml.) and sulfuric acid (30 ml.) or suspended in water, diazotized at 5~10°C and converted into the iodo-*p*-terphenyl with 40~60% yield. 2'-Chloro and 2'-bromo were also prepared by the Sandmeyer reaction, but the yield was lower. On the other hand, 4-chloro and 4-bromo were synthesized with 40~60% yield. 2-Iodo: colorless needles from ethanol (Found: C, 60.61; H, 3.80; I, 35.79. Calcd. for $C_{18}H_{13}I$: C, 60.69; H, 3.68; I, 35.63%). 3-Iodo; colorless plates from ethanol (Found: C, 60.54; H, 3.51; I, 35.45%. Calcd.: the same with 2-iodo). 2'-Iodo: colorless plates from ethanol (Found: C, 60.62; H, 3.91; I, 35.76%. Calcd: the same with 2-iodo). 2'-Chloro: colorless needles or plates from ethanol (Found: C, 81.80; H, 5.13; Cl, 13.46. Calcd. for $C_{18}H_{13}Cl$: C, 81.65; H, 4.95; Cl, 13.39%). 2'-Bromo: colorless plates from ethanol (Found: C, 69.84; H, 4.38; Br, 26.06. Calcd. for $C_{18}H_{13}Br$: C, 69.92; H, 4.24; Br, 25.84%).

Synthesis of 2'-Chloro-*p*-terphenyl from 3-Chloro-4-acetamidobiphenyl.—3-Chloro-4-acetamidobiphenyl (20 g.) dissolved in a mixture of acetic acid (150 ml.) and acetic anhydride (50 ml.) was nitrosated by passing nitrous fumes for 2 hr. at 10~15°C. Stirring the solution into ice water resulted in formation of a milky suspension, from which yellowish hydrophobic powder gradually precipitated. The precipitate was dried and allowed to react with benzene (300 ml.) at 35°C overnight. After benzene was removed from the solution, the residue was distilled under reduced pressure, and the distillate recrystallized from ethanol to give 2'-chloro compound (9 g.).

Preparation of 2'-Bromo-*p*-terphenyl from 4-Acetamidobiphenyl.—4-Acetamidobiphenyl (20 g.) in acetic acid (200 ml.) was treated with bromine (30 g.) at 30~35°C and poured into water. The separated solid was digested with a mixture of ethanol (100 ml.) and water (100 ml.), the insoluble solid removed, and the solution poured into a large quantity of water. From the precipitate (10 g.), 2'-bromo compound (3 g.) was obtained by a similar process to that for 2'-chloro followed by column-chromatographic separation.

Measurement of the Physical Constants.—Melting point was measured in a capillary tube dipped in a sulfuric acid bath, and the value was corrected with reference to several standard substances. The solubility in a given solvent was measured by weighing the solid that was obtained by drying up a definite volume of the saturated solution. For the measurement of the specific gravity, a small crystal of the compound was prepared using a Bridgeman-type furnace. A portion of the crystal was immersed in water, to which a concentrated aqueous solution of a heavy metal salt was added until the specific gravity of the liquid became equal to that of the crystal.

We acknowledge with thanks the aid given to us during the course of the synthesis by Mr. Jun-ichi Shimada, Mr. Takashi Yamamoto and Mr. Kunio Sakai.

The Electrical Communication Laboratory
Musashino, Tokyo

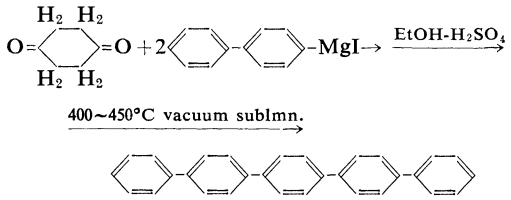
Synthesis and Purification of Quinquiphenyl for Scintillator

By Tadashi NOZAKI

(Received May 21, 1962)

It has been pointed out that quinquiphenyl and sexiphenyl are interesting organic semiconductors and promissing scintillators for charged particles[1]. Previously, we reported on the synthesis and purification of sexiphenyl[2]. Preparation of a large crystal of high-purity quinquiphenyl, however, has not been substantiated owing to the difficulty in the synthesis by older methods and in the purification. A convenient process for preparing quinquiphenyl of high purity is presented in this paper.

Mayer and Schiffner[3] briefly reported that *p*-terphenyl was formed when a reaction product of cyclohexanedione-1, 4 with phenylmagnesium bromide was sublimed under reduced pressure. A similar process has been found to be convenient for the synthesis of quinquiphenyl:



Cyclohexanedione-1, 4 is highly soluble in benzene, which keeps the compound mostly in keto-form. When the reaction product of cyclohexanedione-1, 4 in benzene with the etherial Grignard reagent is treated with a mineral acid, pale yellow powder containing quinquiphenyl precipitates gradually from the solution. None of the intermediates such as 1, 4-bisbiphenylylcyclohexanediol-1, 4 and 1, 4-bisbiphenylylcyclohexadiene has separated in pure state. They must be quite unstable and convert themselves into quinquiphenyl. The conversion is very slow at an ordinary temperature, but much faster at a higher temperature or in the presence of a mineral acid. Therefore, a rapid synthesis of quinquiphenyl can be substantiated by heating the Grignard reaction product to 400~450°C afterteatmeat with a boiling mixture of sulfuric acid and ethanol.

This heat treatment serves also for the purification, since most of the impurity by-products suffer thermal decomposition more easily than quinquiphenyl to give products which are easily removed. Too high a temperature or a prolonged heating, however, causes considerable decomposition of quinquiphenyl itself. Three other processes are also useful for the purification: i. e. vacuum sublimation, recrystallization and segregation. Slow sublimation at about 300°C (ca. 10^{-3} mmHg) is much more effective than rapid sublimation at a higher temperature. Since quinquiphenyl is quite sparingly soluble in any solvent under 100°C, a large quantity of a solvent having a high boiling point, such as nitrobenzene, tetraline or diethyl succinate should be used for recrystallization. Segregation with a Bridgeman-type furnace is especially effective for further purification of the sample already purified by other methods. The same process is also useful for single-crystal preparation. Yield of the purified quinquiphenyl was about 20% based on cyclohexanedione-1, 4 or 15% based on 4-iodobiphenyl.

A large crystal of purified quinquiphenyl is completely colorless, transparent, hard and tough, and gives an intense violet fluorescence. It has no marked habit to cleave into thin plates. It melts at 388°C into liquid crystal, which becomes transparent at 423°C. (These constants in literature[4] are 401°C (observed, 375°C) and 445°C (observed, 413°C) respectively, while in another literature[5] the melting point is 388.5°C). Specific gravity of quinquiphenyl at 25°C is 1.284 (terphenyl, 1.236; quarterphenyl, 1.262; sexiphenyl, 1.287).

Physical properties of pure quinquiphenyl, such as infrared, ultraviolet and fluorescence spectrum and scintillator efficiency are now under measurement. The results will be reported with those of quarterphenyl and sexiphenyl.

Experimental

Synthesis.—To a warm solution of 4-iodobiphenyl (40 g.) in diethyl ether (250 ml.) containing magnesium ribon (ca. 10 g.) was added a crystal or two of iodine, and the mixture refluxed for 3 hr. and filtered through asbestos fibers.

1) R. C. Sangster et al., *J. Chem. Phys.*, **24**, 713 (1956).
2) T. Nozaki et al., This Bulletin, **33**, 1329 (1960).
3) F. Mayer et al., *Ber.*, **65**, 1337 (1932).
4) D. Vorländer, *Z. phys. Chem.*, **126**, 472 (1927).
5) O. Gerngross et al., *Ber.*, **57**, 745 (1924).

Cyclohexanedione-1, 4 (5 g.) in benzene (100 ml.) was slowly stirred into the Grignard solution during 10 min., and the mixture refluxed for 20 min. and treated with hydrochloric acid. Most part of the solvent being removed, the residue was boiled in a mixture of sulfuric acid (50 ml.) and ethanol (50 ml.) for 30 min., cooled, collected by filtration and sublimed in vacuo to give two kinds of sublimate: (1) yellowish powder (7 g.) melting at ca. 300°C, (2) colorless material of a higher vapor pressure, melting at 180~185°C, which seemed to be a derivative of biphenylylcyclohexane. Sublimate 1 was placed in a narrow-necked glass tube and heated to 400°C in a furnace. Gas evolved vigorously form the molten product. When the evolution became feeble, the temperature was gradually raised to 450°C during 20 min. The dark grey massive product was sublimed (10^{-3} mmHg, 300°C) to give yellowish powder with black residue. The heat treatment and the vacuum sublimation of this sublimate were repeated once again to give crude quinquiphenyl (4 g.) in almost colorless powder, which melted at 350~360°C into liquid crystal.

Purification.—The crude quinquiphenyl (ca. 4g.) was recrystallized from diethyl succinate (800 ml.) into thin plates, which were sealed in an evacuated Telex-glass tube (9 mm. diameter) and purified by segregation with a Bridgeman-type furnace as in the case of sexiphenyl[2] (maximum temperature, 405°C; rate of downward movement, 8 mm. per hr.). The brownish segregate was removed, and the yellowish mass slowly sublimed in vacuo (10^{-3}~10^{-4} mmHg, 290~300°C) into colorless fluorescent powder, which was again subjected to the segregation and sublimation. The sublimate was recrystallized from tetralin, sublimed in vacuo and submitted to single-crystal formation by the same technique used for the segregation. Large colorless crystals were obtained (10×5×2 mm.) with a small amount of faintly yellowish segregate. Found: C, 94.26; H, 5.90. Calcd. for $C_{30}H_{22}$: C, 94.20; H, 5.85%.

Measurement of Melting Point and Specific Gravity.—The sample in a glass capillary was placed along the central axis of a transparent quartz tube (3.5 cm. diameter) together with an Almel-Chromel thermocouple. The tube was heated from outside with nichrome wire, and the temperature was read with a calibrated millivoltmeter. Melting point was measured with the sample obtained as mentioned above and also after further purification; no difference was observed. For the measurement of specific gravity, the crystal was immersed in water, to which a concentrated solution of a heavy metal salt was added until specific gravity of the liquid became equal to that of the crystal, and the former was measured.

The Electrical Communication Laboratory
Musashino, Tokyo

*On the Solubility and the Velocity of Dissolution of Corundum under Hydrothermal Conditions**

By Goro YAMAGUCHI, Hiroaki YANAGIDA and Shigeo SOEJIMA**

(Received May 23, 1962)

The fact that the dehydration of boehmite under hydrothermal conditions gives corundum directly has been noted by Laubengayer and Weisz[1], Ervin and Osborn[2] and Kennedy[3]. Using this reaction, the present authors obtained grains consisting of separated single crystals of corundum of a uniform size and habits[4]. The grains showed excellent qualities as abrasives for germanium, silicon and glass materials[5]. The uniformity in the grain size and habits may be attributed to a proper reaction mechanism under hydrothermal conditions. The mechanism, however, has not been clarified yet. In order to obtain some basic and important data for a discussion of the mechanism, the present authors have measured the solubilitiy of corundum under hydrothermal conditions.

The solubilities of aluminum hydroxides and aluminas as measured by Russell, Edwards and Taylor[6] have been widely accepted. It is, however, almost impossible to extrapolate these values to the temperature at which boehmite may be transformed into corundum. Yalman, Shaw and Corwin have presented

* This investigation was reported on at the 15th Annual Meeting of the Chemical Society of Japan, No. 3314 (Kyoto, April, 1962).

** Presnt address: Nihon Gaishi Kaisha, Ltd., Mizuho, Nagoya.

1) A. W. Laubengayer and R. S. Weisz, *J. Am. Chem. Soc.*, **65**, 247 (1943).

2) G. Ervin, Jr. and E. F. Osborn, *J. Geol.*, **59**, 391 (1951).

3) G. C. Kennedy, *Am. J. Sci.*, **257**, 563 (1953).

4) G. Yamaguchi and H. Yanagida, 13th Annual Meeting of the Chemical Society of Japan, No. 5A27 (Tokyo, April, 1960).

5) G. Yamaguchi, H. Yanagida, Y. Suwa and S. Soejima, Congress on Artificial Minerals, No. 2-2 (Osaka, November, 1961).

6) A. S. Russell, J. D. Edwards and C. S. Taylor, *Transaction AIME J. Metals*, 1123 (1955).

some data about the solubility of corundum[7], but they are insufficient to discuss the transformation of boehmite into corundum without the seed crystal, which has been observed practically only above 440°C[4]. The data above 420°C have not been included in their paper[7]. In the present work, the solubility of corundum has been measured up to 500°C under different conditions of hydrothermal pressure, alkaline solution and reaction period.

Experiments

Procedure.—Fused corundum grains of a uniform size, over 99 per cent pure and weighing 0.40 mg. on the average, were weighed and laid in a Morey-type reactor with an aqueous solution of sodium hydroxide or sodium carbonate. They were heated from room temperature to an appointed temperature within 15 min. and then kept at that temperature for some hours in an electric furnace. The hydrothermal pressure at that temperature was calculated from Kennedy's table showing the relations among pressure, density and temperature of water[8]. They were also quenched to room temperature within 15 min. The quenched contents, the solution and the residue were washed out completely with distilled water into a glass beaker. The residue was then washed with hot hydrochloric acid, and the gelatinous precipitate of aluminum hydroxide was eliminated by decantation, leaving only the corundum residue in the beaker.

Analysis.—Aluminum dissolved in a solution is usually analyzed by the EDTA titration method, with an indicator such as chromazurol S[9]. This method, however, cannot applied when an aluminum hydroxide is precipitated. A hydrothermal solution may become supersaturated through cooling it to room temperature, and aluminum hydroxide may be newly precipitated. In this case, the solubility obtained by the titration method may show a lower value. Actually, the gelatinous precipitate was observed in some runs in the present work. The true corundum residue was separated from the gelatinous precipitate by the above-mentioned procedure, and the difference in the weight of corundum between that placed in the reactor and that which remained after hydrothermal treatment was considered to indicate the dissolved alumina in the solution.

Results and Discussion

Effects of the Sample Quantity on the Solubility and Velocity of Dissolution.—0.5 or 1.0 g. of the corundum grain was treated with 3 normal sodium carbonate aqueous solutions at 450°C under a 1000 atmospheric pressure; the results of this experiment are shown in Table I and Fig. 1. It can be seen there that the time derivative of dissolved corundum has

Table I. Solubility of corundum in sodium carbonate aqueous solution

(Corundum grain; 0.40 mg. per each grain, 33 cm^2/g.; Hydrothermal condition; 450°C, 1000 atm., 3 N Na_2CO_3 5 cc.)

Initial corundum grain wt.	Reaction period	Dissolved corundum wt.		g. eq. / g. eq. of Na_2CO_3
g.	hr.	g.	g./cc.	
1.000	0.5	0.065	0.013	0.25
1.000	1.0	0.131	0.026	0.51
1.000	1.5	0.132	0.026	0.52
1.000	2.0	0.177	0.035	0.69
1.000	4.0	0.155	0.031	0.61
1.000	5.0	0.145	0.029	0.57
1.000	9.0	0.126	0.025	0.49
1.000	12.0	0.121	0.024	0.47
1.000	26.0	0.120	0.024	0.47
0.500	1.5	0.085	0.017	0.33
0.500	2.0	0.090	0.018	0.35
0.500	3.0	0.152	0.030	0.60
0.500	4.0	0.205	0.041	0.80
0.500	8.0	0.139	0.028	0.54
0.500	10.0	0.130	0.026	0.51
0.500	40.0	0.123	0.025	0.48

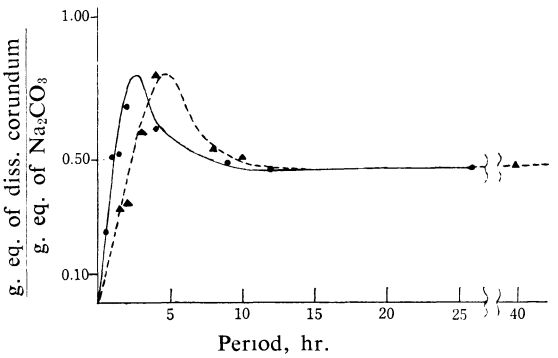


Fig. 1. Dissolution curve of corundum in sodium carbonate aqueous solution at 450°C (1000 atm.).
● —— 1.000 g. ▲ ---- 0.500 g.

a term proportional to the surface area of the sample. This may mean that the rate-determinant process of the dissolution is an elementary process occurring on or near the surface of the grain and that the diffusion velocity in space is sufficiently large. After being supersaturated, the dissolved alumina recrystallizes into corundum and the concentration of dissolved alumina approaches 0.024 g. per 1 cc. of the solution regardless of the sample quantity. This value corresponds to a 0.47 g. equiv. of dissolved alumina per 1 g. equiv. of sodium carbonate in the solution and can be considered as an equilibrium solubility. Here, the 1 g. equiv. of corundum 1/6 Al_2O_3, is 17 g. and that of sodium carbonate 1/2 Na_2CO_3, is 53 g.

7) R. G. Yalman, E. R. Shaw and J. F. Corwin, *J. Phys. Chem.*, **64**, 300 (1960).
8) G. C. Kennedy, *Am. J. Sci.*, **248**, 540 (1950).
9) M. Z. Theis, *Anal. Chem.*, **144**, 106 (1955).

TABLE II. SOLUBILITY OF CORUNDUM IN SODIUM HYDROXIDE AQUEOUS SOLUTION AT 400°C

Initial corundum wt.	Reaction period	g. eq. of NaOH	Liquid volume	Press.	Dissolved corundum	g. eq. / g. eq. of NaOH
g.	hr.		cc.	atm.	g.	
1.000	2.0	0.005	4.9	500	0.171	2.01
1.000	6.0	0.005	4.9	500	0.218	2.57
1.000	41.0	0.005	4.9	500	0.218	2.57
1.000	2.0	0.005	5.9	1000	0.172	2.02
1.000	4.0	0.005	5.9	1000	0.202	2.38
1.000	18.0	0.005	5.9	1000	0.230	2.70
1.000	42.0	0.005	5.9	1000	0.223	2.62
1.000	2.0	0.005	6.4	1500	0.173	2.03
1.000	3.0	0.005	6.4	1500	0.219	2.58
1.000	3.0	0.010	5.9	1000	0.376	2.21
1.000	8.0	0.010	5.9	1000	0.424	2.49
1.000	12.0	0.010	5.9	1000	0.420	2.47
1.000	17.5	0.010	5.9	1000	0.435	2.56
1.000	0.8	0.010	6.4	1500	0.187	1.10
1.000	2.0	0.010	6.4	1500	0.281	1.61
1.000	4.0	0.010	6.4	1500	0.343	2.02
1.000	8.0	0.010	6.4	1500	0.434	2.55
1.000	18.0	0.010	6.4	1500	0.444	2.61

TABLE III. SOLUBILITY OF CORUNDUM IN SODIUM HYDROXIDE AQUEOUS SOLUTION AT 450°C

Initial corundum wt.	Reaction period	g. eq. of NaOH	Liquid volume	Press.	Dissolved corundum	g. equiv. / g. eq. of NaOH
g.	hr.		cc.	atm.	g.	
1.000	0.5	0.005	3.4	500	0.185	2.18
1.000	1.0	0.005	3.4	500	0.161	1.98
1.000	2.0	0.005	3.4	500	0.221	2.60
1.000	12.0	0.005	3.4	500	0.232	2.73
1.000	1.0	0.005	5.2	1000	0.191	2.25
1.000	2.4	0.005	5.2	1000	0.221	2.60
1.000	3.0	0.005	5.2	1000	0.228	2.69
1.000	12.0	0.005	5.2	1000	0.237	2.79
1.000	1.0	0.005	5.9	1500	0.192	2.26
1.000	8.0	0.005	5.9	1500	0.227	2.68
1.000	1.0	0.010	5.2	1000	0.377	2.22
1.000	1.6	0.010	5.2	1000	0.431	2.54
1.000	4.0	0.010	5.2	1000	0.439	2.56
1.000	12.0	0.010	5.2	1000	0.445	2.62
1.000	20.0	0.010	5.2	1000	0.457	2.69
1.000	2.0	0.010	5.9	1500	0.383	2.25
1.000	2.0	0.010	5.9	1500	0.411	2.42
1.000	8.0	0.010	5.9	1500	0.442	2.60
5.000	18.0	0.020	2.0	100	0.948	2.28
5.000	20.0	0.020	2.0	100	0.910	2.68

Effects of Pressure, Alkaline Concentration and Temperature on the Solubility and Velocity of Dissolution.—The solubility of corundum at 400°C and at 450°C were measured under atmospheric pressures of 100, 500, 1000 and 1500 with 0.005, 0.010 and 0.020 g. equiv. of sodium hydroxide in an aqueous solution for various reaction periods. Table II and Fig. 2 show the results at 400°C, and Table III and Fig. 3 those at 450°C. The supersaturation which was found in the sodium carbonate solution could not be observed here in this sodium hydroxide solution. The total gram equivalent of alumina in a saturated solution may be expressed in terms of temperature, total gram equivalent of sodium hydroxide in the solution, and hydrothermal pressure as follows:

$$x_{\infty}^{\mathrm{cor}} = f(T) \cdot g(x_{\mathrm{OH}}) \cdot h(P_{\mathrm{H_2O}}) \qquad (1)$$

where, $x_{\infty}^{\mathrm{cor}}$ is the total gram equivalent of dissolved alumina in the saturated solution, $f(T)$, the temperature term, $g(x_{\mathrm{OH}})$, a function of

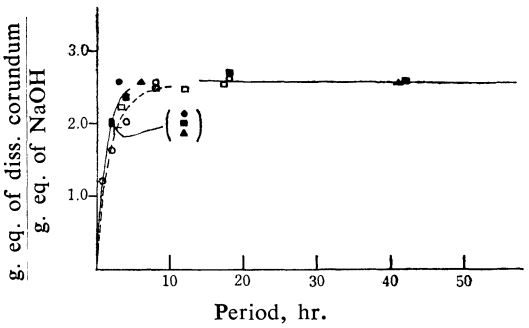
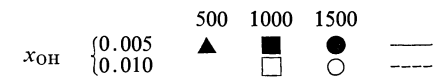


Fig. 2. Dissolution curve of corundum in sodium hydroxide aqueous solution at 400°C.



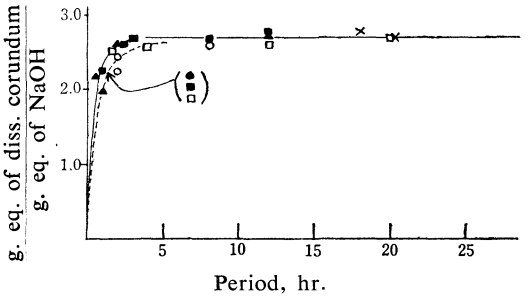
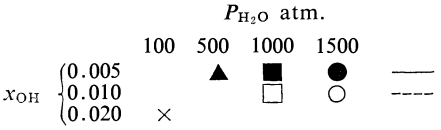


Fig. 3. Dissolution curve of corundum in sodium hydroxide aqueous solution at 450°C.



the total gram equivalent of sodium hydroxide in the solution, and $h(P_{H_2O})$, the pressure factor. In the present work, x_∞^{cor} appeared nearly proportional to x_{OH} independently of pressure. This means that

$$g(x_{OH}) \simeq x_{OH} \tag{2}$$

$$h(P_{H_2O}) \simeq 1 \tag{3}$$

Substituting 2 and 3 into 1, the present authors obtained the temperature term as:

$$f(T) = \begin{cases} 2.58_8 \pm 0.02 & \text{at } 400°C \quad (4) \\ 2.70_0 \pm 0.05 & \text{at } 450°C \quad (5) \end{cases}$$

From the fact that the velocity of dissolution appeared proportional to the total gram equivalent of sodium hydroxide in the solution independently of the hydrothermal pressure, it can be considered that the rate-determinant process of dissolution is an elementary process occurring on or near the sample surface and that the diffusion velocity in space is sufficiently large, as the sodium carbonate solution.

$$\frac{d(x_{cor}/x_{OH})}{dt} = kS(x_\infty^{cor}/x_{OH} - x_{cor}/x_{OH}) \tag{6}$$

may be proposed as a general equation of dissolution in the present case; here k is a velocity constant dependent on the temperature, S, the total surface area of corundum grains at t, and x_{cor} the total gram equivalent of dissolved alumina in the solution, also at t. In Eq. 6, $d(x_{cor}/x_{OH})/dt$ indicates the relative velocity of dissolution and $(x_\infty^{cor}/x_{OH} - x_\infty^{cor}/x_{OH})$, a driving force to a saturated solution instead of a term of the concentration gradient. Two variables, S and x_{cor}, are included in 6. The total surface area of the initial corundum grains before hydrothermal treatment is expressed as

$$S_0 = N_0\theta_0\left(\frac{17}{4}a_0\right)^{2/3} \tag{7}$$

where S_0 indicates the initial surface area in cm^2, N_0, the numbers of corundum grains, θ_0, a factor depending on the shape, and a_0, the gram equivalent of corundum per each initial grain. It is assumed that N_0 and θ_0 are invariants throughout the hydrothermal dissolution treatment. Therefore, it may be also expressed as

$$S = N_0\theta_0\left(\frac{17}{4}a\right)^{2/3} \tag{8}$$

where S is the total surface area of corundum grains during dissolution at t and a, the gram equivalent of corundum per each grain during dissolution, also at t. A_0, the total gram equivalent of the initial corundum grains, can be expressed as:

$$A_0 = N_0a_0 \tag{9}$$

and A, that of the corundum residue during dissolution at t, as:

$$A = N_0a \tag{10}$$

From the mass balance in the corundum,

$$A_0 \equiv A + x_{cor} \tag{11}$$

Substituting 7, 8, 9, 10 and 11 into 6, an equation including only one variable, x_{cor}/x_{OH}, is obtained:

$$\frac{d(x_{cor}/x_{OH})}{dt} = kS_0\left(\frac{A_0}{x_{OH}}\right)^{-2/3}\left(\frac{A_0}{x_{OH}} - \frac{x_{cor}}{x_{OH}}\right)^{2/3} \times\left(\frac{x_\infty^{cor}}{x_{OH}} - \frac{x_{cor}}{x_{OH}}\right) \tag{12}$$

This can be solved as follows;

$$\frac{2}{3}\ln\left\{\frac{\left(\frac{A_0}{x_{OH}}\right)^{1/3}-\left(\frac{A_0}{x_{OH}}-\frac{x_\infty^{cor}}{x_{OH}}\right)^{1/3}}{\left(\frac{A_0}{x_{OH}}-\frac{x_{cor}}{x_{OH}}\right)^{1/3}-\left(\frac{A_0}{x_{OH}}-\frac{x_\infty^{cor}}{x_{OH}}\right)^{1/3}}\right\}$$

$$+\frac{1}{3}\ln\left\{\frac{\left(\frac{x_\infty^{cor}}{x_{OH}}\right)-\left(\frac{x_{cor}}{x_{OH}}\right)}{\left(\frac{x_\infty^{cor}}{x_{OH}}\right)}\right\}$$

$$+\sqrt{3}\left\{\left(\frac{A_0}{x_{OH}}\right)-\left(\frac{x_\infty^{cor}}{x_{OH}}\right)\right\}^{1/3}$$

$$\times\left\{\tan^{-1}\frac{\left(\frac{A_0}{x_{OH}}-\frac{x_{cor}}{x_{OH}}\right)^{1/3}+\frac{1}{2}\left(\frac{A_0}{x_{OH}}-\frac{x_\infty^{cor}}{x_{OH}}\right)^{1/3}}{\frac{\sqrt{3}}{2}}\right.$$

$$\left.-\tan^{-1}\frac{\left(\frac{A_0}{x_{OH}}\right)^{1/3}+\frac{1}{2}\left(\frac{A_0}{x_{OH}}-\frac{x_\infty^{cor}}{x_{OH}}\right)^{1/3}}{\frac{\sqrt{3}}{2}}\right\}$$

$$=k(T)S_0\left(\frac{A_0}{x_{OH}}\right)^{-2/3}\left(\frac{A_0}{x_{OH}}-\frac{x_\infty^{cor}}{x_{OH}}\right)^{2/3}t \qquad (13)$$

The velocity constant, $k(T)S_0$, can be calculated according to 13 by comparison with the experimental results as follows;

$$k(T)S_0=\begin{cases}0.80/\text{hr.} & \text{at } 400^\circ\text{C} \quad (14)\\ 1.90/\text{hr.} & \text{at } 450^\circ\text{C} \quad (15)\end{cases}$$

The surface area of the initial corundum grains is estimated to be 33 cm^2/g. assuming the shape of corundum grain to be a tetragonal prism 1 : 1 : 2 in edge length. Putting this value into S_0 of 14 and 15, the present authors calculated the general velocity constant, not including the S_0 term, to be:

$$k(T)=\begin{cases}0.024/\text{cm}^2\,\text{hr.} & \text{at } 400^\circ\text{C} \quad (16)\\ 0.056/\text{cm}^2\,\text{hr.} & \text{at } 450^\circ\text{C} \quad (17)\end{cases}$$

From the velocity constant ratio, 0.056/0.024, with the temperature difference between 400°C and 450°C, the activation energy for the rate-determinant process is considered to be of the order of 3.8 kcal.

Effect of Temperature on the Equilibrium Solubility.—From 2 and 3, the equilibrium solubility can be considered in the term of $f(T)$ independently of pressure. The $f(T)$ term was obtained at 350°C and at 500°C in addition as at 400°C and 450°C. The $f(T)$ value at 350°C was measured for more than 70 hr. under an atmospheric pressure at 500 and that at 500°C for more than 12 hr. under an atmospheric pressure of from 500 to 1500. These are summarized in Table IV and are illustrated in Fig. 4.

TABLE IV. TEMPERATURE DEPENDENCE OF THE SOLUBILITY OF CORUNDUM

Temp. °C	g. eq. of diss. corundum / g. eq. of NaOH
350	2.46 ±0.09
400	2.58_8±0.02
450	2.70_0±0.05
500	2.85 ±0.10

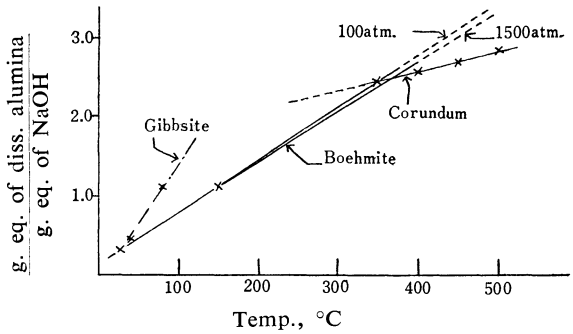


Fig. 4. Solubility curves of aluminas in sodium hydroxide aqueous solution ($Na_2O < 100$ g./l.).

Russell et al.[6] showed boehmite to be dissolved by 5.6% as alumina in 90 g. of sodium oxide per 1 l. aqueous solution at 150°C. This corresponds to a 1.14 g. equivalent of boehmite to be dissolved in a 1 g. equiv. of a sodium hydroxide aqueous solution. Here, the 1 g. equiv. of boehmite, 1/3 AlOOH, is 20 g. Russell et al. proposed that the equilibrium point between boehmite and gibbsite should be 27°C with extrapolation of the solubility. Near this temperature of 30°C, gibbsite is dissolved by 1.82% as alumina in 96.8 g. of sodium oxide per 1 l. of an aqueous solution[10]. This corresponds to a 0.34 g. equiv. of gibbsite to be dissolved in a 1 g. equivalent of a sodium hydroxide aqueous solution. Here, the 1 g. equiv. of gibbsite, 1/3 $Al(OH)_3$, is 26 g. In these alkaline concentrations lower than 100 g. of sodium oxide per 1 l., the ratio of the gram equivalent of dissolved alumina to that of sodium hydroxide in the solution may be considered to be invariant with the concentrations at the same temperature[11]. The solubility of gibbsite at 40°C is 0.45, and that at 80°C is 1.11 in the ratio.

The equilibrium point between boehmite and corundum varies with the pressure[3]; 355°C under 100 atm., 360°C under 500 atm., 365°C under 1000 atm. and 370°C under 1500 atm. The solubility curves of boehmite and corundum may intersect each other at these points. This indicates that the supersaturation

10) "Kagaku-Binran," Ed. by the Chemical Society of Japan, Maruzen Co., Tokyo (1958), p. 610.
11) J. Shimozato, Ph. D. Thesis, Tokyo Univ. (1961).

factor seems to be about 0.12 at the temperature where boehmite can be transformed into corundum without seed.

The curves illustrated in Fig. 4 give the basic information for a discussion about the transformation mechanism and for the growth of a single crystal of corundum under hydrothermal conditions. The present authors will discuss the mechanism in a later paper.

Summary

The solubility of corundum was measured under hydrothermal conditions. The equilibrium solubility seems independent of the pressure. The temperature term, $f(T)$, the ratio of the gram equivalent of dissolved corundum to that of sodium hydroxide in the solution, was as follows:

$$f(T)=\begin{cases} 2.46 \pm 0.09 & \text{at } 350^\circ\text{C} \\ 2.58_8 \pm 0.02 & \text{at } 400^\circ\text{C} \\ 2.70_0 \pm 0.05 & \text{at } 450^\circ\text{C} \\ 2.85 \pm 0.10 & \text{at } 500^\circ\text{C} \end{cases}$$

The velocity of dissolution was proportional to the surface area of the corundum crystal and the total gram equivalent of sodium hydroxide in the solution. This is shown as

$$\frac{\mathrm{d}(x_{\mathrm{cor}}/x_{\mathrm{OH}})}{\mathrm{d}t}=kS(x_{\infty}^{\mathrm{cor}}/x_{\mathrm{OH}}-x_{\mathrm{cor}}/x_{\mathrm{OH}})$$

The velocity constant was as follows:

$$k(T)=\begin{cases} 0.024/\mathrm{cm}^2\,\mathrm{hr.} & \text{at } 400^\circ\text{C} \\ 0.056/\mathrm{cm}^2\,\mathrm{hr.} & \text{at } 450^\circ\text{C} \end{cases}$$

The nucleation of corundum may be initiated at the supersaturation ratio of 0.12 without seed.

Department of Industrial Chemistry
Faculty of Engineering
The University of Tokyo
Hongo, Tokyo

Statistical Thermodynamics of Solutions of Optically Active Substances. III. Influence of an Optically Active Substance on the Equilibrium between Interconvertible d- and l-Optical Isomers

By Kazuo AMAYA

(Received June 1, 1962)

If an optically active substance is added to a mixture of d- and l-optical isomers which are interconvertible to each other, the original equilibrium between d- and l-isomers is expected to change. This seems to cause a new type of solvent effect on the optical rotation, the feature of which is that the solvent molecules themselves contribute to the optical rotation. Before the addition of an optically active substance there exist an equal number of the molecules of d- and l-isomers in the mixture, so it shows no optical rotation, but after that addition, the number of molecules of d- and l-isomers in equilibrium is expected to become unequal; this unbalanced number of molecules of either d- or l-isomer contribute to the total optical rotation.

This problem also seems to be important for studying asymmetric synthesis in an optically active solvent, because it is intimately related to the optical purity of the product.

In order to clarify the fundamental features of these problems, the statistical mechanics of such systems have been developed and the influence of the addition of optically active substances on the equilibrium between interconvertible d- and l-optical isomers has been examined.

Theory

Consider a system consisting of N_A molecules of either d- or l-isomer of an optically active substance of species A and of N_B molecules of a mixture of interconvertible d- and l-isomers of species B, namely, $N_B = N_{B_d} + N_{B_l}$ where N_{B_d} and N_{B_l} denote the number of molecules of d- and l-isomers respectively.

For the sake of simplicity, assumptions similar to those described in previous papers[1] are made. These are briefly summarized here again:

1) K. Amaya, This Bulletin, **34**, 1689, 1803 (1961).

1) The molecules of species A and B are covered by z planes. One of them consists of 3 different subelements; the arrangement of these three subelements for d- and l-isomers are mirror images of one another (this plane will be called the optically active plane). The remaining z-1 planes, composed of one uniform element and the pair of optically active planes in contact, can take three sets of configuration of a different energies.

2) The molecules of A and B have the same molecular volume; these molecules occupy the lattice points of the quasi-crystalline lattice of the nearest neighbors of z, and the molecule at a given site posseses $3z$ orientational freedom.

3) The configurational energy of the system is the sum of the potential energy of the $1/2 \cdot z(N_A+N_B)$ pairs of the surface plane of the molecules in contact.

To make the fundamental features of the problem as clear as possible, mathematical rigorousness is abandoned and we now introduce a concept of effective potential energy for a pair of optically active planes and attribute any difference between two optical isomers to it. Here "effective" means that we take the weighted mean of the potential energy of a given pair of planes in contact by averaging three different configurations by multiplying each Boltzmann factor.

Following the above assumptions, it can easily be expected that the non-zero value of the effective interchange energy of B_d and B_l molecules, w_{dl}, arises only from the pair of optically active planes, and that the differences in the effective interchange energy of A and B_d molecules, w_{AB_d}, and that of A and B_l, w_{AB_l}, also arise from the difference in the potential energy of the pairs of optically active planes of the A and B_d molecules and those of the A and B_l molecules.

Following the model described above, $w_{AB_d} - w_{AB_l}$ and w_{dl} will be estimated. If the potential energy of the i-th configuration of a pair of optically active planes from the pairs of molecules A–A, B_d–B_d, B_l–B_l, A–B_d, A–B_l and B_d–B_l are denoted by $U^{aa}_{AA_i}$, $U^{dd}_{BB_i}$, $U^{ll}_{BB_i}$, $U^{ad}_{AB_i}$, $U^{al}_{AB_i}$ and $U^{ld}_{BB_i}$ respectively, the weighted mean potential energy of each pair over three different configurations may be represented as:

$$\bar{U}^{aa}_{AA} = \sum_{i=1}^{3} U^{aa}_{AA_i} e^{-U^{aa}_{AA_i}/kT} \Big/ \sum_{i=1}^{3} e^{-U^{aa}_{AA_i}/kT}$$

$$\bar{U}^{dd}_{BB} = \sum_{i=1}^{3} U^{dd}_{BB_i} e^{-U^{dd}_{BB_i}/kT} \Big/ \sum_{i=1}^{3} e^{-U^{dd}_{BB_i}/kT}$$

$$\bar{U}^{ll}_{BB} = \sum_{i=1}^{3} U^{ll}_{BB_i} e^{-U^{ll}_{BB_i}/kT} \Big/ \sum_{i=1}^{3} e^{-U^{ll}_{BB_i}/kT}$$

$$\bar{U}^{ab}_{AB} = \sum_{i=1}^{3} U^{ad}_{AB_i} e^{-U^{ad}_{AB_i}/kT} \Big/ \sum_{i=1}^{3} e^{-U^{ad}_{AB_i}/kT}$$

$$\bar{U}^{al}_{AB} = \sum_{i=1}^{3} U^{al}_{AB_i} e^{-U^{al}_{AB_i}/kT} \Big/ \sum_{i=1}^{3} e^{-U^{al}_{AB_i}/kT}$$

$$\bar{U}^{dl}_{AB} = \sum_{i=1}^{3} U^{dl}_{AB_i} e^{-U^{dl}_{AB_i}/kT} \Big/ \sum_{i=1}^{3} e^{-U^{dl}_{AB_i}/kT}$$

Since each term of $U^{ad}_{AB_i}$ has a different value, from the corresponding term in $U^{al}_{AB_i}$, the effective potential energies, $\bar{U}^{ad}_{AB}$ and $\bar{U}^{al}_{AB}$, have different values. In a similar way, it is deduced that $\bar{U}^{dl}_{BB}$ and U^{dd}_{BB} or $\bar{U}^{dl}_{BB}$ and U^{ll}_{BB} have different values. In this way, d and l optical isomers in the system can be made distinguishable energetically.

Further, we define the following quantity:

$$\chi_A = \frac{1}{2z}\left\{(z-1)^2 U^{bb}_{AA} + 2(z-1)\bar{U}^{ab}_{AA} + U^{aa}_{AA}\right\}$$

$$\chi_{B_d} = \frac{1}{2z}\left\{(z-1)^2 U^{bb}_{BB} + 2(z-1)\bar{U}^{ab}_{BB} + \bar{U}^{dd}_{BB}\right\}$$

and

$$\chi_{B_l} = \frac{1}{2z}\left\{(z-1)^2 U^{bb}_{BB} + 2(z-1)\bar{U}^{ab}_{BB} + U^{ll}_{BB}\right\}$$

where χ_A, χ_{B_d}* and χ_{B_l}* indicate the mean potential energy per molecule of the A, B_d and B_l molecules respectively; U^{bb}_{AA} and U^{bb}_{BB} are the potential energies of a pair of planes which are not optically active of the A and B molecules respectively, and U^{ab}_{AA} and U^{ab}_{BB} are those of a pair of** planes, one of which is optically active and the other of which is optically inactive for A and B molecules respectively.

The interchange energy of A and B_d, w_{AB_d}, that of A and B_l, w_{AB_l}, and that of B_d and B_l, w_{dl}, molecules are, by definition, expressed as follows:

$$2\bar{w}_{AB_d} = \frac{2}{z}\left\{(z-1)^2 U^{bb}_{AB} + (z-1) \times (\bar{U}^{ab}_{AB} + U^{ba}_{AB}) + \bar{U}^{ad}_{AB}\right\} - 2\chi_A - 2\chi_{B_d}$$

$$2\bar{w}_{AB_l} = \frac{2}{z}\left\{(z-1)^2 U^{bb}_{AB} + (z-1) \times (\bar{U}^{ab}_{AB} + U^{ba}_{AB}) + \bar{U}^{al}_{AB}\right\} - 2\chi_A - 2\chi_{B_l}$$

$$2w_{dl} = \frac{2}{z}\left\{(z-1)^2 U^{bb}_{AB} + 2(z-1) + U^{ab}_{BB} + \bar{U}^{dl}_{BB}\right\} - 2\chi_{B_d} - 2\chi_{B_l}$$

---

* χ_{B_d} and χ_{B_l} are imaginary because B_d and B_l are interconvertible and an assembly of pure B_d or B_l molecule cannot exist.

** The suffix "a" denotes optically active and "b" denotes optically inactive.

Since $\bar{\bar{U}}_{BB}^{dd}=\bar{\bar{U}}_{BB}^{ll}$ $(=\bar{\bar{U}}_{BB}^{aa})$ and, hence, $\chi_{B_d}=\chi_{B_l}$ $(=\chi_B)$, it follows that

$$\Delta\bar{\bar{w}}=\bar{\bar{w}}_{AB_d}-\bar{\bar{w}}_{AB_l}=\frac{1}{z}(\bar{U}_{AB}^{ad}-\bar{U}_{AB}^{al})$$

$$\bar{w}_{dl}=\frac{1}{z}(U_{BB}^{dl}-\bar{U}_{BB}^{aa})$$

Having thus defined these quantities, we can proceed to the next step.

Before considering the ternary system, we must first consider the pure solvent system, a binary system composed of N_{B_d} molecules of B_d and N_{B_l} molecules of B_l.

The configurational free energy of the system F_C^B is represented as:

$$F_C^B=-kT\ln\frac{(N_{B_d}+N_{B_l})!}{N_{B_d}!\,N_{B_l}!}+\frac{N_{B_d}N_{B_l}}{N_B^2}\bar{\bar{w}}_{dl}-\chi_B N_B-kT N_B\ln 3z$$

In the equilibrium state, F_C^B must be the minimum.

Then, the first derivative of F_C^B with respect to N_{B_d} under the condition that $N_B=N_{B_d}+N_{B_l}$ =constant must be zero, we have

$$\left(\frac{\delta F_C^B}{\delta N_{B_d}}\right)_{N_B}=kT\ln N_{B_d}/(N_B-N_{B_d})+(N_B-2N_{B_d})w_{dl}=0$$

Since the B_d and B_l molecules are equivalent, the same relation must hold for N_{B_l}. Therefore, we obtain, by using the relation $N_{B_l}=N_B-N_{B_d}$;

$$\left(\frac{\delta F_C^B}{\delta N_{B_l}}\right)_{N_B}=kT\ln(N_B-N_{B_d})/N_{B_d}+(2N_{B_d}-N_B)\bar{\bar{w}}_{dl}=0$$

For the simultaneous satisfaction of these two relations both terms must always be zero; it follows that

$$N_{B_d}=N_{B_l}=\frac{1}{2}N_B$$

Next, we consider the solution, a ternary system composed of A, B_d and B_l molecules.

The configurational free energy of the system F_C is represented by

$$F_C=-N_A\chi_A-N_B\chi_B-kT\ln\frac{(N_A+N_B)!}{N_A!\,N_{B_d}!\,N_{B_l}!}+\frac{N_A N_{B_d}}{N_A+N_B}\bar{\bar{w}}_{AB_d}+\frac{N_A N_{B_l}}{N_A+N_B}(\bar{\bar{w}}_{AB_d}-\Delta\bar{\bar{w}})+\frac{N_{B_d}N_{B_l}}{(N_A+N_B)}\bar{\bar{w}}_{dl}-(N_A+N_B)kT\ln 3z$$

The equilibrium concentration of B_d or B_l molecules is the one that minimizes F_C. This can be obtained by differentiating F_C with respect to N_{B_d} or N_{B_l}, under the condition that $N_B=N_{B_d}+N_{B_l}$ is constant, and by then equating it with zero. Thus, we obtain

$$\delta F_C/\delta N_{B_d}=Tk\ln\frac{N_{B_d}}{N_B-N_{B_d}}+N_A/(N_A+N_B)\Delta w+(N_B-2N_{B_d})/(N_A+N_B)w_{dl}=0$$

By introducing the notations y and x_A defined by the following equations:

$$y=\frac{N_{B_d}}{N_B},\qquad x_A=N_A/(N_A+N_B)$$

the above equation may be rewritten as:

$$kT\ln y/(1-y)+x_A\Delta w-(1-x_A)(1-2y)w_{dl}=0$$

When y is close to 0.5, y can be replaced by $0.5+\Delta$. The logarithmic term is expanded in the power series in Δ and, by neglecting terms higher than the second, we can obtain the following approximate solution for Δ:

$$\Delta=-\frac{x_A\cdot\Delta w}{4kT-(1-x_A)w_{dl}}$$

Discussion

Since the value of Δ is usually different from zero, the equilibrium is shifted in either direction. If the sign of Δ is positive, the D isomers increase, and vice versa.

The absolute value of Δ increases as x_A increases, and the maximum value of $|\Delta|$ is $|\Delta w/4kT|$. Usually $w_{dl}\ll kT$, and w_{dl} can be neglected as too small, and the $|\Delta|$ is approximated to $\Delta w/4kT\cdot x_A$. Since Δw is nearly proportional to $1/T$, $|\Delta|$ is nearly proportional to $1/T^2$. The extent of the shift from the original equilibrium state become greater as the temperature decreases. This indicates that, in order to get optically active polymers of a large optical rotatory power by the polymerization of monomers in an optically active solvent, it is desirable to perform polymerization at as low temperatures and as low concentrations (large value of x_A) as possible.

In order to get direct evidence of this predicted phenomena, it seems to be most suitable to measure the optical rotatory dispersion of these mixtures, since, by the measurement of optical rotation with the light of a single wavelength, it is difficult to distinguish the contributions of the solute from that of the solvent in the observed optical rotation.

However, if the optical rotatory dispersion is measured, the contributions from each species can easily be distinguished, for usually the dispersion curve is different and the maxima of optical rotation appear at different wavelengths. Humps may be observed on the optical rotatory dispersion curve of the solute. (No such hump is expected for optically inactive solvents.) Another indirect evidence

may be obtained by the study of polymerization in an optically active medium. This kind of study has already been done[2], but the effect of the temperature of polymerization is not apparent.

Government Chemical Industrial Research Institute
Shibuya-ku, Tokyo

2) G. Natta, M. Farina, M. Peraldo and G. Bressan, *Makromol. Chem.*, **43**, 68 (1961).

Effects of Nonelectrolytes on the Temperature of the Maximum Density of Water. II. Organic Compounds with Polar Groups

By Goro WADA and Saburo UMEDA*

(Received June 4, 1962)

Water normally shows its maximum density at 3.98°C under atmospheric pressure, although "the temperature of the maximum density" (abbreviated as T. M. D.) is altered by foreign substances dissolved in it. In the preceding paper[1], the T. M. D.'s of dilute aqueous solutions of various alcohols were determined and several monovalent alkyl alcohols were found to elevate the T. M. D. of water when present in a low concentration. The effects of these substances on the T. M. D. of water were ascribed to the mutual interaction between the solute and water, such as the hydration and the hydrogen bondings formed between dipolar molecules. In this paper, some polar substances other than alcohols, i. e., amines, nitriles, ketones and cyclic ethers, are mainly examined in order to elucidate their influence upon the T. M. D. of water and to compare the results with those concerning alcohols already reported on[1].

Experimental

The experiments were carried out by means of dilatometry in a manner quite similar to that described in the previous report[1]. Fourteen species were used, all of which were thoroughly purified enough for the present purpose. Pure water was prepared by distillation and by the ion-exchange method.

The elevation of the T. M. D., ΔT, is defined by the following equation, in which T_m indicates the T. M. D. of a solution of mole fraction x of a solute and T_{m_0} is that of water, namely 3.98°C.

$$\Delta T = T_m - T_{m_0} \tag{1}$$

The observed values of ΔT at various concentrations are listed in Table I. The experimental errors are within ±0.02°C.

* Present address: Toppan Printing Co., Ltd., Fukushima-ku, Osaka.

1) G. Wada and S. Umeda, This Bulletin, 35, 646 (1962).

Discussion

Generally surveying Table I, the ΔT's are all negative, in contrast with the case of the alcohols previously observed[1]. Particularly, urea, pyridine, acetonitrile, propionitrile and 1, 4-dioxane are seen to exhibit superior abilities in lowering the T. M. D. of water.

The Excessive Elevation of the T. M. D. of an Aqueous Solution Caused by Mutual Interaction.—If there occur no change in volume and no interaction between a solute and water on mixing the two, the T. M. D. of water should be elevated as high as ΔT_n shown by the next equation[1]. As a matter of course, judging from the equation, ΔT_n should always be negative.

$$\Delta T_n = -\frac{x}{1-x} \cdot \frac{\alpha}{2\beta} \cdot \frac{V_{s_0}}{V_{w_m}} \tag{2}$$

Here, V_{s_0} and V_{w_m} are the molar volumes of the solute at 0°C and of water at T_{m_0} respectively, and α and β are the respective coefficients of thermal expansion. The molar volumes at θ°C are, therefore, expressed as:

$$V_s = V_{s_0}(1+\alpha\theta) \tag{3}$$

$$V_w = V_{w_m}\{1+\beta(\theta-T_{m_0})^2\} \tag{4}$$

Therefore, the excessive elevation of the T. M. D. of an aqueous solution, $\Delta T'$, is defined as follows:

$$\Delta T' = \Delta T - \Delta T_n \tag{5}$$

The necessary data on α and V_{s_0} for calculating the ΔT_n for each substance are collected in Table II. For water, the following values are adopted[1,2]: $\beta = 7.80\times10^{-6}$ deg^{-2}, and $V_{w_m} = 18.016$ cc. mol^{-1}. The values of $\Delta T'$ derived from Eq. 5 are also shown in Table I, together

2) G. Wada, This Bulletin, 34, 955 (1961).

TABLE I. ΔT AND $\Delta T'$ AT VARIOUS MOLE FRACTIONS x

Substance	$x\times10^2$	ΔT	$\Delta T'$
Monomethylamine			
	0.15	−0.14	0.21
	0.44	−0.28	0.78
	0.72	−0.48	1.26
	0.99	−0.92	1.46
	1.25	−1.28	1.73
	1.51	−1.64	2.03
	1.68	−1.98	2.10
	2.01	−2.41	2.49
	2.25	−2.87	2.64
Dimethylamine			
	0.14	−0.02	0.71
	0.36	−0.08	1.71
	0.44	−0.10	2.08
	0.91	−0.50	3.98
	1.16	−1.00	4.76
	1.40	−1.42	5.51
	1.63	−1.94	6.15
	1.85	−2.50	6.30
	2.09	−3.08	7.34
n-Butylamine			
	0.08	−0.25	0.11
	0.22	−0.65	0.32
	0.36	−1.08	0.52
	0.51	−1.68	0.59
	0.64	−2.15	0.62
Acetamide			
	0.08	−0.25	−0.12
	0.26	−0.70	−0.25
	0.44	−1.16	−0.40
	0.61	−1.65	−0.59
	0.81	−2.17	−0.70
Urea			
	0.09	−0.42	—
	0.21	−0.94	—
	0.43	−1.92	—
	0.57	−2.45	—
	0.68	−2.89	—
	0.86	−3.77	—
Pyridine			
	0.08	−0.33	−0.10
	0.20	−0.90	−0.34
	0.36	−1.54	−0.52
	0.52	−2.26	−0.79
	0.67	−3.03	−1.14
Acetonitrile			
	0.15	−0.56	−0.21
	0.38	−1.42	−0.51
	0.68	−2.52	−0.87
	0.81	−3.11	−1.13
	1.03	−4.03	−1.52
	1.19	−4.77	−1.87
Propionitrile			
	0.10	−0.42	−0.12
	0.28	−0.22	−0.38
	0.42	−1.83	−0.52
	0.65	−2.97	−0.98
	0.82	−3.86	−1.38
Formaldehyde			
	0.38	−0.69	—
	0.76	−1.49	—
	1.07	−2.30	—
	1.41	−3.07	—
	1.74	−3.97	—
	2.06	−4.77	—
Acetone			
	0.17	−0.32	0.27
	0.41	−0.96	0.46
	0.63	−1.58	0.61
	0.88	−2.51	0.59
	1.14	−3.49	0.52
	1.41	−4.42	0.55
Tetrahydrofuran			
	0.19	−0.48	0.22
	0.36	−0.88	0.46
	0.57	−1.47	0.65
	0.76	−2.06	0.78
	1.00	−2.85	0.90
	1.21	−3.72	0.83
1,4-Dioxane			
	0.17	−0.76	−0.10
	0.35	−1.43	−0.07
	0.52	−2.18	−0.16
	0.70	−3.06	−0.35
	0.93	−4.39	−0.75
Benzene			
	0.007	−0.04	0.00
	0.026	−0.09	0.01
	0.038	−0.12	0.01
Tetraethylammonium bromide			
	0.03	−0.19	—
	0.07	−0.41	—
	0.16	−0.97	—
	0.24	−1.51	—
	0.34	−2.14	—
	0.44	−2.77	—
	0.53	−3.28	—

with those of ΔT for comparison, and the relationships between $\Delta T'$ and x are pictured separately for three groups of substances in Figs. 1—3. Since $\Delta T'/x$ holds an approximate linearity with x in any solute substance, $\Delta T'$ may be expressed as a second order equation with respect to x, both the a and b parameters being shown in Table II as well.

$$\Delta T' = ax + bx^2 \qquad (6)$$

TABLE II. THE CHARACTERISTIC DATA FOR SUBSTANCES; COEFFICIENT OF THERMAL EXPANSION α, MOLAR VOLUME AT 0°C V_{so}, PARAMETERS IN Eq. 6 a AND b, AND DIPOLE MOMENT μ

Substance	$\alpha\times10^{3}$ deg^{-1}	V_{so} cc. mol^{-1}	$a\times10^{-1}$ deg.	$b\times10^{-3}$ deg.	μ D. U.
Monomethylamine	1.49	45.14	18.0	− 2.9	1.32
Dimethylamine	2.07	66.27	51.5	− 8.5	1.02
n-Butylamine	1.31	95.4	17.3	−12.0	—
Acetamide	0.81	59.152	− 9.4	− 0.6	—
Urea	—	—	—	—	4.56
Pyridine	1.00	78.860	−11.5	− 7.7	2.22
Acetonitrile	1.32	51.089	− 9.4	− 5.4	3.94
Propionitrile	1.24	68.678	−11.7	− 5.9	4.00
Formaldehyde	—	—	—	—	2.27
Acetone	1.36	71.485	17.3	−11.5	2.85
Tetrahydrofuran	1.3	78.96	15.4	− 6.7	1.71
1,4-Dioxane	1.310	83.03	1.8	−10.6	0.43
Benzene	1.187	86.784	0.0	0.0	0

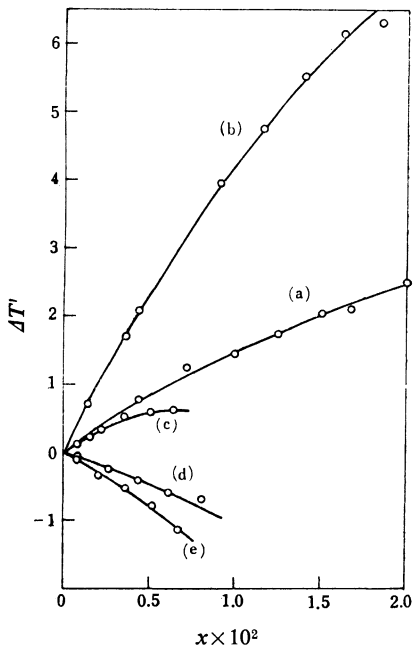


Fig. 1. Variation of $\Delta T'$ with the concentration of (a) monomethylamine, (b) dimethylamine, (c) *n*-butylamine, (d) acetamide and (e) pyridine.

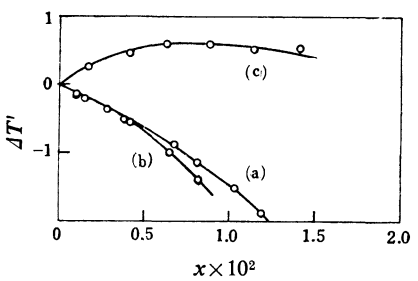


Fig. 2. Variation of $\Delta T'$ with the concentration of (a) acetonitrile, (b) propionitrile and (c) acetone.

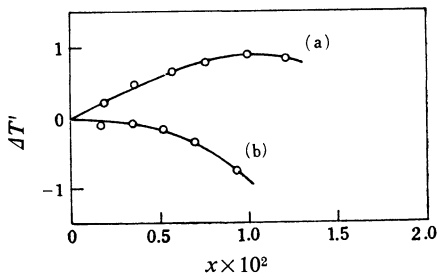


Fig. 3. Variation of $\Delta T'$ with the concentration of (a) tetrahydrofuran and (b) 1,4-dioxane.

In the cases of urea, formaldehyde and tetraethylammonium bromide, a and b are not known because of the lack of appropriate data for α and V_{so} in the liquid state.

The Nature of *a*.—Since, as was mentioned in the previous paper[1], $\Delta T'$ is caused by an appreciable change in the molar volume and in the coefficient of the thermal expansion of the solute (ΔV_{so} and $\Delta\alpha$) on mixing a solute and water, a has a nature expressed as follows:

$$a\equiv\lim_{x\to0}\left(\frac{\mathrm{d}\Delta T'}{\mathrm{d}x}\right)=-k(\alpha\Delta V_{so}+V_{so}\Delta\alpha) \tag{7}$$

As $k=(1/2)\,\beta V_{wm}$ is taken to be constant, any changes in the volume or the coefficient of the thermal expansion of water accompanied by a transition of states in the sheaths of the hydration layer attached to the solute molecules are entirely included in ΔV_{so} or $\Delta\alpha$ respectively.

A polar substance in question may overcome the association between the molecules themselves and may newly establish the hydration sphere around the individual molecules when it is dissolved in water. Since water is as much compressed in the hydration sphere as in "the packed state" of pure water, the coefficient of

the thermal expansion of water in this state is larger than that in the free state[1,2]. Consequently, the second term in the parenthesis on the right-hand side of Eq. 7, $V_{s_0}\Delta\alpha$, may be reasonably regarded as positive in most cases. On the other hand, ΔV_{s_0} may be either positive or negative according to whether or not the degree of the contraction of volume caused by the association of the solute due to its cohesive force in the separated state is superior to that resulting from the formation of the hydration sphere in the dissolved system. Thus, the magnitudes of a are dependent upon the signs and the absolute values of $\alpha\Delta V_{s_0}$ and $V_{s_0}\Delta\alpha$ in Eq. 7.

As is illustrated in Fig. 1, the a values for monomethylamine, dimethylamine and *n*-butylamine are all positive; the a for dimethylamine especially is as high as that for *t*-butyl alcohol*. In the case of dimethylamine, the $|\alpha\Delta V_{s_0}| \gg |V_{s_0}\Delta\alpha|$ relation may hold because it would be least associative with a very small dipole moment (Table II); consequently, $\Delta V_{s_0}<0$ and $\Delta\alpha$ would be nearly equal to zero, as it has an extraordinarily large α.

On the other hand, a becomes negative for acetamide; this is because both α and V_{s_0} are essentially small due to the strong formation of the intermolecular hydrogen bondings. Since this tendency occurs more severely in urea than in acetamide on account of its molecular structure, the ΔT of urea appears far lower than that of acetamide at the same mole fraction**. Unfortunately, the a value for urea can not be known, for it is not liquidous. Pyridine also exhibits an excellent ability to lower the T. M. D. of water, probably due to its good hydrophilic nature.

In Fig. 2, acetonitrile and propionitrile show large negative a values because of their large dipole moments. In Fig. 3, on the contrary, tetrahydrofuran and 1, 4-dioxane, which are both cyclic ethers, have positive a's as in the cases of amines and acetone; this is because they have comparatively many alkyl radicals in the molecule which are of rather a hydrophobic nature and are likely to diminish the degree of hydration.

In the case of benzene, $\Delta T'$ is zero within the range of experimental error; therefore, $a=b=0$. This fact shows that benzene is a perfect non-polar liquid and that it behaves quite independently in its aqueous solution with no mutual interaction with water.

Since tetraethylammonium bromide is a kind of electrolyte, its ability to lower the T. M. D. of water is much greater than that of any polar nonelectrolyte. The relation between ΔT and x shows a features similar to those of ammonium bromide[4]. Generally speaking, the lowering of the T. M. D. of water by 1-1 type electrolytes, composed of monatomic ions, seems to become greater as the size of the ion grows larger; moreover, this trend appears more effective in anions than in cations. In spite of such a tendency, it is quite strange that $N(C_2H_5)_4^+$ ion exhibits behavior similar to that of the simple NH_4^+ ion.

Additivity of a.—When an assumption is made that the total effect of a substance to lower the T. M. D. of water is approximately the additive sum of the nature of its individual component radicals according to their polarity, the a values assigned to several radicals can be obtained by the least square method based on the observed data of relatively simple compounds, including alcohols[1], such as are taken up in Table IV. Table III shows the a values thus calculated for various radicals and, as well, their radical dipole moments, between which a good parallelism is easily recognized; namely, the more polar a radical, the more negative a becomes. By using the a values for radicals in Table III, the a values for compounds are calculated in Table IV, the agreement with the observed a values being satisfactory, with errors of less than ± 0.3.

TABLE III. a AND DIPOLE MOMENT FOR RADICALS

Radical	$a\times10^{-1}$	μ, D. U.
$-CH_3$	27.8	0.3
$-CH_2-$	3.4	0
$-O-$	− 4.3	—
$>NH$ (or $-NH_2$)	− 4.4	1.31
$-OH$	− 7.6	1.53
$>CO$	−37.7	2.5
$-CN$	−40.0	3.6

The Nature of b.—In dilute solutions of some electrolytes, an approximate linearity is established between ΔT and x (Despretz's rule), but in the case of nonelectrolytes, the deviation from this linearity is considerable, from which fact the b parameter in Eq. 6 originates and always exhibits a negative value. As b is the coefficient of the second-order term with respect to the mole fraction, it may be related to some solute-solute interaction. When b values for various substances are

* In the case of *t*-butyl alcohol, $a=60.5$ and $\alpha=1.295$, both of which are the largest values among the observed alcohols[1].

** Urea and acetamde are far more likely to form hydrogen bondings than alcohol and acetone; the dielectric constants of their aqueous solutions are larger than that of water itself[3].

3) J. Wymann, Jr., *J. Am. Chem. Soc.*, **55**, 4116 (1933); H. Baba, *Chem. & Chem. Ind.*, **12**, 1001 (1959).

4) International Critical Tables, Vol. III, p. 107.

TABLE IV. ADDITIVITY OF a FROM RADICALS

Substance		$a_{calcd} \times 10^{-1}$	$a_{obs} \times 10^{-1}$
Methyl alcohol	CH_3OH	20.2	17.3
Ethyl alcohol	C_2H_5OH	23.6	27.3
Ethylene glycol	CH_2OH | CH_2OH	− 8.4	− 8.9
Monomethylamine	CH_3NH_2	23.4	18.0
Dimethylamine	$(CH_3)_2NH$	51.2	51.5
Acetone	CH_3COCH_3	17.9	17.3
Acetamide	CH_3CONH_2	−14.3	− 9.4
Acetonitrile	CH_3CN	−12.2	− 9.4
Propionitrile	C_2H_5CN	− 8.8	−11.7
Tetrahydrofuran	CH_2-CH_2 | CH_2-CH_2 >O	9.3	15.4
1, 4-Dioxane	O<CH_2-CH_2 CH_2-CH_2>O	5.0	1.8

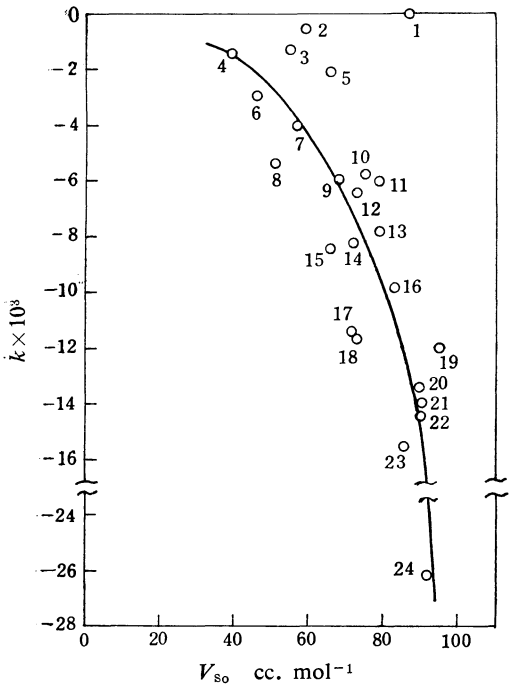


Fig. 4. Relation of b against V_{so}. 1: Benzene, 2: Acetamide, 3: Ethylene glycol, 4: Methyl alcohol, 5: Ethylene chlorohydrin, 6: Monomethylamine, 7: Ethyl alcohol, 8: Acetonitrile, 9: Propionitrile, 10: Isopropyl alcohol, 11: Tetrahydrofuran, 12: *n*-Propyl alcohol, 13: Pyridine, 14: Glycerin, 15: Dimethylamine, 16: 1,4-Dioxane, 17: Acetone, 18: Propylene glycol, 19: *n*-Butylamine, 20: *n*-Butyl alcohol, 21: Isobutyl alcohol, 22: *sec*-butyl alcohol, 23: Phenol, 24: *t*-Butyl alcohol.

plotted against their molar volumes, as in Fig. 4, the explicit correlation is indicated, with the exception of benzene, that the larger the molar volume, the greater negative value b has. Nevertheless, the mechanism of the solute-solute interaction can not be made clear at present.

Summary

The temperature of the maximum density (T. M. D.) of aqueous solutions of various organic polar substances at various concentrations were measured dilatometrically, and the degrees of elevating the T. M. D., ΔT, were estimated. The information derived from the experimental results includes:

1) At any concentration, the values of ΔT for all substances used in the present study are inevitably negative, in contrast with the cases of alkyl monovalent alcohols, reported on in the preceding paper[1].

2) $\Delta T'$, defined as the difference between the actual elevation of T. M. D. and that when the solution is assumed to be an ideal mixture, is given by an empirical formula, $\Delta T' = ax + bx^2$, where a is a characteristic constant of the solute, indicating the degree of the interaction between the solute and water; it generally has a more negative value as the substance is more polar.

3) Benzene does not interact with water; therefore, $\Delta T' = 0$ and $a = b = 0$ in so far as it is soluble in water.

4) An additivity correlation concerning a is realized from the composing radicals, and the a values assigned to respective radicals show a simple parallelism with their own polarities.

5) The b parameter is negative for all substances; the absolute value of this is greater as the molar volume becomes larger.

Department of Chemistry
Faculty of Science
Kobe University
Mikage, Kobe

Polarographic Study of the Rate of the Dissociation Reaction of the Zinc(II)-Nitrilotriacetate Complex in Ammonia-Ammonium Nitrate Buffer Solutions

By Mutsuo KODAMA and Mitsuo HASHIMOTO

(Received June 8, 1962)

It has been known that the cadmium-nitrilotriacetate complex in ammonia-ammonium nitrate buffer solutions gives a reversible kinetic wave due to the dissociation of the complex and that the height of the limiting current of the kinetic wave increases with the concentration of ammonia[1,2]. A similar phenomena can also be observed in the case of zinc(II)-nitrilotriacetate[3]. In this study, the nature of the kinetic wave due to the dissociation of zinc(II)-nitrilotriacetate complex ions has been investigated more thoroughly from both theoretical and experimental viewpoints.

Experimental

Apparatus.—Direct current (D. C.) polarograms were measured by a manual polarograph similar to that of Kolthoff and Lingane[4]. The current was calculated from the ohmic potential drop, measured by a potentiometer, across a 10000-ohm resistance which was in series with the polarographic cell. A Yanagimoto Model GA-103 galvarecorder equipped with an automatically-scanning potentiometer was employed for the measurements of all alternating current (A. C.) polarograms.

A dropping mercury electrode, which has an m value of 1.23_7 mg./sec. and a drop time of 4.02 sec./drop in air-free 0.1 M potassium chloride solutions with an open circuit at 70 cm. of mercury column at 25.0 ± 0.1°C, was used for all measurements. A saturated calomel electrode (S. C. E.) of a large area was used as the reference electrode and was connected to the cell solution through a Hume and Harris-type[5] salt bridge.

The dissolved oxygen in the solution was removed by bubbling pure nitrogen gas through the solution. All D. C. polarograms given in this paper were measured at 25.0 ± 0.1°C unless otherwise stated and are corrected for residual currents. The pH value of the solution was measured with a glass electrode pH meter (Toyoroshi Kaisha Model G).

Reagent.—A standard solution of zinc(II) was prepared by dissolving pure zinc sulfate crystals in redistilled water. The concentration of zinc(II) was determined accurately by titrating it with standard nitrilotriacetate volumetrically[6]. Nitrilotriacetic acid (NTA) of an analytical reagent grade (Wako Pure Chemical Industries, Ltd.) was used without further purification. The stock solution of NTA was standardized with a standard nickel(II) solution[7]. The ammonia-ammonium nitrate buffer solutions were prepared by the method described in a previous paper[6]. All other chemicals were of an analytical reagent grade and were used without further purification. The ionic strength of the solution was adjusted to 0.4 by adding appropriate amounts of potassium nitrate.

Results and Discussion

In order to simplify the theoretical treatment, it is desirable to keep the concentration of NTA ions at the electrode surface constant during the reaction. This is ordinarily attained by adding a large excess of NTA ions. In the present case, however, it is advantegeous to keep the concentration of NTA ions fairly low, because the kinetic wave decreases with the increase in the concentration of free NTA ions. As an alternative, the above condition may be satisfied by adding a large excess of calcium ions to the solution; these ions react with free NTA ions to form stable complex ions. Therefore, all experiments were carried out in a solution containing a large excess of calcium ions, in other words, in a solution well-buffered with respect to free NTA ions.

The zinc(II)-nitrilotriacetate complex ion in a 0.1 M potassium nitrate medium does not show a reduction wave at less negative potentials than those where the supporting electrolyte is reduced. The system containing $2.11_6\times10^{-3}$ M NTA, $9.15_2\times10^{-4}$ M zinc(II) and 0.1 M calcium nitrate, however, exhibits a reduction wave in the ammonia buffer medium of a pH value of 8.25 (ionic strength 0.4), which corresponds to the reduction of zinc(II)-ammine complex

1) J. Koryta, *Collection Czechoslov. Chem. Commun.*, **24**, 2903 (1959).
2) J. Koryrta, ibid., **24**, 3057 (1956).
3) M. Brezina, kandidatur-Dissertationsarbeit, Polarographisches Institut, Tschecholowakische Akademie der Wissenschaften, Prague 1956.
4) I. M. Kolthoff and J. J. Lingane, "Polarography", Vol. I, Interscience, New York (1952), p. 297.
5) D. N. Hume and W. E. Harris, *Ind. Eng. Chem. Anal. Ed.*, **15**, 465 (1943).
6) G. Numaziri, M. Kodama and A. Shimizu, *J. Chem. Soc. Japan, Pure Chem. Sec. (Nippon Kagaku Zasshi)*, **81**, 454 (1960).
7) M. Kodama, A. Shimizu and H. Terakado, ibid., **81**, 1545 (1960).

ions (see Fig. 1). The limiting current of the polarogram is much larger than that which would be expected from the calculated concentration of the free ions which are in equilibrium with the zinc(II)-nitrilotriacetate complex at a pH value of 8.25. The numerical values for the equilibrium constants of NTA, ammonia, and their complexes, which were used for the calculation of the concentration of zinc(II)-ammine complex ions, the ZnX^-, NH_3 and X^{3-} listed in Table III, are given in Table II. These values were also used for the various calculations discussed below.

The relation between the limiting current of the reduction wave, i_t, and the effective pressure, H_c, was examined. The limiting current was found to be independent of H_c within the range of experimental error (Table I).

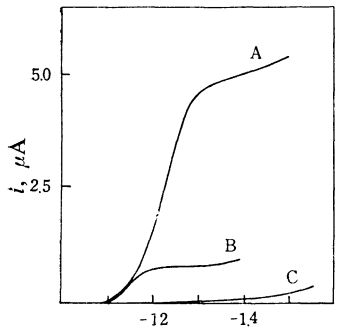


Fig. 1. The reduction wave of $9.15_2\times10^{-4}$ M Zn(II).

A: Ammonia-buffer of pH 9.2_5
B: Ammonia-buffer of pH 8.2_6 containing $2.11_6\times10^{-3}$ M NTA and 0.1 M $Ca(NO_3)_2$
C: 0.1 M KNO_3 medium containing $2.11_6\times10^{-3}$ M NTA

TABLE I. RELATION BETWEEN THE LIMITING CURRENT AND THE EFFECTIVE PRESSURE OF MERCURY ON THE DME

($9.15_2\times10^{-4}$ M Zn(II), $2.11_6\times10^{-3}$ M NTA, 0.1 M $Ca(NO_3)_2$, ionic strength 0.4, 25°C)

Height of mercury column, H cm.	Limiting current i_l, μA	$i_l/H_c^{1/2}\times10$
55	0.74_5	1.02_1
70	0.75_1	0.91_0
90	0.75_5	0.80_5

H_c: Effective pressure in cm.

The effect of the pH value of the solution on i_l was studied over the pH range of 8.26 to 9.36 in ammonia buffer solutions containing $2.11_6\times10^{-3}$ M NTA, $9.15_2\times10^{-4}$ M zinc(II) and 0.1 M or 0.05 M calcium(II), the ionic strength of which was adjusted to 0.4. The total concentration of ammonia in the solution was 0.1 M or 0.05 M. The expeimental results show that the limiting current increases with the pH value of the solution, provided the other conditions are kept constant (Table III). The concentration of ammonia was calculated by successive approximation. Similar results were also obtained at 15 and 33°C.

TABLE II

i) Dissociation constants of NTA (hybrid constants; ionic strength: 0.4)[8]
$pK_1=1.82_1$ $pK_2=2.30_6$ $pK_3=9.44_5$
ii) Dissociation constants of zinc-ammine complex (ionic strength: 0.4)[9]
$pK_1=2.18$ $pK_2=2.25$ $pK_3=2.31$ $pK_4=1.96$
iii) Formation constant of Zn(II)-NTA (ionic strength: 0.4)[10]
$K_{ZnX}=C_{ZnX}/C_{Zn}\cdot C_X=10^{10.09}$
iv) Formation constant of Ca(II)-NTA (ionic strength: 0.4)[8]
$K_{CaX}=C_{CaX}/C_{Ca}\cdot C_X=10^{5.83_4}$
v) Dissociation constant of ammonia (hybrid constant; ionic strength: 0.4)[11]
$pK=9.30$

In this table, the C's, represent the concentration of the corresponding ionic species.

As these values had not been determined experimentally, they were calculated from the related formation constants in the solution of an ionic strength of 0.1 at 20°C. The activity coefficients of the ions were calculated by means of the Debye-Hückel equation, using the proper values of ionic radii given in Kielland's table[12]. The temperature coefficients of these formation constants were assumed to be zero between 15° and 33°C in these calculations.

The relation between $\log(i/(i_l-i))$ and E, where i_l indicates the limiting current, and i, the current at a potential of E, was analyzed with some typical examples. This relation gave a straight line with a slope of 57 mV. (Fig. 2), which is greater than the value of 45 mV. obtained for the zinc(II) ion in the ammonia buffer solution[13].

The value for the degree of reversibility, K, defined by Eq. 1, was 0.03 for the reduction of the zinc(II) ions in the ammonia buffer solution. This value is much smaller than that for the reduction of cadmium(II) in a potassium nitrate medium.

$$K=I/n\cdot t_d^{1/2}\cdot i_d \qquad (1)$$

8) G. Schwarzenbach, H. Ackermann and P. Ruckstuhl, *Helv. Chim. Acta*, **32**, 1175 (1949).
9) J. Bjerrum, *Chem. Revs*, **46**, 681 (1950).
10) E. J. Wheelwright, F. H. Spedding and G. Schwarzenbach, *J. Am. Chem. Soc.*, **75**, 4196 (1953).
11) R. G. Bates and G. D. Pinchirg,ibid., **72**, 1393 (1950).
12) J. Kielland, ibid., **59**, 1675 (1937).
13) M. Senda M Senda and I. Tachi, *J. Electrochem. Soc. Japan (Denki Kagaku)*, **27**, 83 (1959).

TABLE III. EFFECT OF pH ON THE REDUCTION WAVE (IONIC STRENGTH 0.4)

pH	C°_{ZnX} M×10⁴	C°_{X} M×10⁷	$C^{\circ}_{NH_3}$ M×10²	i_l μA	$E_{1/2}$ V. vs. S. C. E.
8.26[a,b]	9.15_2	39.8_3	0.83_5	0.76	−1.155
8.56[a,d]	9.15_2	52.0_1	0.76_8	0.77	−1.152
8.60[c,d]	9.15_2	20.5_6	0.83_1	0.60	−1.165
8.68[a,b]	9.15_2	23.5_6	1.93	1.99	−1.156
8.76[a,d]	9.15_2	36.5_3	1.11	1.24	−1.154
8.82[b,c]	9.15_2	10.3_9	2.46	2.04	
8.94[c,d]	9.15_2	17.5_6	1.51	1.24	−1.166
9.05[a,b]	9.15_2	6.19_1	3.50	3.77	
9.16[b,c]	9.15_2	2.03_3	2.05	2.75	
9.21[a,d]	9.15_2	2.69_6	4.36	4.15	
9.36[c,d]	9.15_2	9.74_0	2.60	2.77	−1.168

a) Total concentration of Ca(II), 0.1 M
b) Total concentration of NH_3, 0.1 M
c) Total concentration of Ca(II), 0.05 M
d) Total concentration of NH_3, 0.05 M

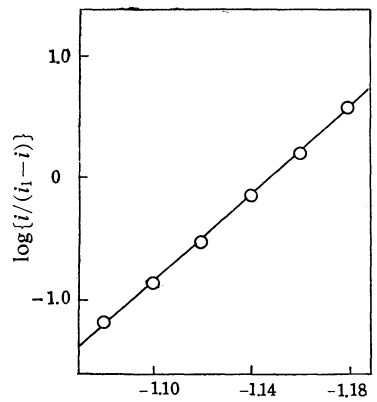


Fig. 2. Log-plot analysis of the reduction wave of Zn(II)-NTA complex in an ammonia buffer of pH 8.2_6 containing 0.1 M $Ca(NO_3)_2$ (Zn(II), $9.15_2\times10^{-4}$ M; NTA, $2.11_6\times10^{-3}$ M; $\mu=0.4$).

In Eq. 1, I indicates the A.C. peak current and t_d, the drop time.

In view of the experimental facts that K for the reduction of zinc(II) ions in the ammonia buffer solution corresponds to the value of the irreversible electrode reaction and that the slope of the log-plots for the reduction wave of the zinc(II)-NTA system is greater than that of the zinc(II) ions in the ammonia buffer solution, we can conclude that the electrode reaction of the zinc(II)-NTA system proceeds irreversibly in a usual polarographic sense.

The effect of temperature on the limiting current was also examined. The results show that the i_l increases in an appreciable degree with the temperature and that the value of the temperature coefficient was 5%, which is larger than that expected for the diffusion-controlled case (Table IV).

TABLE IV. THE RELATION BETWEEN THE LIMITING CURRENT AND THE TEMPERATURE OF THE SOLUTION

($9.15_2\times10^{-4}$ M Zn(II), $2.11_6\times10^{-3}$ M NTA
0.1 M $Ca(NO_3)_2$, ionic strength 0.4)

Temp. T, °C	Limiting current i_l, μA	$\Delta i_l/\Delta T$ %
15	0.38_2	4.8
25	0.75_1	5.8
33	1.10_1	

The experimental results on the relation between the limiting current and the effective pressure of mercury on the DME clearly indicate that the limiting current is kinetic in nature. This explanation is also supported by the experimental finding on the relation between the limiting current and the temperature of the solution.

Under the experimental conditions employed, ZnX^-, zinc ammine complex ions and zinc(II) ions coexist in the bulk of the solution; their concentrations are determined according to the following chemical equilibria:

$$ZnX^- + m\,NH_3 \rightleftharpoons Zn(NH_3)_m^{2+} + X^{3-} \quad (2)$$

$$Zn(NH_3)^{2+} \rightleftharpoons Zn^{2+} + NH_3 \quad (3)$$

$$Zn(NH_3)_2^{2+} \rightleftharpoons Zn(NH_3)^{2+} + NH_3 \quad (4)$$

$$Zn(NH_3)_3^{2+} \rightleftharpoons Zn(NH_3)_2^{2+} + NH_3 \quad (5)$$

$$Zn(NH_3)_4^{2+} \rightleftharpoons Zn(NH_3)_3^{2+} + NH_3 \quad (6)$$

In an ammonia buffer of a value from pH 8.3 to 9.5 and containing a large excess of calcium(II) ions with respect to the total concentration of NTA, the equilibrium between ZnX^- and zinc ammine-complex ions is greatly in favor of ZnX^-; i.e., the concentration of

ZnX^- is virtually equal to the total concentration of zinc in the bulk of the solution.

It is a well-known fact that the electrode reaction of zinc ions at mercury electrodes in ammonia buffer solutions corresponds to the direct reduction of zinc ammine complex ions[14]. From the above consideration, and from the fact that the limiting current increases with the concentration of ammonia in the solution provided that the other conditions are kept constant (Table III), it is very reasonable to conclude that the reaction at the electrode surface proceeds according to the following equations:

$$(I_a)\quad \begin{cases} ZnX^- + m\,NH_3 \rightleftharpoons Zn(NH_3)_m{}^{2+} + X^{3-} \text{ (slow)} & (2) \\ Zn(NH_3)_m{}^{2+} + 2\,e^- + Hg \rightleftharpoons Zn(Hg) + m\,NH_3 & (7) \end{cases}$$

where the forward reaction rate of process 2 is assumed to be nearly equal to or smaller than the rate of the diffusion process of the ordinary ionic species and where the electron transfer reaction 7 proceeds irreversibly.

The theoretical equation of the kinetic current derived for the simple electrode reaction by Delahay[15] can not be applied without modification to the kinetic current obtained in the electrode reaction, where the complicated chemical reaction precedes the irreversible electron-transfer process. Therefore, we tried to derive a theoretical equation of the current-voltage curve obtained under such a mechanism as Ia by using the concept of the reaction layer[17], as in the case of cadmium(II)-EDTA complex ions[16].

When the concentrations of hydrogen ions, ammonia and X^{3-} ions at the electrode surface are kept constant by using buffer solutions containing a large excess of calcium ions which readily react with X^{3-} ions and form stable complex ions, reaction (I_a) can be written in a simpler form:

$$(II)\quad \begin{cases} Y \underset{\vec{k_8}}{\overset{\vec{k_8}}{\rightleftharpoons}} O & \text{slow} \quad (8) \\ O + 2\,e \underset{\vec{\kappa}}{\overset{\vec{\kappa}}{\rightleftharpoons}} R & (9) \end{cases}$$

where the $(m+1)$-th order reaction 2 is replaced by the pseudo-first order reaction 8. O represents the oxidized form, and R, the reduced form, both of which concern the electron-transfer process. The terms k and κ are the reaction rate constants corresponding to each process, the former of which is a usual rate constant of the first order homogeneous reaction expressed in sec^{-1}, while the latter is a rate constant of an electron-transfer process expressed in cm. sec^{-1}. In the present case, $\vec{\kappa}$ and $\overleftarrow{\kappa}$ are represented by the following relations:

$$\vec{\kappa} = \vec{\kappa}_0 \exp\left(\frac{-2\,\alpha EF}{RT}\right)$$

$$\overleftarrow{\kappa} = \overleftarrow{\kappa}_0 \exp\left(\frac{+2(1-\alpha)EF}{RT}\right) \qquad (10)$$

where E is the electrode potential, α, the transfer coefficient, F, the Faraday constant, R, the gas constant, T, the absolute temperature, and κ_0, the value of κ at $E=0$.

Taking into consideration the diffusion process of Y from the bulk of the solution to the electrode surface and assuming the condition of the stationary state with respect to the concentrations of Y, O and R at the electrode surface, the following equations are obtained:

$$dC_Y/dt = K^D{}_Y(C^\circ{}_Y - C_Y) - (\vec{k_8}'C_Y - \overleftarrow{k_8}'C_O) = 0 \qquad (11)$$

$$dC_O/dt = (\vec{k_8}'C_Y - \overleftarrow{k_8}'C_O) - (\vec{\kappa}C_O - \overleftarrow{\kappa}C_R) = 0 \qquad (12)$$

$$dC_R/dt = (\vec{\kappa}C_O - \overleftarrow{\kappa}C_R) - K^D{}_R C_R = 0 \qquad (13)$$

$$\vec{k_8}' = \mu_8 \vec{k_8}$$

$$\overleftarrow{k_8}' = \mu_8 \overleftarrow{k_8}$$

where the C°'s represent the concentrations in the bulk of the solution, the C's, the concentrations at the electrode surface, the K's, the rate constants corresponding to the diffusion processes, and the μ's, the thicknesses of the reaction layer of the corresponding chemical reactions expressed in cm^{-1}. In the above equations, the diffusion process of O is neglected, because, in the present case, the concentration of O in the bulk of the solution can be assumed to be negligibly small.

The average current, i, can be represented by the equation:

$$i = 2\,AF(\vec{\kappa}C_O - \overleftarrow{\kappa}C_R) \qquad (14)$$

where A is the mean surface area of DME. From Eqs. 11, 12, 13 and 14, we can obtain the following equation for the limiting current, i_l:

$$i_l = 2\,AF\left\{\frac{\vec{k_8}' \cdot C^\circ{}_Y}{1 + \vec{k_8}'/K^D}\right\} \qquad (15)$$

14) H. Matsuda and Y. Ayabe, *Z. Elektrochem.*, **63**, 1164 (1959).
15) p. Delahay, "New Instrumental Methods in Electrochemistry", Interscience Publishers, New York (1954), p. 87.
16) N. Tanaka, R. Tamamushi and M. Kodama, *Z. physik. Chem. N. F.*, **14**, 141 (1958).
17) For example, see Ref. 15, p. 94.

under the assumption that K_Y^D and K_R^D are the same ($=K^D$).

By introducing the relation $\mu_8=K_8^{1/2}\cdot D^{1/2}\cdot(\vec{k_8})^{-1/2}$ [17], Eq. 15 can be rearranged to:

$$\frac{1}{i_l}=\frac{1}{2AFK_8^{1/2}D^{1/2}\vec{k_8}^{1/2}C^\circ}+\frac{1}{2AFK^D C^\circ_Y} \tag{16}$$

where D is the diffusion coefficient of Y and O, and $K_8=C^\circ_O/C^\circ_Y$. On the right-hand side of Eq. 16, the first and the second terms represent the contribution of the kinetic and the diffusion currents respectively to the limiting current. If $K^{1/2}D^{1/2}\vec{k_8}^{1/2}C^\circ_Y$ is much larger than $K^D C^\circ_Y$, the limiting current comes to be completely diffusion-controlled, which state is represented by the well-known Ilkovic equation.

If the electron-transfer process is assumed to be irreversible, i. e., $\vec{\kappa}\gg\overleftarrow{\kappa}$, as in the present case of the zinc(II)-NTA system, we can obtain the following equation, which represents the current-voltage relation of the so-called irreversible reduction wave corresponding to reaction II by combining Eqs. 11, 12, 13 and 14.

$$i=\frac{\vec{\kappa}}{\overleftarrow{k_8}}(i_l-i)\left(1+\frac{\vec{k_8}'}{K^D}\right) \tag{17}$$

When the limiting current is kinetic in nature, as in the case of the zinc(II)-NTA system, $\vec{k_8}'$ is assumed to be much smaller than K^D. For this reason, the term $\vec{k_8}'/K^D$ is negligibly small in comparison with 1 and Eq. 17 can be simplified as follows at 25°C:

$$E=\frac{0.0591}{2}\left\{\log\vec{\kappa}_0-\log\left(\frac{i}{i_l-i}\right)-\log\overleftarrow{k_8}'\right\} \tag{18}$$

The experimental results on the zinc(II)-NTA system were analyzed with the aid of Eqs. 16 and 18. When these equations are applied to the electrode Eq. Ia, Y and O correspond to ZnX^- and $Zn(NH_3)_m^{2+}$ respectively, and the rate constants and equilibrium constants in these equations must be replaced by the corresponding terms, as in the following way:

$$\vec{k_8}=\vec{k_2}(C^\circ_{NH_3})^m$$

$$\overleftarrow{k_8}=\overleftarrow{k_2}C^\circ_X$$

$$K_8=\frac{C^\circ_{Zn(NH_3)_m}}{C^\circ_{ZnX}}=K\times\frac{(C^\circ_{NH_3})^m}{C^\circ_X}$$

$$K=K_{Zn(NH_3)_m}/K_{ZnX}$$

$$K_{Zn(NH_3)m}=\frac{C^\circ_{Zn(NH_3)_m}}{(C^\circ_{NH_3})^m C^\circ_X}$$

$$K_{ZnX}=\frac{C^\circ_{ZnX}}{C^\circ_{Zn}\cdot C^\circ_X}$$

Therefore, Eq. 16 can be written as

$$\frac{1}{i_l}=\frac{1}{2AFD^{1/2}K^{1/2}\vec{k_2}^{1/2}}\cdot\frac{(C^\circ_X)^{1/2}}{C^\circ_{ZnX}\cdot(C^\circ_{NH_3})^m}+\frac{1}{2AFK^D\cdot C^\circ_{ZnX}} \tag{19}$$

This equation indicates that, if the electrode reaction proceeds according to the Ia mechanism, the relation between $1/i_l$ and $(C^\circ_X)^{1/2}/C^\circ_{ZnX}\cdot(C^\circ_{NN_3})^m$ must be linear. The above relations were examined in connection with the experimental data in Table III. Linear relations were found between $1/i_l$ and $(C^\circ_X)^{1/2}/C^\circ_{ZnX}\cdot(C^\circ_{NN_3})^2$, but not between $1/i_l$ and $(C^\circ_X)^{1/2}/C^\circ_{ZnX}$, $(C^\circ_X)^{1/2}/C^\circ_{ZnX}\cdot C^\circ_{NN_3}$ or $(C^\circ_X)^{1/2}/C^\circ_{ZnX}\cdot(C^\circ_{NN_3})^3$ (Figs. 3, 4, 5 and 6). Similar results were also obtained at 15 and 33°C. Therefore, it can be concluded that the electrode reaction

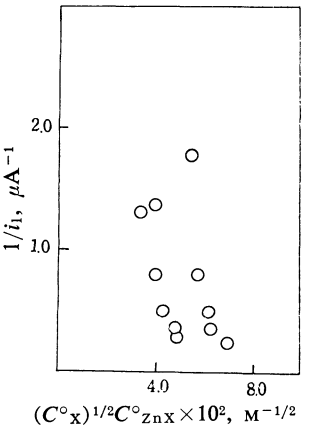


Fig. 3. Relation between $1/i_l$ and $(C^\circ_X)^{1/2}/C^\circ_{ZnX}$.

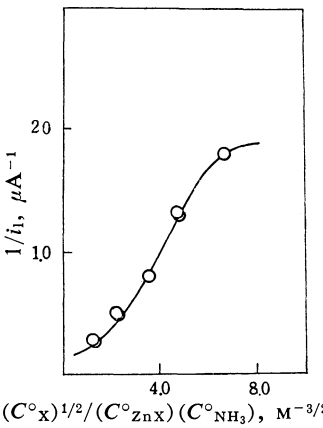


Fig. 4. Relation between $1/i_l$ and $(C^\circ_X)^{1/2}/(C^\circ_{ZnX}\cdot C^\circ_{NH_3})$.

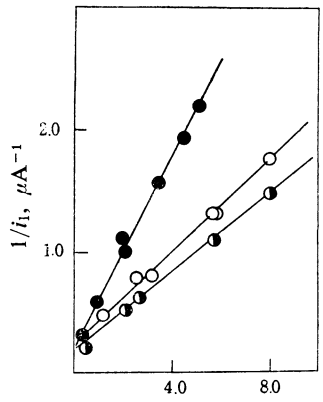


Fig. 5. Relation between $1/i_l$ and $(C^\circ_X)^{1/2}/(C^\circ_{Zn^X})(C^\circ_{NH_3})^2$.

● 15°C ○ 25°C
◐ 33°C

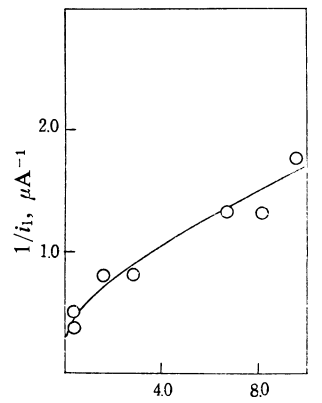


Fig. 6. Relation between $1/i_l$ and $(C^\circ_X)^{1/2}/(C^\circ_{ZnX})(C^\circ_{NH_3})^3$.

of the zinc(II)-NTA system proceeds according to the following mechanism:

$$\text{(Ib)}\begin{cases} ZnX^- + 2\,NH_3 \\ \quad \rightleftharpoons Zn(NH_3)_2^{2+} + X^{3-} & (2) \\ Zn(NH_3)_2^{2+} + 2\,e + Hg \\ \quad \rightleftharpoons Zn(Hg) + 2NH_3 & (7) \end{cases}$$

By remembering the fact, mentioned by Matsuda and Ayabe[14], that the reduction wave of zinc-ammine complex ions at the dropping mercury electrode is due to the direct reduction of $Zn(NH_3)_2^{2+}$, it is very plausible to propose the I_b electrode reaction mechanism, where the dissociation reaction of ZnX^- precedes the electron transfer process.

The fact that linear relations between $1/i_l$ and $(C^\circ_X)^{1/2}/C^\circ_{ZnX}(C^\circ_{NN_3})^2$ were found at 15, 25 and 33°C clearly show that the concentration of calcium(II) employed was high enough to keep the concentration of X^{3-} constant at the electrode surface.

Figure 5 clearly shows the existence of a small contribution of the diffusion-controlled current to the total limiting current, which must be equal to $(2\,AFK^DC^\circ_{ZnX})^{-1}$, according to Eq. 19. Theretically, this term must be equal to $(2\times6.07\times10^4\times m^{2/3}\,t^{1/6}\,D^{1/2}\,C^\circ)^{-1}$ in comparison with the Ilkovic equation, where m is expressed in g./sec. and t_d, in sec., and where D is the deffusion coefficient of Zn^{2+}, ZnX^- or $Zn(NH_3)_m^{2+}$ expressed in cm. sec^{-2} [18]. The current is expressed in ampere and the concentration, in mol./cc. The observed value of $(2\,AFK^DC^\circ_{ZnX})^{-1}$ was 1.8×10^3 amp^{-1}, whereas the calculated value is 2×10^3 amp^{-1}. It could be said that the observed value agrees with the calculated value.

The tangent of the relation of $1/i_l$ vs. $(C^\circ_X)^{1/2}/C^\circ_{ZnX}(C^\circ_{NN_3})^2$ was found to be 2.4×10^{-3}. According to Eq. 22, this value must be equal to $(2\,AFK^{1/2}\,D^{1/2}\,\vec{k}_2^{1/2})^{-1}$, which can be written as $(2.51+10^5\,m^{2/3}\,t^{2/3}\,D^{1/2}\,K^{1/2}\,k_2^{1/2})^{-1}$. If we use the values of $10^{10.09}$ for K_{ZnX} and $10^{4.43}$ for $K_{Zn(NH_3)_2}$, $\vec{k}_2$ in Eq. 22 is calculated to be 0.85_0 $(mol./l.)^{-2}\,sec^{-1}$, which corresponds to the rate constant of the forward reaction of $ZnX^- + 2\,NH_3 = Zn(NH_3)_2^{2+} + X^{3-}$ at 25°C in the medium with the ionic strength of 0.4 containing a large excess of calcium(II) ions. The rate constant of the backward reaction, $\overleftarrow{k}_2$, is also found to be equal to 2.42×10^5 $(mol./l.)^{-1}\,sec^{-1}$ from the $K=\vec{k}_2/\overleftarrow{k}_2$ relation.

The experimental data on the limiting current obtained at 15 and 33°C at various pH values were analyzed by using Eq. 22. The linearity between $1/i_l$ and $(C^\circ_X)^{1/2}/C^\circ_{ZnX}(C^\circ_{NH_3})^2$ was satisfied also in these cases. If we assume that the value of the equilibrium constant, K, is independent of the temperature, the values of $\vec{k}_2$ are calculated as 0.22 $(mol./l.)^{-2}\,sec^{-1}$ and 5.52 $(mol./l.)^{-2}\,sec^{-1}$ for 15 and 33°C respectively. From the values of $\vec{k}_2$ at 15, 25 and 33°C, the heat of activation, ΔH^*, and the entropy of activation, ΔS^*, of the forward reaction of $ZnX^- + 2NH_3 = Zn(NH_3)_2^{2+} + X^{3-}$, are obtained as 31.1 kcal. and -25.4 e. u. respectively. These thermodynamic values, however, are not so accurate partly because of the approximate estimation of the equilibrium constants, K_{ZnX} and $K_{Zn(NH_3)_2}$.

When the mechanism of the electrode reaction is represented by Ib, the natures of the current-voltage curve must satisfy Eq. 18. This equation predicts that the log-plot analysis will give a straight line with a slope of 57 mV. at

18) In this calculation, the diffusion coefficients of Zn^{2+}, ZnX^- and $Zn(NH_3)_2^{2+}$ were assumed to be the same, 8.40×10^{-6} cm. sec^{-2}.

25°C; this is in agreement with the experimental results when we employ the value of 0.53_0 for (see Fig. 2).

The expression of the half-wave potential, $E_{1/2}$, is obtained from Eqs. 10 and 18 as:

$$E_{1/2}=\frac{0.0591}{2\alpha}\left\{\log\vec{\kappa}_0-\log\overleftarrow{k_2}'\right\} \quad (20)$$

By remembering the nature of $\overleftarrow{k_2}'$, Eq. 20 can be written as

$$E_{1/2}=\text{const}-\frac{0.0591}{4\alpha}\log C^\circ \quad (21)$$

This relation was examined by using some typical data from Table III, the results of which are shown in Fig. 6. The tangent of the relation between $E_{1/2}$ and C°_X is 35 mV. and is in agreement with the theoretical prediction of 29 mV.

It can be concluded from the results of the theoretical analysis of the experimental data that the reduction wave of the zinc(II)-NTA system under the presence of an excess of calcium ions is of a kinetic nature, the mechanism of which is represented by the I_b reaction.

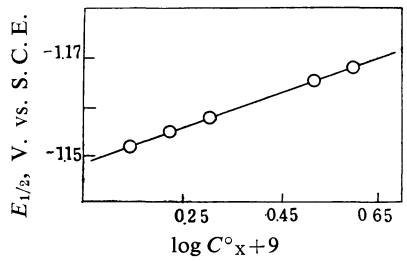


Fig. 7. Relation between $E_{1/2}$ ang $\log C^\circ_X$.

Summary

The kinetic current due to the dissociation of zinc-nitrilotriacetate complexes has been investigated in buffers with pH values from 8.3 to 9.5 and containing a large excess of calcium ions with respect to the total concentration of nitrilotriacetate. The ionic strength was kept at 0.4.

It was confirmed that the electrode reaction at the surface of the dropping mercury electrode proceeds according to the mechanism:

$$ZnX^- + 2\,NH_3 \rightleftarrows Zn(NH_3)_2^{2+} + X^{3-} \quad \text{(slow)}$$

$$Zn(NH_3)_2^{2+} + 2\,e + Hg \rightleftarrows Zn(Hg) + 2\,NH_3 \quad \text{(fast)}$$

The rate constants were calculated as 0.85_0 $(\text{mol./l.})^{-2}\,\text{sec}^{-1}$ for the dissociation reaction of $ZnX^- + 2\,NH_3 = Zn(NH_3)_2^{2+} + X^{3-}$ and $2.42\times 10^5(\text{mol./l.})^{-1}\,\text{sec}^{-1}$ for the association reaction at 25°C. in buffer solutions of pH values from 8.3 to 9.5 with an ionic strength of 0.4 and containg 0.1 M calcium nitrate. The heat of activation and the entropy of activation of the dissociation reaction were calculated as 31.1 kcal. and −25.4 e. u. respectively.

Department of Chemistry
Faculty of Arts and Sciences
Ibaraki University
Mito, Ibaraki

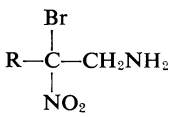
Die Darstellung und Charakterisierung von 2-Brom-2-nitroalkylaminen

Von Mitsuo MASAKI und Masaki OHTA

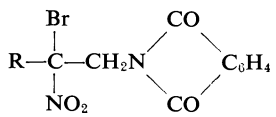
(Eingegangen am 14 Juni, 1962)

Kürzlich berichteten wir[1], dass durch neue Darstellungsmethode der Umsetzung von 1, 2-Dibrom-2-nitropentan (III-a) mit Phthalimidkalium und nachfolgender Behandlung der entstandenen Phthalimid-Körper (II-a) mit Hydrazinhydrat 2-Brom-nitropentylamin (I-a) dargestellt werden kann.

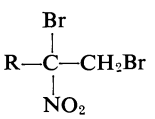
Zur Prüfung auf die Anwendungsfähigkeit



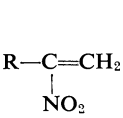
(I)



(II)



(III)



(IV)

R = C_3H_7 (a)
n-C_4H_9 (b)
iso-C_4H_9 (c)

1) M. Masaki und M. Ohta, Dieses Bulletin, 35, 1418 (1962).

dieser Methode versuchten wir weiter auch andere Nitroolefine (IV) in 2-Brom-2-nitroalkylamine (I) überzuführen, weil diese Verbindungsklasse in der erst wenigen Literatur beschrieben worden ist[2].

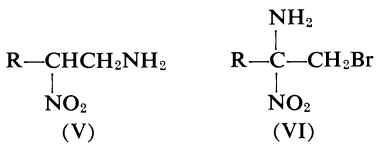
In analoger Weise wie bei I-a konnten wir 2-Brom-2-nitrohexylamin (I-b) und 2-Brom-2-nitro-4-methylpentylamin (I-c) mit befriedigender Ausbeute herstellen.

Nitroolefine lassen sich gewöhnlich nach der von Hass und Mitarbb.[3] angegebenen Methode, die in Erhitzen von 2-Nitroalkylacetat mit Alkalicarbonat besteht, darstellen. Bei unserem Fall jedoch konnte in der Ausbeute kein befriedigenes Resultat erhalten werden. Die direkte Dehydratisierung von Nitroalkohol mittels Phthalsäureanhydrid zu Olefin ist schon von Buckley und Scaife[4] sowie von Khannanov und Mitarbb.[5] berichtet worden. Nach dieser Methode erhielten wir[1] auch 2-Nitropenten (IV-a) in guter Ausbeute und ferner konnten wir durch Erhitzen von 2-Nitrohexanol und 2-Nitro-4-methylpentanol mit Phthalsäureanhydrid die entsprechenden Nitroolefine (IV) darstellen.

Die auf diese Weise erhaltenen Nitroolefine (IV) liessen sich in 1,2-Dibrom-Körper (III) überführen, welche bei 30 stdg. Erhitzen mit Phthalimidkalium in Aceton 1-Phthalimid-2-brom-2-nitroalkane (II) lieferten, die sich mit Hydrazinhydrat zu der Aminen I zersetzen liessen.

Die so erhaltenen 2-Brom-2-nitroalkylamine (I) wurden durch Infrarot-Spektren und Elementaranalysen von den Hydrochloriden und den Pikraten, sowie durch Umsetzung mit Phenylisocyanat charakterisiert.

In Infrarot Absorptionsspektrum des Hydrochlorids von I tritt die für aktive Methylengruppe, d. h. an NH_3^+ benachbartes CH_2 charakteristische Bande[6] bei 1440 cm^{-1} intensiv auf, welche in demjenigen des freien Amins I verschwindet. Vergleicht man ferner die Absorptionsbanden der Nitrogruppe in I mit denjenigen in 2-Nitroalkylamine (V) (s. Tabelle I), so kann man einen Effekt des α-Substituent finden, welcher mit dem Bericht Haszeldines[7] übereinstimmt und darauf hinweist, dass Bromatom in I an α-Kohlenstoff der Nitrogruppe gebunden ist. Somit lässt sich beweisen, dass I nicht das alternative Nitroamin, d. h. 1-Brom-2-amino-2-nitro-Körper (VI) ist.



(V) (VI)

Durch Umsetzung mit Phenylisocyanat lieferten die Amine I die entsprechenden Derivate des Harnstoffes und mit Benzoylchlorid konnte die Benzoylierung erreicht werden. Dagegen ist uns die Umsetzung von I mit Chlor- bzw. Brom-essigester nicht gelungen. Auch bei der Reaktion mit verschiedenen Carbonylverbindungen konnte kein definiertes Produkt erhalten werden.

Im Infrarot-Spektrum von I-a beobachtet man zwei schwache Banden bei 3420 und 3345 cm^{-1}, welche man zu den asymmetrischen und symmetrischen NH_2-Valenzschwingungen zurückführen kann, weil die Wellenzahl-Beziehung dieser zwei Banden in guter Übereinstimmung mit der Gleichung von Bellamy-Williams[8] ist. Doch ist die Lage dieser Banden einigermassen in niedriger Wellenzahl verschoben als diejenige eines freien primären Amins[9]. Diese Verschiebung

Tabelle I. IR-Spektren

	$-NH_2$ bzw. $-NH_3^+$ cm^{-1}	$-NO_2$ cm^{-1}
1-Amino-2-brom-	*3420	1560
2-nitropentan (I-a)	3345	1330
	(3341)	845
	1620	
Hydrochlorid von I-a	2800~3050	1560
	1900	1340
	1580	845
	1500	
1-Amino-2-nitropentan	*3410	1555
(V, $R=C_3H_7$)	3330	1365
	(3333)	855
	1620	
Hydrochlorid von V	2800~3050	1558
($R=C_3H_7$)	1980	1359
	1600	850
	1519	

( )···Die aus asymm. Valenzschwingung* nach der Gleichung[8] berechnete symm. Valenzschwingung.

2) Die Umsetzung von β-Brom-β-nitrostyren mit Ammoniak ergibt 2-Brom-2-nitro-1-phenylethylamin (J. Loevenich und H. Gerber, *Ber.*, **63**, 1707 (1930).) und bei der Umsetzung von 1-Brom-2-nitro-1-buten mit Aminen oder Ammoniak werden unbestätige Addukte erhalten (J. Loevenich, J. Koch und U. Pucknet, *Ber.*, **63**, 636 (1930).).

3) H. B. Hass, A. C. Susie und R. L. Heider, *J. Org. Chem.*, **15**, 8 (1950).

4) G. D. Buckley und C. W. Scaife, *J. Chem. Soc.*, **1947**, 1471.

5) T. M. Khannanov, L. M. Kozlov und V. I. Burmistow, *Chem. Abstr.*, **54**, 24345 (1960).

6) K. Nakanishi, T. Goto und M. Ohashi, Dieses Bulletin, **30**, 403 (1957).

7) R. N. Haszeldine, *J. Chem. Soc.*, **1953**, 2525.

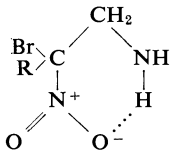
8) L. J. Bellamy und R. L. Williams, *Spectrochim. Acta*, **9**, 341 (1957).

9) L. J. Bellamy, "The Infra-red Spectra of Complex Molecules", 2nd Ed., Methuen, London; Wiley, New York (1958), s. 250.

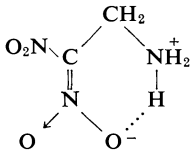
mag möglicherweise auf Wasserstoffbindung beruhen.

Ferner weist es auf die Bildung der intramolekularen Wasserstoffbindung in diesem Nitro-amin I-a hin, dass die Lage der NH_2-Valenzschwingungsbanden von Konzentration unabhängig ist und die Bande von der symmetrischen NO_2-Valenzschwingung in I-a um 10 cm^{-1} in niedriger Wellenzahl verschoben wird als diejenige in Hydrochlorid von I-a.

Vor einiger Zeit stellten Kamlet und Dacons[10] 2, 2-Dinitroethylamin (V, R=NO_2) her und beobachteten, dass Formylierung, Mannich-Reaktion oder Michael-Kondensation des Dintro-amins nicht auftrat und dies auf die Bildung der intramolekularen Wasserstoffbindung VIII, die Zwitterion enthält, zurückzuführen ist.



(VII)



(VIII)

Im Infrarot-Spektrum von 2-Nitropentylamin (V, R=C_3H_7), das durch die Anlagerung von Ammoniak an 2-Nitropenten hergestellt wurde, erscheinen auch die zwei Banden bei 3410 und 3330 cm^{-1}, die zur NH_2-Valenzschwingung gehören, und dafür kann man die analogen Verhältnisse wie bei I-a beobachten.

Aus den oben erwähnten Tatsachen wird es klar, dass die 2-Nitroalkylamine auf jeden Fall die intramolekulare Wasserstoffbindung auszubilden scheinen.

Jedoch kann man es nicht durch Wasserstoffbindung erklären, dass die Aminogruppe in 2-Brom-2-nitroalkylamin (I) reaktionsträge ist, was vielmehr auf sterische Grüde zurückzuführen sein dürfte.

Beschreibung der Versuche

2-Nitro-1-hexen (IV-b).—Ein Gemisch von 42 g 2-Nitro-1-hexanol und 41 g Phthalsäureanhydrid wurde im Destillierkolben unter vermindertem Druch von ca. 45 mmHg bei 160～170°C erhitzt und das erzeugte Olefin kam durch 15 cm Kolonne mit wenigem Wasser sehr langsam über. Nach 5～6 Stdn. war das Destillieren beendet, das Destillat wurde mit Äther versetzt und nach der Befreiung von der Wasserschicht mit Calciumchlorid getrocknet. Nach dem Abdampfen des Äther wurde der Rückstand unter vermindertem Druck destilliert. Ein gelbliches, Augen stechendes Öl vom Sdp. 93.5～94.5°C/47.5 mmHg. Ausb. 24 g.

Gef.: N, 10.45. Ber. für $C_6H_{11}O_2N$: N, 10.85%.

1, 2-Dibrom-2-nitrohexan (III-b).—Eine Lösung von 60 g IV-b in 80 ccm Chloroform wurde mit 24.8 g Brom in 45 ccm Chloroform langsam versetzt. Die Reaktion verlief langsam unter mässiger Wärmeerzeugung. Nach 3 stdg. Stehenlassen bei Raumtemperatur wurde das Lösungsmittel entfernt und der Rückstand unter vermindertem Druck destilliert. Sdp. 108～109°C/7 mmHg. Ausb. 41 g.

Gef.: C, 25.05; H, 3.91; N, 4.56. Ber. für $C_6H_{11}O_2NBr_2$: C, 24.91; H, 3.86; N, 4.84%.

1-Phthalimid-2-brom-2-nitrohexan (II-b).—Ein Gemisch von 28.9 g III-b und 18.5 g Phthalimidkalium in 100 ccm des mit Kupfersulfat getrockneten Acetons wurde 30 Stdn. unter Rühren und Rückfluss erhitzt. Nach dem Abkühlen filtrierte man Kaliumbromid ab, dampfte das Filtrat unter vermindertem Druck ein und versetzte das verbliebene Öl mit 30 ccm Äthanol, woraus sich beim Stehenlassen der Phthalimid-Körper (II-b) auskristallisierte. Dieser wurde mit verdüunnter Natronlauge, dann mit Wasser gewaschen und aus Äthanol umkristallisiert. Farblose Prismen vom Schmp. 88°C. Ausb. 24 g.

Gef.: C, 47.29; H, 4.33; N, 8.03. Ber. für $C_{14}H_{15}O_4N_2Br$: C, 47.32; H, 4.23; N, 7.89%.

1-Amino-2-brom-2-nitrohexan-hydrochlorid. — In 50 ccm Äthanol wurden 5 g II-b mit 1 g Hydrazinhydrat (80%) versetzt, 6 Stdn auf dem Wasserbad auf 40～50°C erwärmt und dann über Nacht stehengelassen. Am nächsten Tag wurde das Reaktionsgemisch mit 2.5 ccm konz. Salzsäure versetzt und noch 2 Stdn. bei 30°C stehengelassen. Das ausgeschiedene Phthalsäureanhydrid wurde abfiltriert und das Filtrat nach Einengen auf ca. 5 ccm mit 50 ccm Wasser versetzt, wobei weiteres Phthalsäurehydrazid ausfiel, das abfiltriert wurde. Das Filtrat wurde weiter unter vermindertem Druck eingedampft. Der Rückstand wurde aus Äthanol-Äther in Nadelchen vom Schmp. 134～138°C umkristallisiert. Ausb. 2.3 g. Zur Analyse wurden diese noch zweimal umkristallisiert. Farblose Nadelchen vom Schmp. 147～148°C.

Gef.: C, 27.14; H, 5.17; N, 10.31. Ber. für $C_6H_{13}O_2N_2Br \cdot HCl$: C, 27.55; H, 5.19; N, 10.71%.

Pikrat.—Gelbe Nadeln vom Schmp. 147°C.

Gef.: C, 31.70; H, 3.68; N, 15.58. Ber. für $C_{12}H_{16}O_9N_5Br$: C, 31.72; H, 3.52; N, 15.42%.

Zur Aufnahme des Infrarot-Spektrum liess sich die Lösung des freien Amins I-b in Chloroform dadurch erhalten, dass man eine Lösung von 0.5 g Hydrochlorid von I-b in 20 ccm Wasser in einem Scheidetrichter mit 20 ccm Chloroform und 0.16 g Natrium Hydrogencarbonat versetzte und die nach dem Durchschütteln abgetrennte Chloroformschicht dreimal mit Wasser wäscht, und anschliessend mit Natriumsulfat trocknet.

***N*-(2-Brom-2-nitrohexyl-1)-*N'*-phenylharnstoff.** — Die Lösung von I-b in Chloroform (aus 1 g Hydrochlorid von I-b und 30 ccm Chloroform dargestellt) wurde mit 0.45 g Phenylisocyanat versetzt, 2 Stdn. unter Rückfluss erwärmt und unter vermindertem Druck eingeengt. Beim Versetzen mit Ligroin und Stehenlassen kristallisierte sich der Rückstand. Ausb. 0.9 g. Aus Ligroin umkristallisiert, farblose Nadelchen vom Schmp. 110～112°C.

Gef.: N, 12.21. Ber. für $C_{13}H_{18}O_3N_3Br$.: N, 12.21%.

10) M. J. Kamlet und J. C. Dacons, *J. Org. Chem.*, **26**, 3005 (1961).

2-Nitro-4-methyl-1-penten (IV-c).—Ein Gemisch von 26 g 2-Nitro-isohexanol (aus 1-Nitro-isopentan nach der Methode von Vanderbilt und Hass[11] dargestellt) und 25.5 g. Phthalsäureanhydrid wurde analog wie bei IV-b aufgearbeitet. Ein gelbliches, Augen stechendes Öl vom Sdp. 82~83°C/42 mmHg. Ausb. 17.5 g (77%).

Gef.: N, 10.99. Ber. für $C_6H_{11}O_2N$: N, 10.85%.

1,2-Dibrom-2-nitro-4-methylpentan (III-c).—Eine Lösung von 15 g IV-c in 60 ccm Chloroform wurde mit 18.6 g Brom in 35 ccm Chloroform langsam versetzt. Dann wude das Gemisch analog wie bei III-b aufgearbeitet. Sdp. 106~108°C/7 mmHg. Ausb. 31 g (92%).

Gef.: N, 4.94. Ber. für $C_6H_{11}O_2NBr_2$: N, 4.84%:

1-Phthalimid-2-brom-2-nitro-4-methylpentan (II-c).—Ein Gemisch von 29 g III-c und 20 g Phthalimidkalium in 120 ccm des mit Kupfersulfat getrocknetens Acetons wurde 30 Stdn. unter Rühren und Rückfluss erhitzt, und dann wurde das Reaktionsgemisch analog wie bei II-b aufgearbeitet. Ausb. 22 g. Farblose Prismen vom Schmp. 111°C (aus Äthanol).

Gef.: N, 7.74. Ber. für $C_{14}H_{15}O_4N_4Br$: N, 7.89%.

1-Amino-2-brom-2-nitro-4-methylpentan-hydrochlorid.—Ein Gemisch von 5 g II-c und 1 g Hydrazinhydrat (80%) in 50 ccm Äthanol wurde 5~6 Stdn. auf 40~50°C erwärmt und dann über Nacht bei Raumtemperatur stehengelassen. Am nächsten Tag wurde das Reaktionsgemisch aufgearbeitet, wie bei Hydrochlorid von I-b beschrieben. Farblose Nadelchen vom Schmp. 150~153°C (aus Äthanol-Äther).

Gef.: C, 27.74; H, 5.49; N, 10.51. Ber für $C_6H_{13}O_2N_2Br \cdot HCl$: C, 27.55; H, 5.19; N, 10.71%.

***N*-(2-Brom-2-nitro-4-methylpentyl-1)-*N'*-phenylharnstoff.**—Analog wie bei *N*-(2-Brom-2-nitrohexyl-1)-*N'*-phenylharnstoff wurde eine Lösung von I-c und Phenylisocyanat in Chloroform aufgearbeitet. Farblose Nadelchen vom Schmp. 106°C.

Gef.: N, 12.43. Ber. für $C_{13}H_{18}O_3N_3Br$: N, 12.21%.

1-Benzoylamino-2-brom-2-nitro-4-methylpentan.—Bei Umsetzung von I-c mit Benzoylchlorid erhielt man farblose Nadeln, die aus Ligroin umkristallisiert wurden. Schmp. 110°C.

Gef.: N, 8.64. Ber für $C_{13}H_{17}O_3N_2Br$: N, 8.51%.

1-Amino-2-nitropentan (V, R=C_3H_7).—Eine Lösung von 9 g 2-Nitro-1-penten[1] in 30 ccm Methanol liess sich unter Rühren und Kühlung im Eis/Kochsalz-Bad zu 70 ccm des mit Ammoniak gesättigten Methanols hinzutropfen. Nach der zugabe der Olefin-Lösung wurde die Mischung 2 Stdn. bei 0°C und noch 1 Std bei Raumtemperatur weitergerührt, und dann unter vermindertem Druck eingeengt. Nach der vollständigen Entfernung von Ammoniak wurde das verbliebene Öl mit Äther versetzt und mit verd. Salzsäure durchgeschüttelt, dabei scheidet ein Kristallbrei ab. Die abgetrennte Wasserschicht wurde unter vermindertem Druck zur Trockenheit eingedampft. Durch Umkristallisieren des festen Rück standes aus Äthanol-Äther erhielt man 2.5 g 1-Amino-2-nitropentan-hydrochlorid. Schmp. 143~145°C.

Gef.: N, 16.69. Ber. für $C_5H_{12}O_2N_2 \cdot HCl$: N, 16.62%.

Der oben erwähnte, beim Durchschütteln des Reaktionsgemisches mit verd. Salzsäure erhaltene Kristallbrei wiegt 2.5 g und wird aus Äthanol umkristallisiert. Farblose Nadeln vom Schmp. 160°C scheinen uns nach Elementaranalyse bis(2-Nitropentyl)amin-hydrochlorid zu sein.

Gef.: C, 42.62; H, 7.56; N, 15.21. Ber. für $C_{10}H_{21}O_4N_3 \cdot HCl$: C, 42.33; H, 7.66; N, 14.82%.

Laboratorium für Organische Chemie
Tokyo Institut für Technologie
Meguro-ku, Tokyo

11) B. M. Vanderbilt und H. B. Hass, *Ind. Eng. Chem.*, **32**, 34 (1940).

Carbon-14 in a Biological Environment. I. Annual Variation of Carbon-14 Concentration in Thymol

By Yosihiko KASIDA, Mikio YAMAZAKI, Tetsuo IWAKURA, Naoko MAGINU and Joju HAGINIWA*

(Received June 15, 1962)

Since 1954, the concentration level of C-14 in the atmosphere has remarkably increased as a result of the artificial production of C-14 by the successive nuclear testings; this tendency was confirmed by many investigators[1].

Recently, two excellent methods have become available for the measurement of the concentration level of C-14, i. e., gas sample counting with a proportional counter and liquid scintillation counting. Although the latter is very useful for the measurement of

* Pharmaceutical Faculty, Chiba University, Yahagi-cho, Chiba-shi.

1) Scientific Committee on the Effect of Atomic Radiation, A/AC. 82/R. 105; K. Kigoshi, This Bulletin, 33, 1576 (1960).

the radioactivity of many liquid samples, it has the characteristic weakness that the counting efficiency is strongly influence by the quenching of the sample. Unfortunately, many organic compounds act as quenching agents. Therefore, the solvent system which is used for this method can only measure the radioactivity of a limited number of organic compounds[2].

In the present work, the concentration of C-14 in thymol was measured by the liquid scintillation counting method; its annual variation was observed from 1954 to 1961.

Althouth thymol and other phenolic compounds could not be measured directly by this method because of the strong quenching effect arising from their phenolic nature, it was found that the quenching effect of phenols could be masked by the methylation of their phenolic hydroxyl group. Moreover, the methylation of thymol was carried out with a good yield.

Experimental

Sample Materials.—Thymol was obtained by the usual method[3] from the essential oil of *Orthodon japonicum* Benth (Labiatae). The plant, cultivated every year from 1954 to 1961, was harvested in October in the Experimental Field of Chiba University, located in Chiba city (35°35'N, 140°08'E). The methylation of the thymol was carried out according to the method used in the preparation of anisol[4]. Table I shows the yields of thymol from the essential oil and the yields arising from the methylation of the thymol thus obtained.

TABLE I. THE YIELDS OF THYMOL FROM ESSENTIAL OIL AND OF METHYLATION OF THE THYMOL THUS OBTAINED

Year	Oil	Thymol		Thymol methyl ether	
	g.	g.	(%)	g.	(%)
Pre-war[a]	84	41.4	(49.2)	24.0	(58.0)
1954	100	53.2	(53.2)	27.7	(75.6)
1955	—	—	—	—	—
1956	100	44.3	(44.3)	25.0	(71.4)
1957	90	49.2	(54.7)	25.2	(78.2)
1958	100	52.4	(52.4)	27.3	(81.4)
1959	100	46	(46.0)	28.9	(82.5)
1960	100	52	(52.0)	26.5	(75.7)
1961	150	80	(53.3)	30.3	(37.9)[b]

a) This was probably harvested during 1930—1940.

b) Raw product was used for methylation.

Preparation of Counting Samples. — 2,5-Diphenyloxazol (PPO) and 1,4-bis-(5-phenyl-2-oxazolyl)-benzene (POPOP) were dissolved in the thymol methyl ether obtained in concentrations of 0.4 and 0.01% respectively. Eighteen grams of these solutions were then put in low potassium glass vials (obtained from the Wheaton Glass Co., N. J., U. S. A).

Preparation of "Dead Carbon" Standard Samples. — *p*-Cymene and thymol methyl ether, consisting of the so-called "dead carbons" from petroleum products, were synthesized as standard samples in order to estimate the background counting rate. *p*-Cymene was prepared by the Friedel-Crafts reaction of toluene and isopropyl alcohol. Thymol synthesized from *m*-cresol and isopropyl chloride was obtained from the Koso Chemical Co., Tokyo, Japan, while its methyl ether was prepared in this laboratory.

Counting Procedure.—The measurement of radioactivity was carried out using a scintillation spectrometer Tri-Carb Model 314 A (Packard Instrument Co. Inc., Ill., U. S. A.) which incorporated a coincidence circuit and a two-channel pulse height analyzer. Each sample was counted 4 times for every 100 min. at a balance point operation with a 10~100 V. window setting. The counting efficiency of C-14 was calibrated by an internal standard of 5 mg. of benzoic acid (1-C-14). The specific activity is 5080 d. p. m. per mg. (Standard Source Compound, Packard).

Results and Discussion

Hayes et al.[5] recently reported the measurement of C-14 in *p*-cymene obtained from lemongrass oil with the aid of liquid scintillation counting, thereby proving that *p*-cymene could be used as an excellent liquid scintillation solvent. It is possible to synthesize *p*-cymene from thymol by elimination of its phenolic group[6], but the chemical yield of this dehydroxylation is poor (Chart 1).

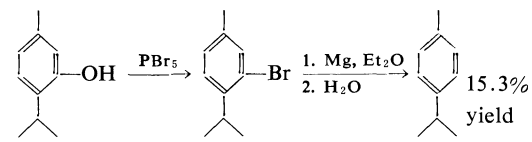


Chart 1. Synthesis of *p*-cymene from thymol.

On the other hand, the methylation of thymol is possible, giving a 70~80% yield (Table I); the strong quenching effect of thymol is almost masked by the methylation (Fig. 1). The counting efficiency of thymol methyl ether was found to be about 86% of that of toluene when it was used as a scintillation solvent.

The counting rates of samples prepared from natural products and from a "dead carbon"

2) F. N. Hayes, B. S. Rogers and P. C. Sanders, *Nucleonics*, **13**, 46 (1955); Y. Kasida, M. Yamazaki and T. Iwakura, *Radioisotopes*, **10**, 27 (1961).

3) T. Kariyone and K. Atsumi, *Yakugaku Zasshi*, **40**, 707 (1920).

4) L. Gattermann, "Die Praxis des Organischen Chemikers", 37 Aufl., Walter de Gruyter Berlin (1956), p. 212.

5) F. N. Hayes, E. Hansburry, V. N. Kerr and D. L. Williams, *Z. für Physik*, **158**, 374 (1960).

6) C. G. Le Fèvre, R. J. W. Le Fèvre and K. W. Robertson, *J. Chem. Soc.*, **1935**, 481.

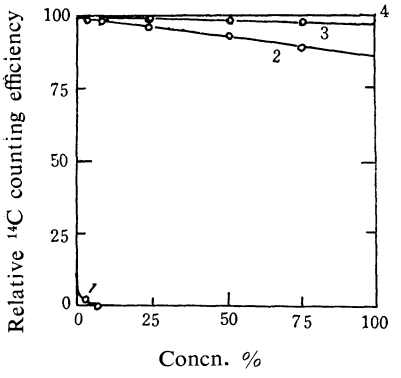


Fig. 1. Quenching curves of thymol and its related compounds.
1 Thymol 2 Thymol methyl ether
3 *p*-Cymene 4 Toluene

TABLE II. ANNUAL VARIATION OF C-14 CONCENTRATION IN THYMOL

Year	n_s	d. p. m./g. of carbon
Pre-war	123.47	13.62±0.14
1954	126.90	14.05±0.16
1955	—	—
1956	120.85	13.28±0.17
1957	140.85	15.84±0.17
1958	135.67	15.16±0.17
1959	148.89	16.82±0.17
1960	151.60	17.21±0.17
1961	154.29	17.49±0.17

$$\text{d. p. m./g. carbon} = \frac{n_s - n_b \pm 2sd}{C_g \times E}$$

$$sd = \sqrt{\frac{n_s + n_b}{t}}$$

n_s=Counts of samples, c. p. m.
n_b=Counts of natural background, 16.96 c. p. m.
$t = t_s = t_b$=Counting time, 400 min.
C_g=Carbon weight in thymol, 18 g. 13.16 g.
E=Counting efficiency, 59.4%

standard were 120~150 c. p. m. and 17 c .p. m. respectively.

The data of measurement are listed in Table II. All the values of radioactivity are indicated in d. p. m./g. of carbon.

As is shown in this table, it was observed that the concentration of C-14 in thymol increased 18.4% from 1954 to 1961. This values was rather lower than the 26.8% which was reported by Hayes for the northern hemisphere[5]. This difference suggests that the dilution effect by the "dead carbon" from fossil fuels probably contributes somewhat to the depression of the C-14 concentration. In fact, steel-manufacturing and other heavy industrial plants have gone into operation in the suburbs of Chiba city, and the consumption of coal in one of the big steel factories last year was about eight times that in 1953. Therefore, a considerable amount of "dead carbon" has been added to the atmosphere by the combustion of coal or oil; the C-14 concentration level might have been thereby reduced.

The pre-war sample shown in Table II was supplied from the Kasukabe Experimental Field of the National Institute of Hygienic Sciences, in Saitama prefecture (35°59'N, 139°45'E). This was harvested during the 1930—1940 period, but no definite harvesting data are known. The sample is used in the data as a supplemental reference to the level before the beginning of World War II.

The authors wish to thank Dr. Toyohiko Kawatani of the Kasukabe Experimental Field of the National Institute of Hygienic Sciences, for his kind assistance in obtaining the pre-war sample, and Professor Eizo Tajima, a Scientific Consultant of this Institute, for his kind advice.

Division of Environmental Hygiene
National Institute of
Radiological Sciences
Kurosuna-cho, Chiba-shi

MO Interpretation of Some Physico-chemical Properties of Alkyl Compound

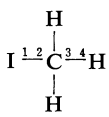
By Teijiro YONEZAWA, Hiroshi KATO, Hazime SAITO and Kenichi FUKUI

(Received July 2, 1962)

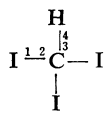
A few quantum-mechanical investigations of the electronic structure of halomethane molecules have been made by the VB method, discussing the ionic character of carbon-halogen bonds in these compounds[1], and also by a simple two-center LCAO MO treatment[2].

In a previous paper[3], we discussed the electronic structures and reactivities of some halomethane molecules using the simple LCAO MO treatment for saturated compounds we had previously reported. In this treatment, the molecular orbitals of halomethanes are given by the linear combinations of the atomic (or of hybridized) orbitals of the composite atoms in a molecule. It has been made clear by the microwave spectral data that the bond lengths, especially that of the C–X bond, and also the valence angles vary remarkably among CH_3X, CH_2X_2, CHX_3 and CX_4. Also, the double bond character, which has been particularly recognized in CX_4 molecules, has been disregarded, since the main purpose of our paper is to a verification of the validity of our simple LCAO MO treatment. For the sake of simplicity, overlap integrals are neglected and the same values as in the previous paper[3] are adopted in the present paper for Coulomb and resonance integrals. These values

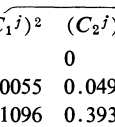
TABLE I. THE CALCULATED ORBITAL ENERGIES AND ELECTRON DISTRIBUTIONS IN IODOMETHANES



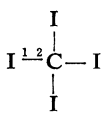
Orbital energy	Electron distribution $(C_1^j)^2$	$(C_2^j)^2$	$(C_3^j)^2$	$(C_4^j)^2$
$\alpha-1.37223\beta$*	0	0	0.3545	0.3122
$\alpha-1.08150\beta$	0.0183	0.1430	0.1093	0.1702
$\alpha-0.33688\beta$	0.2739	0.5249	0.0010	0.0646
$\alpha+0.69454\beta$	0.6854	0.2117	0.0137	0.0207
$\alpha+0.83223\beta$*	0	0	0.3122	0.3545
$\alpha+1.60384\beta$	0.0255	0.1160	0.2093	0.0778



Orbital energy	Electron distribution $(C_1^j)^2$	$(C_2^j)^2$	$(C_3^j)^2$	$(C_4^j)^2$
$\alpha-1.29580\beta$	0.4745	0.4708	0.0166	0.0016
$\alpha-0.61637\beta$*	0	0	0.5241	0.1455
$\alpha-0.02709\beta$	0.1004	0.0025	0.1177	0.1813
$\alpha+0.67638\beta$*	0	0	0.1455	0.5241
$\alpha+0.76110\beta$	0.2870	0.2191	0.0522	0.1124
$\alpha+1.44152\beta$	0.1378	0.3074	0.1469	0.0380



Orbital energy	Electron distribution $(C_1^j)^2$	$(C_2^j)^2$	$(C_3^j)^2$	$(C_4^j)^2$
$\alpha-1.37223\beta$	0	0	0.2659	0.2341
$\alpha-1.20359\beta$	0.0055	0.0499	0.2020	0.2427
$\alpha-0.61637\beta$	0.1096	0.3931	0	0
$\alpha-0.16738\beta$	0.1944	0.2227	0.0001	0.0828
$\alpha+0.67638\beta$	0.3931	0.1069	0	0
$\alpha+0.72067\beta$	0.2721	0.0996	0.0528	0.0754
$\alpha+0.83223\beta$	0	0	0.2341	0.2659
$\alpha+1.53029\beta$	0.0281	0.1278	0.2451	0.0991



Orbital energy	Electron distribution $(C_1^j)^2$	$(C_2^j)^2$
$\alpha-0.61637\beta$**	0.1603	0.5897
$\alpha+0.09500\beta$	0.1881	0.0619
$\alpha+0.67637\beta$**	0.5897	0.1603
$\alpha+1.32401\beta$	0.0619	0.1881

* Doubly degenerate

** Three fold degenerate

1) E. Hamano, *J. Chem. Soc. Japan, Pure Chem. Sec.* (*Nippon Kagaku Zassi*), **77**, 985 (1956); **79**, 362 (1958).

2) G. Del Re, *J. Chem. Soc.*, **1958**, 4031.

3) K. Fukui, H. Kato and T. Yonezawa, This Bulletin, **34**, 442, 1111 (1961).

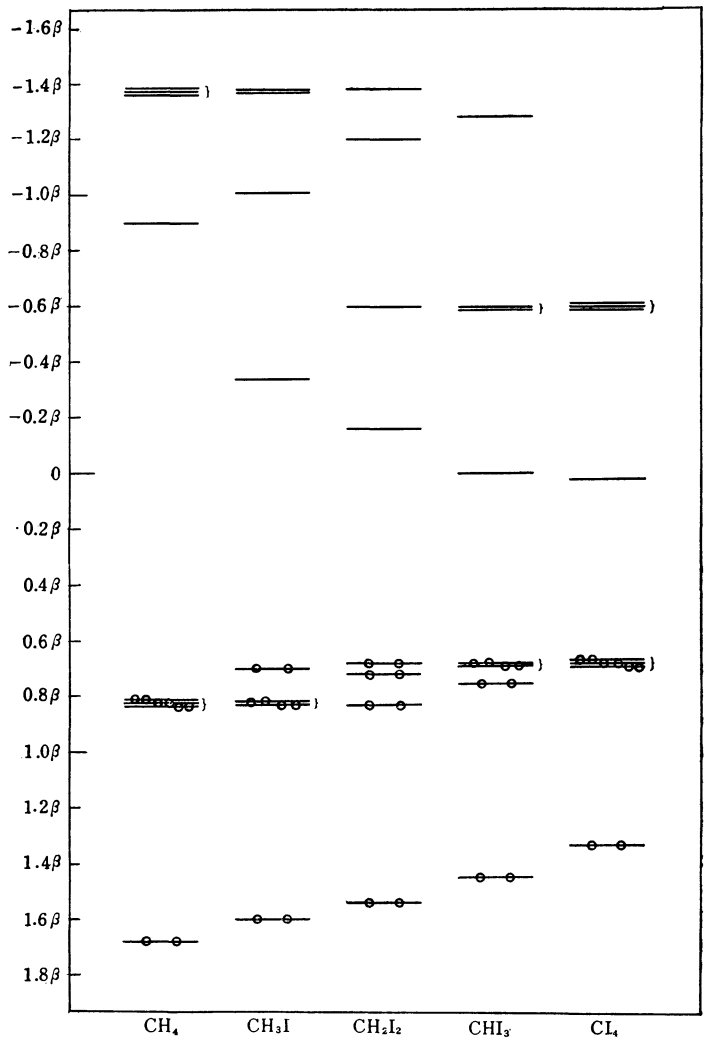


Fig. 1. The orbital energies of iodomethanes.

are summarized as follows:

$\alpha_C=\alpha$	$\beta_{CC}=\beta$
$\alpha_H=\alpha-0.2\beta$	$\beta_{-C-}=0.34\beta$
$\alpha_F=\alpha+0.9\beta$	$\beta_{CH}=1.1\beta$
$\alpha_{Cl}=\alpha+0.5\beta$	$\beta_{CF}=0.5\beta$
$\alpha_{Br}=\alpha+0.45\beta$	$\beta_{CCl}=0.65\beta$
$\alpha_I=\alpha+0.4\beta$	$\beta_{CBr}=0.58\beta$
	$\beta_{CI}=0.53\beta$

Since the lone pair electrons at halogen atoms are not explicitly taken into account in the present treatment, the energy of this non-bonding orbital is estimated from the experimental values of the ionization potentials assigned by McDowell[4]. The estimated energies of non-bonding orbitals at fluorine, chlorine, bromine and iodine atoms are represented in terms of α and β, which are the standard Coulomb and resonance integrals respectively in σ-electronic systems*.

Electronic Structure of Halomethanes

The calculated energy levels and electronic distributions for iodine derivatives of methane are listed in Table I, while a diagram indicating the change in the energy levels is given in Fig. 1. As was mentioned in our previous paper[3], the bonding electrons tend to be

4) D. C. Frost and C. A. McDowell, *Proc. Roy. Soc.*, **A241**, 194 (1957).

* The estimated values of the lone pair orbital energy of halogen atoms (ε_X) are:

$\varepsilon_F=\alpha+1.1\beta$
$\varepsilon_{Cl}=\alpha+0.5\beta$
$\varepsilon_{Br}=\alpha+0.4\beta$
$\varepsilon_I=\alpha+0.2\beta$

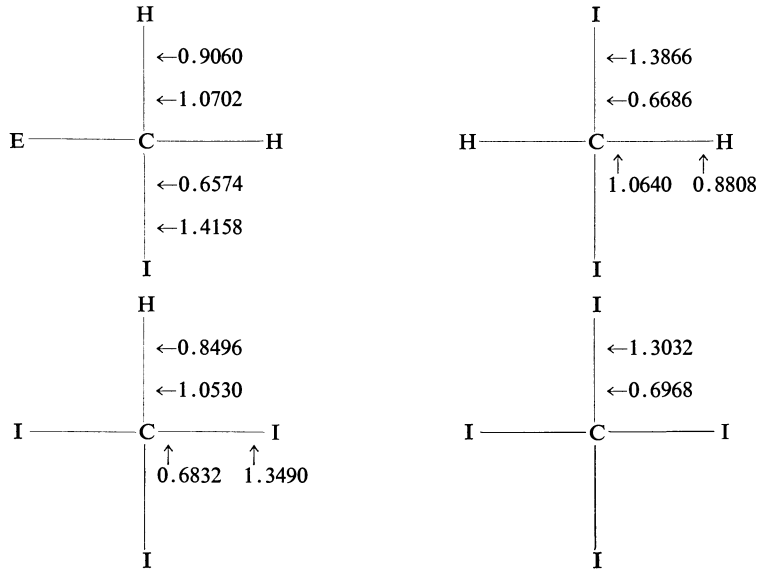


Fig. 2. The σ electronic densities of iodomethanes.

localized in the particular bonds in each molecular orbital; the bonding electrons in the highest occupied and the lowest vacant orbital are localized mainly in the C–I bond, and those in the next highest occupied orbital, in the C–H bond.

As to the orbital energies, it is seen that the larger the number of substituted halogen atoms, the lower the lowest vacant orbital energy, as is shown in Fig. 1.

In Fig. 2, the calculated total σ-electron densities in iodomethanes are presented.

As a general tendency, the ionic character interpreted from the present molecular orbital treatment decreases in the order: $CH_3X > CH_2X_2 > CHX_3 > CX_4$. This order agree with that indicated by the experimental results of pure quadrupole coupling constants.

Based upon these findings, a molecular orbital interpretation of such physico-chemical properties of halomethane molecules as n-σ^* absorption, PQR coupling constants, and proton chemical shifts are presented.

***n*-σ^* Absorption.**—The theoretical interpretation of the n-σ^* absorption of halomethane molecules, especially of iodine and chlorine compounds, has been argued by Mulliken[5], Walsh[6], and Nagakura et al.[7] The longest-wavelength absorption in halomethanes is due to the excitation of an electron from the lone pair electron orbital to the lowest vacant orbital. The calculated energy differences between the lone pair electron orbital and the vacant orbital in these compounds are listed in Table II, together with the observed wavelengths[8]. In the series of halomethanes substituted for by a certain number of halogen atoms of the same kind, a parallelism is found between experimental and calculated values; the calculated values show a tendency for the wavelength of the absorption spectrum to increase with the number of halogen atoms in halomethanes, all in accordance with experimental findings. When a comparison is made among the molecules with different halogen atoms, however, a discrepancy between the observed and the calculated results is found. This discrepancy may

TABLE II. THE CALCULATED VALUES OF ENERGY DIFFERENCE BETWEEN TRANSITION AND OBSERVED WAVELENGTHS

Compound	Calcd. (in unit of $-\beta$)	Obs. (Å)[8]
CH_3Cl	0.8998	1610∼1540
CH_2Cl_2	0.7287	—
$CHCl_3$	0.5810	1830<2200
CCl_4	0.4401	—
CH_3Br	0.7611	2040
CH_2Br_2	0.5897	2190 (2208)
$CHBr_3$	0.4446	2290 (2497)
CBr_4	0.3112	— (2558)
CH_3I	0.5369	2577 —
CH_2I_2	0.3674	2900 (3096)
CHI_3	0.2271	3490 (3497)
CI_4	0.1450	— (3891)

5) R. S. Mulliken, *J. Chem. Phys.*, **8**, 234, 382 (1940).
6) A. D. Walsh, *Quart. Revs.*, **2**, 73 (1948).
7) K. Kimura and S. Nagakura, *Spectrochim. Acta*, **17**, 166 (1961).
8) Mortiner J. Kamlet, "Organic Spectral Data", Vol. I, Interscience, N. Y. (1960); M. Ito, P. C. Huang and E. M. Koswer, *Trans. Faraday Soc.*, **57**, 1662 (1961).

TABLE III. OSCILLATOR STRENGTH

Compound	Calcd. by Nagakura et al.		Present	Obs.[7]
	AO	non polar		
CH_3Br	0.0262	0.0422	0.0276	0.0106
CH_3I	0.0105	0.0264	0.0169	0.0087
CH_3Cl	—	—	0.0346	—

partly be ascribed to the values of the parameters adopted.

The oscillator strengths of n-σ^* transitions in bromo-methane and iodo-methane have been calculated by Kimura and Nagakura both by the VB method and by a localized molecular orbital method in which the molecular orbital is constructed in terms of two AO's of the C–X bond[7]. Their results are listed in Table III for the sake of comparison. In the table, one can see that the results obtained by the VB method are much better than those by the localized molecular orbital method. In the present treatment, where the molecular orbital is delocalized, we can see that a considerable improvement in the value of oscillator strength is achieved, as is shown in the same table.

The $CH_3I \rightarrow CH_3 + I$[6] bond dissociation and the continuous absorption spectrum are observed after the light absorption takes place in these compounds.

These results might well be explained by our calculated results; that is, in the lowest vacant orbital in these compounds, electrons are localized mainly in the carbon-halogen bonds, and this orbital is strongly anti-bonding. This result is recognized in terms of the partial σ bond order* (p_{rs}) between the r-th atoms and the s-th atom in the lowest vacant orbitals of these compounds; that is, the p_{rs} values of methyl iodide are the largest among the methyl halides. These calculated values are listed in Table IV.

TABLE IV. THE CALCULATED VALUES OF PARTIAL BOND ORDER IN THE LOWEST VACANT ORBITAL OF HALOMETHANES

X	p_{C-H}	p_{C-X}
I	−0.0160	−0.7616
Br	−0.0202	−0.7504
Cl	−0.0264	−0.7370

PQR Coupling Constant.—PQR coupling constants of some halomethanes have been discussed theoretically by Hamano[1]. He calculated the ionic character of C–X bond by VB method. A satisfactory parallelism was observed between experimental coupling constants and his results. In the present paper, a molecular orbital procedure to discuss coupling constants is presented. We estimate the magnitude of the coupling constant by the total σ density (q_X) of halogen atoms in these compounds. Neglecting the s-character of the bonding orbital of halogen atoms, the equation connecting the coupling constant, eQq, with the total electron density, q_X, is given as[9]:

$$|eQq| = (2 - q_X)|eQq_{atm}|$$

The calculated values of $|eQq|$ of some halomethanes are listed, together with the observed values[10], in Table V, which shows that the results obtained by our present procedure seem almost satisfactory. Hence, it may be stressed that the observed coupling constants in halomethane molecules are explained well by the magnitude of the total σ electron density.

TABLE V. THE CALCULATED AND OBSERVED VALUES OF eQq (MC) IN HALOMETHANES

Compound	Calcd.	Obs.
CH_3Cl	63.85	68.4
CH_2Cl_2	66.27	72.47
$CHCl_3$	69.56	76.98
CCl_4	74.75	81.85
CH_3Br	443.24	442
CH_2Br_2	462.67	470
$CHBr_3$	489.29	501
CBr_4	526.32	—
CH_3I	1245	1753
CH_2I_2	1321	1912
CHI_3	1401	—
CI_4	1500	2130

Proton Nuclear Magnetic Shielding in Halomethanes.—It has been pointed out that the proton chemical shift depends upon the local diamagnetic shielding, due to the electron cloud around the nucleus, and to long-range shielding due to the magnetic anisotropies of halogen and carbon atoms which are remote from the nucleus[11]. The proportion of the contribution of these two effects in propane was discussed by Narasimhan et al.[12] In the present paper, we indicate that a qualitative interpretation of the chemical shifts in halomethanes may be possible on the basis of the local diamagnetic shielding. This nuclear magnetic shielding constant in a molecule can be represented by the equation

$$\sigma_{dia} = -Aq_r \quad \text{(in units of p. p. m.)}$$

* This indicates the product of the molecular orbital coefficients $2C_rjC_sj$.

9) C. H. Towens and B. P. Dailey, *J. Chem. Phys.*, **17**, 782 (1949).
10) H. Robinson, H. G. Dehmelt and W. Gorday, ibid., **22**, 511 (1954): R. Livingston, *J. Phys. Chem.*, **57**, 496 (1953).
11) J. A. Pole, *Proc. Roy. Soc.*, **A239**, 541, 55 (1957).
12) P. T. Narasimhan and M. T. Rogers, *J. Chem. Phys.*, **31**, 1302 (1959).

Table VI. The calculated values of electron densities at hydrogen atom and observed chemical shift in halomethanes

Compound	q_H	Chemical shift[a] (in p.p.m. from CH_4)
CH_4	0.9264	0
CH_3F	0.8912	− 7.1
CH_2F_2	0.8308	− 8.8
CHF_3	0.6948	−10.3
CH_3Cl	0.9006	− 7.1
CH_2Cl_2	0.8613	− 9.9
$CHCl_3$	0.7927	−11.8
CH_3Br	0.9058	− 7.3
CH_2Br_2	0.8784	−10.1
$CHBr_3$	0.8428	−12.4
CH_3I	0.9060	− 7.6 (−2.14)[b]
CH_2I_2	0.8808	− 9.9 (−3.85)[b]
CHI_3	0.8496	− 6.5 (−4.88)[b]

a) L. H. Meyer and H. S. Gutowsky, *J. Phys. Chem.*, **57**, 481 (1953).
b) A. A. Bothner-By and C. Naar-Colin, *J. Am. Chem. Soc.*, **80**, 1728 (1958).

where A is the constant and q_r is the total σ-electron density at the r-th hydrogen atom.

Hence, the resonance magnetic field of a proton is expected to increase with the total σ density. In fact, in Table VI, there exists a parallelism between the magnitude of chemical shifts and the values of the total σ density. Some further experimental investigation has been carried out on iodo-methanes and so forth. The observed chemical shifts in these molecules (written in parenthesis in Table VI) support our interpretation based upon the total σ electron density. The apparent discrepancies found in methyl fluoride, methyl chloride, methyl bromide and methyl iodide are shown to be in a reasonable order according to the values, −3.99, −2.71, −2.32 and −1.85 p.p.m. respectively, observed by Spieseck and Schneider[13]. Hence, it may be concluded that the parallelism between the observed shift and the total electron density is rather satisfactory. Regarding the quantitative interpretation, the following points should be remarked:

1. The deformation of the valence angle in these compounds is not considered.
2. The magnetic anisotropy of the neighboring atom is omitted in the present consideration.
3. The lone pair electron is considered to be thoroughly isolated in a molecule.

A further interpretation of the fluorine chemical shifts in fluoromethanes has been successfully made by the present authors; it will be published in the near future.

In the present paper, we have investigated some physico-chemical properties of halomethanes by the simple LCAO MO treatment. In spite of the extreme simplicity of our method, the calculated results are almost parallel with the observed values. If one may further adopt the modified Coulomb integrals of halogen atoms, a more comprehensive explanation of the physico-chemical properties of saturated and unsaturated σ-electron systems may be possible in the future.

Faculty of Engineering
Kyoto University
Sakyo-ku, Kyoto

13) H. Spieseck and W. G. Schneider, ibid., 35, 722 (1961).

The Gelation of Lead Aldose-cysteinate. The Properties of Gel and the Structure of Lead Aldose-cysteinate

By Fujio TAKAHASHI and Jun MIZUGUCHI

(Received July 6, 1962)

The authors have studied the preparation and utilization of cysteine and have already reported on the electrolytic preparation of cysteine[1], and on the preparation and properties of glucose-cysteine[2]. The organo- and physicochemical properties of the metal salts of

1) J. Mizuguchi, S. Suzuki, F. Takahashi and Y. Kawasaki, Annual Meeting of the Electrochemical Society of Japan, 1958.

2) J. Mizuguchi, S. Suzuki and F. Takahashi, 13th Annual Meeting of the Chemical Society of Japan, Tokyo, April, 1960.

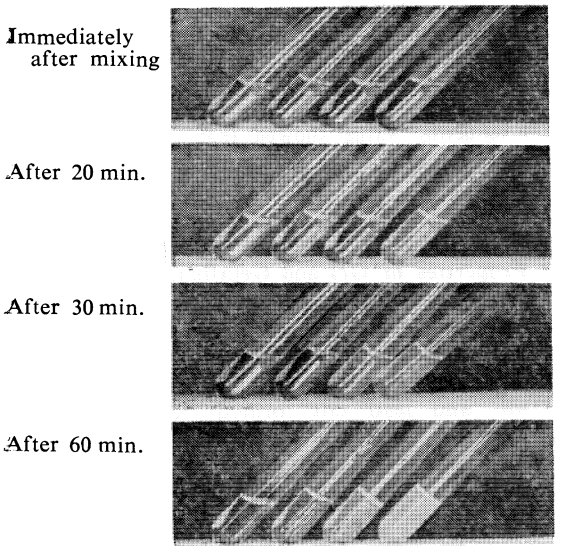


Photo. 1. The solution containing equimolar NaGC and lead acetate.
Concn.; distilled water, 0.01, 0.03, 0.05 M from left to right of test tubes. Temp. 16.5°C

HGC* have now been studied. When a solution containing HGC and lead salt was allowed to stand for some time, it was found to form gel[3], as is shown in photographs attached. This gel is stable, and no syneresis is observed. This gel has a heat-reversible property.

It has been known that the gelation of a solution containing such high molecular substance as agar-agar, gelatin, silicic acid occurs because of the formation of an infinite three-dimentional network in the solution by means of intermolecular cross-linking[4]. Most of the gels of such inorganic substances as hydrous oxides of iron and aluminum have been found to expel liquids.

The gel composed of HGC and lead salt was different from the other gels because of its stability. Furthermore, high molecular compounds were unexpectedly found in this gel.

This investigation was carried out to elucidate the mechanism and kinetics of the gelation of a solution containing HGC and lead salt. In this paper, we report on an extensive study of the properties of the gel and gelation and on the structure of lead aldose-cysteinate.

Experimental

Materials.—HSCs were prepared by the condensation reaction of cysteine hydrochloride and an aldose such as glucose, galactose, mannose, arabinose and xylose in a methanol or aqueous solution after the addition of pyridine[5]. The products precipitated were washed with methanol after filtration.

Apparatus and Procedure. — The turbidity was measured by a Coleman spectrophotometer, universal model. The turbidity was measured from the time a solution of lead salt was added to a solution of HSC. On the basis of these measurements, we got the relative values of turbidity based on the definition that the turbidity of distilled water is 0%. The turbidity measured 3 hr. after the time a solution containing 40 mM of NaGC and 40 mM of lead acetate formed a gel is 100%.

The rigidity of the gel was determined by an apparatus** measuring gel rigidity. The amount of weight which sank into the gel with a velocity of 2 cm./20~40 sec. was adopted as the rigidity of the gel. Each 100 ml. of a solution containing HGC and lead salt was poured into several 100 ml. beakers and allowed to stand at 25°C. The rigidity of the gel was measured at intervals from the time when a solution of lead salt was added to a solution of HGC.

Preparation of Lead Aldose-cysteinates. — *$PbGCNO_3$*—a) 2.83 g. of HGC and 0.84 g. sodium bicarbonate were dissolved in 20 ml. of water; 10 ml. of 1 M lead nitrate was then added. On the addition of 60 ml. of methanol or ethanol before the gelation of the mixture, sticky precipitates soon separated. The precipitates were crystallized in alcohol after an hour or so. The product was filtered and washed with methanol; yield, 5.3 g. (96%).

Found: C, 19.6; H, 3.0; N, 5.1; Pb, 37.3; NO_3, 9.9. Calcd. for $C_9H_{16}NO_7SPbNO_3$: C, 19.6; H, 2.9: N, 5.1; Pb, 37.5; NO_3, 11.3%.

b) 10 ml. of 1 M NaGC was added to 10 ml. of 1 M lead nitrate. The mixture formed at gel after a few minutes at room temperature; then fine crystals separated from this gel. After two days, the product was filtered and washed with 50% aqueous ethanol, and then with ethanol; yield, 5.0 g. The crystalline product melted at 193.5°C with decomposition.

Found: C, 19.7; H, 2.6; Pb, 37.2. Calcd. for $C_9H_{16}NO_7SPbNO_3$: C, 19.6; H, 2.9; Pb, 37.5%.

$PbGCNO_3$ is soluble in water (1.2~1.3 g./dl.) The solution of $PbGCNO_3$ formed a gel when it was allowed to stand at room temperature for a while. $PbGCNO_3$ is insoluble in methanol, ethanol,

* All the aldose-cysteines and their sodium salts are abbreviated as follows:

Aldose-cysteine	HSC
Glucose-cysteine	HGC
Galactose-cysteine	HGaC
Mannose-cysteine	HMC
Xylose-cysteine	HXC
Arabinose-cysteine	HAC
Various HSC	HSCs
Sodium aldose-cysteinate	NaSC
Sodium glucose-cysteinate	NaGC
Sodium galactose-cysteinate	NaGaC
Sodium mannose-cysteinate	NaMC
Sodium xylose-cysteinate	NaXC
Sodium arabinose-cysteinate	NaAC

3) J. Mizuguchi, F. Takahashi and S. Suzuki, *J. Chem. Soc. Japan, Pure Chem. Sec.* (*Nippon Kagaku Zasshi*), 81, 1627 (1960).

4) P. J. Flory, "Principles of Polymer Chemistry", Cornell Univ. Press, New York (1953).

5) M. P. Schubert, *J. Biol. Chem.*, 130, 601 (1939); G. Weitzel, J. Engelmann and A-M. Fretzdorff, *Z. physiol. Chem.*, 315, 236 (1959).

** A Nikkansui-shiki apparatus measuring agar-agar gel rigidity.

benzene, acetic acid, pyridine, acetone and chloroform.

$PbGaCNO_3$.—A mixture of NaGaC and lead nitrate was prepared in the same manner as has been described in the preparation of $PbGCNO_3$. On the addition of 200 ml. of ethanol, sticky precipitates separated. When it was allowed to stand overnight at room temperature, sticky precipitates were crystallized in alcohol. The product was filtered and washed with ethanol; yield, 4.5 g. (76%).

Found: C, 19.0; H, 3.6; N, 4.6; Pb, 36.4; NO_3, 9.8; H_2O, 3.3. Calcd. for $C_9H_{16}NO_7SPbNO_3 \cdot 2H_2O$: C, 19.0; H, 3.2; N, 4.9; Pb, 36.4; NO_3, 10.9; H_2O, 3.2%.

PbGCOH.—2.83 g. of HGC and 0.84 g. of sodium bicarbonate were dissolved in 20 ml. of water; 10 ml. of 1 M lead acetate was added. On the addition of 300 ml. of ethanol, fine precipitates soon separated. The product was filtered and washed with ethanol; yield, 4.2 g. (75%). The product was dried on phosphorus pentoxide at 100°C under reduced pressure.

Found: C, 21.9; H, 3.3; N, 2.7; Pb, 40.7. Calcd. for $C_9H_{17}NO_8SPb$: C, 21.3; H, 3.4; N, 2.8; Pb, 40.9%.

It was found, from the result of alkaline titration, that the filtrate contained 8.5 mmol. (85%) of acetic acid. PbGCOH is slightly soluble in water. When it was allowed to stand at room temperature for a while, the suspension of PbGCOH formed a gel.

$PbGC \cdot CH_3COO \cdot PbGCOH$.—To a solution in which 2.83 g. of HGC and 0.84 g. of sodium bicarbonate were dissolved in 20 ml. of water, 5 ml. of acetic acid and 10 ml. of 1 M lead acetate were added. A hundred mililiters of methanol and 100 ml. of acetic acid were added before the gelation of the mixture. After a week, precipitates were filtered and washed with methanol; yield, 1.78 g.

Found: C, 22.5; H, 3.0; N, 2.6; Pb, 39.0. Calcd. for $C_{18}H_{36}N_2O_{17}S_2Pb_2$: C, 22.8; H, 3.4; N, 2.7; Pb, 39.3%.

$PbMCNO_3$ and $PbACNO_3$.—It was difficult to obtain pure $PbMCNO_3$ and $PbACNO_3$ prepared in the same manner as $PbGCNO_3$. When the solution containing lead nitrate or acetate and NaMC or NaAC was allowed to stand for a few days, white precipitates separated. The precipitates were found to be crude lead cysteinate from the following results: 1.41 g. of HMC and 0.42 g. of sodium bicarbonate were dissolved in 10 ml. of water; 5 ml. of 1 M lead acetate was added. The mixture was allowed to stand at room temperature for a few days. The precipitates were filtered and washed with distilled water; yield, 1.5 g.

Found: Pb, 61.6; N, 4.1. Calcd. for $PbC_3H_5NO_2S$: Pb, 63.3; N, 4.3%.

The determination of the reducing value showed that the filtrate contained 4.4 mM (97%) of mannose.

The Preparation of Lead Cysteinate from Gel.—Fifty milliliters of 0.2 M NaGC was added to 50 ml. of 0.2 M lead acetate. The mixtue formed a gel. An hour after the beginning of the gelation, the gel was heated at 100°C for 6 hr. The gel melted, and then gray precipitates separated. The precipitates were filtered and washed with water; yield 3.1 g. (94%).

Found: C, 11.3; H, 1.6; N, 4.3; Pb, 62.2. Calcd. for $PbC_3H_5NO_2S$: C, 11.0; H, 1.5; N, 4.3; Pb, 63.3%.

The alkaline titration and the determination of the reducting value showed that the filtrate contained 9.7 mM (97%) of acetic acid and 9.5 mM. of glucose.

Results and Discussion

Properties of Gel and Gelation.—*Gel-forming HSC*.—A solution containing HGaC and lead salt also yielded gel in the same manner as HGC. However, in the case of HXC and HAC, flocculation occured. A solution containing HMC and lead salt formed neither gel nor fluocculent precipitates.

Turbidity.—The transparent solution containing HGC and lead salt became turbid gel rapidly upon gelation. The turbidity of the gel increased with the lapse of time for a few hours, and then the turbidity approached to almost constant values. The turbidity of this gel was greater than that of agar-agar gel. The results are shown in Fig. 1.

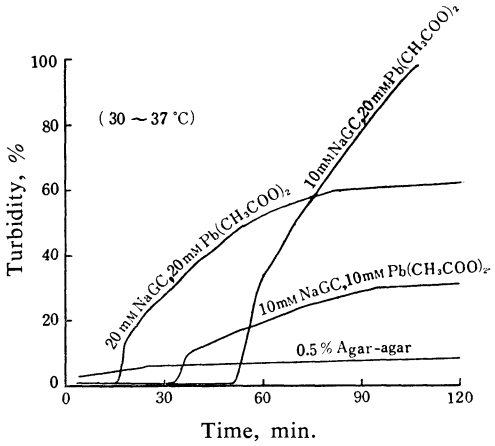


Fig. 1. Development of turbidity.

Rigidity.—The rigidity of the gel increased rapidly with gelation. The rigidity of gel depends on the pH value and the concentration. The rigidity of this gel was smaller than that of agar-agar gel (Figs. 2, 3 and 4).

The Range of pH Values and Concentrations.—The lowest concentration of a solution which was able to yield gel was the 5 mM (0.3%) of a lead glucose-cysteinate solution (Fig. 3). The pH range of the formation of gel was between 3.8 and 11 (Fig. 4). When a solution of NaGC was added to a solution of lead salt in the pH range of 8～11, precipitation occured immediately. The precipitates redissolved gradually, and then the solution set to gel after a certain time, whether precipitates redissolved perfectly or not.

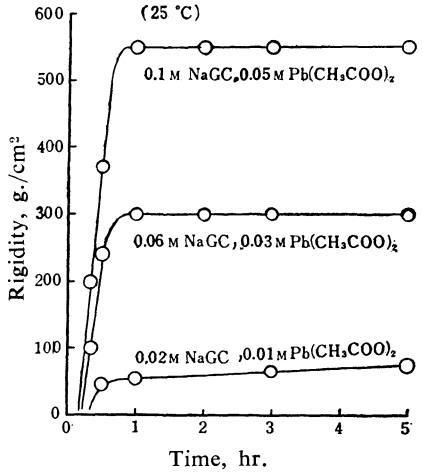


Fig. 2. Development of rigdity.

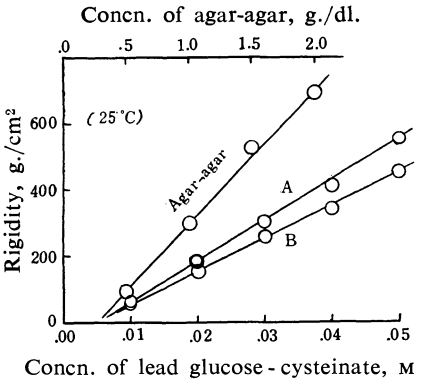


Fig. 3. Rigidity and concentration of gel.
A NaGC : $Pb(CH_3COO)_2$=2 : 1 (mol. ratio)
B NaGC : $Pb(NO_3)_2$ =2 : 1 (mol. ratio)
Measuring after 3 hr. from the gelation time

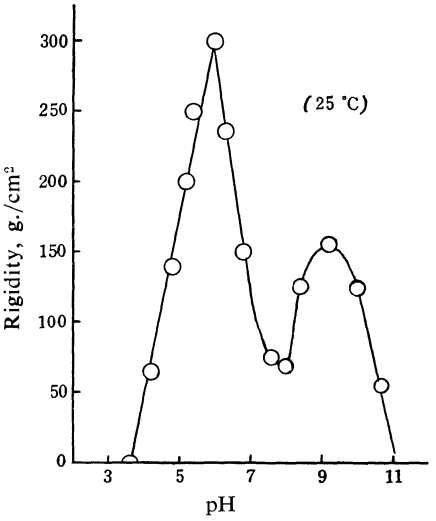


Fig. 4. Rigidity and pH of gel.
0.06 M NaGC, 0.03 M lead nitrate or acetate measuring after 3 hr. from the gelation time.

Heat-reversible Property.—As it was warmed, this gel melted above 70°C. The liquified gel yielded gel containing a small amount of white precipitates when it was allowed to stand at room temperature. The amount of precipitates increased with the lapse of the time of heating. Re-gelation could not occur when the heating of the gel was continued further.

Properties of the Solution before Gelation.—*Chemical Reactions of Lead Ion in Solution.*—Insoluble lead salt was precipitated by the addition of hydrogen sulfide, phosphoric acid, or potassium chromate or iodide into the HGC-lead acetate solution. Lead sulfate, however, was not found to precipitate when sodium sulfate was added.

Stability of Lead Glucose-cysteinate.—The stability constant, $\log k = 4.5$, was given from the method of pH titration, as is shown in Table I.

TABLE I. STABILITY CONSTANT

To 50.0 ml. of the solution (4.00×10^{-3} M HGC, 3.79×10^{-3} M $Pb(NO_3)_2$) 0.973 N NaOH solution was titrated. 30°C. Ionic strength 0.1 (KNO_3) $K_{COOH}=6.6_1\times10^{-3}$, $K_{NH_2}=8.3_2\times10^{-6}$ (reference value[5]: $K_{COOH}=7.24\times10^{-3}$, $K_{NH_2}=4.27\times10^{-6}$)

pH	NaOH, ml.	$\bar{n}$	pA
3.00	0.000	0.41	4.8_5
3.13	0.030	0.45	4.7_3
3.31	0.060	0.50	4.5_7
3.50	0.100	0.63	4.4_8
3.75	0.130	0.72	4.3_4
4.11	0.160	0.83	4.1_6

$pA_{\bar{n}=0.5}=4.5$

Structure and Properties of the Lead Aldose-cysteinate.—*Structure of Lead Aldose-cysteinate.* It was found that the lead aldose-cysteinates isolated ($PbGCNO_3$, PbGCOH and $PbGaCNO_3$), which are the essential materials for gelation, are composed of one atom of lead, one molecule of HSC, and one univalent anion (e. g., NO_3^-, OH^-, etc.).

The infrared spectra of NaGC and $PbGCNO_3$ show peaks at 1600 and 1400 cm^{-1} which arise from the antisymmetric and symmetric carbon-oxygen stretching vibration in the carboxylate ion[6]. The $PbGCNO_3$ bands and lead nitrate bands observed at about 820 and 730 cm^{-1} arise from the deforming vibrations of the nitrate ion, which does not coordinate with the lead atom (Fig. 5).

It was found, from the study of ultraviolet absorption spectra[7], that the sulfur atom and

6) D. N. Sen, S. Mizushima, C. Curran and J. V. Quagliano, *J. Am. Chem. Soc.*, **77**, 211 (1955).
7) The results of ultraviolet spectra will be described in the next paper. F. Takahashi and J. Mizuguchi, This Bulletin, **35**, 1823 (1962).

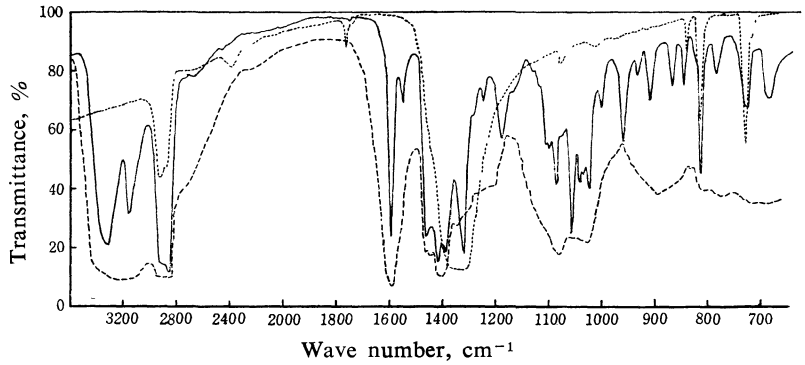
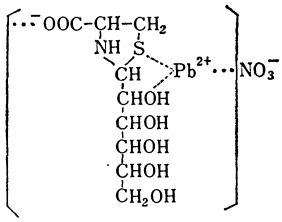


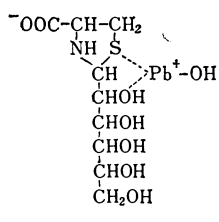
Fig. 5. Infrared spectra (Nujol method). —— $PbGCNO_3$, --- NaGC, ····· $Pb(NO_3)_2$

one hydroxyl group of HGC coordinate with the lead atom in solution.

Based on the infrared and ultraviolet absorption spectra, structural formulae (I, II) were suggested for lead aldose-cysteinate:



(I)



(II)

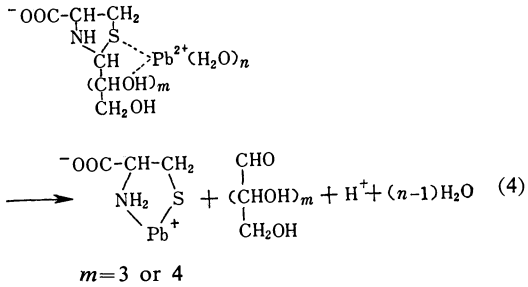
Properties of Lead Aldose-cysteinate. — Pure $PbGC \cdot CH_3COO$ could not be prepared from the solution of NaGC and lead acetate. Judging from this fact, it is presumed that the following reactions occur in solution.

$$NaGC + Pb(CH_3COO)_2 \rightarrow PbGC \cdot CH_3COO + CH_3COONa \quad (1)$$

$$PbGC \cdot CH_3COO + nH_2O \rightarrow [PbGC(H_2O)_n]^+ + CH_3COO^- \quad (2)$$

$$[PbGC(H_2O)_n]^+ \rightarrow PbGCOH(H_2O)_{n-1} + H^+ \quad (3)$$

It is suggested that the lead complex ion of HSC in solution converts to lead cysteinate and aldose as shown in Eq. 4:



$$m=3 \text{ or } 4$$

Summary

When a solution containing HGC or HGaC and lead acetate on nitrate was allowed to stand for sometime, it was found to form a stable gel like agar-agar in the pH range between 3.8 and 11 and with a concentration over 0.3%. The turbidity and rigidity of the gel began to increase rapidly with gelation. A solution containing HMC and lead salt did not form a gel, but precipitated lead cysteinate with the liberation of mannose.

It was found that the lead aldose-cysteinates isolated, which are the essentials materials for gelation, are composed of one atom of lead, one molecule of HSC, and one univalent anion, and that the sulfur atom and one hydroxyl group HGC coordinate with the lead atom, but that the carboxyl group of HGC does not coordinate to the lead atom.

Research Laboratory of Resources Utilization
Tokyo Institute of Technology
Meguro-ku, Tokyo

*Ultraviolet Absorption Spectra of Lead Aldose-cysteinate**

By Fujio TAKAHASHI and Jun MIZUGUCHI

(Received July 6, 1962)

When the present authors studied metal complexes of HGC**, lead glucose-cysteinates in solution were found to form a gel like agar-agar and to have an ultraviolet absorption maximum at 270 mμ[1]. The other HSCs** with lead acetate in solution also show the same absorption spectra as HGC. These absorption spectra have not been known thus far. Moreover, no absorption spectrum of lead cysteinate has been reported.

In the study of the mechanism of gelation, one of the most important projects is to clarify the structure of lead aldose-cysteinate in solution.

In this paper, the results of spectrophotometric study related to the structure of lead aldose-cysteinates are described.

Experimental

HSCs were prepared in the same manner as was described in the previous paper[1]. Cysteine was prepared by the addition of pyridine to cysteine hydrochloride (monohydrate) in hot ethanol, filtration, and washing with ethanol until the pyridine odor had vanished; d. p., 218°C. The cysteine methyl ester was prepared by the electrolytic reduction of the cystine dimethyl ester which had been obtained by the usual method. Thiazolidine carboxylic acid-4 was prepared by the treatment of cysteine hydrochloride in an aqueous solution with formalin.

The spectrophotometric measurements were carried out in an aqueous solution with a Hitachi spectrophotometer, model EPU-2.

The pH value of the solution was adjusted by the addition of an appropriate amount of nitric acid or sodium hydroxide.

Results and Discussion

The absorption spectra in the solution containing different HSCs and lead acetate, and HGC and different metal salts are shown in Figs. 1 and 2 respectively. Only the lead complex of HSC in solution shows an absorption maximum at 270 mμ. Neither HSCs nor metal salts in solution show an absorption in the range between 250 and 600 mμ.

The lead complexes of different amino acids, except cysteine, show no absorption in the range between 250 and 300 mμ (Fig. 3). On the other hand, the lead complexes of various thiol-containing compounds have an absorption maximum at about 270 mμ (Fig. 4). From

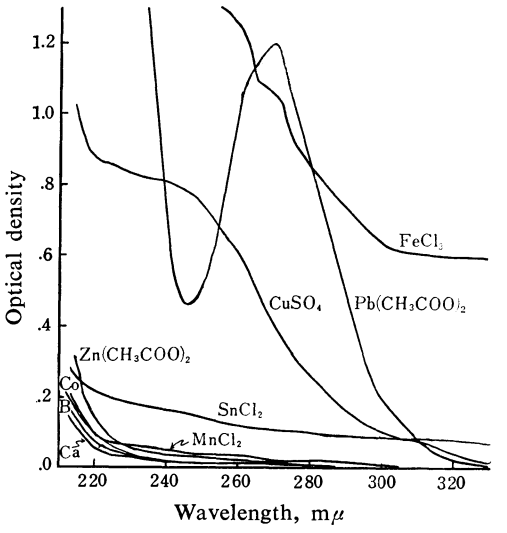


Fig. 1. HGC-various metal salts
0.5 mM HGC, 0.5 mM metal salt.
B: Only HGC (metal free)
Co: $CoCl_2$+HGC
Ca: $CaCl_2$+HGC

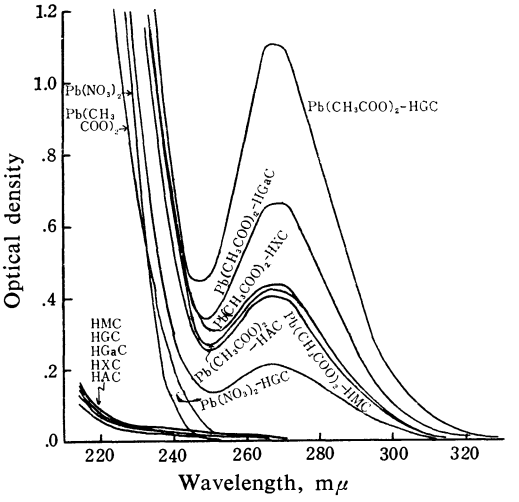


Fig. 2. HSC-lead salt.
0.5 mM HSC, 0.5 mM $Pb(CH_3COO)_2$ or $Pb(NO_3)_2$

* Gelation of Lead Aldose-cysteinate Part II.

** See this Bulletin 35, 1819 (1962).

1) F. Takahashi and J. Mizuguchi, This Bulletin 35, 1818 (1962).

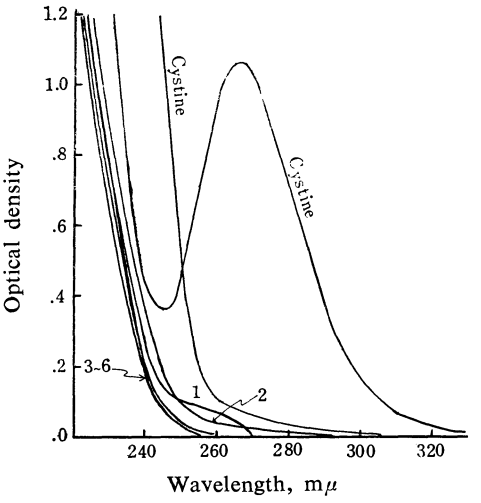


Fig. 3. Various amino acids-$Pb(CH_3COO)_2$.
0.5 mM amino acid, 0.5 mM $Pb(CH_3COO)_2$.
1 Phenylalanine
2 Thiazolidine carboxylic acid-4
3 Glycine
4 Glutamic acid
5 Serine
6 Lysine-HCl

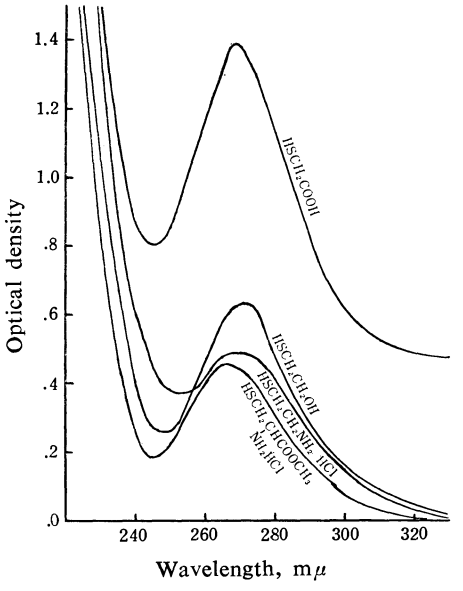


Fig. 4. $Pb(CH_3COO)_2$-thiol containing compounds.
0.5 mM $Pb(CH_3COO)_2$, 0.5 mM thiol-containing compounds

these results, it can be concluded that lead is coordinated through the sulfur atom of thiol-containing compounds.

The lead complexes of HSCs, which have a thiazolidine ring and no thiol group, show the same absorption spectra as that of thiol-containing compounds. In the beginning of this

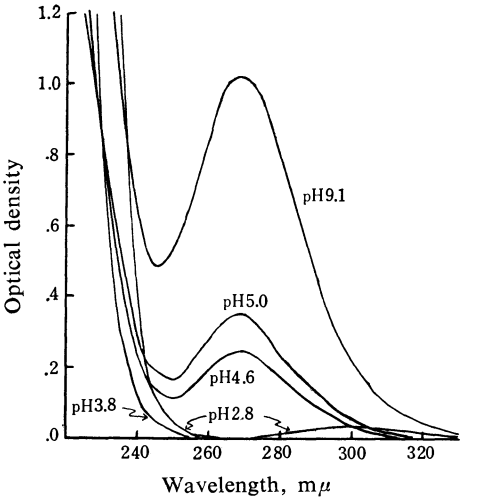


Fig. 5. HGC-lead salt in various pH.
0.25 mM HGC, 0.25 mM lead salt.

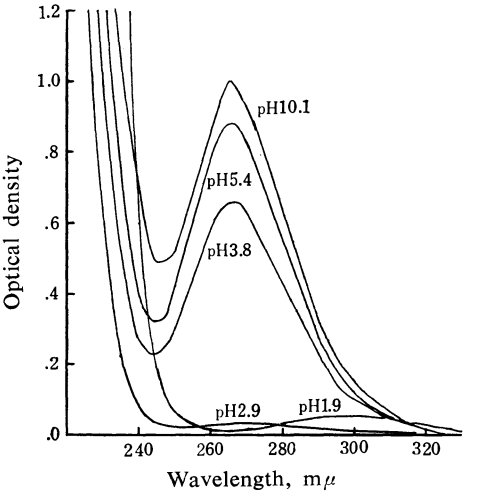


Fig. 6. Cysteine-lead salt in various pH.
0.5 mM cysteine, 0.25 mM lead salt

work, it was thought that the material which shows an absorption maximum was not the lead complexes of HSC but lead cysteinate, because HSC can be hydrolized to form cysteine in an aqueous solution. However, from the results of iodide-iodate determination[2], it was found to show no cysteine in the solution prepared for the determination of absorption spectra. Therefore, it is suggested that lead is doubtless coordinated through the sulfur atom of HSC and that the absorption maximum appears by means of this Pb–S bond.

Lead aldose-cysteinate, which has hydroxyl groups, shows the absorption maximum, but thiazolidine carboxylic acid, which has no

2) M. Sato, T. Hirano and T. Kan, *J. Agr. Chem. Soc. (Japan)*, **15**, 783 (1938).

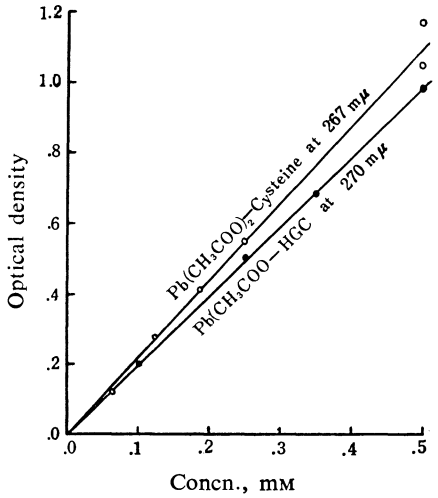


Fig. 7. $Pb(CH_3COO)_2$-HGC or cysteine in various concentration.
(Molar ratio 1 : 1)

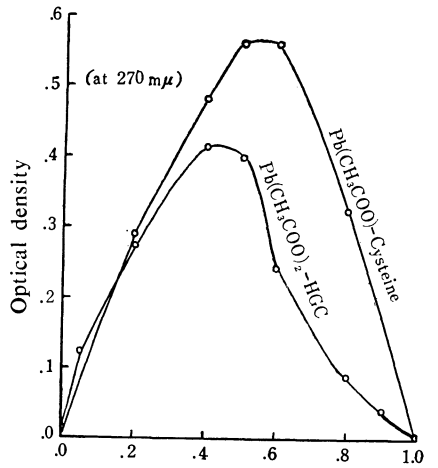


Fig. 8. Graphical determination of the composition of lead glucose-cysteinate or cysteinate.
Total concn. 0.5 mM

hydroxyl group, does not show it, as is shown in Fig. 3. It is suggested that an absorption maximum appears when lead is coordinated through not only the sulfur atom but also hydroxyl groups of HSC.

It seems that these coordinations exist in the pH range between 3 and 10. In this pH range, the curves exhibit the same general contour and the same peak, as is shown in Fig. 5. The characteristic absorption spectra could not be observed in the pH range of 6 to 8 because the solution became turbid. In the lower pH range below 3, an absorption maximum was found to shift from 270 to 300 mμ. This fact presumably means that the complex is transformed.

Lead cysteinate was found to show the same absorption spectra as lead glucose-cysteinate (Fig. 6).

The absorption spectra of lead glucose-cysteinate was found to obey Beer's law in the range of 250 to 300 mμ (Fig. 7). When the absorption spectra were measured according to Job's method[3], the optical density at 270 mμ was found to be at a maximum at the molar ratio of about 1 : 1 (Fig. 8). It can be concluded that the highest order lead aldose-cysteinates and lead cysteinate are 1 : 1. These results can be supported by the suggestion obtained from the potentiometric study of Li and Manning[4].

Summary

Lead Aldose-cysteinates in solution were found to show an ultraviolet absorption maximum at 270 mμ. Moreover, lead complexes of various thiol-containing compounds were found to show the same absorption spectra as aldose-cysteine. From these results, it has been suggested that the absorption maximum appears when lead is coordinated through the sulfur atom.

Research Laboratory of Resources Utilization
Tokyo Institute of Technology
Meguro-ku, Tokyo

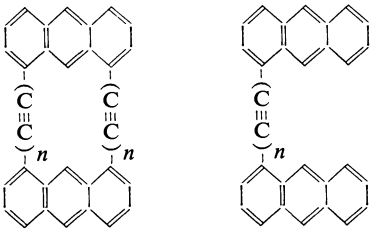
3) P. Job, *Ann. chim.*, **9**, 113 (1928).
4) N. C. Li and R. A. Manning, *J. Am. Chem. Soc.*, **77**, 5225 (1955).

Cyclic Acetylenes. VIII. Synthesis of 1, 1'-Dianthryltetraacetylene. A Model Substance of a Cyclic Octaacetylene Containing Anthracene Nuclei*

By Shuzo AKIYAMA, Soichi MISUMI and Masazumi NAKAGAWA

(Received July 10, 1962)

The synthesis of the macrocyclic tetraacetylene (I) in which two anthracene nuclei constitute a part of the fully conjugated planar macroring has been reported by the present authors[1]. It is of interest to prepare the higher homologue of I in view of the unusual stability and



I (n=2)
II (n=4)

III (n=2)
IV (n=4)

the characteristic spectroscopic properties of I. The present paper concerns with the synthesis of 1, 1'-dianthryltetraacetylene (IV) which is a model substance of the cyclic octaacetylene (II), a higher homologue of I. The structural units of IV can be regarded as the same with that of II. Also a lower homologue of IV, 1 1'-dianthryldiacetylene (III) has been synthesized by the present authors[2]. Therefore, the comparison of the physical and chemical properties of these compounds with those of IV is also of interest.

Benzanthrone was converted into 1-carboxyanthracene via two steps[2] and the carboxylic acid was esterified yielding the methyl ester (V). Reduction of the ester V by means of lithium aluminum hydride afforded 1-hydroxymethylanthracene (VI) in a good yield. 1-Bromomethylanthracene (VII) derived from VI was converted to 1-formylanthracene (VIII) by the Sommelet's method[3]. The aldehyde VIII was also prepared directly by the oxidation of the alcohol VI with chromium trioxide-pyridine[4] in a yield of 88%. The reaction of the aldehyde VIII with the Grignard derivative of tetrahydropyranyl ether of propargyl alcohol yielded the acetylenic glycol (IX). The glycol IX was treated with thionyl chloride and pyridine, and the dichloride X thus obtained was dehydrochlorinated without further purification with sodium amide in liquid ammonia. 1-Butadiynylanthracene (XI) was obtained in yellow needles. The diacetylene XI was found to be fairly stable substance and could be kept without decomposition for periods of days in a refrigerator. A dilute solution of XI in an organic solvent exhibits an intense lilac fluorescence. XI gave orange cuprous and orange-yellow silver salts indicating the presence of terminal acetylene. Also the infrared spectrum of XI exhibits strong bands at 3250 and 2210 cm^{-1} indicating the presence of ethynyl group and disubstituted carbon-carbon triple bond (Fig. 1). The electronic spectrum of XI was illustrated in Fig. 2.

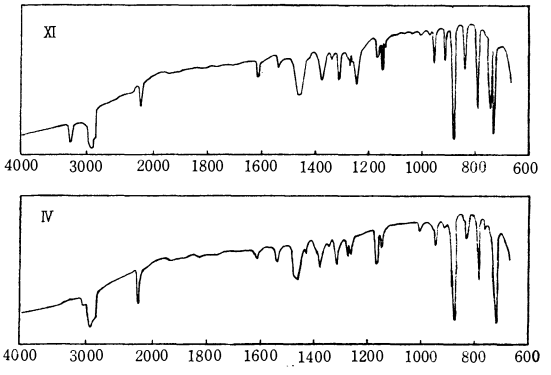


Fig. 1. The infrared spectra of 1-butadiynylanthracene (XI) and 1, 1'-dianthryltetraacetylene (IV) (Nujol mull).

The oxidative coupling of XI according to the procedure of Eglinton[5] yielded golden-yellow leaflets or needles. The structure of

* Although the present paper is concerned with acyclic acetylenes, it has been included in this series since the compounds and the reaction described here served as models for the synthesis of analogous cyclic derivative.

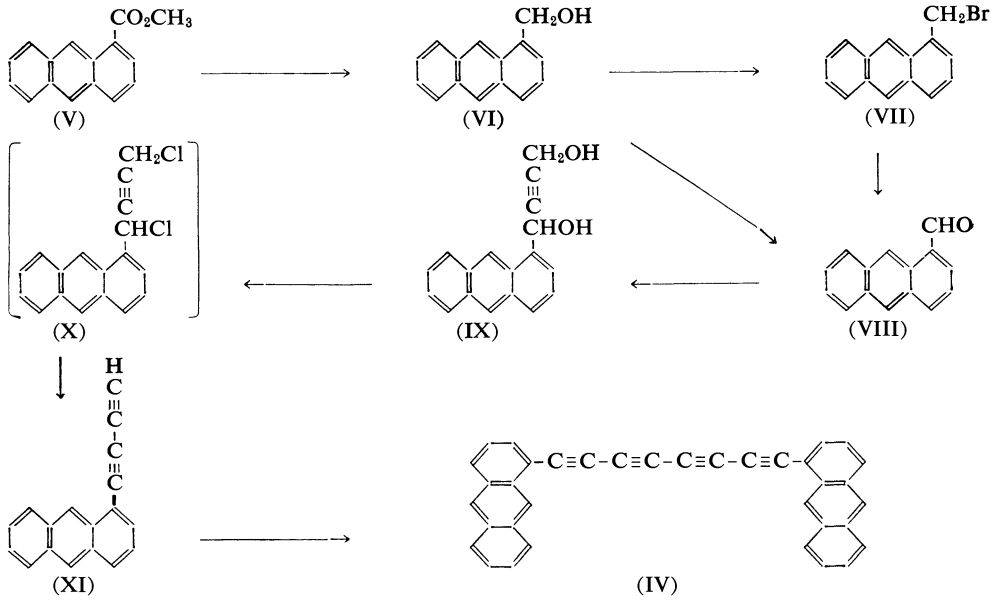
1) S. Akiyama, S. Misumi and M. Nakagawa, This Bulletin, 33, 1293 (1960).

2) S. Akiyama and M. Nakagawa, This Bulletin, 33, 1291 (1960).

3) Cf., M. Sommelet, *Compt. rend.*, **157**, 852 (1913); *Bull. soc. chim. France*, [4] **13**, 1085 (1913); S. J. Angyal, "Org. Reactions", Vol. VIII, J. Wiley & Sons, Inc., New York (1954), p. 197.

4) Cf., G. I. Poos, G. E. Arth, R. E. Beyler and L. H. Sarett, *J. Am. Chem. Soc.*, **72**, 422 (1953).

5) G. Eglinton and A. R. Galbraith, *J. Chem. Soc.*, **1959**, 886.



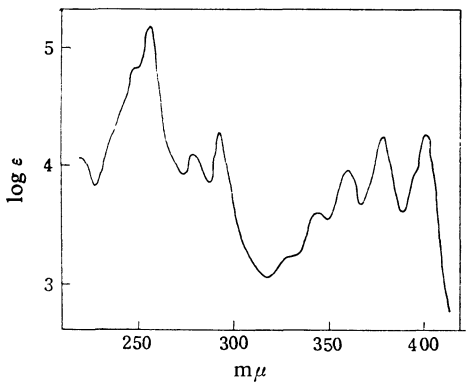


Fig. 2. The electronic spectrum of 1-butadiynylanthracene (XI).

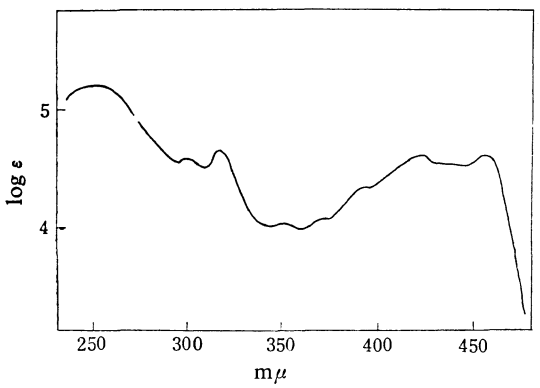


Fig. 3. The electronic spectrum of 1, 1'-dianthryltetraacetylene (IV).

1, 1'-dianthryltetraacetylene (IV) was given to the substance on the bases of its analytical data and the infrared spectroscopic evidences (the absence of free ethynyl absorption and the presence of acetylenic absorption at 2205 cm^{-1} (Fig. 1)). IV was found to be a very stable substance. IV showed no melting point, it decomposed on heating to ca. 245°C forming a black substance without the change of its crystal form. Like I and III, the tetraacetylene (IV) is slightly soluble or almost insoluble in common organic solvents. The electronic spectrum of IV was shown in Fig. 3. The electronic spectral properties of XI, IV and related compounds will be discussed in the following paper[6].

Experimental*

1-Methoxycarbonylanthracene (V).—1-Carboxyanthracene was refluxed with methanol in the presence of sulfuric acid yielding V, m. p. 104°C, (lit., m. p. 108°C[7]; m. p. 104°C[8]).

1-Hydroxymethylanthracene (VI).—The methyl ester (V, 30.6 g., 0.13 mol.) was reduced with lithium aluminum hydride (4.8 g.) in boiling ether (1.2 l.) using a Soxhlet type extractor. The refluxing of the reaction mixture was continued for further 1 hr. to complete the reduction after all of the ester V had been extracted (3 hr.). Ethyl acetate (6 ml.) and 5% aqueous sodium hydroxide (100 ml.) were added successively to the ice-cooled reaction mixture under vigorous stirring. The ether layer was separated and the residue obtained by the removal of the solvent was stirred with 10% aqueous sodium hydroxide (100 ml.) for 1 hr. The insoluble material was collected by filtration,

6) S. Akiyama, S. Misumi and M. Nakagawa, This Bulletin, 35, 1829 (1962).

* All melting points were not corrected.

7) E. A. Coulson, *J. Chem. Soc.*, **1930**, 1931.

8) A. Sonoda, F. Ogura and M. Nakagawa, This Bulletin, 35, 853 (1962).

washed with water, 6 N hydrochloric acid and water, successively, yielding colorless fine fibrous crystals, m. p. 124~125°C, (26.0 g., 96%). This was recrystallized from ethanol to give pure VI, colorless long needles, m. p. 125~126°C.

Found: C, 86.63; H, 5.99. Calcd. for $C_{15}H_{12}O$: C, 86.51; H, 5.81%.

IR: 3215 (O-H), 1030 cm^{-1} (C-O), (KBr-disk).

1-Bromomethylanthracene (VII).—To an ice-cooled mixture of VI (1.1 g., 5 mmol.), chloroform (20 ml.) and pyridine (0.2 ml.) was added phosphorus tribromide (0.6 g., 2.2 mmol.). The mixture was allowed to warm up to room temperature and kept at the temperature for 1 hr. with occasional shaking and then water was added. The chloroform layer was washed with water and dried over sodium sulfate. Evaporation of the solvent yielded crude VII, yellow needles, m. p. 111~113°C, (1.3 g., 93%). The crude material was recrystallized twice from carbon tetrachloride to give pure VII, yellow needles, m. p. 114~115°C. VII could not be kept without decomposition for a long time.

Found: C, 66.05; H, 4.04; Br, 29.30. Calcd. for $C_{15}H_{11}Br$: C, 66.04; H, 4.09; Br, 29.47%.

The Pyridinium Bromide.—Pale yellow leaflets, m. p. 225~227°C (decomp.).

Found: C, 68.27; H, 4.64; N, 3.92. Calcd. for $C_{20}H_{16}NBr$: C, 68.53; H, 4.60; N, 4.00%.

The Pyridinium Perchlorate.—Pale yellow leaflets, m. p. 235~237°C (decomp.).

Found: C, 64.94; H, 4.43; N, 3.93, Cl, 9.07. Calcd. for $C_{20}H_{16}O_4NCl$: C, 64.96; H, 4.36; N, 3.79, Cl, 9.59%.

An accurate analysis of chlorine could not be performed owing to an explosive decomposition of the salt in the combustion tube.

1-Formylanthracene (VIII).—*a) By the Sommelet Method.*—The hydroxymethyl derivative (VI, 2.2 g., 0.01 mol.) was treated with phosphorus tribromide according to the above-mentioned procedure and the chloroform solution was washed with water and dried (sodium sulfate). A solution of hexamethylenetetramine (1.7 g., 0.012 mol.) in chloroform (15 ml.) was added to the dried solution and the mixture was refluxed for 3 hr. About half of the solvent was removed and the concentrated solution was chilled with ice. The hexamine-adduct deposited was filtered and washed with a small amount of chloroform affording pale yellow crystalline solid (3.3 g.). Water (30 ml.) was added to a solution of the adduct (3.3 g.) in acetic acid (30 ml.) and the mixture was refluxed for 1 hr., then 12 N hydrochloric acid (0.7 ml.) was added and refluxed for 5 min. The mixture was poured into water (200 ml.), extracted with benzene (100 ml.), and the extract washed with water and dried (sodium sulfate). Evaporation of the solvent under reduced pressure afforded yellow leaflets, m. p. 126~130°C (from ethanol), (1.1 g., 53%). Further recrystallization from the same solvent gave pure VIII, m. p. 131~132°C, (lit., m. p. 131~133°C[9], m. p. 126.5~127.5°C[10]).

Found: C, 87.16; H, 4.97. Calcd. for $C_{15}H_{10}O$: C, 87.35; H, 4.89%.

b) By the Oxidation of VI with Chromium Trioxide-pyridine.—A solution of VI (4.2 g., 0.02 mol.) in dry pyridine (30 ml.) was added in one portion to an ice-cooled mixture of chromium trioxide (3.8 g., 0.08 mol.) and dry pyridine (80 ml.). The mixture was shaken for 30 min. in the cooling bath, then for 2 hr. at room temperature and then poured into water (1.5 l.); leaflets precipitated. The crystals were extracted with benzene (100 ml.) employing a Soxhlet type extractor. Evaporation of the solvent afforded VIII, yellow leaflets, m. p. 123~129°C, (3.6 g., 88%). Analytical specimen (m. p. 131~132°C) was prepared by one recrystallization from benzene.

Found: C, 87.36; H, 4.93. Calcd. for $C_{15}H_{10}O$: C, 87.35; H, 4.89%.

IR: 2710 (-CHO), 1690 cm^{-1} (C=O), (KBr-disk).

UV λ_{max}^{MeOH} mμ (log ε): 241.5 (4.80), 259.5 (4.63), 334† (3.16), 348 (3.48), 366 (3.69), 392 (3.76), 405† (3.71).

1-(1', 4'-Dihydroxybut-2'-ynyl)-anthracene (IX).—To a solution of ethylmagnesium bromide (prepared from magnesium, 9.7 g., 0.4 g. atom and ethyl bromide, 49 g., 0.45 mol.) in tetrahydrofuran (150 ml.) was added a solution of tetrahydropyranyl ether of propargyl alcohol[11] (56 g., 0.4 mol.) in tetrahydrofuran (50 ml.) over a period of 30 min. under cooling with water and then the mixture was refluxed for 1.5 hr. A solution of the aldehyde (VIII, 20.6 g., 0.1 mol.) in the same solvent (460 ml.) was introduced during 1 hr. under cooling with water. After stirring for 10 hr. at 10°C, 4 N sulfuric acid (800 ml.) was added into the reaction mixture under cooling with water and stirred for 1.5 hr. The mixture was extracted with benzene (300 ml.). The extract was washed with 4 N sulfuric acid (100 ml.) and water, successively and dried (sodium sulfate). The most part of the solvent was removed under reduced pressure. The crystals deposited were filtered and washed with a small amount of benzene yielding crude IX, pale yellow fine crystals, m. p. 192~196°C, (18.4 g., 70%). This material was recrystallized from ethanol-benzene (4:1) to give pure IX, yellowish white leaflets, m. p. 204~205°C.

Found: C, 82.20; H, 5.50. Calcd. for $C_{15}H_{14}O_2$: C, 82.42; H, 5.38%.

IR: 3220 (O-H), 1015, 1030 cm^{-1} (C-O), (KBr-disk).

UV $\lambda_{max}^{95\%EtOH}$ mμ (log ε): 254 (5.13), 302† (2.76), 312 (3.15), 327 (3.51), 342 (3.78), 359 (3.95), 378 (3.87).

1-Butadiynylanthracene (XI).—To an ice-cooled mixture of the acetylene glycol (IX, 3.15 g., 0.012 mol.) in dry pyridine (4 g., 0.05 mol.) and tetrahydrofuran (100 ml.) was added under stirring a solution of thionyl chloride (6 g., 0.05 mol.) in tetrahydrofuran (10 ml.) over a period of 1 hr. The mixture was stirred for 0.5 hr. at 40°C and then refluxed for 1.5 hr. resulting in a dark red solution.

9) R. Walker, "Documentation of Molecular Spectroscopy", English Ed., 4504, 3/59, Butterworth Scientific Publications (London).

10) P. H. Gore, *J. Chem. Soc.*, **1959**, 1616.

† Dagger on the figures of the spectral data denotes shoulder.

11) H. B. Henbest, E. R. H. Jones and I. M. S. Walls, *J. Chem. Soc.*, **1950**, 3646.

Crushed ice was added to the solution and extracted with benzene (100 ml.). The extract was washed with aqueous sodium hydrogen carbonate and dried (sodium sulfate). The solvent was removed under reduced pressure in an atmosphere of nitrogen yielding the crude dichloride X as tarry viscous oil. A solution of the crude dichloride in tetrahydrofuran (25 ml.) was added dropwise into a solution of sodium amide (prepared from sodium, 5.8 g., 0.25 g. atom) in liquid ammonia (250 ml.) in the course of 1 hr. After stirring for 3 hr., ammonium chloride (10 g.) was introduced to the mixture and the ammonia was allowed to evaporate. The residue was repeatedly extracted with petroleum benzine (b. p. 60~80°C, total 1000 ml.). The extract was condensed, after being washed with water and dried (sodium sulfate), to ca. 300 ml. under reduced pressure in nitrogen atmosphere. The condensed extract was filtered through a thin layer of alumina (10 g.). The filtrate was again condensed under reduced pressure in nitrogen atmosphere to yield XI, yellow needles, (0.89 g., 33%) which decomposed at ca. 130°C forming a black solid without fusion.

Found: C, 95.38; H, 4.44. Calcd. for $C_{18}H_{10}$: C, 95.54; H, 4.46%.

IR: 3250 (≡C-H), 2210 cm^{-1} (-C≡C-), (Nujol mull).

UV $\lambda_{max}^{n\text{-Hexane}}$ $m\mu$ (log ε): 249.5 (4.85), 257.5 (5.19), 279 (4.10), 294.5 (4.27), 330 (3.23), 345 (3.60), 361 (3.97), 380 (4.22), 402 (4.25).

Formation of IV by the Oxidative Coupling of XI.—Cupric acetate monohydrate (15 g.) was added to a solution of the diacetylene (XI, 0.79 g., 0.0035 mol.) in pyridine (100 ml.) and the mixture was stirred for 4 hr. at 45°C. The solid obtained by filtrating the reaction mixture was washed thoroughly with water affording tiny yellow crystals, 0.65 g. (82%). The crystals were found to be free from inorganic substance. The residue obtained by the concentration of the filtrate under reduced pressure was dissolved in benzene (80 ml.) and passed through a thin layer of alumina. Benzene was removed by evaporation yielding crude orange-yellow crystals, 0.05 g. (6%). The combined crystals were recrystallized thrice from benzene to give pure IV, golden yellow leaflets or needles. The crystals decomposed at ca. 245°C without fusion forming a black solid.

Found: C, 95.90; H, 4.10. Calcd. for $C_{36}H_{18}$: C, 95.97; H, 4.03%.

IR: 2205 cm^{-1} (-C≡C-), (Nujol mull).

UV λ_{max} $m\mu$ (log ε): 250 (5.20), (in tetrahydrofuran), 301 (4.59), 316.5 (4.65). 351† (4.05), 371† (4.30), 422 (4.60), 457 (4.61), (in benzene).

The authors are grateful to the Ministry of Education for the financial support. The microanalyses were performed by Messrs. Masakazu Okumiya and Osamu Saiki in the Microanalytical Laboratory of this Department, to whom the authors' thanks are also due.

Department of Chemistry
Faculty of Science
Osaka University
Nakanoshima, Osaka

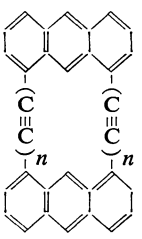
Cyclic Acetylenes. IX. Synthesis of a Cyclic Octaacetylene Containing Anthracene Nuclei

By Shuzo AKIYAMA, Soichi MISUMI and Masazumi NAKAGAWA

(Received July 10, 1962)

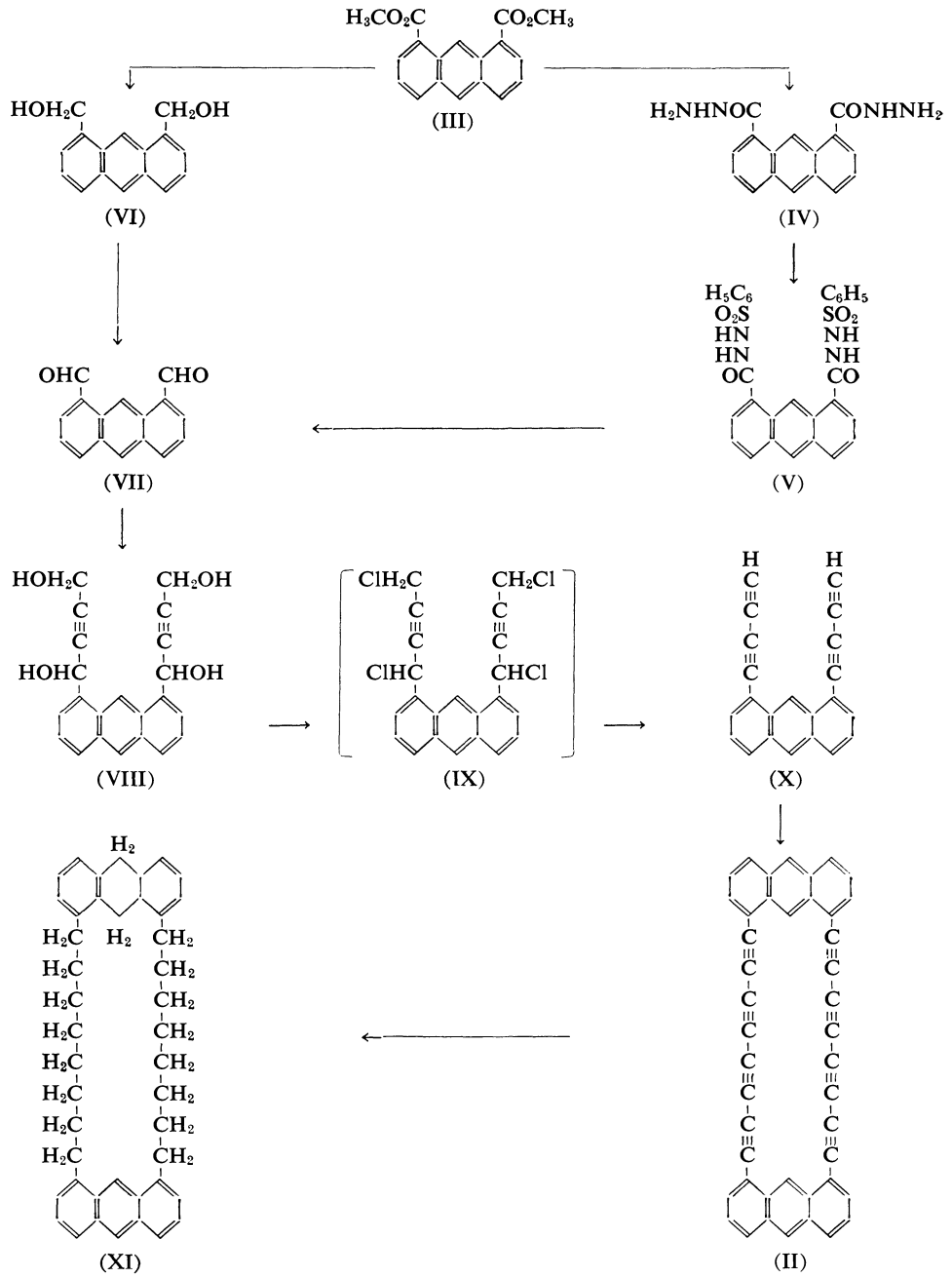
As reported in a previous paper[1] of this series, we have synthesized a fully conjugated cyclic tetraacetylene containing anthracene nuclei. The extremely stable nature of the cyclic acetylene (I) urged the present authors to the synthesis of a higher homologue of I. The present paper deals with the synthesis of the same type cyclic octaacetylene (II).

1, 8-Dicarboxyanthracene which was derived from 1, 8-dichloroanthraquinone[1] was converted to the corresponding dimethyl ester (III). The ester III was treated with hydrazine hydrate yielding the bishydrazide (IV). The decomposition of the benzenesulfonyl derivative of IV (V) in ethylene glycol in the presence



I ($n=2$)
II ($n=4$)

1) S. Akiyama, S. Misumi and M. Nakagawa, This Bulletin, 33, 1293 (1960).



of sodium carbonate afforded 1, 8-diformylanthracene (VII)[2]. But the procedure was found to be scarcely feasible for the preparation of VII owing to its highly sensitive nature to reaction conditions which makes impossible to improve the low yield and the poor reproducibility. The reduction of the dimethyl ester III with lithium aluminum hydride yilded 1, 8-bis-hydroxymethylanthracene (VI). The attempts to convert VI into 1, 8-bis-bromomethyl derivative which is the potential starting material of the preparation of the dialdehyde VII according to the Sommelet[3] or the Kröhnke method[4], were prevented due to the poor solubility of VI in chloroform or carbon tetrachloride. Finally we have found

2) Cf., J. S. McFadyen and T. S. Stevens, *J. Chem. Soc.*, **1936**, 584.

3) Cf., M. Sommelet, *Compt. rend.*, **157**, 852 (1913); *Bull. soc. chim. France*, [4] **13**, 1083 (1913); S. J. Angyal, "Org. Reactions", Vol. VIII, J. Wiley & Sons, Inc., New York (1954), p. 197.

4) F. Kröhnke and H. Schmeiss, *Ber.*, **72**, 440 (1939).

that the oxidation of VI by means of chromium trioxide in pyridine[5] results in the formation of VII in a reasonable yield.

The reaction of the lithium derivative of the tetrahydropyranyl ether of propargyl alcohol, 2-(prop-2'-yn-1'-yloxy)-tetrahydropyran with the dialdehyde VII was studied to obtain the tetraol VIII. The lithium derivative obtained by the action of lithium on the mercuric acetylide of the tetrahydropyranyl ether gave the tetraol VIII in a low yield. According to this result, the tetrahydropyranyl ether in tetrahydrofuran was treated with phenyllithium to attain a complete metalation. The reaction of the resulting lithium salt with the aldehyde VII at low temperature followed by the hydrolysis of the tetrahydropyranyl ether yielded the tetraol VIII in a reasonable yield. The tetrachloro-compound IX which was obtained by the treatment of VIII in tetrahydrofuran with thionyl chloride and pyridine was dehydrochlorinated without purification by the action of sodium amide in liquid ammonia yielding 1, 8-bis-butadiynylanthracene (X) as bright yellow fine needles in a reasonable yield. The terminal bis-diacetylene X was found to be fairly unstable substance. The crystals lose their bright surface lustre on exposure to air and form a brown material insoluble in common organic solvents. A dilute solution of X exhibits an intense, beautiful lilac fluorescence. The infrared spectrum of X showed absorptions at 2280 and 3200 cm^{-1} indicating the presence of ethynyl group and disubstituted carbon-carbon triple bond (Fig. 1). X forms red cuprous and orange-yellow silver acetylides.

In the course of the oxidative coupling of X to the cyclic octaacetylene II according to the method of Eglinton[6], we have encountered

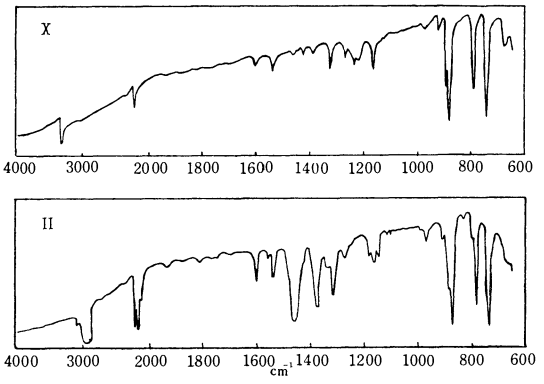


Fig. 1. The infrared spectra of 1, 8-bis-butadiynylanthracene (X) (KBr-disk) and cyclic-octaacetylene (II) (Nujol mull).

5) Cf., G. I. Poos, G. E. Arth, R. E. Beyler and L. H. Sarett, *J. Am. Chem. Soc.*, **75**, 422 (1953).

6) G. Eglinton and A. R. Galbraith, *Chem. & Ind.*, **1956**, 737; *J. Chem. Soc.*, **1959**, 886.

unexpected difficulty. A large amount of a decomposition product soluble in pyridine was formed when the oxidative coupling was carried out under ordinary conditions for several ten minutes at a slightly elevated temperature. In these cases, the isolation of the cyclic dimer II was practically impossible. Finally it was found that the oxidation had to be carried out at a temperature of ca. 20°C and be interrupted within 1 min. The cyclic octaacetylene II thus obtained was deep red fine needles which decomposed at ca. 160°C into brown solid keeping the shape of the crystals. The octaacetylene II was found to be a stable substance and could be kept without decomposition for a long time. No change of the electronic spectrum was observed after a benzene or a tetrahydrofuran solution of II was exposed to a direct sunlight or a mercury are lamp for some several hours. The analytical data and the infrared spectrum are consistent with the structure of II. The infrared spectrum of II exhibits strong absorptions at 2190, 2140 and 2110 cm^{-1} indicating the presence of polyacetylenic linkage and lacks the absorption arising from the C–H streching of ethynyl group (Fig. 1). Also a solution of II gave a negative test against alcoholic silver nitrate solution. The molecular weight of II could not be determined owing to its poor solubility in organic solvents. The Rast method also gave unsatisfactory result as a result of decomposition of II at the elevated temperature. The catalytic reduction of II in benzene over a large amount of palladium-on-charcoal afforded stable pale yellow crystals. The empirical formula of this substance was determined to be $(C_{22}H_{25})_n$. The molecular weight determination of this substance by Rast's method in camphor (found, 613) revealed that the molecular formula should be $(C_{22}H_{25})_2$, (calcd., 579). The dimeric nature of the coupling product II was unequivocally confirmed by this result.

The infrared spectroscopy of the hydrogenated product revealed the presence of 1, 2, 4, 5-tetrasubstituted benzene nucleus. Also the presence of anthracene nucleus was inferred from the characteristic ultraviolet absorption. The structure of XI was tentatively assigned to the reduction product on the bases of the above-mentioned evidences.

As stated above, the oxidative coupling of X gave II in a poor yield under the restricted conditions. This fact makes a sharp contrast with fact that the oxidative coupling of 1, 8-diethynylanthracene[1] yields the cyclic tetraacetylene I in a quantitative yield. This difference seems to be rather surprising in view of their similar molecular geometry which

is most favorable to the cyclic dimerization. It was confirmed that II was stable in the reagent of Eglinton's oxidative coupling. A solution of II in the reagent was diluted with a large amount of water and extracted with benzene. After treatment according to the usual manner, the benzene solution was subjected to a spectroscopic examination. An identical electronic spectrum was obtained. On the other hand, the cuprous salt of X readily decomposed in pyridine forming a decomposition product. This behavior makes a contrast with the stable nature of the cuprous salt of 1,8-diethynylanthracene in the same solvent. The details of the oxidative coupling of X is not clear, but it seemed to be related with the enhanced flexibility of the diacetylenic groups in X as compared with the rigid ethynyl groups in 1, 8-diethynylanthracene.

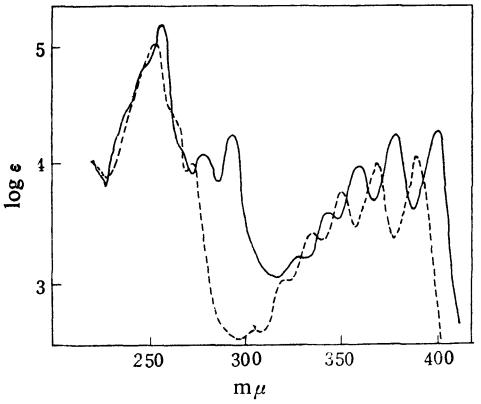


Fig. 2. The electronic spectra of 1-ethynylanthracene (------) and 1-butadiynylanthracene (XI, ——).

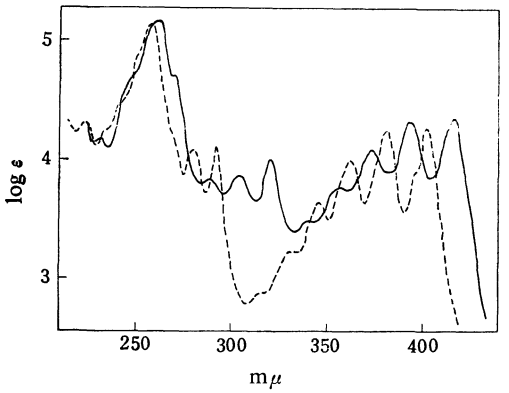


Fig. 3. The electronic spectra of 1, 8-diethynylanthracene (------) and 1, 8-bis-butadiynylanthracene (X, ——).

As illustrated in Figs. 2 and 3, the electronic spectra of 1-ethynyl-[7], 1-butadiynyl-[8], 1, 8-diethynyl-[1] and 1, 8-bis-butadiynylanthracene exhibit absorption curves characteristic to anthracene nucleus excepting the wavelength region of 270~320 mμ. The characteristic feature of the electronic spectra of these acetylenic compounds appears in this wavelength. 1-Ethynylanthracene has an absorption peak in this region. 1-Butadiynyl- and 1, 8-diethynylanthracene exhibit two absorption peaks. Whereas three absorption maxima appeared in the case of 1, 8-bis-butadiynylanthracene (X). The spectra of 1, 1'-dianthryldiacetylene[6], 1, 1'-dianthryltetraacetylene[7], the cyclic tetraacetylene I[1] and the cyclic octaacetylene II were summarized in Fig. 4. The fine structures in the spectra of 1, 1'-dianthryltetraacetylene and II are much more indistinct as compared with those of 1, 1'-dianthryldiacetylene and the cyclic tetraacetylene I. It is of interest to note that the fine structure in the spectra of α, ω-diphenyl- or α, ω-dialkylpolyynes become more and more distinct with the increasing number

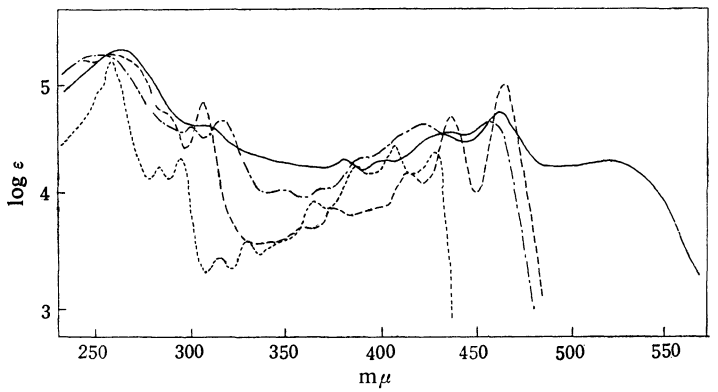
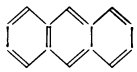
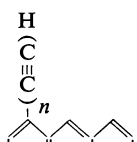
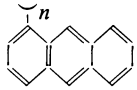
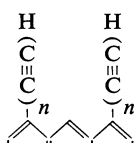
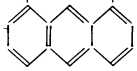
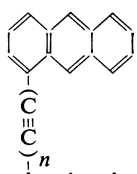
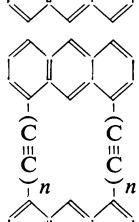
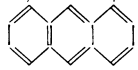


Fig. 4. The electronic spectra of 1, 1'-dianthryldiacetylene (------), 1, 1'-dianthryltetraacetylene (—·—·—·) cyclictetraacetylene (I, ------) and cyclicoctaacetylene (II, ——).

7) S. Akiyama and M. Nakagawa, This Bulletin, 33, 1293 (1960).

8) S. Akiyama, S. Misumi and M. Nakagawa, This Bulletin, 35, 1826 (1962).

TABLE I. THE BATHOCHROMIC SHIFTS OF THE ELECTRONIC SPECTRA OF THE ACETYLENES

	Compound	λ_{max} (mμ)	ε	Shifts in mμ from 1	2	3	4	5	6	7	8	Solvent
1		374	7400	—	—	—	—	—	—	—	—	C
2	 $n=1$	391	11500	17	—	—	—	—	—	—	—	C
3	 $n=2$	402	17800	28	11	—	—	—	—	—	—	H
4	 $n=1$	402	17400	28	11	0	—	—	—	—	—	C
5	 $n=2$	416	19950	42	25	14	14	—	—	—	—	E
6	 $n=2$	428	24600	54	37	26	26	12	—	—	—	C
7	 $n=4$	457	40700	83	66	55	55	41	29	—	—	B
8	 $n=2$	465	91200	91	74	63	63	49	37	8	—	B
9	 $n=4$	520	20420	146	129	118	118	104	92	63	55	T

Solvent: C=cyclohexane; H=n-hexane; E=ethanol; B=benzene; T=tetrahydrofuran

of the acetylenic linkage making a contrast with the case of the acetylenic derivatives of anthracene[9].

The position of absorption maxima, their ε-values and the relative shifts of the maxima of the above-mentioned acetylenic derivatives as compared with anthracene are tabulated in Table I. The comparison of the spectra of 1, 1'-dianthryltetraacetylene and the cyclic tetraacetylene I indicates that the red-shift of the maximum at the longest wavelength of I from the acyclic analogue is only 8 mμ, but the ε-value of I is over twice as large as that of the acyclic tetraacetylene. The large difference in the ε-values is remarkable, because these two compounds have the same structural units. The five absorption peaks at the longer wavelength region in the spectrum of II correspond well with those of the spectrum of the cyclic tetraacetylene I*, but the magnitude of red-shifts of the corresponding absorption peaks increases with the increasing wavelength of the maxima (4, 11, 17, 25 and 55 mμ). The characteristic of the spectrum of the cyclic octaacetylene II is the relatively low absorption intensity at the maximum of the longest wavelength, but the absorption intensities of other peaks are found to be higher than those of the corresponding peaks of I. Another remarkable feature of the spectrum of II is its high absorption intensity over a wide range of wavelength. It was found that the log ε-value was over 4.0 from 230 to 550 mμ.

9) Cf., M. Nakagawa, *Proc. Japan Acad.*, **26** (10), 38, 43 (1950); H. H. Schlubach, *Ann.*, **537**, 110 (1951); F. Bohlmann, *Chem. Ber.*, **84**, 545, 785 (1951).

* The absorption peaks of I are as follows: λ_{max} 258 mμ (logε, 5.22) (in *n*-hexane), 307 (4.82), 340 (3.66), 358 (3.79), 376 (3.93), 392 (3.90, shoulder), 413 (4.22), 437 (4.67), 465 (4.96) (in benzene).

Experimental*

1, 8-Dimethoxycarbonylanthracene (III). — A stirred mixture of 1, 8-dicarboxyanthracene[1] (50 g., 0.188 mol.), (methanol 1000 ml.) and concentrated sulfuric acid (20 g.) was refluxed for 8 hr. The reaction mixture was chilled with ice precipitating crystalline solid. The solid was washed with a small amount of methanol and water, successively, yielding yellow needles, m. p. 104~105°C (34 g.). The filtrate was concentrated under reduced pressure. The residue was poured into water (100 ml.) and extracted with benzene (60 ml.). Further crop of yellow needles, m. p. 104~105°C (10.5 g.) was obtained from the benzene extract. The combined yield was found to be 81%. Crystallization from methanol gave pure III, long yellow needles, m. p. 104~105°C.

Found: C, 73.41; H, 4.68. Calcd. for $C_{18}H_{14}O_4$: C, 73.46; H, 4.80%.

Anthracene-1, 8-bis-carbohydrazide (IV.). — A solution of the methyl ester (III, 85 g., 0.28 mol.) in 99% ethanol (430 ml.) containing 80% hydrazine hydrate (170 ml.) was refluxed for 4 hr. Deposition of crystals was observed after 30 min. The reaction mixture was cooled in an ice-bath, and the crystals deposited were filtered, washed with ethanol (100 ml.) and water (300 ml.), successively, yielding crude IV, yellow needles, m. p. 279~288°C (decomp.), 75 g., (92%). The crude material was recrystallized twice from ethanol to give pure IV, yellow needles, m. p. 292~293°C (decomp.).

Found: C, 64.86; H, 4.87; N, 18.97. Calcd. for $C_{16}H_{14}O_2N_4$: C, 65.29; H, 4.80; N, 19.04%.

Bis-benzenesulfonyl Derivative of IV (V). — The hydrazide (IV, 73 g., 0.25 mol.) and benzenesulfonyl chloride (146 g.) were dissolved in dry pyridine (365 ml.) and the mixture was stirred at 0°C. Gradual deposition of light yellow crystals was observed. After 3 hr., the reaction mixture was allowed to warm up to room temperature and the stirring was continued for further 5 hr. The solid deposited was filtered, washed successively with a small amount of pyridine, diluted hydrochloric acid and water yielding light yellow crystalline powder, m. p. 260~264°C (decomp.), 133 g. (92%). This substance was recrystallized 3 times from pyridine yielding pure V, light yellow fine crystals, m. p. 263~264°C (decomp.).

Found: N, 9.71. Calcd. for $C_{28}H_{22}N_4O_6S_2$: N, 9.75%.

1, 8-Bis-hydroxymethylanthracene (VI). — The methyl este (III, 29.4 g., 0.10 mol.) was placed in a Soxhlet type extractor and extracted with ether (1.4 l.) containing lithium aluminum hydride (3.8 g., 0.10 mol.). The ester III was completely extracted during 4 hr. The reflux was continued for further 3 hr. to complete the reduction. Ethyl acetate (9 ml.) was added to the ice-cooled reduction mixture and the solvent was distilled out. 6 N-Hydrochloric acid (250 ml.) was added to the residue and the insoluble substance was collected, washed successively with diluted hydrochloric acid and water yielding crude VI, light yellow fine needles, m. p. 215~217°C, 23.0 g. (97%). Crystallization from ethanol gave pure VI, light yellow cubes, m. p. 217~218°C.

Found: C, 80.31; H, 5.93. Calcd. for $C_{16}H_{14}O_2$: C, 80.64; H, 5.92%.

IR: 3260 (-OH), 1010 cm^{-1} (C-O), (KBr-disk).

1, 8-Diformylanthracene (VII). — *a) By the Alkaline Decomposition of V.* — A solution of the bis-benzenesulfonyl derivative (V, 11.5 g., 0.02 mol.) in anhydrous ethylene glycol (240 ml.) was heated to 165°C. Finely powdered anhydrous sodium carbonate (25 g.) was added in one portion to the solution accompanying vigorous frothing. After 10 sec., the solution was poured into water (600 ml.) and the precipitate formed was filtered, washed with water yielding yellowish brown solid (1.8 g.). The solid was digested with hot benzene. Concentration of the benzene solution resulted in the crude dialdehyde (VII), yellow needles, m. p. 181~185°C, 0.7 g. (15%). Recrystallization from benzene gave pure VII, m. p. 189~191°C.

Found: C, 81.83; H, 4.29. Calcd. for $C_{16}H_{10}O_2$: C, 82.04; H, 4.30%.

b) By the Oxidation of the Bis-hydroxymethyl Derivative VI. — A solution of VI (4.8 g., 0.02 mol.) in dry pyridine (120 ml.) was added in one portion to an ice-cooled solution of chromium trioxide (16 g., 0.16 mol.) in dry pyridine (160 ml.) and the mixture was shaken. The cooling-bath was removed after 20 min. The mixture was shaken for 2 hr. at room temperature and poured into water. The precipitate formed was filtered, washed with water affording a brown powder (4.4 g.). The powder thus obtained was extracted with benzene (100 ml.) employing Soxhlet type extractor. Evaporation of the solvent gave yellow leaflets, m. p. 187~190°C, 3.5 g. (75%). Recrystallization from benzene yielded pure VII, yellow cubes, m. p. 189~191°C.

Found: C, 82.06; H, 4.29. Calcd. for $C_{16}H_{10}O_2$: C, 82.04; H, 4.30%.

IR: 2710 (-CHO), 1675 cm^{-1} (-C=O), (KBr-disk).

UV $\lambda_{max}^{Tetrahydrofuran}$ $m\mu$ (log ε): 235.5 (4.45), 259.5 (4.87), 330 (3.73), 352 (3.62), 371 (3.77), 397 (3.87), 418 (3.79).

1, 8-Bis (1', 4'-dihydroxybut-2'-ynyl)-anthracene (VIII). — *a) Via 2-(Prop-2'-yn-1'-yloxy)-tetrahydropyran Mercuric Salt.* — The mercuric acetylide of tetrahydropyranyl ether of propargyl alcohol (11.5 g., 0.024 mol.) was prepared according to the method of Johnson[10] was refluxed for 1.5 hr. with an excess of lithium in dry dioxane (120 ml.) in an atmosphere of nitrogen. The solution of the lithium acetylide thus prepared was transferred into another reaction vessel, and was mixed with a solution of the dialdehyde (VII, 0.94 g., 0.004 mol.) in dioxane (50 ml.) and tetrahydrofuran (120 ml.). The mixture was stirred for 4 hr. at 10°C and then 4 N sulfuric acid (100 ml.) was added under ice-cooling. After stirring for 1 hr., the mixture was extracted with benzene (200 ml.), washed successively with saturated solutions of sodium chloride, sodium hydrogen carbonate and sodium chloride, and dried (sodium sulfate). Removal of the solvent under reduced pressure resulted in a dark red oil. Light brown

* All melting points are not corrected.

10) J. R. Johnson and W. L. McEwen, *J. Am. Chem. Soc.*, 48, 469 (1926).

amorphous solid, m. p. ca. 170°C, 0.26 g. (19%) was obtained on addition of benzene (20 ml.) to the dark red oil. This substance was recrystallized 3 times from benzene-methanol to give pure VIII, light yellow leaflets. This material decomposed at ca. 210°C.

Found: C, 75.89; H, 5.24. Calcd. for $C_{22}H_{18}O_4$: C, 76.28; H, 5.24%.

b) By the Method of Metalation with Phenyllithium.—An ethereal solution of phenyllithium (1.66 N, 90 ml.) was added during 20 min. to an ice-cooled solution of tetrahydropyranyl ether of propargyl alcohol (21.0 g., 0.15 mol.) in ether (20 ml.) under nitrogen atmosphere. The mixture was stirred for 30 min. at room temperature, then for 1 hr. under reflux. A solution of the dialdehyde (VII, 7.0 g., 0.03 mol.) in tetrahydrofuran (750 ml.) was added to the ice-cooled mixture and stirred for 4.5 hr. resulting in a dark red solution. At this stage, an aliquot of the reaction mixture gave negative test against carbonyl reagents. 4 N Sulfuric acid (300 ml.) was introduced to the reaction mixture under ice-cooling and the mixture was stirred for 3 hr. at 10°C. The organic layer separated was washed with saturated solutions of sodium chloride, sodium hydrogen carbonate and sodium chloride, successively, and dried over sodium sulfate. Evaporation of the solvent under reduced pressure gave a dark red viscous oil. Benzene (100 ml.) was added to the oil precipitating a light brown amorphous solid, 4.4 g. (42%). The solid was recrystallized twice from tetrahydrofuran-benzene to give pure VIII, m. p. ca. 210°C (decomp.), light yellow leaflets.

Found: C, 76.31; H, 5.24. Calcd. for $C_{22}H_{18}O_4$: C, 76.28; H, 5.24%.

The infrared and ultraviolet spectra were proved to be entirely identical with those of the specimen prepared by the above-mentioned method a).

IR: 3260 (O-H), 1055, 1020 cm^{-1} (C-O) (KBr-disk).

UV $\lambda_{max}^{90\%EtOH}$ mμ (log ε): 254 (5.10), 300† (2.54), 315† (3.05), 329 (3.42), 345 (3.70), 362 (3.88), 381.5 (3.80).

1, 8-Bis-butadiynylanthracene (X).—A mixture of thionyl chloride (5.0 g., 0.042 mol.), dry pyridine (0.5 g., 6 mmol.) and tetrahydrofuran (10 ml.) was added dropwise during 1 hr. to an ice-cooled solution of the tetraol (VIII, 2.10 g., 6 mmol.) in tetrahydrofuran (100 ml.) under stirring. Stirring was continued for 30 min. at the same temperature, for 1.5 hr. at 20°C and finally for 10 min. under reflux. The dark red reaction mixture was concentrated to ca. 20 ml. under reduced pressure in an atmosphere of nitrogen. The solution of the crude tetrachloride thus obtained was added dropwise during 30 min. into a solution of sodium amide (prepared from sodium, 7 g., 0.3 g. atom) in liquid ammonia (250 ml.) at −70°C. After stirring for 2 hr., ammonium chloride (15 g.) was added and the ammonia was allowed to evaporate. The residual solid was repeatedly digested with petroleum benzine (b. p. 60~80°C, total 1.8 l.). The extract was washed with water and dried (sodium sulfate). The solvent was removed under reduced pressure in nitrogen atmosphere resulting in crude crystals, which were dissolved in benzene (40 ml.). The solution was passed through a thin layer of alumina (20 g.). Concentration of the filtrate afforded X, bright yellow fine needles, m. p. ca. 110°C (decomp.), 0.38 g. (23%). Crystallization from benzene-petroleum benzine gave the analytical sample with m. p. ca. 110°C (decomp.).

Found: C, 96.54; H, 3.79. Calcd. for $C_{22}H_{10}$: C, 96.33; H, 3.67%.

IR: 3280 (≡CH), 2200 cm^{-1} (-C≡C-), (KBr-disk).

Electronic spectrum, $\lambda_{max}^{95\%EtOH}$ mμ (log ε): 230.5 (4.13), 262 (5.16), 270.5 (4.71), 287.5 (3.84), 304 (3.90), 320 (4.01), 339† (3.46), 356 (3.75), 374 (4.09), 394 (4.30), 417 (4.30).

The Oxidative Coupling of X.—To a mixture of finely powdered cupric acetate monohydrate (9 g.) and dry pyridine (30 ml.) was added a solution of the tetraacetylene (X, 0.35 g., 0.0013 mol.) in pyridine (10 ml.) and methanol (10 ml.) in one portion at 20°C. The color of the reaction mixture changed immediately to brownish black. The mixture was vigorously shaken for 1 min., and petroleum ether (100 ml.) was added to quench the reaction. The solid formed was filtered, washed with a small amount of petroleum ether and ethanol, and then thororoughly with water. The solid thus obtained was triturated successively with a minor amount of ethanol and benzene yielding reddish black powder (0.18 g.). The substance was digested with chlorobenzene (1.2 l.). The chlorobenzene solution was passed twice through a short column of alumina (15 g.) resulting in deep orange-red filtrate with fluorescence. Concentration of the solution under reduced pressure in an atmosphere of nitrogen resulted in deep red crystals. This was filtered, washed with a small amount of benzene yielding II, deep red fine needles, 0.06 g., (17%). II changed to a brownish black solid at ca. 160°C without fusion.

Found: C, 96.73; H, 3.31. Calcd. for $C_{44}H_{16}$: C, 97.04; H, 2.96%.

IR: 2190, 2140, 2110 cm^{-1} (-C≡C-), (Nujol mull).

Electronic spectrum $\lambda_{max}^{Tetrahydrofuran}$ mμ (log ε): 262 (5.26), 330† (4.41), 380 (4.33), 403† (4.30), 430 (4.53), 462 (4.71), 520 (4.31).

Catalytic Reduction of the Octaacetylene (II).—A suspension of II (0.04 g.) in pure benzene (500 ml.) was shaken in an atmosphere of hydrogen in the presence of 10% palladium-on-charcoal (0.1 g.). The progress of hydrogenation was followed by the change of the electronic spectrum. After 72 hr., no more change in the spectrum was observed. The catalyst was removed by filtration, and washed with benzene (250 ml.). The combined benzene solution was concentrated to 150 ml. and hydrogenated for 24 hr. in the presence of the fresh catalyst (0.05 g.). Further change of the spectrum could not be detected. The catalyst was removed and washed with the same solvent. The solvent was removed under reduced pressure giving light yellow solid. The solid was dissolved in petroleum benzine (10 ml.) and chromatographed on alumina (2.0 g.). Elution with petroleum benzine-benzene (3:1) afforded a light yellow

† Dagger on the figure of the electronic spectral data denotes shoulder.

solution. After concentration of the eluate, a small amout of ethanol was added yielding a faint yellow amorphous substance. A benzene solution (2 ml.) of this substance was passed through a thin layer of alumina (1 g.) and eluted with benzene resulting in a light yellow eluate with blue fluorescence. The most part of the solvent was removed under reduced pressure and a minor quantity of ethanol was added yielding light yellow crystals. Recrystallization from benzene-ethanol gave XI, light yellow fine crystals, m. p. 122~125°C (0.01 g.).

Found: C, 91.27; H, 8.49. Mol. wt., 613 (Rast, in camphor). Calcd. for $C_{44}H_{50}$: C, 91.29; H, 8.71%. Mol. wt., 579.

IR: 2935, 2870, 1470 ($-CH_2-$), 770 (1, 2, 3-trisubstituted benzene), 875 cm^{-1} (1, 2, 4, 5-tetrasubstituted benzene), (KBr-disk).

UV $\lambda_{max}^{Tetrahydrofuran}$ $m\mu$ (log ε): 235 (4.85), 259 (4.55), 284 (3.86), 295 (3.85), 308† (3.69), 327 (2.32), 334† (3.17), 351 (3.27), 369 (3.40), 389 (3.36).

The present study was partly supported by the grant-in-aid of the Ministry of Education, to which grateful acknowledgment is made. The present authors are also indebted to Messrs. Masakazu Okumiya and Osamu Saiki for performing the microanalyses.

Department of Chemistry
Faculty of Science
Osaka University
Nakanoshima, Osaka

Polarographic and Chronopotentiometric Studies on the Dissociation Reaction of Nitrilotriacetatocadmate(II) Complexes

By Nobuyuki TANAKA, Kazuko EBATA, Tomoo TAKAHARI* and Tsutomi KUMAGAI**

(Received July 17, 1962)

The kinetic current due to the dissociation of nitrilotriacetatocadmate(II) complexes has been investigated by several researchers[1-4]. In early works, however, the effect of acetate ion on the kinetic current was not taken into consideration, though the measurements were made in acetic acid - sodium acetate buffer solutions. Koryta[4] was the first to consider this effect and to assume the kinetic current as due to the reduction of the free (hydrated) ions and acetato complexes of cadmium. Similar treatments of the effect of acetate and/or other coexisting ions have been approved when applied to the equilibrium and kinetic studies on the substitution or complex-forming reactions in solutions.

Since the application of the treatment to the kinetic current has not been proved, it seems worth while to investigate the dissociation reaction of nitrilotriacetatocadmate(II) in the presence and absence of acetate ions. Because of the limitations of polarographic and chronopotentiometric methods, the reaction rate was determined polarographically in the presence of acetate and chronopotentiometrically in the absence of acetate.

Experimental

Reagents. — A standard solution of cadmium nitrate was obtained by the same procedure as reported previously[5]. A stock solution of disodium nitrilotriacetate (NTA) was prepared from the commercial nitrilotriacetic acid, the concentration of which was determined against the standardized copper(II) nitrate solution by amperometric titration with a dropping mercury electrode. All chemicals used were of analytical reagent grade and all solutions were prepared with redistilled water.

Apparatus and Procedure. — Polarographic current-voltage curves were obtained with a Yanagimoto pen-recording polarograph (Polarorecorder Model PR-2 with an automatic potential scanner) and a dropping mercury electrode. The measurements were carried out in solutions containing 0.4 mM of cadmium nitrate, 0.01 M of NTA and 0.05 M of sodium acetate - acetic acid buffers. The

* Present address: Tokyo Research Institute, Yawata Iron and Steel Co., Ltd., Ida, Kawasaki.
** Present address: Research Laboratory, Sony Corp., Fujitsuka-cho, Hodogaya, Yokohama.

1) J. Koryta, Sbornik Mezinarod. Polarog. Sjezdu Praze, 1st Congr., 1951, Part I., p. 798.
2) K. Morinaga and T. Nomura, *J. Chem. Soc. Japan, Pure Chem. Sec.* (*Nippon Kagaku Zassi*), **79**, 200 (1958).
3) P. Papoff, *J. Am. Chem. Soc.*, **81**, 3254 (1958).
4) J. Koryta, *Collection Czechoslov. Chem. Communs.*, **24**, 3057 (1959).
5) N. Tanaka, M. Kamada, H. Osawa and G. Satô, This Bulletin, **33**, 1412 (1960).

ionic strength was adjusted to be 0.2 with potassium nitrate. The pH of the solution was measured, immediately after the measurement of the current-voltage curve, with a Hitachi EHP-1 pH meter with a glass electrode.

For chronopotentiometric study, an apparatus similar to that reported in the previous paper[6] was used. The hanging mercury drop electrode served as a cathode and a saturated calomel electrode with a large surface area (SCE) as an anode. Controlled electrolysis current was supplied by five 90 V. dry cells connected in series and resistors of 0.1 to 100 megohms. The electrolysis current was measured by means of a standard resistance and potentiometer. The potential difference between the working electrode and the SCE was fed to the Y-axis of a cathode-ray oscillograph (Toshiba ST-1747A) through a direct-current preamplifier. The alternating voltage of 100 to 1000 cycles/sec. from an oscillator (Yokogawa OV 21 A) was supplied for the beam modulation. Thus, chronopotentiograms were obtained as dotted curves as shown in Fig. 1, of which the transition

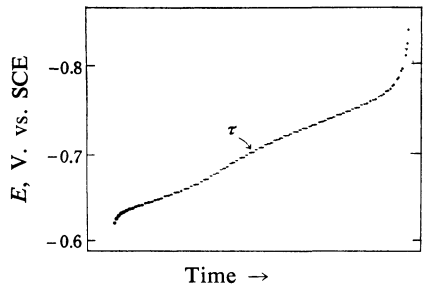


Fig. 1. Chronopotentiogram of Cd(II)-NTA complex. $[Cd^{2+}]_t$, 1.04 mM; $[NTA]_t$, 0.0202 M; pH, 3.19; μ, 0.2 (KNO_3); current density, 5.25 μamp./mm^2; surface area, 3.65 mm^2. The interval of every two dots corresponds to 1/140 sec.

time was determined by counting the number of dots. The measurements of chronopotentiograms were made with the solutions containing 1.04 mM of cadmium nitrate and 0.0202 M of NTA. The ionic strength was adjusted to be 0.2 with potassium nitarte and the pH, to be of an appropriate value between 2.8 and 3.4 with nitric acid. In this range of pH's, nitrilotriacetate itself served as a buffer. All chronopotentiometric measurements were carried out at 25°C.

Results

a) Polarographic Study. — In acetate buffer solution of an appropriate pH containing NTA in excess, cadmium(II) gave a doublet wave. As has been reported previously[1-4], the first wave is kinetic in nature and considered as due to the reduction of cadmium(II) which is dissociated from Cd(II)-NTA complex. The over-all electrode reaction at the dropping mercury electrode is written as

$$CdX^- + jH^+ \overset{k_j}{\rightleftharpoons} Cd^{2+} + H_jX^{(3-j)-} \quad (j=0, 1, \cdots\cdots, n) \tag{1}$$

$$Cd^{2+} + OAc^- \rightleftharpoons CdOAc^+ \tag{2}$$

$$\left\{\begin{matrix} Cd^{2+} \\ \uparrow\downarrow \\ CdOAc^+ \end{matrix}\right\} + 2e + Hg \rightleftharpoons \left\{\begin{matrix} Cd(Hg) \\ Cd(Hg) + OAc^- \end{matrix}\right\} \tag{3}$$

where X^{3-} denotes a tervalent NTA anion and k_j the rate constant of the dissociation reaction given by Eq. 1. Assuming that reactions 2 and 3 are rapid enough to attain the equilibria and that the hydrated ions and the acetato complex ions of cadmium are both reduced at the potentials under consideration where the Cd(II)-NTA complexes are not reduced, the following equation is derived according to Koryta[4],

$$\frac{\bar{i}_l}{\bar{i}_d - \bar{i}_l} = 0.886\sqrt{\frac{kK_{CdX}[X^{3-}]t_d}{1+K_{CdOAc}[OAc^-]}} \tag{4}$$

$$k = \sum_{j=0}^{n} k_j [H^+]^j$$

where $\bar{i}_l$ and $\bar{i}_d$ mean the kinetic current and the hypothetical diffusion current of total electro-inactive species respectively, K_{CdOAc} and K_{CdX} the formation constants of $CdOAc^+$ and CdX^- respectively, and t_d the drop time. Equation 4 holds only when NTA exists in a large excess over cadmium(II) in the solution.

The rate constants were calculated with the observed values of $\bar{i}_l$ at various pH's using Eq. 4. The concentration of X^{3-} at the given hydrogen ion concentration was calculated with the total concentration ($[NTA]_t$) and the dissociation constants of NTA. The values of $10^{-1.89}$, $10^{-2.49}$ and $10^{-9.73}$ were used for the first, second and third dissociation constants, respectively, which were determined by Schwarzenbach et al.[7] at 20°C and 0.1 ionic strength. For the formation constants of CdX^- and $CdOAc^+$, $10^{9.83}$(K_{CdX}) obtained by Schwarzenbach et al.[7] and 16(K_{CdOAc}) determined in this laboratory[5] were used, respectively.

In Fig. 2, the rate constants at 5, 15 and 25°C are plotted against hydrogen ion concentration. Those linear plots clearly indicate that the rate constants can be expressed as linear functions of hydrogen ion concentration as shown in Table I, where the rate constants obtained by other researchers are also given. Our values at 25°C may be compared with those by Koryta, though the experimental

6) T. Murayama, *Sci. Repts. Tohoku Univ. Ser. I*, **45**, 84 (1961).

7) G. Schwarzenbach, H. Anderegg, W. Schneider and H. Senn, *Helv. Chim. Acta*, **38**, 1147 (1955).

TABLE I. THE DISSOCIATION RATE CONSTANTS OF Cd(II)-NTA COMPLEX OBTAINED POLAROGRAPHICALLY IN ACETATE BUFFER SOLUTIONS

Conditions for measurement			Rate constants sec^{-1}	Investigators
Temp., °C	pH range	Ionic strength		
25	5.3~5.9	0.2	$3.4+2.5\times10^5[H^+]$	The present authors
15	5.2~5.8	0.2	$1.5+0.4\times10^5[H^+]$	
5	5.2~5.8	0.2	$0.64+0.2\times10^5[H^+]$	
25	4.5~6.0	0.1	$1.6+3.0\times10^5[H^+]$	Koryta[4]
25	4.6~5.7	3	$(1.5\pm0.3)\times10^6[H^+]$	Papoff[3]
25		0.3	$(1.3\pm0.3)\times10^6[H^+]$	
25	4.2~4.9	0.1	$(6.5\pm1.7)\times10^4[H^+]$	Morinaga et al.[2]

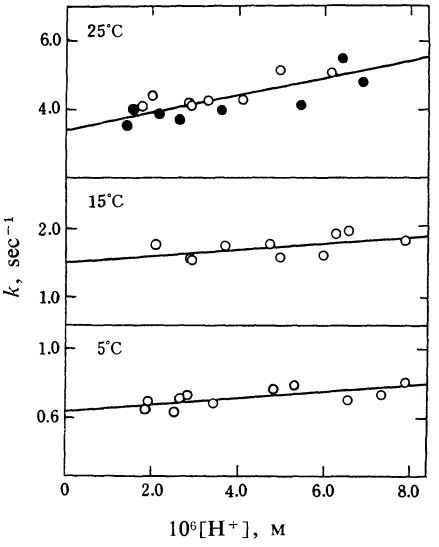


Fig. 2. Dissociation rate constants as a function of hydrogen ion concentration at various temperatures. $[Cd^{2+}]_t$, 0.4 mM; $[NTA]_t$, 0.01 M; $[OAc^-]$, 0.05 M; μ, 0.2 (KNO_3). ○ 1st run, ● 2nd run.

conditions and the values of various constants used in the calculation are not the same.

b) Chronopotentiometric Study. — Chronopotentiometric potential-time curves were obtained with the solutions of pH 2.8 to 3.4 in the absence of acetate. An example of those curves is given in Fig. 1, which shows the separation of two steps to be ambiguous. Therefore, the transition time was determined by measuring the time that was required for the given change in potential from the beginning of electrolysis. Such a potential change was not the same at different pH's and, consequently, was determined preliminarily at every pH with the chronopotentiogram which is relatively well-defined. Examples of the transition times obtained at varied current densities are given in Table II.

TABLE II. EXAMPLES OF CHRONOPOTENTIOMETRIC MEASUREMENTS

$Cd(NO_3)_2$ 1.04 mM; NTA 0.0202 M; pH 3.12; ionic strength 0.2; 25°C

i_0, μamp./mm²	τ, sec.	$i_0\tau^{1/2}$
4.06	0.68_0	3.3_5
5.23	0.36_5	3.1_6
5.74	0.25_5	2.9_0
7.02	0.15_2	2.7_4
8.65	0.09_0	2.6_0
9.30	0.07_3	2.5_1

The relation between the transition time and the current density for the electrochemical reaction which is preceded by a first order chemical reaction was derived first by Delahay and Berzins[8] for a linear diffusion and later by Murayama[6] for a spherical diffusion. Although the measurements were made with the hanging mercury drop electrode, the observed values of transition time were not accurate enough for the Murayama's rigorous treatment. In this study, therefore, the equation derived by Delahay and Berzins for a linear diffusion was employed.

When NTA is present in the solution in a large excess over cadmium(II), the relation,

$$i_0\tau^{1/2}=\pi^{1/2}FD^{1/2}[Cd^{2+}]_t - \frac{\pi^{1/2}K_{CdX}[X^{3-}]}{2k^{1/2}(1+K_{CdX}[X^{3-}])^{1/2}}i_0 \qquad (5)$$

holds, where i_0 is the current density, τ the transition time for the reduction of free cadmium ion, F the Faraday, D the common value of the diffusion coefficients of various species which are assumed to be equal, and $[Cd^{2+}]_t$ the total concentration of cadmium. Equation 5 indicates that the plot of $i_0\tau^{1/2}$ against i_0 should give a straight line with a negative slope. In Fig. 3, the values of $i_0\tau^{1/2}$ calculated with the observed transition times at pH 2.99 and 3.35 are plotted against current

8) P. Delahay and T. Berzins, *J. Am. Chem. Soc.*, 75, 2486 (1953).

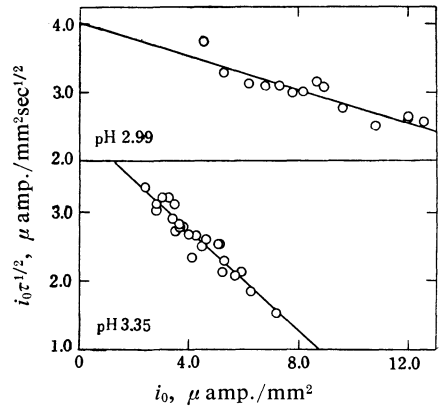


Fig. 3. $i_0\tau^{1/2}$ as a function of i_0 at various pH's.

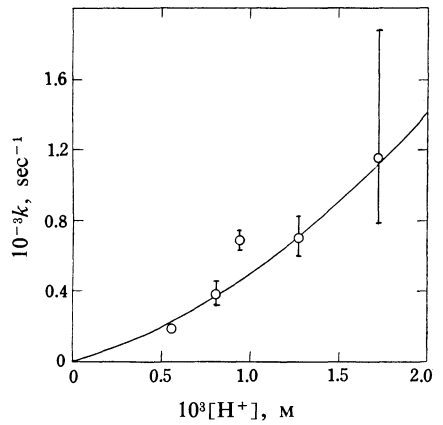


Fig. 4. Dependence of the dissociation rate constant on the hydrogen ion concentration. The solid curve represents the relation, $k=3\times10^5[H^+]+2\times10^8[H^+]^2$.

density. The negative slopes of those plots clearly indicate that the electrode processes are kinetic in nature. The rate constants at various pH's were calculated from the slopes, and are plotted against hydrogen ion concentration with the standard deviation (Fig. 4). The solid curve in Fig. 4 represents a relation given by the equation,

$$k=3\times10^5[H^+]+2\times10^8[H^+]^2 \qquad (6)$$

At lower pH's the contribution of the term independent of the hydrogen ion concentration is so small compared to other terms that it can be hardly determined.

Discussions

Inaccuracy of the present chronopotentiometric measurement is due to mainly the fact that the reduction potentials for hydrated ion and NTA complex of cadmium are not sufficiently separated. In addition, the chronopotentiogram of cadmium is considerably affected by the presence of surface-active substance, and this may be another cause of the inaccuracy of the measurement. Murayama[6] reported that the presence of 0.001% gelatin decreased the transition time and deteriorated the shape of the chronopotentiogram of hydrated cadmium ion. In the present experiment, redistilled water was used and no surface-active substance was added, but an effect of aging of the hanging mercury drop electrode was clearly observed. Transition time was measured as a function of time after the formation of a mercury drop (θ) and the values of $i_0\tau^{1/2}$ were plotted against θ (Fig. 5). Those linear plots in Fig. 5 suggest that an abrupt decrease in $i_0\tau^{1/2}$ in the region of small values of θ would be most unlikely.

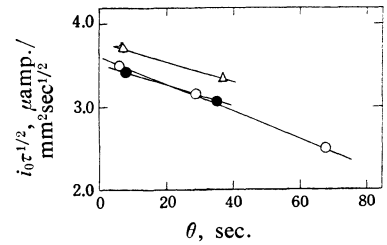


Fig. 5. Variations of $i_0\tau^{1/2}$ with θ.
-△-△-, pH 3.19 and i_0 3.64 μamp./mm^2;
-○-○-, pH 3.12 and i_0 4.06 μamp./mm^2;
-●-●-, pH 2.86 and i_0 5.87 μamp./mm^2.

The over-all rate constant k obtained from the kinetic current was a linear function of the hydrogen ion concentration. The chronopotentiometric study, on the other hand, showed that at lower pH's the over-all rate involves a second-order term with respect to the hydrogen ion concentration. The first-term of Eq. 6 obtained by the chronopotentiometric method, $3\times10^{-5}[H^+]$, is in good agreement with the values obtained polarographically by the authors and by Koryta (see Table I). This proves clearly that the Koryta's treatment of the effect of acetate ion on the kinetic current is appropriate.

In conclusion, the rate constant of the dissociation of Cd(II)-NTA complex is a function of hydrogen ion concentration, and expressed as

$$k=3.4+2.5\times10^5[H^+]+2\times10^8[H^+]^2$$

at 25°C, from the results obtained polarographically and those obtained chronopotentiometrically. The dissociation reaction, therefore, is considered to proceed through three simultaneous reaction paths,

$$CdX^- \rightarrow Cd^{2+}+X^{3-}$$
$$CdX^-+H^+ \rightarrow Cd^{2+}+HX^{2-}$$
$$CdX^-+2H^+ \rightarrow Cd^{2+}+H_2X^-$$

Summary

The dissociation reaction of nitrilotriacetatocadmate(II) complexes has been investigated polarographically and chronopotentiometrically in the presence and the absence of acetate ions. The results indicate that the treatment reported by Koryta for the effect of acetate ion on the kinetic current is appropriate.

The rate constant of the dissociation reaction of nitrilotriacetatocadmate(II) complexes is a function of hydrogen ion concentration and expressed as

$$k = 3.4 + 2.5 \times 10^5 [H^+] + 2 \times 10^8 [H^+]^2$$

at 25°C.

The authors thank the Ministry of Education for the financial support granted for this research.

Department of Chemistry
Faculty of Science
Tohoku University
Katahira-cho, Sendai

*Preparation of Some Tricyclohexylsilyl Derivatives**

By Motonori KANAZASHI and Michio TAKAKURA

(Received July 25, 1962)

Preparation of organosilicon compounds containing cyclohexyl groups has been studied by several workers[1-5] from a viewpoint of steric effect. Nebergall and Johnson[3] synthesized a wide variety of tricyclohexylsilyl compounds through the reaction of cyclohexyllithium with silicon tetrachloride. Lately it was reported by Eaborn[4] and Petrov[5] that the use of silicon tetrafluoride or fluorosilanes was more effective than that of silicon tetrachloride in the reaction. However, substitution or condensation reaction of a compound carrying two or three bulky cyclohexyl groups has an unavoidable difficulty in approaching of a reagent. We overcame the difficulty and prepared tetracyclohexylsilane and three cyclohexylmethylsilanes by hydrogenation of the corresponding phenyl-silicon compounds[1].

Hexacyclohexyldisilane was not obtained by the reaction of tricyclohexylchlorosilane with metallic sodium[3], whereas the corresponding digermane was obtained by a similar treatment[6]. It has been also reported by Nebergall and Johnson[3] that the hydrolysis product of chlorosilane was tricyclohexylsilanol, m. p. 177°C. The compound reported by Jenkins and Post[7] as "probably hexacyclohexyldisiloxane", m. p. 178°C, seems to be the same compound.

In the present paper hydrogenations of hexaphenyldisilane, hexaphenyldisiloxane and triphenylsilanol are reported.

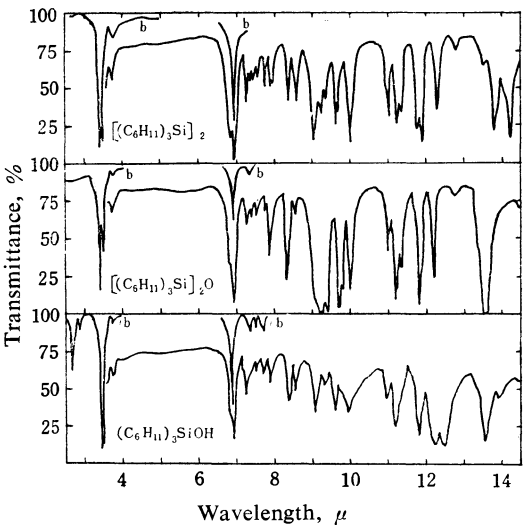


Fig. 1 (A). Infrared spectra of cyclohexyl-compounds.
(a) Absorption bands of Nujol appear at 3.4~3.5, 6.80 and 7.23 μ.
(b) Parts of spectra obtained with CCl_4 soluare shown by curve b.

* This work was presented at the 9th Annual Meeting of the Chemical Society of Japan, Kyoto, April, 1956.

1) The first paper of this series, M. Kanazashi and M. Takakusa, This Bulletin, **27**, 441 (1954).

2) N. W. Cusa and F. S. Kipping, *J. Chem. Soc.*, **1933**, 1040.

3) W. H. Nebergall and O. H. Johnson, *J. Am. Chem. Soc.*, **71**, 4022 (1949).

4) C. Eaborn, *J. Chem. Soc.*, **1952**, 2840.

5) A. D. Petrov and T. I. Chernysheva, *Zhur. Obshcheĭ* Khim., **24**, 1189 (1954).

6) O. H. Johnson and W. H. Nebergall, *J. Am. Chem. Soc.*, **70**, 1706 (1948).

7) J. W. Jenkins and H. W. Post, *J. Org. Chem.*, **15**, 556 (1950).

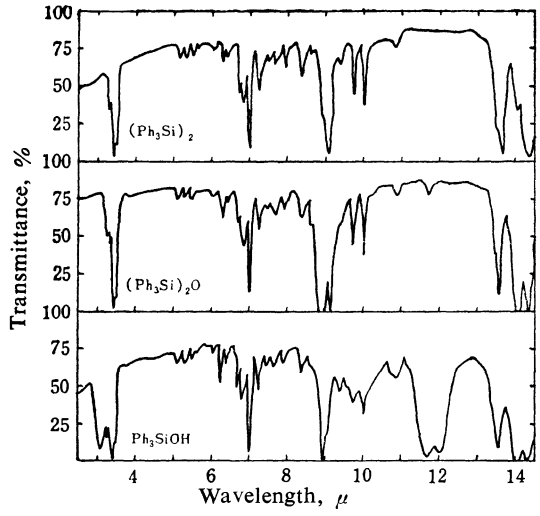


Fig. 1 (B). Infrared spectra of phenyl-silicon compounds measured in Nujol mull.

Each compound absorbed the calculated amount of hydrogen, and hexacyclohexyldisilane, m. p. 351°C, hexacyclohexyldisiloxane, m. p. 308°C, and tricyclohexylsilanol, m. p. 177°C, were obtained. As was expected, hydrogenation of triphenylsilanol proceeded more smoothly than those of tetraphenylsilane, hexaphenyldisilane and hexaphenyldisiloxane.

The infrared spectra of the hydrogenation products show none of the absorption bands associated with the phenyl group or phenyl-silicon bond but, instead, clearly show the strong bands characteristic to the cyclohexyl group at 10.0, 11.2 and 11.8 μ[8].

Experimental

All melting points and boiling points are uncorrected.

Hexaphenyldisilane. —Triphenylchlorosilane was treated with sodium in xylene solution at reflux temperature. The precipitate was washed with benzene, treated with methanol, and then washed with hot water and methanol, to give hexaphenyldisilane, m. p. 342~350°C.

Hexaphenyldisiloxane. — Triphenylchlorosilane was hydrolyzed in aqueous ethanol by refluxing for thirty hours with a small amount of hydrochloric acid. The precipitate of hexaphenyldisiloxane was washed with benzene repeatedly and recrystallized. M. p. 221~222.5°C.

Triphenylsilanol.—Hydrolysis of triphenylchlorosilane was carried out in neutral acetone solution. Recrystallization from petroleum ether (50~70°) of triphenylsilanol thus obtained gave white crystals melting at 152°C.

Methylcyclohexane. — Methylcyclohexane was dried over calcium chloride and fractionated through a 30 cm. column packed with single turn helices. B. p. 98~98.5°C.

Raney Nickel Catalyst.—The catalyst was prepared from Raney nickel alloy (Ni content, 42%) in the same way as reported in a previous paper[1]. It was kept under absolute alcohol in a refrigerator, and the alcohol was substituted by methylcyclohexane before use.

Hydrogenation. — A sample in about 50 cc. of methylcyclohexane was hydrogenated in a stainless steel autoclave (capacity, 100 cc.) equipped with a magnetic inner agitator. The initial hydrogen pressure was 100~110 atm., and the conditions are listed in Table I.

Separation of Products. Disilane (Table I, No. 1).—A solid part was separated from the reaction mixture, and the solid was extracted with about 500 cc. of cyclohexane. Recrystallization of a white material, 1.7 g., obtained from the extract gave 0.8 g. of hexacyclohexyldisilane, m. p. 339~343°C. The melting point of hexacyclohexyldisilane was raised to 349~351.5°C by recrystallization from cyclohexane-petroleum ether (9 : 1).

Found: C, 78.04, 78.09; H, 11.86, 11.75; mol. wt. (Rast), 539~559. Calcd. for $C_{36}H_{66}Si_2$: C, 77.90; H, 11.99%; mol. wt., 555.

From the liquid part of the reaction mixture an additional 2.4 g. of hexacyclohexyldisilane was obtained. The solvent recovered was carefully fractionated, but cyclohexane was not detected; the fact shows that silicon-carbon cleavage did not occur during the course of hydrogenation. Another run carried out under forced conditions gave also hexacyclohexyldisilane as a sole product.

TABLE I. HYDROGENATION CONDITIONS

Exp. No.	Material	g.	Catalyst[a] g.	Reaction temp. °C	Hydrogen[c] absorbed l.	Hydrogen[c] calcd. l.
1	Ph_6Si_2	9.35	12~15	110~200	7.7	7.3
2	Ph_6Si_2O	8.0	4	110~160	6.0	6.1
3	Ph_3SiOH	6.9	5	100~130[b]	4.9	5.0

a) The catalyst was added in 3~5 portions.
b) The reaction started at 70~80°C.
c) The initial pressure of hydrogen was 100~110 atm.

8) A study on the infrared spectra of organosilicon compounds containing cyclohexyl groups was presented at the Fall Meeting of the Chemical Society of Japan in 1956 by T. Yoshimoto and M. Takakusa; the paper will be published shortly.

Disiloxane (Table I, No. 2). — From the solid part of the reaction mixture, there was obtained 3.1 g. of crude material melting at 300～308°C. Recrystallizations from cyclohexane-ethanol and from petroleum ether gave 0.95 g. of hexacyclohexyldisiloxane, m. p. 305～308°C. Further recrystallization from petroleum ether, carbon tetrachloride or benzene did not raise the melting point.

Found: C, 76.22, 76.41, 76.44; H, 11.65, 11.75, 11.69; mol. wt. (Rast), 558～592, 575. Calcd. for $C_{36}H_{66}OSi_2$: C, 75.71; H, 11.65%; mol. wt., 571.

From the liquid part, 1.6 g. of hexacyclohexyldisiloxane was separated. Cyclohexane was not detected in the recovered reaction solvent.

Silanol (Table I, No. 3). — By a similar treatment, 6.2 g. of tricyclohexylsilanol was obtained from the reaction mixture. M. p. 174～176°C. Duplicated recrystallization from petroleum ether raised the melting point to 176～177°C (Reported[3], 177°C).

Found: C, 73.50, 73.57; H, 11.81, 11.78. Calcd. for $C_{18}H_{34}OSi$: C, 73.40; H, 11.64%.

Infrared Spectra.—The absorption spectra were measured in Nujol mull and in carbon tetrachloride solution with a Shimadzu AR-275-I infrared spectrophotometer equipped with a sodium chloride prism. Solubility in carbon tetrachloride of hexacyclohexyldisilane (less than 1%) or hexacyclohexyldisiloxane (ca. 2%) was not sufficient to give good spectra.

Summary

Hydrogenations of hexaphenyldisilane, hexaphenyldisiloxane and triphenylsilanol were carried out in the presence of Raney nickel catalyst (W-6), and hexacyclohexyldisilane**, hexacyclohexyldisiloxane** and tricyclohexylsilanol were obtained (41, 56, 84%, respectively). Infrared spectra of the products and the starting materials were measured.

The authors are grateful to Dr. Toshio Yoshimoto for valuable suggestions in the analysis of the infrared spectra of the compounds.

Electrotechnical Laboratory
Agency of Industrial
Science and Technology
Kitatama-gun, Tokyo

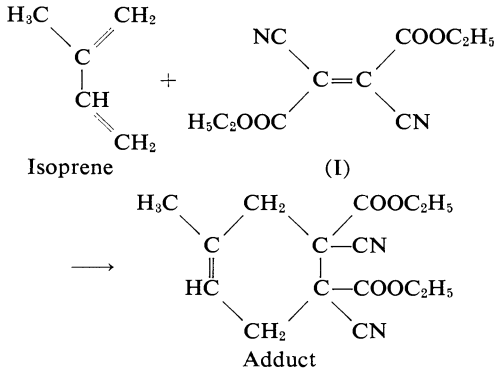
** New compounds.

Studies on trans-Dicyanodiethoxycarbonylethylene. III. Diels-Alder Reaction

By Ken-ichi KUDO

(Received July 31, 1962)

Knowledge in various addition reactions of tetracyanoethylene[1] and the properties of *trans*-dicyanodiethoxycarbonylethylene (I) described in the previous papers[2] suggest that I might also undergo Diels-Alder additions with conjugated dienes with unusual ease. However, such vigorous and exothermic reactions as expected were not observed in the additions of I with conjugated dienes. Namely, the addition of I with cyclopentadiene proceeded in tetrahydrofuran slowly at room temperature. Furthermore, to obtain a condensation product of I with butadiene or isoprene, it was necessary to heat them in an autoclave under pressure at 180~190°C for several hours.



In the reaction with cyclopentadiene, the reaction mixture showed a transient yellow color, which would be attributed to the formation of a π-complex between I and cyclopentadiene.

The proposed structures of the adducts were supported by the infrared absorption spectra and the elemental analyses.

Experimental

Adduct with Isoprene. — A mixture of 4 g. (0.06 mol.) of isoprene and 13 g. (0.06 mol.) of I in

1) W. J. Middleton et al., *J. Am. Chem. Soc.*, **80**, 2783 (1958).
2) Parts I and II: K Kudo, This Bulletin, **35**, 1490, 1730 (1962).

100 ml. of benzene was heated in an autoclave at 180～188°C for 5 hr. After cooling, benzene was removed by vacuum distillation to obtain the syrupy residue which changed to crystals. The crystals were collected by filtration, washed with benzene-petroleum benzine, and recrystallized to give 17 g. (100%) of 1-methyl-4,5-dicyano-4,5-diethoxycarbonylcyclohexene, m. p. 77～79°C, as colorless crystals.

Found: C, 62.30; H, 6.36; N, 9.73. Calcd. for $C_{15}H_{18}O_4N_2$: C, 62.05; H, 6.25; N, 9.65%.

Its infrared absorption spectrum had bands at 2252 cm^{-1} (C≡N) and at 1761 cm^{-1} (C=O).

Adduct with Butadiene. — A mixture of 13 g. (0.06 mol.) of I and 100 ml. of benzene in a flask was chilled to −40°C. The flask was tarred, charged with 3.2 g. (0.06 mol.) of butadiene by distillation, and placed in an autoclave. The mixture was heated at 170～190°C for 5 hr. After cooling, benzene was removed by distillation and the residue solidified. After recrystallization from benzene-petroleum benzine, there was obtained 11 g. (70%) of 4,5-dicyano-4,5-diethoxycarbonylcyclohexene, m. p. 109～110°C, as colorless crystals.

Found: C, 61.11; H, 5.76; N, 10.15. Calcd. for $C_{14}H_{16}O_4N_2$: C, 60.86; H, 5.84; N, 10.14%.

Its infrared absorption spectrum had a C≡N band at 2247 cm^{-1} and a C=O band at 1757 cm^{-1}.

Adduct with Cyclopentadiene. — A mixture of 6.5 g. (0.03 mol.) of I and 20 ml. of tetrahydrofuran in a flask was chilled to 0°C. The flask was tarred, charged with 2.3 g. (0.03 mol.) of cyclopentadiene by distillation, capped, and allowed to stand at room temperature for 24 hr. The mixture was evaporated to expel benzene at room temperature and the residue crystallized to give 8 g. (90%) of the adduct, m. p. 70～71°C, as colorless crystals.

Found: C, 62.40; H, 5.34; N, 9.52. Calcd. for $C_{15}H_{16}O_4N_2$: C, 62.49; H, 5.59; N, 9.72%.

Its infrared absorption spectrum had a C≡N band at 2247 cm^{-1} and a C=O band at 1761 cm^{-1}.

Adduct with Anthracene. — A mixture of 13 g. (0.06 mol.) of I and 8 g. (0.06 mol.) of anthracene was heated at 130～150°C for 5 min. After cooling, the mixture was crystallized by trituration with acetone to give 12 g. (57%) of the adduct, m. p. 168～169°C, as colorless crystals.

Found: C, 72.20; H, 5.01; N, 7.37. Calcd. for $C_{24}H_{20}O_4N_2$: C, 71.98; H, 5.03; N, 7.00%.

Its infrared absorption spectrum had a C≡N band at 2242 cm^{-1} and a C=O band at 1764 cm^{-1}.

The author wishes to express profound gratitude to Professor Risaburo Nakai of the Institute for Chemical Research of Kyoto University for his cordial encouragement and direction throughout this work. He also desires to give sincere thanks to Professor Ryozo Goto of Kyoto University for his invaluable advice and criticism throughout the investigation.

Institute for Chemical Research
Kyoto University
Takatsuki, Osaka

New Addition Reactions. IV. The Addition of Schiff Bases to Diketene

By Ryohei ODA, Shunichi TAKASHIMA and Masaya OKANO

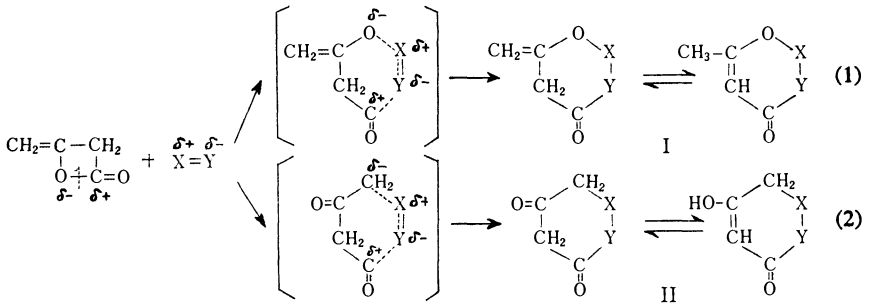
(Received August 13, 1962)

For the cyclic addition of unsaturated components to diketene, two possible paths may be considered.

The type 1 reaction including the reaction of diketene with ketones[1], carbodiimides[2] and enamines[3], and the formation of dimeric dehydroacetic acid[4] are already known, but examples of the type 2 addition have not been reported. We wish to report the formation of type II adduct by the reaction of diketene with some Schiff bases.

Treatment of diketene with *N*-benzylidene-*t*-butylamine in chloroform gave a cyclic adduct, 1-*t*-butyl-6-phenyl-2, 4-piperidinedione (III), in an excellent yield. The structural assignment was made on the basis of its elementary analysis, infrared spectrum, dinitrophenylhydrazone formation, and a positive ferric chloride test. No evidence for the formation of a type I adduct was observed. Similar reactions with *N*-methylene-*t*-butylamine and *N*-methylenecyclohexylamine also gave the corresponding piperidinediones, but the yields were very low. In the spectra (Nujol) of all adducts obtained, two sharp bands at 1700～1725 cm^{-1} (keto CO) and 1633～1650 cm^{-1} (lactam CO) regions, along with two other bands (conjugated C=C, 1550 cm^{-1} and OH,

1) M. F. Carroll and A. R. Bader, *J. Am. Chem. Soc.*, **75**, 5400 (1953).
2) R. N. Lacey and W. R. Ward, *J. Chem. Soc.*, **1958**, 2134.
3) B. B. Millward, *J. Chem., Soc.*. **1960**, 26; S. Hünig, E. Benzing and K. Hübner, *Chem. Ber.*, **94**, 486 (1961).
4) A. B. Boese, Jr., *Ind. Eng. Chem.*, **32**, 21 (1940); T. Isozima, *J. Chem. Soc. Japan, Ind. Chem. Sec.* (*Kogyo Kagaku Zassi*), **57**, 773 (1954).



3290～3300 cm^{-1}) assigned to the enolic structure of II, were observed.

In cases where *N*-benzylideneaniline and *N*-benzylidenecyclohexylamine were used as Schiff bases, the desired adduct could not be isolated from the resinous reaction mixtures. On the other hand, when diketene was treated with *N*-isopropylidenecyclohexylamine, the formation of a polymer of diketene was observed. Its melting point and infrared spectrum were essentially in accord with those of a polyester obtained by the aluminum isopropoxide-[5] or potassium *t*-butoxide-[6]catalyzed polymerizations of diketene.

The failure of the desired cyclization appears to depend largely on the nature of the Schiff base used, especially its degree of dimerization or trimerization[7], its basicity and its bulkiness; but a detailed explanation is not possible at the present time.

Experimental[8]

1-*t*-Butyl-6-phenyl-2, 4-piperidinedione (III).—A mixture of 30 g. (0.19 mol.) of *N*-benzylidene-*t*-butylamine (prepared by the procedure of Emmons[9]) and 17 g. (0.19 mol.) of diketene in 100 ml. of chloroform was refluxed for 5 hr. After removal of the solvent, there was obtained 37 g. (80%) of crude 1-*t*-butyl-6-phenyl-2,4-piperidinedione. Recrystallization from benzene gave the pure product which melted at 108～109°C. This adduct gave a dark-red color with ethanolic ferric chloride on standing for several hours.

Found: C, 73.68; H, 7.85; N, 5.53. Calcd. for $C_{15}H_{19}NO_2$: C, 73.34; H, 7.81; N, 5.71%.

The 2,4-dinitrophenylhydrazone after recrystallization from ethanol melted at 230°C with decomposition.

Found: C, 59.23; H, 5.61; N, 16.24. Calcd. for $C_{21}H_{24}N_5O_5$: C, 59.14; H, 5.67; N, 16.42%.

1-*t*-Butyl-2, 4-piperidinedione.—To a stirred solution of 6 g. (0.07 mol.) of freshly distilled *N*-methylene *t*-butylamine[9] in 100 ml. of ether was added slowly 6.7 g. (0.08 mol.) of diketene at room temperature. After completion of the addition, the mixture was heated at 30°C for 3 hr. The resultant precipitate was collected, and weighed 1 g. (8%). An analytical sample was obtained by recrystallization from benzene, m. p. 159～160°C.

Found: C, 63.87; H, 9.23; N, 8.52. Calcd. for $C_9H_{15}NO_2$: C, 63.88; H, 8.94; N, 8.28%.

1-Cyclohexyl-2, 4-piperidinedione.—A mixture of 11 g. (0.10 mol.) of *N*-methylenecyclohexylamine[10] and 300 ml. of ether was stirred and cooled to −15°C, 25 g. (0.30 mol.) of diketene was added dropwise to this solution at such a rate so as to maintain that temperature. After the addition of diketene, the stirring was continued at the same temperature for 1 hr. and at 0°C for 5 hr. The tar-like product that separated was extracted with petroleum ether. Removal of the solvent by distillation gave 0.5 g. (3%) of the crude adduct. After one recrystallization from toluene, the adduct melted at 182～186°C. The analysis was somewhat unsatisfactory, but the infrared spectrum was quite similar to that of III.

Found: C, 66.75; H, 9.04; N, 7.14. Calcd. for $C_{11}H_{17}NO_2$: C, 67.66; H, 8.78; N, 7.17%.

The authors wish to express their gratitude to Dainippon Celluloid Co., Ltd., for the gift of diketene.

Department of Synthetic Chemistry
Faculty of Engineering
Kyoto University
Sakyo-ku, Kyoto (R. O. & S. T.)

Institute for Chemical Research
Kyoto University
Takatsuki-shi, Osaka (M. O.)

5) J. Furukawa et al., ibid., 65, 254 (1962).
6) Our data, unpublished.
7) Cf. M. M. Sprung, *Chem. Revs.*, 26, 311 (1940).
8) All temperatures are uncorrected.
9) W. D. Emmons *J. Am. Chem. Soc.*, 79, 5748 (1957).
10) J. Graymove, *J. Chem. Soc.*, 1947, 1118.

Study on Unimolecular Decomposition of Excited Olefin Ions

By Itiro OMURA

(Received June 29, 1962)

Since Eyring and his co-workers[1] first used statistical theory in the interpretation of the mass spectra of polyatomic molecules, several authors[2-5] have reported applications of the theory. They have adopted some alkanes, esters as well as aliphatic alcohols, and discussed mass spectra, appearance potentials, yields of fragment ions, frequency factors, decomposition processes and such other things. The present author reported in a previous paper[6] on his experimental results concerning the mass spectra of some paraffins and olefins and discussed the bond dissociation of molecular ions.

In this paper, frequency factors, rate constants and decomposition probabilities are estimated from the mass spectra of olefins by the quasi-equilibrium theory, and the decomposition processes of olefins are briefly discussed in comparison with those of paraffins.

Theory

According to the quasi-equilibrium theory[1], the rate constant for the unimolecular dissociation of a polyatomic ion with the excitation energy of E is given by:

$$K(E)=\int_{\circ}^{E-\varepsilon_{\circ}} \frac{1}{h}\cdot\frac{\rho^{+}(E,\varepsilon_{\circ},\varepsilon_t)}{\rho(E)}\mathrm{d}\varepsilon_t \qquad (1)$$

where $\rho(E)$ is the density of the states of the ion with an energy of E, $\rho^{+}(E,\varepsilon_{\circ},\varepsilon_t)$ is the density of the states of the ion in the activated complex configuration with the potential energy of $\varepsilon_{\circ}$ and the translational energy of ε_t, and h is Planck's constant. The internal energy of the transition complex is, then, $E-\varepsilon_{\circ}$. Neglecting the contribution of the electronic state to the state density function, and assuming the oscillations in normal and activated complex configurations of the molecular ion to be harmonic, Eq. 1 can be rewritten as:

$$K(E)=z\left(1-\frac{\varepsilon_{\circ}}{E}\right)^{p}(E-\varepsilon_{\circ})^{q} \qquad (2)$$

Here, z is the frequency factor; the exponents p and q are defined by the following equations:

$$p=(3N'-6)-L/2-1$$
$$q=(L-L^{*})/2$$

where N' is the number of atoms in the parent ion, L is the number of internal rotational degree of freedom, and the symbol* indicates the quantities relating to the activated complex.

In such a system of unimolecular reaction, the amount of parent ions left at time t is given by:

$$n_t=n_{\circ}\exp(-\sum_{i}^{n}K_i t) \qquad (3)$$

Here, $n_{\circ}$ is the amount of parent ions at the beginning. In practical calculation, the time, t, is usually assumed to be a certain constant value of the order of 10^{-5} sec. according to the dimension of the ion source as well as of the ion-accelerating voltage. The relative abundance of fragment ions is given by:

$$(I_i)_j=\frac{K_j}{\sum_{i}K_i(E)} \qquad (4)$$

It is very difficult to calculate theoretically the frequecy factor. In general, the frequency factor is estimated from the experimental data concerning the reactant and activated complex states in spectroscopy. In other cases, the frequency factor is determined inversely from the relative yields of the principal ions in mass spectrometry. Thus, low-energy reaction paths for the unimolecular decomposition of the polyatomic ion have been studied through mass spectrometry[1,4-8].

Experimental

The instrument used was a Hitachi mass spectrometer, RMS-3, of a single focusing, 60°-sector type with a radius of 100 mm. Ionization is carried out by electron impact. The appearance potentials and the relative yields of the principal ions produced from some paraffins and olefins were measured and reported on in the previous paper[6].

For the case of propylene, a block diagram for the unimolecular decomposition is shown in Fig. 1.

1) H. M. Rosenstock, M. B. Wallenstein, A. L. Wahrhaftig and H. Eyring, *Proc. Natl. Acad. Sci.*, **38**, 667 (1952).
2) A. Krope, E. M. Eyring, A. L. Wahrhaftig and H. Eyring, *J. Chem. Phys.*, **32**, 149 (1960).
3) L. Friedman, F. A. Long and M. Wolfsberg, ibid., **27**, 613 (1957).
4) A. B. King and F. A. Long, ibid., **29**, 374 (1958).
5) L. Friedman, F. A. Long and M. Wolfsberg, ibid., **30**, 1605 (1959).
6) I. Omura, This Bulletin, **34**, 1227 (1961).
7) W. A. Chupka, *J. Chem. Phys.*, **30**, 191 (1951).
8) B. Steiner, C. F. Ciese and M. G. Inghram, ibid., **34**, 189 (1961).

TABLE I. LOW VOLTAGE PATTERNS AND APPEARANCE POTENTIALS FOR OLEFINS

Mass	Propylene ion yield	Propylene A. P., eV.	1-Butene ion yield	1-Butene A. P., eV.	*cis*-2-Butene ion yield	*cis*-2-Butene A. P., eV.
$C_4H_8^+$			34.5	9.72	42.5	9.25
$C_4H_7^+$			9.5	12.01	6.3	11.20
$C_3H_6^+$	57.4	9.74				
$C_3H_5^+$	30	12.11	34.5	11.73	29.5	11.60
$C_3H_4^+$	8.5	12.52				
$C_3H_3^+$	4.5	14.21	2.5		3.0	
$C_2H_5^+$					1.5	12.25
$C_2H_4^+$		12.85	9.0	12.38	6.8	12.19
$C_2H_3^+$	2.6	13.80		13.6		

V_e—I: 4 eV.

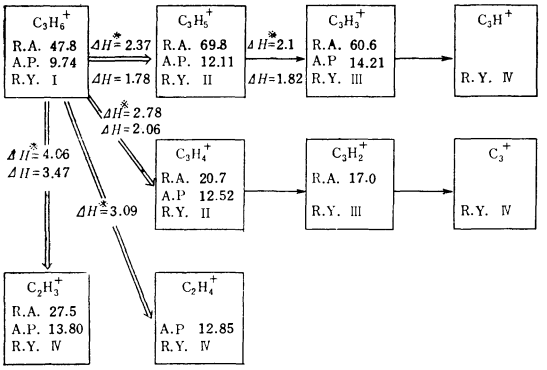


Fig. 1. Unimolecular decomposition scheme for propylene ion by electron impact.
R.A. Relative abundance (%)
A.P. Appearance potential (eV.)
R.Y. Type of relative yield curve[6]
ΔH^* Heat of activation (eV.)
ΔH Heat of reaction (eV.)

In each block are shown the chemical formula of the ion, the relative abundance (R. A.), and the type of relative yield curve (R. Y.)[6]. The bold lines connecting two blocks show primary reaction paths, fine lines, secondary or higher reaction paths, and broken lines, energetically impossible paths. Over and along the arrow are shown the heat of activation (ΔH^*) and the heat of reaction (ΔH). Table I shows the appearance potentials of principal fragment ions from propylene, 1-butene and *cis*-2-butene, and also the relative abundances at the ionizing voltage four volts higher than the ionization potantial of the parent molecule.

Figure 2 shows the decomposition probability of the parent ion calculated from the following equation:

$$F_p = \frac{\sum_j (I_f)_j}{I_p + \sum_j (I_f)_j} \qquad (5)$$

where I_p is the intensity of the undecomposed parent ions and $\sum_j (I_f)_j$ is the total sum of all the other fragment ions in the mass spectrum. Abscissa, V_e-I, is the excess energy of the ionizing electron over the ionization potential of the parent

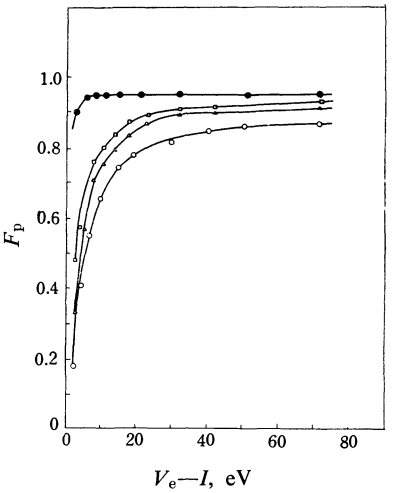


Fig. 2. Decomposition probability of parent ions.
○ Propylene
△ 1-Butene
□ *cis*-2-Butene
● *n*-Butane.

molecule. The curve for *n*-butane is taken as an example of paraffins.

Similarly, the probability of the secondary decomposition of $C_3H_5^+$ ions is shown in Fig. 3. In this case, the $C_3H_5^+$ ion intensity corresponds to I_p in Eq. 6, while the total sum of fragment ions expected from the decomposition of $C_3H_5^+$ ions corresponds to $\sum (I_f)$. The ratio of the intensity of the $C_3H_5^+$ ion to that of the parent ion, as well as the ratio of the intensity of the $C_3H_3^+$ ion produced from the $C_3H_5^+$ ion by secondary decomposition to that of the $C_3H_5^+$ ion, are shown in Fig. 4.

TABLE II. RATE CONSTANT FOR OLEFIN IONS

Molecule	Ion	Rate constant 10^5 sec^{-1}
C_2H_4	$C_2H_4^+$	1.39
C_3H_6	$C_3H_6^+$	4.21
1-C_4H_8	1-$C_4H_8^+$	7.59
cis-2-C_4H_8	*cis*-2-$C_4H_8^+$	4.78

TABLE III. FREQENCY FACTORS FOR DECOMPOSITION PROCESSES

Parent ion	Primary decomposition H	CH_3	C_2H_4	C_2H_5	H_2
$C_3H_6^+$	1.74×10^{11}	4.07×10^{18}			1.13×10^{14}
$1\text{-}C_4H_8^+$	1.25×10^{15}	1.35×10^{13}	5.62×10^{17}	1.0×10^{14}	
cis-$2\text{-}C_4H_8^+$	8.65×10^{12}	1.55×10^{15}	6.4×10^{20}	3.54×10^{20}	

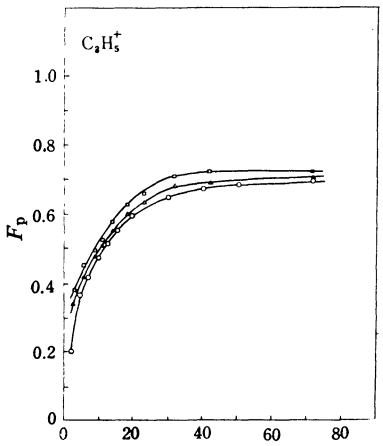


Fig. 3. Decomposition probability of $C_3H_5^+$ ions.
○ $C_3H_5^+$ from propylene
△ $C_3H_5^+$ from 1-butene
□ $C_3H_5^+$ from *cis*-2-butene

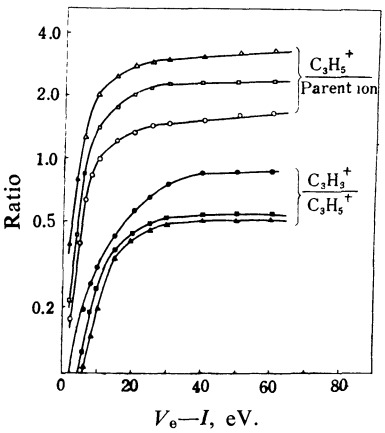


Fig. 4. Ratios of yields.
○, ● Propylene
△, ▲ 1-Butene
□, ■ *cis*-2-Butene

The rate constants for the $C_3H_6^+$, $C_3H_5^+$ and $C_3H_3^+$ ions from propylene are calculated from the mass spectrometric data and are shown in Fig. 5, where the time is assumed to be 1×10^{-5} sec. In Table II are listed the rate constants of the parent ions of some olefins at an ionizing voltage four volts higher than the ionization potential. The frequency factors are also calculated and listed in Table III.

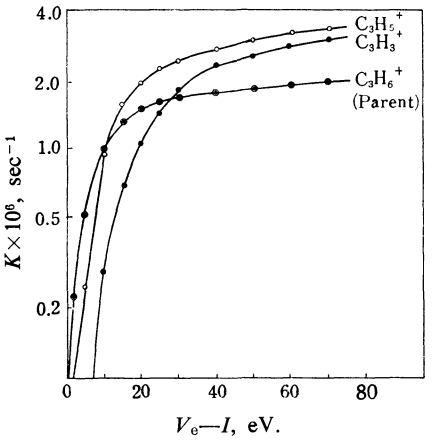


Fig. 5. Unimolecular decomposition rate constant — propylene —.

Discussion

In the estimation of the rate constant, the time, t, in Eq. 3 is assumed to be 1×10^{-5} sec. because the time between the formation of the ions and their entering the focusing system is presumed to be of the order of 10^{-5} sec. The absolute value of the rate constant obtained depends greatly on this assumption and is not very important. It should be discussed in relation with the assumption as well as with the value obtained from theory or other kinds of experiment. The frequency factor is of the same type.

The frequency factor obtained for the hydrogen atom abstraction from propane ion and that obtained for the methyl radical abstraction are in the ratio of about $1:10^3$, as has been reported by Friedman[5]. It seem there are no gross mistakes in the present experiment.

The rate constant of the parent ion in a homologous series seems to increase with the size of the ion, as is shown in Table II. This may be due to the increase in possible reaction paths.

It might be simply considered that the character of the fragment ion, $C_3H_5^+$, is independent of the parent ion. Contrary to this simple expectation, the secondary decomposition probabilities of the $C_3H_5^+$ ion in the cases of propylene, 1-butene, and *cis*-2-butene are slightly different from each other,

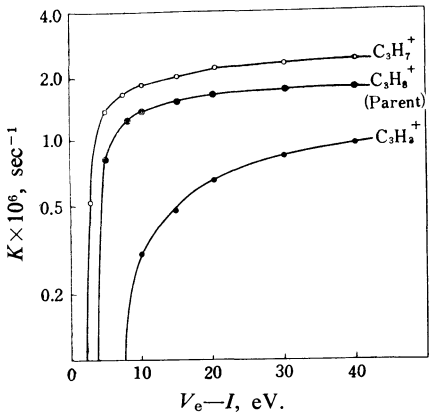


Fig. 6. Unimolecular decomposition rate constant — propane —.

as is shown in Fig. 3. The $C_3H_3^+/C_3H_5^+$ ratio for the ions from propylene considerably differs from those for the ions from 1-butene and *cis*-2-butene, as is shown in Fig. 4. The cause remains to be further investigated.

The rate constants of the principal ions from propane are shown in Fig. 6 in comparison with those of propylene, as in Fig. 5. The decomposition paths of the propane ion are as follows:

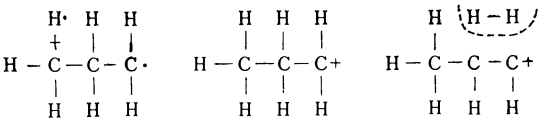
$$C_3H_8^+ \xrightarrow[\text{primary}]{\text{H abstraction}} C_3H_7^+ \begin{cases} \xrightarrow[\text{secondary}]{H_2\text{ abstraction}} C_3H_5^+ \\ \longrightarrow C_2H_3^+ \\ \longrightarrow CH_3^+ \end{cases}$$

Here, bold lines indicate principal paths and fine lines, reaction paths energetically possible but of secondary importance. The secondary decomposition path from $C_3H_7^+$ to $C_3H_5^+$ in the case of propane corresponds to the path from $C_3H_5^+$ to $C_3H_3^+$ in the case of propylene. Comparing Fig. 5 with Fig. 6, we can see that the rate constant for the secondary decomposition probability is larger in the case of propylene than in the case of propane. This may be caused by the fact that the probability of the abstraction of the hydrogen molecule is closely related with the distribution of the positive charge or the ionic structure of the activated complex. According to the quasi-equilibrium theory, the density of the positive charge associated with the bonds has an effect on the bond rupture, and the relative yield of ions is related with the distribution of the positive charge[6]. Inversely, the effect of positive charge distribution may be presumed from the rate constant or the activation energy.

The decomposition paths to the $C_3H_3^+$ ion from the propylene ion are as follows:

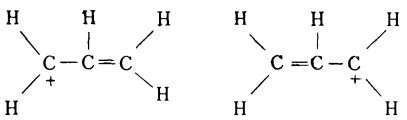
$$C_3H_6^+ \xrightarrow[\text{primary}]{\text{H abstraction}} C_3H_5^+ \xrightarrow[\text{secondary}]{H_2\text{ abstraction}} C_3H_3^+$$

The ionic structure of the $C_3H_7^+$ ion from propane is presumed to be of the last type of the follwing three structures;

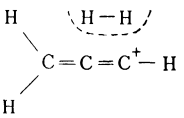


I II III

Similarly, the ionic structure of the $C_3H_5^+$ ion from propylene is presumed to be of the last type of the following three structures:



I' II'



III'

In the case of propylene, the activation energy for the secondary reaction (hydrogen molecule abstraction) is smaller than twice the activation energy for the primary reaction (hydrogen atom abstraction), as is shown in Table IV. In the case of propane, on the other hand, the energy for the secondary reaction (hydrogen molecule abstraction) is larger than twice the energy for the primary reaction (hydrogen atom abstraction). These interesting results seem to be very important for the study of the dissociation of these molecular ions.

TABIE IV. ENERGY FOR THE ABSTRACTION OF A HYDROGEN ATOM AND A HYDOGEN MOLECULE

Parent ion	Primary H, eV.	Secondary H_2, eV.	H_2-2H eV.
$C_3H_6^+$	2.37	2.10	−2.64
1-$C_4H_8^+$	2.29	2.09	−2.49
cis-2-$C_4H_8^+$	1.95	2.15	−1.75
$C_3H_8^+$	0.56	3.2	+2.08
n-$C_4H_{10}^+$	0.78	2.54	+0.98
iso-$C_4H_{10}^+$	1.37	3.39	+0.65

Summary

The decomposition probabilities, rate constants, and frequency factors for some olefins have been calculated on the basis of mass spectrometric data and the quasi-equilibrium theory.

The rate constant of the parent ion in a homologous series increases with the size of the ion. Fragment ions of the same form but from different parent ions sometimes reveal different rate constants.

The scheme of hydrogen molecule abstraction in the secondary decomposition processes of propane is analogous to that of propylene, and reasonable ionic structures of primary ions can be presumed.

For a more quantitative discussion, however, there remain some indistinct points in the application of the quasi-equilibrium theory. For instance, the time of reaction along with the rate constant is assumed to be 1×10^{-5} sec. and to be constant for all ions. Further studies should be carried out both in theory and experiments.

The author wishes to thank Dr. Nozomu Morito and the members of the mass spectrometry section of Hitachi Central Research Laboratory for their helpful discussions throughout this work.

Thanks are also due to Professor Keniti Higasi of Hokkaido University, as well as Professor Itiro Kanomata of Tokyo Metropolitan University, for their discussions regarding the broader of the problems treated.

Hitachi Central Research Laboratory
Kokubunji, Tokyo

The cis-trans Photoisomerization of Azobenzene

By Shigeru YAMASHITA, Hiroshi ONO and Osamu TOYAMA

(Received July 7, 1962)

The cis-trans photoisomerization of azobenzene in solution has been investigated by a number of workers[1-3]. For both of the isomers of azobenzene, n-π^* bands have been observed in the visible wavelength region and π-π^* bands in the near-ultraviolet region. However, the quantum yield values reported by the previous workers show some inconsistency concenrning the relative efficiencies of n-π^* and π-π^* absorption for the isomerization.

The present paper reports on a reinvestigation of these quantum yield values as well as on a kinetic study of the isomerization reaction. All the experiments have been carried out with *n*-hexane as the solvent.

Experimental

Materials.—*cis-Azobenzene.*—The method of preparation described by Hartley[4] was followed.

trans-Azobenzene.—A commercial reagent was used after repeated recrystallization. The absorption curves of the two azobenzene isomers were in good agreement with those in the literature.

n-Hexane.—A commercial reagent of a chemically pure grade was treated with fuming sulfuric acid, concentrated sulfuric acid, and an aqueous solution of potassium permanganate successively. After having been dried over anhydrous calcium chloride, the product was fractionally distilled.

Apparatus and Procedure.—In Fig. 1 are shown the absorption curves of *cis*- and *trans*-azobenzene in *n*-hexane at 15°C. The light source for the photoisomerization was a Mazda SHL-100 mercury lamp. A combined filter consisting of Mazda UV-D2 and a potassium chromate solution was used to isolate the 313 mμ line, which gives rise to π-π^* transitions in both the isomers of azobenzene. To study the effect of the n-π^* absorption of *cis*-azobenzene, a combintation of Mazda V-P 1.5 and Walz UV was used; the 405 mμ line was thereby isolated. To study the effect of the n-π^* absorption of *trans*-azobenzene, a Walz Y-1 filter was used; this allowed mercury lines of longer wavelengths

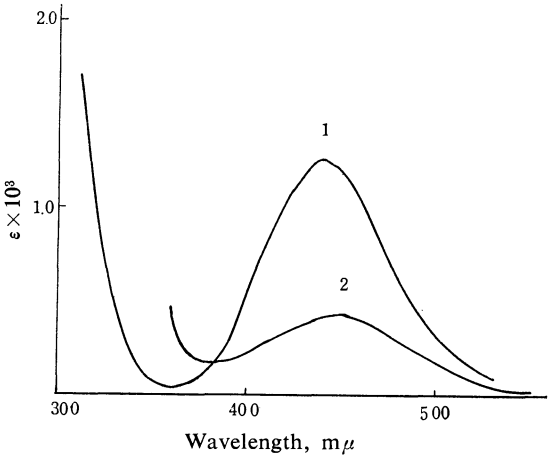


Fig. 1. Molar extinction coefficients of *cis*-azobenzene (curve 1) and *trans*-azobenzene (curve 2).

1) P. P. Birnbaum and D. W. G. Style, *Trans. Faraday Soc.*, **50**, 1192 (1954).
2) G. Zimmerman, L. Chow and U. Paik, *J. Am. Chem. Soc.*, **80**, 3528 (1958).
3) E. Fischer, ibid., **82**, 3249 (1960).
4) G. S. Hartley, *J. Chem. Soc.*, **1938**, 633.

than about 420 mμ to enter the reaction cell, although the only strongly absorbed lines of these, in view of the absorption curve in Fig. 1, was 436 mμ. Through the collimating quartz lens and the filters, a parallel light beam of a desired wavelength was projected upon a quartz reaction cell 4 cm. in diameter and 2 cm. thick immersed in a thermostat which had a window for the exciting light beam. For experiments at −78°C, the thermostat was replaced by a Dewar vessel containing dry ice-ethanol.

In the present study the rate of isomerization reaction was measured only in the initial stage of reaction so that the reverse reaction could be neglected. The change in concentration of *cis*- and *trans*-azobenzene caused by isomerization was determined by a Hitachi EPB-U type spectrophotometer.

For determination of the exciting light intensity, a potassium ferrioxalate actinometer was used[5]. Taking the actinometric result and transmittancy of the reaction mixture into account, quantum yields for the isomerization reaction under various conditions were obtained. Other details of the procedure have been described in a previous paper on the photochemical cis-trans isomerization of stilbene[6].

Results and Discussion

The results obtained are shown in Tables I—V. The kinetic results obtained with dilute solutions approximately conform to the rate expression:

$$-\mathrm{d(A)}/\mathrm{d}t=\phi I_a=kI_0(\mathrm{A})$$

where A represents *cis*- or *trans*-azobenzene, and I_0, the incident light intensity. This rate equation implies that the rate of isomerization is simply proportional to the light quanta absorbed per unit time, I_a, since I_a is proportional

TABLE I. PHOTOISOMERIZATION OF *trans*-AZOBENZENE CAUSED BY n-π^* ABSORPTION

Reaction temp., 0°C; irradiation, 436 mμ. Reaction time, 5 min.

Initial concn. of *trans*-azobenzene ×10⁴ mol./l.	Light intensity ×10⁸ einstein/sec.	Light quanta absorbed ×10⁹ einstein/sec.	Rate of isomerization ×10⁹ mol./sec.	Quantum yield
1.0	9.37	3.33	0.693	0.21
2.0	9.37	6.23	1.22	0.19
3.0	9.37	8.77	1.70	0.19
4.0	9.37	11.0	2.11	0.19
5.0	9.37	13.0	2.51	0.19
6.0	9.37	14.7	2.83	0.19
7.0	9.37	16.3	3.14	0.19
8.0	9.37	17.6	3.39	0.19
9.0	9.37	18.9	3.69	0.19
10.0	9.37	20.0	4.23	0.21
1.0	4.57	1.63	0.36	0.22
2.0	4.57	3.04	0.61	0.20
3.0	4.57	4.29	0.85	0.20
4.0	4.57	5.38	1.04	0.19
5.0	4.57	6.34	1.25	0.20
6.0	4.57	7.19	1.42	0.20
7.0	4.57	7.95	1.56	0.20
8.0	4.57	8.62	1.72	0.20
9.0	4.57	9.22	1.82	0.20
10.0	4.57	9.76	1.90	0.19
1.0	1.96	0.70	0.16	0.20
2.0	1.96	1.31	0.25	0.20
3.0	1.96	1.84	0.35	0.19
4.0	1.96	2.31	0.45	0.20
5.0	1.96	2.72	0.55	0.20
6.0	1.96	3.09	0.60	0.20
7.0	1.96	3.41	0.66	0.20
8.0	1.96	3.70	0.74	0.20
9.0	1.96	3.96	0.77	0.20
10.0	1.96	4.19	0.82	0.20

5) C. A. Parker, *Proc. Roy. Soc.*, **A220**, 104 (1955); C. G. Hatchard and C. A. Parker, ibid., **A235**, 518 (1956).

6) S. Yamashita, This Bulletin, **34**, 490 (1961).

TABLE II. EFFECT OF TEMPERATURE ON THE trans-cis PHOTOISOMERIZATION OF AZOBENZENE CAUSED BY n-π^* ABSORPTION

Irradiation wavelength, 436 mμ. Reaction time, 1.0 hr.

Initial concn. of *trans*-azo benzene $\times 10^3$ mol./l.	Reaction temp., °C	Light quanta absorbed $\times 10^{10}$ einstein/sec.	Rate of isomerization $\times 10^{10}$ mol./sec.	Activation energy kcal./mol.
1.0	0	12.37	2.13	0.71
1.0	−78	12.37	1.32	
0.8	0	11.15	1.85	0.70
0.8	−78	11.15	1.13	
0.6	0	9.59	1.40	0.64
0.6	−78	9.59	0.89	

TABLE III. PHOTOISOMERIZATION OF *trans*-AZOBENZENE CAUSED BY π-π^* ABSORPTION

Recation temp., 3~4°C; irradiation, 313 mμ; light intensity, 1.67×10^{-10} einstein/sec.

Initial concn. of *trans*-azo-benzene $\times 10^3$ mol./l.	Reaction time hr.	Light quanta absorbed $\times 10^{10}$ einstein/sec.	Rate of isomerization $\times 10^{11}$ mol./sec.	Quantum yield
1.0	1.0	1.67	1.66	0.10
1.0	2.0	1.67	1.64	0.10
1.0	8.0	1.67	1.59	0.095

TABLE IV. PHOTOISOMERIZATION OF *cis*-AZOBENZENE CAUSED BY n-π^* ABSORPTION

Reaction temp., 0°C; irradiation, 405 mμ; reaction time, 30 min.

Initial concn. of *cis*-azo-benzene $\times 10^4$ mol./l.	Light intensity $\times 10^9$ einstein/sec.	Light quanta absorbed $\times 10^{10}$ einstein/sec.	Rate of isomerization $\times 10^{10}$ mol./sec.	Quantum yield
2.0	1.71	5.49	3.81	0.70
3.0	1.71	7.36	5.06	0.69
4.0	1.71	8.83	5.96	0.68
5.0	1.71	9.98	6.47	0.65
2.0	1.15	3.70	2.57	0.69
3.0	1.15	4.97	3.44	0.69
4.0	1.15	5.96	4.02	0.67
5.0	1.15	6.74	4.39	0.65
4.0	0.84	4.32	2.92	0.68
4.0	0.48	2.51	1.70	0.68

TABLE V. PHOTOISOMERIZATION OF *cis*-AZOBENZENE CAUSED BY π-π^* ABSORPTION

Reaction temp., 3~4°C; irradiation, 313 mμ; light intensity, 1.67×10^{-10} einstein/sec.

Initial concn. of *cis*-azo-benzene $\times 10^3$ mol./l.	Reaction time hr.	Light quanta absorbed $\times 10^{10}$ einstein/sec.	Rate of isomerization $\times 10^{11}$ mol./sec.	Quantum yield
2.0	1.0	1.66	7.55	0.45
2.0	3.0	1.66	7.32	0.44
0.5	1.0	1.55	6.84	0.44

to the product, $I_0(A)$, for dilute solutions. The constancy of the quantum yield values, the ϕ's, given in each table proves the validity of such an interpretation.

Fischer[3], on the basis of measurements of photoequilibrium at varied temperatures, argues that the trans→cis photoisomerization of azobenzene and its derivatives is dependent on temperature. In the present work, such a temperature dependence has really been found, as

is shown in Table II, for the trans → cis conversion of azobenzene caused by n-π^* absorption. The effect of the temperature, however, is rather small, the activation energy being as low as 0.7 kcal./mol. For the trans → cis conversion caused by π-π^* absorption and for the conversion in the reverse direction caused by either n-π^* or π-π^* absorption, similar rate measurements have shown that these are all independent of temperature within the range of experimental error.

TABLE VI. SUMMARY OF QUANTUM YIELDS

Reaction	Temp. °C	Light wave-length mμ	Absorption	Quantum yield
cis→trans	3∼4	313	π-π^*	0.44
				0.42[a]
				0.69[b]
	0	405	n-π^*	0.68
				0.55[a]
				0.45[b]
trans→cis	3∼4	313	π-π^*	0.10
				0.10[a]
				0.22[b]
	0	436	n-π^*	0.20
				0.25[a]
				0.36[b]

a) Values obtained by Zimmerman et al. (Ref. 2) at 25°C.
b) Values obtained by Birnbaum and Style (Ref. 1) at room temperature.

The quantum yield values obtained in this work are summarized in Table IV, together with those reported by previous workers. As may be seen in the table, Zimmerman et al. report that n-π^* absorption is more efficient than π-π^* in both directions of conversion, while according to Birnbaum and Style π-π^* absorption is more efficient in the cis→trans conversion. The results obtained in the present work confirm the observations of the former workers.

The sum of the quantum yields for the cis→trans and trans → cis isomerization reactions is frequently found to be approximately unity; the mechanism of isomerization in such a case is usually supposed to be:

$$C \rightleftarrows E \rightleftarrows T \qquad (1)$$

where C and T denote normal molecules of cis and trans-forms respectively, and E is the excited state reached by light absorption, where the two isomeric forms are assumed to be indistinguishable. The assumption of such an excited state may not be improbable, since there are theoretical grounds for supposing the potential barrier separating the two isomeric forms in the excited state to be much lower than that in the ground state[7]. The sum of quantum yields obtained in the present work, with n-π^* absorption at 0°C, is about 0.9; the mechanism in this case may be supposed to be approximately as described above.

However, the conversion due to π-π^* absorption cannot be interpreted in the same way, since the sum of the quantum yields is here distinctly lower than unity. Zimmerman et al. have proposed the following mechanism as an interpretation:

$$C \underset{k_1}{\overset{h\nu}{\rightleftarrows}} C^* \underset{k_4}{\overset{k_3}{\rightleftarrows}} T^* \underset{h\nu}{\overset{k_2}{\rightleftarrows}} T \qquad (2)$$

Here the two isomeric forms in the exited state, C* and T*, are assumed to be separated by a potential barrier of an appreciable magnitude —say, 5 kcal./mol. Scheme 2 explains the sum of quantum yields lower than unity, since they are represented by:

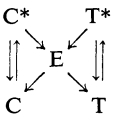
$$1/\phi_{C\to T} = 1 + (k_1/k_3)\,[1 + (k_4/k_2)]$$

and

$$1/\phi_{T\to C} = 1 + (k_2/k_4)\,[1 + (k_3/k_1)]$$

where the k's are the respective rate constants given in the scheme. These expressions for the quantum yields are, however, incompatible with the experimental findings in the present work, for the quantum yields obtained with 313 mμ are $\phi_{C\to T} = 0.44$ and $\phi_{T\to C} = 0.10$, both being independent of temperature; it follows from these figures that neither k_3 nor k_4 can have an appreciable activation energy.

An alternative interpretation reconcilable with the experimental results may be presented as follows:



(3)

Here E denotes an excited state similar to the one assumed in scheme 1, which lies lower than either state C* or T*. Scheme 3 leads to a sum of quantum yields, $\phi_{C\to T} + \phi_{T\to C}$, less than unity, where neither $\phi_{C\to T}$ nor $\phi_{T\to C}$ now needs to be dependent on temperature.

Summary

The photoisomerization of *cis*- and *trans*-azobenzene in an *n*-hexane solution has been studied in the n-π^* and π-π^* absorption wavelength regions. The rate of isomerization has always been found to be proportional to the

7) For example, the bond order of the ethylenic double bond in stilben, calculated for the first excited state, is markedly lower than that for the ground state. (C. A. Coulson and J. Jacobs, *J. Chem. Soc.*, **1949**, 1983)

product of the incident light intensity and the concentration of *cis*- or *trans*-azobenzene. This simply means that the rate of isomerization is proportional to that of light absorption. Quantum yields of isomerization are independent of the temperature except for the trans → cis conversion caused by n-π^* absorption, where the quantum yield is slightly dependent on temperature. The sum of quantum yields for cis → trans and trans → cis conversions caused by n-π^* absorption is approximately unity, while the sum obtained with π-π^* absorption is much smaller than unity. The mechanism of photoisomerization has been discussed with reference to these results.

The authors are grateful to Professor Teruo Hayakawa for his valuable discussions.

Department of Applied Chemistry
College of Engineering
(O. T. & H. O.)
and
Department of Chemistry
College of General Education
(S. Y)

The University of Osaka Prefecture
Sakai, Osaka

Relations between the Electronic Absorption Spectra and the Spatial Configurations of Conjugated Systems. XIII. Phenyl-carbonyl and Vinyl-carbonyl Systems

By Hiroshi SUZUKI

(Received July 7, 1962)

As is well known, Braude[1] classified the steric effects in the ultraviolet absorption spectra of conjugated compounds into two types. Type 1, exemplified by the substituted phenyl- and vinyl-carbonyl compounds, is characterized by a decrease in the absorption intensity alone, with no appreciable accompanying change in the position of the absorption maximum. Type 2, exemplified by the *o*-alkylated biphenyls, is characterized by a hypsochromic shift as well as by a decrease in the absorption intensity.

Braude ascribed the difference between the two types to the difference in the underlying mechanism. According to him, while the type 2 effect occurs when the steric hindrance to the planarity of the conjugated system is relatively strong, the type 1 effect occurs when the steric hindrance is relatively weak, and while in the former case the maximum absorption originates in electronic transitions in those molecules with the most probable non-planer configuration in the electronic ground state, in the latter case it originates in transitions in those molecules with the less probable planar or near-planar configuration in the ground state. He therefore ascribed the decrease in the intensity of the absorption maximum in the case of type 1 to the decrease in the population ratio, r, of the planar or near-planar configuration in the electronic ground state (i.e., the probability in which molecules in the electronic ground state assume the planar or near-planar configuration); further, he assumed that the population ratio, r, and hence the molar extinction coefficient of the absorption maximum, ε, would be proportional to $\cos\theta$, where θ is the interplanar angle between moieties of the conjugated system linked to each other by a formally single bond, i.e., the angle of twist of the bond, in the most probable configuration[2,3]. Afterwards[4,5], he replaced the cosine of θ in the above assumption by the cosine-square of θ; that is, he assumed the following relation:

$$\varepsilon/\varepsilon_0=\cos^2\theta \qquad (1)$$

1) E. A. Braude, E. R. H. Jones, H. P. Koch, R. W. Richardson, F. Sondheimer and J. B. Toogood, *J. Chem. Soc.*, **1949**, 1890.

2) E. A. Braude, F. Sondheimer and W. F. Forbes, *Nature*, **173**, 117 (1954).

3) E. A. Braude and E. S. Waight, in W. Klyne, "Progress in Stereochemistry, I.", Butterworths Scientific Publications, London (1954), p. 126.

4) E. A. Braude, in E. A. Braude and F. C. Nachod, "Determination of Organic Structures by Physical Methods", Academic Press, Inc., New York (1955), p. 131.

5) E. A. Braude and F. Sondheimer, *J. Chem. Soc.*, **1955**, 3754.

where ε_0 is the molar extinction coefficient of the absorption maximum of the sterically unhindered reference compound.

As has been mentioned in Parts XI[6] and XII[7] of this series, Braude's interpretation of steric effects is unacceptable. Although the border line between the two types of steric effect is not distinct in practice, the classification may be provisionally admitted. However, the difference between the two types is due neither to a difference in the underlying mechanism nor to a difference in the magnitude of steric hindrance. The sensibility of the transition energy to a change in the spatial configuration of the conjugated system depends on the nature of the electronic upper state to which the transition leads. According to Murrell[8], the energy of the transition to a perturbed, locally-excited state is relatively sensitive to a change in the configuration, while, on the other hand, that of the transition to a perturbed, intramolecular electron-transfer state is relatively insensitive. Roughly, it may be said that the steric effect in the former case corresponds to type 2, and that in the latter case to type 1. At any rate, in both cases, the maximum absorption is considered to originate in transitions in those molecules with the most probable configuration in the electronic ground state, contrary to the theory of Braude.

In this way, the untenability of the theory of Braude may be said to have been established. However, Eq. 1 itself, assumed by Braude on the wrong grounds, seems to have some plausibility. Thus, the values of θ calculated by the use of this relation for some benzaldehydes and acetophenones are generally in quite good agreement with the values deduced from the dipole moment data, although the latter values themselves seem also to be unreliable, because their deduction was based on a rather arbitrary assumption bearing a certain similarity to Eq. 1. Furthermore, a relation similar to Eq. 1 was found by Klevens and Platt[9] to hold in the case of *o*-substituted dimethylanilines. Thus, according to them, the oscillator strength, f, of each band varies with the cosine-square of the minimum angle of twist of the dimethylamino group with respect to the benzene ring estimated from the van der Waals radius of the ortho substituent.

It may, therefore, be of some interest to examine to what extent the relation assumed by Braude can be validated by theoretical considerations. In the present paper, with special emphasis on this problem, it is attempted, on the same ground as in the previous papers of this series, to clarify the relation between the conjugation band and the spatial configuration of the conjugated system in the cases of the phenyl-carbonyl (C_6–C=O) and vinyl-carbonyl (C=C–C=O) systems as representatives of systems exhibiting the so-called type 1 steric effect.

Transition Energy as a Function of the Angle of Twist

It has already been pointed out by Nagakura and Tanaka[10-12] that the intense band near 240 mμ, i. e., the conjugation band, of acetophenones as well as of benzaldehydes has the nature of an intramolecular electron-transfer band. According to them, the band is due to electronic transition between two π-orbitals, ψ_{-1} and ψ_{+1}, which arise primarily from the interaction of the lowest antibonding π-orbital of the carbonyl group, $\phi_{-1(C)}$, and the highest bonding π-orbital of the benzene ring, $\phi_{+1(B)}$. Since the interaction of two orbitals is always in the sense of a repulsion, the energy separation between ψ_{-1} and ψ_{+1} will become greater as the interaction between $\phi_{-1(C)}$ and $\phi_{+1(B)}$ becomes greater. Therefore, this theory leads to a surmise that the steric hindrance to coplanarity of the benzene nucleus and the carbonyl group would result in a bathochromic shift of the band. As was pointed out in Part X[13] of this series, this surmise is contrary to observed facts. Thus, with the acetophenone system, the steric effect should be considered to cause a hypsochromic shift of the band. It is evident that the omission of interactions among orbitals other than $\phi_{-1(C)}$ and $\phi_{+1(B)}$ is an over-simplification. Therefore, in the first place, the dependence of the transition energy on the angle of twist of the formally single bond is examined by the use of the perturbation theory, all the π-orbitals being taken into account.

Notation.—A conjugated system is represented by R–S and is regarded as being composed of two mesomeric systems, R and S, linked to each other by a formally single bond between the atoms r and s, which belong to R and S respectively. In the phenyl-carbonyl and vinyl-carbonyl systems, R represents the benzene nucleus or the ethylenic bond and S represents the carbonyl bond.

The following notation is used: ϕ_m: m-th MO of R. $\phi_{n'}$: n'-th MO of S. ϕ_k: k-th

6) H. Suzuki, This Bulletin, **33**, 619 (1960).
7) H. Suzuki, ibid., **35**, 1715 (1962).
8) J. N. Murrell, *J. Chem. Soc.*, **1956**, 3779.
9) H. B. Klevens and J. R. Platt, *J. Am. Chem. Soc.*, **71**, 1714 (1949).
10) S. Nagakura and J. Tanaka, *J. Chem. Phys.*, **22**, 236 (1954).
11) J. Tanaka, S. Nagakura and M. Kobayashi, ibid., **24**, 311 (1956).
12) J. Tanaka and S. Nagakura, ibid., **24**, 1274 (1956).
13) H. Suzuki, This Bulletin, **33**, 613 (1960).

MO of R–S. $F_m=\alpha-v_m\beta$: energy of ϕ_m. $F_{n'}=\alpha-v_{n'}\beta$: energy of $\phi_{n'}$. $E_k=\alpha-w_k\beta$: energy of ϕ_k. χ_i: AO of atom i. $b_{m,r}$: coefficient of χ_r in ϕ_m. $b_{n',s}$: coefficient of χ_s in $\phi_{n'}$. $c_{k,i}$: coefficient of χ_i in ϕ_k. $p_{k,i-j}=c_{k,i}c_{k,j}$: partial π-bond order of the i–j bond in ϕ_k, i.e., the contribution to the π-bond order of the bond by an electron occupying ϕ_k. $\alpha_i=\alpha+\delta_i\beta$: coulomb integral of χ_i. $\rho_{i-j}\beta$: resonance integral between χ_i and χ_j.

By the way, α is the coulomb integral of the 2 pπ atomic orbital of a carbon atom, and β is the resonance integral of the 2 pπ atomic orbitals of adjacent carbon atoms in the benzene ring. That is, v or w represents the energy of the orbital in a unit of $-\beta$ relative to the energy of the 2 pπ atomic orbital of a carbon atom.

In each of the mesomeric systems, the highest bonding π-orbital is designated as $+1$, and the lower orbitals in the order of decreasing energy are designated as $+2$, $+3$, and so on. Quite analogously, the lowest antibonding π-orbital is designated as -1, and the higher orbitals in the order of increasing energy are designated as -2, -3, and so on. Thus, for example, ϕ_{+1}, $\phi_{+1'}$, and ψ_{+1} refer to the highest bonding π-orbitals of R, S, and R–S respectively.

The parameter ρ_{i-j} can be expressed as follows, on the basis of the usual assumption of the proportionality of the resonance integral to the overlap integral:

$$\rho_{i-j}=\cos\theta_{ij}\cdot S(R_{i-j}, 0^\circ)/S(\text{benz.}) \qquad (2)$$

In this expression, θ_{ij} is the angle of twist of the bond (i.e., the angle by which the axes of χ_i and χ_j are twisted with respect to each other), R_{i-j} is the length of the bond, $S(R_{i-j}, 0^\circ)$ is the overlap integral of χ_i and χ_j when the interatomic distance is R_{i-j} and the angle of twist is 0°, and S(benz.) is the π–π overlap integral for adjacent carbon atoms in the benzene nucleus.

Classification of Conjugated Systems.—With respect to the heights of the energies of $\phi_{-1'}$ and $\phi_{+1'}$ relative to the energies of ϕ_{-1} and ϕ_{+1}, the following three typical cases are distinguished:

(A) $v_{-1}=v_{-1'}$; $v_{+1}=v_{+1'}$

(B) $v_{-1}<v_{-1'}$; $v_{+1}>v_{+1'}$

(C) $v_{-1}>v_{-1'}$; $v_{+1}>v_{+1'}$

These cases are exemplified by the following conjugated systems: (A), butadiene and biphenyl; (B), styrene; and (C), phenyl-carbonyl and vinyl-carbonyl.

In the case of A, ψ_{-1} and ψ_{+1} are regarded as orbitals arising from the perturbation of $1/\sqrt{2}\cdot(\phi_{-1}+\phi_{-1'})$ and of $1/\sqrt{2}\cdot(\phi_{+1}-\phi_{+1'})$ respectively, and the transition from ψ_{+1} to ψ_{-1} corresponds to the transition to a so-called charge-resonance state[14]. In the case of B, ψ_{-1} and ψ_{+1} are regarded as originating from ϕ_{-1} and ϕ_{+1} respectively, and the transition from ψ_{+1} to ψ_{-1} is the transition to a so-called perturbed, locally-excited state.

In general, the π-orbitals in any even-alternant hydrocarbon system occur in pairs. Thus, for such a system, $v_{+m}=-v_{-m}$, and $|b_{+m,i}|=|b_{-m,i}|$. Therefore, any system in which both fragments, R and S, are even-alternant hydrocarbon systems belongs to either case A or case B; moreover, in such a system, not only in case A but also in case B, the interaction of ϕ_{-1} with $\phi_{-1'}$ and that of ϕ_{+1} with $\phi_{+1'}$ make predominant contributions to the formation of ψ_{-1} and of ψ_{+1} respectively. Accordingly, as the value of ρ_{r-s} becomes larger, the energies of ψ_{-1} and ψ_{+1} become lower and higher respectively, and, consequently, the energy separation between them becomes smaller. This means that a deviation from coplanarity of R and S by a twist of the formally single r–s bond in any even-alternant hydrocarbon system, R–S, results in a hypsochromic shift of the conjugation band. In particular, in case A, the interaction of ϕ_{-1} with ϕ_{-1}, as well as that of ϕ_{+1} with $\phi_{+1'}$, depends on the ρ_{r-s} in the first order. Therefore, in this case, the transition energy increases to a first approximation linearly with the decreasing value of ρ_{r-s}. Representative alternant hydrocarbon systems have been discussed in some detail in the preceding parts of this series.

In case C, the transition from ψ_{+1} to ψ_{-1} corresponds to the transition to a perturbed electron-transfer state. The present paper is concerned chiefly with this case.

Treatment of Case C by Means of the Perturbation Theory.—In case C, ψ_{-1} and ψ_{+1} are regarded as orbitals arising from the perturbation of $\phi_{-1'}$ and ϕ_{+1} respectively, interaction between ϕ_m's and $\phi_{n'}$'s being regarded as a pertubation. Thus, if the $|A_{m,n}\rho_{r-s}|\ll 1$ relation holds for each pair of orbitals of R and S, where $A_{m,n'}=b_{m,r}b_{n',s}/(v_m-v_{n'})$, the first order perturbation theory gives the following expressions for ψ_{-1} and ψ_{+1}:

$$\psi_{-1}=N_{-1}(\phi_{-1'}-\sum_m A_{-1',m}\rho_{r-s}\phi_m) \qquad (3)$$

$$\psi_{+1}=N_{+1}(\phi_{+1}-\sum_{n'} A_{+1,n'}\rho_{r-s}\phi_{n'}) \qquad (4)$$

where N_{-1} and N_{+1} are normalization factors. The second order approximation to the energy of these orbitals is given by:

14) J. N. Murrell, *Quart. Revs.*, **15**, 191 (1961).

$$w_{-1}=v_{-1'}+\sum_{m} G_{-1',\,m}\,\rho^2_{r-s} \equiv v_{-1'}+g_{-1}\,\rho^2_{r-s} \quad (5)$$

$$w_{+1}=v_{+1}+\sum_{n'} G_{+1,\,n'}\,\rho^2_{r-s} \equiv v_{+1}+g_{+1}\,\rho^2_{r-s} \quad (6)$$

where $G_{m,n'}=b^2_{m,r}b^2_{n',s}/(v_m-v_{n'})$. Accordingly, the energy separation between ψ_{-1} and ψ_{+1}, $\Delta E_{-1,+1}$(in $-\beta$), is expressed as:

$$\Delta E_{-1,+1}=\Delta w_{-1,+1}=\Delta v_{-1',+1}+\Delta g_{-1,+1}\,\rho^2_{r-s}$$

where $\Delta v_{-1',+1}$ and $\Delta g_{-1,+1}$ represent $v_{-1'}-v_{+1}$ and $g_{-1}-g_{+1}$ respectively. (The subscript -1, $+1$, which refers to quantities concerning the transition from ψ_{+1} to ψ_{-1}, is subsequently omitted for the sake of brevity.) The partial π-bond orders are given by:

$$p_{-1,\,r-s}=-g_{-1}\,\rho_{r-s}\,N^2_{-1}$$

$$p_{+1,\,r-s}=-g_{+1}\,\rho_{r-s}\,N^2_{+1}$$

The change in the π-bond order of the r–s bond on the one-electron transition from ψ_{+1} to ψ_{-1}, ΔP_{r-s}, is $p_{-1,\,r-s}-p_{+1,\,r-s}$.

When R is an alternant hydrocarbon system, and when $v_{-1'}$ is positive, $-G_{-1',\,-m}$ is greater than $G_{-1',\,+m}$; that is, the contribution of the antibonding orbitals of R to ψ_{-1} is greater than that of the bonding orbitals of R. In this case, g_{-1} is negative, and $p_{-1,\,r-s}$ is positive.

S is taken to represent an unsaturated group, C=X, in which X may represent a hetero-atom such as oxygen or nitrogen. The coulomb integral of the pπ atomic orbital of atom X, α_X, is expressed as $\alpha+\delta_X\beta$. As may easily be proved, according as $\delta_X \lessgtr -v_{+1}$, $-G_{+1,\,-1'} \lessgtr G_{+1,\,+1'}$, and, consequently, $g_{+1} \gtrless 0$ and $p_{+1,\,r-s} \gtrless 0$. Thus, if δ_X is smaller than $-v_{+1}$, the contribution of ϕ_{+1} to $\psi_{+1'}$ as a perturbed orbital of ϕ_{+1} surpasses that of $\phi_{-1'}$. As δ_X becomes greater, the contribution of $\phi_{+1'}$ decreases owing to an increase in the energy separation of $v_{+1}-v_{+1'}$ as well as to a decrease of $b_{+1',\,s}$, and the contribution of $\phi_{-1'}$ increases owing to a decrease in the energy separation of $v_{-1'}-v_{+1}$ as well as to an increase of $b_{-1',\,s}$. This situation may be stated in terms of the resonance theory as follows: With the increasing value of δ_X, the contribution of the ionic structure, $R^+=S^-$, to the electronic ground state increases, resulting in an increase of the π-bond order of the r–s bond in the state.

Putting the above discussions together, the situation can be expressed as follows. If $\delta_X \leqslant -v_{+1}$, Δg is negative and ΔP_{r-s} is positive. In this case, a decrease in ρ_{r-s} results in an increase in Δw. This means that a twist of the r–s bond will cause a hypsochromic shift of the absorption band due to the transition from ψ_{+1} to ψ_{-1}. Of course, the smaller the value of δ_X, the larger the absolute value of Δg and, hence, the more effective the steric hypsochromic effect. The extreme case in which δ_X is zero reduces to case A or B. If δ_X has a moderately larger value than $-v_{+1}$, Δg may be nearly zero. In this case, a steric distortion will result in substantially no shift of the band. In the case where δ_X is much larger than $-v_{+1}$, Δg is positive and, accordingly, a twist of the bond will cause a bathochromic shift of the band.

Calculation and Discussion.—The length of the carbonyl bond in a number of compounds has an average value of 1.23±0.01 Å[15]. By the use of the value of 1.23 Å, the ρ-value for this bond is estimated at 0.844.

In the C_6–C=O and the C=C–C=O systems, the r–s bond is the 1–1′ bond linking the carbonyl group to the phenyl or the vinyl group. The length of this bond, $R_{1-1'}$, is assumed for the sake of convenience to be 1.48 Å when the angle of twist of the bond, $\theta_{1,\,1'}$, is 0°. Then the value of $\rho_{1-1'}$ is 0.858 when $\theta_{1,\,1'}$ is 0°, and the same relation among ρ, θ, and R as the one assumed tentatively for the cases of styrene[6] and biphenyl[16] can be used.

In application of the perturbation theory, the forms of ϕ's and the values of v's obtained by the simple LCAO MO method were used. When R is the benzene ring, for example, $v_{-1}=-v_{+1}=1$, and $b_{-1,\,1}=b_{+1,\,1}=1/\sqrt{3}$. By the way, in the C=C–C=O system, the δ-value for the ethylenic bond was taken to be 1.080, as in the cases of butadiene[7], styrene[6] and stilbene[17].

In Fig. 1, the following quantities as functions of δ_X for the C_6–C=X system, calculated by the use of th above parameter values, are

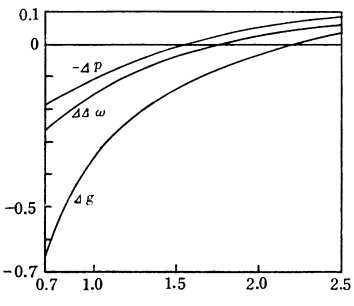


Fig. 1. ΔP_{r-s}, $\Delta\Delta w$, and Δg as functions of δ_X in the C_6–C=X system.

15) "Tables of Interatomic Distances and Configuration in Molecules and Ions", The Chemical Society, London (1958).
16) H. Suzuki, This Bulletin, 32, 1340 (1959).
17) H. Suzuki, ibid., 33, 379 (1960).

shown graphically: the value of Δg calculated from Eqs. 5 and 6; the difference between the value of Δw at $\theta_{rs}=0°$ and the value at $\theta_{rs}=90°$, $\Delta\Delta w$, and the value of ΔP_{r-s} at $\theta_{rs}=0°$, calculated by an application of the simple LCAO MO method to the whole conjugated system. The foregoing trends of the dependence of a change in the transition energy associated with a change in the angle of twist of the pivot bond, and of the change in the π-bond order of the bond, on the transition on the value of δ_X are clearly shown. In the case of C=C-C=X, the situation is quite similar.

After Matsen[18], the α/β ratio is assumed to be about 2.4. Then, on the basis of the assumption that the value of α_X should be proportional to the ionization energy of an electron occupying the pπ atomic orbital in the pertinent valence state of atom X, the value of δ for the 2pπ orbital of oxygen is estimated at 1.27, by the use of the ionization energy data collected by Pritchard and Skinner[19]. Of course, this numerical value is not conclusive, but approximately this value, probably 1.2~1.3, seems to be pertinent. (By the way, the value of δ for the 2pπ orbital of nitrogen is estimated at 0.60 by a similar procedure.)

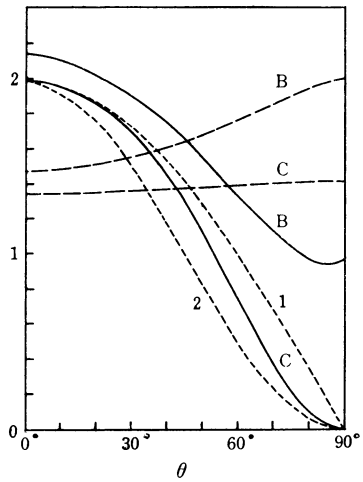


Fig. 2. The transition energy (in $-\beta$), Δw, and the dipole strength of the transition (in Å^2), M^2, as functions of the angle of twist of the formally single bond, θ, in the phenyl-carbonyl system as well as in the styrene system.

Broken lines, Δw; Solid lines: M^2;
B, C_6-C=C; C, C_6-C=O
Dotted lines: 1, $M^2(0°)\cdot\cos\theta$;
2, $M^2(0°)\cdot\cos^2\theta$

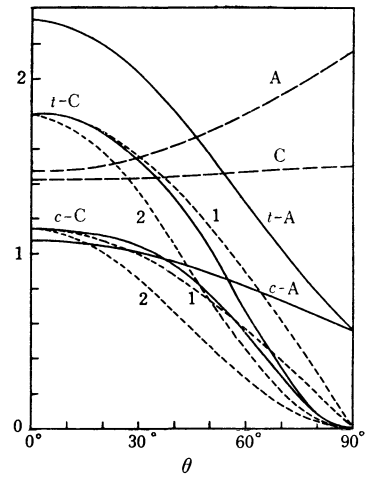


Fig. 3. The transition energy (in $-\beta$), Δw, and the dipole strength of the transition (in Å^2), M^2, as functions of the angle of twist of the formally single bond, θ, in the vinyl-carbonyl system as well as in the butadiene system.

Broken lines, Δw; Solid lines, M^2;
A, C=C-C=C; C, C=C-C=O
t, s-trans; *c*, s-cis.
Dotted lines: 1, $M^2(0°)\cdot\cos\theta$;
2, $M^2(0°)\cdot\cos^2\theta$

When δ_X is 1.2~1.3, Δg, as well as $\Delta\Delta w$, has a small negative value. This means that a deviation from planarity of the conjugated system, of C_6-C=O as well as of C=C-C=O, will cause a small hypsochromic shift of the socalled conjugation band, in accordance with observations.

In Figs. 2 and 3, the Δw values for $\delta_X=1.3$, calculated by the simple LCAO MO method for the phenyl-carbonyl and vinyl-carbonyl systems, are plotted against θ_{rs} with broken lines. In these figures, the corresponding curves for the styrene and the butadiene system are also shown for the sake of comparison.

If X is N instead of O, the steric hypsochromic shift will be somewhat more effective, δ_N being smaller than δ_O. Experimental data pertinent to test this surmise is not available. However, for example, the fact that the steric hypsochromic effect in the case of the semicarbazones of acetophenones is appreciably more effective than in tha case of acetophenones[5] seems to suggest the validity of this surmise.

According to Heilbronner and Gerdil[20], the weak longest-wavelength band at 546 mμ ($\varepsilon_{max}=440$) (A-band) of 1-acetylazulene undergoes a bathochromic shift as well as a reduction of intensity by substitution of a methyl group

18) F. A. Matsen, *J. Am. Chem. Soc.*, **72**, 5243 (1950).
19) H. O. Pritchard and H. A. Skinner, *Chem. Revs.*, **55**, 745 (1955).
20) E. Heilbronner and R. Gerdil, *Helv. Chim. Acta*, **39**, 1996 (1956).

at the 2- or the 8-position of the azulene nucleus, which will prevent the coplanar arrangement of the azulene nucleus and the carbonyl group. This band has been considered to correspond to the α-band ($\lambda_{max}=580\,m\mu$; $\varepsilon_{max}=329$) of azulene, and the latter has been assigned as a band due to the $N \rightarrow V_1$ transition[21]. Thus, if R and S are taken to refer to the azulene nucleus and the carbonyl group respectively, the $v_{-1} < v_{-1'}$ and $v_{+1} > v_{+1'}$ relations probably exist, and the A-band of the 1-acetylazulenes may be regarded as a band due to the transition from ϕ_{+1} as a perturbed orbital of ϕ_{+1} to ψ_{-1} as a perturbed orbital of ϕ_{-1}. The transition may be said to be one to a perturbed locally-excited state, and the situation may be considered to belong to case B. Therefore, a bathochromic effect of a twist of the bond linking the azulene nucleus and the carbonyl group to each other would be rather surprising. Heilbronner and Gerdil correlated this effect to a possible decrease in the π-bond order of the bond upon excitation. This effect can be interpreted as below on the basis of the above considerations.

According to Pariser[22], the energies of the lowest vacant and the highest occupied orbital of azulene and the coefficients of the $2p\pi$ atomic orbital χ_1 in these orbitals in the simple LCAO MO approximation are as follows: $v_{-1}=+0.40039$, $v_{+1}=-0.47726$; $b_{-1,1}=0.06321$, $b_{+1,1}=0.54285$. On the other hand, if the values $\delta_0=1.3$ and $\rho=0.844$ are used for the carbonyl bond, the following values are obtained: $v_{-1'}=+0.415$, $v_{+1'}=-1.715$; $b_{-1',1'}=0.897$, $b_{+1',1'}=0.441$. Thus, since $-v_{+1}$ is smaller than δ_0, g_{+1} is negative. That is, of the effects of the two orbitals of the carbonyl group on ϕ_{+1}, the depressing effect of $\phi_{-1'}$ outweighs the raising effect of $\phi_{+1'}$. In addition, since $b_{+1,1}$ is much larger than $b_{-1,1}$, $|G_{+1,-1'}|$ is larger than $|G_{-1,-1'}|$, notwithstanding the fact that the energy separation of $v_{-1'}-v_{+1}$ is larger than that of $v_{-1'}-v_{-1}$. That is, the depression of the energy of ϕ_{+1} due to the interaction with $\phi_{-1'}$ is probably greater than that of ϕ_{-1}. Thus, the energy separation between ψ_{-1} as a perturbed orbital of ϕ_{-1} and ψ_{+1} as a perturbed orbital of ϕ_{+1} will become greater as the $\rho_{1-1'}$ parameter becomes greater.

Absorption Intensity as a Function of the Angle of Twist

The moment of the one-electron transition from ψ_{+1} to ψ_{-1} is denoted by $M_{-1,+1}$, which is subsequently abbreviated to M, the subscript being omitted. In the case of C, on the basis of Eqs. 3 and 4, the square of this transition moment, i.e., the dipole strength of the transition, can be expressed as follows:

$$M^2=2\left(\int \psi_{-1}\, q\, \psi_{+1}\, d\tau\right)^2$$
$$=2\,\rho^2_{r-s}\,N^2_{-1}\,N^2_{+1}\times\left(\sum_m A_{-1',m}\,I_{+1,m}+\sum_{n'} A_{+1,n'}\,I_{-1',n'}\right)^2$$

where $I_{m,n}$ represents the integral $\int \phi_m\, q\, \phi_n\, d\tau$, q being a general symbol for the position coordinate of the electron. To a first approximation, $I_{m,n'}=0$. Accordingly, when ρ_{r-s} is zero, M^2 is zero.

If the assumption is made that N_{-1}, N_{+1}, and I's do not vary in magnitude to any appreciable extent with changes in the value of ρ_{r-s}, the oscillator strength, f, can be considered to be approximately proportional to ρ^2_{r-s}, since Δw, and hence ν_{max}, are comparatively insensitive to a change in the value of ρ_{r-s}. Further, if it is assumed that the length of the pivot bond remains unchanged when the angle of twist of the bond, θ_{rs}, does vary, ρ_{r-s} can be taken to be proportional to $\cos\theta_{rs}$; hence, the oscillator strength can be considered to be proportional to $\cos^2\theta_{rs}$. Furthermore, if the molar extinction coefficient at the absorption maximum can be taken to be proportional to the oscillator strength of the band, its proportionality to the cosine-square of the angle of twist, i.e., the relation assumed by Braude, is reached.

It should be noted that many assumptions have been needed to reach this relation by the present approach. Above all, the assumption of the insensibility of $N_{-1}\,N_{+1}$ to ρ_{r-s} seems not to be permissible. Accordingly, insofar as it depends on the present approach based on the perturbation theory, the relation of Braude can be admitted only as a very rough approximation.

The dipole strength of the transition as a function of θ_{rs} has been calculated for the phenyl-carbonyl system, as well as for the vinyl-carbonyl system, by taking the value of δ_0 to be 1.3 and by applying the simple LCAO MO method to the whole conjugated system. In these calculations, all the valence angles at carbon atoms have been assumed to be 120°. In Figs. 2 and 3, the results of the calculation are shown graphically with solid lines, together with the analogous data for the styrene and butadiene systems for the sake of comparison.

21) C. A. Coulson, *Proc. Phys. Soc.*, **65**, 933 (1952).
22) R. Pariser, *J. Chem. Phys.*, **25**, 1112 (1956).

It is seen that the transition probability of the electron-transfer band of the phenyl-carbonyl system, as well as of the vinyl-carbonyl system, is slightly more sensitive to the steric hindrance than that of the conjugation band of the corresponding conjugated hydrocarbon system.

By the way, the calculated values (in Å^2) of M^2 at $\theta=0°$, i.e., $M^2(0°)$, are as follows: C_6–C=O, 1.984; C=C–C=O, s-trans, 1.794; s-cis, 1.140. The prefix s denotes that the steric arrangement is about the formally single bond between the ethylenic bond and the carbonyl bond. From the value of $M^2(0°)$, the oscillator strength (the f_{theor}-value) for the planar phenyl-carbonyl system, for example, is calculated to be 0.909. This value is to be compared with the f_{exp}-value of 0.310 for benzaldehyde estimated from the absorption curve reported in Part X[13] of this series. In this case, the ratio of f_{theor} to f_{exp} is 2.93, a value which is reasonable in view of the general trend of this ratio observed for some conjugated hydrocarbons in Part XII[7] of this series.

In Figs. 2 and 3, curves for $M^2(0°)\cdot\cos\theta$ and $M^2(0°)\cdot\cos^2\theta$ are also shown with dotted lines. It is seen that, for each system, the $M^2(\theta)$ curve lies between the cosine curve and the cosine-square curve, largely approaching the former.

As was mentioned in Part XII of this series, however, there seems to be a trend, the smaller the f-value, for the ratio of f_{theor} to f_{exp} to be slightly the greater, and also a trend, the greater the most probable angle of twist, for the ratio of f_{exp} to the molar extinction coefficient at the absorption maximum, ε_{max}, to be the greater. If these trends can be considered as holding in general, it may be expected that the value of ε_{max} decreases somewhat more rapidly with an increasing value of θ than would be anticipated from the calculated value of $M^2(\theta)$. Therefore, it is not imposible thet ε_{max} is approximately proportional to $\cos^2\theta$ rather than to $\cos\theta$.

Thus, it may be said that the relation, proposed by Braude on a quite unreasonable ground, has been given a theoretical support here to some extent. At any rate, such a relation should, of course, be considered to be a rough approximation, since it is an approximation to correlate the observed ε-value or the f_{exp}-value with the steric effect alone, neglecting the possible hyperchromic effect of an electronic origin of the substituent and the uncertainty of the values due to the probably poor resolvability of the band concerned from the neighboring bands.

Summary

It has been shown that the characteristic feature of the steric effect on the conjugation band in the case of the phenyl-carbonyl and vinyl-carbonyl systems, i.e., the relatively small hypsochromic shift and the relatively large decrease in the intensity of the band, as compared with that in the case of the conjugated hydrocarbon systems, can be adequately interpreted using the simple MO approach. From theoretical considerations it has especially been concluded that the proportionality of the intensity of the band to the cosine-square of the angle of twist of the formally single bond in these systems, formerly assumed by Braude, may be admitted as a rough approximation in spite of the invalidity of its original reasoning.

Department of Chemistry
College of General Education
The University of Tokyo
Meguro-ku, Tokyo

Photoreduction of Methylene Blue by Some Derivatives of N-Phenylglycine. Relation between the Structure and the Reactivity of the Electron Donors

By Shiro MATSUMOTO

(Received July 11, 1962)

It has been reported[1] that the photoreduction of methylene blue was effected in deaerated solutions by some chelating agents, including *N*-phenylglycine. To elucidate the mechanism of the photoreduction of dyestuffs and to understand, in general, the nature of the reactions of photo-excited species, it may be useful to investigate systematically the effects of changes in the structure of the reducing agent (the electron donor). *N*-Phenylglycine was chosen as a suitable starting material for this purpose, as its homologues and benzene ring-substituted derivatives are well characterized (loc. cit.) and are prepared easily in a fairly good crystalline state.

N-Phenylglycine becomes unstable to air-oxidation upon the introduction of electropositive substituents into the ortho- and para-positions of the benzene ring, while the introduction of electronegative substituents has the opposite effect. A solution of *N*-*p*-oxyphenylglycine soon assumes a brown color, especially when it is alkaline, while *N*-*p*-nitrophenylglycine can be heated in boiling water without any appreciable decomposition. It seems, therefore, that the rate of the photoreduction of the dyestuff in the presence of various benzene ring-substituted *N*-phenylglycines should increase in proportion to the order of the electron-repelling tendency of the substituents. The highest rate was observed, however, with unsubstituted *N*-phenylglycine. Both positive and negative substituents reduced the efficiency of the *N*-phenylglycine as a photoreductant.

This apparent contradiction can be explained by taking into account the possibility of the deactivation of the excited dye ions by the reductant ions. In fact, *N*-*p*-methoxyphenylglycine was found to have a remarkable retarding effect, comparable to that of *p*-phenylenediamine[1], upon the photoreduction of the dye by other reducing agents. It is shown in this paper that, if a customary reaction scheme is assumed, certain of its rate constants parallel Hammett's σ[2] value for the substituent.

Other kinds of derivatives of *N*-phenylglycine were also examined; it was found that the replacement of the hydrogen atom, either on the nitrogen or on the α-carbon atom of *N*-phenylglycine, by the methyl group did not deprive it of the ability to photoreduce the dye. These hydrogen atoms, therefore, do not take part in the photoreduction. On the other hand, the insertion of a methylene unit between the amino and the carboxyl group greatly reduced the ability.

Experimental

Benzene ring-substituted *N*-phenylglycines were prepared from the corresponding anilines either by the action of haloacetic acid or by Knoevenagel's[3] or Schwalbe's[4] method. *N*-Methyl-*N*-phenylglycine was prepared by the action of ethyl bromoacetate on dimethylaniline[5], followed by hydrolysis. It was separated as hydrochloride and purified in this form. α-Methyl-*N*-phenylalanine was prepared by the hydrolysis of the nitrile, which had been obtained by the action of potassium cyanide on the acetone in acetic acid[6]. *N*-Acetyl-*N*-phenylglycine was prepared by the acetylation of *N*-phenylglycine with acetic anhydride[7]. *N*-phenyl-β-alanine was prepared by the action of 3-bromopropanoic acid on aniline[8].

Methylene blue was a G. R. grade reagent from the Koso Chem. Co. and was used without further purification. Its molar extinction coefficient at 665 mμ was 8.16×10^4. *p*-Phenylenediamine hydrochloride was a G. R. grade reagent from the Kanto Chem. Co.

Photobleaching was followed, in an apparatus which was similar to that used by Pestemer[9], by some practical modification. The light source for the reaction was a 200 W./100 V. incandescent lamp operated at 78 V. This voltage was regulated to within 0.03 V. during a run. The light, filtered through a layer of water and an interference filter ($\lambda_{max.}$ 665 mμ, band width 12 mμ), fell on a reaction

1) G. Oster and N. Wotherspoon, *J. Am. Chem. Soc.*, **79**, 4836 (1957).

2) L. P. Hammett, "Physical Organic Chemistry", McGraw-Hill Book Co., New York, N. Y. (1940), Chap. 7.

3) E. Knoevenagel, *Ber.*, **37**, 4065 (1904).

4) C. G. Schwalbe, W. Schulz and H. Jochheim, ibid., **41**, 3790 (1908).

5) J. F. Thorpe and A. S. Wood, *J. Chem. Soc.*, **103**, 1601 (1913).

6) R. v. Walther and R. Hübner, *J. prak. Chem.*, [2] **93**, 119 (1916).

7) C. A. Bischoff and A. Hausdörfer, *Ber.*, **25**, 2270 (1892).

8) C. A. Bischoff and N. Mintz, ibid., **25**, 2345 (1892).

9) M. Pestemer, *Z. Elektrochem.*, **58**, 121 (1954).

cell in a thermostat kept to 40±0.1°C. The transmitted light was measured by a photocell to follow the change in the optical density. The thickness of the liquid layer was 15.5 mm., while the light intensity was estimated to be 2.2×10^{14} photons per cm^2 per sec. A metal net was inserted between the light source and the cell to reduce the light intensity if necessary. Deaeration was achieved by flushing with nitrogen as in Pestemer's[9] experiment.

Absorption spectra and total fluorescence intensity were measured by a Shimadzu Spectrophotometer QR 50.

Results and Discussion

A qualitative test showed that *N*-*p*-chlorophenylglycine (*p*-Cl-ϕ·G) would be more suitable than unsubstituted *N*-phenylglycine (ϕ·G) as a reference substance. The former was found to be more stable in air, though it caused the photobleaching nearly as effectively as the latter. Therefore, all the preliminary experiments to inspect various factors were performed with this substance as the electron donor.

1. Time Course of the Bleaching.—The change in the optical density, *D*, with time could be expressed quite well by the superposition of two exponential terms, as in the case of methylamines reported by Obata and Koizumi[10]. An example is shown in Fig. 1, in which the curve is drawn according to $D=0.1099\times10^{-0.00344t}+0.0220\times10^{-0.000787t}$. This fact may be explained most simply by assuming an intermediate that slowly accumulates during the course of the reaction[10]. However, to avoid complexity in treating the kinetic data and to minimize special assumptions, it may be convenient to consider, for the moment, only the early stage of the photoreduction.

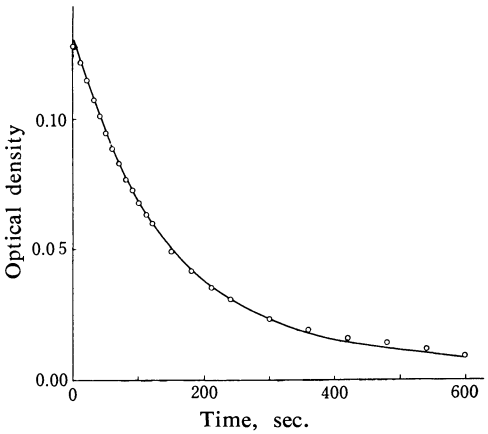


Fig. 1. Photobleaching of M.B.
M.B. 1.1×10^{-6} M, *p*-Cl-ϕ·G 1.0×10^{-4} M
pH 7.0 40°C

At this stage, such intermediates, if any, can safely be neglected. Therefore, Bodenstein's stationary state method may be used to derive the rate equation. Accordingly, tangents were drawn at time zero to the log *D* versus time curves, which were usually convex to an ordinate showing the deviations from the first order kinetics; the initial values of quautum yield Φ[11] were calculated from the slopes.

2. Effect of Light Intensity on Φ.—As is shown in Table I, a two-to three-fold variation in light intensity has little effect on Φ.

Table I. Effect of light intensity on ϕ
M.B. 1.5×10^{-6} M, *p*-Cl-ϕ·G 1.0×10^{4} M pH 7.0

Relative intens.*	1.00	0.55	0.34
Φ	0.150	0.157	0.147

* Stand. intens. 2.2×10^{14} photons/cm^2·sec.

3. Effect of Dye Concentration.—Table II shows that Φ is practically independent of the dye concentration in the $(1\sim5)\times10^{-6}$ mol./l. range.

Table II. Effect of dye concn. on Φ
p-Cl-ϕ·G 1.0×10^{-4} M. pH 7.0

Dye concn. $\times10^{6}$ M	0.92	1.53	3.13	5.47
Φ	0.141	0.150	0.150	0.130

4. Effect of the pH Value.—The points in Fig. 2 are taken from some preliminary experiments, where the concentrations of the methylene blue and *p*-Cl-ϕ·G were fixed arbitrarily at 1.5×10^{-6} and 1.0×10^{-4} mol./l. respectively. A maximum is observed at a pH value near 7.8. However, Φ depends also on the concentration of the electron donor. This matter will be described more fully in the next paper, together with the effect of buffer solutions.

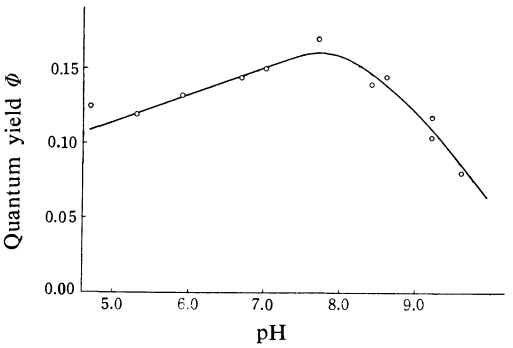


Fig. 2. pH dependence of quantum yield.
M. B. 1.5×10^{-6} M, *p*-Cl-ϕ·G 1.0×10^{-4} M 40°C

10) H. Obata and M. Koizumi, This. Bulletin, **30**, 136, 142 (1957).

11) Any inaccuracy in the determination of the absolute light intensity does affect the absolute values of Φ, but their relative values are of main interest here.

5. Dependence of Φ on the Concentration of the Electron Donor.—The dependence is expressed by the equation:

$$1/\Phi = 1/\Phi_0 + b/[E] \quad (1)$$

where Φ_0 and b are constants and [E] is the concentration of the electron donor. An example is shown in Fig. 3.

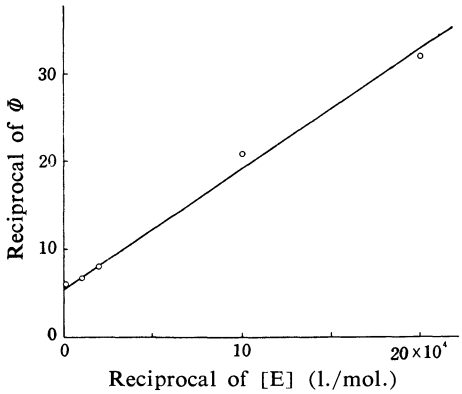


Fig. 3. Dependence of Φ on electron donor concn.
E: p-Cl-ϕ·G, pH 7.0 40°C

6. Dependence of Φ on the Structure of the Electron Donor.—In Table III are summarized the Φ's of the photoreduction by various *N*-phenylglycines and related compounds of the same molarity (10^{-4} mol./l. except for *N*-phenyl-β-alanine, for which 10^{-3} mol./l.). It is seen that the replacement of the hydrogen atom on the nitrogen or α-carbon atom of *N*-phenylglycine by a methyl group does not deprive it of its ability as a photoreductant. These hydrogen atoms are therefore, not included in photoreduction process; and reduction is probably initiated by electron transfer from the reducing ions to the excited dye cations. *N*-Acetylation reduces the ability, but this may be due either to steric effects or to the electron-attracting influence of the acetyl group (see below). The insertion of a methylene unit between the amino and the carboxyl group greatly reduces the ability as a photoreductant.

Table III also shows that both electropositive and electronegative substituents in the ortho- and para-positions reduce the effectiveness of the *N*-phenylglycine. Moreover, bromine-substitution in these positions has a much more pronounced effect than chlorine-substitution, though these two elements have nearly the same substituent effects in ordinary thermal reactions, as is seen in their similar Hammett σ[2] values. It may be added here that slow bleaching is observed even in the absence of any reducing agent (the quantum yield is of the order of 10^{-3} at a pH value of 7). Such slow bleaching is completely absent in the presence of *N*-*p*-methoxyphenylglycine (p-MeO-ϕ·G), while it is at least preserved in the case of *N*-*p*-nitrophenylglycine (p-NO_2-ϕ·G). These facts suggest the parallel occurrence of the retardation by the reductants themselves. It is also interesting that the effect of substituents is much smaller in meta-substitution than in ortho- and para-substitutions. It is especially ramarkable that *N*-*m*-methoxyphenylglycine (m-MeO-ϕ·G) normally photoreduces the dye.

In regard to the high efficiencies of *N*-phenylglycines in the photoreduction, a question arises whether any complex is formed between *N*-phenylglycines and the dye in its ground state, the complex being ready to undertake inner oxidation-reduction upon the absorption of light. To check this point, the absorption spectra of the reaction mixtures were examined, together with those of the components from the ultraviolet end to the red end of the

TABLE III. INITIAL QUANTUM YIELD Φ OF PHOTOREDUCTIONS BY VARIOUS DERIVATIVES OF *N*-PHENYLGLYCINE

M. B. 1.5×10^{-6} M, ϕ·G's 1.0×10^{-4} M pH 7.0

a) Benzene ring-substituted *N*-phenylglycines

Substituent	HO	MeO	Me	H	Cl
ortho	0.000	0.003			0.092
Position meta		0.169		0.230	0.147
para	0.000	0.000	0.076		0.150
	Br	COOH	MeCO	CN	NO_2
	0.018				0.001
	0.063	0.167			0.022
	0.010		0.041	0.010	0.001

b) Other derivatives

$\phi N(CH_3)\cdot CH_2\cdot COOH$	0.235	$\phi N(COCH_3)\cdot CH_2\cdot COOH$	0.003
$\phi NH\cdot C(CH_3)_2\cdot COOH$	0.305	$\phi NH\cdot(CH_2)_2\cdot COOH$†	0.009

† 10^{-3} M

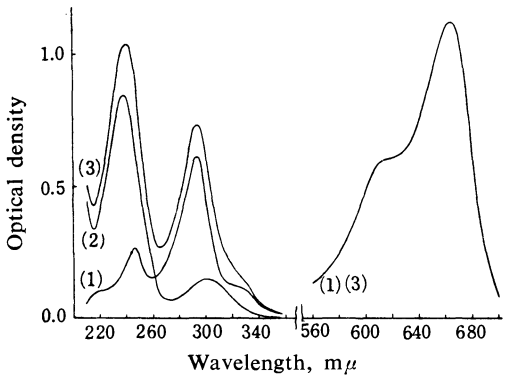


Fig. 4. Absorption curves of solns. of M. B., *p*-MeO-ϕ·G and their mixture. (1) M. B. 1.44×10^{-5} M (2) *p*-MeO-ϕ·G 7.65×10^{-5} M (3) M. B. 1.44×10^{-5} M, *p*-MeO-ϕ·G 7.65×10^{-5} M pH 7.0. In the visible region, where the ϕ·G does not absorb, curve (3) coinsides with (1).

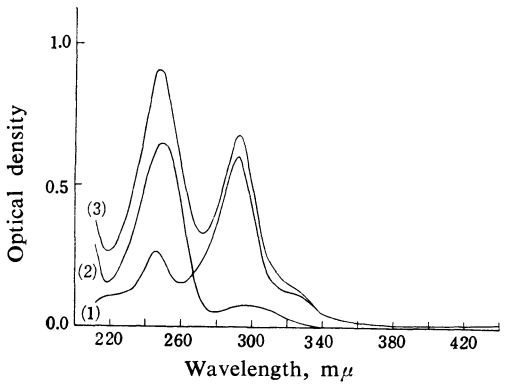


Fig. 5. Absorption curves of solns. of M. B., *p*-Cl-ϕ·G and their mixture. (1) M. B. 1.44×10^{-5} M (2) *p*-Cl-ϕ·G 4.92×10^{-5} M (3) M. B. 1.44×10^{-5} M, *p*-Cl-ϕ·G 4.92×10^{-5} pH 7.0. Absorption in longer-wavelength region is the same as that in Fig. 4.

visible region. As may be seen in Figs. 4 and 5, a good additivity holds in the entire region. No sign of complex formation is observed.

The following scheme may tentatively be assumed as the simplest for describing the reaction sequences:

$$\begin{array}{ccccccc} & & \overset{k_2}{\longrightarrow} & & \overset{k_r[E]}{\longrightarrow} & & \\ D^{+*} & & & D^{+t} & & M & \longrightarrow \text{Red. Prod.} \\ h\nu \uparrow\downarrow k_1 & & & k_s+k_d[E] & & \gamma_E & \\ D^{+} & \longleftarrow & & \longleftarrow & & & \end{array}$$

where D^+ is the dye cation in the ground state, and D^{+*} is that in its first electronically-excited singlet state. A second metastable excited state, D^{+t}, is assumed for the same reason as in some other cases[9,12]. It was confirmed that the fluorescence intensity of methylene blue was little affected by the addition of *p*-Cl-ϕ·G or *p*-MeO-ϕ·G up to a concentration of 10^{-4} mol./l.

The rate constants of deactivation, k_1 and k_s, may contain terms that correspond to the deactivation by the emission of radiation, as well as terms corresponding to radiationless deactivation. The deactivation of D^{+t} must be enhanced by E (an electron donor), as is stated above, which is represented by the term, $k_d[E]$. Adding a term representing the deactivation of D^{+*} by E is not justifiable because that will lead to a rate equation that has not the simple form of Eq. 1. The reduction of D^{+t} may take place via intermediate, M, some fraction of which may foil to give the reduction product. The fraction of M's that succeeds in getting to the final product is denoted by γ_E.

Therefore, Φ may be expressed according to Bodenstein's approximation:

$$\Phi=\varphi\cdot\frac{k_r[E]}{k_s+(k_d+k_r)[E]}\cdot\gamma_E \qquad (2)$$

where $\varphi=k_2/(k_1+k_2)$ may be said to be the quantum yield of the first stage. Equation 2 is identical with Eq. 1, if $\Phi_\infty=\varphi\cdot\gamma_E\cdot k_r/(k_d+k_r)$ and $1/b=\varphi\gamma_E\cdot k_r/k_s$. Φ_∞ is the quantum yield extrapolated for infinite electron

Table IV. Φ_∞ and $1/b$ for various electron donors

a) Benzene ring-substituted *N*-phenylglycines

Substituent	Φ_∞	$1/b$ (l./mol.)
p-MeO*		(0)
m-MeO	0.236	7.59×10^3
p-Me	0.077	1.73×10^4
H	0.274	1.17×10^4
o-Cl	0.206	1.64×10^3
m-Cl	0.260	3.57×10^3
p-Cl	0.185	7.39×10^3
o-Br	0.023	5.51×10^2
m-Br	0.087	2.04×10^3
p-Br	0.014	9.50×10^2
m-COOH	0.229	4.97×10^3
p-COMe	0.218	5.07×10^2
p-CN	0.227	1.07×10^2
m-NO_2	0.212	2.68×10^2
p-NO_2	0.05	6.7

b) Other derivatives

	Φ_∞	$1/b$ (l./mol.)
$\phi N(CH_3)\cdot CH_2\cdot COOH$	0.278	2.71×10^4
$\phi N(COCH_3)\cdot CH_2\cdot COOH$	0.039	4.99×10
$\phi NH\cdot C(CH_3)_2\cdot COOH$	0.388	1.31×10^4
$\phi NH\cdot CH_2\cdot CH_2\cdot COOH$†	(0.032)	(1.40×10^2)

* $B=1/(\Phi_\infty b)=5.29\times10^5$ l./mol. † $B=4.31\times10^3$ l./mol. These values and the values in ( ) were obtained from retardation experiments (section 7).

12) G. Oster and A. H. Adelman, *J. Am. Chem. Soc.*, **78**, 913 (1956).

donor concentration and is naturally the Φ when k_s is neglected compared with (k_d+k_r) [E]. In this kinetic scheme, $1/b$ represents the relative effectiveness of ϕ·G's as a photoreductant, if k_s is independent of the nature of the added substances. These quantities can be obtained from plots similar to those in Fig. 3.

The results are summarized in Table IV. As is seen in the table, *o*- and *p*-Br-ϕ·G, for which unexpectedly small Φ values were observed, have small Φ_∞ values, which implies large k_d values.

7. Direct Measurement of the Retardation by *N*-Phenylglycines.—The retarding action of *N*-phenylglycines is demonstrated in the plots of Fig. 6, where Φ is measured in a system containing 1.5×10^{-6} mol./l. of methylene blue and 1.0×10^{-4} mol./l. of *p*-Cl-ϕ·G, to which are added various concentrations [E'] of retarding ϕ·G's. When [E'] $=0$, the system bleaches with $\Phi=0.150$. Φ decreases, in general, by the addition of ϕ·G's, which were above suspected of retarding action. The effect of *p*-MeO-ϕ·G is most remarkable; it shows only a retarding action. The efficiency is comparable to that of the well-known retarder *p*-phenylenediamine (PPD)[1]. The retarding ratio $R_{ret}=\Phi_0/\Phi$ (Φ_0 and Φ are the quantum yields in the absence and in the presence of retarders respectively) with 10^{-5} mol./l. of PPD was 1.88, whereas that with *p*-MeO-ϕ·G was 1.79. It is interesting that *p*-MeO-ϕ·G is isoelectronic with PPD. Other ϕ·G's, e. g., *p*-Br-ϕ·G, cause photobleaching by themselves. If it is assumed that these ϕ·G's compete with *p*-Cl-ϕ·G in reacting with D^{+t}, the equation for Φ is modified as follows:

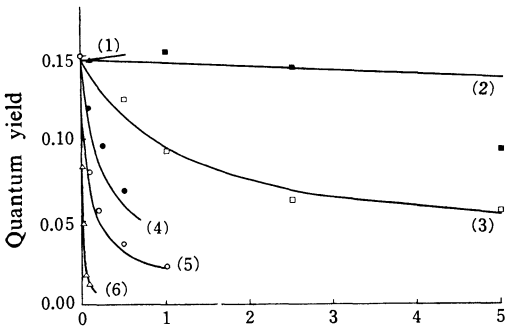


Fig. 6. Retardation by *N*-phenylglycines.
Test soln. contains: *p*-Cl-ϕ·G 1.0×10^{-4} M, retdg.
ϕ·G's [E'] M and M. B. 1.5×10^{-6} M pH 7.0
(1) *m*-NO_2-ϕ·G (2) *p*-NO_2-ϕ·G (3) *N*-ϕ-β-alanine (4) *o*-Br-ϕ·G (5) *p*-Br-ϕ·G (6) *p*-MeO-ϕ·G

$$\Phi=\varphi\cdot(\gamma_E\cdot k_r[E]+\gamma_E' k_r'[E'])/\{k_s+(k_d+k_r)[E]+(k_d'+k_r')[E']\}$$

where k_d', k_s' and γ_E' are the quantities corresponding to k_d, k_s and γ_E respectively for the second ϕ·G.

Or

$$\Phi=\varphi\cdot\frac{[E]/b+[E']/b'}{1+[E]/(b\cdot\Phi_\infty)+[E']/(b'\cdot\Phi_\infty')} \quad (3)$$

Again, b' and Φ_∞' correspond to b and Φ_∞ respectively. This relation could be checked by the insertion of the values of b, Φ_∞, b' and Φ_∞' given in Table IV. The curves in Fig. 6 are drawn to show this calculation. They coincide, at least qualitatively, with the experimental results. Φ_∞ and b could not be determined directly for *p*-MeO-ϕ·G and *N*-phenyl-β-alanine. In these cases, the insertion of the b and Φ_∞ values of *p*-Cl-ϕ·G into Eq. 3 gave:

$$\Phi=(0.739+A[E'])/(5.00+B[E'])$$

where $A=1/b'$ and $B=1/(b'\cdot\Phi_\infty')$. A and B were then determined, so that the best fit was obtained in Fig. 6. This required $B=5.29\times10^5$ and $A\fallingdotseq0$ for *p*-MeO-ϕ·G and $B=4.31\times10^3$ and $A=1.40\times10^2$ for *N*-phenyl-β-alanine respectively.

8. Reactivities of *N*-Phenylglycines and Hammett's σ Value.—The B quantity given above has a simpler kinetic meaning than either $1/b$ or Φ_∞ has; i. e., $B=1/(b\cdot\Phi_\infty)=(k_d+k_r)/k_s$. It is the sum of the rate constants for the reduction and deactivation of D^{+t} by the ϕ·G concerned, divided by the rate constant for the spontaneous deactivation. The value of k_s may be independent of the nature of the ϕ·G. Thus, B represents the relative total reactivity of the ϕ·G with D^{+t}.

Some relation might be sought between this value and Hammett's σ for the substituent in the benzene ring. The plots of $\log(B/B_0)$ versus σ are given in Fig. 7, where B_0 is the B

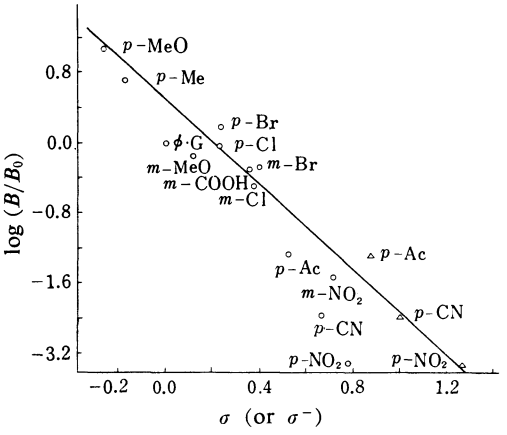
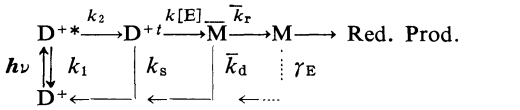


Fig. 7. Hammett's σ and the reactivity of *N*-phenylglycines.
○: σ △: σ^- pH 7.0 40°C

for the unsubstituted *N*-phenylglycine. It is seen that the points arrange near a straight line, the σ^- values giving better fits for the +E substituents. This might indicate the importance of the lone pair of electrons on the nitrogen atom of *N*-phenylglycine in the first stage of interaction with D^{+t} [13]. Although the detailed reason must be kept unspecified until other physico-chemical studies throw light from other angles on this problem, it is, nevertheless, interesting that a relation like Hammett's rule is found in a photochemical process.

The above considerations may be consistent with a kinetic scheme written in a more detailed form than the previous one:



where a step is imagined in which D^{+t} forms a loose complex, M, with E before it is either reduced or deactivated by E. Then,

$$\Phi=\varphi\{k[E]/(k_s+k[E])\}\times\{\bar{k}_r/(\bar{k}_d+\bar{k}_r)\}\ \gamma_E \quad (4)$$

and $k_d=k\cdot\bar{k}_d/(\bar{k}_d+\bar{k}_r)$ and $k_r=k\cdot\bar{k}_r/(\bar{k}_d+\bar{k}_r)$ correspond; i. e., Eq. 4 becomes identical with Eq. 2 with these substitutions. B becomes simply k/k_s, and the rate constant of the complex formation k bears a regular relation to δ irrespective of the $\bar{k}_r/\bar{k}_d$ ratio.

9. Evaluation of the Life-time of D^{+t}.— The retardation data with PPD may be used to estimate the lower limit of $1/k_s$, the life-time of the metastable state D^{+t}, using the method described by Oster and Adelman[12], in which it is assumed that the reaction is diffusion-controlled and that every collision of a PPD molecule with D^{+t} effectively deactivates the latter. It is easy to derive

$$R_{ret}=\Phi_0/\Phi=1+\frac{k_q/k_s}{1+\{(k_d+k_r)/k_s\}[E]}\cdot[X] \quad (5)$$

where X represents PPD or another quencher molecule and [X] is its concentration. The rate of the deactivation of D^{+t} is supposed to increase by a term of $k_q[X]$. Φ_0 is the Φ when $[X]=0$. As is stated above, $R_{ret}=1.88$ for $[X]=10^{-5}$ mol./l. and $[p\text{-Cl-}\phi\cdot G]=10^{-4}$ mol./l. As $(k_d+k_r)/k_s=1/(b\cdot\Phi_\infty)=4.00\times10^4$ l./mol. for p-Cl-$\phi\cdot$G (Table IV), Eq. 5 gives $k_q/k_s=4.4\times10^5$ l./mol. The number of collisions of a D^{+t} with X molecules in a unit of time is given as $(8RT/3\eta)\cdot[X]\times10^{-3}$ [12] by the use of Smoluchowski's theory of diffusional collisions and Einstein's theory of diffusion, together with the simplifying assumptions that the reacting species are spherical and equal in size, with encounter radii equal to their diffusional radii. R and η are the gas constant and the viscosity of the medium respectively. Hence, $k_q\leqq(8RT/3\eta)\times10^{-3}$. If $T=313$ and $\eta=6.56\times10^{-3}$ poise, this gives $k_q\leqq1.06\times10^{10}$ sec^{-1}, so that $\tau=1/k_s\geqq4.2\times10^{-5}$ sec., which is of a reasonable order of magnitude for a triplet of the dye in aqueous solutions at ordinary temperatures. If $1/k_s=4.2\times10^{-5}$ sec., then k_d+k_r is determined. For example, it is 9.6×10^8 l./mol. for p-Cl-$\phi\cdot$G.

13) M. Kotake, "Dai-yūkikagaku", Asakura Book Co., Tokyo (1958), p. 310.

Summary

The photobleaching of methylene blue in the presence of various derivatives of *N*-phenylglycine has been examined to investigate the relation between the structure and the reactivity of the electron donor and to get information about the nature of the photoreaction. The time course of the photobleaching is well expressed by the superposition of two terms decreasing exponentially with time.

The hydrogen atom on the nitrogen or α-carbon atom of the *N*-phenylglycine molecule seems to take no part in the photoreduction process, and the first stage is probably the electron transfer between the interacting species.

As judged from the initial quantum yield, Φ, of the photoreductions, the influence of substituents in the ortho- and para-positions of the benzene ring is much larger than that in the meta-position. Both electropositive and electronegative substituents reduce Φ. The small Φ in the former cases is attributed to the ability of such $\phi\cdot$G's to deactivate the excited dye ions. From spectral data, no sign of complex formation between $\phi\cdot$G's and unexcited dye molecules can be inferred. The fluorescence of methylene blue is not quenched by $\phi\cdot$G's in the range of concentrations used in the photochemical reaction. In view of these results, the kinetic data are treated by use of a current kinetic scheme, when a relation akin to Hammett's rule is found between a certain rate constant and the σ value of the substituent in the benzene ring of the *N*-phenylglycine.

Kinetic data are also used to estimate the life-time of the metastable excited state of the dye, which is calculated to be about 4.2×10^{-5} sec. or longer. This value is in a range reasonable to be interpreted as that of the lowest triplet state of the dye.

The author is indebted to Professor Ikuzo Tanaka of the Tokyo Institute of Technology

and to Professor Masao Koizumi of Tohoku University for their constant encouragement and many helpful discussions.

Faculty of Agriculture
Kagawa University
Kita-gun, Kagawa-ken

Effect of the pH Value on the Rate of the Photoreduction of Methylene Blue by N-Phenylglycines

By Shiro MATSUMOTO

(Received July 11, 1962)

In the preceding paper, a preliminary result was described as to the dependence of the initial quantum yield, Φ, of the photoreduction of methylene blue by *N*-phenylglycines on the pH value of the medium. As Φ does not vary linearly with the concentration of electron donors, it is not sufficient to investigate the problem only at a definite electron donor concentration. The ionization of the *N*-phenylglycines is another factor to be studied. Moreover, Φ will also depend on the nature and concentrations of the buffer solutions. It is the object of this paper to investigate these factors in some detail.

Experimental

The photobleaching apparatus and the experimental method were the same as those described in the preceding paper. A Shimadzu Glass Electrode Potentiometric Titrator PT-1 was used to measure the pH value of solutions. Reagents for the buffer solutions were obtained from the Kanto Chem. Co., Inc. The phosphates were of the G. R. grade "for pH determination," while the others were of E. P. grades. The borax was recrystallized once from water. Corrections for ionic strength were made with sodium chloride which was also a G. R. reagent from the Kanto Chem. Co., Inc.

Results and Discussion

1.—First, two orienting experiments were carried out.

a. Dissociation of N-Phenylglycines.—Figure 1 shows the titration curve of *N*-phenylglycine (10^{-2} mol./l.) with a 0.0553 N sodium hydroxide solution. The points agree fairly well with the calculated curve for monobasic acid of pK_a 4.3, except in alkaline regions, where the deviation is probably due to the effect of atmospheric carbon dioxide. It is evident, therefore, that *N*-phenylglycine exists only in a definite form, $C_6H_5NH\cdot CH_2\cdot COO^-$, in aqueous solutions with pH values within the 5.9~10.5 range, where the experiments were performed.

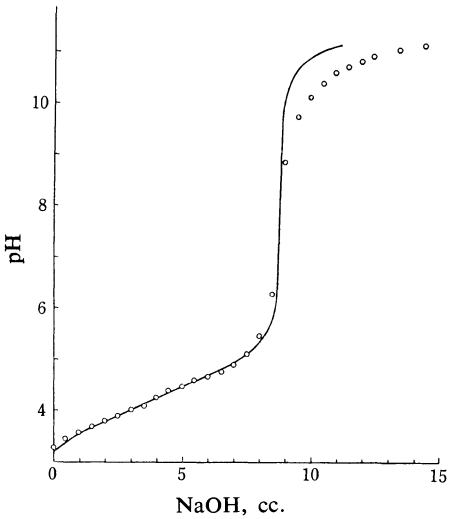


Fig. 1. Base titration of *N*-phenylglycine.

TABLE I. pK_a OF SUBSTITUTED *N*-PHENYLGLYCINES

$\phi\cdot$G	*p*-Cl-$\phi\cdot$G	*p*-CH_3-$\phi\cdot$G
4.3	3.9	5.0
p-CN-$\phi\cdot$G	*p*-Ac-$\phi\cdot$G	*m*-COOH-$\phi\cdot$G
3.8	3.7	(3.7)*

* The pH of half titrated soln. Ionization of the two COOH-groups cannot be separated titrimetrically.

Such other forms as $C_6H_5NH\cdot CH_2\cdot COOH$ and $C_6H_5NH_2^+\cdot CH_2\cdot COO^-$ may be neglected in this study. Similar experiments gave the pK_a values of various *N*-phenylglycines; these are listed in Table I.

b. Effect of the Concentration of Buffer Solutions and Ionic Strength. — The quantum yield, Φ, of the photoreduction was measured in buffer solutions of three different concentrations at various pH values. The ionic strength, μ, was designed to be constant. The results are shown in Fig. 2, which clearly shows the effect of buffer concentration. It is

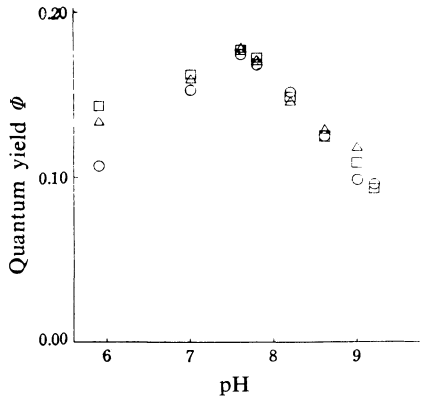


Fig. 2. Effect of buffer concentration on Φ.
Electr. donor p-Cl-ϕ·G 1.0×10^{-4},
M. B. 2.5×10^{-6} M

	Buff. concn., mol./l.			
pH	5.9*	7.0*	7.8*	7.6†
○	0.102	0.056	0.044	0.088
△	0.061	0.033	0.026	0.053
□	0.020	0.011	0.009	0.018
pH	8.2†	8.6†	9.0†	9.2†
○	0.097	0.109	0.131	0.140
△	0.058	0.065	0.078	
□	0.019	0.022	0.026	0.028

* KH_2PO_4-Na_2HPO_4 buff. $\mu=0.122$ g. ion./l.
† $Na_2B_4O_7$-HCl buff. $\mu=0.071$ g. ion./l.

TABLE II. EFFECT OF IONIC STRENGTH ON Φ

μ (g. ion./l.)	0.049	0.074	0.149	0.449
Φ	0.159	0.162	0.144	0.139

especially marked at the lower end of the pH region. The effect of ionic strength at a constant buffer concentration is shown in Table II. It is seen that the effect is within the range of experimental error for $\mu<0.1$ g. ion/l.

To avoid the above complexity, it would be best, theoretically, to use the Φ's extraporated to those in infinitely dilute buffer solutions. However, this procedure would be too troublesome to be practicable, and the errors in the extrapolation might be appreciable. Accordingly, the following experiments were performed in buffer solutions in which the total phosphate, borate or carbonate concentration and the ionic strength were maintained at constant and minimum practical values.

2. Dependence of Φ_∞, $1/b$ and B on pH Value. —At every pH value the following relation[1] holds:

$$1/\Phi=1/\Phi_\infty+b/[\mathrm{E}]$$

where [E] is the concentration of the electron donor and Φ_∞ and b are constants for the particular conditions. Φ_∞ and b naturally

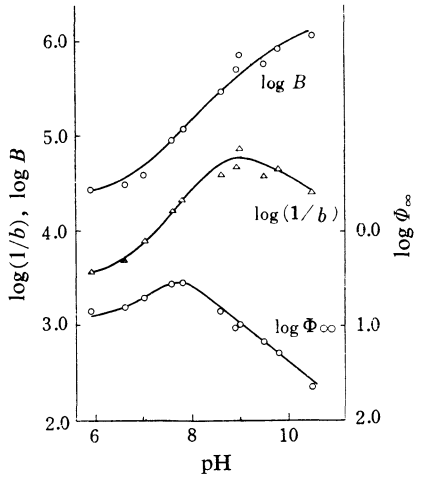


Fig. 3. Dependence of Φ_∞, $1/b$ and B on pH.
Electr. donor p-Cl-ϕ·G M. B. 2.5×10^{-6} M
40°C

depend on the pH value. In Fig. 3 their values and the $B=1/(\Phi_\infty\cdot b)$ value[1] for *N*-*p*-chlorophenylglycine are plotted on a logarithmic scale against the pH values. The dependence of Φ_∞ on the pH value is similar to that of Φ measured at a definite electron donor concentration. This is in contrast to Oster's[2] results with EDTA, where Φ_∞ was independent of the pH value. On the other hand, $\log(1/b)$ and $\log B$ increase markedly with an increase in the pH value. $\log B$ increases especially steadily and is linear with the pH value in the 7~9 range[3]. The slope is approximately 0.51. Figure 4 shows similar results with *N*-phenylglycine. In this case, the variation of Φ_∞ is smaller, but the slope of $\log B$ against the pH value is nearly the same. Figure 5 shows the results with *N*-*p*-acetylphenylglycine, which has a much smaller reactivity[1] than the above two *N*-phenylglycines. The slope of $\log B$ is approximately 0.45.

To see whether the linear dependence of $\log B$ on the pH value is a general occurrence, it is desirable to investigate also with other simple molecules. Methylamines are the simplest, but their dissociation constants are comparatively large, and for the study with uniform ionic species[4], the bleaching must be measured in a region of higher pH value,

1) Cf. (the preceding paper) S. Matsumoto, 35, 1860 (1962).

2) G. Oster and N. Wotherspoon, *J. Am. Chem. Soc.*, 79, 4836 (1957).

3) At higher pH values, the photobleaching of methylene blue occurs appreciably in the absence of any reductant, and rigorous treatment of the data is more difficult, unless the nature of such bleaching is definitely established, than at a low pH value where the photobleaching is negligible in the absence of a reductant. In the above calculation of Φ, such a bleaching rate was merely subtracted, for the moment, as 'blanck' from the total bleaching rate.

4) Cf. section 1, a of this paper.

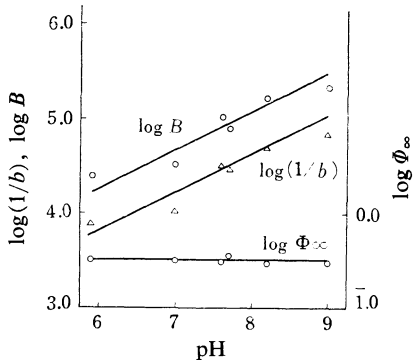


Fig. 4. Dependence of Φ_∞, $1/b$ and B on pH. Electr. donor ϕ·G M. B. 2.5×10^{-6} M 40°C

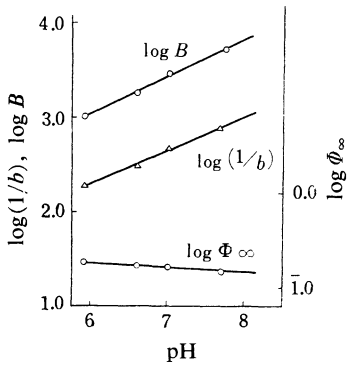
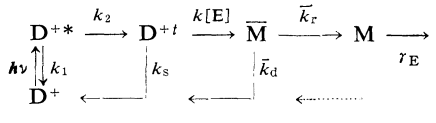


Fig. 5. Dependence of Φ_∞, $1/b$ and B on pH. Electr. donor *p*-Ac-ϕ·G M. B. 2.5×10^{-6} M 40°C

where another complexity arises[3]. Among the several substances tested, semicarbazide was found to have ability as a photoreductant and also to have a low ionization constant: $pK_b=10.6$[5]. Its effectiveness was, however, very much smaller than that of the *N*-phenylglycines. The results are shown in Fig. 6. It is interesting that the pH value dependences of Φ_∞, $1/b$ and B are similar for this different kind of substance. The slope of log B against the pH value is, however, much smaller (ca. 0.1) than those in the preceding cases.

Let the following scheme be assumed as in the preceding paper:



Then,

$$\Phi=\varphi\cdot\gamma_E\{k[E]/(k_s+k[E])\}\{\bar{k}_r/(\bar{k}_d+\bar{k}_r)\}$$

$$\Phi_\infty=\varphi\cdot\gamma_E\cdot\bar{k}_r/(\bar{k}_d+\bar{k}_r)$$

$$1/b=\varphi\cdot\gamma_E(k/k_s)\{\bar{k}_r/(\bar{k}_d+\bar{k}_r)\}$$

5) N. A. Lange, "Handbook of Chemistry", 8th Ed., Handbook Publishers, Inc., Sandusky, Ohio (1952), p. 1235.

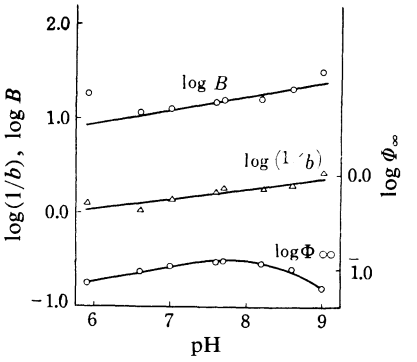


Fig. 6. Dependence of Φ_∞, $1/b$ and B on pH. Electr. donor $NH_2\cdot CO\cdot NH\cdot NH_2$ M. B. 2.5×10^{-6} M 40°C

and $$B=k/k_s$$

The simpler dependence of B is in accord with the simpler expression of B than those of Φ_∞ and $1/b$.

If k_s is independent of the pH value, then

$$\partial \log B/\partial pH=\partial \log k/\partial pH$$

In most of the cases described above, this slope is approximately 0.5, so that $k\propto\sqrt{[OH^-]}$. This may suggest the contribution of OH^- in the reaction: $D^{+t}+E\rightarrow\bar{M}$, though the true nature is uncertain as yet.

Summary

The effect of the pH value on the rate of the photoreduction of methylene blue by *N*-phenylglycines was studied in detail in the range between 5.9 and 10.5, attention being paid to the effects of buffer solutions and to a possible change in the ionic species of *N*-phenylglycines with the change in pH value. *N*-Phenylglycine behaved as a monobasic acid of pK_a 4.3 to base titration, so that it existed solely as a univalent anion $C_6H_5NH\cdot CH_2COO^-$ in this pH value range. The pK_a of several other *N*-phenylglycines was given also. The concentration and ionic strength of the buffer solutions had some effect; they must be kept constant and as small as possible.

With these precautions, the pH value dependences of Φ_∞, $1/b$ and $B=1/(\Phi_\infty\cdot b)$, which characterize the quantum yield of the photoreduction, were determined for several electron donors. They were similar in all cases. Semicarbazide was found to be effective as an electron donor for this photoreduction. Log B varied linearly with the pH value in the pH range between 7.0 and 9.0. The slopes were nearly 0.5 for all the *N*-phenylglycines studied. This means that, if the excited metastable state of the dye formed a complex before the oxidation-reduction reaction, the rate constant of

its formation must vary as the root of the hydroxide ion concentration.

The auther is indebted to Professor Ikuzo Tanaka of the Tokyo Institute of Technology and to Professor Masao Koizumi of Tohoku University for their helpful discussions and constant encouragement during this work.

Faculty of Agriculture
Kagawa University
Kita-gun Kagawa-ken

Reactions of Active Methylene Compounds. VIII. A New Route to 3-Alkyl-4-hydroxycoumarins

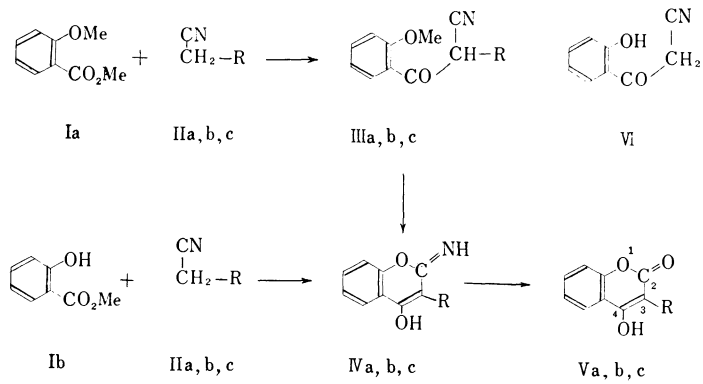
By Yoshiyuki KAWASE and Kazuko SAKASHITA

(Received July 16, 1962)

In previous papers[1], one of the present authors has reported the synthesis of 3-aryl-4-hydroxycoumarins by the ester condensation of methyl *o*-methoxy- or *o*-hydroxy-benzoate and phenylacetonitriles, followed by the ring closure of the condensation products. Now the method has been applied, with some modifications, to the synthesis of 3-alkyl-4-hydroxycoumarins (V).

For the preparation of 3-alkyl-4-hydroxycoumarins, several methods have hitherto been reported: (a) by the reaction of *o*-acetoxybenzoyl chlorides with ethyl alkylmalonates, alkylacetoacetates or alkylcyanoacetates, followed by hydrolysis[2], (b) by the ring closure of *o*-acyloxybenzoates[3], (c) by the reaction of alkyl *o*-hydroxyphenyl ketones with ethyl carbonate[4] or with carbon dioxide and potassium carbonate[5], and (d) by the reaction of phenols with ethyl alkylmalonates[6] or by the ring closure of phenyl alkylmalonates[7].

For the present paper the authors synthesized 3-alkyl-4-hydroxycoumarins (Va, b, c) by two similar routes. In one route, the ester condensation of methyl *o*-methoxybenzoate (Ia) and nitriles (IIa, b, c) gave α-(*o*-methoxybenzoyl)-nitriles (IIIa, b, c) in a good yield by a method analogous to that reported by Hauser et al.[8] for ester condensation; one mole of ester Ia was made to react with the sodio compound prepared from 2.5 mol. of sodium amide and 2 mol. of nitrile II in liquid ammonia. In this procedure, care was taken to prevent the formation of *o*-methoxybenzamide and the



For II—V: a) R=H, b) R=Me, c) R=Et

1) Y. Kawase, This Bulletin, **31**, 390, 440 (1958); **32**, 9, 11, (1959).
2) R. Anschütz, *Ber.*, **36**, 465 (1903).
3) H. Pauli and K. Lockemann, ibid., **48**, 32 (1915); M. A. Stahmann et al., *J. Am. Chem. Soc.*, **65**, 2285 (1943).
4) J. Boyd and A. Robertson, *J. Chem. Soc.*, **1948**, 174.
5) P. Da Re and E. Sandri, *Chem. Ber.*, **93**, 1085 (1960).
6) G. Urbain and C. Mentzer, *Bull. Soc. Chim.*, **11**, 171 (1944).
7) E. Ziegler and H. Junek, *Montatsh.*, **86**, 29 (1955).
8) R. Levine and C. R. Hauser, *J. Am. Chem. Soc.*, **68**, 760 (1946); C. J. Eby and C. R. Hauser, ibid., **79**, 723 (1957).

self-condensation of the nitrile. On the other hand, only poorer yields were obtained by the method reported previously for phenylacetonitriles[1] in which sodium hydride was used in benzene. The nitriles III were then demethylated by anhydrous aluminum chloride in nitrobenzene to give 3-alkyl-4-hydroxycoumarin-2-imides (IVa, b, c), which were readily hydrolyzed by dilute hydrochloric acid to 3-alkyl-4-hydroxycoumarins (Va, b, c). The intermediate *o*-hydroxybenzoyl-acetonitrile (VI) was isolated in the case of *o*-methoxybenzoylacetonitrile (IIa).

By another route, the ester condensation of methyl salicylate (Ib) and nitriles IIa, b, c directly gave the imides IVa, b, c in a fairly good yield by means of sodium amide in liquid ammonia.

Attempted condensations of Ia or Ib and dinitriles (e. g., malono-, succino-, glutaro- and adipo-nitriles) failed, furnishing only the self-condensed products of nitriles.

Experimental*

o-Methoxybenzoylacetonitrile (IIIa). — *a) By Sodium Amide in Liquid Ammonia.*—A solution of acetonitrile IIa (3 g., 0.072 mol.) in an equal volume of anhydrous ether was stirred over a period of 5 min. into a solution of sodium amide in liquid ammonia (prepared from 2.1 g. (0.09 mol.) of sodium and 50 ml. of ammonia) and then cooled in dry ice-acetone. After 5 min., a solution of *o*-methoxybenzoate (Ia) (6 g., 0.036 mol.) in an equal volume of ether was added rapidly, and the stirring and cooling were continued for one hour The ammonia was then removed, and the residue was treated with ice water. The aqueous solution obtained was washed with ether, filtered and acidified with dilute hydrochloric acid. The crystalline product obtained was washed with aqueous sodium bicarbonate and then recrystallized from ethanol to give IIIa in the form of colorless needles; m. p., 86~87°C; yield, 5.3 g. (84%). The reported m. p. is 87°C[9].

Found: N, 8.28. Calcd. for $C_{10}H_9O_2N$: N, 8.00%.

b) By Sodium Hydride in Benzene.—A mixture of Ia (8.4 g., 0.05 mol.), sodium hydride (1.8 g., 0.075 mol.) and anhydrous benzene (100 ml.) was refluxed for 2 hr., and for a further 5 hr. after the addition of IIa (3.1 g., 0.075 mol.). The cooled mixture was treated with water, and the aqueous layer obtained was acidified with hydrochloric acid. The crystalline product formed was washed with aqueous sodium bicarbonate and recrystallized from ethanol; m. p., 84.5~85.5°C; yield, 2.4 g. (27.4%).

α-(o-Methoxybenzoyl)propionitrile (IIIb). —*a) By Sodium Amide.* — Ia (7.5 g., 0.045 mol.) was made to react in a manner similar to that described for IIIa, with the sodio compound prepared from 2.6 g. (0.11 mol.) of sodium and 5 g. (0.09 mol.) of propionitrile (IIb) in liquid ammonia; the oily product formed by acidifying the aqueous alkaline solution was taken up in ether. The ether solution was washed with aqueous sodium bicarbonate, the solvent was removed, and the residual product was distilled in a high vacuum to give IIIb as colorless oil; b. p., 100~150°C/0.003 mmHg; yield, 6.8 g. (80%). 2,4-Dinitrophenylhydrazone: yellow microcrystals; m. p., 167~168°C (from ethanol).

Found: C, 55.48; H, 4.20; N, 19.08. Calcd. for $C_{17}H_{15}O_5N_5$: C, 55.28; H, 4.09; N, 18.96%.

b) By Sodium Hydride.—By the same procedure, 4.5 g. (36.8%) of IIIb (b. p., 100~124°C/0.001 mmHg) were obtained from Ia (10.7 g., 0.065 mol.), sodium hydride (3.3 g., 0.13 mol.) and IIb (3.5 g., 0.065 mol.).

α-(o-Methoxybenzoyl)butyronitrile (IIIc). — *a) By Sodium Amide.*—By the same procedure, 1.4 g. (57%) of IIIc (a colorless oil; b. p., 150~160°C/0.0035 mmHg) were obtaind from sodium (0.7 g., 0.03 mol.), IIc (1.7 g., 0.024 mol.) and Ia (2 g., 0.012 mol.). 2,4-Dinitrophenylhydrazone: yellow microcrystals; m. p., 128~129°C (from ethanol).

Found: C, 56.41; H, 4.55; N, 18.56. Calcd. for $C_{18}H_{17}O_5N_5$: C, 56.39; H, 4.47; N, 18.27%.

b) By Sodium Hydride.—By the same procedure, 0.9 g. (35%) of IIIc was obtained from Ia (2.1 g., 0.0125 mol.), sodium hydride (0.6 g., 0.025 mol.) and IIc (0.9 g., 0.0125 mol.).

4-Hydroxycoumarin-2-imide (IVa). — *a) From Methyl Salicylate (Ib) and IIa.*—Ib (2.5 g., 0.0165 mol.) was made to react in a manner similar to that described for IIIa with the sodio compound prepared from 1.3 g. (0.058 mol.) of sodium and 1.4 g. (0.033 mol.) of IIa in liquid ammonia. The ammonia was removed, and the residue was treated with water; the aqueous solution was filtered, washed with ether, and warmed for a while. The crystalline product separated was collected and recrystallized from ethanol to give IVa as colorless needles (m. p. 275°C (decomp.)), which were soluble in dilute hydrochloric acid; yield, 1 g. (38%).

Found: C, 66.81; H, 4.43; N, 8.97. Calcd. for $C_9H_7O_2N$: C, 67.07; H, 4.38; N, 8.69%.

b) From IIIa.—Powdered anhydrous aluminum chloride (3 g.) was added to a solution of IIIa (1 g.) in nitrobenzene (10 ml.), and the mixture was heated on a steam-bath for 1.5 hr. The cooled solution was then treated with ice water, the nitrobenzene was removed by steam-distillation, and the residual product was dissolved in ethyl acetate. The ethyl acetate solution was washed with aqueous sodium bicarbonate and then extracted with aqueous sodium hydroxide. From the ethyl acetate solution, 0.2 g. (23%) of IVa was obtained (m. p., 272~273°C (decomp.), identical with the other sample). The crystals obtained by acidifying the sodium hydroxide solution were recrystallized from ethanol to give 0.1 g. of *o*-hydroxybenzoylacetonitrile (VI) as colorless microcrystals (m. p., 108~109°C), which gave a red ferric chloride reaction in ethanol.

Found: C, 66.90; H, 4.75; N, 8.32. Calcd. for $C_9H_7O_2N$: C, 67.07; H, 4.38; N, 8.69%.

This VI was readily converted into IVa by warming its sodium hydroxide solution for a while.

* Melting and boiling points are uncorrected.

9) R. S. Long, *Chem. Abstr.*, **40**, 2634 (1946).

3-Methyl-4-hydroxycoumarin-2-imide (IVb).—*a) From Ib and IIb.*—By the same procedure, 5.9 g. (74.4%) of IVb were obtained from Ib (7 g., 0.046 mol.) and the sodio compound prepared from 3.7 g. (0.161 mol.) of sodium and 5.1 g. (0.092 mol.) of IIb in liquid ammonia (colorless microcrystals; m. p., 238~241°C (from dilute ethanol)).

Found: C, 68.47; H, 5.37; N, 7.93. Calcd. for $C_{10}H_9O_2N$: C, 68.56; H, 5.18; N, 8.00%.

b) From IIIb.—By the same procedure, 0.3 g. (37.7%) of IVb (m. p., 235~239°C) was obtained from 1 g. of IIIb.

3-Ethyl-4-hydroxycoumarin-2-imide (IVc).—*a) From Ib and IIc.*—By the same procedure, 0.6 g. (16.5%) of IVc was obtained from Ib (2.9 g., 0.019 mol.) and the sodio compound prepared from 1.5 g. (0.065 mol.) of sodium and 2.6 g. (0.038 mol.) of IIc in liquid ammonia (colorless microcrystals; m. p., 192~193.5°C (from dilute ethanol)).

Found: C, 69.39; H, 5.77; N, 7.80. Calcd. for $C_{11}H_{11}O_2N$: C, 69.82; H, 5.86; N, 7.40%.

b) From IIIc.—By the same procedure, 0.1 g. (21.5%) of IVc (m. p., 185~186°C) was obtained from IIIc (0.5 g.) and aluminum chloride (1.5 g.).

4-Hydroxycoumarin (Va).—*a) From IVa.*—A solution of IVa (0.5 g.) in 2 N hydrochloric acid (20 ml.) was heated on a steam-bath for 2 hr. The crystalline product separated from the cooled solution was recrystallized from dilute ethanol to give Va in the form of colorless needles; m. p., 208.5~209.5°C, identical with the authentic sample; yield, 0.3 g. (60%). The reported m. p. is 204~206°C[2] or 214~216°C[3].

Found: C, 66.61; H, 3.84. Calcd. for $C_9H_6O_3$: C, 66.67; H, 3.73%.

b) From IIIa.—Powdered anhydrous aluminum chloride (3 g.) was added to a solution of IIIa (1 g.) in nitrobenzene (10 ml.), and the mixture was heated on a steam-bath for 1.5 hr. The cooled solution was treated with ice water and hydrochloric acid, and the nitrobenzene was removed by steam-distillation. The crystalline product obtained from the cooled residue was recrystallized from ethanol; m. p., 205~207°C; yield, 0.5 g. (54.3%).

3-Methyl-4-hydroxycoumarin (Vb).—*a) From IVb.*—By the same procedure, 0.35 g. (70%) of Vb was obtained from IVb (0.5 g.); colorless crystals; m. p., 225~227°C (from dilute ethanol). The reported m. p. is 227~228°C[3] or 230°C[6].

Found: C, 68.10; H, 4.53. Calcd. for $C_{10}H_8O_3$: C, 68.18; H, 4.58%.

b) From IIIb.—By the same procedure, 0.4 g. (43%) of Vb was obtained from 1 g. of IIIb.

3-Ethyl-4-hydroxycoumarin (Vc).—*a) From IVc.*—By the same procedure, 0.2 g. (66.7%) of Vc was obtained from IVc (0.3 g.); colorless crystals; m. p., 157~158°C (from benzene). The reported m. p. is 155~156°C[3].

Found: C, 69.52; H, 5.25. Calcd. for $C_{11}H_{10}O_3$: C, 69.46; H, 5.30%.

b) From IIIc.—By the same procedure, 0.2 g. (43%) of Vc (m. p., 156~157°C) was obtained from 0.5 g. of IIIc and 1.5 g. of aluminum chloride.

The authors are grateful to the members of the Faculty of Pharmacology of this University and to the members of the Faculty of Science of Osaka University for their microanalyses.

Faculty of Literature and Science
Toyama University
Gofuku, Toyama

Photosensitized Oxidation of Leuco-uranine. I. Qualitative Studies of the Nature of the Reaction in the Deaerated Solution

By Kengo UCHIDA and Masao KOIZUMI

(Received March 12, 1962)

In a previous paper[1], the present authors joined in studying some properties of leuco-uranine prepared by reducing uranine with the use of sodium amalgam. It was found that the aqueous solution of it is rather stable in the presence of dissolved oxygen but that it is easily oxidized to the colored form by adding some suitable sensitizer to the solution and by then irradiating with the light appropriate to the sensitizer. A remarkable result then found was that the restoration of the color also takes place in the absence of oxygen and, moreover, faster and more completely. Besides, it has been established that the photoproduct obtained by the irradiation of the deaerated alcoholic solution of xanthene dyes[2] shows similar behavior; this affords definite evidence that it consists mostly of the reduced form of the dye.

The purpose of the present paper is to

1) K. Uchida, S. Kato and M. Koizumi, This Bulletin, 35, 16 (1962).

2) M. Imamura and M. Koizumi, ibid., 28, 117 (1955); 29, 899 (1956); M. Imamura, ibid., 30, 249 (1957).

clarify the nature of this sensitized oxidation in the deaerated condition; this oxidation is peculiar because the oxidation of the leuco dye may take place accompanied by no eventual reduction of the sensitizer. Thus no even slight change in the spectrum of acridine, used as a sensitizer, was perceived; a more definite fact was that uranine itself is efficient as a sensitizer. For the present research, acridine and uranine were chosen as sensitizers; the former, which absorbs light in the 400~330 mμ region where neither leuco-uranine nor uranine has any absorption, can afford an unequivocal interpretation of the results, while the latter has no possibility of promoting the reaction by being itself reduced to the leuco form. The nature of the reaction is studied rather qualitatively, the quantitative treatment being postponed to the next report.

Experimental

Materials.—*Leuco-uranine.*—Uranine was reduced by sodium amalgam and, after repeated recrystallization from an ethanol solution, was desiccated in a vacuum. The details of the procedure were the same as reported on in the previous paper. The solution is rather stable in the dark, but it gradually gets colored due to the formation of the oxidized form of uranine. For example, in several months the oxidation proceeds to the extent of more than half in the case of a 10^{-2} M solution. The coloration is less in the dilute solution, the magnitude being less than 20% for a 10^{-4} M solution.

Acridine.—Tokyo Kasei special-grade acridine was recrystallized twice from the water-ethanol mixture.

Uranine. — Commercial material was repeatedly recrystallized from ethanol.

Sodium Hydroxide.—The saturated solution was prepared from the G. R. reagent of the Wakojunyaku Co. The supernatant liquid was diluted to the desired concentration.

Disodium Hydrogen Phosphate and Potassium Dihydrogen Phosphate. — The G. R. Wakojunyaku reagents were recrystallized three times from the aqueous solution.

Sodium Carbonate, Barium Hydroxide, Ethanol and Sodium Thiosulfate.—Special grade reagents were used without further purification.

Procedure.—The stock solution of leuco-uranine 9.5×10^{-5} M was ordinarily diluted ten times. The evacuation of the solution was usually performed five to six times by the use of a mercury diffusion pump, melting and freezing being repeated each time.

When acridine was used as a sensitizer, 365 mμ light from a mercury lamp was used for exciting the acridine, which has an absorption maximum at 355 mμ. Neither uranine nor leuco-uranine has any absorption in this region. The concentration of acridine is usually 1.3×10^{-4} M. The apparatus specially designed for kinetic study was used; details will be described in the next paper. A high-pressure mercury lamp (Matsuda SHL-100UV) was used as the light source.

When uranine was used as a sensitizer, 1×10^{-6} M of uranine was added in some experiments, but in most experiments, especially in later ones, uranine was not added purposely, since the solution of leuco-uranine already had a small quantity of uranine produced during its storage. The apparatus for the photochemical reaction was similar to those used for other experiments in our laboratory. The reaction cell was the one for a spectrophotometer, $1\times1\times4$ cm., especially designed for evacuation. As a light source, a 75 V. 500 W. tungsten lamp was used at 55 V. The ultraviolet part was removed by a Waltz yellow filter Y1 (> 430 mμ).

Results and Discussion

I. Possibility of the Evolution of Hydrogen Gas. — On the basis of the results already reported, it seemed most natural to infer that molecular hydrogen is evolved accompanying the production of the oxidized dye; first this was examined.

One-hundred milliliters of the aqueous solution of leuco-uranine 6×10^{-5} M was irradiated using uranine or acridine as a sensitizer. When the oxidation of leuco dye had almost completely taken place, the water was distilled to another trap in vacuum and, at the same time, the gas non-condensable by liquid nitrogen was gathered by the use of a small mercury diffusion pump and a Toepler-pump. The quantity of the gas obtained was about 9.8 ml. at 1 mmHg, this quantity being about one-tenth of that expected stoichiometrically. The gas was examined spectroscopically by the use of a small Geissler tube. Faint hydrogen lines were detected in one experiment (sensitizer: acridine), but in the other two experiments no trace of hydrogen could be found.

The above tests do not seem conclusive, however, because the discharge rapidly declined in strength; it is suspected that a small quantity of hydrogen might be fixed in that metallic film which had been spattered from the molybden electrode on to the wall of the tube.

II. Scrutiny of Any Impurity which Might Act as an Oxidizing Agent.—Since the above results were not conclusive, all possibilities of the contamination of a small quantity of the oxidizing agent were examined.

a) Utmost Exclusion of Molecular Oxygen.— The following procedure was adopted for this purpose. First, nitrogen gas which had been purified by bubbling it through the aqueous solution of vanadous sulfate[3] was passed through for more than 30 min. After extensive evacuation, the water was sublimed into another ampoule and it was further evacuated, melting and freezing being repeated for five times. Finally, the water was distilled back to the

3) L. Meites and T. Meites, *Anal. Chem.*, **20**, 984 (1948).

Table I. The effect of the addition of sodium carbonate

Concn. of Na_2CO_3	0	4.0×10^{-3} M	0	4.7×10^{-3} M
Initial rate (M. min^{-1})	0.55×10^{-5}	0.46×10^{-5}	0.63×10^{-5}	0.49×10^{-5}

reaction cell. The experiment using this sample showed that the reaction proceeded and with a rate not so much lower than that of the sample evacuated in the ordinary way.

b) The Effect of the Addition of Sodium Thiosulfate.—The results described above strongly establish the impossibility of molecular oxygen participating in the reaction.

However, oxygen might be loosely attached to leuco dye or some other compound in such a way that it can not be eliminated by mere evacuation. Furthermore, there might exist a trace of some other unknown oxidant which induces the reaction in question. In order to examine such a possibility, the effect of the addition of sodium thiosulfate was studied. If the reaction were due to some unknown oxidant, it would not proceed at all in the presence of sodium thiosulfate, or it would proceed at a much lower rate.

An amount of sodium thiosulfate about equal to that of leuco dye was added; the result was that the reaction took place at a rate about 75% of that for the solution to which no sodium thiosulfate was added.

III. Scrutiny of the Contamination of Any Small Quantity of a Reducible Substance.—From the results in a) and b), it can be said with confidence that no conceivable oxidant takes part in the present reaction.

Another possibility to be examined is that the reaction might be induced by some easily reducible substance contaminating the solution. Since the oxidation-reduction potential of uranine is quite low, the reduction of the carbonate ion may be possible, at least energetically, if the light energy absorbed by a sensitizer is utilized for the reaction. If this be the case, the effect of the addition to the solution or of the elimination of sodium carbonate from it ought to be carefully studied, since there is no doubt that a sample contains more or less sodium carbonate.

c) The Effect of the Addition or of the Elimination of Sodium Carbonate.—The addition of the salt up to 4×10^{-3} M did not essentially affect the rate, although the rate decreased somewhat, as may be seen from Table I.

There is, however, another possibility, that the original solution already contains an appreciable quantity of carbonate ions and, so, further addition of them scarcely affects the rate. Hence, the effect of an extensive elimination of carbonate ions was next examined. Barium hydroxide was added to the concentration of 0.1 M; this should decrease the concentration of carbonate ions down to one-hundredth that of leuco dye. The precipitate of barium carbonate was eliminated by passing the solution through a glass-filter and by repeated decantation, all procedures being done in vacuo. The experiment with the solution thus treated showed about the same rate as that of the solution not so treated.

If the carbonate ion were to be reduced, the formation of the formaldehyde would be expected. Hence, the solution was, after a long irradiation, tested by Tollens' reagent, by Schiff's reagent and by a method based on the catalytic action of aldehyde on the oxidation of *p*-phenylenediamine by means of hydrogen peroxide[4]. All the results proved to be negative. From the above results, it can be concluded that carbonate ions are indifferent to the reaction.

d) The Effect of Ethanol on the Rate.—The contamination of a small quantity of ethanol is inevitable, since it was used for repeated crystallization. Hence, the effect of the elimination or addition of ethanol was tested, though its reduction seems rather improbable. Leuco-uranine was prepared by treating an alkaline (0.5 N sodium hydroxide) solution of uranine 1×10^{-5} M with sodium amalgam. When the experiment was made utilizing the above solution, it was found that a similar reaction occurs and that the addition of 10 vol.% ethanol does not affect the rate at all.

Thus it is clear that ethanol does not participate in the reaction.

IV. Reaction in the Presence of Palladium Asbestos.—All these results, a)—d), led once more to the view that hydrogen is to be evolved as a reaction product in spite of a rather negative result of part I above. To test this from a different view-point, the experiment was undertaken in the presence of palladium asbestos suspended in the solution. If the reaction were to proceed under such conditions, the hydrogen which might be evolved would be arrested by the palladium. The oxidized dye, when kept in the dark, would be expected to be reduced, and this cycle would be repeated again and again. The above test would, in addition, completely eliminate the possibility of any oxidizing agent taking part in the reaction.

Uranine 1.0×10^{-5} M in the alkaline solution

4) F. Feigl, "Spot Tests", Vol. II, Elsevier, Amsterdam (1956), p. 208.

of 0.5 N sodium hydroxide was reduced by hydrogen in the presence of a small quantity of palladium asbestos to the extent that a small quantity of uranine was left behind to take the role of sensitizer. The sample was then evacuated and irradiated as usual. The recovery of color went on at about the same as in the case of the leuco dye prepared by the sodium amalgam method.

The sample when kept in the dark (in the presence of palladium asbestos) became almost colorless, but when irradiated once more it regained its color. This could be repeated more than three times.

An analogous experiment could be performed in the presence of sodium amalgam.

The above experiment definitely demonstrates that no impurity takes part in the oxidation of leuco-uranine and that the uranine $\rightleftharpoons$ leuco-uranine process is accompanied by no other side reaction of an appreciable magnitude.

Thus, the oxidation of leuco-uranine is most probably due to the detachment of hydrogen, although this had not yet been proved successfully by the experiment described in part I.

The evolution of the hydrogen gas is to be examined by a different method in the near future.

V. Semiquinone as an Intermediate of the Reaction.—During the course of the reaction in which uranine was used as a sensitizer, the existence of semiquinone was clearly observed spectroscopically. A typical result, which was obtained by a Hitachi recording spectrophotometer, is shown in Fig. 1.

The concentration of leuco-uranine in this case is 1×10^{-5} M, while that of sodium hydroxide is 0.10 N. About 1×10^{-6} M uranine was existent in the original solution. It is seen that, after 3 min. of irradiation, the absorption with a maximum ca. 393 mμ clearly appears. This maximum declines gradually, as is shown in the figure, when kept in the dark. There is no doubt, judging from the findings of some previous workers[5] that the absorption in the 350~420 mμ region is due to semiquinone. The molar extinction coefficient at the maximum was reported to be 6.5×10^{4}. Although the details of the reaction mechanism must await further examination, it seems certain that semiquinone is formed in the early stage of the reaction and that this changes into an oxidized form of uranine either by dismutation or by evolving hydrogen through the intermolecular reaction. If only the dismutation were to occur in the dark, the rise of the maximum at 490 mμ ought to be much smaller.

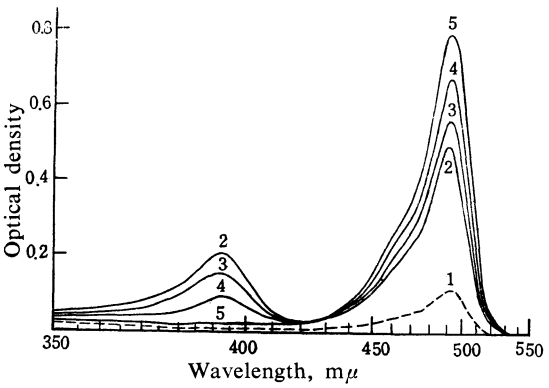


Fig. 1. Behavior of the intermediate which is produced by the irradiation of an alkaline solution of leuco-uranine (uranine used as a sensitizer).
1: Initial
2: 1.5 min. after irradiation (3 min.)
3: 6 min. after irradiation
4: 12 min. after irradiation
5: About 2.5 hr. after irradiation

VI. Reexamination of the Spectral Change of Acridine During the Reaction. — In view of the results described in part V, there is the distinct possibility of the formation of semi-hydrogenated acridine when acridine is used as a sensitizer. If this were the case, more or less acridan would be produced according to the experimental conditions. From such a viewpoint, the spectra of acridine during the course of the reaction was reexamined more carefully under various conditions*. No definite evidence for the formation of either acridan or semi-hydrogenated acridine was obtained, but in some cases, especially at a low concentration of acridine, a clear drop of the maximum at 355 mμ was perceived. Its magnitude fluctuates from one experiment to another; the reason for this is not clear.

All the above facts suggest that, to some extent, acridine is partially hydrogenated at an earlier stage of the reaction and that some of it changes into acridine with the formation of molecular hydrogen while the remaining part dismutes into acridine and acridan.

Summary

The nature of the photosensitized oxidation of leuco-uranine (in the deaerated condition), using uranine or acridine as a sensitizer, was investigated from various viewpoints. The possibility of either an oxidizing or a reducing impurity taking part in the reaction was definitely ruled out. The uranine $\underset{\text{dark}}{\overset{\text{light}}{\rightleftharpoons}}$ leuco-

5) M. Imamura, This Bulletin, **31**, 962 (1958); L. Lindqvist, *Arkiv. Kemi.*, **16**, 79 (1960).

* Thus, the concentration of leuco was varied from 1×10^{-5} to 2×10^{-5}M and that of acridine from 1.8×10^{-5} to 13×10^{-5}M. The concentration of sodium hydroxide was always 0.122 N.

uranine reaction could be repeatedly carried out in the presence of palladium asbestos. When uranine was used as a sensitizer (alkaline solution), an appreciable quantity of semiquinone could be detected as an intermediate. Reexamination of the spectra of acridine (when acridine was used as a sensitizer) showed that in some cases acridine takes part in the eventual reaction.

It is concluded from various pieces of indirect evidence that the overall reaction is the evolution of hydrogen gas from the leuco dye, although the direct detection of hydrogen formation has not yet been successful.

The authors wish to thank Dr. Shunji Kato for his illuminating discussions.

Department of Chemistry
Faculty of Science
Tohoku University
Katahira-cho, Sendai

Photosensitized Oxidation of Leuco-uranine. II. Kinetics of an Acridine-sensitized Photoöxidation in the Deaerated Solution

By Kengo UCHIDA and Masao KOIZUMI

(Received March 12, 1962)

As has been reported in a preceding paper[1], leuco-uranine is oxidized to the colored form when its deaerated aqueous solution is irradiated by 365 mμ in the presence of acridine. There was some ambiguity as to the role which acridine plays in this reaction, since, although its quantity remained almost constant in most cases, in a few experiments it decreased a little, as judged from its spectra. In spite of this finding, preliminary experiments showed that the rate of restoration of the dye is quite reproducible under given conditions, suggesting that the process in question does not essentially affect the overall rate of the reaction.

As described in the preceding paper, acridine is a suitable sensitizer for a quantitative study of the reaction; the objective of the present paper is to report on investigations into the influence of various factors upon this reaction. They may be summarized as follows. The triplet state of acridine reacts with leuco-uranine, producing perhaps the semi-hydrogenated form of both species. The various ionic forms of leuco-uranine (mono-, di- and tri-valent anions) have different reactivities towards the triplet state of acridine, which can be evaluated quantitatively from the pH dependence of the overall rate constant. The rate constants of various steps have been obtained with moderate accuracy.

1) K. Uchida and M. Koizumi, This Bulletin, 35, 1871 (1962).

Apparatus and Procedure

The apparatus is shown in Fig. 1.

The light source, L, is a high-pressure mercury lamp (Mazuda SHL 100 UV) operating at 100 V. The power was supplied through a voltage stabilizer, Volco H. T. A remarkable feature is that the same light source, L, was made use of in a specific manner both for inducing the reaction (excitation) and for tracing the reaction (measurement). This technique, which was suggested by Dr. Kato, is described below.

F_1 is an aqueous solution of copper sulfate designed to remove the thermal radiation. F_2 is a specially-designed interference filter (manufactured by the Shonan Komaku Co.), the second order interference of which is 727 mμ; accordingly, the

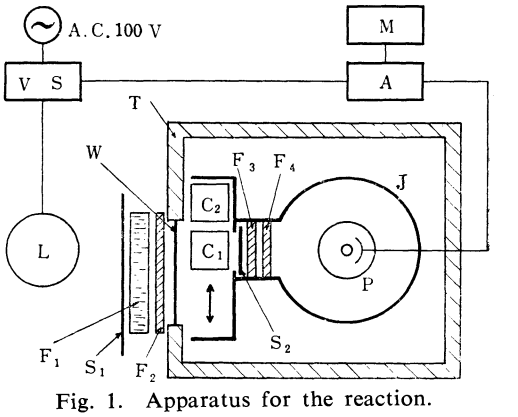


Fig. 1. Apparatus for the reaction.

V. S.: Voltage stabilizer A: Amplifier
M: Micro-ammeter W: Glass window

third and the fourth interference are, respectively, 490 and 375 mμ (half width 18 mμ), transmitted light being chiefly limited in the region near the above three wavelengths. The 365 mμ of the mercury lamp can pass through the above filter with a transmission of about 19%. 490 mμ corresponds just to the absorption maximum of the aqueous uranine solution and, since the present mercury lamp has a weak continuous emission, the light in the region of 490 mμ passing through F_2 can be utilized for measuring the quantity of uranine produced. The light of 490 mμ passing through the solution is received by a photocell, P (Mazuda No. 7211). The optical density of the solution at this wave length can easily be evaluated. The fact that its intensity is very weak does not affect the reaction. Between the sample-solution and the photocell are inserted an opaque glass, F_3, and a cut-off filter, F_4 (>450 mμ), in order to remove the light of 365 mμ.

C_1 and C_2 are, respectively, the reaction cell and the reference cell for optical density. Both are set tightly in a movable cell-holder. They are made from Terex, are 1×1×4 cm, and are fitted with a side tube for evacuation. The reading of the meter, M, was calibrated by the use of a Hitachi spectrophotometer (EPU-2A). J is a brass tube with an air-tight glass window, F_3; it contains a photocell and a part of circuit for multiplication, C_1, C_2 and J being immersed in a water-thermostat, T. S_1 and S_2 are shutters. The reaction temperature is 30°C unless otherwise denoted.

The intensity of the irradiating light was controlled by changing the distance between the light source and the cell, or by the use of neutral density filters (manufactured by the Hoya Co.), and it was measured each time by means of a potassium ferrioxalate actinometer.

Results

Rate Formula for a Run. — Under certain experimental conditions, i. e., when the intensity of light, I_0, the concentration of acridine, [A], the initial concentration of leuco-uranine, $[L]_0$, and the temperature, T, are in proper range, the reaction proceeds as of first order with regard to [L]:

$$\frac{d[U]}{dt}=k'[L] \qquad (1)$$

Hence,

$$\ln\frac{[L]_0}{[L]}=k't \qquad (2)$$

Equation 2 fits the experimental results quite satisfactorily, and the reproducibility is moderately good. Typical examples are shown in Fig. 2. The conditions of the reaction for these examples are $[A]=1.3\times10^{-4}$ M, $[L]_0=9.5\times10^{-6}$ M, $I_0\sim5.5\times10^{-8}$ mol. min^{-1} cm^{-2}, and temperature, 30°C. When [A] becomes less and $[L]_0$ larger than the above values, the applicability of the first order rate formula becomes gradually less satisfactory (see below).

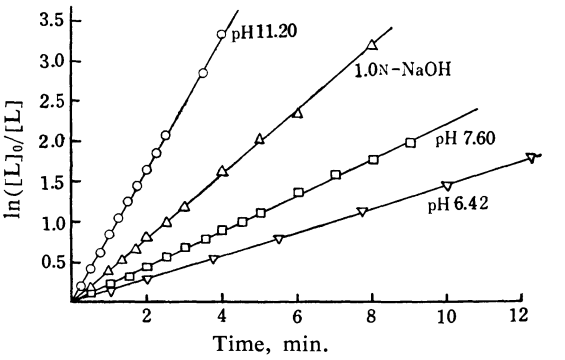


Fig. 2. Plots of $\ln([L]_0/[L])$ against time for typical examples.
$[L]_0=9.5\times10^{-6}$ M, $[A]=1.3\times10^{-4}$ M

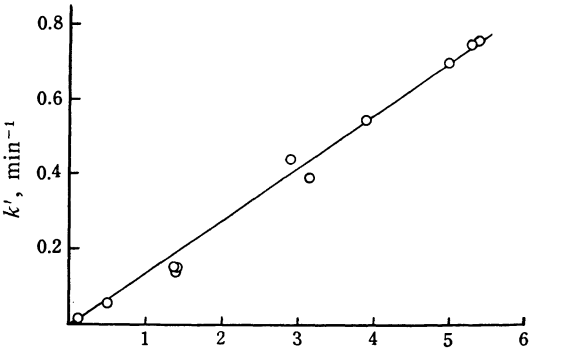


Fig. 3. Dependence of k' on the light intensity.
pH=11.1, $[A]=1.7\times10^{-4}$ M, $[L]_0=9.5\times10^{-6}$ M

In this paper, most of the experiments were performed under the above conditions.

The Effect of Light Intensity.—The results are shown in Fig. 3. k' increases proportionally to the light intensity.

The Effect of the Concentration of Acridine. —The values of k' for various [A]-values are listed in Table I.

In this table, D is the optical density at 365 mμ; hence, $1-10^{-D}$ is a fraction of the light absorbed by acridine. The concentration of acridine was calculated from the optical density of the solution at 365 mμ using the value of $\varepsilon_{365}=0.455\times10^4$.

If the rate is proportional to the absorbed light, Eq. 1 can be rewritten as follows with a new constant, k;

$$\frac{d[U]}{dt}=-\frac{d[L]}{dt}=k'[L]$$
$$=10^3\frac{k}{d}I_{abs}[L]$$
$$=10^3\frac{k}{d}I_0(1-10^{-D})[L] \qquad (3)$$

TABLE I. THE EFFECT OF THE CONCENTRATION OF ACRIDINE

0.010 N NaOH $[L]_0=9.5\times10^{-6}$ M

Exp. No.	$[A]\times10^4$ M	$I_0\times10^8$ mol. cm^{-2} min^{-1}	$1-10^{-D}$	k' min^{-1}	$k'/(I_0\times10^7)$ cm^2 mol^{-1}	$\frac{10^{-3}k'\cdot d}{(1-10^{-D})I_0}\times10^{-4}$
145	1.92	6.08	0.867	0.749	1.23	1.42
146	1.46	6.08	0.784	0.75	1.23	1.57
154	1.05	6.70	0.667	0.835	1.25	1.88
147	0.835	6.90	0.583	0.898	1.30	2.23
162	0.651	6.25	0.494	0.617	0.988	2.00
155	0.525	6.54	0.425	0.576	0.882	2.07
148	0.319	6.90	0.284	0.456	0.662	2.33
158	0.233	6.35	0.217	0.293	0.462	2.12
150	0.132	6.2	0.129	0.161	0.260	2.01

TABLE II. THE EFFECT OF THE INITIAL CONCENTRATION OF LEUCO-URANINE

$[A]\sim0.6\times10^{-4}$ M, $[NaOH]=0.010$ N

Exp. No.	$[L]_0\times10^5$ M	$(1/[L]_0)\times10^{-5}$ M^{-1}	$I_0\times10^8$ mol. cm^{-2} min^{-1}	$1-10^{-D}$	Init. rate $\times10^6$ min^{-1} M	$\frac{10^3I_0(1-10^{-D})}{\text{Initial rate}}$	k' min^{-1}
157	0.475	2.11	6.52	0.462	3.56	8.46	0.968
161	0.713	1.40	6.35	0.457	4.33	6.70	0.738
155	0.950	1.05	6.54	0.425	4.70	5.91	0.576
162	0.950	1.05	6.25	0.494	4.82	6.40	0.617
156	1.90	0.526	6.52	0.435	5.42	5.23	0.339
159	6.89	0.145	6.35	0.480	6.34	4.81	—
160	23.8	0.042	6.35	0.504	8.17	3.92	—

where I_{abs} is the number of photons (in the mole) absorbed ($cm^{-2}.min^{-1}$), d is the light path length (=1 cm.), and D is the optical density at 365 mμ. $k[L]_0$ gives the quantum yield at the initial stage.

As may be seen from Table I, $k'd/10^3I_0(1-10^{-D})=k$ begins to decrease beyond about 0.8×10^{-4} M of acridine. This is most plausibly due to the self-quenching of the singlet or triplet excited state of acridine.

It can be said from the above results that the rate is proportional to the absorbed light up to ca. 0.8×10^{-4} M, whence the self-deactivation of the excited acridine molecule becomes appreciable.

The Effect of the Initial Concentration of Leuco-uranine. — Equation 1—3 hold when $[L]_0\leqq10^{-5}$ M and $[A]\geqq10^{-4}$ M. To examine the general applicability of the first order rate formula, $[L]_0$ was increased from 0.475×10^{-5} to 2.38×10^{-4} M, keeping [A] constant (0.6×10^{-4} M, about half of the usual value). The results are listed in Table II.

As may be seen from Table II, the initial rate increases with the rise of $[L]_0$. Each run can be approximately treated as of the first order with respect to [L] up about 1×10^{-5} M. However, it is evident that k' decreases appreciably with the increase in $[L]_0$. For the highest concentrations of $[L]_0$ (6.89 and 23.8 $\times10^{-5}$ M), the zeroth order rate formula is rather better than that of the first order.

All these facts suggest that the order of the reaction is generally between zero and one, the first order rate formula holding only for the limited conditions under which most of the experiments happen to have been performed. The interpretation of this will be given in the discussion of the 7th column, $10^3 I_0(1-10^{-D})/$(initial rate), of the table.

The Effect of the pH Value.—When the pH value of the solution was changed from ca. 6.4 to 14 by the use, for example, of the phosphate buffer, $[L]_0$ and [A] being given the values of 9.5×10^{-6} M and 1.3×10^{-4} M respectively, it was found that the rate changes in a curious manner.

Figure 4 shows the plot of k against the pH value, where k is the constant introduced in Eq. 3. Equations 1 to 3 hold satisfactorily throughout the whole pH region. It is evident that the rate constant has a maximum near the pH value of 11~12. The full line represents the calculated values, which will be described in the discussion below.

It is to be noted that below a pH value of 6, the oxidized form of uranine exists as a neutral molecule, of which the absorption in the visible region at 490 mμ is quite small.

Under the present experimental conditions, no coloration could be perceived in situation below a pH value of 6.0, but preliminary experiments showed that the solution, after being irradiated, becomes colored when made alkaline. As to the higher alkaline solution, the solubility of acridine decreases with the

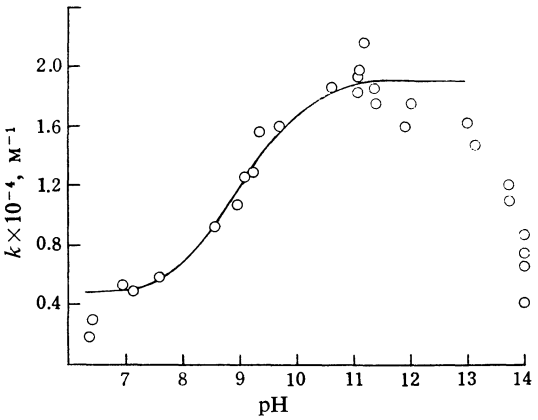


Fig. 4. Dependence of k on pH. The line corresponds to the calculated values.
$I_0=5.5\sim7.0\times10^{-8}$ mol./cm^2 min.
$[A]=1.3\times10^{-4}$ M, $[L]_0=9.5\times10^{-6}$ M

alkalinity, and the experiments could not be carried out beyond 1.5 N.

The Effect of Temperature.—The rate was measured from 10° to 52°C. The results are listed in Table III.

These data are not very accurate, and the following Arrhenius formula only serves to show an approximate relation between k and T:

$$k=8.1\times109\exp(-8000/RT)$$

TABLE III. THE EFFECT OF TEMPERATURE

pH=11.0, $[A]=1.5\times10^{-4}$ M, $[L]_0=9.5\times10^{-6}$ M
$I_0\simeq6\times10^{-8}$ mol. cm^{-2} min^{-1}

Exp. No.	Temp., °C	k' min^{-1}	k l./mol.$\times10^{-4}$
79	10.0	0.270	0.546
80	20.0	0.336	0.680
81	30.0	0.766	1.55
82	40.0	1.00	2.03
83	51.0	1.01	2.04
19*	25.0	0.933	1.07
37*	52.	1.85	3.83

* pH=13.14, $[A]=1.3\times10^{-4}$ M

Discussion

The first problem to be solved is the exact determination of the excited species of acridine (singlet or triplet) which actually reacts with leuco-uranine. This can be judged from the experiment concerning the effect of leuco-uranine on the fluorescence of acridine. The fluorescence intensity of the aqueous solution of acridine (1.3×10^{-4} M) was measured by a fluorescence accessory attached to a Hitachi spectrophotometer. The addition of leuco-uranine (9.5×10^{-6} M) to the above solution scarcely affected the intensity of the fluorescence, showing that the quenching effect of the former is within the range of experimental error.

From this result, it can be inferred that leuco-uranine does not appreciably attack the singlet excited state, because the opposite assumption leads, as is shown below, to a relation contradicting the experimental result.

Let the quantum yield of the fluorescence be designated as η_E and η_E', in the absence and in the presence of leuco-uranine respectively. If leuco-uranine attacks the singlet excited state as the first step of the reaction, η_E and η_E' can be expressed as follows:

$$\eta_E=\frac{v_E}{v_E+v_Q} \qquad \eta_E'=\frac{v_E}{v_E+v_Q+v_R} \tag{4}$$

where v_E, v_Q and v_R are, respectively, the rate of emission, the inner quenching, and the process leading to the reaction.

The quantum yield of the reaction, on the other hand, can be written as follows:

$$\eta_R=\frac{v_R}{v_E+v_Q+v_R}\cdot\alpha \tag{5}$$

where $\alpha<1$. Equations 4 and 5 lead to the following relation:

$$\frac{\eta_E-\eta_E'}{\eta_E}=\frac{\eta_R}{\alpha} \tag{6}$$

Now, since the addition of leuco-uranine does not affect the intensity of fluorescence beyond the range of experimental error, the left side of the above equation can safely be said to be smaller than 1/10, perhaps, a few hundredths or so. Thus, $1/10>\eta_R/\alpha$ must hold. The quantum yield of the reaction being in favorable conditions, ~0.2, η_R must >0.2; hence, $\alpha>2$, which never holds in any case. Thus one can safely conclude that leuco-uranine does not appreciably react with the singlet state, its contribution to the entire reaction, even if it exists, being less than 10%.

In the following, we assume that the entire reaction proceeds via the triplet state of acridine, which attacks leuco-uranine.

In general, it must be taken into account that the triplet state returns to the ground state, dissipating its excess energy. Therefore, $k[L]$ in Eq. 3 must be represented as follows:

$$k[L]=\varphi\frac{k_r[L]}{k_d+k_r[L]}\ ^* \tag{7}$$

where φ gives the fraction of the singlet excited state that goes to the triplet, and k_d and k_r are, respectively, the rate constant of deactivation and the reaction with leuco-uranine. The rate formula should be of the first order or zeroth order according as $k_r[L]\ll k_d$ or $k_r[L]\gg k_d$. The general applicability of Eq.

* The mere deactivation by leuco-uranine in this case may be ignored.

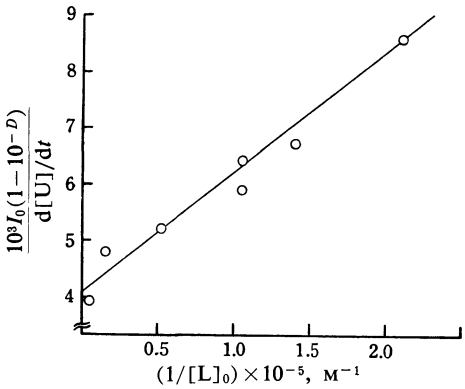


Fig. 5. Plot of $10^3 I_0(1-10^{-D})/(d[U]/dt)$ against $1/[L]_0$.

7 can be tested from the data in Table II. Based on Eqs. 3 and 7, the initial rate can be written as follows:

$$\frac{d[U]}{dt}=10^3 I_0(1-10^{-D})\varphi\frac{k_r[L]_0}{k_r[L]_0+k_d} \qquad (8)$$

whence

$$\frac{10^3 I_0(1-10^{-D})}{d[U]/dt}=\frac{1}{\varphi}+\frac{1}{\varphi}\times\frac{k_d}{k_r[L]_0}$$

As is shown in Fig. 5, the plot of $10^3 I_0(1-10^{-D})/(d[U]/dt)$ against $1/[L]_0$ gives a satisfactory straight line. From the slope and the intercept, the values of φ and k_d/k_r can be set at 0.24 and 0.51×10^{-5} mol./l. φ gives the intersystem crossing probability ($S'\rightarrow T$); this value reconfirms that the reaction involves the triplet state of acridine.

In most experiments the initial concentration of leuco-uranine is $\sim1\times10^{-5}$ M; hence, $k_d/k_r[L]_0\sim0.51$. Thus, the rate of deactivation is rather smaller than that of the reaction. Integrating Eq. 8, one gets an exact rate formula as follows:

$$\frac{k_r}{k_d}\{[L]_0-[L]\}+\ln\frac{[L]_0}{[L]}=10^3\frac{k_r}{k_d}I_0(1-10^{-D})\varphi t \qquad (9)$$

Equation 9 can reproduce quite satisfactorily most of the runs for which the first order rate formula fails. Examples are shown in Fig. 6.

In most of the experiments, [A] was chosen as $\geqq1.3\times10^{-4}$ M, where the deactivation of the triplet state is rather large (see Table I); hence, k_d becomes more than twice as large as the above value. Thus, the situation in this case is more favorable for the first order rate formula; yet it is unlikely that the $k_r[L]$ term is negligible in comparison with the k_d term. Therefore, the possibility of the quenching action of uranine (produced) on the triplet state of acridine was examined. Thus, if

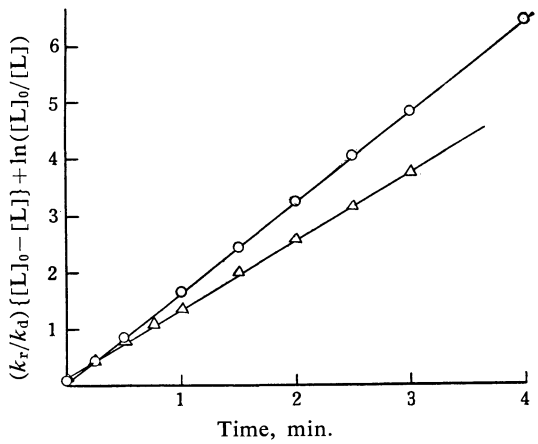


Fig. 6. Plots of $(k_r/k_d)\{[L]_0-[L]\}+\ln([L]_0/[L])$ against t.
○: [A]$=0.6\times10^{-4}$ M, [L]$=0.95\times10^{-5}$ M, [NaOH]$=0.01$ N
△: [A]$=0.6\times10^{-4}$ M, [L]$=1.9\times10^{-5}$ M, [NaOH]$=0.01$ N

uranine were to deactivate the triplet of acridine about a rate constant equal to that with which leuco-uranine attacks the triplet state of acridine, then the denominator of Eq. 7 would be expected to be approximately constant during the course of the reaction. In this case, Eq. 7 can be replaced by:

$$k[L]=\varphi\frac{k_r[L]}{k_d+k_r[L]_0} \qquad (7a)$$

and the run is to proceed as of the first order in [L]. However, it was found that the addition of uranine up to 8×10^{-6} M never affects the rate beyond the range of experimental error. Taking all the above facts into account, there still remains some question as to the reason why the first order rate formula fits most of the experimental results quite well.

We will next discuss the actual molecular species which participates in the reaction. First, acridine is a base, and in an acidic solution it exists as acridinium cation; it must be determined which species is really involved in the reaction. However, according to Jackson and Porter[2], the pK value of acridine in the triplet state is 5.6 and, in the present pH range, it can be said that acridine exists only as a neutral molecule.

On the other hand, due attention must be paid to the various ionic forms of leuco-uranine. Information as to the reactivity of various species can be obtained from an analysis of the pH effect. In other words, the results depicted in Fig. 4 can be satisfactorily

2) G. Jackson and G. Porter, *Proc. Roy. Soc.*, **A260**, 13 (1961).

interpreted on the basis of the four species of leuco-uranine, L, L^-, L^{2-} and L^{3-}, having different reactivities and, accordingly, different rate constants.

All the processes to be considered (taking the deactivation process into account) are:

$A + h\nu \rightarrow A^*$	$10^3\varphi I_{abs}$	(i)
$A^* + L^{3-} \rightarrow AH + UH^{3-}$	k_1	(ii)
$A^* + L^{2-} \rightarrow AH + UH^{2-}$	k_2	(iii)
$A^* + L^- \rightarrow AH + UH^-$	k_3	(iv)
$A^* + L \rightarrow AH + UH$	k_4	(v)
$A^* \rightarrow A$	k_q	(vi)
$A^* + OH^- \rightarrow A + OH^-$	k_{OH}	(vii)

In this scheme, A* is the triplet state of acridine. ii~v are tentatively expressed as formations of the semi-reduced forms of acridine and uranine. This is plausible, as has been described in the preceding paper, but it has not yet been decided definitely. vii was added for the sake of completeness (see below).

The application of the steady state method leads at once to the following equation:

$$\frac{d[U]}{dt}=10^3\varphi I_{abs}\times\frac{k_1[L^{3-}]+k_2[L^{2-}]+k_3[L^-]+k_4[L]}{k_1[L^{3-}]+k_2[L^{2-}]+k_3[L^-]+k_4[L]+k_q+k_{OH}[OH^-]} \quad (10)$$

As long as the first order rate formula holds, $k_1[L^{3-}]+k_2[L^{2-}]+k_3[L^-]+k_4[L]+k_q$ may be put approximately as

$$k_r[L]_m+k_q=k_t$$

in which $[L]_m$ is the mean value of [L] during the course of the reaction and k_r depends on the pH value. Furthermore, one may assume that:

$$k_t \gg k_{OH}[OH^-]$$

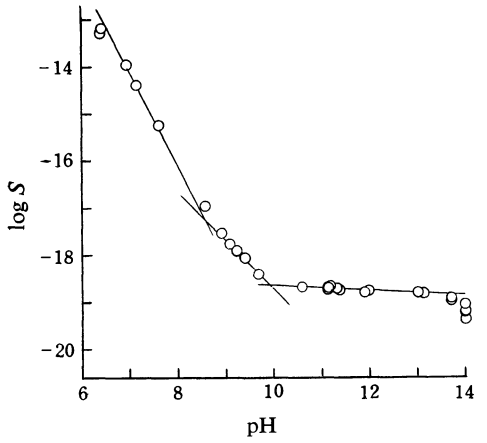


Fig. 7. Plot of log S against the pH value.

so long as $[OH^-]$ is not very great.

By the use of the successive dissociation constants of leuco-uranine (K_1, K_2 and K_3), Eq. 8 can be rewritten as follows:

$$\frac{d[U]}{dt}=10^3\frac{\varphi}{k_t}I_{abs}\times\frac{k_4[H^+]^3+k_3K_1[H^+]^2+k_2K_1K_2[H^+]+k_1K_1K_2K_3}{[H^+]^3+K_1[H^+]^2+K_1K_2[H^+]+K_1K_2K_3}[L]_s \quad (11)$$

where $[L]_s$ is the analytical concentration of leuco-uranine.

Thus, the experimentally-obtained k-value in Eq. 3 can be related to the rate constants of various species in the following way:

$$k\{[H^+]^3+K_1[H^+]^2+K_1K_2[H^+]+K_1K_2K_3\}(=S)=\frac{\varphi}{k_t}\{k_4[H^+]^3+k_3K_1[H^+]^2+k_2K_1K_2[H^+]+k_1K_1K_2K_3\} \quad (12)$$

The left side of this equation is experimentally determined, since K_1, K_2 and K_3 have already been evaluated as $pK_1=3.8$, $pK_2\approx$, and $pK_3=9.6$[3].

Plotting log S against the pH value, it is expected that in the region where the pH value is so small that the first term of the right side overwhelms the other terms, the curve should be a straight line with a slope of -3. As the pH value increases, the straight line gradually curves and connects with another straight part having a slope of -2, then further to a part with slopes of -1 and of 0.

The results obtained by the use of the above K-values and the experimentally determined k-values are shown in Fig. 7. It is seen that the curve really consists of three linear sections with slopes of -2, -1 and approximately 0, although the second range is very short and is not quite clear. The most plausible values of k_1 to reproduce the experimental curve are $\varphi k_1/k_t=1.9\times10^4$, $\varphi k_2/k_t=1.4\times10^4$ and $\varphi k_3/k_t=0.48\times10^4$ (l./mol.)*. The calculated values of k at various pH values are compared with the experimental values in Fig. 4. The line with a slope of -3 having not been obtained, $\varphi k_4/k_t$ can not be obtained under the present experimental conditions.

In the highest pH value region, the line has a little negative slope; this can be attributed to the quenching of the triplet state due to the hydroxyl ion.

Thus, one can write in this region:

3) K. Uchida, S. Kato and M. Koizumi, This Bulletin, 35, 16 (1962).

* As pK, the pH values at the points of intersection in Fig. 7 are employed: $pK_1=3.8$, $pK_2=8.6$ and $pK_3=9.9$.

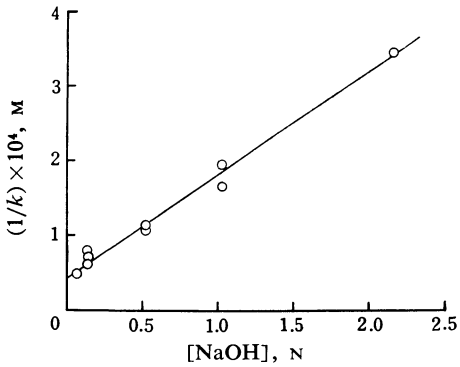


Fig. 8. Plot of $1/k$ against [NaOH].
$[L]_0=9.5\times10^{-6}$ M, $[A]=1.3\times10^{-4}$ M

$$k=\frac{\varphi k_1}{k_t+k_{OH}[OH^-]}$$

or

$$\frac{1}{k}=\frac{k_t}{\varphi k_1}+\frac{k_{OH}}{\varphi k_1}[OH^-] \qquad (13)$$

The plot of $1/k$ against $[OH^-]$ gives a straight line, as is shown in Fig. 8. From the slope and the intercept, one can evaluate k_{OH}/k_t at ~3 l./mol. Furthermore, the value of $\varphi k_1/k_t$ obtained from the intercept is 2.3×10^4 l./mol., with a fair agreement with that obtained from the analysis of Eq. 12.

At this point, it is to be noted that the fluorescence of acridine is also quenched by the hydroxyl ion. The quantitative investigation has shown that the effect is satisfactorily reproduced by Stern-Volmer's equation, the value of the quenching constant K being 0.50 ~0.69 l./mol. K is given by

$$K=\frac{k'_{OH}}{k'_q+k_f}$$

where k_f, k'_q and k'_{OH} are, respectively, the rate constant of emission, of self-quenching and of the reaction between the singlet excited state of acridine and the hydroxyl ion.

In view of the quenching action of the hydroxyl ion on the fluorescence, the above-mentioned value of k_{OH}/k_t ~3 is, of course, an apparent one, pertaining to the action on the singlet excited state as well as on the triplet state. However, the fact that k_{OH}/k_q is much larger than K shows that the latter predominates, reconfirming again that the reaction chiefly takes place via the triplet state of acridine.

In concluding the discussion, it must be added that the absolute value of each rate constant can be estimated with moderate accuracy for a high alkaline region. In this region one may take the value of φ as 0.24; then one can get the value of k_r/k_t as follows:

from the relation between the initial rate and $[L]_0$, 6.6×10^4

from the pH effect on k, 7.9×10^4

from the effect of $[OH^-]$ on k, 9.5×10^4

Perhaps the first value is the most accurate. From this, the value of k_d/k_1 can be evaluated as 0.51×10^{-5} (as has already been described). Although this is not very reliable, chiefly because of the assumption about k_t and φ, it is certain that the reaction between leuco-uranine and the triplet state of acridine occurs quite rapidly, the quantum yield in favorable conditions, being chiefly determined by φ. If one tentatively assumes $k_d=10^4$ sec^{-1}, then k_1 is ca. 2×10^9 sec^{-1} l. mol^{-1}.

Summary

The acridine-sensitized photoöxidation of leuco-uranine in the deareated aqueous solution was studied kinetically. It was established that about 0.24 of the excited acridine molecules goes to the triplet state and then reacts with leuco-uranine. In favorable conditions, the quantum yield is near 0.20, which shows that the genuine reaction rather predominates over the deactivation process of the triplet state.

The pH value dependence of the rate was successfully interpreted from the assumption that each of the different molecular species has a different rate constant.

The authors wish to thank Dr. Shunji Kato for his illuminating discussion.

Department of Chemistry
Faculty of Science
Tohoku University
Katahira-cho, Sendai

Infrared Absorption Spectra of Hydrazides. IV Some Monoacid Hydrazides

By Mitsuo MASHIMA

(Received July 18, 1962)

Although Jensen[1] studied the infrared absorption spectra of some monoacid hydrazides, he examined the bands in the 6 and 3 μ regions only. The infrared spectrum of benzoylhydrazine was previously observed by the present author[2], but the absorption bands obtained could not be interpreted with confidence.

In the present study the spectra of some monoacid hydrazides in the solid state and in acetonitrile solutions are examined in the rock salt region and the frequencies characteristic of the $-CONHNH_2$ group are considered.

Experimental

Formyl-[3], acetyl-[4], cyanoacetyl-[5], propionyl-[6], butyryl-[7] and isovaleryl-hydrazine[8] were synthesized with ethyl esters of corresponding acids and hydrazinehydrate and were purified by recrystallization from ethanol or ether; m. p., 54, 67, 110, 40, 45, 68°C, respectively. *N*-Deuterated cyanoacetylhydrazine was prepared in sealed tubes in the presence of heavy water (99.8%), the excess of which was evaporated in vacuum.

The spectra were taken with a double-beam Hitachi infrared spectrophotometer, type EPI-2, with rock salt prisms. Potassium bromide disks were employed for taking the spectra of solids, and the solution spectra were examined in acetonitrile.

Results and Discussion

Cyanoacetylhydrazine (CAH). — The solid spectra of CAH and *N*-deuterated CAH (CAH-d_3) and the solution spectrum of CAH are illustrated in Fig. 1. The absorption bands of CAH are interpreted without much difficulty by comparing the spectrum with those of cyanoacetyl-acetylhydrazine (CAAH)[9], hydrazine[10] and its derivatives[11,12].

The 3000 cm^{-1} Region. — The most intense band among the bands in this region is found at 3180 cm^{-1} for solid CAH, while a corresponding band is observed at 2380 cm^{-1} for solid CAH-d_3, the value of ν_H/ν_D being 1.336. This is probably due to the N–H stretching vibration of the –CONH– group, because CAAH[9] has also a NH band at 3190 cm^{-1} which is displaced by a band at 2370 cm^{-1} on *N*-deuteration, the ν_H/ν_D ratio being 1.346. The NH_2 stretching vibrations ($\nu(NH_2)$) of the hydrazine residue will also give rise to bands in this region. Hydrazine[10] in the solid state has two bands, ascribed to $\nu_a(NH_2)$ at 3315 cm^{-1} and to $\nu_s(NH_2)$ at 3204 cm^{-1}. Monomethylhydrazine[11] in the liquid state shows three Raman lines, 3317, 3245 and 3177 cm^{-1}, which have been ascribed to NH or NH_2 stretching

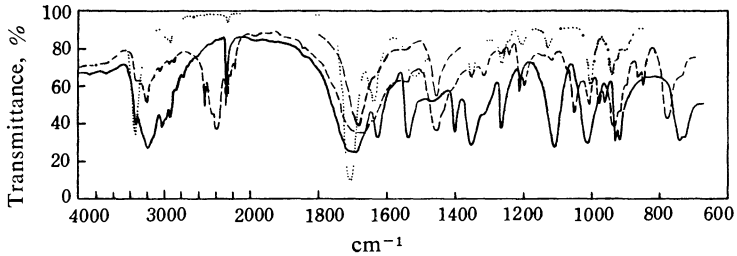


Fig. 1. Infrared spectra of cyanoacetylhyrazine (solid curve) and its *N*-deuterated derivative (dashed curve) in KBr disks and cyanoacetylhydrazine in the CH_3CN solution (dotted curve).

1) J. B. Jensen, *Acta Chem. Scand.*, **10**, 667 (1956).
2) M. Mashima, This Bulletin, **35**, 332 (1962).
3) G. Pellizzari, *Gazz. chim. ital.*, **24**, II, 225 (1894).
4) T. Curtius and T. S. Hofmann, *J. prakt. Chem.*, [2] **53**, 524 (1897).
5) V. Rothenburg, *Ber.*, **27**, 687 (1894).
6) T. Curtius and H. Hille, *J. prakt. Chem.*, [2] **64**, 404 (1901).
7) R. Stolle and G. Zinsser, ibid., [2] **69**, 489 (1904).
8) T. Curtius and H. Hille, ibid., [2] **64**, 411 (1901).
9) M. Mashima, This Bulletin, **35**, 423 (1962).
10) D. A. Giguere and I. D. Liu, *J. Chem. Phys.*, **20**, 136 (1952).
11) D. W. E. Axford, G. J. Janz and K. E. Russell, ibid., **19**, 704 (1951).
12) E. R. Shull, J. L. Wood, J. G. Aston and D. H. Rank, ibid., **22**, 1191 (1954).

vibrations, while 1,1-dimethylhydrazine[12] shows two Raman lines, 3330 and 3141 cm^{-1}, assigned to $\nu(NH_2)$. In this region, CAH has a band at 3320 cm^{-1} and CAH-d_3 has an isolated band at 2510 cm^{-1} and a shoulder band at 2430 cm^{-1}. The 3320 cm^{-1} band is very close in frequency to the 3315 cm^{-1} band ($\nu_a(NH_2)$) of solid hydrazine; its counterpart is found at 2510 cm^{-1} in the CAH-d_3 spectrum, the ν_H/ν_D ratio being 1.323. Therefore, the 3320 cm^{-1} band may be ascribed to $\nu_a(NH_2)$. On the other hand, the $\nu_s(NH_2)$ absorption is expected to appear near 3200 cm^{-1} because solid hydrazine has a corresponding band at 3204 cm^{-1}. However, we can not observe the corresponding band because of the overlap of the intense band at 3180 cm^{-1}, which was already ascribed to $\nu(NH)$. CAH-d_3 has, however, a band at 2430 cm^{-1} which is probably to be ascribed to $\nu_s(ND_2)$. For phenylacetic acid hydrazide, Jensen[1] obtained three bands, at 3300, 3175 and 3000 cm^{-1}, in the solid state, but he did not make detailed assignments of them. The former two bands are very close in frequency to the 3320 and 3180 cm^{-1} bands of CAH respectively. In the present study the assignment of the 3180 cm^{-1} band to the NH stretching vibration of the -CONH- group depends also on the fact that CAH in acetonitrile has a band at 3320 cm^{-1} which is very close in frequency to the $\nu(NH)$ band at 3310 cm^{-1} of CAAH[9] in the same solvent

In this region, CAH has several more weak bands. Of these, three bands are shifted to lower frequencies on *N*-deuteration, but a reasonable interpretation of them is not easy on the basis of the present observations only. On the other hand, a sharp band at 2925 cm^{-1} and a shoulder band at 2860 cm^{-1} are probably to be ascribed to the CH_2 stretching vibrations, because the corresponding bands are found at 2930 and 2870 cm^{-1} for CAH-d_3.

A band at 2265 cm^{-1} of CAH is easily assigned to $\nu(C\equiv N)$, because CAH-d_3 has a corresponding band at 2270 cm^{-1} and CAAH[9] absorbs at 2270 cm^{-1}.

The 1700~700 cm^{-1} Region. — The amide group, -CONH-, is contained in a CAH molecule, so CAH will show amide I, II, III and IV absorptions in this region[13]. CAH has a very strong and broad band with a center at 1698 cm^{-1} and CAH-d_3 has a corresponding band at 1680 cm^{-1}, the ν_H/ν_D ratio being 1.010. Therefore, the 1698 cm^{-1} band of solid CAH may surely be assigned to the amide I band. In the acetonitrile solution, CAH has the corresponding band at 1704 cm^{-1}.

CAH has a band at 1534 cm^{-1} which corresponds in intensity to the band of CAH-d_3 at 1451 cm^{-1}, the ν_H/ν_D ratio being 1.057. A corresponding band is also found at 1513 cm^{-1} for CAH in acetonitrile. CAAH[9] has an amide II band at 1497 cm^{-1}, and CAAH-d_2 has an amide II′ band at 1413 cm^{-1}, the ν_H/ν_D ratio being 1.059. Thus, the 1534 cm^{-1} band of CAH is undoubtedly to be ascribed to the amide II band.

Although the amide III band is expected to appear in the 1300~1250 cm^{-1} range, its identification will be considered with the assignments of the NH_2 deformation vibrations.

Let us now consider the location of the NH_2 deformation vibrations. Yamaguchi[14] has shown that the deformation vibrational modes of the non-planar $-NH_2$ group (e. g., of methylamine and hydrazine) are composed of bending, twisting and wagging vibrations and that the absorption bands due to them occur near 1600, 1300 and 800 cm^{-1} respectively. On the other hand, the deformation vibrations of the planar $-NH_2$ group are composed of bending, rocking, wagging and twisting vibrations. Urea[15] in the solid state has the bands at 1629 and 1603 cm^{-1} (bending), 1150 cm^{-1} (rocking), 719 cm^{-1} (wagging) and 500 cm^{-1} (twisting). Oxamide[16] in the solid state has these four bands at 1608, 1103, 792 and 678 cm^{-1} respectively. Therefore, the presence of the non-planar $-NH_2$ group may probably be detected by the presence of the NH_2 deformation band near 1300 cm^{-1}. Yamaguchi[14] has assigned the 1275 cm^{-1} band of hydrazine vapor to the NH_2 twisting vibration. For solid hydrazine Giguere and Liu[10] have obtained the 1320 cm^{-1} band, which corresponds to the 1275 cm^{-1} band of hydrazine vapor. Axford and others[11] obtained an absorption band at 1308 cm^{-1} for methylamine in the liquid state, but they could not reasonably assign the band. For liquid 1, 1-dimethylhydrazine, Shull and others[12] have observed a strong band at 1321 cm^{-1} which they ascribed to a CH_3 bending vibration. However, this assignment is doubtful because liquid trimethylhydrazine[12] has no band corresponding to it. The band of these hydrazine derivatives near 1300 cm^{-1} is probably due to the non-planar NH_2 deformation vibration.

In the region below 1650 cm^{-1}, CAH has five band which disappear on *N*-deuteration; they are the bands at 1625 (s), 1347 (s), 1258 (m), 1105 (s) and 1009 (s) cm^{-1}. On the other hand, CAH-d_3 has five new bands at 1192 (m), 1044 (m), 973 (m), 928 (s) and 842

13) See, for example, T. Miyazawa, T. Shimanouchi and S. Mizushima, ibid., **24**, 408 (1956).

14) A. Yamaguchi, *J. Chem. Soc. Japan, Pure Chem. Sec.* (*Nippon Kagaku Zasshi*), **80**, 1105, 1109 (1959).

15) A. Yamaguchi, ibid., **78**, 1467 (1957).

16) T. A. Scott, Jr. and E. L. Wagner, *J. Chem. Phys.*, **30**, 465 (1959); see also T. Miyazawa, *J. Chem. Soc. Japan, Pure Chem. Sec.* (*Nippon Kagaku Zassi*), **75**, 86 (1954).

(w) cm^{-1}. Of these, the 1625 cm^{-1} band of CAH will correspond to the 1192 cm^{-1} band of CAH-d_3, the ν_H/ν_D ratio being 1.363. This band is close in frequency to the band due to the NH_2 (planar or non-planar) bending vibration and, acoordingly, it is surely to be ascribed to the NH_2 bending vibration of the $-CONHNH_2$ group. The corresponding band is observed at 1636 cm^{-1} for CAH in acetonitrile.

The 1313 cm^{-1} band of CAH probably corresponds to the 1044 cm^{-1} band of CAH-d_3 ($\nu_H/\nu_D=1.257$). This is close in frequency to the 1320 cm^{-1} band of solid hydrazine[10]. As was mentioned above, the 1320 cm^{-1} band of solid hydrazine corresponds to the 1275 cm^{-1} band of hydrazine vapor[10], and the latter has been assigned to the NH_2 (non-planar) twisting vibration[14]. Therefore, the 1313 cm^{-1} band of CAH may probably be ascribed to the NH_2 twisting vibration of the $-CONHNH_2$ group. It is further concluded that the NH_2 group of CAH has the non-planar structure, because only such a group has the band near 1300 cm^{-1} indicated above.

Next, the 1258 cm^{-1} band of CAH is considered to correspond to the 973 cm^{-1} of CAH-d_3 ($\nu_H/\nu_D=1.293$). Its value of frequency lies in the normal 1250~1300 cm^{-1} range in which the amide III band is usually found for the secondary amides. CAAH[9] has also amide III bands at 1281 and 1235 cm^{-1}. Therefore, the 1258 cm^{-1} band of CAH is undoubtedly to be ascribed to the amide III band. CAH in acetonitrile has also a corresponding band at 1258 cm^{-1}.

The 1105 cm^{-1} band of CAH probably corresponds to the 928 cm^{-1} band of CAH-d_3, the ν_H/ν_D ratio being 1.190. CAH in acetonitrile has a corresponding band at 1122 cm^{-1}. Such a strong band as the 1105 cm^{-1} one may not be observed near 1100 cm^{-1} for CAAH[9] and cyanoacetate acid amide*1. It is, therefore, concluded that the 1105 cm^{-1} band is not due to a vibration of the $N\equiv C-CH_2-CO-$ group, which is the group contained in CAH, CAAH and cyanoacetic acid amide. In consequence, the 1105 cm^{-1} band has to be due to a vibration of the hydrazine residue. Hydrazine in the vapor state has the bands at 966, 933 cm^{-1} (doublet) and 780 cm^{-1} which have been ascribed[14] to the NH_2 wagging vibrations of different species (B and A) respectively. The bands corresponding to the former have been observed at 1078, 1072 cm^{-1} for solid hydrazine by Giguere and Liu[10]. The 1105 cm^{-1} band of CAH is close in frequency to the 1078, 1072 cm^{-1} bands of solid hydrazine. Therefore, it is probably to be ascribed to the NH_2 wagging vibration of the hydrazine residue.

The band at 1009 cm^{-1} of CAH probably corresponds to the 842 cm^{-1} band of CAH-d_3 ($\nu_H/\nu_D=1.198$); it is probably due to an NH_2 deformation vibration (perhaps rocking).

As was mentioned above, it is seen that CAH has four bands ascribed to the NH_2 deformation vibrations. This is not consistent with Yamaguchi's conclusion[14], that the deformation modes of the non-planar NH_2 group are composed of three fundamental vibrations. However, it is of interest to note that four NH_2 deformation frequencies are obtained for other monoacid hydrazides the absorption bands of which will be considered later. In spite of some doubtfulness in the assignments, we can regard these frequencies as characteristic of the $-CONHNH_2$ group.

The $CH_2<$ deformation vibrations are probably to be found in this region. For the $CH_2<$ deformation frequencies, Nakagawa[17] has proposed the following ranges: 1450~1350 cm^{-1} for bending, 1350~1100 cm^{-1} for wagging, 1250~1000 cm^{-1} for twisting, and 1000~700 cm^{-1} for rocking. CAH has 1396, 1347, 1205 and 1009*2 cm^{-1} bands, which are scarcely changed in frequency on *N*-deuteration. CAH-d_3 has corresponding bands at 1397, 1347, 1206 and 1000 cm^{-1}. These four bands lie in the four ranges indicated above; accordingly, they are ascribed to the CH_2 bending, wagging, twisting and rocking vibrations respectively. The bending and wagging frequencies are not observed for CAH in acetonitrile because of interference due to solvent absorption, but the bands due to the latter two vibrations are found at 1197 and 997 cm^{-1} respectively.

Bands ascribed to the skeletal (CH_2–CO, NC–CH_2 and N–N) stretching vibrations and the O=C–N deformation vibration (amide IV) are expected to appear in this region. The N–N stretching frequency of 1143 cm^{-1} has been obtained for CAAH[9], but no band corresponding to it is observed for CAH because of its location on the sloping back ground of the much more intense band at 1105 cm^{-1}. On the other hand, CAH-d_3 has a very weak band at 1112 cm^{-1} which is probably to be ascribed to the N–N stretching vibration. Hydrazine[10] absorbs at 1098 cm^{-1} (vapor) and 1124 cm^{-1} (solid). The 1098 cm^{-1} band has been ascribed to the N–N stretching vibration[14]. The corresponding band was observed at 1110 cm^{-1} for HCONDNHCOH[18], at 1165 cm^{-1} for

*1 Its infrared absorption spectrum will be published elsewhere.

17) I. Nakagawa, *J. Chem. Soc. Japan, Pure Chem. Sec.* (*Nippon Kagaku Zassi*), **76**, 540 (1955).

*2 It seems probable that this band arises from the NH_2 deformation band overlapping the CH_2 deformation band.

18) T. Miyazawa, *J. Chem. Soc. Japan, Pure Chem. Sec.* (*Nippon Kagaku Zassi*), **76**, 341 (1955).

TABLE I. INFRARED FREQUENCIES OF CYANOACETYLHYDRAZINE AND ITS *N*-DEUTERATED DERIVATIVE (in cm^{-1})

Assignment	Cyanoacetylhydrazine		Its *N*-deuterated derivative
	Solid	in CH_3CN	Solid
$\nu_a(NH_2)$	3320 (m)		
$\nu(NH)$, $\nu_s(NH_2)$	3180 (vs)	3320	
	3020 (m)		
	2970 (sh)		
$\nu(CH_2)$	2925 (m)	2910	2930 (w)
	2860 (w)		2870 (w)
	2770 (w)		
$\nu_a(ND_2)$			2510 (m)
$\nu_s(ND_2)$			2430 (sh)
$\nu(ND)$			2380 (vs)
$\nu(C\equiv N)$	2265 (m)	2250	2270 (m)
			2240 (w)
			2200 (w)
			2150 (w)
Amide I	1698 (vs)	1704	1680 (vs)
$\beta(NH_2)$	1625 (s)	1636	
Amide II	1534 (s)	1513	
	1464 (b, w)		
Amide II'			1451 (s)
$\beta(CH_2)$	1396 (m)		1397 (sh)
$\omega(CH_2)$	1347 (s)	1347	1347 (w)
$\tau(NH_2)$	1313 (sh)		1312 (w)
Amide III	1258 (m)	1258	
$\tau(CH_2)$	1205 (w)	1197	1206 (m)
$\beta(ND_2)$			1192 (m)
$\omega(NH_2)$?	1105 (s)	1122	
ν(N-N)			1112 (vw)
			1069 (sh)
$\tau(ND_2)$			1044 (m)
$\gamma(NH_2)$?, $\gamma(CH_2)$	1009 (s)	997	1000 (m)
Amide III'			973 (m)
$\omega(ND_2)$?			928 (s)
	932 (w)	935	
ν(C-C)	924 (s)	920	912 (sh)
	913 (s)	892	892 (sh)
$\gamma(ND_2)$			857, 842 (w)
Amide IV	738 (s)		772 (s)
	723 (sh)		729 (sh)

ν; stretching; a, asymmetric; s, symmetric; β, bending; τ, twisting; ω, wagging; γ, rocking

$(CH_3CONH-)_2 \cdot H_2O$[19] and at 1133 cm^{-1} for formyl-acetylhydrazine[9].

CAH has bands at 932 (w), 924 (s), 913 (s), 738 (s) and 723 (sh) cm^{-1} not yet accounted for. CAH-d_3 also has four bands at 912 (sh), 892 (sh), 772 (s) and 729 (sh) cm^{-1}. Of these, the bands near 900 cm^{-1} are probably due to the C–C stretching vibrations and a band near 750 cm^{-1} can be assigned to amide IV, although their detailed assignments are not easy.

The infrared frequencies of CAH and their tentative assignments are summarised in Table I.

Formylhydrazine (FH).—The infrared spectra of FH in the solid state and in acetonitrile are illustrated in Fig. 2. Although the spectrum of *N*-deuterated FH could not be observed*3, absorption bands of FH were interpreted without much difficulty by comparing the spectrum with those of diformylhydrazine (DFH)[18], formamide(FA)[20]and *N*-methylformamide (MFA)[21]. The infrared frequencies of DFH, FA and MFA have reasonably been explained with a model of a trans-planar configuration of the HCONH– group. Therefore, it will be assumed that an FH molecule also contains such a planar HCONH– group. This assumption is supported by the fact that FH has six bands very close in frequency to the bands of DFH; accordingly, these bands are immediately assigned to vibrational modes of the HCONH– group, as is indicated in Table II (upper part).

The amide I absorption will be shown near 1600 cm^{-1} because DFH has a band at 1610 cm^{-1}. FH in the solid state has a very strong band at 1674 cm^{-1} which corresponds to the band at 1689 cm^{-1} of FH in acetonitrile. The value of 1674 cm^{-1} is rather higher than that of the amide I band of DFH, but it is surely taken to be an amide I band because MFA in the solid state also has a band at 1672 cm^{-1} [21].

DFH[18] has a 3100 cm^{-1} band ascribed to the NH stretching vibration. In this region, FH in the solid state shows very intense and broad absorption with a maximum near 3210 cm^{-1}, while FH in acetonitrile has the band at 3330 cm^{-1}. FA[20] in the solide state also has a broad and strong band near 3250 cm^{-1}, which has been ascribed to the NH_2 assym. or sym. stretching vibration. The rock salt optics employed are not suitable for measurements in this region because of low resolution, but it is seen that the band near 3210 cm^{-1} of solid FH is really composed of three bands, i. e., it is accompanied by a shoulder band which could not be defined on both the high- and low-frequencies sides. Therefore, these bands are due to the NH_2 and NH stretching vibrations.

The out-of-plane CH deformation vibration may also be located in the region examined here. No band corresponding to it has been observed for DFH[18], but its sodium salt[22] has

19) A. Yamaguchi, ibid., 79, 880 (1958).

*3 *N*-Deuterated FH could not be prepared by the usual exchange reaction.

20) T. Miyazawa, *J. Chem. Soc. Japan, Pure Chem. Sec.* (*Nippon Kagaku Zassi*), 76, 821 (1955).

21) T. Miyazawa, ibid., 77, 321, 619 (1956); see also I. Suzuki, This Bulletin, 35, 540 (1962).

22) M. Mashima, ibid., 35, 338 (1962).

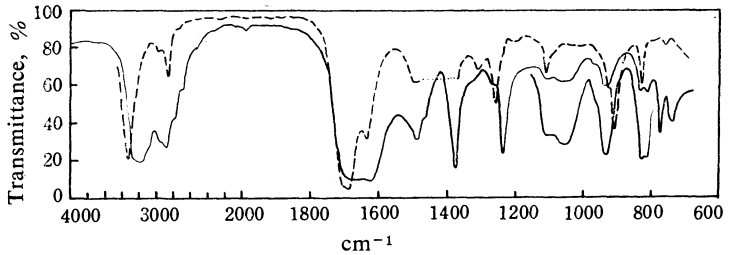


Fig. 2. Infrared spectra of formylhydrazine in the solid state (solid curve) and in the CH_3CN solution (dashed curve).

Table II. Infrared frequencies of formylhydrazine (in cm^{-1})

Assignment	DFH[a] Solid	DFH-d_2[a] Solid	FH Solid	FH in CH_3CN
ν(CH)	2900	2920	2880 (s)	2860 (w)
Amide II	1480	1338	1488 (m)	—[b]
δ(CH)	1368	1389	1373 (s)	—[b]
Amide III (III′)	1229	985	1233 (s)	1255 (m)
π(NH)	770	—	772 (m)	
Amide IV	753	751	737 (m)	753 (vw)
ν(NH) or $\nu(NH_2)$	3100		3210 (vs)	3330 (s)
			2790 (sh)	
			2700 (sh)	
Amide I	1610	1605	1674 (vs)	1689 (vs)
$\beta(NH_2)$			1632 (vs)	1635 (m)
			1463 (sh)	
NH_2 deformation			1262 (vw)	1305 (w)
NH_2 deformation			1104 (vw)	1106 (w)
π(CH)			1050 (w)	
ν(N-N) ?			927 (w)	921 (w)
				907 (m)
NH_2 deformation			826 (w)	826 (w)
			807	

ν, stretching; δ, in-plane deformation; π, out-of-plane deformation; β, bending
a See Ref. 18
b Could not observe because of interference due to solvent absorption

a band at 1026 cm^{-1}. FA[20] and MFA[21] in the solid states have a CH band at 1060 cm^{-1} and 1015 cm^{-1} respectively. In this region FH has a weak band at 1050 cm^{-1} which is probably to be ascribed to the out-of-plane CH deformation vibration.

Let us now consider the location of the NH_2 deformation vibrations and the N–N stretching vibration of the hydrazine residue. Solid FH has a strong band at 1632 cm^{-1} which is very close in frequency to the 1625 cm^{-1} band (ascribed to the NH_2 bending vibration) of CAH. FH in acetonitrile has a corresponding band at 1635 cm^{-1}. Thus, the 1632 cm^{-1} band may be ascribed to the bending vibration.

The infrared frequencies of FA have been reasonably explained[20] by use of the model of the planar structure of the $-CONH_2$ group; the compound shows the NH_2 deformation frequencies as follows: 1610 cm^{-1} (bending), 1110 cm^{-1} (rocking), and 800 cm^{-1} (wagging). As has been indicated already, CAH has the end group $-NH_2$, being non-planar in structure, and it has four bands, 1625, 1347, 1105 and 1009 cm^{-1}, due to the NH_2 deformation vibrations. FH has several weak or shoulder bands not yet accounted for. Of these, the very weak band at 1262 cm^{-1} is expected to be due to a fundamental vibrational mode because the band corresponding to it is observed at 1305 cm^{-1} for FH in acetonitrile. This band probably corresponds to the 1347 cm^{-1} band of CAH; it will be ascribed to the NH_2 deformation vibration. Two further bands at 1104 and 927 cm^{-1} and the doublet band (826, 807 cm^{-1}) have their respective counterparts in the solution spectrum as represented in Table II. Of these three, the 1104 cm^{-1} band and the doublet

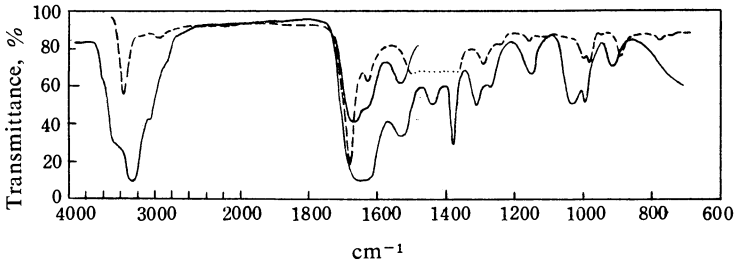


Fig. 3. Infrared spectra of acetylhydrazine in the solid state (solid curve) and in the CH_3CN solution (dashed curve).

band are very close in frequency to the 1110 cm^{-1} (NH_2 rocking) and 800 cm^{-1} (NH_2 wagging) bands of FH respectively. These two bands are probably to be ascribed to the NH_2 deformation vibratios and the band at 927 cm^{-1}, to the N–N stretching vibration, but these assignments, of course, are not certain.

The infrared frequencies of FH and their tentative assignments are summarized in Table II, in which the frequencies of DFH are also indicated for the sake of comparison.

Acetyl-, Propionyl-, *n*-Butyryl- and Isovaleryl-hydrazine. — The infrared spectra of acetylhydrazine (AH) in the solid state and in the acetonitrile solution are illustrated in Fig. 3. The spectrum of its *N*-deuterated species could not be observed*4, but the absortion bands of AH were interpreted by a comparison of the spectrum with those of diacetylhydrazine[19], *N*-methylacetamide[23] and cyanoacetylhydrazine. The infrared frequencies of AH and their tentative assignments are summarized in Table III.

In the solid state, AH has a very strong band at 3270 cm^{-1}, which is accompanied by two shoulder bands at 3420 and 3050 cm^{-1}. These bands are probably to be ascribed to the NH_2 or NH stretching vibrations. The band corresponding to them is found at 3360 cm^{-1} for AH in acetonitrile.

The very strong band at 1673 cm^{-1} of solid AH corresponds to the 1684 cm^{-1} band of AH in acetonitrile; it may surely be taken as an amide I band. The band at 1535 cm^{-1} is easily taken as an amide II band. Further, it is expected that an amide III band will appear near 1300 cm^{-1}. Solid AH has two bands at 1316 and 1276 cm^{-1}. They will correspond to the band at 1295 cm^{-1} of AH in acetonitrile. An amide III band has been obtained at 1261 cm^{-1} for diacetylhydrazine[19], 1258 cm^{-1} for cyanoacetylhydrazine and 1312 cm^{-1} for *N*-methylacetamide[23]. Therefore, one of the two bands, 1316 and 1276 cm^{-1}, is probably to be taken as an amide III band.

TABLE III. INFRARED FREQUENCIES OF AH (in cm^{-1})

Assignment	$CH_3CONHNH_2$	
	Solid	in CH_3CN
$\nu(NH_2)$ or $\nu(NH)$	3420 (sh)	
	3270 (vs)	3360 (s)
	3050 (sh)	
	2860 (w)	
Amide I	1673 (vs)	1684 (vs)
$\beta(NH_2)$	1633 (sh)	1633 (m)
Amide II	1535 (s)	
$\delta_a(CH_3)$	1443 (b, m)	
$\delta_s(CH_3)$	1382 (s)	
Amide III or	1316 (m)	1295 (m)
NH_2 deformation	1276 (sh)	
NH_2 deformation	1154 (m)	1163 (w)
NH_2 deformation	1034 (m)	998 (m)
$\gamma(CH_3)$	994 (m)	986 (m)
$\nu(C\text{-}CH_3)$	909 (m)	894 (m)
		780 (w)

ν, stretching; β, bending; δ, deformation; γ, rocking; a, asymmetric; s, symmetric

AH in the solid state has two bands at 1443 and 1382 cm^{-1}. They may surely be ascribed to the CH_3 asym. and sym. deformation vibrations, for the corresponding bands have been found at 1433 and 1368 cm^{-1} for solid diacetylhydrazine[19] and at 1413 and 1373 cm^{-1} for *N*-methylacetamide[23] in the carbon tetrachloride solution.

The CH_3 rocking and C–CH_3 stretching vibrations may be located without difficulty in the spectrum of AH. *N*-Methylacetamide[23] in carbon tetrachloride has two bands, at 1040 and 987 cm^{-1}, which have been ascribed to the CH_3 rocking vibrations. They correspond to the bands at 1050 and 1001 cm^{-1} for solid *N*-methylacetamide[23]. The compound has, further, a C–CH_3 stretching band at 881 cm^{-1} in carbon tetrachloride solution and at 892 cm^{-1} in the solid state[23]. Diacetylhydrazine[19] also has

*4 *N*-Deuterated acetylhydrazine could not be prepared by the usual exchange reaction.

23) T. Miyazawa, T. Shimanouchi and S. Mizushima, *J. Chem. Phys.*, **29**, 611 (1958); see also T. Miyazawa, *J. Chem. Soc. Japan, Pure Chem. Sec.* (*Nippon Kagaku Zassi*), **77**, 171, 321, 619 (1956).

CH_3 rocking bands at 1029 and 1019 cm^{-1} and a C–CH_3 stretching band at 921 cm^{-1}. In the region of 1100~800 cm^{-1}, solid AH has three bands at 1034, 994 and 909 cm^{-1}; bands corresponding to them are found at 998, 986 and 894 cm^{-1} respectively for AH in acetonitrile. The value of 909 cm^{-1} is considered to be basis enough for ascribing the band to the C–CH_3 stretching vibration, because in the solid state *N*-methylacetamide and diformylhydrazine have the C–CH_3 stretching band at 892 and 921 cm^{-1} respectively, as has been mentioned above. This assignment is also supported by the fact that a similar frequency shift in the change of states is seen between the 909 cm^{-1} band of AH and the C–CH_3 stretching band at 892 cm^{-1} of solid *N*-methylacetamide. Two other bands, 1034 and 994 cm^{-1}, may be interpreted as follows: if the 1034 cm^{-1} band of solid AH corresponds to the 998 cm^{-1} band of the compound in solution, the value of the frequency shift is 36 cm^{-1}, which value is relatively larger than that of the CH_3 rocking vibration of *N*-methylacetamide. On the other hand, the 994 cm^{-1} band of solid AH is, in the value of frequency, 8 cm^{-1} larger than its 986 cm^{-1} band in solution. This value of the frequency shift is in accordance with that of the CH_3 rocking bands of *N*-methylacetamide. In consequence, the 994 cm^{-1} band of AH is ascribed to the CH_3 rocking vibration and the 1034 cm^{-1} band is due to another vibrational mode.

Solid AH has four more bands, at 1633, 1316 (or 1276), 1154 and 1034 cm^{-1}, not yet acounted for. These four bands correspond, respectively, to the bands at 1625, 1347, 1105 and 1009 cm^{-1} of cyanoacetylhydrazine. The 1633 cm^{-1} band is surely to be ascribed to the NH_2 bending vibration, while the latter three bands are due to the NH_2 deformation vibrations.

Let us next consider the absorption spectra of propionyl-, *n*-butyryl- and isovaleryl-hydrazine. They are illustrated in Fig. 4, in which the spectra of corresponding symmetric diacid

TABLE IV. INFRARED FREQUENCIES OF PROPIONYL-, *n*-BUTYRYL- AND ISOVALERYLHYDRAZINE (in cm^{-1})

$CH_3CH_2\cdot CONHNH_2$ Solid (KBr disk)	$CH_3CH_2CH_2\cdot CONHNH_2$ Solid (KBr disk)	$CH_3>CH_3>CHCH_2\cdot CONHNH_2$ Solid (KBr disk)
3250 (vs)	3230 (vs)	3300 (vs)
	3160 (sh)	3190 (m)
3030 (m)	3000 (m)	3050 (w)
2965 (m)	2920 (s)	2950 (s)
2880 (sh)	2840 (m)	2875 (w)
1640 (b, vs)	1645 (b, vs)	1682 (sh)
		1632 (vs)
1523 (s)	1532 (s)	1542 (s)
1464 (m)	1467 (m)	1473 (m)
1436 (sh)	1439 (sh)	1441 (w)
		1392 (sh)
1374 (m)	1380 (m)	1378 (s)
		1337 (sh)
	1331 (m)	1321 (m)
1280 (m)	1288 (m)	
1242 (m)	1261 (m)	1269 (w)
	1222 (m)	1226 (m)
1150 (w)	1158 (m)	1159 (sh)
		1124 (vw)
	1085 (b, m)	1087 (m)
	1055 (w)	
1067 (m)	1044 (m)	
1027 (m)	1016 (s)	1017 (s)
		998 (sh)
954 (s)	932 (b, m)	955 (m)
		933 (m)
899 (w)	898 (w)	887 (m)
	877 (sh)	
801 (w)	806 (vw)	837 (m)
	772 (vw)	762 (w)
	748 (w)	
	696 (w)	

TABLE V. INFRARED FREQUENCIES CHARACTERISTIC TO THE GROUP -$CONHNH_2$ (in cm^{-1})

Assignment	H-X[a]	CH_3-X	$CNCH_2$-X	CH_3CH_2-X	$CH_3CH_2CH_2$-X	$CH_3>CH_3>CHCH_2$-X
NH_2 or NH stretching	3210	3270	3320	3250	3230	3300
			3180			
Amide I	1674	1673	1698			1682
				1640[b]	1645[b]	
NH_2 bending	1632	1633	1625			1632
Amide II	1488	1535	1534	1523	1532	1542
NH_2 deformation	1262	1316	1313	1280	1331	1321
Amide III	1233	1276	1258	1242	1288	1269
NH_2 deformation	1050	1154	1105	1150	1158	1159
NH_2 deformation	826	1034	1009	954	1006	1017
	807					

a X is the group -$CONHNH_2$
b Observed the very strong band with a center near those

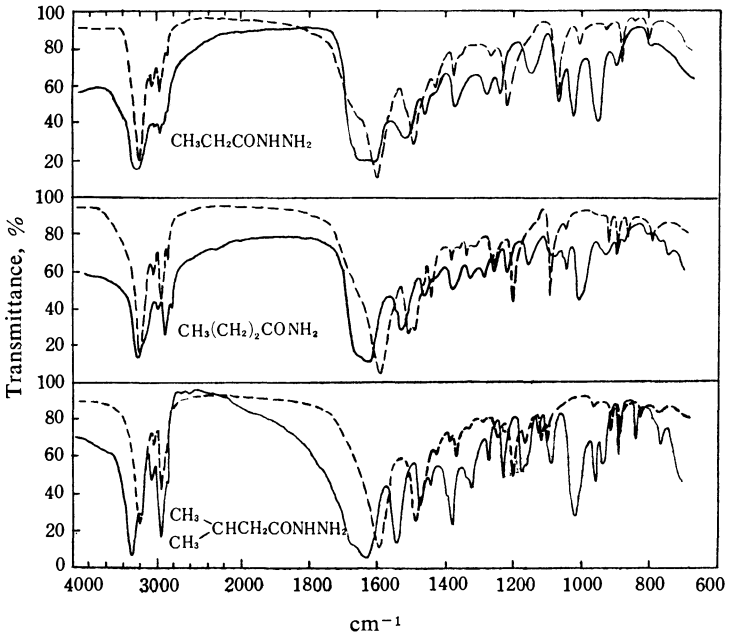


Fig. 4. Infrared spectra of the monoacid hydrazides being indicated (in KBr disks). Solid curves show the spectra of the monoacid hydrazides and dashed curves show the spectra (represented for comparison) of the corresponding diacid hydrazides.

hydrazides are represented for purposes of comparison; the infrared frequencies of these monoacid hydrazides are summarized in Table IV.

All of these hydrazides have a very strong band near 3250 cm^{-1}, which may be ascribed to the NH_2 or NH stretching vibrations. In the 1630~1680 cm^{-1} range, these hydrazides are expected to have an amide I band and a band due to the NH_2 bending vibration. These two bands are not separated from each other for propionyl- and *n*-butyrylhydrazine; i. e., they have a very broad and strong band with a center near 1640 cm^{-1}. On the other hand, isovalerylhydrazine has a very strong band at 1632 cm^{-1} which is accompanied with a shoulder band at 1682 cm^{-1}; these two bands are taken, respectively, as a band due to the NH_2 bending vibration and an amide I band. In the region below 1350 cm^{-1}, the spectral patterns of these hydrazides are rather complex, but we can find four bands corresponding to the 1316, 1276, 1154 and 1034 cm^{-1} bands of AH. They are summarized, with other frequencies characteristic of the $-CONHNH_2$ group, in Table V.

Characteristic Frequencies.—As may be seen from Table V, the frequencies characteristic of the $-CONHNH_2$ group were obtained as follows: 1) An amide I band is found near 1670 cm^{-1} for the monoacid hydrazides when examined in the solid state. 2) An amide II band is also shown near 1530 cm^{-1}. 3) All the monoacid hydrazides examined here have a band near 1630 cm^{-1} ascribed to the NH_2 bending vibration. 4) In the region below 1350 cm^{-1}, these hydrazides have four bands which may also be taken as bands characteristic of the $-CONHNH_2$ group. Of these four, one band near 1250 cm^{-1} is probably to be taken as an amide III band. However, the detailed assignment of these four bands is difficult on the basis of the present observations only. The present author plans to examine the infrared absorptions for other monoacid hydrazides and related compounds. 5) A strong band due to the NH_2 or NH stretching vibrations is found near 3250 cm^{-1}.

The author is grateful to Professor Sunao Imanishi of Kyushu University for his generous permission to use the University's spectrophotometer.

Department of Literature and Science
Saga University
Saga

*The Reaction of cis-2-α-Carboxyethylcyclopentanol Lactone**

By Tsuguo TANAKA

(Received July 23, 1962)

It is of some interest to synthesize nor-nepetalactone and nor-nepetalic acid through the stereospecific route starting from a compound of an identified structure. The author attempting such a synthesis, has examined some reactions of *cis*-2-α-carboxyethylcyclopentanol lactone[1].

First, in order to obtain cyanoacid III, *cis*-2-α-carboxyethylcyclopentanol lactone (I) was heated with potassium cyanide[2] at 250~260°C for 24 hr., and the products were isolated and fractionally distilled. Two compounds were obtained as the main products. One was a lactone, $C_8H_{12}O_2$ (II), and the other, a cyanoacid, $C_9H_{13}O_2N$ (III). Many differences were observed between the infrared spectra as well as the ultraviolet spectra of lactone II and those of *cis*-2-α-carboxyethylcyclopentanol lactone I, although the molecular formulas of these two lactones are identical.

The 5.83 μ band of the carbonyl stretching vibration of II, as compared with the 5.70 μ band of that of I[1], seems to indicate that the five-membered γ-lactone ring of I is expanded to a six-membered δ-lactone ring[3] linked to the same cyclopentane unit, producing structure (II) of *cis*-3-α-carboxyethylcyclopentanol lactone as a result of the rearrangement[4] induced by potassium cyanide. Lactone II is easily hydrolysed by aqueous sodium hydroxide into the hydroxyacid, which is easily reconverted into the original lactone on acidification. We are dealing with *cis*-lactone in this case. In order to obtain further evidence for structure II, lactone II was hydrolysed with a 10% aqueous sodium hydroxide solution and the sodium salt of hydroxyacid was thoroughly oxidised with potassium permanganate. Two compounds were isolated from the reaction mixture. The one, a tricarboxylic acid, $C_8H_{12}O_6$ (IV), (m. p., 180°C), was identified as α-methyl-β-carboxyadipic acid[5] both by mixed melting point determination and by its infrared spectra, substantially supporting structure II for new lactone. The other, a tricarboxylic acid, $C_8H_{12}O_6$ (m. p., 140°C), was not identified. It might be the lower melting modification of α-methyl-β-carboxyadipic acid, but its identity was not examined because the author could not convert α-methyl-β-carboxyadipic acid (m. p., 180°C[5]) into an acid of m. p. 140°C, either by heating the aqueous solution at 200°C for 10 hr. or by heating it in acetyl chloride[6]. Another possibility is β-(α-carboxyethyl)glutaric acid[7]. But mixed melting of tricarboxylic acid V with it shows a melting point depression.

In order to see whether or not there exists another modification of β-(α-carboxyethyl)-glutaric acid, the synthesis of this acid was attempted.

The condensation of diethyl β-bromoglutarate with diethyl methylmalonate produced diethyl glutaconate (VI) and tetraethyl 2, 3-bis(carboxymethyl)adipate (VII) ; the latter on hydrolysis yielded tetracarboxylic acid (m. p., 203°C) which was proved to be 2, 3-bis(carboxymethyl)adipic acid (VIII), reported previously to have been obtained from diethyl β-bromoglutarate by a different procedure[8]. Another condensation of diethyl malonate with diethyl β-bromoglutarate resulted in the same products. The original aim was no attained. The hydrolysis of cyanoacid III with hydrochloric acid yielded a dicarboxylic acid, $C_9H_{14}O_4$ (IX) (m. p., 130°C).

Cyanoacid III was treated with oxalyl chloride and warmed on the water bath. The cyanoacid chloride X obtained was, very unstable. The distillation of the raw material was accompanied by extensive degradation and resinification and was not considered to be an convenient intermediate for further synthesis.

In the second scheme, attention was centered on the reduction of *cis*-lactone I into hydroxyaldehyde (XII).

The reduction of *cis*-lactone I with lithium

* The Synthesis of Cyclopentane Derivatives. II. Parts of this paper were presented in a preliminary way in This Bulletin, 34, 888 (1961).

1) T. Tanaka, This Bulletin, 32, 1320 (1959).

2) Cf. G. Komppa, *Ber.*, 41, 4472 (1908); M. A. Haller, *Compt. rend.*, 112, 446 (1896).

3) L. J. Bellamy, "Infrared Spectra of Complex Molecules," Methuen, London (1954), pp. 153, 159; R. N. Jones, P. Humphries and K. Dobriner, *J. Am. Chem. Soc.*, 72, 956 (1950); G. Stork and R. Breslow, ibid., 75, 3291 (1953).

4) Cf. C. C. Price and W. Kaplan, ibid., 66, 477 (1944).

5) W. N. Haworth and W. H. Perkin, *J. Chem. Soc.*, 93, 581 (1908).

6) A. Küster, *Ann.*, 345, 39 (1906).

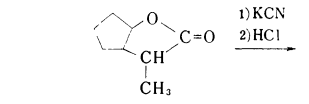
7) Z. H. Skraup, *Monatsh.*, 21, 1907 (1900).

8) Ch. Grundmann and H. Paul, *Ber.*, 86, 186 (1953); C. T. Blood, N. J. Cartwright and R. P. Linstead, *J. Chem., Soc.*, 1952, 2268.

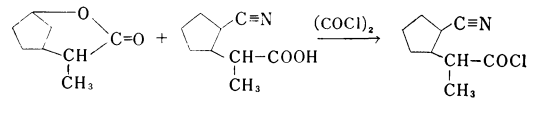
aluminum hydride at a low temperature[9] was not satisfactory. It is liable to produce diol (XIII) and unreacted recoveries. The reduction of methylanilide of hydroxyacid XI with lithium aluminum hydride[10] is also a possible route to a hydroxyaldehyde. It is realized in this case that the reduction of methylanilide XI proceeds in as much as a 50~55% yield. However, the yield of the methylanilide in the reaction of *cis*-lactone with methylanilinomagnesium bromide[11] as well as with methylanilinomagnesium iodide is not satisfactory. When the *cis*-lactone is treated with an equivalent amount of a fresh colorless reagent (immediately after methylaniline has been added), plates (m. p., 130°C (a)) are obtained in a low yield but in a very pure state. However, in the usual procedures using an excess amount of an aged (20 min.), purple-colored methylanilinomagnesium bromide solution, although the yield is improved the products are crystal needles (m. p., 110~120°C) from which, after repeated crystallization from ethyl acetate, a lower yield of crystals (m. p., 130°C (a)) is obtained. The chromatography of a tetrahydrofuran solution of crystals (m. p., 110~120°C) through alumina produced in a 64% yield, crystals (m. p., 130°C (b)), the 14.14 μ band of the infrared spectra of which differs from the corresponding 14.35 μ band of that of crystal with a m. p. of 130°C (a) although the mixed melting of these two methylanilides does not show any melting point depression.

The configuration of the carbon atom adjacent to the carbonyl group of *cis*-lactone I is considered to be that formulated by Ia, whereas for *trans*-2-α-carboxyethylcyclopentanol lactone, either XIVa or XIVb is possible. In accordance with this, the singlet infrared band (10.50; 11.13 μ) of *cis*-lactone appears as a doublet band (10.50, 10.64; 11.13, 11.25 μ) of *trans*-lactone[1]. However, whether or not modifications a and b correspond to XIa and XIb respectively has not been ascertained. It seems probable that the colorless methylanilinomagnesium bromide which is produced immediately by reacting the ethylmagnesium bromide with methylaniline is a covalented $C_6H_5(CH_3)$-N-MgBr and that the aged, purple-colored solution of the reagent is an ionic conjugate, $C_6H_5(CH_3)N^{\ominus}Mg^{\oplus}Br[O(C_2H_5)_2]_2$ which is an effective reagent for the aldol type condensation[12] and which can also act to induce the dissociation of the hydrogen attached to the carbon atom adjacent to the carbonyl group, resulting in the inversion or racemization at a carbon atom adjacent to the carbonyl. For methylanilinomagnesium iodide, however, no such ionic conjugate form seems possible.

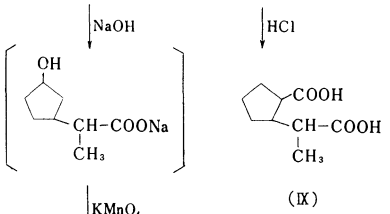
By the reaction of hydroxyaldehyde XII with ethylene glycol a high yield to product is obtained, although it is not the ordinary form of the ethylenedioxy derivative but a cyclic acetal formulated in XV[9b].



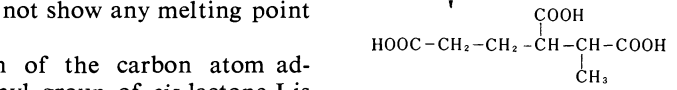
(I)



(II) (III) (X)



(IX)

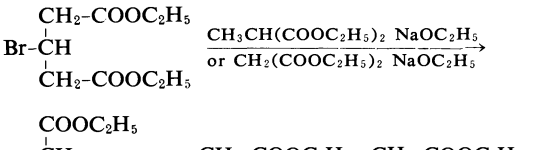


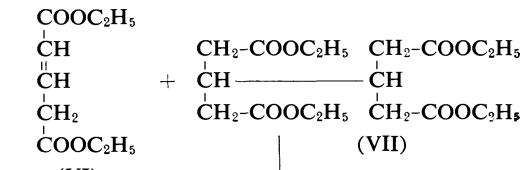
(IV)

+

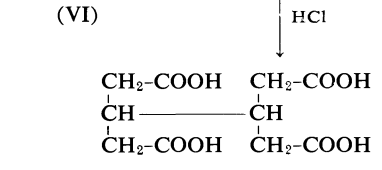
$C_8H_{12}O_6$ (m.p.140°C)

(V)



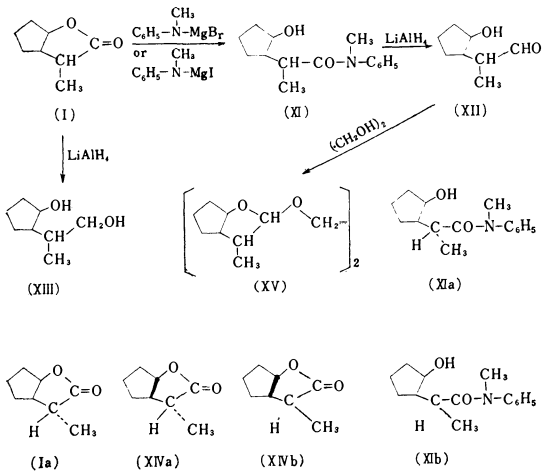


(VI) (VII)



(VIII)

9a) Cf. G. E. Arth, *J. Am. Chem. Soc.*, **75**, 2413 (1953).
9b) Cf. H. Ohara, *J. Chem. Soc. Japan, Pure Chem. Sec. (Nippon Kagaku Zasshi)*, **82**, 65 (1961).
10) F. Weygand, G. Eberhardt, H. Linden, F. Schäfer and I. Eigen, *Angew. Chem.*, **65**, 525 (1953).
11) Cf. F. Bodroux, *C. r. d. l'Acad. des Sciences*, **138**, 1427 (1904).
12) A. T. Nielsen, C. Gibbons and C. A. Zimmermann, *J. Am. Chem. Soc.*, **73**, 4696 (1951); W. G. Garden and F. D. Gunstone, *J. Chem. Soc.*, **1952**, 2651.



Experimental

***cis*-3-α-Carboxyethylcyclopentanol Lactone (II) and 2-α-Carboxyethylcyclopentyl Cyanide (III).**—Eight grams of *cis*-2-α-carboxyethylcyclopentanol lactone (I) and 6.4 g. of potassium cyanide are sealed in a glass tube and heated at 250~260°C for 24 hr. The mass becomes a dark solid. After cooling, the tube is opened (a slight pressure is observed) and the reaction mass is dissolved in 60 ml. of water. When 10 ml. of 6 N hydrochloric acid is added to the solution, it becomes turbid and some tarry substance separates. The suspension is made alkaline by the addition of an excess of a saturated sodium bicarbonate solution, and a small amount of active charcoal is added and filtered. The tarry residue is further extracted with a sodium bicarbonate solution. The filtrates are joined and acidified with 30 ml. of concentrated hydrochloric acid and extracted with ether. The ether layer is separated and washed with water. Ethereal solutions obtained from six batches of such a reaction (treating 48 g. of *cis*-lactone) are joined and then dried with sodium sulfate. The ether is evaporated, and the residue is distilled in a vacuum. Two fractions are obtained as the main distillate.

Fraction 1: 15 g. of oil (b. p., 48~85°C/3 mmHg), the redistillation of which gives 13 g. of the fraction (b. p. 85~86°C/3.5 mmHg). Yield, 27.1%. λ_{max}^{EtOH} 211 mμ, IR 5.83 μ (C=O), 8.24 μ (C-O).

Found: C, 68.05; H, 8.80. Calcd. for $C_8H_{12}O_2$: C, 68.54; H, 8.63%.

Fraction 2: 11 g. of oil (b. p., 126~127°C/0.6 mmHg. Yield, 22.9%. λ_{max}^{EtOH} 212.5 mμ, IR 5.84 μ (C=O), 4.42 μ (C≡N).

Found: C, 64.12; H, 8.22; N, 6.99. Calcd. for $C_9H_{13}O_2N$: C, 64.65; H, 7.84; N, 8.38%.

Oxidation of *cis*-3-α-Carboxyethylcyclopentanol Lactone (II) with Potassium Permanganate.—To a stirred and ice-cooled solution of 3g. of lactone (II) dissolved in aqueous sodium hydroxide (1.1 g. sodium hydroxide in 9 ml. water), a saturated aqueous solution of 12 g. of potassium permanganate is added for 30 min.; the mixture is then left to stand overnight. Copious precipitates of manganese dioxide are filtered out, and the mother liquor is evaporated to a syrup, acidified with concentrated hydrochloric acid, and evaporated to dryness; the residue is then extracted with ether. Evaporation of the ether produces crystals (m. p., 120°C) which are dissolved in ethyl acetate and precipitated by adding petroleum ether. The procedure is repeated again, and the precipitate thus obtained is recrystallized twice from ethyl acetate. M. p., 140°C. 300 mg. Melting point depression was observed by mixed melting with authentic β-(α-carboxyethyl)-glutaric acid synthesized by the method of Skraup[7]. IR 5.86, 5.81 (shoulder) μ (C=O)[13].

Found: C, 47.26; H, 6.21. Calcd. for $C_8H_{12}O_6$: C, 47.06; H, 5.92%.

The filtered manganese dioxide is extracted three times with 100 ml. of a 3% aqueous sodium hydroxide solution. The combined filtrates are evaporated to a syrup, acidified with concentrated hydrochloric acid and evaporated to dryness. The residue is extracted with ether; the evaporation of ether from the ether extract produces crystals with a m. p. of 160°C which, after recrystallization twice from ethyl acetate, give crystals with a m. p. of 180°C, the mixed melting of which with authentic α-methyl-α-β-carboxyadipic acid does not show any melting point depression; also the infrared spectra of this acid is superimposable with that of α-methyl-β-carboxyadipic acid synthesized by Perkin's method. IR 5.89, 5.83 (shoulder) μ (C=O).

Found: C, 47.05; H, 6.28. Calcd. for $C_8H_{12}O_6$: C, 47.06; H, 5.92%.

2-α-Carboxyethylcyclopentanecarboxylic Acid (IX).—One gram of cyanoacid III is dissolved in 7 ml. of concentrated hydrochloric acid and refluxed for 8 hr. Hydrochloric acid is evaporated on the water bath, and from the concentrated hydrochloric acid solution crystals separate out on cooling. Recrystallized from ethyl acetate. M. p., 130°C. Yield, 150 mg.

Found: C, 57.77; H, 7.62. Calcd. for $C_9H_{14}O_4$: C, 58.05; H, 7.58%.

α-(2-Cyanocyclopentyl)propionic Acid Chloride (X).—Three grams of cyanoacid III, 3.5 g. of oxalyl chloride and 6 ml. of benzene are mixed and refluxed on the water bath for 2 hr. Benzene and excess oxalyl chloride are evaporated off, and the residue is distilled in vacuum. 2.1 g. of the fraction with a b. p. of 90~105°C/3 mmHg is obtained, from which on redistillation there emerges a fraction with a b. p. of 96.5~99.5°C/0.6 mmHg. IR 5.60, 5.91 μ (C=O); 4.44 μ (C≡N).

Found: C, 58.63; H, 6.49; N, 5.76. Calcd. for $C_9H_{12}ONCl$: C, 58.22; H, 6.52; N, 7.55%.

Tetraethyl 2,3-Bis(carboxymethyl)adipate (VII).—(1) 0.7 g. of sodium is dissolved in 25 ml. of absolute alcohol, to which after cooling is added 5.2 g. of diethyl methylmalonate. The solution is stirred and kept at 20°C, and 8 g. of diethyl-β-bromoglutarate is added to it over the period of

13) Those of synthetic β-(α-caboxyethyl)glutaric acid are 5.73, 5.87 and 5.95 (shoulder) μ. Many differences are observed between the infrared spectra of the acid (m. p., 140 C°) isolated and those of β-(α-carboxyethyl)glutaric acid and α-methyl-β-carboxyadipic acid.

an hour. Stirring is continued at 20°C for an hour more, and then the solution is refluxed on a water bath for an hour. The alcohol is distilled off, the reaction mixture is poured into ice-water, and the product is extracted with ether. The ether layer is washed with water and dried with sodium sulfate. The ether is distilled off, and the residue is distilled in vacuum. Three fractions are obtained. Fraction I. B. p., 60°C/2.5 mmHg (obtained by redistillation of the fraction with a b. p. of 63~120°C/4 mmHg). 3.6 g. Diethyl methylmalonate. By reaction with ammonia, it gives methylmalonamide (m. p., 206°C). Fraction II, B. p., 83~85°C/2.5 mmHg (obtained by redistillation of the fraction with a b. p. of 63~120°C/4 mmHg). Diethyl glutaconate. IR 5.8 μ (C=O), 6.05 μ (C=C), 2.90 μ (very weak, OH)[14].

Found: C, 57.74; H, 7.71. Calcd. for $C_9H_{14}O_4$: C, 58.05; H, 7.58%. Fraction III. B. p., 155~165°C/2.5 mmHg. 2.4 g. Tetraethyl 2,3-bis(carboxymethyl)adipate.

Found: C, 57.77; H, 7.83. Calcd. for $C_{18}H_{30}O_8$: C, 57.74; H, 8.08%.

(2) 0.6 g. of sodium is dissolved in 17 ml. of absolute alcohol, to which is added 4.2 g. of diethyl malonate. The solution is stirred and cooled in an ice bath, and 7 g. of diethyl β-bromoglutarate is added to it over a 30-min. period. After the addition is over, stirring is continued for 2.5 hr.; then the solution is refluxed on a water bath for 2 hr. more. After cooling, the reaction mixture is poured into ice-water and dried with sodium sulfate. The ether is distilled off, and the residue on distillation in vacuum yields three fractions. Fraction I. B. p., 60~65°C/2.5 mmHg. 4 g. Diethyl malonate. By reaction with ammonia it gives malonamide (m. p., 168°C). Fraction II. B. p., 82~85°C/2.5 mmHg. 2.3 g. Identified as diethyl glutaconate by comparison of infrared spectra. Fraction III. B. p., 153~155°C/2.5 mmHg. 1 g. Tetraethyl 2,3-bis(carboxymethyl)adipate.

Found: C, 57.87; H, 7.89. Calcd. for $C_{18}H_{30}O_8$: C, 57.74; H, 8.08%.

2,3-Bis(carboxymethyl)adipic Acid (VIII).—Two grams of tetraester VII is mixed with 18 ml. of concentrated hydrochloric acid and refluxed for 10 hr. After evaporation of the hydrochloric acid and cooling, crystals separate out which are three times recrystallized from ethyl acetate. M. p., 203°C. On further recrystallization from acetone, it shows a m. p. of 206°C. Yield, 200 mg.

Found: C, 45.92; H, 4.99. Calcd. for $C_{10}H_{14}O_8$; C, 45.80; H, 5.38%.

Diethyl β-Bromoglutarate.—7.2 g. of β-bromoglutaric acid[15], 36 ml. of absolute alcohol and 1.8 g. of concentrated sulfuric acid are mixed and refluxed for 5 hr. Thirty milliliters of benzene is added to it, the benzene and alcohol are distilled off, and the residue is poured into ice-water and extracted with ether. The ether layer is separated, washed with an aqueous sodium bicarbonate solution and water, dried with sodium sulfate, and distilled. B. p., 114~115°C/2.5 mmHg. 7.3 g.

Found: C, 40.67; H, 5.84. Calcd. for $C_9H_{15}O_4Br$: C, 40.46; H, 5.66%.

Reduction of *cis*-Lactone I with Lithium Aluminum Hydride.—Twenty-one grams of *cis*-lactone I is dissolved in 40 ml. of tetrahydrofuran and cooled to −15~−13.5°C, while 1.8 g. of lithium aluminum hydride dissolved in 60 ml. of tetrahydrofuran is efficiently stirred in at this temperature over a 40-min. period. Stirring is continued at that temperature for 30 min., and then the solution is left to stand to raise the temperature to 7°C. The reaction mixture is poured into ice-colled aqueous hydrochloric acid (concentrated hydrochloric acid 110 ml. in 200 ml. of water), and extracted with ether. The ether layer is separated, washed with water, and dried with sodium sulfate. The ether is distilled off and, on fractionation of the residue, the following fractions are obtained. Fraction I. B. p., 72~82°C/5.5 mmHg. 0.2 g. Fraction II. 82~89°C/5.5 mmHg. 3.8 g. The infrared spectra of these fractions show a band of 2.98 μ (OH stretching), but it lacks many of the characteristic bands of hydroxyaldehyde XII and is considered to be an unreacted lactone contaminated with some hydroxylic compounds. Fraction III. B. p., 89~93°C/5.5 mmHg. Recovered lactone. Fraction IV. B. p., 132~135°C/3 mmHg. 6 g. *cis*-Diol XIII.

Methylanilide of *cis*-2-α-Carboxyethylcyclopentanol (XI).—Into a solution of ethylmagnesium bromide (prepared by the reaction of 48 g. of magnesium with 24 g. of ethyl bromide in 200 ml. of ether) is efficiently stirred a solution of 18.2 g. of methylaniline in 50 ml. of ether (nitrogen atmosphere; moisture is avoided) over a 10-min. period in an ice bath. After stirring is continued for 25 min., a deep purple solution of methylanilinomagnesium bromide is produced, to which is added 11 g. of *cis*-lactone I in 50 ml. ether for 5 min. The ice bath is removed, and the reaction mixture is refluxed for one and a half hours with stirring. After the reaction is over, the mixture is cooled in an ice bath and decomposed by the addition of dilute hydrochloric acid (30 ml. of concentrated hydrochloric acid in 300 ml. of water). The products are thoroughly extracted with ether, and the ether layers are separated, washed with an aqueous sodium bicarbonate solution and water, and dried with sodium sulfate. The ether is distilled off, and the residue, which separates as a yellow solid, is washed with a small amount of ethyl acetate. Crystals with a m. p. of 110°C are obtained. Yield, 11 g. After recrystallization six times from ethyl acetate, 3.2 g. of plates (m. p., 130°C) are obtatined. IR 6.18 μ (C=O), 2.99 μ (OH).

Found: C, 72.75; H, 8.52; N, 5.66. Calcd. for $C_{15}H_{21}O_2N$: C, 72.84; H, 8.56; N, 5.66%.

From the mother liquor, needles with a m. p. of 110~118°C are obtained.

Found: C, 72.72; H, 8.48; N, 5.76. Calcd. for $C_{15}H_{21}O_2N$: C, 72.84; H, 8.56; N, 5.66%.

In an analogous procedure using 12 g. of *cis*-lactone I, 9.8 g. of methylaniline, 2.4 g. magnesium and 12 g. of ethylbromide, 9.8 g. of raw crystals with a m. p. of 110°C are obtained; from these, after repeated recrystallization from ethyl acetate, 4.6 g. of

14) F. Henrich, *Ber.*, **35**, 1663 (1902).
15) Obtained by the method of Semenow, *Chem. Zentr.*, **11**, 28 (1899).

plates (m. p., 130°C) are obtained. However, when the reaction is conducted in such a way as *cis*-lactone I is added to a fresh colorless methylanilinomagnesium bromide solution (immediately after methylaniline has been added), the yield of the raw methylanilide is 6.5 g.; from these, after one recrystallization from ethyl acetate, 4.8 g. of plates (m. p., 130°C) are obtained.

By the use of 6 g. of *cis*-lactone I, 11.5 g. of methylaniline, 2.5 g. of magnesium and 14.2 g. of methyl iodide, 4.4 g. of the raw methylanilide is obtained; after recrystallization from ethyl acetate this gives 2.8 g. of crystals with a m. p. of 130°C. Methylanilinomagnesium iodide consists of crystals insoluble in ether. A tetrahydrofuran solution of methylanilide with a m. p. of 110~118°C is chromatographed on alumina. From an tetrahydrofuran effluent plates with a m. p. of 130°C are obtained in a 64% yield after one recrystallization from ethyl acetate. However, the 14.14 μ band of the infrared spectra of these plates differs from the 14.35 μ band of that of crystals with a m. p. of 130°C obtained by direct crystallization of the reaction product.

***cis*-2-α-Formylethylcyclopentanol (XII).**—11.5 g. of methylanilide of *cis*-2-α-carboxyethylcyclopentanol is dissolved in 110 ml. of tetrahydrofuran and cooled in an ice-salt bath. 1.1 g. of powdered lithium aluminum hydride is efficiently stirred into it for 30 min. After the addition is over, the ice-salt bath is replaced by an ice bath and stirring is continued for 7.5 hr. 200 ml. of hydrochloric acid (1 : 4) is added, the mixture is left to stand overnight and then extracted with ether. The ether layer is separated, washed with water and dried with sodium sulfate. The ether is distilled off, and the residue is distilled in vacuum. 3.5 g. of an oil b. p. 89~90°C/5 mmHg are obtained. *cis*-2-α-Formyl ethylcyclopentanol. IR 2.93, 2.85 μ (OH), 5.70 μ (C=O).

Found: C, 68.00; H, 8.94. Calcd. for $C_8H_{14}O_2$: C, 67.57; H, 9.93%.

Ethylenedioxy Derivative XV.—Four grams of 2-α-formylethylcyclopentanol and 2.5 g. of ethyleneglycol, together with 20 mg. of *p*-toluenesulfonic acid, are dissolved in 15 ml. of benzene and refluxed for 3 hr. 50 ml. of benzene is gradually added while the amount of benzene and water formed in the reaction are distilled off over a 4-hr. period. After cooling, the reaction mixture is diluted with ether, washed with an aqueous sodium bicarbonate solution and water, dried with sodium sulfate, and distilled. 3.1 g. of an oil (b. p., 76~78°C/3 mmHg) are obtained.

Found: C, 68.65; H, 8.86. Calcd. for $C_{18}H_{30}O_4$: C, 69.64; H, 9.74%.

The author is grateful to Mr. H. Kotsuma*1 and Dr. Y. Kanda*2 for the determination of the infrared spectra and to Mr. M. Shito*2 for his microanalysis.

Faculty of Liberal Arts
Saga University
Honjo, Saga City

*1 Present address: Shin Nihon-Chisso Fertilizers Company, Minamata, Kumamoto.
*2 Present address: Faculty of Science, Kyushu University.

NOTES

A Supplementary Note on the Author's Equation of State

By Tetsuya ISHIKAWA

(Received June 4, 1962)

Bentley's mass spectral study at room temperature of carbon dioxide gas[1] seems to give a concrete meaning to the ε of the author's equation of state: $p+a/V^{2-\varepsilon}=RT/(V-b)$, where $a=3p_cV_c^2$, $b=V_c/3$, and ε is a parameter depending upon molecular association[2]. Since ε is presumably the concentration of associated molecules (cybotactic groups) as judged from the deduction of the equation from the kinetic theory of gases[3], the $(2-\varepsilon)$ parameter should be the concentration of unassociated molecules. If this is really so, $\varepsilon/(2-\varepsilon)$ may correspond to the total intensities of CO_2^+, $(CO_2)_2^+$, $(CO_2)_3^+$, ……, and $(CO_2)_{23}^+$ relative to CO_2^+, which is numerically equal to 0.0442 as estimated from the graph given by Bentley. In his graph the point for $(CO_2)_{23}^+$ is lacking, probably because experimental errors for polymers above $(CO_2)_{22}^+$ become too great for actual values to be decided.

For the test of this postulation, the author has quoted PVT measurements on carbon dioxide at the critical temperature (30.98°C) from the I. C. T.[4] and those at 32.075, 31.037, 25.053 and 0°C from Michels and Michels' data[5], using 44.011 for the molecular weight and 1.9768 g. cm^{-3} for the density at 0°C.

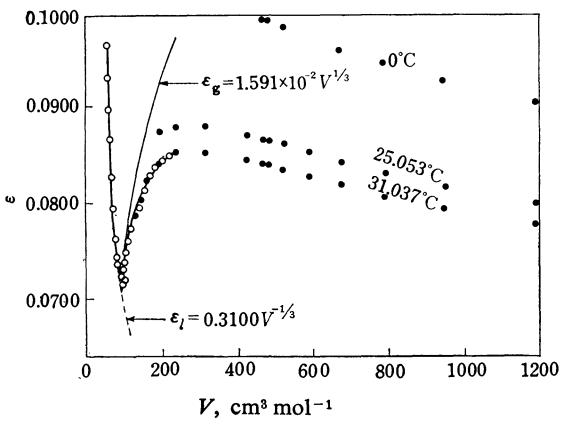


Fig. 1. ε-V Diagrams of carbon dioxide at 30.98, 31.037, 25.053 and 0°C.

ε-V relations are shown in Fig. 1, in which the values from the former data are denoted by white circles and those from the latter data by black circles. The analysis of ε at the critical temperature is quite similar to that already made in the case of isopentane[6].

We obtain for the liquid portion $\varepsilon=5.046\ V^{-1}$ ($V=52.59\sim63.72$) and $\varepsilon_l=0.3100\ V^{-1/3}$ ($V=67.93\sim73.38$); for the liquid and gaseous coexisting portion $\varepsilon_l+\varepsilon_g=0.1406$ ($V=81.40\sim106.36$) and $\varepsilon_g=1.591\times10^{-2}\ V^{1/3}$; and, for the gaseous portion, $\varepsilon=\varepsilon_g-cV^n$, $n=4$, $c=7.130\times10^{-12}$ ($V=113.59\sim139.71$), $n=3$, $c=1.116\times10^{-9}$ ($V=156.54\sim190.63$), and $n=2$, $c=2.284\times10^{-7}$ ($V=207.37\sim224.15$), the numbers in parentheses indicating volume ranges in $cm^3\ mol^{-1}$. The calculated pressures from these values have an average deviation of $\pm0.52\%$ from the observed pressures[7].

Granting that the ε values at the lowest pressure, 16.5~19.0 atm., listed in Michels and Michels' data are not so much different from those for 5 atm., at which the pressure of the beam of gas molecules passing through a small orifice and a series of larger orifices from a reservoir was maintained in Bentley's measurements, we can guess at what temperature his measurements were made: Bentley's value, 0.0442, will lie on a straight line passing through the four values of $\varepsilon/(2-\varepsilon)$ at 32.075, 31.037, 25.053 and 0°C, namely, 0.0403 at 19.0843 atm., 0.0405 at 19.0023 atm., 0.0417 at 18.5374 atm., and 0.0474 at 16.5488 atm., if his measurements were made at 14.2°C. However, as Bentley remarked, cooling of the bulk gas occurs as a result of the Joule-Thomson effect, which is less than 6°C for 5 atm.; his so-called room temperature seems, therefore, to have been about 20°C.

In Bentley's reply to the author's request, he

1) P. G. Bentley, *Nature*, **190**, 432 (1961).
2) T. Ishikawa, This Bulletin, **26**, 78 (1953).
3) T. Ishikawa, ibid., **27**, 573 (1954).
4) "International Critical Tables", Vol. 3, McGraw-Hill Book Co., New York (1928), p. 12.
5) A. Michels and C. Michels, *Proc. Roy. Soc.*, A153, 201 (1935—6).
6) T. Ishikawa and M. Ikeda, This Bulletin, **34**, 1329 (1961).
7) Presented by T. Ishikawa and M. Ikeda at the Meeting of the Chemical Society of Japan, Tokyo, November, 1961.

said the room temperature was indeed about 20°C; it is difficult to give a more precise figure as the work was done over a long period during which the temperature altered by several degrees.

The above consideration leads us to the following conclusion: $\varepsilon/(2-\varepsilon)$ corresponds to the ratio of the total sum of ion intensities of polymers to that of monomers, at least so far as the present data are concerned.

Junior College of Commerce
Nagasaki University
Nagasaki

On the Relation among γ-, η- and δ-Al_2O_3 under Hydrothermal Condition

By Goro YAMAGUCHI and Hiroaki YANAGIDA

(Received June 19, 1962)

What was formerly called simply γ-Al_2O_3 may in truth consist of the three forms of γ-, η- and δ-Al_2O_3. The γ-Al_2O_3 is usually obtained by dehydration of good crystalline boehmite γ-$Al_2O_3 \cdot H_2O$ in air over 500°C[1]. The crystal structure is considered to be closely related to that of spinel $MgO \cdot Al_2O_3$[2,3] with a small amount of strongly bound water[4,5], but slightly deformed tetragonally with a lattice constant $a=b=7.96$ and $c=7.82$ Å[6,7]; the (400) peak in the spinel indice in the X-ray diffraction diagram is slightly split into a doublet. The η-Al_2O_3 has been proposed[8] as a product of the dehydration of bayerite α-$Al_2O_3 \cdot 3H_2O$. Its X-ray diffraction diagram seems extremely similar to that of γ-Al_2O_3 except for the (400) peak being hardly split at all[9]. The δ-Al_2O_3 has been proposed as a product of the further heating of γ-Al_2O_3[10]; the peaks in the X-ray diffraction diagram are somewhat sharp and have, except for the weak ones, mostly been attributed to the spinel indice. The existence of η- and of δ-Al_2O_3 as discrete forms independent of γ-Al_2O_3 has been doubted[11]. The present authors have therefore investigated the relation among γ-, η- and δ-Al_2O_3 under hydrothermal conditions.

The starting material was obtained by the dehydration of good crystalline boehmite at 700°C in air. The X-ray diffraction diagram is that of γ-Al_2O_3. This was treated hydrothermally under 20 to 100 atm. at 450 to 500°C. One of the X-ray diffraction diagrams of the products is shown in Fig. 1. There can easily be noticed a remarkable split about the peak (400) in the spinel indice. The diagram about the (400) peak was examined by slow-scanning X-ray diffraction (Geigerflex, Ni filtered Cu$K\alpha$ 30 kV. 10 mamp. irradiation; 1° 1° 0.2 mm. slit system; rate meter, 16; time constant, 4 sec.; scanning speed, 1°/2 min.). The results of the products under various hydrothermal conditions are as shown in Fig. 2 and as summarized in Table I. Under such condition, γ-Al_2O_3 was more deformed tetragonally. The degree of deformation increased as

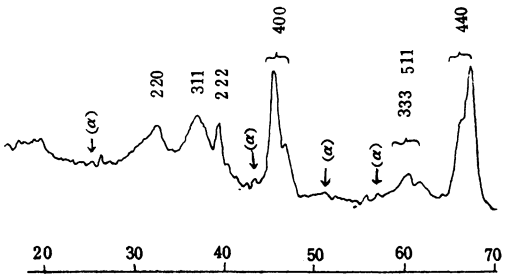


Fig. 1. (γ-Al_2O_3 treated under 50 atm. at 500°C for 15 hr.) No. 9 (α) indicates α-Al_2O_3.

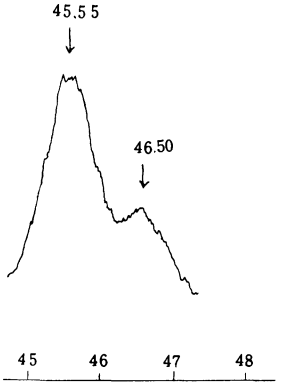


Fig. 2. (400) peak of (γ-Al_2O_3 treated under 100 atm. at 450°C for 13 hr.) No. 7.

1) G. Weitbrecht and R. Fricke, *Z. anorg. Chem.*, **253**, 9 (1945).
2) F. Rinne, *N. Jb. Miner.*, **58**, 43 (1928).
3) H. Jagozinski and H. Saalfeld, *Z. Krist.*, **110**, 197 (1958).
4) J. H. deBoer and G. M. M. Houben, *Proc. Intern. Symp. React. Solids*, 237 (1952).
5) E. Kordes, *Z. Krist.*, **91**, 193 (1935).
6) G. W. Brindley and M. Nakahira, ibid., **112**, 136(1959).
7) B. C. Lippens, "Structure and Texture of Aluminas", Ph. D. Thesis of Tech. Hogeschool, Delft. (1961).
8) H. C. Stumpf, A. S. Russell, J. W. Newsome and J. W. Tucker, *Ind. End. Chem.*, **42**, 1398 (1950).
9) H. Ginsberg,. W. Hüttig and G. S. Lichtenberg, *Z. anorg. Chem.*, **293**, 204 (1957).
10) R. Tertian and D. Papée, *J. Chim. Phys.*, **55**, 341 (1958).
11) H. Saalfeld, *N. Jb. Miner.*, **95**, 1 (1962).

TABLE I. TETRAGONAL DEFORMATION OF γ-Al_2O_3 UNDER HYDROTHERMAL CONDITION

Specimen No.	Treatment	2θ and d spacing, Å (400) and (040)	(004)	Lattice constant, Å $a=b=$	$c=$	a/c	Remark
1	Starting Material	45.72 1.983	(46.38) (1.956)	7.93	(7.82)	(1.014)	
2	after B. C. Lippens[7]			7.96	7.82	1.018	
3	450°C 20 atm. 15 hr.	45.62 1.987	46.44 1.954	7.95	7.81	1.018	
4	450°C 20 atm. 20 hr.	45.51 1.992	(46.52) (1.951)	7.97	(7.80)	(1.022)	
5	450°C 50 atm. 17 hr.	45.58 1.989	(46.45) (1.953)	7.95	(7.81)	(1.018)	
6	450°C 50 atm. 45 hr.	45.40 1.996	(46.55) (1.949)	7.98	(7.80)	(1.023)	
7	450°C 100 atm. 13 hr.	45.44 1.990	46.50 1.951	7.96	7.81	1.019	
8	450°C 100 atm. 18 hr.	45.32 2.000	46.58 1.948	8.00	7.79	1.027	
9	500°C 50 atm. 15 hr.	45.21 2.004	46.79 1.940	8.02	7.76	1.033	Fig. 1. Small amount of α-Al_2O_3 included

TABLE II. TETRAGONAL DEFORMATION DECREASE DUE TO RE-HEATING IN AIR

Specimen No.	Treatment	2θ and d spacing, Å (400) and (040)	(004)	Lattice constant, Å $a=b=$	$c=$	a/c	Remark
3′	Heated No. 3 at 800°C	45.58 1.989	46.33 1.958	7.95	7.83	1.015	cf. No. 3. ig. loss 3.3%
6′	Heated No. 6 at 800°C	45.46 1.993	46.33 1.958	7.97	7.83	1.018	cf. No. 6.
9′	Heated No. 9 at 800°C	45.40 1.996	46.46 1.953	7.98	7.81	1.022	Fig. 2 ig. loss 7.6% cf. No. 9

the hydrothermal pressure became high and as the reaction period lengthened. Corundum α-Al_2O_3 was directly obtained from γ-Al_2O_3, while good crystalline γ-Al_2O_3 or δ-Al_2O_3 was not found in the present work.

The tetragonally-deformed γ-Al_2O_3 were re-heated in air at 800°C. The results are summarized in Table II. The degree of tetragonal deformation decreased with re-heating.

The present authors were able to prepare γ-Al_2O_3 with various degrees of tetragonal deformation. The lattice constant could not be determined precisely, for it varied with the conditions of formation. This led us to conclude that there may be η-Al_2O_3 as an extrapolated form of γ-Al_2O_3 with little tetragonal deformation. Good crystalline γ-Al_2O_3 or δ-Al_2O_3 was not found under the hydrothermal conditions.

Department of Industrial Chemistry
Faculty of Engineering
The University of Tokyo
Hongo, Tokyo

Deformation Vibration of SiOH

By Reisuke SODA

(Received July 14, 1962)

When crystalline silica is ground into fine particles which have a particle size of about 1 μ, its surface is destroyed and its original structure is modified into an irregular one. On this layer, which is easily soluble in an aqueous alkaline solution, the silanol group is formed by the reaction between atmospheric water vapor and the Si–O$^-$ or Si$^-$ which is produced by the cleavage of the Si–O–Si bond. A parallel exists between the grinding process and the infrared absorption spectrum of the particle; i. e., the spectrum of the ground particle gives rise to a band at 950

cm^{-1} band, and the band group near 1100 cm^{-1} becomes more diffuse. The present author[1,2] has previously assigned the band near 1100 cm^{-1} to the SiO stretching vibration which appeared on the new surface layer and the band at 950 cm^{-1} to the SiOH deformation vibration. On the basis of the experimental finding that the band at 950 cm^{-1} diminishes or decreases in intensity by ethylation of the ground particle, his assignment has been considered to be correct[3]. Recently, however, Takamura et al.[4] assigned the band at 950 cm^{-1} to the SiO stretching vibration of the silicate structure which is produced on the new surface layer and the band near 1120 cm^{-1} to the SiOH deformation vibration on the basis of the results of the deuteration and other treatments of the particle. The experimental results described above can be explained according to the assignments made by Takamura et al. Ethylation of the SiOH of the silicate structure produces SiOEt, and then the SiO structure of the silicate decreases; therefore, the band at 950 cm^{-1} decreases in intensity. The fact that the ethylation is more difficult than the deuteration can be also explained, considering that the SiO in the silicate structure has an ionic bond character, while the SiO in SiOEt has a homopolar bond character and that the reaction from SiOH in the silicate structure to that in SiOEt must pass over a relatively high activated-energy level. Therefore, the present author wishes here to correct his assignment of the 950 cm^{-1} band to the SiO stretching vibration and the band near 1100 cm^{-1} to the SiOH deformation vibration.

Shimadzu[5] has found a resemblance between the infrared absorption bands near 1100 cm^{-1} of the leached particle, the size of which is less than 0.1 μ, and that of the ground particle, but he found no band at 950 cm^{-1} for the leached particle. The surface of the particle is a terminal structure of the SiO_2 frame, and, therefore, it normally consists of Si–O–H and Si–O–Si bonds, the former being particularly dominant. Fine particles have a larger surface area, and the SiOH group increases in proportion to the particle size. The leached particle apparently does not have a silicate structure which is easily soluble in an aqueous solution of sodium hydroxide. These facts are only explainable by the assignments made by Takamura et al. Though the structure of the surface layer of the particle which is considered to be silicate-like SiO by Takamura et al. should be further reexamined, their assignment of the SiOH deformation vibration is correct.

National Institute of Industrial Health
Kawasaki-shi

1) H. Sakabe, K. Kawai, K. Koshi, R. Soda, A. Hamada, M. Shimadzu and H. Hayashi, *Bull. Nat. Inst. Ind. Health*, No. 4, 1 (1960).
2) R. Soda, This Bulletin, **34**, 1491 (1961).
3) R. Soda, presented at the 15th Annual Meeting of the Chemical Society of Japan, Kyoto, April, 1962.
4) T. Takamura, H. Yoshida and K. Inezuka, presented at the same meeting as above.
5) M. Shimadzu, unpublished data (in this Institute).

SHORT COMMUNICATIONS

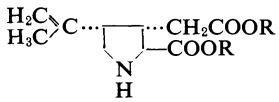
Nuclear Magnetic Resonance Spectra of Isopropenyl Groups

By Kazue KONDO, Yoshikazu KONDO, Tsunematsu TAKEMOTO and Tsuneo IKENOUE

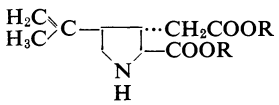
(Received August 6, 1962)

Definition of structures on α-kainic acid and α-allokainic acid as anthelmintic agent of *Digenea simplex* has been presented by Takemoto et al.[1] and by Morimoto et al.[2] In this report nuclear magnetic resonance (NMR) spectra of these compounds were observed by a Varian V-4300B NMR spectrometer at a fixed frequency 40 Mc.

Since both α-kainic acid (I) and α-allokainic acid (III) did not have a sufficient solubility in organic solvents to measure their NMR spectra at 40 Mc., their dimethyl esters, dimethyl α-kainate (II) and dimethyl α-allokainate (IV), were employed for the measurement of their spectra.



(I) R=H
(II) R=CH_3



(III) R=H
(IV) R=CH_3

The interesting patterns of olefinic protons, doublet in the case of II and singlet in IV respectively, are illustrated in Fig. 1. It is considered that there is difference in degree of receiving steric hindrance dynamically when isopropenyl group makes rotation. In other words, H_b of olefinic protons and methyl group of isopropenyl receive a steric hindrance at

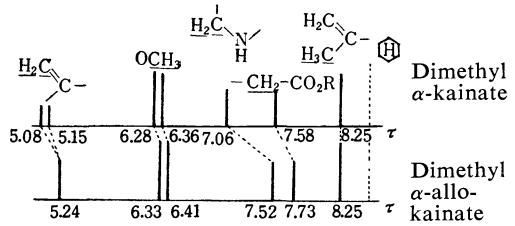


Fig. 1

TABLE I. DOUBLET IN OLEFINIC PROTONS OF ISOPROPENYL GROUP

Compound	τ
2,2,4-Trimethyl-4-pentene	
Lupeol acetate	5.17
Dimethyl cianothiate	5.4
1,5-Dimethyl-2-isopropenyl-1-cyclohexene	5.31
1,6-Dimethyl-2-isopropenyl-1-cyclohexene	5.25
1,5-Dimethyl-2-isopropenyl-1-cyclopentene	
2'-Methyl-allylidenecyclohexane	5.20

TABLE II. SINGLET IN OLEFINIC PROTONS OF ISOPROPENYL GROUP

Compound	τ
2-Methyl-1-propene	5.40
Isoprene	5.06
Limonene	5.34
Carvone	5.22
1-Acetyl-4-isopropenyl-1-cyclopentene	4.87
1-Acetoxyl-1-methyl-2-hydroxyl-4-isopropenylcyclohexane	5.37

C_5 protons when they are rotated. Further, in the case of II they also receive steric hindrance from the protons of methylene group in C_3 side chain, so that the dynamic steric hindrance is greatly increased. Therefore, H_b shifts to low field considerably. H_a also shifts very slightly. The C_5 protons and methylene of C_3 side chain in II both shift to lower field in comparison with IV. These results may be also explained as follows; when isopropenyl group is rotated, the olefinic proton H_b is locating in high probability between C_5 protons and the methylene protons of C_3 side chain which are affected by the long-range shielding of double bond of isopropenyl group.

It is of interest that olefinic protons, methylene protons of C_3 side chain and C_5 protons are all broad compared with the spectrum of

1) T. Takemoto, Z. Tei and K. Daigo, *J. Pharm. Soc. Japan* (*Yakugaku Zassi*), **76**, 298 (1956).
2) H. Morimoto and R. Nakamori, *Proc. Japan Acad.*, **32**, 41 (1956): *J. Pharm. Soc. Japan* (*Yakugaku Zassi*), **76**, 294 (1956).

other groups and fine splittings greater than 1 c. p. s. were not observed in each of them. It is considered that the broadening are due to the asymmetry of their electron cloud caused by the dynamic steric hindrance.

Doublet patterns of NMR spectra is also observed in olefinic protons of isopropenyl group of other compounds (Table I)[3-5]. When its adjacent group is polar group or aromatic ring[3,6] its patterns shows doublet. This is thought to be caused by different degree of inductive effect or long-range shielding one. On the contrary, when the effects of polar group and of imhomogeneous magnetic field are both weak, and the effect of dynamic steric hindrance is considered small, singlet structure is observed in olefinic protons (Table II)[3,5-7].

The authors wish to thank Dr. J. Wolinsky for his kindly supply of the NMR data of 1-acetyl-4-isopropenyl-1-cyclopentene and several other compounds.

Institute of Pharmacy
School of Medicine
Tohoko University
Kitayomban-cho, Sendai
(*K. K., Y. K. & T. T.*)
and
Chemical Research Institute of
Non-Aqueous Solutions
Tohoku University
Katahira-cho, Sendai (*T. I.*)

3) L. M. Jackman, "Applications of Nuclear Magnetic Resonance Spectroscopy in Organic Chemistry", Pergamon Press, London, New York (1959), p. 120.
4) P. de Mayo and A. N. Starratt, *Tetrahedron Letters*, No. 7, 259 (1961).
5) Private communication from Dr. J. Wolinsky.
6) G. Van Dyke Tiers, "Characteristic Nuclear Magnetic Resonance 'Shielding Values' (Spectral Position) for Hydrogen in Organic Structures" (1958).
7) J. Wolinsky and W. Barker, *J. Am. Chem. Soc.*, **82**, 636 (1960).

The Geometric Factor of Catalysts in the Isotopic Exchange Reaction of Paraxylene with Deuterium Oxide

By Kozo HIROTA and Tomiko UEDA

(Received August 8, 1962)

Since two decades ago, the geometric factor of catalysts have been discussed by Horiuti[1], Beeck[2] and others as an interesting problem in catalysis. However, it is difficult to investigate this factor extensively for lack of such convenient reactions as to fulfill the requirement of investigation.

According to our former reports[3], it has been found promising to use the isotopic exchange reaction of *p*-xylene with deuterium oxide for such purpose, because some catalysts (nickel, nickel-silica, nickel-kieselguhr) can exchange only methyl hydrogen with deuterium while others (platinum, palladium and nickel-alumina) can exchange hydrogen of benzene ring as well as of methyl groups. Such a selectivity now observed can be determined without any knowledge of exchange activities per unit area of each metal. Moreover, the reaction suits the present purpose, by the reason that it is unnecessary to take the electronic factor of metals into consideration. Because even if work function has some connection with the mechanism of both exchange reactions, the selectivity above mentioned would be invariant, as far as their ratio of velocities is concerned.

The research has, therefore, been extended to other metals since the former papers, adopting the same method of research, and a relation was found between the selectivity and the geometric factor of catalysts; i. e., if the ratios of the exchanged degree* of ring hydrogen to that of methyl hydrogen are plotted against lattice constants** of the catalysts, a

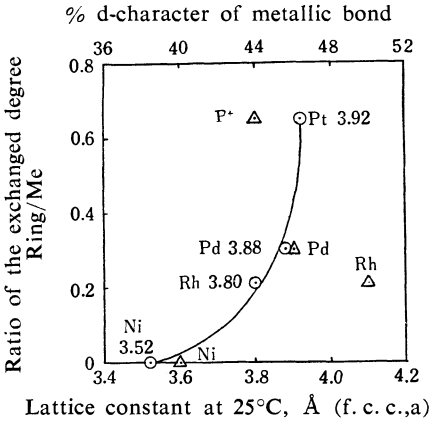


Fig. 1. Relations between exchanged degree and lattice constant or/and d-character of metallic bond (Pauling) for Pt, Pd, Ph and Ni.

⊙ Lattice constans △ d-Character

1) G. Okamoto, J. Horiuti and K. Hirota, *Sci. Pap. Inst. Phys. Chem. Res.*, **29**, 223 (1936).
2) O. Beeck, *Rev. Mod. Phys.*, **17**, 61 (1945).
3) K. Hirota, K. Kuwata and T. Ueda, *J. Chem. Soc. Japan, Pure Chem. Sec.* (*Nippon Kagaku Zasshi*), **81**, 362 (1960); K. Hirota and T. Ueda, This Bulletin, **33**, 423 (1960); **35**, 228 (1962).

* The exchanged degree was determined by the mass-spectrometric and NMR methods.

** R. W. G. Wykoff, "Crystal Structures", Vol. I, Interscience, New York (1948—1958).

monotonous curve is obtained between the two quantities, as shown by the curve in Fig. 1. For the sake of reference the ratios are plotted against Pauling's d-characters of the metals as triangles as shown in Fig. 1. As might be expected, it seems that no relation exists between them.

It will be mentioned here that this relation is perfectly different from the one found by Beeck[2] in the hydrogenation of ethylene with films of similar metals; i.e., he found a maximum in the curve of logarithms of velocity constant vs. lattice constants of these metals. The present result resembles, however, that of Balandin[4], who found a linear relation between interatomic distance and activation energy in the dehydrogenation of isopropanol.

Any explanation is not given here to the discrepancy found above, because such an attempt would not be so easy, considering the situation that the reactions to be discussed are not the same in the cases of Beeck, Balandin and the present authors.

We express our thanks to Professor Ryoiti Kiriyama, Osaka University, who kindly taught us the recent data of lattice constants.

Department of Chemistry
Faculty of Science
Osaka University
Nakanoshima, Osaka

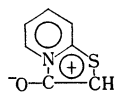
4) A. A. Balandin, "Actes de II Congrès International de Catalyse", Technip, Paris (1960), p. 1135.

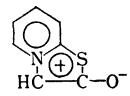
Preparation of Meso-ionic ψ-Pyrido[2,1-b]-3,4-dihydro-4-keto-(and imino)-thiazole[1] *by a New Mode of Formation**

By Hiroshi KATO, Kazuo TANAKA and Masaki OHTA

(Received August 29, 1962)

Duffin and Kendall[2] have prepared a meso-ionic compound I[3] by the reaction of (2-pyridylthio)-acetic acid and acetic anhydride. In an attempt to prepare meso-ionic compounds of the type II, in which the positions of CH and CO groups in the meso-ionic ring are reversed, the authors have carried out the reaction between *S*-acetyl-2-mercaptopyridine (yellow liquid, b.q. 96~99°C/3.5 mmHg; absence of band between 1600 and 1700 cm^{-1} due to non-benzenoid double bond system[4], ν_{CO} 1050, 952, 770 cm^{-1} [5]; Found: C, 54.56; H, 4.86; N, 9.30. Calcd. for C_7H_7NOS: C, 54.90; H, 4.61; N, 9.15%.) and chloroacetic acid. The reaction product was, quite unexpectedly, identical with I instead of the expected quaternary salt.





The same compound I was formed by the following reactions: i) *S*-benzoyl-2-mercaptopyridine (white needles, m.p. 44~45°C, b.p. 172°C/3 mmHg; Found: C, 66.76; H, 4.39; N, 6.48. Calcd. for $C_{12}H_9NOS$: C, 66.97; H, 4.22; N, 6.51%.) and chloroacetic acid (accompanied by benzoic acid); ii) *S*-acetyl- or *S*-benzoyl-2-mercaptopyridine and chloroacetamide; iii) (2-pyridylthio)-acetamide (white leaflets, m.p. 80°C; Found: C, 49.88; H, 4.88; N, 16.68. Calcd. for $C_7H_8N_2OS$: C, 50.00; H, 4.80; N, 16.66%.) and acetyl chloride (accompanied by acetamide)[6]; iv) sodium 2-pyridylmercaptide and chloroacetyl chloride, followed by acetic anhydride and sodium acetate.

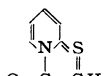
This type of ring formation was further extended to the preparation of the unknown corresponding meso-ionic acyl-imino derivatives III by the reaction with chloroacetonitrile: the reaction of *S*-acetyl-2-mercaptopyridine with chloroacetonitrile in benzene gave III (R=Me yellow needles, m.p. 73~74°C; absence of ν_{CN} in 2200~2300 cm^{-1}; Found: C, 51.52; H, 5.06; N, 13.58. Calcd. for $C_9H_8N_2OS+H_2O$: C, 51.42; H, 4.80; N, 13.33%;

* Presented at the 15th Annual Meeting of The Chemical Society of Japan, Kyoto, April, 1962.

1) The authors have adopted the nomenclature and symbol proposed by Baker. (W. Baker, W. D. Ollis and V. D. Poole, *J. Chem. Soc.*, **1949**, 311; W. Baker and W. D. Ollis, *Chem. & Ind.*, **1955**, 910.)

2) G. F. Duffin and J. D. Kendall, *J. Chem. Soc.*, **1951**, 734.

3) Duffin and Kendall (*J. Chem. Soc.*, **1956**, 361) are now of the opinion that compounds of this type can be satisfactorily represented by the structural formula V, and that they should no longer be regarded as meso-ionic. The present authors belive that structure V certainly would contribute to some extent to resonance, but it is more probable that several dipolar canonical forms play important role in the resonance. Discussion on the structure of these types of compounds will be given in a detailed report.

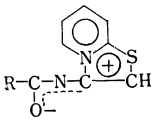


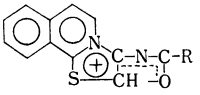
4) E. Spinner, *J. Chem. Soc.*, **1960**, 1237.

5) R. Sairs et al., *J. Am. Oil Chemists' Soc.*, **35**, 192 (1958).

6) Duffin et al.[2] reported that when (2-quinolythio)-acetamide was treated with acetic anhydride, the starting material was recovered unchanged.

hydrochloride: yellow prisms; m. p. 250°C; Found: N, 12.04. Calcd. for $C_9H_9N_2OSCl$: N, 12.25%), and the reaction of *S*-benzoyl-2-mercaptopyridine gave III (R=Ph; yellow needles, m. p. 206°C. Found: C, 66.14; H, 3.75; N, 10.76. Calcd. for $C_{14}H_{10}N_2OS$: C, 66.13; H, 3.96; N, 11.02%.). Compound III was also prepared by the reaction of (2-pyridylthio)-acetonitrile (unstable yellow liquid, b. p. 118 ~120°C/3 mmHg; Found: C, 55.03; H, 3.90; N, 18.26. Calcd. for $C_7H_6N_2S$: C, 56.00; H, 4.03; N, 18.66%.) and acetyl or benzoyl chloride. The corresponding acyl-imino derivative (IV, R=Me; yellow needles, m. p. 215°C, absence of ν_{CN}, Found: C, 64.25; H, 4.40; N, 11.59. Calcd. for $C_{13}H_{10}N_2OS$: C, 64.46; H, 4.16; N, 11.59%. R=PhCO; yellow leaflets, m. p. 273°C, no ν_{CN}, Found: C, 71.30; H, 3.81; N, 9.49. Calcd. for $C_{18}N_{12}N_2OS$: C, 71.04; H, 3.98; N, 9.21%.) was prepared by treatment of (1-isoquinolylthio)-acetonitrile (white plates, m. p. 95.5°C, ν_{CN} 2240 cm^{-1}, Found: C, 65.91; H, 3.84; N,14.27: Calcd. for $C_{11}H_8N_2S$: C, 65.99; H, 4.03; N, 13.99%.) with acetyl or benzoyl chloride, but when (4-lepidyl-2-thio)-acetonitrile (colorless needles, m. p. 65°C, Found: C, 67.28; H, 4.71; N, 13.09. Calcd. for $C_{12}H_{10}N_2S$: C, 67.28; H, 4.71; N, 13.08%.) was treated with acyl chloride by the same method, the starting material was recovered unchanged. The failure of ring formation in this case might be ascribed to the steric hindrance by the hydrogen at 8 position of quinoline nucleus.





The starting material, 1-mercaptoisoquinoline and 2-mercapto-4-lepidine were prepared in almost quantitative yield and in high purity by treatment of the corresponding chloro derivatives with thioacetic acid.

The preparation of intermediate compounds, discussions on the mechanism of formation and the structure, properties and reactions of III and IV and the extension of this type of ring formation to the syntheses of other new meso-ionic ring systems will be reported shortly.

The authors are indebted to the Kawakami Foundation for partial support of this study, and to Kyorin Pharmaceutical Co. for measurement of UV and IR spectra.

Laboratory of Organic Chemistry
Tokyo Institute of Technology
Meguro-ku, Tokyo

Polymerization of Styrene in Liquid Sulfur Dioxide Initiated by Alkyl or Aralkyl Chloride

By Niichiro TOKURA and Tetsuyo KAWAHARA

(Received September 4, 1962)

Alkyl chloride catalyzed polymerization has never hitherto been reported in the literature. Triphenylmethyl chloride has been shown to be a catalyst for a cationic polymerization of vinyl ether in cresol[1]; no detailed information, however, on the mechanism has been indicated. The role of alkyl chloride such as methyl chloride, ethyl chloride or ethyl bromide as a cocatalyst in a cationic polymerization with a Lewis acid catalyst has been the subject of controversy in recent years. While Plesch and his collaborators[2] have indicated in several experiments that alkyl halides are no more an effective cocatalyst for polymerization of isobutene with titanium(IV) chloride, Kennedy et al.[3] have suggested methyl chloride could be a cocatalyst in the same polymerization with aluminum chloride.

In this article, the present authors would like to report on the alkyl or aralkyl chloride catalyzed polymerization (without any Lewis acid) of styrene in liquid sulfur dioxide. It was found that ethyl, *n*-propyl, isopropyl, *n*-butyl, *t*-butyl, α-phenethyl, and benzyl chlorides are all effective catalysts for the cationic polymerization of styrene. No Lewis acid catalyst has been used with the alkyl chloride in the polymerization.

Initial over-all rates were estimated. The viscosity of the polymer was measured in ethyl methyl ketone and the number average molecular weight was calculated from the viscosity using Outer, Carr and Zimm's equation[4],

$$[\eta]_{\mathrm{dl./g.}} = 3.9 \times 10^{-4} \ [\mathrm{M}]^{0.58}$$

The polymerization may be of cationic nature, since (1), no styrene-polysulfone was found in the polymer and (2) any anionic polymerization may be inhibited in liquid sulfur dioxide

1) D. D. Eley and A. W. Richards, *Trans. Faraday Soc.*, **45**, 425 (1949).
2) a) R. H. Biddulph and P. H. Plesch, *J. Chem. Soc.*, **1960**, 3913; b) W. R. Longworth, P. H. Plesch and P. P. Rutherford, *Proc. Chem. Soc.*, Feb., 68 (1960); c) P. H. Plesch et al., *Symposium on Makromol. Wiesbaden* (1959).
3) J. P. Kennedy and R. M. Thomas, *J. Polymer Sci.*, **45**, 227 (1959); **46**, 233, 481 (1960).
4) P. Outer, C. Carr and B. Zimm, *J. Chem. Phys.*, **18**, 830 (1950).

TABLE I. ALKYL CHLORIDE INITIATED POLYMERIATION IN LIQUID SULFUR DIOXIDE

Chloride	Initial rate $-dM/dt$ $\times 10^4$ mol. l^{-1} sec^{-1}	$[\eta]_{dl}$/g. in ethyl methyl ketone	$\bar{P}_n \times 10^{-2}$	Conversion % (150 min.)
Benzyl	3.95	0.118	1.82	13.5
α-Phenethyl	1.84	0.132	2.20	14
n-Propyl	1.70	0.151	2.78	13
Isopropyl	1.45	0.165	3.24	9
t-Butyl	0.99	0.088	1.10	4
Ethyl	0.82	0.152	2.80	9
n-Butyl	0.44	0.132	2.20	10
Triphenylmethyl	Trace			
HCl	0			

$[styrene]_0 = 1.32$ mol./l. $[RCl]_0 = 0.366$ mol./l.
Total volume = 100 ml. Reaction temp. 25°C

because of its acid nature. The elementary analysis and the infrared[5] spectrum of the polymer indicated that the polymer was a polystyrene.

As is listed in Table I, the initial rates of the polymerization initiated by various chlorides seem to follow neither the order of the inductive effect of the respective alkyl groups nor the order of the ionization tendency of the alkyl chloride in liquid sulfur dioxide. Triphenylmethyl chloride has been said to be a good electrolyte in the solvent[6], and an extensive ionization is to be expected in the solvent, but no reproducible result on the polymerization was obtained and the rate was approximately zero. A steric inhibition of the triphenylmethyl carbonium ion may perhaps be partly responsible for the restriction of polymerization. An alternative explanation for the failure of polymerization by triphenylmethyl carbonium ion may exist in the fact that this ion is too stable in liquid sulfur dioxide to initiate the cationic polymerization.

The attempted polymerization with hydrogen chloride as catalyst failed to suggest that the formation of α-phenethyl cation is impossible in liquid sulfur dioxide, since the addition of a proton to styrene, as the following,

$$C_6H_5CH{=}CH_2 + H^+ \rightarrow \underset{\alpha\text{-Phenethyl cation}}{C_6H_5\overset{+}{C}H{-}CH_3}$$

should yield an α-phenethyl cation which might be able to initiate the polymerization as is the case in α-phenethyl chloride. It should be also reminded that α-phenethyl cation[7] has been shown as an acting species for the initiation of the ordinary cationic polymerization of styrene. Inadequacy of hydrogen chloride as a catalyst may be verified by a few studies in our laboratory. The association of hydrogen chloride in liquid sulfur dioxide has already been suggested by one of the present authors[8]. No deuterium exchange in liquid sulfur dioxide between a growing polymer cation and heavy water has also been reported earlier[9]. These facts are well consistent with the protophobic nature of liquid sulfur dioxide.

The fastest rate is attained by benzyl chloride catalysis, however the authors have no appropriate explanation for such a phenomenon at present. As is seen in the table, the polymerization has also been conducted by ethyl, *n*-propyl or *n*-butyl chloride. The production of free carbonium ions of them is not conceivable in ordinary solvent, but a strong solvation of chloride anion with liquid sulfur dioxide may be operative during the polymerization in liquid sulfur dioxide. The ionized carbonium ion may initiate and conduct the polymerization, however, the mechanism of initiation needs a further study.

The authors wish to thank the Seitetsu Kagaku K. K. for the donation of liquid sulfur dioxide.

The Chemical Research Institute of Non-Aqueous Solutions
Tohoku University
Katahira-cho, Sendai

5) C. Y. Liang and S. Krimm, *J. Polymer Sci.*, **27**, 241 (1958).
6) L. P. Hammett, "Physical Organic Chemistry", McGraw-Hill Co., New York (1940), p. 53.
7) D. Jordan and F. E. Treloar, *J. Chem. Soc.*, **1961**, 729.
8) N. Tokura, K. Shiina and T.Terashima, This Bulletin, in press.
9) N. Tokura, M. Matsuda and I. Shirai, ibid., **35**, 371 (1962).

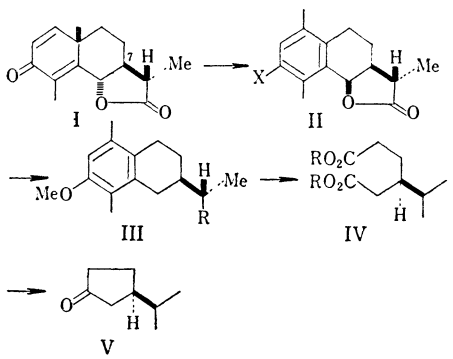
The Absolute Configuration of the Asymmetric Center at Position of 7 of α- and β-Desmotroposantonin

By Masao Nakazaki

(Received September 13, 1962)

Although the bulk of the evidence[1] mainly deduced from the stereochemistry of α-(II: X, OH) and β-desmotroposantonin strongly favors R-configuration at position 11 of (−)-α-santonin (I), recent publications[2,3] confirmed Abe's assignment[4] of the s-configuration at this center. To settle this discrepancy, the determination of the absolute configuration of α- and β-desmotroposantonin seemed necessary.

The methyl ester of (+)-α-desmotroposantonous acid methyl ether (III: R, CO_2Me) was reduced with lithium aluminum hydride to the alcohol (III: R, CH_2OH), b.p. 160~180°C/10^{-2} mmHg, $[\alpha]_D^{27}$ +60.8° (*c* 2.90 in ethanol), (phenylurethane: m.p. 125~126°C, $[\alpha]_D^{27}$ +47.3° (*c* 0.65 in ethanol)), which was converted with phosphorus tribromide/pyridine to the bromide (III: R, CH_2Br), b.p. 150~160°C/10^{-2}mmHg, $[\alpha]_D^{28}$ +66.4° (*c* 2.24 in ethanol). The bromide was refluxed with lithium aluminum hydride in tetrahydrofuran to afford the methyl ether (III: R, Me), b.p.



145~155°C/3 mmHg, n_D^{29} 1.5328, $[\alpha]_D^{25}$ +60.0° (*c* 2.52 in ethanol), (Found: C, 83.0; H, 10.4. Calcd. for $C_{16}H_{24}O$: C, 82.70; H, 10.41%). Exhaustive ozonolysis (30 hr.) of III (R, Me) followed by peracetic acid oxidation gave crude β-isopropyladipic acid (IV: R, H) which was purified via the dimethyl ester (IV: R, Me), b.p. 100~150°C (bath temp.)/5 mmHg. Heating IV (R, H) with barium hydroxide at 280~300°C gave 3-isopropylcyclopentan-1-one (V) which was directly converted into the semicarbazone, m.p. 181~183°C, $[\alpha]_D^{31}$ +43.8° (*c* 0.48 in ethanol), (Found: C, 59.2; H, 8.9: N, 22.7. Calcd. for $C_9H_{17}ON_3$: C, 58.98; H, 9.35; N, 22.93%). Its identity with R-(+)-3-isopropylcyclopentan-1-one semicarbazone[5,6], m.p. 186~187°C, $[\alpha]_D^{26}$ +65.2° (*c* 0.62 in ethanol) prepared from R-(+)-dihydrolimonene[7] was established by mixed melting point (181~183°C) and comparison of infrared absorption (in chloroform).

This correlation established the R-configuration of (−)-α-desmotroposantonin (II: X, OH) at position 7. Since (−)-α-desmotroposantonin may be derived from (−)-α-santonin via isohyposantonin (II: X, H) without affecting the configuration at C_7[8], the R-configuration of (−)-α-santonin at this center is also confirmed.

The fact that (+)-β-desmotroposantonin has the opposite configuration from (−)-α-desmotroposantonin at C_7 was established by the conversion of the former into the enantiomer of III (R, Me), b.p. 110~120°C/0.1 mmHg, n_D^{29} 1.5322, $[\alpha]_D^{28}$ −65.1° (*c* 1.51 in ethanol), (Found: C, 82.6; H, 10.3. Calcd. for $C_{16}H_{24}O$: C, 82.70; H, 10.41%), whose infrared absorption spectrum was found superimposable on that of III (R, Me).

Department of Chemistry
Osaka City University
Kita-ku, Osaka

1) W. Cocker and T. B. H. McMurry, *Tetrahedron*, **8**, 181 (1960).
2) D. H. R. Barton, T. Miki, J. T. Pinhey and R. J. Wells, *Proc. Chem. Soc.*, **1962**, 112; J. D. M. Asher and G. A. Sim, ibid., **1962**, 111.
3) M. Nakazaki and H. Arakawa, ibid., **1962**, 151.
4) Y. Abe, T. Miki, M. Sumi and T. Toga, *Chem. & Ind.*, **1956**, 953.
5) J. v. Braun and G. Werner, *Ber.*, **62**, 1050 (1929).
6) G. Burger and K. Macbeth, *J. Chem. Soc.*, **1946**, 145.
7) A. J. Birch, *Ann. Reports*, **47**, 191 (1950).
8) Y. Asahina and T. Momose, *Ber.*, **71**, 1421 (1938), and our unpublished observation on the conversion of (−)-3-amino-isohyposantonin (II: X, NH_2) back to isohyposantonin (II: X, H).

High-resolution NMR Spectra of Crystalline Cyclohexanol

By Hiroshi SUGA and Syûzô SEKI

(Received September 22, 1962)

Usually, broad line NMR spectral study gives some important informations on the nature of molecular motion in the crystalline state by observing so-called motional narrowing. On the other hand, high-resolution NMR spectrometer has been generally applied to the study of chemical shift only when the samples are in their liquid or solution states.

We have been studying for a long time the behavior of molecular motion in the plastic crystals[1], mainly by use of X-ray and thermal methods[2]. This kind of crystals has been known to exhibit self-diffusion phenomenon even at the temperatures considerably below their melting points[3]. These things led us to expect strongly that the high-resolution NMR techniques would disclose their usefulness for investigating molecular motion in these crystals in more details and also for observing directly chemical shifts of the protons involved in the constituent molecule. We have chosen cyclohexanol crystal for the study of this purpose and found it was indeed the case.

Measurement were carried out with the Varian Associates Model V-4311 high-resolution NMR spectrometer. Comparison of the entropy of transition[4], $\Delta S_{tr}=7.44$ e. u. ($T_{tr}=263.5°K$), and entropy of fusion[4], $\Delta S_f=1.37$ e. u. ($T_f=297.0°K$) of the present material with the entropies of fusion of rare gases, such as argon: $\Delta S_f=3.4$ e. u.[5] and krypton: $\Delta S_f=3.38$ e. u.[6] and also broad line NMR study by Averbuch[7] below the transition point suggest strongly the possibility of occurrence of the self-diffusion above the transition point.

As we have expected, the line width is sufficiently narrow to give well-separated peaks originated from different protons even just above the transition point. The area under the peaks stand roughly in the ratio 1 : 1 : 10, as would be expected if each peak in the order

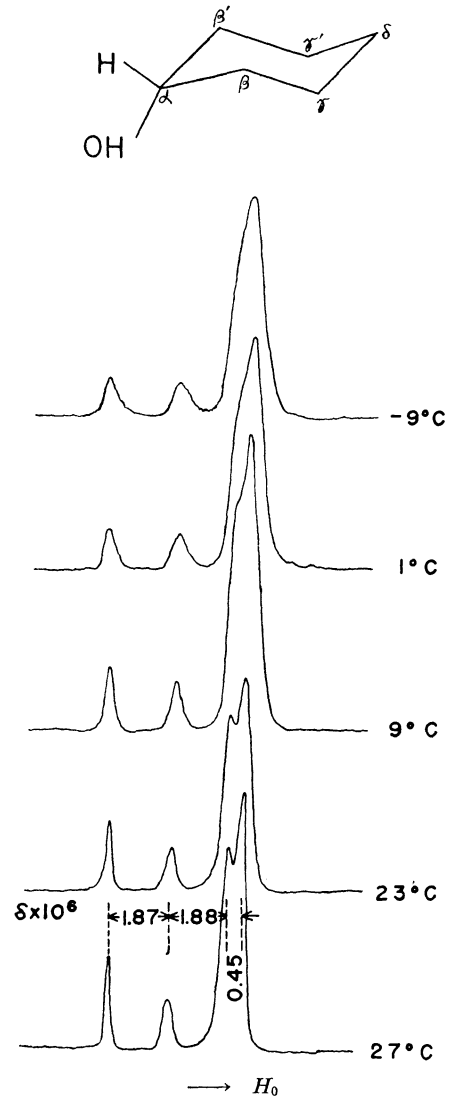


Fig. 1. Temperature variation of high-resolution NMR spectra of cyclohexanol.

of increasing field corresponded to the chemically different OH, H_α and the other ring protons (see figure). As the temperature rises and the line width of each peak narrows by the self-diffusion process, the main peak gives a further splitting in the approximate intensity ratio 2 : 3. These two peaks may not be due to chemical shifts between the axial and the equatorial ring protons, since there are equal number of protons in each species, and rather may be interpreted as the chemical shift between H_β (or $H_{\beta'}$) and H_γ (or $H_{\gamma'}$) plus H_δ. The rate at which the change from one conformation to the other of the cyclohexanol isomers will be faster[8] than the inverse of the chemical shift

1) J. Timmermans, *J. Phys. Chem. Solids*, **18**, 1 (1961).
2) I. Nitta, *Z. Krist.*, **112**, 234 (1959).
3) E. R. Andrew "Nuclear Magnetic Resonance", Cambridge Univ. Press, New York (1955); T. Yukitoshi, H. Suga, S. Seki and J. Itoh, *J. Phys. Soc. Japan*, **12**, 506 (1957).
4) K. K. Kelley, *J. Am. Chem. Soc.*, **51**, 1400 (1929).
5) P. Flubacher, A. J. Leadbetter and J. A. Morrison, *Proc. Phys. Soc. (London)*, **78**, 1449 (1961).
6) R. H. Beaumont, H. Chihara and J. A. Morrison, ibid., **78**, 1462 (1961).
7) P. Averbuch, *C. R. Acad. Sci. Paris*, **2**, 3147 (1957).
8) L. Reinisch, *Compt. rend.*, **243**, 1032 (1956).

difference between the axial and the equatorial protons attached to the same carbon atom. There is no discernible change in the line width at the melting point.

In conclusion, it was revealed that the high-resolution NMR spectrometers were also useful for investigating the molecular motions and also for detecting the chemical shifts in the plastic crystals. Similar results were also obtained for crystalline trimethylacetic acid[9]. A full discussion will be published elsewhere in near future.

We wish to express their sincere thanks to Dr. Eiichi Nagai and Mr. Shiro Satō of Kureha Bōseki Co. for their kindness of allowing the use of the Varian Associates spectrometer for our purposes and also for their collaboration in the measurements.

Department of Chemistry
Faculty of Science
Osaka University
Nakanoshima, Osaka

9) H. Suga and S. Seki, *J. Phys. Chem. Solid.*, to be published.

*Electrochemical Fluorination of Aldehydes**

By Shunji NAGASE, Hajime BABA and Rimpei KOJIMA

(Received January 16, 1962)

It has been shown in previous papers[1,2] that perfluorocarboxylic acids are prepared by electrochemical fluorination from alcohols and esters in a significant yield. A possible mechanism for the formation of perfluorocarboxylic acid fluorides from alcohols was suggested to involve the first attack by fluorine on the α-carbon atom of the alcohols, and dehydrofluorination followed by exhaustive fluorination of the acid fluorides formed into perfluorocarboxylic acid fluorides. In this process, it is possible to consider the formation of aldehydes as an intermediate, though not actually isolated, at the next step of the dehydrofluorination, before the formation of the acid fluorides.

With esters, the mechanism was assumed to start with the hydrofluorolysis of the esters in hydrogen fluoride to form acid fluorides and alcohols. The latter would then be converted into acid fluorides by the mechanism involving dehydrofluorination at the α-carbon atom. Perfluorocarboxylic acid fluorides would be formed by exhaustive fluorination of these two kinds of acid fluorides.

On the basis of these previous works and from the results of the fluorination of ketone[3], which gave perfluorocarboxylic acids in a reasonable yield, the electrochemical fluorination of aldehydes was attempted with the expectation that perfluorocarboxylic acids could be prepared from aldehydes.

So far, very little attention has been paid to the fluorination of aldehydes. Simons[4] carried out the electrochemical fluorination of butyraldehyde and obtained perfluoropropane. In the present work, acetaldehyde, propionaldehyde, butyraldehyde and aldol, as well as paraldehyde, were fluorinated under various anodic current densities (2.5~3.5 amp./dm^2). This treatment afforded trifluoroacetic acid, a mixture of trifluoroacetic acid and perfluoropropionic acid, or a mixture of trifluoroacetic acid, perfluoropropionic acid, and perfluorobutyric acid. Generally, however, the yield and current efficiency were relatively lower than those obtained in alcohols[1], esters[2], ketones[3] and some unsaturated compounds[5], because of considerable fragmentation or polymerization. No formation of a detectable amount of partially fluorinated aldehydes or perfluoroaldehydes could be confirmed throughout the reaction. Acid fluorides, unreacted aldehydes, and a tarry polymeric substance were found in the residue in the electrolytic cell.

The possible major route of the formation of perfluorocarboxylic acid fluorides from aldehydes may involve the fluorination-fragmentation of the ringed para-type polymer of the aldehyde which is in equilibrium with the aldehyde in hydrogen fluoride.

Experimental

Materials. — *Aldehydes.* — Special or first grade commercial reagents were used after distillation, but aldol (first grade) in a glass ampoule (25 g.) was used without further purification. Acetaldehyde was prepared in the usual manner from paraldehyde.

Hydrogen Fluoride.—Hydrogen fluoride of 99.4% purity was supplied from a commercial cylinder.

Apparatus.—The apparatus used for this work essentially consisted of an electrolytic cell provided with a reflux condenser at the top and a drain at the bottom, a sodium fluoride tube, and a pair of polyethylene bottle absorbers. The details have been described in previous papers[1,2].

Standard Procedure.—One liter of hydrogen fluoride was placed in the cell and, prior to the addition of the sample, in order to remove a trace of water in hydrogen fluoride, electrolysis was carried out in a nitrogen atmosphere, with an anodic current density of 2.7 amp./dm^2 until the cell voltage rose to 5.5 V. Twenty-five grams of the sample were then introduced into the cell, and electrolysis was carried out with an anodic current density of 3.3 amp./dm^2 at about 4.8~5.2 V. until the cell voltage again rose to 5.5 V.

The same amount of electricity as used under this current density was supplied for electrolysis under different current densities. The reaction temperature was kept at 4~6°C by the circulation of ice water through the copper tubing in the cell.

The gaseous product generated from the cell, containing perfluorocarboxylic acid fluorides, was passed through the reflux condenser and the sodium

* Presented in part at the Nagoya Regional Meeting of the Chemical Society of Japan, Nagoya, November, 1961.

1) S. Nagase and R. Kojima, *J. Chem. Soc. Japan, Ind. Chem. Sec.* (*Kogyo Kagaku Zasshi*), **64**, 1397 (1961).

2) S. Nagase and R. Kojima, This Bulletin, **34**, 1468 (1961).

3) S. Nagase, H. Baba and R. Kojima, *J. Chem. Soc. Japan, Ind. Chem. Sec.* (*Kogyo Kagaku Zasshi*), **64**, 2126 (1961).

4) J. H. Simons, U. S. Pat. 2519983 (1950).

5) S. Nagase, H. Baba and R. Kojima, *J. Chem. Soc. Japan, Ind. Chem. Sec.* (*Kogyo Kagaku Zasshi*), **65**, 38 (1962).

fluoride tube and bubbled through water in then polyethylene absorber. The perfluorocarboxylic acid formed in the absorber was neutralised with sodium carbonate and filtered; the filtrate was the evaporated to dryness. The sodium perfluorocarboxylate thus formed was then extracted with absolute ethanol and dried. Quantitative analysis of the product thus prepared was made by means of the base line method of infrared absorption spectrum, as was previously described in detail[1].

A pair of glass traps, cooled by ice and by dry ice-acetone respectively, was connected with the absorber to collect the low-boiling fluorocarbons for the reaction under this current density.

Results and Discussion

Trifluoroacetic acid was obtained in a reasonable yield from acetaldehyde. The product from propionaldehyde was a mixture of trifluoroacetic acid and perfluoropropionic acid, while that from butyraldehyde and aldol consisted of trifluoroacetic acid, perfluoropropionic acid, and perfluorobutyric acid. However, the yield of these products was relatively low compared with those from alcohols[1], esters[2], ketones[3], or esters of unsaturated carboxylic acids[5], because of the great fragmentation or polymerization in the fluorination reaction. A considerable part of the perfluorocarboxylic acids obtained consisted of degraded acid, the number of whose carbon atoms was less than that of the starting aldehydes.

The results of the fluorination of acetaldehyde, propionaldehyde, butyraldehyde, and aldol are given in Tables I, II, III and IV. The calculation of the current efficiencies shown was based on the amount of electricity assumed to be required to form fluorine by discharging the fluoride ion which would substitute for hydrogen in the aldehyde and combine with it to form hydrogen fluoride.

This means that electricity enough to make 4, 6, 8 and 9 mol. of fluorine would be required for the fluorination of 1 mol. of acetaldehyde, propionaldehyde, butyraldehyde, and aldol respectively to yield perfluorocarboxylic acid fluorides the number of whose carbon atoms corresponds to those of the starting aldehydes.

In the case of the fluorination of alcohols[1] and in the majority of ketones[3], the highest yield of perfluorocarboxylic acids was found at the anodic current density of 3.3 amp./dm^2, irrespective of the kind of the sample used; with aldehydes, however, the yield appeared not to be much affected within the range of anodic current densities applied, although the highest yield was also found at 3.3 amp./dm^2 for most of the aldehydes.

It is interesting to note that the composition of the perfluorocarboxylic acids prepared was

TABLE I. FLUORINATION OF ACETALDEHYDE

Electricity passed: 181 amp. hr.

D_A[a] amp./dm^2	Product obtained g.	Yield mol. %	Current efficiency %
2.5	12.8	16.6	11.2
2.7	13.1	17.0	11.5
3.0	14.0	18.1	12.3
3.3	16.9	22.0	14.8
3.5	12.9	16.7	11.3

a) D_A: Anodic current density

TABLE II. FLUORINATION OF PROPIONALDEHYDE

Electricity passed: 160 amp. hr.

D_A amp./dm^2	Product obtained g.	Composition, wt. %		Yield, mol. %			Current efficiency %
		CF_3COONa	C_2F_5COONa	CF_3COONa	C_2F_5COONa	Total	
2.5	9.2	43	57	6.8	6.5	13.3	10.0
2.7	8.9	42	58	6.4	6.4	12.8	9.7
3.0	9.1	41	59	6.4	6.7	13.1	9.9
3.3	9.6	41	59	6.7	7.1	13.8	10.4
3.5	8.5	38	62	5.5	6.6	12.1	9.3

TABLE III. FLUORINATION OF BUTYRALDEHYDE

Electricity passed: 103 amp. hr.

D_A amp./dm^2	Product obtained g.	Composition, wt. %			Yield, mol. %				Current efficiency %
		CF_3COONa	C_2F_5COONa	C_3F_7COONa	CF_3COONa	C_2F_5COONa	C_3F_7COONa	Total	
2.5	2.6	23	32	45	1.3	1.3	1.4	4.0	4.6
2.7	2.8	23	31	46	1.4	1.4	1.6	4.4	5.0
3.0	2.4	23	28	49	1.2	1.0	1.4	3.6	4.3
3.3	3.1	22	28	50	1.5	1.3	1.9	4.7	5.5
3.5	3.0	19	32	49	1.2	1.5	1.8	4.5	5.3

Table IV. Fluorination of aldol

Electricity passed: 154 amp. hr.

D_A amp./dm²	Product obtained g.	Composition, wt. %			Yield, mol. %				Current efficiency %
		CF_3COONa	C_2F_5COONa	C_3F_7COONa	CF_3COONa	C_2F_5COONa	C_3F_7COONa	Total	
3.0	5.6	66	17	17	1.0	1.8	1.4	4.2	7.5
3.3	5.1	64	14	22	0.9	1.4	1.7	4.0	6.8
3.5	4.9	60	18	22	0.8	1.7	1.6	4.1	6.5

Table V. Fluorination of paraldehyde

Electricity passed: 191 amp. hr.

D_A amp./dm²	Product obtained g.	Yield I mol. %	Yield II mol. %	Current efficiency I %	Current efficiency II %
3.0	14.4	56.1	18.7	35.4	11.8
3.3	17.5	68.1	22.7	42.9	14.3
3.5	15.7	60.9	20.3	38.7	12.9

not changed and was almost independent of the anodic current densities within the range of experimental conditions used, as was seen in the fluorination of alcohols[1], esters[2], ketones[3], and unsaturated alcohols, esters and ketones[5].

In the cold trap, about 5, 3, 1 and 1 ml. of a solution were collected at the anodic current density of 3.3 amp./dm² by the fluorination of acetaldehyde, propionaldehyde, butyraldehyde and aldol respectively. These solutions were identified as a mixture of fluorocarbons by their infrared absorption spectra, but they were not separated into their individual components. In the case of acetaldehyde, a considerable amount of perfluorodiethyl ether was found in the mixture.

In about 50 ml. of the residue remaining in the bottom of the cell after the distillation of hydrogen fluoride, a tarry polymeric substance was found which was soluble in such organic solvents as acetone, ethanol, ether, and carbon tetrachloride, and in hydrogen fluoride, but which was insoluble in water. This was extracted by the method described previously[5]. In the fluorination of acetaldehyde, propionaldehyde, butyraldehyde, and aldol, 1.0, 4.3, 6.0, and 6.0 g. of the tarry substance were yielded, respectively, at the anodic current density of 3.3 amp./dm².

The presence of a carboxylic acid formed through acid fluoride in the residue was also identified by its formation of a sodium carboxylate (0.5~1 g.) in the same way as has been mentioned earlier[1], and a small amount of unreacted aldehyde was identified by its formation of a 2,4-dinitrophenylhydrazone with hydrazine in 1:4 hydrochloric acid solution. An examination of the formation of partially fluorinated aldehydes was attempted by the zirconium-alizarine test[6], which was carried out after combustion treatment of the hydrazones, obtained as described above, with fused metallic potassium, but the presence of fluoride could not be confirmed. No evidence could be obtained either for the formation of perfluoroaldehydes throughout the fluorination reactions. For example, in the case of acetaldehyde, the gaseous product generated from the cell was collected in the cold trap, without bubbling through water, and the condensate was examined by its infrared absorption spectrum; however, no perfluoroacetaldehyde was found.

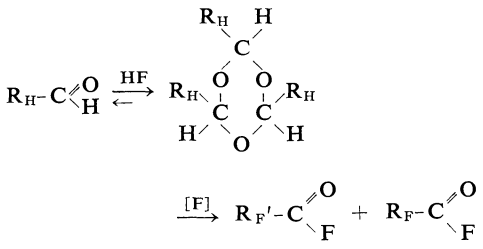
As a polymeric aldehyde having a six-membered oxide ring, paraldehyde was fluorinated with anodic current densities of 3.0, 3.3 and 3.5 amp./dm². Trifluoroacetic acid was obtained. The results are shown in Table V.

Yield I and current efficiency I were calculated in the same way as for other aldehydes, while yield II and current efficiency II were calculated on the assumption that 1 mol. of paraldehyde would give 3 mol. of sodium trifluoroacetate. The amount of fluorocarbon mixture containing perfluorodiethyl ether obtained, as in the case of acetaldehyde, was 5 ml., and the tarry polymeric substance in the residue was 1.0 g. at an anodic current density of 3.3 amp./dm². Although the amount of electricity required for the fluorination of paraldehyde was a little more than that for required for acetaldehyde, the overall results appeared to be similar in these two cases.

The mechanism for the formation of perfluorocarboxylic acid fluorides from aldehydes may

6) F. Feigl (Translated by R. E. Oesper), "Spot Tests", Vol. I, Elsevier Pub. Co., New York (1954), p. 252.

be explained by the following representative scheme, although the reaction could, and probably did, follow different routes simultaneously:



where R_H is the hydrocarbon radical, and R_F and $R_{F'}$ are fluorocarbon radicals.

When aldehydes are dissolved into hydrogen fluoride, they undergo rapid polymerization into para-type ringed aldehydes to reach a condition of equilibrium. The perfluorocarboxylic acid fluorides are probably formed through the process of the fluorination-fragmentation of the para-type aldehydes. The postulated mechanism should explain the bulk of the experimental evidence described above involving a low yield and a greatly degraded product of perfluorocarboxylic acids (a considerable part of which consisted of acids having a smaller number of carbon atoms than those of the starting aldehydes), the presence of a carboxylic acid fluoride in the residue, and the very similar feature fluorination reactions between acetaldehyde and paraldehyde including the formation of perfluorodiethyl ether, etc.

If alcohol has been fluorinated through the route involving the formation of intermediate aldehyde, the aldehyde thus formed would be fluorinated into acid fluoride, immediately and successively, on the surface of the electrodes, without accumulation to any considerable extent in hydrogen fluoride.

Summary

Aldehydes were fluorinated electrochemically to prepare prefluorocarboxylic acids. The results were compared with those obtained from the fluorination of alcohols, esters, ketones and unsaturated compounds.

Generally, the yield of perfluorocarboxylic acids was considerably lower in aldehydes because of a great fragmentation or polymerization in the fluorination reaction. No evidence could be obtained for the formation of a detectable amount of partially fluorinated aldehydes or perfluoroaldehydes in the reaction. The mechanism for the formation of perfluorocarboxylic acid fluorides from aldehydes was discussed.

The authors are much indebted to Professor Ikumi Kagawa of Nagoya University for his invaluable advice and encouragement throughout this work. They wish to express their thanks also to the Osaka Metal Industries Co. for supplying the hydrogen fluoride used in this work.

Government Industrial Research Institute, Nagoya
Kita-ku, Nagoya

Studies of 2-Oxazolidinones. II. Products of the Pyrolysis of Some 2-Oxazolidinones

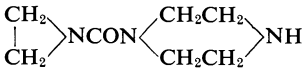
By Ryohei ODA, Masahiko MIYANOKI and Masaya OKANO

(Received February 2, 1962)

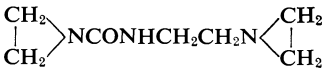
Among the various earlier studies of 2-oxazolidinones, some recent observations on the formation of ethylenimine and its polymer from 2-oxazolidinone[1-3] have been of great interest to us. Jones[3], studying the pyrolysis of 2-oxazolidinone at 210~235°C without a catalyst, isolated the following six products from ca. 42 g. of 2-oxazolidinone: ca. 11 g. of a polymer (A); 12.5 g. of a hygroscopic substance (B), b. p. 231~236°C/13 mmHg; 1.5 g. of a basic substance having the empirical formula of $C_7H_{13}N_3O$ (C), m. p. 244°C; 1 g. each of two distillates D and E, b. p. 86°C/13 mmHg and 136~160°C/13 mmHg respectively, and ca. 1 g. of ethanolamine. On the basis of infrared analysis, Jones suggested a poly(ethylenimine)

1) O. Sundén, Swed. Pat. 148559; *Chem. Abstr.*, **50**, 2679 (1956).
2) M. Crowther and W. R. Nummy, U. S. Pat. 2806839; *Chem. Abstr.*, **52**, 3405 (1958).
3) J. I. Jones, *Chem. & Ind.*, **1956**, 1454.

structure having a certain carbonyl group for A, and a tri- or tetrasubstituted urea structure such as I or II for C. However, there are some doubtful points in his assignments of A and C, and no information on the structure of B, one of the major products, has yet been obtained.



I



II

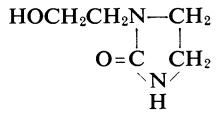
It is the purpose of this investigation to provide more detailed information on the structures of the pyrolysates from some 2-oxazolidinones and also to discuss a possible mechanism of the pyrolysis.

Results and Discussion

Products of the Pyrolysis of 2-Oxazolidinone.—2-Oxazolidinone was pyrolyzed at 230°C until the evolution of carbon dioxide ceased completely, this was done under the same conditions as Jones'[3], i. e., under the atmospheric pressure of dry nitrogen in the absence of a catalyst. Somewhat unexpectedly, the evolution of carbon dioxide ceased at ca. 61% of the theoretical amount. Moreover, in the infrared spectrum of the pyrolysate, the disappearance of the carbonyl band at 1760 cm^{-1}, which was found in 2-oxazolidinone, was accompanied by the formation of a new carbonyl band at the 1686 cm^{-1} position. These facts suggest that ca. 39 mol. % of 2-oxazolidinone was converted to another carbonyl compound which was thermally stable.

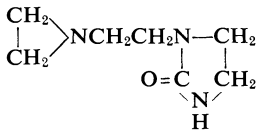
By careful fractionation, the pyrolysate (21 g.) could be separated into the following four fractions; probably ethanolamine (fraction 1), 1 g.; a hygroscopic product of b. p. 180~185°C/3.5 mmHg and m. p. 51.5°C, $C_5H_{10}N_2O_2$ (fraction 2), 11 g.; a basic powder of m. p. 234°C, $C_7H_{13}N_3O$ (fraction 3), 1 g.; and a semi-solid polymeric residue (fraction 4), 8 g. In comparison with Jones's results, our fractions 2 and 3 seem to correspond to his substances B and C respectively.

In the infrared spectrum of fraction 2 shown in Fig. 1A, three strong bands corresponding to amide I, II and III appeared at 1690, 1495 and 1279 cm^{-1} respectively; they are in nearly the same positions as in unsubstituted 2-imidazolidinone (1660, 1508 and 1270 cm^{-1})[4]. A characteristic hydroxyl band can also be found at 1067 cm^{-1}. Based on spectral and analytical data, formula III was proposed as the structure of fraction 2. This structure was further confirmed by a mixed melting point determination with an authentic sample prepared by an independent method.



III

As is shown in Fig. 1B, fraction 3 also has three bands, corresponding to amide I, II and III, at 1690, 1500 and 1279 cm^{-1}. Their positions and intensities are just the same as those in fraction 2; this suggests a 1-substituted 2-imidazolidinone structure for fraction 3[5]. Futhermore, an absorption which is probably due to the C–H stretching vibration of a strained ethylenimine ring[6] is found at 3080 cm^{-1}. These data suggest that the most probable structure of fraction 3 is represented by formula IV. If Jones' tentative structure I or II were correct, its carbonyl frequency (amide I) should be lower than that of normal tri- or tetrasubstituted urea (cf. footnote 5) under the influence of a strained, three-membered ring[7]. Therefore, it is obvious that Jones's structures for fraction 3, which shows an amide I absorption in such a higher frequency region (near 1690 cm^{-1}), are erroneous.



IV

In polymeric fraction 4, the infrared spectrum was measured after its low boiling portion had been distilled off as completely as possible; the absorption curve is shown in Fig. 1C. Three amide absorptions (1695, 1495 and 1275 cm^{-1}) agreed with those in fractions 2 and 3. This would imply that the 2-imidazolidinone

4) R. Mecke, Jr. and R. Mecke, Sr., *Chem. Ber.*, **89**, 343 (1956).

5) Judging from the position of the amide I of the product, the possibility of some other carbonyl structure may be excluded. The amide I absorption of acyclic urethanes usually occurs in the 1705~1722 cm^{-1} region, while in cyclic systems such as 2-oxazolidinone, the carbonyl frequency falls in the range 1745~1760 cm^{-1} [e. g., S. Pinchas and D. Ben-Ishai, *J. Am. Chem. Soc.*, **79**, 4099 (1957).]. In acyclic *N,N'*-disubstituted ureas, the amide I absorption appears at a lower frequency than 1660 cm^{-1} [e. g., H. J. Becher, *Chem. Ber.*, **89**, 1953 (1956).], and in tri- or tetrasubstituted ureas, a further decrease in the frequency would be expected. However, the amide I band of fraction 3 was observed in another region. This is equally true for fraction 4.

6) H. T. Hoffman, Jr., G. E. Evans and G. Glockler, *J. Am. Chem. Soc.*, **73**, 3028 (1951).

7) Cf. L. J. Bellamy, "Infra-Red Spectra of Complex Molecules", Methuen, London (1958), p. 387.

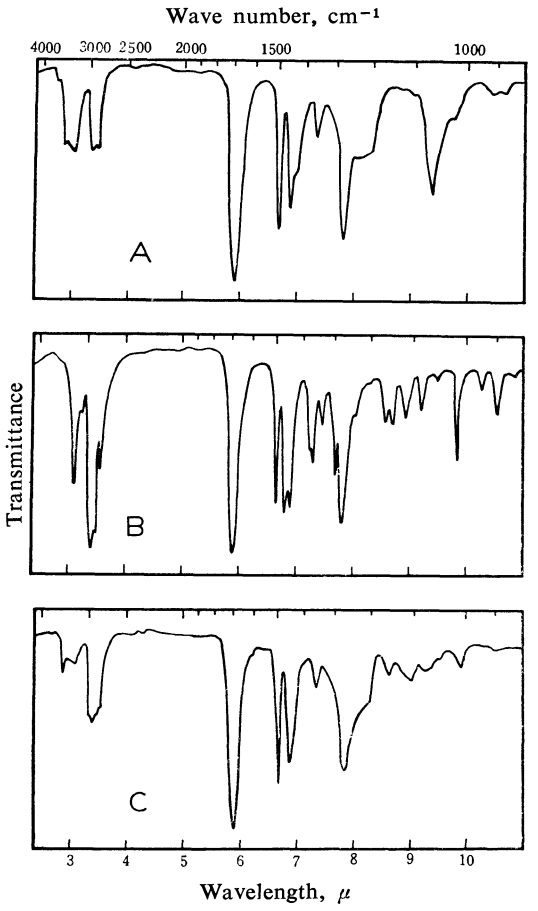
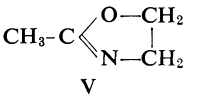


Fig. 1. Infrared spectra of each fraction of the pyrolysate from 2-oxazolidinone: A, fraction 2 (in $CHCl_3$ sol.); B, fraction 3 (in Nujol); C, fraction 4 (in $CHCl_3$ sol.).

rings are joined at the 1-position with the chain ends of some part, if not all, of the poly(ethylenimine) molecules[8].

Products of the Pyrolysis of 3-Substituted 2-Oxazolidinones.—3-*p*-Chlorophenyl-2-oxazolidinone, which was less reactive than 2-oxazolidinone itself, was completely decarboxylated at 230°C. In the infrared spectrum of the pyrolysate, the carbonyl absorption which is found at 1740 cm^{-1} in the starting oxazolidinone completely disappears. This coincides with the fact that quantitative decarboxylation was observed. It therefore appears that the basic residue on the pyrolysis of this oxazolidinone is mainly composed of poly(*N*-*p*-chlorophenylethylenimine), in contrast with the polymeric product from unsubstituted 2-oxazolidinone. The pyrolysis of 3-*p*-nitrophenyl-2-oxazolidinone at 230°C gave essentially the same results. After half one of the theoretical amount of carbon dioxide had been evolved, the pyrolysis was stopped and the reaction mixture was examined by infrared analysis. The 1767 cm^{-1} absorption (in chloroform) due to the carbonyl group in 2-oxazolidinone was decreased to just half in transmittance, and no new carbonyl absorption was found.

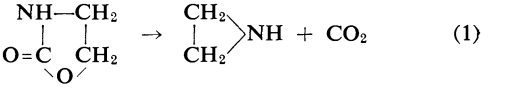
As a particular case, the pyrolytic decarboxylation of 3-acetyl-2-oxazolidinone at 195°C afforded a basic distillate of b. p. 110°C in addition to a polymeric residue. The infrared spectrum suggested that the distillate was 2-methyl-2-oxazoline V[9]. The structural assignment was established by a mixed melting point determination of its picrate with an authentic sample prepared by an independent route. This substance probably results from the rearrangement of *N*-acetylethylenimine, which seems to be an intermediate in pyrolysis. The above



V

consideration appears reasonable in view of the fact that *N*-benzoylethylenimine thermally rearranged to 2-phenyl-2-oxazoline with ease[10].

Mechanism of the Pyrolysis of 2-Oxazolidinones.—All experimental results, including our data, seem to indicate that the pyrolysis proceeds through the intermediate formation of ethylenimine.



(1)

It is well known that ethylenimine is rather stable in strong alkaline media, but that in the presence of acids (including carbon dioxide) it easily polymerizes to give poly(ethylenimine) according to a step-wise mechanism[11,12] promoted by the ethylenimmonium cation. In connection with our work, an initiation by carbon dioxide is interesting; it seems to arise from the following equilibrium:

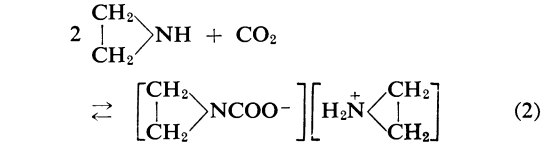
8) It is known that the shift of amide I frequency is of the order of 20 cm^{-1} to the lower side, with the structure varying from secondary to tertiary amide (Ref. 7, p. 211), from secondary to tertiary urethane [S. Pinchas and D. Ben-Ishai, *J. Am. Chem. Soc.*, **79**, 4099 (1957).], and from *N*-monosubstituted to *N*,*N*-disubtituted urea [H. J. Becher et al., *Chem. Ber.*, **89**, 1593 (1956); *Naturwiss.*, **43**, 467 (1956).]. If fraction 3 or 4 had any 1, 3-disubstituted 2-imidazolidinone structure, a similar frequency decrease would be expected. Therefore, there is no possibility that the 2-imidazolidinone ring is sandwiched in between two poly(ethylenimine) residues.

9) The same compound has been obtained as a by-product in the preparation of 3-acetyl-2-oxazolidinone from *N*-(2-hydroxyethyl)-acetamide and methyl trichloroacetate. [G. Y. Lesher and A. R. Surrey, *J. Am. Chem. Soc.*, **77**, 639 (1955)].

10) S. Gabriel and R. Stelzner, *Ber.*, **28**, 2933 (1895).

11) G. D. Jones et al., *J. Org. Chem.*, **9**, 125 (1944).

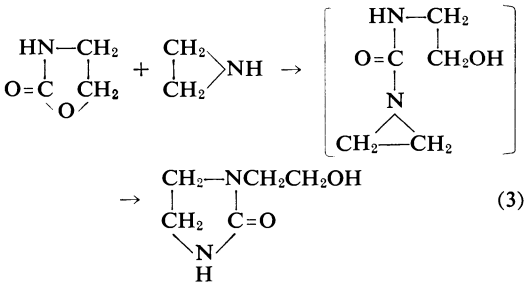
12) W. G. Barb, *J. Chem. Soc.*, **1955**, 2564, 2577.



(2)

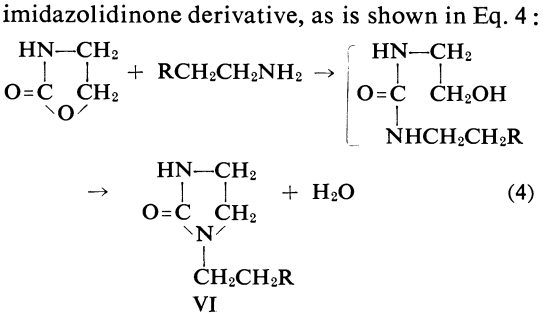
The same reaction path would be expected in the formation of ethylenimine polymer by pyrolysis. In default of equilibrium 2, however, the pyrolytic polymerization of 3-aryl- or 3-acyl-2-oxazolidinone seems to be initiated by some acidic impurity (e. g., traces of water).

Furthermore, the fact that, in the pyrolysis of unsubstituted 2-oxazolidinone, some 1-substituted 2-imidazolidinones including the polymer were isolated, as has been described above, is strikingly different from the result in other cases, so that some explanation seems to be necessary. First, the formation of 1-(β-hydroxyethyl)-2-imidazolidinone could be understood in terms of a nucleophilic attack of ethylenimine having active hydrogen on a cyclic



(3)

urethane, 2-oxazolidinone, followed by cyclization of the resulting adduct. However, in this mechanism, it is necessary for the reactants to be unsubstituted at the 3-position of 2-oxazolidinone and the 1-position of ethylenimine; this requirement is fulfilled in 2-oxazolidinone itself. Secondary, a similar attack of the terminal amino group of the polymer on 2-oxazolidinone, followed by dehydration of the adduct, may also lead to the formation of a 2-imidazolidinone derivative, as is shown in Eq. 4:



(4)

(R: Any group derived from ethylenimine)

Actually, a compound corresponding to R=$-\underset{|}{N}CH_2CH_2\underset{|}{-}$ in VI, as well as a polymer having a VI type structure, was isolated as described above. In this connection, Gabriel and Eschenbach[13] long ago investigated a similar reaction, which involved the formation of 1-phenyl-2-imidazolidinone from 2-oxazolidinone and aniline. Further, the water formed in Eq. 4 seems to be consumed by the ring-cleavage of ethylenimine itself and by the terminal ethylenimine ring of the polymer.

Under such severe conditions as bulk pyrolysis, the contribution of more complicated reactions may also be considered. However, the discussion above seems to be sufficient to explain all the products of the pyrolysis.

Finally, we wish to point out the difference in mechanism between this reaction and the formation of polypeptide from 2, 5-oxazolidinedione (Leuchs' anhydride), which involves a similar decarboxylative polymerization. On the formation of ethylenimine from 2-oxazolidinone, the ethylenimine and its polymer act only as a catalyst for the decarboxylation[14] and cannot directly initiate the polymerization, so the decarboxylation and the polymerization are two entirely independent steps. On the other hand, in the formation of polypeptide, the reaction proceeds by the repeated attack of the propagating chain on the monomer (Leuchs' anhydride); that is, the decarboxylation and the polymerization occur simultaneously.

Experimental

Materials.—2-Oxazolidinone was prepared by the condensation of ethanolamine with diethyl carbonate according to Homeyer's procedure[15]. The yield was 70%. It melted at 89~90°C after recrystallization from tetrahydrofuran.

3-Acetyl-2-oxazolidinone was prepared from acetylchloride and 2-oxazolidinone by the method of Close[16]. The yield was 70%. It melted at 69°C after recrystallization from benzene. 3-*p*-Chlorophenyl- and 3-*p*-nitrophenyl-2-oxazolidinone were prepared as previously desribed[17]. The *p*-chlorophenyl derivative, m. p. 121°C; the *p*-nitrophenyl derivative, m. p. 154.5°C.

General Procedure of Pyrolysis. — The material was placed in a small flask fitted with a nitrogen inlet and a delivery tube which was connected with a potash-bulb through a trap, and then heated under a stream of dry nitrogen in a silicone oil bath maintained at the descired temperature. The extent of pyrolysis was determined from the amount of absorbed carbon dioxide. After the evolution of carbon dioxide has ceased completely, the syrupy or resinous mass remaining in the flask was cooled and examined by infrared analysis. The amount

13) S. Gabriel and G. Eschenbach, *Ber.*, **30**, 2495 (1897).
14) A detailed study of the catalytic action of bases will be presented in a following paper.
15) A. H. Homeyer, U. S. Pat. 2399188; *Chem. Abstr.*, **40**, 4084 (1946).
16) W. J. Close, *J. Am. Chem. Soc.*, **73**, 97 (1951).
17) R. Oda, M. Miyanoki and M. Okano, This Bulletin, **35**, 1309 (1962).

of evolved carbon dioxide was 61.4% of the theoretical value in the case of 2-oxazolidinone and quantitative in the case of its 3-substituted derivative (e. g., *p*-chlorophenyl, 101%). The pyrolysate from 2-oxazolidinone was further fractionated (as described below). However, the fractionation of no other pyrolysate was undertaken. Their molecular weights were not very high, this may be due to the simultaneous depolymerization cited by Barb[12].

Fractionation of the Pyrolysate from 2-Oxazolidinone.—The pyrolysate (21 g.) obtained by the decomposition of 2-oxazolidinone (30.5 g.) at 230°C under the atmospheric pressure of nitrogen was distilled under reduced pressure to yield 1 g. of a water-soluble base boiling below 100°C at 4 mmHg, probably ethanolamine (fraction 1), and 11 g. of a viscous liquid, b. p. 185°C/3.5 mmHg (fraction 2). The addition of chloroform to the resulting residue gave 1 g. of a white powder, m. p. 234°C (fraction 3) which was removed by filtration; the filtrate was then evaporated to yield 8 g. of a polymeric residue (fraction 4). Treatment of this fraction at 240°C/3 mmHg for a short time to remove its low boiling portion gave a pale yellow mass which solidified on cooling.

Redistillation of fraction 2 gave hygroscopic crystals, m. p. 51.5°C, having an empirical formula of $C_5H_{10}N_2O_2$ (Found: C, 45.96; H, 8.51; N, 21.27. Calcd. C, 45.79; H, 8.45; N, 21.36%.). This compound was presumed to be 1-(β-hydroxyethyl)-2-imidazolidinone, and no depression in melting point was observed when it was mixed with an authentic sample, which had been prepared in a 68% yield according to Wilson's procedure[18] except that diethyl carbonate was used instead of urea as a carbonyl source.

In basic fraction 3, its empirical formula $C_7H_{13}N_3O$ (Found: C, 53.41; H, 8.57; N, 27.13. Calcd. C, 54.17; H, 8.44; N, 27.08%.) agreed with Jones' result, but its melting point was 10°C lower than that he reported. A higher value was not obtained by repeated recrystallizations from chloroform. This fraction is believed to be 1-(β-aziridinylethyl)-2-imidazolidinone.

Fraction 4 was strongly basic and hygroscopic. On the basis of infrared analysis, it was assumed to be a mixture of low molecular weight poly(ethylenimine) partially terminated with 2-imidazolidinone ring.

On the pyrolysis of 2-oxazolidinone under a reduced pressure of 20 mmHg at 170°C a similar result was obtained.

Distillate of the Pyrolysis of 3-Acetyl-2-oxazolidinone.—When 16.5 g. of 3-acetyl-2-oxazolidinone was thermally decarboxylated at 195°C, 4.4 g. of a basic oil having a pyridine-like odor was distilled out in addition to a polymeric residue. The redistilled liquid boiled at 110°C. Its picrate recrystallized from absolute ethanol melted at 151°C. The infrared spectrum of the free base is identical with that of 2-methyl-2-oxazoline. Furthermore, a mixed melting point of its picrate with an authentic sample prepared according to Wenker's procedure[19] showed no depression.

Summary

The products obtained by the pyrolytic decarboxylation of 2-oxazolidinones have been investigated, chiefly by infrared analysis. In the case of 2-oxazolidinone, the products are 1-(β-hydroxyethyl)-2-imidazolidinone, 1-[β-(1-azilidinyl)ethyl]-2-imidazolidinone (somewhat uncertain), and poly(ethylenimine) having a 2-imidazolidinone ring at the chain end. On the other hand, the only products from 3-*p*-chlorophenyl- and 3-*p*-nitrophenyl-2-oxazolidinone are believed to be low molecular weight polymers of the corresponding ethylenimines. From 3-acetyl-2-oxazolidinone, a considerable amount of 2-methyl-2-oxazoline, which seems to arise from the rearrangement of *N*-acetylethylenimine, is isolated, in addition to the corresponding poly(ethylenimine). On the basis of the products obtained, a possible mechanism for the pyrolysis has been proposed.

The authors wish to thank Dr. Tōru Takenaka and Mr. Shōzō Iida for their infrared measurements.

Department of Synthetic Chemistry
Faculty of Engineering
Kyoto University
Sakyo-ku, Kyoto (R. O. & M. M.)

Institute for Chemical Research
Kyoto University
Takatsuki, Osaka (M. O.)

18) A. L. Wilson, U. S. Pat. 2517750; *Chem. Abstr.*, **45**, 1627 (1951).

19) H. Wenker, *J. Am. Chem. Soc.*, **57**, 1079 (1935).

Studies of 2-Oxazolidinones. III. Kinetics of the Pyrolytic Decarboxylation of 2-Oxazolidinones

By Ryohei ODA, Masahiko MIYANOKI and Masaya OKANO

(Received February 2, 1962)

Studies of the thermal decomposition of 2-oxazolidinones are important not only in order to synthesize ethylenimines or their polymers, but also in order to consider the thermal stability in some applications of 2-oxazolidinone derivatives to polymer chemistry[1]. In the second paper of this series[2], the authors examined the pyrolysates from 3-substituted 2-oxazolidinones by means of infrared spectroscopy and discussed a two-step process, in which decarboxylation was followed polymerization. The present kinetic study has been undertaken to provide further insight into the mechanism of the decarboxylation step in this reaction. The effect of a 3-substituent on the decarboxylation rate and the rate-accelerating effect of various amines have been especially studied in detail.

Results and Discussion

Autocatalytic Nature of the Reaction. — The decarboxylation rates of some 2-oxazolidinones without either catalyst or solvent were measured. Figure 1 shows the results of plotting the decarboxylation rate, dx/dt, against the conversion x, for two representative 2-oxazolidinones. As is illustrated in this figure, the rate first increases as the reaction proceeds, but it comes to a maximum and then decreases[3]. The basic products of the reaction —the corresponding ethylenimines and/orth eir polymers—appear to at as an auto-catalyst; this will be proved experimentally below.

Effect of the 3-Substituent on the Decarboxylation Rate.—The decarboxylation rates of various 3-substituted 2-oxazolidinones are summarized in Table I. Each of these values indicates a relative rate at 25% conversion taking as a standard the rate of the 3-phenyl

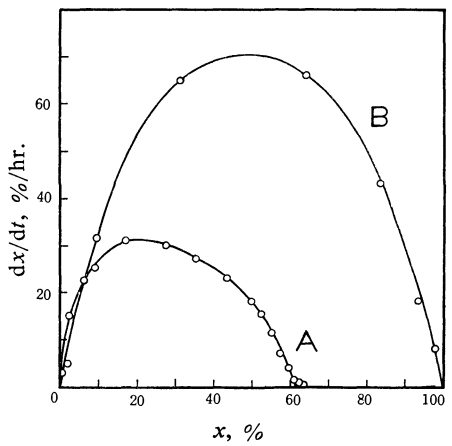


Fig. 1. Rate vs. conversion curves for the bulk decarboxylation of 2-oxazolidinones (0.02 mol.) without catalyst: A, 2-Oxazolidinone (at 200°C); B, 3-*o*-Nitrophenyl-2-oxazolidinone (at 230°C).

TABLE I. RELATIVE RATES FOR BULK DECARBOXYLATION OF 3-SUBSTITUTED 2-OXAZOLIDINONES WITHOUT CATALYST AT 230°C[a]

Run	Oxazolidinone[b]	Relative rate[c]
1	C_6H_5-Ox	1
2	*p*-CH_3-C_6H_4-Ox	0.7
3	*p*-C_2H_5OOC-C_6H_4-Ox	1.3
4	*p*-Cl-C_6H_4-Ox	1.9
5	*p*-NO_2-C_6H_4-Ox	130
6	*o*-NO_2-C_6H_4-Ox	140
7	$CH_3(CH_2)_3$-Ox	2.3
8	Ox-Ox	33[d]
9	Ox-$(CH_2)_2$-Ox	8.6[d]
10	Ox-$(CH_2)_4$-Ox	15[d]

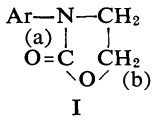
a) In each run, 0.02 mol. of oxazolidinones was used.
b) The oxazolidinonyl group, -N-CH_2CH_2OCO-, abbreviated as Ox.
c) The volume of the compounds differs, but no correction for this is made, so that it is impossible to compare each rate value exactly.
d) This value has been divided by a statistical correction factor of two.

1) e. g., J. R. Caldwell, U. S. Pat. 2656328 [*Chem. Abstr.*, 48, 2415 (1954)]; W. H. Schuller and E. J. Kerle, U. S. Pat. 2786043 [*Chem. Abstr.*, 51, 11758 (1957)]; R. Oda et al., *Chem. High Polymer Japan* (*Kōbunshi Kagaku*), 17, 72 (1960): G. P. Speranza and W. J. Peppel, *J. Org. Chem.*, 23, 1922 (1958); E. K. Drechsel, ibid., 22, 849 (1957).

2) R. Oda, M. Miyanoki and M. Okano, This Bulletin, 35, 1910 (1962).

3) In the decarboxylation of such 3-substituted 2-oxazolidinones as the 3-*o*-nitrophenyl or 3-*p*-chlorophenyl derivatives, the evolution of the theoretical amount of carbon dioxide was observed. In the case of unsubstituted 2-oxazolidinone, however, the evolution of carbon dioxide ceased at 61.4% of the theoretical amount; this is attributed to the fixation of the part corresponding to 38.6 mol.% as 1-substituted 2-imidazolidinones [see Ref. 2].

derivative. The results from runs 1—6 in Table I show that the reactivity of various 3-aryl derivatives depends on the electronic effect of the substitutent on the benzene ring; that is, an electron-attracting group such as *p*-nitro accelerates the decarboxylation, while an electron-releasing group such as *p*-methyl retards it. It may be inferred from this observation that the rate-determining step for this ring-cleavage is the fission of the N–C bond, (a) in I, rather than that of the O–C bond, (b) in I.



I

As is seen in runs 8–10, all bis-oxazolidinones showed high decomposition rates compared with that of *n*-butyl-2-oxazolidinone (run 7). This may be partially accounted for by the participation of the steric effect[4], but at present no complete solution is possible.

Aromatic Amine-Catalyzed Decarboxylation of 3-Aryl-2-oxazolidinone. — In both the presence and absence of *N*, *N*-diethyl-*p*-nitroaniline, the decarboxylation rates of 3-*p*-nitrophenyl-2-oxazolidinone in *o*-nitroanisole were measured. Rate vs. conversion curves are shown in Fig. 2[5]. Since the structure of the amine used is similar to that of *N*-*p*-nitrophenylethylenimine, which seems to be an initial product in this decomposition, and since the amount of the amine added is equivalent to that of the oxazolidinone, rate maximum would be expected to appear at the beginning of the reaction. As is shown in curve B, however, the rate increases gradually at first and comes to a maximum only after some conversion has occurred. This means that the pyrolysate formed, rather than the amine added, acts as the more effective catalyst.

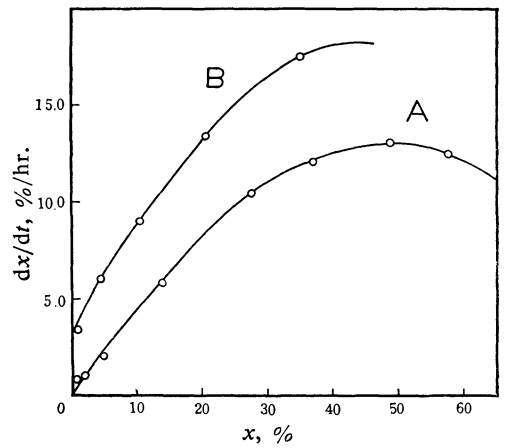


Fig. 2. Rate vs. conversion curves for the decarboxylation of 3-*p*-nitrophenyl-2-oxazolidinone (1 mol./l.) in the absence (A) and presence (B) of *N*, *N*-diethyl-*p*-nitroaniline in *o*-nitroanisole at 230°C. $[Ox]_0=[I]_0=1.00$ mol./l.

The rates of decarboxylation catalyzed by some *N*-ethylaniline derivatives for the same oxazolidinone were also measured. A comparison between the rates at 25% conversion are given in Table II. The order of the rates disagrees with that which would be expected judging from the basicities of the catalysts[6]. The larger accelerating effects of a polyamine (run 5) and of a small ring monoamine (run 4) as compared with an ordinary monoamine (run 2) suggest that the rates depend considerably on the steric requirements of amines.

TABLE II. RATE-ACCELERATING EFFECT OF ANILINE SERIES ON DECARBOXYLATION OF 3-*p*-NITROPHENYL-2-OXAZOLIDINONE IN *o*-NITROANISOLE AT 230°C[a]

Run	Catalyst added	Concn. mol./l.	Rate, dx/dt %/hr.
1	None	—	9.5
2	$C_6H_5N(C_2H_5)_2$	1.00	20
3	$C_6H_5NHCH_2CH_2NHC_6H_5$	0.50	30
4	$C_6H_5NCH_2CH_2$ (ring)	0.75	31
5	$(-NCH_2CH_2-)_n$ (C$_6$H$_5$ on N)	0.20/*n*	23

a) In each run, $[Ox]_0=1.00$ mol./l.

Aliphatic Amine-Catalyzed Decarboxylation of 3-Aryl-2-oxazolidinones.—Using high boiling aliphatic amines as catalysts for the decarboxylation of 3-*p*-nitrophenyl- and 3-*p*-chlorophenyl-2-oxazolidinone, the kinetic order with respect to the catalysts and the rate constants have been determined. In all cases, there was a rate maximum at the beginning of the reaction, as expected. Figure 3 shows the rate vs. conversion curves for the *n*-dodecylamine-catalyzed decarboxylation in dibenzyl ether. From this

4) In the contiguous existence of two rings (intermolecular or intramolecular), the imino group resulting from one oxazolidinone ring would lie in a suitable position for promoting the decomposition of the other ring, though it appears to depend on the number of carbons in the polymethylene linkage.

5) In this figure and hereafter, $[Ox]_0$ and $[I]_0$ represent the initial concentrations of oxazolidinone and amine respectively.

6) The basicity constants of $(C_2H_5)_2NH$, $NH_2CH_2CH_2NH_2$, and HN(CH$_2$CH$_2$) at 25°C are estimated to be 9.6×10^{-4}, 8.5×10^{-5}, 1.1×10^{-7} respectively. [a) "Handbook of Chemistry (Kagaku Binran)", New Ed., compiled by the Chemical Sociehy of Japan, Maruzen, Tokyo, (1958) p. 871; b) S. Searles et al., *J. Am. Chem. Soc.*, 78, 4918 (1959).] Presumably, those of $C_6H_5N(C_2H_5)_2$, $C_6H_5NHCH_2CH_2NHC_6H_5$, and C_6H_5N(CH$_2$CH$_2$) would decrease in this order.

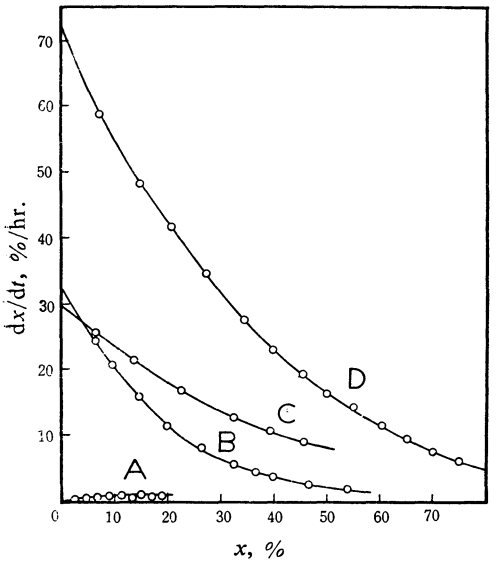
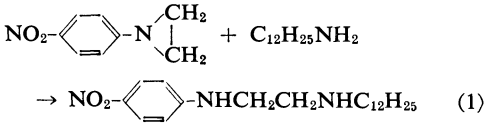


Fig. 3. Rate vs. conversion curves for the *n*-dodecylamine-catalyzed decarboxylation of 3-*p*-nitrophenyl- and 3-*p*-chlorophenyl-2-oxazolidinones in dibenzyl ether at 230°C: A, *p*-NO_2, non-catalyzed; B and D, *p*-NO_2, amine-catalyzed; C, *p*-Cl, amine-catalyzed. $[Ox]_0=1.00$ mol./l.; $[I]_0=1.00$ mol./l. in C and D, and 0.50 mol./l. in B.

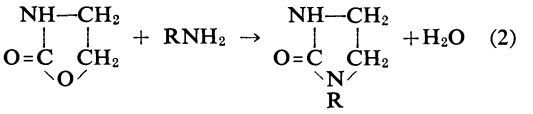
figure, it can be seen that the rate of the decarboxylation of the *p*-nitrophenyl compound in the absence of a catalyst is very slow in comparison with that in the presence of the amine; hence, the participation of the non-catalyzed term is possibly negligible for the latter case.

If the amine concentration remains constant during a run, the reaction will be in pseudo-first-order; hence, a plot of dx/dt vs. x should be linear. However, first-order plots with a downward curvature were obtained, as is shown in B, C and D of Fig. 3. This observation may be interpreted as follows: By the reaction with the *N*-arylethylenimines formes as reaction intermediates, *n*-dodecylamine is partially converted to the less effective *N*-aryl-*N'*-*n*-dodecylethylenediamines, and the low catalytic activity of these amines may lead to a slower rate. Judging from the experimental data (see below), it is appearent that a secondary aliphatic amine is less effective than a primary one as a catalyst. Additionally, no appreciable rate acceleration by the aromatic amine in dibenzyl ether was observed in a preliminary test.



(1)

Another consumption of the amine which is due to the condensation with oxazolidinone to afford 1-substituted 2-imidazolidinone may also be considered[7] (cf. our previous paper[2]). In



(2)

another experiment[8], however, it has been found that the existence of a 3-substituent on the oxazolidinone ring makes this condensation difficult. Therefore, such consumption would be negligible.

Since the rate did not fit the simple pseudo-first-order rate equation, as has been mentioned above, the initial second-order rate constants, k, were computed from the values of the initial rate, $(dx/dt)_{x=0}$, which were extrapolated graphically in Fig. 3, using the following equation:

$$(dx/dt)_{x=0}=k[Ox]_0[I]_0 \qquad (3)$$

In Table III-A, a little increase of k with an increase in the amine concentration is observed; this may be ascribed to a small contribution of the second-order term with respect to amine.

Table III. Rate constants of decarboxylation of 3-*p*-nitrophenyl-2-oxazolidinone catalyzed by various amines in dibenzyl ether at 230°C[a]

Amine added	Concn. of amine mol./l.	Initial second-order rate constant, l. mol^{-1} min^{-1} $k\times10^3$
A series		
n-Dodecylamine	0.50	10.7
n-Dodecylamine	1.00	12.0
N-Ethyl-*n*-dodecylamine	1.00	8.75
Bis(2-ethylhexyl)-amine	1.00	1.40
N,*N*-Diethyl-*n*-dodecylamine	1.00	1.90
B series		
Tetraethylenepentamine	0.125	73
Triethanolamine	0.20; 0.40	33[b]

a) In each run, $[Ox]_0=1.00$ mol./l.
b) Mean value for two different amine concentrations.

Rate vs. conversion curves for similar decarboxylations in the presence of aliphatic secondary or tertiary amines (e.g., *N*-ethyl-*n*-dodecylamine, bis(2-ethylhexyl)-amine and *N*,*N*-diethyl-*n*-dodecylamine) are shown in Fig. 4. In contrast with Fig. 3, the plots of A and B in Fig. 4 are very close to straight lines; hence, it appears that the concentration of the catalyst remains constant, at least in the range

7) S. Gabriel and G. Eschenbach, *Ber.*, 30, 2495 (1879).
8) R. Oda and K. Yamamoto, Unpublished data.

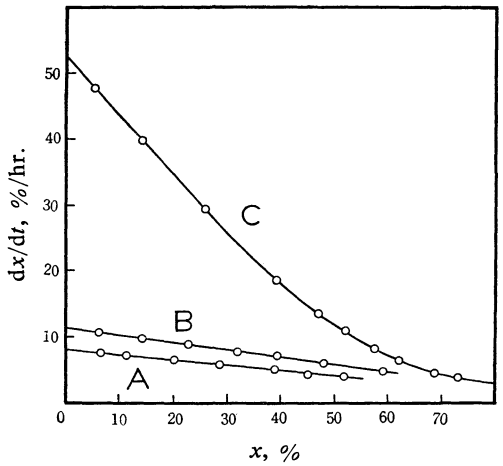


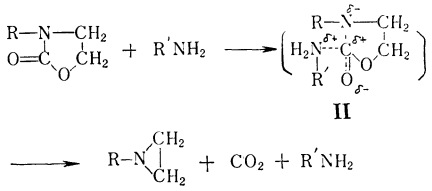
Fig. 4. Rate vs. conversion curves for the aliphatic amine-catalyzed decarboxylation of 3-*p*-nitrophenyl-2-oxazolidinone in dibenzyl ether at 230°C: A, Bis(2-ethylhexyl)-amine; B, *N*,*N*-Diethyl-*n*-dodecylamine; C, *N*-Ethyl-*n*-dodecylamine. $[Ox]_0=[I]_0=1.00$ mol./l.

of ca. 50% conversion. Probably this means that these amines react only slowly with the intermediate *N*-aryl-ethylenimine. The initial second-order rate constants calculated from Eq. 3 are also listed in Table III-A. In a series of amines, a variation in structure from primary to secondary and from secondary to tertiary leads to a decrease in the catalytic effect; this order disagrees with that of their basicities[9]. Such behavior would be caused by steric hindrance to the approach of the oxazolidinone molecule. Actually, in the case of highly hindered bis(2-ethylhexyl)-amine, an unexpectedly low rate was observed.

It can be seen from Table III that a polyamine is more effective as a catalyst than a monoamine in the aliphatic as well as in the aromatic series (cf. Table II). In order to make the rate constant for the tetraethylenepentamine-catalyzed reaction comparable with the value obtained from monoamine-catalyzed decomposition, a statistical correction factor of 5 has to be applied. The calculated rate constant per amino group, 14.6×10^{-3} mol.$^{-1}$·min^{-1}, is somewhat larger than the observed values in other cases. Considering that this polyamine contains three secondary amino groups, which are less effective than primary groups, the larger value would be expected. Therefore it seems, clear that polyamine acts as a bi-functional (or polyfunctional) catalyst in this decarboxylation. This suggests a push-pull mechanism which involves the nucleophilic attack of one amino group on the positive carbon of the carbonyl group in oxazolidinone and the simultaneous electrophilic attack of the hydrogen of the other amino group on the nitrogen of the urethane group in the same molecule of oxazolidinone. Since the hydroxyl group is known to be more acidic than the amino group, triethanolamine, which has both groups, may be expected to be a more powerful catalyst[10]. As is shown in Table III-B, the decomposition rate in the presence of this amine is much larger than that for the ordinary tertiary amine-catalyzed reaction. Additionally, it was ascertained experimentally that just aliphatic alcohols such as *n*-dodecyl alcohol showed no accelerating effect on the rate. Therfore, the first-order dependence with respect to triethanolamine strongly supports a concerted mechanism, in which the hydroxyl group in the catalyst acts as electrophile and the amino group act as a nucleophile simultaneously.

The above considerations may also be applied to the problem of two amino groups in separate molecules; that is, the slight second-order dependence with respect to amine, which has been observed in the monoamine-catalyzed reaction, can be understood by a similar explanation.

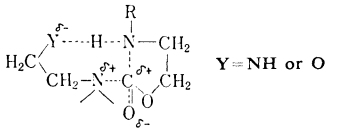
In summary, it may be concluded that amine-catalyzed decarboxylations proceed by two different mechanisms depending on the structure of the amine. When simple monoamine is used as a catalyst, the reaction occurs mainly through transition state II, as is shown in Eq. 4. On the other hand, in the reaction catalyzed



II

(4)

by an amine having an active hydrogen group, such as NH_2 or OH, on the β-carbon, the activated complex may be approximated by structure III:



III

9) e.g., the basicity constants of $C_2H_5NH_2$, $(C_2H_5)_2$-NH, and $(C_2H_5)_3N$ at 25°C are estimated to be 3.4×10^{-4}, 9.6×10^{-4} and 5.65×10^{-4} respectively (Ref. 6a).

10) In fact, it has been reported in patent literature [O. Sunden, Swed. Pat. 148559; *Chem. Abstr.*, **50**, 2679 (1956)] that the use of triethanolamine on the decarboxylation of 2-oxazolidinone leads to a satisfactory yield of ethylenimine.

TABLE IV. RATE CONSTANTS OF DECARBOXYLATION OF 2-OXAZOLIDINONE CATALYZED BY *n*-DODECYLAMINE IN DIBENZYL ETHER AT 230°C

Initial concn. of oxazolidinone mol./l.	Initial concn. of amine mol./l.	Initial second-order rate constant l. mol^{-1} min^{-1} $k \times 10^3$	Initial third-order rate constant l. mol^{-1} min^{-1} $k' \times 10^3$
0.50	0.50	1.00	2.00
0.50	0.75	0.98	1.96
1.00	0.50	2.33	2.33
1.00	0.75	2.37	2.37

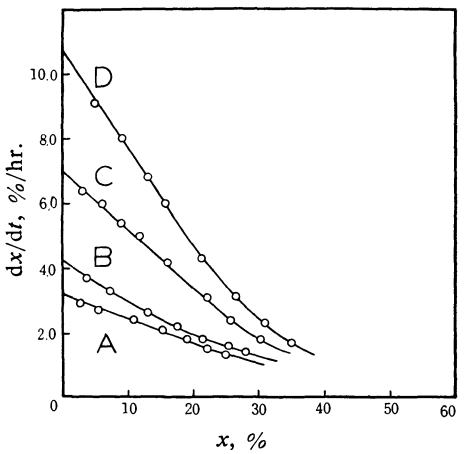


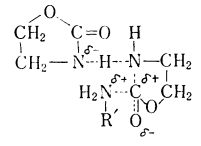
Fig. 5. Rate vs. conversion curves for the *n*-dodecylamine-catalyzed decarboxylation of 2-oxazolidinone in dibenzyl ether at 230°C. $[Ox]_0=1.00$ mol./l. in C and D, and 0.50 mol./l. in A and B. $[I]_0=0.75$ mol./l. in A and C, and 0.50 mol./l. in B and D.

Aliphatic Amine-Catalyzed Decarboxylation of 2-Oxazolidinone. — Finally, in the presence of an amine catalyst, the rate of the decarboxylation of 2-oxazolidinone itself was measured. As is shown in Fig. 5, rate vs. conversion curves for the *n*-dodecylamine-catalyzed reaction in dibenzyl ether tend to converge at a point near 60%-conversion; similar behavior has also been observed in the non-catalyzed reaction (cf. Fig. 1).

The initial second-order and third-order rate constants, k and k', for various concentrations of oxazolidinone and amine, were evaluated by using Eqs. 3 and 5 respectively. These values are listed in Table IV.

$$(dx/dt)_{x=0}=k'[Ox]_0^2[I]_0 \qquad (5)$$

In the table, the k value changes for the two initial concentrations of oxazolidinone, while the k' value becomes nearly constant, though one can not overlook a slight increase in k' with an increase in the oxazolidinone concentration. Therefore, the amine-catalyzed decarboxylation of 2-oxazolidinone would proceed mainly by a concerted mechanism, in which the added amine attacks oxazolidinone as a nucleophile and, simultaneously, another oxazolidinone molecule attacks it as an electrophile. The transition state may be represented as IV[11]:



IV

Experimental

Materials. — All 2-oxazolidinones used in this work were prepared by methods previously described[2,12]. The following constants were observed: 3-substituent, b. p. or m. p.; none, m. p. 90°C; *n*-butyl, b. p. 113°C/4.3 mmHg; phenyl, m. p. 49°C; *p*-tolyl, m. p. 61°C; *p*-nitrophenyl, m. p. 116°C; *o*-nitrophenyl, m. p. 70.5°C; *p*-carbethoxyphenyl, m. p. 145°C; *p*-chlorophenyl, m. p. 69°C; bis, m. p. 97°C; ethylene-bis, m. p. 136°C; tetramethylene-bis, m. p. 118°C. The solvents (*o*-nitroanisole and dibenzyl ether) and the aliphatic and aromatic amines, except those described below, were of the best grade commercially available and were used after sufficient purification.

N, N-Diethyl-p-nitroaniline. — The amine was prepared according to the procedure of Behr et al.[13] from *p*-chloronitrobenzene and diethylamine in a 94.5% yield. Recrystallization from ethanol afforded the pure product, m. p. 77°C.

N-Phenylethylenimine and its Polymer.—*N*-(β-Bromoethyl)-aniline was treated with aqueous sodium hydroxide according to the method of Heine et al.[14] The *N*-phenylethylenimine thus obtained boiled at 62~65°C/10 mmHg. The polymer was purified by reprecipitation using dimethylformide as a solvent and water as a precipitator.

N-Ethyl-n-dodecylamine. — A mixture of 25 g. of

11) Though the existence of an oxazolidione dimer has been known [Cf. S. Pinchas and D. Ben-Ishai, *J. Am. Chem. Soc.*, 79, 4102 (1956); E. Fischer, *J. Chem. Soc.*, **1952**, 4525], the dimer seems to be inferior in reactivity because of the lower reactivity of the carbon atoms of its carbonyl groups. Therefore, the possibility of the nucleophilic attack of amine on the dimer may be eliminated from the main route of the reaction. However, the appearance of a third order term with respect to oxazolidinone, though in a slight degree, seems to indicate the participation of such an attack.

12) R. Oda, M. Miyanoki and M. Okano, This Bulletin, 35, 1309 (1962).

13) L. C. Behr, E. J. Kirby, R. N. MacDonald and C. W. Todd, *J. Am. Chem. Soc.*, 68, 1296 (1946).

n-dodecylbromide and 25.8 g. of 70% aqueous ethylamine was allowed to stand in a sealed tube at 80°C for 24 hr. The resulting mixture was gradually made acidic with hydrochloric acid. After the extraction of the organic layer with ether, the aqueous layer was made strongly alkaline with aqueous potassium hydroxide, and the amine formed was extracted with ether. After the resulting ethereal solution had been dried over anhydrous potassium carbonate and the ether had then been evaporated, distillation in vacuo gave 19 g. (90%) of the fraction of *N*-ethyl-*n*-dodecylamine, b. p. 107~110°C/2 mmHg. The redistilled product boiled at 108°C/2 mmHg.

Found: C, 78.59; H, 14.43; N, 6.69. Calcd. for $C_{14}H_{31}N$: C, 78.79; H, 14.64; N, 6.56%.

N,N-Diethyl-n-dodecylamine.—The amine was prepared according to the method of Coan et al.[15] in an 87% yield by the reaction of *n*-dodecylbromide with diethylamine. The product boiled at 155°C/16.5 mmHg, and its hydrochloride melted at 116°C.

Kinetic Measurement.—Pyrolytic decarboxylation was carried out in glass tubes of ca. 5 or 10 ml. volume for bulk and solution experiments respectively; these tubes were immersed in a constant temperature bath of silicone oil. The evolved carbon dioxide was swept out by a stream of purified nitrogen and absorbed in a potash-bulb. Figure 6 shows an outline of the apparatus. After the immersion of the reaction vessel, a period of 10 min. was allowed for establishment of the temperature equilibrium, and then the rate was measured by weighing the potash-bulb at appropriate time intervals.

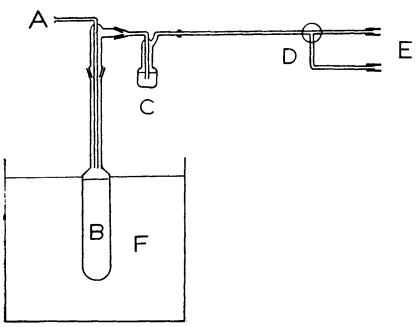


Fig. 6. Apparatus.
A: Dry nitrogen inlet
B: Reactor (Pyrex tube)
C: Trap containing concd. sulfuric acid
D: Switching cook
E: To potash-bulb
F: Thermo-regulated silicone oil bath

In the complete decarboxylation of 3-*p*-chlorophenyl- and 3-*o*-nitrophenyl-2-oxazolidinone, the amounts of evolved carbon dioxide were nearly quantitative (101 and 98% respectively). Therefore, it is believed that the above estimation method leads to responsible results.

Summary

The kinetics of the pyrolytic decarboxylation of 3-substituted 2-oxazolidinones have been studied and the following results obtained. (1) This decomposition is an autocatalytic reaction, in which the amine formed acts as a catalyst. (2) In the decarboxylation of 3-aryl-2-oxazolidinones, the electronic effect of the substituent on the benzene ring indicates that the fission of the N–C bond of the urethane group in the 2-oxazolidinone ring is rate-determining. (3) The initial rate of the aliphatic amine-catalyzed decarboxylation of 3-aryl-2-oxazolidinones is of the pseudo-first-order; it also depends on the concentration and structure of the amine. A mechanism has been proposed which involves a nucleophilic attack of amine on the carbonyl-carbon atom. An amine having an hydroxyl or amino group on the β-carbon shows a large rate-acceleration; this suggests the simultaneous electrophilic participation by the active hydrogen of these groups. (4) The initial rate of the decarboxylation of 2-oxazolidinone itself, catalyzed by aliphatic amine, is of the second-order in oxazolidinone and of the first-order in amine. From this a concerted mechanism has been inferred, in which the amine acts as a nucleophile and the other oxazolidinone acts as an electrophile.

Department of Synthetic Chemistry
Faculty of Engineering
Kyoto University
Sakyo-ku, Kyoto (R. O. & M. M.)

Institute for Chemical Research
Kyoto University
Takatsuki, Osaka (M. O.)

14) H. W. Heine, B. L. Kapur and C. S. Mitch, ibid., 76, 1173 (1954).
15) S. B. Coan and D. Papa, ibid., 77, 2404 (1955).

The Behavior of Heat-treated Graphitizing Carbons in Wet Oxidation[1)]

By Hiroaki TAGAWA and Hitoshi NAKAJIMA

(Received April 17, 1962)

The chemical property of carbon may vary considerably according to the nature of the original carbonaceous material and the conditions under which it has been carbonized. Although the problem of the chemical reactivity of solid carbon is very complex, the reactivity of carbon which is free of ash and appreciable amounts of hydrogen and oxygen may be thought to depend mainly on such structural factors as the crystallinity and the state of the condensed system of aromatic carbon.

The wet oxidizability of carbon in a solution of potassium dichromate in phosphoric acid has been studied by Riley et al.[2-5)], Akamatu et al.[6)], Tamaru[7)], and Honda and Hirose[8)]. It has been reported by Riley et al.[2-5)] that differences in the oxidation rate for various cokes are due largely to differences in graphite content and give a semiquantitative measure of the degree of graphitization. Akamatu et al.[6)] have investigated the reactivity of various kinds of carbon in wet oxidation and have concluded that the rate of reaction depends on the type of carbon and on the modes of the aggregation of crystallites.

The relationship between the chemical reactivity of carbon and its structure has been studied only from the standpoint of carbon species of different degrees of graphitization. In order to obtain a general view of that relationship, the wet oxidation of three kinds of graphitizing carbon graphitized by heat treatment is here examined in the solution of potassium dichromate in phosphoric acid.

Experimental

Materials and Heat Treatments.—Petroleum coke (Union Oil Co., U. S. A.), coal coke used as the industrial raw material of calcium carbide (Kinki Cokes Co., Japan) and anthracite (Hongay, Vietnam). The proximate analysis of these substances and the chemical analysis of ashes are listed in Tables I and II respectively. The specimens were prepared by preheating these substances for 2 hr. at 900°C in a laboratory electric furnace in a nitrogen atmosphere and by then heating them, in vacuo, to the higher temperatures of 1100, 1380, 1660, 1950 and 2250°C. The maximum temperature for each preparation was maintained for 2 hr. Heat treatments at 2600 and 2800°C were also made in the industrial graphitizing furnace for about 15 min. This latter procedure was undertaken in the Nagoya Factory of the Tokai Electrode Manufacturing Company to which our thanks are due. The heat-treated specimens were pulverized and graded for wet oxidation between a 180~200 tyler mesh sieve. The ashes in the carbon decreased with the rise in temperature, showing 6.4 and 2.0% at 1660°C and 0.3 and 0.04% at 2250°C for coal coke and anthracite respectively.

TABLE I. PROXIMATE ANALYSIS OF CARBONS (%)

	Petroleum coke	Coal coke	Anthracite
Moisture	6.7	1.4	1.8
VM	11.5	2.3	6.6
Ash	0.7	7.9	6.9
Fixed carbon	81.7	88.4	84.7

TABLE II. CHEMICAL ANALYSIS OF ASHES (%)

	Petroleum coke	Coal coke	Anthracite
SiO_2	12.89	49.02	50.83
Fe_2O_3	45.84	13.90	5.43
Al_2O_3	9.63	27.27	37.51
CaO	14.67	5.93	4.37
MgO	2.87	2.65	1.28
P_2O_5	0.20	0.90	—
SO_3	4.86	0.69	0.74
MnO	0.51	—	—
Cr_2O_3	0.51	—	—
NiO	6.83	—	—
TiO_2	0.84	—	—

X-Ray Measurements.—Changes in the interlayer spacing and crystallite growth were observed as a function of the heat treatment temperature. The X-ray diffraction patterns were recorded by an automatic recording X-ray spectrometer (Rigaku Denki Co., Japan) and were calibrated by reference to a standard quartz specimen. As the diffraction

1) This investigation was already published partly in *J. Chem. Soc. Japan, Ind. Chem. Sec.* (*Kogyo Kagaku Zasshi*), **63**, 1690 (1960); **65**, 1220 (1962).
2) H. E. Blayden and H. L. Riley, *J. Soc. Chem. Ind. London*, **54**, 195T (1935).
3) A. E. Balfour and H. L. Riley, *J. Chem. Soc.*, **1935**, 1723.
4) A. E. Balfour, H. E. Blayden, A. H. Charter and H. L. Riley, *J. Soc. Chem. Ind. London*, **57**, 1 (1938).
5) H. L. Riley, *Trans. Faraday Soc.*, **34**, 1011 (1938).
6) H. Akamatu, R. Takahashi and K. Tamaru, This Bulletin, **24**, 27 (1951).
7) K. Tamaru, *Kolloid-Z.*, **133**, 97 (1953).
8) H. Honda and Y. Hirose, *Fuel*, **37**, 323 (1958).

maxima did not directly give the true interlayer spacing in the case of low graphitic carbon, the correction factors given by Ruston were used[9]. These factors were negligibly small for the specimens treated above 2250°C.

The crystallite size was obtained from the broadening of the X-ray diffraction lines according to the procedure described by Klug and Alexander[10]. The crystallite dimension was calculated according to the following equation;

$$L = K\lambda/\beta\cos\theta$$

where L is the average effective dimension of the crystallite in the direction perpendicular to the reflecting plane at the glancing angle θ, λ is the wavelength of the X-ray, K is a shape factor, and β is defined as the half-value breadth. The L_c-dimension, the thickness of the parallel packets of layers, was obtained from the (002) line using $K=0.9$, while the L_a-dimension, the width of the graphite-like layer, was obtained from the (10) band using $K=1.84$, as well as from the (110) lines using $K=0.9+(1.84-0.9)p$ for highly graphitizing specimens[11], where p as defined by Franklin[12] meant the fraction of the amorphous part in graphitic carbon and was given as the following equation; $d_{002}=3.44-0.086(1-p^2)$.

The diffration conditions employed were as follows: The target, copper, filtered by nickel; filament voltage and current, 40 kV. and 15 mamp. respectively; divergent slit 1°; receiving slit 1° and 0.1 mm.; time constant, 4 sec., and scanning speed, 1/4°/min.

Wet Oxidation Procedure. — Carbon is oxidized to carbon dioxide in the solution of potassium dichromate in phosphoric acid. The reactivity of carbon can be known from the quantity of carbon dioxide evolved per unit time or of the carbon decomposed, which is calculated from the quantity of carbon dioxide evolved. The author used the volumetric method, which gives reproducible results.

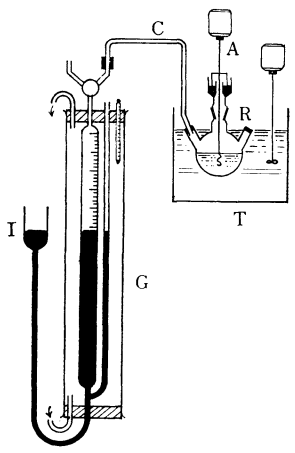


Fig. 1. Apparatus.

The apparatus used in these experiments is shown in Fig. 1. It consists of the temperature-controlled bath, T, a reaction vessel, R, and a gas burette, G. The reaction vessel was a 100 cc. three-necked flask with a mercury-sealed stirrer, S, of the constant speed. The gas burette, 80 cc. in volume, was kept at a constant temperature with flowing water in order to avoid the effect of any change in room temperature. The gas burette was connected to the levelling bulb I, filled with mercury, and to the reaction vessel with a glass capillary tube, C. The bath temperature was measured with a mercury thermometer and was maintained at a desired value within 0.1°C by the aid of an automatic temperature controller, although this is not shown in the figure.

The experimental procedure was as follows: 1 g. of the sample was added to the reaction flask already containing 10 g. of potassium dichromate (G. R. Grade, Wako Chemicals Co.) and 50 cc. of concentrated phosphoric acid (d 1.70 g./cc.; E. P. Grade, Wako Chemicals Co.). While the water bath was being heated to the desired temperature, the three-way cock of the gas burette was opened to the air. When the vessel was dipped in the bath, the meniscus was adjusted to the zero mark of the burette and the stopcock was closed. The volume of gas evolved was measured with the burette as a function of time. It was found, by means of gas chromatography analysis, that all the gas evolved was carbon dioxide. The volume of gas was converted to the value in the standard state. Fifty cubic centimeters of carbon dioxide (N. T. P.) is equivalent to 2.68% of consumed carbon. The reaction temperatures were 62, 67, 73, 79, 85 and 89°C.

Results and Discussion

Graphitization.—The graphitization states of the specimens heated at several temperatures from 1100 to 2800°C were determined by means of the X-ray diffractometer.

The interlayer spacings obtained from the (002) line are plotted against the temperature of heat treatment in Fig. 2. The crystallite sizes determined from the breadth of the diffraction patterns of the (002) line and the (10) band or the (110) line are given against the heating temperature in Figs. 3 and 4. It has been found that the developement of crystallinity by heat treatment varies among different carbon species. The growth of crystallite proceeds with the most facility in petroleum coke. No remarkable difference, however, could be found between these three materials in the general features of graphitization.

Wet Oxidation. — The results for petroleum coke and anthracite at 85°C are shown in Figs. 5 and 6 respectively, where the gas evolved is plotted as a function of time. In Fig. 5, all the curves of the gas evolved vs. time are

9) W. R. Ruston, ibid., 31, 52 (1953).
10) H. P. Klug and L. E. Alexander, "X-ray Diffraction Procedure", John Wiley, New York (1954), p. 491.
11) H. Akamatu, H. Inokuchi, H. Takahashi and Y. Matsunaga, This Bulletin, 29, 574 (1956).
12) R. E. Franklin, *Acta Cryst.*, 4, 253 (1951).

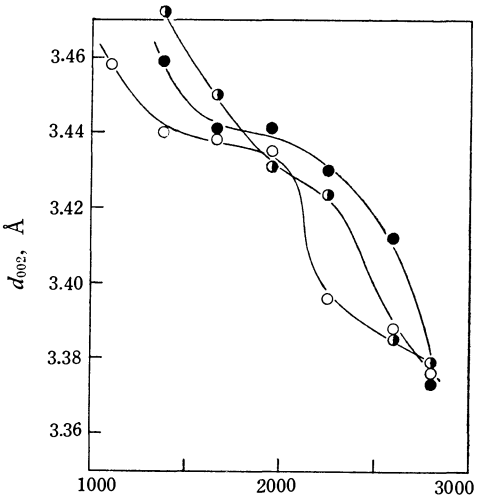


Fig. 2. Interlayer spacing of carbons as a function of the heat treatment temperature.

○ Petroleum coke ● Coal coke
◑ Anthracite

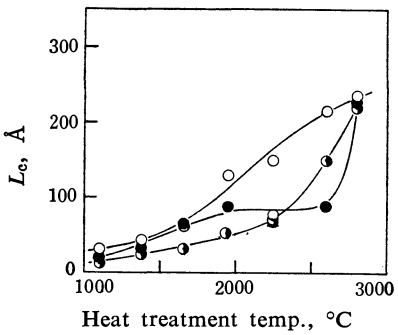


Fig. 3. L_c-Dimension vs. heat treatment temperature.

○ Petroleum coke ● Coal coke
◑ Anthracite

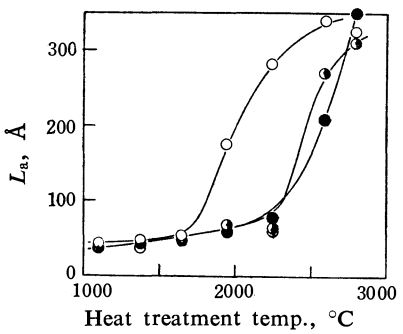


Fig. 4. L_a-Dimension vs. heat treatment temperature.

○ Petroleum coke ● Coal coke
◑ Anthracite

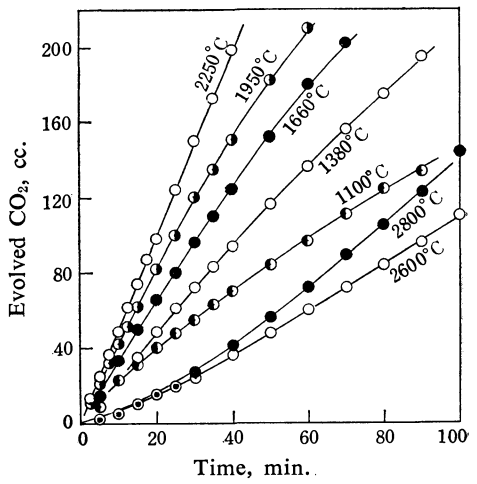


Fig. 5. Oxidation curve of petroleum coke at 85°C.

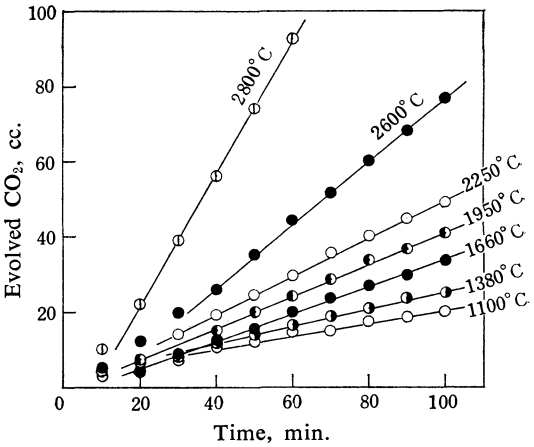


Fig. 6. Oxidation curve of anthracite at 85°C.

seemingly linear; however, the oxidation velocity for the petroleum cokes heat-treated below 1950°C decreased as the oxidation proceeded, while that for the specimens heat-treated above 2600°C increased with time.

These curves may be roughly classified into the following three types according to the heat treatment temperature:

(1) The oxidation rate decreases as the reaction proceeds for the specimens heat-treated below 1950°C.

(2) The rate is almost constant during the whole course of the reaction for the specimens heat-treated near 2250°C.

(3) The rate increases as the oxidation proceeds for the specimens heat-treated above 2600°C.

To examine whether these phenomena are expressed by a quantitative measure, all the curves in Fig. 5 are replotted in the logarithm

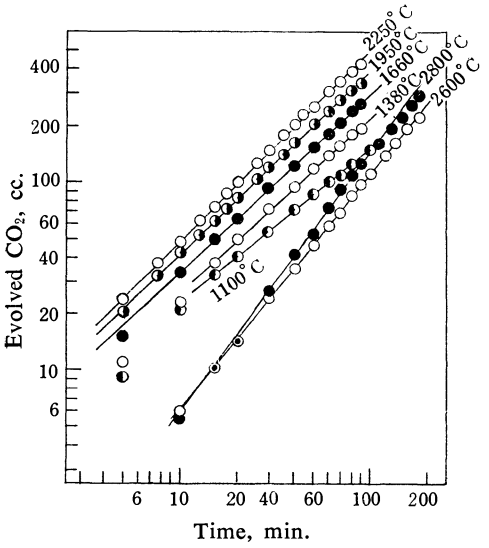


Fig. 7. Evolved carbon dioxide vs. reaction time.

scale in Fig. 7. The logarithm of the quantity of carbon dioxide evolved, V, becomes linear with that of time, t, and is expressed as the following equation at any reaction temperature:

$$V=at^b$$

where a and b are constant. The b-value depends on only the heat treatment temperature. Moreover, that value does not depend on the oxidation temperature; e. g., the values for petroleum coke treated at 2600°C were 1.49, 1.39, 1.43, 1.44 and 1.44 at the oxidation temperatures of 62, 67, 73, 79 and 85°C respectively.

As is shown in Fig. 6, the curves of carbon dioxide evolved vs. the time for anthracite were more linear than those for petroleum coke. The quantity of the gas evolved per unit time for anthracite and coal coke was much less than that for petroleum coke; therefore, the curve of three types. i. e., $b<1$, $b=1$ and $b>1$ in $V=at^b$, is not explicitly shown in Fig. 6 as in the case of petroleum coke in Fig. 5. Anthracite and coal coke heat-treated at 2250°C and below were oxidized at 100°C in order to obtain the b-value. The b-values for anthracite and coal coke heat-treated at 2600 and 2800°C were the average values at the reaction temperatures from 65 to 89°C.

The b-values for three kinds of carbon are plotted as a function of the interlayer spacing in Fig. 8. It is interesting that these b-values of all specimens compose one curve which increases monotonically as graphitization proceeds.

The oxidation velocity was obtained as follows: the reaction velocity for petroleum

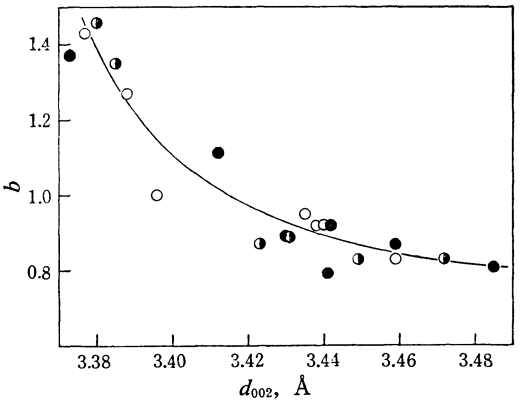


Fig. 8. b-Value vs. interlayer spacing.
○ Petroleum coke ● Coal coke
◑ Anthracite

coke was measured from the time which it took for initial 50 cc. of carbon dioxide to evolve; for anthracite and coal coke, this was decided from the slope of each straight line which related the carbon dioxide evolved and the reaction time. The curve of the gas evolved vs. the time was apparently linear when the less reactive carbons such as anthracite and coal coke were oxidized.

The reaction velocities at 85°C of three heat-treated carbon are plotted against the interlayer spacing in Fig. 9. Of the three, petroleum coke was oxidized with the highest rate; the reactivity of coal coke was of the same order as that of anthracite. The velocity for petroleum coke heat-treated at 2600 and 2800°C was smaller than that heat-treated below 2250°C, but the reason can not be

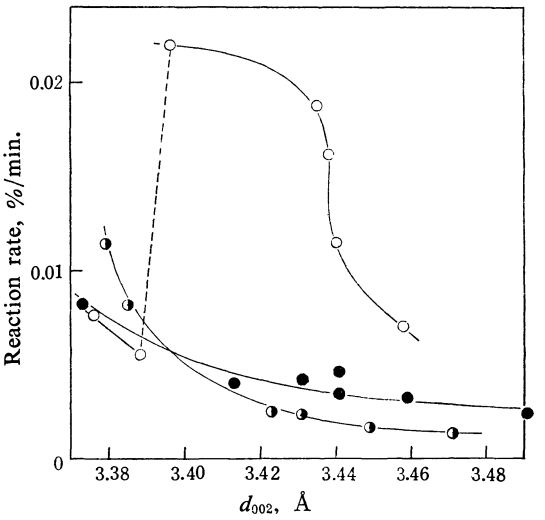


Fig. 9. Reaction velocity at 85°C vs. interlayer spacing.
○ Petroleum coke ● Coal coke
◑ Anthracite

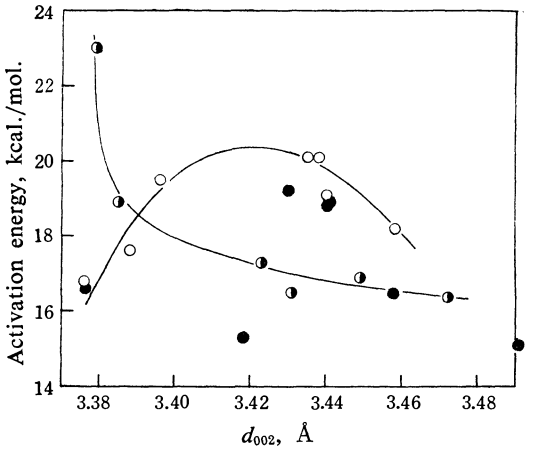


Fig. 10. Activation energy in wet oxidation vs. interlayer spacing.
○ Petroleum coke ● Coal coke
◑ Anthracite

understood from only the standpoint of the graphitization.

The activation energy obtained from the Arrhenius plot is shown as a function of the interlayer distance in Fig. 10. The standard deviation of activation energy for the three carbons obtained from the method of least squares was 0.7 kcal./mol. at most, although this is not shown in the figure. The activation energy for anthracite increased monotonically with the decrease of d_{002}, but for petroleum coke and coal coke there was a maximum at about 3.42Å of the interlayer spacing. The different behavior of the activation energy mentioned above seems to come from the nature of the original carbonaceous materials.

It has been reported that petroleum coke, anthracite and coal coke are non-graphitic graphitizing carbons. These carbons graphitize easily upon heat treatment. The difference of the graphitization between petroleum coke and anthracite and coal coke seems to be attributable to the original carbonaceous materials. As is shown in Fig. 2, of the three specimens, the graphitization of these carbons proceeds with the most facility in petroleum coke. The structure of anthracite is seemingly similar to that of coal coke, although anthracite has been carbonized naturally.

The difference in structure between petroleum coke and anthracite and coal coke appears in the wet oxidation, as is shown in Fig. 9. As far as our experiments show, the oxidation velocity of the carbon graphitized increases toward graphite. Of the three kinds of carbon, the dioxidation velocity of petroleum coke is five times as large as that of the other, and coal coke is of the same order as anthracite in oxidation velocity.

As has been mentioned above, the behavior of the oxidation velocity of three different types of carbon in accordance with the reaction time has been classified. For non-graphitizing carbon of d_{002} 3.44Å, the oxidation velocity decreases as the reaction proceeds.

As for the graphitic carbon of d_{002} 3.44Å, the oxidation velocity, which increases with the degree of graphitization, has a tendency to increase as the reaction proceeds. The reason for the increase in the reaction velocity may be thought to be that the carbon heat-treated disperses into the colloidal state in the process of the wet oxidation and that its surface area in contact with the oxidizing solution increases progressively. It seems that the increase in the surface area is closely connected with the rigidity of the cross-linkage bridged between crystallites. Moreover, the linkage between them weakens as the graphitization proceeds.

It is considered that the *b*-value, which is a unique function of the degree of graphitization, as is shown in Fig. 8, becomes one measure of the rigidity of the crystallite linkage. Akamatu et al.[6] have found that such carbons as carbon black and graphitic carbon disperse into the colloidal state during the wet oxidation, whereas no colloidal dispersion occurs in the case of charcoal and pitch coke. It is shown that their conclusion is in good agreement with our experimental results given in Fig. 8.

Summary

The wet oxidation of three kinds of heat-treated graphitizing carbons, petroleum coke, anthracite and coal coke, in a solution of potassium dichromate in phosphoric acid has been studied in order to clarify the relationship between the chemical reactivity and the carbon structure.

Changes in the interlayer spacing and crystallite size, which are used as a measure of graphitization, have been examined by X-ray diffraction method for each specimen over the range of heat treatment temperatures from 1100 to 2800°C.

The oxidation velocity increases with the degree of graphitization. The quantity of carbon dioxide evolved, V, is generally expressed by the following equation, $V=at^b$. The *b*-value depends on only the degree of graphitization and varies from 0.8 to 1.5 according to the increase of graphitization, but it does not depend on the oxidation temperatures.

Research Laboratory
Nippon Carbide Industries Co., Inc.
Uozu, Toyama

*3-Aryl-2, 4-thiazolidindiones. New Local Anaesthetics. IV**

By Prithwi Nath BHARGAVA and Suresh Chandra SHARMA

(Received June 2, 1962)

In viw of close relationship between thiazolidones and thiazolidiones and reported uses of thiazolidone compounds as local anaesthetics*,[1,2], amoebacidal agents[3], and anticonvulsants[4], it was considered worthwhile to prepare 3-aryl-2, 4-thiazolidindiones under the conditions laid down by earlier workers[5-8]. The compounds having piperazino group connected to the heterocyclic nucleus as a lipophylic moiety confer greater activity and less toxicity than the benzene analogues[9-11].

3-Aryl-2, 4-thiazolidindiones have been obtained in good yields by interaction of *S*-diarylthiourea with monochloroacetic acid and glacial acetic acid. An amino group has been introduced at 5-position in the thiazolidindionyl nucleus at the reactive methylene group[12,13] through coupling[14] with benzenediazonium chloride and subsequent reduction[15,16] with sodium hydrosulfite. 5-Chloroacetyl-amino-3-aryl-2, 4-thiazolidindiones, prepared from the chloroacetyl chloride and respective 5-amino compounds, have been further condensed with piperazine to give the required piperazino-1, 4-bis(5-acetylamino-3-aryl-2, 4-thiazolidindiones). These bases have been converted into their hydrochlorides by the usual method.

These compounds have also been tested for the local anaesthetic activity by frog's sciatic plexus method[17] which has shown that the hydrochlorides of piperazino-1, 4-bis(5-chloroacetylamino-3-*p*-chlorophenyl-, -3-*m*-tolyl-, -3-*p*-tolyl-, -3-*p*-anisyl-, -3-*p*-phenetyl-2, 4-thiazolidindiones) have been found most effective local anaesthetics in this class of compounds.

Experimental

5-Phenylazo-3-phenyl-2, 4-thiazolidindione. — A solution of 5 g. of 3-phenyl-2, 4-thiazolidindione in 30 cc. of glacial acetic acid was slowly added to a solution of benzenediazonium chloride (prepared from 4 cc. of aniline), cooled with the freezing mixture at 0°C, with stirring and kept for an hour at 0~5°C. The precipitate formed was filtered, washed with water and dilute ethanol and crystallized from absolute ethanol, m. p. 122°C.

Similarly other thiazolidindiones were coupled with benzenediazonium chloride. Their properties and analytical data are recorded in Table I.

5-Amino-3-phenyl-2, 4-thiazolidindione. — A solution of 8 g. of sodium hydrosulfite in 20 cc. of water was added to the solution of 5 g. of azo compound dissolved in 20 cc. of ethanol. The product which separated, was filtered, washed with hot water and finally crystallized from absolute ethanol into a colorless form, m. p. 133°C.

Similarly, 5-amino derivatives of other 5-phenylazo-3-aryl-2, 4-thiazolidindiones were prepared. Their properties and analytical data are mentioned in Table II.

5-Chloroacetylamino-3-phenyl-2, 4-thiazolidindione.—Chloroacetyl chloride (0.5 cc.) and 5-amino compound (4 g.) were refluxed in 45 cc. of dry benzene for 2 hr. on a water bath at 70°C. Benzene and excess of chloroacetyl chloride were distilled off and the residue washed with the solution of sodium bicarbonate and water. The product was crystallized from absolute ethanol, m. p. 146°C.

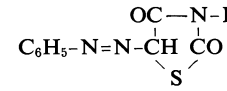
Chloroacetylamino derivatives of other 5-amino-3-aryl-2, 4-thiazolidindiones were prepared similarly and their properties and analytical data are shown in Table III.

Piperazino-1, 4-bis(5-acetylamino-3-phenyl-2, 4-thiazolidindione).—A mixture of 5.6 g. of 5-chloroacetylamino-3-phenyl-2, 4-thiazolidindione and 0.84 g. of piperazine in 40 cc. of absolute ethanol was refluxed on a water bath at 60°C for 4 hr. Ethanol was recovered by distillation and the residue subsequently washed with sodium bicarbonate solution and water. The product was crystallized from ethanol and recrystallized from benzene, m. p. 304°C.

* Part III of this series: P. N. Bhargava and S. C. Sharma, *J. Ind. Chem. Soc.*, **39**, 319 (1962).

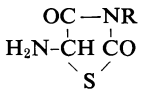
1) A. R. Surrey, *J. Am. Chem. Soc.*, **71**, 3105 (1949).
2) P. N. Bhargava and P. R. Singh, *J. Sci. & Ind. Res.*, **20c**, 209 (1961).
3) A. R. Surrey and R. A. Cutler, *J. Am. Chem. Soc.*, **76**, 758 (1954).
4) H. D. Troutman and L. M. Long, ibid., **70**, 3436 (1948).
5) K. S. Markley and E. E. Reid., ibid., **52**, 2137 (1930).
6) P. N. Bhargava and G. C. Goswami, *J. Ind. Chem. Soc.*, **32**, 763 (1955).
7) P. N. Bhargava, R. P. Rao and M. S. Sastry, ibid., **33**, 596 (1956).
8) P. N. Bhargava, A. J. Pantulu and R. P. Rao, ibid., **34**, 475 (1957).
9) P. N. Bhargava and M. G. R. Nair, ibid., **34**, 42 (1957).
10) I. S. Gupta, M. K. Shah and K. N. Gaind, ibid., **31**, 845 (1954).
11) A. M. Mattocks and O. S. Hutchinson, *J. Am. Chem. Soc.*, **70**, 3474 (1948).
12) M. T. Bogert and M. Chertcoff, ibid., **46**, 2864 (1924).
13) M. T. Bogert and M. Chertcoff, *Proc. Nat. Acad. Sci.*, **10**, 418 (1924).
14) P. N. Bhargava and M. Nagabhusanam, *J. Ind. Chem. Soc.*, **34**, 776 (1957).
15) E. Grandmougin, *J. Prakt. Chem.*, **76**(2), 124 (1907).
16) B. K. Patnaik and M. K. Rout, *J. Ind. Chem. Soc.*, **32**, 563 (1955).
17) E. Bülbring and I. Wajda, *J. Pharmacol.*, **85**, 78 (1945).

TABLE I. 5-PHENYLAZO-3-ARYL-2,4-THIAZOLIDINDIONES



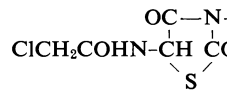
R	Yield %	M. p. °C	Molecular formula	N, % Found	N, % Calcd.	S, % Found	S, % Calcd.
Phenyl-	60	122	$C_{15}H_{11}N_3O_2S$	14.03	14.14	10.82	10.77
p-Chlorophenyl-	53	137	$C_{15}H_{10}N_3O_2SCl$	15.56	12.67	9.69	9.65
o-Tolyl-	45	150	$C_{16}H_{13}N_3O_2S$	13.35	13.50	10.08	10.29
m-Tolyl-	50	89	$C_{16}H_{13}N_3O_2S$	13.31	13.50	10.21	10.29
p-Tolyl-	59	148	$C_{16}H_{13}N_3O_2S$	13.40	13.50	10.17	10.29
o-Anisyl-	41	107	$C_{16}H_{13}N_3O_3S$	12.69	12.84	9.74	9.79
p-Anisyl-	39	111	$C_{16}H_{13}N_3O_3S$	12.72	12.84	9.78	9.79
p-Phenetyl-	57	98	$C_{17}H_{15}N_3O_3S$	12.17	12.32	9.42	9.38

TABLE II. 5-AMINO-3-ARYL-2,4-THIAZOLIDINDIONES



R	Yield %	M. p. °C	Molecular formula	N, % Found	N, % Calcd.	S, % Found	S, % Calcd.
Phenyl-	40	133	$C_9H_8N_2O_2S$	13.29	13.46	15.41	15.38
p-Chlorophenyl-	49	131	$C_9H_7N_2O_2SCl$	11.47	11.55	13.12	13.19
o-Tolyl-	39	156	$C_{10}H_{10}N_2O_2S$	12.53	12.61	14.29	14.41
m-Tolyl-	32	91	$C_{10}H_{10}N_2O_2S$	12.45	12.61	14.33	14.41
p-Tolyl-	50	157	$C_{10}H_{10}N_2O_2S$	12.42	12.61	14.44	14.41
o-Anisyl-	43	90	$C_{10}H_{10}N_2O_3S$	11.64	11.76	13.51	13.45
p-Anisyl-	55	117	$C_{10}H_{10}N_2O_3S$	11.61	11.76	13.38	13.45
p-Phenetyl-	40	102	$C_{11}H_{12}N_2O_3S$	11.08	11.11	12.47	12.50

TABLE III. 5-CHLOROACETYLAMINO-3-ARYL-2,4-THIAZOLIDINDIONES



R	Yield %	M. p. °C	Molecular formula	N, % Found	N, % Calcd.	S, % Found	S, % Calcd.
Phenyl-	75	146	$C_{11}H_9N_2O_3SCl$	9.66	9.84	11.32	11.29
p-Chlorophenyl-	62	148	$C_{11}H_8N_2O_3SCl_2$	8.71	8.78	10.11	10.06
o-Tolyl-	59	158	$C_{12}H_{11}N_2O_3SCl$	9.27	9.38	10.74	10.76
m-Tolyl-	78	157	$C_{12}H_{11}N_2O_3SCl$	9.25	9.38	10.85	10.76
p-Tolyl-	51	160	$C_{12}H_{11}N_2O_3SCl$	9.28	9.38	10.81	10.76
o-Anisyl-	76	103	$C_{12}H_{11}N_2O_4SCl$	8.82	8.90	10.09	10.21
p-Anisyl-	53	113	$C_{12}H_{11}N_2O_4SCl$	8.79	8.90	10.16	10.21
p-Phenetyl-	49	101	$C_{13}H_{13}N_2O_4SCl$	8.41	8.52	9.73	9.77

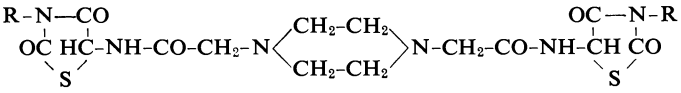
The hydrochloride of the base was prepared by dissolving in dry ether and passing into it dry hydrochloric acid gas. The mass was crystallized from absolute ethanol, m. p. 305°C.

The properties and analytical data of the piperazino derivatives and hydrochlorides of the bases prepared similarly from other 5-chloroacetylamino compounds are reported in Tables IV and V respectively.

Pharmacological Screening.—Adopting the procedure of Bülbring and Wajda[17], the local anaesthetic activity of these hydrochlorides was tested on frogs and the time of onset of anaesthesia i. e. the time for which a given concentration (0.1%) of the local anaesthetic failed to provoke withdrawal of feet is also recorded in Table V.

Pharmacological screening of these compounds

TABLE IV. PIPERAZINO-1,4-BIS(5-ACETYLAMINO-3-ARYL-2,4-THIAZOLIDINDIONES)



R	Yield %	M. p. °C	Molecular formula	N, % Found	N, % Calcd.	S, % Found	S, % Calcd.
Phenyl-	57	304	$C_{26}H_{26}N_6O_6S_2$	14.32	14.43	11.07	10.99
p-Chlorophenyl-	69	311	$C_{26}H_{24}N_6O_6S_2Cl_2$	12.81	12.90	9.94	9.83
o-Tolyl-	54	135	$C_{28}H_{30}N_6O_6S_2$	13.63	13.77	10.53	10.49
m-Tolyl-	62	174	$C_{28}H_{30}N_6O_6S_2$	13.68	13.77	10.46	10.49
p-Tolyl-	59	273	$C_{28}H_{30}N_6O_6S_2$	13.71	13.77	10.51	10.49
o-Anisyl-	71	168	$C_{28}H_{30}N_6O_8S_2$	13.00	13.08	9.86	9.97
p-Anisyl-	70	99	$C_{28}H_{30}N_6O_8S_2$	12.94	13.08	9.92	9.97
p-Rhenetyl-	58	95	$C_{30}H_{34}N_6O_8S_2$	12.45	12.54	9.63	9.55

TABIE V. HYDROCHLORIDES OF PIPERAZINO-1,4-BIS(5-ACETYLAMINO-3-ARYL-2,4-THIAZOLIDINDIONES) AND THEIR LOCAL ANAESTHETIC ACTIVITY

R	M. p. °C	Molecular formula	N, % Found	N, % Calcd.	Onset of anaesthesis (min.) with administration of anaesthetic* in hydrochloric acid of strength 0.05 N	0.1 N	0.2 N
Phenyl-	305	$C_{26}H_{26}N_6O_6S_2 \cdot 2HCl$	12.72	12.82	22.0	23.0	23.5
p-Chlorophenyl-	313	$C_{26}H_{24}N_6O_6S_2Cl_2 \cdot 2HCl$	11.41	11.60	14.5	15.0	16.0
o-Tolyl-	145	$C_{28}H_{30}N_6O_6S_2 \cdot 2HCl$	12.17	12.30	15.0	16.5	17.5
m-Tolyl-	183	$C_{28}H_{30}N_6O_6S_2 \cdot 2HCl$	12.23	12.30	8.5	9.5	10.0
p-Tolyl-	278	$C_{28}H_{30}N_6O_6S_2 \cdot 2HCl$	12.19	12.30	11.0	12.0	12.5
o-Anisyl-	185	$C_{28}H_{30}N_6O_8S_2 \cdot 2HCl$	11.61	11.75	13.5	15.5	17.0
p-Anisyl-	168	$C_{28}H_{30}N_6O_8S_2 \cdot 2HCl$	11.68	11.75	10.5	11.5	12.0
p-Phenetyl-	162	$C_{30}H_{34}N_6O_8S_2 \cdot 2HCl$	11.22	11.31	11.5	12.0	13.0
Procaine hydrochloride**					16.0	17.0	17.5

* Concn. of anaesthetic, 0.1%

** Procaine hydrochloride was used as such.

has shown that the hydrochlorides of piperazino-1,4-bis(5-acetylamino-3-*p*-chlorophenyl-, -3-*m*-tolyl-, -3-*p*-tolyl-, -3-*p*-anisyl-, -3-*p*-phenetyl-2,4-thiazolidindiones) were the most potent local anaesthetics amongst the compounds reported, as they required less time for the onset of anaesthesia than the standard substance, procaine hydrochloride, at 0.1% concentration in 0.7% of saline solution.

Thanks are due to Professor Gurbakhsh Singh, Head of the Department of Chemistry and other authorities of Banaras Hindu University for providing necessary facilities and also to the Council of Scientific and Industrial Research, New Delhi, India, for the award of a Junior Research Fellowship to one of us (S. C. S.).

Department of Chemistry
College of Science
Banaras Hindu University
Varanasi, India

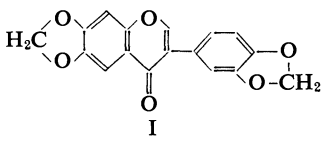
Synthesis of Maxima Substance B

By Kenji FUKUI, Mitsuru NAKAYAMA and Masayuki HATANAKA

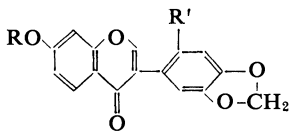
(Received June 18, 1962)

In 1954 Rangaswami and Sastry reported the isolation of three colorless substances from the roots of *Tephrosia maxima* Aers[1]. The substances were called maxima substance A, B and C[1], and later were assigned as isoflavones[2-4]. Degradative work with three crystalline, which shows that they all have the same isoflavone skeletons including the methylenedioxy group, has led to the following structures being proposed for them, maxima substance A (I)[2], B (II)[3] and C (III)[4].

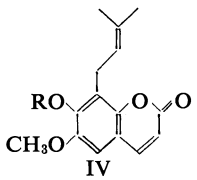
Maxima substance B was of interest as it is one of the naturally occuring γ,γ-dimethylallylethers of chromone derivatives. These ethers have been isolated and known as maxima substance C (III)[4], brayleyanin (IV)[5] and 5-hydroxy-4'-γ,γ-dimethylallyloxy-3',7-dimethoxyflavanone (V)[6]. None of these substances has so far been synthesized. We were led by our interest in the oxygen heterocyclics synthesis to attempt their synthesis and our initial aim was to prepare maxima substance B.



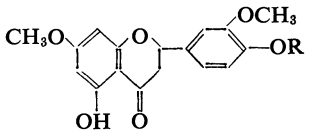
I



II; R', H
III; R', OCH_3



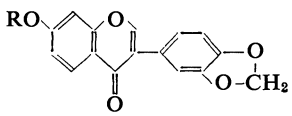
IV



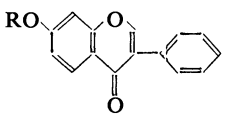
V

For II—V; R, $\begin{matrix}CH_3\\CH_3\end{matrix}\!\!>\!C{=}CH{-}CH_2$

In the present communication, we now record the synthesis of maxima substance B and related compounds. A key intermediate in our proposed synthesis was pseudobaptigenin (VI), an isoflavone which has been obtained by Späth and Schmidt[7] and synthesized by Späth[8], Venkataraman[9], Baker[10-11] and Farkas[12-13]. The reaction of pseudobaptigenin (VI), which was prepared by the Farkas' method[13], and γ,γ-dimethylallylbromide[14] with potassium carbonate gave an ether in good yield. It formed colorless needles, having an empirical formula of $C_{21}H_{18}O_5$, m. p. 134~135°C.



II; R, $\begin{matrix}CH_3\\CH_3\end{matrix}\!\!>\!C{=}CH{-}CH_2$
VI; R, H
VII; R, $\begin{matrix}CH_3\\CH_3\end{matrix}\!\!>\!CH{-}CH_2{-}CH_2$



VIII; R, $\begin{matrix}CH_3\\CH_3\end{matrix}\!\!>\!C{=}CH{-}CH_2$
X; R, H
IX; R, $\begin{matrix}CH_3\\CH_3\end{matrix}\!\!>\!CH{-}CH_2{-}CH_2$

Cleavage of an etheral linkage with sulfuric acid in acetic acid took place smoothly to give pseudobaptigenin (VI), m. p. 288~290°C, which was used as a key intermediate. Hydrogenation

1) S. Rangaswami and B. V. Rama Sastry, *Current Sci. (India)*, **23**, 397 (1954): *Chem. Abstr.*, **49**, 8568 (1955).
2) S. Rangaswami and B. V. Rama Sastry, *Proc. Indian Acad. Sci.*, **44A**, 279 (1956): *Chem. Abstr.*, **51**, 8083 (1957).
3) S. Rangaswami and B. V. Rama Sastry, *Current Sci. (India)*, **24**, 337 (1955): *Chem. Abstr.*, **50**, 13008 (1956).
4) S. Rangaswami and B. V. Rama Sastry, *Arch. Pharm.*, **292**, 170 (1959).
5) F. A. L. Anet, G. K. Hughes and E. Ritchie, *Australian J. Sci. Research*, **2A**, 608 (1949): *Chem. Abstr.*, **45**, 2938 (1951).
6) T. A. Geissman, *Australian J. Chem.*, **11**, 376 (1958): *Chem. Abstr.*, **53**, 1320 (1959).
7) E. Späth and O. Schmidt, *Monatsh. Chem.*, **53-54**, 454 (1929).
8) E. Späth and E. Lederer, *Ber.*, **63**, 743 (1930).
9) H. S. Mahal, H. S. Rai and K. Venkataraman, *J. Chem. Soc.*, **1934**, 1769.
10) W. Baker, R. Robinson and N. M. Simpson, ibid., **1937**, 805.
11) W. Baker, J. Chadderton, J. B. Harborne and W. D. Ollis, ibid., **1953**, 1852.

of the ether in the presence of platinum oxide catalyst in acetic acid afforded a dihydrocompound, m. p. 138~139°C, after one mole of hydrogen was absorbed. Pseudobaptigenin (VI) and isoamylbromide with potassium carbonate gave the 7-isoamyloxypseudobaptigenin (VII), m. p. 139~140°C, which was identical with the above dihydrocompound as shown by the infrared spectrum and the mixed melting point determination. It was shown to have structure II of the ether. The ether II was identical with the natural substance in the mixed melting point determination by Rangaswami. The structure assigned to maxima substance B has, therefore, been fully confirmed. The infrared and ultraviolet spectra of II and VII were shown in Figs. 1 and 2.

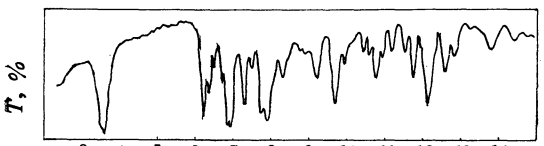


Fig. 1a. Infrared spectrum of maxima substancce B (II) (Nujol).

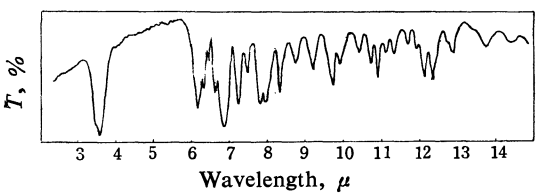


Fig. 1b. Infrared spectrum of 7-isoamyloxypseudobaptigenin (VII) (Nujol).

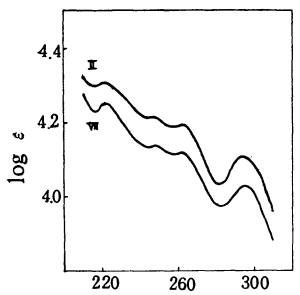


Fig. 2. Ultraviolet spectra of maxima substance B (II) and 7-isoamyloxypseudobaptigenin (VII).

By model experiment with a simple analogue, 7-γ, γ-dimethylallyloxyisoflavone (VIII) and 7-isoamyloxyisoflavone (IX), respectively m. p. 157~158°C and 149~150°C, were obtained from 7-hydroxyisoflavone (X)[15].

Experimental*

Maxima Substance B (7-γ, γ-Dimethylallyloxypseudobaptigenin) (II).—To a solution of pseudobaptigenin[13] (VI, m. p. 288~290°C, 1.0 g.) and γ, γ-dimethylallylbromide[14] (1.1 g.) in anhydrous acetone (250 ml.) was added anhydrous potassium carbonate (5.0 g.), and the mixture was refluxed for 20 hr. in a steam bath. The resulting mixture was filtered from precipitates and the solvent was distilled off. The residual product was recrystallized from ethanol to give II in the form of colorless needles, m. p. 134~135°C; yield 0.9 g. (75%). The natural substance is m. p. 126~128°C[1]. This substance showed no depression of the meltint point on admixture with the natural specimen by Rangaswami.

Found; C, 71.85; H, 5.23. Calcd. for $C_{21}H_{18}O_5$: C, 71.99; H, 5.18%.

UV λ_{max}^{EtOH} mμ (log ε): 222 (4.32), 249 (4.21), 264 (4.19), 295 (4.12).

7-Isoamyloxypseudobaptigenin (VII).—*a) From II.*—The mixture of maxima substance B (II) (300 mg.) and platinum oxide (50 mg.) in glacial acetic acid (80 ml.) was shaken in the atmosphere of hydrogen until 1.2 mol. of hydrogen was absorbed. After separation of the catalyst, the filtrate was evaporated under reduced pressure. The residual product was recystallized from ethanol to give VII in the form of colorless needles, m. p. 138~139°C; yield 150 mg. (50%).

b) From VI.—By a similar method as described for II, VII was obtained from VI (1.5 g), isoamylbromide (2.0 g.), anhydrous potassium carbonate (5.0 g.) and acetone (150 ml.); colorless needles, m. p. 139~140°C; yield 1.5 g. (76%). This substance showed no depression of the melting point on admixture with the specimen derived by the above-mentioned method a).

Found: C, 71.77; H, 5.76. Calcd. for $C_{21}H_{20}O_5$: C, 71.58; H, 5.72%.

UV λ_{max}^{EtOH} mμ (log ε): 223 (4.26), 249 (4.14), 261 (4.12), 295 (4.04).

Degradation of Maxima Substance B (II).—To maxima substance B (II) (2.0 g.) in acetic acid (100 ml.) was added concentrate sulfuric acid (1 ml.). After standing of the mixture for two days at room temperature, the solids appeared and were collected by filtration. The product was recrystallized from ethanol to give VI in the form of colorless microcrystals, m. p. 288~290°C; yield 1.4 g. (86%). Reported m. p. is 296°C[13].

Acetate of VI was prepared quantitatively by refluxing VI and acetic anhydride with anhydrous sodium acetate, m. p. 175~175.5°C. Reported m. p. is 176°C[13].

12) L. Farkas, A. Major, L. Pallos and J. Várady, *Chem. Ber.*, **91**, 2858 (1958).
13) L. Farkas and V. Szánthó, *Acta Chim. Acad. Sci. Hung.*, **19**, 217 (1959): *Chem. Abstr.*, **54**, 3398 (1960).
14) A. Bolleter, K. Eiter and H. Schmidt, *Helv. Chim. Acta*, **34**, 186 (1951).
15) V. R. Sathe and K. Venkataraman, *Current Sci. (India)*, **18**, 378 (1949): *Chem. Abstr.*, **44**, 8916 (1950).
* All melting points are uncorrected.

These substances showed no depression of the melting point on admixture with the authentic specimens.

7-γ,γ-Dimethylallyloxyisoflavone (VIII).—By a similar method as described for II, VIII was obtained from 7-hydroxyisoflavone[15] (X, m. p. 211~212°C, 1.0 g.), γ,γ-dimethylallylbromide (1.3 g.), anhydrous potassium carbonate (2.5 g.) and acetone (100 ml.); colorless plates, m. p. 157~158°C; yield 0.9 g. (70%).

Found: C, 78.61; H, 5.95. Calcd. for $C_{20}H_{18}O_3$: C, 78.41; H, 5.92%.

7-Isoamyloxyisoflavone (IX).—By a similar method as described for II, IX was obtained from X (0.5 g.), isoamylbromide (0.7 g.), anhydrous potassium carbonate (2.0 g.) and acetone (50 ml.); colorless needles, m. p. 149~150°C; yield 0.6 g. (92%).

Found: C, 77.78; H, 6.62. Calcd. for $C_{20}H_{20}O_3$: C, 77.90; H, 6.54%.

We are grateful to Professor S. Rangaswami, Andhra University, India, for measurement of the mixed melting point with the natural substances and ours and to Professor Minoru Nakajima and Professor Tetsuo Mitsui, Kyoto University, for measurements of infrared spectroscopy and microanalysis. This work is being partially supported by the grant-in-aid for Scientific Research from the Ministry of Education.

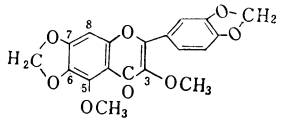
Department of Chemistry
Faculty of Science
Hiroshima University
Higashi-Sendamachi, Hiroshima

Synthetic Studies of the Flavone Derivatives. I. Syntheses of Some 3-Methoxy-6, 7-methylenedioxyflavones

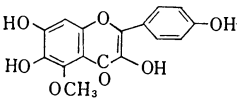
By Kenji FUKUI and Takashi MATSUMOTO

(Received July 6, 1962)

There have been only a few investigations of flavones which possess a methylenedioxy group in the chromone nucleus. Meliternatin (3, 5-dimethoxy-6, 7; 3', 4'-bismethylenedioxyflavone) (I) and wharangin have been isolated from the bark of *Melicope ternata*[1] and *M. mantelli*[2]. 3, 4'-Dihydroxy-5-methoxy-6, 7-methylenedioxyflavone have been obtained from naturally occurring vogoletin (3, 6, 7, 4'-tetrahydroxy-5-methoxyflavone) (II)[3]. 7, 8-Methylenedioxyflavone, 6, 7-methylenedioxyflavone and 3', 4'-dimethoxy-6,7-methylenedioxyflavone have been synthesized[4-5]. However, 3-methoxy-6, 7-methylenedioxyflavone derivatives and 3, 5-dimethoxy-6, 7-methylenedioxyflavone derivatives have not yet been synthesized.



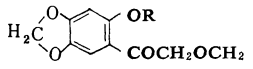
(I)



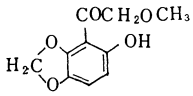
(II)

In the present paper, the syntheses of 3-methoxy-6, 7-methylenedioxyflavone (VIII) and its analogues are described. The Hoesch reaction of sesamol (3, 4-methylenedioxyphenol) and methoxyacetonitrile yielded a ketone, $C_{10}H_{10}O_5$ (m. p., 136~138°C). At this stage, the reaction could give either 2-hydroxy-4, 5-methylenedioxy-ω-methoxyacetophenone (III) or 2-hydroxy-5, 6-methylenedioxy-ω-methoxyacetophenone (VI). The oxidation of the ω-methoxyacetophenone to a benzoic acid derivative was used to settle this question. The ketone was methylated to monomethyl ether (m. p., 99~100°C), which was then converted into 2-methoxy-4, 5-methylenedioxybenzoic acid (VII)[6-7] by potassium permanganate oxidation. The acid VII was identified by direct comparison with an authentic sample. From this fact, the structure of 2-hydroxy-4, 5-methylenedioxy-ω-methoxyacetophenone (III) was established for the ketone.

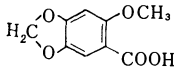
1) L. H. Briggs and R. H. Locker, *J. Chem. Soc.*, **1949**, 2157; **1951**, 3131.
2) R. C. Cambie, ibid., **1960**, 2376.
3) S. Rangaswami and K. H. Rao, *Proc. Indian Acad. Sci.*, **49A**, 241 (1959).
4) K. Viswesware Rao and N. Viswanadham, ibid., **29A**, 218 (1949).
5) A. Romeo and G. Bargellini, *Ann. Chim. (Rome)*, **42**, 361 (1952): *Chem. Abstr.*, **47**, 10529e (1953).
6) R. T. Arnold and N. Bortnick, *J. Am. Chem. Soc.*, **67**, 1798 (1945).
7) K. N. Campbell, P. F. Hopper and B. K. Campbell, *J. Org. Chem.*, **16**, 1741 (1951).



(III) R=H (IV) R=Ac
(V) R=CH_3



(VI)



(VII)

According to Allan and Robinson's flavone synthesis[8], the condensation of the ketone III with benzoic anhydride in the presence of potassium benzoate, followed by treatment with alcoholic potassium hydroxide, afforded 3-methoxy-6, 7-methylenedioxyflavone (VIII) (m. p., 180.5~182.5°C). By a similar reaction, 3, 4'-dimethoxy-6, 7-methylenedioxyflavone (IX) (m. p., 238.5~239°C), 3, 3', 4'-trimethoxy-6, 7-methylenedioxyflavone (X) (m. p., 171~172°C), 3-methoxy-6, 7; 3', 4'-bismethylenedioxyflavone (XI) (m. p., 247~248°C), 3, 3', 4', 5'-tetramethoxy-6,7-methylenedioxyflavone (XII) (m. p., 224~225°C) and 3-methoxy-3', 4'-dibenzyloxy-6, 7-methylenedioxyflavone (XIII) (m. p., 123.5~125°C) were obtained. These compounds gave a negative ferric reaction and were soluble in concentrated sulfuric acid to a yellow solution. The debenzylation of XIII with hydrogen afforded 3-methoxy-3', 4'-dihydroxy-6, 7-methylenedioxy-flavone (XIV) (m. p., 293~295°C) (decomp.), which was then converted into 3, 3', 4'-trimethoxy-6, 7-methylenedioxyflavone (X) by methylation. The ultraviolet spectra of these compounds are shown in Figs. 1 and 2. In most cases there are two peaks, ca. 245 and ca. 335 mμ, but the absorption maxima of VIII and IX is observed ca. 255 mμ in addition to these two peaks.

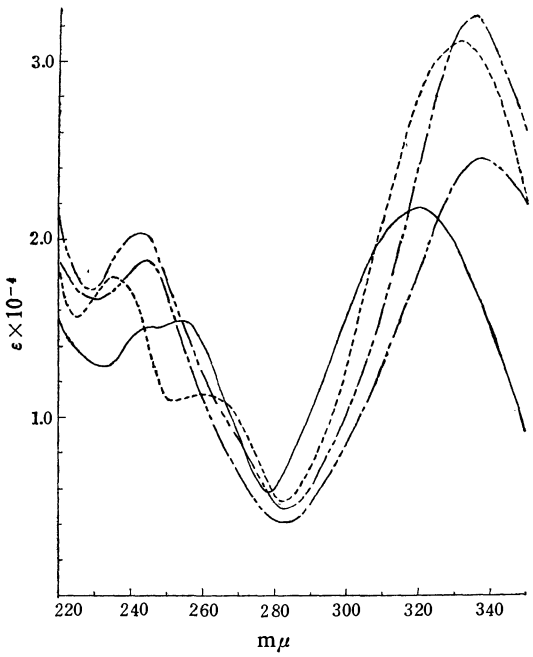


Fig. 1. Ultraviolet spectra of VIII (——), IX (----), X (– – –) and XI (–·–·–) in ethanol.

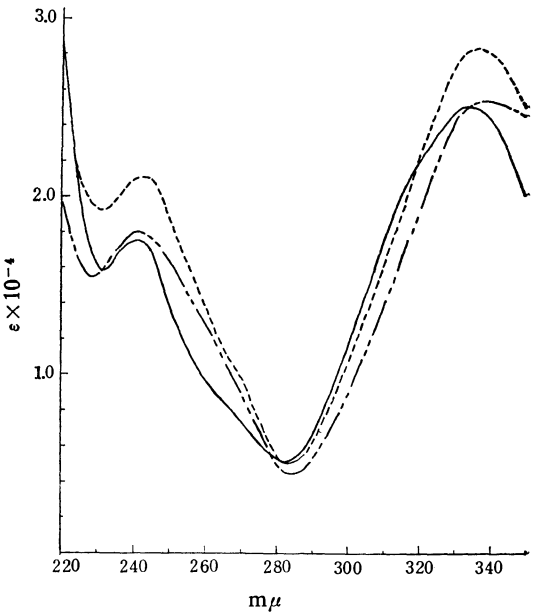
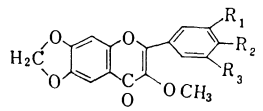


Fig. 2. Ultraviolet spectra of XII (——), XIII (----) and XIV (– – –) in ethanol.



(VIII) $R_1=R_2=R_3=H$
(IX) $R_1=R_3=H$ $R_2=OCH_3$
(X) $R_1=R_2=OCH_3$ $R_3=H$
(XI) R_1, $R_2=O-CH_2-O$ $R_3=H$
(XII) $R_1=R_2=R_3=OCH_3$
(XIII) $R_1=R_2=OCH_2C_6H_5$ $R_3=H$
(XIV) $R_1=R_2=OH$ $R_3=H$

Experimental*

2-Hydroxy-4, 5-methylenedioxy-ω-methoxyacetophenone (III).—A mixture of sesamol (3.1 g.),

8) J. Allan and R. Robinson, *J. Chem. Soc.*, **1924**, 2192.

* All melting points were uncorrected. The ultraviolet spectra were determined with a Shimadzu model SV-50A spectrophotometer, while the infrared spectra were determined with a Hilger model 800 spectrophotometer.

which had been obtained from piperonal by Baeyer-Villiger oxidation[9], methoxyacetonitrile (1.9 g.) and anhydrous zinc chloride (0.6 g.) in anhydrous ether (20 ml.) was saturated with dried hydrogen chloride in an ice-bath and allowed to stand overnight. The ether solution was decanted from the ketimine hydrochloride-zinc chloride complex which had separated. The residue was washed twice with dry ether and then heated on a steam bath with water (20 ml.) for 30 min. After this had cooled and stood, the precipitated ketone was collected. Recrystallization from ethanol gave colorless needles (m. p., 136~138°C) which gave a dark blue color with ferric chloride; yield, 1.2 g. (26%). IR 1636 (C=O), 1025 (=C-O-C), 915 cm^{-1} ($O-CH_2-O$) (Nujol).

Found: C, 57.17; H, 4.84. Calcd. for $C_{10}H_{10}O_5$: C, 57.14; H, 4.80%.

III was acetylated with acetic anhydride and pyridine. The acetate IV formed colorless needles from aqueous methanol (m. p., 87~89°C) which gave a negative ferric reaction. IR 1753, 1675 (C=O), 1028 (=C-O-C), 925 cm^{-1} ($O-CH_2-O$) (Nujol).

Found: C, 57.08; H, 4.79. Calcd. for $C_{12}H_{12}O_6$: C, 57.14; H, 4.80%.

2-Methoxy-4, 5-methylenedioxy-ω-methoxyacetophenone (V). — The ketone III (1.0 g.), dissolved in acetone (40 ml.), was heated under reflux with methyl iodide (1.0 g.) and anhydrous potassium carbonate (3.0 g.) for 6 hr. on a steam bath. The solution was then filtered and evaporated to dryness. The residue was collected, washed with a dilute alkaline solution and recrystallized from aqueous ethanol to give colorless needles (m. p., 99~100°C) which gave a negative ferric reaction; yield, 0.45 g. (42%). IR 1663 (C=O), 1030 (=C-O-C), 915 cm^{-1} ($O-CH_2-O$) (Nujol).

Found: C, 58.65; H, 5.36. Calcd. for $C_{11}H_{12}O_5$: C, 58.92; H, 5.40%.

2-Methoxy-4,5-methylenedioxybenzoic Acid (VII). —A suspension of 2-methoxy-4, 5-methylenedioxy-ω-methoxyacetophenone (V) (0.4 g.) in water (15 ml.) was treated under reflux with small portions of a 2% potassium permanganate solution until the consumption of the oxidant subsided. After the excess permanganate had been reduced with sodium bisulfite, the precipitate was separated by filtration and washed with hot water. The combined filtrates were acidified with dilute sulfuric acid and extracted with ethyl acetate. The organic layer was washed with water and dried over anhydrous sodium sulfate. The solvent was evaporated, and the residue was recrystallized from aqueous methanol to give pale yellow needles (m. p., 150~151°C) (reported 148~149°C[6] and 147~147.5°C[7]); yield, 0.1 g. Its identity with an authentic sample of 2-methoxy-4,5-methylenedioxybenzoic acid (VII) was established by mixed melting point determination and infrared spectral comparison. IR 1710, 1625 (C=O), 1026 (=C-O-C), 920 cm^{-1} ($O-CH_2-O$) (Nujol).

Found: C, 55.31; H, 4.10. Calcd. for $C_9H_8O_5$: C, 55.10; H, 4.11%.

3-Methoxy-6, 7-methylenedioxyflavone (VIII).— The ketone III (0.7 g.), benzoic anhydride (1.5 g.) and potassium benzoate (0.8 g.) were ground together and heated at 170~180°C under reduced pressure for 3 hr. The reaction mixture was ground and boiled with 8% aqueous alcoholic (1 : 4) potassium hydroxide (25 ml.) for 15 min. After the removal of the solvent in vacuo, water (60 ml.) was added to the pasty mass. The precipitated solid was collected, washed with water and recrystallized from ethanol to give colorless needles m. p., 180.5~182.5°C) which gave a negative ferric reaction and a yellow colored solution with concentrated sulfuric acid; yield, 0.35 g. (35%). IR 1618 (C=O), 1023 (=C-O-C), 928 cm^{-1} ($O-CH_2-O$) (Nujol). UV λ_{max}^{EtOH} mμ ($\varepsilon \times 10^{-4}$); 247** (1.51), 254 (1.55), 320 (2.18).

Found: C, 68.95; H, 4.07. Calcd. for $C_{17}H_{12}O_5$: C, 68.91; H, 4.08%.

3, 4'-Dimethoxy-6, 7-methylenedioxyflavone (IX). —A mixture of the ketone III (1.0 g.), anisic anhydride (2.8 g.) and potassium anisate (1.4 g.) was treated in a way similar to that used for VIII. Yield, 0.8 g. of colorless needles (m. p., 238.5~239°C) from acetic acid and then from ethyl acetate. This substance gave a negative ferric reaction and a yellow colored solution with concentrated sulfuric acid. IR 1629 (C=O), 1025 (=C-O-C), 928 cm^{-1} ($O-CH_2-O$) (Nujol). UV λ_{max}^{EtOH} mμ ($\varepsilon \times 10^{-4}$); 235 (1.80), 260 (1.14), 332 (3.12).

Found: C, 66.04; H, 4.15. Calcd. for $C_{18}H_{14}O_6$: C, 66.25; H, 4.32%.

3, 3', 4' - Trimethoxy - 6, 7 - methylenedioxyflavone (X).—From the ketone III (0.5 g.), veratric anhydride (1.7 g.) and potassium veratrate (0.8 g.), synthesis was carried out by a method similar to that used for VIII. Yield, 0.35 g. of pale yellow needles (m. p., 171~172°C) from ethanol. This substance gave a negative ferric reaction and showed a yellow color in a concentrated sulfuric acid solution. IR 1630 (C=O), 1020 (=C-O-C), 923 cm^{-1} ($O-CH_2-O$) (Nujol). UV λ_{max}^{EtOH} mμ ($\varepsilon \times 10^{-4}$); 243 (2.05), 336 (3.27).

Found: C, 64.31; H, 4.69. Calcd. for $C_{19}H_{16}O_7$: C, 64.04; H, 4.53%.

3-Methoxy-6, 7; 3', 4'-bismethylenedioxyflavone (XI). — From the ketone III (1.0 g.), piperonylic anhydride (3.9 g.) and potassium piperonylate (1.5 g.), synthesis was carried out by a method similar to that used for VIII. Yield, 0.56 g. of colorless needles (m. p., 247~248°C) from acetic acid. This substance gave a negative ferric reaction and showed a yellow color in a concentrated sulfuric acid solution. IR 1635 (C=O), 1025 (=C-O-C), 925 cm^{-1} ($O-CH_2-O$) (Nujol). UV λ_{max}^{EtOH} mμ ($\varepsilon \times 10^{-4}$); 244.5 (1.89), 337 (2.46).

Found: C, 63.54; H, 3.67. Calcd. for $C_{18}H_{12}O_7$: C, 63.53; H, 3.55%.

3, 3', 4', 5' - Tetramethoxy - 6, 7 - methylenedioxyflavone (XII). — From the ketone (III) (1.0 g.), trimethylgallic anhydride[10] (4.0 g.) and potassium trimethylgallate (1.9 g.), synthesis was carried out by a method similar to that used for VIII. Yield,

9) J. Böesken, W. D. Coden and C. J. Kip, *Rec. trav. Chim.*, **55**, 815 (1936): *Chem. Abstr.*, **31**, 1017 (1937).

** Inflexion point.

10) J. Kalff and R. Robinson, *J. Chem Soc.*, **1925**, 182.

11) M. Shimizu and G. Ohta, *J. Pharm. Soc. Japan*, **71**, 1485 (1951).

0.8 g. of pale yellow needles (m. p., 224~225°C) from acetone. This substance gave a negative ferric reaction and showed a yellow color in a concentrated sulfuric acid solution. IR 1628 (C=O), 1023 (=C-O-C), 930 cm^{-1} (O-CH_2-O) (Nujol). UV λ_{max}^{EtOH} mμ ($\varepsilon \times 10^{-4}$) ; 242 (1.76), 335 (2.50).

Found : C, 61.98 ; H, 4.61. Calcd. for $C_{20}H_{18}O_8$; C, 62.17 ; H, 4.70%.

3-Methoxy-3', 4'-dibenzyloxy-6,7-methylenedioxyflavone (XIII). — From the ketone III (1.0 g.), 3,4-dibenzyloxybenzoic anhydride[11] (6.5 g.) and potassium 3,4-dibenzyloxybenzoate (2.8 g.), synthesis was carried out by a method similar to that used for VIII. Yield, 1.0 g. of pale yellow needles (m. p., 123.5~125°C) from aqueous acetone and then from ethanol. This substance gave a negative ferric reaction and showed a yellow color in a concentrated sulfuric acid solution. IR 1610 (C=O), 1035 (=C-O-C), 943 cm^{-1} (O-CH_2-O) (Nujol). UV λ_{max}^{EtOH} mμ ($\varepsilon \times 10^{-4}$) ; 243 (2.11), 337 (2.83).

Found : C, 73.16 ; H, 4.83. Calcd. for $C_{31}H_{24}O_7$: C, 73.22 ; H, 4.76%.

3-Methoxy-3', 4'-dihydroxy-6, 7-methylenedioxyflavone (XIV). — A solution of 3-methoxy-3', 4'-dibenzyloxy-6,7-methylenedioxyflavone (XIII) (600 mg.) in acetic acid (30 ml.) was submitted to catalytic reduction in the presence of a 10% Pd-C catalyst (1.0 g.) at room temperature. The precipitate was collected and extracted with dilute aqueous sodium hydroxide. After the alkaline extract had been acidified with dilute sulfuric acid, the precipitate was collected, washed with water and recrystallized from ethanol to give yellow needles (m. p., 293~295°C) (decomp.) which gave a green color with ferric chloride ; yield, 170 mg. IR 1630 (C=O), 1028 (=C-O-C), 928 cm^{-1} (O-CH_2-O) (Nujol). UV λ_{max}^{EtOH} mμ ($\varepsilon \times 10^{-4}$) ; 242 (1.80), 338 (2.53).

Found : C, 61.99 ; H, 3.85. Calcd. for $C_{17}H_{12}O_7$: C, 62.20 ; H, 3.68%.

A solution of 3-methoxy-3', 4'-dihydroxy-6, 7-methylenedioxyflavone (XIV) (100 mg.) in acetone (50 ml.) was heated under reflux with methyl iodide (0.3 g.) and anhydrous potassium carbonate (0.5 g.) for 5 hr. The acetone solution was filtered and evaporated to dryness. The residue was washed with water and recrystallized from ethanol to give colorless needles (m. p., 171~172°C, undepressed on admixture with X).

Found : C, 64.00 ; H, 4.53. Calcd. for $C_{19}H_{16}O_7$: C, 64.04 ; H, 4.53%.

The authors wish to express their gratitude to the members of the Microanalytical Center of Kyoto University for their microanalyses. The cost of this research was partly defrayed by the Scientific Research Expenditure Fund of the Ministry of Education, to which the authors' thanks are due.

Department of Chemistry
Faculty of Science
Hiroshima University
Higashi-Sendamachi, Hiroshima

*The Mechanism of the Gelation of a Lead Aldose-cysteinate Solution**

By Fujio TAKAHASHI and Jun MIZUGUCHI

(Received July 6, 1962)

Previous papers have described studies of the properties of the gel and the structure of lead aldose-cysteinate[1]. On measuring the rigidity of the gel, the pH value of a lead glucose-cysteinate solution was found to vary with the lapse of time, as is shown in Table I. From this fact, it was suggested that the internal structure of a lead glucose-cysteinate solution, which appeared to be transparent initially, might also change with the lapse of time.

In this paper, the study of the mechanism of gelation deals with the measurement of such various developments as the pH value, the conductivity, the optical density, and the gelation time.

* Gelation of Lead Aldose-cysteinate: Part III.

1) F. Takahashi and J. Mizuguchi, This Bulletin 35, 1823 (1962).

Experimental

Materials.—All materials used are the same as have been described in the previous papers[1].

Apparatus.—The measurements of the pH value, the conductivity, and the optical density were carried out with a portable pH meter, a Yanagimoto conductometer, model MY-6, and an Erma Lippich Polarimeter respectively. The measurements of volume change were carried out with a 25 ml. pycnometer with an attached, graduated glass tube (0.0~0.1 ml.) shown in Fig. 1.

Procedure.—All the measurements were carried out from the time when a solution of lead salt was mixed with a solution of HSC at a constant temperature in the thermostats. The different pH value of the solution was adjusted by the addition of an appropriate amount of nitric acid or sodium hydroxide. Re-distilled water ($2.0\times10^5\ \Omega\cdot$cm.) was used for conductivity water measurements.

TABLE I. pH CHANGE

0.06 M NaGC, 0.03 M $Pb(CH_3COO)_2$ or $Pb(NO_3)_2$, appropriate amount of HNO_3 or NaOH. 25°C. Rigidity was measured after 3 hr. from the gelation time.

pH		The gelation time	Rigidity
Initial	Final (after gelation)	min.	g./cm²
3.6	3.3	Not form gel	—
4.2	3.3	5.5	65
4.8	3.5	4	140
5.2	3.7	5	200
5.5	4.4	8	260
6.0	5.3	9	300
6.8	6.6	8.5	150
7.6	7.5	10	75
8.0	8.5	5	70
8.4	8.7	3	125
9.2	9.9	4	155
10.0	10.3	10	125
10.7	10.6	1 day	55

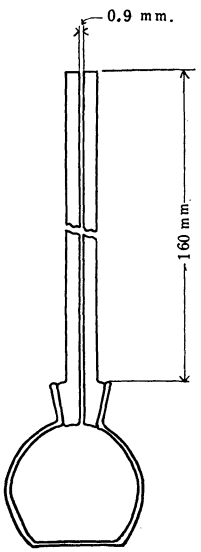


Fig. 1

All the measurements of the gelation time were carried out with test tubes in which a solution containing 0.15 to 2.5 ml. of 0.2 M NaGC** or 0.05 M NaGaC** and 0.15 to 2.5 ml. of 0.1 or 0.2 M lead acetate or nitrate was diluted to 5.0 ml. with distilled water. The mixtures were allowed to stand for a while. The time when a mixture lost fluidity was adopted as the gelation time.

Precipitates obtained in the pH Range between 8 and 10. — White precipitates were obtained when 10 ml. of 0.2 M lead acetate was added to a mixture of 10 ml. of 0.2 M NaGC and 30 ml. of 0.1 M sodium hydroxide. The precipitates were filtered and washed with a little amount of water and then with methanol as fast as possible for fear that precipitates might redissolved; yield, 0.40 g.

Found: C, 13.1; H, 2.1; N, 1.6; ash, 71.2%.

Results

pH Value. — In the pH range below 8, the lower the initial pH value, the more this pH

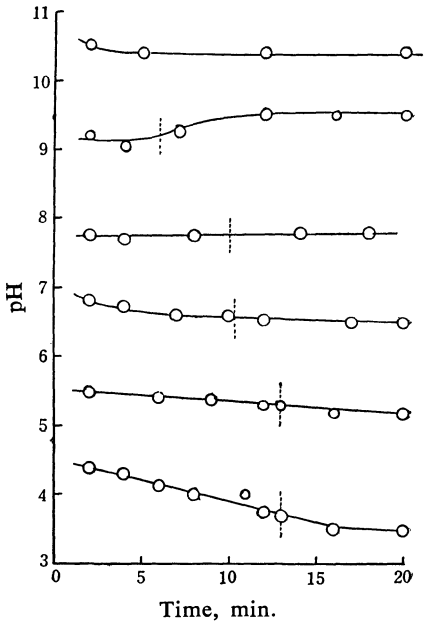


Fig. 2. pH change.
0.04 M NaGC, 0.04 M lead salt
The sign ⋮ denotes the gelation time.

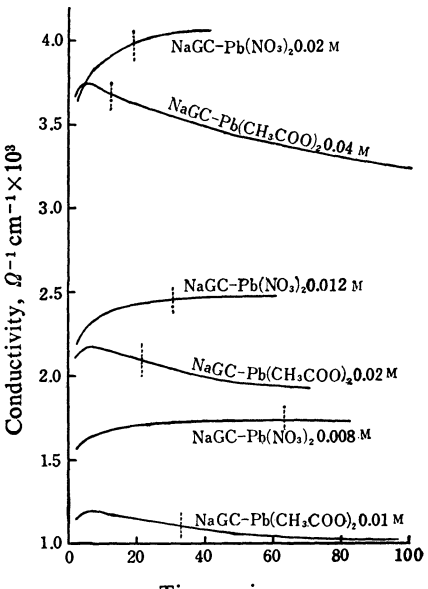


Fig. 3. Conductivity change.
The sign ⋮ denotes the gelation time.
25°C.

** See This Bulletin 35, 1819 (1962).

value gradually decreased with the lapse of time. In the pH range between 8 and 10, white precipitates were obtained. These precipitates were gradually redissolved with the rise of the pH value. The results are shown in Fig. 2.

From the analytical results, the precipitates were found to be neither pure lead glucose-cysteinates, the lead content of which is less than 41%, nor pure lead hydroxide. It is seen that the precipitates presumably consist of lead hydroxide and lead glucose-cysteinate co-precipitated.

Conductivity and Optical Density.—The conductivity of the mixture of NaGC and lead acetate gradually. In the mixture of NaGC and lead nitrate, the conductivity increased initially and then stayed constant (Fig. 3).

The mutarotation toward dextrorotary occurred in every case. Optical rotation could not determined after gelation (Fig. 4).

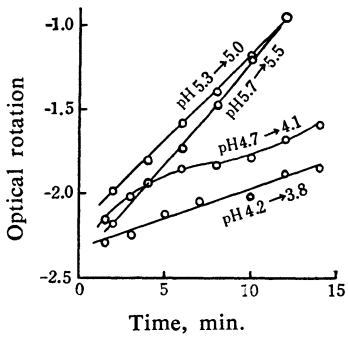


Fig. 4. Optical rotation change.
0.04 M NaGC, 0.04 M lead salt.
4 dm. tube, 20~24°C.

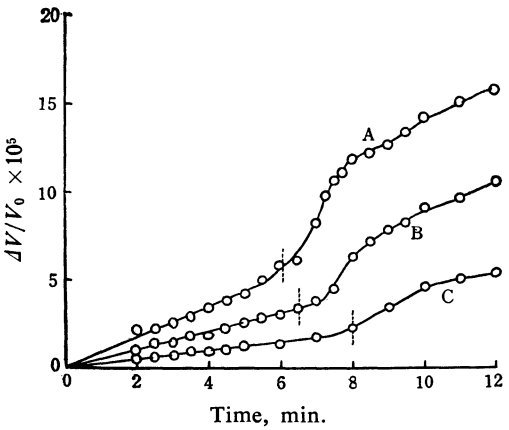


Fig. 5. Volume change. 20°C
The sign : denotes the gelation time.

	NaGC	$Pb(CH_3COO)_2$
A	0.50 M	0.50 M
B	0.33 M	0.33 M
C	0.20 M	0.20 M

Volume Change.—In the case of the mixture of NaGC and lead acetate, the volume of the mixture increased proportionally with the lapse of time before gelation. The rate of increase of the volume rose remarkably after gelation. After about an hour, however, the rate of increase slowed down. The results are shown in Fig. 5.

In the case of the mixture of NaGC and lead nitrate, the increase also occurs, but it was not proportional to the lapse of time.

The Gelation Time.—In every case, the gelation time was proportional to the reciprocal

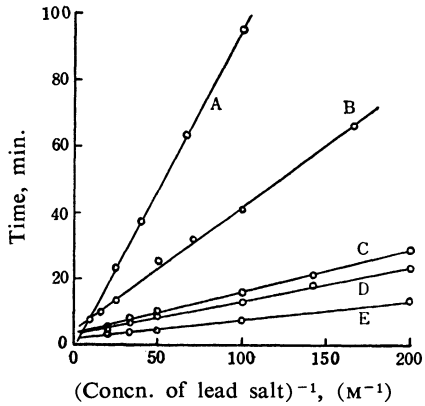


Fig. 6. Effect of concentration on the gelation time.
A NaG_aC : $Pb(CH_3COO)_2$=1 : 1, 25°C
B NaGC : $Pb(CH_3COO)_2$=1 : 1, 25°C
C NaGC : $Pb(CH_3COO)_2$=2 : 1, 25°C
D NaGC : $Pb(NO_3)_2$=2 : 1, 25°C
E NaGC : $Pb(CH_3COO)_2$=2 : 1, 35°C

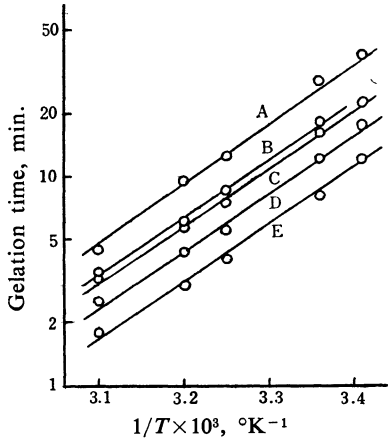
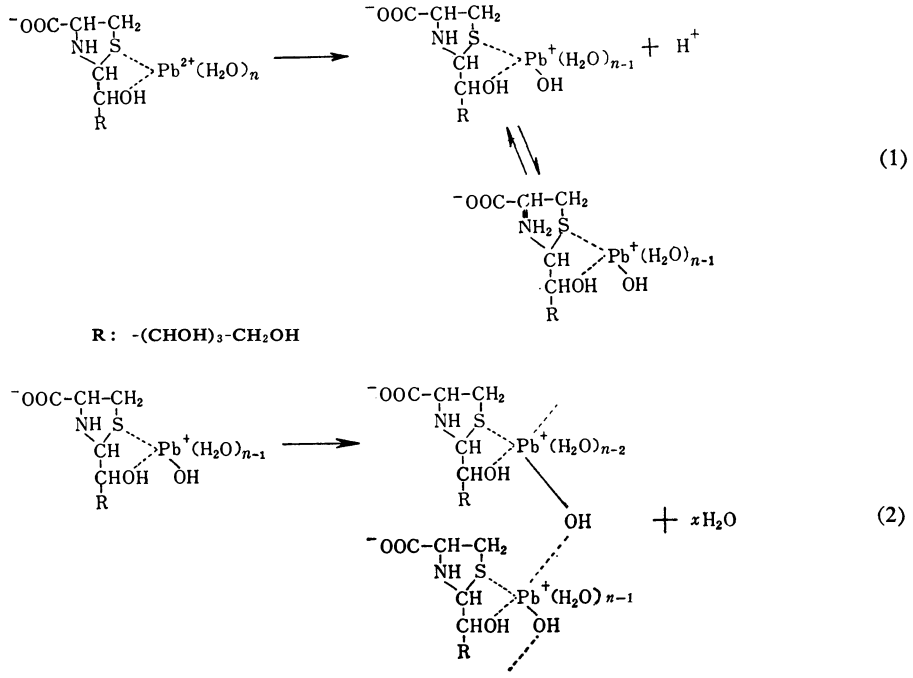


Fig. 7. Effect of temperature on the gelation time.

	NaGC	$Pb(CH_3COO)_2$
A	0.03 M	0.06 M
B	0.03 M	0.03 M
C	0.02 M	0.01 M
D	0.03 M	0.01 M
E	0.06 M	0.03 M



(1)

R: $-(CHOH)_3-CH_2OH$

(2)

of the concentration of lead salt (Fig. 6). Regarding temperatures between 20 to 50°C, straight lines are given in Fig. 7.

Discussion

In the previous paper[1], Eq. 1 was assumed from the fact that lead glucose-cysteinate hydroxide was isolated from the solution of NaGC and lead acetate.

The "ol" structure has been proposed by Hall and Eyring[2], who have studied the conductance of chromic salts in solution. It can be assumed that the "olation" of lead glucose-cysteinate occurs by the same mechanism as that of the hexaaquo chromic ion. Accordingly, the complex ion of hydrated lead glucose-cysteinate may be transformed into an "ol" structure with dehydration (Eq. 2). Perhaps the gelation occurs when an infinite three-dimensional structure is formed by olation.

The "olated" lead glucose-cysteinate so formed has to be removed from the system of an equilibrium state. Equation 1 may transfer to the right side in the pH value range between 3.8 and 8, and the concentration of protons may increase. In the pH value range between 8 and 10, the pH value of the solution may rise because of a reaction as is shown in the following equation:

$$Pb(OH)_2 + GC^- \rightarrow PbGCOH + OH^- \quad (3)$$

In the solution containing NaGC and lead acetate, the acetate ion shows the buffer action against the proton liberated by the olation:

$$CH_3COO^- + H^+ \rightleftharpoons CH_3COOH \quad (4)$$

In the solution containing NaGC and lead nitrate, the nitrate ion does not show any buffer action, so that the pH value of the solution may vary downward because of the liberation of the proton.

It is presumably seen that the optical rotation varies also because the olation occurs.

To verify the above assumptions, the kinetics of gelation was studied by determining the gelation time. The olation of the complex ion of hydrated lead glucose-cysteinate, accompanied with dehydration, was considered to be a process which follows the laws of ordinary chemical reaction. The reaction of the intermolecular combination is of the second order. Therefore, this reaction was expressed as follows:

$$-dC/dt = kC^2 \quad (5)$$

where C is the concentration against the time, t, of the complex ion of lead glucose-cysteinate not "olated"; k is the velocity constant. From 5 and Arrhenius' equation, $k = A \cdot e^{-\Delta E/RT}$, Eq. 6 was derived:

$$-(1/C_0)\cdot(C_0/C-1) = Kt\cdot e^{-\Delta E/RT} \quad (6)$$

where C_0 is the initial concentration of the complex ions of lead glucose-cysteinate and K is constant. This equation has already been

2) H. T. Hall and H. Eyring, *J. Am. Chem. Soc.*, 72, 782 (1950).

reported by Hurd and Letteron[3]. They permitted themselves to make an assumption in which C_0/C was constant. Therefore, the following equation was derived:

$$1/C_0 = K't \cdot e^{-\Delta E/RT} \quad (7)$$

where K' is constant. The experimental results were found to obey Eq. 7.

It has been known that the volume occupied by a molecule of free water is larger than that occupied by one of bound water[4]. Therefore, it can be suggested that the dehydration makes for a volume increase of the solution and that the rate of olation is parallel to the amount of volume increase. Regarding the gelation time, the concentration of olated lead glucose-cysteinate, C_0-C, is parallel to the ratio of the volume increase to the initial volume; that is,

$$C_0 - C = B(\Delta V_t/V_0) \quad (8)$$

where B is constant, ΔV_t is the amount of volume increase at the gelation time, and V_0 is the initial volume. Both sides of Eq. 8 may be divided by C_0. Therefore,

$$1 - C/C_0 = B(\Delta V_t/V_0)/C_0 \quad (9)$$

The $(\Delta V_t/V_0)/C_0$ calculated from the data of Fig. 5 shows almost constant values (Table II).

TABLE II. VOLUME CHANGE

Concn. of lead aldose-cysteinate C_0, M	$\frac{\Delta V_t}{V_0}$	$\frac{\Delta V_t}{V_0} \cdot \frac{1}{C_0}$
0.50	5.7×10^{-4}	$1.1_4\times10^{-3}$
0.33	3.4×10^{-4}	$1.0_3\times10^{-3}$
0.20	2.1×10^{-4}	$1.0_5\times10^{-3}$

3) C. B. Hurd and H. A. Letteron, *J. Phys. Chem.*, **36**, 604 (1932).
4) T. Yasunaga and T. Sasaki, *J. Chem. Soc. Japan, Pure Chem. Sec.* (*Nippon Kagaku Zassi*), **70**, 379 (1949).

The assumptions concerning the mechanism of gelation seem to have been verified by the determination of the gelation time.

Summary

The mechanism of the gelation of a solution containing aldose-cysteine and lead salt was studied by measuring various developments such as the pH value, the conductivity, the optical density, and the gelation time. From these results, it was suggested that the gelation occurred when the complex ion of hydrated lead glucose-cysteinate was transformed into an "ol" structure with dehydration. The process of this olation was found to follow the laws of ordinary chemical reaction. The reaction was of the second order.

The authors wish to express their sincere thanks to Professor Ikuzo Tanaka, Professor Kunio Kojima, Professor Koemon Funaki and Dr. Hiroshi Kobayashi of Tokyo Institute of Technology, and Director Kiyoshi Morikawa of the Research Laboratory of Resources Utilization, Tokyo Institute of Technology, for their invaluable advice on the structure of lead aldose-cysteinates and the mechnism of gelation. The authors are also indebted to Dr. Shoji Matsumoto of Tanabe Pharmaceutical Co., Ltd., who has provided facilities for elementary and infrared spectra analyses, and to Mr. Kaoru Matsuzaki and Miss Satoko Miyashita for their assistance in the experiments.

Research Laboratory of Resources Utilization
Tokyo Institute of Technology
Meguro-ku, Tokyo

Thermometric Studies on the Reaction between Silver Nitrate and Sodium Thiosulfate

By Mahendra Singh BHADRAVER

(Received June 19, 1962)

Thermometric titrations between silver nitrate and sodium thiosulfate with varying concentrations of two salts in solution were performed. Reactions are indicated when Ag^+ and $S_2O_3^{2-}$ ions are present in solution in the molar ratio of 1 : 2, 1 : 1, 3 : 4 and 2 : 1 (in the direct method) and 1 : 2 and 1 : 1 (in the reverse method) respectively, indicating the formation of the complexes $Na_3Ag(S_2O_3)_2$, $NaAgS_2O_3$, $Na_5Ag_3(S_2O_3)_4$ and $Ag_2S_2O_3$ whereas in the reverse titrations $NaAgS_2O_3$ and $Ag_2S_2O_3$. The results support and throw more light on the reaction between silver nitrate and sodium thiosulfate.

There is meager amount of literatures on the study of this reaction. The possibility of formation of silver thiosulfate complexes was discovered by Herschel[1]. More recently Rosenheim and Steinhäuser[2] and Meyer and Eggeling[3] and lastly Rosenheim and Trewendt[4] carried out the study on the silver thiosulfate complexes. No attempt has so far been made by applying thermometric studies on this reaction. It was therefore considered worthy of interest to carry out study this reaction by thermometric method to throw more light on the nature of this reaction.

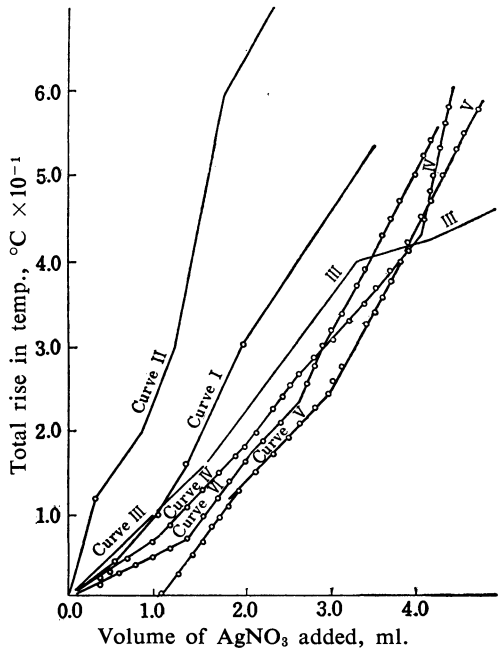


Fig. 1. Direct thermometric titrations curves for silver nitrate against sodium thiosulfate.
Curves I, II, III; M/5 $AgNO_3$ and M/100 $Na_2S_2O_3$
Curves IV, V, VI; M/10 $AgNO_3$ and M/100 $Na_2S_2O_3$ for curve IV, V, VI scale 1″=2 ml.

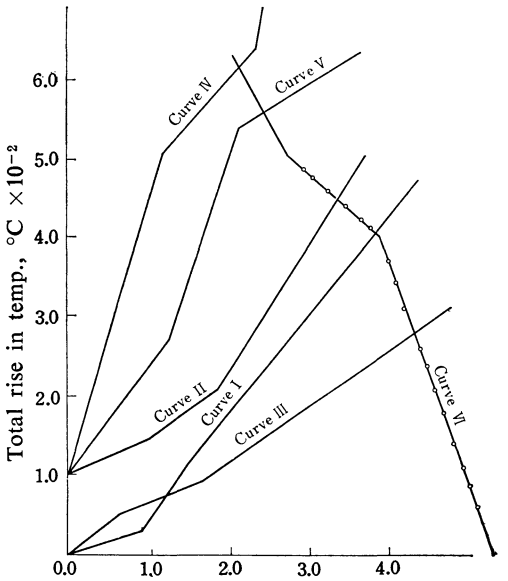


Fig. 2. Thermometric titrations curves for silver nitrate against sodium thiosulfate. (Reverse titrations) [Ag^+] conc. (molality or M)
Curve I, II, III; M/10 $Na_2S_2O_3$, M/200 $AgNO_3$
Curve IV, V, VI; M/40 $AgNO_3$; M/5 Na_2SO_3

Experimental

Silver nitrate and sodium thiosulfate employed for the preparation of solutions were of E. Merck quality. Thermometric titrations were carried out in the apparatus described by Dutoit[5]. Titrations

1) J. F. W. Herschel, *Edinb. Phil. Journal*, **26**, 2, 154 (1819).

2) A. Rosenheim and S. Steinhäuser, *Z. anorg. Chem.*, **25**, 72 (1900).

3) J. Meyer and H. Eggeling, *Ber.*, **40**, 1351 (1907).

4) A. Rosenheim and G. Trewendt, ibid., **61**, 1731 (1928).

5) P. Dutoit and E. Grobet, *J. Chim. Phys.*, **19**, 324 (1922).

were performed by the direct and reverse methods. Titrations were also carried out in varying percentage of alcohol upto a total concentration of 20% by volume. A correction was applied by carrying out 'blank' experiment using water instead of either reactants to account for the dilution effect.

Discussion

From the summary of observations in Table I it is clear that when silver nitrate is added to sodium thiosulfate, the reaction involves the formation of four different compounds $Na_3Ag(S_2O_3)_2$, $NaAgS_2O_3$, $Na_5Ag_3(S_2O_3)_4$ and $Ag_2S_2O_3$ respectively where the molar ratio of the reactants (silver nitrate and sodium thiosulfate) is 1 : 2, 1 : 1, 3 : 4 and 2 : 1 respectively. The reverse thermometric titration curves suggest that when the order of addition of reagents is reversed, the formation of the complexes $Ag_2S_2O_3$ and $NaAgS_2O_3$ takes place.

Rosenheim and Trewendt[4] have reported

TABLE I. SUMMARY OF THERMOMETRIC TITRATIONS

$AgNO_3$ concn.	$Na_2S_2O_3$ concn.	Med.	Point showing breaks		Formula supported	Ratio
			Calcd.	Obs.		
Direct titrations						
M/5	M/100	Aq.	0.50	0.50	$Na_3Ag(S_2O_3)_2$	1 : 2
			1.00	1.00	$NaAgS_2O_3$	1 : 1
			1.33	1.33	$Na_5Ag_3(S_2O_3)_4$	3 : 4
			2.0	2.0	$Ag_2S_2O_3$	2 : 1
M/5	M/100	Alc. 10%	0.45	0.40	$Na_3Ag(S_2O_3)_2$	1 : 2
			0.90	0.90	$NaAgS_2O_3$	1 : 1
			1.2	1.2	$Na_5Ag_3(S_2O_3)_4$	3 : 4
			1.8	1.8	$Ag_2S_2O_3$	2 : 1
M/5	M/100	Alc. 20%	0.8	0.8	$Na_3Ag(S_2O_3)_2$	1 : 2
			1.6	1.6	$NaAgS_2O_3$	1 : 1
			2.13	2.0	$Na_5Ag_3(S_2O_3)_4$	3 : 4
			3.2	3.2	$Ag_2S_2O_3$	2 : 1
M/10	M/100	Aq.	1.0	1.0	$Na_3Ag(S_2O_3)_2$	1 : 2
			2.0	2.0	$NaAgS_2O_3$	1 : 1
			2.66	2.6	$Na_5Ag_3(S_2O_3)_4$	3 : 4
			4.0	4.0	$Ag_2S_2O_3$	2 : 1
M/10	M/100	Alc. 10%	0.9	0.9	$Na_3Ag(S_2O_3)_2$	1 : 2
			1.8	1.8	$NaAgS_2O_3$	1 : 1
			2.4	2.4	$Na_5Ag_3(S_2O_3)_4$	3 : 4
			3.6	3.6	$Ag_2S_2O_3$	2 : 1
M/10	M/100	Alc. 20%	0.8	0.8	$Na_3Ag(S_2O_3)_2$	1 : 2
			1.6	1.6	$NaAgS_2O_3$	1 : 1
			2.13	2.1	$Na_5Ag_3(S_2O_3)_4$	3 : 4
			3.2	3.2	$Ag_2S_2O_3$	2 : 1
Reverse titrations						
M/200, 20 cc.	M/10	Aq.	0.5	0.45	$Ag_2S_2O_3$	1 : 2
			1.0	1.0	$NaAgS_2O_3$	1 : 1
M/200, 18 cc.	M/10	Alc. 10%	0.45	0.42	$Ag_2S_2O_3$	1 : 2
			0.9	0.9	$NaAgS_2O_3$	1 : 1
M/200, 16 cc.	M/10	Alc. 20%	0.4	0.33	$Ag_2S_2O_3$	1 : 2
			0.8	0.8	$NaAgS_2O_3$	1 : 1
M/40, 20 cc.	M/5	Aq.	1.25	1.2	$Ag_2S_2O_3$	1 : 2
			2.5	2.5	$NaAgS_2O_3$	1 : 1
M/40, 18 cc.	M/5	Alc. 10%	1.12	1.1	$Ag_2S_2O_3$	1 : 2
			2.25	2.2	$NaAgS_2O_3$	1 : 1
M/40, 16 cc.	M/5	Alc. 20%	1.0	1.0	$Ag_2S_2O_3$	1 : 2
			2.0	2.0	$NaAgS_2O_3$	1 : 1

the formation of the complexes $NaAgS_2O_3 \cdot 1/2\ H_2O$, $Na_3Ag(S_2O_3)_2 \cdot H_2O$, and $Na_5Ag_3(S_2O_3)_4$. The formation of these complexes have been confirmed by our thermometric studies.

The possibility of the formation of the complexes $NaAg(S_2O_3)_2 \cdot H_2O$ as reported by Basset and Lemon[6] and $Ag_2S_2O_3 \cdot 4Na_2S_2O_3$ by Dey and Mushran[7] (by analysis) is ruled out by our thermometric studies.

Other physico-chemical methods are being tried for the study of this reaction and the results will be communicated in future.

Thanks of author are due to Professor Dr. J. N. Gaur, Head of Chemistry Department, Maharaja College, Jaipur, for his constant help and keen interest in this piece of investigation.

Chemical Laboratories
Lohia College
Churu, India

6) H. Basset, J. T. Lamon and Fritz Ephraim, "Text Book of Inorganic Chemistry", p. 584.
7) A. K. Dey and S. P. Mushran, *Proc. Nat. Acad. Sci.*, **16A**, 37 (1947).

Synthesis of Tetramic Acids

By Yoshikazu Isowa and Masaki Ohta

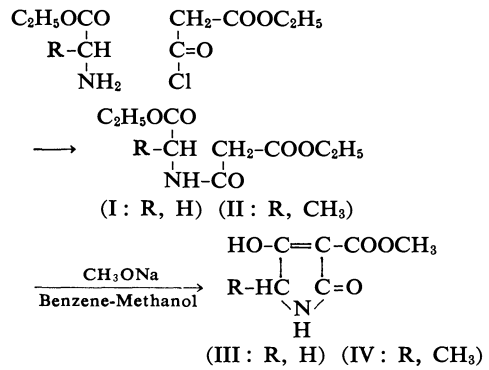
(Received July 10, 1962)

Recent interest has been shown in the study of acids concerning tetramic acid nucleus which was found to be a metabolic product obtained by micro-organisms[1].

There is only one report concerning the synthesis of tetramic acid in the case of α-acetyltetramic acids[2] which was prepared from α-amino acid esters and diketene. It was shown there that α-acetyltetramic acid is not a desirable intermediate for the preparation of tetramic acid itself because α-acetyl derivatives are resistant to alkaline hydrolysis.

In the present study, the synthesis of some tetramic acids was tried and the ultraviolet spectra of tetramic acid derivatives were measured.

In the first place, ethyl ethoxycarbonylacetaminoacetate (I) was prepared from ethyl α-aminoacetate and ethoxycarbonylacetyl chloride in the hope that the activation of the methylene group by the adjacent carboxyl group would facilitate the cyclisation to yield tetramic acid.



When the acetate I was refluxed in benzene-metanol solution in the presence of the sodium methoxide, α-methoxycarbonyltetramic acid (III) was obtained in a 80% yield by the self-ester condensation. The formation of methyl ester may be attributed to the ester exchange between the ester and solvent methanol.

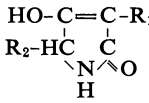
When ethyl α-aminopropionate was treated with ethoxycarbonylacetyl chloride in a cold alkaline solution, ethyl α-(ethoxycarbonylacetamino)propionate (II) was obtained as an oil. The treatment of the crude oily product with sodium methoxide in benzene-methanol gave α-methoxycarbonyl-γ-methyltetramic acid (IV).

Tetramic acid (V) was prepared from III by hydrolysis with aqueous barium hydroxide, followed by neutralisation. Similarly hydrolysis of IV gave γ-methyltetramic acid (VI). Tetramic acid and γ-methyltetramic acid liberated carbon dioxide from sodium hydrogen carbonate and gave a red color with ferric chloride.

The light-absorption properties of tetramic acid derivatives resemble that of tetronic acids and the spectrum of α-methoxycarbonyl-γ-methyl tetramic acid in aqueous solution exhibits pH dependence.

1) T. Rosett et al., *Biochem. J.*, **67**, 390 (1957); C. E. Stickings, ibid., **74**, 232 (1959); C. E. Stickings and R. J. Townsent, ibid., **74**, 36 (1960).
2) R. N. Racey, *J. Chem. Soc.*, **1954**, 850.

Table I. Ultraviolet light absorption



Compound		Short wavelength		Long wavelength	
R_1	R_2	λ_{max}, mμ	ε_{max}	λ_{max}, mμ	ε_{max}
H	H (in water)	239	5.69×10^3	320	6.99×10^3
H	H (in 0.1 N NaOH)	240	6.57×10^3	312	8.00×10^3
$COOCH_3$	H (in water)	228	1.23×10^4	262	1.05×10^4
$COOCH_3$	CH_3 (in water)	228	1.31×10^4	263	1.04×10^4
$COCH_3$	H*	239	9.55×10^3	277	1.35×10^4
$COCH_3$	CH_3*	240	9.25×10^3	280	1.09×10^4
$COCH_3$	C_6H_5 (in 0.001 N NaOH)	242	1.04×10^4	282	1.35×10^4
$COCH_3$	$COOC_2H_5$** (in EtOH)	241	1.50×10^4	281	1.20×10^4

* Lacey (1954)
** The details of this compound will be published in the near future.

The absorption maximum of tetramic acid displays two bands at 239 mμ and 320 mμ, and the introduction of an α-alkoxycarbonyl group displaces the maximum to shorter wavelength.

The introduction of α-acetyl group has little influence on the peak at 239 mμ, but the group causes a shift of the absorption maximum at 320 mμ to shorter wavelength.

Although the introduction of the γ-alkyl or aryl group has little influence on the absorption maximum and its intensity of the two bands, yet the presence of an γ-alkoxycarbonyl group shows an increase in intensity of the peak at 240 mμ.

In position and intensity of the absorption maximum α-methoxycarbonyl-γ-methyltetramic acid exhibits the two characteristic bands at 228 mμ and 263 mμ in aqueous solution at different pH value as follows.

Table II. The pH value effect on the light absorption of α-methoxycarbonyl-γ-methyltetramic acid in water

pH	Short wavelength		Long wavelength	
	λ_{max}, mμ	ε_{max}	λ_{max}, mμ	ε_{max}
	228	1.31×10^4	263	1.05×10^4
11	229	2.63×10^4	263	2.14×10^4
3	230	2.08×10^4	257.5	1.34×10^4

Experimental

Ethyl Ethoxycarbonylacetaminoacetate (I).—Ethoxycarbonylacetyl chloride (22.5 g.) was added during 2 hr. to a mixture of ethyl α-aminoacetate hydrochloride (21 g.) and 50% potassium carbonate (100 ml.) at 0°C, and the mixutre set aside overnight, then extracted with chloroform. The chloroform-extracts were washed with cold water, dried over anhydrous sodium sulfate, and the solvent was evaporated. The residue crystallized, m. p. 60~61°C, 27 g. (84%). Chromatography of this product on alumina afforded a pure crystalline substance, m. p. 64~65°C, on elution with benzene.

Found: C, 50.03; H, 7.21; N, 6.59. Calcd. for $C_9H_{15}O_5N$: C, 49.76; H, 6.96; N, 6.45%.

α-Methoxycarbonyltetramic Acid (III).—Ethyl ethoxycarbonylacetaminoacetate (21 g.) in benzene (100 ml.) was refluxed with agitation with a solution of sodium methoxide (from 2.3 g. of sodium and 40 ml. of methanol) for 3.5 hr. and set aside overnight. Water was added and the solvent layer extracted with water (2×60 ml.). The aqueous extracts were carefully acidified with concentrated sulfuric acid and then precipitated a crystalline product. This material was dissolved with aqueous sodium hydrogen carbonate, acidification of the solution with sulfuric acid precipitated α-methoxycarbonyltetramic acid. The white micro-crystals were washed with cold water, m. p. above 360°C (decomp.).

Found: C, 45.80; H, 4.46; N, 8.64. Calcd. for $C_6H_7O_4N$: C, 45.86; H, 4.49; N, 8.92%.

α-Methoxycarbonyl-γ-methyltetramic Acid (IV).—Ethoxycarbonylacetyl chloride (22.5 g.) was added during 2 hr. to a mixture of ethyl α-aminopropionate hydrochloride (23 g.) and 50% potassium carbonate (100 ml.) at 0°C, and the mixture set aside overnight, then extracted thoroughly with chloroform. The chloroform extracts were washed with cold water, dried on anhydrous sodium sulfate and the solvent evaporated at reduced pressure. The product was a pale yellow oil (28 g. 80%).

In order to remove traces of water from this product, it was dissolved in benzene, dried over anhydrous magnesium sulfate, filtered, and evaporated to yield 27.7 g. of the oil product which was used directly in the next step.

The above crude product (23 g.) in benzene (100 ml.) was refluxed with agitation with a solution of sodium methoxide (from 2.4 g. of sodium and 30 ml. of methanol) for 3 hr. and set aside overnight.

Water was added and the benzene layer was extracted with water.

The combined extracts were carefully neutralized with concentrated sulfuric acid and extracted thoroughly with chloroform. The organic extracts

were washed with water, dried over anhydrous sodium sulfate, filtered and evaporated to yield 15 g. of crude acidic product.

Recrystallization from ethyl acetate (or, better, methanol) yielded 13.5 g. (61%), m. p. 135~136°C.

Found: C, 49.64; H, 5.28; N, 8.11. Calcd. for $C_7H_9O_4N$: C, 49.12; H, 5.30; N, 8.18%.

Tetramic Acid (V).—α-Methoxycarbonyltetramic acid (1.5 g.) and 0.2 N barium hydroxide (50 ml.) were boiled under reflux for 3 hr., after cooling carefully concentrated hydrochloric acid was added to the mixture and then carbon dioxide was evolved.

The mixture was filtered and evaporated to a small volume at reduced pressure. After standing overnight tetramic acid separated as microcrystals from the solution. The product was washed with cold water, m. p. above 360°C. Yield, 0.65 g. (66%).

Found: C, 48.39; H, 5.15; N, 13.97. Calcd. for $C_4H_5O_2N$: C, 48.48; H, 5.09; N, 14.14%.

γ-Methyltetramic Acid (VI). — α-Methoxycarbonyl-γ-methyltetramic acid (1.7 g.) and 0.2 N barium hydroxide (50 ml.) were boiled under reflux for 2.5 hr. After cooling the mixture carefully neutralized with concentrated hydrochloric acid and then carbon dioxide evolution was observed. The solution was filtered, was concentrated in vacuo and microcrystals were obtained. Yield, about 0.67 g. (60%).

Found: N, 12.34: Calcd. for $C_5H_7O_2N$: N, 12.38%.

α-Acetyl-γ-phenyltetramic Acid. — Prepared by the use of Lacey's procedure from phenylglycine ester: m. p. 126°C.

Found: C, 66.36; H, 5.20; N, 6.38. Calcd. for $C_{12}H_{11}O_3N$: C, 66.35; H, 5.10; N, 6.45%.

2,4-dinitrophenylhydrazone, m. p. 246°C.

Found: C, 54.66; H, 4.06; N, 17.24. Calcd. for $C_{18}H_{15}O_6N_5$: C, 54.41; H, 3.81; N, 17.63%.

The authors wish to express their gratitude to Dainippon Celluloid Co., Ltd., for the gift of ketene dimer. Thanks are also due to Mr. Keiji Naruse for the microanalysis.

Laboratory of Organic Chemistry
Tokyo Institute of Technology
Meguro-ku, Tokyo

*Synthesis of Histidyl Peptides. II. Synthesis and Properties of Dicarbobenzyloxyhistidylamino Acid Esters**

By Fumio SAKIYAMA

(Received July 11, 1962)

In the previous paper[1], a report was made of the snythesis of some *N*-α-*N*-*Im*-dicarbobenzyloxy-L-histidyl-L-amino acid esters including neutral, acidic, hydroxyl and sulfur-containing amino acids from dicarbobenzyloxyhistidine and respective amino acid esters by the dicyclohexylcarbodiimide method and it was observed that this reagent was useful for the preparation of these peptide derivatives. However, other possible methods for the synthesis of the dicarbobenzyloxyhistidyl peptide ester have not yet been investigated. In the present communication, some recent studies on the application of the other peptide bond forming methods for the preparation of dicarbobenzyloxy peptide esters are described, and additional syntheses of some of dicarbobenzyloxyhistidyl-amino acid esters by the dicylohexylcarbodiimide method are also included.

In order to find the most suitable method to prepare dicarbobenzyloxyhistidylamino acid ester from its constituent, three different methods (the mixed anhydride, the *p*-nitrophenyl ester and the dicyclohexylcarbodiimide methods) were compared in points of easiness of purification, purity and yield of the product. Because of the relative ease in the preparation of crystalline material, dicarbobenzyloxy-L-histidyl-L-phenylalanine methyl ester was chosen as a model peptide in the present investigation.

In the first place, the mixed anhydride method using alkylchloroformate[2] was employed as a synthetic method.

When dicarbobenzyloxy derivative of L-histidine is recrystallized from methyl alcohol, this material is known to contain one molecule of methyl alcohol which is the essential factor in getting stable crystals[1]. Since methyl alcohol was known to react with alkylchloroformate, twice molar amounts of the reagent were brought to reaction with dicarbobenzyl-

* Part I; The previous report (Ref. 1) was Part I of this series. Preliminary study was presented at the 14th Annual Meeting of the Chemical Society of Japan, Tokyo, April, 1961.

1) S. Akabori, K. Okawa and F. Sakiyama, *Nature*, **181**, 772 (1958); F. Sakiyama, K. Okawa, T. Yamakawa and S. Akabori, This Bulletin, **31**, 926 (1958).

2) J. R. Vaughan, *J. Am. Chem. Soc.*, **73**, 3547 (1951); Th. Wieland, H. Bernhard, *Ann.*, **572**, 190 (1951); R. A. Boissonas, *Helv. Chim. Acta*, **34**, 884 (1951).

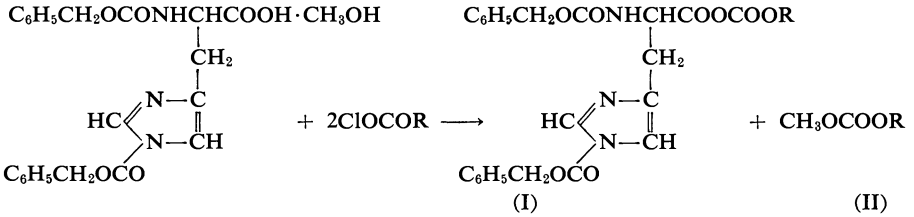


Fig. 1. Reaction of *N*-α-*N*-*Im*-dicarbobenzyloxyhistidine methanolate with alkyl chloroformate.

oxy-L-histidine methanolate[3] in dry tetrahydrofuran to prepare the mixed anhydride (I). Both the mixed anhydride (I) and alkyl-methyl carbonate (II) were formed in the reaction mixture (Fig. 1). By the coupling of the ester component with the mixed anhyride (I), the crystalline model peptide derivative was obtained in a 46% yield when isobutyl chloroformate was used. The same product was also obtained in a 35% yield by using ethyl chloroformate in place of the isobutyl derivative. When the reaction mixture was immediately warmed up to the refluxing point, after completion of the addition of L-phenylalanine methyl ester to the mixed anhydride (I), the yield increased significantly higher (50%).

After the first crop of the model peptide derivative was collected, no ninhydrin positive substances was detected in the mother liquor by paper chromatography.

It seems that no side reaction of alkyl methyl carbonate (II) with the methyl ester of L-phenylalanine occurs at this temperature. Therefore the absence of a free amino group might be due to the acylation of the amino group of phenylalanine ester with an excess of alkyl chloroformate. Next, the model peptide was prepared using a reduced amount of the reagent, one and a half equivalents of alkyl-chloroformate to a unit amount of disubstituted histidine, in stead of two, by a similar refluxed procedure. The yield of the model peptide derivative in this experiment was much higher than the previous. This fact suggested that the methyl alcohol was partly liberated from dicarbobenzyloxyhistidine methanolate[4] and the amount of the reagent was sufficient even under the above conditions, or that the reagent was preferably reacted with phenylalanine ester than alcohol.

In the second place, *p*-nitrophenyl ester of dicarbobenzyloxy-L-histidine was prepared in an 85% yield in chloroform by the Bodanszky's procedure[5] and also obtained by the procedure via the mixed anhydride[6]. This *p*-nitrophenyl ester could not be obtained in a crystalline state, in contrast to those of the other amino acid derivatives. Coupling of this ester with L-phenylalanine methyl ester afforded the model peptide derivative in a yield of 58%. This relatively low yield of the product might be attributed to the presence of another unsubstituted tertiary nitrogen in the imidazole nucleus and partly to the steric hindrance by the bulky substituent adjacent to the carboxyl group in the histidine residue.

Thirdly the model peptide derivative was prepared by the condensation using dicyclohexylcarbodiimide[7]. No difficulties were encountered in the procedure of the peptide synthesis by this reagent as mentioned in the previous paper. The most satisfactory result was given in the present case.

Some pysico-chemical properties of this model peptides obtained by the above described different methods were compared as is shown in Table I and Fig. 2.

It was concluded from the above results that the dicyclohexylcarbodiimide method was the most suitable for the formation of the peptide bond in which dicarbobenzyloxyhistidine was concerned. By this method additional dicarbobenzyloxy-L-histidyl-L-amino acid esters containing alanine, valine, aspartic acid, tyrosine, *S*-benzylcysteine, methionine and serine were synthesized. The author also describes the preparation of the benzyl ester of dicarbobenzyloxy-L-histidyl-L-threonine. The benzyl ester of the threonine was prepared by an esterification procedure similar to that of L-histidine benzyl ester[8]. The DL-isomer of threonine benzyl ester tosylate was obtained in fine crystals. Efforts to crystallize the L-isomer failed, but L-threonine benzyl ester could be obtained in fine needles[9]. *N*-α-Carbobenzyloxy-L-histidyl-L-threonine hydrazide from this benzl ester was identical with same compound obtained from the methyl ester.

3) Dicarbobenzyloxy-L-histidine methanolate represents crystalline dicarbobenzyloxy-L-histidine with one molecule of methyl alcohol.

4) A. Patchornik, A. Berger and E. Katchalski, *J. Am. Chem. Soc.*, **79**, 6416 (1957).

5) D. F. Elliot, D. W. Russel, *Biochem. J.*, **66**, 49P (1957); M. Bodanszky and V. du Vigneaud, *J. Am. Chem. Soc.*, **81**, 5688 (1959).

6) M. Rothe and F. W. Kunitz, *Ann.*, **609**, 97 (1957); Details by this procedure will be presented elsewhere.

7) J. C. Sheehan and G. P. Hess, *J. Am. Chem. Soc.*, **77**, 1067 (1955).

8) S. Akabori. S. Sakakibara and S. Shiina, This Bulletin, **31**, 784 (1958).

9) F. Sakiyama, unpublished data.

TABLE I. DICARBOBENZYLOXY-L-HISTIDYL-L-PHENYLALANINE METHYL ESTER OBTAINED BY MEANS OF VARIOUS METHODS

Method	Reaction solvent	Yield	M. p. °C	$[\alpha]_D^{20}$ *8	Anal.*9 C	H	N
DCCD*1	Chloroform	93	123~124, 132	+54.2	65.74	5.58	9.56
Mixed anhydride with *iso*-BuOCOCl*2	THF*4	46*5, 50*6, 71*7	123~124, 132~133	+53.5	65.86	5.49	9.52
Mixed anhydride with EtOCOCl*3	THF	35	123~124, 132~133	—	65.53	5.56	9.55
p-Nitrophenol	Chloroform	58	123~124, 132~133	+54.4	65.90	5.48	9.58

*1 DCCD: dicyclohexylcarbodiimide
*2 *iso*-BuOCOCl: isobutyl chloroformate
*3 EtOCOCl: ethyl chloroformate
*4 THF: tetrahydrofuran
*5 The molar ratio between dicarbobenzyloxy-L-histidine and alkyl chloroformate is 1 to 2 and the reaction mixture of the mixed anhydride and phenylalanine methyl ester was not warmed.
*6 The molar ratio is similar to *5, but the reaction mixture was warmed to reflux.
*7 The molar ratio is 1 to 1.5 and the reaction mixture was transiently warmed to reflux.
*8 *c* 2.5 in chloroform
*9 Calcd. for $C_{32}H_{32}O_7N_4$: C, 65.74; H, 5.52; N, 9.59%

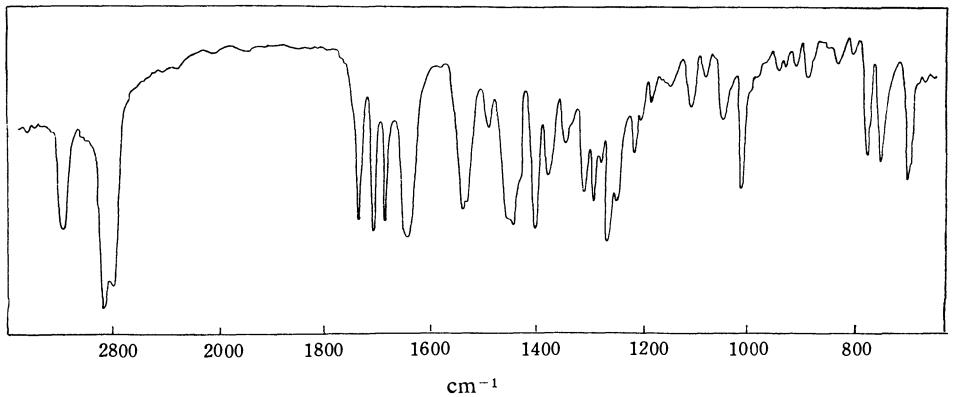


Fig. 2. IR-Spectrum of *N*-α-*N*-*Im*-dicarbobenzyloxy-L-histidyl-L-phenylalanine methyl ester obtained by the DCCD method.

It is interesting to note that the imidazole linked carbobenzyloxy group of dicarbobenzyloxyhistidine is relatively less stable than that of dicarbobenzyloxyhistidylamino acid ester, when the crystalline material is allowed to stand in the atmosphere for a long time.

When the dicarbobenzyloxyhistidine was exposed to alkaline media, the labile imidazole-linked carbobenzyloxy group was eliminated and *N*-α-carbobenzyloxyhistidine was produced. Therefore it was expected that some difficulties would be encountered during the alkaline hydrolysis of the disubstituted histidyl peptide ester owing to the presence of the labile carbobenzyloxy group. In the present paper, the problems concerning the alkaline hydrolysis of the dicarbobenzyloxy-L-histidylamino acid ester are also investigated.

As has been reported[10], *N*-α-carbobenzyloxyhistidylamino acid esters, which were prepared by means of the azide method, were thoroughly hydrolyzed by an equimolar amount of alkali in aqueous alcoholic solution. The alkaline hydrolysis of dicarbobenzyloxyhistidylamino acid esters was thus explored under similar conditions. But only low yield of the hydrolysis product was obtained. Since no detectable cleavage of the peptide bond and no destruction of the imidazole nucleus were found, it appears probable that the low yield was based on the incomplete hydrolysis.

It seems probable that the incompleteness of the hydrolysis reaction was due to the presence of the alkaline labile carbobenzyloxy group. For example, a hydrolysis product of dicarbobenzyloxy-L-histidyl-L-phenylalanine

10) R. Holley and E. Sondhemer, *J. Am. Chem. Soc.*, **76**, 1326 (1954).

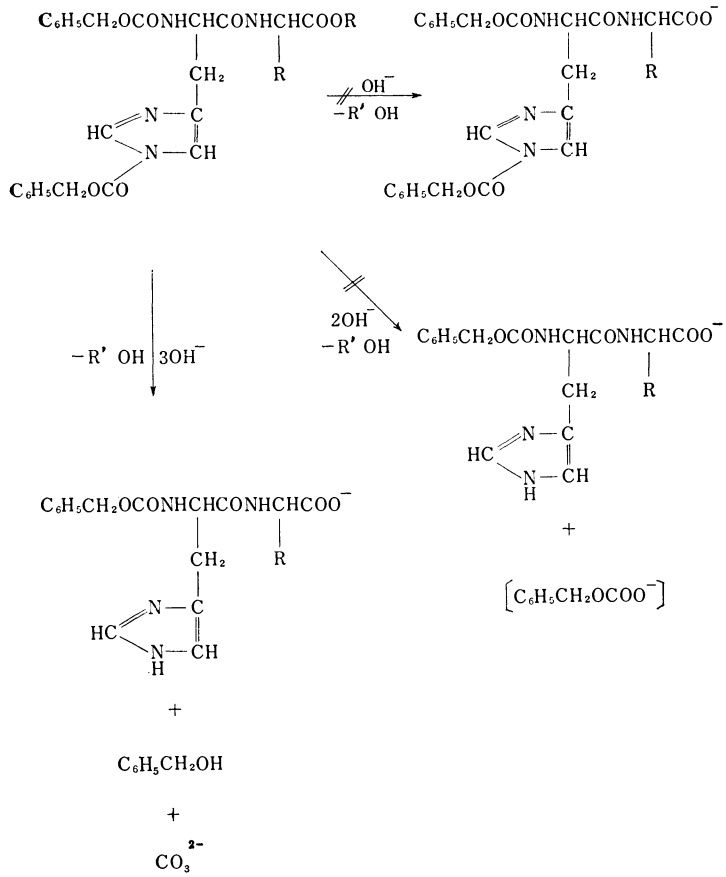


Fig. 3. Alkaline hydrolysis of the dicarbobenzyloxyhistidyl amino acid ester.

ethyl ester was identified to be *N*-α-carbobenzyloxy-L-histidyl-L-phenylalanine and not the dicarbobenzyloxy dipeptide. The carbobenzyloxy group linked to the nitrogen of the imidazole nucleus in the histidyl peptide derivative was quite stable comparing with that of dicarbobenzyloxy histidine in the crystalline state. However, in the alkaline or basic medium, this carbobenzyloxy group was also unstable. In alkaline media, hydroxide ions might simultaneously attack both the labile carbobenzyloxy group and the carboxyl ester group. Generally, the active acyl group linked to imidazole was readily convertible to the acyl anion and imidazole by hydroxdie ions. Thus the formation of the acyl anion might result in the consumption of hydroxide ions. If the acyl anion produced was stable in alkaline media, twice molar amounts of alkali would be sufficient for the hydrolysis reaction as is shown in Fig. 3. But the use of twice molar amounts of alkali also brought the incomplete hydrolysis of the ester group. For example, *N*-α-carbobenzyloxy-L-histidyl-L-leucine, which used to be readily obtained as crystals, was not crystallized merely by acidification of the reaction mixture but the isolation yield was 60%.

The complete hydrolysis was finally obtained by the use of three-fold molar equivalents of alkali in alcohol, dioxane or acetone. Thus the following mechanism for the hydrolysis of dicarbobenzyloxyhistidylamino acid ester with aqueous alkali would be considered: hydroxide ions attacked not only the –CO–N= bond in the imidazole-linked carbobenzyloxy group but also the –CO–O– bond in the carboxyl ester group, and the intermediate monobenzyl carbonate ions produced from the former might be converted into benzyl alcohol and carbonate ions by the action of hydroxide ions as is shown in Fig. 3. This carbonate forming reaction would prevent the complete hydrolysis of the ester group when equi- or twice molar amounts of alkali are used.

The infrared spectra of these *N*-α-carbobenzyloxy-L-histidylamino acids showed the absence of the absorption band at near 1750 cm^{-1}.

N-α-N-Im-Dicarbobenzyloxy-L-histidyl-L-phenylalanine prepared by the direct carbobenzyloxylation of the *N-α*-carbobenzyloxy dipeptide revealed the above characteristic absorption[11] owing to the presence of the imidazole-linked carbobenzyloxy group as is shown in Fig. 4.

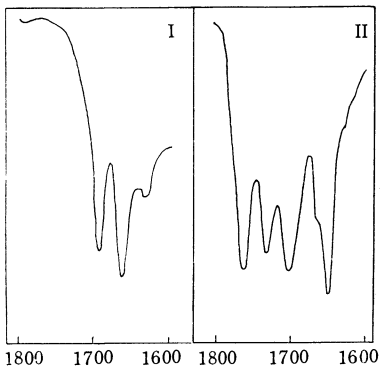


Fig. 4. Infrared spectra of *N-α*-monocarbobenzyloxy- and *N-α-N-Im*-dicarbobenzyloxy-L-histidyl-L-phenylalanine.

I *N-α*-Carbobenzyloxy-L-histidyl-L-phenylalanine.
II *N-α-N-Im*-Dicarbobenzyloxy-L-histidyl-L-phenylalanine.
(Nujol mull. Rock-salt optics. Hitachi infrared spectrophotometer)

A few of *N-α*-carbobenzyloxyl-L-histidylamino acids were obtained by this hydrolysis procedure. The threonine derivative was obtained in a poor yield in contrast to the *O*-benzylserine derivative. The fact seems to be due to the presence of a free hydroxyl group in threonine residue. It was observed that the carbobenzyloxyhistidylamino acids are generally hardly soluble in ordinary oranic solvents, as is expected from their dipolar properties.

Experiental

All melting points were uncorrected. The R_f values described were those by *n*-butanol-acetic acid-water (4 : 1 : 1, by volume) and the spot of *N-α*-carbobenzyloxyhistidylamino acid was detected by the use of Pauly's reagent.

***N-α-N-Im*-Dicarbobenzyloxy-L-histidyl-L-phenylalanine Methyl Ester.**—*A) By the Mixed Anhydride Method.* — i) The mixed anhydride method with isobutyl chloroformate:

Dicarbobenzyloxy-L-histidine methanolate (4.5 g., 0.01 M) was dissolved in anhydrous tetrahydrofuran (10 ml.) and triethylamine (3 ml.). Then isobutyl chloroformate (2.7 g., 0.02 M) was added dropwise to the above solution with vigorous stirring at −16 ∼−10°C and the temperature was maintained at −10°C for 15 min. L-Phenylalanine methyl ester was added to the above mixed anhydride solution at −15∼−20°C with vigorous stirring. After being kept overnight at room temperature, white precipitates were filtered off and the filtrate was evaporated to syrup, which was first dissolved in methyl alcohol and then gradually crystallized out. The fine needles were collected. Yield 2.5 g. The second crop (0.2 g.) was obtained from the mother liquor. Total yield was 2.7 g. (46%). Recrystallization was performed from methyl alcohol.

ii) The mixed anhydride method with isobutyl chloroformate under heating:

After the addition of the ester component to the anhydride solution was complete, the mixture was warmed to the refluxing point and then immediately cooled to room temperature. The filtrate, after triethylamine hydrochloride had been removed, was concentrated and treated with methyl alcohol. The yields were 50% (when dicarbobenzyloxy-L-histidine methanolate/isobutyl chloroformate=1/2), and 71% (when the above ratio=2/3), respectively.

iii) The mixed anhydride method with ethyl chloroformate:

The procedure of synthesis was similar to i).

B) By the p-Nitrophenyl Ester Method. — i) Dicarbobenzyloxy-L-histidine *p*-nitrophenyl ester: A solution of dicyclo hexylcarbodiimide (1.1 g.) in chloroform (6 ml.) was added into a chloroform solution (20 ml.) containing dicarbobenzyloxy-L-histidine methanolate (2.3 g.) and *p*-nitrophenol (0.83 g.). After being kept at room temperature for 5 hr., two drops of glacial acetic acid was added to the above mixture. After one hour, dicyclohexylurea was separated and filtered off. The filtrate was evaporated to syrup in vacuo. By the addition of ether, a gelatinous product was precipitated, filtered off and thoroughly washed with ether. The removal of ether gave a powder-like *p*-nitrophenyl ester with slight yellowish color. Yield 2.4 g. (85%). Sample for analysis was reprecipitated from ethyl alcohol but could not be obtained in fine crystals, m. p. 86∼90°C.

Found: C, 61.53; H, 4.55; N, 10.35. Calcd. for $C_{28}H_{24}O_8N_4$: C, 61.76; H, 4.44; N, 10.29%.

ii) Dicarbobenzyloxy-L-histidyl-L-phenylalanine methyl ester: Dicarbobenzyloxy-L-histidine *p*-nitrophenyl ester (2.2 g.) was dissolved in warm chloroform (7 ml.) and the chloroform solution was mixed with L-phenylalanine methyl ester which was prepared from its hydrochloride (1.1 g.) and triethylamine in chloroform. After being kept at room temperature overnight, the solvent was removed and resulting syrup was treated with methyl alcohol, and then chilled as was described in A i). Yield 1.35 g. (58%).

C) By the Dicyclohexylcarbodiimide Method.—Dicarbobenzyloxy-L-histidine methanolate (2.3 g.) was dissolved in chloroform (7 ml.). A solution of L-phenylalanine methyl ester, which was prepared from its hydrochloride (1.4 g.) and triethylamine, was added into the above solution. After the addition of dicyclohexylcarbodiimide (1.1 g.) in chloroform was complete, the reaction mixture was

11) In general, dicarbobenzyloxyhistidine and dicarbobenzyloxyhistidyl amino acid esters show strong absorption at 1750∼1760 cm⁻¹.

TABLE II. DICARBOBENZYLOXY-L-HISTIDYLAMINO ACID ESTERS OBTAINED BY THE DCCD METHOD

Dicarbobenzyloxy derivative of L-histidyl-	Yield %	M. p. °C	$[\alpha]_D^{20}$*	Solvent for recrystallization	Anal. Found C	Found H	Found N	Calcd. C	Calcd. H	Calcd. N
L-Alanine ethyl ester	77	131~132	+42.0	Ethyl acetate-petroleum ether	62.30	5.90	10.97	62.05	5.79	10.72
L-Valine methyl ester	76	120~121	+37.6	Ethyl acetate	62.87	6.07	10.82	62.65	6.01	10.44
L-Aspartic acid dimethyl ester	72	100~102	+40.9	Ethyl acetate-petroleum ether	59.46	5.39	9.93	59.34	5.34	9.89
S-Benzyl-L-cysteine methyl ester	66	137~137.5	+27.6	Methyl alcohol-ether	62.99	5.39	9.55	62.83	5.42	9.09
L-Threonine ethyl ester	65	106~108	+21.3	Ethyl acetate	60.43	5.90	10.18	60.83	5.84	10.14
L-Phenylalanine ethyl ester	94	159~161	+50.0	Ethyl alcohol	65.91	5.70	9.77	66.21	5.89	9.39
L-Tyrosine methyl ester	—	129~131	+41.6	Ethyl alcohol-ether	64.18	5.55	9.15	63.98	5.37	9.33
L-Serine methyl ester	50	152~152.5	+25.6	Ethyl alcohol	59.31	5.44	11.11	59.53	5.38	10.68
Glycine benzyl ester	82	112.5~113.5	+21.7	Ethyl acetate	65.50	5.33	9.94	65.25	5.30	9.82
L-Methionine benzyl ester	72	125	+32.9	Ethyl alcohol	63.56	5.70	8.72	63.34	5.63	8.69
L-Glutamic acid dibenzyl ester	79	117~118	+24.5	Ethyl alcohol-petroleum ether	67.26	5.60	7.45	67.20	5.50	7.63

* *c* 2, in chloroform

allowed to stand overnight at room temperature. The cyclohexylurea precipitated was filtered off and the filtrate was evaporated. The syrupy material was dissolved in a small amount of methyl alcohol and chilled. The fine needles precipitated were collected and weighed. Yield, 2.7 g. (93%). By recrystallization from methyl alcohol 2.3 g. of pure materials were obtained (80%).

This peptide derivative has double melting points. The crystal melted at 123~124°C after softening at 117~119°C and meanwhile (within from thirty seconds to a few minutes) the molten materials solidified and melted again at 131~132°C.

Dicarbobenzyloxy-L-histidylamino acid esters described in Table II were synthesized by the carbodiimide method[1] from dicarbobenzyloxy-L-histidine methanolate and respective amino acid esters.

DL-Threonine Benzyl Ester *p*-Toluenesulfonate. —DL-Threonine (5 g.), *p*-toluenesulfonic acid monohydrate (10 g.) and benzyl alcohol (50 ml.) were dissolved in chloroform (100 ml.). The mixture was refluxed for thirty hours by using Wieland's esterification apparatus, in which silica gel was used as a desiccant. The solvent and excess benzyl alcohol were removed under reduced pressure and the oily product obtained was gradually crystallized by a minute trituration in ether (200 ml.) under cooling. After being kept in a refrigerator overnight, the crystals were filtered and washed thoroughly with ether until no smell of benzaldehyde was detected. Recrystallization of the crude product (12.5 g., 89%) from methyl alcohol-ether gave fine crystals. m. p. 113°C. R_f 0.72, yellow spot with ninhydrin.

Found: C, 57.46; H, 5.82; N, 3.59. Calcd. for $C_{18}H_{23}O_6NS$: C, 56.68; H, 6.08; N, 3.67%.

Since an attempt to crystallize the L-isomer by the same procedure failed, and a slightly brownish paperchromatographically pure L-threonine benzyl ester *p*-toluenesulfonate was used as a starting material for the peptide synthesis without further purification.

Dicarbobenzyloxy-L-histidyl-L-threonine Benzyl Ester. — Dicarbobenzyloxy-L-histidyl-L-threonine benzyl ester was prepared in a 71% yield. Recrystallization from ethyl alcohol or ethyl alcohol-petroleum ether gave fine crystals. M. p. 130~131°C. $[\alpha]_D^{20}$ +22.5° (*c* 2, in chloroform).

Found: C, 64.46; H, 5.66; N, 9.40. Calcd. for $C_{33}H_{34}O_8N_4$: C, 64.47; H, 5.57; N, 9.11%.

***N*-α-Carbobenzyloxy-L-histidyl-L-threonine Hydrazide.**—Warm methanolic solution of dicarbobenzyloxy-L-histidyl-L-threonine benzyl ester (600 mg.) was cooled to room temperature and 80% hydrazine hydrate (0.3 ml.) was added. After 42 hr. at room temperature, white crystals (350 mg., 82%) precipitated, and were collected, washed with water and recrystallized from ethyl alcohol. M. p. 185.5~186°C (decomp.).

Found: C, 51.20; H, 6.29; N, 19.72. Calcd. for $C_{18}H_{24}O_5N_6 \cdot H_2O$: C, 51.18; H, 6.20; N, 19.90%.

The same product was also obtained from the methyl ester of dicarbobenzyloxy-L-histidyl-L-threonine by a similar procedure.

***N*-α-Carbobenzyloxy-L-histidylglycine.**—Into dicarbobenzyloxy-L-histidylglycine methyl ester (478 mg.) suspended in methyl alcohol (4 ml.), N sodium

hydroxide (3 ml.) was portionwise added with shaking. By the addition of the first 2 ml. of alkali the suspension became clear. After being kept for half an hour at room temperature, the clear solution was diluted with water (5 ml.) and acidified with N hydrochloric acid to pH 4.8~5.0. Yield, 300 mg. (83%). Recrystallization from hot dimethylformamide-ether gave pure *N*-α-carbobenzyloxy-L-histidyl-glycine, m. p. 230°C (decomp.); lit.[12], 230~231°C (decomp.). $[\alpha]_D^{31.2}$ −20.5° (*c* 1.05, in 5% aqueous hydrogen carbonate), R_f, 0.78.

Found: C, 55.00; H, 5.34; N, 16.39. Calcd. for $C_{16}H_{18}O_6N_4$: C, 55.48; H, 5.24; N, 16.17%.

This procedure is referred to below as method-i-a.

***N*-α-Carbobenzyloxy-L-histidyl-L-alanine.**—Into a suspension of dicarbobenzyloxy-L-histidyl-L-alanine ethyl ester (600 mg.) in ethyl alcohol (3 ml.), N sodium hydroxide (3 ml.) was added. The resulting solution was allowed to stand for half an hour at room temperature and then acidified with N hydrochloric acid to pH 4.8~5.0. Fine white needles (285 mg.) were obtained by scratching and chilling, m. p. 214~216.5°C (decomp.). Additional crystals (30 mg.) were obtained from the mother liquor. Total yield, 87%. Pure materials recrystallized from water melted at 218~219°C with decomposition after sintering at 215°C. $[\alpha]_D^{31.2}$ −25.5° (*c* 1.00, in 5% sodium hydrogen carbonate).

Found: C, 56.36; H, 5.60; N, 15.81. Calcd. for $C_{17}H_{21}O_5N_4Cl$: C, 56.65; H, 5.59; N, 15.55%.

This procedure is referred to below as method-i-b.

***N*-α-Carbobenzyloxy-L-histidyl-L-valine.**—A solution of dicarbobenzyloxy-L-histidyl-L-valine methyl ester (536 mg.) in methyl alcohol (4 ml.) was treated with N sodium hydroxide (3 ml.) at room temperature for half an hour and then the resulting solution was acidified. In this case, contrary to the other dipeptide derivative no precipitates were produced. The solution then evaporated to dryness under reduced pressure. The residues were dissolved in ethyl alcohol and the insoluble material (probably sodium chloride) was filtered off. The filtrate was diluted with ether. Fine crystals were collected (385 mg., 95%), m. p. 196~197.5°C (decomp.). Recrystallization from ethyl alcohol-ether gave fine crystals after being kept in a refrigerator about three weeks, m. p. 187~187.5°C (decomp.) sintered at 175°C. $[\alpha]_D^{31.2}$ −20.0° (*c* 1.08, in water).

Found: C, 56.52; H, 6.23; N, 13.95. Calcd. for $C_{19}H_{25}O_5N_4 \cdot H_2O$: C, 56.17; H, 6.45; N, 13.79%.

This procedure is referred to below as method-ii.

***N*-α-Carbobenzyloxy-L-histidyl-L-leucine.**—By method-i-b *N*-α-carbobenzyloxy-L-histidyl-L-leucine was obtained from dicarbobenzyloxy dipeptide ester in a 90% yield. Recrystallization from ethyl alcohol-water gave pure materials, m. p. 188~189°C (decomp.) $[\alpha]_D^{31.2}$ −9.9° (*c* 1.00 in 5% aqueous sodium hydrogen carbonate).

Found: C, 57.09; H, 6.87; N, 13.42. Calcd. for $C_{20}H_{26}O_5N_4 \cdot H_2O$: C, 57.13; H, 6.87; N, 13.33%.

***N*-α-Carbobenzyloxyl-L-histidyl-L-phenylalanine.**—Dicarbobenzyloxy-L-histidyl-L-phenylalanine ethyl ester (600 mg.) was hydrolyzed by method-i-a and *N*-α-carbobenzyloxy-L-histidyl-L-phenylalanine (420 mg.) was obtained in an almost theoretical yield. Recrystallization from a large amount of 25% aqueous ethyl alcohol gave fine crystals, m. p. 231~232°C (decomp.) (lit., 227~228[13]).

Found: C, 63.28; H, 5.58; N, 13.15. Calcd. for $C_{24}H_{26}O_6N_4$: C, 63.29; H, 5.54; N, 12.84%.

The alkaline hydrolysis in aqueous dioxane solution also proceeded smoothly in a homogeneous solution but only colloidal precipitates resulted from acidification. The hydrolysis in the acetone solution was, at first, in a heterogeneous state and after a few minutes the solution became clear but the sodium carbonate was precipitated at the end of the reaction.

By method-i-a the dipeptide derivatives mentioned below were also prepared.

***N*-α-Carbobenzyloxy-L-histidyl-*O*-benzyl-L-serine.**—Yield, 80%. M. p. 210~211°C (decomp.). Recrystallization from dimethylformamide-ether.

Found: C, 61.51; H, 5.72; N, 12.04. Calcd. for $C_{24}H_{26}O_6N_4$: C, 61.79; H, 5.61; N, 12.01%.

***N*-α-Carbobenzyloxy-L-histidyl-L-tyrosine.**—Yield, 88%. M. p. 240°C (decomp.). Recrystallization from ethyl alcohol-water.

Found: C, 61.05; H, 5.35; N, 12.38. Calcd. for $C_{24}H_{26}O_7N_4$: C, 60.89; H, 5.52; N, 12.30%.

***N*-α-Carbobenzyloxy-L-histidyl-*S*-benzyl-L-cysteine.**—Yield, 94%. M. p. 197~199°C. (lit., 191~192°C[14]).

Found: C, 59.87; H, 5.35; N, 11.63. Calcd. for $S_{24}H_{26}O_5N_4S$: C, 59.58; H, 5.43; N, 12.09%.

***N*-α-Carbobenzyloxy-L-histidyl-L-aspartic Acid.**—By method-i-b, dicarbobenzyloxy-L-histidyl-L-aspartic acid dimethyl ester (2.3 g.) in methyl alcohol (8 ml.) was treated with four molar equivalents of alkali because of the presence of two carboxyl groups in the aspartic acid residue. Yield, 1.3 g. (75%). M. p. 222~222.5°C (decomp.). Recrystallization from dimethylformamide did not raise the melting point. $[\alpha]_D^{31.2}$ −16.9° (*c* 1.05, 5% aqueous sodium hydrogen carbonate) (lit., m. p. 222°C[14]).

Found: C, 53.15; H, 5.19; N, 13.83. Calcd. for $C_{18}H_{20}O_7N_4$: C, 53.47; H, 4.98; N, 13.86%.

***N*-α-Carbobenzyloxy-L-histidyl-L-glutamic Acid.**—By the procedure mentioned above, *N*-α-carbobenzyloxy-L-histidyl-L-glutamic acid was prepared in an 83% yield and recrystallized from water, m. p. 169~172°C. $[\alpha]_D^{31.2}$ −21.1 (*c* 1.00, in a 5% aqueous sodium hydrogen carbonate) (lit., 169~171°C[14]).

Found: C, 53.19; H, 5.48; N, 12.98. Calcd. for $C_{19}H_{22}O_7N_4 \cdot (1/2)H_2O$: C, 53.40; H, 5.42; N, 13.11%.

***N*-α-Carbobenzyloxy-L-histidyl-L-threonine.**—The *N*-α-carbobenzyloxy derivative of this dipeptide was isolated in a 50% yield by method-ii and recrystallized from ethyl alcohol-ether, m. p. 189.5~190°C (decomp.). $[\alpha]_D^{16}$ −23.6° (*c*, 1.00, in 5% aqueous sodium hydrogen carbonate).

Found: C, 55.38; H, 5.68; N, 14.35. Calcd. for $C_{18}H_{22}O_6N_4$: C, 55.24; H, 5.66; N, 14.32%.

12) G. Weitzel, F. Schneider and A-M. Fretzdorff, *Z. physiol. Chem.*, **307**, 23 (1957).

13) K. Hofmann, H. Kappeler, A. E. Furlenmeier, M. E. Wooner, E. T. Schwartz and T. A. Thompson, *J. Am. Chem. Soc.*, **79**, 1641 (1957).

14) F. Schneider, *Z. physiol. Chem.*, **320**, 82 (1960).

Dicarbobenzyloxy-L-histidyl-L-phenylalanine.—*N*-α-Carbobenzyloxy-L-histidyl-Lphenylalanine (420 mg.) was dissolved in a mixture of sodium hydroxide (1 ml.), water (7 ml.) and solid sodium carbonate (100 mg.). Into the above solution, carbobenzyloxychloride (171 mg.) was portionwise added under cooling and stirring. An oily product was separated, then gradually solidified, and finally gelled. After half an hour, the solution was acidified to Congo red and the gel was filtered, washed with alcohol and dried. White powders (300 mg.) were obtained and reprecipitated from the mixture of ethyl alcohol and ethyl acetate-ether. M. p. 123°C.

Found: C, 63.84; H, 5.40; N, 9.31. Calcd. for $C_{31}H_{30}O_7N_4 \cdot H_2O$: C, 63.25; H, 5.48; N, 9.52%.

Summary

Three different methods for the synthesis of dicarbobenzyloxy-L-histidylamino acid esters were studied. The general procedure of the hydrolysis of dicarbobenzyloxyhistidylamino acid esters were reported and the mechanism of this hydrolysis reaction was also discussed.

The author wishes to express his sincere thanks to Professor Shiro Akabori, Professor Kozo Narita, Institute for Protein Research, Osaka University, and Dr. Kenji Okawa, Faculty of Science, Kwansei-Gakuin University, for their guidances, and he is also indebted to Mr. Tsuneo Sowa and Mr. Yasuhiro Murase for their assistance.

Division of Protein Chemistry
Institute for Protein Research
Osaka University
Kita-ku, Osaka

Molecular Rotations of Glucides in Relation to their Structures. X[1]. *On the ζ-Coefficient of the Hydroxyl Group in Pentose and Methylpentose*

By Shukichi YAMANA

(Received July 14, 1962)

In the analysis of the $[M]_D^{20}$(W) by using the PM-method reported on in previous papers[1,2], the following two facts became apparent:

(1) The product of the ζ-coefficients of the hydroxyl and methyl groups, $\zeta_{OH}\zeta_{CH_3}$, is nearly definite and constant, regardless either of the kind of ring or of the number of hydroxyl groups in the molecule in which they are contained.

(2) When there are only two hydroxyl groups in a molecule, the value of ζ_{OH}^2 is also nearly constant, regardless of the kind of ring in the molecule.

On the other hand, the value of ζ_{OH}^2 when there are more than three hydroxyl groups in a molecule does not seem to be so simple. That value was calculated as $3.6402\{3/(n^2+2)\}$ (for polyhydroxycyclohexane[3]) and $2.4897\{3/(n^2+2)\}$ (for pentose, etc.[4]).

These two values show that the value of ζ_{OH}^2 is not nearly constant in this case. Therefore, it is necessary in this article to examine the value of ζ_{OH}^2 in pentose, etc.

New Treatment Applied

The value of ζ_{OH}^2 in pentose, etc., $2.4897\cdot\{3/(n^2+2)\}$, was obtained in a previous paper[5] on the assumption that every one of the hydroxyl groups in a carbohydrate molecule has the same ζ_{OH} value. However, it is well-known that the chemical character of the hydroxyl group which combines with the C^1-atom of the aldopyranose-ring, $(OH)^1$[6], is quite different from that of the other hydroxyl groups in the carbohydrate molecule. Therefore, it may be appropriate to presume that the optical character of $(OH)^1$ may also be different from that of the other hydroxyl group[7]. In

1) Part IX: S. Yamana, This Bulletin, 35, 1421 (1962).
2) S. Yamana, ibid., 35, 1269 (1962).
3) S. Yamana, ibid., 33, 1741 (1960).
4) Eq. 11 in a previous paper[5].
5) S. Yamana, This Bulletin, 31, 558 (1958).
6) The reducing group, $(OH)^1$, of a cyclic sugar, although alcoholic in form, is in fact a cyclic semi-acetal group ("Advances in Carbohydrate Chemistry", Vol. 5, Academic Press, New York (1950), p. 145).
7) In his own method of the calculation of the $[M]_D^{20}$(W) of carbohydrates, Whiffen treated the glycosidic O-atom, O_g, as of a different optical character from the other O-atom (D. H. Whiffen, *Chem. & Ind.*, 1956, 964).

Table I

Name	Unit group	$[M]_D^{20}$(W)	Ref.
β-L-Arabinose	[$(OH)^{1\alpha}$, $(OH)^{2\alpha}$, $(OH)^{3\beta}$, $(OH)^{4\beta}$, Ring]	303.3°	9
α-L-Arabinose	[$(OH)^{1\beta}$, $(OH)^{2\alpha}$, $(OH)^{3\beta}$, $(OH)^{4\beta}$, Ring]	133.6°	9
α-D-Xylose	[$(OH)^{1\alpha}$, $(OH)^{2\alpha}$, $(OH)^{3\beta}$, $(OH)^{4\alpha}$, Ring]	140.5°	10
β-D-Xylose	[$(OH)^{1\beta}$, $(OH)^{2\alpha}$, $(OH)^{3\beta}$, $(OH)^{4\alpha}$, Ring]		
α-D-Fucose	[$(OH)^{1\alpha}$, $(OH)^{2\alpha}$, $(OH)^{3\beta}$, $(OH)^{4\beta}$, $(CH_3)^{5\beta}$, Ring]	251.0°	10
β-D-Fucose	[$(OH)^{1\beta}$, $(OH)^{2\alpha}$, $(OH)^{3\beta}$, $(OH)^{4\beta}$, $(CH_3)^{5\beta}$, Ring]		
α-D-Isorhamnose	[$(OH)^{1\alpha}$, $(OH)^{2\alpha}$, $(OH)^{3\beta}$, $(OH)^{4\alpha}$, $(CH_3)^{5\beta}$, Ring]	163.7°	11
β-D-Isorhamnose	[$(OH)^{1\beta}$, $(OH)^{2\alpha}$, $(OH)^{3\beta}$, $(OH)^{4\alpha}$, $(CH_3)^{5\beta}$, Ring]		
α-D-Rhamnose	[$(OH)^{1\alpha}$, $(OH)^{2\beta}$, $(OH)^{3\beta}$, $(OH)^{4\alpha}$, $(CH_3)^{5\beta}$, Ring]	15.7°	10
β-D-Rhamnose	[$(OH)^{1\beta}$, $(OH)^{2\beta}$, $(OH)^{3\beta}$, $(OH)^{4\alpha}$, $(CH_3)^{5\beta}$, Ring]	−63.0°	10
α-D-Talomethylose	[$(OH)^{1\alpha}$, $(OH)^{2\beta}$, $(OH)^{3\beta}$, $(OH)^{4\beta}$, $(CH_3)^{5\beta}$, Ring]		
β-D-Talomethylose	[$(OH)^{1\beta}$, $(OH)^{2\beta}$, $(OH)^{3\beta}$, $(OH)^{4\beta}$, $(CH_3)^{5\beta}$, Ring]		
α-D-Galactose	[$(OH)^{1\alpha}$, $(OH)^{2\alpha}$, $(OH)^{3\beta}$, $(OH)^{4\beta}$, $(CH_2)^{5\beta}$, $(OH)^6$, Ring]	271.5°	10
β-D-Galactose	[$(OH)^{1\beta}$, $(OH)^{2\alpha}$, $(OH)^{3\beta}$, $(OH)^{4\beta}$, $(CH_2)^{5\beta}$, $(OH)^6$, Ring]	95.1°	10
α-D-Glucose	[$(OH)^{1\alpha}$, $(OH)^{2\alpha}$, $(OH)^{3\beta}$, $(OH)^{4\alpha}$, $(CH_2)^{5\beta}$, $(OH)^6$, Ring]	202.1°	10
β-D-Glucose	[$(OH)^{1\beta}$, $(OH)^{2\alpha}$, $(OH)^{3\beta}$, $(OH)^{4\alpha}$, $(CH_2)^{5\beta}$, $(OH)^6$, Ring]	33.7°	10
α-D-Mannose	[$(OH)^{1\alpha}$, $(OH)^{2\beta}$, $(OH)^{3\beta}$, $(OH)^{4\alpha}$, $(CH_2)^{5\beta}$, $(OH)^6$, Ring]	52.8°	10
β-D-Mannose	[$(OH)^{1\beta}$, $(OH)^{2\beta}$, $(OH)^{3\beta}$, $(OH)^{4\alpha}$, $(CH_2)^{5\beta}$, $(OH)^6$, Ring]	−30.6°	10
α-D-Talose	[$(OH)^{1\alpha}$, $(OH)^{2\beta}$, $(OH)^{3\beta}$, $(OH)^{4\beta}$, $(CH_2)^{5\beta}$, $(OH)^6$, Ring]	122.5°	10
β-D-Talose	[$(OH)^{1\beta}$, $(OH)^{2\beta}$, $(OH)^{3\beta}$, $(OH)^{4\beta}$, $(CH_2)^{5\beta}$, $(OH)^6$, Ring]	23.8°	10

Note: In order to simplify the calculations, all of these aldopyranoses may be assumed to be entirely of C1 conformation

this article, the ζ-coefficient of $(OH)^1$ is symbolized as $\zeta_{(OH)^1}$ and is distinguished from the general ζ_{OH}.

Molecular Model and Data Used

McGeachin and Beevers' molecular model[8] of C1 conformation, used in a previous paper[2], is again employed here. The unit groups in the molecules of several aldopyranoses and the corresponding values of molecular rotations are shown in Table I.

A part of Table I is a repetition of Table I of a previous paper[2]. The optical properties of the unit groups (except for the value of the ζ-coefficient) used in a previous paper[2] are adopted here without any correction. The optical center of a unit group is located at the center of the mass of its corresponding bond.

Method Proposed

$[\mu]^{20}_{D\,calcd}\{3/(n^2+2)\}$, caused by the dynamical coupling effect between any two members of the unit groups (except the ring) has already been calculated; it is given in Table III of a previous paper[2]. That table is applicable for this article without any correction.

Moreover, the equation which indicates the relation between ζ_{OH} and ζ_{CH_3} in pentose and methylpentose has already been obtained in a previous paper[2]:

$$\zeta_{OH}\zeta_{CH_3}=1.5440\{3/(n^2+2)\} \quad (1)^{12}$$

Now, some new equations concerning $\zeta_{(OH)^1}$ can be obtained as follows:

$$[\mu]^{20}_{D\,obs} \text{ of the An. Diff. of D-rhamnose}^{13}$$
$$=\{(1\alpha)-(1\beta)\}\,\text{Å}\,\{(2\beta)+(3\beta)+(4\alpha)+(CH_3)^{5\beta}+R\}^{15}=\{(1\alpha)\,\text{Å}\,(2\beta)+(1\alpha)\,\text{Å}\,(3\beta)+(1\alpha)\,\text{Å}\,(4\alpha)+(1\alpha)\,\text{Å}\,(CH_3)^{5\beta}+(1\alpha)\,\text{Å}R\}-\{(1\beta)\,\text{Å}\,(2\beta)+(1\beta)\,\text{Å}\,(3\beta)+(1\beta)\,\text{Å}\,(4\alpha)+(1\beta)\,\text{Å}\,(CH_3)^{5\beta}+(1\beta)\,\text{Å}R\}=[\{1.51\zeta_{(OH)^1}\zeta_{OH}+2.54\zeta_{(OH)^1}\zeta_{OH}+0.02\zeta_{(OH)^1}\zeta_{OH}-5.57\zeta_{(OH)^1}\zeta_{CH_3}\}-\{12.60\zeta_{(OH)^1}\zeta_{OH}-0.82\zeta_{(OH)^1}\zeta_{OH}+0.02\zeta_{(OH)^1}\zeta_{OH}+1.26\zeta_{(OH)^1}\zeta_{CH_3}\}]\{(n^2+2)/3\}+(1\alpha)\,\text{Å}R-(1\beta)\,\text{Å}R^{16}=(-7.73\zeta_{(OH)^1}\zeta_{OH}-6.83\zeta_{(OH)^1}\zeta_{CH_3})\{(n^2+2)/3\}+(1\alpha)\,\text{Å}R-(1\beta)\,\text{Å}R$$

8) H. Mc. D. McGeachin and C. A. Beevers, *Acta Crys.*, **10**. 227 (1957).
9) E. Montgomery and C. S. Hudson, *J. Am. Chem. Soc.*, **56**, 2074 (1934).
10) F. J. Bates et al., "Polarimetry, Saccharimetry and the Sugars", United States Government Printing Office, Washington (1942).
11) E. Zissis, N. K. Richtmyer and C. S. Hudson, *J. Am. Chem. Soc.*, **73**, 4714 (1951).
12) Eq. 4′ in a previous paper[2].
13) Cf. Ref. *21 in a previous paper[14].
14) S. Yamana, This Bulletin, **31**, 564 (1958).
15) Table I is used.
16) Table III in a previous paper[2] is used.

TABLE II. $[\mu]^{20}_{D\,obs}$, CAUSED BY THE DYNAMICAL COUPLING EFFECT BETWEEN ANY TWO MEMBERS OF UNIT GROUPS (EXCEPT RING) IN McGEACHIN AND BEEVERS' MOLECULAR MODEL

	$(CH_3)^{5\beta}$	4β	4α	3β	3α	2β	2α
1α	− 5.6	0.1	0.0	6.0	− 4.5	3.6	28.6
1β	1.3	− 0.6	0.0	− 1.9	− 3.5	29.6	−28.7
2α	− 0.9	7.1	− 0.5	40.2	−40.5		
2β	2.0	− 2.4	− 6.6	−41.1	1.1		
3α	5.6	0.6	45.4				
3β	0.4	41.9	−43.7				
4α	37.9						
4β	−37.6						

The corresponding ovserved value is given by, $\{[M]^{20}_{D}(W)$ of α-D-rhamnose$\}$ minus $\{[M]^{20}_{D}(W)$ of β-D-rhamnose$\}$. This is $15.7-(-63.0)$[15] $=78.7$. As these two values should be equal to each other,

$$(-7.73\zeta_{(OH)^1}\zeta_{OH}-6.83\zeta_{(OH)^1}\zeta_{CH_3})\{(n^2+2)/3\}+(1\alpha)\text{Ä}R-(1\beta)\text{Ä}R\equiv 78.7 \quad (2)$$

By using a method similar to that mentioned above, another equation is obtained for $[\mu]^{20}_{D\,obs}$ of the An. Diff. of L-arabinose:

$$28.06\zeta_{(OH)^1}\zeta_{OH}\{(n^2+2)/3\}+(1\alpha)\text{Ä}R-(1\beta)\text{Ä}R\equiv 169.7 \quad (3)$$

From Eq. 3 minus Eq. 2[17]:

$$(35.79\zeta_{(OH)^1}\zeta_{OH}+6.83\zeta_{(OH)^1}\zeta_{CH_3})\times\{(n^2+2)/3\}=91.0 \quad (4)$$

Now, in order to calculate the values of ζ_{OH}, ζ_{CH_3}, and of $\zeta_{(OH)^1}$ in pentose and methylpentose, another new equation (besides Eqs. 1 and 4) is necessary.

On the other hand, it has already been pointed out that the values of ζ_{OH} in the carbohydrate which has only two hydroxyl groups in its molecule (i. e., hydro-D-xylal) is nearly equal to that in the polyhydroxycyclohexane which has only two hydroxyl groups in the molecule (i. e., (−)1/2-cyclohexanediol)[1]. Therefore, it may be presumed that the ζ_{OH} value of some hydroxyl groups in pentose or methylpentose may be nearly equal to that in the polyhydroxycyclohexane which has more than three hydroxyl groups in the molecule, $1.9079\{3/(n^2+2)\}^{1/2}$ [3]. Therefore, in order to simplify the calculations, the author assumes, in pentose and methylpentose, the next equation:

$$\zeta_{OH}=1.9079\{3/(n^2+2)\}^{1/2} \quad (5)$$

or

$$\zeta_{OH}^2=3.6402\{3/(n^2+2)\} \quad (6)$$

Combining Eqs. 1, 4 and 5, the following values of ζ-coefficients can be obtained:

$$\zeta_{CH_3}=0.8093\{3/(n^2+2)\}^{1/2} \quad (7)$$

$$\zeta_{(OH)^1}=1.2329\{3/(n^2+2)\}^{1/2} \quad (8)$$

$$\zeta_{(OH)^1}\zeta_{OH}=2.3522\{3/(n^2+2)\}$$[18] $\quad (9)$

$$\zeta_{(OH)^1}\zeta_{CH_3}=0.9978\{3/(n^2+2)\} \quad (10)$$

By combining Eqs. 1, 6, 9 and 10 with Table III of a previous paper[2], a table of $[\mu]^{20}_{D\,obs}$ in pentose and methylpentose can be produced[19]. This is Table II.

In order to test the correctness of Table II, the $[M]^{20}_{D}(W)$ values of some carbohydrates have been calculated by using it, and those calculated values have then been tested by using Hudson's methyl glycoside rule[20] or another new method, devised by the author.

Calculation of $[M]^{20}_{D}(W)$

Pentose[21].—At first, by using the experimental data of $[M]^{20}_{D}(W)$ of β- and α-L-arabinoses, the value of $\{(1\alpha)\text{Ä}R-(1\beta)\text{Ä}R\}$ can be calculated as below:

$$[\mu]^{20}_{Dob} \text{ of the An. Diff. of L-arabinose} = \{(1\alpha)-(1\beta)\}\text{Ä}\{(2\alpha)+(3\beta)+(4\beta)+R\}$$[13] $$=(1\alpha)\text{Ä}(2\alpha)+(1\alpha)\text{Ä}(3\beta)+(1\alpha)\text{Ä}(4\beta)+(1\alpha)\text{Ä}R-\{(1\beta)\text{Ä}(2\alpha)+(1\beta)\text{Ä}(3\beta)+(1\beta)\text{Ä}(4\beta)+(1\beta)\text{Ä}R\}$$

17) Eq. 3 is used for the purpose of cancelling the $\{(1\alpha)\text{Ä}R-(1\beta)\text{Ä}R\}$ term in Eq. 2.

18) According to the conception that $\zeta_{(OH)^1}$ is different from ζ_{OH}, Eq. 11 in a previous paper[5] is rewritten as follows: $\zeta_{(OH)^1}\ \zeta_{OH}=2.4897\{3/(n^2+2)\}$. Note: This value was calculated by using McDonald and Beevers' molecular model (T. R. R. McDonald and C. A. Beevers, *Acta Cryst.*, **5**, 654 (1952)) and the $[M]^{20}_{D}(W)$ value of four hexoses (i. e., α-D-glucose, β-D-glucose, α-D-mannose and β-D-mannose) on the assumption that the internal conformation of the C^6-O bond is definite and similar in those four hexoses.

19) Concerning the making of the table of $[\mu]^{20}_{D\,obs}$, cf. Eq. 3 in a previous paper[5].

20) Cf. Ref. 20 in a previous paper[2].

21) There are four kinds of pentose, arabinose, xylose, lyxose and ribose. However, the exact $[M]^{20}_{D}(W)$ value of ribose has never been observed, and lyxose is of C1 and 1C conformations in an aqueous solution (R.E.Reeves, *J. Am. Chem. Soc.*, **72**, 1499 (1950)). Ribose and lyxose will be discussed by the author in detail in a future paper. Therefore, these two pentoses are not discussed in this article.

$$=28.6+6.0+0.1+(1\alpha)\lambda R-\{-28.7-1.9-0.6+(1\beta)\lambda R\}=65.9+(1\alpha)\lambda R-(1\beta)\lambda R^{22)}\equiv 169.7^{23)}$$

or

$$(1\alpha)\lambda R-(1\beta)\lambda R=103.8 \qquad (11)$$

In a like manner, by using Table II and Eq. 11, the $[\mu]^{20}_{D\,obs}$ value of the An. Diff. of D-xylose can be calculated as 169.0. Therefore, if the $[M]^{20}_{D}$(W) of β-D-xylose is x, $\{[M]^{20}_{D}(W)$ of α-D-xylose$\}-\{[M]^{20}_{D}(W)$ of β-D-xylose$\}=140.5-x^{15)}\equiv 169.0$

$$\therefore \quad x=-28.5$$

This calculated value is approximately equal to Hudson's figure, $-30°$ [24].

Methylpentose. — When the H atom which is combined with the C^5-atom of pentose is replaced by $(CH_3)^{5\beta}$ [15], methyl pentose can be obtained. This process can be shown schematically by the following equation:

$$(\text{pentose})-H^{5\beta}+(CH_3)^{5\beta}=(\text{methylpentose})$$

Because of its small polarizability, the $[\mu]^{20}_{D\,obs}$ of $H^{5\beta}$ can be neglected. Then, concerning the molecular rotations, the next equation can be obtained:

$$\{[M]^{20}_{D}(W) \text{ of pentose}\}+\{[\mu]^{20}_{D\,obs} \text{ of } (CH_3)^{5\beta}\}\simeq\{[M]^{20}_{D}(W) \text{ of methylpentose}\} \qquad (12)$$

Next, the value of $(CH_3)^{5\beta}\lambda R$ is calculated quasi-empirically as follows: The unit groups which can couple with $(CH_3)^{5\beta}$ in α-D-fucose are $(OH)^{1\alpha}$, $(OH)^{2\alpha}$, $(OH)^{3\beta}$, $(OH)^{4\beta}$ and ring [15]. Then,

$$[\mu]^{20}_{D\,obs} \text{ of } (CH_3)^{5\beta} \text{ in } \alpha\text{-D-fucose}=(CH_3)^{5\beta}\lambda\{(1\alpha)+(2\alpha)+(3\beta)+(4\beta)+R\}=(CH_3)^{5\beta}\lambda(1\alpha)+(CH_3)^{5\beta}\lambda(2\alpha)+(CH_3)^{5\beta}\lambda(3\beta)+(CH_3)^{5\beta}\lambda(4\beta)+(CH_3)^{5\beta}\lambda R=-5.6-0.9+0.4-37.6+(CH_3)^{5\beta}\lambda R=-43.7+(CH_3)^{5\beta}\lambda R$$

The corresponding observed value is given by the following equation:

$$\{[M]^{20}_{D}(W) \text{ of } \alpha\text{-D-fucose}\} \text{ minus } \{[M]^{20}_{D}(W) \text{ of } \beta\text{-L-arabinose}\}=251.0-303.3^{15)}=-52.3$$

$$\therefore \quad -43.7+(CH_3)^{5\beta}\lambda R\equiv -52.3$$

or

$$(CH_3)^{5\beta}\lambda R=-8.6 \qquad (13)$$

Referring to Eq. 12 and the unit groups in the molecules of α-D-xylose and of α-D-isorhamnose, the next equation can be obtained:

$$\{[M]^{20}_{D} \text{ of } \alpha\text{-D-xylose}\}+\{[\mu]^{20}_{D\,obs} \text{ of } (CH_3)^{5\beta}\}\simeq\{[M]^{20}_{D}(W) \text{ of } \alpha\text{-D-isorhamnose}\}$$

In this equation, $[\mu]^{20}_{D\,obs}$ of $(CH_3)^{5\beta}$ can be given by the following equation:

$$(CH_3)^{5\beta}\lambda\{(1\alpha)+(2\alpha)+(3\beta)+(4\alpha)+R\}^{15)}=(CH_3)^{5\beta}\lambda(1\alpha)+(CH_3)^{5\beta}\lambda(2\alpha)+(CH_3)^{5\beta}\lambda(3\beta)+(CH_3)^{5\beta}\lambda(4\alpha)+(CH_3)^{5\beta}\lambda R=-5.6-0.9+0.4+37.9-8.6^{22,25)}=23.2$$

Combining this value with Eq. 14, the $[M]^{20}_{D}$ of α-D-isorhamnose is calculated as 163.7. This is just equal to the observed value, 163.7 [15]. By using a method similar to that mentioned above, the $[M]^{20}_{D}$(W) values of two methylpentoses (β-D-fucose and β-D-isorhamnose) which have never been observed are calculated as 88.2 and 1.6 respectively from the $[M]^{20}_{D}$(W) values of their corresponding pentoses. As the $[M]^{20}_{D}$(W) values of methyl-β-D-fucoside and of methyl-β-D-isorhamnoside are $-25.3^{26)}$ and $-97.3^{27)}$, their respective $[M]^{20}_{D}$(W)-Diff. < methyl glycoside − cor. al.[28] pyranose > [29] values become −113.5 and −98.9. Therefore, the above expected values of β-D-fucose and β-D-isorhamnose satisfy Hudson's methyl glycoside rule [20]; accordingly, these two expected values seem to be reliable.

Next, by using the experimental data of the $[M]^{20}_{D}$(W) values of α-D-xylose and β-L-arabinose, the value of $\{(4\alpha)\lambda R-(4\beta)\lambda R\}$ can be calculated as follows:

$$[\mu]^{20}_{D\,obs} \text{ of Yo. Diff.}^{30)} < \alpha\text{-D-xylose} - \beta\text{-L-arabinose} >^{29)}=\{(4\alpha)-(4\beta)\}\lambda\{(1\alpha)+(2\alpha)+(3\beta)+R\}^{31,15)}=(4\alpha)\lambda(1\alpha)+(4\alpha)\lambda(2\alpha)+(4\alpha)\lambda(3\beta)+(4\alpha)\lambda R-\{(4\beta)\lambda(1\alpha)+(4\beta)\lambda(2\alpha)+(4\beta)\lambda(3\beta)+(4\beta)\lambda\}^{22)}=-93.3+(4\alpha)\lambda R-(4\beta)\lambda R$$

The corresponding observed value is given by the next equation:

$$\{[M]^{20}_{D}(W) \text{ of } \alpha\text{-D-xylose}\}-\{[M]^{20}_{D}(W) \text{ of } \beta\text{-L-arabinose}\}=140.5-303.3^{15)}=-162.8$$

Then, $-93.3+(4\alpha)YR-(4\beta)\lambda R\equiv -162.8$

$$\therefore \quad (4\alpha)\lambda R-(4\beta)\lambda R=-69.5 \qquad (15)$$

22) Table II is used.
23) Cf. Eq. 3.
24) This is the $[M]^{20}_{D}$ in an 80% alcoholic solution (E. Yanovsky and C. S. Hudson, *J. Am. Chem. Soc.*, 39, 1013 (1917)).
25) Eq. 13 is used.
26) R. C. Hockett, F. P. Phelps and C. S. Hudson, *J. Am. Chem. Soc.*, 61, 1658 (1939).
27) W. D. Maclay, R. M. Hann and C. S. Hudson, ibid., 61, 1660 (1939).
28) "cor." and "al." mean "corresponding" and "aldo-".
29) Cf. Ref. 17 in a previous paper [2].
30) Cf. Ref. *10 in a previous paper [14].
31) Cf. Ref. *12 in a previous paper [14].

TABLE III. $[M]_D^{20}$(W)-DIFF. ⟨HEXOSE−COR. METHYLPENTOSE⟩

Series	$[M]_D^{20}$(W) of hexose[15]	$[M]_D^{20}$(W) of cor. methyl pentose[15]	$[M]_D^{20}$(W)-Diff.
I	α-D-Glucose (202.1)	α-D-Isorhamnose (163.7)	38.4
	α-D-Mannose (52.8)	α-D-Rhamnose (15.7)	37.1
II	β-D-Glucose (33.7)	β-D-Isorhamnose ((1.6))	32.1
	β-D-Mannose (−30.6)	β-D-Rhamnose (−63.0)	32.4
III	α-D-Galactose (271.5)	α-D-Fucose (251.0)	20.5
	α-D-Talose (122.5)	α-D-Talomethylose ((99.6))	22.9
IV	β-D-Galactose (95.1)	β-D-Fucose ((88.2))	6.9
	β-D-Talose (23.8)	β-D-Talomethylose ((20.2))	3.6

Note: The value in (( )) is the calculated value in this article.

By using Eq. 15, the $[M]_D^{20}$(W) of α-D-talomethylose can be calculated as follows:

$$[\mu]_{D\,obs}^{20} \text{ of Yo. Diff}\langle\alpha\text{-D-rhamnose} - \alpha\text{-D-talomethylose}\rangle = \{(4\alpha)-(4\beta)\}\lambda \{(1\alpha)+(2\beta)+(3\beta)+(CH_3)^{5\beta}+R\}^{15,31)} = -83.9^{22)}$$

If the $[M]_D^{20}$(W) value of α-D-talomethylose is y, the corresponding observed value is given by {$[M]_D^{20}$(W) of α-D-rhamnose} minus {$[M]_D^{20}$(W) of α-D-talomethylose} $= 15.7^{15)} - y$

$$-83.9 \equiv 15.7 - y$$

or

$$y = 99.6$$

By using a similar method, the $[M]_D^{20}$(W) value of β-D-talomethylose is calculated as 20.2. However, in these cases, as the $[M]_D^{20}$(W) values of their corresponding methyl glycosides have not yet been observed, examinations by using Hudson's methyl glycoside rule are impossible. Therefore, in order to test the validity of these presumed $[M]_D^{20}$(W) values of methylpentoses, a new method has been devised as follows:

When an $(H)^6$ [32] in $(CH_3)^{5\beta}$ of methylpentose is replaced by $(OH)^6$ [32], hexose can be obtained. This process can be shown schematically by the next equation:

$$(\text{methylpentose}) - (H)^6 + (OH)^6 = (\text{hexose})$$

Owing to its small polarizability, the $[\mu]_{D\,obs}^{20}$ value of $(H)^6$ can be neglected; the following equation on molecular rotations is obtained:

$$\{[M]_D^{20}(\text{W}) \text{ of methylpentose}\} + \{[\mu]_{D\,obs}^{20} \text{ of } (OH)^6\} \simeq \{[M]_D^{20}(\text{W}) \text{ of hexose}\}$$

or

$$[M]_D^{20}\text{(W)-Diff.}\langle\text{hexose} - \text{cor. methylpentose}\rangle \equiv \{[M]_D^{20}(\text{W}) \text{ of hexose}\} - \{[M]_D^{20}(\text{W}) \text{ of methylpentose}\} \simeq [\mu]_{D\,obs}^{20} \text{ of } (OH)^6 \quad (16)$$

On the other hand, $(OH)^2$ is situated at the opposite end of a diameter of the aldopyranose-ring in relation to the C^5-atom with which $(CH_2OH)^{5\beta}$ is combined, and the distance between $(OH)^2$ and $(OH)^6$ is fairly large[34]. Therefore, referring to Tschúgaeff's Entfernungssatz[35] and Freudenberg's Verschiebungssatz[36], the following anticipation is possible:

The value, expressed in Eq. 16, should be almost indifferent to the orientation-change of $(OH)^2$. In short, the $[M]_D^{20}$(W)-Diff.⟨hexose-cor. methylpentose⟩ of the epimer[37] should be nearly equal to each other. (Anticipation 3)

Therefore, if a $[M]_D^{20}$(W) value does not satisfy Anticipation 3, it should be doubtful. Thus, Anticipation 3 can be a new instrument to test the validity of any $[M]_D^{20}$(W) value of hexose or methylpentose.

The concrete values of $[M]_D^{20}$(W)-Diff. ⟨hexose−cor. methylpentose⟩ now available are shown in Table III.

It is apparent in Table III that $[M]_D^{20}$(W)-Diff.⟨hexose−cor. methylpentose⟩ can be classified into approximately four series and that, moreover, when considering the orientation of $(OH)^2$ [15], the hexoses (or methylpentoses) which belong to the same series are the empimers of each other. Therefore, the values of $[M]_D^{20}$(W) in Table III satisfy Anticipation 3. This fact indicates that the $[M]_D^{20}$(W) values in Table III are almost completely reliable.

32) Cf. Ref. *10 in a previous paper[33].

33) S. Yamana, This Bulletin, 30, 920(1957).
34) Cf. Ref. *17 in a previous paper[33].
35) L. Tschúgaeff, *Ber.*, 31, 360 (1898).
36) K. Freudenberg and W. Kuhn, ibid., 64, 726 (1931).
37) Cf. Ref. *9 in a previous paper[14].

Summary

As there are four hydroxyl groups in the pentose and methylpentose molecules, the ζ_{OH} values in some of them may be nearly equal to that in the polyhydroxycyclohexane which has four hydroxyl groups in the molecule. In order to satisfy this condition, the ζ-coefficient of $(H)^1$, $\zeta_{(OH)^1}$, was distinguished from that of the other (OH), ζ_{OH}. Next, by using the PM-method, the values of $\zeta_{(OH)}$, ζ_{OH} and ζ_{CH_3} were calculated. Making use of these ζ-coefficients, a table of $[\mu]^{20}_{D\,obs}$ values was made. By using this table, the $[M]^{20}_{D}(W)$ values of some carbohydrates, hitherto unknown, were calculated. The validity of the presumed values was then tested by applying Hudson's methyl glycoside rule and a new anticipation proposed by the author.

Department of Chemistry
Kyoto Gakugei University
Fushimi-ku, Kyoto

Decomposition of Peroxybenzoic Acid in Solution. III. Decomposition in Ethers

By Katsumi TOKUMARU and Osamu SIMAMURA

(Received July 24, 1962)

In previous papers[1,2], an account has been given of the decomposition of peroxybenzoic acid in alcohols and hydrocarbons and a radical chain mechanism has been proposed for the decomposition. This part deals with the decomposition of peroxybenzoic acid in diethyl, diisopropyl, and di-*n*-butyl ether.

Experimental

Materials.—Peroxybenzoic acid was prepared as previously described[1].

Diethyl ether was shaken with cold 50% sulphuric acid, followed by aqueous sodium hydroxide, dried with calcium chloride and then with sodium metal, and distilled under an atmosphere of nitrogen. Diisopropyl ether and di-*n*-butyl ether were similarly purified. Dioxan was refluxed with sodium metal in a stream of nitrogen and distilled.

Kinetic Measurements.—Rate of decomposition of peroxybenzoic acid was measured under an atmosphere of nitrogen by the same method as in Part I[1].

Product Study. — The general procedure was essentially the same as that described in Part II[2].

1) Decomposition in Diisopropyl Ether. — Peroxybenzoic acid (5.0 g., 36 mmol.) was decomposed in diisopropyl ether (150 ml.), in a stream of nitrogen at 65°C for 6 hr. Carbon dioxide (4 mmol.) was caught by absorption in a potash bulb. The reaction mixture was distilled, with occasional addition of fresh diisopropyl ether to the distilling flask to remove volatile matter completely. The distillate and the condensate in a trap cooled with solid carbon dioxide were combined and shown to contain isopropyl alcohol and acetone by gas chromatography. This mixture was extracted repeatedly with water, and the aqueous extract, on treatment with 2, 4-dinitrophenylhydrazine, gave 2, 4-dinitrophenylhydrazone of acetone (24 mmol.), melting point and mixed melting point with an authentic sample, 126°C. The residue from the distillation was extracted with water, and the aqueous extract, on treatment with 2, 4-dinitrophenylhydrazine, gave no appreciable precipitate; the organic layer was extracted with aqueous sodium hydrogen carbonate, and the extract gave benzoic acid (3.8 g., 31 mmol.), m. p. 121°C, on acidification.

In an experiment intended to investigate gaseous products, peroxybenzoic acid (2.8 g., 20 mmol.) was decomposed in diisopropyl ether (50 ml.) at 65°C in a closed system. Analysis of the gaseous products by absorption method showed formation of carbon dioxide (2 mmol.) and oxygen (3 mmol.).

2) Decomposition in Diethyl Ether.—Peroxybenzoic acid (2.8 g., 20 mmol.) was decomposed in boiling diethyl ether under an atmosphere of nitrogen. The reaction mixture was distilled. The distillate and the condensate in a trap chilled with solid carbon dioxide were combined and the mixture shown by gas chromatography to contain ethyl alcohol and acetaldehyde, on treatment with 2, 4-dinitrophenylhydrazine, gave 2, 4-dinitrophenylhydrazone of acetaldehyde (7 mmol.), melting point and mixed melting point with an authentic sample, 168°C. The distillation of the remaining reaction mixture at reduced pressure gave acetic acid (trace), which was identified by the infrared spectrum. The residue from the distillation consisted of almost pure benzoic acid (2.2 g., 18 mmol.), m. p. 121°C.

1) K. Tokumaru, O. Simamura and M. Fukuyama, This Bulletin, 35, 1673 (1962).
2) K. Tokumaru and O. Simamura, ibid., 35, 1678 (1962).

3) Decomposition in Di-n-butyl Ether. — Peroxybenzoic acid (2.1 g., 15 mmol.) was decomposed in di-*n*-butyl ether at 60°C in a stream of nitrogen. The reaction mixture was distilled, and the distillate, treated with 2, 4-dinitrophenylhydrazine, gave 2, 4-dinitrophenylhydrazone of *n*-butyraldehyde (3 mmol.), melting point (from ethyl alcohol) and mixed melting point with an authentic sample, 122°C. Gas chromatographic analysis of the distillate showed the presence of *n*-butyraldehyde and *n*-butyl alcohol. Benzoic acid (1.7 g., 14 mmol.), m. p. 121°C, was obtained from the residue of the distillation.

Results and Discussion

Peroxybenzoic acid decomposed rapidly in ethers. The initial rapid decomposition often was followed by decomposition with decreasing speed as shown in Fig. 1, and the rate of decomposition did not conform to a simple first-order kinetics. Therefore, only percentage decomposition of peroxybenzoic acid is shown in Table I. The results of the product study are summarized in Table II.

If peroxybenzoic acid decomposes in ethers by the radical chain mechanism postulated previously[1,2], the reaction paths in ethers will be represented as follows.

$$PhCO_3H \rightarrow PhCO_2\cdot + HO\cdot \quad (1)$$

$$PhCO_2\cdot \rightarrow Ph\cdot + CO_2 \quad (1')$$

$$ROCHR'R'' + \text{Radical} \rightarrow ROC\dot{R}'R'' + \text{Stable molecule} \quad (2)$$

$$PhCO_3H + ROC\dot{R}'R'' \rightarrow ROCR'R''OH + PhCO_2\cdot \quad (3)$$

$$ROC\dot{R}'R'' \rightarrow R\cdot + R'R''CO \quad (4)$$

$$ROCR'R''OH \rightarrow ROH + R'R''CO \quad (5)$$

In the above mechanism, the radicals formed from peroxybenzoic acid abstract a hydrogen atom α to the oxygen of ether (reaction 2). Solvent radicals thus formed, that is, 1-alkoxyalkyl radicals, attack peroxybenzoic acid, producing 1-hydroxyalkyl ether and the benzoyloxy radical (reaction 3), which in turn abstracts a hydrogen atom from ether, propagating the chain. 1-Hydroxyalkyl ether will be unstable, decomposing to an alcohol and a carbonyl compound (reaction 5). There exists the alternative possibility of thermal decomposition of the solvent radical (reaction 4), but it does not seem important, since, in the first place, in the decomposition of benzoyl peroxide in ethers, its induced decomposition by 1-alkoxyalkyl radicals is reported to take place to an appreciable extent[3-5], and, secondly, peroxybenzoic acid is more readily attacked by radicals than benzoyl peroxide is, as will be shown in a subsequent paper. The alcohols formed by reaction 5 may suffer further oxidation by peroxybenzoic acid as described in Part I of this series. In fact, the production of acetone and isopropyl alcohol from diisopropyl ether can be explained on the basis of the above reaction scheme, and some part of the acetone may have been formed by further oxidation of isopropyl alcohol. The products from diethyl and di-*n*-butyl ether listed in Table II are explained similarly.

The isolation of benzoic acid in a yield ranging from 80 to 93% indicates that the benzoyloxy radical underwent only a slight thermal decomposition and mainly abstracted an α-hydrogen of ethers. This conclusion is well in accord with the behaviour of the benzoyloxy radical in the decomposition of benzoyl peroxide in ethers [3-5].

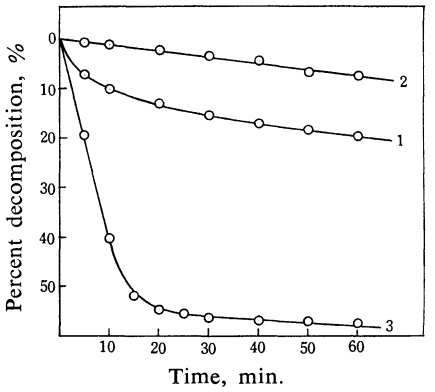


Fig. 1. Decomposition of peroxybenzoic acid in ethers at 50°C (initial concentration of peroxybenzoic acid, 0.1 mol./l.).

1 Diisopropyl ether
2 Di-*n*-butyl ether
3 Dioxan

TABLE I. DECOMPOSITION OF PEROXYBENZOIC ACID IN ETHERS AT 50°C

Solvent	Percent decomposition in 10 min.	30 min.	1 hr.
Diisopropyl ether	10.3	15.6	19.6
Di-*n*-butyl ether	1.2	3.4	7.4
Dioxan	40.5	56.5	57.5
Isopropyl alcohol*	17.8	44.5	62.1
Cumene**	4.1	7.5	13.9

*k_1 at 50°C: 3.4×10^{-4} sec^{-1} [1]
**k_1 at 60°C: 3.8×10^{-5} sec^{-1} [2]

3) W. E. Cass, *J. Am. Chem. Soc.*, **69**, 500 (1947).
4) E. H. Drew and J. C. Martin, *Chem. and Ind.*, **1959**, 925.
5) D. B. Denny and G. Feig, *J. Am. Chem. Soc.*, **81**, 5322 (1959).

TABLE II. PRODUCTS FORMED IN DECOMPOSITION OF PEROXYBENZOIC ACID IN ETHERS

Ether	Temp.	Product and yield (% based on peroxybenzoic acid)			
		Products from ether	Benzoic acid	Carbon dioxide	Oxygen
Diethyl	under reflux	Acetaldehyde, 35; Ethyl alcohol, Acetic acid	90		
Diisopropyl	65°C	Acetone, 67; Isopropyl alcohol	80	11	
Diisopropyl	65°C			10	15
Di-*n*-butyl	60°C	*n*-Butyraldehyde, 20; *n*-Butyl alcohol	93		

Peroxybenzoic acid has been thought[6,7] to exist in a monomeric form with an intramolecular hydrogen bond in a non-polar solvent, but in polar solvents like alcohols and ethers, it can form an intermolecular hydrogen bond with an oxygen atom of the solvent molecule. This view has been supported by a spectroscopic study of peroxybenzoic acid made in this laboratory[7]. Thus it is reasonable to suppose that the acidic dissociation of peroxybenzoic acid will be favoured in polar solvents like alcohols and ethers with a basic oxygen atom, producing peroxybenzoate anions. These anions will attack peroxybenzoic acid with electron transfer, giving radicals according to the mechanism suggested by Kirmse and Horner[8] as follows:

$$PhCO_3^- + PhCO_3H \rightarrow PhCO_3\cdot + PhCO_2^- + HO\cdot$$

This process will contribute, as an initial radical forming process, to the rapid decomposition of peroxybenzoic acid in ethers and alcohols. Some part of the benzoylperoxy radicals thus formed may give rise to molecular oxygen by some mechanism such as:

$$2PhCO_3\cdot \rightarrow 2PhCO_2\cdot + O_2$$

For the production of oxygen an alternative mechanism similar to that postulated by Kharasch and coworkers[9] in the case of α-cumyl hydroperoxide cannot be excluded, thus:

$$RO_2^- + ROOH \rightarrow RO^- + ROH + O_2$$

Summary

Decomposition of peroxybenzoic acid was studied in diethyl, diisopropyl and di-*n*-butyl ether and explained in terms of the same radical mechanism that was postulated previously. Besides ready induced decomposition of peroxybenzoic acid by solvent radicals and facile abstraction of a hydrogen atom from ether by radicals, attack of peroxybenzoate anions on peroxybenzoic acid was pointed out to be an important contributing factor for the relatively rapid decomposition in ethers.

Department of Chemistry
Faculty of Science
The University of Tokyo
Hongo, Tokyo

6) W. H. T. Davison, *J. Chem. Soc.*, **1951**, 2456.
7) T. Mitsuhashi, O. Simamura and K. Tokumaru, unpublished observation.
8) W. Kirmse and L. Horner, *Chem. Ber.*, **89**, 836 (1956).
9) M. S. Kharasch, A. Fono and W. Nudenberg, *J. Org. Chem.*, **16**, 113 (1951); M. S. Kharasch, A. Fono, W. Nudenberg and B. Bischof, ibid., **17**, 207 (1952).

*Reaction of Benzoyl Peroxide with Phenols Substituted with Electron-Withdrawing Groups**

By Hakuai INOUE, Osamu SIMAMURA and Kanichiro TAKAMIZAWA

(Received September 4, 1962)

Ever since benzoyl peroxide was recognized as a typical radical generator in solution[1], a great many investigations have been made to elucidate the nature of the reactions which ensue from the homolytic rupture of benzoyl peroxide in various solvents[2]. The detailed reaction pattern depends on the nature of a substrate compound in which benzoyl peroxide is allowed to decompose. Among other substrates phenols are of particular interest, since they act as efficient inhibitor or retarder of free-radical reactions, especially of autoxidation. Studies[3-6] carried out on the reaction with phenols show that the reaction of benzoyl peroxide takes place quite differently in phenols than in other solvents; a marked feature in phenols is that carbon dioxide is evolved in very much smaller amounts than in other solvents, and that the yield of benzoic acid is correspondingly higher, thus:

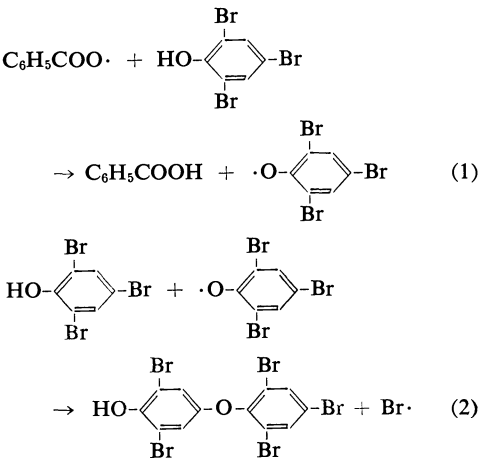
$$(C_6H_5COO)_2 \rightarrow 2C_6H_5COO\cdot$$

$$C_6H_5COO\cdot + ArOH \rightarrow C_6H_5COOH + ArO\cdot$$

The aryloxy radical ArO· produced from phenols by abstraction of a hydrogen atom of the hydroxyl group is comparatively stable because of the conjugation of the odd electron on the oxygen atom with the π-electron system of the nucleus and consequently tends to dimerize giving dihydroxybiphenyls rather than to attack some other molecules. The aryloxy radical may also cause, according to its reactivity, the induced decomposition of benzoyl peroxide giving a benzoyloxy derivative of the phenol and a benzoyloxy radical. Recently, on the basis of kinetic evidence, Walling and Hodgdon[7] have put forward a simple bimolecular "four-center" mechanism without radical formation for the reaction between benzoyl peroxide and phenols at 30°C.

Except for Walling and Hodgdon's work which included *m*-chloro-, *p*-chloro-, and *p*-bromo-phenol, previous studies have been carried out on phenol and phenols substituted with electron-releasing groups. We now report the results of a study on the reaction of benzoyl peroxide with various phenols with electron-withdrawing groups such as halogens and nitro group.

The Reaction of Benzoyl Peroxide with 2,4,6-Tribromophenol. — Benzoyl peroxide was refluxed with 2, 4, 6-tribromophenol in carbon tetrachloride and there were isolated as major products benzoic acid and a polymeric material of an approximate molecular weight of 3600~4800, whose chemical constitution was shown to be polydibromophenylene oxide $H(OC_6H_2\cdot Br_2)_nBr$. Minor products are shown in Table I. In one experiment 2, 6-dibromo-4-(2, 4, 6-tribromophenoxy)-phenol ($n=2$ in the above formula) was isolated. The structure of this compound suggests the following mechanism in which a benzoyloxy radical generated by unimolecular decomposition of benzoyl peroxide abstracts a hydrogen atom from the hydroxy group of 2, 4, 6-tribromophenol and the resulting 2, 4, 6-tribromophenoxy radical then attacks 2, 4, 6-tribromophenol to give 2, 6-dibromo-4-(2, 4, 6-tribromophenoxy)phenol and a bromine atom.



(1)

(2)

* Most of the material of this paper was presented in parts at the 6th, the 7th, and the 9th Annual Meeting of the Chemical Society of Japan held in Kyoto in 1953, in Tokyo in 1954, and in Kyoto in 1956, respectively.

1) D. H. Hey and W. A. Waters, *Chem. Revs.*, **21**, 169 (1937).

2) For reviews see C. Walling, "Free Radicals in Solution", John Wiley & Sons, Inc., New York (1957), p. 474, and T. Suehiro, "Yukihannokiko no Simpo", Vol. 1, Maki Syoten, Tokyo (1958), p. 119.

3) C. Walling, *J. Am. Chem Soc.*, **66**, 1602 (1944).

4) P. D. Bartlett and K. Nozaki, ibid., **69**, 2299 (1947).

5) S. L. Cosgrove and W. A. Waters, *J. Chem. Soc.*, **1949**, 3189; **1951**, 388.

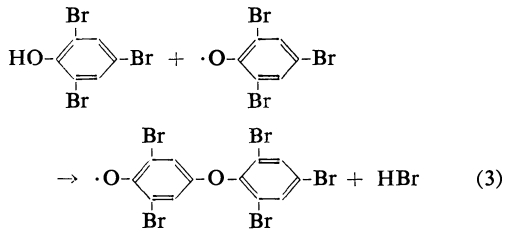
6) T. Suehiro, *J. Chem. Soc. Japan, Pure Chem. Sec.* (*Nippon Kagaku Zassi*), **72**, 301 (1951).

7) C. Walling and R. B. Hodgdon, *J. Am. Chem. Soc.*, **80**, 228 (1958).

TABLE I. REACTION OF BENZOYL PEROXIDE WITH 2,4,6-TRIBROMOPHENOL

	Reactant	mol.	Product	mol./mol. peroxide
(a)	$HOC_6H_2Br_3$	0.024~0.05	CO_2	0.1~0.26
	$(C_6H_5COO)_2$	0.015	Br_2	0.2~0.4
			C_6H_5COOH	1.7~1.8
	Refluxed 22 hr. in CCl_4 (40 cc.)		C_6H_6	trace
			C_6H_5Br	trace
			$H(C_6H_2Br_2O)_nBr$	(5~6.7 g.)
(b)	$HOC_6H_2Br_3$	0.276	CO_2	not measured
	$(C_6H_5COO)_2$	0.056	HBr	0.11
			Br_2	0.48
	Refluxed 17 hr. in CCl_4 (400 cc.)		C_6H_6	trace
			C_6H_5Br	0.1
			$(C_6H_5)_2$	trace
			C_6H_5COOH	1.89
			$C_6H_5COOC_6H_5$	0.002
			$H(C_6H_2Br_2O)_2Br$	0.14
			$H(C_6H_2Br_2O)_nBr$	(34 g.)
			$HOC_6H_2Br_3$ (recovered)	2.5

It may be plausible to suppose that in step 2 a 2,6-dibromo-4-(2,4,6-tribromophenoxy)-phenoxy radical and hydrogen bromide are produced without liberation of any bromine atoms:



(3)

This view is supported by the fact that no chlorine was formed at all in the reaction of benzoyl peroxide with 2,4,6-trichlorophenol under similar experimental conditions.

The bromine atoms produced in step 2 may combine to give molecular bromine or react with phenols (ArOH), affording aryloxy radicals including 2,4,6-tribromophenoxy-, 2,6-dibromo-4-(2,4,6-tribromophenoxy)phenoxy radicals etc.:

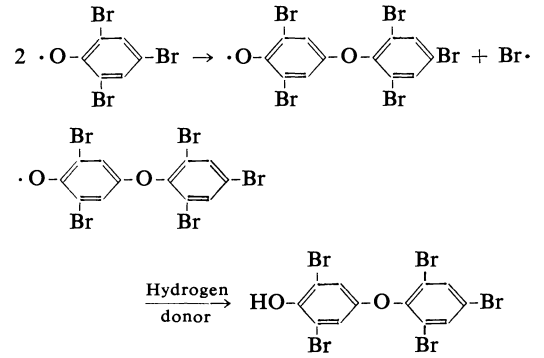
$$2Br\cdot \longrightarrow Br_2$$

$$Br\cdot + ArOH \rightleftarrows HBr + ArO\cdot$$

Bromine can also be produced from hydrogen bromide by oxidation with benzoyl peroxide.

Obviously, successive attack by aryloxy radicals on phenols at a nuclear position carrying a bromine atom according to the above mechanism (step 2 or 3) leads to the formation of polymeric $H(OC_6H_2Br_2)_nBr$.

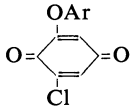
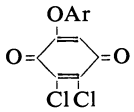
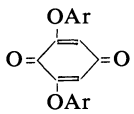
However, the possibility cannot be excluded that two of the tribromophenoxy radical react with each other with expulsion of a bromine atom giving a 2,6-dibromo-4-(2,4,6-tribromophenoxy)phenoxy radical, which then affords a molecule of the corresponding phenol by abstracting an atom of hydrogen from a hydrogen donor, that is, presumably from another molecule of phenols or from a molecule of hydrogen bromide, one of the reaction products:



Continuation of such a reaction between two aryloxy radicals may similarly result in the formation of the polydibromophenylene oxide $H(OC_6H_2Br_2)_nBr$.

As for the minor products there scarcely seems to be any need of comments, since these are the usual products in the decomposition of benzoyl peroxide in solvents. Carbon dioxide was evolved in much larger amount than in the decomposition in phenol itself and in phenols with an electron-releasing group. This fact seems to indicate that the benzoyloxy radical has a little more difficulty in abstracting a hydrogen atom from tribromophenol.

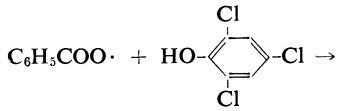
TABLE II. REACTION OF BENZOYL PEROXIDE WITH 2,4,6-TRICHLOROPHENOL

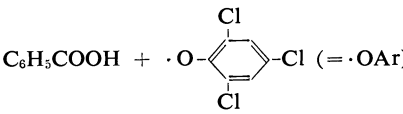
Reactant	mol.	Product	mol./mol. peroxide
$HOC_6H_2Cl_3$	0.426	C_6H_5COOH	0.60
$(C_6H_5COO)_2$	0.15	HCl	a large amount but not determined
		C_6H_6	0.04
Refluxed 30 hr. in CCl_4 (360 cc.)		C_6H_5Cl	0.087
		$HOC_6H_2Cl_2COOCH_3$	0.018
			0.002
			0.005
			0.0013
		C_6H_5COCl	0.113
		$HOC_6H_2Cl_3$ (recovered)	0.162

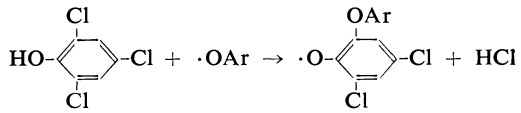
Ar=2,4,6-Trichlorophenyl

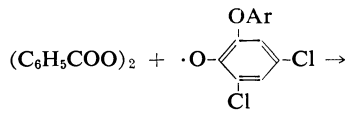
Hunter and his coworkers[8] had observed that in the presence of trace amount of bromine vapour potassium or silver 2,4,6-tribromophenoxide decomposes to give poly-dibromophenylene oxide. This fact indicates that bromine and tribromophenoxide can give tribromophenoxy radicals, which then start the chain reaction to give the polymeric material similarly to the case initiated by benzoyl peroxide. Recently Price[9] has reported the formation of polyphenylene oxides by oxidation of substituted *p*-bromophenols and proposed a mechanism involving the aryloxy radical.

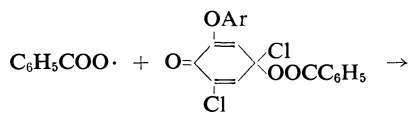
The Reaction of Benzoyl Peroxide with 2, 4, 6-Trichlorophenol.—The results of the reaction of benzoyl peroxide with 2,4,6-trichlorophenol in boiling carbon tetrachloride are tabulated in Table II. Although a considerable amount of tar was formed, a polymeric material corresponding to polydibromophenylene oxide could not be isolated. Among other products, however, 2-chloro-6-(2,4,6-trichlorophenoxy)-, 2,3-dichloro-6-(2,4,6-trichlorophenoxy)-, and 2,6-bis-(2,4,6-trichlorophenoxy)-*p*-benzoquinone are worth mentioning. Obviously their isolation indicates the formation of 2,4,6-trichlorophenoxy radicals by attack of the benzoyloxy radical on 2,4,6-trichlorophenol. Further the formation of benzoyl chloride is remarkable, and a separate experiment showed that it is formed even in the absence of carbon tetrachloride as solvent. These findings immediately suggest the following steps for the mechanism of the formation of the quinones:

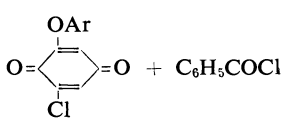












8) W. H. Hunter, A. O. Olson and E. A. Daniels, *J. Am. Chem. Soc.*, **38**, 1761 (1916); W. A. Hunter and G. H. Woollett, ibid., **43**, 135 (1921).

9) G. D. Staffin and C. C. Price, ibid., **82**, 3632 (1960); C. J. Kurian and C. C. Price, *J. Polymer Sci.*, **49**, 267 (1961).

TABLE III. PRODUCTS FROM REACTION OF 2,4,6-TRICHLOROPHENOL (1.0 g.) WITH LEAD DIOXIDE (7.0 g.)

Reactant	g.	Product, g.	In the Presence of 2,6-dichloro-*p*-benzoquinone (1.0 g.)	In the Absence
PbO_2	7.0	2,6-Dichloroquinone	1.1	0.01
$HOC_6H_2Cl_3$	1.0	2-Chloro-6-(2,4,6-trichlorophenoxy)-*p*-benzoquinone	0.8	0.8
		2,6-Bis-(2,4,6-trichlorophenoxy)-*p*-benzoquinone	0.07	0.07

TABLE IV. REACTION OF BENZOYL PEROXIDE WITH 2,6-DIHALOGENOPHENOLS

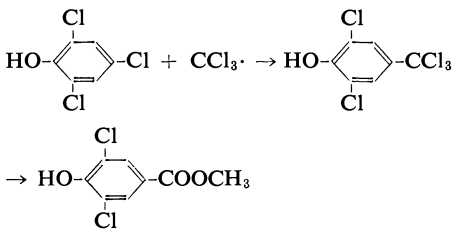
	Reactant,	mol.	Product	mol./mol. peroxide
(a)	$HOC_6H_3Cl_2$	0.1	C_6H_5COOH	1.13
	$(C_6H_5COO)_2$	0.05	$HOC_6H_2Cl_2C_6H_2Cl_2OH$	0.012
	Refluxed 20 hr. in CCl_4 (100 cc.)		C_6H_5COCl	detected
			HCl	detected
(b)	$HOC_6H_3Br_2$	0.074	C_6H_5COOH	1.72
			CO_2	0.13
	$(C_6H_5COO)_2$	0.021	$HOC_6H_2Br_2C_6H_2Br_2OH$	0.01
	Refluxed 25 hr. in CCl_4 (100 cc.)		Br_2	0.48
			$HOC_6H_2Br_3$	0.04
			$HOC_6H_3Br_2$ (recovered)	0.04

Similar steps will explain the formation of the other quinones. 2,3-Dichloro-6-(2,4,6-trichlorophenoxy)-*p*-benzoquinone seems to have been produced by chlorination of 2-chloro-6-(2,4,6-trichlorophenoxy)-*p*-benzoquinone, as is supported by an experiment described in the experimental part.

The isolation of methyl 3,5-dichloro-4-hydroxybenzoate suggests the involvement of trichloromethyl radicals derived from carbon tetrachloride, thus:

$$C_6H_5COO\cdot \rightarrow C_6H_5\cdot + CO_2$$

$$C_6H_5\cdot + CCl_4 \rightarrow C_6H_5Cl + CCl_3\cdot$$



Any substituted *o*-benzoquinones could not be isolated; such compounds would have decomposed under the present experimental conditions because of their instability. No chlorine was detected at all; since benzoyl peroxide does not oxidize hydrochloric acid to chlorine, this fact suggests that either the substitution of trichlorophenol by the trichlorophenoxy radical takes place without producing free chlorine atoms or these atoms, if produced at all, are very quick to abstract a hydroxyl hydrogen atom from the phenol.

Another mechanism for the production of aryloxyquinones from trichlorophenol is initial formation of 2,6-dichloro-*p*-benzoquinone followed by substitution of chlorine with 2,4,6-trichlorophenoxy radicals. The following findings, however, rule out this possibility. Since the same aryloxyquinones, viz., 2-chloro-6-(2,4,6-trichlorophenoxy)- and 2,6-bis-(2,4,6-trichlorophenoxy)-*p*-benzoquinone, are formed by oxidation of 2,4,6-trichlorophenol with lead dioxide at room temperature[10], it is reasonable to suppose that the same mechanism should be operative in the oxidation with lead dioxide as well as with benzoyl peroxide. In order to examine the effect of 2,6-dichloro-*p*-benzoquinone oxidation of 2,4,6-trichlorophenol with lead dioxide was carried out both in the presence and in absence of the dichloroquinone; the results tabulated in Table III show that the yield of aryloxyquinones were nearly equal in both experiments and that the dichloroquinone added beforehand was recovered unchanged, eliminating the formation of this compound as an intermediate.

The Reaction of Benzoyl Peroxide with 2,6-Dihalogenophenols.—The results of the reaction are summarized in Table IV. In the reaction with 2,6-dibromophenol bromine and 2,4,6-tribromophenol were formed, whereas hydrogen chloride and benzoyl chloride were detected in the reaction with 2,6-dichlorophenol. The formation of these products indicates that at

10) W. H. Hunter and H. Morse, *J. Am. Chem. Soc.*, **48**, 1615 (1926).

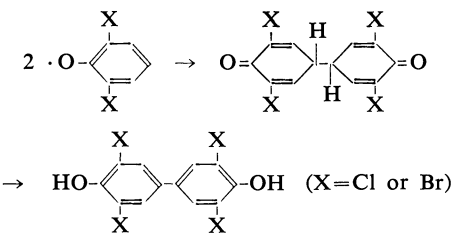
TABLE V. REACTIONS OF BENZOYL PEROXIDE WITH *p*-HALOGENOPHENOLS

	Reactant	mol.	Product	mol./mol. peroxide
(a)	*p*-ClC_6H_4OH	0.195	C_6H_5COOH	1.32
	$(C_6H_5COO)_2$	0.067	HCl	detected
	Refluxed 12.5 hr. in CCl_4 (100 cc.)		$ClC_6H_3(OH)OCOC_6H_5$	0.545
(b)	*p*-BrC_6H_4OH	0.302	C_6H_5COOH	1.45
	$(C_6H_5COO)_2$	0.1	$BrC_6H_3(OH)OCOC_6H_5$	0.284
	Refluxed 35.5 hr. in CCl_4 (100 cc.)		BrC_6H_4OH	0.121
(c)	*p*-IC_6H_4OH	0.08	C_6H_5COOH	0.94
	$(C_6H_5COO)_2$	0.039	$IC_6H_3(OH)OCOC_6H_5$	0.18
	Refluxed 13 hr. in CCl_4 (80 cc.)		I_2	0.24
			IC_6H_4OH	0.017

TABLE VI. REACTION OF BENZOYL PEROXIDE WITH NITROPHENOLS

	Reactant	mol.	Product	mol./mol. peroxide
(a)	*p*-$NO_2C_6H_4OH$	0.10	C_6H_5COCl	detected
	$(C_6H_5COO)_2$	0.05	HCl, CO_2	detected
	Refluxed 15 hr. in CCl_4 (400 cc.)		*p*-$NO_2C_6H_4OH$, (recovered)	2.0
(b)	*p*-$NO_2C_6H_4OH$	0.10	C_6H_5COOH	1.65
	$(C_6H_5COO)_2$	0.05	CO_2	0.22
	at 100°C		$C_6H_5COOC_6H_4NO_2$	trace
			$HOC_6H_4NO_2$, (recovered)	0.073
(c)	*o*-$NO_2C_6H_4OH$	0.20	CO_2	0.59
	$(C_6H_5COO)_2$	0.10	C_6H_5COOH	0.93
	at 100°C		4-$C_6H_5C_6H_4COOH$	0.02
			$HOC_6H_3(NO_2)C_6H_5$	0.11
			$C_6H_5COOC_6H_5$	0.019

least part of the reaction mechanism is essentially similar to that in the case of tribromo- or trichloro-phenol, although any substances containing a diphenyl ether linkage could not be isolated. In contrast to the case with trihalogenophenols 2, 6-dibromophenol gave 3, 5, 3', 5'-tetrabromo - 4, 4' - dihydroxybiphenyl, and 2, 6-dichlorophenol, the corresponding tetrachloro-compound. Evidently dimerization of the dihalogenophenoxy radical gave the tetrahalogenodihydroxybiphenyl:



The Reaction of Benzoyl Peroxide with *p*-Halogenophenols. — Products from these reactions are listed in Table V.

The formation of benzoic acid and 2-benzoyloxy-4-halogenophenols is in line with the observations by Suehiro[6] and by Cosgrove and Waters[5] with phenol and its homologues.

The Reaction of Benzoyl Peroxide with *o*- and *p*-Nitrophenols. — The results are shown in Table VI.

When a mixture of benzoyl peroxide and *p*-nitrophenol was refluxed in carbon tetrachloride, benzoyl peroxide reacted only with carbon tetrachloride and the whole of the *p*-nitrophenol used was recovered. However, when both components were allowed to react at 100°C in the absence of any solvent, an appreciable amount of carbon dioxide was evolved in contrast to the reactions with other phenols. The isolated products were *p*-nitrophenyl benzoate and benzoic acid.

Similarly, *o*-nitrophenol gave at 100°C carbon dioxide, benzoic acid, 4-biphenylcarboxylic acid, phenyl-*o*-nitrophenol, and phenyl benzoate. In this case phenylation of *o*-nitrophenol occurred; no such reaction has ever been observed with phenols. These results show that the benzoyloxy radical abstracts a hydrogen atom from nitrophenols only with difficulty and therefore has to decompose into carbon dioxide and a phenyl radical.

Experimental

Materials.—Benzoyl peroxide was recrystallized twice from chloroform and methanol, m. p. 106°C

(decomp.), purity 99.8% as determined by iodometry. 2,4,6-Tribromophenol, prepared according to Vanino[11], had m. p. 96°C. 2,4,6-Trichlorophenol was prepared by chlorination of phenol with sodium hypochlorite solution[12], m. p. 66~67°C. 2,6-Dibromophenol was synthesized according to Huston and Neeley's method[13], m. p. 56°C. 2,6-Dichlorophenol was synthesized from *t*-butyl *p*-hydroxybenzoate by chlorination with sulphuryl chloride followed by hydrolysis and decarboxylation[14]. *p*-Chlorophenol was obtained from phenol and sulphuryl chloride[15], b. p. 99°C/11 mmHg, m. p. 44°C. *p*-Bromophenol was prepared by bromination of phenol in carbon disulphide[16], m. p. 64°C, b. p. 145~150°C/25 mmHg. *p*-Iodophenol was synthesized from *p*-aminophenol by diazotization followed by action of potassium iodide[17], m. p. 94°C. *o*- and *p*-Nitrophenols were prepared by nitration of phenol[18], m. p. 46.5~47.5° and 114°C, respectively.

Reaction of Benzoyl Peroxide with 2,4,6-Tribromophenol.—a) Benzoyl peroxide (3.63 g.) and 2,4,6-tribromophenol (8.00 g.) were heated in boiling carbon tetrachloride (40 cc.) for 22 hr., nitrogen being passed through the reaction mixture. The effluent nitrogen was passed through aqueous potassium hydroxide solution to determine the carbon dioxide formed. From the red-coloured reaction mixture carbon tetrachloride was distilled, and the bromine formed came over with it. The distillate, boiled with concentrated nitric acid and concentrated sulphuric acid, gave trace of *m*-dinitrobenzene indicating the formation of benzene. The residue from the distillation was extracted with aqueous sodium hydrogen carbonate solution, and the aqueous solution, on acidification, precipitated benzoic acid, which was then collected and weighed (2.23~2.36 g.). Then the residue was subjected to steam distillation to give tribromophenol. The resulting light brown residue was dissolved in chloroform, and addition of ethanol to the solution gave a precipitate. The precipitate was collected and dried to give white powder. This material is soluble in chloroform, ether, and benzene, but insoluble in methanol and petroleum ether, begins to soften at 240°C and melts at 260~285°C. It had molecular weight 3600~4800 (cryoscopy in bromoform or benzene) contained no benzoyloxy group, and strongly resisted hydrolysis in aqueous alkaline solution. The results of elemental analysis (Found: C, 26.75; H, 1.19; Br, 63.78, 64.05. Calcd. for $C_6H_2Br_2O$: C, 28.80; H, 0.80; Br, 64.00%) show that this compound must be a polymer consisting of many units of the dibromophenoxy group, $H(OC_6H_2Br_2)_nBr$. The same polymeric material was also obtained in the reaction in ligroin (b. p. 150°C).

b) Benzoyl peroxide (13.5 g.) was gradually added in small portions during 15 hr. to a boiling solution of 2,4,6-tribromophenol (91.5 g.) in carbon tetrachloride (400 cc.). After the addition of benzoyl peroxide was over, the solution was kept boiling for a further 15 hr. The gas evolved during the reaction was passed through a trap cooled with dry ice-ethanol, and then through acidic silver nitrate solution. The weight of the silver bromide precipitated gave the amount of hydrogen bromide formed (0.49 g.). The carbon tetrachloride was distilled from the reaction vessel and the bromine which came over with it was determined by the usual method (0.027 mol.). The carbon tetrachloride was treated with a mixture of nitric acid and sulphuric acid giving traces of dinitrobenzene. The residue was further distilled under reduced pressure (2 mmHg) and treatment of the distillate with a mixture of nitric acid and sulphuric acid gave 2,4-dinitrobromobenzene (1.14 g.). The residue was extracted with aqueous sodium carbonate and the extract acidified to pH 6 to give 2,4,6-tribromophenol (45.0 g.), which was filtered off. The filtrate, on acidification to Congo red, yielded benzoic acid (12.8 g.). The neutral residue was extracted with warm petroleum ether, giving polydibromophenylene oxide as insoluble part, and the extract was distilled in vacuo to yield phenyl benzoate (40 mg.) and a new compound (b. p. 200°C/5×10^{-4} mmHg) melting at 167~168°C (from methanol) (3.8 g.). This compound was identified with 2,4,6,3',5'-pentabromo-4'-hydroxydiphenyl ether on the basis of molecular weight measurement (Found: 583 (Rast). Calcd. for $H(OC_6H_2Br_2)_2Br$: 581) and the results of the following debromination: In the presence of palladium-calcium carbonate catalyst in ethanol the compound absorbed five moles of hydrogen, affording the corresponding amount of bromide ions and one mole of *p*-hydroxydiphenyl ether, melting point and mixed melting point with an authentic specimen, 85°C. Incidentally another debromination by Raney alloy in aqueous alkaline solution brought about splitting of the ether linkage as well as debromination, and produced two molecules of phenol.

The Reaction of Benzoyl Peroxide with 2,4,6-Trichlorophenol.—Benzoyl peroxide (36.4 g.) was allowed to react with 2,4,6-trichlorophenol (85.0 g.) in boiling carbon tetrachloride for 30 hr. with purified nitrogen being passed. Evolution of hydrogen chloride was observed during the reaction. After the reaction was over, the solvent was removed by distillation on a water bath. The distillate, boiled with a mixture of concentrated nitric acid and concentrated sulphuric acid gave *m*-dinitrobenzene. The residue was further distilled at 170 mmHg to afford benzoyl chloride, which on hydrolysis gave 0.2 g. of benzoic acid, and chlorobenzene, which on nitration gave 2.65 g. of 2,4-dinitrochlorobenzene. The residue was extracted with methanol and the extract was distilled in steam to give trichlorophenol (32 g.), benzoic acid (11 g.), and methyl benzoate (2 g.). Vacuum distillation

11) L. Vanino, "Handbuch der Präparativen Chemie", 3rd Ed., Ferdinand Enke, Stuttgart (1937), p. 432.
12) W. H. Hunter and L. M. Seyfried, *J. Am. Chem. Soc.*, **43**, 151 (1921).
13) R. C. Huston and A. N. Neeley, ibid., **57**, 2176 (1935).
14) D. S. Tarbell, J. W. Wilson and P. E. Fanta, "Organic Syntheses", **29**, 35 (1949).
15) H. F. Fierz-David and L. Blangey, "Grundlegende Operationen der Farbenchemie", 4th Ed., Julius Springer, Wien (1938), p. 98.
16) R. Adams and C. S. Marvel, "Organic Syntheses", Coll. Vol. I (1948), p. 128.
17) F. B. Dains and F. Eberly, ibid., Coll. Vol. II (1950), p. 355.
18) J. B. Fischman, *J. Am. Chem. Soc.*, **42**, 2291 (1920).

of the residue gave methyl 3,5-dichloro-4-hydroxybenzoate (0.6 g.), m. p. 122°C (from petroleum ether) (Found: mol. wt., 198 (Rast); Cl, 31.63. Calcd. for $C_8H_6Cl_2O_3$: mol. wt., 221; Cl, 32.12%). The identification was done by hydrolyzing it with alkali to 3,5-dichloro-4-hydroxybenzoic acid, melting point and mixed melting point with an authentic specimen 256°C, and by converting the ester into the known acetyl derivative, m. p. 70~71°C. When the residue from the vacuum distillation was dissolved in ether and the solution left to stand, 2,6-bis-(2,4,6-trichlorophenoxy)-*p*-benzoquinone (1.0 g.), m. p. 241~243°C, mixed m. p. 240°C with authentic specimen[10], was obtained. Ether was removed from the filtrate and vacuum distillation at 10^{-3} mmHg of the residue gave 2-chloro-6-(2,4,6-trichlorophenoxy)-*p*-benzoquinone (0.1 g.), melting point and mixed melting point with an authentic specimen[10] 120.5~121°C, and 2,3-dichloro-6-(2,4,6-trichlorophenoxy)-*p*-benzoquinone (2.79 g.), m. p. 155~156°C (Found: mol. wt., 387 (Rast); Cl, 47.85. Calcd. for $C_{18}H_3O_3Cl_5$: mol. wt., 372; Cl, 47.64%). The structure of the latter quinone was established both by its preparation by chlorination of the former quinone with hydrochloric acid and potassium bichromate on a boiling water bath and by its conversion into 2,5-dianilino-6-chloro-*p*-benzoquinone, melting point and mixed melting point with an authentic specimen 263°C, and trichlorophenol on treatment with aniline and aniline hydrochloride on a boiling water bath.

The residual tarry material (mol. wt., 650 by cryoscopy in benzene) contained 47.0% of chlorine and 3.5% of the benzoyloxy group.

Reaction of Benzoyl Peroxide with 2,4,6-Trichlorophenol in the Absence of Solvent.—Benzoyl peroxide (12.2 g.) and 2,4,6-trichlorophenol (39.0 g.) were allowed to react in the absence of solvent at 100°C on a water bath for 20 hr. After the reaction was over, vacuum distillation (2 mmHg) gave benzoyl chloride in a trap which was cooled in dry ice-ethanol mixture, and it was characterized by the formation of benzanilide, m. p. and mixed m. p. 162°C.

Reaction of 2,4,6-Trichlorophenol with Lead Dioxide.—2,4,6-Trichlorophenol (1.0 g.) was allowed to react with lead dioxide (7.0 g.) in the presence of anhydrous sodium sulphate in benzene (40 cc.) with and without 2,6-dichloro-*p*-benzoquinone (1.0 g.) at room temperature for 30 hr. The lead dioxide was filtered off and extracted with benzene, the filtrate and the benzene extract were combined and distilled, and the residue was subjected to sublimation on a boiling water bath to give 2,6-dichloro-*p*-benzoquinone (1.1 g. in the reaction in the presence of 2,6-dichloro-*p*-benzoquinone; 0.1 g. in the absence of the quinone). When the residue from the sublimation was dissolved in small amount of ether, 2,6-bis-(2,4,6-trichlorophenoxy)-*p*-benzoquinone precipitated (0.07 g. each in both experiments), and the filtered ether solution gave on condensation 2-chloro-6-(2,4,6-trichlorophenoxy)-*p*-benzoquinone (0.8 g. each in both experiments).

The Reaction of Benzoyl Peroxide with 2,6-Dibromophenol.—Benzoyl peroxide (5 g.) was allowed to react with 2,6-dibromophenol (20.0 g.) in boiling carbon tetrachloride (100 cc.) for 25 hr., with purified nitrogen being passed. As in the case of tribromophenol, bromine (0.14 g.) was produced during the reaction, and the amount of carbon dioxide evolved was 0.12 g. Benzoic acid (4.3 g.) was obtained from the reaction mixture by extracting with aqueous sodium hydrogen carbonate. On distillation of the residue, 2,6-dibromophenol (10.1 g.) was recovered, and 2,4,6-tribromophenol (0.3 g.) and 3,5,3',5'-tetrabromo-4,4'-dihydroxybiphenyl (0.2 g., m. p. and mixed m. p. 268°C) were isolated.

The Reaction of Benzoyl Peroxide with 2,6-Dichlorophenol.—Benzoyl peroxide (12.1 g.) was allowed to react with 2,6-dichlorophenol (16.3 g.) in boiling carbon tetrachloride (100 cc.) for 20 hr., during which period evolution of hydrogen chloride was observed. Extraction of the reaction mixture with aqueous sodium hydrogen carbonate followed by acidification gave benzoic acid (7.4 g.). The residue from distillation of the carbon tetrachloride solution was subjected to distillation in vacuo to give 2,6-dichlorophenol (6.0 g.). The distillation residue was dissolved in ether, and the solution extracted with dilute sodium hydroxide solution. On acidification of the extract 3,5,3',5'-tetrachloro-4,4'-dihydroxybiphenyl (0.2 g.) was isolated, m. p. and mixed m. p. 234°C.

The Reaction of Benzoyl Peroxide with *p*-Chlorophenol.—Benzoyl peroxide (16.2 g.) and *p*-chlorophenol (25.0 g.) in carbon tetrachloride solution were boiled on a water bath for 12.5 hr. with purified nitrogen being passed. The effluent gas was passed through a trap cooled with dry ice-ethanol and then through potassium hydroxide solution. Weight increase of the alkali solution was 0.256 g. This value and the amount of chloride ions (0.22 g.) in the solution determined by argentometry show that only hydrogen chloride evolved and evolution of carbon dioxide was very slight. Benzoic acid (11.5 g.) was separated from the reaction mixture by extraction with aqueous sodium hydrogen carbonate, and carbon tetrachloride was removed by distillation. The crystalline residue was recrystallized from benzene to give 2-benzoyloxy-4-chlorophenol, m. p. 147.5~149.5°C (Found: mol. wt., 253 (Rast); Cl, 14.05. Calcd. for $C_{13}H_9O_3Cl$: mol. wt., 249; Cl, 14.28%). Its structure was established by its preparation by chlorination of catechol monobenzoate with sulphuryl chloride.

The Reaction of Benzoyl Peroxide with *p*-Bromophenol.—Benzoyl peroxide (24.2 g.) and *p*-bromophenol (52.0 g.) in carbon tetrachloride were refluxed for 35.5 hr. with purified nitrogen being passed. No gas was evolved during the reaction. The solvent was distilled, and in the distillate no benzene could be detected. When benzoic acid (17.6 g.) and *p*-bromophenol (21.0 g.) were separated as before, the residue changed to crystalline solid, which recrystallized from benzene gave 2-benzoyloxy-4-bromophenol, m. p. 156~157°C (Found: mol. wt., 308, 284 (Rast); Br, 27.18, 27.36. Calcd. for $C_{13}H_9O_3Br$: mol. wt., 293; Br, 27.30%). The structure of this compound was proved by mixed

melting point determination with the bromocatechol monobenzoate which was prepared by bromination of catechol monobenzoate with bromine in glacial acetic acid.

The Reaction of Benzoyl Peroxide with *p*-Iodophenol.—Benzoyl peroxide (9.5 g.) and *p*-iodophenol (17.5 g.) were boiled in carbon tetrachloride for 13 hr. with purified nitrogen being passed. No gas was evolved, but iodine (2.38 g.) was liberated. Vacuum distillation of the reaction mixture gave benzoic acid (4.43 g.) and *p*-iodophenol (3.78 g.). The solid residue, recrystallized from methanol, gave a white crystalline compound, m. p. 165~169°C (Found: C, 45.86; H, 2.81. Calcd. for $C_{13}H_9O_3I$: C, 45.88; H, 2.65%), which was thought to be 2-benzoyloxy-4-iodophenol.

The Reaction of Benzoyl Peroxide with *p*-Nitrophenol.—Benzoyl peroxide (12.1 g.) and *p*-nitrophenol (13.8 g.) were refluxed in carbon tetrachloride solution (100 cc.) on a water bath for 15 hr. Vigorous evolution of hydrogen chloride was observed during the reaction. The solvent was removed and vacuum distillation of the residue gave benzoyl chloride and a crystalline residue, which, on recrystallization from water, gave almost all the original *p*-nitrophenol unchanged.

A mixture of powdered *p*-nitrophenol (13.8 g.) and powdered benzoyl peroxide (12.1 g.) was gently heated with stirring on a water bath with nitrogen being passed. At about 90°C, the mixture melted into a viscous fluid and the melt was kept at 100°C for 13 hr. with stirring. During that period 0.484 g. of carbon dioxide evolved. A small amount of carbon tetrachloride was added to the reaction mixture and the mixture was distilled. In the distillate benzene (25 mg.) was detected (as *m*-dinitrobenzene). Steam distillation of the residue gave benzoic acid (10 g.) and codistillation with purified ligroin (b. p. 100~165°/25 mmHg) yielded *p*-nitrophenol (10.1 g.). The residue was extracted with warm petroleum ether, the extract condensed and the residue recrystallized from benzene to give *p*-nitrophenyl benzoate (20 mg.).

The Reaction of Benzoyl Peroxide with *o*-Nitrophenol.—A mixture of *o*-nitrophenol (27.5 g.) and benzoyl peroxide (24.2 g.) was heated on a boiling water bath for 17 hr. with agitation with purified nitrogen being passed. Carbon dioxide (2.6 g.) was evolved. To the reaction mixture carbon tetrachloride was added and the mixture distilled. Nitration of the distillate gave *m*-dinitrobenzene (0.2 g.). Steam distillation of the residue yielded phenyl benzoate (0.66 g.), *o*-nitrophenol (17.3 g.), benzoic acid (11.2 g.) and a yellow crysalline compound (2.35 g.). This yellow compound, recrystallized from methanol, melted at 103~104.5°C (Found: C, 67.14; H, 4.63; N, 6.40. Calcd. for $C_{13}H_9NO_3$: C, 66.98; H, 4.19; N, 6.51%) and seems to be phenyl-*o*-nitrophenol. The residue, distilled in super-heated steam, gave 4-biphenylcarboxylic acid (0.37 g.), m. p. and mixed m. p. 219~221°C.

Summary

Benzoyl peroxide has been allowed to react with various halogenophenols in boiling carbon tetrachloride and the nature of the products has been examined.

2,4,6-Tribromophenol gave benzoic acid, polydibromophenylene oxide $H(OC_6H_2Br_2)_nBr$, 4-hydroxy-3,5,2',4',6'-pentabromodiphenyl ether, carbon dioxide and bromine, whereas in the case of 2, 4, 6-trichlorophenol the corresponding polymeric material could not be isolated, but *p*-benzoquinones substituted with chlorine and the 2, 4, 6-trichlorophenoxy group were formed. The reaction with 2, 6-dichloro- and 2, 6-dibromophenol gave a small amount of the corresponding 3, 5, 3', 5'-tetrahalogeno-4, 4'-dihydroxybiphenyls, a type of product which were not obtained in the other cases. *p*-Halogenophenols yielded an appreciable amount of halogenocatechol monobenzoates.

p-Nitrophenol did not react with benzoyl peroxide in boiling carbon tetrachloride, but at 100°C in the absence of any solvent this phenol as well as the ortho isomer underwent reaction with evolution of considerable amount of carbon dioxide. These observations are discussed in terms of mechanisms involving free radicals.

Department of Chemistry
Faculty of Science
The University of Tokyo
Hongo, Tokyo

*Studies on the Synthesis of Peptides Containing Glutamine as the C-Terminal. I. Protection of Amide-nitrogen with Xanthyl Group during Peptide Synthesis**

By Yasutsugu SHIMONISHI, Shumpei SAKAKIBARA and Shiro AKABORI

(Received July 26, 1962)

To date reports on the synthesis of glutaminyl peptides have been rare, because the chemically unstable amide group in glutamine makes preparation of these peptides difficult. Therefore the development of a practical method for synthesizing these peptides would be of particular interest in the study of the synthesis of peptides. The authors have attempted to find a new method especially for the synthesis of *C*-terminal glutaminyl peptides, as well as to improve earlier methods.

It is known that troublesome side reactions[1] occur during the synthesis of asparagine- and glutamine-peptides because of the instability of the β- and γ-amide groups respectively. For example, Sondheimer and Holley[2] synthesized peptides such as L-glutaminyl-L-leucine by the carbobenzoxy azide method, but their method could not be used to prepare peptides containing *C*-terminal glutamine. They reported also[3] that carbobenzoxyglutamine and its isomer, namely carbobenzoxyisoglutamine, could be obtained by normal alkaline saponification of carbobenzoxyglutamine methyl ester. During this treatment α-carbobenzoxyaminoglutarimide was found to be an intermediate; consequently the product was a mixture of α- and γ-amides. Similar reactions took place in the synthesis of asparagine series. It was also reported[4] that peptide derivatives, when treated in the same way, gave rise to a mixture of α- and γ-peptide derivatives.

Glutamine or glutaminyl peptides are labile even in neutral solution and are cyclized to pyrrolidonecarboxylic acid or to pyrroglutamyl peptides, respectively, merely by heating their aqueous solutions[5,6] or by passing them through a strongly acidic ion-exchange resin[7]. It has been found[8-10] that the application of tetraethylpyrrophosphite or *N,N'*-dicyclohexylcarbodiimide as a condensing reagent gave the cyano-compound as one of the products by intramolecular dehydration of the amide group during the formation of asparaginyl peptide bonds and, to a lesser extent, during the formation of glutaminyl peptide bonds.

Hofmann et al.[11] prepared L-methionyl-L-glutamine, intermediate for melanocite stimmulating hormone, from carbobenzoxy-L-methionine and L-glutamine by the mixed anhydride procedure. By the same method, Shiba et al.[5,12] and Rudinger et al.[13] synthesized L-pyrroglutamyl-L-glutaminyl-L-glutamine (fastigiatin) from carbobenzoxy-L-glutamic acid γ-methyl ester and L-glutaminyl-L-glutamine, and L-glutaminyl-L-glutamine (its intermediate) starting with carbobenzoxy-L-glutamic acid γ-methyl ester and L-glutamine. Vigneaud et al.[14] synthesized tosyl-L-isoleucyl-L-glutamine from tosyl-L-isoleucyl chloride and L-glutamine, but this procedure has not been used generally. These methods are limited to the reaction in which unprotected glutamine can be used.

In developing a method of preparation of these peptides which does not involve side reactions, the following considerations must be investigated. It is desirable to protect the amide nitrogen by a protective group which is easily removable after the formation of peptide bonds. This protective group should not be attacked by the reagents used for synthesis of the peptide. The optical activity of the amino acids or peptides should be maintained during the introduction and removal of the protective group.

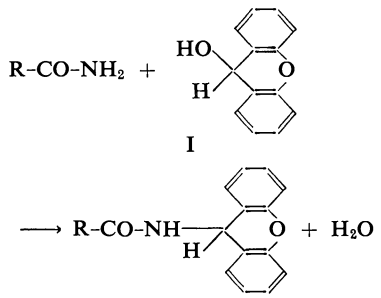
The author first tried the benzyl group as a

* Preliminary report, This Bulletin, **34**, 739 (1961).

1) J. Rudinger, *Angew. Chem.*, **71**, 742 (1959).
2) E. Sondheimer and R. W. Holley, *J. Am. Chem. Soc.*, **76**, 2816 (1954).
3) E. Sondheimer and R. W. Holley, ibid., **76**, 2467 (1954).
4) V. Bruckner, J. Kovacs and K. Medzihradszky, *Naturwiss.*, **42**, 96 (1955).
5) T. Shiba, S. Imai and T. Kaneko, This Bulletin, **31**, 244 (1958).
6) J. Melville, *Biochem. J.*, **29**, 179 (1935).
7) K. Narita, *Biochem. et Biophys. Acta*, **30**, 352 (1958).
8) D. T. Gish, P. G. Katsoyannis, G. P. Hess and R. J. Stedmann, *J. Am. Chem. Soc.*, **78**, 5954 (1956).
9) C. Ressler, ibid., **78**, 5956 (1956).
10) P. G. Katsoyannis, D. T. Gish, G. P. Hess and V. du Vigneaud, ibid., **80**, 2558 (1958).
11) K. Hofmann, T. A. Thompson and E. T. Schwarz, ibid., **79**, 6087 (1957).
12) T. Shiba and S. Imai, *J. Chem. Soc. Japan, Pure Chem. Sec.* (*Nippon Kagaku Zasshi*), **80**, 497 (1959).
13) J. Rudinger and Z. Pravoa, *Chem. Listy*, **52**, 120 (1958).
14) P. G. Katsoyannis and V. du Vigneaud, *J. Am. Chem. Soc.*, **76**, 3113 (1954).

protective group and prepared N^{α}-carbobenzoxy-N^{γ}-benzyl-L-glutamine from carbobenzoxy-L-glutamic acid γ-hydrazide, but the benzyl group could not be removed. Frankel et al.[15] also reported that they prepared poly-N^{β}-benzyl-asparagine in order to obtain poly-asparagine, but that the removal of the benzyl group was very difficult because of its unexpected stability.

Phillips et al.[16] reported that unsubstituted acyl amide reacted with xanthydrol (I) to give acyl xanthyl amide. The present authors applied the reaction to carbobenzoxy-L-glutamine (II) and N^{α}-carbobenzoxy-N^{γ}-xanthyl-L-glutamine (III) was obtained in a good yield.



The authors found that the N^{γ}-xanthyl group was comparatively stable in caustic alkalis, but very unstable in mineral acids. Both decarbobenzoxylation and dexanthylation took place, when III was treated with glacial acetic acid containing hydrogen bromide. From the reaction mixture, L-glutamine was recovered in a 55% yield by the usual procedures, and it had the same optical activity as glutamine which had been obtained directly from II. By catalytic reduction with Pd-charcoal only decarbobenzoxylation occurred, and N^{γ}-xanthyl-L-glutamine (IV) was obtained. Moreover, IV could not be prepared from glutamine and I in acetic acid. The xanthyl derivative III, obtained from carbobenzoxy-L-glutamine (II) with xanthydrol (I), was esterified to N^{α}-carbobenzoxy-N^{γ}-xanthyl-L-glutamine methyl ester (V) by means of diazomethane. After catalytic hydrogenation of V by Pd-charcoal in the presence of acetic acid, the acetate ester (VI) obtained was coupled with carbobenzoxy-glycine *p*-nitrophenyl ester[17] (VII, R=H) to form carbobenzoxy-glycyl-N^{γ}-xanthyl-L-glutamine methyl ester (VIII). Glycyl-L-glutamine

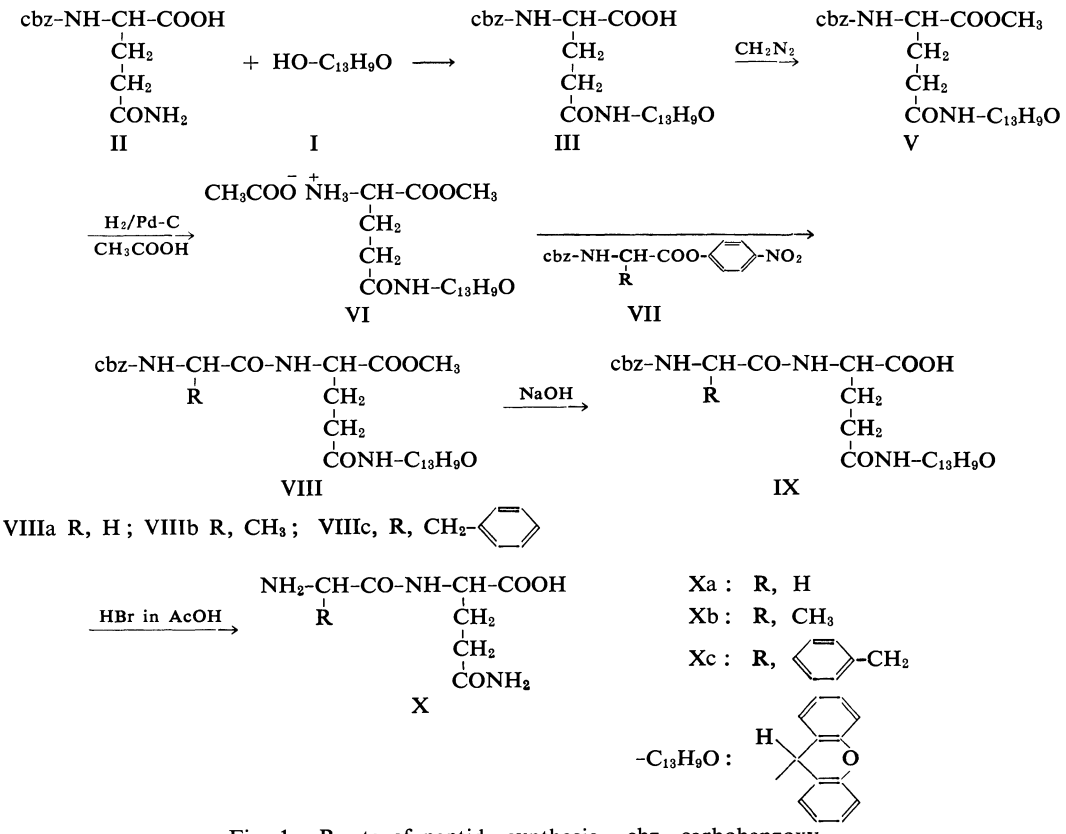


Fig. 1. Route of peptide synthesis. cbz=carbobenzoxy

15) M. Frankel, Y. Liwschitz and A. Zilkha, ibid., **75**, 3270 (1953).

16) R. F. Phillips et al., *J. Org. Chem.*, **8**, 1355 (1943).

17) R. Schwyzer and P. Sieber, *Angew. Chem.*, **68**, 518 (1956).

(Xa) was obtained by treatment of carbobenzoxy-glycyl-N^{γ}-xanthyl-L-glutamine (IX, R=H) with hydrogen bromide, which had been prepared by saponification of VIII (R=H). The yield at each step of these reactions was more than 70%. The above synthetic route is shown in Fig. 1. Carbobenzoxy-L-alanyl- (VIIIb), -L-phenylalanyl (VIIIc) N^{γ}-xanthyl-L-glutamine methyl ester were synthesized from N^{γ}-xanthyl-L-glutamine methyl ester acetate (VI) and the respective carbobenzoxyamino acid *p*-nitrophenyl esters (VII) prepared by the procedure of Bodanszky et al.[18] After saponification of VIII, followed by treatment with hydrogen bromide, L-alanyl-L-glutamine (Xb) and L-phenylalanyl-L-glutamine (Xc) were obtained. This method, using the xanthyl derivatives, was superior to the methods used in earlier work in that there was less possibility of the occurrence of side reactions. A weak point is that the solubility of xanthyl derivatives in organic solvents is low. Therefore, it was difficult to observe the rotation of the xanthyl derivatives of peptides. An attempt was made to apply the protection resulting from the xanthyl group to asparagine derivative; however, N^{β}-xanthyl-L-asparagine methyl ester acetate, a starting material in peptide synthesis, could not be obtained from the catalytic hydrogenation of carbobenzoxy-N^{β}-xanthyl-L-asparagine methyl ester, which had been previously obtained by the reaction of carbobenzoxy-N^{β}-xanthyl-L-asparagine with diazomethane.

Experimental*

N^{α}-Carbobenzoxy-N^{γ}-xanthyl-L-glutamine.—Xanthydrol[19] (9.8 g., 0.050 mol.) and carbobenzoxy-L-glutamine (13.9 g., 0.050 mol.) were dissolved in 200 ml. of glacial acetic acid and the solution was allowed to stand for 2 days at room temperature. The gelatinous solid product was drained, filtered and dried in an alkali desiccator. The resulting white powder was recrystallized from tetrahydrofran to give colorless needles with a melting point at 182~183°C. The yield was 18.5 g. (80% of the theoretical amount). $[\alpha]_D^{17}=-5.7°$ (*c* 5.7, dimethylformamide).

Found: C, 66.36; H, 5.55; N, 6.13. Calcd. for $C_{26}H_{24}O_6N_2 \cdot 1/2H_2O$ C, 66.52; H, 5.37; N, 5.97%.

N^{α}-Carbobenzoxy-N^{γ}-xanthyl-L-glutamine Methyl Ester.—*Preparation of an Ethereal Solution of Diazomethane*[20]. — In a 200 ml. round bottomed flask were placed 12 ml. of 50% aqueous potassium hydroxide solution and 35 ml. of ether. The mixture was cooled to 5°C in an ice-bath, and 4.0 g. of nitrosomethylurea was slowly added with shaking. The upper layer was colored yellow by diazomethane. After the complete decomposition of nitrosomethylurea by alkali to diazomethane, the upper layer was decanted and dried over pellets of potassium hydroxide for two hours. A measured portion of this solution was allowed to react at 0°C with a solution of an accurately weighed excess of pure benzoic acid dissolved in absolute ether. The unreacted benzoic acid was titrated with standard N alkali. The yield of diazomethane was found to be about 70 per cent.

Preparation of the Ester (V).—The dry ethereal solution of diazomethane was slowly dropped, with stirring, into a suspension of 6.0 g. (0.013 mol.) of N^{α}-carbobenzoxy-N^{γ}-xanthyl-L-glutamine in 100 ml. of dioxane at 0~10°C. With the evolution of nitrogen gas the reaction proceeded smoothly. The mixture was kept overnight at room temperature in a flask, to which was attached a tube of mercury seal. The precipitate was filtered by suction, washed with ether and dried on sodium hydroxide in a vacuum desiccator. After recrystallization of the crude product (5.2 g., m. p. 235°C) from 150 ml. of dioxane, colorless needles were obtained, m. p. 235~235.5°C. The yield was 81% of the theoretical (5 g.). Titration by sodium methoxide solution showed the absence of free carboxylic acid.

Found: C, 68.21; H, 5.50; N, 5.94. Calcd. for $C_{27}H_{26}O_6N_2$: C, 68.34; H, 5.52; N, 5.90%.

N^{γ}-Xanthyl-L-glutamine. — N^{α}-Carbobenzoxy-N^{γ}-xanthyl-L-glutamine (4.6 g., 0.01 mol.) was hydrogenated in 150 ml. of ethanol under 70~80 atm. of H_2 at 75~80°C in the presence of Pd-charcoal catalyst, which was prepared from 10% palladium chloride in dilute hydrochloric acid (15 ml.) and charcoal (3 g.). The hydrogenated product was deposited on the catalyst. After 3 hr. the reaction mixture was cooled to room temperature. The mixture was filtered and washed three times with 20 ml. of hot ethanol. The residue on the filter paper was suspended in 60 ml. of water containing 1.5 ml. of triethylamine to dissolve the product deposited on the charcoal. After filtration, the filtrate and aqueous washings were combined and brought to pH 4.5~5.0 with 2 N hydrochloric acid. The precipitate was separated by centrifugation and washed with methanol and then with ether. 2.2 g. of N^{γ}-xanthyl-L-glutamine was obtained after drying in a desiccator, and purified by reprecipitation from 2 N ammonium hydroxide and 2 N hydrochloric acid. This compound melted at 218~220°C (60% of the theoretical).

Found: C, 65.17; H, 5.60; N, 8.94. Calcd. for $C_{18}H_{18}O_4N_2$: C, 66.24; H, 5.56; N, 8.58%.

N^{γ}-Xanthyl-L-glutamine Methyl Ester Acetate.—Five grams (0.01 mol.) of N^{α}-carbobenzoxy-N^{γ}-xanthyl-L-glutamine methyl ester were suspended in 130 ml. of methanol and palladium-charcoal catalyst, prepared freshly from 25 ml. of 1% palladium chloride solution, and 5 g. of charcoal were added. Three milliliters of glacial acetic acid were dropped into the above mixture. Hydrogen gas was allowed to bubble through the mixture for

18) M. Bodanszky and V. du Vigneaud, *J. Am. Chem. Soc.*, **81**, 5688 (1959).

* Melting points are uncorrected.

19) R. Meyer and E. Saul, *Ber.*, **26**, 1276 (1893).

20) F. Arndt, "Orgnic Syntheses", Coll. Vol. II (1948), pp. 165—167.

6 hr. at room temperature. The filtrate was concentrated under reduced pressure, at low temperature. The residue was dissolved in a small amount of methanol and the undissolved part was filtered off. Ether was added to the filtrate and a colorless crystalline product was obtained in a 67% yield (2.8 g.) which melted at 148~148.5°C. This material was ninhydrin positive and had an R_f value of 0.85 on paper chromatography in a solvent system of *n*-butanol : acetic acid : water (4 : 1 : 1).

Found: C, 62.72; H, 6.07; N, 6.90. Calcd. for $C_{21}H_{24}O_6N_2$: C, 62.99; H, 6.04; N, 7.00%.

Carbobenzoxy-glycyl-N^{γ}-xanthyl-L-glutamine Methyl Ester.—Carbobenzoxy-glycine *p*-nitrophenyl ester (3.5 g., 0.011 mol.) was added to an anhydrous solution of N^{γ}-xanthyl-L-glutamine methyl ester acetate (3.5 g., 0.0087 mol.) and triethylamine (1.2 ml., 0.0087 mol.) in chloroform according to the description of du Vigneaud[18]. The clear pale yellow solution was allowed to stand overnight at room temperature. The crystalline precipitate was filtered and washed with chloroform. After recrystallization of crude material (4.0 g.) from dioxane, fine colorless needles, which melted at 184°C, (3.5 g.) were obtained in a 76% yield.

Found: C, 65.49; H, 5.64; N, 7.89. Calcd. for $C_{29}H_{29}O_7N_3$: C, 65.52; H, 5.50; N, 7.91%.

Carbobenzoxy-L-alanyl-N^{γ}-xanthyl-L-glutamine Methyl Ester. — N^{γ}-Xanthyl-L-glutamine methyl ester, prepared from its acetate (2.0 g., 0.0050 mol.), was treated with carbobenzoxy-L-alanine *p*-nitrophenyl ester (2.4 g., 0.0070 mol.). Carbobenzoxy-L-alanyl-N^{γ}-xanthyl-L-glutamine methyl ester (2.4 g.) was obtained as a precipitate. Recrystallization from ethanol yielded colorless needles (1.4 g., 52% of the theoretical yield) with a melting point at 208°C (decomp.).

Found: C, 65.17; H, 5.69; N, 7.79. Calcd. for $C_{30}H_{31}O_7N_3$: C, 66.04; H, 5.73; N, 7.70%.

Carbobenzoxy-L-phenylalanyl-N^{γ}-xanthyl-L-glutamine Methyl Ester. — By the same treatment as above, crystalline precipitates (5.9 g.) were obtained in an 80% yield from N^{γ}-xanthyl-L-glutamine methyl ester acetate (4.8 g., 0.012 mol.) and carbobenzoxy-L-phenylalanine *p*-nitrophenyl ester (6.0 g., 0.014 mol.). M. p. 215~216°C.

Found: C, 69.60; H, 5.59; N, 6.59. Calcd. for $C_{36}H_{35}O_7N_3$: C, 69.55; H, 5.68; N, 6.76%

Carbobenzoxy-glycyl-N^{γ}-xanthyl-L-glutamine.— To a solution of 1.6 g. (0.003 mol.) of carbobenzoxy-glycyl-N^{γ}-xanthyl-L-glutamine methyl ester in 100 ml. of dioxane 30 ml. of 0.1 N sodium hydroxide was added (1.0 equiv.). After standing for an hour at room temperature (25°C), the solution was acidified to about pH 3.5 with N hydrochloric acid and concentrated under reduced pressure at low temperature. The residue was suspended in water and filtered. The resulting precipitate was dried in a desiccator and then dissolved in a warm mixture of methanol and toluene (4 : 1) and the insoluble material was filtered off. A small quantity of water was slowly added to the filtrate whereby IX (R=H) deposited in colorless needles. M. p. 198°C. The yield was 77% of the theoretical.

Found: C, 65.17; H, 5.39; N, 8.04. Neut. eq. 516. Calcd. for $C_{28}H_{27}O_7N_3$: C, 64.98; H, 5.26; N, 8.12%; mol. wt. 517.5.

Glycyl-L-glutamine. — Carbobenzoxyglycyl-N^{γ}-xanthyl-L-glutamine (1.5 g., 0.0029 mol.) was treated with 4.2 g. (5.0 equiv.) of 28.1 per cent glacial acetic acid containing hydrogen bromide. This solution was kept for about an hour at room temperature and dry ether was added where a colored material precipitated. Then the precipitate was washed with ether and the ether was decanted. The residue was dissolved in water and the undissolved material was filtered. The filtrate was passed through a weakly basic resin (Amberlite IR-4B) column, and the product was washed out of the column with a sufficient volume of water. The effluent was lyophilized, and the residue was dissolved in a small amount of water. On addition of ethanol to the solution, the final product was obtained as fine colorless crystals of the monohydrate (0.44 g., 70%), m. p. 260°C (decomp.). $[\alpha]_D^{15}=-1.8\pm0.5°$ (*c* 3.8, water). R_f value was 0.17 in solvent system (*n*-BuOH : AcOH : H_2O=4 : 1 : 1).

Found: C, 38.02; H, 7.02; N, 19.12. Calcd. for $C_7H_{13}O_4N_3\cdot H_2O$: C, 38.00; H, 6.84; N, 19.00%.

Thierfelder reported; m. p. 199~200°C. $[\alpha]_D^{15}=-2.47°$ (*c* 4.20, water).

L-Alanyl-L-glutamine. — One gram (1.83×10^{-3} mol.) of carbobenzoxy-L-alanyl-N^{γ}-xanthyl-L-glutamine methyl ester was saponified with 2.8 ml. (1.5 equiv.) of N sodium hydroxide in 100 ml. of dioxane for about 4 hr. at room temperature (15~20°C). The reaction mixture was concentrated to dryness after neutralization with dilute hydrochloric acid. The residue was crystallized from dioxane to yield a product (0.7 g.) having m. p. 138°C. This product was treated with 2.7 g. of 20% glacial acetic acid containing hydrogen bromide. This mixture was kept for 2 hr. at room temperature, and then dry ether (100 ml.) was added. A precipitate was obtained and the upper solution was decanted. The precipitate was dissolved in a small amount of water and the undissolved material was filtered. The filtrate was passed through an Amberlite IR-4B (OH-form) column. The effluent was lyophilized and the residue was recrystallized from water-ethanol as fine needles. One hundred milligrams of L-alanyl-L-glutamine were obtained as the monohydrate in about a 30% yield which melted at 214~215°C with decomposition. On paper chromatography it had an R_f value of 0.14 in the solvent system (*n*-BuOH : AcOH : H_2O=4 : 1 : 1). $[\alpha]_D^{14}=+11.4\pm0.5°$ (*c* 3.7, water).

Found: C, 40.42; H, 7.52; N, 17.82. Calcd. for $C_8H_{15}O_4N_3\cdot H_2O$: C, 40.84; H, 7.28; N, 17.86%.

Carbobenzoxy-L-phenylalanyl-N^{γ}-xanthyl-L-glutamine. — Carbobenzoxy-L-phenylalanyl-N^{γ}-xanthyl-L-glutamine methyl ester (2.6 g., 0.0042 mol.) was dissolved in 130 ml. of dimethylformamide and 6.3 ml. (1.5 equiv.) of N sodium hydroxide were added. After standing for 3 hr. at room temperature, the solution was neutralized with aqueous hydrochloric acid and then concentrated under reduced pressure. The residue was suspended in water, finely crushed with a rod, filtered by suction and dried in vacuo. Recrystallization of crude material (2.4 g., 188~

189.5° with decomposition) from methanol-water gave a crystalline product (1.7 g.) in a 68% yield. M. p. 188~189.5°C (decomp.). Neut. eq. 601, (mol. wt. 604).

L-Phenylalanyl-L-glutamine. — Carbobenzoxy-L-phenylalanyl-N^{γ}-xanthyl-L-glutamine (1.6 g., 0.0027 mol.) was treated with 5.0 g. (5 equiv.) of 21.4% glacial acetic acid solution containing hydrogen bromide. After the mixture was allowed to stand for 2 hr. at room temperature, a precipitate was obtained by adding 150 ml. of dry ether. The upper layer was decanted, and the residue was washed with dry ether and dissolved in a small amount of water. After filtration, the filtrate was passed through an Amberlite IR-4B (OH-form) column. The effluent was lyophilized and the residue was dissolved in water. Fine crystals were obtained in a 35% yield 0.26 g.) by adding ethanol. These melted at 209~210°C. $[\alpha]_D^{17} = +51.9 \pm 0.5°$ (c 4.0, in water).

Found: C, 57.55; H, 6.78; N, 14.45. Calcd. for $C_{14}H_{19}O_4N_3$: C, 57.32; H, 6.53; N, 14.33%.

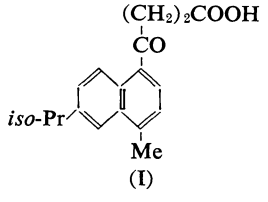
Division of Organic Chemistry
Institute for Protein Research
Osaka University
Kita-ku, Osaka

*7-Isopropyl-2, 9-dimethylphenanthrene and 2-Isopropyl-10-methylphenanthrene**

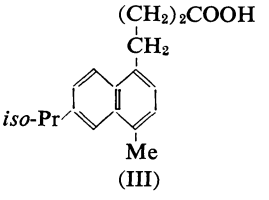
By Hiroshi KOBAYASHI

(Received August 2, 1962)

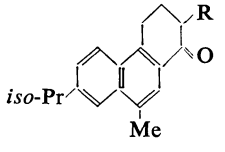
During degradative studies on the constitution of the conifer diterpene thunbergene[1], 7-isopropyl-2, 9-dimethylphenanthrene and 2-isopropyl-10-methylphenanthrene have been synthesized as reference compounds by standard methods.



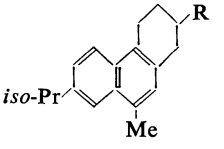
(I)



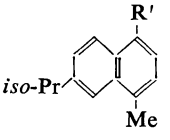
(III)



(IV) R, H
(V) R, Me



(VI) R, Me
(VII) R, H



(VIII) R', COOH
(IX) R', CH_2OH
(X) R', Me

The Friedel-Crafts succinoylation of 7-isopropyl-1-methylnaphthalene furnished 4-(6-isopropyl-4-methyl-1-naphthyl)-4-oxobutyric acid (I) along with a minor product, which was considered to be 4-(6-isopropyl-4-methyl-2-naphthyl)-4-oxobutyric acid (II) as mentioned below.

Reduction of the ketoacid (I) by the Wolff-Kishner method as modified by Huang-Minlon gave 4-(6-isopropyl-4-methyl-1-naphthyl)-butyric

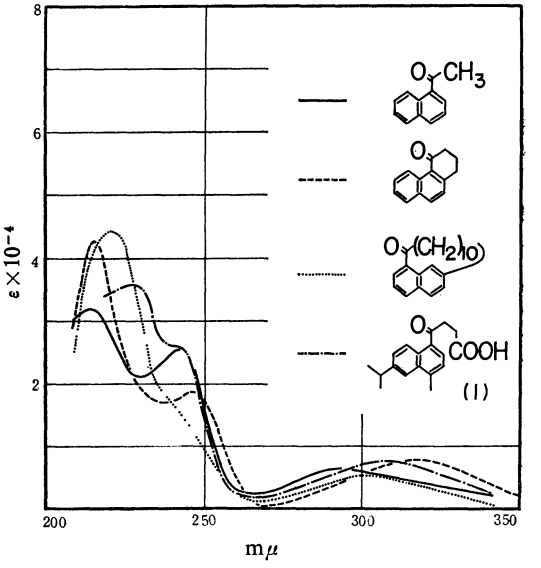


Fig. 1. UV Absorptions of α-naphthyl-keto systems in ethanol.

* Contribution No. 32 from the Deparment of Organic Synthesis, Faculty of Engineering, Kyushu University, Fukuoka.

1) H. Kobayashi and S. Akiyoshi, This Bulletin, 35, 1044 (1962).

acid (III), which was cyclized 1, 2, 3, 4-tetrahydro-7-isopropyl-9-methyl-1-oxophenanthrene (IV). Introduction of a methyl group at the 2-position of this cyclic ketone (IV) yielded 1, 2, 3, 4-tetrahydro-7-isopropyl-2, 9-dimethyl-1-oxophenanthrene (V). Wolf-Kishner reduction of the last ketone (V) yielded 1, 2, 3, 4-tetrahydro-7-isopropyl-2, 9-dimethylphenanthrene (VI) which furnished 7-isopropyl-2, 9-dimethylphenanthrene on dehydrogenation.

Similarly 2-isopropyl-10-methylphenanthrene was prepared from the cyclic ketone IV via VII.

In accordance with general principles[2], the succinoylation of 7-isopropyl-1-methylnaphthalene should occur at the 3- and 4-positions. This expectation was supported by the ultraviolet absorption spectra[3] which showed that one of the two isomeric naphthyl-oxobutyric acids I and II, had 1-naphthoyl chromophore (Fig. 1) while the other had 2-naphthoyl one (Fig. 3).

The structure of the 4-substituted product I was confirmed by obtaining 6-isopropyl-1, 4-dimethylnaphthalene (X)[4], via intermediates, VIII and IX. If the 5-substitution had occurred, instead, the reaction sequence should lead to 3-isopropyl-1, 5-dimethylnaphthalene[5].

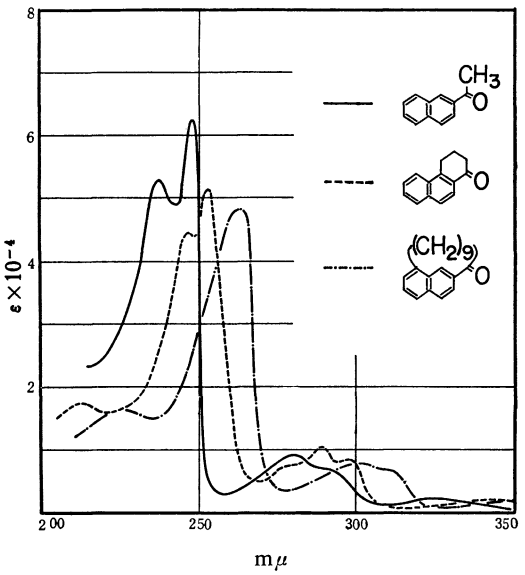


Fig. 2. UV Absorptions of 2-naphthoyl systems in ethanol.

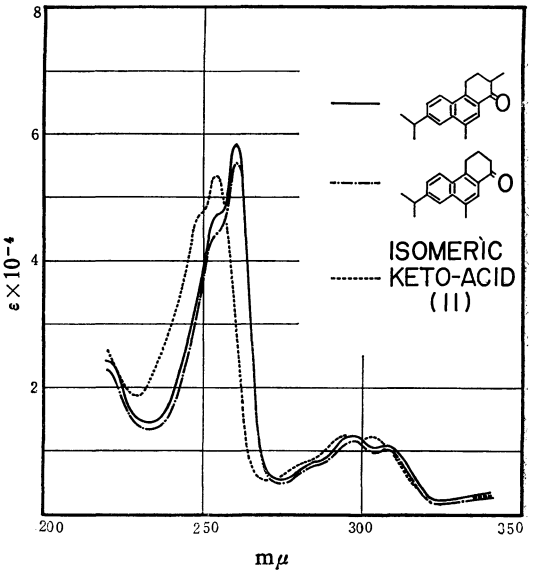


Fig. 3. UV Absorptions of the naphthoyl systems in this study.

Additional evidences for the assignments are that the cyclic ketones formulated as IV and V show similar ultraviolet spectra (Fig. 3) to those of the 2-naphthoyl system (Fig. 2)[3] and that final tricyclic hydrocarbons are phenanthrenes but not anthracenes. The 3-substituted naphthalene II has not been further investigated.

Experimental

Melting points are uncorrected and were measured on a Kofler micro hot stage. The ultraviolet spectra were recorded on a Hitachi EPS-2 type spectrophotometer. 7-Isopropyl-1-methylnaphthalene (eudalene) was synthesized according to the method of Ruzicka and Stoll[6] via 1,2,3,4-tetrahydro-7-isopropyl-1-oxonaphthalene[7]. The picrate, m. p. 92°C, was identical with that of eudalene prepared from eudesmol which occurred naturally. Pure eudalene was regenerated from the picrate by elution from alumina column.

7-Isopropyl-2, 9-dimethylphenanthrene. — Finely powdered aluminum chloride (28.0 g.) was added slowly to a stirred solution of eudalene (18.4 g.) and succinic anhydride (11.0 g.) in nitrobenzene (130 ml.) at 0°C, and after 30 hr. of a reaction period at room temperature the mixture was treated with ice (150 g.) and excess of hydrochloric acid (30 ml.). The removal of the nitrobenzene by steam-distillation furnished a resinous acid which was dissolved in 5% sodium carbonate and treated with activated charcoal. The resulting alkaline solution was acidified with dilute hydrochloric acid. A mixture of keto-acids (18.0 g.) was precipitated.

2) E. Berliner, "Organic Reactions", Vol. V, p. 229 (1949).
3) a) R. Huisgen and U. Rietz, *Ber.*, **90** 2768 (1957); b) R. Huisgen and U. Rietz, *Tetrahedron*, **2**, 271 (1958).
4) a) S. Dev, *J. Indian Chem. Soc.*, **33**, 561 (1956); b) L. Ruzicka, P. P. Th. Reichstein and L. Ehmann, *Helv. Chim. Acta*, **16**, 268 (1933).
5) A. S. Pfau and Pl. Plattner, *Helv. Chim. Acta*, **19**, 857 (1936).
6) L. Ruzicka and M. Stoll, ibid., **5**, 936 (1922).
7) E. Ochiai, T. Okamoto, M. Sekigawa, M. Nishikawa and K. Shono, *Pharm. Bull. (Tokyo)*, **5**, 48 (1957).

Repeated crystallization from ethanol gave 4-(6-isopropyl-4-methyl-1-naphthyl)-4-oxobutyric acid (I) (6.5 g.) as plates, m. p. 133.7~134.4°C.

Found: C, 75.85; H, 7.09. Calcd. for $C_{18}H_{20}O_3$: C, 76.03; H, 7.09%.

The mother liquor from this acid slowly deposited a crystalline acid (1.6 g.) which on repeated crystallization from ethanol gave the isomeric naphthyl-oxobutyric acid II (0.85 g.) m. p. 179.5~181.0°C.

Found: C, 75.77; H, 7.11. Calcd. for $C_{18}H_{20}O_3$: C, 76.03; H, 7.09%.

A mixture of 4-(6-isopropyl-4-methyl-1-naphthyl)-4-oxobutyric acid (I) (2.90 g.), 80% hydrazine hydrate (1.5 ml.), potassium hydroxide (2.0 g.) and diethylene glycol (15 ml.) was refluxed at 170~180°C for 2 hr., then excess of hydrazine and water were removed by distillation until the reaction temperature was 220°C and this temperature was maintained for an additional 3 hr. After acidification of the cooled reaction mixture, the product was purified by recrystallization from ethanol to give 4-(6-isopropyl-4-methyl-1-naphthyl)-butyric acid (III) as needles, m. p. 151.5~153.5°C (2.45 g.).

Found: C, 79.94; H, 8.18. Calcd. for $C_{18}H_{22}O_2$: C, 79.96; H, 8.20%.

4-(6-Isopropyl-4-methyl-1-naphthyl)-butyric acid (III) (950 mg.) was added with stirring to a cooled 80% sulfuric acid (6.5 ml.) and then heated to 100°C for 1.5 hr. with occasional swirling. The cooled reaction mixture was added to ice and water and extracted with ether. The extract was washed with aqueous sodium carbonate, dried and evaporated to yield a crystalline solid IV which was purified by recrystallization from ethanol, m. p. 125.5~127.0°C, (750 mg.).

Found: C, 85.53; H, 8.02. Calcd. for $C_{18}H_{20}O$: C, 85.67; H, 7.99%.

The semicarbazone formed white glittering plates decomposing at about 220°C. The crystals melted at 255°C with immediate decomposition upon rapid heating.

Found: C, 73.65; H, 7.59; N, 13.47, 13.45. Calcd. for $C_{18}H_{20}O \cdot CH_3N_3$: C, 73.75; H, 7.49; N, 13.58%.

Finely powdered sodium amide (250 mg.) suspended in dry benzene (10 ml.) was added to the cyclic ketone IV (1450 mg.) dissolved in dry benzene (5 ml.). After refluxing for 45 min., the evolution of ammonia ceased and a solid sodio-derivative separated. Addition of methyl iodide (1.0 g.) to the cooled solution resulted in an exothermic reaction, which was completed by refluxing for 30 min. The mixture was treated with dilute hydrochloric acid. Extraction with ether followed by crystallization from ethanol gave cycloketone V (650 mg.), m. p. 101~103°C.

Found: C, 85.69; H, 8.19. Calcd. for $C_{19}H_{22}O$: C, 85.67; H, 8.33%.

Semicarbazone could not be prepared in the usual way.

Reduction of the methylated cycloketone V (620 mg.) with 80% hydrazine hydrate (0.5 ml.), potassium hydroxide (500 mg.) and diethylene glycol (10 ml.) was carried out at 150°C for 2 hr., and then at 220°C for 4 hr. after removal of excess of hydrazine and water. The product VI was extracted with ether and then purified by elution with petroleum ether from an alumina column. A mixture of this tetrahydrophenanthrene VI (540 mg.) and 30% palladium on charcoal (50 mg.) was heated under reflux at 300°C for 2 hr. and then at 350°C for half an hour. The cooled mixture was extracted with petroleum ether and the crude product purified by chromatography from the same solvent on activated alumina, to give 7-isopropyl-1,9-dimethylphenanthrene which separated from ethanol in plates m. p. 77~79°C. λ_{max} (in hexane): 224, 250(shoulder), 257, 274, 281, 288, 299, 319, 328 and 355 mμ. log ε 4.44, 4.84, 5.00, 4.44, 4.37, 4.19, 4.08, 2.46, 2.40 and 2.45 respectively.

Found: C, 91.90; H, 8.19. Calcd. for $C_{19}H_{20}$: C, 91.88: H, 8.12%.

The picrate separated from ethanol in orange yellow needles melting at 133.5~134.5°C.

2-Isopropyl-10-methylphenanthrene.—The Wolff-Kishner reduction of 1,2,3,4-tetrahydro-7-isopropyl-9-methyl-1-oxophenanthrene (IV) (250 mg.) furnished 1,2,3,4-tetrahydro-7-isopropyl-9-methylphenanthrene (VII) (210 mg.), which could not be crystallized. Dehydrogenation of this tetrahydrophenanthrene with 30% palladium on charcoal as before furnished 2-isopropyl-10-methylphenanthrene, which separated from ethanol in white needles melting at 49.0~49.5°C. λ_{max} (in hexane): 223, 248(shoulder), 255, 272, 279, 285, 298, 318, 327 and 334 mμ.

log ε 4.37, 4.75, 4.88, 4.25, 4.21, 4.09, 4.01, 2.37, 2.35 and 2.38 respectively.

Found: C, 92.15; H, 7.75. Calcd. for $C_{18}H_{18}$: C, 92.26; H, 7.74%.

The picrate separated from ethanol as orange yellow needles melting at 123~124°C.

6-Isopropyl-1,4-dimethylnaphthalene via 6-Isopropyl-4-methyl-1-naphthoic Acid.—To a solution of sodium hypochlorite (30 ml. of 10% available chlorine) and sodium hydroxide (6 g.) in water (250 ml.) was dissolved 4-(6-isopropyl-4-methyl-1-naphthyl)-4-oxobutyric acid (I) in aqueous sodium hydroxide (20 ml. of 5%) and the mixture was heated at 65°C for 20 min. and then at 100°C under reflux for 20 min. The cooled solution was washed with ether and the aqueous solution was completely freed from ether by heating and then recooled. Acidification of this solution with sulfur dioxide furnished a solid which after recrystallization from benzene, gave 6-isopropyl-4-methyl-1-naphthoic acid (VIII) (470 mg.), m. p. 179.5~181.0°C.

Found: C, 79.05; H, 7.05. Calcd. for $C_{15}H_{16}O_2$: C, 78.92; H, 7.06%.

The naphthoic acid VIII (141 mg.) was methylated with diazomethane in ether. Excess of diazomethane was removed together with ether by evaporation. Residual oily methyl ester dissolved in dry ether was reduced with lithium alminum hydride (40 mg.). Excess of the hydride was decomposed by addition of dilute hydrochloric acid. Recrystallization from petroleum ether gave 1-hydroxymethyl-6-isopropyl-4-methylnaphthalene (IX) (129 mg.) m. p. 52.5~53.5°C.

Found: C, 83.99; H, 8.28. Calcd. for $C_{15}H_{18}O$: C, 84.07; H, 8.47%.

The carbinol IX (129 mg.) and ethanol (120 mg.)

were dissolved together in liquid ammonia (3.5 ml.) and sodium (70 mg.) was added in small pieces with stirring[8]. A deep blue-colored mixture was obtained. Further ethanol was then added, and after the blue color had disappeared most of the ammonia was allowed to evaporate. The residue was cautiously decomposed by addition of dilute hydrochloric acid, and then extracted with ether. The ether extract was washed with water, and dried. Removal of the solvent followed by chromatography on an alumina column yielded 6-isopropyl-1,4-dimethylnaphthalene (62 mg.) which gave a picrate melting at 103.5~105°C (from ethanol). The mixed melting point of the picrate with that of the authentic sample[9] was undepressed and the infrared spectrum was superimposable on that of the authentic picrate.

Department of Organic Synthesis
Faculty of Engineering
Kyushu University
Hakozaki, Fukuoka

8) A. J. Birch, *J. Chem. Soc.*, **1945**, 809.

9) The author is indebted to Dr S. Dev for his kindly offering trinitrobenzene adduct of the authentic sample.

*The Behavior of Various Inorganic Ions in the Separation of Calcium Carbonate from a Bicarbonate Solution**

By Yasushi KITANO

(Received July 11, 1962)

Calcium carbonate has three different crystal forms: calcite, aragonite and vaterite. Many studies have been made of the conditions under which calcium carbonate is formed in various forms[1-14]. No definite conclusion has yet been reached, however, as to the exactness and the significance of the results.

The factors influencing the mineralogy of carbonate sediments include: (1) the presence of certain inorganic ions, including hydrogen ions, hydroxide ions and carbon dioxide, in the mother solution; (2) the influence of organic material; (3) enzymes (carbonic anhydrase) and bacteria; (4) the mechanical conditions; (5) the temperature, and (6) the transformation of the crystal type after calcium carbonate has been formed.

Experiments on the effects of the materials in the mother solution have been few and inconclusive compared with those on the other factors. The purpose of this study is to cover one phase of this problem: the influence of various inorganic ions on the polymorphic crystallization of calcium carbonate.

In the experiments, calcium carbonate was formed from a calcium bicarbonate solution as carbon dioxide gas escaped. This reaction was used, because it is typical for the formation of calcium carbonate by inorganic processes in the hydrosphere, because it is one of the "homogeneous precipitation" reactions and reproducible precipitation is easily achieved, because no ions other than the calcium, the bicarbonate, and the carbonate ions are present in the mother solution.

Experimental

Materials and Solutions.—The effects of the following alkali and alkaline earth salts (analytical grade reagents) were investigated, since most of them are expected to be found in nature: lithium chloride, sodium chloride, potassium chloride, ammonium chloride, rubidium chloride, cesium chloride, sodium nitrate, sodium sulfate, sodium

* This study was begun at Water Research Laboratory of Nagoya University and completed at the Department of Oceanography, A & M College of Texas, College Station, Texas, U. S. A.

1) W. L. Dekeyser and L. Dugueldre, *Bull. soc. chim. Belges.*, **59**, 40 (1950).
2) J. Johnston, H. E. Merwin and E. D. Williamson, *Am. J. Sci.*, **41**, 473 (1916).
3) Y. Kitano, *J. Chem. Soc. Japan, Pure Chem. Sec. (Nippon Kagaku Zassi)*, **76**, 581 (1955).
4) Y. Kitano, *J. Chem. Soc. Japan, Ind. Chem. Sec. (Kogyo Kagaku Zassi)*, **59**, 1346 (1956).
5) Y. Kitano and N. Kawasaki, *J. Earth Sciences, Nagoya Univ.*, Vol. **16** No. 2, 63 (1958).
6) H. A. Lowenstam, *J. Geol.*, **62**, 284 (1954).
7) H. A. Lowenstam, *Proc. Natl. Acad. Sci. U. S.*, **40**, 39 (1954).
8) J. W. Mellor, "A Comprehensive Treatise on Inorganic and Theoretical Chemistry", Vol. 3, Longmans, Green and Co., London (1925).
9) J. W. Murray, *J. Geol.*, **62**, 481 (1954).
10) H. U. Sverdrup, M. W. Johnson and R. H. Fleming, "The Oceans", Prentice-Hall, Inc., New York (1959), p. 997.
11) N. Watabe and K. M. Wilbur, *Nature*, **188**, 4747, 334 (1960).
12) K. M. Wilbur, *Am. Assoc. Adv. Sci., Washington D. C.*, 15 (1960).
13) J. L. Wray and F. Daniels, *J. Am. Chem. Soc.*, **79**, 2031 (1957).
14) E. J. Zeller and J. L. Wray, *Bull. Am. Petrol. Geol.*, **40**, 140 (1956).

bicarbonate, sodium carbonate, sodium hydroxide, magnesium chloride, calcium chloride, strontium chloride, barium chloride, magnesium sulfate, magnesium bicarbonate, strontium bicarbonate and barium bicarbonate.

For the preparation of the bicarbonate solution of alkaline earth elements, the carbonate was pulverized and suspended in distilled water, and then carbon dioxide gas was bubbled through the suspension for approximately one day at room temperature. After having been allowed to stand for 30 min., the suspension was filtered. The filtrate was aerated for another hour with carbon dioxide.

Procedure.—Different amounts (0~6 g.) of the salts were placed in one liter flasks with a small amount of distilled water, and 300 ml. portions of a calcium bicarbonate solution (prepared according to the above procedure) were added to each. The flasks were left to stand at room temperature for two or three weeks, during which time carbon dioxide gas escaped from the solution and calcium carbonate crystals were separated. As the carbon dioxide gas escaped, portions of the supernatant solution were withdrawn to determine the change in the pH value and the decrease in the calcium content. The rate of calcium carbonate precipitation was estimated from these data. Eventually, the remaining precipitate of carbonate was filtered off and washed with distilled water until it was free from any trace of the mother solution. After having been dried in an air bath and ground in an agate mortar, a fraction of the crystals was used for the determination of the chemical composition, while another fraction was used for the identification of the crystal form by X-ray diffraction.

Calcium carbonate was formed at room temperature. The pH value and the calcium content in the mother solution changed during the process of calcium carbonate precipitation; therefore, it is considered that calcium carbonate precipitates were formed from solution of varying pH values and varying calcium concentrations. The author studied whether there was a difference in the polymorphic composition among the calcium carbonate crystals after different lapses of time. Under the given conditions, the difference was not significant.

Results and Discussion

The Effect of Alkali Chlorides.—Table I and Fig. 1 show that alkali chlorides in the mother

TABLE I. $Ca(HCO_3)_2$-ALKALI CHLORIDE-CO_2-H_2O SYSTEM (28±3°C)

Composition of solutions (total volume, 300 ml.)										Crystal form* of $CaCO_3$ formed during 14 days	
at the start				on the 2nd day		on the 5th day		on the 14th day			
Ca-bicarbonate solution**	Salt added		pH	Ca	pH	Ca	pH	Ca	pH	Aragonite	Calcite
Ca mg.	Salt	meq. of cation		mg.		mg.		mg.		%	
85	—	—	6.7	40	7.5	11	7.9	7	7.9	15	85
85	LiCl	7	6.7	58	7.4	21	7.8	9	7.8	2	98
85	LiCl	24	6.8	68	7.6	26	7.9	12	7.9	0	100
85	LiCl	70	6.8	73	7.9	35	8.0	15	8.1	0	100
85	NaCl	5	6.7	60	7.4	25	7.8	9	7.8	4	96
85	NaCl	17	6.8	64	7.6	30	7.9	12	7.9	0	100
85	NaCl	50	6.8	70	7.9	36	8.0	13	8.1	0	100
85	KCl	4	6.7	61	7.6	20	7.8	10	7.9	10	90
85	KCl	14	6.8	64	7.8	24	7.9	11	7.9	1	99
85	KCl	40	6.8	70	7.8	30	8.0	13	8.0	0.5	99.5
85	NH_4Cl	6	6.7	65	7.4	25	7.8	18	7.9	0	100
85	NH_4Cl	19	6.8	70	7.5	35	7.8	27	7.9	0	100
85	NH_4Cl	57	6.8	75	7.6	47	7.8	45	7.9	0	100
85	RbCl	3	6.8	60	7.4	20	7.8	9	7.8	11	89
85	RbCl	8	6.8	66	7.5	25	7.9	10	7.9	10	90
85	CsCl	2	6.7	57	7.4	18	7.8	9	7.8	10	90
85	CsCl	6	6.8	61	7.5	19	7.8	10	7.8	9	91
85	CsCl	18	6.8	67	7.8	22	7.9	10	7.9	9	91
85	$NaNO_3$	4	6.7	59	7.5	21	7.8	9	7.8	11	89
85	$NaNO_3$	12	6.8	64	7.6	25	7.9	12	7.9	10	90
85	$NaNO_3$	40	6·8	69	7.8	30	7.9	13	7.9	7	93

* No vaterite was found.

** A solution containing $Ca(HCO_3)_2$, H_2CO_3, CO_2 and H_2O as shown in "materials and solutions" in Experimental of this report.

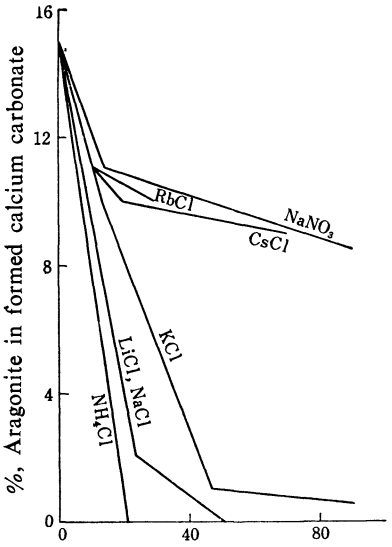


Fig. 1. Effect of alkali chloride in a mother solution on crystal type of formed calcium carbonate.

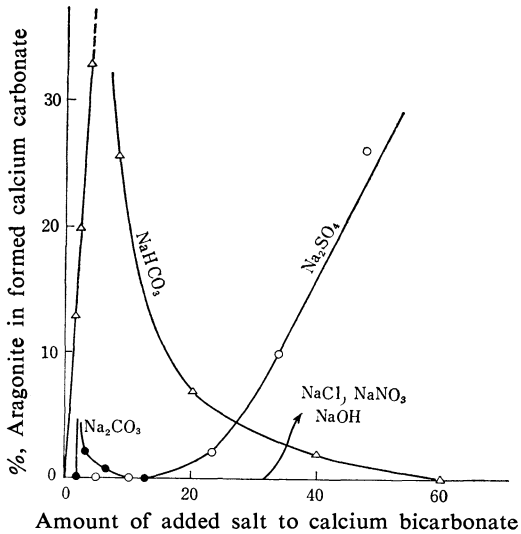


Fig. 2. Effect of sodium salts in a mother solution on crystal type of formed calcium carbonate.

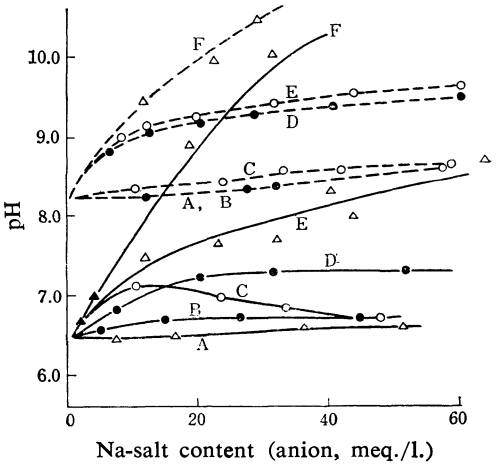


Fig. 3. pH of calcium bicarbonate solution containing sodium salt.
—— pH at the start
--- pH on the 21st day
A, NaCl B, $NaNO_3$ C, Na_2SO_4
D, $NaHCO_3$ E, Na_2CO_3 F, NaOH

solution inhibited the formation of aragonite favored the formation of calcite. Furthermore, Table I shows that alkali chlorides had little influence on the pH value of the mother solution. The extent of the inhibition of the aragonite formation decreased in the sequence: ammonium chloride>lithium chloride, sodium chloride>potassium chloride>rubidium chloride, cesium chloride, (sodium nitrate).

Previous reports[4,8] showed that the presence of alkali chlorides favored aragonite formation. This report, covering a large number of samples in various amounts, shows, in every case, a definite decrease in the percentage of aragonite formation with an increase in the concentration of alkali chloride. The precipitate consisted only of calcium and carbonate.

The Effect of Anions.—Calcium carbonate was formed from the calcium bicarbonate solution containing sodium salt. The crystal form of the calcium carbonate was identified (Fig. 2), and the change in the pH value of the mother solution with time was measured (Fig. 3). The following results were obtained concerning the effect of anions on the crystallization of calcium carbonate:

Sodium Chloride and Nitrate.—The presence of both sodium chloride and sodium nitrate inhibited aragonite formation, although the effect of sodium chloride was stronger than that of sodium nitrate (Fig. 1).

Sodium Bicarbonate and Carbonate.—With a moderate increase in the amount of sodium bicarbonate (sodium carbonate) added to the mother bicarbonate solution, the percentage of aragonite formation increased. With a further increase in amount, however, the percentage began to decrease and reached zero (Fig. 2). The present author has previously joined to show[15] that calcium carbonate was not formed directly from a solution highly concentrated in calcium, bicarbonate or carbonate ions, but that a gelatinous, unstable compound having a

15) Y. Inoue, Y. Kitano and E. Yagyu, *J. Chem. Soc. Japan, Pure Chem. Sec.* (*Nippon Kagaku Zassi*), **96**, 19 (1955).

definite chemical composition was first formed. Furthermore, the present author[16-17] has reported that the unstable compound was then transformed into a calcium carbonate precipitate, and that with an increase in the concentrations of the calcium ions and the carbonate ions in the original, highly-concentrated solution, the stability of the unstable compound increased; consequently, the rate of calcium carbonate separation decreased. Therefore, one can say that the rate of calcium carbonate separation is moderate when the concentration of calcium ions or carbonate ions is either very high or very low. When calcium carbonate separation is moderate, the most stable form, calcite, is predominant. This finding helps qualitatively to explain the maximum percentage of aragonite formation for a certain value of the added carbonate salt.

Sodium Hydroxide.—When sodium hydroxide was added, only calcite was formed (Fig. 2). Aragonite was never formed from the solution which had been made alkaline (up to a pH value of 10) with sodium hydroxide. It has been reported by many researchers[3,4,8] that aragonite formation was favored in a solution having a pH value of more than 8. However, as can be seen from Figs. 2 and 3, aragonite was not always formed from an alkaline solution; the previous conclusion, therefore, is not always reliable.

The ease of aragonite formation does not seem always to depend upon the pH value, but upon the carbonate ion* content of the mother solution. Since the pH value and the total carbonate content changed with time in the mother solution, the estimation of the carbonate ion content in the mother solution was difficult. A more detailed study is under way on the effect of sodium bicarbonate, sodium carbonate and sodium hydroxide.

Sodium Sulfate.—The presence of sulfate ions favored aragonite formation.

The Effect of Alkaline Earth Salts.—*Magnesium Chloride, Bicarbonate and Sulfate.*—On the basis of the following facts, it can be supposed that the presence of magnesium bicarbonate or magnesium sulfate in the mother solution is more conducive to aragonite formation than is the presence of magnesium chloride. (1) Magnesium ions, bicarbonate ions and sulfate ions favored aragonite formation (Figs. 2 and 4), but chloride ions inhibited aragonite formation (Table I). (2) According to the previous conclusion[3,4], aragonite in general was formed

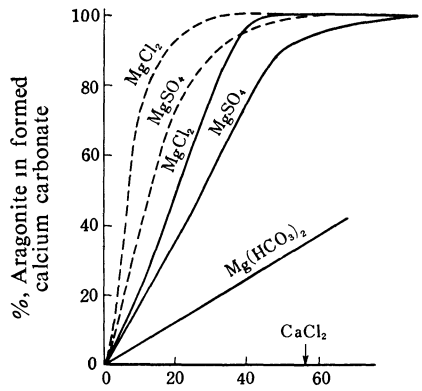


Fig. 4. Effect of calcium and magnesium salts in mother solution on crystal type of formed calcium carbonate.
—— 10±2°C
--- 28±3°C

when the rate of calcium carbonate precipitation was large, while calcite was formed when the rate was small, provided that the mechanism of calcium carbonate formation was similar. It must be noted that the rate was larger in a mother solution containing magnesium bicarbonate than in that containing magnesium chloride (Fig. 5). However, in the experiment, the presence of magnesium chloride in the mother solution was more favorable to aragonite formation than that of magnesium bicarbonate or magnesium sulfate (Fig. 4). The presence of the magnesium salts had little influence on the pH value of the solution. The result shows that the presence of magnesium ions in the mother solution seems to favor aragonite formation very strongly. Working with solutions of a low and a nearly constant ionic strength ($\mu=0.15$), Greenwald[18] concluded that following equilibria exist at 22°C:

$$\frac{M_{Ca^{2+}}\, M_{HCO_3^-}}{M_{CaHCO_3^+}} = K'_{CaHCO_3^+} = 1.6\times10^{-1}$$

$$\frac{M_{Mg^{2+}}\, M_{HCO_3^-}}{M_{MgHCO_3^+}} = K'_{MgHCO_3^+} = 1.7\times10^{-1}$$

$$\frac{M_{Ca^{2+}}\, M_{CO_3^{2-}}}{M_{CaCO_3^0}} = K'_{CaCO_3^0} = 1\times10^{-3}$$

$$\frac{M_{Mg^{2+}}\, M_{CO_3^{2-}}}{M_{MgCO_3^0}} = K'_{MgCO_3^0} = 4.3\times10^{-3}$$

and Garrels[19] concluded $K'_{MgCO_3^0}=4.0\times10^{-4}$.

The concentration of magnesium ions in the mother solution was calculated by the use of

16) Y. Inoue, Y. Kitano and S. Koyama, ibid., **76**, 22 (1955).
17) Y. Inoue, Y. Kitano and S. Konaka, ibid., **76**, 124 (1955).
* Carbonate ion concentration is estimated from the pH value and the total carbonate content in a solution.
18) I. Greenwald, *J. Biol. Chem.*, **141**, 789 (1941).
19) R. M. Gerrels, M. E. Thompson and R. Silver, *Am. J. Sci.*, **259**, 24 (1961).

TABLE II. $Ca(HCO_3)_2$-Mg SALT-CO_2-H_2O SYSTEM (10±2°C)

Composition of solution at the start: Ca-bicarbonate solution ml.	Ca mg.	Salt added: Salt	ml.	Mg mg.	on the 15th day: Ca mg.	Mg mg.	on the 50th day: Ca mg.	Mg mg.	Precipitate: Mg content (%) in precipitate during 15 days	during 50 days	Crystal form** of $CaCO_3$ separated during 15 days: Aragonite %	Calcite
250	106	—	—	—	9	—	7	—	0.00	0.00	0.0	100
250	106	$MgCl_2$	50	48	18	48	11	48	0.00	0.00	33	67
250	106	$MgCl_2$	150	145	29	145	20	145	0.00	0.00	78	22
250	106	$MgCl_2$	250	242	42	247	31	247	0.00	0.00	99	1
250	106	$MgCl_2$	400	394	53	397	40	399	0.00	0.00	100	0
250	106	$MgSO_4$	50	60	—	—	—	—	0.00	0.00	28	72
250	106	$MgSO_4$	150	100	—	—	—	—	0.00	0.00	37	63
250	106	$MgSO_4$	250	200	—	—	—	—	0.00	0.00	63	37
250	106	$MgSO_4$	400	400	—	—	—	—	0.00	0.00	92	8
250	106	$Mg(HCO_3)_2$	50	61	0.0	61	0.0	61	0.00	0.00	8	92
250	106	$Mg(HCO_3)_2$	150	184	0.0	183	0.0	185	0.00	0.00	21	79
250	106	$Mg(HCO_3)_2$	250	307	0.0	308	0.0	304	0.00	0.3*	31	69
250	106	$Mg(HCO_3)_2$	400	491	0.0	493	0.0	485	0.00	1.2*	43	57

* Mg is contained as $MgCO_3 \cdot 3H_2O$.
** No vaterite was formed.

the dissociation constants of the complexes, $MgHCO_3^+$ and $CaHCO_3^+$, because the concentration of carbonate ions is very small compared with that of bicarbonate ions at the given pH value; even when the calculated concentration of magnesium ions was the same, aragonite formation was much more favored in the solution containing magnesium chloride than in the solution containing magnesium bicarbonate.

Figure 5 shows the rate constants* in the reaction of calcium carbonate separation from a calcium bicarbonate solution containing various amounts of salts. Magnesium and sodium were not co-precipitated with calcium carbonate (Table II). The presence of magnesium chloride (which aided aragonite formation) lowered the rate of calcium carbonate separation to a greater extent than did sodium chloride (which aided calcite formation).

It must be said that the percentage of aragonite (unstable crystal) formation does not always increase with an increase in the rate of calcium carbonate separation and that the mechanism of the effect of ions in the mother solution upon the polymorphic crystallization is probably be different from ion group to ion

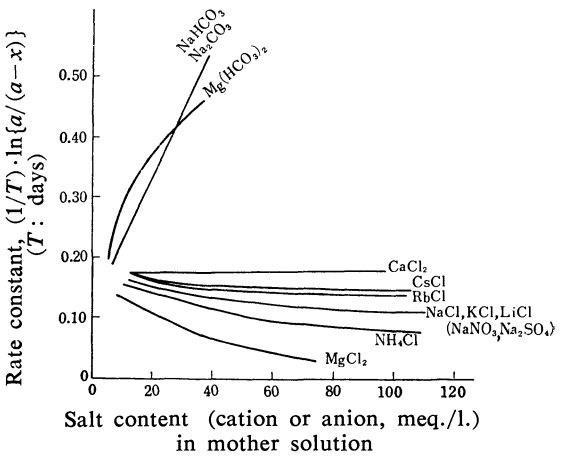


Fig. 5. Rate constant in reaction of calcium carbonate separation from calcium bicarbonate solution containing salt.

group. Work is under way to investigate the mechanisms whereby magnesium chloride favors aragonite formation more than magnesium bicarbonate or magnesium sulfate and whereby magnesium chloride favors aragonite formation while sodium chloride favors calcite formation at room temperature.

Calcium Chloride.—Calcium chloride was added to the mother solution to accelerate calcium carbonate precipitation; its addition did not aid aragonite formation (Fig. 4).

Strontium Chloride and Bicarbonate.—The significant behavior of strontium ions in the

* The decrease in the calcium content of the mother solution was measured during the process of calcium carbonate precipitation. On the basis of the measurements, the rate constant, $(1/T)\cdot\ln\{a/(a-x)\}$, of the first order reaction, and the constant, $[1/2T]\cdot[1/(a-x)^2-1/a^2]$, of the third order reaction were calculated. Judging from these calculations, the reaction seemed to be a first order reaction; therefore, in Fig. 5, the rate constants of the first order reaction are given.

separation of calcite or aragonite has been clarified previously[5]: (1) With an increase in the amount of strontium bicarbonate added to the original calcium bicarbonate solution, the percentage of aragonite formation increased to a maximum (optimum strontium content: approximately 2 mg./l.). The percentage began to decrease with a further increase in the strontium concentration (Fig. 6). When strontium chloride was added to the mother solution, aragonite formation was inhibited. (2) The strontium was always entrained in the calcium carbonate precipitate, even when the strontium concentration in the mother solution was very low.

Barium Chloride and Bicarbonate.—Calcium carbonate was formed from the calcium bicarbonate solution containing barium bicarbonate or barium chloride; it was also formed from the calcium bicarbonate solution containing magnesium chloride and barium bicarbonate or barium chloride (Table III and Fig. 7), judging from the fact that calcium carbonate consisting of increasing percentages of aragonite could be obtained from calcium bicarbonate solutions containing increasing amounts of magnesium chloride (Fig. 3). Table III shows the barium content in the carbonate prepared. The barium content was obtained by first adding different amounts of barium ions labeled with ^{140}Ba to the mother bicarbonate solutions. Measured volumes of the original solution, and of the residual solution from which the calcium carbonate crystals had been collected, were dried in planchets. The radioactivities of the two samples were measured at the same time, sixteen days after the residual solution had been dried. The ratio of the distribution of barium between the precipitate and the residual solution was calculated. From this ratio, the

TABLE III. $Ca(HCO_3)_2$-$MgCl_2$-Ba SALT-CO_2-H_2O SYSTEM (12±3°C)

Composition of solutions at the start						Composition of solutions on the 15th day	Precipitate formed duaring 15 days			
Ca-bicarbonate solution		$MgCl_2$	Ba salt				Crystal form			Fractionation factor ((Ba/Ca) in ppt.)/((Ba/Ca) in soln.)
ml.	Ca mg.	m. M	Salt	ml.	Ba mg.	Ca, mg.	Vaterite %	Aragonite %	Calcite %	
300	75	0	0	0	0	14	0	0	100	—
300	75	0	$BaCl_2$	0.05	0.05	18	0	0	100	0.40
300	75	0	$BaCl_2$	0.1	0.1	19	0	0	100	0.40
300	75	0	$BaCl_2$	0.3	0.3	20	0	0	100	0.41
300	75	0	$BaCl_2$	0.7	0.7	21	0	0	100	0.36
300	75	0	$BaCl_2$	2	2	21	0	0	100	0.33
300	75	0	$BaCl_2$	10	10	26	0	0	100	0.33
300	75	0	$BaCl_2$	50	50	—	94	0	6	—
300	75	0	$BaCl_2$	75	75	—	100	0	0	—
300	75	0	$BaCl_2$	100	100	—	100	0	0	—
300	75	0	$Ba(HCO_3)_2$	0.05	0.04	20	0	0	100	0.35
300	75	0	$Ba(HCO_3)_2$	0.1	0.07	20	0	0	100	0.33
300	75	0	$Ba(HCO_3)_2$	0.3	0.2	20	0	0	100	0.34
300	15	0	$Ba(HCO_3)_2$	0.7	0.5	21	0	0	100	0.34
300	75	0	$Ba(HCO_3)_2$	2	1.5	22	0	0	100	0.31
300	75	0	$Ba(HCO_3)_2$	10	6	23	0	0	100	0.32
300	75	0	$Ba(HCO_3)_2$	50	28	—	0	0	100	—
300	75	0	$Ba(HCO_3)_2$	75	42	—	46	0	54	—
300	75	0	$Ba(HCO_3)_2$	100	60	—	96	0	4	—
300	75	1.5	0	0	0	20	0	30	70	—
300	75	4	0	0	0	26	0	70	30	—
300	75	5	0	0	0	37	0	95	5	—
300	75	1.5	$BaCl_2$	5	5	24	0	0	100	0.41
300	75	4	$BaCl_2$	5	5	29	0	0	100	0.49
300	75	5	$BaCl_2$	5	5	37	0	0	100	0.67
300	75	1.5	$Ba(HCO_3)_2$	5	3	20	0	0	100	0.35
300	75	4	$Ba(HCO_3)_2$	5	3	27	0	0	100	0.48
300	75	5	$Ba(HCO_3)_2$	5	3	35	0	0	100	0.63

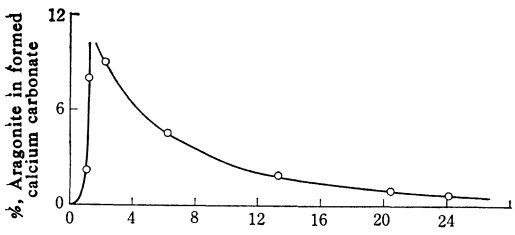


Fig. 6. Effect of strontium ions on the crystal type of formed calcium carbonate.

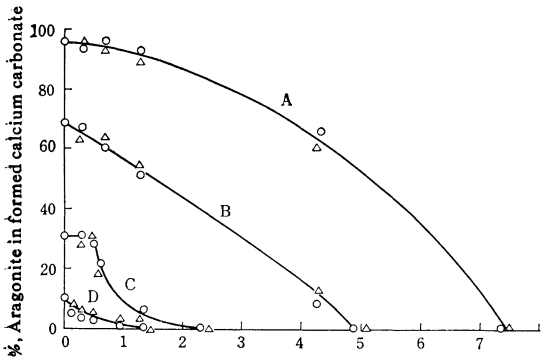


Fig. 7. Effect of barium ions in mother solution on crystal type of formed calcium carbonate (36±3°C).
○ $BaCl_2$ △ $Ba(HCO_3)_2$
A $MgCl_2$ 12 mmol./l.
B $MgCl_2$ 4.5 mmol./l.
C $MgCl_2$ 2.5 mmol./l.
D $MgCl_2$ none

original and the residual calcium content and the original barium content in the solution, the barium content of the precipitated carbonate was calculated.

The behavior of barium ions in the separation of calcium carbonate from a bicarbonate solution has been clarified. (1) Contrary to previous findings[4,9,14] that the presence of a small number of barium ions in the mother solution favored aragonite formation, the presence of barium ions favored calcite formation (Table III, and Fig. 7). (2) The presence of a large amount of barium ions favored vaterite formation[2] (Table III). (3) Even at a low concentration in the mother solution, barium was always entrapped in the precipitates (Table III). The behavior of barium ions did not follow the law of solubility. (4) With an increase in the barium concentration of the mother solution, the amount of barium entrapped in the calcium carbonate increased and the specific peak for calcite configuration became diffuse when measured with an X-ray diffractometer. Therefore, it can be expected that barium is present in calcium carbonate as a form of $(Ca, Ba)CO_3$. As can be seen from Table III, the amount of entrapped barium in calcium carbonate increased with an increase in the magnesium chloride concentration of the mother solution. The presence of the barium salts had little influence on the pH value of the solution.

Summary

The author has shown the effect of various inorganic ions on the polymorphic crystallization of calcium carbonate from a bicarbonate solution. No definite conclusion regarding the mechanism to give calcite, aragonite or vaterite can yet be made, but these data help to give a pattern of the influence of inorganic ionic species and the concentration of the mother solution on the polymorphic crystallization of calcium carbonate.

(1) Alkali chlorides in the mother solution inhibited aragonite formation and favored calcite formation. The extent of the inhibition of the aragonite formation decreases in the sequence: ammonium chloride>lithium chloride, sodium chloride>potassium chloride >rubidium chloride, >cesium chloride (sodium nitrate).

(2) (a) Sodium chloride and sodium nitrate in the mother solution inhibited aragonite formation, sodium chloride more strongly than sodium nitrate. (b) With a moderate increase in the amount of sodium bicarbonate (sodium carbonate) added to the mother solution, the percentage of aragonite formation increased to a maximum. With a further increase in the amount, however, the percentage began to decrease and reached zero. (c) When sodium hydroxide was added to the mother solution, only calcite was formed. Aragonite was never formed from the solution which had made alkaline with sodium hydroxide. (d) The presence of sulfate ions favored aragonite formation.

(3) (a) Magnesium ions in the mother solution favored aragonite formation very strongly. The presence of magnesium chloride in the mother solution was more favorable to aragonite formation than that of magnesium bicarbonate or magnesium sulfate. Magnesium was not co-precipitated with calcium carbonate. (b) The presence of calcium chloride in the mother solution had no effect on the crystallization. (c) With an increase in the strontium concentration in the original solution, the percentage of aragonite formation increased to a maximum (optimum strontium content: approximately 2 mg./l.). The percentage began to decrease with a further increase in strontium

concentration. The strontium was always entrained in calcium carbonate precipitates, even when the strontium concentration was very low. (d) The presence of a small number of barium ions in the mother solution favored calcite formation. The presence of a large number of barium ions favored vaterite formation. Even at a low concentration in the mother solution, barium was always entrapped in the precipitates.

The author wishes to express his deep appreciation to Mrs. Nobuko Kanamori of Nagoya University for her help in the experiment on the behavior of barium, and to Professor Donald W. Hood, Mr. Edward R. Ibert and Miss. Lela M. Jeffery of Texas A & M College and Professor Ken Sugawara of Nagoya University for their encouragement throughout this work.

Water Research Laboratory
Faculty of Science
Nagoya University
Chikusa-ku, Nagoya

A Study of the Polymorphic Formation of Calcium Carbonate in Thermal Springs with an Emphasis on the Effect of Temperature

By Yasushi KITANO

(Received July 16, 1962)

The conditions which determine the polymorphic crystallization of calcium carbonate have been discussed by many researchers[1-9]; however, many questions still remain unsolved. The temperature of the mother solution should be considered as one of the most important factors controlling the polymorphic formation. It has been reported that aragonite was formed easily from a solution at a temperature above 50°C, but this conclusion is not always reliable[3]. In the following discussion of the conditions of the polymorphic formation of calcium carbonate, the combined effect of the temperature and of the materials in the mother solution is examined. The author has attempted to show this combined effect on the formation of the various crystal forms of calcium carbonate in the thermal springs of Japan, such springs being typical areas of calcium carbonate deposition.

Crystal Forms of Calcium Carbonate Deposited in Thermal Springs of Japan.—Table I shows the chemical constituents of the thermal spring waters in Japan from which calcium carbonate deposits have been formed and the crystal forms of this calcium carbonate. Related articles have showen that the presence of sodium chloride, magnesium chloride and carbon dioxide in the mother solution greatly affects the polymorphic crystallization of calcium carbonate[10,11]. On the basis of their sodium, magnesium and chloride ion content, the spring waters are classified in two typical groups, A and B, as is shown in Table I.

Experimental and Results

When thermal waters come to the surface of the earth, they are subjected to a sudden environmental change, exposure to the air at an atmospheric pressure. Then, on the one hand, carbon dioxide gas escapes from the water to precipitate calcium carbonate, and on the other, some of the ferrous and manganous ions begin to be oxidized by the air.

Calcium carbonate is formed in thermal springs according to the following reaction : $Ca^{2+}+2HCO_3^- \rightarrow CaCO_3+CO_2+H_2O$. Therefore, the effect of temperature upon the polymorphic formation of calcium carbonate formed from a calcium bicarbonate solution has been studied in the laboratory. For the preparation of the calcium bicarbonate solution,

1) W. L. Dekeyser and L. Dugueldre, *Bull. soc. chim. Belges*, **59**, 40 (1950).
2) J. Johnston, H. E. Merwin and E. D. Williamson, *Am. J. Sci.*, **41**, 473 (1916).
3) Y. Kitano, *J. Chem. Soc. Japan, Pure Chem. Sec. (Nippon Kagaku Zassi)*, **76**, 581 (1955).
4) Y. Kitano, *J. Chem. Soc. Japan, Ind. Chem. Sec. (Kogyo Kagaku Zassi)*, **59**, 1346 (1956).
5) H. A. Lowenstam, *J. Geol.*, **62**, 284 (1954).
6) J. W. Mellor, "A Comprehensive Treatise on Inorganic and Theoretical Chemistry", Vol. 3, Longmans, Green and Co., London (1923).
7) J. W. Murray, *J. Geol.*, **62**, 481 (1954).
8) J. L. Wray and F. Daniels, *J. Am. Chem. Soc.*, **79**, 2031 (1957).
9) E. J. Zeller and J. L. Wray, *Bull. Am. Petrol. Geol.*, **40**, 140 (1956).
10) Y. Kitano, This Bulletin, **35**, 1973 (1962).
11) Y. Kitano and D. W. Hood, *J. Ocea. Soc. Japan*, **18**, 141 (1962).

TABLE I. CHEMICAL CONSTITUENTS OF THERMAL SPRING WATERS AND THE CRYSTAL FORMS OF DEPOSITED CALCIUM CARBONATE

Thermal springs	Temp. °C	pH	Ions, g./l. Na^+	K^+	Ca^{2+}	Mg^{2+}	Cl^-	SO_4^{2-}	HCO_3^-		Vaterite %	Calcite %	Aragonite %
Futamata	35～50	6.5～6.6	1.5～2.5	0.42～0.73	0.54～0.83	0.11～0.16	3.3～5.3	0.09～0.13	1.2～1.7	A***	0	100*	0
Yunokawa	66	6.7	2.2	0.17	0.61	0.19	4.1	0.82	0.88	A	0	3～0	97～100
Yatsu	100	8.6	0.4	0.009	0.056	0.13	0.53	0.64	0.16	A	0	8	92
Masutomi	26～32	6.0～6.3	2.4～3.3	0.04～0.23	0.30	0.02	3.9～4.2	0.51～0.63	1.2～2.0	B	0	100	0
Senami	?～100	7.9	1.3	0.03	0.11	0.002	2.0	0.25	0.15	B	0	100	0**
Shirahama	64～79	7.4～7.9	1.5～3.7	0.07～0.26	0.04～1.1	0.01～0.57	1.0～4.4	0.25～0.94	2.3～4.7	A/B	0	0	100
Teshikaga	50～70	8.3～8.5	0.56～0.78	0.01～0.02	0.07～0.23	0.002～0.005	0.92～1.3	0.09～0.18	0.14～0.22	B	0	3～1	97～99
Shiobara	66		0.44	0.04	0.08	0.02	0.62	0.07	0.40	B?	0	100	0
Ikaho	40～50	5.2～6.1	0.06～0.09	0.006～0.02	0.10～0.25	0.02～0.05	0.07～0.18	0.19～0.39	0.28～0.70	B?	0	100	0
Hisayoshi	42	5.8	0.18	0.008	0.48	0.05	0.29	0.66	0.88	B?	0	100	0
Shikabe	80～100	7.0～8.1	0.7～1.2	0.04～0.09	0.07～0.10	0.008～0.013	0.73～1.6	0.40～0.48	0.23～0.46	B?	0	16～0	84～100
Mine	100	8.6	0.73	0.04	0.06	0.0007	1.1	0.16	0.080	B?	0	1～0	99～100
Atakawa	?～100	8.2～8.5	0.5～0.74	0.09～0.11	0.11～0.13	0.004～0.016	0.4～1.2	0.27～0.46	0.05～0.11	B?	0	100	0
Nigorikawa	50～90	5.9～7.3	0.4～1.4	0.04～0.14	0.1～0.16	0.04～0.05	0.5～2.3	0.007～0.04	0.8～1.4	B?	0	100～77	0～23
Fushime	100	7.2	3.8	0.32	0.63	0.012	7.3	0.11	0.06	B	0	13	87

* Aragonite was observed in some special stations (Table IV).

** Qnly one sample was of pure aragonite configuration.

*** Group A: NaCl, 5 g./l.; $MgCl_2$, 0.7 g./l.
Group B: NaCl, 5 g./l.; $MgCl_2$, 0.07 g./l.

carbon dioxide gas was bubbled into a suspension of 40 g. of calcium carbonate in 20 l. of distilled water for 48 hr. at room temperature and filtered (Whatman No. 3 filter paper); and then carbon dioxide gas was bubbled again into the filtrate for 2 hr. The calcium content was 300 mg. per liter. The bicarbonate solution prepared at room temperature was used throughout the present experiments. When the solution was left to stand at various temperatures, carbon dioxide gas escaped from the solution and calcium carbonate crystals appeared; even when carbon dioxide gas was passed continuously through the bicarbonate solution at high temperatures, calcium carbonate was precipitated because of the decrease in the solubilities of carbon dioxide and calcium carbonate with the increase in the temperature of the solution.

Experiment A.—Calcium carbonate was precipitated from the calcium bicarbonate solution in order to examine the effect of temperature change.

1) A 300 ml. portion of the bicarbonate solution was allowed to stand (20 min. to 3 weeks) at varying temperatures, with occasional stirring so that carbon dioxide gas escaped from the solution and calcium carbonate crystals appeared. The crystals were filtered off and washed several times with distilled water. After the crystals had been dried in an air bath and ground in an agate mortar, their crystal forms were identified by the use of an X-ray diffractometer (Fig. 1). At temperatures below 25°C, only calcite was formed. At around 30°C, both calcite and aragonite were formed, but no vaterite was. Between 40 and 60°C, all three forms were formed, but the proportion of calcite was small. At around 40°C the proportion of vaterite was large. With a rise in the temperature, the proportion of aragonite increased, and at around 60°C aragonite predominated. Between 70 and 90°C, only aragonite was formed. At the boiling point, aragonite predominated, but a small amount of vaterite was formed.

2) Calcium carbonate was formed from 300 ml. of the calcium bicarbonate solution through which carbon dioxide gas was bubbled continuously at high temperatures. The carbon dioxide content controls the pH value of the solution, and the pH value is an important factor in determining the crystal form of the resulting calcium carbonate. The experiments were conducted at various temperatures above 70°C because at lower temperatures the formation of calcium carbonate was difficult from the solution bubbled with carbon dioxide gas. When calcium carbonate was formed from the solution bubbled with carbon dioxide gas, even at a high temperature, calcite and vaterite were formed with aragonite, as is shown in Fig. 2. With a rise in the temperature, the formation of aragonite increased.

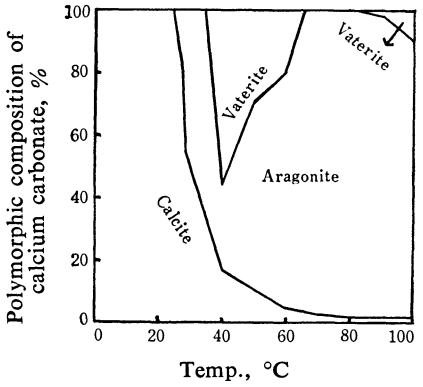


Fig. 1. Polymorphic composition of calcium carbonate formed from calcium bicarbonate solution at various temperatures.

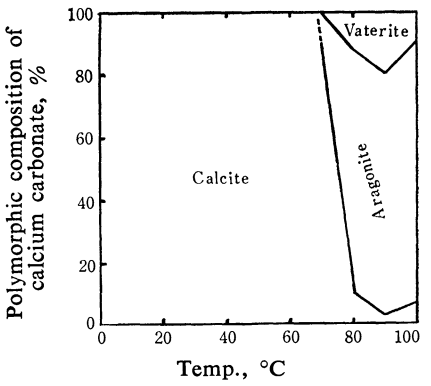


Fig. 2. Polymorphic composition of calcium carbonate formed from calcium bicarbonate solution bubbled with carbon dioxide gas at various temperatures.

Experiment B.—Calcium carbonate was precipitated from 300 ml. of the calcium bicarbonate solution containing sodium chloride and/or magnesium chloride, in order to investigate the effect of these salts on the polymorphic formation of calcium carbonate.

1) Sodium Chloride.—a) Calcium carbonate was formed as in Experiment A-1 from the calcium bicarbonate solution containing various amounts of sodium chloride (Table II). With an increase in the temperature and in the concentration of sodium chloride in the solution, the proportion of vaterite increased. At the boiling point, vaterite predominated. From Fig. 1 and Table II, it can be concluded that the presence of sodium chloride favors the formation of vaterite at a high temperature, while it favors calcite formation at a low temperature[10]. b) When calcium carbonate was formed from the solution containing sodium chloride and bubbled with carbon dioxide gas, only calcite was formed (Table II).

2) Magnesium Chloride.—a) Calcium carbonate was formed from the calcium bicarbonate solution containing various amounts of magnesium chloride according to the same procedure as in Experiment A-1 (Table III). Table III and Fig. 1 indicate that the presence of magnesium chloride in the solution favored aragonite formation and hindered vaterite formation. b) When calcium carbonate was formed from the solution containing magnesium chloride and bubbled with carbon dioxide gas continuously, only calcite was formed (Table III).

TABLE II. CRYSTAL FORMS OF CALCIUM CARBONATE FORMED FROM THE CALCIUM BICARBONATE SOLUTION CONTAINING SODIUM CHLORIDE

Mother solution		Crystal forms of $CaCO_3$		
Temp.	NaCl in calcium bicarbonate solution	Vaterite	Calcite	Aragonite
°C	g./l.	%	%	%
30	1.5	0	100	0
50	1.5	12	14	74
60	1.5	40	10	50
70	1.5	35	5	60
80	1.5	40	8	52
100	1.5	63	10	27
80	0.3	14	8	78
80	1.0	40	10	50
80	1.5	40	8	52
80	3	52	10	38
80	10	55	20	35
80	15	49	9	42
100	1.5	63	10	27
100	3	78	9	13
100	10	91	6	3
100	25	91	8	1
Solution aerated with carbon dioxide gas				
80	3	0	100	0
80	6	0	100	0
80	10	0	100	0
80	15	0	100	0

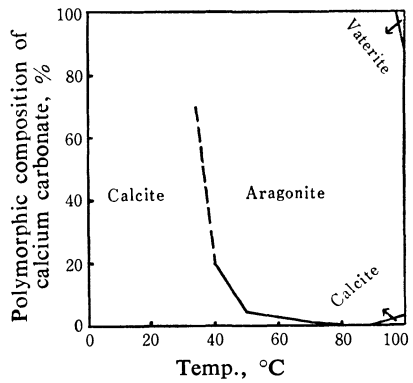


Fig. 3. Polymorphic composition of calcium carbonate formed from calcium bicarbonate solution containing sodium chloride (5 g./l.) and magnesium chloride (0.7 g./l.).

3) Sodium Chloride and Magnesium Chloride.— A) When calcium carbonate was formed from the calcium bicarbonate solution containing both sodium chloride (5 g./l.) and magnesium chloride (0.7 g./l.) (group A in Table I), vaterite was not formed at a lower temperature than the boiling point (Fig. 3). At a temperature above 50°C, aragonite predominated. This indicates that the magnesium chloride in the solution had a greater effect than the sodium chloride, so that the composition of

TABLE III. CRYSTAL FORMS OF CALCIUM CARBONATE FORMED FROM THE CALCIUM BICARBONATE SOLUTION CONTAINING MAGNESIUM CHLORIDE

Mother solution		Crystal forms of $CaCO_3$		
Temp.	$MgCl_2$ in calcium bicarbonate solution	Vaterite	Calcite	Aragonite
°C	g./l.	%	%	%
10	0.6	0	88	12
10	1.8	0	40	60
10	3~4.5	0	0	100
30	0.5	0	30	70
30	0.8	0	23	77
30	1.5	0	0	100
50	0.15	0	7	93
50	4.5	0	0	100
60	0.15	0	5	95
60	4.5	0	0	100
70	0.15	0	5	95
70	4.5	0	0	100
80	0.15	0	0	100
80	4.5	0	0	100*
100	0.15	0	0	100*
100	4.5	0	0	100*
Solution aerated with carbon dioxide gas				
70	3	0	100	0
80	3	0	100	0

* A small amount of magnesium carbonate was precipitated with calcium carbonate. (The details are; Y. Kitano, K. Park and D. W. Hood, "Pure Aragonite Synthesis," *J. Geophys. Research*, in press).

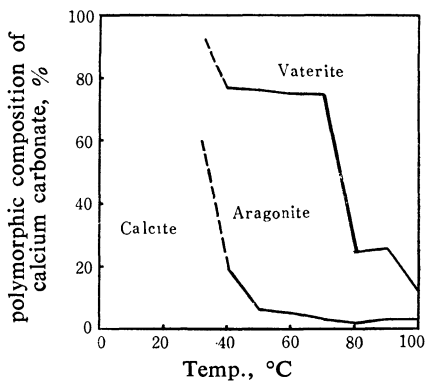


Fig. 4. Polymorphic composition of calcium carbonate formed from calcium bicarbonate solution containing sodium chloride (5 g./l.) and magnesium chloride (0.07 g./l.).

the crystal forms was dependent upon the magnesium chloride content (Fig. 3, Tables II and III). When calcium carbonate was formed from the calcium bicarbonate solution containing both sodium chloride (5 g./l.) and magnesium chloride (0.07 g./l.) (group B in Table I), vaterite was always

TABLE IV. CRYSTAL FORMS OF CALCIUM CARBONATE IN FUTAMATA THERMAL SPRINGS

Station No.	Distance from orifice to station, m.	Water		Crystal forms of $CaCO_3$		
		Temp. °C	pH	Vaterite %	Calcite %	Aragonite %
1	0	42	6.6	0	100	0
2	15	38	7.0	0	95~90	5~10
3	40	27	7.3	0	80~35	20~65

formed (Fig. 4). At a temperature above 50°C the proportion of calcite was very small, at below 70°C aragonite predominated, and at above 70°C vaterite predominated and its proportion increased with a rise in the temperature. Apparently the magnesium chloride content in the solution was too small to affect the polymorphic formation of calcium carbonate, so that the composition of the crystal forms of calcium carbonate was dependent upon the sodium chloride content (Fig. 4, Tables II and III).

b) When calcium carbonate was formed from the calcium bicarbonate solution containing sodium chloride and magnesium chloride and bubbled with carbon dioxide gas continuously during the formation of the calcium carbonate, only calcite was formed, even at a high temperature.

Discussion

Calcium carbonate formed in the laboratory from the calcium bicarbonate solution bubbled with carbon dioxide gas continuously during the formation of calcium carbonate is comparable to calcium carbonate deposited in the original orifice of thermal spring waters where carbon dioxide gas gushes forth, while calcium carbonate formed from the solution without aeration of carbon dioxide gas is comparable to calcium carbonate deposited with the escape of carbon dioxide gas from spring waters during the flow.

The following facts were observed in thermal springs:

1) When the temperature of thermal spring waters was very high, aragonite was usually formed (Table I). Futamata spring waters were made to flow through an open wooden conduit from the orifice to a bath[12,13]. As carbon dioxide gas escaped from the waters, calcium carbonate was deposited. The crystals of calcium carbonate formed at various locations in the flow were sampled and their crystal forms were identified (Table IV). The data indicate that calcite was formed readily at the original location of thermal springs despite a high temperature, where carbon dioxide gas was supplied to the water. Aragonite was formed at a location where carbon dioxide gas was not supplied, despite a low temperature. These observations were supported by the experimental results in the laboratory (Fig. 2, Tables II and III, Experiment B-3-b). The content of carbon dioxide controls the pH value of the solution. The solution bubbled with carbon dioxide gas is acid. It can be said that even at a high temperature calcite was formed from the solution containing carbon dioxide, sodium chloride and/or magnesium chloride, in other words, from an acid solution. This appears to be attributable to the facts that the solubility of calcium carbonate is very large in the acidic solution containing carbon dioxide, sodium chloride and/or magnesium chloride[14] and that the rate of the calcium carbonate formation is very small, because calcite (a stable crystal) is formed easily when the rate of calcium carbonate formation is very small. It can also be said that, even at a low temperature, aragonite is formed from the basic solution which does not contain a large amount of carbon dioxide.

2) Calcite was formed from Futamata spring waters running still, while aragonite was formed when the same waters struck a rock so strongly that carbon dioxide gas escaped rapidly; calcium carbonate was also formed rapidly. In the laboratory, calcite was formed from Futamata water which was kept still so that carbon dioxide gas could gradually escape from the water with a slow separation of calcium carbonate crystals, at 30 and 35°C; a mixture of calcite and aragonite was formed from the same Futamata water which was repeatedly stirred, whereby the escape of the carbon dioxide gas and calcium carbonate formation were accelerated, at the same temperatures, 30 and 35°C. The result makes it possible to conclude that, in waters with the same chemical constituents, pH value, and temperature, with an increase in the rate of carbon dioxide gas escape from the waters and in the rate of calcium carbonate formation, the proportion of aragonite (an unstable crystal) increases and that of calcite (a stable crystal) decreases.

3) Vaterite has not been found in thermal

12) Y. Uzumasa and Y. Kitano, *J. Chem. Soc. Japan, Pure Chem. Sec.* (*Nippon Kagaku Zassi*), 73, 901 (1951).
13) Y. Uzumasa and Y. Kitano, ibid., 73, 720 (1952).
14) Y. Seidell, "Solubilities of Inorganic and Metal Organic Compounds", Van Nostrand, New York (1940), pp. 273-275.

springs. On the basis of the laboratory results, possible explanations for this are: a) The spring waters contain a rather large amount of magnesium chloride (Tables II and III, Fig. 3), or calcium carbonate is formed near the orifice where carbon dioxide gas is supplied (Fig. 2, Tables II and III, Experiment B-3-b). b) When vaterite is formed, it changes to calcite or aragonite because of its high instability in a solution. It seems probable, however, that vaterite can be found in thermal springs when calcium carbonate is formed at a high temperature from the waters of group B in Table I (NaCl 5 g./l., $MgCl_2$ 0.07 g./l.), at a location where carbon dioxide gas is not supplied to the waters (Fig. 4).

4) The mechanical and physical conditions and the minor elements in the waters have an influence on the polymorphic formation of calcium carbonate in thermal springs. Aragonite was found in precipitates which were floating on the surface of the waters, but it was not found in precipitates deposited on the wall or on the bottom in the same waters[3]. In addition, strontium ions[7,10,15] and barium ions[10] are minor elements affecting the polymorphic formation. The presence of strontium ions favored aragonite formation and that of barium ions favored calcite formation, but the effects of these factors are less significant than those of carbon dioxide (pH), sodium ions, magnesium ions, and chloride ions and the temperature of the mother solution.

Summary

1) When calcium carbonate was formed in the laboratory from the calcium bicarbonate solution through which carbon dioxide gas had not been bubbled during the process of the calcium carbonate formation: a) Only calcite was formed at a temperature below 25°C; aragonite was formed above 25°C, and vaterite was formed above 40°C. Between 40 and 60°C a large amount of vaterite was formed. With a rise in the temperature of the mother solution, the proportion of calcite decreased. b) Vaterite was easily formed from the calcium bicarbonate solution containing sodium chloride at a high temperature. With an increase in the temperature and in sodium chloride concentration, the proportion of vaterite increased. c) With an increase in both temperature and magnesium chloride concentration, the proportion of aragonite increased but that of calcite decreased. The presence of magnesium chloride in the mother solution hindered the formation of vaterite.

2) When calcium carbonate was formed in the laboratory from the calcium bicarbonate solution containing sodium chloride (or magnesium chloride) and bubbled with carbon dioxide gas continuously during the calcium carbonate formation, only calcite was formed despite a high temperature.

3) When calcium carbonate was deposited in thermal spring waters of a high temperature, aragonite was formed. However, from the waters into which carbon dioxide gas was supplied, in other words, from the acidic solution, calcite was formed despite a high temperature, and aragonite was formed from the waters to which carbon dioxide was not supplied, in other words, from the basic waters, despite a low temperature.

4) Up to the present time, vaterite has not been found in the deposits of thermal springs because: a) Calcium carbonate deposits of thermal springs were either formed at a location where carbon dioxide gas was supplied to the mother waters or where the concentration of magnesium ions in the waters was rather high, or b) even if vaterite had been formed, it would have changed to calcite or aragonite very quickly because of its low stability in solution.

5) In spring waters with the same chemical constituents, pH value, and temperature, the proportion of aragonite increased and that of calcite decreased with an increase in the rate of carbon dioxide gas escape from the waters and in the rate of calcium carbonate formation.

6) Aragonite was readily found in calcium carbonate precipitates formed floating on the surface of thermal spring waters, but it was not likely to be found in the precipitates deposited on the wall or bottom in the same waters.

The polymorphic formation of calcium carbonate formed in thermal springs depends mainly on the temperature, the concentrations of sodium ions, magnesium ions and carbon dioxide (pH) in the waters, and on the rate of calcium carbonate formation when calcium carbonate is formed from a similar water.

The author wishes to express his deep appreciation to Professor Ken Sugawara of Nagoya University and to Professor Donald W. Hood and Mr. Edward R. Ibert of Texas A & M College for their encouragement throughout this work.

Water Research Laboratory
Faculty of Science
Nagoya University
Chikusa-ku, Nagoya

15) Y. Kitano and N. Kawasaki, *J. Earth Sciences, Nagoya Univ.*, **6**, 63 (1958).

The Acid-Catalyzed Isomerization of Cyclohexyl Phenyl Ketoxime in Liquid Sulfur Dioxide[1]

By Niichiro TOKURA, Katsuo SHIINA and Tetsuo TERASHIMA

(Received July 18, 1962)

It has been previously demonstrated that the Beckmann rearrangement of a geometrical isomer of a ketoxime in liquid sulfur dioxide at −70°C results in the trans-migrated products exclusively[2]. Although the slow syn-anti isomerization of the ketoxime in liquid sulfur dioxide has also been observed in the same medium, the rate of the Beckmann rearrangement has been too fast to be competitive against the rate of the isomerization[2]. According to Tokura and Shiina[3], the sulfur dioxide-catalyzed isomerization is accelerated by light and retarded by hydroquinone, and the rate is of the first order with respect to the concentration of the oxime.

Since the isomerization of the oxime may also be undertaken by an acid and since such an acid may often be present in the medium by the decomposition of the Lewis acid (the reagent of the Beckmann rearrngement) with a trace of water in liquid sulfur dioxide, the acid-catalyzed isomerization of β-cyclohexyl phenyl ketoxime has been carried out in order to obtain further information about the competition of the isomerization versus the Beckmann rearrangement. Such hydrohalogenic acids as hydrochloric acid, hydrobromic acid and hydroiodic acid have been used as the catalyst.

The acid-catalyzed isomerization experiment has been preceded by an NMR spectrometry to confirm the intrinsic structures of the respective geometrical isomers, the α- and the β-ketoxime, since the previous establishment of the structures of the ketoximes has only been proved by the results of the Beckmann rearrangement[2]. The experience of Lustig[4] has also prompted the present writers to this procedure.

Experimental

Materials. — β-Cyclohexyl phenyl ketoxime was prepared and separated as described in a preceding paper[2]. Commercial sulfur dioxide was dehydrated with phosphorus pentoxide and distilled. The hydrogen halogenide (Cl, Br or I) solution of liquid sulfur dioxide was prepared by passing a dry hydrogen halide gas into liquid sulfur dioxide cooled to −70°C. From the increase in the weight and by volumetric analysis, the strength of the acid was determined. An acid solution of liquid sulfur dioxide of a definite concentration was prepared by adding liquid sulfur dioxide to this parent mixture. The DCl solution of liquid sulfur dioxide was prepared by the following reaction in liquid sulfur dioxide:

$$SOCl_2 + D_2O \rightarrow 2DCl + SO_2$$

Method of Analysis. — The analysis of the α-oxime produced and of the unchanged β-oxime was made by infrared spectroscopy using a Perkin-Elmar model 21 doule-beam spectrophotometer[3]. The specimen in carbon disulfide was analyzed at the absorption maxima, with 762 and 957 cm^{-1} as key bands. The contents of the oximes were calculated by the following equations:

$$E_m^{762} = C_\alpha E_\alpha^{762} + C_\beta E_\beta^{762} \quad (1)$$

$$E_m^{957} = C_\alpha E_\alpha^{957} + C_\beta E_\beta^{957} \quad (2)$$

where E_α^{762}, E_β^{762}, E_α^{957} and E_β^{957} are the molar absorption coefficients of α- and β-oxime at 762 and 957 cm^{-1} respectively, E_m^{762} and E_m^{957} are those of the sample for analysis, and C_α and C_β are the content of the α- and β-oximes in the sample.

TABLE I. A TYPICAL KINETIC RUN

Oxime, 0.05 M/l.; HCl, 0.15 M/l., at 0°C

t, min.	E_m^{762}	E_m^{957}	Conversion α-oxime, %	$a/(a-x)$	$\ln a/(a-x)$	$k \times 10^5$ sec^{-1}
45	49.8	76.9	3.56	1.0367	0.0363	1.343
90	50.1	75.6	7.12	1.0767	0.0739	1.369
135	50.6	74.0	11.63	1.1316	0.1237	1.526
180	50.5	73.6	12.37	1.1412	0.1321	1.223
						Mean 1.36

1) The Beckmann Rearrangement in Liquid Sulfur Dioxide. Part XI.
2) R. Tada, Y. Masubuchi and N. Tokura, This Bulletin 34, 209 (1961).
3) N. Tokura and K. Shiina, ibid.. 35, 1779 (1962).
4) E. Lustig, *J. Phys. Chem*, 65, 491 (1961).

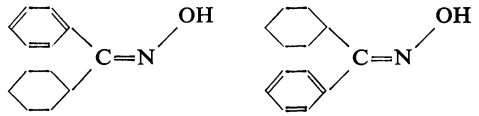
Beer's law was obeyed throughout this experiment, and the range of experimental error was within three percent.

Kinetic Procedure. — The β-oxime was dissolved into a sulfur dioxide solution of an acid at −70°C to make a 50 ml. solution of the reaction mixture. The mixture was then placed in a thermostat. A 10 ml. aliquot was taken off after a definite time interval, and the mixture was mixed with ice water, neutralyzed with ammonia water, and filtered. The precipitate was well rinsed with water, dried in vacuo, and analyzed for the oxime content. A typical run is listed in Table I. No symptom of the Beckmann rearrangement was observed during the course of the isomerization experiment.

NMR Spectrometer.—A Varian Associates' type V-4300B (60 Mc.) was used.

Results and Discussion

NMR Spectrometry of the Geometrical Isomers.—The geometrical structures of the cyclohexyl phenyl ketoximes were assigned as below in a previous paper[2], the hydroxyl group in the α-oxime being syn-positioned to the phenyl groups. If the Beckmann rearrangement in liquid sulfur dioxide should take place in the migration of the group trans to the hydroxyl group, such a conclusion must be accepted. Moreover, no contamination by another acidamide which might be derivable by a competitive isomerization of the ketoxime was observed.



α-Oxime β-Oxime

However, Lustig[4] has recently disclosed that the assignments of the isomeric ketoximes by the Beckmann rearrangement are not always safe since the oximes considered as single materials were often found by the NMR spectrometry to be contaminated by another isomers. Since no contamination of acidamides other than the authentic trans-migrated product was seen after the rearrangement in liquid sulfur dioxide, and since the oximes afforded only the corresponding acidamides, which were proved to be the proper (trans-migrated) ones[2], further examination into the purity of the respective oximes may not be needed.

An NMR study of the α- and β-oximes was undertaken in order to confirm the previous assignments for the geometrical structures of the respective oximes; the results are listed in Table II.

As is seen in Table II, the Tau values assigned for the cyclohexyl and phenyl groups coincide well with the literature values[5] of cyclohexane and benzene, 8.564 and 2.734 respectively.

Table II. NMR chemical shift of α- and β-ketoximes

Assigned	Oxime α	Oxime β
in CCl_4 in Tau value (T.M.S. as reference)		
Cyclohexyl	8.76	8.76
	8.27	8.27
Phenyl	2.91	2.90
=N-O-H	1.04	1.37
in Dioxane in c. p. s.		
Cyclohexyl	−2.28	−2.26
	−2.21	−2.21
	−1.81	−1.91
Phenyl	+3.72	+3.70
=N-O-H	+5.48	+5.95

The NMR spectrum of the hydroxyl proton of the α-oxime always shifts to a lower field than that of the β-oxime. This may be interpreted as being caused by the interaction of the hydroxyl proton with the benzene ring. In addition, no anisotropic effect may be anticipated from the Fischer-Hilschfelder model of the oxime. Moreover, our calculation, by the method of Johnson and Bovey[6], of the difference in the shifts between the two ketoximes on the hydroxyl proton, the results of which will be published elswhere in the near future, supports the above explanation.

Effect of Temperature.—The reaction rate of the acid-catalyzed isomerization was a faster reaction than the isomerization by sulfur dioxide itself. The concentrations of the β-oxime and of hydrochloric acid were 0.05 M/l.

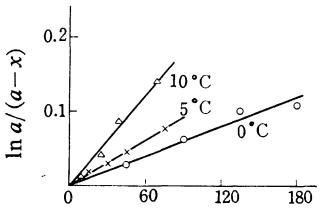


Fig. 1

Table III. Rate constant k, for $R=k$[oxime]

Temp., °C	$k\times10^5$ sec^{-1}
0	1.36
5	1.87
10	3.44

The Arrhenius parameters
Activation energy, $E_a=13.1$ kcal./mol.
Frequency factor, $A=3.5\times10^5$ sec^{-1}

5) G. van Dyke Tiers, *J. Phys. Chem.*, **62**, 1151 (1958).

6) C. E. Johnston, Jr. and F. A. Bovey, *J. Chem. Phys.*, **29**, 1012 (1958).

and 0.15 M/l. respectively. The order of the reaction is of the first order with respect to the concentration of the oxime, as may be seen in the $\ln a/(a-x)$ vs. time plots at 0, 5 and 10°C in Fig. 1. The rate constant k and the Arrhenius parameters calculated are listed in Table III.

Effect of Light. — The isomerization of the ketoxime in liquid sulfur dioxide has been reported to be effected by diffused daylight in the room[2]. In the acid-catalyzed isomerization, the reaction in diffused daylight was compared with the reaction in the dark. (Table IV)

TABLE IV. EFFECT OE DIFFUSED DAYLIGHT ON ACID-CATALYZED ISOMERIZATION

[oxime] = 0.05 M/l. ; [HCl] = 0.15 M/l. Temp. 10°C

k(dark) $= 3.20 \times 10^{-5}$ sec^{-1}

k $= 3.44 \times 10^{-5}$ sec^{-1}

where, k (dark) and k are the constants in the dark and in diffused room daylight respectively.

The reaction was slightly accelerated by daylight, but the effect was not significant.

Effect of Salts and Deuteriochloric Acid. — Tetraethylammonium halides, $(C_2H_5)_4NX$, X = Cl, Br or I, were used as the salts. The salt, 0.005 M/l., was added to the reaction mixture. Table V lists the results. The results of Table V agree with the general trend of ionic catalysis. The depression of the rate by the addition of the chloride may be explained by a mass law effect, while the increase of the rate by the bromide and iodide may be due to the ionic strength effect[7].

TABLE V. THE EFFECT OF SALT ON THE HCl-CATALYZED ISOMERIZATION

[oxime] = 0.05 M/l., [HCl] = 0.15 M/l. Temp. 0°C

Salt, $(C_2H_5)_4NX$ salt	$k \times 10^5$ sec^{-1}
None	1.36
X=Cl	1.07
Br	1.95
I	2.04

The isomerization experiment using DCl as the catalyst resulted in the isotope effect;

$$k_{HCl}/k_{DCl} = 1.21 \quad (\text{at } 30°C)$$

Both the salt and isotope effect suggest the importance of the dissociation equilibrium of the acid catalyst in liquid sulfur dioxide.

Acid-Catalyzed Reaction with Hydrogen Bromide or Hydrogen Iodide. — Neither hydrogen bromide nor hydrogen iodide has had any reproducible effect on the isomerization. In both cases the color of the reaction mixture gradually changed to a yellowish red, suggesting the slow decomposition of the reagent in liquid sulfur dioxide. The gradual decomposition of hydrogen iodide to iodine in liquid sulfur dioxide has already been noticed by Steele and Bagster[8]. Moreover, the result may have been complicated also by an accompanying Beckmann rearrangement if the bromine or iodine produced was present[9].

The Effect of the Concentration of Hydrogen Chloride.—No symptom of the Beckmann rearrangement was observed by hydrogen chloride in liquid sulfur dioxide. The reason for this has been discussed in a preceding paper[10]. The isomerization reaction was carried out at various concentrations of [HCl], 0.05, 0.15 and 0.27 M/l., with [oxime], 0.05 M/l. at 0°C.

From the log-log plot of the initial rate, R, and the concentration of hydrogen chloride, [HCl], the order of the [HCl] is obtained as 1.43 (approximately 1.5) (Fig. 2). Because the linear plot of $\log R$ vs. log[HCl] does not pass through the origin and because the simultaneous catalysis by sulfur dioxide itself must be considered, the overall rate expression may be as follows:

$$R = A + k_{HCl}[\text{oxime}] \cdot [\text{HCl}]^{1.5} \qquad (3)$$

where k_{HCl} is the rate constant catalyzed by hydrogen chloride and A is the rate when [HCl] = 0, i. e., the rate of the isomerization by liquid sulfur dioxide itself, as has been reported in a previous paper[2]. Judging from previous results[2].

$$A = k_{SO_2}[\text{oxime}] \qquad (4)$$

Therefore,

$$R = k_{SO_2}[\text{oxime}] + k_{HCl}[\text{oxime}] \cdot [\text{HCl}]^{1.5} \qquad (5)$$

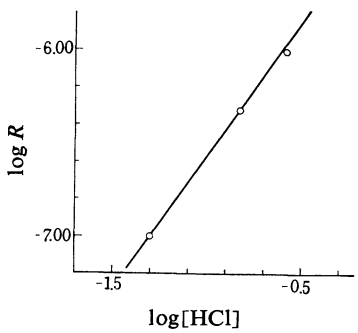


Fig. 2. Plot of $\log R$ vs. log[HCl].

7) C. K. Ingold, "Structure and Mechanism in Organic Chemistry", Cornell University Press, Ithaca, New York (1953), p. 362.

8) B. D. Steele and L. S. Bagster, *J. Chem. Soc.*, **97**, 2607 (1910).

9) N. Tokura, R. Asami and R. Tada, *J. Am. Chem. Soc.*, **79**, 3135 (1957).

10) N. Tokura, R. Tada and K. Yokoyama, This Bulletin, **34**, 1812 (1961).

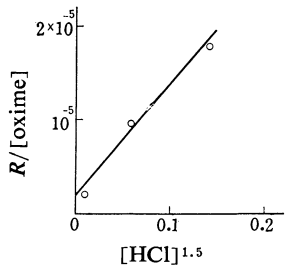


Fig. 3

Eq. 5 is transformed to 6 by dividing it with [oxime]:

$$R/[\text{oxime}] = k_{SO_2} + k_{HCl}[HCl]^{1.5} \quad (6)$$

From the linear plot of $R/[\text{oxime}]$ vs. $[HCl]^{1.5}$, as shown in Fig. 3, k_{SO_2} and k_{HCl} are obtained from the intercept and the slope of the plot as:

$$k_{SO_2} = 0.23 \times 10^{-5}\ \text{sec}^{-1}$$

$$k_{HCl} = 1.04 \times 10^{-4}\ \text{l}^{1.5}\,\text{mol}^{-1.5}\,\text{sec}^{-1}$$

The value of k_{SO_2} agrees well with the rate constant of the liquid sulfur dioxide-catalyzed isomerization (0.65×10^{-5})[2] in its order, when the accuracy of the treatment is considered. Although the rate as catalyzed by hydrogen chloride is over three times as fast as the rate by sulfur dioxide, yet the order of both rates is of $10^{-4}-10^{-5}$. When the β-oxime, [oxime] $=5.0 \times 10^{-2}$ M/l., was subject to the Beckmann rearrangement in liquid sulfur dioxide with thionyl chloride, $[SOCl_2] = 5.0 \times 10^{-2}$ M/l., the reaction was completed within 5 and 3 min. at 0 and -75°C respectively, the rate being so fast that no accurate kinetic measurement was possible[2].

A discussion should be added on the reason of the order of hydrogen chloride, 1.5, in rate expression 5. For the mechanism of the acid-catalyzed isomerization, the following scheme may be considered:

$$HCl \underset{K_{HCl}}{\rightleftharpoons} H^+ + Cl^- \quad (7)$$

$$\begin{matrix} R \\ R' \end{matrix}\!\!>\!C{=}N\!-\!OH + H^+ \xrightarrow[k_H]{} \left[\begin{matrix} R \\ R' \end{matrix}\!\!>\!C{=}\overset{+}{N}\!<\!\begin{matrix} OH \\ H \end{matrix}\right]$$

$$\longrightarrow \begin{matrix} R \\ R' \end{matrix}\!\!>\!\overset{+}{C}\!-\!N\!<\!\begin{matrix} OH \\ H \end{matrix} \quad (8)$$

$$\begin{matrix} R \\ R' \end{matrix}\!\!>\!\overset{+}{C}\!-\!N\!<\!\begin{matrix} OH \\ H \end{matrix} \xrightarrow[k]{\text{R.D.}} \begin{matrix} R' \\ R \end{matrix}\!\!>\!\overset{+}{C}\!-\!N\!<\!\begin{matrix} OH \\ H \end{matrix} \quad (9)$$

$$\begin{matrix} R' \\ R \end{matrix}\!\!>\!\overset{+}{C}\!-\!N\!<\!\begin{matrix} OH \\ H \end{matrix} \longrightarrow \begin{matrix} R' \\ R \end{matrix}\!\!>\!C{=}N\!-\!OH + H^+ \quad (10)$$

If Eq. 9 is selected as the rate-determining step, the rate expression is found to be:

$$R = k\left[\begin{matrix} R \\ R' \end{matrix}\!\!>\!\overset{+}{C}\!-\!N\!<\!\begin{matrix} OH \\ H \end{matrix}\right] = k \cdot k_H[\text{oxime}] \cdot [H^+]$$

$$= k \cdot k_H \cdot K_{HCl}^{0.5}[\text{oxime}] \cdot [HCl]^{0.5}$$

$$= k'[\text{oxime}][HCl]^{0.5} \quad (11)$$

when the value of K_{HCl} is very small. Thus, in the above scheme the order of hydrogen should be 0.5, whereas in reality the order is 1.5 in this experiment.

In such a non-aqueous solvent as sulfur dioxide, the association of ion pairs is a phenomenon of considerable importance. If the three associated molar hydrochloric acids could give one set of cations and anions, and if the cation could behave as the catalyst for the oxime isomerization, the order for hydrogen chloride, 1.5 may be derived; however, the kinetics can give no detailed information on the nature of the active species for the isomerization. The following dissociation equilibria may be considered as examples:

$$3\,HCl \rightleftharpoons H^+ + (HCl)_2 \cdot Cl^-$$

$$3\,HCl \rightleftharpoons HCl \cdot H^+ + Cl \cdot HCl^-$$

In conclusion, sulfur dioxide-catalyzed or acid catalyzed-isomerization is not competitive against the Beckmann rearrangement of the oxime in liquid sulfur dioxide.

Summary

1. The hydrochloric acid-catalyzed isomerization of β-cyclohexyl phenyl ketoxime has been carried out in liquid sulfur dioxide. The effects of temperature, light, deuterium chloride and the concentrations of hydrogen chloride have been examined.

2. The overall rate may be expressed as;

$$R = k_{SO_2}[\text{oxime}] + k_{HCl}[\text{oxime}] \cdot [HCl]^{1.5}$$

and the k_{SO_2} and the k_{HCl} have been estimated. The reason for the order of hydrogen chloride, 1.5 has also been discussed.

The present authors would like to express their appreciation to Professor G. Hazato and Mr. K. Takahashi for their NMR spectrometry. The authors are also indebted to the Seitetsu Kagaku K. K., Ltd., for its donation of liquid sulfur dioxide.

The Chemical Research Institute of Non-Aqueous Solutions
Tohoku University
Katahira-cho, Sendai

*Synthesis of 2-Substituted Azulenes by Nucleophilic Substitution Reactions of 2-Haloazulene Derivatives**

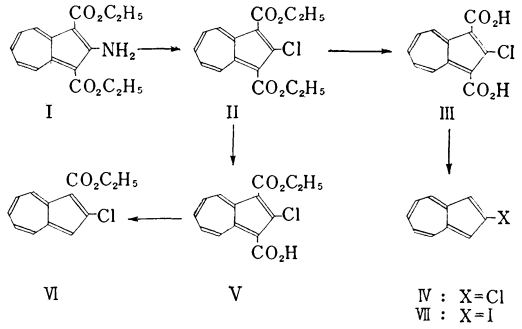
By Tetsuo NOZOE, Shuichi SETO** and Shingo MATSUMURA**

(Received March 3, 1962)

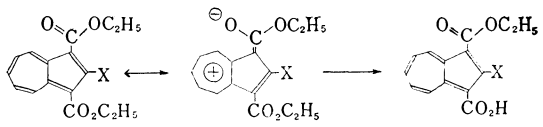
Quantum mechanical calculation as to the position of attack on azulenes by nucleophilic reagents, first made by Brown[1], showed that such reactions should result in substitution in the 4- (or 8-) and 6-positions. The susceptibility of the 4-position to nucleophilic attack was proved by an ether exchange reaction converting ethyl 4-methoxyazulenecarboxylate into 4-ethoxyazulenecarboxylate[2]. According to the result of the ground state electron density calculation made by Julg[3] using the SCF-method, it has been shown that the density in the 2-position has comparatively lower values.

In the preceding papers[4], we reported that the reaction of 2-halo- or 2-methoxytropone with ethyl cyanoacetate resulted in the novel condensation to form diethyl 2-aminoazulene-1, 3-dicarboxylate (I) and other related azulene derivatives. In the present series of experiments, we wish to report on nucleophilic substitution at 2-position in 2-haloazulene derivatives, obtained from the compound I by Sandmeyer reaction.

Passage of dry hydrogen chloride gas through the benzene solution of I precipitated reddish orange salt[4b], and addition of isoamyl nitrite to this suspension resulted in the color change from green, blue, violet, to red, and the reaction mixture afforded diethyl 2-chloroazulene-1, 3-dicarboxylate (II), m. p. 78°C, in over 90% yield. The use of hydrogen bromide in place of hydrogen chloride resulted in the formation of a small amount of deaminated product, diethyl azulene-1, 3-dicarboxylate, but not of the anticipated 2-bromo compound. Hydrolysis of II with an excess of 10% ethanol - water solution of potassium hydroxide afforded 2-chloroazulene-1, 3-dicarboxylic acid (III), very sparingly soluble in organic solvents, and its decarboxylation by heating at 265~270°C under a partially reduced pressure gave 2-chloroazulene (IV) as violet crystals of m. p. 92°C, in a fairly good yield. Hydrolysis of II with one molar equivalent of potassium hydroxide produced a crystalline monobasic acid (V), whose decarboxylation by heating at 250°C afforded ethyl 2-chloroazulene-1-carboxylate (VI) as reddish violet oil (picrate, m. p. 92°C). It is



interesting to note that one of two ethoxycarbonyl groups in II is somewhat more resistant to alkali, and monobasic acid (V) is obtained in a good yield. This probably means that one of two ethoxycarbonyl groups is stabilized by the resonance with the following ionic structure.



The halide interchange reaction was studied in connection with the preparation of 2-iodo- and 2-bromoazulene. 2-Iodoazulene (VII) as violet crystals of m. p. 126°C could be prepared conveniently form 2-chloro compound IV by treatment with potassium iodide in wet acetic acid. 2-Bromoazulene (VIII), however, could

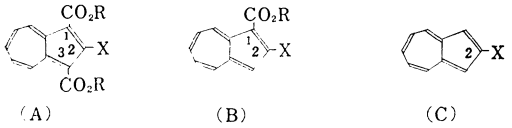
* Presented at the 9th Annual Meeting of the Chemical Society of Japan, Kyoto, April, 1956; General outline of this paper is already described in some review articles. Cf. T. Nozoe, *Croat. Chem. Acta*, 29, 201 (1957); T. Nozoe and T. Asao, in "Dai Yuki Kagaku (Comprehensive Organic Chemistry)", Vol. 13, Asakura Shoten, Tokyo (1960), p. 439; T. Nozoe and S. Ito, *Frotschr. Chem. org. Naturstoffe*, 19, 33 (1961).

** Present address: The Chemical Research Institute of Non-Aqueous Solutions, Tohoku Univ., Katahira-cho, Sendai.

1) R. D. Brown, *Trans. Faraday Soc.*, 44, 984 (1948).
2) D. H. Reid, W. H. Stafford and J. P. Ward, *J. Chem. Soc.*, 1958, 1100.
3) A. Julg, *J. Chim. Phys.*, 52, 377 (1955).
4) a) T. Nozoe, S. Matsumura, Y. Murase and S. Seto, *Chem. & Ind.*, 1955, 1257; b) This Bulletin, 35, 1179 (1962); c) T. Nozoe, S. Seto, S. Matsumura and T. Asano, *Proc. Japan Acad.*, 32, 339 (1956); d) T. Nozoe, S. Seto and S. Matsumura, *Chem. & Ind.*, 1961, 1715; e) S. Matsumura, *Chem. Pharm. Bull.*, in press.

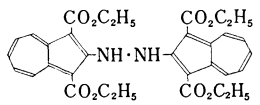
not be obtained by the action of potassium bromide in similar condition.

By the use of these compounds (II—VII), we had been able to synthesize various new azulene derivatives of the types A, B and C.



(A) (B) (C)

1, 2, 3,-Trisubstituted Azulene (A).—Reaction of II with sodium methoxide in methanol afforded dimethyl 2-methoxyazulene-1, 3-dicarboxylate (IX) and monomethyl ester of 2-methoxyazulene-1, 3-dicarboxylic acid (X). Ester group in azulene nucleus, in the presence of alkali or alcoholate, is easily exchanged by alcoholysis. Treatment of II with ammonia, methylamine, dimethylamine, aniline and *p*-bromoaniline, respectively afforded 2-amino- (I), 2-methylamino- (XI), dimethylamino- (XII), anilino- (XIII) and 2-(4'-bromoanilino)-azulene derivatives (XIV). Reaction of II with hydrazine hydrate afforded, besides diethyl 2-hydrazinoazulene-1, 3-dicarboxylate (XV), bis-1, 3-diethoxycarbonylazulen-2-yl) hydrazine (XVI).

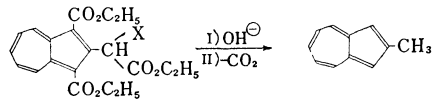


XVI

Treatment of II with sodiocompound of diethyl malonate, ethyl cyanoacetate, and ethyl acetoacetate respectively afforded the anticipated diethyl 2-diethoxycarbonylmethyl-(XVII), 2-(cyano-ethoycarbonylmethyl)- (XVIII), and 2-(acetyl-ethoxycabonylmethyl)-azulene-1,3-dicarboxylate (XIX).

1, 2-Disubstituted Azulenes (B).—Ethyl 2-chloroazulenl-1-carboxylate (VI) may be generally used to synthesize 1,2-disubstituted azulenes of the type (B). For example, reaction of VI with sodium ethoxide afforded ethyl 2-ethoxyazulene-1-carboxylate (XX), and reaction of VI with ethyl cyanoacetate, in the presence of sodium ethoxide, also afforded XX, besides a small amount of violet crystals (XXI) of unknown structure. Trisubstituted azulene (A) also could be converted to disubstituted derivatives (B) without difficulty. Thus, hydrolysis of XIII with one molar equivalent of potassium hydroxide afforded crystalline carboxylic acid, whose decarboxylation gave ethyl 2-anilinoazulene-1-carboxylate (XXII).

2-Substituted Azulenes (C).—2-Monosubstituted azulenes can be obtained as follows: 1) By saponification followed by decarboxylation of di- or trisubstituted derivatives, 2) by nucleophilic substitution of 2-iodoazulene (VII), or 3) more conveniently by nucleophilic substitution of 2-chloroazulene-1, 3-dicarboxylic acid (III) accompanied by simultaneous decarboxylation. Hydrolysis of IX, XX and XIII followed by decarboxylation respectively afforded 2-methoxy- (XXIII), 2-ethoxy- (XXIV) and 2-anilinoazulene (XXV). Heating of 2-chloroazulene (IV) with a methanolic solution of sodium methoxide in a sealed tube, however, gave only a trace of XXIII, while most of the original compound were recovered. Under the same condition, 2-iodoazulene (VII) afforded XXIII in a fairly good yield. Similarly, 2-cyanoazulene (XXVI) was obtained from VII by treatment with cuprous cyanide in pyridine over 85% yield. Heating of 2-chloroazulene-1, 3-dicarboxylic acid (III) with aniline, hydrazine and dimethylamine, respectively, resulted in facile substitution and simultaneous decarboxylation to form 2-anilino- (XXV), 2-hydrazino- (XXVII) and 2-dimethylaminoazulene (XXVIII). Hydrolysis of XVII and XVIII followed by decarboxylation produced 2-methylazulene (XXIX).



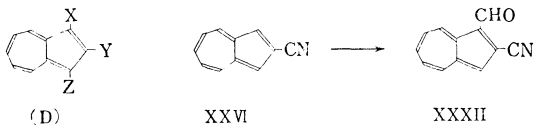
XVII : X=$CO_2C_2H_5$
XVIII : X=CN

XXIX

Cyano group in the 1- and 3-position is quite stable to attempted saponification with strong acid or alkali[4b], 2-cyanoazulene, however, are susceptible to such reagent, affording methyl azulene-2-carboxylate (XXX), on heating with absolute methanol containing hydrogen chloride. Hydrolysis of XXVI and XXX with alkali gave azulene-2-carboxylic acid (XXXI).

Further Substitution of Azulene Derivatives.—The fact that azulenes are liable to electrophilc substitution in the 1- and 3-positions is generally well known, and various azulene derivatives have been obtained by this method[5]. Combination of this electrophilic substitution and our nucleophilic substitution would give various azulene derivatives (D) having different substituents in the 1-, 2- and 3-positions. For example, application of Vilsmeier method to 2-cyanoazulene (XXVI) gave 2-cyano-1-formylazulene (2-cyanoazulene-1-carboxyaldehyde) (XXXII). This compound has been substituted further to give the compound of the type D[6].

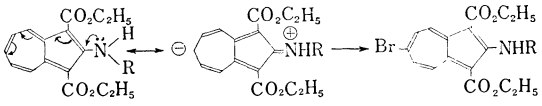
5) A. G. Anderson, Jr., J. A. Nelson and J. J. Tazuma, *J. Am. Chem. Soc.*, 75, 4980 (1953).
6) T. Nozoe and A. Sato, to be published.



(D) XXVI XXXII

Julg[3] predicted that the elctron density of the 5-position of azulene nucleus has the next highest values after 1- and 3-positions. More recently Anderson et al.[7] have reported that the acetylation of 1, 3-dichloroazulene by means of acetyl chloride in carbon tetrachloride in the presence of stannic chloride gave 5-acetyl-1, 3-dichloroazulene.

In the case of 2-amino- substituted azulenes

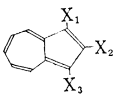


(E) (F)

R=H, CH_3, Ph.

(I, XI—XIII), the 4- (or 8-) and 6-positions would have higher electron density than the 5-position by the electron releasing mesomeric effect of the amino group in the 2-position. Accordingly, the electrophilic substitution of these compounds is likely to occur in the 4- (or 8-) and 6-positions, because 1- and 3-positions are already blocked by ethoxycarbonyl groups. Furthermore, it may be presumed that the 4- or 8-position is sterically hindered by the ethoxycarbonyl groups in the 1- and 3-positions and is less easily attacked than the 6-position. The bromination of 2-amino- (I), 2-methylamino- (XI) and 2-anilinoazulene derivatives (XIII) respectively afforded monobromo derivatives, XXXIII, XXXIV and XXXV (type F), while 2-dimethylaminoazulene derivative XII was inert to bromine. Diethyl 2-(4'-bromoanilino)azulene-1, 3-dicarboxylate (XIV) and the brominated product XXXV showed the closs melting point, but

TABLE I. SOME PROPERTIES OF THE REACTION PRODUCTS



Compd. No.	X_1	X_2	X_3	M. p., °C	Color
II	CO_2Et	Cl	CO_2Et	77～ 78	R
III	CO_2H	Cl	CO_2H	260～265(d)	R
IV	H	Cl	H	91～ 92	V
VI	CO_2Et	Cl	H	Oil (pic. 92)	R
VII	H	I	H	125～126	V
IX	CO_2Me	OMe	CO_2Me	61～ 62	O
X	CO_2H	OMe	CO_2Me	145(d)	O
XI	CO_2Et	NHMe	CO_2Et	Oil (TNB 102)	O
XII	CO_2Et	NMe_2	CO_2Et	81～ 82	O
XIII	CO_2Et	NHPh	CO_2Et	141～142	O
XIV	CO_2Et	NHPhBr	CO_2Et	166～168	O
XV	CO_2Et	$NHNH_2$	CO_2Et	Oil (acetate 132)	O
XVI	CO_2Et	NHNHAz	CO_2Et	163～164	O
XVII	CO_2Et	$CH(CO_2Et)_2$	CO_2Et	Oil	R
XVIII	CO_2Et	$CH(CN)CO_2Et$	CO_2Et	116～117	R
XIX	CO_2Et	$CH(Ac)CO_2Et$	CO_2Et	53～ 54	R
XX	CO_2Et	OEt	H	84～ 85	P
XXII	CO_2Et	NHPh	H	Oil (TNB 112)	O
XXIII	H	OMe	H	82～ 83	R.V
XXIV	H	OEt	H	Oil	R.V
XXV	H	NHPh	H	144～145	R.O
XXVI	H	CN	H	77～ 78	B
XXVII	H	$NHNH_2$	H	127～128	R.O
XXVIII	H	HMe_2	H	98～ 99	O
XXX	H	CO_2Me	H	110～111	B
XXXI	H	CO_2H	H	200～203	G
XXXII	CHO	CN	H	180～182	R.V

pic.=picrate, TNB=Trinitrobenzene compound, R=Red, V=Violet, P=Pink, O=Orange, B=Blue, G=Green, Az=1,3-Diethoxycarbonylazulen-2-yl

7) A. G. Anderson and L .L. Replogle, *J. Org. Chem.*, 25, 1275 (1960).

a distinct depression of the melting point occurred on their admixture. As the 2'- (or 6'-) position of benzene ring in XIII is sterically hindered by two ethoxycarbonyl groups in the 1- and 3-positions, the possibility of the substitution of benzene ring would be excluded. From these considerations, it was assumed that XXXIII, XXXIV and XXXV were likely to be 6-bromo derivatives of I, XI and XIII respectively. Resistance of dimethylamino compound XII in bromination reaction would be due to the steric interference between two ethoxycarbonyl groups and a dimethylamino group. More recently, one of us (Matsumura)[4e] established the structure of the compound (XXXIII) as diethyl 2-amino-6-bromoazulene-1, 3-dicarboxylate, by synthesizing this compound from 5-bromo-2-methoxytropone and ethyl cyanoacetate.

Visible Absorption Spectra.—The visible absorption spectra[8] of the compounds IV, VII, XXIII, XXVI, XXVIII, and XXX are shown in Fig. 1. It was found that substitution of *o, p*-directing group in the 2-position of azulene ring caused a shift toward shorter wavelengths and substitution of *m*-directing group in the same position, a shift toward longer wavelengths in the spectra.

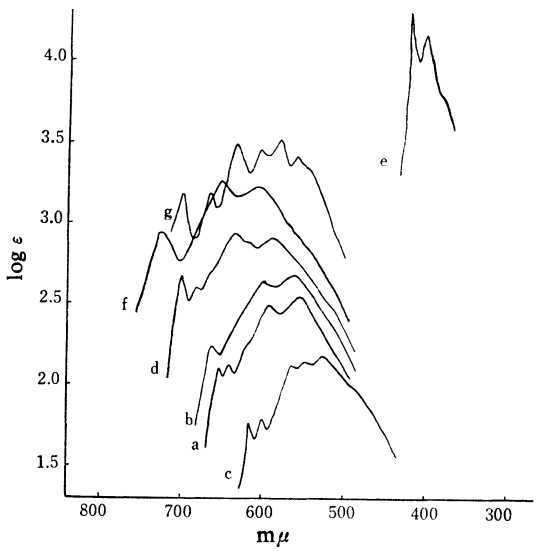


Fig. 1. Visible absorption spectra of IV, VII, XXIII, XXVI, XXVIII and XXX in cyclohexane.

IV(a) $Y = \log\varepsilon + 0$
VII(b) $Y = \log\varepsilon + 0.1$
XXIII(c) $Y = \log\varepsilon + 0$
XXVI(d) $Y = \log\varepsilon + 0.2$
XXVIII(e) $Y = \log\varepsilon + 0$
XXX(f) $Y = \log\varepsilon + 0.5$
Azulene(g) $Y = \log\varepsilon + 1.0$

8) Visible absorption spectra were measured with a Beckman DK spectrophotometer.

Experimental[9]

Diethyl 2-Chloroazulene-1, 3-dicarboxylate (II).—Dry hydrogen chloride gas passed through a solution of 6 g. of diethyl 2-aminoazulene-1, 3-dicarboxylate (I) dissolved in 200 ml. of dehydrated benzene under cooling and reddish orange precipitates began to separate out. Addition of 2.7 g. of isoamyl nitrite to this suspension resulted in the color change form green, blue, violet, to red gradually and the reaction mixture was allowed to stand overnight at room temperature. The solution was washed with water. After being dried over anhydrous sodium sulfate, the solvent was evaporated. The crystalline residue that formed was recrystallized from ethanol to afford 5.4 g. of II as red prisms, m. p. 77~78°C.

Found: C, 62.96; H, 4.91. Calcd. for $C_{16}H_{15}O_4Cl$: C, 62.54; H, 4.92%.

UV λ_{max}^{MeOH} mμ (logε): 237 (4.50), 272 (4.36), 296 (4.65), 306 (4.75), 310 (4.58), 344 (3.90), 349 (3.89), 357 (3.68).

Diethyl Azulene-1, 3-dicarboxylate.—To a solution of 600 mg. of I dissolved in 20 ml. of dehydrated benzene saturated with dry hydrogen bromide, 270 mg. of isoamyl nitrite was added at room temperature. The color of the mixture changed to reddish brown gradually. After allowing to stand overnight at room temperature, the solution was washed with water and dried over anhydrous sodium sulfate and the solvent was removed under a reduced pressure. The oily residue was dissolved in benzene and the solution was passed through a column of alumina. The column was eluted with benzene and the solvent was evaporated. The crystalline residue was recrystallized from ethanol to give 150 mg. of diethyl azulene-1, 3-dicarboxylate, m. p. 120~121°C

2-Chloroazulene-1, 3-dicarboxylic Acid (III).—A solution of 5 g. of II dissolved in 50 ml. of 10% ethanol-water (4 : 1) solution of potassium hydroxide was refluxed in a water bath for 15~30 min. The solution colored from red to reddish violet. After being cooled, the solution was acidified with 6 N nitric acid. The precipitate thereby formed was collected by filtration and repeatedly washed with water, by which 4 g. of sparingly soluble 2-chloroazulene-1, 3-dicarboxylic acid (III), m. p. 260 ~265°C (decomp.), was obtained.

2-Chloroazulene (IV).—Low-pressure (200 mmHg) sublimation of 1 g. of III by heating at 265~270°C produced violet crystals. The crystals were dissolved in petroleum ether (b. p. 50~60°C) and the solution was passed through a column of alumina. The column was eluted with petroleum ether and the solvent was cautiously removed. The crystalline residue was recrystallized from methanol to give 600 mg. of IV as violet needles, m. p. 91~92°C.

Found: C, 74.16; H, 4.13. Calcd. for $C_{10}H_7Cl$: C, 74.07; H, 4.32%.

9) All melting points are uncorrected. The microanalyses were carried out by Mr. S. Ohyama, Miss. A. Iwanaga and Mr. S. Azumi, to whom the authors are deeply indebted.

UV λ_{max}^{MeOH} mμ (logε): 226 (4.36), 275 (4.87), 284 (4.88), 290 (4.35), 328 (3.76), 343 (3.85), 350 (3.53); $\lambda_{max}^{Cyclohexane}$ mμ (logε): 552 (2.55), 593 (2.49), 619 (2.22), 638 (2.11), 653 (2.10).

Ethyl 2-Chloroazulene-1-carboxylate (VI).—To a solution of 200 mg. of potassium hydroxide dissolved in 10 ml. of ethanol-water (4 : 1) mixture, 1 g. of II was added and the mixture was refluxed in a water bath for 15 min., by which the color of solution turned clearly reddish violet. The solution was acidified with 6 N nitric acid. The precipitate was collected by filtration and repeatedly washed with water, by which 500 mg. of crude crystalline carboxylic acid (V), m. p. 193~195°C (decomp.), was obtained. Five hundred milligrams of V was decarboxylated by treatment as in the foregoing case. The oily substance thereby obtained was dissolved in petroleum ether (b. p. 50~60°C) and the solution was passed through a column of alumina, by which the product separated into violet and reddish violet bands. Elution of the violet band with petroleum ether afforded ca. 20 mg. of IV. Elution of the reddish violet band with benzene gave 300 mg. of reddish violet oil (VI).

Picrate of VI.—Red needles, m. p. 91~92°C, as recrystallized from ethanol. Found: C, 48.97; H, 3.15; N, 9.26. Calcd. for $C_{19}H_{14}O_9N_3Cl$: C, 49.20; H, 3.02; N, 9.07%.

2-Iodoazulene (VII).—A mixture of 10 g. of IV and 200 g. of potassium iodide in 600 ml. of acetic acid containing 50 ml. of water was refluxed at 130~140°C for 3.5 hr. and diluted with 1000 ml. of water. The violet crystals thet separated out were collected by filtration. The collected crystals were dissolved in benzene to separate from inorganic salt and the solution was passed through a column of alumina. The column was eluted with benzene and the solvent was removed. The violet crystals thereby obtained were recrystallized from a large quantity of methanol to afford 12 g. of violet needles (VII), m. p. 125~126°C.

Found: C, 47.08; H, 2.69. Calcd. for $C_{10}H_7I$: C, 47.24; H, 2.75%.

UV $\lambda_{max}^{Cyclohexane}$ mμ (logε): 558 (2.58), 601 (2.54), 660 (2.13).

Attempted Synthesis of 2-Bromoazulene (VIII).—A mixture of 100 mg. of IV and 1.5 g. of potassium bromide was refluxed with 6 ml. of glacial acetic acid and 0.5 ml. of water for 4 hr. The reaction mixture was diluted with 10 ml. of water. The black precipitates that separated out were collected by filtration. The precipitates were very sparingly soluble in organic solvents.

Action of Sodium Methoxide on II.—To a solution of 300 mg. of sodium methoxide dissolved in 3 ml. of absolute methanol, 200 mg. of II was added and the mixture was refluxed on a water bath for 2 hr. After evaporation of methanol, the residue was dissolved in water to separate into water-insoluble and soluble portions. The water-insoluble portion was recrystallized from methanol to give 120 mg. of orange needles (IX), m. p. 61~62°C.

Found: C, 65.53; H, 5.12. Calcd. for $C_{15}H_{14}O_5$: C, 65.69; H, 5.15%.

The water-soluble portion produced, upon neutralization with dilute nitric acid, 20 mg. of orange precipitates and recrystallization from methanol afforded micro scales (X), m. p. 143~145°C (decomp.).

Found: C, 64.82; H, 4.58. Calcd. for $C_{14}H_{12}O_5$: C, 64.61, H, 4.65%.

Diethyl 2-Aminoazulene-1, 3-dicarboxylate (I).—A mixture of 100 mg. of II, 1 ml. of ethanol and 1 ml. of 28% ammonia water was sealed in a tube and heated at 100°C for 1 hr. The mixture was allowed to cool and crystals that formed were collected by filtration. The recrystallization from ethanol afforded 60 mg. of orange prisms (I), m. p. 93~94°C.

Diethyl 2-Methylaminoazulene-1, 3-dicarboxylate (XI).—To a solution of 200 mg. of II dissolved in 3 ml. of ethanol, 3 ml. of 10% aqueous solution of methylamine was added and refluxed on a water bath for 2 hr. After removal of ethanol, the reaction mixture was diluted with water and extracted with benzene and the benzene extract was passed through a column of alumina, by which the product separated into red and orange bands. Elution of the red band with benzene recovered 40 mg. of II. Further elution of the orange band with benzene-ethyl acetate mixture afforded 160 mg. of orange oil (XI).

UV λ_{max}^{MeOH} mμ (logε): 230 (4.13), 253 (4.25), 275 (4.23), 325 (4.62), 405 (3.82).

1, 3, 5-Trinitrobenzene Compound of XI.—Orange needles, m. p. 100~102°C, as recrystallized from ethanol.

Found: C, 53.92; H, 4.56; N, 10.76. Calcd. for $C_{23}H_{22}O_{10}N_4$: C, 53.70; H, 4.31; N, 10.89%.

Diethyl 2-Dimethylaminoazulene-1, 3-dicarboxylate (XII).—A mixture of 200 mg. of II, 3 ml. of 40% aqueous solution of dimethylamine and 3 ml. of ethanol was refluxed on a water bath for 2 hr. and the reaction mixture was diluted with water. The orange crystals that separated out were collected by filtration. The collected crystals were recrystallized from petroleum ether (b. p. 80~90°C) to afford 160 mg. of orange leaflets (XII), m. p. 81~82°C.

Found: C, 68.77; H, 6.49; N, 4.83. Calcd. for $C_{18}H_{21}O_4N$: C, 68.55; H, 6.71; N, 4.44%.

UV λ_{max}^{MeOH} mμ (logε): 223 (4.20), 265 (4.30), 323 (4.58), 430 (4.04).

Diethyl 2-Anilinoazulene-1,3-dicarboxylate (XIII).—A mixture of 100 mg. of II dissolved in 2 ml. of ethanol and 60 mg. of aniline was heated in a water bath for 3 hr. and the reaction mixture was diluted with water and extracted with benzene. After removal of the solvent, the residue was recrystallized from ethanol to give 70 mg. of orange needles (XIII), m. p. 141~142°C.

Found: C, 72.81; H, 5.83; N, 3.69. Calcd. for $C_{22}H_{21}O_4N$: C, 72.71; H, 5.82; N, 3.85%.

UV λ_{max}^{MeOH} mμ (logε): 230 (4.25), 237 (4.25), 260 (4.28), 270 (4.40), 310 (4.62), 327 (4.68), 420 (4.09).

Diethyl 2-(4'-Bromoanilino)-azulene-1, 3-dicarboxylate (XIV).—A mixture of 100 mg. of II dissolved in 2 ml. of ethanol and 100 mg. of *p*-bromoaniline was treated as in the foregoing case, by which 60 mg. of orange needles (XIV), m. p. 166~168°C was obtained.

Found: C, 59.58; H, 4.77; N, 3.16. Calcd. for $C_{22}H_{20}O_4NBr$: C, 59.73; H, 4.52; N, 3.16%.

Diethyl 2-Hydrazinoazulene-1, 3-dicarboxylate (XV).—To a solution of 100 mg. of II dissolved in 3 ml. of ethanol, 100 mg. of 80% aqueous solution of hydrazine hydrate was added and the mixture was refluxed for 2 hr. When cooled, crystals formed, they were collected by filtration and recrystallized from ethanol to give 30 mg. of orange scales of bis-(1, 3-diethoxycarbonylazulen-2-yl)hydrazine (XVI), m. p. 163~164°C.

Found: C, 67.37; H, 5.59; N, 4.68. Calcd. for $C_{32}H_{32}O_5N_2$: C, 67.12; H, 5.63; N, 4.89%.

The mother liquor after separation of above product was evaporated. The oily residue thereby formed was dissolved in benzene and the solution was passed through a column of alumina, by which the product separated into red, yellow and orange bands. Elution of the red band with benzene recovered II. Further elution of the orange band with benzene afforded 30 mg. of orange oil (XV).

Isopropylidine Compound of XV.—A solution of 30 mg. of XV dissolved in 0.3 ml. of acetone was warmed on a water bath for 10 min. After removal of the solvent, the residue was dissolved in benzene and chromatographically purified through a column of alumina. Isopropylidine compound was obtained as orange leaflets, m. p. 133~134°C.

Found: C, 67.15; H, 6.34; N, 8.33. Calcd. for $C_{19}H_{22}O_4N_2$: C, 66.65; H, 6.48; N, 8.18%.

Acetate of XV.—A solution of 50 mg. of XV dissolved in 0.5 ml. of acetic anhydride was warmed on a water bath for 50 min. Evaporation of excess acetic anhydride left crystals which were recrystallized from ethanol and acetate of XV, m. p. 130~132°C, was obtained.

Found: C, 62.61; H, 5.83; N, 8.25. Calcd. for $C_{18}H_{20}O_5N_2$: C, 62.78; H, 5.85; N, 8.14%.

Diethyl 2-(Diethoxycarbonylmethyl)-azulene-1, 3-dicarboxylate (XVII).—To a suspension of diethyl sodiomalonate prepared from 30 mg. of metallic sodium, 250 mg. of diethyl malonate and 1 ml. of absolute ethanol, 100 mg. of II was added and the mixture was warmed on a water bath for 1 hr. The color of reaction mixture turned into dark reddish violet. After removal of the solvent, the residue was dissolved in water and the solution was acidified with acetic acid and the dark red oil that formed was extracted with benzene. The benzene extract was dried over anhydrous sodium sulfate and passed through a column of alumina, by which the product separated into red and dark red bands. Elution of the red band with benzene afforded ca. 10 mg. of II. Further elution of the dark red band with ethyl acetate gave 60 mg. of red oil (XVII).

Found: C, 64.57; H, 6.83. Calcd. for $C_{23}H_{26}O_8$: C, 64.17; H, 6.09%.

Diethyl 2-(Cyano-ethoxycarbonylmethyl)-azulene-1, 3-dicarboxylate (XVIII).—To a suspension of ethyl sodiocyanoacetate prepared from 75 mg. of metallic sodium, 370 mg. of ethyl cyanoacetate and 5 ml. of absolute ethanol, 500 mg. of II was added and the mixture was heated at 90°C for 1 hr. and small amount of precipitate separated gradually. Ethanol was evaporated from the mixture, the residue was dissolved in water and the solution was acidified with 6 N nitric acid by which red crystalline precipitate was produced. The precipitate was dissolved in benzene and chromatographically purified through an alumina column. The crystals thereby obtained were recrystallized from ethanol to give 470 mg. of XVIII as red prisms, m. p. 116~117°C.

Found: C, 65.63; H, 5.68; N, 3.92. Calcd. for $C_{21}H_{21}O_6N$: C, 65.78; H, 5.52; N, 3.65%.

UV λ_{max}^{MeOH} mμ (logε): 235 (4.50), 277 (4.51), 300 (4.72), 335 (3.87), 355 (3.86), 363 (3.97).

Diethyl 2-(Acetyl-ethoxycarbonylmethyl)-azulene-1, 3-dicarboxylate (XIX).—To a suspension of ethyl sodioacetoacetate prepared from 50 mg. of metallic sodium, 400 mg. of ethyl acetoacetate and 4 ml. of absolute ethanol, 200 mg. of II was added and the mixture was warmed in a water bath for 1 hr. The reaction mixture changed the color from reddish purple to dark purple and the precipitates began to separate out gradually. After removal of the solvent, the residue was dissolved in water and the aqueous solution was acidified with 6 N nitric acid. The red oil thereby produced was extracted with benzene and the benzene extract was dried over anhydrous sodium sulfate. The solution was passed through a column of alumina. The column was eluted with ethyl acetate and 120 mg. of red crystals was obtained. Recrystallization from cyclohexane afforded 100 mg. of red prisms (XIX), m. p. 53~54°C.

Found: C, 66.03; H, 5.25. Calcd. for $C_{22}H_{24}O_7$: C, 65.98; H, 6.04%.

UV λ_{max}^{MeOH} mμ (logε): 235 (4.55), 267 (4.41), 305 (4.80), 340 (3.90).

Ethyl 2-Ethoxyazulene-1-carboxylate (XX).—To a solution of 100 mg. of sodium ethoxide dissolved in 3 ml. of absolute ethanol, 200 mg. of VI was added and the mixture was refluxed for 3 hr. After evaporation of ethanol, the residue was dissolved in benzene and the solution was passed through a column of alumina, by which the product separated into red and pink bands. Elution of the red band with benzene recovered 60 mg. of VI. Further elution of the pink band with benzene afforded 90 mg. of pink crystals. Recrystallization from ethanol afforded pink prisms (XX), m. p. 84~85°C.

Found: C, 73.68; H, 6.49. Calcd. for $C_{15}H_{16}O_3$: C, 73.75; H, 6.60%.

UV $\lambda_{max}^{Cyclohexane}$ mμ (logε): 464 (2.09), 488 (2.11), 527 (1.92), 574 (1.17).

Reaction of VI with Ethyl Cyanoacetate.—To a suspension of ethyl sodiocyanoacetate prepared from 40 mg. of metallic sodium, 200 mg. of ethyl cyanoacetate and 4 ml. of absolute ethanol, 150 mg. of VI was added and the mixture was heated at 120~130°C for 1.5 hr. The reaction occurred gradually and dark violet precipitate began to separate out. After removal of ethanol, the residue was dissolved in water and the solution was acidified with 6 N nitric acid. The dark oil thereby formed was extracted with benzene. The benzene extract was dried over anhydrous sodium sulfate and the solution was passed through a column of alumina, by which the product separated into red, pink and dark violet bands. Elution of the red band with

benzene recovered 90 mg. of VI. Further elution of the pink band with benzene afforded crystalline substance. Recrystallization from ethanol gave ca. 20 mg. of XX, m. p. 84~85°C. Further elution of the dark violet band with ethyl acetate afforded a small amount of violet needles (XXI), m. p. 115~116°C. The yield of XXI was so poor that further examination of this product was not made.

Ethyl 2-Anilinoazulene-1-carboxylate (XXII).—To a solution of 15 mg. of potassium hydroxide dissolved in 1.5 ml. of ethanol, 100 ml. of XIII was added and the mixture was refluxed in a water bath for 3 hr. After being cooled, the solution was acidified with 6N hydrochloric acid. The crystalline carboxylic acid thereby formed was collected by filtration and washed with water and benzene. The thermal decomposition of the carboxylic acid by heating at 160°C produced orange oil and the oil was dissolved in petroleum ether (b. p. 70~80°C). The solution was passed through a column of alumina. The column was eluted with benzene and 50 mg. of orange oil (XXII) was obtained.

Trinitrobenzene Compound of XXII.—Brownish orange needles, m. p. 111~112°C, as recrystallized from ethanol.

Found: C, 60.41; H, 3.52; N, 10.86. Calcd. for $C_{25}H_{20}O_8N_4$: C, 59.52; H, 4.00; N, 11.11%.

2-Methoxyazulene (XXIII).—a) A mixture of 50 mg. of VII and 100 mg. of sodium methoxide dissolved in 1 ml. of absolute methanol was sealed in a tube and heated at 100°C for 30 hr. The reaction occurred gradually and the color changed from violet to reddish violet. Evaporation of methanol left crystalline residue. The residue was dissolved in petroleum ether (b. p. 50~60°C) and the solution was passed through a column of alumina. The column was eluted with petroleum ether and a small amount of VII was recovered. Further elution of the column with petroleum ether-benzene (1 : 1) mixture afforded 20 mg. of reddish violet crystals which were crystallized from methanol to give reddish violet needles (XXIII), m. p. 82~83°C, with an aroma.

Found: C, 83.46; H, 6.21. Calcd. for $C_{11}H_{10}O$: C, 83.51; H, 6.37%.

UV λ_{max}^{MeOH} mμ (logε): 237 (4.07), 275 (4.76), 300 (4.72), 335 (3.87), 355 (3.86), 363 (3.97). $\lambda_{max}^{Cyclohexane}$ mμ (logε): 524 (2.19), 544 (2.14), 550 (2.13), 561 (2.12), 592 (1.77), 613 (1.75).

b) A mixture of 100 mg. of IV and 200 mg. of sodium methoxide dissolved in 2 ml. of absolute methanol was treated as in the foregoing case. One-hundred and seventy milligrams of IV was recovered and a small amount of XXIII was obtained.

c) To a solution of 50 mg. of IX dissolved in 0.5 ml. of ethanol, 1 ml. of 10% aqueous solution of potassium hydroxide was added and the solution was refluxed in a water bath for 2 hr. The color of the solution changed from orange to reddish violet. After cooling, the solution was acidified with 6N sulfuric acid and the precipitate was washed with water and 30 mg. of crude acid substance sparingly soluble in organic solvents was obtained. Low-pressure (100 mmHg) sublimation of the acid substance by heating at 200°C produced red oily substance. Purification by chromatography over alumina gave 10 mg. of XXIII.

2-Ethoxyazulene (XXIV).—To a solution of 50 mg. of XX dissolved in 1 ml. of 10% aqueous solution of potassium hydroxide was added and the mixture was treated as in the case of above procedure c). The oil thereby obtained was chromatographically purified through an alumina column, by which 20 mg. of reddish violet oil (XXIV) was obtained.

UV λ_{max}^{MeOH} mμ (logε): 237 (3.99), 275 (4.69), 285 (4.81), 315 (3.65), 340 (3.45), 355 (3.59), 370 (3.48).

2-Anilinoazulene (XXV).—a) A solution of 100 mg. of XIII dissolved in 2 ml. of 10% ethanol-water (4 : 1) solution of potassium hydroxide was warmed in a water bath for 2.5 hr. After cooling, the solution was acidified with 6N hydrochloric acid. The acid substance thereby formed was collected by filtration, washed with water and completely dried in a desiccator. The acid substance was heated at 160°C under a reduced pressure (10 mmHg) to effect decarboxylation, by which reddish orange crystals were obtained. The crystals were recrystallized from petroleum ether (b. p. 50~60°C) to give 40 mg. of XXV as reddish orange scales, m. p. 144~145°C.

Found: C, 87.53; H, 6.07; N, 6.43. Calcd. for $C_{16}H_{13}N$: C, 87.64; H, 5.98; N, 6.39%.

UV λ_{max}^{MeOH} mμ (logε): 256 (4.14), 310 (4.75), 352(3.78), 420 (4.35).

b) To a solution of 50 mg. of III dissolved in 0.5 ml. of pyridine, 100 mg. of aniline was added and the mixture was heated at 120~130° for 1 hr. After removal of pyridine, the residue was dissolved in benzene and the solution was passed through a column of alumina, by which the product separated into yellow and brown bands. Elution of the yellow band with benzene recovered aniline. Further elution of the brown band with benzene afforded reddish orange crystals which were recrystallized from petroleum ether to give ca. 15 mg. of XXV, m. p. 144~145°C.

2-Cyanoazulene (XXVI).—a) A mixture of 5 g. of VII, 5 g. of cuprous cyanide and 50 ml. of pyridine, dried over solid potassium hydroxide, was heated at 140~150°C for 30 min. The color of the solution changed from violet to deep blue. Pyridine was distilled off under a reduced pressure and the residue was dissolved in benzene to separate from inorganic substance. Evaporation of benzene left deep blue crystalline solid. The crystalline solid was dissolved in a large quantity of cyclohexane and the solution was passed through a column of alumina, by which the product separated into violet and deep blue bands. Elution of the violet band with cyclohexane recovered 600 mg. of VII. Further elution of the deep blue band with benzene afforded 2 g. of blue crystals which were recrystallized from methanol to give deep blue leaflets (XXVI), m. p. 77~78°C.

Found: C, 86.31; H, 4.43; N, 9.36. Calcd. for $C_{11}H_7N$: C, 86.25; H, 4.61; N, 9.15%.

UV $\lambda_{max}^{Cyclohexane}$ mμ (logε): 586 (2.72), 621 (2.71), 635 (2.73), 660 (2.50), 679 (2.40), 697 (2.47).

b) A mixture of 500 mg. of IV, 500 mg. of cuprous cyanide and 5 ml. of pyridine was treated as in the foregoing case, by which 430 mg. of IV was recovered and 10 mg. of XXVI was obtained.

2-Hydrazinoazulene (XXVII).—A solution of 100 mg. of III dissolved in 3 ml. of 80% aqueous solution of hydrazine hydrate was heated in a water bath for 30 min. The leaflet crystals began to separate out. The crystals were collected by filtration and recrystallized from benzene to afford 30 mg. of reddish orange leaflets (XXVII), m. p. 127~128°C.

Found: C, 75.89; H, 6.54; N, 17.83. Calcd. for $C_{10}H_{10}N_2$: C, 75.92; H, 6.37; N, 17.71%.

UV λ_{max}^{MeOH} mμ (logε): 240 (4.12), 285 (4.82), 296 (4.92), 347 (3.76), 389 (3.94), 405 (3.86).

2-Dimethylaminoazulene (XXVIII).—A solution of 100 mg. of III dissolved in 3 ml. of 40% aqueous solution of dimethylamine was sealed in a tube and heated at 100°C for 3 hr. The leaflet crystals formed on cooling were collected by filtration and dissolved in benzene. The solution was passed through a column of alumina. The column was eluted with benzene and 50 mg. of orange crystals was obtained. Recrystallization from ethanol afforded 30 mg. of XXVIII as orange leaflets, m. p. 98~99°C.

Found: C, 84.21; H, 7.85; N, 8.43. Calcd. for $C_{12}H_{13}N$: C, 84.17; H, 7.65; N, 8.18%.

UV λ_{max}^{MeOH} mμ (logε): 247 (4.05), 292 (4.75); 302 (4.83), 335 (3.69), 355 (3.74), 400 (4.06), 424 (4.23).

2-Methylazulene (XXIX).—A solution of 200 mg. of XVII or XVIII dissolved in 30% ethanol-water (4:1) solution of potassium hydroxide was heated at 100°C for 6 hr. After cooling, the solution was acidified with 6 N hydrochloric acid. The precipitate thereby formed was collected by filtration and repeatedly washed with water. After being dried, low pressure sublimation (100 mmHg) of the precipitate by heating at 260~270°C produced violet oil with an odor of naphthalene. The oil was dissolved in petroleum ether (b. p. 50~60°C) and chromatographically purified through an alumina column, by which 70 mg. of the crystalline residue was obtained. Recrystallization from methanol-water mixture gave 50 mg. of violet needles (XXIX), m. p. 49~50°C. The ultraviolet and visible absorption spectra of XXIX and its melting point were in good agreement with those reported in the literature.

Methyl Azulene-2-carboxylate (XXX).—Hydrogen chloride gas was passed through the solution of 100 mg. of XXVI dissolved in 3 ml. of absolute methanol and the solution was heated on a water bath for 8 hr. Methanol was evaporated from the solution and residual crystals were dissolved in petroleum ether-benzene (1:1) mixture. The solution was passed through a column of alumina. The column was eluted with benzene-petroleum ether mixture and 60 mg. of blue crystals was obtained. Recrystallization from methanol afforded blue needles (XXX), m. p. 110~111°C.

Found: C, 77.19; H, 5.40. Calcd. for $C_{12}H_{10}O_2$: C, 77.40; H, 5.41%.

UV $\lambda_{max}^{Cyclohexane}$ mμ (logε): 604 (2.71), 656 (2.73), 713 (2.37), 728 (2.42).

Azulene-2-carboxylic Acid (XXXI).—a) A solution of 100 mg. of XXVI dissolved in 2 ml. of 10% ethanol-water (4:1) solution of potassium hydroxide was warmed in a water bath for 3 hr. Black substance began to precipitate out. The filtrate obtained after isolation of the black substance was concentrated and the residue was dissolved in water. The solution was neutralized with dilute sulfuric acid, from which green precipitate was obtained. Recrystallization of this precipitate from benzene afforded 20 mg. of XXXI as green needles, m. p. 200~203°C (decomp.).

Found: C, 76.67; H 5.00. Calcd. for $C_{11}H_8O_2$: C, 76.73; H, 4.68%.

UV λ_{max}^{MeOH} mμ (logε): 610 (2.62), 661 (2.65), 732 (2.35).

b) A solution of 100 mg. of XXX dissolved in 2 ml. of 10% ethanol-water (4:1) solution of potassium hydroxide was treated as the above procedure, by which 40 mg. of XXXI was obtained.

2-Cyano-1-formylazulene (XXXII).—To a solution of 100 mg. of XXVI dissolved in 0.3 ml. of dimethylformamide, 120 mg. of phosphorus oxychloride was added under ice-cooling. The reaction mixture was poured into ice-water, by which reddish violet crystals began to precipitate out. The crystals were recrystallized from methanol to afford 80 mg. of XXXII as reddish violet scales, m. p. 180~182°C.

Found: C, 79.46; H, 4.05; N, 7.62. Calcd. for $C_{12}H_7ON$: C, 79.55; H, 3.89; N. 7.73%.

UV $\lambda_{max}^{Cyclohexane}$ mμ (logε): 543 (2.88), 583 (2.90), 629 (2.57), 645 (2.51).

Bromination of Diethyl 2-Aminoazulene-1, 3-dicarboxylate (I).—To a solution of 100 mg. of I dissolved in 2 ml. of chloroform, 60 mg. of bromine was added and the mixture was allowed to stand at room temperature for 2 hr. A large amount of orange crystals began to precipitate out. The crystals were collected by filtration and repeatedly washed with water. Recrystallization from benzene afforded 130 mg. of orange prisms (XXXIII), m. p. 163~164°C.

Found: C, 52.65; H, 4.23; N, 3.72. Calcd. for $C_{16}H_{16}O_4NBr$: C, 52.35; H, 4.37; N, 3.87%.

UV λ_{max}^{MeOH} mμ (logε): 245 (4.33), 320 (4.55), 332 (4.66), 410 (3.38), 473 (3.50).

Bromination of Diethyl 2-Methylaminoazulene-1, 3-dicarboxylate (XI).—To a solution of 100 mg. of XI dissolved in 1.5 ml. of acetic acid, 60 mg. of bromine was added, by which brownish red oil separated out and later crystallized. The mixture was allowed to stand overnight at room temperature. Acetic acid removed and the residual oil was extracted with chloroform. The chloroform extract was washed with an aqueous solution of sodium hydrogencarbonate and water. After removal of chloroform, the residue was dissolved in benzene and the solution was passed through a column of alumina. The column was eluted with benzene and 120 mg. of brown oil which was crystallized from cyclohexane to crystals of melting point, 98~105°C.

Recrystallization from ethanol afforded 90 mg. of orange scales (XXXIV), m. p. 117~118°C.

Found: C, 53.79; H, 4.65; N, 3.46. Calcd. for $C_{17}H_{18}O_4NBr$: C, 53.54; H, 4.73; N, 3.67%.

Bromination of Diethyl 2-Anilinoazulene-1, 3-dicarboxylate (XIII).—To a solution of 100 mg. of XIII dissolved in 2 ml. of chloroform, 60 mg. of bromine was added and the mixture was allowed to stand at room temperature for 2 hr. The chloroform solution was washed with water and dried over anhydrous sodium sulfate. After removal of the solvent, the residue was dissolved in benzene and the solution was passed through a column of alumina. The column was eluted with benzene and 60 mg. of orange crystals was obtained. Recrystallization from ethanol afforded orange scales (XXXV), m. p. 173~174°C, which showed a distinct depression of the melting point on admixture with XIV.

Found: C, 59.64; H, 4.82; N, 3.27. Calcd. for $C_{22}H_{20}O_4NBr$: C, 59.73; H, 4.52; N, 3.16%.

The authors wish to take this opportunity to express their gratitude for the donation of the grant-in-aid for Scientific Research from the Ministry of Education and for financial assistance from the Sankyo Pharmaceutical Co., Ltd. The authors gratefully acknowledge their debts to Messrs Yasohiro Murase and Akira Sato for their co-operations in carrying out the experiments.

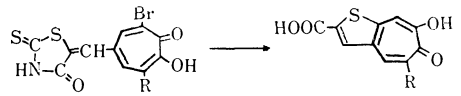
Department of Chemistry
Faculty of Science
Tohoku University
Katahira-cho, Sendai

Cycloheptathiazole Derivatives. I. Synthesis of 7-Hydroxycyclohepta-[d]thiazol-6-one and its Derivatives

By Shuichi SETO, Yukio NISHIYAMA and Kyozo OGURA

(Received April 16, 1962)

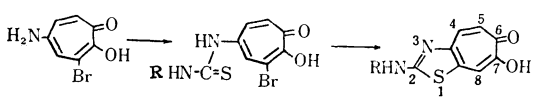
Tropolone derivatives with fused thiazole ring would be interesting compounds from the point of biology and pharmacology, but none has been reported to date. One of the authors (K. O.) found a noteworthy phenomenon during studies on 5-formyltropolone derivatives[1] that the treatment of a condensation product I of 5-formyltropolone derivative and rhodanine with alkali resulted in facile cyclization with liberation of bromide ion to form a thiophene derivative II.



I : R=Br or *i*-Pr II

It was thought that this type of reaction might be utilizable for the synthesis of tropolone derivatives with a fused thiazole ring. Therefore, thiourea derivatives obtained from 3-bromo-5-aminotropolone (III) were treated with a base and structure of the products was examined. It was thereby found that the reaction had proceeded as expected and tropolone derivatives with a fused thiazole ring could certainly be obtained. The cyclization was effected in one step by the reaction of III and carbon disulfide, and a tropolone derivative with a fused thiazole ring was obtained. This cyclization reaction and structural determination of its products will be described herein.

Treatment of III with benzoyl isothiocyanate and ethoxycarbonyl isothiocyanate in methanol respectively affords *N*-(3-bromotropolon-5-yl)-*N'*-benzoylthiourea (IV) and *N*-(3-bromotropolon-5-yl)-*N'*-ethoxycarbonylthiourea (V). By stirring IV in aqueous alkali solution at room temperature, the substance dissolves once to form an orange-yellow solution and yellow alkali salt begins to precipitate out after a few hours. The filtrate left after removal of this salt contains one atom equivalent of bromide ion. Treatment of this salt with an acid gives pale yellow crystals (VI), whose analytical values correspond to the formula of $C_{15}H_{10}O_3N_2S$. The ultraviolet spectrum of VI (Fig. 1) suggests the presence of a tropolone ring in VI. Compound VI is also obtained on treatment of IV with pyridine.



III IV : R=COC_6H_5 VI : R=COC_6H_5
V : R=$COOC_2H_5$ VII : R=$COOC_2H_5$
VIII : R=H

1) K. Ogura, This Bulletin, 35, 808 (1962).

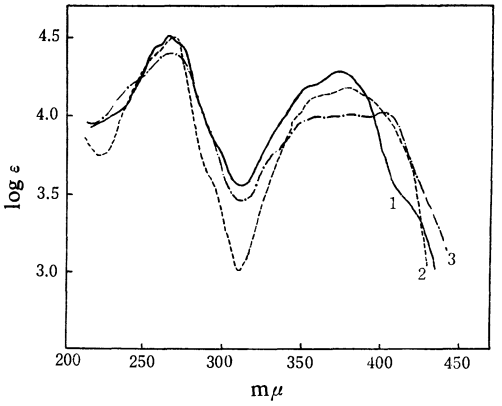
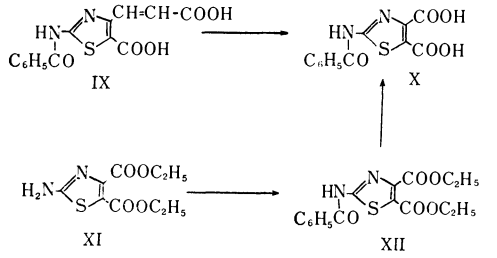


Fig. 1. The ultraviolet absorption spectra in methanol.
1 : VI 2 : VIII 3 : XIX

Thiourea derivative V undergoes similar reactions with alkali to form VII whose ultraviolet spectrum is similar to that of VI, indicating that VI and VII have a common skeleton. In fact, heating of VI and VII with concentrated sulfuric acid results in the formation of identical yellow crystals (VIII). While VI is stable to alkali and is recovered unchanged even when heated at 200°C, VII forms VIII on being heated with alkali.

In order to prove the presence of a thiazole ring in VI, its oxidative degradation was carried out. Oxidation of VI with alkaline hydrogen peroxide afforded a dicarboxylic acid (IX). If a cleavage had occurred in this case as in the oxidation of fused-ring tropolones with alkaline hydrogen peroxide[1,2], IX should be 2-benzamido-4-(β-carboxyvinyl)-5-carboxythiazole. Further oxidation of IX with alkaline potassium permanganate afforded a dicarboxylic acid (X), which was assumed to be 2-benzamido-4, 5-dicarboxythiazole.

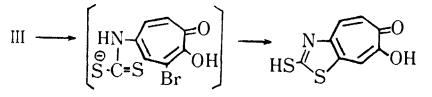


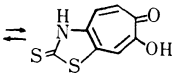
In order to confirm this assumption, the known 2-amino-4, 5-bis(ethoxycarbonyl)thiazole[3] was benzoylated to XII which was hydrolyzed to form the structurally reliable 2-benzamido-4, 5-dicarboxythiazole. The product (X) was found to be completely identical with this 2-benzamido-4, 5-dicarboxythiazole through mixed melting point and by comparison of infrared and ultraviolet spectra.

The foregoing facts have shown that VI has a thiazole ring, as anticipated, and VI, VII and VIII were proved respectively as the 2-benzamido, 2-ethoxycarbamido, and 2-amino derivatives of 7-hydroxycyclohepta[d]thiazol-6-one.

Reaction of III and carbon disulfide, in the presence of a tertiary amine, will now be described. In this case, as in the reaction of amines in general and carbon disulfide, formation of a dithiocarbamate XIII may be expected.

However, as was witnessed in the case of IV and V, formation of a thiazole ring by the liberation of hydrogen bromide is very facile and there is a possibility that the reaction would proceed on to XIV without stopping at XIII.



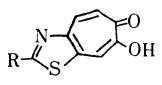


XIVb

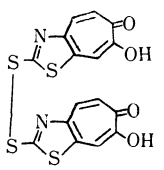
Reaction of III and carbon disulfide in pyridine, evaporation of pyridine and excess carbon disulfide from the reaction mixture, and addition of dilute sulfuric acid to its residue precipitated yellow crystals (XIV). The filtrate left after removal of XIV contained one atom equivalent of bromide ion. The analytical values of XIV corresponded to the molecular formula of $C_8H_5O_2NS_2$. This fact supports the assumption that the reaction had progressed to cyclization and that XIV would be a 2-mercaptothiazole derivative. Ultraviolet spectrum of XIV is different from that of VI and exhibits absorption in a longer wavelength region. The ultraviolet spectrum of the *S*-methyl derivative XV, obtained by application of dimethyl sulfate to XIV in the presence of alkali, is similar to that of VI. Consequently, XIV may be assumed to have a thiazole ring. This assumption was found to be correct from following facts. Oxidation of XIV with hydrogen peroxide gives sparingly soluble substance (XVI) and easily soluble pale yellow crystals (XVII). Analytical values of XVII correspond to $C_8H_5O_2NS$ and the substance is assumed to be 7-hydroxycyclohepta[d]thiazol-6-one. It is known that application of hydroxylamine to

2) H. Fernholz, E. Hartwig and J. C. Salfeld, *Ann.*, **576**, 131 (1952); J. W. Cook, A. R. M. Gibb, R. A. Raphael and A. R. Sommerville, *J. Chem. Soc.*, **1952**, 603.
3) L. H. Conover and D. S. Tarbell, *J. Am. Chem. Soc.*, **72** 5222 (1950).

benzothiazole in the presence of alkali results in the formation of 2-aminobenzothiazole[4]. If XVII were a thiazole derivative as



XV: R=SCH_3
XVII: R=H
XVIII: R=SCH_2COOH



XVI

anticipated it should form a 2-aminothiazole derivative VIII by reaction with hydroxylamine, as in the case of benzothiazole. Experimental result showed that this assumption had been correct and the structure of XVII and XIV was therefore proved.

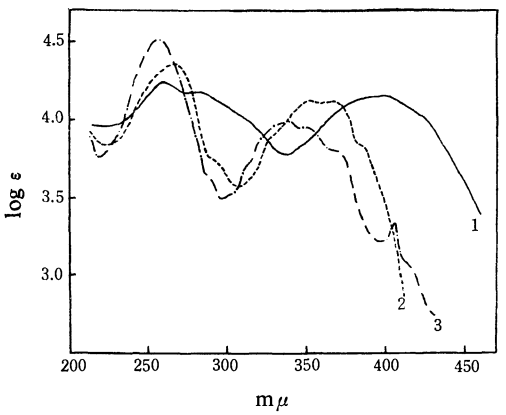
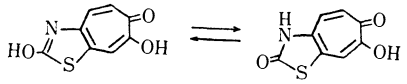


Fig. 2. The ultraviolet absorption spectra in methanol.
1: XIV 2: XV 3: XVII

Compound XVI is assumed to be a disulfide derivative from its analytical values, and ultraviolet and infrared spectra.

Application of chloroacetic acid to XIV in the presence of sodium hydrogencarbonate gives a 2-carboxymethylthio derivative XVIII, which remains unchanged on treatment with liquid ammonia at room temperature but forms a 2-hydroxyderivative XIX on being heated with an acid.



XIXa XIXb

Experimental[5]

***N*-(3-Bromotropolon-5-yl)-*N'*-benzoylthiourea (IV).**—A solution of 1.2 g. of benzoyl isothiocyanate dissolved in 10 ml. of methanol was added dropwise into 1.2 g. of 3-bromo-5-aminotropolone (III) suspended in 50 ml. of methanol, maintained at 50°C, while stirring, during ca. 1 hr. The mixture was stirred for subsequent 3 hr., cooled to room temperature, and crystals that precipitated out were collected by filtration. The crystals were washed with a small amount of methanol and was obtained as pale yellow needles, m. p. 340°C (decomp.). Yield, 1.5 g.

Found: C, 47.75; H, 3.02; N, 6.60. Calcd. for $C_{15}H_{11}O_3N_2BrS$: C, 47.48; H, 2.92; N, 7.39%.

UV λ_{max}^{MeOH} mμ(log ε): 258(4.54), 350(4.07).

***N'*-(3-Bromotropolon-5-yl)-*N*-ethoxycarbonylthiourea (V).**—To a suspension of 0.8 g. of III in 40 ml. of methanol, 1.5 g. of ethoxycarbonyl isothiocyanate was added dropwise during 30 min., while the suspension was stirred at 40°C, and the mixture was stirred at the same temperature for subsequent 1 hr. The mixture was cooled, precipitated crystals were collected, and washed a small amount of methanol to pale yellow scales (V), m. p. 280°C (decomp.). Yield, 1.1 g.

Found: C, 38.31; H, 3.23; N, 7.60. Calcd. for $C_{11}H_{11}O_4N_2BrS$: C, 38.03; H, 3.19; N, 8.07%.

UV λ_{max}^{MeOH} mμ (log ε): 254 (4.51), 350 (4.05).

2-Benzamido-7-hydroxycyclohepta[d]thiazole-6-one (VI).—a) A mixture of 0.1 g. of IV and 4 ml. of 2 N sodium hydroxide was stirred, by which the mixture went into solution, coloring orange yellow. After about 10 min., orange-yellow crystals began to separate out. The mixture was stirred for 1 hr. at room temperature and the orange-yellow crystals were collected by filtration. The crystals were suspended in 4 ml. of water, the solution was adjusted to pH 3 with 6 N sulfuric acid, by which the solid became pale yellow, and the mixture was stirred for about 20 min. The solid was collected and washed with water to VI as pale yellow microcrystals, m. p. 340°C (decomp.). Yield, 75 mg.

Found: C, 60.36; H, 3.20; N, 9.27; S, 10.51. Calcd. for $C_{15}H_{10}O_3N_2S$: C, 60.37; H, 3.38; N, 9.40; S, 10.79%.

UV λ_{max}^{MeOH} mμ (log ε): 264 (4.51), 375 (4.27).

b) A mixture of 0.1 g. of IV and 0.4 ml. of pyridine was warmed at 40°C for 2 hr., 3 ml. of water was added, and the solution was adjusted to pH 3 with 6 N sulfuric acid. The crystals of VI that separated out were collected and washed with water. Yield, 70 mg.

2-Ethoxycarbamido-7-hydroxycyclohepta[d]thiazol-6-one (VII).—A mixture of 0.8 g. of V in a solution of 1.2 g. of sodium hydroxide in 4 ml. of water was stirred for 1 hr. at room temperature and the orange yellow crystals sodium salt that separated out was collected by filtration. This sodium salt was suspended in 10 ml. of water, the solution was adjusted to pH 3 with 6 N sulfuric acid, and the mixture was stirred for 30 min. The solid that separated was collected by filtration and washed with water to give VII as pale yellow

4) S. Skraup, *Ann.*, **419**, 1 (1920).

5) All melting points are uncorrected. Microanalyses were carried out by Misses Yôko Endô and Yukiko Endô of this Institute, and microanalyses of sulfur were made in Takamine Research Laboratory of Sankyo Co., Ltd., to whom the present authors are indebted. Ultraviolet spectra were measured with a Hitachi EPU-2A type spectrophotometer.

microcrystals, m. p. 313°C (decomp.). Yield, 0.57 g.

Found: C, 49.89; H, 4.02; N, 10.32. Calcd. for $C_{11}H_{10}O_4N_2S$: C, 49.63; H, 3.79; N, 10.52%.

UV λ_{max}^{MeOH} mμ (log ε): 268 (4.45), 371 (4.11).

2-Amino-7-hydroxycyclohepta [d] thiazol-6-one (VIII).—a) A mixture of 40 mg. of VI in 0.2 g. of concentrated sulfuric acid was heated at 120°C for 5 hr. and 3 g. of ice was added to the mixture, by which the sulfate of VIII separated out as colorless crystals. Without collecting these crystals, the mixture was adjusted to pH 4 with ammonia water and cooled in ice. The yellow crystals that separated out were collected and washed with water to give VIII as yellow crystals, m. p. 280~285°C (decomp.). Yield, 20 mg.

Found: C, 49.65; H, 2.98; N, 13.85. Calcd. for $C_8H_5O_2N_2S$: C, 49.47; H, 3.12; N, 14.43%.

UV λ_{max}^{MeOH} mμ (log ε): 272 (4.52), 383 (4.17).

VIII colors brown with ferric chloride in methanol.

b) A mixture of 50 mg. of VII in 0.2 g. of concentrated sulfuric acid was heated at 110°C for 1 hr. and treated as in above method a), from which 30 mg. of VIII was obtained.

c) A mixture of 100 mg. of VII, 300 mg. of potassium hydroxide, and 1 ml. of water was heated at 130°C for 2 hr., diluted with 5 ml. of water, and adjusted to pH 4 with 6 N sulfuric acid. The crystals that separated out were collected and washed with water to 70 mg. of VIII.

d) A mixture of 20 mg. of XVII, 0.4 ml. of 2 N sodium hydroxide, 0.6 ml. of water, and 10 mg. of hydroxylamine hydrochloride was heated at 110°C for 1 hr., cooled, and yellow crystals (sodium salt of VIII) that separated out were collected by filtration. The crystals were suspended in water, the mixture was adjusted to pH 4 with acetic acid, and the free VIII that separated out were collected by filtration and washed with water. Yield, 18 mg.

This substance was found to be identical with VIII, obtained by the foregoing methods a), b) and c), through mixed melting point and by comparison of thier ultraviolet and infrared spectra.

Oxidation of VI with Hydrogen Peroxide.—A mixture of 100 mg. of VI, 200 mg. of potassium hydroxide, and 10 ml. of water, in which the potassium salt of VI is sparingly soluble in water and the majority remains as a solid in suspension, was stirred and 30% hydrogen peroxide was added in drops. One milliliter of hydrogen peroxide was added every 12 hr. until a total of 4 ml. was added, when the reaction mixture formed a pale yellow solution. 6 N Sulfuric acid was added to the mixture under ice-cooling to adjust the solution to pH 2 and 40 mg. of crystals, m. p. 220~223°C (decomp.), that separated out was collected. Recrystallization from methanol gave 2-benzamido-4-(β-carboxyvinyl)-5-carboxythiazole (IX) as colorless crystals, m. p. 229~230°C (decomp.) Yield, 20 mg.

Found: C, 50.48; H, 2.99; N, 8.53. Calcd. for $C_{14}H_{10}O_5N_2S$: C, 52.83; H, 3.17; N, 8.80%.

UV λ_{max}^{MeOH} mμ (log ε): 240 (4.23), 301 (4.24).

2-Benzamido-4, 5-dicarboxythiazole (X).—a) To a solution of 15 mg. of IX dissolved in 0.08 ml. of 2 N sodium hydroxide, 0.6 ml. of 5% aqueous solution of potassium permanganate was added and the mixture was allowed to stand at room temperature. After 1 hr., manganese dioxide that separated out was filtered off, the filtrate was adjusted to pH 2 with dilute sulfuric acid, and the mixture was allowed to stand overnight in an ice box. The colorless crystals that separated out were collected by filtration, washed with water, and recrystallized from hydrous methanol to X as colorless crystals, m. p. 283~285°C (decomp.). Yield, 5 mg. This substance was identical with X obtained by the following method b), through mixed melting point and by comparison of ultraviolet and infrared spectra.

b) To a solution of 60 mg. of 2-amino-4, 5-bis-(ethoxycarbonyl)thiazole (XI) dissolved in 0.35 ml. of pyridine, 0.15 ml. of benzoyl chloride was added dropwise with stirring at room temperature, the mixture was stirred for further 15 min., and allowed to stand at room temperature. Pyridine was evaporated in a reduced pressure, 2 g. of ice was added to the residue, and colorless crystals that separated out were recrystallized from 50% methanol to 2-benzamido-4, 5-bis(ethoxycarbonyl)thiazole (XII) as colorless crystals, m. p. 151~153°C. Yield, 60 mg.

Found: C, 55.42; H, 4.51; N, 7.67. Calcd. for $C_{16}H_{16}O_5N_2S$: C, 55.17; H, 4.63; N, 8.04%.

UV λ_{max}^{MeOH} mμ (log ε): 232 (4.18), 301 (4.25).

A mixture of 50 mg. of XII, 3 ml. of ethanol, and 230 mg. of potassium hydroxide was allowed to stand overnight at room temperature, ethanol was evaporated in reduced pressure, and the residue was dissolved in 3 ml. of water. The solution was adjusted to pH 2 with dilute sulfuric acid, the crystals that separated out were collected by filtration, and washed with water. Recrystallization from hydrous methanol gave X as colorless crystals, m. p. 285°C (decomp.). Yield, 35 mg.

Found: C, 49.47; H, 2.86; N, 9.29. Calcd. for $C_{12}H_6O_5N_2S$: C, 49.32; H, 2.76; N, 9.59%.

UV λ_{max}^{MeOH} mμ (log ε): 235 (4.25), 301 (4.17).

2-Mercapto-7-hydroxycyclohepta[d]thiazol-6-one (XIV).—a) A mixture of 1 g. of 3-bromo-5-aminotropolone (III), 8 ml. of pyridine, and 1.2 ml. of carbon disulfide was stirred at room temperature for 1 hr., and then maintained at 45°C for 1 hr., and pyridine and excess carbon disulfide were evaporated in a reduced pressure. Water was added to the residue, the solution was adjusted to pH 2 with 6 N sulfuric acid, and the yellowish brown solid (XIV), m. p. 305~310°C (decomp.), was collected by filtration and washed with water. Yield, 0.95 g.

Found: C, 44.34; H, 2.59; N, 6.24. Calcd. for $C_8H_5O_2NS_2$: C, 45.51; H, 2.39; N, 6.63%.

UV λ_{max}^{MeOH} mμ (log ε): 258 (4.23), 280 (4.17), 390 (4.14), 400 (4.14).

b) A mixture of 30 mg. of III, 1 ml. of triethylamine, and 0.1 ml. of carbon disulfide was maintained at 50°C for 2 hr. and excess of the reagents was evaporated in a reduced pressure. The residue was added with 2 ml. of water, adjusted to pH 2 with 6 N sulfuric acid, and the yellowish brown solid (XIV) that separated out was collected. Yield, 26 mg.

2-Methylthio-7-hydroxycyclohepta[d]thiazol-6-one (XV).—To a solution of 200 mg. of XIV dissolved in a mixture of 6 ml. of 2 N sodium hydroxide and 4 ml. of water, 380 mg. of dimethyl sulfate was added with stirring under ice-cooling and yellowish orange crystals began to separate out after 1 hr. The mixture was stirred for 2 hr., diluted with 15 ml. of water to dissolved the crystals and treated with activated carbon. The filtrate was adjusted to pH 2 with 6 N sulfuric acid by which yellow precipitate formed. After standing the mixture in an ice box over night, the precipitate was collected and washed with water. This precipitate was sublimed at 140°C (bath temp.)/2 mmHg and the sublimate was redrystallized from ether to XV as pale yellow crystals, m. p. 191~193°C. Yield, 190 mg.

Found: C, 47.76; H, 3.11; N, 6.35. Calcd. for $C_9H_7O_2NS_2$: C, 48.01; H, 3.13; N, 6.22%.

UV λ_{max}^{MeOH} mμ (log ε): 267 (4.35), 355 (4.10), 365 (4.11).

2-Carboxymethylthio-7-hydroxycyclohepta[d]thiazol-6-one (XVIII).—To a mixture of 200 mg. of XIV, 400 mg. of sodium hydrogen carbonate, and 5 ml. of water, 200 mg. of monochloroacetic acid was added with stirring, and the mixture was stirred for subsequent 3 hr. at room temperature. The reaction mixture remained a suspension at first but went completely into solution 2 hr. later. The solution was adjusted to pH 2 with 6 N sulfuric acid, by which a precipitate formed, and the mixture was allowed to stand in an ice box overnight. The precipitate was collected by filtration, washed with water, and XVIII was obtained as a pale yellow solid, m. p. 245~250°C (decomp.). Yield, 250 mg.

Found: C, 43.67; H, 2.56; N, 5.01. Calcd. for $C_{10}H_7O_4NS_2$: C, 44.62; H, 2.62; N, 5.20%:

UV λ_{max}^{MeOH} mμ (log ε): 268 (4.44), 370 (4.22).

Reaction of XIV and Hydrogen Peroxide.—A mixture of 80 mg. of XIV, 3 ml. of *t*-butanol, and 0.4 ml. of 30% hydrogen peroxide was heated at 90°C for 15 hr. When cooled, 40 mg. of yellow insoluble matter (XVI), m. p. 230°C (decomp.), was collected by filtration.

Found: C, 44.88; H, 2.48; N, 6.55. Calcd. for $C_{16}H_8O_4N_2S_4$: C, 45.51; H, 2.28; N, 6.63%.

t-Butanol was evaporated in a reduced pressure from the filtrate left after removal of XVI, a small amount of water was added to the residue, and the solution was adjusted to pH 3 with sodium hydrogen carbonate. This was extracted with ethyl acetate, the solvent was evaporated from the extract, and the residue was sublimed at 120°C (bath temp.)/1 mmHg. The sublimate was recrystallized from methanol to 7-hydroxycyclohepta[d]thiazol-6-one (XVII) as pale yellow needles, m. p. 162~163°C. Yield, 20 mg.

Found: C, 53.86; H, 2.76; N, 7.77; S, 17.68. Calcd. for $C_9H_5O_2NS$: C, 53.64; H, 2.81; N, 7.82; S, 17.90%.

UV λ_{max}^{MeOH} mμ (log ε): 258 (4.50), 340 (3.96).

The benzene solution of XVII colored brownish red in the organic layer with ferric chloride.

2,7-Dihydroxycyclohepta[d]thiazol-6-one (XIX).—a) A mixture of 30 mg. of XIV and 0.1 ml. of 85% phosphoric acid was heated at 160~170°C for 11 hr., cooled and diluted with a small amount of water. The mixture was adjusted to pH 4 with ammonia water under ice-cooling, the black precipitate that formed was collected, and washed with water. The precipitate was sublimed at 200°C (bath temp.)/1 mmHg and the yellow sublimate was recrystallized from ethyl acetate. m. p. 275~278°C (decomp). Yield, 10 mg.

Found: C, 49.20; H, 2.92; N, 7.12. Calcd. for $C_8H_5O_3NS$: C, 49.24; H, 2.58; N, 7.18%.

UV λ_{max}^{MeOH} mμ (log ε): 265.5 (4.43), 355 (3.99), 370 (3.99), 384 (4.00), 402 (4.01).

The ethyl acetate solution of XIX colors green in the aqueous layer by addition of aqueous solution of ferric chloride.

b) A mixture of 100 mg. of XVIII, 9 ml. of concentrated hydrochloric acid, and 3 ml. of water was heated at 120°C for 8 hr., cooled and insoluble matter was filtered off. The filtrate was evaporated to dryness in a reduced pressure, the residue was dissolved in water, and the solution was adjusted to pH 4 with ammonia water. The solid (A) that separated out was collected by filtration.

The filtrate left after removal of A was extracted with ethyl acetate and the solvent was evaporated from this extract. This residue was combined with A and sublimed at 200°C (bath temp.)/1 mmHg. The yellow crystalline sublimate was recrystallized from ethyl acetate. Yield, 40 mg.

Summary

It has been found that treatment of 3-bromotropolon-5-yl-thiourea derivatives with a base resulted in facile formation of 7-hydroxycyclohepta[d]thiazol-6-one derivatives, with liberation of hydrogen bromide. Out of such products, 2-benzamido derivative was submitted to oxidative degradation and its structure was confirmed.

Reaction of 3-bromo-5-aminotropolone and carbon disulfide, in the presence of a tertiary amine, was found to form a 2-mercapto derivative. Correlation of this product with the foregoing products proved the structure.

A part of the expenses for the present work was supported by a fund from the Sankyo Co., Ltd., which is gratefully acknowledged.

The Chemical Research Institute of Non-Aqueous Solutions
Tohoku University
Katahira-cho, Sendai

*2-Phenylthiazolo[4, 5-b]tropones**

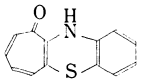
By Tetsuo NOZOE, Toyonobu ASAO and Kazuko TAKAHASHI

(Received August 8, 1962)

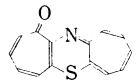
The authors have been reported[1] the synthesis of benzo-1,4-thiazino[3,2-b]tropone (cyclohepta[b]benzo-1,4-thiazin-10(11*H*)-one) (I) and its various derivatives by the reaction of 3-halotropolones and *o*-aminothiophenol. In anticipation of the sythesis of the similar compound II having 7–6–7 ring system, the reaction of 2-amino-3-bromotropones and 2-mercaptotropones was carried out, but in this reaction 2-phenylthiazolo[4,5-b]tropones, instead of II, were obtained by rearrangement of mercaptotropone nucleus, the results of which will be described herein.

When 2-amino-3-bromotropone (III)[2] and 2-mercaptotropone (2-hydroxytropothione[3]) (IV)[4] was refluxed in ethanol, the starting materials were recovered with a minute amout of disulfide V. However, heating of the mixture of III and IV in ethanol in the presence of sodium ethoxide in a sealed tube at 125°C for 10 hr., which is the same conditon as in the synthesis of 3-alkylthiotropolones from 3-bromotropolone[4], gave yellow prisms (VI), m.p. 183°C, with the correct analytical values for II. In a similar reaction of IV and 2-amino-3-bromo-6-isopropyltropone (VII), which was obtained from 3-bromo-6-isopropyl-2-methoxytropone[5] and liquid ammonia, yellow plates (VIII), m.p. 145°C, were obtained, analysis being agreed with isopropyl derivative of VI.

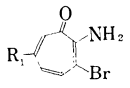
Reaction of III with 6-isopropyl-2-mercaptotropone (IX)[6] or 4-isopropyl-2-mercaptotropone (X)[6] were carried out. Although the reaction of III and IX at 125°C in the presence of sodium ethoxide gave no definite product except disulfide XI and some starting materials, the reaction at 110°C afforded yellow prisms (XII), m.p. 142°C, having the same molecular formula with VIII. X also gave yellow prisms by the reaction with III, but the product proved to be identical with XII. This fact clearly showed that the reactions in both cases underwent a quite different fashion from our anticipation and the product (XII) could not be the homologs of II. These unexpected reaction can be explained by assuming XII



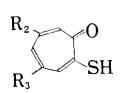
I



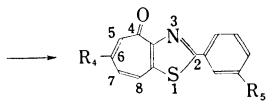
II



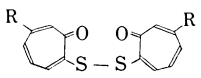
III R_1=H
VII R_1=*iso*-Pr



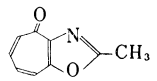
IV R_2=R_3=H
IX R_2=*iso*-Pr, R_3=H
X R_2=H, R_3=*iso*-Pr



VI R_4=R_5=H
VIII R_4=*iso*-Pr, R_5=H
XII R_4=H, R_5=*iso*-Pr



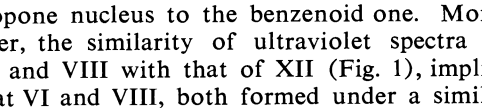
V R=H
XI R=*iso*-Pr



XIII

is 2(3'-isopropylphenyl)-thiazolo[4,5-b]tropone produced by rearrangement of the mercaptotropone nucleus to the benzenoid one. Moreover, the similarity of ultraviolet spectra of VI and VIII with that of XII (Fig. 1), implies that VI and VIII, both formed under a similar reaction condition, are not II and its isopropyl derivative but 2-phenylthiazolo[4,5-b]tropone and its 6-isopropyl derivatives.

These hypotheses were confirmed by the formation of VI from the condensation reaction of thiobenzoic acid and III.



III VI

* Presented at the Local Meeting of the Chemical Society of Japan, Yonezawa, Octorber, 1961.

1) T. Nozoe, T. Asao and K. Takahashi, This Bulletin, **34**, 146 (1961).
2) T. Nozoe, S. Seto, H. Takeda, S. Morosawa and K. Matsumoto, *Proc. Japan Acad.*, **27**, 556 (1951); *Sci. Repts. Tohoku Univ., First Ser.*, **36**, 126 (1952).
3) T. Nozoe and K. Matsui, This Bulletin, **34**, 616 (1961).
4) T. Nozoe, M. Sato and K. Matsui, *Proc. Japan Acad.*, **28**, 407 (1952); *Sci. Repts. Tohoku Univ., First Ser.*, **37**, 211 (1953).
5) S. Seto, ibid., **37**, 297 (1953).
6) K. Matsui, This Bulletin, **33**, 1448 (1960).

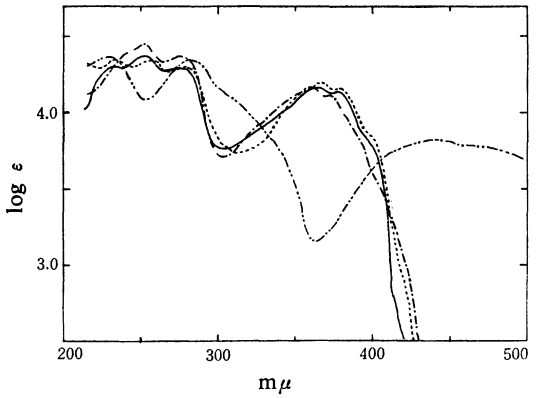
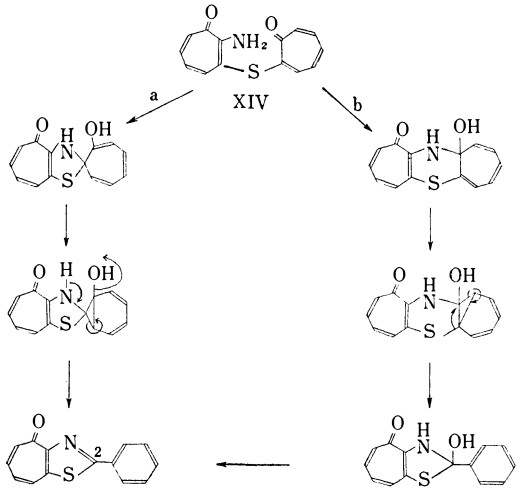


Fig. 1. Ultraviolet absorption spectra of I (—··—··), VI (———), VIII (—·—·) and XII (·····) in methanol.

Ultraviolet spectra of these thiazolotropones show considerable hypsochromic shift compared with I and rather resemble that of 2-methyloxazolo[4,5-b]tropone (XIII)[7]. While, in their infrared spectra, absorption band of N–H or O–H do not appear and C=O stretching bands appear at 1627 cm^{-1} in VI and 1622 cm^{-1} in VIII, and these values seem to be reasonably corresponding to the C=O band of tropones[8] VI, VIII and XII are very stable toward heat, acid or alkali and do not give any molecular compound such as picrate. However, they give 2,4-dinitrophenylhydrazones, m. p. 251, 259 and 218°C, respectively.

Since it was found that 2-mercaptotropone was stable under the condition employed in these condensation reactions, the reaction path to these 2-phenylthiazolo[4,5-b]tropones involves the initial formation of thio ether XIV which undergoes rearrangement by one of the following routes.

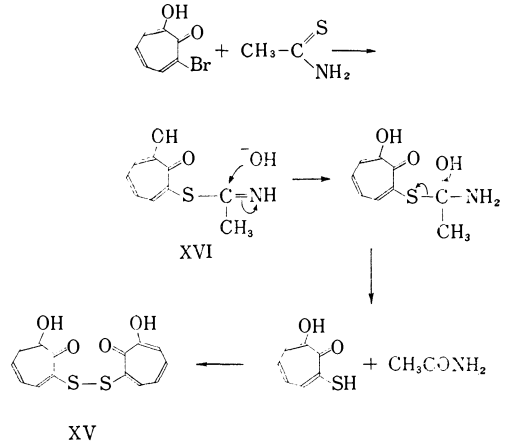


In path a, carbon at 2-position in the product, thiazolotropone, is originated from carbon-2 of mercaptotropone, while the same carbon in the product is carbonyl carbon if path b has been followed. It is considered that b is the more favorable path than a, since the aromatization of 2-substituted tropones is accepted to be initiated by attack of bases on the carbonyl-carbon, a similar attack on carbon-2 resulting in the replacement of the substituent at the same carbon[9]. A more detailed examination would, however, be desirable before any difinite conclusion is drawn.

Attempted synthesis of other thiazolotropones will be described in the following. Attempted reaction of III and thioacetic acid gave an oily substance, whose ultraviolet spectrum is similar to that of VI. However, the closer investigation on the structure was interrupted by minuteness of the yield.

It has been known that the reaction of 3-bromotropolone and thioacetamide gave an undifined compound[10]. This reaction was duplicated in various condions. The compound, m. p. 236°C, was obtained which was identical with the one previously obtained. However, it became clear that this compound is, in fact, 3,3'-ditropolonyl disulfide (XV)[4]. It is considered that this reaction proceeds through the initial formation of thio ether XVI followed by its decomposition to acetamide and 3-mercaptotropolone, which is oxidized to XV as is depicted below[11].

The reaction of thiourea with isomeric methyl



7) A. W. Johnson and M. Tisler, *J. Chem. Soc.*, **1955**, 1841.

8) Cf. Y. Ikegami, *Kagaku-no-Ryoiki, Extra*, No. **38**, 33 (1959).

9) Cf. T. Nozoe, "Non-Benzenoid Aromatic Compounds", Ed. by D. Ginsburg, Interscience Publishers, Inc., New York (1959), p. 339.

10) K. Matsui, *Sci. Repts. Tohoku Univ., First Ser.*, **43**, 223 (1959).

11) 3-Mercaptotropolone has not been obtained due to its facile oxidation to give the corresponding disulfide under neutral or acidic conditions (cf. Ref. 4).

ethers obtained from 3-bromotropolone was attempted. Heating of 2-bromo-7-methoxytropone with thiourea in ethanol gave yellow needles (XVII), m. p. 152°C. By the same way, pale yellow needles (XVIII), m. p. 108°C, were obtained from 3-bromo-2-methoxytropone. From the fact that original bromomethoxytropones were obtained by treatment of these products with silver nitrate and their ultraviolet spectra resemble those of original tropones, together with their analyses, it is concluded that XVII is a molecular compound of 2-bromo-7-methoxytropone and thiourea with a ratio of 2 : 1, and XVIII is 1 : 1 molecular compound of 3-bromo-2-methoxytropone and thiourea. These molecular compounds are quite stable and always only products obtained from the above-menthioned reactions under more severe conditions.

Experimental*

2-Phenylthiazolo[4, 5-b]tropone (VI).—a) To a sodium ethoxide solution prepared from sodium (51.7 mg.) and anhydrous ethanol (15 ml.), 2-mercaptotropone (IV) (310 mg.) and 2-amino-3-bromotropone (III) (300 mg.) were added, and the mixture was heated in a sealed tube at 125°C for 10 hr. After cooling, the precipitate was filtered off, the solvent was removed from the filtrate in vacuo. To the dark oily residue, water (50 ml.) was added, adjusted to slightly alkaline and extracted with chloroform. Recrystallization from benzene of the crude crystals (159 mg.) obtained from the extract afforded yellow prisms (VI), m. p. 182~183°C.

Found: C, 70.02; H, 3.77; N, 5.56. Calcd. for $C_{14}H_9ONS$: C, 70.29; H, 3.79; N, 5.86%.

UV: λ_{max}^{MeOH} mμ (log ε): 233 (4.29), 252 (4.37), 273 (4.29), 363 (4.16), 380 (4.13).

2,4-Dinitrophenylhydrazone; violet needles, m. p. 251°C.

Found: C, 57.18; H, 2.87; N, 16.37. Calcd. for $C_{20}H_{13}O_4N_5S$: C, 57.28; H, 3.12; N, 16.70%.

b) To a solution of sodium (26 mg.) in anhydrous ethanol (10 ml.), III (150 mg.) and thiobenzoic acid (155 mg.) were added and the mixture was treated in the same way as in a). Sixty milligrams of yellow prisms obtained showed no depression of the melting point on admixture with VI obtained by method a) and their ultraviolet and infrared spectra were identical.

2 (3' - Isopropylphenyl) - thiazolo [4, 5 - b] tropone (XII).—a) Heating of a solution of III (300 mg.) and 6-isopropyl-2-mercaptotropone (IX) (405 mg.) in a sodium ethoxide solution prepared from 57 mg. of sodium and 15 ml. of ethanol in a sealed tube at 110°C for 10 hr., followed by the same procedure described in the preceeding section yielded 227 mg. of yellow prisms (XII) (from acetone), m. p. 141~142°C.

Found: C, 72.51; H, 5.09; N, 4.85. Calcd. for $C_{17}H_{15}ONS$: C, 72.58; H, 5.37; N, 4.98%.

UV: λ_{max}^{MeOH} mμ (log ε): 235 (4.35), 256 (4.35), 275 (4.29), 365 (4.19), 380 (4.15).

2,4-Dinitrophenylhydrazone; violet needles, m. p. 218°C.

Found: C, 60.15; H, 3.93; N, 15.02. Calcd. for $C_{23}H_{19}O_4N_5S$: C, 59.87; H, 4.15; N, 15.18%.

b) The reaction of III (300 mg.) and 4-isopropyl-2-mercaptotropone (X) (405 mg.) according to the above mentioned procedure afforded 265 mg. of yellow prisms, m. p. 142°C, which is identical with XII (mixed melting point, and ultraviolet and infrared spectra).

6-Isopropyl-2-phenylthiazolo[4,5-b]tropone (VIII).—The reaction of IV (857 mg.) and 2-amino-3-bromo-6-isopropyltropone (VII) (752 mg.) in ethanol contained 143 mg. of sodium followed by the above-mentioned procedure resulted in 300 mg. of yellow plates (XIII), m. p. 144~145°C.

Found: C, 72.89; H, 5.59; N, 4.82. Calcd. for $C_{17}H_{15}ONS$: C, 72.58; H, 5.37; N, 4.98%.

UV: λ_{max}^{MeOH} mμ (log ε): 253 (4.45), 275 (4.38), 359 (4.16), 375 (4.10).

2,4-Dinitrophenylhydrazone; violet needles, m. p. 259°C.

Found: C, 59.61; H, 3.95; N, 15.14. Calcd. for $C_{23}H_{19}O_4N_5S$: C, 59.87; H, 4.15; N, 15.18%.

2-Amino-3-bromo-6-isopropyltropone (VII).—After a solution of 3-bromo-6-isopropyl-2-methoxytropone (1.16 g.) in liquid ammonia (20 ml.) was allowed to stand at room temperature for 3 days, ammonia was evaporated, the residual yellow oil was dissolved in chloroform, washed with water, dried (sodium sulfate) and passed through an alumina column, and 812 mg. of yellow oil was obtained, which was crystallized by adding ethanol. Recrystallization from ethanol gave yellow crystals, m. p. about 35°C.

Found: C, 48.80; H, 4.69; N, 5.99. Calcd. for $C_{10}H_{12}ONBr$: C, 49.60; H, 4.99; N, 5.79%.

Reaction of 3-Bromotropolone with Thioacetamide.—a) A solution of 3-bromotropolone (600 mg.) and thioacetamide (600 mg.) in pyridine (12 ml.) was refluxed for 3.5 hr. To the residue left after removal of pyridine, water was added and the precipitate (484 mg.) was recrystallized from ethanol affording 3,3'-ditropolonyl disulfide, m. p. 235°C, which was identified by the mixed melting point with authentic sample[4].

b) A solution of sodium salt (300 mg.) of 3-bromotropolone and thioacetamide (250 mg.) in anhydrous pyridine (8 ml.) was heated in a sealed tube at 120°C for 3 hr., from which 127 mg. of 3, 3'-ditropolonyl disulfide was obtained.

Molecular Compounds (XVII and XVIII) of 3-Bromotropolone Methyl Ethers and Thiourea.—a) A solution of 2-bromo-7-methoxytropone (500 mg.) and thiourea (266 mg.) in ethanol (13 ml.) was refluxed for 1 hr. By cooling the mixture, yellow needles (432 mg.) were obtained and recrystallized from methanol giving yellow needles (XVII), m. p. 152°C.

Found: C, 40.27; H, 3.56; N, 5.58. Calcd. for $C_{17}H_{18}O_4N_2SBr_2$: C, 40.33; H, 3.66; N, 5.54%.

b) Heating of a solution of 3-bromo-2-methoxytropone (600 mg.) and thiourea (213 mg.) in ethanol

* All melting points were not corrected.

(15 ml.) afforded XVIII (213 mg.) pale yellow needles, m. p. 108°C.

Found: C, 36.69; H, 3.71; N, 9.56. Calcd. for $C_9H_{11}O_2N_2SBr$: C, 37.13; H, 3.81; N, 9.63%.

Department of Chemistry
Faculty of Science
Tohoku University
Katahira-cho, Sendai

Syntheses of DL-Hydroxylysine and DL-Allohydroxylysine

By Nobuo IZUMIYA, Yoshimasa FUJITA and Motonori OHNO

(Received August 13, 1962)

Although the separation of normal and allo form of DL-hydroxylysine derivatives were performed by Fones[1] through fractional recrystallizations of two diastereomeric α-chloroacetyl-ε-carbobenzoxy lactones and by Zahn and Zürn[2] in the same way through α, ε-dicarbobenzoxy lactones, none of them were considered satisfactory because of their poor yields. This paper describes the separation of α, ε-dicarbobenzoxyhydroxylysine lactones into the two diastereomers with good yield by a new method which was based on the fact that the normal form of dicarbobenzoxy lactone is saponified by alkali faster than its allo form.

For the synthesis of diastereomeric mixture of hydroxylysine hydrochlorides, the methods of the literatures[2-3] were slightly modified. To reduce an intermediate diethyl (γ-hydroxy-δ-nitro-*n*-butyl)-acetamidomalonate (I) to the δ-amino derivative, Van Zyl et al.[3] used platinum black as a catalyst and Zahn et al.[2] employed Raney-nickel catalyst under high pressure of hydrogen. However, both procedures seemed not to be practical for a large scale experiment. We studied with palladium catalyst on the reduction of the δ-nitro group in I in several different solvents and found acetic acid to be an excellent solvent. Some results were shown in Fig. 1. In this way, 300 g. of I were reduced to diethyl (γ-hydroxy-δ-amino-*n*-butyl)-acetamidomalonate which was then hydrolyzed with acid giving 158 g. of hydroxylysine hydrochloride. Thus, the yield was improved and the procedure was remarkably simplified. Chromatographic analysis[4] revealed that the ratio of normal to allo form of this synthetic hydroxylysine hydrochloride was 46 : 54. In the next steps of carbobenzoxylation and lactonization, although Zahn and Zürn[2] reported the synthesis of diastereomeric dicarbobenzoxy lactones with the yield of 61%, we improved the yield until 91% applying an azeotropic distillation technique with benzene for the completion of lactonization. For the separation of the diastereomers, a solution of dicarbobenzoxy lactones in dioxane was first treated with sodium hydroxide equivalent to an amount of normal form which was estimated on free hydroxylysine by chromatographic analysis. Sodium salt of dicarbobenzoxyhydroxylysine thus obtained by partial saponification gave pure normal dicarbobenzoxy lactone while unsaponified lactone extracted into ethyl acetate was purified, giving the pure allo form. The two diastereomers of hydroxylysine hydrobromide were obtained from the corresponding dicarbobenzoxy lactones by the treatment of hydrogen bromide in acetic acid, and their purities were ascertained by the elution analysis from a column of Dowex 50[4] (see Figs. 5, 6 and 7).

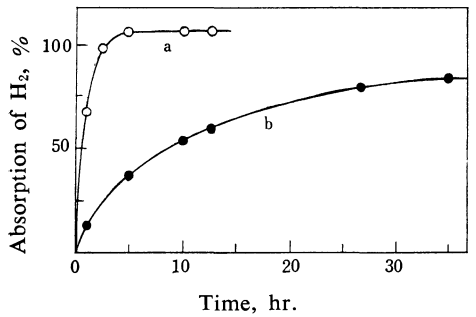


Fig. 1. Reduction of diethyl (γ-hydroxy-δ-nitro-*n*-butyl)-acetamidomalonate (I) : a, I (1 g.) and 10% Pd charcoal (0.2 g.) in acetic acid (10 ml.) ; b, I (1 g.) and 10% Pd charcoal (0.2 g.) in methanol (10 ml.) containing HCl equivalent to I.

The rates of saponification of the pure dicarbobenzoxy lactones were determined using a pH-Stat. As shown in Fig. 2, the normal

1) W. S. Fones, *J. Am. Chem. Soc.*, **75**, 4865 (1953).
2) H. Zahn and L. Zürn, *Chem. Ber.*, **91**, 1359 (1958).
3) G. Van Zyl, E. E. Van Tan Tamelen and G. D. Zuidema, *J. Am. Chem. Soc.*, **73**, 1765 (1951).
4) B. Witkop and T. Beiler, ibid., **78**, 2882 (1956).

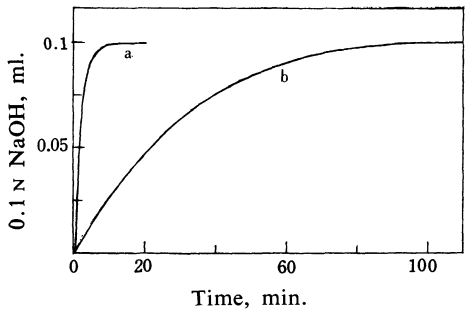
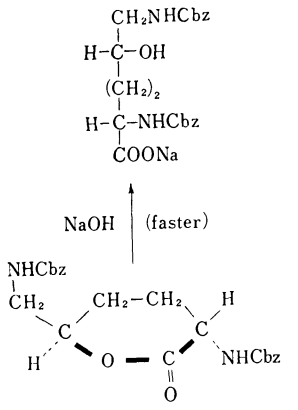
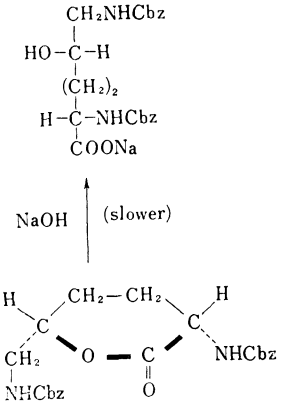


Fig. 2. Saponification of dicarbobenzoxyhydroxylysine lactones by pH-Stat: a, the normal lactone (III); b, the allo lactone (IV).



Hydroxylysine series



Allohydroxylysine series

Fig. 3. Configurations and correlations of hydroxylysine and allohydroxylysine derivatives.

form was saponified about 10 times faster than the allo form. Recently Witkop reported that the normal hydroxylysine and its lactone have erythro and trans configuration, respectively[5]. Taking this view into consideration, it is concluded that the lactone with trans configuration is easily saponified as shown in Fig. 3. In this connection, it should be noted that Wisiger reported that dibenzoyl derivative of L-allohydroxylysine was obtained as the lactone, whereas that of D-hydroxylysine as free acid[6]. In a preliminary experiment in this laboratory in collaboration with Dr. Bernhard Witkop, diastereomeric dicarbobenzoxy-DL-hydroxyornithine lactones, unlike the case of dicarbobenzoxyhydroxylysine lactones, could not be separated with the use of sodium hydroxide equivalent to an amount of the trans form.

Experimental

Diethyl (γ-Hydroxy-δ-nitro-*n*-butyl)-acetamidomalonate (I).—Diethyl acetamidomalonate (760 g., 3.5 mol.) and acrolein (257 ml., 3.86 mol.) were condensed in ethanol (1.4 l.) containing metallic sodium (1.1 g.)[7]. The solution containing γ-acetamido-γ,γ-diethoxycarbonylbutyraldehyde was added during 30 min. under stirring to an ice-cooled solution of nitromethane (0.88 l.), dioxane (0.088 l.) and 5 N sodium hydroxide (0.088 l.). After being stirred for 16 hr. at room temperature, 5 N sodium hydroxide (0.025 l.) was added and the stirring was continued for another 24 hr. After being neutralized with acetic acid (0.039 l.), the solution was evaporated in vacuo and the residue was added to a mixture of benzene (1.5 l.) and petroleum ether (0.15 l.). The mixture was allowed to stand for several days in a refrigerator to cause the separation of crystals which were filtered and washed with water. After being dried well and recrystallized from benzene (2.5 l.), it was dissolved in ethanol (1.5 l.) and the solution was evaporated in vacuo. The addition of water (1.5 l.) and the shaking of mixture caused the formation of crystals, yield 620 g. (53%), m. p. 68~71°C. This was saved for the next step. Two recrystallizations from aqueous ethanol gave an analytical sample, m. p. 76°C (Found: C, 46.70; H, 6.52; N, 8.34%). The reported values are m. p. 95.2~96°C[8] and 77°C[8].

Hydroxylysine Monohydrochloride (Diastereomeric Mixture).—I (300 g., 0.9 mol.) in acetic acid (1.5 l.) containing 10% palladium charcoal (30 g.) was reduced for 6 hr. at room temperature under 1 atm. of hydrogen in a 5 l. three-neck flask, fitted with a sealed stirrer, an inlet tube for hydrogen, and an outlet tube which was in contact with a surface of mercury. The catalyst was removed by filtration, the filtrate was added to concentrated hydrochloric acid (1.5 l.), and the solution was refluxed for 10 hr. It was evaporated to dryness in vacuo and the excess of acids was removed by repeated addition of water and evaporation. The residue was taken up in water, treated with triethylamine (0.4 l.) and the solution was evaporated to dryness in vacuo. After being washed with a mixture of ethanol (1.5 l.) and acetone (0.3 l.) by the method of decantation, the residue was taken

5) B. Witkop, *Experientia*, **12**, 372 (1956).

6) J. R. Wisiger, *J. Biol. Chem.*, **186**, 591 (1950).

7) O. A. Moe and D. T. Warner, *J. Am. Chem. Soc.*, **70**, 2763 (1948).

8) H. Zahn and E. Umlauf, *Z. physiol. Chem.*, **297**, 127 (1954).

up in water. The solution was decolorized with charcoal and concentrated in vacuo to a small volume. The addition of ethanol (1.8 l.) effected the precipitation of a powdery substance, yield 158 g. (88%). This was saved for the next step. The paper chromatography of this compound showed only one spot by means of the ninhydrin test with several solvent systems. As shown in Fig. 4, ion-exchange analysis of the compound gave a ratio, normal to allohydroxylysine, of 46 : 54. Two recrystallizations from water-ethanol gave a sample, m. p. 212~218°C (decomp.). (Found: C, 35.99; H, 7.72; N, 14.31%).

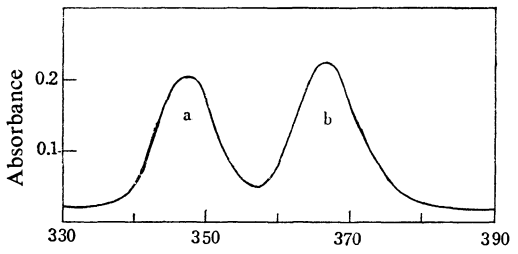


Fig. 4. Chromatography of diastereomeric hydroxylysine monohydrochloride: a, hydroxylysine; b, allohydroxylysine.

Chromatographic Assay of Normal and Allohydroxylysine. — The method of Stein and Moore as modified by Witkop and Beiler[4] was utilized to assay the composition of hydroxylysine. A 100× 0.9 cm. column of Dowex 50×8 (200~400 mesh) was treated with 0.1 M sodium citrate buffer of pH 3.4. An aqueous solution containing 1.0 mg. of hydroxylysine monohydrochloride was passed through the column and eluted with 0.1 M sodium phosphate buffer of pH 7.6. Slight pressure was applied to keep the flow rate at 4 ml. per hr. One-ml. samples were collected with an automatic fraction collector and analyzed by the ninhydrin method[9] at 570 mμ.

Dicarbobenzoxyhydroxylysine Lactone (Diastereomeric Mixture) (II).—The powdery hydroxylysine monohydrochloride (39.8 g., 0.2 mol.) obtained above was treated with carbobenzoxy chloride (89 ml., 0.52 mol.) and 2 N sodium hydroxide (0.52 l.) by Schotten-Baumann's procedure. An oil separated upon acidification with 5 N hydrochloric acid (0.21 l.) was extracted with chloroform. The chloroform solution was dried over sodium sulfate and evaporated in vacuo to an oil to which benzene (1 l.) was added. The mixture was heated under reflux for 3 hr., the liberated water being removed azeotropically using a Dean and Stark distilling apparatus[10]. After the filtration of some insoluble material, the filtrate was evaporated to an oil which was crystallized by the addition of petroleum ether. It was filtered and washed with petroleum ether, yield 75.4 g. (91%). This was used without further purification. We supposed that a ratio of normal to allo form in this compound should have been close to 46 : 54 because the yield of dicarbobenzoxy derivative from diastereomeric hydroxylysine, the ratio of which was 46 : 54, was excellent (91%).

Dicarbobenzoxy-DL-hydroxylysine Lactone (III). To a solution of II (41.2 g., 0.1 mol.) in dioxane (400 ml.) was added 1 N sodium hydroxide (46 ml.)* at room temperature. After standing for 1 hr., the solution was evaporated in vacuo to dryness. The residue was shaken with a mixture of ethyl acetate (600 ml.) and water (400 ml.) (the ethyl acetate layer was saved for the recovery of IV), the aqueous layer was acidified with 5 N hydrochloric acid (10 ml.) and an oil separated was extracted with ethyl acetate. The solution was dried over sodium sulfate and evaporated in vacuo to an oil to which benzene was added. The benzene solution was refluxed for 3 hr., the liberated water being removed azeotropically. Benzene was removed by evaporation in vacuo and the residue was recrystallized twice from ethyl acetate, yield 10.4 g. (55% based on the supposed amount (46%) of normal form in II), m. p. 135~136°C.

Found: C, 64.01; H, 5.97; N, 6.67. Calcd. for $C_{22}H_{24}O_6N_2$: C, 64.06; H, 5.87; N, 6.79%.

The reported value is m. p. 137~141°C[2].

Dicarbobenzoxy-DL-allohydroxylysine Lactone (IV).—After the ethyl acetate layer described above was kept in a refrigerator, crystals appearing were filtered and washed with cold ethyl acetate. The combined filtrate and washings were dried over sodium sulfate and evaporated in vacuo to dryness. The crystals and dried residue were recrystallized twice from ethanol, yield 17.8 g. (80% based on the supposed amount (54%) of allo form in II), m. p. 151°C.

Found: C, 63.96; H, 5.86; N, 6.74. Calcd. for $C_{22}H_{24}O_6N_2$: C, 64.06; H, 5.87; N, 6.79%.

The reported value is m. p. 154~155.5°C[2].

DL-Hydroxylysine Monohydrobromide (V). — A saturated solution of hydrogen bromide in acetic acid[11] (30 ml.) was added at room temperature to III (6.17 g., 0.015 mol.) which had been previously pulverized. III was dissolved within 2~3 min. and different crystals appeared after 5~6 min. The mixture was allowed to stand with occasional shakings for 1 hr., and then treated with ether (120 ml.) and petroleum ether (30 ml.). The crystals were filtered and washed with ether, but changed instantly to a gummy product because of its highly hygroscopic character. Second crop of the gummy product was obtained from the filtrate and washings by the addition of petroleum ether. The combined products were dissolved in water and triethylamine (9 ml.) was added**. The solution was evaporated in vacuo

9) H. Rosen, *Arch. Biochem. Biophys.*, **67**, 10 (1957).

10) J. P. Greenstein and M. Winitz, "Chemistry of the Amino Acids", J. Wiley & Sons, Inc., New York (1961), p. 940.

* In another run of the same experiment, a half mole of 1 N sodium hydroxide (50 ml.) was used, III and IV being obtained with the yields of 9.5 g. and 17.1 g., respectively.

11) D. Ben-Ishai and A. Berger, *J. Org. Chem.*, **17**, 1564 (1952).

** In another run of the same experiment, silver carbonate was added to the aqueous solution until pH 6.5 and pure DL-hydroxylysine monohydrobromide was obtained from the filtrate with a similar yield in the case of the use of triethylamine.

to dryness and the residue was filtered with the aid of ethanol. It was recrystallized from water (7 ml.)-ethanol (20 ml.), yield 3.17 g. (87%), m. p. 230~231°C (decomp.).

Found: C, 29.66: H, 6.31; N, 11.39. Calcd. for $C_6H_{15}O_3N_2Br$: C, 29.64; H, 6.22; N, 11.52%.

The product (1.0 mg.) was analyzed by the method of ion-exchange chromatography, the procedure being described before. The curves of absorbance of V itself and a mixture of V and L-allohydroxylysine monhydrochloride[12] were shown in Figs. 5 and 6, respectively. These results indicate that V is a pure normal form.

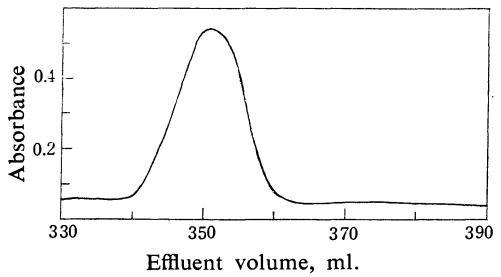


Fig. 5. Chromatography of DL-hydroxylysine monohydrobromide.

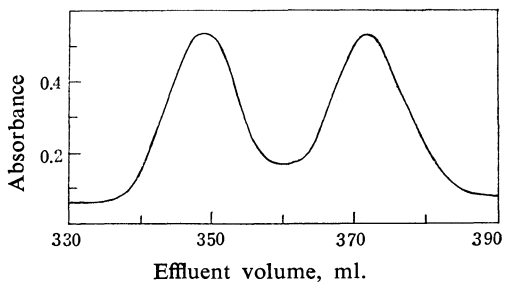


Fig. 6. Chromatography of a mixture of DL-hydroxylysine monohydrobromide and L-allohydroxylysine monohydrochloride.

DL-Allohydroxylysine Monohydrobromide (VI).—IV (6.17 g.) was treated with hydrogen bromide in acetic acid in the same way as described above. The yield of the recrystallized product was 2.61 g. (71%), m. p. 219°C (decomp.)

Found: C, 29.74; H, 6.26; N, 11.21. Calcd. for $C_6H_{15}O_3N_2Br$: C, 29.64; H, 6.22; N, 11.52%.

As shown in Fig. 7, the product is a pure allo form. Zahn and Zürn reported the preparation of DL-hydroxylysine and DL-allohydroxylysine monohydrochloride[2].

12) W. S. Fones, *Biochem. Preparation*, **8**, 62 (1961).

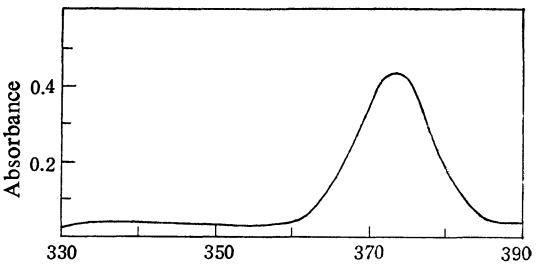


Fig. 7. Chromatography of DL-allohydroxylysine monohydrobromide.

Saponification of Dicarbobenzoxy Derivatives, III and IV.—A solution of III or IV (4.12 mg., 0.01 mmol.) in a mixture of dimethylformamide (1.5 ml.) and water (1.5 ml.) was saponified at 40°C with 0.1 N sodium hydroxide using Radiometer's pH-Stat (type TTTl) which was set at a constant pH of 10.0. The curves recorded automatically were shown in Fig. 2, indicating that III was saponified completely within about 10 min., while IV needed about 100 min. for complete saponification.

Summary

A diastereomeric mixture of DL-hydroxylysine hydrochlorides was obtained with a good yield through hydrogenation of diethyl (γ-hydroxy-δ-nitro-*n*-butyl)-acetamidomalonate with palladium catalyst in a solvent of acetic acid, which was followed by hydrolysis of the reduced product. Dicarbobenzoxy lactone was prepared with a yield of 91% from hydroxylysine hydrochloride obtained above. A solution of diastereomeric dicarbobenzoxy lactones in dioxane was treated with sodium hydroxide equivalent to the amount of normal form. The salt obtained after saponification converted into a pure normal dicarbobenzoxy lactone, a pure allo compound being isolated from the unsaponified portion. The two lactones were converted into chromatographically pure normal and allohydroxylysine monohydrobromides by the action of hydrogen bromide in acetic acid.

Laboratory of Biochemistry
Faculty of Science
Kyushu University
Fukuoka

Synthesis of DL-*Lysine from 1, 1, 1, 5-Tetrachloropentane*

By Kazuo SAOTOME and Yasuto KODAIRA

(Received August 23, 1962)

In a previous paper[1], the synthesis of DL-lysine from 1, 1, 1, 5-tetrachloropentane which was prepared by the telomerization of ethylene and carbontetrachloride via benzoylaminocaproic acid as the intermediate was reported.

The present work is concerned with another process for the synthesis of DL-lysine from 1, 1, 1, 5-tetrachloropentane involving seven steps as shown below.

$Cl(CH_2)_4CCl_3$ (I) $\longrightarrow$ $Cl(CH_2)_3CH{=}CCl_2$ (II) $\longrightarrow$ $CN(CH_2)_3CH{=}CCl_2$ (III) $\longrightarrow$ $H_2N(CH_2)_4CH{=}CCl_2$ (IV) $\longrightarrow$ $C_6H_4(CO)_2N(CH_2)_4CH{=}CCl_2$ (V) $\longrightarrow$ $C_6H_4(CO)_2N(CH_2)_4CHCl\text{-}COOH$ (VI) $\longrightarrow$ $C_6H_4(CO)_2N(CH_2)_4CHNH_2\text{-}COOH$ (VII) $\longrightarrow$ DL-Lysine·HCl

In the first step, I was dehydrochlorinated to 1, 1, 5-trichloropentene-1 (II) in the presence of anhydrous ferric chloride as the catalyst[2]. Since the dichlorovinyl group in II is inert towards nucleophilic reagents, II was treated with potassium cyanide in dimethylformamide (DMF) solution to prepare 1, 1-dichloro-5-cyanopentene-1 (III). In the hydrogenation of III under a high pressure of hydrogen, the Raney cobalt was found to be a favorable catalyst for attacking the nitrile group selectively. 1, 1-Dichloro-6-aminohexene-1 (IV) was acylated by heating with phthalic anhydride to give 1, 1-dichloro-6-phthaliminohexene-I (V).

Some examples of the reaction between the dichlorovinyl group and chlorine in a sulfuric acid solution to obtain α-chlorocarboxylic derivatives were reported by Russian authors[3]. The reaction mechanisms are explained as follows.

$$C_6H_4(CO)_2N(CH_2)_4CH{=}CCl_2 \xrightarrow[H_2SO_4]{Cl_2} C_6H_4(CO)_2N(CH_2)_4\underset{Cl}{CH}\text{—}\underset{OSO_3H}{CCl_2} \xrightarrow{H_2O} C_6H_4(CO)_2N(CH_2)_4\underset{Cl}{CH}\text{—}COOH$$

A chlorine atom and a sulfuric acid residue are added to the double bond of V, and the resulting adduct decomposes with water to give 2-chloro-6-phthaliminocaproic acid (VI). The resulting VI was aminated with aqueous ammonia. Since phthaliminolysine could not be crystallized, the reaction mixture was concentrated, and without further purification it was hydrolyzed by hydrochloric acid to give DL-lysine. DL-Lysine monohydrochloride was separated and purified as in the previous paper[1].

Experimental

1, 1, 5-Trichloropentene-1 (II).—Dehydrochlorination of I was investigated using several Friedel-Crafts type catalysts. After the evolution of hydrogen chloride had ceased, the reaction mixture was

TABLE I. DEHYDROCHLORINATION OF 1, 1, 1, 5-TETRACHLOROPENTANE

$Cl(CH_2)_4CCl_3$ g.	Catalyst	g.	Temp. ×Time °C×hr.	$Cl(CH_2)_3\cdot CH{=}CCl_2$ g.	Unreacted $Cl(CH_2)_4CCl_3$ g.	Yield* %
126	$ZnCl_2$	3.0	120×4	26.0	69.0	83
126	$AlCl_3$	2.0	60×2	85.0	8.0	87
126	$SnCl_4$	3.0	130×3	37.5	76.0	91
210	$FeCl_3$	3.0	55×3	148.0	10.0	90
420	$FeCl_3$	(6+2)**	55×3	318.0	—	92

* The yield was calculated taking the recovered tetrachloropentane into account.
** The catalyst was added in two portions 2 g. of ferric chloride was added after 2 hr. reaction.

1) K. Saotome, *J. Chem. Soc. Japan, Ind. Chem. Sec.* (*Kogyo Kagaku Zasshi*), **65**, 1061 (1962).
2) A. N. Nesmeyanov and L. I. Zakharkin, *Izv. Akad. Nauk SSSR, Otd. Khim. Nauk*, **1951**, 505; A. N. Nesmeyanov et al., ibid., **1955**, 657.
3) A. N. Nesmeyanov, V. N. Kost and R. Kh. Freidlina, *Dakl. Akad. Nauk SSSR*, **103**, 1029 (1955).

TABLE II. HYDROGENATION OF 1, 1-DICHLORO-5-CYANOPENTENE-1

$CN(CH_2)_3CH=CCl_2$ g.	(mol.)	Catalyst	g.	EtOH ml.	NH_3 g.	H_2 kg./cm²	Temp. ×Time °C hr.	$H_2N(CH_2)_4CH=CCl_2$ g.	%
33.0	(0.2)	Co	3.0	100	12.5	80	80×6	16.5	49.1
33.0	(0.2)	Co	3.0	100	satu.	85	80×5	17.4	51.8
33.0	(0.2)	Co	6.0	200	16.0	80	80×3	19.0	56.0
33.0	(0.2)	Co	6.0	100	satu.	80	80×5	19.8	58.8
33.0	(0.2)	Ni	3.0	100	10.0	80	80×3	7.8	22.9

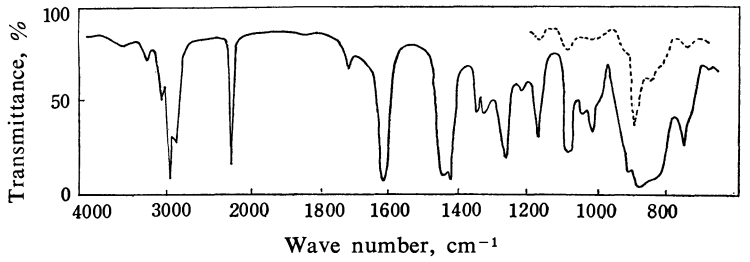


Fig. I. Infrared spectrum of 1, 1-dichloro-5-cyanopentene.

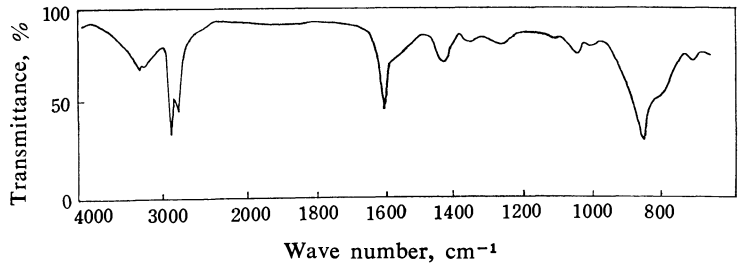


Fig. 2. Infrared spectrum of 1, 1-dichloro-6-aminohexene.

washed with water, then distilled under reduced pressure to afford II, b. p. 48~50°C/4 mmHg, n_D^{20} 1.4892 (lit. b. p. 68~69°C/7 mmHg, n_D^{20} 1.4892). The reaction conditions and the yields are shown in Table I.

When aluminum chloride which is a stronger catalyst than ferric chloride was used for the reaction, the reaction proceeded smoothly at a lower temperature. But the resinous by-product was observed to increase in the distillation residue.

However, in the case of a weaker catalyst such as zinc chloride or stannic chloride, the reaction proceeded only slowly even at an elevated temperature. The best result was obtained when ferric chloride was added in two portions. The infrared spectrum of II showed a strong absorption band at 1620 cm^{-1} due to C=C double bond.

1, 1-Dichloro-5-cyanopentene-1 (III).—Into a solution of 82 g. of potassium cyanide in 500 ml. of DMF maintained at 115°C was added dropwise 174 g. of II over one hour with stirring. The reaction was continued for additional two hours. Potassium chloride was filtered and the solvent was evaporated under reduced pressure. Distillation of the residue under reduced pressure afforded 142 g. of III (88% yield), b. p. 99~101°C/5 mmHg, n_D^{20} 1.4818 (lit.[4] b. p. 80~81°C/3 mmHg, n_D^{20} 1.4815).

1, 1-Dichloro-6-aminohexene-1 (IV).—Hydrogenation of III was carried out using the Raney cobalt and nickel (prepared according to the recipe W-7[4]) as a catalyst in an alcoholic solution containing ammonia. An autoclave (500 ml.) equipped with a magnetic stirrer was used for the reaction. After removal of the catalyst and the solvent, the reaction product was washed with water and extracted with ether. Distillation of the extract under reduced pressure afforded IV, b. p. 77~80°C/5 mmHg, n_D^{20} 1.4860. Details of the reaction are shown in Table II.

From Table II, the Raney cobalt is shown to be the preferable catalyst to the Raney nickel for the selective hydrogenation of III. On the other hand, the hydrogenation of 1, 1, 5-trichloropentene-1 was attempted under the same conditions, but no absorption of hydrogen was observed. An attempt to hydrogenate the nitrile group in III by metallic sodium in an alcoholic solution was also made. But the product was resinous, and no IV was obtained.

Infrared Spectra.—The spectra of III and IV are shown in Figs. 1 and 2. The characteristic band

4) A. N. Nesmeyanov, L. I. Zakharkin and R. Kh. Freidlina, *Izv. Akad. Nauk SSSR, Otd. Kim. Nauk*, **1954**, 34.
5) H. Adkins and H. R. Billica, *J. Am. Chem. Soc.*, **70**, 695 (1948).

at 2220 cm^{-1} due to cyano group in Fig. 1 disappears in Fig. 2, and a new band at 3250 cm^{-1} (NH) appears in Fig. 2. While the band at 1620 cm^{-1} assigned to carbon-carbon double bond is observed both in Fig. 1 and Fig. 2.

1, 1-Dichloro-6-phthaliminohexene-1 (V).—A mixture of IV (16.4 g.) and phthalic anhydride (29 g.) was heated under nitrogen atomosphere at 145~150°C in an oil bath for 4 hr. Aqueous solution of sodium hydroxide (5%, 120 ml.) was poured to the reaction mixture to dissolve the excess phthalic anhydride. The precipitate was separated, powdered and washed several times with water. Its recrystallization from ethanol afforded white crystals. Yield, 27.4 g. (96%); m. p., 56°C.

Found: C, 56.56; H, 4.70; N, 4.59. Calcd. for $C_{14}H_{13}O_2NCl_2$: C, 56.39; H, 4.39; N, 4.70%.

2-Chloro-6-phthaliminocaproic Acid (VI).—Into 70 ml. of sulfuric acid (96%) cooled with ice-water, V (15 g.) was added slowly to make a clear solution. Chlorine gas was passed through this solution at 5°C with stirring. The reaction was continued for 3 hr. until the evolution of hydrogen chloride had ceased. The reaction mixture was poured into ice-water, and the solidified product was washed with water. Recrystallization from benzene afforded white crystals. Yield, 14.1 g. (95%); m. p., 124~125°C.

Found: C, 56.83; H, 4.72; N, 5.01. Calcd. for $C_{14}H_{14}O_4NCl$: C, 56.82; H, 4.73; N, 4.73%.

DL-Lysine Monohydrochloride.—Into an autoclave (200 ml.) equipped with a magnetic stirrer, were taken VI (10 g.), ammonium carbonate (15 g.) and 100 ml. of 28% aqueous ammonia. The reaction was carried out at 60~65°C for 8 hr. The reaction mixture was concentrated to about 30 ml. to remove free ammonia. To this solution was added 80 ml. of 20% hydrochloric acid and the mixture was refluxed for 12 hr. Phthalic acid precipitated was filtered off and the solution was concentrated to dryness under reduced pressure. The solid product was dissolved in 200 ml. of water. The solution was treated with anion exchange resin (Amberlite IR-4B) to remove the excess hydrochloric acid. The solution was concentrated and cooled. DL-Lysine monohydrochloride was precipitated by adding acetone. The pure sample (3.3 g.) was obtained by recrystallization from an acetone-water mixture. The yield was 53.4% of the theoretical amount. This was identified by paper chromatography with the authentic sample and shown to be one-spot.

Found: C, 39.21; H, 8.06; N, 15.46. Calcd. for $C_6H_{15}O_2N_2Cl$: C, 39.45; H, 8.23; N, 15.34%.

Summary

DL-Lysine was synthesized from 1, 1, 1, 5-tetrachloropentane. The process involves seven steps; 1, 1, 5-trichloropentene-1 (92%), 1, 1-dichloro-5-cyanopetene-1 (88%), 1, 1-dichloro-6-aminohexene-1 (59%), 1, 1-dichloro-6-phthaliminohexene-1 (96%), 2-chloro-6-phthaliminocaproic acid (95%), DL-lysine monohydrochloride (53%). The over-all yield from 1, 1, 1, 5-tetrachloropentane to DL-lysine monohydrochloride was 23%.

In the hydrogenation of 1, 1-dichloro-5-cyanopentene-1 to 1, 1-dichloro-6-aminohexene-1; the Raney cobalt was found to be a favorable catalyst for attacking the nitrile group selectively.

Technical Research Laboratory
Asahi Chemical Industry Co., Ltd.
Itabashi-ku, Tokyo

Vinyl Polymerization. LXIV. Graft Copolymerization of Vinyl Monomers to Starch*

By Shoichi KIMURA**, Takehiro TAKITANI and Minoru IMOTO

(Received August 6, 1962)

Many authors have reported on the synthesis of graft copolymers of starch. The methods described were chain transfer reaction[1,2], high energy radiation[3], oxidation with ozone[4], oxidation with ceric salt[5], and polymer blend[6]. In order to obtain a graft copolymer of starch with high efficiency, we used the method of the polymerization of the monomer in the presence of oxidized starch. Kargin et al. peroxidized starch with ozone and initiated vinyl polymerization with it to obtain a graft

* LXIII of this series: M. Kinoshita, *Chem. High Polymers, Japan.*, in press.

** Present address: Meiji Sugar Mfgr. Co., Ltd., Kawasaki, Japan.

1) Brit. Pat. 715194 (1959).

2) Brit. Pat. 809745 (1959).

3) A. Mishina, *J. Agr. Chem. Soc. Japan*, 35, 40 (1961).

4) V. A. Kargin, P. V. Kozlov, N. A. Plate and I. I. Konoreva, *Vysokomol. Soed.*, 1, 114 (1959); V. A. Kargin, N. A. Plate and E. P. Rebinder, ibid., 1, 1547 (1959).

5) S. Kimura and M. Imoto, *Makromol. Chem.*, 42, 140 (1960).

6) R. F. Ceresa, IUPAC Simposium (1960); A. A. Berlin, Je. A. Penskaja and G. I. Wolkova; IUPAC Simposium (1960).

copolymer. They obtained grafted starch with polymethyl methacrylate or polystyrene. However, the efficiency of their reaction was not stated[4].

The present paper concerns the stability of ozone-oxidized starch, the graft copolymerization of methyl methacrylate, acrylonitrile or vinyl chloride with the oxidized starch, and the fractionations of the grafted copolymer and their properties.

Experimental

Oxidation of Starch.—Starch was purified by reprecipitation from an aqueous solution with ethanol. It was charged into a four-necked flask which contained water or carbon tetrachloride. Ozonized oxygen generated by an ozonizer of the Japan Ozonizer Co. (Type 03-5-2) was introduced at the velocity of 6 l./hr. at room temperature while the mixture was vigorously stirred. A stirrer, as shown in Fig. 1, was made from a glass-tube; it had two gas-outlets, of which one opened near the bottom in the liquid layer and the other just above the liquid surface. After a definite time, the reaction mixture was filtered in order to obtain oxidized starch.

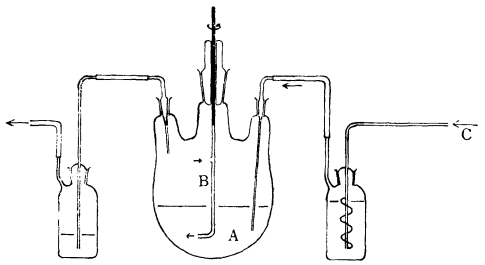


Fig. 1. Equipment for the ozonization of starch.

A Suspension of starch
B A glass-tube stirrer
C O_3 (in O_2)

Determination of the Content of the Peroxide Group in Oxidized Starch. — The content of the peroxide group in the oxidized starch was determined as follows. A definite quantity of the oxidized starch was immersed in a 10% aqueous solution of potassium iodide for 10 min. at room temperature (29°C) or for 3 min. at 70 and 100°C. The content of the peroxide group was expressed by the number of peroxide groups per anhydroglucose unit (AGU) of starch. The quantity of starch in the filtrate was estimated on the basis of the amount of glucose which was liberated by hydrolysis in 1.0 N hydrochloric acid at 95°C for 3 hr. The determination of the glucose was made by Somogyi's method.

Polymerization Procedure.—The polymerization of methyl methacrylate (MMA), acrylonitrile (AN), and vinyl chloride (VC) was carried out under the conditions described in Table I.

In Experiments I, III, V and VI, a mixture of a monomer, starch and solvent was charged in a test tube, cooled in a dry ice-methanol bath, and sealed in vacuum. The sealed tube was shaken at 90°C in a thermostat for a given time; the contents were then poured into methanol to precipitate the polymer mixtures. In Experiments II and IV, the mixture was charged into a three-necked flask, and nitrogen was then introduced into it at room temperature for 15 min. Then, the mixture was heated while being stirred. After a given time, the contents were poured into methanol to precipitate all the polymers.

Fractionation of Polymerization Products. — *Copolymerization Product with Methyl Methacrylate.*— Copolymerization product with MMA was extracted with benzene for 30 hr., using a Soxlhet extractor. The benzene solution was poured into methanol to precipitate polymer I. The residue of the extraction was dissolved or swelled in dimethyl sulfoxide. It was then poured into warm water (about 50°C) to precipitate polymer II. As will be discussed below, it was assumed that polymer I was pure PMMA and that polymer II was a starch-PMMA graft copolymer.

The grafting efficiency and grafting ratio were computed as follows:

$$\text{Grafting efficiency} = \frac{\text{Wt. of vinyl polymer in grafts}}{\text{Total wt. of vinyl polymer formed}} \times 100$$

$$\text{Grafting ratio} = \frac{\text{Wt. of vinyl polymer in grafts}}{\text{Wt. of starch in grafts}}$$

The intrinsic voiscosities of PMMA and hydrolyzed graft copolymer were measured in benzene at 30°C.

Copolymerization Product with Vinyl Chloride. — Copolymerization product with vinyl chloride was

Table I. Polymerization procedure

Exp. No.	Oxi-starch g.	Monomer	ml.	Water ml.	Emulsifier* g.	Procedure
I	1	MMA	15	0	0	In sealed tube
II	1	MMA	5	60	0.15	In flask, under N_2 atmosphere
III	0.2**	MMA	3	15	0.08	In sealed tube
IV	1	AN	9	90	0	In flask, under N_2 atmosphere
V	1	VC	10	0	0	In sealed tube
VI	1	VC	4	15	0.1	In sealed tube

* "Emulgen-120", polyoxymethylene deriv.
** Starch deriv. See Table IX

extracted with tetrahydrofuran for 30 hr., using a Soxlhet extractor. The solution was poured into methanol to precipitate polymer III. The residue of the extraction was dissolved in dimethylsulfoxide and poured into warm water (about 50°C) to precipitate polymer IV. Polymers III and IV were assumed to be pure polyvinyl chloride and its graft copolymer respectively. The grafting efficiency and grafting ratio were computed according to the above equations. The intrinsic viscosities of polymer III and hydrolysed polymer IV were measured in a tetrahydrofuran solution at 30°C.

Acetylation of Graft Copolymer.—The acetylation of the graft copolymer of starch was carried out with acetic anhydride in pyridine, according to Pacsu's method[7]. The pyridine solution was poured into methanol to obtain the acetylated polymer. The infrared spectra of the resulting acetate no longer showed hydroxyl band.

Melting Points of Polymers.—An apparatus with a hot plate and a microscope (Shimadzu Seisakusho) was used for the measurement of the melting points of polymers.

Results and Discussion

Oxidation of Starch with Ozone.—During the oxidation with ozone in water, the oxidized starch was separated into water-soluble and water-insoluble parts. Figures 2 and 3 show the relationships between the contents of the peroxide group and the oxidation durations. The insoluble oxidized starch in water (abbr. as insoluble "oxi-starch-W") was used for syntheses of graft copolymers.

Oxi-starch-W was colored red purple with an iodine solution. Since the coloration of non-oxidized starch is blue, it was assumed that partial hydrolysis occured in the course of oxidation.

However, when ozonization was carried out in carbon tetrachloride, starch remained in-

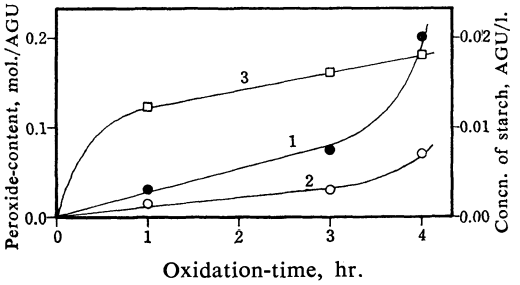


Fig. 2. Peroxide-content of soluble oxi-starch-W.

1 Determination by treating with KI solution at room temp. for 10 min.
2 Determination by treating with KI solution at 100°C for 3 min.
3 Concentration of starch

7) E. Pacsu and W. Mullen, *Ind. Eng. Chem.*, **34**, 1209 (1942).

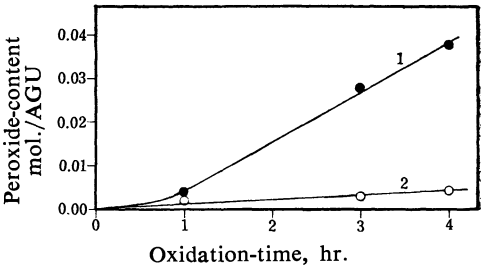


Fig. 3. Peroxide-content of insoluble oxi-starch-W.

1 Determination by treating with KI solution at room temp. for 10 min.
2 Determination by treating with KI solution at 70°C for 3 min.

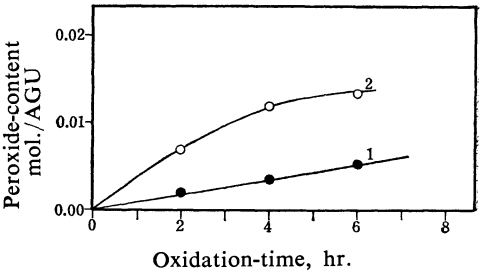


Fig. 4. Peroxide-content of oxi-starch-C.

1 Determination by treating at room temp. for 10 min.
2 Determination by treating at 100°C for 3 min.

soluble in the medium and was not hydrolyzed. This was abbreviated in "oxi-starch-C". Figure 4 shows the relationship between the contents of the peroxide group of oxi-starch-C and the oxidation time.

The figures for the contents of the peroxide group of oxi-starch-W, as determined by treating it at room temperature for 10 min., were higher than those determined by treating it at 70°C for 3 min. Conversely, the figures for the contents of the peroxide group of oxi-starch-C, as determined by treating it at room temperature for 10 min., were lower than those determined at 100°C for 3 min. During the oxidation, starch particles swelled in water but not in carbon tetrachloride. Accordingly, it was assumed that the swelled particles were oxidized more uniformly, and that the unswelled particles were oxidized only on the surface. The differences in the contents of peroxide group according to the temperature of determination may be explained by the consideration that the peroxide groups located within the strach particles were inactivated at a higher temperature, before potassium iodide molecules diffused to the reaction centers. The following determination of the peroxide group of oxi-starch was

TABLE II. BULK POLYMERIZATION OF MMA IN THE PRESENCE OF OXI-STARCH

Exp. No.	Polymerization: Oxi-starch: Type	Polymerization: Oxi-starch: Peroxy-content mol./AGU	Polymerization: Polymn. temp. °C	Polymerization: Polymn. time hr.	Polymers: Total yield g.	Polymers: Conversion %	Polymers: Homopolymer: Yield g.	Polymers: Homopolymer: [η]	Polymers: Graft: Yield g.	Polymers: Graft: Starch-cont. %	Polymers: Graft: [η]	Graft eff. %	Graft ratio
I-1	W	0.002	90	4	1.2631	5.6	0.3384		0.0060				
I-2	W	0.014	90	4	1.7521	16.0	0.9418		0.0069				
I-3	W	0.019	90	4	1.2958	6.3	0.3096		0.0070				
I-4	—	—	90	4	0.3638	7.7	0.3638						
I-5	C	0.0040	60	1	2.7593	37.4	1.6302	2.43	0.1374	2.9	2.43	7.5	33.4
I-6	C	0.0050	60	1	3.0026	42.6	1.9601	2.43	0.1028	2.9	2.43	4.9	33.4
I-7	—	—	60	1	0.0778	1.7	0.0778						
I-8	C	0.0040	60	2	3.7493	58.7	2.5737	3.17	0.1431	2.8	3.10	5.0	34.7
I-9	C	0.0050	60	2	3.8076	59.8	2.7858	2.57	0.0774	3.1	2.57	3.0	31.3
I-10	—	—	60	2	0.1230	2.6	0.1230						

Polymerization mixture: 1 g. of oxi-starch, and 15 ml. of MMA

TABLE III. EMULSION POLYMERIZATION OF PMMA IN THE PRESENCE OF OXI-STARCH

Exp. No.	Polymerization: Starch: Type	Polymerization: Starch: Peroxy-content mol./AGU	Polymerization: Polymn. temp. °C	Polymerization: Polymn. time hr.	Polymers: Yield g.	Polymers: Conversion %	Polymers: Homopolymer: Yield g.	Polymers: Homopolymer: [η]	Polymers: Graft copolymer: Yield	Polymers: Graft copolymer: Starch content %	Polymers: Graft copolymer: [η]	Polymers: Free starch %	Graft eff. %	Graft ratio
II-1	C	0.0024	90	3	4.877	82.3	1.712	2.60	1.960	6.0	2.90	87.0	57.0	15.7
II-2	C	0.0024	60	3	1.237	5.0	0.323	3.70	0.368	31.0	3.06	81.6	47.9	2.2
II-3	C	0.0024	30	3	0.992	0								
II-4	W	0.0016	90	3	5.121	87.7	1.299	3.45	2.590	4.0	4.75	88.5	68.5	24.0
II-5	W	0.0016	60	3	1.136	2.8	0.180							
II-6	W	0.0016	30	3	0.956	0								
II-7	N	—	90	3	1.7817	16.6	0.4746	5.10	1.110	63.7	6.20	29.2	39.3	0.6
II-8	N	—	60	3	1.0288	0.6								
II-9	N	—	30	3	0.9820	0								
II-10	—	—	90	3	0.4128	8.9	0.4128							
II-11	—	—	60	3	0.1630	3.5	0.1630							
II-12	—	—	30	3	0									

Polymerization mixture: Type of starch, C, W and N mean oxi-starch-C, oxi-starch-W and non oxidized starch, respectively. 5 ml. of MMA, 60 ml. of water, 0.15 g. of emulsifier and 1 g. of starch or the derivatives. In Expt. No. II-10, 11 and 12, starch was absent.

TABLE IV. SOLUBILITY OF ACETYLATED STARCH-PMMA GRAFT COPOLYMER

Solvent	Polymer			
	Starch	Acetyl-starch	PMMA	Acetyl-starch-PMMA graft
Tetrachloroethane	ins	s	ins	s
Pyridine	sw	s	ins	vs
Chloroform	ins	ss	s	vs
Dioxane	ins	ss	s	s
Dimethylsulfoxide	s	ss	ins	s
Acetone	ins	sw	s	vs
Tetrahydrofuran	ins	sw	s	s
Ethyl Acetate	ins	sw	s	s
Dimethy formamide	ins	sw	s	ss
Benzene	ins	sw	s	s
Methanol	ins	ins	ins	ins
Water	ss	ins	ins	ins

vs: very soluble; ss: slightly soluble; ins: insoluble; sw: swell

carried out by treating it at room temperature.

Figure 4 shows that oxi-starch was decomposed during the preservation at a different temperature. Oxi-starch-W was more stable than oxi-starch-C. The half life of oxi-starch-W was 4 and 12 days at 29 and 5°C respectively. That of oxi-starch-C was 4 days at 29°C.

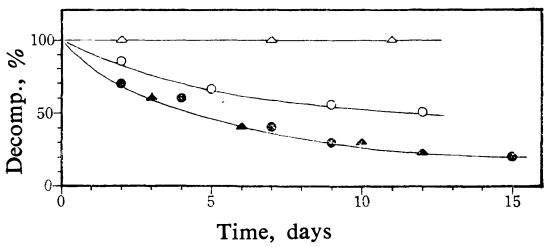


Fig. 5. Decomposition of peroxide group of oxi-starch.

△▲ Oxi-starch-C, peroxide-content 0.0023 mol./AGU
○● Oxi-starch-W, peroxide-content 0.0038 mol./AGU
△○ Preservation at 5°C
▲● Preservation at 29°C

Bulk Polymerization of MMA in the Presence of Oxi-Starch. — The results of the bulk copolymerization of MMA with oxi-starch, and of the fractionation of the products, are summarized in Table II. Polymer I was not colored by the iodine solution and was so assumed to be pure PMMA. Polymer II contained starch and was insoluble in most organic solvents. However, after hydrolysis in an acidic medium, the product dissolved in benzene. Polymer II was therefore assumed to be a starch-PMMA graft copolymer.

The polymerization of MMA initiated with oxi-starch gave a large amount of the homopolymer of PMMA and a small amount of grafted PMMA.

From this table, it can be seen that the intrinsic viscosities of grafted PMMA were slightly higher than those of free PMMA.

Emulsion Polymerization of MMA in the Presence of Oxi-Starch or Non-oxidized Starch. —The polymerization of MMA in the presence of oxi-starch was carried out in an aqueous emulsion. The results of the polymerization and of the fractionation of the products are summarized in Table III. At 90°C, the polymerization proceeded smoothly. The grafting efficiency and the grafting ratio were quite high. At 60°C, the graft copolymer was obtained.

The graft copolymer was insoluble in most organic solvents, but the acetylated graft copolymer dissolved in some solvents, as is shown in Table IV. It was also shown that its solubility lay between PMMA and starch triacetate. From this solubility, it was assumed that polymer II is a starch-PMMA graft copolymer.

The differences between the cases of oxi-starch-W and of oxi-starch-C were only with difficulty observed with regard to the conversion of MMA and the free starch content of the products. The degrees of polymerization of free PMMA and of grafted PMMA were the same. However, the grafting efficiency with oxi-starch-C was slightly higher than that with oxi-starch-W.

Unexpectedly, non-oxidized starch could initiate the polymerization of MMA to yield a graft copolymer in an aqueous emulsion state. It is clear from Table III that the initiation of polymerization is not due to the heat. However, in the absence of water, no initiation by starch itself as is shown in Table II, was observed. The results of the interesting

TABLE V. EMULSION POLYMERIZATION OF MMA IN THE PRESENCE OF STARCH OR THE DERIVATIVES

Exp. No.	Polymerization: Starch or the deriv.	Polymerization: Polymn. time hr.	Polymer: Total yield g.	Polymer: Conversion %	Polymer: Fractionation: PMMA g.	Polymer: Fractionation: Graft and starch deriv.	Graft. eff. %
III-1	—	3	0.1480	5.3			
III-2	—	3	0.2533	9.0			
III-3	—	3	0.2713	9.7			
III-4	—	4	0.3577	12.7			
III-5	Starch[a]	3	2.2760	73.9	1.0910	1.1850	47.4
III-6	Starch[a]	3	1.4670	45.1			
III-7	Starch refined[b]	3	1.2733	38.2			
III-8	Starch refined[b]	3	1.5469	48.0			
III-9	Soluble starch[c]	3	1.1164	32.6			
III-10	Soluble starch[c]	3	0.9475	26.6			
III-11	Starch-KI[d]	3	2.1924	71.0			
III-12	Heated starch[e]	3	0.9191	25.5	0.2597	0.6594	63.9
III-13	Heated starch[e]	3	0.8866	24.5			
III-14	Dialdehyde starch[f]	3	2.9438	97.7			
III-15	Maltose[g]	3	0.1762	6.3			
III-16	Maltose[h]	3	2.0099	64.2			
III-17	Maltose[h]	3	1.9693	70.0			
III-18	Maltose[i]	3	1.5056	53.8			
III-19	Maltose[j]	3	1.8149	64.8			
III-20	Sucrose[k]	3	0.1025	3.7			
III-21	Sucrose[k]	3	0.1132	4.0			
III-22	Glucose[l]	3	0.0723	2.6			
III-23	Glucose[l]	4	0.2381	8.5			

Polymerization mixture: 0.2 g. of starch or its deriv., 3 ml. of MMA, 15 ml. of water and 0.08 g. of emulsifier

a Potato starch, from Japanese Pharmacopeia
b Purified starch by reprecipitation from aqueous solution of starch (a) with ethanol
c Soluble starch from Merck Co.
d Starch (a) was immersed in 20% solution of KI for a day, and was filtered, washed and dried.
e Starch (a) was treated by heat in air at 150°C for 5 hr.
f Oxidized starch by $NaIO_4$
g Maltose, from Difco Co.
h Maltose, from Wako Pure Chemicals Co.
i Recrystallized maltose of maltose (h)
j Solid substance from mother liquor of the recrystallization of maltose (h)
k Cane sugar, commercial pure, purity 99.9%
l Glucose, from Wako Pure Chemicals Co.

TABLE VI. MELTING POINTS OF STARCH-PMMA GRAFT COPOLYMER

Exp. No.	Graft copolymer: Starch content %	Graft copolymer: $[\eta]$	Graft copolymer: M. p. °C	Hydrolysates* M. p. °C	Homopolymer: $[\eta]$	Homopolymer: M. p. °C	Acetates** M. p. °C
II-4	4.0	4.75	230~274	230~255	3.45	250~264	150~240
II-1	6.0	2.90	240~278	241~259	2.60	233~264	
II-2	31.0	3.06	265~280	235~255	3.70	235~255	
II-7	63.7	6.20	260~281		5.20	240~283	

Hydrolysates*: Hydrolysis product of the graft copolymer
Acetates** : Acetylation product of the graft copolymer

TABLE VII. POLYMERIZATION OF AN IN THE PRESENCE OF OXI-STARCH

Exp. No.	Polymerization: Starch Type[a]	Polymerization: Starch Peroxy-content mol./AGU	Polymerization: AN ml.	Polymerization: H_2O ml.	Polymerization product: Total yield g.	Polymerization product: Conversion %	Polymerization product: Starch-content %	Polymerization product: [η] of hydrolysates	Acetylated polymer: Insoluble in pyridine: Yield g.	Acetylated polymer: Insoluble in pyridine: Starch-content %	Acetylated polymer: Soluble in pyridine: Yield g.	Acetylated polymer: Soluble in pyridine: Starch-content %
IV-1	C	0.0031	9	90	2.0230	17.1	39.3	5.10	1.468	20.3	0.554	89.5
IV-2	N	—	9	90	0.9100	0.0						
IV-3	—	—	9	90	0.0	0.0						

Polymerization mixture: 9 ml. of AN, 90 ml. of water and 1 g. of starch
Polymerization temp., 90°C; Time, 1 hr.
a. C: Oxi-starch-C, N: Non oxidized starch

TABLE VIII. SOLUBILITY OF ACETYLATED STARCH-PAN GRAFT COPOLYMER

Solvent	Polymer: Starch triacetate	Polymer: Acetate*: Soluble part	Polymer: Acetate*: Insoluble part	Polymer: PAN
Tetrachloroethane	s	s	sw	ins
Pyridine	s	s	sw	ins
Chloroform	ss	ss	sw	ins
Dioxane	ss	sw	sw	ins
Dimethylsulfoxide	ss	sw	s	s
Acetone	sw	sw	sw	ins
Tetrahydrofuran	sw	sw	sw	ins
Ethyl acetate	sw	sw	sw	ins
Dimethylformamide	sw	sw	s	s
Benzene	sw	sw	sw	ins
Methanol	ins	ins	ins	ins
Water	ins	ins	ins	ins

* "Acetates" were separated to soluble and insoluble parts in pyridine.
s: soluble, ss: slightly soluble, sw: swell, ins: insoluble

graft-copolymerizations are tabulated in Table V.

Even starch treated with a solution of potassium iodide could initiate the polymerization of MMA. In this case, it is clear that starch had no peroxide group.

Dialdehyde starch, which was prepared by the oxidization of starch with periodic acid, could initiate the polymerization of MMA at a greatly increased rate. When starch was preheated, the rate of polymerization decreased. Glucose and purified maltose had no abilities to initiate the polymerization. However, when impure maltose was used, the polymerization of MMA started. Accordingly, the polymerization was initiated by some impurities existing in starch. The exact process still remains unexplained.

The melting points of starch-PMMA graft copolymers are shown in Table VI. They are slightly higher than the values of the homopolymer.

Polymerization of AN in the Presence of Oxi-Starch. — The polymerization of AN in the presence of oxi-starch was carried out in an aqueous suspension at 90°C. The results are shown in Table VII. The polymerization product dissolved with difficulty in most organic solvents. After its hydrolysis with 1 N hydrochloric acid at 95°C for 3 hr., a polymer soluble in dimethyl formamide was obtained. It contained no free starch.

After the acetylation of the polymerization product, it was separable into two parts: soluble and insoluble polymers in pyridine. The former was 89.5% starch, and the latter, 20.3% starch. It was assumed that the former was a mixture of PAN and starch acetate-PAN graft copolymers and that the latter was a mixture of starch acetate and a small number of the graft copolymers. The isolation of the graft copolymer was too difficult to accomplish. The solubilities of these polymers are shown in Table VIII.

No polymerization of AN by non-oxidized starch in an aqueous suspension was observed.

Polymerization of Vinyl Chloride (VC) in the Presence of Oxi-Starch. — The polymerization of VC in the presence of oxi-starch was carried out in bulk or in an aqueous

TABLE IX. POLYMERIZATION OF VC IN THE PRESENCE OF OXI-STARCH

Exp. No.	Polymerization: Starch: Type	Polymerization: Starch: Peroxy-content mol./AGU	Polymerization: VC ml.	Polymerization: H_2O ml.	Polymerization: Emulsifier g.	Polymerization: Time hr.	Polymer: Total yield g.	Polymer: Conversion %
V-1	C	0.0031	10	0	0	7	1.0145	0.2
V-2	C	0.0031	10	0	0	7	1.0050	0.1
V-3	N	—	10	0	0	7	0.9710	0
V-4	N	—	10	0	0	7	0.9580	0
V-5	—	—	10	0	0	7	0.0000	0
V-6	C	0.0031	4	15	0.1	2	1.6123	17.1
V-7	C	0.0031	4	15	0.1	2	1.6075	16.1
V-8	N	—	4	15	0.1	2	1.0483	0.9
V-9	—	—	4	15	0.1	2	0.0000	0

Exp. No.	Polymerization: Homopolymer: Yield g.	Polymerization: Homopolymer: $[\eta]$	Polymerization: Graft copolymer: Yield g.	Polymerization: Graft copolymer: Starch-content %	Polymerization: Free starch %	Grafting eff. %	Grafting ratio
V-6	0.520	0.49	0.321	67.6	78.0	23.5	0.5

Polymerization temp.: 60°C

emulsion, as is shown in Table IX. Only in aqueous emulsion was the polymerization observed. Polymer III did not contain starch and was assumed to be PVC. Polymer IV was 67.6% starch and was soluble in dimethyl sulfoxide. It was considered to be a starch-PVC graft copolymer. The degree of polymerization of PVC was lower. The grafting efficiency and the grafting ratio were lower than in the case of PMMA. The solubility of the graft copolymer is shown in Table X.

TABLE X. SOLUBILITY OF STARCH-PVC GRAFT COPOLYMER

Solvent	Polymer: Starch	Polymer: Graft	Polymer: PVC
Dimethylformamide	ins	sw	vs
Acetone	ins	sw	sw
Dimethylsulfoxide	s	s	s
Tetrahydrofuran	ins	ins	vs
Chloroform	ins	ins	ins
Dioxane	ins	ins	ins
Benzene	ins	ins	ins

vs: very soluble, s: soluble, sw: swell, ins: insoluble

Summary

1) Starch was oxidized with ozone in a medium of water or carbon tetrachloride to yield per-oxidized starch (abbreviated as oxi-starch-W or oxi-starch-C).

2) The stabilities of the peroxide-group of oxi-starchs were measured.

3) In the present of oxi-starch, polymerizations of methyl methacrylate (MMA), acrylonitrile (AN) and vinyl chloride were carried out. Graft copolymers of starch with vinyl polymers were obtained. Their properties were described.

4) It was confirmed that commercial starch, dialdehyde starch oxidized with periodic acid, starch treated with potassium iodide, and commercial maltose could also initiate the polymerization of methyl acrylate, yielding graft copolymers and vinyl homo-polymers.

Department of Applied Chemistry
Faculty of Engineering
Osaka City University
Kita-ku, Osaka

Infrared Absorption Spectra of Hydrazides. V. Oxal-, Malon- and Succin-Hydrazides

By Mitsuo MASHIMA

(Received August 11, 1962)

In a previous paper[1] the infrared frequencies characteristic of the $-CONHNH_2$ group have been reported on. The present investigation has aimed at obtaining further evidence about the characteristic frequencies of the $-CONHNH_2$ group. The infrared absorption spectra of oxal-, malon- and succin-hydrazides and their *N*-deuterated species in the solid state were examined in the rock salt region. For the sake of comparison, the infrared absorption spectra of hydrazioxlyl, hydrazimalonyl, hydrazisuccinyl and oxamide acide hydrazide were also examined. The results of these measurements are reported in this paper, and the frequencies characteristic of the $-CONHNH_2$ group are considered on the basis of these experimental results.

Experimental

Oxal-, malon- and succin-hydrazides were synthesized with ethyl esters of corresponding acids and hydrazine hydrate and were purified by recrystallization from ethanol (m. p., 236, 150, 167°C respectively). Oxamide acid hydrazide was synthesized by the reaction of oxalic acid ethylester amide and hydrazine hydrate and was purified by recrystallization from water (m. p., 220°C). Hydrazioxalyl and hydrazisuccinyl were synthesized by the reactions of oxal- and succin-hydrazides respectively, with sodium nitrite in the acetic acid solution. Hydrazimalonyl was prepared by heating malon-hydrazide with acetic acid. These compounds were purified by repeatedly washing the precipitates obtained with a quantity of ethanol; they were neither melted nor decomposed up to 280°C. The *N*-deuterated derivatives examined were prepared in sealed tubes in the presence of heavy water (99.8%), the excess of which was evaporated in a vacuum.

The infrared spectrophotometer used to obtaining the absorption spectra is an Hitachi infrared spectrophotometer Type EPI-2 with rock salt prisms. Potassium bromide disks were used to obtain the solid spectra.

Results and Discussion

Oxalhydrazide (OxH) and Oxamide Acid Hydrazide (OAH).—The infrared spectra of OxH, its *N*-deuterated species (OxH-d_6), and OAH are illustrated in Fig. 1. The absorption bands of these compounds were interpreted by comparison of the spectra with those of oxamide[2] and *NN'*-dimethyloxamide[3].

In the 3000 cm^{-1} region, oxamide* has two very strong bands, at 3363 and 3185 cm^{-1}, which have been ascribed to the asymmetric and symmetric NH_2 stretching vibrations. *NN'*-Dimethyloxamide[3] has a band at 3290 cm^{-1} which has been ascribed to the NH stretching vibration. OAH has three bands at 3340, 3250, and 3190 cm^{-1}. Of these three, the first and the third bands are very close in frequency to the two bands due to the NH_2 stretching vibrations for oxamide, while the second one is close in frequency to the ν(NH) band of *NN'*-dimethyloxamide. Therefore, the 3340 and 3190 cm^{-1} bands are probably to be ascribed to $\nu(NH_2)$, and the 3250 cm^{-1} band, to ν(NH).

OxH has a relatively sharp band at 3260 cm^{-1}, two broad bands at 3160 and 3000 cm^{-1}, and a shoulder band at 2780 cm^{-1}. These bands are probably due to $\nu(NH_2)$ and ν(NH), but further, detailed assignments of them are not easy. OxH-d_6 has two bands, at 2640 and 2300 cm^{-1}, which are due to $\nu(ND_2)$ or ν(ND).

The 1662 and 1606 cm^{-1} bands of OxH correspond in frequency, respectively, to the 1656 cm^{-1} band ascribed to the C=O stretching vibration and the 1608 cm^{-1} band ascribed to the NH_2 bending vibration for oxamide[2]. OxH-d_6 has a broad and intense absorption band with a centre near 1650 cm^{-1}; this band corresponds to the 1662 cm^{-1} band of OxH, the ratio of ν_H/ν_D being 1.01. The 1606 cm^{-1} band of OxH corresponds to the band at 1202 cm^{-1} for OxH-d_6, $\nu_H/\nu_D=1.336$. From these facts, the 1662 and 1606 cm^{-1} bands can surely be ascribed to the C=O stretching and the NH_2 bending vibrations respectively. These assignments are also supported by the fact that *NN'*-dimethyloxamide[3] has an amide I band at 1658 cm^{-1}, while the compound has

1) M. Mashima, This Bulletin, 35, 1882 (1962).

2) a) J. A. Scott, Jr. and E. L. Wagner, *J. Chem. Phys.*, 30, 465 (1959); see also b) T. Miyazawa, *J. Chem. Soc. Japan, Pure Chem. Sec.* (*Nippon Kagaku Zassi*), 75, 86 (1954).

3) T. Miyazawa, ibid., 76, 1018 (1955).

* The infrared frequencies of this compound are taken from the data published by J. A. Scott, Jr. and E. L. Wagner (Ref. 2a).

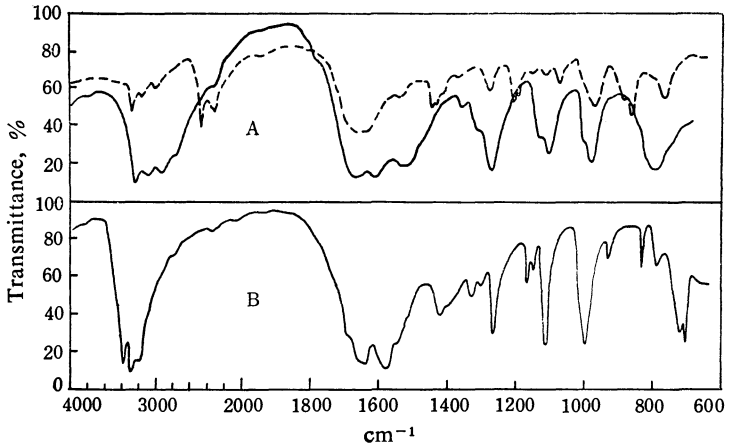


Fig. 1. Infrared absorption spectra of oxalhydrazide (curves A's) and oxamide acid hydrazides (curve B). Of the curves A's the dashed curve indicates the spectrum of *N*-deuterated specy of oxalhydrazide.

no band corresponding to the 1606 cm^{-1} band of OxH. On the other hand, OAH shows rather different absorptions in this region; i. e., it has two intense bands, at 1637 and 1583 cm^{-1}, both of which are associated with a shoulder band, at 1684 and 1532 cm^{-1} respectively. These bands are probably due to the C=O stretching and NH_2 bending vibrations, but detailed interpretations of them are not easy.

The 1522 cm^{-1} band of OxH has its counterpart at 1440 cm^{-1} in the OxH-d spectrum, the value of ν_H/ν_D being 1.057. These two bands are, respectively, very close in frequency to the amide II band at 1532 cm^{-1} for *NN'*-dimethyloxamide[3] and the amide II' band at 1445 cm^{-1} for its *N*-deuterated specy[3]. In consequence, the 1522 cm^{-1} and 1440 cm^{-1} bands can surely be taken as the amide II and amide II' bands respectively. In this region, oxamide[2] has no band corresponding to the amide II band, while the compound has a 1348 cm^{-1} band which has been ascribed to the C–N stretching vibration. For OAH, the 1417 and 1326 cm^{-1} bands can also be ascribed to the C–N stretching vibrations, but the assignments are not certain.

In the 1300~900 cm^{-1} range, OxH has three bands, at 1267, 1097 and 973 cm^{-1}, which correspond in frequency to the bands at 1261, 1107 and 991 cm^{-1} respectively for OAH. The three bands of OxH are apparently weakened on *N*-deuteration; they correspond, respectively, to the bands at 1067, 966 and 858 cm^{-1} for OxH-d_6. They are, therefore, due to the NH_2 or NH deformation vibrations. For OxH, the band at 1307 cm^{-1} corresponds to the band at 1108 cm^{-1} for OxH-d_6. OAH also has a band at 1296 cm^{-1}. For monoacid hydrazides, the present author has obtained three frequencies due to the NH_2 deformation vibrations, e. g., 1347, 1105 and 1009 cm^{-1} for cyanoacetylhydrazine[1]. Consequently, the bands at 1307, 1097 and 973 cm^{-1} for OxH and 1296, 1107 and 991 cm^{-1} for OAH are taken as characteristic of the $-CONHNH_2$ group. The 1267 cm^{-1} (for OxH) and 1261 cm^{-1} (for OAH) bands are close in frequency to the amide III band at 1239 cm^{-1} for *NN'*-dimethyloxamide[3]. They will, therefore, be taken as the amide III band.

OxH has a strong band at 792 cm^{-1} which has not yet been accounted for. This band shifts to 757 cm^{-1} on *N*-deuteration. OAH has a band with two peaks (713 and 702 cm^{-1}); this band corresponds to the 792 cm^{-1} band for OxH. *NN'*-Dimethyloxamide[3] has an amide IV band at 765 cm^{-1}, the frequency value of which is close to that of the 792 cm^{-1} band for OxH. Therefore, the 792 cm^{-1} band of OxH will be taken as an amide IV band. On the other hand, oxamide[2] has a 629 cm^{-1} band which has been ascribed to the in-plane N–C=O deformation vibration. For OAH the appearance of two peaks, 713 and 702 cm^{-1}, will depend on the reduced symmetry of the molecule.

The 1124 cm^{-1} band of OxH has its counterpart at 1146 cm^{-1} in the OxH-d_6 spectrum. OAH also has corresponding bands at 1159 and 1144 cm^{-1}. They are probably dut to the N–N stretching vibration, but the assignments are not sure. OxH has more two weak bands, at 834 and 815 cm^{-1}, while no band corresponding to them has been found for OxH-d_6 in the region examined here. These two bands correspond in frequency to the bands at 824 and 783 cm^{-1} of OAH, but these can

TABLE I. INFRARED FREQUENCIES OF OXALHYDRAZIDE AND OXAMIDE ACID HYDRAZIDE (in cm^{-1})

Assignment[a]	Oxamide[b]	*NN'*-Dimethyloxamide[c]	Oxamide acid hydrazide	Oxalhydrazide	Its *N*-deuterated specy
$\nu_{as}(NH_2)$	3363	—	3340 (vs)		
ν(NH)	—	3290	3250 (vs)	3260 (s)	
$\nu_s(NH_2)$	3185	—	3190 (vs)	3160 (s) 3000 (s) 2780 (sh)	
$\nu(ND_2)$ or ν(ND)					2640 (s) 2300 (s)
Amide I	1656	1658	1684 (sh) 1637 (vs)	1662 (vs)	1650 (b vs)
$\beta(NH_2)$ or $\beta(ND_2)$	1608	—	1583 (vs)	1606 (s)	1202 (m)
Amide II (or II')	—	1532	1532 (sh)	1522 (s)	1440 (s)
ν(C-N)	1348	—	1417 (m) 1326 (m)		
$NH_2(ND_2)$ def.	—	—	1296 (w)	1307 (m)	1108 (w)
Amide III, III'	—	1239	1261 (s)	1267 (s)	1067 (w)
ν(N-N)	—	—	1159 (w) 1144 (w)	1124 (w)	1146 (vw)
$NH_2(ND_2)$ def.	—	—	1107 (s)	1097 (m)	966 (s)
$NH_2(ND_2)$ def.	792	—	991 (s)	973 (s)	858 (s)
ν(C-C)	—	—	925 (w) 824 (w) 783 (w)	 834 (sh) 815 (sh)	
Amide IV (O=C-N def.)	629	765	713 (s) 702 (s)	792 (s)	757 (m)

a ν and β denote stretching and bending vibrations respectively
b See Ref. 2
c See Ref. 3

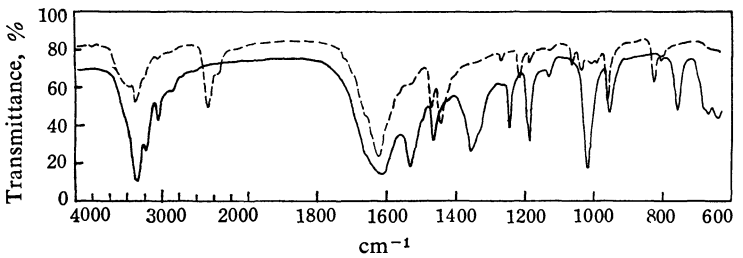


Fig. 2. Infrared absorption spectra of succinhydrazide (solid curve) and its *N*-deuterated specy (dashed curve).

not be interpreted with confidence. For OAH a weak band at 925 cm^{-1} is probably to be attributed to the C-C stretching vibration, which is infrared active because of the asymmetric character of the molecule.

The observed frequencies for OxH and OAH and their tentative assignments are summarized in Table I, in which the infrared frequencies of oxamide and *NN'*-dimethyloxamide are also represented for the sake of comparison.

Succinhydrazide (SH).—For this compound the frequencies characteristic of the $-CONHNH_2$ group were rather easily obtained. The solid spectra of SH and its *N*-deuterated specy (SH-d_6) are illustrated in Fig. 2, and the tentative assignments of the absorption bands are given in Table II.

In the 3000 cm^{-1} region, SH has three strong or moderately strong bands, at 3270, 3160 and 3030 cm^{-1}, all of which are apparently weakened on *N*-deuteration. Their counterparts are found at 2440 and 2340 cm^{-1} in the SH-d_6 spectrum. They can, therefore, be ascribed to NH_2 or NH stretching vibrations. Since an SH molecule has a hydrazine residue, it can reasonably be expected that three bands due to the N-H bond stretching vibrations appear in this region. However, detailed assignments of the observed bands are impossible on the basis of present observations only.

Next, we will concern ourselves with the location of the CH_2 deformation vibrations. For $X-XH_2-CH_2-X$ type molecules, Nakagawa[4]

4) I. Nakagawa, *J. Chem. Soc. Japan, Pure Chem. Sec.* (*Nippon Kagaku Zassi*), **77**, 602 (1956).

Table II. Infrared frequencies of SH and SH-d_6 in the rock salt region (in cm^{-1})

Assignment	SH	SH-d_6
$\nu(NH_2)$ or $\nu(NH)$	3270 (s) 3160 (m) 3030 (m)	
$\nu(ND_2)$ or $\nu(ND)$		2440 (s) 2340 (m)
Amide I or $\beta(NH_2)$	1624 (vs)	1620 (vs)
Amide II (II')	1528 (s)	1441 (s)
$\beta(CH_2)$	1462 (m)	1466 (m)
NH_2 deformation	1353 (s) 1328 (sh)	
$\omega(CH_2)$	1258 (m)	1265 (w)
Amide III	1240 (m)	
$\beta(ND_2)$		1212 (m)
NH_2 deformation	1181 (s)	
$\tau(CH_2)$	1126 (w)	1128 (vw)
ND_2 deformation or Amide III'		1059 (w) 1032 (w)
NH_2 deformation	1012 (s)	
ν(C-C)	948 (m)	957 (m)
ND_2 deformation		820 (m)
$\gamma(CH_2)$	800 (vw)	798 (w)
Amide IV ?	751 (m) 674 (sh) 662 (m) 638 (m)	

ν; stretching, β; bending, ω; wagging, τ; twisting, γ; rocking

has obtained the following ranges for the CH_2 deformation frequencies; 1400~1450 cm^{-1} for bending, 1200~1350 cm^{-1} for wagging, 1050~1250 cm^{-1} for twisting, and 700~1000 cm^{-1} for rocking. For SH, the band at 1462 cm^{-1} is near the range for CH_2 bending vibrations, and its value of frequency is scarcely changed on *N*-deuteration. In consequence, it may be assigned to the CH_2 bending vibration. The band at 1258 cm^{-1} corresponds to the band at 1265 cm^{-1} of SH-d_6 and they both fall in the range for the CH_2 wagging vibrations; accordingly, they are assigned to the CH_2 wagging vibration. SH has a further weak band at 1126 cm^{-1} which is scarcely changed in frequency on *N*-deuteration and which falls in the range for the CH_2 twisting vibrations. Thus, the 1126 cm^{-1} band may be assigned to the CH_2 twisting vibration. The weak band at 800 cm^{-1}, which also is scarcely changed in frequency on *N*-deuteration, falls in the range for the CH_2 rocking vibration. Consequently, the 800 cm^{-1} band is assigned to the CH_2 rocking vibration. However, SH has a further band falling in the 700~1000 cm^{-1} range. This is the band at 948 cm^{-1}, which is also scarcely changed in frequency on *N*-deuteration. Although the 948 cm^{-1} band is tentatively assigned to the C–C stretching vibration, an alternative assignment (to the CH_2 rocking vibration) is also possible.

Let us now consider the location of vibrations relating to the $-CONHNH_2$ group. This group contains the –CONH– group, so the amide I, II, III and IV bands may be expected to appear in the region examined here. In fact, very strong band at 1624 cm^{-1} is surely assigned to amide I because it corresponds in frequency and intensity to the band at 1620 cm^{-1} of SH-d_6. SH has a band at 1528 cm^{-1} which can easily be assigned to the amide II band. This assignment is supported by the observation that SH-d_6 has a corresponding band (amide II') at 1441 cm^{-1}, the ratio of ν_H/ν_D being 1.060. The amide III band is expected to appear near 1300 cm^{-1}, but its identification will be considered with those of the bands due to the NH_2 deformation vibrations. SH apparently shows absorptions below 700 cm^{-1} and the amide IV band will apparently appear near 700 cm^{-1}, but no definite evidence can be observed in the spectra of SH-d_6 in the region examined here.

In the 700 to 1700 cm^{-1} region, five absorption bands (with the exception of the amide I and II bands) have been found for some monoacid hydrazides; these have been taken as characteristic of the $-CONHNH_2$ group[1]; e. g., for cyanoacetylhydrazine they have been observed at 1625, 1347, 1258, 1105 and 1009 cm^{-1}. Of these five the first band has been ascribed to the NH_2 bending vibration. For SH no band corresponding to it is observed because of its location near the amide I band at 1624 cm^{-1}, while SH-d_6 has a band at 1212 cm^{-1} which is probably due to the ND_2 bending vibration. SH has bands corresponding to the latter four at 1353, 1240, 1181 and 1012 cm^{-1}, all of which disappear on *N*-deuteration. The 1258 cm^{-1} band of cyanoacetylhydrazine has been taken as the amide III band; accordingly, the 1240 cm^{-1} band of SH can be assigned similarly. In the SH-d_6 spectrum, the counterpart of the 1012 cm^{-1} band is easily found at 820 cm^{-1} ($\nu_H/\nu_D=1.234$), but definite identifications of the counterparts of the other three are not easy. SH-d_6 has a further two bands at 1059 and 1032 cm^{-1} which are not present in the SH spectrum. These two bands probably correspond to two of the bands at 1353, 1240 and 1181 cm^{-1} for SH.

Malonhydrazide (MH). — The absorption spectra of MH and its *N*-deuterated specy (MH-d_6) are illustrated in Fig. 3. The obserevd frequencies of MH and MH-d_6 and their tentative assignments are summarized in Table III.

In the 3000 cm^{-1} region, a strong band at 3290 cm^{-1} and two moderately strong bands

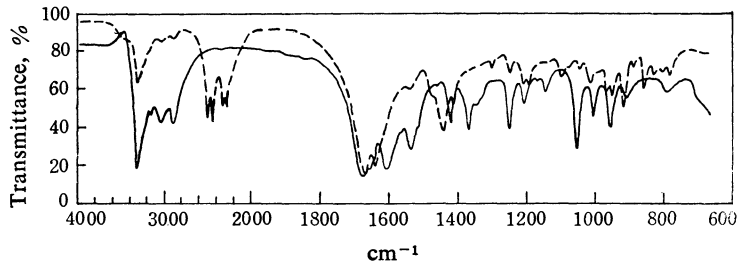


Fig. 3. Infrared absorption spectra of malonhydrazide (solid curve) and its *N*-deuterated specy (dashed curve) in the rock salt region.

at 3020 and 2870 cm^{-1} are found for MH. For MH-d_6 two doublet bands are found at 2480 and 2430 cm^{-1} and at 2310 and 2260 cm^{-1}. They are probably due to NH_2 (ND_2) or NH(ND) stretching vibrations; more detailed assignments are difficult on the basis of present observations only.

MH has two very strong bands at 1669 cm^{-1} (accompanied by two ill-defined shoulder bands on the lower frequency side) and 1602 cm^{-1}. The two bands correspond to the bands at 1664 and 1636 cm^{-1} for MH-d_6 and are taken as amide I bands. The appearance of two bands taken as amide I bands is due to coupling two vibrations which are localized mainly on two C=O bonds. Although the NH_2 bending vibration is also expected to give rise to bands near 1600 cm^{-1}, definite identification is impossible because of its location near the amide I band. For MH-d_6, the band at 1189 cm^{-1} is probably to be ascribed to the ND_2 bending vibration. The 1532 cm^{-1} band of MH shifts to 1435 cm^{-1} (ν_H/ν_D= 1.068) on *N*-deuteration; it may be taken as an amide II band. For monoacid hydrazides[1], an amide III band has been observed near 1250 cm^{-1}. MH has a band at 1247 cm^{-1} which shifts to 1036 cm^{-1} on *N*-deuteration (ν_H/ν_D=1.203) and which hence may be taken as an amide III band.

Let us next consider the locations of the NH_2 deformation vibrations other than the bending one already accounted for. For monoacid hydrazides[1] such vibrations have been observed near 1300, 1150 and 1000 cm^{-1}. MH has three bands, at 1365 (accompanied by a shoulder band on its lower frequency side), 1139 and 1051 cm^{-1}. All these three disappear on *N*-deuteration; their counterparts are found at 1093, 962 and 918 cm^{-1} in the MH-d_6 spectrum, the values of ν_H/ν_D being 1.249, 1.184 and 1.145 respectively. They may, therefore, be ascribed to the NH_2 deformation vibrations.

In the region examined here, the CH_2 deformation vibrations are also expected to give rise to bands. For them Nakagawa[5] has obtained the ranges of 1350~1450 cm^{-1} (bending), 1100~1350 cm^{-1} (wagging), 1000~1250 cm^{-1} (twisting) and 700~1000 cm^{-1} (rocking) for the molecules of the CH_2XY type. MH has corresponding bands at 1418, 1202, 1002 and 785 cm^{-1}. None of these four is greatly changed in frequency on *N*-deuteration; i.e., MH-d_6 has the four bands at 1408, 1203, 1008 and 775 cm^{-1}. In consequence, they may easily be ascribed to the CH_2 bending, wagging, twisting and rocking vibrations respectively.

TABLE III. INFRARED FREQUENCIES OF MH AND MH-d_6 (in cm^{-1})

Assignment	MH	MH-d_6
$\nu(NH_2)$ or ν(NH)	3290 (vs)	
	3210 (sh)	
	3020 (m)	
	2870 (m)	
$\nu(ND_2)$ or ν(ND)		2480 (s)
		2430 (s)
		2310 (s)
		2260 (s)
Amide I	1669 (vs)	1664 (vs)
	1602 (s)	1636 (vs)
Amide II (II′)	1532 (s)	1435 (s)
$\beta(CH_2)$	1418 (m)	1408 (m)
NH_2 deformation	1365 (m)	
	1340 (sh)	
Amide III (III′)	1247 (m)	1036 (w)
$\omega(CH_2)$	1202 (w)	1203 (w)
$\beta(ND_2)$		1189 (m)
NH_2 deformation	1139 (w)	
ND_2 deformation		1093 (w)
		1072 (sh)
NH_2 deformation	1051 (s)	
$\tau(CH_2)$	1002 (m)	1008 (w)
ND_2 deformation		962 (w)
ν(C-C)	952 (m)	948 (m)
	903 (w)	850 (m)
ND_2 deformation		918 (m)
$\gamma(CH_2)$	785 (w)	775 (w)

ν; stretching, β; bending, ω; wagging, τ; twisting, γ; rocking

5) I. Nakagawa, ibid., **76**, 540 (1955).

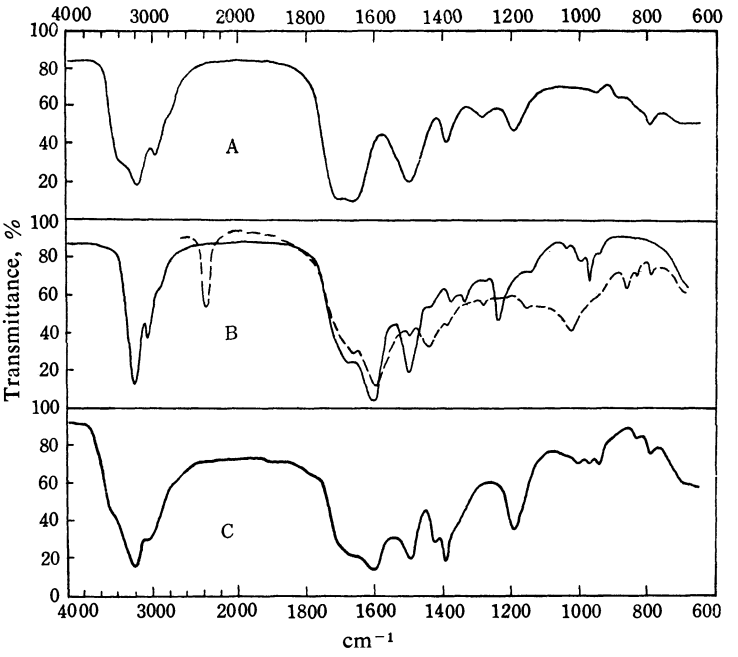


Fig. 4. Infrared absorption spectra of hydrazioxalyl (curve A), hydrazimalonyl (curves B's), and hydrazisuccinyl (curve C). Of the curves B's the dashed curve indicates the spectrum of *N*-deuterated specy of hydrazimalonyl.

For MH, two bands, at 952 and 903 cm^{-1}, are not yet accounted for. In the MH-d_6 spectrum, the former has its counterpart at 948 cm^{-1}, but the band corresponding to the latter can not be identified because of its location on the sloping background of the more intense band at 918 cm^{-1}. MH-d_6 has a rather stronger band at 850 cm^{-1}. These are probably due to the C–C stretching vibrations.

Hydrazioxalyl (HO), $(C_2H_2O_2N_2)_x$, Hydrazimalonyl (HM), $(C_3H_4O_2N_2)_x$ and Hydrazisuccinyl (HS), $(C_4H_6O_2N_2)_x$. — The solid spectra of these compounds are illustrated in Fig. 4. For HM the absorption spectrum of its *N*-deuterated specy (HM-d_2) was also examined. The so-called amide bands were identified without difficulty.

For HM, two, very strong bands are found at 1662 and 1593 cm^{-1} which correspond in intensity to the bands at 1655 and 1590 cm^{-1} for HM-d_2. The two bands, therefore, may easily be taken as amide I bands; corresponding bands are found at 1655 and 1590 cm^{-1} for HS and at 1705 and 1656 cm^{-1} for HO.

HM has a strong band at 1486 cm^{-1} which shifts to 1432 cm^{-1} on *N*-deuteration, ν_H/ν_D= 1.038. The corresponding band is found at 1492 cm^{-1} for HO and 1485 cm^{-1} for HS. In consequence, they may surely be taken as amide II bands.

The amide III band is also expected to appear in the region examined here. For HM, the band at 1230 cm^{-1} shifts to 1009 cm^{-1} on *N*-deuteration, ν_H/ν_D=1.219. This band corresponds to the 1185 cm^{-1} band for HO and the 1184 cm^{-1} band for HS; these are taken as amide III bands.

For all these compounds, a strong band is found near 3160 cm^{-1}; this band is probably due to the NH stretching vibration.

The present author[6] has obtained the frequencies characteristic of the –CONHNHCO– group of some diacid hydrazides; e. g., formylacetylhydrazine in the solid state absorbs at 3020 and 3200 cm^{-1} (NH stretching), 1580 and 1613 cm^{-1} (amide I), 1483 cm^{-1} (amide II), and 1232 and 1279 cm^{-1} (amide III). In the present study, bands similar to these were obtained for HO, HM and HS as is summarized in Table IV.

Characteristic Frequencies. — Oxal-, malon- and succin-hydrazide show the frequencies characteristic of the $-CONHNH_2$ group, as

Table IV. Frequencies characteristic of HO, HM and HS (in cm^{-1})

	HO	HM	HS
ν(NH)	3160	3160	3170
Amide I	1656, 1705	1593, 1662	1590, 1655
Amide II	1492	1486	1485
Amide III	1185	1230	1184

6) M. Mashima, This Bulletin, 35, 423 (1962).

summarized in Table V. The characteristic frequencies of HO, HM and HS are represented in Table IV.

Amide Bands.—In the 600~1800 cm^{-1} region mono-substituted amides[7] usually show the following bands characteristic of the trans-planar –CONH– group; the amide I band ca. 1650 cm^{-1}, the amide II band ca. 1550 cm^{-1}, the amide III band in the 1200~1300 cm^{-1} range, and the amide IV band ca. 760 or 630 cm^{-1}. As may be seen from Table V*, the –CONH– group contained in the $-CONHNH_2$ group also exhibits the characteristic bands indicated above.

On the other hand, *NN'*-diacid hydrazides[6] show amide I, II and III bands having rather low frequency values. Further, two values of frequencies have been obtained for the amide I and III bands. In the present study also, amide bands of rather low frequencies were obtained for HO, HM and HS, while two frequency values were obtained for the amide I band, as may be seen from the Table IV. The spectroscopic evidence, therefore, suggests that the –CONHNHCO– group of HO, HM and HS has a structure similar to that of *NN'*-diacidhydrazides. The presence of two frequencies, taken as amide I bands, is probably due to the coupling of two vibrations which are localized mainly on the C=O group, as was postulated in an earlier paper[6].

TABLE V. CHARACTERISTIC FREQUENCIES OF THE $-CONHNH_2$ GROUP

	Oxal-hydrazide	Malon-hydrazide	Succin-hydrazide
Amide I	1662	1669	(1624)*
Amide II	1522	1532	1528
Amide III	1267	1247	1240
Amide IV	792	—	670
$\nu(NH_2)$ or $\nu(NH)$	3260 3160 3000	3290 3210 3020	3270 3160 3030
NH_2 deformation	1606	1602	(1624)*
NH_2 deformation	1307	1365	1353
NH_2 deformation	1097	1139	1181
NH_2 deformation	973	1051	1012

* For these see the Table II

NH_2 Deformation Absorptions. — For some aliphatic acid hydrazides[1], four frequencies characteristic of the $-CONHNH_2$ group have been obtained, in addition to the amide I, II, and III absorptions and the $\nu(HN_2)$ or $\nu(NH)$ absorptions. The highest one of the four was found ca. 1630 cm^{-1} and the second highest one in the 1260~1350 cm^{-1} range. The other two bands were observed ca. 1150 and ca. 1000 cm^{-1}. In the present study for dicarboxylic acid hydrazides, bands corresponding to them were obtained (cf. Table V), while HO, HM and HS have no band corresponding to them. Thus, they may surely be taken as the characteristic frequencies of the $-CONHNH_2$ group. They are probably due to the NH_2 deformation vibrations, but, of course, no definite assignments can be made without a theoretical investigation of the normal vibrations.

The author is grateful to Professor Sunao Imanishi of Kyushu University for his generous permission to use the University's spectrophotometer. He is also indebted to the Ministry of Education for its financial support.

Department of Literature and Science
Saga University
Saga-city Saga

7) T. Miyazawa, T. Shimanouchi and S. Mizushima, *J. Chem. Phys.*, **24**, 408 (1956).
* See also Ref. 1.

$\Delta^{9(10)}$-Octal-1-one and its Molecular Compound[1]

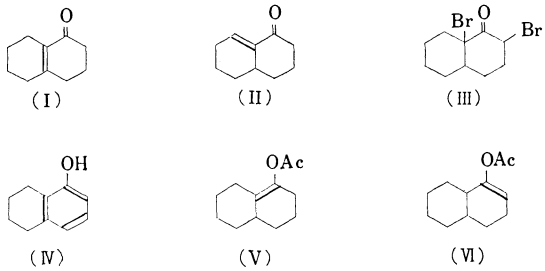
By Akira SUZUKI* and Takeshi MATSUMOTO

(Received August 16, 1962)

In the course of a study on the synthesis of a certain diterpenoid[2] the authors stood in need of the synthesis of $\Delta^{2(3)}$-octal-1-one from decal-1-one. It is well known that the bromination of 6-ketocholestanyl acetate[3] at low temperature gives a 5-bromo-derivative, which is converted into an isomeric 7-bromoketone on heating in acetic acid containing hydrogen bromide. Although there have been few papers[4] reporting the bromination of decal-1-one at the time this work was initiated, the authors attempted to synthesize $\Delta^{2(3)}$-octal-1-one through bromination of *trans*-decal-1-one, followed by conversion of thus obtained 9-bromo-derivative into 2-bromo-isomer, and then by dehydrobromination.

The reaction of *trans*-decal-1-one with an equivalent of bromine in chloroform at low temperature led to a mixture of bromoketones, from which a dibromodecalone, melting at 94~95°C and being designated as " dibromide ", was isolated. The yield of dibromoketone depended upon the rate of addition of bromine. The NMR spectrum (40 Mc.) of a mixture of bromoketones contained resonance lines centered at 5.41τ[5] attributable to the hydrogen atom at the C_2 position of 2-bromodecal-1-ones. It was, however, found that the quantity of 2-bromo-derivatives was several per cent by the estimation of the relative peak area. At the time such results were ascertained, Zimmerman and Mais[6] reported that the monobromination product of *trans*-decal-1-one in acetic acid containing hydrogen bromide at low temperature consists of ca. 80% of 9-bromodecalones (cis and trans) and ca. 20% of 2-bromo-isomers.

The crude bromination product, which appeared to be chiefly composed of 9-bromodecalones, was treated with hydrogen bromide in acetic acid solution, but the isomerization shown in 6-ketocholestanyl acetate[3] could not be effected. The first attempt to synthesize $\Delta^{2(3)}$-octal-1-one from *trans*-decal-1-one was thus unsuccessful. However, the dehydrobromination product of bromodecalones described above is expected to be either $\Delta^{8(9)}$-octal-1-one (II) or $\Delta^{9(10)}$-octal-1-one (I). The literature describes[7-23] a variety of reactions leading to an octal-1-one, to which usually the structure I is assigned.



Although the chemical properties of this substance were in accord with structure I, the observation[13] that the compound exhibited an ultraviolet absorption maximum at 243 mμ led Campbell and Harris to assign structure II to this octalone. The present authors therefore undertook the elucidation of the structure of the unsaturated ketone, which is also a

* Present address: Chemical Process Engineering Department, Faculty of Engineering, Hokkaido University, Sapporo.

1) Read in part before the 14th Annual Meeting of the Chemical Society of Japan, Tokyo, April, 1961.
2) T. Matsumoto and A. Suzuki, This Bulletin, **34**, 274 (1961).
3) I. M. Heilbron, E. R. H. Jones and F. S. Spring, *J. Chem. Soc.*, **1937**, 801.
4) F. Galinovsky, *Ber.*, **76**, 230 (1943).
5) H. Conroy and R. A. Raphael's " Advances in Organic Chemistry, Methods and Results ", Vol. II, Interscience Publishers, Inc., New York (1960), pp. 287—291.
6) H. E. Zimmerman and A. Mais, *J. Am. Chem. Soc.*, **81**, 3644 (1959).
7) W. Hückel, R. Danneel, A. Schwartz and A. Gercke, *Ann.*, **474**, 121 (1929).
8) W. Hückel and M. Blohm, ibid., **502**, 114 (1933).
9) W. Hückel and H. Naab, ibid., **502**, 136 (1933).
10) J. W. Cook and C. A. Lawrence, *J. Chem. Soc.*, **1935**, 1637.
11) J. W. Cook and C. A. Lawrence, ibid., **1937**, 817.
12) C. D. Nenitzescu and V. Przemetzky, *Ber.*, **74**, 676 (1941).
13) W. P. Campbell and G. C. Harris, *J. Am. Chem. Soc.*, **63**, 2721 (1941).
14) G. C. Harris, ibid., **64**, 720 (1942).
15) A. J. Birch, *J. Chem. Soc.*, **1944**, 430.
16) A. J. Birch, A. R. Murray and H. Smith, ibid., **1951**, 1945.
17) M. I. Bowman, C. C. Ketterer and A. U. Chamberlain, *J. Org. Chem.*, **18**, 905 (1953).
18) A. S. Dreiding and R. J. Pratt, *J. Am. Chem. Soc.*, **75**, 3717 (1953).
19) A. L. Wilds and N. A. Nelson, ibid., **75**, 5360 (1953).
20) K. Schenker and V. Prelog, *Helv. Chim. Acta*, **36**, 896 (1953).
21) R. K. Hill and R. T. Conley, *Chem. & Ind.*, **1956**, 1314.
22) R. K. Hill and R. T. Conley, *J. Am. Chem. Soc.*, **82**, 645 (1960).
23) M. F. Ansell and J. W. Ducker, *J. Chem. Soc.*, **1960**, 5219.

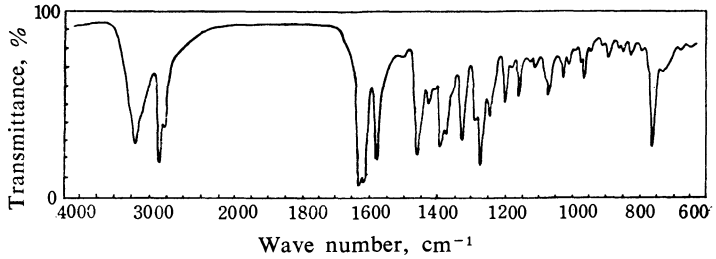


Fig. 1. Infrared spectrum of "solid octalone" (KBr Tablet).

possible intermediate for the synthesis of certain diterpenes. The crude 9-bromodecalones, previously described, could be converted into an octalone, b. p. 133~136°C/14 mmHg, by thermal dehydrobromination at 145°C; the octalone was tentatively named "liquid octalone". The identity of this product with that described in the literature was established by conversion to the 2, 4-dinitrophenylhydrazone, oxime, and semicarbazone. At the same time, there could be obtained a crystalline compound which had m. p. 58~59°C and was designated as "solid octalone". The latter compound afforded the same 2, 4-dinitrophenylhydrazone, oxime and semicarbazone as the those from "liquid octalone". The authors supposed at this stage that though the chemical and physical properties of "liquid octalone" are similar to the octalone which was previously reported[7-23], the "solid octalone" is a purer sample. Contrary to expectation, the elemental composition of the latter compound corresponded to $(C_{10}H_{13}O)_n$ rather than to that of the expected octalone, $C_{10}H_{14}O$ (see Experimental). Moreover, the infrared spectrum of the "solid octalone" (Fig. 1.) exhibited absorption bands at 3200, 1637, 1623, 1587 and 760 cm^{-1}. These bands suggest presence of a hydroxyl group and aromatic ring.

That the octal-1-one afforded the corresponding 2, 4-dinitrophenylhydrazone in a quantitative yield, was described by Campbell and Harris[13]. The "solid octalone", however, could only afford the same derivative in about a 50% yield.

From the above results, the authors next supposed that the "solid octalone" was a molecular compound of the octalone I or II, and a phenolic substance, perhaps, 5, 6, 7, 8-tetrahydronaphth-1-ol, because the presence of 2, 9-dibromodeca-1-one in the reaction mixture of the bromination of *trans*-decalone was indicated, as will be shown later. The obtained experimental data seem to support this assumption, which can be summarized as follows:

(1) The elemental composition completely agrees with that of the molecular complex $C_{20}H_{26}O_2 (=C_{10}H_{14}O+C_{10}H_{12}O)$.

(2) In the infrared spectrum, the bands at 1587 and 760 cm^{-1} correspond to aromatic ring, 1637 cm^{-1} to the conjugated carbonyl group, 1623 cm^{-1} to a conjugated double bond, and 3200 cm^{-1} to the bonded hydroxyl group.

(3) The "solid octalone" affords the same 2, 4-dinitrophenylhydrazone, oxime and semicarbazone obtained from the "liquid octalone" which is regarded as the octalone I or II.

(4) The yield of the 2, 4-dinitrophenylhydrazone is about 50%.

(5) Furthermore, through the aid of NMR spectroscopy, the "solid octalone" was suggested to be a molecular compound consisting of hydronaphthol V and octalone I rather than II. The absorption spectrum[24] (Fig. 2) is roughly divided into two parts, at a low and high applied magnetic field. The former, part A, is characteristic of proton resonance for aromatic, vinyl, and phenolic hydroxyl hydrogens[25], and the latter, part B, for other alicyclic hydrogens[25]. The intensity ratio between parts A and B, I_A/I_B which is given by the area ratio, is 5.3. The calculation value is 5.5 for the molecular compound made up of IV and I, while it is 4.2 for that composed of IV and II.

In hope confirming the structure, the authors next attempted the separation of components. After chromatography on alumina, there could

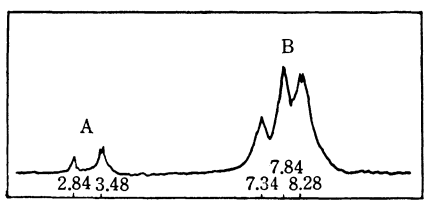


Fig. 2. The NMR spectrum of "solid octalone" in CCl_4.

24) The NMR spectra were taken on a Varian 40 Mc. instrument at Tohoku University through the courtesy of Prof. Genjiro Hazato, Drs. Tsuneo Ikenoue and Kensuke Takahashi, to whom the authors are pleased to express their sincere thanks.

25) H. S. Gutowsky, D. S. McCall, B. R. McGarvey and L. H. Meyer, *J. Am. Chem. Soc.*, **74**, 4809 (1952); L. M. Jackman, "Applications of Nuclear Magnetic Resonance Spectroscopy in Organic Chemistry", Pergamon Press, London (1959), pp. 50—71; see also Ref. 5.

be quantitatively isolated from the "solid octalone", a crystalline compound, m. p. 70~71°C and a liquid fraction. The former compound was characterized, as expected, as 5, 6, 7, 8-tetrahydronaphth-1-ol (V) and the latter compound as the "liquid octalone" by comparison with authentic sample. Conversely, the "solid octalone" could be obtained by mixing the two components in the proportion of one to one in mole.

Next, the authors discuss the structure of the "liquid octalone". The ultraviolet spectrum shows a maximum at 245 mμ (ε 12000) (lit., House and Thompson[29], 245.5 mμ (ε 12400); Campbell and Harris[13], 243 mμ (ε 11000)) characteristic of an α,β-unsaturated ketone. The basis on which Campbell and Harris[13] considered the structure to be octalone II, is that the maximum at 243 mμ falls within the range (234 to 244 mμ) which was shown by Woodward[26] to be characteristic of α,β-unsaturated ketones having one hydrogen on the doubly bound carbon atoms, and the only octal-1-one which meets this requirement is the $\Delta^{8(9)}$-derivative II. However, according to Woodward's calculation rule[26,27] for ultraviolet spectrum, the most probable maximum for $\Delta^{9(10)}$-octalone I ought to be situated at about 247 mμ[28]. Further evidence, therefore, is needed before a definite decision between the 8, 9 and 9, 10 positions of the double bond can be made. In the present work, the question was solved by the aid of NMR spectroscopic method. The NMR spectrum (40 Mc.) of the "liquid octalone" exhibited no absorption below 7 τ. It has been therefore confirmed that the structure of the "liquid octalone" is $\Delta^{9(10)}$-octal-1-one (I). Recently, the same result had been reported by House and Thompson[29]. Consequently the "solid octalone" is the molecular compound of I and 5, 6, 7, 8-tetrahydronaphth-1-ol (IV).

Moreover, the dibromodecalone, m. p. 94~95°C, which was previously named "dibromide", is probably 2, 9-dibromodecal-1-one (III) for the reason that the bromide, on heating with collidine, gives 5, 6, 7, 8-tetrahydronaphth-1-ol (IV). The "dibromide" appears to correspond to a dibromodecalone reported by Galinovsky[4] and by Zimmerman and Mais[6]. The infrared spectrum of III showed an absorption at 1726 cm^{-1} characteristic of carbonyl vibration, whereas that of parent decal-1-one at 1705 cm^{-1}. Considering Corey's observation[30] for α,α'-dibromocyclohexanone derivative, this wave number between the two ketones indicates that one bromine atom is axial and the other is equatorial in the dibromodecalone III. Further evidence, however, is necessary for determination of the complete stereochemistry.

In order to introduce a functional group only at the 2 position of decal-1-one, the authors next undertook to prepare the enol acetate VI. The reaction of *cis*-decal-1-one with acetic anhydride in the presence of *p*-toluenesulfonic acid was reported by Zimmerman and Mais[6] to yield an enol acetate. However, that the enol acetate prepared from *trans*-decal-1-one by tehir method has no absorption below 7τ in the NMR spectrum, has been ascertained in the course of the present work[31]. The product therefore may be regarded as practically pure $\Delta^{1(9)}$-enol acetate V.

Experimental[32]

By the procedure of Johnson[33], *trans*-decal-1-one was prepared. The infrared spectrum of the decalone differed markedly from that of the cis compound[6]. For example, at 950 cm^{-1}, where the former showed a minimum, the latter exhibited a maximum. Conversely, at 907 cm^{-1}, *cis*-decalone had a minimum while trans-isomer showed a maximum. It was found through the infrared analysis that the decalone prepared in the above manner is an almost pure trans compound.

Bromination of *trans*-Decal-1-one.—A solution of 30.0 g. (0.2 mol.) of *trans*-decalone in 100 ml. of chloroform was kept at −20 to −10°C while a solution of 32.0 g. (0.2 mol.) of bromine in 100 ml. of chloroform was added dropwise with stirring over a period of 3 hr. The resulting solution was further stirred for 2 hr. under cooling and then washed successively with water, aqueous sodium bicarbonate, and saturated aqueous sodium chloride. After the organic layer was dried over anhydrous sodium sulfate and concentrated under reduced pressure at room temperature, 45.0 g. of crude 9-bromodecalone was obtained.

In the case of rapid addition of bromine to chloroform, the "dibromide" III was obtained. For example, 10.4 g. (0.065 mol.) of bromine in 30 ml. of chloroform was added to the decalone, 10.0 g. (0.065 mol.) in 30 ml. of chloroform for 20 min. After the reaction mixture was treated by the procedure described above, removal of the solvent in vacuo left an oily residue from which

26) R. B. Woodward, *J. Am. Chem. Soc.*, **63**, 1123 (1941).
27) R. B. Woodward, ibid., **64**, 76 (1942).
28) According to Fieser's modified calculation rule, this value is 249 mμ. L. F. Fieser and M. Fieser, "Steroids", Reinhold Publishing Co., New York (1959), p. 19.
29) H. O. House and H. W. Thompson, *J. Org. Chem.*, **26**, 3729 (1961).
30) E. J. Corey, *J. Am. Chem. Soc.*, **75**, 3297 (1953).
31) Independently, House and Thompson also obtained the same conclusion. See Ref. 29.
32) All melting and boiling points are uncorrected. Unless otherwise specified, infrared spectra were taken on a Koken model DS-301 infrared spectrophotometer with sodium chloride optics. Ultraviolet spectra were measured in 95% ethanol solution by means of a Beckman model DK-2 spectrophotometer. The authors are indebted to Mr. K. Narita for microanalysis.
33) W. S. Johnson, *J. Am. Chem. Soc.*, **65**, 1322 (1943).

on cooling 1.0 g. of crystalline material, m. p. 88～93°C, was obtained. The sample for analysis was prepared by recrystallization from petroleum ether (b. p. 30～60°C) ; it had m. p. 94～95°C, IR(KBr) 1726 cm^{-1} (ketone group).

Found: C, 38.96; H, 4.66. Calcd. for $C_{10}H_{14}OBr_2$: C, 38.73; H, 4.64%.

Thermal Dehydrobromination of 9-Bromodecal-1-one.—The crude 9-bromodecalone, 45.0 g., was heated at 145°C under slightly reduced pressure (ca. 85 mmHg) for 2 hr. and then cooled. Distillation of the residue gave 13.5 g. of "liquid octalone" and 2.0 g. of "solid octalone".

"Liquid Octalone", Namely $\Delta^{9(10)}$-Octal-1-one (I).—This ketone has the following physical properties; b. p. 133～136°C/14 mmHg (lit., ca. 140°C/9 mmHg[10]), 127～128°C/10 mmHg[13]), 134～136°C/13 mmHg[16]), 85～92°C/3 mmHg[17]), 60～70°C/0.3 mmHg[23]), n_D^{25} 1.5234 (lit., n_D^{14} 1.4996[10]), n_D 1.4931[23]), n_D^{25} 1.5267[29]). The material had infrared absorption bands at 1660 (conjugated C=O) and 1632 cm^{-1} (cojugated C=C). The NMR spectrum in carbon tetrachloride solution has a series of partially resolved bands in the region 7.5 to 8.6 τ with no absorption attributable to a vinyl hydrogen atom.

Found: C, 80.24; H. 9.45. Calcd. for $C_{10}H_{14}O$: C, 79.95; H 9.39%.

Reaction of a sample of the ketone with 2, 4-dinitrophenyl hydrazine yielded, after several recrystallizations from *n*-butyl alcohol dark red needles, m. p. 263°C decomp. (lit., m. p. 262°C[16]), 266.5～267.5°C[17]), 268°C[19]), 264～266°C[20]), 264.5～265.5°C[22]), 271～272°C[23]), 266～266.5°C[29]).

Found: C, 58.10; H, 5.31. Calcd. for $C_{16}H_{18}O_4N_4$: C, 58.17; H, 5.49%.

The melting point of the semicarbazone which was recrystallized from ethanol as colorless plates, was 240°C decomp. (lit., m. p. 242～243°C[11]), 241～242°C[13,17]), 246～247°C[23]).

Found: C, 63.64; H, 8.00. Calcd. for $C_{11}H_{17}ON_3$: C, 63.74; H, 8.27%.

The oxime of I, recrystallized from methanol, was colorless needles, melted at 147.5～128°C (lit., 144～145°C[10]), 146～147°C[13]), 148～149°C[23]).

Found: C, 72.37; H, 9.15. Calcd. for $C_{10}H_{15}ON$: C, 72.69; H, 9.15%.

"Solid Octalone", viz. Molecular Compound of 5, 6, 7, 8-Tetrahydronaphth-1-ol (IV) and $\Delta^{9(10)}$-Octal-1-one (I).—The complex, distilled at 145～147°C/14 mmHg, crystallized after standing at room temperature. Recrystallization from petroleum ether (b. p. 30～60°C) gave a pure sample as colorless needles, m. p. 58～59°C.

Found: C, 80.61, 80.72, 80.40, 80.57; H, 8.78, 8.88, 8.94, 9.01. Calcd. for $C_{20}H_{26}O$(=$C_{10}H_{12}O$+$C_{10}H_{14}O$) : C, 80.49; H, 8.78%.

Ultraviolet absorption bands (Fig. 3) were found at 246 mμ (ε 7160), and infrared absorption bands (Fig. 1) at 3200 (phenolic OH), 1637 (conjugated C=O), 1623 (conjugated C=C), and 1587 cm^{-1} (aromatic ring). The NMR spectrum was reproduced in Fig. 2.

Separation of Each Component from the Molecular Compound by Chromatography.—Two hundred milligrams of the molecular compound was chromatographed on alumina (10 g.) packed and washed with ether. Forty fractions were collected as in the following table.

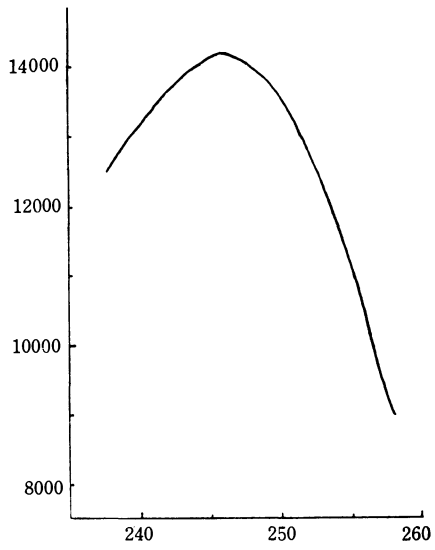


Fig. 3

Fraction No.	Eluant	Residue
1—10	Ether; 50 ml.	Colorless oil, 95 mg.
11—40	Ether; 150 ml.	Colorless crystal, 102 mg. m. p. 65～68°C

The colorless liquid, $n_D^{25.7}$ 1.5270, was identified by comparison of infrared spectra with $\Delta^{9(10)}$-octal-1-one (I). The colorless crystal afforded a pure sample by recrystallization from petroleum ether (b. p. 30～60°C), m. p. 70～71°C.

Found: C, 80.93; H, 8.02. Calcd. for $C_{10}H_{12}O$: C, 81.04; H, 8.16%.

The latter compound was characterized as 5, 6, 7, 8-tetrahydronaphth-1-ol (V) on the basis of mixed melting point determination with the authentic sample prepared by Papa's procedure[34]).

Conversely, the molecular compound was yielded by mixing an equivalent amount of the former component with the latter. The identity of these two complex compounds was proved by melting and mixed melting point determinations.

Dehydrobromination of 2, 9-Dibromodecal-1-one (III) with Collidine.—A mixture of 100 mg. of the dibromodecalone (III) and 5 ml. of collidine was heated at 150°C for 20 min. under a nitrogen atmosphere. The resulting mixture was diluted with 6 N hydrochloric acid and then extracted with ether. The ether extracts were washed successively with 2 N hydrochloric acid, 5% aqueous sodium bicarbonate and water, and dried over anhydrous sodium sulfate. The solution was concentrated in vacuo to leave a pale brown oil, which on trituration with petroleum ether completely crystallized. Upon recrystallization from petroleum ether, it

34) D. Papa, E. Schwenk and B. Whitman, *J. Org. Chem.* 7, 587 (1942).

formed colorless needles, m. p. 70~71°C. This compound was confirmed to be 5, 6, 7, 8-tetrahydronaphth-1-ol (IV) by the observation of mixed melting point with an authentic sample.

Preparation of the Enol acetate (V).—A mixture of 6.0 g. of *trans*-decal-1-one, 1.3 g. of *p*-toluenesulfonic acid and 150 ml. of acetic anhydride was heated under reflux in such a way that the acetic acid formed was allowed to distil from the reaction mixture. After 7 hr. 1.24 g. of anhydrous potassium acetate was added and the excess of acetic anhydride was almost completely evaporated under reduced pressure. The residue was cooled, diluted with benzene and washed successively with water, 5% aqueous sodium bicarbonate and water. The organic layer was concentrated and distilled to give 6.1 g. of enol acetate as a colorless liquid, b. p. 60~65°C/0.7 mmHg (lit., b. p. 63~66°C/0.75 mmHg[6], 68~79°C/0.6 mmHg[29]).

Found: C, 74.42; H, 9.30. Calcd. for $C_{12}H_{18}O_2$: C, 74.19; H, 9.34%.

IR (film) 1751 (C=O stretching) and 1217 cm^{-1} (C−O stretching).

According to the report by House and Thompson [29], the enol acetate fraction prepared by a similar method was a mixture of $\Delta^{1(9)}$-enol acetate (V) (90%), *trans*-$\Delta^{1(2)}$-enol acetate (VI) (5%), and a component believed to be the *cis*-$\Delta^{1(2)}$-enol acetate. The product in the present experiment, however, has no absorption below 7τ in the NMR spectrum and may be regarded as practically pure $\Delta^{1(9)}$-enol acetate (V).

Department of Chemistry
Faculty of Science
Hokkaido University
Sapporo

Studies on the Chemical Decomposition of Simple Sugars. XIII. Separation of the So-called Glutose (a 3-Ketohexose)

By Akira SERA

(Received August 3, 1962)

In 1895 Lobry de Bruyn and Alberda van Ekenstein[1] found that glucose, when treated with a dilute alkaline solution, gave a equilibrium mixture containing original glucose, mannose, and fructose. This isomerization of reducing sugars is well known as the Lobry de Bruyn-Alberda van Ekenstein transformation[2,3]. Through this transformation, all of the known reducing sugars and some non-carbohydrate substances such as α-hydroxy-ketones and -aldehydes have been converted into their epimers or diastereomers through the action of inorganic or organic bases, or, in some cases, enzymes.

According to present thinking[2,3], this classical transformation is base-catalysed; it has usually been supposed to proceed through an enolization which gives rise to an 1, 2-enediol or enediolate anion intermediate. The 1, 2-enediol or enediolate anion so produced may either revert to the starting aldose (i. e., glucose), be converted into the epimeric aldose (i. e., mannose), or be further transformed to the corresponding ketose (i. e., fructose).

The transformation, however, may further proceed and, if so, the 2, 3-enediol or enediolate anion can be produced; this is probably converted into the corresponding 2-ketoses (i. e., fructose and allulose) or 3-ketohexoses. Lobry de Bruyn and Alberda van Ekenstein[1] could separate an unfermentable, reducing substance from the equilibrium mixture which was produced by the action of alkalis on glucose or fructose. They mistakenly considered allulose to be a fermentable sugar, so they described the unfermentable, reducing substance as a 3-ketose and named it "glutose", though they did not provide any supporting experimental evidence.

Their unfermentable, reducing substance was imagined to be the same as the unfermentable portion of cane molasses. Goto[4] prepared an osazone from the unfermentable, reducing substance obtained from invert sugar by the action of dibasic sodium phosphate. After repeated fractional recrystallization, he obtained; osazone A, m. p. 172~176°C* (163

1) C. A. Lobry de Bruyn and W. Alberda van Ekenstein, *Rec. trav. chim.*, **14**, 203 (1895); **15**, 92 (1896), **16**, 257, 262, 274, 282 (1897), **18**, 72 (1899).

2) J. C. Speck, Jr., "Advances in Carbohydrate Chemistry", **13**, 63 (1958).

3) R. L. Whistler and J. N. BeMiller, ibid., **13**, 289 (1958).

4) R. Goto, Graduation Thesis, Kyoto Univ. (1931) unpublished.

* Further recrystallization gave osazones: A_1, m. p. 178~180°C and A_2, m. p., 185~186°C.

parts); osazone B, m. p. 190~194°C (325 parts; after recrystallization, m. p. 193~194°C); and others (about 170 parts). He also considered that the so-called "glutose" was not 3-keto-hexose but a more complex mixture which was produced from sugar by means of rearrangements, dehydrations, decompositions and polymerizations. Sattler and Zarban[5] observed that the "glutose" from fructose was a mixture of fructose anhydride and difructose dianhydride.

In accordance with the research program in our laboratory on the decomposition of simple sugars, the separation of "glutosazone" has been investigated. When D-glucose was treated with oxygen-free saturated lime-water, an unfermentable, reducing substance was obtained (about 11%); the osazone of this, prepared in the usual way, melted at 194°C. The "glutosazone" from cane molasses* also melted at 192~193°C. With liquid chromatography by silica-gel-Celite (5 : 1, wt./wt.), using petroleum ether (40~70°C) as a developer, the osazone of m. p. 194°C was separated into 3 parts. From the top zone D-glucosazone (m. p., 207~208°C) and from the lower zone methylglyoxal bisphenylhydrazone (m. p. and mixed m. p., 152°C) were isolated. The composition of these two was 37 : 1 in a typical run. The middle zone contained a trace of an unidentified substance. From these results, it is claimed that the so-called "glutosazone" is substantially glucosazone contaminated with among other things, methylglyoxal bisphenylhydrazone; this is consistent with the results of Sattler and Zarban[5].

Experimental

Preparation of the Unfermentable, Reducing Substance.—Thirty grams of D-glucose was dissolved in oxygen-free, saturated lime-water (100 ml.), and the solution (initial pH 10.0) was allowed to stand or to boil gently. After 22 hr. at room temperature, the solution turned yellow in color and the pH value of the solution fell to 9.2. The solution was neutralized with 0.1 N oxalic acid, and the precipitated calcium oxalate was filtered off with the aid of Celite**. Then the filtrate was diluted with distilled water to about 600 ml. To this aqueous solution (pH 7.15), 90 g. of baker's yeast*** was added, and the mixture was kept in an incubator at 30°C. After 72 hr. the yeast was removed by filtration, and the filtrate was neutralized with dilute sodium hydroxide and freed from protein by the addition of a slight exess of lead acetate solution. After filtration, the filtrate was bubbled with hydrogen sulfide gas to remove any dissolved lead salt. The precipitate was filtered and the filtrate was concentrated under reduced pressure at 40~50°C to about 100 ml. of syrup. To this syrup, an equal volume of alcohol was added, and the mixture was heated on a water bath for 15 min., whereupon the flocculent precipitate appeared. After filtration, the filtrate was concentrated as above. After this purification process with alcohol had been repeated three times, the resulting filtrate was decolorized with active carbon and concentrated under reduced pressure at 40~50°C to a syrup.

This syrup was freed from water by repeated azeotropic distillation by adding a benzene-alcohol mixture. The syrup obtained was slight yellow in color and was not fermented by baker's yeast; yield, 3.5 g. With repeated reprecipitations of this syrup from methanol-acetone, a light yellow, hygroscopic solid was obtained. The reducing power of this unfermentable substance was 10.3% of that of D-fructose (Fehling's solution).

Treatment of the unfermentable, reducing substance with phenylhydrazine hydrochloride and sodium acetate, under the usual conditions, produced a yellow osazone which melted at 148~152°C when crude. After three recrystallizations from aqueous alcohol, yellow crystals were obtained; m. p., 194°C.

Found: N, 15.8%. Calcd. for $C_{18}H_{22}O_4N_4$: N, 15.6%.

Many authors have reported on the melting points of the so-called "glutosazone": 194~195[5], 165[1,5], 207[6] and 163~166°C[7].

Chromatographic Separation of the So-called "Glutosazone".—A portion of "glutosazone" (720 mg.) was dissolved in a minimum volume of ethanol, and the solution was placed at the top of a chromatographic column (2.6×30 cm.) in which acid-washed silica gel-Celite (5 : 1, wt./wt.) had been packed. The development was carried on with petroleum ether (40~70°C) until the separation of the yellow zones was complete. The content was extruded, and each zone was cut and extracted with boiling ethanol. The solvent was distilled off, and the residual crystalline mass was weighed, and recrystallized from aqueous ethanol. The results obtained are shown in Table I.

Table I. Chromatographic separation of "glutosazone"

No.	Zone	Wt., mg.	Remark
1	Top	630	D-Glucosazone, m. p. 208~209°C*
2	Middle	trace	Orange yellow powder
3	Lower	17	Methylglyoxal bisphenylhydrazone, yellow crystal; m. p. and mixed m. p., 152°C*,**

* Recrystallized from aqueous ethanol.
** Found: N, 22.0%. Calcd. for $C_{15}H_{16}N_4$: N, 22.2%.

* Research laboratory, Taito Co. Ltd., Odawara. Japan.
5) L. Sattler and F. W. Zarban, *Ind. Eng. Chem.*, 37, 1133 (1945).
** Johns-Manville Co., New York, N. Y.
*** Kaneka No. 2612409, Kanegahuti Chem. Ind. Co., Ltd.
6) H. A. Spoehr et al., *J. Biol. Chem.*, 85, 305 (1929).
7) H. A. Spoehr and P. C. Wilbur, ibid., 69. 421 (1926).

The author wishes to express his thanks to Professor Ryozo Goto for his kind guidance and encouragement throughout the course of the present work, and also to Mr. Shiro Fujimoto, Taito Co., Ltd., for supplying a sample of cane molasses.

Institute of Chemistry
Faculty of Science
Kyoto University
Sakyo-ku, Kyoto

*Studies on the Chemical Decomposition of Simple Sugars. XIV. 3-Xylulose (a 3-Ketopentose)**

By Akira SERA

(Received August 24, 1962)

In a previous communication, the present author has shown that so-called "glutosazone" is not an osazone of 3-ketose but is substantially glucosazone contaminated by a small amount of methylglyoxal bisphenylhydrazone and other substances. On the other hand, D-allulose[1], DL- and D-sorbose[2,3] had been obtained from D-glucose (or from D-fructose) by the action of bases. Although the production of these sugars indicates that the transformation** of carbohydrates may proceed through 2, 3- or 3, 4-enediol intermediates under suitable conditions, no 3-ketose is isolated from any transformation mixture. The absence of a 3-ketose in a mixture obtained from hexose by means of this transformation suggests that a 3-ketose or its equivalents are unstable under the conditions employed and are converted into the corresponding 2-ketoses.

Recently, attempts to prepare a 3-ketose have been carried out by many authors. Jones[4] obtained 2-*O*-methyl-L-*xylo*-3-hexulose from an L-ascorbic acid derivative. Sugihara and Yuen[5,6] oxidized 3-*O*-benzoyl-1, 2; 5, 6-di-*O*-isopropylidene-D-mannitol and 6-*O*-benzoyl-1, 2; 4, 5-di-*O*-isopropylidene-DL-galactitol with chromium trioxide and obtained 4-*O*-benzoyl-1, 2; 5, 6-di-*O*-isopropylidene-D-*arabo*-3-hexulose and 6-*O*-benzoyl-1, 2; 4, 5-di-*O*-isopropylidene-DL-*xylo*-3-hexulose respectively. After the protecting substituents had been removed, the former gave a mixture of ketoses produced via an enediol intermediate during the debenzoylation procedure. The latter, however, gave a crystalline DL-*xylo*-3-hexulose after saponification of a benzoyl group followed by hydrolysis of isopropylidene groups. Schaffer[7] prepared D-manno-3-heptulose from 3-*O*-formyl-D-*glycero*-D-*talo*heptitol. From the products formed on the oxidation of ribitol with mercuric acetate, Stoodley[8] isolated *erythro*-3-pentulose in addition to D-*threo*- and D-*erythro*-2-pentulose.

In the biological field, some 3-ketoses are produced from suitable precursors. Thus, *Acetobacter suboxydans* transforms L-fucitol into 1-deoxy-D-*xylo*-3-hexulose[9]. D-Ribose-5-phosphate, when incubated with a mouse spleen extract, gave a mixture of phosphorylated pentoses. From the dephosphorylated pentose mixture, Ashwell and Hickman[10] isolated a small amount of *erythro*-3-pentulose besides D-*threo*- and D-*erythro*-2-pentulose.

In the present paper, a new synthesis of 3-xylulose and related preliminary examinations are described. The synthesis of 3-xylulose resulted in success in the following manners.

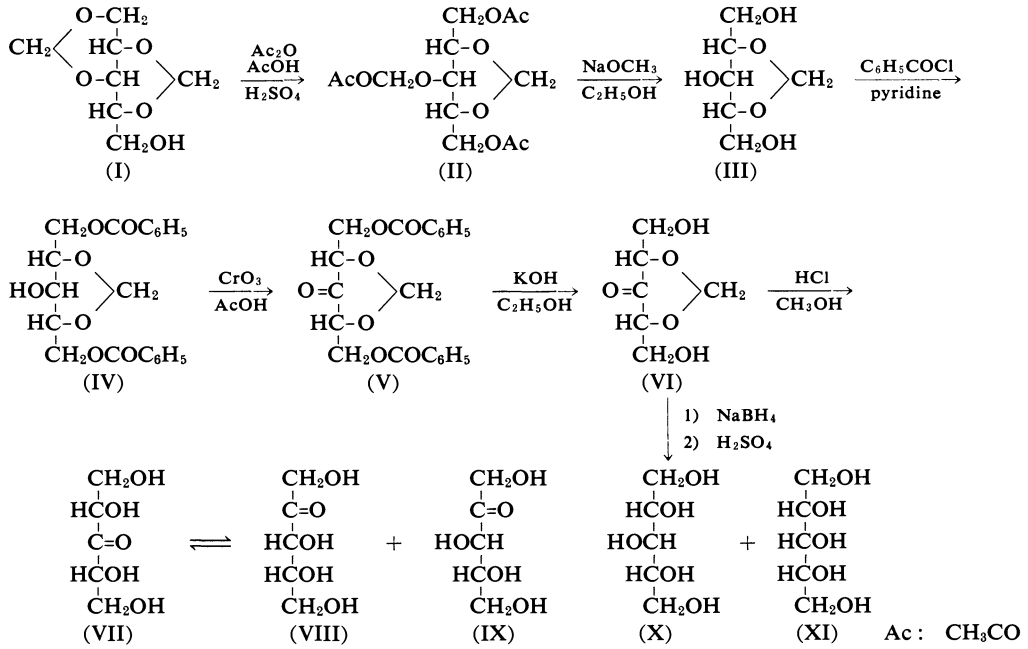
Results and Discussion

The oxidation of a secondary hydroxyl group to a carbonyl group may be realized by using a variety of agents. However, in the presence

* Presented at the 15th Annual Meeting of the Chemical Society of Japan, Kyoto, April, 1962.

** Lobry de Bruyn-Alberda van Ekenstein transformation; C. A. Lobry de Bruyn and W. Alberda van Ekenstein, *Rec. trav. chim.*, **14**, 156, 203 (1895) **15**, 92 (1896); **16**, 241, 257, 262, 274, 282 (1897); **18**, 72, 147 (1899); **19**, 1 (1900); J. C. Speck, Jr., "Advances in Carbohydrate Chemistry", **13**, 63 (1958).

1) L. Hough et al., *J. Chem. Soc.*, **1953**, 2005.
2) M. G. Blair and J. C. Sowden, *J. Am. Chem. Soc.*, **77**, 3323 (1955).
3) M. L. Wolfrom and J. N. Schumacher, ibid., **77**, 3318 (1955).
4) J. K. N. Jones, ibid., **78**, 2855 (1956).
5) J. M. Sugihara and G. U. Yuen, ibid., **79**, 5780 (1957).
6) G. U. Yuen and J. M. Sugihara, *J. Org. Chem.*, **26**, 1598 (1961).
7) R. Schaffer, *J. Am. Chem. Soc.*, **81**, 2838 (1959).
8) R. J. Stoodley, *Can. J. Chem.*, **39**, 2593 (1961).
9) The first recorded 3-ketose. L. E. Stewart et al., *J. Am. Chem. Soc.*, **72**, 4934 (1950).
10) G. Ashwell and J. Hickman, ibid., **77**, 1062 (1955).



of acid- and base-sensitive groups in the starting material, chromium trioxide in pyridine or acetic acid is the most suitable oxidant. For preparing 3-ketose from polyol, the hydroxyl groups attached at other carbons than carbon 3 in polyol must be protected by suitable substituents (i. e., isopropylidene, benzylidene, methylene, and/or ester groupings); then the remaining free hydroxyl group on carbon 3 may be oxidized with chromium trioxide. After the protecting groups have been removed, the oxidized polyol may give an unsubstituted 3-ketose. α-Ketol, however, when dissolved in an alkaline solution in the presence of oxygen, gives acidic products produced by autoxidation[11] and carbon chain fission. In the case of the synthesis of 3-ketoses, the products are easily transformed through an enediol intermediate (Lobry de Bruyn—Alberda van Ekenstein transformation) into a mixture of ketoses through the action of alkalis.

The behavior of some acetoxyketones as model compounds in a dilute alkaline solution are shown in Fig. 1. As is shown α-ketols were autoxidized easily, even in a dilute solution (such as 0.05 N) in the presence of oxygen. Furthermore, α, α'-diacetoxyketones gave the corresponding dicarbonyl derivatives in an alkaline solution in accordance with the β-hydroxy-carbonyl elimination mechanism[12,13].

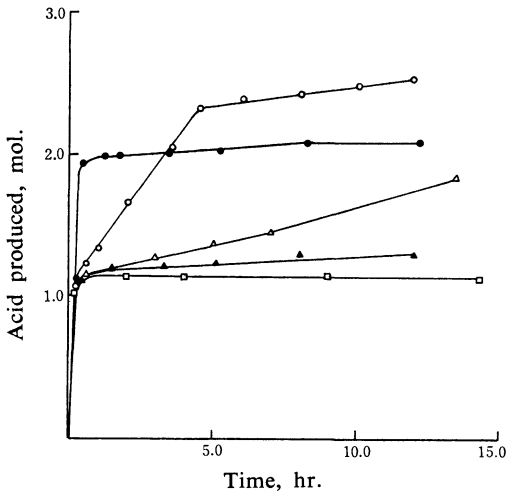


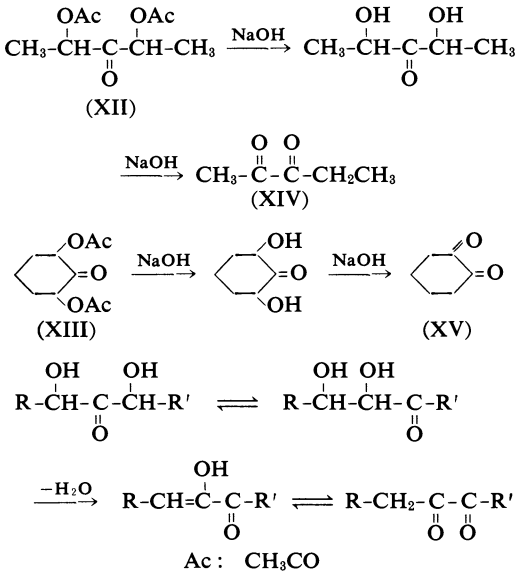
Fig. 1. Production of acid from acetoxyketones.
- ○ 2-Acetoxycyclohexanone in 0.5 N NaOH under aeration
- ● 2,6-Diacetoxycyclohexanone in 0.046 N NaOH under N_2 atmosphere
- △ 2-Acetoxycyclohexanone in 0.045 N NaOH
- ▲ 2-Acetoxypentan-3-one in 0.051 N NaOH under N_2 atmosphere
- □ 2-Acetoxycyclohexanone in 0.045 N NaOH under N_2 atmosphere

Wallach[14] has reported that the corresponding α-dicarbonyl compounds were obtained either when α, β-dibromoketones were treated with potassium hydroxide or when α, β-unsaturated

11) C. Walling, "Free Radicals in Solution," John Wiley & Sons, Inc., New York (1957), p. 461.
12) J. C. Sowden, "Advances in Carbohydrate Chemistry", 12, 36 (1957).
13) R. L. Whistler and J. N. BeMiller, ibid., 13, 289 (1958).
14) O. Wallach, *Ann.*. 437, 148 (1924).

ketones were oxidized with potassium permanganate. The α,β-dihydroxyketones produced through above-mentioned treatments seemed smoothly to eliminate their β-hydroxy groups under alkaline conditions in both cases.

When 2,4-diacetoxypentan-3-one (XII) and 2,6-diacetoxycyclohexanone (XIII) were treated with an ethanolic sodium hydroxide solution under a nitrogen atmosphere, pentan-2,3-dione (XIV) and cyclohexan-1,2-dione (XV) were produced respectively. In these reactions it is considered that the α,α'-dihydroxyketone produced by means of the saponification rearranges itself to an α,β-dihydroxyketone* which easily eliminates its β-hydroxyl group and gives rise to an enolic form of dicarbonyl compounds.



Sugihara and Yuen[5,6] failed to obtain crystalline products from 4-*O*-benzoyl-1,2;5,6-di-*O*-isopropylidene-D-*arabo*-3-hexulose after debenzoylation and deacetonation. They mentioned that the enediol produced by saponification of benzoyl group would provide a mixture of four isomeric ketoses. Consequently, in the final stage during the synthetic route of unsubstituted 3-ketose, alkaline treatment must be avoided, if possible.

In attempting to synthesize 3-xylulose, 1,3;2,4-di-*O*-methylene-xylitol (I) was used as a starting substance. The preparation of this compound was carried out by a modification of the procedure of Hann, Ness and Hudson[15]. The acetolysis of 1,3;2,4-di-*O*-methylene-xylitol gave crystalline 3-*O*-acetoxymethyl-1,5-di-*O*-acetyl-2,4-*O*-methylene-xylitol (II) in a good yield (96%). All attempts to obtain 1,5-di-*O*-acetyl-2,4-*O*-methylene-xylitol by the limited hydrolysis of the *O*-acetyl group on carbon 3 failed. The saponification of all ester linkages in 3-*O*-acetoxymethyl-1,5-di-*O*-acetyl-2,4-*O*-methylene-xylitol, followed by the benzoylation of the resulting 2,4-*O*-methylene-xylitol (III) with two molar equivalents of benzoyl chloride, gave 1,5-di-*O*-benzoyl-2,4-*O*-methylene-xylitol (IV) in a 79% yield. The infrared spectrum of IV shows the presence of benzoyl groups (conjugated carbonyl absorptions at 1685 and 1715 cm^{-1}, and phenyl group absorptions at 1580 and 1595 cm^{-1} respectively). The 1 and 5 positions for the benzoyl groups were assigned because of the well-known preferential benzoylation of primary hydroxyl groups under the conditions employed.

After being oxidized with chromium trioxide in anhydrous pyridine, 1,5-di-*O*-benzoyl-2,4-*O*-methylene-xylitol was recovered unchanged, but when pyridine was replaced with glacial acetic acid, the oxidation afforded crystalline 1,5-di-*O*-benzoyl-2,4-*O*-methylene-3-xylulose (V) in a 30% yield. In the infrared spectrum, V shows an absorption peak at 1725 cm^{-1}, indicating the presence of a carbonyl group. No absorption, however, is observed near 3420 cm^{-1}, where the parent compound IV had an absorption because of its free hydroxyl group.

The saponification of the substituted 3-xylulose (V) with an alcoholic potassium hydroxide solution gave crystalline 2,4-*O*-methylene-3-xylulose (VI) in a 64% yield. The sodium borohydride reduction of the product VI, followed by the hydrolysis of the methylene group with sulfuric acid, gave an excepted mixture containing xylitol (X) and ribitol (XI) (paper chromatographic separation), confirming that the parent compound VI is of a 3-ketose structure. 2,4-*O*-Methylene-3-xylulose (VI) has an absorption at 3317 cm^{-1} (hydroxyl groupings), but it has no peaks at 1580~1600 cm^{-1} (phenyl groupings), indicating the completeness of saponification. However, no absorption at 1700~1735 cm^{-1} is observed because of its carbonyl grouping. Hence, in 2,4-*O*-methylene-3-xylulose, the carbonyl group must be masked, presumably by a dimer formation, in which the carbonyl group of the ketose may be combined with the free hydroxyl groups of the other to form acetal linkage. Späth and his co-workers[16] established that β-hydroxy-aldehyde, in general, took a dimeric form containing a 1,3-dioxane ring structure. Schaffer and

* According to the acyloin rearrangement or to the Lobry de Bruyn-Alberda van Ekenstein transformation, in the sense of carbohydrate chemistry.

15) R. M. Hann, A. T. Ness and C. S. Hudson, *J. Am. Chem. Soc.*, **66**, 670 (1944).

16) E. Späth et al., *Ber.*, **74**, 859 (1941); **76**, 57, 949, 1196 (1943).

Isbell[17] found that 5-aldo-1, 2-*O*-isopropylidene-D-*xylo*-pentofuranose existed in the form of a dimer, as has been mentioned above.

The demethylenation of 2, 4-*O*-methylene-3-xylulose (VI) with methanolic hydrogen chloride gave a syrup which did not crystallize. The acid hydrolysis of the syrup gave a viscous syrup which also did not give a crystalline product. Paper chromatographic investigations of this syrup showed that it was composed of 3-xylulose (VII), *erythro*-2-pentulose (VIII*), and of *threo*-2-pentulose (IX)* (R_f values: 0.369, 0.359 and 0.347 respectively). The R_f value of 3-xylulose (0.369) corresponds to 1.26 in R_{rib}** value. Stoodley[8] has recorded the R_{rib} of 1.23 for 3-xylulose obtained from ribitol. The observation that the syrup obtained by removing the methylene group was a mixture of 3-ketose and corresponding 2-ketoses suggests that isomerization plays a leading role during acid treatment. It is suggested also that the unsubstituted 3-ketose does, in general, not exist in a stable form but is transformed into its isomers according to the Lobry de Bruyn—Alberda van Ekenstein transformation.

Further investigations related to those described in this communication are in progress.

Experimental

All melting points and boiling points are corrected. All concentrations were carried out under reduced pressure at 30~40°C (bath temp.) unless otherwise stated. Paper chromatographic analyses were carried out on Toyo Roshi No. 50 filter paper by the descending method at 30°C, using a *n*-butanol—ethanol—acetic acid—water mixture (40 : 10 : 5 : 15, vol./vol.) as a developer. Spots were located on chromatograms by the following color reagents: a) silver nitrate in ammonium hydroxide, b) lead tetraacetate in anhydrous benzene, c) naphthoresorcinol in hydrochloric acid and d) aniline hydrogenphthalate in *n*-butanol saturated with water. Multiple developments were employed for the complete separation of spots, if necessary. Infrared spectra were determined by using an infrared recording spectrophotometer (Model D. S. 301, Nippon Bunko Co., Ltd.).

Acetoxyketones.—Acetoxyketones were prepared by the method of Cavill and Solomon[18]. The samples obtained were as follows: 2-acetoxycyclohexanone, b. p., 103~104°C/6 mmHg, n_D 1.4598 (Cavill and Solomon reported a b. p. of 123~126°C/16 mmHg); 2, 6-diacetoxycyclohexanone***, b. p., 140~142°C/1 mmHg, m. p., 147~148°C (leaflets, recrystallized from ethanol—petroleum ether) (Cavill and Solomon reported a b. p. of 158~160°C/10 mmHg and m. p. 145~146°C); 2-acetoxypentan-3-one, b. p., 58~60°C/3 mmHg, n_D 1.4181; and 2, 4-diacetoxypentan-3-one, b. p., 81~82°C/2 mmHg (Cavill and Solomon reported a b. p. of 80°C/1 mmHg).

Behavior of Acetoxyketones in a Dilute Alkaline Solution.—*In the Presence of Oxygen.*—In a 0.05 N sodium hydroxide solution (70% aqueous ethanol*), each acetoxyketone was dissolved and allowed to stand at room temperature. When the solution was aerated with a stream of gas, a dry ice—acetone condenser was fitted to the reaction flask to prevent the evaporation loss of the solvent. At suitable intervals, an aliquot of the reaction mixture was pipetted out and titrated with 0.05 N hydrochloric acid, using phenolphthalein as an indicator.

b) In the Absence of Oxygen. — The above-mentioned procedure was carried out using an oxygen-free alkaline solution. Nitrogen gas was passed through the mixture during the reaction period. The results obtained (a) and b)) are shown in Fig. 1.

c) Cyclohexan-1, 2-dione (XV) from 2, 6-Diacetoxycyclohexanone (XIII).— 2, 6-Diacetoxycyclohexanone was dissolved in a 0.28 N sodium hydroxide solution (70% aqueous ethanol) under nitrogen gas bubbling for 3 hr. at room temperature. After the solution had been neutralized with dilute hydrochloric acid to a slightly alkaline state, phenylhydrazine hydrochloride and sodium acetate were added and the mixture was allowed to stand overnight. The precipitate was then filtered and recrystallized from ethanol. Cyclohexane-1, 2-dione bisphenylhydrazone was obtained as golden yellow needles; m. p. 150.5~151.0°C.

Found: N, 19.08. Calcd. for $C_{18}H_{20}N_4$: N, 19.16%.

d) Pentan-2, 3-dione (XIV) from 2, 4-Diacetoxypentan-3-one (XII). — After the treatment of 2, 4-diacetoxypentan-3-one in a 0.048 N sodium hydroxide solution (70% aqueous ethanol), as mentioned above, bisphenylhydrazone of pentane-2, 3-dione was obtained in the form of yellow needles (recrystallized from benzene—ethanol); m. p., 170~171°C.

Found: N, 20.30. Calcd. for $C_{17}H_{20}N_4$: N, 19.99%.

e) Analysis of the Reaction Mixture.— From the reaction mixture (2-acetoxycyclohexanone in 0.5 N sodium hydroxide, under aeration), an aliquot was pipetted ont at suitable intervals, neutralized with dilute acetic acid, and deionized by Amberlite IR-120*. The resulting aqueous solution** was concentrated under reduced pressure. To the distillate, which was collected in a cold trap, a 2 N hydrochloric acid solution of 2, 4-dinitrophenylhydrazine was added. After the whole solution had been allowed to stand overnight, cyclohexane-1, 2-dione bisphenylhydrazone was obtained (m. p., 225~226.5°C), after recrystallization from ethyl acetate—ethanol. From the distillation residue, adipic

17) R. Schaffer and H. S. Isbell, *J. Am. Chem. Soc.*, **79**, 3864 (1957).

* Both the sugars showed R_f values similar to that of the authentic specimens prepared by the pyridine epimerization of D-xylose and of D-ribose respectively.

** The rate of movement relative to that of D-ribose.

*** Two moles of lead tetraacetate were employed for one mole of ketone.

18) G. W. K. Cavill and D. H. Solomon, *J. Chem. Soc.*, 1955, 4426.

* Aldehyde free, freshly distilled.

** Rohm and Haas Co., Philadelphia, Pa., U. S. A.

*** Periodate oxidation of this aqueous solution gave only a trace of adipic acid semialdehyde, indicating the absence of 2-hydroxycyclohexanone in the solution.

TABLE I. RESULTS OF THE ALKALI TREATMENT OF 2-ACETOXYCYCLOHEXANONE

Time hr.	Yield of products from 1 g. of ketone: Cyclohexane-1,2-dione mg.	Adipic acid mg.
6	660	85
10	210	125
15	140	325

acid was isolated, by recrystallizing from ethanol, in the form of crystals (m. p. and mixed m. p. 150~151°C). The results obtained are shown in Table I.

1,5-Di-*O*-acetyl-3-*O*-acetoxymethyl-2,4-*O*-methylene-xylitol (II).—Twenty grams of finely powdered 1,3; 2,4-di-*O*-methylene-xylitol (I) was added into an ice-cold acetylating mixture containing 140 ml. of acetic anhydride, 60 ml. of glacial acetic acid, and 4 ml. of sulfuric acid. The diacetal dissolved slowly, and, after standing 15 min. at 5°C, the reaction mixture was poured into 500 ml. of ice and water. The precipitate was filtered by suction and washed with a small amount of cold water (first crop). The filtrate and the washings were combined, and the whole solution was neutralized with aqueous sodium carbonate to a slightly alkaline state; then the produced precipitate was collected by filteration (second crop). The filtrate was extracted with chloroform (150 ml. ×3), and the chloroform layer was washed with water and dried over magnesium sulfate. After removal of the solvent, a yellow solid was obtained (third crop). After recrystallizing from water, the combined product (34.8 g., 95.6%) gave crystalline 1,5-di-*O*-acetyl-3-*O*-acetoxymethyl-2,4-*O*-methylene-xylitol (II); yield, 31.5 g., m. p., 136~137.5°C. After two recrystallizations from water, an analytical sample was obtained, m. p., 139.5~140.0°C.

Found: CH_3CO, 39.0. Calcd. for $C_{13}H_{20}O_9$: CH_3CO, 40.3%.

After being treated with boiling 70% acetic acid for 2 hr., or after being stirred with Amberlite IR-45 for 2 hr., II was recovered unchanged.

2,4-*O*-Methylene-xylitol (III). — In 25 ml. of chloroform (dried over phosphorous pentoxide), 5.9 g. of 1,5-di-*O*-acetyl-3-*O*-acetoxymethyl-2,4-*O*-methylene-xylitol (II) was dissolved and the solution was cooled with an ice-bath. Into the cold solution, 20 ml. of absolute ethanol and 20 ml. of 0.1 N sodium methoxide in methanol were added. The ice-bath was removed after 1 hr., and the solution was allowed to stand overnight at room temperature. The solvent was distilled off under reduced pressure, the residue obtained was dissolved in 5 ml. of water, and the solution was decolorized with active carbon. The resulting pale yellow solution was evaporated under reduced pressure to dryness. After being recrystallized from 5 ml. of ethanol, the residue gave a crystalline solid (2.1 g.). An additional 0.5 g. of the product was obtained from the mother liquor after it had been left standing for a few days. Yield, 2.6 g. (86.1%). After several recrystallizations from ethanol, 2,4-*O*-methylene-xylitol (III) was obtained as needles which melted at 110~110.5°C. The infrared spectrum is shown in Fig. 2.

1,5-Di-*O*-benzoyl-2,4-*O*-methylene-xylitol (IV).—Ten grams of 2,4-*O*-methylene-xylitol (III) was dissolved in 100 ml. of ice-cooled anhydrous pyridine (dried over barium oxide and stored over calcium hydride); 14 ml. (2 mol. equiv.) of benzoyl chloride was then added with agitation into the solution. The reaction mixture, which after being stirred for 2.5 hr. at room temperature became slushy, was poured into 700 ml. of ice and water. The amorphous precipitate was filtered by suction, washed with cold water, and dried. Yield, 18.0 g. (79.3%); recrystallizations from absolute ethanol gave pure 1,5-di-*O*-benzoyl-2,4-*O*-methylene-xylitol (IV) in the form of long needles (m. p., 140.5~141.0°C).

Found: C, 64.64; H, 5.59; C_6H_5CO, 55.9. Calcd. for $C_{20}H_{20}O_7$: C, 64.51; H, 5.41; C_6H_5CO, 56.4%.

The infrared spectrum is shown in Fig. 3.

A solution of 1,5-di-*O*-benzoyl-2,4-*O*-methylene-xylitol (1.0 g.) in 3 ml. of glacial acetic acid and 7 ml. of acetic anhydride was treated with the above-mentioned acetylating mixture (10 ml.) for 1 hr. at room temperature, and the resulting slushy mixture was poured into 250 ml. of ice and water. The resulting precipitate, after filtration, washing with water, and drying, weighed 850 mg. Two recrystallizations from absolute ethanol gave 1,5-di-*O*-benzoyl-3-*O*-acetyl-2,4-*O*-methylene-xylitol in the form of long needles (m. p., 174.5~175.0°C).

Found: C, 63.96; H, 5.49; acyl groups, 60.3.

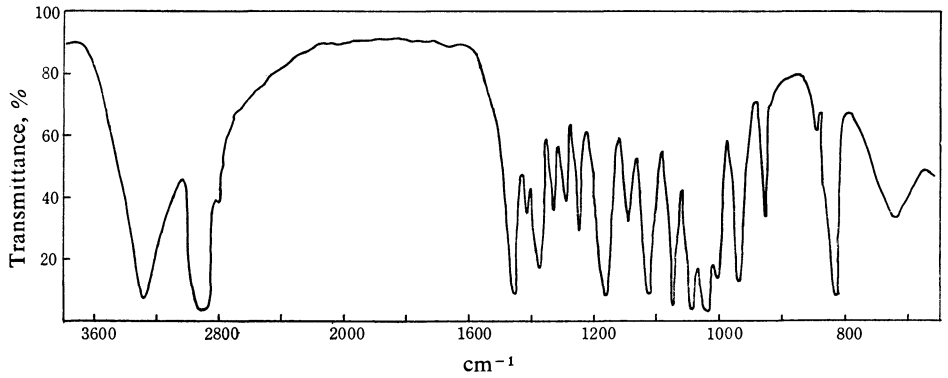


Fig. 2. Infrared spectrum of 2,4-*O*-methylene-xylitol (III), in Nujol.

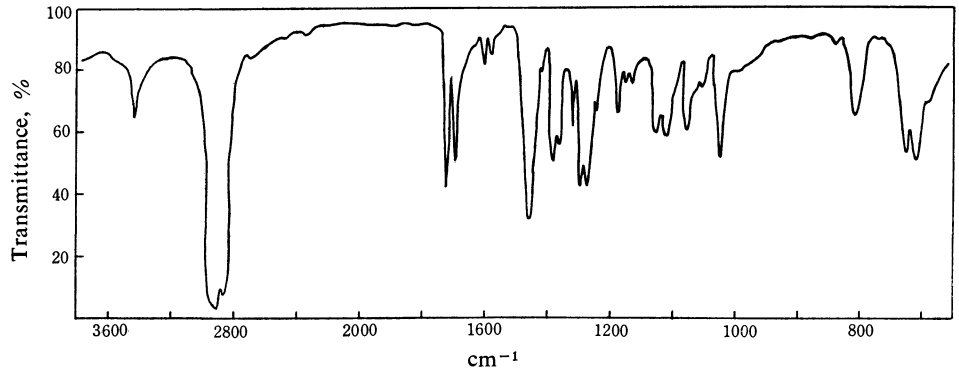


Fig. 3. Infrared spectrum of 1,5-di-*O*-benzoyl-2,4-*O*-methylene-xylitol (IV), in Nujol.

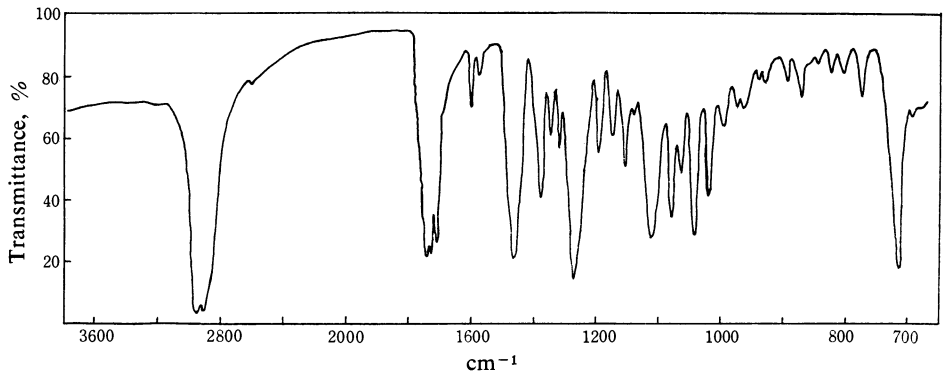


Fig. 4. Infrared spectrum of 1,5-di-*O*-benzoyl-2,4-*O*-methylene-3-xylulose (V), in Nujol.

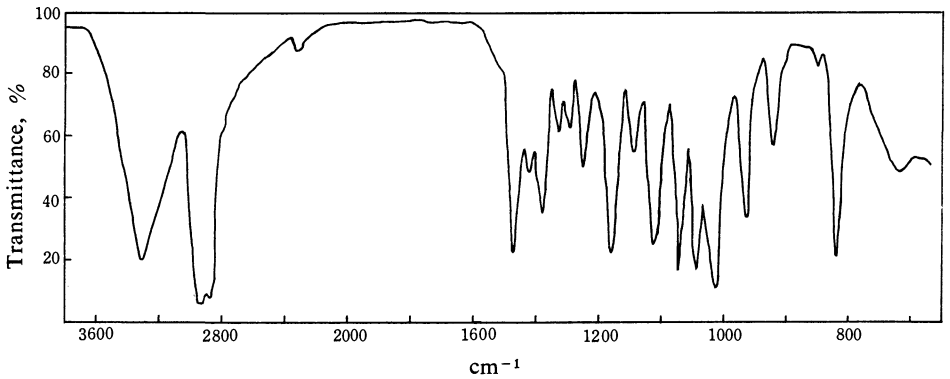


Fig. 5. Infrared spectrum of 2,4-*O*-methylene-3-xylulose (VI), in Nujol.

Calcd. for $C_{22}H_{22}O_8$: C, 63.76; H, 5.35; acyl groups, 61.1%.

1, 5-Di-*O*-benzoyl-2,4-*O*-methylene-3-xylulose (V). — A portion (4.4 g.) of 1,5-di-*O*-benzoyl-2,4-*O*-methylene-xylitol (IV) was dissolved in 200 ml. of glacial acetic acid (treated with chromium trioxide and distilled). To the resulting solution maintained at 15°C, 5.0 g. of chromium trioxide in 300 ml. of acetic acid was added with agitation. After this addition, the mixture was stirred for 1 hr. and then allowed to stand overnight at room temperature. The excess of the oxidant was decomposed by adding methanol, and the mixture was evaporated under reduced pressure to a black residue. The residue was extracted three times with warm diisopropyl ether (100 ml. portions). The combined ethereal solution was washed successively with water, 5% aqueous sodium bicarbonate, and again with water, and then dried over anhydrous magnesium sulfate. The solvent was distilled off under reduced pressure, and the resulting thick syrup was dissolved in 30 ml. of warm ethanol and decolorized with active carbon. When the solvent was evaporated under reduced pressure, a crystalline mass

TABLE II. PAPER CHROMATOGRAPHIC SEPARATION OF THE SYRUP

Spot No.	R_f	Color with Reagent a)	Color with Reagent b)	Coloration with reagent a)	Remarks
1	0.12~0.14	Black	——	Strong	Unknown
2	0.25~0.27	Black	Pink	Weak	Aldose (?)
3	0.347	Black	Light brown	Strong	*threo*-2-Pentulose
4	0.357	Black	Light brown	Strong	*erythro*-2-Pentulose
5	0.369	Black	Brown	Strong	3-Xylulose
6	0.54~0.56	Black	Faint	Variable	Unchanged substance

Spot 2 gave a blue color with reagent c).

To confirm spots 3 and 4 as *threo*- and *erythro*-2-pentulose, authentic specimens prepared by the pyridine epimerization of the corresponding aldoses, were dotted on the side of the paper and then developed.

Spot 6 was negative against reagent b).

was obtained (1.3 g. (29.3%); m. p., 111~112°C). After repeated recrystallizations from diisopropyl ether, an analytical sample of 1,5-di-*O*-benzoyl-2,4-*O*-methylene-3-xylulose (V) was obtained as long needles (m. p., 115.5~116.5°C).

Found: C, 64.44; H, 4.96; C_6H_5CO, 56.9. Calcd. for $C_{20}H_{18}O_7$: C, 64.86; H, 4.90; C_6H_5CO, 56.8%.

The infrared spectrum is shown in Fig. 4.

2,4-*O*-Methylene-3-xylulose (VI). — In 20 ml. of ethanol, 480 mg. of 1,5-di-*O*-benzoyl-2,4-*O*-methylene-xylulose (V) was dissolved, and to this solution, 30 ml. of 95% ethanol containing 0.5 g. of potassium hydroxide was then added. The solution was allowed to stand overnight, after which the solvent was evaporated by a jet of dry air. The residual syrup was dissolved in 10 ml. of water and deionized by passing it through a column containing ion exchange resins (5 ml. of Amberlite IR-45 and of IR-120). The effluent and the washings were decolorized with active carbon, concentrated under reduced pressure to dryness. After recrystallization from ethanol—diisopropyl ether (1 : 1, vol./vol.), the resulting white solid gave 2,4-*O*-methylene-3-xylulose (VI) as fine needles (80 mg.; m. p., 90~92°C). After further recrystallizations from the same solvent, an analytical sample was obtained (m. p., 95.5~97.5°C).

Found: C, 43.97; H, 6.10. Calcd. for $C_6H_{10}O_5$: C, 44.44; H, 6.22%.

The infrared spectrum is shown in Fig. 5.

Reduction of 2,4-*O*-Methylene-3-xylulose (VI). —In 5 ml. of water, 120 mg. of 2,4-*O*-methylene-3-xylulose was dissolved; this solution was then cooled and maintained at 5°C. Ten milliliters of a 1.5% sodium borohydride aqueous solution was added drop by drop under agitation. After being allowed to stand for 1.5 hr., the reaction mixture was acidified by dilute acetic acid to a slightly acid state and concentrated under reduced pressure to 5 ml. To the resulting solution, 0.5 ml. of concentrated sulfuric acid was added, and the solution was heated on a water bath for 4 hr. The hydrolysate was neutralized with barium carbonate and filtered through a layer of Celite*, and the filtrate and the washings were deionized by passing it through a column (Amberlite IR-45 and IR-120), decolorizing it by active carbon, and dried under reduced pressure to a thick syrup. Paper chromatographic separation of the syrup, using reagent a) and b) as detectors, showed the presence of xylitol (X) and ribitol (XI) (R_f 0.243 and 0.281 respectively).

Hydrolysis of 2,4-*O*-Methylene-3-xylulose (VI) into 3-Xylulose (VII). — In 10 ml. of a 9.3% methanolic hydrogen chloride solution was dissolved 620 mg. of 2,4-*O*-methylene-3-xylulose (VI); the solution was then allowed to stand for 48 hr. at room temperature (about 15°C). The resultant mixture was evaporated under reduced pressure to a thick syrup, which was then dissolved in 5 ml. of water, followed by deionizing (Amberlite IR-45) and by decolorizing by a small amount of active carbon. The clear solution obtained was concentrated under reduced pressure to a thick syrup which did not crystallize. When the methanolysis was carried out for 10, 24, and 72 hr., the resulting syrups also failed to yield a crystalline product. The syrup obtained was hydrolyzed in 0.1 N hydrochloric acid for 24 hr. at room temperature. After the removal of acid with Amberlite IR-45, the solution was concentrated under reduced pressure to a thick syrup, which reduced a warm Fehling's solution. Paper chromatographic investigations of this syrup gave the results shown in Table II.

The author wishes to express his thanks to Professor Ryozo Goto for his kind guidance and encouragement throughout the course of the present work.

Institute of Chemistry
Faculty of Science
Kyoto University
Sakyo-ku, Kyoto

* A filter-aid; Johns-Manville Co., New York, N. Y., U. S. A.

Gouy Magnetic Balance for Use at Low Temperatures

By Yoshiaki SHIRAIWA*, Katsunari KIKUCHI**, Eichi KISHI, Hiroshi NAGANO and Keichi OSHIMA

(Received June 25, 1962)

A magnetic balance of the Gouy type has been constructed in our laboratory for making absolute measurements of the magnetic susceptibility of paramagnetic salts which are to be used as working substances in adiabatic demagnetization experiments; the construction of the balance was very simple, and its performance has proved to be very satisfactory. The paramagnetic susceptibility of potassium chromium alum was measured over the temperature range between room temperature and liquid nitrogen temperatures.

When a cylindrical specimen is suspended between the magnet poles so that the lower end of the specimen is at the center of the magnet, where the field strength, H, is strongest, and the other end in a weaker field, the specimen is influenced by a longitudinal force, f, with a magnitude[1] in which

$$f=1/2\,\chi A(H_1^2-H_2^2) \qquad (1)$$

χ is the volume susceptibility of the specimen, H_1, H_2 are the maximum and minimum values of the field strength respectively, and A is the cross sectional area of the specimen.

Construction of the Apparatus

A chemical balance of the standard type (as shown in Fig. 1) was used for measuring the body force, f. For the measurements in the low temperature region, the magnetic balance was set as a whole in a large, glass bell-jar so as to avoid the condensation of air and vapors on the surface of a quartz tube containing the specimen. The helium which filled the bell-jar served as a heat exchange gas. The balance was placed on the thick aluminum plate (600 mm.×600 mm.×20 mm.) with leveling screws.

The beam arrest of the balance was achieved by pushing an O-ring-sealed metal bar below the pillar of the balance. The compensation[2] of the body force being exerted upon the specimen was adjusted by the electromagnetic force between a needle-shaped permanent magnet suspended from an end of the beam and a solenoid with 2500 turns of copper wire wound on an ebonite pipe (30 mm.×8 mm.ϕ×5 mm.ϕ). A storage battery of 2 volts was used as the current source of the solenoid. A "Kovar seal" was used for electrical lead connections from the storage battery to the solenoid set on the aluminum plate.

Powdered potassium chromium alum was filled in a long quartz tube, which was suspended at one end of the beam by a nylon string. This tube was enclosed in a pyrex glass tube in a Dewar flask, as shown in Fig. 1. A number of compression nuts with O-ring seals were used so as to avoid leakage of the helium gas.

The magnet used was a highly homogeneous permanent magnet with a 30 mm. pole gap, a 150 mm. pole diameter and a 5820 gauss field intensity. The homogeneity of this magnet, which has previously been used in nuclear magnetic resonance studies in this laboratory, is very high to the degree that the fluctuation is less than 0.1 gauss in the 2.54 cm. square area at the center of the pole face.

The ball bearing used in the wheels of the truck on which the permanent magnet was mounted was satisfactory enough to free the balance system from vibrations when the permanent magnet slides on the rails. For the determination of the specimen temperature, a copper-constantan thermocouple was used. It was, however, necessary not to set the leads in the suspended specimen, because the leads may influence the smooth swinging of the beam. Three thermocouples, the upper, the middle, and the lower, were set quite near the specimen, as is shown in Fig. 1, so that the temperature gradient could be checked. From this measurement, it was proved that the temperature difference was within 0.3 degree centigrade over the specimen when the liquid nitrogen filled the Dewar flask. These copper-constantan thermocouples have been calibrated by the melting point of several pure liquids (water, carbon tetrachloride, and ethyl alcohol). The sample of potassium chromium alum was

* Present address: Toa Denpa Kogyo Co. Ltd., Suwa-cho, Shinjuku-ku, Tokyo.
** Present address: Pennsylvania State University, Park, Pennsylvania, U. S. A.

1) P. W. Selwood, "Magnetochemistry", Interscience publishers, (1943).
2) T. Hirone et al., *Sci. Rept. Research Institute of Tohoku University*, A, 67 (1954).

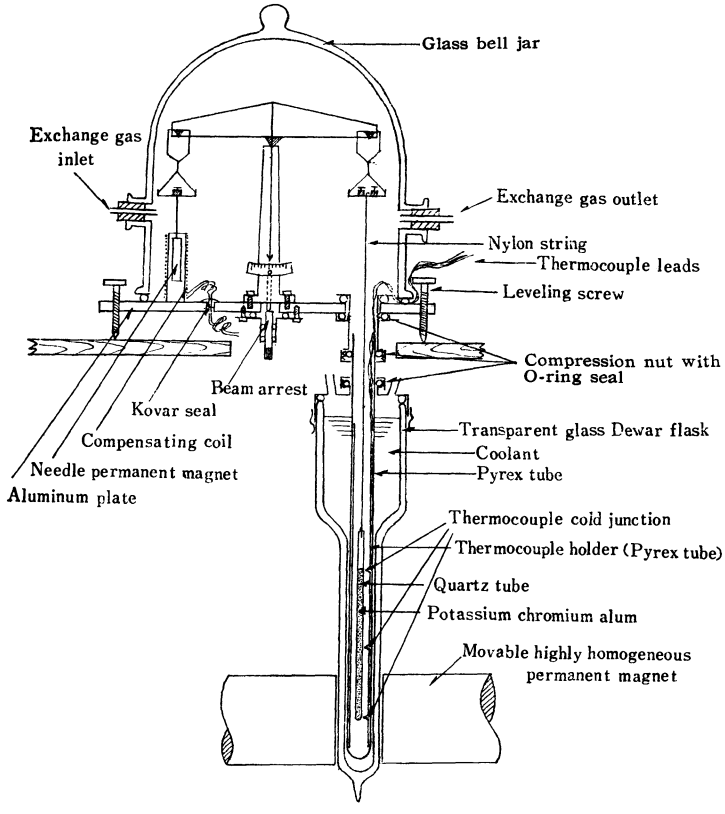


Fig. 1. Sketch of the Gouy magnetic balance.

the same as that which was previously used by us as a cooling substance in adiabatic demagnetization experiments*. The weight of the powdered specimen was approximately 2.77 g. in the present experiments.

Experimental

After filling the refrigerant into the Dewar flask, the temperature equilibrium of the whole system containing the specimen was attained in 10 min. Then, the pointer of the magnetic balance was adjusted to come to rest at the zero mark. Thereafter, the specimen was subjected to the magnetic field by setting the permanent magnet at the position of the specimen. The force acting on the specimen was measured by the compensating system explained above.

No linear relation was obtained between the force and the compensating current. Therefore, several approximate experimental expressions for the relation between the body force and compensating current were set up. The compensating current was read by a precise milliammeter. The magnetic field measurement was made using a magnetic fluxmeter of Yokogawa Electric Works which had been calibrated by the nuclear magnetic resonance frequency of protons. The field intensity at the lower end of the specimen tube was 5820 gauss, while that at the upper end was 25 gauss. H_2 (25 gauss) in Eq. 1, therefore, is negligible as compared with H_1 (5820 gauss), and Eq. 1 reduces to this relation:

$$f=1/2\,\chi AH_1^2 \qquad (2)$$

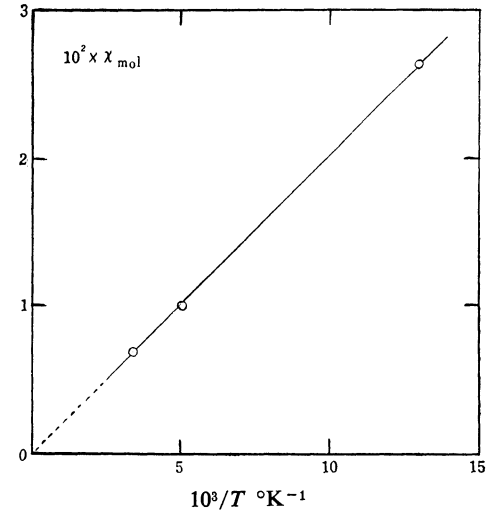


Fig. 2. Plot of susceptibility per mol. vs. reciprocal temperature for potassium chromium alum.

* To be published shortly.

TABLE I. THE MEASURED VALUES OF THE BODY FORCE AND MOLAR SUSCEPTIBILITY OF POTASSIUM CHROMIUM ALUM VS. ABSOLUTE TEMPERATURE

	T°K		
	285	195	77
f, dyne	21.7	31.6	85.0
$\chi_{mol} \times 10^3$	6.73	9.76	26.4

The cross-sectional area of the powdered specimen was determined gravimetrically by assuming that the powder is uniformly filled in the quartz tube. The diamagnetic susceptibility of a quartz tube was measured over the range from room temperature to liquid nitrogen temperature and was found to be suitable for the present work, because its variation with the temperature was very small. The observed susceptibility is the sum of the susceptibility of a quartz tube and the powdered specimen. The diamagnetic fraction of the quartz tube was about 1.5% of the total susceptibility at the liquid nitrogen temperature, and about 6% at room temperature. In Table I, the measured values of the body force and the molar susceptibility of potassium chromium alum are given. The Curie constant of potassium chromium alum, which was determined from the data in Fig. 2, was $C=1.86$. This value is comparable with the theoretical value, $C=1.84$, which is calculated by assuming the "spin only paramagnetism" for the Cr^{+3} ion[3].

3) C. Kittel, "Introduction to Solid State Physics", John wiley (1953).

Summary

This paper has reported on the performance, in the range between room and liquid nitrogen temperatures, of a Gouy-type magnetic balance, which had been constructed for absolute measurements of the magnetic susceptibility of paramagnetic salts. As a magnetic field, we used a highly homogeneous permanent magnet which was easily movable by hand. Therefore, precise measurement of the susceptibily is possible. With this balance, the susceptibility of 10^{-5} c. g. s. units was measurable within a range of error of 5%.

The authors are indebted to the members of the technical staff of the cryogenic laboratory of the Institute for Solid State Physics for their invaluable cooperation.

Institute for Solid State Physics
The University of Tokyo
Minato-ku, Tokyo

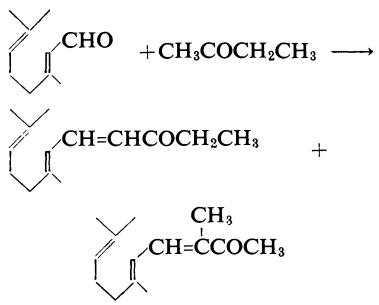
NOTES

Synthesis of Pseudoionone and its Homologues Using the Wittig Reaction

By Kazuyoshi FUJIWARA, Hidetaka TAKAHASHI and Masaki OHTA

(Received May 1, 1962)

Pseudoionone and its homologues are prepared by the condensation of citral with ketone in the presence of alkali; in the case of unsymmetrical alkyl ketones, however, a mixture of isomers is produced. For example, ethyl methyl ketone gives a mixture of *n*-methylpseudoionone and isomethylpseudoionone, and the separation of these isomers is very difficult. In order to obtain pure *n*-methylpseudoionone and isomethylpseudoionone separately, the



Wittig olefin synthesis[1], in which the olefinic double bond is to be located in a given position, was adopted. For this paper pseudoionone and three of its homologues were synthesized by means of the Wittig reaction, i. e., the reaction of citral with triphenylphosphine-acylmethylene. The products were identified as their 2, 4-dinitrophenylhydrazones.

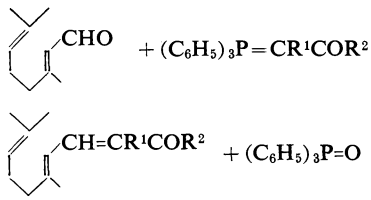
1) U. Schöllkopf, *Angew. Chem.*, **71**, 260 (1959).

TABLE I. $(C_6H_5)_3P=CR^1COR^2$

R^1	R^2	M. p. °C	Yield		Anal. Calcd. %	Anal. Found %	M. p. °C
H	CH_3	205~206 (from MeOH+H_2O)	71%				205~206[2]
H	C_6H_5	190~192 (from C_6H_6+petr. ether)	58%	$C_{26}H_{21}OP$	C: 82.10 H: 5.57	81.74 5.81	178~180[2]
H	C_2H_5	221~222 (from MeOH+H_2O)	82%	$C_{22}H_{21}OP$	C: 79.50 H: 6.37	79.71 6.38	
CH_3	CH_3	193~195 (from MeOH+H_2O)	55%	$C_{22}H_{21}OP$	C: 79.50 H: 6.37	79.67 6.56	

TABLE II. 2, 4-DINITROPHENYLHYDRAZONE OF PSEUDOIONONE AND ITS HOMOLOGUES

R^1	R^2	M. p. °C		Anal. Calcd. %	Anal. Found %	M. p. °C
H	CH_3	144~145	$C_{19}H_{24}N_4O_4$	C: 61.27 H: 6.48 N: 15.05	60.94 6.74 15.18	143
H	C_6H_5	126~127	$C_{24}H_{26}N_4O_4$	C: 66.34 H: 6.03 N: 12.90	65.69 6.16 12.92	
H	C_2H_5	149~150	$C_{20}H_{26}N_4O_4$	C: 62.16 H: 6.78 N: 14.50	61.83 6.91 14.56	151~151.5[5]
CH_3	CH_3	113~115	$C_{20}H_{26}N_4O_4$	C: 62.16 H: 6.78 N: 14.50	62.37 6.43 14.51	113~113.5[6]



Triphenylphosphineacylmethylenes were prepared by Ramirez's method[2] through the phosphonium salts obtained from triphenylphosphine with appropriated α-halogenoketones. Different structures have been suggested for the triphenylphosphineacylmethylenes by Michaelis[3], Wittig[4] and Ramirez[2]. The elementary analysis of carbon and hydrogen for the triphenylphosphineacylmethylenes obtained favored the formulae $(C_6H_5)_3P=CR^1 \cdot COR^2$) which Ramirez suggested.

Pseudoionone and its homologues were obtained by the reaction of citral with triphenylphosphineacylmethylenes in *n*-butyl ether at 100°C for 4~5 hr. and thereafter treated with 2, 4-dinitrophenylhydrazonium sulfate to give their hydrazones (see Table II). Moreover, the pseudoionone obtained above gave α-ionone by the usual method, heating with 85% phosphoric acid: this α-ionone was identified as its 2, 4-dinitrophenylhydrazone (m. p., 144~145°C, Found: N, 15.28; Calcd. for $C_{19}H_{24} \cdot N_4O_4$: N, 15.05%).

Experimental

Triphenylphosphineacylmethylenes. — Triphenylphosphineacylmethylenes were prepared according to the methods described in Ramirez's paper. A solution of triphenylphosphine and α-haloketone was allowed to stand at room temperature for 1 day; then triphenylphosphineacylmethylene was obtained as a crystal by shaking the obtained phosphonium salt with 10% aqueous sodium carbonate.

Pseudoionone and its Homologues.—A solution of citral (0.01 mol.) and triphenylphosphineacylmethylene (0.01 mol.) in *n*-butyl ether (10 cc.) was heated at 100°C for 4~5 hr. The solvent was removed in vacuo, ether was added to the residue, and then the crystallized triphenylphosphine oxide was filtered off. The oily residue obtained on the removal of the solvent from the ether solution was

2) F. Ramirez and S. Dershowitz, *J. Org. Chem.*, **22**, 41 (1957).
3) A. Michaelis and E. Kohler, *Ber.*, **32**, 1566 (1899).
4) G. Wittig and U. Schöllkopf, ibid., **87**, 1318 (1954).
5) Y. Naves, *Bull. soc. chim. France*, **1951**, 640.
6) H. Barbier, et al., ibid., **1951**, 254.

taken up in ethanol and then treated with an aqueous ethanolic solution of 2, 4-dinitrophenylhydrazonium sulfate. The crude 2, 4-dinitrophenylhydrazones were recrystallized from ethanol.

Laboratory of Organic Chemistry
Tokyo Institute of Technology
Meguro-ku, Tokyo

Steroid Studies. III. A New Route for the Preparation of Cholestane-3β, 5α, 6α-triol 3, 6-Diacetate from Cholesterol*

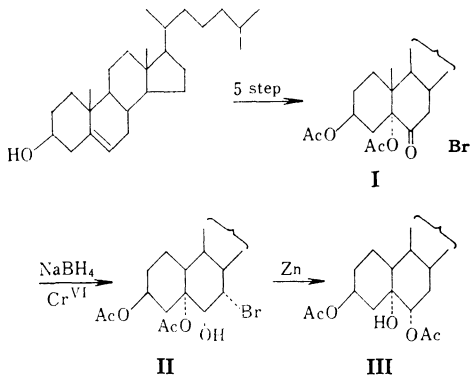
By Toshio GOTO and Yoshito KISHI

(Received May 30, 1962)

Several methods have been reported for the preparation of cholestane-3β, 5α, 6α-triol from cholesterol, but none of them are practicable for large-scale preparation because of their low yields[1,2] or because of the necessity for an expensive reagent[3]. Recently, Mori and Yoshida[4] reported a stereospecific synthesis of this triol in a 36.5% yield from cholesterol, the method involving a treatment of 6β-chlorocholestane-3β, 5α-diol diacetate with silver acetate.

Fieser and Rajagopalan have converted cholesterol in a good yield (52%) to 7α-bromocholestane-3β, 5α-diol-6-one diacetate (I)[5]. This procedure consists of no less than five steps, but each step is conducted without difficulty and is not time-consuming. We found that this bromodiolone diacetate I is convertible to cholestane-3β, 5α, 6α-triol 3, 6-diacetate (III) simply by borohydride reduction and by debromination with zinc. The over-all yield of triol diacetate III from cholesterol is about 32%.

Thus, the bromodiolone diacetate (I) obtained from cholesterol is reduced with sodium borohydride in methanol-dioxane to give exclusively a *cis*-bromohydrin[6], 7α-bromocholestane-3β, 5α, 6α-triol 3, 5-diacetate (II), the configuration of which will be discussed below. The solvents used in this reduction must be purified carefully to exclude a trace of heavy-metal impurities, especially those of lead, since its catalytic action alters the reaction course and produces cholestane-3β, 5α-diol-6-one diacetate[8].



The *cis*-bromohydrin II thus obtained was debrominated on refluxing with zinc dust in ethanol. During the reaction, the acetyl group at the C_5 position migrates to the C_6 position to produce cholestane-3β, 5α, 6α-triol 3, 6-diactate (III). Bromohydrins, both cis and trans, when refluxed with zinc dust in ethanol or in acetic acid, usually give monoenes[9]. However, not even in boiling acetic acid was bromohydrin II reduced to Δ^6-cholestene-3β, 5α-diol diacetate; on the contrary, it afforded, though in a lower yield, the same triol diacetate III.

The formation of the known 5, 6-cis compound III indicates that the hydroxyl group at the C_6 position in bromohydrin II must have α-configuration. Although an attempted acetylation with acetic anhydride and pyridine at room temperature was unsuccessful, bromohydrin II gave, by dichromate oxidation, bromodiolone diacetate I. This means that the acetyl

* Part II; T. Goto and Y. Kishi, *J. Chem. Soc. Japan, Pure Chem. Sec.* (*Nippon Kagaku Zasshi*), **83**, 1135 (1962).

1) A. Windaus, *Ber.*, **40**, 257 (1907).

2) M. Shiota, *J. Chem. Soc. Japan, Pure Chem. Sec.* (*Nippon Kagaku Zassi*), **77**, 1245 (1956).

3) M. I. Ushakov and A. I. Lyutenberg, *J. Gen. Chem.*, **9**, 69 (1939),

4) S. Mori and M. Yoshida, *Proc. Japan Acad.*, **34**, 612 (1958).

5) L. F. Fieser and S. Rajagopalan, *J. Am. Chem. Soc.*, **71**, 3938 (1949).

6) On borohydride reduction, 3β-acetoxycholestan-6-one gives exclusively the corresponding 6β-ol, whereas 5α-bromo- and 7α-bromo-3β-acetoxycholestan-6-one afford mixtures of *cis*- and *trans*-bromohydrins[7]. The greater the shielding of the α-side of 6-ketone, the more the corresponding 6α-ol is produced. Although, therefore, it is quite reasonable that the bromodiolone diacetate (I) gives the corresponding 6α-ol, it is curious that cholestane-3β, 5α-diol-6-one diacetate is not reduced under the same reaction conditions. The difference in those reactivities may be due to the inductive effect of the bromine atom.

7) D. R. James and C. W. Shoppee, *J. Chem. Soc.*, **1954**, 4224.

8) 4γ Lead acetate/200 mg. bromoketone (I) is still effective for debromination: T. Goto and Y. Kishi, *Tetrahedron Letters*, 513 (1961).

9) For example, 7α-bromo-3β-acetoxycholestane-6β-ol, 7α-bromo-6α-ol, and 6β-bromo-7α-ol all afford the same ethylenic compound, 3β-acetoxy-Δ^6-cholestene; D. R. James, R. W. Rees and C. W. Shoppee, *J. Chem. Soc.*, **1955**, 1370.

group migration occurred during the debromination reaction and not during the borohydride reduction.

Experimental

7α-Bromocholestane-3β, 5α-diol-6-one Diacetate (I) from Cholesterol. — Essentially according to Fieser and Rajagopalan's procedure[3]. Cholestane-3β, 5α, 6β-triol: m. p., 236~238°C (not recrystallized); 90% yield. Cholestane-3β, 5α-diol-6-one: m. p., 232~233°C (not recrystallized.); 95% yield. Cholestane-3β, 5α-diol-6-one 3-acetate: m. p., 233~234°C (not recrystallized); 95% yield. 7α-Bromocholestane-3β, 5α-diol-6-one 3-acetate: m. p., 160~165°C (recrystallized from methanol); 80% yield. 7α-Bromocholestane-3β, 5α-diol-6-one diacetate; m. p. 215~216°C (recrystallized from methanol); 80% yield. The overall yield from cholesterol is 52%. In the last step, the diolone monoacetate was brominated and then acetylated since in the alternate procedure the brominated product of the diolone 3, 5-diacetate was very difficult to purify.

7α-Bromocholestane-3β, 5α, 6α-triol 3, 5-Diacetate (II).—Two milliliters of EDTA solution (1 mol./l. in methanol) and 2.0 g. of sodium borohydride were added to a solution of 3.0 g. of the bromoketone I in 450 ml. of dioxane and 300 ml. of methanol. After having been allowed to stand at room temperature for 45 min., the mixture was acidified with acetic acid and diluted with 700 ml. of water. The precipitates obtained were crystallized from methanol to give plates melting at 148~149°C (2.4 g., 80%); IR 3380, 1740, 1720 cm^{-1} (in carbon disulfide).

Found: C, 63.72; H, 8.64. Calcd. for $C_{31}H_{51}O_5Br$: C, 63.79; H, 8.67%.

After having been treated with acetic anhydride and pyridine at room temperature overnight, the bromohydrin was recovered unchanged.

Dichromate Oxidation of Bromohydrin II.—To a solution of 110 mg. of bromohydrin II in 3 ml. of acetic acid was added a solution of 50 mg. of sodium dichromate in 1 ml. of acetic acid; the mixture was allowed to stand overnight at room temperature. The addition of water and extraction with ether in the usual way gave a crystalline solid which on several recrystallizations from methanol gave needles (m. p., 208~209°C), the mixed melting point of which with ketone I was 210~214°C and the infrared spectra of which are superimposable. From the mother liquor, a small quantity of starting material was recovered.

Cholestane-3β, 5α, 6α-triol 3, 6-Diacetate (III).—A solution of 3.0 g. of bromohydrin II in 70 ml. of ethanol was refluxed with 5.0 g. of zinc dust for 30 hr. and then filtered. The filtrate was diluted with water and extracted with ether in the usual way, and the ether solution was evaporated to dryness. The solid residue was crystallized from methanol to give prisms (2.0 g., 77%) (m. p., 186~187°C); no melting point depression was observed when this was admixed with an authentic sample.

Found: C, 73.74; H, 10.19. Calcd. for $C_{31}H_{52}O_5$: C, 73.76; H, 10.38%.

When treated with acetic anhydride and pyridine, diacetate III was recovered unchanged.

The authors are indebted to Professor Yoshimasa Hirata for his interest in this research. They are also grateful for a grant from the Ministry of Education.

Chemical Institute
Faculty of Science
Nagoya University
Chikusa-ku, Nagoya

Radioactivation Analysis of Bromine and Iodine in Organic Compounds Using a Low-level Neutron Source

By Haruo Tsuji, Yuzuru Kusaka and Yasuo Namikawa

(Received June 6, 1962)

This paper describes some experimental results on the activation analysis of bromine and iodine in various organic compounds using a 50 mg.-radium-plus-beryllium-neutron source.

The sample solution to be analyzed was put in a polyethylene capsule (length, 86 mm.; diameter, 16 mm.; thickness, 1 mm.) and irradiated with neutrons at the sample hole of the irradiation apparatus shown in Fig. 1. The thermal neutron flux at the sample position,

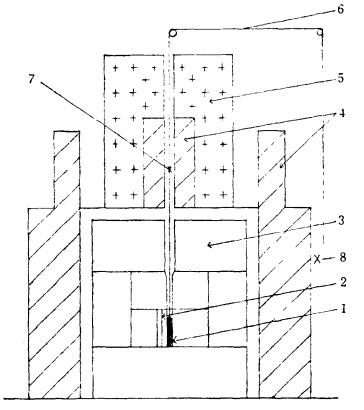


Fig. 1. Irraditation apparatus.

1 Neutron source
2 Sample hole
3 Paraffin
4 Lead
5 Paraffin containg boric acid
6 String
7 Position A
8 Position B

TABLE I. RADIOACTIVATION ANALYSIS OF BROMINE BY 1.0 hr. IRRADIATION

Sample	Weight g./5 ml.	Solvent	Bromine content in sample, %	
			Determined value	Theoretical value
Bromoform	0.527	Benzene	93.96±2.85	94.85
Bromoform	0.527	Methyl alcohol	93.59±2.85	94.85
Ethylene dibromide	0.763	Benzene	86.06±2.10	85.07
Ethylene dibromide	0.748	Methyl alcohol	84.04±2.14	85.07
Acetylene tetrabromide	0.469	Benzene	93.25±3.20	92.47
n-Butyl bromide	0.710	Benzene	60.99±2.11	58.32
Bromoacetic acid	0.826	Methyl alcohol	55.20±1.82	57.51
Bromobenzene	1.176	Benzene	51.64±1.36	50.90
Bromobenzene	1.204	Methyl alcohol	49.56±1.33	50.90
α-Bromonaphthalene	1.063	Benzene	35.34±1.32	38.59

TABLE II. RADIOACTIVATION ANALYSIS OF BROMINE BY 16.0 hr. IRRADIATION

Sample	Weight g./5 ml.	Solvent	Bromine content in sample, %	
			Determined value	Theoretical value
Ethylene dibromide	0.956	Benzene	84.32±0.84	85.07
Acetylene dibromide	0.481	Benzene	93.56±1.25	92.47
Bromoacetic acid	0.869	Methyl alcohol	55.04±0.69	57.51
Bromobenzene	1.204	Benzene	48.39±0.58	50.90
α-Bromonaphthalene	1.017	Benzene	38.74±0.59	38.59

TABLE III. RADIOACTIVATION ANALYSIS OF IODINE BY 1.0 hr. IRRADIATION

Sample	Weight g./5 ml.	Solvent	Iodine content in sample, %	
			Determined value	Theoretical value
Iodoform	0.411	Benzene	95.44±3.41	96.69
Methyl iodide	0.783	Benzene	90.65±2.04	89.41
Ethyl iodide	0.616	Benzene	81.17±2.44	81.37
n-Propyl iodide	0.415	Benzene	77.51±3.13	74.66
Iodoacetic acid	0.954	Water	65.20±1.68	68.25
o-Iodobenzoic acid	0.828	Methyl alcohol	53.30±1.69	51.17
p-Iodoaniline	0.578	Benzene	59.23±2.23	57.94

where the paraffin thickness between the neutron source and the sample hole was 7 mm., was approximately 1×10^3 neutrons/cm^2/sec. (The accuracy of this value will be estimated in another report). When the source was at position A in Fig. 1, the radiation dosage at position B, which was just in front of the lead shield, was about 2 mr./hr. When the source was set at the irradiation position, it was about 1 mr./hr.

A known amount of the sample to be analyzed was dissolved in an appropriate solvent, such as benzene, methyl alcohol or water, adjusted to 5.00 ml. in 30°C, and then irradiated. The irradiation times were 1.0 and 16.0 hr. in the bromine analysis and 1.0 hr. in the iodine analysis. After the end of the irradiation, the neutron source was pulled up to position A in Fig. 1 and the sample capsule was taken out rapidly. Then, after a 2.5 min. interval, the radioactivity induced in the sample was measured by a well-type NaI scintillation counter (1.75''$\phi\times$2''h. hole; 0.75''$\phi\times$1.5'' deep) for 30.0 min.

The induced radioactivities in the bromine analysis were due to ^{80}Br, ^{80m}Br and ^{82}Br, whose counting rate ratio at the beginning of the counting was 1000 : 80 : 66 in the 1.0 hr. irradiation. In the iodine analysis, the induced radioactivity was due only to ^{128}I.

Among the irradiation samples of a water, a methyl alcohol and a benzene solution of a compound to be analyzed, and even of a solid mixture of the compound and cane sugar, no appreciable difference in the induced radioactivity strength could be found.

Using the solution of *p*-dibromobenzene in benzene or hydrogen bromide in water as a standard substance in the bromine analysis, the bromine content in various organic compounds was determined. The analytical results obtained are shown in Tables I and II, along with the

theoretical values. Iodine analysis was done using a solution of iodobenzene in benzene as a standard. The results are shown in Table III.

As is shown in these tables, the results of the non-destructive activation analysis of bromine and iodine in various organic compounds were satisfactory. Although the sensitivities of both the analyses in this report were low, but it is expected that the use of a stronger neutron source will improve the sensitivities and will also make possible the use of smaller amounts of the sample.

Department of Chemistry
Faculty of Science
Konan University
Higashinada-ku, Kobe

A Kinetic Study of the Reaction from Tetramethyl-p-benzoquinone to Tetramethylhydroquinone

By Chie MIYAKE, Takasuke MORI and Tadao SANO

(Received June 25, 1962)

The semiquinone free radical which appears during course of the oxidation-reduction reaction between quinone and hydroquine has been widely studied to ascertain the relation between the formation of the free radical and the condition of the reacting solution[1], as well as its electronic structure. However, there is little conclusive information about the nature of these reactions because they are confused with fairly complicated side reactions.

The measurement of the magnetic susceptibility of the solution during the course of reaction was carried out with systems having duroquinone and various monosaccharides applied as reducing agents, considering that in these systems the side reactions need not be taken into account[2]. The results have already been reported but are now dealt with from the view-point of chemical kinetics. The rates of the formation and decomposition of the tetramethyl-*p*-benzosemiquinone radical are empirically found to follow such simultaneous differential equations as:

$$dx/dt = -(k_1 + k_2 y)x$$
$$dy/dt = (k_1 + k_2 y)x - k_3 y$$
$$dz/dt = k_3 y$$

where x, y and z are the concentrations of tetramethyl-*p*-benzoquinone, tetramethyl-*p*-benzosemiquinone and tetramethyl-*p*-hydroquinone, respectively, after time t. k_1, k_2 and k_3 are rate constants. Figure 1 shows the relation between the experimental and calculated values using the equation as representative. The dependency of the rate constants k_1, k_2 and k_3 on the temperature at which the measurement was performed is represented in Fig. 2, which shows a good linearity. k_1 and k_3 are found to be proportional to the concentrations of such monosaccharide used as glucose, mannose or fructose, while k_2 is in parabolic proportion to those of every monosaccharide. The activation energy necessary for the formation of the free radical by the reaction of tetramethyl-*p*-benzoquinone with monosaccharide, that for the formation of the free radical by a reaction like the auto-reduction reaction between the

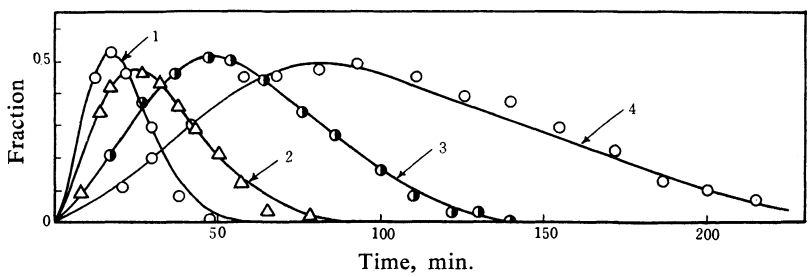


Fig. 1. Relation between experimental values and those calculated from equation.
—— calcd.; ○, ◑ and △ experimental
1 65 mg. of glucose, at 25.2°C
2 10 mg. of fructose, at 25.4°C
3 100 mg. of mannose, at 24.0°C
4 10 mg. of glucose, at 25.2°C

1) J. E. LuValle et al., "Technical Note on the Chemistry of Quinone", ASTIA Document Service Center, Arlington Hall Station, Arlington, Virginia, Report No. TOI 58-29 (1958).

2) H. Takaki, N. Kawai, C. Miyake and T. Morita, *J. Phys. Soc. Japan*, 13 629 (1958).

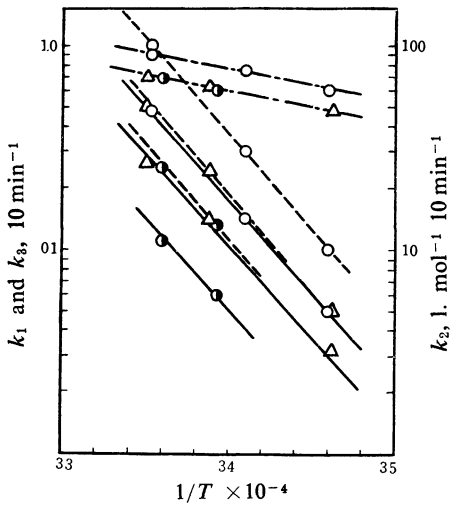


Fig. 2. Dependency of rate constants k_1, k_2 and k_3 upon temperature.
—— for k_1; —·— for k_2; ------ for k_3
○ 80 mg. of glucose
◑ 100 mg. of mannose
△ 10 mg. of fructose

free radical and tetramethyl-*p*-benzoquinone, and that for the decomposition of the free radical producing tetramethyl-*p*-benzohydroquinone are 40, 8 and 41 kcal./mol., respectively.

The details of this report will be published in the Technology Reports of Osaka University.

Department of Nuclear Engineering
Faculty of Engineering
Osaka University
Miyakojima-ku, Osaka

*Some Reactions of Pentamethylenediaziridine**

By Hiroshi KATO and Masaki OHTA

(Received July 16, 1962)

Increasing attention has been attracted to diaziridines, and it would be worth while to report some preliminary results on the reactions of pentamethylenediaziridine (I).

Schmitz and Ohme[1] reported that diaziridines are readily dehydrogenated with silver oxide to give diazirines. The present authors have attempted the preparation of diazirines by the action of bromine on diaziridines, and have found that when pentamethylenediaziridine (I) was treated with bromine in the presence of triethylamine, bromination-dehydrobromination took place to afford pentamethylenediazirine (II), which was identified by addition of cyclohexylmagnesium bromide and conversion to urea derivative III by treatment with phenylisocyanate.

As to the reaction with acyl chloride, Abendroth et al.[2] reported that when 3,3-dimethyldiaziridine was treated with an excess of benzoyl chloride in an aqueous medium, acetone and *N*,*N'*-dibenzoylhydrazine were formed. The present authors have studied the reaction of I with an equivalent amount of benzoyl chloride in tetrahydrofuran in the presence of pyridine. In this case also, *N*,*N'*-dibenzoylhydrazine was obtained. When diaziridine I was treated with *p*-tosyl chloride in benzene in the presence of triethylamine, the reaction product was not a diaziridine derivative but an open ring isomer, *N*-cyclohexylidene-*N'*-*p*-tosylhydrazine (IV). The structure of IV was determined by comparison with a specimen of IV, prepared by the reaction between *p*-tosyl hydrazine and cyclohexanone.

Diaziridine I could neither be metalated with sodium amide, sodium hydride, or Grignard reagent, nor be alkylated directly with cyclohexyl bromide.

Experimental[3]

Pentamethylenediaziridine (I)[4]. — Finely powdered hydroxylamine-*O*-sulfonic acid (11.4 g.) was added portionwise under cooling, to a stirred mixture of concentrated ammonia (34 ml.), cyclohexanone (15 g.) and methanol (10 ml.). After two hours, the mixture was extracted with chloroform. The chloroform extracts were dried over potassium carbonate, concentrated and the residue was collected and washed with ether, to give white plates, m. p. 102°C (5.7 g.). Reported m. p.[6], 102~104°C.

Found: N, 25.20. Calcd. for $C_6H_{12}N_2$: N, 24.98%.

Reaction of Pentamethylenediaziridine with Bromine.—A solution of bromine (3.2 g.) in hexane (5 ml.) was added dropwise to a stirred suspension of pentamethylenediaziridine (2.24 g.) in a mixture of triethylamine (4.04 g.) and ether (20 ml.), while the mixture was maintained at 0~10°C. Stirring was continued for two hours after the addition of bromine was complete. The precipitate of triethylamine hydrobromide (6.6 g.) was filtered off;

* Presented at the 15th Annual Meeting of the Chemical Society of Japan, Kyoto, April, 1962.

1) E. Schmitz and R. Ohme, *Chem. Ber.*, **94**, 2166 (1961).

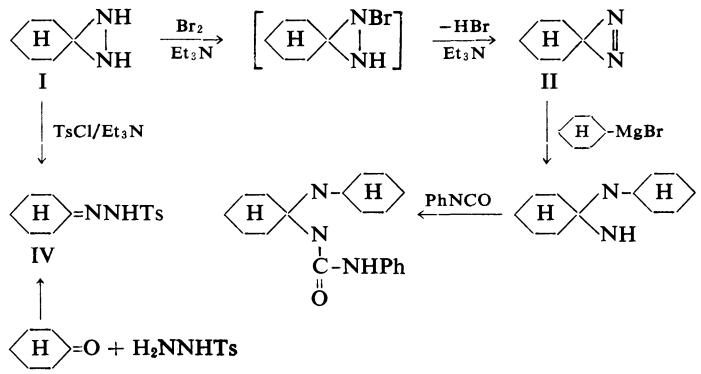
2) H. J. Abendroth and G. Henrich, *Angew. Chem.*, **71**, 283 (1959).

3) All the melting points reported are micro-melting points corrected.

4) After the experiment had been performed, detailed descriptions of preparative method of I has appeared[1,5].

5) E. Schmitz and D. Habisch, *Chem. Ber.*, **95**, 680 (1962).

6) H. J. Abendroth, *Angew. Chem.*, **73**, 67 (1961).



the filtrate was washed with 1 N hydrochloric acid (5 ml.), and was dried over potassium carbonate. Distillation under reduced pressure gave colorless liquid (0.6 g.) which distilled at 28°C/35 mmHg[7].

To a solution of Grignard reagent prepared from cyclohexyl bromide (1.8 g.) and magnesium (0.27 g.) in ether, was added a solution of the above described distillate in ether (10 ml.) with stirring and cooling. After an hour, the mixture was decomposed with water and was extracted with ether (100 ml.). The ether layer was extracted with ice-cooled 2 N sulfuric acid (30 ml.); the acid extracts were neutralized with aqueous sodium hydroxide and again extracted with ether (50 ml.). The ether extracts were dried over potassium carbonate and was concentrated. Phenylisocyanate (0.3 ml.) was added to the residue and the crystals which separated out were collected. Recrystallization from *n*-hexane afforded white needles (0.4 g.), m. p. 146°C. Reported m. p.[1] for *N*-(1-cyclohexylaminocyclohexyl)-*N'*-phenylurea is 147~148°C.

Found: N, 13.24. Calcd. for $C_{19}H_{27}N_3O$: N, 13.42%.

Reaction of Pentamethylenediaziridine with Benzoyl Chloride. — Benzoyl chloride (0.7 g.) was added under cooling to a stirred solution of pentamethylenediaziridine (0.56 g.) and pyridine (0.4 ml.) in tetrahydrofuran (10 ml.). Stirring was continued for two hours; the precipitate of pyridine hydrochloride was filtered off and the filtrate was concentrated under reduced pressure. The oily residue which slowly solidified on cooling was recrystallized from ethanol to give white silky needles, m. p. 241°C. Its melting point was undepressed on admixture with an authentic specimen of *N,N'*-dibenzoylhydrazine.

Found: N, 11.68. Calcd. for $C_{14}H_{12}N_2O_2$: N, 11.66%.

Reaction of Pentamethylenediaziridine with *p*-Tosyl Chloride.—To a stirred solution of pentamethylenediaziridine (2.24 g.) and triethylamine (4.04 g.) in benzene (20 ml.), was added *p*-tosyl chloride (3.82 g.) under cooling, and the mixture was allowed to stand overnight. The crystals of triethylamine hydrochloride (1.8 g.) were filtered off and the filtrate was concentrated under reduced pressure. The colorless prisms which separated out were collected (4.7 g., m. p. 155~156°C) and recrystallized from ethanol to afford colorless prisms, m. p. 160°C. Its melting point was undepressed on admixture with a sample of *N*-cyclohexylidene-*N'*-*p*-tosylhydrazine, prepared by the following method.

Found: C, 58.33; H, 6.60; N, 10.52. Calcd. for $C_{13}H_{18}N_2O_2S$: C, 58.63; H, 6.81; N, 10.52%.

***N*-Cyclohexylidene-*N'*-*p*-tosylhydrazine (IV).** — A solution of *p*-tosylhydrazine (1.86 g.) and cyclohexanone (0.98 g.) in ethanol (30 ml.) was refluxed for an hour. The colorless prisms which separated out on cooling were collected (1.35 g.), m. p. 160°C.

Found: N, 10.79. Calcd. for $C_{13}H_{18}N_2O_2S$: N, 10.52%.

Attempted Metalation and Alkylation of Pentamethylenediaziridine. — When pentamethylenediaziridine was treated with ethylmagnesium iodide in ether at room temperature, or with sodium amide or sodium hydride in benzene at reflux temperature in an atmosphere of nitrogen, and then with cyclohexyl bromide, unchanged starting material was recovered.

Laboratory of Organic Chemistry
Tokyo Institute of Technology
Meguro-ku, Tokyo

7) Uncorrected. Reported b. p.[1], 33°C/30mmHg.

*The Selective Adsorption of Optical Antipodes as Revealed by the Chromatographic Techniques**

By Masaaki CHARA, Isao FUJITA and Takao KWAN

(Received July 21, 1962)

A number of attempts for the optical resolution by adsorption have been so far made, using various optically active adsorbents such

* Presented at the 15th Annual Meeting of the Chemical Society of Japan, Kyoto, April, 1962.

as protein[1], starch[2], lactose[3], alumina coated with L-(+)-tartaric acid,[4] optically active quartz powder[5], ion exchange resins[6] and so on. Most of these observations, with the use of batch technique, appear to give too small a rotation to draw any definite conclusion while some using the chromatographic one seem to give a partial yet definite resolution[2,4]. Even for the latter case there are conflicting observations and uncertainties, suggesting that the phenomenon is extremely sensitive to the environment of the adsorbate-adsorbent system, particularly to the surface structure of the adsorbent.

We undertook this problem by utilizing both gas chromatographic and Tswett type column chromatographic techniques and by using starch, (−)-quartz, cellulose, alumina coated with various optically active substances as column packings.

Particular interest was first in the gas chromatographic separation of DL-*sec*-butanol on starch due to Karagounis et al.[7] We prepared *specific starch* according to the method kindly communicated by Karagounis and followed their work.

Helium was the carrier when the thermal conductivity cell was used as the detector, while nitrogen was the carrier when the hydrogen flame ionization gauge was employed as the detector*1. In both cases we had nothing but single peaks on the chart, however. Other optically active packings were investigated without success.

On the other hand the passage of DL-mandelic acid through Tswett column packed with starch—the one first studied by Krebs et al.[2]—was found to give a distinct resolution of the racemate: the initial fractions of the eluate as well as those close to the final stage gave rise to almost 100% optical purity differing in the direction of rotation.

Experiments were made as follows. A potato starch column 149×1.6 cm. was employed. Mandelic acid was chosen as the adsorbate because of its large specific rotation. Sample of 0.25~2.00 g. mandelic acid in a 5% aqueous methanol was adsorbed on top of the column and then eluted with water through the column kept at room temperature. The eluate from the column was fractionated with the automatic fraction collector. The rotation of each fraction amounting 2.2 cc. was determined by Zeiss-Kreis polarimeter. The amount of mandelic acid in each fraction was weighed out after evaporating the solvent up to dryness.

The specific rotation $[\alpha]_D$ was now calculated according to the expression:

$$[\alpha]_D = (100 \times \alpha)/(d \times c)$$

where c is the number of grams of mandelic acid in 100 cc. of the solution, α the observed angle of rotation and d the cell length (usually 1 dm.). In Fig. 1 $[\alpha]_D$ is shown against fraction numbers.

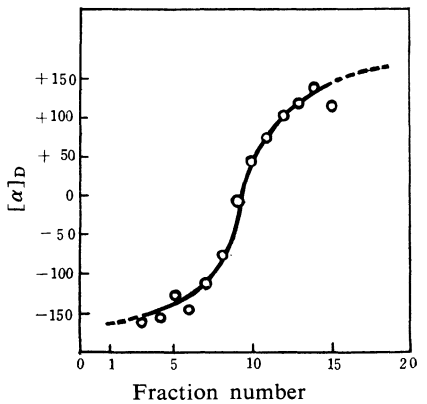


Fig. 1. The plot of the specific rotation $[\alpha]_D$ against fraction numbers.

Figure 1 shows that mandelic acid having a negative angle of rotation is eluted first, then followed by the one with the positive angle of rotation. It is apparent therefore that the latter, denoted by L-(+)-mandelic acid, is adsorbed on the starch more strongly than D-(−)-isomer. Now assuming that the additivity rule holds between the specific rotation and the composition of each optical isomer and that $[\alpha]_D$ of mandelic acid is independent of the concentration at ±157 at room temperature, the concentration of D- or L-isomer was calculated against each fraction. The chromatogram obtained in this way is shown in Fig. 2.

Figure 2 shows that the initial fractions as well as those close to the final stage are highly enriched or almost pure with regard to D- or L-mandelic acid respectively. None of the previous reports ever achieved such high resolution*2. The efficiency of resolution, judged

1) W. Bradley and G. C. Easty, *J. Chem. Soc.*, **1951**, 499.
2) H. Krebs, J. Diewald and J. A. Wagner, *Chem. Ber.*, **89**, 1875 (1956).
3) G. M. Henderson and H. G. Rule, *J. Chem. Soc.*, **1939**, 1568.
4) G. Karagounis, E. Charbonnier and E. Floss, *J. Chromatography*, **2**, 84 (1959).
5) G. M. Schwab and L. Rudolph, *Naturwissenschaften*, **20**, 363 (1932). R. Tsuchida, A. Nakamura and M. Kobayashi, *J. Chem. Soc. Japan*, **56**, 1339 (1935); G. Karagounis and G. Coumoulos, *Nature*, **142**, 162 (1938).
6) N. Grubhofer and L. Schleith, *Naturwissenschaften*, **40**, 508 (1953).
7) G. Karagounis and G. Lippold, ibid., **46**, 145 (1959).
*1 Karagounis used Scott type detector using hydrogen as the carrier.

*2 Using a starch column 45 cm. long, Krebs et al. were able to enrich D- or L-mandelic acid only partially. Our satisfactory results may perhaps be due partially to the comparatively long column length 149 cm., which has much more plate numbers effective in the resolution.

TABLE I. AMOUNT OF D-MANDELIC ACID (%) IN THE FIRST THREE FRACTIONS

Run	Amount of racemate g.	Recovery %	% D-Mandelic acid in fraction number			Ratio of V_R L/D
			1	2	3	
1	2.00	83	65	57	52	
2	2.00	97	96	90	87	1.04
3	1.00	99	100	99	89	1.04
4	0.50	100	93	94	100	1.04
5	0.25	96	100	100	79	1.04

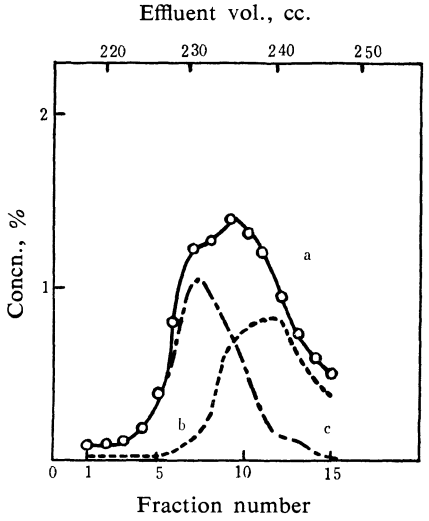


Fig. 2. Chromatograms of D- and L-mandelic acid. Flow rate of effluent: 2.5 cc./hr.

a Total amount of mandelic acid
b L-(+)-Mandelic acid
c D-(−)-Mandelic acid

from the optical rotation of the initial fractions, was found unexpectedly to be little affected by preheating the starch in the air around 110°C or by the pretreatment with ether.

Table I shows the concentration of D-mandelic acid calculated for the first three fractions respectively.

It is noted from the third column of the table that fresh starch i. e. the one used in run 1 adsorbs mandelic acid irreversibly or results in an imperfect material balance. This was not the case with the subsequent runs: run 2—5 gave almost perfect material balance. Thus, a sample of starch pretreated with dilute mandelic acid solution was packed in the column and subjected to experiment which was found to give reasonable recovery of mandelic acid with high resolution similar to those of run 2—5 of the table. The resolution of racemate on the *pretreated* starch may perhaps be associated with some physical modification of the adsorbent due to the irreversibly occluded mandelic acid molecules.

To estimate the degree of resolution of the racemate, the ratio of the retention volume V_R*3 of each isomer was calculated except run 1 and compared in the last column of the table. The ratio was invariable at 1.04 with varying the amount of mandelic acid eluted.

Several homologues of mandelic acid were also subjected to experiment for resolution on the starch column and found to be resolved definitely but to a less extent. The details of the experiments will be presented and discussed in the near future.

Division of Physicochemical Technology
Faculty of Pharmaceutical Sciences
The University of Tokyo
Hongo, Tokyo

*3 V_R was defined as the volume of the effluent that passed through the column until the highest concentration of L- or D-mandelic acid was collected in the fraction.

Hafnyl Ion - Sodium Alizarin 3-Sulfonate Chelate : A Spectrophotometric Study

By Samir K. BANERJI* and Arun K. DEY

(Received August 18, 1962)

Considerable work on metal chelates involving sodium alizarin-3-sulfonate (trivial name Alizarin Red S, abbr. ARS), and their analytical applications have been reported from these

* Present address: Chemistry Department, Birla Engineering College, Pilani, India.

laboratories[1-9]. From electrical conductance measurements[10] it has been concluded that the reagent behaves as a colloidal electrolyte and aqueous solutions of ARS show the characteristics of a true solution, only when very dilute.

Chelate formation of sodium alizarin-3-sulfonate with quadrivalent metals like zirconium and hafnium[11,12], and thorium[13] has been studied mainly with reference to the nature of lakes formed and position of the chelate ring in the structures. This paper describes the composition and stability of the hafnium chelate.

Experimental

Materials.—BDH reagent grade sodium alizarin-3-sulfonate (Alizarin Red S reagent) was used for the studies without any further purification. A solution of suitable concentration was prepared and standardized by determining the sulfur in the compound. Hafnyl chloride, obtained from M/S A. D. Mackay & Co. Inc., N. Y., was dissolved in water, hydrochloric acid being added to prevent hydrolysis and the hafnium in the solution was determined as hafnia. Freshly prepared solutions in redistilled water, free from carbon dioxide, were employed to avoid effects due to the hydrolysis of the metal salt.

Experimental Procedure. — A Unicam SP 500 spectrophotometer, operated by Doran mains unit on 220 V./50 cycl., single phase stabilized mains was used. Matched glass cells of 10 mm. thickness were used for absorbance measurements, which were noted against distilled water blanks.

pH measurements were made with a Leeds and Northrup pH meter with a glass-calomel electrode system. The experiments were performed in a room maintained at 25°C. The pH of all solutions were adjusted to 2.0±0.2, by the addition of hydrochloric acid.

Results

Nature of the Complex in Solution. — The method described by Vosburgh and Cooper[14] was adopted. Mixtures were prepared containing various proportions of hafnyl chloride and sodium alizarin-3-sulfonate and the absorbances were measured at different wavelengths. The λ_{max} of each mixture is found to lie at the same spectral region of 520 mμ, which shows that only one complex is formed, under the conditions of study, in the system investigated here.

Stoichiometry of the Components.—The ratio of the metal : reagent in the complex has been established by the method of continuous variations. The total volume in each case was 50 ml. The absorbances were measured at 500 and 520 mμ. Various concentrations of the reactants were used and the results are summarized in Table I and some are graphically represented in Fig. 1. In Fig. 1, the difference of the absorbance of the mixture and that which would be shown by the chelating agent alone, if no chelation occurred, is plotted against the composition of the mixture. In Table I and in the legends of Fig. 1, c represents the concentration of hafnyl chloride and

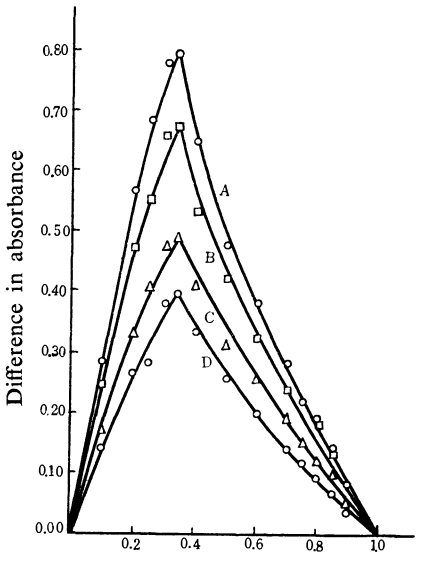


Fig. 1. Determination of the composition from absorption spectra studies at 500 mμ (equimolecular solutions).
Curve A $c=4.0\times10^{-4}$ M, $p=1$
Curve B $c=3.33\times10^{-4}$ M, $p=1$
Curve C $c=2.5\times10^{-4}$ M, $p=1$
Curve D $c=2.0\times10^{-4}$ M, $p=1$

1) A. K. Mukherji and A. K. Dey, *Proc. Natl. Acad. Sci. (India)*, **26A**, 242 (1957).
2) A. K. Mukherji and A. K. Dey, This Bulletin, **31**, 521 (1958).
3) A. K. Mukherji and A. K. Dey, *Z. anal. Chem.*, **160**, 98 (1958).
4) A. K. Mukherji and A. K. Dey, *J. Ind. Chem. Soc.*, **34**, 461 (1957).
5) A. K. Mukherji and A. K. Dey, *Proc. Natl. Acad. Sci. (India)*, **26A**, 20 (1957).
6) A. K. Mukherji and A. K. Dey, *Vijñana Pari. Anu. Patrika*, **1**, 23 (1958).
7) S. K. Banerji and A. K. Dey, *J. Ind. Chem. Soc.*, **38**, 121 (1961).
8) S. K. Banerji and A. K. Dey, *Z. anorg. Chem.*, **309**, 226 (1961).
9) S. K. Banerji and A. K. Dey, *J. sci. industr. Research, India*, **20B**, 375 (1961).
10) A. K. Mukherji and A. K. Dey, *Kolloid-Z.*, **158**, 147 (1958).
11) H. A. Leibhafsky and E. H. Winslow, *J. Am. Chem. Soc.*, **60**, 1776 (1938).
12) E. M. Larson and S. T. Hirozawa, *J. Inorg. Nucl. Chem.*, **3**, 198 (1956).
13) D. V. N. Sarma and Bh. S. V. Raghava Rao, *Anal. Chim. Acta*, **13**, 142 (1955).
14) W. C. Vosburgh and G. R. Cooper, *J. Am. Chem. Soc.*, **63**, 437 (1941).

TABLE I. COMPOSITION OF HAFNIUM - ARS CHELATE

Fig.	Curve	$c \times 10^4$ M	p	Wavelength mμ	Vol. of $HfOCl_2$ ml. at peak	Composition of the chelate Hf : ARS
1	A	4.00	1.0	500	16.7	1 : 2
	B	3.33	1.0	500	16.7	1 : 2
	C	2.50	1.0	500	16.7	1 : 2
	D	2.00	1.0	500	16.7	1 : 2
Not	A	4.00	1.0	520	16.7	1 : 2
shown	B	3.33	1.0	520	16.7	1 : 2
	C	2.50	1.0	520	16.7	1 : 2
	D	2.00	1.0	520	16.7	1 : 2
Not	A	3.33	1.5	500	21.4	1 : 2
shown	B	2.00	2.0	500	25.0	1 : 2
Not	A	3.33	1.5	520	21.4	1 : 2
shown	B	2.00	2.0	520	25.0	1 : 2

$p = c'/c$, where c' is the concentration of sodium alizarin sulfonate.

From the above table it is evident that the composition of the chelate is $HfO(ARS)_2$.

Influence of pH on the Stability of the Chelate.—The absorbances of mixtures containing 0.00009 M of hafnyl chloride and 0.00018 M of the reagent at different pH were measured at different wavelengths and it is seen that the λ_{max} lies at 520 mμ in the case of solutions having pH of 1.0 to 4.0, showing thereby that the chelate is stable in this range of pH.

Evaluation of the Stability Constant. — The stability constant has been calculated by the modified method of Anderson et al.[15] as described earlier[7-9]. In this case the stability constant K is given by

$$K = \frac{x}{(a-x)(b-2x)^2} \qquad (1)$$

where x is the concentration of the complex at equilibrium and a and b are the initial concentration of the metal ion and the chelating agent, respectively. Taking two sets of concentrations with the same absorbance, i. e. the same value of x, we have:

$$K = \frac{x}{(a_1-x)(b_1-2x)^2} = \frac{x}{(a_2-x)(b_2-2x)^2} \qquad (2)$$

Hence, from a knowledge of two sets of initial concentrations of a and b, the value of x can be calculated and therefrom K may be evaluated.

The value of $\log K$ in the system hafnyl chloride-sodium alizarin-3-sulfonate works out to be 10.4 ± 0.3 at 25°C, and the corresponding free energy of formation ΔF° is -14.4 ± 0.4 kcal.

Chemical Laboratories
University of Allahabad
Allahabad, India

15) R. C. Anderson and R. T. Foley, ibid., **70**, 1195 (1948); **71**, 909 (1949).

SHORT COMMUNICATIONS

On the ESR Study of Quinquevalent Chromium Complexes

By Hideo KON

(Received August 24, 1962)

The author has been interested in the four characteristic ESR lines observed at room temperature of the chromium(VI) oxide (or potassium bichromate) - concentrated sulfuric acid system. As is shown in Fig. 1, a very remarkable feature of the absorption is that all the four lines are very narrow (ca. 1~5 gauss), even narrower than the Cr^{3+} absorption lines which can be observed at room temperature. Observations of the same solution doped with Cr^{3+} show that the narrow lines in question are definitely different from that of Cr^{3+}. Also, careful purifications of concentrated sulfuric acid and potassium bichromate do not alter the signal intensity and the number of lines. It is suspected, therefore, that the paramagnetic species responsible for the narrow absorption lines be some chromium oxides of intermediate valence state, the best possiblity being chromium(V) oxide.

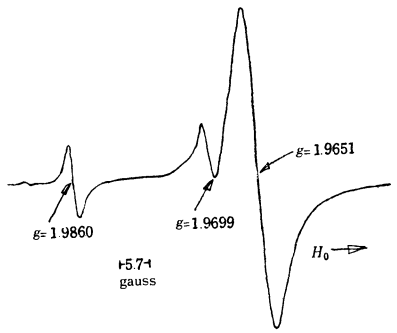


Fig. 1. ESR absorption of a CrO_3 - conc. H_2SO_4 solution. Observed g-value is accurate to ± 0.0005.

The transition metal ions with one 3d electron (for example, Cr^{5+}, Ti^{3+}, etc.) usually show the electron spin resonance absorption which is so broad that the observation is sometimes prohibitively difficult, particularly at ambient temperatures. In fact, Ti^{3+} absorption was observed only at 4 to 8°K with remarkably anisotropic g-value and with very short relaxation time[1]. This is explained as due to the fact that the combined effect of the microcrystalline field and the spin orbit coupling is not so great as to lift the degeneracy of the ground spin orbitals very much and so, there is always an excited state fairly close to the lowest Kramer's doublet. A quinquevalent chromium compound was shown to behave in a similar fashion; its electron spin resonance was observed in CrO_4^{3-} at 20°K with very broad and temperature dependent absorption lines. Thus the assumption of quinquevalent chromium in chromium oxide-concentrated sulfuric acid system seems to be in conflict with the above consideration on the line width.

However, if the crystalline field perturbation would be greater and the deviation from the cubic symmetry extreme, then, there could be further decrease in the spin-lattice relaxation, and so the reduction in the ESR line width. In order to see if such is the case actually, a few complexes of quinquevalent chromium, such as K_2CrOCl_5, $HCrOCl_4X$ (where X is the base; pyridine, quinoline tetramethylamine) were prepared and their ESR absorption observed in solution and in polycrystalline form. If the structural unit of these compounds would be CrO^{3+}, the microcrystalline field symmetry would have a strong axial component and the line width could be smaller than in, for example, CrO_4^{3-}. A

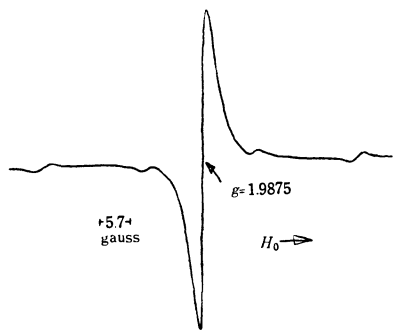


Fig. 2. ESR absorption of a $HCrOCl_4$-pyr. solution. The four satellites are the hyperfine components due to ^{53}Cr nucleus.

1) B. Bleaney and K. W. H. Stevens, *Rep. Prog. Phys.*, **16**, 108 (1953).
2) A. Carrington, D. J. E. Ingram, D. Shonland and M. C. R. Symons, *J. Chem. Soc.*, **1956**, 4710.

typical solution spectrum shown in Fig. 2 indicates that this is the case at least in solution, and the peak to peak line width there, is only 2.7 $\pm$0.2 gauss, a value much smaller than VO^{2+} which has an analogous structure. Though not conclusive, this result may lend a strong support to the assumption of chromium(V) existing in chromium(VI) oxide-concentrated sulfuric acid system. Several other ESR absorptions with even narrower line widths and with different *g*-values were also observed transiently during the course of the reaction of the chromium(VI) compounds with various acids (acetic, trifluroacetic, phosphoric, oxalic, lactic, citric, malonic acid and so on), and the paramagnetic species may be considered here again as some quinquevalent chromium oxyions.

Details of the result of these ESR observation will be published soon with the visible and infrared absorption data.

NAIG Nuclear Research Laboratory
Kawasaki

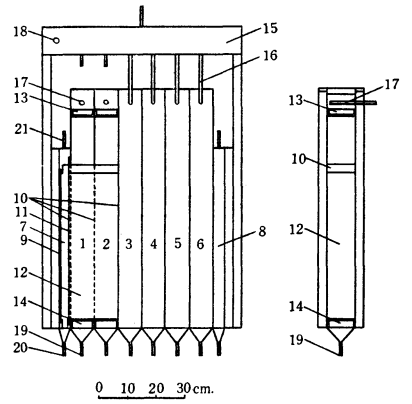


Fig. 1. Essential part of enrichment apparatus.

1—6: Resin compartments
7: Cathode compartment
8: Anode compartment
9: Pt electrode
10: Cation exchange membrane
11: Supporter
12: Cation exchange resin
13: Perforated plate
14: Resin holder
15: Feed conduit
16: P. V. C. tube
17: Solution distributor
18: Feed solution inlet
19: Discharge solution outlet
20: Electrode solution inlet
21: Electrode solution outlet

Continuous Isotope Enrichment by a Simultaneous Use of Ion Exchange and Electromigration

By Hidetake KAKIHANA, Yoshihiro MORI and Tadaya HOSHINO*

(Received October 8, 1962)

For a continuous isotope enrichment a new type of apparatus (Fig. 1) was devised on the basis of a simultaneous use of ion exchange and electromigration. The principle of the continuous enrichment is schematized in Fig. 2.

If an ion of isotope I moving down through an ion exchange bed with velocity of v_1 is placed under the horizontal supply of an electric field, the movement of the ion should be the addition of vectors v_1, the vertical velocity, and h_1, the horizontal velocity caused by the electric field. Similarly the movement of isotope II ion is the addition of vectors v_2, and h_2. If $v_1 > v_2$ and $h_1 < h_2$, the movement of the two ions can be expressed by the vectors R_1 and R_2. As R_1 and R_2 are different each other not only in their magnitude but also in their direction, the continuous enrichment of the isotopes should be possible by the continuous feed of the isotope solution from the top (Fig. 2).

After the compartments (1, 2, 3, 4, 5 and 6 in Fig. 1) had been filled with ion exchange resin, a lithium solution was introduced at the top and drawn from the bottom, and at the same time a electric current was horizontally passed through the apparatus. To the electrode compartments electrolyte solutions were circulated.

To find whether any isotopic enrichment can be experimentally detected, a number of runs were carried out. Data for a run are given in Table I. In 35 hr. the run reached the stationary state, where the potential gradient

TABLE I. OPERATING CONDITIONS

Ion exchange resin: 50~60 mesh Diaion SK 1
Potential across resin: 60~140 V., D. C.
Current through resin: 9.0~12.0 amp.
Temperature of solution at the bottom: 40.0~50.0°C
Feed solution: 0.043 N Li_2CO_3 aq. solution
Feed rate: 60 ml./cm²/hr.
Electrode solution: 0.5 N $(NH_4)_2SO_4$ aq. solution
Flow rate: 10 l./hr.

* Present address: Atomic Fuel Cooperation, Chiyoda-ku, Tokyo.

TABLE II. RESULTS OF ANALYSIS

Position	Samples of 38hr10min after the start				Samples of 43hr40min after the start			
	L. concn. γ/cc. samp. solution	$^7Li/^6Li$	Li flow rate g./hr.	Li distribution, %	Li concn. γ/cc. samp solution	$^7Li/^6Li$	Li flow rate g./hr.	Li distribution, %
Cathode	189	12.10	0.58	8.0	205	12.11	0.29	4.6
1	646	12.16	3.23	44.7	428	12.14	2.14	33.6
2	311	12.22	1.56	21.6	369	12.23	1.85	29.0
3	252	12.20	1.26	17.4	291	12.21	1.42	22.3
4	90.4	12.19	0.47	6.5	97.2	12.17	0.49	7.7
5	16.3	12.31	0.08	1.1	28.7	12.27	0.14	2.2
6	4.9	12.26	0.03	0.4	6.1	12.43	0.03	0.5
Anode	3.3		0.02	0.3	2.6		0.01	0.2
Feed	300.0	12.20	7.23	100.0	300.0	12.20	6.37	100.1

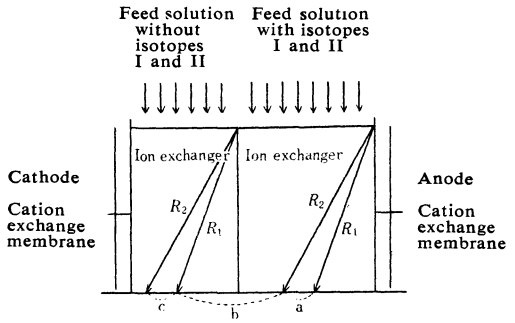


Fig. 2. Principle of the continuous isotope enrichment.

a: Pure isotope I comes out
b: The solution same as feed solution comes out
c: Pure isotope II comes out

was 2V./cm., the current density was 18 mamp./cm^2 and the thermal convection and gas evolution were effectively reduced. The samples of solution drawn off from each bottom of the six compartments were analyzed. Lithium concentration in the samples was determined by colorimetry with thoron[1]. Another portion of the sample solutions was evaporated to dryness, and sulfate ion was separated with anion exchange resin column in the hydroxide form. Then the lithium was converted to iodide by the addition of hydroiodic acid and evaporation to dryness, the lithium in the feed solution was also converted to lithium iodide in the similar manner. Isotopic ratios of the lithium iodide samples were determined with a Nier-type 60 degree mass spectrometer, Atlas CH-4 using the thermionic method[2].

The analytical results are given in Table II. The ratios $^7Li/^6Li$ were decreased in the solutions from the compartment 1 and the cathode, and increased in the solutions from the compartment 5 and 6. At the stationary state about 38.2 per cent of the lithium came out continuously from the compartment 1 to the cathode compartment and the bottom of the compartment, while 2.7 per cent of the lithium could be continuously collected in the outputs from the compartments 5 and 6. The values for the ratio of $^7Li/^6Li$ in both products are estimated 12.14 and 12.30 respectively.

Tokyo Institute of Technology
Meguro-ku, Tokyo

1) P. F. Thomason, *Anal. Chem.*, **28**, 1527 (1956).
2) H. Kakihana, T. Nomura and Y. Mori, *J. Inorg. Nucl. Chem.*, in press.

Micro-wave Absorption in Benzene Solution of Cyclohexane-1, 4-dione

By Ariyuki AIHARA*, Kazuo CHITOKU and Ken-ichi HIGASI

(Received October 13, 1962)

With an aim of checking the polarity of cyclohexane-1, 4-dione molecule, dielectric absorption of this substance in micro-wave region (0.446 molar benzene solution) has been measured with use of a resonant cavity which was originally designed by Dr. Hatori of this Institute. The results obtained at a frequency of 9.4 Gc/sec. (3.2 cm.) are shown in the following table:

* On leave from the University of Electro-Communications, Chofu, Tokyo.

TABLE I. DIELECTRIC LOSS AND DIELECTRIC CONSTANT AT 3.2 cm. (20°C)

Substance	$\tan\delta\cdot10^4$	ε'
Benzene	5.8	2.282
Cyclohexane-1, 4-dione in benzene	22.3	2.383
Chlorobenzene in benzene	28.6	2.286

For the sake of comparison, the results obtained with the solution of chlorobenzene in benzene (0.049 molar) are also shown in Table I.

Considering the fact that a fairly large value of the dipole moment has been reported so far for cyclohexane-1, 4-dione (1.2~1.5 Debye)[1-5], the $\tan\delta$ value for this compound as listed in Table I is unexpectedly small, being less than that of chlorobenzene solution, the concentration of which is almost one tenth of the former, while the increment of dielectric constant with the former is much more appreciable. This seems to indicate that either the actual dipole moment of this compound should be much smaller than those so far obtained by other investigators or that we must seek for the mechanism of dielectric absorption which differs from that of usual Debye absorption.

If we assume the magnitude of relaxation time for cyclohexane-1, 4-dione as 7×10^{-12} sec.[6], we can calculate an apparent dipole moment of the compound with use of the following equation:

$$\mu^2=6750\,\varepsilon'\boldsymbol{k}T(1+\omega^2\tau^2)\tan\delta/(\varepsilon'+2)^2\pi c\boldsymbol{N}\omega\tau$$

where ε', $\boldsymbol{k}$, T, c, $\boldsymbol{N}$, ω, and τ are the dielectric constant of the solution, Boltzmann's constant, absolute temperature, molar concentration, Avogadro's number, angular frequency, and the relaxation time of the molecule, respectively. The value of dipole moment thus calculated is 0.43 Debye, suggesting that the molecule of cyclohexane-1, 4-dione exists almost in a non-polar conformation.

We may conclude, therefore, that 1) the larger values of dipole moment so far reported for this compound by a number of investigators are due to their underestimation of atom polarization or "vibration polarization" in calculating μ value from the observed molar polarization, and 2) the "libration" of two carbonyl groups attached at the opposite ends of flexible ring, or "puckering" should be responsible for such a high value of atom polarization (Chiba's estimation is ~33 cc.)[5], and 3) consequently, cyclohexane-1, 4-dione exists predominantly in the flexible form with two carbonyl groups directed almost in opposite sense: libration of the groups may give rise to a small apparent dipole moment.

Details will be published later in this Bulletin.

Research Institute of Applied Electricity
Hokkaido University, Sapporo

1) C. G. Le Fèvre and R. J. W. Le Fèvre, *J. Chem. Soc.* **1935**, 1696.
2) K. Hayasaki and K. Kozima, *Bull. Tokyo Inst. Tech.*, **1952**, 1.
3) M. Rogers and J. M. Canon, *J. Phys. Chem.*, **65**, 1417 (1961).
4) N. L. Allinger and L. A. Freiburg, *J. Am. Chem. Soc.*, **83**, 5028 (1961).
5) T. Chiba, private communication.
6) τ values for chlorobenzene and cyclohexanone are 8×10^{-12} sec. and 6×10^{-12} sec., respectively.

Mechanism of Chemiluminescence of 2, 4, 5-Triphenylimidazole

By Taro HAYASHI and Koko MAEDA

(Received October 12, 1962)

Radziszewsky[1] found that lophine exhibits a whitish greenish blue luminescence in an ethanolic solution of potassium hydroxide with molecular oxygen or several oxidizing agents. We have been studying the mechanism of the chemiluminescence of 2, 4, 5-triphenylimidazole (lophine) for several years[2,3], and have found that substitution of its imino-hydrogen[4] prevented luminescence. This fact suggests that the anion produced by the dissociation of the imino-hydrogen is the active agent of chemiluminescence.

The chemiluminescence of lophine with an ethanolic solution of bromine or an aqueous solution of potassium ferricyanide was inhibited by the removal of dissolved oxygen in the solutions and the luminescence was restored immediately upon passing oxygen into the reaction mixture. This indicates that molecular oxygen is necessary for chemiluminescence. When an ethanolic solution of bromine

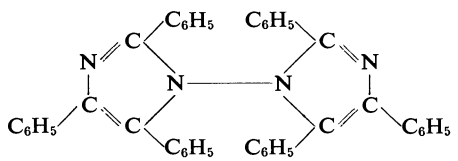
1) B. Radziszewsky (*Ber.*, **10**, 70 (1877)) found that benzoic acid and ammonia were produced with the chemiluminescence of lophine.

2) T. Hayashi and K. Maeda, 1st Joint Meeting of the Societies of Chemistry in Japan, Tokyo, November, 1957; 11th Annual Meeting of the Chemical Society of Japan, Tokyo, April, 1958; T. Hayashi, K. Maeda and H. Ojima, Symosium on Mechanism of Organic Reactions, Chem. Soc. Japan, Tokyo, 1959; Shirahama, 1960; Sendai, 1961.

3) The spectrum of luminescence extending over the visible region with a maximum at about 540 mμ will be reported soon.

4) *N*-Methyllophine (m. p. 149~150°C), *N*-ethyllophine (m. p. 125~126°C) and *N*-*n*-butyllophine (m. p. 122~123°C were investigated.

was mixed with a solution of lophine in ethanolic potassium hydroxide, a reddish violet color was produced and soon faded. When an aqueous solution of potassium ferricyanide was mixed with the solution of lophine, a grayish white precipitate was produced[5]. The precipitate was recrystallized from benzene at a temperature below room temperature to give fine pale yellow prisms of $C_{42}H_{30}N_4$, m. p. 199~201°C (decomp.)[5]. Its benzene solution turned reddish violet with ultraviolet irradiation or heating. Electron spin resonance[6], formation of yellow nitroso compound, m. p. 110~113°C (decomp.)[5], molecular weight determination and spectroscopic investigation revealed that the color was due to the free radical 2, 4, 5-triphenylimidazyl $C_{21}H_{15}N_2$ produced by the dissociation of the N–N bond in the dimeric compound $C_{42}H_{30}N_4$[7] (I). The dissociation was increased with ultraviolet radiation or heating.



(I)

These findings suggest that the free radical is the essential intermediate in the process of chemiluminescence. The reddish violet benzene solution showed a luminescence, similar to that of lophine, with the addition of hot ethanolic potassium hydroxide, yielding benzoic acid and ammonia. When the solutions of lophine and potassium ferricyanide or bromine were mixed in the absence of oxygen, no luminescence was observed, although the reddish violet color did appear; and when oxygen was passed into the solution, a luminescence was immediately produced. This fact shows that molecular oxygen is necessary for the luminescence of the free radical. When the solution of the dimeric compound in carbon disulfide was exposed to air in direct sunlight, the reddish violet color, first produced, gradually faded to yellow, giving a yellow solid residue by evaporation of the solvent at room temperature. It melted at about 110~120°C with evolution of gas, presumably oxygen, and it oxidized potassium iodide in acetic acid to iodine. Thus it seems probable that the yellow solid contains the peroxide produced from the free radical and molecular oxygen[8]. The benzene solution of the yellow solid exhibited luminescence, similar to that of lophine, with hot ethanolic potassium hydroxide in the absence of oxygen.

From the facts mentioned above, the probable mechanism of the chemiluminescence of lophine is suggested[9] to be as follows: the anion of lophine formed in ethanolic potassium hydroxide yields the free radical 2, 4, 5-triphenylimidazyl by oxidation, from which the peroxide is produced with molecular oxygen and finally the peroxide emits light to yield benzoic acid and ammonia[10].

Department of Chemistry
Faculty of Science
Ochanomizu University
Bunkyo-ku, Tokyo

5) T. Hayashi and K. Maeda, This Bulletin, 33, 566 (1960). This compound exhibits photochromism in solid and in solutions and also thermochromism in solutions.

6) T. Hayashi, K. Maeda, S. Shida and K. Nakada, *J. Chem. Phys.*, 32, 1568 (1960).

7) The investigation of the constitution by spectroscopy and molecular weight determination will be reported soon.

8) Eosine, exhibited a weak photosensitizing effect on the photo-oxidation and zinc oxide suspended in the solution, also exhibited a weak catalytic action on the photo-oxidation.

9) T. Hayashi, *Chemistry and Industry (Kagaku to Kogyo)*, 14, 225 (1960).

10) The mechanism of the luminescence of the peroxide has not yet been ascertained.

Chemiluminescence of 2, 3, 4, 5-Tetraphenylpyrrole

By Taro HAYASHI and Koko MAEDA

(Received October 13, 1962)

We have been studying[1] the mechanism of the chemiluminescence of 2, 4, 5-triphenylimidazole (lophine) and have already proposed a mechanism involving free radical and peroxide[2]. Recently an investigation of the electron spin resonance of the free radical 2, 3, 4, 5-tetraphenylpyrryl, a solution of which was prepared by oxidation of tetraphenylpyrrole, was reported[3].

Lophine and tetraphenylpyrrole resemble each other in several aspects. They are both nitrogen-containing, unsaturated, five-membered heterocyclic compounds in which each of the carbon atoms of the ring combines with a phenyl group; and they both produce a free

1) T. Hayashi and K. Maeda, This Bulletin, **33**, 566 (1960) : T. Hayashi, K. Maeda, S. Shida and K. Nakada, *J. Chem. Phys*, **32**, 1568 (1960).

2) T. Hayashi, *Chemistry and Industry* (*Kagaku to Kogyo*), **14**, 225 (1960); T. Hayashi and K. Maeda, This Bulletin, **35**, 2057 (1962).

3) S. M. Blinder. M. L. Peller, N. W. Lord, L. L. Aamodt and N. S. Ivanchukov, *J. Chem. Phys.*, **36**, 540 (1962).

radical by oxidation, which reacts with molecular oxygen to produce a peroxide. Tetraphenylpyrrole was therefore expected to exhibit chemiluminescence on oxidation as lophine does. As expected, a solution of tetraphenylpyrrole (0.1 g.) in 20 cc. of 2 N ethanolic solution of potassium hydroxide produced a weak greenish blue luminescence[4] at about 60°C upon addition of 3% aqueous hydrogen peroxide solution followed by 2% aqueous potassium ferricyanide solution, or 2% aqueous potassium ferricyanide solution only, or 2% ethanolic solution of bromine. When dissolved oxygen in the solutions in the latter two cases was removed by a stream of nitrogen, no luminescence was shown, and when oxygen was passed into the reaction mixture, a luminescence appeared immediately. Therefore it seems probable that molecular oxygen is necessary for the luminescence of tetraphenylpyrrole.

By oxidation of the benzene solution of tetraphenylpyrrole containing 2 N ethanolic potassium hydroxide with 2% aqueous solution of potassium ferricyanide in nitrogen, a pink benzene solution was obtained containing the free radical 2, 3, 4, 5-tetraphenylpyrryl, with optical absorption maxima at 524 mμ and 563 mμ[3]. The benzene solution containing the free radical produced a weak greenish blue luminescence when 2 N ethanolic potassium hydroxide was added with a stream of oxygen at about 60°C. Thus it appears probable that the free radical tetraphenylpyrryl is the intermediate stage of the chemiluminescence process of tetraphenylpyrrole.

The pink solution of the free radical tetraphenylpyrryl in benzene reacted with molecular oxygen to turn yellow. The reaction was promoted markedly by irradiation with ultraviolet light. The yellow solution was evaporated under reduced pressure to leave a yellow solid residue which melted at about 70~80°C with evolution of gas, presumably oxygen, and proved positive in the starch test for iodine when treated with potassium iodide. Hence the yellow residue seemed sure to contain the peroxide. When 2 N ethanolic potassium hydroxide was added to the benzene solution of this yellow residue at about 60°C in the absence of oxygen, a weak greenish blue luminescence was produced. This fact shows that the peroxide of tetraphenylpyrryl produces a luminescence in ethanolic potassium hydroxide in the absence of oxygen.

Accordingly, the mechanism of the chemiluminescence of tetraphenylpyrrole appears probable that tetraphenylpyrrole in the first step produces the free radical tetraphenylpyrryl with oxidizing agent, and then the free radical produces the peroxide with molecular oxygen and the peroxide exhibits a luminescence without molecular oxygen. This free radical-peroxide mechanism is analogous to that of lophine[2,5]. It is considered that this mechanism would be general for luminescence, at least for that of nitrogen-containing unsaturated heterocyclic compounds requiring molecular oxygen, and would be involved in the mechanism of bioluminescence.

When the solution of the peroxide in ethanolic potassium hydroxide was heated at about 60°C in nitrogen atmosphere for several hours, ammonia, benzoic acid and 2, 3, 4, 4-tetraphenyl-5-oxo-2-pyrroline were detected. The mechanism of the luminescence of the peroxide has not yet been determined.

Department of Chemistry
Faculty of Science
Ochanomizu University
Bunkyo-ku, Tokyo

4) The luminescence was far weaker than that of lophine. No luminescence of tetraphenylpyrrole was observed with molecular oxygen.

5) For the chemiluminescence of 3-amino-phthalhydrazide (luminol) and 10, 10'-dimethyl-9, 9'-biacridium dinitrate (lucigenin), speculative mechanisms involving free radical and peroxide have been proposed. (T. Bremer, *Bull. soc. chim. Belg.*, 62, 569 (1953); H. Eyring et al., "The Luminescence of Biological Systems", A. A. A. S. (1955), p. 75); B. Tamamushi and H. Akiyama, *Trans. Faraday Soc.*, 35, 491 (1939).

Polarographic Determination of Lignosulfonic Acid in Sulfite Spent Liquor

By Akira HAYASHI, Hiroko YAMAJO and Yoshikazu KOJIMA

(Received October 18, 1962)

Determination of lignosulfonic acid in sulfite spent liquor is very troublesome, because in sulfite spent liquor there are many impurities which behave very similarly to lignosulfonic acid in its physical and chemical behavior.

The present communication deals with the rapid and accurate determination of lignosulfonic acid in sulfite spent liquor with polarographic method. Lignosulfonic acid does not show any d. c. polarographic waves. It was found, however, that lignosulfonic acid combines quantitatively with polarographically active methylene blue to give polarographically inactive form, leaving excess methylene blue active.

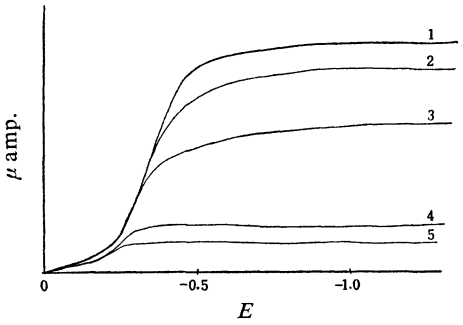


Fig. 1. Polarogram of methylene blue with lignosulfonate.
KCl : 0.5 N. Methylene blue : 0.00125 mol.
1 Lignosulfonate : 0%
2 Lignosulfonate : 0.01%
3 Lignosulfonate : 0.02%
4 Lignosulfonate : 0.05%
5 Lignosulfonate : 0.06%

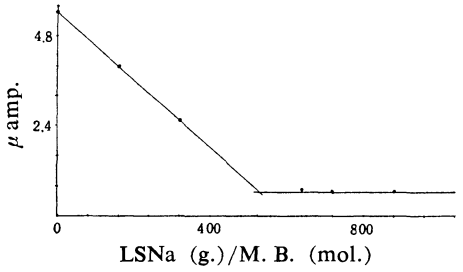


Fig. 2. The relation of wave-height to lignosulfonate concentration.
KCl : 0.5 N, Methylene blue : 0.00125 mol., Sodium lignosulfonate : 0~900 g./mol. M.B.

The polarograms of methylene blue and the combination of methylene blue and purified lignosulfonic acid are shown in Fig. 1. The wave height of methylene blue is depressed linearly by addition of lignosulfonic acid and after a certain point it becomes constant as shown in Fig. 2. This equivalent point was 530 g. of lignosulfonic acid per 1 mol. of methylene blue, being in good agreement with the sulfonic acid equivalence of lignosulfonic acid. Diluted and neutralized sulfite spent liquor, which contained 12.0% of lignosulfonic acid by β-naphthylamine method and 11.4% by methoxyl method, was analyzed by this method, and it was found that 11.6% of lignosulfonic acid was contained.

In order to simplify this method, the amperometric titration of methylene blue by sulfite spent liquor was carried out at −0.8 V. of mercury electrode potential. 11.6% of lignosulfonic acid was found again in the sulfite spent liquor.

These results show that in sulfite spent liquor only lignosulfonic acid combines quantitatively with methylene blue and is precipitated in polarographically inactive form. This method is very useful for the rapid and accurate determination of lignosulfonic acid in sulfite spent liquor.

Department of Chemistry
Faculty of Science and Engineering
Ritsumeikan University
Kita-ku, Kyoto (A. H. & H. Y.)

Marubishi Oil Co.
Miyakojima-ku, Osaka (Y. K.)